ISSN 1007-9327 (print)
ISSN 2219-2840 (online)

World Journal of *Gastroenterology*

World J Gastroenterol 2023 May 7; 29(17): 2515-2703



Published by Baishideng Publishing Group Inc

World Journal of Gastroenterology

Contents

Weekly Volume 29 Number 17 May 7, 2023

REVIEW

2515 Novel biomarkers for early detection of gastric cancer

Matsuoka T, Yashiro M

2534 Non-invasive evaluation of liver steatosis with imaging modalities: New techniques and applications

Zeng KY, Bao WYG, Wang YH, Liao M, Yang J, Huang JY, Lu Q

2551 Alcohol-related hepatitis: A review article

Chaudhry H, Sohal A, Iqbal H, Roytman M

2571 Current and novel approaches in the pharmacological treatment of hepatocellular carcinoma

Villarruel-Melquiades F, Mendoza-Garrido ME, García-Cuellar CM, Sánchez-Pérez Y, Pérez-Carreón JI, Camacho J

MINIREVIEWS

2600 Difficult colorectal polypectomy: Technical tips and recent advances

Pattarajierapan S, Takamaru H, Khomvilai S

ORIGINAL ARTICLE

Basic Study

2616 Cryptotanshinone induces apoptosis of activated hepatic stellate cells *via* modulating endoplasmic reticulum stress

Hou XX, Li YW, Song JL, Zhang W, Liu R, Yuan H, Feng TT, Jiang ZY, Li WT, Zhu CL

2628 *Lafoensia pacari* alleviates intestinal damage by modulating cyclooxygenase-2: *In silico* and *in vivo* evaluation in a colitis model

Peiter GC, Moesch Queiroz TK, Michalkiewicz Jr EL, Chappuis RH, Luz JS, Casagrande Piovezani LH, Ferreira Silva C, Nozomi Tsutumi M, Fernandes Chaves A, Luiz RM, Façanha Wendel C, Zarpelon-Schutz AC, Teixeira KN

2642 Establishment and characterization of a new human ampullary carcinoma cell line, DPC-X1

Xu H, Chai CP, Miao X, Tang H, Hu JJ, Zhang H, Zhou WC

Retrospective Study

2657 Mucosal patterns change after *Helicobacter pylori* eradication: Evaluation using blue laser imaging in patients with atrophic gastritis

Nishikawa Y, Ikeda Y, Murakami H, Hori SI, Yoshimatsu M, Nishikawa N

Randomized Controlled Trial

2666 Fecal microbiota transplantation for the maintenance of remission in patients with ulcerative colitis: A randomized controlled trial

Lahtinen P, Jalanka J, Mattila E, Tillonen J, Bergman P, Satokari R, Arkkila P

SYSTEMATIC REVIEWS

2679 Different types of fruit intake and colorectal cancer risk: A meta-analysis of observational studies

Wu ZY, Chen JL, Li H, Su K, Han YW

LETTER TO THE EDITOR

2701 T cells in pancreatic cancer stroma: Tryptophan metabolism plays an important role in immunoregulation

Yang T, Li QQ, Liu YM, Yang B

World Journal of Gastroenterology

Weekly Volume 29 Number 17 May 7, 2023

Contents

ABOUT COVER

Editorial Board Member of *World Journal of Gastroenterology*, Mohamad Amin Pourhoseingholi, PhD, Associate Professor, Gastroenterology and Liver Diseases Research Center, Research Institute for Gastroenterology and Liver Diseases, Shahid Beheshti University of Medical Sciences, Tehran 19835, Iran. aminphg@gmail.com

AIMS AND SCOPE

The primary aim of *World Journal of Gastroenterology* (*WJG*, *World J Gastroenterol*) is to provide scholars and readers from various fields of gastroenterology and hepatology with a platform to publish high-quality basic and clinical research articles and communicate their research findings online. *WJG* mainly publishes articles reporting research results and findings obtained in the field of gastroenterology and hepatology and covering a wide range of topics including gastroenterology, hepatology, gastrointestinal endoscopy, gastrointestinal surgery, gastrointestinal oncology, and pediatric gastroenterology.

INDEXING/ABSTRACTING

The *WJG* is now abstracted and indexed in Science Citation Index Expanded (SCIE, also known as SciSearch®), Current Contents/Clinical Medicine, Journal Citation Reports, Index Medicus, MEDLINE, PubMed, PubMed Central, Scopus, Reference Citation Analysis, China National Knowledge Infrastructure, China Science and Technology Journal Database, and Superstar Journals Database. The 2022 edition of Journal Citation Reports® cites the 2021 impact factor (IF) for *WJG* as 5.374; IF without journal self cites: 5.187; 5-year IF: 5.715; Journal Citation Indicator: 0.84; Ranking: 31 among 93 journals in gastroenterology and hepatology; and Quartile category: Q2. The *WJG*'s CiteScore for 2021 is 8.1 and Scopus CiteScore rank 2021: Gastroenterology is 18/149.

RESPONSIBLE EDITORS FOR THIS ISSUE

Production Editor: *Ying-Yi Yuan*; **Production Department Director:** *Xu Guo*; **Editorial Office Director:** *Jia-Ru Fan*.

NAME OF JOURNAL
World Journal of Gastroenterology

ISSN
ISSN 1007-9327 (print) ISSN 2219-2840 (online)

LAUNCH DATE
October 1, 1995

FREQUENCY
Weekly

EDITORS-IN-CHIEF
Andrzej S Tarnawski

EDITORIAL BOARD MEMBERS
http://www.wjgnet.com/1007-9327/editorialboard.htm

PUBLICATION DATE
May 7, 2023

COPYRIGHT
© 2023 Baishideng Publishing Group Inc

INSTRUCTIONS TO AUTHORS
https://www.wjgnet.com/bpg/gerinfo/204

GUIDELINES FOR ETHICS DOCUMENTS
https://www.wjgnet.com/bpg/GerInfo/287

GUIDELINES FOR NON-NATIVE SPEAKERS OF ENGLISH
https://www.wjgnet.com/bpg/gerinfo/240

PUBLICATION ETHICS
https://www.wjgnet.com/bpg/GerInfo/288

PUBLICATION MISCONDUCT
https://www.wjgnet.com/bpg/gerinfo/208

ARTICLE PROCESSING CHARGE
https://www.wjgnet.com/bpg/gerinfo/242

STEPS FOR SUBMITTING MANUSCRIPTS
https://www.wjgnet.com/bpg/GerInfo/239

ONLINE SUBMISSION
https://www.f6publishing.com

© 2023 Baishideng Publishing Group Inc. All rights reserved. 7041 Koll Center Parkway, Suite 160, Pleasanton, CA 94566, USA
E-mail: bpgoffice@wjgnet.com https://www.wjgnet.com

World Journal of Gastroenterology

Submit a Manuscript: https://www.f6publishing.com

World J Gastroenterol 2023 May 7; 29(17): 2515-2533

DOI: 10.3748/wjg.v29.i17.2515

ISSN 1007-9327 (print) ISSN 2219-2840 (online)

REVIEW

Novel biomarkers for early detection of gastric cancer

Tasuku Matsuoka, Masakazu Yashiro

Specialty type: Gastroenterology and hepatology

Provenance and peer review: Invited article; Externally peer reviewed.

Peer-review model: Single blind

Peer-review report's scientific quality classification

Grade A (Excellent): 0
Grade B (Very good): B, B
Grade C (Good): C, C
Grade D (Fair): 0
Grade E (Poor): 0

P-Reviewer: Chen X, China; Li DH, China; Zhang Y, China; Zhao Q, China

Received: November 19, 2022
Peer-review started: November 19, 2022
First decision: January 2, 2023
Revised: January 31, 2023
Accepted: April 13, 2023
Article in press: April 13, 2023
Published online: May 7, 2023

Tasuku Matsuoka, Masakazu Yashiro, Molecular Oncology and Therapeutics, Osaka Metropolitan University Graduate School of Medicine, Osaka 5458585, Japan

Corresponding author: Masakazu Yashiro, MD, PhD, Assistant Professor, Molecular Oncology and Therapeutics, Osaka Metropolitan University Graduate School of Medicine, 1-4-3 Asahi-machi, Abeno-ku, Osaka 5458585, Japan. i21496f@omu.ac.jp

Abstract

Gastric cancer (GC) remains a leading cause of cancer-related death worldwide. Less than half of GC cases are diagnosed at an advanced stage due to its lack of early symptoms. GC is a heterogeneous disease associated with a number of genetic and somatic mutations. Early detection and effective monitoring of tumor progression are essential for reducing GC disease burden and mortality. The current widespread use of semi-invasive endoscopic methods and radiologic approaches has increased the number of treatable cancers: However, these approaches are invasive, costly, and time-consuming. Thus, novel molecular noninvasive tests that detect GC alterations seem to be more sensitive and specific compared to the current methods. Recent technological advances have enabled the detection of blood-based biomarkers that could be used as diagnostic indicators and for monitoring postsurgical minimal residual disease. These biomarkers include circulating DNA, RNA, extracellular vesicles, and proteins, and their clinical applications are currently being investigated. The identification of ideal diagnostic markers for GC that have high sensitivity and specificity would improve survival rates and contribute to the advancement of precision medicine. This review provides an overview of current topics regarding the novel, recently developed diagnostic markers for GC.

Key Words: Gastric cancer; Diagnostic biomarkers; Early detection; Liquid biopsy

©The Author(s) 2023. Published by Baishideng Publishing Group Inc. All rights reserved.

Core Tip: Gastric cancer (GC) is a major unsolved clinical problem. It is the fifth most diagnosed cancer in the world, and the fourth most frequent cause of cancer-related deaths worldwide. The outcome of advanced GC remains tremendously poor despite the use of surgery and adjuvant therapy. Therefore, the detection new biomarkers for early diagnosis will be potential therapeutic strategies for improving survival of GC patients. The aim of this review is to summarizes the current status and approaches for novel biomarkers, which could be useful for early diagnosis.

Citation: Matsuoka T, Yashiro M. Novel biomarkers for early detection of gastric cancer. *World J Gastroenterol* 2023; 29(17): 2515-2533
URL: https://www.wjgnet.com/1007-9327/full/v29/i17/2515.htm
DOI: https://dx.doi.org/10.3748/wjg.v29.i17.2515

INTRODUCTION

Gastric cancer (GC) is the fifth most common cancer and the fourth most common cause of cancer-related death worldwide[1]. The overall survival rate of individuals with GC remains poor, because it is often diagnosed at an advanced stage or even as metastasis. One strategy for lowering the burden of GC is early screening and diagnosis. Even though upper gastrointestinal endoscopy has been well established as the standard for GC screening, capturing a concealed tumor in the stomach requires higher sensitivity and specificity. Upper gastrointestinal endoscopies also involve high costs with regard to cost and human resources, requiring experienced endoscopists and patient understanding.

To achieve large-scale GC screening among healthy individuals in the future, a more general and cost-effective approach is needed. Cancer biomarkers (tumor markers) are molecules indicative of the presence and progression of cancer; as such, they play a crucial role in cancer diagnoses and treatment selection[2]. Their applications are rapidly expanding owning to advances in genetic analysis technology and molecular targeting. There are at present no biomarkers with sufficient sensitivity and specificity for the diagnosis of GC that could be applied in clinical settings. Biomarkers are needed for every stage of GC to improve its clinical course. The emergence of liquid biopsy technology, which enables the detection of specific molecular information of solid tumors from body fluids, has provided major changes in cancer diagnosis and treatment[3]. There are many studies on biomarkers for GC screening. However, many of these candidate biomarkers identified thus far are preferentially expressed at advanced stages, and thus unsuitable for early detection. Moreover, a comprehensive review focusing on early detection of GC is still lacking. Herein, we review novel candidates of biomarkers focusing on early detection of GC comprehensively, from the laboratory to the clinical prevalence and the future prospects. This information will contribute to further research on GC biomarkers and their clinical applications.

METHODS

A non-systematic review was performed based on an electronic search through the medical literature using PubMed and Google Scholar. The keywords "biomarker", "gastric cancer", "early detection", "diagnostics", "liquid biopsy" were used. Review articles and guidelines investigating the values of biomarker for early detection of GC from gastroenterology, oncology and genetics were included in this review. When more than one guideline concerning the same subject was available, the most up-to-date one was selected. Only full articles in the English language published in the last ten years were considered for further review. Great importance was also given to "Clinical study" and "Review" articles dealing with the topic. The exclusion criteria comprised duplicated articles, studies absent of diagnostic outcomes. Case reports, correspondences, letters, and non-human research were not included.

LIQUID BIOPSY

Various diverse molecules in blood (serum/plasma) have been said to be correlated with GC carcinogenesis. Among them, DNA, proteins, and noncoding RNA (ncRNA) molecules have been focused. These molecules allow the dependable finding of new noninvasive biomarkers for GC in plasma/serum. Liquid biopsy has shown good potential in detecting circulating tumor cells (CTCs) from any bodily fluid, including peripheral blood, urine and cerebrospinal fluid, ascites, pleural effusion, *etc*., and includes a genomic, proteomic and metabolite assessment. It is a quick, easy and inexpensive method

with minimal invasiveness, making it widely accepted by patients, without major side effects[4]. Liquid biopsy (using mainly peripheral blood) can be used as a screening method to detect early GC (EGC) and minimal residual disease (MRD) after surgery and can create an appropriate treatment plan in GC patients.

CTCs/circulating tumor DNA

CTCs defined as tumor cells that have been detached from the primary tumor or metastases and shed in patient's bloodstream, characterize an easily attainable sample of cancer specimens. As a liquid biopsy, emerging technologies for CTC isolation have enabled the research on the pathology of CTCs and have prompted the clinical uses of CTCs in the diagnosis of malignancies[5]. Although many researchers have come to the same conclusion that CTCs positivity was associated with prognosis, few researches were found for the early diagnosis, especially in the last several years.

Circulating cell-free DNA (cfDNA) consists of fragments of extracellular DNA that can be found in the blood[6]. cfDNA changes across different pathological states have been successfully exploited as noninvasive biomarkers for liquid biopsies. Particularly, the cfDNA that is identified from tumors and shows tumor-specific mutations is named circulating tumor DNA (ctDNA)[7]. The analysis of ctDNA has been predominantly of interest over a decade as its remarkable stability in body fluids. Besides, accumulating evidences showed that ctDNA is useful for early incidence during disease progress after surgical procedure. Further improvement of the ctDNA detection system is progressing. The cfDNA-based liquid biopsy for early diagnosis is mostly restrained by the low signals shed from early-stage cancer, which directly influence the sensitivity of sequencing analyses.

Recent paper has described that the circulating biomarkers, such as cfDNA was highly expressed in stage I GC patients compared with those in benign gastric disease patients and health controls, suggesting the potential for their use for the early detection of GC[8,9]. The human epidermal growth factor receptor 2 (HER2) gene copy number detected in ctDNA was higher in GC patients compared to healthy control. Elucidation of HER2 copy number variation could distinguish healthy individuals and patients with GCs with 58% sensitivity and 98% specificity [area under curve (AUC) = 0.707, 95% confidence interval (CI): 0.593-0.821][10]. ctDNA sequencing identifies fibroblast growth factor receptor 2 (FGFR2) amplification missed by tissue testing in patients with advanced GC, and these patients may respond to FGFR inhibition. ctDNA can detect plasma *FGFR2* alterations, occasionally at a higher frequency than tissue testing, identify patients and these patients may respond to FGFR inhibition[11].

Current cancer biomarkers can be categorized into two groups: (1) Biomarkers generally used for the detection of specific cancer types; and (2) Biomarkers to be aimed to decide personalized medicine, such as companion diagnostics. Even when surgical procedure is successfully carried out, detecting MRD after surgery is still challenging for doctors, and it is difficult to detect MRD in time using radiologic imaging or tissue biopsy. Recent studies presented that ctDNA-based testing were able to detect MRD several weeks earlier than imaging[12]. Another study monitoring ctDNA in postoperative blood has verified that, the median duration from positive ctDNA detection to relapse was 4.05 mo[13]. Moreover, the postoperative positive ctDNA was significantly correlated with tumor recurrence within 12 mo after surgery, suggesting that postoperative ctDNA monitoring possess clinical application value in the prediction of postoperative GC recurrence[13]. In a similar, ctDNA positivity preceded radiographic recurrence by a median of 6 mo, suggesting that, ctDNA is a sensitive and specific biomarker for finding patients at high risk for relapse after curative treatment[14]. ctDNA-positive patients were at higher risk of relapse and exhibited worse outcome compared to the ctDNA-negative group, implying that ctDNA monitoring in the post-treatment setting is predicted to offer knowledge about necessity for further therapy[15]. The clinical usefulness of ctDNA as biomarker for longitudinal disease monitoring and identification of MRD in GC was assessed by ultra-deep sequencing methods. The occurrence of relapse was 100% (7 of 7), 100% (5 of 5), and 94% (16 of 17), respectively in patients with measurable ctDNA at the post-operative, post-adjuvant chemotherapy, and consequent longitudinal time spots. To date, novel high throughput sequencing techniques such as next-generation sequencing (NGS) or whole exosome sequence can identify mutations in multiple genetic regions[16]. Recent study conducted surveillance for recurrent disease after curative surgical resection analyzed by whole genome sequence. For 1630 patients with GC and esophageal adenocarcinomas, detection of MRD after successful surgical procedure is intensely correlated with an enhanced risk of relapse by utilizing a Guardant 360, ctDNA-NGS assay[17]. These studies elucidate that risk stratification of patients for adjuvant chemotherapy escalation/de-escalation could be predicted by incorporation of ctDNA. ctDNA-guided treatment strategy in post-surgery surveillance for patients with GC is a novel emerging strategy that will likely replace the current treatment decision, as outlined in Figure 1.

NC RNA

Diverse ncRNAs, such as microRNA (miRNA), circular RNA (circRNA), and long ncRNA (lncRNA), are implicated in GC carcinogenesis[18]. MiRNAs are small ncRNA molecules of approximately 18-22 nucleotides that regulate cell differentiation, proliferation, apoptosis and gene regulation[19]. Currently, due to the stability and specificity of expression in circulation, accumulating evidences suggest that miRNAs can serve as novel biomarkers with a prospective clinical significance tool for patient with GC. MiRNAs are very stable in blood and can be identified by various assays such as reverse transcription

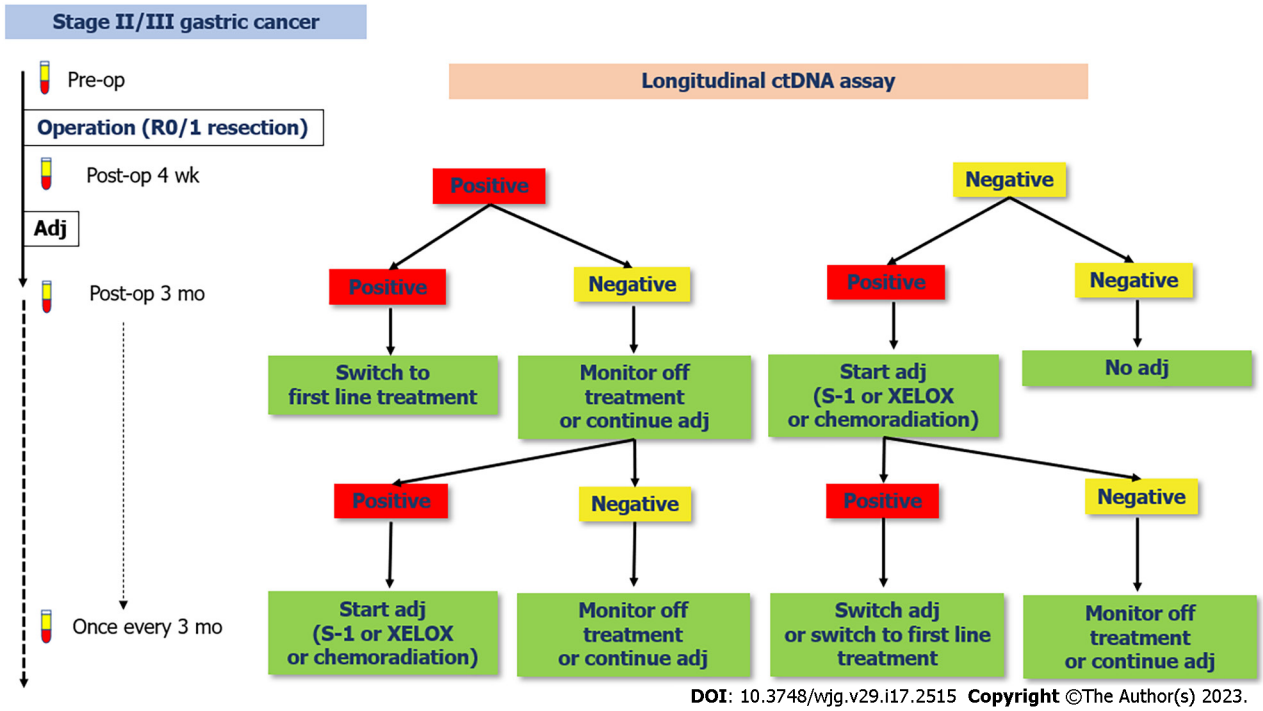


Figure 1 Proposed design of circulating tumor DNA-guided treatment strategy in gastric cancer. Schematic presentation of proposed circulating tumor DNA (ctDNA) guided treatment strategy in gastric cancer evaluating tailored treatment based on ctDNA detection. ctDNA positivity was determined by accessing the presence of plasma mutations, which indicates the existence of minimal residual disease. Adapted from Chakrabarti *et al*[100], and Kasi *et al*[101]. ctDNA: Circulating tumor DNA; Op: Operative; Adj: Ajuvant chemotherapy.

quantitative real-time polymerase chain reaction, and NGS. Recent studies challenged to verify the importance of various miRNAs in human plasma/serum as diagnostic markers for early-stage GC, including miR-17, miR-25, and miR-133b[20], miR-425-5p, miR-1180-3p, miR-122-5p, miR-24-3p, and miR-4632-5p[21]. A recent distinctive expression study of miRNA profiles utilizing two datasets from plasma samples identified hsa-miR-320a, hsa-miR-1260b, and hsa-miR-6515.5p as potential biomarkers for primary diagnosis of GC, with an AUC higher than 0.95 in all cases. Furthermore, hsa-miR-320a and hsa-miR-1260b was more stable in all the discovery and validation datasets[22]. Similarly, a recent study developed an EGC index to differentiate EGC from non-cancer controls based on the serum levels of four miRNAs (miR-4257, miR-6785-5p, miR-187-5p, and miR-5739). This index provided a sensitivity of 0.996 and a specificity of 0.953, with an AUC of 0.998 for the detection of EGC in a large sample size study (n = 1417)[23]. These results suggest that miRNAs could act as promising biomarkers for the early detection of GC. Nevertheless, further research is needed to optimize their detection methods and reproducibility of accrued results to meet the rigorous requirements for clinical setting.

LncRNAs are the transcripts of more than 200 nucleotides that have been found to participate widely in various pathological processes of organisms[24]. In colon cancer, LncRNA small nucleolar RNA host gene 11 has been presented as a promising biomarker for early detection of this malignancy[25]. Meanwhile, hepatocellular carcinoma upregulated lncRNA and ZNFX1 antisense RNA 1 have been shown to distinguish GC patients from healthy subjects and proposed as novel diagnostic biomarkers of GC[26]. LncRNAs promoter of CDKN1A antisense DNA damage activated RNA, FOXD2 adjacent opposite strand RNA 1, and SWI/SN F related, matrix associated, actin dependent regulator of chromatin subfamily c member 2 in plasma may serve as novel biomarkers for early detection of GC. The combined these three lncRNAs offer a high sufficient diagnostic sensitivity[27]. LncRNA B3GALT5 antisense RNA 1 was shown to be better than carcinoembryonic antigen (CEA) and carbohydrate antigen 19-9 (CA19-9) and may serve as a diagnostic biomarker of GC[28]. Distinct levels of serum C5orf66 antisense RNA 1 (C5orf66-AS1) were shown between patients with GC and gastritis. A risk of gastric dysplasia and GC negatively associated with serum expression of C5orf66-AS1, implying that C5orf66-AS1 a potential biomarker for predicting EGC[29]. Combined lncRNAs have been displayed to improve biomarker values for early detection of GC. LncRNA HLA Complex P5 (HCP5) is a kind of RNA gene without protein-coding. The AUC of serum lncRNA HCP5 was 0.818 (95%CI: 0.757-0.880, 80% sensitivity, and 70% specificity) in distinguishing between GC and healthy controls. Besides, the highest AUC of 0.870 (95%CI: 0.819-0.921) with 81% sensitivity and 79% specificity were revealed by the combination of three diagnoses, HCP5, CEA, and CA19-9[30]. Thus, the results above indicate that lncRNAs possess the diagnostic potential for early diagnosis of GC.

CircRNAs are also generally categorized as a ncRNA and physically vigorous nucleic acid molecules that construct closed loop RNA and require polyadenylated tails unlike messenger RNAs[31]. CircRNAs are more stable in tissues, have a superior life period and are more resistant to Ribonuclease R compared with linear RNAs[32]. In a recent, the rapid development of high-throughput sequencing has promoted the detection of circRNAs and their roles in physiological and pathological processes, including GC carcinogenesis, have been evaluated. A recent study found circRNA Has_circ_0000745 was downregulated in GC tissues and in plasma from patients with GC. Therefore, the use of these circRNAs has great potential as a new biomarker for diagnosis of GC[33]. The expression of hsa_circ_0001789 in 24 paired of cancerous and paracancerous plasma specimens were examined. A down-regulated expression of hsa_circ_0001789 was detected in GC plasma samples in comparison to the healthy controls, indicating that hsa_circ_0001789 has the potential to be a novel GC diagnostic biomarker[34]. CircPTPN22 is an outstanding diagnostic marker for GC. Utilizing receiver operator characteristic (ROC) analysis of circPTPN22 expression in GC patients, gastritis patients, and healthy controls, showed that its AUC was higher than that of traditional tumor markers CEA and CA19-9, and the AUC reached 0.892 after combined use[35]. 8-circRNA biomarker panel (hsa_circ_0001013, hsa_circ_0052001, hsa_circ_0034398, circ_0006089, hsa_circ_0002019, hsa_circ_0007380, hsa_circ_0008768, hsa_circ_0045602) discriminated patients with GC from normal control tissues, with an AUC value of 0.87 (95%CI: 0.82-0.93, sensitivity 78.3%, specificity 78.3%). Interestingly, 7 of 8 circRNA markers significantly lower expressed in serum specimens after surgery. Furthermore, 8-circRNA panel showed a greater specificity for the identification of patients with GC *vs* all other gastrointestinal cancers, such as colorectal cancer, pancreatic cancer, esophageal cancer, and hepatocellular carcinoma[36]. Studies using ncRNAs in screening/diagnostics of GC in the past 5 years are collected in Table 1.

Exosome

Exosomes are lipid bilayer-enclosed extracellular vehicles (EVs) approximately 30-150 nm in size, consist of a lipid bilayer interspersed with various membrane proteins, and which contain a variety of nucleic acids, proteins, and lipids[37]. Exosomes are secreted continuously by all cells and offer distinct prospects for clinically relevant diagnostic content, including DNA, RNA, and proteins[37]. Exosomes have been said to be associated with driving key features of cancer activity, including facilitation of tumor cell proliferation, suppression of the immune response, stimulation of tumor cell migration, initiation of angiogenesis, and formation of metastases[38]. Recently, growing evidences have established the latent diagnostic value of EVs or circulating exosomes for early diagnosis of GC. Due to the easiness to isolate exosomes compared with CTCs and cfDNA in malignant tumors, an growing number of studies will be highlighted on exosomes in the diagnosis of EGC in the next several decades. Exosomal lncUEGC1 exhibited an AUC of 0.8760 and 0.8406 in distinguishing EGC patients from normal subjects and those with atrophic gastritis, respectively, implying that exosomal lncUEGC1 had higher diagnostic reliability compared with CEA[39]. Circulating exosomal lncRNA proprotein convertase subtilisin/kexin type 2-2:1, G protein subunit alpha q-6:1 and GC-associated lncRNA1 (lncRNA-GC1) have been reported as better biomarkers for distinguishing GC patients from healthy people, compared with CEA, CA19-9, and CA72-4[40-42]. Similarly, serum four exosoms, miR-92b-3p, miR-146b-5p, miR-9-5p, and miR-let-7g-5p have been shown to be latent biomarkers for early detection of GC[43]. Likewise, the ROC showed that serum exosomal miR-590-5p showed a good classifier with an AUC of 0.810 (95%CI: 0.751-0.860) with a sensitivity of 63.7% and specificity of 86.0%, suggesting that serum exosomal miR-590-5p expression may be a noninvasive diagnostic biomarker of GC[44]. MiR-195-5p and miR-211-5p in GC patients' plasma exosomes have shown to be upregulated compared to healthy controls. The AUC values of plasma exosomal 2-miRNAs signature was 0.820, which was more meaningful to discriminate the GC patients from the healthy samples, compared to the AUC values obtained for combined CEA, CA19-9[45]. circ_0065149 levels in plasma exosomes from EGC patients were significantly lower than those from healthy individuals. Thus, circ_0065149 revealed distinguished diagnostic accuracy, with an AUC of 0.64, sensitivity of 48.7%, and specificity of 90.2%[46]. Piwi-interacting RNAs (piRNAs) are another class of small ncRNAs that are 26-31 nucleotides in length, and quite comparable in size to miRNAs. PiRNAs are distinctly different from miRNA counterparts because they lack the sequence conservation present in miRNAs. As a source for liquid biopsy, piRNAs have similar properties to miRNAs and stabile in the blood flow and resistant to ribonuclease mediated degradation. Therefore, piRNAs can be used as effective biomarkers for the early detection of GC. Serum exosomal piR-019308, piR-004918 and piR-018569 can be utilized for the diagnosis of GC with the AUC value of 0.820, 0.754 and 0.732, respectively. Diagnostic value of these piRNAs were much better than that of CEA, CA19-9 and alpha-fetoprotein[47]. Collectively, circulating exosome has clinical potentials in the early diagnosis of GC, which may lead to the identification of cancer subtypes. Exosome investigated as potential diagnostic GC markers are listed in Table 2.

Collectively, this section highlights the developments in the ncRNAs as a source for the development of non-invasive diagnostic biomarkers for GC patients. NcRNAs appear to have a crucial potential to be implemented into biomarker development for early detection of GC. On the other hand, a variety of circulating biomarkers have been reported in different research team. The clinical value of all these factors is not still defined. Some discrepancies among different studies can be caused by the hetero-

Table 1 Overview of non-coding RNAs for early detection of GC in the past 5 years

Circulating biomarkers	Alterations	Patients	Controls (normal)	Sample	Methods	Sensitivity (%)	Specificity (%)	AUC	Ref.
miRNA									
miR-25	Upregulated	65	65	Plasma	qRT-PCR	87.6	76.9	0.817	[102]
miR-214	Downregulated	168	74	Plasma	qRT-PCR	73.2	91.9	0.880	[103]
miR-376c	Upregulated	47	67	Plasma	qRT-PCR	71.0	78.0	0.77	[104]
miR-381	Downregulated	40	40	Serum	qRT-PCR	83.6	97.5	0.931	[105]
miR-200c	Upregulated	200	250	Tissue and blood	Micoarrayand qRT-PCR	74.0	66.0	0.75	[106]
miR-551b-5p	Downregulated	40	40	Serum	qRT-PCR	77.5	80.0	0.84	[107]
Combination of miR-21, miR-93, miR-106a, and miR-196b	Upregulated	11	17	Plasma	qRT-PCR	84.8	79.2	0.887	[108]
Combination of miR-16, miR-25, miR-92a, miR-451 and miR-486-5p	Upregulated	40	40	Plasma	qRT-PCR	72.9	89.2	0.812	[109]
Combination of miR-4257, miR-6785-5p, miR-187-5p and miR-5739	Upregulated	1417	1417	Serum	microarray analysis	0.996 (index)	0.953 (index)	0998	[23]
Combination of miR-18a, miR-181b, and miR-335	Upregulated	176	173	Serum	qRT-PCR	71.6	87.9	0.86	[95]
Combination of miR-425-5p, miR-1180-3p. miR-122-5p, miR-24-3p and miR-4632-5p	Downregulated	30	90	Plasma	qRT-PCR	NA	NA	0829	[21]
Combination of miRNA-3185, miRNA-6083, miRNA-6792-3p, and miRNA-659-3p	Upregulated	52	30	Plasma	qRT-PCR	NA	NA	0.825	[110]
Combination of miRNA-936, miRNA-1306-3p	Downregulated	52	30	Plasma	qRT-PCR	NA	NA	0.730	[110]
Long non-coding RNAs									
ZNFX1-AS1	Upregulated	50	50	Plasma	qRT-PCR	84	68	0.85	[26]
LINC00978	Upregulated	38	31	Serum	qRT-PCR	80	70	0.831	[111]
CTC-501O10.1	Upregulated	100	100	Plasma	qRT-PCR	90	51	0.74	[112]
AC100830.4	Upregulated	100	100	Plasma	qRT-PCR	84	58	0.73	[112]
RP11-210K20.5	Upregulated	100	100	Plasma	qRT-PCR	89	55	0.737	[112]
CTC-497E21.4	Upregulated	110	84	Serum	qRT-PCR	81.8	75.0	0.896	[113]
SNHG17	Upregulated	67	67	Plasma	qRT-PCR	NA	NA	0.748	[114]
ARHGAP27P1	Downregulated	53	53	Plasma	qRT-PCR	75,5	60.4	0.732	[115]
PANDAR	Upregulated	109	106	Plasma	qRT-PCR	NA	NA	0.767	[27]
FOXD2-AS1	Upregulated	109	106	Plasma	qRT-PCR	NA	NA	0.700	[27]
SMARCC2	Upregulated	109	106	Plasma	qRT-PCR	NA	NA	0.748	[27]
LINC00086	Downregulated	168	74	Plasma	qRT-PCR	72.6	83.8	0.86	[103]
B3GALT5-AS1	Upregulated	107	87	Serum	qRT-PCR	87.4	74.7	0.816	[28]
C5orF66-AS1	Downregulated	200	278	Serum	qRT-PCR	77.5	53.6	0.668	[29]

HCP5	Upregulated	98	82	Serum	qRT-PCR	80	70	0.818	[30]
Combined of lnc-MB21D1-3:5, lnc-PSCA-4:2 and lnc-ABCC5-2:1	Upregulated	52	30	Plasma	qRT-PCR	NA	NA	0904	[110]
circular RNAs									
has_circ_0000745	Downregulated	60	60	Plasma	qRT-PCR	85.5	45,0	0.683	[33]
circPTPN22	Upregulated	120	104	Plasma	qRT-PCR	78.0	84.0	0.857	[35]
hsa_circ_0001789	Downregulated	24	24	Plasma	qRT-PCR	84.0	50.0	0.82	[34]
8-circRNA biomarker panel	Upregulated	92	46	Serum	qRT-PCR	78.3	78.3	0.87	[36]

miRNA: Micro RNA; qRT-PCR: Quantitative reverse transcriptase polymerase chain reaction; AUC: Area under curve; HCP5: HLA Complex P5; lncRNA: Long non-coding RNA; circ RNA: Circular RNA; NA: Not applicable; ZNFX1-AS1: ZNFX1 antisense RNA 1; PANDAR: Promoter of CDKN1A antisense DNA damage activated RNA; FOXD2-AS1: FOXD2 adjacent opposite strand RNA 1; SMARCC2: SWI/SN F related, matrix associated, actin dependent regulator of chromatin subfamily c member 2; B3GALT5-AS1: B3GALT5 antisense RNA 1; C5orf66-AS1: C5orf66 antisense RNA 1.

Table 2 Overview of exosome associated with early detection of gastric cancer

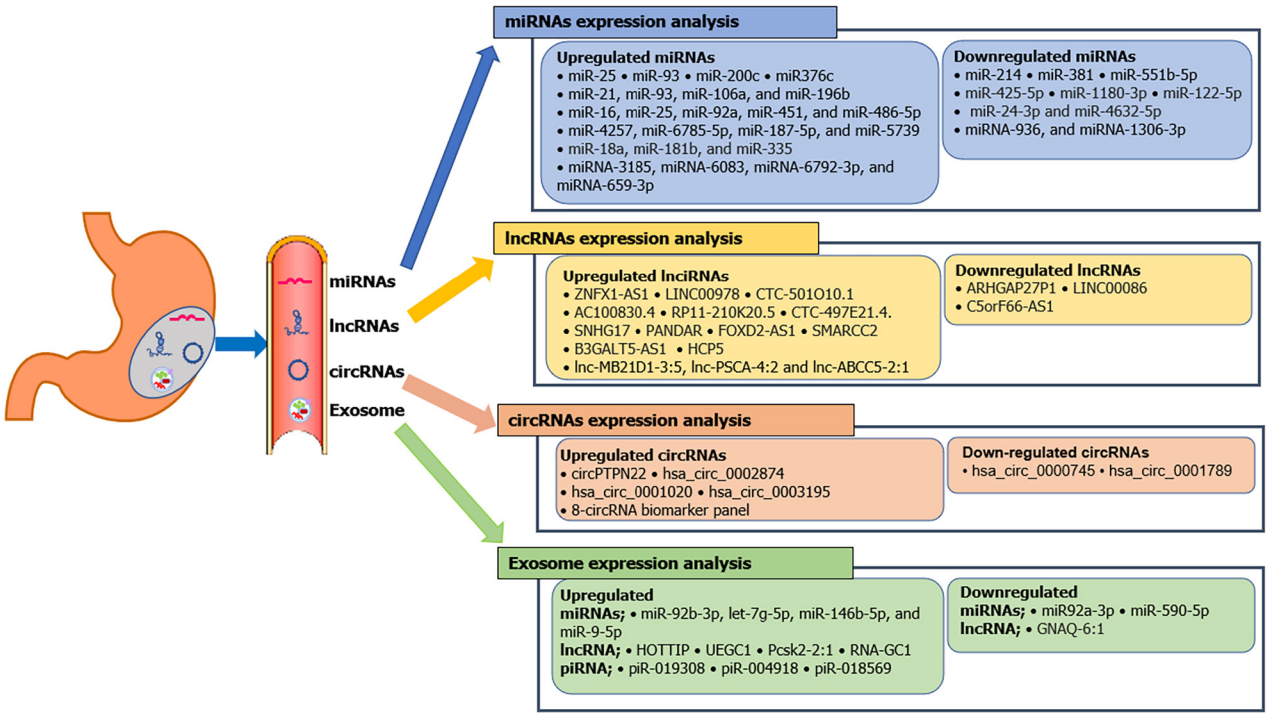
Marker	Alterations	Patients	Controls (normal)	Sample	Methods	Sensitivity (%)	Specificity (%)	AUC	Ref.
miRNA									
miR-590-5p	Downregulated	168	50	Serum	qRT-PCR	63.7	86.0	0.810	[44]
miR-92a-3p	Downregulated	131	122	Serum	qRT-PCR	NA	NA	0.829	[116]
Combination of miR-92b-3p, let-7g-5p, miR-146b-5p, and miR-9-5p	Upregulated	36	12	Serum	qRT-PCR	60	84	0.773	[43]
LncRNA									
HOTTIP	Upregulated	126	120	Serum	qRT-PCR	69.8	85.0	0.827	[117]
UEGC1	Upregulated	51	60	Plasma	qRT-PCR	NA	NA	0.876	[39]
Pcsk2-2:1	Upregulated	63	29	Serum	qRT-PCR	84	86.5	0.896	[40]
GNAQ-6:1	Downregulated	43	27	Serum	qRT-PCR	83.7	55.6	0.736	[41]
RNA-GC1	Upregulated	522	219	Serum	qRT-PCR	88.2	82.3	0.90	[42]
piRNAs									
piR-019308	Upregulated	70	60	Serum	qRT-PCR	57.14	91.67	0.820	[47]
piR-004918	Upregulated	70	60	Serum	qRT-PCR	42.86	95.0	0.754	
piR-018569	Upregulated	70	60	Serum	qRT-PCR	44.29	96.67	0.732	

miRNA: MicroRNA; lncRNA: Long non-coding RNA; circRNA: Circular RNA; piRNA: Piwi-interacting RNAs; qRT-PCR: Quantitative reverse transcriptase polymerase chain reaction; NA: Not applicable; GNAQ-6:1: G protein subunit alpha q-6:1.

geneity of GC. Thus, a more precise patient inclusion criteria or enlarging of the cohort size could overcome the differences in ncRNAs expression caused by the intrinsic heterogeneity of the disease. More multicenter, greater, longer-term studies are warranted to apply liquid biopsies in clinical settings, in terms of early diagnosis of GC. We systematically summarized the ncRNAs as biomarker for early detection of GC in Figure 2.

DNA METHYLATION

DNA methylation is an epigenetic mechanism which lead to oncogenesis in GC through activation of oncogenes and silencing of tumor-suppressor genes[48]. In a recent, a variety of studies demonstrated that aberrant epigenetic regulations, such as DNA methylation, histone posttranslational modifications,



DOI: 10.3748/wjg.v29.i17.2515 **Copyright** ©The Author(s) 2023.

Figure 2 The summary of non-coding RNAs as biomarker for early detection of gastric cancer. Schematic of the non-coding RNAs composition. Liquid biopsy obtained from peripheral blood is composed of different tumoral components such as micro-RNA, long non-coding RNAs, and circular RNAs. miRNA: MicroRNA; lncRNA: Long non-coding RNA; circRNA: Circular RNA; piRNA: Piwi-interacting RNAs.

ncRNAs and chromatin remodeling, have a pivotal influence on the pathogenesis of GC. DNA methylation is well-investigated epigenetic change among the epigenetic modifications[49]. Nowadays, the importance of aberrant DNA methylation is identified by liquid biopsy, including plasma/serum and gastric juice. Tumor suppressor genes methylation in peripheral blood has been examined most broadly. Aberrant gene methylation identified in body fluids could be a useful biomarker for the early detection of GC, likewise SEPT9 in CRC. Numerous methylated gene promoters detected in ctDNA have been proposed for GC detection as a latent diagnostic marker[50]. Among them, aberrant methylation of Reprimo, RUNX3, RASSF1A, SFRP2, PCDH10, H19, and MALAT1 show high sensitivity and specificity, suggesting that they have superiority in the early detection of GC[51-55]. A recent study elucidated the association of aberrant DNA methylation with the risk of GC. Hypermethylation of SOCS3 promoter in blood extensively facilitated GC risk[56]. Genome-wide hypomethylation commonly occurs in repeated components that are normally hypermethylated to keep genomic stability. Long interspersed nucleotide element 1, Alu repetitive elements and human endogenous retroviruses are the main components of scattered repeated sequences[57]. Although a number of studies examined the perspective of DNA methylation as a biomarker in GC, the methylation levels in those studies were mainly shown from the tissues. Thus, novel aberrantly methylated genes whose roles in GC should be investigated, especially those detected by non-invasive methods.

DNA methylation is major epigenetic changes when pathogens invade to gastric mucosa, which allows the infection to persist and promotes the development of GC[58]. *Helicobacter pylori* (*H. pylori*) is one of the most important pathogens for GC. Previous studies have demonstrated that Alu and Satα hypomethylation was significantly correlated with *H. pylori* infection in patients with GC[59]. Although numerous studies were examined to elucidate the mechanism of epigenetic changes induced by *H. pylori* infection, useful biomarker for early detection in GC is still not applied in clinical setting. Most recent report demonstrated that FGFR4 activation was interacted with signal transducer and activator of transcription 3 thorough steroid receptor coactivator in response to *H. pylori* infection, suggesting that FGFR4 could be a candidate of biomarker for early detection of GC[60].

NOVEL BIOMAKER IDENTIFIED FROM MULTI-OMICS DATA

Previous classifications of GC have quite restricted achievement in advocating the advancement of subtype-specific treatment applies due to the heterogeneity of GC and their incapacity to detect latent molecular targets. With NGS, omics technologies have offered beneficial tools to examine the molecular basis of GC. Multiple omics-based studies have been used to evaluate the biofluids of GC patients,

which resulted in numerous novel biomarkers due to rapid progress in machine learning approaches [61]. A number of mutations, gene alteration, protein abundance differences, epigenetic mutations, and metabolite concentrations which is linked to GC heterogeneity and staging, leading to improve our understanding of GC, have been successfully identified. NGS has high throughput and can screen unknown variants. A variety of methods are applying NGS to target panel, namely Tagged-Amplicon deep sequencing, Safe-Sequencing System, and Cancer Personalized Profiling by deep sequencing. The developments of NGS enable many applications in both DNA and RNA sequencing (RNA-seq), such as whole-genome, whole-exome, and targeted sequencing of DNA, and total RNA, mRNA, and small RNA [62].

Proteins contribute to determine the identity of a cell[63]. Cell function can be affected by aberrant protein expression, or altered post-translational arrangements. Proteomic signatures can afford complementary information for patient stratification to genetic signature. Besides, proteins can be a useful tool as a biomarker for malignances[63]. The development of proteomics technologies, such as mass-spectrometry (MS), has made it easier to identify protein biomarkers applied to tumor diagnosis. Liquid chromatography-MS (LC-MS) of digested proteins conducted with high-resolution instruments enable to quantitate thousands of proteins from complex biological specimens. Study using LC-MS/MS combined with TMT labeling, found that 11 proteins differentially expressed in plasma from EGC patients and healthy controls identified from the total of 2040 proteins. This model presented that the altered proteins found by plasma proteomics could provide a resource of potential biomarkers for diagnosis of EGC[64]. Isobaric tags for relative and absolute quantification (iTRAQ) are said to be the most widely used method for high-throughput protein quantification. The study using iTRAQ-labeled quantitative proteomics revealed that NAD(P)-dependent steroid dehydrogenase-like (NSDHL) and neutral cholesterol ester hydrolase 1 (NCEH1), key enzymes in cholesterol metabolism, were aberrantly expressed in patients with GC. Moreover, the combined analysis of NSDHL and NCEH1 showed high sensitivity compared with a single marker in detecting GC, indicating that NSDHL and NCEH1 may be adequate for novel biomarkers in the screening[65]. Identically, thioredoxin reductase 1 was aberrantly expressed in GC by using Itraq-labelling and/or LC-MS, supporting that these proteins are an important target for early determining and follow-up monitoring for GC[66]. Integration of phosphoproteome data with other types of omics data from young diffuse-type GC patients provided links of somatic mutations to phosphorylation changes in signaling pathways, association of mRNA-protein abundance correlations with survivals, and four subtypes of young diffuse-type GC patients characterized by genomic and proteomic signatures, which may contribute to have a deep insight into diffuse-type GCs[67]. More recent study using proteomics methods of serum based on high-resolution MS with ion mobility separation followed by multivariate statistics and network analysis presented that a 29-protein marker panel containing, integrin β6 and glutathione peroxidase, and ten serum markers specific for GC (ITIH1, FZD6, DPP10, SERPINA4, AKAP12, S100A9, POTEF, CACNB1, CRP KIAA1328), which were independent of *H. pylori* infection[68]. Multi-omic analysis characterizing the intricate relationships between the intragastric microbiome and gastric mucosal gene expression revealed higher abundances in several bacterial taxa (*Pasteurellaceae*, *Enterococcaceae*, *Helicobacteraceae*, *Gemellales* and *Neisseriaceae*) and genes (*SOCS3* and *ITM2A*) were shown in GC patients. In turn, *Lachnospiraceae* was closely associated with the expression of *Ubiquitin D*, which regulates mitosis and cell cycle time in GC [69]. Besides, lower abundances of B cell signatures in GC compared to gastritis may suggest a previously unidentified immune evasion process in gastric carcinogenesis. These results suggest that a combined analysis of microbiome and gene expression may help to devise a diagnostic kit that screens for high-risk patients of GC who require surveillance endoscopy.

STOMACH SPECIFIC BIOMARKER

The measurement of a biomarker in a gastric juice sample should be specific for early-stage GC than the same biomarker measured in plasma/serum because it is obtained directly from the area of the lesion, which would lead to avoid dilution of the biomarkers and their lack of specificity[70]. Because DNA is easily degraded due to gastric juice acidity, the main part of biomarkers identified in gastric juice are ncRNAs and some proteins. A significantly increased miR-135b-3p and miR-199a-3p, and a decreased miR-451a levels in gastric juice-derived EVs from GC patients was shown compared to non-cancer individuals[71]. LncRNAs in gastric juice and urine have also been reported as biomarkers of GC and urinary system cancer, respectively[72]. On the other hand, a recent study revealed that the levels of SNCG in gastric juice detected by enzyme-linked immunosorbent assay were significantly higher in the GC group compared with the control group[73]. Analysis using gastric juice-derived exosomal DNA samples presented that BARHL2 methylation had an area under the curve of 0.923 with 90% sensitivity and 100% specificity which suggested the feasibility of the application of BARHL2 methylation for screening for GC biomarker[74]. Although a number of studies elucidating the value of gastric juice as a biomarker for early detection of GC were carried out, the limitation is the tolerance of the patients as a usual examination due to the discomfort of gastroscopy.

Serological examinations, which are noninvasive and relatively convenient. can offer efficient indicators of gastrointestinal diseases. Markers of gastric function such as pepsinogen (PG)-I, PG-II, PG-I/PG-II ratio, gastrin 17, anti-*H. pylori* antibodies are used to cooperatively diagnose chronic atrophic gastritis (CAG)[75]. A recent meta-analysis has presented the use of serum pepsinogens revealed significant diagnostic accuracy for the early detection of gastric CAG or GC[76]. Among the various cut-off values investigation, PG rate ≤ 3 and PG-I ≤ 70 ng/mL have been proposed for CAG and GC prediction. Although there are numerous studies for evaluating PG as biomarker for early detection of GC, the potential use of pepsinogens in GC prevention is still not well-established.

DISCUSSION AND FUTURE PERSPECTIVE

Biomarkers are biological molecules implicated in the initiation and progression of cancer, and determination of their levels can clarify abnormal molecular changes in patients[77]. Morphological detection of diseased gastric epithelial cells using upper gastrointestinal endoscopy has always been the standard method for diagnosis of GC. However, the false-positive rates for endoscopic screening in the first round are said to be 14.9%. Notably, endoscopy is easily missed during screening, even when it is performed by qualified endoscopists. In this review, we describe the comprehensive and systematic search for and development of blood-based biomarkers for early detection of GC. Identification of highly sensitive biomarkers for GC screening might render upper gastrointestinal endoscopy unnecessary. Biomarker has assisted in the advancement of new DNA, RNA, and protein-based cancer biomarkers that can be detected from noninvasive, sensitive, specific, and cost-effective body fluids. These include the OncoBEAM™ RAS CRC liquid biopsy assay approved by the European Commission as an *in vitro* diagnostic tool for colorectal cancer therapy, and this has led to the early detection of emergent resistance to anti-epidermal growth factor receptor treatment and the assessment of genomic profile during treatment in clinical settings[78]. Such assays may also enable us to abandon approved but useless treatments for patients resistant to molecular targeted agents or immunosuppressants. For instance, with this technology the future patients with stage II or III GC with a low risk of postoperative recurrence may be simply monitored under active surveillance without adjuvant chemotherapy and possibly be started to treat from when MRD is detected (Figure 1). Although ctDNA for detection of MRD can be an emerging clinical biomarker for disease monitoring in GC, applications of ctDNA in clinical practice require more comprehensive examination in prospective trials.

However, several technical factors are hindering the use of liquid biopsy biomarkers in clinical use. A major challenge is the very low levels of peripheral DNA/RNA[79]. In 2022, ESMO published recommendations on the use of ctDNA in genomic testing and clinical practice. Based on its review of the different aspects of ctDNA, the ESMO Precision Medicine Working Group provides some outlook on the future of ctDNA examination. Considering deficient sensitivity in clinical practice for gene fusions and copy number variations and advancing tests to discriminate accurate results for more progressive genotyping are included in their recommendations[80]. To overcome these issues, several upgraded liquid biopsy approaches for cancer diagnosis are under development. It is likely that precancerous and cancerous lesions can be detected by combinations of biomarkers with superior sensitivity and specificity, fulfilling an unmet need in clinical practice. Combining biomarkers, such as ncRNAs, can enhance the sensitivity and specificity for detecting EGC. However, it would be difficult to identify the ideal combination of other biomarkers that can enhance the overall detection performance. Correlations between different types of biomarkers like the association pattern to guide the choice of panels can be effectively identified using biostatistical approaches. For example, a serum biomarker miRNA panel consisting of 12 miRNAs was developed for risk assessment in patients with GC. With the use of a multitarget miRNA assay in more than 5000 individuals in Singapore and Korea, this panel showed an AUC of 0.848 and 87% sensitivity and 68.4% specificity values to distinguish GC patients from healthy controls. Moreover, upgrading of the AUC to 0.884 and specificity to 69.4% for GC detection were achieved by the combination of this 12-miRNA panel with patient age, *H. pylori* serology, and the plasminogen I:II ratio[81]. Combinations of ctDNA mutations with other biomarkers, such as protein or methylation have been examined toward the goal of improving the overall sensitivity. It has been demonstrated that the combination of ctDNA and protein biomarkers can markedly increase the sensitivity[82]. Genome-wide methylation and protein marker profiles have been validated for a combination of *mSEPT9*, *mRNF180* and CA724 for the detection of GC, and the combination of all three markers detected 68.6% of GC cases[83].

Another important strategy for improving the sensitivity and specificity of GC detection is the use of innovative bioinformatic algorithms. Machine learning involves various computational techniques that are used to simplify large numbers of measurements into lower-dimensional outputs that are more explainable[84]. In the case of GC, a combination of artificial intelligence (AI)-based endoscopy and miR148a methylation has been evaluated for the diagnosis of gastric indefinite dysplasia[85]. Interestingly, a recent study using the microbial compositions of the Cancer Genome Atlas (TCGA) of 18116 human blood samples across 33 cancer types and stochastic gradient-boosting machine learning models effectively discriminated cancer-free individuals, patients with cancer, and patients with

multiple types of cancer[86]. A new concept of cfDNA is also expected to be applied to cancer diagnoses in the near future.

Unfortunately, there is a lack of standardized technique for isolation, amplification and detection in the use liquid biopsies for early diagnoses in clinical settings. One of the most meaningful accomplishments regarding biomarkers for early cancer detection is the emergence of high-throughput technological platforms such as NGS, which allows comprehensive quantification of whole genome or transcriptome. The cost of NGS has greatly declined over the past several decades, which has allowed the sequencing of a larger number of clinical biospecimens, as well as the ability to generate datasets with higher depth of coverage. The opportunity to generate higher resolution data for low expressing transcripts improves the ability to detect rare cancer-derived transcripts in circulation. A study aiming to found the latent miRNA for predicting GC by AI in the Gene Expression Omnibus (GEO) datasets, particularly with several states of the machine learning methods and the Boruta algorithm, demonstrated that the use of hsa-miR-1343-3p could predict GC with the AUC of 100% (sensitivity 100%, specificity 100%, ROC 100%)[87]. In a recent study using high-throughput RNA-seq, the expression profiles of circRNAs in serum EV between GC patients and healthy individuals were examined. The results demonstrated that the circRNA, Chr10q11, Chr1p11, and Chr7q11 were upregulated in GC; the AUC of the three combined circRNAs was 0.839 (95%CI: 0.772-0.893) with 73.2% sensitivity and 84.1% specificity. The construction of a circRNA-miRNA-mRNA network predicted that the three identified circRNAs interact with 13 miRNAs and 91 mRNAs. These findings suggest that panels of EV circRNAs may provide new insights into the early diagnosis of GC[88]. With the use of publicly available gene expression profiles from the TCGA and GEO datasets, a recent study explored the circRNA-miRNA-mRNA interaction axis by constructing a competing endogenous (ce)RNA network. On the basis of the hub RNAs included in ceRNA, the screening of the model for predicting the mRNA signature and miRNA signature by LASSO regression analysis found that both five mRNA-based signatures (CTF1, FKBP5, RNF128, GSTM2 and ADAMTS1) and five miRNA-based signatures (miR-145-5p, miR-615-3p, miR-6507-5p, miR-937-3p and miR-99a-3p) had superior capacity to predict the diagnosis of GC patients with the AUC of 0.9975[89]. Similarly, a study using regulatory networks for circRNA-miRNA-immune-related mRNA validated in the new GEO and TCGA datasets identified various ceRNA (circRNA-miRNA-immune-related mRNA) regulatory networks in GC constructed by hsa_circ_0050102–hsa-miR-4537-NRAS-Tgd cells, hsa_circ_0001013-hsa-miR-485-3p-MAP2K1-Tgd cells, hsa_circ_0003763-hsa-miR-145-5p-FGF10-StromaScore, hsa_circ_0001789-hsa-miR-1269b-MET-adipocytes, hsa_circ_0040573-hsa-miR-3686-RAC1-Tgd cells, and hsa_circ_0006089-hsa-miR-5584-3p-LYN-neurons, among which FGF10, MET, NRAS, RAC1, MAP2K1, and LYN showed promising diagnostic significance for GC patients[90]. In a study based solely on bioinformatics models constructed a circRNA-miRNA-mRNA network based on three circRNAs, 43 miRNAs, and 119 mRNAs, and upregulations of hsa_circ_0001013, hsa_circ_0007376, and hsa_circ_0043947 were observed, which may offer a new pathway for mechanical examinations and provide possible biomarkers for early detection of GC[91]. Likewise, in a bioinformatics circRNA-miRNA-gene interaction network analysis, two circRNAs (CircCEACAM5 and CircCOL1A1) cooperated with GC correlated miRNAs and their host genes were suggested as the pivotal diagnostic biomarker for GC[92]. The emergence of single-cell sequencing technologies has markedly improved the resolution of low-input sequencing. The recent introduction of single-cell DNA/RNA-seq provides an opportunity to detect cell types and cell status. For example, a single-cell expression atlas of gastric premalignant gastric lesions and EGC identified the expression signatures of multiple cell types across different lesions, as well as a panel of six high-confidence markers that could serve as specific biomarkers for early diagnosis of GC[93]. A weighted gene co-expression network analysis (WGCNA) aims to: (1) Identify co-expressed modules in multiple biological samples based on correlations between different gene expression profiles; and (2) Explore the relationship between gene networks and phenotypes of interest, as well as the hub genes in the network[94]. Performing a WGCNA can prevent the false-negative and false-positive results of previous biological methods. WGCNA data from the GEO database revealed hub genes involved in GC and identified four functional genes (*ITGAX*, *CCL14*, *ADHFE1*, and *HOXB13*) that were differentially expressed in tumor and normal gastric samples. Another study applying a WGCNA to screen potential biomarkers for EGC using RNA-seq and clinical data from the TCGA database identified five hub genes, *MS4A1*, *THBS2*, *VCAN*, *PDGFRB*, and *KCNA3*[94]. These technological developments will allow more researchers to conduct comprehensive assessment of molecular profiles in the human circulatory system.

Systematic studies applying the molecular profiling of ncRNAs for cancer biomarker have been developed. Several investigations have used tissue profiling data to identify ncRNA as a potential biomarker, leading to the evaluation of these cancer-associated ncRNA signatures in blood cohorts. Multiple tissue sequencing datasets were recently used to identify highly overexpressed miRNAs in GC tissues. Risk probabilities using quantitative reverse transcriptase polymerase chain reaction data for three miRNAs (miR-18a, miR-181b, and miR-335) were validated and showed much better diagnostic performance than the conventional tumor markers CEA and CA19-9 currently in use. Moreover, the three-miRNA signature discriminated between patients with stage I GC and cancer-free individuals. More importantly, using the miRNA signature was significantly more cost-effective relative to the current clinical practice of endoscopic screening, suggesting the robustness of a GC associated miRNA signature in multiple cohorts[95].

Table 3 Clinical trials of blood-based biofluid biomarkers for gastric cancer detection

Clinical trials	Type of trial	Phase	Results	Participants (estimated)	Assay	Comments
ctDNA						
NCT05027347	Cohort	NA	Recruiting	200	Ultradeep massive parallel sequencing assay	Development of a protocol for detection of ctDNA in plasma of patients with early stages of GC
NCT04511559	Cohort	NA	Not yet recruiting	540	ctDNA methylation sequencing	The correlation between the plasma ctDNA methylation status and the diagnosis of patients with early GC
NCT05208372	Case-control	NA	Recruiting	200	CTC and ctDNA test	Investigation of the value of CTCs and ctDNA in the diagnosis of metastasis of GC in peritoneal flushing fluid and blood
NCT04665687	Cohort	NA	Recruiting	1730	Illumina HiSeq2000/2500-based, MiSeq NGS targeted sequencing	Identification whether tumor's molecular profiling based on blood could be used for diagnosis of EGC and precancerous gastric adenoma
NCT05029869	Cohort	NA	Recruiting	100	NGS technologies	Study aims to evaluate the use of NGS to detect ctDNA in GC patients after gastrectomy
NCT05224596	Case-control	NA	Recruiting	498	Blood draw and blood-based biomarkers analyses	Multi-omics 498 study aimed at detecting GC by combined assays for serum protein markers, deep sequencing of cfDNA, ctDNA mutation and RNA
miRNAs						
NCT04329299	Cohort	NA	Completed	6862	Blood-based biomarkers analyses	Validation of the predictive value of various blood biomarkers, such as miRNA
lncRNAs						
NCT05397548	Cohort	NA	Recruiting	700	RT-PCR	Study to investigate the predictive value of circulating exosomal lncRNA-GC1 for early-detection and monitoring progression of GC
Methylation						
NCT04511559	Cohort	NA	Not yet recruiting	540	ctDNA methylation sequencing	Methylation analysis of ct DNA in early diagnosis in patients with GC
NCT03076567	Observational	NA	Completed	440	NA	Discovery and validation of plasma DNA methylation biomarker for detection of GC
NCT05336058	Cohort	NA	Recruiting	1240	Multi-target PCR	Exploration of the clinical performance of polygene methylation in the adjunctive diagnosis of GC
NCT04253106	Non-randomized	NA	Recruiting	10	NGS	Activating methylation profiles identified by liquid biopsies could identify CDH1 and CTNNA1 pathogenic variants carriers with DGC
Multi-omics						
NCT04947995	Case-control	NA	Recruiting	450	ctDNA multi-omics test	Exploration of a blood-based multi-omics assay and computational model for early detection of GC
NCT05347524	Observational	NA	Recruiting	384	Blood draw and blood-based biomarkers analyses	Detection of peritoneal metastasis of GC by combined assays for methylation of cfDNA and other blood-based biomarkers

GC: Gastric cancer; NGS: Next generation sequencing; PCR: Polymerase chain reaction; DGC: Diffuse gastric cancer; ctDNA: Circulating tumor DNA; cfDNA: Cell-free DNA; miRNA: MicroRNA; lncRNA: Long non-coding RNA; NA: Not applicable; lncRNA-GC1: Gastric cancer-associated lncRNA1.

More multicenter studies and prospective evaluations in large clinical trials are necessary for the integrations of such biomarkers into GC screening platforms supporting the daily clinical treatments of GC patients. Several clinical trials have explored the use of a liquid biopsy for early diagnosis of setting for patients with GC (Table 3). However, all of the trials were either observational, case-control, or cohort trials; no randomized control trial assessing liquid biopsy have been conducted to date. Hence, incorporating liquid biopsies into clinical practice for GC may be difficult.

Regarding the development of a circulating non-invasive biomarkers for early detection of GC, specificity for stomach would provide an additional confidence and suggested robustness of GC biomarkers. Biomarkers that are highly specific to GC will reduce the false positive rates, and thus are helpful in clinical practice. The detection of dysregulated genes that are highly expressed specifically in distinct organ could make it easier to find the locations of cancer. For example, KRAS mutations are rarely identified in healthy individuals, which makes these mutations highly cancer-specific. Nevertheless, detecting KRAS mutations in the circulation does not help identify the location of cancer as KRAS mutations can occur in multiple cancer types. Using candidates for GC specific driver genes, such as CDH1 and RhoA, may be possible to increase the specificity as diagnostic biomarkers of GC [96]. Growing evidences suggest that some EVs released from specific organs retain tissue-specific molecular features. It was recently reported that tumor cell-specific molecules, *i.e.*, circulating exosome-derived lncRNA-GC1 can be used as a biomarker to detect EGC and monitor disease progression[42]. Interestingly, a clinical study (ClinicalTrials.gov identifier NCT05397548) investigated whether circulating exosomal lncRNA-GC1 could support the early-detection and progression monitoring of GC. It is thus possible to measure ncRNA content of cancer-specific exosomes to further increase cancer specificity as biomarkers for GC diagnosis. The status of acquired DNA methylation can be tissue-specific and maintained during carcinogenesis, and examination of this status could allow the discovery of the tumor of origin[97], suggesting that biomarkers based on DNA methylation could have the additional potential to provide key information to guide follow-up clinical decision making. Multiple cancer types have been identified *via* high-depth, targeted bisulfite sequencing analysis of a large panel of methylation sites that have signals specific to certain organs; these panels include DEEPGEN™, CancerSEEK, PanSEER, cfMeDIP-se,q GRAIL, IvyGene®, and stMCEDs. Using these panels, excellent rates of detection in individuals with cancer were obtained[98]. However, the specificity of GC in individuals with early disease have been limited. A cost-effective experimental assay, called cell-free DNA Methylome Sequencing (cfMethyl-Seq) profiles the genome-wide methylation of cfDNA, offering > 12 × enrichment over whole-genome bisulfite sequencing in CpG islands[99]. By integrating four marker types, namely cancer-specific hypermethylation markers, tissue hypermethylation markers, cancer-specific hypomethylation markers types, and tissue hypomethylation markers, a cfMethyl-Seq model showed an AUR of 0.974 (95%CI: 0.926-0.998), yielding a sensitivity of 80.7% (95%CI: 68.6%-90.7%) at 97.9% specificity in multiple organs, including those with GC.

Collectively, the combination of multiple parameters and multiple analytes obtained by emerging machine learning methods will help address the challenges of EGC detection. Overcoming the limitation of cancer biomarker translation into clinical practice will require the development of high throughput, multiplexing techniques that can be easily incorporated into clinical settings as well as large-scale prospective research and interventional clinical trials with standardized specimen processing and data collection procedures.

CONCLUSION

Increased understanding of the molecular genetics and epigenetics of GC has led to the progress of molecular marker assays for GC screening. Liquid biopsy is emerging as a promising future screening technique for clinical testing owing to the use of a single sample and ease of specimen collection. The advancement of new technologies with improved sensitivity, such as methylation sequencing and multi-omics analysis, and rapid, global detection capacities that allowed the identification of novel potential biomarkers for early detection of GC.

FOOTNOTES

Author contributions: Matsuoka T and Yashiro M performed literature research; Matsuoka T wrote the manuscript and performed the revision and approval of the final version; Yashiro M designed research, coordinated and corrected the writing of the paper.

Supported by the National Cancer Center Research and Development Fund, No. 23-A-9.

Conflict-of-interest statement: All the authors report no relevant conflicts of interest for this article.

Open-Access: This article is an open-access article that was selected by an in-house editor and fully peer-reviewed by external reviewers. It is distributed in accordance with the Creative Commons Attribution NonCommercial (CC BY-NC 4.0) license, which permits others to distribute, remix, adapt, build upon this work non-commercially, and license their derivative works on different terms, provided the original work is properly cited and the use is non-commercial. See: https://creativecommons.org/Licenses/by-nc/4.0/

Country/Territory of origin: Japan

ORCID number: Tasuku Matsuoka 0000-0001-5019-8519; Masakazu Yashiro 0000-0001-5743-7228.

S-Editor: Wang JJ
L-Editor: A
P-Editor: Yu HG

REFERENCES

1 **Siegel RL**, Miller KD, Fuchs HE, Jemal A. Cancer statistics, 2022. *CA Cancer J Clin* 2022; **72**: 7-33 [PMID: 35020204 DOI: 10.3322/caac.21708]
2 **Matsuoka T**, Yashiro M. Biomarkers of gastric cancer: Current topics and future perspective. *World J Gastroenterol* 2018; **24**: 2818-2832 [PMID: 30018477 DOI: 10.3748/wjg.v24.i26.2818]
3 **Alix-Panabières C**, Pantel K. Liquid Biopsy: From Discovery to Clinical Application. *Cancer Discov* 2021; **11**: 858-873 [PMID: 33811121 DOI: 10.1158/2159-8290.CD-20-1311]
4 **Heitzer E**, Haque IS, Roberts CES, Speicher MR. Current and future perspectives of liquid biopsies in genomics-driven oncology. *Nat Rev Genet* 2019; **20**: 71-88 [PMID: 30410101 DOI: 10.1038/s41576-018-0071-5]
5 **Joosse SA**, Gorges TM, Pantel K. Biology, detection, and clinical implications of circulating tumor cells. *EMBO Mol Med* 2015; **7**: 1-11 [PMID: 25398926 DOI: 10.15252/emmm.201303698]
6 **Wan JCM**, Massie C, Garcia-Corbacho J, Mouliere F, Brenton JD, Caldas C, Pacey S, Baird R, Rosenfeld N. Liquid biopsies come of age: towards implementation of circulating tumour DNA. *Nat Rev Cancer* 2017; **17**: 223-238 [PMID: 28233803 DOI: 10.1038/nrc.2017.7]
7 **Pessoa LS**, Heringer M, Ferrer VP. ctDNA as a cancer biomarker: A broad overview. *Crit Rev Oncol Hematol* 2020; **155**: 103109 [PMID: 33049662 DOI: 10.1016/j.critrevonc.2020.103109]
8 **Qian C**, Ju S, Qi J, Zhao J, Shen X, Jing R, Yu J, Li L, Shi Y, Zhang L, Wang Z, Cong H. Alu-based cell-free DNA: a novel biomarker for screening of gastric cancer. *Oncotarget* 2017; **8**: 54037-54045 [PMID: 28903321 DOI: 10.18632/oncotarget.11079]
9 **Lan YT**, Chen MH, Fang WL, Hsieh CC, Lin CH, Jhang FY, Yang SH, Lin JK, Chen WS, Jiang JK, Lin PC, Chang SC. Clinical relevance of cell-free DNA in gastrointestinal tract malignancy. *Oncotarget* 2017; **8**: 3009-3017 [PMID: 27936467 DOI: 10.18632/oncotarget.13821]
10 **Grenda A**, Wojas-Krawczyk K, Skoczylas T, Krawczyk P, Sierocińska-Sawa J, Wallner G, Milanowski J. HER2 gene assessment in liquid biopsy of gastric and esophagogastric junction cancer patients qualified for surgery. *BMC Gastroenterol* 2020; **20**: 382 [PMID: 33198632 DOI: 10.1186/s12876-020-01531-5]
11 **Jogo T**, Nakamura Y, Shitara K, Bando H, Yasui H, Esaki T, Terazawa T, Satoh T, Shinozaki E, Nishina T, Sunakawa Y, Komatsu Y, Hara H, Oki E, Matsuhashi N, Ohta T, Kato T, Ohtsubo K, Kawakami T, Okano N, Yamamoto Y, Yamada T, Tsuji A, Odegaard JI, Taniguchi H, Doi T, Fujii S, Yoshino T. Circulating Tumor DNA Analysis Detects FGFR2 Amplification and Concurrent Genomic Alterations Associated with FGFR Inhibitor Efficacy in Advanced Gastric Cancer. *Clin Cancer Res* 2021; **27**: 5619-5627 [PMID: 34376535 DOI: 10.1158/1078-0432.CCR-21-1414]
12 **Reinert T**, Schøler LV, Thomsen R, Tobiasen H, Vang S, Nordentoft I, Lamy P, Kannerup AS, Mortensen FV, Stribolt K, Hamilton-Dutoit S, Nielsen HJ, Laurberg S, Pallisgaard N, Pedersen JS, Ørntoft TF, Andersen CL. Analysis of circulating tumour DNA to monitor disease burden following colorectal cancer surgery. *Gut* 2016; **65**: 625-634 [PMID: 25654990 DOI: 10.1136/gutjnl-2014-308859]
13 **Kim YW**, Kim YH, Song Y, Kim HS, Sim HW, Poojan S, Eom BW, Kook MC, Joo J, Hong KM. Monitoring circulating tumor DNA by analyzing personalized cancer-specific rearrangements to detect recurrence in gastric cancer. *Exp Mol Med* 2019; **51**: 1-10 [PMID: 31395853 DOI: 10.1038/s12276-019-0292-5]
14 **Yang J**, Gong Y, Lam VK, Shi Y, Guan Y, Zhang Y, Ji L, Chen Y, Zhao Y, Qian F, Chen J, Li P, Zhang F, Wang J, Zhang X, Yang L, Kopetz S, Futreal PA, Zhang J, Yi X, Xia X, Yu P. Deep sequencing of circulating tumor DNA detects molecular residual disease and predicts recurrence in gastric cancer. *Cell Death Dis* 2020; **11**: 346 [PMID: 32393783 DOI: 10.1038/s41419-020-2531-z]
15 **Chae YK**, Oh MS. Detection of Minimal Residual Disease Using ctDNA in Lung Cancer: Current Evidence and Future Directions. *J Thorac Oncol* 2019; **14**: 16-24 [PMID: 30296486 DOI: 10.1016/j.jtho.2018.09.022]
16 **Koldby KM**, Mortensen MB, Detlefsen S, Pfeiffer P, Thomassen M, Kruse TA. Tumor-specific genetic aberrations in cell-free DNA of gastroesophageal cancer patients. *J Gastroenterol* 2019; **54**: 108-121 [PMID: 30242476 DOI: 10.1007/s00535-018-1508-5]
17 **Maron SB**, Chase LM, Lomnicki S, Kochanny S, Moore KL, Joshi SS, Landron S, Johnson J, Kiedrowski LA, Nagy RJ, Lanman RB, Kim ST, Lee J, Catenacci DVT. Circulating Tumor DNA Sequencing Analysis of Gastroesophageal Adenocarcinoma. *Clin Cancer Res* 2019; **25**: 7098-7112 [PMID: 31427281 DOI: 10.1158/1078-0432.CCR-19-1704]
18 **Zhang M**, Du X. Noncoding RNAs in gastric cancer: Research progress and prospects. *World J Gastroenterol* 2016; **22**: 6610-6618 [PMID: 27547004 DOI: 10.3748/wjg.v22.i29.6610]
19 **Finnegan EF**, Pasquinelli AE. MicroRNA biogenesis: regulating the regulators. *Crit Rev Biochem Mol Biol* 2013; **48**: 51-68 [PMID: 23163351 DOI: 10.3109/10409238.2012.738643]
20 **ZiaSarabi P**, Sorayayi S, Hesari A, Ghasemi F. Circulating microRNA-133, microRNA-17 and microRNA-25 in serum and its potential diagnostic value in gastric cancer. *J Cell Biochem* 2019; **120**: 12376-12381 [PMID: 30861177 DOI: 10.1002/jcb.28503]
21 **Zhu XL**, Ren LF, Wang HP, Bai ZT, Zhang L, Meng WB, Zhu KX, Ding FH, Miao L, Yan J, Wang YP, Liu YQ, Zhou WC, Li X. Plasma microRNAs as potential new biomarkers for early detection of early gastric cancer. *World J Gastroenterol* 2019; **25**: 1580-1591 [PMID: 30983818 DOI: 10.3748/wjg.v25.i13.1580]

22 **Yao Y**, Ding Y, Bai Y, Zhou Q, Lee H, Li X, Teng L. Identification of Serum Circulating MicroRNAs as Novel Diagnostic Biomarkers of Gastric Cancer. *Front Genet* 2020; **11**: 591515 [PMID: 33597967 DOI: 10.3389/fgene.2020.591515]

23 **Abe S**, Matsuzaki J, Sudo K, Oda I, Katai H, Kato K, Takizawa S, Sakamoto H, Takeshita F, Niida S, Saito Y, Ochiya T. A novel combination of serum microRNAs for the detection of early gastric cancer. *Gastric Cancer* 2021; **24**: 835-843 [PMID: 33743111 DOI: 10.1007/s10120-021-01161-0]

24 **Fang XY**, Pan HF, Leng RX, Ye DQ. Long noncoding RNAs: novel insights into gastric cancer. *Cancer Lett* 2015; **356**: 357-366 [PMID: 25444905 DOI: 10.1016/j.canlet.2014.11.005]

25 **Xu W**, Zhou G, Wang H, Liu Y, Chen B, Chen W, Lin C, Wu S, Gong A, Xu M. Circulating lncRNA SNHG11 as a novel biomarker for early diagnosis and prognosis of colorectal cancer. *Int J Cancer* 2020; **146**: 2901-2912 [PMID: 31633800 DOI: 10.1002/ijc.32747]

26 **Xian HP**, Zhuo ZL, Sun YJ, Liang B, Zhao XT. Circulating long non-coding RNAs HULC and ZNFX1-AS1 are potential biomarkers in patients with gastric cancer. *Oncol Lett* 2018; **16**: 4689-4698 [PMID: 30197680 DOI: 10.3892/ol.2018.9199]

27 **Yang Z**, Sun Y, Liu R, Shi Y, Ding S. Plasma long noncoding RNAs PANDAR, FOXD2-AS1, and SMARCC2 as potential novel diagnostic biomarkers for gastric cancer. *Cancer Manag Res* 2019; **11**: 6175-6184 [PMID: 31308753 DOI: 10.2147/CMAR.S201935]

28 **Feng W**, Zong W, Li Y, Shen X, Cui X, Ju S. Abnormally expressed long noncoding RNA B3GALT5-AS1 may serve as a biomarker for the diagnostic and prognostic of gastric cancer. *J Cell Biochem* 2020; **121**: 557-565 [PMID: 31338903 DOI: 10.1002/jcb.29296]

29 **Zhou Q**, Li H, Jing J, Yuan Y, Sun L. Evaluation of C5orf66-AS1 as a Potential Biomarker for Predicting Early Gastric Cancer and Its Role in Gastric Carcinogenesis. *Onco Targets Ther* 2020; **13**: 2795-2805 [PMID: 32308414 DOI: 10.2147/OTT.S239965]

30 **Qin S**, Yang L, Kong S, Xu Y, Liang B, Ju S. LncRNA HCP5 : A Potential Biomarker for Diagnosing Gastric Cancer. *Front Oncol* 2021; **11**: 684531 [PMID: 34222007 DOI: 10.3389/fonc.2021.684531]

31 **Li X**, Yang L, Chen LL. The Biogenesis, Functions, and Challenges of Circular RNAs. *Mol Cell* 2018; **71**: 428-442 [PMID: 30057200 DOI: 10.1016/j.molcel.2018.06.034]

32 **Enuka Y**, Lauriola M, Feldman ME, Sas-Chen A, Ulitsky I, Yarden Y. Circular RNAs are long-lived and display only minimal early alterations in response to a growth factor. *Nucleic Acids Res* 2016; **44**: 1370-1383 [PMID: 26657629 DOI: 10.1093/nar/gkv1367]

33 **Huang M**, He YR, Liang LC, Huang Q, Zhu ZQ. Circular RNA hsa_circ_0000745 may serve as a diagnostic marker for gastric cancer. *World J Gastroenterol* 2017; **23**: 6330-6338 [PMID: 28974900 DOI: 10.3748/wjg.v23.i34.6330]

34 **Lu H**, Zhang Z, Yuan X, Song H, Li P. The role of circular RNA hsa_circ_0001789 as a diagnostic biomarker in gastric carcinoma. *Scand J Gastroenterol* 2023; **58**: 248-253 [PMID: 36111683 DOI: 10.1080/00365521.2022.2122865]

35 **Ma S**, Kong S, Gu X, Xu Y, Tao M, Shen L, Shen X, Ju S. As a biomarker for gastric cancer, circPTPN22 regulates the progression of gastric cancer through the EMT pathway. *Cancer Cell Int* 2021; **21**: 44 [PMID: 33430866 DOI: 10.1186/s12935-020-01701-1]

36 **Roy S**, Kanda M, Nomura S, Zhu Z, Toiyama Y, Taketomi A, Goldenring J, Baba H, Kodera Y, Goel A. Diagnostic efficacy of circular RNAs as noninvasive, liquid biopsy biomarkers for early detection of gastric cancer. *Mol Cancer* 2022; **21**: 42 [PMID: 35139874 DOI: 10.1186/s12943-022-01527-7]

37 **Yu W**, Hurley J, Roberts D, Chakrabortty SK, Enderle D, Noerholm M, Breakefield XO, Skog JK. Exosome-based liquid biopsies in cancer: opportunities and challenges. *Ann Oncol* 2021; **32**: 466-477 [PMID: 33548389 DOI: 10.1016/j.annonc.2021.01.074]

38 **Xu R**, Rai A, Chen M, Suwakulsiri W, Greening DW, Simpson RJ. Extracellular vesicles in cancer - implications for future improvements in cancer care. *Nat Rev Clin Oncol* 2018; **15**: 617-638 [PMID: 29795272 DOI: 10.1038/s41571-018-0036-9]

39 **Lin LY**, Yang L, Zeng Q, Wang L, Chen ML, Zhao ZH, Ye GD, Luo QC, Lv PY, Guo QW, Li BA, Cai JC, Cai WY. Tumor-originated exosomal lncUEGC1 as a circulating biomarker for early-stage gastric cancer. *Mol Cancer* 2018; **17**: 84 [PMID: 29690888 DOI: 10.1186/s12943-018-0834-9]

40 **Cai C**, Zhang H, Zhu Y, Zheng P, Xu Y, Sun J, Zhang M, Lan T, Gu B, Li S, Ma P. Serum Exosomal Long Noncoding RNA pcsk2-2:1 As A Potential Novel Diagnostic Biomarker For Gastric Cancer. *Onco Targets Ther* 2019; **12**: 10035-10041 [PMID: 31819499 DOI: 10.2147/OTT.S229033]

41 **Li S**, Zhang M, Zhang H, Hu K, Cai C, Wang J, Shi L, Ma P, Xu Y, Zheng P. Exosomal long noncoding RNA lnc-GNAQ-6:1 may serve as a diagnostic marker for gastric cancer. *Clin Chim Acta* 2020; **501**: 252-257 [PMID: 31730812 DOI: 10.1016/j.cca.2019.10.047]

42 **Guo X**, Lv X, Ru Y, Zhou F, Wang N, Xi H, Zhang K, Li J, Chang R, Xie T, Wang X, Li B, Chen Y, Yang Y, Chen L. Circulating Exosomal Gastric Cancer-Associated Long Noncoding RNA1 as a Biomarker for Early Detection and Monitoring Progression of Gastric Cancer: A Multiphase Study. *JAMA Surg* 2020; **155**: 572-579 [PMID: 32520332 DOI: 10.1001/jamasurg.2020.1133]

43 **Tang S**, Cheng J, Yao Y, Lou C, Wang L, Huang X, Zhang Y. Combination of Four Serum Exosomal MiRNAs as Novel Diagnostic Biomarkers for Early-Stage Gastric Cancer. *Front Genet* 2020; **11**: 237 [PMID: 32256526 DOI: 10.3389/fgene.2020.00237]

44 **Zheng GD**, Xu ZY, Hu C, Lv H, Xie HX, Huang T, Zhang YQ, Chen GP, Fu YF, Cheng XD. Exosomal miR-590-5p in Serum as a Biomarker for the Diagnosis and Prognosis of Gastric Cancer. *Front Mol Biosci* 2021; **8**: 636566 [PMID: 33681295 DOI: 10.3389/fmolb.2021.636566]

45 **Yang J**, Li X, Wei S, Peng L, Sang H, Jin D, Chen M, Dang Y, Zhang G. Evaluation of the Diagnostic Potential of a Plasma Exosomal miRNAs Panel for Gastric Cancer. *Front Oncol* 2021; **11**: 683465 [PMID: 34422636 DOI: 10.3389/fonc.2021.683465]

46 **Ni D**, Zhang Z, Liu X. Benthic ecological quality assessment of the Bohai Sea, China using marine biotic indices. *Mar*

Pollut Bull 2019; **142**: 457-464 [PMID: 31232324 DOI: 10.1016/j.marpolbul.2019.03.055]
47 **Ge L**, Zhang N, Li D, Wu Y, Wang H, Wang J. Circulating exosomal small RNAs are promising non-invasive diagnostic biomarkers for gastric cancer. *J Cell Mol Med* 2020; **24**: 14502-14513 [PMID: 33169519 DOI: 10.1111/jcmm.16077]
48 **Puneet**, Kazmi HR, Kumari S, Tiwari S, Khanna A, Narayan G. Epigenetic Mechanisms and Events in Gastric Cancer-Emerging Novel Biomarkers. *Pathol Oncol Res* 2018; **24**: 757-770 [PMID: 29552712 DOI: 10.1007/s12253-018-0410-z]
49 **Skvortsova K**, Stirzaker C, Taberlay P. The DNA methylation landscape in cancer. *Essays Biochem* 2019; **63**: 797-811 [PMID: 31845735 DOI: 10.1042/EBC20190037]
50 **Zeng Y**, Rong H, Xu J, Cao R, Li S, Gao Y, Cheng B, Zhou T. DNA Methylation: An Important Biomarker and Therapeutic Target for Gastric Cancer. *Front Genet* 2022; **13**: 823905 [PMID: 35309131 DOI: 10.3389/fgene.2022.823905]
51 **Alarcón MA**, Olivares W, Córdova-Delgado M, Muñoz-Medel M, de Mayo T, Carrasco-Aviño G, Wichmann I, Landeros N, Amigo J, Norero E, Villarroel-Espíndola F, Riquelme A, Garrido M, Owen GI, Corvalán AH. The Reprimo-Like Gene Is an Epigenetic-Mediated Tumor Suppressor and a Candidate Biomarker for the Non-Invasive Detection of Gastric Cancer. *Int J Mol Sci* 2020; **21** [PMID: 33322837 DOI: 10.3390/ijms21249472]
52 **Wen J**, Zheng T, Hu K, Zhu C, Guo L, Ye G. Promoter methylation of tumor-related genes as a potential biomarker using blood samples for gastric cancer detection. *Oncotarget* 2017; **8**: 77783-77793 [PMID: 29100425 DOI: 10.18632/oncotarget.20782]
53 **Wu S**, Zhang Y, Zhang L, Ma JL, Zhou T, Li ZX, Liu WD, Li WQ, You WC, Pan KF. Methylation and Expression of Nonclustered Protocadherins Encoding Genes and Risk of Precancerous Gastric Lesions in a High-Risk Population. *Cancer Prev Res (Phila)* 2018; **11**: 717-726 [PMID: 30213786 DOI: 10.1158/1940-6207.CAPR-18-0119]
54 **Miao J**, Liu Y, Zhao G, Liu X, Ma Y, Li H, Li S, Zhu Y, Xiong S, Zheng M, Fei S. Feasibility of Plasma-Methylated SFRP2 for Early Detection of Gastric Cancer. *Cancer Control* 2020; **27**: 1073274820922559 [PMID: 32379490 DOI: 10.1177/1073274820922559]
55 **Hu D**, Lou X, Meng N, Li Z, Teng Y, Zou Y, Wang F. Peripheral Blood-Based DNA Methylation of Long Non-Coding RNA H19 and Metastasis-Associated Lung Adenocarcinoma Transcript 1 Promoters are Potential Non-Invasive Biomarkers for Gastric Cancer Detection. *Cancer Control* 2021; **28**: 10732748211043667 [PMID: 34615385 DOI: 10.1177/10732748211043667]
56 **Han Q**, Zhou H, Xie W, Sun T, Wei R, Nie C, Hong J, Zhu L, Tian W. Association between the methylation of the STAT1 and SOCS3 in peripheral blood and gastric cancer. *J Gastroenterol Hepatol* 2020; **35**: 1347-1354 [PMID: 32108380 DOI: 10.1111/jgh.15021]
57 **Chansangpetch S**, Prombhul S, Tantisevi V, Sodsai P, Manassakorn A, Hirankarn N, Lin SC. DNA Methylation Status of the Interspersed Repetitive Sequences for LINE-1, Alu, HERV-E, and HERV-K in Trabeculectomy Specimens from Glaucoma Eyes. *J Ophthalmol* 2018; **2018**: 9171536 [PMID: 29651348 DOI: 10.1155/2018/9171536]
58 **Fattahi S**, Kosari-Monfared M, Ghadami E, Golpour M, Khodadadi P, Ghasemiyan M, Akhavan-Niaki H. Infection-associated epigenetic alterations in gastric cancer: New insight in cancer therapy. *J Cell Physiol* 2018; **233**: 9261-9270 [PMID: 30076708 DOI: 10.1002/jcp.27030]
59 **Yoshida T**, Yamashita S, Takamura-Enya T, Niwa T, Ando T, Enomoto S, Maekita T, Nakazawa K, Tatematsu M, Ichinose M, Ushijima T. Alu and Satα hypomethylation in Helicobacter pylori-infected gastric mucosae. *Int J Cancer* 2011; **128**: 33-39 [PMID: 20602342 DOI: 10.1002/ijc.25534]
60 **Zhang X**, Soutto M, Chen Z, Bhat N, Zhu S, Eissmann MF, Ernst M, Lu H, Peng D, Xu Z, El-Rifai W. Induction of Fibroblast Growth Factor Receptor 4 by Helicobacter pylori *via* Signal Transducer and Activator of Transcription 3 With a Feedforward Activation Loop Involving Steroid Receptor Coactivator Signaling in Gastric Cancer. *Gastroenterology* 2022; **163**: 620-636.e9 [PMID: 35588797 DOI: 10.1053/j.gastro.2022.05.016]
61 **Shi XJ**, Wei Y, Ji B. Systems Biology of Gastric Cancer: Perspectives on the Omics-Based Diagnosis and Treatment. *Front Mol Biosci* 2020; **7**: 203 [PMID: 33005629 DOI: 10.3389/fmolb.2020.00203]
62 **Morganti S**, Tarantino P, Ferraro E, D'Amico P, Viale G, Trapani D, Duso BA, Curigliano G. Complexity of genome sequencing and reporting: Next generation sequencing (NGS) technologies and implementation of precision medicine in real life. *Crit Rev Oncol Hematol* 2019; **133**: 171-182 [PMID: 30661654 DOI: 10.1016/j.critrevonc.2018.11.008]
63 **Ren AH**, Diamandis EP, Kulasingam V. Uncovering the Depths of the Human Proteome: Antibody-based Technologies for Ultrasensitive Multiplexed Protein Detection and Quantification. *Mol Cell Proteomics* 2021; **20**: 100155 [PMID: 34597790 DOI: 10.1016/j.mcpro.2021.100155]
64 **Zhou B**, Zhou Z, Chen Y, Deng H, Cai Y, Rao X, Yin Y, Rong L. Plasma proteomics-based identification of novel biomarkers in early gastric cancer. *Clin Biochem* 2020; **76**: 5-10 [PMID: 31765635 DOI: 10.1016/j.clinbiochem.2019.11.001]
65 **Xiao Y**, Xie J, Liu L, Huang W, Han Q, Qin J, Liu S, Jiang Z. NAD(P)-dependent steroid dehydrogenase-like protein and neutral cholesterol ester hydrolase 1 serve as novel markers for early detection of gastric cancer identified using quantitative proteomics. *J Clin Lab Anal* 2021; **35**: e23652 [PMID: 33219617 DOI: 10.1002/jcla.23652]
66 **Zhu Y**, Hu Y, Zhu X, Zhang J, Yuwen D, Wei X, Tang C, Zhang W. Plasma thioredoxin reductase: a potential diagnostic biomarker for gastric cancer. *Carcinogenesis* 2022; **43**: 736-745 [PMID: 35709525 DOI: 10.1093/carcin/bgac052]
67 **Mun DG**, Bhin J, Kim S, Kim H, Jung JH, Jung Y, Jang YE, Park JM, Lee H, Bae J, Back S, Kim SJ, Kim J, Park H, Li H, Hwang KB, Park YS, Yook JH, Kim BS, Kwon SY, Ryu SW, Park DY, Jeon TY, Kim DH, Lee JH, Han SU, Song KS, Park D, Park JW, Rodriguez H, Kim KP, Yang EG, Kim HK, Paek E, Lee S, Lee SW, Hwang D. Proteogenomic Characterization of Human Early-Onset Gastric Cancer. *Cancer Cell* 2019; **35**: 111-124.e10 [PMID: 30645970 DOI: 10.1016/j.ccell.2018.12.003]
68 **Aziz S**, Rasheed F, Zahra R, König S. Gastric Cancer Pre-Stage Detection and Early Diagnosis of Gastritis Using Serum Protein Signatures. *Molecules* 2022; **27** [PMID: 35566209 DOI: 10.3390/molecules27092857]
69 **Park CH**, Hong C, Lee AR, Sung J, Hwang TH. Multi-omics reveals microbiome, host gene expression, and immune landscape in gastric carcinogenesis. *iScience* 2022; **25**: 103956 [PMID: 35265820 DOI: 10.1016/j.isci.2022.103956]
70 **Kon OL**, Yip TT, Ho MF, Chan WH, Wong WK, Tan SY, Ng WH, Kam SY, Eng AKh, Ho P, Viner R, Ong HS,

Kumarasinghe MP. The distinctive gastric fluid proteome in gastric cancer reveals a multi-biomarker diagnostic profile. *BMC Med Genomics* 2008; **1**: 54 [PMID: 18950519 DOI: 10.1186/1755-8794-1-54]

71 **Skryabin GO**, Vinokurova SV, Galetsky SA, Elkin DS, Senkovenko AM, Denisova DA, Komelkov AV, Stilidi IS, Peregorodiev IN, Malikhova OA, Imaraliev OT, Enikeev AD, Tchevkina EM. Isolation and Characterization of Extracellular Vesicles from Gastric Juice. *Cancers (Basel)* 2022; **14** [PMID: 35884376 DOI: 10.3390/cancers14143314]

72 **Shao Y**, Ye M, Li Q, Sun W, Ye G, Zhang X, Yang Y, Xiao B, Guo J. LncRNA-RMRP promotes carcinogenesis by acting as a miR-206 sponge and is used as a novel biomarker for gastric cancer. *Oncotarget* 2016; **7**: 37812-37824 [PMID: 27192121 DOI: 10.18632/oncotarget.9336]

73 **Pan Y**, Zheng Y, Yang J, Wei Y, Wu H, Liu S, Yin A, Hu J, Zeng Y. A new biomarker for the early diagnosis of gastric cancer: gastric juice- and serum-derived SNCG. *Future Oncol* 2022; **18**: 3179-3190 [PMID: 35947016 DOI: 10.2217/fon-2022-0253]

74 **Yamamoto H**, Watanabe Y, Oikawa R, Morita R, Yoshida Y, Maehata T, Yasuda H, Itoh F. BARHL2 Methylation Using Gastric Wash DNA or Gastric Juice Exosomal DNA is a Useful Marker For Early Detection of Gastric Cancer in an H. pylori-Independent Manner. *Clin Transl Gastroenterol* 2016; **7**: e184 [PMID: 27441821 DOI: 10.1038/ctg.2016.40]

75 **Botezatu A**, Bodrug N. Chronic atrophic gastritis: an update on diagnosis. *Med Pharm Rep* 2021; **94**: 7-14 [PMID: 33629042 DOI: 10.15386/mpr-1887]

76 **Bang CS**, Lee JJ, Baik GH. Prediction of Chronic Atrophic Gastritis and Gastric Neoplasms by Serum Pepsinogen Assay: A Systematic Review and Meta-Analysis of Diagnostic Test Accuracy. *J Clin Med* 2019; **8** [PMID: 31083485 DOI: 10.3390/jcm8050657]

77 **Sarhadi VK**, Armengol G. Molecular Biomarkers in Cancer. *Biomolecules* 2022; **12** [PMID: 35892331 DOI: 10.3390/biom12081021]

78 **Nakajima H**, Kotani D, Bando H, Kato T, Oki E, Shinozaki E, Sunakawa Y, Yamazaki K, Yuki S, Nakamura Y, Yamanaka T, Yoshino T, Ohta T, Taniguchi H, Kagawa Y. REMARRY and PURSUIT trials: liquid biopsy-guided rechallenge with anti-epidermal growth factor receptor (EGFR) therapy with panitumumab plus irinotecan for patients with plasma RAS wild-type metastatic colorectal cancer. *BMC Cancer* 2021; **21**: 674 [PMID: 34098908 DOI: 10.1186/s12885-021-08395-2]

79 **Ignatiadis M**, Sledge GW, Jeffrey SS. Liquid biopsy enters the clinic - implementation issues and future challenges. *Nat Rev Clin Oncol* 2021; **18**: 297-312 [PMID: 33473219 DOI: 10.1038/s41571-020-00457-x]

80 **Pascual J**, Attard G, Bidard FC, Curigliano G, De Mattos-Arruda L, Diehn M, Italiano A, Lindberg J, Merker JD, Montagut C, Normanno N, Pantel K, Pentheroudakis G, Popat S, Reis-Filho JS, Tie J, Seoane J, Tarazona N, Yoshino T, Turner NC. ESMO recommendations on the use of circulating tumour DNA assays for patients with cancer: a report from the ESMO Precision Medicine Working Group. *Ann Oncol* 2022; **33**: 750-768 [PMID: 35809752 DOI: 10.1016/j.annonc.2022.05.520]

81 **So JBY**, Kapoor R, Zhu F, Koh C, Zhou L, Zou R, Tang YC, Goo PCK, Rha SY, Chung HC, Yoong J, Yap CT, Rao J, Chia CK, Tsao S, Shabbir A, Lee J, Lam KP, Hartman M, Yong WP, Too HP, Yeoh KG. Development and validation of a serum microRNA biomarker panel for detecting gastric cancer in a high-risk population. *Gut* 2021; **70**: 829-837 [PMID: 33028667 DOI: 10.1136/gutjnl-2020-322065]

82 **Cohen JD**, Li L, Wang Y, Thoburn C, Afsari B, Danilova L, Douville C, Javed AA, Wong F, Mattox A, Hruban RH, Wolfgang CL, Goggins MG, Dal Molin M, Wang TL, Roden R, Klein AP, Ptak J, Dobbyn L, Schaefer J, Silliman N, Popoli M, Vogelstein JT, Browne JD, Schoen RE, Brand RE, Tie J, Gibbs P, Wong HL, Mansfield AS, Jen J, Hanash SM, Falconi M, Allen PJ, Zhou S, Bettegowda C, Diaz LA Jr, Tomasetti C, Kinzler KW, Vogelstein B, Lennon AM, Papadopoulos N. Detection and localization of surgically resectable cancers with a multi-analyte blood test. *Science* 2018; **359**: 926-930 [PMID: 29348365 DOI: 10.1126/science.aar3247]

83 **Xu J**, Song J, Wang T, Zhu W, Zuo L, Wu J, Guo J, Yang X. A combination of methylation and protein markers is capable of detecting gastric cancer detection by combined markers. *Epigenomics* 2021; **13**: 1557-1570 [PMID: 34632818 DOI: 10.2217/epi-2021-0080]

84 **Ko J**, Baldassano SN, Loh PL, Kording K, Litt B, Issadore D. Machine learning to detect signatures of disease in liquid biopsies - a user's guide. *Lab Chip* 2018; **18**: 395-405 [PMID: 29192299 DOI: 10.1039/c7lc00955k]

85 **Watanabe Y**, Oikawa R, Agawa S, Matsuo Y, Oda I, Futagami S, Yamamoto H, Tada T, Itoh F. Combination of artificial intelligence-based endoscopy and miR148a methylation for gastric indefinite dysplasia diagnosis. *J Clin Lab Anal* 2022; **36**: e24122 [PMID: 34811809 DOI: 10.1002/jcla.24122]

86 **Poore GD**, Kopylova E, Zhu Q, Carpenter C, Fraraccio S, Wandro S, Kosciolek T, Janssen S, Metcalf J, Song SJ, Kanbar J, Miller-Montgomery S, Heaton R, Mckay R, Patel SP, Swafford AD, Knight R. Microbiome analyses of blood and tissues suggest cancer diagnostic approach. *Nature* 2020; **579**: 567-574 [PMID: 32214244 DOI: 10.1038/s41586-020-2095-1]

87 **Gilani N**, Arabi Belaghi R, Aftabi Y, Faramarzi E, Edgünlü T, Somi MH. Identifying Potential miRNA Biomarkers for Gastric Cancer Diagnosis Using Machine Learning Variable Selection Approach. *Front Genet* 2021; **12**: 779455 [PMID: 35082831 DOI: 10.3389/fgene.2021.779455]

88 **Xiao K**, Li S, Ding J, Wang Z, Wang D, Cao X, Zhang Y, Dong Z. Expression and clinical value of circRNAs in serum extracellular vesicles for gastric cancer. *Front Oncol* 2022; **12**: 962831 [PMID: 36059681 DOI: 10.3389/fonc.2022.962831]

89 **Ding W**, Wu L, Li X, Chang L, Liu G, Du H. Comprehensive analysis of competitive endogenous RNAs network: Identification and validation of prediction model composed of mRNA signature and miRNA signature in gastric cancer. *Oncol Lett* 2022; **23**: 150 [PMID: 35350591 DOI: 10.3892/ol.2022.13270]

90 **Wu Z**, Liu P, Zhang G. Identification of circRNA-miRNA-Immune-Related mRNA Regulatory Network in Gastric Cancer. *Front Oncol* 2022; **12**: 816884 [PMID: 35280778 DOI: 10.3389/fonc.2022.816884]

91 **Gong Y**, Jiao Y, Qi X, Fu J, Qian J, Zhu J, Yang H, Tang L. Construction of a circRNA-miRNA-mRNA network based on differentially co-expressed circular RNA in gastric cancer tissue and plasma by bioinformatics analysis. *World J Surg Oncol* 2022; **20**: 34 [PMID: 35164778 DOI: 10.1186/s12957-022-02503-7]

92 **Hossain MT**, Li S, Reza MS, Feng S, Zhang X, Jin Z, Wei Y, Peng Y. Identification of circRNA Biomarker for Gastric Cancer through Integrated Analysis. *Front Mol Biosci* 2022; **9**: 857320 [PMID: 35359600 DOI: 10.3389/fmolb.2022.857320]

93 **Zhang P**, Yang M, Zhang Y, Xiao S, Lai X, Tan A, Du S, Li S. Dissecting the Single-Cell Transcriptome Network Underlying Gastric Premalignant Lesions and Early Gastric Cancer. *Cell Rep* 2019; **27**: 1934-1947.e5 [PMID: 31067475 DOI: 10.1016/j.celrep.2019.04.052]

94 **Tan R**, Zhang G, Liu R, Hou J, Dong Z, Deng C, Wan S, Lai X, Cui H. Identification of Early Diagnostic and Prognostic Biomarkers *via* WGCNA in Stomach Adenocarcinoma. *Front Oncol* 2021; **11**: 636461 [PMID: 34221961 DOI: 10.3389/fonc.2021.636461]

95 **Izumi D**, Zhu Z, Chen Y, Toden S, Huo X, Kanda M, Ishimoto T, Gu D, Tan M, Kodera Y, Baba H, Li W, Chen J, Wang X, Goel A. Assessment of the Diagnostic Efficiency of a Liquid Biopsy Assay for Early Detection of Gastric Cancer. *JAMA Netw Open* 2021; **4**: e2121129 [PMID: 34427680 DOI: 10.1001/jamanetworkopen.2021.21129]

96 **Dong Y**, Song N, Wang J, Shi L, Zhang Z, Du J. Driver Gene Alterations in Malignant Progression of Gastric Cancer. *Front Oncol* 2022; **12**: 920207 [PMID: 35903675 DOI: 10.3389/fonc.2022.920207]

97 **Flavahan WA**, Gaskell E, Bernstein BE. Epigenetic plasticity and the hallmarks of cancer. *Science* 2017; **357** [PMID: 28729483 DOI: 10.1126/science.aal2380]

98 **Liu MC**, Oxnard GR, Klein EA, Swanton C, Seiden MV; CCGA Consortium. Sensitive and specific multi-cancer detection and localization using methylation signatures in cell-free DNA. *Ann Oncol* 2020; **31**: 745-759 [PMID: 33506766 DOI: 10.1016/j.annonc.2020.02.011]

99 **Stackpole ML**, Zeng W, Li S, Liu CC, Zhou Y, He S, Yeh A, Wang Z, Sun F, Li Q, Yuan Z, Yildirim A, Chen PJ, Winograd P, Tran B, Lee YT, Li PS, Noor Z, Yokomizo M, Ahuja P, Zhu Y, Tseng HR, Tomlinson JS, Garon E, French S, Magyar CE, Dry S, Lajonchere C, Geschwind D, Choi G, Saab S, Alber F, Wong WH, Dubinett SM, Aberle DR, Agopian V, Han SB, Ni X, Li W, Zhou XJ. Cost-effective methylome sequencing of cell-free DNA for accurately detecting and locating cancer. *Nat Commun* 2022; **13**: 5566 [PMID: 36175411 DOI: 10.1038/s41467-022-32995-6]

100 **Chakrabarti S**, Kasi AK, Parikh AR, Mahipal A. Finding Waldo: The Evolving Paradigm of Circulating Tumor DNA (ctDNA)-Guided Minimal Residual Disease (MRD) Assessment in Colorectal Cancer (CRC). *Cancers (Basel)* 2022; **14** [PMID: 35804850 DOI: 10.3390/cancers14133078]

101 **Kasi PM**, Fehringer G, Taniguchi H, Starling N, Nakamura Y, Kotani D, Powles T, Li BT, Pusztai L, Aushev VN, Kalashnikova E, Sharma S, Malhotra M, Demko ZP, Aleshin A, Rodriguez A, Billings PR, Grothey A, Taieb J, Cunningham D, Yoshino T, Kopetz S. Impact of Circulating Tumor DNA-Based Detection of Molecular Residual Disease on the Conduct and Design of Clinical Trials for Solid Tumors. *JCO Precis Oncol* 2022; **6**: e2100181 [PMID: 35263168 DOI: 10.1200/PO.21.00181]

102 **Kong Y**, Ning L, Qiu F, Yu Q, Cao B. Clinical significance of serum miR-25 as a diagnostic and prognostic biomarker in human gastric cancer. *Cancer Biomark* 2019; **24**: 477-483 [PMID: 30909187 DOI: 10.3233/CBM-182213]

103 **Ji B**, Huang Y, Gu T, Zhang L, Li G, Zhang C. Potential diagnostic and prognostic value of plasma long noncoding RNA LINC00086 and miR-214 expression in gastric cancer. *Cancer Biomark* 2019; **24**: 249-255 [PMID: 30689553 DOI: 10.3233/CBM-181486]

104 **Hung PS**, Chen CY, Chen WT, Kuo CY, Fang WL, Huang KH, Chiu PC, Lo SS. miR-376c promotes carcinogenesis and serves as a plasma marker for gastric carcinoma. *PLoS One* 2017; **12**: e0177346 [PMID: 28486502 DOI: 10.1371/journal.pone.0177346]

105 **Li Y**, Sun H, Guan J, Ji T, Wang X. Serum microRNA-381: A Potential Marker for Early Diagnosis of Gastric Cancer. *Yonsei Med J* 2019; **60**: 720-726 [PMID: 31347326 DOI: 10.3349/ymj.2019.60.8.720]

106 **Huang ZS**, Guo XW, Zhang G, Liang LX, Nong B. The Diagnostic and Prognostic Value of miR-200c in Gastric Cancer: A Meta-Analysis. *Dis Markers* 2019; **2019**: 8949618 [PMID: 31089400 DOI: 10.1155/2019/8949618]

107 **Jiang X**, Jiang M, Xu M, Xu J, Li Y. Identification of diagnostic utility and molecular mechanisms of circulating miR-551b-5p in gastric cancer. *Pathol Res Pract* 2019; **215**: 900-904 [PMID: 30732916 DOI: 10.1016/j.prp.2019.01.035]

108 **Zhao G**, Jiang T, Liu Y, Huai G, Lan C, Li G, Jia G, Wang K, Yang M. Droplet digital PCR-based circulating microRNA detection serve as a promising diagnostic method for gastric cancer. *BMC Cancer* 2018; **18**: 676 [PMID: 29929476 DOI: 10.1186/s12885-018-4601-5]

109 **Herrera-Pariente C**, Montori S, Llach J, Bofill A, Albeniz E, Moreira L. Biomarkers for Gastric Cancer Screening and Early Diagnosis. *Biomedicines* 2021; **9** [PMID: 34680565 DOI: 10.3390/biomedicines9101448]

110 **Yu Z**, Rong Z, Sheng J, Luo Z, Zhang J, Li T, Zhu Z, Fu Z, Qiu Z, Huang C. Aberrant Non-Coding RNA Expressed in Gastric Cancer and Its Diagnostic Value. *Front Oncol* 2021; **11**: 606764 [PMID: 34295803 DOI: 10.3389/fonc.2021.606764]

111 **Fu M**, Huang Z, Zang X, Pan L, Liang W, Chen J, Qian H, Xu W, Jiang P, Zhang X. Long noncoding RNA LINC00978 promotes cancer growth and acts as a diagnostic biomarker in gastric cancer. *Cell Prolif* 2018; **51** [PMID: 29271006 DOI: 10.1111/cpr.12425]

112 **Liu J**, Wang J, Song Y, Ma B, Luo J, Ni Z, Gao P, Sun J, Zhao J, Chen X, Wang Z. A panel consisting of three novel circulating lncRNAs, is it a predictive tool for gastric cancer? *J Cell Mol Med* 2018; **22**: 3605-3613 [PMID: 29700972 DOI: 10.1111/jcmm.13640]

113 **Zong W**, Feng W, Jiang Y, Ju S, Cui M, Jing R. Evaluating the diagnostic and prognostic value of serum long non-coding RNA CTC-497E21.4 in gastric cancer. *Clin Chem Lab Med* 2019; **57**: 1063-1072 [PMID: 30763257 DOI: 10.1515/cclm-2018-0929]

114 **Zhang G**, Xu Y, Wang S, Gong Z, Zou C, Zhang H, Ma G, Zhang W, Jiang P. LncRNA SNHG17 promotes gastric cancer progression by epigenetically silencing of p15 and p57. *J Cell Physiol* 2019; **234**: 5163-5174 [PMID: 30256413 DOI: 10.1002/jcp.27320]

115 **Zhang G**, Xu Y, Zou C, Tang Y, Lu J, Gong Z, Ma G, Zhang W, Jiang P. Long noncoding RNA ARHGAP27P1 inhibits gastric cancer cell proliferation and cell cycle progression through epigenetically regulating p15 and p16. *Aging (Albany NY)* 2019; **11**: 9090-9110 [PMID: 31665700 DOI: 10.18632/aging.102377]

116 **Lu X**, Lu J, Wang S, Zhang Y, Ding Y, Shen X, Jing R, Ju S, Chen H, Cong H. Circulating serum exosomal miR-92a-3p as a novel biomarker for early diagnosis of gastric cancer. *Future Oncol* 2021; **17**: 907-919 [PMID: 33533649 DOI: 10.2217/fon-2020-0792]

117 **Zhao R**, Zhang Y, Zhang X, Yang Y, Zheng X, Li X, Liu Y. Exosomal long noncoding RNA HOTTIP as potential novel diagnostic and prognostic biomarker test for gastric cancer. *Mol Cancer* 2018; **17**: 68 [PMID: 29486794 DOI: 10.1186/s12943-018-0817-x]

World Journal of Gastroenterology

Submit a Manuscript: https://www.f6publishing.com

World J Gastroenterol 2023 May 7; 29(17): 2534-2550

DOI: 10.3748/wjg.v29.i17.2534

ISSN 1007-9327 (print) ISSN 2219-2840 (online)

REVIEW

Non-invasive evaluation of liver steatosis with imaging modalities: New techniques and applications

Ke-Yu Zeng, Wu-Yong-Ga Bao, Yun-Han Wang, Min Liao, Jie Yang, Jia-Yan Huang, Qiang Lu

Specialty type: Gastroenterology and hepatology

Provenance and peer review: Invited article; Externally peer reviewed.

Peer-review model: Single blind

Peer-review report's scientific quality classification

Grade A (Excellent): A, A
Grade B (Very good): B, B
Grade C (Good): C
Grade D (Fair): 0
Grade E (Poor): 0

P-Reviewer: Losurdo G, Italy; Tai DI, Taiwan; Uhlmann D, Germany

Received: December 23, 2022
Peer-review started: December 23, 2022
First decision: February 16, 2023
Revised: February 26, 2023
Accepted: April 11, 2023
Article in press: April 11, 2023
Published online: May 7, 2023

Ke-Yu Zeng, Wu-Yong-Ga Bao, Yun-Han Wang, Min Liao, Jie Yang, Jia-Yan Huang, Qiang Lu, Department of Medical Ultrasound, West China Hospital of Sichuan University, Chengdu 610041, Sichuan Province, China

Corresponding author: Qiang Lu, MD, Professor, Department of Medical Ultrasound, West China Hospital of Sichuan University, No. 37 Guoxue Xiang, Chengdu 610041, Sichuan Province, China. luqiang@scu.edu.cn

Abstract

In the world, nonalcoholic fatty liver disease (NAFLD) accounts for majority of diffuse hepatic diseases. Notably, substantial liver fat accumulation can trigger and accelerate hepatic fibrosis, thus contributing to disease progression. Moreover, the presence of NAFLD not only puts adverse influences for liver but is also associated with an increased risk of type 2 diabetes and cardiovascular diseases. Therefore, early detection and quantified measurement of hepatic fat content are of great importance. Liver biopsy is currently the most accurate method for the evaluation of hepatic steatosis. However, liver biopsy has several limitations, namely, its invasiveness, sampling error, high cost and moderate intraobserver and interobserver reproducibility. Recently, various quantitative imaging techniques have been developed for the diagnosis and quantified measurement of hepatic fat content, including ultrasound- or magnetic resonance-based methods. These quantitative imaging techniques can provide objective continuous metrics associated with liver fat content and be recorded for comparison when patients receive check-ups to evaluate changes in liver fat content, which is useful for longitudinal follow-up. In this review, we introduce several imaging techniques and describe their diagnostic performance for the diagnosis and quantified measurement of hepatic fat content.

Key Words: Non-alcoholic fatty liver disease; Hepatic steatosis; Imaging techniques; Quantitative evaluation; Ultrasound; Quantitative ultrasound

©The Author(s) 2023. Published by Baishideng Publishing Group Inc. All rights reserved.

Core Tip: Accurate evaluation of the hepatic steatosis is important. The conventional gray scale ultrasound has the limitation of low diagnostic accuracy for mild hepatic steatosis and inability to make quantification evaluations. Quantification imaging techniques including ultrasound-based techniques and magnetic resonance imaging-based techniques can provide objective continuous numbers associated with liver fat content and past records can be found when patients receiving check-ups to evaluate change of liver fat content, which is useful for the longitudinal follow-up to monitor the impact of clinical interventions.

Citation: Zeng KY, Bao WYG, Wang YH, Liao M, Yang J, Huang JY, Lu Q. Non-invasive evaluation of liver steatosis with imaging modalities: New techniques and applications. *World J Gastroenterol* 2023; 29(17): 2534-2550
URL: https://www.wjgnet.com/1007-9327/full/v29/i17/2534.htm
DOI: https://dx.doi.org/10.3748/wjg.v29.i17.2534

INTRODUCTION

There are several types of chronic liver diseases, but nonalcoholic fatty liver disease (NAFLD) is the broadest state[1,2]. NAFLD represents a wide range of liver abnormalities[3]. Over 25% of general population is influenced by NAFLD, while affected proportion of type 2 diabetes population is 55%-80% [1]. Simple fatty liver may progress to non-alcoholic steatohepatitis (NASH), which is a severe form of fatty liver characterized by inflammation of hepatocyte. This form may result in cirrhosis with portal hypertension or liver dysfunction or even to hepatocellular carcinoma (HCC)[4]. Notably, there is an annual incidence of 0.4 cases of HCC per 1000 population-years among patients with NAFLD, making it the third most common cause of HCC in the United States[5]. A diagnosis of NAFLD is associated with not only adverse effects on the liver, but also an increased risk of type 2 diabetes and cardiovascular disease[6,7]. A study suggested that there was a significant increase in mortality associated with liver-specific diseases or cardiovascular diseases in patients with NAFLD compared to controls[8]. For patients who received hepatectomy, hepatic steatosis can increase incidence of postoperative complications and death[9]. The risk of graft failure for patients undergoing liver transplantation increases when hepatic steatosis exceeds 30%[10].

As NAFLD poses substantial risks of HCC, liver-associated complications and other adverse events to patients, it is of great importance to diagnose and quantify hepatic fat content early[4]. NAFLD is likely to be reversible in its early stage even with simple treatments, for example, lifestyle changes[11]. In addition, the main factor contributing to disease progression in patients with NAFLD is liver fibrosis[1, 3]. Abundant liver fat accumulation can trigger and accelerate hepatic fibrosis, thus contributing to disease progression[12,13]. Therefore, in patients with NAFLD, quantitative measurements of liver steatosis could be useful for prognostic assessment and treatment[4]. Although high level of liver fat can lead to fibrosis progression, it is of note that the level of liver fat is not always parallel to the grade of fibrosis. It has been suggested that patients without fibrosis or in the early stages of fibrosis may demonstrate obvious disease progression with high level of liver fat content; however, the fat content decreases when disease progresses to advanced fibrosis or cirrhosis[14-16]. Therefore, when evaluating the value of measuring hepatic steatosis for assessing disease progression and prognosis, the fibrosis status should first be taken into account[17].

When it comes to diagnosing diffuse hepatic disease, liver histopathologic examination is the most precise method. With liver biopsy, quantification of the liver fat level is classified into four grades (grade 0, < 5%; grade 1, 5%-33%; grade 2, 33%-66%; grade 3, > 66%)[18]. Although the use of liver biopsy correctly evaluates liver steatosis, its limitations include its invasiveness, sampling error, which make biopsy impractical for patients who have only simple steatosis[19,20]. Therefore, noninvasive methods to diagnose the presence of steatosis and to monitor changes in hepatic steatosis are needed (Table 1). Conventional gray-scale ultrasound can be applied to diagnose liver steatosis. However, its inability to provide accurate quantification of liver fat has limited its use in the diagnostic pathway of liver steatosis[21]. At present, a number of imaging techniques for the evaluation of hepatic fat content, including MR- and ultrasound-based methods, have been developed. In this review, we summarize the available imaging methods for the quantified measurement of hepatic fat content. In addition, we briefly discuss the clinical performance of these methods.

ULTRASOUND-BASED METHODS TO DIAGNOSE AND QUANTIFY HEPATIC STEATOSIS

Table 2 summarizes published diagnostic utility metrics and optimal cutoff values of quantitative ultrasound methods for quantified measurement of hepatic fat content.

Table 1 Characteristics of imaging techniques for hepatic steatosis evaluation

Techniques	Clinical characteristics	Limitations
CAP	Low cost; High availability; Time-saving	High measurement failure rate
	Allows simultaneous evaluation of steatosis and fibrosis	Measurement without B-mode ultrasound image
	Moderate to high diagnostic accuracy for detecting and grading steatosis	The cutoff value for diagnosing steatosis is poorly standardized
	Moderate to high repeatability and reproducibility	
	Well validated	
ATI, ATT and UGAP	Outperform or have comparable diagnostic accuracy compared with CAP	The measurement may be influenced by liver fibrosis
	High repeatability and reproducibility	Fairly small number of studies
	Strong correlation with liver histology or MRI-PDFF	
	Low measurement failure rate	
	Measured on B-mode ultrasound images	
Att. PLUS	Measurement is obtained at the same time as the sound speed measurement	Fairly small number of studies
	Comparable diagnostic accuracy with CAP	No study comparing this technique with liver histology or MRI-PDFF
TAI and TSI	High diagnostic accuracy for detecting and grading steatosis	Fairly small number of studies
	Strong correlation with MRI-PDFF	
	High repeatability and reproducibility	
BSC	Uses a reference phantom to reduce sources of variability due to ultrasound systems or operators	Fairly small number of studies
	High diagnostic accuracy for detecting and grading steatosis	
	Strong correlation with liver histology or MRI-PDFF	
	High repeatability and reproducibility	
UDFF	Is a combination of both attenuation coefficient and backscatter coefficient	Fairly small number of studies
	UDFF approximates MRI-PDFF	
ASQ and NLV	Moderate to high diagnostic accuracy for detecting and grading steatosis	Weak correlation with liver histology
	Strong correlation with CAP	The correlation with MR-based techniques is controversial
		The influence of fibrosis on measurement is controversial
		Fairly small number of studies
SS	Moderate to high diagnostic accuracy for detecting and grading steatosis	Fairly small number of studies
	Strong correlation with CAP	
MRS and MRI-PDFF	High diagnostic accuracy for detecting and grading steatosis	High cost; low availability
	Considered as the reference standard	Time-consuming

CAP: Controlled attenuation parameter; ATI: Attenuation imaging; ATT: Attenuation measurement function; UGAP: Ultrasound-guided attenuation parameter; Att. PLUS: Attenuation plane-wave ultrasound; TAI: Tissue attenuation imaging; TSI: Tissue scatter distribution imaging; BSC: Backscatter coefficient; UDFF: Ultrasound-derived fat fraction; ASQ: Acoustic structure quantification; NLV: Normalized local variance; SS: Speed of sound; MRS: Magnetic resonance spectroscopy; MRI-PDFF: Magnetic resonance imaging-proton density fat fraction.

Conventional gray scale ultrasound

Due to its low price and availability, gray scale ultrasound is a traditional diagnostic method for diagnosing and monitoring liver steatosis[22]. When using this method, fatty infiltration is indicated by the following signs: Hyperechogenicity of the liver parenchyma, liver-to-kidney comparison, ultrasound beam attenuation, and impaired visualization of the intrahepatic structures[23]. However, it is difficult for operators to grade liver steatosis solely based on the gray scale ultrasound[24]. Degree of liver fat content can be classified into 4 grades (normal, mild, moderate, and severe)[22]. For moderate to severe hepatic steatosis, gray scale ultrasound has a high diagnostic accuracy. A meta-analysis enrolling a total of 2815 patients and using hepatic histopathologic results as the golden standard demonstrated that the overall sensitivity and specificity of gray scale ultrasound to distinguish normal liver and moderate steatosis were 85% and 93%[25]. However, gray scale ultrasound has restricted diagnostic performance for mild steatosis[24]. Another limitation is that gray scale ultrasound is based on qualitative visual features, and the intraobserver and interobserver reproducibility vary with different operators[26,27].

Hepatorenal index

To improve the diagnostic performance of using gray scale ultrasound for the measurement of liver content, hepatorenal index (HRI) was developed[28] (Figure 1). This metric calculates the rate of parenchymal echo of the liver and the renal cortex[28]. Previous studies found that HRI had a significant correlation with histologic steatosis[29-31]. Marshall *et al*[32] reported a sensitivity, confirmed by liver biopsy, of 100% with an HRI cutoff of 1.27 for detecting more than 5% steatosis. Borges *et al*[33] reported for diagnosing fatty liver, the cutoff value of 1.24 revealed 93% sensitivity and specificity, but this study only used healthy volunteers as the control group. Stahlschmidt *et al*[34] suggested in livers with advanced fibrosis, HRI should not be used to measure steatosis because fibrosis replaces fat as NAFLD progresses. Similarly, patients suffering from chronic kidney disease may present increased echo of the renal cortex, which makes the HRI unreliable for grading steatosis[35]. Furthermore, Kjaergaard *et al*[36] found that HRI presented a higher incidence of failure (12%) compared to controlled attenuation parameter (CAP, 2%). In addition, it can be challenging to diagnose mild steatosis by HRI[33].

Quantitative ultrasound techniques

Mechanism of quantitative ultrasound techniques: Conventional gray scale ultrasound and HRI cannot provide quantitative information about liver fat content. Essentially, quantitative methods are used to model the relationship between physical properties of hepatic tissue and the echo signals that are scattered by it. The impedance difference of fat vesicles in hepatocytes causes increased scattering magnitudes and signal attenuation. A frequency-dependent analysis of signal attenuation and backscatter is performed on signals returned by tissue[37].

The quantitative ultrasound techniques used for the measurement of hepatic fat quantification included the spectral-based techniques and the techniques based on envelope statistics. Estimation of either attenuation coefficient (AC) or the backscatter coefficient (BSC) is used for spectral based techniques. The AC measures energy loss as ultrasound wave passes through tissue and the BSC measures the returned ultrasound energy when ultrasound wave strikes the microstructure of tissue. Techniques based on the envelope statistics of the backscattered ultrasound include the acoustic structure quantification (ASQ), normalized local variance (NLV), and estimation of sound speed[38]. Techniques according to envelope statistics are relatively novel. Microstructural characteristics of tissues can be determined by the shape and attributes of backscattered ultrasound[38].

Current commercial techniques and their mechanism of hepatic steatosis quantification are presented in Table 3.

CAP: CAP was the initial available technique for quantified measurement of hepatic fat content. Attenuation of the ultrasound beam is applied to generate the CAP amount[39,40]. Typically, two types of probes, the medium probe and the extra-large probe, can be utilized. The choice of optimal probe is automatically controlled according to skin-to-liver capsule distance (SCD). When the SCD exceeds 2.5 cm, the extra-large probe is more effective than the M probe. The CAP is presented in units of decibels per meter (dB/m)[41].

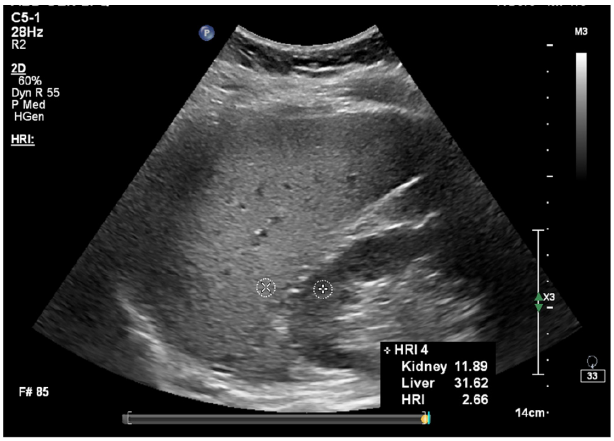
More than 160 studies have discussed the efficacy of CAP as a metric for quantified measurement of liver fat content, and acceptable accuracy was found. The general diagnostic accuracy evaluated by the area under the receiver operating curve (AUROC) of CAP for detecting presence of steatosis has been displayed to range from 0.64 to 0.97[42-44]. A meta-analysis including 19 studies found that CAP had good diagnostic performance with AUROCs of 0.823 for distinguishing steatosis grade > S0, 0.865 for distinguishing steatosis grade > S1, 0.882 for distinguishing steatosis grade > S2. The corresponding optimal cutoff values for > S0, > S1, > S2 were 248, 268 and 280 dB/m. Moreover, they found that there was a potential link between NAFLD, diabetes mellitus, and body mass index with the CAP value[45]. Although the diagnostic utility of CAP for differentiating patients with and without hepatic steatosis has been fully validated, the optimal cutoff value to determine the presence of steatosis varies significantly between studies[17]. A meta-analysis of 2346 participants with different diffused hepatic diseases demonstrated that CAP cutoffs varied according to the etiology of the hepatic diseases,

Table 2 Summary of studies using ultrasound methods to evaluate hepatic steatosis

Ref.	No.	Method	Reference standard	Grade of steatosis	Optimal cutoff value	AUROC
Bae *et al*[59], 2019	108	ATI	LB	≥ S1	0.64	0.84
				≥ S2	0.70	0.89
				≥ S3	0.75	0.93
Bae *et al*[60], 2022	120	ATI	LB	≥ S1	0.66	0.91
				≥ S2	0.66	0.91
Tada *et al*[62], 2019	148	ATI	LB	≥ S1	0.66	0.85
				≥ S2	0.67	0.91
				≥ S3	0.68	0.91
Tada *et al*[63], 2020	119	ATI	MRI-PDFF	≥ S1	0.63	0.81
				≥ S2	0.73	0.87
				≥ S3	0.75	0.94
Jeon *et al*[61], 2019	87	ATI	MRI-PDFF	≥ S1	0.59	0.76
Ferraioli *et al*[65], 2019	129	ATI	MRI-PDFF	≥ S1	0.63	0.91
				≥ S2	0.72	0.95
Ferraioli *et al*[66], 2021	72	ATI-GEN	MRI-PDFF	≥ S1	0.62	0.92
		ATI-PEN	MRI-PDFF	≥ S1	0.69	0.90
Sugimoto *et al*[67], 2021	111	ATI	LB	≥ S1	0.67	0.88
				≥ S2	0.72	0.86
				≥ S3	0.86	0.79
Hsu *et al*[70], 2021	28	ATI	LB	≥ S1	0.69	0.97
				≥ S2	0.78	0.99
				≥ S3	0.82	0.97
Kwon *et al*[57], 2021	100	ATI	MRI-PDFF	≥ S1	0.62	0.91
				≥ S2	0.72	0.94
Jang *et al*[58], 2022	57	ATI	LB	≥ S1	0.62	0.81
Koizumi *et al*[73], 2019	89	ATT	LB	≥ S1	0.68	0.74
				≥ S2	0.72	0.80
				≥ S3	0.78	0.96
Tamaki *et al*[54], 2018	351	ATT	LB	≥ S1	0.63	0.79
				≥ S2	0.69	0.87
				≥ S3	0.85	0.96
Fujiwara *et al*[75], 2018	163	UGAP	LB	≥ S1	0.53	0.90
				≥ S2	0.60	0.95
				≥ S3	0.65	0.96
Imajo *et al*[76], 2022	1010	UGAP	MRI-PDFF	≥ S1	0.65	0.91
				≥ S2	0.71	0.91
				≥ S3	0.77	0.89
Kuroda *et al*[79], 2021	202	UGAP	LB	≥ S1	0.49	0.89
				≥ S2	0.65	0.91

				≥ S3	0.69	0.92
Tada *et al*[80], 2019	126	UGAP	MRI-PDFF	≥ S1	0.60	0.92
				≥ S2	0.69	0.87
				≥ S3	0.69	0,89
Jeon *et al*[83], 2021	120	TAI	MRI-PDFF	≥ S1	0.88	0.86
		TSI	MRI-PDFF	≥ S1	91.2	0.96
Rónaszéki *et al*[84], 2022	110	TAI	MRI-PDFF	≥ S1	0.59	0.92
		TSI	MRI-PDFF	≥ S1	99.7	0.91
Şendur *et al*[85], 2023	80	TAI	MRI-PDFF	≥ S1	0.75	0.95
				≥ S2	0.86	0.97
				≥ S3	0.96	0.97
		TSI	MRI-PDFF	≥ S1	92.44	0.96
				≥ S2	96.64	0.91
				≥ S3	99.45	0.94
Lin *et al*[91], 2015	204	BSC	MRI-PDFF	≥ S1	0.0038	0.98
Dillman *et al*[94], 2022	56	UDFF	MRI-PDFF	≥ S1	5%	0.90
Labyed *et al*[37], 2020	101	UDFF	LB	≥ S1	8.1%	0.94
				≥ S2	15.9%	0.88
				≥ S3	16.1%	0.83

AUROC: Area under the receiver operating characteristic curve; LB: Liver biopsy; MRI-PDFF: Magnetic resonance imaging-proton density fat fraction; ATI: Attenuation imaging; ATT: Attenuation measurement function; UGAP: Ultrasound-guided attenuation parameter; TAI: Tissue attenuation imaging; TSI: Tissue scatter distribution imaging; BSC: Backscatter coefficient; UDFF: Ultrasound-derived fat fraction.



DOI: 10.3748/wjg.v29.i17.2534 **Copyright** ©The Author(s) 2023.

Figure 1 Hepatorenal index. In this case, the result was 2.66, indicating severe hepatic steatosis.

including NAFLD, chronic viral hepatitis, alcoholic liver disease[46].

The CAP value demonstrated a moderate to strong correlation with magnetic resonance (MR)-based techniques for liver steatosis quantification[47,48]. However, compared with MR-based methods, the CAP has inferior diagnostic ability in grading liver steatosis. Diagnostic effectiveness of MR spectroscopy (MRS) over CAP for diagnosing S1 was significantly higher (AUROC, 0.77 *vs* 0.99)[49]. Imajo *et al*[50] demonstrated suboptimal diagnostic performance of CAP compared to MRI-proton density fat fraction (MRI-PDFF) in grading liver steatosis.

However, CAP has the limitation of failure rate up to 7.7%. According to previous reports, an association was found between measurement failure and sex, body mass index, and metabolic syndrome[51]. Use of the extra-large probe can reduce the failure rate because it is designed for patients

Table 3 Summary of techniques for liver fat quantification and their mechanisms

Technique	Mechanism for liver fat quantification	Principle of the techniques
CAP	Spectral based technique (AC)	CAP measures the attenuation of or reduction in the amplitude of the ultrasound waves on their way through the liver
ATI	Spectral based technique (AC)	ATI quantifies the degree of the ultrasound beam attenuation. The attenuation of the ultrasound beam is calculated by analyzing echo signals received by the transducer
ATT	Spectral based technique (AC)	Two ultrasonic waves of different frequencies (F0, F1; F0 < F1) are transmitted to the same beamline and the received signal is obtained. ATT estimates the attenuation coefficient it by calculating the slope of the received signal ratio (F0/F1)
UGAP	Spectral based technique (AC)	UGAP compares the measured liver signal and the referential signal (measured on the reference phantom with known attenuation and backscatter coefficients)
Att. PLUS	Spectral based technique (AC)	Att. PLUS measures the decrease in amplitude of ultrasound waves as they propagate throughout the tissue
TAI	Spectral based technique (AC)	TAI is determined based on the attenuation properties of different frequency components in the tissue, and the spectrum of radiofrequency signals provides a downshift of the center frequency according to depth. The TAI parameter indicates the slope of the ultrasound center frequency downshift
BSC	Spectral based technique (BSC)	BSC measures the ultrasound energy returned from the tissue
UDFF	Spectral based technique (BSC)	UDFF is obtained by combining both AC and BSC and the result is presented as the percentage of hepatic steatosis. Reference phantom data is integrated into the ultrasound system and fixed-acquisition region of interest is applied
TSI	Envelope Statistic based technique	The TSI is based on the shape parameter of the Nakagami distribution which reflects the local concentration and arrangement of ultrasound scatterers
ASQ	Envelope Statistic based technique	ASQ measures the FD ratio, which is based on the difference between theoretical and real echo amplitude distributions
NLV	Envelope Statistic based technique	NLV parameter was derived from ASQ, which analyzed ultrasound amplitudes sampled from gray-scale ultrasound images
SS	Envelope Statistic based technique	SS calculates the speed of sound through the liver
SSp.PLUS	Envelope Statistic based technique	SSp.PLUS is a novel technique that allows quantification of the intrahepatic speed of sound which is correlated with the liver fat content

AC: Attenuation coefficient; BSC: Backscatter coefficient; CAP: Controlled attenuation parameter; ATI: Attenuation imaging; ATT: Attenuation measurement function; UGAP: Ultrasound-guided attenuation parameter; Att.PLUS: Attenuation plane-wave ultrasound; TAI: Tissue attenuation imaging; UDFF: Ultrasound-derived fat fraction; TSI: Tissue scatter distribution imaging; ASQ: Acoustic structure quantification; NLV: Normalized local variance; SS: Speed of sound; SSp.PLUS: Sound speed plane-wave ultrasound; FD: Focal disturbance.

with obesity[4].

Quantification of attenuation using ultrasound imaging: Several techniques aiming to evaluate the attenuation coefficient applying ultrasound guidance have been exploited, including attenuation imaging (ATI), attenuation measurement function (ATT), and ultrasound guided attenuation parameter (UGAP). CAP has a disadvantage that it lacks the guidance of gray scale ultrasound images in choosing the area for measurement. In contrast, the ATI, ATT, and UGAP techniques are characterized by evaluating liver steatosis on gray scale ultrasonography images with accurate placement of region of interest[17]. When using these techniques, conventional gray scale ultrasound images can be evaluated simultaneously, and the exact region of interest can be placed to avoid the vessels, bile duct, masses or cysts. Therefore, the technical success rate using these methods is high[52-55]. Another advantage of ATI, ATT, and UGAP is that these techniques have high intraobserver and interobserver agreement. A range of 0.81 to 0.98 is found for the intraobserver agreement of ATI, and a range of 0.79 to 0.92 is found for the interobserver agreement. Although there are few studies investigating the topic, the intraobserver and interobserver agreement of UGAP is reported to be 0.86 and 0.84, respectively. In addition, ATI measurements among different operators demonstrated high agreement (intraclass correlation coefficients: 0.91)[17,44,56].

ATI is a kind of two-dimensional attenuation imaging technique (Figure 2)[57,58]. ATI assesses the attenuation of ultrasound beams in a region of interest using color-coded maps in real time. dB/cm/MHz is the unit of measurement for the attenuation coefficient[35]. In addition, to ensure a high technique success rate, the ATI is equipped with a reliability index (R^2), and an R^2 value ≥ 0.80 is considered a reliable measurement[59-61]. In the reported measurements, the cutoff values ranged from 0.63 to 0.69 dB/cm/MHz for detecting ≥ S1, 0.66-0.72 dB/cm/MHz for detecting ≥ S2, and 0.68-0.86 dB/

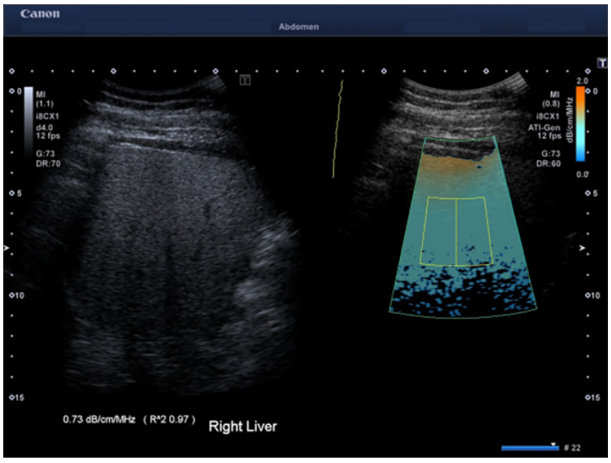


Figure 2 Attenuation imaging technique by Canon with reliability indicator (R^2)[40]. The Gray scale image and the corresponding attenuation imaging image are shown side by side. The attenuation coefficient measurement of the images shown here is 0.73 dB/cm/MHz with an R^2 of 0.97, indicating a valid measurement. Citation: Seneviratne N, Fang C, Sidhu PS. Ultrasound-based hepatic fat quantification: current status and future directions. *Clin Radiol* 2023; 78: 187-200. Copyright© The Author(s) 2023. Published by Elsevier Ltd. The authors have obtained the permission for figure using (Supplementary material).

cm/MHz for detecting = S3. The reported AUROCs were 0.80-0.97 for detecting ≥ S1, 0.86-0.99 for detecting ≥ S2, and 0.79-0.99 for detecting = S3[59-70]. It has been found that ATI measurements have a significant correlation with histological steatosis grade determined by liver biopsy[59,60,67]. Additionally, in case where MRI-PDFF was applied as the gold standard, the ATI demonstrated positive correlation with it (r = 0.70-0.83)[57,65,66]. The ATI also outperformed the CAP in evaluating the grades of hepatic steatosis. A study including 72 consecutive adult patients found that the AUROC for detecting S0 *vs* S1-S3 of CAP was lower than that of ATI (0.85 *vs* 0.92, respectively)[66].

ATT is a technique developed by Fujifilm Health Care company (previously Hitachi Medical Systems, Japan) (Figure 3). In ATT, a beamline is connected to an ultrasonic transmitter with two ultrasonic waves of different frequencies (F0, F1) at once. The received signal is obtained, and attenuation coefficients are determined by the slope of the received signal ratio (F0/F1). The results are presented in units of dB/cm/MHz[54,55,71-73]. A study enrolled 351 patients and biopsy specimens were examined quantitatively for fat content. In terms of fat area, ATT had a significant correlation (r = 0.50, P < 0.001). The cutoff values were 0.62 dB/cm/MHz for S ≥ 1, 0.67 dB/cm/MHz for S ≥ 2 and 0.73 dB/cm/MHz for S ≥ 3 and corresponding AUROCs were 0.79, 0.87 and 0.96[54]. An analysis of 94 patients who received both ATT and CAP examinations when undergoing liver histopathologic examination revealed that ATT exhibited diagnostic accuracy equivalent to that of CAP for grading histological steatosis[73].

With known attenuation and BSC, an ultrasound system uses a phantom method to calculate attenuation coefficients measurement implemented in UGAP (Figure 4). Using this method, the US system's transmitting and receiving beamforming characteristics can be compensated. The result is presented in units of dB/cm/MHz[4,74-76]. Several studies reported good diagnostic efficacy of UGAP for liver fat content quantification applying hepatic histological results as the gold standard, and a positive association was found between UGAP and steatosis percentage (correlation coefficient: 0.78-0.81). The reported AUROCs were 0.89-0.92 for detecting steatosis grade ≥ S1, 0.90–0.95 for detecting steatosis grade ≥ S2, and 0.88-0.96 for detecting steatosis grade = S3[75,77-79]. Several other studies compared UGAP with MR-based methods, and a significant correlation between MR-based methods and attenuation coefficient values by UGAP was found (correlation coefficient: 0.72-0.77)[76,80]. Imajo *et al*[76] conducted a multicentric study with 1010 patients and reported that UGAP had good diagnostic efficacy for making quantified measurement of liver fat content. In their study, the AUROCs were 0.910 for detecting MRI-PDFF ≥ 5.2%, 0.912 for MRI-PDFF ≥ 11.3%, and 0.894 for MRI-PDFF ≥17.1%[76]. Fujiwara *et al*[75] reported that as compared to CAP, UGAP achieved significantly higher AUROCs for identifying ≥ S2 (0.950 *vs* 0.841) and ≥ S3 (0.959 *vs* 0.817). In addition, they also reported 5.2% of CAP patients had measurement failures, while no UGAP patients did. Tada *et al*[81] reported that there was no effect of liver stiffness on UGAP attenuation coefficient values.

Attenuation plane-wave ultrasound: Attenuation Plane-Wave Ultrasound (Att. PLUS) presents information on ultraphonic beam attenuation through a region of interest. The ultrasound beam attenuation is calculated in a region of interest at a constant depth. The attenuation coefficient results are displayed in units of dB/cm/MHz[56]. The Att. PLUS measurement is combined with the sound speed measurement for each acquisition. It is the median of five measurements taken consecutively that determines the final result[35]. Only one published study regarding this method was found. Popa *et al*[82] carried out a study aiming to assess the clinical value of Att. PLUS of noninvasive measurement of fatty liver with the CAP value considered as control. They reported that the cutoff value to detect S2-S3

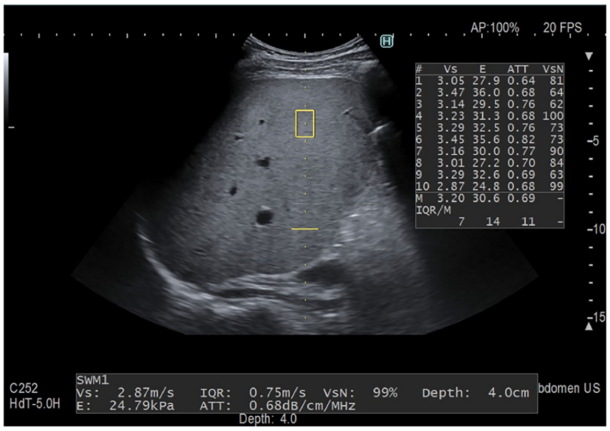


Figure 3 The attenuation measurement function technique was developed by Fujifilm Health Care company[4]. The attenuation coefficient (0.68 dB/cm/MHz) is measured in a fixed area (yellow box) along the same axis as the liver stiffness measurement. Ten acquisitions are performed, and the median value is utilized as the final metric. Citation: Ferraioli G, Berzigotti A, Barr RG, Choi BI, Cui XW, Dong Y, Gilja OH, Lee JY, Lee DH, Moriyasu F, Piscaglia F, Sugimoto K, Wong GL, Wong VW, Dietrich CF. Quantification of Liver Fat Content with Ultrasound: A WFUMB Position Paper. *Ultrasound Med Biol* 2021; 47: 2803-2820. Copyright© The Author(s) 2021. Published by Elsevier Ltd. The authors have obtained the permission for figure using (Supplementary material).

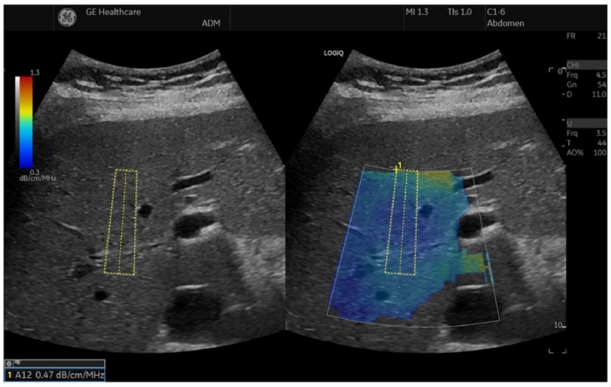


Figure 4 The ultrasound-guided attenuation parameter method implemented in the LOGIQ E9 XDclear 2.0 US scanner[4]. The attenuation coefficient is 0.47 dB/cm/MHz, indicating less than 5% steatosis. Citation: Ferraioli G, Berzigotti A, Barr RG, Choi BI, Cui XW, Dong Y, Gilja OH, Lee JY, Lee DH, Moriyasu F, Piscaglia F, Sugimoto K, Wong GL, Wong VW, Dietrich CF. Quantification of Liver Fat Content with Ultrasound: A WFUMB Position Paper. *Ultrasound Med Biol* 2021; 47: 2803-2820. Copyright© The Author(s) 2021. Published by Elsevier Ltd. The authors have obtained the permission for figure using (Supplementary material).

was 0.5 dB/cm/MHz (sensitivity 53.1%, specificity 82.0%), and the AUROC was 0.72.

Tissue attenuation imaging and tissue scatter distribution imaging: Tissue attenuation imaging (TAI) parameter indicates slope of the ultrasound central frequency downshift along depth, which is able to be utilized to calculate acoustic attenuation. The tissue scatter distribution imaging (TSI) parameter is a measurement of the Nakagami parameters in the region of interest, which reflects the concentration of ultrasound scatterers and their arrangement locally[35,83].

We found three studies comparing TAI and TSI with MRI-PDFF, and these studies revealed that both TAI and TSI revealed correlation with MRI-PDFF[84-86]. Jeon *et al*[86] enrolled 120 patients to assess feasibility of TAI and TSI for hepatic steatosis quantification utilizing MRI-PDFF as the reference. According to MRI-PDFF, the participants were classified into three groups (≤ 5%, 5%-10%, and ≥ 10%). They found that both methods had excellent utility for diagnosing and evaluating the degree of hepatic steatosis. For diagnosing fatty quantification of ≥ 5% and ≥ 10%, the AUROCs of TAI were 0.861 and 0.835, and those of TSI were 0.964 and 0.935, respectively[86]. Rónaszéki *et al*[84] compared TAI with TSI utilizing MRI-PDFF as gold standard enrolling 101 participants and found that TAI provided better diagnostic performance than TSI for diagnosing ≥ 5% MRI-PDFF (AUROC: 0.89 *vs* 0.87) and ≥ 10% (AUROC: 0.93 *vs* 0.86). TAI and TSI revealed good intra- and interobserver agreement. In TAI, the intra- and interobserver ICCs were reported at 0.994 and 0.975, respectively, while in TSI, they were reported at 0.991 and 0.947[87].

Techniques based on ultrasound BSC: Using the BSC, we can determine amount of ultrasound energy reflected by the tissue. Applying computer algorithm and a reference phantom, the BSC can be

estimated with less changeability resulted from ultrasound systems and operators. The right liver lobe was used to obtain gray scale images, and in the same liver region, a continuous series of 10 frames of transducer signals was captured. Then, in the tissue-imitating reference phantom, which mimics the acoustic properties of human hepatic tissue, consecutive frames were noted without changing scanner settings[35,88-90].

The diagnostic accuracy of the BSC has been evaluated by Lin *et al*[91] by analyzing 204 participants. They found that BSC was positively correlated with MRI-PDFF (Spearman's $\rho = 0.80$; $P < 0.0001$). BSC had an AUROC of 0.98 with a cutoff value of 0.00381/cm-steradian for detecting patients with hepatic steatosis. In addition, when using the optimal BSC cutoff value, in the training group, hepatic steatosis was detected with 93% sensitivity and 97% specificity, while in the validation group, it was detected with 87% sensitivity and 91% specificity[91].

Han *et al*[89,90,92,93] published several studies focusing on the use of the BSC. In a study including 102 participants, they revealed moderate correlation of the BSC with MRI-PDFF (Pearson's $r = 0.58$, $P < 0.001$)[93]. In addition, they enrolled 41 participants to study the repeatability and reproducibility of BSC and found that ICC were 0.87-0.95 for BSC acquired without participant repositioning and 0.69-0.82 with participant repositioning, suggesting that BSC measurement is repeatable and reproducible in patients with NAFLD[89].

Ultrasound-derived fat fraction

The ultrasound-derived fat fraction (UDFF) technique is a coalition of attenuation coefficient and BSC, and a percentage of liver fat content is reported as the result. Data from reference phantoms is integrated into the ultrasound system, and a fixed-acquisition region of interest is utilized[4] (Figure 5). Labyed and Milkowski[37] designed the UDFF method and conducted a study including 101 participants. They found that the UDFF was positively correlated with the MRI-PDFF (Pearson's $r = 0.87$). Using the histology results as the gold standard, the AUROCs of UDFF were 0.94 for detecting S ≥ 1, 0.88 for S ≥ 2 and 0.83 for S = 3. When using MRI-PDFF to be the gold standard, AUROCs of UDFF were 0.97 for diagnosing MRI-PDFF higher than 5%, 0.95 for diagnosing MRI-PDFF higher than 10% [37]. Similarly, Dillman *et al*[94] reported that liver fat content quantification applying UDFF showed a significant correlation with MRI-PDFF (Spearman's $\rho = 0.82$; $P < 0.001$).

ASQ: Quantifying the acoustic structure of an environment by comparing theoretical and real echo amplitude distributions is referred to as ASQ. In order to compute the theoretical echo amplitude distribution of the hepatic section imaged, the Rayleigh distribution function, assuming that solely ultrasound beam interference from small scattering objects generates the speckle pattern, is applied. However, actual echo amplitude distribution of the liver parenchyma does not follow the Rayleigh distribution. Because ultrasound beams are scattered by small structures, for example the walls of hepatic vessels, resulting in heterogeneity in echo amplitudes[95,96]. However, when diffuse liver diseases cause changes in parenchymal echotexture, ASQ can provide quantitative information by comparing theoretical echo amplitude distribution to a real distribution[97]. Kuroda *et al*[98] tested the ASQ-derived focal disturbance ratio (FD ratio) with 9 Leptin-deficient mice in comparison with histopathological results and found that the FD ratio had significant negative correlations with the fat droplet area (Spearman $r = -0.72$, $P = 0.0017$) and fat droplet size (Spearman $r = -0.98$, $P = 0.0052$), suggesting that the FD ratio can be used to quantify steatosis grade in an animal model and may be a quantitative metric of hepatic steatosis[98]. Karlas *et al*[95] conducted a cohort study to compare ASQ with MRS, and negative correlation was found between FD ratio and MRS (Spearman $r = -0.43$, $P = 0.004$). Similarly, in a prospective study including 36 patients with suspected fatty liver disease, the FD ratio showed a strong, negative correlation with the MRS in 36 patients[99]. Son *et al*[100] also reported FD ratio is comparable to hepatic fat fraction by MRS to make quantified measurement of liver fat content and diagnose liver fat content more than 10% in donor liver patients. Keller *et al*[96] found significant negative correlation between ASQ and steatosis level obtained by histological examination ($r = -0.55$, $P < 0.0001$). Nevertheless, they found no correlation between histologically determined fibrosis stage and any measurements of ASQ.

NLV: The NLV is derived from ASQ and analyzes ultrasound amplitudes sampled from grayscale ultrasound images[4,101]. Bae *et al*[102] assessed the clinical value of the NLV in the measurement of liver fat content in comparison with MRS in 40 male mice using histopathology as the golden standard and found that the AUROCs for diagnosing mild, moderate, and severe hepatic steatosis were 0.953, 0.896, and 0.735, and the NLV value performed similarly to MRS in detecting mild or moderate hepatic steatosis. The same authors also conducted a study with 194 patients to assess the diagnostic efficacy of the NLV for diagnosing and grading liver fat content using liver histopathology as the reference standard. They demonstrated the NLV had excellent diagnostic efficacy in detecting and grading fatty liver with AUROCs of 0.911 for ≥ steatosis grade 1, 0.974 for ≥ steatosis grade 2, and 0.954 ≥ steatosis grade 3[103].

Speed of sound: A speed of sound (SS) estimation is based on the fact that sound speed varies with fat content in soft tissues, and that the relationship between sound speed and liver fat percentage can be

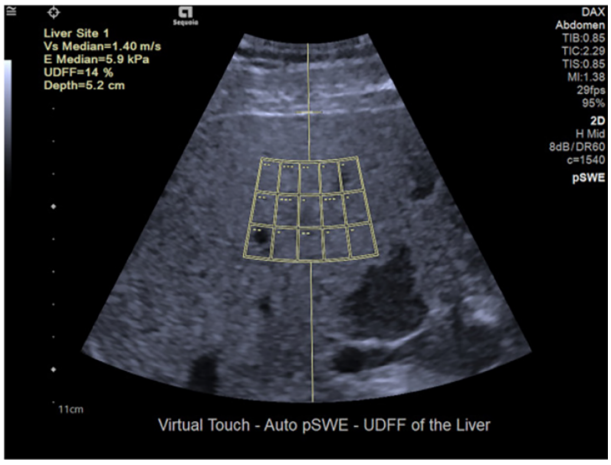


Figure 5 Ultrasound-derived fat fraction method[40]. The ultrasound-derived fat fraction method approximates the magnetic resonance imaging-derived proton density fat fraction and is based on the combination of the attenuation and backscatter coefficient. The method provides both liver stiffness measurement (5.9 kPa in this case) and the percentage of fat accumulation (14% in this case). Citation: Seneviratne N, Fang C, Sidhu PS. Ultrasound-based hepatic fat quantification: current status and future directions. *Clin Radiol* 2023; 78: 187-200. Copyright© The Author(s) 2023. Published by Elsevier Ltd. The authors have obtained the permission for figure using (Supplementary material).

identified[104]. Dioguardi Burgio *et al*[104] carried out a study aiming to explore the value of SS for detecting and quantifying liver steatosis and included 100 patients who underwent both SS and abdominal MR. They found that, in the training cohort, a cut-off value of less than 1.537mm/s led to 87% sensitivity and 95.7% specificity for diagnosing any steatosis with an AUROC of 0.882%. Based on an SS cut-off value of 1.511mm/s, the sensitivity was 100% and specificity was 95.6% for detecting moderate to severe steatosis and the AUROC was 0.989[104].

Sound speed plane-wave ultrasound (SSp.PLUS) is a novel technique for measuring intrahepatic sound speed which is correlated with the liver fat content. The measurement of SSp.PLUS is expressed in m/s[82]. Popa *et al*[82] performed a study with 215 patients to test the value of SSp.PLUS in detecting and grading hepatic fat level applying the CAP value as the gold standard. As a first finding, SSp.PLUS is more closely correlated with CAP values than Att.PLUS: (r = -0.74) *vs* (r = 0.45). Furthermore, the SSp.PLUS cut-off of less than 1516 m/s indicated 98.36% specificity and 58.74% sensitivity for predicting the presence of significant steatosis (S2-S3)[82].

CONCLUSION

Quantification ultrasound techniques can provide objective continuous number associated with liver fat content and past records can be found when patients receiving check-ups to evaluate change of degree of fatty liver, which is useful for follow-up to monitor the impact of any clinical interventions. Besides, as hepatic steatosis may pose adverse effects to prognosis of patients, quantification of liver fat holds clinical significance. For example, substantial hepatic fat accumulation may contribute to rapid disease progression toward NASH or liver fibrosis[105]. Patients with liver resections are more likely to suffer postoperative complications and die due to liver fat accumulation. Compared with patients without steatosis, those with ≤ 30% steatosis have a significantly increased risk of postoperative complications and patients with > 30% steatosis have an increased risk of postoperative death[9,106,107]. It is worth to be mentioned that simple steatosis may lead to poor prognosis. A study carried out in a nationwide Swedish cohort from 1966 to 2017 including 10568 patients found that simple steatosis, non-fibrotic NASH, non-cirrhotic fibrosis, and cirrhosis were associated with significant higher hazard ratio for mortality risk compared with controls. The all-cause mortalities of cohorts with simple steatosis, non-fibrotic NASH, non-cirrhotic fibrosis, and cirrhosis were 2.52% person-years, 3.03% person-years, 3.53% person-years, and 7.05% person-years respectively whereas the mortality of population comparators was 1.69% person-years[108]. Association between imaging quantification method and clinical prognosis is another issue. In patients with chronic hepatitis C, CAP value ≤ 221 dB/m is associated with higher risk of HCC and in patients with NAFLD, CAP value ≤ 265 dB/m is associated with higher risk of HCC[109]. Similarly, in another cross-sectional study including 130 patients (HCC) and 54 patients (chronic hepatitis C), the authors reported that CAP value of chronic hepatitis C group was significantly higher than that of HCC group (259.96 dB/m *vs* 209.57 dB/m, P < 0.001)[110].

While serving as the conventional reference standard, liver histopathologic test has the limitations of invasiveness, sampling error, and high cost. Issues including availability, cost, accuracy and reliability should be taken into consideration when choosing the optimal noninvasive methods. The further

application of noninvasive methods is desirable for detecting and grading hepatic steatosis at the initial diagnosis and monitoring changes in liver fat content during follow-up after receiving clinical therapies.

MRS and MRI-PDFF are reported to be the most accurate imaging modalities for quantified measurement of liver fat content. However, their low accessibility and high cost make it impossible to use MR-based techniques as repeatable methods to monitor the process of liver steatosis. Therefore, ultrasound-based techniques are more desirable with the advantages of portability and cost-effectiveness. CAP is the first method based on attenuation of the ultrasound beam, and its performance has been validated in several studies. However, the limitations of CAP are nonnegligible in that due to its blindness, it has a high rate of measurement failures because it cannot determine the exact location of the region of interest. UGAP, ATT and ATI have been developed to improve this situation, and these metrics can be used to evaluate degree of fatty liver on gray scale ultrasonography in real-time with a correct region of interest. The CAP measurement also showed suboptimal performance in quantifying liver fat content especially in mild steatosis, which limited its use as a golden standard to evaluate the efficacy of novel imaging methods for liver fat content quantification. In addition, techniques derived from other principles, such as ASQ, TSI and UDFF, have been developed. These techniques are reported to have nice clinical efficacy for liver fat quantification. Nevertheless, studies exploring value of such techniques enrolled a small number of participants. Therefore, future studies enrolling more participants are needed to test the utility of such techniques. Besides, imaging-based techniques may have some limitations. For example, CAP, ATI and MRI-PDFF may be unable to differentiate grade 2 with grade 3 liver steatosis.

Several hepatic steatosis quantification tools are launched by commercial platforms. Larger clinical studies are needed to compare the efficacy among different products. For patients with NAFLD, except for steatosis, inflammation and fibrosis are also significant features which are associated with prognosis. The steatosis measurement is able to be obtained together with the stiffness value by some tools. In this way, comprehensive evaluation of patients with NAFLD can be made. Except for elastography tools, ASQ has also been studied to evaluate liver stiffness. Hepatic steatosis measurement and stiffness measurement, in conjunction with other ultrasound methods, are promising tools for patients with diffuse liver disease to supervise curative effect and disease progression. Developing such a multiparametric ultrasound modality will require future studies.

ACKNOWLEDGEMENTS

We thank all medical staff and technicians who agreed to participate in this review.

FOOTNOTES

Author contributions: Lu Q conceived and designed the protocol; Zeng KY performed the literature search; Bao WYG and Wang YH selected the studies and extracted relevant information; Liao M, Yang J and Huang JY prepared the figures and tables; Zeng KY wrote the first version of draft; Lu Q critically revised successive drafts of the paper and approved the final version.

Conflict-of-interest statement: The authors have no financial relationships to disclose.

Open-Access: This article is an open-access article that was selected by an in-house editor and fully peer-reviewed by external reviewers. It is distributed in accordance with the Creative Commons Attribution NonCommercial (CC BY-NC 4.0) license, which permits others to distribute, remix, adapt, build upon this work non-commercially, and license their derivative works on different terms, provided the original work is properly cited and the use is non-commercial. See: https://creativecommons.org/Licenses/by-nc/4.0/

Country/Territory of origin: China

ORCID number: Ke-Yu Zeng 0000-0002-0836-3186; Wu-Yong-Ga Bao 0000-0001-7693-5804; Yun-Han Wang 0000-0002-5885-1356; Min Liao 0000-0002-0923-9419; Jie Yang 0000-0002-6819-146X; Jia-Yan Huang 0000-0002-1918-2874; Qiang Lu 0000-0002-4057-1997.

S-Editor: Yan JP
L-Editor: A
P-Editor: Zhao S

REFERENCES

1 **Younossi Z**, Anstee QM, Marietti M, Hardy T, Henry L, Eslam M, George J, Bugianesi E. Global burden of NAFLD and NASH: trends, predictions, risk factors and prevention. *Nat Rev Gastroenterol Hepatol* 2018; **15**: 11-20 [PMID: 28930295 DOI: 10.1038/nrgastro.2017.109]

2 **Powell EE**, Wong VW, Rinella M. Non-alcoholic fatty liver disease. *Lancet* 2021; **397**: 2212-2224 [PMID: 33894145 DOI: 10.1016/S0140-6736(20)32511-3]

3 **Chalasani N**, Younossi Z, Lavine JE, Charlton M, Cusi K, Rinella M, Harrison SA, Brunt EM, Sanyal AJ. The diagnosis and management of nonalcoholic fatty liver disease: Practice guidance from the American Association for the Study of Liver Diseases. *Hepatology* 2018; **67**: 328-357 [PMID: 28714183 DOI: 10.1002/hep.29367]

4 **Ferraioli G**, Berzigotti A, Barr RG, Choi BI, Cui XW, Dong Y, Gilja OH, Lee JY, Lee DH, Moriyasu F, Piscaglia F, Sugimoto K, Wong GL, Wong VW, Dietrich CF. Quantification of Liver Fat Content with Ultrasound: A WFUMB Position Paper. *Ultrasound Med Biol* 2021; **47**: 2803-2820 [PMID: 34284932 DOI: 10.1016/j.ultrasmedbio.2021.06.002]

5 **Younossi ZM**, Koenig AB, Abdelatif D, Fazel Y, Henry L, Wymer M. Global epidemiology of nonalcoholic fatty liver disease-Meta-analytic assessment of prevalence, incidence, and outcomes. *Hepatology* 2016; **64**: 73-84 [PMID: 26707365 DOI: 10.1002/hep.28431]

6 **El-Serag HB**, Tran T, Everhart JE. Diabetes increases the risk of chronic liver disease and hepatocellular carcinoma. *Gastroenterology* 2004; **126**: 460-468 [PMID: 14762783 DOI: 10.1053/j.gastro.2003.10.065]

7 **Adams LA**, Lymp JF, St Sauver J, Sanderson SO, Lindor KD, Feldstein A, Angulo P. The natural history of nonalcoholic fatty liver disease: a population-based cohort study. *Gastroenterology* 2005; **129**: 113-121 [PMID: 16012941 DOI: 10.1053/j.gastro.2005.04.014]

8 **Musso G**, Gambino R, Cassader M, Pagano G. Meta-analysis: natural history of non-alcoholic fatty liver disease (NAFLD) and diagnostic accuracy of non-invasive tests for liver disease severity. *Ann Med* 2011; **43**: 617-649 [PMID: 21039302 DOI: 10.3109/07853890.2010.518623]

9 **Leandro G**, Mangia A, Hui J, Fabris P, Rubbia-Brandt L, Colloredo G, Adinolfi LE, Asselah T, Jonsson JR, Smedile A, Terrault N, Pazienza V, Giordani MT, Giostra E, Sonzogni A, Ruggiero G, Marcellin P, Powell EE, George J, Negro F; HCV Meta-Analysis (on) Individual Patients' Data Study Group. Relationship between steatosis, inflammation, and fibrosis in chronic hepatitis C: a meta-analysis of individual patient data. *Gastroenterology* 2006; **130**: 1636-1642 [PMID: 16697727 DOI: 10.1053/j.gastro.2006.03.014]

10 **Linares I**, Hamar M, Selzner N, Selzner M. Steatosis in Liver Transplantation: Current Limitations and Future Strategies. *Transplantation* 2019; **103**: 78-90 [PMID: 30418431 DOI: 10.1097/TP.0000000000002466]

11 **Hossain N**, Kanwar P, Mohanty SR. A Comprehensive Updated Review of Pharmaceutical and Nonpharmaceutical Treatment for NAFLD. *Gastroenterol Res Pract* 2016; **2016**: 7109270 [PMID: 27006654 DOI: 10.1155/2016/7109270]

12 **Ajmera V**, Park CC, Caussy C, Singh S, Hernandez C, Bettencourt R, Hooker J, Sy E, Behling C, Xu R, Middleton MS, Valasek MA, Faulkner C, Rizo E, Richards L, Sirlin CB, Loomba R. Magnetic Resonance Imaging Proton Density Fat Fraction Associates With Progression of Fibrosis in Patients With Nonalcoholic Fatty Liver Disease. *Gastroenterology* 2018; **155**: 307-310.e2 [PMID: 29660324 DOI: 10.1053/j.gastro.2018.04.014]

13 **Stine JG**, Munaganuru N, Barnard A, Wang JL, Kaulback K, Argo CK, Singh S, Fowler KJ, Sirlin CB, Loomba R. Change in MRI-PDFF and Histologic Response in Patients With Nonalcoholic Steatohepatitis: A Systematic Review and Meta-Analysis. *Clin Gastroenterol Hepatol* 2021; **19**: 2274-2283.e5 [PMID: 32882428 DOI: 10.1016/j.cgh.2020.08.061]

14 **Vilar-Gomez E**, Calzadilla-Bertot L, Wai-Sun Wong V, Castellanos M, Aller-de la Fuente R, Metwally M, Eslam M, Gonzalez-Fabian L, Alvarez-Quiñones Sanz M, Conde-Martin AF, De Boer B, McLeod D, Hung Chan AW, Chalasani N, George J, Adams LA, Romero-Gomez M. Fibrosis Severity as a Determinant of Cause-Specific Mortality in Patients With Advanced Nonalcoholic Fatty Liver Disease: A Multi-National Cohort Study. *Gastroenterology* 2018; **155**: 443-457.e17 [PMID: 29733831 DOI: 10.1053/j.gastro.2018.04.034]

15 **Permutt Z**, Le TA, Peterson MR, Seki E, Brenner DA, Sirlin C, Loomba R. Correlation between liver histology and novel magnetic resonance imaging in adult patients with non-alcoholic fatty liver disease - MRI accurately quantifies hepatic steatosis in NAFLD. *Aliment Pharmacol Ther* 2012; **36**: 22-29 [PMID: 22554256 DOI: 10.1111/j.1365-2036.2012.05121.x]

16 **Wildman-Tobriner B**, Middleton MM, Moylan CA, Rossi S, Flores O, Chang ZA, Abdelmalek MF, Sirlin CB, Bashir MR. Association Between Magnetic Resonance Imaging-Proton Density Fat Fraction and Liver Histology Features in Patients With Nonalcoholic Fatty Liver Disease or Nonalcoholic Steatohepatitis. *Gastroenterology* 2018; **155**: 1428-1435.e2 [PMID: 30031769 DOI: 10.1053/j.gastro.2018.07.018]

17 **Tamaki N**, Ajmera V, Loomba R. Non-invasive methods for imaging hepatic steatosis and their clinical importance in NAFLD. *Nat Rev Endocrinol* 2022; **18**: 55-66 [PMID: 34815553 DOI: 10.1038/s41574-021-00584-0]

18 **Kleiner DE**, Brunt EM, Van Natta M, Behling C, Contos MJ, Cummings OW, Ferrell LD, Liu YC, Torbenson MS, Unalp-Arida A, Yeh M, McCullough AJ, Sanyal AJ; Nonalcoholic Steatohepatitis Clinical Research Network. Design and validation of a histological scoring system for nonalcoholic fatty liver disease. *Hepatology* 2005; **41**: 1313-1321 [PMID: 15915461 DOI: 10.1002/hep.20701]

19 **Davison BA**, Harrison SA, Cotter G, Alkhouri N, Sanyal A, Edwards C, Colca JR, Iwashita J, Koch GG, Dittrich HC. Suboptimal reliability of liver biopsy evaluation has implications for randomized clinical trials. *J Hepatol* 2020; **73**: 1322-1332 [PMID: 32610115 DOI: 10.1016/j.jhep.2020.06.025]

20 **Wong VW**, Adams LA, de Lédinghen V, Wong GL, Sookoian S. Noninvasive biomarkers in NAFLD and NASH - current progress and future promise. *Nat Rev Gastroenterol Hepatol* 2018; **15**: 461-478 [PMID: 29844588 DOI: 10.1038/s41575-018-0014-9]

21 **Castera L**, Friedrich-Rust M, Loomba R. Noninvasive Assessment of Liver Disease in Patients With Nonalcoholic Fatty Liver Disease. *Gastroenterology* 2019; **156**: 1264-1281.e4 [PMID: 30660725 DOI: 10.1053/j.gastro.2018.12.036]

22 **Barr RG**. Ultrasound of Diffuse Liver Disease Including Elastography. *Radiol Clin North Am* 2019; **57**: 549-562 [PMID:

30928077 DOI: 10.1016/j.rcl.2019.01.003]
23 **Saadeh S**, Younossi ZM, Remer EM, Gramlich T, Ong JP, Hurley M, Mullen KD, Cooper JN, Sheridan MJ. The utility of radiological imaging in nonalcoholic fatty liver disease. *Gastroenterology* 2002; **123**: 745-750 [PMID: 12198701 DOI: 10.1053/gast.2002.35354]
24 **Dasarathy S**, Dasarathy J, Khiyami A, Joseph R, Lopez R, McCullough AJ. Validity of real time ultrasound in the diagnosis of hepatic steatosis: a prospective study. *J Hepatol* 2009; **51**: 1061-1067 [PMID: 19846234 DOI: 10.1016/j.jhep.2009.09.001]
25 **Hernaez R**, Lazo M, Bonekamp S, Kamel I, Brancati FL, Guallar E, Clark JM. Diagnostic accuracy and reliability of ultrasonography for the detection of fatty liver: a meta-analysis. *Hepatology* 2011; **54**: 1082-1090 [PMID: 21618575 DOI: 10.1002/hep.24452]
26 **Strauss S**, Gavish E, Gottlieb P, Katsnelson L. Interobserver and intraobserver variability in the sonographic assessment of fatty liver. *AJR Am J Roentgenol* 2007; **189**: W320-W323 [PMID: 18029843 DOI: 10.2214/AJR.07.2123]
27 **Cengiz M**, Sentürk S, Cetin B, Bayrak AH, Bilek SU. Sonographic assessment of fatty liver: intraobserver and interobserver variability. *Int J Clin Exp Med* 2014; **7**: 5453-5460 [PMID: 25664055]
28 **Osawa H**, Mori Y. Sonographic diagnosis of fatty liver using a histogram technique that compares liver and renal cortical echo amplitudes. *J Clin Ultrasound* 1996; **24**: 25-29 [PMID: 8655663 DOI: 10.1002/(SICI)1097-0096(199601)24:1<25::AID-JCU4>3.0.CO;2-N]
29 **Mancini M**, Prinster A, Annuzzi G, Liuzzi R, Giacco R, Medagli C, Cremone M, Clemente G, Maurea S, Riccardi G, Rivellese AA, Salvatore M. Sonographic hepatic-renal ratio as indicator of hepatic steatosis: comparison with (1)H magnetic resonance spectroscopy. *Metabolism* 2009; **58**: 1724-1730 [PMID: 19716568 DOI: 10.1016/j.metabol.2009.05.032]
30 **Webb M**, Yeshua H, Zelber-Sagi S, Santo E, Brazowski E, Halpern Z, Oren R. Diagnostic value of a computerized hepatorenal index for sonographic quantification of liver steatosis. *AJR Am J Roentgenol* 2009; **192**: 909-914 [PMID: 19304694 DOI: 10.2214/AJR.07.4016]
31 **Shiralkar K**, Johnson S, Bluth EI, Marshall RH, Dornelles A, Gulotta PM. Improved method for calculating hepatic steatosis using the hepatorenal index. *J Ultrasound Med* 2015; **34**: 1051-1059 [PMID: 26014325 DOI: 10.7863/ultra.34.6.1051]
32 **Marshall RH**, Eissa M, Bluth EI, Gulotta PM, Davis NK. Hepatorenal index as an accurate, simple, and effective tool in screening for steatosis. *AJR Am J Roentgenol* 2012; **199**: 997-1002 [PMID: 23096171 DOI: 10.2214/AJR.11.6677]
33 **Borges VF**, Diniz AL, Cotrim HP, Rocha HL, Andrade NB. Sonographic hepatorenal ratio: a noninvasive method to diagnose nonalcoholic steatosis. *J Clin Ultrasound* 2013; **41**: 18-25 [PMID: 22997020 DOI: 10.1002/jcu.21994]
34 **Stahlschmidt FL**, Tafarel JR, Menini-Stahlschmidt CM, Baena CP. Hepatorenal index for grading liver steatosis with concomitant fibrosis. *PLoS One* 2021; **16**: e0246837 [PMID: 33577616 DOI: 10.1371/journal.pone.0246837]
35 **Bozic D**, Podrug K, Mikolasevic I, Grgurevic I. Ultrasound Methods for the Assessment of Liver Steatosis: A Critical Appraisal. *Diagnostics (Basel)* 2022; **12** [PMID: 36291976 DOI: 10.3390/diagnostics12102287]
36 **Kjaergaard M**, Lindvig KP, Hansen CD, Detlefsen S, Krag A, Thiele M. Hepatorenal Index by B-Mode Ratio Versus Imaging and Fatty Liver Index to Diagnose Steatosis in Alcohol-Related and Nonalcoholic Fatty Liver Disease. *J Ultrasound Med* 2023; **42**: 487-496 [PMID: 35475550 DOI: 10.1002/jum.15991]
37 **Labyed Y**, Milkowski A. Novel Method for Ultrasound-Derived Fat Fraction Using an Integrated Phantom. *J Ultrasound Med* 2020; **39**: 2427-2438 [PMID: 32525261 DOI: 10.1002/jum.15364]
38 **Oelze ML**, Mamou J. Review of Quantitative Ultrasound: Envelope Statistics and Backscatter Coefficient Imaging and Contributions to Diagnostic Ultrasound. *IEEE Trans Ultrason Ferroelectr Freq Control* 2016; **63**: 336-351 [PMID: 26761606 DOI: 10.1109/TUFFC.2015.2513958]
39 **Sasso M**, Beaugrand M, de Ledinghen V, Douvin C, Marcellin P, Poupon R, Sandrin L, Miette V. Controlled attenuation parameter (CAP): a novel VCTE™ guided ultrasonic attenuation measurement for the evaluation of hepatic steatosis: preliminary study and validation in a cohort of patients with chronic liver disease from various causes. *Ultrasound Med Biol* 2010; **36**: 1825-1835 [PMID: 20870345 DOI: 10.1016/j.ultrasmedbio.2010.07.005]
40 **Seneviratne N**, Fang C, Sidhu PS. Ultrasound-based hepatic fat quantification: current status and future directions. *Clin Radiol* 2023; **78**: 187-200 [PMID: 36411088 DOI: 10.1016/j.crad.2022.10.003]
41 **Ferraioli G**, Soares Monteiro LB. Ultrasound-based techniques for the diagnosis of liver steatosis. *World J Gastroenterol* 2019; **25**: 6053-6062 [PMID: 31686762 DOI: 10.3748/wjg.v25.i40.6053]
42 **de Lédinghen V**, Vergniol J, Foucher J, Merrouche W, le Bail B. Non-invasive diagnosis of liver steatosis using controlled attenuation parameter (CAP) and transient elastography. *Liver Int* 2012; **32**: 911-918 [PMID: 22672642 DOI: 10.1111/j.1478-3231.2012.02820.x]
43 **Caussy C**, Brissot J, Singh S, Bassirian S, Hernandez C, Bettencourt R, Rizo E, Richards L, Sirlin CB, Loomba R. Prospective, Same-Day, Direct Comparison of Controlled Attenuation Parameter With the M vs the XL Probe in Patients With Nonalcoholic Fatty Liver Disease, Using Magnetic Resonance Imaging-Proton Density Fat Fraction as the Standard. *Clin Gastroenterol Hepatol* 2020; **18**: 1842-1850.e6 [PMID: 31843596 DOI: 10.1016/j.cgh.2019.11.060]
44 **Park J**, Lee JM, Lee G, Jeon SK, Joo I. Quantitative Evaluation of Hepatic Steatosis Using Advanced Imaging Techniques: Focusing on New Quantitative Ultrasound Techniques. *Korean J Radiol* 2022; **23**: 13-29 [PMID: 34983091 DOI: 10.3348/kjr.2021.0112]
45 **Karlas T**, Petroff D, Sasso M, Fan JG, Mi YQ, de Lédinghen V, Kumar M, Lupsor-Platon M, Han KH, Cardoso AC, Ferraioli G, Chan WK, Wong VW, Myers RP, Chayama K, Friedrich-Rust M, Beaugrand M, Shen F, Hiriart JB, Sarin SK, Badea R, Jung KS, Marcellin P, Filice C, Mahadeva S, Wong GL, Crotty P, Masaki K, Bojunga J, Bedossa P, Keim V, Wiegand J. Individual patient data meta-analysis of controlled attenuation parameter (CAP) technology for assessing steatosis. *J Hepatol* 2017; **66**: 1022-1030 [PMID: 28039099 DOI: 10.1016/j.jhep.2016.12.022]
46 **Petroff D**, Blank V, Newsome PN, Shalimar, Voican CS, Thiele M, de Lédinghen V, Baumeler S, Chan WK, Perlemuter G, Cardoso AC, Aggarwal S, Sasso M, Eddowes PJ, Allison M, Tsochatzis E, Anstee QM, Sheridan D, Cobbold JF, Naveau S, Lupsor-Platon M, Mueller S, Krag A, Irles-Depe M, Semela D, Wong GL, Wong VW, Villela-Nogueira CA,

Garg H, Chazouillères O, Wiegand J, Karlas T. Assessment of hepatic steatosis by controlled attenuation parameter using the M and XL probes: an individual patient data meta-analysis. *Lancet Gastroenterol Hepatol* 2021; **6**: 185-198 [PMID: 33460567 DOI: 10.1016/S2468-1253(20)30357-5]

47 **Caussy C**, Alquiraish MH, Nguyen P, Hernandez C, Cepin S, Fortney LE, Ajmera V, Bettencourt R, Collier S, Hooker J, Sy E, Rizo E, Richards L, Sirlin CB, Loomba R. Optimal threshold of controlled attenuation parameter with MRI-PDFF as the gold standard for the detection of hepatic steatosis. *Hepatology* 2018; **67**: 1348-1359 [PMID: 29108123 DOI: 10.1002/hep.29639]

48 **Shao CX**, Ye J, Dong Z, Li F, Lin Y, Liao B, Feng S, Zhong B. Steatosis grading consistency between controlled attenuation parameter and MRI-PDFF in monitoring metabolic associated fatty liver disease. *Ther Adv Chronic Dis* 2021; **12**: 20406223211033119 [PMID: 34408822 DOI: 10.1177/20406223211033119]

49 **Runge JH**, Smits LP, Verheij J, Depla A, Kuiken SD, Baak BC, Nederveen AJ, Beuers U, Stoker J. MR Spectroscopy-derived Proton Density Fat Fraction Is Superior to Controlled Attenuation Parameter for Detecting and Grading Hepatic Steatosis. *Radiology* 2018; **286**: 547-556 [PMID: 28915103 DOI: 10.1148/radiol.2017162931]

50 **Imajo K**, Kessoku T, Honda Y, Tomeno W, Ogawa Y, Mawatari H, Fujita K, Yoneda M, Taguri M, Hyogo H, Sumida Y, Ono M, Eguchi Y, Inoue T, Yamanaka T, Wada K, Saito S, Nakajima A. Magnetic Resonance Imaging More Accurately Classifies Steatosis and Fibrosis in Patients With Nonalcoholic Fatty Liver Disease Than Transient Elastography. *Gastroenterology* 2016; **150**: 626-637.e7 [PMID: 26677985 DOI: 10.1053/j.gastro.2015.11.048]

51 **de Lédinghen V**, Vergniol J, Capdepont M, Chermak F, Hiriart JB, Cassinotto C, Merrouche W, Foucher J, Brigitte le B. Controlled attenuation parameter (CAP) for the diagnosis of steatosis: a prospective study of 5323 examinations. *J Hepatol* 2014; **60**: 1026-1031 [PMID: 24378529 DOI: 10.1016/j.jhep.2013.12.018]

52 **Yoo J**, Lee JM, Joo I, Lee DH, Yoon JH, Kang HJ, Ahn SJ. Reproducibility of ultrasound attenuation imaging for the noninvasive evaluation of hepatic steatosis. *Ultrasonography* 2020; **39**: 121-129 [PMID: 31693842 DOI: 10.14366/usg.19034]

53 **Yuri M**, Nishimura T, Tada T, Yoshida M, Fujiwara A, Kawata S, Yoshihara K, Yoshioka R, Ota S, Nakano R, Yuri Y, Takashima T, Aizawa N, Ikeda N, Shiomi H, Ide YH, Enomoto H, Yasuhiro F, Yano H, Iijima H. Diagnosis of hepatic steatosis based on ultrasound attenuation imaging is not influenced by liver fibrosis. *Hepatol Res* 2022; **52**: 1009-1019 [PMID: 36018852 DOI: 10.1111/hepr.13831]

54 **Tamaki N**, Koizumi Y, Hirooka M, Yada N, Takada H, Nakashima O, Kudo M, Hiasa Y, Izumi N. Novel quantitative assessment system of liver steatosis using a newly developed attenuation measurement method. *Hepatol Res* 2018; **48**: 821-828 [PMID: 29679473 DOI: 10.1111/hepr.13179]

55 **Tamaki N**, Kurosaki M, Yasui Y, Tsuchiya K, Izumi N. Attenuation coefficient (ATT) measurement for liver fat quantification in chronic liver disease. *J Med Ultrason (2001)* 2021; **48**: 481-487 [PMID: 34165645 DOI: 10.1007/s10396-021-01103-4]

56 **Ferraioli G**, Kumar V, Ozturk A, Nam K, de Korte CL, Barr RG. US Attenuation for Liver Fat Quantification: An AIUM-RSNA QIBA Pulse-Echo Quantitative Ultrasound Initiative. *Radiology* 2022; **302**: 495-506 [PMID: 35076304 DOI: 10.1148/radiol.210736]

57 **Kwon EY**, Kim YR, Kang DM, Yoon KH, Lee YH. Usefulness of US attenuation imaging for the detection and severity grading of hepatic steatosis in routine abdominal ultrasonography. *Clin Imaging* 2021; **76**: 53-59 [PMID: 33549920 DOI: 10.1016/j.clinimag.2021.01.034]

58 **Jang JK**, Kim SY, Yoo IW, Cho YB, Kang HJ, Lee DH. Diagnostic performance of ultrasound attenuation imaging for assessing low-grade hepatic steatosis. *Eur Radiol* 2022; **32**: 2070-2077 [PMID: 34549325 DOI: 10.1007/s00330-021-08269-y]

59 **Bae JS**, Lee DH, Lee JY, Kim H, Yu SJ, Lee JH, Cho EJ, Lee YB, Han JK, Choi BI. Assessment of hepatic steatosis by using attenuation imaging: a quantitative, easy-to-perform ultrasound technique. *Eur Radiol* 2019; **29**: 6499-6507 [PMID: 31175413 DOI: 10.1007/s00330-019-06272-y]

60 **Bae JS**, Lee DH, Suh KS, Kim H, Lee KB, Lee JY, Han JK. Noninvasive assessment of hepatic steatosis using a pathologic reference standard: comparison of CT, MRI, and US-based techniques. *Ultrasonography* 2022; **41**: 344-354 [PMID: 34852424 DOI: 10.14366/usg.21150]

61 **Jeon SK**, Lee JM, Joo I, Yoon JH, Lee DH, Lee JY, Han JK. Prospective Evaluation of Hepatic Steatosis Using Ultrasound Attenuation Imaging in Patients with Chronic Liver Disease with Magnetic Resonance Imaging Proton Density Fat Fraction as the Reference Standard. *Ultrasound Med Biol* 2019; **45**: 1407-1416 [PMID: 30975533 DOI: 10.1016/j.ultrasmedbio.2019.02.008]

62 **Tada T**, Iijima H, Kobayashi N, Yoshida M, Nishimura T, Kumada T, Kondo R, Yano H, Kage M, Nakano C, Aoki T, Aizawa N, Ikeda N, Takashima T, Yuri Y, Ishii N, Hasegawa K, Takata R, Yoh K, Sakai Y, Nishikawa H, Iwata Y, Enomoto H, Hirota S, Fujimoto J, Nishiguchi S. Usefulness of Attenuation Imaging with an Ultrasound Scanner for the Evaluation of Hepatic Steatosis. *Ultrasound Med Biol* 2019; **45**: 2679-2687 [PMID: 31277922 DOI: 10.1016/j.ultrasmedbio.2019.05.033]

63 **Tada T**, Kumada T, Toyoda H, Nakamura S, Shibata Y, Yasuda S, Watanuki Y, Tsujii K, Fukuda N, Fujioka M, Takeshima K, Niwa F, Ogawa S, Hashinokuchi S, Kataoka S, Ichikawa H, Iijima H. Attenuation imaging based on ultrasound technology for assessment of hepatic steatosis: A comparison with magnetic resonance imaging-determined proton density fat fraction. *Hepatol Res* 2020; **50**: 1319-1327 [PMID: 32876367 DOI: 10.1111/hepr.13563]

64 **Jeon SK**, Lee JM, Joo I, Yoon JH. Assessment of the inter-platform reproducibility of ultrasound attenuation examination in nonalcoholic fatty liver disease. *Ultrasonography* 2022; **41**: 355-364 [PMID: 34933319 DOI: 10.14366/usg.21167]

65 **Ferraioli G**, Maiocchi L, Raciti MV, Tinelli C, De Silvestri A, Nichetti M, De Cata P, Rondanelli M, Chiovato L, Calliada F, Filice C. Detection of Liver Steatosis With a Novel Ultrasound-Based Technique: A Pilot Study Using MRI-Derived Proton Density Fat Fraction as the Gold Standard. *Clin Transl Gastroenterol* 2019; **10**: e00081 [PMID: 31609745 DOI: 10.14309/ctg.0000000000000081]

66 **Ferraioli G**, Maiocchi L, Savietto G, Tinelli C, Nichetti M, Rondanelli M, Calliada F, Preda L, Filice C. Performance of the Attenuation Imaging Technology in the Detection of Liver Steatosis. *J Ultrasound Med* 2021; **40**: 1325-1332 [PMID:

32960457 DOI: 10.1002/jum.15512]
67 **Sugimoto K**, Abe M, Oshiro H, Takahashi H, Kakegawa T, Tomita Y, Yoshimasu Y, Takeuchi H, Itoi T. The most appropriate region-of-interest position for attenuation coefficient measurement in the evaluation of liver steatosis. *J Med Ultrason (2001)* 2021; **48**: 615-621 [PMID: 34453648 DOI: 10.1007/s10396-021-01124-z]
68 **Lee DH**. Quantitative assessment of fatty liver using ultrasound attenuation imaging. *J Med Ultrason (2001)* 2021; **48**: 465-470 [PMID: 34453237 DOI: 10.1007/s10396-021-01132-z]
69 **Hsu PK**, Wu LS, Su WW, Su PY, Chen YY, Hsu YC, Yen HH, Wu CL. Comparing the controlled attenuation parameter using FibroScan and attenuation imaging with ultrasound as a novel measurement for liver steatosis. *PLoS One* 2021; **16**: e0254892 [PMID: 34653177 DOI: 10.1371/journal.pone.0254892]
70 **Hsu PK**, Wu LS, Yen HH, Huang HP, Chen YY, Su PY, Su WW. Attenuation Imaging with Ultrasound as a Novel Evaluation Method for Liver Steatosis. *J Clin Med* 2021; **10** [PMID: 33801163 DOI: 10.3390/jcm10050965]
71 **Cerit M**, Şendur HN, Cindil E, Erbaş G, Yalçın MM, Cerit ET, Allahverdiyeva S, Oktar SÖ, Yücel C. Quantification of liver fat content with ultrasonographic attenuation measurement function: Correlation with unenhanced multidimensional computerized tomography. *Clin Imaging* 2020; **65**: 85-93 [PMID: 32387801 DOI: 10.1016/j.clinimag.2020.04.028]
72 **Ferraioli G**, Raimondi A, Maiocchi L, De Silvestri A, Filice C. Quantification of Liver Fat Content with the iATT Algorithm: Correlation with Controlled Attenuation Parameter. *Diagnostics (Basel)* 2022; **12** [PMID: 35892497 DOI: 10.3390/diagnostics12081787]
73 **Koizumi Y**, Hirooka M, Tamaki N, Yada N, Nakashima O, Izumi N, Kudo M, Hiasa Y. New diagnostic technique to evaluate hepatic steatosis using the attenuation coefficient on ultrasound B mode. *PLoS One* 2019; **14**: e0221548 [PMID: 31454369 DOI: 10.1371/journal.pone.0221548]
74 **Bende F**, Sporea I, Şirli R, Bâldea V, Lazăr A, Lupușoru R, Fofiu R, Popescu A. Ultrasound-Guided Attenuation Parameter (UGAP) for the quantification of liver steatosis using the Controlled Attenuation Parameter (CAP) as the reference method. *Med Ultrason* 2021; **23**: 7-14 [PMID: 33220028 DOI: 10.11152/mu-2688]
75 **Fujiwara Y**, Kuroda H, Abe T, Ishida K, Oguri T, Noguchi S, Sugai T, Kamiyama N, Takikawa Y. The B-Mode Image-Guided Ultrasound Attenuation Parameter Accurately Detects Hepatic Steatosis in Chronic Liver Disease. *Ultrasound Med Biol* 2018; **44**: 2223-2232 [PMID: 30077415 DOI: 10.1016/j.ultrasmedbio.2018.06.017]
76 **Imajo K**, Toyoda H, Yasuda S, Suzuki Y, Sugimoto K, Kuroda H, Akita T, Tanaka J, Yasui Y, Tamaki N, Kurosaki M, Izumi N, Nakajima A, Kumada T. Utility of Ultrasound-Guided Attenuation Parameter for Grading Steatosis With Reference to MRI-PDFF in a Large Cohort. *Clin Gastroenterol Hepatol* 2022; **20**: 2533-2541.e7 [PMID: 34768008 DOI: 10.1016/j.cgh.2021.11.003]
77 **Ogino Y**, Wakui N, Nagai H, Igarashi Y. The ultrasound-guided attenuation parameter is useful in quantification of hepatic steatosis in non-alcoholic fatty liver disease. *JGH Open* 2021; **5**: 947-952 [PMID: 34386604 DOI: 10.1002/jgh3.12615]
78 **Kuroda H**, Abe T, Fujiwara Y, Nagasawa T, Takikawa Y. Diagnostic accuracy of ultrasound-guided attenuation parameter as a noninvasive test for steatosis in non-alcoholic fatty liver disease. *J Med Ultrason (2001)* 2021; **48**: 471-480 [PMID: 34415481 DOI: 10.1007/s10396-021-01123-0]
79 **Kuroda H**, Fujiwara Y, Abe T, Nagasawa T, Oguri T, Noguchi S, Kamiyama N, Takikawa Y. Two-dimensional shear wave elastography and ultrasound-guided attenuation parameter for progressive non-alcoholic steatohepatitis. *PLoS One* 2021; **16**: e0249493 [PMID: 33826669 DOI: 10.1371/journal.pone.0249493]
80 **Tada T**, Kumada T, Toyoda H, Kobayashi N, Sone Y, Oguri T, Kamiyama N. Utility of Attenuation Coefficient Measurement Using an Ultrasound-Guided Attenuation Parameter for Evaluation of Hepatic Steatosis: Comparison With MRI-Determined Proton Density Fat Fraction. *AJR Am J Roentgenol* 2019; **212**: 332-341 [PMID: 30476453 DOI: 10.2214/AJR.18.20123]
81 **Tada T**, Kumada T, Toyoda H, Yasuda S, Sone Y, Hashinokuchi S, Ogawa S, Oguri T, Kamiyama N, Chuma M, Akita T, Tanaka J. Liver stiffness does not affect ultrasound-guided attenuation coefficient measurement in the evaluation of hepatic steatosis. *Hepatol Res* 2020; **50**: 190-198 [PMID: 31661724 DOI: 10.1111/hepr.13442]
82 **Popa A**, Bende F, Şirli R, Popescu A, Bâldea V, Lupușoru R, Cotrău R, Fofiu R, Foncea C, Sporea I. Quantification of Liver Fibrosis, Steatosis, and Viscosity Using Multiparametric Ultrasound in Patients with Non-Alcoholic Liver Disease: A "Real-Life" Cohort Study. *Diagnostics (Basel)* 2021; **11** [PMID: 33926073 DOI: 10.3390/diagnostics11050783]
83 **Jeon SK**, Lee JM, Joo I. Clinical Feasibility of Quantitative Ultrasound Imaging for Suspected Hepatic Steatosis: Intra- and Inter-examiner Reliability and Correlation with Controlled Attenuation Parameter. *Ultrasound Med Biol* 2021; **47**: 438-445 [PMID: 33277108 DOI: 10.1016/j.ultrasmedbio.2020.11.009]
84 **Rónaszéki AD**, Budai BK, Csongrády B, Stollmayer R, Hagymási K, Werling K, Fodor T, Folhoffer A, Kalina I, Győri G, Maurovich-Horvat P, Kaposi PN. Tissue attenuation imaging and tissue scatter imaging for quantitative ultrasound evaluation of hepatic steatosis. *Medicine (Baltimore)* 2022; **101**: e29708 [PMID: 35984128 DOI: 10.1097/MD.0000000000029708]
85 **Şendur HN**, Özdemir Kalkan D, Cerit MN, Kalkan G, Şendur AB, Özhan Oktar S. Hepatic Fat Quantification With Novel Ultrasound Based Techniques: A Diagnostic Performance Study Using Magnetic Resonance Imaging Proton Density Fat Fraction as Reference Standard. *Can Assoc Radiol J* 2023; **74**: 362-369 [PMID: 36113064 DOI: 10.1177/08465371221123696]
86 **Jeon SK**, Lee JM, Joo I, Park SJ. Quantitative Ultrasound Radiofrequency Data Analysis for the Assessment of Hepatic Steatosis in Nonalcoholic Fatty Liver Disease Using Magnetic Resonance Imaging Proton Density Fat Fraction as the Reference Standard. *Korean J Radiol* 2021; **22**: 1077-1086 [PMID: 33739636 DOI: 10.3348/kjr.2020.1262]
87 **Şendur HN**, Cerit MN, Ibrahimkhanli N, Şendur AB, Özhan Oktar S. Interobserver Variability in Ultrasound-Based Liver Fat Quantification. *J Ultrasound Med* 2023; **42**: 833-841 [PMID: 35778902 DOI: 10.1002/jum.16048]
88 **Coila A**, Oelze ML. Effects of acoustic nonlinearities on the ultrasonic backscatter coefficient estimation. *J Acoust Soc Am* 2019; **146**: 85 [PMID: 31370607 DOI: 10.1121/1.5115355]
89 **Han A**, Andre MP, Deiranieh L, Housman E, Erdman JW Jr, Loomba R, Sirlin CB, O'Brien WD Jr. Repeatability and Reproducibility of the Ultrasonic Attenuation Coefficient and Backscatter Coefficient Measured in the Right Lobe of the

Liver in Adults With Known or Suspected Nonalcoholic Fatty Liver Disease. *J Ultrasound Med* 2018; **37**: 1913-1927 [PMID: 29359454 DOI: 10.1002/jum.14537]

90 **Han A**, Zhang YN, Boehringer AS, Andre MP, Erdman JW Jr, Loomba R, Sirlin CB, O'Brien WD Jr. Inter-platform reproducibility of ultrasonic attenuation and backscatter coefficients in assessing NAFLD. *Eur Radiol* 2019; **29**: 4699-4708 [PMID: 30783789 DOI: 10.1007/s00330-019-06035-9]

91 **Lin SC**, Heba E, Wolfson T, Ang B, Gamst A, Han A, Erdman JW Jr, O'Brien WD Jr, Andre MP, Sirlin CB, Loomba R. Noninvasive Diagnosis of Nonalcoholic Fatty Liver Disease and Quantification of Liver Fat Using a New Quantitative Ultrasound Technique. *Clin Gastroenterol Hepatol* 2015; **13**: 1337-1345.e6 [PMID: 25478922 DOI: 10.1016/j.cgh.2014.11.027]

92 **Han A**, Labyed Y, Sy EZ, Boehringer AS, Andre MP, Erdman JW Jr, Loomba R, Sirlin CB, O'Brien WD Jr. Inter-sonographer reproducibility of quantitative ultrasound outcomes and shear wave speed measured in the right lobe of the liver in adults with known or suspected non-alcoholic fatty liver disease. *Eur Radiol* 2018; **28**: 4992-5000 [PMID: 29869170 DOI: 10.1007/s00330-018-5541-9]

93 **Han A**, Zhang YN, Boehringer AS, Montes V, Andre MP, Erdman JW Jr, Loomba R, Valasek MA, Sirlin CB, O'Brien WD Jr. Assessment of Hepatic Steatosis in Nonalcoholic Fatty Liver Disease by Using Quantitative US. *Radiology* 2020; **295**: 106-113 [PMID: 32013792 DOI: 10.1148/radiol.2020191152]

94 **Dillman JR**, Thapaliya S, Tkach JA, Trout AT. Quantification of Hepatic Steatosis by Ultrasound: Prospective Comparison With MRI Proton Density Fat Fraction as Reference Standard. *AJR Am J Roentgenol* 2022; **219**: 784-791 [PMID: 35674351 DOI: 10.2214/AJR.22.27878]

95 **Karlas T**, Berger J, Garnov N, Lindner F, Busse H, Linder N, Schaudinn A, Relke B, Chakaroun R, Tröltzsch M, Wiegand J, Keim V. Estimating steatosis and fibrosis: Comparison of acoustic structure quantification with established techniques. *World J Gastroenterol* 2015; **21**: 4894-4902 [PMID: 25945002 DOI: 10.3748/wjg.v21.i16.4894]

96 **Keller J**, Kaltenbach TE, Haenle MM, Oeztuerk S, Graeter T, Mason RA, Seufferlein T, Kratzer W. Comparison of Acoustic Structure Quantification (ASQ), shearwave elastography and histology in patients with diffuse hepatopathies. *BMC Med Imaging* 2015; **15**: 58 [PMID: 26637242 DOI: 10.1186/s12880-015-0100-1]

97 **Lin YH**, Wan YL, Tai DI, Tseng JH, Wang CY, Tsai YW, Lin YR, Chang TY, Tsui PH. Considerations of Ultrasound Scanning Approaches in Non-alcoholic Fatty Liver Disease Assessment through Acoustic Structure Quantification. *Ultrasound Med Biol* 2019; **45**: 1955-1969 [PMID: 31130411 DOI: 10.1016/j.ultrasmedbio.2019.04.018]

98 **Kuroda H**, Kakisaka K, Kamiyama N, Oikawa T, Onodera M, Sawara K, Oikawa K, Endo R, Takikawa Y, Suzuki K. Non-invasive determination of hepatic steatosis by acoustic structure quantification from ultrasound echo amplitude. *World J Gastroenterol* 2012; **18**: 3889-3895 [PMID: 22876042 DOI: 10.3748/wjg.v18.i29.3889]

99 **Lee DH**, Lee JY, Park MS, Han JK. Non-invasive monitoring of hepatic steatosis *via* acoustic structure quantification of ultrasonography with MR spectroscopy as the reference standard. *Ultrasonography* 2020; **39**: 70-78 [PMID: 31639886 DOI: 10.14366/usg.19002]

100 **Son JY**, Lee JY, Yi NJ, Lee KW, Suh KS, Kim KG, Lee JM, Han JK, Choi BI. Hepatic Steatosis: Assessment with Acoustic Structure Quantification of US Imaging. *Radiology* 2016; **278**: 257-264 [PMID: 26121121 DOI: 10.1148/radiol.2015141779]

101 **Zhao Y**, Zhang C, Xu S, Zhang H, Wei S, Huang P, Zhang L, Wong YN, Xu W. Quantitative evaluation of hepatic steatosis using novel ultrasound technology normalized local variance (NLV) and its standard deviation with different ROIs in patients with metabolic-associated fatty liver disease: a pilot study. *Abdom Radiol (NY)* 2022; **47**: 693-703 [PMID: 34958409 DOI: 10.1007/s00261-021-03394-0]

102 **Bae JS**, Lee JY, Lee DH, Kim H, Lee Y, Han JK. Quantitative Evaluation of Hepatic Steatosis Using Normalized Local Variance in a Rat Model: Comparison with Histopathology as the Reference Standard. *Korean J Radiol* 2019; **20**: 1399-1407 [PMID: 31464118 DOI: 10.3348/kjr.2019.0068]

103 **Bae JS**, Lee DH, Lee JY, Kim H, Yu SJ, Lee JH, Cho EJ, Lee YB, Han JK, Choi BI. Quantitative Assessment of Fatty Liver using Ultrasound with Normalized Local Variance Technique. *Ultraschall Med* 2021; **42**: 599-606 [PMID: 32323278 DOI: 10.1055/a-1143-3091]

104 **Dioguardi Burgio M**, Imbault M, Ronot M, Faccinetto A, Van Beers BE, Rautou PE, Castera L, Gennisson JL, Tanter M, Vilgrain V. Ultrasonic Adaptive Sound Speed Estimation for the Diagnosis and Quantification of Hepatic Steatosis: A Pilot Study. *Ultraschall Med* 2019; **40**: 722-733 [PMID: 30396216 DOI: 10.1055/a-0660-9465]

105 **Suliman I**, Abdelgelil N, Kassamali F, Hassanein TI. The Effects of Hepatic Steatosis on the Natural History of HBV Infection. *Clin Liver Dis* 2019; **23**: 433-450 [PMID: 31266618 DOI: 10.1016/j.cld.2019.05.001]

106 **Abdalla EK**, Vauthey JN. Steatosis as a risk factor in liver surgery. *Ann Surg* 2007; **246**: 340-1; author reply 341 [PMID: 17667519 DOI: 10.1097/SLA.0b013e31811ea9d2]

107 **Spitzer AL**, Lao OB, Dick AA, Bakthavatsalam R, Halldorson JB, Yeh MM, Upton MP, Reyes JD, Perkins JD. The biopsied donor liver: incorporating macrosteatosis into high-risk donor assessment. *Liver Transpl* 2010; **16**: 874-884 [PMID: 20583086 DOI: 10.1002/lt.22085]

108 **Simon TG**, Roelstraete B, Khalili H, Hagström H, Ludvigsson JF. Mortality in biopsy-confirmed nonalcoholic fatty liver disease: results from a nationwide cohort. *Gut* 2021; **70**: 1375-1382 [PMID: 33037056 DOI: 10.1136/gutjnl-2020-322786]

109 **Izumi T**, Sho T, Morikawa K, Shigesawa T, Suzuki K, Nakamura A, Ohara M, Kawagishi N, Umemura M, Shimazaki T, Kimura M, Nakai M, Suda G, Natsuizaka M, Ogawa K, Kudo Y, Nishida M, Ono K, Baba M, Furuya K, Sakamoto N. Assessing the risk of hepatocellular carcinoma by combining liver stiffness and the controlled attenuation parameter. *Hepatol Res* 2019; **49**: 1207-1217 [PMID: 31219667 DOI: 10.1111/hepr.13391]

110 **Abdelaziz AO**, Shousha HI, Said EM, Soliman ZA, Shehata AA, Nabil MM, Abdelmaksoud AH, Elbaz TM, Abdelsalam FM. Evaluation of liver steatosis, measured by controlled attenuation parameter, in patients with hepatitis C-induced advanced liver fibrosis and hepatocellular carcinoma. *Eur J Gastroenterol Hepatol* 2018; **30**: 1384-1388 [PMID: 30179227 DOI: 10.1097/MEG.0000000000001196]

World Journal of Gastroenterology

Submit a Manuscript: https://www.f6publishing.com

World J Gastroenterol 2023 May 7; 29(17): 2551-2570

DOI: 10.3748/wjg.v29.i17.2551

ISSN 1007-9327 (print) ISSN 2219-2840 (online)

REVIEW

Alcohol-related hepatitis: A review article

Hunza Chaudhry, Aalam Sohal, Humzah Iqbal, Marina Roytman

Specialty type: Gastroenterology and hepatology

Provenance and peer review: Invited article; Externally peer reviewed.

Peer-review model: Single blind

Peer-review report's scientific quality classification

Grade A (Excellent): 0
Grade B (Very good): 0
Grade C (Good): C, C, C
Grade D (Fair): 0
Grade E (Poor): 0

P-Reviewer: Li M, China; Liu W, China

Received: December 26, 2022
Peer-review started: December 26, 2022
First decision: March 8, 2023
Revised: March 10, 2023
Accepted: April 13, 2023
Article in press: April 13, 2023
Published online: May 7, 2023

Hunza Chaudhry, Humzah Iqbal, Department of Internal Medicine, University of California, San Francisco, Fresno, CA 93701, United States

Aalam Sohal, Department of Hepatology, Liver Institute Northwest, Seattle, WA 98105, United States

Marina Roytman, Department of Gastroenterology and Hepatology, University of California, San Francisco, Fresno, CA 93701, United States

Corresponding author: Hunza Chaudhry, MD, Staff Physician, Department of Internal Medicine, University of California, San Francisco, 155 N. Fresno St, Fresno, CA 93701, United States. hunza.chaudhry@ucsf.edu

Abstract

Alcohol-related hepatitis (ARH) is a unique type of alcohol-associated liver disease characterized by acute liver inflammation caused by significant alcohol use. It ranges in severity from mild to severe and carries significant morbidity and mortality. The refinement of scoring systems has enhanced prognostication and guidance of clinical decision-making in the treatment of this complex disease. Although treatment focuses on supportive care, steroids have shown benefit in select circumstances. There has been a recent interest in this disease process, as coronavirus disease 2019 pandemic led to substantial rise in cases. Although much is known regarding the pathogenesis, prognosis remains grim due to limited treatment options. This article summarizes the epidemiology, genetics, pathogenesis, diagnosis and treatment of ARH.

Key Words: Alcohol; Hepatitis; Epidemiology; Prevalence; Treatment; Clinical trials

©The Author(s) 2023. Published by Baishideng Publishing Group Inc. All rights reserved.

Core Tip: The aim of this article is to review alcohol-related hepatitis (ARH). Despite the increased understanding of the pathogenesis of this disease process, treatment options remain limited. Our review article focuses on epidemiology, genetics, pathogenesis, diagnosis and treatment. We also discuss complications of ARH along with their optimal management and ongoing clinical trials. Further research evaluating therapeutic targets for its management are warranted.

Citation: Chaudhry H, Sohal A, Iqbal H, Roytman M. Alcohol-related hepatitis: A review article. *World J Gastroenterol* 2023; 29(17): 2551-2570
URL: https://www.wjgnet.com/1007-9327/full/v29/i17/2551.htm
DOI: https://dx.doi.org/10.3748/wjg.v29.i17.2551

INTRODUCTION

The burden of alcohol-associated liver disease continues to grow with rising cases during and even after the coronavirus disease 2019 (COVID-19) pandemic[1-2]. Some experts believe that the rise in cases during the COVID-19 pandemic will have long lasting effects on society and healthcare. Alcohol is an integral part of American culture and its widespread use cuts across socioeconomic and racial lines. Alcohol-related liver disease (ALD) can range from hepatic steatosis to end-stage liver disease. Alcohol-related hepatitis (ARH), a form of ALD, is an acute inflammatory syndrome of jaundice and liver injury occurring in patients with significant alcohol use. The severity can range from subclinical to acute severe illness, which is associated with high mortality. The recent trends in ARH hospitalizations in the United States suggest its importance in the current realm of clinical practice[1-4].

The prevalence of ARH has been on a rise even prior to COVID-19 pandemic[4]. Studies have shown a 53% increase in ARH from 2019 to 2020 with a 64% increase in the latter phase of the pandemic[2]. Multiple other studies have shown that the societal disruptions associated with the pandemic have further intensified the rise in cases of ARH. ARH can resolve with abstinence and supportive therapy; however, these measures do not guarantee recovery in all patients. Acute-on-chronic liver failure (ACLF) and development of cirrhosis are the most feared complications of ARH and is associated with significant morbidity and mortality. Thus, identifying patients early during the course of the disease is critical.

PREVALENCE

The true prevalence of ARH is difficult to assess as patients can be asymptomatic and remain undiagnosed. A study by Jinjuvadia *et al*[5] evaluating the temporal trends in ARH hospitalizations reported an increase in patients with ARH from 249884 in 2002 to 326403 in 2010. Their study included hospitalizations with a primary and secondary diagnosis of ARH. To estimate true prevalence, Ali *et al* [4] included patients only with a primary diagnosis of ARH and reported an increase in the total hospitalizations from 67070 in 2009 to 125540 in 2019. They also reported an increase in inpatient mortality from 2.48% in 2009 to 3.78% in 2019. The increase in the cases of ARH has been further intensified during the COVID-19 pandemic, especially in younger patients and in women.

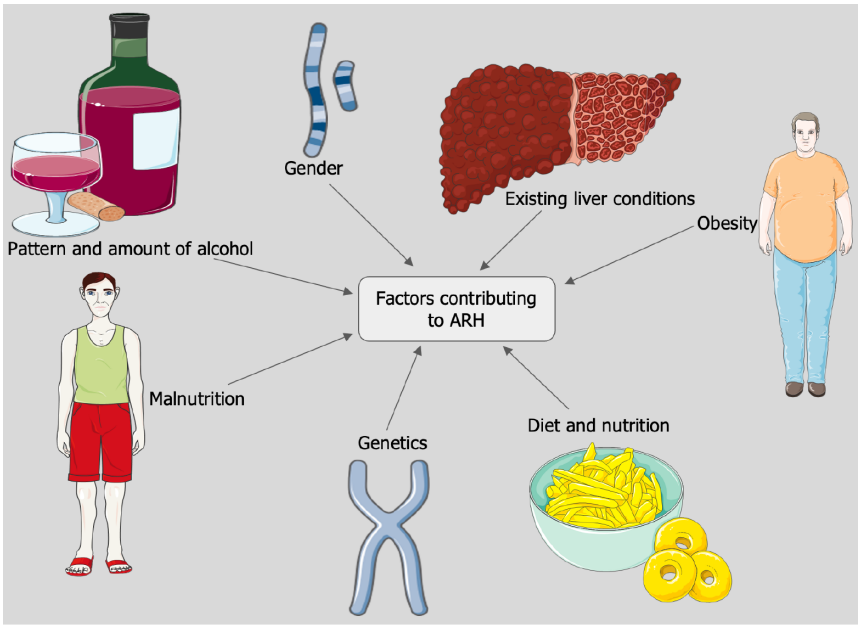
ARH is also associated with a significant risk of mortality. Mortality has been estimated to be around 15% at 30 d and 39% at 1 year and has been linked to the severity of the disease[5]. Patients with mild liver injury have a 20% mortality, while patients with severe liver injury have an overall 40% mortality [6]. Mortality in patients with higher Maddrey's discriminant function (MDF) score (> 30), a surrogate marker of severity, is estimated to be between 30%-50%[7-8].

In previous years, there has also been an increase in the healthcare burden of ARH hospitalizations. An increase was noted in the mean inpatient cost for ARH hospitalizations from $31189 in 2009 to $62229 in 2019[4]. A study by Thompson *et al*[9], using commercial insurance claims, examined hospitalized patients between 2006-2013 and reported the average cost per patient is $145000 in their cohort of 15546 patients. They also reported the cost surrounding death of ARH was 200%-300% higher than the average cost surrounding death.

EPIDEMIOLOGY

Alcohol intake: The amount of alcohol consumption that places patients at risk of ARH is largely unknown. The estimates of the amount of alcohol consumed by patients may not be accurate as they are based on interviewing patients and family members[9]. The majority of patients with ARH consume more than 100 g/d of alcohol[10]. American Association for the Study of Liver Disease (AASLD) practice guidelines recommend suspecting ARH in women who consume > 40 g of alcohol and in men who consume > 60 g/d for ≥ 6 mo[11-12]. It is also pertinent to note that not all patients who drink heavily develop ALD. In a study by Friedman *et al*[13], 35% of the patients developed steatohepatitis and ARH, while only 10% of the patient's developed cirrhosis.

The pattern of drinking as well as the type of alcohol consumed also contributes to the risk of developing ARH. Drinking spirits or beer, binge drinking as well as drinking outside of the typical mealtimes has been associated with a higher risk of developing ALD[13-15] (Figure 1).



DOI: 10.3748/wjg.v29.i17.2551 **Copyright** ©The Author(s) 2023.

Figure 1 Risk factors of alcohol-related hepatitis. ARH: Alcohol-related hepatitis.

Gender: There are significant differences based on gender. Women are at a higher risk of developing ARH at a lower threshold compared to men. This is attributed to differences in the variability of alcohol dehydrogenase activity, sex hormones, body fat distribution and liver volume between the two genders [16-18]. There has been an increase in the cases of ARH in women in recent years. A study conducted between 2009-2019 showed an increase in the proportion of women being admitted with ARH from 29.1% to 34.1%[4].

Malnutrition: Patients who consume alcohol excessively are often malnourished and can suffer from vitamin deficiencies[19]. Mortality has been closely related to the severity of protein-energy malnutrition. Patients with severe malnutrition and ARH have an estimated mortality of 80%[20]. Additionally, depletion of hepatic vitamin A and vitamin E can aggravate liver disease[21]. Zinc deficiency in patients with excessive alcohol can lead to disruption of mucosal permeability which may play a role in the pathogenesis of ARH.

Concurrent liver disease: It is well established that the combination of alcohol misuse and chronic hepatitis C (HCV) increases the incidence of cirrhosis and hepatocellular carcinoma (HCC) and is associated with reduced survival compared to patients with either HCV or alcohol use alone[22]. Consuming upward of 50 g/d of alcohol increases the relative risk of liver disease compared to patients with HCV who do not consume alcohol[23]. Patients with chronic HCV have been noted to have worse outcomes and higher in-hospital mortality when admitted with ARH[24].

While the literature clearly demonstrated worse outcomes in patients with concomitant alcohol misuse and chronic HCV, the data regarding the effect of alcohol use on patients with chronic hepatitis B (HBV) remains understudied. A study by Iida-Ueno *et al*[25] revealed that patients with light to moderate alcohol consumption had a 1.5-fold increase of chronic HBV infection while patients with heavy alcohol consumption had significantly accelerated progression to cirrhosis and HCC with 1.3 to 8.4-fold increased risk. Although the mechanism by which alcohol enhances disease progression is less studied in patients with chronic HBV in comparison to patients with HCV, patients with either chronic HCV and HBV should be counseled to avoid alcohol consumption to minimize chances of liver disease progression.

Obesity, diabetes mellitus and metabolic syndrome-underlying non-alcoholic fatty liver disease, a hepatic manifestation of metabolic syndrome, can be additive to the damage sustained through alcohol misuse and lead to worse outcomes. A study by Siddiqui *et al*[26] reported obesity to be an independent predictor of mortality in ARH.

Seasonality: Studies have shown that there might be a seasonal trend to admissions with alcohol use. We have previously reported that in the United States, ARH was highest in the summer months, as compared to the common opinion that ARH hospitalizations are higher in the winter season[27].

GENETICS

Significant variability has been noted among patients in regard to the susceptibility of developing ARH as well as the severity of symptoms. This variability has prompted several studies exploring a possible genetic basis for individual response to ARH. Studies have found an alteration in the expression of claudins, osteopontin, CD209, selenoprotein, and bile duct proliferation genes in patients with ARH compared to patients with alcoholic steatosis and healthy controls without liver disease[28]. Colmenero *et al*[29] identified several genes that were upregulated in ARH including extracellular matrix proteins, fibrogenesis mediators, inflammatory cytokines, and apoptosis regulators. Cytochrome p450 2E1 and angiotensinogen were found to be downregulated. Additionally, certain genes were found to be correlated with the severity of disease features including tissue inhibitors of metalloproteinases-1 and growth-related oncogene α. Epigenetic studies have also shown that a liver affected by ARH has significant alterations in HNF4α-dependent genes, which play a role in impairing metabolic and synthetic function[30]. A cohort study by Beaudoin *et al*[31] demonstrated an increased risk for developing ARH with a higher total bilirubin in patients with variants in the patatin-like phospholipase domain-containing protein 3 (*PNPLA3*) and the haptoglobin genes as compared to other genetic variants associated with chronic liver disease states[32].

The *PNPLA3* gene in particular has been identified to play a significant role in the pathogenesis of several liver diseases, as it belongs to a group of lipid-metabolizing enzymes. The I148M variant, a single-nucleotide polymorphism of the gene, is associated with an increased risk for developing hepatic steatosis, non-alcoholic steatohepatitis (NASH), ALD, cirrhosis, and HCC[33]. Despite these correlations, the precise function of the *PNPLA3* gene is yet to be fully understood. Palmer *et al*[33] demonstrated that variants in the *PNPLA3* gene in Hispanic-American and African-American patients is significantly associated with the development of hepatic steatosis, and other studies have shown that these groups suffer from higher mortality rates due to ALD. Levy *et al*[34] reported that patients of Hispanic ancestry presented with ALD at a significantly earlier age than patients of Caucasian or African-American background, though the mechanisms remain unclear and may be related to the gene variants described by Palmer *et al*[33] as well as health care disparities. Future studies can help to elucidate the underlying mechanisms of these discrepancies and the potential of gene-targeted therapy in the management of ARH.

PATHOGENESIS

The pathogenesis of ARH involves acute inflammation superimposed on chronic ALD. Initial hepatic injury results from the metabolism of ethanol into acetaldehyde by alcohol dehydrogenase and cytochrome P450 2E1 (CYP2E1). As ethanol builds up as a result of increased consumption, acetaldehyde also accumulates in the liver and begins to exert toxic effects[35]. Acetaldehyde leads to the formation of adducts, in the form of bonds with proteins, lipids, and DNA. This in turn impairs the normal function of the affected proteins and lipids and leads to DNA damage. CYP2E1 further contributes to liver injury by the production of reactive oxygen species which leads to hepatocyte injury [36]. This is thought to occur as a result of lipid peroxidation and interaction with proteins and nucleic acids, leading to hepatocyte necrosis[37] (Figure 2).

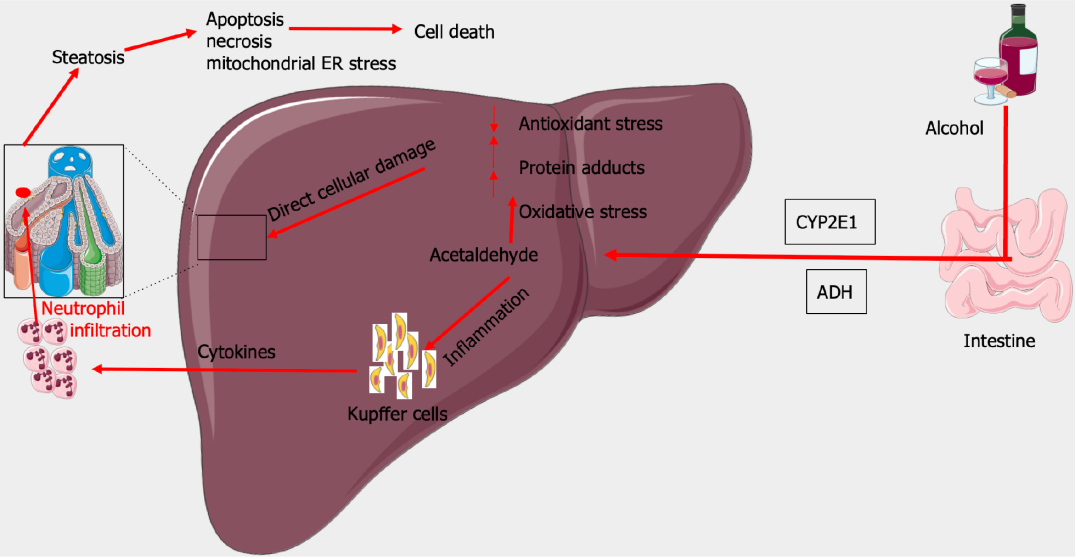
The oxidation of ethanol and acetaldehyde leads to an increase in the levels of nicotinamide adenine dinucleotide, which enhances lipogenesis in the liver[38]. Fatty infiltration of the liver is also a result of increased gut permeability due to alcohol ingestion, leading to higher levels of lipopolysaccharides present in the portal circulation[39]. Endotoxin, a lipopolysaccharide present in cell walls of gut microbiota, forms a protein complex and binds to the CD14 receptor on Kupffer cells in the liver[40]. The activation of Kupffer cells leads to the release of tumor necrosis factor-α (TNF-α), a pro-inflammatory cytokine[41]. TNF-α exerts its hepatotoxic effects by causing hepatocyte apoptosis and stimulating the release of other cytokines[42]. Higher levels of TNF-α are correlated with increased severity of ARH, demonstrating the significance of the cytokine in the pathogenesis of ARH[43].

The stimulation of Kupffer cells also lead to an increase in polymorphonuclear leukocyte infiltrate in the liver, as a result of chemotactic factors such as interleukin-8[44]. The multifactorial process of inflammation superimposed on alcohol-induced hepatic damage leads to the impairment of liver function observed as systemic illness and laboratory abnormalities in ARH. A thorough understanding of the pathogenesis of ARH can aid in its treatment, and further studies elucidating the precise mechanisms involved may improve treatment modalities and outcomes.

DIAGNOSIS

Physical Examination

Physical examination can range from benign to profoundly abnormal[45]. Patients may have signs of



DOI: 10.3748/wjg.v29.i17.2551 **Copyright** ©The Author(s) 2023.

Figure 2 Pathogenesis of alcohol-related hepatitis. ADH: Alcohol dehydrogenase.

malnutrition/sarcopenia manifested as temporal or thenar muscle wasting. Jaundice and scleral icterus may be apparent in patients with more severe disease while subtle signs of jaundice can be noted sublingually or in the tympanic membranes in patients with less severe disease. The presence of spider angiomas, gynecomastia in men and caput medusa is uncommon in patients with ARH in the absence of cirrhosis. Right upper quadrant tenderness to palpation along the enlarged hepatic border is common, with the liver edge extending into the pelvis and crossing the midline in severe cases. Some studies have reported a bruit over the liver as a feature of severe ARH in > 50% of patients[46]. Splenomegaly can often be appreciated as well even in the absence of cirrhosis. Fluid wave, shifting dullness and frank abdominal distention signifying large-volume ascites can be seen in severe cases. Lower extremity swelling progressing to anasarca can also be seen in severe cases. Finally, asterixis can be seen in patients with significant hepatic dysfunction.

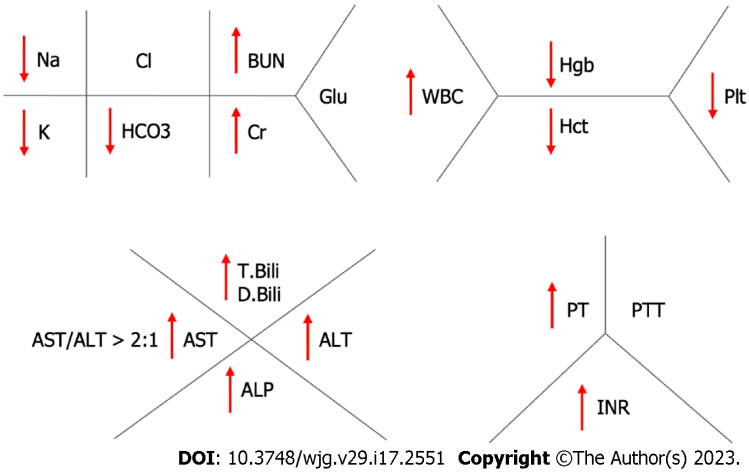
Laboratory findings

Patients with suspected ARH should undergo a broad laboratory workup including comprehensive metabolic panel, complete blood count, international normalized ratio (INR), and gamma glutamyl transferase (GGT). Serologies for HAV, HBV and HCV should also be obtained to rule out alternative/concomitant infectious causes. Typical laboratory findings in ARH consist of elevated white blood cell count, thrombocytopenia, low sodium, potassium and magnesium. Other findings include total bilirubin > 3 mg/dL, elevated alanine transaminase (ALT) and aspartate transaminase (AST) with levels usually < 400 U/L, AST:ALT ratio > 2, GGT > 100 U/mL, INR > 1.5, and albumin < 3.0 g/L[47]. Other sequelae of chronic alcohol use such as macrocytic anemia can also be seen (Figure 3).

It is pertinent to rule out alternative/concomitant causes of liver disease such as Wilson's disease, autoimmune liver diseases and iron overload syndromes. This is especially important in patients with severe disease who may be considered for liver transplantation, as these diagnoses will have significant implications on patient's ability to qualify for an urgent transplant as well as pre-and post-transplant management. Making these diagnoses can be challenging as patients with ARH may have multiple metabolic derangements. For example, patients with ARH may have decreased ceruloplasmin levels in the setting of hepatic dysfunction leading to suspicion of Wlison's disease. If there is a significant clinical concern for Wilson's disease, patients should undergo a slit lamp examination for Kayser-Fleischer rings as well as a 24-h urine copper collection. Ferritin levels as well as iron saturations in patients with ARH can be markedly elevated in ARH therefore genetic testing for *HFE* gene mutation should be considered[48]. A clinical suspicion of autoimmune liver disease, especially in the setting of elevated autoimmune markers [antinuclear antibody (ANA), anti-smooth muscle antibody (SMA), antimitochondrial antibody, anti-liver kidney microsomal antibody], should prompt consideration of liver biopsy. Alpha-1-antitrypsin levels can be artificially elevated in the setting of acute illness; genetic testing should be considered if clinical suspicion is sufficiently high.

Imaging

Abdominal imaging can be effective in the initial evaluation of suspected ARH however, it cannot serve as the sole basis for the diagnosis. Abdominal ultrasound (US) computed tomography scan and/or magnetic resonance imaging will likely reveal and enlarged liver with smooth contours and decreased



DOI: 10.3748/wjg.v29.i17.2551 **Copyright** ©The Author(s) 2023.

Figure 3 Fishnet diagram showing laboratory abnormalities, commonly seen in patients with alcohol-related hepatitis. BUN: Blood urea nitrogen; WBC: White blood cell; Glu: Glucose; Hgb: Hemoglobin; Hct: Hematocrit; Plt: Platelet; T.Bili: Total bilirubin; D.Bili: Direct bilirubin; AST: Aspartate transaminase; ALT: Alanine transaminase; ALP: Alkaline phosphatase; PT: Prothrombin time; PTT: Partial thromboplastin time; INR: International normalized ratio.

attenuation, and in more severe cases, an enlarged spleen, ascites and other sequelae of portal hypertension. The presence of smooth hepatic borders, as opposed to the nodular contour, can help to differentiate ARH from cirrhosis[49] (Figure 4).

BIOPSY

The European Association for the Study of the Liver clinical practice guideline in 2014 stated that the "presence of acute steatohepatitis can be suspected on the clinical and biochemical grounds, but a definitive diagnosis of acute steatohepatitis requires liver biopsy"[50]. AASLD practice guidelines in 2019 recommend performing biopsy for confirmation if there are potential confounding factors such as [11]: (1) Ischemic hepatitis (*e.g.* severe upper GI bleed, cocaine use within 7 d or hypotension); (2) Suspected drug-induced liver disease; (3) Uncertain alcohol use assessment; and (4) Atypical laboratory tests (AST < 50 or > 400 IU/L, AST/ALT < 1.5), ANA > 1:160 or SMA > 1:80. Liver biopsy is controversial, especially in patients with coagulopathy and ascites. Percutaneous biopsy may be performed in most patients, but transjugular biopsy is preferred in patients with severe thrombocytopenia and prolonged INR. Liver biopsy is also recommended in patients suspected of having additional etiology for ACLF.

HISTOLOGY

Histology in patients with ALD can range from steatosis to steatofibrosis[51-52]. Steatofibrosis is defined as steatosis with fibrosis, with or without hepatitis. Histological features include steatosis, hepatocyte ballooning, neutrophil-rich inflammation in the lobular parenchyma, necrosis, apoptosis and Mallory-Denk bodies (MDB)[53]. The predominant mode of hepatocyte injury is *via* ballooning degeneration, followed by lytic necrosis and apoptosis. The hepatocytes become swollen, with clumping of intermediate filaments and loss of cytokeratin 8 and 18[51]. The swelling in hepatocytes can be attributed to severe ATP depletion and an increase in intra-cellular calcium, resulting in loss of plasma membrane volume control, oncotic necrosis and disruption of the intermediate filament network. The majority of changes in ALD are seen in the centrilobular region of hepatic lobe as they contain enzymes such as alcohol dehydrogenase, which are critical in alcohol metabolism[54].

It is pertinent to note there are histological similarities between NASH and ARH[53]. The differentiation is based on clinical information regarding alcohol intake; however some features are seen more commonly in ARH as compared to NASH (Table 1).

Apoptosis can be triggered by oxidative stress. Apoptotic hepatocytes, also known as councilman bodies or acidophil bodies, are visualized as shrunken cells, chromatin condensation and cellular fragmentation[55]. MDB contain eosinophilic material, located primarily in the perinuclear location in the cytoplasm of hepatocytes[56]. They are formed due to the misfolding of aggregated keratin filaments. MDB demonstrate immunoreactivity with antibodies to keratin 8, 18 and p62. Portal inflammation is milder as compared to other etiologies of liver disease. Portal inflammation, when present, is accompanied by ductular reaction and periportal inflammation[57]. Other features of this disease

Table 1 Histological differences between non-alcoholic steatohepatitis and alcohol-related hepatitis

Histological features	NASH	ARH
Canalicular cholestasis	Less common	More common
Mallory denk body	Less common	More common
Ductular reaction	Less common	More common
Fibrosis in portal tract	Less common	More common
Sclerosing hyaline necrosis	Less common	More common
Veno-occlusive lesions	Less common	More common
Severe steatosis	More common	Less common
Glycogenated nuclei	More common	Less common
Lipogranulomas	More common	Less common
Fibrosis	Lattice pattern	Solid pattern

NASH: Non-alcoholic steatohepatitis; ARH: Alcohol-related hepatitis.



DOI: 10.3748/wjg.v29.i17.2551 **Copyright** ©The Author(s) 2023.

Figure 4 Computerized tomography showing enlarged liver with smooth contour.

include glycogenated nuclei, megamitochondria, cholestasis and hemosiderin deposits[58]. Iron deposition can also occur in patients with ALD[59-60]. Based on the index of suspicion, concomitant hereditary hemochromatosis should be ruled out.

As the disease progresses, fibrosis begins in perivenular region (Zone 3) and extends to the perisinusoidal region in patients giving classic "chicken-wire fibrosis". Trichrome stain visualizes the fibrosis. If the injury continues, fibrosis progresses resulting in nodule formation and finally cirrhosis. An orcein stain, can be beneficial in later stages to differentiate broad bands of fibrosis from areas of collapse, which can occur in superimposed ARH[54].

A histological severity score including cytokeratin 8 and 18, has shown good accuracy in predicting 90-d survival[61]. Alcoholic hepatitis histologic score was created using parameters such as degree of fibrosis, degree of neutrophil inflammation, type of bilirubin stasis, and presence of mitochondria[62]. This score has been shown to be predictive of 90-d mortality. Trépo *et al*[63] combined the expression patterns of 123 genes with the model for end-stage liver disease (MELD) score to create gene-signature

plus MELD scoring system. This helped in discriminating patients with poor and good 90-d survival with an area under the curve of 0.86. This score outperformed other models including MELD plus Lille. This is not yet commercially available for use, however, may hold promise for the future.

COMPLICATIONS

Complications of ARH include infection, kidney injury, gastrointestinal bleeding, and acute liver failure amongst others (Figure 5).

Infection

Patients with ascites are at risk for developing spontaneous bacterial peritonitis (SBP), a life-threatening infection of the peritoneal cavity. SBP is almost exclusively seen in patients with ascites and is a result of bacterial translocation of enteric microflora into the ascitic fluid with concurrent failure of liver-related defensive mechanisms due to cirrhosis[64]. Additionally, patients with ARH are often treated with corticosteroids, further suppressing the immune response and increasing the risk of serious infection. Treatment of SBP is usually with a third-generation cephalosporin, such as ceftriaxone, which can also be used prophylactically in patients with decompensated cirrhosis or known patient with cirrhosis who presents with gastrointestinal bleeding.

Despite the well-known association of SBP with ALD, several studies demonstrate that infection due to pneumonia and urinary tract infection (UTI) is more common in severe ARH than SBP[65]. Infection overall is a major cause of mortality in severe ARH, with the majority being bacterial in nature[66-67]. A recent meta-analysis[68] found pneumonia to be the most common infection in severe ARH at 23%, followed by UTI at 10%. In comparison, SBP accounted for only 7% of infections. Patients with acute severe ARH have also been shown to have a greater level of immunosuppression compared to patients with cirrhosis, as they were found to have reduced T-lymphocyte and neutrophil activity[69]. Furthermore, obesity has been associated with increased susceptibility to infection in patients with ARH [70]. A high index of suspicion is needed in monitoring infectious signs and symptoms in patients with ARH as these patients often lack typical signs of infection such as fever or abdominal pain and may present instead with progressive hepatic decompensation. A low threshold for initiation of antibiotic therapy is advised and can be initiated empirically while infectious work-up is in progress.

Acute kidney injury

Acute kidney injury (AKI) is a common complication in hospitalized patients with ARH and can be due to pre-renal, intrinsic renal and post-renal causes. Pre-renal AKI continues to be the most common etiology, while the most feared etiology is hepatorenal syndrome (HRS). These entities can be differentiated *via* volume expansion challenge (25% albumin 1 g/kg for 48 h). Renal US can be used to rule out post-renal causes. Diuretics should be discontinued in patients with AKI.

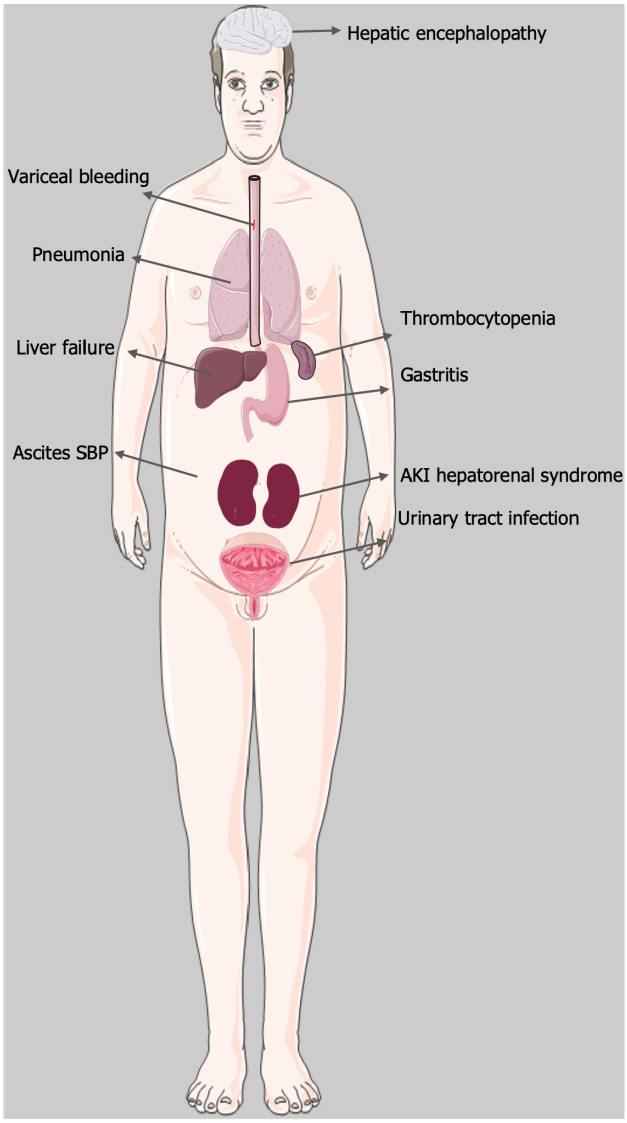
Another etiology that should be considered in patients with ARH is acute tubular necrosis (ATN) secondary to cholemic nephrosis, or bile salt nephropathy and should be suspected in patients with prolonged severe cholestasis. Hyperbilirubinemia can also lead to formation of tubular casts, which can lead to ATN[71]. Evaluation of fractional excretion of sodium/urea as well as urine microscopy is beneficial to identify the etiology of kidney disease. Workup for AKI in patients with ARH is presented in Figure 6.

The most feared complication, HRS, results from renal artery vasoconstriction secondary to splanchnic vasodilation seen in liver disease[72]. Patients with ARH and other ALD often develop dilation of the splanchnic vasculature in response to increased hepatic resistance, which in turn leads to activation of the renin-angiotensin-aldosterone system, sympathetic nervous system, and arginine vasopressin system. The activation of these vasoconstrictor systems leads to constriction of the renal arteries and subsequent AKI due to decreased renal blood flow often in the setting of decreased cardiac output[73]. The development of AKI in patients with ARH is associated with a significantly higher mortality rate compared to patients without AKI, 65% *vs* 7% ($P < 0.0001$) respectively[74].

Treatment of HRS is complex, with most studies supporting the use of vasoconstrictors in combination with albumin administration. Terlipressin, a vasopressin analogue, has shown promising results in the treatment of HRS as it was found to be superior to both placebo and octreotide[75]. It has recently been approved in the United States by the Food and Drug Administration for the management of HRS. Liver transplantation (LT) is the treatment of choice in patients with HRS as renal dysfunction is potentially reversible with the correction of hepatic failure[76]. Interestingly, obesity has been found to be associated with decreased survival in acute ARH, and this is thought to be due to an increased risk of developing renal failure[77].

Acute on chronic liver failure

Severe ARH can lead to ACLF, a condition that is associated with increased mortality in patients with ARH and is commonly seen during the course of the disease[78]. ACLF manifests as worsening jaundice and coagulopathy and is usually triggered by a precipitating event. Current literature shows that ARH



DOI: 10.3748/wjg.v29.i17.2551 **Copyright** ©The Author(s) 2023.

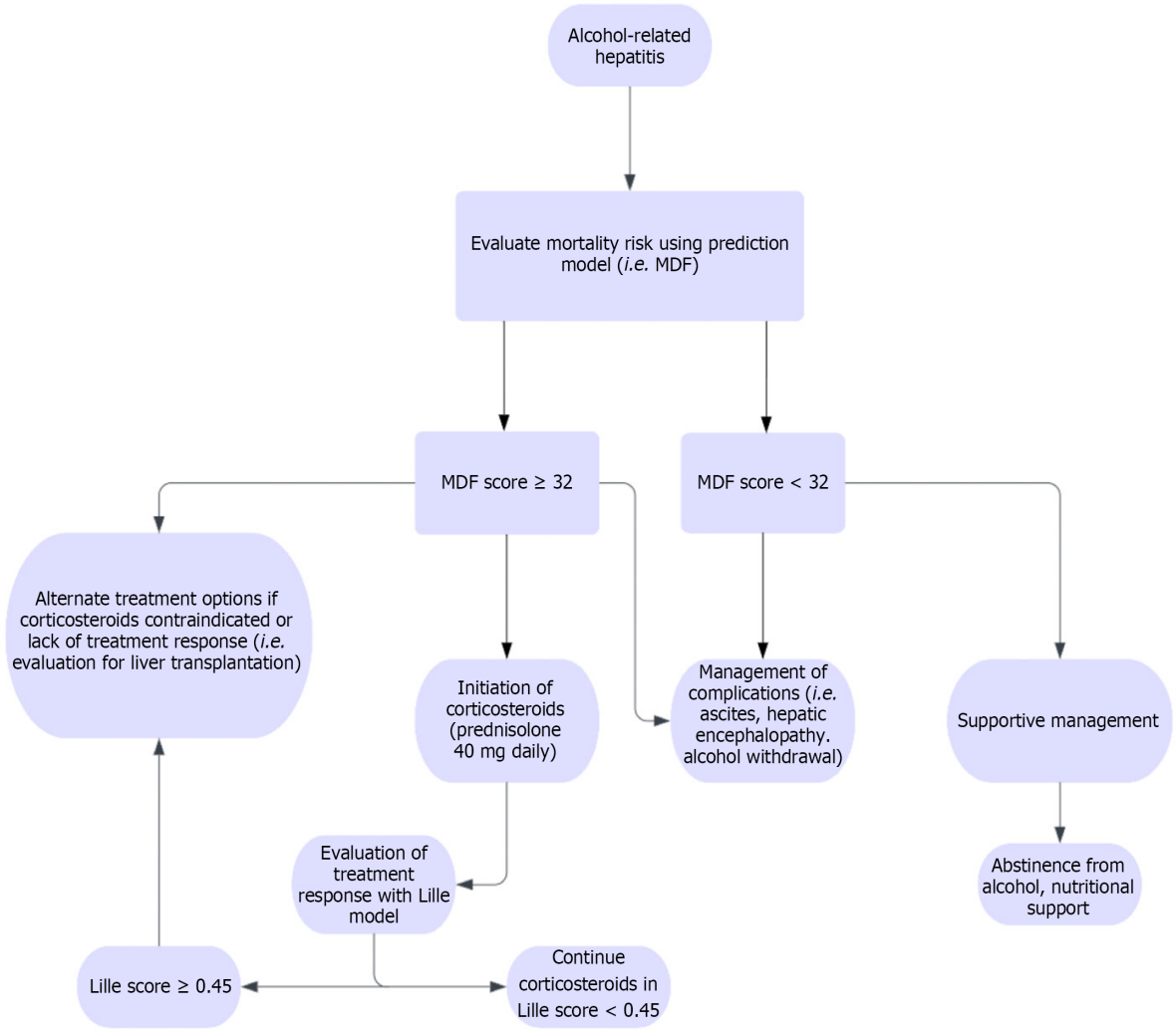
Figure 5 Complications and clinical features in patients with alcohol-related hepatitis. SBP: Spontaneous bacterial peritonitis; AKI: Acute kidney injury.

serves as a common precipitating event for the development of ACLF[76]. Studies have demonstrated that 65% of patients with severe ARH had ACLF at the time of diagnosis or within a 6-mo follow-up period[77]. Given the poor prognosis of ACLF, early liver transplantation is becoming more commonplace in the treatment of severe ARH, with recent literature supporting its use with stringent patient selection criteria[79-80].

Portal hypertension and cirrhosis

Many patients with ARH also have portal hypertension or will develop portal hypertension at some point during their disease course potentially leading to variceal hemorrhage. Overall one-month mortality in moderate to severe ARH is 23%, with the most common causes of death being liver failure, gastrointestinal bleeding, and infection[81] The one-month mortality in non-severe ARH is 6%, however the rate increases to 13% after one year[82].

Long-term follow-up in patients with ARH over 4 years revealed the probability of developing cirrhosis to be 10%-20% per year and up to 70% of patients will ultimately develop cirrhosis[83]. In another study, about 40% of the patients were diagnosed with cirrhosis on biopsy, 5 years after the episode of ARH[84]. The probability of developing cirrhosis is associated with continued alcohol use, as Rehm *et al*[85] demonstrated in a meta-analysis that there is a close dose-dependent relationship between ongoing alcohol use and the risk of progression of ALD to liver cirrhosis. Parés *et al*[86] found an 18% risk of progression to cirrhosis in patients who abstained from alcohol after 20 mo compared to 23% in patients with continued alcohol consumption.



DOI: 10.3748/wjg.v29.i17.2551 **Copyright** ©The Author(s) 2023.

Figure 6 Diagnostic workup for acute kidney injury in patients with alcohol-related hepatitis. MDF: Maddrey's discriminant function.

PREDICTION MODELS

MDF is a commonly used prognostic indicator in the management of ARH as it is specific for ARH and has shown to be relatively accurate in predicting short-term outcomes[87]. The MDF score incorporates two of the major indices of liver function, prothrombin time (PT) and total bilirubin with the formula 4.6 × (prolongation of PT in seconds) + bilirubin (μmol/L)/17. MDF score of < 32 signifies mild to moderate ARH with 30-d survival estimated at 80%-100%. MDF score ≥ 32 is considered to be severe ARH with a 30-d survival of only 50%, and these patients warrant corticosteroid administration for treatment of their disease[87] (Table 2).

Lille Model is used to evaluate treatment response to corticosteroids and includes age, initial serum albumin, change in total serum bilirubin at day 7 of treatment, renal insufficiency, and initial MDF score [88]. Patients with a Lille score of < 0.45 had an average 6-mo survival rate of 85%, compared to just 25% in patients who scored ≥ 0.45 after 7 d of treatment (P < 0.0001). The Lille model is primarily used in conjunction with the MDF to guide treatment of ARH. Patients who score ≥ 0.45 after receiving corticosteroid therapy for 7 d are considered for discontinuation of steroids and initiation of alternative treatment modalities, as continuation of steroids is of little benefit in these patients.

MELD was initially created to assess the mortality risk in patients with portal hypertension undergoing transjugular intrahepatic portosystemic shunts procedure however, it has now become a validated tool in assessing patients with a variety of liver pathologies[89]. MELD differs from MDF in that it incorporates serum creatinine and uses INR rather than PT. The formula for MELD is 9.57 × loge (creatinine) + 3.78 × loge (total bilirubin) + 11.2 × loge (INR) + 6.43. In comparison to the MDF, the MELD has been shown to be superior in predicting outcomes of patients with ARH. Several studies have demonstrated this effect, further supporting the use of MELD in patients with ARH[90-94]. Patients with a MELD score ≤ 11 have mild disease associated with a very low mortality rate. Patients who score > 21 are considered to have severe ARH.

Table 2 Prediction models for alcohol-related hepatitis

Score	Variables	Mortality rate
MDF	PT, total bilirubin	50% at 30 d for score ≥ 32
Lille model	Age, albumin, change in total bilirubin, renal insufficiency, MDF score	75% at 6 mo for score ≥ 0.45
Model for end-stage liver disease	Creatinine, total bilirubin, INR	20% at 90 d for score > 21
Glasgow alcoholic hepatitis score	Age, white blood cell count, BUN, total bilirubin, PT	48% at 28 d for score ≥ 9
ABIC score	Age, total bilirubin, creatinine, INR	75% at 90 d for score > 9

PT: Prothrombin time; BUN: Blood urea nitrogen; INR: International normalized ratio; ABIC: Age, serum bilirubin, international normalized ratio, serum creatinine; MDF: Maddrey discriminant function.

Glasgow alcoholic hepatitis score (GAHS) was developed in order to present a model with increased specificity than MDF and a more accurate cutoff score than MELD. The GAHS incorporates many of the same parameters as the MDF and MELD, but differs in its inclusion of the peripheral white blood cell count[95]. The inclusion of an inflammatory component is thought to provide a more accurate predictor of mortality in ARH and has been shown to be superior to MDF in predicting 28-d and 84-d mortality. The cutoff point delineating severe ARH from non-severe is a GAHS score of ≥ 9.

Age, serum bilirubin, INR, serum creatinine (ABIC) score is another scoring system that was developed to predict mortality in patients with ARH[96]. The ABIC score includes liver function as well as kidney function and has a formula of (age × 0.1) + (serum bilirubin × 0.08) + (serum creatinine × 0.3) + (INR × 0.8). This model is validated for predicting 3-mo survival rates in ARH based on stratification of the severity of disease. Patients are classified based on their ABIC score into low (< 6.71), intermediate (6.71-8.99), and high (> 9.0) mortality risk. These classes correspond to a 90-d mortality of 0%, 30%, and 75%, respectively. Despite its efficacy in death risk stratification, the ABIC score does not play a major role in treatment or in determining whether corticosteroid administration is indicated.

TREATMENT

The management of ARH involves reducing hepatic inflammation by targeting pro-inflammatory and immunologic substances acutely and reversing alcohol-induced hepatotoxicity in the long term. The mainstay of treatment in ALD is abstinence from alcohol. A retrospective study by Lackner *et al*[97] demonstrated a 5-year mortality rate of 13% in early ALD and 43% in decompensated ALD. Abstaining from alcohol showed an improvement in survival in patients with both early and decompensated ALD. A meta-analysis by Xie *et al*[98] determined that patients with ALD see an improvement in survival rates after approximately 1.5 years of abstinence. However, studies have also shown that histological improvements in ALD can be observed in patients as soon as 2 wk after discontinuation of alcohol consumption[99].

Many of the traditional pharmacologic agents used to promote abstinence from alcohol such as disulfiram, naltrexone, acamprosate, and topiramate are of limited use in ALD as they may be hepatotoxic and lack data supporting their usage[100]. Baclofen, a selective gamma-aminobutyric acid B receptor agonist, has been studied as a potential agent of choice in patients with ALD as it has minimal hepatic clearance. A recent multi-site randomized control trial[101] of patients with and without ALD demonstrated that low-medium dose baclofen at 30-75 mg daily led to a significant improvement in alcohol abstinence.

Nutritional supplementation is a vital component in the treatment of ALD. Malnutrition is common in patients with ALD, and the severity of malnourishment is correlated with the severity of liver disease [102]. The AASLD recommends a diet of at least 2000 kcal/d with at least 1.5 g protein/kg/d in patients with ALD[103]. These patients suffer from nutritional deficiencies and appropriate nutritional supplementation should be provided as nutritional deficiencies have been shown to be associated with worse outcomes[104].

Treatment of mild to moderate ARH, as defined by an MDF score < 32, consists mainly of supportive care and management of complications such as ascites, hepatic encephalopathy, and acute alcohol withdrawal syndrome[105]. Ascites is managed primarily through sodium restriction and diuresis. Patients with ascites generally have decreased sodium excretion, warranting a daily sodium restriction of 2-4 g/d. AASLD guidelines recommend that for the first episode of ascites, aldosterone antagonists alone can generate an adequate response with few side effects[106]. On the contrary, if the patient has long-standing ascites, anasarca or hepatic hydrothorax, the recommended regimen is a combination of an aldosterone antagonist and loop diuretic.

Hepatic encephalopathy is managed primarily with lactulose and rifaximin in order to promote the excretion of toxic metabolites *via* stool and improve the biodiversity of gut flora. Acute alcohol withdrawal is treated with benzodiazepines such as lorazepam on a scheduled regimen or symptom-triggered dose in accordance with protocols such as the Clinical Institute Withdrawal Assessment. Lorazepam has been shown to be the safest agent in its class in patients with liver disease due to minimal hepatotoxicity and is therefore the drug of choice[107]. Use of long-acting benzodiazepines, such as chlordiazepoxide, should be avoided in patients with significant hepatic dysfunction due to decreased rate of hepatic metabolism and potential for rapid accumulation leading to progressive decline in mental status[108].

The most well-studied treatment modality in severe ARH, classified as an MDF score ≥ 32, is the use of corticosteroids. Its use was validated in the "Steroids or pentoxifylline for alcoholic hepatitis" (STOPAH)[109] trial, which included 1053 subjects with ARH. There was a 28-d mortality benefit in patients treated with prednisolone. On the contrary, no mortality benefit was observed in the prednisolone group after 90 d or 1 year, adding further evidence that the positive effects of steroids in severe ARH are limited to short-term (Figure 7).

A meta-analysis of 5 randomized control trials[110] revealed a significant improvement in 28-d survival among patients with severe ARH treated with corticosteroids (79.97% ± 2.8% *vs* 65.7% ± 3.4%, $P = 0.0005$). A more recent meta-analysis[111] of 11 randomized control trials found similar results in short-term mortality benefit, however also demonstrated that corticosteroid treatment did not decrease mortality rate after 6 mo. The primary mechanism by which corticosteroids exert their effect in severe ARH is by blunting the immune response and inflammation that contributes to mortality[112]. The standard regimen for treatment of severe ARH is administration of prednisolone 40 mg daily[113]. Contraindications to steroid administration include active infection, gastrointestinal bleeding, acute pancreatitis, and renal failure, as steroids can acutely exacerbate these conditions[114].

STOPAH109 trial reported that incidence of serious infections occurred in 13% of patients in the prednisolone group compared to 7% in patients who were not treated with prednisolone ($P = 0.002$). However, a recent meta-analysis[115] found that corticosteroid administration in severe ARH reduced 28-d mortality from liver-related death with no significant change in mortality from bacterial infection or gastrointestinal bleeding. The study also found a higher incidence of fungal infection in steroid-treated patients. Pentoxifylline was previously used in the management of ARH. Its use has been limited based on the results of STOPAH trial, in which use of pentoxifylline was not associated with mortality benefit.

LT has been controversial in the treatment of ARH, as patients with ALD have historically been considered poor candidates for transplantation due to concern for continued alcohol use after transplantation. However, recent trends have shown an opportunity for LT to gain a larger role in the treatment of ARH with strict selection criteria for candidates, as demonstrated in several studies[116]. A prospective trial by Mathurin *et al*[117] showed a significantly improved 6-mo survival rate in patients with severe ARH (MDF > 32, Lillie > 0.45) who received LT compared to controls without LT (77% and 23% respectively, $P < 0.001$). However, selection criteria were remarkably strict, as only patients with no prior episodes of hepatic decompensation, strong family support, complete commitment to abstinence, and consensus among all care providers were accepted for LT, which was less than 2% of all patients admitted with ARH during the study period. A more recent trial by Weeks *et al*[118] demonstrated a 97% 1-year survival rate in patients who received LT for severe ARH, however had an alcohol use relapse rate at 17% due to less strict inclusion requirements (including patients with recent hepatic decompensation). A recent large multi-center retrospective analysis (ACCELERATE-AH)[119] found a 94% 1-year survival rate and 84% 3-year survival rate with a 11% relapse rate. Of note, median MELD score was 39 and median Lille score was 0.82 for patients who received LT.

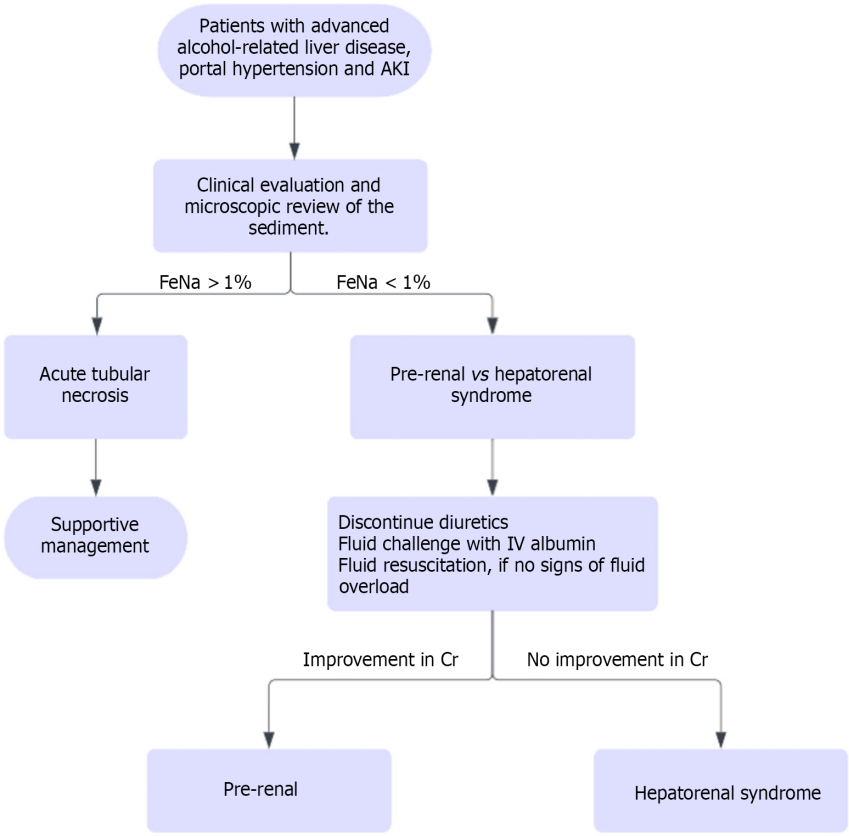
In summary, LT should be considered for patients with life-threatening ARH who have failed medical therapy and who have a low likelihood of alcohol relapse based on predetermined medical and social criteria. The proportion of candidates meeting these criteria may be relatively low, however stringent patient selection can aid in avoiding improper use of donor organs while dramatically improving survival rates. A study reported that the rates of relapse-free survival and hazardous relapse-free survival did not differ between the patients who received early transplantation compared to those who were transplanted after 6 mo of abstinence[120].

THERAPIES/CLINICAL TRIALS UNDER INVESTIGATION

Multiple therapies are currently under clinical trial for the management of ARH. While the discussion regarding all the therapies under investigation is beyond the scope of this article, information regarding the various mechanisms and clinical trials currently targeting this disease is presented in Table 3 below.

Table 3 Clinical trials under investigation

Drugs	Mechanisms	Clinical trials
Anakinra and Canakinumab	Reduce hepatic inflammation	NCT01809132[121], NCT04072822[122], NCT03775109[123]
N-acetyl cysteine, S-adenosyl methionine (SAM-E)	Reduce oxidative stress	NCT03069300[124], NCT00851981[125], NCT02024295[126]
DUR-928	Epigenetic modulation of lipid homeostasis, inflammation, cell survival, tissue regeneration	NCT03432260[127], NCT03917407[128]
Granulocyte colony stimulating growth factors, interleukin-22 and obeticholic acid	Boosts liver regeneration	NCT02442180[129], NCT03703674[130], NCT04066179[131], NCT02655510[132], NCT01918462[133], NCT02039219[134]
Rifaximin, zinc supplementation, bovine colostrum, probiotics, and fecal microbiota transplant	Targets the gut-liver axis	NCT02116556[135], NCT02485106[136], NCT01968382[137], NCT02473341[138], NCT01922895[139], NCT02335632[140], NCT02458079[141], NCT03091010[142], NCT03827772[143]



DOI: 10.3748/wjg.v29.i17.2551 **Copyright** ©The Author(s) 2023.

Figure 7 Treatment algorithm for alcohol-related hepatitis. AKI: Acute kidney injury.

CONCLUSION

ARH remains a disease process with high morbidity and mortality. Despite research advances in pathogenesis of this disease process, limited progress has been made in management of this condition. Abstinence remains critical in maximizing the chances of hepatic recovery; corticosteroids continue to play a role in select populations. Given the grim prognosis and increasing prevalence of ARH, research efforts are aiming at inhibiting inflammatory cytokine pathways that lead to progressive hepatic damage. In the meantime, many centers around the world are resorting to liver transplantation as salvage therapy. The COVID-19 pandemic exacerbated the pre-existing trend of rising cases of ARH. Urgent societal and government interventions are needed to prevent the ongoing rise in ARH cases in addition to intensifying research efforts in identifying and testing therapeutic targets for this complex disease process.

ACKNOWLEDGEMENTS

We thank Dino Dukovic for his expertise and assistance in writing the manuscript.

FOOTNOTES

Author contributions: Chaudhry H, Sohal A and Iqbal H reviewed the literature, drafted the manuscript, revised it for important intellectual content and were involved in the final approval of the version to be published; Roytman M revised the article for important intellectual content and was involved in the final approval of the version to be published; All authors have read and approved the final manuscript.

Conflict-of-interest statement: All the authors report no relevant conflicts of interest for this article.

Open-Access: This article is an open-access article that was selected by an in-house editor and fully peer-reviewed by external reviewers. It is distributed in accordance with the Creative Commons Attribution NonCommercial (CC BY-NC 4.0) license, which permits others to distribute, remix, adapt, build upon this work non-commercially, and license their derivative works on different terms, provided the original work is properly cited and the use is non-commercial. See: https://creativecommons.org/Licenses/by-nc/4.0/

Country/Territory of origin: United States

ORCID number: Hunza Chaudhry 0000-0001-7769-0394.

S-Editor: Li L
L-Editor: A
P-Editor: Zhang XD

REFERENCES

1 **Moon AM**, Curtis B, Mandrekar P, Singal AK, Verna EC, Fix OK. Alcohol-Associated Liver Disease Before and After COVID-19-An Overview and Call for Ongoing Investigation. *Hepatol Commun* 2021; **5**: 1616-1621 [PMID: 34510833 DOI: 10.1002/hep4.1747]
2 **Sohal A**, Khalid S, Green V, Hagino J, Chaudhry H, Gulati A, Roytman M. Soaring rates of alcohol-related hepatitis in the latter phase of the COVID-19 pandemic: A new normal? *JGH Open* 2023; **7**: 148-151 [PMID: 36852146 DOI: 10.1002/jgh3.12864]
3 **Gonzalez HC**, Zhou Y, Nimri FM, Rupp LB, Trudeau S, Gordon SC. Alcohol-related hepatitis admissions increased 50% in the first months of the COVID-19 pandemic in the USA. *Liver Int* 2022; **42**: 762-764 [PMID: 35094494 DOI: 10.1111/liv.15172]
4 **Ali H**, Pamarthy R, Bolick NL, Farooq MF. Ten-year trends and prediction model of 30-day inpatient mortality for alcoholic hepatitis in the United States. *Ann Gastroenterol* 2022; **35**: 427-433 [PMID: 35784634 DOI: 10.20524/aog.2022.0718]
5 **Jinjuvadia R**, Liangpunsakul S; Translational Research and Evolving Alcoholic Hepatitis Treatment Consortium. Trends in Alcoholic Hepatitis-related Hospitalizations, Financial Burden, and Mortality in the United States. *J Clin Gastroenterol* 2015; **49**: 506-511 [PMID: 25198164 DOI: 10.1097/MCG.0000000000000161]
6 **Mathurin P**, Duchatelle V, Ramond MJ, Degott C, Bedossa P, Erlinger S, Benhamou JP, Chaput JC, Rueff B, Poynard T. Survival and prognostic factors in patients with severe alcoholic hepatitis treated with prednisolone. *Gastroenterology* 1996; **110**: 1847-1853 [PMID: 8964410 DOI: 10.1053/gast.1996.v110.pm8964410]
7 **Morgan MY**. The prognosis and outcome of alcoholic liver disease. *Alcohol Alcohol Suppl* 1994; **2**: 335-343 [PMID: 8974353]
8 **Shah NJ**, Royer A, John S. Alcoholic Hepatitis. 2023. In: StatPearls [Internet]. Treasure Island (FL): StatPearls Publishing; 2023 [PMID: 29262136]
9 **Thompson JA**, Martinson N, Martinson M. Mortality and costs associated with alcoholic hepatitis: A claims analysis of a commercially insured population. *Alcohol* 2018; **71**: 57-63 [PMID: 30048829 DOI: 10.1016/j.alcohol.2018.02.003]
10 **Midanik L**. The validity of self-reported alcohol consumption and alcohol problems: a literature review. *Br J Addict* 1982; **77**: 357-382 [PMID: 6762224 DOI: 10.1111/j.1360-0443.1982.tb02469.x]
11 **Naveau S**, Giraud V, Borotto E, Aubert A, Capron F, Chaput JC. Excess weight risk factor for alcoholic liver disease. *Hepatology* 1997; **25**: 108-111 [PMID: 8985274 DOI: 10.1002/hep.510250120]
12 **Crabb DW**, Im GY, Szabo G, Mellinger JL, Lucey MR. Diagnosis and Treatment of Alcohol-Associated Liver Diseases: 2019 Practice Guidance From the American Association for the Study of Liver Diseases. *Hepatology* 2020; **71**: 306-333 [PMID: 31314133 DOI: 10.1002/hep.30866]
13 **Friedman SL**, Neuschwander-Tetri BA, Rinella M, Sanyal AJ. Mechanisms of NAFLD development and therapeutic strategies. *Nat Med* 2018; **24**: 908-922 [PMID: 29967350 DOI: 10.1038/s41591-018-0104-9]
14 **Barrio E**, Tomé S, Rodríguez I, Gude F, Sánchez-Leira J, Pérez-Becerra E, González-Quintela A. Liver disease in heavy drinkers with and without alcohol withdrawal syndrome. *Alcohol Clin Exp Res* 2004; **28**: 131-136 [PMID: 14745311 DOI: 10.1097/01.ALC.0000106301.39746.EB]

15 **Wechsler H**, Austin SB. Binge drinking: the five/four measure. *J Stud Alcohol* 1998; **59**: 122-124 [PMID: 9498324 DOI: 10.15288/jsa.1998.59.122]

16 **Mezey E**, Kolman CJ, Diehl AM, Mitchell MC, Herlong HF. Alcohol and dietary intake in the development of chronic pancreatitis and liver disease in alcoholism. *Am J Clin Nutr* 1988; **48**: 148-151 [PMID: 3389321 DOI: 10.1093/ajcn/48.1.148]

17 **Bellentani S**, Saccoccio G, Costa G, Tiribelli C, Manenti F, Sodde M, Saveria Crocè L, Sasso F, Pozzato G, Cristianini G, Brandi G. Drinking habits as cofactors of risk for alcohol induced liver damage. The Dionysos Study Group. *Gut* 1997; **41**: 845-850 [PMID: 9462221 DOI: 10.1136/gut.41.6.845]

18 **Lu XL**, Luo JY, Tao M, Gen Y, Zhao P, Zhao HL, Zhang XD, Dong N. Risk factors for alcoholic liver disease in China. *World J Gastroenterol* 2004; **10**: 2423-2426 [PMID: 15285035 DOI: 10.3748/wjg.v10.i16.2423]

19 **Mendenhall CL**, Moritz TE, Roselle GA, Morgan TR, Nemchausky BA, Tamburro CH, Schiff ER, McClain CJ, Marsano LS, Allen JI. Protein energy malnutrition in severe alcoholic hepatitis: diagnosis and response to treatment. The VA Cooperative Study Group #275. *JPEN J Parenter Enteral Nutr* 1995; **19**: 258-265 [PMID: 8523623 DOI: 10.1177/0148607195019004258]

20 **Mendenhall C**, Roselle GA, Gartside P, Moritz T. Relationship of protein calorie malnutrition to alcoholic liver disease: a reexamination of data from two Veterans Administration Cooperative Studies. *Alcohol Clin Exp Res* 1995; **19**: 635-641 [PMID: 7573786 DOI: 10.1111/j.1530-0277.1995.tb01560.x]

21 **Leevy CM**, Moroianu SA. Nutritional aspects of alcoholic liver disease. *Clin Liver Dis* 2005; **9**: 67-81 [PMID: 15763230 DOI: 10.1016/j.cld.2004.11.003]

22 **Singal AK**, Anand BS. Mechanisms of synergy between alcohol and hepatitis C virus. *J Clin Gastroenterol* 2007; **41**: 761-772 [PMID: 17700425 DOI: 10.1097/MCG.0b013e3180381584]

23 **Poynard T**, Bedossa P, Opolon P. Natural history of liver fibrosis progression in patients with chronic hepatitis C. The OBSVIRC, METAVIR, CLINIVIR, and DOSVIRC groups. *Lancet* 1997; **349**: 825-832 [PMID: 9121257 DOI: 10.1016/S0140-6736(96)07642-8]

24 **Singal AK**, Sagi S, Kuo YF, Weinman S. Impact of hepatitis C virus infection on the course and outcome of patients with acute alcoholic hepatitis. *Eur J Gastroenterol Hepatol* 2011; **23**: 204-209 [PMID: 21258239 DOI: 10.1097/MEG.0b013e328343b085]

25 **Iida-Ueno A**, Enomoto M, Tamori A, Kawada N. Hepatitis B virus infection and alcohol consumption. *World J Gastroenterol* 2017; **23**: 2651-2659 [PMID: 28487602 DOI: 10.3748/wjg.v23.i15.2651]

26 **Siddiqui T**, Trieu J, Bilal M, Mehta D, Gollapudi LA, Nabors C, Wolf DC. Obesity Has Significant Impact on Mortality in Patients With Acute Alcoholic Hepatitis. *Am. J. Gastroenterol***113**: S591-S593 [DOI: 10.14309/00000434-201810001-01037]

27 **Sohal A**, Bains K, Dhaliwal A, Chaudhry H, Sharma R, Singla P, Gupta G, Dukovic D, Sandhu S, Roytman M, Tringali S. Seasonal Variations of Hospital Admissions for Alcohol-Related Hepatitis in the United States. *Gastroenterology Res* 2022; **15**: 75-81 [PMID: 35572478 DOI: 10.14740/gr1506]

28 **Seth D**, Gorrell MD, Cordoba S, McCaughan GW, Haber PS. Intrahepatic gene expression in human alcoholic hepatitis. *J Hepatol* 2006; **45**: 306-320 [PMID: 16797773 DOI: 10.1016/j.jhep.2006.04.013]

29 **Colmenero J**, Bataller R, Sancho-Bru P, Bellot P, Miquel R, Moreno M, Jares P, Bosch J, Arroyo V, Caballería J, Ginès P. Hepatic expression of candidate genes in patients with alcoholic hepatitis: correlation with disease severity. *Gastroenterology* 2007; **132**: 687-697 [PMID: 17258719 DOI: 10.1053/j.gastro.2006.12.036]

30 **Argemi J**, Latasa MU, Atkinson SR, Blokhin IO, Massey V, Gue JP, Cabezas J, Lozano JJ, Van Booven D, Bell A, Cao S, Vernetti LA, Arab JP, Ventura-Cots M, Edmunds LR, Fondevila C, Stärkel P, Dubuquoy L, Louvet A, Odena G, Gomez JL, Aragon T, Altamirano J, Caballeria J, Jurczak MJ, Taylor DL, Berasain C, Wahlestedt C, Monga SP, Morgan MY, Sancho-Bru P, Mathurin P, Furuya S, Lackner C, Rusyn I, Shah VH, Thursz MR, Mann J, Avila MA, Bataller R. Defective HNF4alpha-dependent gene expression as a driver of hepatocellular failure in alcoholic hepatitis. *Nat Commun* 2019; **10**: 3126 [PMID: 31311938 DOI: 10.1038/s41467-019-11004-3]

31 **Beaudoin JJ**, Liang T, Tang Q, Banini BA, Shah VH, Sanyal AJ, Chalasani NP, Gawrieh S. Role of candidate gene variants in modulating the risk and severity of alcoholic hepatitis. *Alcohol Clin Exp Res* 2021; **45**: 709-719 [PMID: 33616244 DOI: 10.1111/acer.14581]

32 **Bruschi FV**, Tardelli M, Claudel T, Trauner M. PNPLA3 expression and its impact on the liver: current perspectives. *Hepat Med* 2017; **9**: 55-66 [PMID: 29158695 DOI: 10.2147/HMER.S125718]

33 **Palmer ND**, Musani SK, Yerges-Armstrong LM, Feitosa MF, Bielak LF, Hernaez R, Kahali B, Carr JJ, Harris TB, Jhun MA, Kardia SL, Langefeld CD, Mosley TH Jr, Norris JM, Smith AV, Taylor HA, Wagenknecht LE, Liu J, Borecki IB, Peyser PA, Speliotes EK. Characterization of European ancestry nonalcoholic fatty liver disease-associated variants in individuals of African and Hispanic descent. *Hepatology* 2013; **58**: 966-975 [PMID: 23564467 DOI: 10.1002/hep.26440]

34 **Levy R**, Catana AM, Durbin-Johnson B, Halsted CH, Medici V. Ethnic differences in presentation and severity of alcoholic liver disease. *Alcohol Clin Exp Res* 2015; **39**: 566-574 [PMID: 25702770 DOI: 10.1111/acer.12660]

35 **Setshedi M**, Wands JR, Monte SM. Acetaldehyde adducts in alcoholic liver disease. *Oxid Med Cell Longev* 2010; **3**: 178-185 [PMID: 20716942 DOI: 10.4161/oxim.3.3.12288]

36 **Lieber CS**. Cytochrome P-4502E1: its physiological and pathological role. *Physiol Rev* 1997; **77**: 517-544 [PMID: 9114822 DOI: 10.1152/physrev.1997.77.2.517]

37 **Gao B**, Bataller R. Alcoholic liver disease: pathogenesis and new therapeutic targets. *Gastroenterology* 2011; **141**: 1572-1585 [PMID: 21920463 DOI: 10.1053/j.gastro.2011.09.002]

38 **Osna NA**, Donohue TM Jr, Kharbanda KK. Alcoholic Liver Disease: Pathogenesis and Current Management. *Alcohol Res* 2017; **38**: 147-161 [PMID: 28988570]

39 **Abenavoli L**, Masarone M, Federico A, Rosato V, Dallio M, Loguercio C, Persico M. Alcoholic Hepatitis: Pathogenesis, Diagnosis and Treatment. *Rev Recent Clin Trials* 2016; **11**: 159-166 [PMID: 27457347 DOI: 10.2174/1574887111666160724183409]

40 **Su GL**, Klein RD, Aminlari A, Zhang HY, Steinstraesser L, Alarcon WH, Remick DG, Wang SC. Kupffer cell activation

by lipopolysaccharide in rats: role for lipopolysaccharide binding protein and toll-like receptor 4. *Hepatology* 2000; **31**: 932-936 [PMID: 10733550 DOI: 10.1053/he.2000.5634]

41 **Morgan TR**, McClain CJ. Pentoxifylline and alcoholic hepatitis. *Gastroenterology* 2000; **119**: 1787-1791 [PMID: 11113103 DOI: 10.1053/gast.2000.20826]

42 **Bradham CA**, Plümpe J, Manns MP, Brenner DA, Trautwein C. Mechanisms of hepatic toxicity. I. TNF-induced liver injury. *Am J Physiol* 1998; **275**: G387-G392 [PMID: 9724248 DOI: 10.1152/ajpgi.1998.275.3.G387]

43 **McClain C**, Hill D, Schmidt J, Diehl AM. Cytokines and alcoholic liver disease. *Semin Liver Dis* 1993; **13**: 170-182 [PMID: 8337603 DOI: 10.1055/s-2007-1007347]

44 **Bird G**. Interleukin-8 in alcoholic liver disease. *Acta Gastroenterol Belg* 1994; **57**: 255-259 [PMID: 7810274]

45 **Dugum M**, Zein N, McCullough A, Hanouneh I. Alcoholic hepatitis: Challenges in diagnosis and management. *Cleve Clin J Med* 2015; **82**: 226-236 [PMID: 25955457 DOI: 10.3949/ccjm.82a.14048]

46 **Hardison JE**. Auscultation of the Liver. In: Clinical Methods: The History, Physical, and Laboratory Examinations. Boston: Butterworths; 1990 [PMID: 21250262]

47 **Keating M**, Lardo O, Hansell M. Alcoholic Hepatitis: Diagnosis and Management. *Am Fam Physician* 2022; **105**: 412-420 [PMID: 35426628]

48 **Atkinson SR**, Hamesch K, Spivak I, Guldiken N, Cabezas J, Argemi J, Theurl I, Zoller H, Cao S, Mathurin P, Shah VH, Trautwein C, Bataller R, Thursz MR, Strnad P. Serum Transferrin Is an Independent Predictor of Mortality in Severe Alcoholic Hepatitis. *Am J Gastroenterol* 2020; **115**: 398-405 [PMID: 31985531 DOI: 10.14309/ajg.0000000000000492]

49 **Grillet F**, Calame P, Cervoni JP, Weil D, Thevenot T, Ronot M, Delabrousse E. Non-invasive diagnosis of severe alcoholic hepatitis: Usefulness of cross-sectional imaging. *Diagn Interv Imaging* 2021; **102**: 247-254 [PMID: 33069642 DOI: 10.1016/j.diii.2020.09.009]

50 **European Association for the Study of the Liver**. EASL Clinical Practice Guidelines: Management of alcohol-related liver disease. *J Hepatol* 2018; **69**: 154-181 [PMID: 29628280 DOI: 10.1016/j.jhep.2018.03.018]

51 **Crawford JM**. Histologic findings in alcoholic liver disease. *Clin Liver Dis* 2012; **16**: 699-716 [PMID: 23101978 DOI: 10.1016/j.cld.2012.08.004]

52 **Lefkowitch JH**. Morphology of alcoholic liver disease. *Clin Liver Dis* 2005; **9**: 37-53 [PMID: 15763228 DOI: 10.1016/j.cld.2004.11.001]

53 **Sakhuja P**. Pathology of alcoholic liver disease, can it be differentiated from nonalcoholic steatohepatitis? *World J Gastroenterol* 2014; **20**: 16474-16479 [PMID: 25469015 DOI: 10.3748/wjg.v20.i44.16474]

54 **Theise ND**. Histopathology of alcoholic liver disease. *Clin Liver Dis (Hoboken)* 2013; **2**: 64-67 [PMID: 30992826 DOI: 10.1002/cld.172]

55 **Feldstein AE**, Gores GJ. Apoptosis in alcoholic and nonalcoholic steatohepatitis. *Front Biosci* 2005; **10**: 3093-3099 [PMID: 15970563 DOI: 10.2741/1765]

56 **Denk H**, Stumptner C, Zatloukal K. Mallory bodies revisited. *J Hepatol* 2000; **32**: 689-702 [PMID: 10782920 DOI: 10.1016/S0168-8278(00)80233-0]

57 **Yeh MM**, Brunt EM. Pathology of nonalcoholic fatty liver disease. *Am J Clin Pathol* 2007; **128**: 837-847 [PMID: 17951208 DOI: 10.1309/RTPM1PY6YGBL2G2R]

58 **Tiniakos DG**. Liver biopsy in alcoholic and non-alcoholic steatohepatitis patients. *Gastroenterol Clin Biol* 2009; **33**: 930-939 [PMID: 19646834 DOI: 10.1016/j.gcb.2009.05.009]

59 **Kowdley KV**. Iron Overload in Patients With Chronic Liver Disease. *Gastroenterol Hepatol (N Y)* 2016; **12**: 695-698 [PMID: 28035198]

60 **Eng SC**, Taylor SL, Reyes V, Raaka S, Berger J, Kowdley KV. Hepatic iron overload in alcoholic end-stage liver disease is associated with iron deposition in other organs in the absence of HFE-1 hemochromatosis. *Liver Int* 2005; **25**: 513-517 [PMID: 15910487 DOI: 10.1111/j.1478-3231.2005.01004.x]

61 **Mookerjee RP**, Lackner C, Stauber R, Stadlbauer V, Deheragoda M, Aigelsreiter A, Jalan R. The role of liver biopsy in the diagnosis and prognosis of patients with acute deterioration of alcoholic cirrhosis. *J Hepatol* 2011; **55**: 1103-1111 [PMID: 21376092 DOI: 10.1016/j.jhep.2011.02.021]

62 **Altamirano J**, Miquel R, Katoonizadeh A, Abraldes JG, Duarte-Rojo A, Louvet A, Augustin S, Mookerjee RP, Michelena J, Smyrk TC, Buob D, Leteurtre E, Rincón D, Ruiz P, García-Pagán JC, Guerrero-Marquez C, Jones PD, Barritt AS 4th, Arroyo V, Bruguera M, Bañares R, Ginès P, Caballería J, Roskams T, Nevens F, Jalan R, Mathurin P, Shah VH, Bataller R. A histologic scoring system for prognosis of patients with alcoholic hepatitis. *Gastroenterology* 2014; **146**: 1231-9.e1 [PMID: 24440674 DOI: 10.1053/j.gastro.2014.01.018]

63 **Trépo E**, Goossens N, Fujiwara N, Song WM, Colaprico A, Marot A, Spahr L, Demetter P, Sempoux C, Im GY, Saldarriaga J, Gustot T, Devière J, Thung SN, Minsart C, Sersté T, Bontempi G, Abdelrahman K, Henrion J, Degré D, Lucidi V, Rubbia-Brandt L, Nair VD, Moreno C, Deltenre P, Hoshida Y, Franchimont D. Combination of Gene Expression Signature and Model for End-Stage Liver Disease Score Predicts Survival of Patients With Severe Alcoholic Hepatitis. *Gastroenterology* 2018; **154**: 965-975 [PMID: 29158192 DOI: 10.1053/j.gastro.2017.10.048]

64 **Koulaouzidis A**, Bhat S, Saeed AA. Spontaneous bacterial peritonitis. *World J Gastroenterol* 2009; **15**: 1042-1049 [PMID: 19266595 DOI: 10.3748/wjg.15.1042]

65 **Karakike E**, Moreno C, Gustot T. Infections in severe alcoholic hepatitis. *Ann Gastroenterol* 2017; **30**: 152-160 [PMID: 28243035 DOI: 10.20524/aog.2016.0101]

66 **Orntoft NW**, Sandahl TD, Jepsen P, Vilstrup H. Short-term and long-term causes of death in patients with alcoholic hepatitis in Denmark. *Clin Gastroenterol Hepatol* 2014; **12**: 1739-44.e1 [PMID: 24780287 DOI: 10.1016/j.cgh.2014.04.020]

67 **Markwick LJ**, Riva A, Ryan JM, Cooksley H, Palma E, Tranah TH, Manakkat Vijay GK, Vergis N, Thursz M, Evans A, Wright G, Tarff S, O'Grady J, Williams R, Shawcross DL, Chokshi S. Blockade of PD1 and TIM3 restores innate and adaptive immunity in patients with acute alcoholic hepatitis. *Gastroenterology* 2015; **148**: 590-602.e10 [PMID: 25479137 DOI: 10.1053/j.gastro.2014.11.041]

68 **Falagas ME**, Kompoti M. Obesity and infection. *Lancet Infect Dis* 2006; **6**: 438-446 [PMID: 16790384 DOI: 10.1016/S1473-3099(06)70523-0]

69 **Leclerc M**, Lanot A, Béchade C, Le Naoures C, Comoz F, Lobbedez T. [Bile salt nephropathy/cholemic nephrosis]. *Nephrol Ther* 2016; **12**: 460-462 [PMID: 27262935 DOI: 10.1016/j.nephro.2016.03.002]

70 **Ginès P**, Solà E, Angeli P, Wong F, Nadim MK, Kamath PS. Hepatorenal syndrome. *Nat Rev Dis Primers* 2018; **4**: 23 [PMID: 30213943 DOI: 10.1038/s41572-018-0022-7]

71 **Francoz C**, Durand F, Kahn JA, Genyk YS, Nadim MK. Hepatorenal Syndrome. *Clin J Am Soc Nephrol* 2019; **14**: 774-781 [PMID: 30996046 DOI: 10.2215/CJN.12451018]

72 **Altamirano J**, Fagundes C, Dominguez M, García E, Michelena J, Cárdenas A, Guevara M, Pereira G, Torres-Vigil K, Arroyo V, Caballería J, Ginès P, Bataller R. Acute kidney injury is an early predictor of mortality for patients with alcoholic hepatitis. *Clin Gastroenterol Hepatol* 2012; **10**: 65-71.e3 [PMID: 21946124 DOI: 10.1016/j.cgh.2011.09.011]

73 **Wang H**, Liu A, Bo W, Feng X, Hu Y. Terlipressin in the treatment of hepatorenal syndrome: A systematic review and meta-analysis. *Medicine (Baltimore)* 2018; **97**: e0431 [PMID: 29668606 DOI: 10.1097/MD.0000000000010431]

74 **Parker R**, Kim SJ, Im GY, Nahas J, Dhesi B, Vergis N, Sinha A, Ghezzi A, Rink MR, McCune A, Aithal GP, Newsome PN, Weston CJ, Holt A, Gao B. Obesity in acute alcoholic hepatitis increases morbidity and mortality. *EBioMedicine* 2019; **45**: 511-518 [PMID: 31278069 DOI: 10.1016/j.ebiom.2019.03.046]

75 **Liang W**, Chikritzhs T, Pascal R, Binns CW. Mortality rate of alcoholic liver disease and risk of hospitalization for alcoholic liver cirrhosis, alcoholic hepatitis and alcoholic liver failure in Australia between 1993 and 2005. *Intern Med J* 2011; **41**: 34-41 [PMID: 20546060 DOI: 10.1111/j.1445-5994.2010.02279.x]

76 **Jalan R**, Gines P, Olson JC, Mookerjee RP, Moreau R, Garcia-Tsao G, Arroyo V, Kamath PS. Acute-on chronic liver failure. *J Hepatol* 2012; **57**: 1336-1348 [PMID: 22750750 DOI: 10.1016/j.jhep.2012.06.026]

77 **Michelena J**, Altamirano J, Abraldes JG, Affò S, Morales-Ibanez O, Sancho-Bru P, Dominguez M, García-Pagán JC, Fernández J, Arroyo V, Ginès P, Louvet A, Mathurin P, Mehal WZ, Caballería J, Bataller R. Systemic inflammatory response and serum lipopolysaccharide levels predict multiple organ failure and death in alcoholic hepatitis. *Hepatology* 2015; **62**: 762-772 [PMID: 25761863 DOI: 10.1002/hep.27779]

78 **Arroyo V**, Moreau R, Jalan R. Acute-on-Chronic Liver Failure. *N Engl J Med* 2020; **382**: 2137-2145 [PMID: 32459924 DOI: 10.1056/NEJMra1914900]

79 **Bodzin AS**, Baker TB. Liver Transplantation Today: Where We Are Now and Where We Are Going. *Liver Transpl* 2018; **24**: 1470-1475 [PMID: 30080954 DOI: 10.1002/lt.25320]

80 **Jadlowiec CC**, Taner T. Liver transplantation: Current status and challenges. *World J Gastroenterol* 2016; **22**: 4438-4445 [PMID: 27182155 DOI: 10.3748/wjg.v22.i18.4438]

81 **Yu CH**, Xu CF, Ye H, Li L, Li YM. Early mortality of alcoholic hepatitis: a review of data from placebo-controlled clinical trials. *World J Gastroenterol* 2010; **16**: 2435-2439 [PMID: 20480532 DOI: 10.3748/wjg.v16.i19.2435]

82 **Bennett K**, Enki DG, Thursz M, Cramp ME, Dhanda AD. Systematic review with meta-analysis: high mortality in patients with non-severe alcoholic hepatitis. *Aliment Pharmacol Ther* 2019; **50**: 249-257 [PMID: 31231848 DOI: 10.1111/apt.15376]

83 **Bird GL**, Williams R. Factors determining cirrhosis in alcoholic liver disease. *Mol Aspects Med* 1988; **10**: 97-105 [PMID: 3067028 DOI: 10.1016/0098-2997(88)90017-9]

84 **Alexander JF**, Lischner MW, Galambos JT. Natural history of alcoholic hepatitis. II. The long-term prognosis. *Am J Gastroenterol* 1971; **56**: 515-525 [PMID: 5134879]

85 **Rehm J**, Taylor B, Mohapatra S, Irving H, Baliunas D, Patra J, Roerecke M. Alcohol as a risk factor for liver cirrhosis: a systematic review and meta-analysis. *Drug Alcohol Rev* 2010; **29**: 437-445 [PMID: 20636661 DOI: 10.1111/j.1465-3362.2009.00153.x]

86 **Parés A**, Caballería J, Bruguera M, Torres M, Rodés J. Histological course of alcoholic hepatitis. Influence of abstinence, sex and extent of hepatic damage. *J Hepatol* 1986; **2**: 33-42 [PMID: 3950362 DOI: 10.1016/S0168-8278(86)80006-X]

87 **Maddrey WC**, Boitnott JK, Bedine MS, Weber FL Jr, Mezey E, White RI Jr. Corticosteroid therapy of alcoholic hepatitis. *Gastroenterology* 1978; **75**: 193-199 [PMID: 352788]

88 **Louvet A**, Naveau S, Abdelnour M, Ramond MJ, Diaz E, Fartoux L, Dharancy S, Texier F, Hollebecque A, Serfaty L, Boleslawski E, Deltenre P, Canva V, Pruvot FR, Mathurin P. The Lille model: a new tool for therapeutic strategy in patients with severe alcoholic hepatitis treated with steroids. *Hepatology* 2007; **45**: 1348-1354 [PMID: 17518367 DOI: 10.1002/hep.21607]

89 **Kamath PS**, Kim WR; Advanced Liver Disease Study Group. The model for end-stage liver disease (MELD). *Hepatology* 2007; **45**: 797-805 [PMID: 17326206 DOI: 10.1002/hep.21563]

90 **Morales-Arráez D**, Ventura-Cots M, Altamirano J, Abraldes JG, Cruz-Lemini M, Thursz MR, Atkinson SR, Sarin SK, Kim W, Chavez-Araujo R, Higuera-de la Tijera MF, Singal AK, Shah VH, Kamath PS, Duarte-Rojo A, Charles EA, Vargas V, Jager M, Rautou PE, Rincon D, Zamarripa F, Restrepo-Gutiérrez JC, Torre A, Lucey MR, Arab JP, Mathurin P, Louvet A, García-Tsao G, González JA, Verna EC, Brown RS Jr, Argemi J, Fernández-Carrillo C, Clemente A, Alvarado-Tapias E, Forrest E, Allison M, Bataller R. The MELD Score Is Superior to the Maddrey Discriminant Function Score to Predict Short-Term Mortality in Alcohol-Associated Hepatitis: A Global Study. *Am J Gastroenterol* 2022; **117**: 301-310 [PMID: 34962498 DOI: 10.14309/ajg.0000000000001596]

91 **Srikureja W**, Kyulo NL, Runyon BA, Hu KQ. MELD score is a better prognostic model than Child-Turcotte-Pugh score or Discriminant Function score in patients with alcoholic hepatitis. *J Hepatol* 2005; **42**: 700-706 [PMID: 15826720 DOI: 10.1016/j.jhep.2004.12.022]

92 **Dunn W**, Jamil LH, Brown LS, Wiesner RH, Kim WR, Menon KV, Malinchoc M, Kamath PS, Shah V. MELD accurately predicts mortality in patients with alcoholic hepatitis. *Hepatology* 2005; **41**: 353-358 [PMID: 15660383 DOI: 10.1002/hep.20503]

93 **Sheth M**, Riggs M, Patel T. Utility of the Mayo End-Stage Liver Disease (MELD) score in assessing prognosis of patients with alcoholic hepatitis. *BMC Gastroenterol* 2002; **2**: 2 [PMID: 11835693 DOI: 10.1186/1471-230X-2-2]

94 **Peng Y**, Qi X, Guo X. Child-Pugh Versus MELD Score for the Assessment of Prognosis in Liver Cirrhosis: A Systematic

Review and Meta-Analysis of Observational Studies. *Medicine (Baltimore)* 2016; **95**: e2877 [PMID: 26937922 DOI: 10.1097/MD.0000000000002877]

95 **Forrest EH**, Evans CD, Stewart S, Phillips M, Oo YH, McAvoy NC, Fisher NC, Singhal S, Brind A, Haydon G, O'Grady J, Day CP, Hayes PC, Murray LS, Morris AJ. Analysis of factors predictive of mortality in alcoholic hepatitis and derivation and validation of the Glasgow alcoholic hepatitis score. *Gut* 2005; **54**: 1174-1179 [PMID: 16009691 DOI: 10.1136/gut.2004.050781]

96 **Dominguez M**, Rincón D, Abraldes JG, Miquel R, Colmenero J, Bellot P, García-Pagán JC, Fernández R, Moreno M, Bañares R, Arroyo V, Caballería J, Ginès P, Bataller R. A new scoring system for prognostic stratification of patients with alcoholic hepatitis. *Am J Gastroenterol* 2008; **103**: 2747-2756 [PMID: 18721242 DOI: 10.1111/j.1572-0241.2008.02104.x]

97 **Lackner C**, Spindelboeck W, Haybaeck J, Douschan P, Rainer F, Terracciano L, Haas J, Berghold A, Bataller R, Stauber RE. Histological parameters and alcohol abstinence determine long-term prognosis in patients with alcoholic liver disease. *J Hepatol* 2017; **66**: 610-618 [PMID: 27894795 DOI: 10.1016/j.jhep.2016.11.011]

98 **Xie YD**, Feng B, Gao Y, Wei L. Effect of abstinence from alcohol on survival of patients with alcoholic cirrhosis: A systematic review and meta-analysis. *Hepatol Res* 2014; **44**: 436-449 [PMID: 23607793 DOI: 10.1111/hepr.12131]

99 **Diehl AM**. Alcoholic liver disease: natural history. *Liver Transpl Surg* 1997; **3**: 206-211 [PMID: 9346741 DOI: 10.1002/Lt.500030303]

100 **Dugum M**, McCullough A. Diagnosis and Management of Alcoholic Liver Disease. *J Clin Transl Hepatol* 2015; **3**: 109-116 [PMID: 26356792 DOI: 10.14218/JCTH.2015.00008]

101 **Morley KC**, Baillie A, Fraser I, Furneaux-Bate A, Dore G, Roberts M, Abdalla A, Phung N, Haber PS. Baclofen in the treatment of alcohol dependence with or without liver disease: multisite, randomised, double-blind, placebo-controlled trial. *Br J Psychiatry* 2018; **212**: 362-369 [PMID: 29716670 DOI: 10.1192/bjp.2018.13]

102 **McClain CJ**, Barve SS, Barve A, Marsano L. Alcoholic liver disease and malnutrition. *Alcohol Clin Exp Res* 2011; **35**: 815-820 [PMID: 21284673 DOI: 10.1111/j.1530-0277.2010.01405.x]

103 **Bertha M**, Choi G, Mellinger J. Diagnosis and Treatment of Alcohol-Associated Liver Disease: A Patient-Friendly Summary of the 2019 AASLD Guidelines. *Clin Liver Dis (Hoboken)* 2021; **17**: 418-423 [PMID: 34386207 DOI: 10.1002/cld.1129]

104 **DiCecco SR**, Francisco-Ziller N. Nutrition in alcoholic liver disease. *Nutr Clin Pract* 2006; **21**: 245-254 [PMID: 16772542 DOI: 10.1177/0115426506021003245]

105 **Mitchell MC**, Friedman LS, McClain CJ. Medical Management of Severe Alcoholic Hepatitis: Expert Review from the Clinical Practice Updates Committee of the AGA Institute. *Clin Gastroenterol Hepatol* 2017; **15**: 5-12 [PMID: 27979049 DOI: 10.1016/j.cgh.2016.08.047]

106 **Biggins SW**, Angeli P, Garcia-Tsao G, Ginès P, Ling SC, Nadim MK, Wong F, Kim WR. Diagnosis, Evaluation, and Management of Ascites, Spontaneous Bacterial Peritonitis and Hepatorenal Syndrome: 2021 Practice Guidance by the American Association for the Study of Liver Diseases. *Hepatology* 2021; **74**: 1014-1048 [PMID: 33942342 DOI: 10.1002/hep.31884]

107 Benzodiazepines. 2017. In: LiverTox: Clinical and Research Information on Drug-Induced Liver Injury [Internet]. Bethesda (MD): National Institute of Diabetes and Digestive and Kidney Diseases; 2012 [PMID: 31643176]

108 **Peppers MP**. Benzodiazepines for alcohol withdrawal in the elderly and in patients with liver disease. *Pharmacotherapy* 1996; **16**: 49-57 [PMID: 8700792]

109 **Thursz MR**, Richardson P, Allison M, Austin A, Bowers M, Day CP, Downs N, Gleeson D, MacGilchrist A, Grant A, Hood S, Masson S, McCune A, Mellor J, O'Grady J, Patch D, Ratcliffe I, Roderick P, Stanton L, Vergis N, Wright M, Ryder S, Forrest EH; STOPAH Trial. Prednisolone or pentoxifylline for alcoholic hepatitis. *N Engl J Med* 2015; **372**: 1619-1628 [PMID: 25901427 DOI: 10.1056/NEJMoa1412278]

110 **Mathurin P**, O'Grady J, Carithers RL, Phillips M, Louvet A, Mendenhall CL, Ramond MJ, Naveau S, Maddrey WC, Morgan TR. Corticosteroids improve short-term survival in patients with severe alcoholic hepatitis: meta-analysis of individual patient data. *Gut* 2011; **60**: 255-260 [PMID: 20940288 DOI: 10.1136/gut.2010.224097]

111 **Louvet A**, Thursz MR, Kim DJ, Labreuche J, Atkinson SR, Sidhu SS, O'Grady JG, Akriviadis E, Sinakos E, Carithers RL Jr, Ramond MJ, Maddrey WC, Morgan TR, Duhamel A, Mathurin P. Corticosteroids Reduce Risk of Death Within 28 Days for Patients With Severe Alcoholic Hepatitis, Compared With Pentoxifylline or Placebo-a Meta-analysis of Individual Data From Controlled Trials. *Gastroenterology* 2018; **155**: 458-468.e8 [PMID: 29738698 DOI: 10.1053/j.gastro.2018.05.011]

112 **Levitsky J**, Mailliard ME. Diagnosis and therapy of alcoholic liver disease. *Semin Liver Dis* 2004; **24**: 233-247 [PMID: 15349802 DOI: 10.1055/s-2004-832937]

113 **Sohail U**, Satapathy SK. Diagnosis and management of alcoholic hepatitis. *Clin Liver Dis* 2012; **16**: 717-736 [PMID: 23101979 DOI: 10.1016/j.cld.2012.08.005]

114 **Sougioultzis S**, Dalakas E, Hayes PC, Plevris JN. Alcoholic hepatitis: from pathogenesis to treatment. *Curr Med Res Opin* 2005; **21**: 1337-1346 [PMID: 16197651 DOI: 10.1185/030079905X56493]

115 **Hmoud BS**, Patel K, Bataller R, Singal AK. Corticosteroids and occurrence of and mortality from infections in severe alcoholic hepatitis: a meta-analysis of randomized trials. *Liver Int* 2016; **36**: 721-728 [PMID: 26279269 DOI: 10.1111/liv.12939]

116 **Im GY**, Cameron AM, Lucey MR. Liver transplantation for alcoholic hepatitis. *J Hepatol* 2019; **70**: 328-334 [PMID: 30658734 DOI: 10.1016/j.jhep.2018.11.007]

117 **Mathurin P**, Moreno C, Samuel D, Dumortier J, Salleron J, Durand F, Castel H, Duhamel A, Pageaux GP, Leroy V, Dharancy S, Louvet A, Boleslawski E, Lucidi V, Gustot T, Francoz C, Letoublon C, Castaing D, Belghiti J, Donckier V, Pruvot FR, Duclos-Vallée JC. Early liver transplantation for severe alcoholic hepatitis. *N Engl J Med* 2011; **365**: 1790-1800 [PMID: 22070476 DOI: 10.1056/NEJMoa1105703]

118 **Weeks SR**, Sun Z, McCaul ME, Zhu H, Anders RA, Philosophe B, Ottmann SE, Garonzik Wang JM, Gurakar AO, Cameron AM. Liver Transplantation for Severe Alcoholic Hepatitis, Updated Lessons from the World's Largest Series. *J*

Am Coll Surg 2018; **226**: 549-557 [PMID: 29409981 DOI: 10.1016/j.jamcollsurg.2017.12.044]

119 **Lee BP**, Mehta N, Platt L, Gurakar A, Rice JP, Lucey MR, Im GY, Therapondos G, Han H, Victor DW, Fix OK, Dinges L, Dronamraju D, Hsu C, Voigt MD, Rinella ME, Maddur H, Eswaran S, Hause J, Foley D, Ghobrial RM, Dodge JL, Li Z, Terrault NA. Outcomes of Early Liver Transplantation for Patients With Severe Alcoholic Hepatitis. *Gastroenterology* 2018; **155**: 422-430.e1 [PMID: 29655837 DOI: 10.1053/j.gastro.2018.04.009]

120 **Herrick-Reynolds KM**, Punchhi G, Greenberg RS, Strauss AT, Boyarsky BJ, Weeks-Groh SR, Krach MR, Anders RA, Gurakar A, Chen PH, Segev DL, King EA, Philosophe B, Ottman SE, Wesson RN, Garonzik-Wang JM, Cameron AM. Evaluation of Early vs Standard Liver Transplant for Alcohol-Associated Liver Disease. *JAMA Surg* 2021; **156**: 1026-1034 [PMID: 34379106 DOI: 10.1001/jamasurg.2021.3748]

121 **Mitchell M**. Efficacy study of anakinra, pentoxifylline, and zinc compared to methylprednisolone in severe acute alcoholic hepatitis. [accessed 2022 Dec 16]. In: ClinicalTrials.gov [Internet]. Bethesda (MD): U.S. National Library of Medicine. Available from: https://clinicaltrials.gov/ct2/show/NCT01809132 ClinicalTrials.gov Identifier: NCT01809132

122 **Gawrieh S**. Trial of Anakinra (Plus Zinc) or Prednisone in Patients With Severe Alcoholic Hepatitis. [accessed 2022 Dec 16]. In: ClinicalTrials.gov [Internet]. Bethesda (MD): U.S. National Library of Medicine. Available from: https://clinicaltrials.gov/ct2/show/NCT04072822 ClinicalTrials.gov Identifier: NCT04072822

123 **Imperial College London**. IL-1 Signal Inhibition in Alcoholic Hepatitis [accessed 2022 Dec 16]. In: ClinicalTrials.gov [Internet]. Bethesda (MD): U.S. National Library of Medicine. Available from: https://clinicaltrials.gov/ct2/show/NCT03775109 ClinicalTrials.gov Identifier: NCT03775109

124 **Imperial College London**. N-ACetylcysteine to Reduce Infection and Mortality for Alcoholic Hepatitis [accessed 2022 Dec 16]. In: ClinicalTrials.gov [Internet]. Bethesda (MD): U.S. National Library of Medicine. Available from: https://clinicaltrials.gov/ct2/show/NCT03069300 ClinicalTrials.gov Identifier: NCT03069300

125 **Mendler MH**. Randomized, Controlled Trial of S-adenosylmethionine in Alcoholic Liver Disease. [accessed 2022 Dec 16]. In: ClinicalTrials.gov [Internet]. Bethesda (MD): U.S. National Library of Medicine. Available from: https://clinicaltrials.gov/ct2/show/NCT00851981 ClinicalTrials.gov Identifier: NCT00851981

126 **Cheng J**. Efficacy and Safety of S-adenosyl-l-methionine in Treatment of Alcoholic Hepatitis With Cholestasis. [accessed 2022 Dec 16]. In: ClinicalTrials.gov [Internet]. Bethesda (MD): U.S. National Library of Medicine. Available from: https://clinicaltrials.gov/ct2/show/NCT02024295 ClinicalTrials.gov Identifier: NCT02024295

127 **Gordon R**. A Research Study to Assess the Safety, Pharmacokinetics and Pharmacodynamics of DUR-928 in Patients With Alcoholic Hepatitis. [accessed 2022 Dec 16]. In: ClinicalTrials.gov [Internet]. Bethesda (MD): U.S. National Library of Medicine. Available from: https://clinicaltrials.gov/ct2/show/NCT03432260 ClinicalTrials.gov Identifier: NCT03432260

128 **McClain CJ**. DUR-928 in Patients With Alcoholic Hepatitis. [accessed 2022 Dec 16]. In: ClinicalTrials.gov [Internet]. Bethesda (MD): U.S. National Library of Medicine. Available from: https://clinicaltrials.gov/ct2/show/NCT03917407 ClinicalTrials.gov Identifier: NCT03917407

129 **Kim DJ**. Efficacy and Safety of G-CSF in Patients With Severe Alcoholic Hepatitis With Null or Partial Response to Steroid. [accessed 2022 Dec 16]. In: ClinicalTrials.gov [Internet]. Bethesda (MD): U.S. National Library of Medicine. Available from: https://clinicaltrials.gov/ct2/show/NCT02442180 ClinicalTrials.gov Identifier: NCT02442180

130 **Singh V**. GCSF in Alcoholic Hepatitis. [accessed 2022 Dec 16]. In: ClinicalTrials.gov [Internet]. Bethesda (MD): U.S. National Library of Medicine. Available from: https://clinicaltrials.gov/ct2/show/NCT03703674 ClinicalTrials.gov Identifier: NCT03703674

131 **Mishra A**. Efficacy of Monotherapy vs Combination Therapy of Corticosteroids With GCSF in Severe Alcoholic Hepatitis Patients. [accessed 2022 Dec 16]. In: ClinicalTrials.gov [Internet]. Bethesda (MD): U.S. National Library of Medicine. Available from: https://clinicaltrials.gov/ct2/show/NCT04066179 ClinicalTrials.gov Identifier: NCT04066179

132 **Shah V**. Use of F-652 in Patients With Alcoholic Hepatitis [accessed 2022 Dec 16]. In: ClinicalTrials.gov [Internet]. Bethesda (MD): U.S. National Library of Medicine. Available from: https://clinicaltrials.gov/ct2/show/NCT02655510 ClinicalTrials.gov Identifier: NCT02655510

133 **Stoy S**. Protective Immune Mechanisms in Alcoholic Hepatitis. [accessed 2022 Dec 16]. In: ClinicalTrials.gov [Internet]. Bethesda (MD): U.S. National Library of Medicine. Available from: https://clinicaltrials.gov/ct2/show/NCT01918462 ClinicalTrials.gov Identifier: NCT01918462

134 **Chalasani N**. Trial of Obeticholic Acid in Patients With Moderately Severe Alcoholic Hepatitis (AH). [accessed 2022 Dec 16]. In: ClinicalTrials.gov [Internet]. Bethesda (MD): U.S. National Library of Medicine. Available from: https://clinicaltrials.gov/ct2/show/NCT02039219 ClinicalTrials.gov Identifier: NCT02039219

135 **Vargas V**. Effects of Rifaximin in Patients With Acute Alcoholic Hepatitis. [accessed 2022 Dec 16]. In: ClinicalTrials.gov [Internet]. Bethesda (MD): U.S. National Library of Medicine. Available from: https://clinicaltrials.gov/ct2/show/NCT02116556 ClinicalTrials.gov Identifier: NCT02116556

136 **Song DS**. Rifaximin Use in Severe Alcoholic Hepatitis. [accessed 2022 Dec 16]. In: ClinicalTrials.gov [Internet]. Bethesda (MD): U.S. National Library of Medicine. Available from: https://clinicaltrials.gov/ct2/show/NCT02485106 ClinicalTrials.gov Identifier: NCT02485106

137 **Sanyal A**. Safety and Efficacy of IMM 124-E for Patients With Severe Alcoholic Hepatitis. [accessed 2022 Dec 16]. In: ClinicalTrials.gov [Internet]. Bethesda (MD): U.S. National Library of Medicine. Available from: https://clinicaltrials.gov/ct2/show/NCT01968382 ClinicalTrials.gov Identifier: NCT01968382

138 **Sidhu S**. Comparison of Bovine Colostrum Versus Placebo in Treatment of Severe Alcoholic Hepatitis: A Randomized Double Blind Controlled Trial. [accessed 2022 Dec 16]. In: ClinicalTrials.gov [Internet]. Bethesda (MD): U.S. National Library of Medicine. Available from: https://clinicaltrials.gov/ct2/show/NCT02473341 ClinicalTrials.gov Identifier: NCT02473341

139 **Mitchell M**. Novel Therapies in Moderately Severe Acute Alcoholic Hepatitis. [accessed 2022 Dec 16]. In: ClinicalTrials.gov [Internet]. Bethesda (MD): U.S. National Library of Medicine. Available from: https://clinicaltrials.gov/ct2/show/NCT01922895 ClinicalTrials.gov Identifier: NCT01922895

140 **Suk KT**. Effect of Probiotics on Gut-Liver Axis of Alcoholic Hepatitis. [accessed 2022 Dec 16]. In: ClinicalTrials.gov [Internet]. Bethesda (MD): U.S. National Library of Medicine. Available from: https://clinicaltrials.gov/ct2/show/NCT02335632 ClinicalTrials.gov Identifier: NCT02335632

141 **Institute of Liver and Biliary Sciences**. Pentoxyphilline Versus Fecal Microbiota Therapy in Severe Alcoholic Hepatitis. [accessed 2022 Dec 16]. In: ClinicalTrials.gov [Internet]. Bethesda (MD): U.S. National Library of Medicine. Available from: https://clinicaltrials.gov/ct2/show/NCT02458079 ClinicalTrials.gov Identifier: NCT02458079

142 **Institute of Liver and Biliary Sciences**. A Comparison of Fecal Microbiota Transplantation and Steroid Therapy in Patients With Severe Alcoholic Hepatitis. [accessed 2022 Dec 16]. In: ClinicalTrials.gov [Internet]. Bethesda (MD): U.S. National Library of Medicine. Available from: https://clinicaltrials.gov/ct2/show/NCT03091010 ClinicalTrials.gov Identifier: NCT03091010

143 **Dhiman RK**. Fecal Microbiota Transplantation in Severe Alcoholic Hepatitis- Assessment of Impact on Prognosis and Short-term Outcome. [accessed 2022 Dec 16]. In: ClinicalTrials.gov [Internet]. India: U.S. National Library of Medicine. Available from: https://clinicaltrials.gov/ct2/show/NCT03827772 ClinicalTrials.gov Identifier: NCT03827772

World Journal of Gastroenterology

Submit a Manuscript: https://www.f6publishing.com

World J Gastroenterol 2023 May 7; 29(17): 2571-2599

DOI: 10.3748/wjg.v29.i17.2571

ISSN 1007-9327 (print) ISSN 2219-2840 (online)

REVIEW

Current and novel approaches in the pharmacological treatment of hepatocellular carcinoma

Fernanda Villarruel-Melquiades, María Eugenia Mendoza-Garrido, Claudia M García-Cuellar, Yesennia Sánchez-Pérez, Julio Isael Pérez-Carreón, Javier Camacho

Specialty type: Gastroenterology and hepatology

Provenance and peer review: Invited article; Externally peer reviewed.

Peer-review model: Single blind

Peer-review report's scientific quality classification

Grade A (Excellent): 0
Grade B (Very good): B, B
Grade C (Good): C
Grade D (Fair): 0
Grade E (Poor): 0

P-Reviewer: Bao YZ, China; Han J, China; Wang C, China

Received: December 27, 2022
Peer-review started: December 27, 2022
First decision: January 11, 2023
Revised: January 19, 2023
Accepted: April 11, 2023
Article in press: April 11, 2023
Published online: May 7, 2023

Fernanda Villarruel-Melquiades, Javier Camacho, Departamento de Farmacología, Centro de Investigación y de Estudios Avanzados del Instituto Politécnico Nacional (CINVESTAV-IPN), Mexico City 07360, Mexico

María Eugenia Mendoza-Garrido, Departamento de Fisiología, Biofísica y Neurociencias, Centro de Investigación y de Estudios Avanzados del Instituto Politécnico Nacional (CINVESTAV-IPN), Mexico City 07360, Mexico

Claudia M García-Cuellar, Yesennia Sánchez-Pérez, Subdirección de Investigación Básica, Instituto Nacional de Cancerología (INCan), Mexico City 14080, Mexico

Julio Isael Pérez-Carreón, Instituto Nacional de Medicina Genómica, Instituto Nacional de Medicina Genómica (INMEGEN), Mexico City 14610, Mexico

Corresponding author: Javier Camacho, BSc, MSc, PhD, Research Scientist, Departamento de Farmacología, Centro de Investigación y de Estudios Avanzados del Instituto Politécnico Nacional (CINVESTAV-IPN), Avenida Instituto Politécnico Nacional 2508, Mexico City 07360, Mexico. fcamacho@cinvestav.mx

Abstract

Hepatocellular carcinoma (HCC) is one of the most lethal malignant tumours worldwide. The mortality-to-incidence ratio is up to 91.6% in many countries, representing the third leading cause of cancer-related deaths. Systemic drugs, including the multikinase inhibitors sorafenib and lenvatinib, are first-line drugs used in HCC treatment. Unfortunately, these therapies are ineffective in most cases due to late diagnosis and the development of tumour resistance. Thus, novel pharmacological alternatives are urgently needed. For instance, immune checkpoint inhibitors have provided new approaches targeting cells of the immune system. Furthermore, monoclonal antibodies against programmed cell death-1 have shown benefits in HCC patients. In addition, drug combinations, including first-line treatment and immunotherapy, as well as drug repurposing, are promising novel therapeutic alternatives. Here, we review the current and novel pharmacological approaches to fight HCC. Preclinical studies, as well as approved and ongoing clinical trials for liver cancer treatment, are discussed. The pharmacological opportunities analysed here should lead to significant improvement in HCC therapy.

Key Words: Liver cancer; Systemic therapy; Immunotherapy; Drug repurposing; Drug combinations; Hepatocellular carcinoma

©The Author(s) 2023. Published by Baishideng Publishing Group Inc. All rights reserved.

Core Tip: Hepatocellular carcinoma (HCC) is one of the most lethal malignant tumours worldwide. Unfortunately, most HCC cases are diagnosed at an advanced stage, and "curative" options are not suggested for these patients. The best option is to start with drug therapy, with sorafenib and lenvatinib as the first-choice drugs. However, most patients do not respond to these treatments; therefore, new therapeutic strategies are urgently needed. Here, we review current potential and novel pharmacological approaches, including immunotherapy, drug combination, and drug repositioning, that should help to improve the prognosis of HCC patients.

Citation: Villarruel-Melquiades F, Mendoza-Garrido ME, García-Cuellar CM, Sánchez-Pérez Y, Pérez-Carreón JI, Camacho J. Current and novel approaches in the pharmacological treatment of hepatocellular carcinoma. *World J Gastroenterol* 2023; 29(17): 2571-2599
URL: https://www.wjgnet.com/1007-9327/full/v29/i17/2571.htm
DOI: https://dx.doi.org/10.3748/wjg.v29.i17.2571

INTRODUCTION

Liver cancer ranks seventh in incidence and fourth in mortality worldwide. It is one of the malignancies with the highest mortality-to-incidence ratio, reaching up to 91.6%, according to the World Health Organization[1]. This cancer frequently occurs in association with chronic liver disease and is classified according to the cells of origin of the tumour. Hepatocellular carcinoma (HCC) is the most common, originating in hepatocytes and accounting for 75%-85% of all cases[2].

The main risk factors for developing HCC are chronic liver disease, such as non-alcoholic fatty liver disease and non-alcoholic steatohepatitis, as well as hepatitis B (HBV) and C virus (HCV) infections[3]. In addition, some habits, including excessive alcohol consumption and smoking, are also considered major risk factors for developing HCC[2].

The most appropriate management in clinical practice depends on the stage of the disease. At an early or even intermediate stage, the treatment options currently available are surgical methods (liver resection and transplantation), locoregional therapy (radiofrequency ablation), and transarterial chemoembolization therapy[4]. The 5-year survival rate for patients at these stages is 14%, and only 30% can be subjected to curative treatment. Unfortunately, most diagnoses are made when HCC is at an advanced stage, and treatment options are no longer viable[5,6]; pharmacological therapy is suggested in these cases. Chemotherapy is a potential treatment for these patients, but the main disadvantage is that such agents target both cancer and healthy cells, leading to unwanted events that can even endanger the life of the patient. The use of chemotherapeutic agents in monotherapy is ineffective; therefore, more effective and directed drugs are urgently needed. A new generation of treatments called “targeted therapy” (also known as “systemic therapy”) aims to specifically target some molecular features that provide malignant advantages to cancer cells while having low toxicity to non-cancerous cells[7,8]. Table 1 summarizes the recommended HCC management based on the Barcelona Clinic Liver Cancer strategy (BCLC), the most widely used liver cancer staging system. This system has five stages depending on disease extension, liver function, and performance status (Table 1)[9-11].

Systemic therapy is the standard treatment for advanced-stage disease (BCLC stage C). This type of treatment is classified into first- and second-line therapies, and its use in clinical practice depends on the individual patient characteristics. To date, many potential drug targets for the treatment of HCC have been investigated; the most critical targets are listed below and represented in Figure 1[8].

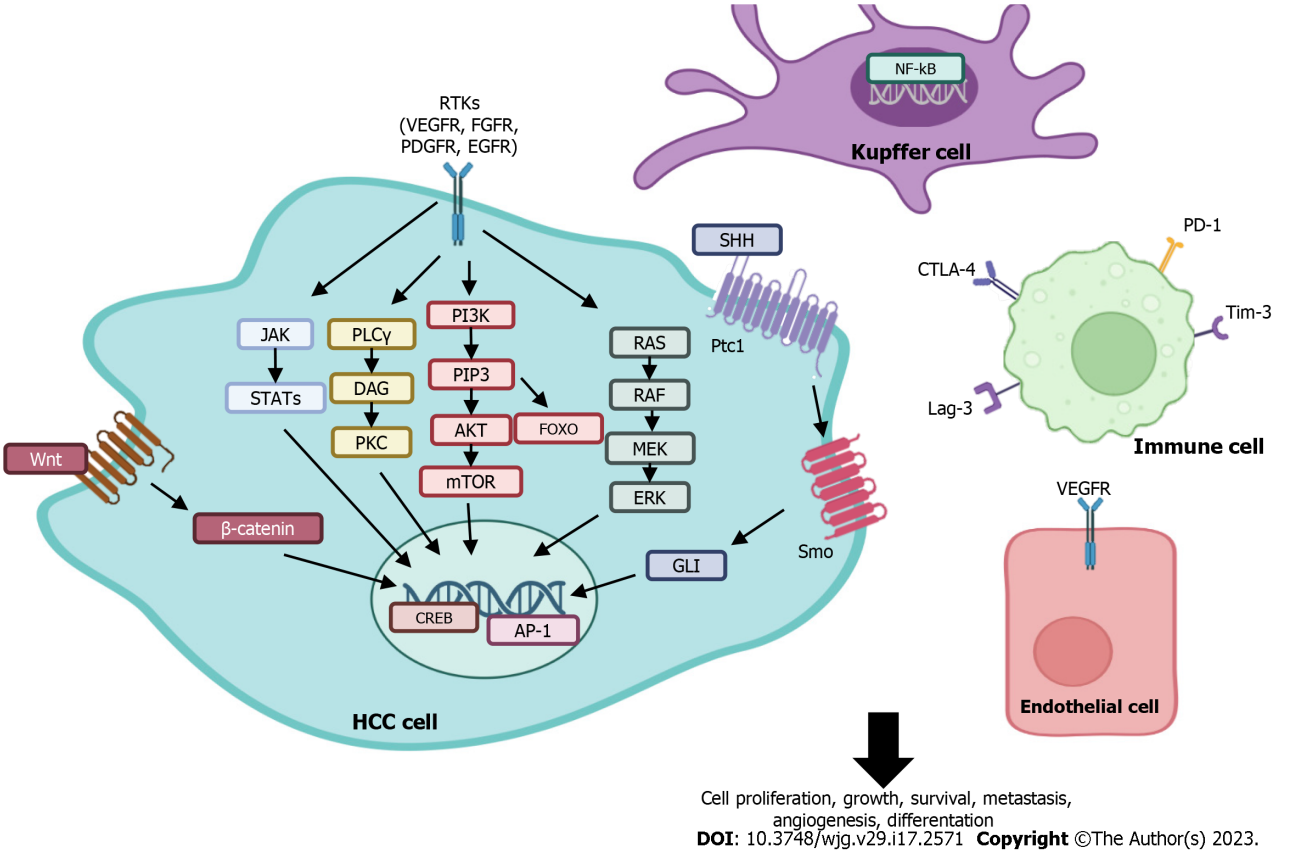
Growth factors and their receptors include vascular endothelial growth factor (VEGF), fibroblast growth factor (FGF), platelet-derived growth factor (PDGF), epidermal growth factor (EGF), mesenchymal-epithelial transition factor (c-Met), insulin-like growth factor, and transforming growth factor α (TGF-α).

Intracellular signalling pathways include phosphoinositide 3-kinase (PI3K)/Akt/mechanistic target of rapamycin (mTOR), RAS/RAF/MEK/ERK, Janus kinase (JAK)/signal transducer and activator of transcription (STAT), and Wnt/β-catenin and the Hedgehog pathway. There are also cell cycle regulators such as CDKs. Transcription factors include nuclear factor kB (NF-kB), activating protein-1 and cyclic AMP response element binding (CREB).

Table 1 Barcelona Clinic Liver Cancer staging system and treatment strategy

Stage	Very early stage (0)	Early stage (A)	Intermediate stage (B)	Advanced stage (C)	Terminal stage (D)
Characteristics	Single nodule < 2 cm, preserved liver function, ECOG PS 0	Single or 2-3 nodules < 3 cm, preserved liver function, ECOG PS 0	Multinodular, unresectable, preserved liver function, ECOG PS 0	Portal invasion/extrahepatic spread, preserved liver function, ECOG PS 1-2	Not transplantable HCC, end-stage liver function, ECOG PS 3-4
Treatment	Ablation, resection, transplant		Chemoembolization	Systemic therapy	Best supportive care
Survival	> 5 yr		> 2.5 yr	> 2 yr	3 mo

ECOG PS: Eastern Cooperative Oncology Group performance status; HCC: Hepatocellular carcinoma.



DOI: 10.3748/wjg.v29.i17.2571 **Copyright** ©The Author(s) 2023.

Figure 1 Critical signalling pathways involved in hepatocellular carcinoma progression. Systemic therapy primarily targets signalling pathways triggered by tyrosine kinase receptors expressed on tumour cells, which are known to play an essential role in liver carcinogenesis. However, Wnt/B-catenin and Smo (hedgehog pathway) signalling are also important components in liver cancer development. Furthermore, Kupffer cells, immune cells, and endothelial cells are part of the tumour microenvironment, and activation of critical signalling pathways in these cells may also contribute to cancer development. Indeed, the expression of immune checkpoint molecules (cytotoxic T-lymphocyte-associated protein 4, programmed cell death protein 1, Lag-3, Tim-3) on the surface of immune cells play an essential role in the development of hepatocellular carcinoma (discussed in the main text). RTK: Receptor tyrosine kinase; VEGFR: Vascular endothelial growth factor receptor; FGFR: Fibroblast growth factor receptor; PDGFR: Platelet-derived growth factor receptors; EGFR: Endothelial growth factor receptor; JAK: Janus kinase; STAT: Signal transducer and activator of transcription; PLCγ: Phospholipase C-γ; DAG: Diacylglycerol; PKC: Protein kinase C; PI3K: Phosphoinositide 3-kinase; PIP3: phosphatidylinositol 3,4,5-trisphosphate; mTOR: Mechanistic target of rapamycin; FOXO: Forkhead box O; AP-1: Activating protein-1; CREB: Cyclic AMP response element binding; NF-kB: Nuclear factor kB; CTLA-4: Cytotoxic T-lymphocyte-associated protein 4; PD-1: Programmed cell death protein 1.

Next, first- and second-line systemic therapies approved for advanced HCC, as well as those drugs and targets under investigation for treating the disease, are described and discussed in detail and summarized in Table 2.

Table 2 Summary of first and second-line drugs approved for the treatment of advanced hepatocellular carcinoma

Drug	Pharmacological target	Trial (NCT)	Treatment arm	Control arm
First-line				
Systemic therapy				
Sorafenib	VEGF 1-3, PDGF, KIT, FLT3, BRAF, RAF	SHARP (NCT00105443)	Sorafenib (400 mg twice daily)	Placebo
Lenvatinib	VEGFR1-3, FGFR 1-4, PDGR, RET and KIT	REFLECT (NCT01761266)	Lenvatinib (12 mg/day for bodyweight ≥ 60 kg or 8 mg/day for bodyweight < 60 kg)	Sorafenib (400 mg twice-daily in 28-d cycles)
Immunotherapy				
Atezolizumab plus bevacizumab	PD-L1, vEGF	IMbrave150 (NCT03434379)	1200 mg of atezolizumab plus 15 mg per kilogram of body weight of bevacizumab intravenously every 3 wk	Sorafenib (400 mg orally twice daily)
Tremelimumab plus durvalumab	CTLA-4, PD-L1	HIMALAYA (NCT03298451)	STRIDE: Tremelimumab plus durvalumab or durvalumab alone (300 mg, one dose of tremelimumab plus 1500 mg every 4 wk for durvalumab)	Sorafenib (400 mg orally twice daily)
Second-line[1]				
Systemic therapy				
Regorafenib	VEGFR 1-3, PDGFR, FGFR 1-2, RET, RAF	RESORCE (NCT01774344)	Regorafenib (160 mg once daily during weeks 1-3 of each 4-wk cycle)	Placebo
Cabozantinib	VEGFR 1-3, MET and AXL	CELESTIAL (NCT01908426)	Cabozantinib (60 mg once daily)	Placebo
Ramucirumab	VEGFR	REACH-2 (NCT02435433)	Ramucirumab 8 mg/kg intravenous ramucirumab every 2 wk	Placebo
Immunotherapy				
Nivolumab	PD-1	CheckMate-459 (NCT02576509)	Nivolumab (240 mg intravenously every 2 wk)	Sorafenib(400 mg orally twice daily)
Nivolumab plus ipilimumab	PD-1, CTLA-4	CheckMate-040 (NCT01658878)	Nivolumab 1 mg/kg plus ipilimumab 3 mg/kg, administered every 3 wk (4 doses), followed by nivolumab 240 mg every 2 wk (arm A); nivolumab 3 mg/kg plus ipilimumab 1 mg/kg, administered every 3 wk (4 doses), followed by nivolumab 240 mg every 2 wk (arm B); or nivolumab 3 mg/kg every 2 wk plus ipilimumab 1 mg/kg every 6 wk (arm C)	Placebo
Pembrolizumab	PD-1	KEYNOTE-240 (NCT02702401)	Pembrolizumab (200 mg intravenously every 3 wk for at least 35 cycles during approximately 2 yr)	Placebo

[1]Eligible patients who had received previous treatment with sorafenib.

CTLA-4: Cytotoxic T-lymphocyte-associated protein 4; PD-1: Programmed cell death protein 1; VEGFR: Vascular endothelial growth factor receptor; FGFR: Fibroblast growth factor receptor; PDGFR: Platelet-derived growth factor receptors; OS: Overall survival; PFS: Progression-free survival; PD-L1: Programmed death ligand-1.

FIRST-LINE SYSTEMIC THERAPIES

Sorafenib

The need for new and better treatments for patients in advanced stages has led researchers to develop molecules to specifically target components of the carcinogenesis process. Sorafenib was the first oral multikinase inhibitor drug approved by the Food and Drug Administration (FDA) in 2007 to treat advanced HCC. *In vitro* experiments found that this drug inhibited HCC cell line growth and angiogenesis by inhibiting the RAF/MEK/ERK signalling pathway, as well as tyrosine and serine/threonine kinase receptors, including those for VEGF, PDGF, c-KIT, FLT3 and BRAF[12]. This drug is indicated in patients with preserved liver function who are not candidates for surgical or locoregional therapies and those with advanced tumours according to the BCLC classification and the Child-Pugh scale[9].

Sorafenib was the first drug to significantly improve the survival of patients with advanced HCC in the Asia-Pacific region. The median overall survival (OS) was 6.5 mo [95% confidence interval (CI): 5.56-7.56] in patients treated with sorafenib compared to 4.2 mo (3.75-5.46) in patients treated with placebo [13]. Similar results in terms of improved survival were observed in the SHARP clinical trial (ClinicalTrials.gov identifier: NCT00105443), a phase III, double-blind, placebo-controlled study that evaluated the effect of sorafenib on OS and time to symptomatic progression in patients diagnosed with advanced HCC. Here, the median OS was 10.7 mo in the sorafenib group and 7.9 mo in the placebo group. The most frequent adverse events in the sorafenib group were weight loss, diarrhoea, hypophosphataemia, and hand-foot skin reactions. Based on these trials, sorafenib became the first targeted therapy drug to be approved for the treatment of advanced HCC and has been the first-choice drug since its approval. Currently, the treatment of patients with sorafenib until significant radiographic progression and simultaneous treatment with regorafenib (discussed below) are recommended[9]. Unfortunately, only 30% of sorafenib users benefit, and within a short period of time, resistance to sorafenib often develops, rendering further use ineffective[14].

Lenvatinib

Following the approval of sorafenib, research led to the recognition of lenvatinib as another drug targeting important receptors and pathways in HCC. Lenvatinib is an oral receptor tyrosine kinase inhibitor and was approved in 2018 by the FDA as a first-line treatment for unresectable HCC[15]. VEGF receptor (VEGFR), FGF receptor (FGFR), PDGRα, RET, and KIT[16,17] are among its therapeutic targets. In preclinical models, lenvatinib was shown to selectively inhibit the proliferation of human HCC cell lines and *in vivo* tumour growth in xenograft models[18]. The approval of this molecule was based on the REFLECT clinical trial (ClinicalTrials.gov identifier: NCT01761266), a phase III, multicentre, open-label, non-inferiority trial that evaluated the OS of patients diagnosed with advanced HCC treated with lenvatinib *vs* patients treated with sorafenib. Lenvatinib met non-inferiority criteria against sorafenib, as the median survival for lenvatinib was 13.6 mo (95%CI: 12.1-14.9) *vs* 12.3 mo for the sorafenib group [12.3 mo, 10.4-13.9; hazard ratio (HR): 0.92, 95%CI: 0.79-1.06][19]. The most common adverse events in the lenvatinib group in this study were diarrhoea, loss of appetite, and weight loss.

Atezolizumab plus bevacizumab

Atezolizumab is a monoclonal antibody that selectively targets programmed death ligand-1 (PD-L1) to reverse the suppression of T-cell activity[20]. Its activity was assessed through an assay that determined predictive correlates of response to this antibody in cancer patients. According to Herbst *et al*[20], who studied various types of cancer, responses were observed in patients with tumours expressing high levels of PD-L1, mainly when it was expressed on tumour-infiltrating immune cells[20].

Conversely, the monoclonal antibody bevacizumab interferes with angiogenesis and tumour growth by inhibiting VEGF activity[21]. Finn *et al*[22] demonstrated the potential of bevacizumab as a promising anti-VEGF treatment for liver cancer in preclinical trials. They evaluated the effect of this humanized antibody in an orthotopic mouse model of HCC using the Hep3B cell line and found that bevacizumab treatment significantly reduced tumour microvessel density and alpha-fetoprotein (AFP) levels and prolonged time to progression compared to the control group[22].

The combination of atezolizumab and bevacizumab is a therapeutic strategy aiming to simultaneously inhibit PD-L1 (atezolizumab) and VEGF (bevacizumab) signalling in patients with advanced HCC. This combination was evaluated in the Imbrave150 clinical trial (ClinicalTrials.gov identifier: NCT03434379), a global, open-label, phase III study that evaluated the effect of the combination of these two antibodies in patients with unresectable HCC against the effect of sorafenib as a single drug, resulting in improved OS and progression-free survival (PFS) for the combination group [67. 2% (95%CI: 61.3-73.1) and 54.6% for the sorafenib group (95%CI: 45.2-64.0)][23]. A few years later, a longer follow-up of these patients was performed, reporting that the combination maintained the improvement in patients over the effect of sorafenib[24]. Accordingly, atezolizumab plus bevacizumab combination therapy was very recently approved by the FDA (2020) as the initial treatment for advanced HCC, adding a targeted drug combination to the first-line treatment strategies for these patients[25].

Tremelimumab plus durvalumab

In October 2022, the FDA approved the combination of tremelimumab plus durvalumab for treating

patients with unresectable HCC, which could form part of the first-line treatment for this cancer[26].

Tremelimumab is a fully human immunoglobulin G (IgG)2 monoclonal antibody against cytotoxic T-lymphocyte-associated protein 4 (CTLA-4), a receptor that inhibits T-cell activity[27]. Duffy *et al*[28] subjected patients diagnosed with HCC to a study evaluating the efficacy of treatment with tremelimumab plus an ablative procedure performed during week 6 (ClinicalTrials.gov identifier: NCT01853618). The authors observed that such a combination led to the accumulation of intratumoural CD8+ T-cells and suggested it as a potential new treatment for patients with advanced HCC[28]. In contrast, dirvalumab is another human monoclonal antibody that binds to the PD-L1 protein and has been shown to be effective in liver cancer and in small-cell lung cancer, especially when used in combination with another therapeutic agent[29,30].

A phase I/II clinical trial (ClinicalTrials.gov identifier: NCT02519348) evaluated the safety and efficacy of monotherapy and combination treatment of tremelimumab plus durvalumab (300 mg and 1500 mg, respectively) in patients with HCC who had progressed on, were intolerant to, or refused sorafenib. The objective response rates (ORRs) were 24.0% (95%CI: 14.9-35.3) for the combination, 10.6% for durvalumab (5.4-18.1), and 7.2% (2.4-16.1) for tremelimumab, while the median OS was 18.7 (10.8-27.3), 13.6 (8.7-17.6), and 15.1 (11.3-20.5) months, respectively[31]. However, the clinical study that led to the approval of this combination was HIMALAYA (ClinicalTrials.gov identifier: NCT03298451), a phase III and global study with a heterogeneous population representative of HCC patients and no previous systemic treatment, which also evaluated the effect of durvalumab monotherapy and compared it to sorafenib. Here, the median OS was 16.43 mo for the combination (95%CI: 14.16-19.58), 16.56 mo (95%CI: 14.06-19.12) with durvalumab, and 13.77 mo (95%CI: 12.25-16.13) with sorafenib. The combination significantly improved OS over sorafenib, and durvalumab was not inferior to sorafenib in these patients, suggesting that it could be used as a first-line treatment[32].

SECOND-LINE SYSTEMIC THERAPIES AND IMMUNOTHERAPY

Although approximately 30% of patients receiving sorafenib show improvement, resistance to treatment can develop after prolonged use (approximately 6 mo), rendering it ineffective after this period[14]. Therefore, second-line treatments are indicated for patients who either have progressed on previous sorafenib or do not respond to it. Notably, to date, no clinical trials have evaluated second-line therapy after lenvatinib[33].

Regorafenib

Regorafenib is another oral multikinase inhibitor that primarily targets VEGFR, PDGF receptors, FGFR, RET, and RAF and, in preclinical trials, was shown to significantly inhibit liver tumour development [34]. In addition, it activates proteins involved in MAPK signalling, apoptosis, and autophagy[35]. The FDA approved this drug as a second-line treatment for patients who have already been treated with sorafenib. The safety and efficacy of this drug in humans were tested in a multinational, randomized, double-blind, placebo-controlled, phase III clinical trial (RESORCE, ClinicalTrials.gov identifier: NCT01774344), in which the median OS was 10.6 mo (95%CI: 9.1-12.1) for the regorafenib group *vs* 7.8 mo (6.3-8.8) in the placebo group[36]. The most common adverse events reported in this study were hypertension, hand-foot skin reactions, fatigue, and diarrhoea. Thus, because of the survival benefit of regorafenib in HCC patients unresponsive to sorafenib, it was approved by health agencies in several countries, including the United States, Japan, and China.

Cabozantinib

Cabozantinib is a multikinase inhibitor suppressor of tumour growth, metastasis, and angiogenesis that primarily targets VEGFR but also targets MET and AXL, which in addition to being implicated in HCC progression are involved in sorafenib resistance[37]. Initially, this drug showed clinical activity in a phase II study in previously untreated HCC patients and those with progression or no response to sorafenib, resulting in a median OS of 5.5 mo with no significant radiographic responses[38]. However, its approval was based on the results of the CELESTIAL clinical trial (ClinicalTrials.gov identifier: NCT01908426), a randomized, double-blind, phase III trial evaluating cabozantinib *vs* placebo in patients diagnosed with advanced HCC, in which cabozantinib demonstrated significant benefit over placebo in OS and tumour PFS. The median OS was 10.2 mo with cabozantinib and 8.0 mo with placebo (95%CI: 0.63-0.92). The median PFS was 5.2 mo with cabozantinib and 1.9 mo with placebo (95%CI: 0.36-0.52)[39]. In 2019, the FDA approved cabozantinib for treating patients with advanced HCC who were previously treated with sorafenib[40].

Interestingly, this drug is involved in tyrosine kinase inhibition and has also been reported to be an immunomodulator since some of its targets are involved in the immune response. Indeed, in combination with anti-programmed cell death protein 1 (PD-1) therapy, cabozantinib showed a greater antitumour effects than monotherapy or placebo in animal models of HCC. On its own, cabozantinib significantly increased neutrophil infiltration and reduced intratumoural CD8+ PD-1+ T-cell ratios, while the combination further stimulated this effect[41].

Ramucirumab

Ramucirumab is an antiangiogenic anti-VEGFR2 monoclonal antibody[42,43]. The efficacy of this drug was tested in the REACH clinical trial, a randomized, placebo-controlled, double-blind, multicentre, phase III trial (ClinicalTrials.gov identifier: NCT01140347). Here, ramucirumab was tested against placebo in patients diagnosed with advanced HCC who were previously treated with sorafenib and who experienced either progression or intolerance. The median OS for the ramucirumab group was 9.2 mo (95%CI: 8.0-10.6) *vs* 7.6 mo (6.0-9.3) for the placebo group (HR: 0.87; 95%CI: 0.72-1.05; $P = 0.14$). Consistent with these results, second-line treatment with ramucirumab did not significantly improve survival over placebo in patients with advanced HCC[44]. A follow-up trial, REACH-2, was a randomized, double-blind, placebo-controlled, phase III trial comparing ramucirumab *vs* placebo at a 2:1 ratio in the same population, but this time for a preselected population with AFP concentrations ≥ 400 ng/mL. The median OS was 8.5 mo (95%CI: 7.0-10.6) *vs* 7.3 mo (5.4-9.1); HR: 0.71 (95%CI: 0.53-0.95; $P = 0.0199$) and PFS [2.8 mo (2.8-4.1) *vs* 1.6 mo (1.5-2.7); 0.452 (0.33-0.60); $P < 0.0001$] were significantly improved in the ramucirumab group compared with the placebo group. This trial showed improved OS with ramucirumab compared to placebo in patients with HCC and AFP concentrations of at least 400 ng/mL who had previously received sorafenib[45].

Very recently, the clinical relevance of rechallenge treatment with previously administered drugs was evaluated, with five consecutive patients with advanced HCC who received rechallenge treatment with lenvatinib and with failure after treatment with ramucirumab. Here, the radiological findings using the modified Response Evaluation Criteria in Solid Tumours showed stable disease in four patients and a partial response in one. This trial demonstrated that re-exposure to lenvatinib treatment after ramucirumab might be effective for treating advanced HCC[46].

IMMUNOTHERAPY

Unfortunately, cancer cells can develop resistance to systemic therapies. Thus, more and better drug treatments must be devised for these patients. Potential strategies include combination approaches and immunological therapy. In fact, immunotherapy has now been postulated as a possible therapeutic strategy to treat different types of cancer.

Cancer cells can escape the defence mechanisms of immune cells in the tumour microenvironment, thus avoiding detection and elimination by host lymphocytes by downregulating stimulatory immunoreceptors and stimulating inhibitory immunoreceptors. For example, in the case of T cells, tumour cells can modulate stimulatory activity by downregulating MHC-I on the surface. Conversely, inhibitory activity can be modulated by these cells through upregulation of PD-L1 on the surface[47-49]. Such molecules are known as immune checkpoints, which act as modulators of immune responses. These molecules can be used as pharmacological targets to generate various monoclonal antibodies that modulate their activity. Among the most studied immune receptors are PD-1, CTLA-4, LAG3, TIM3, TIGIT, and BTLA[49].

Immunotherapy has been shown to have significant efficacy in the treatment of different types of cancer, including HCC[50], making it an excellent option for patients with cancer progression or for whom systemic therapy with sorafenib was ineffective. Several immune checkpoint inhibitors that primarily target CTLA-4, PD-1, and its ligand PD-L1 have been tested to date. Some ICIs have also been approved by the FDA for the treatment of HCC. PD-L1, also called B7-H1 or CD274, is expressed in many cancer and immune cells and plays an essential role in blocking the "cancer immunity cycle" by binding to PD-1 and B7.1 (CD80), both of which are negative regulators of T-cell activation[51,52].

Antibody-based therapy is the main strategy designed to modulate the tumour immune response, but other cancer immunotherapeutic strategies, such as adoptive cell therapy, chimeric antigen receptor-modified immune cells, engineered cytokines, and therapeutic cancer vaccines, are still under development[53,54].

Nivolumab

Nivolumab is a human IgG4 monoclonal antibody that binds to the PD-1 receptor, inhibiting its interaction with PD-L1 and PD-L2 and restoring T-cell activity[55]. Nivolumab has been shown to be effective in several malignancies, including melanoma, renal Hodgki''s lymphoma, lung cancer, and gastric cancer[56-60].

Nivolumab was evaluated in HCC patients in a study called CheckMate-040 (ClinicalTrials.gov identifier: NCT01658878), a phase I/II, open-label, non-comparative, multicentre trial that included patients with advanced HCC who either had also reported progression after treatment with sorafenib or were sorafenib naive. Patients received intravenous nivolumab 240 mg every 2 wk until unacceptable toxicity or disease progression occurred. In this study, nivolumab showed favourable clinical activity and safety with manageable toxicities, suggesting that it could be suitable for patients with advanced HCC[61].

Subsequently, the activity of nivolumab (240 mg intravenously every 2 wk) was compared to that of sorafenib (400 mg orally twice daily) in a randomized, open-label, phase III trial (CheckMate 459, ClinicalTrials.gov identifier: NCT02576509) until disease progression or unacceptable toxicity. OS was improved from 14.7 mo for sorafenib to 16.4 mo with nivolumab but did not reach statistical significance (P = 0.0752). In addition, there was no significant difference in PFS (3.7 *vs* 3.8 mo). The ORRs for nivolumab and sorafenib were 15% and 7%, respectively. Nivolumab showed relevant clinical activity and a favourable safety profile for patients with advanced HCC. However, nivolumab administered for the first time in these patients was not significantly better than sorafenib in terms of OS[62]. Thus, in September 2017, nivolumab was approved by the FDA as a second-line treatment for patients with advanced HCC. It is worth mentioning that this antibody has only been approved by this institution[63].

Recently, the effect of the combination of nivolumab plus ipilimumab, a fully human IgG1 monoclonal antibody that binds to CTLA-4 on T cells[64], was evaluated. The efficacy of this combination was tested in the CheckMate 040 study (ClinicalTrials.gov identifier: NCT01658878), a multicentre, open-label, multicohort, phase I/II study in which it was shown that the combination of nivolumab plus ipilimumab led to high OS rates and had a manageable safety profile[65]. Based on the results of this trial, in March 2020, the FDA approved the combination of nivolumab plus ipilimumab as a second-line treatment for patients with HCC who had been previously treated with sorafenib[66].

Pembrolizumab

Pembrolizumab is an anti-PD-1 monoclonal antibody that demonstrated clinical efficacy in patients with advanced HCC. This antibody was evaluated in a non-randomized, multicentre, open-label, phase II study in patients with BCLC B-C HCC pre-treated with sorafenib (ClinicalTrials.gov identifier: NCT02702414), and it showed antineoplastic activity with an ORR of 17% and a manageable safety profile[67]. Based on these results, in November 2018, the FDA granted accelerated approval to pembrolizumab for patients with HCC who had been previously treated with sorafenib[68]. A subsequent study was then conducted evaluating pembrolizumab in a randomized, double-blind, phase III study in patients with advanced HCC previously treated with sorafenib (KEYNOTE-240, ClinicalTrials.gov identifier: NCT02702401). Here, the median OS was 13.9 mo (95%CI: 11.6-16.0 mo) for pembrolizumab *vs* 10.6 mo (95%CI: 8.3-13.5 mo) for placebo (HR: 0.781; 95%CI: 0.611-0.998; P = 0.0238). The median PFS for pembrolizumab was 3.0 mo (95%CI: 2.8-4.1 mo) *vs* 2.8 mo (95%CI: 1.6 to 3.0 mo) for placebo[69].

Additionally, the KEYNOTE-394 trial (ClinicalTrials.gov identifier: NCT03062358), a randomized, double-blind, phase III study, evaluated the efficacy of pembrolizumab plus best supportive care *vs* placebo in Asian HCC patients as second-line therapy. Overall, the results were consistent with those seen in previous trials, further supporting the use of pembrolizumab in patients with advanced HCC. Here, the median OS was 14.6 mo (12.6-18.0) for pembrolizumab and 13.0 mo (10.5-15.1) for placebo (95%CI); furthermore, pembrolizumab showed significant improvement of PFS (HR: 0.74, 95%CI: 0.60-0.92, P = 0.0032)[70].

INNOVATIVE STRATEGIES FOR HCC TREATMENT

Drug combination and repurposing

Currently, monotherapies are ineffective in fighting cancer mainly due to the development of resistance of cancer cells to available drugs[71], and preclinical findings may not be replicated in patients. For instance, the monoclonal antibody bortezomib demonstrated promising antineoplastic activity in preclinical assays, but in humans, it did not show notable single-agent activity compared to sorafenib [72]. Thus, more and better treatment options are needed for these patients, and drug combinations are promising options. This strategy consists of simultaneously administering two or more drugs aimed at different cancer-specific drug targets and has shown significant benefits compared to monotherapy[73]. However, combining drugs must become a rational strategy that guarantees significant pharmacological responses, especially for those patients who either did not respond to current therapy or developed resistance.

Several tools have been developed for the identification of potentially useful drug combinations; these tools include dose-response matrices, RNA interference technology, and the wide adaptation of clustered regularly interspaced short palindromic repeats (CRISPR) systems, as well as more novel techniques such as patient-derived xenograft (PDX) models and *ex vivo* primary cell and organoid models[74]. For instance, Lim *et al*[75] used PDXs of HCC, PDX-derived organoids and a hybrid experimental-computational approach–namely, the quadratic phenotypic optimization platform–and found that the combination of the second-generation proteasome inhibitor ixazomib and the CDK inhibitor dinaciclib (Dina), which they tested *in vitro* and *in vivo*, is effective against HCC[75]. Another example of the usefulness of these strategies is CRISPR-Cas9 combinatorial screening, a technique that accelerated the discovery of combination treatment with the approved drug ifenprodil (an NMDA receptor antagonist) and sorafenib as a new therapeutic alternative for advanced HCC[76].

Therefore, implementing the abovementioned strategies should aid the discovery of potentially useful drug combinations. In this manner, medical staff may have different choices and establish a selection order more suitable for each HCC patient in a personalized manner[77,78].

Conversely, it is well known that the discovery of new molecules with pharmacological activity is a process with two main disadvantages: Time and cost. It takes at least 10 years to bring a new drug to the market, and the approximate cost ranges from $314 million to $2.8 billion[79]. Furthermore, in emergency situations such as cancer, the demand for effective treatments is extremely high, and additional strategies are required to obtain novel therapies in an expedited manner. Thanks to advances in pharmacology and genomics, several non-cancer drugs have been shown to have great potential for use in treating multiple cancers. Drug repurposing is a strategy that involves the discovery of already known drugs initially used to treat other diseases but with the potential to treat various malignancies. The main advantage of this approach is that it allows an accelerated and less costly process to identify new cancer treatments since it focuses on the selection of drugs already approved by relevant health institutions[80,81]. Some non-cancer drugs showing antineoplastic activity against HCC and with high repurposing potential are described below and summarized in Table 3.

One of the differences between repositioned drugs and existing drugs approved to treat HCC is that the latter target relatively few signalling pathways; in contrast, repositioned drugs have the enormous advantage of targeting a surprisingly wide variety of signalling pathways involved in liver carcinogenesis (Table 3). For instance, Nair *et al*[82] identified CDC20 as a marker of poor prognosis during the development of early and advanced HCC. Through molecular docking studies, it was determined that labetalol, a beta blocker, binds with high affinity to CDC20[82], suggesting that the effect of labetalol against the development of HCC should be tested. The same research group further investigated this possibility by *in vitro* cytotoxicity studies, in which labetalol significantly inhibited the growth of the HepG2 cell line[83]. Subsequent application of bioinformatics analysis tools to repositioned drugs provides an incredible advantage for the identification of unknown drug targets and signalling pathways potentially involved in liver carcinogenesis.

Antihistamines

Histamine exerts a variety of physiological activities *via* its G protein-coupled receptors, the activation of which has been associated with the progression of different types of cancer[84,85]. It is well known that histamine favours the development of different types of cancer, including liver cancer[86]. Accordingly, overexpression of the histamine H1 receptor (H1HR) is associated with HCC cell proliferation and metastasis by inducing cell cycle progression, lamellipodia production, matrix metalloprotease 2 (MMP2) production and inhibition of apoptosis. Furthermore, suppressing H1HR activity significantly inhibited tumour growth and metastasis in mouse xenograft models[86]. Interestingly, very recently, it was shown that antihistamine consumption is associated with a significant decrease in the developing of liver cancer in patients diagnosed with HBV, HCV or both viruses[87].

Astemizole

Ellegaard *et al*[88] analysed cohort studies and reported that the use of cationic amphiphilic antihistamines, including astemizole (an H1-antihistamine), was associated with a significant reduction in mortality in lung cancer patients[88]. It is worth mentioning that astemizole might affect cancer cell proliferation *via* different molecular mechanisms, including ion channels.

The ether à-go-go-1 (Eag1) potassium channel has been reported to play an important role in the development of several types of cancer, such as liver, cervical, breast, lung and colon cancer[89-93], suggesting that this channel is a potential early biomarker and drug target for these tumours[94]. Eag1 overexpression has been implicated in cell cycle progression and cancer cell proliferation[95], and inhibition of this channel has reduced tumour progression in both *in vitro* and *in vivo* assays in leukaemia and gastric cancer[86-97]. De Guadalupe Chávez-López *et al*[98] found that astemizole inhibited cell proliferation and induced apoptosis in human HCC cell lines[98]. In the same study using an HCC model induced by diethylnitrosamine (DEN) in mice, they found that astemizole inhibited tumour development and decreased Eag1 mRNA and protein levels[98].

Cytochrome P450 2J2 (CYP2J2) is implicated in the development of different types of cancer. In HCC, CYP2J2 is overexpressed, and its activity promotes cell proliferation[99-101]. Interestingly, astemizole and loratadine inhibit CYP2J2 activity[102]. Ellegaard *et al*[88] proposed the possibility that this drug targets this protein, which would partially explain the effect of reduced mortality in lung cancer patients [88].

TRPV2 is a calcium channel expressed in and associated with several types of cancer, including HCC progression. Both mRNA and protein levels of this channel are increased in well-differentiated HCC tumour tissue compared to undifferentiated tissue. There is a strong association between its expression and portal vein invasion. Van den Eynde *et al*[103] reported that TRPV2 is related to endometrial cancer progression and identified astemizole, loratadine, and clemizole as TRPV2 blockers, with loratadine being the most potent antagonist, leading to inhibition of cell proliferation and migration in *in vitro* assays in HEK293 cells[103].

Table 3 Identified drugs and their targets for drug repurposing in hepatocellular carcinoma

Drug	Original therapeutic indication	Molecular targets in HCC	Ref.
Antihistamines	Allergy	H1R-H4R, Eag1, CYP2J2, TRPV2, AP-1, NF-B	[88,91,96,98,102,103,105,109,111,113,115,116]
Raloxifene, bazedoxifene	Breast cancer (raloxifene), osteoporosis	ER-, ER-, GPER, IL-6R, aHR, NF-B, STAT3, PI3K/AKT, MAPK	[135-137,141,142]
Disulfiram	Alcoholism	NF-B, TGF-β, ROS-JNK	[149-151,157]
Clofazimine	Antimycobacterial used to treat leprosy	Wnt/-catenin pathway	[166-178]
Albendazole	Anthelmintic	Tubulin, ERK1/2-HIF-1α-p300/CREB	[175]
Pimozide	Antipsychotic used to manage Tourette's Disorder	STAT3, Wnt/-catenin	[185,188]
Natamycin	Macrolide antifungal	PRDX1	[191]
Metformin	Glycemic control in type 2 diabetes mellitus	PI3K-mTOR pathway, AMPK	[200-202,206,207]
Valproate	Anticonvulsant	HDAC, Notch-1, MAPK pathway, -catenin pathway	[220,221,223]
Atorvastatin	Lower lipid levels and reduce the risk of cardiovascular disease	Mevalonate pathway	[231]
Celebrex	NSAID	COX-2, PNO1	[237,243]
Hydroxychloroquine	Antimalarial	Autophagy inhibition, TLR9 pathway	[247]

NSAID: Non-steroidal anti-inflammatory drug; mTOR: Mechanistic target of rapamycin; HCC: Hepatocellular carcinoma; NF-kB: Nuclear factor kB; AP-1: Activating protein-1; CYP2J2: Cytochrome P450 2J2; ER: Oestrogen receptor; IL-6R: Interleukin-6R; STAT3: Signal transducer and activator of transcription 3; PI3K: Phosphoinositide 3-kinase; TGF-β: Transforming growth factor-β; PRDX1: Peroxiredoxin 1; HDAC: Histone deacetylase; aHR: Adjusted hazard ratio.

Loratadine

Loratadine is a second-generation antihistamine indicated for the treatment of allergic rhinitis and urticaria. It is a selective H1HR receptor antagonist[104]. Fritz *et al*[105,106] evaluated the effect of loratadine through retrospective studies in patients diagnosed with breast cancer and melanoma and found that loratadine use was associated with improved OS[105,106]. In patients diagnosed with lung cancer, a cohort study found that the use of loratadine or its metabolite desloratadine was associated with a significant reduction in mortality; the authors proposed that cancer-related changes in lysosomal membranes could favour the entry of these antihistamines[88,107]. To date, there has been scarce evidence studying the effect of loratadine in HCC. In a thesis from a few years ago, the cytotoxic effect of the combination of loratadine and cisplatin in HCC cell lines was evaluated; loratadine alone had a concentration-dependent cytotoxic effect on liver cancer cell lines, and the combination of loratadine with cisplatin had a synergistic effect[108]. The same thesis showed that loratadine alone and in combination also induced apoptosis and cell cycle arrest in the G2/M phase. Loratadine targets proteins that have been suggested to be involved in the development of HCC. As in the case of astemizole, loratadine might exert antineoplastic effects through H1HR antagonism, lysosomal membrane sensitization, TRPV2 calcium channel blockade and inhibition of CYP2J2 activity[86,88,102,103]. Furthermore, it has been reported that loratadine could exert anti-inflammatory activity by inhibiting the inflammatory response triggered by NF-kB signalling[109], an effect that reduces the levels of proinflammatory components, including interleukin (IL)-6 and tumour necrosis factor (TNF)-α. The effect of loratadine on HCC and its potential mechanisms of action deserve further investigation.

Deptropine

Deptropine is a first-generation H1HR antihistamine indicated to treat asthma[110]. This drug has activity against cancer cells. For example, *in vitro* assays in human liver cancer cells showed that, compared to the activity of other first- and second-generation antihistamines, deptropine was more potent in inhibiting cell proliferation and inducing autophagosome formation by significantly increasing the expression of light chain 3B-II. In mouse xenograft models, deptropine potently inhibited the tumour effect[111].

Cyproheptadine

This antihistamine is a potential anti-HCC agent. Feng *et al*[112] evaluated the activity of cyproheptadine in liver cancer cell viability and found that this drug had a potent inhibitory effect on cell proliferation through cell cycle arrest. Interestingly, a minimal cytotoxic effect was observed in healthy

hepatocytes[112]. Subsequently, a cohort study in Taiwanese patients at different stages of HCC compared patients who received cyproheptadine treatment and those who did not. The adjusted HR (aHR) of all-cause mortality significantly decreased in all stages in the patients who received palliative treatments with cyproheptadine use compared with those who received palliative treatments without cyproheptadine use (all $P < 0.0001$ and aHR = 0.76, 0.80, 0.66, and 0.66 for stages I, II, III, and IV, respectively). The authors suggested that cyproheptadine could improve survival in patients with HCC at any stage[113]. The same research group conducted a case report documenting that a 62-year-old woman with suspected advanced HCC and bone metastases showed disease remission after cyproheptadine monotherapy[114]. A dose of 4 mg of this drug three times daily for 17 mo reduced serum AFP concentrations from 17697.62 ng/mL to 4.3 ng/mL in only 3 mo. A liver biopsy performed two months after starting cyproheptadine treatment showed no malignancy. This outcome was previously observed in another case report in which two patients with HCC and lung metastases were treated with a combination of cyproheptadine plus thalidomide (it should be noted that the cyproheptadine prescription was indicated for skin itching). Computed tomography imaging showed complete remission of HCC in both patients after 6 mo and 6 wk of treatment[115].

A cohort study evaluated the efficacy of the combination of cyproheptadine with sorafenib compared to sorafenib alone in patients with advanced HCC. The median OS was 11 mo in the combination group (95%CI: 6.8-15.1 mo) and 4.8 mo in the sorafenib group (95%CI: 3.1-6.6 mo), while the median PFS time was 7.5 mo (95%CI: 5.1-10.0 mo) in the combination group compared with 1.7 mo (95%CI: 1.4-2.1 mo) in the sorafenib group[116].

Roles of other histamine receptors and antihistamines in HCC

Histamine 2 receptor: Histamine receptor 2 (H2HR) activation has an inhibitory effect on tumour progression in colorectal cancer; gene expression profiling studies in tumour samples from colorectal cancer patients described the elevated expression of this receptor, associated with improved OS outcomes[117]. In human liver cancer cells, H2HR activation leads to the inhibition of IL-6 expression and signalling, arresting cell proliferation[118]. In contrast, there is evidence that H2HR activation in HCC favours the expression of β-catenin and survivin, leading to cell survival[119]. Cimetidine, an H2 antihistamine, decreases intracellular cAMP concentrations, as well as EGF-induced cell proliferation and migration, and it has been suggested as an HCC chemopreventive agent[120]. Additionally, cimetidine treatment was shown to inhibit liver carcinogenesis in rats with DEN-induced HCC[121]. Recently, Crouchet *et al*[122] developed a system in human liver cells that models a clinical prognostic liver signature predicting long-term liver disease progression to HCC, and they identified nizatidine, an H2HR antihistamine, for the treatment of advanced liver disease and prevention of HCC[122].

Histamine 3 receptor: The H3HR receptor has been described to participate in the carcinogenesis of different types of cancer, including colorectal and pancreatic cancer[123,124]. In tumour tissues from HCC patients, H3HR was overexpressed and associated with poor prognosis, and its activation promoted the growth and metastasis of HCC cell lines by inducing lamellipodia formation[125,126]. Zhang *et al*[126] reported that H3HR activation favours HCC progression through an acceleration of the G1-S phase transition, inhibition of apoptosis, and activation of the AMPc/PKA/CREB signalling pathway to downregulate the expression of CDKN1A, a cyclin-dependent kinase inhibitor that has anti-oncogene activity[126]. Thus, the oncogenic role of H3HR might be antagonized as a potential therapy in HCC.

Histamine 4 receptor: Analysis of cancer genomic data from The Cancer Genome Atlas showed that the histamine H4 receptor (H4HR) is slightly but significantly overexpressed in human HCC tumour tissues compared to healthy tissue[84]. Furthermore, patients with increased H4HR protein expression in tumour cells also had increased tumour sizes and more metastasis compared to those with lower receptor expression, suggesting that H4HR levels could be used as a prognostic marker for liver cancer [127]. However, to date, there have been insufficient studies demonstrating the role of H4HR in HCC and its clinical relevance, so it is crucial to investigate its association with this cancer.

ESTROGEN RECEPTOR MODULATORS

According to the Global Cancer Observatory, liver cancer ranks fifth in incidence in men, while in women, it ranks ninth[1]. This fact has attracted the attention of researchers, who have argued that oestrogens explain this difference. Accordingly, oestrogens play a protective role against liver damage and prevent the development of HCC[128-130]. Epidemiological data have indicated that oestrogen deficiency in peri- and postmenopausal women increases the risk of developing liver damage and increases HCC incidence in postmenopausal women; in concordance, oestrogen treatment suppresses this phenomenon[131,132].

Both isoforms of the nuclear oestrogen receptor (ER), ER-α and ER-β, are involved in the development of liver cancer; however, the functions of ER-β have not yet been fully described. Both ER-α and ER-β are expressed in the liver under normal conditions, but their expression is modified during inflammatory

processes. Both are decreased in HCC patients compared to healthy tissue samples[133] and are believed to lose their function during disease progression; indeed, the ER-α isoform might even be considered a predictor of poor prognosis in HCC[128,134]. Conversely, Matsushima *et al*[135] reported that the selective oestrogen receptor modulators (SERMs) raloxifene and bazedoxifene inhibited HCC progression through their specific interaction with ER-β. They proposed that both drugs could activate the ER-β receptor in the liver, which through downstream signal transduction suppresses TGF-induced HCC cell migration *via* inhibition of Akt[135].

Raloxifene is indicated for the treatment of osteoporosis and is used for the treatment and prevention of breast cancer[136]. Raloxifene is a potent inhibitor of the IL-6/GP130 signalling pathway, which is involved in the process of oncogenesis of various cancers, including HCC[137]. This research group observed that raloxifene inhibited cell viability in human liver cancer cell lines. Furthermore, using an *in vivo* model, they also demonstrated that it could inhibit tumour growth.

Because liver cancer frequently develops in the context of chronic inflammatory liver disease, proinflammatory cytokines and immune cells play important roles in carcinogenesis. One of the most relevant cytokines in the development of HCC is IL-6; when overproduced, it has a strong effect on liver carcinogenesis, and its high expression is related to a high rate of metastasis and poor prognosis in HCC [138-140]. Naugler *et al*[141] reported in an animal model that oestrogen administration inhibited IL-6 secretion and significantly reduced DEN-induced injury in males[141]. When IL-6 binds to its receptor, it recruits JAK, leading to activation of STAT3, a transcription factor that favours proliferative processes, angiogenesis, invasion, *etc*[142]. In addition, ER-α could interact directly with NF-kB and inhibit IL-6 secretion, and raloxifene could interact with ER-α and inhibit IL-6 secretion and thus tumour progression[142].

OTHER DRUGS

Disulfiram

Disulfiram is an FDA-approved drug from several years ago and has been extensively used in the treatment of alcoholism[143]. This drug has potential anticancer activity in different types of cancer, including lymphoma[144], breast cancer[145,146], and pancreatic cancer[147]. A phase II, multicentre, randomized, double-blind trial (ClinicalTrials.gov identifier: NCT00312819) evaluated the safety and efficacy of the combination of disulfiram with cisplatin and vinorelbine in patients diagnosed with lung cancer. Interestingly, a significant increase in survival was observed in patients given this combined treatment[148]. Intracellular copper (Cu) levels are significantly elevated in HCC cells and are associated with poor patient prognoses[149,150]. Surprisingly, the increase in Cu concentration might be harnessed for therapeutic use since disulfiram has Cu-dependent anticancer properties. Li *et al*[151] found that disulfiram inhibited the proliferation, migration, and invasion of liver cancer cells; interestingly, Cu enhanced this activity when combined with disulfiram; however, Cu alone did not [151]. In this regard, a phase I clinical trial determined the maximum tolerated dose of Cu administered with disulfiram in patients with liver cancer and found that 250 mg of daily Cu gluconate were well tolerated by these patients[152]. In the same study, temporary disease stabilization was observed in some patients, but there were no objective responses. Disulfiram can penetrate cancer cells and chelate intracellular Cu because Cu levels are elevated in many cancers. This action provides the advantage of specificity for cancer cells compared to healthy cells. Disulfiram might work as a Cu ionophore that induces oxidative stress by promoting reactive oxygen species (ROS) production, resulting in the inhibition of NF-kB[151], a transcription factor involved in the regulation of inflammatory processes and the development of liver injury, as well as HCC progression[153,154]. Blocking NF-kB signalling leads to an increase in ROS-induced toxicity and consequent cell apoptosis[155]. Furthermore, Thiery[156] found that inhibition of NF-kB signalling also resulted in inhibition of liver cancer cell metastasis by reversing the epithelial-to-mesenchymal transition (EMT), an important process in cancer metastasis in which NF-kB and TGF-β are important components[156]. Indeed, in this same study, disulfiram was found to inhibit TGF-kβ signalling. Interestingly, disulfiram plus Cu reversed EMT more effectively than disulfiram alone[151].

Most recently, Zhang *et al*[157] reported that disulfiram plus copper in combination with sorafenib resulted in increased anticancer activity against HCC under *in vitro* and *in vivo* conditions. Moreover, this combination synergistically inhibited the proliferation of human HCC cell lines and significantly increased autophagy and apoptosis compared to sorafenib alone. In addition, in a mouse orthotopic HCC xenograft model, the combination effectively inhibited tumour growth compared to the effect of sorafenib alone[157].

Clofazimine

The canonical Wnt/β-catenin signalling pathway is a crucial component during embryonic development and normal adult homeostasis because it participates in processes such as cell differentiation, polarity, migration, and apoptosis[158]. However, abnormal activation of this pathway (especially of the transcription factor β-catenin) has been linked to cellular malignant transformation

and promotion of carcinogenesis, and it is present in many types of cancer, including HCC[159-161]. Notably, mutations in the *CTNNB1* gene, which codes for β-catenin, are the most frequent mutations during HCC[162,163]. Interestingly, clofazimine, an anti-leprosy agent, could be useful for treating Wnt-dependent cancers. For instance, it has been shown to be effective against triple-negative breast cancer, both *in vitro* and *in vivo*, through inhibition of Wnt/β-catenin signalling[164,165]. Furthermore, Xu *et al* [166] demonstrated that clofazimine could effectively suppress HCC cell growth, inhibiting Wnt/β-catenin canonical signalling[166]. This drug has been evaluated for some years, and the results have suggested that it might work successfully as an antitumour agent. For example, Van Rensburg *et al*[167] found that it inhibited HCC cell line proliferation *in vitro*[167]. In addition, in a phase II clinical trial in patients with unresectable or metastatic liver cancer, 600 mg of this drug were administered daily for two weeks, followed by a dose reduction to 400 mg until progression or death. In this trial, 13 of 30 treated patients had disease stability for up to 20 mo, and the median OS was 13 wk[168]. Furthermore, a phase II clinical trial evaluated the combination of clofazimine plus doxorubicin in patients diagnosed with HCC. Although no patients showed complete or partial response, this combination showed only mild toxic effects, and the authors recommended further studies involving this antileprosy agent[169]. Overall, these trials provided strong evidence to suggest that clofazimine might be useful in treating HCC.

Albendazole

Albendazole is an antiparasitic agent used to treat parenchymal neurocysticercosis and other helminth infections by blocking parasite microtubules, leading to the inhibition of glucose uptake and transport and, ultimately, cell death[170]. Interestingly, this drug has been reported to possess antitumour activity and has been studied in different malignancies, including liver, lung, breast, prostate, and colorectal cancers and melanoma[171-175]. Pourgholami *et al*[176] evaluated the effect of this drug in several liver cancer cell lines and in mouse xenograft models (human SKHEP-1 tumour growth in nude mice), reporting that the drug induced dose-dependent inhibition of [^{3}H] thymidine incorporation in all the cell lines studied and a significant decrease in the number of SKHEP-1 cells significantly inhibiting tumour growth[176].

Pimozide

Pimozide is a dopamine receptor antagonist neuroleptic drug[177] that was approved by the FDA for the treatment of Tourette's syndrome and schizophrenia[178] and it has shown efficacy for the treatment of different types of cancer, such as breast cancer[179,180], prostate cancer[181], brain tumours[182], colorectal cancer[183], and chronic myelogenous leukaemia[184]. In liver cancer, pimozide effectively inhibited cell proliferation of HCC cell lines through disruption of Wnt/β-catenin signalling and reduction of epithelial cell adhesion molecule expression, a marker of both liver stem cells[185] and HCC tumour-initiating cells[186,187]. Furthermore, Chen *et al*[188] found that pimozide was able to inhibit cell proliferation, migration, colony formation, and sphere formation *in vitro* in HCC cell lines and stem-like cells by suppressing STAT3 activity. Additionally, pimozide reduced the tumour burden in a xenograft model in nude mice[188]. Moreover, the same research group found that the antiproliferative effects of pimozide on HCC cell lines were reversible and in line with the involvement of cell quiescence and ROS production. Interestingly, pimozide combined with sorafenib synergistically inhibited HCC cell proliferation *in vitro*[188].

Natamycin

Natamycin is a natural polyene amphoteric macrolide antibiotic with antifungal properties[189]. It has been reported to significantly inhibit the proliferation of prostate cancer cells[190]. Conversely, An *et al* [191] found that natamycin induced apoptosis and inhibited the proliferation of HCC cells by triggering excessive ROS production through the downregulation of peroxiredoxin 1 (PRDX-1). Additionally, they found that the combination of natamycin plus sorafenib exerted a synergistic effect on cell growth suppression compared to the effect of monotherapy[191].

Dysregulation of cellular redox systems is a critical feature of many types of cancer. Increased ROS play a fundamental role in the tumour microenvironment, activating important signalling pathways in carcinogenesis, such as MAPK/ERK, JNK, and PI3K/AKT, and in turn activating NF-kB, MMPs, and VEGF, consequently affecting angiogenesis, metastasis and cell survival in many types of cancer[192-194]. However, at significantly elevated ROS concentrations, cancer cells are able to develop antioxidant defence systems to maintain redox homeostasis and survive[195]. An example of this situation is the participation of the peroxiredoxin family, which consists of peroxidases that break down hydrogen peroxide, protecting the cancer cell from oxidative stress and consequently providing a survival advantage; thus, this family of enzymes are potential targets for tumour growth arrest and cancer therapy[196,197]. It is worth mentioning that the PRDX-1 isoform is the most abundant and positively regulated protein in different types of cancer, and its expression is associated with poor prognosis[198].

Valproic acid

Valproic acid is a drug that possesses anticonvulsant activity and is primarily indicated for the

treatment of epilepsy. However, it is also useful for treating migraine, bipolar disorder, anxiety, and psychiatric disorders[199]. The interest in testing the activity of this drug as an antineoplastic agent came from findings in human neuroblastoma models. This molecule was able to inhibit proliferation and induce differentiation of primitive neuroectodermal tumour cells *in vivo*, providing evidence for using valproic acid as a treatment for neuroblastoma patients[200]. Machado *et al*[201] reported the effect of this drug on human liver cancer cells both *in vitro* and *in vivo*. Valproic acid significantly inhibited cell proliferation in a dose-dependent manner, while in mouse xenograft models, it reduced tumour growth, in addition to negatively regulating Notch-1 mRNA levels[201]. Very recently, Bai *et al*[202] evaluated the effect of valproate in animal models of HCC in rats treated with DEN and found that this drug significantly reduced liver nodules and AFP levels, as well as other important liver enzymes, compared to rats treated with DEN alone. Additionally, valproate reduced inflammatory cytokines, such as TNF-α, IL-6, IL-1β, NF-kB and TGF-β1, in liver tissue[202].

Lee *et al*[203] took advantage of the benefits of combination therapy to evaluate the effects of cytokine-induced killer (CIK) cells with valproic acid. CIK cells are *ex vivo* expanded T lymphocytes expressing natural killer and T-cell markers that are used as adjuvant therapy to reduce HCC recurrence, yet CIK cell monotherapy is insufficient to treat advanced HCC[203-205]. Therefore, this research group determined whether treatment with CIK cells and valproic acid synergized to inhibit tumour growth in mouse models of HCC. After seven days of the combined treatment, there was a synergistic effect on relative tumour volume in the animals since the relative tumour volume in control animals was significantly increased[206].

Additionally, Yu *et al*[207] implemented a therapeutic strategy in HCC cells *in vitro* and *in vivo* that consisted of testing the combined effect of valproic acid with proton and photon irradiation. Histone deacetylase (HDAC) inhibitors, including valproic acid, have shown promising results in the treatment of different cancers[208-210]. However, their use as monotherapy has not been satisfactory, so using them in combination with another therapy is an appealing strategy. HDAC inhibitors can sensitize human cancer cells to ionizing radiation[211], which is a therapeutic strategy for cancer[212]. In a study by Yu *et al*[207], valproic acid prolonged DNA damage and increased proton-induced apoptosis and ROS formation while suppressing the expression of nuclear factor erythroid 2–related factor 2, a transcription factor involved in cellular antioxidant regulation. In tumour xenograft models, valproic acid significantly enhanced tumour growth retardation[207]. In addition, An *et al*[213] reported that valproic acid could induce cellular senescence in HCC cells through its role as an HDAC inhibitor[213].

ONGOING CLINICAL TRIALS USING ONCOLOGY AND NON-ONCOLOGY DRUGS

Table 4 summarizes the ongoing clinical trials for HCC patients. Immunotherapy is currently positioned as the most innovative pharmacological strategy to treat different types of cancer, including liver cancer. In addition, it is interesting to note that most of the ongoing HCC clinical trials are evaluating the effects of combination therapy and that drug repurposing is gaining tremendous interest, as non-oncology molecules are now being tested. Next, the non-oncology drugs used in ongoing clinical trials (Tables 3 and 4) are discussed.

Metformin

This drug is commonly used for the treatment of type 2 diabetes and was approved by the FDA in 1994. Metformin lowers glucose levels and improves insulin sensitivity[214]. Surprisingly, metformin has been shown to have antineoplastic activity in different types of cancer[83,215]. It is one of the most successful non-cancer drugs used in oncology. Several clinical trials are currently investigating the therapeutic potential of this drug in various cancers, including breast, prostate, endometrial, and colorectal cancer[216-219]. In the case of liver cancer, metformin has gained interest as an antineoplastic agent, given the increased risk of developing liver cancer in diabetic patients. Meta-analyses have reported that metformin has a beneficial effect on the incidence and/or survival of patients with liver cancer. For example, Ma *et al*[220] reported the association between metformin use and improved survival in diabetic patients with liver cancer[220]. Afterwards, the same research group reported a meta-analysis of 19 studies in diabetic subjects and suggested that metformin use reduced the proportion of liver cancer by 48% compared to non-users[221]. At the molecular level, metformin reduces insulin levels, activating the PI3K-mTOR signalling pathway and inhibiting cell proliferation in cancers expressing the insulin receptor[222]. Other mechanisms include negative regulation of mTOR *via* AMPK activation[223].

Ongoing clinical trials in HCC patients are evaluating the use of metformin in combination with other molecules, such as vitamin C (ClinicalTrials.gov identifier: NCT04033107), statins (ClinicalTrials.gov identifier: NCT02819869) and Celebrex (ClinicalTrials.gov identifier: NCT03184493).

Statins (atorvastatin)

Statins are agents that decrease the level of low-density lipoprotein cholesterol in the blood. They are specific inhibitors of the mevalonate pathway through inhibition of the conversion of 3-hydroxy-3-

Table 4 Ongoing clinical trials involving monotherapy, drug combination and non-oncology drugs

Study title	NTC number	Study design	Drugs	Status
Monotherapy				
Study of Pembrolizumab (MK-3475) as Monotherapy in Participants With Advanced Hepatocellular Carcinoma (MK-3475-224/KEYNOTE-224)	NCT02702414	Phase II, non-randomized, parallel assignment, open label	Pembrolizumab	Active, not recruiting
An Investigational Immuno-therapy Study of Nivolumab Compared to Sorafenib as a First Treatment in Patients With Advanced Hepatocellular Carcinoma	NCT02576509	Phase III, randomized, parallel assignment, open label	Nivolumab. Sorafenib	Active, not recruiting
Exploratory Study on Combined Conversion Immuno-therapy for Liver Metastasis of MSS Type Initial Unresectable Colorectal Cancer Based on Gene Status	NCT05409417	Phase II, III, single group assignment, open label	Experimental drug	Recruiting
First-in-Human Safety, Tolerability and Antitumour Activity Study of MTL-CEBPA in Patients With Advanced Liver Cancer	NCT02716012	Phase I, non-randomized, parallel assignment, open label	MLT-CEBPA. Sorafenib (200 mg)	Active, not recruiting
Drug combination				
A Phase III, Open-Label, Randomized Study of Atezol-izumab in Combination With Bevacizumab Compared With Sorafenib in Patients With Untreated Locally Advanced or Metastatic Hepatocellular Carcinoma (IMbrave150)	NCT03434379	Phase III, randomized, parallel assignment, open label	Atezolizumab. Bevacizumab. Sorafenib	Active, not recruiting
A Trial of Lenvatinib Plus Pembrolizumab in Participants With Hepatocellular Carcinoma	NCT03006926	Phase I, single group, open label	Lenvatinib. Pembrol-izumab (200 mg)	Active, not recruiting
A Study of Durvalumab or Tremelimumab Monotherapy, or Durvalumab in Combination With Tremelimumab or Bevacizumab in Advanced Hepatocellular Carcinoma	NCT02519348	Phase II, randomized, parallel assignment, open label	Tremelimumab. Durvalumab. Bevacizumab	Active, not recruiting
Pembrolizumab With or Without Elbasvir/Grazoprevir and Ribavirin in Treating Patients With Advanced Refractory Liver Cancer	NCT02940496	Phase II, non-randomized, parallel assignment, open label	Elbasvir/Grazoprevir. Pembrolizumab. Ribavirin	Active, not recruiting
Clinical Recruitment of Patients With First-line Targeted Drug Resistance or Intolerance to Hepatocellular Cancer With PD-1 Inhibitor (Toripalimab, JS001) Detected on the NGS Platform Combined With Anlotinib	NCT05453383	Phase II, single group assignment, open label	Anlotinib. Toripalimab	Recruiting
TACE Combined With Camrelizumab and Apatinib in the Treatment of Advanced Liver Cancer	NCT05550025	Phase II, single group assignment, open label	Camrelizumab. Apatinib	Recruiting
IBR900 Cell Injection Combined With Lenvatinib or Bevacizumab in the Treatment of Advanced Primary Liver Cancer	NCT05411757	Phase I, single group assignment, open label	IBR900. Lenvatinib. Bevacizumab	Not recruiting yet
Trial to Evaluate the Safety of Talimogene Laherparepvec Injected Into Tumors Alone and in Combination With Systemic Pembrolizumab MK-3475-611/Keynote-611	NCT02509507	Phase I, II, non-randomized, sequential assignment, open label	Talimogene. Laherparepvec. Pembrol-izumab	Active, not recruiting
HAIC Sequential TAE Combined With Lenvatinib and Tislelizumab in Unresectable HCC	NCT05532319	Phase II, single group assignment, open label	HAIC sequential TAE. Lenvatinib. Tislelizumab	Not recruiting yet
A Study of E7386 in Combination With Other Anticancer Drug in Participants With Solid Tumor	NCT04008797	Phase I, non-randomized, sequential assignment, open label	E7386. Lenvatinib	Recruiting
An Immuno-therapy Study to Evaluate the Effectiveness, Safety and Tolerability of Nivolumab or Nivolumab in Combination With Other Agents in Patients With Advanced Liver Cancer	NCT01658878	Phase I, II, parallel assignment, open label	Nivolumab. Sorafenib. Ipilimumab. Cabozantinib	Active, not recruiting
A Phase I Clinical Study of Recombinant Humanized Anti-BTLA Monoclonal Antibody (JS004) Injection Combined With Toripalimab Injection in Patients With Advanced Solid Tumors	NCT05427396	Phase I, single group assignment, open label	JS004. Toripalimab	Recruiting
mFOLFOX7 Plus Camrelizumab and Apatinib for Advanced HCC	NCT05412589	Phase II, single group assignment, open label	mFOLFOX7. Camrel-izumab. Apatinib	Recruiting
Trial of PXS-5505 Combined With First Line Atezolizumab Plus Bevacizumab For Treating Patients With Unresectable Hepatocellular Carcinoma	NCT05109052	Phase II, III, single group assignment, open label	PXS-5505. Atezolizumab. Bevacizumab	Not recruiting yet

Combination of Regorafenib and Nivolumab in Unresectable Hepatocellular Carcinoma	NCT04310709	Phase II, single group assignment, open label	Regorafenib. Nivolumab	Recruiting
Phase Ib Trial of Infigratinib In Combination With Atezolizumab And Bevacizumab for The Second-Line Treatment of Advanced Cholangiocarcinoma With FGFR2 Fusion/Amplification	NCT05510427	Phase I, randomized, single group assignment, open label	Infigratinib. Atezolizumab. Bevacizumab	Recruiting
A Study of TAK-500 With or Without Pembrolizumab in Adults With Select Locally Advanced or Metastatic Solid Tumors	NCT05070247	Phase I, non-randomized, parallel assignment, open label	TAK-500. Pembrolizumab	Recruiting
A Study of Nivolumab and Relatlimab in Combination With Bevacizumab in Advanced Liver Cancer	NCT05337137	Phase I, II, randomized, parallel assignment, quadruple (participant care, provider, investigator, outcomes assessor)	Relatlimab. Nivolumab. Bevacizumab	Recruiting
Drug repurposing				
High Dose Vitamin C Combined With Metformin in the Treatment of Malignant Tumors	NCT04033107	Phase II, single group assignment, open label	Vitamin C. Metformin	Recruiting
Statin Combination Therapy in Patients Receiving Sorafenib for Advanced Hepatocellular Carcinoma	NCT03275376	Phase II, randomized, parallel assignment, Quadruple (Participant, Care Provider, Investigator, Outcomes Assessor)	Atorvastatin	Terminated
The Combination Effect of Statin Plus Metformin on Relapse-free	NCT02819869	Phase II, randomized, parallel assignment	Statin. Metfotmin	Terminated
Statin for Preventing Hepatocellular Carcinoma Recurrence After Curative Treatment	NCT03024684	Phase IV, randomized, parallel assignment, triple masking (Participant, Care Provider, Investigator)	Atorvastatin	Recruiting
Meclizine for Hepatocellular Carcinoma	NCT03253289	Phase I, single group assignment, open label	Meclizine	Recruiting
Celebrex and Metformin for Postoperative Hepatocellular Carcinoma	NCT03184493	Phase III, non- randomized, parallel assignment	Celebrex plus metformin	Recruiting
Sorafenib Induced Autophagy Using Hydroxychloroquine in Hepatocellular Cancer	NCT03037437	Phase II, non-randomized, parallel assignment, open label	Sorafenib. Hydroxychloroquine	Recruiting

PD-1: Programmed cell death protein 1; HCC: Hepatocellular carcinoma.

methylglutaryl coenzyme A into mevalonate, which is responsible for cholesterol synthesis[224]. Interestingly, mevalonate signalling is deregulated in several types of cancer and is also involved in the process of tumorigenesis[225,226], making it a potentially useful target for cancer treatment. Preclinical trials have demonstrated that statins can be used as antitumour agents in colorectal cancer[227-229]. It was suggested that statins might reduce the risk of developing HCC[230]. Kim *et al*[231] reported that atorvastatin inhibited the activation of YAP (*via* the mevalonate pathway) and AKT (*via* stabilization of the truncated retinoid X receptor alpha pathway), which are involved in cancer development[231].

Ongoing clinical trials are evaluating the effects of statins in patients with advanced HCC, such as a trial evaluating atorvastatin in patients receiving treatment with sorafenib (ClinicalTrials.gov identifier: NCT03275376) and a clinical trial studying two non-oncology drugs-statins and metformin-either alone or in combination (ClinicalTrials.gov identifier: NCT03024684).

Celebrex

Celebrex (celecoxib) is a cyclooxygenase-2 (COX-2) selective non-steroidal anti-inflammatory drug indicated for the treatment of pain and inflammation caused by osteoarthritis, rheumatoid arthritis, and ankylosing spondylitis[232]. Interestingly, celecoxib anticancer activity is presumed to occur by inhibiting COX-2[233-235] because this cyclooxygenase isoform is frequently expressed in many types of cancer and promotes carcinogenesis and resistance of cancer cells to chemotherapy[236]. Dai *et al*[237] found that celecoxib also targets the RNA-binding protein ""partner of NOB1"" (PNO1) and exerts antitumour activity through the AKT/mTOR pathway[237]. In addition, PNO1 has been reported to participate in the progression of lung, oesophageal, breast, bladder, and colorectal cancer[238-242]. Targeting PNO1 (which is overexpressed in HCC tissues) can inhibit cell apoptosis by promoting autophagy through the ERK/MAPK signalling pathway[243].

A clinical trial is currently ongoing to compare the effect of Celebrex alone, metformin alone, and the combination of both drugs in preventing HCC recurrence after hepatic resection (ClinicalTrials.gov identifier: NCT03184493). In preclinical trials, it was shown that the combination of the two *in vitro* and

in vivo inhibited HCC proliferation more effectively than the effect of each drug alone[244].

Hydroxychloroquine

Hydroxychloroquine is an antimalarial drug that has been evaluated as an antitumour agent in HCC and has even been used for the treatment of other cancers, either alone or in combination with other therapeutic agents[215,245]. This drug targets cancer cells and the tumour microenvironment; among its molecular mechanisms of action, it inhibits autophagosome-lysosome fusion and Toll-like receptor 9 (TLR9) signalling, along with TLR7, which are overexpressed in HCC and are involved in cell proliferation and inhibition of apoptosis[246]. Furthermore, Chen *et al*[247] reported that hydroxychloroquine and miRNA (hsa-miR-30a-5p) target and resensitize sorafenib-resistant HCC cells to sorafenib through impairment of autophagy and DNA damage by oxidative stress *via* the TLR9/SOD1/hsa-miR-30a-5p/Beclin-1 pathway[247]. Since one of the mechanisms of sorafenib resistance is the induction of autophagy, a prospective, phase II clinical trial is currently under way to evaluate the efficacy of sorafenib and hydroxychloroquine treatment in patients with advanced HCC (ClinicalTrials.gov identifier: NCT03037437).

PERSPECTIVES

The high mortality caused by liver cancer remains an important concern in oncology. Therefore, there is an urgent need to implement new therapeutic strategies to provide significant benefits in patients with advanced HCC.

Immunotherapy is a tool that has shown great promise in treating HCC. Nevertheless, it is necessary to continue developing immunotherapy agents, which increase understanding of the role of the immune response in the tumour and take advantage of this process.

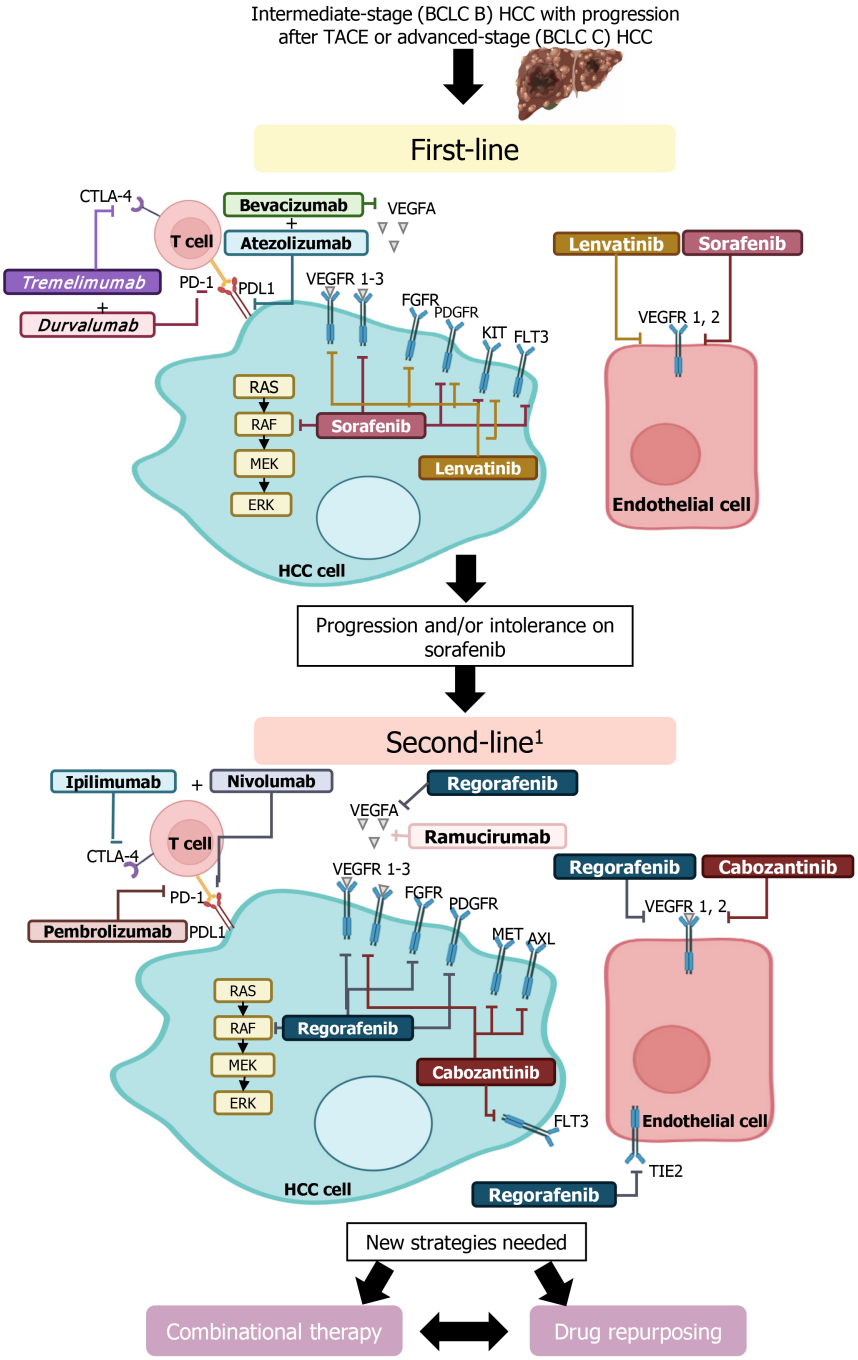
In contrast, the use of combination therapy has shown very favourable results compared to the effect of monotherapy, reflected by the diversity of current clinical trials evaluating the impact of the combination of two or more agents in HCC. Drug combinations simultaneously targeting relevant signalling pathways in liver carcinogenesis provide at least four potential advantages: (1) Anticancer synergistic effects; (2) minimization of treatment resistance; (3) reduction of individual drug doses; and (4) the occurrence of minimal adverse events. These advantages should facilitate HCC treatment, making it extremely important to consider possible future drug combinations to achieve greater benefits for HCC patients.

Furthermore, growing evidence has supported that non-cancer drugs possess antineoplastic activity. In emergency situations such as cancer, drug repurposing can be a very useful strategy. Compared to the traditional process of developing new drugs, drug repurposing allows for the rapid and less costly discovery of new treatments, increasing the likelihood of success with the advantage that safety issues in humans have already been described. It is crucial to mention that drug repurposing does not replace the traditional process; both are extremely important. However, repurposing non-oncology drugs is an attractive strategy to obtain more treatment options for advanced HCC.

Simultaneously, implementing non-oncology drug repurposing and proposing combinations of non-oncology drugs with systemic therapy or immunotherapy are very attractive strategies to generate significant benefits in patients with unresectable HCC. In addition, new relevant signalling pathways, critical drug targets, and biomarkers of this cancer might be identified along the way, providing significant advantages for understanding liver carcinogenesis.

CONCLUSION

Currently, approved drug options for treating advanced HCC are limited, and the likelihood of generating resistance is high, making the use of novel pharmacological approaches urgent (Figure 2). Compared to monotherapy, this review demonstrated that combining therapies has resulted in more significant benefits for HCC patients. Furthermore, evidence has been provided indicating that several non-oncology drugs are potentially useful for the treatment of this cancer. In addition, immunotherapy has significant effects in some cases compared to current systemic therapy, making this approach, along with repositioning and combination therapy, promising for the pharmacological treatment of advanced liver cancer.



DOI: 10.3748/wjg.v29.i17.2571 **Copyright** ©The Author(s) 2023.

Figure 2 Pharmacological strategies for the treatment of advanced hepatocellular carcinoma. When a patient is diagnosed with hepatocellular carcinoma either intermediate (BCLC B) or advanced (BCLC C) stage, surgical and locoregional therapeutic options are no longer indicated. In these cases, the most appropriate treatment option is systemic therapy with first-line treatments with sorafenib and lenvatinib as the initial drugs. However, if the patient develops resistance to sorafenib or disease progression after therapy, treatment with second-line drugs indicated in the schedule is initiated. It is important to note that immunotherapy using monoclonal antibodies is already part of the current and approved drug options. Because current drug treatments are limited and monotherapy is ineffective, the implementation of combination and drug repositioning are two therapeutic strategies to achieve more and better treatments. [1]All agents require prior sorafenib use. BCLC: Barcelona Clinic Liver Cancer; TACE: Transarterial chemoembolization; CTLA-4: Cytotoxic T-lymphocyte-associated protein 4; PD-1: Programmed cell death protein 1; VEGFR: Vascular endothelial growth factor receptor; FGFR: Fibroblast growth factor receptor; PDGFR: Platelet-derived growth factor receptors; HCC: Hepatocellular carcinoma.

FOOTNOTES

Author contributions: Villarruel-Melquiades F and Camacho J wrote the paper and made substantial contributions to conception of the manuscript; Mendoza-Garrido ME, García-Cuellar CM, Sánchez-Pérez Y and Pérez-Carreón JI made critical revisions related to important intellectual content of the manuscript; all authors read and approved the final version of the article to be published.

Supported by CONACyT Fellowship (FV-M), No. 787907.

Conflict-of-interest statement: All the authors report no relevant conflicts of interest for this article.

Open-Access: This article is an open-access article that was selected by an in-house editor and fully peer-reviewed by external reviewers. It is distributed in accordance with the Creative Commons Attribution NonCommercial (CC BY-NC 4.0) license, which permits others to distribute, remix, adapt, build upon this work non-commercially, and license their derivative works on different terms, provided the original work is properly cited and the use is non-commercial. See: https://creativecommons.org/Licenses/by-nc/4.0/

Country/Territory of origin: Mexico

ORCID number: María Eugenia Mendoza-Garrido 0000-0003-2037-0618; Claudia M García-Cuellar 0000-0001-8080-5797; Yesennia Sánchez-Pérez 0000-0003-0103-9188; Julio Isael Pérez-Carreón 0000-0001-9284-7775; Javier Camacho 0000-0002-8886-086X.

S-Editor: Fan JR
L-Editor: A
P-Editor: Zhao S

REFERENCES

1 **Ferlay J**, Ervik M, Lam F, Colombet M, Mery L, Piñeros M, Znaor A, Soerjomataram I, Bray F (2022). Global Cancer Observatory: Cancer Today. Lyon, France: International Agency for Research on Cancer. [cited 14 October 2022]. Available from: https://gco.iarc.fr/today

2 **Massarweh NN**, El-Serag HB. Epidemiology of Hepatocellular Carcinoma and Intrahepatic Cholangiocarcinoma. *Cancer Control* 2017; **24**: 1073274817729245 [PMID: 28975830 DOI: 10.1177/1073274817729245]

3 **Sung H**, Ferlay J, Siegel RL, Laversanne M, Soerjomataram I, Jemal A, Bray F. Global Cancer Statistics 2020: GLOBOCAN Estimates of Incidence and Mortality Worldwide for 36 Cancers in 185 Countries. *CA Cancer J Clin* 2021; **71**: 209-249 [PMID: 33538338 DOI: 10.3322/caac.21660]

4 **Bruix J**, Han KH, Gores G, Llovet JM, Mazzaferro V. Liver cancer: Approaching a personalized care. *J Hepatol* 2015; **62**: S144-S156 [PMID: 25920083 DOI: 10.1016/j.jhep.2015.02.007]

5 **Khalaf N**, Ying J, Mittal S, Temple S, Kanwal F, Davila J, El-Serag HB. Natural History of Untreated Hepatocellular Carcinoma in a US Cohort and the Role of Cancer Surveillance. *Clin Gastroenterol Hepatol* 2017; **15**: 273-281.e1 [PMID: 27521507 DOI: 10.1016/j.cgh.2016.07.033]

6 **Zhu XD**, Li KS, Sun HC. Adjuvant therapies after curative treatments for hepatocellular carcinoma: Current status and prospects. *Genes Dis* 2020; **7**: 359-369 [PMID: 32884990 DOI: 10.1016/j.gendis.2020.02.002]

7 **Baudino TA**. Targeted Cancer Therapy: The Next Generation of Cancer Treatment. *Curr Drug Discov Technol* 2015; **12**: 3-20 [PMID: 26033233 DOI: 10.2174/1570163812666150602144310]

8 **Chow AK**, Yau SW, Ng L. Novel molecular targets in hepatocellular carcinoma. *World J Clin Oncol* 2020; **11**: 589-605 [PMID: 32879846 DOI: 10.5306/wjco.v11.i8.589]

9 **European Association for the Study of the Liver**. EASL Clinical Practice Guidelines: Management of hepatocellular carcinoma. *J Hepatol* 2018; **69**: 182-236 [PMID: 29628281 DOI: 10.1016/j.jhep.2018.03.019]

10 **Reig M**, Forner A, Rimola J, Ferrer-Fàbrega J, Burrel M, Garcia-Criado Á, Kelley RK, Galle PR, Mazzaferro V, Salem R, Sangro B, Singal AG, Vogel A, Fuster J, Ayuso C, Bruix J. BCLC strategy for prognosis prediction and treatment recommendation: The 2022 update. *J Hepatol* 2022; **76**: 681-693 [PMID: 34801630 DOI: 10.1016/j.jhep.2021.11.018]

11 **Raoul JL**, Sangro B, Forner A, Mazzaferro V, Piscaglia F, Bolondi L, Lencioni R. Evolving strategies for the management of intermediate-stage hepatocellular carcinoma: available evidence and expert opinion on the use of transarterial chemoembolization. *Cancer Treat Rev* 2011; **37**: 212-220 [PMID: 20724077 DOI: 10.1016/j.ctrv.2010.07.006]

12 **Abdelgalil AA**, Alkahtani HM, Al-Jenoobi FI. Sorafenib. *Profiles Drug Subst Excip Relat Methodol* 2019; **44**: 239-266 [PMID: 31029219 DOI: 10.1016/bs.podrm.2018.11.003]

13 **Cheng AL**, Kang YK, Chen Z, Tsao CJ, Qin S, Kim JS, Luo R, Feng J, Ye S, Yang TS, Xu J, Sun Y, Liang H, Liu J, Wang J, Tak WY, Pan H, Burock K, Zou J, Voliotis D, Guan Z. Efficacy and safety of sorafenib in patients in the Asia-Pacific region with advanced hepatocellular carcinoma: a phase III randomised, double-blind, placebo-controlled trial. *Lancet Oncol* 2009; **10**: 25-34 [PMID: 19095497 DOI: 10.1016/S1470-2045(08)70285-7]

14 **Tang W**, Chen Z, Zhang W, Cheng Y, Zhang B, Wu F, Wang Q, Wang S, Rong D, Reiter FP, De Toni EN, Wang X. The mechanisms of sorafenib resistance in hepatocellular carcinoma: theoretical basis and therapeutic aspects. *Signal Transduct Target Ther* 2020; **5**: 87 [PMID: 32532960 DOI: 10.1038/s41392-020-0187-x]

15 **U.S. Food & Drug Administration**. FDA approves lenvatinib for unresectable hepatocellular carcinoma. 2018 Ago 16 [Internet]. [cited 30 October 2022]. Available from: https://www.fda.gov/drugs/resources-information-approved-drugs/fda-approves-lenvatinib-unresectable-hepatocellular-carcinoma

16 **Al-Salama ZT**, Syed YY, Scott LJ. Lenvatinib: A Review in Hepatocellular Carcinoma. *Drugs* 2019; **79**: 665-674 [PMID: 30993651 DOI: 10.1007/s40265-019-01116-x]

17 **Vogel A**, Bathon M, Saborowski A. Advances in systemic therapy for the first-line treatment of unresectable HCC. *Expert Rev Anticancer Ther* 2021; **21**: 621-628 [PMID: 33499684 DOI: 10.1080/14737140.2021.1882855]

18 **Matsuki M**, Hoshi T, Yamamoto Y, Ikemori-Kawada M, Minoshima Y, Funahashi Y, Matsui J. Lenvatinib inhibits angiogenesis and tumor fibroblast growth factor signaling pathways in human hepatocellular carcinoma models. *Cancer*

Med 2018; **7**: 2641-2653 [PMID: 29733511 DOI: 10.1002/cam4.1517]

19 **Kudo M**, Finn RS, Qin S, Han KH, Ikeda K, Piscaglia F, Baron A, Park JW, Han G, Jassem J, Blanc JF, Vogel A, Komov D, Evans TRJ, Lopez C, Dutcus C, Guo M, Saito K, Kraljevic S, Tamai T, Ren M, Cheng AL. Lenvatinib versus sorafenib in first-line treatment of patients with unresectable hepatocellular carcinoma: a randomised phase 3 non-inferiority trial. *Lancet* 2018; **391**: 1163-1173 [PMID: 29433850 DOI: 10.1016/S0140-6736(18)30207-1]

20 **Herbst RS**, Soria JC, Kowanetz M, Fine GD, Hamid O, Gordon MS, Sosman JA, McDermott DF, Powderly JD, Gettinger SN, Kohrt HE, Horn L, Lawrence DP, Rost S, Leabman M, Xiao Y, Mokatrin A, Koeppen H, Hegde PS, Mellman I, Chen DS, Hodi FS. Predictive correlates of response to the anti-PD-L1 antibody MPDL3280A in cancer patients. *Nature* 2014; **515**: 563-567 [PMID: 25428504 DOI: 10.1038/nature14011]

21 **Ferrara N**, Hillan KJ, Novotny W. Bevacizumab (Avastin), a humanized anti-VEGF monoclonal antibody for cancer therapy. *Biochem Biophys Res Commun* 2005; **333**: 328-335 [PMID: 15961063 DOI: 10.1016/j.bbrc.2005.05.132]

22 **Finn RS**, Bentley G, Britten CD, Amado R, Busuttil RW. Targeting vascular endothelial growth factor with the monoclonal antibody bevacizumab inhibits human hepatocellular carcinoma cells growing in an orthotopic mouse model. *Liver Int* 2009; **29**: 284-290 [PMID: 18482274 DOI: 10.1111/j.1478-3231.2008.01762.x]

23 **Finn RS**, Qin S, Ikeda M, Galle PR, Ducreux M, Kim TY, Kudo M, Breder V, Merle P, Kaseb AO, Li D, Verret W, Xu DZ, Hernandez S, Liu J, Huang C, Mulla S, Wang Y, Lim HY, Zhu AX, Cheng AL; Imbrave150 Investigators. Atezolizumab plus Bevacizumab in Unresectable Hepatocellular Carcinoma. *N Engl J Med* 2020; **382**: 1894-1905 [PMID: 32402160 DOI: 10.1056/NEJMoa1915745]

24 **Cheng AL**, Qin S, Ikeda M, Galle PR, Ducreux M, Kim TY, Lim HY, Kudo M, Breder V, Merle P, Kaseb AO, Li D, Verret W, Ma N, Nicholas A, Wang Y, Li L, Zhu AX, Finn RS. Updated efficacy and safety data from Imbrave150: Atezolizumab plus bevacizumab vs. sorafenib for unresectable hepatocellular carcinoma. *J Hepatol* 2022; **76**: 862-873 [PMID: 34902530 DOI: 10.1016/j.jhep.2021.11.030]

25 **U.S. Food & Drug Administration**. FDA approves atezolizumab plus bevacizumab for unresectable hepatocellular carcinoma. 2020 Jun 01 [Internet]. [cited 30 October 2022]. Available from: https://www.fda.gov/drugs/resources-information-approved-drugs/fda-approves-atezolizumab-plus-bevacizumab-unresectable-hepatocellular-carcinoma

26 **U.S. Food & Drug Administration**. FDA approves tremelimumab in combination with durvalumab for unresectable hepatocellular carcinoma. 2022 Oct 10 [Internet]. [cited 30 October 2022]. Available from: https://www.fda.gov/drugs/resources-information-approved-drugs/fda-approves-tremelimumab-combination-durvalumab-unresectable-hepatocellular-carcinoma

27 **Tarhini AA**. Tremelimumab: a review of development to date in solid tumors. *Immunotherapy* 2013; **5**: 215-229 [PMID: 23444951 DOI: 10.2217/imt.13.9]

28 **Duffy AG**, Ulahannan SV, Makorova-Rusher O, Rahma O, Wedemeyer H, Pratt D, Davis JL, Hughes MS, Heller T, ElGindi M, Uppala A, Korangy F, Kleiner DE, Figg WD, Venzon D, Steinberg SM, Venkatesan AM, Krishnasamy V, Abi-Jaoudeh N, Levy E, Wood BJ, Greten TF. Tremelimumab in combination with ablation in patients with advanced hepatocellular carcinoma. *J Hepatol* 2017; **66**: 545-551 [PMID: 27816492 DOI: 10.1016/j.jhep.2016.10.029]

29 **Al-Salama ZT**. Durvalumab: A Review in Extensive-Stage SCLC. *Target Oncol* 2021; **16**: 857-864 [PMID: 34731446 DOI: 10.1007/s11523-021-00843-0]

30 **Antonia SJ**, Villegas A, Daniel D, Vicente D, Murakami S, Hui R, Yokoi T, Chiappori A, Lee KH, de Wit M, Cho BC, Bourhaba M, Quantin X, Tokito T, Mekhail T, Planchard D, Kim YC, Karapetis CS, Hiret S, Ostoros G, Kubota K, Gray JE, Paz-Ares L, de Castro Carpeño J, Wadsworth C, Melillo G, Jiang H, Huang Y, Dennis PA, Özgüroğlu M; PACIFIC Investigators. Durvalumab after Chemoradiotherapy in Stage III Non-Small-Cell Lung Cancer. *N Engl J Med* 2017; **377**: 1919-1929 [PMID: 28885881 DOI: 10.1056/NEJMoa1709937]

31 **Kelley RK**, Sangro B, Harris W, Ikeda M, Okusaka T, Kang YK, Qin S, Tai DW, Lim HY, Yau T, Yong WP, Cheng AL, Gasbarrini A, Damian S, Bruix J, Borad M, Bendell J, Kim TY, Standifer N, He P, Makowsky M, Negro A, Kudo M, Abou-Alfa GK. Safety, Efficacy, and Pharmacodynamics of Tremelimumab Plus Durvalumab for Patients With Unresectable Hepatocellular Carcinoma: Randomized Expansion of a Phase I/II Study. *J Clin Oncol* 2021; **39**: 2991-3001 [PMID: 34292792 DOI: 10.1200/JCO.20.03555]

32 **Abou-Alfa GK**, Lau G, Kudo M, Chan SL, Kelley RK, Furuse J, Sukeepaisarnjaroen W, Kang YK, Van Dao T, De Toni EN, Rimassa L, Breder V, Vasilyev A, Heurgué A, Tam VC, Mody K, Thungappa SC, Ostapenko Y, Yau T, Azevedo S, Varela M, Chrng AL, Qin S, Galle PR, Ali S, Marcovitz M, Makowsky M, He P, Kurland JF, Negro A, Sangro B. Tremelimumab plus Durvalumab in Unresectable Hepatocellular Carcinoma. *NEJM Evidence* 2022; 1 [DOI: 10.1056/EVIDoa2100070]

33 **Frenette C**, Blanc JF, Cheng AL, Finn R, Galle, P, Pfiffer T, Sun HC. The importance of systemic treatment sequencing in improving survival for patients with hepatocellular carcinoma. Bayer. [cited 10 September 2020]. Available from: https://www.bayer.com/sites/default/files/Bayer_HCC_Expert_Statement_1.pdf

34 **Wilhelm SM**, Dumas J, Adnane L, Lynch M, Carter CA, Schütz G, Thierauch KH, Zopf D. Regorafenib (BAY 73-4506): a new oral multikinase inhibitor of angiogenic, stromal and oncogenic receptor tyrosine kinases with potent preclinical antitumor activity. *Int J Cancer* 2011; **129**: 245-255 [PMID: 21170960 DOI: 10.1002/ijc.25864]

35 **Carr BI**, Cavallini A, Lippolis C, D'Alessandro R, Messa C, Refolo MG, Tafaro A. Fluoro-Sorafenib (Regorafenib) effects on hepatoma cells: growth inhibition, quiescence, and recovery. *J Cell Physiol* 2013; **228**: 292-297 [PMID: 22777740 DOI: 10.1002/jcp.24148]

36 **Bruix J**, Qin S, Merle P, Granito A, Huang YH, Bodoky G, Pracht M, Yokosuka O, Rosmorduc O, Breder V, Gerolami R, Masi G, Ross PJ, Song T, Bronowicki JP, Ollivier-Hourmand I, Kudo M, Cheng AL, Llovet JM, Finn RS, LeBerre MA, Baumhauer A, Meinhardt G, Han G; RESORCE Investigators. Regorafenib for patients with hepatocellular carcinoma who progressed on sorafenib treatment (RESORCE): a randomised, double-blind, placebo-controlled, phase 3 trial. *Lancet* 2017; **389**: 56-66 [PMID: 27932229 DOI: 10.1016/S0140-6736(16)32453-9]

37 **Yakes FM**, Chen J, Tan J, Yamaguchi K, Shi Y, Yu P, Qian F, Chu F, Bentzien F, Cancilla B, Orf J, You A, Laird AD, Engst S, Lee L, Lesch J, Chou YC, Joly AH. Cabozantinib (XL184), a novel MET and VEGFR2 inhibitor, simultaneously suppresses metastasis, angiogenesis, and tumor growth. *Mol Cancer Ther* 2011; **10**: 2298-2308 [PMID: 21926191 DOI:

10.1158/1535-7163.MCT-11-0264]
38 **Kelley RK**, Verslype C, Cohn AL, Yang TS, Su WC, Burris H, Braiteh F, Vogelzang N, Spira A, Foster P, Lee Y, Van Cutsem E. Cabozantinib in hepatocellular carcinoma: results of a phase 2 placebo-controlled randomized discontinuation study. *Ann Oncol* 2017; **28**: 528-534 [PMID: 28426123 DOI: 10.1093/annonc/mdw651]
39 **Abou-Alfa GK**, Meyer T, Cheng AL, El-Khoueiry AB, Rimassa L, Ryoo BY, Cicin I, Merle P, Chen Y, Park JW, Blanc JF, Bolondi L, Klümpen HJ, Chan SL, Zagonel V, Pressiani T, Ryu MH, Venook AP, Hessel C, Borgman-Hagey AE, Schwab G, Kelley RK. Cabozantinib in Patients with Advanced and Progressing Hepatocellular Carcinoma. *N Engl J Med* 2018; **379**: 54-63 [PMID: 29972759 DOI: 10.1056/NEJMoa1717002]
40 **U.S. Food & Drug Administration**. FDA approves cabozantinib for hepatocellular carcinoma. 2019 Mar 03 [Internet]. [cited 30 October 2022]. Available from: https://www.fda.gov/drugs/fda-approves-cabozantinib-hepatocellular-carcinoma
41 **Esteban-Fabró R**, Willoughby CE, Piqué-Gili M, Montironi C, Abril-Fornaguera J, Peix J, Torrens L, Mesropian A, Balaseviciute U, Miró-Mur F, Mazzaferro V, Pinyol R, Llovet JM. Cabozantinib Enhances Anti-PD1 Activity and Elicits a Neutrophil-Based Immune Response in Hepatocellular Carcinoma. *Clin Cancer Res* 2022; **28**: 2449-2460 [PMID: 35302601 DOI: 10.1158/1078-0432.CCR-21-2517]
42 **Syed YY**. Ramucirumab: A Review in Hepatocellular Carcinoma. *Drugs* 2020; **80**: 315-322 [PMID: 32034692 DOI: 10.1007/s40265-020-01263-6]
43 **Turkes F**, Chau I. Ramucirumab and its use in the treatment of hepatocellular carcinoma. *Future Oncol* 2019; **15**: 979-988 [PMID: 30644314 DOI: 10.2217/fon-2018-0822]
44 **Zhu AX**, Park JO, Ryoo BY, Yen CJ, Poon R, Pastorelli D, Blanc JF, Chung HC, Baron AD, Pfiffer TE, Okusaka T, Kubackova K, Trojan J, Sastre J, Chau I, Chang SC, Abada PB, Yang L, Schwartz JD, Kudo M; REACH Trial Investigators. Ramucirumab versus placebo as second-line treatment in patients with advanced hepatocellular carcinoma following first-line therapy with sorafenib (REACH): a randomised, double-blind, multicentre, phase 3 trial. *Lancet Oncol* 2015; **16**: 859-870 [PMID: 26095784 DOI: 10.1016/S1470-2045(15)00050-9]
45 **Zhu AX**, Kang YK, Yen CJ, Finn RS, Galle PR, Llovet JM, Assenat E, Brandi G, Pracht M, Lim HY, Rau KM, Motomura K, Ohno I, Merle P, Daniele B, Shin DB, Gerken G, Borg C, Hiriart JB, Okusaka T, Morimoto M, Hsu Y, Abada PB, Kudo M; REACH-2 study investigators. Ramucirumab after sorafenib in patients with advanced hepatocellular carcinoma and increased α-fetoprotein concentrations (REACH-2): a randomised, double-blind, placebo-controlled, phase 3 trial. *Lancet Oncol* 2019; **20**: 282-296 [PMID: 30665869 DOI: 10.1016/S1470-2045(18)30937-9]
46 **Komatsu S**, Yano Y, Kido M, Kuramitsu K, Gon H, Fukushima K, Urade T, So S, Yanagimoto H, Toyama H, Kodama Y, Fukumoto T. Lenvatinib Rechallenge After Ramucirumab Treatment Failure for Hepatocellular Carcinoma. *Anticancer Res* 2021; **41**: 4555-4562 [PMID: 34475083 DOI: 10.21873/anticanres.15268]
47 **Das S**, Johnson DB. Immune-related adverse events and anti-tumor efficacy of immune checkpoint inhibitors. *J Immunother Cancer* 2019; **7**: 306 [PMID: 31730012 DOI: 10.1186/s40425-019-0805-8]
48 **Franzin R**, Netti GS, Spadaccino F, Porta C, Gesualdo L, Stallone G, Castellano G, Ranieri E. The Use of Immune Checkpoint Inhibitors in Oncology and the Occurrence of AKI: Where Do We Stand? *Front Immunol* 2020; **11**: 574271 [PMID: 33162990 DOI: 10.3389/fimmu.2020.574271]
49 **He X**, Xu C. Immune checkpoint signaling and cancer immunotherapy. *Cell Res* 2020; **30**: 660-669 [PMID: 32467592 DOI: 10.1038/s41422-020-0343-4]
50 **Keilson JM**, Knochelmann HM, Paulos CM, Kudchadkar RR, Lowe MC. The evolving landscape of immunotherapy in solid tumors. *J Surg Oncol* 2021; **123**: 798-806 [PMID: 33595890 DOI: 10.1002/jso.26416]
51 **Onuma AE**, Zhang H, Huang H, Williams TM, Noonan A, Tsung A. Immune Checkpoint Inhibitors in Hepatocellular Cancer: Current Understanding on Mechanisms of Resistance and Biomarkers of Response to Treatment. *Gene Expr* 2020; **20**: 53-65 [PMID: 32340652 DOI: 10.3727/105221620X15880179864121]
52 **Xu F**, Jin T, Zhu Y, Dai C. Immune checkpoint therapy in liver cancer. *J Exp Clin Cancer Res* 2018; **37**: 110 [PMID: 29843754 DOI: 10.1186/s13046-018-0777-4]
53 **Lai E**, Astara G, Ziranu P, Pretta A, Migliari M, Dubois M, Donisi C, Mariani S, Liscia N, Impera V, Persano M, Tolu S, Balconi F, Pinna G, Spanu D, Pireddu A, Saba G, Camera S, Musio F, Puzzoni M, Pusceddu V, Madeddu C, Casadei Gardini A, Scartozzi M. Introducing immunotherapy for advanced hepatocellular carcinoma patients: Too early or too fast? *Crit Rev Oncol Hematol* 2021; **157**: 103167 [PMID: 33271389 DOI: 10.1016/j.critrevonc.2020.103167]
54 **Liu Z**, Liu X, Liang J, Liu Y, Hou X, Zhang M, Li Y, Jiang X. Immunotherapy for Hepatocellular Carcinoma: Current Status and Future Prospects. *Front Immunol* 2021; **12**: 765101 [PMID: 34675942 DOI: 10.3389/fimmu.2021.765101]
55 **Finkelmeier F**, Waidmann O, Trojan J. Nivolumab for the treatment of hepatocellular carcinoma. *Expert Rev Anticancer Ther* 2018; **18**: 1169-1175 [PMID: 30304963 DOI: 10.1080/14737140.2018.1535315]
56 **Ansell SM**, Lesokhin AM, Borrello I, Halwani A, Scott EC, Gutierrez M, Schuster SJ, Millenson MM, Cattry D, Freeman GJ, Rodig SJ, Chapuy B, Ligon AH, Zhu L, Grosso JF, Kim SY, Timmerman JM, Shipp MA, Armand P. PD-1 blockade with nivolumab in relapsed or refractory Hodgkin's lymphoma. *N Engl J Med* 2015; **372**: 311-319 [PMID: 25482239 DOI: 10.1056/NEJMoa1411087]
57 **Borghaei H**, Paz-Ares L, Horn L, Spigel DR, Steins M, Ready NE, Chow LQ, Vokes EE, Felip E, Holgado E, Barlesi F, Kohlhäufl M, Arrieta O, Burgio MA, Fayette J, Lena H, Poddubskaya E, Gerber DE, Gettinger SN, Rudin CM, Rizvi N, Crinó L, Blumenschein GR, Antonia SJ, Dorange C, Harbison CT, Finckenstein FG, Brahmer JR. Nivolumab vs Docetaxel in Advanced Nonsquamous Non–Small-Cell Lung Cancer. *N Engl J Med* 2015; **373**: 1627-1639 [PMID: 26412456 DOI: 10.1056/NEJMoa1507643]
58 **Kang YK**, Boku N, Satoh T, Ryu MH, Chao Y, Kato K, Chung HC, Chen JS, Muro K, Kang WK, Yeh KH, Yoshikawa T, Oh SC, Bai LY, Tamura T, Lee KW, Hamamoto Y, Kim JG, Chin K, Oh DY, Minashi K, Cho JY, Tsuda M, Chen LT. Nivolumab in patients with advanced gastric or gastro-oesophageal junction cancer refractory to, or intolerant of, at least two previous chemotherapy regimens (ONO-4538-12, ATTRACTION-2): a randomised, double-blind, placebo-controlled, phase 3 trial. *Lancet* 2017; **390**: 2461-2471 [PMID: 28993052 DOI: 10.1016/S0140-6736(17)31827-5]
59 **Motzer RJ**, Escudier B, McDermott DF, George S, Hammers HJ, Srinivas S, Tykodi SS, Sosman JA, Procopio G, Plimack ER, Castellano D, Choueiri TK, Gurney H, Donskov F, Bono P, Wagstaff J, Gauler TC, Ueda T, Tomita Y,

Schutz FA, Kollmannsberger C, Larkin J, Ravaud A, Simon JS, Xu LA, Waxman IM, Sharma P; CheckMate 025 Investigators. Nivolumab versus Everolimus in Advanced Renal-Cell Carcinoma. *N Engl J Med* 2015; **373**: 1803-1813 [PMID: 26406148 DOI: 10.1056/NEJMoa1510665]

60 **Weber JS**, D'Angelo SP, Minor D, Hodi FS, Gutzmer R, Neyns B, Hoeller C, Khushalani NI, Miller WH Jr, Lao CD, Linette GP, Thomas L, Lorigan P, Grossmann KF, Hassel JC, Maio M, Sznol M, Ascierto PA, Mohr P, Chmielowski B, Bryce A, Svane IM, Grob JJ, Krackhardt AM, Horak C, Lambert A, Yang AS, Larkin J. Nivolumab versus chemotherapy in patients with advanced melanoma who progressed after anti-CTLA-4 treatment (CheckMate 037): a randomised, controlled, open-label, phase 3 trial. *Lancet Oncol* 2015; **16**: 375-384 [PMID: 25795410 DOI: 10.1016/S1470-2045(15)70076-8]

61 **Kudo M**, Matilla A, Santoro A, Melero I, Gracián AC, Acosta-Rivera M, Choo SP, El-Khoueiry AB, Kuromatsu R, El-Rayes B, Numata K, Itoh Y, Di Costanzo F, Crysler O, Reig M, Shen Y, Neely J, Tschaika M, Wisniewski T, Sangro B. CheckMate 040 cohort 5: A phase I/II study of nivolumab in patients with advanced hepatocellular carcinoma and Child-Pugh B cirrhosis. *J Hepatol* 2021; **75**: 600-609 [PMID: 34051329 DOI: 10.1016/j.jhep.2021.04.047]

62 **Yau T**, Park JW, Finn RS, Cheng AL, Mathurin P, Edeline J, Kudo M, Harding JJ, Merle P, Rosmorduc O, Wyrwicz L, Schott E, Choo SP, Kelley RK, Sieghart W, Assenat E, Zaucha R, Furuse J, Abou-Alfa GK, El-Khoueiry AB, Melero I, Begic D, Chen G, Neely J, Wisniewski T, Tschaika M, Sangro B. Nivolumab versus sorafenib in advanced hepatocellular carcinoma (CheckMate 459): a randomised, multicentre, open-label, phase 3 trial. *Lancet Oncol* 2022; **23**: 77-90 [PMID: 34914889 DOI: 10.1016/S1470-2045(21)00604-5]

63 **U.S. Food & Drug Administration**. FDA grants accelerated approval to nivolumab for HCC previously treated with sorafenib. 2017 Sep 25 [Internet]. [cited 30 October 2022]. Available from: https://www.fda.gov/drugs/resources-information-approved-drugs/fda-grants-accelerated-approval-nivolumab-hcc-previously-treated-sorafenib

64 **Tsang J**, Wong JSL, Kwok GGW, Li BCW, Leung R, Chiu J, Cheung TT, Yau T. Nivolumab + Ipilimumab for patients with hepatocellular carcinoma previously treated with Sorafenib. *Expert Rev Gastroenterol Hepatol* 2021; **15**: 589-598 [PMID: 33666530 DOI: 10.1080/17474124.2021.1899808]

65 **Yau T**, Kang YK, Kim TY, El-Khoueiry AB, Santoro A, Sangro B, Melero I, Kudo M, Hou MM, Matilla A, Tovoli F, Knox JJ, Ruth He A, El-Rayes BF, Acosta-Rivera M, Lim HY, Neely J, Shen Y, Wisniewski T, Anderson J, Hsu C. Efficacy and Safety of Nivolumab Plus Ipilimumab in Patients With Advanced Hepatocellular Carcinoma Previously Treated With Sorafenib: The CheckMate 040 Randomized Clinical Trial. *JAMA Oncol* 2020; **6**: e204564 [PMID: 33001135 DOI: 10.1001/jamaoncol.2020.4564]

66 **U.S. Food & Drug Administration**. FDA grants accelerated approval to nivolumab and ipilimumab combination for hepatocellular carcinoma. 2020 Mar 03 [Internet]. [cited 31 October 2022]. Available from: https://www.fda.gov/drugs/resources-information-approved-drugs/fda-grants-accelerated-approval-nivolumab-and-ipilimumab-combination-hepatocellular-carcinoma

67 **Zhu AX**, Finn RS, Edeline J, Cattan S, Ogasawara S, Palmer D, Verslype C, Zagonel V, Fartoux L, Vogel A, Sarker D, Verset G, Chan SL, Knox J, Daniele B, Webber AL, Ebbinghaus SW, Ma J, Siegel AB, Cheng AL, Kudo M; KEYNOTE-224 investigators. Pembrolizumab in patients with advanced hepatocellular carcinoma previously treated with sorafenib (KEYNOTE-224): a non-randomised, open-label phase 2 trial. *Lancet Oncol* 2018; **19**: 940-952 [PMID: 29875066 DOI: 10.1016/S1470-2045(18)30351-6]

68 **U.S. Food & Drug Administration**. FDA grants accelerated approval to pembrolizumab for hepatocellular carcinoma. 2018 Dic 14 [Internet]. [cited 31 October 2022]. Available from: https://www.fda.gov/drugs/fda-grants-accelerated-approval-pembrolizumab-hepatocellular-carcinoma

69 **Finn RS**, Ryoo BY, Merle P, Kudo M, Bouattour M, Lim HY, Breder V, Edeline J, Chao Y, Ogasawara S, Yau T, Garrido M, Chan SL, Knox J, Daniele B, Ebbinghaus SW, Chen E, Siegel AB, Zhu AX, Cheng AL; KEYNOTE-240 investigators. Pembrolizumab As Second-Line Therapy in Patients With Advanced Hepatocellular Carcinoma in KEYNOTE-240: A Randomized, Double-Blind, Phase III Trial. *J Clin Oncol* 2020; **38**: 193-202 [PMID: 31790344 DOI: 10.1200/JCO.19.01307]

70 **Qin S**, Chen Z, Fang W, Ren Z, Xu R, Ryoo BY, Meng Z, Bai Y, Chen X, Liu X, Xiao J, Ho GF, Mao Y, Ye X, Ying J, Li J, Zhong WY, Zhou Y, Siegel AB, Hao C. Pembrolizumab plus best supportive care vs placebo plus best supportive care as second-line therapy in patients in Asia with advanced hepatocellular carcinoma (HCC): Phase 3 KEYNOTE-394 study. *J Clin Oncol* 2022; **40** Suppl 4: 383-383 [DOI: 10.1200/JCO.2022.40.4_suppl.383]

71 **Bayat Mokhtari R**, Homayouni TS, Baluch N, Morgatskaya E, Kumar S, Das B, Yeger H. Combination therapy in combating cancer. *Oncotarget* 2017; **8**: 38022-38043 [PMID: 28410237 DOI: 10.18632/oncotarget.16723]

72 **Kim GP**, Mahoney MR, Szydlo D, Mok TS, Marshke R, Holen K, Picus J, Boyer M, Pitot HC, Rubin J, Philip PA, Nowak A, Wright JJ, Erlichman C. An international, multicenter phase II trial of bortezomib in patients with hepatocellular carcinoma. *Invest New Drugs* 2012; **30**: 387-394 [PMID: 20839030 DOI: 10.1007/s10637-010-9532-1]

73 **He B**, Lu C, Zheng G, He X, Wang M, Chen G, Zhang G, Lu A. Combination therapeutics in complex diseases. *J Cell Mol Med* 2016; **20**: 2231-2240 [PMID: 27605177 DOI: 10.1111/jcmm.12930]

74 **Pemovska T**, Bigenzahn JW, Superti-Furga G. Recent advances in combinatorial drug screening and synergy scoring. *Curr Opin Pharmacol* 2018; **42**: 102-110 [PMID: 30193150 DOI: 10.1016/j.coph.2018.07.008]

75 **Lim JJ**, Hooi L, Dan YY, Bonney GK, Zhou L, Chow PK, Chee CE, Toh TB, Chow EK. Rational drug combination design in patient-derived avatars reveals effective inhibition of hepatocellular carcinoma with proteasome and CDK inhibitors. *J Exp Clin Cancer Res* 2022; **41**: 249 [PMID: 35971164 DOI: 10.1186/s13046-022-02436-9]

76 **Xu F**, Tong M, Tong CSW, Chan BKC, Chu HY, Wong TL, Fong JHC, Cheung MSH, Mak KH, Pardeshi L, Huang Y, Wong KH, Choi GCG, Ma S, Wong ASL. A Combinatorial CRISPR-Cas9 Screen Identifies Ifenprodil as an Adjunct to Sorafenib for Liver Cancer Treatment. *Cancer Res* 2021; **81**: 6219-6232 [PMID: 34666996 DOI: 10.1158/0008-5472.CAN-21-1017]

77 **Canzoneri R**, Lacunza E, Abba MC. Genomics and bioinformatics as pillars of precision medicine in oncology. *Medicina (B Aires)* 2019; **79**: 587-592 [PMID: 31864231]

78 **Suwinski P**, Ong C, Ling MHT, Poh YM, Khan AM, Ong HS. Advancing Personalized Medicine Through the Application

of Whole Exome Sequencing and Big Data Analytics. *Front Genet* 2019; **10**: 49 [PMID: 30809243 DOI: 10.3389/fgene.2019.00049]

79 **Wouters OJ**, McKee M, Luyten J. Estimated Research and Development Investment Needed to Bring a New Medicine to Market, 2009-2018. *JAMA* 2020; **323**: 844-853 [PMID: 32125404 DOI: 10.1001/jama.2020.1166]

80 **Corsello SM**, Nagari RT, Spangler RD, Rossen J, Kocak M, Bryan JG, Humeidi R, Peck D, Wu X, Tang AA, Wang VM, Bender SA, Lemire E, Narayan R, Montgomery P, Ben-David U, Garvie CW, Chen Y, Rees MG, Lyons NJ, McFarland JM, Wong BT, Wang L, Dumont N, O'Hearn PJ, Stefan E, Doench JG, Harrington CN, Greulich H, Meyerson M, Vazquez F, Subramanian A, Roth JA, Bittker JA, Boehm JS, Mader CC, Tsherniak A, Golub TR. Discovering the anti-cancer potential of non-oncology drugs by systematic viability profiling. *Nat Cancer* 2020; **1**: 235-248 [PMID: 32613204 DOI: 10.1038/s43018-019-0018-6]

81 **Shah RR**, Stonier PD. Repurposing old drugs in oncology: Opportunities with clinical and regulatory challenges ahead. *J Clin Pharm Ther* 2019; **44**: 6-22 [PMID: 30218625 DOI: 10.1111/jcpt.12759]

82 **Nair G**, Saraswathy GR, Hema Sree GNS. 48P Target mining and drug repurposing for hepatocellular carcinoma *via* bioinformatic and computational approaches. *Ann Oncol* 2021; **32**: S19 [DOI: 10.1016/j.annonc.2021.01.063]

83 **Nair G**, Hema Sree GNS, Saraswathy GR, Marise VLP, Krishna Murthy TP. Application of comprehensive bioinformatics approaches to reconnoiter crucial genes and pathways underpinning hepatocellular carcinoma: a drug repurposing endeavor. *Med Oncol* 2021; **38**: 145 [PMID: 34687371 DOI: 10.1007/s12032-021-01576-w]

84 **Massari NA**, Nicoud MB, Medina VA. Histamine receptors and cancer pharmacology: an update. *Br J Pharmacol* 2020; **177**: 516-538 [PMID: 30414378 DOI: 10.1111/bph.14535]

85 **Nguyen PL**, Cho J. Pathophysiological Roles of Histamine Receptors in Cancer Progression: Implications and Perspectives as Potential Molecular Targets. *Biomolecules* 2021; **11** [PMID: 34439898 DOI: 10.3390/biom11081232]

86 **Zhao J**, Hou Y, Yin C, Hu J, Gao T, Huang X, Zhang X, Xing J, An J, Wan S, Li J. Upregulation of histamine receptor H1 promotes tumor progression and contributes to poor prognosis in hepatocellular carcinoma. *Oncogene* 2020; **39**: 1724-1738 [PMID: 31740780 DOI: 10.1038/s41388-019-1093-y]

87 **Shen YC**, Hsu HC, Lin TM, Chang YS, Hu LF, Chen LF, Lin SH, Kuo PI, Chen WS, Lin YC, Chen JH, Liang YC, Chang CC. H1-Antihistamines Reduce the Risk of Hepatocellular Carcinoma in Patients With Hepatitis B Virus, Hepatitis C Virus, or Dual Hepatitis B Virus-Hepatitis C Virus Infection. *J Clin Oncol* 2022; **40**: 1206-1219 [PMID: 35044851 DOI: 10.1200/JCO.21.01802]

88 **Ellegaard AM**, Dehlendorff C, Vind AC, Anand A, Cederkvist L, Petersen NHT, Nylandsted J, Stenvang J, Mellemgaard A, Østerlind K, Friis S, Jäättelä M. Repurposing Cationic Amphiphilic Antihistamines for Cancer Treatment. *EbioMedicine* 2016; **9**: 130-139 [PMID: 27333030 DOI: 10.1016/j.ebiom.2016.06.013]

89 **Ortiz CS**, Montante-Montes D, Saqui-Salces M, Hinojosa LM, Gamboa-Dominguez A, Hernández-Gallegos E, Martínez-Benítez B, Del Rosario Solís-Pancoatl M, Garcia-Villa E, Ramírez A, Aguilar-Guadarrama R, Gariglio P, Pardo LA, Stühmer W, Camacho J. Eag1 potassium channels as markers of cervical dysplasia. *Oncol Rep* 2011; **26**: 1377-1383 [PMID: 21887469 DOI: 10.3892/or.2011.1441]

90 **Chen J**, Xuan Z, Song W, Han W, Chen H, Du Y, Xie H, Zhao Y, Zheng S, Song P. EAG1 enhances hepatocellular carcinoma proliferation by modulating SKP2 and metastasis through pseudopod formation. *Oncogene* 2021; **40**: 163-176 [PMID: 33097858 DOI: 10.1038/s41388-020-01522-6]

91 **García-Quiroz J**, Camacho J. Astemizole: an old anti-histamine as a new promising anti-cancer drug. *Anticancer Agents Med Chem* 2011; **11**: 307-314 [PMID: 21443504 DOI: 10.2174/187152011795347513]

92 **Hemmerlein B**, Weseloh RM, Mello de Queiroz F, Knötgen H, Sánchez A, Rubio ME, Martin S, Schliephacke T, Jenke M, Heinz-Joachim-Radzun, Stühmer W, Pardo LA. Overexpression of Eag1 potassium channels in clinical tumours. *Mol Cancer* 2006; **5**: 41 [PMID: 17022810 DOI: 10.1186/1476-4598-5-41]

93 **Toplak Ž**, Hendrickx LA, Abdelaziz R, Shi X, Peigneur S, Tomašič T, Tytgat J, Peterlin-Mašič L, Pardo LA. Overcoming challenges of HERG potassium channel liability through rational design: Eag1 inhibitors for cancer treatment. *Med Res Rev* 2022; **42**: 183-226 [PMID: 33945158 DOI: 10.1002/med.21808]

94 **Rodríguez-Rasgado JA**, Acuña-Macías I, Camacho J. Eag1 channels as potential cancer biomarkers. *Sensors (Basel)* 2012; **12**: 5986-5995 [PMID: 22778627 DOI: 10.3390/s120505986]

95 **Asher V**, Sowter H, Shaw R, Bali A, Khan R. Eag and HERG potassium channels as novel therapeutic targets in cancer. *World J Surg Oncol* 2010; **8**: 113 [PMID: 21190577 DOI: 10.1186/1477-7819-8-113]

96 **Smith GA**, Tsui HW, Newell EW, Jiang X, Zhu XP, Tsui FW, Schlichter LC. Functional up-regulation of HERG K+ channels in neoplastic hematopoietic cells. *J Biol Chem* 2002; **277**: 18528-18534 [PMID: 11893742 DOI: 10.1074/jbc.M200592200]

97 **Shao XD**, Wu KC, Hao ZM, Hong L, Zhang J, Fan DM. The potent inhibitory effects of cisapride, a specific blocker for human ether-a-go-go-related gene (HERG) channel, on gastric cancer cells. *Cancer Biol Ther* 2005; **4**: 295-301 [PMID: 15846098 DOI: 10.4161/cbt.4.3.1500]

98 **de Guadalupe Chávez-López M**, Pérez-Carreón JI, Zuñiga-García V, Díaz-Chávez J, Herrera LA, Caro-Sánchez CH, Acuña-Macías I, Gariglio P, Hernández-Gallegos E, Chiliquinga AJ, Camacho J. Astemizole-based anticancer therapy for hepatocellular carcinoma (HCC), and Eag1 channels as potential early-stage markers of HCC. *Tumour Biol* 2015; **36**: 6149-6158 [PMID: 25783527 DOI: 10.1007/s13277-015-3299-0]

99 **Gui L**, Xu Q, Huang J, Wu G, Tang H, Hui L, Hua P, Zhang L, Zhu Y. CYP2J2 promotes the development of hepatocellular carcinoma by increasing the EETs production to improve HIF-1α stability. *Am J Transl Res* 2020; **12**: 7923-7937 [PMID: 33437370]

100 **Hwang GH**, Park SM, Han HJ, Baek KM, Kim JS, Chang W, Lee HJ, Yun SP, Ryu JM, Lee MY. Role of cytochrome P450 2J2 on cell proliferation and resistance to an anticancer agent in hepatocellular carcinoma HepG2 cells. *Oncol Lett* 2017; **14**: 5484-5490 [PMID: 29098037 DOI: 10.3892/ol.2017.6846]

101 **Jeon YJ**, Kim JS, Hwang GH, Wu Z, Han HJ, Park SH, Chang W, Kim LK, Lee YM, Liu KH, Lee MY. Inhibition of cytochrome P450 2J2 by tanshinone IIA induces apoptotic cell death in hepatocellular carcinoma HepG2 cells. *Eur J Pharmacol* 2015; **764**: 480-488 [PMID: 26209360 DOI: 10.1016/j.ejphar.2015.07.047]

102 **Lee CA**, Jones JP 3rd, Katayama J, Kaspera R, Jiang Y, Freiwald S, Smith E, Walker GS, Totah RA. Identifying a selective substrate and inhibitor pair for the evaluation of CYP2J2 activity. *Drug Metab Dispos* 2012; **40**: 943-951 [PMID: 22328583 DOI: 10.1124/dmd.111.043505]

103 **Van den Eynde C**, Held K, Ciprietti M, De Clercq K, Kerselaers S, Marchand A, Chaltin P, Voets T, Vriens J. Loratadine, an antihistaminic drug, suppresses the proliferation of endometrial stromal cells by inhibition of TRPV2. *Eur J Pharmacol* 2022; **928**: 175086 [PMID: 35714693 DOI: 10.1016/j.ejphar.2022.175086]

104 **Sidhu G**, Akhondi H. Loratadine. In StatPearls. StatPearls Publishing 2022. [cited 31 October 2022]. Available from: http://www.ncbi.nlm.nih.gov/books/NBK542278/

105 **Fritz I**, Wagner P, Broberg P, Einefors R, Olsson H. Desloratadine and loratadine stand out among common H(1)-antihistamines for association with improved breast cancer survival. *Acta Oncol* 2020; **59**: 1103-1109 [PMID: 32459128 DOI: 10.1080/0284186X.2020.1769185]

106 **Fritz I**, Wagner P, Olsson H. Improved survival in several cancers with use of H(1)-antihistamines desloratadine and loratadine. *Transl Oncol* 2021; **14**: 101029 [PMID: 33550204 DOI: 10.1016/j.tranon.2021.101029]

107 **Kallunki T**, Olsen OD, Jäättelä M. Cancer-associated lysosomal changes: friends or foes? *Oncogene* 2013; **32**: 1995-2004 [PMID: 22777359 DOI: 10.1038/onc.2012.292]

108 **Adly N**. Evaluation of cytotoxic potential of loratadine and the combination of loratadine and cisplatin on hepatocellular carcinoma cell lines [American University in Cairo (AUC)] 2018. [cited 31 October 2022]. Available from: https://fount.aucegypt.edu/etds/418

109 **Hunto ST**, Kim HG, Baek KS, Jeong D, Kim E, Kim JH, Cho JY. Loratadine, an antihistamine drug, exhibits anti-inflammatory activity through suppression of the NF-(k)B pathway. *Biochem Pharmacol* 2020; **177**: 113949 [PMID: 32251678 DOI: 10.1016/j.bcp.2020.113949]

110 **de Vries TW**, Tobi H, Schirm E, van den Berg P, Duiverman EJ, de Jong-van den Berg LT. The gap between evidence-based medicine and daily practice in the management of paediatric asthma. A pharmacy-based population study from The Netherlands. *Eur J Clin Pharmacol* 2006; **62**: 51-55 [PMID: 16365748 DOI: 10.1007/s00228-005-0065-z]

111 **Liang YC**, Chang CC, Sheu MT, Lin SY, Chung CC, Teng CT, Suk FM. The Antihistamine Deptropine Induces Hepatoma Cell Death through Blocking Autophagosome-Lysosome Fusion. *Cancers (Basel)* 2020; **12** [PMID: 32570749 DOI: 10.3390/cancers12061610]

112 **Feng YM**, Feng CW, Chen SY, Hsieh HY, Chen YH, Hsu CD. Cyproheptadine, an antihistaminic drug, inhibits proliferation of hepatocellular carcinoma cells by blocking cell cycle progression through the activation of P38 MAP kinase. *BMC Cancer* 2015; **15**: 134 [PMID: 25886177 DOI: 10.1186/s12885-015-1137-9]

113 **Hsieh MC**, Lee WH, Wu AT, Chow JM, Chang CL, Yuan KS, Wu SY. Cyproheptadine use in hepatocellular carcinoma. *Am J Cancer Res* 2017; **7**: 584-602 [PMID: 28401014]

114 **Feng YM**, Chen TH, Berman D, Chou CK, Liao KS, Hsieh MC, Chen CY. Efficacy of Cyproheptadine Monotherapy in Hepatocellular Carcinoma With Bone Metastasis: A Case Report. *Front Oncol* 2021; **11**: 620212 [PMID: 34745929 DOI: 10.3389/fonc.2021.620212]

115 **Feng YM**, Feng CW, Chen SC, Hsu CD. Unexpected remission of hepatocellular carcinoma (HCC) with lung metastasis to the combination therapy of thalidomide and cyproheptadine: report of two cases and a preliminary HCC cell line study. *BMJ Case Rep* 2012; **2012** [PMID: 23076705 DOI: 10.1136/bcr-2012-007180]

116 **Feng YM**, Feng CW, Lu CL, Lee MY, Chen CY, Chen SC. Cyproheptadine significantly improves the overall and progression-free survival of sorafenib-treated advanced HCC patients. *Jpn J Clin Oncol* 2015; **45**: 336-342 [PMID: 25646358 DOI: 10.1093/jjco/hyv007]

117 **Shi Z**, Fultz RS, Engevik MA, Gao C, Hall A, Major A, Mori-Akiyama Y, Versalovic J. Distinct roles of histamine H1- and H2-receptor signaling pathways in inflammation-associated colonic tumorigenesis. *Am J Physiol Gastrointest Liver Physiol* 2019; **316**: G205-G216 [PMID: 30462522 DOI: 10.1152/ajpgi.00212.2018]

118 **Merétey K**, Falus A, Taga T, Kishimoto T. Histamine influences the expression of the interleukin-6 receptor on human lymphoid, monocytoid and hepatoma cell lines. *Agents Actions* 1991; **33**: 189-191 [PMID: 1680274 DOI: 10.1007/BF01993163]

119 **Lampiasi N**, Azzolina A, Montalto G, Cervello M. Histamine and spontaneously released mast cell granules affect the cell growth of human hepatocellular carcinoma cells. *Exp Mol Med* 2007; **39**: 284-294 [PMID: 17603279 DOI: 10.1038/emm.2007.32]

120 **Fujikawa T**, Shiraha H, Nakanishi Y, Takaoka N, Ueda N, Suzuki M, Shiratori Y. Cimetidine inhibits epidermal growth factor-induced cell signaling. *J Gastroenterol Hepatol* 2007; **22**: 436-443 [PMID: 17295779 DOI: 10.1111/j.1440-1746.2006.04541.x]

121 **Furuta K**, Sato S, Miyake T, Okamoto E, Ishine J, Ishihara S, Amano Y, Adachi K, Kinoshita Y. Anti-tumor effects of cimetidine on hepatocellular carcinomas in diethylnitrosamine-treated rats. *Oncol Rep* 2008; **19**: 361-368 [PMID: 18202782]

122 **Crouchet E**, Bandiera S, Fujiwara N, Li S, El Saghire H, Fernández-Vaquero M, Riedl T, Sun X, Hirschfield H, Jühling F, Zhu S, Roehlen N, Ponsolles C, Heydmann L, Saviano A, Qian T, Venkatesh A, Lupberger J, Verrier ER, Sojoodi M, Oudot MA, Duong FHT, Masia R, Wei L, Thumann C, Durand SC, González-Motos V, Heide D, Hetzer J, Nakagawa S, Ono A, Song WM, Higashi T, Sanchez R, Kim RS, Bian CB, Kiani K, Croonenborghs T, Subramanian A, Chung RT, Straub BK, Schuppan D, Ankavay M, Cocquerel L, Schaeffer E, Goossens N, Koh AP, Mahajan M, Nair VD, Gunasekaran G, Schwartz ME, Bardeesy N, Shalek AK, Rozenblatt-Rosen O, Regev A, Felli E, Pessaux P, Tanabe KK, Heikenwälder M, Schuster C, Pochet N, Zeisel MB, Fuchs BC, Hoshida Y, Baumert TF. A human liver cell-based system modeling a clinical prognostic liver signature for therapeutic discovery. *Nat Commun* 2021; **12**: 5525 [PMID: 34535664 DOI: 10.1038/s41467-021-25468-9]

123 **Tanaka T**, Kochi T, Shirakami Y, Mori T, Kurata A, Watanabe N, Moriwaki H, Shimizu M. Cimetidine and Clobenpropit Attenuate Inflammation-Associated Colorectal Carcinogenesis in Male ICR Mice. *Cancers (Basel)* 2016; **8** [PMID: 26907350 DOI: 10.3390/cancers8020025]

124 **Cricco GP**, Mohamad NA, Sambuco LA, Genre F, Croci M, Gutiérrez AS, Medina VA, Bergoc RM, Rivera ES, Martín

GA. Histamine regulates pancreatic carcinoma cell growth through H3 and H4 receptors. *Inflamm Res* 2008; **57** Suppl 1: S23-S24 [PMID: 18345506 DOI: 10.1007/s00011-007-0611-5]

125 **Yu D**, Zhao J, Wang Y, Hu J, Zhao Q, Li J, Zhu J. Upregulated histamine receptor H3 promotes tumor growth and metastasis in hepatocellular carcinoma. *Oncol Rep* 2019; **41**: 3347-3354 [PMID: 31002350 DOI: 10.3892/or.2019.7119]

126 **Zhang C**, Yu Y, Ma L, Fu P. Histamine H3 Receptor Promotes Cell Survival *via* Regulating PKA/CREB/CDKN1A Signal Pathway in Hepatocellular Carcinoma. *Onco Targets Ther* 2020; **13**: 3765-3776 [PMID: 32440145 DOI: 10.2147/OTT.S250655]

127 **Nicoud MB**, Formoso K, Medina VA. Pathophysiological Role of Histamine H4 Receptor in Cancer: Therapeutic Implications. *Front Pharmacol* 2019; **10**: 556 [PMID: 31231212 DOI: 10.3389/fphar.2019.00556]

128 **Shi L**, Feng Y, Lin H, Ma R, Cai X. Role of estrogen in hepatocellular carcinoma: is inflammation the key? *J Transl Med* 2014; **12**: 93 [PMID: 24708807 DOI: 10.1186/1479-5876-12-93]

129 **Villa E**. Role of estrogen in liver cancer. *Womens Health (Lond)* 2008; **4**: 41-50 [PMID: 19072450 DOI: 10.2217/17455057.4.1.41]

130 **Wei Q**, Guo P, Mu K, Zhang Y, Zhao W, Huai W, Qiu Y, Li T, Ma X, Liu Y, Chen X, Han L. Estrogen suppresses hepatocellular carcinoma cells through Erβ-mediated upregulation of the NLRP3 inflammasome. *Lab Invest* 2015; **95**: 804-816 [PMID: 26006022 DOI: 10.1038/labinvest.2015.63]

131 **Brady CW**. Liver disease in menopause. *World J Gastroenterol* 2015; **21**: 7613-7620 [PMID: 26167064 DOI: 10.3748/wjg.v21.i25.7613]

132 **Shimizu I**. Impact of oestrogens on the progression of liver disease. *Liver Int* 2003; **23**: 63-69 [PMID: 12640729 DOI: 10.1034/j.1600-0676.2003.00811.x]

133 **Sukocheva OA**. Estrogen, estrogen receptors, and hepatocellular carcinoma: Are we there yet? *World J Gastroenterol* 2018; **24**: 1-4 [PMID: 29358876 DOI: 10.3748/wjg.v24.i1.1]

134 **Villa E**, Colantoni A, Cammà C, Grottola A, Buttafoco P, Gelmini R, Ferretti I, Manenti F. Estrogen receptor classification for hepatocellular carcinoma: comparison with clinical staging systems. *J Clin Oncol* 2003; **21**: 441-446 [PMID: 12560432 DOI: 10.1200/JCO.2003.11.051]

135 **Matsushima-Nishiwaki R**, Yamada N, Hattori Y, Hosokawa Y, Tachi J, Hori T, Kozawa O. SERMs (selective estrogen receptor modulator), acting as estrogen receptor β agonists in hepatocellular carcinoma cells, inhibit the transforming growth factor-α-induced migration *via* specific inhibition of AKT signaling pathway. *PloS One* 2022; **17**: e0262485 [PMID: 35007301 DOI: 10.1371/journal.pone.0262485]

136 **Pinkerton JV**. Selective Estrogen Receptor Modulators in Gynecology Practice. *Clin Obstet Gynecol* 2021; **64**: 803-812 [PMID: 34310353 DOI: 10.1097/GRF.0000000000000647]

137 **Wang Y**, Ma H, Zhao C, Liu T, Yan D, Jou D, Li H, Zhang C, Lü J, Li C, Lin J, Li S, Lin L. Growth-suppressive activity of raloxifene on liver cancer cells by targeting IL-6/GP130 signaling. *Oncotarget* 2017; **8**: 33683-33693 [PMID: 28430601 DOI: 10.18632/oncotarget.16898]

138 **Hsia CY**, Huo TI, Chiang SY, Lu MF, Sun CL, Wu JC, Lee PC, Chi CW, Lui WY, Lee SD. Evaluation of interleukin-6, interleukin-10 and human hepatocyte growth factor as tumor markers for hepatocellular carcinoma. *Eur J Surg Oncol* 2007; **33**: 208-212 [PMID: 17140760 DOI: 10.1016/j.ejso.2006.10.036]

139 **Nakagawa H**, Maeda S, Yoshida H, Tateishi R, Masuzaki R, Ohki T, Hayakawa Y, Kinoshita H, Yamakado M, Kato N, Shiina S, Omata M. Serum IL-6 levels and the risk for hepatocarcinogenesis in chronic hepatitis C patients: an analysis based on gender differences. *Int J Cancer* 2009; **125**: 2264-2269 [PMID: 19585572 DOI: 10.1002/ijc.24720]

140 **Xu J**, Lin H, Wu G, Zhu M, Li M. IL-6/STAT3 Is a Promising Therapeutic Target for Hepatocellular Carcinoma. *Front Oncol* 2021; **11**: 760971 [PMID: 34976809 DOI: 10.3389/fonc.2021.760971]

141 **Naugler WE**, Sakurai T, Kim S, Maeda S, Kim K, Elsharkawy AM, Karin M. Gender disparity in liver cancer due to sex differences in MyD88-dependent IL-6 production. *Science* 2007; **317**: 121-124 [PMID: 17615358 DOI: 10.1126/science.1140485]

142 **Svinka J**, Mikulits W, Eferl R. STAT3 in hepatocellular carcinoma: new perspectives. *Hepat Oncol* 2014; **1**: 107-120 [PMID: 30190945 DOI: 10.2217/hep.13.7]

143 **Mutschler J**, Grosshans M, Soyka M, Rösner S. Current Findings and Mechanisms of Action of Disulfiram in the Treatment of Alcohol Dependence. *Pharmacopsychiatry* 2016; **49**: 137-141 [PMID: 26987743 DOI: 10.1055/s-0042-103592]

144 **Zha J**, Chen F, Dong H, Shi P, Yao Y, Zhang Y, Li R, Wang S, Li P, Wang W, Xu B. Disulfiram targeting lymphoid malignant cell lines *via* ROS-JNK activation as well as Nrf2 and NF-kB pathway inhibition. *J Transl Med* 2014; **12**: 163 [PMID: 24915933 DOI: 10.1186/1479-5876-12-163]

145 **Liu P**, Kumar IS, Brown S, Kannappan V, Tawari PE, Tang JZ, Jiang W, Armesilla AL, Darling JL, Wang W. Disulfiram targets cancer stem-like cells and reverses resistance and cross-resistance in acquired paclitaxel-resistant triple-negative breast cancer cells. *Br J Cancer* 2013; **109**: 1876-1885 [PMID: 24008666 DOI: 10.1038/bjc.2013.534]

146 **Wang Y**, Li W, Patel SS, Cong J, Zhang N, Sabbatino F, Liu X, Qi Y, Huang P, Lee H, Taghian A, Li JJ, DeLeo AB, Ferrone S, Epperly MW, Ferrone CR, Ly A, Brachtel EF, Wang X. Blocking the formation of radiation-induced breast cancer stem cells. *Oncotarget* 2014; **5**: 3743-3755 [PMID: 25003837 DOI: 10.18632/oncotarget.1992]

147 **Cong J**, Wang Y, Zhang X, Zhang N, Liu L, Soukup K, Michelakos T, Hong T, DeLeo A, Cai L, Sabbatino F, Ferrone S, Lee H, Levina V, Fuchs B, Tanabe K, Lillemoe K, Ferrone C, Wang X. A novel chemoradiation targeting stem and nonstem pancreatic cancer cells by repurposing disulfiram. *Cancer Lett* 2017; **409**: 9-19 [PMID: 28864067 DOI: 10.1016/j.canlet.2017.08.028]

148 **Nechushtan H**, Hamamreh Y, Nidal S, Gotfried M, Baron A, Shalev YI, Nisman B, Peretz T, Peylan-Ramu N. A phase Iib trial assessing the addition of disulfiram to chemotherapy for the treatment of metastatic non-small cell lung cancer. *Oncologist* 2015; **20**: 366-367 [PMID: 25777347 DOI: 10.1634/theoncologist.2014-0424]

149 **Davis CI**, Gu X, Kiefer RM, Ralle M, Gade TP, Brady DC. Altered copper homeostasis underlies sensitivity of hepatocellular carcinoma to copper chelation. *Metallomics* 2020; **12**: 1995-2008 [PMID: 33146201 DOI: 10.1039/d0mt00156b]

150 **Denoyer D**, Masaldan S, La Fontaine S, Cater MA. Targeting copper in cancer therapy: 'Copper That Cancer'. *Metallomics* 2015; **7**: 1459-1476 [PMID: 26313539 DOI: 10.1039/c5mt00149h]

151 **Li Y**, Wang LH, Zhang HT, Wang YT, Liu S, Zhou WL, Yuan XZ, Li TY, Wu CF, Yang JY. Disulfiram combined with copper inhibits metastasis and epithelial-mesenchymal transition in hepatocellular carcinoma through the NF-κB and TGF-β pathways. *J Cell Mol Med* 2018; **22**: 439-451 [PMID: 29148232 DOI: 10.1111/jcmm.13334]

152 **Kelley KC**, Grossman KF, Brittain-Blankenship M, Thorne KM, Akerley WL, Terrazas MC, Kosak KM, Boucher KM, Buys SS, McGregor KA, Werner TL, Agarwal N, Weis JR, Sharma S, Ward JH, Kennedy TP, Sborov DW, Shami PJ. A Phase 1 dose-escalation study of disulfiram and copper gluconate in patients with advanced solid tumors involving the liver using S-glutathionylation as a biomarker. *BMC Cancer* 2021; **21**: 510 [PMID: 33957901 DOI: 10.1186/s12885-021-08242-4]

153 **Czauderna C**, Castven D, Mahn FL, Marquardt JU. Context-Dependent Role of NF-κB Signaling in Primary Liver Cancer-from Tumor Development to Therapeutic Implications. *Cancers (Basel)* 2019; **11** [PMID: 31349670 DOI: 10.3390/cancers11081053]

154 **Luedde T**, Schwabe RF. NF-κB in the liver–linking injury, fibrosis and hepatocellular carcinoma. *Nat Rev Gastroenterol Hepatol* 2011; **8**: 108-118 [PMID: 21293511 DOI: 10.1038/nrgastro.2010.213]

155 **Yip NC**, Fombon IS, Liu P, Brown S, Kannappan V, Armesilla AL, Xu B, Cassidy J, Darling JL, Wang W. Disulfiram modulated ROS-MAPK and NFκB pathways and targeted breast cancer cells with cancer stem cell-like properties. *Br J Cancer* 2011; **104**: 1564-1574 [PMID: 21487404 DOI: 10.1038/bjc.2011.126]

156 **Thiery JP**. Epithelial-mesenchymal transitions in tumour progression. *Nat Rev Cancer* 2002; **2**: 442-454 [PMID: 12189386 DOI: 10.1038/nrc822]

157 **Zhang G**, Wang Y, Fuchs BC, Guo W, Drum DL, Erstad DJ, Shi B, DeLeo AB, Zheng H, Cai L, Zhang L, Tanabe KK, Wang X. Improving the Therapeutic Efficacy of Sorafenib for Hepatocellular Carcinoma by Repurposing Disulfiram. *Front Oncol* 2022; **12**: 913736 [PMID: 35912209 DOI: 10.3389/fonc.2022.913736]

158 **Komiya Y**, Habas R. Wnt signal transduction pathways. *Organogenesis* 2008; **4**: 68-75 [PMID: 19279717 DOI: 10.4161/org.4.2.5851]

159 **Duchartre Y**, Kim YM, Kahn M. The Wnt signaling pathway in cancer. *Crit Rev Oncol Hematol* 2016; **99**: 141-149 [PMID: 26775730 DOI: 10.1016/j.critrevonc.2015.12.005]

160 **Zhan T**, Rindtorff N, Boutros M. Wnt signaling in cancer. *Oncogene* 2017; **36**: 1461-1473 [PMID: 27617575 DOI: 10.1038/onc.2016.304]

161 **Zhang Y**, Wang X. Targeting the Wnt/β-catenin signaling pathway in cancer. *J Hematol Oncol* 2020; **13**: 165 [PMID: 33276800 DOI: 10.1186/s13045-020-00990-3]

162 **Arzumanian VA**, Kiseleva OI, Poverennaya EV. The Curious Case of the HepG2 Cell Line: 40 Years of Expertise. *Int J Mol Sci* 2021; **22** [PMID: 34884942 DOI: 10.3390/ijms222313135]

163 **He S**, Tang S. WNT/β-catenin signaling in the development of liver cancers. *Biomed Pharmacother* 2020; **132**: 110851 [PMID: 33080466 DOI: 10.1016/j.biopha.2020.110851]

164 **Ahmed K**, Koval A, Xu J, Bodmer A, Katanaev VL. Towards the first targeted therapy for triple-negative breast cancer: Repositioning of clofazimine as a chemotherapy-compatible selective Wnt pathway inhibitor. *Cancer Lett* 2019; **449**: 45-55 [PMID: 30771433 DOI: 10.1016/j.canlet.2019.02.018]

165 **Koval AV**, Vlasov P, Shichkova P, Khunderyakova S, Markov Y, Panchenko J, Volodina A, Kondrashov FA, Katanaev VL. Anti-leprosy drug clofazimine inhibits growth of triple-negative breast cancer cells *via* inhibition of canonical Wnt signaling. *Biochem Pharmacol* 2014; **87**: 571-578 [PMID: 24355563 DOI: 10.1016/j.bcp.2013.12.007]

166 **Xu J**, Koval A, Katanaev VL. Beyond TNBC: Repositioning of Clofazimine Against a Broad Range of Wnt-Dependent Cancers. *Front Oncol* 2020; **10**: 602817 [PMID: 33363033 DOI: 10.3389/fonc.2020.602817]

167 **Van Rensburg CE**, Van Staden AM, Anderson R. The riminophenazine agents clofazimine and B669 inhibit the proliferation of cancer cell lines in vitro by phospholipase A2-mediated oxidative and nonoxidative mechanisms. *Cancer Res* 1993; **53**: 318-323 [PMID: 7678073]

168 **Ruff P**, Chasen MR, Long JE, van Rensburg CE. A phase II study of oral clofazimine in unresectable and metastatic hepatocellular carcinoma. *Ann Oncol* 1998; **9**: 217-219 [PMID: 9553669 DOI: 10.1023/a:1008204911774]

169 **Sato B**. Can an autocrine loop explain sex-hormone-dependent tumor growth? *Oncology* 1999; **57** Suppl 2: 3-6 [PMID: 10545797 DOI: 10.1159/000012036]

170 **Venkatesan P**. Albendazole. *J Antimicrob Chemother* 1998; **41**: 145-147 [PMID: 9533454 DOI: 10.1093/jac/41.2.145]

171 **Kim U**, Shin C, Kim CY, Ryu B, Kim J, Bang J, Park JH. Albendazole exerts antiproliferative effects on prostate cancer cells by inducing reactive oxygen species generation. *Oncol Lett* 2021; **21**: 395 [PMID: 33777218 DOI: 10.3892/ol.2021.12656]

172 **Patel K**, Doudican NA, Schiff PB, Orlow SJ. Albendazole sensitizes cancer cells to ionizing radiation. *Radiat Oncol* 2011; **6**: 160 [PMID: 22094106 DOI: 10.1186/1748-717X-6-160]

173 **Petersen JSSM**, Baird SK. Treatment of breast and colon cancer cell lines with anti-helmintic benzimidazoles mebendazole or albendazole results in selective apoptotic cell death. *J Cancer Res Clin Oncol* 2021; **147**: 2945-2953 [PMID: 34148157 DOI: 10.1007/s00432-021-03698-0]

174 **Zhou F**, Du J, Wang J. Albendazole inhibits HIF-1α-dependent glycolysis and VEGF expression in non-small cell lung cancer cells. *Mol Cell Biochem* 2017; **428**: 171-178 [PMID: 28063005 DOI: 10.1007/s11010-016-2927-3]

175 **Zhu L**, Yang Q, Hu R, Li Y, Peng Y, Liu H, Ye M, Zhang B, Zhang P, Liu-Smith F, Li H, Liu J. Novel therapeutic strategy for melanoma based on albendazole and the CDK4/6 inhibitor palbociclib. *Sci Rep* 2022; **12**: 5706 [PMID: 35383224 DOI: 10.1038/s41598-022-09592-0]

176 **Pourgholami MH**, Woon L, Almajd R, Akhter J, Bowery P, Morris DL. In vitro and in vivo suppression of growth of hepatocellular carcinoma cells by albendazole. *Cancer Lett* 2001; **165**: 43-49 [PMID: 11248417 DOI: 10.1016/S0304-3835(01)00382-2]

177 **Smyj R**, Wang XP, Han F. Pimozide. *Profiles Drug Subst Excip Relat Methodol* 2012; **37**: 287-311 [PMID: 22469321 DOI: 10.1016/B978-0-12-397220-0.00007-6]

178 **Egolf A**, Coffey BJ. Current pharmacotherapeutic approaches for the treatment of Tourette syndrome. *Drugs Today (Barc)* 2014; **50**: 159-179 [PMID: 24619591 DOI: 10.1358/dot.2014.50.2.2097801]

179 **Dakir el-H**, Pickard A, Srivastava K, McCrudden CM, Gross SR, Lloyd S, Zhang SD, Margariti A, Morgan R, Rudland PS, El-Tanani M. The anti-psychotic drug pimozide is a novel chemotherapeutic for breast cancer. *Oncotarget* 2018; **9**: 34889-34910 [PMID: 30405882 DOI: 10.18632/oncotarget.26175]

180 **Li J**, Qu P, Zhou XZ, Ji YX, Yuan S, Liu SP, Zhang QG. Pimozide inhibits the growth of breast cancer cells by alleviating the Warburg effect through the P53 signaling pathway. *Biomed Pharmacother* 2022; **150**: 113063 [PMID: 35658233 DOI: 10.1016/j.biopha.2022.113063]

181 **Kim U**, Kim CY, Lee JM, Ryu B, Kim J, Shin C, Park JH. Pimozide Inhibits the Human Prostate Cancer Cells Through the Generation of Reactive Oxygen Species. *Front Pharmacol* 2019; **10**: 1517 [PMID: 32009948 DOI: 10.3389/fphar.2019.01517]

182 **Ranjan A**, Kaushik I, Srivastava SK. Pimozide Suppresses the Growth of Brain Tumors by Targeting STAT3-Mediated Autophagy. *Cells* 2020; **9** [PMID: 32971907 DOI: 10.3390/cells9092141]

183 **Ren Y**, Tao J, Jiang Z, Guo D, Tang J. Pimozide suppresses colorectal cancer *via* inhibition of Wnt/β-catenin signaling pathway. *Life Sci* 2018; **209**: 267-273 [PMID: 30107167 DOI: 10.1016/j.lfs.2018.08.027]

184 **Nelson EA**, Walker SR, Weisberg E, Bar-Natan M, Barrett R, Gashin LB, Terrell S, Klitgaard JL, Santo L, Addorio MR, Ebert BL, Griffin JD, Frank DA. The STAT5 inhibitor pimozide decreases survival of chronic myelogenous leukemia cells resistant to kinase inhibitors. *Blood* 2011; **117**: 3421-3429 [PMID: 21233313 DOI: 10.1182/blood-2009-11-255232]

185 **Fako V**, Yu Z, Henrich CJ, Ransom T, Budhu AS, Wang XW. Inhibition of wnt/β-catenin Signaling in Hepatocellular Carcinoma by an Antipsychotic Drug Pimozide. *Int J Biol Sci* 2016; **12**: 768-775 [PMID: 27313491 DOI: 10.7150/ijbs.14718]

186 **Noh CK**, Wang HJ, Kim CM, Kim J, Yoon SY, Lee GH, Cho HJ, Yang MJ, Kim SS, Hwang JC, Cho SW, Roh J, Kim YB, Kim SJ, Kim BW, Cheong JY. EpCAM as a Predictive Marker of Tumor Recurrence and Survival in Patients Who Underwent Surgical Resection for Hepatocellular Carcinoma. *Anticancer Res* 2018; **38**: 4101-4109 [PMID: 29970536 DOI: 10.21873/anticanres.12700]

187 **Vasanthakumar S**, Sasikala P, Padma M, Balachandar V, Venkatesh B, Ganesan S. EpCAM as a novel therapeutic target for hepatocellular carcinoma. *J Oncol Sci* 2017; **3**: 71-76 [DOI: 10.1016/j.jons.2017.04.002]

188 **Chen JJ**, Zhang LN, Cai N, Zhang Z, Ji K. Antipsychotic agent pimozide promotes reversible proliferative suppression by inducing cellular quiescence in liver cancer. *Oncol Rep* 2019; **42**: 1101-1109 [PMID: 31322218 DOI: 10.3892/or.2019.7229]

189 **National Center for Biotechnology Information (2022)**. PubChem Compound Summary for CID 5284447, Natamycin. [cited 9 November 2022]. Available from: https://pubchem.ncbi.nlm.nih.gov/compound/Natamycin

190 **Vasquez JL**, Lai Y, Annamalai T, Jiang Z, Zhang M, Lei R, Zhang Z, Liu Y, Tse-Dinh YC, Agoulnik IU. Inhibition of base excision repair by natamycin suppresses prostate cancer cell proliferation. *Biochimie* 2020; **168**: 241-250 [PMID: 31756402 DOI: 10.1016/j.biochi.2019.11.008]

191 **An Y**, Jiang J, Zhou L, Shi J, Jin P, Li L, Peng L, He S, Zhang W, Huang C, Zou B, Xie N. Peroxiredoxin 1 is essential for natamycin-triggered apoptosis and protective autophagy in hepatocellular carcinoma. *Cancer Lett* 2021; **521**: 210-223 [PMID: 34428517 DOI: 10.1016/j.canlet.2021.08.023]

192 **Aggarwal V**, Tuli HS, Varol A, Thakral F, Yerer MB, Sak K, Varol M, Jain A, Khan MA, Sethi G. Role of Reactive Oxygen Species in Cancer Progression: Molecular Mechanisms and Recent Advancements. *Biomolecules* 2019; **9** [PMID: 31766246 DOI: 10.3390/biom9110735]

193 **Reczek CR**, Chandel NS. The Two Faces of Reactive Oxygen Species in Cancer. *Annu Rev Cancer Biol* 2017; **1**: 79-98 [DOI: 10.1146/annurev-cancerbio-041916-065808]

194 **Singh R**, Manna PP. Reactive oxygen species in cancer progression and its role in therapeutics. *Explor Med* 2022; 43-57 [DOI: 10.37349/emed.2022.00073]

195 **Harris IS**, DeNicola GM. The Complex Interplay between Antioxidants and ROS in Cancer. *Trends Cell Biol* 2020; **30**: 440-451 [PMID: 32303435 DOI: 10.1016/j.tcb.2020.03.002]

196 **Hampton MB**, Vick KA, Skoko JJ, Neumann CA. Peroxiredoxin Involvement in the Initiation and Progression of Human Cancer. *Antioxid Redox Signal* 2018; **28**: 591-608 [PMID: 29237274 DOI: 10.1089/ars.2017.7422]

197 **Kim Y**, Jang HH. The Role of Peroxiredoxin Family in Cancer Signaling. *J Cancer Prev* 2019; **24**: 65-71 [PMID: 31360686 DOI: 10.15430/JCP.2019.24.2.65]

198 **Sun YL**, Cai JQ, Liu F, Bi XY, Zhou LP, Zhao XH. Aberrant expression of peroxiredoxin 1 and its clinical implications in liver cancer. *World J Gastroenterol* 2015; **21**: 10840-10852 [PMID: 26478675 DOI: 10.3748/wjg.v21.i38.10840]

199 **Ghodke-Puranik Y**, Thorn CF, Lamba JK, Leeder JS, Song W, Birnbaum AK, Altman RB, Klein TE. Valproic acid pathway: pharmacokinetics and pharmacodynamics. *Pharmacogenet Genomics* 2013; **23**: 236-241 [PMID: 23407051 DOI: 10.1097/FPC.0b013e32835ea0b2]

200 **Cinatl J Jr**, Cinatl J, Driever PH, Kotchetkov R, Pouckova P, Kornhuber B, Schwabe D. Sodium valproate inhibits in vivo growth of human neuroblastoma cells. *Anticancer Drugs* 1997; **8**: 958-963 [PMID: 9436639 DOI: 10.1097/00001813-199711000-00007]

201 **Machado MC**, Bellodi-Privato M, Kubrusly MS, Molan NA, Tharcisio T Jr, de Oliveira ER, D'Albuquerque LA. Valproic acid inhibits human hepatocellular cancer cells growth in vitro and in vivo. *J Exp Ther Oncol* 2011; **9**: 85-92 [PMID: 21699015]

202 **Bai X**, Liu L, Wang Y. Valproate Ameliorates Diethylnitrosamine/Phenobarbital- Induced Hepatic Cancer *via* the Role of TNF-α and TGF-β1. *Int J Pharmacol* 2021; **17**: 156-168 [DOI: 10.3923/ijp.2021.156.168]

203 **Lee JH**, Lee JH, Lim YS, Yeon JE, Song TJ, Yu SJ, Gwak GY, Kim KM, Kim YJ, Lee JW, Yoon JH. Adjuvant immunotherapy with autologous cytokine-induced killer cells for hepatocellular carcinoma. *Gastroenterology* 2015; **148**: 1383-91.e6 [PMID: 25747273 DOI: 10.1053/j.gastro.2015.02.055]

204 **Lee JH**, Lee JH, Lim YS, Yeon JE, Song TJ, Yu SJ, Gwak GY, Kim KM, Kim YJ, Lee JW, Yoon JH. Sustained efficacy of adjuvant immunotherapy with cytokine-induced killer cells for hepatocellular carcinoma: an extended 5-year follow-up.

Cancer Immunol Immunother 2019; **68**: 23-32 [PMID: 30232520 DOI: 10.1007/s00262-018-2247-4]

205 **Ma Y**, Xu YC, Tang L, Zhang Z, Wang J, Wang HX. Cytokine-induced killer (CIK) cell therapy for patients with hepatocellular carcinoma: efficacy and safety. *Exp Hematol Oncol* 2012; **1**: 11 [PMID: 23210562 DOI: 10.1186/2162-3619-1-11]

206 **Lee DH**, Nam JY, Chang Y, Cho H, Kang SH, Cho YY, Cho E, Lee JH, Yu SJ, Kim YJ, Yoon JH. Synergistic effect of cytokine-induced killer cell with valproate inhibits growth of hepatocellular carcinoma cell in a mouse model. *Cancer Biol Ther* 2017; **18**: 67-75 [PMID: 28055304 DOI: 10.1080/15384047.2016.1276132]

207 **Yu JI**, Choi C, Shin SW, Son A, Lee GH, Kim SY, Park HC. Valproic Acid Sensitizes Hepatocellular Carcinoma Cells to Proton Therapy by Suppressing NRF2 Activation. *Sci Rep* 2017; **7**: 14986 [PMID: 29118323 DOI: 10.1038/s41598-017-15165-3]

208 **Lane AA**, Chabner BA. Histone Deacetylase Inhibitors in Cancer Therapy. *J Clin Oncol* 2009; **27**: 5459-5468 [PMID: 19826124 DOI: 10.1200/JCO.2009.22.1291]

209 **Li G**, Tian Y, Zhu WG. The Roles of Histone Deacetylases and Their Inhibitors in Cancer Therapy. *Front Cell Dev Biol* 2020; **8**: 576946 [PMID: 33117804 DOI: 10.3389/fcell.2020.576946]

210 **West AC**, Johnstone RW. New and emerging HDAC inhibitors for cancer treatment. *J Clin Invest* 2014; **124**: 30-39 [PMID: 24382387 DOI: 10.1172/JCI69738]

211 **Munshi A**, Tanaka T, Hobbs ML, Tucker SL, Richon VM, Meyn RE. Vorinostat, a histone deacetylase inhibitor, enhances the response of human tumor cells to ionizing radiation through prolongation of gamma-H2AX foci. *Mol Cancer Ther* 2006; **5**: 1967-1974 [PMID: 16928817 DOI: 10.1158/1535-7163.MCT-06-0022]

212 **Chen W**, Chiang CL, Dawson LA. Efficacy and safety of radiotherapy for primary liver cancer. *Chin Clin Oncol* 2021; **10**: 9 [PMID: 32576017 DOI: 10.21037/cco-20-89]

213 **An HM**, Xue YF, Shen YL, Du Q, Hu B. Sodium valproate induces cell senescence in human hepatocarcinoma cells. *Molecules* 2013; **18**: 14935-14947 [PMID: 24304587 DOI: 10.3390/molecules181214935]

214 **Pernicova I**, Korbonits M. Metformin–mode of action and clinical implications for diabetes and cancer. *Nat Rev Endocrinol* 2014; **10**: 143-156 [PMID: 24393785 DOI: 10.1038/nrendo.2013.256]

215 **Zhang Z**, Zhou L, Xie N, Nice EC, Zhang T, Cui Y, Huang C. Overcoming cancer therapeutic bottleneck by drug repurposing. *Signal Transduct Target Ther* 2020; **5**: 113 [PMID: 32616710 DOI: 10.1038/s41392-020-00213-8]

216 **Akce M**, Rupji M, Switchenko JM, Shaib WL, Wu C, Alese OB, Diab M, Lesinski GB, El-Rayes BF. Phase II trial of nivolumab and metformin in patients with treatment refractory microsatellite stable metastatic colorectal cancer. *J Clin Oncol* 2021; **39** Suppl 3: 95 [DOI: 10.1200/JCO.2021.39.3_suppl.95]

217 **Goodwin PJ**, Chen BE, Gelmon KA, Whelan TJ, Ennis M, Lemieux J, Ligibel JA, Hershman DL, Mayer IA, Hobday TJ, Bliss JM, Rastogi P, Rabaglio-Poretti M, Mukherjee SD, Mackey JR, Abramson VG, Oja C, Wesolowski R, Thompson AM, Rea DW, Stos PM, Shepherd LE, Stambolic V, Parulekar WR. Effect of Metformin vs Placebo on Invasive Disease-Free Survival in Patients With Breast Cancer: The MA.32 Randomized Clinical Trial. *JAMA* 2022; **327**: 1963-1973 [PMID: 35608580 DOI: 10.1001/jama.2022.6147]

218 **Soliman PT**, Westin SN, Iglesias DA, Fellman BM, Yuan Y, Zhang Q, Yates MS, Broaddus RR, Slomovitz BM, Lu KH, Coleman RL. Everolimus, Letrozole, and Metformin in Women with Advanced or Recurrent Endometrioid Endometrial Cancer: A Multi-Center, Single Arm, Phase II Study. *Clin Cancer Res* 2020; **26**: 581-587 [PMID: 31628143 DOI: 10.1158/1078-0432.CCR-19-0471]

219 **Wilson BE**, Armstrong AJ, de Bono J, Sternberg CN, Ryan CJ, Scher HI, Smith MR, Rathkopf D, Logothetis CJ, Chi KN, Jones RJ, Saad F, De Porre P, Tran N, Hu P, Gillessen S, Carles J, Fizazi K, Joshua AM. Effects of metformin and statins on outcomes in men with castration-resistant metastatic prostate cancer: Secondary analysis of COU-AA-301 and COU-AA-302. *Eur J Cancer* 2022; **170**: 296-304 [PMID: 35568679 DOI: 10.1016/j.ejca.2022.03.042]

220 **Ma SJ**, Zheng YX, Zhou PC, Xiao YN, Tan HZ. Metformin use improves survival of diabetic liver cancer patients: systematic review and meta-analysis. *Oncotarget* 2016; **7**: 66202-66211 [PMID: 27494848 DOI: 10.18632/oncotarget.11033]

221 **Ma S**, Zheng Y, Xiao Y, Zhou P, Tan H. Meta-analysis of studies using metformin as a reducer for liver cancer risk in diabetic patients. *Medicine (Baltimore)* 2017; **96**: e6888 [PMID: 28489794 DOI: 10.1097/MD.0000000000006888]

222 **Pollak M**. Overcoming Drug Development Bottlenecks With Repurposing: Repurposing biguanides to target energy metabolism for cancer treatment. *Nat Med* 2014; **20**: 591-593 [PMID: 24901568 DOI: 10.1038/nm.3596]

223 **Howell JJ**, Hellberg K, Turner M, Talbott G, Kolar MJ, Ross DS, Hoxhaj G, Saghatelian A, Shaw RJ, Manning BD. Metformin Inhibits Hepatic mTORC1 Signaling *via* Dose-Dependent Mechanisms Involving AMPK and the TSC Complex. *Cell Metab* 2017; **25**: 463-471 [PMID: 28089566 DOI: 10.1016/j.cmet.2016.12.009]

224 **Stancu C**, Sima A. Statins: mechanism of action and effects. *J Cell Mol Med* 2001; **5**: 378-387 [PMID: 12067471 DOI: 10.1111/j.1582-4934.2001.tb00172.x]

225 **Clendening JW**, Pandyra A, Boutros PC, El Ghamrasni S, Khosravi F, Trentin GA, Martirosyan A, Hakem A, Hakem R, Jurisica I, Penn LZ. Dysregulation of the mevalonate pathway promotes transformation. *Proc Natl Acad Sci U S A* 2010; **107**: 15051-15056 [PMID: 20696928 DOI: 10.1073/pnas.0910258107]

226 **Mullen PJ**, Yu R, Longo J, Archer MC, Penn LZ. The interplay between cell signalling and the mevalonate pathway in cancer. *Nat Rev Cancer* 2016; **16**: 718-731 [PMID: 27562463 DOI: 10.1038/nrc.2016.76]

227 **Jiang W**, Hu JW, He XR, Jin WL, He XY. Statins: a repurposed drug to fight cancer. *J Exp Clin Cancer Res* 2021; **40**: 241 [PMID: 34303383 DOI: 10.1186/s13046-021-02041-2]

228 **Kodach LL**, Jacobs RJ, Voorneveld PW, Wildenberg ME, Verspaget HW, van Wezel T, Morreau H, Hommes DW, Peppelenbosch MP, van den Brink GR, Hardwick JC. Statins augment the chemosensitivity of colorectal cancer cells inducing epigenetic reprogramming and reducing colorectal cancer cell 'stemness' *via* the bone morphogenetic protein pathway. *Gut* 2011; **60**: 1544-1553 [PMID: 21551187 DOI: 10.1136/gut.2011.237495]

229 **Longo J**, van Leeuwen JE, Elbaz M, Branchard E, Penn LZ. Statins as Anticancer Agents in the Era of Precision Medicine. *Clin Cancer Res* 2020; **26**: 5791-5800 [PMID: 32887721 DOI: 10.1158/1078-0432.CCR-20-1967]

230 **Mansourian PG**, Yoneda M, Krishna Rao M, Martinez FJ, Thomas E, Schiff ER. Effects of statins on the risk of

hepatocellular carcinoma. *Gastroenterol Hepatol (N Y)* 2014; **10**: 417-426 [PMID: 25904829]

231 **Kim MH**, Kim MY, Salloum S, Qian T, Wong LP, Xu M, Lee Y, Shroff SG, Sadreyev RI, Corey KE, Baumert TF, Hoshida Y, Chung RT. Atorvastatin favorably modulates a clinical hepatocellular carcinoma risk gene signature. *Hepatol Commun* 2022; **6**: 2581-2593 [PMID: 35712812 DOI: 10.1002/hep4.1991]

232 **Krasselt M**, Baerwald C. Celecoxib for the treatment of musculoskeletal arthritis. *Expert Opin Pharmacother* 2019; **20**: 1689-1702 [PMID: 31339385 DOI: 10.1080/14656566.2019.1645123]

233 **Khafaga AF**, Shamma RN, Abdeen A, Barakat AM, Noreldin AE, Elzoghby AO, Sallam MA. Celecoxib repurposing in cancer therapy: molecular mechanisms and nanomedicine-based delivery technologies. *Nanomedicine (Lond)* 2021; **16**: 1691-1712 [PMID: 34264123 DOI: 10.2217/nnm-2021-0086]

234 **Sobolewski C**, Legrand N. Celecoxib Analogues for Cancer Treatment: An Update on OSU-03012 and 2,5-Dimethyl-Celecoxib. *Biomolecules* 2021; **11** [PMID: 34356673 DOI: 10.3390/biom11071049]

235 **Tołoczko-Iwaniuk N**, Dziemiańczyk-Pakieła D, Nowaszewska BK, Celińska-Janowicz K, Miltyk W. Celecoxib in Cancer Therapy and Prevention – Review. *Curr Drug Targets* 2019; **20**: 302-315 [PMID: 30073924 DOI: 10.2174/1389450119666180803121737]

236 **Hashemi Goradel N**, Najafi M, Salehi E, Farhood B, Mortezaee K. Cyclooxygenase-2 in cancer: A review. *J Cell Physiol* 2019; **234**: 5683-5699 [PMID: 30341914 DOI: 10.1002/jcp.27411]

237 **Dai H**, Zhang S, Ma R, Pan L. Celecoxib Inhibits Hepatocellular Carcinoma Cell Growth and Migration by Targeting PNO1. *Med Sci Monit* 2019; **25**: 7351-7360 [PMID: 31568401 DOI: 10.12659/MSM.919218]

238 **Li J**, Liu L, Chen Y, Wu M, Lin X, Shen Z, Cheng Y, Chen X, Weygant N, Wu X, Wei L, Sferra TJ, Han Y, Shen A, Peng J. Ribosome assembly factor PNO1 is associated with progression and promotes tumorigenesis in triplenegative breast cancer. *Oncol Rep* 2022; **47** [PMID: 35445733 DOI: 10.3892/or.2022.8319]

239 **Lin C**, Yuan H, Wang W, Zhu Z, Lu Y, Wang J, Feng F, Wu J. Importance of PNO1 for growth and survival of urinary bladder carcinoma: Role in core-regulatory circuitry. *J Cell Mol Med* 2020; **24**: 1504-1515 [PMID: 31800162 DOI: 10.1111/jcmm.14835]

240 **Liu D**, Lin L, Wang Y, Chen L, He Y, Luo Y, Qi L, Guo Y, Han Z, Li G, Li Q, Liu Z, Chen P, Guo H. PNO1, which is negatively regulated by miR-340-5p, promotes lung adenocarcinoma progression through Notch signaling pathway. *Oncogenesis* 2020; **9**: 58 [PMID: 32483111 DOI: 10.1038/s41389-020-0241-0]

241 **Shen Z**, Chen Y, Li L, Liu L, Peng M, Chen X, Wu X, Sferra TJ, Wu M, Lin X, Cheng Y, Chu J, Shen A, Peng J. Transcription Factor EBF1 Over-Expression Suppresses Tumor Growth in vivo and in vitro *via* Modulation of the PNO1/p53 Pathway in Colorectal Cancer. *Front Oncol* 2020; **10**: 1035 [PMID: 32676457 DOI: 10.3389/fonc.2020.01035]

242 **Wang G**, Li Q, Li C, Duan G, Sang H, Dong H, Yang Y, Ma C, Tao T. Knockdown of PNO1 inhibits esophageal cancer progression. *Oncol Rep* 2021; **45** [PMID: 33864661 DOI: 10.3892/or.2021.8036]

243 **Han Z**, Liu D, Chen L, He Y, Tian X, Qi L, Luo Y, Chen Z, Hu X, Li G, Zhan L, Wang Y, Li Q, Chen P, Liu Z, Guo H. PNO1 regulates autophagy and apoptosis of hepatocellular carcinoma *via* the MAPK signaling pathway. *Cell Death Dis* 2021; **12**: 552 [PMID: 34050137 DOI: 10.1038/s41419-021-03837-y]

244 **Hu JW**, Chen B, Zhang J, Qi YP, Liang JH, Zhong JH, Xiang BD. Novel combination of celecoxib and metformin improves the antitumor effect by inhibiting the growth of Hepatocellular Carcinoma. *J Cancer* 2020; **11**: 6437-6444 [PMID: 33033527 DOI: 10.7150/jca.47532]

245 **Levy JMM**, Towers CG, Thorburn A. Targeting autophagy in cancer. *Nat Rev Cancer* 2017; **17**: 528-542 [PMID: 28751651 DOI: 10.1038/nrc.2017.53]

246 **Mohamed FE**, Al-Jehani RM, Minogue SS, Andreola F, Winstanley A, Olde Damink SW, Habtesion A, Malagó M, Davies N, Luong TV, Dhillon AP, Mookerjee RP, Dhar DK, Jalan R. Effect of toll-like receptor 7 and 9 targeted therapy to prevent the development of hepatocellular carcinoma. *Liver Int* 2015; **35**: 1063-1076 [PMID: 24990399 DOI: 10.1111/liv.12626]

247 **Chen MY**, Yadav VK, Chu YC, Ong JR, Huang TY, Lee KF, Lee KH, Yeh CT, Lee WH. Hydroxychloroquine (HCQ) Modulates Autophagy and Oxidative DNA Damage Stress in Hepatocellular Carcinoma to Overcome Sorafenib Resistance *via* TLR9/SOD1/hsa-miR-30a-5p/Beclin-1 Axis. *Cancers (Basel)* 2021; **13** [PMID: 34203465 DOI: 10.3390/cancers13133227]

World Journal of Gastroenterology

Submit a Manuscript: https://www.f6publishing.com

World J Gastroenterol 2023 May 7; 29(17): 2600-2615

DOI: 10.3748/wjg.v29.i17.2600

ISSN 1007-9327 (print) ISSN 2219-2840 (online)

MINIREVIEWS

Difficult colorectal polypectomy: Technical tips and recent advances

Sukit Pattarajierapan, Hiroyuki Takamaru, Supakij Khomvilai

Specialty type: Gastroenterology and hepatology

Provenance and peer review: Invited article; Externally peer reviewed.

Peer-review model: Single blind

Peer-review report's scientific quality classification

Grade A (Excellent): 0
Grade B (Very good): B, B, B
Grade C (Good): C
Grade D (Fair): D
Grade E (Poor): 0

P-Reviewer: Argyriou K, Greece; Gao SG, China; Ichita C, Japan; Rasa K, Turkey

Received: January 29, 2023
Peer-review started: January 29, 2023
First decision: February 14, 2023
Revised: February 24, 2023
Accepted: April 12, 2023
Article in press: April 12, 2023
Published online: May 7, 2023

Sukit Pattarajierapan, Supakij Khomvilai, Surgical Endoscopy Colorectal Division, Department of Surgery, Faculty of Medicine, Chulalongkorn University, Bangkok 10330, Thailand

Hiroyuki Takamaru, Endoscopy Division, National Cancer Center Hospital, Tokyo 104-0045, Japan

Corresponding author: Sukit Pattarajierapan, MD, Doctor, Surgeon, Surgical Endoscopy Colorectal Division, Department of Surgery, Faculty of Medicine, Chulalongkorn University, 1873 Rama IV Road, Pathumwan, Bangkok 10330, Thailand. sukit.p@chulahospital.org

Abstract

Colonoscopy has been shown to be an effective modality to prevent colorectal cancer (CRC) development. CRC reduction is achieved by detecting and removing adenomas, which are precursors of CRC. Most colorectal polyps are small and do not pose a significant challenge for trained and skilled endoscopists. However, up to 15% of polyps are considered "difficult", potentially causing life-threatening complications. A difficult polyp is defined as any polyp that is challenging for the endoscopist to remove owing to its size, shape, or location. Advanced polypectomy techniques and skills are required to resect difficult colorectal polyps. There were various polypectomy techniques for difficult polyps such as endoscopic mucosal resection (EMR), underwater EMR, Tip-in EMR, endoscopic submucosal dissection (ESD), or endoscopic full-thickness resection. The selection of the appropriate modality depends on the morphology and endoscopic diagnosis. Several technologies have been developed to aid endoscopists in performing safe and effective polypectomies, especially complex procedures such as ESD. These advances include video endoscopy system, equipment assisting in advanced polypectomy, and closure devices/techniques for complication management. Endoscopists should know how to use these devices and their availability in practice to enhance polypectomy performance. This review describes several useful strategies and tips for managing difficult colorectal polyps. We also propose the stepwise approach for difficult colorectal polyps.

Key Words: Adenoma; Colonic polyps; Colonoscopy; Endoscopic mucosal resection; Endoscopic submucosal dissection; Polypectomy

©The Author(s) 2023. Published by Baishideng Publishing Group Inc. All rights reserved.

Core Tip: Most colorectal polyps are small and do not pose a significant challenge to resection. However, up to 15% of polyps are considered "difficult" because of their size, shape, or location. Advanced polypectomy techniques and skills are required for the resection of difficult colorectal polyps. Recent advancements in techniques and devices for endoscopic mucosal resection, endoscopic submucosal dissection, and endoscopic full-thickness resection allow curative therapy of these difficult polyps and avoid unnecessary surgery that carries the risk of morbidity and mortality. However, the proper selection of adjunct endoscopic devices/techniques and stepwise training for skill improvement are critical for successful advanced polypectomy.

Citation: Pattarajierapan S, Takamaru H, Khomvilai S. Difficult colorectal polypectomy: Technical tips and recent advances. *World J Gastroenterol* 2023; 29(17): 2600-2615
URL: https://www.wjgnet.com/1007-9327/full/v29/i17/2600.htm
DOI: https://dx.doi.org/10.3748/wjg.v29.i17.2600

INTRODUCTION

In 2020, colorectal cancer (CRC) was the fourth most common malignancy worldwide, with 1.9 million new cases recorded[1]. Colonoscopy has been shown to be an effective modality to prevent CRC development. Previous studies have shown a 60%-90% reduction in CRC incidence after screening colonoscopy[2,3]. CRC reduction is achieved by detecting and removing adenomas, which are precursors of CRC. Most colorectal polyps detected during colonoscopy are small, benign, and easily resected by skilled endoscopists. However, 10%-15% of colorectal polyps are classified as "difficult" colorectal polyps[4,5]. Generally, difficult colorectal polyps are defined as any polyps that are technically challenging for endoscopic resection because of their size (> 20 mm), morphology (pedunculated polyp with a thick stalk, laterally spreading tumor), or location (ileocecal valve, appendiceal orifice, dentate line)[5,6].

Endoscopic resection of difficult polyps is associated with an increased risk of incomplete resection and serious adverse events, including intra-procedural massive bleeding and perforation. Therefore, difficult polypectomy should be performed or supervised by an experienced endoscopist. This review describes helpful strategies and tips for dealing with difficult colorectal polyps.

THE STEPWISE APPROACH FOR DIFFICULT COLORECTAL POLYPS

Lesion assessment

The first step in managing colorectal polyps is lesion assessment. Dye-based chromoendoscopy and image-enhanced endoscopy (IEE) with magnifying observation should be used to distinguish benign lesions, adenomas, and adenocarcinomas. Dye-based chromoendoscopy with indigo carmine and crystal violet enables pit pattern diagnosis based on Kudo's classification[7]. However, IEE techniques such as narrow-band imaging (NBI) and blue laser imaging are more common than chromoendoscopy in clinical practice outside Japan. IEE can diagnose lesions by visualizing surface patterns and microvessels based on the NBI International Colorectal Endoscopic (NICE) and Japan NBI Expert Team (JNET) classification[8,9] (Table 1). The accuracy of discriminating non-neoplastic from neoplastic lesions was 95% for magnifying observation with IEE and 96%-98% for pit pattern observation with chromoendoscopy, while the accuracy for discriminating adenomas from adenocarcinomas was 70%-90% for both IEE and chromoendoscopy[10].

Colorectal cancers with submucosal invasion have a 7%-14% risk of lymph node metastasis[11-14]. For submucosal cancers, it is crucial to differentiate between superficial (< 1000 μm) and deep submucosal invasive (≥ 1000 μm) cancer. Current evidence strongly supports the theory that superficial cancer with submucosal invasion < 1000 μm without lymphovascular invasion, grade 2/3 tumor budding, or poorly differentiated component have no risk of lymph node metastasis[15,16]. A Japanese study suggested that magnifying chromoendoscopy with crystal violet is the best modality for estimating the invasion depth in early colorectal lesions. Matsuda *et al*[17] found that the diagnostic accuracy of the invasive pattern in magnifying chromoendoscopy with crystal violet to differentiate superficial (< 1000 μm) and deep submucosal invasive (≥ 1000 μm) cancers was 98.8%. Patients with submucosal invasive cancer should undergo radical colectomy considering the risk of nodal metastasis, whereas patients with adenoma or cancer with submucosal superficial invasion are candidates for endoscopic resection. It should be noted that experienced examiners performed magnifying chromoendoscopy in this study; therefore, the effectiveness of magnifying chromoendoscopy should be revalidated in general endoscopists. Togashi *et al*[18] reported a minimum experience of observing 200

Table 1 The Japan Narrow-band Imaging Expert Team classification[8]

	Type 1	Type 2A	Type 2B	Type 3
Vessel pattern	Invisible	Regular caliber, regular distribution (meshed/spiral pattern)	Variable caliber, irregular distribution	Loose vessel areas, interruption of thick vessels
Surface pattern	Regular dark or white spots, similar to surrounding normal mucosa	Regular (tubular/branched/papillary)	Irregular or obscure	Amorphous areas
Suspected pathology	Hyperplastic polyp/sessile serrated polyp	Low grade intramucosal neoplasia	High grade intramucosal neoplasia/shallow submucosal invasive cancer	Deep submucosal invasive cancer

lesions with magnifying chromoendoscopy is needed to understand pit pattern diagnosis. Moreover, the limited availability of crystal violet outside Japan makes this approach difficult to apply in clinical practice.

Identification of the causes of difficult polypectomy

Table 2 shows the causes of difficult polypectomy. The difficulty might arise from the size, location, morphology, or other specific conditions. Possible solutions for each complex polyp character or situation are described in the following subsections.

The Size, Morphology, Site, Access (SMSA) classification system has been proposed by Gupta *et al*[19] for stratifying lesion complexity (Table 3). This stratifies polyps into 4 levels of difficulty, with level 1 being the easiest to resect by all endoscopists and level 4 being very difficult to resect. Longcroft-Wheaton *et al*[20] validated the SMSA system in a prospective study of 220 lesions ≥ 20 mm in diameter. They found that lesions with SMSA level 4 had higher complication rates (8.6% *vs* 0%, $P = 0.007$) and lower complete resection rates (87.5% *vs* 97.5%, $P = 0.009$) than the lesions with SMSA level 2 and 3. European Society of Gastrointestinal Endoscopy guideline for colorectal polypectomy and endoscopic mucosal resection (EMR) recommends using the SMSA system to assess large and complex polyps. If the lesions have SMSA level 4, they should be resected by experts at a high-volume tertiary care center [21].

Basic techniques of colorectal polypectomy

Endoscopists should have the appropriate basic skills to conduct a colorectal polypectomy. First, looping on the colonoscope should be unwound by shortening before performing polypectomy; otherwise, colonoscope manipulation would be paradoxical and troublesome. Second, endoscopists should position the polyp at 5-6 o'clock on the monitor because the instrument exits the colonoscope channel at 5 o'clock (Figure 1A). Finally, the base of the polyp, particularly that of a pedunculated polyp, should lie opposite to gravity. Polyp stretching by gravity improves the visualization of the polyp base, and this maneuver prevents blood pooling at the resected site (Figure 1B and C).

Selection of therapeutic modality for large colorectal polyps

The selection of the appropriate modality from various polypectomy techniques depends on the morphology and endoscopic diagnosis. Large pedunculated polyps are mainly resected by polypectomy with a prophylactic strategy against bleeding. The selection of a therapeutic modality for large non-pedunculated polyps, mostly laterally spreading tumors (LSTs), is highly debated. LST is defined as a lesion ≥ 10 mm in diameter, extending laterally with a low vertical axis[22]. The comparison between EMR and endoscopic submucosal dissection (ESD) is an important issue for large LSTs. ESD has higher *en bloc* resection and lower recurrence rates than EMR because the snare EMR method tends to result in piecemeal resection for large lesions[23,24]. Moreover, ESD allows accurate histopathologic diagnosis regarding the depth of invasion without segmentation of the carcinomatous part, which compromises the pathological diagnosis[25]. Nevertheless, colorectal ESD is one of the most challenging endoscopic procedures with high complications. The learning curve of colorectal ESD is steep, with approximately 80 procedures required to gain proficiency in large polyp resection[26]. Recently, Tip-in EMR was proposed as a promising modified EMR technique for the resection of large nonpedunculated polyps [27,28]. After the submucosal injection, the snare tip with a cut current was used to make a spot-shaped mucosal incision at the proximal side of the tumor. The small incision helps fix the snare tip in the submucosal layer during the snare placement; therefore, endoscopists could place the snare flexibly and repeatedly in the appropriate position. Takada *et al*[29] compared Tip-in EMR with ESD for the resection of 20- to 30-mm nonpedunculated polyp using propensity score matching. They found that Tip-in EMR had a lower *en bloc* resection (85% *vs* 99%, $P < 0.001$) and R0 resection rates (63% *vs* 91%, $P < 0.001$) than ESD; however, Tip-in had a shorter procedural time (8 min *vs* 60 min, $P < 0.001$) and comparable local recurrence rate (2% *vs* 0%, $P = 0.386$). They concluded that Tip-in EMR could be a feasible alternative to ESD for 20- to 30-mm nonpedunculated polyps.

Table 2 Characteristics of the difficult colorectal polyps

Size	> 20 mm
Location	Near or involving the appendiceal orifice
	Ileocecal valve
	Anorectal junction
	Behind the fold
	Angulated segment
Morphology	Pedunculated polyp with thick stalk and large head
	Laterally spreading tumor
	Submucosal fibrosis or positive non-lifting sign
Special situation	Recurrent lesion
	Strong colonic peristalsis

Table 3 Size/Morphology/Site/Access scoring system[19]

Parameter	Range	Score
Size	< 1 cm	1
	1.0-1.9 cm	3
	2.0-2.9 cm	5
	3.0-3.9 cm	7
	> 4 cm	9
Morphology	Pedunculated	1
	Sessile	2
	Flat	3
Site	Left	1
	Right	2
Access	Easy	1
	Difficult	3

Size/Morphology/Site/Access (SMSA) level 1: 4-5 points, level 2: 6-8 points, level 3: 9-12 points, level 4: > 12 points.

LST is classified as granular type (LST-G), which has a nodular surface, or non-granular type (LST-NG), which has a smooth surface. These two types have different patterns of submucosal invasion. In a large retrospective cohort study by Yamada *et al*[30], 19% of the LST-G cases had submucosal invasion; the invasion site was the large nodule in 56%, the depression area in 28%, and multifocal in 16%. LST-NG showed 39% submucosal invasion, and the invasion site was 10% at submucosal mass-like elevation, 45% at depression, or 45% multifocal. Because of the substantial risk of multifocal submucosal invasion, ESD is warranted for LST-NG, and *en bloc* resection is required for large LST-G nodules. Table 4 shows the indications for colorectal ESD suggested by the 2020 Japan Gastroenterological Endoscopy Society (JGES) guidelines for colorectal ESD and EMR[10].

APPROACHES TO DIFFICULT POLYPECTOMY IN SPECIFIC SITUATIONS

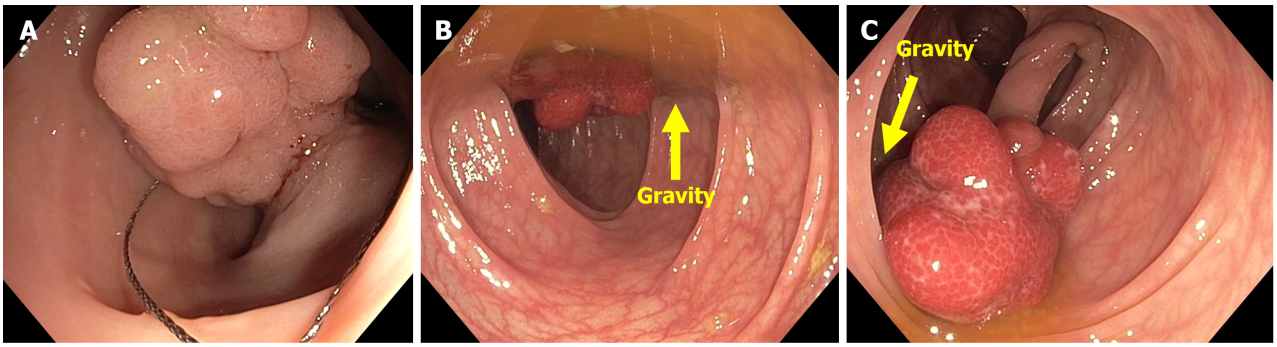
Pedunculated polyp with thick stalk and large head

The risk of bleeding after polypectomy of large pedunculated polyps with thick stalk increases due to the possibility of large blood vessels in the stalk. A prospective study found that pedunculated polyps with stalk diameter > 5 mm and polyp size > 17 mm are risk factors for post-polypectomy bleeding[31]. Therefore, prophylactic strategies against bleeding should be implemented prior to polypectomy.

Table 4 Indications for colorectal endoscopic submucosal dissection[10]

	Lesions requiring *en bloc* resection
1	Lesions which *en bloc* resection with EMR is difficult
	LST-NG, particularly LST-NG with pseudo-depressed type
	Lesions with V_I-type pit pattern
	Carcinoma with shallow T1 invasion
	Large depressed-type tumor
	Large protruded-type lesions suspected to be carcinoma
2	Mucosal tumors with submucosal fibrosis
3	Sporadic tumors in conditions of chronic inflammation such as ulcerative colitis
4	Local residual or recurrent early carcinomas after endoscopic resection

EMR: Endoscopic mucosal resection; LST-NG: Laterally spreading tumor non-granular type.



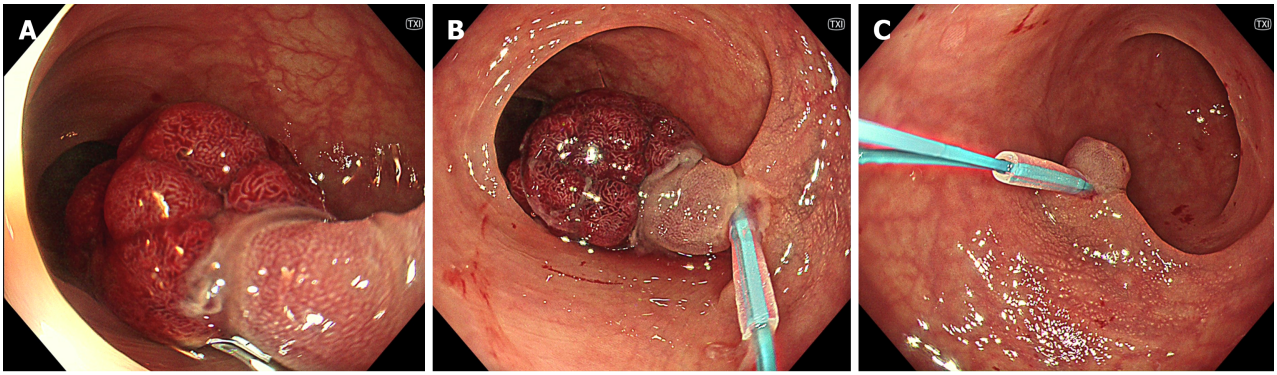
DOI: 10.3748/wjg.v29.i17.2600 **Copyright** ©The Author(s) 2023.

Figure 1 Basic maneuvers of polypectomy. A: Positioning the polyp at 5-6 o'clock on the monitor before polypectomy; B: The polyp's base lying on gravity, this leads to poor visualization of the resection area; therefore, the patient's position should be altered; C: The polyp's base lying opposite to gravity after changing the patient's position. This position change allows polyp stretching and avoids blood pooling on the resected site.

A randomized controlled trial (RCT) by Dobrowolski *et al*[32] found that colorectal polyps ≥ 1 cm that underwent prophylactic adrenaline injection at the stalk before polypectomy had a lower immediate bleeding rate than conventional polypectomy (2% *vs* 16%, $P < 0.05$). In contrast, another RCT by Lee *et al*[33] revealed no statistical difference in immediate and delayed post-polypectomy bleeding rates between the prophylactic adrenaline injection and control groups.

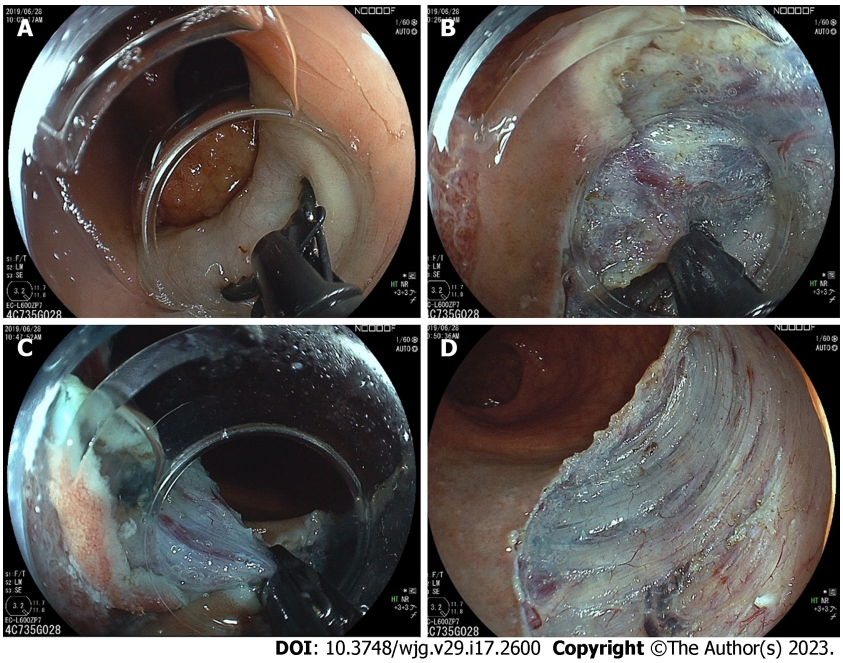
A detachable snare (endoloop) was developed by Hachisu to prevent post-polypectomy bleeding from large pedunculated polyps[34]. A nylon-thread loop is tightened around the polyp stalk to ensure hemostasis before polypectomy (Figure 2). Three RCTs confirmed that a detachable snare effectively prevents post-polypectomy bleeding in large colorectal polyps[35-37]. However, endoloop placement might not be possible for all polyps, especially those with a large head or a short stalk. A previous study reported an 8.3% failure rate in endoloop placement[37]. Although the largest available endoloop has an opening diameter of 30 mm, it is floppy and challenging to place at the stalk of large polyps. Moreover, the polyp stalk will be shortened after endoloop tightening; therefore, endoloop-assisted polypectomy might not be suitable for polyps with short stalks due to the possibility of incomplete resection. A case series reported successful ESD for large pedunculated polyps with failed endoloop placement using a scissor-type knife[38], which allows precise dissection with targeted hemostasis. With a scissor-type knife, the tissue and vessels could be grasped between two blades and pre-coagulated before cutting (Figure 3). In addition, a case report described successful ESD with a scissor-type knife for a large pedunculated polyp with a short, thick stalk[39].

Prophylactic clip application at the thick stalk before polypectomy may prevent post-polypectomy bleeding (Figure 4). Soh *et al*[40] conducted an RCT of 137 pedunculated polyps ≥ 1 cm in 116 patients and found that prophylactic clip application before polypectomy significantly decreased immediate bleeding compared with conventional polypectomy [odds ratio (OR): 0.22; 95% confidence interval (95%CI): 0.08-0.57]. The delayed bleeding rate did not differ between the two groups. However, this technique is difficult to apply to polyps with a short thick stalk due to the risk of incomplete resection, and endoscopists should be aware of transmural burns from electrical current conducted by the



DOI: 10.3748/wjg.v29.i17.2600 **Copyright** ©The Author(s) 2023.

Figure 2 Endoloop-assisted polypectomy. A: A pedunculated polyp with a thick stalk; B: Endoloop tightening around the stalk before snaring, the polyp's color turned deep purple due to the ischemia; C: No bleeding evidence after the resection.



DOI: 10.3748/wjg.v29.i17.2600 **Copyright** ©The Author(s) 2023.

Figure 3 Endoscopic submucosal dissection with a scissor-type knife for a large subpedunculated polyp. A: After submucosal injection, a scissor-type knife could be used to perform mucosal incision; B: The tissue and vessels could be grasped between two blades and precoagulated before cutting; C: Final cut of the procedure; D: Mucosal defect after completed endoscopic submucosal dissection.

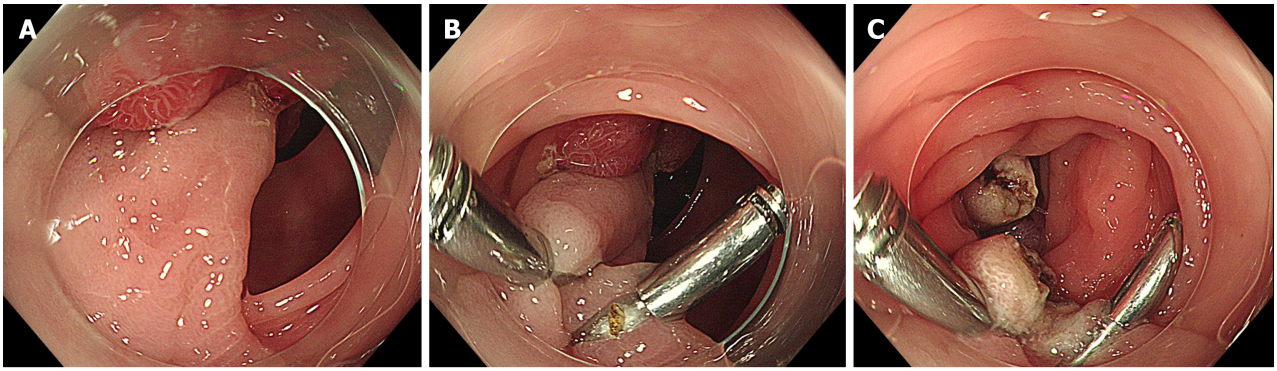
endoscopic clip.

A meta-analysis of 15 RCTs involving 3,462 patients found that both prophylactic adrenaline injection and mechanical therapy reduced the risk of early post-polypectomy bleeding [injection therapy, risk ratio (RR): 0.32; 95%CI: 0.11-0.67; mechanical therapy: RR: 0.13; 95%CI: 0.03-0.37], although no prophylactic therapy decreased the risk of delayed bleeding[41]. In conclusion, prophylactic therapy, including adrenaline injection, detachable snare, or clipping, should be performed before the resection of a pedunculated polyp with a thick stalk or large head. However, detachable snare placement or prophylactic clipping may not be possible for polyps with a short, thick stalk, which may be suitably resected using ESD.

Polyps involving the appendiceal orifice

Endoscopic resection of polyps involving the appendiceal orifice is technically challenging because of the poor-lifting nature of submucosal fibrosis, thin cecal wall, and inability to access the lesion extending deep into the appendiceal orifice. Traditionally, these polyps have been managed surgically. However, recent advances have allowed endoscopists to perform a safe endoscopic resection for these polyps.

A Japanese retrospective study revealed the safety and effectiveness of ESD for the treatment of polyps involving the appendiceal orifice. For a total of 76 lesions, the authors reported a 95.0% *en bloc*



DOI: 10.3748/wjg.v29.i17.2600 **Copyright** ©The Author(s) 2023.

Figure 4 Prophylactic clip application at the stalk before polypectomy. A: A pedunculated polyp with a thick stalk and large head. There were failed attempts placing the endoloop due to the large polyp head; B: Clip application before snaring; C: No bleeding evidence after the resection.

resection rate, 1.3% perforation, and 2.6% post-ESD appendicitis rate. However, they excluded patients with lesions deeply involving the orifice and without a history of appendectomy. The authors emphasized that ESD should be performed by experienced and skilled endoscopists in this situation[42].

Binmoeller *et al*[43] suggested the usefulness of underwater endoscopic mucosal resection (UEMR) without submucosal injection for polyps involving the appendiceal orifice. With a water-filled lumen, the floating effect facilitated snare capture (Figure 5). They reported an 89% success ratio for UEMR in 27 polyps involving the appendiceal orifice (rim, 5 patients; extending deep inside, 22 patients). There was no perforation or post-resection appendicitis; however, 7% of the patients had post-polypectomy syndrome. During surveillance, 10% of the patients had residual adenomas that could be treated endoscopically.

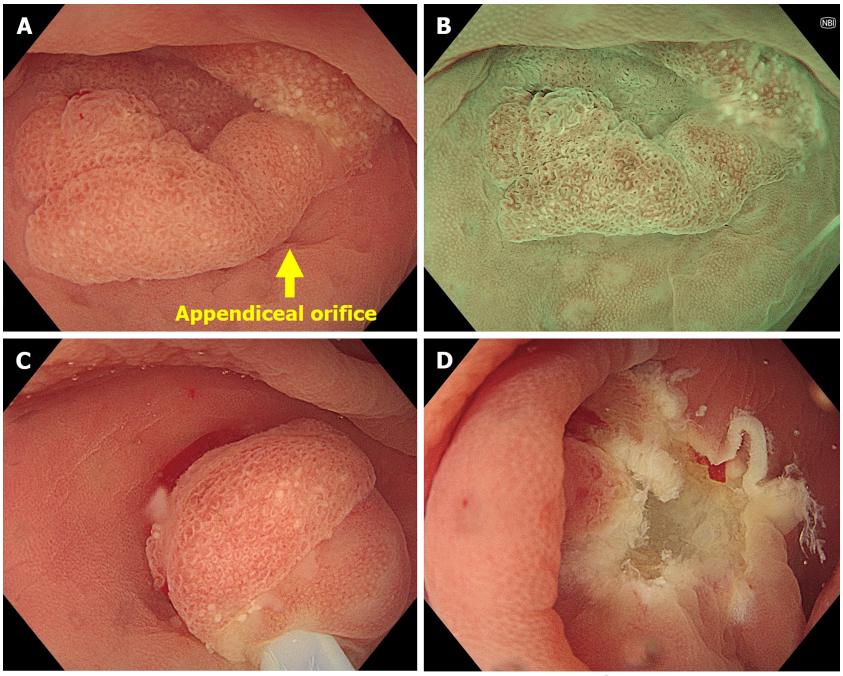
Endoscopic full-thickness resection (EFTR) has recently been employed for difficult polyps and is another suitable modality for polyps involving the appendiceal orifice. In a multicenter retrospective study, Schmidbaur *et al*[44] found that EFTR achieved R0 resection in 64% of 50 lesions involving the appendiceal orifice. However, 14% of patients developed acute appendicitis, and 42% of those with appendicitis required appendectomy. Similarly, a multicenter retrospective study by Ichkhanian *et al*[45], including 66 appendiceal orifice lesions (61% polyps extending deep into the appendiceal lumen) with a mean size of 14.5 mm, found that EFTR achieved an 89% technical success ratio and 93% R0 resection of the neoplastic lesions. Post-resection appendicitis occurred in 17% of patients without a prior history of appendectomy, and 60% (six patients) required appendectomy. Even with the promising outcomes of EFTR, the authors of both studies emphasized that patients must be counseled about the risk of post-resection appendicitis.

In summary, ESD is a viable option for polyps involving the rim of the appendiceal orifice for experienced endoscopists. However, ESD may not be feasible for lesions with a deep extension into the appendiceal orifice. UEMR is also a decent modality that is less technically demanding and has a high success rate. For lesions with deep extension into the appendiceal orifice, EFTR is the suitable option due to the high R0 resection rate. However, patients must be counseled regarding the risk of post-resection appendicitis.

Polyps on the ileocecal valve

Polyps on the ileocecal valve are technically challenging for endoscopic resection because the valve shape and orifice make it difficult to approach the lesions. Moreover, lesions may extend from the valve orifice to the terminal ileum. Therefore, resection is extremely difficult and associated with a high risk of recurrence[46]. A large retrospective study revealed a high complete resection rate (76.3%) of piecemeal EMR for polyps on the ileocecal valve, and the rate increased to 93.0% in the most recent eight years. Delayed bleeding and perforation occurred in 3.3% and 0% of the patients, and residual polyps were found in 16.5% and 18.6% during the first and second surveillance, respectively. They suggested four EMR keys for polyps on the ileocecal valve: (1) Use of a high-definition colonoscope; (2) use of a cap on the distal end of the scope; (3) inclusion of a dye in the injection fluid; and (4) initiating injection at the margin of the polyp with the valve orifice[47].

ESD for polyps on the ileocecal valve may be necessary for lesions suspected to be early carcinomas. However, ESD in this area is technically challenging because of the valve anatomy and composition. The ileocecal valve has abundant submucosal fatty tissue; consequently, the colonoscope lens often becomes cloudy during dissection. Yoshizaki *et al*[48] found no difference in the *en bloc* resection and perforation rates between ESD of lesions involving the ileocecal valve and lesions that did not involve it. Lesions involving the ileocecal valve were reported to have a 97% *en bloc* resection rate without perforation. The authors highlighted the critical steps for successful ESD. The mucosal incision should be started on the ileal side of the tumor to prevent the tumor from prolapsing into the terminal ileum.



DOI: 10.3748/wjg.v29.i17.2600 **Copyright** ©The Author(s) 2023.

Figure 5 Underwater endoscopic mucosal resection for a polyp involving appendiceal orifice. A: Endoscopic image showing a 15-mm sessile polyp involving the appendiceal orifice; B: Magnifying narrow-band image showing a type 1 polyp of the Japan Narrow-band Imaging Expert Team classification with open pit pattern. The most likely diagnosis was sessile serrated lesion; C: Underwater snaring without submucosal injection; D: Mucosal defect after completed underwater endoscopic mucosal resection.

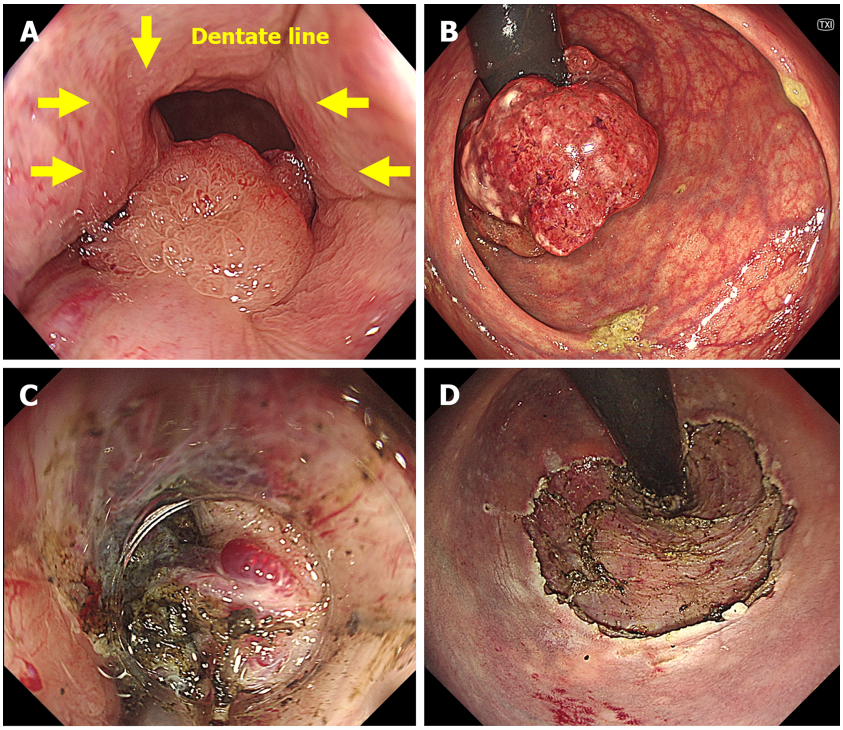
For areas with abundant submucosal fatty tissue, the electrical setting should be changed from the forced coagulation mode to the endocut or swift coagulation mode to enhance tissue cutting. Recently, Tanaka *et al*[49] conducted a study to evaluate the outcomes of ESD for polyps of the ileocecal valve with extension into the terminal ileum. They found that ESD of lesions with or without extension into the terminal ileum showed no difference in the *en bloc* resection rate (95% *vs* 94%, $P = 0.79$), R0 resection rate (90% *vs* 89%, $P = 0.89$), postoperative bleeding (5% *vs* 3%, $P = 0.79$), intraoperative perforation (0% *vs* 4%, $P = 0.34$), or delayed perforation (0% *vs* 0%, respectively). Therefore, ESD for polyps involving the ileocecal valve with extension into the terminal ileum is safe and effective in expert hands.

Polyps at the anorectal junction

Polyps close to the dentate line can be challenging to resect because of the risk of bleeding from the hemorrhoids. Polypectomy in this area is painful due to the sensory nerves in the squamous epithelium below the dentate line. Moreover, the anatomy of the anal sphincter makes it difficult to maintain good visualization[50]. For polyps at the anorectal junction that are indicated for ESD, Imai *et al*[51] proposed the following strategies: (1) Using a cap on the distal end of the scope to maintain good visualization in the narrow space of the anal canal; (2) addition of 1% lidocaine to the submucosal injection solution to prevent pain; (3) employing a horizontal approach with an endoscopic knife to minimize thermal damage to the muscular layer; and (4) performing preventive hemostasis when thick hemorrhoidal vessels are observed. With these strategies, they reported an *en bloc* resection rate of 95.6% and an R0 resection rate of 53.3%. The low R0 resection rate was due to burning artifacts on the anal side of the specimens. They reported a 4.4% perforation and a 2.2% postoperative bleeding rate. Tamaru *et al*[52] investigated the outcomes of ESD for polyps at the anorectal junction in patients with and without hemorrhoids. They found no differences in *en bloc* resection (93% *vs* 95%) or postoperative bleeding (16% *vs* 11%) rates between patients with and without hemorrhoids. Therefore, ESD is safe and effective for patients with lesions near the anorectal junction and hemorrhoids. Similarly, several studies have shown the safety and effectiveness of ESD for polyps at the anorectal junction[53-55]. In conclusion, ESD for polyps at the anorectal junction is safe even in the presence of hemorrhoids, and special strategies to prevent bleeding and pain should be implemented (Figure 6).

Locally recurrent colorectal polyps

Locally recurrent polyps mostly result from incomplete resections. A systematic review and meta-analysis found that local recurrence after EMR of non-pedunculated polyps occurred in 3% of *en bloc* resections and 20% of piecemeal resections, and 90% of recurrences were detected within 6 mo after EMR[56]. Locally recurrent polyps without risk factors for lymph node metastasis and positive vertical margins can be resected endoscopically[57]. However, endoscopic resection of locally recurrent polyps



DOI: 10.3748/wjg.v29.i17.2600 **Copyright** ©The Author(s) 2023.

Figure 6 Endoscopic submucosal dissection for a polyp involving the anorectal junction. A: Endoscopic image showing a 6-cm laterally spreading tumor involving the dentate line; B: Retroflexed view of the same polyp; C: Hemorrhoidal plexus at the anus makes the endoscopic submucosal dissection (ESD) challenging with the bleeding risk; D: Mucosal defect after completed ESD.

is extraordinarily challenging because it is associated with poor lifting with submucosal injection from submucosal fibrosis[58].

The 2020 JGES guidelines for colorectal ESD and EMR suggest that local recurrence of early carcinoma after endoscopic resection is an indication of ESD[10]. A Japanese retrospective study revealed that ESD had a higher *en bloc* resection rate than EMR for locally recurrent lesions (56% *vs* 39%, respectively), although the lesions in the ESD group were significantly larger than those in the EMR group (mean size; 25.3 mm *vs* 7.8 mm, $P = 0.001$)[59]. Perforations were not observed in the ESD group. However, this study was conducted at a single center with expertise in ESD. ESD for locally recurrent lesions is technically demanding and requires high operator skills. It is noted that the *en bloc* resection rate of locally recurrent polyps was much lower than their previous report of colorectal ESD (168/200 patients, 84%)[60]. Ide *et al*[61] conducted a retrospective study comparing ESD with the pocket-creation method using a traction device and conventional ESD for locally recurrent lesions. They found that ESD using the pocket-creation method with a traction device had higher *en bloc* resection and R0 resection rates than conventional ESD (100% *vs* 78%, $P = 0.008$, and 97% *vs* 66%, $P=0.001$, respectively). Therefore, the combination of the pocket creation method and traction device is a promising strategy for the resection of locally recurrent polyps.

UEMR without submucosal injection has been reported as a promising technique for the salvage treatment of recurrent adenomas. Fibrosis prevents elevation of the recurrent lesion after submucosal injection, while the surrounding normal mucosa still elevates around the non-lifting lesion after the injection. This makes snare capture difficult. The floating effect after UEMR facilitates snare capture with minimal risk of perforation because the colonic muscularis propria remains circular with a water-filling lumen. Kim *et al*[62] conducted a retrospective, cross-sectional study involving patients with recurrent adenomas after piecemeal resection of colorectal LSTs. They found that the *en bloc* resection and complete resection rates were higher in the UEMR group than in the EMR group (47.2% *vs* 15.9%, $P = 0.002$, and 88.9% *vs* 31.8%, $P < 0.001$, respectively). The recurrence rate on surveillance colonoscopy was lower in the UEMR group than in the EMR group (10.0% *vs* 39.4%, $P = 0.020$). In this study, UEMR was an independent predictor of *en bloc* resection and complete removal.

In summary, ESD and UEMR are the appropriate modalities for treating locally recurrent colorectal polyps. Previous studies have shown a higher *en bloc* resection rate with ESD than with UEMR and ESD using the pocket-creation method and a traction device is a promising strategy for locally recurrent polyps. However, ESD for locally recurrent lesions is only suitable for centers with high ESD expertise because it is technically difficult, even with advances in ESD devices and techniques. In extremely difficult cases, endoscopists may consider surgery if the anticipated risk of complications is too high.

Polypectomy in patients with strong colonic peristalsis

Strong colonic spasm is a common obstacle during colorectal polypectomy, limiting visualization and scope manipulation. In this situation, endoscopists generally use antispasmodic drugs. Hyoscine butylbromide is the most common antispasmodic agent in practice, and the recommended dose is 20 mg *via* intravenous injection. Hyoscine butylbromide exerts an antimuscarinic anticholinergic effect that reduces the smooth muscle tone at multiple sites in the gastrointestinal tract. Contraindications of hyoscine butylbromide include cardiovascular disease, glaucoma, myasthenia gravis, and hypersensitivity to the drug[63]. In patients with these contraindications, other antispasmodic agents, including glucagon or peppermint oil, should be administered. The dose of glucagon is 1 mg *via* intravenous injection, which is contraindicated in patients with pheochromocytoma[64]. Peppermint oil was administered *via* intraluminal application of 20 mL of 1.6% L-menthol solution without contraindications[65]. Topical lidocaine, a local anesthetic, also functions as an antispasmodic agent by blocking the Na^+ channels. It was administered *via* the intraluminal application of 30 mL of 2% lidocaine hydrochloride. An RCT found no difference in the inhibitory duration between topical lidocaine and peppermint oil; however, topical lidocaine significantly decreased rebound spasm[66].

In specific situations with intense colonic spasms, even with the administration of antispasmodic drugs, UEMR may be a decent modality. Another advantage of the water-filled lumen in UEMR is the stabilized visualization of the lumen. Pattarajierapan *et al*[67] reported successful UEMR for rectal adenoma in the non-distensible rectum due to severe fecal incontinence and intense colonic peristalsis. Therefore, UEMR may be a suitable option for patients with intense colonic spasms who have failed medication.

RECENT ADVANCES IN POLYPECTOMY DEVICES AND TECHNIQUES

Several technologies have been developed to aid endoscopists in performing safe and effective polypectomies, especially complex procedures such as ESD. These advances include video endoscopy system, equipment assisting in advanced polypectomy, and closure devices/techniques for complication management. Endoscopists should know how to use these devices and their availability in practice to enhance polypectomy performance, particularly in challenging cases.

Video endoscopy system

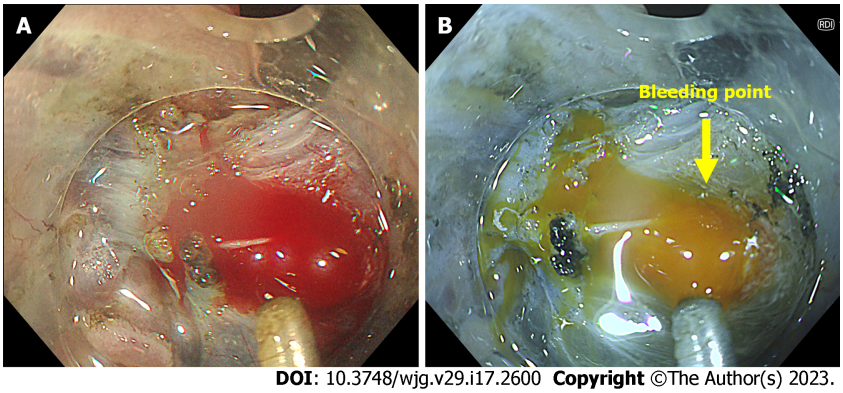
Red dichromatic imaging (RDI) was recently installed in the latest Olympus endoscopy system EVIS X1. RDI utilizes two long-wavelength lights (600 nm and 630 nm), which improve the visibility of thick blood vessels in deep tissues[68,69]. Therefore, easier identification of bleeding sources during polypectomy is expected in the RDI mode (Figure 7). Fujimoto *et al*[69] conducted an RCT comparing hemostatic procedures using RDI and white-light imaging (WLI). Although they found that RDI did not shorten the hemostatic time, it significantly reduced psychological stress compared to WLI. They concluded that it is safe and reasonable to use the RDI during hemostatic procedures to reduce the psychological stress experienced by endoscopists.

Equipment assisting advanced polypectomy

Although ESD has been widely accepted as a standard procedure for colorectal polyps that require *en bloc* resection, a limited number of endoscopists outside East Asia are competent owing to the difficulty of the method[70]. Colorectal ESD is more technically demanding than gastric or esophageal ESD because of its thin colonic wall and narrow colonic lumen, as well as peristalsis and respiratory movement. In addition to good training with experienced endoscopists, the recent development of traction devices and techniques may facilitate the procedure. The lack of traction during dissection contributes to the technical difficulty of ESD; therefore, various traction devices and techniques have been proposed (Figure 8). These devices include the clip-line method[71], S-O clip[72], double clips and rubber band traction[73], and traction wire[74]. To date, there have been no head-to-head comparisons of these traction devices, and the traction method has been selected based on tumor location and preference[75]. The clip-line method is helpful for rectal lesions but may not be feasible for colon lesions. For colonic ESD, endoscopists can use an S-O clip, double clips and rubber band traction, or traction wire. Without traction devices, ESD using the pocket creation method is a special technique that maintains a stable scope position inside the pocket while sustaining good traction[76,77]. This technique starts with an initial small mucosal incision, the creation of a submucosal pocket under most of the tumor, and then the completion of opening the pocket in a step-by-step manner.

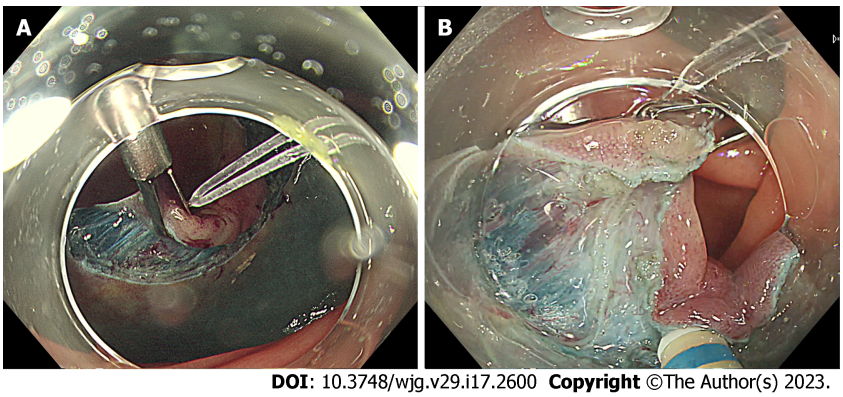
Closure devices and techniques for complication management

Perforation is the most feared complication of polypectomy. With advances in closure devices, most perforations after polypectomy can be closed endoscopically, thereby eliminating the need for surgery, which is associated with morbidity and mortality[78]. Endoscopic closure devices can be classified into through-the-scope clips (TTSC), over-the-scope clips (OTSC), and suturing devices. Useful modified



DOI: 10.3748/wjg.v29.i17.2600 **Copyright** ©The Author(s) 2023.

Figure 7 Bleeding during endoscopic submucosal dissection. A: Endoscopic image in white light imaging showing the bleeding from the large vessels of the polyp; B: Identification of bleeding sources during polypectomy is easier in the Red Dichromatic Imaging (RDI) mode. RDI mode also reduces the endoscopists' psychological stress by turning the blood color yellow.



DOI: 10.3748/wjg.v29.i17.2600 **Copyright** ©The Author(s) 2023.

Figure 8 Traction device during endoscopic submucosal dissection. A: Rubber band traction clip facilitating endoscopic submucosal dissection of a laterally spreading tumor with submucosal fibrosis; B: Traction force from the device helping during the submucosal dissection.

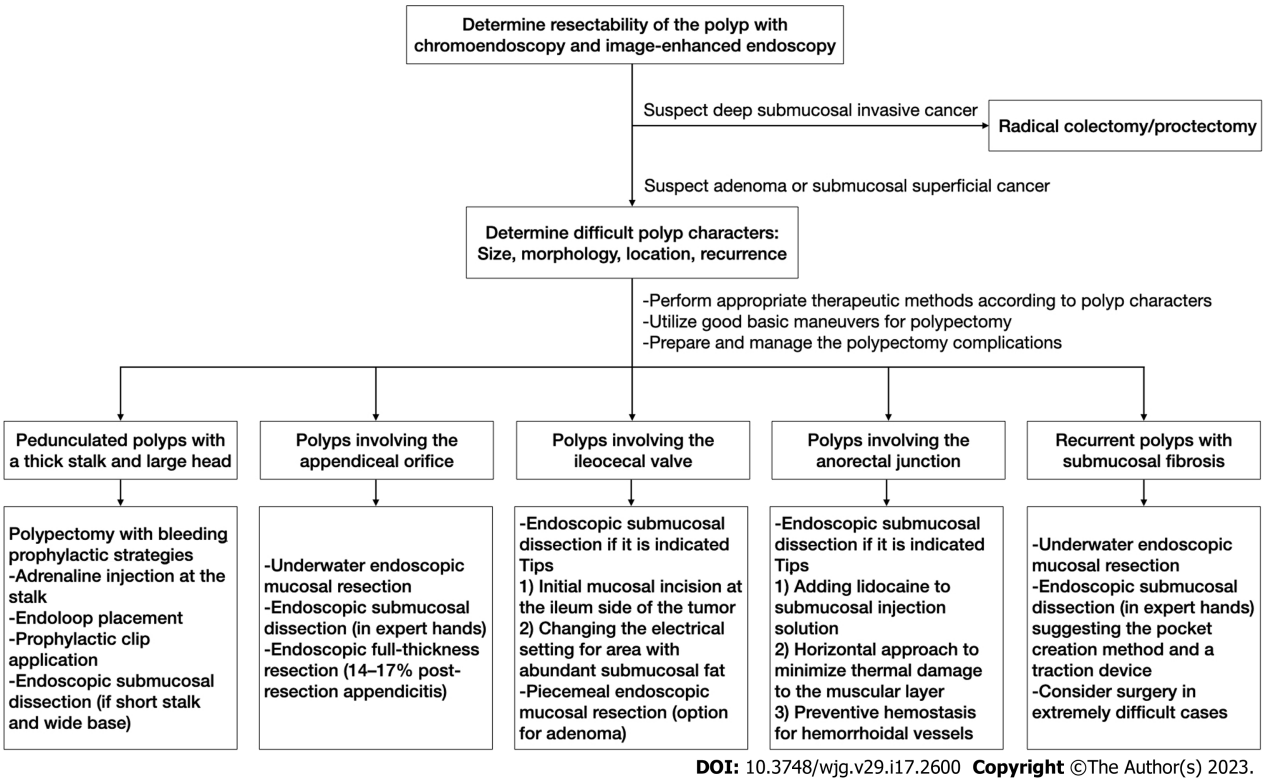
techniques in TTSC include the hold-and-drag closure technique using reopenable clips[78], mucosal incision method[79], endoloop-assisted clip closure[80], over-the-line clip method[80], and dual-action clip closure[81]. To date, no RCT has compared these closure techniques after colorectal polypectomy. Modified techniques in TTSC help close defects larger than the width of the clips. Therefore, endoscopists should learn these modified techniques, which are feasible for their centers because they may occasionally be necessary.

The OTSC system is a super-elastic nitinol clip that must be mounted at the end of an endoscope before deployment. This results in full-thickness closure of the teeth arranged in a bear-trap shape[78]. The reported successful closure rate for iatrogenic colon perforation for OTSC is 89%-100%[82-85]. However, the limitations of OTSC include lower success rates in the right colon compared with the left side and limited availability.

Endoscopic suturing is a promising method for defect closure with a 100% success rate in a report of 16 patients[86]. The endoscopic suturing device consists of a curved needle placed on the endoscope tip, a catheter-based suture anchor, and an operating handle attached to the neck of the instrument channel of the endoscope[87]. Limitations to the suturing device include the requirement of a double-channel endoscope and special training in endoscopic suturing to become competent in this technique. In addition, endoscopic suturing devices are expensive and limited in availability.

CONCLUSION

Recent advancements in EMR, ESD, and EFTR techniques and devices allow curative therapy of difficult colorectal polyps and prevent unnecessary surgery that carries the risk of morbidity and mortality. Moreover, these advancements also help endoscopists cope with feared complications, such as massive intra-procedural bleeding and perforation. However, proper selection of adjunct endoscopic devices/techniques according to polyp characteristics and step-by-step training for skill improvement are critical for successful advanced polypectomies. Based on current evidence, we summarize the stepwise



DOI: 10.3748/wjg.v29.i17.2600 **Copyright** ©The Author(s) 2023.

Figure 9 Stepwise approach for difficult colorectal polyps.

approach (Figure 9) that might help endoscopists make better decisions for the treatment of difficult colorectal polyps.

FOOTNOTES

Author contributions: Pattarajierapan S wrote the article; Takamaru H and Khomvilai S made substantial contributions to the content, offered critical revisions, and approved the final version of the article.

Conflict-of-interest statement: The authors have no conflicts of interest or financial ties to disclose.

Open-Access: This article is an open-access article that was selected by an in-house editor and fully peer-reviewed by external reviewers. It is distributed in accordance with the Creative Commons Attribution NonCommercial (CC BY-NC 4.0) license, which permits others to distribute, remix, adapt, build upon this work non-commercially, and license their derivative works on different terms, provided the original work is properly cited and the use is non-commercial. See: https://creativecommons.org/Licenses/by-nc/4.0/

Country/Territory of origin: Thailand

ORCID number: Sukit Pattarajierapan 0000-0003-1042-8476; Hiroyuki Takamaru 0000-0002-7019-6331; Supakij Khomvilai 0000-0002-9703-9627.

Corresponding Author's Membership in Professional Societies: American Society for Gastrointestinal Endoscopy, No. 162994.

S-Editor: Chen YL
L-Editor: A
P-Editor: Cai YX

REFERENCES

1 **Sung H**, Ferlay J, Siegel RL, Laversanne M, Soerjomataram I, Jemal A, Bray F. Global Cancer Statistics 2020: GLOBOCAN Estimates of Incidence and Mortality Worldwide for 36 Cancers in 185 Countries. *CA Cancer J Clin* 2021; **71**: 209-249 [PMID: 33538338 DOI: 10.3322/caac.21660]

2 **Winawer SJ**, Zauber AG, Ho MN, O'Brien MJ, Gottlieb LS, Sternberg SS, Waye JD, Schapiro M, Bond JH, Panish JF. Prevention of colorectal cancer by colonoscopic polypectomy. The National Polyp Study Workgroup. *N Engl J Med* 1993; **329**: 1977-1981 [PMID: 8247072 DOI: 10.1056/NEJM199312303292701]

3 **Baxter NN**, Warren JL, Barrett MJ, Stukel TA, Doria-Rose VP. Association between colonoscopy and colorectal cancer mortality in a US cohort according to site of cancer and colonoscopist specialty. *J Clin Oncol* 2012; **30**: 2664-2669 [PMID: 22689809 DOI: 10.1200/JCO.2011.40.4772]

4 **Gallegos-Orozco JF**, Gurudu SR. Complex colon polypectomy. *Gastroenterol Hepatol (N Y)* 2010; **6**: 375-382 [PMID: 20733940]

5 **Ngamruengphong S**, Pohl H, Haito-Chavez Y, Khashab MA. Update on Difficult Polypectomy Techniques. *Curr Gastroenterol Rep* 2016; **18**: 3 [PMID: 26714965 DOI: 10.1007/s11894-015-0476-7]

6 **Mann R**, Gajendran M, Umapathy C, Perisetti A, Goyal H, Saligram S, Echavarria J. Endoscopic Management of Complex Colorectal Polyps: Current Insights and Future Trends. *Front Med (Lausanne)* 2021; **8**: 728704 [PMID: 35127735 DOI: 10.3389/fmed.2021.728704]

7 **Kudo S**, Tamura S, Nakajima T, Yamano H, Kusaka H, Watanabe H. Diagnosis of colorectal tumorous lesions by magnifying endoscopy. *Gastrointest Endosc* 1996; **44**: 8-14 [PMID: 8836710 DOI: 10.1016/s0016-5107(96)70222-5]

8 **Sano Y**, Tanaka S, Kudo SE, Saito S, Matsuda T, Wada Y, Fujii T, Ikematsu H, Uraoka T, Kobayashi N, Nakamura H, Hotta K, Horimatsu T, Sakamoto N, Fu KI, Tsuruta O, Kawano H, Kashida H, Takeuchi Y, Machida H, Kusaka T, Yoshida N, Hirata I, Terai T, Yamano HO, Kaneko K, Nakajima T, Sakamoto T, Yamaguchi Y, Tamai N, Nakano N, Hayashi N, Oka S, Iwatate M, Ishikawa H, Murakami Y, Yoshida S, Saito Y. Narrow-band imaging (NBI) magnifying endoscopic classification of colorectal tumors proposed by the Japan NBI Expert Team. *Dig Endosc* 2016; **28**: 526-533 [PMID: 26927367 DOI: 10.1111/den.12644]

9 **Hayashi N**, Tanaka S, Hewett DG, Kaltenbach TR, Sano Y, Ponchon T, Saunders BP, Rex DK, Soetikno RM. Endoscopic prediction of deep submucosal invasive carcinoma: validation of the narrow-band imaging international colorectal endoscopic (NICE) classification. *Gastrointest Endosc* 2013; **78**: 625-632 [PMID: 23910062 DOI: 10.1016/j.gie.2013.04.185]

10 **Tanaka S**, Kashida H, Saito Y, Yahagi N, Yamano H, Saito S, Hisabe T, Yao T, Watanabe M, Yoshida M, Saitoh Y, Tsuruta O, Sugihara KI, Igarashi M, Toyonaga T, Ajioka Y, Kusunoki M, Koike K, Fujimoto K, Tajiri H. Japan Gastroenterological Endoscopy Society guidelines for colorectal endoscopic submucosal dissection/endoscopic mucosal resection. *Dig Endosc* 2020; **32**: 219-239 [PMID: 31566804 DOI: 10.1111/den.13545]

11 **Tateishi Y**, Nakanishi Y, Taniguchi H, Shimoda T, Umemura S. Pathological prognostic factors predicting lymph node metastasis in submucosal invasive (T1) colorectal carcinoma. *Mod Pathol* 2010; **23**: 1068-1072 [PMID: 20473277 DOI: 10.1038/modpathol.2010.88]

12 **Yamaoka Y**, Shiomi A, Kagawa H, Hino H, Manabe S, Chen K, Nanishi K, Notsu A. Lymph node metastasis in T1 colorectal cancer with the only high-risk histology of submucosal invasion depth ≥ 1000 μm. *Int J Colorectal Dis* 2022; **37**: 2387-2395 [PMID: 36283994 DOI: 10.1007/s00384-022-04269-6]

13 **Suh JH**, Han KS, Kim BC, Hong CW, Sohn DK, Chang HJ, Kim MJ, Park SC, Park JW, Choi HS, Oh JH. Predictors for lymph node metastasis in T1 colorectal cancer. *Endoscopy* 2012; **44**: 590-595 [PMID: 22638780 DOI: 10.1055/s-0031-1291665]

14 **Kikuchi R**, Takano M, Takagi K, Fujimoto N, Nozaki R, Fujiyoshi T, Uchida Y. Management of early invasive colorectal cancer. Risk of recurrence and clinical guidelines. *Dis Colon Rectum* 1995; **38**: 1286-1295 [PMID: 7497841 DOI: 10.1007/BF02049154]

15 **Kitajima K**, Fujimori T, Fujii S, Takeda J, Ohkura Y, Kawamata H, Kumamoto T, Ishiguro S, Kato Y, Shimoda T, Iwashita A, Ajioka Y, Watanabe H, Watanabe T, Muto T, Nagasako K. Correlations between lymph node metastasis and depth of submucosal invasion in submucosal invasive colorectal carcinoma: a Japanese collaborative study. *J Gastroenterol* 2004; **39**: 534-543 [PMID: 15235870 DOI: 10.1007/s00535-004-1339-4]

16 **Nakadoi K**, Tanaka S, Kanao H, Terasaki M, Takata S, Oka S, Yoshida S, Arihiro K, Chayama K. Management of T1 colorectal carcinoma with special reference to criteria for curative endoscopic resection. *J Gastroenterol Hepatol* 2012; **27**: 1057-1062 [PMID: 22142484 DOI: 10.1111/j.1440-1746.2011.07041.x]

17 **Matsuda T**, Fujii T, Saito Y, Nakajima T, Uraoka T, Kobayashi N, Ikehara H, Ikematsu H, Fu KI, Emura F, Ono A, Sano Y, Shimoda T, Fujimori T. Efficacy of the invasive/non-invasive pattern by magnifying chromoendoscopy to estimate the depth of invasion of early colorectal neoplasms. *Am J Gastroenterol* 2008; **103**: 2700-2706 [PMID: 18853968 DOI: 10.1111/j.1572-0241.2008.02190.x]

18 **Togashi K**, Konishi F, Ishizuka T, Sato T, Senba S, Kanazawa K. Efficacy of magnifying endoscopy in the differential diagnosis of neoplastic and non-neoplastic polyps of the large bowel. *Dis Colon Rectum* 1999; **42**: 1602-1608 [PMID: 10613481 DOI: 10.1007/BF02236215]

19 **Gupta S**, Miskovic D, Bhandari P, Dolwani S, McKaig B, Pullan R, Rembacken B, Riley S, Rutter MD, Suzuki N, Tsiamoulos Z, Valori R, Vance ME, Faiz OD, Saunders BP, Thomas-Gibson S. A novel method for determining the difficulty of colonoscopic polypectomy. *Frontline Gastroenterol* 2013; **4**: 244-248 [PMID: 28839733 DOI: 10.1136/flgastro-2013-100331]

20 **Longcroft-Wheaton G**, Duku M, Mead R, Basford P, Bhandari P. Risk stratification system for evaluation of complex polyps can predict outcomes of endoscopic mucosal resection. *Dis Colon Rectum* 2013; **56**: 960-966 [PMID: 23838864 DOI: 10.1097/DCR.0b013e31829193e0]

21 **Ferlitsch M**, Moss A, Hassan C, Bhandari P, Dumonceau JM, Paspatis G, Jover R, Langner C, Bronzwaer M, Nalankilli K, Fockens P, Hazzan R, Gralnek IM, Gschwantler M, Waldmann E, Jeschek P, Penz D, Heresbach D, Moons L, Lemmers A, Paraskeva K, Pohl J, Ponchon T, Regula J, Repici A, Rutter MD, Burgess NG, Bourke MJ. Colorectal polypectomy and endoscopic mucosal resection (EMR): European Society of Gastrointestinal Endoscopy (ESGE) Clinical Guideline. *Endoscopy* 2017; **49**: 270-297 [PMID: 28212588 DOI: 10.1055/s-0043-102569]

22 **Kudo Se**, Lambert R, Allen JI, Fujii H, Fujii T, Kashida H, Matsuda T, Mori M, Saito H, Shimoda T, Tanaka S, Watanabe H, Sung JJ, Feld AD, Inadomi JM, O'Brien MJ, Lieberman DA, Ransohoff DF, Soetikno RM, Triadafilopoulos G, Zauber

A, Teixeira CR, Rey JF, Jaramillo E, Rubio CA, Van Gossum A, Jung M, Vieth M, Jass JR, Hurlstone PD. Nonpolypoid neoplastic lesions of the colorectal mucosa. *Gastrointest Endosc* 2008; **68**: S3-47 [PMID: 18805238 DOI: 10.1016/j.gie.2008.07.052]

23 **Hotta K**, Fujii T, Saito Y, Matsuda T. Local recurrence after endoscopic resection of colorectal tumors. *Int J Colorectal Dis* 2009; **24**: 225-230 [PMID: 18972121 DOI: 10.1007/s00384-008-0596-8]

24 **Oka S**, Tanaka S, Saito Y, Iishi H, Kudo SE, Ikematsu H, Igarashi M, Saitoh Y, Inoue Y, Kobayashi K, Hisabe T, Tsuruta O, Sano Y, Yamano H, Shimizu S, Yahagi N, Watanabe T, Nakamura H, Fujii T, Ishikawa H, Sugihara K; Colorectal Endoscopic Resection Standardization Implementation Working Group of the Japanese Society for Cancer of the Colon and Rectum, Tokyo, Japan. Local recurrence after endoscopic resection for large colorectal neoplasia: a multicenter prospective study in Japan. *Am J Gastroenterol* 2015; **110**: 697-707 [PMID: 25848926 DOI: 10.1038/ajg.2015.96]

25 **Tanaka S**, Saitoh Y, Matsuda T, Igarashi M, Matsumoto T, Iwao Y, Suzuki Y, Nozaki R, Sugai T, Oka S, Itabashi M, Sugihara KI, Tsuruta O, Hirata I, Nishida H, Miwa H, Enomoto N, Shimosegawa T, Koike K. Evidence-based clinical practice guidelines for management of colorectal polyps. *J Gastroenterol* 2021; **56**: 323-335 [PMID: 33710392 DOI: 10.1007/s00535-021-01776-1]

26 **Hotta K**, Oyama T, Shinohara T, Miyata Y, Takahashi A, Kitamura Y, Tomori A. Learning curve for endoscopic submucosal dissection of large colorectal tumors. *Dig Endosc* 2010; **22**: 302-306 [PMID: 21175483 DOI: 10.1111/j.1443-1661.2010.01005.x]

27 **Chien H**, Imai K, Hotta K, Ito S, Yamaguchi Y, Kawata N, Tanaka M, Takizawa K, Kakushima N, Matsubayashi H, Ono H. Tip-in EMR for R0 resection for a large flat colonic tumor. *Gastrointest Endosc* 2016; **84**: 743 [PMID: 27207826 DOI: 10.1016/j.gie.2016.05.017]

28 **Sato Y**, Ozawa SI, Yasuda H, Kato M, Kiyokawa H, Yamashita M, Matsuo Y, Yamamoto H, Itoh F. Tip-in endoscopic mucosal resection for large colorectal sessile polyps. *Surg Endosc* 2021; **35**: 1820-1826 [PMID: 32356110 DOI: 10.1007/s00464-020-07581-w]

29 **Takada K**, Hotta K, Imai K, Ito S, Kishida Y, Minamide T, Yamamoto Y, Yabuuchi Y, Yoshida M, Maeda Y, Kawata N, Takizawa K, Ishiwatari H, Matsubayashi H, Kawabata T, Ono H. Tip-in EMR as an alternative to endoscopic submucosal dissection for 20- to 30-mm nonpedunculated colorectal neoplasms. *Gastrointest Endosc* 2022; **96**: 849-856.e3 [PMID: 35798055 DOI: 10.1016/j.gie.2022.06.030]

30 **Yamada M**, Saito Y, Sakamoto T, Nakajima T, Kushima R, Parra-Blanco A, Matsuda T. Endoscopic predictors of deep submucosal invasion in colorectal laterally spreading tumors. *Endoscopy* 2016; **48**: 456-464 [PMID: 26919264 DOI: 10.1055/s-0042-100453]

31 **Dobrowolski S**, Dobosz M, Babicki A, Głowacki J, Nałecz A. Blood supply of colorectal polyps correlates with risk of bleeding after colonoscopic polypectomy. *Gastrointest Endosc* 2006; **63**: 1004-1009 [PMID: 16733117 DOI: 10.1016/j.gie.2005.11.063]

32 **Dobrowolski S**, Dobosz M, Babicki A, Dymecki D, Hać S. Prophylactic submucosal saline-adrenaline injection in colonoscopic polypectomy: prospective randomized study. *Surg Endosc* 2004; **18**: 990-993 [PMID: 15108107 DOI: 10.1007/s00464-003-9214-6]

33 **Lee SH**, Chung IK, Kim SJ, Kim JO, Ko BM, Kim WH, Kim HS, Park DI, Kim HJ, Byeon JS, Yang SK, Jang BI, Jung SA, Jeen YT, Choi JH, Choi H, Han DS, Song JS. Comparison of postpolypectomy bleeding between epinephrine and saline submucosal injection for large colon polyps by conventional polypectomy: a prospective randomized, multicenter study. *World J Gastroenterol* 2007; **13**: 2973-2977 [PMID: 17589949 DOI: 10.3748/wjg.v13.i21.2973]

34 **Hachisu T**. A new detachable snare for hemostasis in the removal of large polyps or other elevated lesions. *Surg Endosc* 1991; **5**: 70-74 [PMID: 1948617 DOI: 10.1007/BF00316840]

35 **Di Giorgio P**, De Luca L, Calcagno G, Rivellini G, Mandato M, De Luca B. Detachable snare *vs* epinephrine injection in the prevention of postpolypectomy bleeding: a randomized and controlled study. *Endoscopy* 2004; **36**: 860-863 [PMID: 15452780 DOI: 10.1055/s-2004-825801]

36 **Kouklakis G**, Mpoumponaris A, Gatopoulou A, Efraimidou E, Manolas K, Lirantzopoulos N. Endoscopic resection of large pedunculated colonic polyps and risk of postpolypectomy bleeding with adrenaline injection *vs* endoloop and hemoclip: a prospective, randomized study. *Surg Endosc* 2009; **23**: 2732-2737 [PMID: 19430833 DOI: 10.1007/s00464-009-0478-3]

37 **Paspatis GA**, Paraskeva K, Theodoropoulou A, Mathou N, Vardas E, Oustamanolakis P, Chlouverakis G, Karagiannis I. A prospective, randomized comparison of adrenaline injection in combination with detachable snare *vs* adrenaline injection alone in the prevention of postpolypectomy bleeding in large colonic polyps. *Am J Gastroenterol* 2006; **101**: 2805; quiz 2913 [PMID: 17026560 DOI: 10.1111/j.1572-0241.2006.00855.x]

38 **Jawaid S**, Draganov PV, Yang D. Endoscopic resection of large pedunculated colon polyps using only a scissor-type knife: a case series. *VideoGIE* 2020; **5**: 264-266 [PMID: 32529165 DOI: 10.1016/j.vgie.2020.02.016]

39 **Yamamoto S**, Shafazand M. Endoscopic submucosal dissection with scissor-type knife for pedunculated polyp with short and thick stalk. *VideoGIE* 2018; **3**: 189-190 [PMID: 30128383 DOI: 10.1016/j.vgie.2018.04.001]

40 **Soh JS**, Seo M, Kim KJ. Prophylactic clip application for large pedunculated polyps before snare polypectomy may decrease immediate postpolypectomy bleeding. *BMC Gastroenterol* 2020; **20**: 68 [PMID: 32164613 DOI: 10.1186/s12876-020-01210-5]

41 **Park CH**, Jung YS, Nam E, Eun CS, Park DI, Han DS. Comparison of Efficacy of Prophylactic Endoscopic Therapies for Postpolypectomy Bleeding in the Colorectum: A Systematic Review and Network Meta-Analysis. *Am J Gastroenterol* 2016; **111**: 1230-1243 [PMID: 27402502 DOI: 10.1038/ajg.2016.287]

42 **Jacob H**, Toyonaga T, Ohara Y, Tsubouchi E, Takihara H, Baba S, Yoshizaki T, Kawara F, Tanaka S, Ishida T, Hoshi N, Morita Y, Umegaki E, Azuma T. Endoscopic submucosal dissection of cecal lesions in proximity to the appendiceal orifice. *Endoscopy* 2016; **48**: 829-836 [PMID: 27467815 DOI: 10.1055/s-0042-110396]

43 **Binmoeller KF**, Hamerski CM, Shah JN, Bhat YM, Kane SD. Underwater EMR of adenomas of the appendiceal orifice (with video). *Gastrointest Endosc* 2016; **83**: 638-642 [PMID: 26375437 DOI: 10.1016/j.gie.2015.08.079]

44 **Schmidbaur S**, Wannhoff A, Walter B, Meier B, Schäfer C, Meining A, Caca K. Risk of appendicitis after endoscopic

full-thickness resection of lesions involving the appendiceal orifice: a retrospective analysis. *Endoscopy* 2021; **53**: 424-428 [PMID: 32894866 DOI: 10.1055/a-1227-4555]

45 **Ichkhanian Y**, Barawi M, Seoud T, Thakkar S, Kothari TH, Halabi ME, Ullah A, Edris W, Aepli P, Kowalski T, Shinn B, Shariaha RZ, Mahadev S, Mosko JD, Andrisani G, Di Matteo FM, Albrecht H, Giap AQ, Tang SJ, Naga YM, van Geenen E, Friedland S, Tharian B, Irani S, Ross AS, Jamil LH, Lew D, Nett AS, Farha J, Runge TM, Jovani M, Khashab MA. Endoscopic full-thickness resection of polyps involving the appendiceal orifice: a multicenter international experience. *Endoscopy* 2022; **54**: 16-24 [PMID: 33395714 DOI: 10.1055/a-1345-0044]

46 **Nanda KS**, Tutticci N, Burgess NG, Sonson R, Williams SJ, Bourke MJ. Endoscopic mucosal resection of laterally spreading lesions involving the ileocecal valve: technique, risk factors for failure, and outcomes. *Endoscopy* 2015; **47**: 710-718 [PMID: 25763831 DOI: 10.1055/s-0034-1391732]

47 **Ponugoti PL**, Broadley HM, Garcia J, Rex DK. Endoscopic management of large ileocecal valve lesions over an 18-year interval. *Endosc Int Open* 2019; **7**: E1646-E1651 [PMID: 31788547 DOI: 10.1055/a-0990-9035]

48 **Yoshizaki T**, Toyonaga T, Tanaka S, Ohara Y, Kawara F, Baba S, Tsubouchi E, Takihara H, Watanabe D, Ishida T, Hoshi N, Morita Y, Umegaki E, Azuma T. Feasibility and safety of endoscopic submucosal dissection for lesions involving the ileocecal valve. *Endoscopy* 2016; **48**: 639-645 [PMID: 26990510 DOI: 10.1055/s-0042-102783]

49 **Tanaka H**, Oka S, Kunihiro M, Nagata S, Kitamura S, Kuwai T, Hiraga Y, Furudoi A, Tanaka S. Endoscopic submucosal dissection for tumors involving the ileocecal valve with extension into the terminal ileum: a multicenter study from the Hiroshima GI Endoscopy Research Group. *Surg Endosc* 2023; **37**: 958-966 [PMID: 36070146 DOI: 10.1007/s00464-022-09542-x]

50 **Nakadoi K**, Tanaka S, Hayashi N, Ozawa S, Terasaki M, Takata S, Kanao H, Oka S, Chayama K. Clinical outcomes of endoscopic submucosal dissection for rectal tumor close to the dentate line. *Gastrointest Endosc* 2012; **76**: 444-450 [PMID: 22817799 DOI: 10.1016/j.gie.2012.04.004]

51 **Imai K**, Hotta K, Yamaguchi Y, Shinohara T, Ooka S, Shinoki K, Kakushima N, Tanaka M, Takizawa K, Matsubayashi H, Oishi T, Ono H. Safety and efficacy of endoscopic submucosal dissection of rectal tumors extending to the dentate line. *Endoscopy* 2015; **47**: 529-532 [PMID: 25502418 DOI: 10.1055/s-0034-1391078]

52 **Tamaru Y**, Oka S, Tanaka S, Hiraga Y, Kunihiro M, Nagata S, Furudoi A, Ninomiya Y, Asayama N, Shigita K, Nishiyama S, Hayashi N, Chayama K. Endoscopic submucosal dissection for anorectal tumor with hemorrhoids close to the dentate line: a multicenter study of Hiroshima GI Endoscopy Study Group. *Surg Endosc* 2016; **30**: 4425-4431 [PMID: 26895899 DOI: 10.1007/s00464-016-4761-9]

53 **Tanaka S**, Toyonaga T, Morita Y, Hoshi N, Ishida T, Ohara Y, Yoshizaki T, Kawara F, Umegaki E, Azuma T. Feasibility and safety of endoscopic submucosal dissection for lower rectal tumors with hemorrhoids. *World J Gastroenterol* 2016; **22**: 6268-6275 [PMID: 27468216 DOI: 10.3748/wjg.v22.i27.6268]

54 **Matsumoto S**, Mashima H. The efficacy of endoscopic submucosal dissection for colorectal tumors extending to the dentate line. *Int J Colorectal Dis* 2017; **32**: 831-837 [PMID: 28188417 DOI: 10.1007/s00384-017-2775-y]

55 **Probst A**, Ebigbo A, Märkl B, Ting S, Schaller T, Anthuber M, Fleischmann C, Messmann H. Endoscopic submucosal dissection for rectal neoplasia extending to the dentate line: European experience. *Endosc Int Open* 2018; **6**: E1355-E1362 [PMID: 30410957 DOI: 10.1055/a-0749-8735]

56 **Belderbos TD**, Leenders M, Moons LM, Siersema PD. Local recurrence after endoscopic mucosal resection of nonpedunculated colorectal lesions: systematic review and meta-analysis. *Endoscopy* 2014; **46**: 388-402 [PMID: 24671869 DOI: 10.1055/s-0034-1364970]

57 **Shichijo S**, Takeuchi Y, Uedo N, Ishihara R. Management of local recurrence after endoscopic resection of neoplastic colonic polyps. *World J Gastrointest Endosc* 2018; **10**: 378-382 [PMID: 30631401 DOI: 10.4253/wjge.v10.i12.378]

58 **Sato K**, Ito S, Kitagawa T, Kato M, Tominaga K, Suzuki T, Maetani I. Factors affecting the technical difficulty and clinical outcome of endoscopic submucosal dissection for colorectal tumors. *Surg Endosc* 2014; **28**: 2959-2965 [PMID: 24853849 DOI: 10.1007/s00464-014-3558-y]

59 **Sakamoto T**, Saito Y, Matsuda T, Fukunaga S, Nakajima T, Fujii T. Treatment strategy for recurrent or residual colorectal tumors after endoscopic resection. *Surg Endosc* 2011; **25**: 255-260 [PMID: 20559661 DOI: 10.1007/s00464-010-1169-9]

60 **Saito Y**, Uraoka T, Matsuda T, Emura F, Ikehara H, Mashimo Y, Kikuchi T, Fu KI, Sano Y, Saito D. Endoscopic treatment of large superficial colorectal tumors: a case series of 200 endoscopic submucosal dissections (with video). *Gastrointest Endosc* 2007; **66**: 966-973 [PMID: 17524403 DOI: 10.1016/j.gie.2007.02.053]

61 **Ide D**, Ohya TR, Ishioka M, Enomoto Y, Nakao E, Mitsuyoshi Y, Tokura J, Suzuki K, Yakabi S, Yasue C, Chino A, Igarashi M, Nakashima A, Saruta M, Saito S, Fujisaki J. Efficacy of the pocket-creation method with a traction device in endoscopic submucosal dissection for residual or recurrent colorectal lesions. *Clin Endosc* 2022; **55**: 655-664 [PMID: 35636748 DOI: 10.5946/ce.2022.009]

62 **Kim HG**, Thosani N, Banerjee S, Chen A, Friedland S. Underwater endoscopic mucosal resection for recurrences after previous piecemeal resection of colorectal polyps (with video). *Gastrointest Endosc* 2014; **80**: 1094-1102 [PMID: 25012560 DOI: 10.1016/j.gie.2014.05.318]

63 **Sanagapalli S**, Agnihotri K, Leong R, Corte CJ. Antispasmodic drugs in colonoscopy: a review of their pharmacology, safety and efficacy in improving polyp detection and related outcomes. *Therap Adv Gastroenterol* 2017; **10**: 101-113 [PMID: 28286563 DOI: 10.1177/1756283X16670076]

64 **Hosseinnezhad A**, Black RM, Aeddula NR, Adhikari D, Trivedi N. Glucagon-induced pheochromocytoma crisis. *Endocr Pract* 2011; **17**: e51-e54 [PMID: 21324811 DOI: 10.4158/EP10388.CR]

65 **Inoue K**, Dohi O, Gen Y, Jo M, Mazaki T, Tokita K, Yoshida N, Okayama T, Kamada K, Katada K, Uchiyama K, Ishikawa T, Handa O, Takagi T, Konishi H, Wakabayashi N, Yagi N, Naito Y, Itoh Y. L-menthol improves adenoma detection rate during colonoscopy: a randomized trial. *Endoscopy* 2014; **46**: 196-202 [PMID: 24573731 DOI: 10.1055/s-0034-1365035]

66 **Nemoto D**, Utano K, Isohata N, Endo S, Kumamoto K, Koshimizu TA, Lefor A, Togashi K. Topical lidocaine inhibits spasm during colonoscopy: a double-blind, randomized controlled trial (with video). *Endosc Int Open* 2017; **5**: E402-E407 [PMID: 28573171 DOI: 10.1055/s-0043-105489]

67 **Pattarajierapan S**, Khomvilai S. Underwater endoscopic mucosal resection of a rectal adenoma in the nondistensible rectum from severe fecal incontinence. *VideoGIE* 2021; **6**: 275-276 [PMID: 34141972 DOI: 10.1016/j.vgie.2021.02.014]

68 **Uraoka T**, Igarashi M. Development and clinical usefulness of a unique red dichromatic imaging technology in gastrointestinal endoscopy: A narrative review. *Therap Adv Gastroenterol* 2022; **15**: 17562848221118302 [PMID: 36082177 DOI: 10.1177/17562848221118302]

69 **Fujimoto A**, Saito Y, Abe S, Hoteya S, Nomura K, Yasuda H, Matsuo Y, Uraoka T, Kuribayashi S, Tsuji Y, Ohki D, Maehata T, Kato M, Yahagi N. Clinical usefulness of red dichromatic imaging in hemostatic treatment during endoscopic submucosal dissection: First report from a multicenter, open-label, randomized controlled trial. *Dig Endosc* 2022; **34**: 379-390 [PMID: 34775648 DOI: 10.1111/den.14191]

70 **Ma MX**, Bourke MJ. Endoscopic submucosal dissection in the West: Current status and future directions. *Dig Endosc* 2018; **30**: 310-320 [PMID: 28884493 DOI: 10.1111/den.12960]

71 **Yamasaki Y**, Takeuchi Y, Uedo N, Kanesaka T, Kato M, Hamada K, Tonai Y, Matsuura N, Akasaka T, Hanaoka N, Higashino K, Ishihara R, Okada H, Iishi H. Efficacy of traction-assisted colorectal endoscopic submucosal dissection using a clip-and-thread technique: A prospective randomized study. *Dig Endosc* 2018; **30**: 467-476 [PMID: 29424030 DOI: 10.1111/den.13036]

72 **Sakamoto N**, Osada T, Shibuya T, Beppu K, Matsumoto K, Shimada Y, Konno A, Kurosawa A, Nagahara A, Ohkusa T, Ogihara T, Watanabe S. The facilitation of a new traction device (S-O clip) assisting endoscopic submucosal dissection for superficial colorectal neoplasms. *Endoscopy* 2008; **40** Suppl 2: E94-E95 [PMID: 19085712 DOI: 10.1055/s-2007-995603]

73 **Oung B**, Rivory J, Chabrun E, Legros R, Faller J, Léger-Nguyen F, Rostain F, Ber CE, Hervieu V, Saurin JC, Ponchon T, Jacques J, Pioche M. ESD with double clips and rubber band traction of neoplastic lesions developed in the appendiceal orifice is effective and safe. *Endosc Int Open* 2020; **8**: E388-E395 [PMID: 32118111 DOI: 10.1055/a-1072-4830]

74 **Bhatt A**, Hwang JH, Sharma NR, Waxman I. Traction wire endoscopic submucosal dissection: tips and techniques from 4 institutions. *VideoGIE* 2022; **7**: 21-22 [PMID: 35059534 DOI: 10.1016/j.vgie.2021.08.011]

75 **Abe S**, Wu SYS, Ego M, Takamaru H, Sekiguchi M, Yamada M, Nonaka S, Sakamoto T, Suzuki H, Yoshinaga S, Matsuda T, Oda I, Saito Y. Efficacy of Current Traction Techniques for Endoscopic Submucosal Dissection. *Gut Liver* 2020; **14**: 673-684 [PMID: 31887810 DOI: 10.5009/gnl19266]

76 **Hayashi Y**, Sunada K, Takahashi H, Shinhata H, Lefor AT, Tanaka A, Yamamoto H. Pocket-creation method of endoscopic submucosal dissection to achieve en bloc resection of giant colorectal subpedunculated neoplastic lesions. *Endoscopy* 2014; **46** Suppl 1 UCTN: E421-E422 [PMID: 25314173 DOI: 10.1055/s-0034-1377438]

77 **Hayashi Y**, Miura Y, Yamamoto H. Pocket-creation method for the safe, reliable, and efficient endoscopic submucosal dissection of colorectal lateral spreading tumors. *Dig Endosc* 2015; **27**: 534-535 [PMID: 25708068 DOI: 10.1111/den.12465]

78 **Raju GS**. Closure of Defects and Management of Complications. *Gastrointest Endosc Clin N Am* 2019; **29**: 705-719 [PMID: 31445692 DOI: 10.1016/j.giec.2019.06.005]

79 **Otake Y**, Saito Y, Sakamoto T, Aoki T, Nakajima T, Toyoshima N, Matsuda T, Ono H. New closure technique for large mucosal defects after endoscopic submucosal dissection of colorectal tumors (with video). *Gastrointest Endosc* 2012; **75**: 663-667 [PMID: 22341112 DOI: 10.1016/j.gie.2011.10.037]

80 **Nomura T**, Sugimoto S, Temma T, Oyamada J, Ito K, Kamei A. Suturing techniques with endoscopic clips and special devices after endoscopic resection. *Dig Endosc* 2023; **35**: 287-301 [PMID: 35997063 DOI: 10.1111/den.14427]

81 **Wei MT**, Friedland S. Use of a novel dual-action clip for closure of complex endoscopic resection defects. *VideoGIE* 2022; **7**: 389-391 [PMID: 36407049 DOI: 10.1016/j.vgie.2022.08.005]

82 **Verlaan T**, Voermans RP, van Berge Henegouwen MI, Bemelman WA, Fockens P. Endoscopic closure of acute perforations of the GI tract: a systematic review of the literature. *Gastrointest Endosc* 2015; **82**: 618-28.e5 [PMID: 26005015 DOI: 10.1016/j.gie.2015.03.1977]

83 **Voermans RP**, Le Moine O, von Renteln D, Ponchon T, Giovannini M, Bruno M, Weusten B, Seewald S, Costamagna G, Deprez P, Fockens P; CLIPPER Study Group. Efficacy of endoscopic closure of acute perforations of the gastrointestinal tract. *Clin Gastroenterol Hepatol* 2012; **10**: 603-608 [PMID: 22361277 DOI: 10.1016/j.cgh.2012.02.005]

84 **Gubler C**, Bauerfeind P. Endoscopic closure of iatrogenic gastrointestinal tract perforations with the over-the-scope clip. *Digestion* 2012; **85**: 302-307 [PMID: 22614286 DOI: 10.1159/000336509]

85 **Kirschniak A**, Subotova N, Zieker D, Königsrainer A, Kratt T. The Over-The-Scope Clip (OTSC) for the treatment of gastrointestinal bleeding, perforations, and fistulas. *Surg Endosc* 2011; **25**: 2901-2905 [PMID: 21424197 DOI: 10.1007/s00464-011-1640-2]

86 **Kantsevoy SV**, Bitner M, Hajiyeva G, Mirovski PM, Cox ME, Swope T, Alexander K, Meenaghan N, Fitzpatrick JL, Gushchin V. Endoscopic management of colonic perforations: clips *versus* suturing closure (with videos). *Gastrointest Endosc* 2016; **84**: 487-493 [PMID: 26364965 DOI: 10.1016/j.gie.2015.08.074]

87 **Staudenmann D**, Choi KKH, Kaffes AJ, Saxena P. Current endoscopic closure techniques for the management of gastrointestinal perforations. *Ther Adv Gastrointest Endosc* 2022; **15**: 26317745221076705 [PMID: 35252863 DOI: 10.1177/26317745221076705]

World Journal of Gastroenterology

Submit a Manuscript: https://www.f6publishing.com

World J Gastroenterol 2023 May 7; 29(17): 2616-2627

DOI: 10.3748/wjg.v29.i17.2616

ISSN 1007-9327 (print) ISSN 2219-2840 (online)

ORIGINAL ARTICLE

Basic Study

Cryptotanshinone induces apoptosis of activated hepatic stellate cells *via* modulating endoplasmic reticulum stress

Xiao-Xue Hou, Yu-Wen Li, Jia-Li Song, Wen Zhang, Rui Liu, Hui Yuan, Tian-Tong Feng, Zheng-Yi Jiang, Wen-Ting Li, Chuan-Long Zhu

Specialty type: Gastroenterology and hepatology

Provenance and peer review: Unsolicited article; Externally peer reviewed.

Peer-review model: Single blind

Peer-review report's scientific quality classification

Grade A (Excellent): 0
Grade B (Very good): 0
Grade C (Good): C, C, C, C
Grade D (Fair): 0
Grade E (Poor): 0

P-Reviewer: Maslennikov R, Russia; Perazzo JC, Argentina

Received: November 4, 2022
Peer-review started: November 4, 2022
First decision: February 18, 2023
Revised: February 28, 2023
Accepted: April 10, 2023
Article in press: April 10, 2023
Published online: May 7, 2023

Xiao-Xue Hou, Jia-Li Song, Wen Zhang, Hui Yuan, Tian-Tong Feng, Zheng-Yi Jiang, Chuan-Long Zhu, Department of Infectious Disease, The First Affiliated Hospital of Nanjing Medical University, Nanjing 210009, Jiangsu Province, China

Yu-Wen Li, Department of Pediatrics, The First Affiliated Hospital of Nanjing Medical University, Nanjing 210009, Jiangsu Province, China

Rui Liu, Wen-Ting Li, Department of Infectious and Tropical Diseases, The Second Affiliated Hospital of Hainan Medical University, Haikou 570000, Hainan Province, China

Corresponding author: Chuan-Long Zhu, Founder, Professor, Department of Infectious Disease, The First Affiliated Hospital of Nanjing Medical University, No. 300 Guangzhou Road, Nanjing 210009, Jiangsu Province, China. zhuchuanlong@jsph.org.cn

Abstract

BACKGROUND

Cryptotanshinone (CPT) has wide biological functions, including anti-oxidative, antifibrosis, and anti-inflammatory properties. However, the effect of CPT on hepatic fibrosis is unknown.

AIM

To investigate the effects of CPT treatment on hepatic fibrosis and its underlying mechanism of action.

METHODS

Hepatic stellate cells (HSCs) and normal hepatocytes were treated with different concentrations of CPT and salubrinal. The CCK-8 assay was used to determine cell viability. Flow cytometry was used to measure apoptosis and cell cycle arrest. Reverse transcription polymerase chain reaction (RT-PCR) and Western blot analyses were used to measure mRNA levels and protein expression of endoplasmic reticulum stress (ERS) signaling pathway related molecules, respectively. Carbon tetrachloride (CCL_4) was used to induce *in vivo* hepatic fibrosis in mice. Mice were treated with CPT and salubrinal, and blood and liver samples were collected for histopathological examination.

RESULTS

We found that CPT treatment significantly reduced fibrogenesis by modulating

the synthesis and degradation of the extracellular matrix *in vitro*. CPT inhibited cell proliferation and induced cell cycle arrest at the G2/M phase in cultured HSCs. Furthermore, we found that CPT promoted apoptosis of activated HSCs by upregulating expression of ERS markers (CHOP and GRP78) and activating ERS pathway molecules (PERK, IRE1α, and ATF4), which were inhibited by salubrinal. Inhibition of ERS by salubrinal partially eliminated the therapeutic effect of CPT in our CCL_4-induced hepatic fibrosis mouse model.

CONCLUSION
CPT can promote apoptosis of HSCs and alleviate hepatic fibrosis through modulating the ERS pathway, which represents a promising strategy for treating hepatic fibrosis.

Key Words: Hepatic fibrosis; Endoplasmic reticulum stress; Cryptotanshinone; Hepatic stellate cells; Apoptosis

©The Author(s) 2023. Published by Baishideng Publishing Group Inc. All rights reserved.

Core Tip: Hepatic fibrosis is a necessary stage of liver cirrhosis, and there is currently no effective treatment. Cryptotanshinone (CPT), one of the extracts of Chinese herbal medicine Radix Salviae Miltiorrhizae, has a good anti-fibrosis effect. Through this study, we found that CPT can treat hepatic fibrosis by activating endoplasmic reticulum stress and leading to apoptosis of hepatic stellate cells, which provides a new method for the treatment of hepatic fibrosis.

Citation: Hou XX, Li YW, Song JL, Zhang W, Liu R, Yuan H, Feng TT, Jiang ZY, Li WT, Zhu CL. Cryptotanshinone induces apoptosis of activated hepatic stellate cells *via* modulating endoplasmic reticulum stress. *World J Gastroenterol* 2023; 29(17): 2616-2627
URL: https://www.wjgnet.com/1007-9327/full/v29/i17/2616.htm
DOI: https://dx.doi.org/10.3748/wjg.v29.i17.2616

INTRODUCTION

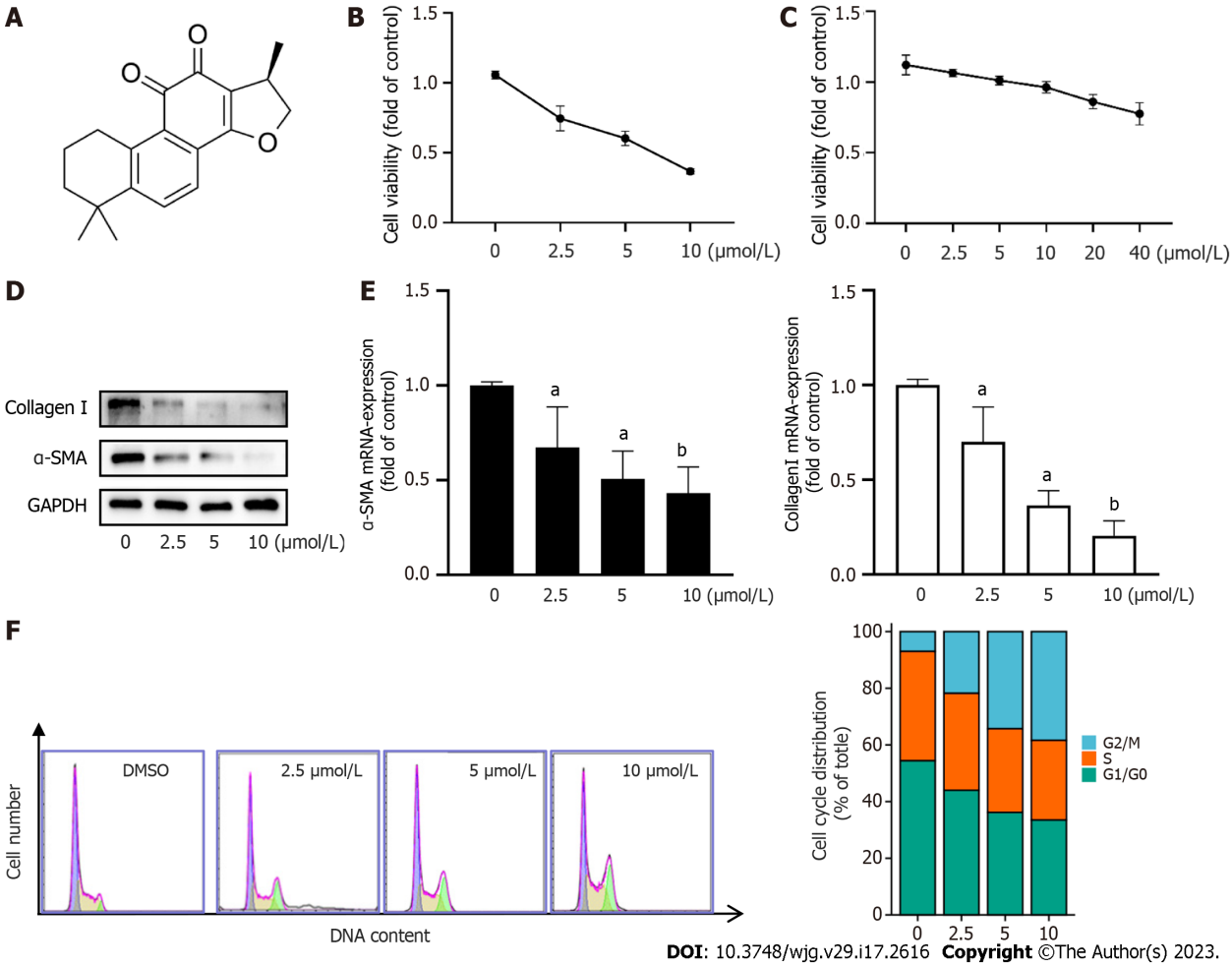
Hepatic fibrosis is a reversible liver injury that occurs in response to viruses, drugs, inflammation, fat deposition, and other causes. The underlying pathological mechanism of hepatic fibrosis involves the deposition of extracellular matrix (ECM), which leads to the replacement of functional liver parenchyma by scar tissue, proliferation and activation of hepatic stellate cells (HSCs), and increased production of collagen and unfolded proteins[1-3]. The endoplasmic reticulum (ER) is an important organelle in eukaryotic cells that is involved in a variety of biological processes, including protein synthesis, processing, modification, folding, and transport, lipid and carbohydrate metabolism, and Ca^{2+} maintenance, among others[4-6]. In some cases, when the physiological function of the ER is disturbed, ER stress (ERS) will be activated to promote cell survival. However, persistent ERS can lead to apoptosis [7,8], which can either promote the occurrence and development of hepatic fibrosis or lead to the activation of HSCs, which can reverse the transformation of hepatic fibrosis[2,9-11].

Cryptotanshinone (CPT) is a diterpene quinone compound that is isolated from Salvia miltiorrhiza. CPT has been shown to have anti-oxidant, anti-inflammatory, and antibacterial properties[12]. Studies have also reported that CPT antifibrotic effects on cardiac and renal tissues[13-15]. These findings suggest that CPT plays a protective role in fibrotic disease. Therefore, we hypothesized that CPT might also protect against hepatic fibrosis. In this study, we treated LX2 cells with different concentrations of CPT and found that cell viability decreased and apoptosis increased in a dose-dependent manner. We also found that expression of proteins related to ERS increased, and inhibiting ERS decreased the apoptosis rate. Based on our findings, we speculate that CPT promotes apoptosis of HSCs through modulating the ERS pathway.

MATERIALS AND METHODS

Reagents and antibodies

CPT (purity ≥ 98% purity by HPLC, Cat No. HY-N0174), were purchased from Med Chem Express LLC (Shanghai, China) (Figure 1A). Primary antibodies for α-SMA, Collagen I, eIF2α, p-eIF2α, p-PERK, PERK, IRE1-α, BAX, BCL2, CHOP, and GRP78/BIP and all secondary antibodies were purchased from Proteintech (China). ATF4, and XBP1 were purchased from Sigma (United States). The primers used in



DOI: 10.3748/wjg.v29.i17.2616 **Copyright** ©The Author(s) 2023.

Figure 1 Cryptotanshinone reduces collagen deposition and induces cell cycle arrest at the G2/M checkpoint. A: Chemical structure of cryptotanshinone; B: CCK8 assay for LX2 cell viability; C: CCK8 assay for cell viability of LO2; D: Protein levels of collagen I and α-SMA were determined using Western blot analysis; E: mRNA levels of α-SMA and collagen I were determined using reverse transcription polymerase chain reaction (RT-PCR); F: The percentage of cell cycle distribution was determined using flow cytometry. Data are presented as mean ± SD. $^{a}P < 0.05$, $^{b}P < 0.01$ versus control.

quantitative reverse transcription polymerase chain reaction (qRT-PCR) were purchased from Qingke Co. Ltd. (China) (Table 1).

Animals and experimental procedures

All experiments were approved by institutional and local committees. All mice were provided humane care according to the National Institutes of Health (NIH, United States) guidelines[16]. Male C57BL/6 mice (20-25 g) were randomly divided into five groups (n = 8 per group). Group 1 (vehicle control) did not receive carbon tetrachloride (CCL_4) or CPT treatment. Group 2 (model group) received CCL_4. Group 3 received intraperitoneal injections of salubrinal (1 mg/kg). Group 4 received CCL_4 followed by intraperitoneal injections of CPT (40 mg/kg). Group 5 received simultaneous intraperitoneal injections of salubrinal and CPT. Groups 2, 3, 4, and 5 were administered CCL_4 twice a week for 8 wk to induce hepatic fibrosis. Groups 3, 4, and 5 were intraperitoneally injected with CPT or salubrinal every day from 5 wk to 8 wk. CPT and salubrinal were dissolved in physiological saline. After 8 wk of treatment, blood samples and livers were collected. Livers were fixed in 4% buffered paraformaldehyde for histological (hematoxylin and eosin) and Western blot analyses.

Cell culture

The HSC LX2 cell line was donated by Professor Wenting Li. Cells were cultured in high-sugar DMEM medium with 10% fetal bovine serum (FBS) in an incubator at 37 °C[17].

qRT-PCR analysis

RNA was extracted from the LX2 cells using an RNA extraction kit (Biyuntian, China) according to the kit's instructions. The Stepone system was used for qRT-PCR, and the experiment was repeated three times to calculate the mRNA levels of the target genes.

Table 1 Primer sequences

Primer	Sequence
GAPDH-F (human)	AAATCCCATCACCATCTTCCAG
GAPDH-R (human)	AGGGGCCATCCACAGTCTTCT
Bax-F (human)	TGAGCAGATCATGAAGACAGGG
Bax-R (human)	TGAGACACTCGCTCAGCTTC
BCL2-F (human)	TCACTTGTGGCCCAGATAGG
BCL2-R (human)	GATAACGGAGGCTGGGATGC
GRP78-F (human)	CATCACGCCGTCCTATGTCG
GRP78-R (human)	CGTCAAAGACCGTGTTCTCG
CHOP-F (human)	ACCTGAAAGCAGATGTGCT
CHOP-R (human)	GTCCTCATACCAGGCTTCC
α-SMA-F (human)	AAAAGACAGCTACGTGGGTGA
α-SMA-R (human)	GCCATGTTCTATCGGGTACTTC
Col1a1-F (human)	GAGCCAAGACGAAGACATC
Col1a1-R (human)	CAGATCACGTCATCGCACAAC
GAPDH-F (mouse)	TGTCGTGGAGTCTACTGGTG
GAPDH-R (mouse)	ACACCCATCACAAACATGG
α-SMA-F (mouse)	TGACGCTGAAGTATCCGATAGA
α-SMA-R (mouse)	CGAAGCTCGTTATAGAAAGAGTGG
Col1a1-F (mouse)	GATCCTGCCGATGTCGCTAT
Col1a1-R (mouse)	TGTAGGCTAGCTGTTCTTGCA

Western blot analysis

RIPA buffer containing protease and phosphatase inhibitors was used to lyse cells and tissues on ice. Proteins were electrophoresed and transferred to PVDF membranes (Millipore, United States), which were blocked with 5% bovine serum albumin for 2 h. Subsequently, the membranes were incubated with primary antibodies at 4 °C overnight, followed by incubation with second antibodies at room temperature for 2 h. Finally, the PVDF membranes were washed using 1% TBST and detected by the Bio-Rad ChemiDoc Touch Imaging System.

Enzyme-linked immunosorbent assay

Serum levels of interleukin (IL)-6 and IL-10 were determined using enzyme-linked immunosorbent assay (ELISA) kits (LinkTech Biotechnology, China) according to the manufacturer's instructions. The absorbance was observed at 450 nm using a full-wavelength microplate reader.

Transmission electron microscopy

LX2 cells were treated with CPT for 24 h, gently scraped with a cell scraper, washed with PBS three times, precipitated, centrifuged, and fixed overnight with an electron microscopy fixative. The fixed cells were imaged using a transmission electron microscope (Tokyo, Japan).

Biochemical analysis

Serum levels of aspartate aminotransferase (AST) and alanine aminotransferase (ALT) were measured using a liver function analysis kit (Nanjing Chengjian Institute of Bioengineering, China) according to the kit's instructions. The absorbance was measured using an enzyme-labeled instrument.

Cell proliferation assay

The Cell Counting Kit 8 (CCK-8) kit (Biyuntian, China) was used to assay cell proliferation. LX2 cells were inoculated into a 96-well plate at 3000 cells per well and cultured overnight at 37 °C. After 24 h cells were treated with CPT at different concentrations, and 10 μL of the CCK-8 solution was added to each well. The cells were cultured at 37 °C for 2 h. The absorbance of each well was measured at 450 nm using a microplate reader.

TUNEL staining

LX2 cells were inoculated into a 24-well plate. After the cells attached, DMSO, CPT, or salubrinal was added for 24 h. A TUNEL staining kit (Biyuntian, China) was used to detect apoptotic cells according to the kit's instructions. Cell apoptosis was observed with a fluorescent microscope (Nikon).

Flow cytometry analysis of cell cycle and apoptosis

LX2 cells were inoculated into a 6-well plate at a density of 2×10^4 cells/well. On the following day, the cells were treated with CPT at different concentrations for 24 h. Cell cycle was measured using a cell cycle kit (KeyGen Biotech). Cell apoptosis was determined using Annexin V and propidium iodide double staining with fluorescein isothiocyanate. The percentage of apoptotic cells was determined using flow cytometry (FACS Calibur)[17].

Statistical analysis

Experimental data were graphed using Prism 9.0 and statistically analyzed using SPSS26.0. Statistical significance of differences was determined using one-way analysis of variance with the post-hoc Dunnett's test. A P value of <0.05 was considered statistically significant.

RESULTS

CPT inhibits the proliferation of LX2 cells

Hepatic fibrosis is characterized by progressive and excess accumulation of ECM, leading to disruption of normal liver structure and function. HSC activation is a key cellular event in the pathogenesis of hepatic fibrosis[18,19]. In this study, we sought to determine the effects of CPT on hepatic fibrosis. To do so we first investigated the effect of CPT on cell viability. We treated LX2 cells with varying concentrations of CPT (0, 2.5, 5, 10, and 20 μmol/L) for 24 h and assessed cell proliferation using the CCK-8 assay. The results showed that CPT significantly reduced cell viability in a dose-dependent manner (Figure 1B). We also observed that CPT inhibited the vitality of normal hepatocytes (L02) at 40 μm (Figure 1C), which was far in excess of the concentration that affected HSC viability. To further observe the inhibitory effect of CPT on activated LX2 cells *in vitro*, we examined ECM accumulation under different concentrations of CPT. We found that CPT reduced ECM deposition (Figure 1D and E). To further investigate the inhibitory effect of CPT on cell growth, we measured cell cycle distribution using flow cytometry. Cell cycle analysis showed that the number of cells in the G2/M phase significantly increased while those in the G1 phase significantly decreased with higher concentrations of CPT (Figure 1F). Collectively, these findings suggest that CPT can induce HSC growth.

CPT stimulates apoptosis of activated HSCs

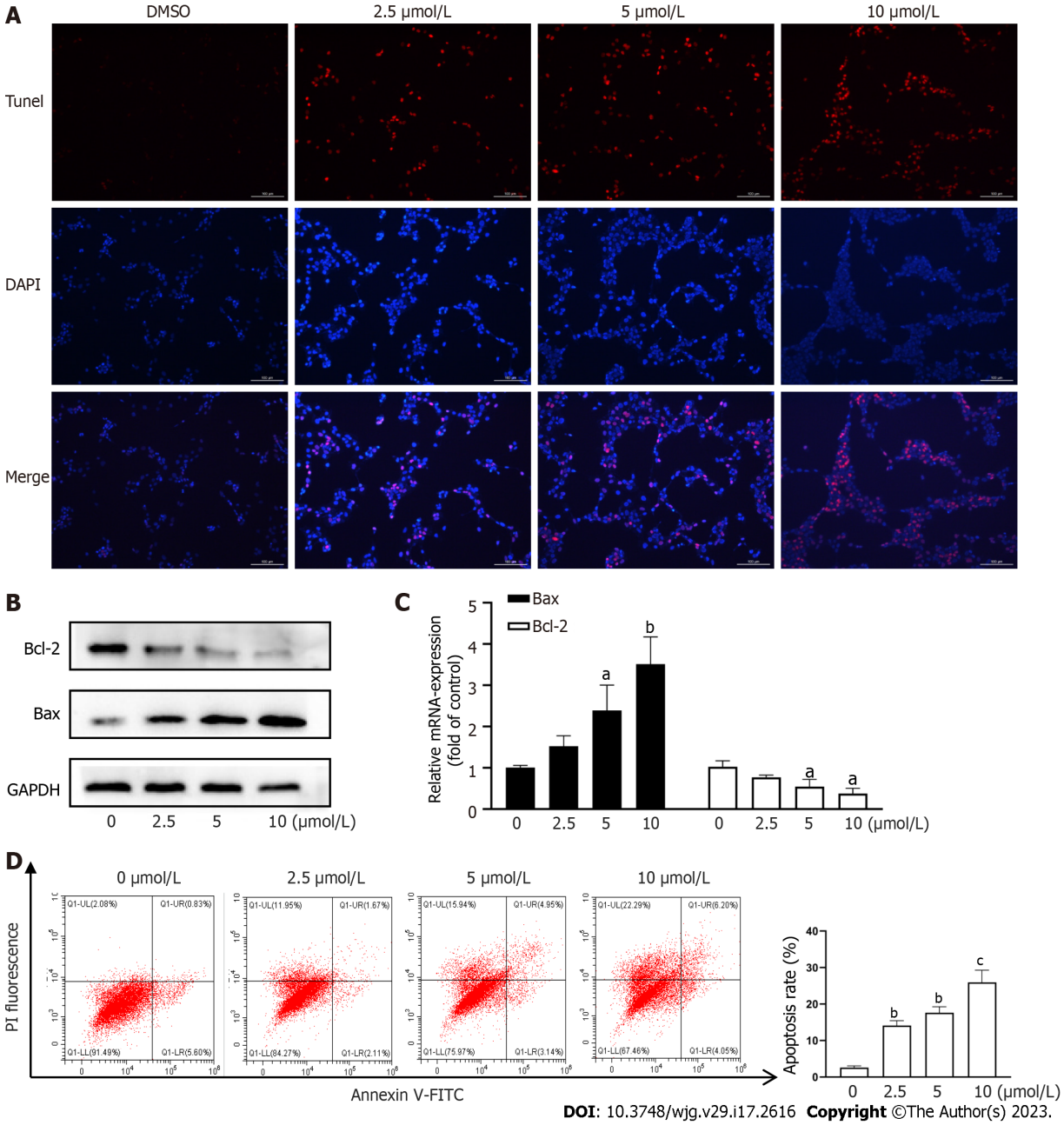
Apoptosis of activated HSCs has been shown to reduce the degree of hepatic fibrosis[2,3]. We assessed HSC apoptosis using TUNEL staining and found that CPT induced activated HSC apoptosis in a dose-dependent manner (Figure 2A). We next explored the pathway underlying CPT-induced HSC apoptosis. We observed that CPT dose-dependently reduced Bcl-2/Bax expression in HSCs (Figure 2B and C). We quantitatively evaluated the apoptotic rate using flow cytometry, which demonstrated that CPT dose-dependently increased the apoptotic rate in activated HSCs (Figure 2D). These data indicate that CPT activates HSC apoptosis.

CPT activates the ERS pathway

ERS is a signaling response pathway intended to protect against cell death. However, if the stress response is very strong or prolonged, it can cause cellular damage[20]. We investigated the underlying mechanism of CPT-induced HSC apoptosis by detecting ERS-related mediators. We found that CPT significantly upregulated the mRNA levels and protein expression of GFR78 and CHOP in LX2 cells, resepectively (Figure 3A and B). Subsequently, we examined the expression of GFR78 and CHOP in L02 cells and found that their expression was not significantly altered (Figure 3C and D). These results suggest that CPT promotes ERS in activated HSCs without triggering ERS in normal liver cells. Western blot analysis revealed that CPT significantly upregulated protein expression of ERS regulatory molecules (Figure 3E and F). We also observed the expansion and swelling of the ER lumen in CPT-treated HSCs using electron microscopy. More specifically, we observed a disappearance of the normal sheet-like folded structure and the formation of numerous vacuoles within the ER (Figure 3G).

CPT-induced apoptosis of HSCs requires ERS activation

Salubrinal, an inhibitor of ERS, can protect HSCs from ERS-induced apoptosis[20]. Based on the above experimental results, we next investigated if activation of ERS by CPT leads to apoptosis of LX2 cells. To test this hypothesis, we treated LX2 cells with both CPT and salubrinal and found that CPT did not significantly upregulate the mRNA and Western blot levels of GFR78 and CHOP (Figure 4A and B). We also measured the expression of ECM components at the mRNA and protein levels. Interestingly, The



DOI: 10.3748/wjg.v29.i17.2616 Copyright ©The Author(s) 2023.

Figure 2 Cryptotanshinone induces apoptosis of activated hepatic stellate cells. A: TUNEL staining to assess LX2 apoptosis. Red fluorescence indicates apoptotic cells. Scale baes: 100μm; B: Western blot analysis of Bcl-2 and Bax protein expression in LX2 cells; C: Reverse transcription polymerase chain reaction analysis of Bcl-2 and Bax mRNA levels in LX2 cells; D: Flow cytometric analysis of LX2 cell apoptosis using fluorescein isothiocyanate-labeled Annexin-V/propidium iodide staining. Cells located in the right two quadrants of each figure were considered apoptotic cells. $^{a}P < 0.05$, $^{b}P < 0.01$, $^{c}P < 0.001$ versus control.

decrease of ECM accumulation following CPT treatment was prevented by salubrinal (Figure 4C and D). These results suggest that CPT can activate ERS, leading to apoptosis of LX2 cells, which may be a mechanism to promote HSC clearance. We found that the apoptotic effect of CPT on activated LX2 cells could be reversed by salubrinal (Figure 4E-H). Taken together, these findings suggest that CPT can induce apoptosis of HSCs through modulating ERS, which may be a mechanism for promoting HSCs clearance.

CPT protects mice from CCL_4-induced hepatic fibrosis

CCl_4-induced hepatic fibrosis is a well-established model to investigate hepatic fibrosis *in vivo*. We used this model to confirm the protective effect of CPT in mice(Figure 5A). To this end, we measured protein expression of major markers of hepatic fibrosis including α-SMA and collagen I. CPT effectively diminished expression of these proteins in the CCL_4-induced model of hepatic fibrosis (Figure 5B). In addition, we analyzed biochemical markers of liver injury after 8 wk of CCL_4 treatment. Levels of AST and ALT increased in the model group but were reduced in the CPT groups (Figure 5C and D). During chronic liver disease, hepatic fibrogenesis is commonly accompanied by inflammation. As demonstrated

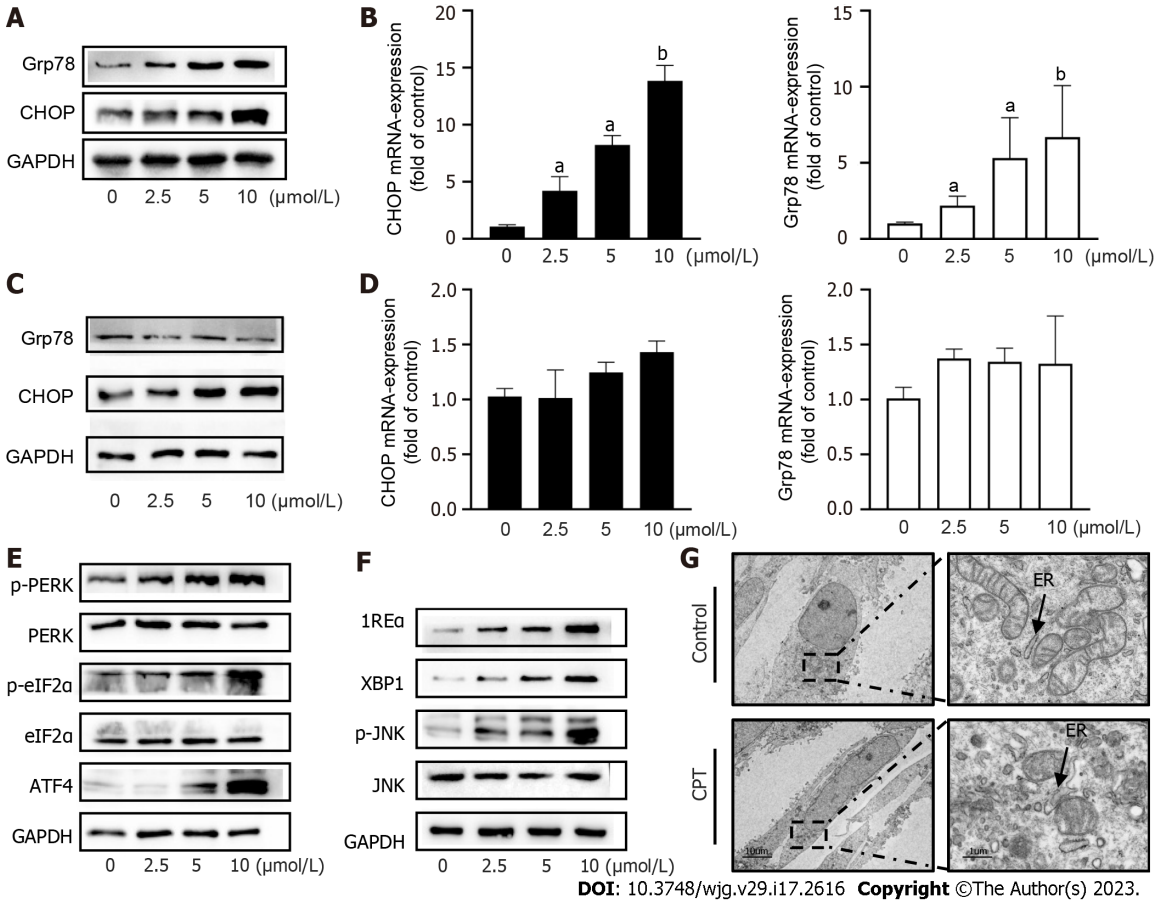


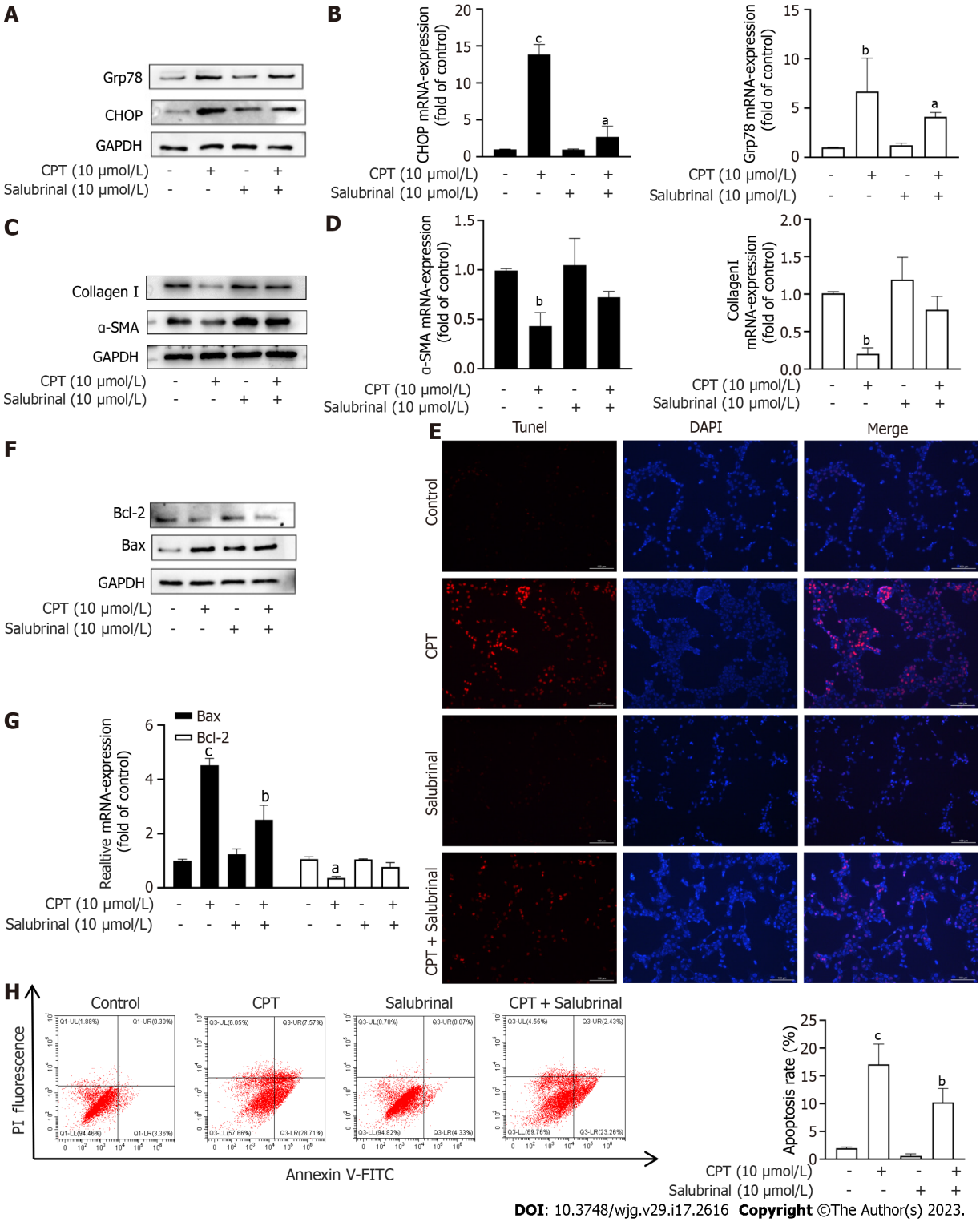
Figure 3 Cryptotanshinone activates the endoplasmic reticulum stress pathway in activated LX2 cells. A: Western blot analysis of endoplasmic reticulum stress (ERS)-related protein expression in LX2 cells; B: Reverse transcription polymerase chain reaction (RT-PCR) analysis of Grp78 and CHOP mRNA levels in LX2 cells; C: Western blot analysis of ERS-related protein expression in LO2 cells; D: RT-PCR analysis of Grp78 and CHOP mRNA levels in LO2 cells; E and F: Western blot analyses of ATF4, PERK, and IRE1 signaling pathways in hepatic stellate cells; G: Transmission electron microscopy showing that CPT caused ER swelling and destruction of the mitochondrial membrane integrity. Data are presented as mean ± SD. $^{a}P < 0.05$, $^{b}P < 0.01$ versus control. ER: Endoplasmic reticulum.

by ELISA, CPT decreased serum levels of IL-6 and IL-10 (Figure 5E and F). Furthermore, the inhibitory effect of CPT on the secretion of pro-inflammatory cytokines was diminished by salubrinal. Thus, we propose that CPT protects against CCL_4-induced liver injury by suppressing inflammation. Next, we analyzed the pathological changes in the liver tissue after CPT treatment. Histological staining showed that treatment with CPT significantly improved morphological changes in liver tissue (Figure 5G). As fibrogenesis is accompanied by accumulation of collagen, liver tissue sections were stained with Masson's reagent and Sirius red to detect collagen deposition. The results showed that collagen was markedly deposited in the CCL_4-injured livers but reduced in the livers of mice in the CPT-treated groups, which was further suppressed by salubrinal (Figure 5G). Taken together, these data provide *in vivo* evidence that activation of ERS signaling can result in reduced collagen accumulation and attenuation of fibrotic damage in a hepatic fibrosis mouse model.

DISCUSSION

Due to their diverse sources and high safety profiles, there has recently been a widespread increase in the use of natural bioactive components from plants for the prevention and treatment of diseases. Salvia miltiorrhiza is a traditional Chinese medicine that has been used to treat many diseases. CPT is one of the main tanshinones extracted from Salvia miltiorrhiza Bunge and is considered an important compound with various pharmacological properties. Specifically, recent studies have shown that CPT has antifibrotic properties in the heart, lung, and kidney[14,15]. However, the relationship between CPT and hepatic fibrosis remains unclear.

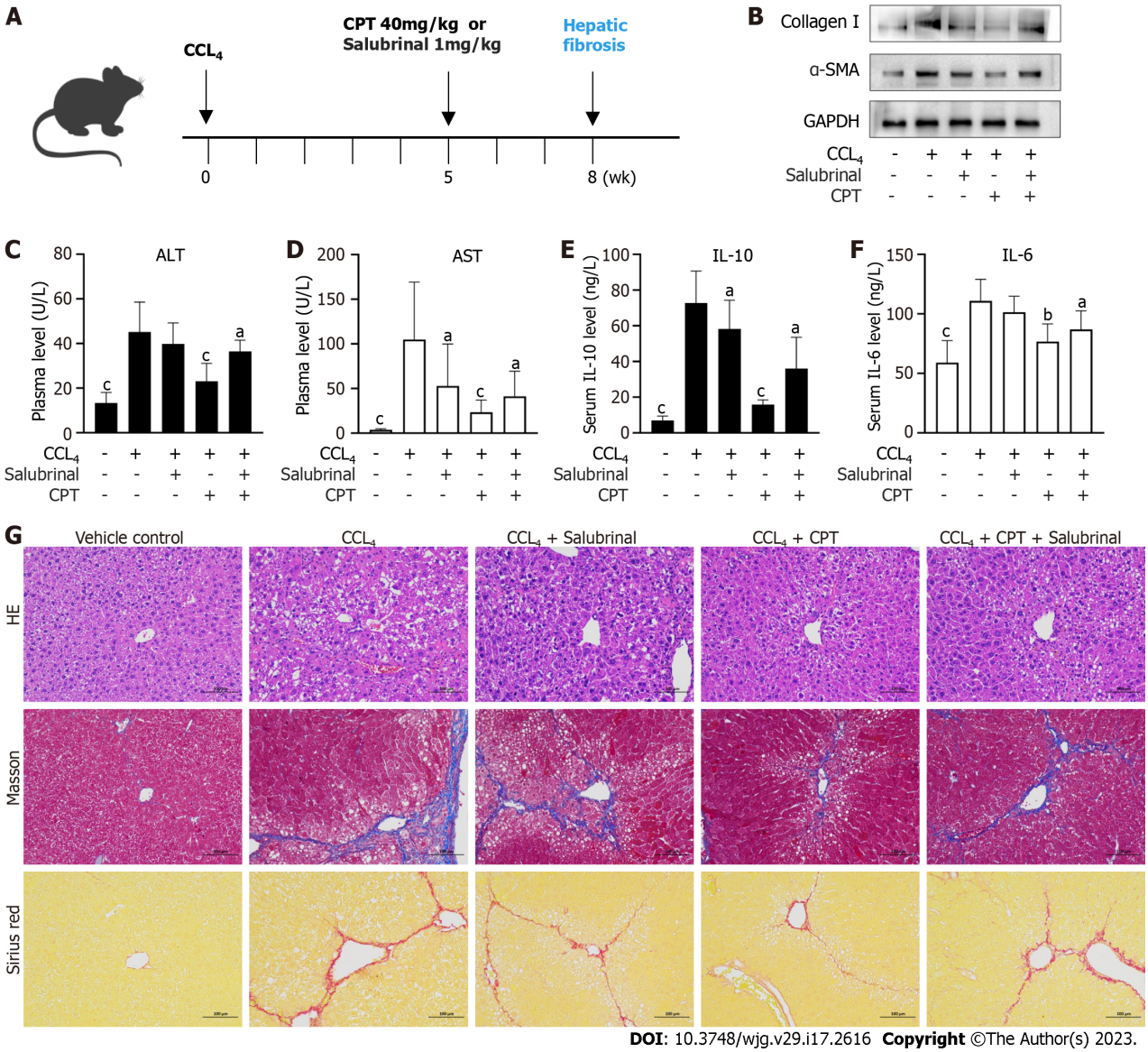
Hepatic fibrosis involves inflammatory responses caused by various acute and chronic liver injuries. If left untreated, hepatic fibrosis can progress to liver cirrhosis or even liver cancer. The production of ECM by activated HSCs plays an important role in hepatic fibrosis and cirrhosis[21]. Hepatic fibrosis might be prevented or even reversed by inducing apoptosis of activated HSCs. In this study, we



DOI: 10.3748/wjg.v29.i17.2616 **Copyright** ©The Author(s) 2023.

Figure 4 The endoplasmic reticulum stress signaling pathway leads to LX2 cell apoptosis and reduces collagen deposition induced by cryptotanshinone. A: Protein expression of Grp78 and CHOP was determined using Western blot analysis; B: mRNA levels of Grp78 and CHOP were determined using reverse transcription polymerase chain reaction (RT-PCR); C: Protein expression of collagen type I and α-SMA was determined using Western blot analysis; D: mRNA levels of α-SMA and collagen I were determined using RT-PCR; E: TUNEL staining was used to assess LX2 cell apoptosis. Red fluorescence indicates apoptotic cells. Scale bars: 100 μm; F: Protein expression of Bax and Bcl2 was determined using Western blot analysis; G: mRNA levels of Bax and Bcl2 were determined using RT-PCR; H: Flow cytometry data are presented as mean ± SD. $^{a}P < 0.05$, $^{b}P < 0.01$, $^{c}P < 0.001$ versus control. CPT: Cryptotanshinone; FITC: Fluorescein isothiocyanate.

established that CPT induces apoptosis through ERS in activated HSCs, which may offer a new strategy for the treatment of hepatic fibrosis. We discovered that CPT decreased both mRNA levels and protein expression of α-SMA and type I collagen in activated HSCs, which resulted in reduced ECM deposition. Furthermore, flow cytometry revealed that CPT dose-dependently induced apoptosis of activated LX2



DOI: 10.3748/wjg.v29.i17.2616 **Copyright** ©The Author(s) 2023.

Figure 5 Cryptotanshinone protects the liver against carbon tetrachloride-induced injury and inflammation. Cryptotanshinone (CPT) alleviates hepatic fibrotic injury in mice. Mice were injected with carbon tetrachloride (CCL_4) for 8 wk to induce liver fibrosis. During weeks 5 through 8, mice in the treatment groups were given CPT (40 mg/kg) or salubrinal (1 mg/kg). A: CPT treatment protocol in the CCL_4-induced hepatic fibrosis mouse model; B: Western blot analysis of α-SMA and collagen I in the liver tissue; C: Determination of serum alanine aminotransferase levels; D: Determination of serum aspartate aminotransferase levels; E: Enzyme-linked immunosorbent assay (ELISA) measurement of IL-6 levels in the serum; F: ELISA measurement of IL-10 levels in the serum; G: Liver sections were stained with hematoxylin and eosin, Masson reagents, and Sirius red. Scale baes: 100 μm. $^aP < 0.05$, $^bP < 0.01$, $^cP < 0.001$ compared with the CCL_4 group. CPT: Cryptotanshinone; CCL_4: Carbon tetrachloride.

cells. Bax is considered an apoptotic factor, while Bcl2 is an anti-apoptotic molecule that inhibits the release of cytochrome C from the mitochondria and inhibits HSC apoptosis[22]. We found that CPT upregulated the expression of the pro-apoptotic protein Bax and downregulated the expression of the anti-apoptotic protein Bcl2 in activated HSCs, increased the Bax/Bcl ratio, and promoted HSC apoptosis. Interestingly, the pro-apoptotic effect of CPT was more specific for activated HSCs than for normal hepatocytes, which did not undergo apoptosis. This finding is important because it indicates that CPT does not affect normal liver cell activity. Thus, we found that CPT is an effective drug that can induce apoptosis of activated HSCs but have no effect on normal hepatocytes during the treatment of hepatic fibrosis.

Our results demonstrated that CPT upregulated expression of ER-resident chaperone proteins, such as CHOP and GRP78, which are significant markers of ERS[23,24]. In addition, the PERK, IRE1, and ATF6 signaling pathways were activated, all of which can phosphorylate the downstream molecules eIF2α, ATF4, and JNK, modulating the ERS response[25,26]. We also observed ultrastructure changes using electron microscopy. The results showed that the ER cavity of the HSCs was swollen, and the integrity of the mitochondrial membrane was damaged after CPT treatment. The ER and mitochondria are important organelles that cooperate to complete a variety of biological functions through their

interactions with various proteins. In the early stage of ERS, GRP78 is translocated to the mitochondria, and the subsequent damage to the integrity of the mitochondrial membrane becomes an early feature of apoptosis[27,28]. Our results indicate that CPT could promote ERS in HSCs to promote apoptosis. Salubrinal is an ERS inhibitor that selectively induces eIF2α phosphorylation and inhibits its dephosphorylation, ultimately protecting cells from ERS-induced apoptosis[29]. To better understand if CPT-induced HSC apoptosis is regulated by activating the ERS pathway, we incubated HSCs with salubrinal to protect cells from ERS-induced apoptosis. In activated HSCs, salubrinal effectively attenuated CPT-induced apoptosis, reducing secretion of apoptotic proteins. Therefore, these results confirm that targeting ERS can trigger HSCs apoptosis.

To further verify the therapeutic effect of CPT on hepatic fibrosis, we conducted *in vivo* experiments using a CCL_4-induced mouse model of hepatic fibrosis. We found that intraperitoneal injection of CPT reversed the development of hepatic fibrosis in mice, and the therapeutic effect of CPT was reduced after by salubrinal. Interestingly, CCL_4 also induces experimental hepatocarcinoma, which shares common features with hepatic fibrosis, such as increased expression of matricellular proteins (SPARC, BM-40, and osteonectin)[30-32]. However, whether or not CPT also has a significant effect on the treatment of liver cancer requires further investigation.

CONCLUSION

In summary, we found that CPT limited HSC activation through an ERS-dependent pathway *in vivo* and *in vitro*, suggesting that CPT should be further investigated as a prospective therapeutic agent for hepatic fibrosis.

ARTICLE HIGHLIGHTS

Research background

Cryptotanshinone (CPT) has been accepted to be an anti-inflammatory molecule.

Research motivation

Hepatic stellate cell (HSC) activation plays an indispensable role in hepatic fibrosis. Inducing apoptosis of activated HSCs can attenuate or reverse fibrogenesis.

Research objectives

This study investigated the effects of CPT treatment on hepatic fibrosis and its underlying mechanism of action.

Research methods

In vitro, we used reverse transcription polymerase chain reaction, Western blot, TUNEL staining and flow cytometry, which demonstrated that CPT can induce HSC apoptosis through the ERS pathway. *In vivo*, we used liver function kit, enzyme-linked immunosorbent assay, pathological section staining a few columns of technical means to prove that CPT has a certain therapeutic effect on hepatic fibrosis.

Research results

In vitro, CPT was considered to activate HSC apoptosis by promoting endoplasmic reticulum stress (ERS) detrimental response to a certain extent. Main molecules came down to the unfolded protein response signaling pathway. *In vivo*, We found CPT protected the Carbon tetrachloride (CCL_4)-induced hepatic fibrosis. Furthermore, CPT inhibited the levels of the downstream inflammatory cytokines, which were triggered by CCL_4-induced hepatic fibrosis.

Research conclusions

CPT can promote apoptosis of HSCs and alleviate hepatic fibrosis through modulating the ERS pathway, which represents a promising strategy for treating hepatic fibrosis.

Research perspectives

Hepatic fibrosis, cirrhosis and liver cancer are typical "trilogy of liver diseases", which seriously endanger human health. Hepatic fibrosis is reversible in the early stage, but it is difficult to reverse in the late stage of liver cirrhosis. Early treatment is therefore essential. CPT is a diterpene quinone compound that is isolated from Salvia miltiorrhiza. CPT has been shown to have anti-oxidant. In this study, we found that CPT could induce apoptosis of activated HSCs and had good prospects for the treatment of hepatic fibrosis.

FOOTNOTES

Author contributions: Zhu CL and Hou XX designed the research; Hou XX, Li YW and Song JL performed the research; Li WT analyzed data and wrote the article; Zhang W and Feng TT checked the statistical calculations; Yuan H, Liu R and Jiang ZY commented on and revised the paper; all authors have read and approved the final paper.

Supported by Science and Technology Plan of Hainan Province (Clinical Research Center), No. LCYX202103 and No. LCYX202204; Hainan Province Science and Technology Special Fund, No. ZDYF2022SHFZ067; and Hainan Province Clinical Medical Center.

Institutional animal care and use committee statement: All procedures involving animals were reviewed and approved by the Institutional Animal Care and Use Committee of The First Affiliated Hospital of Nanjing Medical University (IACUC protocol number: IACUC-2209028).

Conflict-of-interest statement: All the authors report no relevant conflicts of interest for this article.

Data sharing statement: All data generated or analyzed supporting conclusions are included in the current manuscript.

ARRIVE guidelines statement: The authors have read the ARRIVE Guidelines, and the manuscript was prepared and revised according to the ARRIVE Guidelines.

Open-Access: This article is an open-access article that was selected by an in-house editor and fully peer-reviewed by external reviewers. It is distributed in accordance with the Creative Commons Attribution NonCommercial (CC BY-NC 4.0) license, which permits others to distribute, remix, adapt, build upon this work non-commercially, and license their derivative works on different terms, provided the original work is properly cited and the use is non-commercial. See: https://creativecommons.org/Licenses/by-nc/4.0/

Country/Territory of origin: China

ORCID number: Chuan-Long Zhu 0000-0001-6557-1654.

S-Editor: Gao CC
L-Editor: A
P-Editor: Zhao S

REFERENCES

1 **Gan C**, Cai Q, Tang C, Gao J. Inflammasomes and Pyroptosis of Liver Cells in Liver Fibrosis. *Front Immunol* 2022; **13**: 896473 [PMID: 35707547 DOI: 10.3389/fimmu.2022.896473]
2 **Tsuchida T**. [Mechanisms of hepatic stellate cell activation as a therapeutic target for the treatment of non-alcoholic steatohepatitis]. *Nihon Yakurigaku Zasshi* 2019; **154**: 203-209 [PMID: 31597900 DOI: 10.1254/fpj.154.203]
3 **Yang F**, Li H, Li Y, Hao Y, Wang C, Jia P, Chen X, Ma S, Xiao Z. Crosstalk between hepatic stellate cells and surrounding cells in hepatic fibrosis. *Int Immunopharmacol* 2021; **99**: 108051 [PMID: 34426110 DOI: 10.1016/j.intimp.2021.108051]
4 **Duwaerts CC**, Maiers JL. ER Disposal Pathways in Chronic Liver Disease: Protective, Pathogenic, and Potential Therapeutic Targets. *Front Mol Biosci* 2021; **8**: 804097 [PMID: 35174209 DOI: 10.3389/fmolb.2021.804097]
5 **Maiers JL**, Malhi H. Endoplasmic Reticulum Stress in Metabolic Liver Diseases and Hepatic Fibrosis. *Semin Liver Dis* 2019; **39**: 235-248 [PMID: 30912096 DOI: 10.1055/s-0039-1681032]
6 **Bravo R**, Parra V, Gatica D, Rodriguez AE, Torrealba N, Paredes F, Wang ZV, Zorzano A, Hill JA, Jaimovich E, Quest AF, Lavandero S. Endoplasmic reticulum and the unfolded protein response: dynamics and metabolic integration. *Int Rev Cell Mol Biol* 2013; **301**: 215-290 [PMID: 23317820 DOI: 10.1016/B978-0-12-407704-1.00005-1]
7 **Iurlaro R**, Muñoz-Pinedo C. Cell death induced by endoplasmic reticulum stress. *FEBS J* 2016; **283**: 2640-2652 [PMID: 26587781 DOI: 10.1111/febs.13598]
8 **Demirtas L**, Guclu A, Erdur FM, Akbas EM, Ozcicek A, Onk D, Turkmen K. Apoptosis, autophagy & endoplasmic reticulum stress in diabetes mellitus. *Indian J Med Res* 2016; **144**: 515-524 [PMID: 28256459 DOI: 10.4103/0971-5916.200887]
9 **Zhang CY**, Yuan WG, He P, Lei JH, Wang CX. Liver fibrosis and hepatic stellate cells: Etiology, pathological hallmarks and therapeutic targets. *World J Gastroenterol* 2016; **22**: 10512-10522 [PMID: 28082803 DOI: 10.3748/wjg.v22.i48.10512]
10 **Koo JH**, Lee HJ, Kim W, Kim SG. Endoplasmic Reticulum Stress in Hepatic Stellate Cells Promotes Liver Fibrosis *via* PERK-Mediated Degradation of HNRNPA1 and Up-regulation of SMAD2. *Gastroenterology* 2016; **150**: 181-193.e8 [PMID: 26435271 DOI: 10.1053/j.gastro.2015.09.039]
11 **Borkham-Kamphorst E**, Steffen BT, Van de Leur E, Haas U, Tihaa L, Friedman SL, Weiskirchen R. CCN1/CYR61 overexpression in hepatic stellate cells induces ER stress-related apoptosis. *Cell Signal* 2016; **28**: 34-42 [PMID: 26515130 DOI: 10.1016/j.cellsig.2015.10.013]

12 **Li H**, Gao C, Liu C, Liu L, Zhuang J, Yang J, Zhou C, Feng F, Sun C, Wu J. A review of the biological activity and pharmacology of cryptotanshinone, an important active constituent in Danshen. *Biomed Pharmacother* 2021; **137**: 111332 [PMID: 33548911 DOI: 10.1016/j.biopha.2021.111332]

13 **Wang X**, Wan W, Lu J, Zhang Y, Quan G, Pan X, Wu Z, Liu P. Inhalable cryptotanshinone spray-dried swellable microparticles for pulmonary fibrosis therapy by regulating TGF-β1/Smad3, STAT3 and SIRT3 pathways. *Eur J Pharm Biopharm* 2022; **172**: 177-192 [PMID: 35202797 DOI: 10.1016/j.ejpb.2022.02.012]

14 **Wang W**, Zhou PH, Hu W, Xu CG, Zhou XJ, Liang CZ, Zhang J. Cryptotanshinone hinders renal fibrosis and epithelial transdifferentiation in obstructive nephropathy by inhibiting TGF-β1/Smad3/integrin β1 signal. *Oncotarget* 2018; **9**: 26625-26637 [PMID: 29928474 DOI: 10.18632/oncotarget.23803]

15 **Lo SH**, Hsu CT, Niu HS, Niu CS, Cheng JT, Chen ZC. Cryptotanshinone Inhibits STAT3 Signaling to Alleviate Cardiac Fibrosis in Type 1-like Diabetic Rats. *Phytother Res* 2017; **31**: 638-646 [PMID: 28176375 DOI: 10.1002/ptr.5777]

16 **Xu W**, Lu C, Zhang F, Shao J, Yao S, Zheng S. Dihydroartemisinin counteracts fibrotic portal hypertension *via* farnesoid X receptor-dependent inhibition of hepatic stellate cell contraction. *FEBS J* 2017; **284**: 114-133 [PMID: 27896916 DOI: 10.1111/febs.13956]

17 **Bian M**, Chen X, Zhang C, Jin H, Wang F, Shao J, Chen A, Zhang F, Zheng S. Magnesium isoglycyrrhizinate promotes the activated hepatic stellate cells apoptosis *via* endoplasmic reticulum stress and ameliorates fibrogenesis *in vitro* and in vivo. *Biofactors* 2017; **43**: 836-846 [PMID: 29048780 DOI: 10.1002/biof.1390]

18 **Garbuzenko DV**. Pathophysiological mechanisms of hepatic stellate cells activation in liver fibrosis. *World J Clin Cases* 2022; **10**: 3662-3676 [PMID: 35647163 DOI: 10.12998/wjcc.v10.i12.3662]

19 **Kisseleva T**, Brenner DA. Hepatic stellate cells and the reversal of fibrosis. *J Gastroenterol Hepatol* 2006; **21** Suppl 3: S84-S87 [PMID: 16958681 DOI: 10.1111/j.1440-1746.2006.04584.x]

20 **Li X**, Wang Y, Wang H, Huang C, Huang Y, Li J. Endoplasmic reticulum stress is the crossroads of autophagy, inflammation, and apoptosis signaling pathways and participates in liver fibrosis. *Inflamm Res* 2015; **64**: 1-7 [PMID: 25286903 DOI: 10.1007/s00011-014-0772-y]

21 **Li X**, Sun S, Appathurai S, Sundaram A, Plumb R, Mariappan M. A Molecular Mechanism for Turning Off IRE1α Signaling during Endoplasmic Reticulum Stress. *Cell Rep* 2020; **33**: 108563 [PMID: 33378667 DOI: 10.1016/j.celrep.2020.108563]

22 **Wolf P**, Schoeniger A, Edlich F. Pro-apoptotic complexes of BAX and BAK on the outer mitochondrial membrane. *Biochim Biophys Acta Mol Cell Res* 2022; **1869**: 119317 [PMID: 35752202 DOI: 10.1016/j.bbamcr.2022.119317]

23 **Bian M**, He J, Jin H, Lian N, Shao J, Guo Q, Wang S, Zhang F, Zheng S. Oroxylin A induces apoptosis of activated hepatic stellate cells through endoplasmic reticulum stress. *Apoptosis* 2019; **24**: 905-920 [PMID: 31538267 DOI: 10.1007/s10495-019-01568-2]

24 **Dubois V**, Gheeraert C, Vankrunkelsven W, Dubois-Chevalier J, Dehondt H, Bobowski-Gerard M, Vinod M, Zummo FP, Güiza F, Ploton M, Dorchies E, Pineau L, Boulinguiez A, Vallez E, Woitrain E, Baugé E, Lalloyer F, Duhem C, Rabhi N, van Kesteren RE, Chiang CM, Lancel S, Duez H, Annicotte JS, Paumelle R, Vanhorebeek I, Van den Berghe G, Staels B, Lefebvre P, Eeckhoute J. Endoplasmic reticulum stress actively suppresses hepatic molecular identity in damaged liver. *Mol Syst Biol* 2020; **16**: e9156 [PMID: 32407006 DOI: 10.15252/msb.20199156]

25 **Mori K**. Evolutionary Aspects of the Unfolded Protein Response. *Cold Spring Harb Perspect Biol* 2022; **14** [PMID: 35940910 DOI: 10.1101/cshperspect.a041262]

26 **Kishino A**, Hayashi K, Maeda M, Jike T, Hidai C, Nomura Y, Oshima T. Caspase-8 Regulates Endoplasmic Reticulum Stress-Induced Necroptosis Independent of the Apoptosis Pathway in Auditory Cells. *Int J Mol Sci* 2019; **20** [PMID: 31771290 DOI: 10.3390/ijms20235896]

27 **Liu Y**, Pan X, Li S, Yu Y, Chen J, Yin J, Li G. Endoplasmic reticulum stress restrains hepatocyte growth factor expression in hepatic stellate cells and rat acute liver failure model. *Chem Biol Interact* 2017; **277**: 43-54 [PMID: 28844859 DOI: 10.1016/j.cbi.2017.08.015]

28 **Senft D**, Ronai ZA. UPR, autophagy, and mitochondria crosstalk underlies the ER stress response. *Trends Biochem Sci* 2015; **40**: 141-148 [PMID: 25656104 DOI: 10.1016/j.tibs.2015.01.002]

29 **Lan B**, He Y, Sun H, Zheng X, Gao Y, Li N. The roles of mitochondria-associated membranes in mitochondrial quality control under endoplasmic reticulum stress. *Life Sci* 2019; **231**: 116587 [PMID: 31220526 DOI: 10.1016/j.lfs.2019.116587]

30 **Dhar D**, Baglieri J, Kisseleva T, Brenner DA. Mechanisms of liver fibrosis and its role in liver cancer. *Exp Biol Med (Maywood)* 2020; **245**: 96-108 [PMID: 31924111 DOI: 10.1177/1535370219898141]

31 **Zadorozhnii PV**, Pokotylo IO, Kiselev VV, Okhtina OV, Kharchenko AV. Molecular docking studies of salubrinal and its analogs as inhibitors of the GADD34:PP1 enzyme. *ADMET DMPK* 2019; **7**: 140-150 [PMID: 35350543 DOI: 10.5599/admet.632]

32 **Madden E**, Logue SE, Healy SJ, Manie S, Samali A. The role of the unfolded protein response in cancer progression: From oncogenesis to chemoresistance. *Biol Cell* 2019; **111**: 1-17 [PMID: 30302777 DOI: 10.1111/boc.201800050]

World Journal of Gastroenterology

Submit a Manuscript: https://www.f6publishing.com

World J Gastroenterol 2023 May 7; 29(17): 2628-2641

DOI: 10.3748/wjg.v29.i17.2628

ISSN 1007-9327 (print) ISSN 2219-2840 (online)

ORIGINAL ARTICLE

Basic Study

Lafoensia pacari alleviates intestinal damage by modulating cyclooxygenase-2: *In silico* and *in vivo* evaluation in a colitis model

Gabrielle Caroline Peiter, Thayene Kamyli Moesch Queiroz, Edson Luiz Michalkiewicz Jr, Raphael Henrique Chappuis, Jennefer Sousa Luz, Luiz Henrique Casagrande Piovezani, Cleison Ferreira Silva, Matheus Nozomi Tsutumi, Augusto Fernandes Chaves, Rafael Messias Luiz, Cinthia Façanha Wendel, Ana Carla Zarpelon-Schutz, Kádima Nayara Teixeira

Specialty type: Immunology

Provenance and peer review: Invited article; Externally peer reviewed.

Peer-review model: Single blind

Peer-review report's scientific quality classification

Grade A (Excellent): 0
Grade B (Very good): B
Grade C (Good): C, C
Grade D (Fair): D
Grade E (Poor): 0

P-Reviewer: Howarth GS, Australia; Petrovic S, Serbia; Wang WJ, China; Yao SK, China

Received: November 19, 2022
Peer-review started: November 19, 2022
First decision: February 1, 2023
Revised: March 12, 2023
Accepted: April 10, 2023
Article in press: April 10, 2023
Published online: May 7, 2023

Gabrielle Caroline Peiter, Kádima Nayara Teixeira, Programa Multicêntrico de Pós-graduação em Biquímica e Biologia Molecular - Setor Palotina, Universidade Federal do Paraná, Palotina 85.950-000, Paraná, Brazil

Thayene Kamyli Moesch Queiroz, Ana Carla Zarpelon-Schutz, Programa de Pós-graduação em Biotecnologia - Setor Palotina, Universidade Federal do Paraná, Palotina 85.950-000, Paraná, Brazil

Edson Luiz Michalkiewicz Jr, Raphael Henrique Chappuis, Jennefer Sousa Luz, Luiz Henrique Casagrande Piovezani, Cleison Ferreira Silva, Matheus Nozomi Tsutumi, Augusto Fernandes Chaves, Rafael Messias Luiz, Cinthia Façanha Wendel, Ana Carla Zarpelon-Schutz, Kádima Nayara Teixeira, Campus Toledo, Universidade Federal do Paraná, Toledo 85.919-899, Paraná, Brazil

Corresponding author: Kádima Nayara Teixeira, PhD, Professor, Campus Toledo, Universidade Federal do Paraná, Max Planck 3796, Toledo 85.919-899, Paraná, Brazil.
kadimateixeira@ufpr.br

Abstract

BACKGROUND

Inflammatory bowel diseases (IBD) are a worldwide health problem and mainly affect young people, consequently affecting the workforce. Available treatments are often associated with side effects, and new therapeutic options are needed. For centuries, plants have represented important substrates in the field of drug development. *Lafoensia pacari* (*L. pacari*) is a plant whose pharmaceutical potential has been described, and may have biological activity relevant to the treatment of IBD symptoms.

AIM

To investigate the activity of keto-alcoholic extracts of *L. pacari* with respect to ameliorating the inflammatory and nociceptive symptoms of acute experimental colitis in mice.

METHODS

Keto-alcoholic extracts of *L. pacari* leaves and bark were administered to male and

female Swiss mice weighing 25 g to 30 g (n = 8 male mice and n = 8 female mice). The effect of these extracts was observed in an acetic acid-induced acute experimental model of colitis with regard to antinociception/analgesia and inflammatory tissue damage. Recorded macroscopic indices included the Wallace score and the colon weight obtained using a precision scale. Mechanical hyperalgesia was determined using an electronic analgesimeter. Behavior related to overt pain was determined by quantifying the number of writhing instances within 20 min of administration of acetic acid. Molecular docking was performed using human and murine cyclooxygenase-2 (COX-2) with 3 flavonoids (ellagic acid, kaempferol, and quercetin) on the AutoDock Vina software. Analysis of variance followed by Tukey's posttest was used with $P < 0.05$ indicating significance.

RESULTS

In this murine model of colitis, administration of extracts from *L. pacari* ameliorated acetic acid-induced writhing and colitis-associated inflammatory pain. These improvements may be attributable to the reduction in edema, inflammation (*e.g.*, ulcers, hyperemia, and bowel wall damage), and the intensity of abdominal hyperalgesia. The keto-alcoholic extracts of *L. pacari* leaves and bark administered at a dose of either 100 mg/kg or 300 mg/kg significantly reduced the number of writhing events when compared to the negative control ($P < 0.05$). Additionally, extracts of *L. pacari* bark also performed better than Dipyrone. Leaf extracts administered at 10 mg/kg, 30 mg/kg, and 100 mg/kg and bark extracts administered at 30 mg/kg significantly reduced or prevented the development of edema in the colon of treated mice, while mesalazine did not. Moreover, using molecular docking, we observed that the flavonoids present in *L. pacari* extracts bind to COX-2, an event not unique to ellagic acid.

CONCLUSION

The results of this study demonstrate a potential novel application of *L. pacari* extracts for the reduction of inflammation and promotion of antinociception/analgesia as demonstrated by our findings in a murine model of colitis. These findings were also corroborated by *in silico* analyses, and suggest that *L. pacari* extracts may be a promising therapeutic agent in the treatment of IBD.

Key Words: Antinociceptive activity; Anti-inflammatory activity; Cyclooxygenase-2; Flavonoids; Inflammatory bowel disease; *Lafoensia pacari*

©The Author(s) 2023. Published by Baishideng Publishing Group Inc. All rights reserved.

Core Tip: Keto-alcoholic extracts derived from the leaves and bark of *Lafoensia pacari* (*L. pacari*) demonstrate significant analgesic/antinociceptive activity in a murine acetic acid-induced pain model of colitis. These results can likely be extrapolated to humans, as the identities and structures of mouse and human cyclooxygenase-2 (COX-2) are similar. Furthermore, mouse and human COX-2 interacted in a similar fashion with *L. pacari* extract flavonoids when tested *in silico*. Extracts from both the leaves and bark of *L. pacari* were found to improve inflammation and pain symptoms in mice with acetic acid-induced acute colitis.

Citation: Peiter GC, Moesch Queiroz TK, Michalkiewicz Jr EL, Chappuis RH, Luz JS, Casagrande Piovezani LH, Ferreira Silva C, Nozomi Tsutumi M, Fernandes Chaves A, Luiz RM, Façanha Wendel C, Zarpelon-Schutz AC, Teixeira KN. *Lafoensia pacari* alleviates intestinal damage by modulating cyclooxygenase-2: *In silico* and *in vivo* evaluation in a colitis model. *World J Gastroenterol* 2023; 29(17): 2628-2641

URL: https://www.wjgnet.com/1007-9327/full/v29/i17/2628.htm

DOI: https://dx.doi.org/10.3748/wjg.v29.i17.2628

INTRODUCTION

Inflammatory bowel diseases (IBD) represent a wide spectrum of pathologies that manifest with chronic inflammation of the digestive tract and in many cases may not have a defined etiology[1]. The major diseases under the umbrella of IBD are Crohn's disease and ulcerative colitis, which are both characterized by the presence of an inappropriate immune response against gastrointestinal microbiota and other antigens in the digestive tract lumen[2]. Individual genetic susceptibility and other external factors are also important in the pathogenesis of IBD[3].

IBD occurs worldwide and represents a serious health problem, as it affects young people, frequently relapses, and can often be clinically severe. As such, IBD commonly negatively impacts patient quality of life[4,5].

Conventional pharmacological treatment for IBD is associated with many adverse effects[6] and is often associated with long-term resistance[7]. These phenomena are observed with aminosalicylates, corticosteroids, immunosuppressants, immunomodulators, and antibiotics, all of which are commonly used for induction of remission and are also used for disease maintenance as these drugs reduce inflammatory lesions[8]. Therefore, the search for new drugs to treat IBD is critical. Research on medicinal plants could lead to the discovery of bioactives with anti-inflammatory properties that are capable of curbing the symptoms of IBD with the benefit of avoiding adverse reactions associated with current drugs. *Lafoensia pacari* (*L. pacari*) (Lythraceae), a tree from the Brazilian Cerrado popularly known as dedaleiro, mangava-brava, or pacari, is a fever reducer and promoter of healing according to folk knowledge, and is a candidate for an alternative IBD treatment. Pharmacological trials using extracts derived from the leaves and bark of this plant have demonstrated its antifungal, antimicrobial, and anti-free radical properties. *L. pacari* has also been used in the treatment of gastric ulcers and inflammation [9].

Preclinical models of intestinal inflammation are important tools in the study of bioactives, and can assist in the identification of compounds with therapeutic potential, including drugs used in the treatment of IBD such as mesalazine and sulfasalazine[10].

The most common IBD symptom is abdominal pain, and is even reported in individuals in remission. Yet, IBD-associated abdominal pain is undertreated and there is a scarcity of research on this common issue[11]. Therefore, a drug with antinociceptive (reducing pain *via* modulation of nociceptive pathways [12]) and anti-inflammatory activities would be ideal for IBD therapy.

In view of the colloquial sense of the effects of *L. pacari*, it is possible that its components may be able to help improve the symptomatology of IBD through its antinociceptive and anti-inflammatory actions. Here, we tested this hypothesis using an *in vivo* preclinical mouse model and *in silico* analysis of molecular docking to elucidate the bioactive potential of keto-alcoholic extracts of *L. pacari* leaves and bark.

MATERIALS AND METHODS

Keto-alcoholic extracts of L. pacari

Leaves and bark of *L. pacari* were collected in the cerrado of Presidente Olegário, Minas Gerais, Brazil (coordinates 18°24'56" S; 46°25'17" W) in November 2021. The samples were analyzed by a biologist from the Centro Universitário de Patos de Minas (Minas Gerais, Brazil). The material was processed according to a previously published protocol[13] with some modifications. Leaves and bark of *L. pacari* were sanitized, disinfected, washed, dried at 40 ºC for 72 h, and finally ground.

The keto-alcoholic extracts were prepared according to another previously published protocol[14] with modifications. The ground material was mixed in a 1:1 acetone/methanol solution in a 1:10 plant/solution ratio, sonicated (5 cycles of 5 min on/5 min off), incubated at room temperature for 24 h, filtered, and evaporated. The entire extraction process was carried out in the dark. For the *in vivo* experiments, the extracts were solubilized in dimethyl sulfoxide (DMSO) 2% (v/v) in saline [NaCl 0.9% (w/v)].

Determination of total flavonoid content

Keto-alcoholic extracts were submitted for total flavonoid content determination by spectrophotometry using a methanol solution of $AlCl_3$ 5% (w/v). Quercetin was used as the standard with results expressed as quercetin equivalents[15].

Experimental animals

This study was approved by the Ethics Committee for Animal Use of the Setor de Ciências Biológicas at the Universidade Federal do Paraná, Paraná, Brazil (CEUA no. R.O. 07/2022). Male and female Swiss mice weighing 25 g to 30 g were used in the experiments. The animals were kept in the animal house of the Universidade Federal do Paraná - Toledo Campus in polypropylene boxes (41 cm × 33 cm × 16 cm) with pine shavings. Animals had access to rodent food and chlorinated drinking water *ad libitum* and were kept at a controlled temperature (22 ºC ± 2.0 ºC), in a 12 h light/dark cycle.

Writhing test

Female Swiss mice weighing 25 g to 30 g were used (n = 8 per group). The induction of nociceptive response was achieved by intraperitoneal administration of acetic acid [0.8% (v/v)] in saline (10 mL/kg). The noxious stimulus was given 30 min after administration *via* gavage of keto-alcoholic extracts of *L. pacari* leaves and bark (10 mg/kg, 30 mg/kg, 100 mg/kg, or 300 mg/kg), saline (negative control), dipyrone monohydrate 100 mg/kg (positive control), DMSO 2% (v/v), or ellagic acid (a flavonoid found in *L. pacari)* in DMSO 2% (v/v) in saline (1.6 mg/kg)[16]. The mice were individually housed in

glass cylinders and writhing and paw extension events were recorded over a span of 20 min. The intensity of the contortional response was expressed by the cumulative number of contortions over this 20 min period[17,18].

Induction of experimental acute colitis

The following experiment lasted for 14 h. After 24 h of solid fasting, male Swiss mice weighing 25 g to 30 g (*n* = 8 per group) were anesthetized with isoflurane (1.5% in 100% oxygen). At hour 0 and hour 6, the mice were pretreated with keto-alcoholic extracts of *L. pacari* leaves and bark (10 mg/kg, 30 mg/kg, 100 mg/kg, or 300 mg/kg), mesalazine 200 mg/kg (positive control), or saline (negative control). Mice in which colitis was not induced were used as controls. At hour 9, saline enema was performed on all animals. At hour 10, induction of experimental acute colitis was achieved with 7.5% (v/v) acetic acid administered rectally.

The intracolonic injection was performed with a polyethylene cannula measuring 3 cm in length[19]. At hour 12, treatment was administered using the same protocol as for pretreatment. At hour 13, the animals were subjected to mechanical hyperstimulation (Von Frey nociception test). At hour 14, the animals were euthanized by overdose of isoflurane followed by cervical dislocation.

The distal colon of each animal was collected and washed with saline to remove fecal debris. Macroscopic evaluation of each specimen was performed and the severity of lesions was rated using a numerical score (from 0 to 6)[20]. The presence of edema was also evaluated[19,21] by weighing a 2 cm colonic segment using a precision digital scale.

Von Frey test

Visceral mechanical hyperalgesia was assessed using the electronic Von Frey test[22]. Mice were allocated to a box in a temperature-controlled room for at least 45 min prior to testing. Withdrawal reflexes were elicited with a portable force transducer (Digital Algesimeter EFF 310; Insight Ltda, São Paulo, Brazil) fitted to a 0.7 mm^2 polypropylene tip. This apparatus was applied to the lower abdomen up to the mid-abdomen of each animal. After tip removal, the pressure intensity was automatically recorded (recording values from the average of 3 measurements).

Statistical analysis

The means of the values obtained for each group in each experiment were calculated and analyzed using Prism 9.0.1 software. One-way analysis of variance was used to compare groups according to treatment dose followed by Tukey's test. Significance was set at $P < 0.05$.

Bioinformatic analysis by molecular docking

In order to better understand the results of the *in vivo* antinociceptive testing, an *in silico* molecular docking technique was used to evaluate the activity of flavonoids present in *L. pacari*[23] with respect to murine cyclooxygenase-2 (COX-2). The same simulations were performed with human COX-2 for extrapolation of the murine data. Primary sequences of both murine and human COX-2 were analyzed by global alignment using ClustalX 2.1 software[24] for obtaining identity data.

The structure files of the flavonoids (ligands) were obtained from the ZINC database (zinc.docking.org). The 2-dimensional ".sdf" files were converted into 3-dimensional ".pdb" files using the ViewerLite 5.0 software (Accelrys Inc., San Diego, CA, United States). The 3-dimensional structure of murine COX-2 (receptor) was obtained from the Protein Data Bank (PDB) (rcsb.org).

Molecular docking was performed using flexible ligandrigid receptor methodology[25]. For the execution of molecular docking, the AutoDock Tools 4[26] and AutoDock Vina v.1.2.0[27] programs were used. Preparation of molecules was performed, which included the detection of torsion points and calculation of the torsion angles of the ligands, besides the delimitation of the region where the docking was performed (Grid box).

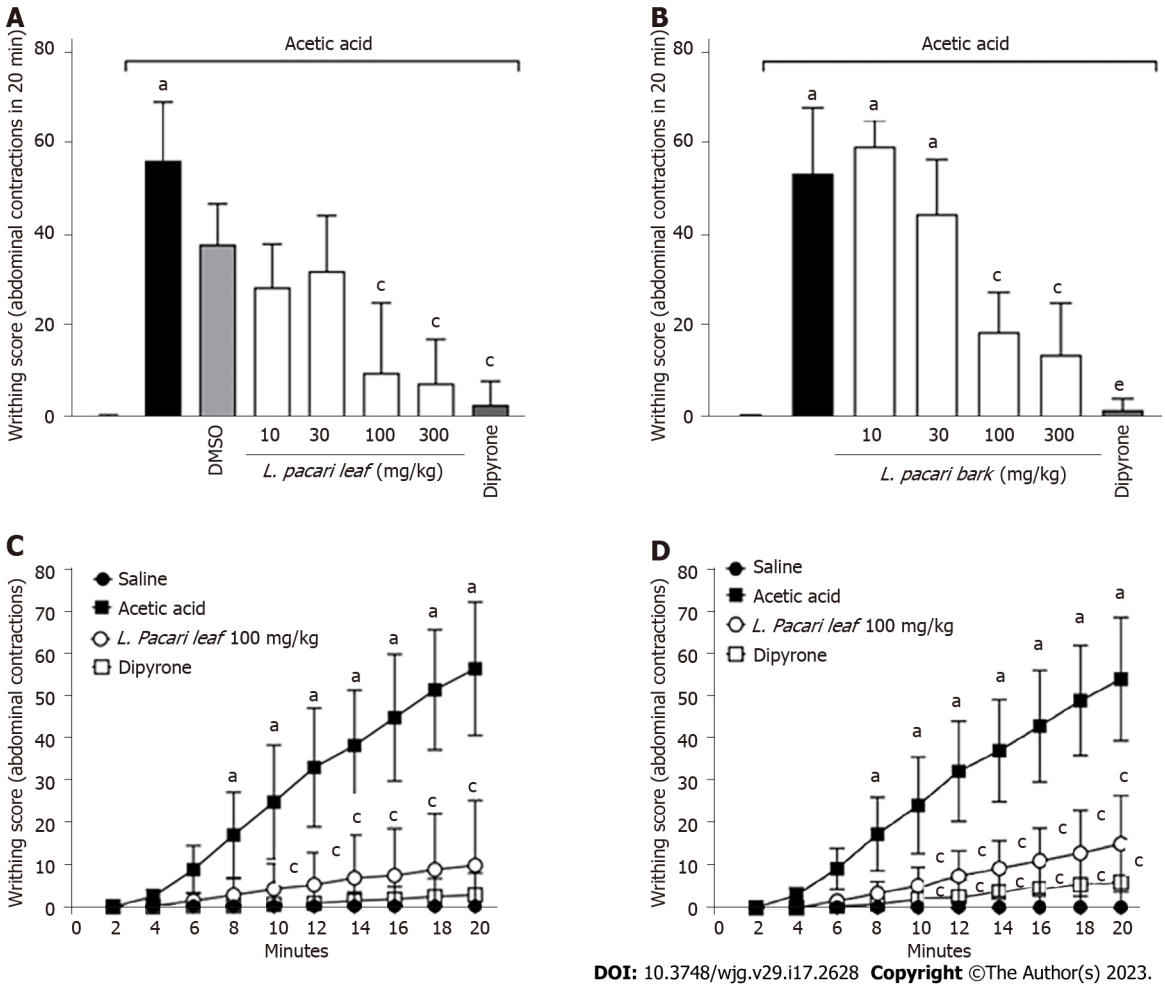
RESULTS

Total flavonoids from L. pacari leaves and bark

The determination of total flavonoid content indicated 97.38 ± 0.0091 (97.38%) and 47.95 ± 0.0035 (47.95%) quercetin/g dry mass equivalents in *L. pacari* leaves or bark, respectively (*i.e.* 97.38 g and 47.95 mg of total flavonoids/g dry mass of leaves or bark, respectively).

Antinociceptive activity of keto-alcoholic extract of L. pacari leaves and bark

The writhing test revealed that DMSO 2% (v/v) did not influence the number of painful contortions when compared to the acetic acid noxious stimulus. A statistically significant decrease in the number of writhing events was observed in mice treated with dipyrone when compared to negative controls (Figure 1).



DOI: 10.3748/wjg.v29.i17.2628 **Copyright** ©The Author(s) 2023.

Figure 1 Antinociceptive activity of keto-alcoholic extracts of *Lafoensia pacari*. A: Keto-alcoholic extracts of leaves; B: Keto-alcoholic extracts of bark; C: Time-dependent action of the keto-alcoholic extract of *Lafoensia pacari* (*L. pacari*) leaves at 100 mg/kg; D: Time-dependent action of the keto-alcoholic extract of *L. pacari* bark at 100 mg/kg. Results presented ± representative error of 8 animals per group. $^{a}P < 0.05$ *vs* saline group; $^{c}P < 0.05$ *vs* DMSO 2% (v/v), acetic acid; $^{e}P < 0.05$ *vs* all groups except the saline group. One-way analysis of variance followed by Tukey's *t*-test. Error bar: Standard error of the mean; *L. pacari*: *Lafoensia pacari*.

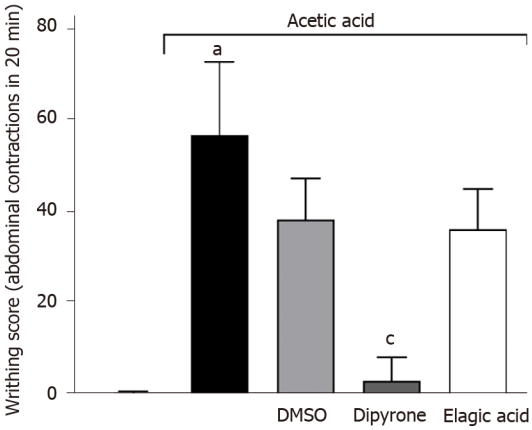
With respect to the keto-alcoholic extracts of *L. pacari* leaves, doses of 100 mg/kg and 300 mg/kg reduced the number of acetic acid-induced writhing events significantly as compared to negative controls, but positive controls (dipyrone-treated; Figure 1A). The keto-alcoholic extracts of *L. pacari* bark at 100 mg/kg and 300 mg/kg significantly reduced the number of acetic-acid induced writhing events as compared to negative controls and also when compared to dipyrone (Figure 1B).

No statistically significant difference was observed between the antinociceptive potential of the low and high *L. pacari* leaves or bark extract doses (100 mg/kg and 300 mg/kg, respectively). The lower dose (100 mg/kg) was found to act in a time-dependent manner, exhibiting effects 10 min after administration (Figure 1C and D). Ellagic acid alone, administered at 1.6 mg/kg, did not significantly reduce the number of contortions (Figure 2).

Activity of keto-alcoholic extracts of L. pacari leaves and bark in acute colitis

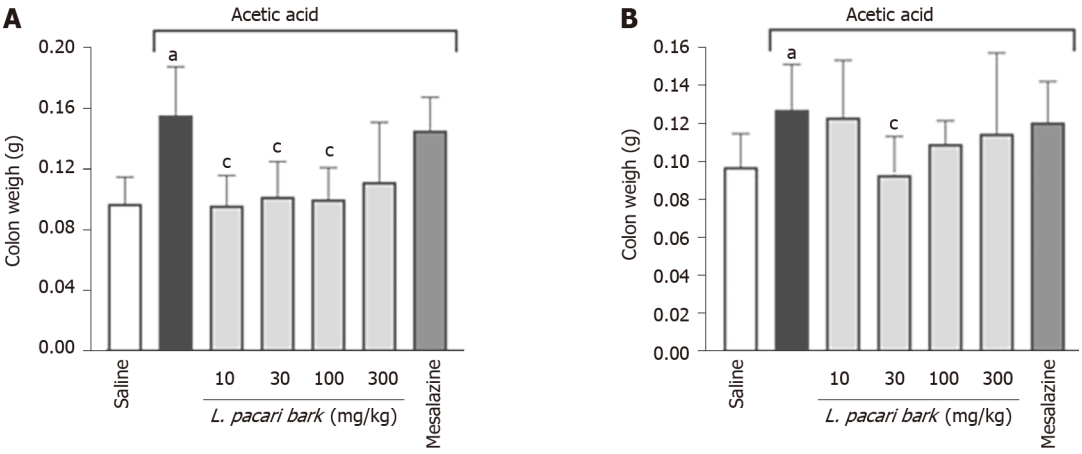
Colitis-induced edema was observed and quantified by weighing the removed colonic segment. Colon segment weight of colitis mice was higher than that of healthy mice with no colitis induction. Keto-alcoholic extracts of *L. pacari* leaves administered at doses of 10 mg/kg, 30 mg/kg, and 100 mg/kg significantly reduced or prevented the development of colonic edema in treated mice (Figure 3A); similar results were observed in mice treated with the keto-alcoholic extracts of *L. pacari* bark administered at 30 mg/kg (Figure 3B), as evidenced by the weight of colonic segments of these animals being similar to that of healthy mice. Treatment with mesalazine did not improve edema.

Numerical lesional severity scores as assigned by gross assessment of colonic segments ranged from 0 to 2 (0 = no lesion; 1 = hyperemia without ulceration; 2 = ulceration without intestinal wall hypertrophy). No control mice were found to have lesions (score 0), and untreated mice with induced colitis demonstrated scores of 1 or 2 (Figure 4). Gross assessment of colonic segments of mice treated with keto-alcoholic extracts of *L. pacari* bark at 30 mg/kg, 100 mg/kg, and 300 mg/kg had fewer lesions



DOI: 10.3748/wjg.v29.i17.2628 **Copyright** ©The Author(s) 2023.

Figure 2 Writhing score for ellagic acid. Results presented ± representative error of 8 animals per group. [a]*P* < 0.05 *vs* saline group, [c]*P* < 0.05 *vs* ellagic acid, DMSO 2% (v/v), acetic acid. One-way analysis of variance followed by Tukey's *t*-test. Error bar: Standard error of the mean.



DOI: 10.3748/wjg.v29.i17.2628 **Copyright** ©The Author(s) 2023.

Figure 3 Anti-inflammatory activity of the keto-alcoholic extract of *Lafoensia pacari* on colonic edema. A: Keto-alcoholic extract of *Lafoensia pacari* (*L. pacari*) leaves; B: Keto-alcoholic extract of *L. pacari* bark. Results presented ± representative error of 8 animals per group. [a]*P* < 0.05 *vs* saline group; [c]*P* < 0.05 *vs* acetic acid and mesalazine. One-way analysis of variance followed by Tukey's *t*-test. Error bar: Standard error of the mean; *L. pacari*: *Lafoensia pacari*.

than untreated mice (Figure 4B); similar results were observed in mice treated with keto-alcoholic extracts of *L. pacari* leaves at 10 mg/kg (scores = 0 or 1; Figure 4A). In general, the keto-alcoholic extracts of *L. pacari* showed anti-inflammatory activity in the colon of animals with acute colitis. Mice treated with mesalazine showed intestinal lesions with scores of 1 or 2, suggesting poorer performance of this drug when compared to keto-alcoholic extracts of *L. pacari* leaves or bark.

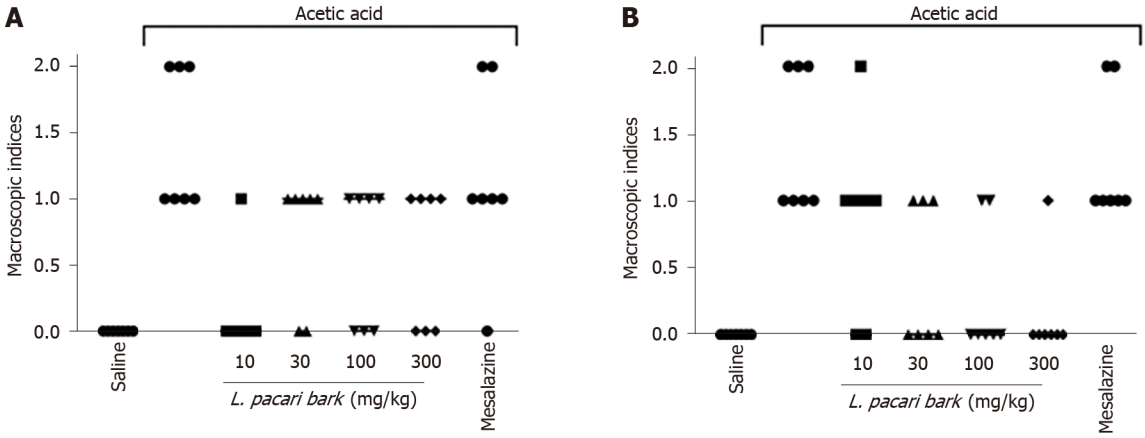
Activity of keto-alcoholic extracts of L. pacari leaves and bark in hyperalgesia

Results of the Von Frey test were expressed as the difference between the intensity required to elicit a positive response before and after the induction of acute colitis by acetic acid. Mice treated with the keto-alcoholic extract of *L. pacari* leaves at 30 mg/kg, 100 mg/kg, or 300 mg/kg or mesalazine showed greater analgesic effect when compared to untreated mice. The keto-alcoholic extract of the leaves administered at 100 mg/kg or 300 mg/kg performed better than the extract administered at 30 mg/kg or mesalazine (Figure 5A).

With respect to the keto-alcoholic extract of *L. pacari* bark, mice treated with 100 mg/kg or 300 mg/kg or mesalazine required a higher intensity of stimulus to elicit a positive response when compared to negative controls. No significant difference was observed among these 3 treatments, although both 100 mg/kg and 300 mg/kg doses of the extract trended toward higher analgesic activity when compared to mesalazine (Figure 5B).

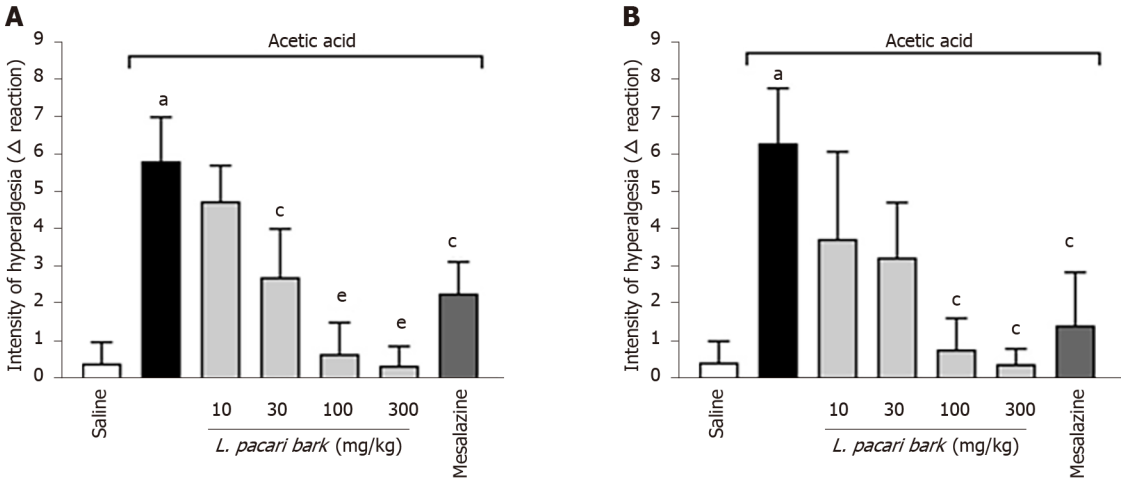
In silico analysis

The 3-dimensional structures of murine COX-2 (PDB: 3LN0) and human COX-2 (PDB: 5 LKQ) were selected from PDB; these were originally complexed to compound 5c-S and meclofenamic acid,



DOI: 10.3748/wjg.v29.i17.2628 **Copyright** ©The Author(s) 2023.

Figure 4 Macroscopic indices of colonic segments from mice with induced colitis post-treatment. Scores: 0 = no lesion; 1 = hyperemia without ulceration; 2 = ulceration without hypertrophy of the intestinal wall, according to Wallace *et al*[20]. Error bar: Standard error of the mean; *L. pacari*: *Lafoensia pacari*.



DOI: 10.3748/wjg.v29.i17.2628 **Copyright** ©The Author(s) 2023.

Figure 5 Antinociceptive activity of the keto-alcoholic extract of *Lafoensia pacari* in the acute colitis model. A: Keto-alcoholic extract of *Lafoensia pacari* (*L. pacari*) leaves; B: Keto-alcoholic extract of *L. pacari* bark. Results presented ± representative error of 8 animals per group. $^{a}P < 0.05$ *vs* saline group; $^{c}P < 0.05$ *vs* acetic acid; $^{e}P < 0.05$ *vs* mesalazine. One-way analysis of variance followed by Tukey's *t*-test. Error bar: Standard error of the mean; *L. pacari*: *Lafoensia pacari*.

respectively. These compounds were removed for analysis in this study. Human and murine COX-2 are homologous and have similar structures. The number of total residues in the primary sequence of both is 604, and the number of residues resolved by X-ray diffraction of human COX-2 and murine COX-2 is 551 and 587, respectively. After global alignment analysis, it was observed that these enzymes have 86.6% primary sequence identity.

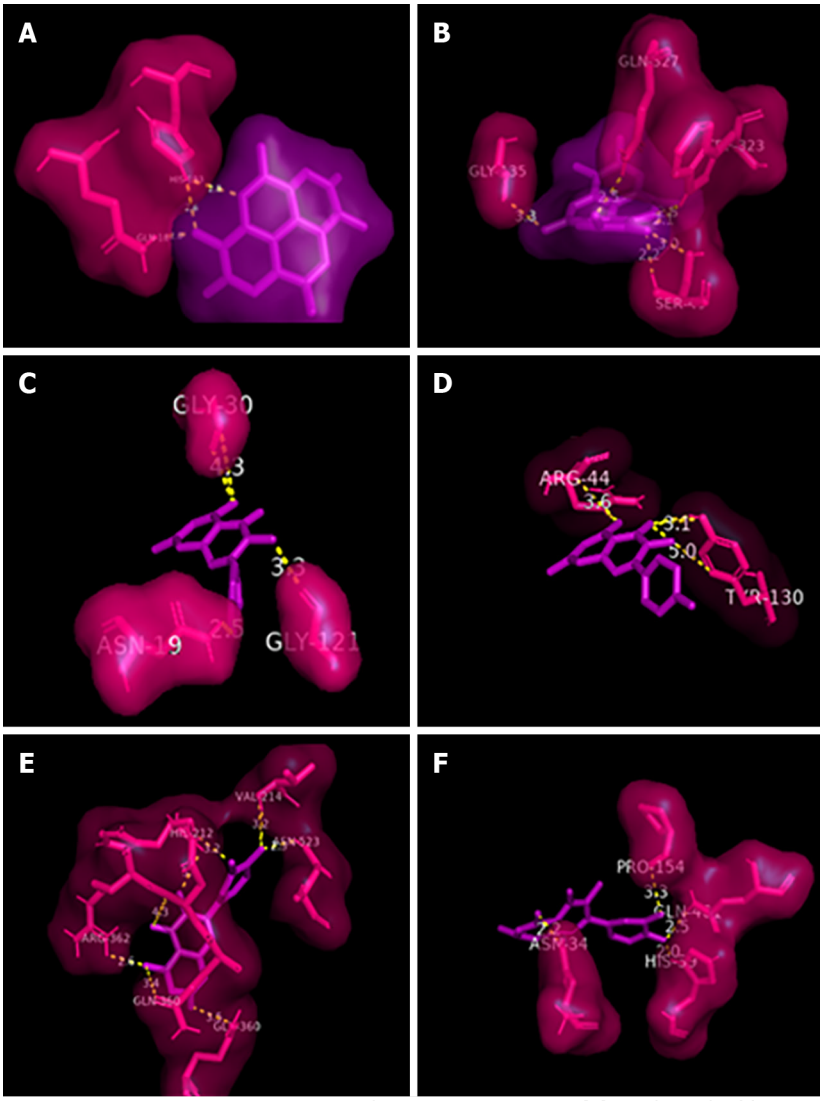
Molecular docking simulations with COX-2 were performed with 3 flavonoids: ellagic acid (ZINC000003872446), kaempferol (ZINC000003869768) and quercetin (ZINC000003869685). It was observed that all flavonoids bind to chain A, the catalytic monomer of COX-2, with significant affinity (Table 1) and possibly, under physiological conditions, the interaction is stable and negatively affects enzyme activity.

Ellagic acid was bound to 2 amino acid residues of murine COX-2 (3 bonds; 2.0-2.8 Å) and to 4 residues of human COX-2 (5 bonds; 2.1-3.3 Å; Figure 6A and B). Kaempferol bound to 3 residues of murine COX-2 (3 bonds; 2.5-4.3 Å) and 2 residues of human COX-2 (3 bonds; 3.1-5.0 Å; Figure 6C and D), and quercetin bound to 6 residues of murine COX-2 (8 bonds; 2.3-4.3 Å) and 4 residues of human COX-2 (4 bonds; 2.0-3.3 Å; Figure 6E and F). None of the flavonoids were bound to the prosthetic group (heme group) of COX-2. The values of the affinity energies are similar to each other, the most significant interactions were between ellagic acid and murine COX-2 and between quercetin and human COX-2.

Table 1 Energy of affinity of cyclooxygenase-2/flavonoid complexes

Flavonoid	Energy of affinity in kcal/mol	
	Human COX-2	Murine COX-2
Ellagic acid	-9.7	-9.9
Kaempferol	-9.9	-8.8
Quercetin	-10.1	-9.5

COX-2: Cyclooxygenase-2.



DOI: 10.3748/wjg.v29.i17.2628 **Copyright** ©The Author(s) 2023.

Figure 6 Complexes formed by cyclooxygenase-2 and flavonoids from *Lafoensia pacari*. A, C and E: Murine cyclooxygenase-2 (COX-2) bound to ellagic acid, kaempferol, and quercetin, respectively; B, D and F: Human COX-2 bound to ellagic acid, kaempferol, and quercetin, respectively. Lilac: Flavonoid; Pink: Amino acid residues; The dashed lines represent chemical interactions. The name of the amino acid is represented by the three-letter code followed by their number in the primary sequence. The numbers next to the dashed lines are the bond lengths in Angstrom.

DISCUSSION

Using extraction in acetone/methanol solution, 97.38 ± 0.0091 mg total flavonoids/g dry mass of the leaves and 47.95 ± 0.0035 mg total flavonoids/g dry mass of the bark of *L. pacari* were obtained; in crude hydroalcoholic and methanolic extracts of leaves, 15.7 ± 0.02 and 14.4 ± 0.04 equivalents of quercetin were obtained, respectively[28]. In another study[29] 13.61% ± 0.72 equivalents of quercetin was obtained from an aqueous extraction of the bark of *L. pacari*. Comparatively, the keto-alcoholic

extraction was more efficient in obtaining total flavonoids from both leaves and bark of *L. pacari*.

The antinociceptive effect of the keto-alcoholic extracts of *L. pacari* leaves and bark was demonstrated by the writhing test, an assay of nociception using injection of a noxious agent[30]. When tissues and cells are exposed to a noxious stimulus, chemical mediators are released, which in turn stimulate C-type nerve fibers causing local pain. Acetic acid has properties that can cause pain, in addition to stimulating the release of cytokines (IL-1β, TNF- and IL-8) by macrophages and basophils present in the abdominal cavity[31]. The writhing test is considered a model for studying visceral pain[32]; keto-alcoholic extracts of *L. pacari* leaves and bark decreased the number of writhing events in this test, suggesting the efficacy of these extracts in treating this type of pain.

The extracts of *L. pacari* leaves and bark administered at 100 mg/kg and 300 mg/kg, reduced the number of painful contortions in the murine colitis model; however, there was no significant difference between these dosages in terms of analgesic effect. However, the extract administered at 300 mg/kg (the highest concentration used in this study) did not exert such a potent antinociceptive effect when compared to the positive control group (dipyrone-treated).

The aqueous extract of *L. pacari* bark administered at 0.5 g/kg and 1.0 g/kg had previously shown an antinociceptive effect in the writhing test[33]. In a study using the ethanolic extract of *L. pacari* leaves administered at 1.0 g/kg, the extract reduced the number of writhing events, especially when it was administered subcutaneously; however, this dose caused toxicity and death in treated animals[31]. Therefore, although the dose of 300 mg/kg is still below the accepted toxic value[31], in order to avoid undesirable adverse effects, the 100 mg/kg dose of keto-alcoholic *L. pacari* extract may be more appropriate.

The choice of oral administration of the extracts was based on the better viability and ease of administration considering future drug development from the plant's bioactive compounds. As we observed analgesic activity when extracts were administered orally, it seems that this route of administration is sufficient for absorption of the active compound at a therapeutic level.

In comparison, one study evaluated the analgesic and anti-inflammatory activity of total flavonoids from the leaves of *Juniperus sabina*, a plant commonly known as sabina native to Europe and Asia. This study indicated significant dose-dependent analgesic activity in the acetic acid-induced writhing test, with the highest dose (500 mg total flavonoids/kg animal mass) showing the greatest inhibition of writhing (22.02%)[34]. In the present study, the most effective inhibitory dose was 100 mg/kg of dry mass of *L. pacari* leaves and bark, which is equivalent to 9.738 mg/kg and 4.795 mg/kg total flavonoids, respectively.

Other studies have investigated the ethanolic extract of white willow as an anti-inflammatory and antinociceptive, with results similar to ours in which the plant extract was effective in an animal model, but the positive control treatment was more effective, even at lower concentrations[35]. Another study aimed to elucidate the effects of an ethanolic extract of *L. pacari* on acute peritonitis in mice[9], and demonstrated significant anti-inflammatory activity of this extract. This finding may be akin to the antinociceptive effect of the keto-alcoholic *L. pacari* extracts demonstrated in the present study.

Although this study does not present the rate of inhibition of writhing, the difference in concentration of total flavonoids used per body mass in each study suggests that flavonoids from *L. pacari* are more effective, as analgesia was observed at lower doses. One possible explanation for this observation may be the types of flavonoids present in each plant species analyzed, and those of *L. pacari* may act more synergistically to produce an analgesic effect.

Fractionation of the *L. pacari* bark extract leads to the isolation of ellagic acid as the main flavonoid compound, suggesting that this compound is responsible for the anti-inflammatory and anti-edema activity of the extract observed in mouse models of asthma. Ellagic acid was also identified in *L. pacari* leaves by high performance liquid chromatography[31]. Recently, evidence regarding the efficacy of ellagic acid in the treatment of acute visceral pain has been growing; its analgesic effects are attributed to the inhibition of COX, which synthesizes prostaglandins at sites of peripheral cell damage[36].

Ellagic acid is reported to have several benefits, such as anti-inflammatory, anticancer, and hepatoprotective actions, and is also a promising agent for the treatment of chronic diseases such as ulcerative colitis, Crohn's disease, Alzheimer's disease, and diabetes[37]. However, according to the results obtained in this study, ellagic acid was not the only phenolic compound present in the extract of the *L. pacari* that may be responsible for the observed analgesic effect. In a statistical comparison, its effect resembles that of the 30 mg/kg dosage of leaf extract in the twitch test. The relatively low efficiency of ellagic acid compared to other doses of extract indicates that this flavonoid likely acts synergistically with other compounds present in the plant to confer a more robust analgesic pharmacological effect.

Regarding acute experimental colitis, the keto-alcoholic extracts of *L. pacari* leaves administered at 10 mg/kg, 30 mg/kg, or 100 mg/kg significantly reduced or prevented the development of colonic in treated mice. The same was observed in mice treated with the keto-alcoholic extract of *L. pacari* bark administered at 30 mg/kg as evidenced by similar colonic segment weights between treated and health mice.

Gross evaluation of colonic segments of mice revealed lower lesional severity scores in mice receiving keto-alcoholic extracts of *L. pacari* leaves and bark, with further reduction in the groups that received a higher dose. The mice that received mesalazine had similar lesional severity scores compared to the saline-treated group; this may be due to the fact that mesalazine typically used in the treatment of

chronic inflammatory bowel disease[38,39], and we used an acute colitis model.

The macroscopic findings suggest that the keto-alcoholic extracts of *L. pacari* leaves and bark have an anti-inflammatory effect on the mucosa of the gastrointestinal tract and reduce tissue destruction in this model of acute colitis. In agreement with these findings, one study showed that a methanolic extract of the bark of *L. pacari* had a potent gastroprotective effect against ethanol-, indomethacin-, and stress-induced ulcers[40].

Another study showed that an ethanolic extract of *L. pacari* possesses healing properties when applied to skin wounds, accelerating healing when compared to controls. This is attributed to the inhibition of the proliferation and inflammation phases of the healing process, corroborating the findings in our acute colitis induction experiments, which showed reduced colonic tissue damage in mice treated with *L. pacari* extracts. These data suggest a negative modulation of tissue inflammatory processes[23].

The anti-inflammatory effects of extracts derived from *L. pacari* leaves have also been demonstrated in a murine model of asthma. One study showed a significant reduction in lung inflammation and tissue damage in animals that received the extract as evidenced by gross tissue damage score analysis[41]. These data corroborate the results of the present study, which also demonstrated the anti-inflammatory effects of keto-alcoholic extracts of *L. pacari* leaves and bark in reducing macroscopic damage to colonic tissue.

Both the Von Frey monofilament and the electronic Von Frey tests are used as quantitative sensory assays to explore mechanical hyperalgesia[42]. In this study, pain stimuli were administered to mice using the electronic Von Frey test, and the keto-alcoholic extracts of *L. pacari* leaves administered at 30 mg/kg, 100 mg/kg, or 300 mg/kg or mezalazine showed greater analgesic effect when compared to untreated mice. Among the treatments, the keto-alcoholic extract administered at 100 mg/kg or 300 mg/kg performed better than the extract at 30 mg/kg or mesalazine.

Regarding the keto-alcoholic extract of *L. pacari* bark, mice treated with the doses 100 mg/kg or 300 mg/kg or mesalazine required a higher intensity stimulus to induce a positive response when compared to the negative controls. No significant difference was observed among these 3 treatments, although the keto-alcoholic extract at 100 mg/kg or 300 mg/kg had greater analgesic effect as compared to mesalazine. It is important to emphasize that, since this is a study based on a model of acute colitis, the findings regarding mesalazine are consistent with what is expected, since this drug has a better effect with long-term use[43]. The Von Frey test was one of the first evoked stimulus tests to be developed and continues to be widely used today[44]. This test is an excellent tool for evaluating hyperalgesia, visceral pain, and inflammation[45].

Molecular docking is an important method to complement and help better understand results obtained by *in vivo* testing. In humans, despite being structurally a homodimer, COX-2 functions as a conformational heterodimer, with 1 monomer being catalytic and the other allosteric[46]. In our experiments, the catalytic monomer, composed of the A chain, was the interaction target of ellagic acid, kaempferol, and quercetin in both human and murine COX-2.

We observed that the evaluated flavonoids bind to COX-2, but also that the interactions are strong. Binding affinity is measured by the affinity energy, which when lower than -6.0 kcal/mol indicates interaction in a biological environment[47]. Although the values are expressive, they are all within a narrow range (-8.8 1 kcal/mol to 10.1 kcal/mol). Our data suggest that COX-2 inhibition after interaction with any of the flavonoids tested should not trigger events other than the expected inhibition of prostaglandin production and consequent decrease in pain sensation.

Our findings also demonstrate that ellagic acid is not the only compound of interest with respect to analgesia found in the keto-alcoholic extracts of *L. pacari* leaves and bark. The affinity energy evaluated by molecular docking represents the strength of interaction between 2 or more interacting molecules. The strength of interaction is favorable when it is negative, and the receptor/ligand interaction is greater when the energy is lower.

Corroborating our study, another demonstrated that quercetin is also effective in inhibiting hyperalgesia[48]. This flavonoid showed an analgesic effect in animal models of inflammatory pain, inhibiting hyperalgesia induced by mechanical or thermal stimuli, and reduced the pain behaviors of studied animals. In addition, it also inhibited the development of inflammation-related edema, cytokine production, myeloperoxidase activity, and cell migration[49].

Nonsteroidal anti-inflammatory agents (NSAIDs) are part of a heterogeneous group of compounds from different chemical classes, and have 3 main actions: Anti-inflammation, analgesia, and fever reduction. NSAIDs are the most commonly used therapeutic agents[50]. Although they are effective, their long-term use is limited in most patients, as they are associated with adverse gastrointestinal effects such as abdominal pain, ulcers, bleeding, and even gastric or duodenal perforation. These effects have been attributed to the low specificity of these compounds for COX-2[51]. Acetylsalicylic acid (ASA) promotes the irreversible inhibition of human COX activity by covalent binding to a serine residue within the active site.

In COX-1, ASA acetylates serine 530, preventing the binding of arachidonic acid to the enzyme's active site, thus suppressing the production of prostaglandins. In COX-2, ASA acetylates serine 516, blocking the activity of this isoform[50,51]. In our study, *in silico* analysis showed that these amino acid residues, which are key to the action of some analgesics, showed no direct interaction with the evaluated flavonoids, demonstrating that in this model there are other residues involved in COX-2

inhibition.

CONCLUSION

We demonstrated the anti-inflammatory effects of keto-alcoholic extracts of *L. pacari* leaves and bark in a murine acetic acid-induced colitis model. Both extracts inhibited colitis-induced tissue damage as assessed using the Wallace score and the development of colonic edema; this effect seems to be COX-2-dependent. The flavonoid content of *L. pacari* extracts has been used to treat many diseases, and shows anti-inflammatory, analgesic, and antioxidant properties. However, the effects of this plant on symptoms related to colitis have not been described. Using molecular docking, we showed a strong interaction between ellagic acid, kaempferol or quercetin with both human and murine COX-2; however, the inflammatory and antinociceptive effects of *L. pacari* are not solely attributable to ellagic acid. Taken together, these results suggest the potential of oral *L. pacari* extract administration in the treatment of inflammatory diseases such as colitis.

ARTICLE HIGHLIGHTS

Research background

Therapeutic activities of *Lafoensia pacari* (*L. pacari*) have been reported in folk medicine, and this plant has been used as an antifungal, an anti-ulcer, an antibacterial, an anti-inflammatory, a fever reducer, in the treatment of pneumonia, and in the treatment of stomach pain. Despite the common use of this plant, the mechanisms by which it achieves medicinal effects have not been elucidated.

Research motivation

L. pacari is a tree found in Brazil thought to have beneficial pharmacological properties, with its main bioactive compounds belonging to the flavonoid class. One of the most studied flavonoids found in this plant is ellagic acid, which has been reported to have anti-inflammatory activity. However, *L. pacari* contains numerous flavonoids, and these compounds may also have similar activity to or act synergistically with ellagic acid.

Research objectives

We aimed to evaluate the activity of keto-alcoholic extracts of *L. pacari* leaves and bark, which contain a significant amount of flavonoids, with respect to the improvement of symptoms related to inflammatory bowel diseases (*e.g.*, inflammation of the intestinal mucosa, edema, and abdominal pain).

Research methods

The methodology used in this study was based on protocols already well established in the scientific literature, and, when necessary, some modifications were made. All experiments were performed with a number of mice that allowed for statistical analysis of the data and were performed in duplicate or triplicate depending on statistical requirements.

Research results

Our results corroborated those described by other studies with respect to the beneficial effects of *L. pacari* extracts; however, to our knowledge, we are the first to evaluate the therapeutic potential of these extracts in a murine model of acute colitis. Antinociception/analgesia in this murine model were observed with respect to treatment with extracts derived from *L. pacari* leaves and bark.

Research conclusions

Our findings suggest that keto-alcoholic extracts of *L. pacari* leaves and bark are beneficial for the reduction of symptoms related to inflammatory bowel disease. These effects are attributed to the decrease or inhibition of inflammation in the intestinal mucosa. Regarding pain, bioinformatics techniques indicated that ellagic acid alone is not responsible for these effects, since other flavonoids interact and inhibit with significant affinity cyclooxygenase-2, an enzyme that produces pain mediators.

Research perspectives

This study is part of a larger research project; follow-up experiments are planned using a rat model of chronic colitis, other antinociception tests. Future experiments will also investigate the histology of intestinal segments after induction and treatment of chronic colitis with *L. pacari* extracts.

FOOTNOTES

Author contributions: Peiter GC, Moesch Queiroz TK, Michalkiewicz Jr EL, Chappuis RH, Luz JS, Casagrande Piovezani LH, Ferreira Silva C, Nozomi Tsutumi M, Fernandes Chaves A, Luiz RM and Façanha Wendel C performed the experiments; Zarpelon-Schutz AC, Peiter GC and Teixeira KN analyzed the results and wrote the manuscript; Zarpelon-Schutz AC and Teixeira KN interpreted the data, performed the critical analysis of the results, corrected the manuscript and coordinated the study; All authors approved the final version of the manuscript.

Institutional review board statement: The Institutional Review Board declares knowledge about the study.

Institutional animal care and use committee statement: The Institutional Animal Care and Use Committee declares knowledge and approval about the study.

Conflict-of-interest statement: All the authors report no relevant conflicts of interest for this article.

Data sharing statement: The authors declare that all data are public and can be shared upon reasonable request.

ARRIVE guidelines statement: The authors have read the ARRIVE guidelines, and the manuscript was prepared and revised according to the ARRIVE guidelines.

Open-Access: This article is an open-access article that was selected by an in-house editor and fully peer-reviewed by external reviewers. It is distributed in accordance with the Creative Commons Attribution NonCommercial (CC BY-NC 4.0) license, which permits others to distribute, remix, adapt, build upon this work non-commercially, and license their derivative works on different terms, provided the original work is properly cited and the use is non-commercial. See: https://creativecommons.org/Licenses/by-nc/4.0/

Country/Territory of origin: Brazil

ORCID number: Gabrielle Caroline Peiter 0000-0001-7965-4434; Thayene Kamyli Moesch Queiroz 0000-0002-2120-4833; Edson Luiz Michalkiewicz Jr 0000-0003-3986-9144; Raphael Henrique Chappuis 0000-0002-1332-4974; Jennefer Sousa Luz 0000-0002-5625-0098; Luiz Henrique Casagrande Piovezani 0000-0003-3526-3292; Cleison Ferreira Silva 0000-0002-2666-3385; Matheus Nozomi Tsutumi 0000-0003-3652-6170; Augusto Fernandes Chaves 0000-0002-1454-0804; Rafael Messias Luiz 0000-0002-5107-7281; Cinthia Façanha Wendel 0000-0003-2183-9748; Ana Carla Zarpelon Schutz 0000-0002-8320-3633; Kádima Nayara Teixeira 0000-0002-2928-9181.

S-Editor: Gong ZM
L-Editor: Filipodia
P-Editor: Yu HG

REFERENCES

1 **Sairenji T**, Collins KL, Evans DV. An Update on Inflammatory Bowel Disease. *Prim Care* 2017; **44**: 673-692 [PMID: 29132528 DOI: 10.1016/j.pop.2017.07.010]
2 **Baumgart DC**, Sandborn WJ. Inflammatory bowel disease: clinical aspects and established and evolving therapies. *Lancet* 2007; **369**: 1641-1657 [PMID: 17499606 DOI: 10.1016/S0140-6736(07)60751-X]
3 **Podolsky DK**. Inflammatory bowel disease. *N Engl J Med* 2002; **347**: 417-429 [PMID: 12167685 DOI: 10.1056/NEJMra020831]
4 **Fakhoury M**, Negrulj R, Mooranian A, Al-Salami H. Inflammatory bowel disease: clinical aspects and treatments. *J Inflamm Res* 2014; **7**: 113-120 [PMID: 25075198 DOI: 10.2147/JIR.S65979]
5 **Figueroa C C**, Quera P R, Valenzuela E J, Jensen B C. [Inflammatory bowel disease: experience of two Chilean centers]. *Rev Med Chil* 2005; **133**: 1295-1304 [PMID: 16446852 DOI: 10.4067/S0034-98872005001100004]
6 **Carter MJ**, Lobo AJ, Travis SP; IBD Section, British Society of Gastroenterology. Guidelines for the management of inflammatory bowel disease in adults. *Gut* 2004; **53** Suppl 5: V1-16 [PMID: 15306569 DOI: 10.1136/gut.2004.043372]
7 **Cai Z**, Wang S, Li J. Treatment of Inflammatory Bowel Disease: A Comprehensive Review. *Front Med (Lausanne)* 2021; **8**: 765474 [PMID: 34988090 DOI: 10.3389/fmed.2021.765474]
8 **Stenson WF**, Korzenik J. Inflammatory bowel disease. In: Yamada T, Alpers DH, Laine L, editors. Yamada's textbook of gastroenterology. 4th ed. Philadelphia: Lippincott Williams & Wilkins Publishers, 2003: 1699–759.
9 **Albuquerque DA**, Juliani JM, Santos JA, Hosida PY, Borges S, Borralho CT. Effect of Lafoensia pacari ethanolic extract on acute peritonitis in mice. In: Program and Proceedings of the 3rd SBPC Special Meeting Coastal Ecosystems - From Knowledge to Management; Santa Catarina, Brazil, 1996: 214
10 **Melo NM da C**, Almeida MVS, Campos DM de O, Oliveira CBS de, Oliveira JIN. Animal models for inducing inflammatory bowel diseases: integrative review. *Revista Ciências em Saúde* 2021; **11**: 80-87 [DOI: 10.21876/rcshci.v11i1.1056]
11 **Norton C**, Czuber-Dochan W, Artom M, Sweeney L, Hart A. Systematic review: interventions for abdominal pain management in inflammatory bowel disease. *Aliment Pharmacol Ther* 2017; **46**: 115-125 [PMID: 28470846 DOI: 10.1111/apt.14108]
12 **Basbaum CB**, Mann JK, Chow AW, Finkbeiner WE. Monoclonal antibodies as probes for unique antigens in secretory

cells of mixed exocrine organs. *Proc Natl Acad Sci U S A* 1984; **81**: 4419-4423 [PMID: 6205396 DOI: 10.1073/pnas.81.14.4419]

13 **Albuquerque ER**, Gossler SC, Piovezan M, Conto LC. Extraction and determination of flavonoids, condensed and total tannins from pine nut bark (Araucaria angustifolia). Educational material. Instituto Federal de Santa Catarina/Brazil. 2017. Available at: http://docente.ifsc.edu.br/michael.nunes/MaterialDidatico/Analises%20Quimicas/TCC%20II/TCC%202017%201/Eduarda%20e%20Sheili.pdf

14 **Oliveira MA**. Extraction of polyphenols from cocoa seed (Theobroma cacao). M.Sc. Thesis, Universidade Federal de Santa Catarina/Brazil. 2005. Available at: https://www.yumpu.com/pt/document/read/10594294/extracao-de-polifenois-da-semente-de-cacau

15 **Dutra RP**, Nogueira AMC, Marques RRO, Costa MCP, Ribeiro MNS. Avaliação farmacognóstica de geoprópolis de *Melipona fasciculata* Smith (tiúba) em municípios da Baixada maranhense, Brasil. *Rev Bras Farmacogn* 2008; **18**: 557-562 [DOI: 10.1590/S0102-695X2008000400010]

16 **Rogerio AP**, Fontanari C, Melo MC, Ambrosio SR, de Souza GE, Pereira PS, França SC, da Costa FB, Albuquerque DA, Faccioli LH. Anti-inflammatory, analgesic and anti-oedematous effects of *Lafoensia pacari* extract and ellagic acid. *J Pharm Pharmacol* 2006; **58**: 1265-1273 [PMID: 16945186 DOI: 10.1211/jpp.58.9.0014]

17 **Valério DA**, Cunha TM, Arakawa NS, Lemos HP, Da Costa FB, Parada CA, Ferreira SH, Cunha FQ, Verri WA Jr. Anti-inflammatory and analgesic effects of the sesquiterpene lactone budlein A in mice: inhibition of cytokine production-dependent mechanism. *Eur J Pharmacol* 2007; **562**: 155-163 [PMID: 17320857 DOI: 10.1016/j.ejphar.2007.01.029]

18 **Verri WA Jr**, Cunha TM, Magro DA, Domingues AC, Vieira SM, Souza GR, Liew FY, Ferreira SH, Cunha FQ. Role of IL-18 in overt pain-like behaviour in mice. *Eur J Pharmacol* 2008; **588**: 207-212 [PMID: 18511039 DOI: 10.1016/j.ejphar.2008.04.010]

19 **Guazelli CF**, Fattori V, Colombo BB, Georgetti SR, Vicentini FT, Casagrande R, Baracat MM, Verri WA Jr. Quercetin-loaded microcapsules ameliorate experimental colitis in mice by anti-inflammatory and antioxidant mechanisms. *J Nat Prod* 2013; **76**: 200-208 [PMID: 23347547 DOI: 10.1021/np300670w]

20 **Wallace JL**, MacNaughton WK, Morris GP, Beck PL. Inhibition of leukotriene synthesis markedly accelerates healing in a rat model of inflammatory bowel disease. *Gastroenterology* 1989; **96**: 29-36 [PMID: 2535830 DOI: 10.1016/0016-5085(89)90760-9]

21 **Colombo BB**. A vimpocetina reduz a colite induzida por ácido acético em camundongos. Universidade Estadual de Londrina, 2017

22 **Cunha TM**, Verri WA Jr, Vivancos GG, Moreira IF, Reis S, Parada CA, Cunha FQ, Ferreira SH. An electronic pressure-meter nociception paw test for mice. *Braz J Med Biol Res* 2004; **37**: 401-407 [PMID: 15060710 DOI: 10.1590/s0100-879x2004000300018]

23 **Pereira LOM**, Vilegas W, Tangerina MMP, Arunachalam K, Balogun SO, Orlandi-Mattos PE, Colodel EM, Martins DTO. *Lafoensia pacari* A. St.-Hil.: Wound healing activity and mechanism of action of standardized hydroethanolic leaves extract. *J Ethnopharmacol* 2018; **219**: 337-350 [PMID: 29501673 DOI: 10.1016/j.jep.2018.02.038]

24 **Thompson JD**, Gibson TJ, Plewniak F, Jeanmougin F, Higgins DG. The CLUSTAL_X windows interface: flexible strategies for multiple sequence alignment aided by quality analysis tools. *Nucleic Acids Res* 1997; **25**: 4876-4882 [PMID: 9396791 DOI: 10.1093/nar/25.24.4876]

25 **Lengauer T**, Rarey M. Computational methods for biomolecular docking. *Curr Opin Struct Biol* 1996; **6**: 402-406 [PMID: 8804827 DOI: 10.1016/s0959-440x(96)80061-3]

26 **Morris GM**, Huey R, Lindstrom W, Sanner MF, Belew RK, Goodsell DS, Olson AJ. AutoDock4 and AutoDockTools4: Automated docking with selective receptor flexibility. *J Comput Chem* 2009; **30**: 2785-2791 [PMID: 19399780 DOI: 10.1002/jcc.21256]

27 **Eberhardt J**, Santos-Martins D, Tillack AF, Forli S. AutoDock Vina 1.2.0: New Docking Methods, Expanded Force Field, and Python Bindings. *J Chem Inf Model* 2021; **61**: 3891-3898 [PMID: 34278794 DOI: 10.1021/acs.jcim.1c00203]

28 **Burque RK**, Francesconi LP, Victorino AT, Mascarenhas MA, Ceresér KM. Determination of phenolic and evaluation of antioxidant activity of *Lafoensia pacari* (Lythraceae). *Revista Eletrônica de Farmácia* 2015; **12**: 1-10 [DOI: 10.5216/ref.v12i1.24645]

29 **Cunha GA**, Bailão EFLC, Borges LL, Almeida LM. Evaluation of the antioxidant potential of Lafoensia pacari. In: Annals of the 5th Congress of Teaching, Research and Extension of the Universidade Estadual de Goiás: Science for reducing inequalities; 2018 Oct 17-19; Goiás, Brazil

30 **Collier HO**, Dinneen LC, Johnson CA, Schneider C. The abdominal constriction response and its suppression by analgesic drugs in the mouse. *Br J Pharmacol Chemother* 1968; **32**: 295-310 [PMID: 4230818 DOI: 10.1111/j.1476-5381.1968.tb00973.x]

31 **Guimarães HA**, Nascimento MVM, Tavares A, Galdino PM, De Paula JR, Costa EA. Effects of ethanolic extract of *Lafoensia pacari* A. St.-Hil., Lythraceae (pacari), in pain and inflammation model. *Brazilian J Pharm* 2010; **20**: 328-333 [DOI: 10.1590/S0102-695X2010000300007]

32 **Silva ABL**, Dias KS, Marques MS, Menezes IAC, Santos TC, Mello ICM, Lisboa ACCD, Cavalcanti SCH, Marçal RM, Antoniolli AR. Evaluation of the analgesic effect and acute toxicity of the aqueous extract of *Hyptis fruticosa* (Salmz. Ex Benth.). *Brazilian J Pharm* 2006; **16**: 475-479 [DOI: 10.1016/j.fct.2019.110940]

33 **de Matos LG**, Santos L da R, Ferreira RN, Pontes IS, de Paula JR, Costa EA. Anti-Inflammatory, Antinociceptive, and Sedating Effects of *Lafoensia pacari*. *Aqueous Extract. Pharm Biol* 2008; **46**: 341-346 [DOI: 10.1080/13880200801887799]

34 **Zhao J**, Maitituersun A, Li C, Li Q, Xu F, Liu T. Evaluation on Analgesic and Anti-Inflammatory Activities of Total Flavonoids from *Juniperus sabina*. *Evid Based Complement Alternat Med* 2018; **2018**: 7965306 [PMID: 30069226 DOI: 10.1155/2018/7965306]

35 **Shara M**, Stohs SJ. Efficacy and Safety of White Willow Bark (Salix alba) Extracts. *Phytother Res* 2015; **29**: 1112-1116 [PMID: 25997859 DOI: 10.1002/ptr.5377]

36 **Naghizadeh B**, Mansouri MT, Ghorbanzadeh B. Ellagic acid enhances the antinociceptive action of carbamazepine in the

acetic acid writhing test with mice. *Pharm Biol* 2016; **54**: 157-161 [PMID: 25898222 DOI: 10.3109/13880209.2015.1025288]

37 **Derosa G**, Maffioli P, Sahebkar A. Ellagic Acid and Its Role in Chronic Diseases. *Adv Exp Med Biol* 2016; **928**: 473-479 [PMID: 27671829 DOI: 10.1007/978-3-319-41334-1_20]

38 **Ministry of Health of Brazil**. Department of Health Care: Clinical protocol and therapeutic guidelines for the treatment of Crohn's disease. In: Diário Oficial da União. Portaria 858/02, 2002; 214: 77-82

39 **Ministry of Health of Brazil**. Department of Health Care: Clinical protocol and therapeutic guidelines for the treatment of ulcerative colitis. In: Diário Oficial da União. Portaria 861/02, 2002; 214: 87-98

40 **Tamashiro Filho P**, Sikiru Olaitan B, Tavares de Almeida DA, Lima JC, Marson-Ascêncio PG, Donizeti Ascêncio S, Rios-Santos F, Martins DT. Evaluation of antiulcer activity and mechanism of action of methanol stem bark extract of *Lafoensia pacari* A. St.-Hil. (Lytraceae) in experimental animals. *J Ethnopharmacol* 2012; **144**: 497-505 [PMID: 23069941 DOI: 10.1016/j.jep.2012.09.019]

41 **Rogerio AP**, Fontanari C, Borducchi E, Keller AC, Russo M, Soares EG, Albuquerque DA, Faccioli LH. Anti-inflammatory effects of *Lafoensia pacari* and ellagic acid in a murine model of asthma. *Eur J Pharmacol* 2008; **580**: 262-270 [PMID: 18021768 DOI: 10.1016/j.ejphar.2007.10.034]

42 **Tena B**, Escobar B, Arguis MJ, Cantero C, Rios J, Gomar C. Reproducibility of Electronic Von Frey and Von Frey monofilaments testing. *Clin J Pain* 2012; **28**: 318-323 [PMID: 22001670 DOI: 10.1097/AJP.0b013e31822f0092]

43 **Sandborn WJ**, Hanauer SB. Systematic review: the pharmacokinetic profiles of oral mesalazine formulations and mesalazine pro-drugs used in the management of ulcerative colitis. *Aliment Pharmacol Ther* 2003; **17**: 29-42 [PMID: 12492730 DOI: 10.1046/j.1365-2036.2003.01408.x]

44 **Deuis JR**, Dvorakova LS, Vetter I. Methods Used to Evaluate Pain Behaviors in Rodents. *Front Mol Neurosci* 2017; **10**: 284 [PMID: 28932184 DOI: 10.3389/fnmol.2017.00284]

45 **Laird JMA**, Martinez-Caro L, Garcia-Nicas E, Cervero F. A new model of visceral pain and referred hyperalgesia in the mouse. *Pain* 2001; **92**: 335-342 [PMID: 11376906 DOI: 10.1016/S0304-3959(01)00275-5]

46 **Dong L**, Vecchio AJ, Sharma NP, Jurban BJ, Malkowski MG, Smith WL. Human cyclooxygenase-2 is a sequence homodimer that functions as a conformational heterodimer. *J Biol Chem* 2011; **286**: 19035-19046 [PMID: 21467029 DOI: 10.1074/jbc.M111.231969]

47 **Pantsar T**, Poso A. Binding Affinity *via* Docking: Fact and Fiction. *Molecules* 2018; **23** [PMID: 30061498 DOI: 10.3390/molecules23081899]

48 **Lin CF**, Leu YL, Al-Suwayeh SA, Ku MC, Hwang TL, Fang JY. Anti-inflammatory activity and percutaneous absorption of quercetin and its polymethoxylated compound and glycosides: the relationships to chemical structures. *Eur J Pharm Sci* 2012; **47**: 857-864 [PMID: 22609526 DOI: 10.1016/j.ejps.2012.04.024]

49 **Souto FO**, Zarpelon AC, Staurengo-Ferrari L, Fattori V, Casagrande R, Fonseca MJ, Cunha TM, Ferreira SH, Cunha FQ, Verri WA Jr. Quercetin reduces neutrophil recruitment induced by CXCL8, LTB4, and fMLP: inhibition of actin polymerization. *J Nat Prod* 2011; **74**: 113-118 [PMID: 21275387 DOI: 10.1021/np1003017]

50 **Malta DJN**. Síntese, elucidação estrutural e atividade biológica de novos derivados imidazolidinônicos. M.Sc. Thesis, Universidade Federal de Pernambuco, 2005. Available at: https://repositorio.ufpe.br/handle/123456789/40873

51 **Carvalho WA**, Carvalho RD, Rios-Santos F. [Specific cyclooxygenase-2 inhibitor analgesics: therapeutic advances.]. *Rev Bras Anestesiol* 2004; **54**: 448-464 [PMID: 19471752 DOI: 10.1590/s0034-70942004000300017]

World Journal of Gastroenterology

Submit a Manuscript: https://www.f6publishing.com

World J Gastroenterol 2023 May 7; 29(17): 2642-2656

DOI: 10.3748/wjg.v29.i17.2642

ISSN 1007-9327 (print) ISSN 2219-2840 (online)

ORIGINAL ARTICLE

Basic Study

Establishment and characterization of a new human ampullary carcinoma cell line, DPC-X1

Hao Xu, Chang-Peng Chai, Xin Miao, Huan Tang, Jin-Jing Hu, Hui Zhang, Wen-Ce Zhou

Specialty type: Gastroenterology and hepatology

Provenance and peer review: Unsolicited article; Externally peer reviewed.

Peer-review model: Single blind

Peer-review report's scientific quality classification

Grade A (Excellent): 0
Grade B (Very good): B, B
Grade C (Good): 0
Grade D (Fair): 0
Grade E (Poor): 0

P-Reviewer: Kode JA, India; Lai SW, Taiwan

Received: December 26, 2022
Peer-review started: December 26, 2022
First decision: February 8, 2023
Revised: February 17, 2023
Accepted: April 13, 2023
Article in press: April 13, 2023
Published online: May 7, 2023

Hao Xu, Chang-Peng Chai, Jin-Jing Hu, The Forth Department of General Surgery, The First Hospital of Lanzhou University, Lanzhou 730000, Gansu Province, China

Xin Miao, State Key Laboratory of Veterinary Etiological Biology, Key Laboratory of Animal Virology of the Ministry of Agriculture, Lanzhou Veterinary Research Institute, Chinese Academy of Agricultural Sciences, Lanzhou 730000, Gansu Province, China

Huan Tang, Wen-Ce Zhou, The Second Clinical Medical College, Lanzhou University, Lanzhou 730000, Gansu Province, China

Hui Zhang, Wen-Ce Zhou, Department of General Surgery, The Second Hospital of Lanzhou University, Lanzhou 730000, Gansu Province, China

Corresponding author: Hao Xu, Doctor, MD, Associate Chief Physician, Surgeon, The Forth Department of General Surgery, The First Hospital of Lanzhou University, No. 1 Donggang West Road, Lanzhou 730000, Gansu Province, China. amoyxu@126.com

Abstract

BACKGROUND

An in-depth study of the pathogenesis and biological characteristics of ampullary carcinoma is necessary to identify appropriate treatment strategies. To date, only eight ampullary cancer cell lines have been reported, and a mixed-type ampullary carcinoma cell line has not yet been reported.

AIM

To establish a stable mixed-type ampullary carcinoma cell line originating from Chinese.

METHODS

Fresh ampullary cancer tissue samples were used for primary culture and subculture. The cell line was evaluated by cell proliferation assays, clonal formation assays, karyotype analysis, short tandem repeat (STR) analysis and transmission electron microscopy. Drug resistances against oxaliplatin, paclitaxel, gemcitabine and 5-FU were evaluated by cell counting kit-8 assay. Subcutaneous injection 1 × 10^6 cells to three BALB/c nude mice for xenograft studies. The hematoxylin-eosin staining was used to detect the pathological status of the cell line. The expression of biomarkers cytokeratin 7 (CK7), cytokeratin 20 (CK20), cytokeratin low molecular weight (CKL), Ki67 and carcinoembryonic antigen

(CEA) were determined by immunocytochemistry assay.

RESULTS

DPC-X1 was continuously cultivated for over a year and stably passaged for more than 80 generations; its population doubling time was 48 h. STR analysis demonstrated that the characteristics of DPC-X1 were highly consistent with those of the patient's primary tumor. Furthermore, karyotype analysis revealed its abnormal sub-tetraploid karyotype. DPC-X1 could efficiently form organoids in suspension culture. Under the transmission electron microscope, microvilli and pseudopods were observed on the cell surface, and desmosomes were visible between the cells. DPC-X1 cells inoculated into BALB/C nude mice quickly formed transplanted tumors, with a tumor formation rate of 100%. Their pathological characteristics were similar to those of the primary tumor. Moreover, DPC-X1 was sensitive to oxaliplatin and paclitaxel and resistant to gemcitabine and 5-FU. Immunohistochemistry showed that the DPC-X1 cells were strongly positive for CK7, CK20, and CKL; the Ki67 was 50%, and CEA was focally expressed.

CONCLUSION

Here, we have constructed a mixed-type ampullary carcinoma cell line that can be used as an effective model for studying the pathogenesis of ampullary carcinoma and drug development.

Key Words: Ampullary carcinoma; Cell line; Xenograft; Drug resistance

©The Author(s) 2023. Published by Baishideng Publishing Group Inc. All rights reserved.

Core Tip: A new ampullary carcinoma cell line has been established, making up for the shortage of Chinese ampullary carcinoma cell lines. And this is the the first study to report a mixed-type ampullary carcinoma cell line. The cell line inoculated into BALB/c nude mice can quickly form xenograft tumors. It is an excellent model for studying the mechanisms of invasion, metastasis and other mechanisms of ampullary carcinoma. The cell line is sensitive to oxaliplatin and paclitaxel but is naturally resistant to gemcitabine and fluorouracil, which can be used for drug resistance mechanism research and new drug development.

Citation: Xu H, Chai CP, Miao X, Tang H, Hu JJ, Zhang H, Zhou WC. Establishment and characterization of a new human ampullary carcinoma cell line, DPC-X1. *World J Gastroenterol* 2023; 29(17): 2642-2656
URL: https://www.wjgnet.com/1007-9327/full/v29/i17/2642.htm
DOI: https://dx.doi.org/10.3748/wjg.v29.i17.2642

INTRODUCTION

Ampullary carcinoma is a relatively rare tumor, accounting for 0.2% of gastrointestinal cancers but 20% of all periampullary cancers[1,2]. Recently, the incidence rate of ampullary cancer has gradually increased[3,4]. Ampullary carcinoma can occur at any age; however, it is more common between 60 and 65 years of age, and the sex ratio is approximately 3:2[1,2]. As biliary obstruction symptoms appear early, the surgical resection rate of ampullary carcinoma is higher than that of other periampullary malignant tumors, and approximately 50% of patients are eligible for surgery on diagnosis[1,5,6]. Its operation amount is over one-third of the total operation amount of pancreatoduodenectomy. The prognosis is good, and the 5-year survival rate exceeds 52.8%[7]. Despite a high potential curative resection rate, most patients with ampullary cancer eventually succumb to tumor recurrence[8,9].

In 1994, Kimura *et al*[10] first classified ampullary carcinoma into intestinal and pancreaticobiliary types according to their histological characteristics. The prevalence of the pancreaticobiliary type was 72%, which is much higher than that of the intestinal type[10]. In 2010, according to the morphological and immunohistochemical characteristics, WHO revised the pathological diagnosis criteria of ampullary carcinoma into three different histopathological subtypes: Intestinal-, pancreaticobiliary-, and mixed-type ampullary carcinoma[11,12].

To date, only eight ampullary cancer cell lines have been included in the official databases of ATCC, JCRB, RIKEN, and DSMZ. One is American, one is Italian, two are Korean, and four are Japanese (three of them are from different lesions of the same patient)[13-17] (Table 1). Among them, SNU-869 is an intestinal-type cell line, whereas the remaining are pancreaticobiliary-type cell lines[18]. No mixed-type ampullary carcinoma cell line has yet been reported.

Table 1 Energy of affinity of cyclooxygenase-2/flavonoid complexes

Cell line	Age (years)	Gender	Source of culture	Race	Differentiation	Primary culture	Ref.
MDAAmp-7	40	Male	Abdominal metastases	American	Well differentiated	1989	[13]
RCB1169/TGBC18TKB	79	Female	Primary tumor	Japanese	-	1995	[14]
RCB1280/TGBC50TKB	52	Male	Liver metastasis	Japanese	Poorly differentiatedadenosquamous carcinoma	1996	[15]
RCB1280/TGBC51TKB	525	Male	Ascites	Japanese	Poorly differentiatedadenosquamous carcinoma	1996	[15]
RCB1280/TGBC52TKB	52	Male	Lymph node	Japanese	Poorly differentiatedadenosquamous carcinoma	1996	[15]
SNU478	-	-	-	Korean	Poorly differentiated with signet ring cell	-	[16]
SNU869	-	-	-	Korean	Well differentiated	-	[16]
AVC1	71	Female	Primary tumor	Italian	Moderately differentiated	1997	[17]

No randomized clinical trial for adjuvant chemotherapy of ampullary carcinoma currently exists, and the data based on which doctors choose treatment methods are limited. Presently, adjuvant therapy for ampullary carcinoma is being tailored according to the histological subtypes. Pancreatic biliary ampullary carcinoma is typically treated similarly to pancreatic adenocarcinoma or biliary tract carcinoma. In contrast, patients with intestinal ampulla receive the usual protocol for colorectal cancer. Based on these premises, the optimal treatment plan for ampullary carcinoma in adjuvant therapy and chemotherapy for advanced patients remains to be determined[19,20].

Based on the aforementioned factors, establishing an ampullary carcinoma cell line, conducting in-depth research on the pathogenesis and biological characteristics of ampullary carcinoma, and then investigating therapeutic targets to formulate effective treatment strategies for patients with ampullary carcinoma are currently required.

In this study, we establish a stable mixed-type ampullary carcinoma cell line named DPC-X1 from the tumor tissue of a patient with ampullary carcinoma. Our study findings underscore the effectiveness of DPC-X1 as an experimental model that can be used to explore the molecular mechanism of ampullary carcinoma and develop therapeutic schemes for disease control.

MATERIALS AND METHODS

Tissue source

The tissue samples were collected from a patient with ampullary cancer who was admitted to the First Hospital of Lanzhou University on November 17, 2021, for pancreatoduodenectomy. The patient was a 60-year-old man who presented with jaundice, had a long history of smoking and drinking, and had no history of carrying hepatitis B or C. His carbohydrate antigen 199 levels exceeded 1000 U/mL (reference range: 0–35 U/mL; Figure 1A), and preoperative magnetic resonance imaging + magnetic resonance cholangiopancreatography indicated ampullary carcinoma (Figure 1B and C). The new organisms growing around the ampulla were grayish-white and were taken from the primary focus for primary culture and subculture (Figure 1D and E).

This study was approved by the Medical Ethics Committee of the First Hospital of Lanzhou University (LDYYLL-2022-487), and signed informed consent was obtained from the patient.

Drugs

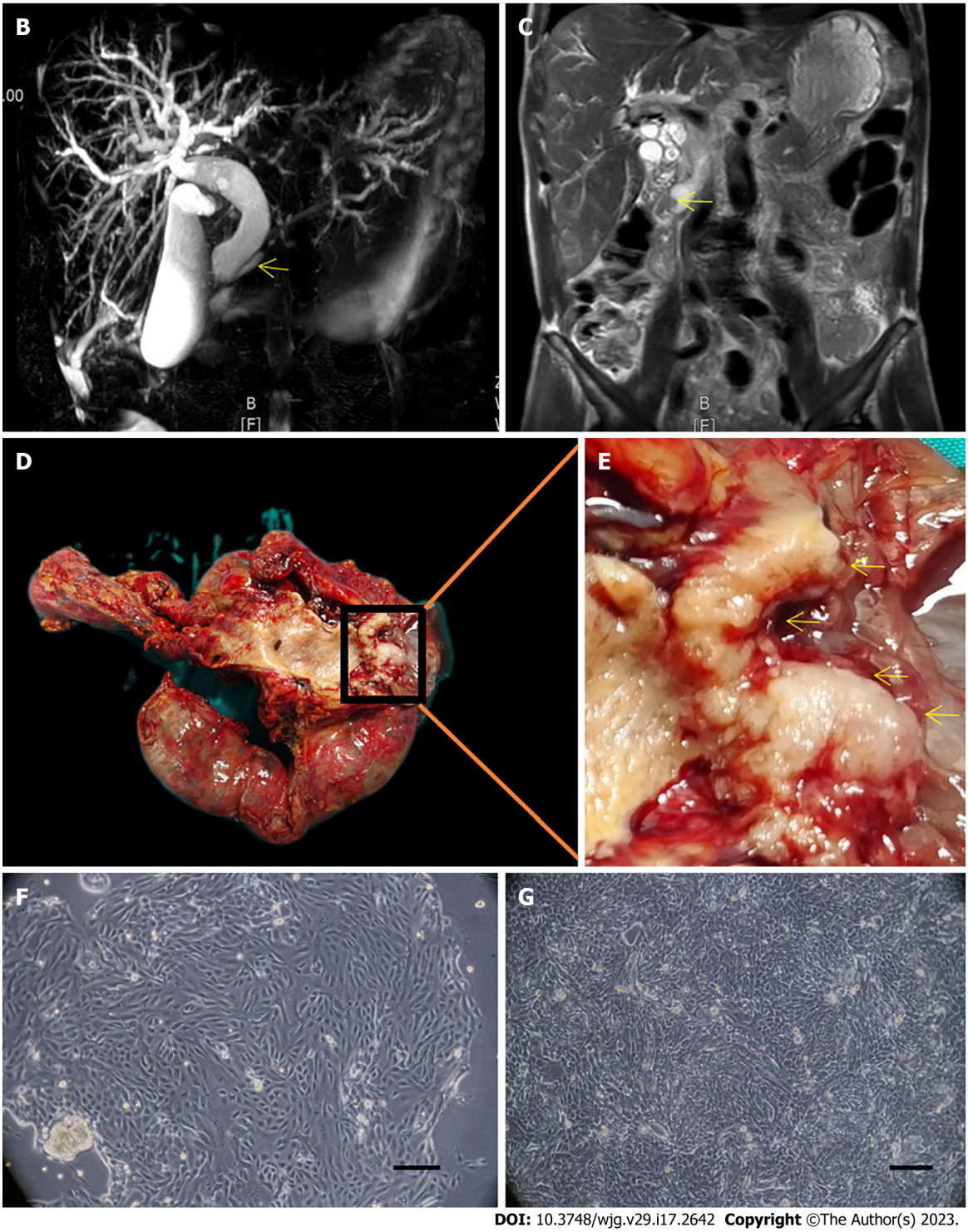
Gemcitabine was obtained from Jiangsu Haosen Pharmaceutical Group Co., Ltd., oxaliplatin from Jiangsu Hengrui Pharmaceutical Co., Ltd., 5-FU from Tianjin Jinyao Pharmaceutical Co., Ltd., and paclitaxel from Jiangsu Aosaikang Pharmaceutical Co., Ltd.

Nude mice

In this study, experiments were conducted on 4–6-week-old BALB/c nude female mice, weighing 16–20 g. They were obtained from Changzhou Kavens Experimental Animal Co., Ltd. and raised in the SPF laboratory of the Animal Experiment Center of Lanzhou University. The animal protocol was designed to minimize pain or discomfort to the animals. The animals were acclimatized to laboratory conditions (23 °C, 12 h/12 h light/dark, 50% humidity, ad libitum access to food and water) for 2 wk prior to experimentation. All animals were euthanized by barbiturate overdose (intravenous injection, 150 mg/

A

Cell line	Patient age/ethnicity	Gender	Current status (days)	Histopathology/differentiation	Tumor size (cm)	Prior therapy	Culture date	Serum		
								AFP IU/mL (0-5.8)	CEA ng/mL (0-5.2)	CA199 U/mL (0-35)
DPC-X1	60/Asian	Male	D (370)	Moderately-poorly	2×1	None	2021-11-17	1.4	4.5	> 1000



DOI: 10.3748/wjg.v29.i17.2642 **Copyright** ©The Author(s) 2023.

Figure 1 Clinical data and cell morphology. A: Clinical data of the patient; B: Magnetic resonance cholangiopancreatography shows the expansion of intrahepatic and extrahepatic bile ducts, gallbladder enlargement, and pancreatic duct expansion (arrow); C: In the coronal view of magnetic resonance imaging, soft tissue shadow (arrow) can be seen in the ampulla, and the upper bile duct is dilated; D: General view of the surgical specimen; E: The enlarged appearance of the ampulla tumor shows the gray-white tumor growing around the ampulla (arrow); F: DPC-X1 primary cell morphology; multinucleated cells and megakaryocytes can be seen; G: DPC-X1 cell morphology of the 80th generation. Scale bars: 100 μm. D: Death; AFP: alpha-fetoprotein; CEA: Carcinoembryonic antigen; CA199:

Carbohydrate antigen 199.

kg pentobarbital sodium) for tissue collection.

All animal experiments were reviewed and approved by the Medical Animal Experiment Ethics Committee of the First Hospital of Lanzhou University (LDYYLL-2022-487). The methods followed in this study were similar or identical to those employed in previous studies[21-23].

Establishment of the cell line

The tumor tissue samples were immersed in sterile phosphate buffered saline (PBS) (Gibco) 3–5 times and sectioned into small pieces. The small woven pieces were mixed with type II collagenase (Gibco) and neutral protease (Invitrogen) and digested in a shaking table at 37 ℃. On digestion of half the tissue block, the supernatant was absorbed, filtered with a 100 mesh filter screen, and centrifuged at 300 × *g* for 3 min. Thereafter, the supernatant was discarded; the sample was resuspended in PBS and centrifugated at 300 × *g* for 3 min. The precipitate was added to a complete medium [RPMI-1640 + 10% fetal bovine serum (FBS) + 1% penicillin–streptomycin, Biological industries (BI)] and uniformly inoculated on a six-well plate (NEST). The medium was refreshed after 48 h. The mixed fibroblasts in the primary culture were removed using differential digestion with 0.25% trypsin. When the cells reached 70% confluency, they were digested and passed on. The cell growth was regularly observed under a light microscope. From the fifth generation, the cells were subcultured in a ratio of 1:2 and frozen with Serum-free rapid cell cryopreservation solution (Mei5 Biotechnology Co., Ltd.).

Cell growth curve

The cell density of DPC-X1 cells in the logarithmic growth phase (P20) was adjusted to 1×10^4/mL after trypsin digestion. After mixing, 0.1 mL of sample was inoculated in each hole in a 96-hole plate cell counting kit-8 (CCK-8) reagent (Dojindo) was added at the same time for 4 consecutive days after inoculation and allowed to react for 2 h. The UV absorbance value at 450 nm wavelength was measured with a microplate reader. The cell doubling time was calculated using the following formula: Td = t × Lg2/Lg (N1/N0). The cell growth curve was plotted with time as the horizontal axis and absorbance value as the vertical axis.

Analysis of short tandem repeats

DPC-X1 cells in the logarithmic growth stage (P10) were collected after trypsin digestion. Together with the primary tumor tissue, they were sent to Suzhou Jianda Biotechnology Company for short tandem repeat (STR) analysis to determine the correlation between the cells and primary tumor tissue.

Karyotype analysis

DPC-X1 cells in the logarithmic growth phase (P40) were treated with 0.25 μg/mL colchicine for 6 h overnight at 37 ℃. The metaphase cells were collected and fixed with methanol glacial acetic acid (3:1). After trypsin digestion, the specimens were stained using Giemsa dye and observed under a microscope. The mitotic phase cells with good dispersion and moderate staining were selected for karyotype analysis.

Organoid culture

DPC-X1 cells in the logarithmic growth phase (P35) were digested, centrifuged, washed twice with PBS, resuspended in a complete culture medium (RPMI-1640 + 10% FBS + 1% penicillin–streptomycin, BI), and inoculated on an ultra-low adsorption cell culture plate (Corning). A thousand cells were added to each well, and 2 mL of culture medium was added for 14 d. The state and number of organ-like cultures were observed under a light microscope.

Transmission electron microscopy

DPC-X1 cells in the logarithmic growth phase (P45) were digested, centrifuged, fixed with an electron microscope fixative, and stored and transported at 4 ℃. Embedding, ultrathin sectioning, and dyeing were performed at Wuhan Servicebio Co., Ltd. Finally, the images were observed under the transmission electron microscope.

Drug sensitivity test

The logarithmically grown DPC-X1 cells (P50) were digested using trypsin to prepare a single-cell suspension. We inoculated 10000 cells/100 μL per well into 96-well plates, and 6 wells in each group were repeated. After the cells adhered to the wall, different concentrations of anti-tumor drugs were added. After 72 h of drug action, 100% X containing 10% (v/v) CCK-8 μL serum-free medium was used to replace the complete medium. The optical density value was measured after 2 h at 450 nm.

Xenograft tumor in nude mice

The cell density of cells in the logarithmic growth phase (P45) was adjusted to 1 × 10^7/mL after trypsin digestion. Thereafter, three BALB/c nude mice each were inoculated with 0.1 mL of this sample. We observed and recorded the tumor growth of the nude mice every alternate day. The mice carrying the tumor were killed after four weeks, and the tumor tissue was excised and fixed with 10% formalin. The surgery was performed under sodium pentobarbital anesthesia, and all efforts were made to minimize suffering. Thereafter, routine histopathological and immunohistochemical examinations were performed.

Immunohistochemical staining

Cells of the 40th generation were digested and inoculated onto sterile slides. After 48 h, the slides were washed with PBS, fixed with 4% paraformaldehyde for 15 min, dried, and treated with 0.5% Triton X-100 for 20 min.

The paraffin sections of primary tumors, transplanted tumors, and organ-like tissues were prepared and incubated at 60 ℃ overnight. The dewaxing, gradient alcohol hydration, and antigen repair processes were completed using Dako's Autostainer Link 48 instrument. Subsequently, 3% hydrogen peroxide solution was incubated at 37 ℃ for 15 min to block the activity of peroxidase; 100 μL of normal goat serum was dripped and then kept sealed at 37 ℃ for 15 min. The first antibody was incubated at 37 ℃ for 1 h with Fuzhou Maxin ready-to-use antibodies [cytokeratin 7 (CK7), cytokeratin 20 (CK20), cytokeratin low molecular weight (CKL), Ki67, and carcinoembryonic antigen (CEA)]. The DAB dye kit (Dako) was used for color development, followed by rinsing with running water for 5 min. Dehydration and xylene transparency were carried out after hematoxylin counterstaining, and the samples were observed under the microscope after neutral resin sealing.

Statistical analyses

All statistical analyses were performed using the SPSS 22.0 software. The data are presented as mean ± SD. Student's *t*-tests and ANOVA were used for group comparisons. Statistical significance was set at $P < 0.05$.

RESULTS

Establishment of the DPC-X1 cell line

Through primary culture and subculture of primary tumor tissue of ampullary carcinoma, an ampullary carcinoma cell line, named DPC-X1, was successfully established. Using light microscopy, we found that DPC-X1 cells adhered to the wall and grew like typical epithelial cells. The cells were mainly short spindle-shaped, with large nuclei and visible nucleoli. The polykaryocytes and megakaryocytes were visible. Loss of contact inhibition between cells likely led to accumulation growth as the cells were closely adherent and grew in clumps and sheets (Figure 1F and Video). The cell morphology and growth mode remained unaltered even though it passed to the 80th generation (Figure 1G).

Cell growth curve

DPC-X1 cells proliferated vigorously and grew stably in RPMI-1640 medium with 10% FBS. Through the CCK-8 method, the doubling time of the DPC-X1 cell population was found to be 48 h using the CCK-8 method. The cell growth curve was plotted using culture time as the abscissa and absorbance values as the ordinate (Figure 2A).

Analysis of STRs

The DNA typing results demonstrated that the two submitted samples were from the same individual with a likelihood ratio = 4.1867 × 10^{20} (Figure 2B and Supplementary material). The results indicate that DPC-X1 is a new human ampullary carcinoma cell line with the same origin as that of the primary tumor tissue and is not contaminated by the existing cell line.

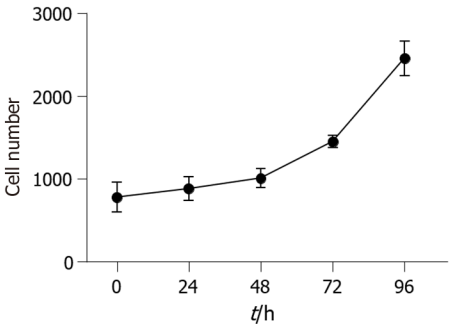
Karyotype analysis

Karyotype analysis showed that DPC-X1 cells were mainly sub-tetraploid, with large differences in chromosome number and morphology. The representative karyotype was 80, XX del (2) (q32) del (5) (p12) del (6) (q24) inv (9) del (10) p (13) del (17) p (12) (Figure 2C).

Organoid culture

After inoculating the DPC-X1 cells on the ultra-low attachment culture plate, the cells were observed to proliferate well and gradually form spherical or cystic organs (Figure 2D). With time, the number of organoid organs gradually increased and appeared spore-like or branch-like (Figure 2E).

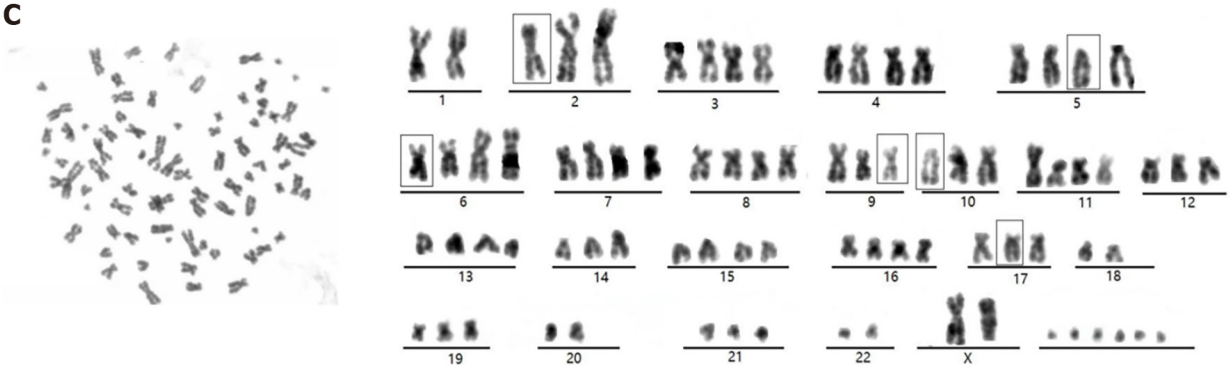
A

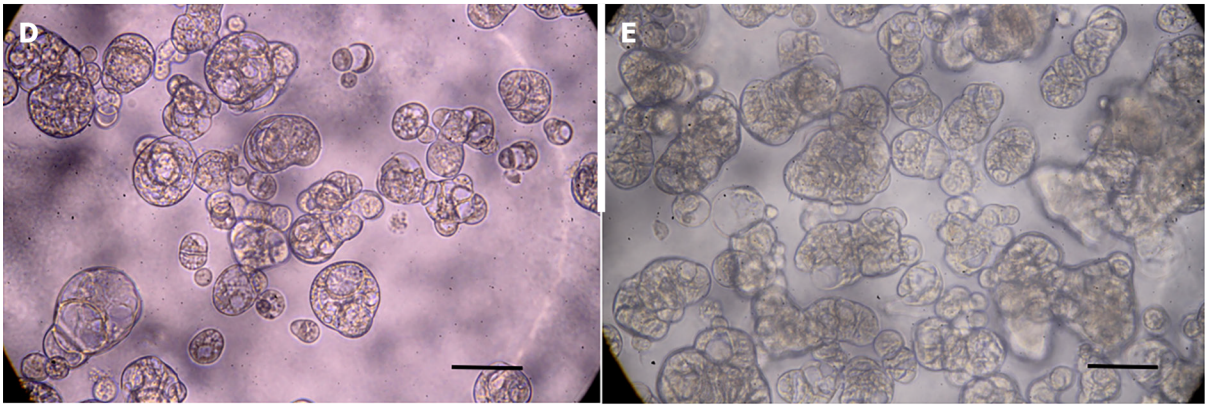


B

Loci	DPC-X1		DPC-X1-tissue		Matching probability
Amelogenin	X	Y	X	Y	/
D3S1358	15		15		0.1225
D13S317	9	10	9	10	0.0338
D7S820	11	12	11	12	0.1538
D16S539	10	13	10	12	-
Penta E	15	16	15	16	0.0109
TPOX	8		8		0.2862
TH01	9		9	9.3	-
D2S1338	18	19	18	19	0.0512
CSF1PO	10		10		0.0420
Penta D	9	10	9	10	0.0744
D19S433	13	15	13	15	0.0244
vWA	16	18	16	18	0.0486
D21S11	29		29		0.0576
D18S51	15		13	15	-
D6S1043	11	19	11	19	0.0330
D8S1179	8	17	8	17	0.0008
D5S818	10	12	10	12	0.0897
D12S391	19	22	19	22	0.0466
FGA	22	25	23	25	-
					4.1867×10^{20}

C





DOI: 10.3748/wjg.v29.i17.2642 **Copyright** ©The Author(s) 2023.

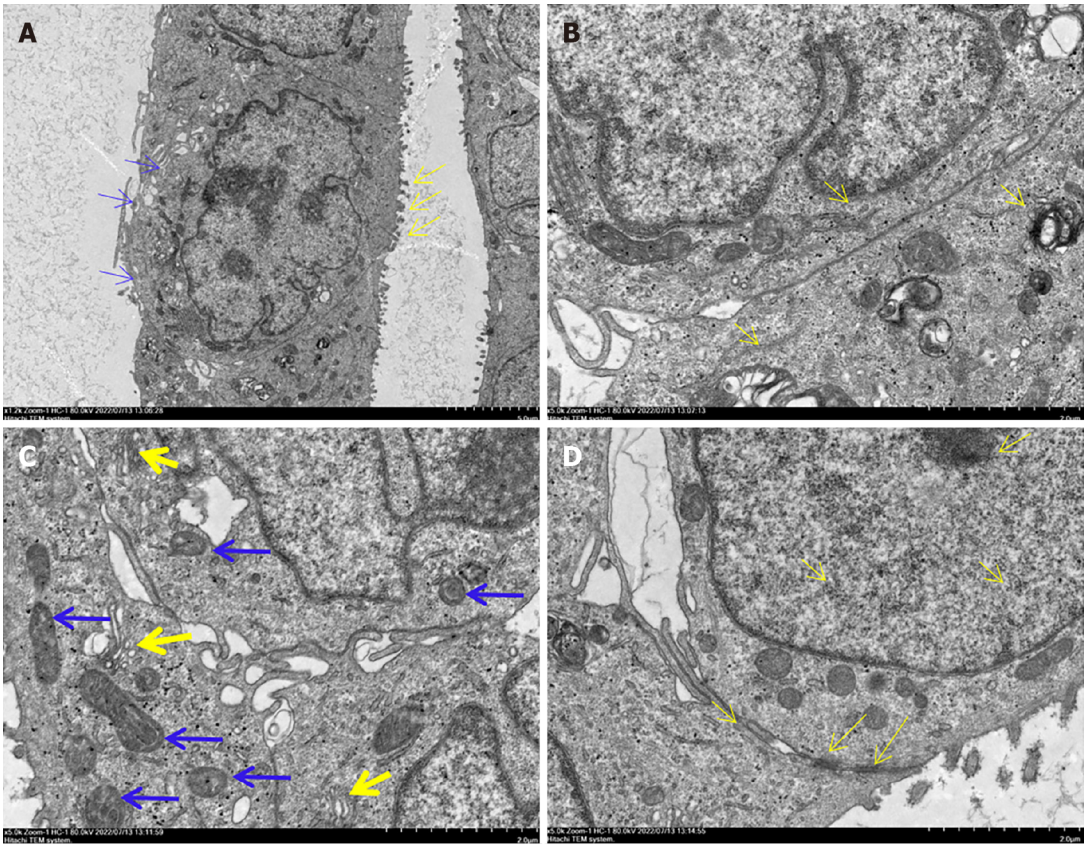
Figure 2 DPC-X1 population doubling time, short tandem repeat detection, karyotype analysis and Organoid culture. A: DPC-X1 growth curve; cell doubling time is 48 h; B: The likelihood ratio between the short tandem repeat results of DPC-X1 and the primary tumor tissue is 4.1867 × 1020. The cells are not contaminated by other cell lines; C: Karyotype analysis shows that DPC-X1 cells are mainly sub-tetraploid, with large differences in chromosome number and morphology. The representative karyotype is 80, XX del (2) (q32) del (5) (p12) del (6) (q24) inv (9) del (10) p (13) del (17) p (12); D: Morphology of DPC-X1organoids after one week. The organoids are spherical or cystic in shape; E: Morphology of DPC-X1 organoids after two weeks. The organoids are spore-like or branch-like in shape. Scale bars: 100 μm.

Transmission electron microscopy

Under the transmission electron microscope, the DPC-X1 nucleus appeared large and deformed, and its number was increased. The nucleolus was clustered in the nuclear membrane, and the cytoplasm was less. Microvilli and pseudopodia were visible on the cell surface (Figure 3A). The endoplasmic reticulum and ribosome were abundantly present in the cells (Figure 3B). Furthermore, the Golgi apparatus was developed, and the mitochondria differed in size and shape (Figure 3C). The desmosome structure was observed between the cells (Figure 3D).

Drug sensitivity test

The chemotherapy drugs gemcitabine and paclitaxel are commonly used for biliary and pancreatic tumors, whereas 5-FU and oxaliplatin are commonly used for gastrointestinal tumors. Our drug



DOI: 10.3748/wjg.v29.i17.2642 **Copyright** ©The Author(s) 2023.

Figure 3 Ultrastructure of DPC-X1 under a transmission electron microscope. A: DPC-X1 has a large and deformed nucleus; it is increased in number. The nucleolus is clustered in the nuclear membrane. There are fewer cytoplasm. Microvilli (yellow arrow) and pseudopodia (blue arrow) were visible on the cell surface; B: DPC-X1 cells are rich in the endoplasmic reticulum (yellow arrow) and ribosome; C: DPC-X1 cells have well-developed Golgi apparatus (yellow arrow), and the size and shape of the mitochondria are different (blue arrow); D: DPC-X1 desmosome structure can be seen between the cells (arrow).

sensitivity test revealed that DPC-X1 was sensitive to oxaliplatin [half maximal inhibitory concentration (IC50) = 13.26 μmol/L; Figure 4A] and paclitaxel (IC50 = 0.014 μmol/L; Figure 4B) and resistant to fluorouracil (IC50 = 144.9 μmol/L; Figure 4C) and gemcitabine (IC50 > 600 μmol/L; Figure 4D).

Xenograft tumor formation experiment

To verify the ability of DPC-X1 to form xenograft tumors *in vivo*, 1 × 10^6 DPC-X1 cells were inoculated subcutaneously in three BALB/c nude mice. The results showed that DPC-X1 was able to rapidly form xenograft tumors under the skin of nude mice, and the tumor formation rate was 100% (Figure 5A). The xenograft tumor grew rapidly and showed invasive growth. New blood vessels were visible on the surface of the xenograft tumor (Figure 5B). At four weeks, the diameter of the tumor body exceeded 1 cm (Figure 5C). No metastatic lesions were found in the liver and lungs of the dissected mice (Figure 5D). Tumor growth curve and mouse weight curve are shown in the figure (Figure 5E and F).

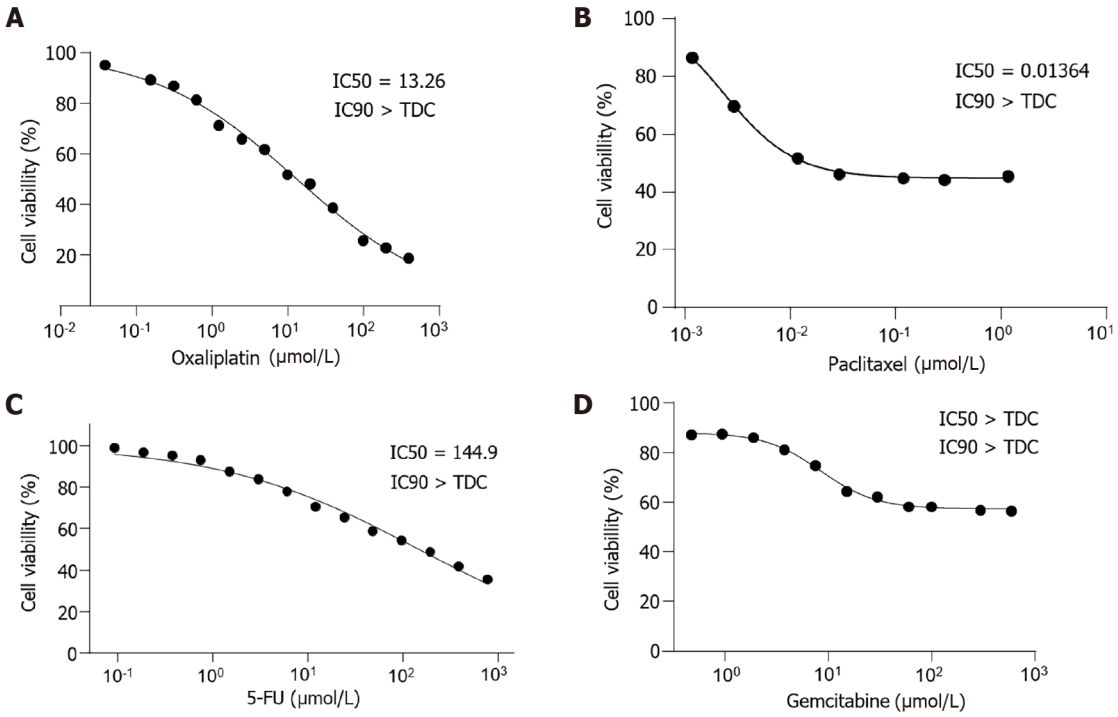
Hematoxylin and eosin and immunohistochemical staining

Hematoxylin-eosin staining showed that DPC-X1 cells were of different shapes, primarily short fusiform, with enlarged nuclei, apparent nucleoli, and less cytoplasm. The polykaryocytes and megakaryocytes were visible, exhibiting typical malignant tumor characteristics (Figure 6A).

The DPC-X1 organoids were observed to form irregular gland-like structures; the cells were closely connected, with a gland cavity-like structure inside. The cells in the organoid organs were highly heterotypic and varied in size (Figure 6B), which is highly similar to the histomorphology of the primary tumor tissue.

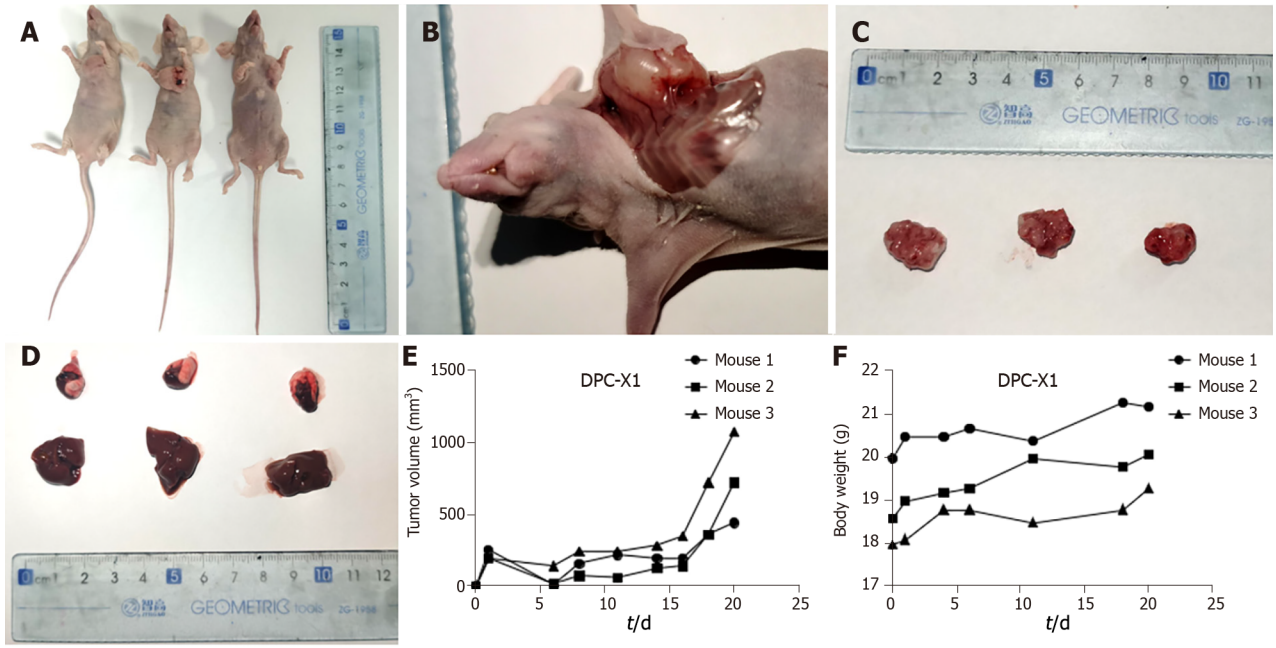
The xenograft tumor formed an irregular gland-like structure, and its histological morphology was similar to that of the primary tumor. The nucleus of the tumor was large and hyperchromatic, and the megakaryocytes were visible. The mitotic images depicted the vigorous proliferation of the DPC-X1 cells (Figure 6C); this observation is consistent with the characteristics of malignant tumors.

The postoperative pathological diagnosis of the patient's primary tumor showed moderately to poorly differentiated, and the tumor cells were arranged in irregular glandular tubes, strips, and nests (Figure 6D).



DOI: 10.3748/wjg.v29.i17.2642 **Copyright** ©The Author(s) 2023.

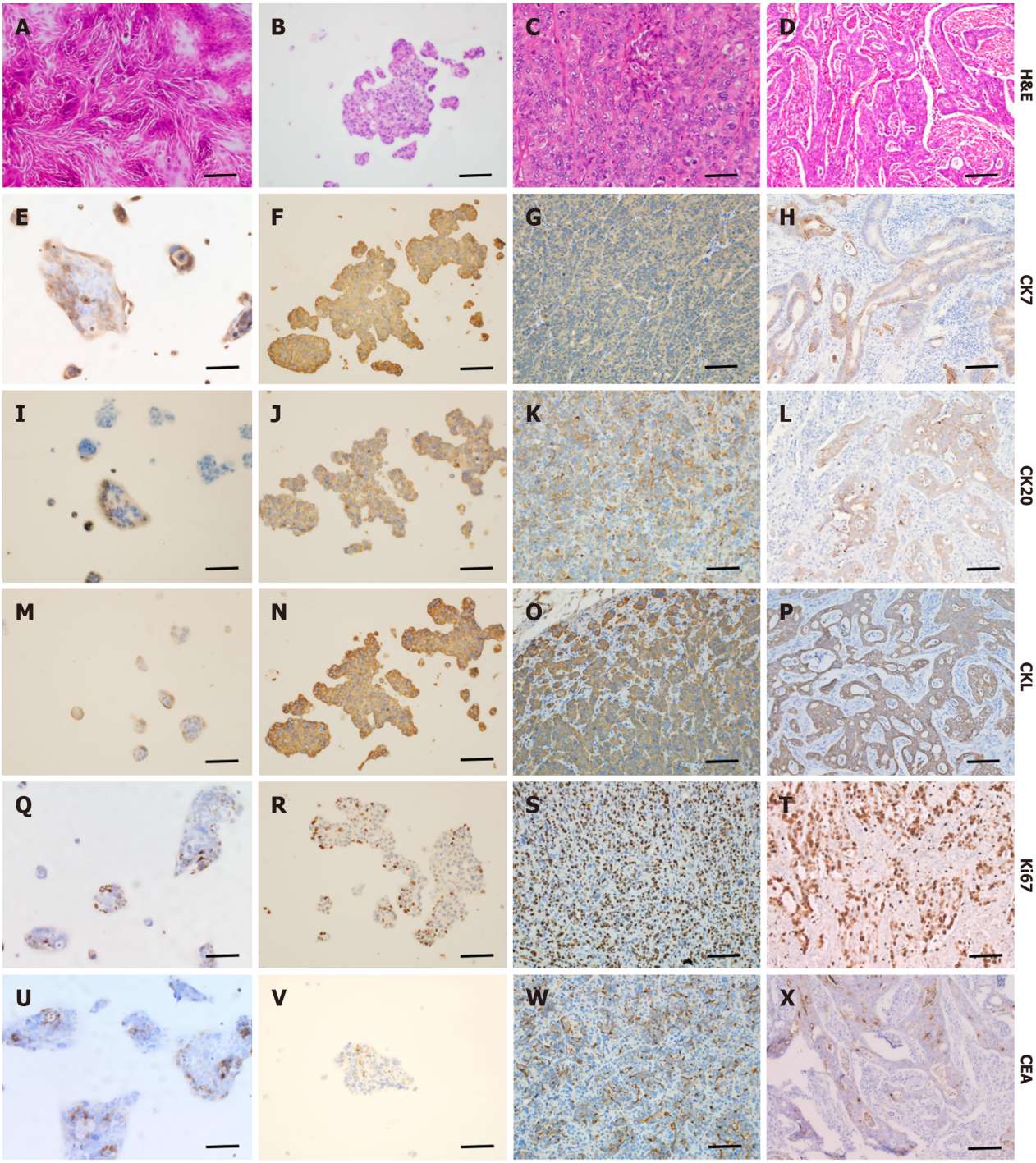
Figure 4 Drug sensitivity test. A: DPC-X1 is sensitive to oxaliplatin; IC50 = 13.26 μmol/L; B: DPC-X1 is sensitive to paclitaxel; IC50 = 0.014 μmol/L; C: DPC-X1 is resistant to fluorouracil; IC50 = 144.9 μmol/L; D: DPC-X1 is resistant to gemcitabine; IC50 > 600 μmol/L. IC50: Half maximal inhibitory concentration; TDC: Test drug concentrations.



DOI: 10.3748/wjg.v29.i17.2642 **Copyright** ©The Author(s) 2023.

Figure 5 Xenograft tumor formation experiment. A: In four weeks, DPC-X1 quickly formed xenograft tumors under the skin of BALB/c nude mice. The tumor formation rate is 100%; B: Anatomically, the xenograft tumor and muscle tissue of the mouse shows invasive growth, and new blood vessels can be seen on the surface of the tumor; C: General view of the xenograft tumor; D: No metastatic lesions were found in the lungs and liver of BALB/c nude mice within four weeks; E: Growth curve of DPC-X1 transplanted tumor; F: Body weight curve of BALB/c nude mice.

Immunohistochemical examination of DPC-X1 cells, organoids, xenograft tumor, and primary tumor showed that CK7 (Figure 6E–H), CK20 (Figure 6I–L), and CKL (Figure 6M–P) were strongly expressed among the four groups, indicating that they had the same origin. Moreover, DPC-X1 cells were found to exhibit both intestinal and pancreaticobiliary characteristics; thus, they were a mixed ampullary carcinoma cell line. Ki67 (Figure 6Q–T) was highly expressed, consistent with the rapid proliferation of



DOI: 10.3748/wjg.v29.i17.2642 **Copyright** ©The Author(s) 2023.

Figure 6 Hematoxylin and eosin and immunohistochemical staining of DPC-X1 cells, organoid, xenograft tumor, and primary tumor. A-D: Hematoxylin and eosin staining of DPC-X1 cells, organoids, xenograft tumor, and primary tumor; E-H: Strong cytokeratin (CK)7 positive staining of DPC-X1 cells, organoids, xenograft tumor, and primary tumor; I-L: Strong CK20 positive staining of DPC-X1 cells, organoids, xenograft tumor, and primary tumor; M-P: Strong cytokeratin low molecular weight positive staining of DPC-X1 cells, organoids, xenograft tumor, and primary tumor; Q-T: Ki67 staining of DPC-X1 cells, organoids, xenograft tumor, and primary tumor; U-X: Carcinoembryonic antigen focal staining of DPC-X1 cells, organoids, xenograft tumor, and primary tumor. Scale bars: 100 μm. H&E: Hematoxylin and eosin; CK7: Cytokeratin 7; CK20: Cytokeratin 20; CKL: Cytokeratin low molecular weight; CEA: Carcinoembryonic antigen.

the tumor, and CEA (Figure 6U–X) showed focal expression. These observations are consistent with the characteristics of malignant tumors.

DISCUSSION

In recent years, with development in endoscopy, imaging equipment, and technological progress, an increasing number of ampullary cancer cases have been diagnosed[24-26]. Owing to the lack of cell lines and related research models of ampullary carcinoma, research on the pathogenesis and biological characteristics of ampullary carcinoma remains limited.

In this study, we successfully established a novel ampullary carcinoma cell line named DPC-X1 from the primary tumor tissue of patients with ampullary carcinoma through primary culture and subculture. This cell line was continuously cultured for more than a year and stably passaged for over 80 generations. DPC-X1 cells adhered to the wall and grew like typical epithelial cells. The cells were chiefly short spindle-shaped, with large nuclei and visible nucleoli, and multinucleated cells and megakaryocytes were visible. The cells were closely adherent and grew in clumps and sheets. The characteristics of DPC-X1 were highly consistent with those of the patient's primary tumor, and it was not contaminated by other cell lines and microorganisms. DPC-X1 could efficiently form organoids in suspension culture. The Ki67 of DPC-X1 was 50%, indicating that DPC-X1 has a vigorous proliferation, which is consistent with its population doubling time of 48 h.

CK7 is typically used as a tumor marker of biliary and pancreatic origin, whereas CK20 and villin are used as tumor markers of gastrointestinal origin[18,20,24,27,28]. In this study, DPC-X1 immunohistochemistry showed that CK7, CK20, and CKL were strongly positive, indicating that DPC-X1 was a mixed ampullary carcinoma cell line. To the best of our knowledge, this is the first study to report a mixed-type ampullary carcinoma cell line. Thus, DPC-X1 may provide a useful model for studying mixed-type ampullary carcinoma.

Chromosome instability and chromosomal aneuploidy are common in human cancers and are important characteristics of tumor cells[29-32]. Aneuploid karyotype of tumor cells is closely related to poor prognosis of patients[33,34]. Triploid karyotype may be related to endogenous drug resistance of tumors, whereas tetraploidy of tumors is associated with acquired drug resistance[35]. Spontaneous chromosomal missegregation events in aneuploid cells promote chromosomal instability, thereby increasing the risk of tumor recurrence[36]. Karyotype analysis showed that DPC-X1 cells had a subtetraploid abnormal karyotype, and the representative karyotype was 80, XX del (2) (q32) del (5) (p12) del (6) (q24) inv (9) del (10) p (13) del (17) p (12). The results of drug sensitivity showed that DPC-X1 was sensitive to oxaliplatin and paclitaxel but was naturally resistant to gemcitabine and fluorouracil. The patient underwent four cycles of chemotherapy with the XELOX regimen and two cycles with the AG regimen after surgery; however, he succumbed to tumor recurrence one year after surgery. Our results are highly consistent with that of earlier studies.

Desmosomes are intercellular junction complexes that anchor the intermediate filaments of adjacent cells and provide them with strong cell adhesion; thus, they are essential in maintaining the organizational structure and structural integrity[37]. Much evidence has substantiated the importance of desmosomes and their components in cancer. Desmosome expression is downregulated in poorly differentiated head and neck transitional and squamous cell carcinoma. In these tissues, desmosomes may have the function of inhibiting invasion and metastasis. In colon cancer, no downregulation has been found[38,39]. The change in desmosome component expression may promote tumor progression by altering the intracellular signal transduction pathway or leading to reduced cell adhesion. The loss of desmosome function is a prerequisite for epithelial-mesenchymal transformation, which is related to the transformation of early tumors to invasive cancer[40-44]. When DPC-X1 cells were subcultured, most of them grew in clumps and sheets, and digesting them into single cells in conventional digestion time was difficult, indicating the strong adhesion between the cells. The presence of intercellular desmosomes under transmission electron microscopy provides some ultrastructural evidence for the aforementioned phenomenon. DPC-X1 cells can be used to further study the relationship between tumors and desmosomes.

Animal models are an intermediate step between cell experiments and human clinical trials. They are a powerful tool for studying canceration and tumor progression and for testing the efficacy and toxicity of therapeutic compounds[45]. Suitable animal models not only help to explore the mechanism of ampullary carcinoma occurrence and development but also provide a good platform for exploring new strategies for early clinical diagnosis and precise treatment[46]. DPC-X1 cells inoculated into BALB/C nude mice could quickly form transplanted tumors, with a tumor formation rate of 100%, and the histology of the xenografts resembled that of the original tumor.

CONCLUSION

In summary, we report a novel human mixed-type ampullary carcinoma cell line DPC-X1 developed from a Chinese patient's tumor. This cell line provides a new experimental model for studying the biological and molecular mechanisms of ampullary carcinoma and developing new therapeutic drugs.

ARTICLE HIGHLIGHTS

Research background

To date, only eight ampullary cancer cell lines have been reported, and a mixed-type ampullary carcinoma cell line has not yet been reported.

Research motivation

There is no ampullary cancer cell line of Chinese origin, and there is no report of mixed ampullary cancer cell line.

Research objectives

To establish a stable mixed-type ampullary carcinoma cell line originating from Chinese.

Research methods

Establish cell lines through primary culture and subculture, and identify their biological characteristics.

Research results

In this study, we successfully established and characterized of a mixed-type ampullary carcinoma cell line, DPC-X1, from the primary tumor of a patient with ampullary carcinoma.

Research conclusions

DPC-X1 can be used as an effective model for studying the pathogenesis of ampullary carcinoma and drug development.

Research perspectives

The establishment of ampullary carcinoma cell lines provides suitable experimental models for further study of ampullary carcinoma.

FOOTNOTES

Author contributions: Xu H designed and coordinated the study; Xu H, Chai CP, Miao X and Tang H performed the experiments, acquired and analyzed data; Xu H, Hu JJ and Zhang H interpreted the data; Xu H, Chai CP and Zhou WC wrote the manuscript; All authors have read and approve the final manuscript.

Supported by National Natural Science Foundation of China, No. 82260555; Gansu Provincial Science and Technology Plan, No. 1606RJZA139, No. 21JR11RA096, No. 21JR1RA099, and No. 21JR1RA113; Gansu Health Industry Project, No. GSWSKY2020-21; Traditional Chinese Medicine Scientific Research Project of Gansu Province, No. GZKP-2020-28; Talent Innovation and Entrepreneurship Project of Lanzhou, No. 2020-RC-46; Intra-Hospital Fund of the First Hospital of Lanzhou University, No. ldyyyn2019-97.

Institutional review board statement: The study was conducted according to the guidelines of the Declaration of Helsinki, and approved by the Ethics Committee of the First Hospital of Lanzhou University, No. LDYYLL-2022-487.

Institutional animal care and use committee statement: The animal study was conducted according to the guidelines of the Declaration of Helsinki, and approved by the Ethics Committee of the First Hospital of Lanzhou University, No. LDYYLL-2022-487.

Informed consent statement: All study participants or their legal guardian provided informed written consent about personal and medical data collection prior to study enrolment.

Conflict-of-interest statement: All the authors report no relevant conflicts of interest for this article.

Data sharing statement: The datasets used and/or analysed during the current study are available from the corresponding author upon reasonable request.

ARRIVE guidelines statement: The authors have read the ARRIVE guidelines, and the manuscript was prepared and revised according to the ARRIVE guidelines.

Open-Access: This article is an open-access article that was selected by an in-house editor and fully peer-reviewed by external reviewers. It is distributed in accordance with the Creative Commons Attribution NonCommercial (CC BY-NC 4.0) license, which permits others to distribute, remix, adapt, build upon this work non-commercially, and license their derivative works on different terms, provided the original work is properly cited and the use is non-commercial. See: https://creativecommons.org/Licenses/by-nc/4.0/

Country/Territory of origin: China

ORCID number: Hao Xu 0000-0001-6459-1063; Chang-Peng Chai 0000-0001-9577-7354; Wen-Ce Zhou 0000-0002-0529-7777.

S-Editor: Fan JR
L-Editor: A
P-Editor: Yu HG

REFERENCES

1 **Ahn DH**, Bekaii-Saab T. Ampullary cancer: an overview. *Am Soc Clin Oncol Educ Book* 2014; 112-115 [PMID: 24857067 DOI: 10.14694/EdBook_AM.2014.34.112]
2 **Zheng-Pywell R**, Reddy S. Ampullary Cancer. *Surg Clin North Am* 2019; **99**: 357-367 [PMID: 30846039 DOI: 10.1016/j.suc.2018.12.001]
3 **Saha SK**, Zhu AX, Fuchs CS, Brooks GA. Forty-Year Trends in Cholangiocarcinoma Incidence in the U.S.: Intrahepatic Disease on the Rise. *Oncologist* 2016; **21**: 594-599 [PMID: 27000463 DOI: 10.1634/theoncologist.2015-0446]
4 **Fischer HP**, Zhou H. Pathogenesis of carcinoma of the papilla of Vater. *J Hepatobiliary Pancreat Surg* 2004; **11**: 301-309 [PMID: 15549428 DOI: 10.1007/s00534-004-0898-3]
5 **de Castro SM**, van Heek NT, Kuhlmann KF, Busch OR, Offerhaus GJ, van Gulik TM, Obertop H, Gouma DJ. Surgical management of neoplasms of the ampulla of Vater: local resection or pancreatoduodenectomy and prognostic factors for survival. *Surgery* 2004; **136**: 994-1002 [PMID: 15523392 DOI: 10.1016/j.surg.2004.03.010]
6 **Yeh CC**, Jeng YM, Ho CM, Hu RH, Chang HP, Tien YW. Survival after pancreaticoduodenectomy for ampullary cancer is not affected by age. *World J Surg* 2010; **34**: 2945-2952 [PMID: 20714897 DOI: 10.1007/s00268-010-0759-y]
7 **Miyakawa S**, Ishihara S, Horiguchi A, Takada T, Miyazaki M, Nagakawa T. Biliary tract cancer treatment: 5,584 results from the Biliary Tract Cancer Statistics Registry from 1998 to 2004 in Japan. *J Hepatobiliary Pancreat Surg* 2009; **16**: 1-7 [PMID: 19110652 DOI: 10.1007/s00534-008-0015-0]
8 **O'Connell JB**, Maggard MA, Manunga J Jr, Tomlinson JS, Reber HA, Ko CY, Hines OJ. Survival after resection of ampullary carcinoma: a national population-based study. *Ann Surg Oncol* 2008; **15**: 1820-1827 [PMID: 18369675 DOI: 10.1245/s10434-008-9886-1]
9 **Partelli S**, Crippa S, Capelli P, Neri A, Bassi C, Zamboni G, Barugola G, Falconi M. Adequacy of lymph node retrieval for ampullary cancer and its association with improved staging and survival. *World J Surg* 2013; **37**: 1397-1404 [PMID: 23546531 DOI: 10.1007/s00268-013-1995-8]
10 **Kimura W**, Futakawa N, Yamagata S, Wada Y, Kuroda A, Muto T, Esaki Y. Different clinicopathologic findings in two histologic types of carcinoma of papilla of Vater. *Jpn J Cancer Res* 1994; **85**: 161-166 [PMID: 7511574 DOI: 10.1111/j.1349-7006.1994.tb02077.x]
11 **Bosman FT**, Carnerio F, Hruban RH, Theise ND. WHO classifcation of tumors of the digestive system. 4th ed. Lyon: IARC, 2010
12 **Sobin LH**, Gospodarowicz MK, Ch W. International Union Against Cancer (UICC). TNM classifcation of malignant tumours, 7th edn. Chichester: Wiley-Blackwell, 2010
13 **Frazier ML**, Brown N, Pathak S, Mackay B, Cleary K, Olive M, Byrd DR, Evans DB, Levin B. Human cell line from an adenocarcinoma of the ampulla of Vater. *In Vitro Cell Dev Biol* 1992; **28A**: 149-153 [PMID: 1582987 DOI: 10.1007/BF02631083]
14 **Liu SQ**, Liu LS, Ohno T. Growth stimulation of tumor-specific cytotoxic T lymphocytes on concanavalin a-immobilized carrier beads. *Cytotechnology* 1998; **26**: 13-21 [PMID: 22359002 DOI: 10.1023/A:1007924430570]
15 **Ghosh M**, Koike N, Tsunoda S, Hirano T, Kaul S, Kashiwagi H, Kawamoto T, Ohkohchi N, Saijo K, Ohno T, Miwa M, Todoroki T. Characterization and genetic analysis in the newly established human bile duct cancer cell lines. *Int J Oncol* 2005; **26**: 449-456 [PMID: 15645130]
16 **Ku JL**, Yoon KA, Kim IJ, Kim WH, Jang JY, Suh KS, Kim SW, Park YH, Hwang JH, Yoon YB, Park JG. Establishment and characterisation of six human biliary tract cancer cell lines. *Br J Cancer* 2002; **87**: 187-193 [PMID: 12107841 DOI: 10.1038/sj.bjc.6600440]
17 **Sorio C**, Moore PS, Ennas MG, Tecchio C, Bonora A, Sartoris S, Balzarini P, Grigolato P, Scarpa A. A novel cell line and xenograft model of ampulla of Vater adenocarcinoma. *Virchows Arch* 2004; **444**: 269-277 [PMID: 14677066 DOI: 10.1007/s00428-003-0936-6]
18 **Lai ZW**, Bolm L, Fuellgraf H, Biniossek ML, Makowiec F, Hopt UT, Werner M, Keck T, Bausch D, Sorio C, Scarpa A, Schilling O, Bronsert P, Wellner UF. Characterization of various cell lines from different ampullary cancer subtypes and cancer associated fibroblast-mediated responses. *BMC Cancer* 2016; **16**: 195 [PMID: 26951071 DOI: 10.1186/s12885-016-2193-5]
19 **Ecker BL**, Vollmer CM Jr, Behrman SW, Allegrini V, Aversa J, Ball CG, Barrows CE, Berger AC, Cagigas MN, Christein JD, Dixon E, Fisher WE, Freedman-Weiss M, Guzman-Pruneda F, Hollis RH, House MG, Kent TS, Kowalsky SJ, Malleo G, Salem RR, Salvia R, Schmidt CR, Seykora TF, Zheng R, Zureikat AH, Dickson PV. Role of Adjuvant Multimodality Therapy After Curative-Intent Resection of Ampullary Carcinoma. *JAMA Surg* 2019; **154**: 706-714 [PMID: 31141112 DOI: 10.1001/jamasurg.2019.1170]
20 **Rizzo A**, Dadduzio V, Lombardi L, Ricci AD, Gadaleta-Caldarola G. Ampullary Carcinoma: An Overview of a Rare Entity and Discussion of Current and Future Therapeutic Challenges. *Curr Oncol* 2021; **28**: 3393-3402 [PMID: 34590592 DOI: 10.3390/curroncol28050293]

21 **Xu H**, Miao X, Chai C, Tang H, Hu J, Zhao Z, Luo W, Zhu K, Zhou W. Establishment and characterization of a new Chinese hepatocellular carcinoma cell line, Hep-X1. *Hum Cell* 2023; **36**: 434-445 [PMID: 36152230 DOI: 10.1007/s13577-022-00797-z]

22 **Peng J**, Xu H, Cai J. Establishment and characterization of a new gastric cancer cell line, XGC-1. *Cancer Cell Int* 2020; **20**: 437 [PMID: 32943986 DOI: 10.1186/s12935-020-01536-w]

23 **Xu H**, Peng JG, Zhuang YF, Chen JJ, Luo QC, Huang WF, Lin CD, Cai JC. Establishment and characterization of an expanding-type gastric cancer cell line by Ming's classification. *Oncol Rep* 2016; **36**: 3030-3036 [PMID: 27633271 DOI: 10.3892/or.2016.5090]

24 **Okano K**, Oshima M, Suto H, Ando Y, Asano E, Kamada H, Kobara H, Masaki T, Suzuki Y. Ampullary carcinoma of the duodenum: current clinical issues and genomic overview. *Surg Today* 2022; **52**: 189-197 [PMID: 33797636 DOI: 10.1007/s00595-021-02270-0]

25 **Albores-Saavedra J**, Schwartz AM, Batich K, Henson DE. Cancers of the ampulla of vater: demographics, morphology, and survival based on 5,625 cases from the SEER program. *J Surg Oncol* 2009; **100**: 598-605 [PMID: 19697352 DOI: 10.1002/jso.21374]

26 **Talamini MA**, Moesinger RC, Pitt HA, Sohn TA, Hruban RH, Lillemoe KD, Yeo CJ, Cameron JL. Adenocarcinoma of the ampulla of Vater. A 28-year experience. *Ann Surg* 1997; **225**: 590-9; discussion 599 [PMID: 9193186 DOI: 10.1097/00000658-199705000-00015]

27 **Perysinakis I**, Minaidou E, Leontara V, Mantas D, Sotiropoulos GC, Tsipras H, Zografos GN, Margaris I, Kouraklis G. Differential Expression of β-Catenin, EGFR, CK7, CK20, MUC1, MUC2, and CDX2 in Intestinal and Pancreatobiliary-Type Ampullary Carcinomas. *Int J Surg Pathol* 2017; **25**: 31-40 [PMID: 27543509 DOI: 10.1177/1066896916664987]

28 **Luchini C**, Veronese N, Nottegar A, Riva G, Pilati C, Mafficini A, Stubbs B, Simbolo M, Mombello A, Corbo V, Cheng L, Yachida S, Wood LD, Lawlor RT, Salvia R, Scarpa A. Perineural Invasion is a Strong Prognostic Moderator in Ampulla of Vater Carcinoma: A Meta-analysis. *Pancreas* 2019; **48**: 70-76 [PMID: 30451797 DOI: 10.1097/MPA.0000000000001194]

29 **Beroukhim R**, Mermel CH, Porter D, Wei G, Raychaudhuri S, Donovan J, Barretina J, Boehm JS, Dobson J, Urashima M, Mc Henry KT, Pinchback RM, Ligon AH, Cho YJ, Haery L, Greulich H, Reich M, Winckler W, Lawrence MS, Weir BA, Tanaka KE, Chiang DY, Bass AJ, Loo A, Hoffman C, Prensner J, Liefeld T, Gao Q, Yecies D, Signoretti S, Maher E, Kaye FJ, Sasaki H, Tepper JE, Fletcher JA, Tabernero J, Baselga J, Tsao MS, Demichelis F, Rubin MA, Janne PA, Daly MJ, Nucera C, Levine RL, Ebert BL, Gabriel S, Rustgi AK, Antonescu CR, Ladanyi M, Letai A, Garraway LA, Loda M, Beer DG, True LD, Okamoto A, Pomeroy SL, Singer S, Golub TR, Lander ES, Getz G, Sellers WR, Meyerson M. The landscape of somatic copy-number alteration across human cancers. *Nature* 2010; **463**: 899-905 [PMID: 20164920 DOI: 10.1038/nature08822]

30 **Gemble S**, Wardenaar R, Keuper K, Srivastava N, Nano M, Macé AS, Tijhuis AE, Bernhard SV, Spierings DCJ, Simon A, Goundiam O, Hochegger H, Piel M, Foijer F, Storchová Z, Basto R. Genetic instability from a single S phase after whole-genome duplication. *Nature* 2022; **604**: 146-151 [PMID: 35355016 DOI: 10.1038/s41586-022-04578-4]

31 **López S**, Lim EL, Horswell S, Haase K, Huebner A, Dietzen M, Mourikis TP, Watkins TBK, Rowan A, Dewhurst SM, Birkbak NJ, Wilson GA, Van Loo P, Jamal-Hanjani M; TRACERx Consortium, Swanton C, McGranahan N. Interplay between whole-genome doubling and the accumulation of deleterious alterations in cancer evolution. *Nat Genet* 2020; **52**: 283-293 [PMID: 32139907 DOI: 10.1038/s41588-020-0584-7]

32 **Bielski CM**, Zehir A, Penson AV, Donoghue MTA, Chatila W, Armenia J, Chang MT, Schram AM, Jonsson P, Bandlamudi C, Razavi P, Iyer G, Robson ME, Stadler ZK, Schultz N, Baselga J, Solit DB, Hyman DM, Berger MF, Taylor BS. Genome doubling shapes the evolution and prognosis of advanced cancers. *Nat Genet* 2018; **50**: 1189-1195 [PMID: 30013179 DOI: 10.1038/s41588-018-0165-1]

33 **Chen Y**, Yang Z, Wang Y, Wang J, Wang C. Karyotyping of circulating tumor cells for predicting chemotherapeutic sensitivity and efficacy in patients with esophageal cancer. *BMC Cancer* 2019; **19**: 651 [PMID: 31269908 DOI: 10.1186/s12885-019-5850-7]

34 **Wang Y**, Liu Y, Zhang L, Tong L, Gao Y, Hu F, Lin PP, Li B, Zhang T. Vimentin expression in circulating tumor cells (CTCs) associated with liver metastases predicts poor progression-free survival in patients with advanced lung cancer. *J Cancer Res Clin Oncol* 2019; **145**: 2911-2920 [PMID: 31646374 DOI: 10.1007/s00432-019-03040-9]

35 **Huang M**, Ma Y, Lv C, Li S, Lu F, Zhang S, Wang DD, Lin PP, Yang Y. Aneuploid Circulating Tumor Cells as a Predictor of Response to Neoadjuvant Chemotherapy in Non-Small Cell Lung Cancer. *Int J Gen Med* 2021; **14**: 6609-6620 [PMID: 34703281 DOI: 10.2147/IJGM.S330361]

36 **Lee AJ**, Endesfelder D, Rowan AJ, Walther A, Birkbak NJ, Futreal PA, Downward J, Szallasi Z, Tomlinson IP, Howell M, Kschischo M, Swanton C. Chromosomal instability confers intrinsic multidrug resistance. *Cancer Res* 2011; **71**: 1858-1870 [PMID: 21363922 DOI: 10.1158/0008-5472.CAN-10-3604]

37 **Brown L**, Wan H. Desmoglein 3: a help or a hindrance in cancer progression? *Cancers (Basel)* 2015; **7**: 266-286 [PMID: 25629808 DOI: 10.3390/cancers7010266]

38 **Garrod DR**. Desmosomes and cancer. *Cancer Surv* 1995; **24**: 97-111 [PMID: 7553665]

39 **Okegawa T**, Li Y, Pong RC, Hsieh JT. Cell adhesion proteins as tumor suppressors. *J Urol* 2002; **167**: 1836-1843 [PMID: 11912444]

40 **Chidgey M**, Dawson C. Desmosomes: a role in cancer? *Br J Cancer* 2007; **96**: 1783-1787 [PMID: 17519903 DOI: 10.1038/sj.bjc.6603808]

41 **Dusek RL**, Attardi LD. Desmosomes: new perpetrators in tumour suppression. *Nat Rev Cancer* 2011; **11**: 317-323 [PMID: 21508970 DOI: 10.1038/nrc3051]

42 **Moh MC**, Shen S. The roles of cell adhesion molecules in tumor suppression and cell migration: a new paradox. *Cell Adh Migr* 2009; **3**: 334-336 [PMID: 19949308 DOI: 10.4161/cam.3.4.9246]

43 **Lamouille S**, Xu J, Derynck R. Molecular mechanisms of epithelial-mesenchymal transition. *Nat Rev Mol Cell Biol* 2014; **15**: 178-196 [PMID: 24556840 DOI: 10.1038/nrm3758]

44 **Davies M**, Robinson M, Smith E, Huntley S, Prime S, Paterson I. Induction of an epithelial to mesenchymal transition in

human immortal and malignant keratinocytes by TGF-beta1 involves MAPK, Smad and AP-1 signalling pathways. *J Cell Biochem* 2005; **95**: 918-931 [PMID: 15861394 DOI: 10.1002/jcb.20458]

45 **Massa A**, Varamo C, Vita F, Tavolari S, Peraldo-Neia C, Brandi G, Rizzo A, Cavalloni G, Aglietta M. Evolution of the Experimental Models of Cholangiocarcinoma. *Cancers (Basel)* 2020; **12** [PMID: 32824407 DOI: 10.3390/cancers12082308]

46 **Li M**, Zhou X, Wang W, Ji B, Shao Y, Du Q, Yao J, Yang Y. Selecting an Appropriate Experimental Animal Model for Cholangiocarcinoma Research. *J Clin Transl Hepatol* 2022; **10**: 700-710 [PMID: 36062286 DOI: 10.14218/JCTH.2021.00374]

World Journal of Gastroenterology

Submit a Manuscript: https://www.f6publishing.com

World J Gastroenterol 2023 May 7; 29(17): 2657-2665

DOI: 10.3748/wjg.v29.i17.2657

ISSN 1007-9327 (print) ISSN 2219-2840 (online)

ORIGINAL ARTICLE

Retrospective Study

Mucosal patterns change after *Helicobacter pylori* eradication: Evaluation using blue laser imaging in patients with atrophic gastritis

Yoshiyuki Nishikawa, Yoshio Ikeda, Hidehiro Murakami, Shin-Ichiro Hori, Megumi Yoshimatsu, Naoki Nishikawa

Specialty type: Gastroenterology and hepatology

Provenance and peer review: Unsolicited article; Externally peer reviewed.

Peer-review model: Single blind

Peer-review report's scientific quality classification

Grade A (Excellent): 0
Grade B (Very good): 0
Grade C (Good): C, C
Grade D (Fair): D
Grade E (Poor): 0

P-Reviewer: Kotelevets SM, Russia; Senchukova M, Russia

Received: February 8, 2023
Peer-review started: February 8, 2023
First decision: February 16, 2023
Revised: March 3, 2023
Accepted: April 7, 2023
Article in press: April 7, 2023
Published online: May 7, 2023

Yoshiyuki Nishikawa, Department of Gastroenterology, Nishikawa Gastrointestinal Clinic, Matsuyama 790-0878, Ehime, Japan

Yoshio Ikeda, Endoscopy Center, Ehime University Hospital, Toon 791-0295, Ehime, Japan

Hidehiro Murakami, Department of Internal Medicine, Saiseikai Matsuyama Hospital, Matsuyama 791-8026, Ehime, Japan

Shin-Ichiro Hori, Department of Gastroenterology, Himeji Red Cross Hospital, Himeji 670-8540, Hyogo, Japan

Megumi Yoshimatsu, Department of Gastroenterology, National Hospital Organization Shikoku Cancer Center, Matsuyama 791-0280, Ehime, Japan

Naoki Nishikawa, Department of Gastroenterology, Matsuyama Shimin Hospital, Matsuyama 790-0067, Ehime, Japan

Corresponding author: Yoshiyuki Nishikawa, MD, PhD, Director, Department of Gastroenterology, Nishikawa Gastrointestinal Clinic, 2-72 Katsuyama-cho, Matsuyama 790-0878, Ehime, Japan. yonishik@ehime.med.or.jp

Abstract

BACKGROUND

Mucosal patterns (MPs) observed on blue laser imaging in patients with atrophic gastritis can be classified as spotty, cracked, and mottled. Furthermore, we hypothesized that the spotty pattern may change to the cracked pattern after *Helicobacter pylori* (*H. pylori*) eradication.

AIM

To further substantiate and comprehensively investigate MP changes after *H. pylori* eradication in a larger number of patients.

METHODS

We included 768 patients who were diagnosed with atrophic gastritis with evaluable MP using upper gastrointestinal endoscopy at the Nishikawa Gas-

trointestinal Clinic, Japan. Among them, 325 patients were *H. pylori*-positive, and of them, 101 patients who underwent upper gastrointestinal endoscopy before and after *H. pylori* eradication were evaluated for post-eradication MP changes. The patients' MPs were interpreted by three experienced endoscopists who were blinded to their clinical features.

RESULTS

Among 76 patients with the spotty pattern before or after *H. pylori* eradication, the pattern disappeared or decreased in 67 patients [88.2%, 95% confidence interval (CI): 79.0%-93.6%), appeared or increased in 8 patients (10.5%, 95%CI: 5.4%-19.4%), and showed no change in 1 patient (1.3%, 95%CI: 0.2%-7.1%). In 90 patients with the cracked pattern before or after *H. pylori* eradication, the pattern disappeared or decreased in 7 patients (7.8%, 95%CI: 3.8%-15.2%), appeared or increased in 79 patients (87.8%, 95%CI: 79.4%-93.0%), and showed no change in 4 patients (4.4%, 95%CI: 1.7%-10.9%). In 70 patients with the mottled pattern before or after *H. pylori* eradication, the pattern disappeared or decreased in 28 patients (40.0%, 95%CI: 29.3%-51.7%), appeared or increased in 35 patients (50.0%, 95%CI: 38.6%-61.4%), and showed no change in 7 patients (10.0%, 95%CI: 4.9%-19.2%).

CONCLUSION

After *H. pylori* eradication, MPs changed from spotty to cracked in most patients, which may help endoscopists easily and precisely evaluate *H. pylori*-related gastritis status.

Key Words: Atrophic gastritis; *Helicobacter pylori*; Gastrointestinal endoscopy; Image enhancement; Classification

©The Author(s) 2023. Published by Baishideng Publishing Group Inc. All rights reserved.

Core Tip: We investigated whether the mucosal patterns on blue laser imaging may change from spotty to cracked after *Helicobacter pylori* (*H. pylori*) eradication. The spotty pattern disappeared or decreased in 88.2% of patients, while the cracked pattern appeared or increased in 87.8% of patients. These suggest that the spotty pattern observed in *H. pylori*-positive patients is likely to disappear after eradication and may be replaced by the cracked pattern. These observations may help endoscopists easily and precisely evaluate *H. pylori*-related gastritis status.

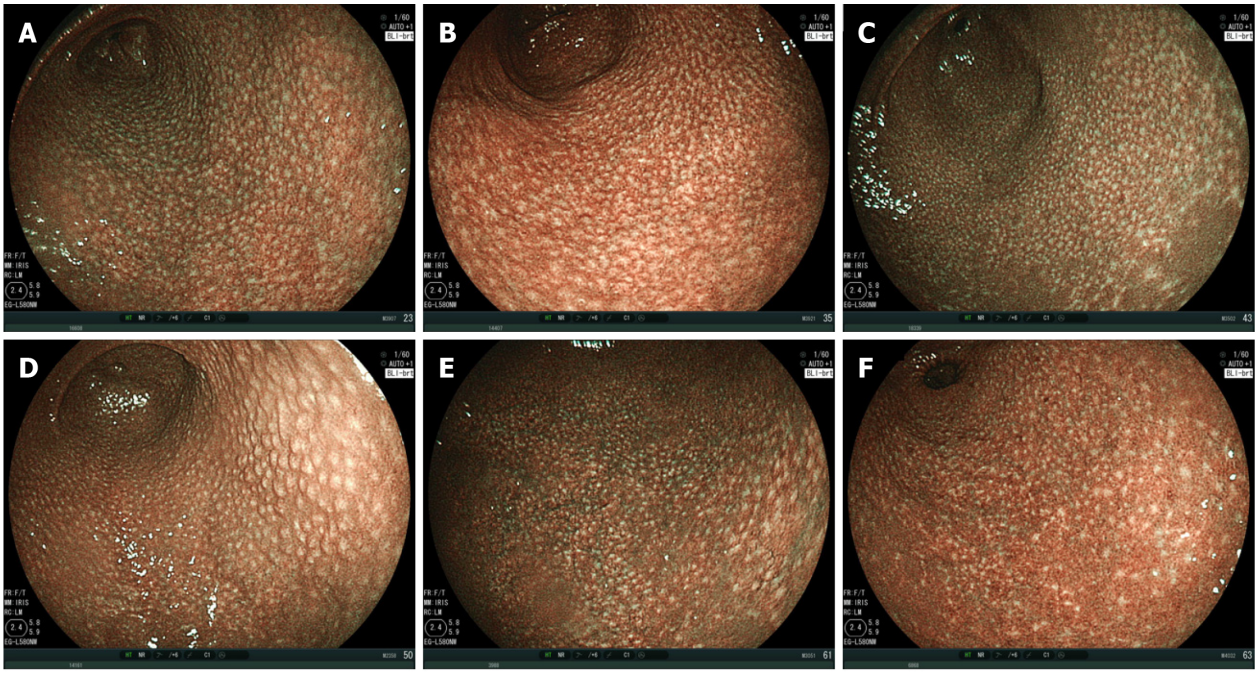
Citation: Nishikawa Y, Ikeda Y, Murakami H, Hori SI, Yoshimatsu M, Nishikawa N. Mucosal patterns change after *Helicobacter pylori* eradication: Evaluation using blue laser imaging in patients with atrophic gastritis. *World J Gastroenterol* 2023; 29(17): 2657-2665
URL: https://www.wjgnet.com/1007-9327/full/v29/i17/2657.htm
DOI: https://dx.doi.org/10.3748/wjg.v29.i17.2657

INTRODUCTION

Helicobacter pylori (*H. pylori*) infection and related atrophic gastritis is closely associated with the development of gastric cancer[1]. Therefore, it is critical to observe the gastric mucosa to precisely judge the infection status as "current," "previous," or "none." Recently, various types of image-enhanced endoscopy have been used to ensure the accurate evaluation of *H. pylori* infection[2-6].

In our previous study[7], we classified mucosal patterns (MPs) into three types (spotty, cracked, and mottled) using blue laser imaging (BLI)[8,9] in patients with *H. pylori*-related gastritis. We found that the spotty pattern indicated the possibility of *H. pylori* infection, the cracked pattern indicated a post-inflammatory change after *H. pylori* eradication, and the mottled pattern indicated an intestinal metaplasia resulting from the progression of *H. pylori*-related gastritis. Thus, we hypothesized that the spotty pattern would disappear or decrease and the cracked pattern would newly appear or increase after *H. pylori* eradication.

To further explore these changes, we quantitatively analyzed the changes to determine whether each pattern would increase, decrease, or remain unchanged. Since little is known concerning the pattern changes after *H. pylori* eradication, clarification of these changes may help endoscopists diagnose the existing pattern as being pre- or post-eradication and understand the MP changes more precisely. Thus, this study aimed to clarify the significance and diagnostic viability of each MP using BLI.



DOI: 10.3748/wjg.v29.i17.2657 **Copyright** ©The Author(s) 2023.

Figure 1 Spotty pattern. Representative images of the spotty pattern shown as white spots of 1-2 mm in diameter in the gastric antrum of 6 patients infected with *Helicobacter pylori* (*H. pylori*) observed using blue laser imaging-bright mode. A: 45-year-old female, *H. pylori*-positive; B: 51-year-old female, *H. pylori*-positive; C: 27-year-old female, *H. pylori*-positive; D: 59-year-old female, *H. pylori*-positive, nodular gastritis; E: 49-year-old male, *H. pylori*-positive; F: 66-year-old female, *H. pylori*-positive.

MATERIALS AND METHODS

Patients and methods

A total of 2242 patients underwent upper gastrointestinal (GI) endoscopy at the Nishikawa Gastrointestinal Clinic, Ehime, Japan from April 1, 2015 to March 31, 2017. Of these, 768 patients were endoscopically diagnosed with atrophic gastritis. The presence or absence of *H. pylori* infection was confirmed. Among them, 325 patients were *H. pylori*-positive, and of them, 101 patients who underwent *H. pylori* eradication and subsequent endoscopy were examined for MP changes.

An EG-L580NW nasal upper GI endoscope (FUJIFILM Medical Co. Ltd., Tokyo, Japan) was used orally or nasally. The BLI bright mode was used to evaluate MPs in the intermediate or distant views.

This study was approved by the Ethics Committee of Ehime University Hospital (No: 1605010; August 22, 2016). Prior to receiving an endoscopic examination, all patients agreed that the data obtained in this study might be published in academic papers.

Classification of MPs

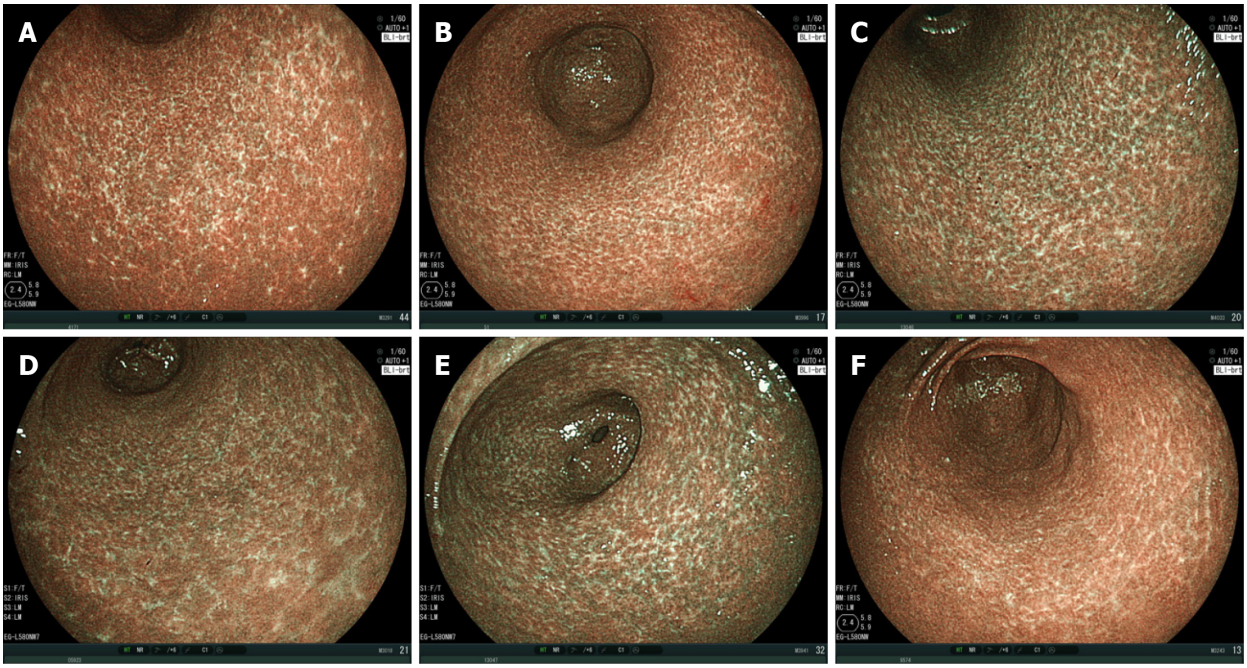
The MPs were classified into three types: The spotty pattern, which consists of 1-2 mm diameter spots (Figure 1); the cracked pattern, which consists of net-like cracks (Figure 2); and the mottled pattern, which has a mottled appearance (Figure 3)[7].

Evaluation of the MP changes after H. pylori eradication

The MP patterns were evaluated as follows: (1) Three expert GI endoscopists, with at least 25 years of experience, evaluated the mucosal changes after *H. pylori* eradication; (2) They were blinded to the patients' endoscopic data, including the patterns obtained before and/or after *H. pylori* eradication; (3) They compared two randomly listed endoscopic image groups and evaluated which image group was dominant, less dominant, equal, or absent for the spotty, cracked, and mottled patterns; (4) When two or all endoscopists agreed on a particular pattern, that pattern was adopted for analysis. When they had conflicting pattern determinations, the final determination was reached through a joint discussion; and (5) *H. pylori* infection was diagnosed using the anti-*H. pylori* IgG antibody serology tests[10,11], urea breath tests[12-15], and biopsies.

Statistical analysis

Student's *t*-test was used for the analysis of age, and the χ^2 test was used for the analyses of other variables. Statistical significance was set at $P < 0.05$. A 95% confidence interval (CI) was calculated to determine the uncertainty of the sample estimates. All statistical analyses were performed using



DOI: 10.3748/wjg.v29.i17.2657 **Copyright** ©The Author(s) 2023.

Figure 2 Cracked pattern. Representative images of the cracked pattern as white net-like cracks consisting of lines in the gastric antrum of 6 patients after *Helicobacter pylori* (*H. pylori*) eradication observed using blue laser imaging-bright mode. A: 69-year-old female, *H. pylori*-negative, 2 years, 11 mo after eradication; B: 75-year-old female, *H. pylori*-negative, 6 years, 0 mo after eradication; C: 63-year-old female, *H. pylori*-negative, 1 year, 2 mo after eradication; D: 72-year-old female, *H. pylori*-negative, 1 year, 0 mo after eradication; E: 63-year-old female, *H. pylori*-negative, 1 year, 2 mo after eradication; F: 52-year-old male, *H. pylori*-negative, 2 years, 1 mo after eradication.

Microsoft Excel 2016, version 1907, Build 11901.20176 (Microsoft Corporation, Redmond, WA, United States), and the statistical methods of this study were reviewed by Dr. Natsumi Yamashita from Clinical Research Center, National Hospital Organization Shikoku Cancer Center.

RESULTS

Patient characteristics

The number of patients evaluated was 768 (480 females and 288 males) with a mean age of 65.8 ± 12.9 (standard deviation) years. The numbers of patients with and without *H. pylori* infection were 325 (204 females and 121 males) and 443 (276 females and 167 males), respectively.

The mean ages of patients with and without *H. pylori* infection were 61.6 ± 14.3 years and 68.9 ± 10.7 years, respectively, with significant differences among them ($P < 0.001$). No significant difference was observed between the proportions of female and male patients with and without *H. pylori* infection ($P = 0.895$; Table 1).

Changes in MPs after H. pylori eradication

Upper GI endoscopy was performed for 101 patients (females: 75; males: 26; mean age: 57.5 ± 14.1 years) who successfully underwent *H. pylori* eradication, and the endoscopic mucosal changes were evaluated. Patients in whom evaluation was difficult because there were no comparable images of the specific parts were excluded from the analysis. The mean interval between *H. pylori* eradication and post-eradication endoscopy was 27.1 ± 13.1 mo.

In our study, multiple patterns commonly coexisted in many patients, with some patients having all three patterns. Of the 101 patients, 38 patients showed all three patterns (spotty, cracked, and mottled), 59 had two patterns (spotty and cracked, 28; spotty and mottled, 7; and cracked and mottled, 24), and 4 patients presented with only one pattern (spotty, 3; cracked, 0; and mottled, 1) either before or after eradication.

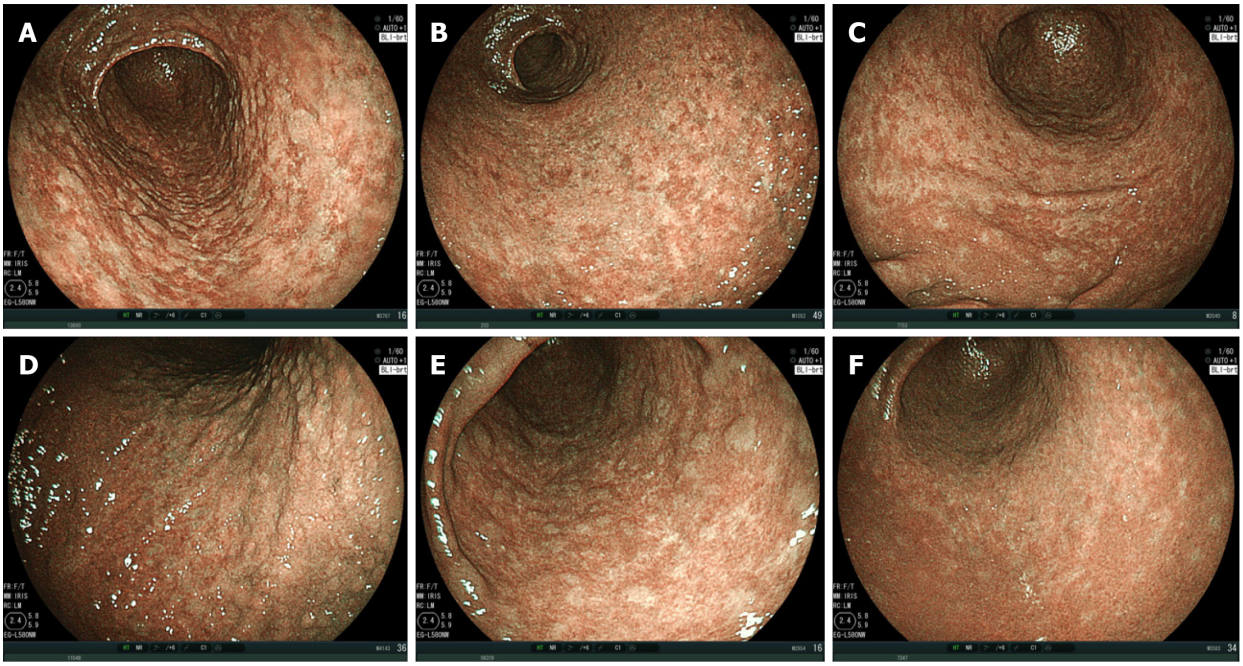
In 76 patients with a spotty pattern before or after *H. pylori* eradication, the pattern disappeared or decreased in 67 patients (88.2%, 95%CI: 79.0%-93.6%) and appeared or increased in 8 patients (10.5%, 95%CI: 5.4%-19.4%). In 1 patient (1.3%, 95%CI: 0.2%-7.1%), no change was observed after *H. pylori* eradication.

In 90 patients with a cracked pattern before or after *H. pylori* eradication, the pattern disappeared or decreased in 7 patients (7.8%, 95%CI: 3.8%-15.2%) and appeared or increased in 79 patients (87.8%,

Table 1 Patient characteristics

Item	Patients with atrophic gastritis	Patients with *H. pylori* infection	Patients underwent both *H. pylori* eradication and follow up endoscopy
No. of patients	768	325	101
Age, mean ± SD	65.8 ± 12.9	61.6 ± 14.3	57.5 ± 14.1
Female	480	204	75
Male	288	121	26

SD: Standard deviation; *H. pylori: Helicobacter pylori*.



DOI: 10.3748/wjg.v29.i17.2657 **Copyright** ©The Author(s) 2023.

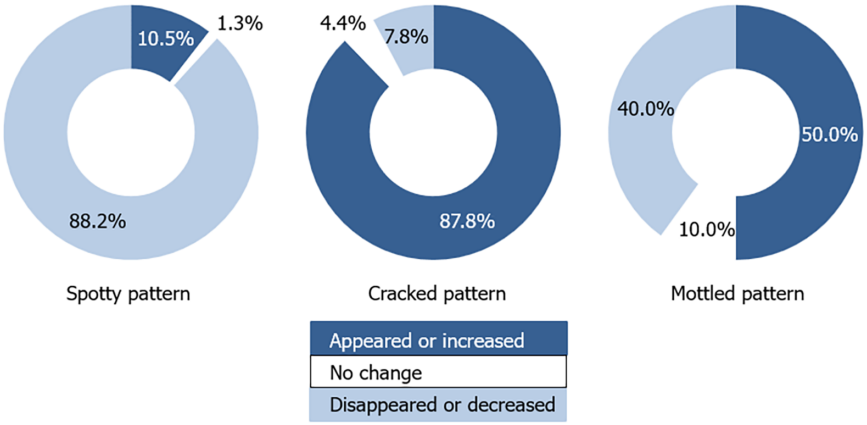
Figure 3 Mottled pattern. Representative images of the mottled pattern observed using blue laser imaging-bright mode in the gastric antrum of 6 patients. The whitish-colored mottled areas varied from small to large. Only panel A shows the pattern of a patient infected with *Helicobacter pylori* (*H. pylori*). A: 67-year-old male, *H. pylori*-positive, before eradication; B: 74-year-old male, *H. pylori*-negative, no eradication; C: 73-year-old female, *H. pylori*-negative, 2 years, 11 mo after eradication; D: 87-year-old male, *H. pylori*-negative, no eradication; E: 83-year-old male, *H. pylori*-negative, 5 years, 2 mo after eradication; F: 60-year-old female, *H. pylori*-negative, 2 years, 2 mo after eradication.

95%CI: 79.4%-93.0%). In 4 patients (4.4%, 95%CI: 1.7%-10.9%), no change was observed after *H. pylori* eradication.

In 70 patients with a mottled pattern before or after *H. pylori* eradication, the pattern disappeared or decreased in 28 patients (40.0%, 95%CI: 29.3%-51.7%) and appeared or increased in 35 patients (50.0%, 95%CI: 38.6%-61.4%). In 7 patients (10.0%, 95%CI: 4.9%-19.2%), no change was observed after *H. pylori* eradication (Figure 4).

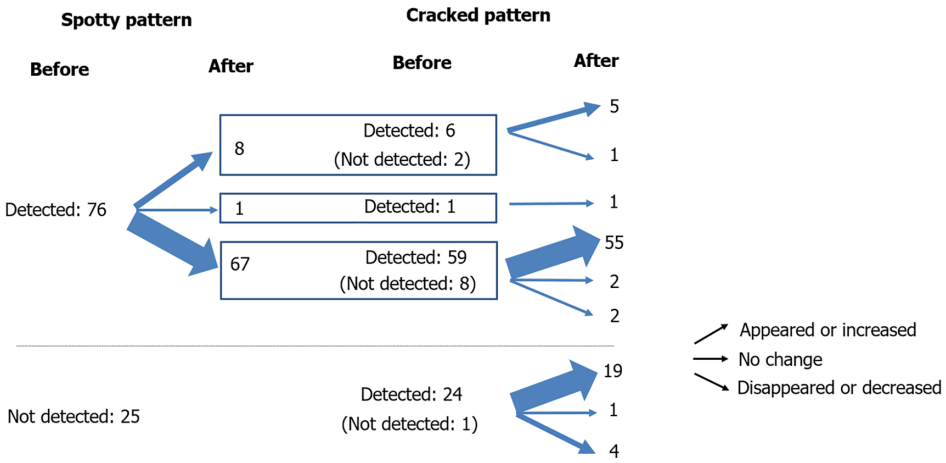
We investigated the relationship between the spotty and cracked patterns before and after eradication. The spotty pattern disappeared or decreased in 67 out of the 76 patients who had a spotty pattern before or after eradication. Of the 67 patients, the cracked pattern appeared or increased in 55 patients. Among the 8 patients with spotty patterns that appeared or increased after eradication, the cracked pattern appeared or increased in 5 patients. The cracked pattern appeared or increased in most of the 25 patients who did not have a spotty pattern before or after eradication (Figure 5).

We further investigated the difference in MP changes due to *H. pylori* eradication between the short-term (8-24 mo) and long-term (25-60 mo) observation groups. The spotty pattern disappeared or decreased in 88.6% and 87.8% (short-term *vs* long-term) of the patients. The cracked pattern newly appeared or increased in 88.9% and 86.7% (short-term *vs* long-term) of the patients. No significant differences were observed between the patients under short-term and long-term observations.



DOI: 10.3748/wjg.v29.i17.2657 **Copyright** ©The Author(s) 2023.

Figure 4 Change in mucosal pattern after *Helicobacter pylori* eradication. The spotty pattern tended to disappear or decrease, the cracked pattern appeared or increased, and the mottled pattern exhibited no specific tendency.



DOI: 10.3748/wjg.v29.i17.2657 **Copyright** ©The Author(s) 2023.

Figure 5 Relationship between the spotty and cracked patterns before and after *Helicobacter pylori* eradication.

DISCUSSION

We investigated the use of BLI, an image-enhanced endoscopy, for the diagnosis of *H. pylori*-related gastritis, with a focus on the MP changes after *H. pylori* eradication. The Kyoto Classification of Gastritis was established in 2014 for the endoscopic diagnosis of *H. pylori*-related gastritis[16,17]. The classification of MPs observed on BLI in this study is simpler and easier to use in endoscopic assessment than the Kyoto classification and thus has the potential to become a new standard method with the addition of new diagnostic information to the Kyoto classification. We previously reported the efficacy of MPs on BLI in an intermediate-to-distant view evaluation of *H. pylori* infection and had the benefits of easy detection of atrophic gastritis and easy diagnosis of infection status (current, previous, or no infection) [7].

The results obtained in the current study indicate that the disappearance of the spotty pattern is evidence of *H. pylori* clearance, while newly-appearing cracked pattern is evidence of post-gastritis healing. The mottled pattern may reflect "intestinal metaplasia," as identified in our previous study using biopsies.

Knowledge of the endoscopic changes after *H. pylori* eradication is helpful in clarifying the meaning of each MP. The spotty pattern disappeared or decreased in 88.2% of patients, whereas the cracked pattern appeared or increased in 87.8% of patients after *H. pylori* eradication. The mottled pattern exhibited no specific tendency. As indicated in Figure 5, the spotty pattern observed in *H. pylori*-positive patients before eradication may disappear and may be replaced by the cracked pattern. Based on these observations, we can diagnose the *H. pylori* infection status as current, previous, or no infection. No difference was detected between the short-term and long-term observations of MP changes after *H. pylori* eradication, suggesting that the changes in MP would occur relatively quickly after eradication. The primary tendency of MP changes after *H. pylori* eradication have been clarified in this study. Irregular pattern changes (those other than spotty to cracked pattern) were observed after eradication in

a limited number of patients. Further verification is necessary.

CONCLUSION

In conclusion, the spotty pattern may indicate *H. pylori* infection, the cracked pattern may indicate post-inflammatory changes after *H. pylori* eradication, and the mottled pattern may indicate intestinal metaplasia resulting from the progression of *H. pylori*-related gastritis. We verified that MPs on BLI may change from a spotty to a cracked pattern after *H. pylori* eradication. These observations may help endoscopists easily and precisely evaluate the status of *H. pylori*-related gastritis. We hope that MP changes on BLI will be routinely used to confirm the diagnosis of *H. pylori*-related gastritis in the future.

ARTICLE HIGHLIGHTS

Research background

Determination of the presence or absence of *Helicobacter pylori* (*H. pylori*) infection is important in the diagnosis of atrophic gastritis. Various studies have been conducted to distinguish these two conditions.

Research motivation

In our previous study, we reported that *H. pylori* eradication may lead to the disappearance of the spotty pattern and the appearance of the cracked pattern.

Research objectives

To further substantiate and comprehensively investigate mucosal pattern changes after *H. pylori* eradication in a larger number of patients.

Research methods

Among the patients with atrophic gastritis in whom *H. pylori* positivity was confirmed, we investigated 101 patients who underwent both *H. pylori* eradication and follow-up endoscopy and evaluated the change of patterns before and after eradication.

Research results

The spotty pattern tended to disappear or decrease, and the cracked pattern tended to appear or increase after *H. pylori* eradication, while the mottled pattern exhibited no specific tendency.

Research conclusions

The spotty pattern likely changes to the cracked pattern after *H. pylori* eradication.

Research perspectives

In future studies, it will be necessary to examine the morphological and histological changes of each mucosal pattern, compare these pattern changes with the Kyoto classification, examine the relationship with other classifications of atrophic gastritis, and clarify the meaning of the mucosal pattern changes.

FOOTNOTES

Author contributions: Nishikawa Y conceived and designed the study; Nishikawa Y, Ikeda Y, Murakami H, Hori S, and Yoshimatsu M analyzed and interpreted the data; Nishikawa Y and Nishikawa N drafted the manuscript; Nishikawa Y, Ikeda Y, Murakami H, Hori S, Yoshimatsu M, and Nishikawa N critically revised the manuscript for important intellectual content; Nishikawa Y gave final approval of the manuscript; all authors approved the final version of the article to be published.

Institutional review board statement: This study was approved by the Ethics Committee of Ehime University Hospital (No. 1605010; August 22, 2016).

Informed consent statement: This study was conducted retrospectively from data obtained for clinical purposes. The study was approved by the institutional review board at the Ethics Committee of Ehime University Hospital. Prior to receiving an endoscopic examination, all patients agreed that the data obtained in this study might be published in academic papers.

Conflict-of-interest statement: None of the authors have any financial relationships to disclose with relevance to this article.

Data sharing statement: Data presented in this study is available on request from the corresponding author.

Open-Access: This article is an open-access article that was selected by an in-house editor and fully peer-reviewed by external reviewers. It is distributed in accordance with the Creative Commons Attribution NonCommercial (CC BY-NC 4.0) license, which permits others to distribute, remix, adapt, build upon this work non-commercially, and license their derivative works on different terms, provided the original work is properly cited and the use is non-commercial. See: https://creativecommons.org/Licenses/by-nc/4.0/

Country/Territory of origin: Japan

ORCID number: Yoshiyuki Nishikawa 0000-0001-8162-9369; Yoshio Ikeda 0009-0009-8832-7852; Hidehiro Murakami 0000-0002-6261-2964; Shin-Ichiro Hori 0000-0002-9393-4413; Megumi Yoshimatsu 0009-0005-8227-0905; Naoki Nishikawa 0009-0003-7489-9071.

S-Editor: Yan JP
L-Editor: A
P-Editor: Chen YX

REFERENCES

1 **Uemura N**, Okamoto S, Yamamoto S, Matsumura N, Yamaguchi S, Yamakido M, Taniyama K, Sasaki N, Schlemper RJ. Helicobacter pylori infection and the development of gastric cancer. *N Engl J Med* 2001; **345**: 784-789 [PMID: 11556297 DOI: 10.1056/NEJMoa001999]

2 **Dohi O**, Majima A, Naito Y, Yoshida T, Ishida T, Azuma Y, Kitae H, Matsumura S, Mizuno N, Yoshida N, Kamada K, Itoh Y. Can image-enhanced endoscopy improve the diagnosis of Kyoto classification of gastritis in the clinical setting? *Dig Endosc* 2020; **32**: 191-203 [PMID: 31550395 DOI: 10.1111/den.13540]

3 **Glover B**, Teare J, Patel N. A systematic review of the role of non-magnified endoscopy for the assessment of H. pylori infection. *Endosc Int Open* 2020; **8**: E105-E114 [PMID: 32010741 DOI: 10.1055/a-0999-5252]

4 **Alaboudy AA**, Elbahrawy A, Matsumoto S, Yoshizawa A. Conventional narrow-band imaging has good correlation with histopathological severity of Helicobacter pylori gastritis. *Dig Dis Sci* 2011; **56**: 1127-1130 [PMID: 20857197 DOI: 10.1007/s10620-010-1414-z]

5 **Tongtawee T**, Kaewpitoon S, Kaewpitoon N, Dechsukhum C, Loyd RA, Matrakool L. Correlation between Gastric Mucosal Morphologic Patterns and Histopathological Severity of Helicobacter pylori Associated Gastritis Using Conventional Narrow Band Imaging Gastroscopy. *Biomed Res Int* 2015; **2015**: 808505 [PMID: 26120585 DOI: 10.1155/2015/808505]

6 **Takeda T**, Asaoka D, Nojiri S, Nishiyama M, Ikeda A, Yatagai N, Ishizuka K, Hiromoto T, Okubo S, Suzuki M, Nakajima A, Nakatsu Y, Komori H, Akazawa Y, Nakagawa Y, Izumi K, Matsumoto K, Ueyama H, Sasaki H, Shimada Y, Osada T, Hojo M, Kato M, Nagahara A. Linked Color Imaging and the Kyoto Classification of Gastritis: Evaluation of Visibility and Inter-Rater Reliability. *Digestion* 2020; **101**: 598-607 [PMID: 31302654 DOI: 10.1159/000501534]

7 **Nishikawa Y**, Ikeda Y, Murakami H, Hori SI, Hino K, Sasaki C, Nishikawa M. Classification of atrophic mucosal patterns on Blue LASER Imaging for endoscopic diagnosis of Helicobacter pylori-related gastritis: A retrospective, observational study. *PLoS One* 2018; **13**: e0193197 [PMID: 29596454 DOI: 10.1371/journal.pone.0193197]

8 **Yoshida N**, Yagi N, Inada Y, Kugai M, Okayama T, Kamada K, Katada K, Uchiyama K, Ishikawa T, Handa O, Takagi T, Konishi H, Kokura S, Yanagisawa A, Naito Y. Ability of a novel blue laser imaging system for the diagnosis of colorectal polyps. *Dig Endosc* 2014; **26**: 250-258 [PMID: 23731034 DOI: 10.1111/den.12127]

9 **Osawa H**, Yamamoto H. Present and future status of flexible spectral imaging color enhancement and blue laser imaging technology. *Dig Endosc* 2014; **26** Suppl 1: 105-115 [PMID: 24373002 DOI: 10.1111/den.12205]

10 **Feldman RA**, Deeks JJ, Evans SJ. Multi-laboratory comparison of eight commercially available Helicobacter pylori serology kits. Helicobacter pylori Serology Study Group. *Eur J Clin Microbiol Infect Dis* 1995; **14**: 428-433 [PMID: 7556232 DOI: 10.1007/BF02114899]

11 **Loy CT**, Irwig LM, Katelaris PH, Talley NJ. Do commercial serological kits for Helicobacter pylori infection differ in accuracy? *Am J Gastroenterol* 1996; **91**: 1138-1144 [PMID: 8651160]

12 **Graham DY**, Klein PD, Evans DJ Jr, Evans DG, Alpert LC, Opekun AR, Boutton TW. Campylobacter pylori detected noninvasively by the 13C-urea breath test. *Lancet* 1987; **1**: 1174-1177 [PMID: 2883491 DOI: 10.1016/s0140-6736(87)92145-3]

13 **Logan RP**, Polson RJ, Misiewicz JJ, Rao G, Karim NQ, Newell D, Johnson P, Wadsworth J, Walker MM, Baron JH. Simplified single sample 13Carbon urea breath test for Helicobacter pylori: comparison with histology, culture, and ELISA serology. *Gut* 1991; **32**: 1461-1464 [PMID: 1773948 DOI: 10.1136/gut.32.12.1461]

14 **Ohara S**, Kato M, Asaka M, Toyota T. Studies of 13C-urea breath test for diagnosis of Helicobacter pylori infection in Japan. *J Gastroenterol* 1998; **33**: 6-13 [PMID: 9497214 DOI: 10.1007/pl00009968]

15 **Gisbert JP**, Pajares JM. Review article: 13C-urea breath test in the diagnosis of Helicobacter pylori infection -- a critical review. *Aliment Pharmacol Ther* 2004; **20**: 1001-1017 [PMID: 15569102 DOI: 10.1111/j.1365-2036.2004.02203.x]

16 **Haruma K**, Kato M, Inoue K, Murakami K, Kamada T. Kyoto Classification of Gastritis. Tokyo: Nihon Medical Center, Ltd., 2014

17 **Toyoshima O**, Nishizawa T, Koike K. Endoscopic Kyoto classification of Helicobacter pylori infection and gastric cancer

risk diagnosis. *World J Gastroenterol* 2020; **26**: 466-477 [PMID: 32089624 DOI: 10.3748/wjg.v26.i5.466]

World Journal of Gastroenterology

Submit a Manuscript: https://www.f6publishing.com

World J Gastroenterol 2023 May 7; 29(17): 2666-2678

DOI: 10.3748/wjg.v29.i17.2666

ISSN 1007-9327 (print) ISSN 2219-2840 (online)

ORIGINAL ARTICLE

Randomized Controlled Trial

Fecal microbiota transplantation for the maintenance of remission in patients with ulcerative colitis: A randomized controlled trial

Perttu Lahtinen, Jonna Jalanka, Eero Mattila, Jyrki Tillonen, Paula Bergman, Reetta Satokari, Perttu Arkkila

Specialty type: Gastroenterology and hepatology

Provenance and peer review: Unsolicited article; Externally peer reviewed.

Peer-review model: Single blind

Peer-review report's scientific quality classification

Grade A (Excellent): 0
Grade B (Very good): 0
Grade C (Good): C, C, C, C
Grade D (Fair): D
Grade E (Poor): 0

P-Reviewer: Triantafillidis J, Greece; Wang LH, China; Zhang Z, China; Zhang F, China

Received: December 27, 2022
Peer-review started: December 27, 2022
First decision: January 22, 2023
Revised: February 6, 2023
Accepted: April 11, 2023
Article in press: April 11, 2023
Published online: May 7, 2023

Perttu Lahtinen, Jyrki Tillonen, Department of Gastroenterology, Päijät-Häme Central Hospital, Lahti 15610, Finland

Perttu Lahtinen, Department of Medicine, University of Helsinki, Helsinki 00014, Finland

Jonna Jalanka, Reetta Satokari, Human Microbiome Research Program, Faculty of Medicine, University of Helsinki, Helsinki 00014, Finland

Eero Mattila, Department of Infectious Diseases, Helsinki University Hospital, Helsinki 00029, Uusimaa, Finland

Paula Bergman, Department of Bioinformatics, Helsinki University Hospital, Helsinki 00014, Finland

Perttu Arkkila, Department of Gastroenterology, University Helsinki, Center Hospital, Helsinki 00029, Uusimaa, Finland

Corresponding author: Perttu Lahtinen, MD, Chief Doctor, Department of Gastroenterology, Päijät-Häme Central Hospital, Keskussairaalankatu 7, Lahti 15610, Finland.
perttu.lahtinen@phhyky.fi

Abstract

BACKGROUND

Fecal microbial transplantation (FMT) is a promising new method for treating active ulcerative colitis (UC), but knowledge regarding FMT for quiescent UC is scarce.

AIM

To investigate FMT for the maintenance of remission in UC patients.

METHODS

Forty-eight UC patients were randomized to receive a single-dose FMT or autologous transplant *via* colonoscopy. The primary endpoint was set to the maintenance of remission, a fecal calprotectin level below 200 μg/g, and a clinical Mayo score below three throughout the 12-mo follow-up. As secondary end-points, we recorded the patient's quality of life, fecal calprotectin, blood chemistry, and endoscopic findings at 12 mo.

RESULTS

The main endpoint was achieved by 13 out of 24 (54%) patients in the FMT group and by 10 out of 24 (41%) patients in the placebo group (log-rank test, P = 0.660). Four months after FMT, the quality-of-life scores decreased in the FMT group compared to the placebo group (P = 0.017). In addition, the disease-specific quality of life measure was higher in the placebo group than in the FMT group at the same time point (P = 0.003). There were no differences in blood chemistry, fecal calprotectin, or endoscopic findings among the study groups at 12 mo. The adverse events were infrequent, mild, and distributed equally between the groups.

CONCLUSION

There were no differences in the number of relapses between the study groups at the 12-mo follow-up. Thus, our results do not support the use of a single-dose FMT for the maintenance of remission in UC.

Key Words: Fecal microbial transplantation; Ulcerative colitis; Quality of life; Maintenance of remission; Inflammatory bowel disease; Fecal calprotectin

©The Author(s) 2023. Published by Baishideng Publishing Group Inc. All rights reserved.

Core Tip: This randomized controlled trial compared the efficacy of fecal microbial transplantation *via* colonoscopy and autologous placebo containing patients' own feces for the maintenance of remission in 48 patients with ulcerative colitis. The colitis activity was measured with the clinical Mayo score and fecal calprotectin. There was no significant difference in relapses between the groups at the 12-mo follow-up. Remission remained in 54% of the patients in the fecal microbial transplantation group compared to 41% in the placebo group. There was no difference in the adverse events between the groups.

Citation: Lahtinen P, Jalanka J, Mattila E, Tillonen J, Bergman P, Satokari R, Arkkila P. Fecal microbiota transplantation for the maintenance of remission in patients with ulcerative colitis: A randomized controlled trial. *World J Gastroenterol* 2023; 29(17): 2666-2678
URL: https://www.wjgnet.com/1007-9327/full/v29/i17/2666.htm
DOI: https://dx.doi.org/10.3748/wjg.v29.i17.2666

INTRODUCTION

Ulcerative colitis (UC) is a chronic inflammatory disease with an uncertain etiology. The symptoms of UC include bloody diarrhea and abdominal cramps. The pathophysiology is thought to involve an altered and exaggerated inflammatory response to commensal bacteria in genetically predisposed individuals[1]. An increasing proportion of the population is affected by UC, and the prevalence is highest in North America and Northern Europe. For example, in Finland, the yearly incidence is over 25/100000 and is growing[2]. The lifelong risk of colectomy remains elevated despite new immune response-targeting treatment options[3]. Patients with UC show a reduced quality of life compared to the general population even if the disease is quiescent[4].

UC is associated with decreased gut microbial diversity and stability as well as altered microbiota composition and function[5]. In conditions such as *Clostridioides difficile* infection (CDI) and irritable bowel syndrome (IBS), fecal microbial transplantation (FMT) has been shown to alter the patients' gut microbiota in the long term to resemble that of healthy donors[6-8]. During the last decade, FMT has become a recommended treatment option for recurrent *Clostridioides difficile* infection (rCDI)[9]. The efficacy of FMT for rCDI exceeds 90% using an optimal protocol[10,11]. On this basis, it is worthwhile to investigate FMT in UC patients.

FMT has shown promising efficacy for active UC in placebo-controlled trials, although the methodology has varied between studies[12-15]. Repetitious FMTs have been the most frequently applied approach among these studies, while the applied treatment protocols have been otherwise diverse. Some studies have applied a multidonor approach and prepared each transplant from the feces of multiple donors[14,15]. Anaerobic conditions for manufacturing the fecal transplant have been investigated and shown to yield good results[15], as has the administration of a transplant to each patient as many as 40 times[14]. One study showed a clear difference in efficacy between donors, as transplants from one donor were more effective than transplants from the other five donors[13].

A recent randomized placebo-controlled trial from India investigated the efficacy of FMT in the maintenance of UC remission[16]. In this study, FMT prevented relapses through the administration of transplants during bimonthly colonoscopies, making the implementation of the applied protocol very

laborious in clinical practice. Additionally, the study population consisted of primary responders to FMT treatment; thus, the patients in the trial were a highly selective group.

Given that a single FMT alters the gut microbiota for the long term in rCDI[6] as well as in IBS[8] patients, we aimed to investigate the efficacy of a single FMT *via* colonoscopy to maintain remission in UC patients. Additionally, we aimed to investigate the potential differences in quality of life, fecal calprotectin, blood chemistry [blood count, liver enzymes, creatinine, and C-reactive protein (CRP)], and endoscopic findings during the 12-mo follow-up period.

MATERIALS AND METHODS

Study design

We randomized patients with UC in remission into two groups in a 1:1 ratio to receive either FMT from a healthy donor ("FMT group") or an autologous transplant made from the patient's own feces ("placebo group"). To ensure blinding, all participants donated their stool for the preparation of the placebo transplant, and the FMT group samples were discarded. Bowel lavage was performed using a macrogol solution prior to colonoscopy. The transplant was administered into the cecum of the patient during colonoscopy at baseline.

After the baseline intervention, the patients were followed until a colonoscopy 12 mo later. During the follow-up period, the participants were contacted at 2 mo, 4 mo, and 8 mo after the intervention, at which times the clinical Mayo score[17] was recorded and blood samples were obtained. The quality of life was assessed at baseline as well as at 4 mo and 12 mo[4]. Fecal calprotectin samples were obtained at seven timepoints (baseline and at 2 mo, 4 mo, 6 mo, 8 mo, 10 mo, and 12 mo).

The primary endpoint was sustained remission through the 12-mo follow-up time. Remission was defined as a clinical Mayo score below three and a fecal calprotectin level below 200 μg/g. Additionally, an overt relapse between the measurement points leading to a course of steroids or escalation of maintenance therapy was considered a failure.

This randomized placebo-controlled study was conducted in Finland in the Gastroenterology Departments of Helsinki University Hospital, Helsinki and Päijät-Häme Central Hospital, Lahti. The ethical review board of Helsinki University Hospital approved the study (29/13/03/01/2014). The principles of the Declaration of Helsinki were followed. The trial was registered at ClinicalTrials.gov (NCT03561532).

Participants

Forty-eight patients (21-70-years-old) diagnosed with UC were recruited for the study. The inclusion criteria stated that the patients had to be in remission, and the eligibility criteria included fecal calprotectin levels below 100 μg/g and a clinical Mayo score < 3 at the time of screening. The exclusion criteria included the use of antibiotics within 3 mo prior to study entry, a history of tumor necrosis factor-α blockers or other biologics, the use of a high dose of corticosteroids (prednisolone ≥ 20 mg/d), and pregnancy. The patients were recruited from primary and secondary health care centers of the Helsinki and Lahti regions. At baseline, the majority of the patients were on mesalazine.

After the screening visit and before the start of the trial, some patients experienced minor activation of the disease; 8 patients, 4 in each group, had a clinical Mayo score ≥ 3, and 10 patients, 3 in the FMT group and 7 in the placebo group, had fecal calprotectin levels ≥ 200 μg/g. At baseline, none of these patients experienced significant symptoms, and they did not require escalation of medication. Participants with fecal calprotectin ≥ 200 μg/g or a clinical Mayo score ≥ 3 were analyzed separately as "subgroup B" (n = 15), and the participants without these signs of disease activity at baseline were included in "subgroup A" (n = 33). Among all the recruited patients, 16 patients had minor endoscopic colitis activity with an endoscopic Mayo score of 1 at baseline, while the rest of the patients had an endoscopic Mayo score of 0 at baseline.

Participant recruitment started in October 2014. At the beginning of the study, the inclusion criteria required a diagnosis of UC within 6 mo. However, due to very slowly proceeding recruitment, an amendment to the study protocol was made and approved by the ethical board in October 2016 (HUS/1652/2016). Thereafter, patients with any disease duration were eligible. Recruitment remained slow even after the amendment. The study proceeded using fewer than the desired 80 participants due to time constraints. The follow-up of the last included patient was completed in May 2020 (CONSORT flow diagram in Supplementary Figure 1).

Donors

Transplants from three healthy donors were used in this study. The donors had normal body weights and were healthy without any diagnosed long-term illnesses or medications. All donors had a healthy lifestyle and a diet that included animal products but was rich in vegetables. They were screened according to the best practice at the time[10]; however, the donor screening guidelines have evolved since the start of the trial[9]. The laboratory tests for donor screening are collectively presented in Supplementary Table 1. We applied transplants from a female in her forties ("Donor 1") and a young

adult male ("Donor 2"), both of whom had previously served as donors in our studies[6,8] and in routine clinical practice of FMT to treat rCDI. A male in his fifties ("Donor 3") was a new donor recruited for this study.

Intervention

Half of the participants, 24 out of 48, received FMT *via* colonoscopy into the cecum as described previously[10]. The fecal transplants were produced from 30 g of feces from a healthy donor. We used three universal donors, and the fecal suspensions were prepared as previously described and stored at -80 °C[10].

Briefly, feces were suspended in sterile saline and mixed with glycerol (final concentration of 10%) in a 250 mL screw cap container by using a spatula. The suspension was frozen at -80 °C immediately after preparation and within 2 h of defecation to minimize the time of exposure to oxygen. For FMT application, the suspension was thawed at 37 °C or room temperature, mixed briefly and loaded into syringes to avoid clogging by unsuspended particles. If necessary, the suspension was passed through a presterilized, stainless steel tea strainer to remove particles before loading the syringes. The remaining 24 participants in the placebo group were treated in an otherwise similar manner, but the fecal suspension was made using the participants' own freshly donated stool. Autologous placebo was prepared from fresh feces for practical reasons to prevent an extra visit and minimize inconvenience to the patients.

Power calculation and estimated sample size

The relapse rates during the 12-mo follow-up period were estimated to be 50% in the placebo group and 15% in the FMT group. Previous studies of FMT for maintenance of remission of UC were not published at the time of study design. Due to the lack of available studies, the estimation of outcomes was based on knowledge concerning the maintenance of remission using mesalazine[18] and extrapolating from FMT studies for rCDI[11], in which over 90% efficacy had been achieved.

The calculated sample size using the z-test (95% confidence interval, $\alpha = 0.05$ and $\beta = 0.1$, 90% power) to find a significant treatment effect was 33 patients in each group, and to cover possible dropouts, we aimed for a sample size of 40 participants per group, 80 participants in total[19].

Randomization and blinding

The participants were randomized 1:1 to receive FMT or placebo. The randomization was executed in blocks of 6 patients by a study nurse not involved in the treatment of the patients. The participants and the treating personnel were blinded to the type of feces transplanted. The randomization was decoded only after all the patients had completed the 12-mo follow-up.

Outcomes

The primary outcome was the maintenance of remission through the 12-mo follow-up period. A relapse of colitis was considered a failure to achieve the primary outcome. The patients were followed until the time of the recorded relapse, after which they were dropped from the follow-up. The patients who remained in remission were followed until the study endpoint of 12 mo after baseline.

The secondary endpoints were quality of life, endoscopic and histologic findings at 12 mo, fecal calprotectin, and blood chemistry. General quality of life was assessed with the 15 dimensions (15D) questionnaire, and disease-specific quality of life was assessed with the Inflammatory Bowel Disease Quality of Life Questionnaire (IBDQ) (McMaster University, Hamilton, Canada, license No. IBDQ22-081)[4]. The histologic activity was graded in four categories: histological remission; mild activity (lamina propria or intraepithelial neutrophils); moderate activity (presence of crypt abscess); and strong activity (presence of erosion or ulcer)[20].

The participants donated stool samples every 2nd mo (months 0, 2, 4, 6, 8, 10, and 12) for the detection of fecal calprotectin. Blood samples were obtained at baseline as well as at months 4, 8, and 12. The blood tests included complete blood counts, liver enzymes, creatinine, and CRP. Fecal calprotectin values below 50 μg/g and CRP values below ten were not reported by the laboratory and were coded as null accordingly.

Statistical methods

Descriptive statistics are presented as the means with standard deviations (SDs) for continuous variables and as frequencies and percentages for qualitative variables. Differences between the study groups in the maintenance of remission during the follow-up were assessed using the Kaplan-Meier method. Associations of baseline characteristics with the maintenance of remission were analyzed with univariate Cox regression models. In addition, 15D scores were presented using profile plots, and differences between groups were assessed by *t* tests. Differences in endoscopic and histological colitis activity between the study groups were analyzed with the χ^2 test. *P* values < 0.05 were considered statistically significant for all analyses. SPSS version 27 (IBM Corp. Released 2020. IBM SPSS Statistics for Windows, Version 27.0. Armonk, NY, United States) was used for the statistical analysis.

RESULTS

Baseline characteristics

Forty-nine patients were recruited for this study. After the screening visit and before randomization, 1 patient had overt activation of colitis and was excluded. This left 48 patients to be randomized, with 24 in each group. The patient flow of the study is presented in Supplementary Figure 1, and the baseline characteristics of the patients are presented in Table 1. The placebo group had a longer duration of disease than the FMT group (114 mo *vs* 39 mo, $P = 0.006$). At baseline, the mean fecal calprotectin level was 115.8 (SD: 184.7) in the placebo group and 66.4 (SD: 108.6) in the FMT group ($P = 0.261$). The majority of the patients were on mesalazine: 21 out of 24 patients in the FMT group and 22 out of 24 in the placebo group. Four patients in the placebo group were on thiopurine, but none were in the FMT group. At the study baseline, 2 patients in both groups were still on lower doses of tapering corticosteroid therapy. There were no statistically significant differences between the randomization groups within subgroups A and B, in which the patients had fecal calprotectin < 200 μg/g and a clinical Mayo score < 3 or fecal calprotectin ≥ 200 μg/g and a clinical Mayo score ≥ 3 at baseline, respectively (Table 1).

The primary endpoint-maintenance of remission

The primary endpoint of the study was the maintenance of remission through the 12-mo follow-up, which was achieved by 13 out of 24 (54%) patients in the FMT group and by 10 out of 24 (41%) patients in the placebo group. The difference between the groups was not statistically significant (log-rank test $P = 0.660$). A Kaplan-Meier survival curve of relapses in the FMT and placebo groups is presented in Figure 1A.

A similar result was obtained when the patients were divided into subgroups according to the clinical Mayo score and fecal calprotectin level at baseline. In subgroup A, 6 out of 16 patients relapsed in the placebo group, and 7 out of 17 patients relapsed in the FMT group ($P = 0.703$, Figure 1B). Similarly, subgroup B showed no difference between the placebo and FMT groups ($P = 0.556$) in the number of relapses; all 8 patients in the placebo group and 5 out of 7 patients in the FMT group relapsed (Figure 1C).

To study the possible effect of a specific donor on the patient's outcome, we divided the patients into three groups according to the donor and compared these to the placebo. There were no statistically significant differences in the number of relapses between the different donors (log-rank, $P = 0.517$). At the 12-mo follow-up, 41.7% (10/24) of the patients in the placebo group remained in remission compared to 33.3% (2/6) from Donor 1, 50.0% (5/10) from Donor 2, and 62.5% (5/8) from Donor 3.

We also analyzed the effect of essential baseline characteristics on the maintenance of remission between these donor groups, which included the duration of disease status, fecal calprotectin, clinical Mayo score, total 15D score, and total IBDQ score (Supplementary Table 2). The mean duration of disease was 114 mo in the placebo group, 5 mo in the Donor 1 group, 52 mo in the Donor 2 group, and 49 mo in the Donor 3 group. The disease duration did not have a statistically significant effect on the maintenance of remission in any of the donor groups. There were some statistically significant relationships between baseline characteristics and maintenance of remission. In the placebo group, lower maintenance of remission time was associated with higher baseline fecal calprotectin [Cox regression, hazard ratio (HR): 1.003; 95% confidence interval (CI): 1.001-1.005; $P = 0.010$) and a higher baseline clinical Mayo score (Cox regression, HR: 1.498; 95%CI: 1.067-2.102; $P = 0.020$). In the Donor 2 group, a lower mean 15D total score at baseline was associated with lower maintenance of remission (Cox regression, HR: 0.000; CI: 0.000-0.374; $P = 0.033$). All other analyzed associations were statistically insignificant (Supplementary Table 2).

Secondary endpoint–changes in patient quality of life

We investigated the impact of FMT on patient quality of life as measured with the 15D questionnaire and disease-specific quality of life as measured with the IBDQ questionnaire.

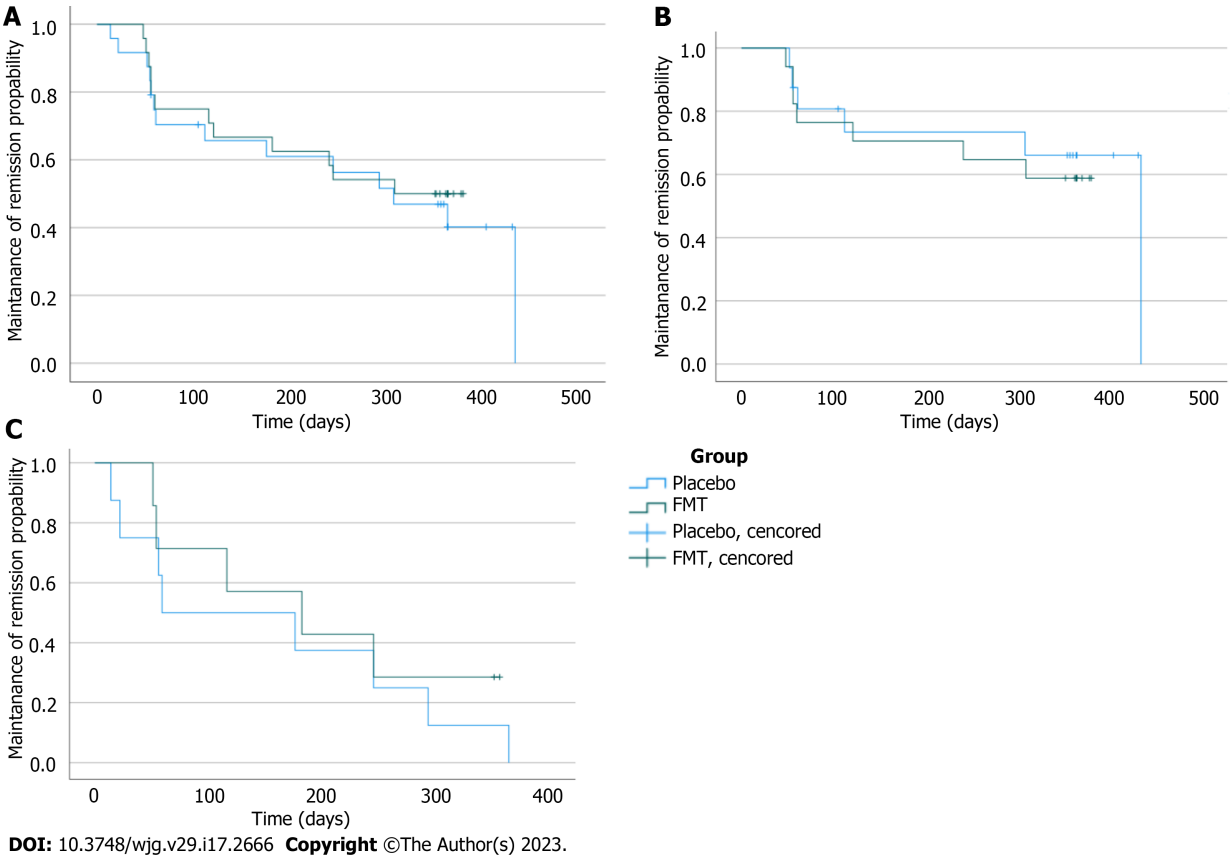
The 15D total score was similar between the placebo and FMT groups at baseline (*t* test, $P = 0.335$) (Figure 2A) and at the 12-mo follow-up after FMT treatment ($P = 0.905$) (Figure 2B). However, there was a significant difference in the 15D total score between the FMT and placebo groups ($P = 0.017$) 4 mo after treatment (Figure 2C). The mean change in the 15D total score from baseline to 4 mo was -0.032 (slightly worse) in the FMT group and -0.009 (no change) in the placebo group. The estimation of the importance of change was performed as presented previously[21]. The mean change in the 15D total score from baseline to 12 mo was -0.008 (no change) in the FMT group and -0.015 (slightly worse) in the placebo group. Additionally, of the 15D, there were statistically significant differences in breathing ($P = 0.049$), usual activities ($P = 0.042$), and vitality ($P = 0.006$), all favoring the placebo group.

The disease-specific quality of life as measured with the IBDQ[22] was also similar between the placebo and FMT groups at baseline ($P = 0.519$) and at 12 mo ($P = 0.868$), but at 4 mo, there was a difference in the IBDQ total score favoring the placebo group ($P = 0.003$). Of the four IBDQ subcategories, there were statistically significant differences in the emotions ($P = 0.008$) and systemic ($P = 0.010$) subcategories.

Table 1 The baseline demographics of patients included in the analysis

Baseline variable	All patients (*n* = 48)		*P* value	Subgroup A (*n* = 33)		*P* value	Subgroup B (*n* = 15)		*P* value
	FMT	Placebo		FMT	Placebo		FMT	Placebo	
Sex as M/F	14/10	12/12	0.562	8/9	8/8	0.866	4/4	5/2	0.608
Age	43.0 (12.9)	43.1 (12.1)	0.982	43.6 (13.0)	44.8 (12.0)	0.781	41.7 (13.6)	39.8 (12.5)	0.775
Disease duration in mo	39.2 (51.0)	114.0 (117.6)	0.006	41.0 (56.2)	125.4 (121.7)	0.015	34.9 (38.7)	91.3 (113.2)	0.233
Fecal calprotectin	66.0 (108.6)	115.8 (184.7)	0.261	34.7 (46.3)	18.9 (44.9)	0.330	142.3 (172.9)	309.6 (208.3)	0.117
15D	0.903 (0.095)	0.928 (0.072)	0.335	0.899 (0.106)	0.939 (0.070)	0.221	0.915 (0.070)	0.907 (0.078)	0.830
IBDQ	169.4 (28.8)	162.7 (39.8)	0.519	166.9 (28.6)	171.4 (32.0)	0.688	175.0 (30.5)	147.4 (49.3)	0.223

Subgroup A included patients with fecal calprotectin < 200 μg/g and a clinical Mayo score < 3 at baseline, and subgroup B included patients with fecal calprotectin ≥ 200 ug/g or a clinical Mayo score ≥ 3 at baseline. Standard deviations are shown in brackets. M: Male; F: Female; 15D: The total score of the 15 dimensions quality of life questionnaire; IBDQ: The total score of the inflammatory bowel disease quality of life questionnaire; FMT: Fecal microbiota transplantation.

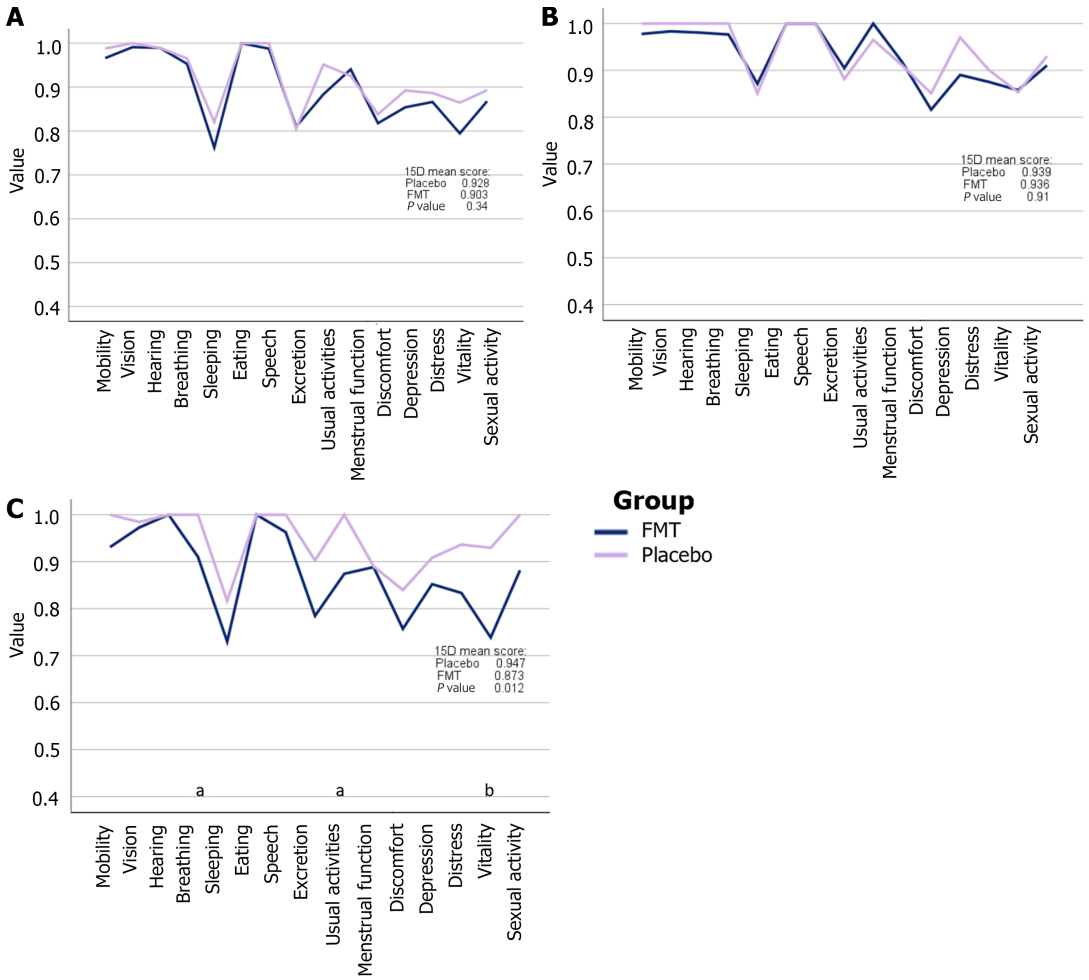


DOI: 10.3748/wjg.v29.i17.2666 **Copyright** ©The Author(s) 2023.

Figure 1 Kaplan-Meier survival curve demonstrating the maintenance of remission defined as fecal calprotectin < 200 μg/g and the clinical Mayo score < 3 or an overt relapse in between the measurement points. A: All patients included in analysis (log rank test *P* = 0.660); B: Subgroup A, *i.e.* the patients with fecal calprotectin < 200 μg/g and clinical Mayo score < 3 at the baseline (*P* = 0.703); C: Subgroup B, *i.e.* the patients with fecal calprotectin ≥ 200 μg/g or the clinical Mayo score ≥ 3 at the baseline (*P* = 0.556). Censored means the end of follow-up without a relapse. FMT: Fecal microbiota transplantation.

Secondary endpoint-blood chemistry and fecal calprotectin

The blood chemistry, complete blood count, liver enzymes, and creatinine and CRP levels were analyzed at four different timepoints. Fecal calprotectin was measured every 2nd mo at six different timepoints. There were no clinically significant changes in any of the blood tests compared to the baseline. All laboratory tests at each timepoint showed no statistically significant differences between the FMT and placebo groups ($P > 0.05$). The blood chemistry and fecal calprotectin values are collectively presented in Supplementary Table 3.



DOI: 10.3748/wjg.v29.i17.2666 **Copyright** ©The Author(s) 2023.

Figure 2 The general quality of life of the complete study group shown according to the 15 dimensions and the mean total score and *P* value as expressed numerically within the picture. A: The total score of the 15 dimensions quality of life questionnaire (15D) profiles at the baseline (n = 48); B: 15D profiles at 12 mo (n = 21); C: 15D profiles at 4 mo (n = 30). [a]$P \leq 0.05$ and [b]$P \leq 0.01$. FMT: Fecal microbiota transplantation; 15D: The total score of the 15 dimensions quality of life questionnaire.

Endoscopic and histologic colitis activity at 12 mo

A colonoscopy was performed at the end of the trial, and pinch biopsies were obtained from all 23 patients who reached the primary endpoint and remained in clinical remission throughout the follow-up period. Endoscopic colitis activity was detected in 2 out of 13 patients in the FMT group and in 2 out of 10 patients in the placebo group. Likewise, mild histological colitis activity was detected in the colon pinch biopsies in 2 out of 13 patients in the FMT group and 2 out of 10 patients in the placebo group, indicating chronic inflammation. Thus, the number of patients who were in endoscopic and histologic remission in the follow-up colonoscopy was 11 out of 13 in the FMT group and 8 out of 10 in the placebo group (χ^2, $P = 0.772$).

Adverse events

A similar number of patients experienced UC activation in the FMT and placebo groups (Figure 1). In addition to colitis activation, other adverse events were recorded in 4 patients in the FMT group and 6 patients in the placebo group.

In the FMT group, the adverse events included fatigue through the follow-up period, gastroenteritis at 8 mo after FMT, constipation at 3 wk after FMT and a diagnosis of primary sclerosing cholangitis. In addition, 1 patient reported fatigue and episodes of atrial fibrillation at the 4-mo timepoint, for which he underwent ablation treatment. This patient subsequently developed pneumonia.

In the placebo group, 1 patient with fibromyalgia reported back pain and colitis symptoms simultaneously. Another patient visited the emergency room 6 mo after the procedure and was diagnosed with mitral valve insufficiency. One patient with spondylarthritis experienced arthralgia during the follow-up. One patient experienced an escalation of bloating after the procedure, and 2 patients experienced a prolonged mild respiratory infection. Possible hospitalizations were monitored in all the participants for 12 mo, but none were attributable to FMT.

DISCUSSION

In this placebo-controlled trial, we examined the effect of a single FMT *via* colonoscopy on the maintenance of remission in UC patients. The primary endpoint was sustained remission over a 12-mo follow-up period. A relapse of UC was regarded as a failure to achieve the primary endpoint. We set the cutoff values to differentiate between remission and relapse to a clinically significant level; thus, a clinical Mayo score above three and fecal calprotectin levels above 200 μg/g were considered to indicate colitis activation. There was no statistically significant difference in the number of patients with a relapse of UC during the follow-up period in the FMT and placebo groups. According to the results, a single FMT *via* colonoscopy was ineffective for maintaining UC in remission.

Previously, the impact of the donor on the outcome of FMT was demonstrated in patients with active UC[13]. Including more than one donor in FMT trials enables comparison between the donors. In this trial, we used three donors. Sustainable remission through the follow-up was achieved by 33.3% of the patients who received FMT from Donor 1, whereas the same was achieved by 62.5% of the patients treated with FMT from Donor 3. However, the number of patients in each group was small, and the differences did not reach statistical significance. Furthermore, the Donor 1 treatment was applied at the beginning of the trial when the inclusion criteria were different, requiring new-onset disease, and consequently the baseline activity markers, fecal calprotectin and clinical Mayo score were higher in the patients of Donor 1 than in the patients of Donor 3. For these reasons, the existence or magnitude of the donor effect could not be proven or disproven.

Studies evaluating FMT for active as well as quiescent UC have been encouraging[13,16], but the present data are not sufficient to justify treating UC patients with FMT in clinical practice. Our goal was to investigate whether manipulation of the gut microbiota with FMT early after UC diagnosis would help in the maintenance of remission and the effect on the course of the disease. When planning this study, we aimed to recruit patients whose UC was diagnosed within 6 mo prior to the study baseline. However, due to slow recruitment, we made a change in the study protocol and started including patients with any duration of the disease. Additionally, another center, Päijät-Häme Central Hospital, joined the study in addition to Helsinki University Hospital. Nevertheless, the recruitment remained slow, and we were only able to recruit 48 of the originally planned 80 patients within a reasonable time.

As a result of the change in the protocol, 31% of the patients fulfilled the initial inclusion criteria and had been diagnosed within the previous 6 mo, of whom 6 patients were in the FMT group and 9 patients were in the placebo group. Coincidentally, the patients with the longest duration of the disease were also randomized into the placebo group, resulting in a statistically significant difference in the duration of disease status between the randomization groups. The groups were similar to each other in all other parameters (Table 1). Patients with biologics were not included in the trial; thus, the participants did not have a history of severe and difficult-to-treat disease.

Previously published randomized, placebo-controlled FMT trials investigating patients with UC have included patients with active colitis or patients who have reached clinical remission after several FMT sessions[15,16,23]. The patients in our study had UC in clinical remission but had not previously received FMT therapy. Between the recruitment and the study baseline, a portion of the patients had elevated calprotectin and clinical Mayo score values without overt colitis symptoms and were included in a subgroup analysis (Table 1). Overall, the population of our study represented UC patients in real-world clinical practice.

As a secondary endpoint, we aimed to investigate the effect of FMT on patient quality of life. We evaluated this outcome with the disease-specific IBDQ questionnaire and with the 15D questionnaire, which measures general health-related quality of life. Both questionnaires measure the quality of life in IBD patients with equal reliability[4]. Interestingly, the placebo group presented higher quality-of-life scores 4 mo after the treatment. This may refer to the extraintestinal influence of the gut microbiota, although the difference between the groups may partly be explained by the longer duration of disease in the placebo group and consequently better adaptation to the fluctuating symptoms of the disease. Indeed, the statistically significant differences concerned vitality, usual activities, and breathing in the 15D questionnaire, while intestinal symptoms did not differ between the groups. Additionally, in the IBDQ questionnaire, the subcategories of emotions and systemic symptoms were statistically significantly better in the placebo group at the 4-mo timepoint. We found disease duration and adaptation to be the most plausible explanation for the observed differences since the subscores of the FMT group increased and the differences between treatment groups disappeared at 12 mo. However, changes in microbiota composition and activity extrapolating to extraintestinal effects should also be addressed in future investigations. Previously, we observed a possible link between microbiota, general mental health, and depression in our FMT studies on IBS and rCDI[8,24].

In line with our previous placebo-controlled FMT trial[8], the reported adverse events in this trial were evenly distributed between groups. There were no severe adverse events attributable to FMT, replicating previous reports stating that FMT was safe when performed with high standards[25]. Even as FMT appears safe in randomized controlled trials[8,13,15] and evidence of long-term safety appears encouraging[24], we find it highly important to continue gathering safety data on FMT from randomized trials as well as collecting registry data from clinical practice. The interindividual variability of donors is high concerning microbiota profiles as well as other characteristics, and therefore the

scientific community and clinicians performing FMT for CDI need to stay alert for infectious complications and for possible rare short-term and long-term adverse effects of FMT[26].

Our study had some limitations. First, the number of studied patients remained rather low, with only 48 patients in total due to slow recruitment. Second, after patients experienced a relapse of UC, further data were not recorded. This decreased the amount of obtained data and complicated the comparison of secondary endpoints between the groups, as there were fewer cases left for the analysis with each successive time point. However, after a relapse, some of the patients were given corticosteroids or the medication was changed, which would have misrepresented the true effects of FMT or placebo. Another drawback was that the patients in the placebo group had UC for a longer duration than those in the FMT group and were likely in a more stable phase of the disease. This may have impacted the results of the primary endpoint as well as secondary endpoints; however, there were no statistically significant correlations between the duration of disease and the time to relapse or quality of life in either study group.

Our study also had clear advantages. Its blinded placebo-controlled design is a definite strength. We applied an autologous placebo, which assures very reliable blinding, and the same method has yielded valid results in FMT trials for rCDI[27] and in other conditions such as IBS[8] and Crohn's disease[28]. However, it must be noted that the composition of the fecal microbiota may change when it is exposed to oxygen, and in the case of patient samples, the duration of oxygen exposure could not be carefully controlled, unlike for the donor samples, which were prepared and frozen within 2 h of defecation. The advantage of applying an autologous placebo is that it assures very reliable blinding. Other forms of placebo may be more easily detected by the patient or treating personnel. Another advantage of our study is the sufficiently long follow-up time, which enabled the treatment effect durability to be monitored.

Unlike in rCDI, clinical efficacy may not be achieved in UC by just a single FMT, possibly due to difficulties in modulating the microbiota in the longer term by only one FMT dose. Repeated FMT treatments could possibly enhance efficacy, as shown by Sood *et al*[16] where repeated FMT treatments were associated with maintenance of remission. In that trial, the study population was selected from responders to FMT given for induction of remission, and bimonthly colonoscopic FMTs for 1 year maintained UC in remission better than placebo. Thus, the positive effects of FMT may be maintained by repeated treatments. Repeated FMT treatments have also shown promising results in the induction of remission of active UC[13-15]. Engraftment of the transplanted microbes may be more difficult in an active colitis environment than in a state of remission. From this perspective, repeated FMT can be more justified in active disease.

Moreover, FMT may also exert its efficacy *via* host-derived biomolecules that exert immunoregulatory action or induce transcriptional changes in the affected intestinal epithelium. Action by nonpersisting biomolecules could also explain why multiple FMTs are needed for the induction of remission. On the other hand, if microbiota modulation is considered critical, a single FMT by colonoscopy with our protocol (applying 30 g of donor feces) can induce prolonged microbial engraftment in rCDI patients as well as in IBS patients[6,8].

To our knowledge, our trial is the first controlled trial to investigate a single FMT for the maintenance of remission in UC patients. In future FMT studies on the maintenance of UC remission, repeated treatments seem reasonable. However, other methods to enhance and prolong the effects should also be considered. For example, combining a dietary intervention may improve results and prolong remission [29]. In one recent trial, a dietary intervention resulted in a superior effect on the induction of remission in UC patients compared to FMT[30].

The optimization of donor selection could possibly improve outcomes even with a single FMT given in remission. Additionally, conditions for the engraftment and functioning of beneficial microbiota may be important, particularly when FMT is given to patients in remission. Diet has a great impact on gut microbiota and is likely an important factor affecting the survival and function of transplanted microbes [31]. We suggest prompt documenting of the diet in future FMT studies. Additionally, the combination of FMT with dietary modulation should be addressed in future studies[29,30].

There are many open questions to be answered before we can determine whether FMT may be applied for the maintenance of remission in UC. More research is needed to define the optimal donor characteristics, patient population, and timing for FMT. Additionally, the best route of FMT administration remains undefined. While the colonoscopic route has shown promise[16], FMT with capsules may be considered when high numbers of patients need to be treated[23]. Finally, we do not yet know which stool components are responsible for the positive effects of FMT, and there is much room for future innovative research.

CONCLUSION

In conclusion, there were no statistically significant differences in the number of UC relapses after a single FMT or placebo treatment; therefore, the main outcome of our study was negative. Our results do not support applying a single FMT for the maintenance of UC remission. However, these results must

be interpreted with caution due to the small sample size, and larger studies are warranted.

ARTICLE HIGHLIGHTS

Research background

Ulcerative colitis (UC) is associated with altered gut microbiota. The pathophysiology of UC is thought to involve an altered and exaggerated inflammatory response to commensal bacteria. Fecal microbiota transplantation has yielded good results in the induction of UC remission.

Research motivation

Despite the development in medications for UC, some patients do not respond sufficiently to current treatment options and new treatment modalities are needed. Modulation of gut microbiota *via* fecal microbial transplantation (FMT) is a potential new treatment option for UC patients.

Research objectives

The goal of this trial was to gather information of the role of gut microbiota in maintenance of remission in UC patients, and the aim was to investigate FMT for the maintenance of UC remission.

Research methods

Forty-eight patients with quiescent UC were randomized 1:1 to receive a single FMT *via* colonoscopy or a placebo made from the patient's own stool. The patients were followed for 12 mo, and colitis symptoms were measured as well as fecal calprotectin. As secondary endpoints, quality of life, blood chemistry, and endoscopic findings at 12 mo were measured.

Research results

UC remission was maintained by 13 out of 24 (54%) patients in the FMT group and by 10 out of 24 (41%) patients in the placebo group (log-rank test, $P = 0.660$). The quality of life was lower in the FMT group at 4 mo after FMT as compared to the placebo group ($P = 0.017$). There were no differences in blood chemistry, fecal calprotectin, or endoscopic findings at 12 mo between the groups.

Research conclusions

There were no significant differences in the maintenance of remission between the groups during the 12-mo follow-up. Thus, our results do not support the use of a single-dose FMT for the maintenance of remission in UC patients.

Research perspectives

Many open questions need to be answered before we can determine whether FMT may be applied for the maintenance of remission in UC. We do not yet know which stool components distribute the positive effects of FMT. More research is needed to define the optimal donor characteristics, patient population, and the optimal number and timing of FMT treatments.

ACKNOWLEDGEMENTS

Study nurses Pirkko Tuukkala (Helsinki University Hospital) and Virve Liukkonen (Päijät-Häme Central Hospital) are acknowledged for their contribution to the study with a high level of expertise and commitment.

FOOTNOTES

Author contributions: Lahtinen P wrote the paper; Lahtinen P and Bergman P analyzed the data and designed the figures; Arkkila P, Satokari R, and Mattila E planned the study; Arkkila P, Satokari R, Lahtinen P, and Tillonen J executed the study and collected most of the data; Arkkila P, Lahtinen P, and Tillonen J assessed the colonoscopies; Satokari R administered fecal banking and FMT treatments; Jalanka J, Mattila E, and Tillonen J provided expertise in the study design and components of the article; All authors contributed to drafting the article and revised the manuscript for important intellectual content; All authors had access to the study data and reviewed and approved the final manuscript.

Supported by Academy of Finland (Reetta Satokari), No. 323156; Sigrid Juselius Foundation and University of Helsinki (A Three-year Grant); The Competitive State Research Financing (Perttu Lahtinen), No. 200230042; The Ella and Georg Ehrnrooth Foundation (Perttu Arkkila).

Institutional review board statement: The study was reviewed and approved by the Helsinki University Hospital Institutional Review Board, No. 29/13/03/01/2014.

Clinical trial registration statement: This study is registered at ClinicalTrials.gov. The registration identification number is NCT03561532.

Informed consent statement: All study participants or their legal guardian provided informed written consent about personal and medical data collection prior to study enrolment.

Conflict-of-interest statement: Dr. Lahtinen reports grants from The Competetive State Research Financing, grants from Academy of Finland, grants from Sigrid Juselius Foundation, grants from University of Helsinki, grants from Ella and Georg Ehrnrooth Foundation, during the conduct of the study.

Data sharing statement: The datasets generated and analyzed during the current study are not publicly available because individual privacy could be compromised. However, they are available from the corresponding author on reasonable request.

CONSORT 2010 statement: The authors have read the CONSORT 2010 statement, and the manuscript was prepared and revised according to the CONSORT 2010 statement.

Open-Access: This article is an open-access article that was selected by an in-house editor and fully peer-reviewed by external reviewers. It is distributed in accordance with the Creative Commons Attribution NonCommercial (CC BY-NC 4.0) license, which permits others to distribute, remix, adapt, build upon this work non-commercially, and license their derivative works on different terms, provided the original work is properly cited and the use is non-commercial. See: https://creativecommons.org/Licenses/by-nc/4.0/

Country/Territory of origin: Finland

ORCID number: Perttu Lahtinen 0000-0001-6430-4642; Jonna Jalanka 0000-0002-3847-8136; Eero Mattila 0000-0001-9787-7674; Jyrki Tillonen 0000-0002-5661-9385; Paula Bergman 0000-0003-4672-2554; Reetta Satokari 0000-0002-4258-3414; Perttu Arkkila 0000-0003-2194-0424.

S-Editor: Fan JR
L-Editor: Filipodia
P-Editor: Cai YX

REFERENCES

1 **Ungaro R**, Mehandru S, Allen PB, Peyrin-Biroulet L, Colombel JF. Ulcerative colitis. *Lancet* 2017; **389**: 1756-1770 [PMID: 27914657 DOI: 10.1016/S0140-6736(16)32126-2]
2 **Jussila A**, Virta LJ, Kautiainen H, Rekiaro M, Nieminen U, Färkkilä MA. Increasing incidence of inflammatory bowel diseases between 2000 and 2007: a nationwide register study in Finland. *Inflamm Bowel Dis* 2012; **18**: 555-561 [PMID: 21425214 DOI: 10.1002/ibd.21695]
3 **Lamb CA**, Kennedy NA, Raine T, Hendy PA, Smith PJ, Limdi JK, Hayee B, Lomer MCE, Parkes GC, Selinger C, Barrett KJ, Davies RJ, Bennett C, Gittens S, Dunlop MG, Faiz O, Fraser A, Garrick V, Johnston PD, Parkes M, Sanderson J, Terry H; IBD guidelines eDelphi consensus group, Gaya DR, Iqbal TH, Taylor SA, Smith M, Brookes M, Hansen R, Hawthorne AB. British Society of Gastroenterology consensus guidelines on the management of inflammatory bowel disease in adults. *Gut* 2019; **68**: s1-s106 [PMID: 31562236 DOI: 10.1136/gutjnl-2019-318484]
4 **Haapamäki J**, Roine RP, Sintonen H, Turunen U, Färkkilä MA, Arkkila PE. Health-related quality of life in inflammatory bowel disease measured with the generic 15D instrument. *Qual Life Res* 2010; **19**: 919-928 [PMID: 20361263 DOI: 10.1007/s11136-010-9650-4]
5 **Manichanh C**, Borruel N, Casellas F, Guarner F. The gut microbiota in IBD. *Nat Rev Gastroenterol Hepatol* 2012; **9**: 599-608 [PMID: 22907164 DOI: 10.1038/nrgastro.2012.152]
6 **Jalanka J**, Mattila E, Jouhten H, Hartman J, de Vos WM, Arkkila P, Satokari R. Long-term effects on luminal and mucosal microbiota and commonly acquired taxa in faecal microbiota transplantation for recurrent Clostridium difficile infection. *BMC Med* 2016; **14**: 155 [PMID: 27724956 DOI: 10.1186/s12916-016-0698-z]
7 **Fuentes S**, van Nood E, Tims S, Heikamp-de Jong I, ter Braak CJ, Keller JJ, Zoetendal EG, de Vos WM. Reset of a critically disturbed microbial ecosystem: faecal transplant in recurrent Clostridium difficile infection. *ISME J* 2014; **8**: 1621-1633 [PMID: 24577353 DOI: 10.1038/ismej.2014.13]
8 **Lahtinen P**, Jalanka J, Hartikainen A, Mattila E, Hillilä M, Punkkinen J, Koskenpato J, Anttila VJ, Tillonen J, Satokari R, Arkkila P. Randomised clinical trial: faecal microbiota transplantation versus autologous placebo administered *via* colonoscopy in irritable bowel syndrome. *Aliment Pharmacol Ther* 2020; **51**: 1321-1331 [PMID: 32343000 DOI: 10.1111/apt.15740]
9 **Cammarota G**, Ianiro G, Tilg H, Rajilić-Stojanović M, Kump P, Satokari R, Sokol H, Arkkila P, Pintus C, Hart A, Segal J, Aloi M, Masucci L, Molinaro A, Scaldaferri F, Gasbarrini G, Lopez-Sanroman A, Link A, de Groot P, de Vos WM,

Högenauer C, Malfertheiner P, Mattila E, Milosavljević T, Nieuwdorp M, Sanguinetti M, Simren M, Gasbarrini A; European FMT Working Group. European consensus conference on faecal microbiota transplantation in clinical practice. *Gut* 2017; **66**: 569-580 [PMID: 28087657 DOI: 10.1136/gutjnl-2016-313017]

10 **Satokari R**, Mattila E, Kainulainen V, Arkkila PE. Simple faecal preparation and efficacy of frozen inoculum in faecal microbiota transplantation for recurrent Clostridium difficile infection--an observational cohort study. *Aliment Pharmacol Ther* 2015; **41**: 46-53 [PMID: 25355279 DOI: 10.1111/apt.13009]

11 **van Nood E**, Vrieze A, Nieuwdorp M, Fuentes S, Zoetendal EG, de Vos WM, Visser CE, Kuijper EJ, Bartelsman JF, Tijssen JG, Speelman P, Dijkgraaf MG, Keller JJ. Duodenal infusion of donor feces for recurrent Clostridium difficile. *N Engl J Med* 2013; **368**: 407-415 [PMID: 23323867 DOI: 10.1056/NEJMoa1205037]

12 **Rossen NG**, Fuentes S, van der Spek MJ, Tijssen JG, Hartman JH, Duflou A, Löwenberg M, van den Brink GR, Mathus-Vliegen EM, de Vos WM, Zoetendal EG, D'Haens GR, Ponsioen CY. Findings From a Randomized Controlled Trial of Fecal Transplantation for Patients With Ulcerative Colitis. *Gastroenterology* 2015; **149**: 110-118.e4 [PMID: 25836986 DOI: 10.1053/j.gastro.2015.03.045]

13 **Moayyedi P**, Surette MG, Kim PT, Libertucci J, Wolfe M, Onischi C, Armstrong D, Marshall JK, Kassam Z, Reinisch W, Lee CH. Fecal Microbiota Transplantation Induces Remission in Patients With Active Ulcerative Colitis in a Randomized Controlled Trial. *Gastroenterology* 2015; **149**: 102-109.e6 [PMID: 25857665 DOI: 10.1053/j.gastro.2015.04.001]

14 **Paramsothy S**, Kamm MA, Kaakoush NO, Walsh AJ, van den Bogaerde J, Samuel D, Leong RWL, Connor S, Ng W, Paramsothy R, Xuan W, Lin E, Mitchell HM, Borody TJ. Multidonor intensive faecal microbiota transplantation for active ulcerative colitis: a randomised placebo-controlled trial. *Lancet* 2017; **389**: 1218-1228 [PMID: 28214091 DOI: 10.1016/S0140-6736(17)30182-4]

15 **Costello SP**, Hughes PA, Waters O, Bryant RV, Vincent AD, Blatchford P, Katsikeros R, Makanyanga J, Campaniello MA, Mavrangelos C, Rosewarne CP, Bickley C, Peters C, Schoeman MN, Conlon MA, Roberts-Thomson IC, Andrews JM. Effect of Fecal Microbiota Transplantation on 8-Week Remission in Patients With Ulcerative Colitis: A Randomized Clinical Trial. *JAMA* 2019; **321**: 156-164 [PMID: 30644982 DOI: 10.1001/jama.2018.20046]

16 **Sood A**, Mahajan R, Singh A, Midha V, Mehta V, Narang V, Singh T, Singh Pannu A. Role of Faecal Microbiota Transplantation for Maintenance of Remission in Patients With Ulcerative Colitis: A Pilot Study. *J Crohns Colitis* 2019; **13**: 1311-1317 [PMID: 30873549 DOI: 10.1093/ecco-jcc/jjz060]

17 **Lewis JD**, Chuai S, Nessel L, Lichtenstein GR, Aberra FN, Ellenberg JH. Use of the noninvasive components of the Mayo score to assess clinical response in ulcerative colitis. *Inflamm Bowel Dis* 2008; **14**: 1660-1666 [PMID: 18623174 DOI: 10.1002/ibd.20520]

18 **Feagan BG**, Macdonald JK. Oral 5-aminosalicylic acid for maintenance of remission in ulcerative colitis. *Cochrane Database Syst Rev* 2012; **10**: CD000544 [PMID: 23076890 DOI: 10.1002/14651858.CD000544.pub3]

19 **Chow SC**. Sample Size Calculations in Clinical Research. 2nd Ed: Chapman & Hall/CRC Biostatistics Series, 2008: 52

20 **D'Haens G**, Sandborn WJ, Feagan BG, Geboes K, Hanauer SB, Irvine EJ, Lémann M, Marteau P, Rutgeerts P, Schölmerich J, Sutherland LR. A review of activity indices and efficacy end points for clinical trials of medical therapy in adults with ulcerative colitis. *Gastroenterology* 2007; **132**: 763-786 [PMID: 17258735 DOI: 10.1053/j.gastro.2006.12.038]

21 **Alanne S**, Roine RP, Räsänen P, Vainiola T, Sintonen H. Estimating the minimum important change in the 15D scores. *Qual Life Res* 2015; **24**: 599-606 [PMID: 25145637 DOI: 10.1007/s11136-014-0787-4]

22 **Guyatt G**, Mitchell A, Irvine EJ, Singer J, Williams N, Goodacre R, Tompkins C. A new measure of health status for clinical trials in inflammatory bowel disease. *Gastroenterology* 1989; **96**: 804-810 [PMID: 2644154]

23 **Haifer C**, Paramsothy S, Kaakoush NO, Saikal A, Ghaly S, Yang T, Luu LDW, Borody TJ, Leong RW. Lyophilised oral faecal microbiota transplantation for ulcerative colitis (LOTUS): a randomised, double-blind, placebo-controlled trial. *Lancet Gastroenterol Hepatol* 2022; **7**: 141-151 [PMID: 34863330 DOI: 10.1016/S2468-1253(21)00400-3]

24 **Jalanka J**, Hillamaa A, Satokari R, Mattila E, Anttila VJ, Arkkila P. The long-term effects of faecal microbiota transplantation for gastrointestinal symptoms and general health in patients with recurrent Clostridium difficile infection. *Aliment Pharmacol Ther* 2018; **47**: 371-379 [PMID: 29226561 DOI: 10.1111/apt.14443]

25 **Baxter M**, Colville A. Adverse events in faecal microbiota transplant: a review of the literature. *J Hosp Infect* 2016; **92**: 117-127 [PMID: 26803556 DOI: 10.1016/j.jhin.2015.10.024]

26 **Osman M**, Budree S, Kelly CR, Panchal P, Allegretti JR, Kassam Z; OpenBiome Collaborators. Effectiveness and Safety of Fecal Microbiota Transplantation for Clostridioides Difficile Infection: Results From a 5344-Patient Cohort Study. *Gastroenterology* 2022; **163**: 319-322 [PMID: 35398345 DOI: 10.1053/j.gastro.2022.03.051]

27 **Kelly CR**, Khoruts A, Staley C, Sadowsky MJ, Abd M, Alani M, Bakow B, Curran P, McKenney J, Tisch A, Reinert SE, Machan JT, Brandt LJ. Effect of Fecal Microbiota Transplantation on Recurrence in Multiply Recurrent Clostridium difficile Infection: A Randomized Trial. *Ann Intern Med* 2016; **165**: 609-616 [PMID: 27547925 DOI: 10.7326/M16-0271]

28 **Sokol H**, Landman C, Seksik P, Berard L, Montil M, Nion-Larmurier I, Bourrier A, Le Gall G, Lalande V, De Rougemont A, Kirchgesner J, Daguenel A, Cachanado M, Rousseau A, Drouet É, Rosenzwajg M, Hagege H, Dray X, Klatzman D, Marteau P; Saint-Antoine IBD Network, Beaugerie L, Simon T. Fecal microbiota transplantation to maintain remission in Crohn's disease: a pilot randomized controlled study. *Microbiome* 2020; **8**: 12 [PMID: 32014035 DOI: 10.1186/s40168-020-0792-5]

29 **Kedia S**, Virmani S, K Vuyyuru S, Kumar P, Kante B, Sahu P, Kaushal K, Farooqui M, Singh M, Verma M, Bajaj A, Markandey M, Sachdeva K, Das P, Makharia GK, Ahuja V. Faecal microbiota transplantation with anti-inflammatory diet (FMT-AID) followed by anti-inflammatory diet alone is effective in inducing and maintaining remission over 1 year in mild to moderate ulcerative colitis: a randomised controlled trial. *Gut* 2022; **71**: 2401-2413 [PMID: 35973787 DOI: 10.1136/gutjnl-2022-327811]

30 **Sarbagili Shabat C**, Scaldaferri F, Zittan E, Hirsch A, Mentella MC, Musca T, Cohen NA, Ron Y, Fliss Isakov N, Pfeffer J, Yaakov M, Fanali C, Turchini L, Masucci L, Quaranta G, Kolonimos N, Godneva A, Weinberger A, Kopylov U, Levine A, Maharshak N. Use of Faecal Transplantation with a Novel Diet for Mild to Moderate Active Ulcerative Colitis: The CRAFT UC Randomised Controlled Trial. *J Crohns Colitis* 2022; **16**: 369-378 [PMID: 34514495 DOI: 10.1093/ecco-jcc/jjab165]

31 **Zmora N**, Suez J, Elinav E. You are what you eat: diet, health and the gut microbiota. *Nat Rev Gastroenterol Hepatol* 2019; **16**: 35-56 [PMID: 30262901 DOI: 10.1038/s41575-018-0061-2]

World Journal of Gastroenterology

Submit a Manuscript: https://www.f6publishing.com

World J Gastroenterol 2023 May 7; 29(17): 2679-2700

DOI: 10.3748/wjg.v29.i17.2679

ISSN 1007-9327 (print) ISSN 2219-2840 (online)

SYSTEMATIC REVIEWS

Different types of fruit intake and colorectal cancer risk: A meta-analysis of observational studies

Zhen-Ying Wu, Jia-Li Chen, Han Li, Ke Su, Yun-Wei Han

Specialty type: Oncology

Provenance and peer review: Unsolicited article; Externally peer reviewed.

Peer-review model: Single blind

Peer-review report's scientific quality classification

Grade A (Excellent): 0
Grade B (Very good): B
Grade C (Good): C, C, C
Grade D (Fair): D
Grade E (Poor): 0

P-Reviewer: Chang YC, Taiwan; Mohamed SY, Egypt; Parthasarathy K, India; Rather AA, India

Received: December 19, 2022
Peer-review started: December 19, 2022
First decision: February 8, 2023
Revised: February 24, 2023
Accepted: March 20, 2023
Article in press: March 20, 2023
Published online: May 7, 2023

Zhen-Ying Wu, Jia-Li Chen, Han Li, Ke Su, Yun-Wei Han, Department of Oncology, The Affiliated Hospital of Southwest Medical University, Luzhou 646099, Sichuan Province, China

Corresponding author: Yun-Wei Han, MD, PhD, Professor, Researcher, Department of Oncology, The Affiliated Hospital of Southwest Medical University, No. 25 Taiping Street, Jiangyang District, Luzhou 646099, Sichuan Province, China. lanpaoxiansheng@126.com

Abstract

BACKGROUND

Multiple studies investigating the relationship between intake of different types of fruit and colorectal cancer (CRC) risk have yielded inconsistent results.

AIM

To perform a meta-analysis of existing studies to assess the association between the intake of different kinds of fruit and the incidence of CRC.

METHODS

We searched online literature databases including PubMed, Embase, WOS, and Cochrane Library for relevant articles available up to August 2022. With data extracted from observational studies, odds ratios (ORs) with 95% confidence intervals (CIs) were assessed using random-effects models. A funnel plot and Egger's test were used to determine publication bias. Furthermore, subgroup analysis and dose-response analysis were performed. All analyses were conducted using R (version 4.1.3).

RESULTS

Twenty-four eligible studies involving 1068158 participants were included in this review. The meta-analysis showed that compared to a low intake, a higher intake of citrus, apples, watermelon, and kiwi reduced the risk of CRC by 9% [OR (95%CI) = 0.91 (0.85-0.97)], 25% [OR (95%CI) = 0.75 (0.66-0.85)], 26% [OR (95%CI) = 0.74 (0.58-0.94)], 13% [OR (95%CI) = 0.87 (0.78-0.96)], respectively. No significant association was observed between the intake of other types of fruit and the risk of CRC. In the dose-response analysis, a nonlinear association was found [R (95%CI) = -0.0031 (-0.0047 to -0.0014)] between citrus intake and CRC risk (P < 0.001), with the risk minimized around 120 g/d (OR = 0.85), while no significant dose-response correlation was observed after continued increase in intake.

CONCLUSION

We found that a higher intake of citrus, apples, watermelon, and kiwi was

negatively associated with the risk of CRC, while the intake of other types of fruits were not significantly associated with CRC. Citrus intake showed a non-linear dose-response relationship with the risk of CRC. This meta-analysis provides further evidence that a higher intake of specific types of fruit is effective in preventing the occurrence of CRC.

Key Words: Colorectal cancer; Fruit; Dose; Systematic review; Meta-analysis

©The Author(s) 2023. Published by Baishideng Publishing Group Inc. All rights reserved.

Core Tip: In this study, we summarized and analyzed existing studies on the association between the intake of different types of fruit and the risk of colorectal cancer (CRC). Some specific types of fruit, such as citrus and apples, were found to reduce the incidence of CRC. We also found a nonlinear association between citrus intake and CRC risk in the dose-response analysis. Finally, this study proposed that people should change their diets to lower the risk of CRC, thereby easing the heavy economic burden of cancer worldwide.

Citation: Wu ZY, Chen JL, Li H, Su K, Han YW. Different types of fruit intake and colorectal cancer risk: A meta-analysis of observational studies. *World J Gastroenterol* 2023; 29(17): 2679-2700
URL: https://www.wjgnet.com/1007-9327/full/v29/i17/2679.htm
DOI: https://dx.doi.org/10.3748/wjg.v29.i17.2679

INTRODUCTION

As the third most common cancer, colorectal cancer (CRC) is the third leading cause of cancer death in both men and women, as well as the second leading cause of cancer death in the United States. when men and women are added together[1]. From 2000-2002 to 2014-2016, the incidence of CRC increased by nearly 15% among adults aged 40 to 49 years[2]. The prognosis of CRC varies which mainly depends on the cancer stage, with a 5-year survival rate of about 90% for stage I patients and only 0%-10% for stage IV patients, making the prevention of cancer of great potential and value.

Important risk factors for early-onset CRC include hyperlipidemia, obesity, alcohol consumption and a history of CRC in first-degree relatives[3], of which dietary habits are modifiable. Up to now, various phytochemicals with the potential to prevent cancer have been found in fruits, such as polysaccharides (modified apple polysaccharides, MAP), resveratrol, and flavonoids[4]. MAP inhibits the binding of galectin-3 to its ligand, which is considered to be the promoter of the inflammatory response[5-7], and this may be part of the mechanism by which MAP promotes apoptosis and prevents tumorigenesis[8]. As suggested by Liu *et al*[9], resveratrol regulates PTEN/PI3K/Akt and Wnt/β-catenin signaling pathways, respectively, and thus exhibits growth inhibitory effects in human colon cancer cells. Anticancer properties of flavonoids include modification or inactivation of enzymes that activate or detoxify carcinogens, free radical scavenging, inhibition of transcription factor induction (*e.g.*, activator protein-1 activity), and induction of apoptosis[10]. Epidemiological studies have also highlighted the protective effect of chemicals present in plants and fruits on the risk of CRC[11-14]. For example, data from Jordan and Italy have shown that high intake of flavonoids can reduce CRC risk. Moreover, a considerable number of studies have demonstrated the association between higher intake of fruits and vegetables and lower mortality[15]. However, results from prospective cohorts began to show nonexistent or weak associations[16,17], and a pooled analysis of 14 studies[18] also showed a weak association. Wang *et al*[19] concluded that mortality was not further reduced in those who consumed five servings of fruits and vegetables daily. A meta-analysis showed that increased intake of vegetables, but not fruits, reduced the risk of liver cancer[20]. This finding was also questioned by a large prospective study[21]. Certain types of fruit may be more strongly associated with cancer risk compared with others due to their particular chemical composition and underlying molecular mechanisms, which may be hidden in epidemiological studies. Here, we systematically reviewed the existing evidence and explored potential sources of heterogeneity between study results and whether study results differ by gender, region, and tumor location in order to elucidate the association between intake of different types of fruits and CRC risk.

MATERIALS AND METHODS

The effect of different types of fruit intake on the risk of CRC was reported in this study according to the

Preferred Reporting Items for Systematic Reviews and meta-analyses (PRISMA) statement[22], and it was previously registered with Prospero (study number: CRD42022354620).

Search strategy

Two researchers (Zhen-Ying Wu and Jia-Li Chen) independently conducted a computerized literature search of PubMed, Cochrane, EMBASE, and Web of Science databases until August 2022 for literature on the association of different types of fruit consumption with CRC risk. Studies were identified with the following medical subject heading (MeSH) terms or keywords: (1) Fruit, berry, and plant; (2) cancer, neoplasm, colorectal tumor, CRC, and colorectal neoplasm; and (3) case-control, cohort, and prospective. Titles, abstracts and citations were exported to Endnote 20. The database search strategy is presented in Supplementary Table 1.

Study selection

Two authors (Zhen-Ying Wu and Jia-Li Chen) independently evaluated the titles and abstracts of potentially eligible studies based on the following inclusion criteria: (1) Original articles; (2) human participants; (3) case-control or cohort design; and (4) studies examining the association between intake of different types of fruit and CRC risk. All full-text articles meeting the inclusion criteria were collected. The following exclusion criteria were applied: (1) Articles with confounding of fruits or other food sources; (2) no specific indication of fruit type; (3) no corresponding 95% confidence interval (95%CI) for the relative risk (RR), odds ratio (OR), or hazard ratio (HR) for estimating the highest to lowest levels of fruit consumption; and (4) systematic reviews, meta-analyses, and reviews. Differences between reviewers were resolved through discussion.

Data extraction

For each included potential study, selection evaluation, data extraction and quality assessment were performed independently by two researchers. We extracted the following data from the included studies: The surname of the first author, study area and design, year of publication, sample size (number of cases and controls; cohort size and incident cases), age, follow-up time of the cohort studies, dietary assessment methods, comparison of exposure levels, OR/RR/HR estimates corresponding to fruit intake, and 95%CIs for the highest and lowest fruit intake. We extracted the estimation models that adjusted the most for confounding factors when multiple estimates were reported in the article. If there were independent risk estimates for men and women in a study, or risk estimates for cancers at different sites such as the colon and rectum, we treated them as separate studies.

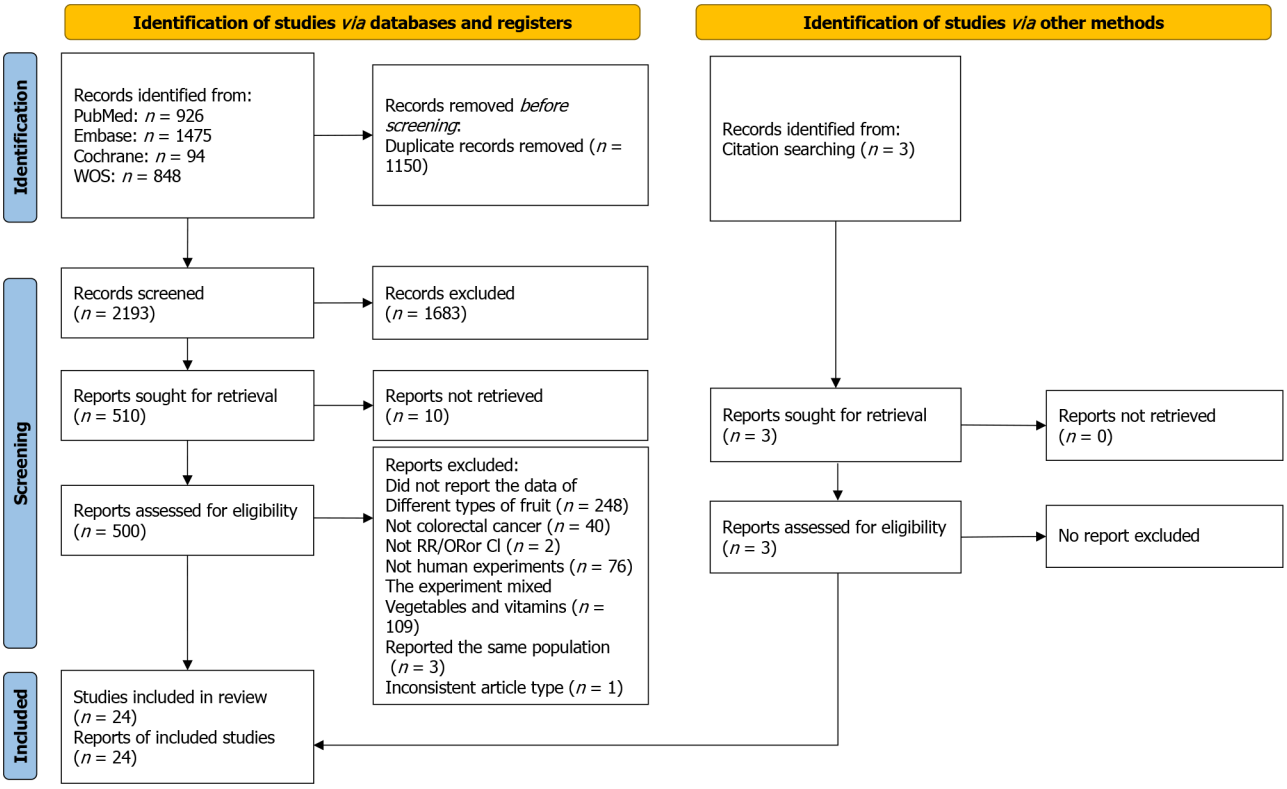
The number of cases and person-years or non-cases for each category of data are required to calculate the slope of the dose-response curve[23]. With citrus intake in each study divided into at least three groups, we took the mean or median consumption under each category and assigned it to the corresponding RR. The midpoint of the upper and lower boundaries was used as the dose for the corresponding category if the study only reported interval ranges for citrus consumption[24]. When the range of intake was unlimited, we assumed the same level as the adjacent category[25]. For instance, the median for the lowest group was 0, while the median for the highest group was 1.5 times the lower limit for that group. For most studies in the meta-analysis, we used 80 g/serving to calculate intake if the study reported intake in servings[26]. Discrepancies between researchers on included studies were resolved through discussion or consultation with the third author.

Assessment of study quality

We assessed the quality of included studies and their potential risk of bias using the Risk of Bias In Non-randomized Studies of Interventions (ROBINS-I) tool[27]. This assessment tool contains seven domains covering pre-intervention (Bias due to confounding, Bias due to selection of participants), at intervention (Bias in classification of interventions) and post-intervention (Bias due to deviations from intended interventions, Bias due to missing data, Bias in measurement of outcomes and Bias in selection of the reported result). The categories for risk of bias judgements are "low risk", "moderate risk", "serious risk", "critical risk", and "no information". The risk of bias was determined independently by two reviewers, and their disagreements were resolved by mutual consensus.

Statistical methods

The meta-analysis was conducted by comparing the risk of CRC reported in the highest and lowest fruit intake groups. Considering a risk of less than 10% for CRC and a small OR, the RR/HR we calculated was approximately equal to the OR[28]. For the overall estimation, the meta-analysis was performed according to the case where all types of rates were OR. The heterogeneity of the results across studies was evaluated with the I^2 test. Since observational study results are inevitably affected by various sources of heterogeneity such as statistical heterogeneity and conceptual heterogeneity in the real world, we followed the Cochrane Handbook for Systematic Reviews of Interventions and used combined results from random-effects models. The effect of individual studies on risk estimates was investigated through sensitivity analyses by omitting each study in turn. We also conducted sensitivity analyses based on quality assessment to improve the reliability of the results. When an outcome indicator was



DOI: 10.3748/wjg.v29.i17.2679 **Copyright** ©The Author(s) 2023.

Figure 1 PRISMA flow chart of literature search and selection. RR: Relative risk; OR: Odds ratio; CI: Confidence intervals.

reported in more than 10 included studies, publication bias analysis was conducted using Egger's linear regression test and funnel plots. Significant publication bias was considered to exist if the intercept of the Egger's regression line deviated from zero and the *P* value < 0.05. In the present study, we performed pre-specified subgroup analyses based on study design type, location of CRC occurrence, geographic region, and gender. To check for possible non-linear relationships, we also carried out pre-specified dose-response analyses by calculating restrictive three-times sample bars for each study for three or more exposure categories[25]. All analyses were performed by R (version 4.1.3), with two-tailed *P* < 0.05 considered statistically significant.

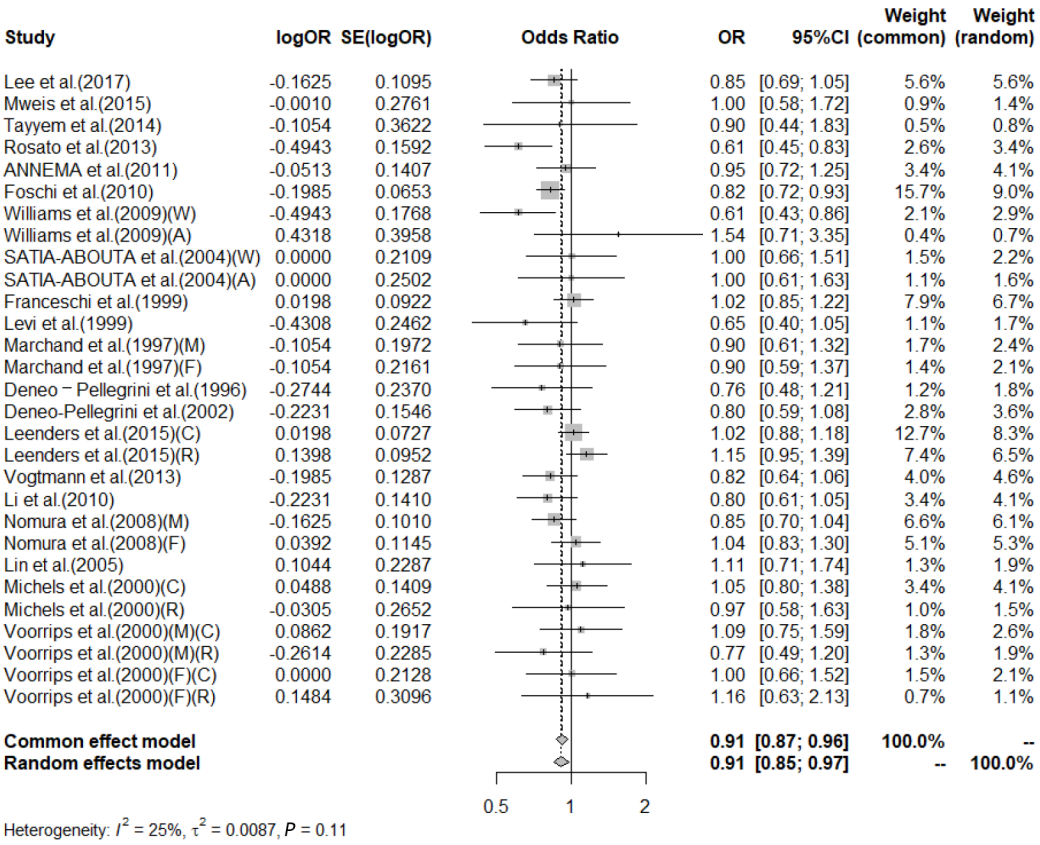
RESULTS

Included studies

A total of 3343 articles were obtained by the initial literature screening, and after removing 1150 duplicate articles, we identified 2193 articles that were potentially eligible for review. Then 1683 irrelevant entries were eliminated by screening titles and abstracts. Of the remaining 510 articles, 486 were eliminated according to the exclusion criteria. In particular, three studies[29-31] were all from the same study, so only the one with the most complete data was included[29]. Another two studies[32,33] were also from the same study, and similarly the one with the most complete data was included[32]. The results of Tuyns *et al*[34] and Tajima *et al*[35] were removed due to lack of OR and corresponding 95%CI for citrus intake and CRC risk. Three additional[36-38] studies that met the inclusion criteria were identified by manually searching the reference list. The 24 articles were ultimately included in the current meta-analysis[29,32,36-57]. The flow chart for study selection is presented in Figure 1.

Characteristics of the studies

Detailed characteristics of the studies investigating the intake of different types of fruit and CRC risk are shown in Table 1. The final analysis included 16 case-control studies[29,32,37-39,41-49,56,57] and 8 cohort studies[36,40,50-55]. The articles were published between 1996 and 2017, with a total of 1068158 participants aged under 80 years. One study involved only men[50] and one study involved only women[55]. Seven articles distinguished between tumor locations such as rectum and colon (even into proximal and distal colon cancer)[29,38,39,44,50,53,54]. Five articles conducted the research with the classification of gender[36,38,39,52,56]. As for the regional distribution of the study population, nine studies were conducted in Europe[29,32,37,40,43,45,47,49,53], two studies in South America[38,57],



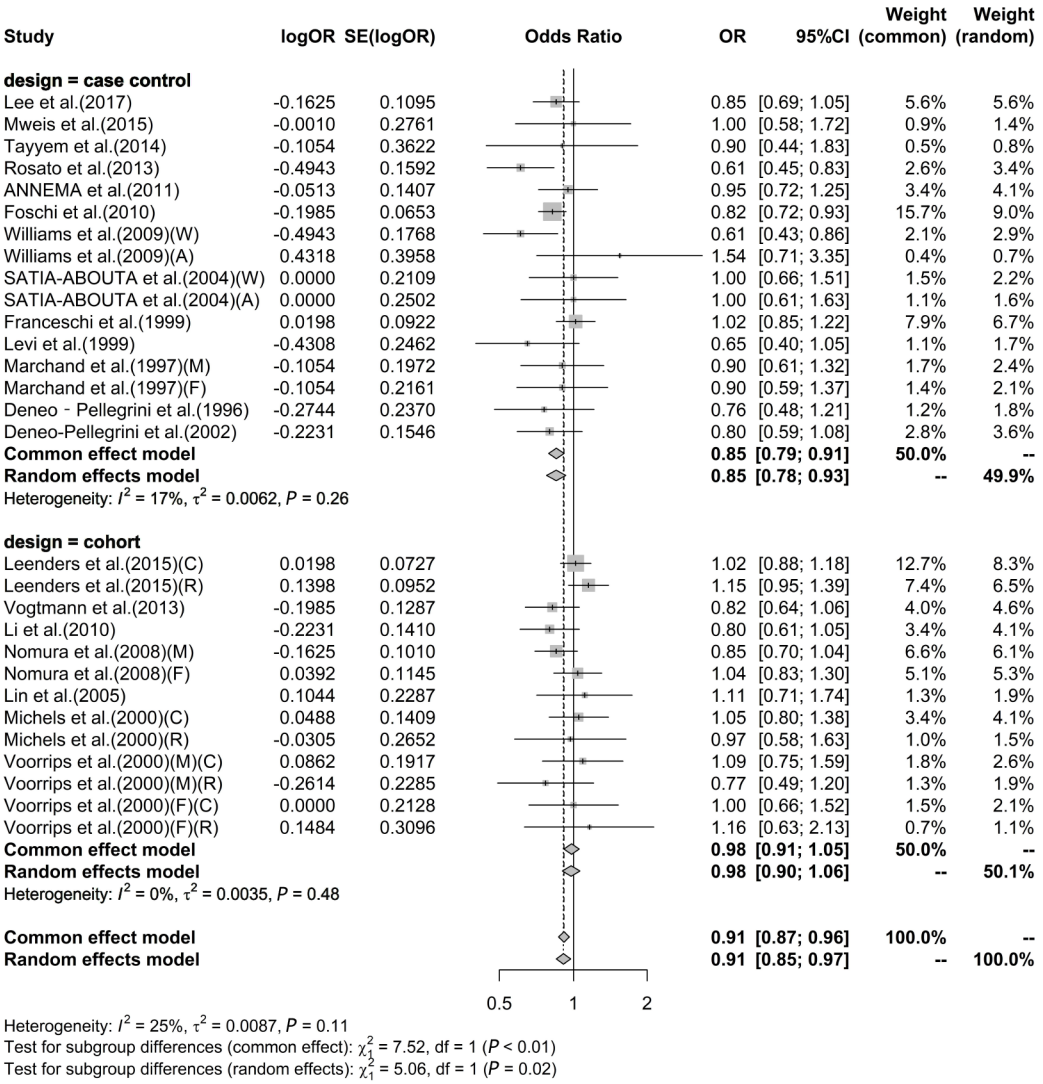
DOI: 10.3748/wjg.v29.i17.2679 **Copyright** ©The Author(s) 2023.

Figure 2 Meta-analysis of the risk of colorectal cancer in the highest *vs* lowest category of Citrus intake. F: Female, M: Male; W: Whites, A: African-Americans; C: Colon cancer, R: Rectal cancer. OR: Odds ratio; CI: Confidence intervals.

seven studies in North America[36,46,48,52,54-56], five studies in Asia[39,41,42,50,51], and one study in Australia[44]. Most studies matched or adjusted for age and energy intake; several studies adjusted for BMI (body mass index), smoking status, alcohol use, history of disease associated with CRC, and physical activity; other adjusting factors included gender, education level, and red meat intake (Table 2). Based on the ROBINS-I tool, we identified all studies as having moderate risk of bias. Most of the problems found were regarding confounding and missing data. There was a moderate bias in the classification of interventions in five studies and a moderate bias in the selection of participants in five studies. Among all observational studies, Bias due to deviations from intended interventions, outcomes measurement bias and selection of reported results were considered low. Risk of bias assessment results are summarized in Table 3.

Heterogeneity and pooled results

High *vs* low analysis: Citrus: For 20 included articles[29,38-46,48-57], the overall outcome analysis found that higher citrus intake was related to a lower risk of CRC [I^2 = 25%, P = 0.11, REM; OR (95%CI) = 0.91 (0.85-0.97), P < 0.01] (Figure 2). Further subgroup analysis based on study design showed that citrus intake may reduce the risk of CRC by 15% in case-control studies [I^2 = 17%, P = 0.26, REM; OR (95%CI) = 0.85 (0.78-0.93)], whereas a similar association was not found in cohort studies [I^2 = 0%, P = 0.48, REM; OR (95%CI) = 0.98 (0.90-1.06)] (Figure 3). We also performed a subgroup analysis of 7 included articles based on the specific location of tumorigenesis, which were divided into a total of four locations, namely distal colon, proximal colon, colon, and rectum, but the results suggested no significant association between citrus intake and proximal colon [I^2 = 0%, P = 0.64, REM; OR (95%CI) = 0.93 (0.65-1.32)], distal colon [I^2 = 0%, P = 0.89, REM; OR (95%CI) = 0.80 (0.57-1.12)], colon [I^2 = 0%, P = 0.60, REM; OR (95%CI) = 0.97 (0.91-1.05)], and rectum [I^2 = 55%, P = 0.03, REM; OR (95%CI) = 0.90 (0.78-1.05)] (Figure 4). In the analysis stratified by region, an association between citrus consumption and lower CRC risk was demonstrated only in studies conducted in Asia [I^2 = 0%, P = 0.96, REM; OR (95%CI) = 0.84 (0.73-0.96)], whereas no association was found in studies conducted in North/South America [I^2 = 1%, P = 0.43, REM; OR (95%CI) = 0.91 (0.83-1.01)] and Europe [I^2 = 60%, P < 0.01, REM; OR (95%CI) = 0.92 (0.81-1.05)] (Figure 5). Finally, our stratified analysis of gender in 6 included articles found the protective effect of citrus was only present in men [I^2 = 30%, P = 0.22, REM; OR (95%CI) = 0.84 (0.75-0.96)] but not in women [I^2 = 47%, P = 0.11, REM; OR (95%CI) = 0.98 (0.78-1.25)] (Figure 6).



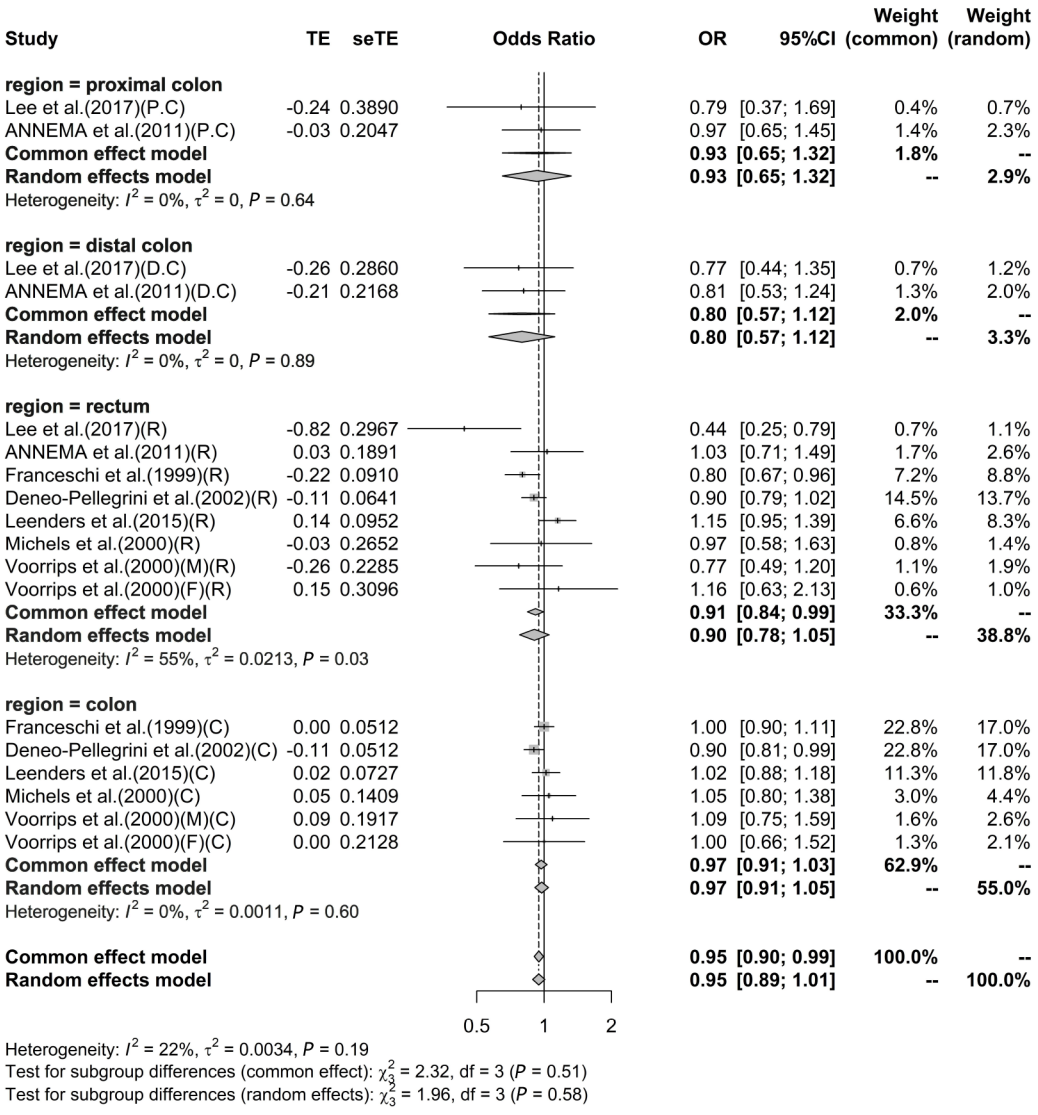
DOI: 10.3748/wjg.v29.i17.2679 **Copyright** ©The Author(s) 2023.

Figure 3 Subgroup analysis of the risk of colorectal cancer in the highest *vs* lowest category of Citrus intake by study type. F: Female; M: Male; W: Whites; A: African-Americans; C: Colon cancer; R: Rectal cancer; OR: Odds ratio; CI: Confidence intervals.

Apple: The analysis of the results in 9 included articles[29,32,36,37,41,42,44,47,57] showed that greater intake of apples led to a significant 25% reduction in CRC risk [I^2 = 49%, P = 0.04, REM; OR (95%CI) = 0.75 (0.66-0.85), P < 0.01] (Figure 7). When studies were stratified by region, a significant association was found between apple intake and reduced risk of CRC in the European population [I^2 = 62%, P = 0.03, REM; OR (95%CI) = 0.77 (0.67-0.90)], while no association was observed in the Asian population [I^2 = 0%, P = 0.69, REM; OR (95%CI) = 0.87 (0.55-1.38)] and the North/South American population [I^2 = 76%, P = 0.04, REM; OR (95%CI) = 0.56 (0.30-1.03)] (Supplementary Figure 1).

Banana: The analysis results of six included articles[29,38,41,42,56,57] demonstrated that consuming more bananas did not contribute to reduced risk of CRC [I^2 = 79%, P < 0.01, REM; OR (95%CI) = 0.74 (0.55-1.00), P = 0.05] (Supplementary Figure 2). When stratified by region, banana intake was found to be related to a lower risk of CRC in North/South American populations [I^2 = 58%, P = 0.07, REM; OR (95%CI) = 0.54 (0.39-0.76)], whereas no association was revealed in European populations [I^2 = 0%, P = 1.00, REM; OR (95%CI) = 1.00 (0.92-1.09)] and Asian populations [I^2 = 0%, P = 0.95, REM; OR (95%CI) = 1.16 (0.70-1.92)] (Supplementary Figure 3). When stratified by gender, we found a protective effect of Bananas for both men [I^2 = 0%, P = 0.59, REM; OR (95%CI) = 0.65 (0.49-0.86)] and women [I^2 = 0%, P = 1.00, REM; OR (95%CI) = 0.60 (0.43-0.83)] (Supplementary Figure 4). In a stratified analysis of tumor sites, high banana intake did not show the association with the risk of malignancy in either the colon [I^2 = 86%, P < 0.01, REM; OR (95%CI) = 0.90 (0.72-1.12)] or the rectum [I^2 = 0%, P = 0.36, REM; OR (95%CI) = 0.95 (0.85-1.06)] (Supplementary Figure 5).

Peach: For the four included articles[29,40,42,57], the total analysis results showed that consuming more peaches did not reduce the risk of CRC [I^2 = 62%, P = 0.02, REM; OR (95%CI) = 0.95 (0.83-1.09), P = 0.50]



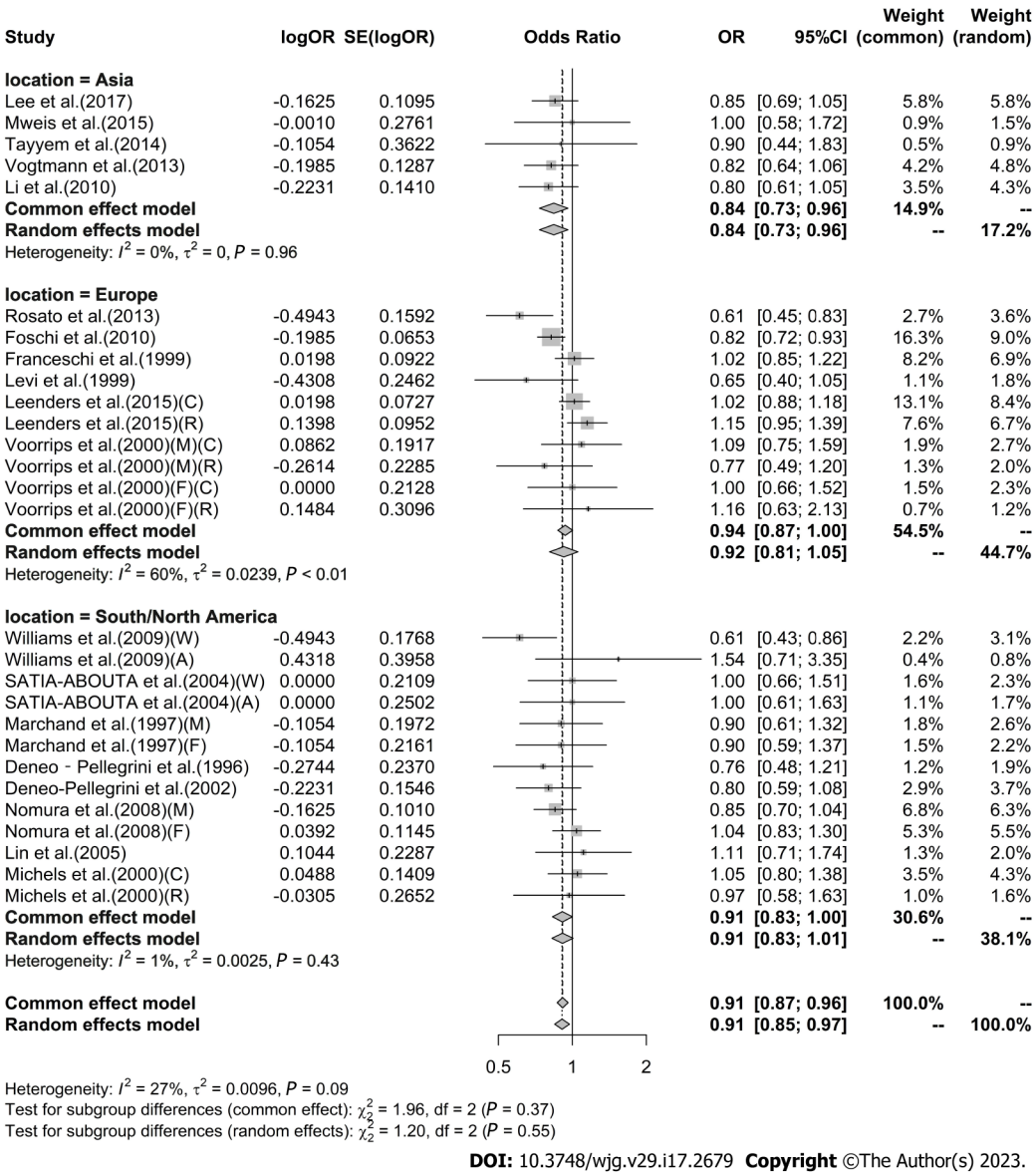
DOI: 10.3748/wjg.v29.i17.2679 **Copyright** ©The Author(s) 2023.

Figure 4 Subgroup analysis of the risk of colorectal cancer in the highest *vs* lowest category of Citrus intake by region of cancer. PC: Proximal colon cancer; DC: Distal colon cancer; C: Colon cancer; R: Rectal cancer; F: Female; M: Male; OR: Odds ratio; CI: Confidence intervals.

(Supplementary Figure 6). When stratified by study type, both case-control studies [I^2 = 86%, P = 0.03, REM; OR (95%CI) = 0.90 (0.75-1.07)] and cohort studies [I^2 = 47%, P = 0.17, REM; OR (95%CI) = 1.06 (0.87-1.29)] indicated that peach intake was not related to CRC risk (Supplementary Figure 7). The subgroup analysis based on tumor sites revealed that greater peach intake was not associated with the risk of malignancy in the colon [I^2 = 0%, P = 0.77, REM; OR (95%CI) = 0.99 (0.91-1.08)] and rectum [I^2 = 88%, P < 0.01, REM; OR (95%CI) = 0.96 (0.65-1.42)] (Supplementary Figure 8).

Strawberry: With three articles included in the analysis[29,40,42], overall results demonstrated no reduction in CRC risk even with higher intake of strawberries [I^2 = 58%, P = 0.05, REM; OR (95%CI) = 0.97 (0.90-1.05)], P = 0.42] (Supplementary Figure 9). In the stratified analysis of tumor sites, strawberry intake was not related to cancer risk in either the rectum [I^2 = 34%, P = 0.22, REM; OR (95%CI) = 0.93 (0.83-1.04)] or colon [I^2 = 0%, P = 0.67, REM; OR (95%CI) = 1.00 (0.95-1.06)] (Supplementary Figure 10). In the stratified analysis by study type, case-control studies [I^2 = 75%, P = 0.02, REM; OR (95%CI) = 0.95 (0.86-1.05)] and cohort studies [I^2 = 0%, P = 1.00, REM; OR (95%CI) = 1.04 (0.91-1.19)] showed that strawberry consumption was not associated with CRC risk (Supplementary Figure 11).

Grape: With four articles included[29,40,42,57], overall analysis results indicated that the intake of large amounts of grapes was not related to a reduced risk of CRC [I^2 = 51%, P = 0.07, REM; OR (95%CI) = 1.00 (0.91-1.10), P = 0.97] (Supplementary Figure 12). Subgroup analysis by tumor site showed that grape intake was not significantly associated with malignancy in both the rectum [I^2 = 0%, P = 0.52, REM; OR (95%CI) = 0.91 (0.83-1.01)] and colon [I^2 = 57%, P = 0.13, REM; OR (95%CI) = 1.05 (0.92-1.19)] (Supplementary Figure 13). Stratified by study type, case-control studies [I^2 = 59%, P = 0.06, REM; OR



DOI: 10.3748/wjg.v29.i17.2679 **Copyright** ©The Author(s) 2023.

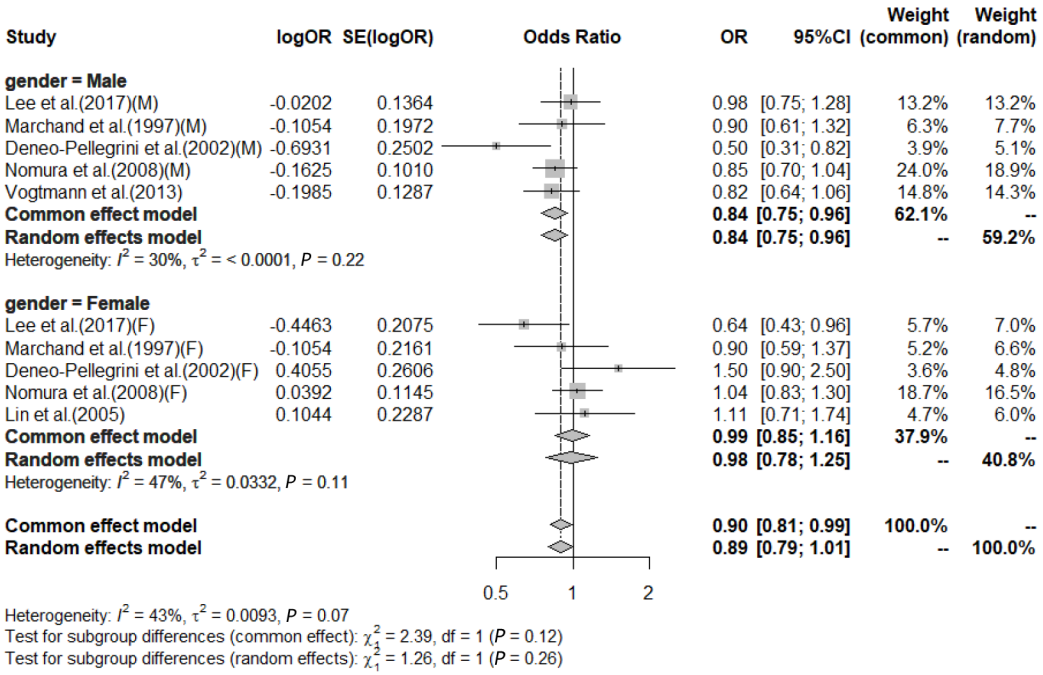
Figure 5 Subgroup analysis of the risk of colorectal cancer in the highest *vs* lowest category of Citrus intake by location. F: Female; M: Male; W: Whites; A: African-Americans; C: Colon cancer; R: Rectal cancer; OR: Odds ratio; CI: Confidence intervals.

(95%CI) = 0.97 (0.87-1.08)] and cohort studies [I^2 = 13%, P = 0.28, REM; OR (95%CI) = 1.08 (0.93-1.26)] revealed no reduction in the risk of CRC with grape consumption (Supplementary Figure 14).

Other fresh Fruits: Watermelon[42,50] [I^2 = 0%, P = 0.37, REM; OR (95%CI) = 0.74 (0.58-0.94), P = 0.02] (Supplementary Figure 15) and kiwi[29,42] [I^2 = 0%, P = 0.51, REM; OR (95%CI) = 0.87 (0.78-0.96), P < 0.01] (Supplementary Figure 16) were related to a reduced risk of CRC. Pears[42,57] [I^2 = 0%, P = 0.88, REM; OR (95%CI) = 1.08 (0.72-1.62), P = 0.70] (Supplementary Figure 17), melons[29,42] [I^2 = 34%, P = 0.22, REM; OR (95%CI) = 0.96 (0.87-1.06), P = 0.39] (Supplementary Figure 18), and figs[42,57] [I^2 = 80%, P = 0.03, REM; OR (95%CI) = 0.83 (0.32-2.17), P = 0.70] (Supplementary Figure 19) were not associated with a reduced risk of CRC.

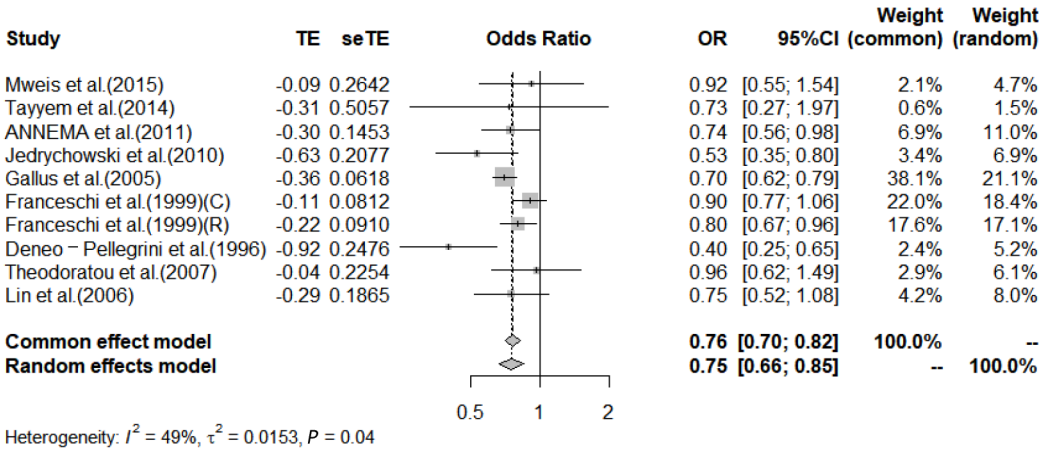
Dose-response meta-analysis

The dose-response analysis of citrus intake included seven articles[39,42,44-46,51,54] (Figure 8). A nonlinear relationship was observed between citrus intake and CRC risk [R (95%CI) = -0.0031 (-0.0047 to -0.0014), P < 0.001]. Based on the above meta-analyses results, a citrus intake of (0 g/d) was used as a reference group and the risk was minimized around 120 g/d (OR = 0.85), whereas no significant dose-response correlation was observed after continuing to increase intake, with correlations only assessed in the range of 0-248 g/d. Dose-response relationships between intake and CRC risk could not be calculated for other types of fruits due to the paucity of available data.



DOI: 10.3748/wjg.v29.i17.2679 **Copyright** ©The Author(s) 2023.

Figure 6 Subgroup analysis of the risk of colorectal cancer in the highest *vs* lowest category of Citrus intake by gender. F: Female; M: Male; OR: Odds ratio; CI: Confidence intervals.

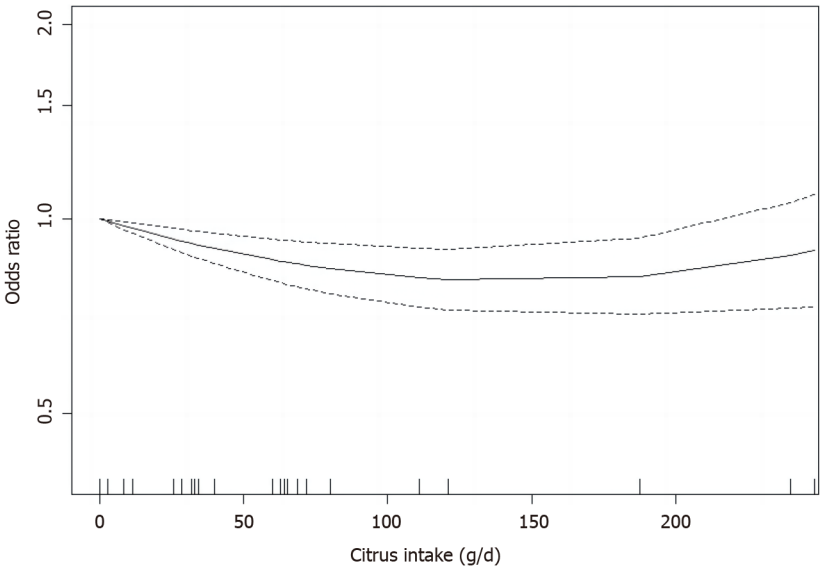


DOI: 10.3748/wjg.v29.i17.2679 **Copyright** ©The Author(s) 2023.

Figure 7 Meta-analysis of the risk of colorectal cancer in the highest *vs* lowest category of Apple intake. C: Colon cancer; R: Rectal cancer; OR: Odds ratio; CI: Confidence intervals.

Sensitivity analysis and publication bias

A sensitivity analysis was conducted for all outcome indicators with more than 50% heterogeneity and P < 0.05, and the results showed that the combined results were stable for heterogeneity. A sensitivity analysis based on quality assessment was also conducted. After articles with relatively low quality of evidence (three domains were graded as moderate risk) were excluded, the remaining data were pooled and analyzed again, and the outcome showed that our combined results were robust (Supplementary Figures 20 and 21). No potential publication bias was found. For the analysis of high and low fruit intake, the P value of the citrus Egger's test was 0.8467 (Figure 9A), and the P value for the apple Egger's test was 0.6068 (Figure 9B). Other types of fruits were not tested for publication bias as the number of articles was less than 10.



DOI: 10.3748/wjg.v29.i17.2679 **Copyright** ©The Author(s) 2023.

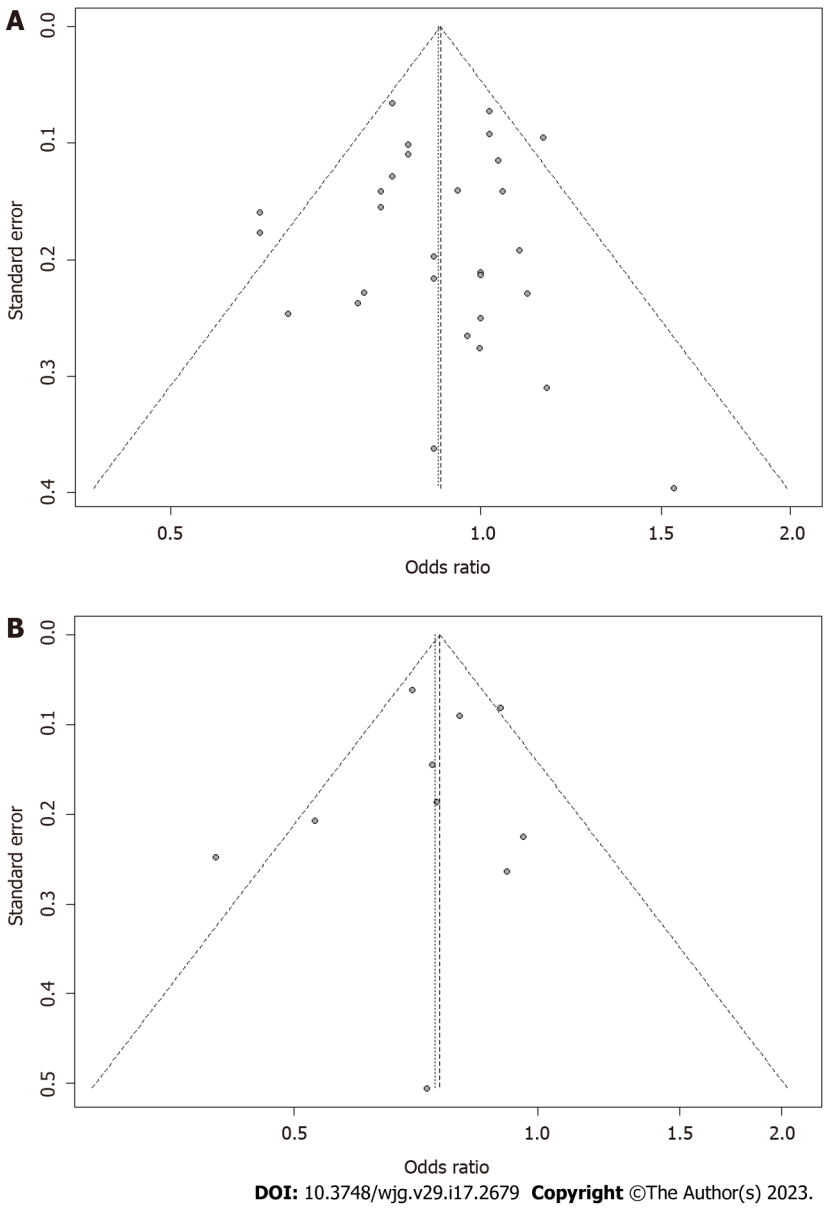
Figure 8 Nonlinear relation between Citrus fruit intake and the risk of colorectal cancer.

DISCUSSION

The main findings of this meta-analysis demonstrated that compared to low intakes, higher intakes of citrus, apples, watermelon, and kiwi reduced the risk of CRC by 9%, 25%, 26%, and 13%, respectively, while bananas, grapes, strawberries, peaches, pears, figs, and other melons did not exhibit an association with CRC risk. A nonlinear dose-response relationship was observed between citrus and CRC risk in the present study. To our knowledge, this study is the first meta-analysis to investigate the association between different fruit intake and CRC risk, and the first to perform a dose-response analysis between citrus intake and CRC risk.

The results of this meta-analysis are supported by relevant biological theories. Citrus has many chemopreventive effects on CRC[58]. Nobiletin, a compound extracted from citrus, blocks the cell cycle, inhibits cell proliferation, induces apoptosis, prevents tumor formation, reduces inflammatory effects and limits angiogenesis[59]. Naringenin, which is rich in citrus, inhibits the proliferation of HT-29 colon cancer cells[60] and also reduces the severity of colorectal adenomas and colitis by inhibiting pro-inflammatory mediators GM-CSF/M-CSF, bone marrow-derived suppressor cells, IL-6 and TNF-α, and NF-κB/IL-6/STAT3 cascade in colorectal tissues[61]. Neohesperidin, derived from citrus fruits, has also been confirmed to prevent colorectal tumors by altering the intestinal microbiota[62]. Moreover, APs contained in apples have been verified to prevent AOM/dss-induced colitis-associated CRC (CACC) in ICR mice. APs modulate intestinal flora composition, reduce infiltration of neutrophils, macrophages and T cells in the colon, and more importantly, inhibit the entry of β-catenin into the nucleus, which in turn retards the Wnt/β-catenin pathway[63]. APs also induce apoptosis in colon cancer cells through microactivating the NF-κB pathway, and inhibit CRC cell migration and invasiveness by targeting the LPS/TLR4/NF-κB pathway[64,65]. It has also been shown that apple polyphenols and apple anthocyanin Cy3Gal inhibit and reduce the appearance of precancerous markers of CRC[66] as well as tumor lesions in AOM-induced CRC mice[67]. In addition, apple polyphenols affect the initiation of apoptosis in human colon cancer cells and the activity of protein kinase C[68]. That other fruits did not show protective effects may be owing to the small number of original studies, resulting in large heterogeneity and wide confidence intervals, which masked their anticancer effects. It could also be possible that the intake was too small to show a protective effect, and more research is needed for verification.

There are many reasons contributing to inconsistent results in several subgroup analyses. In citrus, case-control studies tended to show protective factors, while cohort studies did not. In other types of fruits, no correlation was seen in the subgroup analysis of the study type. Generally speaking, case-control studies have several weaknesses, such as a control group that may not be representative of the general population or more problems with reverse causality and recall bias. On the other side, dietary assessment questionnaires used in a prospective study setting may not be as accurate as those used in a retrospective case-control setting. Meanwhile, it is difficult for individuals to accurately report their fruit intake, and this low correlation has been confirmed in some studies (Spearman's correlation coefficient of 0.6 for fruit consumption[69,70]), which may have weakened the estimates of the associated risk. Thus, the true association may be stronger than what we observed, reinforcing the conclusion of protective effect. In another subgroup analysis of studies' geographic location, a negative association between citrus intake and CRC risk was observed in Asia but not in North/South America or Europe,



DOI: 10.3748/wjg.v29.i17.2679 **Copyright** ©The Author(s) 2023.

Figure 9 Funnel plot. A: Funnel plot of studies evaluating for the association between Citrus fruit intake and risk of colorectal cancer. Dotted lines on both sides indicate 95% pseudo-confidence intervals; B: Funnel plot of studies evaluating for the association between Apple intake and risk of colorectal cancer. OR: Odds ratio; CI: Confidence intervals.

and a negative association for bananas only in North/South America and apples in Europe. These results may be attributed to the varied consumption patterns of fruits and vegetables among countries, leading to errors in the measurement of dietary intake[71]. According to our pooled results, the specific sites of tumor occurrence, such as the distal colon, proximal colon, and rectum, were not significantly associated with the risk and benefit of fruit intake, indicating that fruits improve the function of the entire intestine or regulate the microbial flora of the entire digestive tract, but do not target specific sites, so there is no correlation with the specific location of tumors. No significant risk benefit was seen for men or women in the gender-based subgroup analysis either, possibly due to an insufficient number of included original studies or dietary measurement errors. From the dose-response analysis, the risk of CRC was found to be minimized at a citrus intake of 120 g/d, while the risk of CRC did not decrease further after continuing to increase intake. The underlying mechanism may be related to the availability and digestibility of nutrients from citrus fruits[72,73]. However, further studies are needed to validate our results.

Surgery, chemoradiotherapy and targeted drugs currently used to treat CRC are not only expensive but also highly toxic. Through this Meta-analysis, we can prioritize fruits with proven protective effects to prevent CRC. If cancer prevention can be achieved by changing dietary habits such as fruit supplementation, it will certainly reduce the huge economic burden and mortality of cancer in the world. As for future research directions, we hope to find the key components of anti-cancer through research and make element-specific nutritional preparations to help people better prevent cancer. More prospective

Table 1 Characteristic of eligible studies included in the meta-analysis assessing the relationship between different types of fruit intake and the risk of colorectal cancers

Ref.	Country	No. of cases/controls (age)	Dietary assessment	Comparison of exposure level	Category, OR/RR (95%CI)	Confounding factors
Lee *et al*[39], 2017	-	923 (625 males, 298 females)/1846 (1250 males, 596 females)	SQFFQ, 106 food items	Orange/yellow fruits (g/d); males: T3 (≥ 47.9) *vs* T1 (< 15.9); females: T3 (≥ 90.6) *vs* T1 (< 32.5); proximal colon/distal colon/rectum: T3 (≥ 90.6) *vs* T1 (< 32.5)	Males: 0.98 (0.75-1.28); females: 0.64 (0.43-0.97); total: 0.85 (0.69-1.06); proximal colon: 0.79 (0.37-1.70); distal colon: 0.77 (0.44-1.35); rectum: 0.44 (0.25-0.80)	Age, education, alcohol consumption, BMI, regular exercise, red meat, processed meat, total EI
Leenders *et al* [40], 2015	Ten European countries (Denmark, France, Germany, Greece, Italy, The Netherlands, Norway, Spain, Sweden, and United Kingdom	442961 cohort; 3082 incident cases (2128 colon cancer (954 proximal, 965 distal), 1242 rectal cancer cases); 51.2 (38.3-63.0) years; follow-up 8 years	Center-specific dietary questionnaire	Medians of consumption per quartiles; berries: 21 g/d *vs* 1 g/d; citrus fruits: 110 g/d *vs* 7 g/d; grapes: 32 g/d *vs* 1 g/d; hard fruits: 153 g/d *vs* 10 g/d; stone fruits: 83 g/d *vs* 2 g/d	Colon cancer; berries: 1.04 (0.88-1.24); citrus fruits: 1.02 (0.88-1.17); grapes: 1.15 (0.97-1.37); stone fruits: 0.97 (0.81-1.15); rectal cancer: Berries: 1.04 (0.83-1.30); citrus fruits: 1.15 (0.95-1.38); grapes: 0.98 (0.78-1.25); stone fruits: 1.19 (0.94-1.50)	All other fruit and vegetable consumption, height, weight, dietary calcium consumption, dietary alcohol consumption, dietary cereal fiber consumption, smoking status, time since stopped smoking, duration of smoking, number of cigarettes smoked per day and PA
Abu Mweis *et al*[41], 2015	Jordan	167/240, NA	FFQ, 109 food items	≥ 3 times/wk (high) *vs* ≥ 2 times/wk (low)	Apples: 0.915 (0.545-1.535); bananas: 1.167 (0.670-2.033); oranges: 0.999 (0.581-1.715)	Age, sex, total EI, metabolic equivalent, smoking, education level, marital status, work, income, and family history of CRC
Tayyem *et al* [42], 2014	Jordan	220/281 (248 males, 253 females); males: mean age 55.27 years; females: mean age 48.67 years	NA; 42 food items	Daily (high) *vs* ≤ rarely (low)	Apple: 0.73 (0.27-1.96); banana: 1.12 (0.34-3.67); orange: 0.90 (0.44-1.82); pear: 1.13 (0.56-2.29); peach: 0.64 (0.32-1.25); grape: 0.62 (0.27-1.40); melon: 0.82 (0.38-1.78); watermelon: 0.54 (0.26-1.11); strawberry: 0.75 (0.26-2.13); fig: 0.51 (0.28-0.92); kiwi: 1.14 (0.25-5.06); dried Fruit: 1.42 (0.55-3.67)	Age, sex, total EI, MET minutes/week, tobacco use, education level, marital status, work, income, PA, marital status, family history of CRC
Rosato *et al* [43], 2013	Italia and Swiss	329/1361, median age 40 yr	FFQ; 78 food items	High *vs* Low	Citrus fruit: 0.61 (0.45-0.84)	Age, sex, center, study, year of interview, education, family history, alcohol consumption, EI
Vogtmann *et al*[50], 2013	China	61274 male's cohort (40-74 years); 398 incident cases (236 colon, 162 rectal); follow-up 2002-2006 to 2010	Validated FFQ; 46 food items	Citrus fruit intake g/day: ≥ 12.61 (high) *vs* < 2.70 (low); watermelon intake g/day: ≥ 93.33 (high) *vs* < 33.33 (low)	Citrus fruit: Colorectal cancer: 0.82 (0.64-1.06); colon cancer: 0.86 (0.62-1.19); rectal cancer: 0.76 (0.51-1.14); watermelon: Colorectal cancer: 0.77 (0.59-0.99); colon cancer: 0.76 (0.55-1.06); rectal cancer 0.77 (0.51-1.15)	Age, total EI, red meat intake, total meat intake, education, income, occupation, smoking status, alcohol consumption, BMI, MET hours of exercise participation, history of diabetes mellitus, family history of CRC
Annema *et al* [44], 2011	Western Australia	834 (64.9 yr ± 8.9 yr)/939 (64.6 yr ± 9.4 yr)	FFQ; 74 food items	Servings/d) ≥ 0.50 (high) *vs* < 0.07 (low)	Total: Citrus fruit: 0.95 (0.72-1.25); apples: 0.74 (0.56-0.99); fruit juice: 1.38 (1.08-1.75); citrus fruit: Proximal Colon: 0.97 (0.65-1.45); distal Colon: 0.81 (0.53-1.24); rectum: 1.03 (0.71-1.49); apples: Proximal Colon: 1.13 (0.72-1.77); distal colon: 0.51 (0.34-0.77); rectum: 0.73 (0.49-1.08); fruit	Sex, age, BMI at age 20 yr, EI, multiv-itamin use, alcohol consumption, PA, smoking, diabetes, socioeconomic status

					juice: Proximal Colon: 1.06 (0.74-1.49); distal colon: 1.41 (0.99-2.01); rectum: 1.74 (1.24-2.45)	
Foschi *et al* [45], 2010	Italy and Switzerland	3634 (median age 62 yr)/6804 (median age 57 yr)	Validated FFQ; 78 food items	Citrus fruit or citrus fruit juice intake: ≥ 4 portions/wk *vs* < 1 portion/wk	Citrus: 0.82 (0.72-0.93)	Age, sex, study center, tobacco smoking, alcohol, education, BMI, PA, EI
Li *et al*[51], 2010	Japan	42470 cohort (40-79 yr) (20222 males, 22248 females); 665 incident cases; follow-up 9 years	FFQ; 40 food items	Citrus consumption daily *vs* ≤ 2 times/wk	Citrus: 0.80 (0.61-1.06)	Age, sex, job status, years of education, BMI, time engaging in sports or exercise, time spent walking, cigarette smoking, alcohol drinking, history of hypertension, diabetes mellitus and gastric ulcer, family history of cancer, daily total EI, consumption of rice/miso soup/soybean products/total meat/total fish/dairy products/other fruits/total vegetables/oolong tea/black tea/coffee /green tea
Jedrychowski *et al*[32], 2010	Poland	592/765; NA	EPIC-FFQ148 food items	Apples, servings/d: > 1.50 (Q5; high) *vs* < 0.18 (Q1; low)	Apples: 0.53 (0.35-0.79)	Age, gender, place of residency, marital status, tobacco smoking, total EI, intake of vegetables, fruits excluding apples
Williams *et al* [46], 2009	North Carolina	945/959; 40-79 yr; whites (n = 1520); African-Americans (n = 384)	Diet history questionnaire; 124 food items	Citrus fruit (servings/wk): White: 16.4 Q4 (high) *vs* 1.89 Q1 (low); African-Americans: 21.7 Q4 (high) *vs* 2.3 Q1 (low)	Whites: 0.61 (0.43-0.86); African-Americans: 1.54 (0.71-3.35)	Age, sex, education, income, BMI 1 yr ago, PA, family history, nonsteroidal anti-inflammatory drug use, total EI
Nomura *et al* [52], 2008	Hawaii and Los Angeles	191011 cohort (85903 males, 105108 females); 2110 incident cases (1138 males, 972 females) (1571 of the colon, 515 of the rectum, 24 cases both sites) (45-75 yr); follow-up 7.3 years	Self-administered quantitative FFQ (QFFQ); 180 food items	Citrus fruit were quantified as g × 1000 kcal-1 × d-1; Q5 (high) *vs* Q1 (low)	Citrus fruit: Male: 0.85 (0.70-1.04); female: 1.04 (0.83-1.30)	Ethnicity, age, family history of CRC, history of colorectal polyp, pack-years of cigarette smoking, BMI, hours of vigorous activity, aspirin use, multivitamin use, replacement hormone use (women), log EI, alcohol, red meat, folate, vitamin D, calcium
Gallus *et al* [47], 2005	Italy	1953 (1225 of the colon, 728 of the rectum)/4154	Validated FFQ 78 food items	Average consumption of apples per day ≥ 1 (high) *vs* < 1 (low)	Apples: 0.70 (0.62-0.79)	Age, sex, study center, education, BMI, tobacco smoking, alcohol drinking, total EI, vegetable consumption, PA, other fruit
Lin *et al*[55], 2005	United States	39876 female cohort (mean age 45 years); 240 incident cases; follow-up 10 years	FFQ; 131 food items	Citrus fruit (serving/day) Median intake; 1.6 (Q5) high *vs* 0.1 (Q1) low	Citrus fruit: 1.11 (0.71-1.74)	Age, randomized treatment assignment, BMI, family history of CRC in a first-degree relative, history of

						colon polyps, PA, smoking status, baseline aspirin use, red meat intake, alcohol consumption, total EI, menopausal status and baseline post-menopausal HT use, folate intake, multivitamin use
Satia-Abouta *et al*[48], 2004	United States	613 (337 Caucasians, 276 African-Americans)/996(596 Caucasians, 400 African-Americans) (40-80 years)	Validated FFQ; 100 food items	Citrus fruits and juices: Median g/d: Caucasians: 4th quartile (high) 168 g *vs* 1st quartile 0 g (low); African-Americans: 4th quartile (high) 173 g *vs* 1st quartile 0 g (low)	Caucasians: 1.0 (0.7-1.6); African-Americans: 1.0 (0.6-1.6)	Age, gender, total EI, education, BMI, smoking history, PA, family history of colon cancer, NSAID use, fat, carbohydrates, dietary fiber, vitamin C, vitamin E, beta-carotene, calcium, folate, fruits, vegetables
Voorrips *et al* [53], 2000	Netherlands	4087 cohort; 620 colon cancer cases (332 males, 288 females), 344 rectal cancer cases (217 males, 127 females); follow-up 6.3 years	Validated FFQ; 150 food items	Citrus fruit Median intake (g/d); male: Q5 (167 g/dk) (high) *vs* Q1 (0g/dk) (low); female: Q5 (187 g/dk) (high) *vs* Q1 (8 g/dk) (low)	Male: Colon cancer: 1.09 (0.75-1.59) Rectal cancer: 0.77 (0.49-1.20); female: Colon cancer: 1.00 (0.66-1.52); rectal cancer: 1.16 (0.63-2.12)	Age, family history of CRC, category of alcohol intake
Michels *et al* [54], 2000	United States	136089 cohort (88764 females (30-55 years), 47325 males (40-75years); 1181 incident cases (937 colon cancer, 244 rectal cancer); follow-up 16 years	Validated FFQs; 61 food items	Citrus fruit: Frequencies of intake ≥ 2 servings/d *vs* 1 serving/wk or fewer	Colon cancer: 1.05 (0.80-1.39); rectal cancer: 0.97 (0.58-1.64)	Age, family history of CRC, sigmoidoscopy, height, BMI, pack-years of smoking, alcohol intake, PA, menopausal status, postmenopausal hormone use, aspirin use, vitamin supplement intake, total caloric intake, red meat consumption
Franceschi *et al*[29], 1998	Italy	1953 (1225 colon cancer, 728 rectal cancer)/4154 (2073 males, 2081 females)	Validated FFQ; 78 food items	Mean weekly servings: Citrus fruit Q5 7.5 (high)/Q1 1.0 (low); apples/pears: Q5 15.0 (high)/Q1 3.0 (low); bananas: Q5 3.0 (high)/Q1 0.5 (low); kiwi: Q5 4.0 (high)/Q1 0.5 (low); peaches/apricots/prunes: Q5 5.0 (high)/Q1 0.8 (low); melon: Q5 0.5 (high)/Q1 0.1 (low); grapes: Q5 1.0 (high)/Q1 0.2 (low); Strawberries/cherries: Q5 0.4 (high)/Q1 0.1 (low)	Citrus: Total: 1.02 (0.85-1.22), colon: 1.0 (0.9-1.1), rectal: 0.8 (0.7-1.0); apples/pears: Colon: 0.9 (0.8-1.1) rectal: 0.8 (0.7-1.0); bananas: Colon 1.0 (0.9-1.1), rectal 1.0 (0.8-1.1); kiwi: colon 0.9 (0.8-1.0) rectal 0.8 (0.7-1.0); peaches/apricots/prunes: Colon 1.0 (0.9-1.1) rectal 0.8 (0.7-0.9); melon: Colon 1.0 (0.9-1.0) rectal 0.9 (0.8-1.0); grapes: colon 1.0 (0.9-1.0) rectal 0.9 (0.8-1.0); strawberries/cherries: Colon 1.0 (0.9-1.0) rectal 0.9 (0.9-1.0)	Age, sex, centre, education, PA, total EI
Levi *et al*[49], 1999	Swiss	223 (males 142, females 81) (119 colon cancer, 104 rectal cancer, median age 63 yr)/491 (211 males, 280 females, median age 58 yr)	FFQ; 79 food items	Citrus fruits (Servings per week): Q3 (> 3.5/wk) *vs* Q1 (1.5/wk)	Citrus fruits: 0.65 (0.40-1.05)	Age, sex, education, smoking, alcohol, BMI, PA, meat and vegetable consumption, total EI
Le Marchand *et al*[56], 1997	Hawaii	1192 (698 males, 494 females) (mean age 66 yr)/1192 (698 males, 494 females) (mean age 66 yr)	Validated FFQ; 282 food items	Bananas: Male ≥ 55 g/d (Q4 high) *vs* ≤ 9 g/d (Q1 low), female: ≥ 54 g/d (Q4 high) *vs* ≤ 11 g/d (Q1 low); citrus fruits: Male ≥ 52 g/d (Q4 high) *vs* ≤ 4 g/d (Q1 low), female: ≥ 58 g/d (Q4 high) *vs* ≤ 8 g/d (Q1 low)	Bananas: Male: 0.7 (0.5-1.1), female: 0.6 (0.4-0.9); citrus fruits: Male: 0.9 (0.6-1.3), female: 0.9 (0.6-1.4)	Age, family history of CRC, alcoholic drinks per week, pack-years of cigarette smoking, lifetime recreational activity, Quetelet index 5 years earlier, total calories, egg,

						and calcium
Deneo-Pellegrini *et al*[57], 1996	Uruguay	160 (71 rectal cancer, 89 colon cancer)/221	FFQ; 61 food items	(T3; high) *vs* (T1; low)	Orange: 0.76 (0.47-1.19); apple: 0.40 (0.25-0.66); peach: 1.05 (0.65-1.69); pear: 1.06 (0.65-1.74); grape: 1.61 (0.94-2.74); fig: 1.36 (0.73-2.54); banana: 0.28 (0.16-0.50)	Age, sex, residence, education, BMI, total EI, alcohol intake
Lin *et al*[36], 2006	United States (NHS and HPFS)	71976 female cohort; 498 incident cases (30-55 yr); 35425 male cohort; 380 incident cases (40-75 yr); follow-up 10 yr	Validated FFQ; 131 food items	Apple: ≥ 2 servings/d (Q5; high) *vs* 0-2 servings/wk (Q1; low)	Total: 0.75 (0.52-1.08); NHS females: 0.64 (0.35-1.17); HPFS males: 0.82 (0.51-1.30)	Age, BMI, PA, history of CRC, previous colorectal polyps, prior screening sigmoidoscopy or colonoscopy, smoking, multiv-itamin use, current aspirin use, alcohol, EI, red meat, total Ca, total folate, total fibre
Theodoratou *et al*[37], 2007	United Kingdom	1456 (mean 63.9 yr ± 9.6 yr) yr)/1456 (64.7 yr ± 9.5 yr)	Validated FFQ; 150 food items	Apples: Q4 (high) *vs* Q1 (low)	Apples: 0.96 (0.62-1.50)	Age, sex, residence area, family history of CRC, total EI, fibre, alcohol, NSAID, smoking, BMI, PA
Deneo-Pellegrini *et al*[38], 2002	Uruguay	484 (260 colon cancer, 224 rectal cancer)/1452	FFQ; 64 food items	Citrus fruits estimate: Q4 (high) *vs* Q1 (low); banana estimate: Q4 (high) *vs* Q1 (low)	Total: Citrus fruits: 0.8 (0.6-1.1), banana: 0.6 (0.4-0.8); citrus fruits: Male: 0.5 (0.3-0.8), female: 1.5 (0.9-2.5); colon: 0.9 (0.9-1.1); rectum: 0.9 (0.7-0.9); banana: male: 0.6 (0.4-0.9), female: 0.6 (0.3-0.9); colon: 0.8 (0.7-0.9); rectum: 0.9 (0.8-1.1)	Age, residence, urban/rural status, education, family history of colon cancer for first-degree relatives, BMI, total EI and red meat intakes

NA: Not available; EI: Energy intake; PA: Physical activity; CRC: Colorectal cancer; BMI: Body mass index; MET: Metabolic equivalentr; NSAID: Non-steroidal anti-inflammatory drugs; NHS: Nurses' Health Study; HPFS: Health professionals follow-up study.

studies are also expected to verify the anti-cancer effects of other kinds of fruits.

We observed low heterogeneity between studies. Despite moderate heterogeneity in the studies on bananas and peaches, further sensitivity analysis indicated robust primary outcome and the heterogeneity was acceptable. The funnel plots and Egger's test we adopted produced consistent results, suggesting no publication bias. Moreover, the meta-analysis involved more than 1.06 million subjects, which makes it possible to explore associations between different subgroups, such as gender, geographic location and tumor location. Besides, a significant dose-response relationship was observed between citrus intake and CRC risk, further strengthening the association.

Nevertheless, there are some limitations of our study. First, synthetic results are limited due to the lack of research data on many types of fruits (*e.g.*, grapes, pears, and figs, *etc.*). This is coupled with the fact that dietary assessments of the frequency/amount of fruit intake varies so much that the protective effect against cancer cannot be truly captured. Additional potential bias may exist due to the diversity of designs and inconsistency of adjustment factors in the studies we analyzed. Although we extracted data with the most comprehensive adjustment for confounders, a subset of studies still did not adjust for potential dietary confounding variables (*e.g.*, meat, fiber, income status, and occupation). The limited range of citrus intake in the dose-response meta-analysis may have led to incomplete results. And limited available data for other fruits and the small number of original studies and made it impossible to investigate dose-response relationships between their intake and cancer risk.

CONCLUSION

Taken together, our results support the hypothesis that citrus, apple, watermelon and kiwi intake may contribute to a reduced risk of CRC. A nonlinear dose-response relationship was also observed between citrus intake and CRC risk within a certain range. However, the relationship between other types of fruit intake and CRC risk may be obscured by the various limitations mentioned above. Therefore, future prospective studies are required to further explore the effects of measurement error and control for important confounders, and thus reveal the true relationship between fruit and CRC.

Table 2 The main adjusted factors of studies included in the meta-analysis

Ref.	Adjusted confounders									
	Age	Sex	Energy intake	BMI	Family history of CRC	Alcohol use	Smoking status	Physical activity	Education level	Red meat
Lee *et al*[39], 2017	√		√	√		√		√	√	√
Leenders *et al*[40], 2015				√		√	√	√		
Abu Mweis *et al*[41], 2015	√	√	√		√		√		√	
Tayyem *et al*[42], 2014	√	√	√		√		√	√	√	
Rosato *et al*[43], 2013	√	√	√		√	√			√	
Vogtmann *et al*[50], 2013	√		√	√	√	√	√	√	√	√
Annema *et al*[44], 2011	√	√	√	√		√	√	√		
Foschi *et al*[45], 2010	√	√	√	√		√	√	√	√	
Li *et al*[51], 2010	√	√	√	√	√	√	√	√	√	
Jedrychowski *et al*[32], 2010	√	√	√				√			
Williams *et al*[46], 2009	√	√	√	√	√			√	√	
Nomura *et al*[52], 2008	√		√	√	√	√	√	√		√
Gallus *et al*[47], 2005	√	√	√	√		√	√	√	√	
Lin *et al*[55], 2005	√		√	√	√	√	√	√		√
Satia-Abouta *et al*[48], 2004	√	√	√	√	√		√	√	√	
Voorrips *et al*[53], 2000	√				√	√				
Michels *et al*[54], 2000	√		√	√	√	√	√	√		√
Franceschi *et al*[29], 1998	√	√	√					√	√	
Levi *et al*[49], 1999	√	√	√	√		√	√	√	√	
Le Marchand *et al*[56], 1997	√		√		√	√	√			
Deneo-Pellegrini *et al*[57], 1996	√	√	√	√		√			√	
Lin *et al*[55], 2005	√		√	√	√	√	√	√		√
Theodoratou *et al*[37], 2007	√	√	√	√	√	√	√	√		
Deneo-Pellegrini *et al*[38], 2002	√		√	√	√				√	√

BMI: Body mass index; CRC: Colorectal cancer.

Table 3 Risk of bias of 24 included studies, based on the Risk of Bias In Non-randomized Studies of Interventions-I tool

Ref.	Confounding	Selection of participants	Classification of interventions	Deviations from intended interventions	Bias due to missing data	Measurement of outcomes	Selection of reported result	Overall rating
Lee *et al*[39], 2017	Moderate	Low	Low	Low	Moderate	Low	Low	Moderate
Abu Mweis *et al*[41], 2015	Moderate	Low	Moderate	Low	Moderate	Low	Low	Moderate
Leenders *et al*[40], 2015	Moderate	Moderate	Low	Low	Moderate	Low	Low	Moderate
Tayyem *et al*[42], 2014	Moderate	Low	Low	Low	Low	Low	Low	Moderate
Rosato *et al*[43], 2013	Moderate	Low	Low	Low	Moderate	Low	Low	Moderate
Vogtmann *et al*[50], 2013	Low	Low	Low	Low	Moderate	Low	Low	Moderate
Annema *et al*[44], 2011	Moderate	Low	Low	Low	Moderate	Low	Low	Moderate
Foschi *et al*[45], 2010	Moderate	Moderate	Low	Low	Moderate	Low	Low	Moderate
Jedrychowski *et al*[32], 2010	Moderate	Low	Moderate	Low	Moderate	Low	Low	Moderate
Williams *et al*[46], 2009	Moderate	Low	Low	Low	Moderate	Low	Low	Moderate
Li *et al*[51], 2010	Moderate	Low	Low	Low	Moderate	Low	Low	Moderate
Gallus *et al*[47], 2005	Moderate	Low	Moderate	Low	Moderate	Low	Low	Moderate
Lin *et al*[36], 2006	Low	Moderate	Low	Low	Moderate	Low	Low	Moderate
Satia-Abouta *et al*[48], 2004	Moderate	Low	Low	Low	Moderate	Low	Low	Moderate
Voorrips *et al*[53], 2000	Moderate	Moderate	Low	Low	Moderate	Low	Low	Moderate
Franceschi *et al*[29], 1998	Moderate	Low	Moderate	Low	Moderate	Low	Low	Moderate
Levi *et al*[49], 1999	Moderate	Low	Low	Low	Moderate	Low	Low	Moderate
Le Marchand *et al*[56], 1997	Moderate	Low	Moderate	Low	Moderate	Low	Low	Moderate
Deneo-Pellegrini *et al*[57], 1996	Moderate	Low	Low	Low	Moderate	Low	Low	Moderate
Theodoratou *et al*[37], 2007	Moderate	Low	Low	Low	Moderate	Low	Low	Moderate
Deneo-Pellegrini *et al*[38], 2002	Moderate	Low	Low	Low	Moderate	Low	Low	Moderate
Nomura *et al*[52], 2008	Moderate	Low	Low	Low	Moderate	Low	Low	Moderate
Lin *et al*[55], 2005	Moderate	Low	Low	Low	Moderate	Low	Low	Moderate
Michels *et al*[54], 2000	Moderate	Moderate	Low	Low	Moderate	Low	Low	Moderate

ARTICLE HIGHLIGHTS

Research background

Colorectal cancer (CRC) is the third most prevalent cancer, and the prevalence of CRC in adults aged 40-49 has increased by approximately 15% between 2000-2002 and 2014-2016. However, inconsistent findings have been reported in different studies on the association between the intake of different types of fruits and CRC. Given their different chemical compositions and underlying molecular mechanisms, some types of fruits may have a closer correlation with CRC risk than others. This meta-analysis provides more reliable evidence that a higher intake of certain fruits is more effective in CRC prevention.

Research motivation

The main topic of this study is exploring the association between intake of different types of fruits and CRC risk. The key problem to be solved is to compare the CRC risk in the highest and lowest intake groups and conduct a meta-analysis. The significance of this study is that we have found that certain types of fruits can effectively reduce CRC risk.

Research objectives

To help people improve their lifestyles and dietary habits to live a healthy life. The most important goal is to ease the CRC-related social and economic burden worldwide. In terms of goal realized, through this meta-analysis, we have found that eating more citrus, apple, watermelon and kiwi fruit can effectively reduce CRC risk. Implications of achieving the goals: Further analysis of specific types of fruit is needed to explore key anti-cancer components.

Research methods

This meta-analysis was conducted by comparing the reported CRC risk between the highest and lowest fruit intake groups. Considering that CRC is rare, the risk is less than 10%, and the OR is small, the RR/HR we have calculated is approximately equal to the OR. Heterogeneity of results across studies was assessed by the I^2 test. Publication bias was determined using funnel plots and Egger's linear regression test. A dose-response analysis of citrus fruits was also conducted to examine a possible nonlinear relationship. All analyses were performed using R (version 4.1.3). Characteristics and novelty of the research method: No research has used this method to explore this topic before. This research direction is very suitable for this research method.

Research results

Findings: High intakes of citrus, apple, watermelon, and kiwi reduced CRC risk by 9%, 25%, 26%, and 13%, respectively, compared with low intakes. However, other types of fruit did not show an association with CRC risk. A non-linear dose-response relationship was found between citrus and CRC risk. Contribution to the field: This study performed a meta-analysis of previous data in a scientific context and identified the fruit types most effective in reducing CRC risk. Unresolved issues: More prospective studies are needed in the future to further elucidate the association between fruit and CRC.

Research conclusions

The results of this study underpin the hypothesis that certain types of fruit are effective in preventing CRC. This meta-analysis is based on the reported CRC risk of the highest and lowest fruit intake groups. It convincingly demonstrates the real association between fruit and CRC.

Research perspectives

In future research, we hope to find out the key anti-cancer components of specific types of fruits, so as to help people prevent cancer more effectively.

ACKNOWLEDGEMENTS

We would like to thank the researchers and study participants for their contributions.

FOOTNOTES

Author contributions: Wu ZY and Han YW contributed to conceptualization; Wu ZY contributed to methodology; Chen JL contributed to software; Wu ZY, Chen JL, and Li H contributed to validation; Wu ZY contributed to formal analysis; Su K contributed to investigation; Su K contributed to resources; Li H contributed to data curation; Wu ZY, Chen JL, and Han YW contributed to writing-original draft preparation; all authors contributed to writing-review

and editing; Chen JL contributed to visualization; Han YW contributed to supervision; Han YW contributed to project administration; all authors have read and agreed to the published version of the manuscript.

Conflict-of-interest statement: The authors declare that they have no conflict of interest.

PRISMA 2009 Checklist statement: The authors have read the PRISMA 2009 Checklist, and the manuscript was prepared and revised according to the PRISMA 2009 Checklist.

Open-Access: This article is an open-access article that was selected by an in-house editor and fully peer-reviewed by external reviewers. It is distributed in accordance with the Creative Commons Attribution NonCommercial (CC BY-NC 4.0) license, which permits others to distribute, remix, adapt, build upon this work non-commercially, and license their derivative works on different terms, provided the original work is properly cited and the use is non-commercial. See: https://creativecommons.org/Licenses/by-nc/4.0/

Country/Territory of origin: China

ORCID number: Zhen-Ying Wu 0000-0002-2269-8804; Jia-Li Chen 0000-0002-2692-8179; Han Li 0000-0003-0846-3846; Ke Su 0000-0002-7948-6335; Yun-Wei Han 0000-0002-0942-9095.

S-Editor: Chen YL
L-Editor: A
P-Editor: Yuan YY

REFERENCES

1 **El-Shami K**, Oeffinger KC, Erb NL, Willis A, Bretsch JK, Pratt-Chapman ML, Cannady RS, Wong SL, Rose J, Barbour AL, Stein KD, Sharpe KB, Brooks DD, Cowens-Alvarado RL. American Cancer Society Colorectal Cancer Survivorship Care Guidelines. *CA Cancer J Clin* 2015; **65**: 428-455 [PMID: 26348643 DOI: 10.3322/caac.21286]

2 **Haghighat S**, Sussman DA, Deshpande A. US Preventive Services Task Force Recommendation Statement on Screening for Colorectal Cancer. *JAMA* 2021; **326**: 1328 [PMID: 34609459 DOI: 10.1001/jama.2021.13466]

3 **O'Sullivan DE**, Sutherland RL, Town S, Chow K, Fan J, Forbes N, Heitman SJ, Hilsden RJ, Brenner DR. Risk Factors for Early-Onset Colorectal Cancer: A Systematic Review and Meta-analysis. *Clin Gastroenterol Hepatol* 2022; **20**: 1229-1240.e5 [PMID: 33524598 DOI: 10.1016/j.cgh.2021.01.037]

4 **Li YH**, Niu YB, Sun Y, Zhang F, Liu CX, Fan L, Mei QB. Role of phytochemicals in colorectal cancer prevention. *World J Gastroenterol* 2015; **21**: 9262-9272 [PMID: 26309353 DOI: 10.3748/wjg.v21.i31.9262]

5 **François C**, van Velthoven R, De Lathouwer O, Moreno C, Peltier A, Kaltner H, Salmon I, Gabius HJ, Danguy A, Decaestecker C, Kiss R. Galectin-1 and galectin-3 binding pattern expression in renal cell carcinomas. *Am J Clin Pathol* 1999; **112**: 194-203 [PMID: 10439799 DOI: 10.1093/ajcp/112.2.194]

6 **Piantelli M**, Iacobelli S, Almadori G, Iezzi M, Tinari N, Natoli C, Cadoni G, Lauriola L, Ranelletti FO. Lack of expression of galectin-3 is associated with a poor outcome in node-negative patients with laryngeal squamous-cell carcinoma. *J Clin Oncol* 2002; **20**: 3850-3856 [PMID: 12228204 DOI: 10.1200/jco.2002.01.078]

7 **Nakahara S**, Oka N, Raz A. On the role of galectin-3 in cancer apoptosis. *Apoptosis* 2005; **10**: 267-275 [PMID: 15843888 DOI: 10.1007/s10495-005-0801-y]

8 **Li Y**, Liu L, Niu Y, Feng J, Sun Y, Kong X, Chen Y, Chen X, Gan H, Cao S, Mei Q. Modified apple polysaccharide prevents against tumorigenesis in a mouse model of colitis-associated colon cancer: role of galectin-3 and apoptosis in cancer prevention. *Eur J Nutr* 2012; **51**: 107-117 [PMID: 21516492 DOI: 10.1007/s00394-011-0194-3]

9 **Liu YZ**, Wu K, Huang J, Liu Y, Wang X, Meng ZJ, Yuan SX, Wang DX, Luo JY, Zuo GW, Yin LJ, Chen L, Deng ZL, Yang JQ, Sun WJ, He BC. The PTEN/PI3K/Akt and Wnt/β-catenin signaling pathways are involved in the inhibitory effect of resveratrol on human colon cancer cell proliferation. *Int J Oncol* 2014; **45**: 104-112 [PMID: 24756222 DOI: 10.3892/ijo.2014.2392]

10 **Moon YJ**, Wang X, Morris ME. Dietary flavonoids: effects on xenobiotic and carcinogen metabolism. *Toxicol In Vitro* 2006; **20**: 187-210 [PMID: 16289744 DOI: 10.1016/j.tiv.2005.06.048]

11 **Arafa MA**, Waly MI, Jriesat S, Al Khafajei A, Sallam S. Dietary and lifestyle characteristics of colorectal cancer in Jordan: a case-control study. *Asian Pac J Cancer Prev* 2011; **12**: 1931-1936 [PMID: 22292627]

12 **van Duijnhoven FJ**, Bueno-De-Mesquita HB, Ferrari P, Jenab M, Boshuizen HC, Ros MM, Casagrande C, Tjønneland A, Olsen A, Overvad K, Thorlacius-Ussing O, Clavel-Chapelon F, Boutron-Ruault MC, Morois S, Kaaks R, Linseisen J, Boeing H, Nöthlings U, Trichopoulou A, Trichopoulos D, Misirli G, Palli D, Sieri S, Panico S, Tumino R, Vineis P, Peeters PH, van Gils CH, Ocké MC, Lund E, Engeset D, Skeie G, Suárez LR, González CA, Sánchez MJ, Dorronsoro M, Navarro C, Barricarte A, Berglund G, Manjer J, Hallmans G, Palmqvist R, Bingham SA, Khaw KT, Key TJ, Allen NE, Boffetta P, Slimani N, Rinaldi S, Gallo V, Norat T, Riboli E. Fruit, vegetables, and colorectal cancer risk: the European Prospective Investigation into Cancer and Nutrition. *Am J Clin Nutr* 2009; **89**: 1441-1452 [PMID: 19339391 DOI: 10.3945/ajcn.2008.27120]

13 **Dahm CC**, Keogh RH, Spencer EA, Greenwood DC, Key TJ, Fentiman IS, Shipley MJ, Brunner EJ, Cade JE, Burley VJ, Mishra G, Stephen AM, Kuh D, White IR, Luben R, Lentjes MA, Khaw KT, Rodwell Bingham SA. Dietary fiber and colorectal cancer risk: a nested case-control study using food diaries. *J Natl Cancer Inst* 2010; **102**: 614-626 [PMID: 20407088 DOI: 10.1093/jnci/djq092]

14 **Fung TT**, Hu FB, Wu K, Chiuve SE, Fuchs CS, Giovannucci E. The Mediterranean and Dietary Approaches to Stop

Hypertension (DASH) diets and colorectal cancer. *Am J Clin Nutr* 2010; **92**: 1429-1435 [PMID: 21097651 DOI: 10.3945/ajcn.2010.29242]

15 **Wang DD**, Li Y, Bhupathiraju SN, Rosner BA, Sun Q, Giovannucci EL, Rimm EB, Manson JE, Willett WC, Stampfer MJ, Hu FB. Fruit and Vegetable Intake and Mortality: Results From 2 Prospective Cohort Studies of US Men and Women and a Meta-Analysis of 26 Cohort Studies. *Circulation* 2021; **143**: 1642-1654 [PMID: 33641343 DOI: 10.1161/CIRCULATIONAHA.120.048996]

16 **Fuchs CS**, Giovannucci EL, Colditz GA, Hunter DJ, Stampfer MJ, Rosner B, Speizer FE, Willett WC. Dietary fiber and the risk of colorectal cancer and adenoma in women. *N Engl J Med* 1999; **340**: 169-176 [PMID: 9895396 DOI: 10.1056/nejm199901213400301]

17 **Flood A**, Velie EM, Chaterjee N, Subar AF, Thompson FE, Lacey JV Jr, Schairer C, Troisi R, Schatzkin A. Fruit and vegetable intakes and the risk of colorectal cancer in the Breast Cancer Detection Demonstration Project follow-up cohort. *Am J Clin Nutr* 2002; **75**: 936-943 [PMID: 11976170 DOI: 10.1093/ajcn/75.5.936]

18 **Koushik A**, Hunter DJ, Spiegelman D, Beeson WL, van den Brandt PA, Buring JE, Calle EE, Cho E, Fraser GE, Freudenheim JL, Fuchs CS, Giovannucci EL, Goldbohm RA, Harnack L, Jacobs DR Jr, Kato I, Krogh V, Larsson SC, Leitzmann MF, Marshall JR, McCullough ML, Miller AB, Pietinen P, Rohan TE, Schatzkin A, Sieri S, Virtanen MJ, Wolk A, Zeleniuch-Jacquotte A, Zhang SM, Smith-Warner SA. Fruits, vegetables, and colon cancer risk in a pooled analysis of 14 cohort studies. *J Natl Cancer Inst* 2007; **99**: 1471-1483 [PMID: 17895473 DOI: 10.1093/jnci/djm155]

19 **Wang X**, Ouyang Y, Liu J, Zhu M, Zhao G, Bao W, Hu FB. Fruit and vegetable consumption and mortality from all causes, cardiovascular disease, and cancer: systematic review and dose-response meta-analysis of prospective cohort studies. *BMJ* 2014; **349**: g4490 [PMID: 25073782 DOI: 10.1136/bmj.g4490]

20 **Yang Y**, Zhang D, Feng N, Chen G, Liu J, Zhu Y. Increased intake of vegetables, but not fruit, reduces risk for hepatocellular carcinoma: a meta-analysis. *Gastroenterology* 2014; **147**: 1031-1042 [PMID: 25127680 DOI: 10.1053/j.gastro.2014.08.005]

21 **Norat T**, Aune D, Chan D, Romaguera D. Fruits and vegetables: updating the epidemiologic evidence for the WCRF/AICR lifestyle recommendations for cancer prevention. *Cancer Treat Res* 2014; **159**: 35-50 [PMID: 24114473 DOI: 10.1007/978-3-642-38007-5_3]

22 **Liberati A**, Altman DG, Tetzlaff J, Mulrow C, Gøtzsche PC, Ioannidis JP, Clarke M, Devereaux PJ, Kleijnen J, Moher D. The PRISMA statement for reporting systematic reviews and meta-analyses of studies that evaluate health care interventions: explanation and elaboration. *PLoS Med* 2009; **6**: e1000100 [PMID: 19621070 DOI: 10.1371/journal.pmed.1000100]

23 **Aune D**, Chan DS, Lau R, Vieira R, Greenwood DC, Kampman E, Norat T. Dietary fibre, whole grains, and risk of colorectal cancer: systematic review and dose-response meta-analysis of prospective studies. *BMJ* 2011; **343**: d6617 [PMID: 22074852 DOI: 10.1136/bmj.d6617]

24 **Rong Y**, Chen L, Zhu T, Song Y, Yu M, Shan Z, Sands A, Hu FB, Liu L. Egg consumption and risk of coronary heart disease and stroke: dose-response meta-analysis of prospective cohort studies. *BMJ* 2013; **346**: e8539 [PMID: 23295181 DOI: 10.1136/bmj.e8539]

25 **Vieira AR**, Abar L, Vingeliene S, Chan DS, Aune D, Navarro-Rosenblatt D, Stevens C, Greenwood D, Norat T. Fruits, vegetables and lung cancer risk: a systematic review and meta-analysis. *Ann Oncol* 2016; **27**: 81-96 [PMID: 26371287 DOI: 10.1093/annonc/mdv381]

26 **Riboli E**, Norat T. Epidemiologic evidence of the protective effect of fruit and vegetables on cancer risk. *Am J Clin Nutr* 2003; **78**: 559S-569S [PMID: 12936950 DOI: 10.1093/ajcn/78.3.559S]

27 **Sterne JA**, Hernán MA, Reeves BC, Savović J, Berkman ND, Viswanathan M, Henry D, Altman DG, Ansari MT, Boutron I, Carpenter JR, Chan AW, Churchill R, Deeks JJ, Hróbjartsson A, Kirkham J, Jüni P, Loke YK, Pigott TD, Ramsay CR, Regidor D, Rothstein HR, Sandhu L, Santaguida PL, Schünemann HJ, Shea B, Shrier I, Tugwell P, Turner L, Valentine JC, Waddington H, Waters E, Wells GA, Whiting PF, Higgins JP. ROBINS-I: a tool for assessing risk of bias in non-randomised studies of interventions. *BMJ* 2016; **355**: i4919 [PMID: 27733354 DOI: 10.1136/bmj.i4919]

28 **Localio AR**, Margolis DJ, Berlin JA. Relative risks and confidence intervals were easily computed indirectly from multivariable logistic regression. *J Clin Epidemiol* 2007; **60**: 874-882 [PMID: 17689803 DOI: 10.1016/j.jclinepi.2006.12.001]

29 **Franceschi S**, Parpinel M, La Vecchia C, Favero A, Talamini R, Negri E. Role of different types of vegetables and fruit in the prevention of cancer of the colon, rectum, and breast. *Epidemiology* 1998; **9**: 338-341 [PMID: 9583427]

30 **Franceschi S**, Favero A. The role of energy and fat in cancers of the breast and colon-rectum in a southern European population. *Ann Oncol* 1999; **10** Suppl 6: 61-63 [PMID: 10676554]

31 **Franceschi S**, Favero A, Parpinel M, Giacosa A, La Vecchia C. Italian study on colorectal cancer with emphasis on influence of cereals. *Eur J Cancer Prev* 1998; **7** Suppl 2: S19-S23 [PMID: 9696938 DOI: 10.1097/00008469-199805000-00004]

32 **Jedrychowski W**, Maugeri U, Popiela T, Kulig J, Sochacka-Tatara E, Pac A, Sowa A, Musial A. Case-control study on beneficial effect of regular consumption of apples on colorectal cancer risk in a population with relatively low intake of fruits and vegetables. *Eur J Cancer Prev* 2010; **19**: 42-47 [PMID: 19926998 DOI: 10.1097/CEJ.0b013e328333d0cc]

33 **Jedrychowski W**, Maugeri U, Pac A, Sochacka-Tatara E, Galas A. Reduced risk of colorectal cancer and regular consumption of apples: Hospital based case-control study in Poland. *CEJ Med* 2009; **4**: 320-326 [DOI: 10.2478/s11536-009-0033-6]

34 **Tuyns AJ**, Kaaks R, Haelterman M. Colorectal cancer and the consumption of foods: a case-control study in Belgium. *Nutr Cancer* 1988; **11**: 189-204 [PMID: 3405870 DOI: 10.1080/01635588809513986]

35 **Tajima K**, Tominaga S. Dietary habits and gastro-intestinal cancers: a comparative case-control study of stomach and large intestinal cancers in Nagoya, Japan. *Jpn J Cancer Res* 1985; **76**: 705-716 [PMID: 3930448]

36 **Lin J**, Zhang SM, Wu K, Willett WC, Fuchs CS, Giovannucci E. Flavonoid intake and colorectal cancer risk in men and women. *Am J Epidemiol* 2006; **164**: 644-651 [PMID: 16923774 DOI: 10.1093/aje/kwj296]

37 **Theodoratou E**, Kyle J, Cetnarskyj R, Farrington SM, Tenesa A, Barnetson R, Porteous M, Dunlop M, Campbell H.

Dietary flavonoids and the risk of colorectal cancer. *Cancer Epidemiol Biomarkers Prev* 2007; **16**: 684-693 [PMID: 17416758 DOI: 10.1158/1055-9965.Epi-06-0785]

38 **Deneo-Pellegrini H**, Boffetta P, De Stefani E, Ronco A, Brennan P, Mendilaharsu M. Plant foods and differences between colon and rectal cancers. *Eur J Cancer Prev* 2002; **11**: 369-375 [PMID: 12195164 DOI: 10.1097/00008469-200208000-00009]

39 **Lee J**, Shin A, Oh JH, Kim J. Colors of vegetables and fruits and the risks of colorectal cancer. *World J Gastroenterol* 2017; **23**: 2527-2538 [PMID: 28465637 DOI: 10.3748/wjg.v23.i14.2527]

40 **Leenders M**, Siersema PD, Overvad K, Tjønneland A, Olsen A, Boutron-Ruault MC, Bastide N, Fagherazzi G, Katzke V, Kühn T, Boeing H, Aleksandrova K, Trichopoulou A, Lagiou P, Klinaki E, Masala G, Grioni S, Santucci De Magistris M, Tumino R, Ricceri F, Peeters PH, Lund E, Skeie G, Weiderpass E, Quirós JR, Agudo A, Sánchez MJ, Dorronsoro M, Navarro C, Ardanaz E, Ohlsson B, Jirström K, Van Guelpen B, Wennberg M, Khaw KT, Wareham N, Key TJ, Romieu I, Huybrechts I, Cross AJ, Murphy N, Riboli E, Bueno-de-Mesquita HB. Subtypes of fruit and vegetables, variety in consumption and risk of colon and rectal cancer in the European Prospective Investigation into Cancer and Nutrition. *Int J Cancer* 2015; **137**: 2705-2714 [PMID: 26077137 DOI: 10.1002/ijc.29640]

41 **Abu Mweis SS**, Tayyem RF, Shehadah I, Bawadi HA, Agraib LM, Bani-Hani KE, Al-Jaberi T, Al-Nusairr M. Food groups and the risk of colorectal cancer: results from a Jordanian case-control study. *Eur J Cancer Prev* 2015; **24**: 313-320 [PMID: 25415835 DOI: 10.1097/CEJ.0000000000000089]

42 **Tayyem RF**, Shehadah I, Abu-Mweis SS, Bawadi HA, Bani-Hani KE, Al-Jaberi T, Al-Nusairr M, Heath DD. Fruit and vegetable intake among Jordanians: results from a case-control study of colorectal cancer. *Cancer Control* 2014; **21**: 350-360 [PMID: 25310217 DOI: 10.1177/107327481402100412]

43 **Rosato V**, Bosetti C, Levi F, Polesel J, Zucchetto A, Negri E, La Vecchia C. Risk factors for young-onset colorectal cancer. *Cancer Causes Control* 2013; **24**: 335-341 [PMID: 23224326 DOI: 10.1007/s10552-012-0119-3]

44 **Annema N**, Heyworth JS, McNaughton SA, Iacopetta B, Fritschi L. Fruit and vegetable consumption and the risk of proximal colon, distal colon, and rectal cancers in a case-control study in Western Australia. *J Am Diet Assoc* 2011; **111**: 1479-1490 [PMID: 21963014 DOI: 10.1016/j.jada.2011.07.008]

45 **Foschi R**, Pelucchi C, Dal Maso L, Rossi M, Levi F, Talamini R, Bosetti C, Negri E, Serraino D, Giacosa A, Franceschi S, La Vecchia C. Citrus fruit and cancer risk in a network of case-control studies. *Cancer Causes Control* 2010; **21**: 237-242 [PMID: 19856118 DOI: 10.1007/s10552-009-9454-4]

46 **Williams CD**, Satia JA, Adair LS, Stevens J, Galanko J, Keku TO, Sandler RS. Dietary patterns, food groups, and rectal cancer risk in Whites and African-Americans. *Cancer Epidemiol Biomarkers Prev* 2009; **18**: 1552-1561 [PMID: 19423533 DOI: 10.1158/1055-9965.EPI-08-1146]

47 **Gallus S**, Talamini R, Giacosa A, Montella M, Ramazzotti V, Franceschi S, Negri E, La Vecchia C. Does an apple a day keep the oncologist away? *Ann Oncol* 2005; **16**: 1841-1844 [PMID: 16091428 DOI: 10.1093/annonc/mdi361]

48 **Satia-Abouta J**, Galanko JA, Martin CF, Ammerman A, Sandler RS. Food groups and colon cancer risk in African-Americans and Caucasians. *Int J Cancer* 2004; **109**: 728-736 [PMID: 14999782 DOI: 10.1002/ijc.20044]

49 **Levi F**, Pasche C, La Vecchia C, Lucchini F, Franceschi S. Food groups and colorectal cancer risk. *Br J Cancer* 1999; **79**: 1283-1287 [PMID: 10098773 DOI: 10.1038/sj.bjc.6690206]

50 **Vogtmann E**, Xiang YB, Li HL, Levitan EB, Yang G, Waterbor JW, Gao J, Cai H, Xie L, Wu QJ, Zhang B, Gao YT, Zheng W, Shu XO. Fruit and vegetable intake and the risk of colorectal cancer: results from the Shanghai Men's Health Study. *Cancer Causes Control* 2013; **24**: 1935-1945 [PMID: 23913012 DOI: 10.1007/s10552-013-0268-z]

51 **Li WQ**, Kuriyama S, Li Q, Nagai M, Hozawa A, Nishino Y, Tsuji I. Citrus consumption and cancer incidence: the Ohsaki cohort study. *Int J Cancer* 2010; **127**: 1913-1922 [PMID: 20104526 DOI: 10.1002/ijc.25203]

52 **Nomura AM**, Wilkens LR, Murphy SP, Hankin JH, Henderson BE, Pike MC, Kolonel LN. Association of vegetable, fruit, and grain intakes with colorectal cancer: the Multiethnic Cohort Study. *Am J Clin Nutr* 2008; **88**: 730-737 [PMID: 18779290 DOI: 10.1093/ajcn/88.3.730]

53 **Voorrips LE**, Goldbohm RA, van Poppel G, Sturmans F, Hermus RJ, van den Brandt PA. Vegetable and fruit consumption and risks of colon and rectal cancer in a prospective cohort study: The Netherlands Cohort Study on Diet and Cancer. *Am J Epidemiol* 2000; **152**: 1081-1092 [PMID: 11117618 DOI: 10.1093/aje/152.11.1081]

54 **Michels KB**, Edward Giovannucci, Joshipura KJ, Rosner BA, Stampfer MJ, Fuchs CS, Colditz GA, Speizer FE, Willett WC. Prospective study of fruit and vegetable consumption and incidence of colon and rectal cancers. *J Natl Cancer Inst* 2000; **92**: 1740-1752 [PMID: 11058617 DOI: 10.1093/jnci/92.21.1740]

55 **Lin J**, Zhang SM, Cook NR, Rexrode KM, Liu S, Manson JE, Lee IM, Buring JE. Dietary intakes of fruit, vegetables, and fiber, and risk of colorectal cancer in a prospective cohort of women (United States). *Cancer Causes Control* 2005; **16**: 225-233 [PMID: 15947874 DOI: 10.1007/s10552-004-4025-1]

56 **Le Marchand L**, Hankin JH, Wilkens LR, Kolonel LN, Englyst HN, Lyu LC. Dietary fiber and colorectal cancer risk. *Epidemiology* 1997; **8**: 658-665 [PMID: 9345666 DOI: 10.1097/00001648-199710000-00008]

57 **Deneo-Pellegrini H**, De Stefani E, Ronco A. Vegetables, fruits, and risk of colorectal cancer: a case-control study from Uruguay. *Nutr Cancer* 1996; **25**: 297-304 [PMID: 8771572 DOI: 10.1080/01635589609514453]

58 **Jaganathan SK**, Vellayappan MV, Narasimhan G, Supriyanto E. Role of pomegranate and citrus fruit juices in colon cancer prevention. *World J Gastroenterol* 2014; **20**: 4618-4625 [PMID: 24782614 DOI: 10.3748/wjg.v20.i16.4618]

59 **Goh JXH**, Tan LT, Goh JK, Chan KG, Pusparajah P, Lee LH, Goh BH. Nobiletin and Derivatives: Functional Compounds from Citrus Fruit Peel for Colon Cancer Chemoprevention. *Cancers (Basel)* 2019; **11** [PMID: 31234411 DOI: 10.3390/cancers11060867]

60 **Frydoonfar HR**, McGrath DR, Spigelman AD. The variable effect on proliferation of a colon cancer cell line by the citrus fruit flavonoid Naringenin. *Colorectal Dis* 2003; **5**: 149-152 [PMID: 12780904 DOI: 10.1046/j.1463-1318.2003.00444.x]

61 **Zhang YS**, Wang F, Cui SX, Qu XJ. Natural dietary compound naringin prevents azoxymethane/dextran sodium sulfate-induced chronic colorectal inflammation and carcinogenesis in mice. *Cancer Biol Ther* 2018; **19**: 735-744 [PMID: 29580144 DOI: 10.1080/15384047.2018.1453971]

62 **Gong Y**, Dong R, Gao X, Li J, Jiang L, Zheng J, Cui S, Ying M, Yang B, Cao J, He Q. Neohesperidin prevents colorectal tumorigenesis by altering the gut microbiota. *Pharmacol Res* 2019; **148**: 104460 [PMID: 31560944 DOI: 10.1016/j.phrs.2019.104460]

63 **Li Y**, Wang S, Sun Y, Xu W, Zheng H, Wang Y, Tang Y, Gao X, Song C, Long Y, Liu J, Liu L, Mei Q. Apple polysaccharide protects ICR mice against colitis associated colorectal cancer through the regulation of microbial dysbiosis. *Carbohydr Polym* 2020; **230**: 115726 [PMID: 31887919 DOI: 10.1016/j.carbpol.2019.115726]

64 **Zhang D**, Sun Y, Yue Z, Li Q, Meng J, Liu J, Hekong X, Jiang F, Mi M, Liu L, Mei Q. Apple polysaccharides induce apoptosis in colorectal cancer cells. *Int J Mol Med* 2012; **30**: 100-106 [PMID: 22470124 DOI: 10.3892/ijmm.2012.953]

65 **Zhang D**, Li YH, Mi M, Jiang FL, Yue ZG, Sun Y, Fan L, Meng J, Zhang X, Liu L, Mei QB. Modified apple polysaccharides suppress the migration and invasion of colorectal cancer cells induced by lipopolysaccharide. *Nutr Res* 2013; **33**: 839-848 [PMID: 24074742 DOI: 10.1016/j.nutres.2013.06.004]

66 **Bars-Cortina D**, Martínez-Bardají A, Macià A, Motilva MJ, Piñol-Felis C. Consumption evaluation of one apple flesh a day in the initial phases prior to adenoma/adenocarcinoma in an azoxymethane rat colon carcinogenesis model. *J Nutr Biochem* 2020; **83**: 108418 [PMID: 32592950 DOI: 10.1016/j.jnutbio.2020.108418]

67 **Marzo F**, Milagro FI, Barrenetxe J, Díaz MT, Martínez JA. Azoxymethane-Induced Colorectal Cancer Mice Treated with a Polyphenol-Rich Apple Extract Show Less Neoplastic Lesions and Signs of Cachexia. *Foods* 2021; **10** [PMID: 33921048 DOI: 10.3390/foods10040863]

68 **Kern M**, Pahlke G, Balavenkatraman KK, Böhmer FD, Marko D. Apple polyphenols affect protein kinase C activity and the onset of apoptosis in human colon carcinoma cells. *J Agric Food Chem* 2007; **55**: 4999-5006 [PMID: 17542601 DOI: 10.1021/jf063158x]

69 **Steevens J**, Schouten LJ, Goldbohm RA, van den Brandt PA. Vegetables and fruits consumption and risk of esophageal and gastric cancer subtypes in the Netherlands Cohort Study. *Int J Cancer* 2011; **129**: 2681-2693 [PMID: 21960262 DOI: 10.1002/ijc.25928]

70 **Yamaji T**, Inoue M, Sasazuki S, Iwasaki M, Kurahashi N, Shimazu T, Tsugane S; Japan Public Health Center-based Prospective Study Group. Fruit and vegetable consumption and squamous cell carcinoma of the esophagus in Japan: the JPHC study. *Int J Cancer* 2008; **123**: 1935-1940 [PMID: 18688852 DOI: 10.1002/ijc.23744]

71 **Bae JM**, Lee EJ, Guyatt G. Citrus fruit intake and stomach cancer risk: a quantitative systematic review. *Gastric Cancer* 2008; **11**: 23-32 [PMID: 18373174 DOI: 10.1007/s10120-007-0447-2]

72 **Holst B**, Williamson G. Nutrients and phytochemicals: from bioavailability to bioefficacy beyond antioxidants. *Curr Opin Biotechnol* 2008; **19**: 73-82 [PMID: 18406129 DOI: 10.1016/j.copbio.2008.03.003]

73 **Oh H**, Kim H, Lee DH, Lee A, Giovannucci EL, Kang SS, Keum N. Different dietary fibre sources and risks of colorectal cancer and adenoma: a dose-response meta-analysis of prospective studies. *Br J Nutr* 2019; **122**: 605-615 [PMID: 31495339 DOI: 10.1017/S0007114519001454]

World Journal of Gastroenterology

Submit a Manuscript: https://www.f6publishing.com

World J Gastroenterol 2023 May 7; 29(17): 2701-2703

DOI: 10.3748/wjg.v29.i17.2701

ISSN 1007-9327 (print) ISSN 2219-2840 (online)

LETTER TO THE EDITOR

T cells in pancreatic cancer stroma: Tryptophan metabolism plays an important role in immunoregulation

Ting Yang, Qiao-Qi Li, Yong-Mei Liu, Biao Yang

Specialty type: Gastroenterology and hepatology

Provenance and peer review: Unsolicited article; Externally peer reviewed.

Peer-review model: Single blind

Peer-review report's scientific quality classification

Grade A (Excellent): A
Grade B (Very good): B
Grade C (Good): 0
Grade D (Fair): 0
Grade E (Poor): 0

P-Reviewer: Liu X, China; Zeng C, United States

Received: December 7, 2022
Peer-review started: December 7, 2022
First decision: January 22, 2023
Revised: February 10, 2023
Accepted: April 4, 2023
Article in press: April 4, 2023
Published online: May 7, 2023

Ting Yang, Qiao-Qi Li, Biao Yang, Department of Abdominal Oncology, Division of Medical Oncology, Cancer Center, West China Hospital, Sichuan University, Chengdu 610041, Sichuan Province, China

Yong-Mei Liu, Division of Radiation Oncology, Cancer Center, West China Hospital, Sichuan University, Chengdu 610041, Sichuan Province, China

Corresponding author: Biao Yang, MD, PhD, Professor, Surgeon, Teacher, Department of Abdominal Oncology, Division of Medical Oncology, Cancer Center, West China Hospital, Sichuan University, No. 37 Guoxue Alley, Chengdu 610041, Sichuan Province, China.
landayb@163.com

Abstract

Several studies have shown that the immune system is highly regulated by tryptophan metabolism, which serves as an immunomodulatory factor. The indoleamine 2,3-dioxygenase 1 (IDO1), as an intracellular enzyme that participates in metabolism of the essential amino acid tryptophan in the kynurenine pathway, is an independent prognostic marker for pancreatic cancer (PC). First, overexpression of IDO1 inhibits the maturation of dendritic cells and T-cell proliferation in the liver and spleen. Second, the high expression of kynurenine induces and activates the aryl hydrocarbon receptor, resulting in upregulated programmed cell death protein 1 expression. Third, the induction of IDO1 can lead to loss of the T helper 17 cell/regulatory T cell balance, mediated by the proximal tryptophan catabolite from IDO metabolism. In our study, we found that overexpression of IDO1 upregulated CD8+ T cells and reduced natural killer T cells in pancreatic carcinoma in mice. Hence, it may be essential to pay more attention to tryptophan metabolism in patients, especially those who are tolerant to immunotherapy for PC.

Key Words: Immunosuppression; Pancreatic cancer stroma; T cell; Tryptophan metabolism; Xxx

©The Author(s) 2023. Published by Baishideng Publishing Group Inc. All rights reserved.

Core Tip: There are numerous lines for evidence for tryptophan metabolism, which serves as an immunomodulatory factor. Indoleamine2,3-dioxygenase1 (IDO1) overexpression inhibits the maturation of dendritic cells and T-cell proliferation in the spleen. The high expression of kynurenine induces and activates the aryl hydrocarbon receptor, resulting in upregulated programmed cell death protein 1 expression. The induction of IDO1 can lead to loss of T helper 17 cell/regulatory T cell balance. We also found that overexpression of IDO1 upregulated CD8+ T cells and reduced natural killer T cells in PC in mice.

Citation: Yang T, Li QQ, Liu YM, Yang B. T cells in pancreatic cancer stroma: Tryptophan metabolism plays an important role in immunoregulation. *World J Gastroenterol* 2023; 29(17): 2701-2703
URL: https://www.wjgnet.com/1007-9327/full/v29/i17/2701.htm
DOI: https://dx.doi.org/10.3748/wjg.v29.i17.2701

TO THE EDITOR

We have an interest in the recently published article by Goulart *et al*[1],which summarized the pancreatic cancer (PC) immune landscape, T-cell interactions and immune dysfunction, T-cell phenotype and functions, T-cell exhaustion, and immunotherapy in PC. In this review, Goulart *et al* stated that immune cells including CD8+ T, natural killer (NK) cells, T helper 17 cells (Th17), and regulatory T cells (Tregs) are regulated by different cytokine factors. However, several studies have shown that the immune system is highly regulated by tryptophan metabolism. Indoleamine 2,3-dioxygenase 1 (IDO1), as an intracellular enzyme that participates in the metabolism of the essential amino acid tryptophan in the kynurenine (Kyn) pathway, is an independent prognostic marker for PC. There are numerous lines of evidence for tryptophan metabolism, which serves as an immunomodulatory factor. First, IDO1 overexpression inhibits the maturation of CD11c and dendritic cells, and T-cell proliferation in the liver and spleen[2]. Second, the high expression of Kyn induces and activates the aryl hydrocarbon receptor (AhR), resulting in upregulated programmed cell death protein 1 expression. Inhibition of the Kyn-AhR pathway can enhance the efficacy of antitumor adoptive T-cell therapy and reduce the rate of migration and invasion in both tumor-bearing mice and patients with cancer[3]. In *in vivo* experiments, inactivation of the Kyn-AhR pathway showed amelioration of IDO1-mediated immunosuppression[4]. In a clinical study, high expression of the AhR transcript was correlated with reduced CD8 T-cell infiltration and worse outcomes in patients with PC[5]. Third, the induction of IDO1 can lead to loss of the Th17/Treg balance *in vivo*. Similarly, loss of the Th17/Treg balance is mediated by the proximal tryptophan catabolite from IDO metabolism[6]. In our study, we found that overexpression of IDO1 upregulated CD8+ T cells and reduced NK T cells in both hepatic cancer and PC in mice. Hence, it may be essential to pay more attention to tryptophan metabolism in patients with PC, especially those who are tolerant to immunotherapy.

FOOTNOTES

Author contributions: Yang T, Li QQ, Liu YM, and Yang B designed the research study; Yang T and Li QQ performed the research; Yang T, Li QQ, and Yang B analyzed the data and wrote the manuscript; All authors read and approved the final manuscript.

Supported by National Natural Science Foundation of China, No. 82200695.

Conflict-of-interest statement: The authors have no conflicts of interest to declare.

Open-Access: This article is an open-access article that was selected by an in-house editor and fully peer-reviewed by external reviewers. It is distributed in accordance with the Creative Commons Attribution NonCommercial (CC BY-NC 4.0) license, which permits others to distribute, remix, adapt, build upon this work non-commercially, and license their derivative works on different terms, provided the original work is properly cited and the use is non-commercial. See: https://creativecommons.org/Licenses/by-nc/4.0/

Country/Territory of origin: China

ORCID number: Yong-Mei Liu 0000-0002-0346-1158; Biao Yang 0000-0003-2150-8690.

S-Editor: Liu GL
L-Editor: Filipodia

P-Editor: Liu GL

REFERENCES

1 **Goulart MR**, Stasinos K, Fincham REA, Delvecchio FR, Kocher HM. T cells in pancreatic cancer stroma. *World J Gastroenterol* 2021; **27**: 7956-7968 [PMID: 35046623 DOI: 10.3748/wjg.v27.i46.7956]

2 **Mo C**, Xie S, Liu B, Zhong W, Zeng T, Huang S, Lai Y, Deng G, Zhou C, Yan W, Chen Y, Gao L, Lv Z. Indoleamine 2,3-dioxygenase 1 limits hepatic inflammatory cells recruitment and promotes bile duct ligation-induced liver fibrosis. *Cell Death Dis* 2021; **12**: 16 [PMID: 33414436 DOI: 10.1038/s41419-020-03277-0]

3 **Liu Y**, Liang X, Dong W, Fang Y, Lv J, Zhang T, Fiskesund R, Xie J, Liu J, Yin X, Jin X, Chen D, Tang K, Ma J, Zhang H, Yu J, Yan J, Liang H, Mo S, Cheng F, Zhou Y, Wang J, Li J, Chen Y, Cui B, Hu ZW, Cao X, Xiao-Feng Qin F, Huang B. Tumor-Repopulating Cells Induce PD-1 Expression in CD8(+) T Cells by Transferring Kynurenine and AhR Activation. *Cancer Cell* 2018; **33**: 480-494.e7 [PMID: 29533786 DOI: 10.1016/j.ccell.2018.02.005]

4 **Liang H**, Li T, Fang X, Xing Z, Zhang S, Shi L, Li W, Guo L, Kuang C, Liu H, Yang Q. IDO1/TDO dual inhibitor RY103 targets Kyn-AhR pathway and exhibits preclinical efficacy on pancreatic cancer. *Cancer Lett* 2021; **522**: 32-43 [PMID: 34520819 DOI: 10.1016/j.canlet.2021.09.012]

5 **Newman AC**, Falcone M, Huerta Uribe A, Zhang T, Athineos D, Pietzke M, Vazquez A, Blyth K, Maddocks ODK. Immune-regulated IDO1-dependent tryptophan metabolism is source of one-carbon units for pancreatic cancer and stellate cells. *Mol Cell* 2021; **81**: 2290-2302.e7 [PMID: 33831358 DOI: 10.1016/j.molcel.2021.03.019]

6 **Favre D**, Mold J, Hunt PW, Kanwar B, Loke P, Seu L, Barbour JD, Lowe MM, Jayawardene A, Aweeka F, Huang Y, Douek DC, Brenchley JM, Martin JN, Hecht FM, Deeks SG, McCune JM. Tryptophan catabolism by indoleamine 2,3-dioxygenase 1 alters the balance of TH17 to regulatory T cells in HIV disease. *Sci Transl Med* 2010; **2**: 32ra36 [PMID: 20484731 DOI: 10.1126/scitranslmed.3000632]



Published by **Baishideng Publishing Group Inc**
7041 Koll Center Parkway, Suite 160, Pleasanton, CA 94566, USA
Telephone: +1-925-3991568
E-mail: bpgoffice@wjgnet.com
Help Desk: https://www.f6publishing.com/helpdesk
https://www.wjgnet.com



© 2023 Baishideng Publishing Group Inc. All rights reserved.

ISSN 1007-9327 (print)
ISSN 2219-2840 (online)

World Journal of *Gastroenterology*

World J Gastroenterol 2023 May 14; 29(18): 2704-2887



Published by Baishideng Publishing Group Inc

World Journal of Gastroenterology

Contents

Weekly Volume 29 Number 18 May 14, 2023

REVIEW

2704 Key elements determining the intestinal region-specific environment of enteric neurons in type 1 diabetes

Bagyánszki M, Bódi N

2717 Paediatric gastrointestinal endoscopy in the Asian-Pacific region: Recent advances in diagnostic and therapeutic techniques

Huang JG, Tanpowpong P

2733 Study of tumor necrosis factor receptor in the inflammatory bowel disease

Souza RF, Caetano MAF, Magalhães HIR, Castelucci P

2747 Current trends in acute pancreatitis: Diagnostic and therapeutic challenges

Zerem E, Kurtcehajic A, Kunosić S, Zerem Malkočević D, Zerem O

2764 Wingless/It/β-catenin signaling in liver metastasis from colorectal cancer: A focus on biological mechanisms and therapeutic opportunities

Selvaggi F, Catalano T, Lattanzio R, Cotellese R, Aceto GM

MINIREVIEWS

2784 Infliximab *vs* adalimumab: Points to consider when selecting anti-tumor necrosis factor agents in pediatric patients with Crohn's disease

Kim ES, Kang B

ORIGINAL ARTICLE

Basic Study

2798 Calcitriol attenuates liver fibrosis through hepatitis C virus nonstructural protein 3-transactivated protein 1-mediated TGF β1/Smad3 and NF-κB signaling pathways

Shi L, Zhou L, Han M, Zhang Y, Zhang Y, Yuan XX, Lu HP, Wang Y, Yang XL, Liu C, Wang J, Liang P, Liu SA, Liu XJ, Cheng J, Lin SM

2818 BanXiaXieXin decoction treating gastritis mice with drug-resistant *Helicobacter pylori* and its mechanism

Li XH, Xu JY, Wang X, Liao LJ, Huang L, Huang YQ, Zhang ZF

Retrospective Cohort Study

2836 Endoscopic and pathological characteristics of *de novo* colorectal cancer: Retrospective cohort study

Li SY, Yang MQ, Liu YM, Sun MJ, Zhang HJ

Retrospective Study

2850 Prolonged hyperthermic intraperitoneal chemotherapy duration with 90 minutes cisplatin might increase overall survival in gastric cancer patients with peritoneal metastases

Steinhoff H, Acs M, Blaj S, Dank M, Herold M, Herold Z, Herzberg J, Sanchez-Velazquez P, Strate T, Szasz AM, Piso P

Observational Study

2864 Endoscopic ultrasound-guided fine-needle aspiration pancreatic adenocarcinoma samples yield adequate DNA for next-generation sequencing: A cohort analysis

Bunduc S, Varzaru B, Iacob RA, Sorop A, Manea I, Spiridon A, Chelaru R, Croitoru AE, Becheanu G, Dumbrava M, Dima S, Popescu I, Gheorghe C

2875 Contributory roles of sarcopenia and myosteatosis in development of overt hepatic encephalopathy and mortality after transjugular intrahepatic portosystemic shunt

Yin L, Chu SL, Lv WF, Zhou CZ, Liu KC, Zhu YJ, Zhang WY, Wang CX, Zhang YH, Lu D, Cheng DL

ABOUT COVER

Editorial Board of *World Journal of Gastroenterology*, Octavio Caba, PhD, Professor, Senior Scientist, Department of Human Anatomy and Embriology, University of Granada, Granada 18016, Spain. ocaba@ugr.es

AIMS AND SCOPE

The primary aim of *World Journal of Gastroenterology* (*WJG*, *World J Gastroenterol*) is to provide scholars and readers from various fields of gastroenterology and hepatology with a platform to publish high-quality basic and clinical research articles and communicate their research findings online. *WJG* mainly publishes articles reporting research results and findings obtained in the field of gastroenterology and hepatology and covering a wide range of topics including gastroenterology, hepatology, gastrointestinal endoscopy, gastrointestinal surgery, gastrointestinal oncology, and pediatric gastroenterology.

INDEXING/ABSTRACTING

The *WJG* is now abstracted and indexed in Science Citation Index Expanded (SCIE, also known as SciSearch®), Current Contents/Clinical Medicine, Journal Citation Reports, Index Medicus, MEDLINE, PubMed, PubMed Central, Scopus, Reference Citation Analysis, China National Knowledge Infrastructure, China Science and Technology Journal Database, and Superstar Journals Database. The 2022 edition of Journal Citation Reports® cites the 2021 impact factor (IF) for *WJG* as 5.374; IF without journal self cites: 5.187; 5-year IF: 5.715; Journal Citation Indicator: 0.84; Ranking: 31 among 93 journals in gastroenterology and hepatology; and Quartile category: Q2. The *WJG*'s CiteScore for 2021 is 8.1 and Scopus CiteScore rank 2021: Gastroenterology is 18/149.

RESPONSIBLE EDITORS FOR THIS ISSUE

Production Editor: *Hua-Ge Yu*; **Production Department Director:** *Xu Guo*; **Editorial Office Director:** *Jia-Ru Fan.*

NAME OF JOURNAL
World Journal of Gastroenterology

ISSN
ISSN 1007-9327 (print) ISSN 2219-2840 (online)

LAUNCH DATE
October 1, 1995

FREQUENCY
Weekly

EDITORS-IN-CHIEF
Andrzej S Tarnawski

EDITORIAL BOARD MEMBERS
http://www.wjgnet.com/1007-9327/editorialboard.htm

PUBLICATION DATE
May 14, 2023

COPYRIGHT
© 2023 Baishideng Publishing Group Inc

INSTRUCTIONS TO AUTHORS
https://www.wjgnet.com/bpg/gerinfo/204

GUIDELINES FOR ETHICS DOCUMENTS
https://www.wjgnet.com/bpg/GerInfo/287

GUIDELINES FOR NON-NATIVE SPEAKERS OF ENGLISH
https://www.wjgnet.com/bpg/gerinfo/240

PUBLICATION ETHICS
https://www.wjgnet.com/bpg/GerInfo/288

PUBLICATION MISCONDUCT
https://www.wjgnet.com/bpg/gerinfo/208

ARTICLE PROCESSING CHARGE
https://www.wjgnet.com/bpg/gerinfo/242

STEPS FOR SUBMITTING MANUSCRIPTS
https://www.wjgnet.com/bpg/GerInfo/239

ONLINE SUBMISSION
https://www.f6publishing.com

© 2023 Baishideng Publishing Group Inc. All rights reserved. 7041 Koll Center Parkway, Suite 160, Pleasanton, CA 94566, USA

E-mail: bpgoffice@wjgnet.com https://www.wjgnet.com

World Journal of Gastroenterology

Submit a Manuscript: https://www.f6publishing.com

World J Gastroenterol 2023 May 14; 29(18): 2704-2716

DOI: 10.3748/wjg.v29.i18.2704

ISSN 1007-9327 (print) ISSN 2219-2840 (online)

REVIEW

Key elements determining the intestinal region-specific environment of enteric neurons in type 1 diabetes

Mária Bagyánszki, Nikolett Bódi

Specialty type: Gastroenterology and hepatology

Provenance and peer review: Invited article; Externally peer reviewed.

Peer-review model: Single blind

Peer-review report's scientific quality classification

Grade A (Excellent): 0
Grade B (Very good): B
Grade C (Good): C, C
Grade D (Fair): 0
Grade E (Poor): 0

P-Reviewer: Baccari MC, Italy; Castelucci P, Brazil; Sahin Y, Turkey

Received: December 15, 2022
Peer-review started: December 15, 2022
First decision: March 15, 2023
Revised: March 28, 2023
Accepted: April 17, 2023
Article in press: April 17, 2023
Published online: May 14, 2023

Mária Bagyánszki, Nikolett Bódi, Department of Physiology, Anatomy and Neuroscience, Faculty of Science and Informatics, University of Szeged, Szeged H-6726, Hungary

Corresponding author: Mária Bagyánszki, PhD, Associate Professor, Department of Physiology, Anatomy and Neuroscience, Faculty of Science and Informatics, University of Szeged, Közép Fasor 52, Szeged H-6726, Hungary. bmarcsi@bio.u-szeged.hu

Abstract

Diabetes, as a metabolic disorder, is accompanied with several gastrointestinal (GI) symptoms, like abdominal pain, gastroparesis, diarrhoea or constipation. Serious and complex enteric nervous system damage is confirmed in the background of these diabetic motility complaints. The anatomical length of the GI tract, as well as genetic, developmental, structural and functional differences between its segments contribute to the distinct, intestinal region-specific effects of hyperglycemia. These observations support and highlight the importance of a regional approach in diabetes-related enteric neuropathy. Intestinal large and microvessels are essential for the blood supply of enteric ganglia. Bidirectional morpho-functional linkage exists between enteric neurons and enteroglia, however, there is also a reciprocal communication between enteric neurons and immune cells on which intestinal microbial composition has crucial influence. From this point of view, it is more appropriate to say that enteric neurons partake in multidirectional communication and interact with these key players of the intestinal wall. These interplays may differ from segment to segment, thus, the microenvironment of enteric neurons could be considered strictly regional. The goal of this review is to summarize the main tissue components and molecular factors, such as enteric glia cells, interstitial cells of Cajal, gut vasculature, intestinal epithelium, gut microbiota, immune cells, enteroendocrine cells, pro-oxidants, antioxidant molecules and extracellular matrix, which create and determine a gut region-dependent neuronal environment in diabetes.

Key Words: Enteric neurons; Neuronal environment; Gut region specificity; Type 1 diabetes, Hyperglycemia; Microbiota-gut interactions

©The Author(s) 2023. Published by Baishideng Publishing Group Inc. All rights reserved.

Core Tip: Diabetes-related intestinal motility disturbances result from multifactorial damage to the enteric nervous system. However, the diversity of the neuronal environment in different gut segments basically determines the regionality of diabetic enteric neuropathy. Therefore, in this review, we highlight the role of enteric glial cells, gut circulation, intestinal epithelium, gut microbiota, immune and enteroendocrine cells, pro-oxidants, antioxidant defence and extracellular matrix, which have great impact on the formation and maintenance of a region-specific enteric neuronal environment in diabetes.

Citation: Bagyánszki M, Bódi N. Key elements determining the intestinal region-specific environment of enteric neurons in type 1 diabetes. *World J Gastroenterol* 2023; 29(18): 2704-2716
URL: https://www.wjgnet.com/1007-9327/full/v29/i18/2704.htm
DOI: https://dx.doi.org/10.3748/wjg.v29.i18.2704

INTRODUCTION

In the middle of last century, the general belief was that the neurons within the intestinal wall are parasympathetic neurons[1]. In recent decades, it has become evident that the neurons and glia cells of the gastrointestinal (GI) tract form a third, unique division of the nervous system besides the sympathetic and parasympathetic divisions[2]. The enteric nervous system (ENS) can function independently from the rest of the nervous system and at the same time are in a close, bidirectional connection with it [2,3]. The types and the proportion of enteric neurons were characterized by their morphology, neurochemical code, function and intestinal location in different species[1,4,5]. Nowadays specialized high-throughput "omics" technologies like single cell RNA sequencing even combined with spatially barcoded RNA sequencing can confirm and supplement previous data[6,7].

There is a large body of data on the structure and function of the ENS in physiological state, and it is clear that many pathological conditions strongly affect the enteric plexuses. Since the enteric plexuses are embedded in the histological layers of the intestinal wall (Figure 1), the projections of neurons and glia cells weave through the cross-section of the entire intestine, and because of the lack of blood-brain barrier in the periphery, the role of the environment surrounding the enteric ganglia and neuronal projections is increasingly evident in both health and diseases[2,8].

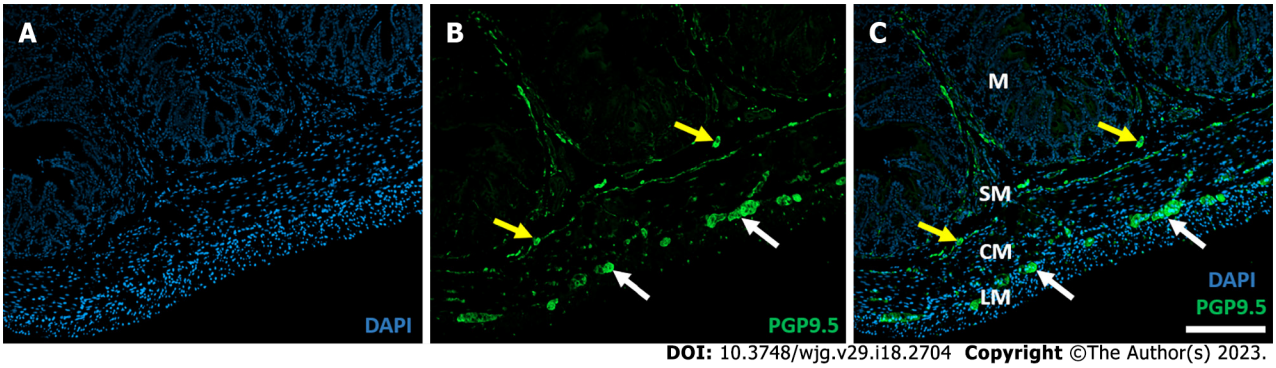
In this review, we provide a brief overview of the effects of type 1 diabetes (T1D) on the intestinal region-specific enteric neuronal environment. Unfortunately, the incidence of T1D is increasing and this incurable disease causes severe GI symptoms[8]. Chronic hyperglycemia influences the structural and functional features of the enteric neurons[9,10], it could change neurochemical code or even can cause neuronal cell death and thus lead to enteric neuropathy described by others and in our former review [11-13]. Hyperglycemia-related enteric neuropathy shows gut-region specific alterations. Therefore, the aim of this paper is to review the main environmental factors (Figure 2) in the intestinal tube from enteric glia cells (EGCs) to the luminal microbiota, which can play a crucial role in the region-specific damage of enteric neurons in the diabetic state. Some key factors like gut microbiota[14-16], GI immune [17-19] or epithelial cells[20-24] are highly emphasized in several papers, so here these are briefly summarized, while other, also critical components of the neuronal environment [*e.g.* EGCs, intestinal vasculature, pro-oxidant/antioxidant balance and extracellular matrix (ECM) molecules], are discussed in more detail.

EGCs AND INTERSTITIAL CELLS OF CAJAL

EGCs are not only supporting their neighboring neurons, but also actively regulate GI barrier function, immune homeostasis, or gut motility[25,26]. They directly interact with numerous cells in the gut wall, like enterocytes, immune cells, muscle cells, enteric neurons and vasculature, and these cross-talks influence their survival and functions in different intestinal layers and gut segments in health and disease[27].

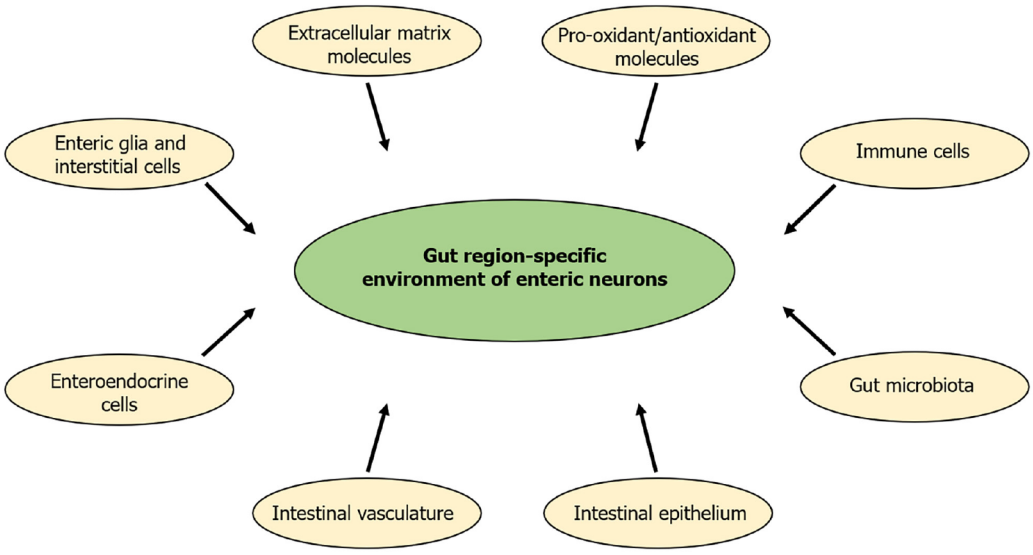
Based on cellular morphology and location within different anatomical layers, EGC subtypes are classified into mucosal, intramuscular, submucosal and myenteric glia cells[28,29]. Glial fibrillary acidic protein (GFAP), S100ß and Sox10 are among the main glial markers, but expression patterns of different EGCs inside and outside the ganglia can be varied and reflect dynamic gene regulation[30]. In summary, the variety of EGCs, as functional heterogeneity and phenotypic plasticity, fundamentally determine the cellular microenvironment within the gut wall[31,32].

Besides gut layer-dependent diversity, intestinal regional heterogeneity of EGCs is also demonstrated among GI segments. Unique developmental patterns derived from different enteric precursors and specialized functions of EGCs are associated with different GI regions (*e.g.* esophagus, stomach or intestine) and result in local environmental properties[32,33]. Different protein expression and transcrip-



DOI: 10.3748/wjg.v29.i18.2704 **Copyright** ©The Author(s) 2023.

Figure 1 Representative fluorescent micrograph of a paraffin section of intestinal wall from control rat colon after Protein gene product 9.5 immunohistochemistry. Protein gene product 9.5 (PGP9.5) (green) was used as a pan-neuronal marker to label neuronal elements and 4',6-diamidino-2-phenylindole (DAPI) (blue) labelled nuclei. A: DAPI; B: PGP9.5; C: DAPI + PGP9.5. M: mucosal layer, SM: Submucosal layer; CM: Circular muscle; LM: Longitudinal muscle; White arrows: Myenteric ganglia, Yellow arrows: Submucous ganglia; PGP9.5: Protein gene product 9.5; DAPI: 4',6-diamidino-2-phenylindole; Scale bar: 200 μm.



DOI: 10.3748/wjg.v29.i18.2704 **Copyright** ©The Author(s) 2023.

Figure 2 Main elements determining the gut region-specific neuronal microenvironment. Enteric glia cells, interstitial cells of Cajal, intestinal vasculature and epithelium, enteroendocrine cells, intestinal microbiota and immune cells, balance of pro-oxidants and antioxidants and extracellular matrix molecules create and determine a strictly regional environment of enteric neurons in diabetes.

tional profiles of myenteric glia cells have observed in mouse ileum and colon[31,34]. EGCs of myenteric ganglia displayed region-dependent responses to neuromodulators and glial regulation of gut contractility was also region- and pathway-specific in the duodenum and colon[35].

Development and function of EGCs and enteric neurons are in close interdependence[36]. Different neurotransmitters can activate EGCs and glial derived neurotrophic factors are crucial for neuronal survival and maintenance[27,37]. EGCs could also act as a critical link in the communication of enteric nervous and immune systems through the modulation of macrophages[38]. Because of the close neuron-glia relationship, it would be beneficial to investigate the involvement of EGCs in diabetes in addition to gut region-specific diabetic neuronal damage[39].

In the duodenum of type 2 diabetic mice with high-fat diet, a decline in the mucosa-associated glial network density was observed, however, neither the glial density and ultrastructure nor the expression of S100ß, Sox10 and GFAP markers were changed in the EGCs of myenteric ganglia[40]. Meanwhile, in a distal direction, an intense reduction in the number of both the enteric neurons and S100-immunoreactive glia cells was seen in diabetic rat jejunum[41]. Expression of GFAP and neurotrophins, like glia cell-derived neurotrophic factor (GDNF) and neurotrophin-3 were decreased in the colon of diabetic rats [42]. Loss of enteric neurons and progressive decrease in GDNF expression was demonstrated with the course of diabetic state both in proximal and distal colon of Sprague-Dawley diabetic rats. Moreover, reduced Akt phosphorylation also accompanied these changes[43]. Also, hyperglycemia stimulated EGC apoptosis in culture by repressing the PI3K/Akt molecular pathway[44]. The down-regulation of

the PI3K/Akt pathway, an important mediator of neuronal survival, is heavily involved in the diabetic damage of enteric neurons[45,46].

Interstitial cells of Cajal (ICCs) are pacemaker cells in GI motility that generate spontaneous and rhythmic slow waves to promote the spontaneous contractions of smooth muscles[47]. The delayed gastric emptying both in diabetic patients and diabetic animal models is associated with ICC depletion [10,48]. Furthermore, damage of ICCs contributes to impaired motility in other GI regions causing constipation[49,50].

INTESTINAL VASCULATURE

Blood vessels enmeshing the small and large intestine are important in nutrient transport and also responsible in supplying enteric cells. Macro- and microvascular anatomy of the GI tract fundamentally determine its regionality. Extramural circulation of the duodenum arises from the coeliac trunk, the jejunum and ileum are supplied by branches of superior mesenteric artery, while different parts of large intestine are supplied by the superior or inferior mesenteric arteries[51]. The impairment of large mesenteric vessels has been described in T1D[52], and substantial heterogeneity of endothelial dysfunction of different large arteries has been observed in a type 2 diabetic animal model[53]. Besides the variability of diabetic macroangiopathy, the impact of diabetes on the intestinal microvasculature can also be region-dependent[54-56].

Investigation of small capillaries in the close vicinity of myenteric ganglia revealed their different susceptibility to diabetic damage along the duodenum-ileum-colon axis[54]. Structural changes such as thickening of the endothelial basement membrane, caveolar hypertrophy and tight junction opening were confirmed in the ileum and colon, whereas only junctional alterations were visible in the duodenal capillaries. In addition, a severely impaired regulation of vascular permeability was shown in ileal and colonic capillaries, while an accelerated, but well-balanced albumin transport was indicated in the duodenum. Immediate insulin treatment prevented most of the diabetes-related changes of the capillary endothelium in the ileum, but not in the colon[54]. Increased thickening of arteriolar wall representing microangiopathy in colonic submucosal vessels was also shown in diabetic patients[56].

Naturally, distinct degrees of capillary damage in different gut segments strongly determine a segment-specific cellular environment and contribute to the diabetic fate of the cells they supply[8]. Close interaction between the capillary endothelial cells and migrating neural crest-derived cells has already been observed in intestinal neurovascular development and has an important role in creating a favorable neuronal microenvironment[57]. Therefore, the diabetes-related regional capillary impairments may greatly contribute to region-dependent enteric neuropathy in T1D[8].

However, not only the structural complications in the vascular system, but also the circulating microparticles can impair the endothelial function in diabetes[58]. Different gut segments feature their distinct microbial compositions and metabolites. Imbalance in the microbial composition accompanying diabetes results in changes of metabolites production, like short-chain fatty acids, bile acids, or tryptophan catabolites[59,60]. Enhancement of gut permeability related to dysbiosis may allow not only the release of different metabolites and endotoxin but also bacterial translocation from the gut to the venous circulation. These elements as integral mediators significantly contribute to vascular inflammation and immune activation[59-62].

INTESTINAL EPITHELIUM

The lining of the GI tract is directly exposed to an ever-changing environment. This single layer of epithelial cells is crucial for preserving gut homeostasis and functions both as barrier and channel for the crosstalk between the GI immune cells and microbiota[23,63].

Epithelial tight junctions are the key components of the physical intestinal barrier along the GI tract [20]. Altered barrier function of enterocytes and colonocytes leads to several pathologic conditions, including obesity or diabetes[20,21,23]. The chronic hyperglycemia-related breakdown of barrier integrity leads to the systemic influx of microbial products and an enhanced incidence of enteric infection[64].

The intestinal epithelium also has an immunological role, as it contains pattern recognition receptors, such as the Toll-like receptors (TLRs)[20]. Recently, several studies demonstrated the expression of TLR4 in metabolic diseases[65-67]. When sensing microbial lipopolysaccharides of Gram-negative bacteria, TLR4 can activate pro-inflammatory pathways in the GI tract[16,22], thus TLRs may play a crucial role in diabetic enteropathy[65]. TLR4 not only affects ENS function, but also modulates neuro-immune interactions by mediating the effects of the intestinal microbiota[65].

GUT MICROBIOTA

In the last two decades it has become clear that the imbalance of microbial species due to a reduction in microbial diversity, known as dysbiosis, is associated with several pathological conditions like autoimmune diseases[68], cancers[69], arteriosclerosis[70] depression[71,72], neurodegenerative diseases[73], obesity or diabetes[74-76]. Dysbiosis contribute to the formation of a proinflammatory milieu and gut leakiness[77,78].

Decreased microbiota diversity has been observed in T1D. At the phyla level, the proportion of *Firmicutes* decreased in patients compared to the healthy individual group, while *Bacteroidetes* abundance increased[16,79].

It is also obvious that the composition of microbiota and the number of microbes is different along the GI tract and each segment contains unique microorganism communities[80,81]. Unfortunately, only a very few studies performed longitudinal comparisons, but results showed that the mode and severity of dysbiosis has also been distinct in different gut segments[82-85]. Besides a longitudinal variability, a horizontal gradient also exists in the gut, with oxygen, redox and mucus gradients from the mucosal surface to the lumen[80] and these variables can contribute to the differences of luminal and mucosal microbiota both in health and disease[83,84,86].

By now, a sufficient amount of evidence has been gathered which show that probiotics have a beneficial influence on diabetes-related dysbiosis[78], and a plethora of studies investigate the effects of prebiotics, synbiotics and fecal microbiota transplantation on hyperglycemia and other diabetes-associated symptoms. Among others, *Roseburia intestinalis, Lactobacillus casei, Akkermansia muciniphila* and *Bacteroides fragilis* have been shown to ameliorate glucose metabolism and insulin sensitivity[75]. In the last 20 years, considerable progress has been made and the intestinal microbiota most certainly represents a promising target for T1D prevention and therapy; however, numerous unresolved concerns require further in-depth investigation.

GI IMMUNITY

The GI tract is the largest immune organ in vertebrates, where the intestinal homeostasis is determined by the gut microbiota, intestinal epithelium and host immunity[21,87].

The complex and enormous amount of information available about the GI immune system is summarized in other reviews[17-19], here we would like to highlight only one aspect. In earlier studies, the GI immune system has been examined as small *vs* large intestine, based on obvious differences in structure and function. Recently it has become apparent that the immunological niches of the GI tract differ between more refined functional compartments, making it necessary to study them separately to understand the consequences on intestinal immune homeostasis[88].

Based on the review of Brown and Esterházy[88], the GI tube can be divided into the following five main parts: Proximal small intestine, gut-draining lymph nodes, distal small intestine, large intestine and mesentery. Each intestinal niche is influenced by a combination of intrinsic tissue properties, extrinsic environmental signals, and immune cell composition.

It would be beneficial if therapies would take into account the regionally different susceptibility of the GI tract to infections and diseases.

ENTEROENDOCRINE CELLS

Enteroendocrine cells (EECs) not only play a role in humoral processes but also act as sensory cells in the GI mucosa next to the neurons and immune cells[89]. Therefore, microbial metabolites could stimulate or suppress hormone secretion by EECs, while endocrine and paracrine factors regulate GI functions and affect several metabolic processes in the body[90]. The diversity of EECs prompts the introduction of a new classification scheme. Earlier, EECs were classified based on producing a single hormone, but in the last decade it was shown that most EECs contain multiple hormones. Several hormones, like secretin and serotonin, are in separate storage vesicles at subcellular level[91]. The hormones produced by EECs might have a big potential in the future as novel microbiota-based therapies to alter metabolically active hormone levels, similarly to the use of the anorectic gut hormone, glucagon-like peptide 1, in the treatment of obesity and type 2 diabetes[90].

It is well established that EEC composition and proportion is different along the GI tract[92,93]. A recently published paper by Martin *et al*[93] has indicated that regional differences in nutrient sensing capability exist in mouse EECs. Colonic EECs has been shown to be more sensitive to glucose, while duodenal EECs to fructose and sucrose.

PRO-OXIDANTS AND ANTIOXIDANTS

The intestinal redox state is critical in maintaining gut homeostasis and functional regulation. The maintenance of this delicate balance in redox state is influenced by the gut microbiota, immune cells and epithelium, which can all produce and respond to redox signals[94]. Numerous genera of bacteria has been identified as biomarkers for gut redox state[95]. Reactive sulfur species-producing bacterial families enhance the host's antioxidant capacity[96], however, sulfur metabolism can be distracted by opportunistic pathogens[94]. Large differences can be observed in different GI segments regarding the quantity and composition of microbiota, intestinal pH or partial pressure of oxygen within the luminal-facing epithelium[80]. There is a richer and more diverse microbial community and deeper anaerobic state from proximal to distal parts of the gut, therefore, it is not surprising that oxidant and antioxidant mechanisms have also been linked to strict region-dependency in health and disease[97]. Foods containing numerous antioxidants, such as vitamins, carotenoids, flavonoids, polyphenols, bioactive peptides or others, however, also include a lot of pro-oxidant molecules[98-100] and all of these can modulate the composition of microbial communities[101]. Consumed and endogenously produced antioxidants have varied strategies at different levels to maintain optimal redox balance[102,103]. Still, the accumulation of reactive oxygen species and/or decrease in antioxidant defence contribute to serious imbalance of intestinal pro-oxidant/antioxidant milieu[104].

Higher mucosal vitamin E and carotenoid concentration, higher total antioxidant activity, superoxide dismutase and catalase activity, as well as glutathione level were observed in the duodenum compared to the ileum and colon of different animal species[105-107]. The presence of probiotic *Lactobacillus* species also reflects a highly beneficial cellular environment in the duodenum[108]. Moreover, in diabetic rats, an increased abundance of the genus *Lactobacillus* has been observed relative to controls [83], which can result in enhanced antioxidant capacity[109]. While no significant changes in peroxynitrite production has been observed, a robust increase of metallothionein 2 and elevated glutathione level has been found in the duodenum of diabetic rats[110], which may contribute to cell survival in this particular gut segments.

In contrast to the duodenum, diabetes increased lipid peroxidation and catalase activity, as well as the percentage of nitrotyrosine-immunoreactive myenteric neurons in the jejunum[111]. Decreased superoxide dismutase and increased myeloperoxidase enzyme concentrations were also demonstrated in the diabetic jejunum[112]. Enhanced lipid peroxidation and protein oxidation accompanied with significantly lower superoxide dismutase levels, catalase and glutathione levels were also observed in the diabetic ileum[113,114]. However, a great increase in the activity of the endogenous heme oxygenase system was shown in myenteric neurons of diabetic ileum[115], maybe as an effect of microbial changes [116]. In the colon of diabetic rats, the doubled peroxynitrite level, reduced superoxide dismutase activity and the induction of the endogenous heme oxigenase system emphasizes the observation that distal gut segments have greater susceptibility to the diabetic oxidative environment, which is in correlation with diabetic neuronal cell loss[97,110,115].

ECM

ECM structures composed of various proteins and polysaccharides are essential in the maintenance and well-regulated remodeling of tissues and have a key role in regulating different cellular events, like cell proliferation, differentiation or migration[117-119]. In the gut, numerous cells (*e.g.* epithelial, mesenchymal, stem cells) participate in the production of matrix molecules, and their precise composition is indispensable for the optimal cellular environment and normal intestinal function. Sensing the stiffness or the porosity of the ECM through specific receptors such as integrins, intestinal cells can change their intracellular state or dynamics[120,121].

Diabetes-related alterations of ECM is demonstrated in all parts of the gut, but with different extent in different regions and intestinal layers. In streptozotocin-induced diabetic rats, a significant increase in the amount of laminin-1 and fibronectin was observed in the small intestine by Western blotting and immunohistochemistry, and the strong labelling was restricted mainly to the intestinal smooth muscle and serous layers[122]. These hyperglycemia-mediated ECM accumulation was reversed by insulin treatment[122]. Additionally, in the distal colon, a marked increase of type 1 collagen was detected with no changes in type 3 and 4 collagen expression[123]. Besides of the well-marked pockets of collagen among the smooth muscle cells, formation of advanced glycation end-products was also observed in diabetic rats. Type 1 collagen deposits and glycation increase stiffness of the diabetic colon muscle, which contribute to limited colonic function[123]. There is a strict association between collagen content and mechanical properties, however, this varied in different parts of the small intestine [124]. Increased ECM deposition, as well as high levels of type 1 and 3 collagen and fibronectin mRNAs were also detected in diabetic colon mucosa[125]. The accumulation of ECM in the mucosa of the diabetic colon was associated with the deregulation of the transforming growth factor (TGF)-β1/Smad signaling pathway[125]. However, TGF-β can also influence deposition of matrix molecules by upregulating several ECM receptors[126].

Structural alterations of basement membranes as specialized ECM structures have been characterized in diabetes mellitus. Thickening of capillary basement membrane is among the first histological hallmarks of the disease. Capillaries located in gut smooth muscle in different gut segments displayed region-specific thickening of their basement membranes in T1D[54]. Additionally, significant increase in mRNA levels of different matrix scaffold proteins, like fibronectin or procollagen type 1, was observed in the aorta and mesenteric artery of type 2 diabetic Goto-Kakizaki rats[127]. Moreover, gene expression was restored in the mesenteric bed but not in the aorta using an endothelin-1 antagonist[127]. Basement membrane thickening of smooth muscle cells was also demonstrated in the small intestine[122] and colon[123]. Moreover, the basement membrane surrounding the myenteric ganglia was also thickened in diabetic rats with strict regionality in different gut segments[128].

ECM accumulation can be due to the enhanced synthesis of matrix components, but also their decreased degradation, which in turn leads to the imbalance of ECM dynamics[129]. Matrix metalloproteinases (MMPs) and their tissue specific inhibitors (TIMPs) mainly produced by macrophages, neutrophils or epithelial cells have an essential role in tissue remodeling as a response to intestinal inflammation[130,131]. Growing molecular evidence support that these proteolytic enzymes are also targets of diabetic damage. In the diabetic ileum, MMP9 expression decreased in myenteric ganglia, capillary endothelial cells and intestinal smooth muscle cells, while these values did not change in the duodenum, which is in perfect agreement with the regionally distinct thickening of the ganglionic basement membrane. However, a specific, but great induction was revealed in MMP9 and TIMP1 at the mRNA level both in duodenum and ileum homogenates of diabetics[128]. Increased early expression of MMP2 and MMP9 mRNAs and MMP1 later on was also demonstrated in the diabetic colon mucosa. On the other hand, increased TIMP1 and TIMP2 expression could be the result of decreased MMPs degrading activities here[125].

CONCLUSION

Because of its various functions, as food intake, mechanical and chemical breakdown, motility, absorption, regulation of blood flow, secretion, water reabsorption and immune functions, the GI tract has unique features. It has three detecting systems, which are more extensive than those of any other organ: (1) The ENS contains as many neurons as the spinal cord and different subpopulations of the EGCs cover all histological layers of the intestinal wall. Intrinsic primary neurons, interneurons and motoneurons can form local reflex circuits in the gut wall[1,2]; (2) There are more than 20 hormones produced by several types of EECs[89]; and (3) The GI tract is the largest immune organ with the cc. 70-80% of the body's immune cells[87,132].

In addition to the three systems listed above, other essential factors such as intestinal epithelial barrier, microcirculation of the gut wall, pro-oxidant/antioxidant milieu, ECM components and gut microbiota also play a crucial role in the formation of the enteric neuronal environment in both physiological and pathological states. Results demonstrated a clear relationship between intestinal microorganisms and the occurrence of T1D, but the correlation or causality remains an important question for several reasons. Altered gut microbiota-mediated redox imbalance and changes in cellular cross-talks may contribute to enteric neuropathy and also influence the function of gut-brain axis[15].

Considering these properties and the size of the GI tract, it is not surprising that it shows profound functional and structural differences along its length. When planning experiments, the gut should be regarded as a multiple organ, and in the case of illness, the applied therapies should take into account the intestinal segment-specific effects[88].

ACKNOWLEDGEMENTS

The authors sincerely thank to their PhD students, Abigél Egyed-Kolumbán, Afnan AL Doghmi, Bence Pál Barta and Benita Onhausz for useful comments on draft of this manuscript.

FOOTNOTES

Author contributions: Bagyánszki M and Bódi N wrote the original draft, they also wrote the review and editing, performed the visualization; all the authors have read and approve the final manuscript.

Supported by Hungarian NKFIH Fund Project (N.B.), No. FK131789; János Bolyai Research Scholarship of The Hungarian Academy of Sciences (N.B.); and New National Excellence Program of The Ministry for Innovation and Technology from The Source of The National Research, Development and Innovation Fund (N.B.); No. ÚNKP-22-5.

Conflict-of-interest statement: All the authors report no relevant conflicts of interest for this article.

Open-Access: This article is an open-access article that was selected by an in-house editor and fully peer-reviewed by external reviewers. It is distributed in accordance with the Creative Commons Attribution NonCommercial (CC BY-NC 4.0) license, which permits others to distribute, remix, adapt, build upon this work non-commercially, and license their derivative works on different terms, provided the original work is properly cited and the use is non-commercial. See: https://creativecommons.org/Licenses/by-nc/4.0/

Country/Territory of origin: Hungary

ORCID number: Mária Bagyánszki 0000-0003-3533-9461; Nikolett Bódi 0000-0002-9774-1387.

S-Editor: Fan JR
L-Editor: A
P-Editor: Yu HG

REFERENCES

1 **Furness JB**. Types of neurons in the enteric nervous system. *J Auton Nerv Syst* 2000; **81**: 87-96 [PMID: 10869706 DOI: 10.1016/s0165-1838(00)00127-2]
2 **Furness JB**. The enteric nervous system and neurogastroenterology. *Nat Rev Gastroenterol Hepatol* 2012; **9**: 286-294 [PMID: 22392290 DOI: 10.1038/nrgastro.2012.32]
3 **Muhammad F**, Fan B, Wang R, Ren J, Jia S, Wang L, Chen Z, Liu XA. The Molecular Gut-Brain Axis in Early Brain Development. *Int J Mol Sci* 2022; **23** [PMID: 36499716 DOI: 10.3390/ijms232315389]
4 **Mongardi Fantaguzzi C**, Thacker M, Chiocchetti R, Furness JB. Identification of neuron types in the submucosal ganglia of the mouse ileum. *Cell Tissue Res* 2009; **336**: 179-189 [PMID: 19326148 DOI: 10.1007/s00441-009-0773-2]
5 **Qu ZD**, Thacker M, Castelucci P, Bagyánszki M, Epstein ML, Furness JB. Immunohistochemical analysis of neuron types in the mouse small intestine. *Cell Tissue Res* 2008; **334**: 147-161 [PMID: 18855018 DOI: 10.1007/s00441-008-0684-7]
6 **Danan CH**, Katada K, Parham LR, Hamilton KE. Spatial transcriptomics add a new dimension to our understanding of the gut. *Am J Physiol Gastrointest Liver Physiol* 2023; **324**: G91-G98 [PMID: 36472345 DOI: 10.1152/ajpgi.00191.2022]
7 **Dharshika C**, Gulbransen BD. Enteric Neuromics: How High-Throughput "Omics" Deepens Our Understanding of Enteric Nervous System Genetic Architecture. *Cell Mol Gastroenterol Hepatol* 2023; **15**: 487-504 [PMID: 36368612 DOI: 10.1016/j.jcmgh.2022.10.019]
8 **Bagyánszki M**, Bódi N. Diabetes-related alterations in the enteric nervous system and its microenvironment. *World J Diabetes* 2012; **3**: 80-93 [PMID: 22645637 DOI: 10.4239/wjd.v3.i5.80]
9 **Santhanam P**, Marashdeh W, Solnes L. Functional Imaging of Evaluation of Diabetic Gastroparesis. *Curr Diabetes Rev* 2018; **14**: 222-226 [PMID: 28128051 DOI: 10.2174/1573399813666170126110932]
10 **Selby A**, Reichenbach ZW, Piech G, Friedenberg FK. Pathophysiology, Differential Diagnosis, and Treatment of Diabetic Diarrhea. *Dig Dis Sci* 2019; **64**: 3385-3393 [PMID: 31541370 DOI: 10.1007/s10620-019-05846-6]
11 **Chandrasekharan B**, Srinivasan S. Diabetes and the enteric nervous system. *Neurogastroenterol Motil* 2007; **19**: 951-960 [PMID: 17971027 DOI: 10.1111/j.1365-2982.2007.01023.x]
12 **Yarandi SS**, Srinivasan S. Diabetic gastrointestinal motility disorders and the role of enteric nervous system: current status and future directions. *Neurogastroenterol Motil* 2014; **26**: 611-624 [PMID: 24661628 DOI: 10.1111/nmo.12330]
13 **Bódi N**, Szalai Z, Bagyánszki M. Nitrergic Enteric Neurons in Health and Disease-Focus on Animal Models. *Int J Mol Sci* 2019; **20** [PMID: 31022832 DOI: 10.3390/ijms20082003]
14 **Del Chierico F**, Rapini N, Deodati A, Matteoli MC, Cianfarani S, Putignani L. Pathophysiology of Type 1 Diabetes and Gut Microbiota Role. *Int J Mol Sci* 2022; **23** [PMID: 36498975 DOI: 10.3390/ijms232314650]
15 **Shandilya S**, Kumar S, Kumar Jha N, Kumar Kesari K, Ruokolainen J. Interplay of gut microbiota and oxidative stress: Perspective on neurodegeneration and neuroprotection. *J Adv Res* 2022; **38**: 223-244 [PMID: 35572407 DOI: 10.1016/j.jare.2021.09.005]
16 **Ye J**, Wu Z, Zhao Y, Zhang S, Liu W, Su Y. Role of gut microbiota in the pathogenesis and treatment of diabetes mullites: Advanced research-based review. *Front Microbiol* 2022; **13**: 1029890 [PMID: 36338058 DOI: 10.3389/fmicb.2022.1029890]
17 **Schill EM**, Floyd AN, Newberry RD. Neonatal development of intestinal neuroimmune interactions. *Trends Neurosci* 2022; **45**: 928-941 [PMID: 36404456 DOI: 10.1016/j.tins.2022.10.002]
18 **Sterling KG**, Dodd GK, Alhamdi S, Asimenios PG, Dagda RK, De Meirleir KL, Hudig D, Lombardi VC. Mucosal Immunity and the Gut-Microbiota-Brain-Axis in Neuroimmune Disease. *Int J Mol Sci* 2022; **23** [PMID: 36362150 DOI: 10.3390/ijms232113328]
19 **Viola MF**, Boeckxstaens G. Niche-specific functional heterogeneity of intestinal resident macrophages. *Gut* 2021; **70**: 1383-1395 [PMID: 33384336 DOI: 10.1136/gutjnl-2020-323121]
20 **Aleman RS**, Moncada M, Aryana KJ. Leaky Gut and the Ingredients That Help Treat It: A Review. *Molecules* 2023; **28** [PMID: 36677677 DOI: 10.3390/molecules28020619]
21 **Lin PY**, Stern A, Peng HH, Chen JH, Yang HC. Redox and Metabolic Regulation of Intestinal Barrier Function and Associated Disorders. *Int J Mol Sci* 2022; **23** [PMID: 36430939 DOI: 10.3390/ijms232214463]
22 **Singh N**, Singh V, Rai SN, Mishra V, Vamanu E, Singh MP. Deciphering the gut microbiome in neurodegenerative diseases and metagenomic approaches for characterization of gut microbes. *Biomed Pharmacother* 2022; **156**: 113958 [PMID: 36411639 DOI: 10.1016/j.biopha.2022.113958]

23 **Stolfi C**, Maresca C, Monteleone G, Laudisi F. Implication of Intestinal Barrier Dysfunction in Gut Dysbiosis and Diseases. *Biomedicines* 2022; **10** [PMID: 35203499 DOI: 10.3390/biomedicines10020289]

24 **Van Spaendonk H**, Ceuleers H, Witters L, Patteet E, Joossens J, Augustyns K, Lambeir AM, De Meester I, De Man JG, De Winter BY. Regulation of intestinal permeability: The role of proteases. *World J Gastroenterol* 2017; **23**: 2106-2123 [PMID: 28405139 DOI: 10.3748/wjg.v23.i12.2106]

25 **Liu C**, Yang J. Enteric Glial Cells in Immunological Disorders of the Gut. *Front Cell Neurosci* 2022; **16**: 895871 [PMID: 35573829 DOI: 10.3389/fncel.2022.895871]

26 **Progatzky F**, Pachnis V. The role of enteric glia in intestinal immunity. *Curr Opin Immunol* 2022; **77**: 102183 [PMID: 35533467 DOI: 10.1016/j.coi.2022.102183]

27 **Grubišić V**, Gulbransen BD. Enteric glia: the most alimentary of all glia. *J Physiol* 2017; **595**: 557-570 [PMID: 27106597 DOI: 10.1113/JP271021]

28 **Coelho-Aguiar Jde M**, Bon-Frauches AC, Gomes AL, Veríssimo CP, Aguiar DP, Matias D, Thomasi BB, Gomes AS, Brito GA, Moura-Neto V. The enteric glia: identity and functions. *Glia* 2015; **63**: 921-935 [PMID: 25703790 DOI: 10.1002/glia.22795]

29 **Gulbransen BD**, Sharkey KA. Novel functional roles for enteric glia in the gastrointestinal tract. *Nat Rev Gastroenterol Hepatol* 2012; **9**: 625-632 [PMID: 22890111 DOI: 10.1038/nrgastro.2012.138]

30 **Grundmann D**, Loris E, Maas-Omlor S, Huang W, Scheller A, Kirchhoff F, Schäfer KH. Enteric Glia: S100, GFAP, and Beyond. *Anat Rec (Hoboken)* 2019; **302**: 1333-1344 [PMID: 30951262 DOI: 10.1002/ar.24128]

31 **Boesmans W**, Lasrado R, Vanden Berghe P, Pachnis V. Heterogeneity and phenotypic plasticity of glial cells in the mammalian enteric nervous system. *Glia* 2015; **63**: 229-241 [PMID: 25161129 DOI: 10.1002/glia.22746]

32 **Seguella L**, Gulbransen BD. Enteric glial biology, intercellular signalling and roles in gastrointestinal disease. *Nat Rev Gastroenterol Hepatol* 2021; **18**: 571-587 [PMID: 33731961 DOI: 10.1038/s41575-021-00423-7]

33 **Espinosa-Medina I**, Jevans B, Boismoreau F, Chettouh Z, Enomoto H, Müller T, Birchmeier C, Burns AJ, Brunet JF. Dual origin of enteric neurons in vagal Schwann cell precursors and the sympathetic neural crest. *Proc Natl Acad Sci U S A* 2017; **114**: 11980-11985 [PMID: 29078343 DOI: 10.1073/pnas.1710308114]

34 **Zeisel A**, Hochgerner H, Lönnerberg P, Johnsson A, Memic F, van der Zwan J, Häring M, Braun E, Borm LE, La Manno G, Codeluppi S, Furlan A, Lee K, Skene N, Harris KD, Hjerling-Leffler J, Arenas E, Ernfors P, Marklund U, Linnarsson S. Molecular Architecture of the Mouse Nervous System. *Cell* 2018; **174**: 999-1014.e22 [PMID: 30096314 DOI: 10.1016/j.cell.2018.06.021]

35 **Seguella L**, McClain JL, Esposito G, Gulbransen BD. Functional Intraregional and Interregional Heterogeneity between Myenteric Glial Cells of the Colon and Duodenum in Mice. *J Neurosci* 2022; **42**: 8694-8708 [PMID: 36319118 DOI: 10.1523/JNEUROSCI.2379-20.2022]

36 **Boesmans W**, Nash A, Tasnády KR, Yang W, Stamp LA, Hao MM. Development, Diversity, and Neurogenic Capacity of Enteric Glia. *Front Cell Dev Biol* 2021; **9**: 775102 [PMID: 35111752 DOI: 10.3389/fcell.2021.775102]

37 **Liu S**. Neurotrophic factors in enteric physiology and pathophysiology. *Neurogastroenterol Motil* 2018; **30**: e13446 [PMID: 30259610 DOI: 10.1111/nmo.13446]

38 **Grubišić V**, McClain JL, Fried DE, Grants I, Rajasekhar P, Csizmadia E, Ajijola OA, Watson RE, Poole DP, Robson SC, Christofi FL, Gulbransen BD. Enteric Glia Modulate Macrophage Phenotype and Visceral Sensitivity following Inflammation. *Cell Rep* 2020; **32**: 108100 [PMID: 32905782 DOI: 10.1016/j.celrep.2020.108100]

39 **Izbéki F**, Wittman T, Rosztóczy A, Linke N, Bódi N, Fekete E, Bagyánszki M. Immediate insulin treatment prevents gut motility alterations and loss of nitrergic neurons in the ileum and colon of rats with streptozotocin-induced diabetes. *Diabetes Res Clin Pract* 2008; **80**: 192-198 [PMID: 18242757 DOI: 10.1016/j.diabres.2007.12.013]

40 **Stenkamp-Strahm C**, Patterson S, Boren J, Gericke M, Balemba O. High-fat diet and age-dependent effects on enteric glial cell populations of mouse small intestine. *Auton Neurosci* 2013; **177**: 199-210 [PMID: 23726157 DOI: 10.1016/j.autneu.2013.04.014]

41 **de Souza SR**, de Miranda Neto MH, Martins Perles JV, Vieira Frez FC, Zignani I, Ramalho FV, Hermes-Uliana C, Bossolani GD, Zanoni JN. Antioxidant Effects of the Quercetin in the Jejunal Myenteric Innervation of Diabetic Rats. *Front Med (Lausanne)* 2017; **4**: 8 [PMID: 28224126 DOI: 10.3389/fmed.2017.00008]

42 **Liu W**, Yue W, Wu R. Effects of diabetes on expression of glial fibrillary acidic protein and neurotrophins in rat colon. *Auton Neurosci* 2010; **154**: 79-83 [PMID: 20042376 DOI: 10.1016/j.autneu.2009.12.003]

43 **Du F**, Wang L, Qian W, Liu S. Loss of enteric neurons accompanied by decreased expression of GDNF and PI3K/Akt pathway in diabetic rats. *Neurogastroenterol Motil* 2009; **21**: 1229-e114 [PMID: 19709371 DOI: 10.1111/j.1365-2982.2009.01379.x]

44 **Chen Y**, Liu G, He F, Zhang L, Yang K, Yu H, Zhou J, Gan H. MicroRNA 375 modulates hyperglycemia-induced enteric glial cell apoptosis and Diabetes-induced gastrointestinal dysfunction by targeting Pdk1 and repressing PI3K/Akt pathway. *Sci Rep* 2018; **8**: 12681 [PMID: 30140011 DOI: 10.1038/s41598-018-30714-0]

45 **Leinninger GM**, Backus C, Uhler MD, Lentz SI, Feldman EL. Phosphatidylinositol 3-kinase and Akt effectors mediate insulin-like growth factor-I neuroprotection in dorsal root ganglia neurons. *FASEB J* 2004; **18**: 1544-1546 [PMID: 15319368 DOI: 10.1096/fj.04-1581fje]

46 **Sariola H**, Saarma M. Novel functions and signalling pathways for GDNF. *J Cell Sci* 2003; **116**: 3855-3862 [PMID: 12953054 DOI: 10.1242/jcs.00786]

47 **Kishi K**, Kaji N, Kurosawa T, Aikiyo S, Hori M. Hyperglycemia in the early stages of type 1 diabetes accelerates gastric emptying through increased networks of interstitial cells of Cajal. *PLoS One* 2019; **14**: e0222961 [PMID: 31596858 DOI: 10.1371/journal.pone.0222961]

48 **Yamamoto T**, Watabe K, Nakahara M, Ogiyama H, Kiyohara T, Tsutsui S, Tamura S, Shinomura Y, Hayashi N. Disturbed gastrointestinal motility and decreased interstitial cells of Cajal in diabetic db/db mice. *J Gastroenterol Hepatol* 2008; **23**: 660-667 [PMID: 18341539 DOI: 10.1111/j.1440-1746.2008.05326.x]

49 **Gotfried J**, Priest S, Schey R. Diabetes and the Small Intestine. *Curr Treat Options Gastroenterol* 2017; **15**: 490-507 [PMID: 28913777 DOI: 10.1007/s11938-017-0155-x]

50 **Jin B**, Ha SE, Wei L, Singh R, Zogg H, Clemmensen B, Heredia DJ, Gould TW, Sanders KM, Ro S. Colonic Motility Is Improved by the Activation of 5-HT(2B) Receptors on Interstitial Cells of Cajal in Diabetic Mice. *Gastroenterology* 2021; **161**: 608-622.e7 [PMID: 33895170 DOI: 10.1053/j.gastro.2021.04.040]

51 **Geboes K**, Geboes KP, Maleux G. Vascular anatomy of the gastrointestinal tract. *Best Pract Res Clin Gastroenterol* 2001; **15**: 1-14 [PMID: 11355897 DOI: 10.1053/bega.2000.0152]

52 **Lee JH**, Bahk JH, Park SH, Huh J. The diabetes-induced functional and distributional changes of the alpha 1-adrenoceptor of the abdominal aorta and distal mesenteric artery from streptozotocin-induced diabetic rats. *Korean J Anesthesiol* 2011; **60**: 272-281 [PMID: 21602978 DOI: 10.4097/kjae.2011.60.4.272]

53 **Sallam NA**, Laher I. Redox Signaling and Regional Heterogeneity of Endothelial Dysfunction in db/db Mice. *Int J Mol Sci* 2020; **21** [PMID: 32858910 DOI: 10.3390/ijms21176147]

54 **Bódi N**, Talapka P, Poles MZ, Hermesz E, Jancsó Z, Katarova Z, Izbéki F, Wittmann T, Fekete É, Bagyánszki M. Gut region-specific diabetic damage to the capillary endothelium adjacent to the myenteric plexus. *Microcirculation* 2012; **19**: 316-326 [PMID: 22296580 DOI: 10.1111/j.1549-8719.2012.00164.x]

55 **De Las Casas LE**, Finley JL. Diabetic microangiopathy in the small bowel. *Histopathology* 1999; **35**: 267-270 [PMID: 10469219 DOI: 10.1046/j.1365-2559.1999.00702.x]

56 **Sasor A**, Ohlsson B. Microangiopathy is common in submucosal vessels of the colon in patients with diabetes mellitus. *Rev Diabet Stud* 2014; **11**: 175-180 [PMID: 25396405 DOI: 10.1900/RDS.2014.11.175]

57 **Hatch J**, Mukouyama YS. Spatiotemporal mapping of vascularization and innervation in the fetal murine intestine. *Dev Dyn* 2015; **244**: 56-68 [PMID: 25138596 DOI: 10.1002/dvdy.24178]

58 **Ishida K**, Taguchi K, Hida M, Watanabe S, Kawano K, Matsumoto T, Hattori Y, Kobayashi T. Circulating microparticles from diabetic rats impair endothelial function and regulate endothelial protein expression. *Acta Physiol (Oxf)* 2016; **216**: 211-220 [PMID: 26235826 DOI: 10.1111/apha.12561]

59 **Thenappan T**, Khoruts A, Chen Y, Weir EK. Can intestinal microbiota and circulating microbial products contribute to pulmonary arterial hypertension? *Am J Physiol Heart Circ Physiol* 2019; **317**: H1093-H1101 [PMID: 31490732 DOI: 10.1152/ajpheart.00416.2019]

60 **Zhu Y**, Shui X, Liang Z, Huang Z, Qi Y, He Y, Chen C, Luo H, Lei W. Gut microbiota metabolites as integral mediators in cardiovascular diseases (Review). *Int J Mol Med* 2020; **46**: 936-948 [PMID: 32705240 DOI: 10.3892/ijmm.2020.4674]

61 **Alarcón Yempén RE**, Venzel R, Paulino Campos MC, de Oliveira LP, Lins RVD, Pessoni AM, Fanaro GB, de Oliveira Souza A, Calaza KDC, de Brito Alves JL, Cavalcanti-Neto MP. Gut microbiota: A potential therapeutic target for management of diabetic retinopathy? *Life Sci* 2021; **286**: 120060 [PMID: 34666038 DOI: 10.1016/j.lfs.2021.120060]

62 **Di Ciaula A**, Baj J, Garruti G, Celano G, De Angelis M, Wang HH, Di Palo DM, Bonfrate L, Wang DQ, Portincasa P. Liver Steatosis, Gut-Liver Axis, Microbiome and Environmental Factors. A Never-Ending Bidirectional Cross-Talk. *J Clin Med* 2020; **9** [PMID: 32823983 DOI: 10.3390/jcm9082648]

63 **Allaire JM**, Crowley SM, Law HT, Chang SY, Ko HJ, Vallance BA. The Intestinal Epithelium: Central Coordinator of Mucosal Immunity. *Trends Immunol* 2018; **39**: 677-696 [PMID: 29716793 DOI: 10.1016/j.it.2018.04.002]

64 **Thaiss CA**, Levy M, Grosheva I, Zheng D, Soffer E, Blacher E, Braverman S, Tengeler AC, Barak O, Elazar M, Ben-Zeev R, Lehavi-Regev D, Katz MN, Pevsner-Fischer M, Gertler A, Halpern Z, Harmelin A, Aamar S, Serradas P, Grosfeld A, Shapiro H, Geiger B, Elinav E. Hyperglycemia drives intestinal barrier dysfunction and risk for enteric infection. *Science* 2018; **359**: 1376-1383 [PMID: 29519916 DOI: 10.1126/science.aar3318]

65 **Bódi N**, Egyed-Kolumbán A, Onhausz B, Barta BP, Doghmi AA, Balázs J, Szalai Z, Bagyánszki M. Intestinal Region-Dependent Alterations of Toll-Like Receptor 4 Expression in Myenteric Neurons of Type 1 Diabetic Rats. *Biomedicines* 2023; **11** [PMID: 36672637 DOI: 10.3390/biomedicines11010129]

66 **Sun Q**, Zhang S, Zhang BY, Zhang Y, Yao L, Hu J, Zhang HH. microRNA-181a contributes to gastric hypersensitivity in rats with diabetes by regulating TLR4 expression. *Mol Pain* 2023; **19**: 17448069231159356 [PMID: 36750423 DOI: 10.1177/17448069231159356]

67 **Zeng F**, Zheng J, Shen L, Herrera-Balandrano DD, Huang W, Sui Z. Physiological mechanisms of TLR4 in glucolipid metabolism regulation: Potential use in metabolic syndrome prevention. *Nutr Metab Cardiovasc Dis* 2023; **33**: 38-46 [PMID: 36428186 DOI: 10.1016/j.numecd.2022.10.011]

68 **Liu X**, Cheng YW, Shao L, Sun SH, Wu J, Song QH, Zou HS, Ling ZX. Gut microbiota dysbiosis in Chinese children with type 1 diabetes mellitus: An observational study. *World J Gastroenterol* 2021; **27**: 2394-2414 [PMID: 34040330 DOI: 10.3748/wjg.v27.i19.2394]

69 **Zhang H**, Chang Y, Zheng Q, Zhang R, Hu C, Jia W. Altered intestinal microbiota associated with colorectal cancer. *Front Med* 2019; **13**: 461-470 [PMID: 31250341 DOI: 10.1007/s11684-019-0695-7]

70 **Anto L**, Blesso CN. Interplay between diet, the gut microbiome, and atherosclerosis: Role of dysbiosis and microbial metabolites on inflammation and disordered lipid metabolism. *J Nutr Biochem* 2022; **105**: 108991 [PMID: 35331903 DOI: 10.1016/j.jnutbio.2022.108991]

71 **Masanetz RK**, Winkler J, Winner B, Günther C, Süß P. The Gut-Immune-Brain Axis: An Important Route for Neuropsychiatric Morbidity in Inflammatory Bowel Disease. *Int J Mol Sci* 2022; **23** [PMID: 36232412 DOI: 10.3390/ijms231911111]

72 **Simpson CA**, Diaz-Arteche C, Eliby D, Schwartz OS, Simmons JG, Cowan CSM. The gut microbiota in anxiety and depression - A systematic review. *Clin Psychol Rev* 2021; **83**: 101943 [PMID: 33271426 DOI: 10.1016/j.cpr.2020.101943]

73 **Kaviyarasan S**, Chung Sia EL, Retinasamy T, Arulsamy A, Shaikh MF. Regulation of gut microbiome by ketogenic diet in neurodegenerative diseases: A molecular crosstalk. *Front Aging Neurosci* 2022; **14**: 1015837 [PMID: 36313018 DOI: 10.3389/fnagi.2022.1015837]

74 **Candon S**, Perez-Arroyo A, Marquet C, Valette F, Foray AP, Pelletier B, Milani C, Ventura M, Bach JF, Chatenoud L. Antibiotics in early life alter the gut microbiome and increase disease incidence in a spontaneous mouse model of autoimmune insulin-dependent diabetes. *PLoS One* 2015; **10**: e0125448 [PMID: 25970503 DOI: 10.1371/journal.pone.0125448]

75 **Iatcu CO**, Steen A, Covasa M. Gut Microbiota and Complications of Type-2 Diabetes. *Nutrients* 2021; **14** [PMID:

35011044 DOI: 10.3390/nu14010166]
76 **Kaiko GE**, Stappenbeck TS. Host-microbe interactions shaping the gastrointestinal environment. *Trends Immunol* 2014; **35**: 538-548 [PMID: 25220948 DOI: 10.1016/j.it.2014.08.002]
77 **Ismail HM**, Evans-Molina C. Does the Gut Microbiome Play a Role in Obesity in Type 1 Diabetes? *Front Cell Infect Microbiol* 2022; **12**: 892291 [PMID: 35873174 DOI: 10.3389/fcimb.2022.892291]
78 **Megur A**, Daliri EB, Baltriukienė D, Burokas A. Prebiotics as a Tool for the Prevention and Treatment of Obesity and Diabetes: Classification and Ability to Modulate the Gut Microbiota. *Int J Mol Sci* 2022; **23** [PMID: 35682774 DOI: 10.3390/ijms23116097]
79 **Pellegrini S**, Sordi V, Bolla AM, Saita D, Ferrarese R, Canducci F, Clementi M, Invernizzi F, Mariani A, Bonfanti R, Barera G, Testoni PA, Doglioni C, Bosi E, Piemonti L. Duodenal Mucosa of Patients With Type 1 Diabetes Shows Distinctive Inflammatory Profile and Microbiota. *J Clin Endocrinol Metab* 2017; **102**: 1468-1477 [PMID: 28324102 DOI: 10.1210/jc.2016-3222]
80 **de Vos WM**, Tilg H, Van Hul M, Cani PD. Gut microbiome and health: mechanistic insights. *Gut* 2022; **71**: 1020-1032 [PMID: 35105664 DOI: 10.1136/gutjnl-2021-326789]
81 **Zheng SJ**, Luo Y, Xiao JH. The Impact of Intestinal Microorganisms and Their Metabolites on Type 1 Diabetes Mellitus. *Diabetes Metab Syndr Obes* 2022; **15**: 1123-1139 [PMID: 35431564 DOI: 10.2147/DMSO.S355749]
82 **Saffouri GB**, Shields-Cutler RR, Chen J, Yang Y, Lekatz HR, Hale VL, Cho JM, Battaglioli EJ, Bhattarai Y, Thompson KJ, Kalari KK, Behera G, Berry JC, Peters SA, Patel R, Schuetz AN, Faith JJ, Camilleri M, Sonnenburg JL, Farrugia G, Swann JR, Grover M, Knights D, Kashyap PC. Small intestinal microbial dysbiosis underlies symptoms associated with functional gastrointestinal disorders. *Nat Commun* 2019; **10**: 2012 [PMID: 31043597 DOI: 10.1038/s41467-019-09964-7]
83 **Wirth R**, Bódi N, Maróti G, Bagyánszki M, Talapka P, Fekete É, Bagi Z, Kovács KL. Regionally distinct alterations in the composition of the gut microbiota in rats with streptozotocin-induced diabetes. *PLoS One* 2014; **9**: e110440 [PMID: 25469509 DOI: 10.1371/journal.pone.0110440]
84 **Wirth R**, Bódi N, Szalai Z, Chandrakumar L, Maróti G, Kovács LK, Bagi Z, Mezei D, Balázs J, Bagyánszki M. Perturbation of the mucosa-associated anaerobic gut microbiota in streptozotocin-induced diabetic rats. *Acta Biol Szegediensis* 2021; **65**: 75-84 [DOI: 10.14232/abs.2021.1.75-84]
85 **Xu SS**, Wang N, Huang L, Zhang XL, Feng ST, Liu SS, Wang Y, Liu ZG, Wang BY, Wu TW, Mu YL, Hou SH, Li K. Changes in the Mucosa-Associated Microbiome and Transcriptome across Gut Segments Are Associated with Obesity in a Metabolic Syndrome Porcine Model. *Microbiol Spectr* 2022; **10**: e0071722 [PMID: 35862956 DOI: 10.1128/spectrum.00717-22]
86 **Zhang L**, Wu W, Lee YK, Xie J, Zhang H. Spatial Heterogeneity and Co-occurrence of Mucosal and Luminal Microbiome across Swine Intestinal Tract. *Front Microbiol* 2018; **9**: 48 [PMID: 29472900 DOI: 10.3389/fmicb.2018.00048]
87 **Margolis KG**, Gershon MD, Bogunovic M. Cellular Organization of Neuroimmune Interactions in the Gastrointestinal Tract. *Trends Immunol* 2016; **37**: 487-501 [PMID: 27289177 DOI: 10.1016/j.it.2016.05.003]
88 **Brown H**, Esterházy D. Intestinal immune compartmentalization: implications of tissue specific determinants in health and disease. *Mucosal Immunol* 2021; **14**: 1259-1270 [PMID: 34211125 DOI: 10.1038/s41385-021-00420-8]
89 **Furness JB**, Kunze WA, Clerc N. Nutrient tasting and signaling mechanisms in the gut. II. The intestine as a sensory organ: neural, endocrine, and immune responses. *Am J Physiol* 1999; **277**: G922-G928 [PMID: 10564096 DOI: 10.1152/ajpgi.1999.277.5.G922]
90 **Arora T**, Vanslette AM, Hjorth SA, Bäckhed F. Microbial regulation of enteroendocrine cells. *Med* 2021; **2**: 553-570 [PMID: 35590233 DOI: 10.1016/j.medj.2021.03.018]
91 **Fothergill LJ**, Furness JB. Diversity of enteroendocrine cells investigated at cellular and subcellular levels: the need for a new classification scheme. *Histochem Cell Biol* 2018; **150**: 693-702 [PMID: 30357510 DOI: 10.1007/s00418-018-1746-x]
92 **Martin AM**, Lumsden AL, Young RL, Jessup CF, Spencer NJ, Keating DJ. The nutrient-sensing repertoires of mouse enterochromaffin cells differ between duodenum and colon. *Neurogastroenterol Motil* 2017; **29** [PMID: 28251760 DOI: 10.1111/nmo.13046]
93 **Martin AM**, Lumsden AL, Young RL, Jessup CF, Spencer NJ, Keating DJ. Regional differences in nutrient-induced secretion of gut serotonin. *Physiol Rep* 2017; **5** [PMID: 28320893 DOI: 10.14814/phy2.13199]
94 **Campbell EL**, Colgan SP. Control and dysregulation of redox signalling in the gastrointestinal tract. *Nat Rev Gastroenterol Hepatol* 2019; **16**: 106-120 [PMID: 30443019 DOI: 10.1038/s41575-018-0079-5]
95 **Ma H**, Zhang B, Hu Y, Wang J, Liu J, Qin R, Lv S, Wang S. Correlation Analysis of Intestinal Redox State with the Gut Microbiota Reveals the Positive Intervention of Tea Polyphenols on Hyperlipidemia in High Fat Diet Fed Mice. *J Agric Food Chem* 2019; **67**: 7325-7335 [PMID: 31184120 DOI: 10.1021/acs.jafc.9b02211]
96 **Uchiyama J**, Akiyama M, Hase K, Kumagai Y, Kim YG. Gut microbiota reinforce host antioxidant capacity *via* the generation of reactive sulfur species. *Cell Rep* 2022; **38**: 110479 [PMID: 35263581 DOI: 10.1016/j.celrep.2022.110479]
97 **Bódi N**, Bagyánszki M. Diabetic enteric neuropathy: Imbalance between oxidative and antioxidative mechanisms. Diabetes: Elsevier, 2020: 25-33
98 **Sotler R**, Poljšak B, Dahmane R, Jukić T, Pavan Jukić D, Rotim C, Trebše P, Starc A. Prooxidant activities of antioxidants and their impact on health. *Acta Clin Croat* 2019; **58**: 726-736 [PMID: 32595258 DOI: 10.20471/acc.2019.58.04.20]
99 **Sun C**, Liu Y, Zhan L, Rayat GR, Xiao J, Jiang H, Li X, Chen K. Anti-diabetic effects of natural antioxidants from fruits. *Trends Food Sci Tech* 2020; 117 [DOI: 10.1016/j.tifs.2020.07.024]
100 **Surai KP**, Surai PF, Speake BK, Sparks NHC. Antioxidant-prooxidant balance in the intestine: Food for thought 2. *Curr Top Nutraceutical Res* 2004; **2**: 27-46
101 **Riaz Rajoka MS**, Thirumdas R, Mehwish HM, Umair M, Khurshid M, Hayat HF, Phimolsiripol Y, Pallarés N, Martí-Quijal FJ, Barba FJ. Role of Food Antioxidants in Modulating Gut Microbial Communities: Novel Understandings in Intestinal Oxidative Stress Damage and Their Impact on Host Health. *Antioxidants (Basel)* 2021; **10** [PMID: 34679698 DOI: 10.3390/antiox10101563]
102 **Bernardi S**, Del Bo' C, Marino M, Gargari G, Cherubini A, Andrés-Lacueva C, Hidalgo-Liberona N, Peron G, González-

Dominguez R, Kroon P, Kirkup B, Porrini M, Guglielmetti S, Riso P. Polyphenols and Intestinal Permeability: Rationale and Future Perspectives. *J Agric Food Chem* 2020; **68**: 1816-1829 [PMID: 31265272 DOI: 10.1021/acs.jafc.9b02283]

103 **Surai PF**, Kochish II, Fisinin VI, Kidd MT. Antioxidant Defence Systems and Oxidative Stress in Poultry Biology: An Update. *Antioxidants (Basel)* 2019; **8** [PMID: 31336672 DOI: 10.3390/antiox8070235]

104 **Rahal A**, Kumar A, Singh V, Yadav B, Tiwari R, Chakraborty S, Dhama K. Oxidative stress, prooxidants, and antioxidants: the interplay. *Biomed Res Int* 2014; **2014**: 761264 [PMID: 24587990 DOI: 10.1155/2014/761264]

105 **Blau S**, Rubinstein A, Bass P, Singaram C, Kohen R. Differences in the reducing power along the rat GI tract: lower antioxidant capacity of the colon. *Mol Cell Biochem* 1999; **194**: 185-191 [PMID: 10391139 DOI: 10.1023/a:1006994800272]

106 **Loguercio C**, Di Pierro M. The role of glutathione in the gastrointestinal tract: a review. *Ital J Gastroenterol Hepatol* 1999; **31**: 401-407 [PMID: 10470601]

107 **McLean JA**, Karadas F, Surai PF, McDevitt RM, Speake BK. Lipid-soluble and water-soluble antioxidant activities of the avian intestinal mucosa at different sites along the intestinal tract. *Comp Biochem Physiol B Biochem Mol Biol* 2005; **141**: 366-372 [PMID: 15927496 DOI: 10.1016/j.cbpc.2005.04.009]

108 **Wang Y**, Wu Y, Wang Y, Xu H, Mei X, Yu D, Li W. Antioxidant Properties of Probiotic Bacteria. *Nutrients* 2017; **9** [PMID: 28534820 DOI: 10.3390/nu9050521]

109 **Mikelsaar M**, Zilmer M. Lactobacillus fermentum ME-3 - an antimicrobial and antioxidative probiotic. *Microb Ecol Health Dis* 2009; **21**: 1-27 [PMID: 19381356 DOI: 10.1080/08910600902815561]

110 **Jancsó Z**, Bódi N, Borsos B, Fekete É, Hermesz E. Gut region-specific accumulation of reactive oxygen species leads to regionally distinct activation of antioxidant and apoptotic marker molecules in rats with STZ-induced diabetes. *Int J Biochem Cell Biol* 2015; **62**: 125-131 [PMID: 25794426 DOI: 10.1016/j.biocel.2015.03.005]

111 **Hermes-Uliana C**, Frez FCV, Sehaber CC, Ramalho FV, de Souza Neto FP, Cecchini R, Guarnier FA, Zanoni JN. Supplementation with l-glutathione improves oxidative status and reduces protein nitration in myenteric neurons in the jejunum in diabetic Rattus norvegicus. *Exp Mol Pathol* 2018; **104**: 227-234 [PMID: 29758186 DOI: 10.1016/j.yexmp.2018.05.002]

112 **Ferreira PEB**, Beraldi EJ, Borges SC, Natali MRM, Buttow NC. Resveratrol promotes neuroprotection and attenuates oxidative and nitrosative stress in the small intestine in diabetic rats. *Biomed Pharmacother* 2018; **105**: 724-733 [PMID: 29906751 DOI: 10.1016/j.biopha.2018.06.030]

113 **Kochar NI**, Umathe SN. Beneficial effects of L-arginine against diabetes-induced oxidative stress in gastrointestinal tissues in rats. *Pharmacol Rep* 2009; **61**: 665-672 [PMID: 19815948 DOI: 10.1016/s1734-1140(09)70118-5]

114 **Shirpoor A**, Ansari MH, Salami S, Pakdel FG, Rasmi Y. Effect of vitamin E on oxidative stress status in small intestine of diabetic rat. *World J Gastroenterol* 2007; **13**: 4340-4344 [PMID: 17708608 DOI: 10.3748/wjg.v13.i32.4340]

115 **Chandrakumar L**, Bagyánszki M, Szalai Z, Mezei D, Bódi N. Diabetes-Related Induction of the Heme Oxygenase System and Enhanced Colocalization of Heme Oxygenase 1 and 2 with Neuronal Nitric Oxide Synthase in Myenteric Neurons of Different Intestinal Segments. *Oxid Med Cell Longev* 2017; **2017**: 1890512 [PMID: 29081883 DOI: 10.1155/2017/1890512]

116 **Onyiah JC**, Sheikh SZ, Maharshak N, Otterbein LE, Plevy SE. Heme oxygenase-1 and carbon monoxide regulate intestinal homeostasis and mucosal immune responses to the enteric microbiota. *Gut Microbes* 2014; **5**: 220-224 [PMID: 24637794 DOI: 10.4161/gmic.27290]

117 **Ahmed M**, Ffrench-Constant C. Extracellular Matrix Regulation of Stem Cell Behavior. *Curr Stem Cell Rep* 2016; **2**: 197-206 [PMID: 27547708 DOI: 10.1007/s40778-016-0056-2]

118 **Hynes RO**. The extracellular matrix: not just pretty fibrils. *Science* 2009; **326**: 1216-1219 [PMID: 19965464 DOI: 10.1126/science.1176009]

119 **Mecham RP**. The Extracellular Matrix: an Overview. Heidelberg: Springer Berlin, 2011

120 **Hageman JH**, Heinz MC, Kretzschmar K, van der Vaart J, Clevers H, Snippert HJG. Intestinal Regeneration: Regulation by the Microenvironment. *Dev Cell* 2020; **54**: 435-446 [PMID: 32841594 DOI: 10.1016/j.devcel.2020.07.009]

121 **Trappmann B**, Gautrot JE, Connelly JT, Strange DG, Li Y, Oyen ML, Cohen Stuart MA, Boehm H, Li B, Vogel V, Spatz JP, Watt FM, Huck WT. Extracellular-matrix tethering regulates stem-cell fate. *Nat Mater* 2012; **11**: 642-649 [PMID: 22635042 DOI: 10.1038/nmat3339]

122 **Sánchez SS**, Genta SB, Aybar MJ, Honoré SM, Villecco EI, Sánchez Riera AN. Changes in the expression of small intestine extracellular matrix proteins in streptozotocin-induced diabetic rats. *Cell Biol Int* 2000; **24**: 881-888 [PMID: 11114237 DOI: 10.1006/cbir.2000.0581]

123 **Siegman MJ**, Eto M, Butler TM. Remodeling of the rat distal colon in diabetes: function and ultrastructure. *Am J Physiol Cell Physiol* 2016; **310**: C151-C160 [PMID: 26561639 DOI: 10.1152/ajpcell.00253.2015]

124 **Storkholm JH**, Villadsen GE, Jensen SL, Gregersen H. Mechanical properties and collagen content differ between isolated guinea pig duodenum, jejunum, and distal ileum. *Dig Dis Sci* 1998; **43**: 2034-2041 [PMID: 9753270 DOI: 10.1023/a:1018855113849]

125 **D'Arpino MC**, Fuchs AG, Sánchez SS, Honoré SM. Extracellular matrix remodeling and TGF-β1/Smad signaling in diabetic colon mucosa. *Cell Biol Int* 2018; **42**: 443-456 [PMID: 29227005 DOI: 10.1002/cbin.10916]

126 **Weston BS**, Wahab NA, Mason RM. CTGF mediates TGF-beta-induced fibronectin matrix deposition by upregulating active alpha5beta1 integrin in human mesangial cells. *J Am Soc Nephrol* 2003; **14**: 601-610 [PMID: 12595495 DOI: 10.1097/01.asn.0000051600.53134.b9]

127 **Song W**, Ergul A. Type-2 diabetes-induced changes in vascular extracellular matrix gene expression: relation to vessel size. *Cardiovasc Diabetol* 2006; **5**: 3 [PMID: 16503991 DOI: 10.1186/1475-2840-5-3]

128 **Bódi N**, Mezei D, Chakraborty P, Szalai Z, Barta BP, Balázs J, Rázga Z, Hermesz E, Bagyánszki M. Diabetes-related intestinal region-specific thickening of ganglionic basement membrane and regionally decreased matrix metalloproteinase 9 expression in myenteric ganglia. *World J Diabetes* 2021; **12**: 658-672 [PMID: 33995853 DOI: 10.4239/wjd.v12.i5.658]

129 **Ra HJ**, Parks WC. Control of matrix metalloproteinase catalytic activity. *Matrix Biol* 2007; **26**: 587-596 [PMID: 17669641 DOI: 10.1016/j.matbio.2007.07.001]

130 **Gao Q**, Meijer MJ, Kubben FJ, Sier CF, Kruidenier L, van Duijn W, van den Berg M, van Hogezand RA, Lamers CB, Verspaget HW. Expression of matrix metalloproteinases-2 and -9 in intestinal tissue of patients with inflammatory bowel diseases. *Dig Liver Dis* 2005; **37**: 584-592 [PMID: 15869913 DOI: 10.1016/j.dld.2005.02.011]
131 **Medina C**, Radomski MW. Role of matrix metalloproteinases in intestinal inflammation. *J Pharmacol Exp Ther* 2006; **318**: 933-938 [PMID: 16644899 DOI: 10.1124/jpet.106.103465]
132 **Silva LM**, Kim TS, Moutsopoulos NM. Neutrophils are gatekeepers of mucosal immunity. *Immunol Rev* 2023; **314**: 125-141 [PMID: 36404627 DOI: 10.1111/imr.13171]

World Journal of Gastroenterology

Submit a Manuscript: https://www.f6publishing.com

World J Gastroenterol 2023 May 14; 29(18): 2717-2732

DOI: 10.3748/wjg.v29.i18.2717

ISSN 1007-9327 (print) ISSN 2219-2840 (online)

REVIEW

Paediatric gastrointestinal endoscopy in the Asian-Pacific region: Recent advances in diagnostic and therapeutic techniques

James Guoxian Huang, Pornthep Tanpowpong

Specialty type: Gastroenterology and hepatology

Provenance and peer review: Invited article; Externally peer reviewed.

Peer-review model: Single blind

Peer-review report's scientific quality classification

Grade A (Excellent): 0
Grade B (Very good): B
Grade C (Good): 0
Grade D (Fair): D
Grade E (Poor): 0

P-Reviewer: Cabezuelo AS, Spain; Maldonado KE, Guatemala

Received: December 29, 2022
Peer-review started: December 29, 2022
First decision: February 1, 2023
Revised: February 12, 2023
Accepted: April 14, 2023
Article in press: April 14, 2023
Published online: May 14, 2023

James Guoxian Huang, Division of Gastroenterology, Hepatology and Nutrition, Department of Paediatrics, Khoo Teck Puat-National University Children's Medical Institute, National University Health System, Singapore 119228, Singapore

James Guoxian Huang, Department of Paediatrics, Yong Loo Lin School of Medicine National University of Singapore, Singapore 119228, Singapore

Pornthep Tanpowpong, Department of Paediatrics, Faculty of Medicine Ramathibodi Hospital, Mahidol University, Bangkok 10400, Thailand

Corresponding author: James Guoxian Huang, MBBS, MRCP, Assistant Professor, Doctor, Division of Gastroenterology, Hepatology and Nutrition, Department of Paediatrics, Khoo Teck Puat-National University Children's Medical Institute, National University Health System, NUHS Tower Block Level 12, 1E Kent Ridge Road, Singapore 119228, Singapore.
paehgj@nus.edu.sg

Abstract

There has been a rapid expansion in the knowledge of paediatric gastroenterology over the recent decade, with a fast-growing repertoire of diagnostic techniques and management strategies for a wide spectrum of childhood gastrointestinal (GI) diseases. Paediatric GI endoscopy is a core competency every paediatric gastroenterologist should possess, and represents one of the most common procedures performed in children for both diagnostic and therapeutic purposes. Yet there remains a dearth of literature on the utility and outcomes of paediatric GI endoscopy in the Asia-Pacific region. Data on the diagnostic value of paediatric GI endoscopy would be an important aspect of discussion, with the emergence of inflammatory bowel disease (IBD) and eosinophilic GI disease as increasingly common endoscopic diagnoses. Time-based trends in paediatric GI endoscopy do point towards more IBD and gastroesophageal reflux disease-related complications being diagnosed, with a declining incidence of GI bleeding. However, the real-world diagnostic value of endoscopy in Asia must be contextualised to the region-specific prevalence of paediatric GI diseases. *Helicobacter pylori* infection, particularly that of multidrug-resistant strains, remains a highly prevalent problem in specific regions. Paediatric functional GI disorders still account for the majority of childhood GI complaints in most centres, hence the diagnostic yield of endoscopy should be critically evaluated in the absence of alarm symptoms. GI therapeutic endoscopy is also occasionally required for children with ingested foreign bodies, intestinal polyposis or oesophageal strictures requiring dilation.

Endoscopic haemostasis is a potentially life-saving skill in cases of massive GI bleeding typically from varices or peptic ulcers. Advanced endoscopic techniques such as capsule endoscopy and balloon-assisted enteroscopy have found traction, particularly in East Asian centres, as invaluable diagnostic and therapeutic tools in the management of IBD, obscure GI bleeding and intestinal polyposis. State of the art endoscopic diagnostics and therapeutics, including the use of artificial intelligence-aided endoscopy algorithms, real-time confocal laser endomicroscopy and peroral endoscopic myotomy, are expected to gain more utility in paediatrics. As paediatric gastroenterology matures as a subspecialty in Asia, it is essential current paediatric endoscopists and future trainees adhere to minimum practice standards, and keep abreast of the evolving trends in the diagnostic and therapeutic value of endoscopy. This review discusses the available published literature on the utility of paediatric GI endoscopy in Asia Pacific, with the relevant clinical outcomes.

Key Words: Endoscopy; Paediatric; Asia; Children; Gastroscopy; Colonoscopy

©The Author(s) 2023. Published by Baishideng Publishing Group Inc. All rights reserved.

Core Tip: Paediatric gastrointestinal (GI) endoscopy has gained traction in Asia as an invaluable tool in the diagnosis and management of chronic GI diseases of current and emerging epidemiological importance. Yet the lack of consensus guidelines and heterogeneity in clinical practice, variability in the referral patterns, healthcare access and prevalence of diseases across the Asian continent, inevitably leads to a wide variance in outcomes for different endoscopic modalities. There is a need for comprehensive and accreditable paediatric endoscopy training in Asia, so that endoscopists adhere to a minimum practice standard and are adequately trained to apply diagnostic and therapeutic endoscopic techniques appropriately and competently.

Citation: Huang JG, Tanpowpong P. Paediatric gastrointestinal endoscopy in the Asian-Pacific region: Recent advances in diagnostic and therapeutic techniques. *World J Gastroenterol* 2023; 29(18): 2717-2732
URL: https://www.wjgnet.com/1007-9327/full/v29/i18/2717.htm
DOI: https://dx.doi.org/10.3748/wjg.v29.i18.2717

INTRODUCTION

Gastrointestinal (GI) symptoms remain a common presenting feature of various ailments in childhood, and the advent of modern GI diagnostic and therapeutic techniques have allowed centres across Asia to utilise GI endoscopy early in the evaluation of a child with suspected GI disease. There remains a lack of consensus statements and guidelines on the utility of paediatric GI endoscopy in the Asian context, leading to a lack of consistency in clinical practice and highly variable clinical outcomes between centres [1]. The epidemiological situation in Asia is unique as rapidly evolving disease trends occur amidst changing lifestyle and environmental factors: Paediatric inflammatory bowel disease (IBD) is of rapidly emerging importance[2], yet its early diagnosis is often complicated by the relatively high prevalence of GI infections such as intestinal tuberculosis[3] and other infectious diseases in certain endemic regions. *Helicobacter pylori* (*H. pylori*) has fallen in prevalence in developed regions of Asia but remains a highly prevalent pathogen in association with peptic ulcer disease and gastric cancer in other regions[4]. There is increasing awareness and knowledge of the role of the gut-brain-axis in disorders of gut-brain interaction or functional GI disorders[5], prompting interest in the actual diagnostic yield of GI endoscopy in childhood abdominal pain syndromes. While Asia remains vastly heterogeneous in socioeconomic status, access to early endoscopy and advanced endoscopy techniques has greatly improved, and has enhanced both the diagnostics and therapeutics in various chronic paediatric GI ailments such as IBD, intestinal polyposis syndromes, varices in portal hypertension and GI strictures.

DIAGNOSTIC ENDOSCOPY

Time-based trends in paediatric endoscopy in Asia: More IBD and gastroesophageal reflux disease-related complications

Improved healthcare access and the maturation of paediatric gastroenterology as a specialty has contributed to the rapid rise in endoscopies performed in children[6]. There are few paediatric

endoscopy consortiums within Asia, with most of the published experience coming from East Asian centres. Data from the Japan Paediatric Endoscopy Society demonstrated a five-fold increase in the number of paediatric endoscopies performed in the latest survey in 2011-2016 *vs* 2000-2004, an increase in advanced endoscopies such as endoscopic retrograde cholangioscopies and balloon-assisted enteroscopies, with a slight rise in adverse events (0.25% from 0.03%) inevitably so from increased procedural complexity[7]. A retrospective review of children undergoing upper GI endoscopy at the Children's Hospital of Philadelphia (CHOP) demonstrated a rapid rise of first-time endoscopes from 107 in 1985 to 1294 in 2005[8]. Interestingly this same study also showed a decline in the proportion of GI bleeding (34% to 5%), a decline in both the overall clinical severity of cases and corresponding endoscopic and histological abnormalities, and yet a rise in the proportion of upper GI endoscopies done for abdominal pain (23% to 43%)[8]. It begets the question if centres are performing more endoscopies in otherwise healthy children, hence the need to examine the diagnostic yield of paediatric GI endoscopies and the impact on clinical management.

There are very limited publications comparing trends in paediatric endoscopy within Asia, to contrast with the aforementioned North American data. In contrast to the significant fall in oesophageal histological abnormalities detected in the CHOP study, a Japanese paediatric study demonstrated a significant rise in the proportion of erosive oesophagitis (9.8% to 18.1%) or endoscopic Barrett's oesophagus (2.5% to 9.6%) between eras 2005-2012 to 2013-2019[9]. It is postulated by the authors that this trend is related to dietary changes and the decreasing prevalence of *H. pylori* amongst the Japanese population. Published adult data from Japan[10] and Malaysia[11] also clearly demonstrates the decline in peptic ulcers and associated upper GI bleeding, with rates of gastroesophageal reflux disease (GERD) increasing on the contrary.

A single centre in Beijing shows a statistically significant rise in the number of colonoscopies performed amongst the 0-3 year age group, from the era 2005-2011 to 2012-2017 (3.0% to 14.1%, $P < 0.001$) but no significant change in diagnostic yield rates between the two eras (36.3% to 38.2%)[12]. The proportions of IBD and colonic polyps detected did not differ between the two eras. A paediatric South Korean cohort study in Busan, however did show a substantial rise in colonoscopies from 2001-2005 to 2011-2015 (200 to 746)[13], with trends in indications somewhat mirroring those in the CHOP study. The number of colonoscopies performed for abdominal pain increased from 27.5% to 43.7%, while those performed for haematochezia fell from 56.0% to 42.5%. There was an actual rise in diagnostic yield with the proportion of Crohn's disease diagnosed doubling from 13.5% (2001-2005) to 26.8% (2011-2015). This is consistent with the rapid rise in paediatric IBD incidence observed in South Korea[14] and the rest of Asia[2].

Diagnostic yield varies widely according to referral indication and regional disease prevalence

Tables 1 and 2 describe the overall diagnostic yield in upper and lower endoscopies (follow-up endoscopies excluded unless stated otherwise). The positive endoscopic yield varies substantially between centres: Between 45%-93% for upper endoscopies (Table 1) and correspondingly 43%-85% (Table 2) for lower endoscopies. The large variability in the diagnostic yields is clearly multifactorial, from varying referral patterns and referral indications, regional differences in disease prevalence and healthcare resource allocation between centres. For instance, in single-centre studies out of Malaysia[15] and India[16], abdominal pain/dyspepsia were indications for just 13.4% and 17.4% of upper GI endoscopies respectively, while upper GI bleeding and variceal surveillance were more common indications. This is in contrast to other cohorts *e.g.*, the North American CHOP[8] and the South Korean cohort[17], where abdominal pain/dyspepsia were the most common indications (43%-64% of upper GI endoscopies) and upper GI bleeding being far less prevalent. These differing trends in GI bleeding rates could be attributed to varying prevalence in *H. pylori*-associated gastroduodenal ulcer disease and upper GI haemorrhage[10], variability in healthcare access, timeliness of referrals for biliary atresia and other childhood liver diseases. Resource-scarce centres also likely prioritise allocation of endoscopy resources for GI emergencies, typically acute GI bleeding, rather than uncomplicated abdominal pain.

Childhood H. pylori infection remains a highly prevalent problem in Southeast Asia and South/West Asia

It must be emphasised that the vast Asian continent is both economically and culturally heterogenous: Peptic ulcerations and *H. pylori* still remain fairly common in certain regions. Jordanian data from 2014-2020 showed *H. pylori* accounted for 66.1% of all abnormal upper GI endoscopies in children[18]; an earlier Israeli paediatric study showed 22.5% of all upper GI endoscopies had peptic ulcerations, of which 66.3% of these were *H. pylo*ri positive[19]. The global trend of increasing antimicrobial resistance in *H. pylori*[20] hinders the implementation of eradication strategies in these regions with high *H. pylori* prevalence. Vietnam has a very high *H. pylori* prevalence rate (> 75%) associated with the highest prevalence of gastric cancer in Southeast Asia[4]. A study of 237 symptomatic Vietnamese children undergoing upper GI endoscopy for suspected *H. pylori*-associated gastroduodenal disease showed 80.6% and 71.7% of *H. pylori* isolates were resistant to clarithromycin and amoxicillin respectively[21]. These figures place Vietnam as one of the regions with the highest rates of *H. pylori* antimicrobial resistance, and emphasises the added importance of upper GI endoscopy to obtain biopsies for a culture

Table 1 Diagnostic yield of oesophagogastroduodenoscopies

Country	Year	Cohort size (*n*)	Indications (top three) (%)	Findings (%)	Ref.
China	2018-2019	2268	Abdominal pain (86.2). Vomiting (31.1). Weight loss (15.1)	62.5% abnormal. Highest yield in dysphagia	[105]
Nepal	2013-2016	270	Abdominal pain (77.3). Vomiting/reflux (8.4). Failure to thrive (7.0)	92.5% abnormal. Gastroduodenitis (28.1). Antral gastritis (18.5). Erosive gastritis (15.9)	[106]
India	2013-2016	822	Variceal surveillance (19.1). Dyspepsia (17.4). Upper GI bleed (16.5)	45.8% abnormal. Duodenal ulcers/varices most common	[16]
Israel	2014	407	Suspected coeliac disease (28.2). Abdominal pain (15.0). Persistent *H. pylori* (10.3)	59.2% abnormal. Coeliac disease (28), *H. pylori* (16.5), Crohn's disease (5.4)	[107]
Jordan	2014-2020	778	Abdominal pain (45.1). Vomiting (21.1). Weight loss (10.3)	47.2% abnormal. *H. pylori* (66.1). Coeliac disease (30.4). Eosinophilic GI disease (3.6)	[18]
Malaysia	2008-2011	231 OGD. 44 OGD and Colonoscopies	Variceal surveillance (50.0). Upper GI bleed (26.0). Abdominal pain (13.4)	79.0% abnormal	[15]
South Korea	2008-2013	554	Abdominal pain (64.1). Dysphagia (9.0). Vomiting (9.0)	88.1% abnormal. Gastritis (53.1). Esophagitis (17.7)	[17]
Thailand	2000-2002	38	Recurrent abdominal pain	45% abnormal. *H. pylori* (26.3)	[108]
United States	2002-2005	454	Recurrent abdominal pain	38.1% abnormal. Reflux esophagitis (23.0). *H. pylori* (5.0). Peptic ulcers (3.0)	[37]

OGD: Oesophagogastroduodenoscopies; *H. pylori*: *Helicobacter pylori*; GI: Gastrointestinal.

and antimicrobial sensitivity-based eradication strategy. This has implications on the feasibility of healthcare access and early endoscopy, as *H. pylori* is typically most prevalent in regions of lower socioeconomic status.

Paediatric IBD: A rapid rise in prevalence with possibly many more undiagnosed cases

While IBD was once considered uncommon in Asia, an emerging number of paediatric publications have documented its meteoric rise in prevalence[2,14] as alluded to earlier. Table 2 describes IBD detection rates between 14%-40% of all abnormal paediatric colonoscopies performed in Asia, emphasising the importance of IBD as an endoscopic diagnosis. Of note, 'non-specific colitis' accounts for a substantial 8%-27% of all abnormal colonoscopic findings across most published studies. It is highly plausible that these unspecified cases may evolve into a more definite diagnosis of IBD on follow-up investigations: These published IBD rates underestimate the true burden of IBD in Asia and may just represent the tip of the iceberg. Paediatric-onset IBD typically has less classical endoscopic features and more subtle histologic findings[22] compared to adult-onset disease, often prompting a diagnosis of 'indeterminate colitis'[23] or 'IBD-unclassified'.

Intestinal tuberculosis, while often considered as an important differential to IBD, was far less common a colonoscopic diagnosis than IBD, even in regions with high tuberculosis burden. Intestinal tuberculosis accounted for 1.5% cases *vs* 14.1% IBD and 27.0% non-specific colitis in a Mainland Chinese paediatric cohort[12]; a Kuwaiti study showed Intestinal tuberculosis in 1.2% *vs* IBD in 21.3% of children undergoing colonoscopy[24]. There is a paucity of epidemiologic data from the Indian subcontinent, where the world's tuberculosis burden is the highest. An Indian publication in 1991 described a cohort of 72 Indian children undergoing colonoscopy: Tuberculous colitis was seen in 2.7%, ulcerative colitis in 5.5% and amoebic colitis in 1.3% of cases[25]. A more recent Bangladeshi study of 332 children undergoing colonoscopy showed intestinal tuberculosis in 1.5% *vs* IBD in 6% and nonspecific colitis in 13.6%[26]. It is not detailed in the aforementioned studies how intestinal tuberculosis is reliably distinguished from IBD, and this distinction remains a diagnostic challenge especially in India. A therapeutic trial of empirical anti-tuberculous therapy is still often practised in cases of diagnostic uncertainty[3].

Paediatric eosinophilic GI disease

There is little published data on the actual prevalence of eosinophilic GI diseases (EGIDs) in Asia, although it is believed the incidence of EGIDs will rise in tandem with the rise of allergic disorders[27]. Symptoms may mimic GERD especially in infants and young children, to recurrent dyspepsia, dysphagia and/or food impaction in the older child. The diagnosis of an EGID hinges greatly on histological findings of significant tissue eosinophilia (> 15 eosinophils per high power field) in the absence of other attributable causes. The increasingly widespread empirical use of proton-pump inhibitors in children[28,29] may reverse the tissue eosinophilia in a subset of patients with acid

Table 2 Diagnostic yield of ileocolonoscopies

Country	Year	Cohort size (*n*)	Indications (top three) (%)	Findings (%)	Ref.
Australia	2001-2010	999 colonoscopies (15.0% done as follow-up)	Suspected IBD (45.0). Haematochezia (20.0). Abdominal pain (5.0)	61.0% abnormal. IBD (28.2). Polyp (3.9)	[109]
China	2005-2017	326	-	62.6% abnormal. IBD (14.1). Nonspecific colitis (27.0). Polyp (12.0)	[12]
China	2013-2016	229	Abdominal pain (35.4). Haematochezia (27.9). Crissum abscess/anal fistula (17.5)	64.2% abnormal. IBD (38.8). Polyp (27.2). Nonspecific colitis (26.5)	[110]
Hong Kong	2003-2008	79	Haematochezia (58.0). Suspected IBD (29.1)	50.6% abnormal. IBD (16.5). Polyp (29.1)	[111]
Japan	2011-2016	275	Haematochezia (75.0). Diarrhoea (13.0). Abdominal pain (2.2)	77.1% abnormal. IBD (18.5). Eosinophilic GI disease (23.0). Polyp (14.0)	[33]
Japan	2007-2015	274	Haematochezia (42.7). Abdominal pain (30.7). Diarrhoea (15.3)	66.8% abnormal. IBD (43.4). Eosinophilic GI disease (2.2). Polyp (5.9). Nonspecific colitis (8.4)	[112]
Malaysia	2010-2015	121	Suspected IBD (30.0). Haematochezia (21.0). Change in bowel habits (17.0)	85.0% abnormal. IBD (42.0). Polyp (7.0). Nonspecific/infective colitis (25.0)	[113]
Saudi Arabia	1993-2002	183	-	44.0% abnormal. Nonspecific colitis or rectal ulcer (71.0). Polyp (20.0)	[114]
South Korea	2008-2013	168	Abdominal pain (37.5). Diarrhoea (28.0). Haematochezia (27.4)	43.5% abnormal. IBD (19.6). Polyp (1.8). Nonspecific inflammation (14.3)	[17]
South Korea	2011-2015	746	Abdominal pain (43.7). Haematochezia (42.5). Diarrhoea (29.1)	72.2% abnormal. IBD (33.9). Polyp (11.5)	[13]
Taiwan, China	1998-2010	192	Haematochezia (53.5). Abdominal pain (20.6). Iron deficiency anaemia (11.8)	75% abnormal. IBD (8.3). Polyp (20.4). Nonspecific colitis (23.4)	[115]

IBD: Inflammatory bowel disease; GI: Gastrointestinal.

suppression-responsive EGID[30], further complicating the diagnostic process. Nevertheless, a short finite trial of acid-suppression is still deemed reasonable, with upper GI endoscopy and/or pH-impedance testing reserved for those refractory to empirical treatment or for those who cannot be weaned off acid-suppressive therapy[31].

In a fairly large study of 910 South Korean children presenting with symptoms of oesophageal dysfunction (vomiting, dysphagia, persistent reflux), 1.5% was diagnosed with eosinophilic oesophagitis (EoE) and 1.3% with eosinophilic gastroenteritis. 30.8% of patients with EGID had normal macroscopic findings, stating the importance of performing biopsies on even normal-appearing segments. The authors commented that the incidence of EoE was similar to a previous Japanese study but much lower than 10%-15% incidence in Western cohorts[32]. A multi-centre study in Japanese children undergoing colonoscopies by Nambu *et al*[33] showed EGIDs accounted for a substantially high proportion (23.0%) of the diagnoses followed by IBD (19.0%), but the authors had included food allergies and food protein-induced proctocolitis within the spectrum of EGIDs. Future studies are required to see if the incidence of EGIDs in Asia would mimic the rising trend seen with IBD.

Low diagnostic yield of endoscopy in uncomplicated abdominal pain

While paediatric endoscopy has high value in the diagnosis and management of IBD, *H. pylori* and EGIDs, most children with GI complaints have a non-organic aetiology yet the prevalence of functional GI disorders in Asian children is largely unknown and seldom described. Functional constipation was the most common condition identified in otherwise healthy Vietnamese (5.6%) and Mainland Chinese (7.0%) children between 7-48 mo of age[34,35]. Recurrent abdominal pain and dyspepsia in children is far more likely to be of a functional aetiology than in adults, prompting one to question the necessity and cost-effectiveness of invasive investigations. El-Matary *et al*[36] evaluated a cohort of 103 British children fulfilling Apley's original criteria of recurrent abdominal pain, *via* a series of blood, stool, imaging investigations with endoscopy done as clinically indicated. Approximately 70% of these children had a non-organic aetiology to their abdominal symptoms, with irritable bowel syndrome being the most common diagnosis. This study was conducted within a hospital setting, and it is likely that the actual prevalence of paediatric functional GI disorders would be much higher if the study were to be repeated in a community setting.

The diagnostic yield of paediatric GI endoscopy in childhood abdominal pain varies widely between published cohorts (Table 1), depending on the referral indication, presence of alarm symptoms[37] and/or index of suspicion guided by abnormal biochemistry (*e.g.*, coeliac serology) or imaging pre-

endoscopy. Moreover, the definition of a 'positive diagnostic yield' can be debatable as positive endoscopic pathology does not equate causality of symptoms *e.g.*, *H. pylori* infection is often asymptomatic and may be an 'innocent bystander' in children with functional abdominal pain[38], especially in the high-prevalence areas. An Israeli study of 329 children undergoing endoscopy for various indications (abdominal pain, diarrhoea, failure to thrive, short stature and iron deficiency anaemia) showed only 36% of children with abdominal pain had a diagnostic finding on endoscopy; if the child had abdominal pain in association with an objective test *e.g.*, positive coeliac serology and/or iron deficiency, the diagnostic yield would be more than 50% while those with subjective symptoms of nausea and constipation would have a positive yield in less than 25%[39]. A Hong Kong-based cohort of 80 children, fulfilling the Rome III criteria of functional dyspepsia and undergoing upper GI endoscopy, showed only 6.3% had ulcerations or erosions. There was a strongly positive correlation between alarm features *e.g.*, nocturnal pain and endoscopic findings[40]. These findings suggest that a risk stratification strategy, combining a clinical assessment for alarm features and the use of non-invasive objective tests, would be potentially helpful in discerning those who would benefit most from diagnostic endoscopy. An example would be the stool calprotectin assay, which is now commonly used globally as a highly sensitive stool biomarker for gut inflammation, both in the diagnosis and monitoring of IBD[41,42].

Advanced paediatric GI endoscopy in Asia

Advanced endoscopy techniques such as video capsule endoscopy (VCE) and balloon-assisted enteroscopy (BAE) can enhance diagnostics especially for obscure small bowel pathology, which would otherwise be inaccessible with standard endoscopy. VCE has been approved in children as young as 2 years old since 2009[43] and remains one of the commonly used modalities to complement standard endoscopy findings or when standard endoscopy has been non-diagnostic. Much of the published Asian experience with VCE has been from large East Asian (China[44], Japan[45] and South Korea[46]) adult and paediatric cohorts. A large Mainland Chinese cohort of 825 children in a single paediatric IBD centre underwent VCE for the main indication of abdominal pain (61.2%) followed by anaemia (17.0%) [44]. The authors noted a much higher diagnostic yield (55.6%) primarily of Crohn's disease-related small bowel pathology, compared to previous studies for similar indications quoting 20%-28%[47,48]; this was ascribed to a higher referral load of suspected IBD patients, further emphasising the strong influence of referral indications on published yields. Other typical VCE findings included idiopathic small bowel ulcers, intestinal polyps, lymphangiectasia and vascular malformations.

While the experience of VCE in adult cohorts has been for obscure GI bleeding, VCE has gained increasing utility for the pan-enteric evaluation of IBD[49]. VCE can be utilised as a non-invasive first-line modality in suspected IBD cases after a patency capsule test, followed by confirmatory endoscopy. VCE may also be advantageous in detecting early mucosal healing in IBD disease monitoring. A Korean paediatric study of Crohn's disease found VCE to be more sensitive than magnetic resonance enterography in detecting mucosal healing and early therapeutic response in the first year post diagnosis[50]. Other indications for VCE include the surveillance of intestinal polyposis, particularly in Peutz-Jeghers' syndrome where small bowel polyps have been known to form a lead point for small bowel intussusception. The use of VCE facilitates the planning of BAE for definitive small bowel polyp clearance[51].

As observed with studies of VCE, much of the published Asian paediatric experience with BAE are from East Asian cohorts[52-54]. Of note, these cohorts may include a varying number of patients undergoing balloon-assisted endoscopic retrograde cholangioscopes primarily for therapy of biliary stenoses. BAE complements the diagnostic value of VCE by providing the means to obtain histological samples and provide therapeutic intervention. Hagiwara *et al*[54] described a multi-centre study of 96 BAEs (both antegrade and retrograde) in 79 paediatric patients. The main indications were for follow-up of IBD, obscure GI bleeding, abdominal pain, and therapy of hereditary polyposis syndromes. The positive diagnostic yield in obscure GI bleeding and abdominal pain was 48%. There were higher reported diagnostic yields of approximately 77% for similar indications in the mainland Chinese paediatric cohorts[53,55], but this variation can be explained by differing referral indications as aforementioned.

State of the art advanced endoscopic diagnostic techniques

While most of these techniques are not in mainstream use at most Asian-Pacific paediatric gastroenterology centres, they are worth discussing in brevity as recent publications have discussed their utility in enhancing current paediatric GI diagnostics.

Transnasal endoscopy: This technique would be useful especially in children with EoE as they commonly require multiple upper GI endoscopies for mucosal surveillance[56]. Transnasal endoscopy may be done as an unsedated office procedure with topical pharyngeal anaesthesia, and significantly save time, costs and endoscopy resources.

Mucosal impedance: This technique measures transmucosal conductivity and thus the mucosal integrity of the oesophageal mucosa, *via* a catheter containing very closely spaced impedance sensors resting close to the mucosa wall. This catheter is inserted through the working channel of a standard upper GI scope, such that the sensors rest directly on the oesophageal mucosa. This has advantages over

standard 24-h pH impedance studies, by directly measuring the barrier function of the oesophageal mucosa in a matter of seconds while the child is sedated[57]. Mucosal impedance can be used to discern between GERD, EoE and non-GERD conditions, as well as to monitor treatment response/disease activity in GERD and EoE[58,59].

Endoluminal functional lumen imaging probe: Endoluminal functional lumen imaging probe (EndoFLIP) is another adjunct technique to measure oesophageal luminal dimensions, distensibility, pressure changes and motility[60], typically while the child is sedated for standard upper GI endoscopy. It involves insertion of a sensor balloon-mounted catheter transorally, and inflating the balloons within the oesophageal and gastric lumens. While high resolution oesophageal manometry is the current gold standard in the assessment of oesophageal function, it is potentially uncomfortable and requires the child to cooperate with swallowing during the manometry. EndoFLIP has utility in the assessment of patients with GERD, EoE[61] and achalasia, as well as patients experiencing persistent symptoms post fundoplication.

Confocal laser endomicroscopy: Confocal laser endomicroscopy is an endoscopic technique that allows for high-resolution histological examination of the GI mucosa at the cellular level. Besides its obvious utility in real-time detection of neoplastic lesions in adults, the group at Sheffield Children's Hospital, United Kingdom has described its usefulness as a biopsy-free method of assessing mucosal pathology in enteropathies, EoE, ileo-colitis and polyposis[62]. This enhances the diagnostic accuracy of GI endoscopy, and reduces the time, risks and costs associated with multiple GI mucosal biopsies.

Artificial intelligence and machine learning in endoscopic diagnostics: Patel *et al*[63] recently reviewed the potential application of artificial intelligence (AI) in paediatric GI pathologies. The aim of utilising machine learning, a form of AI, is to at least semi-automate the process of macroscopic pathology and pattern recognition, which would otherwise be subject to the endoscopist's individual expertise and experience. In paediatrics, AI could potentially automate the process of accurately classifying macroscopic disease severity and extent in IBD and celiac disease, as current endoscopic scoring systems are often time-consuming and subjective. Current AI research in adults is driven by the need for accurate polyp detection: Early published data of the computer-aided detection EYE system demonstrates its AI driven algorithm detects and classifies polyps with excellent sensitivity and specificity[64]. AI would play a major role in standardising endoscopy outcomes across different endoscopists of varying experience levels, especially in units with rotating trainees.

THERAPEUTIC ENDOSCOPY

Foreign body removal

Foreign body ingestion is a common presentation in the ambulatory and emergency department settings. The exploratory behaviour and normal development of young infants and toddlers lead these kids to accidentally grasp and ingest foreign objects. The common age group usually ranges between 6 mo to 6 years[65]. The initial manifestation can range from asymptomatic to significant GI symptoms (drooling, dysphagia, vomiting, obstructive symptoms), coughing, choking, severe respiratory distress, or even death[66,67]. One of the largest cohorts from China reported 1265 children (aged 6 mo to 16 years) admitted with a history of foreign body ingestion, of which 552 (43%) children had detected foreign bodies from endoscopies. The two most common objects were coins (49%) and non-metallic sharp objects (31%)[66]. A systematic review also noted that the coin was the most frequently ingested object in the paediatric population[68]. In contrast to most reports, a medical record review in 105 Iranian children, the button battery was the most commonly found object in 41%[69]. The types of foreign body vary between different countries and geographic locations, that may be likely due to diverse sociocultural and dietary factors[70]. Another study from Khorana *et al*[67] from northern Thailand included 194 patients aged < 15 years (median age of 44 mo) found that most were symptomatic (56%), with vomiting as the commonest complaint. The most common location of impacted foreign bodies was in the oesophagus (37%), similar to most previous reports[68]. Plain radiography can usually confirm the location, size and shape of most radiopaque objects (such as coin, magnets, safety pin, *etc.*), but has little diagnostic value for radiolucent objects such as plastic toys, fishbone, or woods. Contrast studies or computed tomography scans may be needed to locate the radiolucent foreign bodies before deciding on the further management.

Timing of foreign body removal: As most of the ingested objects were coins, which were mostly considered as small and blunt objects, spontaneous passage usually occurred[67,71]. However, endoscopic intervention or even surgical exploration may be needed in some cases especially individuals with symptoms or complications. The timing of endoscopic intervention in paediatric foreign body ingestion has been proposed in various guidelines published from various scientific societies, namely the European Society for Paediatric Gastroenterology Hepatology and Nutrition

(ESPGHAN)/European Society of Gastrointestinal Endoscopy (ESGE)[71], and the North American Society of Paediatric Gastroenterology, Hepatology and Nutrition (NASPGHAN) Endoscopy Committee[72]. The proper timing of endoscopy is mainly based on 3 key factors: The type of ingested objects, the location, and the presence of symptoms. Types of common foreign bodies are button batteries, magnets, sharp objects, long objects, absorptive objects, drug packets, impacted food boluses, and coins.

Button batteries: During the past few decades, major concerns with button battery ingestion have been raised as the integrity of the strong alkali-containing battery can be degraded and cause severe caustic injury to the GI mucosa, especially the oesophagus (*i.e.*, a hollow organ with small lumen). A cohort from the United States reviewing 8648 cases of button and cylindrical battery ingestions, occurring between 1990-2008, found 73 cases with major adverse outcomes (0.8%), including prolonged compromise of feeding and/or breathing that required surgical procedures, tube feedings, tracheostomies. There were 13 deaths (0.15%) related to damage to the oesophagus, major vessels, and/or the airway[73]. Huang *et al*[74] from China reported children with inhaled/ingested button batteries and found that 13 of 116 (11%) cases had button batteries either in the oesophagus or stomach (n = 6 and 7, respectively). One child developed an oesophageal stricture and another one died from sudden cardiac arrest during the perioperative period. A recent Position Paper from ESPGHAN proposed 2 major strategies in the diagnosis and management of button battery ingestion in children. This includes: (1) Computed tomography scan to evaluate injuries to the adjacent organs and blood vessels before endoscopic removal if ingested > 12 h even in asymptomatic children; and (2) Honey (in children > 1 year of age) and sucralfate can be considered in ingestions < 12 h while waiting for endoscopic removal [75].

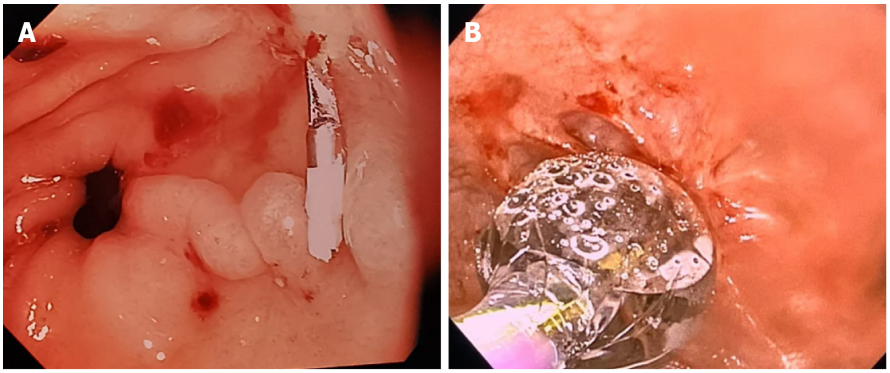
Endoscopic techniques of foreign body removal: Conventional flexible endoscopy is a safe and effective tool for removing most foreign bodies from the GI tract. A high success rate is found when using retrieval nets, polypectomy snares, and the rat-tooth forceps[71]. Opasanon *et al*[76] reported 34 Thai patients with upper GI tract foreign bodies and found that removal was successfully performed in all cases with either rat-tooth forceps, snare, dormia basket or tripods with no procedure-related complications.

Device-assisted enteroscopy for foreign body removal: The challenging cases in paediatric foreign body ingestion are typically the ones with objects beyond the reach of the conventional endoscope, *i.e.*, the depths of the small bowel in the jejunoileal area. Adult-based ESGE guidelines on small bowel endoscopy and device-assisted enteroscopy strongly recommend enteroscopy as an alternative to surgery for retrieving foreign bodies retained in the small bowel in patients without acute intestinal obstruction[77]. Device-assisted enteroscopy refers to any adjunct device used to assist endoscopic advancement into the small bowel (balloon, overtube, stiffening device). As with the use of BAE as an advanced diagnostic tool discussed earlier[54], age- and weight-appropriate device-assisted enteroscopy may be used for foreign body removal and other therapeutic applications within the small bowel.

Haemostasis of GI bleeding

GI bleeding can be divided into upper GI and lower GI bleeding. Upper GI bleeding is defined as bleeding from the GI tract proximal to the ligament of Treitz, while lower GI bleeding is bleeding occurring distal to the aforementioned ligament. Upper GI bleeding can also be further divided into non-variceal bleeding and variceal bleeding which may (or usually) need haemostatic intervention (Figure 1A). On the other hand, for the paediatric population, lower GI bleeding rarely needs endoscopic intervention in the colon or distal small bowel mainly because of the 3 following reasons: (1) Most of the severe GI bleeding occurs up in the upper GI tract; (2) Acute colonic bleeding in children usually stops spontaneously; and (3) Various common aetiologies such as Meckel's diverticulum, intussusception, colitis from infection, inflammation or allergy, or anal fissures rarely need endoscopic intervention to stop bleeding. One of the few exceptions being endoscopic polypectomy for juvenile (colonic) polyps which usually present in a non-urgent setting. After initial haemodynamic stabilization consisting of judicious fluid resuscitation and, if necessary, blood product replacement, endoscopic haemostatic intervention for the lesions causing GI bleeding would need to be justified based on the site and type of the lesion, patient's underlying disease and resource availability/procedural feasibility in conjunction with the potential contraindications.

Haemostasis for acute upper GI bleeding: Non-variceal and variceal bleeding: ESPGHAN/ESGE guidelines suggest early oesophago-gastroduodenoscopy within 12 h in cases presenting with acute upper GI bleeding that require ongoing circulatory support, or those presenting with large volume haematemesis or melena (weak recommendation and low quality of evidence, but a strong recommendation and moderate quality of evidence in cases with a known history of oesophageal varices) [71]. Most recommendations with regards to upper GI bleeding have been adopted from previous adult-dominated studies. An oesophago-gastroduodenoscopy should also be performed in cases with bleeding that require packed red blood cell transfusion due to a haemoglobin value below 8 g/dL and



DOI: 10.3748/wjg.v29.i18.2717 **Copyright** ©The Author(s) 2023.

Figure 1 Images. A: Haemostatic clip applied to a bleeding gastric antral ulcer; B: Balloon dilation in oesophagus with a mucosal tear.

an acute drop of at least 2 g/dL, or a bleeding clinical severity index score above a defined validated threshold such as the Sheffield Scoring System[78]. Furthermore, endoscopy should be performed before discharge from hospital, in children with pre-existing liver disease or portal hypertension.

Endoscopic haemostatic techniques for non-variceal lesions: Overall, lesions causing non-variceal upper GI bleeding such as bleeding ulcers or Dieulafoy lesion should use either thermal techniques such as heater probe, bipolar probe or mechanical techniques such as haemostatic clips, with/without epinephrine injection for controlling bleeding[71,79]. Yabe *et al*[80] reported 36 Japanese children with upper GI bleeding from gastroduodenal ulcers (50%) or gastritis (26%), and 14/36 (39%) underwent haemostatic intervention [clips (n = 12), hypersaline and epinephrine injection and coagulation therapy (n = 1), pure ethanol injections (n = 1)] with 100% initial success rate. Rebleeding occurred only in one patient who was initially treated with ethanol injections.

Endoscopic haemostatic techniques for variceal bleeding: For oesophageal varices, Zargar *et al*[81] demonstrated that endoscopic variceal band ligation is more effective than sclerotherapy in 49 Indian children with extrahepatic portal vein obstruction and variceal bleeding. Band ligation required fewer endoscopic sessions [3.9 (SD 1.1) *vs* 6.1 (SD 1.7) times for sclerotherapy] and had lower rates of rebleeding (4% *vs* 25%)[81]. Since then, studies comparing the efficacy of banding with sclerotherapy in children are sparse. A recent Cochrane Review was initially planned to analyse randomized controlled trials (RCTs) but was eventually unable to find any RCTs comparing band ligation *vs* sclerotherapy as primary variceal prophylaxis (*i.e.*, preventing the first variceal bleeding episode in children with oesophageal varices) in children with chronic liver disease or portal vein thrombosis[82].

Polypectomy

The technique of polypectomy is based on the location, morphology, and size. The ESPGHAN guideline suggests using cold biopsy forceps for small polyps (< 3 mm), hot or cold snaring in polyps diameter 3-8 mm, and hot snaring in the larger polyps[71]. However, hot biopsy forceps induce larger histopathological lesions, increased necrotic depth and submucosal inflammation in a pig's colon model[83], and more cytological artefacts[84]. A retrospective study in 91 Korean children, who underwent endoscopy to find polyps, found that polyp size was the one single factor associated with the presence of any polyps located proximal to the splenic flexure [odds ratio = 2.3, 95% confidence interval (CI): 1.3-4.3]. Polyps proximal to the splenic flexure and sessile morphology were associated with the presence of any adenomatous polyp. Therefore, the authors concluded that a full colonoscopy remains crucial before the occurrence of complications[85]. Another study from Thailand investigated 32 patients with symptoms of colorectal polyps such as haematochezia, rectal mass, or diarrhoea. Most (20/32, 63%) had a single polyp, 6/32 had 2-4 polyps, and a minority (6/32) was diagnosed with polyposis coli. Most had polyps in the rectosigmoid region and only 6 cases had polyps proximal to the splenic flexure. All had pathologically confirmed juvenile polyps without adenomatous changes, which demonstrated an absence of malignant potential[86].

Oesophageal dilation

Dilation of the oesophagus is indicated when symptoms of oesophageal stricture/stenosis occur. Various causes include congenital anomalies, post caustic ingestion, EoE, and GERD[87]. Symptoms of oesophageal stricture include dysphagia, odynophagia, food bolus impaction, vomiting and poor oral intake. Nowadays, the 2 main options for oesophageal dilatation in oesophageal stricture are balloon dilation and bougie dilation.

Balloon dilation (Figure 1B) can be safely performed under both the direct endoscopic and/or fluoroscopic examinations, while most of the bougie dilations are Savary-Gilliard bougies that could dilate up to 12 mm in children age < 5 years and 15 mm in older children. The "rule of 3" has been widely used as dilation to not more than 3 times the stricture diameter with a minimal period of 3 wk between dilation sessions and an average of 3 sessions in total[88,89]. Lan *et al*[90] reported 75 children from Hong Kong with oesophageal strictures [post-oesophageal atresia repair (n = 63), reflux esophagitis (n = 7), caustic ingestion (n = 3) and post-fundoplication (n = 2)], who underwent a total of 260 balloon dilations (mean number of 3.4 sessions per patient). Four oesophageal perforations (1.5%) were noted, with one child required surgical repair; all other patients were asymptomatic after the dilation sessions. Balloon dilation has been reported to be more effective and less traumatic than the bougie dilation, but a study from India reported comparable complications (perforations of 0.9%)[89], and a recent study from China reported a high perforation rate of 4.4% in children undergoing oesophageal balloon dilation[91]. The aforementioned study also reported only a 60% success rate, and found that stricture length was the main determining factor of treatment outcome. Therefore, a universally-agreed dilation choice remains controversial. Furthermore, oesophageal stent placement, intralesional mitomycin C or steroid injections have also been used in refractory oesophageal strictures in children[92].

Bowel preparation of ileocolonoscopy

Low volume bowel preparations preferred: Ileocolonoscopy is an established diagnostic and therapeutic tool in a variety of GI disorders. The optimal bowel preparation is an important key success factor in paediatric ileocolonoscopy[93]. While standardised bowel preparation protocols remain unavailable[94], more recent recommendations propose low-volume preparations using either polyethylene glycol (PEG)[95] along with ascorbate or sodium picosulfate magnesium citrate (SPMC)[71]. The preferable regimen in standard clinical practice should provide optimal colonic cleansing with small volumes of laxatives, acceptable palatability and drinkability and minimal side effects. In 2017, 15 RCTs (n = 1435) from 2124 studies with heterogeneity/bias risk compared PEG with other medications (sodium phosphate enema (n = 2 studies, relative risk = 1.27 with 95%CI: 0.66-2.44), SPMC (n = 3 studies, relative risk = 0.99 with 95%CI: 0.89-1.11), sennasoids (n = 3 studies, relative risk = 0.73 with 95%CI: 0.31-1.76) which showed no difference in the bowel preparation quality. Noninferior efficacy was also noted when comparing low volume PEG with SPMC *vs* standard volume PEG. Children who received PEG regimen also needed nasogastric tube insertions more often than those receiving the SPMC regimen (38% *vs* 1.6%)[96]. Later in 2022, four good quality RCTs (n = 390) showed higher tolerability and acceptability in the SPMC group when compared to the PEG group with comparable efficacy[97].

Split bowel preparation regimens: The newer studies also implement a 'split regimen' of the laxatives at different timepoints prior to GI endoscopy[98-100]. Sriphongphankul *et al*[98] performed an RCT in 45 children aged 2-18 years. The split dose group was given PEG in 2 split doses for 8-12 h apart and at least 6 h before the procedure, and the full single dose was given once the night before scope. Successful preparation (defined as Boston Bowel Preparation Scale ≥ 6) was superior in the split group (95% *vs* 72% in the standard high-volume PEG regimen). Willingness to repeat the same protocol was also much higher (83% *vs* 36%, P = 0.002), but nasogastric tube insertion rates were comparable (57% *vs* 68%). A later meta-analysis, including 4 paediatric studies, also found a trend of significantly higher efficacy in the split dose group (P = 0.07) but significant heterogeneity was noted among studies[99]. Therefore, further high-quality RCTs with low risk of bias are required. With regards to the recommended diet before the procedure, Jiao *et al*[101] studied 321 Chinese children and found that either 1-d or 2-d low residue diet had similar efficacy in bowel preparation but the 1-d low residue diet group had higher acceptability.

State-of-the-art interventions for therapeutic endoscopy

The endoscopic interventions for (esophageal) achalasia, a rare condition with incomplete or lack of normal lower esophageal sphincter relaxation, include pneumatic dilation and botulinum toxin injection. Recently, peroral endoscopic myotomy (POEM) has become another therapeutic intervention in both adults and children that demonstrates satisfactory success rate. The NASPGHAN Endoscopy Committee recently reviewed various aspects of POEM[102]. In brief, the myotomy is made starting from 8-10 cm above to 2-3 cm below the gastroesophageal junction along the cardia. Submucosal injection of the posterior wall is then performed to create a mucosotomy and submucosal tunnel, which would reveal the circular muscle fibers of the lower oesophagus. Complete myotomy of the circular muscle layer is made with longitudinal muscle layer underneath and the clip is finally deployed to close the mucosotomy. However, studies reporting efficacy and complications of POEM in children remain limited. Furthermore, appropriate training and adequate number of the performed procedures would also be required before implementing POEM as a standard of care in paediatric achalasia.

Future training opportunities in paediatric endoscopy in the Asia-Pacific region

ESPGHAN launched a Position Paper on paediatric endoscopy training in 2020[103]. The main content on achievement of training milestones, with regards to competency and procedural numbers including

'Train the trainers' courses, have been mentioned. Educational material such as e-learning, simulator training would also be needed to train the trainees in paediatric endoscopy.

Different scientific societies recommend varying competency thresholds for lower and upper GI endoscopies. NASPGHAN, the Joint Advisory Group in GI Endoscopy Paediatric Certification from the United Kingdom, the Conjoint Committee for Recognition of Training in Gastrointestinal Endoscopy from Australia proposed a minimum of 100-120 lower GI endoscopies with a caecal intubation rate of ≥ 90% (ranges from 15-30 min). NASPGHAN and the Joint Advisory Group from the United Kingdom proposed a minimum of 100 upper GI endoscopies and the Australian Committee proposed a minimum of 200 upper GI endoscopies (≥ 100 in children). Interestingly, ESPGHAN did not specifically define any numbers for endoscopies. The number of therapeutic endoscopies such as foreign body removal, haemostatic intervention, and polypectomy vary greatly across different societies. One of the preprocedure objective outcomes is the rate of adequate bowel preparation before ileocolonoscopy, with a minimum standard of 90% and a target of 95%.

Another important point is that the group suggests endoscopic procedures in children be performed by endoscopists trained in paediatric gastroenterology with established procedure-specific competency. Special consideration must be made to a child requiring GI endoscopy. Physicians need to consider the size of the patient, indications and contraindication of the procedure, proper equipment, bowel preparation, anaesthesia and sedation as well as the psycho-emotional factors of the children and their caregivers throughout the process[104]. Therefore, before implementing training in paediatric endoscopy in the Asia-Pacific region, aforesaid aspects should be carefully considered and implemented in the formal standardized curriculum. The Asian Pan-Pacific Society for Paediatric Gastroenterology, Hepatology and Nutrition conducted its first Paediatric Endoscopy Masterclass on June 2 to 3, 2022 in Bangkok with the purpose of addressing gaps in paediatric endoscopy training within the Asia-Pacific region. The subsequent way forward would be a regionalised set of guidelines and consensus statements, to facilitate standardisation of indications and endoscopic terminology across different paediatric GI centres.

CONCLUSION

Paediatric GI endoscopy has undoubtedly gained utility in the Asia-Pacific region as an invaluable tool in the diagnostics and management of GI diseases of current and emerging epidemiological importance. This is the first article to comprehensively review the evolving epidemiologic trends in paediatric GI endoscopy within Asia-Pacific, and delve into the future directions for paediatric endoscopy training and the advent of state of the art endoscopic techniques which are increasingly applied in the adult population. Yet the lack of consensus guidelines and heterogeneity in clinical practice, variablity in the referral patterns, healthcare access and disease prevalence across the Asian continent, inevitably leads to a wide variance in outcomes for different endoscopic modalities. While it is crucial that early endoscopy is done for a prompt diagnosis and treatment, it must be balanced with avoiding un-necessarily invasive investigations in otherwise benign functional GI conditions. The maturation of paediatric gastroenterology as a subspecialty hence necessitates comprehensive and accreditable endoscopy training, so that paediatric endoscopists in Asia adhere to a minimum practice standard and are adequately trained to apply diagnostic and therapeutic endoscopic techniques appropriately and competently. The inauguration of regular endoscopy masterclasses and workshops by the regional society Asian Pan-Pacific Society for Paediatric Gastroenterology, Hepatology and Nutrition sets the stage for more uniformity in endoscopic practices and outcomes, as well as future inter-regional collaborative efforts in paediatric endoscopic research.

FOOTNOTES

Author contributions: Huang JG and Tanpowpong P involved in the conception of the work, data collection, drafting of the article, critical revision of the article and final approval of the published version.

Conflict-of-interest statement: All the authors report no relevant conflicts of interest for this article.

Open-Access: This article is an open-access article that was selected by an in-house editor and fully peer-reviewed by external reviewers. It is distributed in accordance with the Creative Commons Attribution NonCommercial (CC BY-NC 4.0) license, which permits others to distribute, remix, adapt, build upon this work non-commercially, and license their derivative works on different terms, provided the original work is properly cited and the use is non-commercial. See: https://creativecommons.org/Licenses/by-nc/4.0/

Country/Territory of origin: Singapore

ORCID number: James Guoxian Huang 0000-0002-5869-4194; Pornthep Tanpowpong 0000-0002-3246-8009.

S-Editor: Wang JJ
L-Editor: A
P-Editor: Chen YX

REFERENCES

1 **Jiang MZ**. [Development and thoughts of digestive endoscopy in children]. *Zhongguo Dang Dai Er Ke Za Zhi* 2022; **24**: 350-353 [PMID: 35527406 DOI: 10.7499/j.issn.1008-8830.2203084]
2 **Huang JG**, Wong YKY, Chew KS, Tanpowpong P, Calixto Mercado KS, Reodica A, Rajindrajith S, Chang KC, Ni YH, Treepongkaruna S, Lee WS, Aw MM. Epidemiological characteristics of Asian children with inflammatory bowel disease at diagnosis: Insights from an Asian-Pacific multi-centre registry network. *World J Gastroenterol* 2022; **28**: 1830-1844 [PMID: 35633913 DOI: 10.3748/wjg.v28.i17.1830]
3 **Ma JY**, Tong JL, Ran ZH. Intestinal tuberculosis and Crohn's disease: challenging differential diagnosis. *J Dig Dis* 2016; **17**: 155-161 [PMID: 26854750 DOI: 10.1111/1751-2980.12324]
4 **Quach DT**, Vilaichone RK, Vu KV, Yamaoka Y, Sugano K, Mahachai V. Helicobacter pylori Infection and Related Gastrointestinal Diseases in Southeast Asian Countries: An Expert Opinion Survey. *Asian Pac J Cancer Prev* 2018; **19**: 3565-3569 [PMID: 30583684 DOI: 10.31557/APJCP.2018.19.12.3565]
5 **Mukhtar K**, Nawaz H, Abid S. Functional gastrointestinal disorders and gut-brain axis: What does the future hold? *World J Gastroenterol* 2019; **25**: 552-566 [PMID: 30774271 DOI: 10.3748/wjg.v25.i5.552]
6 **Friedt M**, Welsch S. An update on pediatric endoscopy. *Eur J Med Res* 2013; **18**: 24 [PMID: 23885793 DOI: 10.1186/2047-783X-18-24]
7 **Kudo T**, Abukawa D, Nakayama Y, Segawa O, Uchida K, Jimbo K, Shimizu T. Nationwide survey of pediatric gastrointestinal endoscopy in Japan. *J Gastroenterol Hepatol* 2021; **36**: 1545-1549 [PMID: 33128271 DOI: 10.1111/jgh.15297]
8 **Franciosi JP**, Fiorino K, Ruchelli E, Shults J, Spergel J, Liacouras CA, Leonard M. Changing indications for upper endoscopy in children during a 20-year period. *J Pediatr Gastroenterol Nutr* 2010; **51**: 443-447 [PMID: 20562722 DOI: 10.1097/MPG.0b013e3181d67bee]
9 **Kusakari M**, Nakayama Y, Horiuchi A, Nakazawa Y. Trends in gastroesophageal reflux disease in Japanese children and adolescents. *Pediatr Int* 2020; **62**: 1269-1274 [PMID: 32473087 DOI: 10.1111/ped.14324]
10 **Fujimoto S**, Tsuruoka N, Esaki M, Takamori A, Sakata Y, Shimoda R, Akutagawa T, Node K, Anzai K, Sugisaki N, Iwakiri R, Takagi K, Yamanouchi K, Fujimoto K. Decline incidence in upper gastrointestinal bleeding in several recent years: data of the Japan claims database of 13 million accumulated patients. *J Clin Biochem Nutr* 2021; **68**: 95-100 [PMID: 33536718 DOI: 10.3164/jcbn.20-153]
11 **Leow AH**, Lim YY, Liew WC, Goh KL. Time trends in upper gastrointestinal diseases and Helicobacter pylori infection in a multiracial Asian population--a 20-year experience over three time periods. *Aliment Pharmacol Ther* 2016; **43**: 831-837 [PMID: 26847417 DOI: 10.1111/apt.13550]
12 **Li J**, Gu F, Li ZL, Lu YM. [Pediatric colonoscopy findings and changing patterns from Beijing in one institutional experience over 12 years]. *Beijing Da Xue Xue Bao Yi Xue Ban* 2019; **51**: 819-823 [PMID: 31624383 DOI: 10.19723/j.issn.1671-167X.2019.05.005]
13 **Park JH**. Pediatric Colonoscopy: The Changing Patterns and Single Institutional Experience Over a Decade. *Clin Endosc* 2018; **51**: 137-141 [PMID: 29618177 DOI: 10.5946/ce.2018.051]
14 **Kwak MS**, Cha JM, Lee HH, Choi YS, Seo SI, Ko KJ, Park DI, Kim SH, Kim TJ. Emerging trends of inflammatory bowel disease in South Korea: A nationwide population-based study. *J Gastroenterol Hepatol* 2019; **34**: 1018-1026 [PMID: 30447025 DOI: 10.1111/jgh.14542]
15 **Lee WS**, Zainuddin H, Boey CC, Chai PF. Appropriateness, endoscopic findings and contributive yield of pediatric gastrointestinal endoscopy. *World J Gastroenterol* 2013; **19**: 9077-9083 [PMID: 24379634 DOI: 10.3748/wjg.v19.i47.9077]
16 **Wani MA**, Zargar SA, Yatoo GN, Haq I, Shah A, Sodhi JS, Gulzar GM, Khan M. Endoscopic Yield, Appropriateness, and Complications of Pediatric Upper Gastrointestinal Endoscopy in an Adult Suite: A Retrospective Study of 822 Children. *Clin Endosc* 2020; **53**: 436-442 [PMID: 32252499 DOI: 10.5946/ce.2019.118]
17 **Lee YW**, Chung WC, Sung HJ, Kang YG, Hong SL, Cho KW, Kang D, Lee IH, Jeon EJ. Current status and clinical impact of pediatric endoscopy in Korea. *Korean J Gastroenterol* 2014; **64**: 333-339 [PMID: 25530584 DOI: 10.4166/kjg.2014.64.6.333]
18 **Altamimi E**, Odeh Y, Al-Quraan T, Mohamed E, Rawabdeh N. Diagnostic yield and appropriate indication of upper endoscopy in Jordanian children. *BMC Pediatr* 2021; **21**: 10 [PMID: 33402143 DOI: 10.1186/s12887-020-02470-6]
19 **Egbaria R**, Levine A, Tamir A, Shaoul R. Peptic ulcers and erosions are common in Israeli children undergoing upper endoscopy. *Helicobacter* 2008; **13**: 62-68 [PMID: 18205668 DOI: 10.1111/j.1523-5378.2008.00570.x]
20 **Ghotaslou R**, Leylabadlo HE, Asl YM. Prevalence of antibiotic resistance in Helicobacter pylori: A recent literature review. *World J Methodol* 2015; **5**: 164-174 [PMID: 26413490 DOI: 10.5662/wjm.v5.i3.164]
21 **Le LTT**, Nguyen TA, Nguyen NA, Nguyen YTH, Nguyen HTB, Nguyen LT, Vi MT, Nguyen T. Helicobacter pylori Eradication Efficacy of Therapy Based on the Antimicrobial Susceptibility in Children with Gastritis and Peptic Ulcer in Mekong Delta, Vietnam. *Children (Basel)* 2022; **9** [PMID: 35884002 DOI: 10.3390/children9071019]
22 **Washington K**, Greenson JK, Montgomery E, Shyr Y, Crissinger KD, Polk DB, Barnard J, Lauwers GY. Histopathology of ulcerative colitis in initial rectal biopsy in children. *Am J Surg Pathol* 2002; **26**: 1441-1449 [PMID: 12409720 DOI: 10.1097/00000478-200211000-00006]
23 **Carvalho RS**, Abadom V, Dilworth HP, Thompson R, Oliva-Hemker M, Cuffari C. Indeterminate colitis: a significant

subgroup of pediatric IBD. *Inflamm Bowel Dis* 2006; **12**: 258-262 [PMID: 16633047 DOI: 10.1097/01.MIB.0000215093.62245.b9]

24 **Kalaoui M**, Radhakrishnan S, al Shamali M, Hasan F, al-Nakib B. Findings of colonoscopy in children: experience from Kuwait. *J Trop Pediatr* 1998; **44**: 371-375 [PMID: 9972085 DOI: 10.1093/tropej/44.6.371]

25 **Thapa BR**, Mehta S. Diagnostic and therapeutic colonoscopy in children: experience from a pediatric gastroenterology centre in India. *Indian Pediatr* 1991; **28**: 383-389 [PMID: 1752656]

26 **Begum F**, Nahid KL, Islam F, Majumder W, Rukunuzzaman M, Karim AB. Paediatric Colonoscopy: Experience from Pediatric Gastroenterology and Nutrition Department, BSMMU. *Bangladesh J Child Health* 2021; **45**: 25-28 [DOI: 10.3329/bjch.v45i1.55470]

27 **Gerez IF**, Lee BW, van Bever HP, Shek LP. Allergies in Asia: differences in prevalence and management compared with western populations. *Expert Rev Clin Immunol* 2010; **6**: 279-289 [PMID: 20402390 DOI: 10.1586/eci.09.82]

28 **Yang S**, Trinh NTH, Chalumeau M, Kaguelidou F, Ruemmele FM, Milic D, Lemaitre M, Cohen JF, Taine M. Pediatric Prescriptions of Proton Pump Inhibitors in France (2009-2019): A Time-Series Analysis of Trends and Practice Guidelines Impact. *J Pediatr* 2022; **245**: 158-164.e4 [PMID: 35120983 DOI: 10.1016/j.jpeds.2022.01.041]

29 **Hales CM**, Kit BK, Gu Q, Ogden CL. Trends in Prescription Medication Use Among Children and Adolescents-United States, 1999-2014. *JAMA* 2018; **319**: 2009-2020 [PMID: 29800213 DOI: 10.1001/jama.2018.5690]

30 **Franciosi JP**, Mougey EB, Dellon ES, Gutierrez-Junquera C, Fernandez-Fernandez S, Venkatesh RD, Gupta SK. Proton Pump Inhibitor Therapy for Eosinophilic Esophagitis: History, Mechanisms, Efficacy, and Future Directions. *J Asthma Allergy* 2022; **15**: 281-302 [PMID: 35250281 DOI: 10.2147/JAA.S274524]

31 **Rosen R**, Vandenplas Y, Singendonk M, Cabana M, DiLorenzo C, Gottrand F, Gupta S, Langendam M, Staiano A, Thapar N, Tipnis N, Tabbers M. Pediatric Gastroesophageal Reflux Clinical Practice Guidelines: Joint Recommendations of the North American Society for Pediatric Gastroenterology, Hepatology, and Nutrition and the European Society for Pediatric Gastroenterology, Hepatology, and Nutrition. *J Pediatr Gastroenterol Nutr* 2018; **66**: 516-554 [PMID: 29470322 DOI: 10.1097/MPG.0000000000001889]

32 **Lee K**, Choe BH, Kang B, Kim S, Kim JY, Shim JO, Lee YM, Lee EH, Jang HJ, Ryoo E, Yang HR. Nationwide Multicenter Study of Eosinophilic Esophagitis in Korean Children. *Pediatr Gastroenterol Hepatol Nutr* 2020; **23**: 231-242 [PMID: 32483544 DOI: 10.5223/pghn.2020.23.3.231]

33 **Nambu R**, Hagiwara SI, Kakuta F, Hara T, Shimizu H, Abukawa D, Iwama I, Kagimoto S, Arai K. Current role of colonoscopy in infants and young children: a multicenter study. *BMC Gastroenterol* 2019; **19**: 149 [PMID: 31429721 DOI: 10.1186/s12876-019-1060-7]

34 **Huang Y**, Tan SY, Parikh P, Buthmanaban V, Rajindrajith S, Benninga MA. Prevalence of functional gastrointestinal disorders in infants and young children in China. *BMC Pediatr* 2021; **21**: 131 [PMID: 33731059 DOI: 10.1186/s12887-021-02610-6]

35 **Chia LW**, Nguyen TVH, Phan VN, Luu TTN, Nguyen GK, Tan SY, Rajindrajith S, Benninga MA. Prevalence and risk factors of functional gastrointestinal disorders in Vietnamese infants and young children. *BMC Pediatr* 2022; **22**: 315 [PMID: 35624448 DOI: 10.1186/s12887-022-03378-z]

36 **El-Matary W**, Spray C, Sandhu B. Irritable bowel syndrome: the commonest cause of recurrent abdominal pain in children. *Eur J Pediatr* 2004; **163**: 584-588 [PMID: 15290263 DOI: 10.1007/s00431-004-1503-0]

37 **Thakkar K**, Chen L, Tessier ME, Gilger MA. Outcomes of children after esophagogastroduodenoscopy for chronic abdominal pain. *Clin Gastroenterol Hepatol* 2014; **12**: 963-969 [PMID: 24016631 DOI: 10.1016/j.cgh.2013.08.041]

38 **Jones NL**, Koletzko S, Goodman K, Bontems P, Cadranel S, Casswall T, Czinn S, Gold BD, Guarner J, Elitsur Y, Homan M, Kalach N, Kori M, Madrazo A, Megraud F, Papadopoulou A, Rowland M; ESPGHAN, NASPGHAN. Joint ESPGHAN/NASPGHAN Guidelines for the Management of Helicobacter pylori in Children and Adolescents (Update 2016). *J Pediatr Gastroenterol Nutr* 2017; **64**: 991-1003 [PMID: 28541262 DOI: 10.1097/MPG.0000000000001594]

39 **Fachler T**, Shteyer E, Orlanski Meyer E, Shemasna I, Lev Tzion R, Rachman Y, Bergwerk A, Turner D, Ledder O. Pediatric Gastrointestinal Endoscopy: Diagnostic Yield and Appropriateness of Referral Based on Clinical Presentation: A Pilot Study. *Front Pediatr* 2021; **9**: 607418 [PMID: 34778118 DOI: 10.3389/fped.2021.607418]

40 **Tam YH**, Chan KW, To KF, Cheung ST, Mou JW, Pang KK, Wong YS, Sihoe JD, Lee KH. Impact of pediatric Rome III criteria of functional dyspepsia on the diagnostic yield of upper endoscopy and predictors for a positive endoscopic finding. *J Pediatr Gastroenterol Nutr* 2011; **52**: 387-391 [PMID: 21415670 DOI: 10.1097/MPG.0b013e31820e2026]

41 **Lin WC**, Wong JM, Tung CC, Lin CP, Chou JW, Wang HY, Shieh MJ, Chang CH, Liu HH, Wei SC; Taiwan Society of Inflammatory Bowel Disease Multicenter Study. Fecal calprotectin correlated with endoscopic remission for Asian inflammatory bowel disease patients. *World J Gastroenterol* 2015; **21**: 13566-13573 [PMID: 26730169 DOI: 10.3748/wjg.v21.i48.13566]

42 **Samant H**, Desai D, Abraham P, Joshi A, Gupta T, Dherai A, Ashavaid T. Fecal calprotectin and its correlation with inflammatory markers and endoscopy in patients from India with inflammatory bowel disease. *Indian J Gastroenterol* 2015; **34**: 431-435 [PMID: 26589229 DOI: 10.1007/s12664-015-0608-x]

43 **Fornaroli F**, Gaiani F, Vincenzi F, Bizzarri B, Ghiselli A, Kayali S, Leandro G, Di Mario F, De' Angelis GL. Applications of wireless capsule endoscopy in pediatric age: an update. *Acta Biomed* 2018; **89**: 40-46 [PMID: 30561394 DOI: 10.23750/abm.v89i9-S.7957]

44 **Wu J**, Huang Z, Wang Y, Tang Z, Lai L, Xue A, Huang Y. Clinical features of capsule endoscopy in 825 children: A single-center, retrospective cohort study. *Medicine (Baltimore)* 2020; **99**: e22864 [PMID: 33120825 DOI: 10.1097/MD.0000000000022864]

45 **Ohmiya N**, Oka S, Nakayama Y, Iwama I, Nakamura M, Shimizu H, Sumioka A, Abe N, Kudo T, Osawa S, Honma H, Okuhira T, Mtsufuji S, Imaeda H, Ota K, Matsuoka R, Hotta N, Inoue M, Nakaji K, Takamaru H, Ozeki K, Kobayashi T, Hosoe N, Tajiri H, Tanaka S. Safety and efficacy of the endoscopic delivery of capsule endoscopes in adult and pediatric patients: Multicenter Japanese study (AdvanCE-J study). *Dig Endosc* 2022; **34**: 543-552 [PMID: 34379849 DOI: 10.1111/den.14104]

46 **Lim YJ**, Lee OY, Jeen YT, Lim CY, Cheung DY, Cheon JH, Ye BD, Song HJ, Kim JS, Do JH, Lee KJ, Shim KN, Chang

DK, Park CH, Jang BI, Moon JS, Chun HJ, Choi MG, Kim JO; Korean Gut Image Study Group. Indications for Detection, Completion, and Retention Rates of Small Bowel Capsule Endoscopy Based on the 10-Year Data from the Korean Capsule Endoscopy Registry. *Clin Endosc* 2015; **48**: 399-404 [PMID: 26473123 DOI: 10.5946/ce.2015.48.5.399]

47 **Xue M**, Chen X, Shi L, Si J, Wang L, Chen S. Small-bowel capsule endoscopy in patients with unexplained chronic abdominal pain: a systematic review. *Gastrointest Endosc* 2015; **81**: 186-193 [PMID: 25012561 DOI: 10.1016/j.gie.2014.04.062]

48 **Huang L**, Huang Z, Tai Y, Wang P, Hu B, Tang C. The small bowel diseases detected by capsule endoscopy in patients with chronic abdominal pain: A retrospective study. *Medicine (Baltimore)* 2018; **97**: e0025 [PMID: 29465542 DOI: 10.1097/MD.0000000000010025]

49 **Hilmi I**, Kobayashi T. Capsule endoscopy in inflammatory bowel disease: when and how. *Intest Res* 2020; **18**: 265-274 [PMID: 32623876 DOI: 10.5217/ir.2019.09165]

50 **Hwang JY**, Moon SW, Lee YJ, Park JH, Kim YW, Kim TU, Ryu H. Capsule Endoscopy versus Magnetic Resonance Enterography for Evaluation of Pediatric Small Bowel Crohn's Disease: Prospective Study. *J Clin Med* 2022; **11** [PMID: 35628886 DOI: 10.3390/jcm11102760]

51 **Kirakosyan E**, Lokhmatov M. High-Tech Diagnostic Methods and Enteroscopic Treatment of Children with Peutz-Jeghers Syndrome. *Eur J Pediatr Surg* 2020; **30**: 529-535 [PMID: 31770782 DOI: 10.1055/s-0039-3400286]

52 **Yokoyama K**, Yano T, Kumagai H, Mizuta K, Ono S, Imagawa T, Yamamoto H, Yamagata T. Double-balloon Enteroscopy for Pediatric Patients: Evaluation of Safety and Efficacy in 257 Cases. *J Pediatr Gastroenterol Nutr* 2016; **63**: 34-40 [PMID: 26628449 DOI: 10.1097/MPG.0000000000001048]

53 **Chen H**, Liu Y, Fu L, Lin X, Fan D, Li C. Clinical utility of double-balloon enteroscopy in children: A single-centre experience in South China. *J Paediatr Child Health* 2019; **55**: 188-193 [PMID: 30066974 DOI: 10.1111/jpc.14153]

54 **Hagiwara SI**, Kudo T, Kakuta F, Inoue M, Yokoyama K, Umetsu S, Iwama I, Yodoshi T, Tatsuki M, Shimizu T, Nakayama Y. Clinical Safety and Utility of Pediatric Balloon-assisted Enteroscopy: A Multicenter Prospective Study in Japan. *J Pediatr Gastroenterol Nutr* 2019; **68**: 306-310 [PMID: 30444835 DOI: 10.1097/MPG.0000000000002181]

55 **Liu W**, Xu C, Zhong J. The diagnostic value of double-balloon enteroscopy in children with small bowel disease: report of 31 cases. *Can J Gastroenterol* 2009; **23**: 635-638 [PMID: 19816629 DOI: 10.1155/2009/281040]

56 **Nguyen N**, Lavery WJ, Capocelli KE, Smith C, DeBoer EM, Deterding R, Prager JD, Leinwand K, Kobak GE, Kramer RE, Menard-Katcher C, Furuta GT, Atkins D, Fleischer D, Greenhawt M, Friedlander JA. Transnasal Endoscopy in Unsedated Children With Eosinophilic Esophagitis Using Virtual Reality Video Goggles. *Clin Gastroenterol Hepatol* 2019; **17**: 2455-2462 [PMID: 30708107 DOI: 10.1016/j.cgh.2019.01.023]

57 **Vaezi MF**, Choksi Y. Mucosal Impedance: A New Way To Diagnose Reflux Disease and How It Could Change Your Practice. *Am J Gastroenterol* 2017; **112**: 4-7 [PMID: 27958288 DOI: 10.1038/ajg.2016.513]

58 **Ates F**, Yuksel ES, Higginbotham T, Slaughter JC, Mabary J, Kavitt RT, Garrett CG, Francis D, Vaezi MF. Mucosal impedance discriminates GERD from non-GERD conditions. *Gastroenterology* 2015; **148**: 334-343 [PMID: 25448923 DOI: 10.1053/j.gastro.2014.10.010]

59 **Lowry MA**, Vaezi MF, Correa H, Higginbotham T, Slaughter JC, Acra S. Mucosal Impedance Measurements Differentiate Pediatric Patients With Active Versus Inactive Eosinophilic Esophagitis. *J Pediatr Gastroenterol Nutr* 2018; **67**: 198-203 [PMID: 29543695 DOI: 10.1097/MPG.0000000000001943]

60 **Hoskins B**, Almazan E, Mogul D, Ng K. Endoluminal Functional Lumen Imaging Probe Is Safe in Children Under Five Years Old. *J Pediatr Gastroenterol Nutr* 2022; **74**: e148-e152 [PMID: 35849505 DOI: 10.1097/MPG.0000000000003430]

61 **Hoffmann NV**, Keeley K, Wechsler JB. Esophageal Distensibility Defines Fibrostenotic Severity in Pediatric Eosinophilic Esophagitis. *Clin Gastroenterol Hepatol* 2022 [PMID: 36122653 DOI: 10.1016/j.cgh.2022.08.044]

62 **Venkatesh K**, Cohen M, Evans C, Delaney P, Thomas S, Taylor C, Abou-Taleb A, Kiesslich R, Thomson M. Feasibility of confocal endomicroscopy in the diagnosis of pediatric gastrointestinal disorders. *World J Gastroenterol* 2009; **15**: 2214-2219 [PMID: 19437560 DOI: 10.3748/wjg.15.2214]

63 **Patel V**, Khan MN, Shrivastava A, Sadiq K, Ali SA, Moore SR, Brown DE, Syed S. Artificial Intelligence Applied to Gastrointestinal Diagnostics: A Review. *J Pediatr Gastroenterol Nutr* 2020; **70**: 4-11 [PMID: 31567886 DOI: 10.1097/MPG.0000000000002507]

64 **Neumann H**, Kreft A, Sivanathan V, Rahman F, Galle PR. Evaluation of novel LCI CAD EYE system for real time detection of colon polyps. *PLoS One* 2021; **16**: e0255955 [PMID: 34437563 DOI: 10.1371/journal.pone.0255955]

65 **Reilly BK**, Stool D, Chen X, Rider G, Stool SE, Reilly JS. Foreign body injury in children in the twentieth century: a modern comparison to the Jackson collection. *Int J Pediatr Otorhinolaryngol* 2003; **67** Suppl 1: S171-S174 [PMID: 14662189 DOI: 10.1016/j.ijporl.2003.08.019]

66 **Cheng W**, Tam PK. Foreign-body ingestion in children: experience with 1,265 cases. *J Pediatr Surg* 1999; **34**: 1472-1476 [PMID: 10549750 DOI: 10.1016/s0022-3468(99)90106-9]

67 **Khorana J**, Tantivit Y, Phiuphong C, Pattapong S, Siripan S. Foreign Body Ingestion in Pediatrics: Distribution, Management and Complications. *Medicina (Kaunas)* 2019; **55** [PMID: 31615117 DOI: 10.3390/medicina55100686]

68 **Jayachandra S**, Eslick GD. A systematic review of paediatric foreign body ingestion: presentation, complications, and management. *Int J Pediatr Otorhinolaryngol* 2013; **77**: 311-317 [PMID: 23261258 DOI: 10.1016/j.ijporl.2012.11.025]

69 **Jafari SA**, Khalesi M, Partovi S, Kiani M, Ahanchian H, Kianifar H. Ingested Foreign Bodies Removed by flexible Endoscopy in Pediatric Patients: A 10-year Retrospective Study [corrected]. *Iran J Otorhinolaryngol* 2014; **26**: 175-179 [PMID: 25009808]

70 **Chotigavanich C**, Ballali S, Foltran F, Passali D, Bellussi L, Gregori D; ESFBI Study Group. Foreign bodies injuries in children: analysis of Thailand data. *Int J Pediatr Otorhinolaryngol* 2012; **76** Suppl 1: S80-S83 [PMID: 22341474 DOI: 10.1016/j.ijporl.2012.02.019]

71 **Thomson M**, Tringali A, Dumonceau JM, Tavares M, Tabbers MM, Furlano R, Spaander M, Hassan C, Tzvinikos C, Ijsselstijn H, Viala J, Dall'Oglio L, Benninga M, Orel R, Vandenplas Y, Keil R, Romano C, Brownstone E, Hlava Š, Gerner P, Dolak W, Landi R, Huber WD, Everett S, Vecsei A, Aabakken L, Amil-Dias J, Zambelli A. Paediatric Gastrointestinal Endoscopy: European Society for Paediatric Gastroenterology Hepatology and Nutrition and European

Society of Gastrointestinal Endoscopy Guidelines. *J Pediatr Gastroenterol Nutr* 2017; **64**: 133-153 [PMID: 27622898 DOI: 10.1097/MPG.0000000000001408]

72 **Kramer RE**, Lerner DG, Lin T, Manfredi M, Shah M, Stephen TC, Gibbons TE, Pall H, Sahn B, McOmber M, Zacur G, Friedlander J, Quiros AJ, Fishman DS, Mamula P; North American Society for Pediatric Gastroenterology, Hepatology, and Nutrition Endoscopy Committee. Management of ingested foreign bodies in children: a clinical report of the NASPGHAN Endoscopy Committee. *J Pediatr Gastroenterol Nutr* 2015; **60**: 562-574 [PMID: 25611037 DOI: 10.1097/MPG.0000000000000729]

73 **Litovitz T**, Whitaker N, Clark L. Preventing battery ingestions: an analysis of 8648 cases. *Pediatrics* 2010; **125**: 1178-1183 [PMID: 20498172 DOI: 10.1542/peds.2009-3038]

74 **Huang T**, Li WQ, Xia ZF, Li J, Rao KC, Xu EM. Characteristics and outcome of impacted button batteries among young children less than 7 years of age in China: a retrospective analysis of 116 cases. *World J Pediatr* 2018; **14**: 570-575 [PMID: 30328588 DOI: 10.1007/s12519-018-0188-9]

75 **Mubarak A**, Benninga MA, Broekaert I, Dolinsek J, Homan M, Mas E, Miele E, Pienar C, Thapar N, Thomson M, Tzivinikos C, de Ridder L. Diagnosis, Management, and Prevention of Button Battery Ingestion in Childhood: A European Society for Paediatric Gastroenterology Hepatology and Nutrition Position Paper. *J Pediatr Gastroenterol Nutr* 2021; **73**: 129-136 [PMID: 33555169 DOI: 10.1097/MPG.0000000000003048]

76 **Opasanon S**, Akaraviputh T, Methasate A, Sirikun J, Laohapensang M. Endoscopic management of foreign body in the upper gastrointestinal tract: a tertiary care center experience. *J Med Assoc Thai* 2009; **92**: 17-21 [PMID: 19260238]

77 **Pennazio M**, Rondonotti E, Despott EJ, Dray X, Keuchel M, Moreels T, Sanders DS, Spada C, Carretero C, Cortegoso Valdivia P, Elli L, Fuccio L, Gonzalez Suarez B, Koulaouzidis A, Kunovsky L, McNamara D, Neumann H, Perez-Cuadrado-Martinez E, Perez-Cuadrado-Robles E, Piccirelli S, Rosa B, Saurin JC, Sidhu R, Tacheci I, Vlachou E, Triantafyllou K. Small-bowel capsule endoscopy and device-assisted enteroscopy for diagnosis and treatment of small-bowel disorders: European Society of Gastrointestinal Endoscopy (ESGE) Guideline - Update 2022. *Endoscopy* 2023; **55**: 58-95 [PMID: 36423618 DOI: 10.1055/a-1973-3796]

78 **Thomson MA**, Leton N, Belsha D. Acute upper gastrointestinal bleeding in childhood: development of the Sheffield scoring system to predict need for endoscopic therapy. *J Pediatr Gastroenterol Nutr* 2015; **60**: 632-636 [PMID: 25539193 DOI: 10.1097/MPG.0000000000000680]

79 **Valera JM**, Pino RQ, Poniachik J, Gil LC, O'Brien M, Sáenz R, Quigley EM. Endoscopic band ligation of bleeding dieulafoy lesions: the best therapeutic strategy. *Endoscopy* 2006; **38**: 193-194 [PMID: 16479429 DOI: 10.1055/s-2006-925149]

80 **Yabe K**, Kouchi K, Takenouchi A, Matsuoka A, Kudou W, Nakata C. Current status and future challenges in the endoscopic management of non-variceal upper gastrointestinal bleeding in children. *Pediatr Surg Int* 2020; **36**: 1451-1458 [PMID: 33034717 DOI: 10.1007/s00383-020-04755-4]

81 **Zargar SA**, Javid G, Khan BA, Yattoo GN, Shah AH, Gulzar GM, Singh J, Rehman BU, Din Z. Endoscopic ligation compared with sclerotherapy for bleeding esophageal varices in children with extrahepatic portal venous obstruction. *Hepatology* 2002; **36**: 666-672 [PMID: 12198659 DOI: 10.1053/jhep.2002.35278]

82 **Gana JC**, Cifuentes LI, Gattini D, Torres-Robles R. Band ligation versus sclerotherapy for primary prophylaxis of oesophageal variceal bleeding in children with chronic liver disease or portal vein thrombosis. *Cochrane Database Syst Rev* 2020; **11**: CD011803 [PMID: 33164205 DOI: 10.1002/14651858.CD011803.pub2]

83 **Chino A**, Karasawa T, Uragami N, Endo Y, Takahashi H, Fujita R. A comparison of depth of tissue injury caused by different modes of electrosurgical current in a pig colon model. *Gastrointest Endosc* 2004; **59**: 374-379 [PMID: 14997134 DOI: 10.1016/s0016-5107(03)02712-3]

84 **Mönkemüller KE**, Fry LC, Jones BH, Wells C, Mikolaenko I, Eloubeidi M. Histological quality of polyps resected using the cold versus hot biopsy technique. *Endoscopy* 2004; **36**: 432-436 [PMID: 15100953 DOI: 10.1055/s-2004-814321]

85 **Kim JY**, Kim YB, Choi S, Lee YM, Kim HJ, Kim SC, Jang HJ, Choi SY, Yi DY, Lee Y, Choi YJ, Kang Y, Lee KJ, Hong SJ, Hwang JH, Kwak S, Choe BH, Kang B. Associations of Polyp Characteristics in Children and Adolescents Presenting with Less Than Five Colorectal Polyps: A Full Colonoscopy Is Still Required. *Gut Liver* 2022 [PMID: 36052612 DOI: 10.5009/gnl210404]

86 **Ukarapol N**, Singhavejakul J, Lertprasertsuk N, Wongsawasdi L. Juvenile polyp in Thai children--clinical and colonoscopic presentation. *World J Surg* 2007; **31**: 395-398 [PMID: 17235457 DOI: 10.1007/s00268-005-0686-5]

87 **Pearson EG**, Downey EC, Barnhart DC, Scaife ER, Rollins MD, Black RE, Matlak ME, Johnson DG, Meyers RL. Reflux esophageal stricture--a review of 30 years' experience in children. *J Pediatr Surg* 2010; **45**: 2356-2360 [PMID: 21129544 DOI: 10.1016/j.jpedsurg.2010.08.033]

88 **Cakmak M**, Boybeyi O, Gollu G, Kucuk G, Bingol-Kologlu M, Yagmurlu A, Aktug T, Dindar H. Endoscopic balloon dilatation of benign esophageal strictures in childhood: a 15-year experience. *Dis Esophagus* 2016; **29**: 179-184 [PMID: 25515612 DOI: 10.1111/dote.12305]

89 **Poddar U**, Thapa BR. Benign esophageal strictures in infants and children: results of Savary-Gilliard bougie dilation in 107 Indian children. *Gastrointest Endosc* 2001; **54**: 480-484 [PMID: 11577311 DOI: 10.1067/mge.2001.118253]

90 **Lan LC**, Wong KK, Lin SC, Sprigg A, Clarke S, Johnson PR, Tam PK. Endoscopic balloon dilatation of esophageal strictures in infants and children: 17 years' experience and a literature review. *J Pediatr Surg* 2003; **38**: 1712-1715 [PMID: 14666449 DOI: 10.1016/j.jpedsurg.2003.08.040]

91 **Geng LL**, Liang CP, Chen PY, Wu Q, Yang M, Li HW, Xu ZH, Ren L, Wang HL, Cheng S, Xu WF, Chen Y, Zhang C, Liu LY, Li DY, Gong ST. Long-Term Outcomes of Caustic Esophageal Stricture with Endoscopic Balloon Dilatation in Chinese Children. *Gastroenterol Res Pract* 2018; **2018**: 8352756 [PMID: 30158970 DOI: 10.1155/2018/8352756]

92 **Angelino G**, Tambucci R, Torroni F, De Angelis P, Dall'Oglio L. New therapies for esophageal strictures in children. *Curr Opin Pediatr* 2021; **33**: 503-508 [PMID: 34354006 DOI: 10.1097/MOP.0000000000001049]

93 **Pall H**, Zacur GM, Kramer RE, Lirio RA, Manfredi M, Shah M, Stephen TC, Tucker N, Gibbons TE, Sahn B, McOmber M, Friedlander J, Quiros JA, Fishman DS, Mamula P. Bowel preparation for pediatric colonoscopy: report of the NASPGHAN endoscopy and procedures committee. *J Pediatr Gastroenterol Nutr* 2014; **59**: 409-416 [PMID: 24897169

DOI: 10.1097/MPG.0000000000000447]
94 **Hunter A**, Mamula P. Bowel preparation for pediatric colonoscopy procedures. *J Pediatr Gastroenterol Nutr* 2010; **51**: 254-261 [PMID: 20683200 DOI: 10.1097/MPG.0b013e3181eb6a1c]
95 **Fang S**, Song Y, Liu Y, Wang L. Randomized clinical trial: efficacy and tolerability of two different split dose of low-volume polyethylene glycol electrolytes for bowel preparation before colonoscopy in hospitalized children. *Pediatr Res* 2021; **90**: 171-175 [PMID: 33106606 DOI: 10.1038/s41390-020-01216-5]
96 **Gordon M**, Karlsen F, Isaji S, Teck GO. Bowel preparation for elective procedures in children: a systematic review and meta-analysis. *BMJ Paediatr Open* 2017; **1**: e000118 [PMID: 29637141 DOI: 10.1136/bmjpo-2017-000118]
97 **Dziechciarz P**, Ruszczyński M, Horvath A. Sodium Picosulphate with Magnesium Citrate versus Polyethylene Glycol for Bowel Preparation in Children: A Systematic Review. *Pediatr Gastroenterol Hepatol Nutr* 2022; **25**: 228-239 [PMID: 35611374 DOI: 10.5223/pghn.2022.25.3.228]
98 **Sriphongphankul H**, Tanpowpong P, Lertudomphonwanit C, Treepongkaruna S. Split dose versus full single-dose regimen of polyethylene glycol for bowel preparation in pediatric colonoscopy: a pilot study of randomized controlled trial. *Eur J Gastroenterol Hepatol* 2019; **31**: 1382-1386 [PMID: 31567637 DOI: 10.1097/MEG.0000000000001562]
99 **Cao J**, Zhang W, Hu J, Huang Y, Zhao L, Cai R, Bao Y, Li M. Single versus split dose polyethylene glycol for bowel preparation in children undergoing colonoscopy: a systematic review and meta-analysis. *Ann Palliat Med* 2020; **9**: 3028-3037 [PMID: 32921076 DOI: 10.21037/apm-20-582]
100 **Tripathi PR**, Poddar U, Yachha SK, Sarma MS, Srivastava A. Efficacy of Single- Versus Split-dose Polyethylene Glycol for Colonic Preparation in Children: A Randomized Control Study. *J Pediatr Gastroenterol Nutr* 2020; **70**: e1-e6 [PMID: 31567887 DOI: 10.1097/MPG.0000000000002511]
101 **Jiao L**, Wang J, Zhao W, Zhu X, Meng X, Zhao L. Comparison of the effect of 1-day and 2-day low residue diets on the quality of bowel preparation before colonoscopy. *Saudi J Gastroenterol* 2020; **26**: 137-143 [PMID: 32270774 DOI: 10.4103/sjg.SJG_471_19]
102 **Mencin AA**, Sethi A, Barakat MT, Lerner DG. Peroral Endoscopic Myotomy (POEM) in Children: A State of the Art Review. *J Pediatr Gastroenterol Nutr* 2022; **75**: 231-236 [PMID: 35653433 DOI: 10.1097/MPG.0000000000003503]
103 **Broekaert I**, Tzivinikos C, Narula P, Antunes H, Dias JA, van der Doef H, Isoldi S, Norsa L, Romano C, Scheers I, Silbermintz A, Tavares M, Torroni F, Urs A, Thomson M. European Society for Paediatric Gastroenterology, Hepatology and Nutrition Position Paper on Training in Paediatric Endoscopy. *J Pediatr Gastroenterol Nutr* 2020; **70**: 127-140 [PMID: 31799965 DOI: 10.1097/MPG.0000000000002496]
104 **ASGE Standards of Practice Committee**, Lightdale JR, Acosta R, Shergill AK, Chandrasekhara V, Chathadi K, Early D, Evans JA, Fanelli RD, Fisher DA, Fonkalsrud L, Hwang JH, Kashab M, Muthusamy VR, Pasha S, Saltzman JR, Cash BD; American Society for Gastrointestinal Endoscopy. Modifications in endoscopic practice for pediatric patients. *Gastrointest Endosc* 2014; **79**: 699-710 [PMID: 24593951 DOI: 10.1016/j.gie.2013.08.014]
105 **Wang S**, Qiu X, Chen J, Mei H, Yan H, You J, Huang Y. Pediatric esophagogastroduodenoscopy in china: indications, diagnostic yield, and factors associated with findings. *BMC Pediatr* 2022; **22**: 522 [PMID: 36056317 DOI: 10.1186/s12887-022-03558-x]
106 **Joshi BG**, Ghimire M. Diagnostic Yield of Upper Gastrointestinal Endoscopy in Children: A Three Years Experience. *J Nepal Paediat Society* 2020; **40**: 87-92 [DOI: 10.3126/jnps.v40i2.29321]
107 **Berger TD**, Soffer S, Vurzel-Harel T, Silbermintz A, Fleishaker H, Shamir R, Zevit N. The Yield of Upper Gastrointestinal Endoscopy at a Pediatric Tertiary Care Center. *Isr Med Assoc J* 2020; **22**: 164-168 [PMID: 32147981]
108 **Ukarapol N**, Lertprasertsuk N, Wongsawasdi L. Recurrent abdominal pain in children: the utility of upper endoscopy and histopathology. *Singapore Med J* 2004; **45**: 121-124 [PMID: 15029414]
109 **Kawada PS**, O'Loughlin EV, Stormon MO, Dutt S, Lee CH, Gaskin KJ. Are We Overdoing Pediatric Lower Gastrointestinal Endoscopy? *J Pediatr Gastroenterol Nutr* 2017; **64**: 898-902 [PMID: 26960173 DOI: 10.1097/MPG.0000000000001192]
110 **Chen J**, Yu H, Zhong W, Chen H, Kong X, Sun J, Wang X, Li C. [Pediatric colonoscopy in South China: a single-center experience from 229 cases]. *Zhonghua Wei Chang Wai Ke Za Zhi* 2017; **20**: 1404-1408 [PMID: 29280125]
111 **Tam YH**, Lee KH, Chan KW, Sihoe JD, Cheung ST, Mou JW. Colonoscopy in Hong Kong Chinese children. *World J Gastroenterol* 2010; **16**: 1119-1122 [PMID: 20205284 DOI: 10.3748/wjg.v16.i9.1119]
112 **Morita M**, Takedatsu H, Yoshioka S, Mitsuyama K, Tsuruta K, Kuwaki K, Kato K, Yasuda R, Mizuochi T, Yamashita Y, Kawaguchi T. Utility of Diagnostic Colonoscopy in Pediatric Intestinal Disease. *J Clin Med* 2022; **11** [PMID: 36233615 DOI: 10.3390/jcm11195747]
113 **Lee WS**, Tee CW, Koay ZL, Wong TS, Zahraq F, Foo HW, Ong SY, Wong SY, Ng RT. Quality indicators in pediatric colonoscopy in a low-volume center: Implications for training. *World J Gastroenterol* 2018; **24**: 1013-1021 [PMID: 29531465 DOI: 10.3748/wjg.v24.i9.1013]
114 **El Mouzan MI**, Al-Mofleh IA, Abdullah AM, Al Sanie AM, Al-Rashed RS. Colonoscopy in children. *Saudi J Gastroenterol* 2005; **11**: 35-39 [PMID: 19861845 DOI: 10.4103/1319-3767.33335]
115 **Wu CT**, Chen CA, Yang YJ. Characteristics and Diagnostic Yield of Pediatric Colonoscopy in Taiwan. *Pediatr Neonatol* 2015; **56**: 334-338 [PMID: 25850637 DOI: 10.1016/j.pedneo.2015.01.005]

World Journal of Gastroenterology

Submit a Manuscript: https://www.f6publishing.com

World J Gastroenterol 2023 May 14; 29(18): 2733-2746

DOI: 10.3748/wjg.v29.i18.2733

ISSN 1007-9327 (print) ISSN 2219-2840 (online)

REVIEW

Study of tumor necrosis factor receptor in the inflammatory bowel disease

Roberta Figueiroa Souza, Marcos Antônio Ferreira Caetano, Henrique Inhauser Riceti Magalhães, Patricia Castelucci

Specialty type: Anatomy and morphology

Provenance and peer review: Invited article; Externally peer reviewed.

Peer-review model: Single blind

Peer-review report's scientific quality classification

Grade A (Excellent): 0
Grade B (Very good): B
Grade C (Good): C
Grade D (Fair): 0
Grade E (Poor): 0

P-Reviewer: Xu B, China; Yoo JH, South Korea

Received: December 30, 2022
Peer-review started: December 30, 2022
First decision: January 22, 2023
Revised: February 14, 2023
Accepted: April 4, 2023
Article in press: April 4, 2023
Published online: May 14, 2023

Roberta Figueiroa Souza, Marcos Antônio Ferreira Caetano, Patricia Castelucci, Department of Anatomy, Institute of Biomedical Sciences, University of São Paulo, São Paulo 05508-000, Brazil

Henrique Inhauser Riceti Magalhães, Department of Surgery, School of Veterinary Medicine and Animal Sciences, University of São Paulo, São Paulo 05508-270, Brazil

Corresponding author: Patricia Castelucci, MHSc, PhD, Associate Professor, Associate Research Scientist, Lecturer, Department of Anatomy, Institute of Biomedical Sciences, University of São Paulo, Av. Dr. Lineu Prestes, 2415, São Paulo 05508-000, Brazil.
pcastel@usp.br

Abstract

Ulcerative colitis (UC) and Crohn's disease (CD) are part of Inflammatory Bowel Diseases (IBD) and have pathophysiological processes such as bowel necrosis and enteric neurons and enteric glial cells. In addition, the main inflammatory mediator is related to the tumor necrosis factor-alpha (TNF-α). TNF-α is a mediator of the intestinal inflammatory processes, thus being one of the main cytokines involved in the pathogenesis of IBD, however, its levels, when measured, are present in the serum of patients with IBD. In addition, TNF-α plays an important role in promoting inflammation, such as the production of interleukins (IL), for instance IL-1β and IL-6. There are two receptors for TNF as following: The tumor necrosis factor 1 receptor (TNFR1); and the tumor necrosis factor 2 receptor (TNFR2). They are involved in the pathogenesis of IBD and their receptors have been detected in IBD and their expression is correlated with disease activity. The soluble TNF form binds to the TNFR1 receptor with, and its activation results in a signaling cascade effects such as apoptosis, cell proliferation and cytokine secretion. In contrast, the transmembrane TNF form can bind both to TNFR1 and TNFR2. Recent studies have suggested that TNF-α is one of the main pro-inflammatory cytokines involved in the pathogenesis of IBD, since TNF levels are present in the serum of both patients with UC and CD. Intravenous and subcutaneous biologics targeting TNF-α have revolutionized the treatment of IBD, thus becoming the best available agents to induce and maintain IBD remission. The application of antibodies aimed at neutralizing TNF-α in patients with IBD that induce a satisfactory clinical response in up to 60% of patients, and also induced long-term maintenance of disease remission in most patients. It has been suggested that anti-TNF-α agents inactivate the pro-inflammatory cytokine TNF-α

by direct neutralization, *i.e.*, resulting in suppression of inflammation. However, anti-TNF-α antibodies perform more complex functions than a simple blockade.

Key Words: Tumor necrosis factor 1 receptor; Tumor necrosis factor 2 receptor; Inflammatory bowel diseases; Enteric nervous system; tumor necrosis factor-alpha

©The Author(s) 2023. Published by Baishideng Publishing Group Inc. All rights reserved.

Core Tip: This review summarizes the role of Tumor Necrosis Factor-alpha (TNF-α) in promoting inflammation. Studies have suggested that TNF-α is one of the main pro-inflammatory cytokines involved in the pathogenesis of Inflammatory Bowel Diseases (IBD). In addition, the enteric nervous system is affected by IBD. There are two receptors for TNF: The tumor necrosis factor 1 receptor; and the tumor necrosis factor 2 receptor. They are involved in the pathogenesis of IBD. The application of antibodies aimed at neutralizing TNF-α in patients with IBD induce a satisfactory clinical recovery. This review addresses the main aspects of TNF-α in IBD and anti-TNF therapies.

Citation: Souza RF, Caetano MAF, Magalhães HIR, Castelucci P. Study of tumor necrosis factor receptor in the inflammatory bowel disease. *World J Gastroenterol* 2023; 29(18): 2733-2746
URL: https://www.wjgnet.com/1007-9327/full/v29/i18/2733.htm
DOI: https://dx.doi.org/10.3748/wjg.v29.i18.2733

INTRODUCTION

Inflammatory bowel diseases (IBD) comprise ulcerative colitis (UC) and Crohn's disease (CD), which are chronical and recurrent disorders that affect the gastrointestinal (GI) tract[1-4]. The etiology of IBD is not yet fully understood, but there are reports of a complex relationship between genetic[5,6], immunological and environmental factors[7-10], as well as gut microbiota[11-15]. There is an imbalance between anti- and pro-inflammatory cytokines that cause an exacerbated and inadequate immune response.

The enteric nervous system (ENS) is composed by intrinsic neurons, their axons and enteric glial cells, which constitute a complex of structures responsible for controlling motility of the GI tract, secretion of gastric acid, regulation of fluid movement through the epithelium, local blood flow control, and interactions with the endocrine and immune systems of the gut[16-18]. The ENS is affected by IBD which causes necrosis, apoptosis, degeneration of enteric ganglia and alterations on motility patterns [19-23].

Tumor necrosis factor-alpha (TNF-α) is a mediator in intestinal inflammatory processes, thus being one of the main cytokines involved in pathogenesis of IBD, with high levels in patients with IBD[24,25]. There are two receptors for TNF-α as following: The tumor necrosis factor receptor 1 (TNFR1); and the tumor necrosis factor receptor 2 (TNFR2). After TNF-α binding to these receptors, it activates signaling pathways for cell survival, death and differentiation[26]. An increase in TNF-α expression can lead to mucosal barrier defects in patients with IBD, which increases inflammation and worsens the prognosis [10].

Due to the TNF-α relation with IBD, biological drugs have been used to treat CD and UC with neutralizing monoclonal antibodies used for TNF-α target and blockade, which reduce the development of the inflammatory process and the activation of immune system cells[27]. Anti-TNF-α agents are indicated by various guidelines for the treatment of IBD[28,29] and the use of these agents induces a satisfactory clinical response, and long-term maintenance of disease remission in most patients[24,30]. This review aims to provide the main aspects of IBD and TNF-α relationship, elucidating the role of the TNF-α receptors, anti TNF-α therapy and some perspectives related to the involvement of the ENS.

THE ENS AND IBD

The ENS is a complex of structures responsible for controlling motility of the GI tract, secretion of gastric acid, regulation of fluid movement through the epithelium, changes in local blood flow, and interactions with the endocrine and immune systems of the gut[16-18]. The ENS is located in the intestinal wall and is organized into two ganglionated plexuses: The myenteric plexus; and the submucosal plexus[16-18].

The myenteric plexus (Auerbach's plexus) is situated between the longitudinal muscle layer and the circular muscle layer throughout the entire GI tract, from the esophagus to the rectum. It has three

components as following: A primary plexus; a secondary plexus; and a tertiary plexus. The myenteric plexus is involved with reflex regulation of the contractile activities of the muscle layer[16,17]. The submucosal plexus (Meissner's plexus) is predominantly found in the small and large intestines, with a smaller ganglion and finer interconnected fibers when compared to the myenteric plexus[16,17]. It has a direct role in controlling secretion and absorption through motor neurons that regulate the secretomotor and vasomotor activity of the mucosal layer[16,17].

Enteric neurons can be classified according to their function into motor neurons, interneurons, and Intrinsic Primary Afferent Neurons[16]. Motor neurons are further divided according to their chemical code into excitatory neurons (labeled by the enzyme choline acetyltransferase or by calretinin), inhibitory neurons (labeled by the enzyme neuronal nitric oxide synthase), and secretomotor/vasodilator neurons. Excitatory and inhibitory motor neurons are observed in the myenteric plexus and are involved in motility control, while secretomotor/vasodilator neurons are observed in the submucosal plexus and are responsible for innervating the mucosa and regulating secretion, absorption, and local blood flow[16,17].

Enteric glial cells are small, consisting of numerous processes that do not synthesize myelin, and are also essential for the organization and function of the ENS[31]. These cells have a star shape with numerous branches that surround the neurons. They also exhibit a series of voltage-dependent ion channels that are connected by gap junctions, giving the impression of an intimate and complex intertwining of neurons and glial cells. In addition to their role in supporting neurons, enteric glia cells regulate synaptic transmission, release cytokines, and mediate communication with the immune system [32-34].

Enteric glial cells are identified by immunohistochemical methods such as labeling of cells expressing glial fibrillary acidic protein (GFAP) and/or calcium-binding protein S100/S100β since mature enteric glial cells express these protein types[35,36]. GFAP expression is modulated by enteric glial cell proliferation, differentiation, and inflammation[22]. S100 is a calcium-binding protein that can be found in the nucleus or cytoplasm and acts to regulate the cytoskeleton structure and function as well as the calcium homeostasis in the cytoplasm[35,37,38]. Under inflammatory conditions, enteric glial cells can acquire new functional properties, and in patients with IBD there was an increase in GFAP expression in mucosal inflammation compared to non-inflamed areas[39].

The enteric plexuses are formation of cells that spread throughout the entire GI tract, however, differences in the density and size of enteric neurons and glial cells, as well as in ganglion morphology, may occur in the same segment of the GI tract in different species, or in different experimental models such as undernourishment protein and renutrition[40,41], obesity[42,43], ischemia and reperfusion[44-47], and intestinal inflammation[23,48-52].

About IBD specifically, they are classically classified into UC and CD, disorders that chronically and recurrently affect the GI tract[1-4]. Inflammatory reactions in the intestinal mucosa cause epithelial damage that compromises the intestinal barrier[53]. Although the etiology of IBD is not yet fully understood, they are usually triggered by a complex relationship between genetic[5,6], immunological and environmental factors[7-10], and gut microbiota itself[11-15]. There is, then, an imbalance between anti- and pro-inflammatory cytokines that cause an exacerbated and inadequate immune response. It is emphasized that, in colitis, there are alterations in the neuronal density such as imbalances of contractile and secretory functions associated with diarrhea due to intestinal inflammation[20,49,50,52].

CD is characterized by a segmental and transmural disorder that can affect the entire GI tract, and it could be noted there is also involvement of T-auxiliary cells (TCD4) in the pathogenesis of the disease [54,55]. In contrast, UC is characterized by continuous inflammation of the distal colon and a modification of the cytokine profile coming from Th2 cells, involved in humoral immune response patterns[2,56]. The main clinical manifestations of IBD are abdominal pain, diarrhea, vomiting, weight loss, and the presence of blood in the stool[2,50] and, worryingly, it has been demonstrated that this occurrence has increased worldwide over the years[57-60].

The literature has shown that the ENS may be affected by the IBD, thus presenting necrosis, apoptosis and degeneration of enteric ganglia[19-23]. Similarly, alterations in neurotransmitters and neuropeptides of enteric neurons have been noted in these pathologies[19,48]. Furthermore, injuries in the ENS result in activation of enteric glial cells[61,62], and the onset and/or progression of IBD can be attributed to an immune-mediated damage of enteric glial cells[32]. This activation is pointed to as a signaling mechanism that results in subsequent neuronal death[63].

The diversity of neurotransmitters and receptors found in the ENS makes the intestine one of the main tissue choices for studies of neurotransmitter receptors in pharmacological tests. In turn, several ENS-related treatment strategies have been explored to alter gut function in an effort to improve symptoms, which include drugs targeting opioid, serotoninergic, dopaminergic, and cholinergic receptors[64].

Induced colitis models in the laboratory has been widely used to study intestinal inflammation, especially through dextran sulfate sodium and 2,4,6-trinitrobenzene sulfonic acid[65-69]. Despite this, the cell signaling mechanisms underlying neuronal and tissue damage are poorly understood[49,70], and new therapeutic approaches for IBD are emerging[71-74].

As expected, experimental animal models of colitis, enteric neuronal hyperplasia and hypoplasia may be associated with increased and reduced levels of TNFα production, respectively[75,76]. In addition,

hypertrophy and hyperplasia of enteric neurons have been reported in IBD[77]. Although, the mechanism responsible for neuronal modulation of inflammation severity is still unclear, due to modulations of neuroimmune interactions, it is speculated that enteric neurons could produce and regulate cytokines involved in IBD[76].

TNFR

Specific markers have been identified in GI tract when tissues are affected by injury or disease such as IBD. They are responsible for mucosal injury and tissue damage and consequently may trigger autoimmune disease - specific immune responses in UC[10]. The TNF-α, inducible nitric oxide synthase, heme oxygenase 1, arginase-1 or CD206 in higher levels can lead to massive tissue damage in the intestine[25,54,78].

TNF-α is a mediator in intestinal inflammatory processes, being one of the main cytokines involved in pathogenesis of IBD, since their levels, are frequently high in patients with IBD[24,25]. TNF-α was first described in 1975 by a group in Sloan-Kettering who identified TNF as a promising serum soluble activity[79]. Thus, TNF-α plays roles in promoting inflammation such as the production of interleukins (IL) such as IL-1β and IL-6[10,80]. In the central nervous system (CNS), TNF-α plays homeostatic roles by regulating crucial physiological processes, such as synaptic plasticity, learning and memory, sleep and food and water intake[81]. However, some findings demonstrated that overexpression of TNF in the CNS has negative effects on cognitive functions and TNF deficiency is related to learning processes and poor memory[82]. In addition, it may be involved in gliosis and tissue remodeling and in various processes about mechanisms subserving cognition, such as synaptic scaling, change in neurotransmitter metabolism, and the process of neurodevelopment[82,83]. This observation may pave the way for understand mechanisms of innate immunity and the pathogenesis of infectious diseases which are driven by the same cascade of pro-inflammatory cytokines[79].

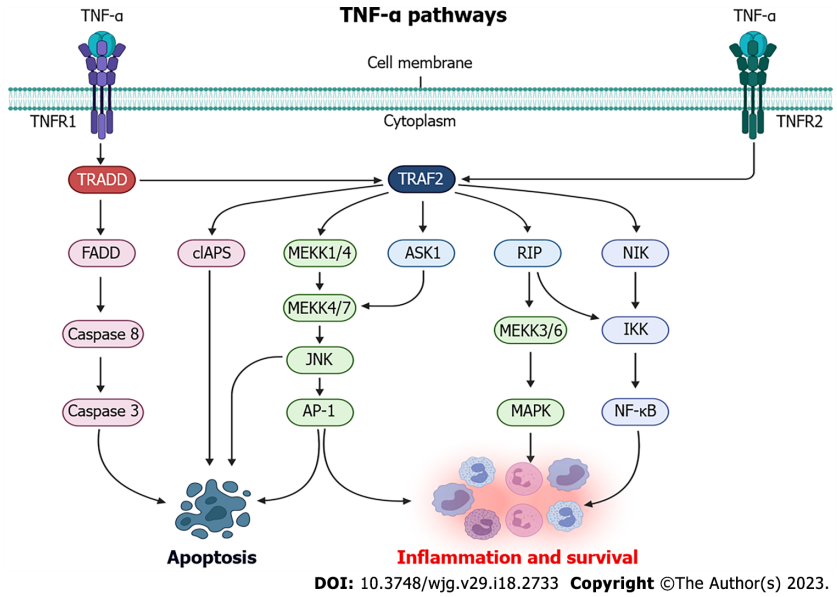
TNF-α is mainly generated by macrophages and monocytes. However, other cells such as some subsets of T cells, NK cells, dendritic cells, B cells, cardiomyocytes, fibroblasts, and astrocytes are also low-level producers of this cytokine[84]. In pathological conditions, astrocytes and microglia release large amounts of TNF-α, seeing that the production of this cytokine is an important component of the neuroinflammatory response that is associated with various neurological disorders such as Alzheimer's, Parkinson's, multiple sclerosis and amyotrophic lateral sclerosis[81].

TNF-α operates significantly in the apoptotic phase increasing the expression of the TNF receptor-associated factor 2 (TRAF2)[53]. Furthermore, TNF-α activates mitogen-activated protein kinase and nuclear factor which contribute to cell differentiation and proliferation and increased expression of pro-inflammatory cytokines[10]. Two distinct forms of TNF-α were identified: 26kDa homotrimeric transmembrane precursor form (mTNF), which is cleaved by the TNF-α-converting enzyme, and matrix metalloproteinase (TACE/Adam17) to its next 17kDa TNF soluble form (sTNF) of monomers[85,86]. Both forms of TNF are biologically active and are signaled through two distinct receptors discussed below.

There are two receptors for TNF being: The 75 kDa TNFR1, ubiquitously expressed and has a cellular death domain; and the 55 kDa TNFR2 has been found in lymphocytes and endothelial cells. Interactions of TNF-α with its receptor activate signaling pathways for cell survival, death and differentiation that control immune function and disease, and various receptors pairs of ligands within TNF family molecules expressed by immune cells that play important roles in T cell Immunity[26].

When TNF-α binds to TNFR1 and TNFR2, several intracellular pathways are activated, thus mediating cell death and/or survival response (Figure 1). When TNF-α binds to TNFR1, TNF receptor associated death domain protein (TRADD) is activated which, in turn, can induce the activation of three signaling pathways. In the first one, after TNFR1 activation, TRADD binds to FAS-associated death domain protein, which recruits caspase 8 proteins, culminating in the activation and cleavage of caspase 3, as well as leading to cell death by apoptosis[87]. The second TNFR1 pathway is related to the recruitment of TRAF2 and receptor-interacting protein (RIP) kinase *via* TRADD. TRAF2, in turn, recruits the IκB kinase (IKK) protein, which will be activated by RIP and will result in the phosphorylation of nuclear factor κB (NF-κB), which will mediate the transcription of proteins involved in the inflammation response and cell survival[87,88]. The third pathway resulting from TNFR1 activation is connected with activation of mitogen-activated protein kinase (MAPK) pathways *via* TRAF2, which activate MAPK kinase kinase 1/4 (MEKK1/4) and, upon phosphorylation, MEKK4/7 leads to activation of c-Jun N-terminal kinase, which is translocated to the nucleus and activate transcription factors such as activator protein 1 (AP-1), that can converge to activate the apoptotic and survival responses[89-91].

Although the pathways behind TNFR2 activation remains poorly understood, when the TNF-α binds to TNFR2, its activation is mediated by TRAF2, and TNFR2 has been widely known as a mediator of the activation of genes related to cell survival and proliferation[91-93]. After TNF-α binds to TNFR2, TRAF2 is activated which, through common signaling pathways to TNFR1 activation, can activate NF-κB through IKK, and AP-1 *via* MEKK, which can also be activated *via* apoptosis signal-regulating kinase 1 [94]. Furthermore, activation of TRAF2 *via* TNFR2 can lead to the recruitment of cellular inhibitor of



DOI: 10.3748/wjg.v29.i18.2733 **Copyright** ©The Author(s) 2023.

Figure 1 Tumor necrosis factor-alpha signaling pathways. TNF-α: Tumor necrosis factor-alpha; TNFR1: Tumor necrosis factor receptor 1; TNFR2: Tumor necrosis factor receptor 2; TRADD: TNF receptor associated protein with death domain; FADD: FAS-associated death domain protein; cIAPS: Cellular inhibitor of apoptosis; MEKK: MAPK kinase kinas; JNK: N-terminal jun kinase; ASK1: Apoptosis signal-regulating kinase 1; IKK: IκB kinase; NF-κB: Nuclear factor κB; RIP: Receptor-interacting protein kinase. Created with BioRender.com.

apoptosis (cIAPS), which will partially inhibit caspase activation and, for this reason, reduce apoptosis response[95]. When both TNFR1 and TNFR2 are activated together, cIAPS recruitment is reduced and the caspase activity, mainly mediated by TNFR1, is activated[91].

These receptors are involved in the pathogenesis of IBD and their expression is correlated with disease activity[96]. The sTNf binds selectively to the TNFR1 receptor, and its activation results in a signaling cascade with effects such as apoptosis, cell proliferation and cytokine secretion[24,97]. In contrast, the mTNF can bind both to TNFR1 and TNFR2[91]. TNFR1 signaling pathways deserve attention, due to cytotoxic effects triggered by activation of TNFR1 *via* sTNF binding and it could be noted that some aspects regarding TNFR2 function are still unclear[91].

Some studies pointed to the presence of a functional cross-talk between TNFR1 and TNFR2, whichever TNFR2 would act as an complement-dependent cytotoxic effect of TNFR1, thus being responsible for the inhibition of anti-apoptotic pathways and for the increase in the cytotoxicity triggered by TNFR1 when both receptors are co-expressed and activated[91,98,99]. This finding could be seen as a distinct situation of the classic phenomenon in which the balance between apoptotic and anti-apoptotic signals triggered by TNF-α determines the accuracy in cell signaling[91].

The TNFR2 pathway does not contain death domains and its stimulation can result in proliferation, migration and production of cytokines such as IL-1 and IL-6. This receptor not only activate an intracellular signaling pathway, but can also induce reverse signaling within the cell expressing TNF-α [100].

TNFR2 is also involved in several autoimmune diseases, playing a protective role or being involved in its development. Thus, TNFR2 is known to be involved in rheumatoid arthritis, CD, erythematosus systemic lupus, UC, scleroderma, among other diseases[10]. It was recognized that the expression of TNFR2 is more limited than that in TNFR1, *i.e.*, this finding suggests that the sTNF-mediating signaling pathway *via* TNFR1 drives a predominantly pro-inflammatory program, whereas mTNF binding to TNFR2 primarily initiates immune modulation and tissue regeneration[84]. Thus, an increase in TNF-α expression can cause mucosal barrier defects in patients with IBD, exacerbating inflammation[10]. However, only a part of the role of TNF-α receptors in the pathogenesis of IBD is understood. It is known that it can be indicated the presence of TNFR2 in the CNS, *i.e.*, in neurons of the cerebral cortex [83], and no data in the literature could identify the presence of TNFR2 in enteric neurons.

ANTI-TNF-α TREATMENT

The immune response plays an important role in the initiation and maintenance of UC[101]. Cytokines play key roles in inflammatory processes, such as targeting cell signaling molecules during inflammation and UC pathogenesis through different roles, such as the production of inflammatory mediators and activation of inflammatory pathways[5,57,102,103]. They are also involved in several biological processes, such as cell activation, differentiation and central factors in the process of developing the

inflammatory and immune response. In addition, studies provide evidence of their involvement in epithelial injury, and consequently, intestinal barrier injury and tissue damage[5,104,105].

The treatment approach in the control of inflamed GI tissue in IBD, including clinical, laboratory conditions, endoscopic and histological remission for a prolonged period, play an important role in its evolution and possibly modifying the natural course of the disease[9,106]. Recent studies have suggested that TNF-α is one of the main pro-inflammatory cytokines involved in the pathogenesis of IBD, as higher TNF-α levels are present in the serum of both patients with UC and CD[25].

For the treatment of IBD, different classes of drugs can be used, respecting the particularities of CD and UC, with the aim of alleviating the symptomatic crisis of patients, as well as inducing and maintaining remission of the disease[107,108]. Generally, the first treatment option for mild to moderate cases of UC and CD involves aminosalicylates, or 5-ASAs, and other treatments include the use of corticosteroids, immunosuppressants, and biological drugs[109,110].

Biological drugs used to treat IBD are monoclonal antibodies that neutralize/block key targets in the development of intestinal[27]. There are biological drugs that target, for example, integrins, interleukins, and cytokines, such as TNF-α, which are related to the development of the inflammatory process and the activation of immune system cells (Figure 2)[111,112].

Currently, four anti-TNF-α agents are indicated by various guidelines for the treatment of IBD: Infliximab; adalimumab; certolizumab pegol; and golimumab[28,29]. Infliximab and adalimumab are indicated for the treatment of both UC and CD, while golimumab is indicated only for the treatment of UC and certolizumab pegol only for CD. American Gastroenterological Association (AGA) and American College of Gastroenterology (ACG) guidelines recommend the use of infliximab, adalimumab, and certolizumab pegol to induce and maintain CD remission in moderate to severe patients unresponsive to corticosteroid or methotrexate treatment, and regarding UC, it could be noted that AGA and ACG recommend the use of infliximab, adalimumab and golimumab in patients who have not responded to conventional therapy[28,29]. These anti-TNF-α antibodies bind to TNF-α, blocking its harmful effects, such as NF-κB activation and increase of pro-inflammatory cytokines, that mediate intestinal inflammation[113,114].

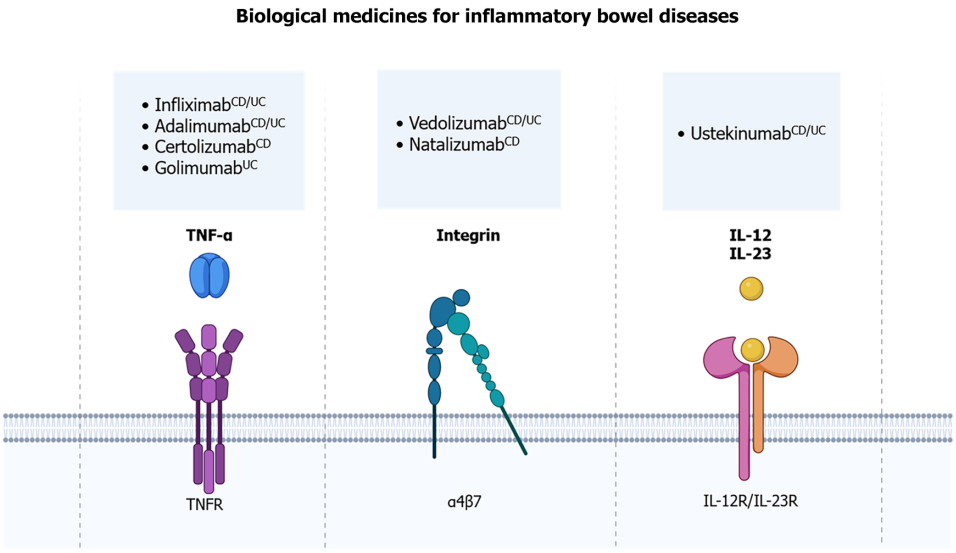
Intravenous and subcutaneous biologics targeting TNF-α have revolutionized the treatment of IBD, becoming the best available agents, when conventional therapy does not work, to induce and maintain IBD remission[115-117]. The application of this type of antibodies in patients with IBD induces a satisfactory clinical response in up to 60% of patients, and induced long-term maintenance of disease remission in most patients[24,30] and also reduces colorectal cancer risks[118]. Despite this, some patients do not improve after the use of these antibodies, some relapses within the first year of treatment and, one alternative used for the management of these cases has been to change the anti-TNF-α used for another one, or even to increase the dosage used[119]. Other alternative option for anti-TNF-α non responsiveness is the use other biological medicines like anti-integrin or anti-interleukin therapies.

Anti-integrin therapy, such as vedolizumab, which can be used for UC and CD treatment, block the integrin α4β7, which is expressed in B and T lymphocytes and interact with mucosal addressin-cell adhesion molecule-1 on intestinal vessels[120-122]. So, vedolizumab blocks lymphocyte trafficking only in the gut, preventing a systemic immunosuppression[123]. Otherwise, natalizumab blocks the integrin α4β7 and α1β7 and blocks lymphocyte trafficking in other organs, for example the brain, which can lead to infections such as progressive multifocal leukoencephalopathy[124]. For this reason, the use of natalizumab is very carefully, considering risk-benefits factors, and it is not available in some countries. Other biological medicine is ustekinumab, an anti-interleukin agent for subunit p40 of IL-12 and IL-23, used for CD and UC. This biological medicine attenuates the immune cell activation by these interleukins and consequently reduces inflammatory response and pro-inflammatory signaling[125-127].

Limitations of therapy with biological drugs include the high cost of adherence to therapy, differences in legislation and availability of these drugs in different countries, and the meticulous risk-benefit analysis related to the choice over treatment alternatives. However, new strategies and medicines have constantly been studied at pre-clinical and clinical instances for treatment of IBD.

ANTI-TNF-α TREATMENT AND APPROACH IN THE ENS

Although the involvement of TNF-α in the ENS is poorly described in the literature, it is reported that the ENS has TNF-α receptors and responds to the inflammatory stimulus, can lead to changes in motility patterns and fluid and electrolyte balance, a condition often found in patients with IBD[128]. When comparing the intestine, under normal conditions, and the intestine in IBD, some aspects must be considered (Figure 3). Under physiological conditions, large populations of microorganisms (bacteria, virus and fungi) inhabit the gut, which constitute the gut microbiota[129]. This microbiota establishes a symbiosis with the host[130]. The intestinal barrier, composed mainly by mucus layer and epithelial, is an intact and functional structure[131]. There is a balance between the levels of pro-inflammatory cytokines TNF-α, IL-12 and IL-23, and anti-inflammatory cytokines such as transforming growth factor-beta and IL-10 by innate immune cells, which leads to a balance between regulatory and effector T cells,



DOI: 10.3748/wjg.v29.i18.2733 **Copyright** ©The Author(s) 2023.

Figure 2 Biological medicines for inflammatory bowel diseases. Biological medicines used for the treatment of inflammatory bowel diseases (IBD) can be classified into anti- Tumor necrosis factor (TNF)-α, anti-integrin and anti-interleukin therapies. Anti-TNF-α binds to TNF-α and inhibits TNF receptor activation. Infliximab, adalimumab, certolizumab pegol and golimumab are examples of anti-TNF-α used in the treatment of IBD. Vedolizumab and natalizumab are anti-integrin agents, which bind to the α4β7 integrin and prevent the migration of inflammatory cells into the intestinal tissue. Ustekinumab is an anti-interleukin that blocks interleukin (IL)-12 and IL-23, which cannot bind to IL-12 receptor and IL-23 receptor on T and B lymphocytes, thus reducing the inflammatory response in the gut. ^{CD}indication only for Crohn's Disease; ^{UC}indication only for Ulcerative Colitis; $^{CD/UC}$indication both for Crohn's Disease and Ulcerative Colitis. TNF-α: Tumor necrosis factor-alpha; IL: Interleukin. Created with BioRender.com.

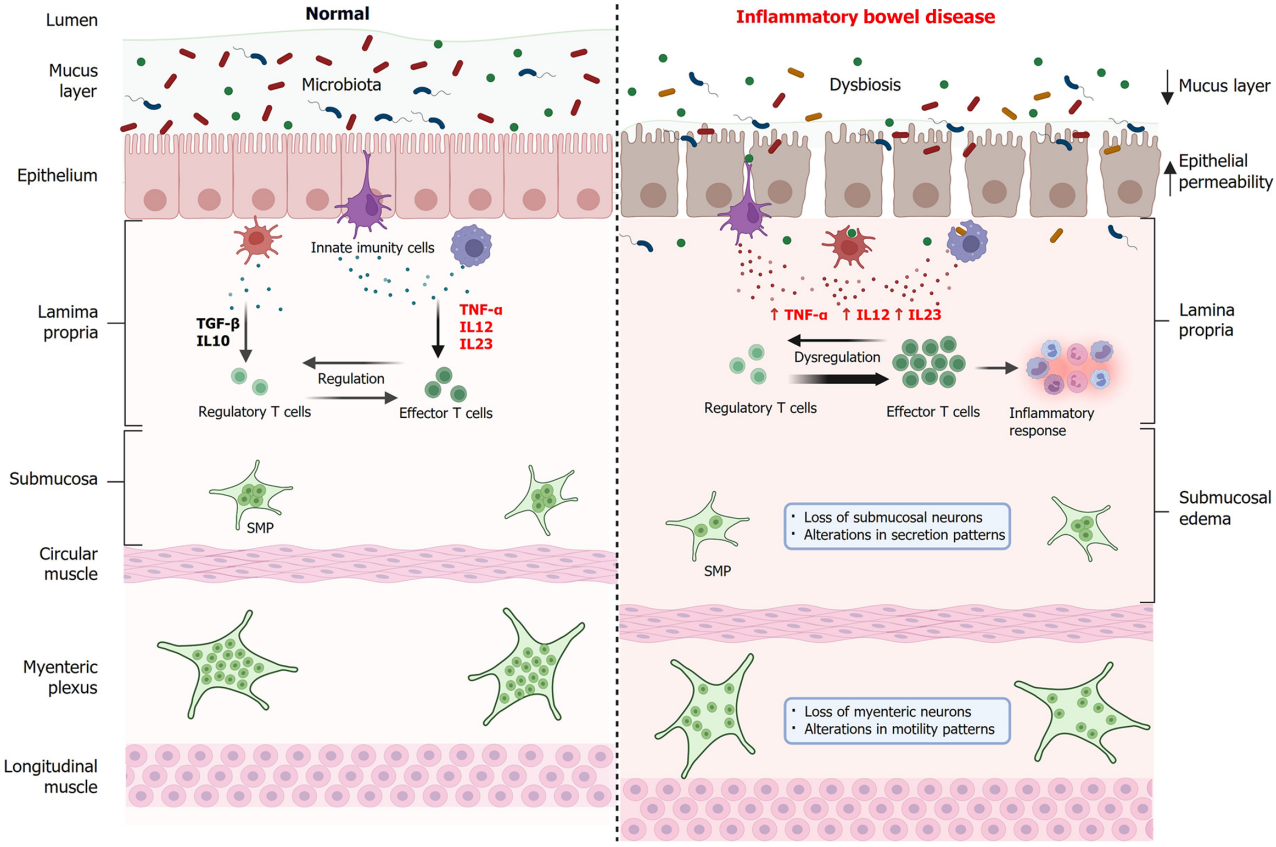
inducing tolerance to microorganisms from the gut microbiota[130,132]. In physiological conditions, both submucosal plexus and myenteric plexus are functional and controls, respectively, fluid secretion and intestinal motility.

In IBD, there is an imbalance in the gut microbiota (dysbiosis), the intestinal barrier is compromised, with a reduction in the mucus layer, weakening of the intercellular junctions and consequently increased epithelial permeability and entry of microorganisms in the lamina propria[15,133]. Innate immune cells increase the secretion of pro-inflammatory cytokines such as TNF-α, IL-12 and IL-23, which leads to a dysregulation of the immune system, which increases the activity of effector T cells which, in turn, recruit cells for the inflammatory response[134]. Morphological findings include submucosal edema, as well as a reduction in the number of neurons in the SMP, causing changes in secretion patterns and loss of neurons in the myenteric plexus, thus changing the motility patterns[51,52,135].

Experimental UC has been shown to affect enteric neurons, causing changes in the number of enteric neurons and glia, as well as changes in intestinal motility and secretion patterns[50-52,136]. As the presence of TNFR1 and TNFR2 have been reported in the ENS, the use of anti-TNF-α agents can exert a series of beneficial effects on ENS levels, improving the inflammatory response, peristalsis and intestinal secretion patterns, relieving symptoms such as diarrhea, fecal bleeding and colic. However, despite the important approach to the ENS and its relationship with IBD, literature data on anti-TNF treatment with analysis focused on the ENS are scarce. Therefore, further studies on the role of mechanisms/signaling pathways of sTNF, mTNF, TNF-α and their receptors in enteric neurons in IBD are needed, since this approach can guide the choice of a more adequate, effective anti-TNF-α agent with lower chances of failure responsiveness.

CONCLUSION

This review provided main details about TNF-α relationship with IBD. The role of TNF receptors in the development of IBD is an issue that deserves attention and may be a key to the treatment of UC and CD. In addition, anti- TNF-α treatments have been very promising in the treatment of IBD unresponsive to conventional therapies. The relationship of the ENS with TNF-α and its response to anti- TNF-α treatment are important aspects to be addressed, as they may direct new therapies and reduce non-responsiveness to specific anti- TNF-α agents.



DOI: 10.3748/wjg.v29.i18.2733 **Copyright** ©The Author(s) 2023.

Figure 3 Comparison of the intestine in normal conditions and in the bowel with inflammatory bowel disease. Under normal conditions (left), the intestinal microbiota establishes a symbiotic condition with the host, the intestinal barrier is intact and functional, and there is a balance between the levels of pro-inflammatory cytokines such as tumor necrosis factor alpha (TNF-α), interleukin (IL)-12 and IL-23 and anti-inflammatory cytokines such as transforming growth factor beta and IL-10 by innate immune cells. In this way, there is a regulation of the immune response through a balance between regulatory T cells and effector T cells. Submucosal plexus (SMP) and myenteric plexus neurons are functional and controlling, respectively, fluid secretion and intestinal motility. In inflammatory bowel diseases (IBD) (right), there is an imbalance in the intestinal microbiota, the intestinal barrier is compromised, with a reduction in the mucous layer, increased epithelial permeability and consequent passage of microorganisms to the lamina propria. Innate immune cells increase the secretion of pro-inflammatory cytokines such as TNF-α, IL-12 and IL-23, which leads to a dysregulation of the immune system mediated by T cells, increasing the activity of effector T cells which, in turn, recruit cells for the inflammatory response. In IBD, submucosal edema is observed, as well as a reduction in the number of neurons in the SMP, causing changes in secretion patterns and loss of neurons in the myenteric plexus, resulting in changes in motility patterns. TNF-α: Tumor necrosis factor-alpha; IL: Interleukin. Created with BioRender.com.

FOOTNOTES

Author contributions: Souza RF, Caetano MAF and Magalhães HIR were responsible for the literature review, and analysis and written; Castelucci P performed the critical interpretation and revised the manuscript for intellectual content; all authors have read and approved the final manuscript.

Supported by Research Support Foundation of the State of São Paulo (FAPESP, Brazil), No. 2014/25927-2, No. 2018/07862-1; National Council for Scientific and Technological Development (CNPq, Brazil); and Higher Education Personnel Improvement Coordination (CAPES, Brazil).

Conflict-of-interest statement: Authors declare no conflict of interests for this article.

Open-Access: This article is an open-access article that was selected by an in-house editor and fully peer-reviewed by external reviewers. It is distributed in accordance with the Creative Commons Attribution NonCommercial (CC BY-NC 4.0) license, which permits others to distribute, remix, adapt, build upon this work non-commercially, and license their derivative works on different terms, provided the original work is properly cited and the use is non-commercial. See: https://creativecommons.org/Licenses/by-nc/4.0/

Country/Territory of origin: Brazil

ORCID number: Roberta Figueiroa Souza 0000-0003-4380-6373; Marcos Antônio Ferreira Caetano 0000-0002-9981-3241; Henrique Inhauser Riceti Magalhães 0000-0001-9151-8160; Patricia Castelucci 0000-0002-7475-5962.

S-Editor: Chang KL

L-Editor: A
P-Editor: Chen YX

REFERENCES

1 **Loddo I**, Romano C. Inflammatory Bowel Disease: Genetics, Epigenetics, and Pathogenesis. *Front Immunol* 2015; **6**: 551 [PMID: 26579126 DOI: 10.3389/fimmu.2015.00551]
2 **Shapiro JM**, Subedi S, LeLeiko NS. Inflammatory Bowel Disease. *Pediatr Rev* 2016; **37**: 337-347 [PMID: 27482063 DOI: 10.1542/pir.2015-0110]
3 **Shivashankar R**, Lichtenstein GR. Mimics of Inflammatory Bowel Disease. *Inflamm Bowel Dis* 2018; **24**: 2315-2321 [PMID: 29947781 DOI: 10.1093/ibd/izy168]
4 **Liu Y**, Zhao J, Zhao Y, Zong S, Tian Y, Chen S, Li M, Liu H, Zhang Q, Jing X, Sun B, Wang H, Sun T, Yang C. Therapeutic effects of lentinan on inflammatory bowel disease and colitis-associated cancer. *J Cell Mol Med* 2019; **23**: 750-760 [PMID: 30472806 DOI: 10.1111/jcmm.13897]
5 **Ahmad T**, Satsangi J, McGovern D, Bunce M, Jewell DP. Review article: The genetics of inflammatory bowel disease. *Aliment Pharmacol Ther* 2001; **15**: 731-748 [PMID: 11380312 DOI: 10.1046/j.1365-2036.2001.00981.x]
6 **Xavier RJ**, Podolsky DK. Unravelling the pathogenesis of inflammatory bowel disease. *Nature* 2007; **448**: 427-434 [PMID: 17653185 DOI: 10.1038/nature06005]
7 **Fiocchi C**. Intestinal inflammation: A complex interplay of immune and nonimmune cell interactions. *Am J Physiol* 1997; **273**: G769-G775 [PMID: 9357817 DOI: 10.1152/ajpgi.1997.273.4.G769]
8 **Ke P**, Shao BZ, Xu ZQ, Chen XW, Liu C. Intestinal Autophagy and Its Pharmacological Control in Inflammatory Bowel Disease. *Front Immunol* 2016; **7**: 695 [PMID: 28119697 DOI: 10.3389/fimmu.2016.00695]
9 **Argollo M**, Fiorino G, Hindryckx P, Peyrin-Biroulet L, Danese S. Novel therapeutic targets for inflammatory bowel disease. *J Autoimmun* 2017; **85**: 103-116 [PMID: 28711286 DOI: 10.1016/j.jaut.2017.07.004]
10 **Tatiya-Aphiradee N**, Chatuphonprasert W, Jarukamjorn K. Immune response and inflammatory pathway of ulcerative colitis. *J Basic Clin Physiol Pharmacol* 2018; **30**: 1-10 [PMID: 30063466 DOI: 10.1515/jbcpp-2018-0036]
11 **Kozik AJ**, Nakatsu CH, Chun H, Jones-Hall YL. Comparison of the fecal, cecal, and mucus microbiome in male and female mice after TNBS-induced colitis. *PLoS One* 2019; **14**: e0225079 [PMID: 31703107 DOI: 10.1371/journal.pone.0225079]
12 **Neurath MF**. Host-microbiota interactions in inflammatory bowel disease. *Nat Rev Gastroenterol Hepatol* 2020; **17**: 76-77 [PMID: 31848474 DOI: 10.1038/s41575-019-0248-1]
13 **Tavakoli P**, Vollmer-Conna U, Hadzi-Pavlovic D, Grimm MC. A Review of Inflammatory Bowel Disease: A Model of Microbial, Immune and Neuropsychological Integration. *Public Health Rev* 2021; **42**: 1603990 [PMID: 34692176 DOI: 10.3389/phrs.2021.1603990]
14 **Vicentini FA**, Keenan CM, Wallace LE, Woods C, Cavin JB, Flockton AR, Macklin WB, Belkind-Gerson J, Hirota SA, Sharkey KA. Intestinal microbiota shapes gut physiology and regulates enteric neurons and glia. *Microbiome* 2021; **9**: 210 [PMID: 34702353 DOI: 10.1186/s40168-021-01165-z]
15 **Caetano MAF**, Castelucci P. Role of short chain fatty acids in gut health and possible therapeutic approaches in inflammatory bowel diseases. *World J Clin Cases* 2022; **10**: 9985-10003 [PMID: 36246826 DOI: 10.12998/wjcc.v10.i28.9985]
16 **Furness JB**. The Enteric Nervous System. Oxford: Blackwell, 2006: 1-102 [DOI: 10.1002/9780470988756]
17 **Furness JB**. The enteric nervous system and neurogastroenterology. *Nat Rev Gastroenterol Hepatol* 2012; **9**: 286-294 [PMID: 22392290 DOI: 10.1038/nrgastro.2012.32]
18 **Furness JB**, Callaghan BP, Rivera LR, Cho HJ. The enteric nervous system and gastrointestinal innervation: Integrated local and central control. *Adv Exp Med Biol* 2014; **817**: 39-71 [PMID: 24997029 DOI: 10.1007/978-1-4939-0897-4_3]
19 **Boyer L**, Ghoreishi M, Templeman V, Vallance BA, Buchan AM, Jevon G, Jacobson K. Myenteric plexus injury and apoptosis in experimental colitis. *Auton Neurosci* 2005; **117**: 41-53 [PMID: 15620569 DOI: 10.1016/j.autneu.2004.10.006]
20 **Linden DR**, Couvrette JM, Ciolino A, McQuoid C, Blaszyk H, Sharkey KA, Mawe GM. Indiscriminate loss of myenteric neurones in the TNBS-inflamed guinea-pig distal colon. *Neurogastroenterol Motil* 2005; **17**: 751-760 [PMID: 16185315 DOI: 10.1111/j.1365-2982.2005.00703.x]
21 **Lomax AE**, Fernández E, Sharkey KA. Plasticity of the enteric nervous system during intestinal inflammation. *Neurogastroenterol Motil* 2005; **17**: 4-15 [PMID: 15670258 DOI: 10.1111/j.1365-2982.2004.00607.x]
22 **Cirillo C**, Sarnelli G, Turco F, Mango A, Grosso M, Aprea G, Masone S, Cuomo R. Proinflammatory stimuli activates human-derived enteroglial cells and induces autocrine nitric oxide production. *Neurogastroenterol Motil* 2011; **23**: e372-e382 [PMID: 21762414 DOI: 10.1111/j.1365-2982.2011.01748.x]
23 **Linden DR**. Colitis is associated with a loss of intestinofugal neurons. *Am J Physiol Gastrointest Liver Physiol* 2012; **303**: G1096-G1104 [PMID: 22997196 DOI: 10.1152/ajpgi.00176.2012]
24 **Billmeier U**, Dieterich W, Neurath MF, Atreya R. Molecular mechanism of action of anti-tumor necrosis factor antibodies in inflammatory bowel diseases. *World J Gastroenterol* 2016; **22**: 9300-9313 [PMID: 27895418 DOI: 10.3748/wjg.v22.i42.9300]
25 **Holtmann MH**, Schütz M, Galle PR, Neurath MF. Functional relevance of soluble TNF-alpha, transmembrane TNF-alpha and TNF-signal transduction in gastrointestinal diseases with special reference to inflammatory bowel diseases. *Z Gastroenterol* 2002; **40**: 587-600 [PMID: 12297983 DOI: 10.1055/s-2002-33418]
26 **So T**, Ishii N. The TNF-TNFR Family of Co-signal Molecules. *Adv Exp Med Biol* 2019; **1189**: 53-84 [PMID: 31758531 DOI: 10.1007/978-981-32-9717-3_3]

27 **de Mattos BR**, Garcia MP, Nogueira JB, Paiatto LN, Albuquerque CG, Souza CL, Fernandes LG, Tamashiro WM, Simioni PU. Inflammatory Bowel Disease: An Overview of Immune Mechanisms and Biological Treatments. *Mediators Inflamm* 2015; **2015**: 493012 [PMID: 26339135 DOI: 10.1155/2015/493012]

28 **Feuerstein JD**, Isaacs KL, Schneider Y, Siddique SM, Falck-Ytter Y, Singh S; AGA Institute Clinical Guidelines Committee. AGA Clinical Practice Guidelines on the Management of Moderate to Severe Ulcerative Colitis. *Gastroenterology* 2020; **158**: 1450-1461 [PMID: 31945371 DOI: 10.1053/j.gastro.2020.01.006]

29 **Lichtenstein GR**, Loftus EV, Isaacs KL, Regueiro MD, Gerson LB, Sands BE. ACG Clinical Guideline: Management of Crohn's Disease in Adults. *Am J Gastroenterol* 2018; **113**: 481-517 [PMID: 29610508 DOI: 10.1038/ajg.2018.27]

30 **Panaccione R**, Colombel JF, Louis E, Peyrin-Biroulet L, Sandborn WJ. Evolving definitions of remission in Crohn's disease. *Inflamm Bowel Dis* 2013; **19**: 1645-1653 [PMID: 23598817 DOI: 10.1097/MIB.0b013e318283a4b3]

31 **Kabouridis PS**, Lasrado R, McCallum S, Chng SH, Snippert HJ, Clevers H, Pettersson S, Pachnis V. Microbiota controls the homeostasis of glial cells in the gut lamina propria. *Neuron* 2015; **85**: 289-295 [PMID: 25578362 DOI: 10.1016/j.neuron.2014.12.037]

32 **Bassotti G**, Villanacci V, Fisogni S, Rossi E, Baronio P, Clerici C, Maurer CA, Cathomas G, Antonelli E. Enteric glial cells and their role in gastrointestinal motor abnormalities: Introducing the neuro-gliopathies. *World J Gastroenterol* 2007; **13**: 4035-4041 [PMID: 17696219 DOI: 10.3748/wjg.v13.i30.4035]

33 **Clarke LE**, Barres BA. Glia keep synapse distribution under wraps. *Cell* 2013; **154**: 267-268 [PMID: 23870116 DOI: 10.1016/j.cell.2013.06.045]

34 **Jensen CJ**, Massie A, De Keyser J. Immune players in the CNS: The astrocyte. *J Neuroimmune Pharmacol* 2013; **8**: 824-839 [PMID: 23821340 DOI: 10.1007/s11481-013-9480-6]

35 **Rühl A**, Nasser Y, Sharkey KA. Enteric glia. *Neurogastroenterol Motil* 2004; **16** Suppl 1: 44-49 [PMID: 15066004 DOI: 10.1111/j.1743-3150.2004.00474.x]

36 **Hagström C**, Olsson C. Glial cells revealed by GFAP immunoreactivity in fish gut. *Cell Tissue Res* 2010; **341**: 73-81 [PMID: 20512593 DOI: 10.1007/s00441-010-0979-3]

37 **Gonzalez-Martinez T**, Perez-Piñera P, Díaz-Esnal B, Vega JA. S-100 proteins in the human peripheral nervous system. *Microsc Res Tech* 2003; **60**: 633-638 [PMID: 12645010 DOI: 10.1002/jemt.10304]

38 **Hsieh HL**, Schäfer BW, Weigle B, Heizmann CW. S100 protein translocation in response to extracellular S100 is mediated by receptor for advanced glycation endproducts in human endothelial cells. *Biochem Biophys Res Commun* 2004; **316**: 949-959 [PMID: 15033494 DOI: 10.1016/j.bbrc.2004.02.135]

39 **Pochard C**, Coquenlorge S, Freyssinet M, Naveilhan P, Bourreille A, Neunlist M, Rolli-Derkinderen M. The multiple faces of inflammatory enteric glial cells: Is Crohn's disease a gliopathy? *Am J Physiol Gastrointest Liver Physiol* 2018; **315**: G1-G11 [PMID: 29517926 DOI: 10.1152/ajpgi.00016.2018]

40 **Misawa R**, Girotti PA, Mizuno MS, Liberti EA, Furness JB, Castelucci P. Effects of protein deprivation and re-feeding on P2X2 receptors in enteric neurons. *World J Gastroenterol* 2010; **16**: 3651-3663 [PMID: 20677337 DOI: 10.3748/wjg.v16.i29.3651]

41 **Girotti PA**, Misawa R, Palombit K, Mendes CE, Bittencourt JC, Castelucci P. Differential effects of undernourishment on the differentiation and maturation of rat enteric neurons. *Cell Tissue Res* 2013; **353**: 367-380 [PMID: 23644765 DOI: 10.1007/s00441-013-1620-z]

42 **Mizuno MS**, Crisma AR, Borelli P, Castelucci P. Expression of the $P2X_2$ receptor in different classes of ileum myenteric neurons in the female obese ob/ob mouse. *World J Gastroenterol* 2012; **18**: 4693-4703 [PMID: 23002338 DOI: 10.3748/wjg.v18.i34.4693]

43 **Mizuno MS**, Crisma AR, Borelli P, Schäfer BT, Silveira MP, Castelucci P. Distribution of the P2X2 receptor and chemical coding in ileal enteric neurons of obese male mice (ob/ob). *World J Gastroenterol* 2014; **20**: 13911-13919 [PMID: 25320527 DOI: 10.3748/wjg.v20.i38.13911]

44 **Palombit K**, Mendes CE, Tavares-de-Lima W, Silveira MP, Castelucci P. Effects of ischemia and reperfusion on subpopulations of rat enteric neurons expressing the P2X7 receptor. *Dig Dis Sci* 2013; **58**: 3429-3439 [PMID: 23990036 DOI: 10.1007/s10620-013-2847-y]

45 **Mendes CE**, Palombit K, Tavares-de-Lima W, Castelucci P. Enteric glial cells immunoreactive for P2X7 receptor are affected in the ileum following ischemia and reperfusion. *Acta Histochem* 2019; **121**: 665-679 [PMID: 31202513 DOI: 10.1016/j.acthis.2019.06.001]

46 **Mendes CE**, Palombit K, Vieira C, Silva I, Correia-de-Sá P, Castelucci P. The Effect of Ischemia and Reperfusion on Enteric Glial Cells and Contractile Activity in the Ileum. *Dig Dis Sci* 2015; **60**: 2677-2689 [PMID: 25917048 DOI: 10.1007/s10620-015-3663-3]

47 **Palombit K**, Mendes CE, Tavares-de-Lima W, Barreto-Chaves ML, Castelucci P. Blockage of the P2X7 Receptor Attenuates Harmful Changes Produced by Ischemia and Reperfusion in the Myenteric Plexus. *Dig Dis Sci* 2019; **64**: 1815-1829 [PMID: 30734238 DOI: 10.1007/s10620-019-05496-8]

48 **Gulbransen BD**, Sharkey KA. Novel functional roles for enteric glia in the gastrointestinal tract. *Nat Rev Gastroenterol Hepatol* 2012; **9**: 625-632 [PMID: 22890111 DOI: 10.1038/nrgastro.2012.138]

49 **Stavely R**, Abalo R, Nurgali K. Targeting Enteric Neurons and Plexitis for the Management of Inflammatory Bowel Disease. *Curr Drug Targets* 2020; **21**: 1428-1439 [PMID: 32416686 DOI: 10.2174/1389450121666200516173242]

50 **da Silva MV**, Marosti AR, Mendes CE, Palombit K, Castelucci P. Differential effects of experimental ulcerative colitis on P2X7 receptor expression in enteric neurons. *Histochem Cell Biol* 2015; **143**: 171-184 [PMID: 25201348 DOI: 10.1007/s00418-014-1270-6]

51 **Magalhães HIR**, Castelucci P. Enteric nervous system and inflammatory bowel diseases: Correlated impacts and therapeutic approaches through the P2X7 receptor. *World J Gastroenterol* 2021; **27**: 7909-7924 [PMID: 35046620 DOI: 10.3748/wjg.v27.i46.7909]

52 **Evangelinellis MM**, Souza RF, Mendes CE, Castelucci P. Effects of a P2X7 receptor antagonist on myenteric neurons in the distal colon of an experimental rat model of ulcerative colitis. *Histochem Cell Biol* 2022; **157**: 65-81 [PMID: 34626216 DOI: 10.1007/s00418-021-02039-z]

53 **Begue B**, Wajant H, Bambou JC, Dubuquoy L, Siegmund D, Beaulieu JF, Canioni D, Berrebi D, Brousse N, Desreumaux P, Schmitz J, Lentze MJ, Goulet O, Cerf-Bensussan N, Ruemmele FM. Implication of TNF-related apoptosis-inducing ligand in inflammatory intestinal epithelial lesions. *Gastroenterology* 2006; **130**: 1962-1974 [PMID: 16762619 DOI: 10.1053/j.gastro.2006.03.022]

54 **Ueno A**, Ghosh A, Hung D, Li J, Jijon H. Th17 plasticity and its changes associated with inflammatory bowel disease. *World J Gastroenterol* 2015; **21**: 12283-12295 [PMID: 26604637 DOI: 10.3748/wjg.v21.i43.12283]

55 **Deepak P**, Fowler KJ, Fletcher JG, Bruining DH. Novel Imaging Approaches in Inflammatory Bowel Diseases. *Inflamm Bowel Dis* 2019; **25**: 248-260 [PMID: 30010908 DOI: 10.1093/ibd/izy239]

56 **Heller F**, Florian P, Bojarski C, Richter J, Christ M, Hillenbrand B, Mankertz J, Gitter AH, Bürgel N, Fromm M, Zeitz M, Fuss I, Strober W, Schulzke JD. Interleukin-13 is the key effector Th2 cytokine in ulcerative colitis that affects epithelial tight junctions, apoptosis, and cell restitution. *Gastroenterology* 2005; **129**: 550-564 [PMID: 16083712 DOI: 10.1053/j.gastro.2005.05.002]

57 **Kaplan GG**, Ng SC. Understanding and Preventing the Global Increase of Inflammatory Bowel Disease. *Gastroenterology* 2017; **152**: 313-321.e2 [PMID: 27793607 DOI: 10.1053/j.gastro.2016.10.020]

58 **Ng SC**, Shi HY, Hamidi N, Underwood FE, Tang W, Benchimol EI, Panaccione R, Ghosh S, Wu JCY, Chan FKL, Sung JJY, Kaplan GG. Worldwide incidence and prevalence of inflammatory bowel disease in the 21st century: A systematic review of population-based studies. *Lancet* 2017; **390**: 2769-2778 [PMID: 29050646 DOI: 10.1016/S0140-6736(17)32448-0]

59 **Quaresma AB**, Kaplan GG, Kotze PG. The globalization of inflammatory bowel disease: The incidence and prevalence of inflammatory bowel disease in Brazil. *Curr Opin Gastroenterol* 2019; **35**: 259-264 [PMID: 30973356 DOI: 10.1097/MOG.0000000000000534]

60 **Kotze PG**, Underwood FE, Damião AOMC, Ferraz JGP, Saad-Hossne R, Toro M, Iade B, Bosques-Padilla F, Teixeira FV, Juliao-Banos F, Simian D, Ghosh S, Panaccione R, Ng SC, Kaplan GG. Progression of Inflammatory Bowel Diseases Throughout Latin America and the Caribbean: A Systematic Review. *Clin Gastroenterol Hepatol* 2020; **18**: 304-312 [PMID: 31252191 DOI: 10.1016/j.cgh.2019.06.030]

61 **Eng LF**, Yu AC, Lee YL. Astrocytic response to injury. *Prog Brain Res* 1992; **94**: 353-365 [PMID: 1337615 DOI: 10.1016/S0079-6123(08)61764-1]

62 **O'Callaghan JP**. Quantitative features of reactive gliosis following toxicant-induced damage of the CNS. *Ann N Y Acad Sci* 1993; **679**: 195-210 [PMID: 8512183 DOI: 10.1111/j.1749-6632.1993.tb18299.x]

63 **Giulian D**, Li J, Leara B, Keenen C. Phagocytic microglia release cytokines and cytotoxins that regulate the survival of astrocytes and neurons in culture. *Neurochem Int* 1994; **25**: 227-233 [PMID: 7833791 DOI: 10.1016/0197-0186(94)90066-3]

64 **Spear ET**, Mawe GM. Enteric neuroplasticity and dysmotility in inflammatory disease: key players and possible therapeutic targets. *Am J Physiol Gastrointest Liver Physiol* 2019; **317**: G853-G861 [PMID: 31604034 DOI: 10.1152/ajpgi.00206.2019]

65 **Kawada M**, Arihiro A, Mizoguchi E. Insights from advances in research of chemically induced experimental models of human inflammatory bowel disease. *World J Gastroenterol* 2007; **13**: 5581-5593 [PMID: 17948932 DOI: 10.3748/wjg.v13.i42.5581]

66 **Brenna Ø**, Furnes MW, Drozdov I, van Beelen Granlund A, Flatberg A, Sandvik AK, Zwiggelaar RT, Mårvik R, Nordrum IS, Kidd M, Gustafsson BI. Relevance of TNBS-colitis in rats: a methodological study with endoscopic, histologic and Transcriptomic [corrected] characterization and correlation to IBD. *PLoS One* 2013; **8**: e54543 [PMID: 23382912 DOI: 10.1371/journal.pone.0054543]

67 **Chassaing B**, Aitken JD, Malleshappa M, Vijay-Kumar M. Dextran sulfate sodium (DSS)-induced colitis in mice. *Curr Protoc Immunol* 2014; **104**: 15.25.1-15.25.14 [PMID: 24510619 DOI: 10.1002/0471142735.im1525s104]

68 **Bramhall M**, Flórez-Vargas O, Stevens R, Brass A, Cruickshank S. Quality of methods reporting in animal models of colitis. *Inflamm Bowel Dis* 2015; **21**: 1248-1259 [PMID: 25989337 DOI: 10.1097/MIB.0000000000000369]

69 **Wirtz S**, Neufert C, Weigmann B, Neurath MF. Chemically induced mouse models of intestinal inflammation. *Nat Protoc* 2007; **2**: 541-546 [PMID: 17406617 DOI: 10.1038/nprot.2007.41]

70 **Wan P**, Liu X, Xiong Y, Ren Y, Chen J, Lu N, Guo Y, Bai A. Extracellular ATP mediates inflammatory responses in colitis *via* P2 × 7 receptor signaling. *Sci Rep* 2016; **6**: 19108 [PMID: 26739809 DOI: 10.1038/srep19108]

71 **Colombel JF**, Sandborn WJ, Rutgeerts P, Enns R, Hanauer SB, Panaccione R, Schreiber S, Byczkowski D, Li J, Kent JD, Pollack PF. Adalimumab for maintenance of clinical response and remission in patients with Crohn's disease: the CHARM trial. *Gastroenterology* 2007; **132**: 52-65 [PMID: 17241859 DOI: 10.1053/j.gastro.2006.11.041]

72 **Sandborn WJ**, Colombel JF, D'Haens G, Van Assche G, Wolf D, Kron M, Lazar A, Robinson AM, Yang M, Chao JD, Thakkar R. One-year maintenance outcomes among patients with moderately-to-severely active ulcerative colitis who responded to induction therapy with adalimumab: subgroup analyses from ULTRA 2. *Aliment Pharmacol Ther* 2013; **37**: 204-213 [PMID: 23173821 DOI: 10.1111/apt.12145]

73 **Eser A**, Colombel JF, Rutgeerts P, Vermeire S, Vogelsang H, Braddock M, Persson T, Reinisch W. Safety and Efficacy of an Oral Inhibitor of the Purinergic Receptor P2X7 in Adult Patients with Moderately to Severely Active Crohn's Disease: A Randomized Placebo-controlled, Double-blind, Phase IIa Study. *Inflamm Bowel Dis* 2015; **21**: 2247-2253 [PMID: 26197451 DOI: 10.1097/MIB.0000000000000514]

74 **Liu Y**, Liu X. Research progress of P2X7 receptor in inflammatory bowel disease. *Scand J Gastroenterol* 2019; **54**: 521-527 [PMID: 31056977 DOI: 10.1080/00365521.2019.1609077]

75 **Margolis KG**, Stevanovic K, Karamooz N, Li ZS, Ahuja A, D'Autréaux F, Saurman V, Chalazonitis A, Gershon MD. Enteric neuronal density contributes to the severity of intestinal inflammation. *Gastroenterology* 2011; **141**: 588-598, 598.e1 [PMID: 21635893 DOI: 10.1053/j.gastro.2011.04.047]

76 **Coquenlorge S**, Duchalais E, Chevalier J, Cossais F, Rolli-Derkinderen M, Neunlist M. Modulation of lipopolysaccharide-induced neuronal response by activation of the enteric nervous system. *J Neuroinflammation* 2014; **11**: 202 [PMID: 25497784 DOI: 10.1186/s12974-014-0202-7]

77 **Geboes K**, Collins S. Structural abnormalities of the nervous system in Crohn's disease and ulcerative colitis. *Neurogastroenterol Motil* 1998; **10**: 189-202 [PMID: 9659662 DOI: 10.1046/j.1365-2982.1998.00102.x]

78 **Cipriani G**, Gibbons SJ, Kashyap PC, Farrugia G. Intrinsic Gastrointestinal Macrophages: Their Phenotype and Role in Gastrointestinal Motility. *Cell Mol Gastroenterol Hepatol* 2016; **2**: 120-130.e1 [PMID: 27047989 DOI: 10.1016/j.jcmgh.2016.01.003]

79 **Clark IA**. How TNF was recognized as a key mechanism of disease. *Cytokine Growth Factor Rev* 2007; **18**: 335-343 [PMID: 17493863 DOI: 10.1016/j.cytogfr.2007.04.002]

80 **Osawa Y**, Banno Y, Nagaki M, Brenner DA, Naiki T, Nozawa Y, Nakashima S, Moriwaki H. TNF-alpha-induced sphingosine 1-phosphate inhibits apoptosis through a phosphatidylinositol 3-kinase/Akt pathway in human hepatocytes. *J Immunol* 2001; **167**: 173-180 [PMID: 11418646 DOI: 10.4049/jimmunol.167.1.173]

81 **Olmos G**, Lladó J. Tumor necrosis factor alpha: a link between neuroinflammation and excitotoxicity. *Mediators Inflamm* 2014; **2014**: 861231 [PMID: 24966471 DOI: 10.1155/2014/861231]

82 **Baune BT**, Wiede F, Braun A, Golledge J, Arolt V, Koerner H. Cognitive dysfunction in mice deficient for TNF- and its receptors. *Am J Med Genet B Neuropsychiatr Genet* 2008; **147B**: 1056-1064 [PMID: 18286589 DOI: 10.1002/ajmg.b.30712]

83 **Richter F**, Lütz W, Eitner A, Leuchtweis J, Lehmenkühler A, Schaible HG. Tumor necrosis factor reduces the amplitude of rat cortical spreading depression in vivo. *Ann Neurol* 2014; **76**: 43-53 [PMID: 24798682 DOI: 10.1002/ana.24176]

84 **Yang S**, Wang J, Brand DD, Zheng SG. Role of TNF-TNF Receptor 2 Signal in Regulatory T Cells and Its Therapeutic Implications. *Front Immunol* 2018; **9**: 784 [PMID: 29725328 DOI: 10.3389/fimmu.2018.00784]

85 **Slevin SM**, Egan LJ. New Insights into the Mechanisms of Action of Anti-Tumor Necrosis Factor-α Monoclonal Antibodies in Inflammatory Bowel Disease. *Inflamm Bowel Dis* 2015; **21**: 2909-2920 [PMID: 26348448 DOI: 10.1097/MIB.0000000000000533]

86 **Tracey D**, Klareskog L, Sasso EH, Salfeld JG, Tak PP. Tumor necrosis factor antagonist mechanisms of action: a comprehensive review. *Pharmacol Ther* 2008; **117**: 244-279 [PMID: 18155297 DOI: 10.1016/j.pharmthera.2007.10.001]

87 **Chen G**, Goeddel DV. TNF-R1 signaling: a beautiful pathway. *Science* 2002; **296**: 1634-1635 [PMID: 12040173 DOI: 10.1126/science.1071924]

88 **Wajant H**, Scheurich P. TNFR1-induced activation of the classical NF-κB pathway. *FEBS J* 2011; **278**: 862-876 [PMID: 21232017 DOI: 10.1111/j.1742-4658.2011.08015.x]

89 **Gan Y**, Long J, Zeng Y, Zhang Y, Tao Y. lncRNA IL-17RA-1 Attenuates LPS-Induced Sepsis *via* miR-7847-3p/PRKCG-Mediated MAPK Signaling Pathway. *Mediators Inflamm* 2022; **2022**: 9923204 [PMID: 36274974 DOI: 10.1155/2022/9923204]

90 **Jurewicz A**, Matysiak M, Tybor K, Selmaj K. TNF-induced death of adult human oligodendrocytes is mediated by c-jun NH2-terminal kinase-3. *Brain* 2003; **126**: 1358-1370 [PMID: 12764057 DOI: 10.1093/brain/awg146]

91 **Cabal-Hierro L**, Lazo PS. Signal transduction by tumor necrosis factor receptors. *Cell Signal* 2012; **24**: 1297-1305 [PMID: 22374304 DOI: 10.1016/j.cellsig.2012.02.006]

92 **MacEwan DJ**. TNF receptor subtype signalling: differences and cellular consequences. *Cell Signal* 2002; **14**: 477-492 [PMID: 11897488 DOI: 10.1016/S0898-6568(01)00262-5]

93 **Wajant H**, Henkler F, Scheurich P. The TNF-receptor-associated factor family: scaffold molecules for cytokine receptors, kinases and their regulators. *Cell Signal* 2001; **13**: 389-400 [PMID: 11384837 DOI: 10.1016/S0898-6568(01)00160-7]

94 **Naudé PJ**, den Boer JA, Luiten PG, Eisel UL. Tumor necrosis factor receptor cross-talk. *FEBS J* 2011; **278**: 888-898 [PMID: 21232019 DOI: 10.1111/j.1742-4658.2011.08017.x]

95 **Zhao Y**, Conze DB, Hanover JA, Ashwell JD. Tumor necrosis factor receptor 2 signaling induces selective c-IAP1-dependent ASK1 ubiquitination and terminates mitogen-activated protein kinase signaling. *J Biol Chem* 2007; **282**: 7777-7782 [PMID: 17220297 DOI: 10.1074/jbc.M609146200]

96 **Walczak H**. TNF and ubiquitin at the crossroads of gene activation, cell death, inflammation, and cancer. *Immunol Rev* 2011; **244**: 9-28 [PMID: 22017428 DOI: 10.1111/j.1600-065X.2011.01066.x]

97 **Grell M**, Wajant H, Zimmermann G, Scheurich P. The type 1 receptor (CD120a) is the high-affinity receptor for soluble tumor necrosis factor. *Proc Natl Acad Sci U S A* 1998; **95**: 570-575 [PMID: 9435233 DOI: 10.1073/pnas.95.2.570]

98 **Weiss T**, Grell M, Hessabi B, Bourteele S, Müller G, Scheurich P, Wajant H. Enhancement of TNF receptor p60-mediated cytotoxicity by TNF receptor p80: requirement of the TNF receptor-associated factor-2 binding site. *J Immunol* 1997; **158**: 2398-2404 [PMID: 9036990]

99 **Fotin-Mleczek M**, Henkler F, Samel D, Reichwein M, Hausser A, Parmryd I, Scheurich P, Schmid JA, Wajant H. Apoptotic crosstalk of TNF receptors: TNF-R2-induces depletion of TRAF2 and IAP proteins and accelerates TNF-R1-dependent activation of caspase-8. *J Cell Sci* 2002; **115**: 2757-2770 [PMID: 12077366 DOI: 10.1242/jcs.115.13.2757]

100 **Eissner G**, Kolch W, Scheurich P. Ligands working as receptors: reverse signaling by members of the TNF superfamily enhance the plasticity of the immune system. *Cytokine Growth Factor Rev* 2004; **15**: 353-366 [PMID: 15450251 DOI: 10.1016/j.cytogfr.2004.03.011]

101 **Kałużna A**, Olczyk P, Komosińska-Vassev K. The Role of Innate and Adaptive Immune Cells in the Pathogenesis and Development of the Inflammatory Response in Ulcerative Colitis. *J Clin Med* 2022; **11** [PMID: 35054093 DOI: 10.3390/jcm11020400]

102 **Shouval DS**, Rufo PA. The Role of Environmental Factors in the Pathogenesis of Inflammatory Bowel Diseases: A Review. *JAMA Pediatr* 2017; **171**: 999-1005 [PMID: 28846760 DOI: 10.1001/jamapediatrics.2017.2571]

103 **Li J**, Jia H, Cai X, Zhong H, Feng Q, Sunagawa S, Arumugam M, Kultima JR, Prifti E, Nielsen T, Juncker AS, Manichanh C, Chen B, Zhang W, Levenez F, Wang J, Xu X, Xiao L, Liang S, Zhang D, Zhang Z, Chen W, Zhao H, Al-Aama JY, Edris S, Yang H, Hansen T, Nielsen HB, Brunak S, Kristiansen K, Guarner F, Pedersen O, Doré J, Ehrlich SD; MetaHIT Consortium, Bork P, Wang J; MetaHIT Consortium. An integrated catalog of reference genes in the human gut microbiome. *Nat Biotechnol* 2014; **32**: 834-841 [PMID: 24997786 DOI: 10.1038/nbt.2942]

104 **Pawłowska-Kamieniak A**, Krawiec P, Pac-Kożuchowska E. Interleukin 6: Biological significance and role in inflammatory bowel diseases. *Adv Clin Exp Med* 2021; **30**: 465-469 [PMID: 33908198 DOI: 10.17219/acem/130356]

105 **Moldoveanu AC**, Diculescu M, Braticevici CF. Cytokines in inflammatory bowel disease. *Rom J Intern Med* 2015; **53**: 118-127 [PMID: 26402980 DOI: 10.1515/rjim-2015-0016]

106 **Nakase H**, Sato N, Mizuno N, Ikawa Y. The influence of cytokines on the complex pathology of ulcerative colitis. *Autoimmun Rev* 2022; **21**: 103017 [PMID: 34902606 DOI: 10.1016/j.autrev.2021.103017]

107 **Fakhoury M**, Negrulj R, Mooranian A, Al-Salami H. Inflammatory bowel disease: clinical aspects and treatments. *J Inflamm Res* 2014; **7**: 113-120 [PMID: 25075198 DOI: 10.2147/JIR.S65979]

108 **Song K**, Wu D. Shared decision-making in the management of patients with inflammatory bowel disease. *World J Gastroenterol* 2022; **28**: 3092-3100 [PMID: 36051346 DOI: 10.3748/wjg.v28.i26.3092]

109 **Yamamoto-Furusho JK**. [Treatment of inflammatory bowel disease]. *Rev Gastroenterol Mex* 2012; **77** Suppl 1: 39-41 [PMID: 22939477 DOI: 10.1016/j.rgmx.2012.07.016]

110 **Rolak S**, Kane SV. Conventional Therapies for Crohn's Disease. *Gastroenterol Clin North Am* 2022; **51**: 271-282 [PMID: 35595414 DOI: 10.1016/j.gtc.2021.12.004]

111 **Moss AC**. Optimizing the use of biological therapy in patients with inflammatory bowel disease. *Gastroenterol Rep (Oxf)* 2015; **3**: 63-68 [PMID: 25567472 DOI: 10.1093/gastro/gou087]

112 **Cheifetz AS**, Abreu MT, Afif W, Cross RK, Dubinsky MC, Loftus EV Jr, Osterman MT, Saroufim A, Siegel CA, Yarur AJ, Melmed GY, Papamichael K. A Comprehensive Literature Review and Expert Consensus Statement on Therapeutic Drug Monitoring of Biologics in Inflammatory Bowel Disease. *Am J Gastroenterol* 2021; **116**: 2014-2025 [PMID: 34388143 DOI: 10.14309/ajg.0000000000001396]

113 **D'Haens GR**, van Deventer S. 25 years of anti-TNF treatment for inflammatory bowel disease: lessons from the past and a look to the future. *Gut* 2021; **70**: 1396-1405 [PMID: 33431575 DOI: 10.1136/gutjnl-2019-320022]

114 **Hanauer SB**, Sandborn WJ, Rutgeerts P, Fedorak RN, Lukas M, MacIntosh D, Panaccione R, Wolf D, Pollack P. Human anti-tumor necrosis factor monoclonal antibody (adalimumab) in Crohn's disease: the CLASSIC-I trial. *Gastroenterology* 2006; **130**: 323-33; quiz 591 [PMID: 16472588 DOI: 10.1053/j.gastro.2005.11.030]

115 **Griffiths OR**, Landon J, Coxon RE, Morris K, James P, Adams R. Inflammatory bowel disease and targeted oral anti-TNF α therapy. *Adv Protein Chem Struct Biol* 2020; **119**: 157-198 [PMID: 31997768 DOI: 10.1016/bs.apcsb.2019.08.009]

116 **Zhu M**, Ran Z. Clinical characteristics of ulcerative colitis in elderly patients. *JGH Open* 2021; **5**: 849-854 [PMID: 34386591 DOI: 10.1002/jgh3.12612]

117 **Little RD**, Ward MG, Wright E, Jois AJ, Boussioutas A, Hold GL, Gibson PR, Sparrow MP. Therapeutic Drug Monitoring of Subcutaneous Infliximab in Inflammatory Bowel Disease-Understanding Pharmacokinetics and Exposure Response Relationships in a New Era of Subcutaneous Biologics. *J Clin Med* 2022; **11** [PMID: 36294494 DOI: 10.3390/jcm11206173]

118 **Alkhayyat M**, Abureesh M, Gill A, Khoudari G, Abou Saleh M, Mansoor E, Regueiro M. Lower Rates of Colorectal Cancer in Patients With Inflammatory Bowel Disease Using Anti-TNF Therapy. *Inflamm Bowel Dis* 2021; **27**: 1052-1060 [PMID: 33051651 DOI: 10.1093/ibd/izaa252]

119 **Papamichael K**, Gils A, Rutgeerts P, Levesque BG, Vermeire S, Sandborn WJ, Vande Casteele N. Role for therapeutic drug monitoring during induction therapy with TNF antagonists in IBD: evolution in the definition and management of primary nonresponse. *Inflamm Bowel Dis* 2015; **21**: 182-197 [PMID: 25222660 DOI: 10.1097/MIB.0000000000000202]

120 **von Andrian UH**, Engelhardt B. Alpha4 integrins as therapeutic targets in autoimmune disease. *N Engl J Med* 2003; **348**: 68-72 [PMID: 12510047 DOI: 10.1056/nejme020157]

121 **Erle DJ**, Briskin MJ, Butcher EC, Garcia-Pardo A, Lazarovits AI, Tidswell M. Expression and function of the MAdCAM-1 receptor, integrin alpha 4 beta 7, on human leukocytes. *J Immunol* 1994; **153**: 517-528 [PMID: 7517418 DOI: 10.4049/jimmunol.153.2.517]

122 **Arihiro S**, Ohtani H, Suzuki M, Murata M, Ejima C, Oki M, Kinouchi Y, Fukushima K, Sasaki I, Nakamura S, Matsumoto T, Torii A, Toda G, Nagura H. Differential expression of mucosal addressin cell adhesion molecule-1 (MAdCAM-1) in ulcerative colitis and Crohn's disease. *Pathol Int* 2002; **52**: 367-374 [PMID: 12100519 DOI: 10.1046/j.1440-1827.2002.01365.x]

123 **Fedyk ER**, Wyant T, Yang LL, Csizmadia V, Burke K, Yang H, Kadambi VJ. Exclusive antagonism of the α4 β7 integrin by vedolizumab confirms the gut-selectivity of this pathway in primates. *Inflamm Bowel Dis* 2012; **18**: 2107-2119 [PMID: 22419649 DOI: 10.1002/ibd.22940]

124 **Ransohoff RM**. Natalizumab and PML. *Nat Neurosci* 2005; **8**: 1275 [PMID: 16189528 DOI: 10.1038/nn1005-1275]

125 **Guillo L**, D'Amico F, Danese S, Peyrin-Biroulet L. Ustekinumab for Extra-intestinal Manifestations of Inflammatory Bowel Disease: A Systematic Literature Review. *J Crohns Colitis* 2021; **15**: 1236-1243 [PMID: 33367674 DOI: 10.1093/ecco-jcc/jjaa260]

126 **Honap S**, Meade S, Ibraheim H, Irving PM, Jones MP, Samaan MA. Effectiveness and Safety of Ustekinumab in Inflammatory Bowel Disease: A Systematic Review and Meta-Analysis. *Dig Dis Sci* 2022; **67**: 1018-1035 [PMID: 33723700 DOI: 10.1007/s10620-021-06932-4]

127 **Sands BE**, Sandborn WJ, Panaccione R, O'Brien CD, Zhang H, Johanns J, Adedokun OJ, Li K, Peyrin-Biroulet L, Van Assche G, Danese S, Targan S, Abreu MT, Hisamatsu T, Szapary P, Marano C; UNIFI Study Group. Ustekinumab as Induction and Maintenance Therapy for Ulcerative Colitis. *N Engl J Med* 2019; **381**: 1201-1214 [PMID: 31553833 DOI: 10.1056/NEJMoa1900750]

128 **Chandrasekharan B**, Jeppsson S, Pienkowski S, Belsham DD, Sitaraman SV, Merlin D, Kokkotou E, Nusrat A, Tansey MG, Srinivasan S. Tumor necrosis factor-neuropeptide Y cross talk regulates inflammation, epithelial barrier functions, and colonic motility. *Inflamm Bowel Dis* 2013; **19**: 2535-2546 [PMID: 24108115 DOI: 10.1097/01.MIB.0000437042.59208.9f]

129 **Milani C**, Duranti S, Bottacini F, Casey E, Turroni F, Mahony J, Belzer C, Delgado Palacio S, Arboleya Montes S, Mancabelli L, Lugli GA, Rodriguez JM, Bode L, de Vos W, Gueimonde M, Margolles A, van Sinderen D, Ventura M. The First Microbial Colonizers of the Human Gut: Composition, Activities, and Health Implications of the Infant Gut Microbiota. *Microbiol Mol Biol Rev* 2017; **81** [PMID: 29118049 DOI: 10.1128/MMBR.00036-17]

130 **Rooks MG**, Garrett WS. Gut microbiota, metabolites and host immunity. *Nat Rev Immunol* 2016; **16**: 341-352 [PMID:

27231050 DOI: 10.1038/nri.2016.42]

131 **Capaldo CT**, Powell DN, Kalman D. Layered defense: how mucus and tight junctions seal the intestinal barrier. *J Mol Med (Berl)* 2017; **95**: 927-934 [PMID: 28707083 DOI: 10.1007/s00109-017-1557-x]

132 **Takiishi T**, Fenero CIM, Câmara NOS. Intestinal barrier and gut microbiota: Shaping our immune responses throughout life. *Tissue Barriers* 2017; **5**: e1373208 [PMID: 28956703 DOI: 10.1080/21688370.2017.1373208]

133 **Chelakkot C**, Ghim J, Ryu SH. Mechanisms regulating intestinal barrier integrity and its pathological implications. *Exp Mol Med* 2018; **50**: 1-9 [PMID: 30115904 DOI: 10.1038/s12276-018-0126-x]

134 **Neurath MF**. Cytokines in inflammatory bowel disease. *Nat Rev Immunol* 2014; **14**: 329-342 [PMID: 24751956 DOI: 10.1038/nri3661]

135 **Bassotti G**, Antonelli E, Villanacci V, Nascimbeni R, Dore MP, Pes GM, Maconi G. Abnormal gut motility in inflammatory bowel disease: an update. *Tech Coloproctol* 2020; **24**: 275-282 [PMID: 32062797 DOI: 10.1007/s10151-020-02168-y]

136 **da Silva MV**, Marosti AR, Mendes CE, Palombit K, Castelucci P. Submucosal neurons and enteric glial cells expressing the P2X7 receptor in rat experimental colitis. *Acta Histochem* 2017; **119**: 481-494 [PMID: 28501138 DOI: 10.1016/j.acthis.2017.05.001]

World Journal of Gastroenterology

Submit a Manuscript: https://www.f6publishing.com

World J Gastroenterol 2023 May 14; 29(18): 2747-2763

DOI: 10.3748/wjg.v29.i18.2747

ISSN 1007-9327 (print) ISSN 2219-2840 (online)

REVIEW

Current trends in acute pancreatitis: Diagnostic and therapeutic challenges

Enver Zerem, Admir Kurtcehajic, Suad Kunosić, Dina Zerem Malkočević, Omar Zerem

Specialty type: Gastroenterology and hepatology

Provenance and peer review: Invited article; Externally peer reviewed.

Peer-review model: Single blind

Peer-review report's scientific quality classification

Grade A (Excellent): 0
Grade B (Very good): B
Grade C (Good): C
Grade D (Fair): 0
Grade E (Poor): 0

P-Reviewer: Matsuo Y, Japan; Tellez-Avila F, United States

Received: January 9, 2023
Peer-review started: January 9, 2023
First decision: February 1, 2023
Revised: February 7, 2023
Accepted: April 18, 2023
Article in press: April 18, 2023
Published online: May 14, 2023

Enver Zerem, Department of Medical Sciences, The Academy of Sciences and Arts of Bosnia and Herzegovina, Sarajevo 71000, Bosnia and Herzegovina

Admir Kurtcehajic, Department of Gastroenterology and Hepatology, Plava Medical Group, Tuzla 75000, Bosnia and Herzegovina

Suad Kunosić, Department of Physics, Faculty of Natural Sciences and Mathematics, University of Tuzla, Tuzla 75000, Bosnia and Herzegovina

Dina Zerem Malkočević, Omar Zerem, Department of Internal Medicine, Cantonal Hospital "Safet Mujić" Mostar, Mostar 88000, Bosnia and Herzegovina

Corresponding author: Enver Zerem, MD, PhD, Professor, Department of Medical Sciences, The Academy of Sciences and Arts of Bosnia and Herzegovina, Bistrik 7, Sarajevo 71000, Bosnia and Herzegovina. zerem@live.com

Abstract

Acute pancreatitis (AP) is an inflammatory disease of the pancreas, which can progress to severe AP, with a high risk of death. It is one of the most complicated and clinically challenging of all disorders affecting the abdomen. The main causes of AP are gallstone migration and alcohol abuse. Other causes are uncommon, controversial and insufficiently explained. The disease is primarily characterized by inappropriate activation of trypsinogen, infiltration of inflammatory cells, and destruction of secretory cells. According to the revised Atlanta classification, severity of the disease is categorized into three levels: Mild, moderately severe and severe, depending upon organ failure and local as well as systemic complications. Various methods have been used for predicting the severity of AP and its outcome, such as clinical evaluation, imaging evaluation and testing of various biochemical markers. However, AP is a very complex disease and despite the fact that there are of several clinical, biochemical and imaging criteria for assessment of severity of AP, it is not an easy task to predict its subsequent course. Therefore, there are existing controversies regarding diagnostic and therapeutic modalities, their effectiveness and complications in the treatment of AP. The main reason being the fact, that the pathophysiologic mechanisms of AP have not been fully elucidated and need to be studied further. In this editorial article, we discuss the efficacy of the existing diagnostic and therapeutic modalities, complications and treatment failure in the management of AP.

Key Words: Pancreatitis; Etiology and pathogenesis; Diagnostic criteria; Nutrition; Antibiotics; Management of complications

©The Author(s) 2023. Published by Baishideng Publishing Group Inc. All rights reserved.

Core Tip: Acute pancreatitis (AP) is an inflammatory disease of the pancreas, with abnormal trypsinogen activation as the primary pathogenesis and varies from clinically mild to fulminant form. Severe forms of AP are a relatively common cause of death. Progress in the establishment of biochemical, imaging and clinical criteria for the severity and prognosis of the disease has markedly influenced the therapeutic approach and the outcome of the disease. This article presents the diagnostic and therapeutic modalities with regard to their effectiveness, complications and treatment failure, as well as discussing some of the controversial issues in the treatment of AP.

Citation: Zerem E, Kurtcehajic A, Kunosić S, Zerem Malkočević D, Zerem O. Current trends in acute pancreatitis: Diagnostic and therapeutic challenges. *World J Gastroenterol* 2023; 29(18): 2747-2763
URL: https://www.wjgnet.com/1007-9327/full/v29/i18/2747.htm
DOI: https://dx.doi.org/10.3748/wjg.v29.i18.2747

INTRODUCTION

Acute pancreatitis (AP) is an inflammatory pancreatic disease affecting all ages, with an annual incidence of 10-50 cases per 100000 persons[1]. The main causes of AP are gallstone migration and alcohol abuse. Among these, predominance of one cause over the other depends on socioeconomic, ethnic, and cultural differences[2-5].

Most patients with AP present with a mild and self-limited disease. Conversely, 15%-20% patients with AP develop local and/or systemic complications, frequently leading in multiple (respiratory, cardiovascular, renal, and hepatic) organ failure (MOF) and death. According to the revised Atlantic classification, the severity of AP is divided into three levels: Mild, moderately severe, and severe, based on organ failure as well as local and systemic complications[3]. However, the pathophysiologic mechanism of AP has not been fully elucidated and there are several controversies regarding the diagnostic and therapeutic modalities due to their effectiveness and complications in the treatment of the disease. These controversies primarily relate to the therapeutic treatment at the early stage of the disease, which includes fluid resuscitation, including the most appropriate type of fluid to use, as well as the time, volume, and rate of administration. Other controversies include the timing of restart and the importance of nutritional support, the role of prophylactic antibiotics, the timing of application of more aggressive methods including surgery, as well as the treatment of complications which can negatively impact the patient's prognosis and quality of life[4-6].

This editorial article presents the most important diagnostic and therapeutic modalities with respect to their efficacy, complications and treatment failure in the treatment of AP.

ETIOLOGY OF AP

There are multiple causes and pathological conditions potentially associated with AP (Table 1). It is generally accepted that gallstones and alcohol abuse are responsible for about 90% of all cases of AP. The role of gallstones is very important in the etiopathogenesis of AP and any finding indicating the presence of gallstones in the gallbladder or biliary tract in patients with AP can be classified as the cause of the disease. Therefore, all patients with AP should be screened by ultrasound for the presence of cholecystolithiasis, common bile duct stones, or diagnose signs of biliary obstruction[2,7,8]. Alcohol-induced pancreatitis is more common in young and middle-aged people in whom an idiosyncratic sensitivity to alcohol may exist at levels of alcohol exceeding 80 g/dL. Other predisposing factors may be the level of alcohol dehydrogenase activity in the gastric mucosa and the liver[2,7,8].

Hypertriglyceridemia (triglycerides > 600 mg) is well-known cause of AP. One of the predominant causes of serum triglycerides elevation is alcohol intake. Therefore, it is sometimes challenging to assess whether the cause of AP is alcohol consumption or hypertriglyceridemia[9-11].

A large variety of drugs have been related to AP. Although, some drugs such as diuretics, azathioprine, sulfonamides, drugs used in the treatment of acquired immunodeficiency syndrome such as didanosine and zalcitabine, and steroids can cause AP through a direct toxic effect, most cases of drug-related pancreatitis are probably triggered by individual sensitivity. In large epidemiological

Table 1 Etiology of acute pancreatitis

Causes of acute pancreatitis
Toxic and metabolic
Alcohol
Hyperlipidemia (triglycerides > 600 mg)
Hypercalcemia (hyperparathyroidism)
Diabetes mellitus
Hypothyroidism
Uremia
Drugs (medicaments)
Scorpion venom
Mechanical
Gallstones, biliary sludge
Ampullary obstruction (Crohn's disease, villous tumors of the ampulla)
Pancreatic obstruction (pancreatic tumor, chronic pancreatitis)
Sphincter of Oddi dysfunction
Pancreas divisium
Post ERCP-pancreatitis
Congenital malformation
Trauma
Others
Ischemia
Organ transplantation (bone marrow transplantation)
Iatrogenic injury
Infection
Hereditary
Autoimmune
Cystic fibrosis
Tropical (Ascaris lumbricoides)
Idiopathic pancreatitis

ERCP: Endoscopic retrograde cholangiopancreatography.

studies, it has been proven that potentially pancreatotoxic drugs are not independent risk factors for the development of AP. The interval from the beginning of drug intake to the development of AP is highly variable and ranges from a few weeks, in a drug-induced immunologic reaction, to several months, when accumulation of toxic metabolites (*e.g.* valporic acid, pentamidine, didanosine) is required. The mechanism of AP for many of these medications is obscure[12-16].

PATHOGENESIS OF AP

AP is predominantly acute inflammatory process which involves the parenchyma of the pancreas, with involvement of other regional tissues or distant organ systems in severe forms of the disease. The pathogenic mechanism of AP is presented by inappropriate activation of trypsinogen and destruction of secretory cells followed by systemic release of cytokines and inflammatory mediators, causing the activation of inflammatory cells, fever and MOF. Calcium overload, mitochondrial dysfunction, impaired autophagy, endoplasmic reticulum stress, and exosomes are other factors in pathogenesis of the disease[16]. Edema of pancreatic and peripancreatic tissues and fat necrosis are common in all forms

of AP (mild, moderately severe and severe) however, in the severe AP (SAP), there is a possibility of hemorrhage within the pancreas[4,7,17,18].

Cellular necrosis elements (acinar cells, duct cell, and islet cells) are considerable in SAP but necrosis is usually absent in mild and moderate forms of the disease. During SAP, pancreatic necrosis (PN) develops due to impairment in pancreatic microcirculation and its complete development takes usually several (approximately 4-7) day after the beginning of the disease but, the development of PN is not strictly fixed in time and may progress during the first 2 wk[4,16-18]. During that period, PN is usual sterile and its infection is extremely rare. After the first 1-2 wk, the development of secondary infection in PN, due to translocation of intestinal flora, is associated with increased morbidity and mortality[4].

Early in the course of AP, acute pancreatic fluid collections (APFC) can occur as amylase-rich and protein-rich pancreatic juice collections and they usually resolve spontaneously. Pancreatic fluid collections, which present for more than 4 wk, are usually caused by disruption of pancreatic duct (PD) with extravasation of pancreatic juice and they are termed as pancreatic pseudocysts (PPC) or pancreatic walled-off necrosis (WON). Extra-pancreatic manifestations of SAP include systemic inflammatory response syndrome (SIRS) following by systemic MOF or exacerbation of serious pre-existing illness related to AP[4,16-18].

DIAGNOSIS OF AP

Diagnosis of AP is based on clinical presentation, laboratory tests, and imaging findings and requires two out of the following three criteria to be present: Clinical (acute pain attack in the upper abdomen spreading to the back), laboratory (serum lipase and/or amylase levels are three or more times higher than normal values) and typical imaging [computed tomography (CT), magnetic resonance imaging, ultrasonography] findings that are characteristic for AP[5].

The most common presenting symptoms of the disease are abdominal pain (80%–95%) followed by nausea and vomiting (40%–80%), rebound tenderness, breathlessness, impaired consciousness with pyrexia, distension and reduced bowel sounds[4,16].

The diagnosis of AP can be supported by serum and urinary laboratory tests to clarify its origin. They usually reflect organ dysfunction and metabolic disturbances. Amylase is traditionally the laboratory test of choice but, given its higher sensitivity and specificity, lipase (serum level greater than three times normal appears) is more valuable test for diagnosing of AP. The elevation of these enzymes in the serum occurs due to the leakage of pancreatic acinar cells into the interstitial space followed by their subsequent absorption into the circulation[19-21]. Some authors consider that the lipase/amylase ratio can be a crucial parameter in establishing alcohol as the etiology of AP. Transaminases are mostly used in differentiation biliary from other causes of AP[22]. The negative predictive value of urinary trypsinogen-2 level is 99%. Therefore, urinary trypsinogen-2 levels accurately diagnose AP and may be considered as useful markers to determine extra-pancreatic inflammation in AP[19,23,24]. Serum immunoreactive trypsin, chymotrypsin, elastase, phospholipase A2, alfa2-macroglobulin, methem-albumin, and carboxipeptides levels have been suggested in diagnosing AP. However, these tests are not in routine use and are not commercially available[25,26].

When the clinical presentation is typical but the laboratory parameters are ambiguous or inconclusive, imaging techniques are necessary. Contrast-enhanced CT (CECT) is the most performed imaging test and the modality of choice for the diagnosis of PN, the determination of its extent, and the diagnosis of local complications[4,27-29]. However, the complete development of PN takes usually several (approximately 4-7) days from the beginning of the disease and CECT cannot be applied to reliably assess the presence and extent of necrosis before that time[1,4].

Magnetic resonance imaging is a good alternative to CECT due to its superiority soft tissue contrast resolution and better evaluation of the biliary tree and PD. Also, this method can be used as a substitute for endoscopic retrograde cholangiopancreatography (ERCP) in the diagnostic evaluation of the PD[4, 30-32].

Ultrasound, endoscopic ultrasound and ERCP are adjuncts to CECT and they are used for the diagnosis of cholelithiasis, disconnected PD, evaluation of the collection contents, and follow-up imaging. Imaging examinations are usually not necessary in an emergency when the clinical presentation and laboratory tests are consistent with features of AP[1,4,28,33,34].

PREDICTION OF SEVERITY AND OUTCOME OF AP

AP varies from clinically mild to fulminating disease and has been recorded as a cause of sudden death. The outcome of acute attack depends in part on the etiology and in part on the severity of the attack. It is generally accepted that death from AP has a bimodal temporal distribution: Early mortality is the consequence of SIRS followed by MOF, while late mortality is caused by superinfection of PNs and peripancreatic fluid collections resulting in sepsis[4,7,34,35].

Advances made in establishing diagnostic criteria for the severity and prognosis of an attack have markedly influenced therapeutic approach. Several multifactorial scoring systems (Ranson, APACHE II, Glasgow-Imrie, SOFA, Balthazar, BISOP, *etc*.) have been extensively applied with the goal of predicting which patients might have a severe clinical course and which of them will recover without major complications[7,20,21,36-41].

A commonly accepted definition of SAP was not established until 1993, when the first version of the Atlanta classification for AP was published. The classification emphasizes the difference between milder interstitial form of AP from SAP related to 'local complications', but do not contain a clear definition of pancreatic and peripancreatic collections that was standardized worldwide[42]. The classification was revised in 2012[1,3], defining early and late AP which can be either edematous interstitial or necrotizing one. According to the severity of the disease, AP is divided into mild, moderately severe, and severe form, based on organ failure as well as local and systemic complications. AP collections are differentiated into APFC, PPC, acute necrotic collection, and pancreatic WON, according to the type of AP[1,3,7] (Figure 1).

However, the value of early prognostic evaluation of AP remains uncertain due to the fact that patients who have the same initial predicting scores often have very different subsequent clinical courses of the disease. Also, the relevance of the prognostic evaluation is markedly affected by the lack of widely accepted definition of severity and outcome of the disease[1,4,7].

INITIAL TREATMENT OF AP

AP is a dynamic disease process in which most attacks are mild (mild and moderately severe forms), AP is a dynamic disease process in which most attacks are mild (mild and moderately severe forms), with ongoing recovery after a few days of conservative supportive therapy. However, some patients with SAP can develop local and/or systemic complications and MOF. There are two treatment periods in AP: Early treatment of the acute attack should be applied in both mild and severe forms of AP, while late management includes treatment of SAP complications. The most important measures of intensive monitoring and supportive therapeutic procedures in AP are presented in Table 2.

In early stage of AP, all patients require appropriate conservative treatment and sufficient nutritional support. Most patients with mild or moderately SAP will recover with conservative treatment that includes correction of hypovolemia and hypoxemia, as well as pain relief. For a long time, correction of hypovolemia, even with mild AP, was carried out by early aggressive hydration with monitoring vital constants and urine output[3,5,6,42-44]. However, there is conflicting evidence regarding the fluid management strategy both in terms of fluid type, optimal volume and rate of administration, as well as severity of AP. Several recent randomized trials showed that early aggressive fluid resuscitation, in patients with AP, resulted in a higher incidence of fluid overload (with potentially increasing risk for acute kidney injury and pulmonary edema) without improvement in clinical outcomes[45-48]. Other, also randomized controlled trials, reported that early aggressive intravenous hydration hastens clinical improvement in patients with AP and that aggressive fluid strategy is beneficial especially for certain subsets of patients and some types of AP[48-51]. Most authors agree that these discrepancies are not fully elucidated and that future studies are needed to investigate which fluid management strategy is optimal for majority of the patients and which subsets of patients with AP may benefit from different management of fluid replacement[6,47].

Pain control is a very important therapeutic measure in the early stage of AP and can be provided by appropriate intravenous administration of a non-opiate analgesic. Opiates (*e.g*., meperidine) may also be given as required[52-54]. Some recent systematic reviews and meta-analysis suggest that epidural anesthesia is safe and effective in reducing pain severity, improving pancreatic perfusion, and decreasing mortality, within the first 24 h of AP onset. However, there is paucity of evidence to guide pain management in AP with small datasets per study[55,56] Hypoxemia is a rare event in mild and moderately SAP but, in severe forms of the disease, respiratory insufficiency with hypoxemia is often present as single organ failure. Hypoxemia could be avoided by ensuring airway patency and supplemental application of humidified oxygen, which would allow maintenance of arterial oxygen saturation above 95%. In case of development of respiratory insufficiency, mechanical ventilation with positive expiratory pressure is mandatory[4-6,43,44].

Conversely, patients with SAP are at high risk of developing PN, MOF, and septic complications. The most important therapeutic goals in the initial treatment of SAP are the provision of supportive therapy and the treatment of specific complications that may occur at the beginning of the disease[4].

Nutritional support

The nutritional management strategy for patients with AP has generated intense debate over the past few decades. Oral nutrition should be restarted immediately in patients with preserved gastrointestinal peristalsis, without abdominal pain, nausea, vomiting, or evidence for intestinal obstruction or ileus[5,18]. Most patients with SAP have increased basal energy needs, pronounced protein catabolism and endogenous gluconeogenesis.

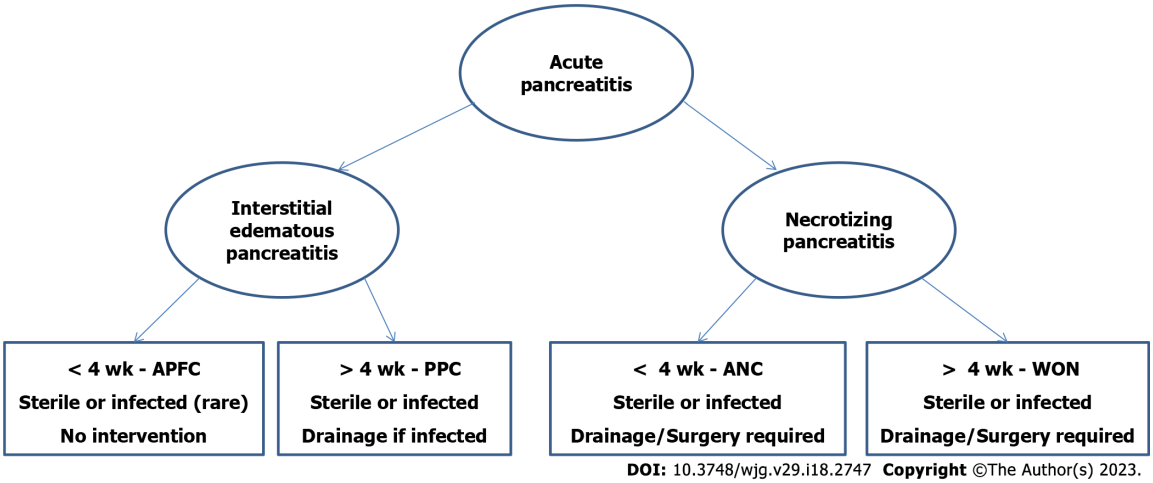
Table 2 Management of acute pancreatitis

Cornerstone treatment measures
Intensive monitoring and support of cardiac, pulmonary, renal, and hepatobiliary functions
Fluid resuscitation with monitoring of vital constants and urine output
Electrolyte solutions and Plasma expanders
Humidified oxygen administration
Catecholamine (dopamine, dobutamine) to prevent renal failure
Appropriate nutritional support
Early treatment of systemic complications
Mechanical ventilation with positive end-expiratory pressure
Catecholamine (epinephrine) if shock develops
Hemofiltration, dialysis
Insulin and calcium substitution to treat metabolic complications
Prevention of infectious complications
Biliary tract management
Management of necrotizing pancreatitis
Conservative, Imaging, Endoscopic, Surgical management
Management of late complications
Pancreatic pseudocysts
Walled-off pancreatic necrosis
Disconnected pancreatic duct syndrome/pancreatic fistula
Acute non-infectious complications in acute pancreatitis
Intra-abdominal hypertension
Pseudoaneurysm
Venous thrombosis
Bowel fistula
Management of special types of acute pancreatitis
Pediatric
Hyperparathyroidism
Hypertriglyceridemia
Post-ERCP pancreatitis
Trauma
Pregnancy
Long term complications and long-term care

ERCP: Endoscopic retrograde cholangiopancreatography.

The purpose of nutritional support is the reduction of wasting, to support the structure and function of organs, and to have a positive influence on the clinical course of the disease. Also, if patients with SAP develop paralytic ileus as a complication of the disease, keeping the pancreas at rest is necessary. Since they require nutritional support to achieve a positive nitrogen balance, parenteral nutrition should be started as soon as possible with the aim to achieve a positive nitrogen balance within the first 72 h after the onset of the disease[4].

However, SAP represents a typical model of septic syndrome due to the gastrointestinal barrier failure, which reduces gastrointestinal motility and damages mucosal integrity with subsequent increases in its permeability. This leads to an increased risk of bacterial overgrowth and their translocation from the intestinal tract to peripancreatic necrosis. Therefore, one of the main therapeutic goals in



DOI: 10.3748/wjg.v29.i18.2747 **Copyright** ©The Author(s) 2023.

Figure 1 The revised Atlanta Classification: Key terms diagram. APFC: Acute pancreatic fluid collection; PPC: Pancreatic pseudo cyst; ANC: Acute necrotic collection; WON: Walled-off necrosis.

SAP is to maintain intestinal integrity to prevent bacterial and endotoxin translocation and improve the immune system of the gastrointestinal tract. Administration of enteral feeding, with or without immunonutrition can maintain mucosal integrity and prevent or decrease bacterial translocation. Therefore, early nutritional support should be prioritized as soon as possible (optimally, within the first 24–72 h)[4,18,57-59].

Role of antibiotics

The presence of infected PN is the most important negative indicator and is the main cause responsible for morbidity and mortality in SAP. The infection organisms that are responsible for PN infection are mostly Gram-negative bacteria of intestinal origin, and they can reach PN through a previously damaged intestinal mucosal barrier[4,18].

Broad-spectrum antibiotics with ability to pass into PN (*e.g.*, carbapenems, quinolones, and metronidazole), should be prescribed only when infected necrosis is confirmed or strongly suspected [18]. However, the administration of antibiotic prophylaxis in order to prevent infection of sterile necrosis is controversial. Some authors advocate the use of prophylactic antibiotics in SAP considering that they can prevent the development of superinfection in necrotic tissues, which is the only measure of initial treatment of PNs, since their development are not preventable[4,18,60-65]. Some authors consider that there is a reduction in pancreatic infection in the subgroup of patients who received broad-spectrum antibiotics, concluding that more evidence is needed[60,61].

However, multiple prospective, randomized, placebo-controlled trials and most important guidelines have demonstrated that the routine use of prophylactic broad-spectrum antibiotics, in patients with SAP, has no influence on the development of infected necrosis, systemic complications, need for surgery, or mortality[18,62-65]. Besides, prolonged antibiotic therapy increases the prevalence of fungal infections[4,18,61]. Evidence supporting the prophylactic use of antifungal agents in patients with PN is lacking. Also, the use of probiotic prophylaxis is not suggested for the prevention of infectious complications in AP[18,62,63].

MANAGEMENT OF NECROTIZING PANCREATITIS

The development of extensive PN is a main cause of complications and mortality in patients with SAP. Therefore, it is very important to apply the best methods to identify patients with PN who require more aggressive interventions than those who could be treated with less aggressive measures. Different clinical entities, such as persistent pancreatic fluid collections, pancreatic fistula, persistent SIRS, obstructive jaundice, and ongoing symptoms can be detected during SAP and they can predict the severity of clinical course of the disease. Their management vary depending on the severity and the type of complication, since different complications require different treatment modalities. The revised Atlanta classification offers useful recommendations to determine the strategy for management of the SAP complications[1,3-5,18,66].

Step-up approach

The step-up approach is used, in the treatment of infected PN, as a less invasive alternative approach compared to early surgical necrosectomy. This approach is based on the statement that surgical

debridement should be delayed until demarcation of necrotic from normal tissue is established, which would reduce the risk of bleeding into the necrotic tissue during or after the surgical intervention. Several studies that have conducted long-term follow-up of clinical outcomes in patients with AP have shown that the step-up approach leads to a reduction in morbidity and mortality and should be preferred over the classic surgical approach if both methods are technically feasible[4,8,18,67-71].

However, there are still certain disagreements regarding the comparison of the endoscopic and surgical step-up approach. In a randomized trial, Bang *et al*[72], compared outcomes of the surgical *vs* endoscopic step-up approach and they reported that the endoscopic was superior to the surgical step-up approach in reducing major complications, lowered costs, and increased quality of life in patients with infected PN[72]. Dutch Pancreatitis Study Group, in the TENSION trial, reported that the endoscopic approach may be more suitable than the surgical step-up approach, in the treatment of infected PN, based on favorable short-term outcomes. However, they presented that the endoscopic was not superior to the surgical step-up approach in reducing death or major complications in patients with infected PN, while the rate of pancreatic fistulas and length of hospital stay were lower in the endoscopy group[73-75]. Most experts in the discussion of this issue point out that the endoscopic approach is the best management for patients with infected PN, but that it is necessary to develop common protocols for endoscopic approach, based on all the observations and suggestions[76-79]. Finally, it can be concluded that, some segments of the step-up approach can be changed and improved, but its basic concept (delay, drain, and debride) remains as the reference standard intervention for PN[71].

The role of abdominal paracentesis drainage in necrotizing pancreatitis

If necrotizing pancreatitis is associated with liquefied necrotic debris in the pancreatic and peripancreatic regions, with the presence of abdominal and/or pelvic fluid several authors[80-85] have advocated the concept of removing the peritoneal fluid. The rationale for removing the peritoneal fluid is to reduce inflammation and disease severity since the intra-abdominal fluid, accumulated during the disease, may contain factors that trigger and increase the severity of AP, including proinflammatory mediators and infection.

In general, abdominal paracentesis drainage (APD) has the role of a preparatory procedure before the application of PCD with the intent to achieve better result than through conventional step-up approach. Therefore, the integration of APD into a step-up approach is beneficial for patients, due to the fact that this procedure removes great number of inflammatory factors from the seroperitoneum[82].

Management of sterile necrosis and acute fluid collections

Early in the course of AP, pancreatic inflammation, manifesting as partial or total PN, causes more liquefied areas and leads to extravasations of enzyme-rich pancreatic juice into the peripancreatic regions, with the consequent development of sterile necrosis and ANC. They usually resolve spontaneously and the vast majority of patients with sterile PN can be treated conservatively and without interventional procedures (*i.e.* catheter drainage or necrosectomy). However, if unresolved spontaneously, they can lead to a poor clinical course and allow active pancreatic enzymes to initiate physiologic pathways leading to MOF and sepsis[4,17].

Therefore, PCD or endoscopic drainage may be required in symptomatic patients with sterile PN and persistent malaise characterized by abdominal pain, nausea, vomiting, and nutritional failure or with associated complications, including gastrointestinal and/or biliary obstruction, persistent SIRS, or fistulas[5]. Continuous PCD may justify this approach based on the concept that elimination of cytokines and inflammatory mediators from initially sterile pancreatic juice collections may avoid or prevent systemic complications in severe forms of AP[4,17,86-90]. Besides, in cases whereby a high output of amylase-rich fluid continues to drain through the catheter, continued prolonged drainage is necessary despite the sterility of the collection[91].

Treatment of infected PN

The development of secondary infection in PN is associated with increased morbidity and mortality (15%–20%) and there is consensus that infected necrotic tissue should be removed in order to prevent the sepsis[4,8,33,92,93]. A small proportion of patients with documented infected PN who remain clinically stable can be managed with only conservative treatment and close monitoring, without intervention[5]. The traditional method of treating patients with infected PN by laparotomy retains its role in the treatment of the disease. However, surgical intervention is performed under general anesthesia and causes significantly greater trauma compared to minimally invasive methods, with possible consequent worsening of organ dysfunction, profuse bleeding and sepsis as well as postoperative mortality[8,94,95]. Therefore, laparotomy should be delayed for as long as possible or avoided in order to decrease mortality and morbidity rates[96]. Although there is no globally accepted treatment modality and it should be tailored to each individual patient, the step-up approach starting with monitoring and conservative measures, followed by PCD or endoscopic drainage and minimally invasive VARD has been shown to produce superior outcomes to the traditional open necrosectomy in the treatment of infected PN[4,8,18,66-72,97-99].

Disconnected PD syndrome

Disconnected PD syndrome (DPDS) is anatomic condition which is usually seen in PN. Early in the course of necrotizing pancreatitis, pancreatic inflammation causes extravasation of pancreatic secretion into the pancreatic and perpancreatic tissues with the consequent development of sterile PN which may lead to the PD disruption and interruption of continuity between the duct in the left sided pancreas and the luminal gastrointestinal tract. In such clinical setting, when the PD has no continuity with the viable tissue of the pancreas, this part no longer drains its contents into the duodenum, but produces a persistent pancreatic fistula, there is a high probability of consequent peripancreatic collection formation [1,18,100-102].

There are three types of DPDS: Concurrent (there is necrosis of the neck and body, but there is perfusion of the tail of the pancreas), delayed (PPC or WON occupy the middle part of the gland but with the perfused left-sided remnant of the pancreas) and DPDS associated with chronic pancreatitis (PD is blocked by a stricture or calculus in the proximal part, leading to atrophy of the distal segment of the duct and resulting in the formation of PPC)[1,102].

Standard treatment for DPDS is operative resection of the disconnected pancreas[103,104]. PN causing DPDS could be initially treated with percutaneous[105], endoscopic, or minimally invasive surgical techniques as temporary measures. However, elective distal pancreatectomy is mandatory in most patients as definitive treatment for DPDS[106-108].

Pancreatic fistula

Pancreatic fistulas are the consequence of pancreatic autodigestion or necrosis that results in a persistent PD disruption. Disruption of the PD secondary to PN causes the lack of continuity between PD and the viable pancreatic tissue, so that this segment of the pancreas no longer drains into the duodenum, but into the surrounding regions (usually in the pancreatic tail area) leading to its accumulation and PPC formation[1,4,18,100]. However, pancreatic secretions can also reach distant sites, causing pancreatic ascites, pleural effusion, distant PPC, or pancreatocutaneous fistula. According to that, pancreatic fistulas can be divided into two groups: (1) Internal, in which the PD communicates with the peritoneal or pleural cavity or some other hollow viscus; and (2) external, where the PD communicates with the skin[1,4,100,105,109].

Treatment of pancreatic fistulas depends on both the site of duct disruption and presence or absence of downstream ductal obstruction or DPDS. In the beginning of the disease, the management is usually conservative including total parenteral nutrition and the administration of pancreatic secretory inhibitor octreotide. However, if this management fails interventional procedures (Figure 2) and surgery are the following options. Surgical intervention, for fistula treatment, is technically challenging and could be followed with major complications[100-102,106-112].

Pancreatic WON

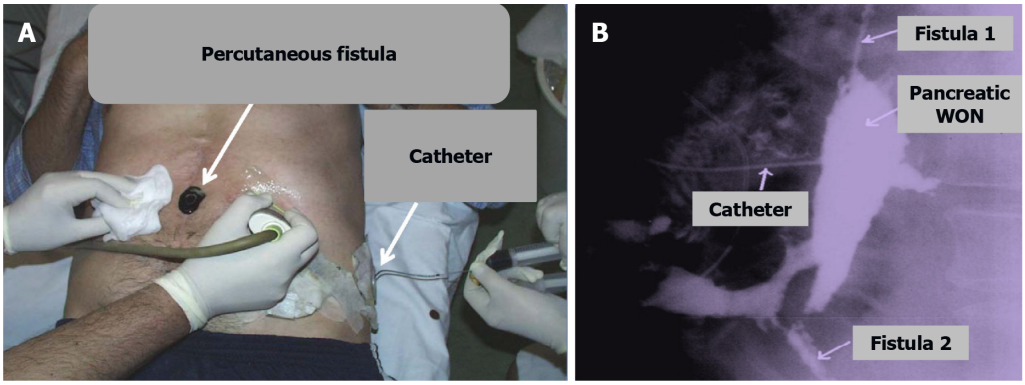
Pancreatic WON is a located WON of pus resulting from liquefaction of necrotic areas or secondary infection of acute PPC, with or without communication with main PD. WON occurs at a relatively late stage, most commonly three to five weeks after of onset of AP. APFCs tend to be poorly walled-off and can leak into retroperitoneum, the peritoneal cavity, the mediastinum, the pleura or the soft tissues. Pancreatic WON is a heterogeneous, low-density collection in a defined cavity containing gas bubbles (Figure 3). CECT scanning is the diagnostic test of choice. Diagnosis may be confirmed by percutaneous or endoscopic aspiration[113]. Asymptomatic WON does not mandate intervention and may resolve spontaneously over a period of time[29]. Symptomatic WON generally requires intervention. The most common treatment modality is PCD (Figure 2) or endoscopic drainage. Surgical drainage is done rarely, only when percutaneous drainage is not successful[114-116].

PPC

A PPC is a fluid collection usually found near the pancreas that is formed by the secretion of pancreatic juice from the inflamed parenchyma or from a disrupted duct. The PPC wall consists of fibrous non-epithelialized tissue[42]. PPC can sometimes appear at a great distance from the pancreas (*e.g.* thorax, groin) when the fluid dissects through tissue planes. At early stage of AP, APFC are common, but majority of them regress spontaneously and need no treatment. About 5% of patients with APFC develop PPCs, which are defined by their ellipsoidal shape and well-formed wall. Treatment for PPCs varies depending on their size and the presence of symptoms. Asymptomatic PPCs, less than 50 mm in diameter, should only be monitored by ultrasound. However, some of them may persist and progress to produce complications such as pain, infection, gastric outlet, intestinal or biliary obstruction. These PPCs are symptomatic and require treatment. The most common treatment modalities for symptomatic PPCs are minimally invasive approaches, such as PCD or endoscopic drainage. Surgical drainage is done rarely, only when percutaneous drainage is not successful[4,97,105,110,115-119].

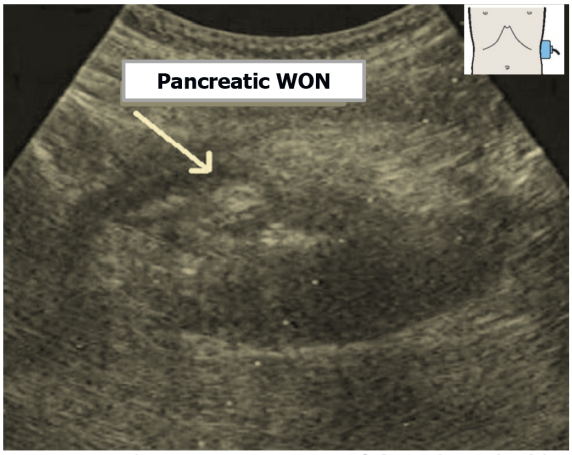
Hemorrhage

Upper gastrointestinal bleeding is common in AP and usually results from stress ulcers, peptic ulcer disease, or hemorrhagic gastroduodenitis. Massive hemorrhage occurs rare in AP, most commonly into



DOI: 10.3748/wjg.v29.i18.2747 **Copyright** ©The Author(s) 2023.

Figure 2 Treatment of pancreatic walled-off necrosis and two fistulas by percutaneous drainage. A: Appearance of iodine *via* cutaneous fistula after its instillation into the walled-off necrosis (WON); B: Retropancreatic WON with two fistulas. Fistula 1: Retropancreatic-percutaneous fistula; Fistula 2: Retropancreatic-sigmoidal fistula. WON: Walled-off necrosis.



DOI: 10.3748/wjg.v29.i18.2747 **Copyright** ©The Author(s) 2023.

Figure 3 Ultrasound appearance of pancreatic walled-off necrosis after acute necrotizing pancreatitis. WON: Walled-off necrosis.

the gastrointestinal tract, the abdominal cavity or into the PD. Erosion of the great pancreatic or peripancreatic vessel leads to rupture or formation of a pseudoaneurysm. The splenic artery is most often affected vessel, followed by the pancreaticoduodenal and gastroduodenal arteries[42,63]. Pseudoaneurysm formation should be suspected if there are repeated episodes of gastrointestinal bleeding, an increasing pulsatile abdominal mass and in patients with bloating and increasing abdominal pain. Unfortunately, aneurysm rupture in these arteries mostly results in severe and life-threatening bleeding. The diagnosis can be made by angiography or angio-CT. Sometimes, arteriography with embolization of bleeding vessel in order to stop the bleeding can be performed as a temporary measure. Otherwise, some patients will require urgent surgery to stop the bleeding[33,63,120].

How to prevent relapses of AP?

The prevention of relapses of AP starts with the current episode treatment. Potential etiologic causes should be determined and adequately treated in order to prevent future relapses of the disease. This implies an adequate and prompt diagnostic and therapeutic approach to patients with biliary stones and sludge, as well as to patients with hyperlipidemia and hypercalcemia[1,5,7,16].

AP caused by hyperlipidemia tend to develop more severe forms of the disease and up to 50% of them develop SAP. Therefore, appropriate diet and drug management of the lipoprotein metabolic disorders as well as alcohol abstinence are crucial in preventing relapses of pancreatitis[9-11]. Morphologic abnormalities and tumors also have to be excluded.

After discharge from the hospital, patients with AP should follow a diet without alcohol and high fat food consumption, eating frequent small meals four to six times per day. A few months after the acute phase of AP, patients can try to introduce a diet with a slightly increased fat content and grilled meat. Patients should be warned that the next attack of AP could be more dangerous than the previous one, so lifestyle changes are necessary to reduce the risk of disease relapse[16,121,122].

CONCLUSION

AP is an inflammatory pancreatic disease that is characterized by inappropriate activation of trypsinogen and destruction of secretory cells which leads to activation of inflammatory cells, fever, and MOF. Diagnosis of AP is based on clinical, laboratory and imaging parameters, which are included into prognostic scoring system, developed with the aim of predicting the severity of the disease. Advances made in establishing diagnostic criteria for the severity and prognosis of AP have markedly influenced therapeutic approach and reduced the mortality rate of the disease.

There are two treatment periods in AP: Initial management remains supportive, consisting of conservative treatment which should be applied in both mild and severe forms of AP, while late management incorporates the treatment of the SAP complications. Currently, the treatment of SAP complications has shifted from early surgical approach to minimally invasive step-up strategy as the reference standard intervention. However, AP is a complex disease and despite the existence of numerous criteria, it is difficult to predict its clinical course. Additional researches, preferably randomized trials or prospective collaborative studies, are required to increase understanding of the pathophysiology of the disease and enable adequate responses to the diagnostic and therapeutic challenges, in order to improve the management of particularly severe forms of AP.

FOOTNOTES

Author contributions: Zerem E contributed to conception and design of the paper, writing of the paper and final revision; Kurtcehajic A, Kunosić S, Zerem Malkočević D and Zerem O contributed to the literature search, writing of the paper and final revision of the paper.

Conflict-of-interest statement: All the authors report no relevant conflicts of interest for this article.

Open-Access: This article is an open-access article that was selected by an in-house editor and fully peer-reviewed by external reviewers. It is distributed in accordance with the Creative Commons Attribution NonCommercial (CC BY-NC 4.0) license, which permits others to distribute, remix, adapt, build upon this work non-commercially, and license their derivative works on different terms, provided the original work is properly cited and the use is non-commercial. See: https://creativecommons.org/Licenses/by-nc/4.0/

Country/Territory of origin: Bosnia and Herzegovina

ORCID number: Enver Zerem 0000-0001-6906-3630; Admir Kurtcehajic 0000-0002-6445-4090; Suad Kunosić 0000-0002-5211-4099; Dina Zerem Malkočević 0000-0003-0347-9881; Omar Zerem 0000-0003-3128-0933.

S-Editor: Fan JR
L-Editor: A
P-Editor: Zhao S

REFERENCES

1 **Sureka B**, Bansal K, Patidar Y, Arora A. Imaging lexicon for acute pancreatitis: 2012 Atlanta Classification revisited. *Gastroenterol Rep (Oxf)* 2016; **4**: 16-23 [PMID: 26224684 DOI: 10.1093/gastro/gov036]

2 **Párniczky A**, Kui B, Szentesi A, Balázs A, Szűcs Á, Mosztbacher D, Czimmer J, Sarlós P, Bajor J, Gódi S, Vincze Á, Illés A, Szabó I, Pár G, Takács T, Czakó L, Szepes Z, Rakonczay Z, Izbéki F, Gervain J, Halász A, Novák J, Crai S, Hritz I, Góg C, Sümegi J, Golovics P, Varga M, Bod B, Hamvas J, Varga-Müller M, Papp Z, Sahin-Tóth M, Hegyi P; Hungarian Pancreatic Study Group. Prospective, Multicentre, Nationwide Clinical Data from 600 Cases of Acute Pancreatitis. *PLoS One* 2016; **11**: e0165309 [PMID: 27798670 DOI: 10.1371/journal.pone.0165309]

3 **Banks PA**, Bollen TL, Dervenis C, Gooszen HG, Johnson CD, Sarr MG, Tsiotos GG, Vege SS; Acute Pancreatitis Classification Working Group. Classification of acute pancreatitis--2012: revision of the Atlanta classification and definitions by international consensus. *Gut* 2013; **62**: 102-111 [PMID: 23100216 DOI: 10.1136/gutjnl-2012-302779]

4 **Zerem E**. Treatment of severe acute pancreatitis and its complications. *World J Gastroenterol* 2014; **20**: 13879-13892 [PMID: 25320523 DOI: 10.3748/wjg.v20.i38.13879]

5 **Working Group IAP/APA Acute Pancreatitis Guidelines**. IAP/APA evidence-based guidelines for the management of acute pancreatitis. *Pancreatology* 2013; **13**: e1-15 [PMID: 24054878 DOI: 10.1016/j.pan.2013.07.063]

6 **Vege SS**, DiMagno MJ, Forsmark CE, Martel M, Barkun AN. Initial Medical Treatment of Acute Pancreatitis: American Gastroenterological Association Institute Technical Review. *Gastroenterology* 2018; **154**: 1103-1139 [PMID: 29421596 DOI: 10.1053/j.gastro.2018.01.031]

7 **Walkowska J**, Zielinska N, Karauda P, Tubbs RS, Kurtys K, Olewnik Ł. The Pancreas and Known Factors of Acute Pancreatitis. *J Clin Med* 2022; **11** [PMID: 36233433 DOI: 10.3390/jcm11195565]

8 **Zerem E**, Imamović G, Sušić A, Haračić B. Step-up approach to infected necrotising pancreatitis: a 20-year experience of percutaneous drainage in a single centre. *Dig Liver Dis* 2011; **43**: 478-483 [PMID: 21478061 DOI:

10.1016/j.dld.2011.02.020]
9 **Cruciat G**, Nemeti G, Goidescu I, Anitan S, Florian A. Hypertriglyceridemia triggered acute pancreatitis in pregnancy - diagnostic approach, management and follow-up care. *Lipids Health Dis* 2020; **19**: 2 [PMID: 31901241 DOI: 10.1186/s12944-019-1180-7]
10 **Wang L**, Xu T, Wang R, Wang X, Wu D. Hypertriglyceridemia Acute Pancreatitis: Animal Experiment Research. *Dig Dis Sci* 2022; **67**: 761-772 [PMID: 33939144 DOI: 10.1007/s10620-021-06928-0]
11 **Yang AL**, McNabb-Baltar J. Hypertriglyceridemia and acute pancreatitis. *Pancreatology* 2020; **20**: 795-800 [PMID: 32571534 DOI: 10.1016/j.pan.2020.06.005]
12 **Chadalavada P**, Simons-Linares CR, Chahal P. Drug-induced acute pancreatitis: Prevalence, Causative agents, and Outcomes. *Pancreatology* 2020; **20**: 1281-1286 [PMID: 32878711 DOI: 10.1016/j.pan.2020.07.401]
13 **Abu-El-Haija M**, Hornung L, Lin TK, Nathan JD, Thompson T, Vitale DS, Nasr A, Husain SZ, Denson L. Drug induced pancreatitis is the leading known cause of first attack acute pancreatitis in children. *Pancreatology* 2020; **20**: 1103-1108 [PMID: 32800650 DOI: 10.1016/j.pan.2020.07.008]
14 **Gagnon AL**, Lavoie A, Frigon MP, Michaud-Herbst A, Tremblay K. A Drug-Induced Acute Pancreatitis Retrospective Study. *Can J Gastroenterol Hepatol* 2020; **2020**: 1516493 [PMID: 33204673 DOI: 10.1155/2020/1516493]
15 **Chocair PR**, Neves PDMM, Mohrbacher S, Neto MP, Sato VAH, Oliveira ÉS, Barbosa LV, Bales AM, da Silva FP, Cuvello-Neto AL, Duley JA. Case Report: Azathioprine: An Old and Wronged Immunosuppressant. *Front Immunol* 2022; **13**: 903012 [PMID: 35757730 DOI: 10.3389/fimmu.2022.903012]
16 **Szatmary P**, Grammatikopoulos T, Cai W, Huang W, Mukherjee R, Halloran C, Beyer G, Sutton R. Acute Pancreatitis: Diagnosis and Treatment. *Drugs* 2022; **82**: 1251-1276 [PMID: 36074322 DOI: 10.1007/s40265-022-01766-4]
17 **Zerem E**, Imamovic G, Omerović S, Imširović B. Randomized controlled trial on sterile fluid collections management in acute pancreatitis: should they be removed? *Surg Endosc* 2009; **23**: 2770-2777 [PMID: 19444515 DOI: 10.1007/s00464-009-0487-2]
18 **Baron TH**, DiMaio CJ, Wang AY, Morgan KA. American Gastroenterological Association Clinical Practice Update: Management of Pancreatic Necrosis. *Gastroenterology* 2020; **158**: 67-75.e1 [PMID: 31479658 DOI: 10.1053/j.gastro.2019.07.064]
19 **Rompianesi G**, Hann A, Komolafe O, Pereira SP, Davidson BR, Gurusamy KS. Serum amylase and lipase and urinary trypsinogen and amylase for diagnosis of acute pancreatitis. *Cochrane Database Syst Rev* 2017; **4**: CD012010 [PMID: 28431198 DOI: 10.1002/14651858.CD012010.pub2]
20 **Zerem D**, Zerem O, Zerem E. Role of Clinical, Biochemical, and Imaging Parameters in predicting the Severity of Acute Pancreatitis. *Euroasian J Hepatogastroenterol* 2017; **7**: 1-5 [PMID: 29201763 DOI: 10.5005/jp-journals-10018-1202]
21 **Zerem E**, Imamović G, Latić F, Mavija Z. Prognostic value of acute fluid collections diagnosed by ultrasound in the early assessment of severity of acute pancreatitis. *J Clin Ultrasound* 2013; **41**: 203-209 [PMID: 22987623 DOI: 10.1002/jcu.21995]
22 **Bougard M**, Barbier L, Godart B, Le Bayon-Bréard AG, Marques F, Salamé E. Management of biliary acute pancreatitis. *J Visc Surg* 2019; **156**: 113-125 [PMID: 30385271 DOI: 10.1016/j.jviscsurg.2018.08.002]
23 **Yasuda H**, Kataoka K, Takeyama Y, Takeda K, Ito T, Mayumi T, Isaji S, Mine T, Kitagawa M, Kiriyama S, Sakagami J, Masamune A, Inui K, Hirano K, Akashi R, Yokoe M, Sogame Y, Okazaki K, Morioka C, Kihara Y, Kawa S, Tanaka M, Andoh A, Kimura W, Nishimori I, Furuse J, Yokota I, Shimosegawa T. Usefulness of urinary trypsinogen-2 and trypsinogen activation peptide in acute pancreatitis: A multicenter study in Japan. *World J Gastroenterol* 2019; **25**: 107-117 [PMID: 30643362 DOI: 10.3748/wjg.v25.i1.107]
24 **Mayumi T**, Inui K, Maetani I, Yokoe M, Sakamoto T, Yoshida M, Ko S, Hirata K, Takada T; Urinary Trypsinogen-2 Dipstick for Acute Pancreatitis Study Group of Japanese Society of Abdominal Emergency Medicine (UtrAP Study Group). Validity of the urinary trypsinogen-2 test in the diagnosis of acute pancreatitis. *Pancreas* 2012; **41**: 869-875 [PMID: 22481290 DOI: 10.1097/MPA.0b013e3182480ab7]
25 **Staubli SM**, Oertli D, Nebiker CA. Laboratory markers predicting severity of acute pancreatitis. *Crit Rev Clin Lab Sci* 2015; **52**: 273-283 [PMID: 26173077 DOI: 10.3109/10408363.2015.1051659]
26 **Staubli SM**, Schäfer J, Rosenthal R, Zeindler J, Oertli D, Nebiker CA. The role of CRP and Pentraxin 3 in the prediction of systemic inflammatory response syndrome and death in acute pancreatitis. *Sci Rep* 2019; **9**: 18340 [PMID: 31798002 DOI: 10.1038/s41598-019-54910-8]
27 **Bastati N**, Kristic A, Poetter-Lang S, Messner A, Herold A, Hodge JC, Schindl M, Ba-Ssalamah A. Imaging of inflammatory disease of the pancreas. *Br J Radiol* 2021; **94**: 20201214 [PMID: 34111970 DOI: 10.1259/bjr.20201214]
28 **Brizi MG**, Perillo F, Cannone F, Tuzza L, Manfredi R. The role of imaging in acute pancreatitis. *Radiol Med* 2021; **126**: 1017-1029 [PMID: 33982269 DOI: 10.1007/s11547-021-01359-3]
29 **Freeman ML**, Werner J, van Santvoort HC, Baron TH, Besselink MG, Windsor JA, Horvath KD, vanSonnenberg E, Bollen TL, Vege SS; International Multidisciplinary Panel of Speakers and Moderators. Interventions for necrotizing pancreatitis: summary of a multidisciplinary consensus conference. *Pancreas* 2012; **41**: 1176-1194 [PMID: 23086243 DOI: 10.1097/MPA.0b013e318269c660]
30 **Ball CG**, Correa-Gallego C, Howard TJ, Zyromski NJ, House MG, Pitt HA, Nakeeb A, Schmidt CM, Akisik F, Lillemoe KD. Radiation dose from computed tomography in patients with necrotizing pancreatitis: how much is too much? *J Gastrointest Surg* 2010; **14**: 1529-1535 [PMID: 20824381 DOI: 10.1007/s11605-010-1314-8]
31 **Arvanitakis M**, Delhaye M, De Maertelaere V, Bali M, Winant C, Coppens E, Jeanmart J, Zalcman M, Van Gansbeke D, Devière J, Matos C. Computed tomography and magnetic resonance imaging in the assessment of acute pancreatitis. *Gastroenterology* 2004; **126**: 715-723 [PMID: 14988825 DOI: 10.1053/j.gastro.2003.12.006]
32 **Pelaez-Luna M**, Vege SS, Petersen BT, Chari ST, Clain JE, Levy MJ, Pearson RK, Topazian MD, Farnell MB, Kendrick ML, Baron TH. Disconnected pancreatic duct syndrome in severe acute pancreatitis: clinical and imaging characteristics and outcomes in a cohort of 31 cases. *Gastrointest Endosc* 2008; **68**: 91-97 [PMID: 18378234 DOI: 10.1016/j.gie.2007.11.041]
33 **Maher MM**, Lucey BC, Gervais DA, Mueller PR. Acute pancreatitis: the role of imaging and interventional radiology.

Cardiovasc Intervent Radiol 2004; **27**: 208-225 [PMID: 15024494 DOI: 10.1007/s00270-003-1907-7]

34 **Vege SS**, Fletcher JG, Talukdar R, Sarr MG. Peripancreatic collections in acute pancreatitis: correlation between computerized tomography and operative findings. *World J Gastroenterol* 2010; **16**: 4291-4296 [PMID: 20818812 DOI: 10.3748/wjg.v16.i34.4291]

35 **Balthazar EJ**. CT diagnosis and staging of acute pancreatitis. *Radiol Clin North Am* 1989; **27**: 19-37 [PMID: 2642273]

36 **Ranson JH**. The timing of biliary surgery in acute pancreatitis. *Ann Surg* 1979; **189**: 654-663 [PMID: 443917 DOI: 10.1097/00000658-197905000-00016]

37 **McKay CJ**, Imrie CW. Staging of acute pancreatitis. Is it important? *Surg Clin North Am* 1999; **79**: 733-743 [PMID: 10470323 DOI: 10.1016/s0039-6109(05)70039-6]

38 **Arif A**, Jaleel F, Rashid K. Accuracy of BISAP score in prediction of severe acute pancreatitis. *Pak J Med Sci* 2019; **35**: 1008-1012 [PMID: 31372133 DOI: 10.12669/pjms.35.4.1286]

39 **Ma X**, Li L, Jin T, Xia Q. [Harmless acute pancreatitis score on admission can accurately predict mild acute pancreatitis]. *Nan Fang Yi Ke Da Xue Xue Bao* 2020; **40**: 190-195 [PMID: 32376542 DOI: 10.12122/j.issn.1673-4254.2020.02.09]

40 **Al-Qahtani HH**, Alam MKh, Waheed M. Comparison of Harmless Acute Pancreatitis Score with Ranson's Score in Predicting the Severity of Acute Pancreatitis. *J Coll Physicians Surg Pak* 2017; **27**: 75-79 [PMID: 28292382]

41 **Kui B**, Pintér J, Molontay R, Nagy M, Farkas N, Gede N, Vincze Á, Bajor J, Gódi S, Czimmer J, Szabó I, Illés A, Sarlós P, Hágendorn R, Pár G, Papp M, Vitális Z, Kovács G, Fehér E, Földi I, Izbéki F, Gajdán L, Fejes R, Németh BC, Török I, Farkas H, Mickevicius A, Sallinen V, Galeev S, Ramírez-Maldonado E, Párniczky A, Erőss B, Hegyi PJ, Márta K, Váncsa S, Sutton R, Szatmary P, Latawiec D, Halloran C, de-Madaria E, Pando E, Alberti P, Gómez-Jurado MJ, Tantau A, Szentesi A, Hegyi P; Hungarian Pancreatic Study Group. EASY-APP: An artificial intelligence model and application for early and easy prediction of severity in acute pancreatitis. *Clin Transl Med* 2022; **12**: e842 [PMID: 35653504 DOI: 10.1002/ctm2.842]

42 **Bradley EL 3rd**. A clinically based classification system for acute pancreatitis. Summary of the International Symposium on Acute Pancreatitis, Atlanta, Ga, September 11 through 13, 1992. *Arch Surg* 1993; **128**: 586-590 [PMID: 8489394 DOI: 10.1001/archsurg.1993.01420170122019]

43 **Crockett SD**, Wani S, Gardner TB, Falck-Ytter Y, Barkun AN; American Gastroenterological Association Institute Clinical Guidelines Committee. American Gastroenterological Association Institute Guideline on Initial Management of Acute Pancreatitis. *Gastroenterology* 2018; **154**: 1096-1101 [PMID: 29409760 DOI: 10.1053/j.gastro.2018.01.032]

44 **Hirota M**, Takada T, Kitamura N, Ito T, Hirata K, Yoshida M, Mayumi T, Kataoka K, Takeda K, Sekimoto M, Hirota M, Kimura Y, Wada K, Amano H, Gabata T, Arata S, Yokoe M, Kiriyama S. Fundamental and intensive care of acute pancreatitis. *J Hepatobiliary Pancreat Sci* 2010; **17**: 45-52 [PMID: 20012652 DOI: 10.1007/s00534-009-0210-7]

45 **de-Madaria E**, Buxbaum JL, Maisonneuve P, García García de Paredes A, Zapater P, Guilabert L, Vaillo-Rocamora A, Rodríguez-Gandía MÁ, Donate-Ortega J, Lozada-Hernández EE, Collazo Moreno AJR, Lira-Aguilar A, Llovet LP, Mehta R, Tandel R, Navarro P, Sánchez-Pardo AM, Sánchez-Marin C, Cobreros M, Fernández-Cabrera I, Casals-Seoane F, Casas Deza D, Lauret-Braña E, Martí-Marqués E, Camacho-Montaño LM, Ubieto V, Ganuza M, Bolado F; ERICA Consortium. Aggressive or Moderate Fluid Resuscitation in Acute Pancreatitis. *N Engl J Med* 2022; **387**: 989-1000 [PMID: 36103415 DOI: 10.1056/NEJMoa2202884]

46 **Cuéllar-Monterrubio JE**, Monreal-Robles R, González-Moreno EI, Borjas-Almaguer OD, Herrera-Elizondo JL, García-Compean D, Maldonado-Garza HJ, González-González JA. Nonaggressive Versus Aggressive Intravenous Fluid Therapy in Acute Pancreatitis With More Than 24 Hours From Disease Onset: A Randomized Controlled Trial. *Pancreas* 2020; **49**: 579-583 [PMID: 32282773 DOI: 10.1097/MPA.0000000000001528]

47 **Gad MM**, Simons-Linares CR. Is aggressive intravenous fluid resuscitation beneficial in acute pancreatitis? *World J Gastroenterol* 2020; **26**: 1098-1106 [PMID: 32206000 DOI: 10.3748/wjg.v26.i10.1098]

48 **Angsubhakorn A**, Tipchaichatta K, Chirapongsathorn S. Comparison of aggressive versus standard intravenous hydration for clinical improvement among patients with mild acute pancreatitis: A randomized controlled trial. *Pancreatology* 2021; **21**: 1224-1230 [PMID: 34215499 DOI: 10.1016/j.pan.2021.06.004]

49 **Buxbaum JL**, Quezada M, Da B, Jani N, Lane C, Mwengela D, Kelly T, Jhun P, Dhanireddy K, Laine L. Early Aggressive Hydration Hastens Clinical Improvement in Mild Acute Pancreatitis. *Am J Gastroenterol* 2017; **112**: 797-803 [PMID: 28266591 DOI: 10.1038/ajg.2017.40]

50 **Park CH**, Paik WH, Park ET, Shim CS, Lee TY, Kang C, Noh MH, Yi SY, Lee JK, Hyun JJ. Aggressive intravenous hydration with lactated Ringer's solution for prevention of post-ERCP pancreatitis: a prospective randomized multicenter clinical trial. *Endoscopy* 2018; **50**: 378-385 [PMID: 29237204 DOI: 10.1055/s-0043-122386]

51 **Wu M**, Jiang S, Lu X, Zhong Y, Song Y, Fan Z, Kang X. Aggressive hydration with lactated ringer solution in prevention of post-endoscopic retrograde cholangiopancreatography pancreatitis: A systematic review and meta-analysis. *Medicine (Baltimore)* 2021; **100**: e25598 [PMID: 33879722 DOI: 10.1097/MD.0000000000025598]

52 **Thompson DR**. Narcotic analgesic effects on the sphincter of Oddi: a review of the data and therapeutic implications in treating pancreatitis. *Am J Gastroenterol* 2001; **96**: 1266-1272 [PMID: 11316181 DOI: 10.1111/j.1572-0241.2001.03536.x]

53 **Peiró AM**, Martínez J, Martínez E, de Madaria E, Llorens P, Horga JF, Pérez-Mateo M. Efficacy and tolerance of metamizole versus morphine for acute pancreatitis pain. *Pancreatology* 2008; **8**: 25-29 [PMID: 18235213 DOI: 10.1159/000114852]

54 **Basurto Ona X**, Rigau Comas D, Urrútia G. Opioids for acute pancreatitis pain. *Cochrane Database Syst Rev* 2013; CD009179 [PMID: 23888429 DOI: 10.1002/14651858.CD009179.pub2]

55 **Al-Leswas D**, Baxter N, Lim WB, Robertson F, Ratnayake B, Samanta J, Capurso G, de-Madaria E, Drewes AM, Windsor J, Pandanaboyana S. The safety and efficacy of epidural anaesthesia in acute pancreatitis: a systematic review and meta-analysis. *HPB (Oxford)* 2023; **25**: 162-171 [PMID: 36593161 DOI: 10.1016/j.hpb.2022.12.004]

56 **Thavanesan N**, White S, Lee S, Ratnayake B, Oppong KW, Nayar MK, Sharp L, Drewes AM, Capurso G, De-Madaria E, Siriwardena AK, Windsor JA, Pandanaboyana S. Analgesia in the Initial Management of Acute Pancreatitis: A Systematic Review and Meta-Analysis of Randomised Controlled Trials. *World J Surg* 2022; **46**: 878-890 [PMID: 34994837 DOI:

10.1007/s00268-021-06420-w]
57 **Oláh A**, Romics L Jr. Enteral nutrition in acute pancreatitis: a review of the current evidence. *World J Gastroenterol* 2014; **20**: 16123-16131 [PMID: 25473164 DOI: 10.3748/wjg.v20.i43.16123]
58 **Takeda K**, Takada T, Kawarada Y, Hirata K, Mayumi T, Yoshida M, Sekimoto M, Hirota M, Kimura Y, Isaji S, Koizumi M, Otsuki M, Matsuno S; JPN. JPN Guidelines for the management of acute pancreatitis: medical management of acute pancreatitis. *J Hepatobiliary Pancreat Surg* 2006; **13**: 42-47 [PMID: 16463210 DOI: 10.1007/s00534-005-1050-8]
59 **Meier R**, Ockenga J, Pertkiewicz M, Pap A, Milinic N, Macfie J; DGEM (German Society for Nutritional Medicine), Löser C, Keim V; ESPEN (European Society for Parenteral and Enteral Nutrition). ESPEN Guidelines on Enteral Nutrition: Pancreas. *Clin Nutr* 2006; **25**: 275-284 [PMID: 16678943 DOI: 10.1016/j.clnu.2006.01.019]
60 **Sharma VK**, Howden CW. Prophylactic antibiotic administration reduces sepsis and mortality in acute necrotizing pancreatitis: a meta-analysis. *Pancreas* 2001; **22**: 28-31 [PMID: 11138967 DOI: 10.1097/00006676-200101000-00005]
61 **Isenmann R**, Rünzi M, Kron M, Kahl S, Kraus D, Jung N, Maier L, Malfertheiner P, Goebell H, Beger HG; German Antibiotics in Severe Acute Pancreatitis Study Group. Prophylactic antibiotic treatment in patients with predicted severe acute pancreatitis: a placebo-controlled, double-blind trial. *Gastroenterology* 2004; **126**: 997-1004 [PMID: 15057739 DOI: 10.1053/j.gastro.2003.12.050]
62 **Kochhar R**, Ahammed SK, Chakrabarti A, Ray P, Sinha SK, Dutta U, Wig JD, Singh K. Prevalence and outcome of fungal infection in patients with severe acute pancreatitis. *J Gastroenterol Hepatol* 2009; **24**: 743-747 [PMID: 19220667 DOI: 10.1111/j.1440-1746.2008.05712.x]
63 **Cruz-Santamaría DM**, Taxonera C, Giner M. Update on pathogenesis and clinical management of acute pancreatitis. *World J Gastrointest Pathophysiol* 2012; **3**: 60-70 [PMID: 22737590 DOI: 10.4291/wjgp.v3.i3.60]
64 **Dellinger EP**, Tellado JM, Soto NE, Ashley SW, Barie PS, Dugernier T, Imrie CW, Johnson CD, Knaebel HP, Laterre PF, Maravi-Poma E, Kissler JJ, Sanchez-Garcia M, Utzolino S. Early antibiotic treatment for severe acute necrotizing pancreatitis: a randomized, double-blind, placebo-controlled study. *Ann Surg* 2007; **245**: 674-683 [PMID: 17457158 DOI: 10.1097/01.sla.0000250414.09255.84]
65 **García-Barrasa A**, Borobia FG, Pallares R, Jorba R, Poves I, Busquets J, Fabregat J. A double-blind, placebo-controlled trial of ciprofloxacin prophylaxis in patients with acute necrotizing pancreatitis. *J Gastrointest Surg* 2009; **13**: 768-774 [PMID: 19082671 DOI: 10.1007/s11605-008-0773-7]
66 **Isaji S**, Takada T, Mayumi T, Yoshida M, Wada K, Yokoe M, Itoi T, Gabata T. Revised Japanese guidelines for the management of acute pancreatitis 2015: revised concepts and updated points. *J Hepatobiliary Pancreat Sci* 2015; **22**: 433-445 [PMID: 25904407 DOI: 10.1002/jhbp.260]
67 **van Santvoort HC**, Besselink MG, Bakker OJ, Hofker HS, Boermeester MA, Dejong CH, van Goor H, Schaapherder AF, van Eijck CH, Bollen TL, van Ramshorst B, Nieuwenhuijs VB, Timmer R, Laméris JS, Kruyt PM, Manusama ER, van der Harst E, van der Schelling GP, Karsten T, Hesselink EJ, van Laarhoven CJ, Rosman C, Bosscha K, de Wit RJ, Houdijk AP, van Leeuwen MS, Buskens E, Gooszen HG; Dutch Pancreatitis Study Group. A step-up approach or open necrosectomy for necrotizing pancreatitis. *N Engl J Med* 2010; **362**: 1491-1502 [PMID: 20410514 DOI: 10.1056/NEJMoa0908821]
68 **da Costa DW**, Boerma D, van Santvoort HC, Horvath KD, Werner J, Carter CR, Bollen TL, Gooszen HG, Besselink MG, Bakker OJ. Staged multidisciplinary step-up management for necrotizing pancreatitis. *Br J Surg* 2014; **101**: e65-e79 [PMID: 24272964 DOI: 10.1002/bjs.9346]
69 **Trikudanathan G**, Tawfik P, Amateau SK, Munigala S, Arain M, Attam R, Beilman G, Flanagan S, Freeman ML, Mallery S. Early (<4 Weeks) Versus Standard (≥ 4 Weeks) Endoscopically Centered Step-Up Interventions for Necrotizing Pancreatitis. *Am J Gastroenterol* 2018; **113**: 1550-1558 [PMID: 30279466 DOI: 10.1038/s41395-018-0232-3]
70 **Aparna D**, Kumar S, Kamalkumar S. Mortality and morbidity in necrotizing pancreatitis managed on principles of step-up approach: 7 years experience from a single surgical unit. *World J Gastrointest Surg* 2017; **9**: 200-208 [PMID: 29109852 DOI: 10.4240/wjgs.v9.i10.200]
71 **Besselink MG**. The 'step-up approach' to infected necrotizing pancreatitis: delay, drain, debride. *Dig Liver Dis* 2011; **43**: 421-422 [PMID: 21531639 DOI: 10.1016/j.dld.2011.04.001]
72 **Bang JY**, Arnoletti JP, Holt BA, Sutton B, Hasan MK, Navaneethan U, Feranec N, Wilcox CM, Tharian B, Hawes RH, Varadarajulu S. An Endoscopic Transluminal Approach, Compared With Minimally Invasive Surgery, Reduces Complications and Costs for Patients With Necrotizing Pancreatitis. *Gastroenterology* 2019; **156**: 1027-1040.e3 [PMID: 30452918 DOI: 10.1053/j.gastro.2018.11.031]
73 **van Brunschot S**, van Grinsven J, Voermans RP, Bakker OJ, Besselink MG, Boermeester MA, Bollen TL, Bosscha K, Bouwense SA, Bruno MJ, Cappendijk VC, Consten EC, Dejong CH, Dijkgraaf MG, van Eijck CH, Erkelens GW, van Goor H, Hadithi M, Haveman JW, Hofker SH, Jansen JJ, Laméris JS, van Lienden KP, Manusama ER, Meijssen MA, Mulder CJ, Nieuwenhuis VB, Poley JW, de Ridder RJ, Rosman C, Schaapherder AF, Scheepers JJ, Schoon EJ, Seerden T, Spanier BW, Straathof JW, Timmer R, Venneman NG, Vleggaar FP, Witteman BJ, Gooszen HG, van Santvoort HC, Fockens P; Dutch Pancreatitis Study Group. Transluminal endoscopic step-up approach versus minimally invasive surgical step-up approach in patients with infected necrotising pancreatitis (TENSION trial): design and rationale of a randomised controlled multicenter trial [ISRCTN09186711]. *BMC Gastroenterol* 2013; **13**: 161 [PMID: 24274589 DOI: 10.1186/1471-230X-13-161]
74 **van Brunschot S**, van Grinsven J, van Santvoort HC, Bakker OJ, Besselink MG, Boermeester MA, Bollen TL, Bosscha K, Bouwense SA, Bruno MJ, Cappendijk VC, Consten EC, Dejong CH, van Eijck CH, Erkelens WG, van Goor H, van Grevenstein WMU, Haveman JW, Hofker SH, Jansen JM, Laméris JS, van Lienden KP, Meijssen MA, Mulder CJ, Nieuwenhuijs VB, Poley JW, Quispel R, de Ridder RJ, Römkens TE, Scheepers JJ, Schepers NJ, Schwartz MP, Seerden T, Spanier BWM, Straathof JWA, Strijker M, Timmer R, Venneman NG, Vleggaar FP, Voermans RP, Witteman BJ, Gooszen HG, Dijkgraaf MG, Fockens P; Dutch Pancreatitis Study Group. Endoscopic or surgical step-up approach for infected necrotising pancreatitis: a multicentre randomised trial. *Lancet* 2018; **391**: 51-58 [PMID: 29108721 DOI: 10.1016/S0140-6736(17)32404-2]
75 **Onnekink AM**, Boxhoorn L, Timmerhuis HC, Bac ST, Besselink MG, Boermeester MA, Bollen TL, Bosscha K,

Bouwense SAW, Bruno MJ, van Brunschot S, Cappendijk VC, Consten ECJ, Dejong CH, Dijkgraaf MGW, van Eijck CHJ, Erkelens WG, van Goor H, van Grinsven J, Haveman JW, van Hooft JE, Jansen JM, van Lienden KP, Meijssen MAC, Nieuwenhuijs VB, Poley JW, Quispel R, de Ridder RJ, Römkens TEH, van Santvoort HC, Scheepers JJ, Schwartz MP, Seerden T, Spanier MBW, Straathof JWA, Timmer R, Venneman NG, Verdonk RC, Vleggaar FP, van Wanrooij RL, Witteman BJM, Fockens P, Voermans RP; Dutch Pancreatitis Study Group. Endoscopic Versus Surgical Step-Up Approach for Infected Necrotizing Pancreatitis (ExTENSION): Long-term Follow-up of a Randomized Trial. *Gastroenterology* 2022; **163**: 712-722.e14 [PMID: 35580661 DOI: 10.1053/j.gastro.2022.05.015]

76 **Rizzatti G**, Rimbaş M, Larghi A. Endoscopic Ultrasound-Guided Drainage for Infected Necrotizing Pancreatitis: Better Than Surgery But Still Lacking Treatment Protocol Standardization. *Gastroenterology* 2019; **157**: 582-583 [PMID: 31102662 DOI: 10.1053/j.gastro.2019.01.274]

77 **Garg PK**, Zyromski NJ, Freeman ML. Infected Necrotizing Pancreatitis: Evolving Interventional Strategies From Minimally Invasive Surgery to Endoscopic Therapy-Evidence Mounts, But One Size Does Not Fit All. *Gastroenterology* 2019; **156**: 867-871 [PMID: 30776344 DOI: 10.1053/j.gastro.2019.02.015]

78 **Boxhoorn L**, Besselink MG, Voermans RP; Dutch Pancreatitis Study Group. Surgery Versus Endoscopy for Infected Necrotizing Pancreatitis: A Fair Comparison? *Gastroenterology* 2019; **157**: 583-584 [PMID: 31103626 DOI: 10.1053/j.gastro.2019.03.073]

79 **Bang JY**, Varadarajulu S. Reply. *Gastroenterology* 2019; **157**: 584-585 [PMID: 31260665 DOI: 10.1053/j.gastro.2019.06.007]

80 **Liu RH**, Wen Y, Sun HY, Liu CY, Zhang YF, Yang Y, Huang QL, Tang JJ, Huang CC, Tang LJ. Abdominal paracentesis drainage ameliorates severe acute pancreatitis in rats by regulating the polarization of peritoneal macrophages. *World J Gastroenterol* 2018; **24**: 5131-5143 [PMID: 30568390 DOI: 10.3748/wjg.v24.i45.5131]

81 **Liu WH**, Wang T, Yan HT, Chen T, Xu C, Ye P, Zhang N, Liu ZC, Tang LJ. Predictors of percutaneous catheter drainage (PCD) after abdominal paracentesis drainage (APD) in patients with moderately severe or severe acute pancreatitis along with fluid collections. *PLoS One* 2015; **10**: e0115348 [PMID: 25659143 DOI: 10.1371/journal.pone.0115348]

82 **Zerem E**, Kunosić S, Zerem D, Boloban A, Zerem O, Zlomužica E. Benefits of abdominal paracentesis drainage performed ahead of percutaneous catheter drainage as a modification of the step-up approach in acute pancreatitis with fluid collections. *Acta Gastroenterol Belg* 2020; **83**: 285-293 [PMID: 32603048]

83 **Liu WH**, Ren LN, Chen T, Liu LY, Jiang JH, Wang T, Xu C, Yan HT, Zheng XB, Song FQ, Tang LJ. Abdominal paracentesis drainage ahead of percutaneous catheter drainage benefits patients attacked by acute pancreatitis with fluid collections: a retrospective clinical cohort study. *Crit Care Med* 2015; **43**: 109-119 [PMID: 25251762 DOI: 10.1097/CCM.0000000000000606]

84 **Wang T**, Liu LY, Luo H, Dai RW, Liang HY, Chen T, Yan HT, Cui JF, Li NL, Yang W, Liu WH, Tang LJ. Intra-Abdominal Pressure Reduction After Percutaneous Catheter Drainage Is a Protective Factor for Severe Pancreatitis Patients With Sterile Fluid Collections. *Pancreas* 2016; **45**: 127-133 [PMID: 26390416 DOI: 10.1097/MPA.0000000000000420]

85 **Liu L**, Yan H, Liu W, Cui J, Wang T, Dai R, Liang H, Luo H, Tang L. Abdominal Paracentesis Drainage Does Not Increase Infection in Severe Acute Pancreatitis: A Prospective Study. *J Clin Gastroenterol* 2015; **49**: 757-763 [PMID: 26053169 DOI: 10.1097/MCG.0000000000000358]

86 **Zhang Y**, Zhang SY, Gao SL, Liang ZY, Yu WQ, Liang TB. Successful Resolution of Gastric Outlet Obstruction Caused by Pancreatic Pseudocyst or Walled-Off Necrosis After Acute Pancreatitis: The Role of Percutaneous Catheter Drainage. *Pancreas* 2015; **44**: 1290-1295 [PMID: 26465954 DOI: 10.1097/MPA.0000000000000429]

87 **Sugimoto M**, Sonntag DP, Flint GS, Boyce CJ, Kirkham JC, Harris TJ, Carr SM, Nelson BD, Bell DA, Barton JG, Traverso LW. Biliary Stenosis and Gastric Outlet Obstruction: Late Complications After Acute Pancreatitis With Pancreatic Duct Disruption. *Pancreas* 2018; **47**: 772-777 [PMID: 29771770 DOI: 10.1097/MPA.0000000000001064]

88 **Bellam BL**, Samanta J, Gupta P, Kumar M P, Sharma V, Dhaka N, Sarma P, Muktesh G, Gupta V, Sinha SK, Kochhar R. Predictors of outcome of percutaneous catheter drainage in patients with acute pancreatitis having acute fluid collection and development of a predictive model. *Pancreatology* 2019; **19**: 658-664 [PMID: 31204261 DOI: 10.1016/j.pan.2019.05.467]

89 **Sugimoto M**, Sonntag DP, Flint GS, Boyce CJ, Kirkham JC, Harris TJ, Carr SM, Nelson BD, Barton JG, Traverso LW. A percutaneous drainage protocol for severe and moderately severe acute pancreatitis. *Surg Endosc* 2015; **29**: 3282-3291 [PMID: 25631111 DOI: 10.1007/s00464-015-4077-1]

90 **Sugimoto M**, Sonntag DP, Flint GS, Boyce CJ, Kirkham JC, Harris TJ, Carr SM, Nelson BD, Bell DA, Barton JG, Traverso LW. Better Outcomes if Percutaneous Drainage Is Used Early and Proactively in the Course of Necrotizing Pancreatitis. *J Vasc Interv Radiol* 2016; **27**: 418-425 [PMID: 26806694 DOI: 10.1016/j.jvir.2015.11.054]

91 **Walser EM**, Nealon WH, Marroquin S, Raza S, Hernandez JA, Vasek J. Sterile fluid collections in acute pancreatitis: catheter drainage versus simple aspiration. *Cardiovasc Intervent Radiol* 2006; **29**: 102-107 [PMID: 16283578 DOI: 10.1007/s00270-004-0220-4]

92 **van Baal MC**, Bollen TL, Bakker OJ, van Goor H, Boermeester MA, Dejong CH, Gooszen HG, van der Harst E, van Eijck CH, van Santvoort HC, Besselink MG; Dutch Pancreatitis Study Group. The role of routine fine-needle aspiration in the diagnosis of infected necrotizing pancreatitis. *Surgery* 2014; **155**: 442-448 [PMID: 24287142 DOI: 10.1016/j.surg.2013.10.001]

93 **van Grinsven J**, van Dijk SM, Dijkgraaf MG, Boermeester MA, Bollen TL, Bruno MJ, van Brunschot S, Dejong CH, van Eijck CH, van Lienden KP, Boerma D, van Duijvendijk P, Hadithi M, Haveman JW, van der Hulst RW, Jansen JM, Lips DJ, Manusama ER, Molenaar IQ, van der Peet DL, Poen AC, Quispel R, Schaapherder AF, Schoon EJ, Schwartz MP, Seerden TC, Spanier BWM, Straathof JW, Venneman NG, van de Vrie W, Witteman BJ, van Goor H, Fockens P, van Santvoort HC, Besselink MG; Dutch Pancreatitis Study Group. Postponed or immediate drainage of infected necrotizing pancreatitis (POINTER trial): study protocol for a randomized controlled trial. *Trials* 2019; **20**: 239 [PMID: 31023380 DOI: 10.1186/s13063-019-3315-6]

94 **van Baal MC**, van Santvoort HC, Bollen TL, Bakker OJ, Besselink MG, Gooszen HG; Dutch Pancreatitis Study Group.

Systematic review of percutaneous catheter drainage as primary treatment for necrotizing pancreatitis. *Br J Surg* 2011; **98**: 18-27 [PMID: 21136562 DOI: 10.1002/bjs.7304]

95 **Horvath K**, Freeny P, Escallon J, Heagerty P, Comstock B, Glickerman DJ, Bulger E, Sinanan M, Langdale L, Kolokythas O, Andrews RT. Safety and efficacy of video-assisted retroperitoneal debridement for infected pancreatic collections: a multicenter, prospective, single-arm phase 2 study. *Arch Surg* 2010; **145**: 817-825 [PMID: 20855750 DOI: 10.1001/archsurg.2010.178]

96 **Bausch D**, Wellner U, Kahl S, Kuesters S, Richter-Schrag HJ, Utzolino S, Hopt UT, Keck T, Fischer A. Minimally invasive operations for acute necrotizing pancreatitis: comparison of minimally invasive retroperitoneal necrosectomy with endoscopic transgastric necrosectomy. *Surgery* 2012; **152**: S128-S134 [PMID: 22770962 DOI: 10.1016/j.surg.2012.05.021]

97 **Mallick B**, Dhaka N, Gupta P, Gulati A, Malik S, Sinha SK, Yadav TD, Gupta V, Kochhar R. An audit of percutaneous drainage for acute necrotic collections and walled off necrosis in patients with acute pancreatitis. *Pancreatology* 2018; **18**: 727-733 [PMID: 30146334 DOI: 10.1016/j.pan.2018.08.010]

98 **van Grinsven J**, van Brunschot S, Bakker OJ, Bollen TL, Boermeester MA, Bruno MJ, Dejong CH, Dijkgraaf MG, van Eijck CH, Fockens P, van Goor H, Gooszen HG, Horvath KD, van Lienden KP, van Santvoort HC, Besselink MG; Dutch Pancreatitis Study Group. Diagnostic strategy and timing of intervention in infected necrotizing pancreatitis: an international expert survey and case vignette study. *HPB (Oxford)* 2015 [PMID: 26475650 DOI: 10.1111/hpb.12491]

99 **Hollemans RA**, Bakker OJ, Boermeester MA, Bollen TL, Bosscha K, Bruno MJ, Buskens E, Dejong CH, van Duijvendijk P, van Eijck CH, Fockens P, van Goor H, van Grevenstein WM, van der Harst E, Heisterkamp J, Hesselink EJ, Hofker S, Houdijk AP, Karsten T, Kruyt PM, van Laarhoven CJ, Laméris JS, van Leeuwen MS, Manusama ER, Molenaar IQ, Nieuwenhuijs VB, van Ramshorst B, Roos D, Rosman C, Schaapherder AF, van der Schelling GP, Timmer R, Verdonk RC, de Wit RJ, Gooszen HG, Besselink MG, van Santvoort HC; Dutch Pancreatitis Study Group. Superiority of Step-up Approach vs Open Necrosectomy in Long-term Follow-up of Patients With Necrotizing Pancreatitis. *Gastroenterology* 2019; **156**: 1016-1026 [PMID: 30391468 DOI: 10.1053/j.gastro.2018.10.045]

100 **van Dijk SM**, Timmerhuis HC, Verdonk RC, Reijnders E, Bruno MJ, Fockens P, Voermans RP, Besselink MG, van Santvoort HC; Dutch Pancreatitis Study Group. Treatment of disrupted and disconnected pancreatic duct in necrotizing pancreatitis: A systematic review and meta-analysis. *Pancreatology* 2019; **19**: 905-915 [PMID: 31473083 DOI: 10.1016/j.pan.2019.08.006]

101 **Sandrasegaran K**, Tann M, Jennings SG, Maglinte DD, Peter SD, Sherman S, Howard TJ. Disconnection of the pancreatic duct: an important but overlooked complication of severe acute pancreatitis. *Radiographics* 2007; **27**: 1389-1400 [PMID: 17848698 DOI: 10.1148/rg.275065163]

102 **Fischer TD**, Gutman DS, Hughes SJ, Trevino JG, Behrns KE. Disconnected pancreatic duct syndrome: disease classification and management strategies. *J Am Coll Surg* 2014; **219**: 704-712 [PMID: 25065360 DOI: 10.1016/j.jamcollsurg.2014.03.055]

103 **Nealon WH**, Bhutani M, Riall TS, Raju G, Ozkan O, Neilan R. A unifying concept: pancreatic ductal anatomy both predicts and determines the major complications resulting from pancreatitis. *J Am Coll Surg* 2009; **208**: 790-9; discussion 799 [PMID: 19476839 DOI: 10.1016/j.jamcollsurg.2008.12.027]

104 **Howard TJ**, Moore SA, Saxena R, Matthews DE, Schmidt CM, Wiebke EA. Pancreatic duct strictures are a common cause of recurrent pancreatitis after successful management of pancreatic necrosis. *Surgery* 2004; **136**: 909-916 [PMID: 15467678 DOI: 10.1016/j.surg.2004.06.028]

105 **Zerem E**, Imširović B, Loga-Zec S, Kunosić S, Hujdurović A, Zerem O. Treatment of Recurrent Pancreatic Pseudocysts with Proven Communication between Pseudocyst and Pancreatic Duct by Long-term Percutaneous Drainage. *Ann Acad Med Singap* 2015; **44**: 542-544 [PMID: 27089962]

106 **Nadkarni NA**, Kotwal V, Sarr MG, Swaroop Vege S. Disconnected Pancreatic Duct Syndrome: Endoscopic Stent or Surgeon's Knife? *Pancreas* 2015; **44**: 16-22 [PMID: 25493375 DOI: 10.1097/MPA.0000000000000216]

107 **Varadarajulu S**, Wilcox CM. Endoscopic placement of permanent indwelling transmural stents in disconnected pancreatic duct syndrome: does benefit outweigh the risks? *Gastrointest Endosc* 2011; **74**: 1408-1412 [PMID: 21981812 DOI: 10.1016/j.gie.2011.07.049]

108 **Rana SS**, Bhasin DK, Rao C, Sharma R, Gupta R. Consequences of long term indwelling transmural stents in patients with walled off pancreatic necrosis & disconnected pancreatic duct syndrome. *Pancreatology* 2013; **13**: 486-490 [PMID: 24075512 DOI: 10.1016/j.pan.2013.07.284]

109 **Zerem E**, Omerović S. Successful percutaneous drainage with iodine irrigation for pancreatic fistulas and abscesses after necrotizing pancreatitis. *Med Princ Pract* 2012; **21**: 398-400 [PMID: 22398319 DOI: 10.1159/000336594]

110 **Varadarajulu S**, Bang JY, Sutton BS, Trevino JM, Christein JD, Wilcox CM. Equal efficacy of endoscopic and surgical cystogastrostomy for pancreatic pseudocyst drainage in a randomized trial. *Gastroenterology* 2013; **145**: 583-90.e1 [PMID: 23732774 DOI: 10.1053/j.gastro.2013.05.046]

111 **Halttunen J**, Kylänpää L. Treatment of Pancreatic Fistulas. *Eur J Trauma Emerg Surg* 2007; **33**: 227-230 [PMID: 26814484 DOI: 10.1007/s00068-007-7067-8]

112 **Seewald S**, Brand B, Groth S, Omar S, Mendoza G, Seitz U, Yasuda I, Xikun H, Nam VC, Xu H, Thonke F, Soehendra N. Endoscopic sealing of pancreatic fistula by using N-butyl-2-cyanoacrylate. *Gastrointest Endosc* 2004; **59**: 463-470 [PMID: 15044879 DOI: 10.1016/s0016-5107(03)02708-1]

113 **van Grinsven J**, van Brunschot S, van Baal MC, Besselink MG, Fockens P, van Goor H, van Santvoort HC, Bollen TL; Dutch Pancreatitis Study Group. Natural History of Gas Configurations and Encapsulation in Necrotic Collections During Necrotizing Pancreatitis. *J Gastrointest Surg* 2018; **22**: 1557-1564 [PMID: 29752684 DOI: 10.1007/s11605-018-3792-z]

114 **Zerem E**, Pavlović-Čalić N, Sušić A, Haračić B. Percutaneous management of pancreatic abscesses: long term results in a single center. *Eur J Intern Med* 2011; **22**: e50-e54 [PMID: 21925043 DOI: 10.1016/j.ejim.2011.01.015]

115 **Nealon WH**, Walser E. Surgical management of complications associated with percutaneous and/or endoscopic management of pseudocyst of the pancreas. *Ann Surg* 2005; **241**: 948-57; discussion 957 [PMID: 15912044 DOI: 10.1097/01.sla.0000164737.86249.81]

116 **Zerem E**, Hauser G, Loga-Zec S, Kunosić S, Jovanović P, Crnkić D. Minimally invasive treatment of pancreatic pseudocysts. *World J Gastroenterol* 2015; **21**: 6850-6860 [PMID: 26078561 DOI: 10.3748/wjg.v21.i22.6850]

117 **Tyberg A**, Karia K, Gabr M, Desai A, Doshi R, Gaidhane M, Sharaiha RZ, Kahaleh M. Management of pancreatic fluid collections: A comprehensive review of the literature. *World J Gastroenterol* 2016; **22**: 2256-2270 [PMID: 26900288 DOI: 10.3748/wjg.v22.i7.2256]

118 **Zerem E**, Imamović G, Omerović S, Ljuca F, Haračić B. Percutaneous treatment for symptomatic pancreatic pseudocysts: Long-term results in a single center. *Eur J Intern Med* 2010; **21**: 393-397 [PMID: 20816592 DOI: 10.1016/j.ejim.2010.06.015]

119 **Will U**, Wegener C, Graf KI, Wanzar I, Manger T, Meyer F. Differential treatment and early outcome in the interventional endoscopic management of pancreatic pseudocysts in 27 patients. *World J Gastroenterol* 2006; **12**: 4175-4178 [PMID: 16830368 DOI: 10.3748/wjg.v12.i26.4175]

120 **Flati G**, Andrén-Sandberg A, La Pinta M, Porowska B, Carboni M. Potentially fatal bleeding in acute pancreatitis: pathophysiology, prevention, and treatment. *Pancreas* 2003; **26**: 8-14 [PMID: 12499910 DOI: 10.1097/00006676-200301000-00002]

121 **Fonseca Sepúlveda EV**, Guerrero-Lozano R. Acute pancreatitis and recurrent acute pancreatitis: an exploration of clinical and etiologic factors and outcomes. *J Pediatr (Rio J)* 2019; **95**: 713-719 [PMID: 30075118 DOI: 10.1016/j.jped.2018.06.011]

122 **Kumar S**, Ooi CY, Werlin S, Abu-El-Haija M, Barth B, Bellin MD, Durie PR, Fishman DS, Freedman SD, Gariepy C, Giefer MJ, Gonska T, Heyman MB, Himes R, Husain SZ, Lin TK, Lowe ME, Morinville V, Palermo JJ, Pohl JF, Schwarzenberg SJ, Troendle D, Wilschanski M, Zimmerman MB, Uc A. Risk Factors Associated With Pediatric Acute Recurrent and Chronic Pancreatitis: Lessons From INSPPIRE. *JAMA Pediatr* 2016; **170**: 562-569 [PMID: 27064572 DOI: 10.1001/jamapediatrics.2015.4955]

World Journal of Gastroenterology

Submit a Manuscript: https://www.f6publishing.com

World J Gastroenterol 2023 May 14; 29(18): 2764-2783

DOI: 10.3748/wjg.v29.i18.2764

ISSN 1007-9327 (print) ISSN 2219-2840 (online)

REVIEW

Wingless/It/β-catenin signaling in liver metastasis from colorectal cancer: A focus on biological mechanisms and therapeutic opportunities

Federico Selvaggi, Teresa Catalano, Rossano Lattanzio, Roberto Cotellese, Gitana Maria Aceto

Specialty type: Gastroenterology and hepatology

Provenance and peer review: Invited article; Externally peer reviewed.

Peer-review model: Single blind

Peer-review report's scientific quality classification

Grade A (Excellent): 0
Grade B (Very good): B, B
Grade C (Good): 0
Grade D (Fair): 0
Grade E (Poor): 0

P-Reviewer: Hashimoto K, Japan; Takemura N, Japan

Received: January 23, 2023
Peer-review started: January 23, 2023
First decision: February 7, 2023
Revised: February 28, 2023
Accepted: April 17, 2023
Article in press: April 17, 2023
Published online: May 14, 2023

Federico Selvaggi, Department of Surgical, ASL2 Lanciano-Vasto-Chieti, Ospedale Clinicizzato SS Annunziata of Chieti, Chieti 66100, Italy

Teresa Catalano, Department of Clinical and Experimental Medicine, University of Messina, Messina 98125, Italy

Rossano Lattanzio, Department of Innovative Technologies in Medicine & Dentistry, University "G. d'Annunzio" Chieti-Pescara, Chieti 66100, Italy

Roberto Cotellese, Department of Medical, Oral and Biotechnological Sciences, University "G. d'Annunzio" Chieti-Pescara, Chieti 66100, Italy

Roberto Cotellese, Villa Serena Foundation for Research, Villa Serena - Del Dott. L. Petruzzi, Città Sant'Angelo 65013, Pescara, Italy

Gitana Maria Aceto, Department of Medical, Oral and Biotechnological Sciences, "G. d'Annunzio" University of Chieti-Pescara, Chieti 66100, Italy

Corresponding author: Gitana Maria Aceto, MSc, PhD, Research Scientist, Senior Lecturer, Department of Medical, Oral and Biotechnological Sciences, "G. d'Annunzio" University of Chieti-Pescara, *Via* dei Vestini, Chieti 66100, Italy. gitana.aceto@unich.it

Abstract

The liver is the most common site of metastases in patients with colorectal cancer. Colorectal liver metastases (CRLMs) are the result of molecular mechanisms that involve different cells of the liver microenvironment. The aberrant activation of Wingless/It (Wnt)/β-catenin signals downstream of Wnt ligands initially drives the oncogenic transformation of the colon epithelium, but also the progression of metastatization through the epithelial-mesenchymal transition/mesenchymal-epithelial transition interactions. In liver microenvironment, metastatic cells can also survive and adapt through dormancy, which makes them less susceptible to pro-apoptotic signals and therapies. Treatment of CRLMs is challenging due to its variability and heterogeneity. Advances in surgery and oncology have been made in the last decade and a pivotal role for Wnt/β-catenin pathway has been recognized in chemoresistance. At the state of art, there is a lack of clear understanding of why and how this occurs and thus where exactly the opportunities for developing anti-CRLMs therapies may lie. In this review, current knowledge on

the involvement of Wnt signaling in the development of CRLMs was considered. In addition, an overview of useful biomarkers with a revision of surgical and non-surgical therapies currently accepted in the clinical practice for colorectal liver metastasis patients were provided.

Key Words: Wingless/It/β-catenin signaling; Colorectal cancer; Epithelial-mesenchymal transition/mesenchymal-epithelial transition; Liver metastasis; Markers; Surgical and non-surgical therapies

©The Author(s) 2023. Published by Baishideng Publishing Group Inc. All rights reserved.

Core Tip: The liver is the most common site of metastasis in patients with colorectal cancer. Wingless/It (Wnt)/β-catenin signals can drive progression and metastatization by epithelial-mesenchymal transition/mesenchymal-epithelial transition. In the hepatic microenvironment, metastatic cells can survive through dormancy and become refractory to therapy. Further studies are needed to elucidate involvement of Wnt signaling in the development of colorectal liver metastases and to improve current surgical and non-surgical therapeutic approaches.

Citation: Selvaggi F, Catalano T, Lattanzio R, Cotellese R, Aceto GM. Wingless/It/β-catenin signaling in liver metastasis from colorectal cancer: A focus on biological mechanisms and therapeutic opportunities. *World J Gastroenterol* 2023; 29(18): 2764-2783
URL: https://www.wjgnet.com/1007-9327/full/v29/i18/2764.htm
DOI: https://dx.doi.org/10.3748/wjg.v29.i18.2764

INTRODUCTION

In patients with colorectal cancer (CRC), the liver and the peritoneum are the most common sites of visceral metastases[1]. Especially in Western countries, CRC appears to be a primary cancer with a predominant ability to metastasize to the liver[2-4]. Although CRC represents the third most common cancer worldwide, it appears to be the leading cause of death in both sexes[1,5,6]. Colorectal liver metastases (CRLMs) develop in 15%-60% of CRC patients[7-9]; at the time of diagnosis, approximately 20%-34% of CRC patients have synchronous liver metastases and more than 50% develop distant metastases within 5 years of primary tumor diagnosis[2,10]. If untreated, median survival of patients with CRC and unresectable CRLM is 5-10 mo[11]. CRLMs are the consequence of sequential molecular events. CRCs are caused by an aberrant Wingless/It (Wnt)/β-catenin pathway, which in 70%-80% of cases is rooted in mutational inactivation of the tumor-suppressor gene adenomatous polyposis coli (*APC*)[12,13]. Aberrant activation of both canonical and non-canonical Wnt/β-catenin signalings, downstream of Wnt ligands, initially drives the process of colon epithelial oncogenic transformation [14]. Particularly in CRC cells, activation of the canonical pathway induces transcriptional regulation of molecules that control cell division, apoptotic evasion, and metabolic demand of the microenvironment, which favor tissue growth. In contrast, in the non-canonical pathway, β-catenin-independent signal transduction controls cytoskeleton activation and invasiveness[14]. Increased nuclear β-catenin has been documented in the invasive front of primary CRC and in the liver metastases; furthermore, this increased expression has been correlated with increased invasive capacity and synchronous CRLM formation[15-17]. Wnt signaling pathway, initially deregulated in CRC tumorigenesis, may crosstalk with RAS-extracellular signal-regulated kinase (ERK)[18], epidermal growth factor receptor (EGFR) cascade[19] and also with vascular endothelial growth factor (VEGF)[19,20]. CRLM differs in *WNT* and *EGFR* gene expression compared with normal liver tissue, showing a high degree of heterogeneity[21]. Treatment of metastatic CRC is challenging because of its variable and heterogeneous characteristics. Advances in the field of oncology have been made in the last decade, and a central role of Wnt/β-catenin pathway has been recognized in CRC chemoresistance[17]. The molecular features of intrahepatic metastatic tissue, including the mutational status of *EGFR* or *VEGF*, may be a therapeutic target to increase the efficacy of neoadjuvant chemotherapy[22]. Current treatments, including radical surgery as well as systemic and localized therapy, achieve clinical results in only a minority of patients with CRLM, who have also a high recurrence rate. Surgical resection appears to be the unique treatment that can offer long-term survival and a better chance of cure, although it applies to only one-third of the patients with CRLM[23]. Unfortunately, about 80% of patients have unresectable metastatic lesions at the time of diagnosis, and for this, 5-year overall survival is low, with a rate of around 48%[24]. For these reasons, development of new integrated treatments has to be advocated to improve CRLM patient clinical outcome. According to these concepts, it is important to remember that early CRC diagnosis remains paramount to achieve a better prognosis[25,26].

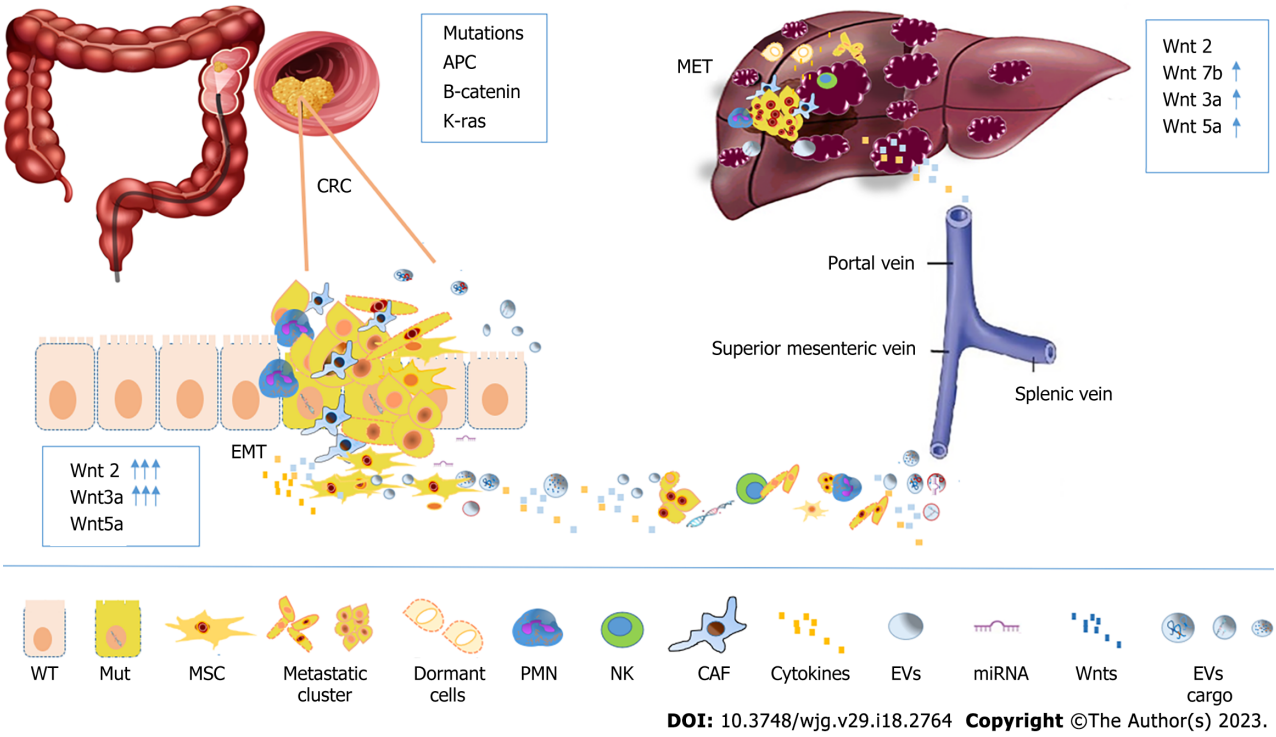
A better understanding of the mechanisms that regulate CRLM holds great potential for both adapting conventional therapies and developing new diagnostic methodologies. In this review, current knowledge on Wnt signaling in the process of CRLM was considered. In addition, an overview of valuable biomarkers with a revision of surgical and non-surgical therapies accepted in the clinical practice for CRLM patients were provided.

WNT SIGNALING: A DRIVER OF LIVER METASTASES FROM CRC

Cancer metastases result from complex selective processes depending on hepatic tissue anatomical, biological and microenvironmental factors. Evidence of metastatic propensity and organ-specific tropism of metastatic tumor cells mirror the concepts of "seed-soil", pre-niche and crosstalk between tumor cells and immune cells. These events allow tumor cells dislocated from the primary site to express their anchoring features on the tissue to be colonized as a site of implantation. Understanding of the interdependence of these biological mechanisms can provide valuable insights into treatment of CRLM[24]. During the metastatic event, tumor cells go through several stages, which include: Epithelial-mesenchymal transition (EMT) process, local tissue and vascular invasion, transition into the vascular system, extravasation process and seeding into the niche of the hepatic tissue. At the end of this multistep and dynamic model, metastatic cells finally have to be able to survive and grow by integrating into the cell community of the metastatic site[27]. Wnts are secreted glycoproteins that regulate multiple signaling pathways through both β-catenin-dependent and -independent mechanisms[28]. Aberrant activation of cellular pathways by Wnt ligands and β-catenin-dependent signaling promotes tumor progression and regulates EMT in CRC[1]. Wnt pathway somatic mutations are present in approximately 80%-90% of CRC patients. Both tumor cells and the surrounding microenvironment can express and release specific hyperactive Wnt ligands that can drive metastases even in cells with APC-inactivating mutations. However, several follow-up studies have revealed that the most aggressive subtypes of CRC do not show the highest levels of Wnt signaling[29]. RNA sequencing has shown that interference with Wnt signaling leads to up-regulation of gene programs that promote cell migration, invasion and downregulation of inflammation signatures in the tumor microenvironment (TME)[29]. Furthermore, it is believed that multiple ligands of Wnts may trigger numerous signaling pathways in addition to the β-catenin-mediated one; some of these alternative pathways have not yet been adequately studied in liver metastases[30]. Alterations in gene and protein expression allow CRC cells to make EMT/mesenchymal-epithelial transition (MET). EMT/MET program generates migrating tumor cells with intermediate phenotypic characteristics (Figure 1). CRC cells with a hybrid EMT/MET program migrate individually or in clusters through local or systemic spread[31]. Wnt signaling dysregulation activates downstream EMT by promoting emergence of migrating cancer stem cells (mCSCs) at the invasive front of the primary lesion. MCSCs invade locally through the driving force of the local TME and form distant metastases (Figure 1)[32].

Tumor progression results from interaction and cooperation between tumor and stromal cells of the hepatic microenvironment. In particular, inflammatory and metabolic signals can significantly influence rooting of metastatic cells in tissue niche, which can lead to reversion from EMT to MET and to their integrated adhesion with the new tissue site (Figure 1). The microenvironmental signals then induce EMT reversal (also called MET) to establish secondary micrometastases (colonization)[33-35].

Recent studies have revealed that cancer cells can follow an intermediate metastatic transition, with a mixture of cells showing features of either epithelial, mesenchymal phenotype or both at the molecular and morphological levels[36,37]. In intermediate stages, "quasi-mesenchymal" cells, which are mobile, more challenging to kill, and aggressive, express the *CDH1* gene (coding for E-cadherin protein) at the transcriptional level without displaying E-cadherin protein on the cell surface[38]. At this intermediate stage the cells have characteristics similar to stem cells and may co-express genes typical of both the epithelial and mesenchymal phenotype[39]. EMT/MET hybrid intermediates can promote metastatic tendency. It is unclear whether EMT/MET hybrid intermediate subpopulations may be responsible for treatment failure (immunotherapy, radiotherapy and/or chemotherapy). EMT can be regulated by different transcription factors and their gene regulatory networks that drive multiple levels of molecular changes. Some key transcription factors, such as Snail family transcriptional repressor 1 (Snail1)/Slug and zinc-finger E-box binding homeobox 1/2 (Zeb1/2), and myocyte enhancer factor 2A, promote the mesenchymal phenotype, while other transcription factors, such as ovol-like zinc finger 1/2 and grainyhead like transcription factor 2, suppress it by promoting the epithelial phenotype[40-43]. These transcription factors can act as either activator or repressor of downstream target gene expression, depending on Wnt signaling pathway activation level. One well-studied example involves the transcriptional activities of zinc finger E-box binding homeobox 1 (ZEB1) and Wnt/β-catenin signaling that mutually modulate each other, as ZEB1 potentiates transcription factor 4/β-catenin-mediated transcription, which in turn transforms ZEB1 from repressor to activator[44]. In addition to modulating its functions as either activator or repressor, Wnt/β-catenin signaling regulates ZEB1 protein expression [44].



DOI: 10.3748/wjg.v29.i18.2764 **Copyright** ©The Author(s) 2023.

Figure 1 Metastatic liver microenvironment in colorectal cancer. Genetic changes such as adenomatous polyposis coli, β-catenin mutations or K-RAS mutations can generate epithelial-mesenchymal transition/mesenchymal-epithelial transition; aberrant activation of Wingless/It (Wnt)2, Wnt7b, Wnt3a and Wnt5a ligands promotes local invasion of mesenchymal stem cell and cell migration from primary lesion to form distant colorectal liver metastases; tumor microenvironment, including extracellular matrix, blood vessels, extracellular vesicles, different types of cells, such as cancer and immune cells, proinflammatory cytokines, chemoattractants, and angiogenic factors, influences the metastatic cell colonization in tissue niches. EMT: Epithelial-mesenchymal transition; MET: Mesenchymal-epithelial transition; APC: Adenomatous polyposis coli; Wnt: Wingless/It; CRC: Colorectal cancer; MSC: Mesenchymal stem cell; CRLMs: Colorectal liver metastases; WT: Wild type; MUT: Mutant; PMNs: Polymorphonuclear neutrophils; CAF: Cancer-associated fibroblast; NK: Natural killer; EVs: Extracellular vesicles; miRNA: MicroRNA.

EMT regulation is also influenced by the action of microRNAs and long noncoding RNAs, as well as chromatid and post-translational modulations[43,45,46]. In the liver, Wnt/β-catenin signaling has physiological functions related to hepatocellular growth, metabolic liver zonation and regeneration[47]. Signal transduction of the canonical pathway mainly involves β-catenin and its ability to modulate T-cell factor (TCF)/lymphoid enhancer-binding factor (LEF)-dependent nuclear transcription factors, together with the activation of genes involved in cell proliferation, survival, differentiation, and migration, such as matrix metalloproteinases and c-Myc[48]. The non-canonical Wnt signals are many and involve calcium-dependent and independent pathways, as well as pathways mediated by c-Jun N-terminal kinase (JNK), protein kinase C, Ca^{2+}, Rho-type GTPases, mitogen-activated protein kinases (MAPK), and nuclear factors such as JUN/FOS and nuclear factor of activated T-cells[28]. While the canonical pathway drives tumor cells towards undifferentiation and growth, the non-canonical pathways appear to be involved in remodeling tissue architecture and mesenchymal differentiation.

Wnt family proteins transduce signals from tissue microenvironment through Frizzled (FZD) and low-density lipoprotein receptor-related protein (LRP) 5/6 receptors to the Wnt/β-catenin signaling as the canonical Wnt pathway and through FZD and/or tyrosine kinases ROR1/ROR2/RYK receptors to the Wnt/planar cell polarity cascade, while Wnt/receptor tyrosine kinase transduces Wnt signals to Wnt/Ca^{2+} signaling called non-canonical pathway[14,28].

Wnt signaling inhibits glycogen synthase kinase-3β (GSK3β) to stabilize β-catenin, which translocates into the nucleus to recruit transcription factors, LEF and TCF, and to promote the expression of SNAIL1 and SLUG, which modulate EMT. Loss of E-cadherin has long been believed to be a hallmark of EMT [49]. Its suppression is mainly attributed to the functions of SNAIL and SLUG expression, which directly bind to the E-box of the promoter region and downregulate its expression[49].

In adult tissue, renewal cell fate decisions appear to be distinct between the opposing Notch/Wnt responses. Crosstalk between Notch and Wnt allows signaling across the two pathways to be resolved into Notch-ON/Wnt-OFF[50]. Notch signaling indirectly activates β-catenin to promote and regulate EMT. Indeed, activation of Notch results in cleavage of Notch intracellular domain, which undergoes nuclear translocation of transcriptional factor, binds to SNAIL promoter, and regulates the mRNA level of SNAIL1/2 and ZEB1/2[35].

Interestingly, Wnt2 mRNA is frequently up-regulated in colorectal polyps, CRC, and CRLM[51]. Wnt2 contributes to CRC-derived cell invasive and metastatic ability by generating genetic changes in fibroblasts. This process seems to occur through extracellular vesicles (EVs) that play a key role in CRC genesis by activating Wnt signaling[17]. Wnt2 protein released from cancer-associated fibroblasts (CAFs) enhances invasion and migration of CRC cells[52]. Activation of Wnt7b may trigger EMT process through Wnt/β-catenin signaling and promote CRLM. Overexpression of the Wnt3a ligand can stimulate Wnt/β-catenin pathway in such a way as to modify cell morphology, regulate EMT and thus favor invasive capacity of tumor cells (Figure 1)[52]. In CRC, Wnt3a and Wnt5a are highly expressed at both primary and metastatic sites. In particular, Wnt3a expression increases at the primary site with a concordance rate higher than 70%. Wnt5a shows no correlation with pathological features or the expression of invasion-related proteins[13]. The expression profile suggests that Wnts might be involved initially when CRC develops and during tumor progression[13]. Recently, several Wnt/β-catenin target genes, including *S100A4*, *p16INK4a* and *BAMBI*, have been identified, showing the ability to promote cell migration *in vitro* and metastases *in vivo*[53]. Interestingly, three Wnt/β-catenin target genes, *5 BOP1* , *CKS2* and *NFIL3* have been found to be correlated with experimental metastases[53].

Increased expression of miR-92a-3p activates the Wnt/β-catenin pathway and promotes stemness, EMT, and metastases from CRC cells[52]. Nuclear β-catenin expression at the invasive front and in CRC tissue vasculature predicts metachronous liver metastases[51]. Both canonical and non-canonical Wnt signaling cascades play a key role in the development and evolution of CSCs. In addition to the classical reversible EMT/MET-driven transport pathway (hybrid-EMT), an alternative cell death process-driven transport pathway [blebbishield metastatic-witch (BMW)] involving a reversible cell death process has been identified[54]. Knowledge of EMT and BMW pathways is important for metastatic tumor therapy, as these pathways confer drug resistance and immune evasion/suppression in the context of coordinated oncogenic, metabolic, immunological, and cell biological events that drive metastases[54]. Specifically, in the tissue microenvironment, cell death signals such as apoptosis, ferroptosis, necroptosis, and neutrophil extracellular traps formation (NETosis) related to BMW or EMT pathways recruit immune cells that may despite themselves promote migration of cancer cells to distant sites to establish metastases[54]. Proinflammatory molecules of the TME may modulate CRC progression. In TME, stromal cells secrete multiple factors, such as chemokines that attract inflammatory cells producing soluble cytokines that promote tumor cell survival. Indeed, high levels of tumor necrosis factor alpha (TNF-α), interleukin (IL)-6, IL-1β and chemokines, such as CXC ligand of chemokines 1 (CXCL1), CXCL2 and CXCL12, counteract host defense mechanisms. Increased levels of IL-6 expression are associated with advanced-stage CRC, since liver metastasis formation is supported by CAFs involved with the creation of a prometastatic microenvironment through IL-6 and monocyte chemo-attractant protein-1 activation. On the other hand, IL-1β activates inflammasome and induces angiogenesis in both the primary colon cancer and metastases[55]. High expression of chemokine receptor type 4 (CXCR4) is observed in patients with liver metastases from CRC, while its ligand CXCL12 is highly expressed in the most frequent metastatic sites of CRC, such as liver, lymph nodes, and lungs, and is a chemoattractant for CXCR4-positive cancer cells[56,57]. Some of these inflammatory mediators, such as TNF-α, may also fulfil the role of tumor suppressors, reconstitute TME by increasing cytotoxic T-cell activity, mature dendritic cells and prevent neoangiogenesis[55].

Immune components of TME may modulate tumor progression and represent interesting therapeutic targets in liver metastases. Indeed, CRLM is also promoted by activating TDO2-kinurenin-AHR pathway, which facilitates programmed cell death protein-1 (PD-1)-mediated immune evasion and maintenance of stemness through Wnt signaling[58]. Recently, in a single-cell analysis on intratumor mutational diversification of CRC cells, a highly heterogeneous tumor immune microenvironment has been found to be enriched with the granulocyte component in CRLMs. Therefore, it was proposed that activation of Wnt signaling coupled with ferroptosis death may promote granulocyte migration into the tumor and metastatic microenvironment (MME)[59].

Metastatic organotropism is believed to be a process that relies on the intrinsic properties of tumor cells and their interactions with molecules and cells in the microenvironment. Even before tumor cells spread, hepatocytes secrete multiple factors to recruit or activate immune cells and stromal cells in the liver to form a favorable premetastatic niche. Liver-resident cells, including Kupffer cells, hepatic stellate cells (HSCs), and hepato-sinusoidal endothelial cells, are co-opted by recruited cells, such as myeloid-derived suppressor cells (MDSCs) and tumor-associated macrophages to establish an immunosuppressive hepatic microenvironment suitable for tumor cell colonization and growth. For these reasons, understanding of the mechanisms that regulate metastasis-prone hepatic immune microenvironment could facilitate immuno-oncology interventions for treating CRLM[27,59,60].

The spread of tumor cells and their ability to survive and grow in a secondary site require intercellular communication pathways with other cells residing in the tissue microenvironment. In recent years, several signaling cascades have been found to use EVs in tumor-stroma interaction. Indeed, modulation of Wnt signaling may also be associated with EVs formation. Tumor cell-derived EVs exert their protumorigenic effects through direct interactions among biologically active surface molecules, transfer of proteins and nucleic acids into recipient cells, or transfer of metabolites that can be used as energy source by the recipient cell; these events induce physiological and phenotypic alterations in tissue environment[61]. Secretion of Wnt proteins through endosomal compartments on

exosomes plays an evolutionarily conserved functional role in extracellular vesicular transport[62]. CRC cells promote angiogenesis through Wnt/β-catenin signaling mediated by Wnt4-enriched exosomes in endothelial cells under hypoxic conditions, which could represent a novel mechanism in the development of CRC and its progression towards CRLM[63]. Moreover, constitutively active mutant β-catenin can be transported through EVs, activate the Wnt pathway in recipient cells and promote cancer progression[64].

Accumulating evidence indicates that EVs have roles in pre-metastatic niche formation and organotropic metastasis. EVs modify the microenvironment to recruit distinct supporting stromal cells, upregulate pro-inflammatory genes, and activate an immunosuppressive state[65]. These signals may mediate the awakening of dormant niches of cancer cells. A minority of disseminated tumor cells (DTCs), surviving as latent entities may take root in the new microenvironment of the recipient organ even years after the removal of a primary CRC. Possibly, over time, the conditions of the recipient organ may change and favor awakening and engrafting of latent tumor cells into the premetastatic niche[66]. Recently, the gut microbiome has also been documented in controlling the metastatic process and premetastatic niche formation[67]. Various bacteria have been implicated in CRC progression by modulating β-catenin pathway[17]. In the liver, CRC premetastatic niche is induced by bacteria dissemination from the primary tumor[10]. Moreover, in CRC patients concomitant chronic hepatitis B virus infection significantly increases the risk of CRLM[68]. Furthermore, in some patients, the same therapeutic programs could induce macro- and micro-environmental changes in the receiving organ, to favor a greater engraftment capacity of cancer cells[69]. Autocrine inhibition of Wnt could promote metastatic latency and immune evasion by deregulating the expression of Dickkopf's Wnt signaling pathway inhibitor 1 (DKK1), in which case the cells arriving to the recipient organ would undergo a slow cell cycle state which would allow them to evade natural killer cell-mediated clearance. By expressing a stem state but actively silencing Wnt signaling, cells could enter quiescence and evade innate immunity to remain dormant for prolonged periods[70]. Finally, cancer cells can actively emit large amounts of EVs with onco-functionality in a variety of contexts such as stromal crosstalk, immune evasion, metastatic site priming and drug resistance. In other cases, tumor cells may remain as latent entities at low cycles and sometimes reactivate following changes in the microenvironment. Currently, there is a lack of clear understanding of why and how this occurs and thus, where exactly the opportunities for developing anti-CRLM therapies may lie.

DORMANT CELLS IN LIVER METASTASES

Cancer cells can enter dormancy, which is a state characterized by either a reversible arrest or a slow cycling[71]. Dormant cells arise from DTCs derived from primary lesion[72]. They acquire new features, becoming non- or slower proliferating cancer cells and resistant to chemo- or targeted therapy, while tumor progression is not clinically visible. A dormant cancer mass (indolent small clusters) includes equilibrium between cell division and apoptosis. Dormant cells can be activated to re-enter cell cycle under particular conditions[72-75]. Micrometastases of CRC can enter a dormant state for years before recurring as metastatic disease[76]. CRC is characterized by two different types of recurrence, the first of which results from reactivation of dormant tumor cells, possibly in distal organs. In contrast, the second type is a relapse after surgical remission due to micrometastatic lesions present in apparently normal tissue adjacent to the tumor. Recurrence implicates changes in TME or immune escape[77]. Indeed, a successful metastasis depends on the dynamic interactions between cancer cells and the host MME[7]. During dissemination and tumor progression, dormant cells show a reduced metabolism associated with constrained growth and can survive under hypoxia and nutritional deprivation[73]. Dormant cells reduce E-cadherin expression and up-regulate activity of the survival pathway through unfolded protein response. This results in down-regulation of major histocompatibility complex class I molecules and immune evasion through undetectability by CD8+ T lymphocytes[78-80]. E-cadherin blocks cell cycle to reduce fraction and velocity of cell proliferation, limiting the effectiveness of therapeutic agents targeting cell cycle. Dormancy-independent resistance stems from E-cadherin signaling pathway and survival kinases, such as AKT, ERK and Janus kinase (JAK)[78]. A high ratio of p38 MAPK/ERK MAPK can induce DTCs into dormancy, while a high ratio of ERK MAPK/p38 MAPK can induce dormant cell awakening and proliferation. These pathways prevent cMET activation, while their downregulation induced by hepatocytes in the MME induces E-cadherin re-expression[73]. Primary CRCs can promote the formation of hepatic pre-niches through microRNA (miRNA)-containing exosomes[24]. Moreover, proinflammatory cytokines, chemoattractants, and angiogenic factors produced by primary tumor induce pre-niche formation by the involvement of bone marrow-derived cells, and marrow-derived granulocytic MDSCs[24]. Activation of HSCs into proliferative myofibroblasts is a significant cause of recurrence of CRLM and hepatic fibrosis[78]. The liver microenvironment offers beneficial conditions for cancer cell dormancy[72].

Surgical procedures can lead to increased levels of pro-angiogenic growth factors, such as VEGF, which could activate dormancy tumor cells by altering their equilibrium through the involvement of the immune system; inhibition of angiogenesis limits tumor growth through increased cancer cell apoptosis

[71,81]. Detection of single-nucleotide polymorphisms in cellular and angiogenic dormancy-related (*NOTCH3* and *NME1*) and dormant CSC related genes (*CD44*) has been associated with treatment response, recurrence and clinical outcome in patients with resected CRLMs[82]. In human CRLMs, quiescence induced by 5-fluorouracil (5-FU) is linked to activation of Yes tyrosine kinase (YES1) and to nuclear depletion of Yes-associated protein (YAP). Moreover, *YES1* silencing decreases nuclear YAP accumulation and induces cell quiescence in 5-FU-free conditions. Increased *YES1* and *YAP* transcript levels in residual CRLMs treated with adjuvant chemotherapy are related to the risk for CRC recurrence and reduced survival[76,83].

The number of resident hepatic $CD25^{-}$ TCR^{+} cells is critical for tumor dormancy in the presence of immunosuppressant cyclosporin A in a rat model. Transformation of growth factor-beta 1 is involved with the acquisition of tumor invasiveness and metastatic spread[84]. Cancer dormancy is poorly understood in its complexity[79]. In disease recurrence and metastases, reactivation of chemotherapy-resistant quiescent cancer cells is the key mechanism that needs to be fully understood. Interestingly, itraconazole-derived subsequent inhibition on suppressor of fused activation in Wnt epithelial tumor cells prevents nuclear localization of β-catenin causing Wnt inhibition. Itraconazole perturbs dormancy by signaling effects on Wnt pathway[85]. Dormant cells are also re-activated through JAK/STAT3 pathway regulation induced by chemokine (C-C motif) ligand 7 (CCL7), which is secreted by monocytic MDSCs[75].

It is of clinical importance to effectively identify and target dormant CRC cells as potential drivers of CRLM with emphasis on Wnt/β-catenin deregulation. Induction of Wnt signaling has been involved with activation of cell cycling of quiescent cells and regulation of stem cell self-renewal[86]. Specifically, Wnt3a alters cell fate program of primitive hematopoietic stem and progenitor cells[86]. Moreover, Wnt pathway is implicated in reactivation of dormant cancer cells induced by extracellular matrix (ECM)[87]. It has been hypothesized that ECM constituents derived from metastasis-initiating cancer cells (stem cell-like properties) and stromal cells may create a suitable microenvironment that activates signaling pathways useful for metastatic cell proliferation and colonization[88]. On the other hand, inhibition of Wnt signaling by DKK1 is a mechanism used by cancer cells to enter quiescence[87]. Several markers can be used to assess CRC cell dormancy state in the liver, such as CK, E-cadherin, Sox-2 and CD133 and cell awakening state such as vimentin, cyclin-D1, Ki-67, c-Myc and VEGF[89]. Some studies have found that tumor cell quiescence can also be induced by metabolic modulation and reactive oxidative species (ROS) *via* miRNAs and peroxisome proliferator-activated receptor γ coactivator 1α, which is a pivotal factor in lipid and metabolic regulation[90,91]. It has recently been suggested that redox mechanisms can control dormant or low-activity tumor cell life cycle, including long-term dormancy and metastatic recurrence. Indeed, quiescent tumor cells overexpressing antioxidant enzymes may survive at low levels of ROS. These cells are strongly involved with cancer recurrence and are able to escape chemotherapy-induced death[92]. On the other hand, increased redox levels associated with oxidative stress may be responsible for a reprogramming process leading to reactivation of dormant cancer cells. Moreover, activation of p38 MAPK signaling is redox-mediated and has priority over ERK1/2 under oxidative stress. In this context, endoplasmic reticulum-stress signaling can induce a dormant state in DTCs[92]. Cooperation between antioxidant enzyme nuclear factor erythroid 2-related factor 2 (Nrf2) and β-catenin has been found in hepatocellular cancer. Nrf2 activation plays a role in oxidative stress as transcriptional regulator of many genes with effects on carcinogenesis suppression[93]. Under acute oxidative distress, CRC cells subjected to growth factor deprivation that mimics cell dormancy show differential gene expression in Wnt/β-catenin-dependent and independent pathways, and cytoplasmic APC modulation[94]. Furthermore, ROS regulate relationships between β-catenin and forkhead box O in JNK signaling activation and cell quiescence[95]. These findings demonstrate that Wnt pathway is a redox-dependent signaling in cancer cellular dormancy and can play an important role in CRLM development and progression.

TUMOR BIOMARKERS AND TARGET THERAPIES IN CRLM

In CRC patients, biomarkers are increasingly needed to improve tumor stratification, detection and prognosis[96]. Biomarkers are both clinical and biochemical, such as the ECOG Performance Status Scale, white blood cell count, alkaline phosphatase, lactate dehydrogenase, CRC staging according to the tumor-nodes-metastasis (TNM) system from the American Joint Committee on Cancer[97].

It is recommended that CRLM patients, especially those considered in a third-line/salvage-therapy setting, should be stratified according to whether their tumors are *RAS* wild-type or *RAS* mutant[98]. Indeed, in metastatic disease setting, the presence of activating *RAS* (*KRAS*/*NRAS*) mutations represents a negative predictive biomarker for cancer cell resistance to monoclonal antibodies directed to EGFR[99], which may detrimentally affect patient health status, specifically when combined with an oxaliplatin-based cytotoxic backbone.

As a result, the European Medicines Agency has restricted chemotherapy and EGFR-directed antibodies, such as cetuximab and panitumumab, only to patients with *RAS* wild-type metastatic CRC. In CRC tumorigenesis, the most frequent mutations are *APC* and *KRAS*[18]. Dysregulation of Wnt/β-

catenin signaling plays a pivotal role in the development and progression of several human cancers, including CRC[17]. A synergistic cooperation between Wnt/β-catenin and RAS-ERK pathways has been observed in CRC with *APC* and *KRAS* mutational status, which has led to stabilization of both β-catenin and RAS[18].

For prognostic assessment of CRLM patients, both the European Society for Medical Oncology and the National Comprehensive Cancer Network guidelines recommend assessing *RAS* and *BRAF* mutation status simultaneously[100,101]. Double mutations in *APC* and *BRAF* are associated with poorer prognosis as compared to single mutations[102]. It has been reported that two-thirds of *BRAF*-mutant primary tumors are located on the right side of the colon and associated with an increased incidence of peritoneal and distant lymph node metastases[103]. *BRAF* gene mutations (most commonly V600E substitution) are present in 8%-12% of patients with CRLM and are considered unfavorable prognostic biomarkers. Indeed, the presence of mutated BRAF correlates with a median survival of 10.4 mo as compared to 34.7 mo in wild-type BRAF[103]. Notably, $BRAF^{V600E}$ mutation, when present, is almost exclusively non-overlapping with *RAS* mutations. $BRAF^{V600E}$ mutation is a negative predictive biomarker for EGFR antibody therapy for CRLM patients, making response to panitumumab or cetuximab treatment highly unlikely. $BRAF^{V600E}$ mutations are present in nearly one-third of CRC patients with microsatellite instability (MSI). Among patients with CRLM, MSI has been documented in less than 10%[104].

Predictive data from treated patients with CRLMs have recently shown that the mismatch repair status can predict an objective response of a tumor to blockade of PD-1[105]. Thus, MSI testing in patients with CRLM has become strongly recommended for its predictive value in treating CRC patients with immune checkpoint inhibitors (with pembrolizumab or nivolumab ± ipilimumab). In terms of response to adjuvant treatment, for CRC patients with *RAS* and *BRAF* wild-type tumors, chemotherapy associated with anti-EGFR antibodies has demonstrated to be significantly more beneficial in the presence of primary left-sided tumors. In contrast, for right-sided tumors, greater survival is associated with chemotherapy combined with bevacizumab[106].

Interactions between the Wnt/β-catenin and RAS-ERK pathways have already been reported in CRC [18]. Combined anti-CSC therapy with drugs targeting both Wnt signaling and tyrosine kinases could be a useful anti-cancer rationale[107]. Tyrosine kinases are aberrantly activated in cancer cells due to genetic alterations. Tyrosine kinase inhibitors can improve CRC prognosis; however, unavoidable drug resistance and cancer relapse are serious problems in clinical practice[107].

Resistance to targeted therapies in CRLM patients exists even among patients whose tumors are wild-type in *KRAS*/*NRAS* and *BRAF* genes, underlining the need to find and better characterize additional resistance biomarkers. A list of biomarkers beyond *RAS*, *BRAF*, and MSI molecular testing is emerging, which may impact the next clinical decisions in targeted therapies. Though they are not recommended for routine patient management outside a clinical trial setting, some of the emerging biomarkers are: *ERBB2* and *MET* gene amplifications, ligands such as amphiregulin (*AREG*), epiregulin (*EREG*), alterations/mutations in phosphoinositide-3-kinase (*PI3KCA*), phosphatase and tensin homolog deleted on chromosome 10 (*PTEN*) and *HER3*.

In CRLM, *MET* amplification is reported to be a potential mechanism of patient acquired resistance to anti-EGFR therapy[108]. However, multiple trials with different types of MET inhibitions have been unsuccessful in proving a predictive value for MET inhibition in CRLM patients previously treated with chemotherapy and EGFR-directed antibodies[109].

EGFR activation is involved with cell survival and proliferation through MAPK and the PI3K pathways[110]. Approximately 20% of *PIK3CA* mutations have been reported in exon 20 of its gene locus on chromosome 3q26.32. The presence of these mutations in tumor tissue has been associated with resistance to anti-EGFR therapies in chemorefractory CRC[111]. However, at the moment, there are no clinical recommendations for detecting mutations in *PIK3CA* exon 20 outside the CRC research field.

Other biomarkers associated with sensitivity to anti-EGFR therapies are gene expression status of *EREG* and *AREG*, which encode for EGFR ligands epiregulin and amphiregulin[112]. *EREG* and *AREG* are strongly regulated by methylation, and their expression is associated with CpG island methylator phenotype status and primary tumor site[113]. It is well documented that high *EREG* and *AREG* expression and left-sided primary colon tumors are associated with efficacy of anti-EGFR therapy[114]. Therefore, assessment of methylation status of *EREG* and *AREG* could be rationally used to predict resistance or susceptibility to anti-EGFR therapies in CRLM patients.

Recently, attention has been placed on the role that HER3 plays in resistance to anti-EGFR therapy. HER3 is overexpressed in several human cancers, including CRC[115]. Somatic mutations in *HER3* have been found in approximately 10% of CRC patients[116], and patients harboring CRC overexpressing HER3 display a worse clinical outcome as compared to those with low expression levels[117]. HER3-targeted therapies based on the use in clinical trials of either monoclonal antibodies, such as patritumab [118] and seribantumab[119], or bispecific monoclonal antibodies against EGFR/HER3, such as duligotuzumab[120], failed to have clinical benefits in CRLM patients.

We need to establish predictive biomarkers that are reliable indicators of activated Wnt signaling. Biomarkers on Wnt activity that show diagnostic, prognostic and therapeutic importance are strongly advocated. Plasmalemma vesicle-associated protein-1, which is a marker of intestine-vascular barrier impairment, is a prognostic marker for CRC recurrence, leading to CRLM[10]. High Wnt6 expression in

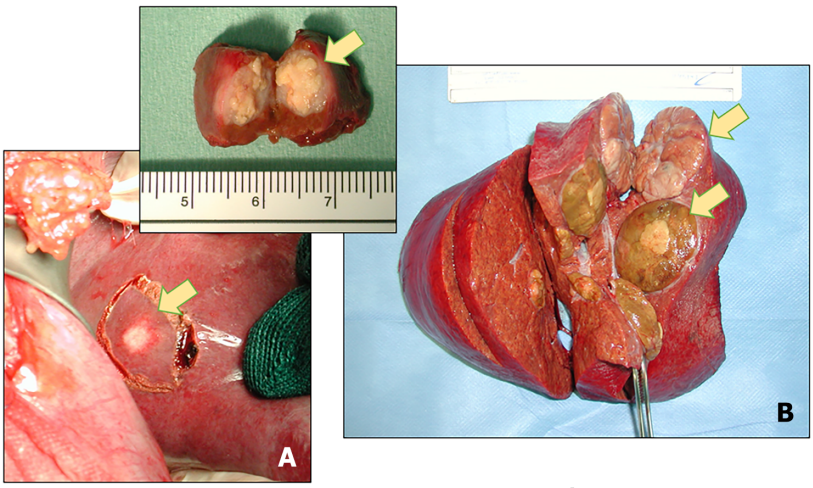
CRC indicates an unfavorable prognosis for patients with CRLM after hepatectomy, suggesting that Wnt6 expression may be a valuable biomarker[51]. Loss of Wnt5a expression is correlated with recurrence reduction and decreased survival in node-negative CRC patients[121]. Serum Wnt4 level may represent a potential biomarker for CRC patients[52]. COX-2 overexpression may have prognostic/diagnostic implications regarding Wnt signaling[121]. In addition, the presence of β-catenin in the nucleus is the only irrefutable proof of Wnt pathway activation. Nuclear β-catenin expression in metastatic lymph node is associated with age, tumor differentiation, TNM stage and liver metastases. Nuclear β-catenin expression may represent a clinically useful marker in differentiating highly metastatic and less invasive CRC[16]. Developing more sensitive antibodies that detect activated (dephosphorylated) β-catenin may represent valid prognostic markers.

THERAPEUTIC STRATEGIES IN CRLMS

Recamier introduced the concept of metastatic cancer cells in 1829 and only in 1952, the first liver metastasis was removed by Lortat-Jacob[81]. The incidence of CRLM is around 12.8%-15% during five years of follow-up after primary CRC diagnosis[7,122]. About 14%-25% of patients have synchronous CRLM at diagnosis, defined as CRLM detected concurrently or before primary CRC, while 7%-40% develop metastatic lesions during the follow-up[6,9,11,122-124]. The occurrence of metachronous CRLMs is related to histopathology and serum-based biomarkers, TME and liquid biopsy[122].

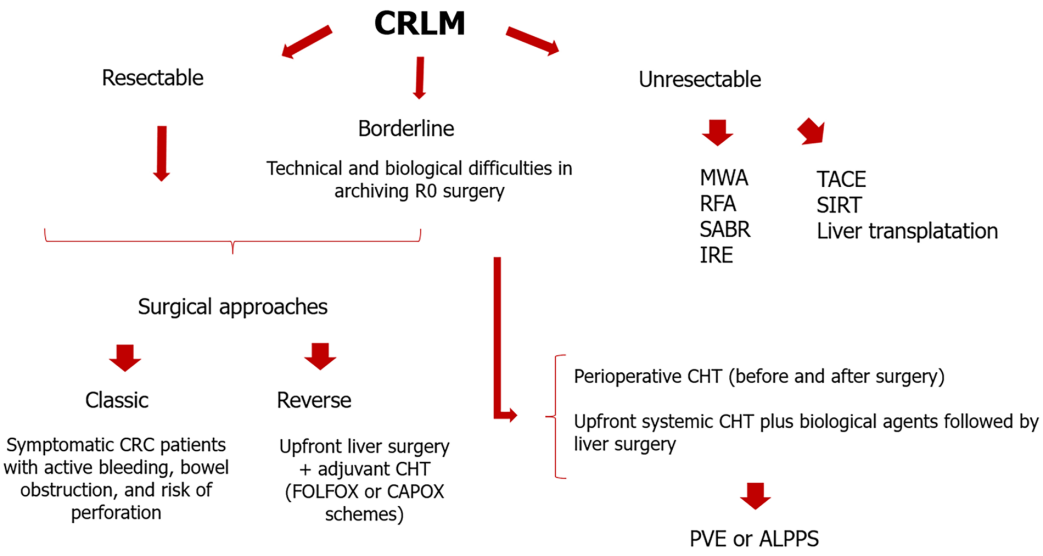
Surgical approaches for CRLM patients

Unfortunately, only 20%-30% of patients are eligible for hepatectomy[9,125,126]. However, after resection, around 65% of patients develop recurrence[127,128]. For patients with only CRLM, surgical resection is still the treatment for curative intent (Figure 2)[6,8,9]. Liver resection has perioperative mortality and morbidity rates of 1%-3% and 30%, respectively[128]. Specifically, major hepatectomy for CRLM has a mortality and major morbidity of 1%-5% and 20%, respectively[9]. In resectability assessment, CRLM patients are considered "resectable", "borderline" or "unresectable" (Figure 3)[6]. The definition of borderline patients concerns technical and biological difficulties that reduce the possibility of achieving an R0 resection. Based on the European Society of Medical Oncology guidelines and multidisciplinary evaluation, three approaches are currently defined: Upfront liver surgery followed by adjuvant chemotherapy (FOLFOX or CAPOX schemes), perioperative chemotherapy (chemotherapy before and after surgery based on FOLFOX or CAPOX scheme), and upfront systemic chemotherapy plus biological agents followed by liver surgery[128]. Surgery planning is based on a "classic" approach with primary CRC resection and a "reverse" approach, where liver metastases are resected first[9,124,128]. The liver-first approach or reversed strategy is more appropriate for either asymptomatic CRC or in locally advanced CRC[6,9]. Classic and reverse surgery showed similar outcomes. In common clinical practice, patients have symptomatic primary tumors with bleeding, obstruction, and a high risk of perforation. For this population of patients, the classic procedure is more often indicated (Figure 3). The reverse approach is performed when the primary tumor is asymptomatic with the aim of reducing the risk of CRLM progression[6,128]. A better prognosis is documented in patients treated with liver resection, which includes a resection margin > 1 mm from the tumor border [128,129]. R1 resection is associated with a higher rate of intra-hepatic local recurrence. Combined colorectal and hepatic resection in one setting is reserved to patients with easy-to-resect primary cancers and limited hepatic disease[9]. Currently, no differences in surgical outcome or survival have been reported when comparing classic, synchronous and liver-first approaches[9,81]. Liver resection combined with chemotherapy offers the best chance of cure with a reported 5-year survival and 10-year survival of 33%-58% and 23%-39%, respectively[123]. Routine chemotherapy improves progression-free survival by 8% at 3 years[130]. Metastatic cancer cells can also remain dormant after obtaining R0 surgical resection[131]. In literature, the percentage of disappearing CRLM ranges from 2.7% to 37%[9]. Although disappearing CRLM cells are of great interest, no consensus on their management has been reached[132]. Disappearing CRLM should be resected whenever feasible because a conservative management of leaving disappearing hepatic lesions results in a local recurrence of 19%[9]. This is a complex topic and the incidence of disappearing CRLM is likely to increase with advances in chemotherapy. The current management of patients with CRLM is multidisciplinary. Current guidelines for major hepatectomy recommend a future liver remnant (FLR) of > 20%-25% in healthy patients, > 30% in patients treated with chemotherapy, and > 40% in cirrhotic patients[6,130]. If FLR is inadequate, a variety of techniques are indicated to induce hepatic hypertrophy, *i.e.,* portal vein embolization, two-stage hepatectomy, association of liver partition and portal vein ligation for staged hepatectomy (ALPPS). Technically, ALPPS consists in liver transection and ligation of the portal vein (first operative approach) followed by resection of metastatic liver segments[9]. Surprisingly, ALPPS causes great hepatic hypertrophy as compared to portal vein ligation with low perioperative risk and satisfactory survival in large hospitals[9]. Laparoscopy has become the gold standard for minor hepatectomies[133]. With implementation of surgical education and minimally invasive techniques, such as laparoscopy and robotic systems, major and extended hepatectomies have been progressively reported. Laparoscopic



DOI: 10.3748/wjg.v29.i18.2764 **Copyright** ©The Author(s) 2023.

Figure 2 Intraoperative images. A: Minor liver resection for colorectal liver metastasis (CRLM); B: Major hepatectomy for multiple CRLMs. Courtesy of Professor Paolo Innocenti, from his personal archive.



DOI: 10.3748/wjg.v29.i18.2764 **Copyright** ©The Author(s) 2023.

Figure 3 Guidelines in colorectal liver metastasis treatments. CHT: Chemotherapy; CRC: Colorectal carcinoma; MWA: Microwave ablation; RFA: Radiofrequency ablation; SABR: Stereotactic ablative body radiotherapy; IRE: Irreversible electroporation; TACE: Transarterial chemoembolization; SIRT: Selective internal radiation therapy; PVE: Portal vein embolization; ALPPS: Associating liver partition and portal vein ligation for staged hepatectomy; CRLM: Colorectal liver metastasis.

liver resection (LLR) improves hospitalization and decreases complications as compared to open surgery[123]. LLR is commonly indicated for tumors located along the liver periphery (segment II, III, IVb, V and VI)[134]. For larger tumors located in superior or posterior hepatic segments, either robotic or hybrid approach (hand-assisted or laparoscopic-assisted open approach) has potential advantages and has overcome the limitations of laparoscopic procedures. After LLR, the reported overall survival at 1-, 3-, and 5-years is 88%, 69%, and 50%, respectively. For disease-free survival, the reported results at 1-, 3-, and 5-years are 65%, 43% and 43%, respectively[134]. Recent data confirm that simultaneous laparoscopic resection of CRC and liver metastases are safe and feasible with the same benefits in terms of oncological outcome compared with open approach[11,124]. Robotic surgery is considered one of the options for CRLM resection to ameliorate the technical limitations of LLR[135]. Robotic systems overcome the disadvantages of laparoscopic approach and facilitate complex surgical procedures such as right hepatectomy, left hepatectomy, central bisegmentectomy, and posterior sectionectomy[136]. Current evidence documents a longer operative time for robotic surgery for CRLM compared with open approach, but a significantly shorter hospital stay[137]. Robotic surgery for CRLM might achieve R0 resection with similar results in terms of overall and disease-free survival compared with open surgery. A multi-institutional analysis of ultrasound-guided robotic surgery for CRLM reported a curative resection rate of 92% in patients with a median tumor size of 2.7 cm (range 0.4-13 cm)[135]. In patients

with CRLM treated with major hepatectomy using robotic systems, 1-, 3-, and 5- year overall survival rates are 87%, 87% and 87%, while disease-free survival rates are 85%, 85% and 85%, respectively[136]. In a multi-center Italian experience, the reported 1- and 3-year disease-free survival is 83.5% and 41.9%, while the 1- and 3-year overall survival is 90.4% and 66.1%, respectively[135]. The open approach has still a role in treating CRLM, especially in patients with a previous history of abdominal open surgery, with synchronous colonic and liver disease and with large liver metastases (Figure 2). Current guidelines consider thermal ablation the gold standard to eliminate small unresectable CRLM[137]. Microwave ablation (MWA), radiofrequency ablation (RFA), irreversible electroporation (IRE) and stereotactic ablative body radiotherapy (SABR) are valid local treatment options for patients with CRLM (Figure 3)[137]. RFA uses alternating electrical current at the frequency of 400 MHz to generate thermal energy, while MWA uses electromagnetic waves with frequencies greater than 900 MHz. Ablative therapies are indicated for patients with unresectable CRLM in combination therapy with hepatectomy, and for patients with comorbidity that are unfit to undergo major surgery. Ablation procedure could be performed using open, laparoscopic or percutaneous approaches[137,138]. The final objective is to obtain complete ablation with 10 mm margins in all directions[9]. While RFA is susceptible to the heat-sink effect with its limits in treating hepatic lesions in close proximity of large vessels, MWA has demonstrated effective in reaching higher tissue temperatures with a more homogeneous tissue heating [138]. Ablative treatments are relatively safe and less invasive methods. The reported morbidity rate is 4%-9% and the mortality rate is 0%-2.0%. Common complications include postoperative bleeding, infections, pneumothorax, hepatic abscess, and biliary tract injury[138,125]. Regarding local tumor control, recurrence after RFA ranges from 4%-40%, while after MWA the reported range is from 6%-10%. Tumor size > 3 cm and ablation margin < 0.5 cm represent predictor factors of local recurrence. Patients with unresectable CRLM have shown a median disease-free survival of 6 mo and median overall survival of 24 mo after laparoscopic RFA[138]. Other studies have reported a median survival of 24-39 mo. 1-, 2-, 3-, and 5-year overall survival ranged from 73%-92%, 41%-72% and 20%-40% in patients with CRLM of 3-5 cm[125]. Median disease-free survival is around 12 mo in patients with CRLM of 4-5 cm. For CRLM > 3 cm, 1-, 2-, 3- and 5-year overall survival ranged from 74%-93%, 30%-70%, and 8%-31%. The reported median disease-free survival in CRLM > 3 cm is 12.4 mo[125]. In patients with difficult-to-reach anatomical lesions, some authors have suggested SABR as an alternative procedure to treat large and unresectable CRLMs[125]. An Italian study reported a 1-, 2-, and 3-year overall survival of 68%, 40% and 17%, respectively, in patients with CRLM > 3 cm. SABR seems to have benefits in local control of larger hepatic lesions compared with MWA. The reported pooled 1- and 2- year control rates are 67% and 59.3%, while 1- and 2-year overall survival are 67.2% and 56.5%, respectively[9,137]. Guidelines have defined SABR as a reasonable therapy for CRLM patients unsuitable for surgery or ablative therapies, but a definitive validation in a large randomized analysis is required[9]. A relatively new non-thermal ablative method for unresectable CRLM is represented by IRE[8]. It is a nonthermal ablation modality using high-voltage electric pulses that induce permanent cell membrane disruption by sparing ECM and preserving critical structures such as blood vessels and biliary ducts[8,9,137]. After IRE treatment, the reported median overall survival ranges from 19.7-32.4 mo[125]. The reported hepatic IRE efficacy varies from 45.5%-100%[8]. A phase II trial (COLDFIRE-2) has reported that IRE is an effective relatively safe treatment for CRLM of 5.0 cm or smaller, with an overall complication rate of 40% (infected biloma, portal vein thrombosis, embolic event, cardiac arrhythmias and acute myocardial infarction). Around 68% of patients are alive one year after IRE treatment, with a median overall survival of 2.7 years after first IRE, and 4.8 years after CRC resection[8]. IRE might be indicated for liver recurrence after previous percutaneous treatment. After repeated IRE, local tumor control is reached in 74% of patients[8]. IRE represents a new and attractive research field and should be considered for patients with oligometastatic CRLM of 5.0 cm or smaller, anatomically unsuitable for surgical procedure or thermal ablation. Although IRE is a promising technique, evidence of IRE in CRLM treatment is still under validation[137]. Liver transplantation is a rare procedure for CRLM patients but mounting evidence suggests survival benefits in selected instances[6]. CRLM prognosis strongly depends on node-positive primary CRC, disease-free interval from primary tumor resection and metastasis detection < 12 mo, hepatic lesion > 5 cm, carcinoembryonic antigen levels > 200 ng/mL and > 1 hepatic lesion. More than two reported prognostic determinants are related to poor prognosis[128]. Surgical resection remains the gold standard for CRLM patients. CRLM distribution, size and number may have prognostic value[6]. CRLM outcome might be improved only if a personalized treatment approach is taken into account, and this has to consider tumor biology, disease staging and patient condition[9].

Chemotherapy for CRLMs

Neoadjuvant chemotherapy has the advantage of down-staging metastatic disease to facilitate curative hepatic resection. It is indicated for patients with borderline resectable or unresectable CRLM with high surgery risk (Figure 3)[129]. First-line schemes consist in fluorouracil-based regimens containing oxaliplatin and/or irinotecan. Neoadjuvant therapy offers no survival advantage in resectable synchronous CRLM with a 5-year overall survival of 42%, which is similar to patients treated with upfront surgery[9,129]. Systemic oxaliplatin- or irinotecan-based chemotherapy constitutes the standard for CRLM patients in many countries[129,139]. Systemic treatments for CRLM consist in a combination of fluorouracil (plus leucovorin) and either irinotecan (FOLFIRI) or oxaliplatin (FOLFOX) plus

bevacizumab, or XELOX (capecitabine and oxaliplatin) and fluorouracil, leucovorin, oxaliplatin, and irinotecan (FOLFOXIRI)[7,129,140]. The choice of a primary line therapy is based on the physician choice and not on drugs, because irinotecan or oxaliplatin lead to similar results. Induction therapy with FOLFOXIRI plus bevacizumab improve CRLM outcome and increase incidence of some adverse events compared with FOLFIRI plus bevacizumab[140]. Several trials have shown that using anti-angiogenic bevacizumab in addition to systemic chemotherapy improves overall survival and progression-free survival[128]. Chemotherapy might downsize CRLM and 12%-54% of unresectable patients become resectable[7,129]. Adjuvant hepatic arterial infusion pump (HAIP) chemotherapy demonstrates promising results. In a phase II study based on the results of two high-volume centers in the Netherlands, the authors have demonstrated that adjuvant HAIP chemotherapy is safe and feasible in resectable CRLM patients[139]. Trans-arterial chemoembolization (TACE) is based on the infusion of high concentration of cytotoxic agents in liver metastases[9]. Usually, mytomycin C and cisplatin/doxorubicin are the conventional drugs for TACE[137]. This selective infusion of tumoricidal agents enhances the effect on liver tumor and minimizes the damage to normal liver. Hepatic arterial infusion chemotherapy (HAIC) represents an attractive strategy to expand resectability and tumor progression. Administration of chemotherapy into the hepatic artery is a selective procedure that allows drug delivery to the tumor with sparing of normal liver parenchyma[126,127]. Systemic side effects of HAIC are limited due to the high first-pass effect in the liver[140]. Most protocols no longer include the use of HAIC alone in favor of a combination therapy with HAIC plus systemic chemotherapy, for patients with initially unresectable CRLM[126]. Floxuridine has been the primary HAIC agent used in several studies by inserting a catheter in the gastroduodenal artery with the tip at the hepatic artery or by subcutaneous port[139]. Floxuridine improves overall survival of HAIC patients treated with concurrent systemic chemotherapy[6,139]. Floxuridine has been approved since 1971, but it is still not registered in Europe[140]. Systemic chemotherapy plus HAIC are associated with a response rate of 85% in patients with previous chemotherapy, and around 100% in chemotherapy naïve patients[6]. The combination of systemic chemotherapy and HAIC induces conversion to resectability in around 52% of patients.

Similar to TACE, selective internal radiation therapy (SIRT) is based on infusion of radiolabeled microspheres (Yttrium-90) in the branches of the hepatic artery (Figure 3)[9]. SIRT associated with systemic 5-FU prolonged progression-free survival in chemo-refractory patients[9]. Currently, data on the efficacy of Yttrium-90 radiotherapy are limited and should be interpreted with caution[137]. The use of irinotecan-loaded drug-eluting beads represents an emergent technique for administration of TACE in liver disease[129]. In addition, immunotherapy represents an alternative option to chemotherapy, for patients with CRLM derived from CRC with high MSI (MSI-H) or mismatch repair deficiency (dMMR)[129]. Pembrolizumab, a monoclonal antibody targeting PD-1 has been found of great interest in patients who had tumors with MSI-H and dMMR. Several trials are needed to evaluate the safety and efficacy of combined immune- and chemotherapy for CRLM patients with dMMR[129].

Wnt/β-catenin signaling pathway as a pharmacological target in CRLM patients

There are currently no approved drugs targeting Wnt/β-catenin pathway available for clinical use in CRLM patients, although several compounds capable of inhibiting Wnt/β-catenin signaling in advanced CRCs have been developed[52]. Inhibitory signaling molecules have been targeted towards the ability to form and secrete Wnt ligands (*e.g.*, PORCN) or towards their receptors and coreceptors (*e.g.*, FZD and LRP5/LRP6), or cytoplasmic proteins (*e.g.*, tankyrase and CK1alpha)[141].

Currently, some drugs that have an inhibitory effect on Wnt signaling are already used for CRC treatment[52]. They include indomethacin, pyrvinium, sulindac, aspirin, celecoxib and rofecoxid. Clinical trials are investigating the role of aspirin as an adjunctive drug for CRLM prevention[52,142,143]. As vitamin D deficiency is a common feature of patients with metastatic rectal cancer, its supplementation could be of great interest. Recently, a pilot study has examined the effect of vitamin D supplementation in patients with stage II-III CRC undergoing chemotherapy. Interestingly, the active form of vitamin D can promote binding of β-catenin to vitamin D receptor and increase expression of E-cadherin. The result is reduction of available β-catenin molecules that can bind to TCF/LEF transcription factors[52].

A phase I/II clinical trial has indicated that genistein combined with chemotherapy is an effective treatment for metastatic CRC. Genistein is a soy-derived isoflavone and phytoestrogen that inactivates Wnt signaling by regulating GSK3β and E-cadherin expression[52,143,144]. Other plant compounds such as curcumin and (-)-epigallocatechin-3-gallate can inhibit Wnt signaling by increasing β-catenin degradation[143,145]. A phase I trial has initially explored the efficacy and safety of curcumin in combination with 5FU in metastatic colon cancer and in combination with irinotecan for metastatic CRC patients[143].

The role of PORCN inhibitor LGK974 is under consideration in a phase II trial in a population of BRAF V600-mutated metastatic CRC patients, since in *vivo* studies have demonstrated that LGK974 inhibits tumor invasion and metastases[143,144]. Vantictumab (OMP-18R5) is a novel monoclonal antibody that interacts with FZD receptors[144]. To date, two phase I/II clinical trials are ongoing with OMP-18R5 modulating ligand/FZD-receptor interfaces, and with PRI-724 molecule interfering with β-catenin transcription[146].

OMP-18R5 inhibits CRC growth by synergizing with irinotecan[143]. OMP-54F28 is a recombinant protein that competes for binding with Fz8 receptor through sequestering Wnt ligands and inhibiting tumor growth[143,144,147,148]. Foxy-5, a Wnt5a peptide mimic, is evaluated in phase I-II clinical trials of metastatic CRC[147]. Secreted R-spondins (RSPO1-3) and their receptors RNF43/ZNRF3 are required to potentiate Wnt signaling in various conditions[144]. Rosmantuzumab (OMP-131R10), a monoclonal antibody against RSPO3 has been evaluated in phase I trial for metastatic CRC, but no results have been published[144]. Currently, phase I studies with anti-LGR5 and anti-RSPO3 therapies are under evaluation for patients with metastatic CRC. The tankyrase inhibitor IWR-1 has the potential to prevent tumor metastases by blocking Wnt/β-catenin pathway[140]. Besides developing new antagonistic molecules, pharmacological research could be directed towards repurposing non-oncology drugs, which are already active for other diseases, and evaluating natural compounds that may have an anti-inflammatory effect on TME. This theoretical concept might be valid for primary and secondary liver cancers. New drugs should be evaluated individually or in combination.

CONCLUSION

Wnt/β-catenin signaling pathway is an emerging target for cancer research and regulates liver metastasis through a complex network of interactions modulated by TME. Immune components of TME can modulate progression and metastatic capacity by promoting CRC cell survival. Proinflammatory molecules and maintenance of stemness through Wnt pathway may be considered potential therapeutic targets. Wnt signaling dysregulation activates downstream EMT by promoting cancer cell migration at the invasive front of the primary lesion. These biological mechanisms are not fully defined. Some evidence of invasive propensity and organ-specific tropism of metastatic tumor cells mirrors the concepts of "seed-soil", pre-niche and crosstalk between tumor and immune cells. Understanding the interdependence of these biological mechanisms can provide useful insight into CRLM treatment. Different cells participate to metastatization, and dormant cells show a leading role. Cancer dormancy is poorly understood in its complexity. It is of clinical importance to effectively identify and target dormant cells as potential drivers of CRLM with emphasis on Wnt/β-catenin deregulation and with the aim to reach a consensus in clinical management. Advances in the field of oncology have been made in the last decade and a central role for Wnt/β-catenin pathway has been recognized in CRC chemoresistance. At the current state of research, there is a lack of clear understanding of why and how CRC chemoresistance occurs, and thus, where exactly the opportunities for developing anti-CRLM therapies may lie. Although several compounds have been developed that inhibit Wnt/β-catenin signaling in advanced CRCs, there are currently no approved drugs targeting Wnt/β-catenin pathway and available for clinical use in CRLM patients. In this review, we considered current knowledge on clinical implication of Wnt signaling in CRLM process, provided the state of the art concerning potential biomarkers with a revision of surgical and non-surgical therapeutic guidelines for CRLM patients. Further efforts in translational medicine are needed to develop and validate novel therapies that antagonize both CRC cell metastatic capacity and their ability to be harbored in liver tissue.

ACKNOWLEDGEMENTS

The authors would like to thank Professor Paolo Innocenti (Fondazione Villa Serena per la Ricerca, Città Sant'Angelo - PE) for the courtesy of the intraoperative images.

FOOTNOTES

Author contributions: Aceto GM conceptualized and designed the study; Selvaggi F and Aceto GM developed the first draft, refined, edited, and revised the manuscript; Catalano T, Lattanzio R and Cotellese R contributed to the content materials and final editing; Aceto GM and Selvaggi F designed the images.

Conflict-of-interest statement: All the authors report no relevant conflicts of interest for this article.

Open-Access: This article is an open-access article that was selected by an in-house editor and fully peer-reviewed by external reviewers. It is distributed in accordance with the Creative Commons Attribution NonCommercial (CC BY-NC 4.0) license, which permits others to distribute, remix, adapt, build upon this work non-commercially, and license their derivative works on different terms, provided the original work is properly cited and the use is non-commercial. See: https://creativecommons.org/Licenses/by-nc/4.0/

Country/Territory of origin: Italy

ORCID number: Federico Selvaggi 0000-0002-7947-5687; Teresa Catalano 0000-0001-6713-3818; Rossano Lattanzio 0000-

0001-9803-4476; Roberto Cotellese 0000-0003-1850-9035; Gitana Maria Aceto 0000-0002-6845-1321.

S-Editor: Wang JJ
L-Editor: A
P-Editor: Chen YX

REFERENCES

1 **Pretzsch E**, Bösch F, Neumann J, Ganschow P, Bazhin A, Guba M, Werner J, Angele M. Mechanisms of Metastasis in Colorectal Cancer and Metastatic Organotropism: Hematogenous versus Peritoneal Spread. *J Oncol* 2019; **2019**: 7407190 [PMID: 31641356 DOI: 10.1155/2019/7407190]
2 **Milette S**, Sicklick JK, Lowy AM, Brodt P. Molecular Pathways: Targeting the Microenvironment of Liver Metastases. *Clin Cancer Res* 2017; **23**: 6390-6399 [PMID: 28615370 DOI: 10.1158/1078-0432.CCR-15-1636]
3 **Enquist IB**, Good Z, Jubb AM, Fuh G, Wang X, Junttila MR, Jackson EL, Leong KG. Lymph node-independent liver metastasis in a model of metastatic colorectal cancer. *Nat Commun* 2014; **5**: 3530 [PMID: 24667486 DOI: 10.1038/ncomms4530]
4 **Knijn N**, van Erning FN, Overbeek LI, Punt CJ, Lemmens VE, Hugen N, Nagtegaal ID. Limited effect of lymph node status on the metastatic pattern in colorectal cancer. *Oncotarget* 2016; **7**: 31699-31707 [PMID: 27145371 DOI: 10.18632/oncotarget.9064]
5 **Sung H**, Ferlay J, Siegel RL, Laversanne M, Soerjomataram I, Jemal A, Bray F. Global Cancer Statistics 2020: GLOBOCAN Estimates of Incidence and Mortality Worldwide for 36 Cancers in 185 Countries. *CA Cancer J Clin* 2021; **71**: 209-249 [PMID: 33538338 DOI: 10.3322/caac.21660]
6 **Ivey GD**, Johnston FM, Azad NS, Christenson ES, Lafaro KJ, Shubert CR. Current Surgical Management Strategies for Colorectal Cancer Liver Metastases. *Cancers (Basel)* 2022; **14** [PMID: 35205811 DOI: 10.3390/cancers14041063]
7 **Dörr NM**, Bartels M, Morgul MH. Current Treatment of Colorectal Liver Metastasis as a Chronic Disease. *Anticancer Res* 2020; **40**: 1-7 [PMID: 31892548 DOI: 10.21873/anticanres.13921]
8 **Meijerink MR**, Ruarus AH, Vroomen LGPH, Puijk RS, Geboers B, Nieuwenhuizen S, van den Bemd BAT, Nielsen K, de Vries JJJ, van Lienden KP, Lissenberg-Witte BI, van den Tol MP, Scheffer HJ. Irreversible Electroporation to Treat Unresectable Colorectal Liver Metastases (COLDFIRE-2): A Phase II, Two-Center, Single-Arm Clinical Trial. *Radiology* 2021; **299**: 470-480 [PMID: 33724066 DOI: 10.1148/radiol.2021203089]
9 **Chow FC**, Chok KS. Colorectal liver metastases: An update on multidisciplinary approach. *World J Hepatol* 2019; **11**: 150-172 [PMID: 30820266 DOI: 10.4254/wjh.v11.i2.150]
10 **Bertocchi A**, Carloni S, Ravenda PS, Bertalot G, Spadoni I, Lo Cascio A, Gandini S, Lizier M, Braga D, Asnicar F, Segata N, Klaver C, Brescia P, Rossi E, Anselmo A, Guglietta S, Maroli A, Spaggiari P, Tarazona N, Cervantes A, Marsoni S, Lazzari L, Jodice MG, Luise C, Erreni M, Pece S, Di Fiore PP, Viale G, Spinelli A, Pozzi C, Penna G, Rescigno M. Gut vascular barrier impairment leads to intestinal bacteria dissemination and colorectal cancer metastasis to liver. *Cancer Cell* 2021; **39**: 708-724.e11 [PMID: 33798472 DOI: 10.1016/j.ccell.2021.03.004]
11 **Lim HK**, Kim M, Park JW, Ryoo SB, Park KJ, Yi NJ, Lee KW, Suh KS, Oh HK, Kim DW, Kang SB, Cho JY, Lee DW, Park SC, Oh JH, Shin A, Jeong SY. Outcomes of simultaneous laparoscopic, hybrid, and open resection in colorectal cancer with synchronous liver metastases: a propensity score-matched study. *Sci Rep* 2022; **12**: 8867 [PMID: 35614070 DOI: 10.1038/s41598-022-12372-5]
12 **Birkenkamp-Demtroder K**, Maghnouj A, Mansilla F, Thorsen K, Andersen CL, Øster B, Hahn S, Ørntoft TF. Repression of KIAA1199 attenuates Wnt-signalling and decreases the proliferation of colon cancer cells. *Br J Cancer* 2011; **105**: 552-561 [PMID: 21772334 DOI: 10.1038/bjc.2011.268]
13 **Lee MA**, Park JH, Rhyu SY, Oh ST, Kang WK, Kim HN. Wnt3a expression is associated with MMP-9 expression in primary tumor and metastatic site in recurrent or stage IV colorectal cancer. *BMC Cancer* 2014; **14**: 125 [PMID: 24564183 DOI: 10.1186/1471-2407-14-125]
14 **Aceto GM**, Catalano T, Curia MC. Molecular Aspects of Colorectal Adenomas: The Interplay among Microenvironment, Oxidative Stress, and Predisposition. *Biomed Res Int* 2020; **2020**: 1726309 [PMID: 32258104 DOI: 10.1155/2020/1726309]
15 **Bandapalli OR**, Dihlmann S, Helwa R, Macher-Goeppinger S, Weitz J, Schirmacher P, Brand K. Transcriptional activation of the beta-catenin gene at the invasion front of colorectal liver metastases. *J Pathol* 2009; **218**: 370-379 [PMID: 19347947 DOI: 10.1002/path.2539]
16 **Cheng H**, Liang H, Qin Y, Liu Y. Nuclear beta-catenin overexpression in metastatic sentinel lymph node is associated with synchronous liver metastasis in colorectal cancer. *Diagn Pathol* 2011; **6**: 109 [PMID: 22053859 DOI: 10.1186/1746-1596-6-109]
17 **Novoa Díaz MB**, Martín MJ, Gentili C. Tumor microenvironment involvement in colorectal cancer progression *via* Wnt/β-catenin pathway: Providing understanding of the complex mechanisms of chemoresistance. *World J Gastroenterol* 2022; **28**: 3027-3046 [PMID: 36051330 DOI: 10.3748/wjg.v28.i26.3027]
18 **Jeong WJ**, Ro EJ, Choi KY. Interaction between Wnt/β-catenin and RAS-ERK pathways and an anti-cancer strategy *via* degradations of β-catenin and RAS by targeting the Wnt/β-catenin pathway. *NPJ Precis Oncol* 2018; **2**: 5 [PMID: 29872723 DOI: 10.1038/s41698-018-0049-y]
19 **Aznar N**, Ear J, Dunkel Y, Sun N, Satterfield K, He F, Kalogriopoulos NA, Lopez-Sanchez I, Ghassemian M, Sahoo D, Kufareva I, Ghosh P. Convergence of Wnt, growth factor, and heterotrimeric G protein signals on the guanine nucleotide exchange factor Daple. *Sci Signal* 2018; **11** [PMID: 29487190 DOI: 10.1126/scisignal.aao4220]
20 **LaFoya B**, Munroe JA, Mia MM, Detweiler MA, Crow JJ, Wood T, Roth S, Sharma B, Albig AR. Notch: A multi-

functional integrating system of microenvironmental signals. *Dev Biol* 2016; **418**: 227-241 [PMID: 27565024 DOI: 10.1016/j.ydbio.2016.08.023]

21 **Menck K**, Wlochowitz D, Wachter A, Conradi LC, Wolff A, Scheel AH, Korf U, Wiemann S, Schildhaus HU, Bohnenberger H, Wingender E, Pukrop T, Homayounfar K, Beißbarth T, Bleckmann A. High-Throughput Profiling of Colorectal Cancer Liver Metastases Reveals Intra- and Inter-Patient Heterogeneity in the EGFR and WNT Pathways Associated with Clinical Outcome. *Cancers (Basel)* 2022; **14** [PMID: 35565214 DOI: 10.3390/cancers14092084]

22 **Morris VK**, Kennedy EB, Baxter NN, Benson AB 3rd, Cercek A, Cho M, Ciombor KK, Cremolini C, Davis A, Deming DA, Fakih MG, Gholami S, Hong TS, Jaiyesimi I, Klute K, Lieu C, Sanoff H, Strickler JH, White S, Willis JA, Eng C. Treatment of Metastatic Colorectal Cancer: ASCO Guideline. *J Clin Oncol* 2023; **41**: 678-700 [PMID: 36252154 DOI: 10.1200/JCO.22.01690]

23 **Van Cutsem E**, Nordlinger B, Adam R, Köhne CH, Pozzo C, Poston G, Ychou M, Rougier P; European Colorectal Metastases Treatment Group. Towards a pan-European consensus on the treatment of patients with colorectal liver metastases. *Eur J Cancer* 2006; **42**: 2212-2221 [PMID: 16904315 DOI: 10.1016/j.ejca.2006.04.012]

24 **Niu Y**, Yang W, Qian H, Sun Y. Intracellular and extracellular factors of colorectal cancer liver metastasis: a pivotal perplex to be fully elucidated. *Cancer Cell Int* 2022; **22**: 341 [PMID: 36348319 DOI: 10.1186/s12935-022-02766-w]

25 **Adam R**, Kitano Y. Multidisciplinary approach of liver metastases from colorectal cancer. *Ann Gastroenterol Surg* 2019; **3**: 50-56 [PMID: 30697610 DOI: 10.1002/ags3.12227]

26 **Wu Q**, Liu Y, Sun D, Wang Y, Wei X, Li J, Liu B, Wang S, Zhou Y, Hu H, Zhang R, Jiao Q, Li Y, Ying T. Protocol of Kupffer phase whole liver scan for metastases: A single-center prospective study. *Front Med (Lausanne)* 2022; **9**: 911807 [PMID: 36017002 DOI: 10.3389/fmed.2022.911807]

27 **Zeng X**, Ward SE, Zhou J, Cheng ASL. Liver Immune Microenvironment and Metastasis from Colorectal Cancer-Pathogenesis and Therapeutic Perspectives. *Cancers (Basel)* 2021; **13** [PMID: 34067719 DOI: 10.3390/cancers13102418]

28 **Selvaggi F**, Catalano T, Cotellese R, Aceto GM. Targeting Wnt/β-Catenin Pathways in Primary Liver Tumours: From Microenvironment Signaling to Therapeutic Agents. *Cancers (Basel)* 2022; **14** [PMID: 35454818 DOI: 10.3390/cancers14081912]

29 **Chen GT**, Tifrea DF, Murad R, Habowski AN, Lyou Y, Duong MR, Hosohama L, Mortazavi A, Edwards RA, Waterman ML. Disruption of β-Catenin-Dependent Wnt Signaling in Colon Cancer Cells Remodels the Microenvironment to Promote Tumor Invasion. *Mol Cancer Res* 2022; **20**: 468-484 [PMID: 34799404 DOI: 10.1158/1541-7786.MCR-21-0349]

30 **Patel S**, Alam A, Pant R, Chattopadhyay S. Wnt Signaling and Its Significance Within the Tumor Microenvironment: Novel Therapeutic Insights. *Front Immunol* 2019; **10**: 2872 [PMID: 31921137 DOI: 10.3389/fimmu.2019.02872]

31 **Teeuwssen M**, Fodde R. Cell Heterogeneity and Phenotypic Plasticity in Metastasis Formation: The Case of Colon Cancer. *Cancers (Basel)* 2019; **11** [PMID: 31540068 DOI: 10.3390/cancers11091368]

32 **Brabletz T**. To differentiate or not--routes towards metastasis. *Nat Rev Cancer* 2012; **12**: 425-436 [PMID: 22576165 DOI: 10.1038/nrc3265]

33 **Seager RJ**, Hajal C, Spill F, Kamm RD, Zaman MH. Dynamic interplay between tumour, stroma and immune system can drive or prevent tumour progression. *Converg Sci Phys Oncol* 2017; **3** [PMID: 30079253 DOI: 10.1088/2057-1739/aa7e86]

34 **Sciacovelli M**, Frezza C. Metabolic reprogramming and epithelial-to-mesenchymal transition in cancer. *FEBS J* 2017; **284**: 3132-3144 [PMID: 28444969 DOI: 10.1111/febs.14090]

35 **Kar R**, Jha NK, Jha SK, Sharma A, Dholpuria S, Asthana N, Chaurasiya K, Singh VK, Burgee S, Nand P. A "NOTCH" Deeper into the Epithelial-To-Mesenchymal Transition (EMT) Program in Breast Cancer. *Genes (Basel)* 2019; **10** [PMID: 31766724 DOI: 10.3390/genes10120961]

36 **Pastushenko I**, Blanpain C. EMT Transition States during Tumor Progression and Metastasis. *Trends Cell Biol* 2019; **29**: 212-226 [PMID: 30594349 DOI: 10.1016/j.tcb.2018.12.001]

37 **Dongre A**, Weinberg RA. New insights into the mechanisms of epithelial-mesenchymal transition and implications for cancer. *Nat Rev Mol Cell Biol* 2019; **20**: 69-84 [PMID: 30459476 DOI: 10.1038/s41580-018-0080-4]

38 **Yu M**, Bardia A, Wittner BS, Stott SL, Smas ME, Ting DT, Isakoff SJ, Ciciliano JC, Wells MN, Shah AM, Concannon KF, Donaldson MC, Sequist LV, Brachtel E, Sgroi D, Baselga J, Ramaswamy S, Toner M, Haber DA, Maheswaran S. Circulating breast tumor cells exhibit dynamic changes in epithelial and mesenchymal composition. *Science* 2013; **339**: 580-584 [PMID: 23372014 DOI: 10.1126/science.1228522]

39 **Pastushenko I**, Brisebarre A, Sifrim A, Fioramonti M, Revenco T, Boumahdi S, Van Keymeulen A, Brown D, Moers V, Lemaire S, De Clercq S, Minguijón E, Balsat C, Sokolow Y, Dubois C, De Cock F, Scozzaro S, Sopena F, Lanas A, D'Haene N, Salmon I, Marine JC, Voet T, Sotiropoulou PA, Blanpain C. Identification of the tumour transition states occurring during EMT. *Nature* 2018; **556**: 463-468 [PMID: 29670281 DOI: 10.1038/s41586-018-0040-3]

40 **Ye GD**, Sun GB, Jiao P, Chen C, Liu QF, Huang XL, Zhang R, Cai WY, Li SN, Wu JF, Liu YJ, Wu RS, Xie YY, Chan EC, Liou YC, Li BA. OVOL2, an Inhibitor of WNT Signaling, Reduces Invasive Activities of Human and Mouse Cancer Cells and Is Down-regulated in Human Colorectal Tumors. *Gastroenterology* 2016; **150**: 659-671.e16 [PMID: 26619963 DOI: 10.1053/j.gastro.2015.11.041]

41 **Xiao Q**, Gan Y, Li Y, Fan L, Liu J, Lu P, Chen A, Shu G, Yin G. MEF2A transcriptionally upregulates the expression of ZEB2 and CTNNB1 in colorectal cancer to promote tumor progression. *Oncogene* 2021; **40**: 3364-3377 [PMID: 33863999 DOI: 10.1038/s41388-021-01774-w]

42 **Balcik-Ercin P**, Cayrefourcq L, Soundararajan R, Mani SA, Alix-Panabières C. Epithelial-to-Mesenchymal Plasticity in Circulating Tumor Cell Lines Sequentially Derived from a Patient with Colorectal Cancer. *Cancers (Basel)* 2021; **13** [PMID: 34771571 DOI: 10.3390/cancers13215408]

43 **Sha Y**, Haensel D, Gutierrez G, Du H, Dai X, Nie Q. Intermediate cell states in epithelial-to-mesenchymal transition. *Phys Biol* 2019; **16**: 021001 [PMID: 30560804 DOI: 10.1088/1478-3975/aaf928]

44 **Sánchez-Tilló E**, de Barrios O, Valls E, Darling DS, Castells A, Postigo A. ZEB1 and TCF4 reciprocally modulate their transcriptional activities to regulate Wnt target gene expression. *Oncogene* 2015; **34**: 5760-5770 [PMID: 26387539 DOI: 10.1038/onc.2015.352]

45 **Khanbabaei H**, Ebrahimi S, García-Rodríguez JL, Ghasemi Z, Pourghadamyari H, Mohammadi M, Kristensen LS. Non-coding RNAs and epithelial mesenchymal transition in cancer: molecular mechanisms and clinical implications. *J Exp Clin Cancer Res* 2022; **41**: 278 [PMID: 36114510 DOI: 10.1186/s13046-022-02488-x]

46 **Gonçalves V**, Pereira JFS, Jordan P. Signaling Pathways Driving Aberrant Splicing in Cancer Cells. *Genes (Basel)* 2017; **9** [PMID: 29286307 DOI: 10.3390/genes9010009]

47 **Liu LJ**, Xie SX, Chen YT, Xue JL, Zhang CJ, Zhu F. Aberrant regulation of Wnt signaling in hepatocellular carcinoma. *World J Gastroenterol* 2016; **22**: 7486-7499 [PMID: 27672271 DOI: 10.3748/wjg.v22.i33.7486]

48 **Nusse R**, Clevers H. Wnt/β-Catenin Signaling, Disease, and Emerging Therapeutic Modalities. *Cell* 2017; **169**: 985-999 [PMID: 28575679 DOI: 10.1016/j.cell.2017.05.016]

49 **Deshmukh AP**, Vasaikar SV, Tomczak K, Tripathi S, den Hollander P, Arslan E, Chakraborty P, Soundararajan R, Jolly MK, Rai K, Levine H, Mani SA. Identification of EMT signaling cross-talk and gene regulatory networks by single-cell RNA sequencing. *Proc Natl Acad Sci U S A* 2021; **118** [PMID: 33941680 DOI: 10.1073/pnas.2102050118]

50 **Acar A**, Hidalgo-Sastre A, Leverentz MK, Mills CG, Woodcock S, Baron M, Collu GM, Brennan K. Inhibition of Wnt signalling by Notch *via* two distinct mechanisms. *Sci Rep* 2021; **11**: 9096 [PMID: 33907274 DOI: 10.1038/s41598-021-88618-5]

51 **Samaržija I**. Wnt Signaling Pathway Is among the Drivers of Liver Metastasis. *Livers* 2021; **1**: 180-200 [DOI: 10.3390/livers1040015]

52 **Zhao H**, Ming T, Tang S, Ren S, Yang H, Liu M, Tao Q, Xu H. Wnt signaling in colorectal cancer: pathogenic role and therapeutic target. *Mol Cancer* 2022; **21**: 144 [PMID: 35836256 DOI: 10.1186/s12943-022-01616-7]

53 **Qi J**, Yu Y, Akilli Öztürk Ö, Holland JD, Besser D, Fritzmann J, Wulf-Goldenberg A, Eckert K, Fichtner I, Birchmeier W. New Wnt/β-catenin target genes promote experimental metastasis and migration of colorectal cancer cells through different signals. *Gut* 2016; **65**: 1690-1701 [PMID: 26156959 DOI: 10.1136/gutjnl-2014-307900]

54 **Jinesh GG**, Brohl AS. Classical epithelial-mesenchymal transition (EMT) and alternative cell death process-driven blebbishield metastatic-witch (BMW) pathways to cancer metastasis. *Signal Transduct Target Ther* 2022; **7**: 296 [PMID: 35999218 DOI: 10.1038/s41392-022-01132-6]

55 **Goodla L**, Xue X. The Role of Inflammatory Mediators in Colorectal Cancer Hepatic Metastasis. *Cells* 2022; **11** [PMID: 35954156 DOI: 10.3390/cells11152313]

56 **Meng W**, Xue S, Chen Y. The role of CXCL12 in tumor microenvironment. *Gene* 2018; **641**: 105-110 [PMID: 29017963 DOI: 10.1016/j.gene.2017.10.015]

57 **Shi Y**, Riese DJ 2nd, Shen J. The Role of the CXCL12/CXCR4/CXCR7 Chemokine Axis in Cancer. *Front Pharmacol* 2020; **11**: 574667 [PMID: 33363463 DOI: 10.3389/fphar.2020.574667]

58 **Miyazaki T**, Chung S, Sakai H, Ohata H, Obata Y, Shiokawa D, Mizoguchi Y, Kubo T, Ichikawa H, Taniguchi H, Aoki K, Soga T, Nakagama H, Okamoto K. Stemness and immune evasion conferred by the TDO2-AHR pathway are associated with liver metastasis of colon cancer. *Cancer Sci* 2022; **113**: 170-181 [PMID: 34714577 DOI: 10.1111/cas.15182]

59 **Zhang Y**, Song J, Zhao Z, Yang M, Chen M, Liu C, Ji J, Zhu D. Single-cell transcriptome analysis reveals tumor immune microenvironment heterogenicity and granulocytes enrichment in colorectal cancer liver metastases. *Cancer Lett* 2020; **470**: 84-94 [PMID: 31610266 DOI: 10.1016/j.canlet.2019.10.016]

60 **Wang M**, Su Z, Amoah Barnie P. Crosstalk among colon cancer-derived exosomes, fibroblast-derived exosomes, and macrophage phenotypes in colon cancer metastasis. *Int Immunopharmacol* 2020; **81**: 106298 [PMID: 32058925 DOI: 10.1016/j.intimp.2020.106298]

61 **Schubert A**, Boutros M. Extracellular vesicles and oncogenic signaling. *Mol Oncol* 2021; **15**: 3-26 [PMID: 33207034 DOI: 10.1002/1878-0261.12855]

62 **Gross JC**, Chaudhary V, Bartscherer K, Boutros M. Active Wnt proteins are secreted on exosomes. *Nat Cell Biol* 2012; **14**: 1036-1045 [PMID: 22983114 DOI: 10.1038/ncb2574]

63 **Huang Z**, Feng Y. Exosomes Derived From Hypoxic Colorectal Cancer Cells Promote Angiogenesis Through Wnt4-Induced β-Catenin Signaling in Endothelial Cells. *Oncol Res* 2017; **25**: 651-661 [PMID: 27712599 DOI: 10.3727/096504016X14752792816791]

64 **Kalra H**, Gangoda L, Fonseka P, Chitti SV, Liem M, Keerthikumar S, Samuel M, Boukouris S, Al Saffar H, Collins C, Adda CG, Ang CS, Mathivanan S. Extracellular vesicles containing oncogenic mutant β-catenin activate Wnt signalling pathway in the recipient cells. *J Extracell Vesicles* 2019; **8**: 1690217 [PMID: 31819794 DOI: 10.1080/20013078.2019.1690217]

65 **Dong Q**, Liu X, Cheng K, Sheng J, Kong J, Liu T. Pre-metastatic Niche Formation in Different Organs Induced by Tumor Extracellular Vesicles. *Front Cell Dev Biol* 2021; **9**: 733627 [PMID: 34616739 DOI: 10.3389/fcell.2021.733627]

66 **Rezaie J**, Ahmadi M, Ravanbakhsh R, Mojarad B, Mahbubfam S, Shaban SA, Shadi K, Berenjabad NJ, Etemadi T. Tumor-derived extracellular vesicles: The metastatic organotropism drivers. *Life Sci* 2022; **289**: 120216 [PMID: 34890589 DOI: 10.1016/j.lfs.2021.120216]

67 **Kim J**, Lee HK. Potential Role of the Gut Microbiome In Colorectal Cancer Progression. *Front Immunol* 2021; **12**: 807648 [PMID: 35069592 DOI: 10.3389/fimmu.2021.807648]

68 **Huo T**, Cao J, Tian Y, Shi X, Wu L, Zhang M, Wong LL, Zhao L. Effect of Concomitant Positive Hepatitis B Surface Antigen on the Risk of Liver Metastasis: A Retrospective Clinical Study of 4033 Consecutive Cases of Newly Diagnosed Colorectal Cancer. *Clin Infect Dis* 2018; **66**: 1948-1952 [PMID: 29293940 DOI: 10.1093/cid/cix1118]

69 **Che LH**, Liu JW, Huo JP, Luo R, Xu RM, He C, Li YQ, Zhou AJ, Huang P, Chen YY, Ni W, Zhou YX, Liu YY, Li HY, Zhou R, Mo H, Li JM. A single-cell atlas of liver metastases of colorectal cancer reveals reprogramming of the tumor microenvironment in response to preoperative chemotherapy. *Cell Discov* 2021; **7**: 80 [PMID: 34489408 DOI: 10.1038/s41421-021-00312-y]

70 **Malladi S**, Macalinao DG, Jin X, He L, Basnet H, Zou Y, de Stanchina E, Massagué J. Metastatic Latency and Immune Evasion through Autocrine Inhibition of WNT. *Cell* 2016; **165**: 45-60 [PMID: 27015306 DOI: 10.1016/j.cell.2016.02.025]

71 **Guba M**, Cernaianu G, Koehl G, Geissler EK, Jauch KW, Anthuber M, Falk W, Steinbauer M. A primary tumor promotes dormancy of solitary tumor cells before inhibiting angiogenesis. *Cancer Res* 2001; **61**: 5575-5579 [PMID: 11454710]

72 **Akkoc Y**, Gozuacik D. Autophagy and Hepatic Tumor Microenvironment Associated Dormancy. *J Gastrointest Cancer* 2021; **52**: 1277-1293 [PMID: 34921672 DOI: 10.1007/s12029-021-00774-z]

73 **Gao XL**, Zhang M, Tang YL, Liang XH. Cancer cell dormancy: mechanisms and implications of cancer recurrence and metastasis. *Onco Targets Ther* 2017; **10**: 5219-5228 [PMID: 29138574 DOI: 10.2147/OTT.S140854]

74 **Jahangiri L**, Ishola T. Dormancy in Breast Cancer, the Role of Autophagy, lncRNAs, miRNAs and Exosomes. *Int J Mol Sci* 2022; **23** [PMID: 35563661 DOI: 10.3390/ijms23095271]

75 **Ren X**, Xiao J, Zhang W, Wang F, Yan Y, Wu X, Zeng Z, He Y, Yang W, Liao W, Ding Y, Liang L. Inhibition of CCL7 derived from Mo-MDSCs prevents metastatic progression from latency in colorectal cancer. *Cell Death Dis* 2021; **12**: 484 [PMID: 33986252 DOI: 10.1038/s41419-021-03698-5]

76 **Heinz MC**, Peters NA, Oost KC, Lindeboom RGH, van Voorthuijsen L, Fumagalli A, van der Net MC, de Medeiros G, Hageman JH, Verlaan-Klink I, Borel Rinkes IHM, Liberali P, Gloerich M, van Rheenen J, Vermeulen M, Kranenburg O, Snippert HJG. Liver Colonization by Colorectal Cancer Metastases Requires YAP-Controlled Plasticity at the Micrometastatic Stage. *Cancer Res* 2022; **82**: 1953-1968 [PMID: 35570706 DOI: 10.1158/0008-5472.CAN-21-0933]

77 **Wang R**, Su Q, Yan ZP. Reconsideration of recurrence and metastasis in colorectal cancer. *World J Clin Cases* 2021; **9**: 6964-6968 [PMID: 34540951 DOI: 10.12998/wjcc.v9.i24.6964]

78 **Ma B**, Wells A, Wei L, Zheng J. Prostate cancer liver metastasis: Dormancy and resistance to therapy. *Semin Cancer Biol* 2021; **71**: 2-9 [PMID: 32663571 DOI: 10.1016/j.semcancer.2020.07.004]

79 **Linde N**, Fluegen G, Aguirre-Ghiso JA. The Relationship Between Dormant Cancer Cells and Their Microenvironment. *Adv Cancer Res* 2016; **132**: 45-71 [PMID: 27613129 DOI: 10.1016/bs.acr.2016.07.002]

80 **Aguirre-Ghiso JA**. How dormant cancer persists and reawakens. *Science* 2018; **361**: 1314-1315 [PMID: 30262486 DOI: 10.1126/science.aav0191]

81 **Govaert KM**, Jongen JMJ, Kranenburg O, Borel Rinkes IHM. Surgery-induced tumor growth in (metastatic) colorectal cancer. *Surg Oncol* 2017; **26**: 535-543 [PMID: 29113675 DOI: 10.1016/j.suronc.2017.10.004]

82 **Stremitzer S**, Zhang W, Yang D, Ning Y, Stintzing S, Sunakawa Y, Sebio A, Yamauchi S, Matsusaka S, Parekh A, Barzi A, El-Khoueiry R, Stift J, Wrba F, Gruenberger T, Lenz HJ. Variations in genes involved in dormancy associated with outcome in patients with resected colorectal liver metastases. *Ann Oncol* 2015; **26**: 1728-1733 [PMID: 25957329 DOI: 10.1093/annonc/mdv224]

83 **Touil Y**, Igoudjil W, Corvaisier M, Dessein AF, Vandomme J, Monté D, Stechly L, Skrypek N, Langlois C, Grard G, Millet G, Leteurtre E, Dumont P, Truant S, Pruvot FR, Hebbar M, Fan F, Ellis LM, Formstecher P, Van Seuningen I, Gespach C, Polakowska R, Huet G. Colon cancer cells escape 5FU chemotherapy-induced cell death by entering stemness and quiescence associated with the c-Yes/YAP axis. *Clin Cancer Res* 2014; **20**: 837-846 [PMID: 24323901 DOI: 10.1158/1078-0432.CCR-13-1854]

84 **Ohsawa I**, Murakami T, Uemoto S, Kobayashi E. In vivo luminescent imaging of cyclosporin A-mediated cancer progression in rats. *Transplantation* 2006; **81**: 1558-1567 [PMID: 16770245 DOI: 10.1097/01.tp.0000209448.50238.de]

85 **Popova SA**, Buczacki SJA. Itraconazole perturbs colorectal cancer dormancy through SUFU-mediated WNT inhibition. *Mol Cell Oncol* 2018; **5**: e1494950 [PMID: 30250932 DOI: 10.1080/23723556.2018.1494950]

86 **Trowbridge JJ**, Guezguez B, Moon RT, Bhatia M. Wnt3a activates dormant c-Kit(-) bone marrow-derived cells with short-term multilineage hematopoietic reconstitution capacity. *Stem Cells* 2010; **28**: 1379-1389 [PMID: 20521329 DOI: 10.1002/stem.457]

87 **Park SY**, Nam JS. The force awakens: metastatic dormant cancer cells. *Exp Mol Med* 2020; **52**: 569-581 [PMID: 32300189 DOI: 10.1038/s12276-020-0423-z]

88 **Høye AM**, Erler JT. Structural ECM components in the premetastatic and metastatic niche. *Am J Physiol Cell Physiol* 2016; **310**: C955-C967 [PMID: 27053524 DOI: 10.1152/ajpcell.00326.2015]

89 **Zhu X**, Wang F, Wu X, Li Z, Wang Z, Ren X, Zhou Y, Song F, Liang Y, Zeng Z, Liao W, Ding Y, Liang L. FBX8 promotes metastatic dormancy of colorectal cancer in liver. *Cell Death Dis* 2020; **11**: 622 [PMID: 32796813 DOI: 10.1038/s41419-020-02870-7]

90 **Ogata R**, Mori S, Kishi S, Sasaki R, Iwata N, Ohmori H, Sasaki T, Nishiguchi Y, Nakashima C, Goto K, Kawahara I, Fujiwara-Tani R, Kuniyasu H. Linoleic Acid Upregulates Microrna-494 to Induce Quiescence in Colorectal Cancer. *Int J Mol Sci* 2021; **23** [PMID: 35008652 DOI: 10.3390/ijms23010225]

91 **Cheng CF**, Ku HC, Lin H. PGC-1α as a Pivotal Factor in Lipid and Metabolic Regulation. *Int J Mol Sci* 2018; **19** [PMID: 30400212 DOI: 10.3390/ijms19113447]

92 **Li B**, Huang Y, Ming H, Nice EC, Xuan R, Huang C. Redox Control of the Dormant Cancer Cell Life Cycle. *Cells* 2021; **10** [PMID: 34685686 DOI: 10.3390/cells10102707]

93 **Tao J**, Krutsenko Y, Moghe A, Singh S, Poddar M, Bell A, Oertel M, Singhi AD, Geller D, Chen X, Lujambio A, Liu S, Monga SP. Nuclear factor erythroid 2-related factor 2 and β-Catenin Coactivation in Hepatocellular Cancer: Biological and Therapeutic Implications. *Hepatology* 2021; **74**: 741-759 [PMID: 33529367 DOI: 10.1002/hep.31730]

94 **Catalano T**, D'Amico E, Moscatello C, Di Marcantonio MC, Ferrone A, Bologna G, Selvaggi F, Lanuti P, Cotellese R, Curia MC, Lattanzio R, Aceto GM. Oxidative Distress Induces Wnt/β-Catenin Pathway Modulation in Colorectal Cancer Cells: Perspectives on APC Retained Functions. *Cancers (Basel)* 2021; **13** [PMID: 34885156 DOI: 10.3390/cancers13236045]

95 **Eijkelenboom A**, Burgering BM. FOXOs: signalling integrators for homeostasis maintenance. *Nat Rev Mol Cell Biol* 2013; **14**: 83-97 [PMID: 23325358 DOI: 10.1038/nrm3507]

96 **Schirosi L**, Mazzotta A, Opinto G, Pinto R, Graziano G, Tommasi S, Fucci L, Simone G, Mangia A. β-catenin interaction with NHERF1 and RASSF1A methylation in metastatic colorectal cancer patients. *Oncotarget* 2016; **7**: 67841-67850 [PMID: 27765918 DOI: 10.18632/oncotarget.12280]

97 **Amin MB**, Edge SB, Greene FL, Byrd DR, Brookland RK, Washington MK, Gershenwald JE, Compton CC, Hess KR, Sullivan DC, Jessup JM, Brierley JD, Gaspar LE, Schilsky RL, Balch CM, Winchester DP, Asare EA, Madera M, Gress DM, Meyer LR. AJCC Cancer Staging Manual. Switzerland: Springer Cham, 2017

98 **Sepulveda AR**, Hamilton SR, Allegra CJ, Grody W, Cushman-Vokoun AM, Funkhouser WK, Kopetz SE, Lieu C, Lindor

NM, Minsky BD, Monzon FA, Sargent DJ, Singh VM, Willis J, Clark J, Colasacco C, Rumble RB, Temple-Smolkin R, Ventura CB, Nowak JA. Molecular Biomarkers for the Evaluation of Colorectal Cancer: Guideline Summary From the American Society for Clinical Pathology, College of American Pathologists, Association for Molecular Pathology, and American Society of Clinical Oncology. *J Oncol Pract* 2017; **13**: 333-337 [PMID: 28350513 DOI: 10.1200/JOP.2017.022152]

99 **Sorich MJ**, Wiese MD, Rowland A, Kichenadasse G, McKinnon RA, Karapetis CS. Extended RAS mutations and anti-EGFR monoclonal antibody survival benefit in metastatic colorectal cancer: a meta-analysis of randomized, controlled trials. *Ann Oncol* 2015; **26**: 13-21 [PMID: 25115304 DOI: 10.1093/annonc/mdu378]

100 **Van Cutsem E**, Cervantes A, Adam R, Sobrero A, Van Krieken JH, Aderka D, Aranda Aguilar E, Bardelli A, Benson A, Bodoky G, Ciardiello F, D'Hoore A, Diaz-Rubio E, Douillard JY, Ducreux M, Falcone A, Grothey A, Gruenberger T, Haustermans K, Heinemann V, Hoff P, Köhne CH, Labianca R, Laurent-Puig P, Ma B, Maughan T, Muro K, Normanno N, Österlund P, Oyen WJ, Papamichael D, Pentheroudakis G, Pfeiffer P, Price TJ, Punt C, Ricke J, Roth A, Salazar R, Scheithauer W, Schmoll HJ, Tabernero J, Taïeb J, Tejpar S, Wasan H, Yoshino T, Zaanan A, Arnold D. ESMO consensus guidelines for the management of patients with metastatic colorectal cancer. *Ann Oncol* 2016; **27**: 1386-1422 [PMID: 27380959 DOI: 10.1093/annonc/mdw235]

101 **Benson AB**, Venook AP, Al-Hawary MM, Arain MA, Chen YJ, Ciombor KK, Cohen S, Cooper HS, Deming D, Farkas L, Garrido-Laguna I, Grem JL, Gunn A, Hecht JR, Hoffe S, Hubbard J, Hunt S, Johung KL, Kirilcuk N, Krishnamurthi S, Messersmith WA, Meyerhardt J, Miller ED, Mulcahy MF, Nurkin S, Overman MJ, Parikh A, Patel H, Pedersen K, Saltz L, Schneider C, Shibata D, Skibber JM, Sofocleous CT, Stoffel EM, Stotsky-Himelfarb E, Willett CG, Gregory KM, Gurski LA. Colon Cancer, Version 2.2021, NCCN Clinical Practice Guidelines in Oncology. *J Natl Compr Canc Netw* 2021; **19**: 329-359 [PMID: 33724754 DOI: 10.6004/jnccn.2021.0012]

102 **Fennell LJ**, Kane A, Liu C, McKeone D, Fernando W, Su C, Bond C, Jamieson S, Dumenil T, Patch AM, Kazakoff SH, Pearson JV, Waddell N, Leggett B, Whitehall VLJ. APC Mutation Marks an Aggressive Subtype of BRAF Mutant Colorectal Cancers. *Cancers (Basel)* 2020; **12** [PMID: 32384699 DOI: 10.3390/cancers12051171]

103 **Tran B**, Kopetz S, Tie J, Gibbs P, Jiang ZQ, Lieu CH, Agarwal A, Maru DM, Sieber O, Desai J. Impact of BRAF mutation and microsatellite instability on the pattern of metastatic spread and prognosis in metastatic colorectal cancer. *Cancer* 2011; **117**: 4623-4632 [PMID: 21456008 DOI: 10.1002/cncr.26086]

104 **Goldstein J**, Tran B, Ensor J, Gibbs P, Wong HL, Wong SF, Vilar E, Tie J, Broaddus R, Kopetz S, Desai J, Overman MJ. Multicenter retrospective analysis of metastatic colorectal cancer (CRC) with high-level microsatellite instability (MSI-H). *Ann Oncol* 2014; **25**: 1032-1038 [PMID: 24585723 DOI: 10.1093/annonc/mdu100]

105 **Le DT**, Uram JN, Wang H, Bartlett BR, Kemberling H, Eyring AD, Skora AD, Luber BS, Azad NS, Laheru D, Biedrzycki B, Donehower RC, Zaheer A, Fisher GA, Crocenzi TS, Lee JJ, Duffy SM, Goldberg RM, de la Chapelle A, Koshiji M, Bhaijee F, Huebner T, Hruban RH, Wood LD, Cuka N, Pardoll DM, Papadopoulos N, Kinzler KW, Zhou S, Cornish TC, Taube JM, Anders RA, Eshleman JR, Vogelstein B, Diaz LA Jr. PD-1 Blockade in Tumors with Mismatch-Repair Deficiency. *N Engl J Med* 2015; **372**: 2509-2520 [PMID: 26028255 DOI: 10.1056/NEJMoa1500596]

106 **Arnold D**, Lueza B, Douillard JY, Peeters M, Lenz HJ, Venook A, Heinemann V, Van Cutsem E, Pignon JP, Tabernero J, Cervantes A, Ciardiello F. Prognostic and predictive value of primary tumour side in patients with RAS wild-type metastatic colorectal cancer treated with chemotherapy and EGFR directed antibodies in six randomized trials. *Ann Oncol* 2017; **28**: 1713-1729 [PMID: 28407110 DOI: 10.1093/annonc/mdx175]

107 **Grassilli E**, Cerrito MG. Emerging actionable targets to treat therapy-resistant colorectal cancers. *Cancer Drug Resist* 2022; **5**: 36-63 [PMID: 35582524 DOI: 10.20517/cdr.2021.96]

108 **Bardelli A**, Corso S, Bertotti A, Hobor S, Valtorta E, Siravegna G, Sartore-Bianchi A, Scala E, Cassingena A, Zecchin D, Apicella M, Migliardi G, Galimi F, Lauricella C, Zanon C, Perera T, Veronese S, Corti G, Amatu A, Gambacorta M, Diaz LA Jr, Sausen M, Velculescu VE, Comoglio P, Trusolino L, Di Nicolantonio F, Giordano S, Siena S. Amplification of the MET receptor drives resistance to anti-EGFR therapies in colorectal cancer. *Cancer Discov* 2013; **3**: 658-673 [PMID: 23729478 DOI: 10.1158/2159-8290.CD-12-0558]

109 **Raghav K**, Bailey AM, Loree JM, Kopetz S, Holla V, Yap TA, Wang F, Chen K, Salgia R, Hong D. Untying the gordion knot of targeting MET in cancer. *Cancer Treat Rev* 2018; **66**: 95-103 [PMID: 29730462 DOI: 10.1016/j.ctrv.2018.04.008]

110 **Bardelli A**, Siena S. Molecular mechanisms of resistance to cetuximab and panitumumab in colorectal cancer. *J Clin Oncol* 2010; **28**: 1254-1261 [PMID: 20100961 DOI: 10.1200/JCO.2009.24.6116]

111 **De Roock W**, Claes B, Bernasconi D, De Schutter J, Biesmans B, Fountzilas G, Kalogeras KT, Kotoula V, Papamichael D, Laurent-Puig P, Penault-Llorca F, Rougier P, Vincenzi B, Santini D, Tonini G, Cappuzzo F, Frattini M, Molinari F, Saletti P, De Dosso S, Martini M, Bardelli A, Siena S, Sartore-Bianchi A, Tabernero J, Macarulla T, Di Fiore F, Gangloff AO, Ciardiello F, Pfeiffer P, Qvortrup C, Hansen TP, Van Cutsem E, Piessevaux H, Lambrechts D, Delorenzi M, Tejpar S. Effects of KRAS, BRAF, NRAS, and PIK3CA mutations on the efficacy of cetuximab plus chemotherapy in chemotherapy-refractory metastatic colorectal cancer: a retrospective consortium analysis. *Lancet Oncol* 2010; **11**: 753-762 [PMID: 20619739 DOI: 10.1016/S1470-2045(10)70130-3]

112 **Jacobs B**, De Roock W, Piessevaux H, Van Oirbeek R, Biesmans B, De Schutter J, Fieuws S, Vandesompele J, Peeters M, Van Laethem JL, Humblet Y, Pénault-Llorca F, De Hertogh G, Laurent-Puig P, Van Cutsem E, Tejpar S. Amphiregulin and epiregulin mRNA expression in primary tumors predicts outcome in metastatic colorectal cancer treated with cetuximab. *J Clin Oncol* 2009; **27**: 5068-5074 [PMID: 19738126 DOI: 10.1200/JCO.2008.21.3744]

113 **Lee MS**, McGuffey EJ, Morris JS, Manyam G, Baladandayuthapani V, Wei W, Morris VK, Overman MJ, Maru DM, Jiang ZQ, Hamilton SR, Kopetz S. Association of CpG island methylator phenotype and EREG/AREG methylation and expression in colorectal cancer. *Br J Cancer* 2016; **114**: 1352-1361 [PMID: 27272216 DOI: 10.1038/bjc.2016.87]

114 **Khambata-Ford S**, Garrett CR, Meropol NJ, Basik M, Harbison CT, Wu S, Wong TW, Huang X, Takimoto CH, Godwin AK, Tan BR, Krishnamurthi SS, Burris HA 3rd, Poplin EA, Hidalgo M, Baselga J, Clark EA, Mauro DJ. Expression of epiregulin and amphiregulin and K-ras mutation status predict disease control in metastatic colorectal cancer patients treated with cetuximab. *J Clin Oncol* 2007; **25**: 3230-3237 [PMID: 17664471 DOI: 10.1200/JCO.2006.10.5437]

115 **Lédel F**, Stenstedt K, Hallström M, Ragnhammar P, Edler D. HER3 expression is correlated to distally located and low-

grade colon cancer. *Acta Oncol* 2016; **55**: 875-880 [PMID: 26863446 DOI: 10.3109/0284186X.2015.1131334]

116 **Littlefield P**, Liu L, Mysore V, Shan Y, Shaw DE, Jura N. Structural analysis of the EGFR/HER3 heterodimer reveals the molecular basis for activating HER3 mutations. *Sci Signal* 2014; **7**: ra114 [PMID: 25468994 DOI: 10.1126/scisignal.2005786]

117 **Lédel F**, Hallström M, Ragnhammar P, Öhrling K, Edler D. HER3 expression in patients with primary colorectal cancer and corresponding lymph node metastases related to clinical outcome. *Eur J Cancer* 2014; **50**: 656-662 [PMID: 24300455 DOI: 10.1016/j.ejca.2013.11.008]

118 **LoRusso P**, Jänne PA, Oliveira M, Rizvi N, Malburg L, Keedy V, Yee L, Copigneaux C, Hettmann T, Wu CY, Ang A, Halim AB, Beckman RA, Beaupre D, Berlin J. Phase I study of U3-1287, a fully human anti-HER3 monoclonal antibody, in patients with advanced solid tumors. *Clin Cancer Res* 2013; **19**: 3078-3087 [PMID: 23591447 DOI: 10.1158/1078-0432.CCR-12-3051]

119 **Cleary JM**, McRee AJ, Shapiro GI, Tolaney SM, O'Neil BH, Kearns JD, Mathews S, Nering R, MacBeath G, Czibere A, Sharma S, Korn WM. A phase 1 study combining the HER3 antibody seribantumab (MM-121) and cetuximab with and without irinotecan. *Invest New Drugs* 2017; **35**: 68-78 [PMID: 27853996 DOI: 10.1007/s10637-016-0399-7]

120 **Hill AG**, Findlay MP, Burge ME, Jackson C, Alfonso PG, Samuel L, Ganju V, Karthaus M, Amatu A, Jeffery M, Bartolomeo MD, Bridgewater J, Coveler AL, Hidalgo M, Kapp AV, Sufan RI, McCall BB, Hanley WD, Penuel EM, Pirzkall A, Tabernero J. Phase II Study of the Dual EGFR/HER3 Inhibitor Duligotuzumab (MEHD7945A) versus Cetuximab in Combination with FOLFIRI in Second-Line RAS Wild-Type Metastatic Colorectal Cancer. *Clin Cancer Res* 2018; **24**: 2276-2284 [PMID: 29506988 DOI: 10.1158/1078-0432.CCR-17-0646]

121 **Pishvaian MJ**, Byers SW. Biomarkers of WNT signaling. *Cancer Biomark* 2007; **3**: 263-274 [PMID: 17917155 DOI: 10.3233/cbm-2007-34-510]

122 **Hao M**, Guo Y, Zhang Z, Zhou H, Gu Q, Xu J. 6-acrylic phenethyl ester-2-pyranone derivative induces apoptosis and G2/M arrest by targeting GRP94 in colorectal cancer. *Bioorg Chem* 2022; **123**: 105802 [PMID: 35436756 DOI: 10.1016/j.bioorg.2022.105802]

123 **Kabir T**, Syn N, Goh BKP. Current status of laparoscopic liver resection for the management of colorectal liver metastases. *J Gastrointest Oncol* 2020; **11**: 526-539 [PMID: 32655931 DOI: 10.21037/jgo.2020.02.05]

124 **Garritano S**, Selvaggi F, Spampinato MG. Simultaneous Minimally Invasive Treatment of Colorectal Neoplasm with Synchronous Liver Metastasis. *Biomed Res Int* 2016; **2016**: 9328250 [PMID: 27294144 DOI: 10.1155/2016/9328250]

125 **Nieuwenhuizen S**, Dijkstra M, Puijk RS, Geboers B, Ruarus AH, Schouten EA, Nielsen K, de Vries JJJ, Bruynzeel AME, Scheffer HJ, van den Tol MP, Haasbeek CJA, Meijerink MR. Microwave Ablation, Radiofrequency Ablation, Irreversible Electroporation, and Stereotactic Ablative Body Radiotherapy for Intermediate Size (3-5 cm) Unresectable Colorectal Liver Metastases: a Systematic Review and Meta-analysis. *Curr Oncol Rep* 2022; **24**: 793-808 [PMID: 35298796 DOI: 10.1007/s11912-022-01248-6]

126 **Datta J**, Narayan RR, Kemeny NE, D'Angelica MI. Role of Hepatic Artery Infusion Chemotherapy in Treatment of Initially Unresectable Colorectal Liver Metastases: A Review. *JAMA Surg* 2019; **154**: 768-776 [PMID: 31188415 DOI: 10.1001/jamasurg.2019.1694]

127 **Buisman FE**, Filipe WF, Galjart B, Grünhagen DJ, Homs MYV, Moelker A, Verhoef C, Groot Koerkamp B. Adjuvant intra-arterial chemotherapy for patients with resected colorectal liver metastases: a systematic review and meta-analysis. *HPB (Oxford)* 2022; **24**: 299-308 [PMID: 34895829 DOI: 10.1016/j.hpb.2021.10.014]

128 **Germani MM**, Borelli B, Boraschi P, Antoniotti C, Ugolini C, Urbani L, Morelli L, Fontanini G, Masi G, Cremolini C, Moretto R. The management of colorectal liver metastases amenable of surgical resection: How to shape treatment strategies according to clinical, radiological, pathological and molecular features. *Cancer Treat Rev* 2022; **106**: 102382 [PMID: 35334281 DOI: 10.1016/j.ctrv.2022.102382]

129 **Guo M**, Jin N, Pawlik T, Cloyd JM. Neoadjuvant chemotherapy for colorectal liver metastases: A contemporary review of the literature. *World J Gastrointest Oncol* 2021; **13**: 1043-1061 [PMID: 34616511 DOI: 10.4251/wjgo.v13.i9.1043]

130 **Primrose JN**. Surgery for colorectal liver metastases. *Br J Cancer* 2010; **102**: 1313-1318 [PMID: 20424612 DOI: 10.1038/sj.bjc.6605659]

131 **D'Andrea V**, Guarino S, Di Matteo FM, Maugeri Saccà M, De Maria R. Cancer stem cells in surgery. *G Chir* 2014; **35**: 257-259 [PMID: 25644725]

132 **Nassar A**, Cimpean S, Abdelhamid A, Jones RP, Wahba R, Fiorentini G, Aldrighetti L, Teh C, Alikhanov R, Hammond J, Silva M, Abdelmabod A, Truant S, Ferrero A, Sturesson C, Ahmed I, Ghazanfar M, Takemura N, Pawlik TM, Bekheit M. The dilemma of the disappeared colorectal liver metastasis: systematic review of reviews and evidence gap map. *BJS Open* 2022; **6** [PMID: 35598157 DOI: 10.1093/bjsopen/zrac051]

133 **Gumbs AA**, Lorenz E, Tsai TJ, Starker L, Flanagan J, Benedetti Cacciaguerra A, Yu NJ, Bajul M, Chouillard E, Croner R, Abu Hilal M. Study: International Multicentric Minimally Invasive Liver Resection for Colorectal Liver Metastases (SIMMILR-CRLM). *Cancers (Basel)* 2022; **14** [PMID: 35326532 DOI: 10.3390/cancers14061379]

134 **Nguyen KT**, Laurent A, Dagher I, Geller DA, Steel J, Thomas MT, Marvin M, Ravindra KV, Mejia A, Lainas P, Franco D, Cherqui D, Buell JF, Gamblin TC. Minimally invasive liver resection for metastatic colorectal cancer: a multi-institutional, international report of safety, feasibility, and early outcomes. *Ann Surg* 2009; **250**: 842-848 [PMID: 19806058 DOI: 10.1097/SLA.0b013e3181bc789c]

135 **Guerra F**, Guadagni S, Pesi B, Furbetta N, Di Franco G, Palmeri M, Annecchiarico M, Eugeni E, Coratti A, Patriti A, Morelli L. Outcomes of robotic liver resections for colorectal liver metastases. A multi-institutional analysis of minimally invasive ultrasound-guided robotic surgery. *Surg Oncol* 2019; **28**: 14-18 [PMID: 30851888 DOI: 10.1016/j.suronc.2018.10.011]

136 **Yang HY**, Rho SY, Han DH, Choi JS, Choi GH. Robotic major liver resections: Surgical outcomes compared with open major liver resections. *Ann Hepatobiliary Pancreat Surg* 2021; **25**: 8-17 [PMID: 33649249 DOI: 10.14701/ahbps.2021.25.1.8]

137 **Kow AWC**. Hepatic metastasis from colorectal cancer. *J Gastrointest Oncol* 2019; **10**: 1274-1298 [PMID: 31949948 DOI: 10.21037/jgo.2019.08.06]

138 **Takahashi H**, Berber E. Role of thermal ablation in the management of colorectal liver metastasis. *Hepatobiliary Surg Nutr* 2020; **9**: 49-58 [PMID: 32140478 DOI: 10.21037/hbsn.2019.06.08]

139 **Buisman FE**, Homs MYV, Grünhagen DJ, Filipe WF, Bennink RJ, Besselink MGH, Borel Rinkes IHM, Bruijnen RCG, Cercek A, D'Angelica MI, van Delden OM, Donswijk ML, van Doorn L, Doornebosch PG, Emmering J, Erdmann JI, IJzerman NS, Grootscholten C, Hagendoorn J, Kemeny NE, Kingham TP, Klompenhouwer EG, Kok NFM, Koolen S, Kuhlmann KFD, Kuiper MC, Lam MGE, Mathijssen RHJ, Moelker A, Oomen-de Hoop E, Punt CJA, Te Riele WW, Roodhart JML, Swijnenburg RJ, Prevoo W, Tanis PJ, Vermaas M, Versleijen MWJ, Veuger FP, Weterman MJ, Verhoef C, Groot Koerkamp B. Adjuvant hepatic arterial infusion pump chemotherapy and resection versus resection alone in patients with low-risk resectable colorectal liver metastases - the multicenter randomized controlled PUMP trial. *BMC Cancer* 2019; **19**: 327 [PMID: 30953467 DOI: 10.1186/s12885-019-5515-6]

140 **Loupakis F**, Cremolini C, Masi G, Lonardi S, Zagonel V, Salvatore L, Cortesi E, Tomasello G, Ronzoni M, Spadi R, Zaniboni A, Tonini G, Buonadonna A, Amoroso D, Chiara S, Carlomagno C, Boni C, Allegrini G, Boni L, Falcone A. Initial therapy with FOLFOXIRI and bevacizumab for metastatic colorectal cancer. *N Engl J Med* 2014; **371**: 1609-1618 [PMID: 25337750 DOI: 10.1056/NEJMoa1403108]

141 **Wang F**, He L, Dai WQ, Xu YP, Wu D, Lin CL, Wu SM, Cheng P, Zhang Y, Shen M, Wang CF, Lu J, Zhou YQ, Xu XF, Xu L, Guo CY. Salinomycin inhibits proliferation and induces apoptosis of human hepatocellular carcinoma cells in vitro and in vivo. *PLoS One* 2012; **7**: e50638 [PMID: 23284640 DOI: 10.1371/journal.pone.0050638]

142 **Xu C**, Xu Z, Zhang Y, Evert M, Calvisi DF, Chen X. β-Catenin signaling in hepatocellular carcinoma. *J Clin Invest* 2022; **132** [PMID: 35166233 DOI: 10.1172/JCI154515]

143 **Chen Y**, Chen M, Deng K. Blocking the Wnt/βcatenin signaling pathway to treat colorectal cancer: Strategies to improve current therapies (Review). *Int J Oncol* 2023; **62** [PMID: 36579676 DOI: 10.3892/ijo.2022.5472]

144 **Kim MJ**, Huang Y, Park JI. Targeting Wnt Signaling for Gastrointestinal Cancer Therapy: Present and Evolving Views. *Cancers (Basel)* 2020; **12** [PMID: 33291655 DOI: 10.3390/cancers12123638]

145 **Nie X**, Liu H, Liu L, Wang YD, Chen WD. Emerging Roles of Wnt Ligands in Human Colorectal Cancer. *Front Oncol* 2020; **10**: 1341 [PMID: 32923386 DOI: 10.3389/fonc.2020.01341]

146 **Vilchez V**, Turcios L, Marti F, Gedaly R. Targeting Wnt/β-catenin pathway in hepatocellular carcinoma treatment. *World J Gastroenterol* 2016; **22**: 823-832 [PMID: 26811628 DOI: 10.3748/wjg.v22.i2.823]

147 **Zhang Y**, Wang X. Targeting the Wnt/β-catenin signaling pathway in cancer. *J Hematol Oncol* 2020; **13**: 165 [PMID: 33276800 DOI: 10.1186/s13045-020-00990-3]

148 **Yu F**, Yu C, Li F, Zuo Y, Wang Y, Yao L, Wu C, Wang C, Ye L. Wnt/β-catenin signaling in cancers and targeted therapies. *Signal Transduct Target Ther* 2021; **6**: 307 [PMID: 34456337 DOI: 10.1038/s41392-021-00701-5]

World Journal of Gastroenterology

Submit a Manuscript: https://www.f6publishing.com

World J Gastroenterol 2023 May 14; 29(18): 2784-2797

DOI: 10.3748/wjg.v29.i18.2784

ISSN 1007-9327 (print) ISSN 2219-2840 (online)

MINIREVIEWS

Infliximab *vs* adalimumab: Points to consider when selecting anti-tumor necrosis factor agents in pediatric patients with Crohn's disease

Eun Sil Kim, Ben Kang

Specialty type: Pediatrics

Provenance and peer review: Invited article; Externally peer reviewed.

Peer-review model: Single blind

Peer-review report's scientific quality classification

Grade A (Excellent): 0
Grade B (Very good): B, B, B
Grade C (Good): 0
Grade D (Fair): 0
Grade E (Poor): 0

P-Reviewer: Govindarajan KK, India; Gravina AG, Italy; Moshref RH, Saudi Arabia

Received: December 28, 2022
Peer-review started: December 28, 2022
First decision: March 8, 2023
Revised: March 20, 2023
Accepted: April 17, 2023
Article in press: April 17, 2023
Published online: May 14, 2023

Eun Sil Kim, Department of Pediatrics, Kangbuk Samsung Hospital, Sungkyunkwan University School of Medicine, Seoul 03181, South Korea

Ben Kang, Department of Pediatrics, School of Medicine, Kyungpook National University, Daegu 41944, South Korea

Corresponding author: Ben Kang, MD, PhD, Associate Professor, Department of Pediatrics, School of Medicine, Kyungpook National University, 680 Gukchaebosang-ro, Jung-gu, Daegu 41944, South Korea. benkang@knu.ac.kr

Abstract

Biologic agents with various mechanisms against Crohn's disease (CD) have been released and are widely used in clinical practice. However, two anti-tumor necrosis factor (TNF) agents, infliximab (IFX) and adalimumab (ADL), are the only biologic agents approved by the Food and Drug Administration for pediatric CD currently. Therefore, in pediatric CD, the choice of biologic agents should be made more carefully to achieve the therapeutic goal. There are currently no head-to-head trials of biologic agents in pediatric or adult CD. There is a lack of accumulated data for pediatric CD, which requires the extrapolation of adult data for the positioning of biologics in pediatric CD. From a pharmacokinetic point of view, IFX is more advantageous than ADL when the inflammatory burden is high, and ADL is expected to be advantageous over IFX in sustaining remission in the maintenance phase. Additionally, we reviewed the safety profile, immunogenicity, preference, and compliance between IFX and ADL and provide practical insights into the choice of anti-TNF therapy in pediatric CD. Careful evaluation of clinical indications and disease behavior is essential when prescribing anti-TNF agents. In addition, factors such as the efficacy of induction and maintenance of remission, safety profile, immunogenicity, patient preference, and compliance play an important role in evaluating and selecting treatment options.

Key Words: Anti-tumor necrosis factor; Infliximab; Adalimumab; Crohn's disease; Pediatric

©The Author(s) 2023. Published by Baishideng Publishing Group Inc. All rights reserved.

Core Tip: In pediatric Crohn's disease (CD), the choice of biologic agents should be made more carefully to achieve the therapeutic goal. This review article focuses on comparing the efficacy of induction and maintenance of remission, safety profile, immunogenicity, preference, and compliance between infliximab and adalimumab in pediatric CD.

Citation: Kim ES, Kang B. Infliximab *vs* adalimumab: Points to consider when selecting anti-tumor necrosis factor agents in pediatric patients with Crohn's disease. *World J Gastroenterol* 2023; 29(18): 2784-2797
URL: https://www.wjgnet.com/1007-9327/full/v29/i18/2784.htm
DOI: https://dx.doi.org/10.3748/wjg.v29.i18.2784

INTRODUCTION

Crohn's disease (CD) has become an important concern of clinicians owing to its rapidly increasing prevalence and incidence worldwide, including in emerging industrial countries[1]. Even though the incidence rate in Western countries has stabilised, most studies have revealed a statistically significant increase in the incidence of pediatric CD[2,3]. Pediatric patients with CD are more likely to have complications such as growth impairment, delayed puberty, psychosocial problems, aggressive disease course, and extensive gastrointestinal involvement than adult patients[4].

After infliximab (IFX) was approved by the Food and Drug Administration (FDA) in 1998[5], biologic agents with various mechanisms have been released and are widely used in clinical practice[6]. Among this broad spectrum of biologics, anti-tumor necrosis factor-α (TNF-α) agents have been classically used as first-line biologics for the treatment of moderate-to-severe CD refractory to conventional therapy[7]. Anti-TNF agents modulate the inflammatory response by binding to the TNF receptor on the cell membrane. IFX is a purified, recombinant DNA-derived chimeric human-mouse immunoglobulin G monoclonal antibody. Adalimumab (ADL) is a human monoclonal antibody that binds specifically to TNF-α[8,9]. Anti-TNF agents, such as IFX and ADL, are the only biologic agents that are currently approved by the FDA for pediatric patients with CD (Table 1)[10,11]. Therefore, the initial biologic agents to modify the disease course of CD and to achieve the therapeutic goal should be chosen more carefully in pediatric patients with CD.

Although head-to-head trials are the gold standard method for determining which treatment option is more effective, to date, no head-to-head trials have directly compared biologic agents. Until direct comparative studies of which biologic agents should be used first are performed, several points must be considered when selecting the initial biologic agent. In this study, we provide practical insights into the choice of anti-TNF therapy in pediatric CD. We reviewed the comparative efficacy, safety profile, immunogenicity, preference, and compliance between IFX and ADL.

MAIN STUDIES IN PEDIATRIC CD ASSESSING THE EFFICACY OF ANTI-TNFα THERAPIES

Anti-TNFα therapies have been well studied in adults and have showed efficacy in both the induction and maintenance of remission[12,13]. Targan *et al*[14] found that after a single 5 mg/kg IFX infusion, more than 80% of patients had a clinical response after four weeks. In the ACCENT-I study in which 58% of 573 patients with CD who had a response after the first dose of IFX were randomised, the IFX 5 mg/kg and 10 mg/kg groups were more effective in achieving clinical remission at week 54 than the placebo group[15].

After IFX and ADL were approved for use in the treatment of pediatric CD in 2006 and 2012, respectively, more than 20 years of data, including those from clinical trials, have been accumulated. There is evidence from randomised controlled trials (RCT) involving open-label induction and randomised dose-ranging maintenance therapies (Table 2). Four RCTs conducted on pediatric CD treated with anti-TNF agents showed the clinical remission rate in both the induction and maintenance periods[16-19].

The first RCT with IFX in pediatric patients with CD showed clinical response and remission in the induction and maintenance phases[16]. Among 112 patients, 99 patients (88.4%) responded to IFX, and 66 patients (58.9%) showed clinical remission at week 10. Patients responding to IFX were randomly assigned to receive IFX 5 mg/kg every 8 or 12 wk. By week 54, 63.5% of patients receiving IFX every eight weeks had a clinical response, and 55.8% achieved clinical remission, which is significantly higher than the clinical remission rate of 23.5% in those who received IFX every 12 wk. Ruemmele *et al*[17] also demonstrated the efficacy of IFX in pediatric patients with CD. Forty patients received IFX according to the induction regimen (weeks 0, 2, and 6) and were then randomly assigned to maintenance therapy of

Table 1 Biologic agents currently used or under study for the treatment of pediatric Crohn's disease

Class	Biologics	FDA approval for CD	Pediatric CD indications
Anti-TNF	Infliximab	Adult: 1998; Pediatric: 2006	Moderate to severe diseases refractory to conventional therapy[10]
	Adalimumab	Adult: 2007; Pediatric: 2012	First-line therapy for patients with CD who are at risk for progressive disease or for whom corticosteroids may exacerbate underlying conditions[10]; Prophylactic therapy for preventing postoperative recurrence in high-risk patients[10]
Anti-α4β7 integrin	Vedolizumab	Adult: 2014; Pediatric: N/A	Guideline recommendations for this pediatric indication are not yet available
IL-12/23 p40 inhibitor	Ustekinumab	Adult: 2016; Pediatric: N/A	Second-line biologic therapy after anti-TNF agent failure[11]

FDA: Food and Drug Administration; CD: Crohn's disease; TNF: Tumor necrosis factor; IL: Interleukin; N/A: Not applicable.

Table 2 Studies evaluating infliximab efficacy in pediatric Crohn's disease in the induction and maintenance phases

Ref.	Study group	Anti-TNF-α	Participants	Study design and aims	Definition of the outcome	Number of patients (*n*)	Age at diagnosis (yr)	Time	Clinical response	Clinical remission
Hyams *et al* [16], 2007	REACH	IFX	CD with a PCDAI > 30	Comparison of IFX maintenance intervals; every 8 *vs* 12 wk. Primary responders were randomised at week 10	Response: ΔPCDAI = -15. Remission: PCDAI ≤ 10	Total: 103. Every 8 wk: 52. Every 10 wk: 51	13.3	Week 10. Week 54	88.4%. Every 8 wk: 63.5%. Every 12 wk: 33.3% (P = 0.002)	58.9%. Every 8 wk: 55.8%. Every 12 wk: 23.5% (P < 0.001)
Ruemmele *et al*[17], 2009	GFHGNP	IFX	CD	Comparison of IFX infusion every 8 wk at maintenance *vs* IFX on demand. Primary responders were randomised at week 10	Remission: Harvey Bradshaw index < 5	Total: 40. Every 8 wk: 18. On demand: 13	13.9	Week 10. Week 60	N/A	85%. Every 8 wk: 83%. On demand: 61% (P = 0.001)
Hyams *et al* [18], 2012	IMAgINE	ADL	Moderate-to-severe CD	Comparison of ADL dose; HD (40 mg or 20 mg for body weight ≥ 40 kg or < 40 kg) *vs* LD (20 mg or 10 mg for body weight ≥ 40 kg or < 40 kg). Primary responders were randomised at week 4	Response: ΔPCDAI = -15. Remission: PCDAI ≤ 10	Total: 188. HD: 93. LD: 95	HD: 13.7 ± 2.52. LD: 13.5 ± 2.47	Week 26. Week 52	HD: 59.1%, LD: 48.4%. HD: 41.9%, LD: 28.4%	HD: 38.7%; LD: 28.4%. HD: 33.3%; LD: 23.2%
Assa *et al* [19], 2019	PAILOT	ADL	Biologic-naïve CD	Comparison of proactive TDM *vs* reactive TDM. Primary responders were randomised at week 4	Remission: PCDAI ≤ 10	Total: 78. Proactive: 38. Reactive: 40	Proactive: 12.9 ± 2.6. Reactive: 13.5 ± 2.7	Week 4. Week 72	NA	NA. Proactive TDM: 82%; Reactive TDM: 48%

CD: Crohn's disease; RCT: Randomised controlled trial; IFX: Infliximab; PCDAI: Pediatric Crohn's disease activity index; NA: Not applicable; ADL: Adalimumab; HD: High dose; LD: Low dose; TDM: Therapeutic drug monitoring.

IFX infusion every two months or an on-demand regimen. Around 85.0% of patients achieved clinical remission during IFX induction therapy. After the induction phase, the relapse rate was significantly higher in the on-demand group (91.7%) than in the IFX-maintenance group (23.1%).

A double-blind RCT evaluating the efficacy and safety of a dose-dependent maintenance regimen with ADL following open-label, weight-adjusted induction therapy (IMAgINE-1) was conducted on both IFX-naïve patients and patients who did not respond to IFX therapy[18]. In patients who had a clinical response in the induction phase, 38.7% and 33.5% of clinical remission was observed at week 26 and week 52, respectively. In addition, there was no statistically significant difference between the high- and low-dose groups. In a recently published RCT conducted in anti-TNF-naïve pediatric patients with CD, the clinical remission rate after the induction phase was much higher than that in the IMAgINE-1 study (48%-82% *vs* 38.7%)[19]. These results are in line with findings from previous adult studies[12,13] and highlight the importance of the choice of initial biologic agents according to risk stratification.

ANTI-TNFα AND ITS INDICATIONS FOR PEDIATRIC CD

The indications for the use of biologic agents have changed over the last two decades since the introduction of anti-TNF agents for the treatment of pediatric CD. Previously, anti-TNF agents were considered when disease activity was not controlled despite conventional therapies such as immunomodulators (IMMs), the so-called step-up strategy[16]. However, the guidelines recently published by the European Society of Pediatric Gastroenterology, Hepatology, and Nutrition (ESPGHAN) recommended early anti-TNF treatment within < 3 mo after diagnosis for the induction of remission in moderate-to-severe pediatric CD with a high risk of complications such as extensive disease, deep colonic ulcers, perianal disease, stricturing (B2), or penetrating disease (B3), growth impairment, the so-called top-down strategy[20]. The RISK study demonstrated that early induction therapy with anti-TNF agents was associated with higher corticosteroid- and surgery-free remission rated at 1 year compared to induction with exclusive enteral nutrition (EEN) and corticosteroids[21]. Kugathasan *et al*[22] also reported that early induction therapy with anti-TNF agents significantly lowered the risk of penetrating (B3) complications, however did not seems to reduce the risk of stricturing (B2) complications. In addition, even in patients with low risk of poor outcome, anti-TNF therapy should be considered in patients with severe growth impairment or who have not achieved clinical (pediatric CD activity index < 10) and biochemical remission (fecal calprotectin < 250 μg/g) despite induction therapy with EEN or corticosteroids[20].

Walters *et al*[21] reported that early anti-TNF therapy was more effective at maintaining remission than IMM monotherapy [relative risk (RR), 1.41; 95%CI: 1.14-1.75; P = 0.0017]. In addition, a prospective study in 76 pediatric patients with CD compared the step-up group and the top-down group in terms of endoscopic healing[23]. Compared with that in the step-up strategy, the rate of achieving endoscopic healing at week 54 was higher in the top-down group of pediatric patients with CD (42% *vs* 72%, P = 0.007), which means that seizing the therapeutic window of opportunity in pediatric CD should be considered earlier than generally accepted[24]. Based on these results, guidelines suggest that either IFX or ADL can be provided to pediatric patients with CD who have not previously received anti-TNF therapy, taking into account the efficacy, route of administration, and preference.

Standard dosing of IFX is weight-based at 5 mg/kg at weeks 0, 2, and 6, followed by maintenance treatment every 8 wk. In the case of ADL, patients weighing < 40 kg received 80/40 mg, and those weighing ≥ 40 kg received 160/80 mg in the first 2 wk. Thereafter, patients weighing < 40 kg were administered 20 mg, and patients weighing ≥ 40 kg were administered 40 mg every 2 wk. Dose escalation is considered in patients who lose response to standard anti-TNF treatment; adjustment of the infusion interval to 4 or 6 wk or an increment in the dose of 10 mg/kg for IFX; and adjustment of the administration interval to every week for ADL. Especially, children at risk for accelerated IFX clearance during induction [*i.e.*, patients < 30 kg, those with extensive disease, and those with low serum albumin] require dose escalation to achieve target trough levels (TLs) or their first proactive therapeutic drug monitoring (TDM) at the second or third anti-TNF infusion[25].

EFFICACY OF ANTI-TNF THERAPY IN PEDIATRIC CD

Comparative efficacy of anti-TNF agents for induction of remission in CD

Head-to-head trials, in which each drug or treatment strategy is compared formally, are the gold standard method for comparing distinct therapies[26]. However, there are currently no head-to-head trials of biologic agents in pediatric or adult CD. Owing to the absence of results, the choice of IFX or ADL relied on expert opinion, real-world data, or indirect comparison of biologic agents. Unfortunately, for pediatric patients with CD, there is a lack of accumulated data, which requires the extrapolation of adult data for the positioning of biologics in pediatric CD.

In 2018, the results of a network meta-analysis that indirectly compared the efficacy of FDA-approved biologic agents in the treatment of CD, which included IFX, ADL, vedolizumab, ustekinumab, and certolizumab pegol, were published[27,28]. When IFX and ADL were compared with respect to the efficacy of remission induction, IFX was ranked higher than ADL [surface under the cumulative ranking (SUCRA) 0.93 *vs* 0.75] for inducing clinical remission in biologic-naïve patients with moderate-to-severe CD. Additionally, IFX was predicted to be more effective in induction therapy than ADL; the rates of achieving clinical remission with induction therapy were 59.6% and 48.7% for IFX and ADL, respectively.

These findings are partly explained by differences in the pharmacokinetics or tissue penetration of IFX and ADL[29]. Drug levels of IFX and ADL show completely different patterns over time after administration. Intravenous (IV) formulations, such as IFX, show the highest concentrations with administration, and the concentrations gradually decrease over time, dropping to the lowest level just before the next administration, that is, to the TLs. In the case of subcutaneous (SC) formulations, including ADL, the concentrations at the time of administration, at the peak point, and at the lowest point are similar[30]. Because IFX has relatively large fluctuations in drug levels according to the drug infusion type, it is necessary to increase drug levels during the induction phase to maintain TLs,

whereas ADL maintains relatively constant drug concentrations.

Post-induction TLs, which can modulate inflammation in patients with high disease and inflammatory burdens, differ according to the type of anti-TNF agent used. In Figure 1A[31], we assumed the threshold of drug levels to control the inflammatory burden in the induction phase as the purple dotted line. IFX exhibits higher TLs than ADL during the induction phase, which is beneficial for maintaining post-induction TLs above the threshold required for treatment in patients with severe inflammation. Therefore, IFX might be more advantageous than ADL in patients with a high inflammatory burden owing to differences in the pharmacokinetics of the two anti-TNF agents during the induction period.

Specifically, a post-hoc analysis of the ACCENT-I study found that high IFX TLs after induction therapy were a key factor in maintaining response after one year of treatment[32]. The study revealed that more than 3.5 μg/mL of post-induction TLs of IFX was associated with a durable, sustained response to maintenance therapy. Feng *et al*[33] reported that post-induction TLs of IFX were correlated with endoscopic healing, and the median TLs in patients who achieved endoscopic healing after the induction of IFX were 7.5 μg/mL.

Similar to adult inflammatory bowel disease (IBD), higher post-induction IFX TLs were the only independent factor that predicted clinical or biochemical remission and durable sustained response during the first year of treatment in pediatric IBD[34]. Singh *et al*[35] reported that cut-off levels of > 3, > 4, > 7 μg/mL of IFX TLs had positive predictive values of 64%, 76%, and 100%, respectively, for predicting persistent remission in pediatric IBD. Recently, El-Matary *et al*[36] showed that higher post-induction IFX TLs had a strong relationship with the healing of the fistula in pediatric perianal CD. The post-induction IFX TLs in the clinical responder group were higher than those in the non-responder group (12.7 μg/mL *vs* 5.4 μg/mL, $P = 0.002$).

Likewise, post-induction TLs of ADL correlated with clinical and biochemical remission[37,38]. Zittan *et al*[37] reported that ADL TLs at week 4 were higher in the biological remission group than in the non-responder group of adult patients with CD (19.8 μg/mL *vs* 10.2 μg/mL, $P = 0.001$). After induction therapy, it was shown that similar to adult CD, there was a positive relationship between ADL TLs and clinical outcomes in pediatric CD[38]. The cut-off values of ADL TLs at weeks 4 and 8 to predict clinical and biological remission at week 24 were 22.5 μg/mL and 12.5 μg/mL, respectively.

Although the cut-off values of post-induction TLs for regulating the inflammatory burden at anti-TNF initiation are different for IFX and ADL, it is anticipated that the higher the post-induction TLs, the higher the clinical and endoscopic remission rate. Considering the pharmacokinetics of the route of administration, IFX can reach drug levels above the threshold in a shorter period of time than ADL and exhibits a rapid response of induction. Therefore, predictions based on the pharmacokinetics of anti-TNF agents and the difference in remission according to post-induction TLs show that IFX is more advantageous than ADL when the inflammatory burden is high.

Comparative efficacy of anti-TNF agents for maintenance of remission in CD

As with the selection of anti-TNF agents for the induction of remission, there are no head-to-head trials comparing the efficacy of maintenance therapy between IFX and ADL. According to a network meta-analysis study conducted in adults, ADL was superior to IFX in the maintenance phase, in contrast to the induction phase. In biologic-naïve adult patients with moderate-to-severe CD, the SUCRA of maintaining remission over one year was 0.97 and 0.68 for ADL and IFX, respectively[27,28].

These results can also be explained by the differences in the pharmacokinetics of IFX and ADL. For IV drugs, a clear distinction can be made among the peak, intermediate, and trough concentrations available for TDM. However, for SC drugs, there is no clear distinction among the peak, intermediate, and trough concentrations. In the case of SC drugs, the sampling time for TDM is less important because the TLs of SC drugs are kept relatively constant because not only is frequent administration required but also the absorption rate is relatively low[29].

Figure 1B shows the concentration changes in IFX and ADL during the maintenance phase, and the purple dotted line indicates the threshold for controlling the inflammatory burden during the maintenance phase[31]. The drug level of IFX tends to be lower than the threshold as it approaches the trough time, whereas the drug level of ADL is continuously maintained above the threshold because of the relatively constant levels of ADL. In the maintenance phase, it is important to keep the drug concentrations above the threshold to not only inhibit the formation of anti-drug antibodies (ADAs) but also to suppress the occurrence of loss of response and increase the durability of anti-TNF agents. Owing to the differences in the pharmacokinetics of the two anti-TNF agents, ADL might be more advantageous than IFX in the maintenance phase.

The association between IFX TLs in the maintenance phase and clinical outcomes has been demonstrated in many studies conducted on adults. One meta-analysis indicated that patients who achieved clinical remission had significantly higher IFX TLs than those who did not achieve remission during the maintenance phase (3.1 μg/mL *vs* 0.9 μg/mL)[39]. In addition, it has been shown in several studies that IFX TLs in the maintenance phase are an important prognostic factor in achieving endoscopic healing. Another study revealed that the only factor associated with endoscopic healing was an increase in IFX TLs > 0.5 μg/mL (likelihood ratio, 2.02; 95%CI: 1.01-4.08; $P = 0.048$) in patients with IBD[40]. Additionally, Yarur *et al*[41] demonstrated a correlation between IFX TLs and fistula healing [area under the curve (AUC), 0.82; $P < 0.0001$]. Likewise, higher maintenance IFX TLs were associated

with clinical and biochemical remission in pediatric patients with CD[42]. Recently, it has been reported that IFX TLs during maintenance treatment are important determinants of endoscopic healing as well as clinical remission in pediatric patients with CD. According to this study, IFX TLs to achieve endoscopic remission with 80% specificity were ≥ 5 μg/mL[43].

Similar to IFX, maintenance TLs of ADL were associated with clinical and laboratory responses in adult patients with CD[44]. The study showed that ADL TLs were associated with clinical remission (AUC, 0.748; $P < 0.001$), with an optimal cut-off value for predicting clinical remission of 5.85 μg/mL (sensitivity, 68%; specificity, 70.6%). In addition, Zittan *et al*[45] conducted a large, homogenous CD cohort study which revealed that patients with endoscopic healing have higher ADL TLs during the maintenance phase than those without endoscopic healing (14.7 μg/mL *vs* 3.4 μg/mL, $P < 0.001$). Similar results were found in studies conducted on pediatric patients with CD. The IMAgINE-1 study showed that patients with clinical remission at week 26 had slightly higher ADL TLs than those without remission (11.3 μg/mL *vs* 10.5 μg/mL, $P = 0.028$)[46]. Choi *et al*[47] reported that pediatric patients with endoscopic healing had significantly higher ADL TLs at week 16 than those without endoscopic healing (13.0 μg/mL *vs* 6.2 μg/mL, $P = 0.023$).

As can be inferred from the above studies, clinical remission and endoscopic healing can be achieved when the drug concentrations are sustained above the threshold despite the difference in the cut-off values for withstanding the inflammatory burden in the maintenance phase between IFX and ADL. Considering the pharmacokinetics of the maintenance phase, ADL maintains drug levels more constantly than IFX; therefore, it is expected that ADL is more advantageous in sustaining remission than IFX in the maintenance phase.

IMMUNOGENICITY OF ANTI-TNF AGENTS

Although anti-TNF agents are effective in patients with CD refractory to conventional therapy, loss of response increases over time, and approximately, half of patients among primary responders require dose escalation[48]. Among patients receiving anti-TNF agents, 60%-87% of patients show clinical remission or partial response in the induction phase, and less than 40% of patients maintain clinical remission at one year[49]. Immunogenicity due to the formation of ADAs to anti-TNF agents as the main reason for the loss of response.

Immunogenicity to anti-TNF agents develops when the immune system of patients recognises drugs as antigens and triggers the formation of ADAs. ADAs accelerate drug clearance by the reticuloendothelial system and neutralise drugs by binding to anti-TNF agents[50]. Additionally, suboptimal TLs of anti-TNF agents are associated with a more immunogenic state, which leads to lower efficacy and greater loss of response[37,51,52]. Higher body weight, the development of ADAs to anti-TNF agents, a low albumin level, and an elevated C-reactive protein level are the covariates that accelerate the clearance of anti-TNF agents[53-56].

Vermeire *et al*[57] reported that the rate of ADA formation in IBD patients receiving IFX was up to 65.3% and that in patients receiving ADL was 38.0%. Theoretically, as ADL is a humanised monoclonal antibody, it is thought that the incidence of immunogenicity in the human body is lower than that for IFX, which is a monoclonal chimeric anti-TNF antibody (partly murine, partly human). Therefore, ADL was superior to IFX in terms of immunogenicity.

ANTI-TNF AGENTS FOR GROWTH IMPROVEMENT

In Selecting Therapeutic Targets in IBD-II, restoration of normal growth was established as an intermediate target for pediatric patients[58]. Therefore, a very important goal in treatment for pediatric patients with CD is to normalise the linear growth.

To date, no study has compared the effects of IFX and ADL on the restoration of linear growth. Studies have shown that each of the two anti-TNF agents has a positive effect on the recovery of normal growth. In the case of IFX, there is a study published on the restoration of growth as well as clinical response and endoscopic healing in 195 pediatric patients with CD[59]. The effect on the recovery of linear growth was greater when IFX was administered at the Tanner 1-2 stage with growth potential than at the Tanner 4-5 stage. Another study showed that early administration of IFX within one month after diagnosis was more effective for linear growth than the conventional step-up therapy ($P = 0.026$) [60]. For Tanner stage 4-5 patients receiving IFX, there was no statistically significant difference in height z-score between patients with early IFX administration and those with the conventional step-up therapy ($P = 0.438$). However, in patients with Tanner 1-2, the restoration of growth was significantly improved in patients with early IFX administration ($P = 0.016$).

Similarly, it was reported that ADL was effective in restoring linear growth at weeks 26 and 52 compared with baseline in patients with growth impairment at diagnosis (median height z-score, baseline, -3.25; 26 wk, -0.34; 52 wk, 0.21, $P < 0.001$)[61]. Additionally, Matar *et al*[62] showed that ADL improves weight as body mass index as well as linear growth after 72 wk of treatment.

SAFETY AND ADVERSE EVENTS DURING ANTI-TNF THERAPY

From an immunological point of view, as TNFα is a cytokine responsible for macrophage activation, neutrophil recruitment, and granuloma formation, anti-TNF agents are associated with an increased risk of infection, especially granulomatous infection[63]. Dulai *et al*[64] reported that the rate of serious infectious disease in pediatric patients with IBD who were treated with anti-TNF agents was similar to that of pediatric patients who received IMMs [352/10000 *vs* 33/10000 patient-years of follow-up evaluation (PYF); 95%CI: 0.83-1.36] but significantly lower than that of adult patients (654/10000 PYF; 95%CI: 0.43-0.67). In addition, the risk of infection is higher when anti-TNF agents are administered in combination with IMMs than with anti-TNF monotherapy (RR, 1.19; 95%CI: 1.03-1.37)[65]. According to a network meta-analysis of adult studies that indirectly compared IFX and ADL, IFX had a lower risk of any infection (SUCRA, 0.83) than ADL (SUCRA, 0.22)[27].

Previous studies have shown the risk of malignancy and lymphoproliferative disorders with IBD treatment, particularly with thiopurine and anti-TNF agents. Based on a meta-analysis of 49 randomised placebo-controlled studies comprising 14590 adult patients, there was no evidence related to an increased risk of malignancy with the use of biologic agents including IFX or ADL (odds ratio, 0.90; 95%CI: 0.54-1.50)[66]. Studies with pediatric patients also showed similar results to those of adult studies. In a study conducted using the DEVELOP registry including 5776 pediatric patients with IBD treated with anti-TNF agents, malignancy occurred in 15 patients[67]. An increased risk of malignancy was found in patients treated with thiopurine when a stratified analysis of thiopurine exposure was performed regardless of biologic agents. Even though the standardised incidence of malignancy for thiopurine exposure was 2.43 when compared to the prevalence in healthy children, no significant increase in the incidence of malignancy was observed in children who were only exposed to IFX.

Recent studies showed that the most common complications in patients with IBD treated with anti-TNF agents were dermatologic complications such as psoriasis, eczema, and skin infection[68]. Similarly, the frequency of skin problems appears to be high in pediatric patients with CD on anti-TNF. When comparing patients treated with IFX and ADL, the rate was much higher in IFX-treated patients than in ADL-treated patients. In a pediatric retrospective, large cohort study comprising 409 patients, 11.5% of patients showed at least one dermatologic complication. Among them, 35 were treated with IFX and 12 with ADL. In particular, among patients who developed psoriasis, the proportion of patients treated with IFX was significantly higher than that of those treated with ADL (84.8% *vs* 15.2%, $P = 0.05$) [69]. Additionally, Hradsky *et al*[70] reported that the only predictive factor for any dermatologic complication in pediatric CD was IFX therapy (*vs* ADL, hazard ratio, 2.07; 95%CI: 1.03-4.17).

EFFECTS OF CONCOMITANT IMM TREATMENT

For patients starting on IFX, combination therapy with IMM including azathioprine (AZA) and methotrexate (MTX) is recommended. As the first RCTs regarding the comparison of combination therapy of IFX and AZA with monotherapy of IFX or AZA, the SONIC trials showed the superiority of combination therapy to monotherapy regarding clinical remission, endoscopic healing, pharmacokinetics, and immunogenicity in adult patients with CD[71]. At week 30, ADAs developed in only 0.9% of patients receiving combination therapy, whereas these were produced in 14.6% of patients receiving IFX monotherapy, leading to higher IFX TLs in the combination therapy group than in the IFX monotherapy group (3.5 μg/mL *vs* 1.6 μg/mL, $P < 0.001$). Additionally, the combination therapy group was more likely than the IFX or AZA monotherapy group to achieve corticosteroid-free clinical remission and endoscopic healing. Likewise, it was revealed that the combination of IFX plus MTX had a lower ADA development (4% *vs* 20%, $P = 0.01$) and higher IFX TLs (6.35 μg/mL *vs* 3.75 μg/mL, $P = 0.08$) than IFX monotherapy in the COMMIT trial conducted in adult[72].

No RCT has compared the effects of combination therapy with IFX and IMM and IFX monotherapy in pediatric CD. A retrospective study conducted on 229 pediatric patients with CD confirmed that combination therapy with IFX and AZA reduced the formation of ADAs and loss of response compared to IFX monotherapy[73]. Moreover, pediatric patients who were treated with IFX monotherapy had a lower probability of remaining ADA than patients with combination therapy at 12, 24, and 36 mo after induction of IFX (72.6% *vs* 93.4%, 57.7% *vs* 91.0%, and 48.1% *vs* 91.0%, respectively). Similarly, pediatric studies comparing combination of IFX plus IMM (including AZA and MTX) and IFX monotherapy reported results similar to those in adult studies[59,74,75]. Therefore, up-front anti-TNF agents in combination with IMMs should be considered in patients with high risk of poor outcomes such as perianal disease, structuring (B2) or penetrating (B3) disease behaviour or severe growth impairment.

A meta-analysis comparing the efficacy of combination therapy of ADL and IMMs and ADL monotherapy in adult CD revealed that the induction of remission rate of ADL monotherapy was lower than that of combination therapy with IMMs, although the maintenance of remission was comparable [76]. In contrast to the results of studies on adults, a post-hoc analysis of the IMAgINE-1 study found that combination therapy of ADL and IMMs is not superior to ADL monotherapy in terms of pharmacokinetics, efficacy, and safety in pediatric patients with CD[77]. Clinical response and remission rates

were comparable in patients treated with combination therapy and ADL monotherapy at weeks 4, 26, and 52. Regarding pharmacokinetics, there were no significant differences in the mean TLs between the two groups. These results are in line with the findings of other studies showing that combination therapy with ADL and IMMs was not more effective than ADL monotherapy in pediatric CD[48,78].

Therefore, the recently updated ESPGHAN guidelines for the medical treatment of CD in children and adolescents recommend combination therapy with IFX and IMMs, whereas ADL monotherapy can be an alternative to combination therapy with IMMs[20].

PREFERENCES OF PATIENTS AND PARENTS

There are several differences between IFX and ADL. However, the primary difference is the mode of administration. The IV delivery of biotherapeutics has the advantage of being able to elicit a relatively rapid induction of response and is suitable for administering a large volume of drugs. On the other hand, SC formulations have the advantage of requiring fewer frequent visits to the clinic and being less invasive than IV administration[79]. Because of these differences in the route of administration, not only the efficacy of anti-TNF agents but also the preference of patients and caregivers for the delivery of drugs should be considered.

In a study conducted on rheumatoid arthritis patients treated with anti-TNF agents, patients under the age of 61 years showed a tendency to prefer SC preparations to IV preparations owing to the convenience of administration[80]. Similarly, a study conducted on adult patients with CD in Switzerland also showed the same results. The patient's choice of a specific anti-TNF agent was influenced by the convenience of use (69%), time required for treatment (34%), frequency of drug administration (31%), scientific evidence for efficacy (19%), and fear of syringes (10%). For these reasons, most patients prefer SC rather than IV injection when choosing anti-TNF agents[81].

However, a recent study conducted on anti-TNF selection in Korea reported the opposite result. Among 189 anti-TNF naïve patients with CD, 63.5% of patients preferred IFX, and 36.5% of patients preferred ADL[82]. In contrast to Western studies, the reason for choosing the IV route of administration over the SC route was the reassurance from the presence of doctors (68.3%).

The differences in results of these studies seem to show differences between Western and Eastern countries in terms of culture and medical environments. Unlike Western countries, Asia has a cultural context in which patients have relative interdependence in the decision-making process during treatment[83]. Therefore, characteristics, daily life, preferences, and cultural differences between patients and caregivers should be considered when selecting biologic agents for the treatment of pediatric patients with CD. Clinicians should discuss the route of administration of biologic agents with patients and their caregivers before prescribing anti-TNF therapy.

ADHERENCE TO ANTI-TNF AGENTS

Low compliance and delayed administration of anti-TNF agents are highly related to the formation of ADAs, which can lead to adverse events and loss of response due to low TLs[84,85]. In the treatment of patients with CD, adherence to anti-TNF agents plays an important role in improving treatment efficacy and patient outcomes. The rate of adherence to anti-TNF agents is known to be approximately 70% in patients with CD[86]. When the adherence rates of IFX and ADL were compared, the adherence rate of IFX was 66%-85%, and that of ADL was 55[87-89], with an RR of 0.76 (95%CI: 0.64-0.91)[86].

The difference in adherence between IFX and ADL is thought to be caused by the route of administration, intervals of injection, and supervision of clinicians during the injection. Adherence could be controlled in favour of IFX because the administration of IV drugs requires patient visits to an outpatient clinic.

However, special circumstances, such as coronavirus disease 2019 (COVID-19), may lead to different results. In 2020, the Pediatric IBD Porto Group of ESPGHAN published a society paper[90]. While investigating and reporting the experience of pediatric IBD management during the COVID-19 situation in China and South Korea, it has been recommended that standard treatment be not stopped or delayed. During the COVID-19 pandemic period, anti-TNF infusion delays were reported in 28% of cases in China and 5% in Korea, and exacerbation of disease among delayers was reported in 21% and 23%, respectively. The difference in infusion delay between the two countries may have been contributed to some extent by social factors such as social distancing or lockdown. However, it can be assumed that the main reason is that self-injectable ADL is not available in China, and only IFX, which requires an outpatient visit and IV infusion, can be administered. Therefore, when contagious diseases such as COVID-19 are spreading, ADL might have an advantage in terms of adherence to IFX.

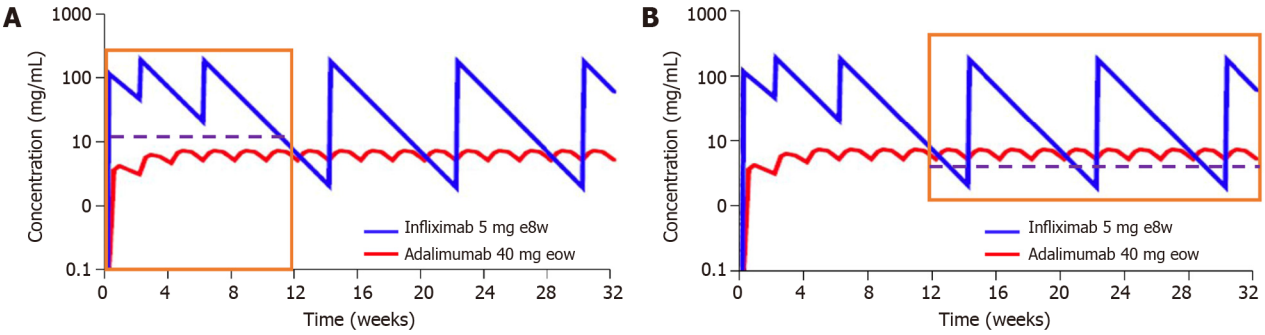
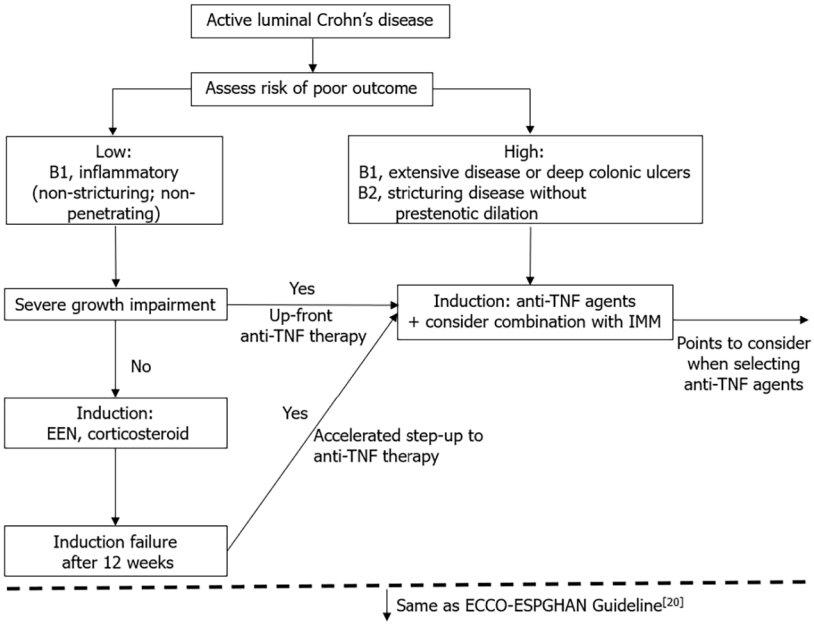


Figure 1 The pharmacokinetic profile of an intravenously or subcutaneously administered anti-tumor necrosis factor agent. A: According to a theoretical induction dosing regimen; B: According to a theoretical maintenance dosing regimen. TNF: tumor necrosis factor. Citation: Gibson DJ, Ward MG, Rentsch C, Friedman AB, Taylor KM, Sparrow MP, Gibson PR. Review article: determination of the therapeutic range for therapeutic drug monitoring of adalimumab and infliximab in patients with inflammatory bowel disease. *Aliment Pharmacol Ther* 2020; 51: 612-628. Copyright ©John Wiley & Sons Ltd. 2020. Published by John Wiley & Sons[31].



Factors	Infliximab	Adalimumab
Inflammatory burden	Superior	Inferior
Rapid response to induction	Superior	Inferior
Any infection	Superior	Inferior
Adherence	Superior	Inferior
Growth improvement	Equivalent	Equivalent
Malignancy	Equivalent	Equivalent
Sustaining remission in maintenance phase	Inferior	Superior
Immunogenicity	Inferior	Superior
Dermatologic complications	Inferior	Superior
Preference	Depend on culture and medical environment	

Figure 2 Summary flowchart of medical management of pediatric luminal Crohn's disease and points to consider when selecting anti-tumor necrosis factor agents. TNF: Tumor necrosis factor; EEN: Exclusive enteral nutrition; IMM: Immunomodulators. Citation: van Rheenen PF, Aloi M, Assa A, Bronsky J, Escher JC, Fagerberg UL, Gasparetto M, Gerasimidis K, Griffiths A, Henderson P, Koletzko S, Kolho KL, Levine A, van Limbergen J, Martin de Carpi FJ, Navas-López VM, Oliva S, de Ridder L, Russell RK, Shouval D, Spinelli A, Turner D, Wilson D, Wine E, Ruemmele FM. The Medical Management of Paediatric Crohn's Disease: an ECCO-ESPGHAN Guideline Update. *J Crohns Colitis* 2020. Copyright ©Oxford University Press 2020. Published by Oxford University Press[20].

CONCLUSION

Anti-TNF agents have proven to be effective in endoscopic, clinical, and biochemical remission in pediatric patients with moderate-to-severe CD. However, careful anti-TNF therapy is required because of the limitations of biologics approved for pediatric patients. Careful evaluation of clinical indications and disease behavior is essential when prescribing anti-TNF agents. In addition, factors such as the efficacy of induction and maintenance of remission, safety profile, immunogenicity, patient preference, and compliance play an important role in evaluating and selecting treatment options (Figure 2)[20]. Larger cohorts and clinical trials comparing groups based on risk stratification are needed to provide more effective and personalised treatment strategies for pediatric patients.

ACKNOWLEDGEMENTS

There are no additional acknowledgments associated with this article. All authors approved the final version of the article.

FOOTNOTES

Author contributions: Kim ES contributed to the literature search, evidence procurement, writing and editing manuscript, revision; Kang B was the guarantor of the article, contributed to the literature search, evidence procurement, writing and editing manuscript, critical review of manuscript, revision and editing of final manuscript. All authors contributed to the article and approved the submitted version.

Conflict-of-interest statement: All authors have no conflicts of interest to declare.

Open-Access: This article is an open-access article that was selected by an in-house editor and fully peer-reviewed by external reviewers. It is distributed in accordance with the Creative Commons Attribution NonCommercial (CC BY-NC 4.0) license, which permits others to distribute, remix, adapt, build upon this work non-commercially, and license their derivative works on different terms, provided the original work is properly cited and the use is non-commercial. See: https://creativecommons.org/Licenses/by-nc/4.0/

Country/Territory of origin: South Korea

ORCID number: Eun Sil Kim 0000-0003-2012-9867; Ben Kang 0000-0002-8516-9803.

S-Editor: Zhang H
L-Editor: A
P-Editor: Yu HG

REFERENCES

1 **Ng SC**, Shi HY, Hamidi N, Underwood FE, Tang W, Benchimol EI, Panaccione R, Ghosh S, Wu JCY, Chan FKL, Sung JJY, Kaplan GG. Worldwide incidence and prevalence of inflammatory bowel disease in the 21st century: a systematic review of population-based studies. *Lancet* 2017; **390**: 2769-2778 [PMID: 29050646 DOI: 10.1016/S0140-6736(17)32448-0]

2 **Benchimol EI**, Fortinsky KJ, Gozdyra P, Van den Heuvel M, Van Limbergen J, Griffiths AM. Epidemiology of pediatric inflammatory bowel disease: a systematic review of international trends. *Inflamm Bowel Dis* 2011; **17**: 423-439 [PMID: 20564651 DOI: 10.1002/ibd.21349]

3 **Sýkora J**, Pomahačová R, Kreslová M, Cvalínová D, Štych P, Schwarz J. Current global trends in the incidence of pediatric-onset inflammatory bowel disease. *World J Gastroenterol* 2018; **24**: 2741-2763 [PMID: 29991879 DOI: 10.3748/wjg.v24.i25.2741]

4 **Rosen MJ**, Dhawan A, Saeed SA. Inflammatory Bowel Disease in Children and Adolescents. *JAMA Pediatr* 2015; **169**: 1053-1060 [PMID: 26414706 DOI: 10.1001/jamapediatrics.2015.1982]

5 US Department of Health & Human Services. Drugs @ FDA-label and approval history. In: Food and Drug Administration. [cited 2022 December 28]. Available from: http://www.accessdata.fda.gov/scripts/cder/drugsatfda/index.cfm?fuseaction=Search.Label_ApprovalHistory#apphis/

6 **Allen PB**, Bonovas S, Danese S, Peyrin-Biroulet L. Evolving primary and secondary endpoints in randomized controlled trials leading to approval of biologics and small molecules in IBD: an historical perspective. *Expert Opin Biol Ther* 2020; **20**: 151-161 [PMID: 31815548 DOI: 10.1080/14712598.2020.1702020]

7 **Nielsen OH**, Ainsworth MA. Tumor necrosis factor inhibitors for inflammatory bowel disease. *N Engl J Med* 2013; **369**: 754-762 [PMID: 23964937 DOI: 10.1056/NEJMct1209614]

8 **Kornbluth A**. Infliximab approved for use in Crohn's disease: a report on the FDA GI Advisory Committee conference. *Inflamm Bowel Dis* 1998; **4**: 328-329 [PMID: 9836088 DOI: 10.1002/ibd.3780040415]

9 **Baker DE**. Adalimumab: human recombinant immunoglobulin g1 anti-tumor necrosis factor monoclonal antibody. *Rev Gastroenterol Disord* 2004; **4**: 196-210 [PMID: 15580154]

10 **Ruemmele FM**, Veres G, Kolho KL, Griffiths A, Levine A, Escher JC, Amil Dias J, Barabino A, Braegger CP, Bronsky J, Buderus S, Martín-de-Carpi J, De Ridder L, Fagerberg UL, Hugot JP, Kierkus J, Kolacek S, Koletzko S, Lionetti P, Miele E, Navas López VM, Paerregaard A, Russell RK, Serban DE, Shaoul R, Van Rheenen P, Veereman G, Weiss B, Wilson D, Dignass A, Eliakim A, Winter H, Turner D; European Crohn's and Colitis Organisation; European Society of Pediatric Gastroenterology, Hepatology and Nutrition. Consensus guidelines of ECCO/ESPGHAN on the medical management of pediatric Crohn's disease. *J Crohns Colitis* 2014; **8**: 1179-1207 [PMID: 24909831 DOI: 10.1016/j.crohns.2014.04.005]

11 **Mack DR**, Benchimol EI, Critch J, deBruyn J, Tse F, Moayyedi P, Church P, Deslandres C, El-Matary W, Huynh H, Jantchou P, Lawrence S, Otley A, Sherlock M, Walters T, Kappelman MD, Sadowski D, Marshall JK, Griffiths A. Canadian Association of Gastroenterology Clinical Practice Guideline for the Medical Management of Pediatric Luminal Crohn's Disease. *Gastroenterology* 2019; **157**: 320-348 [PMID: 31320109 DOI: 10.1053/j.gastro.2019.03.022]

12 **Cholapranee A**, Hazlewood GS, Kaplan GG, Peyrin-Biroulet L, Ananthakrishnan AN. Systematic review with meta-analysis: comparative efficacy of biologics for induction and maintenance of mucosal healing in Crohn's disease and ulcerative colitis controlled trials. *Aliment Pharmacol Ther* 2017; **45**: 1291-1302 [PMID: 28326566 DOI: 10.1111/apt.14030]

13 **Hazlewood GS**, Rezaie A, Borman M, Panaccione R, Ghosh S, Seow CH, Kuenzig E, Tomlinson G, Siegel CA, Melmed GY, Kaplan GG. Comparative effectiveness of immunosuppressants and biologics for inducing and maintaining remission in Crohn's disease: a network meta-analysis. *Gastroenterology* 2015; **148**: 344-54.e5; quiz e14 [PMID: 25448924 DOI: 10.1053/j.gastro.2014.10.011]

14 **Targan SR**, Hanauer SB, van Deventer SJ, Mayer L, Present DH, Braakman T, DeWoody KL, Schaible TF, Rutgeerts PJ. A short-term study of chimeric monoclonal antibody cA2 to tumor necrosis factor alpha for Crohn's disease. Crohn's Disease cA2 Study Group. *N Engl J Med* 1997; **337**: 1029-1035 [PMID: 9321530 DOI: 10.1056/NEJM199710093371502]

15 **Hanauer SB**, Feagan BG, Lichtenstein GR, Mayer LF, Schreiber S, Colombel JF, Rachmilewitz D, Wolf DC, Olson A, Bao W, Rutgeerts P; ACCENT I Study Group. Maintenance infliximab for Crohn's disease: the ACCENT I randomised trial. *Lancet* 2002; **359**: 1541-1549 [PMID: 12047962 DOI: 10.1016/S0140-6736(02)08512-4]

16 **Hyams J**, Crandall W, Kugathasan S, Griffiths A, Olson A, Johanns J, Liu G, Travers S, Heuschkel R, Markowitz J, Cohen S, Winter H, Veereman-Wauters G, Ferry G, Baldassano R; REACH Study Group. Induction and maintenance infliximab therapy for the treatment of moderate-to-severe Crohn's disease in children. *Gastroenterology* 2007; **132**: 863-73; quiz 1165 [PMID: 17324398 DOI: 10.1053/j.gastro.2006.12.003]

17 **Ruemmele FM**, Lachaux A, Cézard JP, Morali A, Maurage C, Giniès JL, Viola S, Goulet O, Lamireau T, Scaillon M, Breton A, Sarles J; Groupe Francophone d'Hépatologie, Gastroentérologie et Nutrition Pédiatrique. Efficacy of infliximab in pediatric Crohn's disease: a randomized multicenter open-label trial comparing scheduled to on demand maintenance therapy. *Inflamm Bowel Dis* 2009; **15**: 388-394 [PMID: 19023899 DOI: 10.1002/ibd.20788]

18 **Hyams JS**, Griffiths A, Markowitz J, Baldassano RN, Faubion WA Jr, Colletti RB, Dubinsky M, Kierkus J, Rosh J, Wang Y, Huang B, Bittle B, Marshall M, Lazar A. Safety and efficacy of adalimumab for moderate to severe Crohn's disease in children. *Gastroenterology* 2012; **143**: 365-74.e2 [PMID: 22562021 DOI: 10.1053/j.gastro.2012.04.046]

19 **Assa A**, Matar M, Turner D, Broide E, Weiss B, Ledder O, Guz-Mark A, Rinawi F, Cohen S, Topf-Olivestone C, Shaoul R, Yerushalmi B, Shamir R. Proactive Monitoring of Adalimumab Trough Concentration Associated With Increased Clinical Remission in Children With Crohn's Disease Compared With Reactive Monitoring. *Gastroenterology* 2019; **157**: 985-996.e2 [PMID: 31194979 DOI: 10.1053/j.gastro.2019.06.003]

20 **van Rheenen PF**, Aloi M, Assa A, Bronsky J, Escher JC, Fagerberg UL, Gasparetto M, Gerasimidis K, Griffiths A, Henderson P, Koletzko S, Kolho KL, Levine A, van Limbergen J, Martin de Carpi FJ, Navas-López VM, Oliva S, de Ridder L, Russell RK, Shouval D, Spinelli A, Turner D, Wilson D, Wine E, Ruemmele FM. The Medical Management of Paediatric Crohn's Disease: an ECCO-ESPGHAN Guideline Update. *J Crohns Colitis* 2020 [PMID: 33026087 DOI: 10.1093/ecco-jcc/jjaa161]

21 **Walters TD**, Kim MO, Denson LA, Griffiths AM, Dubinsky M, Markowitz J, Baldassano R, Crandall W, Rosh J, Pfefferkorn M, Otley A, Heyman MB, LeLeiko N, Baker S, Guthery SL, Evans J, Ziring D, Kellermayer R, Stephens M, Mack D, Oliva-Hemker M, Patel AS, Kirschner B, Moulton D, Cohen S, Kim S, Liu C, Essers J, Kugathasan S, Hyams JS; PRO-KIIDS Research Group. Increased effectiveness of early therapy with anti-tumor necrosis factor-α vs an immunomodulator in children with Crohn's disease. *Gastroenterology* 2014; **146**: 383-391 [PMID: 24162032 DOI: 10.1053/j.gastro.2013.10.027]

22 **Kugathasan S**, Denson LA, Walters TD, Kim MO, Marigorta UM, Schirmer M, Mondal K, Liu C, Griffiths A, Noe JD, Crandall WV, Snapper S, Rabizadeh S, Rosh JR, Shapiro JM, Guthery S, Mack DR, Kellermayer R, Kappelman MD, Steiner S, Moulton DE, Keljo D, Cohen S, Oliva-Hemker M, Heyman MB, Otley AR, Baker SS, Evans JS, Kirschner BS, Patel AS, Ziring D, Trapnell BC, Sylvester FA, Stephens MC, Baldassano RN, Markowitz JF, Cho J, Xavier RJ, Huttenhower C, Aronow BJ, Gibson G, Hyams JS, Dubinsky MC. Prediction of complicated disease course for children newly diagnosed with Crohn's disease: a multicentre inception cohort study. *Lancet* 2017; **389**: 1710-1718 [PMID: 28259484 DOI: 10.1016/S0140-6736(17)30317-3]

23 **Kang B**, Choi SY, Kim HS, Kim K, Lee YM, Choe YH. Mucosal Healing in Paediatric Patients with Moderate-to-Severe Luminal Crohn's Disease Under Combined Immunosuppression: Escalation versus Early Treatment. *J Crohns Colitis* 2016; **10**: 1279-1286 [PMID: 27095752 DOI: 10.1093/ecco-jcc/jjw086]

24 **Kang B**, Choe YH. Early Biologic Treatment in Pediatric Crohn's Disease: Catching the Therapeutic Window of Opportunity in Early Disease by Treat-to-Target. *Pediatr Gastroenterol Hepatol Nutr* 2018; **21**: 1-11 [PMID: 29383299 DOI: 10.5223/pghn.2018.21.1.1]

25 **Clarkston K**, Tsai YT, Jackson K, Rosen MJ, Denson LA, Minar P. Development of Infliximab Target Concentrations During Induction in Pediatric Crohn Disease Patients. *J Pediatr Gastroenterol Nutr* 2019; **69**: 68-74 [PMID: 31232885 DOI: 10.1097/MPG.0000000000002304]

26 **Armstrong K**. Methods in comparative effectiveness research. *J Clin Oncol* 2012; **30**: 4208-4214 [PMID: 23071240 DOI: 10.1200/JCO.2012.42.2659]

27 **Singh S**, Fumery M, Sandborn WJ, Murad MH. Systematic review and network meta-analysis: first- and second-line biologic therapies for moderate-severe Crohn's disease. *Aliment Pharmacol Ther* 2018; **48**: 394-409 [PMID: 29920733 DOI: 10.1111/apt.14852]

28 **Singh S**. Network meta-analysis to inform positioning of biologics in patients with Crohn's disease: Promise and perils. *Best Pract Res Clin Gastroenterol* 2019; **38-39**: 101614 [PMID: 31327401 DOI: 10.1016/j.bpg.2019.05.001]

29 **Nestorov I**. Clinical pharmacokinetics of tumor necrosis factor antagonists. *J Rheumatol Suppl* 2005; **74**: 13-18 [PMID: 15742459]

30 **Vande Casteele N**, Gils A. Pharmacokinetics of anti-TNF monoclonal antibodies in inflammatory bowel disease: Adding value to current practice. *J Clin Pharmacol* 2015; **55** Suppl 3: S39-S50 [PMID: 25707962 DOI: 10.1002/jcph.374]

31 **Gibson DJ**, Ward MG, Rentsch C, Friedman AB, Taylor KM, Sparrow MP, Gibson PR. Review article: determination of the therapeutic range for therapeutic drug monitoring of adalimumab and infliximab in patients with inflammatory bowel disease. *Aliment Pharmacol Ther* 2020; **51**: 612-628 [PMID: 31961001 DOI: 10.1111/apt.15643]

32 **Cornillie F**, Hanauer SB, Diamond RH, Wang J, Tang KL, Xu Z, Rutgeerts P, Vermeire S. Postinduction serum infliximab trough level and decrease of C-reactive protein level are associated with durable sustained response to infliximab: a retrospective analysis of the ACCENT I trial. *Gut* 2014; **63**: 1721-1727 [PMID: 24474383 DOI: 10.1136/gutjnl-2012-304094]

33 **Feng T**, Chen B, Ungar B, Qiu Y, Zhang S, He J, Lin S, He Y, Zeng Z, Ben-Horin S, Chen M, Mao R. Association of Infliximab Levels With Mucosal Healing Is Time-Dependent in Crohn's Disease: Higher Drug Exposure Is Required

Postinduction Than During Maintenance Treatment. *Inflamm Bowel Dis* 2019; **25**: 1813-1821 [PMID: 30934050 DOI: 10.1093/ibd/izz061]

34 **van Hoeve K**, Dreesen E, Hoffman I, Van Assche G, Ferrante M, Gils A, Vermeire S. Adequate Infliximab Exposure During Induction Predicts Remission in Paediatric Patients With Inflammatory Bowel Disease. *J Pediatr Gastroenterol Nutr* 2019; **68**: 847-853 [PMID: 30633108 DOI: 10.1097/MPG.0000000000002265]

35 **Singh N**, Rosenthal CJ, Melmed GY, Mirocha J, Farrior S, Callejas S, Tripuraneni B, Rabizadeh S, Dubinsky MC. Early infliximab trough levels are associated with persistent remission in pediatric patients with inflammatory bowel disease. *Inflamm Bowel Dis* 2014; **20**: 1708-1713 [PMID: 25153505 DOI: 10.1097/MIB.0000000000000137]

36 **El-Matary W**, Walters TD, Huynh HQ, deBruyn J, Mack DR, Jacobson K, Sherlock ME, Church P, Wine E, Carroll MW, Benchimol EI, Lawrence S, Griffiths AM. Higher Postinduction Infliximab Serum Trough Levels Are Associated With Healing of Fistulizing Perianal Crohn's Disease in Children. *Inflamm Bowel Dis* 2019; **25**: 150-155 [PMID: 29912413 DOI: 10.1093/ibd/izy217]

37 **Zittan E**, Steinhart AH, Goldstein P, Milgrom R, Gralnek IM, Silverberg MS. Post-Induction High Adalimumab Drug Levels Predict Biological Remission at Week 24 in Patients With Crohn's Disease. *Clin Transl Gastroenterol* 2021; **12**: e00401 [PMID: 34613952 DOI: 10.14309/ctg.0000000000000401]

38 **Rinawi F**, Ricciuto A, Church PC, Frost K, Crowley E, Walters TD, Griffiths AM. Association of Early Postinduction Adalimumab Exposure With Subsequent Clinical and Biomarker Remission in Children with Crohn's Disease. *Inflamm Bowel Dis* 2021; **27**: 1079-1087 [PMID: 32978946 DOI: 10.1093/ibd/izaa247]

39 **Moore C**, Corbett G, Moss AC. Systematic Review and Meta-Analysis: Serum Infliximab Levels During Maintenance Therapy and Outcomes in Inflammatory Bowel Disease. *J Crohns Colitis* 2016; **10**: 619-625 [PMID: 26763722 DOI: 10.1093/ecco-jcc/jjw007]

40 **Paul S**, Del Tedesco E, Marotte H, Rinaudo-Gaujous M, Moreau A, Phelip JM, Genin C, Peyrin-Biroulet L, Roblin X. Therapeutic drug monitoring of infliximab and mucosal healing in inflammatory bowel disease: a prospective study. *Inflamm Bowel Dis* 2013; **19**: 2568-2576 [PMID: 24013361 DOI: 10.1097/MIB.0b013e3182a77b41]

41 **Yarur AJ**, Kanagala V, Stein DJ, Czul F, Quintero MA, Agrawal D, Patel A, Best K, Fox C, Idstein K, Abreu MT. Higher infliximab trough levels are associated with perianal fistula healing in patients with Crohn's disease. *Aliment Pharmacol Ther* 2017; **45**: 933-940 [PMID: 28211593 DOI: 10.1111/apt.13970]

42 **Choi SY**, Kang B, Choe YH. Serum Infliximab Cutoff trough Level Values for Maintaining Hematological Remission in Pediatric Inflammatory Bowel Disease. *Gut Liver* 2019; **13**: 541-548 [PMID: 30970435 DOI: 10.5009/gnl18129]

43 **Kang B**, Choi SY, Choi YO, Lee SY, Baek SY, Sohn I, Choe BH, Lee HJ, Choe YH. Infliximab Trough Levels Are Associated With Mucosal Healing During Maintenance Treatment With Infliximab in Paediatric Crohn's Disease. *J Crohns Colitis* 2019; **13**: 189-197 [PMID: 30452616 DOI: 10.1093/ecco-jcc/jjy155]

44 **Mazor Y**, Almog R, Kopylov U, Ben Hur D, Blatt A, Dahan A, Waterman M, Ben-Horin S, Chowers Y. Adalimumab drug and antibody levels as predictors of clinical and laboratory response in patients with Crohn's disease. *Aliment Pharmacol Ther* 2014; **40**: 620-628 [PMID: 25039584 DOI: 10.1111/apt.12869]

45 **Zittan E**, Kabakchiev B, Milgrom R, Nguyen GC, Croitoru K, Steinhart AH, Silverberg MS. Higher Adalimumab Drug Levels are Associated with Mucosal Healing in Patients with Crohn's Disease. *J Crohns Colitis* 2016; **10**: 510-515 [PMID: 26783345 DOI: 10.1093/ecco-jcc/jjw014]

46 **Sharma S**, Eckert D, Hyams JS, Mensing S, Thakkar RB, Robinson AM, Rosh JR, Ruemmele FM, Awni WM. Pharmacokinetics and exposure-efficacy relationship of adalimumab in pediatric patients with moderate to severe Crohn's disease: results from a randomized, multicenter, phase-3 study. *Inflamm Bowel Dis* 2015; **21**: 783-792 [PMID: 25723614 DOI: 10.1097/MIB.0000000000000327]

47 **Choi SY**, Choi YO, Choe YH, Kang B. Potential Utility of Therapeutic Drug Monitoring of Adalimumab in Predicting Short-Term Mucosal Healing and Histologic Remission in Pediatric Crohn's Disease Patients. *J Korean Med Sci* 2020; **35**: e114 [PMID: 32329259 DOI: 10.3346/jkms.2020.35.e114]

48 **De Bie CI**, Hummel TZ, Kindermann A, Kokke FT, Damen GM, Kneepkens CM, Van Rheenen PF, Schweizer JJ, Hoekstra JH, Norbruis OF, Tjon A Ten WE, Vreugdenhil AC, Deckers-Kocken JM, Gijsbers CF, Escher JC, De Ridder L. The duration of effect of infliximab maintenance treatment in paediatric Crohn's disease is limited. *Aliment Pharmacol Ther* 2011; **33**: 243-250 [PMID: 21083595 DOI: 10.1111/j.1365-2036.2010.04507.x]

49 **Ding NS**, Hart A, De Cruz P. Systematic review: predicting and optimising response to anti-TNF therapy in Crohn's disease - algorithm for practical management. *Aliment Pharmacol Ther* 2016; **43**: 30-51 [PMID: 26515897 DOI: 10.1111/apt.13445]

50 **Moss AC**, Brinks V, Carpenter JF. Review article: immunogenicity of anti-TNF biologics in IBD - the role of patient, product and prescriber factors. *Aliment Pharmacol Ther* 2013; **38**: 1188-1197 [PMID: 24118102 DOI: 10.1111/apt.12507]

51 **Vermeire S**, Noman M, Van Assche G, Baert F, D'Haens G, Rutgeerts P. Effectiveness of concomitant immunosuppressive therapy in suppressing the formation of antibodies to infliximab in Crohn's disease. *Gut* 2007; **56**: 1226-1231 [PMID: 17229796 DOI: 10.1136/gut.2006.099978]

52 **Kim JY**, Lee Y, Choe BH, Kang B. Factors Associated with the Immunogenicity of Anti-Tumor Necrosis Factor Agents in Pediatric Patients with Inflammatory Bowel Disease. *Gut Liver* 2021; **15**: 588-598 [PMID: 33024062 DOI: 10.5009/gnl20134]

53 **Brandse JF**, Mould D, Smeekes O, Ashruf Y, Kuin S, Strik A, van den Brink GR, D'Haens GR. A Real-life Population Pharmacokinetic Study Reveals Factors Associated with Clearance and Immunogenicity of Infliximab in Inflammatory Bowel Disease. *Inflamm Bowel Dis* 2017; **23**: 650-660 [PMID: 28195852 DOI: 10.1097/MIB.0000000000001043]

54 **Fasanmade AA**, Adedokun OJ, Blank M, Zhou H, Davis HM. Pharmacokinetic properties of infliximab in children and adults with Crohn's disease: a retrospective analysis of data from 2 phase III clinical trials. *Clin Ther* 2011; **33**: 946-964 [PMID: 21741088 DOI: 10.1016/j.clinthera.2011.06.002]

55 **Ternant D**, Aubourg A, Magdelaine-Beuzelin C, Degenne D, Watier H, Picon L, Paintaud G. Infliximab pharmacokinetics in inflammatory bowel disease patients. *Ther Drug Monit* 2008; **30**: 523-529 [PMID: 18641542 DOI: 10.1097/FTD.0b013e318180e300]

56 **Dotan I**, Ron Y, Yanai H, Becker S, Fishman S, Yahav L, Ben Yehoyada M, Mould DR. Patient factors that increase infliximab clearance and shorten half-life in inflammatory bowel disease: a population pharmacokinetic study. *Inflamm Bowel Dis* 2014; **20**: 2247-2259 [PMID: 25358062 DOI: 10.1097/MIB.0000000000000212]

57 **Vermeire S**, Gils A, Accossato P, Lula S, Marren A. Immunogenicity of biologics in inflammatory bowel disease. *Therap Adv Gastroenterol* 2018; **11**: 1756283X17750355 [PMID: 29383030 DOI: 10.1177/1756283X17750355]

58 **Turner D**, Ricciuto A, Lewis A, D'Amico F, Dhaliwal J, Griffiths AM, Bettenworth D, Sandborn WJ, Sands BE, Reinisch W, Schölmerich J, Bemelman W, Danese S, Mary JY, Rubin D, Colombel JF, Peyrin-Biroulet L, Dotan I, Abreu MT, Dignass A; International Organization for the Study of IBD. STRIDE-II: An Update on the Selecting Therapeutic Targets in Inflammatory Bowel Disease (STRIDE) Initiative of the International Organization for the Study of IBD (IOIBD): Determining Therapeutic Goals for Treat-to-Target strategies in IBD. *Gastroenterology* 2021; **160**: 1570-1583 [PMID: 33359090 DOI: 10.1053/j.gastro.2020.12.031]

59 **Church PC**, Guan J, Walters TD, Frost K, Assa A, Muise AM, Griffiths AM. Infliximab maintains durable response and facilitates catch-up growth in luminal pediatric Crohn's disease. *Inflamm Bowel Dis* 2014; **20**: 1177-1186 [PMID: 24865777 DOI: 10.1097/MIB.0000000000000083]

60 **Choi J**, Kang B, Kim MJ, Sohn I, Lee HJ, Choe YH. Early Infliximab Yields Superior Long-Term Effects on Linear Growth in Pediatric Crohn's Disease Patients. *Gut Liver* 2018; **12**: 255-262 [PMID: 29298460 DOI: 10.5009/gnl17290]

61 **Walters TD**, Faubion WA, Griffiths AM, Baldassano RN, Escher J, Ruemmele FM, Hyams JS, Lazar A, Eichner S, Huang B, Li Y, Thakkar RB. Growth Improvement with Adalimumab Treatment in Children with Moderately to Severely Active Crohn's Disease. *Inflamm Bowel Dis* 2017; **23**: 967-975 [PMID: 28301428 DOI: 10.1097/MIB.0000000000001075]

62 **Matar M**, Shamir R, Lev-Zion R, Broide E, Weiss B, Ledder O, Guz-Mark A, Rinawi F, Cohen S, Topf-Olivestone C, Shaoul R, Yerushalmi B, Assa A. The Effect of Adalimumab Treatment on Linear Growth in Children With Crohn Disease: A Post-hoc Analysis of the PAILOT Randomized Control Trial. *J Pediatr Gastroenterol Nutr* 2020; **71**: 237-242 [PMID: 32324651 DOI: 10.1097/MPG.0000000000002728]

63 **Raychaudhuri SP**, Nguyen CT, Raychaudhuri SK, Gershwin ME. Incidence and nature of infectious disease in patients treated with anti-TNF agents. *Autoimmun Rev* 2009; **9**: 67-81 [PMID: 19716440 DOI: 10.1016/j.autrev.2009.08.006]

64 **Dulai PS**, Thompson KD, Blunt HB, Dubinsky MC, Siegel CA. Risks of serious infection or lymphoma with anti-tumor necrosis factor therapy for pediatric inflammatory bowel disease: a systematic review. *Clin Gastroenterol Hepatol* 2014; **12**: 1443-51; quiz e88 [PMID: 24462626 DOI: 10.1016/j.cgh.2014.01.021]

65 **Singh S**, Facciorusso A, Dulai PS, Jairath V, Sandborn WJ. Comparative Risk of Serious Infections With Biologic and/or Immunosuppressive Therapy in Patients With Inflammatory Bowel Diseases: A Systematic Review and Meta-Analysis. *Clin Gastroenterol Hepatol* 2020; **18**: 69-81.e3 [PMID: 30876964 DOI: 10.1016/j.cgh.2019.02.044]

66 **Bonovas S**, Fiorino G, Allocca M, Lytras T, Nikolopoulos GK, Peyrin-Biroulet L, Danese S. Biologic Therapies and Risk of Infection and Malignancy in Patients With Inflammatory Bowel Disease: A Systematic Review and Network Meta-analysis. *Clin Gastroenterol Hepatol* 2016; **14**: 1385-1397.e10 [PMID: 27189910 DOI: 10.1016/j.cgh.2016.04.039]

67 **Hyams JS**, Dubinsky MC, Baldassano RN, Colletti RB, Cucchiara S, Escher J, Faubion W, Fell J, Gold BD, Griffiths A, Koletzko S, Kugathasan S, Markowitz J, Ruemmele FM, Veereman G, Winter H, Masel N, Shin CR, Tang KL, Thayu M. Infliximab Is Not Associated With Increased Risk of Malignancy or Hemophagocytic Lymphohistiocytosis in Pediatric Patients With Inflammatory Bowel Disease. *Gastroenterology* 2017; **152**: 1901-1914.e3 [PMID: 28193515 DOI: 10.1053/j.gastro.2017.02.004]

68 **Fréling E**, Baumann C, Cuny JF, Bigard MA, Schmutz JL, Barbaud A, Peyrin-Biroulet L. Cumulative incidence of, risk factors for, and outcome of dermatological complications of anti-TNF therapy in inflammatory bowel disease: a 14-year experience. *Am J Gastroenterol* 2015; **110**: 1186-1196 [PMID: 26195181 DOI: 10.1038/ajg.2015.205]

69 **Sridhar S**, Maltz RM, Boyle B, Kim SC. Dermatological Manifestations in Pediatric Patients with Inflammatory Bowel Diseases on Anti-TNF Therapy. *Inflamm Bowel Dis* 2018; **24**: 2086-2092 [PMID: 29718343 DOI: 10.1093/ibd/izy112]

70 **Hradsky O**, Kazeka D, Copova I, Lerchova T, Mitrova K, Pospisilova K, Sulovcova M, Zarubova K, Bronsky J. Risk factors for dermatological complications of anti-TNF therapy in a cohort of children with Crohn's disease. *Eur J Pediatr* 2021; **180**: 3001-3008 [PMID: 33876264 DOI: 10.1007/s00431-021-04077-0]

71 **Colombel JF**, Sandborn WJ, Reinisch W, Mantzaris GJ, Kornbluth A, Rachmilewitz D, Lichtiger S, D'Haens G, Diamond RH, Broussard DL, Tang KL, van der Woude CJ, Rutgeerts P; SONIC Study Group. Infliximab, azathioprine, or combination therapy for Crohn's disease. *N Engl J Med* 2010; **362**: 1383-1395 [PMID: 20393175 DOI: 10.1056/NEJMoa0904492]

72 **Feagan BG**, McDonald JW, Panaccione R, Enns RA, Bernstein CN, Ponich TP, Bourdages R, Macintosh DG, Dallaire C, Cohen A, Fedorak RN, Paré P, Bitton A, Saibil F, Anderson F, Donner A, Wong CJ, Zou G, Vandervoort MK, Hopkins M, Greenberg GR. Methotrexate in combination with infliximab is no more effective than infliximab alone in patients with Crohn's disease. *Gastroenterology* 2014; **146**: 681-688.e1 [PMID: 24269926 DOI: 10.1053/j.gastro.2013.11.024]

73 **Kansen HM**, van Rheenen PF, Houwen RHJ, Tjon A Ten W, Damen GM, Kindermann A, Escher JC, Wolters VM; Kids with Crohn's, Colitis (KiCC) Working Group for Collaborative Paediatric IBD Research in the Netherlands. Less Anti-infliximab Antibody Formation in Paediatric Crohn Patients on Concomitant Immunomodulators. *J Pediatr Gastroenterol Nutr* 2017; **65**: 425-429 [PMID: 28945207 DOI: 10.1097/MPG.0000000000001551]

74 **Grossi V**, Lerer T, Griffiths A, LeLeiko N, Cabrera J, Otley A, Rick J, Mack D, Bousvaros A, Rosh J, Grossman A, Saeed S, Kay M, Boyle B, Oliva-Hemker M, Keljo D, Pfefferkorn M, Faubion W, Kappelman MD, Sudel B, Markowitz J, Hyams JS. Concomitant Use of Immunomodulators Affects the Durability of Infliximab Therapy in Children With Crohn's Disease. *Clin Gastroenterol Hepatol* 2015; **13**: 1748-1756 [PMID: 25911120 DOI: 10.1016/j.cgh.2015.04.010]

75 **van Rheenen H**, van Rheenen PF. Long-Term Efficacy of Anti-Tumor Necrosis Factor Agents in Pediatric Luminal Crohn's Disease: A Systematic Review of Real-World Evidence Studies. *Pediatr Gastroenterol Hepatol Nutr* 2020; **23**: 121-131 [PMID: 32206624 DOI: 10.5223/pghn.2020.23.2.121]

76 **Kopylov U**, Al-Taweel T, Yaghoobi M, Nauche B, Bitton A, Lakatos PL, Ben-Horin S, Afif W, Seidman EG. Adalimumab monotherapy versus combination therapy with immunomodulators in patients with Crohn's disease: a

systematic review and meta-analysis. *J Crohns Colitis* 2014; **8**: 1632-1641 [PMID: 25067824 DOI: 10.1016/j.crohns.2014.07.003]

77 **Hyams JS**, Dubinsky M, Rosh J, Ruemmele FM, Eichner SF, Maa JF, Lazar A, Alperovich G, Mostafa NM, Robinson AM. The effects of concomitant immunomodulators on the pharmacokinetics, efficacy and safety of adalimumab in paediatric patients with Crohn's disease: a post hoc analysis. *Aliment Pharmacol Ther* 2019; **49**: 155-164 [PMID: 30506693 DOI: 10.1111/apt.15054]

78 **Matar M**, Shamir R, Turner D, Broide E, Weiss B, Ledder O, Guz-Mark A, Rinawi F, Cohen S, Topf-Olivestone C, Shaoul R, Yerushalmi B, Ben-Horin S, Assa A. Combination Therapy of Adalimumab With an Immunomodulator Is Not More Effective Than Adalimumab Monotherapy in Children With Crohn's Disease: A Post Hoc Analysis of the PAILOT Randomized Controlled Trial. *Inflamm Bowel Dis* 2020; **26**: 1627-1635 [PMID: 31793630 DOI: 10.1093/ibd/izz294]

79 **Bittner B**, Richter W, Schmidt J. Subcutaneous Administration of Biotherapeutics: An Overview of Current Challenges and Opportunities. *BioDrugs* 2018; **32**: 425-440 [PMID: 30043229 DOI: 10.1007/s40259-018-0295-0]

80 **Chilton F**, Collett RA. Treatment choices, preferences and decision-making by patients with rheumatoid arthritis. *Musculoskeletal Care* 2008; **6**: 1-14 [PMID: 17726671 DOI: 10.1002/msc.110]

81 **Vavricka SR**, Bentele N, Scharl M, Rogler G, Zeitz J, Frei P, Straumann A, Binek J, Schoepfer AM, Fried M; Swiss IBDnet and Swiss IBD Cohort Study Group. Systematic assessment of factors influencing preferences of Crohn's disease patients in selecting an anti-tumor necrosis factor agent (CHOOSE TNF TRIAL). *Inflamm Bowel Dis* 2012; **18**: 1523-1530 [PMID: 21987429 DOI: 10.1002/ibd.21888]

82 **Kim ES**, Kim KO, Jang BI, Lee CK, Kim HJ, Lee KM, Kim YS, Eun CS, Jung SA, Yang SK, Lee J, Kim TO, Jung Y, Seo GS, Yoon SM; IBD Study Group of the Korean Association for the Study of the Intestinal Diseases (KASID). Factors Contributing to the Preference of Korean Patients with Crohn's Disease When Selecting an Anti-Tumor Necrosis Factor Agent (CHOICE Study). *Gut Liver* 2016; **10**: 391-398 [PMID: 26347512 DOI: 10.5009/gnl15126]

83 **Alden DL**, Friend JM, Lee AY, de Vries M, Osawa R, Chen Q. Culture and medical decision making: Healthcare consumer perspectives in Japan and the United States. *Health Psychol* 2015; **34**: 1133-1144 [PMID: 26076003 DOI: 10.1037/hea0000229]

84 **Baert F**, Noman M, Vermeire S, Van Assche G, D' Haens G, Carbonez A, Rutgeerts P. Influence of immunogenicity on the long-term efficacy of infliximab in Crohn's disease. *N Engl J Med* 2003; **348**: 601-608 [PMID: 12584368 DOI: 10.1056/NEJMoa020888]

85 **Karmiris K**, Paintaud G, Noman M, Magdelaine-Beuzelin C, Ferrante M, Degenne D, Claes K, Coopman T, Van Schuerbeek N, Van Assche G, Vermeire S, Rutgeerts P. Influence of trough serum levels and immunogenicity on long-term outcome of adalimumab therapy in Crohn's disease. *Gastroenterology* 2009; **137**: 1628-1640 [PMID: 19664627 DOI: 10.1053/j.gastro.2009.07.062]

86 **Fidder HH**, Singendonk MM, van der Have M, Oldenburg B, van Oijen MG. Low rates of adherence for tumor necrosis factor-α inhibitors in Crohn's disease and rheumatoid arthritis: results of a systematic review. *World J Gastroenterol* 2013; **19**: 4344-4350 [PMID: 23885145 DOI: 10.3748/wjg.v19.i27.4344]

87 **Kane SV**, Chao J, Mulani PM. Adherence to infliximab maintenance therapy and health care utilization and costs by Crohn's disease patients. *Adv Ther* 2009; **26**: 936-946 [PMID: 19838649 DOI: 10.1007/s12325-009-0069-7]

88 **Kane S**, Dixon L. Adherence rates with infliximab therapy in Crohn's disease. *Aliment Pharmacol Ther* 2006; **24**: 1099-1103 [PMID: 16984504 DOI: 10.1111/j.1365-2036.2006.03092.x]

89 **Billioud V**, Laharie D, Filippi J, Roblin X, Oussalah A, Chevaux JB, Hébuterne X, Bigard MA, Peyrin-Biroulet L. Adherence to adalimumab therapy in Crohn's disease: a French multicenter experience. *Inflamm Bowel Dis* 2011; **17**: 152-159 [PMID: 21061388 DOI: 10.1002/ibd.21491]

90 **Turner D**, Huang Y, Martín-de-Carpi J, Aloi M, Focht G, Kang B, Zhou Y, Sanchez C, Kappelman MD, Uhlig HH, Pujol-Muncunill G, Ledder O, Lionetti P, Dias JA, Ruemmele FM, Russell RK; Paediatric IBD Porto group of ESPGHAN. Corona Virus Disease 2019 and Paediatric Inflammatory Bowel Diseases: Global Experience and Provisional Guidance (March 2020) from the Paediatric IBD Porto Group of European Society of Paediatric Gastroenterology, Hepatology, and Nutrition. *J Pediatr Gastroenterol Nutr* 2020; **70**: 727-733 [PMID: 32443020 DOI: 10.1097/MPG.0000000000002729]

World Journal of Gastroenterology

Submit a Manuscript: https://www.f6publishing.com

World J Gastroenterol 2023 May 14; 29(18): 2798-2817

DOI: 10.3748/wjg.v29.i18.2798

ISSN 1007-9327 (print) ISSN 2219-2840 (online)

ORIGINAL ARTICLE

Basic Study

Calcitriol attenuates liver fibrosis through hepatitis C virus nonstructural protein 3-transactivated protein 1-mediated TGF β 1/Smad3 and NF-κB signaling pathways

Liu Shi, Li Zhou, Ming Han, Yu Zhang, Yang Zhang, Xiao-Xue Yuan, Hong-Ping Lu, Yun Wang, Xue-Liang Yang, Chen Liu, Jun Wang, Pu Liang, Shun-Ai Liu, Xiao-Jing Liu, Jun Cheng, Shu-Mei Lin

Specialty type: Gastroenterology and hepatology

Provenance and peer review: Unsolicited article; Externally peer reviewed.

Peer-review model: Single blind

Peer-review report's scientific quality classification

Grade A (Excellent): A
Grade B (Very good): B, B
Grade C (Good): 0
Grade D (Fair): 0
Grade E (Poor): 0

P-Reviewer: Andersen JB, Denmark; Heij LR, Germany; Mohamed GA, Egypt

Received: December 13, 2022
Peer-review started: December 13, 2022
First decision: February 23, 2023
Revised: March 8, 2023
Accepted: April 10, 2023
Article in press: April 10, 2023
Published online: May 14, 2023

Liu Shi, Xiao-Jing Liu, Shu-Mei Lin, Department of Infectious Disease Medicine, The First Hospital Affiliated to Xi'an Jiaotong University, Xi'an 710061, Shaanxi Province, China

Li Zhou, China-Japan Friendship Hospital, Department of Infectious Disease China-Japan Friendship Hospital, Beijing 100029, China

Ming Han, Yang Zhang, Xiao-Xue Yuan, Chen Liu, Pu Liang, Shun-Ai Liu, Jun Cheng, Institute of Infectious Diseases, Beijing Ditan Hospital, Capital Medical University, Beijing 100015, China

Yu Zhang, Yun Wang, The Division of Liver Diseases, Beijing Ditan Hospital, Capital Medical University, Beijing 100015, China

Hong-Ping Lu, Institute of Liver Diseases, Beijing Pan-Asia Tongze Institute of Biomedicine Co., Ltd, Beijing 100015, China

Xue-Liang Yang, Department of Rehabilitation Medicine, The First Affiliated Hospital of Xi'an Jiaotong University, Xi'an 710061, Shaanxi Province, China

Jun Wang, Beijing Key Laboratory of Emerging Infectious Diseases, Peking University Ditan Teaching Hospital, Beijing 100015, China

Corresponding author: Shu-Mei Lin, Doctor, MD, PhD, Doctor, Professor, Teacher, Department of Infectious Disease Medicine, The First Hospital Affiliated to Xi'an Jiaotong University, No. 277 Yanta West Road, Yanta, Xi'an 710061, Shaanxi Province, China. lsmxjtu@126.com

Abstract

BACKGROUND

Hepatic fibrosis is a serious condition, and the development of hepatic fibrosis can lead to a series of complications. However, the pathogenesis of hepatic fibrosis remains unclear, and effective therapy options are still lacking. Our group identified hepatitis C virus nonstructural protein 3-transactivated protein 1 (NS3TP1) by suppressive subtractive hybridization and bioinformatics analysis, but its role in diseases including hepatic fibrosis remains undefined. Therefore, additional studies on the function of NS3TP1 in hepatic fibrosis are urgently needed to provide new targets for treatment.

AIM
To elucidate the mechanism of NS3TP1 in hepatic fibrosis and the regulatory effects of calcitriol on NS3TP1.

METHODS
Twenty-four male C57BL/6 mice were randomized and separated into three groups, comprising the normal, fibrosis, and calcitriol treatment groups, and liver fibrosis was modeled by carbon tetrachloride (CCl_4). To evaluate the level of hepatic fibrosis in every group, serological and pathological examinations of the liver were conducted. TGF-β1 was administered to boost the *in vitro* cultivation of LX-2 cells. NS3TP1, α-smooth muscle actin (α-SMA), collagen I, and collagen III in every group were examined using a Western blot and real-time quantitative polymerase chain reaction. The activity of the transforming growth factor beta 1 (TGFβ1)/Smad3 and NF-κB signaling pathways in each group of cells transfected with pcDNA-NS3TP1 or siRNA-NS3TP1 was detected. The statistical analysis of the data was performed using the Student's *t* test.

RESULTS
NS3TP1 promoted the activation, proliferation, and differentiation of hepatic stellate cells (HSCs) and enhanced hepatic fibrosis *via* the TGFβ1/Smad3 and NF-κB signaling pathways, as evidenced by the presence of α-SMA, collagen I, collagen III, p-smad3, and p-p65 in LX-2 cells, which were upregulated after NS3TP1 overexpression and downregulated after NS3TP1 interference. The proliferation of HSCs was lowered after NS3TP1 interference and elevated after NS3TP1 overexpression, as shown by the luciferase assay. NS3TP1 inhibited the apoptosis of HSCs. Moreover, both Smad3 and p65 could bind to NS3TP1, and p65 increased the promoter activity of NS3TP1, while NS3TP1 increased the promoter activity of TGFβ1 receptor I, as indicated by coimmunoprecipitation and luciferase assay results. Both *in vivo* and *in vitro*, treatment with calcitriol dramatically reduced the expression of NS3TP1. Calcitriol therapy-controlled HSCs activation, proliferation, and differentiation and substantially suppressed CCl_4-induced hepatic fibrosis in mice. Furthermore, calcitriol modulated the activities of the above signaling pathways *via* downregulation of NS3TP1.

CONCLUSION
Our results suggest that calcitriol may be employed as an adjuvant therapy for hepatic fibrosis and that NS3TP1 is a unique, prospective therapeutic target in hepatic fibrosis.

Key Words: Nonstructural protein 3-transactivated protein 1; Calcitriol; Liver fibrosis; Hepatic stellate cells; Mouse model; TGFβ1/Smad3; NF-κB; Signaling pathway

©The Author(s) 2023. Published by Baishideng Publishing Group Inc. All rights reserved.

Core Tip: We proved that hepatitis C virus nonstructural protein 3-transactivated protein 1 (NS3TP1) promoted hepatic fibrosis *via* the transforming growth factor beta 1/Smad3 and NF-κB signaling pathways. Calcitriol attenuates liver fibrosis through NS3TP1-mediated above both signaling pathways. These novel findings profoundly expand our knowledge about the mechanisms underlying the role and function of NS3TP1 in hepatic fibrosis. The relationship between NS3TP1 and liver fibrosis was discussed for the first time and provided a foundation for research related to liver fibrosis by targeting NS3TP1. We first showed that calcitriol alleviated hepatic fibrosis through the above signaling pathways *via* NS3TP1.

Citation: Shi L, Zhou L, Han M, Zhang Y, Zhang Y, Yuan XX, Lu HP, Wang Y, Yang XL, Liu C, Wang J, Liang P, Liu SA, Liu XJ, Cheng J, Lin SM. Calcitriol attenuates liver fibrosis through hepatitis C virus nonstructural protein 3-transactivated protein 1-mediated TGF β1/Smad3 and NF-κB signaling pathways. *World J Gastroenterol* 2023; 29(18): 2798-2817
URL: https://www.wjgnet.com/1007-9327/full/v29/i18/2798.htm
DOI: https://dx.doi.org/10.3748/wjg.v29.i18.2798

INTRODUCTION

Hepatic fibrosis is a dynamic process that occurs in any type of chronic liver damage that causes a net increase in the extracellular matrix. Further development of liver fibrosis can lead to liver cirrhosis and a series of complications[1,2]. Early intervention for liver fibrosis is crucial, but currently, there is no

effective treatment. Therefore, additional studies on the mechanism of liver fibrosis are urgently needed to provide new targets for treatment.

The open reading framework region of the hepatitis C virus (HCV) genome consists of a core protein region, envelope protein region and a nonstructural protein region. The NS3 gene is located in the nonstructural protein region of the HCV genome and it has serine protease activity and RNA helicase activity. HCV NS3 is crucial for the maturation and replication of the HCV RNA protein[3]. Moreover, this gene contributes to the occurrence of hepatic fibrosis through interaction with host cell components [4]. In this study, we screened and cloned HCV nonstructural protein 3-transactivated protein 1 (NS3TP1) by suppressive subtractive hybridization and bioinformatics analysis. This protein is also referred to asparagine synthetase domain containing 1 (ASNSD1) and registered in GenBank as NBLA00058. The registration number is AY11696. This gene is located on human chromosome 2q32.2. The total length of the gene coding sequence was 1932 nucleotides, and the coding product was 643 amino acid residues. NS3TP1 is widely distributed in the human body[5-8]. NS3 regulates the occurrence of liver fibrosis by interacting with host cells. Whether NS3TP1, as a trans-activator of NS3, can also affect liver fibrosis should be further investigated. Meienberg *et al*[9] demonstrated that NS3TP1 may interact with type 3 collagen alpha 1 chain (COL3A1). In our studies, we found that the NS3TP1 protein increased the expression levels of transforming growth factor beta receptor I (TGFβRI) by gene chip technology. Moreover, TGFβRI is one of the key molecules involved in the activation of the classic transforming growth factor beta 1 (TGFβ1)/Smad3 pathway in liver fibrosis[10]. Therefore, we speculate that NS3TP1 is related to the occurrence of liver fibrosis.

Furthermore, calcitriol was shown to downregulate the expression of NS3TP1 at the mRNA level in the Comparative Toxicogenomics Database (CTD)[11]. Thus, a correlation was established between calcitriol, NS3TP1, and liver fibrosis. As a conventional drug for treating vitamin D deficiency-related rickets, calcitriol regulates biological effects by binding to the vitamin D receptor (VDR). Pop *et al*[12] discovered that VDR was substantially generated in HSCs and Kupffer cells but weakly expressed in hepatic cells. Moreover, VDR is fully functional in HSCs and Kupffer cells. The role of vitamin D in the emergence of chronic hepatic fibrosis was highlighted by the identification of VDR as a crucial endocrine checkpoint for the fibrogenic activity of HSCs[13,14]. This finding indicated that the active component of vitamin D is a vital regulator of hepatic fibrosis. The activating of VDR in HSCs inhibits liver inflammation and fibrosis through the TGFβ1/Smad3 signaling pathway[15]. Moreover, activation of VDR reduces hepatic fibrosis by alleviating inflammation[16,17]. The activation of hepatic stellate cells (HSCs) has been proven to be a main driving factor of liver fibrosis[18]. The TGFβ1/Smad3 signaling pathway is the classical pathway of liver fibrosis activation[19,20]. In addition, NF-κB regulates cell death, inflammation, and wound healing and is therefore a crucial regulator of the progression of hepatic fibrosis[21,22].

The mechanism and mutual regulation between NS3TP1 and calcitriol in liver fibrosis have not been elucidated. However, based on previous studies, it was speculated that NS3TP1 increases hepatic fibrosis by triggering the TGFβ1/Smad3 and NF-κB signaling pathways. Moreover, calcitriol can regulate NS3TP1, but further studies are necessary for verification.

MATERIALS AND METHODS

Materials

Calcitriol was purchased from MedChemExpress (United States).

Animals

Liver fibrosis was induced by carbon tetrachloride (CCl_4) solubilized in corn oil (Sigma-Aldrich, Germany). Male C57BL/6 mice aged 8 wk were bought from Beijing Weitonglihua Laboratory Corporation (China). They experienced a week in a clean animal room at 24 °C with unrestricted access to food and water prior to the trials. The average weight of mice before modeling was 23-25 g, and mice were given an intraperitoneal (*i.p.*) injection with CCl_4 three times/wk (0.5 μL/g) for 4 wk to induce fibrosis[21,23,24]. Mice with liver fibrosis were successfully established and randomly separated into calcitriol and negative control (NC) groups. Mice in the control group were administered normal saline (10 μL/g/d, 5 times/wk) intragastrically for 4 wk and injected (*i.p.*) with corn oil or CCl_4, while mice in the calcitriol group were intragastrically administered calcitriol (1 μg/kg/d, 5 times/wk) and intraperitoneally injected with CCl_4 for 4 wk. Finally, 48 h after being injected with CCl_4, the mice were sacrificed. Normal saline was used to dilute 100% avertin to a 2.5% solution, and the anesthesia dose for mice was an *i.p.* injection of 100-200 μL/10 g. The mice were euthanized by deep anesthesia, followed by cervical dislocation. The Xi'an Jiaotong University Medical Science Center's specific pathogen free Animal Laboratory Center served as the site for all investigations. The Research Ethics Council of the Xi'an Jiaotong University Medical Science Center (Xi'an, China) gave its approval to all animal trials. All animals were treated humanely, and the experimental protocols were carried out in line with the regulations of the institution.

Cell culture

LX-2 cells are hepatogenic mesenchymal human cells and were obtained from Xiang Ya Central Laboratory (Xiangya Medical College, China). The cells were transfected using jetPRIME reagent (PolyPlus Transfection SA, NY, United States) and treated with calcitriol. Recombinant human TGFβ1 (BioLegend, CA, United States) was administered to the cell cultivation medium at 2.5 ng/mL or 5.0 ng/mL for 24 h[18,25]. All procedures were executed in accordance with the manufacturer's guidelines.

Plasmids and shortinterfering RNA (siRNA) oligonucleotides

PcDNA3.1/mycHis(-)NS3TP1, pGL4.10-NS3TP1 promoter, pGL4.10-p65 promoter, and pGL4.10-TGFβ 1R promoter were constructed by Beijing Genomics Institute (BGI, China). NS3TP1-siRNA was purchased from Gene Pharma (Hong Xun, Suzhou, Jiangsu Province, China).

Real-time quantitative polymerase chain reaction

Total RNA (Total RNA Kit, Omega, United States) was extracted from LX-2 cells and reverse-transcribed into single-stranded cDNA (Prime Script RT Reagent Kit, TaKaRa, China). Real-time quantitative polymerase chain reaction (RT-qPCR) was used to amplify the genes using specific primers (Hong Xun, Suzhou, Jiangsu Province, China), and β-actin was used as the internal control gene. The level of the target gene was estimated using the ΔΔCT method and normalized to that of the control. Supplementary Table 1 includes a list of the primer sequences.

Immunoblot

Proteins were extracted from mouse livers or LX-2 cells and isolated using 10% BIS-Tris gel/MOPS (Invitrogen, NY, United States) in MOPS SDS-PAGE (Thermo Fisher, United States). Transferring the separated proteins to a membrane made of polyvinylidene fluoride (PVDF) (Millipore, United States), which was incubated with secondary antibodies for 1.5 h after being exposed to primary antibodies (Supplementary Table 2) for 12 h at 4 °C. The immunoreactive bands were created using intensified chemiluminescence (Thermo Fisher Scientific) and visualized using the ChemiDoc™ touch imaging system (Bio-Rad, Hercules, CA, United States). ImageJ was used to assess the pictures.

Coimmunoprecipitation

Ice-cold M-PERTM mammalian protein extraction reagent was used to lyse LX-2 cells, and it also contained a mixture of protease and phosphatase inhibitors. Whole cell lysates (500 μL) were incubated with 50 μL protein magnetic beads for 2 h at room temperature and centrifuged, and the supernatant was transferred to a new 1.5 mL centrifuge tube. After that, the beads were mixed for 2 h at room temperature with whole-cell lysates containing 2 μL of anti-HIS antibody and 3 μL of regular mouse IgG antibody. The beads were eluted in DTT-free Laemmli buffer and then washed three times with PBST before being subjected to western blotting analysis.

Proliferation assay

On a 96-well plate, LX-2 cells were exposed to various calcitriol concentrations for 24 h. PBS was used to wash the cells twice after the initial medium was removed. Each well received a 1:100 addition of CCK-8 (Dojindo, Kumamoto, Japan) reagent before being cultured for 1 h at 37 °C. At 450 nm, the optical density was calculated.

Flow cytometry

LX-2 cells were treated with various concentrations of calcitriol for 48 h. The original medium was washed twice with PBS. The cells were collected by flow cytometry, treated with the reagents from an Annexin V-FITC/7-AAD apoptosis detection kit (BioLegend, CA, United States), and measured by a FACSCalibur flow cytometer (Beckman Coulter, CA, United States).

Hematoxylin-eosin staining, Masson staining, Sirius red staining, and oil red O staining

Hematoxylin was obtained from Yili Reagent Company (Beijing, China). Eosin was obtained from Zhongshan Jinqiao Biotechnology Company (Beijing, China). A Masson Tricolor staining kit was bought from Bogoo Corporation (Shanghai, China). A Pico Sirius Red Staining Kit was bought from Ruisai Biologicals (Shanghai, China). Oil red dye was obtained from Sigma-Aldrich (MO, United States). The manufacturer's instructions were strictly adhered to the conduct of every experiment.

Immunohistochemistry

Liver slices underwent an overnight incubation at 4 °C with a primary antibody and a 40-minute incubation at room temperature with an enzyme-labeled anti-rabbit antibody (PV-6001, ZSGB-BIO, Beijing, China). The slices were then developed using DAB substrate (Gene Science and Technology Company, China) after 30 min at room temperature incubation with avidin-biotin complex (PK-6100, Vectastain Elite ABC Standard kit, Vector Laboratories, Burlingame, CA, United States).

Assay of luciferase activity

HepG2 cells were transiently transfected with different promoter plasmids. A renal cell luciferase vector plasmid was used as a control. Dual-luciferase reporter gene activity was evaluated using a dual-luciferase reporter gene detection kit (Promega, United States).

Statistical analysis

Statistical analyses were performed using SPSS 24.0. The Student's *t* test was used to statistically examine all data. A P value < 0.05 was regarded as statistically significant. The data is shown as the mean ± SE.

RESULTS

Upregulated expression of NS3TP1 in HSCs and CCl_4-treated mouse livers

Herein, we confirmed the *in vivo* and *in vitro* roles of NS3TP1 in hepatic fibrosis. The level of NS3TP1 was measured in mice with CCl_4-induced hepatic fibrosis and TGF β1-activated LX-2 cells. Hematoxylin-eosin staining, Masson staining, Sirius red staining, and immunohistochemical staining for α-SMA demonstrated the successful establishment of CCl_4-induced fibrosis models (Supplementary Figure 1). The levels of alanine aminotransferase (ALT) and aspartate aminotransferase (AST) were elevated in mouse plasma (Supplementary Figure 2), suggesting hepatocyte injury. Hepatic fibrosis scores confirmed the disease, and the Ishak score was higher in the CCl_4 group (Supplementary Figure 3).

In vivo, COL1A1, COL3A1, α-SMA, and NS3TP1 were considerably elevated at the mRNA level in CCl_4-treated mouse livers (Figure 1A). The level of α-SMA in the CCl_4-treated mouse livers was upregulated, as indicated by immunofluorescence (Figure 1B). NS3TP1 in CCl_4-handled mouse livers was upregulated, as indicated by immunohistochemistry (Figure 1C and D) and immunofluorescence (Figure 1E).

In vitro, Western blotting was performed to monitor the level of NS3TP1 in various cell lines, such as L02, LX-2, Huh7, and HepG2, and NS3TP1 was significantly raised in LX-2 cells (Figure 1F). In addition, LX-2 cells were administered with recombinant human TGFβ1 protein for 24 h. Then, α-SMA, collagen I, collagen III, and NS3TP1 were found to be significantly upregulated at the protein and mRNA levels (Figure 1G and H).

Therefore, *in vivo* and *in vitro* investigations validated the elevation of NS3TP1 in hepatic fibrosis.

Influence of NS3TP1 overexpression or interference on the progression of hepatic fibrosis in vitro

The pcDNA-NS3TP1 plasmid was constructed and transiently transfected into LX-2 cells. The expression levels of fibrosis-related proteins were detected by Western blotting after 48 h. Compared to those in the negative control group, the levels of collagen I and α-SMA in the NS3TP1 overexpression group were increased (Figure 2A). The mRNA levels of COL1A1, COL2A1, COL3A1, COL4A2, and -SMA were monitored using RT-qPCR, and the results matched those of the Western blotting (Figure 2B). The levels of collagen I, collagen III, collagen IV, and α-SMA in NS3TP1 knockdown LX-2 cells were measured by Western blotting and RT-qPCR after 48 h. The results showed that in the NS3TP1 gene interference group, the expression of collagen I, collagen III, collagen IV, and α-SMA at the protein and mRNA levels was significantly downregulated (Figure 2C and D). This finding was the opposite of that of the NS3TP1 overexpression group.

NS3TP1 was interfered or overexpressed in LX-2 cells, the impact of NS3TP1 on HSC growth was then examined after 24 h, 48 h, and 72 h using a Cell Counting Kit-8 (CCK-8) cell proliferation and activity detection kit. Compared to the control group's results, the proliferation of HSCs in the NS3TP1 interference group decreased, while it increased after NS3TP1 overexpression, indicating that NS3TP1 increased the proliferation of HSCs (Figure 2E and F).

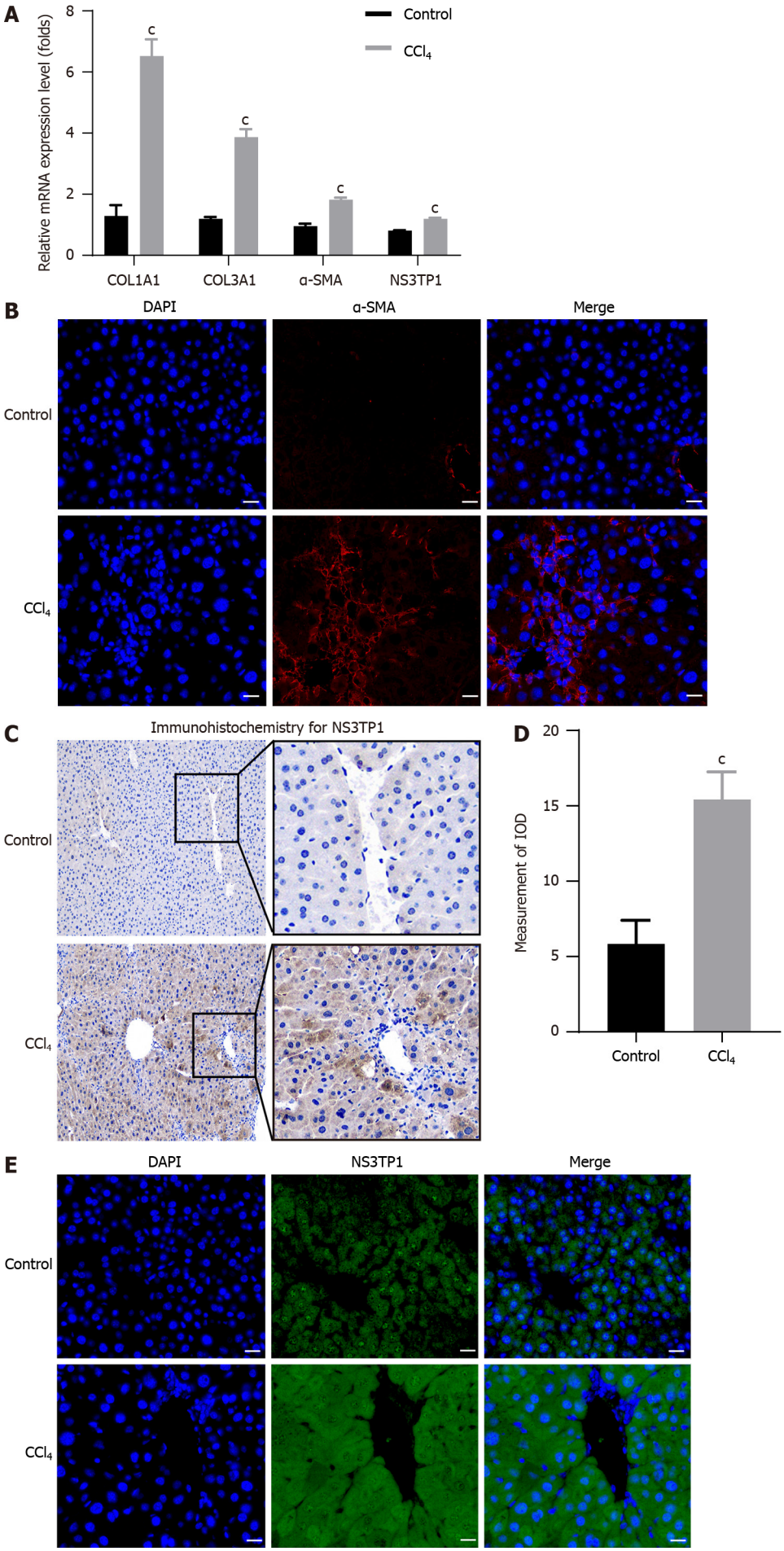
In LX-2 cells, after NS3TP1 was knocked down, the level of Bcl-2 was downregulated, the level of Bax was upregulated, apoptosis was enhanced, and the effects induced by overexpression were reversed. These results indicated that NS3TP1 inhibited the apoptosis of HSCs (Figure 2G and H).

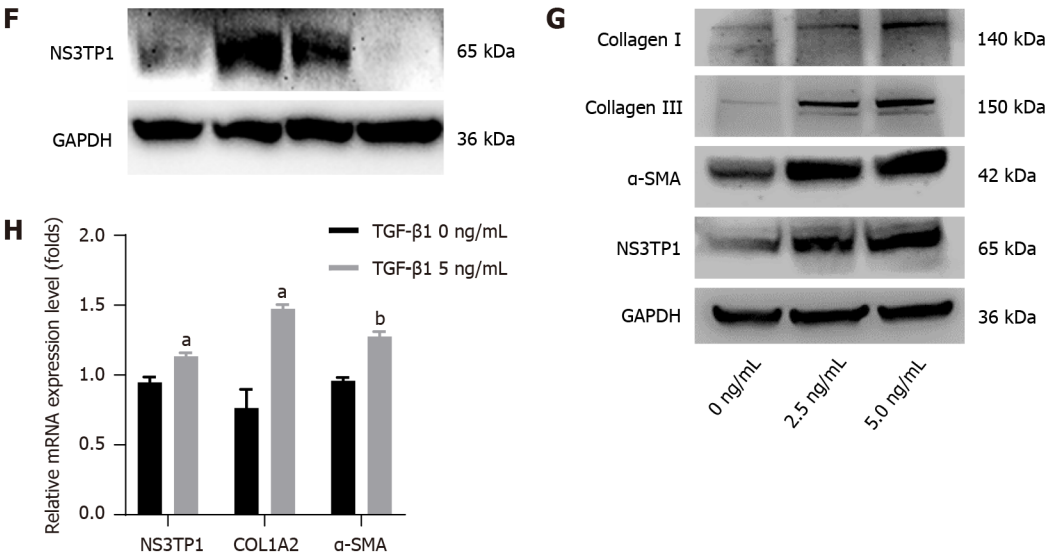
Consequently, *in vitro* research supported NS3TP1's significance in fostering hepatic fibrosis.

Effect of NS3TP1 overexpression or interference on the TGFβ1/Smad3 and NF-kB signaling pathways

After transient transfection of LX-2 cells with the NS3TP1-overexpressing plasmid or siRNA-NS3TP1 for 48 h, the activity of the TGFβ1/Smad3 and NF-κB signaling pathways was evaluated. In comparison to that of the control group, the activity of both signaling pathways was elevated in the NS3TP1 overexpression group and decreased in the gene interference group. These results suggested that NS3TP1 promoted hepatic fibrosis *via* both signaling pathways (Figure 3A and B).

We applied 3 μmol/L Smad3-specific inhibitor (SIS3) and 2 μmol/L licochalcone D (LD, inhibition of the phosphorylation of NF-κB at serine 276) to inhibit the above pathways and then added TGFβ1 (5 ng/mL) or LPS (1 μg/mL). NS3TP1 and downstream collagen I, α-SMA, p-smad3, and p-p65 Levels were decreased, indicating that NS3TP1 was localized downstream of Smad3 and p65 (Figure 3C and


A
Relative mRNA expression level (folds)
Control
CCl4
COL1A1
COL3A1
α-SMA
NS3TP1
B
DAPI
α-SMA
Merge
Control
CCl4
C
Immunohistochemistry for NS3TP1
Control
CCl4
D
Measurement of IOD
Control
CCl4
E
DAPI
NS3TP1
Merge
Control
CCl4



DOI: 10.3748/wjg.v29.i18.2798 **Copyright** ©The Author(s) 2023.

Figure 1 Evaluation of nonstructural protein 3-transactivated protein 1 expression in carbon tetrachloride-induced hepatic fibrosis and Transforming growth factor 1 beta 1-stimulated LX-2 cells. A: Real-time quantitative polymerase chain reaction analysis of fibrosis-related genes in liver tissues (n = 6); B: Immunofluorescence staining for alpha smooth muscle actin (α-SMA); red: α-SMA (n = 3), scale bar = 20 μm; C: Immunohistochemical staining for α-SMA, scale bar = 100 μm; D: Image J analysis of immunohistochemical staining for α-SMA (n = 3); E: Immunofluorescence staining for nonstructural protein 3-transactivated protein 1 (NS3TP1); green: NS3TP1 (n = 3), scale bar = 20 μm; F: Western blot analysis of NS3TP1 in L02, LX-2, Huh7, and G2 cells; G and H: NS3TP1 was overexpressed in LX-2 cells treated with transforming growth factor 1 beta 1 (TGFβ1) for 24 h (n = 3). The data was presented as mean ± SE. ^{a}P < 0.05, ^{b}P < 0.01 *vs* TGFβ1 (0 ng/mL) group; ^{c}P < 0.01 *vs* corn oil control group. NS3TP1: Nonstructural protein 3-transactivated protein 1; TGFβ1: Transforming growth factor 1 beta 1; CCl_4: Carbon tetrachloride; RT-qPCR: Real-time quantitative polymerase chain reaction; α-SMA: Alpha smooth muscle actin.

D).

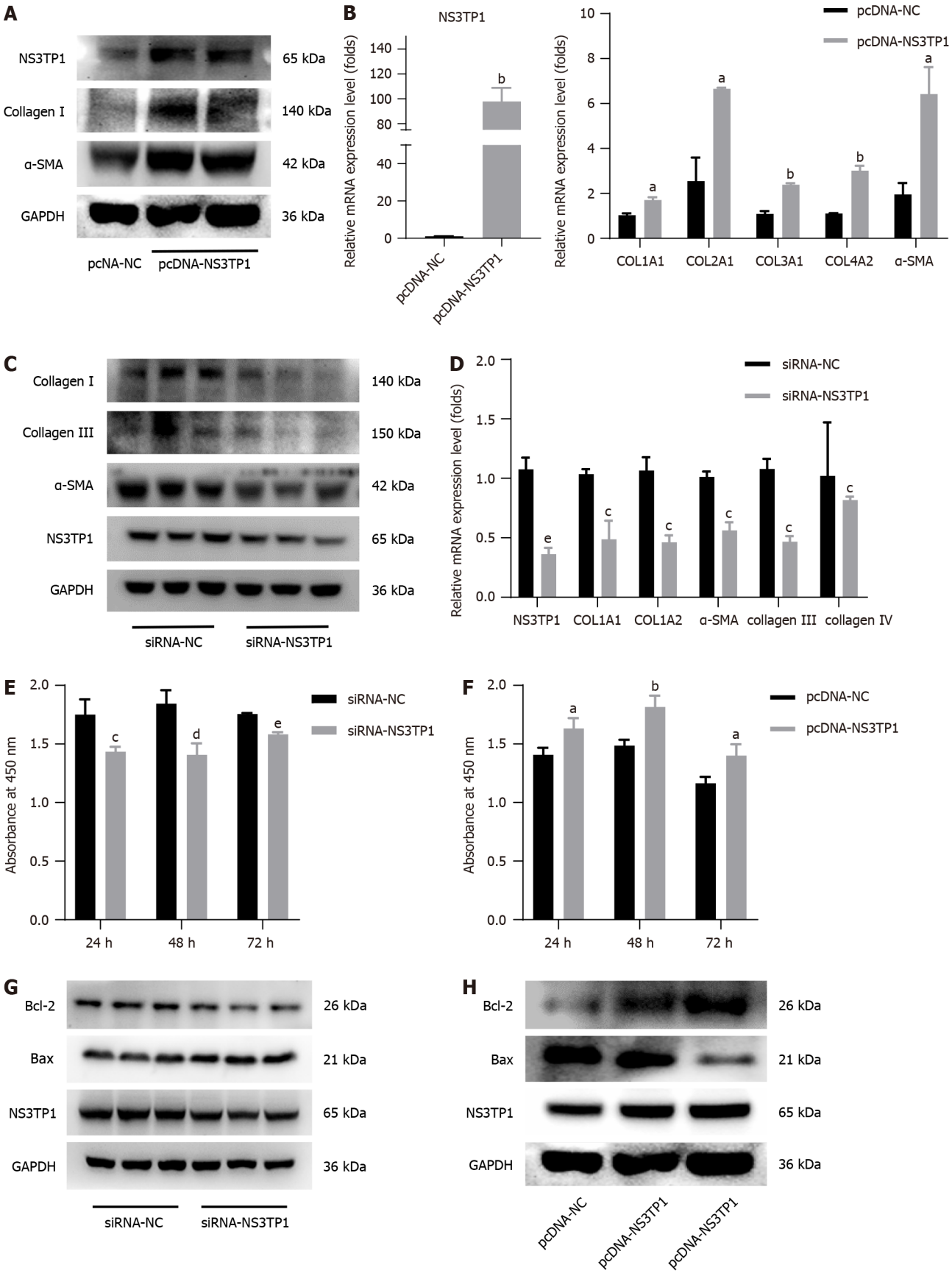
Using coimmunoprecipitation (Co-IP), we found that NS3TP1 could bind to Smad3 and p65 (Figure 3E). The dual luciferase assay revealed that NS3TP1 enhanced TGFβRI promoter activity (Figure 3F), while TGFβ1 had no effect on NS3TP1 promoter activity (Figure 3G). Moreover, NS3TP1 had no effect on p65 promoter activity (Figure 3H), while p65 increased NS3TP1 promoter activity (Figure 3I). Therefore, NS3TP1 may inhibit the activity of both signaling pathways by suppressing the phosphorylation of Smad3 or p65 at the protein level. In addition, NS3TP1 may regulate the TGFβ1/Smad3 signaling pathway at the mRNA level by upregulating the TGFβRI promoter, and the regulation of the NS3TP1 and NF-κB signaling pathways at the mRNA level may be realized through the upregulation of the NS3TP1 promoter by p65.

Calcitriol alleviates liver fibrosis

The CCK-8 kit was used to detect LX-2 cells stimulated with various concentrations of calcitriol. After incubation for 48 h with the CCK-8 reagent, the absorbance value decreased with increasing calcitriol concentration, which could be attributed to calcitriol-inhibited cell proliferation (Supplementary Figure 4). Calcitriol reduced the activation of HSCs in a concentration- and time-dependent manner. The optimum concentration of calcitriol was 16 μmol/L (Figure 4A). The optimum time for calcitriol treatment was 48 h (Figure 4B). Calcitriol promoted the return of TGFβ1-activated HSCs to quiescent HSCs (qHSCs) (Figure 4C). Following calcitriol administration, a Western blot analysis revealed concentration-dependently elevated Bax and diminished Bcl-2 Levels (Figure 4D). Flow cytometry showed that LX-2 cell apoptosis increased with increasing calcitriol concentration (Figure 4E and F). Oil red O staining showed an increased number of fat droplets in LX-2 cells (Supplementary Figure 5). Calcitriol reduced the migration of activated HSCs (Figure 4G and H).

In vivo, the dose and the protocol for this study were chosen based on the results of previous studies [26-28]. The optimal dosage of calcitriol was identified as 1 μg/kg/d, 5 times/wk according to the preliminary experimental results, and subsequent experiments were carried out with this dosage.

Calcitriol treatment reduced CCl_4-induced collagen accumulation in the mouse liver, as shown by hematoxylin-eosin staining, Masson staining, Sirius red staining, immunohistochemistry for α-SMA (Figure 4I), and immunofluorescence for α-SMA (Figure 4J). Western blot results further support these conclusions (Figure 4K and L). Liver fibrosis was improved by calcitriol treatment, according to the Ishak scoring system (Figure 4M). Plasma ALT and AST levels also demonstrated that calcitriol decreased CCl_4-induced inflammation in the mouse liver (Figure 4N). These findings showed that calcitriol prevented hepatic fibrosis both *in vivo* and in a lab setting.



DOI: 10.3748/wjg.v29.i18.2798 **Copyright** ©The Author(s) 2023.

Figure 2 Influence of nonstructural protein 3-transactivated protein 1 on liver fibrosis *in vitro*. A: Western blot analysis of fibrosis-related genes after Nonstructural protein 3-transactivated protein 1 (NS3TP1) overexpression (n = 3); B: Real-time quantitative polymerase chain reaction (RT-qPCR) analysis of fibrosis-related genes after NS3TP1 overexpression (n = 3); C: Western blot analysis of the fibrosis-related genes after NS3TP1 interference (n = 3); D: RT-qPCR analysis of the fibrosis-related genes after NS3TP1 interference (n = 3); E and F: Cell proliferation was measured by cell counting kit-8 assays after interference or

overexpression of NS3TP1 (n = 3); G and H: Western blot analysis of Bcl-2 and Bax after interference or overexpression of NS3TP1 (n = 3). The data was represented as mean ± SE. [a]P < 0.05, [b]P < 0.01 *vs* pcDNA-NS3TP1 group; [c]P < 0.05, [d]P < 0.01, [e]P < 0.001 *vs* siRNA-NS3TP1 group. NS3TP1: Nonstructural protein 3-transactivated protein 1; CCK-8: Cell counting kit-8; COL1A1: Type 1 collagen alpha 1 chain; COL1A2: Type 1 collagen alpha 2 chain; COL3A1: Type 3 collagen alpha 1 chain; COL4A2: Type 4 collagen alpha 2 chain.

Prevention of calcitriol on liver fibrosis through the TGFβ1/Smad3 and NFkB signaling pathways via NS3TP1 in vivo and in vitro

Calcitriol prevented the expression of NS3TP1 at the mRNA level in the CCl_4-treated mouse liver, as shown by RT-qPCR (Figure 5A) and by immunohistochemistry (Figure 5B and C). Moreover, calcitriol inhibited the expression of NS3TP1 at the protein level, as shown by immunofluorescence staining for NS3TP1 (Figure 5D). In LX-2 cells, the inhibition of NS3TP1 by calcitriol at the protein level was time- and concentration dependent, with an optimal concentration of 16 μmol/L and an optimal treatment time of 48 h (Figure 5E and F). In addition, the activity of the NS3TP1 promoter was inhibited by 32 μmol/L calcitriol in HepG2 cells, as validated by dual-luciferase reporter gene assay (Figure 5G).

Both signaling pathways were inhibited in a dose- and time-dependent manner after 12 h of TGFβ1 treatment and 48 h of calcitriol treatment in LX-2 cells (Figure 5H). Calcitriol significantly inhibited the LPS-activated NF-κB signaling pathway in HSCs (Figure 5I). PcDNA 3.1/myC-His(-)-NS3TP1 was transfected into LX-2 cells for 24 h, and then the cells were stimulated with calcitriol for 48 h. Calcitriol inhibited LX-2 cell activation following NS3TP1 overexpression (Figure 5J).

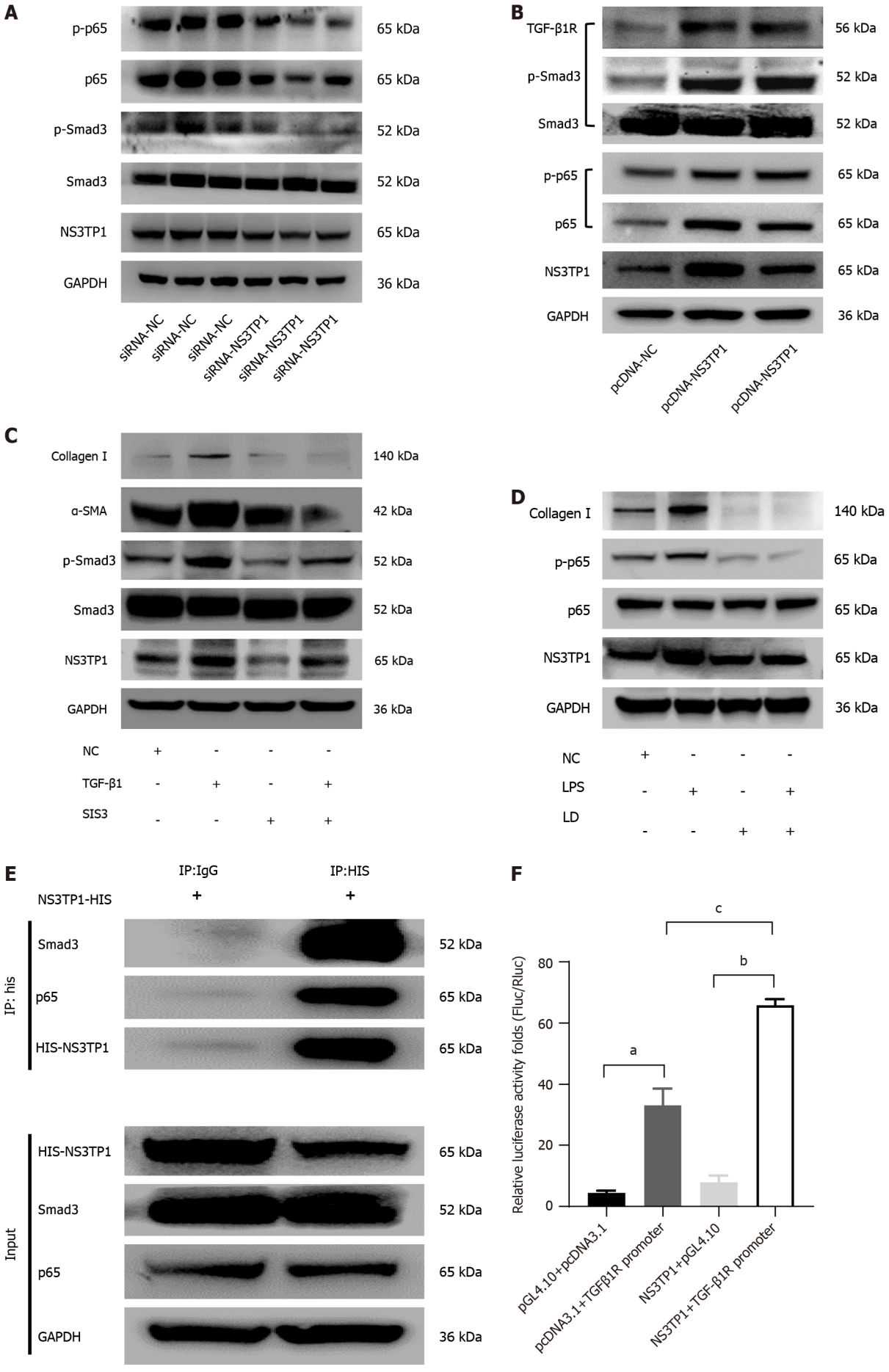
In conclusion, these results confirm that calcitriol prevented hepatic fibrosis through the above signaling pathways *via* NS3TP1.

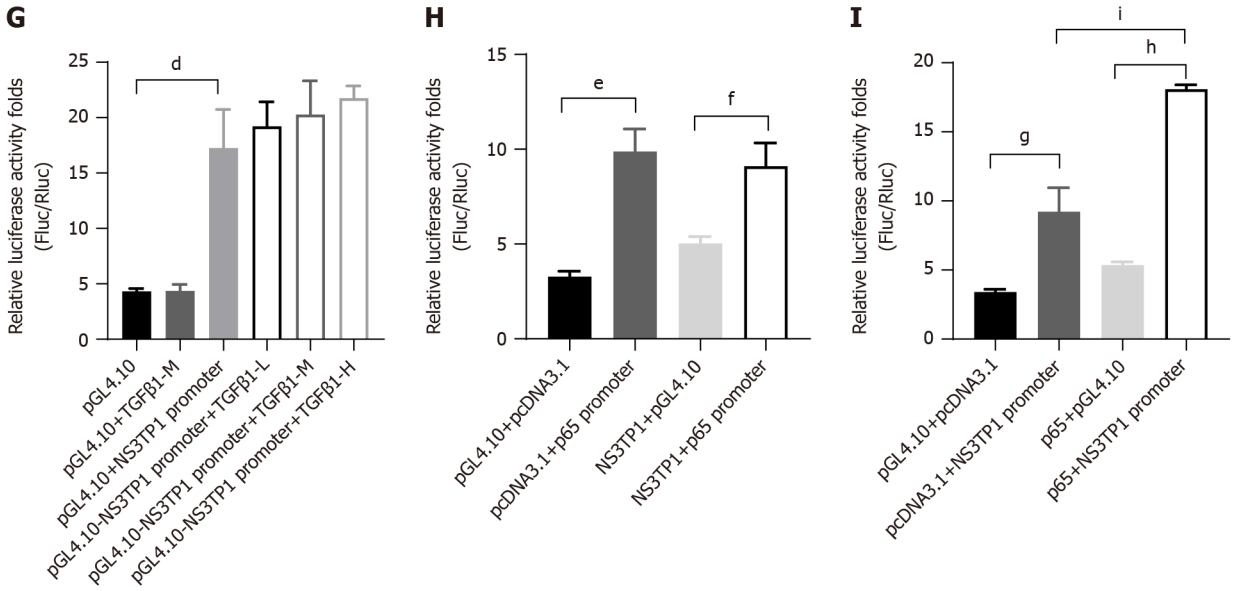
DISCUSSION

The present study first showed that NS3TP1 promoted hepatic fibrosis by enhancing the TGFβ1/Smad3 and NF-κB signaling pathways. NS3TP1 controlled HSC activation, proliferation, and differentiation. These results provide solid proof for the role of NS3TP1 contributing to hepatic fibrosis.

Both *in vivo* and *in vitro* experiments confirmed that NS3TP1 was elevated in liver fibrosis (Figure 1), which was consistent with our group's previous results. TGF-β1 activates hepatic stellate cells effectively[29], and the CCl_4-induced liver fibrosis model is one of the classical models of liver fibrosis [30]. There was an increase in NS3TP1 expression levels in the treated cells and tissues, indicating that NS3TP1 plays a role in liver fibrosis development. Moreover, NS3TP1 promoted the activation and proliferation but inhibited the apoptosis of LX-2 cells (Figure 2), Meienberg *et al*[9] demonstrated that NS3TP1 may interact with COL3A1, which further supports that NS3TP1 regulates the occurrence of hepatic fibrosis. The TGFβ1/Smad3 and NF-κB signaling pathways have been well established as two classical pathways for hepatic stellate cell activation[20,22,31]. To confirm the correlation between NS3TP1 and the activity of both signaling pathways, we overexpressed or interfered with NS3TP1 in LX-2 cells. We found that the activities of both signaling pathways were enhanced in the NS3TP1 overexpression group. However, the activities of both signaling pathways were decreased in the gene interference group, suggesting that NS3TP1 regulated hepatic fibrosis through both the above signaling pathways. To further elucidate the specific mechanisms between NS3TP1 and both signaling pathways, we used Co-IP and dual-luciferase assays. Co-IP analysis demonstrated that Smad3 and p65 could bind to NS3TP1. Therefore, NS3TP1 may decrease the activity of both signaling pathways by inhibiting the phosphorylation of Smad3 or p65. It is necessary to examine the possible colocalization of NS3TP1 and Smad3 or p65 in LX-2 cells by confocal microscopy. The dual-luciferase assay revealed that NS3TP1 increased the activity of the TGFβRI promoter and that p65 increased the activity of the NS3TP1 promoter. Altogether, NS3TP1 regulated both signaling pathways at protein and mRNA levels (Figure 3). The key targets of both signaling pathways are p-smad3 and p65 respectively, and p65 is the classic regulatory factor of the inflammatory pathway[32,33], which further supports our research.

We confirmed that calcitriol inhibited hepatic fibrosis *in vitro* and *in vivo* (Figure 4). This finding is consistent with previous research[26,34,35]. *In vivo* experiments were conducted using CCl_4-induced model mice, wherein calcitriol was found to attenuate liver fibrosis. The optimal dosage of calcitriol to treat liver fibrosis was 1 μg/kg/d, administered five times per week, which also reduced CCl_4-induced inflammation in the mouse liver. Calcitriol decreased the deposition of extracellular matrix following HSC activation, prevented the proliferation, activation, and migration of HSCs, and promoted cell apoptosis, and these *in vitro* experiments were primarily conducted using LX-2 cells. In addition, HSCs were also able to accumulate lipid droplets when exposed to calcitriol, which may be related to the dedifferentiation of activated HSCs into qHSCs, suggesting that calcitriol reversed hepatic fibrosis as described previously[25,36]. In conclusion, calcitriol inhibited liver fibrosis, however, the precise mechanism was uncertain. Therefore, we investigated the mechanisms by which calcitriol prevented hepatic fibrosis.


A
p-p65
p65
p-Smad3
Smad3
NS3TP1
GAPDH
65 kDa
65 kDa
52 kDa
52 kDa
65 kDa
36 kDa
siRNA-NC
siRNA-NC
siRNA-NC
siRNA-NS3TP1
siRNA-NS3TP1
siRNA-NS3TP1
B
TGF-β1R
p-Smad3
Smad3
p-p65
p65
NS3TP1
GAPDH
56 kDa
52 kDa
52 kDa
65 kDa
65 kDa
65 kDa
36 kDa
pcDNA-NC
pcDNA-NS3TP1
pcDNA-NS3TP1
C
Collagen I
α-SMA
p-Smad3
Smad3
NS3TP1
GAPDH
140 kDa
42 kDa
52 kDa
52 kDa
65 kDa
36 kDa
NC + - - -
TGF-β1 - + - +
SIS3 - - + +
D
Collagen I
p-p65
p65
NS3TP1
GAPDH
140 kDa
65 kDa
65 kDa
65 kDa
36 kDa
NC + - - -
LPS - + - +
LD - - + +
E
IP:IgG
IP:HIS
NS3TP1-HIS + +
IP: his
Smad3
p65
HIS-NS3TP1
52 kDa
65 kDa
65 kDa
Input
HIS-NS3TP1
Smad3
p65
GAPDH
65 kDa
52 kDa
65 kDa
36 kDa
F
Relative luciferase activity folds (Fluc/Rluc)
0
20
40
60
80
a
b
c
pGL4.10+pcDNA3.1
pcDNA3.1+TGFβ1R promoter
NS3TP1+pGL4.10
NS3TP1+TGF-β1R promoter



DOI: 10.3748/wjg.v29.i18.2798 **Copyright** ©The Author(s) 2023.

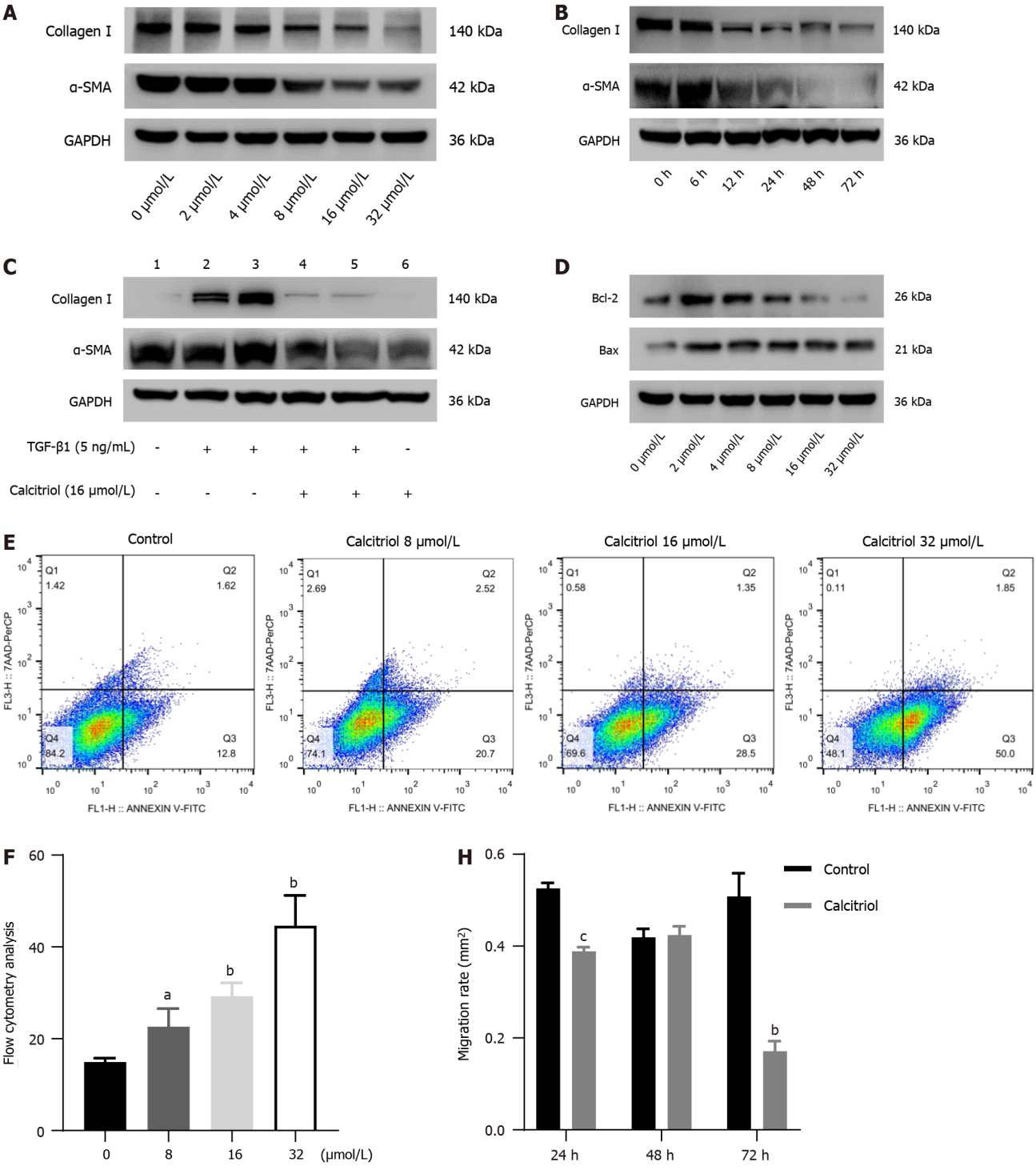
Figure 3 Promotion of nonstructural protein 3-transactivated protein 1 in hepatic fibrosis *via* transforming growth factor beta 1 receptor/Smad3 and NF-kB signaling pathways. A and B: The protein levels of molecules in the transforming growth factor beta 1 (TGFβ1)/Smad3 and NF-kB signaling pathways after nonstructural protein 3-transactivated protein 1 (NS3TP1) interference or overexpression in LX-2 cells were analyzed by Western blot (n = 3); C and D: Western blot analysis of the above signaling pathway molecules in LX-2 cells after Smad3-specific inhibitor or licochalcone D treatment (n = 3); E: Coimmunoprecipitation analysis between NS3TP1 and Smad3 or p65; F: Luciferase activity analysis between NS3TP1 and the TGFβ1 receptor 1 (TGFβRI) promoter (n = 3); G: Luciferase activity analysis between TGFβ1 and the NS3TP1 promoter; TGFβ1 (L: 2.5 ng/mL, M: 5 ng/mL, H: 10 ng/mL) (n = 3); H: Luciferase activity analysis between NS3TP1 and the p65 promoter (n = 3); I: Luciferase activity analysis between p65 and the NS3TP1 promoter (n = 3). The data was represented as mean ± SE. $^{a}P < 0.001$ pcDNA3.1 + TGFβ1R promoter *vs* pGL4.10 + pcDNA3.1, $^{b}P < 0.0001$ NS3TP1 + TGFβ1R promoter *vs* NS3TP1 + pGL4.10; $^{c}P < 0.001$; NS3TP1 + TGFβ1R promoter *vs* pcDNA3.1 + TGFβ1R promoter; $^{d}P < 0.01$ pGL4.10 + NS3TP1 promoter *vs* pGL4.10; $^{e}P < 0.001$ pcDNA3.1 + p65 promoter *vs* pGL4.10 + pcDNA3.1, $^{f}P < 0.01$ NS3TP1 + p65 promoter *vs* NS3TP1 + pGL4.10; $^{g}P < 0.01$ pcDNA3.1 + NS3TP1 promoter *vs* pGL4.10 + pcDNA3.1, $^{h}P < 0.0001$ p65 + NS3TP1 promoter *vs* p65 + pGL4.10; $^{i}P < 0.001$ p65 + NS3TP1 promoter *vs* pcDNA3.1 + NS3TP1 promoter. NS3TP1: Nonstructural protein 3-transactivated protein 1; TGFβ1R: Transforming growth factor beta 1 receptor; p-smad3: Phosphorylated sekelsky mothers against decapentaplegic homolog 3; SIS3: Smad3-specific inhibitor; LD: Licochalcone D; Co-IP: Coimmunoprecipitation.

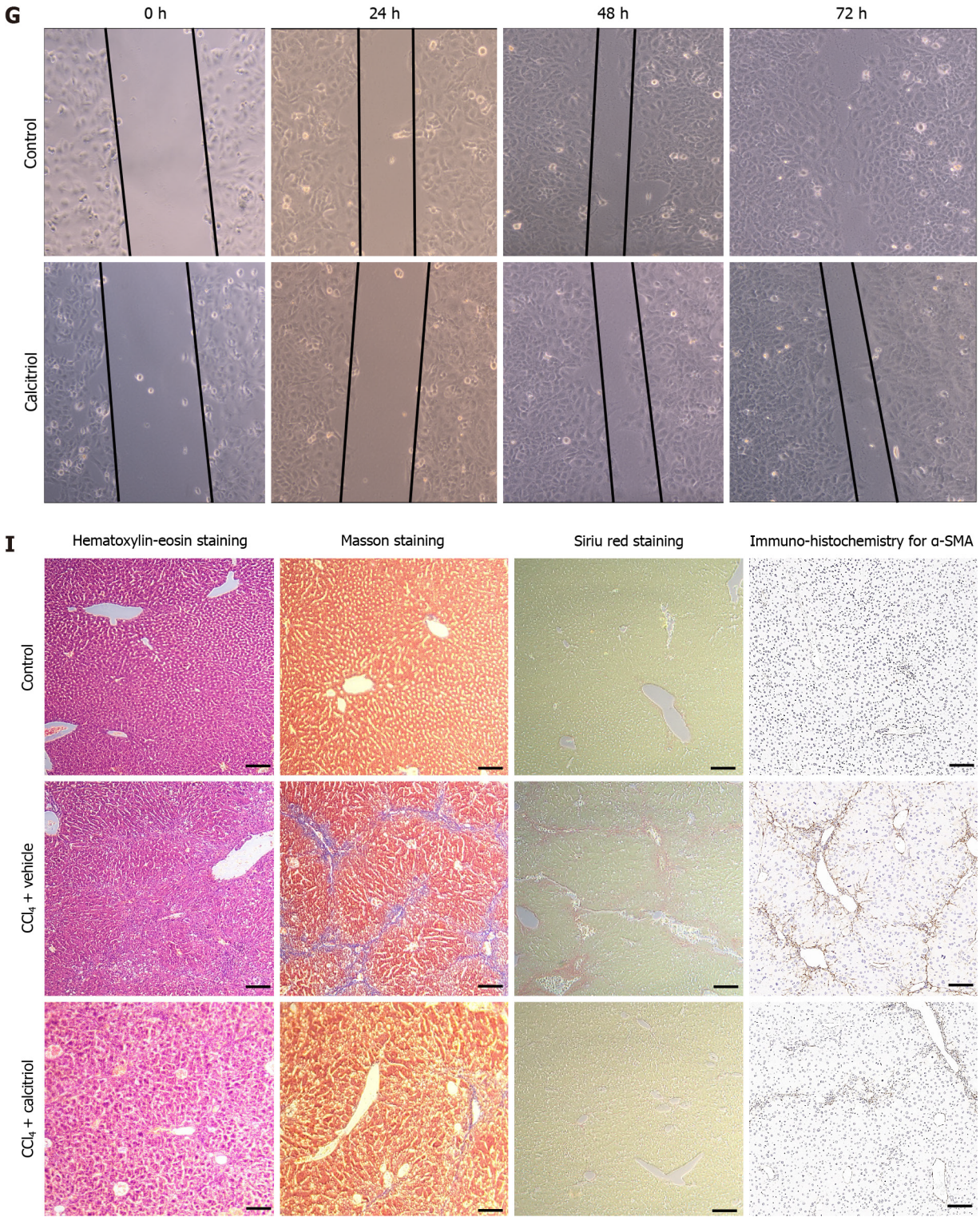
We demonstrated that calcitriol downregulated NS3TP1 at the mRNA level in CTD[11]. Moreover, we first proved that calcitriol inhibited NS3TP1 *in vivo* and *in vitro* (Figure 5) in a dose-dependent manner, and the increased NS3TP1 expression levels were found to be suppressed by calcitriol in mouse liver fibrotic tissues. The dual-luciferase assay showed that calcitriol blocked the promoter activity of NS3TP1, which conforms with the research of Wang *et al*[11]. Finally, we first demonstrated that calcitriol prevented hepatic fibrosis through the above signaling pathways *via* NS3TP1. Calcitriol inhibited liver fibrosis by binding to VDR, and NS3TP1 may be one of the targets. Whether other molecules that can bind to VDR can also reduce the expression of NS3TP1 will be the focus of further research. The results by Hah *et al*[15] supported this phenomenon. It was found that activating VDR in HSCs prevented liver inflammation and fibrosis through the TGFβ1/Smad3 signaling pathway. Activation of the TGFβ1 signaling pathway leads to genome-wide reallocation of VDR binding through TGFβ1-dependent chromatin remodeling in the presence of VDR ligands. By attaching to Smad3, VDR decreases Smad3 occupancy at these locations and inhibits fibrosis[15]. We proved that calcitriol decreased liver fibrosis through the NF-κB signaling pathway *via* NS3TP1. This finding is consistent with previous studies. Calcitriol suppresses the NF-κB signaling pathway, which confirms its anti-inflammatory effect, and activated HSCs are involved in inflammation[37].

Regarding the limitations of this study, animal experiments were not completed on NS3TP1-KO mice. In our research, we discovered that NS3TP1-KO mice could not give birth normally. Combined with the results of GeneCards database retrieval, we found that the NS3TP1 content in the reproductive system is quite rich. We therefore speculated that knocking down NS3TP1 would also have an impact on reproductive functions. To learn more about how the protein contributes to liver fibrosis, we will concentrate on NS3TP1 knockouts that target the liver.

CONCLUSION

In conclusion, NS3TP1 regulates TGFβ1/Smad3 and NF-κB signaling pathways to induce liver fibrosis. These results contribute to NS3TP1 as a novel, prospective therapeutic target for the treatment of


A
Collagen I
α-SMA
GAPDH
140 kDa
42 kDa
36 kDa
0 μmol/L
2 μmol/L
4 μmol/L
8 μmol/L
16 μmol/L
32 μmol/L
B
Collagen I
α-SMA
GAPDH
140 kDa
42 kDa
36 kDa
0 h
6 h
12 h
24 h
48 h
72 h
C
1 2 3 4 5 6
Collagen I
α-SMA
GAPDH
140 kDa
42 kDa
36 kDa
TGF-β1 (5 ng/mL) - + + + + -
Calcitriol (16 μmol/L) - - - + + +
D
Bcl-2
Bax
GAPDH
26 kDa
21 kDa
36 kDa
0 μmol/L
2 μmol/L
4 μmol/L
8 μmol/L
16 μmol/L
32 μmol/L
E
Control
Calcitriol 8 μmol/L
Calcitriol 16 μmol/L
Calcitriol 32 μmol/L
FL3-H :: 7AAD-PerCP
FL1-H :: ANNEXIN V-FITC
Q1 1.42
Q2 1.62
Q4 84.2
Q3 12.8
Q1 2.69
Q2 2.52
Q4 74.1
Q3 20.7
Q1 0.58
Q2 1.35
Q4 69.6
Q3 28.5
Q1 0.11
Q2 1.85
Q4 48.1
Q3 50.0
F
Flow cytometry analysis
0
20
40
60
a
b
b
0
8
16
32
(μmol/L)
H
Migration rate (mm²)
0.0
0.2
0.4
0.6
c
b
Control
Calcitriol
24 h
48 h
72 h


G
0 h
24 h
48 h
72 h
Control
Calcitriol
I
Hematoxylin-eosin staining
Masson staining
Siriu red staining
Immuno-histochemistry for α-SMA
Control
CCl4 + vehicle
CCl4 + calcitriol

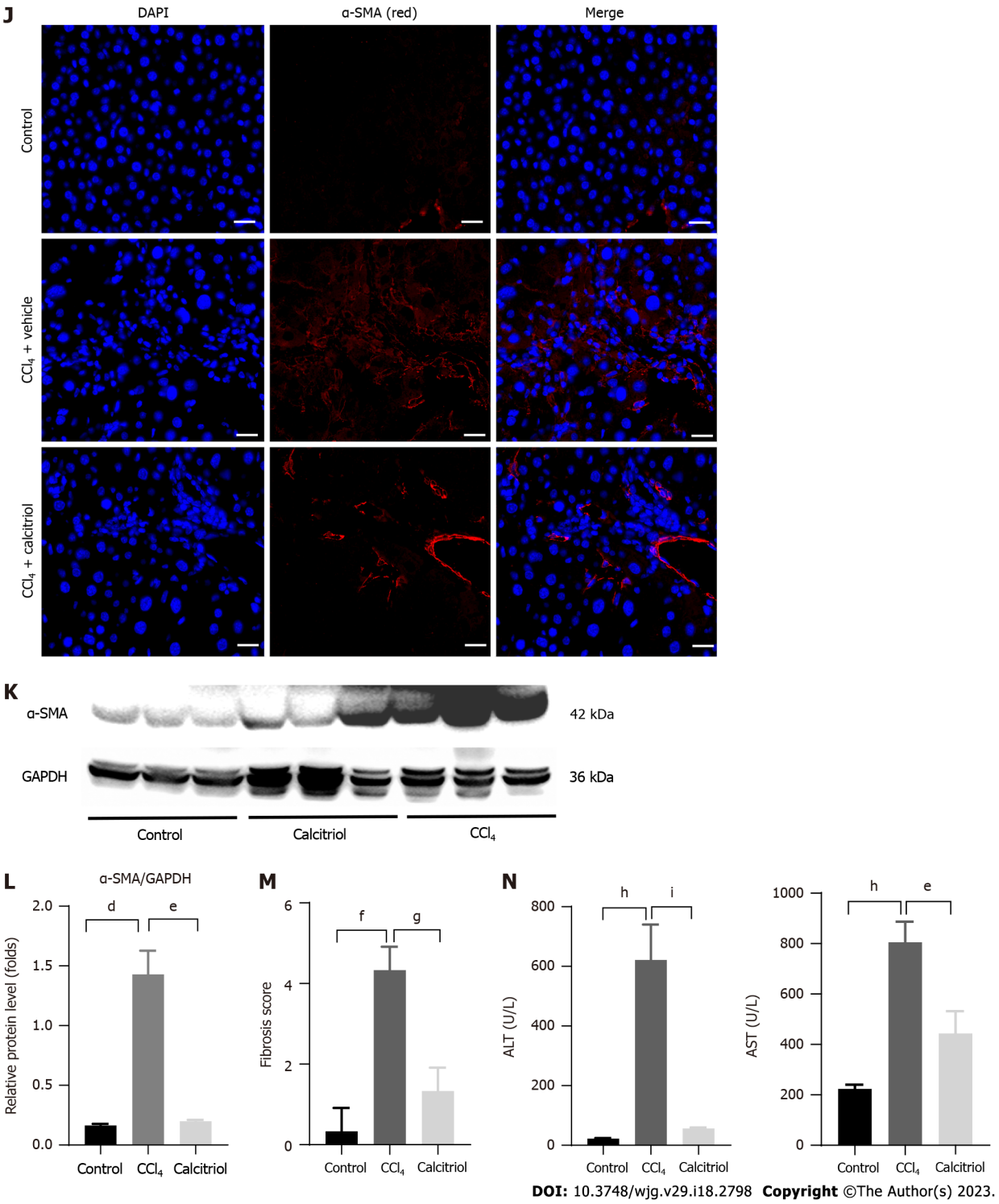
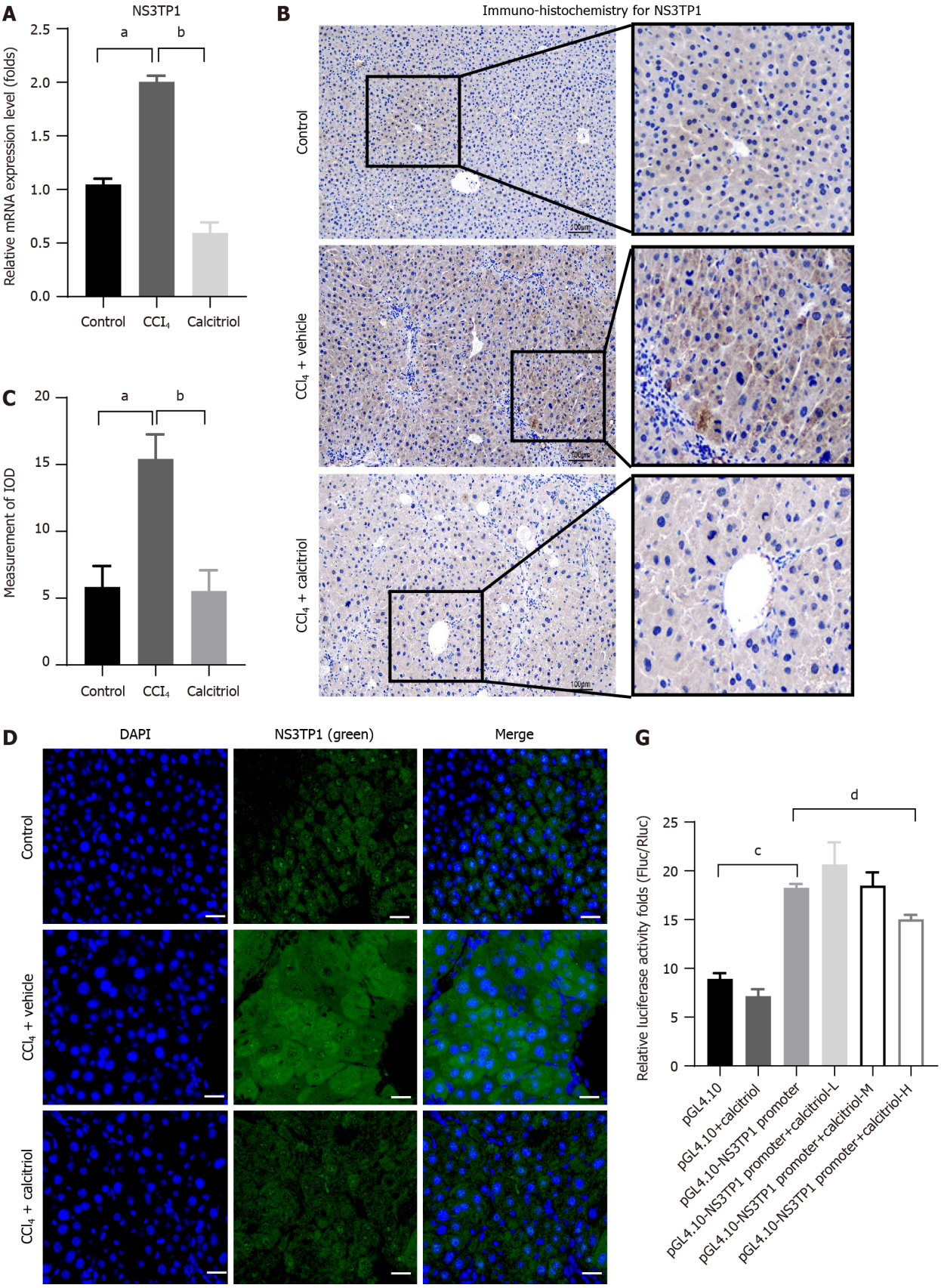
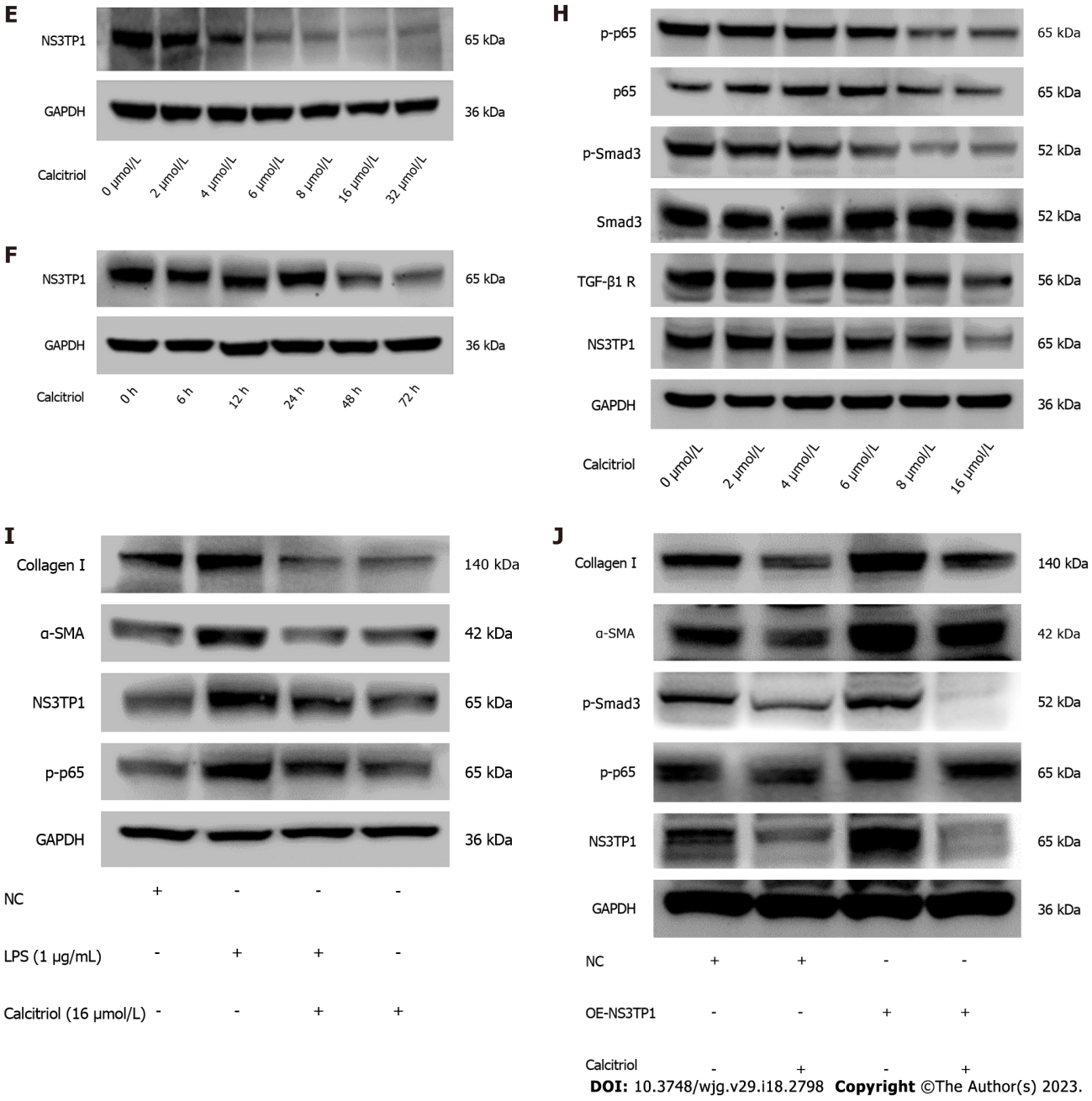


Figure 4 The role of calcitriol in hepatic fibrosis. A: Western blot analysis of collagen I and α-smooth muscle actin (α-SMA) in LX-2 cells treated with different concentrations of calcitriol; B: The protein levels of collagen I and α-SMA after calcitriol treatment at various time points were analyzed by Western blot; C: Calcitriol reduced the transforming growth factor beta 1 (TGFβ1)-induced elevation of collagen I and α-SMA at the protein level (n = 3); D: Western blot analysis of the calcitriol-induced level of Bcl-2 and Bax; E and F: An Annexin V-FITC/7-AAD kit was utilized to measure cellular apoptosis by flow cytometry; G and H: LX-2 cell migration was measured using the wound-healing test at 0 h, 24 h, 48 h, and 72 h (× 100) (n = 3); I: Hematoxylin-eosin, Masson staining, Sirius red staining, and immunohistochemical staining for α-SMA in hepatic tissue, scale bar = 100 μm; J: Immunofluorescence staining for α-SMA in hepatic tissue, red: α-SMA (n = 3), scale bar = 20 μm; K and L: Protein expression of α-SMA in the hepatic tissues was evaluated by Western blot (n = 3); M: The fibrosis score was analyzed according to the Ishak scoring system (n = 6); N: Levels of alanine aminotransferase and aspartate aminotransferase in plasma for the three groups. The carbon tetrachloride (CCl_4) group was contrasted with the corn oil group, while the calcitriol group was contrasted with the CCl_4 group (n = 6). The data was presented as mean ± SE. $^aP < 0.05$, $^bP < 0.01$, $^cP < 0.0001$ *vs* without calcitriol control group; $^dP < 0.001$ CCl_4 group *vs* corn oil control group, $^eP < 0.001$ calcitriol group *vs* CCl_4 group; $^fP < 0.01$ CCl_4 group *vs* corn oil control group, $^gP < 0.01$ calcitriol group *vs* CCl_4 group; $^hP < 0.0001$ CCl_4 group *vs* corn oil control group, $^iP < 0.0001$ calcitriol group *vs* CCl_4 group. ALT: Alanine aminotransferase; AST: Aspartate aminotransferase; CCl_4: Carbon tetrachloride; TGFβ1: Transforming growth factor beta 1.


A
NS3TP1
Relative mRNA expression level (folds)
2.5
2.0
1.5
1.0
0.5
0.0
a
b
Control
CCl4
Calcitriol
B
Immuno-histochemistry for NS3TP1
Control
CCl4 + vehicle
CCl4 + calcitriol
100μm
C
Measurement of IOD
20
15
10
5
0
a
b
Control
CCl4
Calcitriol
D
DAPI
NS3TP1 (green)
Merge
Control
CCl4 + vehicle
CCl4 + calcitriol
G
Relative luciferase activity folds (Fluc/Rluc)
25
20
15
10
5
0
c
d
pGL4.10
pGL4.10+calcitriol
pGL4.10-NS3TP1 promoter
pGL4.10-NS3TP1 promoter+calcitriol-L
pGL4.10-NS3TP1 promoter+calcitriol-M
pGL4.10-NS3TP1 promoter+calcitriol-H



DOI: 10.3748/wjg.v29.i18.2798 **Copyright** ©The Author(s) 2023.

Figure 5 The relationship between calcitriol and nonstructural protein 3-transactivated protein 1. A: RT-qPCR analysis of nonstructural protein 3-transactivated protein 1 (NS3TP1) in mice treated with calcitriol (n = 6); B: Immunohistochemical staining for α-smooth muscle actin (α-SMA) in hepatic tissue, scale bar = 100 μm; C: Image J analysis of immunohistochemical staining for α-SMA, (n = 3); D: Immunofluorescence staining for NS3TP1 in liver tissue, green: NS3TP1 (n = 3), scale bar = 20 μm; E and F: Western blot analysis of NS3TP1 in LX-2 cells stimulated with various concentrations of calcitriol or with 16 μmol/L calcitriol for various durations (n = 3); G: Analysis of luciferase activity between the NS3TP1 promoter and calcitriol in HepG2 cells, calcitriol (L: 8 μmol/L, M: 16 μmol/L, H: 32 μmol/L); H: Western blot analysis of the activity of both above signaling pathways in LX-2 cells treated with different concentrations of calcitriol; I: Collagen I, α-SMA, NS3TP1, and p-p65 in calcitriol-treated LX-2 cells were measured by Western blot and compared to LPS-treated cells; J: Extracellular matrix accumulation was evaluated by Western blot in LX-2 cells stimulated with calcitriol after NS3TP1 overexpression. The data was represented as mean ± SE. $^{a}P < 0.01$ CCl_4 group *vs* corn oil control group, $^{b}P < 0.01$ calcitriol group *vs* CCl_4 group; $^{c}P < 0.0001$ pGL4.10-NS3TP1 promoter *vs* pGL4.10, $^{d}P < 0.0001$ pGL4.10-NS3TP1 promoter + calcitriol (32 μmol/L) *vs* pGL4.10-NS3TP1 promoter. ECM: Extracellular matrix; LPS: Lipopolysaccharide; NS3TP1: Nonstructural protein 3-transactivated protein 1; TGFβ1: Transforming growth factor 1 beta 1; CCl_4: Carbon tetrachloride.

hepatic fibrosis, and calcitriol may be employed as an adjuvant therapy.

ARTICLE HIGHLIGHTS

Research background

Despite the lack of a specific therapeutic medicine, liver fibrosis still constitutes a serious hazard to human health, hence it is critical to identify novel targets for its therapy. After screening using suppressive subtractive hybridization and bioinformatics analysis, our research team discovered that hepatitis C virus nonstructural protein 3-transactivated protein 1 (NS3TP1) may be involved in the occurrence of liver fibrosis. As a result, the role of NS3TP1 in liver fibrosis was investigated to provide a new target for the treatment of liver fibrosis.

Research motivation

A potential new target for the treatment of hepatic fibrosis is provided by this work.

Research objectives

To determine whether NS3TP1 can promote liver fibrosis and whether calcitriol can inhibit the occurrence of liver fibrosis through NS3TP1.

Research methods

In vitro experiments were performed on carbon tetrachloride mouse liver, and NS3TP1 and fibrosis-related indexes were studied through serological and pathological tests. *In vivo* experiments were performed on LX-2 cells, and siRNA-NS3TP1 and pcDNA-NS3TP1 were constructed and transfected into LX-2 cells, respectively. Collagen I, collagen III, α-smooth muscle actin (α-SMA), TGFβ1/Smad3 and NF-κB signaling pathways were detected by western blot, RT-PCR, Co-imunoprecipitation and luciferase assays.

Research results

Collagen I, collagen III, α-SMA, transforming growth factor beta (TGFβ1)/Smad3, and NF-κB signaling pathways were found to be up-regulated following overexpression of NS3TP1, whereas the aforementioned indices were shown to be down-regulated after NS3TP1 interference *in vitro*. Results from Co-IP and Luciferase assays confirmed that Smad3 and p65 could both bind to NS3TP1, and that p65 boosted NS3TP1's promoter activity while NS3TP1 increased the promoter activity of TGFβ receptor I (TGFβ-RI). NS3TP1 and fibrosis-related indicators decreased after calcitriol therapy both *in vitro* and *in vivo*, and calcitriol restrained the expression of TGFβ1/Smad3 and NF-κB signaling pathways *via* NS3TP1.

Research conclusions

NS3TP1 promotes hepatic fibrosis through TGFβ1/Smad3 and NF-κB signaling pathways. Calcitriol further inhibits TGFβ1/Smad3 and NF-κB signaling pathways to reduce liver fibrosis by down-regulating NS3TP1.

Research perspectives

NS3TP1 provides a novel target for the treatment of liver fibrosis and a direction for the research of potential drug targets. Calcitriol is endowed with new functions as an adjunct therapeutic drug for liver fibrosis.

ACKNOWLEDGEMENTS

We would like to thank all the coauthors who participated in this study: Feng Ye, Lei Shi, Yun-Ru Chen, Xi Zhang, Jian-Zhou Li, and Yi-Fan Xu. Thank you to all the teachers at the Institute of Infectious Diseases at Beijing Ditan Hospital.

FOOTNOTES

Author contributions: Shi L, Zhou L, Han M, Zhang Y, Zhang Y, Yuan XX, Lu HP, Wang Y, Yang XL, Liu C, Wang J, Liang P, Liu SA, Liu XJ, Cheng J, and Lin SM contributed to the study conception and design; Liu S, Li Z, Ming H, Yu Z, Yang Z, Xue YX, Ping LH, Yun W, Liang YX, Chen L, Jun W, and Jing LX participated in the design and completion of the experiment; Liu S wrote the original draft; Liu S, Jun C, and Mei LS reviewed and edited the manuscript; Pu L and Ai LS finished the project administration; Jun C and Mei LS have the same contribution to the article; all authors approved the final version of the article.

Supported by the National Key Research and Development Program of China, No. 2017YFC0908104; and National Science and Technology Projects, No. 2017ZX10203201, No. 2017ZX10201201, and No. 2017ZX10202202.

Institutional animal care and use committee statement: All procedures involving animals were reviewed and approved by the Institutional Animal Care and Use Committee at Xi'an Jiaotong University Medical Science Center (approval No. 2020-1739).

Conflict-of-interest statement: The authors declare that they have no competing interests.

Data sharing statement: No additional data are available.

ARRIVE guidelines statement: The authors have read the ARRIVE guidelines, and the manuscript was prepared and revised according to the ARRIVE guidelines.

Open-Access: This article is an open-access article that was selected by an in-house editor and fully peer-reviewed by external reviewers. It is distributed in accordance with the Creative Commons Attribution NonCommercial (CC BY-NC 4.0) license, which permits others to distribute, remix, adapt, build upon this work non-commercially, and license their derivative works on different terms, provided the original work is properly cited and the use is non-commercial. See: https://creativecommons.org/Licenses/by-nc/4.0/

Country/Territory of origin: China

ORCID number: Liu Shi 0000-0001-8952-2144; Li Zhou 0000-0002-6543-1405; Ming Han 0000-0002-8788-1554; Yu Zhang 0000-0002-3469-152X; Yang Zhang 0000-0002-1140-0785; Xiao-Xue Yuan 0000-0002-7981-1863; Hong-Ping Lu 0000-0002-3877-3194; Yun Wang 0000-0003-3256-7397; Xue-Liang Yang 0000-0001-8414-0091; Chen Liu 0000-0002-6248-0797; Jun Wang 0000-0002-6261-8995; Pu Liang 0000-0003-0037-8356; Shun-Ai Liu 0000-0002-5688-8470; Xiao-Jing Liu 0000-0001-5991-792X; Jun Cheng 0000-0001-5579-8353; Shu-Mei Lin 0000-0001-8056-4479.

S-Editor: Chen YL
L-Editor: A
P-Editor: Yuan YY

REFERENCES

1 **Parola M**, Pinzani M. Liver fibrosis: Pathophysiology, pathogenetic targets and clinical issues. *Mol Aspects Med* 2019; **65**: 37-55 [PMID: 30213667 DOI: 10.1016/j.mam.2018.09.002]
2 **Du QH**, Zhang CJ, Li WH, Mu Y, Xu Y, Lowe S, Han L, Yu X, Wang SY, Li Y, Li J. Gan Shen Fu Fang ameliorates liver fibrosis *in vitro* and *in vivo* by inhibiting the inflammatory response and extracellular signal-regulated kinase phosphorylation. *World J Gastroenterol* 2020; **26**: 2810-2820 [PMID: 32550756 DOI: 10.3748/wjg.v26.i21.2810]
3 **Ul Haq A**, Sheikh A, Naeem S, Abidi SH. Molecular docking analysis of fluoroquinolones and other natural and synthetic compounds with the HCV NS3 helicase. *Bioinformation* 2022; **18**: 147-154 [PMID: 36518146 DOI: 10.6026/97320630018147]
4 **Li HC**, Yang CH, Lo SY. Hepatitis C Viral Replication Complex. *Viruses* 2021; **13** [PMID: 33809897 DOI: 10.3390/v13030520]
5 **Powell DR**, Revelli JP, Doree DD, DaCosta CM, Desai U, Shadoan MK, Rodriguez L, Mullens M, Yang QM, Ding ZM, Kirkpatrick LL, Vogel P, Zambrowicz B, Sands AT, Platt KA, Hansen GM, Brommage R. High-Throughput Screening of Mouse Gene Knockouts Identifies Established and Novel High Body Fat Phenotypes. *Diabetes Metab Syndr Obes* 2021; **14**: 3753-3785 [PMID: 34483672 DOI: 10.2147/DMSO.S322083]
6 **Vogel P**, Ding ZM, Read R, DaCosta CM, Hansard M, Small DL, Ye GL, Hansen G, Brommage R, Powell DR. Progressive Degenerative Myopathy and Myosteatosis in ASNSD1-Deficient Mice. *Vet Pathol* 2020; **57**: 723-735 [PMID: 32638637 DOI: 10.1177/0300985820939251]
7 **Vogel P**, Read RW, Hansen GM, Powell DR. Histopathology is required to identify and characterize myopathies in high-throughput phenotype screening of genetically engineered mice. *Vet Pathol* 2021; **58**: 1158-1171 [PMID: 34269122 DOI: 10.1177/03009858211030541]
8 **Theusch E**, Chen YI, Rotter JI, Krauss RM, Medina MW. Genetic variants modulate gene expression statin response in human lymphoblastoid cell lines. *BMC Genomics* 2020; **21**: 555 [PMID: 32787775 DOI: 10.1186/s12864-020-06966-4]
9 **Meienberg J**, Rohrbach M, Neuenschwander S, Spanaus K, Giunta C, Alonso S, Arnold E, Henggeler C, Regenass S, Patrignani A, Azzarello-Burri S, Steiner B, Nygren AO, Carrel T, Steinmann B, Mátyás G. Hemizygous deletion of COL3A1, COL5A2, and MSTN causes a complex phenotype with aortic dissection: a lesson for and from true haploinsufficiency. *Eur J Hum Genet* 2010; **18**: 1315-1321 [PMID: 20648054 DOI: 10.1038/ejhg.2010.105]
10 **Wang T**, Zhang C, Meng X, Zhu B, Wang S, Yuan W, Zhang S, Xu J. Long Noncoding RNA Metastasis-Associated Lung Adenocarcinoma Transcript 1 in Extracellular Vesicles Promotes Hepatic Stellate Cell Activation, Liver Fibrosis and β-Catenin Signaling Pathway. *Front Physiol* 2022; **13**: 792182 [PMID: 35237178 DOI: 10.3389/fphys.2022.792182]
11 **Wang WL**, Chatterjee N, Chittur SV, Welsh J, Tenniswood MP. Effects of 1α,25 dihydroxyvitamin D3 and testosterone on miRNA and mRNA expression in LNCaP cells. *Mol Cancer* 2011; **10**: 58 [PMID: 21592394 DOI: 10.1186/1476-4598-10-58]
12 **Pop TL**, Sîrbe C, Benţa G, Mititelu A, Grama A. The Role of Vitamin D and Vitamin D Binding Protein in Chronic Liver Diseases. *Int J Mol Sci* 2022; **23** [PMID: 36142636 DOI: 10.3390/ijms231810705]

13 **Lu W**, Li X, Liu N, Zhang Y, Li Y, Pan Y, Yang J, Liu Z, Kong J. Vitamin D alleviates liver fibrosis by inhibiting histidine-rich calcium binding protein (HRC). *Chem Biol Interact* 2021; **334**: 109355 [PMID: 33309619 DOI: 10.1016/j.cbi.2020.109355]

14 **Okubo T**, Atsukawa M, Tsubota A, Yoshida Y, Arai T, Iwashita AN, Itokawa N, Kondo C, Iwakiri K. Relationship between serum vitamin D level and sarcopenia in chronic liver disease. *Hepatol Res* 2020; **50**: 588-597 [PMID: 31914479 DOI: 10.1111/hepr.13485]

15 **Hah N**, Sherman MH, Yu RT, Downes M, Evans RM. Targeting Transcriptional and Epigenetic Reprogramming in Stromal Cells in Fibrosis and Cancer. *Cold Spring Harb Symp Quant Biol* 2015; **80**: 249-255 [PMID: 26801159 DOI: 10.1101/sqb.2015.80.027185]

16 **He W**, Ni W, Zhao L, Wang X, Liu L, Fan Z. MicroRNA-125a/VDR axis impaired autophagic flux and contributed to fibrosis in a CCL4-induced mouse model and patients with liver cirrhosis. *Life Sci* 2021; **264**: 118666 [PMID: 33130085 DOI: 10.1016/j.lfs.2020.118666]

17 **Gu L**, Xu Q, Cao H. 1,25(OH)2D3 Protects Liver Fibrosis Through Decreasing the Generation of TH17 Cells. *Med Sci Monit* 2017; **23**: 2049-2058 [PMID: 28455490 DOI: 10.12659/msm.904271]

18 **Chen C**, Li X, Wang L. Thymosinβ4 alleviates cholestatic liver fibrosis in mice through downregulating PDGF/PDGFR and TGFβ/Smad pathways. *Dig Liver Dis* 2020; **52**: 324-330 [PMID: 31542221 DOI: 10.1016/j.dld.2019.08.014]

19 **Zhou MY**, Cheng ML, Huang T, Hu RH, Zou GL, Li H, Zhang BF, Zhu JJ, Liu YM, Liu Y, Zhao XK. Transforming growth factor beta-1 upregulates glucose transporter 1 and glycolysis through canonical and noncanonical pathways in hepatic stellate cells. *World J Gastroenterol* 2021; **27**: 6908-6926 [PMID: 34790014 DOI: 10.3748/wjg.v27.i40.6908]

20 **Tang M**, Guo C, Sun M, Zhou H, Peng X, Dai J, Ding Q, Wang Y, Yang C. Effective delivery of osteopontin small interference RNA using exosomes suppresses liver fibrosis *via* TGF-β1 signaling. *Front Pharmacol* 2022; **13**: 882243 [PMID: 36120332 DOI: 10.3389/fphar.2022.882243]

21 **Luo Q**, Ling Y, Li Y, Qu X, Shi Q, Zheng S, Huang Y, Zhou X. Phosphatidylethanolamine-binding protein 4 deficiency exacerbates carbon tetrachloride-induced liver fibrosis by regulating the NF-κB signaling pathway. *Front Pharmacol* 2022; **13**: 964829 [PMID: 36120358 DOI: 10.3389/fphar.2022.964829]

22 **Masamune A**, Hamada S. Editorial: Mechanisms of Inflammation and Fibrosis Interplays in the Digestive Diseases. *Front Physiol* 2022; **13**: 906742 [PMID: 35492620 DOI: 10.3389/fphys.2022.906742]

23 **Xie S**, Qiu C, Sun Y, Yu Y, Hu Z, Zhang K, Chen L, Cheng Y, Bao M, Zhang Q, Zhu J, Grimm R, Shen W. Assessment of Fibrotic Liver Regeneration After Partial Hepatectomy With Intravoxel Incoherent Motion Diffusion-Weighted Imaging: An Experimental Study in a Rat Model With Carbon Tetrachloride Induced Liver Injury. *Front Physiol* 2022; **13**: 822763 [PMID: 35250624 DOI: 10.3389/fphys.2022.822763]

24 **Higashiyama M**, Tomita K, Sugihara N, Nakashima H, Furuhashi H, Nishikawa M, Inaba K, Wada A, Horiuchi K, Hanawa Y, Shibuya N, Kurihara C, Okada Y, Nishii S, Mizoguchi A, Hozumi H, Watanabe C, Komoto S, Yamamoto J, Seki S, Miura S, Hokari R. Chitinase 3-like 1 deficiency ameliorates liver fibrosis by promoting hepatic macrophage apoptosis. *Hepatol Res* 2019; **49**: 1316-1328 [PMID: 31250532 DOI: 10.1111/hepr.13396]

25 **Udomsinprasert W**, Jittikoon J. Vitamin D and liver fibrosis: Molecular mechanisms and clinical studies. *Biomed Pharmacother* 2019; **109**: 1351-1360 [PMID: 30551386 DOI: 10.1016/j.biopha.2018.10.140]

26 **Reiter FP**, Ye L, Bösch F, Wimmer R, Artmann R, Ziesch A, Kanitz V, Mayr D, Steib CJ, Trauner M, Regel I, Gerbes AL, Mayerle J, Hohenester S, de Toni EN, Denk G. Antifibrotic effects of hypocalcemic vitamin D analogs in murine and human hepatic stellate cells and in the CCl(4) mouse model. *Lab Invest* 2019; **99**: 1906-1917 [PMID: 31467426 DOI: 10.1038/s41374-019-0310-1]

27 **Tsai TH**, Lin CJ, Hang CL, Chen WY. Calcitriol Attenuates Doxorubicin-Induced Cardiac Dysfunction and Inhibits Endothelial-to-Mesenchymal Transition in Mice. *Cells* 2019; **8** [PMID: 31405028 DOI: 10.3390/cells8080865]

28 **Gong J**, Gong H, Liu Y, Tao X, Zhang H. Calcipotriol attenuates liver fibrosis through the inhibition of vitamin D receptor-mediated NF-κB signaling pathway. *Bioengineered* 2022; **13**: 2658-2672 [PMID: 35043727 DOI: 10.1080/21655979.2021.2024385]

29 **Peng D**, Fu M, Wang M, Wei Y, Wei X. Targeting TGF-β signal transduction for fibrosis and cancer therapy. *Mol Cancer* 2022; **21**: 104 [PMID: 35461253 DOI: 10.1186/s12943-022-01569-x]

30 **Delire B**, Stärkel P, Leclercq I. Animal Models for Fibrotic Liver Diseases: What We Have, What We Need, and What Is under Development. *J Clin Transl Hepatol* 2015; **3**: 53-66 [PMID: 26357635 DOI: 10.14218/JCTH.2014.00035]

31 **Zhang YZ**, Yao JN, Zhang LF, Wang CF, Zhang XX, Gao B. Effect of NLRC5 on activation and reversion of hepatic stellate cells by regulating the nuclear factor-κB signaling pathway. *World J Gastroenterol* 2019; **25**: 3044-3055 [PMID: 31293340 DOI: 10.3748/wjg.v25.i24.3044]

32 **Rodríguez MJ**, Sabaj M, Tolosa G, Herrera Vielma F, Zúñiga MJ, González DR, Zúñiga-Hernández J. Maresin-1 Prevents Liver Fibrosis by Targeting Nrf2 and NF-κB, Reducing Oxidative Stress and Inflammation. *Cells* 2021; **10** [PMID: 34943914 DOI: 10.3390/cells10123406]

33 **ShamsEldeen AM**, Al-Ani B, Ebrahim HA, Rashed L, Badr AM, Attia A, Farag AM, Kamar SS, Haidara MA, Al Humayed S, Ali Eshra M. Resveratrol suppresses cholestasis-induced liver injury and fibrosis in rats associated with the inhibition of TGFβ1-Smad3-miR21 axis and profibrogenic and hepatic injury biomarkers. *Clin Exp Pharmacol Physiol* 2021; **48**: 1402-1411 [PMID: 34157155 DOI: 10.1111/1440-1681.13546]

34 **Ma L**, Ishigami M, Honda T, Yokoyama S, Yamamoto K, Ishizu Y, Kuzuya T, Hayashi K, Hirooka Y, Goto H. Antifibrotic Effects of 1,25(OH)(2)D(3) on Nonalcoholic Steatohepatitis in Female Mice. *Dig Dis Sci* 2019; **64**: 2581-2590 [PMID: 30825110 DOI: 10.1007/s10620-019-05560-3]

35 **Arai T**, Atsukawa M, Tsubota A, Koeda M, Yoshida Y, Okubo T, Nakagawa A, Itokawa N, Kondo C, Nakatsuka K, Masu T, Kato K, Shimada N, Hatori T, Emoto N, Kage M, Iwakiri K. Association of vitamin D levels and vitamin D-related gene polymorphisms with liver fibrosis in patients with biopsy-proven nonalcoholic fatty liver disease. *Dig Liver Dis* 2019; **51**: 1036-1042 [PMID: 30683615 DOI: 10.1016/j.dld.2018.12.022]

36 **Megahed A**, Gadalla H, Abdelhamid FM, Almehmadi SJ, Khan AA, Albukhari TA, Risha EF. Vitamin D Ameliorates the Hepatic Oxidative Damage and Fibrotic Effect Caused by Thioacetamide in Rats. *Biomedicines* 2023; **11** [PMID:

36830960 DOI: 10.3390/biomedicines11020424]

37 **Gupta G**, Khadem F, Uzonna JE. Role of hepatic stellate cell (HSC)-derived cytokines in hepatic inflammation and immunity. *Cytokine* 2019; **124**: 154542 [PMID: 30241896 DOI: 10.1016/j.cyto.2018.09.004]

World Journal of Gastroenterology

Submit a Manuscript: https://www.f6publishing.com

World J Gastroenterol 2023 May 14; 29(18): 2818-2835

DOI: 10.3748/wjg.v29.i18.2818

ISSN 1007-9327 (print) ISSN 2219-2840 (online)

ORIGINAL ARTICLE

Basic Study

BanXiaXieXin decoction treating gastritis mice with drug-resistant *Helicobacter pylori* and its mechanism

Xiao-Hua Li, Jia-Yin Xu, Xue Wang, Li-Juan Liao, Liang Huang, Yan-Qiang Huang, Zeng-Feng Zhang

Specialty type: Biochemistry and molecular biology

Provenance and peer review: Unsolicited article; Externally peer reviewed.

Peer-review model: Single blind

Peer-review report's scientific quality classification

Grade A (Excellent): 0
Grade B (Very good): B, B
Grade C (Good): C
Grade D (Fair): 0
Grade E (Poor): 0

P-Reviewer: Lee SC, Korea; Razek AAKA, Japan; Sakamoto S, Egypt

Received: February 28, 2023
Peer-review started: February 28, 2023
First decision: March 14, 2023
Revised: March 16, 2023
Accepted: April 13, 2023
Article in press: April 13, 2023
Published online: May 14, 2023

Xiao-Hua Li, Duate School, Guangxi Medical University, Nanning 5330021, Guangxi Zhuang Autonomous Region, China

Jia-Yin Xu, Xue Wang, Li-Juan Liao, Yan-Qiang Huang, Guangxi Technology Innovation Cooperation Base of Prevention and Control Pathogenic Microbes with Drug Resistance, Youjiang Medical University for Nationalities, Baise 533000, Guangxi Zhuang Autonomous Region, China

Liang Huang, Key Laboratory of the Prevention and Treatment of Drug Resistant Microbial Infecting, Youjiang Medical University for Nationalities, Baise 533000, Guangxi Zhuang Autonomous Region, China

Zeng-Feng Zhang, Department of Microbiology, Guangxi Medical University, Nanning 530021, Guangxi Zhuang Autonomous Region, China

Corresponding author: Zeng-Feng Zhang, professor, Department of Microbiology, Guangxi Medical University,No.22 Shuangyong Road, Nanning, 530021, Guangxi Zhuang Autonomous Region, China. zfzhangphd@163.com

Abstract

BACKGROUND

Helicobacter pylori (*H. pylori*) is the main pathogen that causes a variety of upper digestive diseases. The drug resistance rate of *H. pylori* is increasingly higher, and the eradication rate is increasingly lower. The antimicrobial resistance of *H. pylori* is an urgent global problem. It has been confirmed that Banxia Xiexin decoction (BXXXT) demonstrates the effects of treating gastrointestinal diseases, inhibiting *H. pylori* and protecting gastric mucosa. The purpose of the present study is to further explore the therapeutic effects of BXXXT on drug-resistant *H. pylori*.

AIM

To confirm that BXXXT demonstrates therapeutical effects *in vivo* and *in vitro* on gastritis mice with drug-resistant *H. pylori* and explain its mechanism to provide an experimental basis for promoting the application of BXXXT.

METHODS

The aqueous extract of BXXXT was gained by water decocting method. The inhibitory effect of the aqueous extract on *H. pylori* was detected by dilution *in vitro*; drug-resistant *H. pylori* cells were used to build an acute gastritis model *in*

vivo. Thereafter, the model mice were treated with the aqueous extract of BXXXT. The amount of *H. pylori* colonization, the repair of gastric mucosal damage, changes of inflammatory factors, apoptosis, *etc*., were assessed. In terms of mechanism exploration, the main medicinal compositions of BXXXT aqueous extract and the synergistic bacteriostatic effects they had demonstrated were analyzed using mass spectrometry; the immune function of peripheral blood cells such as $CD3^+$ T and $CD4^+$ T of mice with gastritis before and after treatment with BXXXT aqueous extract was detected using a flow cytometry; the *H. pylori* transcriptome and proteome after treatment with BXXXT aqueous extract were detected. Differently expressed genes were screened and verification was performed thereon with knockout expression.

RESULTS

The minimum inhibitory concentration of BXXXT aqueous extract against *H. pylori* was 256-512 μg/mL. A dose of 28 mg/kg BXXXT aqueous extract treatment produced better therapeutical effects than the standard triple therapy did; the BXXXT aqueous extract have at least 11 ingredients inhibiting *H. pylori*, including berberine, quercetin, baicalin, luteolin, gallic acid, rosmarinic acid, aloe emodin, *etc*., of which berberine, aloe emodin, luteolin and gallic acid have a synergistic effect; BXXXT aqueous extract was found to stimulate the expressions of $CD3^+$ T and $CD4^+$ T and increase the number of $CD4^+$ T/$CD8^+$ T in gastritis mice; the detection of transcriptome and proteome, quantitative polymerase chain reaction, Western blotting and knockout verification revealed that the main targets of BXXXT aqueous extract are *CFAs* related to urea enzymes, and *CagA*, *VacA*, *etc*.

CONCLUSION

BXXXT aqueous extract could demonstrate good therapeutic effects on drug-resistance *H. pylori in vitro* and *in vivo* and its mechanism comes down to the synergistic or additional antibacterial effects of berberine, emodin and luteolin, the main components of the extract; the extract could activate the immune function and enhance bactericidal effects; BXXXT aqueous extract, with main targets of BXXXT aqueous extract related to urease, virulence factors, *etc*., could reduce the urease and virulence of *H. pylori*, weaken its colonization, and reduce its inflammatory damage to the gastric mucosa.

Key Words: Banxia Xiexin decoction; *Helicobacter pylori*; Drug resistance; Therapeutic effects; Mechanism

©The Author(s) 2023. Published by Baishideng Publishing Group Inc. All rights reserved.

Core Tip: The failure rate of treating *Helicobacter pylori* (*H. pylori*) infectious diseases is increasing, leading to an urgent need to study and develop anti-*H. pylori* drugs. Banxia Xiexin decoction (BXXX) has a good effect on Hp infection and Hp-infection-related diseases. However, its pharmacological mechanism remains unclear, and whether it has an effect on drug-resistant *H. pylori* infection has not been confirmed by animal experiments. Our study confirms that BXXX decoction (BXXXT) has good therapeutic effects on drug-resistant *H. pylori* infection through *in vivo* and *in vitro* experiments in mice, then the composition of BXXXT and effective components, the immunomodulatory effect, the main target were verified. We preliminarily explain why BXXXT has a good effects.

Citation: Li XH, Xu JY, Wang X, Liao LJ, Huang L, Huang YQ, Zhang ZF. BanXiaXieXin decoction treating gastritis mice with drug-resistant *Helicobacter pylori* and its mechanism. *World J Gastroenterol* 2023; 29(18): 2818-2835

URL: https://www.wjgnet.com/1007-9327/full/v29/i18/2818.htm

DOI: https://dx.doi.org/10.3748/wjg.v29.i18.2818

INTRODUCTION

Helicobacter pylori (*H. pylori*) is the main pathogen that causes a variety of upper digestive diseases[1], such as chronic gastritis, peptic ulcer, and gastric cancer[2]. At present, the treatment options for *H. pylori* infections include standard triple therapy, bismuth-containing quadruple therapy, and sequential therapy. The drug resistance rate of *H. pylori* is increasingly higher, and the eradication rate is increasingly lower. Clarithromycin-resistant *H. pylori* has been listed as a focus for the research and development of antibiotics by the World Health Organization in 2017. The antimicrobial resistance of *H. pylori* is an urgent global problem. Multiple antibiotic resistance existed in 16847 *H. pylori* strains

isolated in Wenzhou from 2013-2020. Separate statistics on the resistance rates of *H. pylori* to the six commonly used antibiotics revealed that the resistance rates to levofloxacin, clarithromycin and metronidazole were high in the region, respectively 32.81%, 26.02%, and 95.67%. Therefore, how to avoid, overcome and eradicate *H. pylori* and *H. pylori*' s drug resistance brings challenges to the current clinical work. In China, traditional Chinese medicine could be used to treat a variety of refractory diseases, reducing drug resistance and improving the eradication rate of *H. pylori*[3]. "BXXXT" comes from Zhang Zhongjing' s Treatise on Febrile Diseases, which consists of 15 g *Pinellia ternate*, 9 g *Radix scutellariae*, 9 g *Dried ginger*, 9 g *Ginseng*, 9 g *Roasted licorice*, 3 g *Coptis chinensis*, and 4 *Jujubes*. At present, experimental studies and clinical efficacy of this prescription have been reported for gastrointestinal dysfunction, peptic ulcer, chronic gastritis, atrophic gastritis and other digestive system diseases[4-6]. There are numerous studies at home and abroad on the efficacy of this prescription[7-9], and it has been confirmed that BXXXT demonstrates the effects of treating gastrointestinal diseases, inhibiting *H. pylori* and protecting gastric mucosa[10-12]. However, whether it has the same effect on the refractory gastritis caused by drug-resistant *H. pylori* remains unreported.

Therefore, the purpose of the present study is to further explore the therapeutic effects of BXXXT on drug-resistant *H. pylori* through establishing mouse models, and to study the molecular mechanism of BXXXT applied in the treatment of the refractory gastritis caused by drug-resistant *H. pylori* through ingredient analysis, immune regulation, identification of therapeutical targets, *etc*., so as to provide an experimental basis for improving the application efficiency and of this prescription worldwide.

MATERIALS AND METHODS

Strains and culture conditions

H. pylori strains (standard 26695, G27, NSH57, and multi-drug-resistant BHKS159 all provided by Professor Bi Hongkai of Nanjing Medical University) containing the preservation solution and stored at -80 °C, clinical strains HPBS001-HPBS016 that had been isolated by Huang Yanqiang Laboratory, Youjiang Medical College for Nationalities were used. The *H. pylori* strains were cultured in a Columbia (OXOID, United Kingdom) medium with 10% serum or a BHI (OXOID, United Kingdom) medium in a microaerobic environment (85% nitrogen, 5% oxygen, and 10% carbon dioxide) at 37 °C.

Experimental animals

SPF C57BL/6 mice aged six to eight weeks were purchased from Changsha Tianqin Biological Co., Ltd.; the number of SPF animal license: SYXK Gui 2017-0004; animal experiment ethics number: No. 2019112501.

Preparation of BXXXT aqueous extract

The prescription consists of 15 g *Pinellia ternate*, 9 g *Radix scutellariae*, 9 g *Dried ginger*, 9 g *Ginseng*, 9 g *Roasted licorice*, 3 g *Coptis chinensis*, and 4 g *Jujubes*. In the first round, the medical materials used to prepare BXXXT were crashed to crude powder that was placed in a beaker with sterile distilled water at a ratio of 1:10, soaked for 4 h, treated with diluted and boiled for 0.5 h with the liquid filtered out. In the second round, the filtered powder was treated with distilled water in a ratio of 1:5 and boiled for 20 min with the filtrate filtered out; in the third round, the filtered powder was treated following the same steps described in the second round but boiled for 5 min with the liquid filtered out. The liquids prepared during the three rounds were combined, concentrated to crude drug (1 g/mL), evaporated under atmospheric pressure, sterilized, and stored for later use.

Evaluation of MIC of BXXXT against H. pylori in vitro

A medium of BXXXT aqueous extract that had been diluted two-fold was prepared as the treatment group: BXXXT aqueous extract was mixed with BHI and diluted two-fold with berberine set as the positive drug control group. *H. pylori* cells were adjusted at OD^{600} = 0.03 (equivalent to 1.0 × 10^7 CFU/mL). Bacterial solution (100 μL, equivalent to 1.0 × 10^6 CFU/mL) was inoculated into a 96-well plate that contained medicated BHI and incubated at 37 °C for 48 h to determine the results with the lowest concentration of drugs that could inhibit *H. pylori* growth being minimum inhibitory concentration (MIC).

Detection of therapeutic effects of BXXXT aqueous extract on mice with drug-resistant H. pylori gastritis in vivo

BXXXT aqueous extract, amoxicillin (Sigma-Aldrich, Germany), clarithromycin (Sigma-Aldrich, Germany) and omeprazole (Sigma-Aldrich, Germany) were all dissolved and diluted to 10 mg/mL. C57BL/6 model mice (BHKS159) were divided into four groups: The omeprazole + amoxicillin + clarithromycin group (the dose was 138.2 mg/kg of omeprazole, 28.5 mg/kg of amoxicillin, and 14.3 mg/kg of clarithromycin), the omeprazole + BXXXT aqueous extract (28 mg/kg), the omeprazole + BXXXT aqueous extract (7 mg/kg) and the phosphate-buffered saline (PBS) group, with six mice in each group.

Mice were given administration once a day for three consecutive times. Two days after drug withdrawal, the blood was collected from the eyeballs of the mice. The mice were then sacrificed through cervical dislocation with tissues taken from their stomach and broken to acquire *H. pylori* that was then isolated, cultured, and identified with the amount of colonization calculated. Part of the stomach tissues was made into paraffin sections with HE staining, TUNEL immunohistochemistry and fluorescence immunoassay performed thereon.

Main pharmacodynamic components of BXXXT aqueous extract

This analysis was performed by Beijing Bio-Tech Pack Technology Company Ltd using a TripleTOF5600 + and an AB SCIEX™ with the ion source being ESI. The chromatographic column was SHIMADZU InerSustain C18 (100.0 mm × 2.1 mm, 2 μm) with the column temperature being 35 °C and flow rate of 0.300 (mL/min). The mobile phase: (1) Equate = "acetonitrile"; and (2) equate = "0.1% CH3COOH-H2O". The chromatographic conditions were shown in Table 1. The scanning range of mass spectrometry conditions was m/z 100-1500. The scanning mode: DIA. Capillary voltage: 5000 V (positive) and 4500 V (negative). Capillary Temp: 500 °C, DP 60 V, CE 35 V, and CES 15 V.

Synergistic antimicrobial effects of main pharmacodynamic components of BXXXT aqueous extract

According to the protocols of the checkerboard method, drug A in the first row and drug B in the first column were diluted two-fold respectively. Then the transverse and longitudinal drugs were also cross-diluted two-fold and treated with 100 μL bacterial suspension, with the optimal combination effect selected to calculate the antimicrobial concentration index (FICI) after culture for 48 h. FICI= MIC of A drugs used in combination/MIC of A drugs used alone + MIC of B drugs used in combination/MIC of B drugs used alone. Criteria: synergistic effects (FICI ≤ 0.5); additive effect (0.5 < FICI ≤ 1.0); no effect (1.0 < FICI ≤ 2.0); antagonistic effects (FICI > 2.0).

Immunobactericidal effects of BXXXT aqueous extract

During the process of testing the efficacy of BXXXT aqueous extract described previously in section 1.5, the peripheral blood of mice before and after administration was collected and cells thereof were treated with anticoagulant and then with 50 μL antibody mixtures: CD3, CD4, and CD8, *etc*. After the membranes were fixed and broken, the cells were treated with 100 μL antibody mixtures: IFN and IL-4. After filtration, the expressions of immune cells and cytokines were detected using a flow cytometry.

Effect mechanism of BXXXT aqueous extract on H. pylori

BHKS159 bacteria were cultured on a Columbia plate overnight. Thereafter, the single colony was selected and diluted to 0.5 Mcfarland standard (MCF) with 2 μL taken and added to 5 mL BXXXT aqueous extract (1/2 MIC, prepared by being treated with BHI). The negative control group was induced with PBS, shaken at 37 °C and centrifuged to collect the bacteria solutions after it had been treated with the aqueous extract for 4 h and 8 h. The bacteria solutions were delivered to Nanjing Medical University where they were observed under a transmissive electron microscope. *H. pylori* cells were treated with BXXXT aqueous extract at the half inhibitory concentration that had been detected before for 8 h, after which the samples were collected and frozen in liquid nitrogen for 10 min, frozen with dry ice and delivered to Beijing Allwegene Technology Co., Ltd. for detection and analysis of transcriptome and proteome. The transcriptome analysis was performed using the Illumina PE150 sequencing strategy; the length of RNA fragments was detected using Agilent 2100; the alignment and transcript assembly analysis were performed using Boetie2 and the Rockhhoper software; quantitative protein analysis was performed using the ITRAQ labeling quantitative strategy, ITRAQ/TMT labeling performed using isoheavy isotope labeling, and the quantitative detection of target genes performed using a fluorescent polymerase chain reaction (PCR) instrument and Western blotting. Strains with low expressions of related target genes were used to verify MIC changes and mutant strains were constructed with reference to the protocols described in the previous studies[13]. The relevant mRNA amplification primers are shown in Table 2, and the relevant antibody information is displayed in Table 3.

Statistical analysis

Statistical analysis and mapping were performed using the Graphpad Prism software, version 8.0. Continuous data were expressed as mean ± SD. Differences between groups were analyzed using the one-way ANOVA. $P < 0.05$ was considered statistically significant.

RESULTS

The MIC of BXXXT aqueous extract on H. pylori detected in vitro

The MICs of BXXXT aqueous extract on three sensitive *H. pylori* strains and 11 drug-resistant *H. pylori* strains were detected by applying the solid plate method. BXXXT aqueous extract was found to have

Table 1 Chromatographic conditions

Time (min)	Parameter
0	A: 0%, B: 100%
10	A: 50%, B: 50%
13	A: 95%, B: 5%
14	A: 0%, B: 100%
15	A: 0%, B: 100%

Table 2 Primer information

No.	Primer	Sequence (5' to 3')	Company
1	UREA F	GCCAATGGTAAATTAGTT	Shanghai Invitrogen Biotech Co., Lt
2	UREA R	CTCCTTAATTGTTTTTAC	
3	UREB F	TCTATCCCTACCCCACAACC	
4	UREB R	CCATCCACGAACACATGGTA	
5	CagA F	ACCCCTAGTCGGTAATG	
6	CagA R	GCTTTAGCTTCTGATACTGC	
7	VacA F	GTCAGCATCACACCGCAAC	
8	VacA R	CTGCTTGAATGCGCCAAAC	
9	16sRNA F	CTGGAGAGACTAAGCCCTCC	
10	16sRNA R	AGGATCAAGGTTTAAGGATT	

Table 3 Antibody information

Name	Art. No.	Company
CagA (A-10)	sc-32746	Santa Cruz
VacA	sc-28368	Santa Cruz
m-IgGk BP-HRP	sc-516102	Santa Cruz
GAPDH Ab	AF7021	Affinity Biosciences
Goat anti-rabbit IgG (H+L) HPR	S0001	Affinity Biosciences

antibacterial effects on strains, both resistant and sensitive (the MIC was 256-512 μg/mL). The antibacterial effect of BXXXT aqueous extract was compared with that of berberine (the MIC was 512-2048 μg/mL), as shown in Table 4. The results suggested that there was a two-to-four-fold difference between them and that BXXXT aqueous extract produced better antibacterial effects than 98% pure berberine. The reason might be that although berberine accounts for a small portion of the prescription, there might be other antibacterial components, or there might be synergistic or additive effects among these components.

Therapeutic effects of BXXXT aqueous extract were detected in vivo on mice with H. pylori-resistant acute gastritis

Model mice with acute gastritis caused by the drug-resistant strain BHKS159 were constructed and treated with PBS, omeprazole (OPZ) + amoxicillin clarithromycin (AC), OPZ + BXXXT (28 mg/kg) and OPZ + BXXXT (7 mg/kg), respectively. Although *H. pylori* colonization, inflammatory factors IL-1β, IL-6 and tumor necrosis factor-alpha (TNF-α), inflammatory damage, and apoptosis factors Bcl-2 and Bax were improved in OPZ + AC treatment group, there were still significant differences compared with OPZ + BXXXT (28 mg/kg) treatment group. After OPZ + BXXXT (28 mg/kg) treatment, the mice could basically recover to the normal level, implying therapeutical effects significantly better than that of the triple group (Figure 1). However, amoxicillin which does not develop drug resistance, produced therapeutical effects that contributed to the improvement in the OPZ + AC treatment group when

Table 4 Minimum inhibitory concentration of Banxia Xiexin decoction aqueous extract against *Helicobacter pylori* (μg/mL)

Strain	Drug-resistanct strain	BXXXT aqueous extract	Berberine
26695	Sensitive	512	1024
G27	Sensitive	512	1024
NSH57	Sensitive	256	512
BHKS159	Resistant to levofloxacin, clarithromycin and metronidazole	512	1024
HPBS001	Resistant to levofloxacin, clarithromycin and metronidazole	512	1024
HPBS002	Resistant to metronidazole	512	1024
HPBS003	Resistant to clarithromycin	512	1024
HPBS004	Resistant to levofloxacin	512	1024
HPBS005	Resistant to levofloxacin and metronidazole	256	1024
HPBS006	Resistant to clarithromycin and metronidazole	256	1024
HPBS007	Resistant to clarithromycin	512	1024
HPBS010	Resistant to metronidazole, clarithromycin and levofloxacin	512	2048
HPBS011	Resistant to metronidazole and clarithromycin	512	1024
HPBS013	Resistant to metronidazole, clarithromycin and levofloxacin	512	1024
HPBS014	Resistant to metronidazole, clarithromycin, amoxicillin and levofloxacin	512	1024

BXXXT: Banxia Xiexin decoction. The minimum inhibitory concentrations of the drugs for sensitive and drug-resistant strains are amoxicillin ≥ 0.5 μg/mL, clarithromycin ≥ 1.0 μg/mL, levofloxacin ≥ 2.0 μg/mL, and metronidazole ≥ 8.0 μg/mL.

combined with omeprazole. BXXXT, which did not demonstrate good effects *in vitro*, produced obvious therapeutical effects *in vivo*, which might be related to the synergistic and immunomodulatory effects of BXXXT aqueous extract.

Main pharmacodynamic components of BXXXT aqueous extract

MS-DIAL 3.70 (MS-DIAL: Data independent MS/MS deconvolution for comprehensive metabolome analysis) (Nature Methods, 12, 523-526, 2015).The original LC-MS data of BXXXT aqueous extract were imported into MS-DIAL, version 3.70 for preprocessing (MS-DIAL: Data independent MS/MS deconvolution for comprehensive metabolome analysis) (Nature Methods, 12, 523-526, 2015), including peak value extraction, noise-removal, deconvolution and peak alignment, and thereafter the three-dimensional data matrix in comma-separated values format was derived (original data matrix). The peak information extracted was compared with the database, with the full database search of MassBank, Respect and GNPS (14951 records in total). About 428 monomer components were identified, among which, as the related literature suggests, there were a total of 78 major components related to *H. pylori* resistance. Eleven species including berberine, emodin, baicalin, quercetin have been widely reported and demonstrate good antibacterial effects. Their ion additions and molecular structure are displayed in Table 5. It could be suggested that among the components of BXXXT aqueous extract, in addition to berberine, other components such as emodin also have inhibitory effects, which provides experimental basis for the better antibacterial effects *in vitro* BXXXT aqueous extract could produce compared with berberine.

Synergistic antimicrobial effects of main pharmacodynamic components of BXXXT aqueous extract

Six groups of berberine and emodin, berberine and luteolin, luteolin and gallic acid, luteolin and rosmarinic acid, catechuic acid and quercetin, catechuic acid and emodin were selected from 12 main anti-HP components of water extract of BXXXT aqueous extract for combined drug sensitivity detection. The results suggested that the six groups demonstrated additive or synergistic effects on *H. pylori* (Table 6), berberine and emodin, luteolin and gallic acid in particular producing better synergistic effects. Similar effects might also be found in other component combinations that had not been verified, which provides further experimental evidence that BXXXT aqueous extract could produce better antibacterial effects *in vitro* than berberine.

Immunobactericidal effects of BXXXT aqueous extract on mice

The *t*-test was used to analyze the proportion of $CD3^+$ T, $CD4^+$ T, and $CD8^+$ T cells in total lymphocytes

Table 5 Information of main pharmacodynamic components of Banxia Xiexin decoction aqueous extract

Name	Molecular structural formula
Berberine	COC1=C(OC)C2=C[N+]3=C(C=C2C=C1)C1=CC2=C(OCO2)C=C1CC3
Baicalin	C1=CC=C(C=C1)C2=CC(=O)C3=C(C(=C(C=C3O2)O[C@H]4[C@@H]([C@H]([C@@H]([C@H](O4)C(=O)O)O)O)O)O)O
Luteolin	OC1=CC(O)=C2C(=O)C=C(OC2=C1)C1=CC(O)=C(O)C=C1
Gallic acid	OC(=O)C1=CC(O)=C(O)C(O)=C1
Gingerol	CCCCCC(O)CC(=O)CCC1=CC(OC)=C(O)C=C1
Wogonoside	COC1=C(O)C=C(O)C2=C1OC(=CC2=O)C1=CC=CC=C1
Rosmarinic acid	OC(=O)[C@H](CC1=CC(O)=C(O)C=C1)OC(=O)\C=C\C1=CC(O)=C(O)C=C1
Aloe-emodin	OCC1=CC2=C(C(O)=C1)C(=O)C1=C(C=CC=C1O)C2=O
Catechin	CCCCCC(CC(=O)CCC1=CC(=C(C=C1)O)OC)O
Naringenin	OC1=CC=C(C=C1)[C@@H]1CC(=O)C2=C(O)C=C(O)C=C2O1
Quercetin	OC1=CC(O)=C2C(OC(=C(O)C2=O)C2=CC(O)=C(O)C=C2)=C1

before and after administration. After administration, the proportion of $CD3^+$ T and $CD4^+$ T in total lymphocytes increased ($P1 = 0.0009$, $P2 = 0.0115$), as shown in Figure 2A-F; no significant difference was found between $CD8^+$ T cells and TH1 cells ($P3 = 0.1937$, $P4 = 0.8061$), Figure 2A, C, D, and G, and the ratio of $CD4^+$ T/$CD8^+$ T cells was increased ($P5 = 0.0280$) as displayed in Figure 2H. These results indicated that BXXXT aqueous extract could improve the ratio of lymphocytes $CD3^+$ T and $CD4^+$ T to the total number of lymphocytes and the ratio of $CD4^+$ T/$CD8^+$ T cells. However, BXXXT aqueous extract could enhance immune functions, thus helping improve the immunity and antibacterial ability of the body, which might explain why BXXXT could produce better treatment effects *in vivo*.

Mechanism of action of BXXXT aqueous extract on H. pylori

No significant changes were found at × 10000 magnification on the morphological structures of *H. pylori* after 4 h and 8 h of BXXXT treatment (Figure 3A), indicating that BXXXT did not produce antibacterial effects by directly destroying morphological structures. In the samples treated with BXXXT for 8 h, a total of 357 differentially expressed genes were detected after transcriptome analysis, among which 133 genes were up-regulated and 224 genes down-regulated (Figure 3B), mainly concentrating in five metabolic pathways including metabolic pathways, the epithelial cell signaling in *H. pylori* infection and the microbial metabolism in diverse environments (Figure 3C). The epithelial cell signaling in *H. pylori* infection pathway suggested that it is closely related to urease genes and virulence genes, as shown in Figure 3D. The proteome detection found 86 differentially expressed genes, among which 44 were up-regulated and 42 down-regulated (Figure 3E), mainly concentrating in oxidoreductases and transferases pathways (Figure 3F). Among the related genes and proteins found in transcriptome and proteome, respectively, and concentrating in the main pathways, five possible proteins of BXXXT were screened, among which four were urease-related and one was related to the virulence gene *CagA* (Table 7). The quantitative PCR (Q-PCR) and Western blot detection were performed to confirm the correlation between BXXXT action and virulence genes and urease genes. The results suggested that the mRNAs and protein expressions of *CagA* and *VacA* after BXXXT treatment were significantly decreased (Figure 4A-D), providing additional evidence for the obvious effects of BXXXT *in vivo* from the point that BXXXT could reduce virulence of *H. pylori*. The gene *CFAs* related to environmental regulation, urease and drug resistance was mutated (Figure 4E), after which the MIC of the mutant strains increased 2-4 times (Figure 4F), further proving that the urease-related gene *CFAs* might be one of the main targets of BXXXT. However, the decrease of urease could affect the adaptive regulation of stomach acid for which *H. pylori*' s ability to colonize would be significantly reduced.

DISCUSSION

There are about 4.4 billion people with *H. pylori* infections worldwide, with an average infection rate of 62.8%. Southeast Asia could be considered as high-incidence areas, mainly China, Japan, and South Korea[14,15]. The eradication of *H. pylori* has proven to prevent gastric cancer. However, the overuse of antibiotics leads to serious drug resistance. The drug resistance rate varies in different countries and regions and will change over time, indicated by those of clarithromycin, metronidazole, and levloxacin, all increasing over time. For example, the drug resistance rate of clarithromycin rose to 21% between 2012 and 2016[16-18]. Therefore, the failure rate of treating *H. pylori* infectious diseases is increasing,

Table 6 Minimum inhibitory concentrations of main antibacterial components in Banxia Xiexin decoction aqueous extract (μg/mL)

Strain	MIC of drugs used alone		MIC of drugs used in combinations		FIC	Effect
	Berberine	Emodin	Berberine	Emodin		
G27	1024	512	256	256	0.75	Addictive
26695	1024	512	256	128	0.50	Synergistic
BHKS159	1024	512	256	128	0.50	Synergistic
	Berberine	Luteolin	Berberine	Berberine		
G27	1024	1024	512	512	1.00	Addictive
26695	1024	1024	512	256	0.75	Addictive
BHKS159	1024	1024	512	512	1.00	Addictive
	Luteolin	Gallic acid	Luteolin	Gallic acid		
G27	1024	1024	256	256	0.50	Synergistic
26695	1024	1024	256	256	0.50	Synergistic
BHKS159	1024	1024	256	256	0.50	Synergistic
	Luteolin	Rosmarinic acid	Luteolin	Rosmarinic acid		
G27	1024	1024	512	256	0.75	Addictive
26695	1024	1024	512	512	1.00	Addictive
BHKS159	1024	1024	512	256	0.75	Addictive
	Catechuic acid	Quercetin	Catechuic acid	Quercetin		
G27	1024	1024	512	256	0.75	Addictive
26695	1024	1024	512	256	0.75	Addictive
BHKS159	1024	1024	512	256	0.75	Addictive
	Catechuic acid	Emodin	Catechuic acid	Emodin		
G27	1024	512	512	256	1.00	Addictive
26695	1024	512	512	256	1.00	Addictive
BHKS159	1024	512	256	256	0.75	Addictive

MIC: Minimum inhibitory concentration.

leading to an urgent need to study and develop anti-*H. pylori* drugs. In 2018, Hu *et al*[19] from Peking University proposed that non-antibiotic drugs such as traditional Chinese medicine, mucosal protective agents and probiotics could be used to treat *H. pylori* infection. Traditional Chinese medicine, including BXXXT, has a good effect on *H. pylori* infection and *H. pylori*-infection-related diseases[20,21]. However, its pharmacological mechanism remains unclear, and whether it has an effect on drug-resistant *H. pylori* infection or not has not been confirmed by animal experiments.

This study confirms that BXXXT has good therapeutic effects on drug-resistant *H. pylori* infection through *in vivo* and *in vitro* experiments in mice, which provides an experimental basis for elaborating that BXXXT could treat refractory gastritis caused by drug-resistant bacteria. While the efficacy of BXXXT is well established, explaining its mechanism is difficult. Traditional Chinese medicine, especially compound prescriptions, has complex components and a very complex mechanism of action in the body, which might be affected by multiple factors, especially those in stomach. Besides, it produces effects that are multi-target. As the content of the main components of the prescription is not high, the effects on the target may not always appear[22-24], which makes it difficult to elaborate on the mechanism of action. In the present study, the composition of BXXXT was analyzed, the effective anti-HP components were screened out with reference to the related literature and reports, the material basis of the efficacy was identified, and the synergistic effects among some of the effective components was verified. It was found that most of the components had additive or synergistic effects, such as berberine and emodin, luteolin and gallic acid. This indicated that though only accounting for a small portion, the active components of the Chinese medicine prescription, which could produce synergistic or additive effects demonstrated better antibacterial effects. The MIC of BXXXT against *H. pylori* is 256-512 μg/mL, much worse than that of clinical antibiotics but producing better therapeutical effects *in vivo*, especially

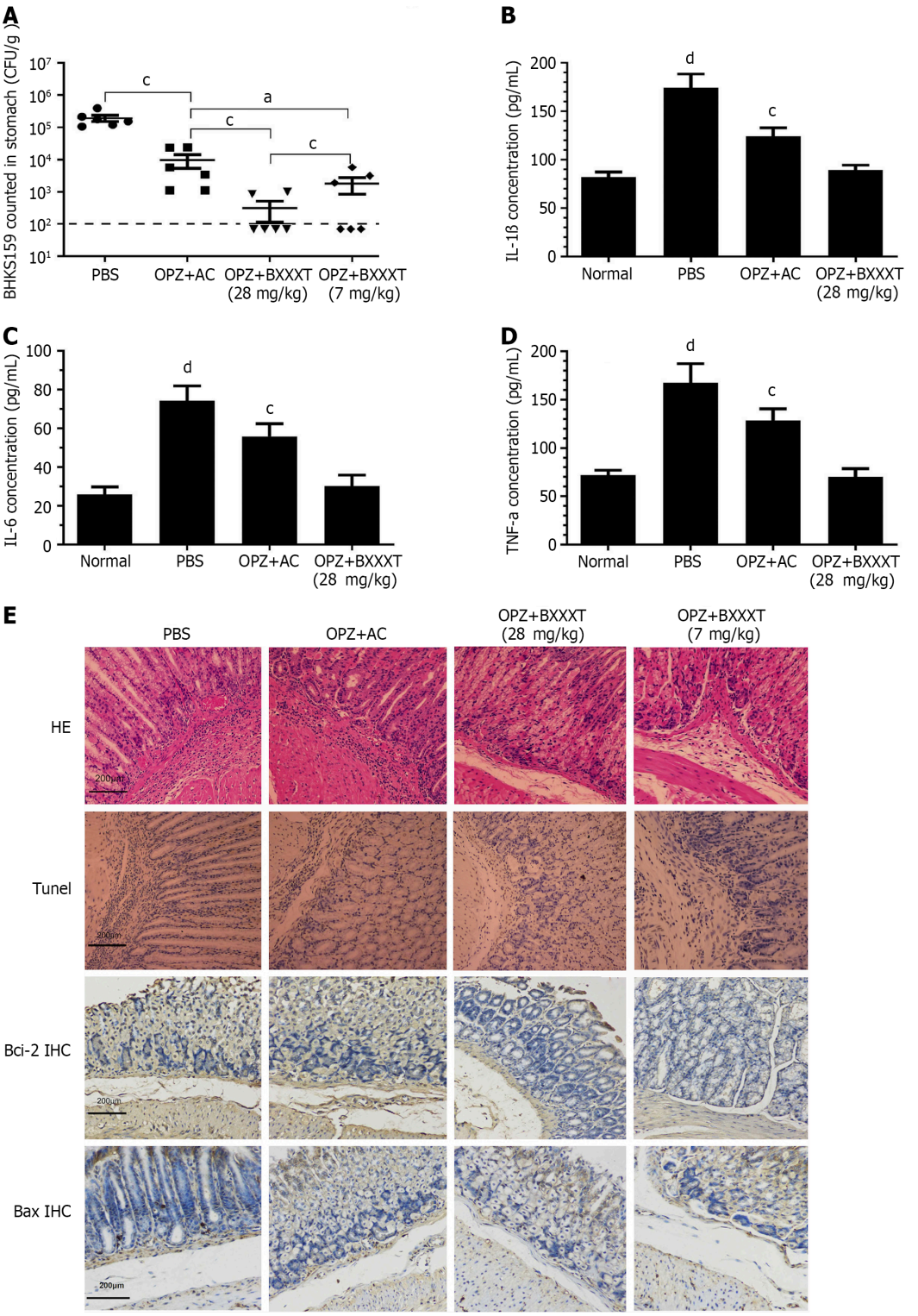
Table 7 Information of related proteins identified by transcriptome analysis after Banxia Xiexin decoction treatment

Uniprot Accession Number	Protein name	Protein amino acid sequence	*P* value	Reliability
E6NPU2	Urease subunit alpha OS = *Helicobacter pylori* (strain F57), OX = 866346, GN = urea, PE = 3, SV = 1	MKLTPKELDKLMLHYAGELARKRKEKGIKLNYVEAVALISAHIMEEARAGKKSAAEL MQEGRTLLKPDDVMDGVASMIHEVGIEAMFPDGTKLVTVHTPIESNGKLVPGELFLK NEDITINEGKKAVSVKVKNVGDRPVQIGSHFHFFEVNRCLDFDREKTFGKRLDIASGT AVRFEPGEEKSVELIDIGGNRRIFGFNALVDRQADNESKKIALHRAKERGFHGAKSDD NYVKTIKE	0.001211988	High
A0A2A6SFH9	Urease (fragment) OS = *Helicobacter pylori*, OX = 210, GN = BB479_08100, PE = 4, SV = 1	MKLTPKELDKLMLHYAGELARKRKEKGIKLNYVEAVALIXAHIMEEARAGKKTAAEL MQEGRTLLKPDDVMDGVASMIHEVGIEAMFPDGTKLVTVHTXIEANGKLVPGELFLKN EDITINEGKKAVSVKVKNVGDRPVQIGSH	0.033815784	High
A0A0L0QH58	Urease subunit alpha OS = *Helicobacter pylori*, OX = 210, GN = urea, PE = 3, SV = 1	MKLTPKELDKLMLHYAGELAKKRKEKGIKLNYVEAVALISAHIMEEARAGKKSAAEL MQEGRTLLKPDDVMDGVASMIHEVGIEAMFPDGTKLVTVHTPIEANGKLVPGELFLKN EDITINEGKKAVSVKVKNVGDRPVQIGSHFHFFEVNRCLDFDREKTFGKRLDIASGTAV RFEPGEEKSVELIDIGGNRRIFGFNALVDRQADNESKKIALHRAKERGFHGAKSDDNY VKTIKE	0.033744196	High
N4TND2	Urease accessory protein UreG OS = *Helicobacter pylori* Hp A-11, OX = 992035, GN = ureG, PE = 3, SV = 1	MVKIGVCGPVGSGKTALIEALTRHMSKDYDMAVITNDIYTKEDAEFMCKNSVMPRER IIGVETGGCPHTAIREDASMNLEAVEEMHGRFPNLELLLIESGGDNLSATFNPELADFTIF VIDVAEGDKIPRKGGPGITRSDLLVINKIDLAPYVGADLKVMERDSKKMRGEKPFIFTNIR AKEGLNDVIAWIKRNALLED	0.016839824	High
Q8RRP6	Cytotoxin associated protein CagA (Fragment), OS = *Helicobacter pylori*, OX = 210, GN = cagA, PE = 4, SV = 1	ALADLKNFSKEQLAQQAQKNESFNAGKKFEFSQSVRNGVNGTLVGNGFSQAEATTL SKNFSDIKKELNAKLGNFNNNNINGLKNSTEPIYAKVNKKETGQAASPEEPIYTQVAKKVN AKIDRLNQIASGLGVVGQAAGFPLKRHDKVDDLSKVGRSVSPEPIYATIDDLGGPFPLKRH DKVDNLSKVGRSVSPEPIYATIDDLGGPFPLKRHDKVDNLSKVGLSRNQELTQKIDNLSQA VSEAKAGFFGNLEQTIDKLKDSTKHNVVNLWAESAKKVPASLSAKLDNYA	0.03652953	High

for drug-resistant *H. pylori*, why?

H. pylori can adhere to the gastrointestinal mucosa, produce virulence factors, damage gastric epithelial cells, and induce, control and regulate inflammatory responses. CagA encodes variety of proteins, including CagA and VacA, *ect*[25]. Karbalaei *et al*[26] found that *CagA* and *VacA* genes were potentially associated with resistance to clarithromycin, metronidazole, amoxicillin, tetracycline and levofloxacin. The VacA can not only destroy mitochondria[27,28], but also reduce the proliferation of T cells, B cells, and the other immune cells, and affect the immune response[29-31]. Among the components of BXXXT, Gingerol, a crude extract containing gingerol, is able to can inhibit the growth of *H. pylori* strains (MIC range is 0.78 μg/mL to 12.5 μg/mL) and has significant activity against $CagA^+$ strains[32]. Kaempferol is able to reduce the transcription of subunit protein A by the type IV secretory system, reduce the expression of pro-inflammatory cytokines (TNF-α, IL-1β) and IL-8 production in cells [33]. Urease can increase the pH value of the stomach and provide a suitable environment for *H. pylori* colonization. Palmatine in Coptis coptitis can act on sulfhydryl at the active site of urease and inhibit the conformational change of the urease molecules, and reduce urease activity[34]. Hesperidin can reduce the expression of UreA and UreB[35].

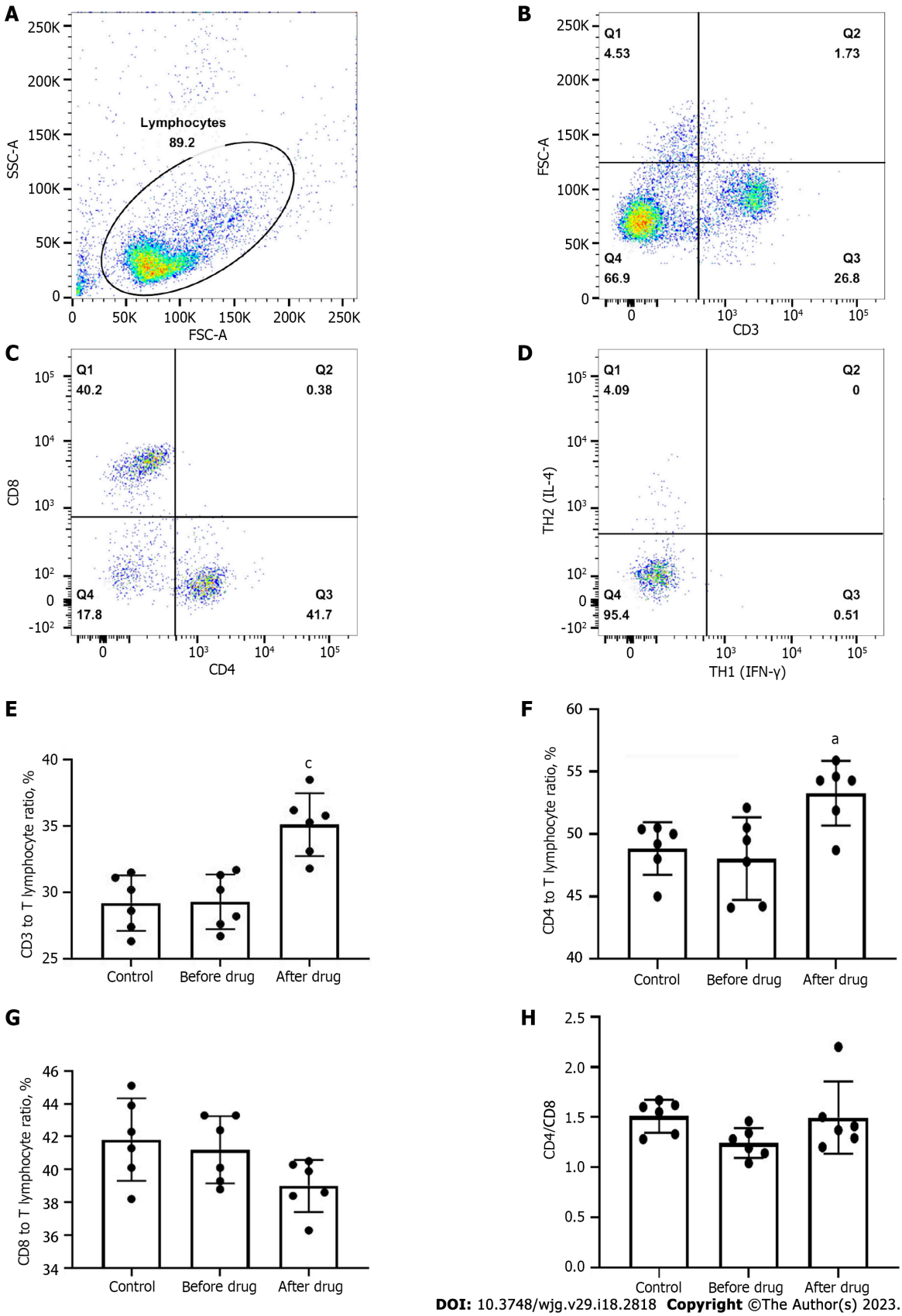
In the present paper, the immunomodulatory effect of BXXXT was analyzed, and it was found that it could up-regulate the expressions of immune factors such as $CD4^+$ T and enhance immunity and the ability of sterilization; the main target of BXXXT was urease-related gene *CFAs*, which was related to the virulence factors *CagA* and *VacA*. When urease was destroyed, *H. pylori* cells could not survive in the gastric acid environment, and its colonization ability would be significantly weakened. With low expressions of *H. pylori* virulence factors, the inflammatory damage caused by *H. pylori* to gastric mucosa would be reduced. The effects of these three aspects could preliminarily explain why BXXXT has good effects *in vivo*. However, clarifying the action mechanism of BXXXT is very complicated and difficult, for there are many components of BXXXT, among which many are anti-*H. pylori*, the



DOI: 10.3748/wjg.v29.i18.2818 **Copyright** ©The Author(s) 2023.

Figure 1 Therapeutic effects of BanXiaXieXin decoction aqueous extract on mice with *Helicobacter pylori*-resistant acute gastritis. A: The amount of *Helicobacter pylori* colonization in model mice infected with drug-resistant strains; B: The expression of inflammatory factor IL-1β in model mice; C: The expression of inflammatory factor IL-6 in model mice; D: The expression of inflammatory factor tumor necrosis factor-alpha in model mice; E: The gastric mucosa injury and the expressions of apoptotic genes Bcl-2 and Bax, × 200. $^{a}P < 0.05$; $^{b}P < 0.01$; $^{c}P < 0.001$; OPZ: Omeprazole; AC: Amoxicillin clarithromycin; PBS: Phosphate-buffered saline.

transcriptome and proteome analyses in this study also suggested that many membrane transporter genes were involved, such as ABC transporter, *etc*. Besides, we also found that berberine and other components of BXXXT could inhibit *HefA* gene to reverse drug resistance[25] and *CFAs* in this study might also be related to drug resistance[36,37]. Therefore, the action mechanism of BXXXT will be further studied.

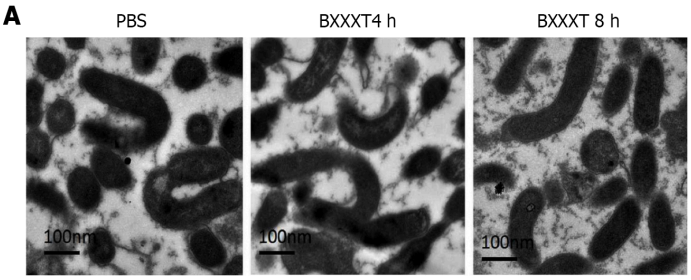


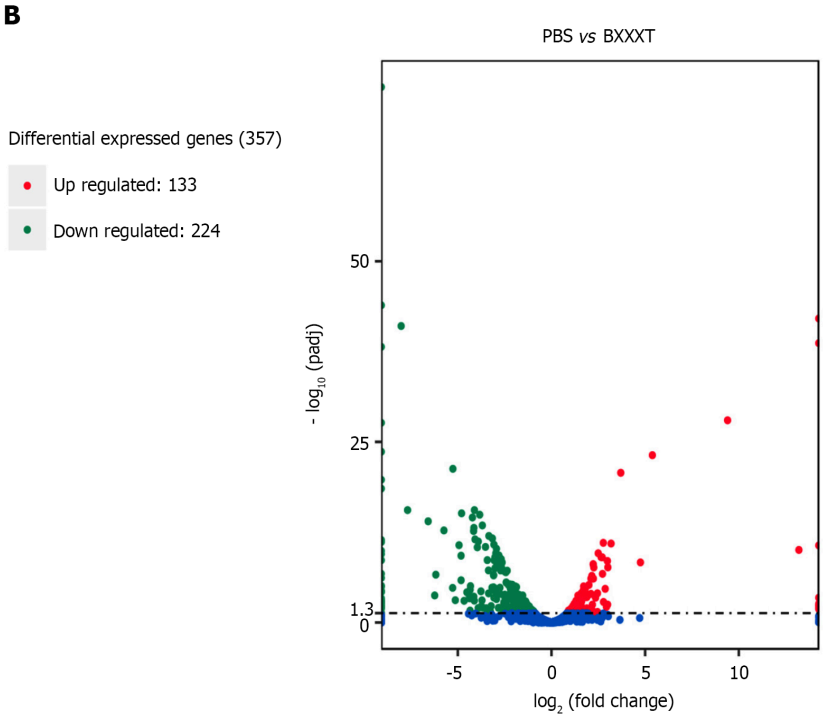
DOI: 10.3748/wjg.v29.i18.2818 **Copyright** ©The Author(s) 2023.

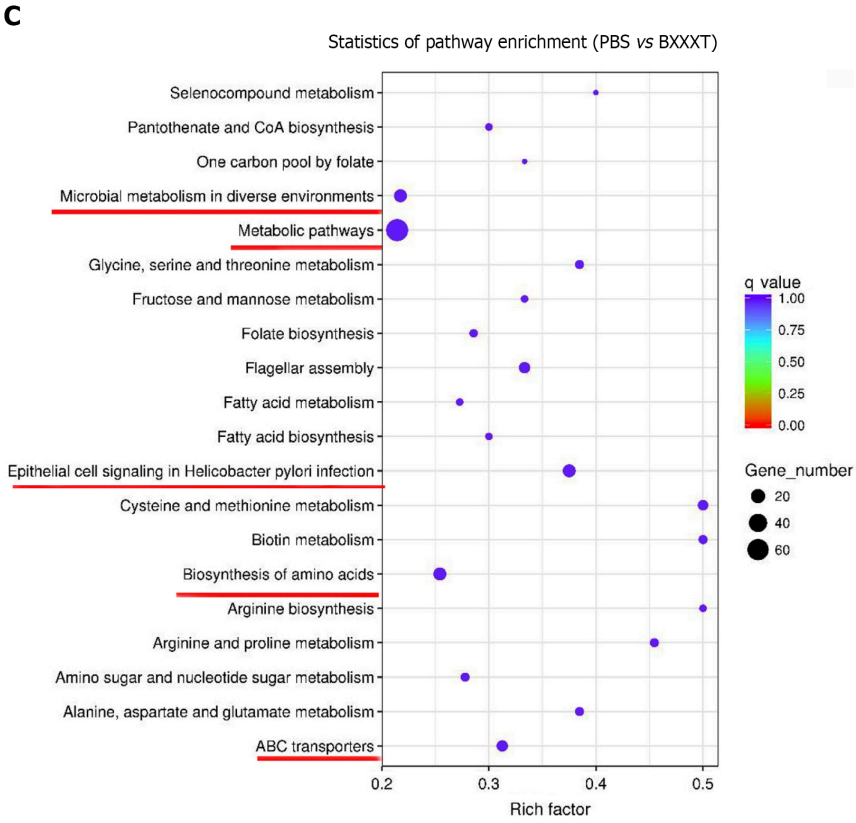
Figure 2 Immunobactericidal effects of BanXiaXieXin decoction aqueous extract on mice. A: Lymphocyte expression; B: CD3T cell expression; C: CD4T and CD8T cell expression; D: TH1 and TH2 expression; E: CD3T to lymphocyte ratio; F: CD4T to lymphocyte ratio; G: CD8T to lymphocyte ratio; H: CD4T /CD8T ratio. $^{a}P < 0.05$; $^{b}P < 0.01$; $^{c}P < 0.001$.

CONCLUSION

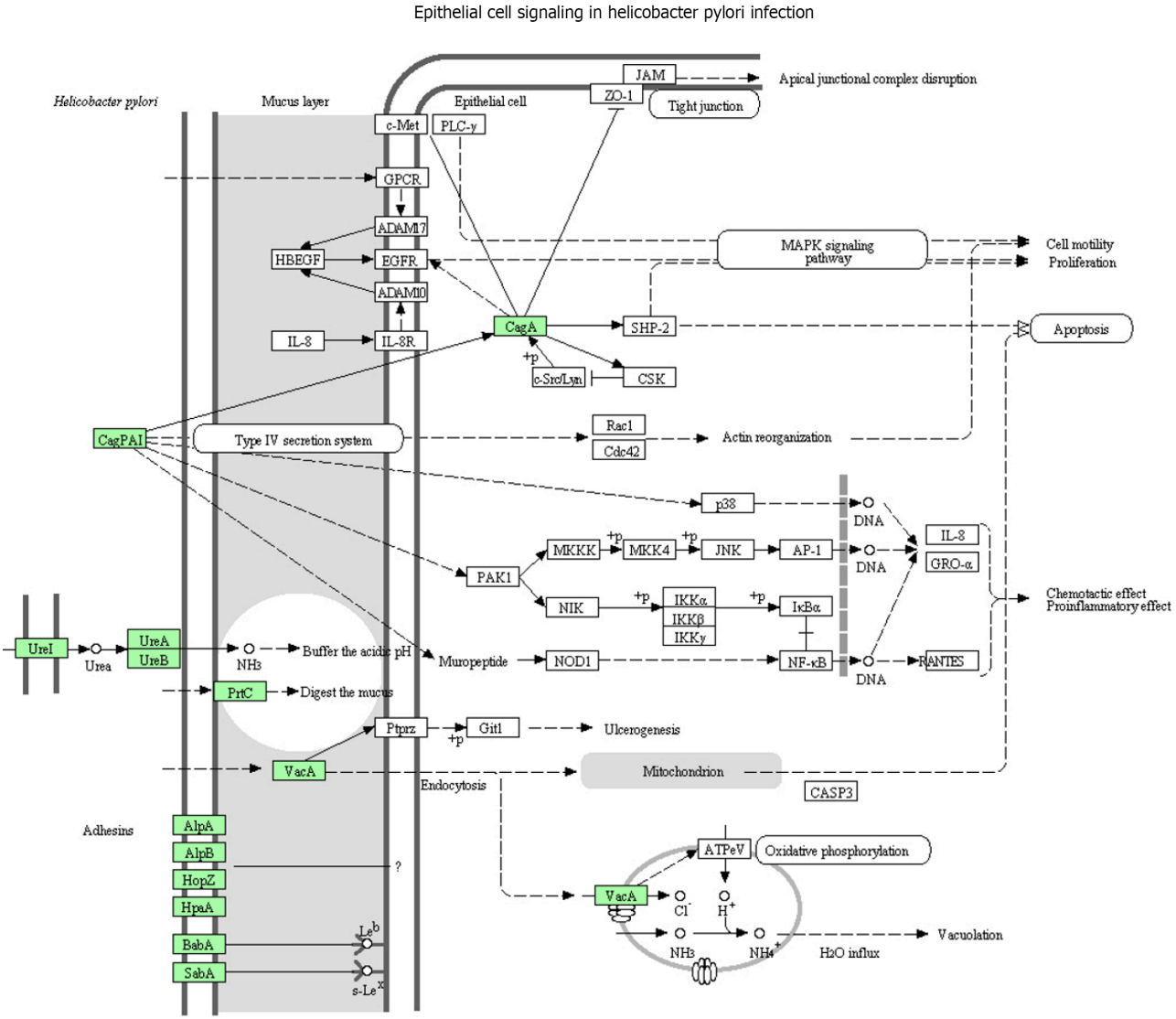
BXXXT aqueous extract could demonstrate good therapeutic effects on drug-resistance *H. pylori in vitro*


A
PBS
BXXXT4 h
BXXXT 8 h
100nm
100nm
100nm

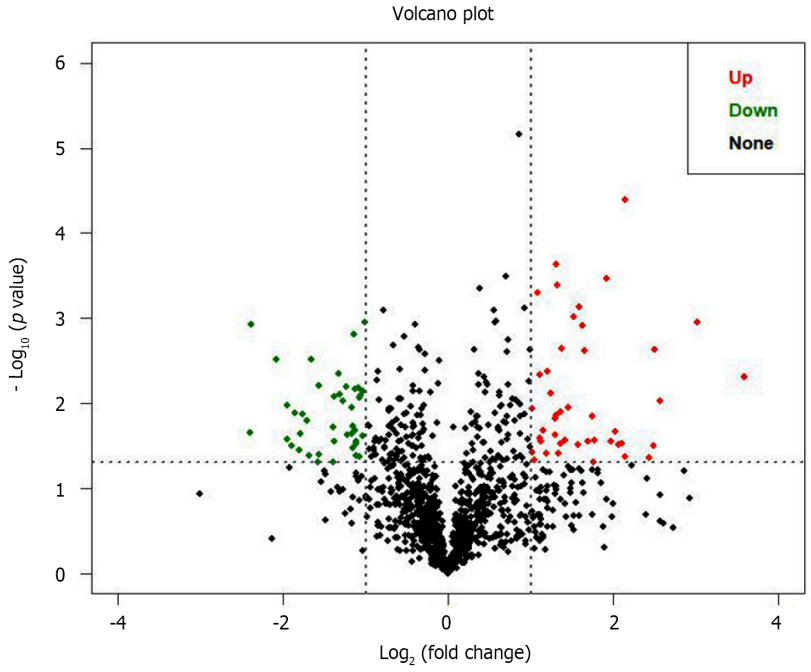

B
PBS *vs* BXXXT
Differential expressed genes (357)
Up regulated: 133
Down regulated: 224
50
25
1.3
0
- log10 (padj)
-5
0
5
10
log2 (fold change)

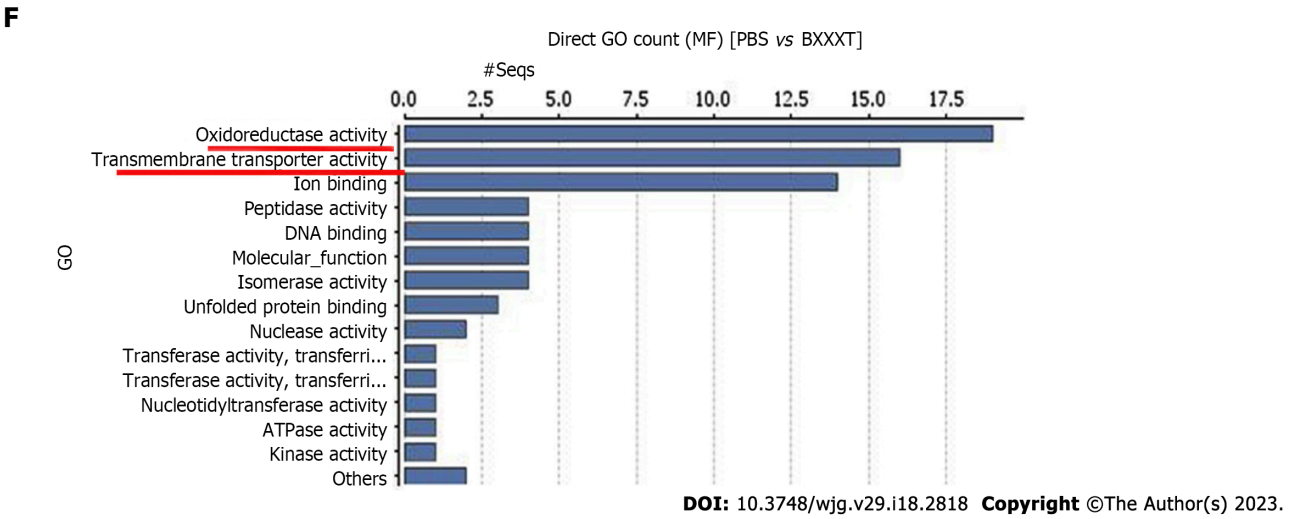

C
Statistics of pathway enrichment (PBS *vs* BXXXT)
Selenocompound metabolism
Pantothenate and CoA biosynthesis
One carbon pool by folate
Microbial metabolism in diverse environments
Metabolic pathways
Glycine, serine and threonine metabolism
Fructose and mannose metabolism
Folate biosynthesis
Flagellar assembly
Fatty acid metabolism
Fatty acid biosynthesis
Epithelial cell signaling in Helicobacter pylori infection
Cysteine and methionine metabolism
Biotin metabolism
Biosynthesis of amino acids
Arginine biosynthesis
Arginine and proline metabolism
Amino sugar and nucleotide sugar metabolism
Alanine, aspartate and glutamate metabolism
ABC transporters
0.2
0.3
0.4
0.5
Rich factor
q value
1.00
0.75
0.50
0.25
0.00
Gene_number
20
40
60

D


Epithelial cell signaling in helicobacter pylori infection
Helicobacter pylori
Mucus layer
Epithelial cell
JAM
ZO-1
Tight junction
Apical junctional complex disruption
c-Met
PLC-γ
GPCR
ADAM17
HBEGF
EGFR
ADAM10
MAPK signaling pathway
Cell motility
Proliferation
IL-8
IL-8R
CagA
SHP-2
Apoptosis
+p
c-Src/Lyn
CSK
CagPAI
Type IV secretion system
Rac1
Cdc42
Actin reorganization
p38
DNA
MKKK
MKK4
JNK
AP-1
IL-8
GRO-α
PAK1
NIK
IKKα
IKKβ
IKKγ
IκBα
Chemotactic effect
Proinflammatory effect
UreI
Urea
UreA
UreB
NH3
Buffer the acidic pH
Muropeptide
NOD1
NF-κB
RANTES
PrtC
Digest the mucus
Ptprz
Git1
Ulcerogenesis
VacA
Endocytosis
Mitochondrion
CASP3
Adhesins
AlpA
AlpB
HopZ
HpaA
BabA
SabA
?
Le^b
s-Le^x
ATPeV
Oxidative phosphorylation
Cl^-
H^+
NH3
NH4^+
H2O influx
Vacuolation

E

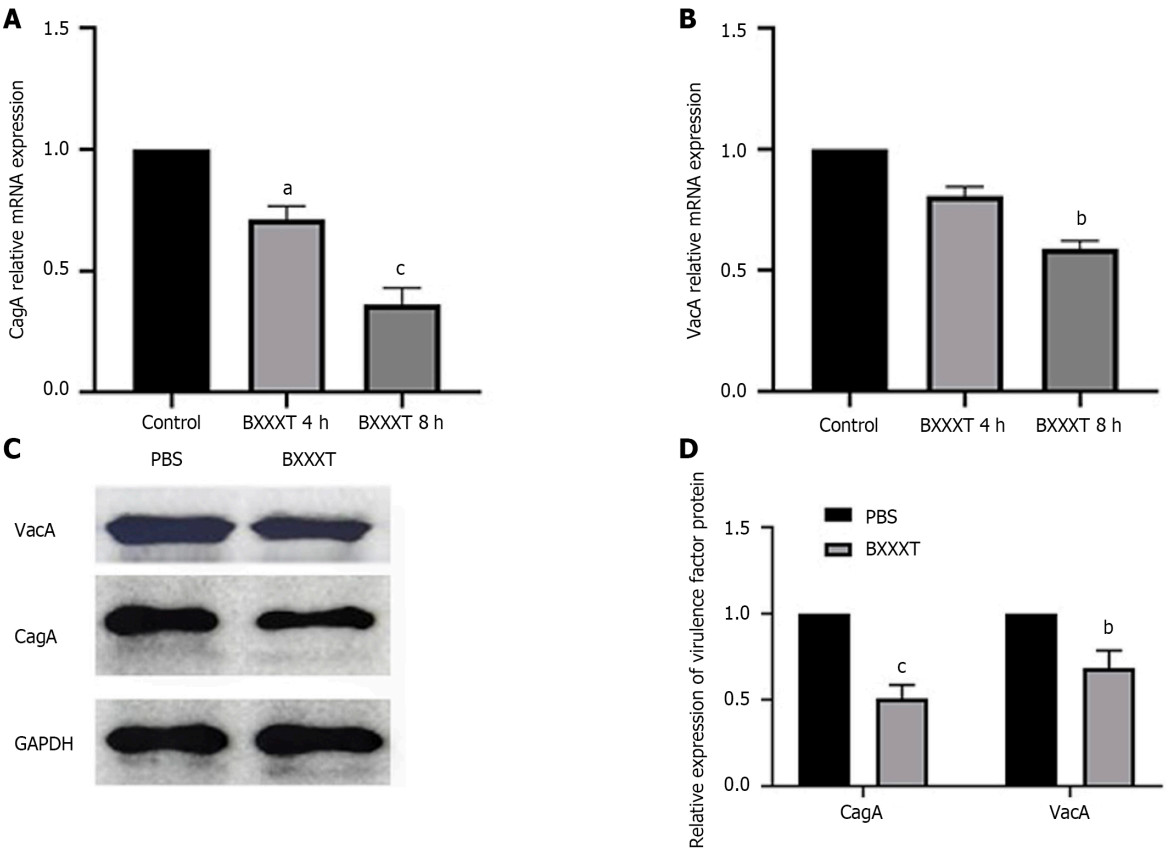

Volcano plot
Up
Down
None
- Log10 (p value)
Log2 (fold change)
6
5
4
3
2
1
0
-4
-2
0
2
4

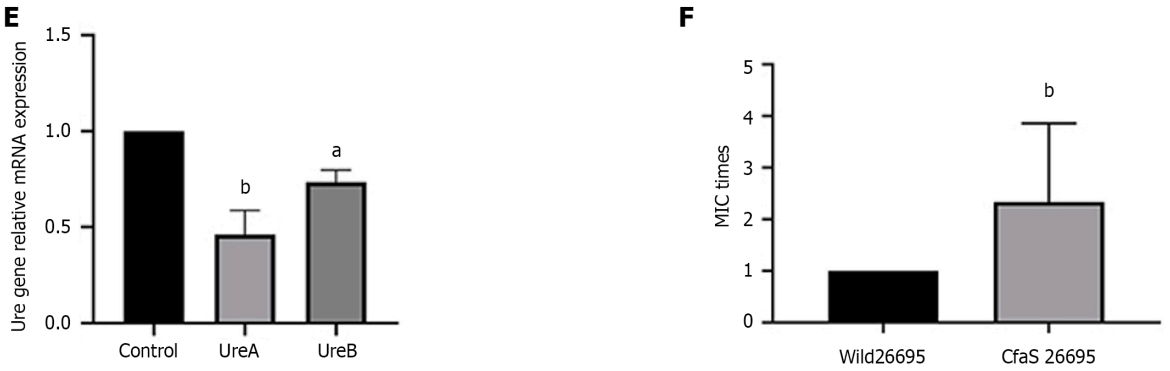


DOI: 10.3748/wjg.v29.i18.2818 **Copyright** ©The Author(s) 2023.

Figure 3 Detection of changes of *Helicobacter pylori* after 8 h treatment with BanXiaXieXin decoction using an electron microscopy, transcriptome, and proteome analyses. A: Observation of changes of *Helicobacter pylori* (*H. pylori*) using an electron microscope; B: The number of significantly differential genes in the transcriptome; C: Significantly differential genes concentrating in the GO enrichment pathway in the transcriptome; D: The epithelial cell signaling in *H. pylori* infection; E: The number of significantly differential genes in the proteome; F: Significantly differential genes concentrating in the GO enrichment pathway in the proteome. BXXXT: BanXiaXieXin decoction; PBS: Phosphate-buffered saline.

and *in vivo* and its mechanism comes down to the synergistic or additional antibacterial effects of berberine, emodin and luteolin, the main components of the extract; the extract could activate the immune function and enhance bactericidal effects; BXXXT aqueous extract, with main targets of BXXXT aqueous extract related to urease, virulence factors, *etc*., could reduce the urease and virulence of *H. pylori*, weaken its colonization, and reduce its inflammatory damage to the gastric mucosa.





DOI: 10.3748/wjg.v29.i18.2818 **Copyright** ©The Author(s) 2023.

Figure 4 Main targets of BanXiaXieXin decoction aqueous extract action. A: mRNA expression of *cagA*; B: mRNA expression of *VacA*; C: Protein expression of *CagA* and *VacA*; D: Quantitative expressions of *CagA* and *VacA* proteins; E: Mutant strain *CFAs* with a low urease expression; F: Changes of minimum inhibitory concentration of BXXXT against mutant strains with a low expression of urease. $^{a}P < 0.05$; $^{b}P < 0.01$; $^{c}P < 0.001$; NS: Not significant. BXXXT: BanXiaXieXin decoction; PBS: Phosphate-buffered saline.

ARTICLE HIGHLIGHTS

Research background

Helicobacter pylori (*H. pylori*)' s drug resistance brings challenges to the current clinical work. In China, traditional Chinese medicine could be used to treat a variety of refractory diseases, reducing drug-resistance, and improving the eradication rate of *H. pylori*. The study is to explore the therapeutic effects of Banxia Xiexin Decoction (BXXXT) on drug-resistant *H. pylori*.

Research motivation

H. pylori' s drug resistance brings challenges to the current clinical work. The study is to explore the therapeutic effects of BXXXT on drug-resistant *H. pylori*, avoid, overcome *H. pylori*' s drug resistance.

Research objectives

To confirm that BXXXT demonstrates therapeutical effects *in vivo* and *in vitro* on gastritis mice with drug-resistant *H. pylori* and explain its mechanism.

Research methods

The aqueous extract of BXXXT was gained by water decocting method. The inhibitory effect of the aqueous extract on *H. pylori* was detected by dilution in vitro. In terms of mechanism exploration, the main medicinal compositions of BXXXT aqueous extract and the synergistic bacteriostatic effects they had demonstrated were analyzed using mass spectrometry; the immune function of peripheral blood cells such as $CD3^+$ T and $CD4^+$ T of mice were detected using a flow cytometry; the *H. pylori* transcriptome and proteome were detected. Differently expressed genes were screened and verification was performed thereon with knockout expression.

Research results

BXXXT aqueous extract against *H. pylori* was better therapeutical effects *in vivo* and *in vitro*; BXXXT aqueous extract was found to stimulate the expressions of $CD3^+$ T and $CD4^+$ T and increase the number of $CD4^+$ T/$CD8^+$ T in gastritis mice; the detection of transcriptome and proteome, quantitative polymerase chain reaction, Western blot and knockout verification revealed that the main targets of BXXXT aqueous extract are *CFAs* related to urea enzymes, and *CagA*, *VacA*, *etc*.

Research conclusions

BXXXT aqueous extract could demonstrate good therapeutic effects on drug-resistance *H. pylori in vitro* and *in vivo* and its mechanism is related to reduce the urease and virulence of *H. pylori*, weaken its colonization, and reduce its inflammatory damage to the gastric mucosa, *etc*.

Research perspectives

BXXXT aqueous extract has good therapeutic effects on drug-resistance *H. pylori*, can overcome *H. pylori* 's drug resistance.

ACKNOWLEDGEMENTS

Thank Professor Bi Hongkai of Nanjing Medical University for the gift of *Helicobacter pylori* strain.

FOOTNOTES

Author contributions: Li XH and Xu JY consulted literature, performed experiments, collected and analyzed data and wrote the first draft, making equal contributions to this work; Wang X and Liao LJ corrected it; Huang L, Huang YQ, and Zhang ZF designed, checked, modified, and completed the manuscript, making equal contributions to this work as co-corresponding authors, Huang L (youyihuangl@163.com) is the first corresponding author; all authors approved the final version of the article.

Supported by the National Natural Science Foundation of China, No. 81760739; Special Fund Projects for Guide Local Science and Technology Development by the China government, No. GUIKEZY20198004; and 2022 Guangxi Graduate Education Innovation Plan Project, No. YCBZ2022071.

Institutional animal care and use committee statement: All procedures involving animals were reviewed and approved by the Youjiang Medical University for Nationalities Institutional Review Board (approval No. 20220110).

Conflict-of-interest statement: The authors declare that they have no conflict of interest.

Data sharing statement: No additional data are available.

ARRIVE guidelines statement: The authors have read the ARRIVE Guidelines, and the manuscript was prepared and revised according to the ARRIVE Guidelines.

Open-Access: This article is an open-access article that was selected by an in-house editor and fully peer-reviewed by external reviewers. It is distributed in accordance with the Creative Commons Attribution NonCommercial (CC BY-NC 4.0) license, which permits others to distribute, remix, adapt, build upon this work non-commercially, and license their derivative works on different terms, provided the original work is properly cited and the use is non-commercial. See: https://creativecommons.org/Licenses/by-nc/4.0/

Country/Territory of origin: China

ORCID number: Xiao-Hua Li 0000-0002-8576-3044; Jia-Yin Xu 0000-0003-0423-5846; Xue Wang 0000-0003-3931-8107; Li-Juan Liao 0000-0003-0547-2026; Liang Huang 0000-0001-7937-8150; Yan-Qiang Huang 0000-0002-0867-0178; Zeng-Feng Zhang 0000-0003-2850-1889.

S-Editor: Chen YL
L-Editor: A
P-Editor: Zhang XD

REFERENCES

1 **Sultan S**, Ahmed SI, Murad S, Irfan SM. Primary *versus* secondary immune thrombocytopenia in adults; a comparative analysis of clinical and laboratory attributes in newly diagnosed patients in Southern Pakistan. *Med J Malaysia* 2016; **71**: 269-274 [PMID: 28064294]
2 **Nagy P**, Johansson S, Molloy-Bland M. Systematic review of time trends in the prevalence of Helicobacter pylori infection in China and the USA. *Gut Pathog* 2016; **8**: 8 [PMID: 26981156 DOI: 10.1186/s13099-016-0091-7]
3 **Du JY**, Pan J, Zhou QJ, Tang QQ, Yang NM, Zhang JZ. The Helicobacter Pylori Antibiotic Resistance in Wenzhou, Zhejiang from 2013 to 2020. *Zhongguo Quanke Yixue* 2023; **26**: 825-829 [DOI: 10.12114/j.issn.1007-9572.2022.0575]
4 **Li RJ**, Dai YY, Qin C, Huang GR, Qin YC, Huang YY, Huang ZS, Luo XK, Huang YQ. Application of traditional Chinese medicine in treatment of Helicobacter pylori infection. *World J Clin Cases* 2021; **9**: 10781-10791 [PMID: 35047590 DOI: 10.12998/wjcc.v9.i35.10781]
5 **Yang M**, Chen J, Xu L, Shi X, Zhou X, An R, Wang X. A Network Pharmacology Approach to Uncover the Molecular Mechanisms of Herbal Formula Ban-Xia-Xie-Xin-Tang. *Evid Based Complement Alternat Med* 2018; **2018**: 4050714 [PMID: 30410554 DOI: 10.1155/2018/4050714]
6 **Li YT**, You J, Song Y, Wang YJ, Wang HB. Meta-analysis of Banxia Xiexin Decoction in the treatment of chronic atrophic gastritis associated with Helicobacter pylori. *Beijing Zhongyiyao* 2021; **40**: 1143-1148 [DOI: 10.16025/j.1674-1307.2021.10.025]
7 **Jong MS**, Hwang SJ, Chen YC, Chen TJ, Chen FJ, Chen FP. Prescriptions of Chinese herbal medicine for constipation under the national health insurance in Taiwan. *J Chin Med Assoc* 2010; **73**: 375-383 [PMID: 20688304 DOI: 10.1016/S1726-4901(10)70081-2]
8 **Jhang JS**, Livneh H, Yang SY, Huang HJ, Chan MWY, Lu MC, Yeh CC, Tsai TY. Decreased risk of colorectal cancer among patients with type 2 diabetes receiving Chinese herbal medicine: a population-based cohort study. *BMJ Open*

Diabetes Res Care 2020; **8** [PMID: 32169932 DOI: 10.1136/bmjdrc-2019-000732]
9 **Murai T**, Matsuo M, Tanaka H, Manabe Y, Takaoka T, Hachiya K, Yamaguchi T, Otsuka S, Shibamoto Y. Efficacy of herbal medicine TJ-14 for acute radiation-induced enteritis: a multi-institutional prospective Phase II trial. *J Radiat Res* 2020; **61**: 140-145 [PMID: 31691810 DOI: 10.1093/jrr/rrz025]
10 **Huang CY**, Lai WY, Sun MF, Lin CC, Chen BC, Lin HJ, Chang CM, Yang CH, Huang KC, Yen HR. Prescription patterns of traditional Chinese medicine for peptic ulcer disease in Taiwan: A nationwide population-based study. *J Ethnopharmacol* 2015; **176**: 311-320 [PMID: 26549268 DOI: 10.1016/j.jep.2015.11.002]
11 **Huang YP**, Zhan DF, Huang H, Chen SF. The effect of Banxia Xiexin Decoction human serum containing drugs on TGF of HP-infected GES-1 cells- β/ Influence of Smad signal pathway. *Zhongguo Shiyan Fangjixue Zazhi* 2018; **14**: 91-96 [DOI: 10.13422/j.cnki.syfjx.20181117]
12 **Ye ZM**, Zhang H. Clinical effect observation of modified Banxia Xiexin Decoction on Hp-related chronic gastritis. *Linchuang Yixue Gongcheng* 2022; **29**: 1515-1516 [DOI: 10.3969/j.issn.1674-4659.2022.11.1515]
13 **Liu XD**. Clinical efficacy observation of Banxia Xiexin Decoction on patients with gastric ulcer. *Zhongguo Yiyao Zhinan* 2021; **19**: 97-99 [DOI: 10.15912/j.cnki.gocm.2021.18.043]
14 **Jiang X**, Duan Y, Zhou B, Guo Q, Wang H, Hang X, Zeng L, Jia J, Bi H. The Cyclopropane Fatty Acid Synthase Mediates Antibiotic Resistance and Gastric Colonization of Helicobacter pylori. *J Bacteriol* 2019; **201** [PMID: 31358615 DOI: 10.1128/JB.00374-19]
15 **Camorlinga-Ponce M**, Gómez-Delgado A, Aguilar-Zamora E, Torres RC, Giono-Cerezo S, Escobar-Ogaz A, Torres J. Phenotypic and Genotypic Antibiotic Resistance Patterns in Helicobacter pylori Strains From Ethnically Diverse Population in México. *Front Cell Infect Microbiol* 2020; **10**: 539115 [PMID: 33643927 DOI: 10.3389/fcimb.2020.539115]
16 **Savoldi A**, Carrara E, Graham DY, Conti M, Tacconelli E. Prevalence of Antibiotic Resistance in Helicobacter pylori: A Systematic Review and Meta-analysis in World Health Organization Regions. *Gastroenterology* 2018; **155**: 1372-1382.e17 [PMID: 29990487 DOI: 10.1053/j.gastro.2018.07.007]
17 **Loffeld RJ**, Werdmuller BF. Changes in Antibiotic Susceptibility of Helicobacter pylori in the Course of Eight Years in the Zaanstreek Region in The Netherlands. *Gastroenterol Res Pract* 2013; **2013**: 625937 [PMID: 23573077 DOI: 10.1155/2013/625937]
18 **Liu DS**, Wang YH, Zeng ZR, Zhang ZY, Lu H, Xu JM, Du YQ, Li Y, Wang JB, Xu SP, Chen Y, Lan CH, Cheng H, Jiang MD, Zhang LX, Huo LJ, Chen SY, Zhang GX, Wu KC, Zhu X, Chen YX, Zhu Y, Shu X, Xie Y, Lu NH. Primary antibiotic resistance of Helicobacter pylori in Chinese patients: a multiregion prospective 7-year study. *Clin Microbiol Infect* 2018; **24**: 780.e5-780.e8 [PMID: 29138101 DOI: 10.1016/j.cmi.2017.11.010]
19 **Hu FL**, Zhang SS. National consensus on integrated treatment of "disease syndrome" related to Helicobacter pylori. *Linchuang Gandanbing Zazhi* 2018; **27**: 1008-1016 [DOI: 10.3969/j.issn.1006-5709.2018.09.012]
20 **Wei P**. Clinical effect of modified Banxia Xiexin Decoction on Helicobacter pylori positive peptic ulcer and its influence on inflammatory factors and gastrointestinal hormones. *Linchuang Heliyongyao Zazhi* 2022; **15**: 73-76 [DOI: 10.15887/j.cnki.13-1389/r.2022.26.022]
21 **Liu Yan**, Ji XQ, Kong LJ, Gao ZH, Xiong X, Zhao YT, Wu JY. Study on the influence of different processing methods on the chemical composition and product quality of Scutellaria baicalensis. *Shi Zhen Guoyi Guoyao* 2019; **3**: 605-608 [DOI: 10.3969/j.issn.1008-0805.2019.03.032]
22 **Zhong JB**, Wang J, Wang YY. The complexity of prescriptions and the development of new drugs of traditional Chinese medicine. *Zhongguo Zhongyiyao Zazhi* 2002; **5**: 321-323 [DOI: 10.3321/j.issn:1001-5302.2002.05.001]
23 **Zhu SN**. The complexity of the material basis of efficacy. *Shandong Zhongyiyao Daxue Xuebao* 2008; **4**: 267-269 [DOI: 10.16294/j.cnki.1007-659x.2008.04.027]
24 **Jin Y**, Lu H, Ge JH, Wang YY, Yu S, Bian HS, Huang LL. Progress in the research on the material basis of Viola yedoensis. *Zhonghua Zhongyiyao Xuekan* 2022; **40**: 21-26 [DOI: 10.13193/j.issn.1673-7717.2022.07.006]
25 **Huang YQ**, Huang GR, Wu MH, Tang HY, Huang ZS, Zhou XH, Yu WQ, Su JW, Mo XQ, Chen BP, Zhao LJ, Huang XF, Wei HY, Wei LD. Inhibitory effects of emodin, baicalin, schizandrin and berberine on hefA gene: treatment of Helicobacter pylori-induced multidrug resistance. *World J Gastroenterol* 2015; **21**: 4225-4231 [PMID: 25892872 DOI: 10.3748/wjg.v21.i14.4225]
26 **Karbalaei M**, Talebi Bezmin Abadi A, Keikha M. Clinical relevance of the cagA and vacA s1m1 status and antibiotic resistance in Helicobacter pylori: a systematic review and meta-analysis. *BMC Infect Dis* 2022; **22**: 573 [PMID: 35752757 DOI: 10.1186/s12879-022-07546-5]
27 **Sharndama HC**, Mba IE. Helicobacter pylori: an up-to-date overview on the virulence and pathogenesis mechanisms. *Braz J Microbiol* 2022; **53**: 33-50 [PMID: 34988937 DOI: 10.1007/s42770-021-00675-0]
28 **McClain MS**, Beckett AC, Cover TL. Helicobacter pylori Vacuolating Toxin and Gastric Cancer. *Toxins (Basel)* 2017; **9** [PMID: 29023421 DOI: 10.3390/toxins9100316]
29 **Djekic A**, Müller A. The Immunomodulator VacA Promotes Immune Tolerance and Persistent Helicobacter pylori Infection through Its Activities on T-Cells and Antigen-Presenting Cells. *Toxins (Basel)* 2016; **8** [PMID: 27322319 DOI: 10.3390/toxins8060187]
30 **Reshetnyak VI**, Burmistrov AI, Maev IV. Helicobacter pylori: Commensal, symbiont or pathogen? *World J Gastroenterol* 2021; **27**: 545-560 [PMID: 33642828 DOI: 10.3748/wjg.v27.i7.545]
31 **Altobelli A**, Bauer M, Velez K, Cover TL, Müller A. Helicobacter pylori VacA Targets Myeloid Cells in the Gastric Lamina Propria To Promote Peripherally Induced Regulatory T-Cell Differentiation and Persistent Infection. *mBio* 2019; **10** [PMID: 30890606 DOI: 10.1128/mBio.00261-19]
32 **Mahady GB**, Pendland SL, Yun GS, Lu ZZ, Stoia A. Ginger (Zingiber officinale Roscoe) and the gingerols inhibit the growth of Cag A+ strains of Helicobacter pylori. *Anticancer Res* 2003; **23**: 3699-3702 [PMID: 14666666]
33 **Yeon MJ**, Lee MH, Kim DH, Yang JY, Woo HJ, Kwon HJ, Moon C, Kim SH, Kim JB. Anti-inflammatory effects of Kaempferol on Helicobacter pylori-induced inflammation. *Biosci Biotechnol Biochem* 2019; **83**: 166-173 [PMID: 30286691 DOI: 10.1080/09168451.2018.1528140]
34 **Lee JW**, Mase N, Yonezawa T, Seo HJ, Jeon WB, Cha BY, Nagai K, Woo JT. Palmatine attenuates osteoclast

differentiation and function through inhibition of receptor activator of nuclear factor-κb ligand expression in osteoblast cells. *Biol Pharm Bull* 2010; **33**: 1733-1739 [PMID: 20930384 DOI: 10.1248/bpb.33.1733]

35 **Kim HW**, Woo HJ, Yang JY, Kim JB, Kim SH. Hesperetin Inhibits Expression of Virulence Factors and Growth of Helicobacter pylori. *Int J Mol Sci* 2021; **22** [PMID: 34576198 DOI: 10.3390/ijms221810035]

36 **Barkan D**, Liu Z, Sacchettini JC, Glickman MS. Mycolic acid cyclopropanation is essential for viability, drug resistance, and cell wall integrity of Mycobacterium tuberculosis. *Chem Biol* 2009; **16**: 499-509 [PMID: 19477414 DOI: 10.1016/j.chembiol.2009.04.001]

37 **Chen YY**, Gänzle MG. Influence of cyclopropane fatty acids on heat, high pressure, acid and oxidative resistance in Escherichia coli. *Int J Food Microbiol* 2016; **222**: 16-22 [PMID: 26828814 DOI: 10.1016/j.ijfoodmicro.2016.01.017]

World Journal of Gastroenterology

Submit a Manuscript: https://www.f6publishing.com

World J Gastroenterol 2023 May 14; 29(18): 2836-2849

DOI: 10.3748/wjg.v29.i18.2836

ISSN 1007-9327 (print) ISSN 2219-2840 (online)

ORIGINAL ARTICLE

Retrospective Cohort Study

Endoscopic and pathological characteristics of *de novo* colorectal cancer: Retrospective cohort study

Shi-Yang Li, Mei-Qi Yang, Yi-Ming Liu, Ming-Jun Sun, Hui-Jing Zhang

Specialty type: Gastroenterology and hepatology

Provenance and peer review: Unsolicited article; Externally peer reviewed.

Peer-review model: Single blind

Peer-review report's scientific quality classification

Grade A (Excellent): 0
Grade B (Very good): B, B
Grade C (Good): 0
Grade D (Fair): 0
Grade E (Poor): 0

P-Reviewer: Schijven MP, Netherlands; Tie J, Australia

Received: March 28, 2023
Peer-review started: March 28, 2023
First decision: April 10, 2023
Revised: April 14, 2023
Accepted: April 19, 2023
Article in press: April 19, 2023
Published online: May 14, 2023

Shi-Yang Li, Mei-Qi Yang, Yi-Ming Liu, Ming-Jun Sun, Hui-Jing Zhang, Department of Endoscopy, The First Affiliated Hospital of China Medical University, Shenyang 110001, Liaoning Province, China

Corresponding author: Hui-Jing Zhang, MD, Professor, Department of Endoscopy, The First Affiliated Hospital of China Medical University, No. 155 Nanjing North Street, Heping District, Shenyang 110001, Liaoning Province, China. hjzhang@cmu.edu.cn

Abstract

BACKGROUND

Endoscopy has rapidly developed in recent years and has enabled further investigation into the origin and features of intestinal tumors. The small size and concealed position of these tumors make it difficult to distinguish them from nonneoplastic polyps and carcinoma in adenoma (CIA). The invasive depth and metastatic potential determine the operation regimen, which in turn affects the overall survival and distant prognosis. The previous studies have confirmed the malignant features and clinicopathological features of *de novo* colorectal cancer (CRC).

AIM

To provide assistance for diagnosis and treatment, but the lack of a summary of endoscopic features and assessment of risk factors that differ from the CIA prompted us to conduct this retrospective study.

METHODS

In total, 167 patients with small-sized CRCs diagnosed by endoscopy were reviewed. The patients diagnosed as advanced CRCs and other malignant cancers or chronic diseases that could affect distant outcomes were excluded. After screening, 63 cases were excluded, including 33 *de novo* and 30 CIA cases. Patient information, including their follow-up information, was obtained from an electronic His-system. The characteristics between two group and risk factors for invasion depth were analyzed with SPSS 25.0 software.

RESULTS

Nearly half of the *de novo* CRCs were smaller than 1 cm (n = 16, 48.5%) and the majority were located in the distal colon (n = 26, 78.8%). The IIc type was the most common macroscopic type of *de novo* CRC. In a Pearson analysis, the differential degree, Sano, JNET, and Kudo types, surrounding mucosa, and chicken skin

mucosa (CSM) were correlated with the invasion depth ($P < 0.001$). CSM was a significant risk factor for deep invasion and disturbed judgment of endoscopic ultrasound. A high degree of tumor budding and tumor-infiltrating lymphocytes are accompanied by malignancy. Finally, *de novo* CRCs have worse outcomes than CIA CRCs.

CONCLUSION

This is the first comprehensive study to analyze the features of *de novo* CRCs to distinguish them from nonneoplastic polyps. It is also the first study paying attention to CSM invasive depth measurement. This study emphasizes the high metastatic potential of *de novo* CRCs and highlights the need for more research on this tumor type.

Key Words: *De novo* colorectal cancer; Carcinoma in adenoma; Endoscopic features; Clinical characteristics; Pathological features

©The Author(s) 2023. Published by Baishideng Publishing Group Inc. All rights reserved.

Core Tip: *De novo* colorectal cancer (CRC) is a specific tumor with a small lesion. Many different features of *de novo* CRCs exist to distinguish them from non-neoplastic polyps. Moreover, the study highlights that *de novo* CRCs have special endoscopic and pathological features that distinguish them from traditional adenocarcinomas. Different pit pattern types indicate various tumor types; for example, the III-type pit pattern often occurs in tubular adenomas. For CRCs, invasion depth evaluation is a vital issue. Computed tomography imaging and endoscopic ultrasound are used for judging invasive depth. Besides, chicken skin mucosa may also be a risk factor.

Citation: Li SY, Yang MQ, Liu YM, Sun MJ, Zhang HJ. Endoscopic and pathological characteristics of *de novo* colorectal cancer: Retrospective cohort study. *World J Gastroenterol* 2023; 29(18): 2836-2849
URL: https://www.wjgnet.com/1007-9327/full/v29/i18/2836.htm
DOI: https://dx.doi.org/10.3748/wjg.v29.i18.2836

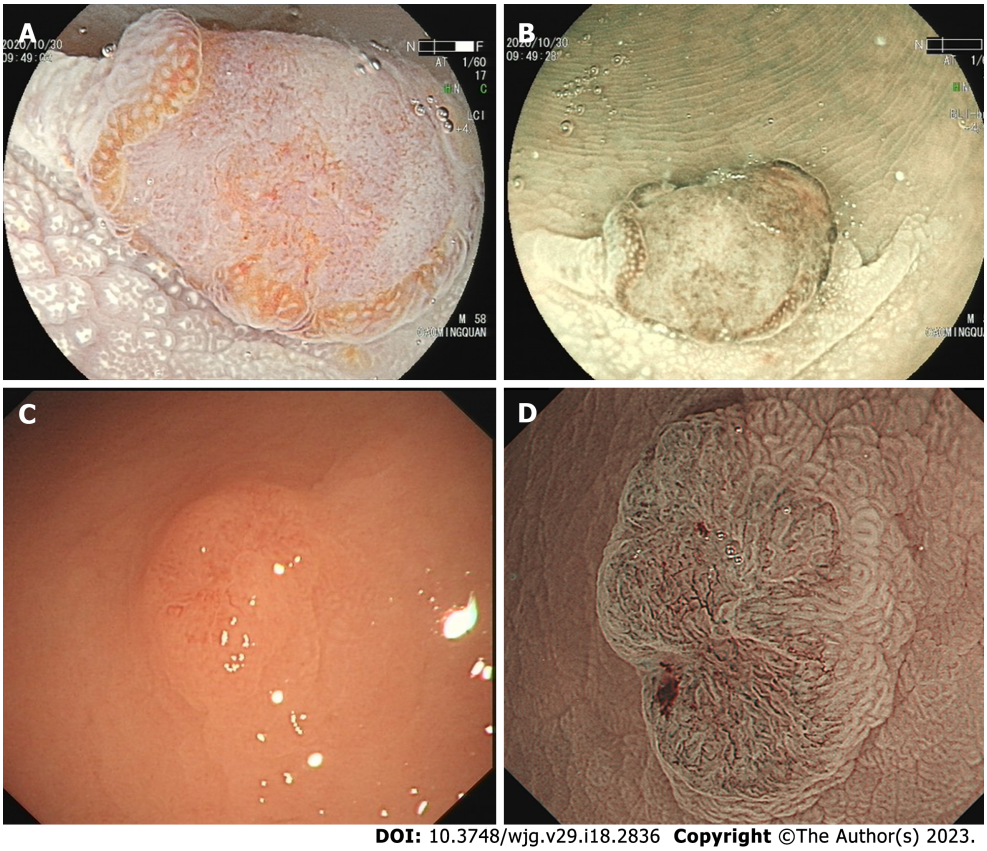
INTRODUCTION

A *de novo* colorectal cancer (CRC) is a unique CRC that represents a significant public health challenge with high morbidity and mortality globally[1,2]. At present, CRCs have four recognized pathways of development: The carcinoma in adenoma (CIA) pathway (aka chromosomal instability pathway), the *de novo* carcinoma pathway, the serrated lesion-carcinoma pathway, and the inflammatory-carcinoma pathway. In the 1950s, *de novo*-originated CRCs emerged increasingly after the definition "de novo" was proposed. In recent decades, the Japanese proposed a *de novo* carcinoma pathway[3]. Unlike other pathways, a *de novo* CRC is a tumor derived from cancer cells without progression of adenomatous changes, as shown in Figure 1, and its true pathway remains unknown. Normal I type around tumor and lack of III or IV type pits is a hallmark of *de novo* CRC under endoscopy[4-6].

For endoscopists, the endoscopic featrures occupied a key position in diagnosis and treatment. Magnified chromoendoscopy and narrow-band imaging (NBI) technology can be used to observe pit pattern and extimate depth of invasion[7-11]. Apart of pit pattern, there existed several indicators could forecast depth of invasion, such as chicken skin mucosa (CSM), mucosa pulling and converging. The CSM is an area of 0.5 mm of pale-yellow speckles adjacent to colonic neoplasms resulting from fat accumulation in the lamina propria[12]. CSM was more common in neoplastic and advanced polyps [13]. In this study, we concentrate on relationship between CSM and depth of invasion. For the whole CRCs, we should get to know three things: Get to know who they are firstly, estimate depth of invasion secondly, and predict the risk of metastasis at last.

Epithelial-mesenchymal transition (EMT) refers to a cellular reprogramming process in which epithelial cells acquire a mesenchymal phenotype[14]. EMT has an important role in development, wound healing, and malignant progression[15]. Mueller *et al*[16] have found that E-cadherin express lower in *de novo* than ex adenoma carcinomas through immunohistochemistry (IHC)[16]. We further want to know the relationship between E-cadherin proportion and distant metastsis.

Until now, there was no a complete study about *de novo* CRC, so we make this study to construct a comprehensive system for diagnosis and treatment of *de novo* CRC.



DOI: 10.3748/wjg.v29.i18.2836 **Copyright** ©The Author(s) 2023.

Figure 1 The *de novo* colorectal cancer under endoscopy. A: A *de novo* colorectal cancer (CRC) under linked color imaging; B and D: The surface structure under the narrow bind imaging pattern; C: A *de novo* CRC under white light.

MATERIALS AND METHODS

We retrospectively reviewed patients diagnosed with CRCs between 2010 to 2020 year. We selected all *de novo* CRC and CIA-type patients on the His Electric System. All lesions were diagnosed by a senior pathologist and confirmed by two pathologists. The results from two pathologists had more than 90% similarity, and discrepant results were determined by a cheif pathologist. These patients did not have other comorbidities that could significantly impact the distant outcomes. Essential clinical information was collected, including endoscopic features and pathological results (size, endoscopic features, macroscopic type, pit pattern, clinical diagnosis, pathologic diagnosis, infiltration (IFN), immunohistology, invasive depth, tumor budding (TB), grading, lymphocyte IFN, perineural IFN, growth pattern, and lymph node metastasis). Pearson and χ^2 tests were performed using SPSS (25.0) software. The difference between each group was statistically significant ($P < 0.05$). Oral informed consent was obtained from all participants *via* telephone calls.

The degree of staining was scored according to the staining intensity (0, no staining; 1, weak; 2, moderate; 3, strong) and the proportion of positive cells (0: 0%; 1: < 25%; 2: < 50%; 3: < 75%; 4: ≥ 75%). The score of each slice was determined by the staining index (staining intensity × proportion of positive cells). A staining index > 4 was classified as high-grade expression, while an index ≤ 4 was defined as low-grade expression.

The pathological film used in the study was IHC, with the patient's consent, and the patient's information was kept confidential; therefore, ethical approval was not required.

RESULTS

Clinical features of de novo CRCs

Nearly half (n = 16, 48.5%) of the *de novo* CRCs were less than 1 cm in size and located in the distal colon (n = 26, 78.8%). In contrast, CIA CRCs were mostly 2 cm (n = 21, 70.0%) and located at the proximal colon (n = 21, 70.0%). There were no significant differences in the other risk factors between the *de novo* and CIA groups ($P > 0.05$). In addition, we focused on the choice of treatment. All submucosa *de novo* CRCs were treated surgically, and seven CIA submucosa CRCs were treated endoscopically. The results are presented in Table 1.

Table 1 The clinical information of *de novo* and carcinoma in adenoma colorectal cancers

		De novo (*n* = 33)	CIA (*n* = 30)	χ^2	*P* value
Clinical information					
Age (%)	> 55	30 (90.9)	25 (83.3)	0.814	> 0.05
	< 55	3 (9.1)	5 (16.7)		
Gender (%)	Male	16 (48.5)	16 (53.3)	0.148	> 0.05
	Female	17 (51.5)	14 (46.7)		
Smoking history (%)	Yes	27 (81.8)	19 (63.3)	2.725	> 0.05
	No	6 (18.2)	11 (36.7)		
Location (%)	Proximal	7 (21.2)	21 (70.0)	15.149	< 0.05
	Distal	26 (78.8)	9 (30.0)		
Depth of invasion	M	8 (24.2)	9 (30.0)	1.504	> 0.05
	SMp	9 (27.3)	11 (36.7)		
	SMd	16 (48.5)	10 (33.3)		
Treatment (%)	Surgery	21 (63.6)	16 (53.3)	0.688	> 0.05
	Endoscopy	12 (36.4)	14 (46.7)		
Supplement chemotherapy (%)	Yes	21 (63.6)	12 (40.0)	3.520	> 0.05
	No	12 (36.4)	18 (60.0)		
Distal metastasis (%)	Yes	5 (15.2)	2 (6.7)	1.145	> 0.05
	No	28 (84.8)	28 (93.3)		
Overall survival (%)	1 yr	33 (100.0)	30 (100.0)		
	3 yr	30 (90.9)	28 (93.3)		
	5 yr	23 (69.7)	28 (93.3)		
DSS	Yes	26 (78.8)	28 (93.3)	2.715	> 0.05
	No	7 (21.2)	2 (6.7)		
Endoscopic gross characteristics					
Size%	1 cm < S ≤ 2 cm	14 (42.4)	9 (30.0)	30.514	< 0.05
	≤ 1 cm	16 (48.5)	0 (0.0)		
	> 2 cm	3 (9.1)	21 (70.0)		
Macroscopic type%	Is	5 (15.2)	6 (20.0)	35.187	< 0.05
	IIa + IIc	11 (33.3)	1 (3.3)		
	IIc	17 (51.5)	4 (13.3)		
	Is + IIc	0 (0.0)	19 (63.3)		
Surface change	Erosion	24 (72.7)	13 (43.3)	9.457	< 0.05
	Ulceration	2 (6.1)	11 (36.7)		
	None	7 (21.2)	6 (20.0)		
Color change	Reddened mucosa	26 (78.8)	2 (6.7)	33.104	< 0.05
	None	7 (21.2)	28 (93.3)		
NICE	Type 1	0 (0.0)	0 (0.0)		> 0.05
	Type 2	0 (0.0)	0 (0.0)		
	Type 3	33 (100.0)	30 (100.0)		
Sano	I	0 (0.0)	0 (0.0)	5.292	< 0.05
	II	0 (0.0)	0 (0.0)		

	IIIA	17 (51.5)	7 (23.3)		
	IIIB	16 (48.5)	23 (76.7)		
JNET	1	0 (0.0)	0 (0.0)	3.094	> 0.05
	2A	0 (0.0)	0 (0.0)		
	2B	12 (36.4)	5 (16.7)		
	3	21 (63.6)	25 (83.3)		
Chemical staining (crystal violet)					
Pit pattern	Vi	1 (3.0)	6 (20.0)	15.774	< 0.05
	Vn	13 (39.4)	15 (50.0)		
	Vi + Vn	19 (57.6)	5 (16.7)		
	IV + Vi	0 (0.0)	4 (13.3)		
Pit pattern at the edge of the tumors	I	33 (100.0)	0 (0.0)	63.000	< 0.05
	III + VI	0 (0.0)	30 (100.0)		
Surrounding mucosa					
Pulling	Yes	9 (27.3)	21 (70.0)	11.501	< 0.05
	No	24 (72.7)	9 (30.0)		
Converging folds	Yes	27 (81.8)	15 (50.0)	7.159	< 0.05
	No	6 (18.2)	15 (50.0)		
CSM	CSM1	11 (33.3)	4 (13.3)	3.553	> 0.05
	CSM2	17 (51.5)	21 (70.0)		
	CSM3	5 (15.2)	5 (16.7)		

CRC: Colorectal cancer; DSS: Disease specific survival; CSM: Chicken skin mucosa; CIA: Carcinoma in adenoma; NICE: Narrow-band imaging International Colorectal Endoscopic.

Endoscopic characteristics of de novo CRCs

Based on endoscopic appearance, small CRCs were classified as type I (polypoid), type IIa (slightly raised), type IIb (flat), or type IIc (depressed)[12]. Type IIa + IIc is the most common type of *de novo* CRC. Notably, 15 (45.5%) *de novo* CRCs were Is type. We showed different macroscopic types of *de novo* CRCs, as shown in Figure 2. For CIA CRCs, the Is + IIc type (polypoid with depression) was the most common presentation (n = 19, 63.3%). Another significant finding was surface changes: We found that erosion and reddened mucosa are hallmark features of *de novo* CRCs. In the CIA group, erosion was the same as ulceration. Furthermore, reddened mucosa was seldom observed in the CIA group (n = 28, 93.3%). The endoscopic results are shown in Table 2.

There was a significant difference in the Sano and pit pattern types (P < 0.05) but no significant difference in the NBI International Colorectal Endoscopic (NICE) classification and JNET types between the two groups (P > 0.05). About half of the *de novo* CRCs were IIIA type (n = 17, 51.5%) with a Vi + Vn type pit pattern (n = 19, 57.6%). The most striking difference was in the pit pattern around the edges of the lesions: I type pit patterns (small and round pits) were observed in all *de novo* CRCs (n = 33, 100%), and III + VI type pit patterns were observed in all CIA CRCs (n = 30, 100%).

We also analyzed the risk factors associated with the invasive depth (Table 3). A third (33.3%) of the *de novo* group had a CSM1 × *vs* 13.3% of the CIA group. CSM was associated with the depth of invasion [r (correlation coefficient) = -0.796, P < 0.001]. CSM1 has a high invasive potential for CRC. In addition to CSM, pulling and converging folds also appear in the mucosa surrounding CRCs. Mucosal pulling appeared more frequently in the CIA group (n = 21, 70.0%) than in the *de novo* group (n = 9, 27.3%). In contrast, the converging fold was more frequent in the *de novo* group (n = 27, 81.8%) than that in the CIA group (n = 15, 50%). After analyzing the relationship between these parameters and invasive depth, we found that mucosal pulling (r = 0.567, P < 0.001) and converging folds (r = 0.620, P < 0.001) were also significantly associated with invasive depth.

Pathological characteristics of de novo CRCs

Pathological results revealed that TB was significantly associated with invasive depth (r = 0.669, P < 0.001) (Table 4). Although there was no significant difference between the two groups, budding grade 3 (BD3) accounted for 33.3% of the *de novo* group, which is far more than that of the CIA group (n = 6,

Table 2 The endoscopic characteristics in *de novo* and carcinoma in adenoma groups

		De novo (*n* = 22)	CIA (*n* = 20)	χ^2	*P* value
Budding	BD1	8 (24.2)	4 (13.3)	6.161	> 0.05
	BD2	8 (24.2)	6 (20.0)		
	BD3	11 (33.3)	6 (20.0)		
	None	5 (18.2)	14 (46.7)		
Grading	G1	6 (18.2)	13 (43.3)	8.878	> 0.05
	G2	11 (33.3)	9 (30.0)		
	G1-2	10 (30.3)	8 (26.7)		
	G3-2	6 (18.2)	0 (0.0)		
TIL	Yes	27 (81.8)	19 (63.3)	2.725	> 0.05
	No	6 (18.2)	11 (36.7)		
Perineural infiltration	Yes	16 (48.5)	3 (10.0)	11.050	< 0.05
	No	17 (51.5)	27 (90.0)		
Lymphovascular invasion	Yes	16 (48.5)	7 (23.3)	4.289	< 0.05
	No	17 (51.5)	23 (76.7)		
Growth pattern	INFa	0 (0.0)	27 (90.0)	63.000	< 0.05
	INFb	0 (0.0)	3 (10.0)		
	INFc	33 (100.0)	0 (0.0)		
Lymph node metastasis	Yes	10 (30.3)	1 (3.3)	7.931	> 0.05
	No	23 (69.7)	29 (96.7)		
Adjacent lesions	Inflammation	33 (100.0)	0 (0.0)	63.000	< 0.05
	Adenoma	0 (0.0)	17 (56.7)		
	Hyperplasia	0 (0.0)	13 (43.3)		
IHC-E-cadherin	No staining	0 (0.0)	0 (0.0)	22.609	< 0.05
	Weak	17 (51.5)	2 (6.7)		
	Moderate	15 (48.5)	19 (63.3)		
	Strong	0 (0.0)	9 (30.0)		
IHC-Vimentin	No staining	0 (0.0)	0 (0.0)	23.182	< 0.05
	Weak	13 (39.4)	18 (60.0)		
	Moderate	1 (3.0)	10 (33.3)		
	Strong	19 (57.6)	2 (6.7)		

CIA: Carcinoma in adenoma; TIL: Tumor Infiltrating Lymphocyte; IHC: Immunohistochemistry; BD: Budding grade.

Table 3 The risk factors are related to the depth of invasion

Depth of invasion	M	SM-S	SM-d and deeper	*r*	*P* value
Size, %				-0.002	> 0.05
1 cm < S ≤ 2 cm	1 (12.5)	0 (0.0)	13 (81.3)		
≤ 1 cm	7 (87.5)	9 (100.0)	0 (0.0)		
> 2 cm	0 (0.0)	0 (0.0)	3 (18.8)		
Growth pattern					> 0.05

IFNa	0 (0.0)	0 (0.0)	0 (0.0)		
IFNb	0 (0.0)	0 (0.0)	0 (0.0)		
IFNc	8 (100.0)	9 (100.0)	16 (100.0)		
Differential degree				0.904	< 0.001
G1	5 (62.5)	1 (11.1)	0 (0.0)		
G2	3 (37.5)	8 (88.9)	0 (0.0)		
G1-2	0 (0.0)	0 (0.0)	10 (62.5)		
G3-2	0 (0.0)	0 (0.0)	6 (37.5)		
Macroscopic type				-0.093	> 0.05
Is	2 (25.0)	0 (0.0)	13 (81.3)		
IIa + IIc	6 (75.0)	9 (100.0)	0 (0.0)		
IIc	0 (0.0)	0 (0.0)	3 (18.8)		
Is + IIc	0 (0.0)	0 (0.0)	0 (0.0)		
NICE					> 0.05
Type 1	0 (0.0)	0 (0.0)	0 (0.0)		
Type 2	0 (0.0)	0 (0.0)	0 (0.0)		
Type 3	8 (100.0)	9 (100.0)	16 (100.0)		
Sano				0.938	< 0.001
I	0 (0.0)	0 (0.0)	0 (0.0)		
II	0 (0.0)	0 (0.0)	0 (0.0)		
IIIA	8 (100.0)	9 (100.0)	0 (0.0)		
IIIB	0 (0.0)	0 (0.0)	16 (100.0)		
JNET				0.649	< 0.001
1	0 (0.0)	0 (0.0)	0 (0.0)		
2A	0 (0.0)	0 (0.0)	0 (0.0)		
2B	5 (62.5)	7 (77.8)	0 (0.0)		
3	3 (37.5)	2 (22.2)	16 (100.0)		
Pit pattern				-0.491	< 0.001
Vi	1 (12.5)	0 (0.0)	0 (0.0)		
Vn	0 (0.0)	0 (0.0)	13 (81.3)		
Vi + Vn	7 (87.5)	9 (100.0)	3 (18.8)		
IV + Vi	0 (0.0)	0 (0.0)	0 (0.0)		
Pit pattern at the edge of the tumors					> 0.05
I	8 (100.0)	9 (100.0)	16 (100.0)		
III + VI	0 (0.0)	0 (0.0)	0 (0.0)		
Surrounding mucosa					
Pulling				-0.567	< 0.001
Yes	0 (0.0)	0 (0.0)	9 (56.3)		
No	8 (100.0)	9 (100.0)	7 (43.8)		
Converging folds				-0.62	< 0.001
Yes	3 (37.5)	8 (88.9)	16 (100.0)		
No	5 (62.5)	1 (11.1)	0 (0.0)		
CSM				-0.796	< 0.001

CSM1	0 (0.0)	0 (0.0)	11 (68.8)
CSM2	3 (37.5)	9 (100.0)	5 (31.3)
CSM3	5 (62.5)	0 (0.0)	0 (0.0)

IFN: Infiltration; CSM: Chicken skin mucosa; NICE: Narrow-band imaging International Colorectal Endoscopic.

Table 4 The risk factors are related to tumor budding

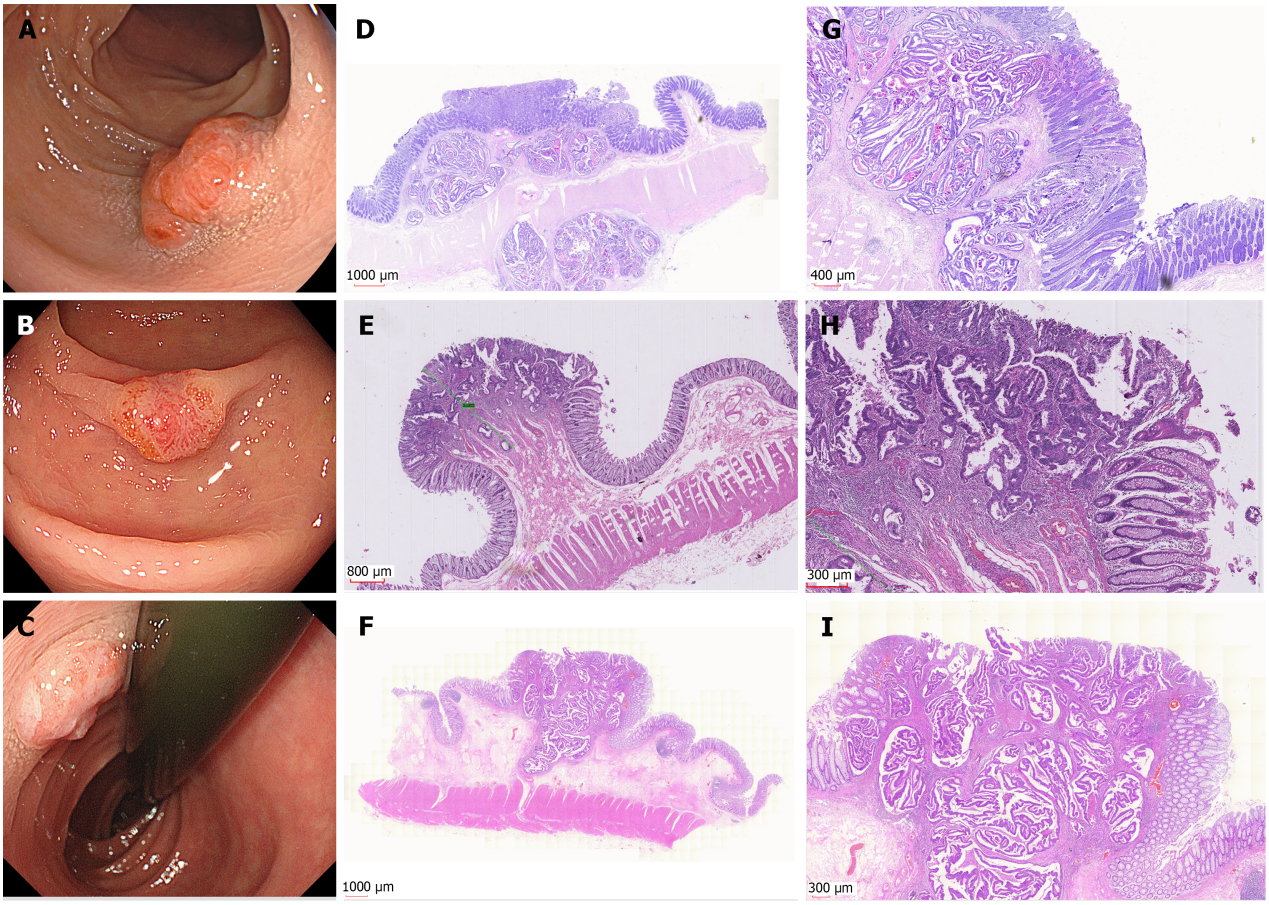
	BD1	BD2	BD3	No budding	*r*	*P* value
Infiltrative depth, %					0.669	< 0.001
M	0 (0.0)	3 (21.4)	0 (0.0)	14 (70.0)		
SMp	10 (83.3)	1 (7.1)	3 (17.6)			
SMd	2 (16.7)	10 (71.4)	14 (82.4)			
Lymphovascular invasion					0.663	< 0.001
Yes	2 (28.6)	4 (21.1)	16 (94.1)	1 (5.0)		
No	5 (71.4)	15 (78.9)	1 (5.9)	19 (95.0)		
Lymph node metastasis					0.489	< -0.001
Yes	1 (14.3)	1 (5.3)	9 (52.9)	0 (0.0)		
No	6 (85.7)	18 (94.7)	8 (41.7)	20 (100.0)		
Perineural infiltration					0.601	< 0.001
Yes	2 (28.6)	4 (21.1)	13 (76.5)	0 (0.0)		
No	5 (71.4)	15 (78.9)	4 (23.5)	20 (100.0)		
Tumor infiltrating lymphocytes					0.476	< 0.001
Yes	7 (100.0)	19 (100.0)	14 (82.4)	6 (30.0)		
No	0 (0.0)	0 (0.0)	3 (17.6)	14 (70.0)		
Differential degree					0.706	< 0.001
G1	0 (0.0)	0 (0.0)	0 (0.0)	19 (95.0)		
G1-2	2 (28.6)	9 (47.4)	7 (41.2)	0 (0.0)		
G2	5 (71.4)	10 (52.6)	4 (23.5)	1 (5.0)		
G3-2	0 (0.0)	0 (0.0)	6 (35.3)	0 (0.0)		

BD: Budding grade.

20%). Regarding other pathological characteristics, perineural IFN, lymph node metastasis, and tumor-infiltrating lymphocytes (TIL) have also emerged in CRC tissues. There was a significant difference in perineural IFN and lymph node metastasis between the two groups ($P < 0.05$).

Another critical issue that deserves attention is IHC. In both groups, approximately 70% of the cases were MLH1 (+), MSH2 (+), MSH6 (+), PMS2 (+), CDX2 (+), Ki67 (+), and P53 (+). We extracted several sections that were stained for E-cadherin and vimentin (VIM). In the *de novo* group, the E-cadherin expression was low in the epithelial regions and VIM was high in the mesenchyma. The CIA group showed opposite results to the *de novo* group, as shown in Figure 3. We analyzed risk factors for distant metastasis in *de novo* group, the results are shown in Supplementary Table 1. Differential degree, Sano classification, expression of E-cad and VIM were correlated with distant metastasis. High expression of E-cad was negatively related with distant metastasis and VIM had an opposite result.

In addition, we explored whether the *de novo* type was correlated with relapse and survival. In the *de novo* group, 11 subjects developed neoplastic polyps again within 5 years, and 10 relapsed within 5 years. The 5-year survival rate was 93.3% for CIA and 69.7% for *de novo* CRCs. Log-rank analysis revealed no significant difference in relapse between the two groups ($\chi^2 = 0.49$, $P = 0.515$); however, there was a significant difference in the survival probability between the two groups ($\chi^2 = 7.08$, $P = 0.020$). Survival curves are shown in Figure 4.



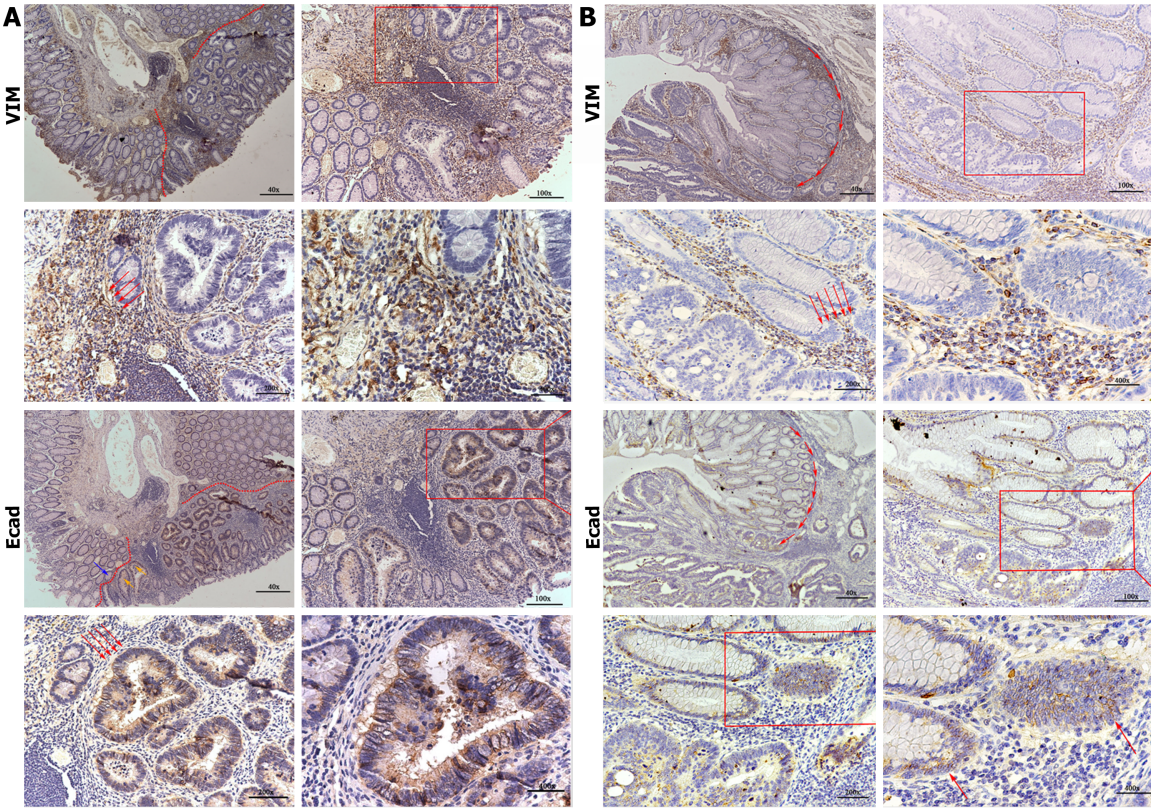
DOI: 10.3748/wjg.v29.i18.2836 **Copyright** ©The Author(s) 2023.

Figure 2 The examples of I-type *de novo* colorectal cancer. A-C: Endoscopic images of different types *de novo* colorectal cancers (CRCs); D-I: Pathological images of *de novo* CRCs.

DISCUSSION

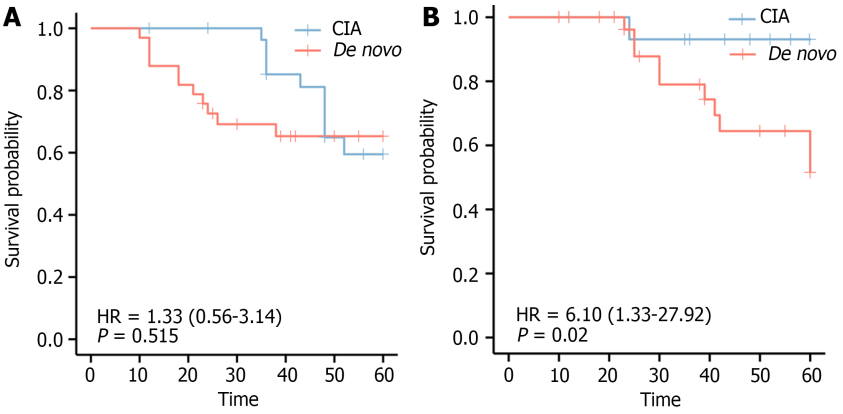
In this study, we present our novel findings pertaining to the characteristics of *de novo* CRC. The key findings included the following: (1) The incidence rate of *de novo* CRCs is considered lower than CIA CRCs, but our study showed that it is related to the classification of CRC. Although some *de novo* CRCs are limited to intramucosal cancer, they are not the same as high-grade dysplasia or cancer with high-grade intraepithelial neoplasia, which could be called advancing adenoma. An advancing adenoma is a precancerous lesion, whereas a *de novo* CRC is a type of early CRC. Some endoscopic physicians misdiagnose advanced adenomas as early CRCs; this will improve the diagnostic rate of CRC but reduce the incidence rate of *de novo* cancer. Therefore, we believe that the diagnostic bias of endoscopic physicians affects the incidence rate. One of the aims of this study was to bolster the standardized diagnostic requirements of endoscopic physicians and to understand *de novo* cancer from the molecular, pathological, and endoscopic perspectives. According to the Vienna classification, category 4 includes advanced adenoma/dysplasia and noninvasive carcinoma. The reason for the lower incidence of *de novo* CRCs in the previous study may be eliminated by comprehensively evaluating the characteristics comprehensively[17-20]; (2) In our study, 48.5% of *de novo* CRCs were < 1 cm in size. Some investigators excluded tumors > 1 cm because they thought that the adenomatous component might be obliterated by the expanding tumor mass[12]. In our study, 42.4% of the *de novo* CRC-derived tumors diagnosed by endoscopists and pathologists were ≥ 1 cm and ≤ 2 cm. In addition, there were three lesions larger than 2 cm. Therefore, warning regarding small lesions without adenomatous components should be escalated; and (3) In addition to platform lift, converging mucosa, pulling, and CSM are significant indicators of invasive depth. Fibroplasia causes surface changes during cancer cell invasion. Converging mucosa was more likely to occur in *de novo* CRCs than that in CIA group, and nearly half of the lesions (n = 16, 48.5%) had deeper invasion. Mucosal pulling may be caused by shrinkage of the mucosa or muscularis mucosa, indicating superficial layer invasion.

The cause of CSM may be fat accumulation in macrophages, which may result from the breakdown of lipids within colonocytes or adjacent tumors. These findings suggest that CSM is a valuable marker for differentiating between neoplastic and advanced polyps using conventional white colonoscopy[21]. Lee *et al*[13] divided CSM into three types based on their characteristics. Type 1 CSM was confirmed before



DOI: 10.3748/wjg.v29.i18.2836 **Copyright** ©The Author(s) 2023.

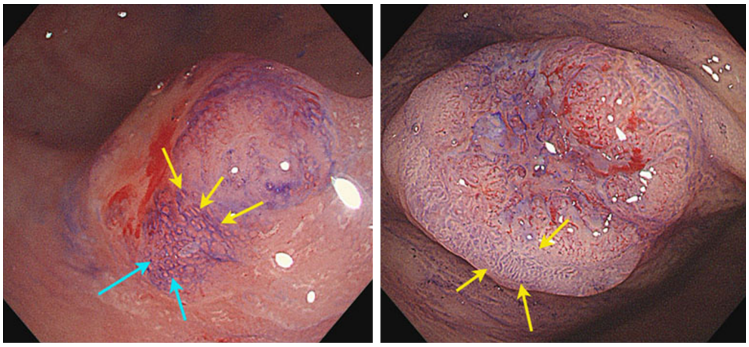
Figure 3 The immunohistory results. A: A *de novo* colorectal cancer (CRC) pathological section stained with E-cad and vimentin (VIM); B: A carcinoma in adenoma CRC pathological section stained with E-cad and VIM. VIM: Vimentin.



DOI: 10.3748/wjg.v29.i18.2836 **Copyright** ©The Author(s) 2023.

Figure 4 The association of *de novo* colorectal cancer and over survival. A: Relationship between relapse rate and colorectal cancer (CRC) types; B: Relationship between rate of death and CRC types. CIA: Carcinoma in adenoma.

injection; type 2 CSM was observed after injection; and type 3 CSM was not observed. Types 1 and 2 were considered positive CSM findings. CSM is accompanied by an increased IFN of foam macrophages in the lamina propria, representing a large-scale inflammatory reaction. The appearance of CSM is also related to the increased expression of Ki-67 and COX2, which suggests that the early appearance of CSM symbolizes a high malignancy. However, whether the appearance of CSM and the IFN of macrophages in the lamina propria affect the determination of the depth of IFN by endoscopic ultrasound (EUS) is unknown. After diagnosing white light endoscopy, magnifying endoscopy, and endoscopic ultrasonography, we concluded that the lesion was a *de novo* cancer with deep invasion, which was no longer suitable for endoscopic treatment. However, after surgical resection, pathology showed that the depth of invasion only reached the M2 layer. After further analysis of the pathology, we found that many inflammatory cells infiltrated the lesion, leading to errors in determining the IFN depth.



DOI: 10.3748/wjg.v29.i18.2836 **Copyright** ©The Author(s) 2023.

Figure 5 The surrounding pit of *de novo* colorectal cancer and carcinoma in adenoma group. The surrounding pit around *de novo* colorectal cancer (CRC) is elongated I-type and IIIL-type around carcinoma in adenoma CRC.

Under NBI and magnifying endoscopy patterns, the surface and vascular microstructures can be clearly evaluated. The NICE classification is a method for assessing the characteristics of lesions under the NBI model, which is based on the color, vessel, and general surface pattern[22]. The NICE classification can help reduce the risk of failing to detect diminutive and small lesions, which are easily regarded as polys[23]. Nevertheless, the NICE classification had no differential ability for *de novo* CRCs and CIA CRCs. The pit pattern of CRC characteristics was categorized according to the Kudo and Tsuruta classification system. Type IIIL and IV patterns are often observed in adenomas and CIA CRCs. Type V is subclassified into Vi and Vn, and occurs in cancers. The surrounding I type pit is a landmark in the diagnosis of *de novo* CRCs. However, the normal I type often deforms and confounds with an abnormal pit due to the extrusion or invasion of cancer. The IIIs type pit was round and smaller than the I type pit, and IIIL was more irregular than the elongated I type pit. An example is shown in Figure 5.

De novo CRCs have greater metastatic potential, and all pathological indicators indicate that *de novo* carcinoma has a higher metastatic potential and worse prognosis. All *de novo* cancers were classified as microsatellite stability (MSS). In the *de novo* group, the degree of TB and lymphocyte IFN was higher than that in the CIA group and was positively correlated with the depth of invasion and poor prognosis. The IHC results also showed that the expression of E-cadherin in the *de novo* group was lower than that in the CIA group. At the same time, the interstitial-related index VIM was higher than that in the CIA group, which means that the metastatic potential of the tumor in the *de novo* group was higher than that in the CIA group. TB is defined as "a single cancer cell or a cell cluster of 5 cancer cells or less". Larger tumors are called poorly differentiated tumor cell nests. TB is closely correlated with disease recurrence and poor prognosis in SM-invasive CRCs[24-27].

In addition, the TB degree had a relationship with other pathological features. In general, tumor tissues with BD2/3 are considered for further surgery[28]. The lymphocytic reaction is another crucial part of pathological changes in CRCs, which includes Crohn's-like reaction, peritumoral reaction, intratumoral periglandular reaction, and TIL[29]. TIL are defined as lymphocytes on the top of cancer cells, which can be used to predict immunotherapy response and survival outcomes. One study reported that tumors with microsatellite instability-high and sufficient CD8+ TIL had better outcomes than those with MSS/microsatellite instability-low and lower CD8+ TIL[30]. Compared to typical pathological indicators, TIL are a better factor for overall survival[29,31,32]. TIL are related to the expression of exhaustion and senescence markers in the tumor microenvironment[33,34].

This study have several promising implications during clinical practice. Due to the highly invasive and metastatic ability of *de novo* CRC, endoscopic mucosal resection or endoscopic submucosal dissection could not be performed without exact observation when we find small protruded or depressed lesions. Observing the lesions with magnified endoscopy and chromoendoscopy is necessary to confirm the diagnosis. If we suspect the lesions may be *de novo* CRCs, it is crucial evaluating invasion depth by magnified endoscopy and chromoendoscopy, or by computed tomography imaging and EUS when necessary. Then, the treatment regimens should be chosen cautiously. In the future, we will further study the molecular biological difference between *de novo* CRC and CIA CRC to find out the molecular mechanism of invasion and metastasis of *de novo* CRCs.

However, there exists some limitations in the study. The sample size appear to be small for deficience of acknowledge of *de novo* CRCs. Moreover, this appears as a single center study, and the pathogenesis/incidence of *de novo* CRC might be different in other countries.

CONCLUSION

This review summarizes the characteristics of *de novo* CRCs and confirms the conclusions of our study.

A *de novo* CRC is a small, but malignant tumor that requires more attention during colonoscopy examination. *De novo* CRCs have special endoscopic and pathological features that distinguish them from the traditional adenocarcinomas. However, more studies are needed to determine the molecular characteristics to explain the genesis mechanism.

ARTICLE HIGHLIGHTS

Research background

The small colorectal small tumors usually be ignored during colonoscopy. However, many depressed or flat lesions have substantial invasion and metastasis. *De novo* colorectal cancer (CRC) is one type of small tumor related to poor prognosis. And some endoscopists could not distinguish *de novo* CRC during the examination.

Research motivation

Some small lesions were cut off directly in the examination without computed tomography imaging and endoscopic ultrasound. This may lead to mistreatment because endoscopists often ignore the judgment of invasion depth. The *de novo* CRC may have a deep invasion layer.

Research objectives

This study aimed to comprehensively review *de novo* CRCs and provide a reference atlas for future studies and analyze the features of *de novo* CRCs to distinguish them from non-neoplastic polyps.

Research methods

This study collected clinical and pathological information on *de novo* patients and stained E-cadherin and vimentin by immunohistochemistry. Based on this information, we analyzed the characteristic of *de novo* CRC and the relative correlation between different indicators.

Research results

This study highlights that *de novo* CRCs have special endoscopic and pathological features that distinguish them from traditional adenocarcinomas. It is also the first study paying attention to chicken skin mucosa invasive depth measurement. More importantly, this study summarized several factors relevant to invasion depth and provide tremendous help in clinical practice to increase diagnostic ability.

Research conclusions

This first study pointed out the relationship between *de novo* CRC and epithelial-mesenchymal transition related genes. And it is the first study put forward that chicken skin mucosa indicates the depth of invasion.

Research perspectives

We will further study the molecular biological difference between *de novo* CRC and carcinoma in adenoma CRC to discover the mechanism of invasion and metastasis of *de novo* CRCs.

FOOTNOTES

Author contributions: Zhang HJ had full access to all the data in the study and takes responsibility for the integrity of the data and the accuracy of the data analysis; Zhang HJ, Li SY, and Yang MQ were responsible for protocol/project development; Li SY, Yang MQ, and Zhang HJ performed data analysis; Li SY, Yang MQ, Liu YM, and Sun MJ performed data collection or management; Yang MQ and Zhang HJ were responsible for manuscript writing/editing; Li SY and Yang MQ, these two authors, contributed equally to this work.

Supported by Natural Science Foundation of Liaoning Province, China, No. 2022-YGJC-71.

Institutional review board statement: The study was reviewed and approved by the Research Ethics Committee of the First Affiliated Hospital of China Medical University Institutional Review Board, No. [2021]2021-68-2.

Informed consent statement: All study participants or their legal guardian provided informed written consent about personal and medical data collection prior to study enrolment.

Conflict-of-interest statement: All the authors report no relevant conflicts of interest for this article.

Data sharing statement: Participants gave informed consent for data sharing.

STROBE statement: The authors have read the STROBE Statement—checklist of items, and the manuscript was prepared and revised according to the STROBE Statement—checklist of items.

Open-Access: This article is an open-access article that was selected by an in-house editor and fully peer-reviewed by external reviewers. It is distributed in accordance with the Creative Commons Attribution NonCommercial (CC BY-NC 4.0) license, which permits others to distribute, remix, adapt, build upon this work non-commercially, and license their derivative works on different terms, provided the original work is properly cited and the use is non-commercial. See: https://creativecommons.org/Licenses/by-nc/4.0/

Country/Territory of origin: China

ORCID number: Hui-Jing Zhang 0000-0002-6322-2335.

S-Editor: Fan JR
L-Editor: A
P-Editor: Cai YX

REFERENCES

1 **Lieberman DA**, Weiss DG, Bond JH, Ahnen DJ, Garewal H, Chejfec G. Use of colonoscopy to screen asymptomatic adults for colorectal cancer. Veterans Affairs Cooperative Study Group 380. *N Engl J Med* 2000; **343**: 162-168 [PMID: 10900274 DOI: 10.1056/NEJM200007203430301]
2 **Bray F**, Ferlay J, Soerjomataram I, Siegel RL, Torre LA, Jemal A. Global cancer statistics 2018: GLOBOCAN estimates of incidence and mortality worldwide for 36 cancers in 185 countries. *CA Cancer J Clin* 2018; **68**: 394-424 [PMID: 30207593 DOI: 10.3322/caac.21492]
3 **Papagiorgis PC**, Zizi AE, Tseleni S, Oikonomakis IN, Nikiteas NI. Clinicopathological differences of colorectal cancers according to tumor origin: Identification of possibly de novo lesions. *Biomed Rep* 2013; **1**: 97-104 [PMID: 24648902 DOI: 10.3892/br.2012.17]
4 **Koga Y**, Hirahashi M, Ohishi Y, Oda Y. Clinicopathological features and phenotypic classification of de novo-type colorectal carcinomas differ from those of colorectal carcinomas derived from flat adenomas. *Pathol Int* 2019; **69**: 331-340 [PMID: 31282116 DOI: 10.1111/pin.12803]
5 **Trinh A**, Lädrach C, Dawson HE, Ten Hoorn S, Kuppen PJK, Reimers MS, Koopman M, Punt CJA, Lugli A, Vermeulen L, Zlobec I. Tumour budding is associated with the mesenchymal colon cancer subtype and RAS/RAF mutations: a study of 1320 colorectal cancers with Consensus Molecular Subgroup (CMS) data. *Br J Cancer* 2018; **119**: 1244-1251 [PMID: 30385823 DOI: 10.1038/s41416-018-0230-7]
6 **Goto H**, Oda Y, Murakami Y, Tanaka T, Hasuda K, Goto S, Sasaki Y, Sakisaka S, Hattori M. Proportion of de novo cancers among colorectal cancers in Japan. *Gastroenterology* 2006; **131**: 40-46 [PMID: 16831588 DOI: 10.1053/j.gastro.2006.04.010]
7 **Matsuda T**, Fujii T, Saito Y, Nakajima T, Uraoka T, Kobayashi N, Ikehara H, Ikematsu H, Fu KI, Emura F, Ono A, Sano Y, Shimoda T, Fujimori T. Efficacy of the invasive/non-invasive pattern by magnifying chromoendoscopy to estimate the depth of invasion of early colorectal neoplasms. *Am J Gastroenterol* 2008; **103**: 2700-2706 [PMID: 18853968 DOI: 10.1111/j.1572-0241.2008.02190.x]
8 **Glover B**, Patel N, Ashrafian H, Teare J. Diagnostic accuracy of i-scan image enhancement for real-time endoscopic diagnosis of small colorectal polyps: a meta-analysis. *Therap Adv Gastroenterol* 2018; **11**: 1756284818814948 [PMID: 30574190 DOI: 10.1177/1756284818814948]
9 **Kuramoto S**, Oohara T. How do colorectal cancers develop? *Cancer* 1995; **75**: 1534-1538 [PMID: 7889487 DOI: 10.1002/1097-0142(19950315)75:6+<1534::aid-cncr2820751525>3.0.co;2-2]
10 **Mueller J**, Mueller E, Hoepner I, Jütting J, Bethke B, Stolte M, Höfler H. Expression of bcl-2 and p53 in de novo and ex-adenoma colon carcinoma: a comparative immunohistochemical study. *J Pathol* 1996; **180**: 259-265 [PMID: 8958802 DOI: 10.1002/(SICI)1096-9896(199611)180:3<259::AID-PATH654>3.0.CO;2-1]
11 **Kinzler KW**, Vogelstein B. Lessons from hereditary colorectal cancer. *Cell* 1996; **87**: 159-170 [PMID: 8861899 DOI: 10.1016/s0092-8674(00)81333-1]
12 **Shatz BA**, Weinstock LB, Thyssen EP, Mujeeb I, DeSchryver K. Colonic chicken skin mucosa: an endoscopic and histological abnormality adjacent to colonic neoplasms. *Am J Gastroenterol* 1998; **93**: 623-627 [PMID: 9576459 DOI: 10.1111/j.1572-0241.1998.177_b.x]
13 **Lee YM**, Song KH, Koo HS, Lee CS, Ko I, Lee SH, Huh KC. Colonic Chicken Skin Mucosa Surrounding Colon Polyps Is an Endoscopic Predictive Marker for Colonic Neoplastic Polyps. *Gut Liver* 2022; **16**: 754-763 [PMID: 35000932 DOI: 10.5009/gnl210271]
14 **Thiery JP**, Acloque H, Huang RY, Nieto MA. Epithelial-mesenchymal transitions in development and disease. *Cell* 2009; **139**: 871-890 [PMID: 19945376 DOI: 10.1016/j.cell.2009.11.007]
15 **Shibue T**, Weinberg RA. EMT, CSCs, and drug resistance: the mechanistic link and clinical implications. *Nat Rev Clin Oncol* 2017; **14**: 611-629 [PMID: 28397828 DOI: 10.1038/nrclinonc.2017.44]
16 **Mueller JD**, Bethke B, Stolte M. Colorectal de novo carcinoma: a review of its diagnosis, histopathology, molecular biology, and clinical relevance. *Virchows Arch* 2002; **440**: 453-460 [PMID: 12021919 DOI: 10.1007/s00428-002-0623-z]
17 **Tsuda S**, Veress B, Tóth E, Fork FT. Flat and depressed colorectal tumours in a southern Swedish population: a prospective chromoendoscopic and histopathological study. *Gut* 2002; **51**: 550-555 [PMID: 12235079 DOI:

10.1136/gut.51.4.550]

18 **Rembacken BJ**, Fujii T, Cairns A, Dixon MF, Yoshida S, Chalmers DM, Axon AT. Flat and depressed colonic neoplasms: a prospective study of 1000 colonoscopies in the UK. *Lancet* 2000; **355**: 1211-1214 [PMID: 10770302 DOI: 10.1016/s0140-6736(00)02086-9]

19 **Gao Z**, Jiang J, Hou L, Zhang B. Dysregulation of MiR-144-5p/RNF187 Axis Contributes To the Progression of Colorectal Cancer. *J Transl Int Med* 2022; **10**: 65-75 [PMID: 35702180 DOI: 10.2478/jtim-2021-0043]

20 **Hornick JL**, Farraye FA, Odze RD. Clinicopathologic and immunohistochemical study of small apparently "de novo" colorectal adenocarcinomas. *Am J Surg Pathol* 2007; **31**: 207-215 [PMID: 17255765 DOI: 10.1097/01.pas.0000213383.17418.a9]

21 **Hayashi N**, Tanaka S, Hewett DG, Kaltenbach TR, Sano Y, Ponchon T, Saunders BP, Rex DK, Soetikno RM. Endoscopic prediction of deep submucosal invasive carcinoma: validation of the narrow-band imaging international colorectal endoscopic (NICE) classification. *Gastrointest Endosc* 2013; **78**: 625-632 [PMID: 23910062 DOI: 10.1016/j.gie.2013.04.185]

22 **Hattori S**, Iwatate M, Sano W, Hasuike N, Kosaka H, Ikumoto T, Kotaka M, Ichiyanagi A, Ebisutani C, Hisano Y, Fujimori T, Sano Y. Narrow-band imaging observation of colorectal lesions using NICE classification to avoid discarding significant lesions. *World J Gastrointest Endosc* 2014; **6**: 600-605 [PMID: 25512769 DOI: 10.4253/wjge.v6.i12.600]

23 **Tanaka S**, Hayashi N, Oka S, Chayama K. Endoscopic assessment of colorectal cancer with superficial or deep submucosal invasion using magnifying colonoscopy. *Clin Endosc* 2013; **46**: 138-146 [PMID: 23614123 DOI: 10.5946/ce.2013.46.2.138]

24 **Landau MA**, Zhu B, Akwuole FN, Pai RK. Histopathological Predictors of Recurrence in Stage III Colon Cancer: Reappraisal of Tumor Deposits and Tumor Budding Using AJCC8 Criteria. *Int J Surg Pathol* 2019; **27**: 147-158 [PMID: 29992847 DOI: 10.1177/1066896918787275]

25 **Liu P**, Zhu H, Zhang X, Feng A, Zhu X, Sun Y. Predicting Survival for Hepatic Arterial Infusion Chemotherapy of Unresectable Colorectal Liver Metastases: Radiomics Analysis of Pretreatment Computed Tomography. *J Transl Int Med* 2022; **10**: 56-64 [PMID: 35702189 DOI: 10.2478/jtim-2022-0004]

26 **Nagata K**, Shinto E, Yamadera M, Shiraishi T, Kajiwara Y, Okamoto K, Mochizuki S, Hase K, Kishi Y, Ueno H. Prognostic and predictive values of tumour budding in stage IV colorectal cancer. *BJS Open* 2020; **4**: 693-703 [PMID: 32472647 DOI: 10.1002/bjs5.50300]

27 **Zhang Y**, Liu Y, Qiu X, Yan B. Concurrent Comparison of the Prognostic Values of Tumor Budding, Tumor Stroma Ratio, Tumor Infiltrating Pattern and Lymphocyte-to-Monocyte Ratio in Colorectal Cancer Patients. *Technol Cancer Res Treat* 2021; **20**: 15330338211045826 [PMID: 34658263 DOI: 10.1177/15330338211045826]

28 **Pan S**, Sun S, Liu B, Hou Y. Pan-cancer Landscape of the RUNX Protein Family Reveals their Potential as Carcinogenic Biomarkers and the Mechanisms Underlying their Action. *J Transl Int Med* 2022; **10**: 156-174 [PMID: 35959452 DOI: 10.2478/jtim-2022-0013]

29 **Ogino S**, Nosho K, Irahara N, Meyerhardt JA, Baba Y, Shima K, Glickman JN, Ferrone CR, Mino-Kenudson M, Tanaka N, Dranoff G, Giovannucci EL, Fuchs CS. Lymphocytic reaction to colorectal cancer is associated with longer survival, independent of lymph node count, microsatellite instability, and CpG island methylator phenotype. *Clin Cancer Res* 2009; **15**: 6412-6420 [PMID: 19825961 DOI: 10.1158/1078-0432.CCR-09-1438]

30 **Zou Q**, Wang X, Ren D, Hu B, Tang G, Zhang Y, Huang M, Pai RK, Buchanan DD, Win AK, Newcomb PA, Grady WM, Yu H, Luo Y. DNA methylation-based signature of CD8+ tumor-infiltrating lymphocytes enables evaluation of immune response and prognosis in colorectal cancer. *J Immunother Cancer* 2021; **9** [PMID: 34548385 DOI: 10.1136/jitc-2021-002671]

31 **Phillips SM**, Banerjea A, Feakins R, Li SR, Bustin SA, Dorudi S. Tumour-infiltrating lymphocytes in colorectal cancer with microsatellite instability are activated and cytotoxic. *Br J Surg* 2004; **91**: 469-475 [PMID: 15048750 DOI: 10.1002/bjs.4472]

32 **Jenkins MA**, Hayashi S, O'Shea AM, Burgart LJ, Smyrk TC, Shimizu D, Waring PM, Ruszkiewicz AR, Pollett AF, Redston M, Barker MA, Baron JA, Casey GR, Dowty JG, Giles GG, Limburg P, Newcomb P, Young JP, Walsh MD, Thibodeau SN, Lindor NM, Lemarchand L, Gallinger S, Haile RW, Potter JD, Hopper JL, Jass JR; Colon Cancer Family Registry. Pathology features in Bethesda guidelines predict colorectal cancer microsatellite instability: a population-based study. *Gastroenterology* 2007; **133**: 48-56 [PMID: 17631130 DOI: 10.1053/j.gastro.2007.04.044]

33 **Newman AM**, Steen CB, Liu CL, Gentles AJ, Chaudhuri AA, Scherer F, Khodadoust MS, Esfahani MS, Luca BA, Steiner D, Diehn M, Alizadeh AA. Determining cell type abundance and expression from bulk tissues with digital cytometry. *Nat Biotechnol* 2019; **37**: 773-782 [PMID: 31061481 DOI: 10.1038/s41587-019-0114-2]

34 **Yang R**, Cheng S, Luo N, Gao R, Yu K, Kang B, Wang L, Zhang Q, Fang Q, Zhang L, Li C, He A, Hu X, Peng J, Ren X, Zhang Z. Distinct epigenetic features of tumor-reactive CD8+ T cells in colorectal cancer patients revealed by genome-wide DNA methylation analysis. *Genome Biol* 2019; **21**: 2 [PMID: 31892342 DOI: 10.1186/s13059-019-1921-y]

World Journal of Gastroenterology

Submit a Manuscript: https://www.f6publishing.com

World J Gastroenterol 2023 May 14; 29(18): 2850-2863

DOI: 10.3748/wjg.v29.i18.2850

ISSN 1007-9327 (print) ISSN 2219-2840 (online)

ORIGINAL ARTICLE

Retrospective Study

Prolonged hyperthermic intraperitoneal chemotherapy duration with 90 minutes cisplatin might increase overall survival in gastric cancer patients with peritoneal metastases

Heinrich Steinhoff, Miklos Acs, Sebastian Blaj, Magdolna Dank, Magdolna Herold, Zoltan Herold, Jonas Herzberg, Patricia Sanchez-Velazquez, Tim Strate, Attila Marcell Szasz, Pompiliu Piso

Specialty type: Gastroenterology and hepatology

Provenance and peer review: Invited article; Externally peer reviewed.

Peer-review model: Single blind

Peer-review report's scientific quality classification

Grade A (Excellent): A
Grade B (Very good): B, B
Grade C (Good): C, C, C
Grade D (Fair): 0
Grade E (Poor): 0

P-Reviewer: Karaca CA, Turkey; Li K, China; Li L, New Zealand; Luo W, China; Segura-Sampedro JJ, Spain

Received: November 18, 2022
Peer-review started: November 18, 2022
First decision: February 15, 2023
Revised: February 27, 2023
Accepted: April 10, 2023
Article in press: April 10, 2023
Published online: May 14, 2023

Heinrich Steinhoff, Miklos Acs, Sebastian Blaj, Pompiliu Piso, Department of General and Visceral Surgery, Hospital Barmherzige Brüder, Regensburg 93049, Germany

Magdolna Dank, Zoltan Herold, Attila Marcell Szasz, Division of Oncology, Department of Internal Medicine and Oncology, Semmelweis University, Budapest 1083, Hungary

Magdolna Herold, Department of Internal Medicine and Hematology, Semmelweis University, Budapest 1088, Hungary

Jonas Herzberg, Tim Strate, Department of Surgery, Krankenhaus Reinbek St. Adolf-Stift, Reinbek 21465, Germany

Patricia Sanchez-Velazquez, Department of General Surgery, Hospital del Mar, Barcelona 08003, Spain

Corresponding author: Heinrich Steinhoff, MD, Doctor, Surgeon, Department of General and Visceral Surgery, Hospital Barmherzige Brüder, Prüfeninger Str. 86, Regensburg 93049, Germany. heinrich.steinhoff@barmherzige-regensburg.de

Abstract

BACKGROUND

Advanced gastric cancer with synchronous peritoneal metastases (GC-PM) is associated with a poor prognosis. Although cytoreductive surgery with hyperthermic intraperitoneal chemotherapy (CRS-HIPEC) is a promising approach, only a limited number of Western studies exist.

AIM

To investigate the clinicopathological outcomes of patients who underwent CRS-HIPEC for GC-PM.

METHODS

A retrospective analysis of patients with GC-PM was conducted. All patients were seen at the Department of General and Visceral Surgery, Hospital Barmherzige Brüder, Regensburg, Germany between January 2011 and July 2021 and underwent CRS-HIPEC. Preoperative laboratory results, the use of neoadjuvant

trastuzumab, and the details of CRS-HIPEC, including peritoneal carcinomatosis index, completeness of cytoreduction, and surgical procedures were recorded. Disease-specific (DSS), and overall survival (OS) of patients were calculated.

RESULTS

A total of 73 patients were included in the study. Patients treated with neoadjuvant trastuzumab (n = 5) showed longer DSS (P = 0.0482). Higher white blood cell counts (DSS: P = 0.0433) and carcinoembryonic antigen levels (OS and DSS: P < 0.01), and lower hemoglobin (OS and DSS: P < 0.05) and serum total protein (OS: P = 0.0368) levels were associated with shorter survival. Longer HIPEC duration was associated with more advantageous median survival times [60-min (n = 59): 12.86 mo; 90-min (n = 14): 27.30 mo], but without statistical difference. To obtain additional data from this observation, further separation of the study population was performed. First, propensity score-matched patient pairs (n = 14 in each group) were created. Statistically different DSS was found between patient pairs (hazard ratio = 0.2843; 95% confidence interval: 0.1119-0.7222; P = 0.0082). Second, those patients who were treated with trastuzumab and/or had human epidermal growth factor receptor 2 positivity (median survival: 12.68 mo *vs* 24.02 mo), or had to undergo the procedure before 2016 (median survival: 12.68 mo *vs* 27.30 mo; P = 0.0493) were removed from the original study population.

CONCLUSION

Based on our experience, CRS-HIPEC is a safe and secure method to improve the survival of advanced GC-PM patients. Prolonged HIPEC duration may serve as a good therapy for these patients.

Key Words: Cytoreductive surgery; Hyperthermic intraperitoneal chemotherapy; Peritoneal metastasis; Stomach neoplasms; Gastric cancer

©The Author(s) 2023. Published by Baishideng Publishing Group Inc. All rights reserved.

Core Tip: Advanced gastric cancer (GC) cases with peritoneal metastases are known for their poor survival rates. It has been previously reported that these patients benefit from cytoreductive surgery (CRS) with hyperthermic intraperitoneal chemotherapy (HIPEC) but available data on this treatment are scarce. In this study, we retrospectively analyzed the clinicopathological and laboratory data of 73 patients with advanced GC and synchronous peritoneal metastases. It was found that prolonged HIPEC duration after macroscopic complete CRS in the scope of multimodal treatment along with advanced perioperative chemotherapy and biologicals may serve as the best currently available therapy for these patients.

Citation: Steinhoff H, Acs M, Blaj S, Dank M, Herold M, Herold Z, Herzberg J, Sanchez-Velazquez P, Strate T, Szasz AM, Piso P. Prolonged hyperthermic intraperitoneal chemotherapy duration with 90 minutes cisplatin might increase overall survival in gastric cancer patients with peritoneal metastases. *World J Gastroenterol* 2023; 29(18): 2850-2863

URL: https://www.wjgnet.com/1007-9327/full/v29/i18/2850.htm

DOI: https://dx.doi.org/10.3748/wjg.v29.i18.2850

INTRODUCTION

Gastric cancer (GC) is the fifth most common cancer, with a worldwide incidence of 1,089,103 new cases and 768,793 deaths based on the 2020 GLOBOCAN results[1,2]. The majority of the new cases are diagnosed in Asia, where occurrence is 6-fold higher than in Europe; a similar distribution is observed in GC mortality[1]. In Germany, 15322 new cases and 9196 deaths were reported in 2020[1]. GC is known for its morphological diversity[3], and the most commonly used classifications are those outlined by Nakamura *et al*[4], Lauren[5], and the World Health Organization (WHO)[6]. The treatment of gastric cancer is multidisciplinary and depends on the clinical staging of the tumor. While early-stage GC (stage T1a) can be endoscopically resected[7], stage T1 with positive lymph node(s) and T2-T4a tumors regardless of lymph node status are treated by surgical resection and peri- or postoperative chemotherapy[8]. Advanced resectable GCs are typically treated with neoadjuvant chemotherapy followed by gastrectomy and adjuvant chemotherapy[9]; if not amenable to resection, then the treatment of choice is chemotherapy[8].

A recent analysis of 18,000 United States patients showed that advanced GC with PM has a median survival of 8.6 mo if treated with chemotherapy only[10], while studies from the United States[11], China[12] and Germany[13] have shown that advanced GCs with peritoneal carcinomatosis benefit significantly from cytoreductive surgery (CRS) and hyperthermic intraperitoneal chemotherapy (HIPEC)[11-15] when complete macroscopic resection of the tumor tissue can be achieved[16]. Nevertheless, the available data regarding the use of CRS and HIPEC in advanced GC with PM is scarce, and this multimodal therapy has infrequently been recommended in any national or international guidelines. To date, the Japanese[17] and the United States[18] guidelines do not include CRS and HIPEC as therapeutic options. In France, the guidelines for treatment of advanced GC with PM[19] are yet to be defined in future randomized phase III studies. The same is true in Germany, where an expert consensus-based recommendation calls for the implementation of CRS and HIPEC in clinical studies[8]. The European Society for Medical Oncology guidelines for the treatment of gastric cancer describe CRS and HIPEC as safe procedures, but with unclear oncological outcomes[20]. Accordingly, the aim of this retrospective study was to investigate the clinical outcome after administration of this multimodal therapy in a tertiary center to treat patients with primary advanced GC with PM.

MATERIALS AND METHODS

Patients and study design

The HIPEC database of a single tertiary care center was analyzed in a retrospective manner. A total of 73 patients seen at the Department of General and Visceral Surgery, Hospital Barmherzige Brüder, Regensburg, Germany between January 2011 and July 2021 with primary GC and synchronous PM were included (Figure 1). All patients gave written and verbal informed consent to be included in the national HIPEC registry, administered by the German Society for General and Visceral Surgery (DGAV), and for the use of their anonymized data for research purposes and quality assurance prior to any study-specific procedures. All 73 patients underwent CRS + HIPEC and were treated according to national or international multidisciplinary recommendations[8,20].

Details of CRS + HIPEC

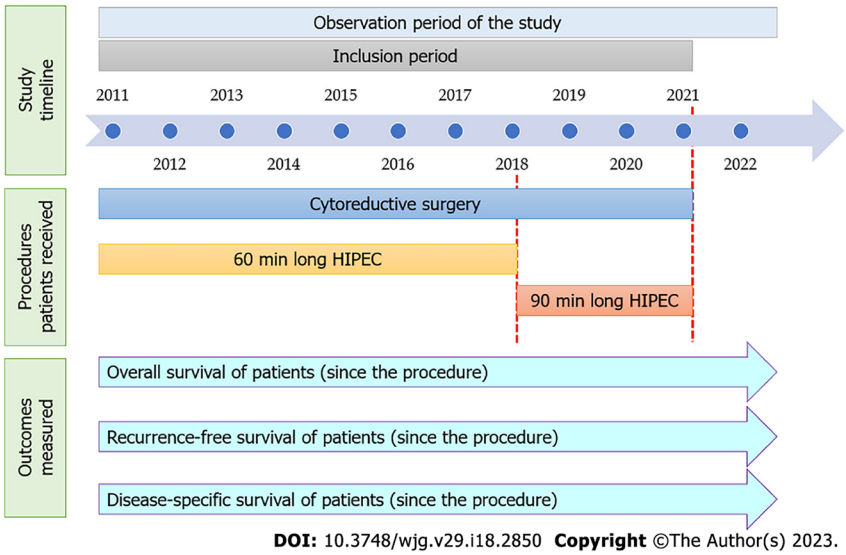
Each of the 73 cases was discussed by a multidisciplinary board of experts (oncologists, surgeons and anesthesiologists) before any treatment decision was made. Preoperatively, the extent of peritoneal dissemination was assessed using abdominal and chest computed tomography (CT) scans. The peritoneal carcinomatosis index (PCI)[21] was calculated based on diagnostic laparoscopy performed on tumors of T3 stage or higher or CT evidence of peritoneal carcinomatosis[22]. Prior to surgery, all patients were preconditioned as per the enhanced recovery after surgery (ERAS) protocol. During CRS, the completeness of cytoreduction (CC) was scored as proposed by Jacquet and Sugarbaker[21]: No residual disease, residual nodules measuring less than 2.5 mm, between 2.5 mm and 2.5 cm, or greater than 2.5 cm were defined as CC-0, CC-1, CC-2, and CC-3, respectively.

Closed HIPEC with a goal temperature of 42 °C with bidirectional HIPEC with cisplatin (75 mg/m^2) and doxorubicin (15 mg/m^2) was administered immediately after CRS for 60 min or 90 min duration (Figure 1). The duration of HIPEC was changed from 60 min to 90 min in 2018 based on the findings of van Driel's study[23]. The cytotoxic agents were added to a 3000 mL-4000 mL isotonic saline solution with a mean flow rate of 1400 mL/min-1800 mL/min. During the treatment, temperature probes for monitoring the 42 °C goal temperature were placed in the right subphrenic and pelvic areas.

Clinicopathological and laboratory data measurements

Clinicopathological and laboratory data were obtained from the DGAV HIPEC registry and the electronic medical system of Hospital Barmherzige Brüder, Regensburg, Germany. The staging of the tumors was unified using the 8th American Joint Committee on Cancer (AJCC) TNM system[24]. Histopathology types of the tumors were categorized as diffuse type adenocarcinoma (ACD), intestinal type adenocarcinoma (ACI), or signet-ring cell adenocarcinoma (SRC)[3]. Neoadjuvant chemotherapeutic treatment of patients was recorded as the latest lineage the patient received prior to CRS + HIPEC. Except for a single patient, all study participants were treated with at least docetaxel-based first-line chemotherapy (FLOT protocol: 5-fluorouracil, leucovorin, oxaliplatin, and docetaxel; or DCF protocol: docetaxel, cisplatin, and 5-fluorouracil). Chemotherapy was administered in accordance with the German guidelines on GC; when recommendation changed from EFC/ECX (Epirubicin, Cisplatin, Fluorouracil/Epirubicin, Cisplatin, Capecitabine) to FLOT after Al-Batran's FLOT-4 study in 2019[25], chemotherapy was accordingly changed. The additional use of trastuzumab (trade name: Herceptin) was also recorded.

Complete blood count, liver enzyme, lipase, creatinine, and tumor marker blood tests were performed at the Department of Laboratory Medicine, Microbiology, and Hospital Hygiene, Hospital Barmherzige Brüder, Regensburg, Germany. The Chronic Kidney Disease Epidemiology Collaboration equations were used to calculate estimated glomerular filtration rate[26]. The Clavien–Dindo Classification[27] was used to assess postoperative adverse events. Although some recent publications have



DOI: 10.3748/wjg.v29.i18.2850 **Copyright** ©The Author(s) 2023.

Figure 1 Timeline of the study. HIPEC: Hyperthermic intraperitoneal chemotherapy.

suggested including all patient deaths within 90 d as post-procedure deaths[28,29], HIPEC-related post-procedure deaths were defined as follows: (1) Those occurring during the observation period at the intensive care unit or at the surgical inpatient unit prior to discharge; or (2) Between discharge and adjuvant chemotherapy. If a patient had started adjuvant chemotherapy, their death was defined as GC-related. Recurrence-free (RFS), disease-specific (DSS), and overall survival (OS) were calculated from the date of surgery (CRS + HIPEC) to the date of tumor recurrence, cancer-related death, or death from any cause, respectively. The follow-up of patients was terminated on 30 September 2022 and the patients alive at this time point were right censored (Figure 1).

Statistical analysis

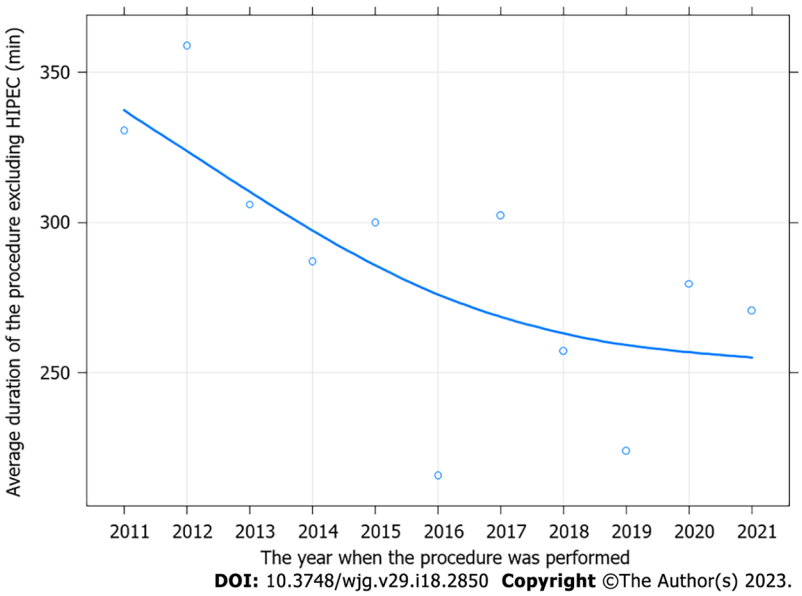
Statistical analyses were performed within the R for Windows version 4.2.1 environment (R Foundation for Statistical Computing, 2022, Vienna, Austria). Wilcoxon rank sum test and Fisher's exact test were used for group comparisons. Linear models were used to investigate whether there was an improvement in the duration of the procedure (learning curve). Matching of patient pairs was done *via* propensity score matching (R-package "Matching" version 4.10-8). DSS, OS, and RFS were determined using the cause-specific competing risk Cox survival model (R packages "survival" version 3.4-0 and "survminer" version 0.4.9). Parameter selection for multivariate survival models was not based on univariate P value, but on literature data and the medical/clinical importance of the given parameter. $P < 0.05$ was considered statistically significant, and P values were corrected with the Holm method[30] for the multiple-comparisons problem. Continuous, survival, and count data were expressed as the mean ± standard deviation (SD), the hazard ratio (HR) with a 95% confidence interval (95%CI), and the number of observations (percentage), respectively.

RESULTS

A total of 73 GC patients with PM were included in the study. Sixty-four cancer-related death events, 13 tumor recurrence events, and 1 death due to postoperative complications occurred. The complete list of pre-, peri- and postoperative clinicopathological characteristics of study participants are listed in Supplementary Table 1. In general, the average operating times (excluding the time for HIPEC) improved significantly over observation period ($P = 0.0097$; Figure 2).

First, it was investigated whether any of the CRS + HIPEC-related or clinicopathological features had a significant effect on patient survival. The need to remove any further organs, such as the removal of the bladder or the appendix during CRS ($n = 9$), was associated with a negative effect on DSS (HR: 2.0538; 95%CI: 1.2715-3.3179; $P = 0.0033$). Those patients who received additional trastuzumab treatment during neoadjuvant chemotherapy ($n = 5$) before the CRS + HIPEC procedure had better DSS (HR: 0.4446; 95%CI: 0.1989-0.9937; $P = 0.0482$). A trend towards longer RFS was found in patients who did not require pelvic peritonectomy (HR: 0.3382; 95%CI: 0.1099-1.0410; $P = 0.0588$). OS was significantly better in patients without pelvic peritonectomy (HR: 0.5459; 95%CI: 0.3152-0.9454; $P = 0.0307$).

Longer HIPEC duration (60 min *vs* 90 min) was associated with more advantageous median survival times: 12.86 mo (95%CI: 11.01-17.31) for the 60 min and 27.30 mo (95%CI: 16.20-NA) for the 90 min cohorts (Supplementary Table 1). However, despite the clinically different median survival times, the



DOI: 10.3748/wjg.v29.i18.2850 **Copyright** ©The Author(s) 2023.

Figure 2 Improvement of the operating times of cytoreductive surgery (excluding hyperthermic intraperitoneal chemotherapy) in our surgical center during the study period. HIPEC: Hyperthermic intraperitoneal chemotherapy.

survival of the groups did not differ based on the results of the statistical models with respect to DSS (HR: 0.6239; 95%CI: 0.3413-1.1410; P = 0.1250; Figure 3), OS (HR: 0.6134; 95%CI: 0.3007-1.2510; P = 0.1790), or RFS (P = 0.9650). Furthermore, the type of histology (ACD *vs* ACI *vs* SRC) did not affect DSS (P = 0.4096; Supplementary Figure 1),OS (P = 0.2422), or RFS (P = 0.2799). However, the RFS survival curves of the different histology types seemed to be visually different (Figure 4).

The effect of pre-HIPEC laboratory results on patient survival was also investigated. Higher white blood cell counts (HR: 1.1319; 95%CI: 1.0037-1.2770; P = 0.0433) and carcinoembryonic antigen (CEA) levels (HR: 1.1490; 95%CI: 1.0422-1.2667; P = 0.0053) were associated with an increased risk for shorter DSS. In contrast, higher hemoglobin (HR: 0.7897; 95%CI: 0.6562-0.9505; P = 0.0125) and serum total protein (HR: 0.6795; 95%CI: 0.4330-1.0660; P = 0.0928) levels were associated with a significant and marginally decreased risk for shorter survival, respectively. The same results were found for OS (white blood cell count: P = 0.0945; CEA: P = 0.0052; hemoglobin: P = 0.0087; serum total protein: P = 0.0368), while shorter RFS times were observed in patients with higher RDW levels (HR: 1.2190; 95%CI: 1.0030-1.4810; P = 0.0466). Moreover, similar to that observed with respect to OS and DSS, marginally advantageous RFS was justified for higher serum total protein levels (P = 0.0875).

The effect of clinicopathological and laboratory data on survival was also further investigated in a multivariate setting (Table 1). DSS was marginally affected by the duration of HIPEC [60 min (ref.) *vs* 90 min: HR: 0.5252; 95%CI: 0.2565-1.0750; P = 0.0781] and by PCI (HR: 1.0630; 95%CI: 0.9982-1.1310; P = 0.0569), and significantly by preoperative serum CEA levels (HR: 1.2220; 95%CI: 1.0880-1.3720; P = 0.0007). Similar trends were observed for OS, while worse RFS was more likely associated with lower preoperative white blood cell count (HR: 0.4616; 95%CI: 0.2270-0.9385; P = 0.0327), lower T stage (HR: 13.1182; 95%CI: 1.0285-167.3080; P = 0.0475), and higher N stage (HR: 5.6893; 95%CI: 0.7616-42.4972; P = 0.0902).

Comparison of the 60 and 90-min-long HIPEC patient groups

Further comparison was performed by creating 2 groups according to the duration of HIPEC. Fifty-nine and 14 study participants were enrolled in the 60 min and 90 min groups, respectively. Except for the above-described median survival differences (12.86 mo *vs* 27.30 mo; Figure 3), no difference was found in any clinicopathological characteristic between the two groups after P value adjustment (Supplementary Table 1).

By investigating the results without P value adjustment, several observations were made. The length of CRS trended toward being shorter in the 90 min group (299 ± 76 min *vs* 264 ± 82 min; crude P = 0.0718). Peritonectomy of the omental bursa was more frequently performed in the 60-min group (30.5% *vs* 0%; crude P = 0.0157), while lesser omentectomy was more common in the 90-min group (33.9% *vs* 71.4%; crude P = 0.0153). Fresh frozen plasma (FFP) transfusion was needed only once in the 90 min group, while in the 60-min group, FFP was administered in 32 patients (7.1% *vs* 54.2%; crude P = 0.0009). On average, the length of hospital stay was shorter in the 90 min group (crude P = 0.0134); a more detailed examination of the data revealed that hospitalization longer than 20 d was more common in the 60 min group (39.0% *vs* 7.1%; crude P = 0.0276). Moreover, abnormal serum levels of gamma-glutamyl transferase (crude P = 0.0407, Figure 5A) and serum total protein (crude P = 0.0570, Figure 5B)

Table 1 *P* values of the multivariate survival model

Parameter	DSS	OS	RFS
HIPEC duration [60 min (ref.) *vs* 90 min]	0.0781	0.1541	0.5578
Age (yr)	0.1870	0.1331	0.3691
Sex [male *vs* female (ref.)]	0.3327	0.2943	0.8681
Stage T [1-2 (ref.) *vs* 3-4]	0.1205	0.1857	0.0475
Stage N [0 (ref.) *vs* 1-3]	0.5071	0.4511	0.0902
Histology			
ACD (ref.) *vs* ACI	0.3092	0.2335	0.2471
ACD (ref.) *vs* SRC	0.9456	0.8638	0.2227
Body-mass index (kg/m^2)	0.6394	0.8365	0.3049
Peritoneal carcinomatosis index	0.0569	0.2530	0.2752
White blood cell count (10^9/L)	0.1843	0.2387	0.0327
Hemoglobin (g/dL)	0.2783	0.2924	0.7656
Carcinoembryonic antigen (ng/mL)	0.0007	0.0005	0.1089

ACD: Diffuse type adenocarcinoma; ACI: Intestinal type adenocarcinoma; DSS: Disease-specific survival; ref.: Reference category; RFS: Recurrence-free survival; OS: Overall survival; SRC: Signet-ring cell adenocarcinoma.

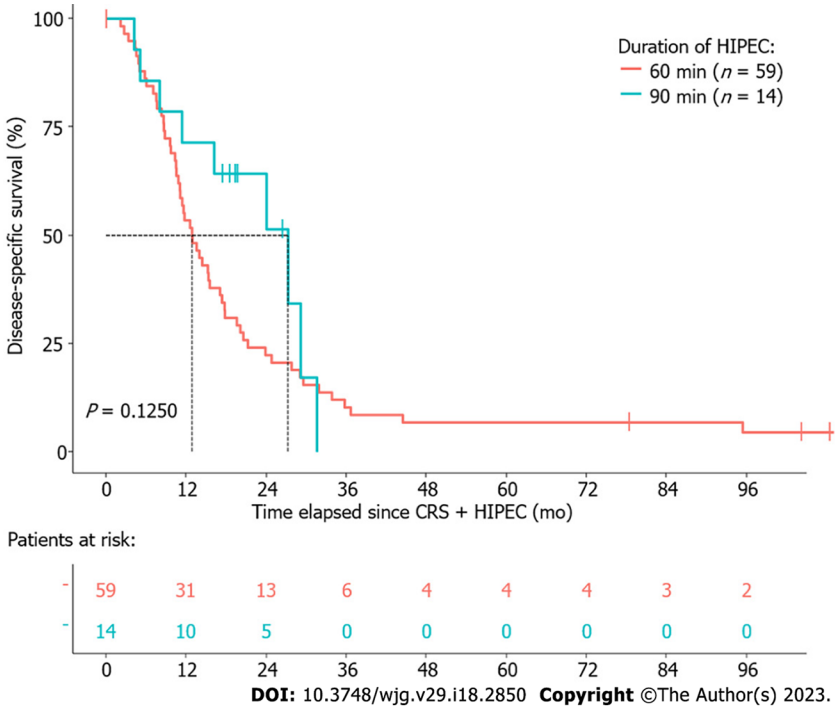
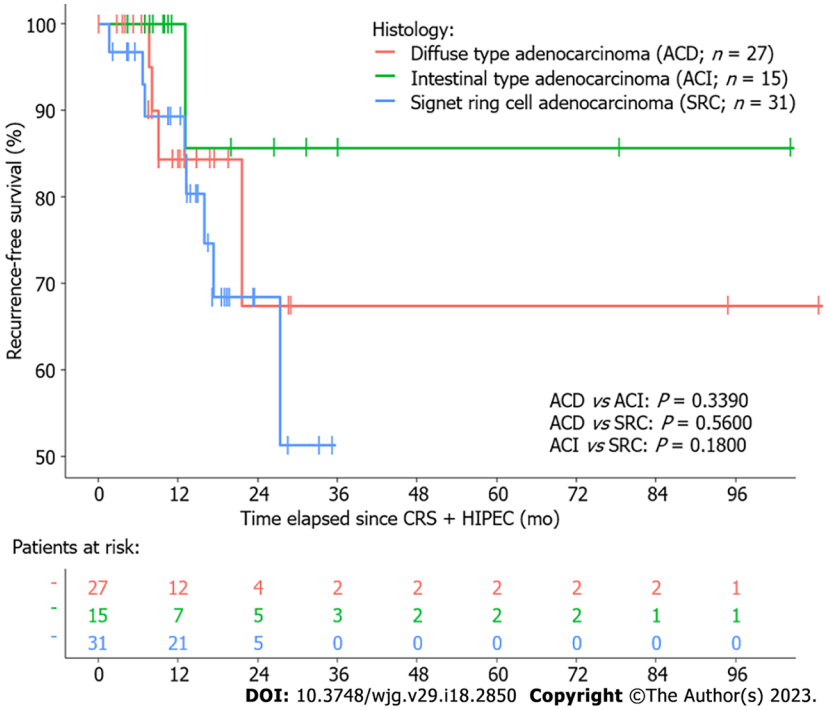


Figure 3 Differences in disease-specific survival between patients with gastric cancer who underwent cytoreductive surgery and 60 min or 90 min hyperthermic intraperitoneal chemotherapy. The dotted line represents median survival. CRS: Cytoreductive surgery; HIPEC: Hyperthermic intraperitoneal chemotherapy.

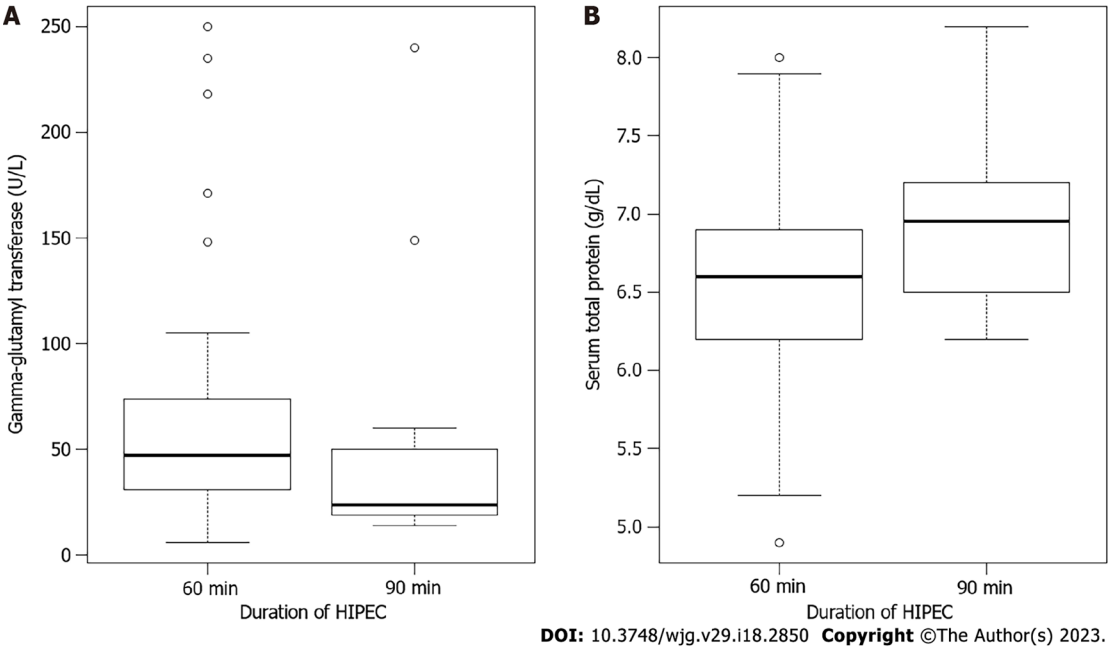
levels were observed more often in the 60-min group (Supplementary Table 1).

To further investigate the cause of the clinically significant difference in median survival, the following adjustments to the groups were performed with consideration of any possible confounding effects. First, propensity score-matched patient pairs (n = 14) were created in which patients were matched by age, sex, PCI score, CC score, time spent in the intensive care unit after CRS + HIPEC, duration of CRS, and the presence of lymph node metastasis (stage N = 0 *vs* stage $N \geq 1$). No differences in adjusted or in crude P values were found in any of the preoperative, perioperative, and postoperative



DOI: 10.3748/wjg.v29.i18.2850 Copyright ©The Author(s) 2023.

Figure 4 Differences in recurrence-free survival between patients with gastric cancer of different histological types who underwent cytoreductive surgery and hyperthermic intraperitoneal chemotherapy. ACD: Diffuse type adenocarcinoma; ACI: Intestinal type adenocarcinoma; CRS: Cytoreductive surgery; HIPEC: Hyperthermic intraperitoneal chemotherapy; SRC: Signet-ring cell adenocarcinoma.



DOI: 10.3748/wjg.v29.i18.2850 Copyright ©The Author(s) 2023.

Figure 5 Gamma-glutamyl transferase and total protein levels in 60 min and 90 min hyperthermic intraperitoneal chemotherapy groups. Clinically abnormal serum levels of gamma-glutamyl transferase (crude $P = 0.0407$) and total protein (crude $P = 0.0570$) were observed more often in those gastric cancer patients who received hyperthermic intraperitoneal chemotherapy (HIPEC) for 60 min after the cytoreductive surgery. Thick lines and hollow circles represent the median and outliers, respectively. A: Gamma-glutamyl transferase; B: Total protein.

parameters between propensity score-matched groups. However, the seemingly different survival between the 2 groups became statistically significant [60 min (ref.) *vs* 90 min: HR = 0.2843; 95%CI: 0.1119-0.7222; $P = 0.0082$; Figure 6] with 10.91 mo (95%CI: 9.56-17.77) and 27.30 mo (95%CI: 16.20-NA) median survivals for the 60 min and 90 min groups, respectively.

We also investigated whether results changed if patients who received trastuzumab and/or had immunohistochemically positive pathological results against human epidermal growth factor receptor 2

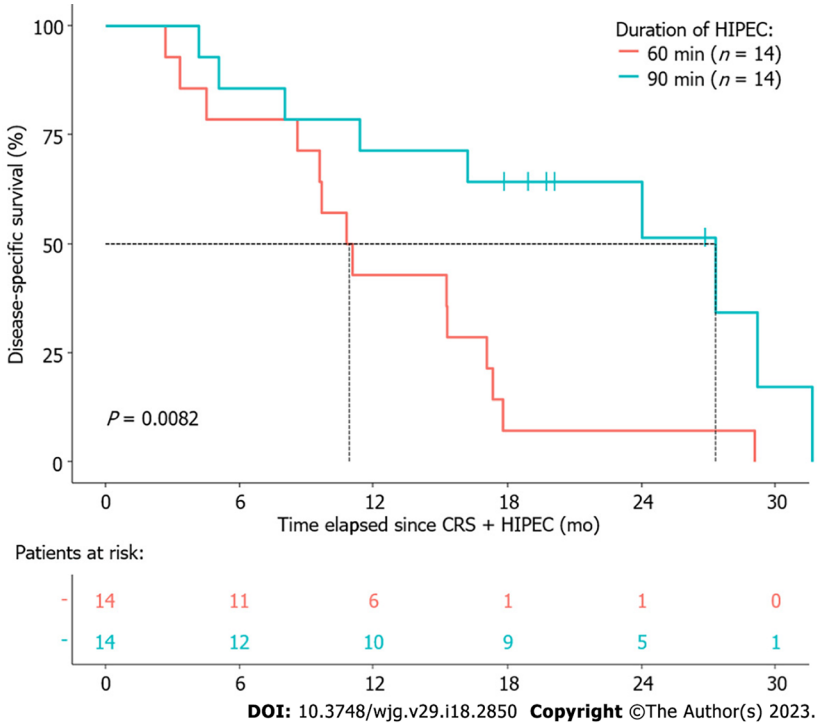


Figure 6 Differences in disease-specific survival between propensity score in matched gastric cancer patient-pairs. Patients were matched by age, sex, peritoneal carcinomatosis index score, Jacquet and Sugarbaker's completeness of cytoreduction score, time spent in the intensive care unit after cytoreductive surgery (CRS) + hyperthermic intraperitoneal chemotherapy (HIPEC), duration of CRS, and presence of lymph node metastasis (stage *N* = 0 *vs* stage *N* ≥ 1). The dotted line represents median survival.

(HER2; *n* = 7) or had the procedure before 2016 (*n* = 44) were removed from the original cohort. For the former, we obtained the same results as those for the full cohort. Median survivals of 12.68 mo and 24.02 mo were observed for the 60-min and 90-min groups, respectively, and no statistical difference was detected in the survival models (DSS: *P* = 0.1540; OS: *P* = 0.2040; Supplementary Figure 2A). However, the same difference was seen for the modified patient population that seen with propensity-matched pairs. Median survivals of 12.52 mo and 27.30 mo were found for the 60 min and 90 min groups, respectively (HR: 0.4225; 95%CI: 0.1789-0.9975; *P* = 0.0493; Supplementary Figure 2B).

DISCUSSION

There are only a few Western studies concerning the treatment of advanced GC with CRS and HIPEC. Although the positive effects of cytoreduction and HIPEC on survival have been described[11-13,31], the practical nonexistence of prospective clinical studies (except for two studies with small sample sizes [12,32]) on CRS and HIPEC highlights the need for additional primary research. Moreover, more randomized trials are required to substantiate the effect of CRS and HIPEC. For example, the results of the German phase III PREVENT study, in which the effect of HIPEC applied for prevention in lieu of FLOT-chemotherapy, is currently recruiting patients, and results are eagerly anticipated[33].

In the current retrospective study, we demonstrated prolonged survival with multimodal therapy in the treatment of primary GC patients with PM. The 27.3 mo median survival that we observed is in line with similar studies. For example, in the phase II trial by Badgwell *et al*[11], the median OS was 24.2 mo from the date of diagnosis and 16.1 mo from the date of CRS and HIPEC. Similarly, a recent Spanish multicenter study found a median survival of 21.2 mo[34], while in the German retrospective HIPEC-register study the median survival times ranged from 7.9 mo to 21.2 mo[35]. The same is true of median PCI-scores; median PCI was 2, 6, 6, and 8 in the studies of Badgwell *et al*[11], Bonnot *et al*[31], Manzanedo *et al*[34], and Rau *et al*[35], respectively; a median PCI of 3 was calculated in the current study. In addition, Rau *et al*[35] reported OS of 18 mo, 12 mo, and 5 mo for the 3 patient groups, with corresponding PCI scores of 0-6, 7-15, and 16-39, respectively; this finding suggests that significantly better outcomes are associated with higher CC. In our study, 93.2% of patients underwent complete macroscopic tumor reduction. An important conclusion of the above presented studies is that patients with small tumor burden (PCI < 6, but maximally 9) benefit the most from this multimodal therapy. Although in the current study we could not confirm the benefit of reduced PCI scores, our results were in line with the previously described observations (*i.e.* patients with higher PCI scores trended toward shorter survival). Furthermore, an interesting observation emerged during the analysis of our data over

time and with an increasing number of cases: The duration of surgery to reach complete cytoreduction became significantly shorter. These findings match with the results of a study outlining the technical aspects and learning curve of CRS/HIPEC by Vining *et al*[36], where the authors describe a steep learning curve and a correlation between CC and surgeon expertise. This observation underscores the idea that treatment of advanced GC with PM should be performed in specialized centers by expert surgeons. Recent studies have also found that sodium thiosulfate can prevent impairment of renal function following HIPEC[37,38]. In the patient population analyzed in the current study, sodium thiosulfate was not used; however, since January 2022, we have started to use it routinely in our center.

There is still no consensus regarding the ideal duration of HIPEC. In the current analysis, the median survival time was 27.30 mo in the 90 min group, which was significantly longer than that of the 60 min group (12.86 mo). Near the publication date of the van Driel *et al*[23] study for ovarian cancer and the PRODIGE-7 trial[39] for HIPEC in colorectal cancer, our institutional HIPEC protocol was changed in favor of the 90 min HIPEC perfusion. Our group has recently described the advantages of prolonged HIPEC duration have been recently described for primary peritoneal carcinoma, primary advanced epithelial carcinoma, and ovarian or fallopian tube carcinoma[40,41]. Longer HIPEC duration does not adversely affect perioperative morbidity and mortality, and a potential survival benefit could be realized by the application of prolonged HIPEC[40]. However, a recent study found that a secondary inflammatory reaction might occur after 90 min HIPEC with mitomycin C/doxorubicin or cisplatin, but not with shorter duration and oxaliplatin[41]. These and the current findings suggest that a prolonged peritoneal perfusion time may be more advantageous after complete cytoreduction; however, as the study of Roth *et al*[41] has shown, gathering additional data is essential.

Another possible reason for better survival in patients with longer HIPEC duration is enhanced cytotoxicity and anti-tumor effects of chemotherapeutic drugs in hyperthermia; the longer exposure may allow for more effective drug action[42]. The effect of cytoreductive surgery with macroscopic complete tumor reduction followed by HIPEC with effective neoadjuvant chemotherapy extends survival time of patients with advanced GC with PM, as recently shown in the CYTO-CHIP study[31]. Since 2016, the most frequently used neoadjuvant chemotherapy for advanced GC with PM is the FLOT-protocol; however, due to differences in cytochrome P450 family 2 subfamily A member 6[43], the S-1 regime (tegafur, gimeracil, and oteracil) is the standard adjuvant treatment in Asia[44,45]. The latest advancements in preoperative chemotherapy with[46] or without[25] biological agents can significantly extend the survival of GC patients. Recently, it has also been demonstrated that the 15%-20% of GC cases that overexpresses HER2 should be treated with monoclonal antibodies like trastuzumab in a neoadjuvant setting due to the positive influence of these drugs on patient survival and fewer side effects than traditional chemotherapies[47]. In the current study, the individual responses to pre- and/or postoperative chemotherapy were not known for most patients, which was one of the biasing factors affecting patient survival in our study.

SRC differentiation is described as a tumor with aggressive growth and a poorer prognosis than non-SRC carcinomas of the stomach[48]. In contrast, we found that the type of histology did not affect DSS, OS, or RFS. A similar finding was reported in an Asian study of 136 advanced GC patients, in which the authors described no difference in median survival between the histopathologic entities after R0-resection[49]. Moreover, we observed that if pelvic peritonectomy during CRS is not necessary, the OS of the patient improved. We hypothesize that the extent of the tumor may have a greater influence on patient survival than the histopathological differentiation. Improvement in patient survival may also be influenced by the experience of the surgical team; this factor may have also introduced additional bias in the current study.

We also investigated whether any preoperative laboratory result was predictive of patient survival. Strong correlations were found between patient survival and white blood cell count, hemoglobin, CEA, and serum total protein. These findings match with previously reported data of non-HIPEC-treated GC patients[50-55]. Furthermore, results of a recent German multi-center study[56] and the WHO urgent call[57] to implement blood management in surgical patients have shown that preoperative anemia is a serious threat to patient survival. Preoperative iron supplementation in preoperative anemia is also an important part of the recently published ERAS protocol for CRS and HIPEC[58]. As such, emphasis should be placed on iron supplementation and normalization of hemoglobin prior to surgery[58].

Limitations

The current study had a few limitations, including the small sample size, the retrospective nature of the study, the fact that data were available from a single center only, and the heterogeneity of the data. Also, during the study period, preoperative chemotherapy protocols changed and surgeon expertise grew. Furthermore, in this small cohort of patients with GC and PM, there were limited data regarding post-HIPEC treatment. Our follow-up data could only differentiate between alive and dead patients and tumor recurrence or no recurrence. Efforts were made to collect post-HIPEC patient data; however, we could not collect these in a timely manner, as routine oncological treatments were often performed in other hospitals. Moreover, the lack of chemotherapy-only control patients should also be mentioned as a limiting factor.

CONCLUSION

In summary, we conducted a single-center retrospective observational study to investigate what factors influence the survival of advanced GC patients with PM who underwent CRS and HIPEC. We confirmed that CRS followed by HIPEC applied over 90 min has a positive impact on DSS in comparison with CRS followed by 60 min of HIPEC. Of note, the learning curve of surgeons may confound the interpretation of this observation. Furthermore, the preparation of patients for surgery based on preoperative laboratory testing according to the current ERAS protocol might optimize the positive effect of CRS and HIPEC. To further expand upon our findings, multi-institutional and cooperative randomized group trials should be organized to further support and confirm survival and safety outcomes.

ARTICLE HIGHLIGHTS

Research background

Cytoreductive surgery (CRS) with hyperthermic intraperitoneal chemotherapy (HIPEC) is one of the last options in the treatment of advanced gastric cancer (GC) with peritoneal metastasis (PM); however, most national and international guidelines only recommend it to be performed within clinical trials. Despite this, CRS with HIPEC is a safe and effective method to treat advanced GC with PM, and recent studies have shown encouraging results with respect to increased patient survival.

Research motivation

CRS and HIPEC are safe and effective therapeutic options for the treatment of advanced GC with PM. To investigate the optimal length of HIPEC procedure, it is important to provide a basis for further research. Improving the composition of HIPEC medications could further improve the outcomes of this modern multimodal therapy. It is expected that ongoing research regarding antibody and checkpoint inhibitor therapies will strongly influence not only perioperative therapy but also the therapeutic agents used during HIPEC itself.

Research objectives

The aim of the study was to explore the effect of CRS and HIPEC in the treatment of advanced GC with PM and find parameters that could further improve patient survival.

Research methods

We conducted a retrospective observational study with the inclusion of 73 GC patients with synchronous PM. Details of CRS + HIPEC, preoperative laboratory results, and pre-, peri-, and postoperative surgical details of the patients were recorded. Overall survival (OS), disease-specific survival (DSS), and recurrence-free survival (RFS) were calculated.

Research results

In line with recently published data, we found that CRS + HIPEC had a measurable impact on the survival of advanced GC patients without significantly elevating the rate of postoperative complications. The effects of longer HIPEC duration, higher white blood cell count, lower hemoglobin and serum total protein, and higher carcinoembryonic antigen levels with respect to the survival of patients were found.

Research conclusions

In general agreement with previously published findings, we concluded that 90 min HIPEC treatment correlates with improvement in the OS and DSS of patients compared to that of 60 min HIPEC. Moreover, more complete cytoreduction also contributes to longer patient survival and better disease management.

Research perspectives

The improvement of CRS and HIPEC with respect to the duration and composition of HIPEC therapeutic agents is a controversial research topic. The current report provides evidence from a single center retrospective study that could be implemented in future randomized multicenter studies.

ACKNOWLEDGEMENTS

We are grateful to Madar-Dank V, research assistant of the Department of the Institute for Dispute Resolution of New Jersey City University, for English proofreading.

FOOTNOTES

Author contributions: Steinhoff H, Acs M, Szasz AM and Piso P built the study design; Steinhoff H, Acs M, Blaj S and Sanchez-Velazquez P were involved in the collection of patient data; Herold Z performed the statistical analysis of data; Steinhoff H, Acs M, Herold Z, Herold M, Herzberg J, Strate T and Szasz AM interpreted the data; Steinhoff H, Blaj S, Acs M, Sanchez-Velazquez P and Piso P were involved in patient selection; Steinhoff H, Acs M and Herold Z prepared the draft of the manuscript; All authors were involved in the manuscript editing and reviewing; Dank M and Piso P supervised the study; all authors have read and agreed to the published version of the manuscript.

Institutional review board statement: The study was conducted according to the guidelines of the Declaration of Helsinki. Ethical review and approval were waived for this study due to the retrospective nature of the study. All the patients had agreed to data recording for the national HIPEC registry and to the use of their anonymized data for quality assurance and research purposes by written and verbal informed consent prior to surgery. Therefore, no institutional or further approval of a review board was necessary.

Informed consent statement: Informed consent was obtained from all subjects before cytoreductive surgery with hyperthermic intraperitoneal chemotherapy (CRS + HIPEC). All patients agreed to their data being recorded for the national HIPEC registry, administered by the German Society for General and Visceral Surgery.

Conflict-of-interest statement: All the authors report having no relevant conflicts of interest for this article.

Data sharing statement: The datasets used and/or analyzed during the current study are available from the corresponding author upon reasonable request.

Open-Access: This article is an open-access article that was selected by an in-house editor and fully peer-reviewed by external reviewers. It is distributed in accordance with the Creative Commons Attribution NonCommercial (CC BY-NC 4.0) license, which permits others to distribute, remix, adapt, build upon this work non-commercially, and license their derivative works on different terms, provided the original work is properly cited and the use is non-commercial. See: https://creativecommons.org/Licenses/by-nc/4.0/

Country/Territory of origin: Hungary

ORCID number: Heinrich Steinhoff 0000-0003-3958-697X; Miklos Acs 0000-0003-4706-5541; Sebastian Blaj 0000-0001-5830-9797; Magdolna Dank 0000-0002-4694-3624; Magdolna Herold 0000-0002-1036-6343; Zoltan Herold 0000-0001-5990-4889; Jonas Herzberg 0000-0003-3562-6575; Patricia Sanchez-Velazquez 0000-0002-7902-3920; Tim Strate 0000-0001-7627-9405; Attila Marcell Szasz 0000-0003-2739-4196; Pompiliu Piso 0000-0001-7146-4505.

S-Editor: Gao CC
L-Editor: Filipodia
P-Editor: Yu HG

REFERENCES

1 **Ferlay J**, Ervik M, Lam F, Colombet M, Mery L, Piñeros M, Znaor A, Soerjomataram I, Bray F. Global Cancer Observatory: Cancer Today. [cited 22 Oct 2022]. In: International Agency for Research on Cancer [Internet]. Available from: https://gco.iarc.fr/today

2 **Sung H**, Ferlay J, Siegel RL, Laversanne M, Soerjomataram I, Jemal A, Bray F. Global Cancer Statistics 2020: GLOBOCAN Estimates of Incidence and Mortality Worldwide for 36 Cancers in 185 Countries. *CA Cancer J Clin* 2021; **71**: 209-249 [PMID: 33538338 DOI: 10.3322/caac.21660]

3 **Berlth F**, Bollschweiler E, Drebber U, Hoelscher AH, Moenig S. Pathohistological classification systems in gastric cancer: diagnostic relevance and prognostic value. *World J Gastroenterol* 2014; **20**: 5679-5684 [PMID: 24914328 DOI: 10.3748/wjg.v20.i19.5679]

4 **Nakamura K**, Sugano H, Takagi K. Carcinoma of the stomach in incipient phase: its histogenesis and histological appearances. *Gan* 1968; **59**: 251-258 [PMID: 5726267]

5 **Lauren P**. The two histological main types of gastric carcinoma: diffuse and so-called intestinal-type carcinoma. An attempt at a histo-clinical classification. *Acta Pathol Microbiol Scand* 1965; **64**: 31-49 [PMID: 14320675 DOI: 10.1111/apm.1965.64.1.31]

6 **Fukayama M**, Rugge M, Washington MK. Tumours of the stomach. In: WHO Classification of Tumours Editorial Board. Digestive System Tumours (WHO Classification of Tumours) 5th ed. Lyon, France: International Agency for Research on Cancer, 2019: 59-104

7 **Pimentel-Nunes P**, Dinis-Ribeiro M, Ponchon T, Repici A, Vieth M, De Ceglie A, Amato A, Berr F, Bhandari P, Bialek A, Conio M, Haringsma J, Langner C, Meisner S, Messmann H, Morino M, Neuhaus H, Piessevaux H, Rugge M, Saunders BP, Robaszkiewicz M, Seewald S, Kashin S, Dumonceau JM, Hassan C, Deprez PH. Endoscopic submucosal dissection: European Society of Gastrointestinal Endoscopy (ESGE) Guideline. *Endoscopy* 2015; **47**: 829-854 [PMID: 26317585 DOI: 10.1055/s-0034-1392882]

8 **Mönig S**, Ott K, Gockel I, Lorenz D, Ludwig K, Messmann H, Moehler M, Piso P, Weimann A, Meyer HJ. [S3 guidelines

on gastric cancer-diagnosis and treatment of adenocarcinoma of the stomach and esophagogastric junction : Version 2.0-August 2019. AWMF register number: 032/009OL]. *Chirurg* 2020; **91**: 37-40 [PMID: 31950198 DOI: 10.1007/s00104-020-01112-y]

9 **Al-Batran SE**, Goetze TO, Mueller DW, Vogel A, Winkler M, Lorenzen S, Novotny A, Pauligk C, Homann N, Jungbluth T, Reissfelder C, Caca K, Retter S, Horndasch E, Gumpp J, Bolling C, Fuchs KH, Blau W, Padberg W, Pohl M, Wunsch A, Michl P, Mannes F, Schwarzbach M, Schmalenberg H, Hohaus M, Scholz C, Benckert C, Knorrenschild JR, Kanngießer V, Zander T, Alakus H, Hofheinz RD, Roedel C, Shah MA, Sasako M, Lorenz D, Izbicki J, Bechstein WO, Lang H, Moenig SP. The RENAISSANCE (AIO-FLOT5) trial: effect of chemotherapy alone vs. chemotherapy followed by surgical resection on survival and quality of life in patients with limited-metastatic adenocarcinoma of the stomach or esophagogastric junction - a phase III trial of the German AIO/CAO-V/CAOGI. *BMC Cancer* 2017; **17**: 893 [PMID: 29282088 DOI: 10.1186/s12885-017-3918-9]

10 **Greco SH**, Chao JC, Heath NG, Lin Y, Gall VA, Grandhi MS, Kennedy TJ, Carpizo DR, Alexander HR, Langan RC, August DA. Surgery is Associated With Improved Overall Survival in Patients With Metastatic Gastric Cancer: A National Cancer Database Analysis. *Am Surg* 2022; **88**: 2637-2643 [PMID: 35649712 DOI: 10.1177/00031348221086800]

11 **Badgwell B**, Ikoma N, Murphy MB, Wang X, Estrella J, Roy-Chowdhuri S, Das P, Minsky BD, Lano E, Song S, Mansfield P, Ajani J. A Phase II Trial of Cytoreduction, Gastrectomy, and Hyperthermic Intraperitoneal Perfusion with Chemotherapy for Patients with Gastric Cancer and Carcinomatosis or Positive Cytology. *Ann Surg Oncol* 2021; **28**: 258-264 [PMID: 32556731 DOI: 10.1245/s10434-020-08739-5]

12 **Yang XJ**, Huang CQ, Suo T, Mei LJ, Yang GL, Cheng FL, Zhou YF, Xiong B, Yonemura Y, Li Y. Cytoreductive surgery and hyperthermic intraperitoneal chemotherapy improves survival of patients with peritoneal carcinomatosis from gastric cancer: final results of a phase III randomized clinical trial. *Ann Surg Oncol* 2011; **18**: 1575-1581 [PMID: 21431408 DOI: 10.1245/s10434-011-1631-5]

13 **Gronau F**, Jara M, Feldbrügge L, Wolf V, Oeff A, Rau B. [Cytoreductive surgery and hyperthermic intraperitoneal chemotherapy in gastric cancer]. *Chirurg* 2021; **92**: 522-527 [PMID: 33620502 DOI: 10.1007/s00104-021-01371-3]

14 **Yan TD**, Black D, Sugarbaker PH, Zhu J, Yonemura Y, Petrou G, Morris DL. A systematic review and meta-analysis of the randomized controlled trials on adjuvant intraperitoneal chemotherapy for resectable gastric cancer. *Ann Surg Oncol* 2007; **14**: 2702-2713 [PMID: 17653801 DOI: 10.1245/s10434-007-9487-4]

15 **Granieri S**, Bonomi A, Frassini S, Chierici AP, Bruno F, Paleino S, Kusamura S, Germini A, Facciorusso A, Deraco M, Cotsoglou C. Prognostic impact of cytoreductive surgery (CRS) with hyperthermic intraperitoneal chemotherapy (HIPEC) in gastric cancer patients: A meta-analysis of randomized controlled trials. *Eur J Surg Oncol* 2021; **47**: 2757-2767 [PMID: 34001385 DOI: 10.1016/j.ejso.2021.05.016]

16 **Di Vita M**, Cappellani A, Piccolo G, Zanghì A, Cavallaro A, Bertola G, Bolognese A, Facchini G, D'Aniello C, Di Francia R, Cardì F, Berretta M. The role of HIPEC in the treatment of peritoneal carcinomatosis from gastric cancer: between lights and shadows. *Anticancer Drugs* 2015; **26**: 123-138 [PMID: 25406023 DOI: 10.1097/CAD.0000000000000179]

17 **Japanese Gastric Cancer Association**. Japanese gastric cancer treatment guidelines 2018 (5th edition). *Gastric Cancer* 2021; **24**: 1-21 [PMID: 32060757 DOI: 10.1007/s10120-020-01042-y]

18 **Ajani JA**, D'Amico TA, Bentrem DJ, Chao J, Cooke D, Corvera C, Das P, Enzinger PC, Enzler T, Fanta P, Farjah F, Gerdes H, Gibson MK, Hochwald S, Hofstetter WL, Ilson DH, Keswani RN, Kim S, Kleinberg LR, Klempner SJ, Lacy J, Ly QP, Matkowskyj KA, McNamara M, Mulcahy MF, Outlaw D, Park H, Perry KA, Pimiento J, Poultsides GA, Reznik S, Roses RE, Strong VE, Su S, Wang HL, Wiesner G, Willett CG, Yakoub D, Yoon H, McMillian N, Pluchino LA. Gastric Cancer, Version 2.2022, NCCN Clinical Practice Guidelines in Oncology. *J Natl Compr Canc Netw* 2022; **20**: 167-192 [PMID: 35130500 DOI: 10.6004/jnccn.2022.0008]

19 **Zaanan A**, Bouché O, Benhaim L, Buecher B, Chapelle N, Dubreuil O, Fares N, Granger V, Lefort C, Gagniere J, Meilleroux J, Baumann AS, Vendrely V, Ducreux M, Michel P; Thésaurus National de Cancérologie Digestive (TNCD). Gastric cancer: French intergroup clinical practice guidelines for diagnosis, treatments and follow-up (SNFGE, FFCD, GERCOR, UNICANCER, SFCD, SFED, SFRO). *Dig Liver Dis* 2018; **50**: 768-779 [PMID: 29886081 DOI: 10.1016/j.dld.2018.04.025]

20 **Lordick F**, Carneiro F, Cascinu S, Fleitas T, Haustermans K, Piessen G, Vogel A, Smyth EC; ESMO Guidelines Committee. Gastric cancer: ESMO Clinical Practice Guideline for diagnosis, treatment and follow-up. *Ann Oncol* 2022; **33**: 1005-1020 [PMID: 35914639 DOI: 10.1016/j.annonc.2022.07.004]

21 **Jacquet P**, Sugarbaker PH. Clinical research methodologies in diagnosis and staging of patients with peritoneal carcinomatosis. *Cancer Treat Res* 1996; **82**: 359-374 [PMID: 8849962 DOI: 10.1007/978-1-4613-1247-5_23]

22 **Segura-Sampedro JJ**, Morales-Soriano R, Pineño Flores C, Craus-Miguel A, Sugarbaker PH. Laparoscopy technique in the setting of peritoneal metastases to avoid port site relapse. *Surg Oncol* 2021; **37**: 101543 [PMID: 33773282 DOI: 10.1016/j.suronc.2021.101543]

23 **van Driel WJ**, Koole SN, Sikorska K, Schagen van Leeuwen JH, Schreuder HWR, Hermans RHM, de Hingh IHJT, van der Velden J, Arts HJ, Massuger LFAG, Aalbers AGJ, Verwaal VJ, Kieffer JM, Van de Vijver KK, van Tinteren H, Aaronson NK, Sonke GS. Hyperthermic Intraperitoneal Chemotherapy in Ovarian Cancer. *N Engl J Med* 2018; **378**: 230-240 [PMID: 29342393 DOI: 10.1056/NEJMoa1708618]

24 **Ajani JA**, In H, Sano T, Gaspar LE, Erasmus JJ, Tang LH, Washington MK, Gerdes H, Wittekind CW, Mansfield PF, Rimmer C, Hofstetter WL, Kelsen D. Stomach. In: Amin M, Edge S, Greene F, Byrd D, Brookland R, Washington M, Gershenwald J, Compton C, Hess K, Sullivan D, Jessup J, Brierley J, Gaspar L, Schilsky R, Balch C, Winchester D, Asare E, Madera M, Gress D, Meyer L. AJCC Cancer Staging Manual. 8th ed. Chicago, IL, United States: Springer International Publishing, 2018: 203-220

25 **Al-Batran SE**, Homann N, Pauligk C, Goetze TO, Meiler J, Kasper S, Kopp HG, Mayer F, Haag GM, Luley K, Lindig U, Schmiegel W, Pohl M, Stoehlmacher J, Folprecht G, Probst S, Prasnikar N, Fischbach W, Mahlberg R, Trojan J, Koenigsmann M, Martens UM, Thuss-Patience P, Egger M, Block A, Heinemann V, Illerhaus G, Moehler M, Schenk M, Kullmann F, Behringer DM, Heike M, Pink D, Teschendorf C, Löhr C, Bernhard H, Schuch G, Rethwisch V, von Weikersthal LF, Hartmann JT, Kneba M, Daum S, Schulmann K, Weniger J, Belle S, Gaiser T, Oduncu FS, Güntner M,

Hozaeel W, Reichart A, Jäger E, Kraus T, Mönig S, Bechstein WO, Schuler M, Schmalenberg H, Hofheinz RD; FLOT4-AIO Investigators. Perioperative chemotherapy with fluorouracil plus leucovorin, oxaliplatin, and docetaxel *vs* fluorouracil or capecitabine plus cisplatin and epirubicin for locally advanced, resectable gastric or gastro-oesophageal junction adenocarcinoma (FLOT4): a randomised, phase 2/3 trial. *Lancet* 2019; **393**: 1948-1957 [PMID: 30982686 DOI: 10.1016/S0140-6736(18)32557-1]

26 **Schwandt A**, Denkinger M, Fasching P, Pfeifer M, Wagner C, Weiland J, Zeyfang A, Holl RW. Comparison of MDRD, CKD-EPI, and Cockcroft-Gault equation in relation to measured glomerular filtration rate among a large cohort with diabetes. *J Diabetes Complications* 2017; **31**: 1376-1383 [PMID: 28711195 DOI: 10.1016/j.jdiacomp.2017.06.016]

27 **Dindo D**, Demartines N, Clavien PA. Classification of surgical complications: a new proposal with evaluation in a cohort of 6336 patients and results of a survey. *Ann Surg* 2004; **240**: 205-213 [PMID: 15273542 DOI: 10.1097/01.sla.0000133083.54934.ae]

28 **Passot G**, Vaudoyer D, Villeneuve L, Kepenekian V, Beaujard AC, Bakrin N, Cotte E, Gilly FN, Glehen O. What made hyperthermic intraperitoneal chemotherapy an effective curative treatment for peritoneal surface malignancy: A 25-year experience with 1,125 procedures. *J Surg Oncol* 2016; **113**: 796-803 [PMID: 27110915 DOI: 10.1002/jso.24248]

29 **Alyami M**, Kim BJ, Villeneuve L, Vaudoyer D, Képénékian V, Bakrin N, Gilly FN, Cotte E, Glehen O, Passot G. Ninety-day post-operative morbidity and mortality using the National Cancer Institute's common terminology criteria for adverse events better describe post-operative outcome after cytoreductive surgery and hyperthermic intraperitoneal chemotherapy. *Int J Hyperthermia* 2018; **34**: 532-537 [PMID: 28838265 DOI: 10.1080/02656736.2017.1367846]

30 **Holm S**. A Simple Sequentially Rejective Multiple Test Procedure. *Scand J Stat* 1979; **6**: 65-70

31 **Bonnot PE**, Piessen G, Kepenekian V, Decullier E, Pocard M, Meunier B, Bereder JM, Abboud K, Marchal F, Quenet F, Goere D, Msika S, Arvieux C, Pirro N, Wernert R, Rat P, Gagnière J, Lefevre JH, Courvoisier T, Kianmanesh R, Vaudoyer D, Rivoire M, Meeus P, Passot G, Glehen O; FREGAT and BIG-RENAPE Networks. Cytoreductive Surgery With or Without Hyperthermic Intraperitoneal Chemotherapy for Gastric Cancer With Peritoneal Metastases (CYTO-CHIP study): A Propensity Score Analysis. *J Clin Oncol* 2019; **37**: 2028-2040 [PMID: 31084544 DOI: 10.1200/JCO.18.01688]

32 **Rudloff U**, Langan RC, Mullinax JE, Beane JD, Steinberg SM, Beresnev T, Webb CC, Walker M, Toomey MA, Schrump D, Pandalai P, Stojadinovic A, Avital I. Impact of maximal cytoreductive surgery plus regional heated intraperitoneal chemotherapy (HIPEC) on outcome of patients with peritoneal carcinomatosis of gastric origin: results of the GYMSSA trial. *J Surg Oncol* 2014; **110**: 275-284 [PMID: 25042700 DOI: 10.1002/jso.23633]

33 **Götze TO**, Piso P, Lorenzen S, Bankstahl US, Pauligk C, Elshafei M, Amato G, Reim D, Bechstein WO, Königsrainer A, Mönig SP, Rau B, Schwarzbach M, Al-Batran SE. Preventive HIPEC in combination with perioperative FLOT *vs* FLOT alone for resectable diffuse type gastric and gastroesophageal junction type II/III adenocarcinoma - the phase III "PREVENT"- (FLOT9) trial of the AIO /CAOGI /ACO. *BMC Cancer* 2021; **21**: 1158 [PMID: 34715810 DOI: 10.1186/s12885-021-08872-8]

34 **Manzanedo I**, Pereira F, Rihuete Caro C, Pérez-Viejo E, Serrano Á, Gutiérrez Calvo A, Regueira FM, Casado-Adam Á, Cascales-Campos PA, Arteaga X, García-Fadrique A, Gómez Sanz R, López García A, Zozaya G, Arjona Á, Gil Martínez J. Cytoreductive Surgery and Hyperthermic Intraperitoneal Chemotherapy (HIPEC) for Gastric Cancer with Peritoneal Carcinomatosis: Multicenter Study of Spanish Group of Peritoneal Oncologic Surgery (GECOP). *Ann Surg Oncol* 2019; **26**: 2615-2621 [PMID: 31115852 DOI: 10.1245/s10434-019-07450-4]

35 **Rau B**, Brandl A, Piso P, Pelz J, Busch P, Demtröder C, Schüle S, Schlitt HJ, Roitman M, Tepel J, Sulkowski U, Uzunoglu F, Hünerbein M, Hörbelt R, Ströhlein M, Beckert S, Königsrainer I, Königsrainer A; Peritoneum Surface Oncology Group and members of the StuDoQ|Peritoneum Registry of the German Society for General and Visceral Surgery (DGAV). Peritoneal metastasis in gastric cancer: results from the German database. *Gastric Cancer* 2020; **23**: 11-22 [PMID: 31228044 DOI: 10.1007/s10120-019-00978-0]

36 **Vining CC**, Izquierdo F, Eng OS, Turaga KK. Cytoreductive surgery and hyperthermic intraperitoneal chemotherapy: Technical considerations and the learning curve. *J Surg Oncol* 2020; **122**: 85-95 [PMID: 32436240 DOI: 10.1002/jso.25939]

37 **Laplace N**, Kepenekian V, Friggeri A, Vassal O, Ranchon F, Rioufol C, Gertych W, Villeneuve L, Glehen O, Bakrin N. Sodium thiosulfate protects from renal impairement following hyperthermic intraperitoneal chemotherapy (HIPEC) with Cisplatin. *Int J Hyperthermia* 2020; **37**: 897-902 [PMID: 32689832 DOI: 10.1080/02656736.2020.1795277]

38 **Kurreck A**, Gronau F, Alberto Vilchez ME, Abels W, Enghard P, Brandl A, Francis R, Föhre B, Lojewski C, Pratschke J, Thuss-Patience P, Modest D, Rau B, Feldbrügge L. Sodium Thiosulfate Reduces Acute Kidney Injury in Patients Undergoing Cytoreductive Surgery Plus Hyperthermic Intraperitoneal Chemotherapy with Cisplatin: A Single-Center Observational Study. *Ann Surg Oncol* 2022; **29**: 152-162 [PMID: 34350529 DOI: 10.1245/s10434-021-10508-x]

39 **Quénet F**, Elias D, Roca L, Goéré D, Ghouti L, Pocard M, Facy O, Arvieux C, Lorimier G, Pezet D, Marchal F, Loi V, Meeus P, Juzyna B, de Forges H, Paineau J, Glehen O; UNICANCER-GI Group and BIG Renape Group. Cytoreductive surgery plus hyperthermic intraperitoneal chemotherapy *vs* cytoreductive surgery alone for colorectal peritoneal metastases (PRODIGE 7): a multicentre, randomised, open-label, phase 3 trial. *Lancet Oncol* 2021; **22**: 256-266 [PMID: 33476595 DOI: 10.1016/S1470-2045(20)30599-4]

40 **Acs M**, Herold Z, Szasz AM, Mayr M, Häusler S, Piso P. Prolonged Exposition with Hyperthermic Intraperitoneal Chemotherapy (HIPEC) May Provide Survival Benefit after Cytoreductive Surgery (CRS) in Advanced Primary Epithelial Ovarian, Fallopian Tube, and Primary Peritoneal Cancer. *Cancers (Basel)* 2022; **14** [PMID: 35884361 DOI: 10.3390/cancers14143301]

41 **Roth L**, Eshmuminov D, Laminger F, Koppitsch C, Schneider M, Graf TR, Gupta A, Kober F, Roka S, Gertsch P, Lehmann K. Systemic inflammatory response after hyperthermic intraperitoneal chemotherapy (HIPEC): The perfusion protocol matters! *Eur J Surg Oncol* 2019; **45**: 1734-1739 [PMID: 30954352 DOI: 10.1016/j.ejso.2019.03.036]

42 **Helderman RFCPA**, Löke DR, Kok HP, Oei AL, Tanis PJ, Franken NAPK, Crezee J. Variation in Clinical Application of Hyperthermic Intraperitoneal Chemotherapy: A Review. *Cancers (Basel)* 2019; **11** [PMID: 30641919 DOI: 10.3390/cancers11010078]

43 **Shimada T**, Yamazaki H, Guengerich FP. Ethnic-related differences in coumarin 7-hydroxylation activities catalyzed by cytochrome P4502A6 in liver microsomes of Japanese and Caucasian populations. *Xenobiotica* 1996; **26**: 395-403 [PMID: 9173680 DOI: 10.3109/00498259609046718]

44 **Shirasaka T**, Shimamato Y, Ohshimo H, Yamaguchi M, Kato T, Yonekura K, Fukushima M. Development of a novel form of an oral 5-fluorouracil derivative (S-1) directed to the potentiation of the tumor selective cytotoxicity of 5-fluorouracil by two biochemical modulators. *Anticancer Drugs* 1996; **7**: 548-557 [PMID: 8862723 DOI: 10.1097/00001813-199607000-00010]

45 **Yamada Y**, Higuchi K, Nishikawa K, Gotoh M, Fuse N, Sugimoto N, Nishina T, Amagai K, Chin K, Niwa Y, Tsuji A, Imamura H, Tsuda M, Yasui H, Fujii H, Yamaguchi K, Hironaka S, Shimada K, Miwa H, Hamada C, Hyodo I. Phase III study comparing oxaliplatin plus S-1 with cisplatin plus S-1 in chemotherapy-naïve patients with advanced gastric cancer. *Ann Oncol* 2015; **26**: 141-148 [PMID: 25316259 DOI: 10.1093/annonc/mdu472]

46 **Högner A**, Moehler M. Immunotherapy in Gastric Cancer. *Curr Oncol* 2022; **29**: 1559-1574 [PMID: 35323331 DOI: 10.3390/curroncol29030131]

47 **Bang YJ**, Van Cutsem E, Feyereislova A, Chung HC, Shen L, Sawaki A, Lordick F, Ohtsu A, Omuro Y, Satoh T, Aprile G, Kulikov E, Hill J, Lehle M, Rüschoff J, Kang YK; ToGA Trial Investigators. Trastuzumab in combination with chemotherapy *vs* chemotherapy alone for treatment of HER2-positive advanced gastric or gastro-oesophageal junction cancer (ToGA): a phase 3, open-label, randomised controlled trial. *Lancet* 2010; **376**: 687-697 [PMID: 20728210 DOI: 10.1016/S0140-6736(10)61121-X]

48 **Zaafouri H**, Jouini R, Khedhiri N, Khanchel F, Cherif M, Mesbahi M, Daghmouri A, Mahmoudi W, Akremi S, Sabbah M, Benzarti Y, Hadded D, Gargouri D, Bader MB, Maamer AB. Comparison between signet-ring cell carcinoma and non-signet-ring cell carcinoma of the stomach: clinicopathological parameters, epidemiological data, outcome, and prognosis-a cohort study of 123 patients from a non-endemic country. *World J Surg Oncol* 2022; **20**: 238 [PMID: 35858903 DOI: 10.1186/s12957-022-02699-8]

49 **Kim KH**, Kim MC, Jung GJ, Kim SJ. The differences in clinicopathological features and prognosis among the subtypes of signet ring cell, mucinous, papillary, and lymphoepithelioma-like carcinoma in advanced gastric cancer. *Hepatogastroenterology* 2014; **61**: 2149-2155 [PMID: 25713922]

50 **Xue W**, Xu X, Tan Y, Qian Y, Wang H, Wang Y, Xu Y, Zhu X, Jiang P, Ding W. Evaluating and validating the predictive ability of preoperative systemic inflammatory/immune cells in gastric cancer following R0 resection. *Oncol Lett* 2019; **18**: 5205-5214 [PMID: 31612031 DOI: 10.3892/ol.2019.10867]

51 **Huang XZ**, Yang YC, Chen Y, Wu CC, Lin RF, Wang ZN, Zhang X. Preoperative Anemia or Low Hemoglobin Predicts Poor Prognosis in Gastric Cancer Patients: A Meta-Analysis. *Dis Markers* 2019; **2019**: 7606128 [PMID: 30719182 DOI: 10.1155/2019/7606128]

52 **Mao MJ**, Wei XL, Sheng H, Wang XP, Li XH, Liu YJ, Xing S, Huang Q, Dai SQ, Liu WL. Clinical Significance of Preoperative Albumin and Globulin Ratio in Patients with Gastric Cancer Undergoing Treatment. *Biomed Res Int* 2017; **2017**: 3083267 [PMID: 28424782 DOI: 10.1155/2017/3083267]

53 **Polat E**, Duman U, Duman M, Derya Peker K, Akyuz C, Fatih Yasar N, Uzun O, Akbulut S, Birol Bostanci E, Yol S. Preoperative serum tumor marker levels in gastric cancer. *Pak J Med Sci* 2014; **30**: 145-149 [PMID: 24639849 DOI: 10.12669/pjms.301.3968]

54 **Wang K**, Jiang X, Ren Y, Ma Z, Cheng X, Li F, Xiao J, Yu Z, Jiao Z. The significance of preoperative serum carcinoembryonic antigen levels in the prediction of lymph node metastasis and prognosis in locally advanced gastric cancer: a retrospective analysis. *BMC Gastroenterol* 2020; **20**: 100 [PMID: 32276616 DOI: 10.1186/s12876-020-01255-6]

55 **Nakane Y**, Okamura S, Akehira K, Boku T, Okusa T, Tanaka K, Hioki K. Correlation of preoperative carcinoembryonic antigen levels and prognosis of gastric cancer patients. *Cancer* 1994; **73**: 2703-2708 [PMID: 8194009 DOI: 10.1002/1097-0142(19940601)73:11<2703::aid-cncr2820731109>3.0.co;2-x]

56 **Judd L**, Hof L, Beladdale L, Friederich P, Thoma J, Wittmann M, Zacharowski K, Meybohm P, Choorapoikayil S; prevalence of pre-operative anaemia in surgical patients (PANDORA) study collaborators. Prevalence of pre-operative anaemia in surgical patients: a retrospective, observational, multicentre study in Germany. *Anaesthesia* 2022; **77**: 1209-1218 [PMID: 36108174 DOI: 10.1111/anae.15847]

57 **World Health Organization**. The urgent need to implement patient blood management: policy brief. [cited 10 Oct 2022]. In: World Health Organization [Internet]. Available from: https://apps.who.int/iris/handle/10665/346655

58 **Hübner M**, Kusamura S, Villeneuve L, Al-Niaimi A, Alyami M, Balonov K, Bell J, Bristow R, Guiral DC, Fagotti A, Falcão LFR, Glehen O, Lambert L, Mack L, Muenster T, Piso P, Pocard M, Rau B, Sgarbura O, Somashekhar SP, Wadhwa A, Altman A, Fawcett W, Veerapong J, Nelson G. Guidelines for Perioperative Care in Cytoreductive Surgery (CRS) with or without hyperthermic IntraPEritoneal chemotherapy (HIPEC): Enhanced recovery after surgery (ERAS®) Society Recommendations - Part I: Preoperative and intraoperative management. *Eur J Surg Oncol* 2020; **46**: 2292-2310 [PMID: 32873454 DOI: 10.1016/j.ejso.2020.07.041]

World Journal of Gastroenterology

Submit a Manuscript: https://www.f6publishing.com

World J Gastroenterol 2023 May 14; 29(18): 2864-2874

DOI: 10.3748/wjg.v29.i18.2864

ISSN 1007-9327 (print) ISSN 2219-2840 (online)

ORIGINAL ARTICLE

Observational Study

Endoscopic ultrasound-guided fine-needle aspiration pancreatic adenocarcinoma samples yield adequate DNA for next-generation sequencing: A cohort analysis

Stefania Bunduc, Bianca Varzaru, Razvan Andrei Iacob, Andrei Sorop, Ioana Manea, Andreea Spiridon, Raluca Chelaru, Adina Emilia Croitoru, Gabriel Becheanu, Mona Dumbrava, Simona Dima, Irinel Popescu, Cristian Gheorghe

Specialty type: Gastroenterology and hepatology

Provenance and peer review: Unsolicited article; Externally peer reviewed.

Peer-review model: Single blind

Peer-review report's scientific quality classification

Grade A (Excellent): 0
Grade B (Very good): B, B
Grade C (Good): 0
Grade D (Fair): D
Grade E (Poor): 0

P-Reviewer: Li JJ, China; Martino A, Italy; Wang D, China

Received: December 31, 2022
Peer-review started: December 31, 2022
First decision: February 28, 2023
Revised: March 14, 2023
Accepted: April 18, 2023
Article in press: April 18, 2023
Published online: May 14, 2023

Stefania Bunduc, Bianca Varzaru, Razvan Andrei Iacob, Gabriel Becheanu, Simona Dima, Cristian Gheorghe, Faculty of Medicine, Carol Davila University of Medicine and Pharmacy, Bucharest 020021, Romania

Stefania Bunduc, Razvan Andrei Iacob, Adina Emilia Croitoru, Gabriel Becheanu, Mona Dumbrava, Simona Dima, Irinel Popescu, Cristian Gheorghe, Digestive Diseases and Liver Transplantation Center, Fundeni Clinical Institute, Bucharest 022328, Romania

Stefania Bunduc, Bianca Varzaru, Razvan Andrei Iacob, Andrei Sorop, Ioana Manea, Andreea Spiridon, Raluca Chelaru, Adina Emilia Croitoru, Gabriel Becheanu, Mona Dumbrava, Simona Dima, Irinel Popescu, Cristian Gheorghe, Center of Excellence in Translational Medicine, Fundeni Clinical Institute, Bucharest 022328, Romania

Corresponding author: Cristian Gheorghe, FASGE, MD, PhD, Professor, Faculty of Medicine, Carol Davila University of Medicine and Pharmacy, No. 258 Fundeni Road, Bucharest 020021, Romania. drcgheorghe@gmail.com

Abstract

BACKGROUND

Genetic tests are increasingly performed for the management of unresectable pancreatic cancer. For genotyping aimed samples current guidelines recommend using core specimens, although based on moderate quality evidence. However, in clinical practice among the endoscopic ultrasound (EUS) guided tissue acquisition methods, fine needle aspiration (FNA) is the most widely performed.

AIM

To assess the adequacy for next generation sequencing (NGS) of the DNA yielded from EUS-FNA pancreatic adenocarcinoma (PDAC) samples.

METHODS

Between November 2018 and December 2021, 105 patients with PDAC confirmed by EUS-FNA were included in the study at our tertiary gastroenterology center. Either 22 gauge (G) or 19G FNA needles were used. One pass was dedicated to

DNA extraction. DNA concentration and purity (A260/280, A260/230) were assessed by spectrophotometry. We assessed the differences in DNA parameters according to needle size and tumor characteristics (size, location) and the adequacy of the extracted DNA for NGS (defined as A260/280 ≥ 1.7, and DNA yield: ≥ 10 ng for amplicon based NGS, ≥ 50 ng for whole exome sequencing [WES], ≥ 100 ng for whole genome sequencing [WGS]) by analysis of variance and *t*-test respectively. Moreover, we compared DNA purity parameters across the different DNA yield categories.

RESULTS

Our cohort included 49% male patients, aged 67.02 ± 8.38 years. The 22G needle was used in 71% of the cases. The DNA parameters across our samples varied as follows: DNA yield: 1289 ng (inter quartile range: 534.75-3101), A260/280 = 1.85 (1.79-1.86), A260/230 = 2.2 (1.72-2.36). DNA yield was > 10 ng in all samples and > 100 ng in 93% of them (one sample < 50 ng). There were no significant differences in the concentration and A260/280 between samples by needle size. Needle size was the only independent predictor of A260/230 which was higher in the 22G samples (P = 0.038). NGS adequacy rate was 90% for 19G samples regardless of NGS type, and for 22G samples it reached 89% for WGS adequacy and 91% for WES and amplicon based NGS. Samples with DNA yield > 100 ng had significantly higher A260/280 (1.89 ± 0.32 *vs* 1.34 ± 0.42, P = 0.013). Tumor characteristics were not corelated with the DNA parameters.

CONCLUSION

EUS-FNA PDAC samples yield DNA adequate for subsequent NGS. DNA amount was similar between 22G and 19G FNA needles. DNA purity parameters may vary indirectly with needle size.

Key Words: Pancreatic adenocarcinoma; Endoscopic ultrasound guided fine needle aspiration; Next generation sequencing; DNA yield; Needle size; Genetic testing

©The Author(s) 2023. Published by Baishideng Publishing Group Inc. All rights reserved.

Core Tip: Genetic testing is increasingly undertaken in pancreatic adenocarcinoma (PDAC). The main diagnostic method is endoscopic ultrasound (EUS)-guided tissue acquisition and fine needle aspiration (FNA) is most frequently performed in clinical practice. However, current guidelines recommend using core specimens for genotyping aimed samples. In our cohort analysis, we show that EUS-FNA PDAC samples yield DNA of adequate amount and purity for subsequent next-generation sequencing (NGS). DNA amount was similar between 22G and 19G FNA needles. DNA purity parameters may vary indirectly with needle size. EUS FNA PDAC samples may be used for NGS.

Citation: Bunduc S, Varzaru B, Iacob RA, Sorop A, Manea I, Spiridon A, Chelaru R, Croitoru AE, Becheanu G, Dumbrava M, Dima S, Popescu I, Gheorghe C. Endoscopic ultrasound-guided fine-needle aspiration pancreatic adenocarcinoma samples yield adequate DNA for next-generation sequencing: A cohort analysis. *World J Gastroenterol* 2023; 29(18): 2864-2874

URL: https://www.wjgnet.com/1007-9327/full/v29/i18/2864.htm

DOI: https://dx.doi.org/10.3748/wjg.v29.i18.2864

INTRODUCTION

Pancreatic cancer (PC) is among the most the most aggressive malignancies with a mortality rate comparable to the incidence[1,2]. In more than 80% of cases it is detected in advanced stages that require systemic treatment[3]. Moreover, there is growing evidence about the benefits of neoadjuvant treatment over upfront surgery for the management of resectable pancreatic cancer[4]. Regardless of stage, anatomopathological confirmation of the disease is mandatory prior to chemo or radiotherapy initiation [5].

Endoscopic ultrasound (EUS) guided tissue acquisition (TA) is the main sampling method for the diagnosis of pancreatic solid lesions with high sensitivity (85%-89%) and specificity (96%-99%)[6]. Among the EUS-TA methods, fine needle aspiration (FNA) is the most widely performed[5].

Despite the high diagnostic accuracy, EUS-TA samples are still associated with an inconclusive diagnosis in 10% to 15% of cases[7]. Detection for KRAS mutations in inconclusive samples could decrease with up to 50% the rates of false negative results[6].

Precision medicine has changed the paradigm in oncologic treatment and although the targeted therapies are not yet routinely used in PC, it is known that up to 25% of the tumors harbor actionable alterations[8]. Molecular testing on tumor tissue for guiding personalized treatment is recommended in the current guidelines for the management of unresectable pancreatic adenocarcinoma (PDAC) amenable for anti-cancer therapy[9].

The roles of EUS-TA in PC have therefore broadened from tumor diagnosis to obtaining adequate samples for further molecular testing that enable the use of targeted therapies and may also increase diagnostic accuracy[6,9,10]. Although according to the current guidelines in pancreatic solid masses core tissue specimens should be used in downstream applications, there is increasing evidence on the feasibility of performing comprehensive genomic profiling based on FNA samples[5,11].

In our study we evaluated the adequacy for NGS [targeted, amplicon based, whole exome sequencing (WES) and whole genome sequencing (WGS)] of the DNA extracted from fresh EUS FNA PDAC samples, in terms of quantity and purity as measured by spectrophotometry. Moreover, we assessed the influence of needle the size and tumor characteristics on the DNA parameters.

MATERIALS AND METHODS

Study design and settings

The research was conducted in Fundeni Clinical Institute-a tertiary gastroenterology referral center in Bucharest, Romania, between November 2018 and December 2021. This prospective observational study was approved by the Internal Review Board of Fundeni Clinical Institute. Patients provided informed consent for EUS-FNA and study enrolment before the procedure.

Study participants

For enrolment, we assessed the cases with pancreatic lesions referred to our department for EUS-TA. The eligibility criterion was-diagnosis of PDAC established by EUS-FNA. We only considered for inclusion in the study patients with a high suspicion of PDAC (as evaluated by clinical, biological, and imaging criteria). Patients with subsequent diagnoses other than PDAC were excluded from our analysis.

Highly experienced endosonographers performed all the procedures and all patients were under propofol sedation. A linear echoendoscope was used (EG-3870UTK, Pentax, equipped with a Hitachi Arietta v70 processor, Tokyo, Japan) and either 19 gauge (G) or 22G FNA needles (EchoTip Ultra Endoscopic Ultrasound Needle; Cook Medical, Bloomington, IN, United States). The endosonographer decided on the needle type. After obtaining the samples for the pathological diagnosis, one pass was dedicated to sample acquisition for DNA extraction. The needle stylet or air flushing were used to facilitate the specimen extrusion. The samples dedicated to diagnosis were smeared onto slides and fixed with ethanol and/or placed into 10% formalin for further paraffin fixation and cell block analysis, FNA yielded small tissue fragments (about 50% of cases). Dedicated pathologists with extensive experience in cytology techniques assessed the samples on site. The diagnosis of PDAC was confirmed if the pathology findings were positive or suspicious for malignancy[12]. The samples purposed for DNA extraction were placed directly in 1.5 mL of RNA later solution, in 2 mL Eppendorf tubes and kept at room temperature until DNA extraction that was performed within 4 h after sampling. For DNA extraction we used a commercially available silica membrane-based column DNA extraction kit (PureLink™ Genomic DNA, Invitrogen™, Waltham, MA, United States) according to the manufacturer's indications.

The purity and quantity of the extracted DNA were assessed immediately after extraction by spectrophotometry (Nanodrop, Thermo Fisher™, Waltham, MA, United States). The DNA concentration was measured in ng/μL and the purity was assessed by the absorbance ratios-A260/280 and A260/230 (the ratios between absorbances of the samples at 260 nm-which is characteristic for nucleic acids, and 280 nm and 230 nm respectively)[13]. The optimal DNA parameters for second generation high throughput sequencing were considered as follows: For DNA yield ≥ 100 ng will be sufficient for NGS of any type (whole genome-WGS, whole exome-WES or amplicon based targeted NGS), for WES at least ≥ 50 ng are required, whereas for amplicon based targeted NGS a minimum of 10 ng is necessary[14-16]. The main purity parameter assessed in terms of NGS adequacy is A260/280 and values ≥ 1.7 are considered optimal[17]. A260/230 is a secondary purity parameter with optimal values ranging between 2.0-2.2 [17]. Abnormal values of the purity parameters reflect mainly a contaminated sample with proteins, phenols, carbohydrates, salts among others[17]. To calculate the DNA yield we multiplied the measured concentration with the elution volume which was 25 μL in all cases. The DNA samples were stored at -80 °C until further analysis. We have successfully performed targeted amplicon based NGS in 20 of the collected samples, using the Illumina NextSeq500 platform.

Data sources

Two investigators, trainees in gastroenterology, collected the data using a customized form. Among the gathered information, we used in our study: Patients demographics (age, gender), tumor characteristics-

size (mm)-the maximum diameter measured during EUS) and location (coded as head/neck or body/tail respectively), if cross-sectional imaging was performed we also collected-TNM (tumor, node, metastasis) stage according to the American Joint Committee on 8th Cancer edition[18], and the vascular invasion status; information about the procedure: total number of passes, needle size (recorded either during the procedure or retrieved from the EUS registry of the department), the parameters for the extracted DNA-concentration and absorbance ratios. We included in our analysis only samples from patients with confirmed PDAC on the FNA specimens.

Outcomes

Our end-points were as follows: To evaluate the adequacy for NGS of the DNA extracted from EUS-FNA PDAC samples we generated several categorical variables based on the previously mentioned criteria: Three of them defining optimal DNA yield for the main types of NGS with the cut-offs: ≥ 100 ng for WGS, ≥ 50 ng for WES and ≥ 10 ng for amplicon based targeted NGS, and one for optimal DNA purity: A260/280 ≥ 1.7. NGS adequacy was defined as optimal parameters for both DNA yield and purity for each type of NGS (WGS, WES and amplicon based NGS adequacy respectively). The definitions of the categorical variables are detailed in Supplementary Table 1. The variables were coded as 1 if the corresponding criteria were accomplished and 0 if not. We also compared the purity parameters between the predefined categories of optimal DNA yield. Furthermore, we assessed the association between the FNA needle size and tumor characteristics (diameter and location) and the DNA parameters (DNA concentration [ng/μL], A260/280, A260/230).

Statistical analysis

Continuous variables are computed as either mean and standard deviation (mean ± SD) or median and inter quartile range. We analyzed the impact of needle size on DNA parameters by one way analysis of variance. We assessed the association between needle size and NGS adequacy using chi-square test. The impact of both needle size and tumor characteristics on the DNA parameters was evaluated by linear regression, while their impact on DNA NGS adequacy was evaluated by logistic regression respectively. The differences in purity parameters across the predefined DNA yield categories were assessed with independent sample *t*-test. Data was normalized using a two-step approach-transforming the variable into a percentile rank and subsequent inverse-normal transformation[19]. Two-tailed alpha of 0.05 defined statistical significance. Data analysis was performed with SPSS (IBM Corp. Released 2020. IBM SPSS Statistics for Windows, Version 27.0. IBM Corp, NY, Armonk, United States). The statistical review of the study was reviewed by Daniel Veres, MD, PhD who is a biomedical statistician at Center for Translational Medicine of Semmelweis University.

RESULTS

Patients characteristics

The characteristics of patients included in our analysis are summarized in Table 1. Out of the 128 patients who accepted to participate in our study, 105 were confirmed with PDAC subsequent to EUS-FNA (Figure 1). Sex distribution was almost equal and the mean age at diagnosis was 67.02 ± 8.38 years. Tumors were more frequently located in the head or neck of the pancreas than in the body or tail, and the tumor diameter was in average 43.66 ± 14.83 mm. More than half of the cases were metastatic at diagnosis. Most of the samples were acquired with 22G FNA needles-75 (71%).

Adequacy of the EUS-FNA PDAC samples for second generation high throughput analysis

In our cohort the DNA yield was in average 1289 ng (inter-quartile range: 534.75-2995). All samples resulted in more than 10 ng of DNA while 98 (93%) of them yielded more than 100 ng of DNA. All 7 samples from which less than 100 ng of DNA were extracted, were acquired with 22G needles, and only one yielded below 50 ng of DNA. In our analysis, needle size was not correlated with DNA NGS adequacy rate regardless of NGS type (Supplementary Table 2). For 19G needles, NGS adequacy rate was 90% for all types of NGS while for the 22 G needles the adequacy rate was 89% for WGS and 91% for both WES and amplicon based NGS. Tumor location and diameter did not significantly influence DNA NGS adequacy regardless of NGS type. When comparing the purity parameters across the predefined DNA yield categories (Table 2), the only significant difference we found was for the A260/280 parameter which was significantly higher in the samples with DNA yield ≥ 100 ng (1.89 ± 0.32 *vs* 1.34 ± 0.42, $P = 0.013$).

Association between FNA needle size and DNA parameters

The DNA parameters across our samples were as follows: median concentration 51.56 ng/μL (21.39-124.04), A260/280 = 1.85 (1.79-1.86), A260/230 = 2.2 (1.72-2.36). The association between FNA needle size and the extracted DNA parameters are summarized in Figure 2. Needle size did not influence the concentration of the extracted DNA nor the A260/280 ratio. The median A260/230 was significantly

Table 1 Characteristics of the enrolled patients

Variable	Amount
Number of PDAC cases	105
Age (yr)	67.02 ± 8.38
Male (number of cases)	51
Tumor diameter (mm)	43.66 ± 14.83
Tumor location (number of cases)	
Head/neck	60
Body/tail	44
Tumor stage (number of cases)[1]	
IA	1
IB	3
IIA	3
IIB	12
III	31
IV	55
Needle size (number of samples)	
22G	75
19G	30

[1]According to American Joint Committee on 8th Cancer edition.
PDAC: Pancreatic adenocarcinoma; FNA: Fine needle aspiration; G: Gauge; NGS: Next generation sequencing. Data is given as: mean ± standard deviation, or median (inter quartile range).

Table 2 Purity parameters across the different DNA yield categories

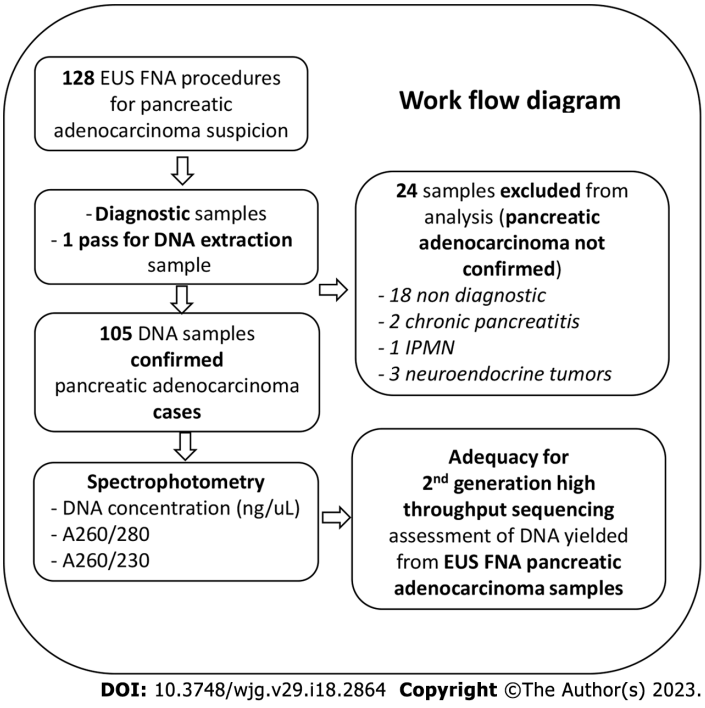
DNA yield	Purity parameters	
	A260/280	A260/230
≥ 100 ng	1.86 (1.80-1.89)	2.23 (1.79-2.35)
≥ 50 ng	1.85 (1.80-1.89)	2.21 (1.7-2.36)
≥ 10 ng	1.85 (1.79-1.86)	2.2 (1.72-2.36)

higher in the 22G samples than in 19G samples (P = 0.038). In multivariate analysis (on needle size, tumor location and tumor diameter) the only independent predictor of A260/230 was needle size (β = 0.36, $t(104)$ = 2.1, P = 0.038). None of the DNA parameters were significantly influenced by the tumor size or location.

DISCUSSION

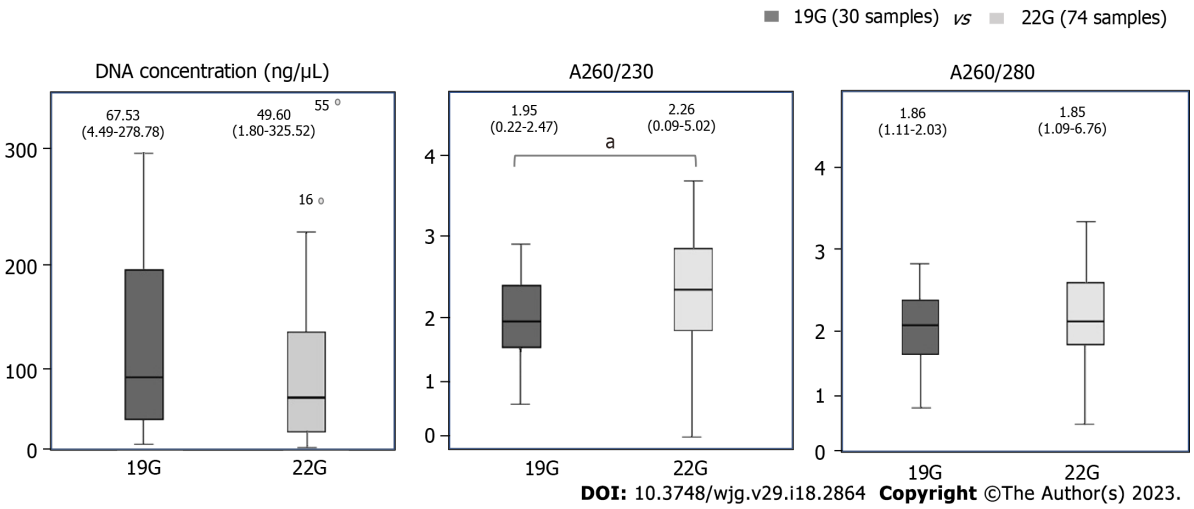
The quantity and quality of the genetic material extracted from tumor samples are essential for their adequacy for downstream genetic analyses performed to further guide the individualized cancer therapy[21]. The requirements for NGS dedicated specimens vary with extraction protocols and testing method, but also with acquisition method, sample manipulation, disease type[22]. Although prior research has demonstrated the suitability of several pancreatic EUS-TA sample types for a range of comprehensive genetic testing techniques, the best sampling protocol for this use is still up for debate [23]. The current guidelines recommend the use of core samples for molecular testing in pancreatic solid lesions based on a moderate level of evidence[6,11].

Our cohort analysis revealed that FNA needle size does not influence the concentration and the primary purity parameter (A260/280) of the DNA extracted from 19G or 22G EUS-FNA PDAC samples. However, needle size was the only independent predictor of A260/230. Tumor diameter and location



DOI: 10.3748/wjg.v29.i18.2864 **Copyright** ©The Author(s) 2023.

Figure 1 Patients recruitment and tumor sampling. EUS FNA: Endoscopic ultrasound guided fine needle aspiration.



DOI: 10.3748/wjg.v29.i18.2864 **Copyright** ©The Author(s) 2023.

Figure 2 The association between needle size and DNA parameters. G: Gauge. To complement the graphical information, the additional data is given as median (min-max). [a]*P* < 0.005.

did not influence the DNA purity and concentration parameters. Based on the purity and DNA yield thresholds there were no significant differences in NGS adequacy rates between the two FNA needle sizes. NGS adequacy rate was 90% for 19G needle samples regardless of NGS type, while for the 22G needle samples it was 89% for WGS and 91% for both WES and amplicon based NGS. Regarding purity parameters, A260/280 was significantly better in samples with DNA yield above 100 ng. We further successfully performed targeted amplicon based NGS on a subgroup of 20 samples.

Park *et al*[24] evaluated which of the EUS-TA related factors and tumor characteristics have a significant impact on the NGS success rate on a cohort of 190 PDAC confirmed cases. They used for DNA analysis the remaining material after acquiring cytologic or histologic specimens for PDAC diagnosis[24]. As needed, 19G, 22G or 25G FNA or Fine needle biopsy (FNB) needles were used[24]. While tumor location in the body or tail of the pancreas was associated with a higher NGS success rate in their cohort than head or uncinate process tumor location, in multivariate analysis the only independent predictor of NGS success was a greater needle size (19G and 22G *vs* 25G)[24]. Although we were able to evaluate only a surrogate marker of NGS success, respectively-the adequacy of the DNA parameters for high throughput analysis, did we did not find a significant impact of tumor character-

istics and neither of needle size on this outcome. Notably, we only used higher gauge needles (19G and 22G and not 25 G).

A group from Johns Hopkins evaluated the concordance of the mutational profiles assessed by targeted NGS between EUS-FNA snap frozen PDAC samples and the corresponding biopsy specimens from the primary tumors that were subsequently resected [25]. Although on a pool of 16 cases only, they detected a 100% concordance between the two sample types for KRAS mutations. They concluded that it is feasible to perform NGS on FNA samples and the results are reliable in complementing pathology results[25].

Besides the parameters of the extracted DNA, the total cellularity and the tumor cell content of the samples are also essential for the assessment of adequacy for NGS[22,26]. We did not evaluate these metrics in our cohort, since we used dedicated FNA samples, processed directly after collection, for DNA extraction. However, we must emphasize that the same needle types were used for the samples dedicated to diagnosis and we only report on confirmed PDAC cases. Moreover, more than 50% of specimens obtained by FNA yielded small tissue fragments and were subjected to cell block techniques to increase the diagnostic accuracy. The most widely used NGS platforms to date require a sample cellularity between 1000 and 5000 cells and a minimum 10% "lesional to-non-lesional cell ratio"[26-28]. A group from MD Anderson compared these parameters between concurrently acquired, percutaneous, image guided FNA and core needle biopsy samples in 24 various malignancy cases. They obtained higher cellularity and better tumor fraction in the cytologic specimens, arguing that by comparison with core biopsies, during FNA the proportion of acquired stromal cells is lower[27].

In their study Berry *et al*[21] performed molecular profiling of 66 snap frozen EUS-FNA pancreatic cancer samples. They revealed a high epithelial and tumor cell content in their specimens and a low contamination with inflammatory, gastric or duodenal cells[21]. Moreover, they compared the DNA yield between the FNA samples dedicated to molecular testing and formalin fixed paraffin embedded cell-block preparations used for PDAC diagnosis, obtaining 10 times higher amounts of DNA from the FNA samples which was in average 4.8 ± 3.7 μg[21]. This could be explained by the degrading effect of formaldehyde on nucleic acids and the cross-links formation between protein and DNA that it determines[22].

Cytologic specimens yield optimal DNA and have adequate cellularity for further NGS. The quality of nucleic acids is altered in samples previously fixed with formalin. More standardized procedures that are focused on specimen sparing and keeping costs and processing times within accessible ranges are needed for the optimization of the sample assessment in the preanalytical phase of NGS.

Implications for practice and research

Regarding the implications for practice our study has shown that both 19G and 22G fresh EUS-FNA PDAC samples yield DNA of adequate amount and purity for next generation high throughput sequencing, regardless of tumor size or location within the pancreas. Overall, the NGS adequacy rates corresponded to the diagnostic accuracy of EUS-FNA samples in PDAC in our cohort[6]. A randomized controlled trial could reliably evaluate the cause-effect relationship between EUS needle G and DNA output from pancreatic cancer samples. Since the technical requirements in various clinical scenarios may limit the feasibility of randomization, prospective cohort studies of greater sizes that allow propensity score matching could decrease the influence of confounders in analyzing this association. Besides targeted NGS, the EUS-FNA samples yielding below 100 ng of DNA could be also used in other downstream applications for genetic testing like droplet digital PCR or TaqMan assays, which, although addressing fewer targets, have the advantage of good sensitivity for samples with low DNA amount.

Strengths and limitations

Even though relatively similar analyses have been previously reported, our study included a high number of samples[21,27]. Besides measuring the yielded DNA concentration and purity ratios, we were able to successfully perform NGS on subgroup of samples, functionality in the downstream application being a reliable method of sample adequacy evaluation[26]. Nevertheless, several limitations should be pointed out: (1) Study design-one of the main limitations of our work-since lack of patients randomization precludes the evaluation of causality between needle size and samples' NGS adequacy; (2) our study was performed in a tertiary gastroenterology center and all involved personnel were experts in their fields (endosonographers, pathologists, biologists); (3) the analysis was not based on a prior sample size calculation therefore our results must be interpreted with caution especially since 71% of the procedures were performed with one EUS-FNA needle type; (4) we did not use 25G needles for our samples therefore our conclusions cannot be extrapolated to all FNA needle sizes; and (5) lack of a comparison group comprising samples obtained by EUS-FNB-another main limitation of our study; to this end however we cite the study of Razzano *et al*[29] that compared the performance for NGS between FNA, FNB and resection PDAC specimens. They obtained similar success rates for mutation and amplification analysis between FNA and FNB samples and proposed FNA material as a source for comprehensive molecular testing[29]. Moreover, the spectrophotometric methods may overestimate the quantity of amplifiable DNA by measuring not only the double stranded fragments, but also single stranded DNA, free and oligonucleotides[22].

CONCLUSION

Acquiring EUS-FNA specimens dedicated for genetic testing is associated with a high adequacy rate for NGS of the extracted DNA. Nineteen and 22G EUS-FNA PDAC samples generate similar amount of DNA. DNA purity may vary indirectly with needle size in EUS-FNA samples. Further standardization in sample handling and cellularity assessment in the pre-analytical phase of NGS will increase reliability of the results for EUS-FNA PDAC samples and hence their usability in current practice.

ARTICLE HIGHLIGHTS

Research background

Due to the opportunities for personalized treatment in pancreatic adenocarcinoma (PDAC), genetic testing is increasingly performed. Fine needle biopsy is the method recommended for endoscopic ultrasound (EUS) guided tissue acquisition to obtain samples dedicated to downstream comprehensive molecular analyses. In current practice however, fine needle aspiration (FNA) is more widely accessible.

Research motivation

We evaluated the EUS-FNA PDAC samples in terms of adequacy for next generation sequencing (NGS) of the yielded DNA to assess the possibility of using this type of samples for genetic testing.

Research objectives

To investigate the association between DNA parameters (amount and purity) measured by spectrophotometry and FNA needle size (19 gauge [G] or 22G), and also tumor characteristics.

Research methods

We performed an observational prospective study on PDAC cases diagnosed through EUS-FNA at a tertiary center of Gastroenterology in Romania. During EUS one pass acquired samples dedicated to genetic testing. NGS adequacy was a dichotomus variable defined based on DNA parameters (purity: A260/280 ≥ 1.7 and DNA amount: ≥ 100 ng for whole genome sequencing, ≥ 50 ng for whole exome sequencing or ≥ 10 ng for amplicon based targeted NGS).

Research results

Our cohort analysis comprised 105 confirmed PDAC cases. The majority of samples were acquired with 22G FNA needles-75 (71%). The DNA amount was in average 1289 ng (inter-quartile range: 534.75-2995). All samples yielded more than 10 ng of DNA while 98 (93%) of them yielded more than 100 ng of DNA. Needle size was not correlated with DNA NGS adequacy rate regardless of NGS type. Needle size did not influence the concentration or A260/280 ratio of the extracted DNA. The median A260/230 was significantly higher in the 22G samples than in 19G samples ($P = 0.038$). In multivariate analysis (on needle size, tumor location and tumor diameter) the only independent predictor of A260/230 was needle size ($\beta = 0.36$, $t(104) = 2.1$, $P = 0.038$).

Research conclusions

Both 22G an 19G EUS-FNA PDAC samples are adequate for downstream NGS. FNA needle size and tumor characteristics did not significantly influence sample NGS adequacy rate. Greater FNA needle size might be associated with decreased sample purity.

Research perspectives

PDAC FNA samples (22 and 19G) yield samples of adequate purity and amount for NGS and can be used both in current practice and for research purposes.

ACKNOWLEDGEMENTS

we would like to give special thanks to Daniel Veres, MD, PhD, for his guidance in performing the formal analysis for the project and Mihaela Topala, MD for her help with patients' enrolment.

FOOTNOTES

Author contributions: Bunduc S contributed to conceptualization, methodology, investigation, formal analysis, original draft, and data visualization; Varzaru B contributed to conceptualization, investigation, data curation, methodology, review and editing; Iacob RA contributed to conceptualization, supervision, review and editing,

methodology, funding acquisition, and resources; Sorop A contributed to methodology, investigation, data curation, review and editing; Manea I contributed to methodology, investigation, data curation, review and editing; Spiridon A contributed to investigation, data curation, review and editing; Chelaru R contributed to investigation, data curation, review and editing; Becheanu G contributed to conceptualization, methodology, investigation, review and editing; Dumbrava M contributed to conceptualization, methodology, investigation, review and editing; Croitoru A contributed to conceptualization, methodology, review and editing, Dima S contributed to conceptualization, supervision, funding acquisition, project administration, review and editing, resources; Popescu I contributed to conceptualization, supervision, funding acquisition, project administration, review and editing, Gheorghe C contributed to guarantor of the article, conceptualization, supervision, funding acquisition, project administration, review and editing; all authors certify that they have participated sufficiently in this work to take public responsibility for the content, including participation in the concept, design, analysis, writing, or revision of the manuscript. All authors have read the journal's authorship agreement, and reviewed and approved the final version of the manuscript.

Supported by The Executive Agency for Higher Education, Research, Development and Innovation Funding-research, No. PN-III-P1-1.2-PCCDI-2017-0797 (PANCNGS).

Institutional review board statement: This prospective observational study was approved by the Internal Review Board of Fundeni Clinical Institute, No. IRB:23878/14.06.2018.

Informed consent statement: Each participant gave informed consent for study enrolment.

Conflict-of-interest statement: All authors confirm they have no conflict of interest in relation to this manuscript.

Data sharing statement: The data underlying this article will be shared upon reasonable request to the corresponding author.

STROBE statement: The authors have read the STROBE Statement-checklist of items, and the manuscript was prepared and revised according to the STROBE Statement-checklist of items.

Open-Access: This article is an open-access article that was selected by an in-house editor and fully peer-reviewed by external reviewers. It is distributed in accordance with the Creative Commons Attribution NonCommercial (CC BY-NC 4.0) license, which permits others to distribute, remix, adapt, build upon this work non-commercially, and license their derivative works on different terms, provided the original work is properly cited and the use is non-commercial. See: https://creativecommons.org/Licenses/by-nc/4.0/

Country/Territory of origin: Romania

ORCID number: Stefania Bunduc 0000-0001-6978-4526; Bianca Varzaru 0000-0002-1428-6439; Razvan Andrei Iacob 0000-0002-8545-310X; Andrei Sorop 0000-0002-2617-4629; Ioana Manea 0000-0002-0226-3037; Andreea Spiridon 0000-0002-2593-709X; Raluca Chelaru 0000-0001-8613-9262; Adina Emilia Croitoru 0000-0003-4216-6570; Gabriel Becheanu 0000-0003-1627-8907; Mona Dumbrava 0000-0002-0788-4473; Simona Dima 0000-0001-5275-8938; Irinel Popescu 0000-0002-2897-1170; Cristian Gheorghe 000000017969628X.

S-Editor: Chang KL
L-Editor: A
P-Editor: Zhao S

REFERENCES

1 **Lu Y**, Gentiluomo M, Macauda A, Gioffreda D, Gazouli M, Petrone MC, Kelemen D, Ginocchi L, Morelli L, Papiris K, Greenhalf W, Izbicki JR, Kiudelis V, Mohelníková-Duchoňová B, Bueno-de-Mesquita B, Vodicka P, Brenner H, Diener MK, Pezzilli R, Ivanauskas A, Salvia R, Szentesi A, Aoki MN, Németh BC, Sperti C, Jamroziak K, Chammas R, Oliverius M, Archibugi L, Ermini S, Novák J, Kupcinskas J, Strouhal O, Souček P, Cavestro GM, Milanetto AC, Vanella G, Neoptolemos JP, Theodoropoulos GE, van Laarhoven HWM, Mambrini A, Moz S, Kala Z, Loveček M, Basso D, Uzunoglu FG, Hackert T, Testoni SGG, Hlaváč V, Andriulli A, Lucchesi M, Tavano F, Carrara S, Hegyi P, Arcidiacono PG, Busch OR, Lawlor RT, Puzzono M, Boggi U, Guo F, Małecka-Panas E, Capurso G, Landi S, Talar-Wojnarowska R, Strobel O, Gao X, Vashist Y, Campa D, Canzian F. Identification of Recessively Inherited Genetic Variants Potentially Linked to Pancreatic Cancer Risk. *Front Oncol* 2021; **11**: 771312 [PMID: 34926279 DOI: 10.3389/fonc.2021.771312]

2 **GLOBOCAN**. Estimated number of deaths in 2020, both sexes, all ages. [cited 31 December 2022]. Available from: https://gco.iarc.fr/today/fact-sheets-cancers

3 **Winter K**, Talar-Wojnarowska R, Dąbrowski A, Degowska M, Durlik M, Gąsiorowska A, Głuszek S, Jurkowska G, Kaczka A, Lampe P, Marek T, Nasierowska-Guttmejer A, Nowakowska-Duława E, Rydzewska G, Strzelczyk J, Śledziński Z, Małecka-Panas E. Diagnostic and therapeutic recommendations in pancreatic ductal adenocarcinoma. Recommendations of the Working Group of the Polish Pancreatic Club. *Prz Gastroenterol* 2019; **14**: 1-18 [PMID: 30944673 DOI: 10.5114/pg.2019.83422]

4 **Ghanem I**, Lora D, Herradón N, de Velasco G, Carretero-González A, Jiménez-Varas MÁ, Vázquez de Parga P, Feliu J.

Neoadjuvant chemotherapy with or without radiotherapy versus upfront surgery for resectable pancreatic adenocarcinoma: a meta-analysis of randomized clinical trials. *ESMO Open* 2022; **7**: 100485 [PMID: 35580504 DOI: 10.1016/j.esmoop.2022.100485]

5 **Elhanafi S**, Mahmud N, Vergara N, Kochman ML, Das KK, Ginsberg GG, Rajala M, Chandrasekhara V. Comparison of endoscopic ultrasound tissue acquisition methods for genomic analysis of pancreatic cancer. *J Gastroenterol Hepatol* 2019; **34**: 907-913 [PMID: 30422342 DOI: 10.1111/jgh.14540]

6 **Dumonceau JM**, Deprez PH, Jenssen C, Iglesias-Garcia J, Larghi A, Vanbiervliet G, Aithal GP, Arcidiacono PG, Bastos P, Carrara S, Czakó L, Fernández-Esparrach G, Fockens P, Ginès À, Havre RF, Hassan C, Vilmann P, van Hooft JE, Polkowski M. Indications, results, and clinical impact of endoscopic ultrasound (EUS)-guided sampling in gastroenterology: European Society of Gastrointestinal Endoscopy (ESGE) Clinical Guideline - Updated January 2017. *Endoscopy* 2017; **49**: 695-714 [PMID: 28511234 DOI: 10.1055/s-0043-109021]

7 **De Palo GM**, De Lena M, Bonadonna G. Adriamycin *vs* adriamycin plus melphalan in advanced ovarian carcinoma. *Cancer Treat Rep* 1977; **61**: 355-357 [PMID: 326402]

8 **Reed JK**, Raftery MA. Properties of the tetrodotoxin binding component in plasma membranes isolated from Electrophorus electricus. *Biochemistry* 1976; **15**: 944-953 [PMID: 3213 DOI: 10.1021/bi00650a002]

9 **Tempero MA**, Malafa MP, Al-Hawary M, Behrman SW, Benson AB, Cardin DB, Chiorean EG, Chung V, Czito B, Del Chiaro M, Dillhoff M, Donahue TR, Dotan E, Ferrone CR, Fountzilas C, Hardacre J, Hawkins WG, Klute K, Ko AH, Kunstman JW, LoConte N, Lowy AM, Moravek C, Nakakura EK, Narang AK, Obando J, Polanco PM, Reddy S, Reyngold M, Scaife C, Shen J, Vollmer C, Wolff RA, Wolpin BM, Lynn B, George GV. Pancreatic Adenocarcinoma, Version 2.2021, NCCN Clinical Practice Guidelines in Oncology. *J Natl Compr Canc Netw* 2021; **19**: 439-457 [PMID: 33845462 DOI: 10.6004/jnccn.2021.0017]

10 **Triplett RG**, Gillmore JD, Armstrong GC. An experimental model for osteomyelitis in the mandible. *J Dent Res* 1977; **56**: 1520 [PMID: 28338 DOI: 10.1177/00220345770560121901]

11 **Pouw RE**, Barret M, Biermann K, Bisschops R, Czakó L, Gecse KB, de Hertogh G, Hucl T, Iacucci M, Jansen M, Rutter M, Savarino E, Spaander MCW, Schmidt PT, Vieth M, Dinis-Ribeiro M, van Hooft JE. Endoscopic tissue sampling - Part 1: Upper gastrointestinal and hepatopancreatobiliary tracts. European Society of Gastrointestinal Endoscopy (ESGE) Guideline. *Endoscopy* 2021; **53**: 1174-1188 [PMID: 34535035 DOI: 10.1055/a-1611-5091]

12 **Saik RP**, Brown D. Lithium: not a sensitive indicator of hydrogen ion diffusion. *J Surg Res* 1978; **25**: 163-165 [PMID: 28450 DOI: 10.1016/0022-4804(78)90071-9]

13 **Thermo Fisher Scientfic**. DNA purification and concentration. 2019. [cited 31 December 2022]. Available from https://assets.thermofisher.com/TFS-Assets/BID/brochures/dna-purification-analysis-brochure.pdf

14 **Asokkumar R**, Yung Ka C, Loh T, Kah Ling L, Gek San T, Ying H, Tan D, Khor C, Lim T, Soetikno R. Comparison of tissue and molecular yield between fine-needle biopsy (FNB) and fine-needle aspiration (FNA): a randomized study. *Endosc Int Open* 2019; **7**: E955-E963 [PMID: 31367675 DOI: 10.1055/a-0903-2565]

15 **Marg-Haufe B**. TECAN. Evaluating the quality of DNA for Next Generation Sequencing, genotyping, and other downstream applications. [cited 31 December 2022]. Available from: https://www.tecan.com/blog/evaluating-the-quality-of-dna-for-next-generation-sequencing

16 How do I determine the concentration, yield and purity of a DNA sample? [Internet]. 2022 Promega Corporation. [cited 20 May 2022]. Available from: https://www.promega.ro/resources/pubhub/enotes/how-do-i-determine-the-concentration-yield-and-purity-of-a-dna-sample/

17 Assessment of Nucleic Acid Purity. Thermo Fisher Scientific – NanoDrop Products. [cited 31 December 2022]. https://tools.thermofisher.com/content/sfs/brochures/TN52646-E-0215M-NucleicAcid.pdf

18 **James D**. Brierley, Mary K. Gospodarowicz, Christian Wittekind BO, Mason, H. Asamura, A. Lee EVE, L. Denny, M.B. Amin SG. TNM Classification of Malignant Tumors. 8th ed. John Wiley & Sons: WILEY Balckwell, 2017: 102-107

19 **Templeton GF**. A two-step approach for transforming continuous variables to normal: Implications and recommendations for IS research. *Commun Assoc Inf Syst* 2011; **28**: 41-58 [DOI: 10.17705/1cais.02804]

20 **Gharaibeh A**, Koppikar S, J. Bonilla-Escobar. F. Strengthening the Reporting of Observational Studies in Epidemiology (STROBE) in the International Journal of Medical Students. *Int J Med Students* 2014; **2**: 36-37 [DOI: 10.5195/ijms.2014.76]

21 **Berry W**, Algar E, Kumar B, Desmond C, Swan M, Jenkins BJ, Croagh D. Endoscopic ultrasound-guided fine-needle aspirate-derived preclinical pancreatic cancer models reveal panitumumab sensitivity in KRAS wild-type tumors. *Int J Cancer* 2017; **140**: 2331-2343 [PMID: 28198009 DOI: 10.1002/ijc.30648]

22 **Mäkinen KK**, Virtanen KK. Effect of 4.5--year use of xylitol and sorbitol on plaque. *J Dent Res* 1978; **57**: 441-446 [PMID: 28341 DOI: 10.1177/00220345780570030401]

23 **Archibugi L**, Testoni SGG, Redegalli M, Petrone MC, Reni M, Falconi M, Doglioni C, Capurso G, Arcidiacono PG. New era for pancreatic endoscopic ultrasound: From imaging to molecular pathology of pancreatic cancer. *World J Gastrointest Oncol* 2019; **11**: 933-945 [PMID: 31798775 DOI: 10.4251/wjgo.v11.i11.933]

24 **Park JK**, Lee JH, Noh DH, Park JK, Lee KT, Lee JK, Lee KH, Jang KT, Cho J. Factors of Endoscopic Ultrasound-Guided Tissue Acquisition for Successful Next-Generation Sequencing in Pancreatic Ductal Adenocarcinoma. *Gut Liver* 2020; **14**: 387-394 [PMID: 31581388 DOI: 10.5009/gnl19011]

25 **Bratfos O**. [Drug therapy of anxiety]. *Tidsskr Nor Laegeforen* 1979; **99**: 333-334 [PMID: 34244]

26 **Fabbri C**, Gibiino G, Fornelli A, Cennamo V, Grifoni D, Visani M, Acquaviva G, Fassan M, Fiorino S, Giovanelli S, Bassi M, Ghersi S, Tallini G, Jovine E, Gasbarrini A, de Biase D. Team work and cytopathology molecular diagnosis of solid pancreatic lesions. *Dig Endosc* 2017; **29**: 657-666 [PMID: 28190274 DOI: 10.1111/den.12845]

27 **Higa HH**, Manzi A, Varki A. O-acetylation and de-O-acetylation of sialic acids. Purification, characterization, and properties of a glycosylated rat liver esterase specific for 9-O-acetylated sialic acids. *J Biol Chem* 1989; **264**: 19435-19442 [PMID: 2808434]

28 **Ronai SE**, Hyman PE. Gianetti v Norwalk Hospital: Connecticut Supreme Court rules on hospital and medical staff

member contractual relationship and judicial review of medical staff termination decisions. *Conn Med* 1989; **53**: 425-426 [PMID: 2758833]

29 **Razzano D**, Bouza SJ, Hernandez PV, Wang M, Robert ME, Walther Z, Cai G. Comprehensive molecular profiling of pancreatic ductal adenocarcinoma in FNA, biopsy, and resection specimens. *Cancer Cytopathol* 2022; **130**: 726-734 [PMID: 35511415 DOI: 10.1002/cncy.22589]

World Journal of Gastroenterology

Submit a Manuscript: https://www.f6publishing.com

World J Gastroenterol 2023 May 14; 29(18): 2875-2887

DOI: 10.3748/wjg.v29.i18.2875

ISSN 1007-9327 (print) ISSN 2219-2840 (online)

ORIGINAL ARTICLE

Observational Study

Contributory roles of sarcopenia and myosteatosis in development of overt hepatic encephalopathy and mortality after transjugular intrahepatic portosystemic shunt

Liang Yin, Sen-Lin Chu, Wei-Fu Lv, Chun-Ze Zhou, Kai-Cai Liu, Yi-Jiang Zhu, Wen-Yue Zhang, Cui-Xia Wang, Yong-Hui Zhang, Dong Lu, De-Lei Cheng

Specialty type: Gastroenterology and hepatology

Provenance and peer review: Unsolicited article; Externally peer reviewed.

Peer-review model: Single blind

Peer-review report's scientific quality classification

Grade A (Excellent): 0
Grade B (Very good): B, B
Grade C (Good): 0
Grade D (Fair): 0
Grade E (Poor): 0

P-Reviewer: Barone M, Italy; Srpcic M, Slovenia

Received: January 29, 2023
Peer-review started: January 29, 2023
First decision: February 22, 2023
Revised: March 8, 2023
Accepted: April 17, 2023
Article in press: April 17, 2023
Published online: May 14, 2023

Liang Yin, Sen-Lin Chu, Wei-Fu Lv, Chun-Ze Zhou, Yi-Jiang Zhu, Wen-Yue Zhang, Cui-Xia Wang, Yong-Hui Zhang, Dong Lu, De-Lei Cheng, Department of Interventional Radiology, The First Affiliated Hospital of University of Science and Technology of China, Division of Life Sciences and Medicine, University of Science and Technology of China, Hefei 230022, Anhui Province, China

Kai-Cai Liu, Infection Hospital, The First Affiliated Hospital of University of Science and Technology of China, Division of Life Sciences and Medicine, University of Science and Technology of China, Hefei 230000, Anhui Province, China

Corresponding author: De-Lei Cheng, MD, Department of Interventional Radiology, The First Affiliated Hospital of University of Science and Technology of China, Division of Life Sciences and Medicine, University of Science and Technology of China, No. 17 Lujiang Road, Luyang District, Hefei 230022, Anhui Province, China. 39055004@qq.com

Abstract

BACKGROUND

Skeletal muscle abnormalities, such as muscle mass depletion (sarcopenia) and fatty infiltration of the muscle (myosteatosis), are frequent complications in cirrhotic patients scheduled for transjugular intrahepatic portosystemic shunt (TIPS).

AIM

To investigate the association and predictive value of sarcopenia and myosteatosis for overt hepatic encephalopathy (HE) and mortality after TIPS.

METHODS

The records of cirrhotic patients who underwent the TIPS procedure at our hospital between January 2020 and June 2021 were retrospectively retrieved. The transversal psoas muscle thickness (TPMT) and psoas muscle attenuation (PMA) measured from the unenhanced abdominal computed tomography (CT) at the level of the third lumbar vertebrae were used to analyze the sarcopenia and myosteatosis, respectively. The area under curve (AUC) was used to evaluate the discriminative power of TPMT, PMA, and relevant clinical parameters. Fur-

thermore, log-rank test was performed to compare the incidence of overt HE and survival between the different groups, and the association of risk factors with overt HE and mortality was analyzed using Cox proportional hazards regression models.

RESULTS

A total of 108 patients were collected. Among these patients, 45.4% of patients developed overt HE after TIPS treatment. Furthermore, 32.4% and 28.7% of these patients were identified to have myosteatosis and sarcopenia, respectively. Myosteatosis (51.0% *vs* 16.9%, $P < 0.001$) and sarcopenia (40.8 *vs* 18.6%, $P = 0.011$) were found to be more frequent in patients with overt HE, when compared to patients without overt HE. The receiver operating characteristics analysis indicated that the predictive power of TPMT and PMA in overt HE (AUC = 0.713 and 0.778, respectively) was higher when compared to the neutrophil lymphocyte ratio (AUC = 0.636). The cumulative incidence of overt HE was the highest in patients with concomitant sarcopenia and myosteatosis, followed by patients with myosteatosis or sarcopenia, while this was the lowest in patients without sarcopenia and myosteatosis. In addition, sarcopenia and myosteatosis were independently associated with overt HE and mortality after adjusting for confounding factors in post-TIPS patients.

CONCLUSION

CT-based estimations for sarcopenia and myosteatosis can be used as reliable predictors for the risk of developing overt HE and mortality in cirrhotic patients after TIPS.

Key Words: Sarcopenia; Myosteatosis; Hepatic encephalopathy; Transjugular intrahepatic portosystemic shunt; Transjugular intrahepatic portosystemic shunt

©The Author(s) 2023. Published by Baishideng Publishing Group Inc. All rights reserved.

Core Tip: Few studies have investigated the relationship among sarcopenia, myosteatosis, and overt hepatic encephalopathy (HE) after transjugular intrahepatic portosystemic shunt (TIPS). The present study revealed that the cumulative incidence of overt HE was the highest in patients with concomitant sarcopenia and myosteatosis, followed by patients with myosteatosis or sarcopenia, and the lowest incidence was found in patients without myosteatosis and sarcopenia. Sarcopenia and myosteatosis were the independent risk factors for overt HE and mortality in patients following TIPS. Therefore, identifying strategies for improving muscle mass (sarcopenia) and muscle fatty infiltration (myosteatosis) may help to reduce the incidence of HE after TIPS.

Citation: Yin L, Chu SL, Lv WF, Zhou CZ, Liu KC, Zhu YJ, Zhang WY, Wang CX, Zhang YH, Lu D, Cheng DL. Contributory roles of sarcopenia and myosteatosis in development of overt hepatic encephalopathy and mortality after transjugular intrahepatic portosystemic shunt. *World J Gastroenterol* 2023; 29(18): 2875-2887
URL: https://www.wjgnet.com/1007-9327/full/v29/i18/2875.htm
DOI: https://dx.doi.org/10.3748/wjg.v29.i18.2875

INTRODUCTION

Transjugular intrahepatic portosystemic shunt (TIPS), which establishes an artificial shunt between the portal and hepatic vein, has been considered an effective method for treating portal hypertension, and can be used to manage refractory ascites and variceal hemorrhage in patients with liver cirrhosis[1]. However, the TIPS procedure leads to a significantly high incidence of overt hepatic encephalopathy (HE), which occurs in approximately 20%-50% of post-TIPS patients[2-4]. Previous studies have suggested that post-TIPS HE is associated with increased hospitalization rates, mortality, and poor quality of life[5]. The use of rifaximin and lactulose remains controversial in treating this pathological entity[6,7]. Thus, studies that can precisely predict post-procedure HE in cirrhotic patients would be beneficial in developing appropriate preventive measures.

More recent studies have revealed that abnormalities in the skeletal muscle, such as sarcopenia (muscle mass depletion) and myosteatosis (fatty infiltration of the muscle), are more prevalent[8,9], and that these are associated with the development of HE in cirrhotic patients[10]. Cirrhosis can lead to the excessive accumulation of ammonia in the skeletal muscle, in which a cascade of molecular alterations and metabolic disturbances may contribute to sarcopenia and myosteatosis. Consequently, both sarcopenia and myosteatosis may, in turn, further increase the circulating ammonia levels to induce

overt HE. These two skeletal muscle abnormalities can hypothetically be targeted for preventing overt HE.

In clinic, both sarcopenia and myosteatosis can be reliably and objectively diagnosed through the computed tomography (CT) image-based measurement of body composition. Compared to the skeletal muscle index (SMI) and total psoas muscle volume, the CT-based measurement of transversal psoas muscle thickness (TPMT) has become an easy-to-use method to diagnose sarcopenia through gauging the psoas diameter, and this has become an independent risk factor for mortality in cirrhotic patients [11]. Furthermore, myosteatosis can be quantitatively graded by CT measurements, which shows that lower muscle radiodensity for designating muscle attenuation can be considered as evidence of fat infiltration in the skeletal muscle[12]. Previous studies have demonstrated that psoas muscle attenuation (PMA) is associated with postoperative complications and mortality in elderly patients[13,14]. The present study employed these CT-based methods to evaluate the association and predictive value of sarcopenia and myosteatosis for overt HE after TIPS.

MATERIALS AND METHODS

The present study retrospectively analyzed the demographic, clinical, laboratory and radiological data of cirrhotic patients who underwent TIPS at our institution between January 2020 and June 2021. A total of 108 patients were included (Supplementary Figure 1). The inclusion criteria were, as follows: (1) Patients diagnosed with cirrhotic portal hypertension; and (2) patients with at least one episode of variceal hemorrhage or refractory ascites after treatment with vasoactive drugs, endoscopic treatment, or large-volume paracentesis. The exclusion criteria were, as follows: (1) Patients < 18 years old; (2) patients with a history of overt HE (grade ≥ 2, according to the West-Haven criteria[7]) within the past six months; (3) patients with hepatocellular carcinoma or other malignancies; (4) patients with no or poor quality preoperative abdominal CT scans; (5) patients with severe medical comorbidities, such as renal failure, pulmonary insufficiency, or extensive cardiovascular and cerebrovascular disease; and (6) patients who were lost to follow-up within three months.

Our institutional ethics review board approved the present retrospective study. According to the Declaration of Helsinki, all data of the study patients remained confidential throughout the study, and the informed consent for the study was waived due to the retrospective nature of the study.

The TIPS procedure

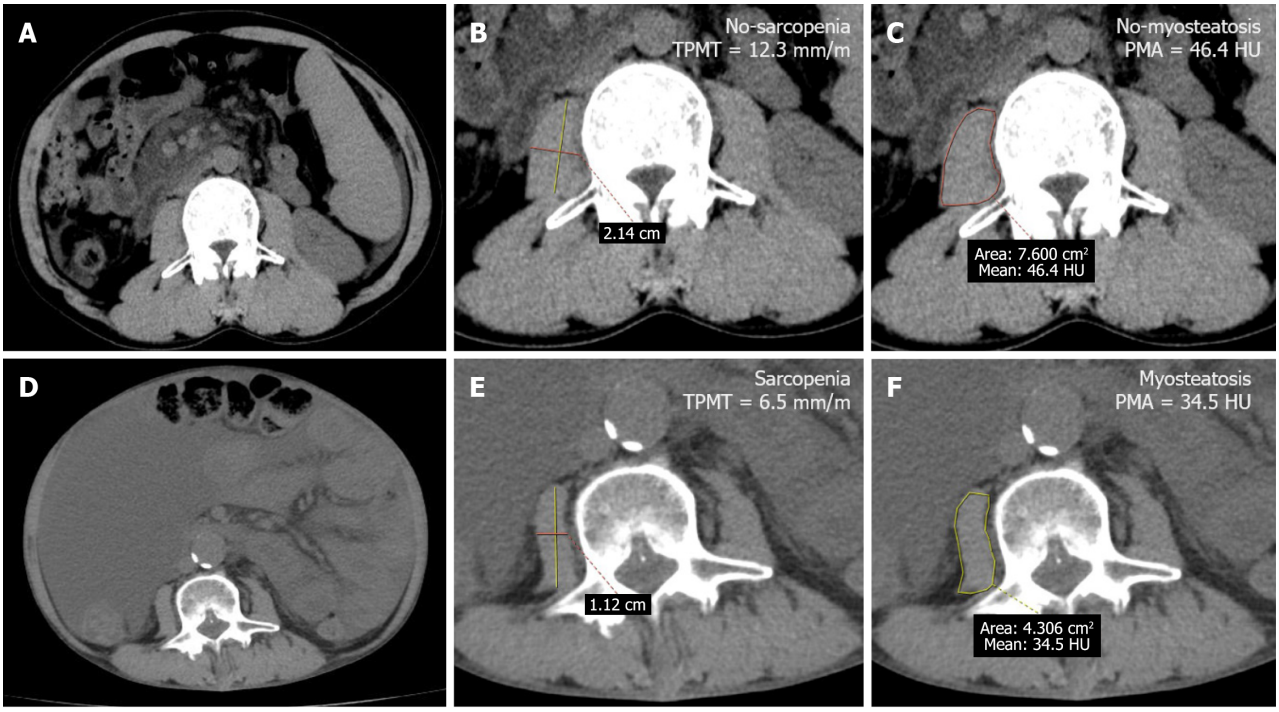
The TIPS procedure was performed based on the following steps: (1) After successfully puncturing the internal jugular vein, a transjugular liver access set (RUPS-100; Cook Incorporated, Bloomington, IN, United States) was introduced over the guidewire into the right hepatic vein; (2) the bifurcation of the left and right branches of the portal vein was punctured from the right hepatic vein; (3) the pre-shunt portosystemic pressure gradient (PPG) was measured; (4) a balloon catheter of 6-7 mm in diameter was passed over the guidewire to dilate the puncture channel; (5) an 8-mm polytetrafluoroethylene-covered stent (Viatorr stent, W. L. Gore & Associates, Flagstaff, AZ, United States) was implanted to establish the portosystemic shunt; (6) an 8-mm balloon catheter was used to further dilate the in-place stent and ensure that the expansion of the stent reaches 8 mm; (7) after the stent insertion, portography was performed to visualize the left and right branches of the portal vein; (8) if the patient was complicated with variceal rebleeding, the esophageal and gastric varicose vessels were embolized at the same time; and (9) finally, the post-shunting PPG was measured again to determine whether the target PPG was ≤ 12 mmHg or reduced by more than 50% from baseline.

CT image analysis

The abdominal CT scans of all studied patients were retrieved from our hospital's Picture Archiving and Communication System (Carestream, Canada). Then, the PMA and TPMT were measured at the level of the third lumbar vertebrae (L3) using the ADW4.4 workstation. In order to standardize the measurement, TPMT was obtained by gauging the transversal diameters of the right psoas muscle, further normalizing these to the body height, and presenting the values in mm/m. PMA was determined as the mean muscle attenuation in Hounsfield unit (HU) of the right psoas muscle at the L3 level (Figure 1). For the present study, sarcopenia was defined as TPMT < 10.7 mm/m in males and TPMT < 7.8 mm/m in females[11], while myosteatosis was defined as PMA < 41 HU for body mass index (BMI) < 25 kg/m^2 and PMA < 33 HU for BMI ≥ 25 kg/m^2[15].

Evaluation and follow-up of overt HE

All patients were followed-up at 1, 3 and 6 mo after TIPS, and every six months thereafter, during the inpatient rounds and outpatient visits. The follow-up evaluation included the following: General clinical manifestations, physical examination, laboratory tests, shunt patency, and HE. The different stages of HE were assessed and classified based on the detailed neurological examination, and according to the clinical criteria (West-Haven criteria). Overt HE was clinically diagnosed according to the grade 2 West-Haven criteria or higher, or based on the evidence of asterixis and disorientation[5].



DOI: 10.3748/wjg.v29.i18.2875 **Copyright** ©The Author(s) 2023.

Figure 1 Abdominal computed tomography images at the level of the third lumbar vertebrae were used to measure the transversal psoas muscle thickness and psoas muscle attenuation in a 45-year-old man without sarcopenia and myosteatosis, and a 51-year-old man with sarcopenia and myosteatosis. A: The axial computed tomography (CT) scan image of a 45-year-old cirrhotic patient (height: 1.74 m, weight: 74 kg) who developed variceal rebleeding; B and C: The patient had normal transversal psoas muscle thickness (TPMT) and psoas muscle attenuation (PMA) levels: 12.3 mm/m (21.4 mm/1.74 m) and 46.4 HU, respectively; D-F: The axial CT scan image of a 51-year-old cirrhotic patient (height: 1.72 m, weight: 55 kg) who developed refractory ascites (D), and had low TPMT and PMA (6.5 mm/m [11.2 mm/1.72 m] and 34.5 HU) (E and F). TPMT: Transversal psoas muscle thickness.

Statistical analysis

The statistical analysis was performed using SPSS v26.0 (IBM, United States). The data were presented as mean ± SE, or in frequency and percentage. Before the analysis, tests were performed to verify the normal distribution of the variables. The comparison of two groups for quantitative variables was performed using Student's *t*-test or Mann-Whitney *U*-test, while the comparison of two groups with qualitative variables was analyzed using χ^2 test. Receiver operating characteristic (ROC) analysis was performed to determine the prognostic significance and precision of various relevant parameters in predicting the development of overt HE. The Kaplan-Meier survival estimates were graphed to plot the survival trends of the patients, and log-rank test was conducted to determine the cumulative rates for overt HE. Univariate and multivariate Cox proportional hazards regression models were used to assess the association of risk factors with HE and mortality, and forward regression analysis was subsequently performed to select the appropriate variables in the multivariate model. A two-sided P value of < 0.05 was considered statistically significant for all statistical tests.

RESULTS

Patient demographics

Among the 108 patients, 84 (77.8%) patients were male, with a mean age of 53.0 ± 10.8 years old. The detailed demographic data and clinical information of these 108 patients are presented in Table 1. The table shows that the most common etiology of cirrhosis was viral hepatitis (67.6%). Furthermore, 74 (68.5%) patients had ascites, and the mean Child-Pugh score, model for end-stage liver disease (MELD) score, and neutrophil-lymphocyte ratio (NLR) was 7.4 ± 1.5, 11.0 ± 4.4 and 4.4 ± 4.1, respectively. The mean levels for hepatic [total bilirubin (TBIL), 22.8 ± 12.9 umol/L; alanine aminotransferase, 27.5 ± 19.7 U/L; aspartate transaminase, 37.8 ± 28.6 U/L] and renal (creatinine, 67.8 ± 25.7 umol/L) function were within the normal range. The mean value for PMA and TPMT was 43.5 ± 6.9 HU and 11.6 ± 3.1 mm/m, respectively. In general, myosteatosis and sarcopenia were found in 35 (32.4%) and 31 (28.7%) patients, respectively, and overt HE was diagnosed in 49 (45.4%) post-TIPS patients.

Table 1 Demographic data, relevant clinical characteristics, and skeletal muscle abnormalities of patients in the study

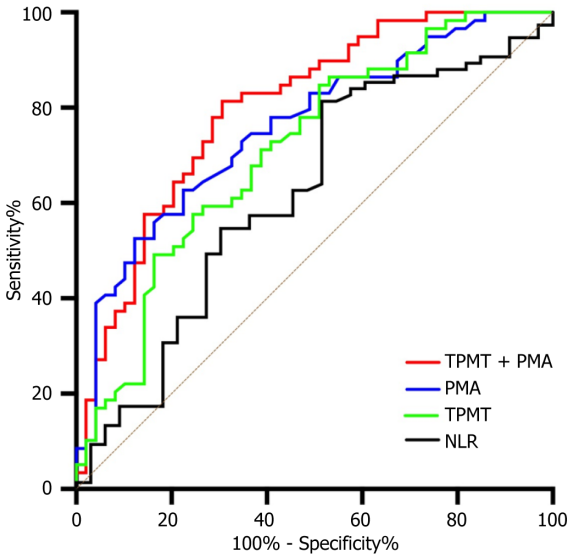
Variables	All patients (*n* = 108)	Non-HE (*n* = 59)	HE (*n* = 49)	*P* value
Age (years)	53.0 ± 10.8	50.3 ± 9.6	56.2 ± 11.5	0.005[a]
Gender (male), *n*, %	84 (77.8)	47 (79.7)	37 (75.5)	0.605
BMI (kg/m^2)	20.99 ± 2.59	21.00 ± 2.58	20.96 ± 2.63	0.856
Etiology (*n*, %)				
Viral hepatitis	74 (68.5)	42 (71.2)	32 (65.3)	0.512
Others	34 (31.5)	17 (28.8)	17 (34.7)	
Ascites (*n*, %)				
Yes	74 (68.5)	41 (69.5)	33 (67.3)	0.811
No	34 (31.5)	18 (30.5)	16 (32.7)	
Child-Pugh score	7.4 ± 1.5	6.9 ± 1.2	7.9 ± 1.8	0.002[a]
Child-Pugh class A/B/C (*n*)	38/59/11	25/30/4	13/29/7	0.155
MELD score	11.0 ± 4.4	9.3 ± 3.8	13.0 ± 4.3	< 0.001[a]
NLR	4.4 ± 4.1	3.9 ± 4.5	4.9 ± 3.5	0.015[a]
TBIL (umol/L)	22.8 ± 12.9	19.1 ± 9.4	27.3 ± 15.0	0.003[a]
ALT (U/L)	27.5 ± 19.7	27.1 ± 16.9	28.0 ± 22.8	0.610
AST (U/L)	37.8 ± 28.6	32.0 ± 16.5	44.9 ± 37.4	0.071
Albumin (g/L)	32.6 ± 5.0	33.2 ± 5.3	31.9 ± 4.7	0.161
Creatinine (umol/L)	67.8 ± 25.7	66.6 ± 23.4	69.1 ± 28.5	0.858
Reduction of PPG (%)	53.7 ± 9.1	51.5 ± 9.1	56.5 ± 8.5	0.004[a]
PMA (HU)	43.5 ± 6.9	46.3 ± 6.6	40.2 ± 5.7	< 0.001[a]
Myosteatosis	35 (32.4)	10 (16.9)	25 (51.0)	< 0.001[a]
No myosteatosis	73 (67.6)	49 (83.1)	24 (49.0)	
TPMT (mm/m)	11.6 ± 3.1	12.6 ± 2.9	10.4 ± 3.1	< 0.001[a]
Sarcopenia	31 (28.7)	11 (18.6)	20 (40.8)	0.011[a]
No sarcopenia	77 (71.3)	48 (81.4)	29 (59.2)	

[a]$P < 0.05$.

HE: Hepatic encephalopathy; BMI: Body mass index; MELD: Model for end-stage liver disease; NLR: Neutrophil-lymphocyte ratio; TBIL: Total bilirubin; ALT: Alanine aminotransferase; AST: Aspartate transaminase; PPG: Portosystemic pressure gradient; PMA: Psoas muscle attenuation; TPMT: Transversal psoas muscle thickness; HU: Hounsfield units.

Features associated with overt HE

The comparison between patients with and without overt HE is presented in Table 1. The table shows that patients with overt HE were older, had higher TBIL, MELD, Child-Pugh scores and reduction of PPG, and had lower NLR, PMA and TPMT values, when compared to patients without overt HE ($P < 0.05$). Furthermore, both myosteatosis (51.0% *vs* 16.9%, $P < 0.001$) and sarcopenia (40.8 *vs* 18.6%, $P = 0.011$) were more common in patients with overt HE, when compared to patients without overt HE. ROC curves were further plotted to determine the area under curve (AUC) values for PMA (AUC = 0.759, 95%CI: 0.669-0.849) and TPMT (AUC = 0.7143, 95%CI: 0.615-0.811), which were similar to the MELD score (AUC = 0.737, 95%CI: 0.642-0.833), but were greater than the NLR (AUC = 0.636, 95%CI: 0.530-0.743). The diagnostic sensitivity and specificity for the combined TPMT and PMA were 81.4% and 69.4%, respectively, and the AUC value was 0.799 (95%CI: 0.715-0.884) (Figure 2). The univariate Cox proportional hazards regression analysis revealed that the following were potentially associated with overt HE: age (HR = 1.044, 95%CI: 1.016-1.071, $P = 0.001$), Child-Pugh score (HR = 1.292, 95%CI: 1.091-1.531, $P = 0.003$), MELD score (HR = 1.137, 95%CI: 1.074-1.203, $P < 0.001$), TBIL (HR = 1.033, 95%CI: 1.014-1.053, $P = 0.001$), reduction of PPG (HR = 1.039, 95%CI: 1.007-1.071, $P = 0.017$), PMA (HR = 0.901, 95%CI: 0.863-0.940; $P < 0.001$), and TPMT (HR = 0.853, 95%CI: 0.774-0.940, $P < 0.001$). The further multivariate Cox proportional hazards regression analysis identified the following as independent predictive variables for overt HE after TIPS: MELD score (HR = 1.083, 95%CI: 1.020-1.449, $P = 0.009$),



DOI: 10.3748/wjg.v29.i18.2875 **Copyright** ©The Author(s) 2023.

Figure 2 Receiver operating characteristic curves for the probability of transversal psoas muscle thickness, psoas muscle attenuation, and neutrophil-lymphocyte ratio in predicting overt hepatic encephalopathy. TPMT: Transversal psoas muscle thickness; PMA: Psoas muscle attenuation; NLR: Neutrophil-lymphocyte ratio.

PMA (HR = 0.930, 95%CI: 0.889-0.974, P = 0.002), and TPMT (HR = 0.895, 95%CI: 0.808-0.992, P = 0.035) (Table 2).

Incidence of overt HE

The 3-mo, 6-mo, 1-year, and 2-year cumulative incidence of overt HE after TIPS was 32.8%, 38.0%, 44.7% and 52.6%, respectively. The incidence of overt HE was significantly higher in patients with sarcopenia (log-rank P = 0.022) or myosteatosis (log-rank P < 0.001), when compared to those without either condition. Furthermore, the 108 studied patients were divided into the following groups: Concomitant sarcopenia and myosteatosis (13.9%, 15/108), myosteatosis alone (18.5%, 20/108), sarcopenia alone (13.0%, 14/108), and normal muscle (54.6%, 59/108) groups (Table 3). It was determined that the cumulative incidence of overt HE was the highest in the concomitant sarcopenia and myosteatosis group, followed by the myosteatosis alone and sarcopenia alone groups, while the incidence was the lowest in the non-myosteatosis and non-sarcopenia groups (Figure 3).

Survival analysis

The univariate Cox proportional hazards regression analysis revealed that age (HR = 1.042, 95%CI: 1.008-1.077, P = 0.016), Child-Pugh score (HR = 1.317, 95%CI: 1.064-1.630, P = 0.011), MELD score (HR = 1.089, 95%CI: 1.013-1.172, P = 0.021), albumin (HR = 0.904, 95%CI: 0.836-0.977, P = 0.011), PMA (HR = 0.887; 95%CI: 0.839-0.938, P < 0.001), and TPMT (HR = 0.851, 95%CI: 0.759-0.954, P = 0.006) were potentially associated with overall mortality. When these above parameters were reprocessed using the multivariate Cox proportional hazards regression model, merely albumin (HR = 0.903, 95%CI: 0.827-0.986, P = 0.023), PMA (HR = 0.901, 95%CI: 0.853-0.951, P < 0.001), and TPMT (HR = 0.867, 95%CI: 0.760-0.988, P = 0.032) were identified as independent predictors for overall mortality (Table 4). Based on the Kaplan-Meier survival analysis, the cumulative survival rate was significantly lower in patients with overt HE (log-rank P < 0.001), sarcopenia (log-rank P = 0.001), and myosteatosis (log-rank P = 0.002), when compared to patients without overt HE. Furthermore, the cumulative survival rate was the lowest in patients with concomitant sarcopenia and myosteatosis, followed by patients with sarcopenia alone and myosteatosis alone, while the cumulative survival rate was the highest in patients without myosteatosis and sarcopenia (Figure 4).

DISCUSSION

Skeletal muscle abnormalities are frequently observed in advanced cirrhosis and cancer, and are associated with unfavorable outcomes[16-18]. Few studies have investigated the relationship between sarcopenia and myosteatosis, and overt HE after TIPS. The present study revealed that the cumulative incidence of overt HE was the highest in patients with concomitant sarcopenia and myosteatosis, followed by patients with myosteatosis alone and sarcopenia alone, while the lowest incidence was identified in patients without myosteatosis and sarcopenia. Furthermore, both myosteatosis and

Table 2 Prognostic factors for overt hepatic encephalopathy in patients treated with transjugular intrahepatic portosystemic shunt

Characteristics	Univariate analysis			Multivariate analysis		
	HR	95%CI	*P* value	HR	95%CI	*P* value
Age (years)	1.044	(1.016-1.071)	0.001[a]	1.043	(1.017-1.069)	0.330
Gender (male)	1.207	(0.629-2.316)	0.572			
BMI (kg/m^2)	1.012	(0.902-1.134)	0.844			
Etiology (viral hepatitis/others)	1.277	(0.706-2.310)	0.418			
Ascites (yes/no)	0.845	(0.465-1.536)	0.580			
Child-Pugh score	1.292	(1.091-1.531)	0.003[a]	1.078	(0.832-1.397)	0.740
MELD score	1.137	(1.074-1.203)	< 0.001[a]	1.083	(1.020-1.449)	0.009[a]
NLR	1.041	(0.984-1.101)	0.161			
TBIL (umol/L)	1.033	(1.014-1.053)	0.001[a]	1.029	(1.000-1.058)	0.768
ALT (U/L)	1.003	(0.989-1.018)	0.681			
AST (U/L)	1.010	(0.998-1.023)	0.107			
Albumin (g/L)	0.956	(0.903-1.013)	0.128			
Creatinine (umol/L)	1.004	(0.993-1.015)	0.454			
Reduction of PPG (%)	1.039	(1.007-1.071)	0.017[a]	1.050	(1.014-1.087)	0.082
PMA (HU)	0.901	(0.863-0.940)	< 0.001[a]	0.930	(0.889-0.974)	0.002[a]
TPMT (mm/m)	0.853	(0.774-0.940)	0.001[a]	0.895	(0.808-0.992)	0.035[a]

[a]$P < 0.05$.

HE: Hepatic encephalopathy; BMI: Body mass index; MELD: Model for end-stage liver disease; NLR: Neutrophil-lymphocyte ratio; TBIL: Total bilirubin; ALT: Alanine aminotransferase; AST: Aspartate transaminase; PPG: Portosystemic pressure gradient; PMA: Psoas muscle attenuation; TPMT: Transversal psoas muscle thickness; HU: Hounsfield units.

Table 3 The different skeletal muscle abnormalities in patients

Skeletal muscle abnormalities (*n* = 108)		PMA	
		Low (*n* = 35); BMI < 25 kg/m^2: < 41 HU; BMI ≥ 25 kg/m^2: < 33 HU	Normal (*n* = 73); BMI < 25 kg/m^2: ≥ 41 HU; BMI ≥ 25 kg/m^2: ≥ 33 HU
TPMT	Low (*n* = 31); Male: < 10.7 mm/m; Female: < 7.8 mm/m	Sarcopenia; Myosteatosis; (*n* = 15)	Sarcopenia; No myosteatosis; (*n* = 14)
	Normal (*n* = 77); Male: ≥ 10.7 mm/m; Female: ≥ 7.8 mm/m	Myosteatosis; No sarcopenia; (*n* = 20)	No myosteatosis; No sarcopenia; (*n* = 59)

BMI: Body mass index; PMA: Psoas muscle attenuation; TPMT: Transversal psoas muscle thickness; HU: Hounsfield units.

sarcopenia were identified as independent risk factors for predicting the occurrence of overt HE and mortality in cirrhotic patients following TIPS.

Overt HE is a frequent complication of decompensated cirrhosis, which is eventually induced and/or aggravated by the TIPS procedure, and this can impact the quality of life and increase the mortality of patients[19]. The present study revealed that the overall incidence of overt HE after TIPS treatment was 45.4%, which is similar to the reports of previous studies[20,21]. However, merely the MELD score (HR = 1.083, 95%CI: 1.020-1.449, $P = 0.009$), myosteatosis (HR = 0.930, 95%CI: 0.889-0.974, $P = 0.002$) and sarcopenia (HR = 0.895, 95%CI: 0.808-0.992, $P = 0.035$) were identified as independent risk factors after adjusting for confounding variables in the present study. Two retrospective studies on 279 and 284 patients with TIPS reported that a unit of increase in the MELD score would lead to a 1.69 higher odds and a 1.06-fold increase in risk of post-TIPS HE development[22,23]. At the same time, a prospective study on 46 patients who underwent the TIPS procedure also reported that the MELD score and sarcopenia were independently associated with the development of HE after TIPS placement[24]. In addition, several studies reported that age, albumin, creatinine, Child-Pugh score, previous HE, PPG, proton pump inhibitors, and shunt size (> 8 mm *vs* 8 mm) are potential risks for developing post-TIPS

Table 4 The univariate and multivariable analysis results for predicting mortality in patients treated with transjugular intrahepatic portosystemic shunt

Characteristics	Univariate analysis			Multivariate analysis		
	HR	95%CI	*P* value	HR	95%CI	*P* value
Age (years)	1.042	(1.008-1.077)	0.016[a]	1.047	(1.012-1.084)	0.278
Gender (male)	1.187	(0.559-2.518)	0.656			
BMI (kg/m^2)	1.000	(0.871-1.148)	0.997			
Etiology (Viral hepatitis/other)	1.187	(0.559-2.518)	0.656			
Ascites (yes/no)	1.652	(0.714-3.823)	0.241			
Child-Pugh score	1.317	(1.064-1.630)	0.011[a]	1.194	(0.903-1.579)	0.740
MELD score	1.089	(1.013-1.172)	0.021[a]	1.050	(0.963-1.146)	0.845
NLR	1.060	(0.994-1.130)	0.075			
TBIL (umol/L)	1.022	(0.996-1.048)	0.096			
ALT (U/L)	1.003	(0.986-1.020)	0.745			
AST (U/L)	1.007	(0.998-1.016)	0.109			
Reduction in PPG (%)	1.030	(0.992-1.069)	0.120			
Albumin (g/L)	0.904	(0.836-0.977)	0.011[a]	0.903	(0.827-0.986)	0.023[a]
Creatinine (umol/L)	1.012	(1.000-1.024)	0.044[a]	1.005	(0.993-1.018)	0.342
PMA (HU)	0.887	(0.839-0.938)	< 0.001[a]	0.901	(0.853-0.951)	< 0.001[a]
TPMT (mm/m)	0.851	(0.759-0.954)	0.006[a]	0.867	(0.760-0.988)	0.032[a]

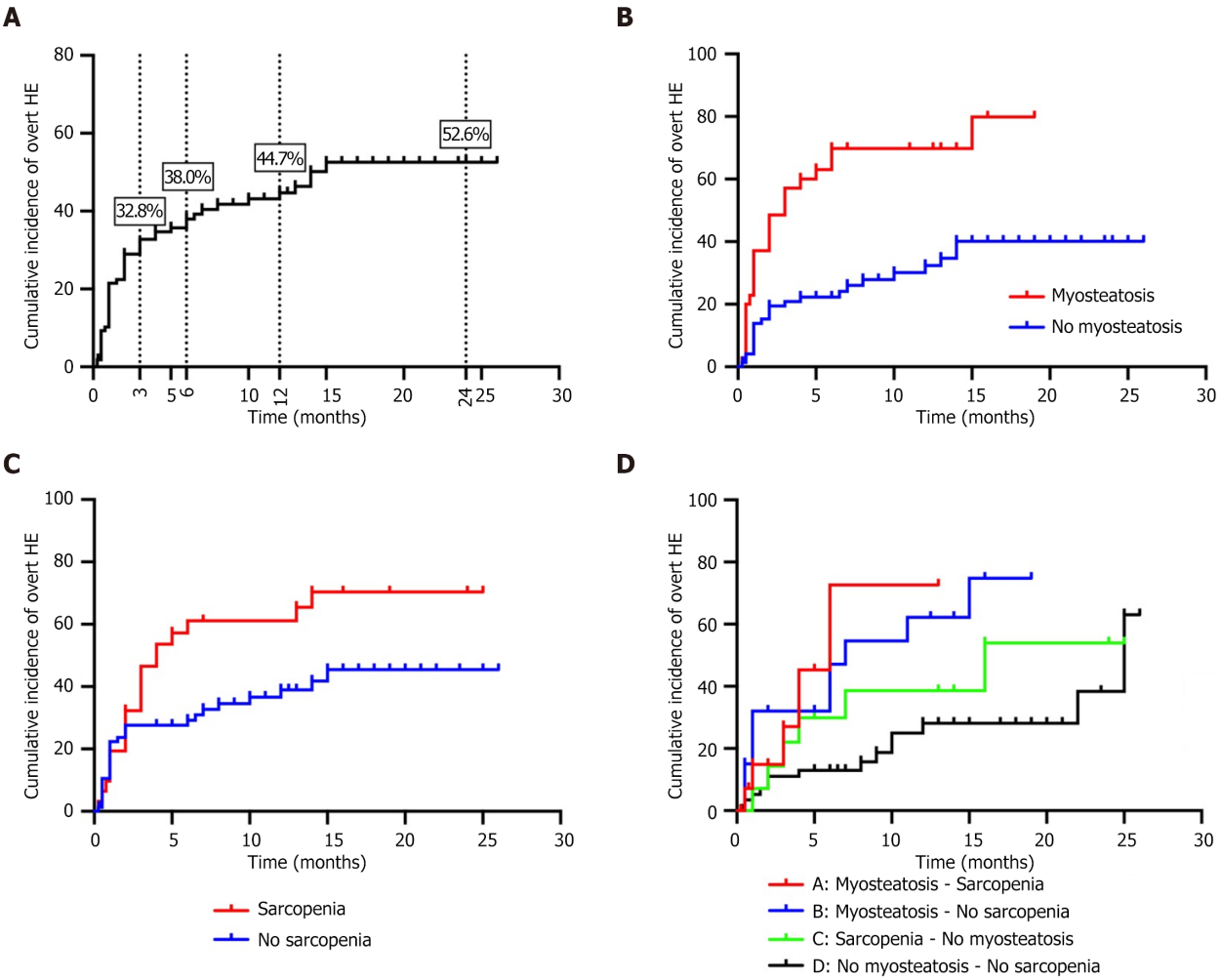
[a]$P < 0.05$.

BMI: Body mass index; MELD: Model for end-stage liver disease; NLR: Neutrophil-lymphocyte ratio; TBIL: Total bilirubin; ALT: Alanine aminotransferase; AST: Aspartate transaminase; PPG: Portosystemic pressure gradient; PMA: Psoas muscle attenuation; TPMT: Transversal psoas muscle thickness; HU: Hounsfield units.

HE[4,23,25-27]. Thus, correct patient selection and early intervention for TIPS based on these potential risk factors may contribute to preventing HE complications, and improving the life quality of patients.

The relationship among myosteatosis, sarcopenia and HE may have different pathophysiological mechanisms. Previous studies have suggested that sarcopenia is caused by impaired protein synthesis and reduced satellite cell function[28]. Furthermore, since the muscle has been considered as an alternative site for the detoxification of ammonia, the accumulation of ammonia may contribute to the development of sarcopenia in cirrhotic patients by interfering with the protein remodeling[29]. On the other hand, myosteatosis may reduce the detoxification of ammonia by inhibiting glutamine synthetase, and increasing inflammatory cytokines[30]. Previous systematic reviews and meta-analyses have revealed that sarcopenia and myosteatosis are highly associated with complications and poor overall survival in patients with various diseases[31,32]. In the present study, patients with sarcopenia (log-rank $P = 0.022$) or myosteatosis (log-rank $P < 0.001$) had a higher cumulative incidence of overt HE after TIPS. In addition, subgroup analysis revealed that the cumulative incidence of overt HE was the highest in patients with concomitant sarcopenia and myosteatosis, followed by patients with myosteatosis alone or sarcopenia alone, while the cumulative incidence was the lowest in patients with normal skeletal muscles. These findings are consistent with those reported by previous studies[10,33], showing that sarcopenia and myosteatosis are independent predictive factors for overt HE in patients with cirrhosis. Furthermore, the relationship between skeletal muscle abnormalities (sarcopenia and myosteatosis) and minimal HE in patients with cirrhosis was further suggested by the Firth's bias-reduced multivariate analysis[33].

Similar to the present study, Liu *et al*[34] observed that the incidence of overt HE after TIPS was higher in patients with sarcopenia, when compared to patients without sarcopenia (29% and 16%, $P = 0.04$). However, that study could only identify sarcopenia as the possible risk factor for post-TIPS HE in the univariate analysis (HR = 1.86, 95%CI: 0.99-3.46, $P = 0.004$), and its significance in the multivariate analysis could not be verified. Another study conducted by Gioia *et al*[35] revealed that the psychometric HE score, ammonia, and occurrence of minimal and overt HE significantly improved in post-TIPS patients, with an amelioration SMI of > 10%, suggesting that the reversal of sarcopenia after TIPS can reduce the risk of occurrence of minimal or overt HE.

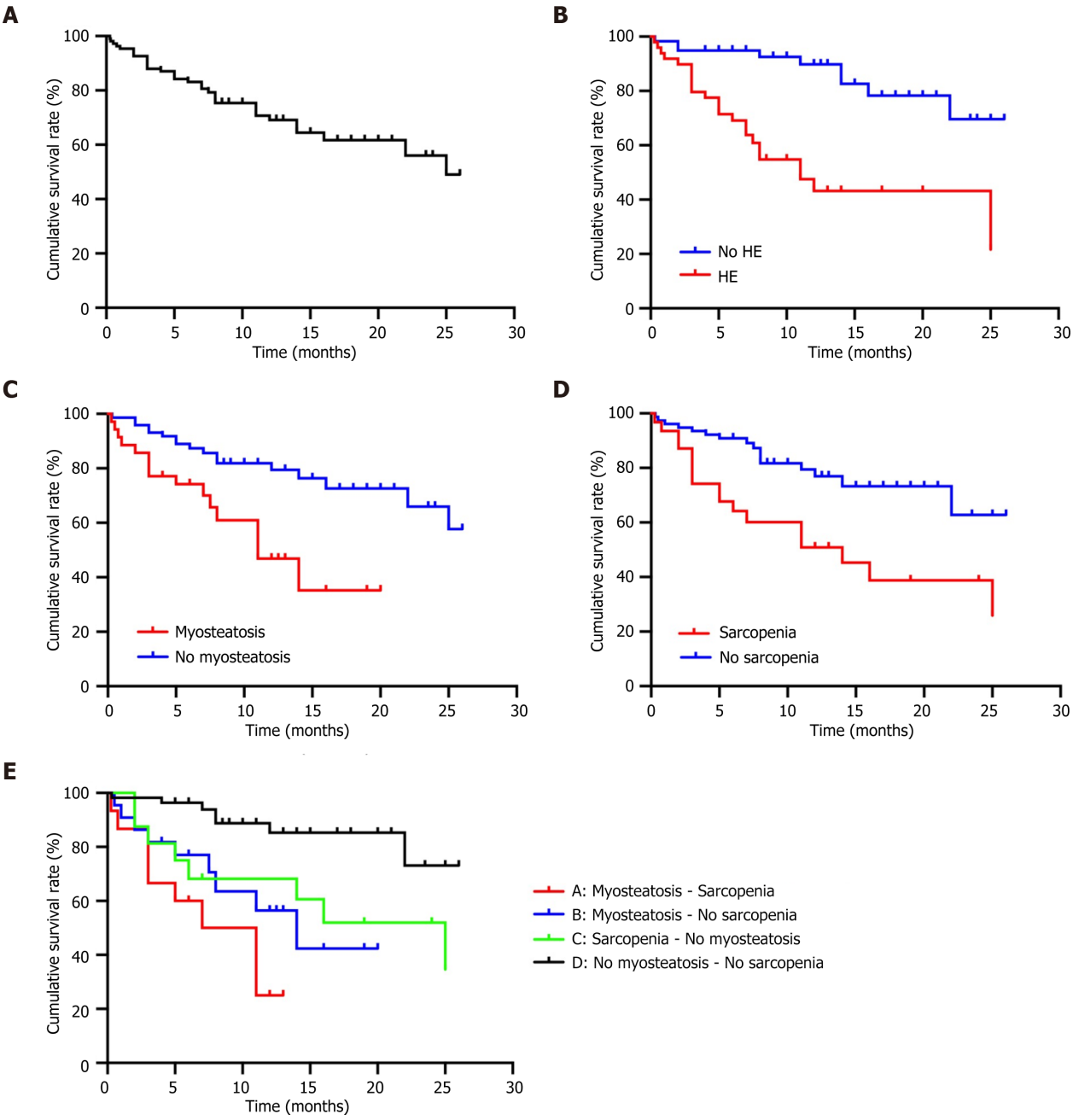


DOI: 10.3748/wjg.v29.i18.2875 **Copyright** ©The Author(s) 2023.

Figure 3 Kaplan-Meier curves for the cumulative incidence of post-transjugular intrahepatic portosystemic shunt overt hepatic encephalopathy. A: For all patients; B: For patients with and without myosteatosis; C: For patients with and without sarcopenia; D: For patients with coexisting sarcopenia and myosteatosis. HE: Hepatic encephalopathy.

Furthermore, the present study revealed that patients with coexisting myosteatosis and sarcopenia had the lowest cumulative survival rate, and it was identified that hypoalbuminemia (HR = 0.903, 95%CI: 0.827-0.986, P = 0.023), sarcopenia (HR = 0.901, 95%CI: 0.853-0.951, P < 0.001) and myosteatosis (HR = 0.867, 95%CI: 0.760-0.988, P = 0.032) are independent predictors of post-TIPS morbidity. Although other relevant factors, including age, creatinine, Child-Pugh score and MELD score, were significant in the present univariate analysis, these lost its significance as independent predictors in the multivariate analysis. A possible explanation is the inherent complexity and heterogeneity of TIPS cohorts, in general, with a high number of factors potentially affecting the clinical outcomes. A retrospective cohort study on 855 patients with cirrhosis reported that myosteatosis and sarcopenia are associated with mortality after adjusting for factors, and it was even quantitatively extrapolated that one HU of increase in muscle radiodensity corresponds to a 2% decrease in mortality risk (HR = 0.98, 95%CI: 0.96-0.99, P < 0.001)[36]. Another recent retrospective study on 224 patients with TIPS also identified sarcopenia (determined by L3 SMI) as an independent risk factor for mortality after TIPS (HR = 3.0, 95%CI: 1.2-7.8), and that patients who converted from sarcopenic to non-sarcopenic had a higher cumulative survival rate, when compared to those who did not convert (96.4% *vs* 82.1%, log-rank P = 0.04)[34]. In the present study, the cumulative survival rates were significantly lower in patients with sarcopenia/myosteatosis, when compared to patients without sarcopenia/myosteatosis (log-rank P = 0.001 and log-rank P = 0.002, respectively), further confirming the predictive value of sarcopenia/myosteatosis in the unfavorable prognosis of cirrhotic patients with TIPS.

There were several limitations in the present study. First, the present study was a single-center retrospective cohort study with a limited number of patients, and the intrinsic limitation of the study design appeared to be inescapable. Second, the diagnostic values for sarcopenia and myosteatosis were heterogeneous across studies in the literature. Thus, more studies and external validation of data are needed to standardize the CT-derived diagnostic criteria for sarcopenia and myosteatosis. Third,



DOI: 10.3748/wjg.v29.i18.2875 **Copyright** ©The Author(s) 2023.

Figure 4 Kaplan-Meier curves for the cumulative survival rate of post-transjugular intrahepatic portosystemic shunt. A: For all patients; B: For patients with and without hepatic encephalopathy; C: For patients with and without myosteatosis; D: For patients with and without sarcopenia; E: For patients with coexisting sarcopenia and myosteatosis. HE: Hepatic encephalopathy.

sarcopenia and myosteatosis were merely evaluated through CT measurements at admission, and these were not re-evaluated through CT imaging during the post-TPS follow-up period[35]. Thus, further well-designed studies are needed to determine whether the improvement in muscle abnormalities after TIPS can reduce the risk of overt HE and variceal rebleeding in post-TIPS patients[34].

CONCLUSION

The present study revealed that patients with coexisting myosteatosis and sarcopenia had the highest incidence of overt HE, and the lowest cumulative survival rate after TIPS placement, when compared to patients with myosteatosis alone or sarcopenia alone, or patients without muscle abnormalities. Sarcopenia and myosteatosis are independent variables for the development of overt HE and mortality in post-TIPS patients.

ARTICLE HIGHLIGHTS

Research background

Skeletal muscle abnormalities, such as muscle mass depletion (sarcopenia) and fatty infiltration of the muscle (myosteatosis), are frequent complications in cirrhotic patients scheduled for a transjugular intrahepatic portosystemic shunt (TIPS) procedure, leading to an incidence of approximately 20%-50% for overt hepatic encephalopathy (HE).

Research motivation

The motivation of the study was to provide computed tomography (CT) image-based methods for predicting overt HE and mortality after TIPS, based on the sarcopenia and myosteatosis.

Research objectives

The study aims to investigate the association and predictive volubility of sarcopenia and myosteatosis for overt HE, and mortality after TIPS.

Research methods

The records of cirrhotic patients, who underwent the TIPS procedure at our hospital, were retrospectively reviewed. Transversal psoas muscle thickness and psoas muscle attenuation, which were measured by unenhanced abdominal CT at the level of the third lumbar vertebrae, were used to diagnose the sarcopenia and myosteatosis, respectively. Then, the incidence of overt HE and mortality were compared based on the sarcopenia and myosteatosis status.

Research results

A total of 108 patients were collected. Myosteatosis (51.0% *vs* 16.9%, $P < 0.001$) and sarcopenia (40.8 *vs* 18.6%, $P = 0.011$) were identified to be more frequent in patients with overt HE, when compared to patients without overt HE. The cumulative incidence of overt HE was the highest in patients with concomitant sarcopenia and myosteatosis, followed by patients with myosteatosis or sarcopenia, while this was the lowest in patients without sarcopenia and myosteatosis. In addition, sarcopenia and myosteatosis were independently associated with overt HE and mortality after adjusting for confounding factors in post-TIPS patients.

Research conclusions

The CT-based diagnostic method of sarcopenia and myosteatosis can be used as a reliable predictor for the risk of developing overt HE and mortality in cirrhotic patients after TIPS.

Research perspectives

In the future, more well-designated trials are required to standardize the CT-derived diagnostic criteria for sarcopenia and myosteatosis. In addition, more validation studies are needed to confirm the predictivities of sarcopenia and myosteatosis in post-TIPS overt HE.

FOOTNOTES

Author contributions: Yin L and Chu SL designed the research, analyzed the data, and wrote the initial draft of the manuscript; Zhou CZ, Liu KC, Zhu YJ and Lu D collected the data, analyzed the data, and designed the study; Zhang WY, Wang CX and Zhang YH performed the research and collected the data; Lv WF and Cheng DL contributed to the central idea, designed the study, and wrote the manuscript.

Supported by Natural Science Foundation of Anhui Province, No. 2108085MH301; and The Key Project of University Research Found of Anhui Province Education Department, No. 2022AH040189.

Institutional review board statement: The retrospective study protocol was approved by the institutional review board of The First Affiliated Hospital of University of Science and Technology of China, No. 2022-RE-461.

Informed consent statement: Informed consent for the study was waived due to the retrospective nature of the study.

Conflict-of-interest statement: All the authors report no relevant conflicts of interest for this article.

Data sharing statement: The datasets generated and analyzed in the study are available from the corresponding author on reasonable request.

STROBE statement: The authors have read the STROBE Statement-checklist of items, and the manuscript was prepared and revised according to the STROBE Statement-checklist of items.

Open-Access: This article is an open-access article that was selected by an in-house editor and fully peer-reviewed by external reviewers. It is distributed in accordance with the Creative Commons Attribution NonCommercial (CC BY-NC 4.0) license, which permits others to distribute, remix, adapt, build upon this work non-commercially, and license their derivative works on different terms, provided the original work is properly cited and the use is non-commercial. See: https://creativecommons.org/Licenses/by-nc/4.0/

Country/Territory of origin: China

ORCID number: Sen-Lin Chu 0000-0001-8153-0430; Wei-Fu lv 0000-0002-3681-639X; Kai-Cai Liu 0000-0002-3561-7209; Yi-Jiang Zhu 0000-0001-6318-2284; Dong Lu 0000-0001-8117-1554; De-Lei Cheng 0000-0001-6528-1163.

S-Editor: Fan JR
L-Editor: A
P-Editor: Chen YX

REFERENCES

1 **Lee HL**, Lee SW. The role of transjugular intrahepatic portosystemic shunt in patients with portal hypertension: Advantages and pitfalls. *Clin Mol Hepatol* 2022; **28**: 121-134 [PMID: 34571587 DOI: 10.3350/cmh.2021.0239]
2 **Dissegna D**, Sponza M, Falleti E, Fabris C, Vit A, Angeli P, Piano S, Cussigh A, Cmet S, Toniutto P. Morbidity and mortality after transjugular intrahepatic portosystemic shunt placement in patients with cirrhosis. *Eur J Gastroenterol Hepatol* 2019; **31**: 626-632 [PMID: 30550458 DOI: 10.1097/MEG.0000000000001342]
3 **Fonio P**, Discalzi A, Calandri M, Doriguzzi Breatta A, Bergamasco L, Martini S, Ottobrelli A, Righi D, Gandini G. Incidence of hepatic encephalopathy after transjugular intrahepatic portosystemic shunt (TIPS) according to its severity and temporal grading classification. *Radiol Med* 2017; **122**: 713-721 [PMID: 28510807 DOI: 10.1007/s11547-017-0770-6]
4 **Riggio O**, Angeloni S, Salvatori FM, De Santis A, Cerini F, Farcomeni A, Attili AF, Merli M. Incidence, natural history, and risk factors of hepatic encephalopathy after transjugular intrahepatic portosystemic shunt with polytetrafluoroethylene-covered stent grafts. *Am J Gastroenterol* 2008; **103**: 2738-2746 [PMID: 18775022 DOI: 10.1111/j.1572-0241.2008.02102.x]
5 **Patidar KR**, Bajaj JS. Covert and Overt Hepatic Encephalopathy: Diagnosis and Management. *Clin Gastroenterol Hepatol* 2015; **13**: 2048-2061 [PMID: 26164219 DOI: 10.1016/j.cgh.2015.06.039]
6 **Bureau C**, Thabut D, Jezequel C, Archambeaud I, D'Alteroche L, Dharancy S, Borentain P, Oberti F, Plessier A, De Ledinghen V, Ganne-Carrié N, Carbonell N, Rousseau V, Sommet A, Péron JM, Vinel JP. The Use of Rifaximin in the Prevention of Overt Hepatic Encephalopathy After Transjugular Intrahepatic Portosystemic Shunt : A Randomized Controlled Trial. *Ann Intern Med* 2021; **174**: 633-640 [PMID: 33524293 DOI: 10.7326/M20-0202]
7 **Vilstrup H**, Amodio P, Bajaj J, Cordoba J, Ferenci P, Mullen KD, Weissenborn K, Wong P. Hepatic encephalopathy in chronic liver disease: 2014 Practice Guideline by the American Association for the Study of Liver Diseases and the European Association for the Study of the Liver. *Hepatology* 2014; **60**: 715-735 [PMID: 25042402 DOI: 10.1002/hep.27210]
8 **Ebadi M**, Montano-Loza AJ. Clinical relevance of skeletal muscle abnormalities in patients with cirrhosis. *Dig Liver Dis* 2019; **51**: 1493-1499 [PMID: 31221549 DOI: 10.1016/j.dld.2019.05.034]
9 **Kim HY**, Jang JW. Sarcopenia in the prognosis of cirrhosis: Going beyond the MELD score. *World J Gastroenterol* 2015; **21**: 7637-7647 [PMID: 26167066 DOI: 10.3748/wjg.v21.i25.7637]
10 **Bhanji RA**, Moctezuma-Velazquez C, Duarte-Rojo A, Ebadi M, Ghosh S, Rose C, Montano-Loza AJ. Myosteatosis and sarcopenia are associated with hepatic encephalopathy in patients with cirrhosis. *Hepatol Int* 2018; **12**: 377-386 [PMID: 29881992 DOI: 10.1007/s12072-018-9875-9]
11 **Paternostro R**, Lampichler K, Bardach C, Asenbaum U, Landler C, Bauer D, Mandorfer M, Schwarzer R, Trauner M, Reiberger T, Ferlitsch A. The value of different CT-based methods for diagnosing low muscle mass and predicting mortality in patients with cirrhosis. *Liver Int* 2019; **39**: 2374-2385 [PMID: 31421002 DOI: 10.1111/liv.14217]
12 **Amini B**, Boyle SP, Boutin RD, Lenchik L. Approaches to Assessment of Muscle Mass and Myosteatosis on Computed Tomography: A Systematic Review. *J Gerontol A Biol Sci Med Sci* 2019; **74**: 1671-1678 [PMID: 30726878 DOI: 10.1093/gerona/glz034]
13 **Margadant CC**, Bruns ER, Sloothaak DA, van Duijvendijk P, van Raamt AF, van der Zaag HJ, Buskens CJ, van Munster BC, van der Zaag ES. Lower muscle density is associated with major postoperative complications in older patients after surgery for colorectal cancer. *Eur J Surg Oncol* 2016; **42**: 1654-1659 [PMID: 27554247 DOI: 10.1016/j.ejso.2016.05.040]
14 **Wagner D**, Büttner S, Kim Y, Gani F, Xu L, Margonis GA, Amini N, Kamel IR, Pawlik TM. Clinical and morphometric parameters of frailty for prediction of mortality following hepatopancreaticobiliary surgery in the elderly. *Br J Surg* 2016; **103**: e83-e92 [PMID: 26604018 DOI: 10.1002/bjs.10037]
15 **Martin L**, Birdsell L, Macdonald N, Reiman T, Clandinin MT, McCargar LJ, Murphy R, Ghosh S, Sawyer MB, Baracos VE. Cancer cachexia in the age of obesity: skeletal muscle depletion is a powerful prognostic factor, independent of body mass index. *J Clin Oncol* 2013; **31**: 1539-1547 [PMID: 23530101 DOI: 10.1200/JCO.2012.45.2722]
16 **Chang KV**, Chen JD, Wu WT, Huang KC, Lin HY, Han DS. Is sarcopenia associated with hepatic encephalopathy in liver cirrhosis? *J Formos Med Assoc* 2019; **118**: 833-842 [PMID: 30279030 DOI: 10.1016/j.jfma.2018.09.011]
17 **Merli M**, Giusto M, Gentili F, Novelli G, Ferretti G, Riggio O, Corradini SG, Siciliano M, Farcomeni A, Attili AF, Berloco P, Rossi M. Nutritional status: its influence on the outcome of patients undergoing liver transplantation. *Liver Int*

2010; **30**: 208-214 [PMID: 19840246 DOI: 10.1111/j.1478-3231.2009.02135.x]

18 **Ryan AM**, Power DG, Daly L, Cushen SJ, Ní Bhuachalla Ē, Prado CM. Cancer-associated malnutrition, cachexia and sarcopenia: the skeleton in the hospital closet 40 years later. *Proc Nutr Soc* 2016; **75**: 199-211 [PMID: 26786393 DOI: 10.1017/S002966511500419X]

19 **Tripathi D**, Stanley AJ, Hayes PC, Travis S, Armstrong MJ, Tsochatzis EA, Rowe IA, Roslund N, Ireland H, Lomax M, Leithead JA, Mehrzad H, Aspinall RJ, McDonagh J, Patch D. Transjugular intrahepatic portosystemic stent-shunt in the management of portal hypertension. *Gut* 2020; **69**: 1173-1192 [PMID: 32114503 DOI: 10.1136/gutjnl-2019-320221]

20 **Li J**, Feng D, Pang N, Zhao C, Gao L, Liu S, Li L. Controlling nutritional status score as a new indicator of overt hepatic encephalopathy in cirrhotic patients following transjugular intrahepatic portosystemic shunt. *Clin Nutr* 2022; **41**: 560-566 [PMID: 35032860 DOI: 10.1016/j.clnu.2021.12.036]

21 **Schindler P**, Heinzow H, Trebicka J, Wildgruber M. Shunt-Induced Hepatic Encephalopathy in TIPS: Current Approaches and Clinical Challenges. *J Clin Med* 2020; **9** [PMID: 33238576 DOI: 10.3390/jcm9113784]

22 **Yao J**, Zuo L, An G, Yue Z, Zhao H, Wang L, Liu F. Risk Factors for Hepatic Encephalopathy after Transjugular Intrahepatic Portosystemic Shunt in Patients with Hepatocellular Carcinoma and Portal Hypertension. *J Gastrointestin Liver Dis* 2015; **24**: 301-307 [PMID: 26405702 DOI: 10.15403/jgld.2014.1121.243.yao]

23 **Lewis DS**, Lee TH, Konanur M, Ziegler C, Hall MD, Pabon-Ramos WM, Suhocki PV, Smith TP, Kim CY, Choi SS, Ronald J. Proton Pump Inhibitor Use Is Associated with an Increased Frequency of New or Worsening Hepatic Encephalopathy after Transjugular Intrahepatic Portosystemic Shunt Creation. *J Vasc Interv Radiol* 2019; **30**: 163-169 [PMID: 30638914 DOI: 10.1016/j.jvir.2018.10.015]

24 **Nardelli S**, Lattanzi B, Torrisi S, Greco F, Farcomeni A, Gioia S, Merli M, Riggio O. Sarcopenia Is Risk Factor for Development of Hepatic Encephalopathy After Transjugular Intrahepatic Portosystemic Shunt Placement. *Clin Gastroenterol Hepatol* 2017; **15**: 934-936 [PMID: 27816756 DOI: 10.1016/j.cgh.2016.10.028]

25 **Nardelli S**, Gioia S, Pasquale C, Pentassuglio I, Farcomeni A, Merli M, Salvatori FM, Nikolli L, Torrisi S, Greco F, Nicoletti V, Riggio O. Cognitive Impairment Predicts The Occurrence Of Hepatic Encephalopathy After Transjugular Intrahepatic Portosystemic Shunt. *Am J Gastroenterol* 2016; **111**: 523-528 [PMID: 26925879 DOI: 10.1038/ajg.2016.29]

26 **Elsaid MI**, Rustgi VK. Epidemiology of Hepatic Encephalopathy. *Clin Liver Dis* 2020; **24**: 157-174 [PMID: 32245524 DOI: 10.1016/j.cld.2020.01.001]

27 **Rowley MW**, Choi M, Chen S, Hirsch K, Seetharam AB. Refractory Hepatic Encephalopathy After Elective Transjugular Intrahepatic Portosystemic Shunt: Risk Factors and Outcomes with Revision. *Cardiovasc Intervent Radiol* 2018; **41**: 1765-1772 [PMID: 29872892 DOI: 10.1007/s00270-018-1992-2]

28 **Dasarathy S**, McCullough AJ, Muc S, Schneyer A, Bennett CD, Dodig M, Kalhan SC. Sarcopenia associated with portosystemic shunting is reversed by follistatin. *J Hepatol* 2011; **54**: 915-921 [PMID: 21145817 DOI: 10.1016/j.jhep.2010.08.032]

29 **Dasarathy S**, Merli M. Sarcopenia from mechanism to diagnosis and treatment in liver disease. *J Hepatol* 2016; **65**: 1232-1244 [PMID: 27515775 DOI: 10.1016/j.jhep.2016.07.040]

30 **Aldridge DR**, Tranah EJ, Shawcross DL. Pathogenesis of hepatic encephalopathy: role of ammonia and systemic inflammation. *J Clin Exp Hepatol* 2015; **5**: S7-S20 [PMID: 26041962 DOI: 10.1016/j.jceh.2014.06.004]

31 **Wijarnpreecha K**, Werlang M, Panjawatanan P, Kroner PT, Cheungpasitporn W, Lukens FJ, Pungpapong S, Ungprasert P. Association between sarcopenia and hepatic encephalopathy: A systematic review and meta-analysis. *Ann Hepatol* 2020; **19**: 245-250 [PMID: 31422030 DOI: 10.1016/j.aohep.2019.06.007]

32 **Ahn H**, Kim DW, Ko Y, Ha J, Shin YB, Lee J, Sung YS, Kim KW. Updated systematic review and meta-analysis on diagnostic issues and the prognostic impact of myosteatosis: A new paradigm beyond sarcopenia. *Ageing Res Rev* 2021; **70**: 101398 [PMID: 34214642 DOI: 10.1016/j.arr.2021.101398]

33 **Nardelli S**, Lattanzi B, Merli M, Farcomeni A, Gioia S, Ridola L, Riggio O. Muscle Alterations Are Associated With Minimal and Overt Hepatic Encephalopathy in Patients With Liver Cirrhosis. *Hepatology* 2019; **70**: 1704-1713 [PMID: 31038758 DOI: 10.1002/hep.30692]

34 **Liu J**, Ma J, Yang C, Chen M, Shi Q, Zhou C, Huang S, Chen Y, Wang Y, Li T, Xiong B. Sarcopenia in Patients with Cirrhosis after Transjugular Intrahepatic Portosystemic Shunt Placement. *Radiology* 2022; **303**: 711-719 [PMID: 35289658 DOI: 10.1148/radiol.211172]

35 **Gioia S**, Merli M, Nardelli S, Lattanzi B, Pitocchi F, Ridola L, Riggio O. The modification of quantity and quality of muscle mass improves the cognitive impairment after TIPS. *Liver Int* 2019; **39**: 871-877 [PMID: 30667572 DOI: 10.1111/liv.14050]

36 **Ebadi M**, Tsien C, Bhanji RA, Dunichand-Hoedl AR, Rider E, Motamedrad M, Mazurak VC, Baracos V, Montano-Loza AJ. Skeletal Muscle Pathological Fat Infiltration (Myosteatosis) Is Associated with Higher Mortality in Patients with Cirrhosis. *Cells* 2022; **11** [PMID: 35456024 DOI: 10.3390/cells11081345]



Published by **Baishideng Publishing Group Inc**
7041 Koll Center Parkway, Suite 160, Pleasanton, CA 94566, USA
Telephone: +1-925-3991568
E-mail: bpgoffice@wjgnet.com
Help Desk: https://www.f6publishing.com/helpdesk
https://www.wjgnet.com



© 2023 Baishideng Publishing Group Inc. All rights reserved.

ISSN 1007-9327 (print)
ISSN 2219-2840 (online)

World Journal of *Gastroenterology*

World J Gastroenterol 2023 May 21; 29(19): 2888-3047



Published by Baishideng Publishing Group Inc

World Journal of Gastroenterology

Contents

Weekly Volume 29 Number 19 May 21, 2023

REVIEW

2888 Radiomics in colorectal cancer patients

Inchingolo R, Maino C, Cannella R, Vernuccio F, Cortese F, Dezio M, Pisani AR, Giandola T, Gatti M, Giannini V, Ippolito D, Faletti R

MINIREVIEWS

2905 Branched chain amino acids in hepatic encephalopathy and sarcopenia in liver cirrhosis: Evidence and uncertainties

Marrone G, Serra A, Miele L, Biolato M, Liguori A, Grieco A, Gasbarrini A

2916 Assessment of delayed bleeding after endoscopic submucosal dissection of early-stage gastrointestinal tumors in patients receiving direct oral anticoagulants

Sugimoto M, Murata M, Kawai T

ORIGINAL ARTICLE

Basic Study

2932 TATA-box-binding protein-associated factor 15 is a novel biomarker that promotes cell proliferation and migration in gastrointestinal stromal tumor

Guo CM, Tang L, Li X, Huang LY

2950 Susceptibility patterns and virulence genotypes of *Helicobacter pylori* affecting eradication therapy outcomes among Egyptian patients with gastroduodenal diseases

Asaad AM, El-Azab G, Abdelsameea E, Elbahr O, Kamal A, Abdel-Samiee M, Abdelfattah A, Abdallah H, Maher D, El-Refaie A, Ghanem SE, Ansari S, Awad SM

2961 *MMP14* is a diagnostic gene of intrahepatic cholangiocarcinoma associated with immune cell infiltration

Wu J, Guo Y, Zuo ZF, Zhu ZW, Han L

Case Control Study

2979 Machine learning model for prediction of low anterior resection syndrome following laparoscopic anterior resection of rectal cancer: A multicenter study

Wang Z, Shao SL, Liu L, Lu QY, Mu L, Qin JC

Retrospective Study

2992 Where is the optimal plane to mobilize the anterior rectal wall in female patients undergoing total mesorectal excision?

Jin W, Yang J, Li XY, Wang WC, Meng WJ, Li Y, Liang YC, Zhou YM, Yang XD, Li YY, Li ST

3003 Association of vitamin D and polymorphisms of its receptor with antiviral therapy in pregnant women with hepatitis B

Wang R, Zhu X, Zhang X, Liu H, Ji YL, Chen YH

World Journal of Gastroenterology

Weekly Volume 29 Number 19 May 21, 2023

Contents

Observational Study

3013 Gastrointestinal manifestations of long-term effects after COVID-19 infection in patients with dialysis or kidney transplantation: An observational cohort study

Chancharoenthana W, Kamolratanakul S, Leelahavanichkul A, Ariyanon W, Chinpraditsuk S, Saelim R, Vadcharavivad S, Phumratanaprapin W, Wilairatana P

META-ANALYSIS

3027 Short *vs* long-course antibiotic therapy in adults with acute cholangitis: A systematic review, meta-analysis, and evidence quality assessment

Kasparian K, Christou CD, Petidis K, Doumas M, Giouleme O

CASE REPORT

3040 Pulmonary hypertension, nephrotic syndrome, and polymyositis due to hepatitis C virus infection: A case report

Zhao YN, Liu GH, Wang C, Zhang YX, Yang P, Yu M

ABOUT COVER

Editorial Board Member of *World Journal of Gastroenterology*, John K Triantafillidis, MD, PhD, FEBGH, Associate Professor of Medicine, Staff Physician, Iasi University of Medicine and Pharmacy, Romania, "Metropolitan General" Hospital, Holargos, Athens 15562, Greece. jktrian@gmail.com

AIMS AND SCOPE

The primary aim of *World Journal of Gastroenterology* (*WJG*, *World J Gastroenterol*) is to provide scholars and readers from various fields of gastroenterology and hepatology with a platform to publish high-quality basic and clinical research articles and communicate their research findings online. *WJG* mainly publishes articles reporting research results and findings obtained in the field of gastroenterology and hepatology and covering a wide range of topics including gastroenterology, hepatology, gastrointestinal endoscopy, gastrointestinal surgery, gastrointestinal oncology, and pediatric gastroenterology.

INDEXING/ABSTRACTING

The *WJG* is now abstracted and indexed in Science Citation Index Expanded (SCIE, also known as SciSearch®), Current Contents/Clinical Medicine, Journal Citation Reports, Index Medicus, MEDLINE, PubMed, PubMed Central, Scopus, Reference Citation Analysis, China National Knowledge Infrastructure, China Science and Technology Journal Database, and Superstar Journals Database. The 2022 edition of Journal Citation Reports® cites the 2021 impact factor (IF) for *WJG* as 5.374; IF without journal self cites: 5.187; 5-year IF: 5.715; Journal Citation Indicator: 0.84; Ranking: 31 among 93 journals in gastroenterology and hepatology; and Quartile category: Q2. The *WJG*'s CiteScore for 2021 is 8.1 and Scopus CiteScore rank 2021: Gastroenterology is 18/149.

RESPONSIBLE EDITORS FOR THIS ISSUE

Production Editor: *Yi-Xuan Cai*; **Production Department Director:** *Xiang Li*; **Editorial Office Director:** *Jia-Ru Fan.*

NAME OF JOURNAL
World Journal of Gastroenterology

ISSN
ISSN 1007-9327 (print) ISSN 2219-2840 (online)

LAUNCH DATE
October 1, 1995

FREQUENCY
Weekly

EDITORS-IN-CHIEF
Andrzej S Tarnawski

EDITORIAL BOARD MEMBERS
http://www.wjgnet.com/1007-9327/editorialboard.htm

PUBLICATION DATE
May 21, 2023

COPYRIGHT
© 2023 Baishideng Publishing Group Inc

INSTRUCTIONS TO AUTHORS
https://www.wjgnet.com/bpg/gerinfo/204

GUIDELINES FOR ETHICS DOCUMENTS
https://www.wjgnet.com/bpg/GerInfo/287

GUIDELINES FOR NON-NATIVE SPEAKERS OF ENGLISH
https://www.wjgnet.com/bpg/gerinfo/240

PUBLICATION ETHICS
https://www.wjgnet.com/bpg/GerInfo/288

PUBLICATION MISCONDUCT
https://www.wjgnet.com/bpg/gerinfo/208

ARTICLE PROCESSING CHARGE
https://www.wjgnet.com/bpg/gerinfo/242

STEPS FOR SUBMITTING MANUSCRIPTS
https://www.wjgnet.com/bpg/GerInfo/239

ONLINE SUBMISSION
https://www.f6publishing.com

© 2023 Baishideng Publishing Group Inc. All rights reserved. 7041 Koll Center Parkway, Suite 160, Pleasanton, CA 94566, USA
E-mail: bpgoffice@wjgnet.com https://www.wjgnet.com

World Journal of Gastroenterology

Submit a Manuscript: https://www.f6publishing.com

World J Gastroenterol 2023 May 21; 29(19): 2888-2904

DOI: 10.3748/wjg.v29.i19.2888

ISSN 1007-9327 (print) ISSN 2219-2840 (online)

REVIEW

Radiomics in colorectal cancer patients

Riccardo Inchingolo, Cesare Maino, Roberto Cannella, Federica Vernuccio, Francesco Cortese, Michele Dezio, Antonio Rosario Pisani, Teresa Giandola, Marco Gatti, Valentina Giannini, Davide Ippolito, Riccardo Faletti

Specialty type: Radiology, nuclear medicine and medical imaging

Provenance and peer review: Invited article; Externally peer reviewed.

Peer-review model: Single blind

Peer-review report's scientific quality classification

Grade A (Excellent): 0
Grade B (Very good): 0
Grade C (Good): C, C
Grade D (Fair): 0
Grade E (Poor): 0

P-Reviewer: Tari DU, Italy; Yang L, China

Received: February 16, 2023
Peer-review started: February 16, 2023
First decision: March 24, 2023
Revised: April 7, 2023
Accepted: April 25, 2023
Article in press: April 25, 2023
Published online: May 21, 2023

Riccardo Inchingolo, Francesco Cortese, Michele Dezio, Unit of Interventional Radiology, F. Miulli Hospital, Acquaviva delle Fonti 70021, Italy

Cesare Maino, Teresa Giandola, Davide Ippolito, Department of Radiology, Fondazione IRCCS San Gerardo dei Tintori, Monza 20900, Italy

Roberto Cannella, Department of Biomedicine, Neuroscience and Advanced Diagnostics (BiND), University of Palermo, Palermo 90127, Italy

Federica Vernuccio, Institute of Radiology, University Hospital of Padova, Padova 35128, Italy

Antonio Rosario Pisani, Interdisciplinary Department of Medicine, Section of Nuclear Medicine, University of Bari "Aldo Moro", Bari 70121, Italy

Marco Gatti, Valentina Giannini, Riccardo Faletti, Department of Surgical Sciences, University of Turin, Turin 10126, Italy

Corresponding author: Riccardo Inchingolo, MD, Director, Doctor, Unit of Interventional Radiology, F. Miulli Hospital, Sp per Santeramo, Acquaviva delle Fonti 70021, Italy. riccardoin@hotmail.it

Abstract

The main therapeutic options for colorectal cancer are surgical resection and adjuvant chemotherapy in non-metastatic disease. However, the evaluation of the overall adjuvant chemotherapy benefit in patients with a high risk of recurrence is challenging. Radiological images can represent a source of data that can be analyzed by using automated computer-based techniques, working on numerical information coded within Digital Imaging and Communications in Medicine files: This image numerical analysis has been named "radiomics". Radiomics allows the extraction of quantitative features from radiological images, mainly invisible to the naked eye, that can be further analyzed by artificial intelligence algorithms. Radiomics is expanding in oncology to either understand tumor biology or for the development of imaging biomarkers for diagnosis, staging, and prognosis, prediction of treatment response and diseases monitoring and surveillance. Several efforts have been made to develop radiomics signatures for colorectal cancer patient using computed tomography (CT) images with different aims: The preoperative prediction of lymph node metastasis, detecting *BRAF* and *RAS* gene mutations. Moreover, the use of delta-radiomics allows the analysis of variations of the radiomics parameters extracted from CT scans performed at different timepoints. Most published studies concerning radiomics and magnetic resonance

imaging (MRI) mainly focused on the response of advanced tumors that under-went neoadjuvant therapy. Nodes status is the main determinant of adjuvant chemotherapy. Therefore, several radiomics model based on MRI, especially on T2-weighted images and ADC maps, for the preoperative prediction of nodes metastasis in rectal cancer has been developed. Current studies mostly focused on the applications of radiomics in positron emission tomogra-phy/CT for the prediction of survival after curative surgical resection and assessment of response following neoadjuvant chemoradiotherapy. Since colorectal liver metastases develop in about 25% of patients with colorectal carcinoma, the main diagnostic tasks of radiomics should be the detection of synchronous and metachronous lesions. Radiomics could be an additional tool in clinical setting, especially in identifying patients with high-risk disease. Nevertheless, radiomics has numerous shortcomings that make daily use extremely difficult. Further studies are needed to assess performance of radiomics in stratifying patients with high-risk disease.

Key Words: Colorectal cancer; Radiomics; Artificial intelligence; Liver metastases; Magnetic resonance imaging; Computed tomography; Positron emission tomography/computed tomography

©The Author(s) 2023. Published by Baishideng Publishing Group Inc. All rights reserved.

Core Tip: Stratifying colorectal cancer patients with high-risk disease and the evaluation of the overall chemotherapy benefit are a clinical challenge. Radiomics through radiological images analysis using automated computer-based techniques allows the extraction of quantitative features from radiological images, mainly invisible to the naked eye, that can be further analyzed by artificial intelligence algorithms. Several efforts have been made to develop radiomics signatures for colorectal cancer patient using computed tomography (CT), magnetic resonance imaging, and positron emission tomography/CT, in particular to understand tumor biology, to develop imaging biomarkers for diagnosis, staging, and prognosis, to predict treatment response and to monitor disease.

Citation: Inchingolo R, Maino C, Cannella R, Vernuccio F, Cortese F, Dezio M, Pisani AR, Giandola T, Gatti M, Giannini V, Ippolito D, Faletti R. Radiomics in colorectal cancer patients. *World J Gastroenterol* 2023; 29(19): 2888-2904
URL: https://www.wjgnet.com/1007-9327/full/v29/i19/2888.htm
DOI: https://dx.doi.org/10.3748/wjg.v29.i19.2888

INTRODUCTION

Colorectal cancer is the fifth-most-common frequent in terms of incidence and mortality, with 1480000 new cases in 2020 worldwide[1]. The TNM staging process itself is widely based on radiological definition of boundaries of primary lesion, nodal and distant metastases. The main therapeutic options for colorectal cancer are surgical resection and adjuvant chemotherapy in non-metastatic patients; however, the evaluation of the overall adjuvant chemotherapy benefit in patients with a high risk of recurrence is a clinical challenge[2]. The decision is based on the TNM staging system[3], which represents the most important parameter: Colorectal cancer patients at stage III are globally recognized as patients who can benefit from chemotherapy, while for those at stage II with other clinical risk factors, the advantages of chemotherapy are still debated[2,4]. In presence of clinical risk factors, the final strategy is often decided by the oncologist or multidisciplinary teams.

Nowadays radiological images can represent a source of data that can be analyzed by using advanced computer-based techniques, working on numerical information coded within the Digital Imaging and Communications in Medicine files[5]: This image numerical analysis has been named "radiomics"[6]. Radiomics might be used as a non-invasive imaging biomarker and be able to provide a quantitative evaluation of medical images, with the chance to shift imaging from a qualitative to a quantitative approach[7,8]. To date, the radiomics approach has been extensively investigated in cancer patients with a specific focus on tumor diagnosis, staging, prognosis prediction, and long-term monitoring[7,9,10]. In this context, radiomics could play a pivotal role in colorectal cancer workup with the expectancy to help clinicians in identifying patients with high-risk disease.

RADIOMICS APPLIED TO CANCER-SUMMARY (PATHOLOGICAL CORRELATION, DIAGNOSIS, PROGNOSIS)

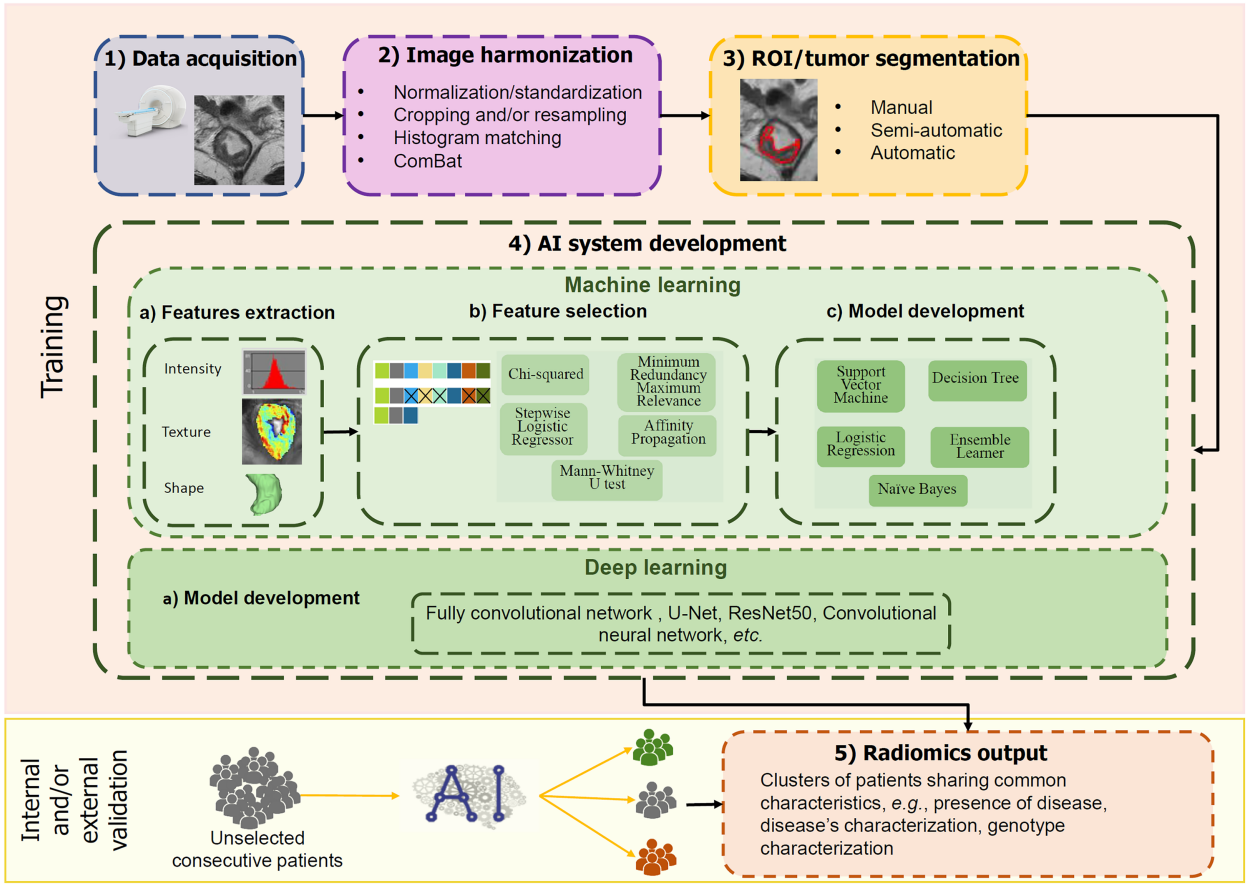
Since its advent in 2012[5], radiomics has been extensively applied in oncology studies and it has been demonstrated as a promising tool that can offer a risk-free and efficient method for diagnosis, classification, and prognosis prediction in oncology[11]. Radiomics, indeed, allows the extraction of quantitative features from radiological images, mainly invisible to the naked eye, that can be further analyzed by machine learning and artificial intelligence (AI) algorithms to produce signatures representing tumor phenotype.

The radiomics pipeline consists of different steps (Figure 1). First, multi-dimensional and multi-institutional data should be collected including high-quality medical images, clinical, and, eventually, molecular data. Once acquired, images should be pre-processed to improve image quality, harmonize raw data, and ensure generalizability across imaging protocols and patient populations, especially if multicentre datasets are acquired. This pre-processing step usually involves image co-registration, image denoising, signal intensity standardization, and/or normalization. Once the image datasets have been pre-processed, tumors should be segmented to extract regions of interest (ROIs) on which subsequent steps will be focused on. This task can be performed either manually, semi- or fully automatically. A big effort in the research field is addressed to the development of AI-based systems to automatically segment lesions and overcomes the most common limitations of manual segmentation. Afterward, from the segmented ROIs a large number of parameters (features) are extracted, including: (1) First-order features, from gray-level intensity histograms and lesion shape; (2) second-order features, related to the spatial relationship between pixels, calculated using different matrices, *e.g.*, gray-level co-occurrence, gray-level run-length, gray-level dependence, gray-level size zone, neighboring gray tone difference; and (3) transform-based features, *e.g.*, Wavelet, Gabor, Laws, Laplacian. However, since the number of extracted features could be much larger than the sample size of patients included in the algorithms' development, it is vital to reduce the number of features through a step called features selection. This step will strongly reduce the risk of overfitting[12], which occurs when the algorithm overadapts its performances based on data in the training set and consequently loses its generalizability. Besides, features selection will ensue to exclude features that are non-reproducible, redundant, and/or non-relevant for the task, and to reduce the computational cost, while improving the performance of the model[13]. Once the most performing features are selected, the radiomics signature is finally developed by using algorithms for classification, such as logistic regression[14,15], k-nearest neighbour[16], naïve Bayes classifier[17], support vector machines (SVM)[18,19], random forest (RF)[20,21], neural network [22,23] and deep learning[24,25]. In this step, is crucial to divide the image dataset into three subgroups: One for training, used to develop the algorithm, the second for testing, to fine-tune the model, and the last for validation, which aims to evaluate the performance on a different dataset. Training and testing could be performed also using a cross-validation approach, *i.e.*, in which different portions of the dataset are iteratively used to train and test the model. Conversely, the validation should be performed using patients that were never seen during the development of the algorithms. The validation step can be internal, when applied in a similar clinical setting and population to the training set, or preferably external, when applied in multiple clinical settings with varying disease prevalence[12,26].

Thanks to the vast number of images routinely used by radiologists and oncologists in their daily workload, radiomics is substantial in oncology to understand tumor biology or develop imaging biomarkers useful for diagnosis, staging, prediction of treatment response, disease monitoring and surveillance[27].

Understanding tumor biology through radiomics can be feasible because it allows the extraction of quantitative information about spatial and temporal heterogeneity in a non-invasively way and using routinely acquired images. This information can be consequently correlated with tumors' phenotype that can either reflects distinct traits (*e.g.*, internal necrosis and proliferation at the periphery) or mirrors genomic and molecular traits or be a signature or different outcomes. Moreover, texture features used in radiomics have been also demonstrated useful in reflecting key oncogenomics processes such as tumor angiogenesis[28], hypoxia[29], tumor invasion[30] and tumor proliferation[31].

The second scope of radiomics in the oncology field is to enhance precision medicine through the implementation of diagnostics and prognostic imaging biomarkers in a variety of solid tumors. Biomarkers for detection and diagnosis are those in a more advanced status since there are many studies that demonstrated their usefulness in discriminating between healthy, benign and malignant cancer in different sites[23,32-34]. However, the most promising applications in which radiomics could truly improve clinical practice are related to the prediction of treatment response and disease monitoring. Indeed, knowing, before or during therapy, which patients would respond might help choosing the best management possible. Moreover, after treatment, radiomics biomarkers may suggest more intense post-treatment surveillance due to a high risk of a tumor recurrence for a particular patient. In parallel to radiomics, it is worthwhile underling that a boost for the development of prognostic biomarkers for precision medicine could be provided by integrating radiomics features to additional layers of -omics information, *i.e.*, pathomics (features derived from digital pathological samples), and genomics. The motivation for this multi-omics approach to disease understanding is that the conventional markers



DOI: 10.3748/wjg.v29.i19.2888 **Copyright** ©The Author(s) 2023.

Figure 1 Radiomics pipeline. ROI: Regions of interest.

discovery which molecularly dissect the disease part by part, if the sum of knowledge of parts will explain the operation of the whole, has mostly failed to understand the causes and cures for complex diseases. On the contrary, recent evidence suggests that patterns discovered from high dimensional, multi-modal data could improve estimation of disease aggressiveness and patient outcomes compared to single modality data.

COMPUTED TOMOGRAPHY

Tumor and nodes

Several efforts have been made to develop radiomics signatures for colorectal cancer patient using computed tomography (CT) images with different aims (Table 1). Li *et al*[35] developed and validated a clinical-radiomics nomogram for the preoperative prediction of nodes metastasis. They validated their algorithm on an internal dataset of 308 patients (136 with and 172 without lymph node metastases) and showed that the model which included clinical parameters, radiomics on both tumor and peripheral nodes was the one reaching the highest accuracy in predicting nodes metastases [area under the curve (AUC) = 0.7509; 95%CI: 0.6901-0.8071; accuracy: 73.70%; sensitivity: 60.29%; specificity: 84.30%; positive predictive value (PPV): 75.23%; and negative predictive value (NPV): 72.86% in the internal validation set]. If further validated, also on an external validation set, this model could be used as an individualized preoperative non-invasive tool, assisting in clinical treatment decision making and achieving precision treatment.

From another point of view, radiomics has also been proven effective in detecting *BRAF* and *RAS* (*KRAS* and *NRAS*) gene mutations, that are genomics signatures usually associated with shorter disease-free and overall survival. These mutations are determined through genetic molecular profiling by sampling the tumor, however biopsy carries several drawbacks, including the risk of adverse events, such as bleeding, physical and psychological discomfort[36].

For these reasons, radiomics could potentially be used to non-invasively predict RAS and BRAF mutation status in patients with colorectal cancer and to further guide treatments with surgery or chemotherapy[16,37]. Shi *et al*[16] validated a combined score that tracks *RAS* (*KRAS* and *NRAS*) and

Table 1 Summary of the most important published papers regarding the usefulness of radiomics in colorectal cancer patients using computed tomography imaging

Ref.	Imaging	Main aim	Patients (*n*)	Main findings
Li *et al*[35], 2020	CT	Prediction of nodes metastases	766	Overall diagnostic values: Sensitivity = 60.3%; specificity = 84.3%; PPV = 75.2%; NPV = 72.9%; AUC = 0.750
Shi *et al*[16], 2020	CT	Detect *RAS* and *BRAF* phenotypes	159	Combined score (semantic features and radiomics) AUC = 0.950; validation cohort AUC = 0.790
Giannini *et al* [41], 2020	CT	Predict response to treatment	38 (141 lesions)	Per-lesion diagnostic values: Sensitivity = 89%; specificity = 85%; PPV = 78%; NPV = 93%
Dercle *et al* [47], 2020	CT	Tumor response to anti-EGFR therapy	667	Sensitivity to therapy: AUCs 0.800 and 0.720 for FOLFIRI and FOLFIRI + cetuximab
Dohan *et al* [48], 2020	CT	Overall survival	491	SPECTRA score > 0.02 has a lower OS; SPECTRA Score at 2 mo has the same prognostic values as RECIST at 6 mo
Giannini *et al* [41], 2020	CT	Predict response to treatment	57 (242 lesions)	Per-lesion diagnostic values: Sensitivity = 99%; specificity = 94%; PPV = 95%; NPV = 99%; the radiomic approach can predict R- wrongly classified by RECIST as R^+
Taghavi *et al* [103], 2021	CT	Prediction of synchronous liver metastases	91	The radiomics model outperformed the clinical model: AUC = 0.93 *vs* 0.64
Rao *et al*[108], 2014	CT	Prediction of synchronous liver metastases	29	The mean entropy of the liver is significantly higher in metastatic patients (P = 0.02); Liver entropy can help the differential between metastatic and non-metastatic patients (AUC = 0.73-0.78)
Li *et al*[109], 2022	CT	Prediction of synchronous liver metastases	323	A combined clinical-radiomics model has a good AUC (= 0.79) in detecting liver metastases
Ng *et al*[111], 2013	CT	Prediction of overall survival	55	Entropy, uniformity, kurtosis, skewness, and standard deviation of the pixel distribution histogram can predict survival; each parameter can be considered an independent predictor of the overall survival state
Mühlberg *et al* [112], 2021	CT	Prediction of overall survival	103	Tumor burden score can discriminate patients with at least 1-year survival (AUC = 0.70); a machine-learning model better predict survival (AUC = 0.73)
Ravanelli *et al* [116], 2019	CT	Prediction of response and prognosis after chemotherapy	43	Uniformity is lower in responders (P < 0.001); uniformity is independently correlated with radiological response (OR = 20.00), overall survival (RR = 6.94) and progression-free survival (RR = 5.05)

PPV: Positive predictive value; NPV: Negative predictive value; AUC: Area under the curve; OS: Overall survival; SPECTRA: Survival PrEdiction in patients treated by FOLFIRI and bevacizumab for mCRC using contrast-enhanced computed tomography TextuRe Analysis; CT: Computed tomography.

BRAF mutant phenotypes in colorectal cancer from multicentre CT image data AUC of 0.79 on the validation cohort.

Recently, efforts have been made to translate radiomics signatures from a patient level to a lesion level, since it has been demonstrated that heterogeneous response, caused by the onset of new resistant tumor clones in some lesions, is a predictor of poor overall survival[38-40]. Differentiating which colorectal liver metastases (CRLM) responds and which lingers and eventually will progress in the same patient could pave the way to truly personalized treatment. Giannini *et al*[41] preliminary demonstrated the feasibility of using radiomics features from baseline CT to predict response of treatment after 3 mo. They validated the signature on an independent cohort of patients obtaining encouraging results especially in identifying patients with outlier lesions, *i.e.*, that do not respond in general condition were most lesions respond. In these cases, a target biopsy on non-responder lesions could have revealed a different genetic makeup or, in absence of extrahepatic lesions, suggested the local ablation of outlier metastases. More recently, another breakthrough has been made using the use of delta-radiomics, whose aim is to assess the treatment-induced change of radiomics features over time that could provide information about prognosis[42,43]. These variations can be measured in different ways, for example as the differences between features computed on the same tumour before and after treatment[44,45] or the net-change (*i.e.*, difference of radiomics features after treatment over the value before treatment)[46]. Other than providing additional information about tumour behaviour, delta-radiomics represents a very interesting approach since it could theoretically allow to adapt and modulate the ongoing treatment approach thanks to the predictive power of this technique[42].

Delta-radiomics has been already proven effective in predicting overall survival in patients with metastatic colorectal cancer[47,48]. Dercle *et al*[47] developed and validated on a multicentre dataset a delta-radiomics associated with tumor sensitivity to anti-EGFR therapy in colorectal cancer patients (AUC = 0.80). Similarly, Dohan *et al*[48] validated a delta-radiomics signature able to predict overall survival and identify good responders better than RECIST1.1 criteria in patients with metastatic colorectal cancer treated by FOLFIRI and bevacizumab as a first-line treatment. From a per-lesion point

of view, Giannini *et al*[45] validated a delta-radiomics signature able to predict long-term response (*i.e.*, more than 8 mo) of individual CRLM with an accuracy of 86% in the validation dataset. Of note, the delta-radiomics signature was able to reliably predict non-responder liver metastases wrongly classified as responder by lesion RECIST at the first time point. This per-lesion approach could strongly impact treatment, since according to the delta-radiomics signature it would be possible to pinpoint lesions with distinct biological and molecular features, thus enabling studies toward lesion-specific personalized treatment in liver-only metastatic colorectal cancer patients.

MAGNETIC RESONANCE IMAGING

Tumor evaluation

The application of radiomics and texture analysis by using magnetic resonance imaging (MRI) images has increased interest in recent years (Table 2), with a specific focus on liver pathology, renal carcinoma, prostate cancer, and, in slight minority of published studies, rectal cancer[49]. As mentioned above, the staging of rectal cancer is mainly based on MRI; however, radiological images analyzed by dedicated software can add important data useful for the best management of patients. In this setting, it is of utmost importance to underline the potentiality of radiomics as a non-invasive biomarker for predicting histopathological data, as demonstrated for different abdominal pathological conditions, related to the liver, pancreas, and colorectal[8]. Even if for many abdominal organs it can be difficult to obtain a useful histological sample, rectal cancer pathological data are easy to collect, considering that colonoscopy or sigmoidoscopy, depending on the location of the lesion, is the reference standard technique[50]. On these bases, most published studies when this search was performed mainly focused on the response of advanced tumors that underwent neoadjuvant therapy.

Recently, Chen *et al*[51], in a single-center prospective study, enrolled 137 patients who underwent neoadjuvant chemotherapy. The Authors demonstrated that the traditional clinical model reported an AUC of 67.6% and 70.1% in the training and validation cohort, respectively, quite similar to the selective clinical model (77.5% and 59.6%, respectively). On the other hand, when combining radiomics with clinical data the AUC raised to 94.9% and 84.4% in the training and validation cohort, respectively.

Similarly, Horvat *et al*[52], by enrolling 114 patients who underwent neoadjuvant chemotherapy, demonstrated that radiomics can help the radiologist determine the pathological complete response. The Authors found that combined clinical and radiomics models increased the agreement compared with radiologist interpretation and can help the less experienced radiologist in increasing diagnostic values, in particular specificity, PPV, and NPV.

Analogously, Dinapoli *et al*[53] analyzed the radiomics data of 221 patients from three different centers and demonstrated that this tool can help the prediction of pathological complete response before starting neoadjuvant chemotherapy. Moreover, the Authors performed an external validation, to test the obtained results, with good diagnostic values.

Even if few studies are published in the literature, to test the robustness of the radiomics approach in rectal cancer patients, Shahzadi *et al*[54], demonstrated that only one study can be used for external validation, underlying the overall lack of reproducibility and the need of further standardization before considered it a useful clinical tool. In this setting, future directions should be focused on multicentre studies with standardized MR protocols to validate and test the feasibility of the radiomics approach and its potential usefulness in current everyday clinical practice.

Node's evaluation

Nodes metastases is the main metastatic site of colorectal cancer and an important cause of post-operative recurrence and death[55]. Nodes status is a key factor in the TNM staging of colorectal cancer and the main determinant of adjuvant chemotherapy[56,57].

Preoperative knowledge of NS can provide valuable information for determining the need for adjuvant therapy and the adequacy of surgical resection, thus aiding in pre-treatment decision making [58].

In clinical practice, CT is the most used preoperative imaging method to detect metastatic lesions and perform tumor staging in patients with colorectal cancer. However, the limitation of CT examination is that it cannot discriminate between benign and malignant nodes[59].

MRI has the highest contrast resolution for soft tissues, allowing the best depiction of neoplastic lesions, their anatomical relationships, the depth of the rectal wall involvement, extramural venous invasion, circumferential resection margins, and the assessment of the N stage. For these reasons, MRI examination is considered the reference standard for locoregional staging and restaging in RC according to the main international guidelines[60-62].

Advances in pattern recognition tools and the increase in data set sizes have facilitated the development of radiomics, which may potentially improve predictive accuracy in oncology[63].

Therefore, in the last decade, several papers have been published, with different imaging techniques, reporting the potential role of radiomics in diagnosis, characterization, and evaluation of the tumor response to treatments[64-67] and nodal assessment[68-70].

Table 2 Summary of the most important published papers regarding the usefulness of radiomics in colorectal cancer patients using magnetic resonance imaging

Ref.	Imaging	Main aim	Patients (*n*)	Main findings
Horvat *et al* [52], 2022	MRI	Response to chemotherapy	114	Combined radiological-radiomics model increased agreement (κ = 0.82 *vs* κ = 0.25)
Dinapoli *et al* [53], 2018	MRI	Pathological complete response	221	Significant covariates, skewness, and entropy can predict pathological complete response, with AUCs = 0.730 and 0.750 for internal and external cohorts
Shahzadi *et al* [50], 2022	MRI	Response to chemotherapy	190	Radiomics combined with the T stage better predict response
Liu *et al*[23], 2021	MRI	Prediction of nodes metastases	186	Clinical-radiomics model improves performance: AUC = 0.827
Chen *et al*[72], 2022	MRI	Tumor differentiation and nodes metastases	37 (487 nodes)	Radiomics features of the primary tumor can predict tumor differentiation: AUC = 0.798
Liu *et al*[73], 2017	MRI	Tumor differentiation	68	Skewness and entropy are lower in pT1-2 in comparison with pT3-4 (P < 0.05)
Yang *et al*[74], 2019	MRI	Prediction of T and N stage	88	Skewness, kurtosis, and energy are higher in metastatic nodes in comparison with non-metastatic ones (P < 0.001)
Ma *et al*[75], 2019	MRI	Prediction of nodes metastases and N staging	152	SVM has higher diagnostic values for T and N stages (AUC = 0.862) in comparison with MLP and RF
Zhu *et al*[76], 2019	MRI	Prediction of nodes metastases	215	Radiomic model AUC = 0.818
Zhou *et al*[77], 2020	MRI	Prediction of nodes metastases	391	The combined model predicts nodes metastases: NPV = 93.7%, AUC = 0.818
Shu *et al*[34], 2019	MRI	Prediction of synchronous liver metastases	194	The Radiomics model combined clinical risk factors and LASSO features and showed a good predictive performance: AUC = 0.921
Liu *et al*[107], 2020	MRI	Prediction of synchronous liver metastases	127	A radiomic nomogram presents an accuracy of 81.6% in predicting liver metastases (AUC = 0.918)
Granata *et al* [115], 2022	MRI	Prediction of overall survival	90	Second-order features can predict infiltrative tumor growth, tumor budding, and mucinous type; a second-order feature can predict the risk of recurrence with an accuracy of 90%
Jalil *et al*[119], 2017	MRI	Prediction of prognosis after chemotherapy	56	MPP can predict overall survival (HR = 6.9) and disease-free survival (HR = 3.36); texture analysis can predict relapse-free survival on pre- and post-treatment analyses

AUC: Area under the curve; SVM: Support vector machine; MLP: Multilayer perceptron; RF: Random forest; NPV: Negative predictive value; HR: Hazard ratio; MPP: Mean positive pixel; MRI: Magnetic resonance imaging.

MRI can provide multiparameter images different from those obtained by CT, so it is of interest whether there exists an association between NS and multiregional radiomics features of multiparametric MR images in rectal cancer patients[71].

Liu *et al*[71] aimed to develop and validate a multiregional radiomics prediction model based on MRI and combine it with clinical-semantic data for the individualized preoperative prediction of lymph node metastasis in rectal cancer patients.

Similarly, the study of Chen *et al*[72] provides two non-invasive and quantitative methods, which respectively predict the tumor differentiation and regional nodes metastases for rectal cancer preoperatively. MRI images of both the primary tumor alongside the lymph nodes and specimens were performed with a node-to-node match and labeling. A prediction model was then successfully developed, which provided AUC values of 84.6% and 73.3% in the training and test cohort, respectively.

Liu *et al*[73] performed a histogram analysis on the ADC map of the whole tumor and reported that entropy was an independent predictor of nodal involvement. Recently, Yang *et al*[74] performed the same analysis on T2-weighted imaging of the whole tumor: They found that a lower skewness was an independent risk factor for lymph node metastases.

In a recent retrospective single-center study, radiomics features were extracted from preoperative high-resolution T2-weighted imaging of different histological RC and analyzed using different algorithms. The RF analysis showed a good diagnostic performance for the N-stage with an AUC of 74.6%. The prediction model was able to differentiate N0 from N1-N2 patients with a sensitivity of 79.0% and a specificity of 72.0%[75].

Zhu *et al*[76] compared the performance of two models based, respectively, on the radiomics signature of the primary tumor and of the lymph nodes, before and after chemoradiotherapy (CRT), for the prediction of nodal involvement in advanced rectal cancer. The authors concluded that the features

from the lymph node model perform better than the tumor features for the prediction of nodal involvement[76].

Similarly, Zhou *et al*[77] evaluated a multi-parametric MRI radiomics model for nodal assessment following CRT by combining the radiomic signature with an experienced radiologist's visual evaluation: stratified analyses indicated that the combined model could predict lymph node metastasis with a NPV of 100 and 87.8% after treatment[77].

Even if current literature is focusing on the importance and applicability of radiomics in rectal cancer, no significant studies have been published in the field of colorectal cancer, mainly because MR is not still validated as imaging technique for local staging and restaging of this kind of tumor.

PET/CT

18F-fluorodeoxyglucose positron emission tomography/computed tomography (18F-FDG PET/CT) is frequently employed in the staging and post-neoadjuvant assessment of patients with rectal cancer. PET/CT provides functional information of the primary tumor, nodes and distant metastases. In patients with colorectal cancer, the combination of texture parameters with the functional information obtained with PET/CT scan can further enhance the predictive power of PET/CT imaging[78]. Current studies mostly focused on the applications of radiomics in PET/CT for the prediction of survival after curative surgical resection and assessment of response following neoadjuvant chemoradiotherapy (Table 3).

For the prediction of prognosis in patients with colorectal cancer, Kang *et al*[79] showed that radiomics score from baseline PET scans was significantly associated with progression-free survival. Similarly, Lovinfosse *et al*[80] and Hotta *et al*[81] correlated the texture features in PET/CT with both progression-free survival and overall survival. Furthermore, a recent study provided a combined clinical-radiomics model with high predictive performance (C-index of 0.780) for recurrence-free survival in 196 patients with PET/CT[82].

Several studies explored the potential of radiomics for the prediction of response and survival after neoadjuvant chemoradiotherapy[83-89]. In an initial study of 27 patients with rectal cancer treated with neoadjuvant chemoradiotherapy, Bundschuh *et al*[83] calculated texture parameters (skewness and kurtosis) on PET/CT, which provided a good performance for late response prediction but no significant predictive capability for the assessment of early response. In a retrospective study performed by Bang *et al*[84], texture parameters extracted from PET images correlated with both tumor regression grading and disease-free survival in patients with rectal cancer undergoing neoadjuvant chemoradiotherapy. Giannini *et al*[85] combined radiomics features from PET and MRI to predict pathological complete response following neoadjuvant chemoradiotherapy with high accuracy (AUC of 0.86) in patients with rectal cancer. Similarly, Schurink *et al*[86] combined pretreatment tumor features on PET/CT and MRI to predict response to chemoradiotherapy in rectal cancer, with an AUC of 0.81. Shen *et al*[87] developed a RF model to predict pathological complete response after neoadjuvant chemoradiotherapy in 169 patients with rectal cancer, which demonstrated a sensitivity of 97.3% and a specificity of 81.8% for the identifications of cancers with complete response. Nevertheless, a study by Karahan Şen *et al*[88] found no superiority of texture features compared to metabolic tumor volume in predicting response to neoadjuvant chemoradiotherapy in patients with locally advanced rectal cancer.

For the prediction of lymph node metastasis, a retrospective study published by He and colleagues [90] analyzed the radiomics score and five machine-learning models to predict metastatic lymph nodes based on the radiomics features of 199 colorectal cancers, with an AUC of 0.747-0.581 in the test set. Additionally, the performance of PET/CT radiomics features for predicting perineural invasion has been explored in a recent retrospective study[91].

Finally, few other studies explored the correlation between radiomics signature extracted from PET/CT and rectal cancer genotypes, such as microsatellite instability status[92], RAS mutational status[93, 94], TP53 and adenomatous polyposis coli mutations[94].

Despite the promising value of radiomics in PET/CT scans of rectal cancer, it should be noted that all current results are based on retrospective single-center studies with heterogeneity on the type of extracted features and analysis. Moreover, several current studies demonstrated insufficient quality according to the radiomics quality score assessment[95].

CRLM

CRLM develop in about 25% of patients with colorectal carcinoma, being more commonly synchronous (14%-17%) rather than metachronous (8%-15%)[96-99]. CT is most adopted to detect CRLM at preoperative staging due to its higher availability compared to MRI, while MRI is usually used in selected doubtful cases particularly in the challenging scenario of the "too small to characterize" hypoattenuating lesion. In addition, chemotherapy regimens may cause focal or diffuse hepatic changes at imaging that can profoundly alter visualization of hepatic metastases on CT, reducing its diagnostic accuracy and MRI proves to be helpful as problem-solving tool in some cases[100]. Therefore, the overall sensitivity, specificity and accuracy for the diagnosis of CRLM are lower for CT compared to

Table 3 Summary of the most important published papers regarding the usefulness of radiomics in colorectal cancer patients using positron emission tomography/computed tomography imaging

Ref.	Imaging	Main aim	Patients (*n*)	Main findings
Lovinfosse *et al* [80], 2018	PET/CT	Progression-free and overall survival	86	SUVmean, dissimilarity, and contrast from the neighborhood intensity-difference matrix are independently associated with overall survival
Hotta *et al*[81], 2021	PET/CT	Progression-free and overall survival	94	MTV, TLG, and GLCM entropy are associated with overall survival; SUVmax, MTV, TLG, and GLCM entropy are associated with progression-free survival
Bundschuh *et al* [83], 2014	PET/CT	Response after neoadjuvant chemotherapy	27	COV can assess histopathologic response during (sensitivity 68%, specificity 88%) and after (sensitivity 79%, specificity 88%) therapy
Bang *et al*[84], 2016	PET/CT	Response after neoadjuvant chemotherapy	74	MV is associated with 3-yr disease-free survival; Kurtosis and kurtosis gradient are associated with 3-yr disease-free survival
Giannini *et al* [85], 2019	PET/CT	Response after neoadjuvant chemotherapy	52	Second-order texture features (five from PET and one from MRI) can help distinguish responder and non-responder patients: Sensitivity = 86%; specificity = 83%; AUC = 0.860
Yuan *et al*[89], 2021	PET/CT	Response after neoadjuvant chemotherapy	66	A radiomics model can predict TRG 0 vs TRG 1-3: Sensitivity = 77.8%, specificity = 89.7%, AUC = 0.858
Schurink *et al* [86], 2021	PET/CT	Response after neoadjuvant chemotherapy	61	Combined baseline and global tumor features better predict response compared to baseline and local texture (AUC = 0.83 *vs* 0.79)
Shen *et al*[87], 2020	PET/CT	Predict pathological complete response	169	RF can predict complete response: Sensitivity = 81.8%; specificity = 97.3%; PPV = 81.8%; NPV = 97.3%; accuracy = 95.3%
He *et al*[90], 2021	PET/CT	Prediction of nodes metastases	199	Logist regression and XGBoost can accurately predict nodes metastases with AUC = 0.866 and 0.903, respectively
Ma *et al*[91], 2022	PET/CT	Prediction of perineural invasion and outcome	131	12 radiomics signatures are associated with peri-neural invasion; a radiomic score can differentiate between perineural positive and negative lesions: AUC = 0.900
Li *et al*[92], 2021	PET/CT	Prediction of microsatellite instability	173	2 radiomics features can predict microsatellite instability: Sensitivity = 83.3%; specificity = 76.3%; accuracy = 76.8%
Lovinfosse *et al* [93], 2016	PET/CT	Prediction of RAS status	151	SUVmax, SUV mean, skewness, SUV standard deviation, and SUV coefficient of variation are associated with RAF mutation (all $P < 0.001$)
Chen *et al*[94], 2019	PET/CT	Prediction of genetic mutations	74	MTV and SUV max are increased in mutated KRAS tumors (all $P < 0.001$); short-run low gray-level emphasis is associated with p53 mutations ($P = 0.001$); gray-level zone emphasis is associated with APC mutations ($P = 0.006$)

PET/CT: Positron emission tomography/computed tomography; PPV: Positive predictive value; NPV: Negative predictive value; AUC: Area under the curve; RF: Random forest; MTV: Metabolic tumor volume; TLG: Total lesion glycolysis; GLCM: Gray-level co-occurrence matrix; COV: Coefficient of variation; MV: Metabolic volume; OR: Odd ratio; MPP: Mean positive pixel.

MRI[100-102]. For this reason, at some center, abbreviated gadoxetate disodium MRI protocols are adopted rather than trusting CT only[103,104].

The adoption of radiomics has been proven successful in diagnostic, prognostic, and therapeutic stages[78].

Diagnosis and risk assessment

In term of diagnosis of synchronous classical logistic regression models (CLRM), it is relevant to highlight that even with MRI the sensitivity may be lower than 80%, particularly in patients with mucinous adenocarcinoma as primary tumor, prior local treatment in the liver or metastases smaller than 1 cm[102]. Therefore, the first main diagnostic task of radiomics should be the identification of CRLM before they can be seen by radiologist's naked eye (*i.e.*, detection of synchronous metastases). In a pilot study, Devoto *et al*[105] proved that radiomics can potentially predict the development of liver metastases on baseline liver CT, by demonstrating a higher heterogeneity of liver texture analysis in patients who developed liver metastases compared to patients who did not develop them. Other authors[34,106] investigated whether radiomics applied to T2-weighted images of the primary tumor on MRI could help in the preoperative prediction of CRLM: Shu *et al*[34] used a region of interest while Liu *et al*[107] used a volume of interest and both demonstrated that a radiomics nomogram constructed by combining radiomics and clinical data achieve AUC higher than 90% in the preoperative prediction of

CRLM.

The second main diagnostic task of radiomics should be preoperative identification of patients at risk of developing CLRM (*i.e.*, detection of metachronous metastases) based on micro-environmental changes in the apparently normal liver. Taghavi *et al*[106] and Rao *et al*[108] designed a prediction model based on liver CT radiomics for the detection of metachronous CRL, with the first study including more patients imaged at three centers and combining radiomics and clinical data achieving AUC of up to 86% in the validation cohort. Other studies tried to achieve the same goal by assessing the primary tumor on CT[109] or MRI[110]. Specifically, Li *et al*[109] obtained an AUC of 0.72 for the prediction of metachronous CLRM by combining clinical data and volumetric radiomics of the primary tumor on CT. In regard of MRI, a systematic review including 1497 patients estimated a pooled sensitivity and specificity of radiomics applied to rectal MRI of 0.76 and 0.85 respectively in predicting metachronous CLRM, and AUC of the included studies ranging from 0.83 to 0.87[110].

Prognosis

In terms of prognostic information, radiomics of CRLM has emerged as a promising tool to preoperatively predict patient survival at diagnosis and after therapy. Ng *et al*[111] suggested that tumors demonstrating less texture tumor heterogeneity using radiomic CT analysis may predict poorer survival at diagnosis[111]. Mühlberg *et al*[112] showed that CT-based geometric distribution and radiomics analysis of whole liver tumor burden from preoperative CT may help for prediction of 1-year survival. Radiomics of CRLM on CT seems also promising for differentiating desmoplastic from replacement histopathological growth patterns[113], and this differentiation may provide an earlier estimate of disease aggressiveness and prognosis as the desmoplastic histopathological growth pattern usually has longer overall survival[114]. As demonstrated by Granata *et al*[115] contrast MR-based radiomics and machine learning analysis may help in the preoperative prediction of the front of tumor growth (expansive or infiltrative), the tumor budding (absent, low grade or high grade) and tumor recurrence after surgery, all of which may affect patient outcome. Studies looking at survival after chemotherapy in patients with CRLMs obtained similar results regarding the role of texture homogeneity/heterogeneity in the prediction of prognosis[116,117]. As an example, Ravanelli *et al*[116] demonstrated that lower uniformity of CRLM on CT texture analysis was independently correlated with overall survival and progression free survival in patients treated with bevacizumab, but not in those treated with standard chemotherapy. Other radiomic features such as entropy, kurtosis, and skewness have been investigated so far on CT and MRI, all providing an additional piece of the puzzle and supporting the concept that the addition of texture analysis in the pre-treatment assessment may provide information on prognosis in patients with primary colorectal cancer and CLRM[118,119].

Treatment response

Finally, the correct assessment of response in the treatment of CLRM and the prompt prediction of early response is of utmost important in defining the success or failure of treatment interventions and in the selection of those patients requiring a change of the therapeutic regimen. Chemotherapy for CLRM in the modern era of oxaliplatin- and irinotecan-containing regimens (*e.g.*, FOLFOX, FOLFIRI, CAPOX/FOLFOXIRI, XELOX) has been implemented with the introduction of targeted biologics and immunotherapeutic agents (*e.g.*, bevacizumab, cetuximab, panitumumab, pembrolizumab), thus expanding the proportion of patients eligible for curative-intent surgery, but their use may lead to side effects or complications[120]. Prediction of tumor response before starting chemotherapy would allow to choose the best treatment, avoiding unnecessary adverse effects of the therapy. Radiomics of CLRM has been proven promising for predicting response to different chemotherapy regimens, but the predictive value of radiomics features seems to be treatment dependent[95]. As shown by two systematic reviews[95,121], most studies performed radiomics on CT rather than MRI. In patients treated with FOLFOX or FOLFIRI, low skewness and narrower standard deviation-both suggesting increased tumor homogeneity-were associated with a high response rate to chemotherapy[122]. Giannini *et al*[41] developed a radiomics signature to predict behaviour of individual CLRMs to targeted treatment in patients with HER2 amplification undergoing dual target therapy; in their model, the two most important radiomics features were difference in variance and homogeneity, thus again highlighting the role of texture analysis homogeneity of CLRM for assessing lesion diagnosis and outcome. Other studies investigated the role of radiomics in assessing tumor response after other targeted biologics and immunotherapeutic agents, such as regorafenib[117], and bevacizumab[116,48].

CONCLUSION

Nowadays much evidence has revealed that not all clinical risk features are equal, not all affect overall survival, and the decision to treat colorectal cancer with adjuvant chemotherapy should be assessed in multidisciplinary approach[123]. In this scenario, radiomics could play a pivotal role in colorectal cancer workup as an additional tool in clinical setting with the expectancy to help clinicians in identifying patients with high-risk disease. In particular, the main fields examined were the preoperative assess-

ment of the differentiation between low- and high-grade colorectal cancer, and the prediction of nodal metastases[124-131]. The results achieved good and consistent efficiency in identifying high-risk clinical factors, reinforcing the idea that radiomics could play a central role in colorectal cancer patient workup. Nevertheless, radiomics has numerous shortcomings that make daily use extremely difficult. Among these, the lack of standardization and validation, poor reproducibility, and missing prospective multicentric studies represent the main drawbacks that must be overcome to introduce the radiomics approach to the clinical routine[7]. Further studies are needed to assess the performance of radiomics in stratifying patients with high-risk disease in patients with non-metastatic colorectal cancer who could benefit from adjuvant chemotherapy.

FOOTNOTES

Author contributions: Inchingolo R, Maino C, Cannella R, Vernuccio F, Cortese F, Dezio M, Pisani AR, Giandola T, Gatti M, Giannini V, Ippolito D, and Faletti R equally contributed to this paper with conception and design of the study, literature review and analysis, drafting and critical revision and editing; and all authors gave final approval of the final version.

Conflict-of-interest statement: All the authors are aware of the content of the manuscript and have no conflict of interest.

Open-Access: This article is an open-access article that was selected by an in-house editor and fully peer-reviewed by external reviewers. It is distributed in accordance with the Creative Commons Attribution NonCommercial (CC BY-NC 4.0) license, which permits others to distribute, remix, adapt, build upon this work non-commercially, and license their derivative works on different terms, provided the original work is properly cited and the use is non-commercial. See: https://creativecommons.org/Licenses/by-nc/4.0/

Country/Territory of origin: Italy

ORCID number: Riccardo Inchingolo 0000-0002-0253-5936; Cesare Maino 0000-0002-5742-802X; Roberto Cannella 0000-0002-3808-0785; Federica Vernuccio 0000-0003-0350-1794; Francesco Cortese 0000-0002-2731-3766; Michele Dezio 0000-0001-6491-4969; Antonio Rosario Pisani 0000-0002-3335-9541; Teresa Giandola 0000-0001-8750-0531; Marco Gatti 0000-0001-8168-5280; Valentina Giannini 0000-0001-5052-8231; Davide Ippolito 0000-0002-2696-7047; Riccardo Faletti 0000-0002-8865-8637.

S-Editor: Chen YL
L-Editor: A
P-Editor: Yuan YY

REFERENCES

1 **Sung H**, Ferlay J, Siegel RL, Laversanne M, Soerjomataram I, Jemal A, Bray F. Global Cancer Statistics 2020: GLOBOCAN Estimates of Incidence and Mortality Worldwide for 36 Cancers in 185 Countries. *CA Cancer J Clin* 2021; **71**: 209-249 [PMID: 33538338 DOI: 10.3322/caac.21660]

2 **Argilés G**, Tabernero J, Labianca R, Hochhauser D, Salazar R, Iveson T, Laurent-Puig P, Quirke P, Yoshino T, Taieb J, Martinelli E, Arnold D; ESMO Guidelines Committee. Electronic address: clinicalguidelines@esmo.org. Localised colon cancer: ESMO Clinical Practice Guidelines for diagnosis, treatment and follow-up. *Ann Oncol* 2020; **31**: 1291-1305 [PMID: 32702383 DOI: 10.1016/j.annonc.2020.06.022]

3 **Weiser MR**. AJCC 8th Edition: Colorectal Cancer. *Ann Surg Oncol* 2018; **25**: 1454-1455 [PMID: 29616422 DOI: 10.1245/s10434-018-6462-1]

4 **Baxter NN**, Kennedy EB, Bergsland E, Berlin J, George TJ, Gill S, Gold PJ, Hantel A, Jones L, Lieu C, Mahmoud N, Morris AM, Ruiz-Garcia E, You YN, Meyerhardt JA. Adjuvant Therapy for Stage II Colon Cancer: ASCO Guideline Update. *J Clin Oncol* 2022; **40**: 892-910 [PMID: 34936379 DOI: 10.1200/JCO.21.02538]

5 **Lambin P**, Rios-Velazquez E, Leijenaar R, Carvalho S, van Stiphout RG, Granton P, Zegers CM, Gillies R, Boellard R, Dekker A, Aerts HJ. Radiomics: extracting more information from medical images using advanced feature analysis. *Eur J Cancer* 2012; **48**: 441-446 [PMID: 22257792 DOI: 10.1016/j.ejca.2011.11.036]

6 **Aerts HJ**, Velazquez ER, Leijenaar RT, Parmar C, Grossmann P, Carvalho S, Bussink J, Monshouwer R, Haibe-Kains B, Rietveld D, Hoebers F, Rietbergen MM, Leemans CR, Dekker A, Quackenbush J, Gillies RJ, Lambin P. Decoding tumour phenotype by noninvasive imaging using a quantitative radiomics approach. *Nat Commun* 2014; **5**: 4006 [PMID: 24892406 DOI: 10.1038/ncomms5006]

7 **Caruso D**, Polici M, Zerunian M, Pucciarelli F, Guido G, Polidori T, Landolfi F, Nicolai M, Lucertini E, Tarallo M, Bracci B, Nacci I, Rucci C, Iannicelli E, Laghi A. Radiomics in Oncology, Part 1: Technical Principles and Gastrointestinal Application in CT and MRI. *Cancers (Basel)* 2021; **13** [PMID: 34063937 DOI: 10.3390/cancers13112522]

8 **Lambin P**, Leijenaar RTH, Deist TM, Peerlings J, de Jong EEC, van Timmeren J, Sanduleanu S, Larue RTHM, Even AJG, Jochems A, van Wijk Y, Woodruff H, van Soest J, Lustberg T, Roelofs E, van Elmpt W, Dekker A, Mottaghy FM,

Wildberger JE, Walsh S. Radiomics: the bridge between medical imaging and personalized medicine. *Nat Rev Clin Oncol* 2017; **14**: 749-762 [PMID: 28975929 DOI: 10.1038/nrclinonc.2017.141]

9 **Caruso D**, Polici M, Zerunian M, Pucciarelli F, Guido G, Polidori T, Landolfi F, Nicolai M, Lucertini E, Tarallo M, Bracci B, Nacci I, Rucci C, Eid M, Iannicelli E, Laghi A. Radiomics in Oncology, Part 2: Thoracic, Genito-Urinary, Breast, Neurological, Hematologic and Musculoskeletal Applications. *Cancers (Basel)* 2021; **13** [PMID: 34072366 DOI: 10.3390/cancers13112681]

10 **Botta F**, Raimondi S, Rinaldi L, Bellerba F, Corso F, Bagnardi V, Origgi D, Minelli R, Pitoni G, Petrella F, Spaggiari L, Morganti AG, Del Grande F, Bellomi M, Rizzo S. Association of a CT-Based Clinical and Radiomics Score of Non-Small Cell Lung Cancer (NSCLC) with Lymph Node Status and Overall Survival. *Cancers (Basel)* 2020; **12** [PMID: 32486453 DOI: 10.3390/cancers12061432]

11 **Fan G**, Qin J, Liu H, Liao X. Commentary: Radiomics in oncology: A 10-year bibliometric analysis. *Front Oncol* 2022; **12**: 891056 [PMID: 35936758 DOI: 10.3389/fonc.2022.891056]

12 **van Timmeren JE**, Cester D, Tanadini-Lang S, Alkadhi H, Baessler B. Radiomics in medical imaging-"how-to" guide and critical reflection. *Insights Imaging* 2020; **11**: 91 [PMID: 32785796 DOI: 10.1186/s13244-020-00887-2]

13 **Defeudis A**, De Mattia C, Rizzetto F, Calderoni F, Mazzetti S, Torresin A, Vanzulli A, Regge D, Giannini V. Standardization of CT radiomics features for multi-center analysis: impact of software settings and parameters. *Phys Med Biol* 2020; **65**: 195012 [PMID: 32575082 DOI: 10.1088/1361-6560/ab9f61]

14 **Pan S**, Ding Z, Zhang L, Ruan M, Shan Y, Deng M, Pang P, Shen Q. A Nomogram Combined Radiomic and Semantic Features as Imaging Biomarker for Classification of Ovarian Cystadenomas. *Front Oncol* 2020; **10**: 895 [PMID: 32547958 DOI: 10.3389/fonc.2020.00895]

15 **Qi Y**, Zhang S, Wei J, Zhang G, Lei J, Yan W, Xiao Y, Yan S, Xue H, Feng F, Sun H, Tian J, Jin Z. Multiparametric MRI-Based Radiomics for Prostate Cancer Screening With PSA in 4-10 ng/mL to Reduce Unnecessary Biopsies. *J Magn Reson Imaging* 2020; **51**: 1890-1899 [PMID: 31808980 DOI: 10.1002/jmri.27008]

16 **Shi R**, Chen W, Yang B, Qu J, Cheng Y, Zhu Z, Gao Y, Wang Q, Liu Y, Li Z, Qu X. Prediction of KRAS, NRAS and BRAF status in colorectal cancer patients with liver metastasis using a deep artificial neural network based on radiomics and semantic features. *Am J Cancer Res* 2020; **10**: 4513-4526 [PMID: 33415015]

17 **Frøkjær JB**, Lisitskaya MV, Jørgensen AS, Østergaard LR, Hansen TM, Drewes AM, Olesen SS. Pancreatic magnetic resonance imaging texture analysis in chronic pancreatitis: a feasibility and validation study. *Abdom Radiol (NY)* 2020; **45**: 1497-1506 [PMID: 32266506 DOI: 10.1007/s00261-020-02512-8]

18 **Petkovska I**, Tixier F, Ortiz EJ, Golia Pernicka JS, Paroder V, Bates DD, Horvat N, Fuqua J, Schilsky J, Gollub MJ, Garcia-Aguilar J, Veeraraghavan H. Clinical utility of radiomics at baseline rectal MRI to predict complete response of rectal cancer after chemoradiation therapy. *Abdom Radiol (NY)* 2020; **45**: 3608-3617 [PMID: 32296896 DOI: 10.1007/s00261-020-02502-w]

19 **Wang JC**, Fu R, Tao XW, Mao YF, Wang F, Zhang ZC, Yu WW, Chen J, He J, Sun BC. A radiomics-based model on non-contrast CT for predicting cirrhosis: make the most of image data. *Biomark Res* 2020; **8**: 47 [PMID: 32963787 DOI: 10.1186/s40364-020-00219-y]

20 **Park S**, Chu LC, Hruban RH, Vogelstein B, Kinzler KW, Yuille AL, Fouladi DF, Shayesteh S, Ghandili S, Wolfgang CL, Burkhart R, He J, Fishman EK, Kawamoto S. Differentiating autoimmune pancreatitis from pancreatic ductal adenocarcinoma with CT radiomics features. *Diagn Interv Imaging* 2020; **101**: 555-564 [PMID: 32278586 DOI: 10.1016/j.diii.2020.03.002]

21 **Gu D**, Hu Y, Ding H, Wei J, Chen K, Liu H, Zeng M, Tian J. CT radiomics may predict the grade of pancreatic neuroendocrine tumors: a multicenter study. *Eur Radiol* 2019; **29**: 6880-6890 [PMID: 31227882 DOI: 10.1007/s00330-019-06176-x]

22 **Bagher-Ebadian H**, Janic B, Liu C, Pantelic M, Hearshen D, Elshaikh M, Movsas B, Chetty IJ, Wen N. Detection of Dominant Intra-prostatic Lesions in Patients With Prostate Cancer Using an Artificial Neural Network and MR Multi-modal Radiomics Analysis. *Front Oncol* 2019; **9**: 1313 [PMID: 31850209 DOI: 10.3389/fonc.2019.01313]

23 **Liu Y**, Fan H, Dong D, Liu P, He B, Meng L, Chen J, Chen C, Lang J, Tian J. Computed tomography-based radiomic model at node level for the prediction of normal-sized lymph node metastasis in cervical cancer. *Transl Oncol* 2021; **14**: 101113 [PMID: 33975178 DOI: 10.1016/j.tranon.2021.101113]

24 **Panic J**, Defeudis A, Mazzetti S, Rosati S, Giannetto G, Vassallo L, Regge D, Balestra G, Giannini V. A Convolutional Neural Network based system for Colorectal cancer segmentation on MRI images. *Annu Int Conf IEEE Eng Med Biol Soc* 2020; **2020**: 1675-1678 [PMID: 33018318 DOI: 10.1109/EMBC44109.2020.9175804]

25 **Barra D**, Nicoletti G, Defeudis A, Mazzetti S, Panic J, Gatti M, Faletti R, Russo F, Regge D, Giannini V. Deep learning model for automatic prostate segmentation on bicentric T2w images with and without endorectal coil. *Annu Int Conf IEEE Eng Med Biol Soc* 2021; **2021**: 3370-3373 [PMID: 34891962 DOI: 10.1109/EMBC46164.2021.9630792]

26 **Riley RD**, Snell KIE, Ensor J, Burke DL, Harrell FE Jr, Moons KGM, Collins GS. Minimum sample size for developing a multivariable prediction model: Part I - Continuous outcomes. *Stat Med* 2019; **38**: 1262-1275 [PMID: 30347470 DOI: 10.1002/sim.7993]

27 **Limkin EJ**, Sun R, Dercle L, Zacharaki EI, Robert C, Reuzé S, Schernberg A, Paragios N, Deutsch E, Ferté C. Promises and challenges for the implementation of computational medical imaging (radiomics) in oncology. *Ann Oncol* 2017; **28**: 1191-1206 [PMID: 28168275 DOI: 10.1093/annonc/mdx034]

28 **Ganeshan B**, Abaleke S, Young RC, Chatwin CR, Miles KA. Texture analysis of non-small cell lung cancer on unenhanced computed tomography: initial evidence for a relationship with tumour glucose metabolism and stage. *Cancer Imaging* 2010; **10**: 137-143 [PMID: 20605762 DOI: 10.1102/1470-7330.2010.0021]

29 **Gevaert O**, Xu J, Hoang CD, Leung AN, Xu Y, Quon A, Rubin DL, Napel S, Plevritis SK. Non-small cell lung cancer: identifying prognostic imaging biomarkers by leveraging public gene expression microarray data--methods and preliminary results. *Radiology* 2012; **264**: 387-396 [PMID: 22723499 DOI: 10.1148/radiol.12111607]

30 **Zhu Y**, Li H, Guo W, Drukker K, Lan L, Giger ML, Ji Y. Deciphering Genomic Underpinnings of Quantitative MRI-based Radiomic Phenotypes of Invasive Breast Carcinoma. *Sci Rep* 2015; **5**: 17787 [PMID: 26639025 DOI:

10.1038/srep17787]
31 **Segal E**, Sirlin CB, Ooi C, Adler AS, Gollub J, Chen X, Chan BK, Matcuk GR, Barry CT, Chang HY, Kuo MD. Decoding global gene expression programs in liver cancer by noninvasive imaging. *Nat Biotechnol* 2007; **25**: 675-680 [PMID: 17515910 DOI: 10.1038/nbt1306]
32 **Reginelli A**, Capasso R, Petrillo M, Rossi C, Faella P, Grassi R, Belfiore MP, Rossi G, Muto M, Muto P, Fiorello A, Serra N, Nizzoli R, De Filippo M, Cappabianca S, Carrafiello G, Brunese L, Rotondo A. Looking for Lepidic Component inside Invasive Adenocarcinomas Appearing as CT Solid Solitary Pulmonary Nodules (SPNs): CT Morpho-Densitometric Features and 18-FDG PET Findings. *Biomed Res Int* 2019; **2019**: 7683648 [PMID: 30733967 DOI: 10.1155/2019/7683648]
33 **Chiappa V**, Bogani G, Interlenghi M, Salvatore C, Bertolina F, Sarpietro G, Signorelli M, Castiglioni I, Raspagliesi F. The Adoption of Radiomics and machine learning improves the diagnostic processes of women with Ovarian MAsses (the AROMA pilot study). *J Ultrasound* 2021; **24**: 429-437 [PMID: 32696414 DOI: 10.1007/s40477-020-00503-5]
34 **Shu Z**, Fang S, Ding Z, Mao D, Cai R, Chen Y, Pang P, Gong X. MRI-based Radiomics nomogram to detect primary rectal cancer with synchronous liver metastases. *Sci Rep* 2019; **9**: 3374 [PMID: 30833648 DOI: 10.1038/s41598-019-39651-y]
35 **Li M**, Zhang J, Dan Y, Yao Y, Dai W, Cai G, Yang G, Tong T. A clinical-radiomics nomogram for the preoperative prediction of lymph node metastasis in colorectal cancer. *J Transl Med* 2020; **18**: 46 [PMID: 32000813 DOI: 10.1186/s12967-020-02215-0]
36 **Purnell SD**, Bloom JB, Valera V, Wood BJ, Turkbey B, Pinto PA. Targeted biopsy: benefits and limitations. *Curr Opin Urol* 2018; **28**: 219-226 [PMID: 29334506 DOI: 10.1097/MOU.0000000000000481]
37 **Negreros-Osuna AA**, Parakh A, Corcoran RB, Pourvaziri A, Kambadakone A, Ryan DP, Sahani DV. Radiomics Texture Features in Advanced Colorectal Cancer: Correlation with BRAF Mutation and 5-year Overall Survival. *Radiol Imaging Cancer* 2020; **2**: e190084 [PMID: 33778733 DOI: 10.1148/rycan.2020190084]
38 **van Kessel CS**, Samim M, Koopman M, van den Bosch MA, Borel Rinkes IH, Punt CJ, van Hillegersberg R. Radiological heterogeneity in response to chemotherapy is associated with poor survival in patients with colorectal liver metastases. *Eur J Cancer* 2013; **49**: 2486-2493 [PMID: 23692811 DOI: 10.1016/j.ejca.2013.03.027]
39 **Russo M**, Siravegna G, Blaszkowsky LS, Corti G, Crisafulli G, Ahronian LG, Mussolin B, Kwak EL, Buscarino M, Lazzari L, Valtorta E, Truini M, Jessop NA, Robinson HE, Hong TS, Mino-Kenudson M, Di Nicolantonio F, Thabet A, Sartore-Bianchi A, Siena S, Iafrate AJ, Bardelli A, Corcoran RB. Tumor Heterogeneity and Lesion-Specific Response to Targeted Therapy in Colorectal Cancer. *Cancer Discov* 2016; **6**: 147-153 [PMID: 26644315 DOI: 10.1158/2159-8290.CD-15-1283]
40 **Piotrowska Z**, Niederst MJ, Karlovich CA, Wakelee HA, Neal JW, Mino-Kenudson M, Fulton L, Hata AN, Lockerman EL, Kalsy A, Digumarthy S, Muzikansky A, Raponi M, Garcia AR, Mulvey HE, Parks MK, DiCecca RH, Dias-Santagata D, Iafrate AJ, Shaw AT, Allen AR, Engelman JA, Sequist LV. Heterogeneity Underlies the Emergence of EGFRT790 Wild-Type Clones Following Treatment of T790M-Positive Cancers with a Third-Generation EGFR Inhibitor. *Cancer Discov* 2015; **5**: 713-722 [PMID: 25934077 DOI: 10.1158/2159-8290.CD-15-0399]
41 **Giannini V**, Rosati S, Defeudis A, Balestra G, Vassallo L, Cappello G, Mazzetti S, De Mattia C, Rizzetto F, Torresin A, Sartore-Bianchi A, Siena S, Vanzulli A, Leone F, Zagonel V, Marsoni S, Regge D. Radiomics predicts response of individual HER2-amplified colorectal cancer liver metastases in patients treated with HER2-targeted therapy. *Int J Cancer* 2020; **147**: 3215-3223 [PMID: 32875550 DOI: 10.1002/ijc.33271]
42 **Nardone V**, Reginelli A, Grassi R, Boldrini L, Vacca G, D'Ippolito E, Annunziata S, Farchione A, Belfiore MP, Desideri I, Cappabianca S. Delta radiomics: a systematic review. *Radiol Med* 2021; **126**: 1571-1583 [PMID: 34865190 DOI: 10.1007/s11547-021-01436-7]
43 **Nasief H**, Zheng C, Schott D, Hall W, Tsai S, Erickson B, Allen Li X. A machine learning based delta-radiomics process for early prediction of treatment response of pancreatic cancer. *NPJ Precis Oncol* 2019; **3**: 25 [PMID: 31602401 DOI: 10.1038/s41698-019-0096-z]
44 **Jeon SH**, Song C, Chie EK, Kim B, Kim YH, Chang W, Lee YJ, Chung JH, Chung JB, Lee KW, Kang SB, Kim JS. Delta-radiomics signature predicts treatment outcomes after preoperative chemoradiotherapy and surgery in rectal cancer. *Radiat Oncol* 2019; **14**: 43 [PMID: 30866965 DOI: 10.1186/s13014-019-1246-8]
45 **Giannini V**, Pusceddu L, Defeudis A, Nicoletti G, Cappello G, Mazzetti S, Sartore-Bianchi A, Siena S, Vanzulli A, Rizzetto F, Fenocchio E, Lazzari L, Bardelli A, Marsoni S, Regge D. Delta-Radiomics Predicts Response to First-Line Oxaliplatin-Based Chemotherapy in Colorectal Cancer Patients with Liver Metastases. *Cancers (Basel)* 2022; **14** [PMID: 35008405 DOI: 10.3390/cancers14010241]
46 **Fave X**, Zhang L, Yang J, Mackin D, Balter P, Gomez D, Followill D, Jones AK, Stingo F, Liao Z, Mohan R, Court L. Delta-radiomics features for the prediction of patient outcomes in non-small cell lung cancer. *Sci Rep* 2017; **7**: 588 [PMID: 28373718 DOI: 10.1038/s41598-017-00665-z]
47 **Dercle L**, Lu L, Schwartz LH, Qian M, Tejpar S, Eggleton P, Zhao B, Piessevaux H. Radiomics Response Signature for Identification of Metastatic Colorectal Cancer Sensitive to Therapies Targeting EGFR Pathway. *J Natl Cancer Inst* 2020; **112**: 902-912 [PMID: 32016387 DOI: 10.1093/jnci/djaa017]
48 **Dohan A**, Gallix B, Guiu B, Le Malicot K, Reinhold C, Soyer P, Bennouna J, Ghiringhelli F, Barbier E, Boige V, Taieb J, Bouché O, François E, Phelip JM, Borel C, Faroux R, Seitz JF, Jacquot S, Ben Abdelghani M, Khemissa-Akouz F, Genet D, Jouve JL, Rinaldi Y, Desseigne F, Texereau P, Suc E, Lepage C, Aparicio T, Hoeffel C; PRODIGE 9 Investigators and PRODIGE 20 Investigators. Early evaluation using a radiomic signature of unresectable hepatic metastases to predict outcome in patients with colorectal cancer treated with FOLFIRI and bevacizumab. *Gut* 2020; **69**: 531-539 [PMID: 31101691 DOI: 10.1136/gutjnl-2018-316407]
49 **Thomas JV**, Abou Elkassem AM, Ganeshan B, Smith AD. MR Imaging Texture Analysis in the Abdomen and Pelvis. *Magn Reson Imaging Clin N Am* 2020; **28**: 447-456 [PMID: 32624161 DOI: 10.1016/j.mric.2020.03.009]
50 **Cunningham D**, Atkin W, Lenz HJ, Lynch HT, Minsky B, Nordlinger B, Starling N. Colorectal cancer. *Lancet* 2010; **375**: 1030-1047 [PMID: 20304247 DOI: 10.1016/S0140-6736(10)60353-4]

51 **Chen BY**, Xie H, Li Y, Jiang XH, Xiong L, Tang XF, Lin XF, Li L, Cai PQ. MRI-Based Radiomics Features to Predict Treatment Response to Neoadjuvant Chemotherapy in Locally Advanced Rectal Cancer: A Single Center, Prospective Study. *Front Oncol* 2022; **12**: 801743 [PMID: 35646677 DOI: 10.3389/fonc.2022.801743]

52 **Horvat N**, Veeraraghavan H, Nahas CSR, Bates DDB, Ferreira FR, Zheng J, Capanu M, Fuqua JL 3rd, Fernandes MC, Sosa RE, Jayaprakasam VS, Cerri GG, Nahas SC, Petkovska I. Combined artificial intelligence and radiologist model for predicting rectal cancer treatment response from magnetic resonance imaging: an external validation study. *Abdom Radiol (NY)* 2022; **47**: 2770-2782 [PMID: 35710951 DOI: 10.1007/s00261-022-03572-8]

53 **Dinapoli N**, Barbaro B, Gatta R, Chiloiro G, Casà C, Masciocchi C, Damiani A, Boldrini L, Gambacorta MA, Dezio M, Mattiucci GC, Balducci M, van Soest J, Dekker A, Lambin P, Fiorino C, Sini C, De Cobelli F, Di Muzio N, Gumina C, Passoni P, Manfredi R, Valentini V. Magnetic Resonance, Vendor-independent, Intensity Histogram Analysis Predicting Pathologic Complete Response After Radiochemotherapy of Rectal Cancer. *Int J Radiat Oncol Biol Phys* 2018; **102**: 765-774 [PMID: 29891200 DOI: 10.1016/j.ijrobp.2018.04.065]

54 **Shahzadi I**, Zwanenburg A, Lattermann A, Linge A, Baldus C, Peeken JC, Combs SE, Diefenhardt M, Rödel C, Kirste S, Grosu AL, Baumann M, Krause M, Troost EGC, Löck S. Analysis of MRI and CT-based radiomics features for personalized treatment in locally advanced rectal cancer and external validation of published radiomics models. *Sci Rep* 2022; **12**: 10192 [PMID: 35715462 DOI: 10.1038/s41598-022-13967-8]

55 **Xue H**, Du X, Xiao C, Yan Y, Zou Z, Xu Y. [Predictive value of lymph node ratio for postoperative distant metastasis of stage III colorectal cancer]. *Nan Fang Yi Ke Da Xue Xue Bao* 2014; **34**: 458-462 [PMID: 24752087]

56 **Watanabe T**, Muro K, Ajioka Y, Hashiguchi Y, Ito Y, Saito Y, Hamaguchi T, Ishida H, Ishiguro M, Ishihara S, Kanemitsu Y, Kawano H, Kinugasa Y, Kokudo N, Murofushi K, Nakajima T, Oka S, Sakai Y, Tsuji A, Uehara K, Ueno H, Yamazaki K, Yoshida M, Yoshino T, Boku N, Fujimori T, Itabashi M, Koinuma N, Morita T, Nishimura G, Sakata Y, Shimada Y, Takahashi K, Tanaka S, Tsuruta O, Yamaguchi T, Yamaguchi N, Tanaka T, Kotake K, Sugihara K; Japanese Society for Cancer of the Colon and Rectum. Japanese Society for Cancer of the Colon and Rectum (JSCCR) guidelines 2016 for the treatment of colorectal cancer. *Int J Clin Oncol* 2018; **23**: 1-34 [PMID: 28349281 DOI: 10.1007/s10147-017-1101-6.]

57 **Sabbagh C**, Mauvais F, Cosse C, Rebibo L, Joly JP, Dromer D, Aubert C, Carton S, Dron B, Dadamessi I, Maes B, Perrier G, Manaouil D, Fontaine JF, Gozy M, Panis X, Foncelle PH, de Fresnoy H, Leroux F, Vaneslander P, Ghighi C, Regimbeau JM; APCD-LNR-2011 study group. A lymph node ratio of 10% is predictive of survival in stage III colon cancer: a French regional study. *Int Surg* 2014; **99**: 344-353 [PMID: 25058763 DOI: 10.9738/INTSURG-D-13-00052.1]

58 **Huang YQ**, Liang CH, He L, Tian J, Liang CS, Chen X, Ma ZL, Liu ZY. Development and Validation of a Radiomics Nomogram for Preoperative Prediction of Lymph Node Metastasis in Colorectal Cancer. *J Clin Oncol* 2016; **34**: 2157-2164 [PMID: 27138577 DOI: 10.1200/JCO.2015.65.9128]

59 **Dighe S**, Purkayastha S, Swift I, Tekkis PP, Darzi A, A'Hern R, Brown G. Diagnostic precision of CT in local staging of colon cancers: a meta-analysis. *Clin Radiol* 2010; **65**: 708-719 [PMID: 20696298 DOI: 10.1016/j.crad.2010.01.024]

60 **Benson AB**, Venook AP, Al-Hawary MM, Arain MA, Chen YJ, Ciombor KK, Cohen S, Cooper HS, Deming D, Garrido-Laguna I, Grem JL, Gunn A, Hoffe S, Hubbard J, Hunt S, Kirilcuk N, Krishnamurthi S, Messersmith WA, Meyerhardt J, Miller ED, Mulcahy MF, Nurkin S, Overman MJ, Parikh A, Patel H, Pedersen K, Saltz L, Schneider C, Shibata D, Skibber JM, Sofocleous CT, Stoffel EM, Stotsky-Himelfarb E, Willett CG, Johnson-Chilla A, Gurski LA. NCCN Guidelines Insights: Rectal Cancer, Version 6.2020. *J Natl Compr Canc Netw* 2020; **18**: 806-815 [PMID: 32634771 DOI: 10.6004/jnccn.2020.0032]

61 **Nicholls RJ**, Zinicola R, Haboubi N. Extramural spread of rectal cancer and the AJCC Cancer Staging Manual 8th edition, 2017. *Ann Oncol* 2019; **30**: 1394-1395 [PMID: 31046085 DOI: 10.1093/annonc/mdz147]

62 **Glynne-Jones R**, Wyrwicz L, Tiret E, Brown G, Rödel C, Cervantes A, Arnold D; ESMO Guidelines Committee. Rectal cancer: ESMO Clinical Practice Guidelines for diagnosis, treatment and follow-up. *Ann Oncol* 2017; **28**: iv22-iv40 [PMID: 28881920 DOI: 10.1093/annonc/mdx224]

63 **Langs G**, Röhrich S, Hofmanninger J, Prayer F, Pan J, Herold C, Prosch H. Machine learning: from radiomics to discovery and routine. *Radiologe* 2018; **58**: 1-6 [PMID: 29922965 DOI: 10.1007/s00117-018-0407-3]

64 **Liu Z**, Wang S, Dong D, Wei J, Fang C, Zhou X, Sun K, Li L, Li B, Wang M, Tian J. The Applications of Radiomics in Precision Diagnosis and Treatment of Oncology: Opportunities and Challenges. *Theranostics* 2019; **9**: 1303-1322 [PMID: 30867832 DOI: 10.7150/thno.30309]

65 **Pinto Dos Santos D**, Dietzel M, Baessler B. A decade of radiomics research: are images really data or just patterns in the noise? *Eur Radiol* 2021; **31**: 1-4 [PMID: 32767103 DOI: 10.1007/s00330-020-07108-w]

66 **Kirienko M**, Ninatti G, Cozzi L, Voulaz E, Gennaro N, Barajon I, Ricci F, Carlo-Stella C, Zucali P, Sollini M, Balzarini L, Chiti A. Computed tomography (CT)-derived radiomic features differentiate prevascular mediastinum masses as thymic neoplasms *vs* lymphomas. *Radiol Med* 2020; **125**: 951-960 [PMID: 32306201 DOI: 10.1007/s11547-020-01188-w]

67 **Karmazanovsky G**, Gruzdev I, Tikhonova V, Kondratyev E, Revishvili A. Computed tomography-based radiomics approach in pancreatic tumors characterization. *Radiol Med* 2021 [PMID: 34386897 DOI: 10.1007/s11547-021-01405-0]

68 **Calabrese A**, Santucci D, Landi R, Beomonte Zobel B, Faiella E, de Felice C. Radiomics MRI for lymph node status prediction in breast cancer patients: the state of art. *J Cancer Res Clin Oncol* 2021; **147**: 1587-1597 [PMID: 33758997 DOI: 10.1007/s00432-021-03606-6]

69 **Benedetti G**, Mori M, Panzeri MM, Barbera M, Palumbo D, Sini C, Muffatti F, Andreasi V, Steidler S, Doglioni C, Partelli S, Manzoni M, Falconi M, Fiorino C, De Cobelli F. CT-derived radiomic features to discriminate histologic characteristics of pancreatic neuroendocrine tumors. *Radiol Med* 2021; **126**: 745-760 [PMID: 33523367 DOI: 10.1007/s11547-021-01333-z]

70 **Qin H**, Que Q, Lin P, Li X, Wang XR, He Y, Chen JQ, Yang H. Magnetic resonance imaging (MRI) radiomics of papillary thyroid cancer (PTC): a comparison of predictive performance of multiple classifiers modeling to identify cervical lymph node metastases before surgery. *Radiol Med* 2021; **126**: 1312-1327 [PMID: 34236572 DOI: 10.1007/s11547-021-01393-1]

71 **Liu X**, Yang Q, Zhang C, Sun J, He K, Xie Y, Zhang Y, Fu Y, Zhang H. Multiregional-Based Magnetic Resonance

Imaging Radiomics Combined With Clinical Data Improves Efficacy in Predicting Lymph Node Metastasis of Rectal Cancer. *Front Oncol* 2020; **10**: 585767 [PMID: 33680919 DOI: 10.3389/fonc.2020.585767]

72 **Chen P**, Wen D, Huang L, Ding J, Yang W, Sun J, Yang L, Zhou Z. Magnetic Resonance Imaging Radiomics-Based Model to Identify the Pathological Features and Lymph Node Metastasis in Rectal Cancer. May 3, 2022. [cited 1 March 2023]. Available from: https://www.medrxiv.org/content/10.1101/2022.05.02.22274247v1

73 **Liu L**, Liu Y, Xu L, Li Z, Lv H, Dong N, Li W, Yang Z, Wang Z, Jin E. Application of texture analysis based on apparent diffusion coefficient maps in discriminating different stages of rectal cancer. *J Magn Reson Imaging* 2017; **45**: 1798-1808 [PMID: 27654307 DOI: 10.1002/jmri.25460]

74 **Yang L**, Liu D, Fang X, Wang Z, Xing Y, Ma L, Wu B. Rectal cancer: can T2WI histogram of the primary tumor help predict the existence of lymph node metastasis? *Eur Radiol* 2019; **29**: 6469-6476 [PMID: 31278581 DOI: 10.1007/s00330-019-06328-z]

75 **Ma X**, Shen F, Jia Y, Xia Y, Li Q, Lu J. MRI-based radiomics of rectal cancer: preoperative assessment of the pathological features. *BMC Med Imaging* 2019; **19**: 86 [PMID: 31747902 DOI: 10.1186/s12880-019-0392-7]

76 **Zhu H**, Zhang X, Li X, Shi Y, Zhu H, Sun Y. Prediction of pathological nodal stage of locally advanced rectal cancer by collective features of multiple lymph nodes in magnetic resonance images before and after neoadjuvant chemoradiotherapy. *Chin J Cancer Res* 2019; **31**: 984-992 [PMID: 31949400 DOI: 10.21147/j.issn.1000-9604.2019.06.14]

77 **Zhou X**, Yi Y, Liu Z, Zhou Z, Lai B, Sun K, Li L, Huang L, Feng Y, Cao W, Tian J. Radiomics-Based Preoperative Prediction of Lymph Node Status Following Neoadjuvant Therapy in Locally Advanced Rectal Cancer. *Front Oncol* 2020; **10**: 604 [PMID: 32477930 DOI: 10.3389/fonc.2020.00604]

78 **Vernuccio F**, Cannella R, Comelli A, Salvaggio G, Lagalla R, Midiri M. [Radiomics and artificial intelligence: new frontiers in medicine]. *Recenti Prog Med* 2020; **111**: 130-135 [PMID: 32157259 DOI: 10.1701/3315.32853]

79 **Kang J**, Lee JH, Lee HS, Cho ES, Park EJ, Baik SH, Lee KY, Park C, Yeu Y, Clemenceau JR, Park S, Xu H, Hong C, Hwang TH. Radiomics Features of (18)F-Fluorodeoxyglucose Positron-Emission Tomography as a Novel Prognostic Signature in Colorectal Cancer. *Cancers (Basel)* 2021; **13** [PMID: 33494345 DOI: 10.3390/cancers13030392]

80 **Lovinfosse P**, Polus M, Van Daele D, Martinive P, Daenen F, Hatt M, Visvikis D, Koopmansch B, Lambert F, Coimbra C, Seidel L, Albert A, Delvenne P, Hustinx R. FDG PET/CT radiomics for predicting the outcome of locally advanced rectal cancer. *Eur J Nucl Med Mol Imaging* 2018; **45**: 365-375 [PMID: 29046927 DOI: 10.1007/s00259-017-3855-5]

81 **Hotta M**, Minamimoto R, Gohda Y, Miwa K, Otani K, Kiyomatsu T, Yano H. Prognostic value of (18)F-FDG PET/CT with texture analysis in patients with rectal cancer treated by surgery. *Ann Nucl Med* 2021; **35**: 843-852 [PMID: 33948903 DOI: 10.1007/s12149-021-01622-7]

82 **Lv L**, Xin B, Hao Y, Yang Z, Xu J, Wang L, Wang X, Song S, Guo X. Radiomic analysis for predicting prognosis of colorectal cancer from preoperative (18)F-FDG PET/CT. *J Transl Med* 2022; **20**: 66 [PMID: 35109864 DOI: 10.1186/s12967-022-03262-5]

83 **Bundschuh RA**, Dinges J, Neumann L, Seyfried M, Zsótér N, Papp L, Rosenberg R, Becker K, Astner ST, Henninger M, Herrmann K, Ziegler SI, Schwaiger M, Essler M. Textural Parameters of Tumor Heterogeneity in ^{1}F-FDG PET/CT for Therapy Response Assessment and Prognosis in Patients with Locally Advanced Rectal Cancer. *J Nucl Med* 2014; **55**: 891-897 [PMID: 24752672 DOI: 10.2967/jnumed.113.127340]

84 **Bang JI**, Ha S, Kang SB, Lee KW, Lee HS, Kim JS, Oh HK, Lee HY, Kim SE. Prediction of neoadjuvant radiation chemotherapy response and survival using pretreatment [(18)F]FDG PET/CT scans in locally advanced rectal cancer. *Eur J Nucl Med Mol Imaging* 2016; **43**: 422-431 [PMID: 26338180 DOI: 10.1007/s00259-015-3180-9]

85 **Giannini V**, Mazzetti S, Bertotto I, Chiarenza C, Cauda S, Delmastro E, Bracco C, Di Dia A, Leone F, Medico E, Pisacane A, Ribero D, Stasi M, Regge D. Predicting locally advanced rectal cancer response to neoadjuvant therapy with (18)F-FDG PET and MRI radiomics features. *Eur J Nucl Med Mol Imaging* 2019; **46**: 878-888 [PMID: 30637502 DOI: 10.1007/s00259-018-4250-6]

86 **Schurink NW**, van Kranen SR, Berbee M, van Elmpt W, Bakers FCH, Roberti S, van Griethuysen JJM, Min LA, Lahaye MJ, Maas M, Beets GL, Beets-Tan RGH, Lambregts DMJ. Studying local tumour heterogeneity on MRI and FDG-PET/CT to predict response to neoadjuvant chemoradiotherapy in rectal cancer. *Eur Radiol* 2021; **31**: 7031-7038 [PMID: 33569624 DOI: 10.1007/s00330-021-07724-0]

87 **Shen WC**, Chen SW, Wu KC, Lee PY, Feng CL, Hsieh TC, Yen KY, Kao CH. Predicting pathological complete response in rectal cancer after chemoradiotherapy with a random forest using (18)F-fluorodeoxyglucose positron emission tomography and computed tomography radiomics. *Ann Transl Med* 2020; **8**: 207 [PMID: 32309354 DOI: 10.21037/atm.2020.01.107]

88 **Karahan Şen NP**, Aksu A, Kaya GÇ. Value of volumetric and textural analysis in predicting the treatment response in patients with locally advanced rectal cancer. *Ann Nucl Med* 2020; **34**: 960-967 [PMID: 32951129 DOI: 10.1007/s12149-020-01527-x]

89 **Yuan Z**, Frazer M, Rishi A, Latifi K, Tomaszewski MR, Moros EG, Feygelman V, Felder S, Sanchez J, Dessureault S, Imanirad I, Kim RD, Harrison LB, Hoffe SE, Zhang GG, Frakes JM. Pretreatment CT and PET radiomics predicting rectal cancer patients in response to neoadjuvant chemoradiotherapy. *Rep Pract Oncol Radiother* 2021; **26**: 29-34 [PMID: 33948299 DOI: 10.5603/RPOR.a2021.0004]

90 **He J**, Wang Q, Zhang Y, Wu H, Zhou Y, Zhao S. Preoperative prediction of regional lymph node metastasis of colorectal cancer based on (18)F-FDG PET/CT and machine learning. *Ann Nucl Med* 2021; **35**: 617-627 [PMID: 33738763 DOI: 10.1007/s12149-021-01605-8]

91 **Ma J**, Guo D, Miao W, Wang Y, Yan L, Wu F, Zhang C, Zhang R, Zuo P, Yang G, Wang Z. The value of (18)F-FDG PET/CT-based radiomics in predicting perineural invasion and outcome in non-metastatic colorectal cancer. *Abdom Radiol (NY)* 2022; **47**: 1244-1254 [PMID: 35218381 DOI: 10.1007/s00261-022-03453-0]

92 **Li J**, Yang Z, Xin B, Hao Y, Wang L, Song S, Xu J, Wang X. Quantitative Prediction of Microsatellite Instability in Colorectal Cancer With Preoperative PET/CT-Based Radiomics. *Front Oncol* 2021; **11**: 702055 [PMID: 34367985 DOI: 10.3389/fonc.2021.702055]

93 **Lovinfosse P**, Koopmansch B, Lambert F, Jodogne S, Kustermans G, Hatt M, Visvikis D, Seidel L, Polus M, Albert A, Delvenne P, Hustinx R. (18)F-FDG PET/CT imaging in rectal cancer: relationship with the RAS mutational status. *Br J Radiol* 2016; **89**: 20160212 [PMID: 27146067 DOI: 10.1259/bjr.20160212]

94 **Chen SW**, Shen WC, Chen WT, Hsieh TC, Yen KY, Chang JG, Kao CH. Metabolic Imaging Phenotype Using Radiomics of [(18)F]FDG PET/CT Associated with Genetic Alterations of Colorectal Cancer. *Mol Imaging Biol* 2019; **21**: 183-190 [PMID: 29948642 DOI: 10.1007/s11307-018-1225-8]

95 **Staal FCR**, van der Reijd DJ, Taghavi M, Lambregts DMJ, Beets-Tan RGH, Maas M. Radiomics for the Prediction of Treatment Outcome and Survival in Patients With Colorectal Cancer: A Systematic Review. *Clin Colorectal Cancer* 2021; **20**: 52-71 [PMID: 33349519 DOI: 10.1016/j.clcc.2020.11.001]

96 **Engstrand J**, Nilsson H, Strömberg C, Jonas E, Freedman J. Colorectal cancer liver metastases - a population-based study on incidence, management and survival. *BMC Cancer* 2018; **18**: 78 [PMID: 29334918 DOI: 10.1186/s12885-017-3925-x]

97 **Hackl C**, Neumann P, Gerken M, Loss M, Klinkhammer-Schalke M, Schlitt HJ. Treatment of colorectal liver metastases in Germany: a ten-year population-based analysis of 5772 cases of primary colorectal adenocarcinoma. *BMC Cancer* 2014; **14**: 810 [PMID: 25369977 DOI: 10.1186/1471-2407-14-810]

98 **Manfredi S**, Lepage C, Hatem C, Coatmeur O, Faivre J, Bouvier AM. Epidemiology and management of liver metastases from colorectal cancer. *Ann Surg* 2006; **244**: 254-259 [PMID: 16858188 DOI: 10.1097/01.sla.0000217629.94941.cf]

99 **Scheele J**, Stangl R, Altendorf-Hofmann A. Hepatic metastases from colorectal carcinoma: impact of surgical resection on the natural history. *Br J Surg* 1990; **77**: 1241-1246 [PMID: 2253003 DOI: 10.1002/bjs.1800771115]

100 **Vernuccio F**, Dioguardi Burgio M, Barbiera F, Cusmà S, Badalamenti G, Midiri M, Vilgrain V, Brancatelli G. CT and MR imaging of chemotherapy-induced hepatopathy. *Abdom Radiol (NY)* 2019; **44**: 3312-3324 [PMID: 31435760 DOI: 10.1007/s00261-019-02193-y]

101 **Schulz A**, Viktil E, Godt JC, Johansen CK, Dormagen JB, Holtedahl JE, Labori KJ, Bach-Gansmo T, Kløw NE. Diagnostic performance of CT, MRI and PET/CT in patients with suspected colorectal liver metastases: the superiority of MRI. *Acta Radiol* 2016; **57**: 1040-1048 [PMID: 26622057 DOI: 10.1177/0284185115617349]

102 **Sivesgaard K**, Larsen LP, Sørensen M, Kramer S, Schlander S, Amanavicius N, Bharadwaz A, Tønner Nielsen D, Viborg Mortensen F, Morre Pedersen E. Diagnostic accuracy of CE-CT, MRI and FDG PET/CT for detecting colorectal cancer liver metastases in patients considered eligible for hepatic resection and/or local ablation. *Eur Radiol* 2018; **28**: 4735-4747 [PMID: 29736846 DOI: 10.1007/s00330-018-5469-0]

103 **Vernuccio F**, Cannella R, Bartolotta TV, Galia M, Tang A, Brancatelli G. Advances in liver US, CT, and MRI: moving toward the future. *Eur Radiol Exp* 2021; **5**: 52 [PMID: 34873633 DOI: 10.1186/s41747-021-00250-0]

104 **Canellas R**, Rosenkrantz AB, Taouli B, Sala E, Saini S, Pedrosa I, Wang ZJ, Sahani DV. Abbreviated MRI Protocols for the Abdomen. *Radiographics* 2019; **39**: 744-758 [PMID: 30901285 DOI: 10.1148/rg.2019180123]

105 **Devoto L**, Ganeshan B, Keller D, Groves A, Endozo R, Arulampalam T, Chand M. Using texture analysis in the development of a potential radiomic signature for early identification of hepatic metastasis in colorectal cancer. *Eur J Radiol Open* 2022; **9**: 100415 [PMID: 35340828 DOI: 10.1016/j.ejro.2022.100415]

106 **Taghavi M**, Trebeschi S, Simões R, Meek DB, Beckers RCJ, Lambregts DMJ, Verhoef C, Houwers JB, van der Heide UA, Beets-Tan RGH, Maas M. Machine learning-based analysis of CT radiomics model for prediction of colorectal metachronous liver metastases. *Abdom Radiol (NY)* 2021; **46**: 249-256 [PMID: 32583138 DOI: 10.1007/s00261-020-02624-1]

107 **Liu M**, Ma X, Shen F, Xia Y, Jia Y, Lu J. MRI-based radiomics nomogram to predict synchronous liver metastasis in primary rectal cancer patients. *Cancer Med* 2020; **9**: 5155-5163 [PMID: 32476295 DOI: 10.1002/cam4.3185]

108 **Rao SX**, Lambregts DM, Schnerr RS, van Ommen W, van Nijnatten TJ, Martens MH, Heijnen LA, Backes WH, Verhoef C, Zeng MS, Beets GL, Beets-Tan RG. Whole-liver CT texture analysis in colorectal cancer: Does the presence of liver metastases affect the texture of the remaining liver? *United European Gastroenterol J* 2014; **2**: 530-538 [PMID: 25452849 DOI: 10.1177/2050640614552463]

109 **Li Y**, Gong J, Shen X, Li M, Zhang H, Feng F, Tong T. Assessment of Primary Colorectal Cancer CT Radiomics to Predict Metachronous Liver Metastasis. *Front Oncol* 2022; **12**: 861892 [PMID: 35296011 DOI: 10.3389/fonc.2022.861892]

110 **Davey MS**, Davey MG, Ryan ÉJ, Hogan AM, Kerin MJ, Joyce M. The use of radiomic analysis of magnetic resonance imaging in predicting distant metastases of rectal carcinoma following surgical resection: A systematic review and meta-analysis. *Colorectal Dis* 2021; **23**: 3065-3072 [PMID: 34536962 DOI: 10.1111/codi.15919]

111 **Ng F**, Ganeshan B, Kozarski R, Miles KA, Goh V. Assessment of primary colorectal cancer heterogeneity by using whole-tumor texture analysis: contrast-enhanced CT texture as a biomarker of 5-year survival. *Radiology* 2013; **266**: 177-184 [PMID: 23151829 DOI: 10.1148/radiol.12120254]

112 **Mühlberg A**, Holch JW, Heinemann V, Huber T, Moltz J, Maurus S, Jäger N, Liu L, Froelich MF, Katzmann A, Gresser E, Taubmann O, Sühling M, Nörenberg D. The relevance of CT-based geometric and radiomics analysis of whole liver tumor burden to predict survival of patients with metastatic colorectal cancer. *Eur Radiol* 2021; **31**: 834-846 [PMID: 32851450 DOI: 10.1007/s00330-020-07192-y]

113 **Starmans MPA**, Buisman FE, Renckens M, Willemssen FEJA, van der Voort SR, Groot Koerkamp B, Grünhagen DJ, Niessen WJ, Vermeulen PB, Verhoef C, Visser JJ, Klein S. Distinguishing pure histopathological growth patterns of colorectal liver metastases on CT using deep learning and radiomics: a pilot study. *Clin Exp Metastasis* 2021; **38**: 483-494 [PMID: 34533669 DOI: 10.1007/s10585-021-10119-6]

114 **Galjart B**, Nierop PMH, van der Stok EP, van den Braak RRJC, Höppener DJ, Daelemans S, Dirix LY, Verhoef C, Vermeulen PB, Grünhagen DJ. Angiogenic desmoplastic histopathological growth pattern as a prognostic marker of good outcome in patients with colorectal liver metastases. *Angiogenesis* 2019; **22**: 355-368 [PMID: 30637550 DOI: 10.1007/s10456-019-09661-5]

115 **Granata V**, Fusco R, De Muzio F, Cutolo C, Setola SV, Dell' Aversana F, Ottaiano A, Avallone A, Nasti G, Grassi F, Pilone V, Miele V, Brunese L, Izzo F, Petrillo A. Contrast MR-Based Radiomics and Machine Learning Analysis to Assess Clinical Outcomes following Liver Resection in Colorectal Liver Metastases: A Preliminary Study. *Cancers*

(Basel) 2022; **14** [PMID: 35267418 DOI: 10.3390/cancers14051110]

116 **Ravanelli M**, Agazzi GM, Tononcelli E, Roca E, Cabassa P, Baiocchi G, Berruti A, Maroldi R, Farina D. Texture features of colorectal liver metastases on pretreatment contrast-enhanced CT may predict response and prognosis in patients treated with bevacizumab-containing chemotherapy: a pilot study including comparison with standard chemotherapy. *Radiol Med* 2019; **124**: 877-886 [PMID: 31172448 DOI: 10.1007/s11547-019-01046-4]

117 **Andersen IR**, Thorup K, Andersen MB, Olesen R, Mortensen FV, Nielsen DT, Rasmussen F. Texture in the monitoring of regorafenib therapy in patients with colorectal liver metastases. *Acta Radiol* 2019; **60**: 1084-1093 [PMID: 30612433 DOI: 10.1177/0284185118817940]

118 **Fiz F**, Viganò L, Gennaro N, Costa G, La Bella L, Boichuk A, Cavinato L, Sollini M, Politi LS, Chiti A, Torzilli G. Radiomics of Liver Metastases: A Systematic Review. *Cancers (Basel)* 2020; **12** [PMID: 33036490 DOI: 10.3390/cancers12102881]

119 **Jalil O**, Afaq A, Ganeshan B, Patel UB, Boone D, Endozo R, Groves A, Sizer B, Arulampalam T. Magnetic resonance based texture parameters as potential imaging biomarkers for predicting long-term survival in locally advanced rectal cancer treated by chemoradiotherapy. *Colorectal Dis* 2017; **19**: 349-362 [PMID: 27538267 DOI: 10.1111/codi.13496]

120 **Albano D**, Benenati M, Bruno A, Bruno F, Calandri M, Caruso D, Cozzi D, De Robertis R, Gentili F, Grazzini I, Micci G, Palmisano A, Pessina C, Scalise P, Vernuccio F, Barile A, Miele V, Grassi R, Messina C; Young SIRM Working Group. Imaging side effects and complications of chemotherapy and radiation therapy: a pictorial review from head to toe. *Insights Imaging* 2021; **12**: 76 [PMID: 34114094 DOI: 10.1186/s13244-021-01017-2]

121 **Wesdorp NJ**, van Goor VJ, Kemna R, Jansma EP, van Waesberghe JHTM, Swijnenburg RJ, Punt CJA, Huiskens J, Kazemier G. Advanced image analytics predicting clinical outcomes in patients with colorectal liver metastases: A systematic review of the literature. *Surg Oncol* 2021; **38**: 101578 [PMID: 33866191 DOI: 10.1016/j.suronc.2021.101578]

122 **Ahn SJ**, Kim JH, Park SJ, Han JK. Prediction of the therapeutic response after FOLFOX and FOLFIRI treatment for patients with liver metastasis from colorectal cancer using computerized CT texture analysis. *Eur J Radiol* 2016; **85**: 1867-1874 [PMID: 27666629 DOI: 10.1016/j.ejrad.2016.08.014]

123 **Babcock BD**, Aljehani MA, Jabo B, Choi AH, Morgan JW, Selleck MJ, Luca F, Raskin E, Reeves ME, Garberoglio CA, Lum SS, Senthil M. High-Risk Stage II Colon Cancer: Not All Risks Are Created Equal. *Ann Surg Oncol* 2018; **25**: 1980-1985 [PMID: 29675762 DOI: 10.1245/s10434-018-6484-8]

124 **Golia Pernicka JS**, Gagniere J, Chakraborty J, Yamashita R, Nardo L, Creasy JM, Petkovska I, Do RRK, Bates DDB, Paroder V, Gonen M, Weiser MR, Simpson AL, Gollub MJ. Radiomics-based prediction of microsatellite instability in colorectal cancer at initial computed tomography evaluation. *Abdom Radiol (NY)* 2019; **44**: 3755-3763 [PMID: 31250180 DOI: 10.1007/s00261-019-02117-w]

125 **Huang X**, Cheng Z, Huang Y, Liang C, He L, Ma Z, Chen X, Wu X, Li Y, Liu Z. CT-based Radiomics Signature to Discriminate High-grade From Low-grade Colorectal Adenocarcinoma. *Acad Radiol* 2018; **25**: 1285-1297 [PMID: 29503175 DOI: 10.1016/j.acra.2018.01.020]

126 **Altini C**, Maggialetti N, Branca A, Pisani AR, Rubini D, Sardaro A, Stabile Ianora AA, Rubini G. 18F-FDG PET/CT in peritoneal tumors: a pictorial review. *Clin Transl Imaging* 2023; **11**: 141-155

127 **Eresen A**, Li Y, Yang J, Shangguan J, Velichko Y, Yaghmai V, Benson AB 3rd, Zhang Z. Preoperative assessment of lymph node metastasis in Colon Cancer patients using machine learning: a pilot study. *Cancer Imaging* 2020; **20**: 30 [PMID: 32334635 DOI: 10.1186/s40644-020-00308-z]

128 **Caruso D**, Zerunian M, Ciolina M, de Santis D, Rengo M, Soomro MH, Giunta G, Conforto S, Schmid M, Neri E, Laghi A. Haralick's texture features for the prediction of response to therapy in colorectal cancer: a preliminary study. *Radiol Med* 2018; **123**: 161-167 [PMID: 29119525 DOI: 10.1007/s11547-017-0833-8]

129 **Coppola F**, Giannini V, Gabelloni M, Panic J, Defeudis A, Lo Monaco S, Cattabriga A, Cocozza MA, Pastore LV, Polici M, Caruso D, Laghi A, Regge D, Neri E, Golfieri R, Faggioni L. Radiomics and Magnetic Resonance Imaging of Rectal Cancer: From Engineering to Clinical Practice. *Diagnostics (Basel)* 2021; **11** [PMID: 33922483 DOI: 10.3390/diagnostics11050756]

130 **Alvarez-Jimenez C**, Antunes JT, Talasila N, Bera K, Brady JT, Gollamudi J, Marderstein E, Kalady MF, Purysko A, Willis JE, Stein S, Friedman K, Paspulati R, Delaney CP, Romero E, Madabhushi A, Viswanath SE. Radiomic Texture and Shape Descriptors of the Rectal Environment on Post-Chemoradiation T2-Weighted MRI are Associated with Pathologic Tumor Stage Regression in Rectal Cancers: A Retrospective, Multi-Institution Study. *Cancers (Basel)* 2020; **12** [PMID: 32722082 DOI: 10.3390/cancers12082027]

131 **Bordron A**, Rio E, Badic B, Miranda O, Pradier O, Hatt M, Visvikis D, Lucia F, Schick U, Bourbonne V. External Validation of a Radiomics Model for the Prediction of Complete Response to Neoadjuvant Chemoradiotherapy in Rectal Cancer. *Cancers (Basel)* 2022; **14** [PMID: 35205826 DOI: 10.3390/cancers14041079]

World Journal of Gastroenterology

Submit a Manuscript: https://www.f6publishing.com

World J Gastroenterol 2023 May 21; 29(19): 2905-2915

DOI: 10.3748/wjg.v29.i19.2905

ISSN 1007-9327 (print) ISSN 2219-2840 (online)

MINIREVIEWS

Branched chain amino acids in hepatic encephalopathy and sarcopenia in liver cirrhosis: Evidence and uncertainties

Giuseppe Marrone, Amato Serra, Luca Miele, Marco Biolato, Antonio Liguori, Antonio Grieco, Antonio Gasbarrini

Specialty type: Gastroenterology and hepatology

Provenance and peer review: Invited article; Externally peer reviewed.

Peer-review model: Single blind

Peer-review report's scientific quality classification

Grade A (Excellent): 0
Grade B (Very good): B, B
Grade C (Good): C
Grade D (Fair): 0
Grade E (Poor): 0

P-Reviewer: Fernandes SA, Brazil; Hong Xiang FK, Singapore; Long X, China

Received: December 28, 2022
Peer-review started: December 28, 2022
First decision: January 10, 2023
Revised: January 24, 2023
Accepted: April 20, 2023
Article in press: April 20, 2023
Published online: May 21, 2023

Giuseppe Marrone, Amato Serra, Luca Miele, Marco Biolato, Antonio Liguori, Antonio Grieco, Antonio Gasbarrini, Medical and Surgical Sciences, Fondazione Policlinico Universitario A. Gemelli-IRCCS, Università Cattolica del Sacro Cuore, Rome 00168, Italy

Corresponding author: Giuseppe Marrone, MD, PhD, Consultant Physician-Scientist, Medical and Surgical Sciences, Fondazione Policlinico Universitario A. Gemelli-IRCCS, Largo Agostino Gemelli 8, Rome 00168, Italy. giuseppe.marrone@policlinicogemelli.it

Abstract

Liver cirrhosis is commonly associated with nutritional alterations, reported in 20% of patients with compensated disease and over 60% of patients with decompensated cirrhosis. Nutritional disturbances are associated with a worse prognosis and increased risk of complication. Serum levels of branched-chain amino acids (BCAAs) are decreased in patients with liver cirrhosis. The imbalance of amino acids levels has been suggested to be associated with the development of complications, such as hepatic encephalopathy and sarcopenia, and to affect the clinical presentation and prognosis of these patients. Several studies investigated the efficacy of BCAAs supplementation as a therapeutic option in liver cirrhosis, but uncertainties remain about the real efficacy, the best route of administration, and dosage.

Key Words: Branched-chain amino acids; Hepatic encephalopathy; Sarcopenia; Liver cirrhosis

©The Author(s) 2023. Published by Baishideng Publishing Group Inc. All rights reserved.

Core Tip: Nutritional perturbance is frequent in liver cirrhosis and has been correlated with the development of complications such as hepatic encephalopathy and sarcopenia. Branched-chain amino acids (BCAAs) have been implicated in the pathophysiology of these two complications and supplementation has been proposed as a therapeutic measure. In this review, we will examine the scientific evidence supporting the clinical use of BCAAs in cirrhotic subjects.

Citation: Marrone G, Serra A, Miele L, Biolato M, Liguori A, Grieco A, Gasbarrini A. Branched chain amino acids in hepatic encephalopathy and sarcopenia in liver cirrhosis: Evidence and uncertainties. *World J Gastroenterol* 2023; 29(19): 2905-2915
URL: https://www.wjgnet.com/1007-9327/full/v29/i19/2905.htm
DOI: https://dx.doi.org/10.3748/wjg.v29.i19.2905

INTRODUCTION

Liver cirrhosis is commonly associated with nutritional alterations, being reported in 20% of patients with compensated disease and over 60% of patients with decompensated cirrhosis[1]. In cirrhotic subjects, nutritional disturbances are associated with a worse prognosis and increased risk of complications such as hepatic encephalopathy (HE) and sarcopenia. On the other hand, serum levels of branched-chain amino acids (BCAAs) are decreased in patients with liver cirrhosis, and this has been associated with the development of complications[2]. Several studies investigated the efficacy of BCAAs supplementation in liver cirrhosis for the treatment and prevention of both HE and sarcopenia. The aim of this review is to analyze scientific evidence supporting the administration of BCAAs in patients with liver cirrhosis affected by HE and sarcopenia (Table 1).

HE

HE is one of the main complications of advanced cirrhosis. It consists of a wide spectrum of non-specific neurological or psychiatric abnormalities, ranging from subclinical alterations to coma, caused by liver failure and/or porto-systemic shunting. According to the West Haven classification HE is classified, as covert HE (CHE), including minimal HE (MHE) and grade 1 HE, and overt HE (OHE), including grade 2, grade 3, and grade 4 HE of the West Haven classification[3]. The prevalence of OHE in liver cirrhosis is 30%-40% at any time during the clinical course of the disease[4] while MHE or CHE occurs in 20%-80% of patients with cirrhosis[5]. HE is associated with a poor prognosis, and high socioeconomic costs and also carries a psychological burden on patients and families[6]. According to the American Association for the Study of Liver Diseases and the European Association for the Study of the Liver (EASL) Clinical Practice Guidelines, episodes of OHE should be actively treated[3]. The therapeutic approach encompasses the active treatment of precipitant factors (*e.g.*, infections, variceal bleeding), administration of non-absorbable disaccharides, such as lactulose, and non-absorbable antibiotics, such as rifaximin[7]. Secondary prophylaxis with oral rifaximin is recommended after an episode of OHE. In case of recurrent and intractable OHE associated with advanced liver disease, the patients should be evaluated for liver transplantation[3]. Other treatments such as metronidazole, neomycin, or intravenous administration of L-ornithine L-aspartate, have been proposed for the treatment of HE, but the evidence supporting their use is still limited or under debate[8]. According to EASL guidelines, despite their limited efficacy, the use of these medications is advocated as an additional treatment for patients -non-responsive to conventional therapies[3].

BCAAS AND HE

In recent years, growing interest in the role of BCAAs in liver cirrhosis has been observed in the scientific literature. A common feature in patients with liver cirrhosis is decreased BCAA plasmatic levels associated with the increase of aromatic amino acids (AAA), namely tyrosine and phenylalanine, thus leading to a low BCAA/AAA ratio, the so-called "Fisher ratio"[9]. This ratio is negatively correlated with the Child-Turcotte-Pugh score (CTP) and the severity of liver disease[10]. A low Fisher ratio is also associated with the development of HE and an excellent correlation has been found between this ratio and the grade of HE[11]. The role of BCAAs in the development of HE was first advocated in the "false neurotransmitters" hypothesis in the 80s[12]. Both AAA and BCAAs compete for the same transporter across blood-brain barrier. According to this hypothesis, the increased concentration of AAA in liver cirrhosis leads to an increased availability of aromatic neurotransmitters precursors, which cause a "false" dopaminergic transmission and inhibition of dopamine synthesis, resulting in neurodepression[13]. Other studies focused on the key role of increased ammonia levels in the development of HE, underling its neurotoxic role[14]. Despite this evidence, mechanisms involved in the pathogenesis of HE remain poorly understood.

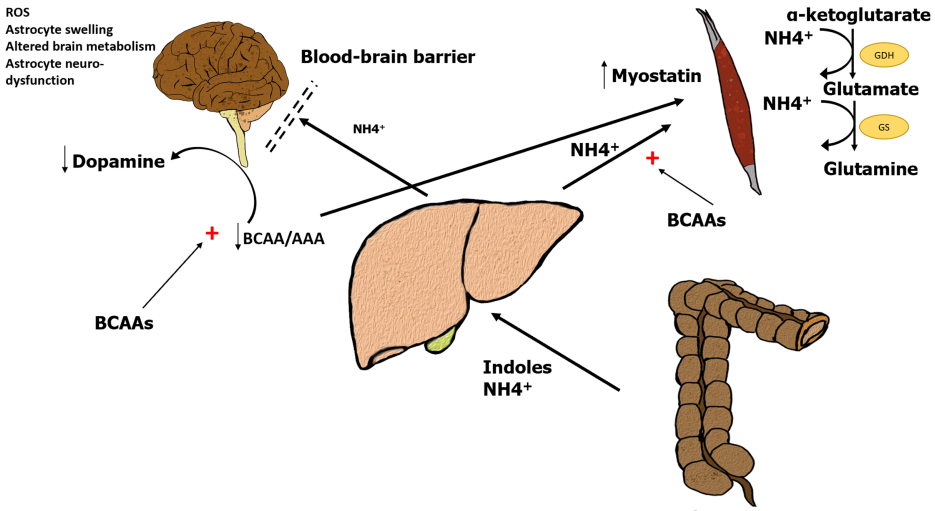
The increase in blood ammonia is a consequence of impaired liver function and portosystemic shunts. Skeletal muscle is a key site of extrahepatic ammonia detoxification by the absorption of plasma ammonia and the conversion of α-ketoglutarate to glutamate, and then of glutamate to glutamine through glutamate dehydrogenase and glutamine synthetase enzymes, which remove two moles of

Table 1 Selected published studies on beneficial effects of branched chain amino acids in liver cirrhosis

Ref.	Study design	Participants	Intervention	Route	Treatment duration	Associated treatments	Outcomes	Results
Horst *et al* [16], 1984	Multicentric RCT	37 cirrhotic patients with OHE	BCAAs (20 g/d increased to 80 g/d) *vs* isonitrogenous diet (placebo)	Oral	4 wk	No	Mortality and hepatic encephalopathy assessed after 4 wk	HE recurrence (decreased). No differences in nitrogen balance
Muto *et al* [17], 2005	Multicentric RCT	646 patients with decompensated cirrhosis	BCAAs (12 g/d) *vs* standard diet (1.0-1.4 protein kg/d	Oral	2 yr	No	Mortality, development of liver cancer, rupture of esophageal varices, or progress of hepatic failure (event-free survival)	EFS (increased), health-related quality of life, mortality (decreased). No differences in improvement of HE
Les *et al*[18], 2011	Double-blind multicentric RCT	40 cirrhotic patients with previous episodes of minimal hepatic encephalopathy	BCAAs (30 g/d) *vs* isocaloric placebo (maltodextrin)	Oral	56 wk	No	Mortality and hepatic encephalopathy assessed after 56 wk	Improvement in MHE symptoms and muscle mass. No reduction of HE recurrence
Gluud *et al* [19], 2017	Meta-analysis of RCT	11 RCT; 14 RCT	BCAAs *vs* diets, antibiotics (neomycin) and non-absorbable disaccharides	Oral and IV	Variable	No	Effect on HE manifestations and prevention of HE episodes	Oral BCAAs improve HE manifestations and prevention of HE episodes. No effects for IV BCAA
Gluud *et al* [20], 2013	Systematic review with meta-analysis	8 RCT: 382 cirrhotic patients with recurrent MHE or OHE	BCAAs (0.25 g/kg body weight/day) *vs* no intervention/placebo/control supplements	Oral	Variable	No	Effect on HE manifestations, mortality, nutritionalstatus, and adverse events in patients with recurrent HE	Improvement in the recurrent HE manifestation (more evident in OHE than MHE). No differences in survival
Gluud *et al* [19], 2017	Cochrane systematic review	16 RCT: 827 cirrhotic patients with OHE or MHE	BCAAs *vs* placebo/no intervention/other (diet, lactulose, neomycicn)	Oral and IV	Variable	No	Beneficial or harmful effects of BCAA versus any control intervention in HE	Oral BCAAs improve HE manifestation (no effect *vs* lactulose or neomycicn). No effect on mortality
Park *et al* [21], 2017	Multicentric retrospective cohort study	307 cirrhotic patients with CTP 8-10	BCAAs (4.15 g/d or 8.3 g/d or 12.45 g/d) *vs* normal diet	Oral	24 wk	No	Changes in MELD score, CP score, incidence of cirrhosis-related complications and event-free survival over 2 yr	Improvement in MELD score, serum bilirubin and CTP score in 12.45/d BCAAs. No differences in HE manifestation
Tajiri *et al* [23], 2018	Retrospective observational study	53 cirrhotic patients with OHE	IV BCAAs and conventional therapies *vs* IV BCAAs and conventional therapies + IV L-carnitine	IV	Median 5 d (range 2-20 d)	L-carnitine conventional therapies (non-absorbable disaccharides and non-absorbable antibiotics)	Effect on HE manifestation, recurrence-free-survival and overall-survival	L-carnitine + BCAAS improve HE manifestation and reduce HE recurrence

BCAAs: Branched chain amino acids; RCT: Randomized control trial; OHE: Overt hepatic encephalopathy; HE: Hepatic encephalopathy; EFS: Early feeding skill; MELD: Model for end stage liver disease; CP: Child-pugh score; CTP: Child-Turcotte-Pugh score.

ammonia for each α-ketoglutarate molecule. Muscle uptake of plasma BCAAs increases with ammonia concentration in patients with liver cirrhosis, suggesting that BCAAs play an important role in ammonia detoxification in muscle and can contribute to preventing HE[13] (Figure 1).



DOI: 10.3748/wjg.v29.i19.2905 **Copyright** ©The Author(s) 2023.

Figure 1 Gut derived ammonia and other aromatic compounds pass into the systemic circulation due to reduced liver function and the presence of porto-systemic shunts. A low plasma branched chain amino acids (BCAA)/aromatic amino acids (AAA) ratio has been observed in liver cirrhosis. BCAA and AAA compete for the same transporter at blood-brain barrier. The increased availability of AAA causes an increase in aromatic neurotransmitter precursors resulting in a false dopaminergic transmission and a reduction in dopamine synthesis. At brain level, ammonia causes astrocyte metabolism changes including reactive oxygen species increase, altered glucose and protein metabolism and astrocyte swelling, resulting in altered neurotransmission. Muscle is a key site of ammonia detoxification by means of the sequential action of glutamate dehydrogenase and glutamine synthetase. Ammonia increases myostatin expression, thus resulting in reduced protein synthesis and inhibition of myogenesis. The administration of BCAAs can increase muscle ammonia uptake from blood and can interfere with amino acids pass throughout the blood brain barrier with beneficial effects on both hepatic encephalopathy and sarcopenia. BCAAs: Branched chain amino acids; AAA: Aromatic amino acids; NH4+: Ammonia; ROS: Reactive oxygen species; GDH: Glutamate dehydrogenase; GS: Glutamine synthetase.

EVIDENCE SUPPORTING THE THERAPEUTIC USE OF BCAAS IN HEPATIC ENCEPHALOPATHY

A possible therapeutic role of BCAAs supplementation in HE was first evaluated in animal models. In dogs with portocaval shunt, which developed HE, neurological manifestations induced by the simultaneous infusion of 1% tryptophan and 1% phenylalanine were prevented by the concomitant infusion of BCAAs (0.63% leucine + 0.4% isoleucine + 0.46% valine)[15]. Subsequently, several clinical studies evaluated the role of BCAAs in the treatment and prevention of HE in cirrhotic subjects. In the early 80s, a randomized study evaluated the effect of BCAAs in protein-intolerant cirrhotic. Enrolled subjects were fed with increasing amounts of either dietary protein or a BCAAs solution until they attained an intake of 80 g protein per day or until they developed stage 2 encephalopathy. Oral BCAAs supplements induced a positive nitrogen balance as an equivalent amount of dietary protein but decreased the risk of HE recurrence[16]. In 2005, a multicenter randomized controlled trial evaluated oral BCAAs (12 g/d for 2 years) compared with diet therapy with defined daily food intake (1.0-1.4 g protein kg/day) in patients with decompensated cirrhosis. The group who received BCCA showed an improvement in event-free survival and consequently, a reduction in mortality, but no statistically significant differences were found in HE[17]. Another randomized, double-blind, multicenter study evaluated subjects with cirrhosis with a previous episode of HE. The two groups of patients received a standard diet and a supplement of 30 g of BCAAs or maltodextrin over 56 wk. BCAAs supplementation was not associated with a reduction in HE recurrence but an improvement in MHE and muscle mass recovery were found in the BCAA-treated group[18]. A meta-analysis of randomized trials, performed by Gluud *et al*[19], confirmed that oral BCAAs administration has a beneficial effect on the clinical manifestation of HE, but no similar results were found for intravenous administration. Based on this evidence, the authors suggested using nonabsorbable disaccharides as the first-line treatment for HE, with a more beneficial effect through the addition of nonabsorbable antibiotics, while oral BCAAs may be considered as a second-line treatment. Another systematic review with meta-analysis evaluated the effects of oral BCAAs compared with placebo or control supplements in patients with HE. The administration of oral BCAAs was found to be associated with an improvement in HE recurrence {87 of 172 patients in the BCAAs group *vs* 56 of 210 in controls, risk ratio (RR) = 1.71 [95% confidence interval (CI): 1.17-2.51]}. The effect of oral BCAAs was higher in patients with OHE rather than in patients with MHE, but no difference in survival was found. These results strengthen the recommendation of oral BCAAs in patients who developed HE during enteral nutrition and in the case of recurrent HE. Most of the analyzed studies used the same dose of oral BCAAs (0.25 g/kg body weight/die) and no adverse events (including nausea and diarrhea) were reported[20]. A Cochrane systematic review, updated in 2017, evaluated the beneficial and harmful effects of BCAAs *vs* any control intervention for people with HE.

The study analyzed 16 randomized clinical trials, including 827 patients with OHE (12 trials) or MHE (4 trials). Control groups received placebo/no intervention in 2 trials, diets in 10 trials, lactulose in 2 trials, or neomycin in 2 trials. BCAAs were administrated orally in 8 trials and intravenous in 7 trials. No differences in mortality were found between BCAAs groups and control groups (RR = 0.88, 95%CI: 0.69-1.11). Reduced mortality was noted only when excluding trials in which control groups were treated with lactulose or neomycin (RR = 0.76, 95%CI: 0.63-0.92). The analysis also showed that BCAAs supplementation was associated with a beneficial effect on HE compared with controls (RR = 0.73, 95%CI: 0.61-0.88). Subgroup analyses showed that oral BCAAs but not intravenous BCAAs had a beneficial effect on overt encephalopathy. These differences were not found for MHE[21]. This systematic review supported the use of oral BCAAs in clinical practice but did not provide enough evidence to evaluate the benefit of BCAAs compared with other interventions. The most adequate dosage and duration of BCAAs supplementation is also a debated issue, since homeostasis of BCAAs in the body is extremely rapid, and circulating values quickly return to baseline after administration. A multicenter retrospective cohort study evaluated the effects of long-term BCAAs supplementation (at least 6 mo) compared with diet in patients with advanced liver disease (CTP 8-10) compared with no BCAAs enriched diet. Patients in the BCAAs group were divided into 3 subgroups according to the dose administrated: 4.15 g, 8.3 g, or 12.45 g/d. Statistical analysis revealed differences in the model for end-stage liver disease (MELD) score, serum albumin levels, and CTP score between the BCAAs group and control group at the baseline. Patients enrolled in the BCAAs group showed lower albumin levels and higher CTP scores, MELD scores, and HE grades (mostly grades 1-2). This was probably related to the propensity of physicians to prescribe BCAAs to patients with a worsened deterioration of hepatic function. Sub-group analysis showed a significant improvement in MELD score, serum bilirubin levels, and CTP score in patients who received the highest dose of BCAAs (12.45 g daily), whereas no significant differences were found in albumin levels. Conversely, only improvement in the serum bilirubin levels was observed in patients who received the lowest dose of BCAAs (4.15 g). This evidence provides a relationship between BCAAs dosage and its beneficial effect on prognostic scores in liver cirrhosis, suggesting high-dose BCAAs supplementation to achieve benefits. The study did not find significant differences in HE manifestations between the two groups. This was probably related to the shorter duration of BCAAs supplementation than in previous studies (about 30% of patients discontinued BCAAs within one year)[22].

A possible synergic role of L-carnitine and BCAAs on HE has been postulated. L-carnitine is a vitamin-like bio-factor that has been shown to induce ureagenesis, and improve energy metabolism leading to a reduction in blood and ammonia levels, thus protecting human astrocytes from ammonia-induced acute cytotoxicity[23]. A study on cirrhotic patients affected by OHE treated with intravenous BCAAs supplementation and conventional therapy (lactulose and non-absorbable antibiotics, showed that the addition of L-carnitine provided an improvement in blood ammonia concentration and Glasgow Coma Scale) with an improvement in HE recurrence. Despite the preliminary nature of the study, these results suggest a possible synergic role between L-carnitine and BCAAs in HE treatment [24].

SARCOPENIA IN LIVER CIRRHOSIS

Patients with chronic liver disease are at risk of malnutrition and sarcopenia[2]. The first definition of sarcopenia was proposed by Rosenberg[25], deriving from the Greek words "sarx" (muscle) and "penia" (reduction), to point out the decline in muscle mass and strength that occurs with healthy aging. The European Working Group on Sarcopenia in Older People in 2019 defined sarcopenia as a progressive and generalized skeletal muscle disorder that consists of decreased muscle quality or quantity and decreased physical function or muscle strength. Sarcopenia is distinguished as primary, or age-related in the absence of other evident specific cause, and secondary when the causal factor is a systemic, neoplastic, or inflammatory disease (*e.g.*, malignancy, inflammatory disease, or organ failure such as liver cirrhosis[26], affecting about 20%-60% of patients in the latter condition)[27]. In cirrhotic patients, the pathogenetic cascade is multifactorial: Since muscle mass is the result of protein anabolism and catabolism balance, reduced liver function, together with portosystemic shunts, causes decreased protein synthesis and ammonia detoxification, thus promoting sarcopenia and hyperammonemia. Hyperammonemia leads to increased muscle expression of the cytokine myostatin, a negative regulator of muscle growth by inhibition of myogenesis[28] (Figure 1). Other involved factors are BCAAs deficiency, which plays a key role in maintaining muscle mass and strength, and perturbation of sex hormone levels, with reduction of testosterone and concomitant increase in estrogen-to-androgen ratio. Hormonal changes suppress myoblast differentiation in skeletal muscle thus promoting sarcopenia[29]. Recently, changes in the intestinal microbiome (reduction of Methanobrevibacter, Prevotella e Akkermansia) and in the intestine-liver-muscle axis with increased bowel inflammation and bacterial translocation have been described in sarcopenic cirrhotic[30]. The role of gut microbiota is crucial for energy extraction from nutrients, in controlling low-grade systemic inflammation and bacterial infections, and has been involved in the genesis of HE, sarcopenia, and hepatocellular carcinoma (HCC) in liver cirrhosis[30-34].

BCAA IN THE TREATMENT OF SARCOPENIA

Despite growing interest in the clinical role of sarcopenia, few evidence-based therapeutic interventions are available to revert this condition in the context of liver cirrhosis. Current literature changed the old concept of protein restriction in patients with liver cirrhosis and daily recommended protein intake has been changed accordingly[35]. According to the European Society for Clinical Nutrition and Metabolism, high protein intake, variable from 1.2 g/kg/d protein in patients with compensated liver cirrhosis to 1.5 g/kg/d protein in patients with malnutrition and/or sarcopenia, is considered safe, well-tolerated, and recommended in liver cirrhosis. Another suggested dietary intervention is to shorten fasting periods by consuming three to five meals per day and taking a late evening snack. The aim of these suggestions is to reduce protein catabolism during overnight fasting and to reverse anabolic resistance and sarcopenia[1].

A nutritional interventional strategy aimed at increasing protein synthesis and preventing sarcopenia is BCAAs exogenous supplementation. BCAAs play a key role in protein synthesis and glucose metabolism. Leucine is involved in the activation of the intracellular mammalian target of rapamycin (mTOR) complex 1 pathway and inhibition of ubiquitin-proteasome signaling, thus resulting in increased protein synthesis, skeletal muscle hypertrophy, and reduced muscle turnover[36].

In experimental animal models of carbon tetrachloride-induced liver cirrhosis, muscle mass loss was described in association with decreased BCAAs and increased AAA plasma levels, while decreased α-ketoglutarate and ATP concentration in muscles was found[37]. A Japanese study evaluating cirrhotic subjects demonstrated a high prevalence of sarcopenia, low serum levels of BCAAs, and insulin-like growth factor 1. Patients with lower baseline levels of BCAAs had also a higher prevalence of CTP class B and C, lower albumin and zinc blood concentration, and lower body mass index (BMI), associated with risk of malnutrition, disease complication, and poor prognosis[38]. The presence of sarcopenia and low plasma levels of total BCAAs have also been associated with a significant reduction of survival in liver cirrhosis[39].

Several studies were performed to evaluate the effect of BCAAs administration to prevent sarcopenia and its complication in cirrhotic patients. In animal models, the administration of BCAAs reversed the metabolic alterations in skeletal muscles, promoting glucose uptake, which improves ATP production and muscle function[40,41]. In patients affected by alcoholic cirrhosis, skeletal muscle biopsy showed increased myostatin expression, dysfunctional mTOR pathway, and increased autophagic proteolysis when compared to well-matched healthy controls. These pathologic alterations were reversed after the administration of a single oral BCAAs mixture enriched with leucine. A monocentric prospective study on adult cirrhotics showed that oral BCAAs powder administration (13.5 g twice a day) for 24-wk was able to improve muscle strength with limited increase in muscle mass. It suggests that BCAAs supplementation alone could not be enough to achieve effective improvement of sarcopenia in cirrhotic patients and that aerobic and resistance exercise could also be necessary to induce protein synthesis response[42]. A prospective, randomized double-blind clinical trial in patients with liver cirrhosis and sarcopenia assessed by computed tomography (CT) scan, showed that BCAAs supplementation, in addition to a nutritional intervention and physical activity, could improve albumin levels and muscle mass. Administration of BCAAs also increased zinc levels after 12 wk of intervention[43]. Zinc is an essential nutrient for human health and its deficiency is often associated with malnutrition and chronic liver disease[44]. Improvement of hypoalbuminemia after BCAAs supplementation is correlated with improved glucose metabolism and a decrease in skeletal muscle fat infiltration, miming exercise training. In these patients, an improvement in liver-related event-free survival (including refractory pleural effusion, ascites, or both, varices rupture or treatment, and hepatocarcinogenesis) was observed and it might contribute to a better prognosis[45]. Today, in liver cirrhosis, an intervention program including physical exercise is considered useful to decelerate sarcopenia progression, but it can't completely prevent skeletal muscle atrophy[46]. The combination of BCAAs supplementation and walking exercise was found to be more effective than exercise alone in improving muscle mass and function and it should be considered a good therapeutic strategy in patients with overt sarcopenia and a prevention strategy in patients at risk of sarcopenia[47]. In a retrospective cohort study, patients with liver cirrhosis were classified into low, intermediate, and high-risk according to the presence of hypoalbuminemia and/or sarcopenia. The high-risk group, including patients with both sarcopenia ad hypoalbuminemia, had significantly lower overall survival than the low-risk group, including patients without both hypoalbuminemia and sarcopenia, regardless of HCC occurrence. The administration of BCAAs improved overall survival and prognosis in treated patients. The survival benefit of BCAAs supplementation was pronounced in the high and intermediate-risk groups[48]. Lastly, in cirrhotic patients, sarcopenia contributes to hyperammonemia due to the reduced capacity of sarcopenic muscle to detoxify circulating ammonia which increases the risk of HE. On the other hand, hyperammonemia through myostatin upregulation, mitochondrial dysfunction, and cellular stress response, induces further muscle depletion, generating a vicious circle. On these bases, nutritional interventions against sarcopenia, including BCAA supplementation, may have a beneficial effect also on HE[49,50].

β-HYDROXY-β-METHYLBUTYRATE SUPPLEMENTATION

A different strategy to counteract muscle mass loss, acting on BCAAs metabolism, is β-Hydroxy-β-methylbutyrate (HMB) supplementation. HMB is a natural derivative of the BCAA leucine, which has shown a positive effect on muscle mass and strength in malnourished subjects. Recently, the randomized, placebo-controlled, double-blind, parallel design strengthening health in the elderly through nutrition trial showed a significant improvement in weight, BMI, mid-arm circumference, and leg strength in elderly subjects receiving an HMB containing oral nutritional supplement along with dietary counseling over six months. Female treated subjects also showed a significant increase in handgrip strength and the whole population showed an improvement in nutritional parameters (including vitamin D levels, fat, protein, and carbohydrate intakes), but no significant difference was found in overall survival and hospital (re)admission rate[51].

A prospective non-randomized interventional cohort study evaluating the effectiveness of HMB supplements in the prehabilitation program of sarcopenic patients undergoing gastrointestinal surgery (HEROS trial, NCT05344313) is ongoing. The effect of HMB supplementation on muscle health and nutritional status has also been evaluated in liver cirrhosis. HMB supplementation in cirrhotic rats was able to increase plasma levels of BCAAs but showed detrimental effects on muscle and liver protein content and was associated with higher mortality and lower weight gain[52].

Despite some conflicting data in the experimental animal, recently, a small pilot randomized controlled clinical trial conducted in Italy demonstrated a significant improvement in muscle mass and performance in cirrhotic subjects receiving HMB supplements as well as dietary and lifestyle counseling. In the HMB-treated group a statistically significant improvement was found in muscle performance assessed through a six-minute walking test and chair stand test. HMB supplementation was also associated with a significant increase in muscle mass at the quadriceps level and with improvement in frailty (evaluated using liver frailty index[53])[54].

In a similar prospective randomized trial, HMB supplementation was evaluated in addition to standard BCAAs supplementation in two matched groups. Both HMB + BCAAs and BCAAs alone treatment have been associated with a significant longitudinal decrease in MELD score, an increase in BMI and fat mass but without significant changes in fat-free mass and handgrip strength. No significant differences were found between the two treated groups[55].

In both studies in cirrhotic subjects HMB supplements were well tolerated and no significant adverse events were reported. HMB supplementation represents an interesting therapeutic approach in the treatment of cirrhotic subjects with sarcopenia, but it is unclear whether it has additional positive effects compared to BCAAs supplementation. Adequately powered prospective studies are needed to assess efficacy, duration, and dose requirements.

THE ROLE OF ZINC IN HEPATIC ENCEPHALOPATHY AND SARCOPENIA

Another condition that can influence protein metabolism and nutritional status in cirrhosis, acting as a bridge between HE and sarcopenia, is zinc deficiency. Zinc is a trace element that is essential for the structure and function of various human proteins and enzymes[56]. Zinc deficiency has been described in cirrhotic subjects, resulting from multiple mechanisms including, among others, reduced dietary intake, reduced intestinal absorption, increased urinary excretion, reduced hepatic extraction, and hypoalbuminemia[57-60]. Ammonia metabolism in the liver requires urea cycle activity, which key enzyme, ornithine transcarbamylase, is a zinc enzyme. It has been reported that zinc supplementation in cirrhotic subjects results in an increase in urea cycle activity with an improvement, though not normalization, of the capacity for ammonia detoxification in the liver[61,62]. The reduction of ammonia detoxification in the liver, at least in part due to zinc deficiency, is associated with increased ammonia uptake in the muscle. In skeletal muscles, BCAAs serve as a glutamate source for glutamine-synthetase reaction to detoxify ammonia. It is therefore possible to link zinc deficiency with reduced plasma BCAAs levels in liver cirrhosis and with the above-described consequences of such condition on HE and sarcopenia [63]. Zinc deficiency has also been associated with taste alterations in elderly individuals and subjects with chronic diseases, including liver cirrhosis[64,65]. Taste alterations in cirrhosis go together with the reduction of appetite caused by abdominal distension due to ascites or osmotic laxatives and with reduced nutrient absorption due to portal hypertensive enteropathy and intestinal dysbiosis. All the described alterations contribute to the worsening of the nutritional status of patients with liver cirrhosis.

BCAAS AND LIVER FUNCTION

As reported above, some evidence exists regarding the effect of BCAA supplementation on overall liver function. Long-term BCAAs supplementation has been associated with improvement in MELD, CPT score, and bilirubin reduction in a retrospective Korean study, but no clear difference was reported in event-free survival[22]. A recent prospective study from the same research group confirmed the

improvement in prognostic scores in subjects receiving long-term BCAAs supplementation, but no differences in albumin and bilirubin levels were found. Interestingly, a significant increase in event-free survival, mainly regarding ascites and HE, was observed in the BCAAs-treated group, but no difference was noted regarding survival[66]. BCAAs supplementation has been investigated also in subjects undergoing treatment for HCC, showing some improvement in liver function after locoregional treatments. Three months of supplementation with a late evening snack enriched with a BCAAs mixture was associated with a rapid improvement in albumin and bilirubin levels and CPT score after radiofrequency ablation[67]. In subjects undergoing trans-arterial chemo-treatment for HCC, BCAAs supplementation was associated with an improvement in albumin but not in bilirubin values. Improved CPT score and survival were also observed in the BCAAs treated group but only in CPT class B patients[68].

CONCLUSION

Today it is widely accepted that low plasma levels of BCAAs levels play a key role in the development of cirrhosis complications such as sarcopenia and HE. The restoration of normal amino acid levels with BCAAs supplementation may improve the clinical course of HE and sarcopenia with few side effects. For these reasons, BCAAs administration should be considered in adult patients with advanced liver disease. BCAAs administration alone improves HE manifestation and reduces HE recurrence but has no significant improvement in mortality. Conversely, the use of BCAAs in addition to conventional therapies, such as non-absorbable disaccharides and non-absorbable antibiotics, shows benefits also in survival. In patients with sarcopenia, the administration of BCAAs improves muscle mass, muscle strength, and albumin levels with a consequent improvement in survival. All these beneficial effects are amplified when BCAAs are used in combination with physical exercise and nutritional intervention. These evidences supports the use of BCAAs supplements in clinical practice, especially in patients affected by concomitant HE and sarcopenia. BCAAs supplements should be used in combination with standard treatments. There is a need to identify patients at high risk of malnutrition and sarcopenia who could have an increased benefit from early nutritional intervention and BCAAs supplementation. According to the scientific literature, oral administration is more effective than intravenous administration and should be preferred. Early discontinuation of BCAAs administration is associated with reduced benefit so a long-term supplementation should be preferred. A minimum dose of 12 g/d of oral BCAAs is more effective than lower doses but further studies are needed to evaluate the most adequate dose and duration of BCAAs treatment.

FOOTNOTES

Author contributions: Marrone G and Serra A were responsible for the conception and writing of the paper; Miele L, Biolato M, and Liguori A reviewed the manuscript; Grieco A and Gasbarrini A performed final editing of the manuscript; and all the authors approved the final version of the manuscript.

Conflict-of-interest statement: All the authors report no relevant conflicts of interest for this article.

Open-Access: This article is an open-access article that was selected by an in-house editor and fully peer-reviewed by external reviewers. It is distributed in accordance with the Creative Commons Attribution NonCommercial (CC BY-NC 4.0) license, which permits others to distribute, remix, adapt, build upon this work non-commercially, and license their derivative works on different terms, provided the original work is properly cited and the use is non-commercial. See: https://creativecommons.org/Licenses/by-nc/4.0/

Country/Territory of origin: Italy

ORCID number: Giuseppe Marrone 0000-0002-9475-3948; Amato Serra 0000-0002-0191-6016; Luca Miele 0000-0003-3464-0068; Marco Biolato 0000-0002-5172-8208; Antonio Liguori 0000-0002-0801-7152; Antonio Grieco 0000-0002-0544-8993; Antonio Gasbarrini 0000-0003-4863-6924.

S-Editor: Wang JJ
L-Editor: A
P-Editor: Cai YX

REFERENCES

1 **Bischoff SC**, Bernal W, Dasarathy S, Merli M, Plank LD, Schütz T, Plauth M. ESPEN practical guideline: Clinical nutrition in liver disease. *Clin Nutr* 2020; **39**: 3533-3562 [PMID: 33213977 DOI: 10.1016/j.clnu.2020.09.001]
2 **Dasarathy S**, Merli M. Sarcopenia from mechanism to diagnosis and treatment in liver disease. *J Hepatol* 2016; **65**: 1232-

1244 [PMID: 27515775 DOI: 10.1016/j.jhep.2016.07.040]
3 **Vilstrup H**, Amodio P, Bajaj J, Cordoba J, Ferenci P, Mullen KD, Weissenborn K, Wong P. Hepatic encephalopathy in chronic liver disease: 2014 Practice Guideline by the American Association for the Study of Liver Diseases and the European Association for the Study of the Liver. *Hepatology* 2014; **60**: 715-735 [PMID: 25042402 DOI: 10.1002/hep.27210]
4 **Amodio P**, Del Piccolo F, Pettenò E, Mapelli D, Angeli P, Iemmolo R, Muraca M, Musto C, Gerunda G, Rizzo C, Merkel C, Gatta A. Prevalence and prognostic value of quantified electroencephalogram (EEG) alterations in cirrhotic patients. *J Hepatol* 2001; **35**: 37-45 [PMID: 11495040 DOI: 10.1016/S0168-8278(01)00129-5]
5 **Groeneweg M**, Moerland W, Quero JC, Hop WC, Krabbe PF, Schalm SW. Screening of subclinical hepatic encephalopathy. *J Hepatol* 2000; **32**: 748-753 [PMID: 10845661 DOI: 10.1016/S0168-8278(00)80243-3]
6 **Montagnese S**, Bajaj JS. Impact of Hepatic Encephalopathy in Cirrhosis on Quality-of-Life Issues. *Drugs* 2019; **79**: 11-16 [PMID: 30706419 DOI: 10.1007/s40265-018-1019-y]
7 **Bass NM**, Mullen KD, Sanyal A, Poordad F, Neff G, Leevy CB, Sigal S, Sheikh MY, Beavers K, Frederick T, Teperman L, Hillebrand D, Huang S, Merchant K, Shaw A, Bortey E, Forbes WP. Rifaximin treatment in hepatic encephalopathy. *N Engl J Med* 2010; **362**: 1071-1081 [PMID: 20335583 DOI: 10.1056/NEJMoa0907893]
8 **Rothenberg ME**, Keeffe EB. Antibiotics in the management of hepatic encephalopathy: an evidence-based review. *Rev Gastroenterol Disord* 2005; **5** Suppl 3: 26-35 [PMID: 17713457]
9 **Fischer JE**, Baldessarini RJ. False neurotransmitters and hepatic failure. *Lancet* 1971; **2**: 75-80 [PMID: 4103986 DOI: 10.1016/S0140-6736(71)92048-4]
10 **Dam G**, Sørensen M, Buhl M, Sandahl TD, Møller N, Ott P, Vilstrup H. Muscle metabolism and whole blood amino acid profile in patients with liver disease. *Scand J Clin Lab Invest* 2015; **75**: 674-680 [PMID: 26243157]
11 **Fischer JE**, Rosen HM, Ebeid AM, James JH, Keane JM, Soeters PB. The effect of normalization of plasma amino acids on hepatic encephalopathy in man. *Surgery* 1976; **80**: 77-91 [PMID: 818729]
12 **James JH**. Branched chain amino acids in heptatic encephalopathy. *Am J Surg* 2002; **183**: 424-429 [PMID: 11975931 DOI: 10.1016/S0002-9610(02)00808-5]
13 **Dam G**, Aamann L, Vistrup H, Gluud LL. The role of Branched Chain Amino Acids in the treatment of hepatic Encephalopathy. *J Clin Exp Hepatol* 2018; **8**: 448-451 [PMID: 30568347 DOI: 10.1016/j.jceh.2018.06.004]
14 **Norenberg MD**, Rama Rao KV, Jayakumar AR. Signaling factors in the mechanism of ammonia neurotoxicity. *Metab Brain Dis* 2009; **24**: 103-117 [PMID: 19104923 DOI: 10.1007/s11011-008-9113-6]
15 **Rossi-Fanelli F**, Freund H, Krause R, Smith AR, James JH, Castorina-Ziparo S, Fischer JE. Induction of coma in normal dogs by the infusion of aromatic amino acids and its prevention by the addition of branched-chain amino acids. *Gastroenterology* 1982; **83**: 664-671 [PMID: 7095369 DOI: 10.1016/S0016-5085(82)80204-7]
16 **Horst D**, Grace ND, Conn HO, Schiff E, Schenker S, Viteri A, Law D, Atterbury CE. Comparison of dietary protein with an oral, branched chain-enriched amino acid supplement in chronic portal-systemic encephalopathy: a randomized controlled trial. *Hepatology* 1984; **4**: 279-287 [PMID: 6706302 DOI: 10.1002/hep.1840040218]
17 **Muto Y**, Sato S, Watanabe A, Moriwaki H, Suzuki K, Kato A, Kato M, Nakamura T, Higuchi K, Nishiguchi S, Kumada H; Long-Term Survival Study Group. Effects of oral branched-chain amino acid granules on event-free survival in patients with liver cirrhosis. *Clin Gastroenterol Hepatol* 2005; **3**: 705-713 [PMID: 16206505 DOI: 10.1016/S1542-3565(05)00017-0]
18 **Les I**, Doval E, García-Martínez R, Planas M, Cárdenas G, Gómez P, Flavià M, Jacas C, Mínguez B, Vergara M, Soriano G, Vila C, Esteban R, Córdoba J. Effects of branched-chain amino acids supplementation in patients with cirrhosis and a previous episode of hepatic encephalopathy: a randomized study. *Am J Gastroenterol* 2011; **106**: 1081-1088 [PMID: 21326220 DOI: 10.1038/ajg.2011.9]
19 **Gluud LL**, Dam G, Borre M, Les I, Cordoba J, Marchesini G, Aagaard NK, Vilstrup H. Lactulose, rifaximin or branched chain amino acids for hepatic encephalopathy: what is the evidence? *Metab Brain Dis* 2013; **28**: 221-225 [PMID: 23275147 DOI: 10.1007/s11011-012-9372-0]
20 **Gluud LL**, Dam G, Borre M, Les I, Cordoba J, Marchesini G, Aagaard NK, Risum N, Vilstrup H. Oral branched-chain amino acids have a beneficial effect on manifestations of hepatic encephalopathy in a systematic review with meta-analyses of randomized controlled trials. *J Nutr* 2013; **143**: 1263-1268 [PMID: 23739310 DOI: 10.3945/jn.113.174375]
21 **Gluud LL**, Dam G, Les I, Marchesini G, Borre M, Aagaard NK, Vilstrup H. Branched-chain amino acids for people with hepatic encephalopathy. *Cochrane Database Syst Rev* 2017; **5**: CD001939 [PMID: 28518283 DOI: 10.1002/14651858.CD001939.pub4]
22 **Park JG**, Tak WY, Park SY, Kweon YO, Jang SY, Lee YR, Bae SH, Jang JY, Kim DY, Lee JS, Suk KT, Kim IH, Lee HJ, Chung WJ, Jang BK, Suh JI, Heo J, Lee WK. Effects of branched-chain amino acids (BCAAs) on the progression of advanced liver disease: A Korean nationwide, multicenter, retrospective, observational, cohort study. *Medicine (Baltimore)* 2017; **96**: e6580 [PMID: 28614215 DOI: 10.1097/MD.0000000000006580]
23 **Wang T**, Suzuki K, Kakisaka K, Onodera M, Sawara K, Takikawa Y. L-carnitine prevents ammonia-induced cytotoxicity and disturbances in intracellular amino acid levels in human astrocytes. *J Gastroenterol Hepatol* 2019; **34**: 1249-1255 [PMID: 30278111 DOI: 10.1111/jgh.14497]
24 **Tajiri K**, Futsukaichi Y, Kobayashi S, Yasumura S, Takahara T, Minemura M, Sugiyama T. L-Carnitine for the Treatment of Overt Hepatic Encephalopathy in Patients with Advanced Liver Cirrhosis. *J Nutr Sci Vitaminol (Tokyo)* 2018; **64**: 321-328 [PMID: 30381621 DOI: 10.3177/jnsv.64.321]
25 **Rosenberg IH**. Summary comments. *Am J Clin Nutr* 1989; **50**: 1231-1233 [DOI: 10.1093/ajcn/50.5.1231]
26 **Cruz-Jentoft AJ**, Bahat G, Bauer J, Boirie Y, Bruyère O, Cederholm T, Cooper C, Landi F, Rolland Y, Sayer AA, Schneider SM, Sieber CC, Topinkova E, Vandewoude M, Visser M, Zamboni M; Writing Group for the European Working Group on Sarcopenia in Older People 2 (EWGSOP2), and the Extended Group for EWGSOP2. Sarcopenia: revised European consensus on definition and diagnosis. *Age Ageing* 2019; **48**: 16-31 [PMID: 30312372 DOI: 10.1093/ageing/afy169]
27 **Meza-Junco J**, Montano-Loza AJ, Baracos VE, Prado CM, Bain VG, Beaumont C, Esfandiari N, Lieffers JR, Sawyer

MB. Sarcopenia as a prognostic index of nutritional status in concurrent cirrhosis and hepatocellular carcinoma. *J Clin Gastroenterol* 2013; **47**: 861-870 [PMID: 23751844 DOI: 10.1097/MCG.0b013e318293a825]

28 **Kumar A**, Davuluri G, Silva RNE, Engelen MPKJ, Ten Have GAM, Prayson R, Deutz NEP, Dasarathy S. Ammonia lowering reverses sarcopenia of cirrhosis by restoring skeletal muscle proteostasis. *Hepatology* 2017; **65**: 2045-2058 [PMID: 28195332 DOI: 10.1002/hep.29107]

29 **Kamimura H**, Sato T, Natsui K, Kobayashi T, Yoshida T, Kamimura K, Tsuchiya A, Murayama T, Yokoyama J, Kawai H, Takamura M, Terai S. Molecular Mechanisms and Treatment of Sarcopenia in Liver Disease: A Review of Current Knowledge. *Int J Mol Sci* 2021; **22** [PMID: 33572604 DOI: 10.3390/ijms22031425]

30 **Ponziani FR**, Picca A, Marzetti E, Calvani R, Conta G, Del Chierico F, Capuani G, Faccia M, Fianchi F, Funaro B, Josè Coelho-Junior H, Petito V, Rinninella E, Paroni Sterbini F, Reddel S, Vernocchi P, Cristina Mele M, Miccheli A, Putignani L, Sanguinetti M, Pompili M, Gasbarrini A; GuLiver study group. Characterization of the gut-liver-muscle axis in cirrhotic patients with sarcopenia. *Liver Int* 2021; **41**: 1320-1334 [PMID: 33713524 DOI: 10.1111/liv.14876]

31 **Patel VC**, Lee S, McPhail MJW, Da Silva K, Guilly S, Zamalloa A, Witherden E, Støy S, Manakkat Vijay GK, Pons N, Galleron N, Huang X, Gencer S, Coen M, Tranah TH, Wendon JA, Bruce KD, Le Chatelier E, Ehrlich SD, Edwards LA, Shoaie S, Shawcross DL. Rifaximin-α reduces gut-derived inflammation and mucin degradation in cirrhosis and encephalopathy: RIFSYS randomised controlled trial. *J Hepatol* 2022; **76**: 332-342 [PMID: 34571050 DOI: 10.1016/j.jhep.2021.09.010]

32 **Ponziani FR**, Bhoori S, Castelli C, Putignani L, Rivoltini L, Del Chierico F, Sanguinetti M, Morelli D, Paroni Sterbini F, Petito V, Reddel S, Calvani R, Camisaschi C, Picca A, Tuccitto A, Gasbarrini A, Pompili M, Mazzaferro V. Hepatocellular Carcinoma Is Associated With Gut Microbiota Profile and Inflammation in Nonalcoholic Fatty Liver Disease. *Hepatology* 2019; **69**: 107-120 [PMID: 29665135 DOI: 10.1002/hep.30036]

33 **Schneider KM**, Mohs A, Gui W, Galvez EJC, Candels LS, Hoenicke L, Muthukumarasamy U, Holland CH, Elfers C, Kilic K, Schneider CV, Schierwagen R, Strnad P, Wirtz TH, Marschall HU, Latz E, Lelouvier B, Saez-Rodriguez J, de Vos W, Strowig T, Trebicka J, Trautwein C. Imbalanced gut microbiota fuels hepatocellular carcinoma development by shaping the hepatic inflammatory microenvironment. *Nat Commun* 2022; **13**: 3964 [PMID: 35803930 DOI: 10.1038/s41467-022-31312-5]

34 **Gómez-Hurtado I**, Santacruz A, Peiró G, Zapater P, Gutiérrez A, Pérez-Mateo M, Sanz Y, Francés R. Gut microbiota dysbiosis is associated with inflammation and bacterial translocation in mice with CCl4-induced fibrosis. *PLoS One* 2011; **6**: e23037 [PMID: 21829583 DOI: 10.1371/journal.pone.0023037]

35 **European Association for the Study of the Liver**. European Association for the Study of the Liver. EASL Clinical Practice Guidelines on the management of hepatic encephalopathy. *J Hepatol* 2022; **77**: 807-824 [PMID: 35724930 DOI: 10.1016/j.jhep.2022.06.001]

36 **Hey P**, Gow P, Testro AG, Apostolov R, Chapman B, Sinclair M. Nutraceuticals for the treatment of sarcopenia in chronic liver disease. *Clin Nutr ESPEN* 2021; **41**: 13-22 [PMID: 33487256 DOI: 10.1016/j.clnesp.2020.11.015]

37 **Holeček M**, Vodeničarovová M. Muscle wasting and branched-chain amino acid, alpha-ketoglutarate, and ATP depletion in a rat model of liver cirrhosis. *Int J Exp Pathol* 2018; **99**: 274-281 [PMID: 30637824 DOI: 10.1111/iep.12299]

38 **Saeki C**, Kanai T, Nakano M, Oikawa T, Torisu Y, Saruta M, Tsubota A. Low Serum Branched-Chain Amino Acid and Insulin-Like Growth Factor-1 Levels Are Associated with Sarcopenia and Slow Gait Speed in Patients with Liver Cirrhosis. *J Clin Med* 2020; **9** [PMID: 33050430 DOI: 10.3390/jcm9103239]

39 **Sano A**, Tsuge S, Kakazu E, Iwata T, Ninomiya M, Tsuruoka M, Inoue J, Masamune A. Plasma free amino acids are associated with sarcopenia in the course of hepatocellular carcinoma recurrence. *Nutrition* 2021; **84**: 111007 [PMID: 33745507 DOI: 10.1016/j.nut.2020.111007]

40 **Nishitani S**, Takehana K, Fujitani S, Sonaka I. Branched-chain amino acids improve glucose metabolism in rats with liver cirrhosis. *Am J Physiol Gastrointest Liver Physiol* 2005; **288**: G1292-G1300 [PMID: 15591158 DOI: 10.1152/ajpgi.00510.2003]

41 **Tsien C**, Davuluri G, Singh D, Allawy A, Ten Have GA, Thapaliya S, Schulze JM, Barnes D, McCullough AJ, Engelen MP, Deutz NE, Dasarathy S. Metabolic and molecular responses to leucine-enriched branched chain amino acid supplementation in the skeletal muscle of alcoholic cirrhosis. *Hepatology* 2015; **61**: 2018-2029 [PMID: 25613922 DOI: 10.1002/hep.27717]

42 **Uojima H**, Sakurai S, Hidaka H, Kinbara T, Sung JH, Ichita C, Tokoro S, Masuda S, Sasaki A, Koizumi K, Egashira H, Kako M, Kobayashi S. Effect of branched-chain amino acid supplements on muscle strength and muscle mass in patients with liver cirrhosis. *Eur J Gastroenterol Hepatol* 2017; **29**: 1402-1407 [PMID: 28984678 DOI: 10.1097/MEG.0000000000000968]

43 **Hernández-Conde M**, Llop E, Gómez-Pimpollo L, Fernández Carrillo C, Rodríguez L, Van Den Brule E, Perelló C, López-Gómez M, Abad J, Martínez-Porras JL, Fernández-Puga N, Ferre C, Trapero M, Fraga E, Calleja JL. Adding Branched-Chain Amino Acids to an Enhanced Standard-of-Care Treatment Improves Muscle Mass of Cirrhotic Patients With Sarcopenia: A Placebo-Controlled Trial. *Am J Gastroenterol* 2021; **116**: 2241-2249 [PMID: 34074812 DOI: 10.14309/ajg.0000000000001301]

44 **Barbara M**, Mindikoglu AL. The role of zinc in the prevention and treatment of nonalcoholic fatty liver disease. *Metabol Open* 2021; **11**: 100105 [PMID: 34337376 DOI: 10.1016/j.metop.2021.100105]

45 **Kitajima Y**, Takahashi H, Akiyama T, Murayama K, Iwane S, Kuwashiro T, Tanaka K, Kawazoe S, Ono N, Eguchi T, Anzai K, Eguchi Y. Supplementation with branched-chain amino acids ameliorates hypoalbuminemia, prevents sarcopenia, and reduces fat accumulation in the skeletal muscles of patients with liver cirrhosis. *J Gastroenterol* 2018; **53**: 427-437 [PMID: 28741271 DOI: 10.1007/s00535-017-1370-x]

46 **Koya S**, Kawaguchi T, Hashida R, Goto E, Matsuse H, Saito H, Hirota K, Taira R, Matsushita Y, Imanaga M, Nagamatsu A, Shirono T, Shimose S, Iwamoto H, Niizeki T, Kuromatsu R, Miura H, Shiba N, Torimura T. Effects of in-hospital exercise on liver function, physical ability, and muscle mass during treatment of hepatoma in patients with chronic liver disease. *Hepatol Res* 2017; **47**: E22-E34 [PMID: 27062043 DOI: 10.1111/hepr.12718]

47 **Hiraoka A**, Michitaka K, Kiguchi D, Izumoto H, Ueki H, Kaneto M, Kitahata S, Aibiki T, Okudaira T, Tomida H,

Miyamoto Y, Yamago H, Suga Y, Iwasaki R, Mori K, Miyata H, Tsubouchi E, Kishida M, Ninomiya T, Kohgami S, Hirooka M, Tokumoto Y, Abe M, Matsuura B, Hiasa Y. Efficacy of branched-chain amino acid supplementation and walking exercise for preventing sarcopenia in patients with liver cirrhosis. *Eur J Gastroenterol Hepatol* 2017; **29**: 1416-1423 [PMID: 29016470 DOI: 10.1097/MEG.0000000000000986]

48 **Hanai T**, Nishimura K, Miwa T, Maeda T, Ogiso Y, Imai K, Suetsugu A, Takai K, Shimizu M. Usefulness of nutritional therapy recommended in the Japanese Society of Gastroenterology/Japan Society of Hepatology evidence-based clinical practice guidelines for liver cirrhosis 2020. *J Gastroenterol* 2021; **56**: 928-937 [PMID: 34533633 DOI: 10.1007/s00535-021-01821-z]

49 **Iqbal U**, Jadeja RN, Khara HS, Khurana S. A Comprehensive Review Evaluating the Impact of Protein Source (Vegetarian vs. Meat Based) in Hepatic Encephalopathy. *Nutrients* 2021; **13** [PMID: 33530344 DOI: 10.3390/nu13020370]

50 **Lattanzi B**, D'Ambrosio D, Merli M. Hepatic Encephalopathy and Sarcopenia: Two Faces of the Same Metabolic Alteration. *J Clin Exp Hepatol* 2019; **9**: 125-130 [PMID: 30765945 DOI: 10.1016/j.jceh.2018.04.007]

51 **Chew STH**, Tan NC, Cheong M, Oliver J, Baggs G, Choe Y, How CH, Chow WL, Tan CYL, Kwan SC, Husain FS, Low YL, Huynh DTT, Tey SL. Impact of specialized oral nutritional supplement on clinical, nutritional, and functional outcomes: A randomized, placebo-controlled trial in community-dwelling older adults at risk of malnutrition. *Clin Nutr* 2021; **40**: 1879-1892 [PMID: 33268143 DOI: 10.1016/j.clnu.2020.10.015]

52 **Holeček M**, Vodeničarovová M. Effects of beta-hydroxy-beta-methylbutyrate supplementation on skeletal muscle in healthy and cirrhotic rats. *Int J Exp Pathol* 2019; **100**: 175-183 [PMID: 31321841 DOI: 10.1111/iep.12322]

53 **Lai JC**, Covinsky KE, Dodge JL, Boscardin WJ, Segev DL, Roberts JP, Feng S. Development of a novel frailty index to predict mortality in patients with end-stage liver disease. *Hepatology* 2017; **66**: 564-574 [PMID: 28422306 DOI: 10.1002/hep.29219]

54 **Lattanzi B**, Bruni A, Di Cola S, Molfino A, De Santis A, Muscaritoli M, Merli M. The Effects of 12-Week Beta-Hydroxy-Beta-Methylbutyrate Supplementation in Patients with Liver Cirrhosis: Results from a Randomized Controlled Single-Blind Pilot Study. *Nutrients* 2021; **13** [PMID: 34371806 DOI: 10.3390/nu13072296]

55 **Espina S**, Sanz-Paris A, Gonzalez-Irazabal Y, Pérez-Matute P, Andrade F, Garcia-Rodriguez B, Carpéné C, Zakaroff A, Bernal-Monterde V, Fuentes-Olmo J, Arbones-Mainar JM. Randomized Clinical Trial: Effects of β-Hydroxy-β-Methylbutyrate (HMB)-Enriched vs. HMB-Free Oral Nutritional Supplementation in Malnourished Cirrhotic Patients. *Nutrients* 2022; **14** [PMID: 35684144 DOI: 10.3390/nu14112344]

56 **Leoni G**, Rosato A, Perozzi G, Murgia C. Zinc proteome interaction network as a model to identify nutrient-affected pathways in human pathologies. *Genes Nutr* 2014; **9**: 436 [PMID: 25367142 DOI: 10.1007/s12263-014-0436-0]

57 **Katayama K**. Zinc and protein metabolism in chronic liver diseases. *Nutr Res* 2020; **74**: 1-9 [PMID: 31891865 DOI: 10.1016/j.nutres.2019.11.009]

58 **Katayama K**, Kawaguchi T, Shiraishi K, Ito T, Suzuki K, Koreeda C, Ohtake T, Iwasa M, Tokumoto Y, Endo R, Kawamura N, Shiraki M, Hanai T, Habu D, Tsuruta S, Sakai H, Miwa Y, Kawada N, Kato A, Takei Y, Mine T, Kohgo Y, Seki T, Sata M, Ito Y, Fukui K, Nishiguchi S, Moriwaki H. The Prevalence and Implication of Zinc Deficiency in Patients With Chronic Liver Disease. *J Clin Med Res* 2018; **10**: 437-444 [PMID: 29581807 DOI: 10.14740/jocmr3374w]

59 **Cousins RJ**. Gastrointestinal factors influencing zinc absorption and homeostasis. *Int J Vitam Nutr Res* 2010; **80**: 243-248 [PMID: 21462106 DOI: 10.1024/0300-9831/a000030]

60 **Chiba M**, Katayama K, Takeda R, Morita R, Iwahashi K, Onishi Y, Kita H, Nishio A, Kanno T, Saito T, Maeda K, Naito M, Michida T, Ito T. Diuretics aggravate zinc deficiency in patients with liver cirrhosis by increasing zinc excretion in urine. *Hepatol Res* 2013; **43**: 365-373 [PMID: 22994500 DOI: 10.1111/j.1872-034X.2012.01093.x]

61 **Riggio O**, Merli M, Capocaccia L, Caschera M, Zullo A, Pinto G, Gaudio E, Franchitto A, Spagnoli R, D'Aquilino E. Zinc supplementation reduces blood ammonia and increases liver ornithine transcarbamylase activity in experimental cirrhosis. *Hepatology* 1992; **16**: 785-789 [PMID: 1505922 DOI: 10.1002/hep.1840160326]

62 **Katayama K**, Saito M, Kawaguchi T, Endo R, Sawara K, Nishiguchi S, Kato A, Kohgo H, Suzuki K, Sakaida I, Ueno Y, Habu D, Ito T, Moriwaki H. Effect of zinc on liver cirrhosis with hyperammonemia: a preliminary randomized, placebo-controlled double-blind trial. *Nutrition* 2014; **30**: 1409-1414 [PMID: 25280421 DOI: 10.1016/j.nut.2014.04.018]

63 **Holecek M**. Ammonia and amino acid profiles in liver cirrhosis: effects of variables leading to hepatic encephalopathy. *Nutrition* 2015; **31**: 14-20 [PMID: 25220875 DOI: 10.1016/j.nut.2014.03.016]

64 **Grüngreiff K**, Reinhold D, Wedemeyer H. The role of zinc in liver cirrhosis. *Ann Hepatol* 2016; **15**: 7-16 [PMID: 26626635 DOI: 10.5604/16652681.1184191]

65 **Stewart-Knox BJ**, Simpson EE, Parr H, Rae G, Polito A, Intorre F, Meunier N, Andriollo-Sanchez M, O'Connor JM, Coudray C, Strain JJ. Zinc status and taste acuity in older Europeans: the ZENITH study. *Eur J Clin Nutr* 2005; **59** Suppl 2: S31-S36 [PMID: 16254578 DOI: 10.1038/sj.ejcn.1602295]

66 **Park JG**, Tak WY, Park SY, Kweon YO, Chung WJ, Jang BK, Bae SH, Lee HJ, Jang JY, Suk KT, Oh MJ, Heo J, Woo HY, Jang SY, Lee YR, Lee JS, Kim DY, Kim SH, Suh JI, Kim IH, Kang MK, Lee WK. Effects of Branched-Chain Amino Acid (BCAA) Supplementation on the Progression of Advanced Liver Disease: A Korean Nationwide, Multicenter, Prospective, Observational, Cohort Study. *Nutrients* 2020; **12** [PMID: 32429077 DOI: 10.3390/nu12051429]

67 **Morihara D**, Iwata K, Hanano T, Kunimoto H, Kuno S, Fukunaga A, Yotsumoto K, Takata K, Tanaka T, Sakurai K, Iwashita H, Ueda S, Hirano G, Yokoyama K, Nakane H, Nishizawa S, Yoshikane M, Anan A, Takeyama Y, Kakumitsu S, Kitamura Y, Sakamoto M, Irie M, Shakado S, Sohda T, Watanabe H, Sakisaka S. Late-evening snack with branched-chain amino acids improves liver function after radiofrequency ablation for hepatocellular carcinoma. *Hepatol Res* 2012; **42**: 658-667 [PMID: 22380706 DOI: 10.1111/j.1872-034X.2012.00969.x]

68 **Kanekawa T**, Nagai H, Kanayama M, Sumino Y. Importance of branched-chain amino acids in patients with liver cirrhosis and advanced hepatocellular carcinoma receiving hepatic arterial infusion chemotherapy. *Cancer Chemother Pharmacol* 2014; **74**: 899-909 [PMID: 25138286 DOI: 10.1007/s00280-014-2564-z]

World Journal of Gastroenterology

Submit a Manuscript: https://www.f6publishing.com

World J Gastroenterol 2023 May 21; 29(19): 2916-2931

DOI: 10.3748/wjg.v29.i19.2916

ISSN 1007-9327 (print) ISSN 2219-2840 (online)

MINIREVIEWS

Assessment of delayed bleeding after endoscopic submucosal dissection of early-stage gastrointestinal tumors in patients receiving direct oral anticoagulants

Mitsushige Sugimoto, Masaki Murata, Takashi Kawai

Specialty type: Gastroenterology and hepatology

Provenance and peer review: Invited article; Externally peer reviewed.

Peer-review model: Single blind

Peer-review report's scientific quality classification

Grade A (Excellent): A
Grade B (Very good): B
Grade C (Good): 0
Grade D (Fair): 0
Grade E (Poor): 0

P-Reviewer: Gu ZC, China; Tharavej C, Thailand

Received: January 24, 2023
Peer-review started: January 24, 2023
First decision: March 21, 2023
Revised: April 3, 2023
Accepted: April 24, 2023
Article in press: April 24, 2023
Published online: May 21, 2023

Mitsushige Sugimoto, Takashi Kawai, Department of Gastroenterological Endoscopy, Tokyo Medical University Hospital, Tokyo 160-0023, Japan

Masaki Murata, Department of Gastroenterology, National Hospital Organization Kyoto Medical Center, Kyoto 612-8555, Japan

Corresponding author: Mitsushige Sugimoto, AGAF, MD, PhD, Professor, Department of Gastroenterological Endoscopy, Tokyo Medical University Hospital, 6-7-1, Nishishinjuku, Shinjuku-ku, Tokyo 160-0023, Japan. sugimo@tokyo-med.ac.jp

Abstract

Delayed bleeding is a major and serious adverse event of endoscopic submucosal dissection (ESD) for early-stage gastrointestinal tumors. The rate of post-ESD bleeding for gastric cancer is higher (around 5%-8%) than that for esophagus, duodenum and colon cancer (around 2%-4%). Although investigations into the risk factors for post-ESD bleeding have identified several procedure-, lesion-, physician- and patient-related factors, use of antithrombotic drugs, especially anticoagulants [direct oral anticoagulants (DOACs) and warfarin], is thought to be the biggest risk factor for post-ESD bleeding. In fact, the post-ESD bleeding rate in patients receiving DOACs is 8.7%-20.8%, which is higher than that in patients not receiving anticoagulants. However, because clinical guidelines for management of ESD in patients receiving DOACs differ among countries, it is necessary for endoscopists to identify ways to prevent post-ESD delayed bleeding in clinical practice. Given that the pharmacokinetics (*e.g.*, plasma DOAC level at both trough and T_{max}) and pharmacodynamics (*e.g.*, anti-factor Xa activity) of DOACs are related to risk of major bleeding, plasma DOAC level and anti-FXa activity may be useful parameters for monitoring the anti-coagulate effect and identifying DOAC patients at higher risk of post-ESD bleeding.

Key Words: Direct oral anticoagulants; Gastrointestinal tumors; Endoscopic submucosal dissection; Delayed bleeding; Adverse events; Anticoagulants

©The Author(s) 2023. Published by Baishideng Publishing Group Inc. All rights reserved.

Core Tip: Recent international clinical guidelines for early-stage gastrointestinal tumors recommend endoscopic submucosal dissection (ESD) as the first-line treatment. Direct oral anticoagulants (DOACs) are a major risk factor for post-ESD bleeding and the pharmacokinetics and pharmacodynamics of DOACs may be related to risk of post-ESD bleeding. Therefore, one way to monitor the anticoagulant effect of DOACs in clinical practice may be to develop a system that effectively measures anti–FXa activity and plasma concentration. In the future, it may be useful to stratify risk of post-ESD delayed bleeding based on a scoring system that includes pharmacological parameters of DOACs.

Citation: Sugimoto M, Murata M, Kawai T. Assessment of delayed bleeding after endoscopic submucosal dissection of early-stage gastrointestinal tumors in patients receiving direct oral anticoagulants. *World J Gastroenterol* 2023; 29(19): 2916-2931
URL: https://www.wjgnet.com/1007-9327/full/v29/i19/2916.htm
DOI: https://dx.doi.org/10.3748/wjg.v29.i19.2916

INTRODUCTION

Endoscopic resection, a minimally invasive endoscopic non-surgical treatment, is now accepted as first-line management for most cases of early-stage esophageal cancer, gastric cancer and colorectal cancer or adenoma around the world[1]. Endoscopic resection mainly includes endoscopic mucosal resection (EMR) and endoscopic submucosal dissection (ESD). Indication for endoscopic resection for EMR and ESD is typically a local mucosal lesion with an extremely low risk of metastasis to lymph nodes (generally less than 1%), and lesions that can be resected *en-bloc*, irrespective of localization in the esophagus, stomach, duodenum or colon. Because ESD enables complete *en-bloc* resection and is associated with a lower recurrence rate than EMR[2,3], recent international clinical guidelines for early-stage gastrointestinal tumors recommend ESD as the first-line treatment over EMR and surgical resection[1,3-7]. To achieve good results and prognosis in ESD for early-stage gastrointestinal tumors, endoscopists and gastroenterologists require excellent skills and knowledge of the diagnosis, indications, actual procedures, and evaluation of curability, complications, long-term postoperative surveillance, and histopathology[3].

ESD often causes adverse events such as intra-operative and delayed bleeding from an artificial ulcer and perforation. The occurrence of such events has been linked to several procedure-, lesion-, physician- and patient-related factors[8-12]. Of the possible risk factors for post-ESD delayed bleeding, use of antithrombotic drugs, especially anticoagulants, is the biggest risk factor[13,14]. Although anticoagulants are mainly divided into warfarin and direct oral anticoagulants (DOACs), no parameters identified to date can be used to accurately monitor the anti-coagulate effect of DOACs in clinical practice or endoscopic/surgical procedures. Thus, it is important to clarify the association between post-ESD delayed bleeding for early-stage gastrointestinal tumors and DOACs, identify risk factors of post-ESD delayed bleeding in patients taking DOACs and methods to prevent bleeding in these patients.

Here, we review delayed bleeding after ESD for gastrointestinal tumors, risk factors for post-ESD bleeding, the pharmacological characteristics of DOACs, international clinical guidelines for endoscopic procedures in patients receiving DOACs, and post-ESD bleeding in patients receiving DOACs.

DELAYED BLEEDING AFTER ESD FOR GASTROINTESTINAL TUMORS

In Japan, upper and lower gastrointestinal tumors are detected in the early stages in many patients, mainly through the use of optimal screening methods, appropriate surveillance and the development of endoscopic diagnostic techniques for early detection and endoscopic equipment[15-17]. In general, evaluation of early-stage gastrointestinal tumors should be performed by expert endoscopists, using a high-definition endoscope by white-light imaging and advanced image-enhanced endoscopy[18]. The experience of the endoscopist may be related to the incidence of adverse events and effective prevention of procedure-related adverse events after ESD. Careful and appropriate coagulation for exposed blood vessels may reduce the gastrointestinal bleeding risk, especially in the stomach[7,19]. The rate of bleeding and its risk factors are known to differ among patients with esophagus, stomach, duodenum and colon cancer.

Esophageal squamous cell carcinoma

The recent development of high-vision endoscopes and techniques for endoscopic diagnosis, including narrow band imaging, has led to more frequent early detection of esophageal esophageal squamous cell carcinoma (SCC)[15,20]. Therefore, ESD is accepted as an effective procedure for detecting superficial

esophageal SCC. In Japan, the Esophageal Cancer Practice Guidelines 2017 weakly recommends endoscopic resection as first-line treatment for preoperatively diagnosed cT1a-MM/T1b-SM1 non-circumferential SCC[6]. In 2014, a meta-analysis of 15 studies with 776 patients with ESD-treated SCC reported pooled estimates of complete resection and *en bloc* resection rates of 89.4% [95%CI: 86.2%–91.9%] and 95.1% (92.6%–96.8%), respectively[21]. In addition, pooled estimates of adverse events such as post-ESD bleeding, perforation, and stenosis were 2.1% (95%CI: 1.2%–3.8%), 5.0% (3.5%–7.2%), and 11.6% (8.2%–16.2%), respectively[21].

Barrett's neoplasia and esophageal adenocarcinoma

The incidence of esophageal adenocarcinoma (EAC) located in Barrett's epithelium has been increasing, especially in Western countries, due to decreases in the *Helicobacter pylori (H. pylori)* infection rate and increases in reflux esophagitis[22]. The European Society of Gastrointestinal Endoscopy (ESGE) recommends using EMR for ≤ 20 mm visible lesions with low probability of submucosal invasion and for larger or multifocal benign dysplastic lesions. In Japan, ESD is strongly recommended over EMR for the radical treatment of superficial EAC with a low risk of metastasis[6]. A meta-analysis of 11 studies investigating the efficacy and safety of ESD for EAC (mean size: 27 mm) reported pooled estimates for *en bloc* resection and pooled R0 resection of 92.9% (95%CI: 90.3%-95.2%) and 74.5% (66.3%-81.9%), respectively[23]. Incidence of recurrence after curative resection was 0.17% (95%CI: 0%-0.3%) at a mean follow-up of 22.9 mo (17.5-28.3 mo)[23]. In adverse events, estimates for bleeding, perforation, and stricture were 1.7% (95%CI: 0.6%-3.4%), 1.5% (0.4%-3.0%) and 11.6% (0.9%-29.6%), respectively. Thus, the rate of post-ESD delayed bleeding in both esophageal SCC and EAC may not be very high (1.7%-2.1%).

Gastric cancer

In the ESGE, gastric cancers that are ≤ 30 mm, submucosal (sm1), and well-differentiated, or ≤ 20 mm, intramucosal, and poorly differentiated, and without ulcerative findings for both sets of criteria can be considered for ESD, although the decision should be individualized[4]. ESD for gastric cancer is associated with high rates of *en bloc* and R0 resection (> 90%), curative resection (75%–80%), low local recurrence (< 5%) and acceptable rates of adverse events (post-ESD bleeding 5%–10% and perforation < 3%)[24,25]. A recent meta-analysis of 22 studies in Western countries reported estimates for *en bloc* resection and R0 resection of 96% (95%CI: 93%-98%) and 84% (79%-89%), respectively[26]. Overall, adverse events occur in 9.5% of patients, including delayed bleeding (5.8%), perforation (3.4%), and stenosis (0.35%)[26]. The odds ratio (OR) indicates that there is no significant difference in risk of post-ESD bleeding between ESD and EMR (OR 1.26, 95%CI: 0.88-1.80)[27]. Another meta-analysis of 74 articles by Libânio *et al*[28] reported post-ESD bleeding rates ranging from 0.6% to 26.9% and a pooled bleeding rate of 5.1% (95%CI: 4.5%-5.7%), with significant heterogeneity across studies (I^2: 84.46, P < 0.001). However, bleeding rates were not significantly different among different study designs (5.9% in randomized clinical trials, 6.1% in prospective studies, and 4.9% in retrospective studies). The elderly Japanese population aged ≥ 85 years has increased from 1.4 to 4.8 million over the last two decades[29] and our investigation of a cohort of 10,320 patients showed that the incidence of bleeding in elderly patients aged > 80 years was 5.7% (95%CI: 4.6%-6.9%), which was significantly higher than in patients aged < 80 years (4.5%, 4.1%-5.0%)[30].

Duodenum

Because ESD for duodenal tumors is associated with high rates of post-ESD bleeding and perforation at both the early and late phases, the ESGE suggests reserving its use for selected cases and tumors in expert centers[4]. In particular, perforation rates are high, with an incidence > 10% in studies involving expert centers[31]. Further, distal location to the ampulla of Vater is a risk factor for delayed perforation [32]. A meta-analysis reported pooled rates of *en bloc* resection, need for surgical intervention, delayed bleeding, intraoperative and delayed perforation of 87%, 4%, 2%, 15% and 2%, respectively[33]. Meanwhile, a recent large retrospective Japanese study reported that the rate of post-ESD adverse events was significantly reduced in cases with complete closure of the mucosal defect compared to partial closure and no closure (1.7%, 25.0% and 15.6%, respectively, P < 0.01)[34].

Colon

In Japan, indications for ESD for colorectal tumors are lesions for which endoscopic *en bloc* resection is required, as follows: (1) Lesions for which *en bloc* resection with snare EMR is difficult to apply; (2) Mucosal tumors with submucosal fibrosis; (3) Sporadic localized tumors in conditions of chronic inflammation such as ulcerative colitis; and (4) Post-EMR local residual or recurrent early-stage cancers[5]. A recent systematic review of 109 studies on 19484 colorectal lesions resected by ESD reported rates of *en bloc* resection of 91%, R0 resection of 82.9%, and local recurrence of 2%. The study also reported a rate of post-ESD bleeding of 2.7% and perforation of 5.2%, and that 1.1% of all patients needed surgical treatment by severe adverse events[35].

Because the rate of post-ESD bleeding may be higher for gastric cancer (5%-8%) than that at other sites (around 2%-4%) due to direct exposure of artificial ulcers to gastric acid and bile, it is necessary for

endoscopists to be aware of and develop countermeasures for gastric ESD.

RISK FACTORS FOR POST-ESD GASTROINTESTINAL DELAYED BLEEDING

Risk factors for post-ESD bleeding are expected to differ among patients with esophagus, stomach, duodenum and colon cancer. Post-ESD bleeding has been shown to be associated with procedure-related factors (*e.g.*, type of knife, coagulation machine and endoscope, and coagulation mode), lesion-related factors (*e.g.*, gastrointestinal organ, large lesion size, location, presence within the ulcerated lesion, scarring, and fibrosis), physician-related factors (*e.g.*, experience with ESD) and patient-related factors [hemodialysis, drugs (antiplatelet drugs, anticoagulants, steroids, and non-steroidal anti-inflammatory drugs), hemostasis ability, and platelet count] (Figure 1)[8-12].

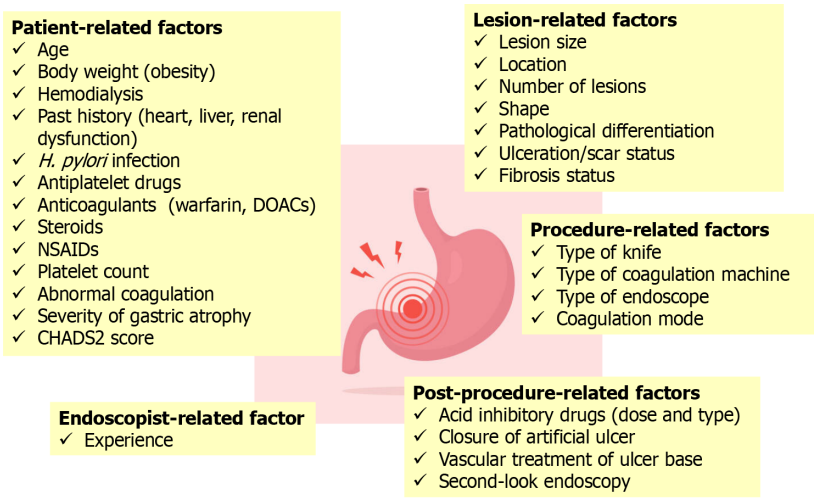
Libânio *et al*[28] showed in a meta-analysis of 74 articles that male sex (OR 1.25), cardiopathy (OR 1.54), antithrombotic drugs (OR 1.63), cirrhosis (OR 1.76), chronic kidney disease (CKD) (OR 3.38), tumor size > 20 mm (OR 2.70), resected specimen size > 30 mm (OR 2.85), localization in the lesser curvature (OR 1.74), flat/depressed morphology (OR 1.43), carcinoma histology (OR 1.46), and ulceration (OR 1.64) were significant risk factors for post-ESD bleeding of gastric cancer, whereas age, hypertension, submucosal invasion, fibrosis, and location (upper, middle, or lower third of stomach) were not. In terms of procedural factors, procedure duration > 60 min (OR, 2.05) and use of histamine-2 receptor antagonists instead of proton pump inhibitors (PPIs) (OR, 2.13) were associated with post-ESD bleeding, whereas endoscopist experience was not. Recently, Hatta *et al*[36] conducted a nationwide multicenter retrospective study focusing on post-ESD bleeding for gastric cancer and used the data to develop a model that applies 10 factors [warfarin, DOAC, hemodialysis, P2Y12 receptor antagonist, aspirin, tumor size > 30 mm, tumor location in the lower third, presence of multiple tumors and interruption of each kind of antithrombotic agent] to predict post-ESD bleeding (BEST-J score). According to the BEST-J score, rates of bleeding in patients categorized as low-risk, intermediate-risk, high-risk, and very high-risk were 2.8%, 6.1%, 11.4%, and 29.7%, respectively[36]. A validation study of the BEST-J score showed that the area under the curve for the BEST-J score at multicenter trials was 0.713 (95%CI: 0.625–0.802), which suggests that the BEST-J score may be useful for predicting post-ESD bleeding in not only expert centers but also general hospitals[37]. In addition, because the healing speed of post-ESD artificial ulcers is related to the post-ESD bleeding rate, factors that affect the healing speed of ulcers, namely *H. pylori* infection status, type of acid inhibitory drug (*e.g.*, PPIs and vonoprazan) and severity of gastric atrophy, may also be risk factors for post-ESD bleeding in gastric cancer[11,12,38]. In today's aging society, the number of patients taking anti-platelet drugs and anticoagulants for the prevention of cardio- and cerebrovascular diseases has risen. That a multicenter study reported a high incidence of post-ESD bleeding in Japanese aged > 80 years, especially in patients receiving hemodialysis and taking warfarin[30], indicates that careful management of ESD is required to prevent bleeding in patients aged > 80 years compared to younger patients.

Major risk factors for post-ESD bleeding for colorectal tumors are generally larger tumor size, location in the rectum or cecum, long procedure time, number of tumors, and taking anti-thrombotic drugs. Recently, Li *et al*[39] reported that post-ESD bleeding for colorectal tumors is observed in 4.7% of patients, and that hypertension (OR 2.829, 95%CI: 1.101-7.265) and using hot biopsy forceps for wound management (OR 2.873, 95%CI: 1.013-8.147) remain significant risk factors for bleeding after multivariate analysis. In another study, Seo *et al*[40] developed a risk-scoring model to predict bleeding after colorectal ESD following identification of the tumor location in the rectosigmoid colon (OR 6.49; 95%CI: 1.96-21.42), large tumor (> 30 mm) (2.10, 1.01-4.40), and use of antiplatelet agents except for aspirin alone (4.04, 1.44-11.30) as risk factors for bleeding[40]. When use of antiplatelet agents except for aspirin alone was scored as 1 point, tumor size > 30 mm as 1 point, and location in the rectosigmoid area as 2 points, the incidence of bleeding in low-risk (score 0-2) and high-risk groups (score 3-4) was 1.5% and 6.0%, respectively.

Thus, current evidence indicates that the use of antithrombotic drugs, especially anticoagulants (DOACs and warfarin) is the biggest risk factor for post-ESD bleeding[13,14].

PHARMACOLOGICAL CHARACTERISTICS OF DOACS

DOACs are currently the first-line drug for the pharmacological prevention of systemic embolism or stroke in atrial fibrillation patients. They are categorized into two main classes: Direct thrombin inhibitors (*i.e.*, dabigatran) and activated coagulation factor X (FXa) inhibitors (*i.e.*, apixaban, edoxaban, rivaroxaban, and betrixaban). Compared with anticoagulation with vitamin K antagonists (*i.e.*, warfarin) or low-molecular-weight heparins, DOACs are new agents that demonstrate superiority or noninferiority to prior standards of care in reducing the risk of thromboembolic complications and major and minor bleeding risk, have fewer monitoring requirements and less frequent follow-up need; and have more immediate drug onset and offset effects and fewer drug and food interactions[41-44]. However, an advantage of using vitamin K antagonist therapy is that a therapeutic international



DOI: 10.3748/wjg.v29.i19.2916 **Copyright** ©The Author(s) 2023.

Figure 1 Post-endoscopic submucosal dissection bleeding-related factors. DOACs: Direct oral anticoagulants; NSAIDs: Non-steroidal anti-inflammatory drugs; CHADS: Congestive heart failure, Hypertension, Age > 75 years, Diabetes mellitus, and Stroke.

normalized ratio range of 2.0-3.0 has been established and is recommended to prevent embolic complications in non-valvular atrial fibrillation in the treatment of deep vein thrombosis and pulmonary embolism. In contrast, a disadvantage of DOACs is that their anticoagulant effects in patients are unclear because there are no Food and Drug Administration (FDA)-approved methods to measure correctly the anticoagulant effect of DOACs. Although qualitative coagulation assays (*e.g.*, thrombin time, activated partial thromboplastin time, and prothrombin time) can be selected as first-line tests, they do not accurately measure the anticoagulant effect of DOACs (Table 1). Quantitative measures for direct assessment of anticoagulant effects do exist, including anti–FXa activity, plasma drug concentration (standard method in preclinical/clinical research and the most accurate method), dilute thrombin time, and ecarin thrombin time[45,46]. In fact, plotting anti–FXa activity against plasma levels of apixaban and rivaroxaban has been confirmed to show a direct linear relationship for both compounds[47].

Pharmacokinetic characteristics such as oral bioavailability, plasma protein binding and relative involvement of renal and non-renal elimination differ substantially among DOACs (Table 2). Pharmacokinetics is influenced by the type of DOAC, dose, renal function, liver function, age, sex, body weight, drug metabolic enzyme gene polymorphisms and drug-drug interactions, but not ethnicity, geographic region, aspirin use, or clopidogrel use[48]. DOACs are relatively safe and effective in patients with moderate CKD [creatinine clearance (Ccr) 30–50 mL/min]. Rivaroxaban, dabigatran and edoxaban will require dose adjustment for renal impairment and patients with severe renal dysfunction (Ccr < 30 mL/min) are recommended to avoid their use[49]. Regulatory agencies such as the FDA and European Medicines Agency have provided guidelines for performing dose adjustments according to the DOAC dose based on Ccr and anticoagulant indications[50]. The International Society on Thrombosis and Hemostasis suggests that use of DOACs are safe in patients of body mass index ≤ 40 kg/m^2 (body weight ≤ 120 kg) at standard doses but does not recommend them for patients of body weight > 120 kg [51]. Compared to warfarin, DOACs are more effective and safer in patients with low body weight (< 50 kg)[52].

DOACs are metabolized by either cytochrome P450 (CYP) metabolic enzymes in the liver or permeability glycoprotein transporters; thus, agents that induce or inhibit CYP metabolic enzymes or glycoprotein transporters can lead to major drug-drug interactions and place the patient at undue risk for adverse events. In fact, concomitant use of apixaban, rivaroxaban, or dabigatran with clarithromycin, a potent inhibitor of CYP3A4, and ATP-binding cassette multidrug transporters increases serum levels of DOACs by 20% to 100% and prolongs coagulation time[53,54]. The pharmacokinetics of DOACs also depend on genetic variations, such as *ABCB1* (ATP-binding cassette multidrug transporters, MDR1) (1236C>T, 2677G>T/A, and 3435C>T), *ABCG2* (421C>A), and *CYP3A5* polymorphisms (6986A>G)[55]. The plasma trough C/D ratio of apixaban is significantly higher in patients with the ABCG2 421A/A genotype and CYP3A5 6986 G allele carriers than in patients with the ABCG2 421C/C genotype and CYP3A5 6986 A/A genotype[55]. Given that CYP3A5 6986A>G and ABCG2 421C>A polymorphisms have allele frequencies of 65%-85%[56] and 29%-36%[57], respectively, in Asians, ABCB1, ABCG2, and CYP3A5 genotypes play pivotal roles in the interindividual variability of apixaban concentrations in Japanese patients.

Although the pharmacodynamic parameters of DOACs differ significantly among individuals and anticoagulant effects also vary widely among patients receiving DOACs, the lack of approved methods to monitor the anticoagulant effect of DOACs makes it unclear whether the effect is adequate in patients

Table 1 Possible methods for monitoring the anticoagulant ability of direct oral anticoagulants[49,71,87]

	Qualitative methods			Quantitative methods					Other	
	aPTT	TT	PT	Anti-FIIa levels	Anti-Fxa levels	Plasma level	dTT	ECT/ECA	CBC	CMP
Dabigatran	[2]	[2]	[2]	[1]		[1]	[2]	[2]	[2]	[2]
Apixaban			[2]		[1]	[1]			[2]	[2]
Edoxaban			[2]		[1]	[1]			[2]	[2]
Rivaroxaban			[2]		[1]	[1]			[2]	[2]

[1]Possible excellent markers.
[2]Possible sensitive markers.
APTT: Activated partial thromboplastin time; CBC: Complete blood count; CMP: Comprehensive metabolic panel; dTT: Dilute thrombin time; ECA: Ecarin chromogenic assay: ECT: Ecarin clotting time; FXa: Activated factor X; PT: Prothrombin time; TT: Thrombin time.

receiving DOAC. Compared with vitamin K antagonist therapy (therapeutic international normalized ratio range: 2.0-3.0), a disadvantage of DOACs is that the dosage of DOAC cannot be controlled according to anticoagulant effect. Therefore, the trough and time to reach maximum plasma concentration (T_{max}) and anti-FXa activity of DOAC-metabolizing enzyme polymorphisms may be useful parameters for accurately monitoring the anti-coagulate effects of DOACs and selecting patients at higher risk of major bleeding. Developing a system that easily measures the anti–FXa activity and plasma level could be an important way to monitor the anticoagulant effect of DOACs in clinical practice.

PHARMACOKINETICS OF DOACS AND MAJOR BLEEDING

Clinical trials have investigated the efficacy of dabigatran (RE-LY trial[58]), apixaban (ARISTOTLE trial [41]), edoxaban (ENGAGE AF TIMI48 trial[59]) and rivaroxaban (ROCKET AF trial[60]) for the prevention of stroke and embolism. According to these trials, adverse events of major bleeding and gastrointestinal bleeding occur at rates of 3.11% and 1.51% for dabigatran 150 mg given twice daily (bid), 2.13% and 0.76% at apixaban 5 mg bid, 2.75% and 1.51% at edoxaban 60 mg given once daily (oid) and 3.6% and 3.2% at rivaroxaban 20 mg oid (Table 3), respectively.

Because the anti-coagulate effects of DOACs are linked to plasma levels of DOAC and anti-FXa activity at trough and T_{max}[48,61,62], these pharmacokinetic and pharmacodynamic parameters are also expected to be related to risk of major bleeding, such as intracerebral and gastrointestinal bleeding. Using multiple logistic regression, Reilly *et al*[48] showed that major bleeding risk increased with dabigatran exposure ($P < 0.0001$), age ($P < 0.0001$), aspirin use ($P < 0.0003$), and diabetes ($P = 0.018$) as significant covariates. Further, patients with major bleeding had higher trough levels (55%) and post-dose levels (36%) than non-bleeding patients[48]. Reilly *et al*[48] also reported a median trough level of 116 ng/mL in 323 major bleeding patients compared with 75.3 ng/mL in 5899 no bleeding patients[48]. Additionally, a Cox regression analysis of time to first major bleeding with trough level, age, and CHADS2 score as covariates showed that, compared with the median trough level of 88 ng/mL, the rate of major bleeding doubled at a level of 210 ng/mL after adjustment for age and CHADS2 score. Moreover, Sakaguchi *et al*[63] showed that, in rivaroxaban-treated patients with major bleeding in Japan, major bleeding is independently predicted to be higher peak rivaroxaban levels and higher anti-FXa activity. Additionally, Sin *et al's* prospective study[64] of rivaroxaban-treated patients with atrial fibrillation with differing severity of CKD (Stage 1–3) showed that trough levels of rivaroxaban were higher in those with bleeding (59.9 ± 35.6 ng/mL) than in those without (41.1 ± 29.2 ng/mL; $P < 0.05$). Therefore, although plasma level and anti–FXa activity may be useful parameters for selecting patients receiving DOACs at higher risk of major bleeding, there is no evidence that patients with higher plasma levels and anti–FXa activity have higher risk of post-ESD bleeding.

A retrospective analysis of 5041 patients demonstrated that concomitant dabigatran–PPI treatment is linked to a significant reduction in bleeding risk compared with dabigatran alone without a PPI[65]. Although dabigatran is an orally administered prodrug, it is rapidly absorbed and converted to its active form, dabigatran. Thus, a potential mechanism for PPI–dabigatran interaction may be reduced dabigatran absorption and availability, which is most probably mediated *via* the effects of PPI on gastric pH, given the poor solubility of dabigatran at pH > 4[66]. Therefore, interactions between PPIs and dabigatran may lead to decreases in dabigatran levels[67].

In terms of gastrointestinal bleeding, unlike warfarin, DOACs remain in the gastrointestinal tract without being absorbed into the blood. Therefore, DOACs may directly inhibit the hemostatic

Table 2 Pharmacological characteristics of direct oral anticoagulant[71,87]

	Dabigatran	Apixaban	Edoxaban	Rivaroxaban
Target factor	Thrombin (Factor IIa)	Factor Xa	Factor Xa	Factor Xa
Half-time (h)	10.7-11.8	6.12-8.11	6.21-6.70	5.7-12.6
Time to peak effect (h)	4	3.0-3.5	1-1.5	1.4-3.3
Distribution volume (L)	50-70	21	107	50
Renal excretion (%)	85	27	35.4-50	50
Fecal excretion (%)	6	25	62.2	50
Hepatic metabolism	No	CYP3A4/5	CYP3A4	CYP3A4 and CYP2J2
Transporter	P-gP	P-gP/BCRP	P-gP	P-gP/BCRP
Protein binding (%)	28.2-31.5	87	40.0-58.9	92-95
Dialyzable	Yes	No	No	No
Prodrug	Yes	No	No	No
Bioavailability (%)	6.5	50	61.8	66-112
Dose for AF (in Japan)	150 mg	5 mg	60 mg	15 mg
Dosing time	Twice daily	Twice daily	Once daily	Once daily
Reversal agent	Idarucizumab	Andexanet alfa	Andexanet alfa	Andexanet alfa
FDA-approved indications	Nonvalvular AF, VTE (T, SP, P)	Nonvalvular AF, VTE (T, SP, P)	Nonvalvular AF, VTE (T)	Nonvalvular AF, VTE (T, SP, P)
Japanese insurance system-approved indications	Nonvalvular AF (P)	Nonvalvular AF (P), VTE (T, SP)	Nonvalvular AF (P), VTE (T, SP)	Nonvalvular AF (P), VTE (T, SP)
Non-pharmacologic interactions	Age, reduced GFR	Age, reduced body weight, reduced GFR, probable severe liver damage	Reduced GFR, probable severe liver damage	Age, reduced GFR, probable severe liver damage
Drug interactions	Dose reduction: Concomitant P-gp inhibitor, gastric acid inhibitory drug	Avoid: Concomitant P-gp and CYP3A4 inhibitors	Avoid: Concomitant rifampin	Avoid: Rivaroxaban with concomitant dual P-gp and CYP3A4 inhibitors
Contraindications	Ccr: < 30mL/min	Nonvalvular AF: Ccr: < 15mL/min, VTE: Ccr: < 30mL/min	Nonvalvular AF: Ccr: < 15mL/min, VTE: Ccr: < 30mL/min	Nonvalvular AF: Ccr: < 15mL/min, VTE: Ccr: < 30mL/min

AF: Atrial fibrillation; P: Prophylaxis; SP: Secondary prevention; T: Treatment; VTE: Venous thromboembolism; FDA: Food and Drug Administration; Ccr: Creatinine clearance.

mechanism in the gastrointestinal tract, thereby aggravating bleeding[68].

CLINICAL GUIDELINES: MANAGEMENT FOR PATIENTS TAKING DOACS IN ENDOSCOPIC PROCEDURES WITH HIGHER RISK FOR BLEEDING (ESD)

During gastrointestinal endoscopy and endoscopic treatment of patients receiving antithrombotic therapy, it is necessary to balance the risk of major and minor bleeding with the risk of thromboembolism resulting from withdrawal of antithrombotic therapy. Therefore, it is important to determine a management strategy (with withdrawal or not) that is optimized for individual patients based on consultation between the endoscopist and physician prescribing the antithrombotic drugs. The risk of thromboembolism is closely related to the underlying disease requiring anticoagulants, and the absolute risk of thromboembolism increases by more than 1% when anticoagulants are withdrawn for more than 4 d[69].

In 2012 the Japan Gastroenterological Endoscopy Society published "Guidelines for gastroenterological endoscopy in patients undergoing antithrombotic treatment" concerning thromboembolism associated with antithrombotic therapy withdrawal and bleeding[70]. The guidelines were updated with a 2017 appendix on anticoagulants in 2017[71]. Although the 2012 version recommends replacing DOACs with heparin during ESD in patients with high risk for post-procedure bleeding as an adverse

Table 3 Comparison of clinical trials on patients receiving direct oral anticoagulant: Major bleeding

	Dabigatran	Apixaban	Edoxaban	Rivaroxaban
Trial name	RE-LY[4]	ARISTOTLE[5]	ENGAGE AF TIMI48[6]	ROCKET AF[7]/J-ROCKET AF
Number of patients	18113	18201	21105	14264
Method	PROBE	RCT	RCT	RCT
Primary endpoints	Stroke or systemic embolism	Ischemic or hemorrhagic stroke or systemic embolism	Stroke or systemic embolism	Stroke or systemic embolism
Period (years)	2.0	1.8	2.8	1.9
$CHADS_2$ score (mean)	2.2	2.1	2.8	3.48 (J-ROCKET: 3.25)
Dosing dose	150 mg/10 mg bid	5 mg bid	60 mg/30 mg qd	20 mg od (J-ROCKET: 15 mg od)
Evaluation				
Thrombus/embolism (*vs* warfarin)	110 mg: Non-inferior, 150 mg: Superior	Superior	60 mg: Similar, 30 mg: Similar	On treatment: Superior, Intention-to-treat: Non-inferior
Outcomes: Stroke or systemic embolism	War: 1.69%/yr, D (110): 1.51%/yr, D (150): 1.11%/yr	War: 1.50%/yr, A: 1.27%/yr	War: 1.81%/yr, E (30): 2.06%/yr, E (60): 1.57%/yr	War: 2.2%/yr, R: 1.7%/yr
Major bleeding (*vs* warfarin)	110 mg: Superior, 150 mg: Similar	Superior	Superior	Similar
Bleeding rate	War: 3.36%/yr, D (110): 2.71%/yr, D (150): 3.11%/yr	War: 3.09%/yr, A: 2.13%/yr	War: 3.43%/yr, E (30): 1.61%/yr, E (60): 2.75%/yr	War: 3.4%/yr, R: 3.6%/yr
Intracranial bleeding	War: 0.74%/yr, D (110): 0.23%/yr, D (150): 0.30%/yr	War: 2.27%/yr, A: 1.79%/yr	War: 0.85%/yr, E (30): 0.26%/yr, E (60): 0.39%/yr	War: 0.7%/yr, R: 0.5%/yr
Gastrointestinal bleeding	War: 1.02%/yr, D (110): 1.12%/yr, D (150): 1.51%/yr	War: 0.86%/yr, A: 0.76%/yr	War: 1.23%/yr, E (30): 0.82%/yr, E (60): 1.51%/yr	War: 2.2%/yr, R: 3.2%/yr1
Minor bleeding (*vs* warfarin)	War: 16.37%/yr, D (110): 13.16%/yr, D (150): 14.84%/yr	War: 6.01%/yr, A: 4.07%/yr	War: 4.89%/yr, E (30): 3.52%/yr, E (60): 4.12%/yr	War: 11.4%/yr, R: 11.8%/yr
Mortality rate	War: 4.13%/yr, D (110): 3.75%/yr, D (150): 3.64%/yr	War: 3.94%/yr, A: 3.52%/yr	War: 4.35%/yr, E (30): 3.80%/yr, E (60): 3.99%/yr	War: 2.2%/yr, R: 1.9%/yr

A: Apixaban; D: Dabigatran; E: Edoxaban; R: Rivaroxaban; war: Warfarin; RCT: Randomized clinical trial; CHADS: Congestive heart failure, Hypertension, Age > 75 years, Diabetes mellitus, and Stroke; PROBE: Prospective randomized open blinded-endpoint.

event, the 2017 version recommends that patients receiving DOACs should continue to take the DOAC orally until the day before ESD and discontinue it on the morning of ESD (Table 4)[71]. Because the anticoagulant effects last 36–48 h for rivaroxaban and edoxaban given oid and 24–36 h for apixaban given bid, and the disappearance of anti-FXa activity and anticoagulant effects increase the risk of thrombosis, DOACs may be resumed the morning after ESD (up to 36 and 48 h when given bid and oid). In addition, when performing ESD, patients receiving concomitant DOAC and antiplatelet agents should be handled with care depending on the individual's condition and needs, while ESD can be performed on patients receiving antiplatelet monotherapy with aspirin or cilostazol[71].

In contrast to the Japanese guidelines, the updated guidelines by the British Society of Gastroenterology and ESGE suggest that patients receiving low-risk procedures for bleeding withdraw from the morning dose of DOAC on the morning of ESD, and recommend that the last dose of DOAC be taken 3 d before ESD for high-risk endoscopic procedures (strong recommendation and low-quality evidence) (Table 4)[72]. For patients receiving dabigatran with a Ccr 30–50 mL/min, this updated version recommends that the last dose be taken 5 d prior to the procedure (strong recommendation and low-quality evidence)[72].

The American Society for Gastrointestinal Endoscopy (ASGE) published a guideline on how to manage patients receiving antithrombotic agents for endoscopy in 2016[73]. This guideline suggests that patients undergoing low-risk procedures should continue taking DOACs (Table 4)[73] and that the resumption of DOACs after ESD be delayed until adequate hemostasis is ensured. If DOACs cannot be resumed within 12 to 24 h post-ESD, thromboprophylaxis should be considered to decrease thromboembolism risk in those with high risk for thromboembolism. However, this version of the ASGE guideline recommends that patients at high risk for thromboembolic events withdraw DOACs and receive bridge therapy to adequately manage patients taking DOACs when ESD is performed (Table 4).

Table 4 Summary of international guidelines concerning withdrawal of direct oral anticoagulants during gastroenterological endoscopy

Ref.	Country	Standard endoscopy	Biopsy	Low risk of bleeding	High risk of bleeding, including ESD
[71]	Japan	[1]	[2]Avoid peak plasma level	[2]Avoid peak plasma level	[3](1) Withdraw on the day of treatment; and (2) Heparin replacement
[72]	Europe	[1]	[3]Withdraw on the day of treatment	[3]Withdraw on the day of treatment	[3](1) Withdraw 3 d before treatment; (2) Withdraw 5 d before treatment for dabigatran patients at Ccr 30–50 mL/min; and (3) No heparin bridging
[73]	United States	[1]	[1]	[1]	[3](1) Withdraw; and (2) Bridge therapy required for patients at high risk for thromboembolic events
[74]	Korea	[1]	[1]	[1]	[3]Withdraw 2 d before treatment
[75]	Asia-Pacific	[1]	[1]	[1]	[3]Withdraw 2 d before treatment

[1]Withdrawal is not required.
[2]Withdrawal is not required but possible.
[3]Withdrawal is required.
ESD: Endoscopic submucosal dissection; Ccr: Creatinine clearance.

In contrast, the Korean clinical practice guideline does not recommend withdrawal of DOACs before low-risk procedures (weak recommendation and low-quality evidence) but suggests withdrawing DOACs > 48 h before high-risk procedures (weak recommendation and low-quality evidence) (Table 4)[74]. The recommendation to withdraw DOACs > 48 h before ESD is based on the fact that the half-life of DOACs is about 12 h and predictions that DOAC levels and anti-FXa activity will be almost undetectable after 48 h[74].

The Asian Pacific Association of Gastroenterology and Asian Pacific Society for Digestive Endoscopy guidelines recommend withholding DOACs at least 48 h before the procedure in DOAC patients receiving gastrointestinal ESD (strong recommendation and low-quality evidence) and do not recommend bridging anticoagulation (strong recommendation and low-quality evidence) (Table 4)[75]. In addition, these guidelines provide recommendations related to the timing of DOAC discontinuation before high-risk procedures according to Ccr[76]. In these guidelines, EMR for large colon polyp (≥ 2 cm) and ESD procedures, which have a higher risk of gastrointestinal bleeding compared with other high-risk endoscopic procedures, are categorized as ultra-high-risk endoscopic procedures[74,75].

Thus, as summarized in Table 4, guidelines for the management of patients undergoing ESD for early-stage gastrointestinal tumors who receive DOACs differ by country. Although subtle differences in the management of DOACs with ESD are important in clinical practice, we consider that these differences are dependent on the year in which the guidelines were published, the different dosage of DOAC in each country, the different numbers of concomitant antithrombotic drugs, and differences in the rate of genetic variations (*e.g.*, CYP3A4/5, ABCG2, and ABCB1 polymorphism).

GASTROINTESTINAL BLEEDING AFTER ESD IN PATIENTS RECEIVING DOACS

Post-ESD bleeding in patients receiving DOACs remains an unpreventable adverse event. Although the combination of heparin-bridging therapy and discontinuation of DOACs is one approach used to prevent thrombosis[70,71], heparin-bridging therapy with discontinuation of any anticoagulants causes an increased risk of delayed bleeding after surgical treatment, interventional procedures and ESD (gastric ESD: 10.8%-61.5%)[77-80] and does not reduce the risk of perioperative arterial thromboembolism[77-79]. In fact, a meta-analysis focused on heparin-bridging therapy with discontinuation of any anticoagulants for ESD found an increased risk of post-ESD bleeding without any benefit for thrombosis [81]. Another meta-analysis reported an increase in thrombosis in patients receiving heparin-bridging therapy with discontinuation of anticoagulants compared with those who discontinued anticoagulation without heparin bridging[82]. In Japan, although the updated guideline recommends discontinuing DOACs on the morning of ESD, most studies conducted on ESD for patients receiving DOACs have been retrospective and enrolled small numbers of patients (Table 5).

However, one study examined a large national database including 16977 patients receiving anticoagulation therapy who underwent high-risk endoscopic procedures. It showed that although warfarin led to a significantly higher post-procedure bleeding rate than DOACs (12.0% *vs* 9.9%, $P = 0.002$), the post-procedure bleeding rate was not significantly different in either upper or lower gastrointestinal ESD between patients receiving DOACs and warfarin[83]. In sub-analyses of procedure types in propensity-matched patients, the gastrointestinal bleeding rate in the DOAC group was 39.6% in

Table 5 Delayed bleeding after endoscopic submucosal dissection in patients receiving direct oral anticoagulants

Ref.	Year	Country	Type	Organ	DOAC patients	Bleeding rate	Non-DOAC patients	Bleeding rate
Nagata *et al*[83]	2018	Japan	Retrospective	Upper GI	275	39.6%	301 (warfarin)	45.8%
Horie *et al*[85]	2022	Japan	Retrospective	Esophagus	16[1]	13%	869[2]	0.3%[1]
Yoshio *et al*[88]	2017	Japan	Retrospective	Stomach	24	20.8%	73 (warfarin)	24.6%
Sanomura *et al*[89]	2018	Japan	Retrospective	Stomach	21	19.0%	40 (warfarin)	17.5%
Saito *et al*[90]	2020	Japan	Retrospective	Stomach	77	19.5%	66 (warfarin)	22.7%
Hatta *et al*[36]	2021	Japan	Retrospective	Stomach	253	17.0%	10,067	4.4%[1]
Tomida *et al*[84]	2021	Japan	Retrospective	Stomach	261	14%	467 (warfarin)	18%
Choi *et al*[91]	2021	Korea	Retrospective	Stomach	23	8.7%	1499	3.0%
Kagawa *et al*[37]	2022	Japan	Retrospective	Stomach	39	15.4%	752	4.3%[1]
Nagata *et al*[83]	2018	Japan	Retrospective	Lower GI	121	13.2%	111 (warfarin)	25.9%
Yamashita *et al*[92]	2018	Japan	Retrospective	Colon	9	22.0%	19 (warfarin)	26.3%
Ogiyama *et al*[93]	2020	Japan	Retrospective	Colon	43	23.3%	44 (warfarin)	11.4%
Harada *et al*[94]	2020	Japan	Retrospective	Colon	25	16.0%	26 (warfarin)	7.7%

[1]Included 2 endoscopic mucosal resection patients.
[2]Included no antithrombotic drug patients.
DOAC: Direct oral anticoagulants.

patients who received upper gastrointestinal ESD and 13.2% in those who received lower gastrointestinal ESD[83].

In a recent retrospective Japanese study of 261 patients with early-stage gastric cancer receiving DOACs, post-ESD bleeding occurred in 14% of patients, which is comparable to that in patients receiving warfarin (18%)[84]. Multivariate analysis demonstrated that age ≥ 65 (OR 2.96, 95%CI: 1.13-7.73), male sex (OR 2.12; 95%CI: 1.01–4.45), receiving multiple antithrombotic agents (OR 2.70, 95%CI: 1.74-4.21) and lesion size ≥ 20 mm (OR 1.67, 95%CI: 1.08-2.59) were independent risk factors for post-ESD bleeding in patients taking anticoagulants, and that cessation of anticoagulants without heparin-bridging therapy was associated with a low risk of bleeding (OR 0.32; 95%CI: 0.14–0.76). However, the multivariate analysis identified no significant independent increased risk factors for post-ESD bleeding and demonstrated that dabigatran was associated with a significantly lower risk of bleeding (OR 0.04, 95%CI: 0.16-0.97)[84]. Further, in a nationwide multicenter retrospective study of 10320 patients, multivariate analysis conducted by Hatta *et al*[36] showed that taking anticoagulants was an independent risk factor for post-ESD bleeding (OR 8.16; 95%CI: 4.74-14.04). Although the number of patients registered in each of these previous studies is relatively small (n = 21-261), both reported post-ESD bleeding in 8.7%-20.8% of gastric cancer patients receiving DOACs, considered to be equivalent to that in patients receiving warfarin (17.5%-22.7%) and higher than that in patients not receiving anticoagulants (Table 5).

Few studies have been conducted on esophageal, duodenal and colorectal ESD in patients receiving DOACs. Horie *et al*[85] reported that the post-endoscopic resection bleeding rate in esophageal cancer patients receiving DOACs (14 patients received ESD and 2 patients received EMR) was significantly higher than that in those not receiving antithrombotic drugs [13% (95%CI: 1.6%–38%) *vs* 0.3% (95%CI: 0.1%–1%), P = 0.003]. Moreover, the post-ESD bleeding rate in colorectal tumor patients receiving DOACs was 16.0%-23.3%, which is equivalent to that in those receiving warfarin (7.7%-26.3%) (Table 5).

Thus, despite the small number of DOAC patients who received ESD in previous studies, the post-ESD delayed bleeding rate appears to vary among different organs in patients not receiving DOACs, but not in patients receiving DOACs.

FUTURE OF ESD FOR PATIENTS RECEIVING DOACS

There is no doubt that patients receiving DOACs are at higher risk of post-ESD bleeding than patients not taking DOACs or receiving antithrombotic drugs. As mentioned above, although examining plasma DOAC level and anti-Xa activity in relation to CYP metabolic enzymes or glycoprotein transporter gene polymorphisms may serve as predictive markers for selecting DOAC patients with higher risk of post-ESD delayed bleeding, no studies have been conducted with such considerations. Although scoring

systems such as the BEST-J score are being developed to assess the risk of post-ESD delayed bleeding by stratifying multiple possible risk factors in clinical practice, we propose the need for a new scoring system that considers pharmacological parameters of DOACs, namely plasma DOAC level and anti-Xa activity.

DOACs is current recommended for not only patients with nonvalvular atrial fibrillation and venous thrombosis (VTE), but also those with cancer due to prevention of VTE by clinical guidelines[86]. Treatment or prophylaxis of VTE for patients with cancer must always balance the risk of incidence or recurrent VTE with the increased risk of major bleeding and take into consideration the consequences of these outcomes (including mortality, financial cost, quality of life)[86]. Developing a system that easily measures the anti–FXa activity and plasma level could be an important way to monitor the anticoagulant effect of DOACs and may help physicians to treat DOAC patients receiving ESD, endoscopic treatment, and surgical treatment and with cancer in clinical practice.

CONCLUSION

Post-ESD delayed bleeding for gastrointestinal tumors is a major adverse event, with an incidence of around 5%-8% for gastric cancer and 2%-4% for esophageal, duodenum and colorectal tumors. Of the many risk factors for bleeding, taking anticoagulants, including DOACs, is currently the biggest. In fact, the post-ESD bleeding rate in DOAC patients is 13% in esophageal cancer, 8.7%-20.8% in gastric cancer and 7.7%-26.3% in colorectal cancer. Compared with warfarin, the anticoagulant effects of which can be monitored using prothrombin time and international normalized ratio tests, there is currently no established method for monitoring the effects of DOACs. Thus, it is important to develop simple and accurate methods to evaluate the pharmacokinetics (*e.g.*, plasma DOAC level at trough and T_{max}) and pharmacodynamics (*e.g.*, anti-factor Xa activity) of DOACs. In the future, a scoring system that includes pharmacological parameters of DOACs may be useful for stratifying risk of post-ESD delayed bleeding in clinical practice.

FOOTNOTES

Author contributions: Sugimoto M wrote the paper; Sugimoto M, Murata M and Kawai T collected the data.

Supported by the Grant-in-Aid for Scientific Research in Japan, No. 21K07949.

Conflict-of-interest statement: All the authors report no relevant conflicts of interest for this article.

Open-Access: This article is an open-access article that was selected by an in-house editor and fully peer-reviewed by external reviewers. It is distributed in accordance with the Creative Commons Attribution NonCommercial (CC BY-NC 4.0) license, which permits others to distribute, remix, adapt, build upon this work non-commercially, and license their derivative works on different terms, provided the original work is properly cited and the use is non-commercial. See: https://creativecommons.org/Licenses/by-nc/4.0/

Country/Territory of origin: Japan

ORCID number: Mitsushige Sugimoto 0000-0002-9194-7392; Masaki Murata 0000-0002-4951-0584; Takashi Kawai 0000-0002-5320-8134.

S-Editor: Li L
L-Editor: A
P-Editor: Zhao S

REFERENCES

1 **Gotoda T**, Yamamoto H, Soetikno RM. Endoscopic submucosal dissection of early gastric cancer. *J Gastroenterol* 2006; **41**: 929-942 [PMID: 17096062 DOI: 10.1007/s00535-006-1954-3]

2 **Tanabe S**, Ishido K, Higuchi K, Sasaki T, Katada C, Azuma M, Naruke A, Kim M, Koizumi W. Long-term outcomes of endoscopic submucosal dissection for early gastric cancer: a retrospective comparison with conventional endoscopic resection in a single center. *Gastric Cancer* 2014; **17**: 130-136 [PMID: 23576197 DOI: 10.1007/s10120-013-0241-2]

3 **Ono H**, Yao K, Fujishiro M, Oda I, Nimura S, Yahagi N, Iishi H, Oka M, Ajioka Y, Ichinose M, Matsui T. Guidelines for endoscopic submucosal dissection and endoscopic mucosal resection for early gastric cancer. *Dig Endosc* 2016; **28**: 3-15 [PMID: 26234303 DOI: 10.1111/den.12518]

4 **Pimentel-Nunes P**, Libânio D, Bastiaansen BAJ, Bhandari P, Bisschops R, Bourke MJ, Esposito G, Lemmers A, Maselli R, Messmann H, Pech O, Pioche M, Vieth M, Weusten BLAM, van Hooft JE, Deprez PH, Dinis-Ribeiro M. Endoscopic

submucosal dissection for superficial gastrointestinal lesions: European Society of Gastrointestinal Endoscopy (ESGE) Guideline - Update 2022. *Endoscopy* 2022; **54**: 591-622 [PMID: 35523224 DOI: 10.1055/a-1811-7025]

5 **Tanaka S**, Kashida H, Saito Y, Yahagi N, Yamano H, Saito S, Hisabe T, Yao T, Watanabe M, Yoshida M, Kudo SE, Tsuruta O, Sugihara KI, Watanabe T, Saitoh Y, Igarashi M, Toyonaga T, Ajioka Y, Ichinose M, Matsui T, Sugita A, Sugano K, Fujimoto K, Tajiri H. JGES guidelines for colorectal endoscopic submucosal dissection/endoscopic mucosal resection. *Dig Endosc* 2015; **27**: 417-434 [PMID: 25652022 DOI: 10.1111/den.12456]

6 **Ishihara R**, Arima M, Iizuka T, Oyama T, Katada C, Kato M, Goda K, Goto O, Tanaka K, Yano T, Yoshinaga S, Muto M, Kawakubo H, Fujishiro M, Yoshida M, Fujimoto K, Tajiri H, Inoue H; Japan Gastroenterological Endoscopy Society Guidelines Committee of ESD/EMR for Esophageal Cancer. Endoscopic submucosal dissection/endoscopic mucosal resection guidelines for esophageal cancer. *Dig Endosc* 2020; **32**: 452-493 [PMID: 32072683 DOI: 10.1111/den.13654]

7 **Draganov PV**, Wang AY, Othman MO, Fukami N. AGA Institute Clinical Practice Update: Endoscopic Submucosal Dissection in the United States. *Clin Gastroenterol Hepatol* 2019; **17**: 16-25.e1 [PMID: 30077787 DOI: 10.1016/j.cgh.2018.07.041]

8 **Fujishiro M**, Yahagi N, Kakushima N, Kodashima S, Muraki Y, Ono S, Kobayashi K, Hashimoto T, Yamamichi N, Tateishi A, Shimizu Y, Oka M, Ogura K, Kawabe T, Ichinose M, Omata M. Successful nonsurgical management of perforation complicating endoscopic submucosal dissection of gastrointestinal epithelial neoplasms. *Endoscopy* 2006; **38**: 1001-1006 [PMID: 17058165 DOI: 10.1055/s-2006-944775]

9 **Tanaka M**, Ono H, Hasuike N, Takizawa K. Endoscopic submucosal dissection of early gastric cancer. *Digestion* 2008; **77** Suppl 1: 23-28 [PMID: 18204258 DOI: 10.1159/000111484]

10 **Cao Y**, Liao C, Tan A, Gao Y, Mo Z, Gao F. Meta-analysis of endoscopic submucosal dissection versus endoscopic mucosal resection for tumors of the gastrointestinal tract. *Endoscopy* 2009; **41**: 751-757 [PMID: 19693750 DOI: 10.1055/s-0029-1215053]

11 **Yoshizawa Y**, Sugimoto M, Sato Y, Sahara S, Ichikawa H, Kagami T, Hosoda Y, Kimata M, Tamura S, Kobayashi Y, Osawa S, Sugimoto K, Miyajima H, Furuta T. Factors associated with healing of artificial ulcer after endoscopic submucosal dissection with reference to Helicobacter pylori infection, CYP2C19 genotype, and tumor location: Multicenter randomized trial. *Dig Endosc* 2016; **28**: 162-172 [PMID: 26331711 DOI: 10.1111/den.12544]

12 **Otsuka T**, Sugimoto M, Ban H, Nakata T, Murata M, Nishida A, Inatomi O, Bamba S, Andoh A. Severity of gastric mucosal atrophy affects the healing speed of post-endoscopic submucosal dissection ulcers. *World J Gastrointest Endosc* 2018; **10**: 83-92 [PMID: 29774087 DOI: 10.4253/wjge.v10.i5.83]

13 **Yano T**, Tanabe S, Ishido K, Suzuki M, Kawanishi N, Yamane S, Watanabe A, Wada T, Azuma M, Katada C, Koizumi W. Different clinical characteristics associated with acute bleeding and delayed bleeding after endoscopic submucosal dissection in patients with early gastric cancer. *Surg Endosc* 2017; **31**: 4542-4550 [PMID: 28378078 DOI: 10.1007/s00464-017-5513-1]

14 **Sato C**, Hirasawa K, Koh R, Ikeda R, Fukuchi T, Kobayashi R, Kaneko H, Makazu M, Maeda S. Postoperative bleeding in patients on antithrombotic therapy after gastric endoscopic submucosal dissection. *World J Gastroenterol* 2017; **23**: 5557-5566 [PMID: 28852315 DOI: 10.3748/wjg.v23.i30.5557]

15 **Muto M**, Minashi K, Yano T, Saito Y, Oda I, Nonaka S, Omori T, Sugiura H, Goda K, Kaise M, Inoue H, Ishikawa H, Ochiai A, Shimoda T, Watanabe H, Tajiri H, Saito D. Early detection of superficial squamous cell carcinoma in the head and neck region and esophagus by narrow band imaging: a multicenter randomized controlled trial. *J Clin Oncol* 2010; **28**: 1566-1572 [PMID: 20177025 DOI: 10.1200/JCO.2009.25.4680]

16 **Dohi O**, Yagi N, Naito Y, Fukui A, Gen Y, Iwai N, Ueda T, Yoshida N, Kamada K, Uchiyama K, Takagi T, Konishi H, Yanagisawa A, Itoh Y. Blue laser imaging-bright improves the real-time detection rate of early gastric cancer: a randomized controlled study. *Gastrointest Endosc* 2019; **89**: 47-57 [PMID: 30189197 DOI: 10.1016/j.gie.2018.08.049]

17 **Ono S**, Kawada K, Dohi O, Kitamura S, Koike T, Hori S, Kanzaki H, Murao T, Yagi N, Sasaki F, Hashiguchi K, Oka S, Katada K, Shimoda R, Mizukami K, Suehiro M, Takeuchi T, Katsuki S, Tsuda M, Naito Y, Kawano T, Haruma K, Ishikawa H, Mori K, Kato M; LCI-FIND Trial Group. Linked Color Imaging Focused on Neoplasm Detection in the Upper Gastrointestinal Tract : A Randomized Trial. *Ann Intern Med* 2021; **174**: 18-24 [PMID: 33076693 DOI: 10.7326/M19-2561]

18 **Sugimoto M**, Koyama Y, Itoi T, Kawai T. Using texture and colour enhancement imaging to evaluate gastrointestinal diseases in clinical practice: a review. *Ann Med* 2022; **54**: 3315-3332 [PMID: 36420822 DOI: 10.1080/07853890.2022.2147992]

19 **Takizawa K**, Oda I, Gotoda T, Yokoi C, Matsuda T, Saito Y, Saito D, Ono H. Routine coagulation of visible vessels may prevent delayed bleeding after endoscopic submucosal dissection--an analysis of risk factors. *Endoscopy* 2008; **40**: 179-183 [PMID: 18322872 DOI: 10.1055/s-2007-995530]

20 **Muto M**, Katada C, Sano Y, Yoshida S. Narrow band imaging: a new diagnostic approach to visualize angiogenesis in superficial neoplasia. *Clin Gastroenterol Hepatol* 2005; **3**: S16-S20 [PMID: 16012987 DOI: 10.1016/s1542-3565(05)00262-4]

21 **Kim JS**, Kim BW, Shin IS. Efficacy and safety of endoscopic submucosal dissection for superficial squamous esophageal neoplasia: a meta-analysis. *Dig Dis Sci* 2014; **59**: 1862-1869 [PMID: 24619279 DOI: 10.1007/s10620-014-3098-2]

22 **Dubecz A**, Solymosi N, Stadlhuber RJ, Schweigert M, Stein HJ, Peters JH. Does the Incidence of Adenocarcinoma of the Esophagus and Gastric Cardia Continue to Rise in the Twenty-First Century? *J Gastrointest Surg* 2013 [PMID: 24234242 DOI: 10.1007/s11605-013-2345-8]

23 **Yang D**, Zou F, Xiong S, Forde JJ, Wang Y, Draganov PV. Endoscopic submucosal dissection for early Barrett's neoplasia: a meta-analysis. *Gastrointest Endosc* 2018; **87**: 1383-1393 [PMID: 28993137 DOI: 10.1016/j.gie.2017.09.038]

24 **Suzuki H**, Takizawa K, Hirasawa T, Takeuchi Y, Ishido K, Hoteya S, Yano T, Tanaka S, Endo M, Nakagawa M, Toyonaga T, Doyama H, Hirasawa K, Matsuda M, Yamamoto H, Fujishiro M, Hashimoto S, Maeda Y, Oyama T, Takenaka R, Yamamoto Y, Naito Y, Michida T, Kobayashi N, Kawahara Y, Hirano M, Jin M, Hori S, Niwa Y, Hikichi T, Shimazu T, Ono H, Tanabe S, Kondo H, Iishi H, Ninomiya M; Ichiro Oda for J-WEB/EGC group. Short-term outcomes of multicenter prospective cohort study of gastric endoscopic resection: 'Real-world evidence' in Japan. *Dig Endosc* 2019; **31**:

30-39 [PMID: 30058258 DOI: 10.1111/den.13246]
25 **Tanabe S**, Ishido K, Matsumoto T, Kosaka T, Oda I, Suzuki H, Fujisaki J, Ono H, Kawata N, Oyama T, Takahashi A, Doyama H, Kobayashi M, Uedo N, Hamada K, Toyonaga T, Kawara F, Tanaka S, Yoshifuku Y. Long-term outcomes of endoscopic submucosal dissection for early gastric cancer: a multicenter collaborative study. *Gastric Cancer* 2017; **20**: 45-52 [PMID: 27807641 DOI: 10.1007/s10120-016-0664-7]
26 **Zullo A**, Manta R, De Francesco V, Manfredi G, Buscarini E, Fiorini G, Vaira D, Marmo R. Endoscopic submucosal dissection of gastric neoplastic lesions in Western countries: systematic review and meta-analysis. *Eur J Gastroenterol Hepatol* 2021; **33**: e1-e6 [PMID: 32804845 DOI: 10.1097/MEG.0000000000001886]
27 **Tao M**, Zhou X, Hu M, Pan J. Endoscopic submucosal dissection versus endoscopic mucosal resection for patients with early gastric cancer: a meta-analysis. *BMJ Open* 2019; **9**: e025803 [PMID: 31874864 DOI: 10.1136/bmjopen-2018-025803]
28 **Libânio D**, Costa MN, Pimentel-Nunes P, Dinis-Ribeiro M. Risk factors for bleeding after gastric endoscopic submucosal dissection: a systematic review and meta-analysis. *Gastrointest Endosc* 2016; **84**: 572-586 [PMID: 27345132 DOI: 10.1016/j.gie.2016.06.033]
29 **Bureau**. MoIAaCS. Population estimates. [cited 3 April 2023]. Available from: http://wwwstatgojp/data/jinsui/
30 **Sugimoto M**, Hatta W, Tsuji Y, Yoshio T, Yabuuchi Y, Hoteya S, Doyama H, Nagami Y, Hikichi T, Kobayashi M, Morita Y, Sumiyoshi T, Iguchi M, Tomida H, Inoue T, Mikami T, Hasatani K, Nishikawa J, Matsumura T, Nebiki H, Nakamatsu D, Ohnita K, Suzuki H, Ueyama H, Hayashi Y, Murata M, Yamaguchi S, Michida T, Yada T, Asahina Y, Narasaka T, Kuribayashi S, Kiyotoki S, Mabe K, Fujishiro M, Masamune A, Kawai T. Risk Factors for Bleeding After Endoscopic Submucosal Dissection for Gastric Cancer in Elderly Patients Older Than 80 Years in Japan. *Clin Transl Gastroenterol* 2021; **12**: e00404 [PMID: 34644281 DOI: 10.14309/ctg.0000000000000404]
31 **Zou J**, Chai N, Linghu E, Zhai Y, Li Z, Du C, Li L. Clinical outcomes of endoscopic resection for non-ampullary duodenal laterally spreading tumors. *Surg Endosc* 2019; **33**: 4048-4056 [PMID: 30756173 DOI: 10.1007/s00464-019-06698-x]
32 **Inoue T**, Uedo N, Yamashina T, Yamamoto S, Hanaoka N, Takeuchi Y, Higashino K, Ishihara R, Iishi H, Tatsuta M, Takahashi H, Eguchi H, Ohigashi H. Delayed perforation: a hazardous complication of endoscopic resection for non-ampullary duodenal neoplasm. *Dig Endosc* 2014; **26**: 220-227 [PMID: 23621427 DOI: 10.1111/den.12104]
33 **Watanabe D**, Hayashi H, Kataoka Y, Hashimoto T, Ichimasa K, Miyachi H, Tanaka S, Toyonaga T. Efficacy and safety of endoscopic submucosal dissection for non-ampullary duodenal polyps: A systematic review and meta-analysis. *Dig Liver Dis* 2019; **51**: 774-781 [PMID: 31014942 DOI: 10.1016/j.dld.2019.03.021]
34 **Kato M**, Ochiai Y, Fukuhara S, Maehata T, Sasaki M, Kiguchi Y, Akimoto T, Fujimoto A, Nakayama A, Kanai T, Yahagi N. Clinical impact of closure of the mucosal defect after duodenal endoscopic submucosal dissection. *Gastrointest Endosc* 2019; **89**: 87-93 [PMID: 30055156 DOI: 10.1016/j.gie.2018.07.026]
35 **Fuccio L**, Hassan C, Ponchon T, Mandolesi D, Farioli A, Cucchetti A, Frazzoni L, Bhandari P, Bellisario C, Bazzoli F, Repici A. Clinical outcomes after endoscopic submucosal dissection for colorectal neoplasia: a systematic review and meta-analysis. *Gastrointest Endosc* 2017; **86**: 74-86.e17 [PMID: 28254526 DOI: 10.1016/j.gie.2017.02.024]
36 **Hatta W**, Tsuji Y, Yoshio T, Kakushima N, Hoteya S, Doyama H, Nagami Y, Hikichi T, Kobayashi M, Morita Y, Sumiyoshi T, Iguchi M, Tomida H, Inoue T, Koike T, Mikami T, Hasatani K, Nishikawa J, Matsumura T, Nebiki H, Nakamatsu D, Ohnita K, Suzuki H, Ueyama H, Hayashi Y, Sugimoto M, Yamaguchi S, Michida T, Yada T, Asahina Y, Narasaka T, Kuribasyashi S, Kiyotoki S, Mabe K, Nakamura T, Nakaya N, Fujishiro M, Masamune A. Prediction model of bleeding after endoscopic submucosal dissection for early gastric cancer: BEST-J score. *Gut* 2021; **70**: 476-484 [PMID: 32499390 DOI: 10.1136/gutjnl-2019-319926]
37 **Kagawa Y**, Fukuzawa M, Sugimoto M, Nemoto D, Muramatsu T, Shinohara H, Matsumoto T, Madarame A, Yamaguchi H, Uchida K, Morise T, Koyama Y, Sugimoto A, Yamauchi Y, Kono S, Naito S, Yamamoto K, Kishimoto Y, Inuyama M, Kawai T, Itoi T. Validation of the BEST-J score, a prediction model for bleeding after endoscopic submucosal dissection for early gastric cancer: a multicenter retrospective observational study. *Surg Endosc* 2022; **36**: 7240-7249 [PMID: 35194665 DOI: 10.1007/s00464-022-09096-y]
38 **Ban H**, Sugimoto M, Otsuka T, Murata M, Nakata T, Hasegawa H, Fukuda M, Inatomi O, Bamba S, Kushima R, Andoh A. Letter: a potassium-competitive acid blocker vs a proton pump inhibitor for healing endoscopic submucosal dissection-induced artificial ulcers after treatment of gastric neoplasms. *Aliment Pharmacol Ther* 2017; **46**: 564-565 [PMID: 28776744 DOI: 10.1111/apt.14202]
39 **Li R**, Cai S, Sun D, Shi Q, Ren Z, Qi Z, Li B, Yao L, Xu M, Zhou P, Zhong Y. Risk factors for delayed bleeding after endoscopic submucosal dissection of colorectal tumors. *Surg Endosc* 2021; **35**: 6583-6590 [PMID: 33237467 DOI: 10.1007/s00464-020-08156-5]
40 **Seo M**, Song EM, Cho JW, Lee YJ, Lee BI, Kim JS, Jeon SW, Jang HJ, Yang DH, Ye BD, Byeon JS. A risk-scoring model for the prediction of delayed bleeding after colorectal endoscopic submucosal dissection. *Gastrointest Endosc* 2019; **89**: 990-998.e2 [PMID: 30521794 DOI: 10.1016/j.gie.2018.11.029]
41 **Granger CB**, Alexander JH, McMurray JJ, Lopes RD, Hylek EM, Hanna M, Al-Khalidi HR, Ansell J, Atar D, Avezum A, Bahit MC, Diaz R, Easton JD, Ezekowitz JA, Flaker G, Garcia D, Geraldes M, Gersh BJ, Golitsyn S, Goto S, Hermosillo AG, Hohnloser SH, Horowitz J, Mohan P, Jansky P, Lewis BS, Lopez-Sendon JL, Pais P, Parkhomenko A, Verheugt FW, Zhu J, Wallentin L; ARISTOTLE Committees and Investigators. Apixaban versus warfarin in patients with atrial fibrillation. *N Engl J Med* 2011; **365**: 981-992 [PMID: 21870978 DOI: 10.1056/NEJMoa1107039]
42 **Hu PT**, Lopes RD, Stevens SR, Wallentin L, Thomas L, Alexander JH, Hanna M, Lewis BS, Verheugt FW, Granger CB, Jones WS. Efficacy and Safety of Apixaban Compared With Warfarin in Patients With Atrial Fibrillation and Peripheral Artery Disease: Insights From the ARISTOTLE Trial. *J Am Heart Assoc* 2017; **6** [PMID: 28096100 DOI: 10.1161/JAHA.116.004699]
43 **Easton JD**, Lopes RD, Bahit MC, Wojdyla DM, Granger CB, Wallentin L, Alings M, Goto S, Lewis BS, Rosenqvist M, Hanna M, Mohan P, Alexander JH, Diener HC; ARISTOTLE Committees and Investigators. Apixaban compared with warfarin in patients with atrial fibrillation and previous stroke or transient ischaemic attack: a subgroup analysis of the

ARISTOTLE trial. *Lancet Neurol* 2012; **11**: 503-511 [PMID: 22572202 DOI: 10.1016/S1474-4422(12)70092-3]
44 **Rose DK**, Bar B. Direct Oral Anticoagulant Agents: Pharmacologic Profile, Indications, Coagulation Monitoring, and Reversal Agents. *J Stroke Cerebrovasc Dis* 2018; **27**: 2049-2058 [PMID: 29753603 DOI: 10.1016/j.jstrokecerebrovasdis.2018.04.004]
45 **Conway SE**, Hwang AY, Ponte CD, Gums JG. Laboratory and Clinical Monitoring of Direct Acting Oral Anticoagulants: What Clinicians Need to Know. *Pharmacotherapy* 2017; **37**: 236-248 [PMID: 27983747 DOI: 10.1002/phar.1884]
46 **Cuker A**, Siegal DM, Crowther MA, Garcia DA. Laboratory measurement of the anticoagulant activity of the non-vitamin K oral anticoagulants. *J Am Coll Cardiol* 2014; **64**: 1128-1139 [PMID: 25212648 DOI: 10.1016/j.jacc.2014.05.065]
47 **Frost C**, Song Y, Barrett YC, Wang J, Pursley J, Boyd RA, LaCreta F. A randomized direct comparison of the pharmacokinetics and pharmacodynamics of apixaban and rivaroxaban. *Clin Pharmacol* 2014; **6**: 179-187 [PMID: 25419161 DOI: 10.2147/CPAA.S61131]
48 **Reilly PA**, Lehr T, Haertter S, Connolly SJ, Yusuf S, Eikelboom JW, Ezekowitz MD, Nehmiz G, Wang S, Wallentin L; RE-LY Investigators. The effect of dabigatran plasma concentrations and patient characteristics on the frequency of ischemic stroke and major bleeding in atrial fibrillation patients: the RE-LY Trial (Randomized Evaluation of Long-Term Anticoagulation Therapy). *J Am Coll Cardiol* 2014; **63**: 321-328 [PMID: 24076487 DOI: 10.1016/j.jacc.2013.07.104]
49 **Chen A**, Stecker E, A Warden B. Direct Oral Anticoagulant Use: A Practical Guide to Common Clinical Challenges. *J Am Heart Assoc* 2020; **9**: e017559 [PMID: 32538234 DOI: 10.1161/JAHA.120.017559]
50 **Derebail VK**, Rheault MN, Kerlin BA. Role of direct oral anticoagulants in patients with kidney disease. *Kidney Int* 2020; **97**: 664-675 [PMID: 32107019 DOI: 10.1016/j.kint.2019.11.027]
51 **Martin K**, Beyer-Westendorf J, Davidson BL, Huisman MV, Sandset PM, Moll S. Use of the direct oral anticoagulants in obese patients: guidance from the SSC of the ISTH. *J Thromb Haemost* 2016; **14**: 1308-1313 [PMID: 27299806 DOI: 10.1111/jth.13323]
52 **Lee SR**, Choi EK, Park CS, Han KD, Jung JH, Oh S, Lip GYH. Direct Oral Anticoagulants in Patients With Nonvalvular Atrial Fibrillation and Low Body Weight. *J Am Coll Cardiol* 2019; **73**: 919-931 [PMID: 30819360 DOI: 10.1016/j.jacc.2018.11.051]
53 **Fralick M**, Juurlink DN, Marras T. Bleeding associated with coadministration of rivaroxaban and clarithromycin. *CMAJ* 2016; **188**: 669-672 [PMID: 26811362 DOI: 10.1503/cmaj.150580]
54 **Mueck W**, Kubitza D, Becka M. Co-administration of rivaroxaban with drugs that share its elimination pathways: pharmacokinetic effects in healthy subjects. *Br J Clin Pharmacol* 2013; **76**: 455-466 [PMID: 23305158 DOI: 10.1111/bcp.12075]
55 **Ueshima S**, Hira D, Fujii R, Kimura Y, Tomitsuka C, Yamane T, Tabuchi Y, Ozawa T, Itoh H, Horie M, Terada T, Katsura T. Impact of ABCB1, ABCG2, and CYP3A5 polymorphisms on plasma trough concentrations of apixaban in Japanese patients with atrial fibrillation. *Pharmacogenet Genomics* 2017; **27**: 329-336 [PMID: 28678049 DOI: 10.1097/FPC.0000000000000294]
56 **Staatz CE**, Goodman LK, Tett SE. Effect of CYP3A and ABCB1 single nucleotide polymorphisms on the pharmacokinetics and pharmacodynamics of calcineurin inhibitors: Part I. *Clin Pharmacokinet* 2010; **49**: 141-175 [PMID: 20170205 DOI: 10.2165/11317350-000000000-00000]
57 **Ieiri I**. Functional significance of genetic polymorphisms in P-glycoprotein (MDR1, ABCB1) and breast cancer resistance protein (BCRP, ABCG2). *Drug Metab Pharmacokinet* 2012; **27**: 85-105 [PMID: 22123128 DOI: 10.2133/dmpk.dmpk-11-rv-098]
58 **Connolly SJ**, Ezekowitz MD, Yusuf S, Eikelboom J, Oldgren J, Parekh A, Pogue J, Reilly PA, Themeles E, Varrone J, Wang S, Alings M, Xavier D, Zhu J, Diaz R, Lewis BS, Darius H, Diener HC, Joyner CD, Wallentin L; RE-LY Steering Committee and Investigators. Dabigatran versus warfarin in patients with atrial fibrillation. *N Engl J Med* 2009; **361**: 1139-1151 [PMID: 19717844 DOI: 10.1056/NEJMoa0905561]
59 **Giugliano RP**, Ruff CT, Braunwald E, Murphy SA, Wiviott SD, Halperin JL, Waldo AL, Ezekowitz MD, Weitz JI, Špinar J, Ruzyllo W, Ruda M, Koretsune Y, Betcher J, Shi M, Grip LT, Patel SP, Patel I, Hanyok JJ, Mercuri M, Antman EM; ENGAGE AF-TIMI 48 Investigators. Edoxaban versus warfarin in patients with atrial fibrillation. *N Engl J Med* 2013; **369**: 2093-2104 [PMID: 24251359 DOI: 10.1056/NEJMoa1310907]
60 **Patel MR**, Mahaffey KW, Garg J, Pan G, Singer DE, Hacke W, Breithardt G, Halperin JL, Hankey GJ, Piccini JP, Becker RC, Nessel CC, Paolini JF, Berkowitz SD, Fox KA, Califf RM; ROCKET AF Investigators. Rivaroxaban versus warfarin in nonvalvular atrial fibrillation. *N Engl J Med* 2011; **365**: 883-891 [PMID: 21830957 DOI: 10.1056/NEJMoa1009638]
61 **Weitz JI**, Connolly SJ, Patel I, Salazar D, Rohatagi S, Mendell J, Kastrissios H, Jin J, Kunitada S. Randomised, parallel-group, multicentre, multinational phase 2 study comparing edoxaban, an oral factor Xa inhibitor, with warfarin for stroke prevention in patients with atrial fibrillation. *Thromb Haemost* 2010; **104**: 633-641 [PMID: 20694273 DOI: 10.1160/TH10-01-0066]
62 **Salazar DE**, Mendell J, Kastrissios H, Green M, Carrothers TJ, Song S, Patel I, Bocanegra TS, Antman EM, Giugliano RP, Kunitada S, Dornseif B, Shi M, Tachibana M, Zhou S, Rohatagi S. Modelling and simulation of edoxaban exposure and response relationships in patients with atrial fibrillation. *Thromb Haemost* 2012; **107**: 925-936 [PMID: 22398655 DOI: 10.1160/TH11-08-0566]
63 **Sakaguchi T**, Osanai H, Murase Y, Ishii H, Nakashima Y, Asano H, Suzuki S, Takefuji M, Inden Y, Sakai K, Murohara T, Ajioka M. Monitoring of anti-Xa activity and factors related to bleeding events: A study in Japanese patients with nonvalvular atrial fibrillation receiving rivaroxaban. *J Cardiol* 2017; **70**: 244-249 [PMID: 28017463 DOI: 10.1016/j.jjcc.2016.11.013]
64 **Sin CF**, Wong KP, Wong HM, Siu CW, Yap DYH. Plasma Rivaroxaban Level in Patients With Early Stages of Chronic Kidney Disease-Relationships With Renal Function and Clinical Events. *Front Pharmacol* 2022; **13**: 888660 [PMID: 35662694 DOI: 10.3389/fphar.2022.888660]
65 **Chan EW**, Lau WC, Leung WK, Mok MT, He Y, Tong TS, Wong IC. Prevention of Dabigatran-Related Gastrointestinal Bleeding With Gastroprotective Agents: A Population-Based Study. *Gastroenterology* 2015; **149**: 586-95.e3 [PMID: 25960019 DOI: 10.1053/j.gastro.2015.05.002]

66 **Ollier E**, Hodin S, Basset T, Accassat S, Bertoletti L, Mismetti P, Delavenne X. In vitro and in vivo evaluation of drug-drug interaction between dabigatran and proton pump inhibitors. *Fundam Clin Pharmacol* 2015; **29**: 604-614 [PMID: 26392328 DOI: 10.1111/fcp.12154]

67 **Bolek T**, Samoš M, Škorňová I, Galajda P, Staško J, Kubisz P, Mokáň M. Proton Pump Inhibitors and Dabigatran Therapy: Impact on Gastric Bleeding and Dabigatran Plasma Levels. *Semin Thromb Hemost* 2019; **45**: 846-850 [PMID: 31537027 DOI: 10.1055/s-0039-1695735]

68 **Desai J**, Granger CB, Weitz JI, Aisenberg J. Novel oral anticoagulants in gastroenterology practice. *Gastrointest Endosc* 2013; **78**: 227-239 [PMID: 23725876 DOI: 10.1016/j.gie.2013.04.179]

69 **Garcia DA**, Regan S, Henault LE, Upadhyay A, Baker J, Othman M, Hylek EM. Risk of thromboembolism with short-term interruption of warfarin therapy. *Arch Intern Med* 2008; **168**: 63-69 [PMID: 18195197 DOI: 10.1001/archinternmed.2007.23]

70 **Fujimoto K**, Fujishiro M, Kato M, Higuchi K, Iwakiri R, Sakamoto C, Uchiyama S, Kashiwagi A, Ogawa H, Murakami K, Mine T, Yoshino J, Kinoshita Y, Ichinose M, Matsui T; Japan Gastroenterological Endoscopy Society. Guidelines for gastroenterological endoscopy in patients undergoing antithrombotic treatment. *Dig Endosc* 2014; **26**: 1-14 [PMID: 24215155 DOI: 10.1111/den.12183]

71 **Kato M**, Uedo N, Hokimoto S, Ieko M, Higuchi K, Murakami K, Fujimoto K. Guidelines for Gastroenterological Endoscopy in Patients Undergoing Antithrombotic Treatment: 2017 Appendix on Anticoagulants Including Direct Oral Anticoagulants. *Dig Endosc* 2018; **30**: 433-440 [PMID: 29733468 DOI: 10.1111/den.13184]

72 **Veitch AM**, Radaelli F, Alikhan R, Dumonceau JM, Eaton D, Jerrome J, Lester W, Nylander D, Thoufeeq M, Vanbiervliet G, Wilkinson JR, Van Hooft JE. Endoscopy in patients on antiplatelet or anticoagulant therapy: British Society of Gastroenterology (BSG) and European Society of Gastrointestinal Endoscopy (ESGE) guideline update. *Gut* 2021; **70**: 1611-1628 [PMID: 34362780 DOI: 10.1136/gutjnl-2021-325184]

73 **ASGE Standards of Practice Committee**, Acosta RD, Abraham NS, Chandrasekhara V, Chathadi KV, Early DS, Eloubeidi MA, Evans JA, Faulx AL, Fisher DA, Fonkalsrud L, Hwang JH, Khashab MA, Lightdale JR, Muthusamy VR, Pasha SF, Saltzman JR, Shaukat A, Shergill AK, Wang A, Cash BD, DeWitt JM. The management of antithrombotic agents for patients undergoing GI endoscopy. *Gastrointest Endosc* 2016; **83**: 3-16 [PMID: 26621548 DOI: 10.1016/j.gie.2015.09.035]

74 **Lim H**, Gong EJ, Min BH, Kang SJ, Shin CM, Byeon JS, Choi M, Park CG, Cho JY, Lee ST, Kim HG, Chun HJ. Clinical Practice Guideline for the Management of Antithrombotic Agents in Patients Undergoing Gastrointestinal Endoscopy. *Clin Endosc* 2020; **53**: 663-677 [PMID: 33242928 DOI: 10.5946/ce.2020.192]

75 **Chan FKL**, Goh KL, Reddy N, Fujimoto K, Ho KY, Hokimoto S, Jeong YH, Kitazono T, Lee HS, Mahachai V, Tsoi KKF, Wu MS, Yan BP, Sugano K. Management of patients on antithrombotic agents undergoing emergency and elective endoscopy: joint Asian Pacific Association of Gastroenterology (APAGE) and Asian Pacific Society for Digestive Endoscopy (APSDE) practice guidelines. *Gut* 2018; **67**: 405-417 [PMID: 29331946 DOI: 10.1136/gutjnl-2017-315131]

76 **Dunn A**. Perioperative management of oral anticoagulation: when and how to bridge. *J Thromb Thrombolysis* 2006; **21**: 85-89 [PMID: 16475048 DOI: 10.1007/s11239-006-5582-9]

77 **Siegal D**, Yudin J, Kaatz S, Douketis JD, Lim W, Spyropoulos AC. Periprocedural heparin bridging in patients receiving vitamin K antagonists: systematic review and meta-analysis of bleeding and thromboembolic rates. *Circulation* 2012; **126**: 1630-1639 [PMID: 22912386 DOI: 10.1161/CIRCULATIONAHA.112.105221]

78 **Beyer-Westendorf J**, Gelbricht V, Förster K, Ebertz F, Köhler C, Werth S, Kuhlisch E, Stange T, Thieme C, Daschkow K, Weiss N. Peri-interventional management of novel oral anticoagulants in daily care: results from the prospective Dresden NOAC registry. *Eur Heart J* 2014; **35**: 1888-1896 [PMID: 24394381 DOI: 10.1093/eurheartj/eht557]

79 **Shindo Y**, Matsumoto S, Miyatani H, Yoshida Y, Mashima H. Risk factors for postoperative bleeding after gastric endoscopic submucosal dissection in patients under antithrombotics. *World J Gastrointest Endosc* 2016; **8**: 349-356 [PMID: 27076874 DOI: 10.4253/wjge.v8.i7.349]

80 **Yamamoto Y**, Kikuchi D, Nagami Y, Nonaka K, Tsuji Y, Fujimoto A, Sanomura Y, Tanaka K, Abe S, Zhang S, De Lusong MA, Uedo N. Management of adverse events related to endoscopic resection of upper gastrointestinal neoplasms: Review of the literature and recommendations from experts. *Dig Endosc* 2019; **31** Suppl 1: 4-20 [PMID: 30994225 DOI: 10.1111/den.13388]

81 **Jaruvongvanich V**, Sempokuya T, Wijarnpreecha K, Ungprasert P. Continued versus interrupted aspirin use and bleeding risk after endoscopic submucosal dissection of gastric neoplasms: a meta-analysis. *Ann Gastroenterol* 2018; **31**: 344-349 [PMID: 29720860 DOI: 10.20524/aog.2018.0251]

82 **Dong J**, Wei K, Deng J, Zhou X, Huang X, Deng M, Lü M. Effects of antithrombotic therapy on bleeding after endoscopic submucosal dissection. *Gastrointest Endosc* 2017; **86**: 807-816 [PMID: 28732709 DOI: 10.1016/j.gie.2017.07.017]

83 **Nagata N**, Yasunaga H, Matsui H, Fushimi K, Watanabe K, Akiyama J, Uemura N, Niikura R. Therapeutic endoscopy-related GI bleeding and thromboembolic events in patients using warfarin or direct oral anticoagulants: results from a large nationwide database analysis. *Gut* 2018; **67**: 1805-1812 [PMID: 28874418 DOI: 10.1136/gutjnl-2017-313999]

84 **Tomida H**, Yoshio T, Igarashi K, Morita Y, Oda I, Inoue T, Hikichi T, Sumiyoshi T, Doyama H, Tsuji Y, Nishikawa J, Hatta W, Mikami T, Iguchi M, Sumiyama K, Yamamoto K, Kitamura K, Kuribayashi S, Yanagitani A, Uraoka T, Yada T, Hasatani K, Kawaguchi K, Fujita T, Nishida T, Hiasa Y, Fujishiro M; FIGHT-Japan Study Group. Influence of anticoagulants on the risk of delayed bleeding after gastric endoscopic submucosal dissection: a multicenter retrospective study. *Gastric Cancer* 2021; **24**: 179-189 [PMID: 32683602 DOI: 10.1007/s10120-020-01105-0]

85 **Horie Y**, Horiuchi Y, Ishiyama A, Tsuchida T, Yoshimizu S, Hirasawa T, Fujisaki J, Maetani I, Yoshio T. The effect of antithrombotic drug use on delayed bleeding with esophageal endoscopic resection. *J Gastroenterol Hepatol* 2022; **37**: 1792-1800 [PMID: 35844140 DOI: 10.1111/jgh.15944]

86 **Lyman GH**, Carrier M, Ay C, Di Nisio M, Hicks LK, Khorana AA, Leavitt AD, Lee AYY, Macbeth F, Morgan RL, Noble S, Sexton EA, Stenehjem D, Wiercioch W, Kahale LA, Alonso-Coello P. American Society of Hematology 2021 guidelines for management of venous thromboembolism: prevention and treatment in patients with cancer. *Blood Adv* 2021; **5**: 927-974 [PMID: 33570602 DOI: 10.1182/bloodadvances.2020003442]

87 **Samoš M**, Bolek T, Stančiaková L, Péč MJ, Brisudová K, Škorňová I, Staško J, Mokáň M, Kubisz P. Tailored Direct Oral Anticoagulation in Patients with Atrial Fibrillation: The Future of Oral Anticoagulation? *J Clin Med* 2022; **11** [PMID: 36362597 DOI: 10.3390/jcm11216369]

88 **Yoshio T**, Tomida H, Iwasaki R, Horiuchi Y, Omae M, Ishiyama A, Hirasawa T, Yamamoto Y, Tsuchida T, Fujisaki J, Yamada T, Mita E, Ninomiya T, Michitaka K, Igarashi M. Effect of direct oral anticoagulants on the risk of delayed bleeding after gastric endoscopic submucosal dissection. *Dig Endosc* 2017; **29**: 686-694 [PMID: 28295638 DOI: 10.1111/den.12859]

89 **Sanomura Y**, Oka S, Tanaka S, Yorita N, Kuroki K, Kurihara M, Mizumoto T, Yoshifuku Y, Chayama K. Taking Warfarin with Heparin Replacement and Direct Oral Anticoagulant Is a Risk Factor for Bleeding after Endoscopic Submucosal Dissection for Early Gastric Cancer. *Digestion* 2018; **97**: 240-249 [PMID: 29421806 DOI: 10.1159/000485026]

90 **Saito H**, Igarashi K, Hirasawa D, Okuzono T, Suzuki K, Abe Y, Nawata Y, Tanaka Y, Tanaka I, Unno S, Nishikawa Y, Tsubokura M, Nakahori M, Chonan A, Matsuda T. The risks and characteristics of the delayed bleeding after endoscopic submucosal dissection for early gastric carcinoma in cases with anticoagulants. *Scand J Gastroenterol* 2020; **55**: 1253-1260 [PMID: 32924673 DOI: 10.1080/00365521.2020.1817542]

91 **Choi J**, Cho SJ, Na SH, Lee A, Kim JL, Chung H, Kim SG. Use of direct oral anticoagulants does not significantly increase delayed bleeding after endoscopic submucosal dissection for early gastric neoplasms. *Sci Rep* 2021; **11**: 9399 [PMID: 33931685 DOI: 10.1038/s41598-021-88656-z]

92 **Yamashita K**, Oka S, Tanaka S, Boda K, Hirano D, Sumimoto K, Mizumoto T, Ninomiya Y, Tamaru Y, Shigita K, Hayashi N, Sanomura Y, Chayama K. Use of anticoagulants increases risk of bleeding after colorectal endoscopic submucosal dissection. *Endosc Int Open* 2018; **6**: E857-E864 [PMID: 29978006 DOI: 10.1055/a-0593-5788]

93 **Ogiyama H**, Inoue T, Maekawa A, Yoshii S, Yamaguchi S, Nagai K, Yamamoto M, Egawa S, Horimoto M, Ogawa H, Nishihara A, Komori M, Kizu T, Tsutsui S, Tsujii Y, Hayashi Y, Iijima H, Takehara T. Effect of anticoagulants on the risk of delayed bleeding after colorectal endoscopic submucosal dissection. *Endosc Int Open* 2020; **8**: E1654-E1663 [PMID: 33140021 DOI: 10.1055/a-1244-2097]

94 **Harada H**, Nakahara R, Murakami D, Suehiro S, Nagasaka T, Ujihara T, Sagami R, Katsuyama Y, Hayasaka K, Tounou S, Amano Y. The effect of anticoagulants on delayed bleeding after colorectal endoscopic submucosal dissection. *Surg Endosc* 2020; **34**: 3330-3337 [PMID: 31482349 DOI: 10.1007/s00464-019-07101-5]

World Journal of Gastroenterology

Submit a Manuscript: https://www.f6publishing.com

World J Gastroenterol 2023 May 21; 29(19): 2932-2949

DOI: 10.3748/wjg.v29.i19.2932

ISSN 1007-9327 (print) ISSN 2219-2840 (online)

ORIGINAL ARTICLE

Basic Study

TATA-box-binding protein-associated factor 15 is a novel biomarker that promotes cell proliferation and migration in gastrointestinal stromal tumor

Cheng-Ming Guo, Li Tang, Xu Li, Liu-Ye Huang

Specialty type: Gastroenterology and hepatology

Provenance and peer review: Unsolicited article; Externally peer reviewed.

Peer-review model: Single blind

Peer-review report's scientific quality classification

Grade A (Excellent): 0
Grade B (Very good): B
Grade C (Good): C
Grade D (Fair): 0
Grade E (Poor): 0

P-Reviewer: Li S, China; Mankotia DS, India

Received: November 28, 2022
Peer-review started: November 28, 2022
First decision: February 15, 2023
Revised: March 6, 2023
Accepted: April 11, 2023
Article in press: April 11, 2023
Published online: May 21, 2023

Cheng-Ming Guo, Li Tang, Xu Li, Liu-Ye Huang, Department of Gastroenterology, The Affiliated Yantai Yuhuangding Hospital of Qingdao University, Yantai 264000, Shandong Province, China

Corresponding author: Liu-Ye Huang, Professor, Academic Research, Chief Doctor, Chief Physician, Research Scientist, Department of Gastroenterology, The Affiliated Yantai Yuhuangding Hospital of Qingdao University, No. 20 Yuhuangding East Road, Yantai 264000, Shandong Province, China. liuye_huang@163.com

Abstract

BACKGROUND

Gastrointestinal stromal tumor (GIST) is a common neoplasm with high rates of recurrence and metastasis, and its therapeutic efficacy is still not ideal. There is an unmet need to find new molecular therapeutic targets for GIST. TATA-box-binding protein-associated factor 15 (TAF15) contributes to the progress of various tumors, while the role and molecular mechanism of TAF15 in GIST progression are still unknown.

AIM

To explore new molecular therapeutic targets for GIST and understand the biological role and underlying mechanisms of TAF15 in GIST progression.

METHODS

Proteomic analysis was performed to explore the differentially expressed proteins in GIST. Western blotting and immunohistochemical analysis were used to verify the expression level of TAF15 in GIST tissues and cell lines. Cell counting kit-8, colony formation, wound-healing and transwell assay were executed to detect the ability of TAF15 on cell proliferation, migration and invasion. A xenograft mouse model was applied to explore the role of TAF15 in the progression of GIST. Western blotting was used to detect the phosphorylation level and total level of RAF1, MEK and ERK1/2.

RESULTS

A total of 1669 proteins were identified as differentially expressed proteins with 762 upregulated and 907 downregulated in GIST. TAF15 was selected for the further study because of its important role in cell proliferation and migration.

TAF15 was significantly over expressed in GIST tissues and cell lines. Overexpression of TAF15 was associated with larger tumor size and higher risk stage of GIST. TAF15 knockdown significantly inhibited the cell proliferation and migration of GIST *in vitro* and suppressed tumor growth *in vivo*. Moreover, the inhibition of TAF15 expression significantly decreased the phosphorylation level of RAF1, MEK and ERK1/2 in GIST cells and xenograft tissues, while the total RAF1, MEK and ERK1/2 had no significant change.

CONCLUSION

TAF15 is over expressed in GIST tissues and cell lines. Overexpression of TAF15 was associated with a poor prognosis of GIST patients. TAF15 promotes cell proliferation and migration in GIST *via* the activation of the RAF1/MEK/ERK signaling pathway. Thus, TAF15 is expected to be a novel latent molecular biomarker or therapeutic target of GIST.

Key Words: Gastrointestinal stromal tumor; Proteomics; TATA-box-binding protein-associated factor 15; Biomarker; Cell proliferation; Cell migration

©The Author(s) 2023. Published by Baishideng Publishing Group Inc. All rights reserved.

Core Tip: TATA-box-binding protein-associated factor 15 (TAF15) was upregulated in gastrointestinal stromal tumor (GIST) cells and tissues and was associated with a poor prognosis in GIST patients. TAF15 promotes cell proliferation and migration of GIST *in vitro* and tumor growth *in vivo via* the activation of the RAF1/MEK/ERK signaling pathway. Therefore, TAF15 is expected to be a novel potential molecular biomarker or therapeutic target of GIST.

Citation: Guo CM, Tang L, Li X, Huang LY. TATA-box-binding protein-associated factor 15 is a novel biomarker that promotes cell proliferation and migration in gastrointestinal stromal tumor. *World J Gastroenterol* 2023; 29(19): 2932-2949

URL: https://www.wjgnet.com/1007-9327/full/v29/i19/2932.htm

DOI: https://dx.doi.org/10.3748/wjg.v29.i19.2932

INTRODUCTION

Gastrointestinal stromal tumor (GIST) is a common neoplasm that arises from the mesenchymal tissue of the gastrointestinal tract and likely originates from the interstitial cells of Cajal[1,2]. Mutations in mast/stem cell growth factor receptor (KIT) and platelet-derived growth factor receptor A (PDGFRA) are considered the primary causes in the pathogenesis of GIST[3]. GIST most commonly occurs in the stomach (50%-60%) and small intestine (30%-35%) but rarely occurs in the colorectum (5%) and esophagus (< 1%)[4]. Previous studies have indicated that GIST accounts for roughly 0.1%-3.0% of gastrointestinal malignances, and 15%-50% of patients present with metastasis at the time of diagnosis [5].

In clinical practice, GIST is liable to recur and distantly metastasize even after the initial tumor excision[6]. In fact, about 40% of patients develop tumor metastasis within 15 years after surgery[7], with a strong tendency to metastasize to the liver and peritoneal surfaces primarily and the lymph nodes and lung less frequently[4,8]. Based on tumor size, mitotic count, tumor site, and tumor rupture, the modified National Institutes of Health (NIH) consensus criteria stratifies GIST into four subgroups: Very low (NIH-VL), low (NIH-L), intermediate (NIH-I), and high risk (NIH-H)[9]. GIST patients with large sized tumors and high mitotic counts are more likely to metastasize to the liver and abdominal cavity and frequently have poor disease-free survival ratios[10].

Before the clinical application of imatinib, a tyrosine kinase inhibitor, surgical resection was the only accepted therapy that could prolong the life of GIST patients who had developed metastasis. Even then, the 5-year overall survival rate of patients was only 27%–34%[11]. Improved treatment with imatinib has been highly effective in advanced or metastatic GIST patients, and approximately 80% of them can reach complete or partial recovery[12,13]. Unfortunately, high rates of drug resistance due to secondary mutations of KIT have rendered imatinib therapy ineffective in recent years[14]. Taken together, the current research shows that the therapeutic efficacy of GIST treatments are still not ideal. Therefore, finding new molecular therapeutic targets for GIST is critical.

In this study, we implemented a proteomic analysis in GIST patients using tandem mass tag (TMT) labeling 10-plex kits to explore potential molecular therapeutic targets for GIST. A total of 4111 proteins were quantified in the GIST samples. Of these, 1669 were identified as significant differentially expressed proteins (DEPs), with 762 upregulated and 907 downregulated proteins. After a systematic

analysis of the top 10 upregulated or downregulated proteins, we selected TATA-box-binding protein-associated factor 15 (TAF15) for further study because of its important role in cell proliferation and migration[15]. TAF15 is a member of the FUS/Ewing sarcoma protein (EWS)/TAF15 (FET) family of RNA- and DNA-binding proteins, which plays an essential role in mRNA transcription, RNA splicing and polyadenylation[16-18].

Previous studies have demonstrated that TAF15 can influence a large number of genes that are closely related to the cell cycle and cell death and that overexpression of TAF15 can promote proliferation in sarcomas, human neuroblastoma and leukemia cells[17,19]. TAF15 mediates resistance to radiation therapy through inhibiting tumor suppressors p53 and p21, and upregulation of TAF15 is closely related to worsened survival in non-small cell lung cancer patients[20]. Additionally, a prior study has described a human anti-TAF15 antibody, PAT-BA4, that targeted a tumor-specific TAF15 antigen and then inhibited cell adhesion and spreading in gastric cancer[21]. Moreover, in a recent study, TAF15 activated the mitogen-activated protein kinase (MAPK) signaling pathway by upregulating the expression of MAPK6 in lung squamous cell carcinoma[22]. Taken together, TAF15 may play an important role in the progression of human cancers. However, the latent functions and molecular mechanism of TAF15 in GIST progression are still unclear and must be further studied.

MATERIALS AND METHODS

Clinical sample collection

One hundred and sixty one patients with GIST were recruited from the Department of Gastrointestinal Surgery, Yantai Yu Huang Ding Hospital of Qing Dao University from March 2020 to June 2022, with ethical permission from the Biomedical Ethics Committee (No.2019–410). All patients were diagnosed with GIST by two independent pathologists based on Chinese clinical guidelines[23]. No patients had received chemotherapy before surgery. Out of the 161 cases, 18 cases had matched tumor (T) and normal (N) tissue samples, and the clinicopathologic features of the paired GIST samples were documented in Table 1. In the remaining 143 cases, only tissue from the tumor site was available. In the beginning we only collected 12 matched samples, which were sent for proteomic analysis, followed by another 6 matched samples. All specimens were immediately frozen in liquid nitrogen within 30 min after excision. All patients provided written informed consent.

Protein extraction and digestion

Tissues from GIST patients were homogenized in RIPA lysis buffer containing protease inhibitors using a mortar and pestle. After homogenizing lightly for 1 min on ice, the lysate was centrifuged twice at 13000 RPM for 10 min at 4 °C, and then the supernatants were transferred to a fresh tube. A BCA assay kit (catalog no.P0010, Beyotime Biotechnology, Shanghai, China) was used to measure the protein concentration of each sample. The protein content of each sample was reduced using 5 mmol/L DL-dithiothreitol at 55 °C for 30 min. Samples were then incubated with 10 mmol/L of iodoacetamide at room temperature for 15 min in the dark to alkylate the protein. Each protein sample was dissolved using triethylammonium bicarbonate buffer and then digested overnight at 37 °C using trypsin.

TMT labeling and fractionation

Tryptic peptides from each sample were labeled with TMT (Thermo Fisher Scientific, Waltham, MA, United States) kits following the manufacturer's protocol. After quenching the reaction using 5% hydroxylamine (Sigma-Aldrich, Saint Louis, MO, United States), the TMT-labeled peptide solution was fractionated using basic pH reversed phase high performance liquid chromatography through an Agilent Zorbax Extend C18 column (5 μm, 150 mm × 2.1 mm). The mobile phase consisted of Buffer A (98% water with 2% acetonitrile) and Buffer B (90% acetonitrile with 10% water). The procedure gradient was run as follows: 0%-8% Buffer B for 0-10 min; 8%-35% Buffer B for 10-80 min; 35%-60% Buffer B for 80-95 min; 60%-70% Buffer B for 95-105 min; 70%-100% Buffer B for 105-120 min. The flow rate was set at 1 mL/min. TMT labeled peptides were separated into 10 fractions by reversed phase high performance liquid chromatography.

Liquid chromatography-tandem mass spectrometry analysis

Liquid chromatography-tandem mass spectrometry (MS) analysis was conducted on a Q Exactive Mass Spectrometer (Thermo Scientific) coupled to an EASY-nanoLC System (Thermo Fisher Scientific). Peptides were loaded onto a reverse-phase C18 column (Thermo Scientific Easy Column, 10 cm long, 75 μm inner diameter, 3μm resin) in Buffer A (0.1% formic acid) and separated with a linear gradient of Buffer B (84% acetonitrile and 0.1% formic acid) at a flow rate of 300 nL/min. The MS was utilized in positive ion mode. MS data were acquired following a data-dependent top10 method, dynamically selecting the most abundant precursor ions from the survey scan (300–1800 m/z). The automatic gain control target was set to $3e^6$ with maximum inject time to 10 ms. Survey scans were acquired from a resolution of 70000 at m/z 200 with an isolation width of 2 m/z.

Table 1 Clinicopathologic features of the collected paired gastrointestinal stromal tumors samples

Case No.	Sex	Age in yr	Location	Tumor size length × width × height in cm	Mitosis count, per 50 HFPs	Risk classification based on NIH
1	Male	74	Stomach	2.8 × 2.8 × 2.0	> 5	High
2	Female	24	Stomach	6.0 × 4.0 × 5.0	> 5	High
3	Male	69	Stomach	7.5 × 5.5 × 4.0	> 10	High
4	Male	46	Small intestine	6.5 × 5.0 × 4.0	> 5	High
5	Female	65	Small intestine	6.5 × 5.5 × 5.0	> 5	High
6	Female	61	Stomach	5.5 × 3.5 × 4.0	> 5	High
7	Female	49	Stomach	8.5 × 8.0 × 7.0	< 5	Intermediate
8	Male	77	Stomach	6.0 × 6.0 × 5.0	< 5	Intermediate
9	Female	54	Stomach	6.0 × 4.5 × 3.5	< 5	Intermediate
10	Female	43	Stomach	5.5 × 4.5 × 3.0	< 5	Intermediate
11	Male	70	Stomach	7.0 × 7.0 × 5.5	< 5	Intermediate
12	Female	55	Stomach	8.0 × 8.0 × 7.0	< 5	Intermediate
13	Male	63	Small intestine	5.0 × 3.5 × 3.0	< 5	Low
14	Male	67	Stomach	2.3 × 1.5 × 1.5	< 5	Low
15	Male	44	Stomach	3.0 × 2.7 × 1.3	< 5	Low
16	Female	49	Stomach	1.0 × 0.8 × 0.8	< 5	Very low
17	Female	66	Stomach	2.0 × 1.8 × 1.0	< 5	Very low
18	Female	57	Stomach	2.0 × 1.8 × 1.5	< 5	Very low

HPF: High-powered field; NIH: National Institutes of Health.

Data processing and analysis

Data for each sample were processed using the Swiss-Prot *Homo sapiens* database (20413 entries, January 14, 2017). The parameters of the procedures were as follows: Cysteine carbamidomethylation was set to fixed modification; oxidation was set to variable modification; peptide mass tolerance was 20 ppm, trypsin digestion, max 2 missed cleavages; and the false discovery rate was less than 1%. Proteins with a fold change of > 1.2 or < 0.83 and a P value < 0.05 were identified as significantly upregulated or downregulated.

Western blotting analysis

Western blot analysis was performed using 10% sodium dodecyl sulfonate-polyacrylamide gel electrophoresis to separate equal amounts (25 μg/load) of protein samples. Protein samples were transferred onto polyvinylidenedifluoride membranes. The membranes were blocked at room temperature for 1 h with 5% nonfat milk in TBS-T buffer and subsequently incubated with primary antibodies at 4 °C overnight. Secondary antibodies were incubated for 1 hat room temperature. Protein samples were visualized using ECL reagents (MA0186, Meilunbio, Dalian, China) using the ChemiScope 6200 Touch Imaging System (CLINX, Shanghai, China). Some membranes were recycled using stripping buffer (SL1340, Coolaber, Beijing, China) and incubated with other primary antibodies. The primary antibodies were used and obtained as follows: TAF15 (1:3000, ab134916, Abcam, United States); GAPDH (1:5000, D110016, Sangon Biotech, Shanghai, China); RAF1 (1:500, D155090, Sangon Biotech, Shanghai, China); p-RAF1 (1:1000, 66592-1-lg, Proteintech, Wuhan, China); MEK1/2 (1:1000, 11049-1-AP, Proteintech, Wuhan, China); p-MEK1 (1:1000, 28930-1-AP, Proteintech, Wuhan, China); ERK1/2 (1:1000, 16443-1-AP, Proteintech, Wuhan, China); and p-ERK1/2 (1:1000, 28733-1-AP, Proteintech, Wuhan, China). The secondary antibodies were used and obtained as follows: HRP goat anti-rabbit immunoglobulin G (IgG) (1:3000, D110058, Sangon Biotech, shanghai, China); and HRP goat anti-mouse IgG (1:3000, D110058, Sangon Biotech, Shanghai, China). Three independent tests were performed.

Immunohistochemistry

Tissue specimens were cut into 4 μm sections and processed by deparaffinization and rehydration. Slides were incubated with 3% hydrogen peroxide for 20 min at room temperature to block endogenous peroxidase activity. Tissue sections were incubated with primary antibody TAF15 (1:100, ab134916, Abcam, United States) at 4 °C in a wet chamber overnight and then incubated with secondary antibody HRP goat anti-rabbit IgG (1:100, D110058, Sangon Biotech, Shanghai, China) for 1 h in a wet chamber at room temperature. Color was developed using diaminobenzidine and hematoxylin. Two independent pathologists evaluated the samples by randomly selecting and evaluating five × 400 microscopic fields per slide. The percentage of stained tumor cells was scored as follows: 0, < 5% positive cells; 1, 5%-24% positive cells; 2, 25%-49% positive cells; 3, 50%-74% positive cells; and 4, ≥ 75% positive cells. The staining intensity was scored as follows: 0 for absence; 1 for weak; 2 for moderate; and 3 for strong. The total stained index was equivalent to intensity score × positive score. A total score ≥ 4 was considered positive expression, and < 4 was treated as negative expression.

Cell lines and culture

GIST-882 and GIST-T1 cell lines were obtained from the Shanghai Cancer Institute, and GIST-48 cell lines were kindly provided by Professor Jonathan Fletcher (Harvard Medical School, United States). GIST-882 and GIST-T1 cells were cultured with RPMI 1640 medium (Gibco, United States), and GIST-48 cells were cultured with DMEM (BioInd, Israel). Both medium preparations contained 10% fetal bovine serum (FBS) (Gibco, United States) and 1% penicillin-streptomycin in a humidified incubator at 37 °C with 5% CO2.

Cell transfection

The lentivirus for knocking down TAF15 (shRNA1, shRNA2, shRNA3) and control scrambled lentivirus (sh-scrambled) were purchased from Genomeditech (Shanghai, China). GIST-882 and GIST-T1 cells were seeded in a 12-well plate(Corning Life Sciences) at 1 × 10^5 cells per well, and the transfection was performed when the cell density reached about 50%. Cells were cultured in fresh medium after being infected with lentivirus for 72 h. The multiplicity of infection of lentivirus to GIST-882 and GIST-T1 was 30. Stable cell lines were generated through selection with puromycin (2 μg/mL). Transfection efficiency was detected using western blot analysis.

Cell immunofluorescence

Transfected cells were cultured in 12-well plates. When the cell density reached 50%-65%, cells were fixed using 4% paraformaldehyde for 30 min to make slides. 0.5% Triton X-100 was added to slides to allow for cell penetration, and 10% goat serum was used to block cells for 2 h at room temperature. Slides were then incubated with the TAF15 primary antibody (1:500, ab134916, Abcam, United States) at 4 °C overnight and then incubated with secondary antibodies for 1 h at room temperature. DAPI was used to stain the cell nuclei, and images were photographed using a fluorescent microscope. The fluorescent intensity of cells were measured using Image J software (version 3.2.0.8).

Cell counting kit-8 assay and colony formation assay

The cell counting kit (CCK)-8 (Dojindo, Tokyo, Japan) assay was performed according to the manufacturer's instructions. Briefly, different groups of cells were seeded onto 96-well plates at 1 × 10^3 cells per well. The CCK-8 reagent was added (10 μL/well) into the individual wells during the last hour. A microplate reader (Bio-Rad) was used to measure the optical density of the samples at 450 nm, as a measure of cell proliferation. With respect to the colony formation assay, different groups of cells were cultured in 6-well plates (500 cells/well) for 2 wk. Cell colonies were fixed with 4% paraformaldehyde for 30 min and stained with 1% crystal violet for 15 min at the room temperature. Colonies consisting of 50 or more cells were counted.

Transwell experiment

GIST-882 and GIST-T1 cells (3 × 10^4 cells/well) were inoculated into the upper polycarbonate membrane chambers of a 12-well plate without FBS, while the lower chamber contained RPMI 1640 medium with 10% FBS. To detect the cell invasion ability, matrix gel was in advance added to the polycarbonate membrane chambers. After being cultured for 48 h, the cells attached to the lower side were fixed with 4% paraformaldehyde for 30 min and stained with 1% crystal violet for 15 min at the room temperature. Five fields were selected randomly to count using an inverted microscope.

Wound healing assay

GIST-882 and GIST-T1 cells were cultured up to 90% confluency and then serum-starved for 12 h. The cell monolayer was scratched using a 1 mL plastic pipette tip. Culture medium was used to wash away the cell debris twice, and then cells were incubated in respective culture medium containing 10% FBS. Samples were photographed at 0 h, 12 h and 24 h post scratch using an Olympus microscope. The percentage of wound healing was evaluated using Image J software.

Modeling of GIST xenografts in nude mice

Nude mice aged 4 wk were purchased from the Beijing Vital River Laboratory Animal Technology Co., Ltd (Beijing, China). All animal care and processing were performed according to the Institutional Animal Care and Use Committee of Qingdao University guidelines. Twenty mice were divided randomly into two groups (10 mice per group) and then subcutaneously injected in the axillary region with stable cells (2×10^6 cells) transfected with sh-TAF15 or sh-scrambled. The volume (volume = length × width × width/2) of tumors were measured every 2 d. The mice were humanely sacrificed using the cervical dislocation method after anesthesia with 0.7% sodium pentobarbital. Tumor tissues were then excised, photographed and weighed.

Statistical analysis

Statistical analyses were performed using GraphPad Prism 9.3.1. The data analyses were conducted using Student's *t*-test, χ^2 test, one-way analysis of variance or Mann-Whitney *U* test. Data were expressed as mean ± standard deviation. $P < 0.05$ was considered statistically significant, and significance was indicated in each graph.

RESULTS

Quantification of DEPs by TMT

In total, 4111 proteins were quantified with a false discovery rate < 0.01 in all 12 GIST matched samples. Of these, 1669 were identified as significant DEPs on the basis of the filtering criteria of fold change > 1.2 or < 0.83 and *P* value < 0.05, including 762 upregulated proteins and 907 downregulated proteins (Figure 1A and Supplementary Table 1). Notably, the key proteins used for diagnosing GIST, including KIT, DOG1 and hematopoietic progenitor cell antigen CD34 (CD34), were all contained in the upregulated protein category (Supplementary Table 1), suggesting that our proteomic data were reliable. Moreover, 667, 686, 840 and 974 significant DEPs were identified in the NIH-H, NIH-I, NIH-L and NIH-VL subgroups, respectively (Figure 1B and Supplemental Table 2). After our systematic analysis of the top 10 upregulated and downregulated proteins (Table 2), we decided to focus on the protein TAF15 due to its important role in cell proliferation and migration.

Identification of TAF15 by western blotting analysis

Western blotting was used to further identify the expression levels of TAF15 in GIST. We detected the extracted proteins from tumor tissues (T) and matched normal tissues (N) of 18 GIST patients, including 6 NIH-H, 6 NIH-I, 3 NIH-L, and 3 NIH-VL cases. The results showed that the expression levels of TAF15 were significantly increased in tumor tissues compared with matched normal tissues (Figure 1C and D), which were in agreement with the results of our quantitative proteomics analysis (Table 2 and Supplemental Table 2).

Validation of TAF15 expression by immunohistochemical analysis

We evaluated the expression level of TAF15 in GIST patients using immunohistochemical (IHC) analysis of tumor tissues (T) from 161 patients and 18 matched normal tissues (N). We found significantly higher levels of expression of TAF15 in tumor tissues compared to matched normal tissues (red arrows, Figure 1E and F, Supplemental Table 3). Moreover, subgroup analyses showed that the expression level of TAF15 was significantly higher in the NIH-H subgroup than in the NIH-I, NIH-L and NIH-VL subgroups and that the expression level of TAF15 was significantly higher in the NIH-I subgroup than the NIH-VL subgroup (Figure 1G and Supplemental Table 3). We found no significant difference in the expression of TAF15 between the NIH-L and NIH-VL subgroups and between the NIH-I and NIH-L subgroups. Furthermore, based on our IHC data, we found that the overexpression level of TAF15 was positively correlated with tumor size and GIST risk stage but was not significantly correlated with gender, age or tumor metastasis (Table 3). These results provided evidence that the higher expression of TAF15 may contribute to malignant progression of GIST and that TAF15 may be a latent promoter or biomarker of GIST.

Knockdown of TAF15 inhibited the proliferation and migration of GIST cells

In order to understand the real role of TAF15 in GIST progression, short-hairpin RNAs (shRNAs) were used to knock down TAF15 in GIST-882 and GIST-T1 cells. GIST-882 and GIST-T1 cells were used instead of GIST-48 cells, as the expression level of TAF15 was higher in the former cell lines (Figure 2A). Three shRNAs targeting TAF15 (sh1, sh2 and sh3) were applied to knock down TAF15 protein. The results showed that sh2 and sh3 could significantly reduce the expression of TAF15 when compared to scrambled shRNA (scr), as tested by western blotting analysis (Figure 2B and C) and cell immunofluorescence assays (Figure 2D and E). Therefore, sh2 and sh3 were used to perform further experiments.

Table 2 The top 10 upregulated and downregulated proteins

Category	Accession	Protein name	FC,T *vs* N	*P* value
Up	P29400	COL4A5	3.129881192	0.001086699
	O94772	LY6H	2.995133385	0.012292301
	P05204	HMGN2	2.92528705	2.10765E-07
	O00479	HMGN4	2.900071252	3.22924E-09
	P20930	FLG	2.87152332	0.002555182
	P52926	HMGA2	2.687785701	0.008942412
	Q6UX72	B3GNT9	2.576105848	4.91404E-09
	Q92804	TAF15	2.456058544	1.54458E-05
	O95081	AGFG2	2.441304592	2.93054E-06
	P09936	UCHL1	2.157884674	7.498E-07
Down	Q96BQ1	FAM3D	0.225135868	0.022611851
	Q5DID0	UMODL1	0.242287446	0.00020958
	P25815	S100P	0.267045455	3.77116E-06
	P13640	MT1G	0.274242	0.0028833
	P42330	AKR1C3	0.290893518	6.40059E-07
	Q9UBU3	GHRL	0.293081189	0.000379102
	Q9NS71	GKN1	0.311488849	6.5931E-06
	O95994	AGR2	0.330784665	9.59846E-06
	P19075	TSPAN8	0.350779233	7.40703E-09
	P55087	AQP4	0.352590936	0.035544439

T: Tumor tissues; N: Matched tumor normal tissues; FC: Fold change.

The results of the CCK-8 assay and the colony formation assay indicated that TAF15 knockdown (sh2 and sh3) exhibited a significant decrease in proliferative and colony forming ability in GIST-882 and GIST-T1 cells when compared with the scr (Figure 3A-D). Transwell assay showed that the sh-TAF15 group (sh2 and sh3) exhibited significantly weaker migratory abilities compared to the scr in GIST-882 and GIST-T1 cells (Figure 3E and F). However, there was no significant difference in the invasion ability of GIST-882 and GIST-T1 cells between the sh-TAF15 group (sh2 and sh3) and sh-scrambled group (Figure 3G and H). The results of the wound healing assay also showed that migratory abilities significantly decreased in the sh-TAF15 group (sh2 and sh3) compared to the scr in GIST-882 and GIST-T1 cells (Figure 3I-K). These findings indicated that TAF15 knockdown can significantly inhibit GIST cell proliferation and migration.

TAF15 promoted GIST progression by activating the RAF1/MEK/ERK signaling pathway

Previous studies have shown that EWS, one of the members of the FET family proteins, forms a fusion oncoprotein EWS-FLI1 whose expression leads to the activation of ERK1/2 signaling in zebrafish embryos and adult tumors[24]. In consideration of the important role of the ERK signaling pathway in many human tumors[25], we speculated that TAF15 could promote cell proliferation and migration directly through the activation of the ERK signaling pathway in GIST. Therefore, we assessed the phosphorylation level of RAF1, MEK and ERK1/2 in GIST-882 and GIST-T1 by western blotting. The results showed that the phosphorylation levels of RAF1, MEK and ERK1/2 were significantly decreased following TAF15 knockdown (sh2 and sh3). However, there was no significant change in levels of total RAF1, MEK and ERK1/2 (Figure 4). Collectively, these findings suggest that TAF15 may promote cell proliferation and migration through the activation of the RAF1/MEK/ERK signaling pathway in GIST.

TAF15 promoted the growth of GIST in vivo

To further confirm the role of TAF15 in the progression of GIST, we established a xenograft mouse model utilizing GIST-882 cells due to their enhanced proliferative and migratory ability. sh2 was used in this experiment because of its higher knockdown efficiency, with scr as a control. Twenty nude female mice were randomly divided into two groups, and each mouse was then subcutaneously injected with

Table 3 Correlation between the expression of TATA-box-binding protein-associated factor 15 and clinicopathological characteristics in gastrointestinal stromal tumors

Characteristics	TAF15 expression		*P* value
	Negative	Positive	
Total number	31	130	
Sex			0.2730[a]
Male	16 (9.9)	53 (32.9)	
Female	15 (9.3)	77 (58.7)	
Age in yr			0.8228[a]
≤ 60	15 (9.3)	60 (37.2)	
> 60	16 (9.9)	70 (43.5)	
Tumor size			
Maximum diameter in cm			
≤ 5	29 (18.0)	74 (46.0)	0.0001[a]
> 5	2 (1.2)	56 (34.8)	
GIST risk stage			0.0021[b]
Very low risk	15 (9.3)	30 (18.6)	
Low risk	11 (6.8)	31 (19.3)	
Intermediate risk	3 (1.9)	29 (18.0)	
High risk	2 (1.2)	40 (24.8)	
Metastasis			0.1316[a]
-	31 (19.3)	121 (75.2)	
+	0 (0.0)	9 (5.6)	

[a]*P* values were calculated by χ^2 test.
[b]*P* values were calculated by Mann-Whitney *U* test.
Total patients of 161. Data are presented as *n*(%). TAF15: TATA-box-binding protein-associated factor 15; GIST: Gastrointestinal stromal tumor.

either sh2 or scr cells. Unfortunately, one mouse in the scr group died on day 7 post-injection for an unknown reason. Ten days after injection, xenograft tumors in the remaining mice were detectable. The results showed that TAF15 knockdown significantly suppressed tumor growth and tumor weight (Figure 5A-C). Furthermore, western blotting analysis was used to confirm the level of TAF15 in the xenograft tumors. The results showed that the levels of TAF15 were significantly decreased in the sh2 group compared to the scr group (Figure 5D and E). Additionally, three xenograft tumors of the sh2 group and three xenograft tumors of the scr group were randomly selected to test the levels of RAF1, MEK and ERK1/2 by western blotting. The results indicated that the phosphorylation levels of RAF1, MEK and ERK also decreased significantly in the sh2 group, while the levels of total RAF1, MEK and ERK showed no significant change (Figure 5F-I). These data indicated that TAF15 may promote the growth of GIST *in vivo via* the activation of the RAF1/MEK/ERK signaling pathway.

DISCUSSION

KIT and PDGFRA mutations are considered to be two major factors in GIST pathogenesis[3,26], and drugs targeting KIT and PDGFRA pathways have achieved great success in the treatment of this disease [27,28]. However, GIST patients gradually become resistant to current targeted drug treatment in recent years[14,28]. Therefore, there is an unmet need to explore other latent targets.

An increasing number of biomarkers or targets have been reported to be important to GIST progression. For example, p53 is a biomarker and potential target in GIST; targeting the p53 pathway is a novel additional treatment strategy for GIST[29]. High expression of carbohydrate antigen 125 is an independent risk factor for GIST progression, and it is a significant biomarker in the overall management of GIST patients[30]. Brain-derived neurotrophic factor is over expressed in high-risk GIST patients, and it may serve as a significant prognostic factor[31].In the present study, proteomic analysis

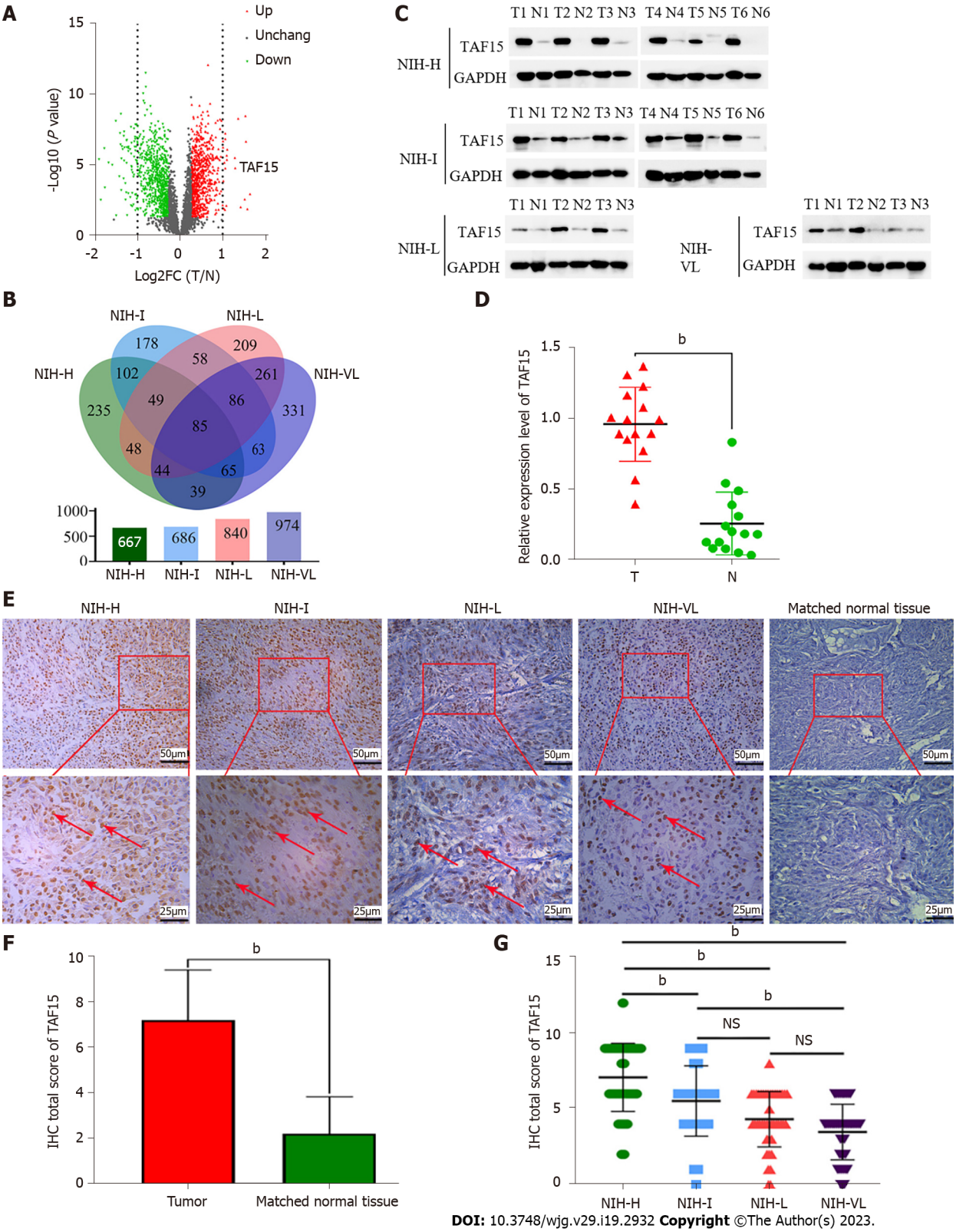
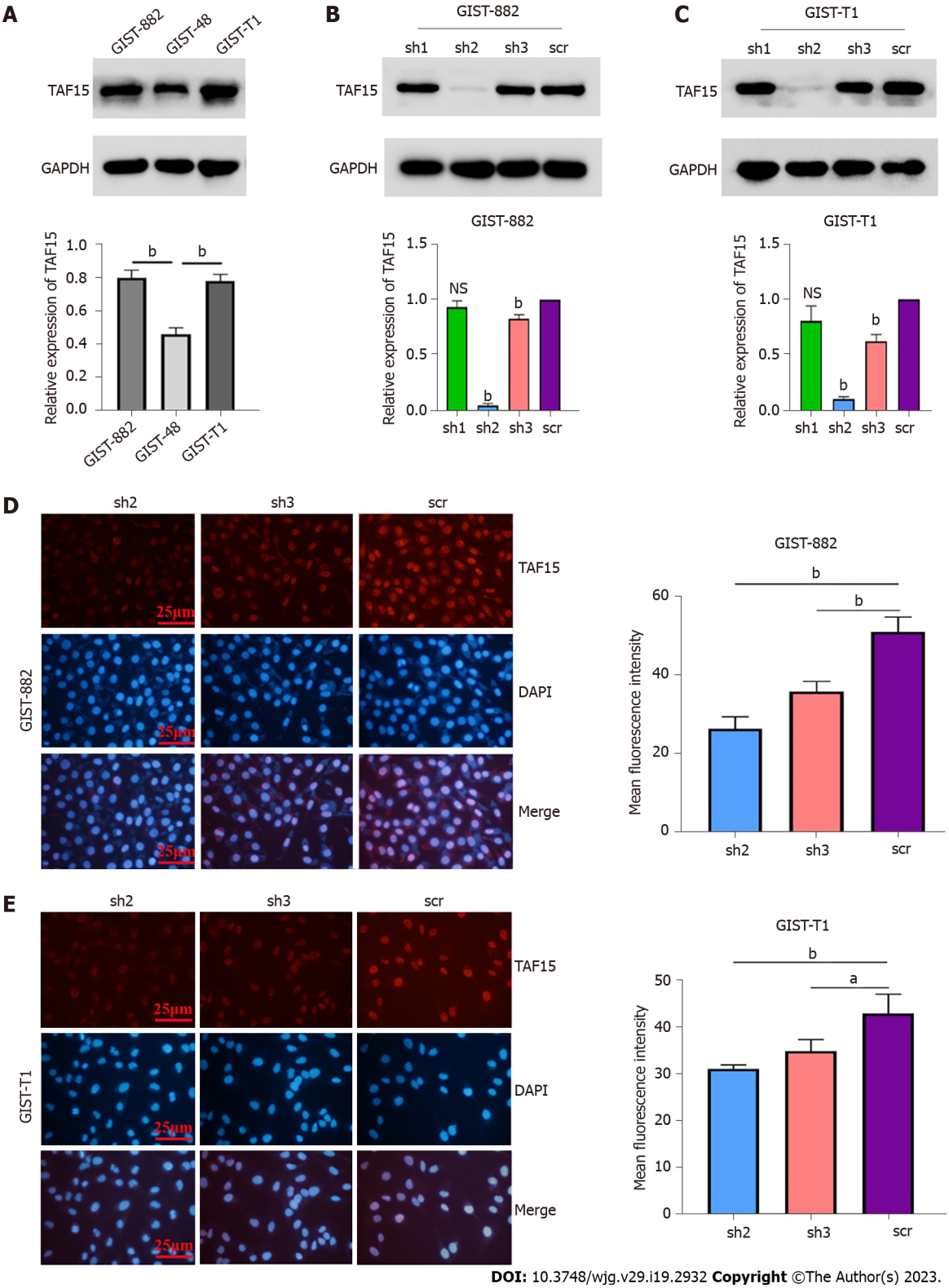
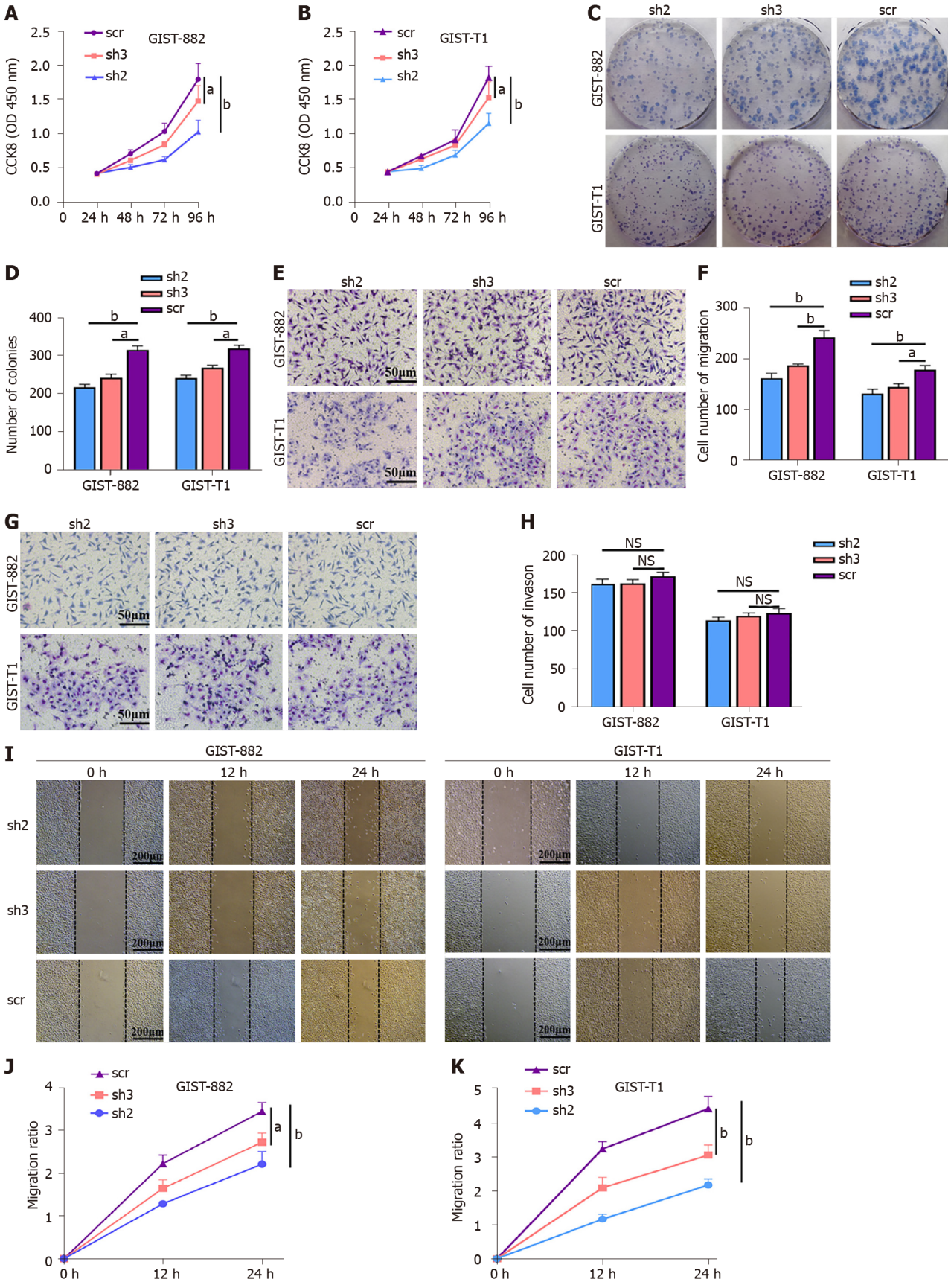


Figure 1 Differentially expressed proteins in gastrointestinal stromal tumor samples. A: Proteomic analysis identified the differentially expressed proteins in gastrointestinal stromal tumor (GIST) patients; B: Venn diagram showed the number of identified differentially expressed proteins in the subgroups of GIST; C and D: Western blotting identified that the expression level of TATA-box-binding protein-associated factor 15 (TAF15) was significantly increased in tumor tissues compared with matched normal tissues in all 18 GIST samples. *P* values were calculated using the Student's *t*-test; E: Immunohistochemical analysis verified the expression of TAF15 using 161 GIST tumor tissues and 18 matched normal tissues (representative images are shown and red arrows indicate positive staining); F: Total immunostaining score of TAF15 protein in tumor tissues and matched normal tissues of GIST; G: Total immunostaining score of TAF15 proteins in the GIST subgroup. *P* values were calculated using the Student's *t*-test or one-way analysis of variance. $^{b}P < 0.01$. NS: No significance between groups; NIH-H: National Institutes of Health high risk; NIH-I: National Institutes of Health intermediate risk; NIH-L: National Institutes of Health low risk; NIH-VL: National Institutes of Health very low risk; IHC: Immunohistochemical; T: Tumor tissues; N: Normal tissues; FC: Fold change; TAF15: TATA-box-binding protein-associated factor 15.



DOI: 10.3748/wjg.v29.i19.2932 **Copyright** ©The Author(s) 2023.

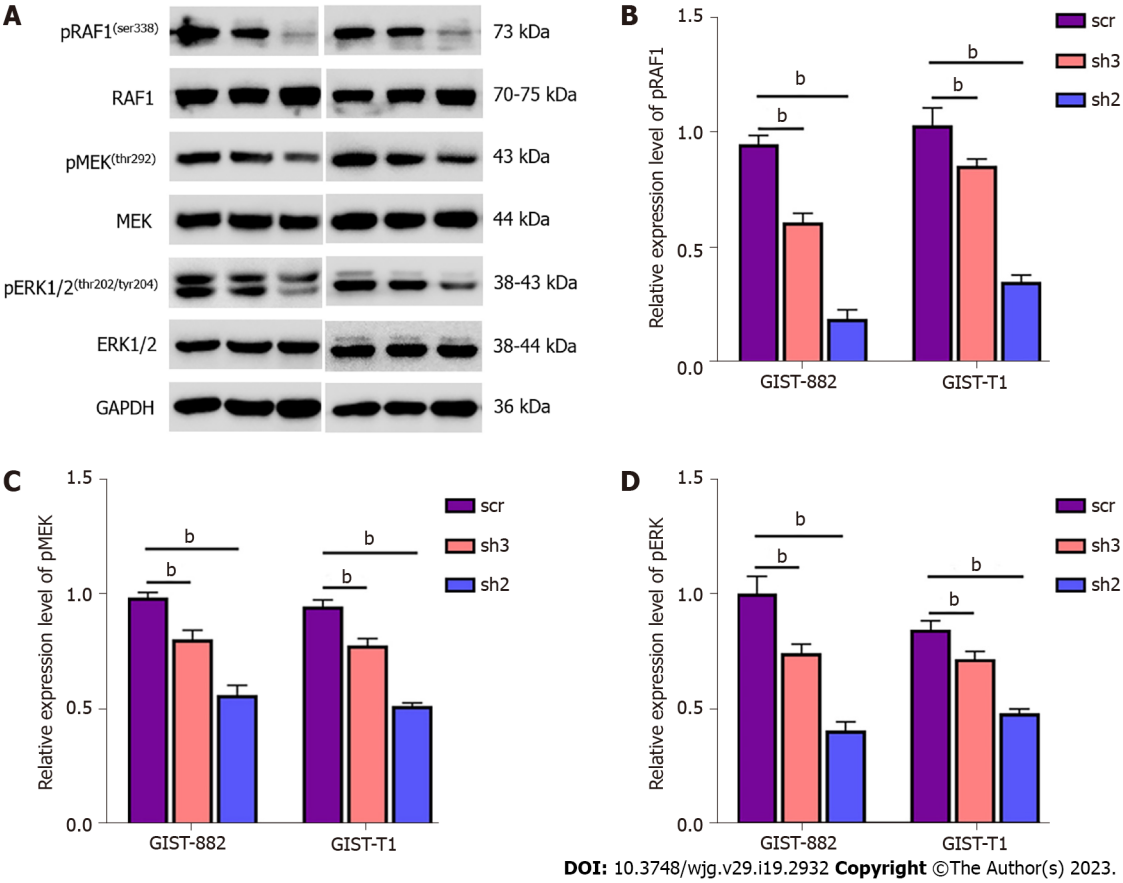
Figure 2 The knockdown efficiency of short hairpin-TATA-box-binding protein-associated factor 15 in gastrointestinal stromal tumor cell lines. A: Western blotting to detect the expression level of TATA-box-binding protein-associated factor 15 (TAF15) in gastrointestinal stromal tumor(GIST) cell lines. *P* values were calculated by one-way analysis of variance; B and C: TAF15 was knocked down using three short hairpin (sh) RNAs (sh1, sh2, and sh3) and scrambled shRNA (scr) as control in GIST-882 and GIST-T1 cells. The results showed that sh2 and sh3 could reduce the expression level of TAF15 significantly when compared to scr as tested by western blotting analysis; D and E: The fluorescence intensity of TAF15 in sh2 and sh3 was reduced significantly when compared to scr in GIST-882 and GIST-T1 cells as tested by a cell immunofluorescence assay. *P* values were calculated using the Student's *t*-test. $^{a}P < 0.05$, $^{b}P < 0.01$. NS: No significance between groups; GIST: Gastrointestinal stromal tumor; TAF15: TATA-box-binding protein-associated factor 15; sh1: shRNA1 targeting TATA-box-binding protein-associated factor 15; sh2: shRNA2 targeting TATA-box-binding protein-associated factor 15; sh3: shRNA3 targeting TATA-box-binding protein-associated factor 15; scr: Scrambled shRNA.



DOI: 10.3748/wjg.v29.i19.2932 **Copyright** ©The Author(s) 2023.

Figure 3 TATA-box-binding protein-associated factor 15 regulated the proliferation and migration of gastrointestinal stromal tumor cells. A and B: Cell counting kit-8 assay was performed to detect the proliferation of gastrointestinal stromal tumor (GIST)-882 and GIST-T1 after cell transfection. *P* values were calculated using the Student's *t*-test; C and D: A colony formation assay identified the proliferative ability of GIST-882 and GIST-T1 after cell transfection. Statistical analyses were performed using the Student's *t*-test; E-H: A transwell assay was performed to analyze the migratory and invasive ability of GIST-882 and

GIST-T1 cells after transfection. *P* values were calculated using the Student's *t*-test; I-K: A wound healing assay was conducted to confirm the migratory ability of GIST-882 and GIST-T1 cells after transfection. *P* values were calculated using the Student's *t*-test. $^{a}P < 0.05$, $^{b}P < 0.01$. GIST: Gastrointestinal stromal tumor; NS: No significance between groups; sh2: shRNA2 targeting TATA-box-binding protein-associated factor 15; sh3: shRNA3 targeting TATA-box-binding protein-associated factor 15; scr: Scrambled shRNA; CCK8: Cell counting kit-8.



DOI: 10.3748/wjg.v29.i19.2932 **Copyright** ©The Author(s) 2023.

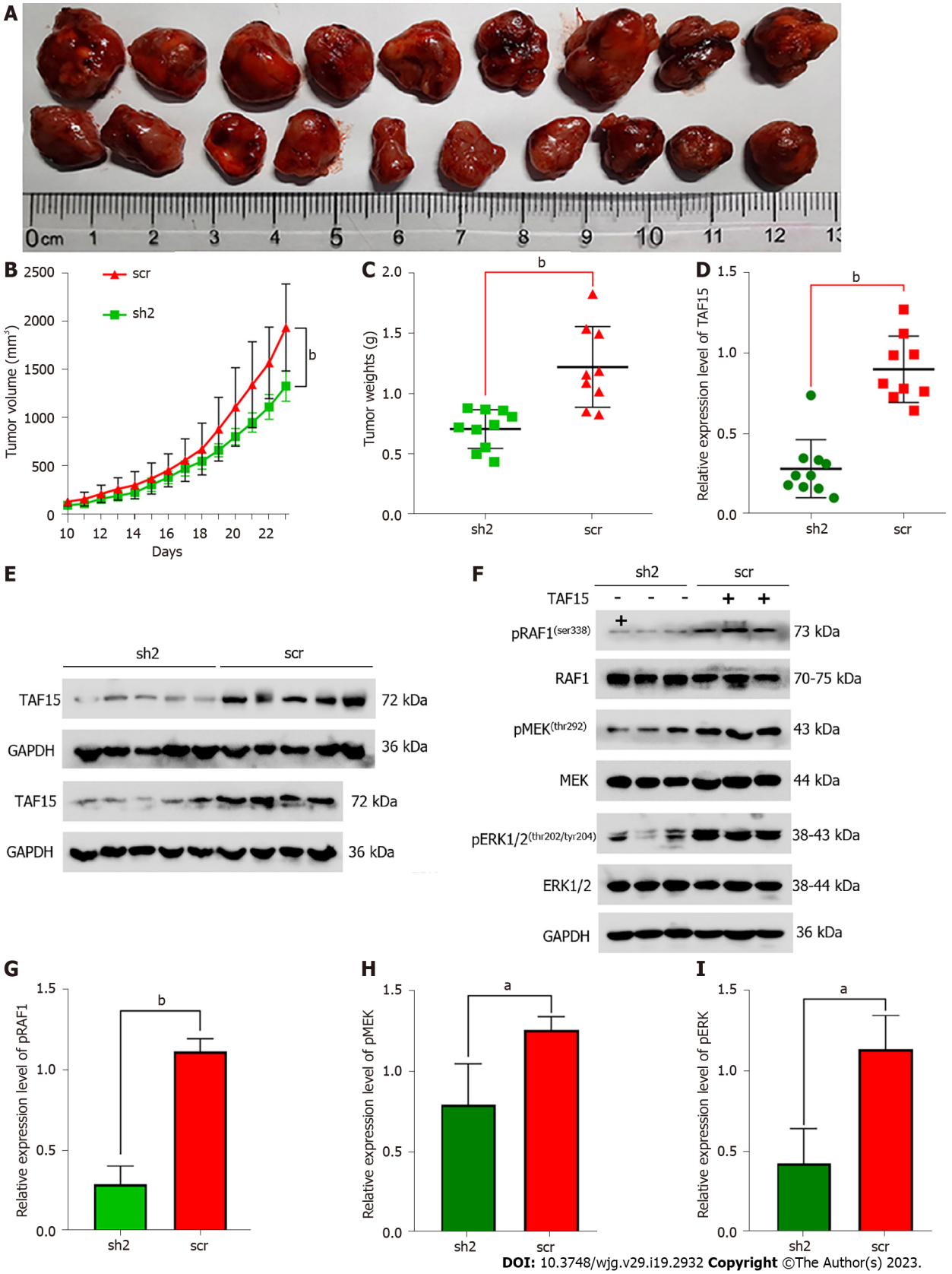
Figure 4 TATA-box-binding protein-associated factor 15 promoted the proliferation and migration of gastrointestinal stromal tumor cells by activating the RAF1/MEK/ERK pathway. A: Western blotting analysis detected the protein level of pRAF1/RAF1, pMEK/MEK and pERK/ERK in gastrointestinal stromal tumor (GIST)-882 and GIST-T1 after cell transfection; B-D: The phosphorylation levels of RAF1, MEK and ERK1/2 were significantly decreased inshRNA2 targeting TATA-box-binding protein-associated factor 15 and shRNA3 targeting TATA-box-binding protein-associated factor 15 when compared to the scrambled shRNA in GIST cell lines. Statistical analyses were executed by the Student's *t*-test. $^{b}P < 0.01$. GIST: Gastrointestinal stromal tumor; sh2: shRNA2 targeting TATA-box-binding protein-associated factor 15; sh3: shRNA3 targeting TATA-box-binding protein-associated factor 15; scr: Scrambled shRNA.

was performed in patients with GIST to explore the potential molecular biomarkers for prediction, early diagnosis or treatment.

A total of 4111 quantified proteins with 1669 DEPs (762 upregulated and 907 downregulated proteins) were revealed in our study. Among the top 10 DEPs identified, TAF15 was interesting due to its key role in promoting growth in other human tumors such as extraskeletalmyxoid sarcomas, leukemia, Ewing's sarcomas, human neuroblastoma and lung squamous cell carcinoma[15,17,19,20,32]. TAF15 was first reported as an RNA or DNA binding protein, while more recent studies have shown that TAF15 also plays important roles in cellular stress responses, cell spreading and cell adhesion[33,34]. GAS5 binding to TAF15 could upregulate expression of HIF1A,thus promoting wound healing in diabetic foot ulcers [35].

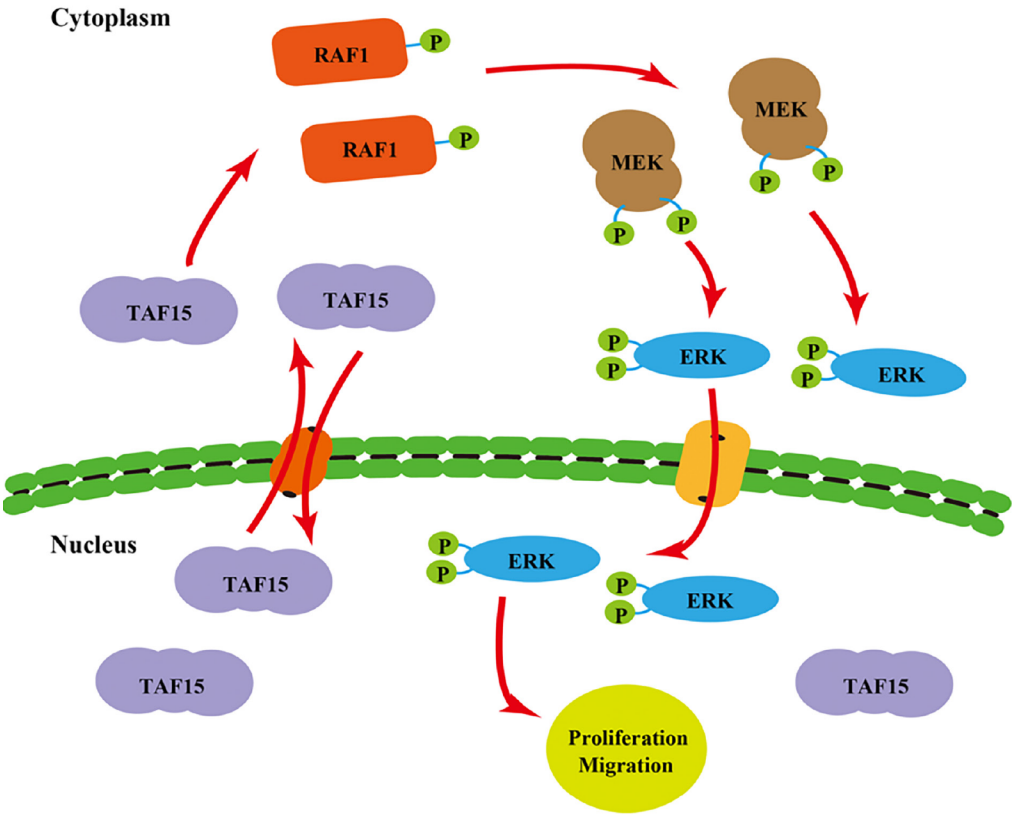
We believe our study is the first to confirm that TAF15 is over expressed in GIST tissues and cell lines and that high expression levels of TAF15 are positively correlated with tumor size and GIST risk stage. Previous studies have shown that the inhibition of TAF15 expression could significantly reduce cellular proliferation in melanoma and lung cancer[20,21]. Similarly, our study demonstrated that TAF15 knockdown could significantly inhibit proliferation and migration of GIST cells *in vitro* and suppress tumor growth *in vivo*. These data provided evidence that overexpression of TAF15 may contribute to the malignant progression of GIST.

The latent molecular mechanism of TAF15 in GIST was also first investigated in this study. Previous studies have shown that FET family proteins are mainly present in the nucleus[34], but it is now known that they also shuttle between the nucleus and cytoplasm[36-38]. They have an extensive functionality



DOI: 10.3748/wjg.v29.i19.2932 **Copyright** ©The Author(s) 2023.

Figure 5 TATA-box-binding protein-associated factor 15 suppressed tumor growth of gastrointestinal stromal tumor cells *in vivo*. A-C: The volumes and weights of tumors in the shRNA2 targeting TATA-box-binding protein-associated factor 15 group were significantly smaller than the scrambled shRNA group. Statistical analyses were performed using the Student's *t*-test; D and E: Western blotting analysis was used to confirm the expression levels of TATA-box-binding protein-associated factor 15 in xenograft tumors; F-I: Western blotting analysis confirmed the protein levels of pRAF1/RAF1, pMEK/MEK and pERK/ERK in xenograft tumors. *P* values were calculated using the Student's *t*-test. $^{a}P < 0.05$, $^{b}P < 0.01$. TAF15: TATA-box-binding protein-associated factor 15; sh2: shRNA2 targeting TATA-box-binding protein-associated factor 15; scr: Scrambled shRNA.



DOI: 10.3748/wjg.v29.i19.2932 **Copyright** ©The Author(s) 2023.

Figure 6 A schematic diagram of the mechanism of action of TATA-box-binding protein-associated factor 15 in gastrointestinal stromal tumors. TATA-box-binding protein-associated factor 15 shuttles between the nucleus and cytoplasm and promotes proliferation and migration of gastrointestinal stromal tumor cells by activating the RAF1/MEK/ERK pathway. TAF15: TATA-box-binding protein-associated factor 15.

including regulation and interaction with various proteins[39,40]. Moreover, recent work demonstrated that EWS-FLI1 fusion protein expression leads to activation of ERK1/2 signaling in zebrafish embryos and adult tumors[24]. Additionally, it is well known that the RAF/MEK/ERK signaling pathway plays an essential role in promoting cellular proliferation and survival[41].

In our study, we found TAF15 knockdown could significantly decrease the phosphorylation levels of RAF1, MEK and ERK, without significantly changing the total amounts of RAF1, MEK and ERK in GIST cell lines and xenograft tumors. Similarly, TAF15 is involved in the promotion of cell proliferation, migration and invasion of lung squamous cell carcinoma by activating the MAPK signaling pathway [22]. These results suggested that the activation of the ERK pathway may represent a new function of the TAF15 protein beyond DNA binding, mRNA splicing and mRNA transport. Taken together, these findings suggested that TAF15 shuttles between the nucleus and cytoplasm and may promote cell proliferation and migration directly through the activation of the RAF1/MEK/ERK signaling pathway in GIST (Figure 6). These observations greatly extend the functional repertoire of TAF15.

However, due to difficulty of obtaining matched tumor tissues after surgery[23], the number of paired samples used in this study for proteomic analysis, western blotting and IHC were small. Thus, we acknowledge that the accuracy of the proteomic analysis, western blotting and IHC in this research may be affected by the sample size and that the statistical analyses may be less robust due to the small sample size. Further studies will help validate some of the important and interesting findings of this study in larger GIST cohorts when available. Additional roles of TAF15 in GIST remain to be explored, as hundreds of genes lie downstream of TAF15[42].

CONCLUSION

In summary, this study utilized a proteomic analysis to find new molecular therapeutic targets for GIST and analyzed the expression level and underlying biological functions of TAF15 in GIST. Moreover, our study may be the first to demonstrate that TAF15 expression may contribute to malignant progression of GIST. TAF15promoted cell proliferation and migration in GIST *via* the RAF1/MEK/ERK signaling pathway. Therefore, TAF15 is expected to be a novel latent molecular biomarker or therapeutic target of GIST.

ARTICLE HIGHLIGHTS

Research background

Gastrointestinal stromal tumors (GIST) are a common neoplasm with high rates of recurrence and metastasis, and its therapeutic efficacy is still not ideal. There is an unmet need to find new molecular therapeutic targets for GIST. TATA-box-binding protein-associated factor 15 (TAF15) contributes to the progress of various tumors, while the role and molecular mechanism of TAF15 in GIST progression are still unknown.

Research motivation

To explore the novel early diagnostic markers or therapeutic targets for the diagnosis and treatment of GIST.

Research objectives

To investigate new molecular therapeutic targets for GIST and explore the role and potential molecular mechanism of TAF15 in GIST progression.

Research methods

Proteomic analysis was performed to explore the differentially expressed proteins in GIST. Western blotting and immunohistochemical analysis were used to verify expression levels of TAF15 in GIST tissues and cell lines. Cell counting kit-8, colony formation, transwell, wound healing and western blotting assays were applied to explore the effect and the molecular mechanism of TAF15 in GIST. The role of TAF15 *in vivo* was confirmed using a xenograft mouse model assay.

Research results

A total of 1669 proteins were identified as differentially expressed proteins with 762 upregulated and 907 downregulated in GIST. TAF15 was significantly upregulated in GIST tissues and cell lines. Overexpression of TAF15 was associated with larger tumor size and higher risk stage of GIST. TAF15 knockdown suppressed proliferation and migration of GIST cells *in vitro* and inhibited the growth of GIST *in vivo*. Moreover, the inhibition of TAF15 expression significantly decreased the phosphorylation level of RAF1, MEK and ERK1/2 in GIST cells and xenograft tissues, while the total levels of RAF1, MEK and ERK1/2 had no significant changes.

Research conclusions

TAF15 may contribute to malignant progression of GIST and promote cell proliferation and migration in GIST *via* the activation of the RAF1/MEK/ERK signaling pathway.

Research perspectives

TAF15 is expected to be a novel latent molecular biomarker or therapeutic target of GIST.

FOOTNOTES

Author contributions: Guo CM and Tang L contributed equally to this work; Guo CM and Tang L performed the data acquisition, drafted the manuscript and executed the *in vitro* experiments; Guo CM completed the statistical analyses; Guo CM and Li X executed the animal experiments; Huang LY designed the work and revised the manuscript.

Supported by National Natural Science Foundation of China, No. 81870453.

Institutional review board statement: The study was conducted according to the guidelines of the Declaration of Helsinki, and approved by Ethics Committee of Yantai Yuhuangding Hospital,No.2019-410.

Institutional animal care and use committee statement: All animal experiments were approved by the Affiliated Yantai Yuhuangding Hospital of Qingdao University for Laboratory Animal Welfare and Ethical Review, No. 2022-A56.

Informed consent statement: All study participants or their legal guardian provided informed written consent about personal and medical data collection prior to study enrolment.

Conflict-of-interest statement: All authors report having no relevant conflicts of interest for this article.

Data sharing statement: The data can be obtained from the corresponding author upon reasonable request.

ARRIVE guidelines statement: The authors have read the ARRIVE guidelines, and the manuscript was prepared and

revised according to the ARRIVE guidelines.

Open-Access: This article is an open-access article that was selected by an in-house editor and fully peer-reviewed by external reviewers. It is distributed in accordance with the Creative Commons Attribution NonCommercial (CC BY-NC 4.0) license, which permits others to distribute, remix, adapt, build upon this work non-commercially, and license their derivative works on different terms, provided the original work is properly cited and the use is non-commercial. See: https://creativecommons.org/Licenses/by-nc/4.0/

Country/Territory of origin: China

ORCID number: Cheng-Ming Guo 0000-0002-6844-6223; Li Tang 0000-0002-1491-2129; Xu Li 0000-0002-4389-0352; Liu-Ye Huang 0000-0002-5016-0331.

S-Editor: Fan JR
L-Editor: Filipodia
P-Editor: Yu HG

REFERENCES

1 **Wu CE**, Tzen CY, Wang SY, Yeh CN. Clinical Diagnosis of Gastrointestinal Stromal Tumor (GIST): From the Molecular Genetic Point of View. *Cancers (Basel)* 2019; **11** [PMID: 31100836 DOI: 10.3390/cancers11050679]

2 **Casali PG**, Abecassis N, Aro HT, Bauer S, Biagini R, Bielack S, Bonvalot S, Boukovinas I, BoveeJVMG, Brodowicz T, Broto JM, Buonadonna A, De Álava E, Dei Tos AP, Del MuroXG, Dileo P, Eriksson M, Fedenko A, Ferraresi V, Ferrari A, Ferrari S, Frezza AM, Gasperoni S, Gelderblom H, Gil T, Grignani G, Gronchi A, Haas RL, Hassan B, Hohenberger P, Issels R, Joensuu H, Jones RL, Judson I, Jutte P, Kaal S, Kasper B, Kopeckova K, Krákorová DA, Le Cesne A, Lugowska I, Merimsky O, Montemurro M, Pantaleo MA, Piana R, Picci P, Piperno-Neumann S, Pousa AL, Reichardt P, Robinson MH, Rutkowski P, Safwat AA, Schöffski P, Sleijfer S, Stacchiotti S, Sundby Hall K, Unk M, Van Coevorden F, van der Graaf WTA, Whelan J, Wardelmann E, Zaikova O, Blay JY; ESMO Guidelines Committee and EURACAN. Gastrointestinal stromal tumours: ESMO-EURACAN Clinical Practice Guidelines for diagnosis, treatment and follow-up. *Ann Oncol* 2018; **29**: iv267 [PMID: 30188977 DOI: 10.1093/annonc/mdy320]

3 **Heinrich MC**, Corless CL, Duensing A, McGreevey L, Chen CJ, Joseph N, Singer S, Griffith DJ, Haley A, Town A, Demetri GD, Fletcher CD, Fletcher JA. PDGFRA activating mutations in gastrointestinal stromal tumors. *Science* 2003; **299**: 708-710 [PMID: 12522257 DOI: 10.1126/science.1079666]

4 **Miettinen M**, Lasota J. Gastrointestinal stromal tumors. *Gastroenterol Clin North Am* 2013; **42**: 399-415 [PMID: 23639648 DOI: 10.1016/j.gtc.2013.01.001]

5 **Xue A**, Gao X, He Y, Shu P, Huang X, Sun J, Lu J, Hou Y, Fang Y, Shen K. Role of Surgery in the Management of Liver Metastases From Gastrointestinal Stromal Tumors. *Front Oncol* 2022; **12**: 903487 [PMID: 35847933 DOI: 10.3389/fonc.2022.903487]

6 **Zhang D**, He C, Guo Y, Li J, Li B, Zhao Y, Yu L, Chang Z, Pei H, Yang M, Li N, Zhang Q, He Y, Pan Y, Zhao ZJ, Zhang C, Chen Y. Efficacy of SCF drug conjugate targeting c-KIT in gastrointestinal stromal tumor. *BMC Med* 2022; **20**: 257 [PMID: 35999600 DOI: 10.1186/s12916-022-02465-3]

7 **Joensuu H**, Vehtari A, Riihimäki J, Nishida T, Steigen SE, Brabec P, Plank L, Nilsson B, Cirilli C, Braconi C, Bordoni A, Magnusson MK, Linke Z, Sufliarsky J, Federico M, Jonasson JG, Dei Tos AP, Rutkowski P. Risk of recurrence of gastrointestinal stromal tumour after surgery: an analysis of pooled population-based cohorts. *Lancet Oncol* 2012; **13**: 265-274 [PMID: 22153892 DOI: 10.1016/S1470-2045(11)70299-6]

8 **Fletcher CD**, Berman JJ, Corless C, Gorstein F, Lasota J, Longley BJ, Miettinen M, O'Leary TJ, Remotti H, Rubin BP, Shmookler B, Sobin LH, Weiss SW. Diagnosis of gastrointestinal stromal tumors: A consensus approach. *Hum Pathol* 2002; **33**: 459-465 [PMID: 12094370 DOI: 10.1053/hupa.2002.123545]

9 **Li S**, Chen D, Li S, Zhao Z, Yang H, Wang D, Zhang Z, Fu W. Novel Prognostic Nomogram for Recurrence-Free Survival of Patients With Primary Gastrointestinal Stromal Tumors After Surgical Resection: Combination of Prognostic Nutritional Index and Basic Variables. *Front Oncol* 2020; **10**: 581855 [PMID: 33585198 DOI: 10.3389/fonc.2020.581855]

10 **Bang YH**, Ryu MH, Kim HD, Lee HE, Kang YK. Clinical outcomes and prognostic factors for patients with high-risk gastrointestinal stromal tumors treated with 3-year adjuvant imatinib. *Int J Cancer* 2022; **151**: 1770-1777 [PMID: 35678337 DOI: 10.1002/ijc.34157]

11 **Nunobe S**, Sano T, Shimada K, Sakamoto Y, Kosuge T. Surgery including liver resection for metastatic gastrointestinal stromal tumors or gastrointestinal leiomyosarcomas. *Jpn J Clin Oncol* 2005; **35**: 338-341 [PMID: 15928191 DOI: 10.1093/jjco/hyi091]

12 **Keung EZ**, Raut CP, Rutkowski P. The Landmark Series: Systemic Therapy for Resectable Gastrointestinal Stromal Tumors. *Ann Surg Oncol* 2020; **27**: 3659-3671 [PMID: 32734368 DOI: 10.1245/s10434-020-08869-w]

13 **Hemming ML**, Heinrich MC, Bauer S, George S. Translational insights into gastrointestinal stromal tumor and current clinical advances. *Ann Oncol* 2018; **29**: 2037-2045 [PMID: 30101284 DOI: 10.1093/annonc/mdy309]

14 **Joensuu H**, Rutkowski P, Nishida T, Steigen SE, Brabec P, Plank L, Nilsson B, Braconi C, Bordoni A, Magnusson MK, Sufliarsky J, Federico M, Jonasson JG, Hostein I, Bringuier PP, Emile JF. KIT and PDGFRA mutations and the risk of GI stromal tumor recurrence. *J Clin Oncol* 2015; **33**: 634-642 [PMID: 25605837 DOI: 10.1200/JCO.2014.57.4970]

15 **Lindén M**, Vannas C, Österlund T, Andersson L, Osman A, Escobar M, Fagman H, Ståhlberg A, Åman P. FET fusion oncoproteins interact with BRD4 and SWI/SNF chromatin remodelling complex subtypes in sarcoma. *Mol Oncol* 2022;

16: 2470-2495 [PMID: 35182012 DOI: 10.1002/1878-0261.13195]
16 **Glisovic T**, Bachorik JL, Yong J, Dreyfuss G. RNA-binding proteins and post-transcriptional gene regulation. *FEBS Lett* 2008; **582**: 1977-1986 [PMID: 18342629 DOI: 10.1016/j.febslet.2008.03.004]
17 **Zuo L**, Zhang G, Massett M, Cheng J, Guo Z, Wang L, Gao Y, Li R, Huang X, Li P, Qi Z. Loci-specific phase separation of FET fusion oncoproteins promotes gene transcription. *Nat Commun* 2021; **12**: 1491 [PMID: 33674598 DOI: 10.1038/s41467-021-21690-7]
18 **Wang J**, Cai Y, Lu H, Zhang F, Zheng J. LncRNA APOA1-AS facilitates proliferation and migration and represses apoptosis of VSMCs through TAF15-mediated SMAD3 mRNA stabilization. *Cell Cycle* 2021; **20**: 1642-1652 [PMID: 34382908 DOI: 10.1080/15384101.2021.1951940]
19 **Ballarino M**, Jobert L, Dembélé D, de la Grange P, Auboeuf D, Tora L. TAF15 is important for cellular proliferation and regulates the expression of a subset of cell cycle genes through miRNAs. *Oncogene* 2013; **32**: 4646-4655 [PMID: 23128393 DOI: 10.1038/onc.2012.490]
20 **Singh AK**, Kapoor V, Thotala D, Hallahan DE. TAF15 contributes to the radiation-inducible stress response in cancer. *Oncotarget* 2020; **11**: 2647-2659 [PMID: 32676166 DOI: 10.18632/oncotarget.27663]
21 **Schatz N**, Brändlein S, Rückl K, Hensel F, Vollmers HP. Diagnostic and therapeutic potential of a human antibody cloned from a cancer patient that binds to a tumor-specific variant of transcription factor TAF15. *Cancer Res* 2010; **70**: 398-408 [PMID: 20048082 DOI: 10.1158/0008-5472.CAN-09-2186]
22 **Zhu H**, Liu Q, Yang X, Ding C, Wang Q, Xiong Y. LncRNA LINC00649 recruits TAF15 and enhances MAPK6 expression to promote the development of lung squamous cell carcinoma *via* activating MAPK signaling pathway. *Cancer Gene Ther* 2022; **29**: 1285-1295 [PMID: 35228660 DOI: 10.1038/s41417-021-00410-9]
23 **Li J**, Ye Y, Wang J, Zhang B, Qin S, Shi Y, He Y, Liang X, Liu X, Zhou Y, Wu X, Zhang X, Wang M, Gao Z, Lin T, Cao H, Shen L; Chinese Society Of Clinical Oncology Csco Expert Committee On Gastrointestinal Stromal Tumor. Chinese consensus guidelines for diagnosis and management of gastrointestinal stromal tumor. *Chin J Cancer Res* 2017; **29**: 281-293 [PMID: 28947860 DOI: 10.21147/j.issn.1000-9604.2017.04.01]
24 **Vasileva E**, Warren M, Triche TJ, Amatruda JF. Dysregulated heparan sulfate proteoglycan metabolism promotes Ewing sarcoma tumor growth. *Elife* 2022; **11** [PMID: 35285802 DOI: 10.7554/eLife.69734]
25 **Ullah R**, Yin Q, Snell AH, Wan L. RAF-MEK-ERK pathway in cancer evolution and treatment. *Semin Cancer Biol* 2022; **85**: 123-154 [PMID: 33992782 DOI: 10.1016/j.semcancer.2021.05.010]
26 **Miettinen M**, Sarlomo-Rikala M, Lasota J. Gastrointestinal stromal tumors: recent advances in understanding of their biology. *Hum Pathol* 1999; **30**: 1213-1220 [PMID: 10534170 DOI: 10.1016/s0046-8177(99)90040-0]
27 **Serrano C**, Mariño-Enríquez A, Tao DL, Ketzer J, Eilers G, Zhu M, Yu C, Mannan AM, Rubin BP, Demetri GD, Raut CP, Presnell A, McKinley A, Heinrich MC, Czaplinski JT, Sicinska E, Bauer S, George S, Fletcher JA. Complementary activity of tyrosine kinase inhibitors against secondary kit mutations in imatinib-resistant gastrointestinal stromal tumours. *Br J Cancer* 2019; **120**: 612-620 [PMID: 30792533 DOI: 10.1038/s41416-019-0389-6]
28 **Demetri GD**, Reichardt P, Kang YK, Blay JY, Rutkowski P, Gelderblom H, Hohenberger P, Leahy M, von Mehren M, Joensuu H, Badalamenti G, Blackstein M, Le Cesne A, Schöffski P, Maki RG, Bauer S, Nguyen BB, Xu J, Nishida T, Chung J, Kappeler C, Kuss I, Laurent D, Casali PG; GRID study investigators. Efficacy and safety of regorafenib for advanced gastrointestinal stromal tumours after failure of imatinib and sunitinib (GRID): an international, multicentre, randomised, placebo-controlled, phase 3 trial. *Lancet* 2013; **381**: 295-302 [PMID: 23177515 DOI: 10.1016/S0140-6736(12)61857-1]
29 **Wu CE**, Chen CP, Huang WK, Pan YR, Aptullahoglu E, Yeh CN, Lunec J. p53 as a biomarker and potential target in gastrointestinal stromal tumors. *Front Oncol* 2022; **12**: 872202 [PMID: 35965531 DOI: 10.3389/fonc.2022.872202]
30 **Sui C**, Lin C, Tao T, Guan W, Zhang H, Tao L, Wang M, Wang F. Prognostic significance of serum CA125 in the overall management for patients with gastrointestinal stromal tumors. *BMC Gastroenterol* 2023; **23**: 25 [PMID: 36703123 DOI: 10.1186/s12876-023-02655-0]
31 **Tian GA**, Xu WT, Sun Y, Wang J, Ke Q, Yuan MJ, Wang JJ, Zhuang C, Gong Q. BDNF expression in GISTs predicts poor prognosis when associated with PD-L1 positive tumor-infiltrating lymphocytes. *Oncoimmunology* 2021; **10**: 2003956 [PMID: 34804639 DOI: 10.1080/2162402X.2021.2003956]
32 **Xiong Y**, Yang C, Yang X, Ding C, Wang Q, Zhu H. LncRNA MIR9-3HG enhances LIMK1 mRNA and protein levels to contribute to the carcinogenesis of lung squamous cell carcinoma *via* sponging miR-138-5p and recruiting TAF15. *Pathol Res Pract* 2022; **237**: 153941 [PMID: 35933883 DOI: 10.1016/j.prp.2022.153941]
33 **de Hoog CL**, Foster LJ, Mann M. RNA and RNA binding proteins participate in early stages of cell spreading through spreading initiation centers. *Cell* 2004; **117**: 649-662 [PMID: 15163412 DOI: 10.1016/s0092-8674(04)00456-8]
34 **Andersson MK**, Ståhlberg A, Arvidsson Y, Olofsson A, Semb H, Stenman G, Nilsson O, Aman P. The multifunctional FUS, EWS and TAF15 proto-oncoproteins show cell type-specific expression patterns and involvement in cell spreading and stress response. *BMC Cell Biol* 2008; **9**: 37 [PMID: 18620564 DOI: 10.1186/1471-2121-9-37]
35 **Peng WX**, He PX, Liu LJ, Zhu T, Zhong YQ, Xiang L, Peng K, Yang JJ, Xiang GD. LncRNA GAS5 activates the HIF1A/VEGF pathway by binding to TAF15 to promote wound healing in diabetic foot ulcers. *Lab Invest* 2021; **101**: 1071-1083 [PMID: 33875793 DOI: 10.1038/s41374-021-00598-2]
36 **Marko M**, Vlassis A, Guialis A, Leichter M. Domains involved in TAF15 subcellular localisation: dependence on cell type and ongoing transcription. *Gene* 2012; **506**: 331-338 [PMID: 22771914 DOI: 10.1016/j.gene.2012.06.088]
37 **Zinszner H**, Sok J, Immanuel D, Yin Y, Ron D. TLS (FUS) binds RNA *in vivo* and engages in nucleo-cytoplasmic shuttling. *J Cell Sci* 1997; **110** (Pt 15): 1741-1750 [PMID: 9264461 DOI: 10.1242/jcs.110.15.1741]
38 **Zakaryan RP**, Gehring H. Identification and characterization of the nuclear localization/retention signal in the EWS proto-oncoprotein. *J Mol Biol* 2006; **363**: 27-38 [PMID: 16965792 DOI: 10.1016/j.jmb.2006.08.018]
39 **Law WJ**, Cann KL, Hicks GG. TLS, EWS and TAF15: a model for transcriptional integration of gene expression. *Brief Funct Genomic Proteomic* 2006; **5**: 8-14 [PMID: 16769671 DOI: 10.1093/bfgp/ell015]
40 **Rual JF**, Venkatesan K, Hao T, Hirozane-Kishikawa T, Dricot A, Li N, Berriz GF, Gibbons FD, Dreze M, Ayivi-

Guedehoussou N, Klitgord N, Simon C, Boxem M, Milstein S, Rosenberg J, Goldberg DS, Zhang LV, Wong SL, Franklin G, Li S, Albala JS, Lim J, Fraughton C, Llamosas E, Cevik S, Bex C, Lamesch P, Sikorski RS, Vandenhaute J, Zoghbi HY, Smolyar A, Bosak S, Sequerra R, Doucette-Stamm L, Cusick ME, Hill DE, Roth FP, Vidal M. Towards a proteome-scale map of the human protein-protein interaction network. *Nature* 2005; **437**: 1173-1178 [PMID: 16189514 DOI: 10.1038/nature04209]

41 **Yaeger R**, Corcoran RB. Targeting Alterations in the RAF-MEK Pathway. *Cancer Discov* 2019; **9**: 329-341 [PMID: 30770389 DOI: 10.1158/2159-8290.CD-18-1321]

42 **Kume K**, Ikeda M, Miura S, Ito K, Sato KA, Ohmori Y, Endo F, Katagiri H, Ishida K, Ito C, Iwaya T, Nishizuka SS. α-Amanitin Restrains Cancer Relapse from Drug-Tolerant Cell Subpopulations *via* TAF15. *Sci Rep* 2016; **6**: 25895 [PMID: 27181033 DOI: 10.1038/srep25895]

World Journal of Gastroenterology

Submit a Manuscript: https://www.f6publishing.com

World J Gastroenterol 2023 May 21; 29(19): 2950-2960

DOI: 10.3748/wjg.v29.i19.2950

ISSN 1007-9327 (print) ISSN 2219-2840 (online)

ORIGINAL ARTICLE

Basic Study

Susceptibility patterns and virulence genotypes of *Helicobacter pylori* affecting eradication therapy outcomes among Egyptian patients with gastroduodenal diseases

Ahmed Morad Asaad, Gasser El-Azab, Eman Abdelsameea, Osama Elbahr, Ahmed Kamal, Mohamed Abdel-Samiee, Ahmed Abdelfattah, Heba Abdallah, Doha Maher, Ahmed El-Refaie, Samar Ebrahim Ghanem, Shamshul Ansari, Samah Mohammed Awad

Specialty type: Gastroenterology and hepatology

Provenance and peer review: Invited article; Externally peer reviewed.

Peer-review model: Single blind

Peer-review report's scientific quality classification

Grade A (Excellent): A
Grade B (Very good): B
Grade C (Good): C, C, C
Grade D (Fair): D
Grade E (Poor): 0

P-Reviewer: Abadi ATB, Iran; Bordin DS, Russia; Kirkik D, Turkey; Koga Y, Japan; Machado NC, Brazil

Received: December 7, 2022
Peer-review started: December 7, 2022
First decision: January 22, 2023
Revised: February 11, 2023
Accepted: April 25, 2023
Article in press: April 25, 2023
Published online: May 21, 2023

Ahmed Morad Asaad, Department of Microbiology, College of Medicine, Zagazig University, Zagazig 44519, Egypt

Gasser El-Azab, Eman Abdelsameea, Osama Elbahr, Ahmed Kamal, Mohamed Abdel-Samiee, Ahmed Abdelfattah, Department of Hepatology and Gastroenterology, National Liver Institute, Menoufia University, Shebin El-Kom 32511, Egypt

Heba Abdallah, Department of Clinical Pathology, National Liver Institute, Menoufia University, Shebin El-Kom 32511, Egypt

Doha Maher, Ahmed El-Refaie, Department of Pathology, National Liver Institute, Menoufia University, Shebin El-Kom 32511, Egypt

Samar Ebrahim Ghanem, Department of Clinical Biochemistry and Molecular Diagnostics, National Liver Institute, Menoufia University, Shebin El-Kom 32511, Egypt

Shamshul Ansari, Department of Health Sciences, Higher Colleges of Technology, Abu Dhabi Women's College, Abu Dhabi 25026, United Arab Emirates

Samah Mohammed Awad, Department of Clinical Microbiology and Immunology, National Liver Institute, Menoufia University, Shebin El-Kom 32511, Egypt

Corresponding author: Shamshul Ansari, MSc, PhD, Assistant Professor, Department of Health Sciences, Higher Colleges of Technology, Abu Dhabi Women's College, Hazza Bin Zayed Street, Al Dhafrah-Abu Dhabi, Abu Dhabi 25026, United Arab Emirates.
shamshulansari483@yahoo.com

Abstract

BACKGROUND

Helicobacter pylori (*H. pylori*) is a significant human pathogen that is responsible for a variety of illnesses, including mucosa-associated lymphoid tissue lymphoma, gastric cancer, peptic ulcers, and gastritis.

AIM

To investigate the frequency of *H. pylori* infection and its resistance patterns among Egyptian patients and to determine the influence of *H. pylori* virulence genetic determinants on the eradication success of 14-d triple therapy regimen.

METHODS

H. pylori infections were investigated in 72 patients with gastroduodenal complications suggestive of *H. pylori* infection. The *cagA* and *vacA* genotypes of cultured strains were studied using polymerase chain reaction. The patients underwent 14 d of triple-therapy treatment. The treatment response was examined using histology and a rapid urease test 6 wk after therapy discontinuation.

RESULTS

The intention-to-treat eradication rate was 59.2% (95%CI: 48.2%–70.3%). Rates of *H. pylori* resistance to clarithromycin, amoxicillin, and metronidazole were 52.8%, 81.9%, and 100%, respectively. Successful eradication of *H. pylori* was more significantly associated with *vacA* s1-positive strains [adjusted odds ratio (aOR) = 0.507, 95%CI: 0.175–0.822]. A significant association was found between failed eradication rate and *H. pylori* strains resistant to clarithromycin (aOR = 0.204, 95%CI: –0.005 to 0.412) and amoxicillin (aOR = 0.223, 95%CI: 0.026–0.537).

CONCLUSION

This study's low *H. pylori* eradication rate following 14-d triple therapy is concerning and worrying. *H. pylori* pan-resistance to metronidazole followed by the high resistance to ciprofloxacin, amoxicillin, and clarithromycin in this research is challenging and of great concern.

Key Words: *Helicobacter pylori*; Eradication therapy; Virulence; Clarithromycin resistance; *cagA* gene; *vacA* gene

©The Author(s) 2023. Published by Baishideng Publishing Group Inc. All rights reserved.

Core Tip: In this study, 72 patients with *Helicobacter pylori* infections were investigated. Half of the *Helicobacter pylori* strains had the *cagA* gene, and more than half of the strains were resistant to antibiotics except tetracycline and clarithromycin (CLR). However, CLR and tetracycline were effective at higher doses to achieve effective eradication by the CLR-based therapy. Most importantly, this study demonstrated that an alternative therapeutic regimen should be adopted to achieve effective infection eradication in Egypt.

Citation: Asaad AM, El-Azab G, Abdelsameea E, Elbahr O, Kamal A, Abdel-Samiee M, Abdelfattah A, Abdallah H, Maher D, El-Refaie A, Ghanem SE, Ansari S, Awad SM. Susceptibility patterns and virulence genotypes of *Helicobacter pylori* affecting eradication therapy outcomes among Egyptian patients with gastroduodenal diseases. *World J Gastroenterol* 2023; 29(19): 2950-2960
URL: https://www.wjgnet.com/1007-9327/full/v29/i19/2950.htm
DOI: https://dx.doi.org/10.3748/wjg.v29.i19.2950

INTRODUCTION

Helicobacter pylori (H. pylori) is a prominent human pathogen and is responsible for a variety of diseases, such as mucosa-associated lymphoid tissue lymphoma, duodenal or peptic ulcer, gastritis, and gastric cancer[1,2]. As a result of its causative relationship to gastric adenocarcinoma, the World Health Organization has identified this pathogen as a class I carcinogen[3]. According to the global estimate, *H. pylori* infects roughly 4.4 billion people with prevalence rates ranging from 20%-90% in developed and underdeveloped nations, accordingly[2].

Pathologically, the existence of gastric mucosa inflammatory changes in areas with abundant *H. pylori* organisms together with the pathognomonic existence of either lymphoid aggregates and/or follicles with germinal centers and neutrophilic infiltration constitutes the definition of chronic *H. pylori* gastritis [2,3].

Previous epidemiological research has produced a long list of microbial virulence factors that have a crucial role in *H. pylori* colonization, persistence, serotype/genotype diversity, host immune responses, pathogenicity, and disease severity. These factors involve the outer inflammatory protein (*oipA*) gene, the cytotoxin-associated gene (*cagA*), the vacuolating cytotoxin gene (*vacA*), the *babA*2 adhesin gene, the epithelium gene A (*iceA*), and the duodenal ulcer-promoting gene (*dupA*)[4-7].

The variability of *H. pylori* strains is believed to be related to the genetic structural diversity with associated polymorphic arrangements of different virulence determinant genes[4]. For example, the *vacA* gene, which encodes a vacuolating toxin, is found in the vast majority of *H. pylori* strains and is an important virulence factor. Because of sequence variability in the middle region (m), m1 and m2 alleles, signal region (s), s1 or s2 alleles, and the intermediate region I subtypes 1 or 2, notable diversity in the vacuolating activity of different strains is found. *iceA1* and *iceA2* are two major alleles of the *iceA* gene, which is another example of microbial genetic variation[8].

Triple therapy for 14 d with proton pump inhibitors and a mixture of two antibiotics, clarithromycin (CLR) and amoxicillin (AMX) or metronidazole (MNZ) is the standard treatment for *H. pylori* infections [9,10]. CLR is the preferred antibiotic in areas in which resistance to this antibiotic is < 15%[10]. However, the continuous surge in antimicrobial resistance, including CLR-resistance, has been accompanied by a failure to eradicate *H. pylori* infections in a significant proportion of cases worldwide. The prevalence of *H. pylori* resistance to CLR ranges from 11.1% in Europe to 92.3% in Africa, reaching 18.9% in Asia and 29.3% in America as described in clinical reports[11-13].

Only a few studies addressing *H. pylori* infections, pathogenicity, and epidemiology among Egyptian patients are available. Besides, data regarding *H. pylori* resistance to CLR is scarce. Therefore, this research aimed to determine the *H. pylori* infection frequency and its resistance patterns among Egyptian patients and to determine the influence of *H. pylori* virulence genetic determinants on the eradication success of a 14-d triple therapy regimen.

MATERIALS AND METHODS

This cross-sectional observational study was completed from August 2021 to June 2022 at the National Liver Institute (NLI), a 760-bed tertiary care hospital in Shebin El-Kom, Egypt. The research adhered to the Helsinki Declaration principles and received ethical approval from the ethics NLI research committee, No. 00308/2022. Written consent was obtained from all participants. The research followed the international principles of strengthening the reporting of observational studies in epidemiology[14]. During the research period, 86 adult cases with different dyspepsia symptoms (vomiting, epigastric, abdominal pain, and/or heartburn) and/or other symptoms indicative of *H. pylori* infection and likely to require *H. pylori* eradication therapy were enrolled in this research.

All cases provided a medical history and underwent a physical examination, a quick urease test, and inspection of the esophagus, stomach, and duodenum using an upper endoscopy.

Endoscopy

Under topical lignocaine anesthesia, each patient underwent an upper gastrointestinal endoscopy (Olympus X Q40; Olympus Optical, Tokyo, Japan). Each patient's antrum and stomach corpus were biopsied during the endoscopy to obtain two sets of biopsy samples. The first set of biopsies was utilized for a rapid urease test utilizing a rapid urease test kit (CLO test; Kimberly-Clark Ltd., Draper, UT, United States). Three hours later, the second set was transferred on ice to the laboratory for bacteriological culture after being packed in 3 mL of sterile normal saline. For histopathological analysis, the third specimen was immediately fixed in 10% formalin. The fourth section was added to a buffered solution (10 mmol/LTris, pH 8, 10 mmol/L ethylenediaminetetraacetic acid, and 0.5% sodium dodecyl sulfate) and then frozen at –80 °C for DNA extraction and polymerase chain reaction (PCR) assays. *H. pylori* was diagnosed using three techniques: (1) *H. pylori* culture; (2) Histopathology using hematoxylin and eosin and Giemsa staining; and (3) Rapid urease test. At baseline, a patient was considered *H. pylori* -positive if he had a positive culture or rapid urease test that was validated by histological features (foveolar-neutrophilic infiltration, lymphoid follicles and/or aggregates, and verified positive Giemsa stained I rods). Six weeks after the triple therapy cessation, a second gastrointestinal endoscopy was completed to determine and confirm the presence of *H. pylori* and whether or not the duodenal ulcer had been successfully cured. Eradication was defined as the absence of histological evidence and a negative result on the rapid urease test.

H. pylori culture and antimicrobial susceptibility testing

Using a tissue grinder, the biopsy specimen was homogenized and plated onto brain-heart infusion agar plates (Difco, Detroit, MI, United States) that were supplemented with vancomycin (6 mg/mL), amphotericin B (8 mg/mL), trimethoprim (5 mg/mL), and 10% glycerol. Under microaerophilic conditions (85% N_2, 5% O_2, and 10% CO_2) in a humid atmosphere, the plates were incubated at 37 °C for 3-5 d. *H. pylori* was recognized based on Gram staining, helical shape, and biochemical assays that were positive for oxidase, catalase, and urease[15].

As suggested by the European committee on antimicrobial susceptibility testing, the E-test minimum inhibitory concentration technique was used to test for antimicrobial susceptibility. Tests were done on Mueller–Hinton agar plates enriched with 7% horse blood (bioMérieux Inc., Marcy-l'Étoile, France) using E-test strips (AB Biodisk, Slona, Sweden)[16]. Tetracycline (TET), CLR, AMX, rifampicin (RIF), and ciprofloxacin (CIP) were among the antibiotics that were evaluated. The isolate was considered

resistant to AMX, CLR, and MNZ if minimal inhibitory concentrations (MICs) were > 0.125 mg/L, > 0.5 mg/L, and > 8 mg/L, respectively. Besides, the isolate was considered resistant to CIP, RIF, and TET if MICs were > 1 mg/L[16].

DNA extraction

Each *H. pylori* isolate was sub-cultured and incubated for 72 h after which 7-10 colonies were pooled together. DNA was extracted according to the manufacturer's instructions using the QIAamp DNA micro kit (Qiagen, Hilden, Germany) and then was eluted in 200 μL of 1x TE buffer (10 mM Tris-HCl, 1 mM ethylenediaminetetraacetic acid; pH 8.0) and stored at –20 °C until PCR amplification.

Molecular identification of cagA and vacA genotypes of H. pylori

As previously disclosed, all isolates were subject to multiplex PCR to determine *cagA* and *vacA* genotypes[17-19]. Table 1 contains a list of all primers utilized for this research. Multiplex PCR was carried out in a thermocycler (Cyclogene; Bio-Techne, Minneapolis, MN, United Kingdom) in a reaction mixture volume of 50 μL. Each reaction contained 25 μL of 2 × multiplex PCR Master mix (Hot start DNA polymerase, multiplex buffer, dNTP mix $MgCl_2$; ThermoScientific, Vilinus, Lithuania), 2 μL of each primer (40 pmol), and 200 ng of template DNA (6 μL) according to DNA concentration in yield. The reaction volume was brought to 50 μL with the addition of nuclease free water. PCR grade water and DNA from *H. pylori* strain American Type Culture Collection 43504 were used as negative and positive controls, respectively. Multiplex PCR was carried out by the simultaneous addition of primers in the same reaction mixture after test of each primer pair separately: (1) 35 cycles of 95 °C for 1 min; (2) Annealing at 54 °C for 1.5 min; (3) Extension at 72 °C for 1 min; and (4) A final extension at 72 °C for 10 min. The amplified PCR products were electrophoresed on 1.5% agarose gels using 1 × TBE after which the gel was stained with ethidium bromide using a 100 bp ladder as the molecular weight standard, visualized under an ultraviolet light source, and photographed using a BioRad Gel Doc device.

H. pylori eradication therapy and follow-up

Patients were given omeprazole (20 mg) and two antibiotics, AMX (1 g) and CLR (500 mg), twice daily for 14 d[9]. Clinical follow-up, including side-effect monitoring, was performed until the medication was completed. Using a rapid urease test, the therapeutic response was examined 6 wk following the termination of therapy. Successful eradication of *H. pylori* was indicated by a negative result from the rapid urease test and microbiological cultures and by the absence of neutrophilic infiltration with a decrease in lymphoid inflammatory changes in the biopsy tissue following treatment[9,20].

Statistical analysis

Coding, validating, and analyzing the data required the use of SPSS version 22 (IBM Corp., Armonk, NY, United States). Data were shown using average, median, and frequencies (%). A χ^2 test or Fisher's exact test was used to compare categorical data, and the Student's *t*-test was used for numerical data. *P* values ≤ 0.05 based on a two-tail test were considered to be significant. Potential risk factors were identified using a binary logistic regression analysis that included an antecedent 95%CI and adjusted odds ratio (aOR).

RESULTS

Patients characteristics and H. pylori infection

Table 2 shows the demographic and clinical characteristics of the patients. The age of the patients ranged from 19 years to 59 years (median: 39.5 years), and 57 (79.2%) were males. Based on endoscopic examination, more than half of the patients (54.2%) had gastritis, while 33.3% and 12.5% of patients had gastric ulcer and duodenitis, respectively. Based on histopathological examination of the tissue biopsy, features of chronic gastritis and rods of *H. pylori* were seen based on Giemsa stain (Figure 1).

Thirty-six (50%) strains were *cagA*-positive among 72 *H. pylori* isolates in this study, and in 50 (69.4%) of the *H. pylori* strains, the *vacA* gene was detected. For the *vacA* gene s and m region sub-typing, 42 and 18 strains were positive for s1 and s2, respectively, while 27 and 33 isolates were positive for m1 and m2, respectively (Figure 2).

Antimicrobial susceptibility test outcomes

During the research period, a total of 86 patients were recruited. Among them, 10 patients were negative for *H. pylori* infection, and 4 patients failed to complete treatment, leaving 72 patients eligible for the study protocol. Among the 72 *H. pylori* isolates, the resistance rates to MNZ, AMX, RIF, CLR, CIP, and TET were 100%, 81.9%, 62.5%, 52.8%, 41.7%, and 37.5%, respectively.

Triple therapy outcomes

The eligible patients underwent 14-d triple therapy with two antibiotics: (1) AMX (1 g); (2) CLR (500

Table 1 Primers used in this study for multiplex polymerase chain reaction for detection of *vacA* and *cagA* genotypes in *Helicobacter pylori* isolates

Primer	Nucleotide sequence, 5'—3'	Gene	Size, bp
vacA			
VA1-F	ATGGAAATACAACAAACACAC	*vacA* s1/s2	259/286
VA1-R	CTGCTTGAATGCGCCAAAC		
VA2-F	CAATCTGTCCAATCAAGCGAG	*vacA* m1/m2	570/645
VA2-R	GCGTCAAAATAATTCCAAGG		
Cag-F	GTTGATAACGCTGTCGCTTC	*cagA*	349
Cag-R	GGGTTGTATGATATTTTCCATAA		

m1/m2: Middle regions; s1/s2: Signal regions.

Table 2 Patient demographic and clinical characteristics

Variable	*n* (%)
Mean age in yr	39.5 ± 12.9
Male sex	57 (79.2)
History of smoking	22 (30.6)
History of upper abdominal pain	48 (66.7)
Endoscopic finding	
Gastritis	39 (54.2)
Gastric ulcer	24 (33.3)
Duodenitis	9 (12.5)
Co-morbid conditions	
Liver cirrhosis	15 (20.8)
Diabetes mellitus	9 (12.5)
Hypertension	3 (4.2)
cagA	36 (50.0)
vacA	60 (83.3)
s1	42 (58.3)
s2	18 (25.0)
m1	27 (37.5)
m2	33 (45.8)

m1/m2: Middle regions; s1/s2: Signal regions.

mg); and (3) Omeprazole (20 mg). In 45 individuals, the 14-d triple therapy was successful in completely eliminating *H. pylori*; however, in the other 27 patients, the infection persisted despite treatment. *H. pylori* eradication rates were 59.2% (95%CI: 48.2–70.3%) for intention-to-treat (ITT) and 62.5% (95%CI: 51.3%–73.7%) for per protocol treatment.

In patients with *vacA* s1-positive (P = 0.02), s2-positive (P = 0.03), or m1-positive (P = 0.01) strains, *H. pylori* eradication occurred more frequently. It was not surprising that the rates of resistance to AMX (P = 0.012) and CLR were higher in *H. pylori* isolates from patients who experienced unsuccessful eradication (P = 0.005). However, no significant association with eradication therapy and resistance rates to CIP, TET, and RIF was found (Table 3).

With 95%CI and aOR the multiple logistic regression analysis revealed possible risk factors associated with *H. pylori* eradication therapy (Table 4). Successful eradication of *H. pylori* was more significantly associated with strains harboring the *vacA* s1 genotype (aOR = 0.507, 95%CI: 0.175–0.822). In contrast,

Table 3 Relationship between risk factors and outcomes of *Helicobacter pylori* eradication therapy, *n* (%)

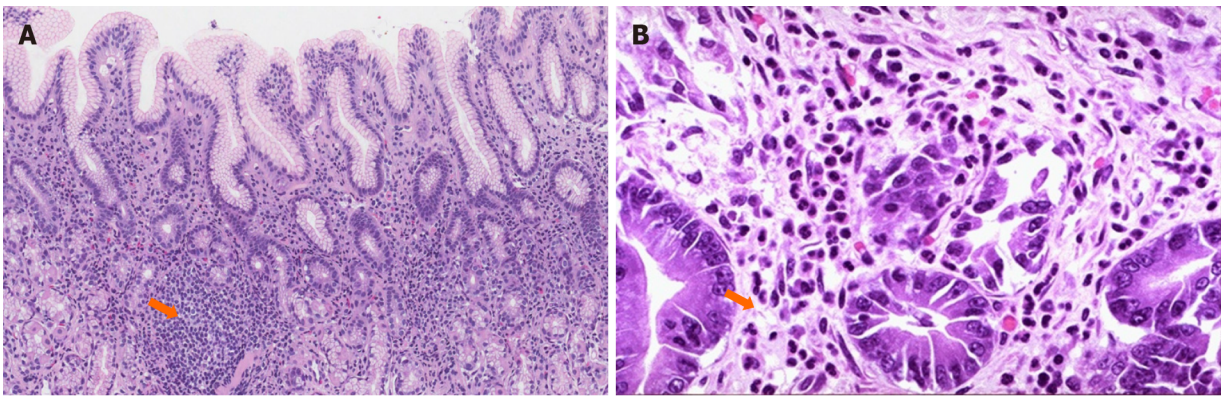
Variable	Successful, *n* = 45	Unsuccessful, *n* = 27	*P* value
Mean age in yr	43.13 ± 12.19	39.22 ± 11.91	0.188
Male sex	36	21	0.524
Smoking	15	12	0.349
cagA	21 (46.7)	15 (55.6)	0.313
s1	31 (68.9)	11 (40.7)	0.022
s2	15 (33.3)	3 (11.1)	0.031
m1	22 (48.9)	5 (18.5)	0.014
m2	21 (46.7)	12 (44.4)	0.525
AMX	33 (73.3)	26 (96.3)	0.012
CIP	18 (40.0)	12 (44.4)	0.45
TET	15 (33.3)	12 (44.4)	0.244
CLR	18 (40.0)	20 (74.1)	0.005
RIF	27 (60.0)	18 (40.0)	0.379

AMX: Amoxicillin; CIP: Ciprofloxacin; CLR: Clarithromycin; m1/m2: Middle region; RIF: Rifampicin; s1/s2: Signal region; TET: Tetracycline.

Table 4 Multivariate analysis of risk factors accompanied with eradication therapy of *Helicobacter pylori*

Variable	aOR (95%CI)	*P* value
s1	0.507 (0.175–0.822)	0.003
s2	0.074 (-0.227 to 0.393)	0.595
m1	-0.028 (-0.291 to 0.234)	0.83
AMX	0.223 (0.026–0.537)	0.032
CLR	0.204 (-0.005 to 0.412)	0.036

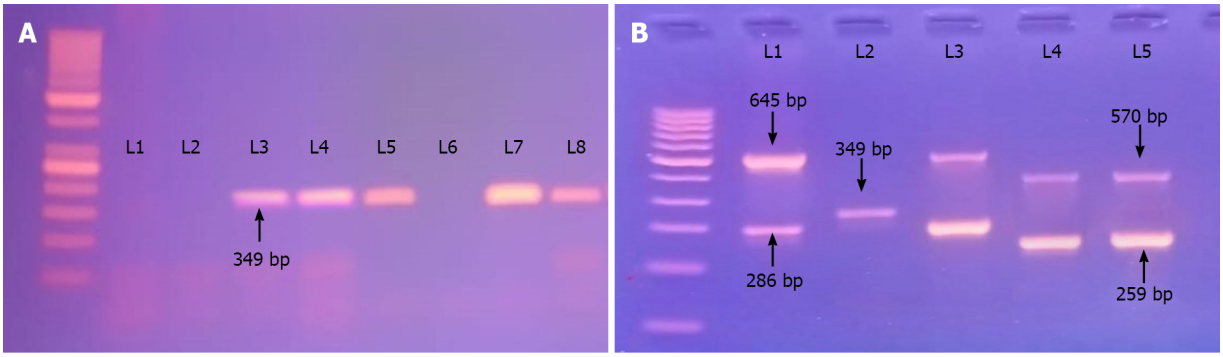
aOR: Adjusted odds ratio; AMX: Amoxicillin; CI: Confidence interval; CLR: Clarithromycin; m1: Middle region; s1/s2: Signal region.



DOI: 10.3748/wjg.v29.i19.2950 **Copyright** ©The Author(s) 2023.

Figure 1 *Helicobacter pylori* associated chronic gastritis with lymphoid aggregates and curved rods of *Helicobacter pylori* carpeting the mucosal surface. A: Hematoxylin and eosin staining, × 200; B: Hematoxylin and eosin staining, × 400.

failed eradication rates were significantly associated with *H. pylori* strains resistant to AMX (aOR = 0.223, 95%CI: 0.026–0.537) and CLR (aOR = 0.204, 95%CI: –0.005 to –0.036).



DOI: 10.3748/wjg.v29.i19.2950 **Copyright** ©The Author(s) 2023.

Figure 2 Polymerase chain reaction amplification of *cagA* and *vacA* genotypes using 100 bp ladder. A: Lanes 1, 2, 6 *cagA*-negative and lanes 3, 4, 5, 7, and 8 *cagA*-positive; B: Lanes 1 and 3 *vacA* genotype s2m2 and lanes 4 and 5 *vacA* genotype s1m1.

DISCUSSION

Eradication therapy of *H. pylori* infections has been deemed beneficial for cases with gastroduodenal disorders, such as gastric MALT lymphoma, peptic ulcer disease history, gastric cancer, dyspepsia, atrophic gastritis, and hyperplastic polyps, and for cases with certain extragastrointestinal disorders, such as unexplained iron-deficiency anemia, chronic idiopathic urticaria, and idiopathic thrombocytopenic purpura[1,21].

Despite establishment of multiple *H. pylori* eradication treatment regimens in different worldwide regions, the usual 14-d triple therapy [piperacillin/AMX/CLR (PAC)] produces adequate eradication rates for both adults and children in Egypt[21-23]. However, cure rates in this study were found to be unsatisfactory and disappointing. Our findings showed that the 14-d triple therapy efficacy of *H. pylori* eradication (59%) was lower than that reported from previous Egyptian studies (ITT range: 72%–83%) [22,23]. A previous meta-analysis investigated the global trend in eradication rates of two different first-line therapeutic regimens (PAC and piperacillin/AMX/MNZ) for 8061 patients infected with *H. pylori* from 30 countries[24]. In this report, the cure rate of PAC (77.1%, 95%CI = 75%–79%) was significantly higher than piperacillin /AMX/MNZ (70%, 95%CI = 67.7%–72.3%) (OR = 0.70, 95%CI = 0.56–0.88; P < 0.002). Previous clinical studies worldwide showed an unacceptable and continuous decrease in *H. pylori* triple eradication therapy-associated cure rates[13,25]. It is noteworthy that the overall global cure rates of these protocols are < 80%, which have recently been considered regimens with disappointing efficacy.

Inadequate treatment duration, antimicrobial resistance, inadequate stomach acid suppression, poor adherence to eradication regimens, and quick metabolism of proton pump inhibitors have all been implicated in the failure of the traditional triple therapy to eradicate a pathogen according to previous ecological research[26,27]. CLR resistance has been recognized as the primary cause of routine triple treatment failure. In a recent meta-analysis investigating 66142 patients from 65 countries, failure to achieve eradication was 7-fold higher in patients with CLR-resistant *H. pylori* infections (OR: 6.97; 95%CI: 5.23–9.01; P = 0.001) when treated with a CLR-containing regimen than patients with susceptible strains[13]. Therefore, in nations with a high prevalence of CLR resistance (> 15%–20%), bismuth quadruple treatment is recommended.

Pooled data from 25 randomized trials including 3990 patients showed that the ITT eradication rate of standard triple therapy (65.7%) was significantly lower than bismuth-containing regimens (74.9%; OR: 1.60; 95%CI: 1.07–2.39). In addition, in the per protocol analysis, the pooled eradication rate for bismuth-containing regimens was 86.7% *vs* 33.3% for the usual triple regimen (OR: 10.64; 95%CI: 2.96–39.53)[28]. It is noteworthy that all isolates in this study were MNZ-resistant, and more than half of the isolates were resistant to AMX and CLR. These findings are not surprising as MNZ has been abused by the public without prescription for various gastrointestinal infections and diarrhea, while both AMX and CLR have been included in empiric therapies for respiratory infections or non-tuberculous mycobacterial infections in our region. Therefore, continuous monitoring of susceptibility patterns of *H. pylori* to various antimicrobials seems crucial as multidrug resistant *H. pylori* strains undoubtedly induce failure of *H. pylori* eradication therapy.

H. pylori cagA and *vacA* genotypes are among the most important factors implicated in the pathogenesis of gastroduodenal diseases and in influencing the sequelae of treatment protocols. The association of *cagA*-positive strains with the *H. pylori* eradication therapy outcomes were demonstrated by former clinical and ecological investigations[4-9]. However, the results from these studies were inconsistent and controversial. In this study, strains with or without *cagA* had no effect on eradication rates, a finding that is similar to previous reports. In a previous meta-analysis including 25 studies, the influence of the virulence factors, *vacA* and *cagA*, on *H. pylori* eradication therapy in 2693 cases was investigated by Wang *et al*[29]. In their report, the pooled *H. pylori* eradication rate was 77% (95%CI:

70%–83%) for *cagA*-negative patients and 85% (95%CI: 81%–89%) for *cagA*-positive with an 8% higher eradication rate among *cagA*-positive strains. In addition, using subgroup analyses based on clinical presentations, eradication detection method, location, and therapeutic regimen types, the authors concluded that *cagA*-negative strains responded to successful *H. pylori* therapy eradication rates than *cagA*-positive strains with pooled risk ratios (RR) of 1.118 (95%CI: 1.051–1.189; $P < 0.001$) for Asia and 1.138 (95%CI: 1.000–1.295; $P = 0.049$) for Europe. In South America, *cagA*-positive strains and *cagA*-negative strains exhibited comparable *H. pylori* treatment rates (RR: 1.104, 95%CI: 0.953–1.279; $P = 0.186$).

The *vacA* s1-positive *H. pylori* strains are typically more virulent and more closely linked to progressive gastroduodenal disorders as reported in many previous studies[29]. An increase in blood flow to the site of infection and stronger inflammatory responses were stimulated by more virulent strains as reported by clinical and epidemiological-based evidence. In addition, the more virulent strains are usually more susceptible to antimicrobials because of faster replication. *H. pylori* strains containing *vacA* s1 were substantially related to a greater *H. pylori* eradication rate in the current investigation.

This result is consistent with earlier findings in which *vacA* s1-positive strains posed a significant risk for the development of gastric illnesses with easier eradication in diseased people. Wang *et al*[29] discovered that the pooled *H. pylori* eradication rate was 73% (95%CI: 61%–85%) for *vacA* s2 and 83% (95%CI: 75%–91%) for *vacA* s1 with a 10% improvement in eradication rates in the *vacA* s1 group compared to the *vacA* s2 group (95%CI: 1.040–1.303; $P = 0.008$). In their meta-analysis, *vacA* s1 status was associated with better eradication rates in the triple therapy subgroup according to an examination of subgroups based on different worldwide locations (RR: 1.175, 95%CI: 1.012–1.360)[29]. Brennan *et al*[7] reported that the incidence of the more virulent s1 genotype was substantially lower among previously treated individuals than among those who had never received therapy (58.3% *vs* 74.3%). A significant increase in the frequency of the least pathogenic s2/m2 genotype was seen in previously treated individuals (36.7% *vs* 21.0%)[7]. Our findings and results of other studies clearly demonstrated that the *vacA* s1 genotype would be useful for predicting successful outcomes of *H. pylori* eradication therapy.

This study had some limitations. First, this research may have been limited in its capability to investigate other virulence marker-associated pathogenic roles due to the lack of molecular analysis beyond PCR and genome sequencing. Second, this study was conducted within a single center. Therefore, our findings cannot be applied to other situations. To further understand the phenotypic and genotypic links between *H. pylori* virulence, antibiotic resistance, and the efficacy of eradication therapy, further molecular-based epidemiological multicenter investigations with longer monitoring durations are required.

CONCLUSION

This low *H. pylori* eradication rate following 14-d triple therapy is concerning and worrying. The pan-resistance of *H. pylori* to MNZ followed by the high resistance to AMX, CLR, and CIP in this research is challenging and of great concern. These findings draw attention to the urgent need for performing *H. pylori* antimicrobial susceptibility testing before starting eradication therapy in addition to continuous surveillance of *H. pylori* resistance patterns in our region to provide data that can guide empirical treatment. In addition, the *vacA* s1-positive *H. pylori* isolates are easier to eradicate and could be used as an indicator to predict the successful outcome of eradication therapy.

ARTICLE HIGHLIGHTS

Research background

Helicobacter pylori (*H. pylori*) has been implicated in the development of gastric cancer and gastric mucosa-associated lymphoid tissue lymphoma. However, the bacterial eradication reduces the risk of theses gastric complications. The therapeutic regimens currently in use and the duration of therapy differ in different countries, which affects the therapy outcomes. The therapeutic outcomes have been found to be affected by the virulence characteristics of the infecting strains. The strains with more virulent characteristics possessing *vacA* s1 and m1 are eradicated more efficiently than the strains harboring less virulent characteristics.

Research motivation

To demonstrate that the infecting strains possessing more virulent characteristics are eradicated efficiently with a 14-d triple therapy. The *vacA* s1-positive *H. pylori* isolates are easier to eradicate and could be used as an indicator to predict the successful outcome of eradication therapy.

Research objectives
To evaluate the *H. pylori* infection frequency and its resistance patterns among Egyptian patients and to determine the *H. pylori* virulence characteristics influencing the eradication success of the 14-d triple therapy regimen.

Research methods
The patients suggestive of *H. pylori* infections were subjected to endoscopy-based biopsy specimen collection. The collected biopsy specimens were used to evaluate the *H. pylori* infection by a combination of diagnostic tests that included urease test, bacterial culture, and histopathological investigation. The extracted DNA was subjected to PCR-based *cagA* and *vacA* genotype investigation. The *H. pylori*-infected patients received triple therapy for 14 d. Six weeks after completion of the therapy, the treatment response was examined utilizing histology and the rapid urease test.

Research results
Among the 86 recruited patients, infection was found in 76 individuals. All of the strains were resistant to metronidazole (MNZ), while 52.8% and 81.9% of the isolates were resistant to clarithromycin (CLR) and amoxicillin (AMX), respectively. Successful eradication of *H. pylori* was significantly associated with *vacA* s1-positive strains [adjusted odds ratio (aOR) = 0.507, 95%CI: 0.175–0.822]. *H. pylori* strains resistant to CLR (aOR = 0.204, 95%CI: -0.005 to 0.412) and AMX (aOR = 0.223, 95%CI: 0.026–0.537) were significantly associated with failed eradication rate.

Research conclusions
The low eradication rate of 14-d triple therapy in this study is worrisome and indicates that an alternative therapy to achieve effective eradication must be identified. The findings of complete failure of MNZ and reduced efficacy of AMX, CLR, and ciprofloxacin draw attention to the urgent need of antimicrobial susceptibility testing-guided eradication therapy. In addition, the strains with virulent properties of *vacA* s1 are easier to eradicate and could be used as an indicator to predict the successful outcome of eradication therapy.

Research perspectives
CLR, AMX, and MNZ-based 14-d eradication therapy is ineffective and discouraged in these populations. Extensive nationwide studies should be considered to document the efficacy and to find alternative therapeutic regimens in respect to the duration. Furthermore, antimicrobial susceptibility testing based therapy should be encouraged to help reduce the development of antimicrobial resistance.

ACKNOWLEDGEMENTS

The authors would like to thank the colleagues in the Department of Laboratory and Microbiology and Endoscopy and the patients in the National Liver Institute who aided this research.

FOOTNOTES

Author contributions: Asaad AM and Awad SM conceived and designed the study; El-Azab G, Abdelsameea E, El-Bahr O, Kamal A, Abdel-Samiee M, and Abdelfattah A collected the data and performed the clinical part of the study; Abdallah H, Maher D, El-Refaie A, Ghanem SE, and Awad SM contributed to the laboratory investigations of the study; Ghanem SE and Awad SM performed the data analysis; Asaad AM, Ansari S, and Awad SM wrote the paper; All authors extensively revised the manuscript.

Institutional review board statement: The study protocol was approved by the local ethics committee of National Liver Institute Menoufia University, No. 00308/2022.

Informed consent statement: Patient consent was taken from all studied patients before the start of the study. The authors affirm that human research participants provided informed consent for publication.

Conflict-of-interest statement: All the authors report having no relevant conflicts of interest for this article.

Data sharing statement: The datasets generated and/or analyzed during the current study are not publicly available due to confidential and institutional ethical issues.

Open-Access: This article is an open-access article that was selected by an in-house editor and fully peer-reviewed by external reviewers. It is distributed in accordance with the Creative Commons Attribution NonCommercial (CC BY-NC 4.0) license, which permits others to distribute, remix, adapt, build upon this work non-commercially, and license their derivative works on different terms, provided the original work is properly cited and the use is non-

commercial. See: https://creativecommons.org/Licenses/by-nc/4.0/

Country/Territory of origin: Egypt

ORCID number: Ahmed Morad Asaad 0000-0002-1422-1117; Eman Abdelsameea 0000-0002-3225-7164; Mohamed Abdel-Samiee 0000-0002-8970-0286; Heba Abdallah 0000-0001-6336-9786; Samar Ebrahim Ghanem 0000-0003-2798-9720; Shamshul Ansari 0000-0003-1846-1377.

S-Editor: Li L
L-Editor: Filipodia
P-Editor: Fan JR

REFERENCES

1 **Leja M**, Axon A, Brenner H. Epidemiology of Helicobacter pylori infection. *Helicobacter* 2016; **21** Suppl 1: 3-7 [PMID: 27531531 DOI: 10.1111/hel.12332]
2 **Atherton JC**. The pathogenesis of Helicobacter pylori-induced gastro-duodenal diseases. *Annu Rev Pathol* 2006; **1**: 63-96 [PMID: 18039108 DOI: 10.1146/annurev.pathol.1.110304.100125]
3 **Herrero R**, Parsonnet J, Greenberg ER. Prevention of gastric cancer. *JAMA* 2014; **312**: 1197-1198 [PMID: 25247512 DOI: 10.1001/jama.2014.10498]
4 **Sukri A**, Hanafiah A, Mohamad Zin N, Kosai NR. Epidemiology and role of Helicobacter pylori virulence factors in gastric cancer carcinogenesis. *APMIS* 2020; **128**: 150-161 [PMID: 32352605 DOI: 10.1111/apm.13034]
5 **Sugimoto M**, Yamaoka Y. Virulence factor genotypes of Helicobacter pylori affect cure rates of eradication therapy. *Arch Immunol Ther Exp (Warsz)* 2009; **57**: 45-56 [PMID: 19219527 DOI: 10.1007/s00005-009-0007-z]
6 **Oktem-Okullu S**, Cekic-Kipritci Z, Kilic E, Seymen N, Mansur-Ozen N, Sezerman U, Gurol Y. Analysis of Correlation between the Seven Important Helicobacter pylori (H. pylori) Virulence Factors and Drug Resistance in Patients with Gastritis. *Gastroenterol Res Pract* 2020; **2020**: 3956838 [PMID: 32908495 DOI: 10.1155/2020/3956838]
7 **Brennan DE**, Dowd C, O'Morain C, McNamara D, Smith SM. Can bacterial virulence factors predict antibiotic resistant Helicobacter pylori infection? *World J Gastroenterol* 2018; **24**: 971-981 [PMID: 29531461 DOI: 10.3748/wjg.v24.i9.971]
8 **Gangwer KA**, Shaffer CL, Suerbaum S, Lacy DB, Cover TL, Bordenstein SR. Molecular evolution of the Helicobacter pylori vacuolating toxin gene *vac*A. *J Bacteriol* 2010; **192**: 6126-6135 [PMID: 20870762 DOI: 10.1128/JB.01081-10]
9 **Malfertheiner P**, Megraud F, Rokkas T, Gisbert JP, Liou JM, Schulz C, Gasbarrini A, Hunt RH, Leja M, O'Morain C, Rugge M, Suerbaum S, Tilg H, Sugano K, El-Omar EM; European Helicobacter and Microbiota Study group. Management of Helicobacter pylori infection: the Maastricht VI/Florence consensus report. *Gut* 2022 [PMID: 35944925 DOI: 10.1136/gutjnl-2022-327745]
10 **De Francesco V**, Bellesia A, Ridola L, Manta R, Zullo A. First-line therapies for Helicobacter pylori eradication: a critical reappraisal of updated guidelines. *Ann Gastroenterol* 2017; **30**: 373-379 [PMID: 28655973 DOI: 10.20524/aog.2017.0166]
11 **Wu W**, Yang Y, Sun G. Recent Insights into Antibiotic Resistance in Helicobacter pylori Eradication. *Gastroenterol Res Pract* 2012; **2012**: 723183 [PMID: 22829809 DOI: 10.1155/2012/723183]
12 **Papastergiou V**, Georgopoulos SD, Karatapanis S. Treatment of Helicobacter pylori infection: meeting the challenge of antimicrobial resistance. *World J Gastroenterol* 2014; **20**: 9898-9911 [PMID: 25110420 DOI: 10.3748/wjg.v20.i29.9898]
13 **Savoldi A**, Carrara E, Graham DY, Conti M, Tacconelli E. Prevalence of Antibiotic Resistance in Helicobacter pylori: A Systematic Review and Meta-analysis in World Health Organization Regions. *Gastroenterology* 2018; **155**: 1372-1382.e17 [PMID: 29990487 DOI: 10.1053/j.gastro.2018.07.007]
14 **Strengthening the reporting of observational studies in epidemiology**. STROBE checklist, version 4. 2007. [cited 22 October 2018]. Available from: http://www.strobe-statement.org/index.php?id=available-checklists
15 **Mégraud F**, Lehours P. Helicobacter pylori detection and antimicrobial susceptibility testing. *Clin Microbiol Rev* 2007; **20**: 280-322 [PMID: 17428887 DOI: 10.1128/CMR.00033-06]
16 **European committee on antimicrobial susceptibility testing**. Breakpoint Tables for Interpretation of MICs and Zone Diameters, Version 9.0. 2019. [cited 1 January 2019]. Available from: http://www.eucast.org
17 **Tummuru MK**, Cover TL, Blaser MJ. Cloning and expression of a high-molecular-mass major antigen of Helicobacter pylori: evidence of linkage to cytotoxin production. *Infect Immun* 1993; **61**: 1799-1809 [PMID: 8478069 DOI: 10.1128/iai.61.5.1799-1809.1993]
18 **Atherton JC**, Cao P, Peek RM Jr, Tummuru MK, Blaser MJ, Cover TL. Mosaicism in vacuolating cytotoxin alleles of Helicobacter pylori. Association of specific *vac*A types with cytotoxin production and peptic ulceration. *J Biol Chem* 1995; **270**: 17771-17777 [PMID: 7629077 DOI: 10.1074/jbc.270.30.17771]
19 **Yamaoka Y**, Kodama T, Gutierrez O, Kim JG, Kashima K, Graham DY. Relationship between Helicobacter pylori *ice*A, cagA, and *vac*A status and clinical outcome: studies in four different countries. *J Clin Microbiol* 1999; **37**: 2274-2279 [PMID: 10364597 DOI: 10.1128/JCM.37.7.2274-2279.1999]
20 **Alboraie M**, Elhossary W, Aly OA, Abbas B, Abdelsalam L, Ghaith D, Shady Z, Gaber Y, Adel E, Peura D, Armstrong D, Esmat G; special interest group; Egyptian Association for Study of Gastrointestinal Diseases and Liver (E A S G L D). Egyptian recommendations for management of Helicobacter pylori infection: 2018 report. *Arab J Gastroenterol* 2019; **20**: 175-179 [PMID: 31564518 DOI: 10.1016/j.ajg.2019.09.001]
21 **Kamboj AK**, Cotter TG, Oxentenko AS. Helicobacter pylori: The Past, Present, and Future in Management. *Mayo Clin Proc* 2017; **92**: 599-604 [PMID: 28209367 DOI: 10.1016/j.mayocp.2016.11.017]
22 **Ismail WA**, Mostafa EF. A comparison between conventional triple therapy and sequential therapy on tolerance of

treatment and eradication of Helicobacter pylori infection in Egyptian patients. *Egy J Int Med* 2018; **30**: 90-95 [DOI: 10.4103/ejim.ejim_6_18]

23 **Abd-Elsalam S**, Kobtan A, El-Kalla F, Elkhalawany W, Nawasany SE, Saif SA, Yousef M, Ali LA, Soliman S, Mansour L, Habba E, Soliman H, Rizk F, Shehata MA. A 2-week Nitazoxanide-based quadruple treatment as a rescue therapy for Helicobacter pylori eradication: A single center experience. *Medicine (Baltimore)* 2016; **95**: e3879 [PMID: 27310977 DOI: 10.1097/MD.0000000000003879]

24 **Puig I**, Baylina M, Sánchez-Delgado J, López-Gongora S, Suarez D, García-Iglesias P, Muñoz N, Gisbert JP, Dacoll C, Cohen H, Calvet X. Systematic review and meta-analysis: triple therapy combining a proton-pump inhibitor, amoxicillin and metronidazole for Helicobacter pylori first-line treatment. *J Antimicrob Chemother* 2016; **71**: 2740-2753 [PMID: 27342548 DOI: 10.1093/jac/dkw220]

25 **Li B**, Lan X, Wang L, Zhao J, Ding J, Ding H, Lei J, Wei Y, Zhang W. Proton-pump inhibitor and amoxicillin-based triple therapy containing clarithromycin *vs* metronidazole for Helicobacter pylori: A meta-analysis. *Microb Pathog* 2020; **142**: 104075 [PMID: 32074497 DOI: 10.1016/j.micpath.2020.104075]

26 **Zullo A**, De Francesco V, Hassan C. Predicting Helicobacter pylori eradication: how to teach an old dog new tricks! *J Clin Gastroenterol* 2012; **46**: 259-261 [PMID: 22395061 DOI: 10.1097/MCG.0b013e318247177e]

27 **Kotilea K**, Mekhael J, Salame A, Mahler T, Miendje-Deyi VY, Cadranel S, Bontems P. Eradication rate of Helicobacter Pylori infection is directly influenced by adherence to therapy in children. *Helicobacter* 2017; **22** [PMID: 28303625 DOI: 10.1111/hel.12383]

28 **Ko SW**, Kim YJ, Chung WC, Lee SJ. Bismuth supplements as the first-line regimen for Helicobacter pylori eradication therapy: Systemic review and meta-analysis. *Helicobacter* 2019; **24**: e12565 [PMID: 30698318 DOI: 10.1111/hel.12565]

29 **Wang D**, Li Q, Gong Y, Yuan Y. The association between *vac*A or cagA status and eradication outcome of Helicobacter pylori infection: A meta-analysis. *PloS One* 2017; **12**: e0177455 [PMID: 28493953 DOI: 10.1371/journal.pone.0177455]

World Journal of Gastroenterology

Submit a Manuscript: https://www.f6publishing.com

World J Gastroenterol 2023 May 21; 29(19): 2961-2978

DOI: 10.3748/wjg.v29.i19.2961

ISSN 1007-9327 (print) ISSN 2219-2840 (online)

ORIGINAL ARTICLE

Basic Study

MMP14 is a diagnostic gene of intrahepatic cholangiocarcinoma associated with immune cell infiltration

Jun Wu, Yang Guo, Zhi-Fan Zuo, Zi-Wei Zhu, Lei Han

Specialty type: Oncology

Provenance and peer review: Unsolicited article; Externally peer reviewed.

Peer-review model: Single blind

Peer-review report's scientific quality classification

Grade A (Excellent): A
Grade B (Very good): B, B
Grade C (Good): 0
Grade D (Fair): 0
Grade E (Poor): 0

P-Reviewer: Bleszynski MS, Canada; Ishii T, Japan; Quaresima S, Italy

Received: February 28, 2023
Peer-review started: February 28, 2023
First decision: March 14, 2023
Revised: March 24, 2023
Accepted: April 23, 2023
Article in press: April 23, 2023
Published online: May 21, 2023

Jun Wu, Zi-Wei Zhu, China Medical University, The General Hospital of Northern Theater Command Training Base for Graduate, Shenyang 110016, Liaoning Province, China

Yang Guo, Lei Han, Department of Hepatobiliary Surgery, The General Hospital of Northern Theater Command, Shenyang 110016, Liaoning Province, China

Zhi-Fan Zuo, Gynecological Radiotherapy Ward, Liaoning Provincial Cancer Hospital, Shenyang 110801, Liaoning province, China

Corresponding author: Lei Han, MD, Associate Chief Physician, Deputy Director, Department of Hepatobiliary Surgery, The General Hospital of Northern Theater Command, No. 83 Wenhua Road, Shenyang 110016, Liaoning Province, China. hanlei1974@sina.com

Abstract

BACKGROUND

Intrahepatic cholangiocarcinoma (ICC) is a malignant tumor of the hepatobiliary system with concealed onset, strong invasiveness and poor prognosis.

AIM

To explore the disease characteristic genes that may be helpful in the diagnosis of ICC and affect immune cell infiltration.

METHODS

We downloaded two ICC-related human gene expression profiles from GEO database as the training group (GSE26566 and GSE32958 datasets) for difference analysis, and performed enrichment analysis on differential genes. The least absolute shrinkage and selection operator (LASSO), support vector machine-recursive feature elimination (SVM-RFE) and random forest (RF), three machine learning algorithms, were used to screen the characteristic genes. Double verification was carried out on GSE107943 and The Cancer Genome Atlas, two verification groups. Receiver operating characteristic curve and area under the curve (AUC) were used to evaluate the diagnostic efficacy of genes for ICC. CIBERSORT and ssGSEA algorithms were used to evaluate the effect of characteristic genes on immune infiltration pattern. Human Protein Atlas (HPA) was used to analyze the protein expression level of the target gene.

RESULTS

A total of 1091 differential genes were obtained in the training group. Enrichment

analysis showed that the above genes were mainly enriched in small molecular catabolism, complement and coagulation cascade, bile secretion and other functions and pathways. Twenty-five characteristic genes were screened by LASSO regression, 19 by SVM-RFE algorithm, and 30 by RF algorithm. Three algorithms were used in combination to determine the characteristic gene of ICC: *MMP14*. The verification group confirmed that the genes had a high diagnostic accuracy (AUC values of the training group and the verification group were 0.960, 0.999, and 0.977, respectively). Comprehensive analysis of immune infiltration showed that *MMP14* could affect the infiltration of monocytes, activated memory CD4 T cells, resting memory CD4 T cells, and other immune cells, and was closely related to the expression of CD200, cytotoxic T-lymphocyte-associated antigen 4, CD14, CD44, and other immune checkpoints. The results of immunohistochemistry in HPA database showed was indeed overexpressed in ICC.

CONCLUSION

MMP14 can be used as a disease characteristic gene of ICC, and may regulate the distribution of immune-infiltrating cells in the ICC tumor microenvironment, which provides a new method for the determination of ICC diagnostic markers and screening of therapeutic targets.

Key Words: Intrahepatic cholangiocarcinoma; MMP14; Machine learning; Immune infiltration; Characteristic gene; Diagnostic markers

©The Author(s) 2023. Published by Baishideng Publishing Group Inc. All rights reserved.

Core Tip: This study demonstrates that a new candidate molecular marker: MMP14 that is important for the diagnosis of intrahepatic cholangiocarcinoma, and MMP14 was related to a variety of immune cell components and participated in the occurrence and development in intrahepatic cholangiocarcinoma.

Citation: Wu J, Guo Y, Zuo ZF, Zhu ZW, Han L. *MMP14* is a diagnostic gene of intrahepatic cholangiocarcinoma associated with immune cell infiltration. *World J Gastroenterol* 2023; 29(19): 2961-2978
URL: https://www.wjgnet.com/1007-9327/full/v29/i19/2961.htm
DOI: https://dx.doi.org/10.3748/wjg.v29.i19.2961

INTRODUCTION

Intrahepatic cholangiocarcinoma (ICC) is the second most common primary tumor of the liver, which originates from intrahepatic bile duct epithelial cells and accounts for about 20% of primary liver malignant tumors[1]. Its incidence is on the rise worldwide, with the highest incidence in Southeast Asia, and the second highest incidence in China after Thailand[2,3]. Pathological changes such as chronic cholangitis, cholestasis, intrahepatic bile duct stones, and liver cirrhosis all increase the incidence of ICC[4]. At present, due to the poor efficacy of radiotherapy and chemotherapy for ICC, surgical treatment is currently the main treatment method for ICC. However, patients with ICC may be asymptomatic in the early stage, and most patients have intrahepatic metastasis, lymph node metastasis, or even distant metastasis at the first time of diagnosis. Only 9% of patients with advanced ICC can survive for 5 years[5-8]. Despite the continuous improvement in imaging and laboratory tests, the early diagnosis of ICC is still not ideal. Currently, the biomarkers of ICC mainly include carcinoembryonic antigen, carbohydrate antigen 19-9 and a-fetoprotein, but the sensitivity and specificity are not satisfactory[9]. Hence, it is crucial to find new biomarkers for early screening and diagnosis of ICC.

Many studies on the tumor microenvironment have confirmed that a variety of immune regulatory mechanisms play an important role in the malignant biological behavior of tumors. Therefore, immunotherapy has gradually been paid attention in various treatments for solid tumors, and as an emerging and effective anticancer treatment, it has also been widely used for ICC. However, the improvement of the efficacy of immunotherapy and the development of effective drugs targeting specific immune targets are still problems to be solved[10].

Machine learning is a part of the field of artificial intelligence, which can find rules through the analysis of data, and can be conducive to the prediction of similar unknown data. And the existing knowledge structure can be constantly updated to improve its own performance[11]. With the continuous progress of machine learning, the development of more accurate machine learning algorithms makes it possible for us to find new disease-related genes[12]. At the same time, second-generation sequencing technology has made convenient screening of ICC diagnostic targets, and provided a solid foundation for precise treatment of patients and selection of personalized drugs[13].

In this study, using the ICC-related data in the GEO and The Cancer Genome Atlas (TCGA) databases, bioinformatics and machine learning algorithms were used to comprehensively analyze and obtain reliable disease-characteristic genes, and in-depth exploration found that this gene may regulate the progression of ICC by mediating the composition of immune-infiltrating cells. The above preliminary research results can provide important references for the identification of early diagnostic markers for ICC and the mining of potential intervention targets for immunotherapy.

MATERIALS AND METHODS

Download of the sample datasets

The gene expression data of ICC cancer tissues and paracancerous tissues were obtained by using the three datasets GSE26566, GSE32958, and GSE107943 in GEO database. The transcriptome gene expression data of cancer and paracancerous samples of ICC patients were obtained from TCGA database. The relevant datasets were sorted, and samples other than cancer and paracancerous tissues of ICC patients were deleted. The two datasets of GSE26566 and GSE32958 were combined as the training group. The GSE107943 dataset was used as the verification group, while the TCCG dataset was used as the external database verification group.

Screening of differential genes

The Limma package was used to analyze the differences between the GSE26566 and GSE32958 datasets after merging the training groups. Genes that met the conditions $|\log2FC| > 2$ and adj. $P < 0.05$ were considered to be differential genes. The first 50 genes with the most significant difference between upregulated and downregulated genes were selected for heat mapping using the pheatmap package. The volcanic map was plotted using ggplot2 and ggrepel packages to visualize significantly different genes.

Functional enrichment analysis

According to the results of differential expression analysis, the org.Hs.eg.db, enrichplot, clusterProfiler, DOSE and GSEABase package were used for GO functional enrichment analysis, KEGG pathway enrichment analysis, DO disease enrichment analysis and GSEA enrichment analysis, respectively. The top 10 most significantly enriched functions in biological processes (BP), CC and molecular functions (MF) were visualized by drawing bubble plots. The top 30 pathways or diseases with the most significant enrichment were selected for KEGG enrichment analysis and DO enrichment analysis bubble diagram drawing. GSEA enrichment analysis was carried out on the experimental group (cancer tissue samples) and the control group (paracancerous tissue samples), and the first five functions and pathways that were most significantly enriched in the experimental group and the control group were visualized respectively.

Screening disease characteristic genes by machine learning

Based on the differential gene expression, least absolute shrinkage and selection operator (LASSO) regression, support vector machine-recursive feature elimination (SVM-RFE) algorithm and random forest (RF) algorithm were used to screen disease characteristic genes. The genes screened by the three algorithms were intersected to obtain the final disease characteristic gene, which was the new characteristic gene for ICC diagnosis. The diagnostic genes obtained by the comprehensive analysis of the above three machine learning algorithms had stronger persuasion and higher accuracy. The LASSO regression algorithm was based on the glmnet package. When the parameters were set to a = 1, type.measure = deviance and nfolds = 10, the number of genes corresponding to the point with the smallest cross-validation error was the target gene. The SVM-RFE algorithm was based on the e1071, kernlab and caret packages. The method adopted was svmRadial, and the number of genes corresponding to the point with the smallest cross-validation error was selected as the disease characteristic gene. The RF algorithm was based on the randomForest package. The differentially expressed genes were used to train the RF model. The number of forest trees was set to 500, and the number of corresponding trees with the smallest cross-verification error was found to reconstruct the RF model for training. The importance score of the gene was obtained. We sorted from high to low according to the scores, and selected the 30 genes with the highest importance scores as the feature gene set.

Assessing the diagnostic value of ICC signature genes

The limma package was used to analyze the differences between the two verification groups of GSE107943 and TCGA to determine whether the differential expression of disease characteristic genes in the verification group was consistent with that of the training group. We used the ggpubr package to visualize and draw a boxplot. The receiver operating characteristic (ROC) curve was drawn based on the pROC package to evaluate the efficiency of characteristic genes in the diagnosis of ICC. Area under the curve (AUC) value was used as an index to evaluate the diagnostic value of characteristic genes in

Table 1 Number of data set samples

Dataset	Number of cancer samples	Number of paracancerous samples	Total
GSE26566	104	59	163
GSE32958	16	7	23
GSE107943	30	27	57
TCGA	33	8	41
Total	183	101	284

TCGA: The Cancer Genome Atlas.

the training and test groups. The 95% confidence interval (CI) of AUC value was extracted and calculated by bootstrap method.

Comprehensive analysis of immune infiltration pattern in ICC

According to the gene expression level of each sample, CIBERSORT algorithm was used to quantify the relative content of immune cells in each sample with the help of e1071 and preprocessCore package, so as to obtain the proportion of different immune cells in each sample, and a bar chart was drawn. The corrplot package was used to analyze the correlation of immune cells and draw the correlation heat map. The vioplot package was used to analyze the difference in immune cell infiltration between cancer tissue and paracancerous tissue of ICC patients, and the violin picture was drawn. The CIBERSORT and ssGSEA algorithms were used to evaluate the relationship between ICC characteristic genes and tumor immune-infiltrating cells, in order to explore the effect of ICC characteristic genes on tumor immune microenvironment. Finally, 46 immune checkpoint related genes (including *CD274*, *PDCD1*, *CTLA4*, *CD14*, *LAG3*, and *TNFRSF9*) were found through the literature. We used the limma and corrplot packages, *etc*. to analyze whether the disease signature genes had a regulatory effect on the expression of immune checkpoints.

Analysis of protein expression level of disease characteristic genes by Human Protein Atlas database

The Human Protein Atlas (HPA) database provides the expression and distribution of all available proteins in human tissues and organs. Therefore, protein expression data of disease-characteristic genes in ICC and paracancerous tissues were obtained from this database for comparative analysis.

Statistical analysis

All statistical analyses in this study were conducted in R version 4.2.0. ICC characteristic genes were screened by LASSO regression, SVM-RFE and RF machine learning algorithms. The diagnostic efficacy of diagnostic biomarkers was evaluated by ROC curve. The relationship between the expression of characteristic genes and immune cell infiltration and immune checkpoint was analyzed by Spearman and Pearson correlation. Statistical significance was identified based on $P < 0.05$.

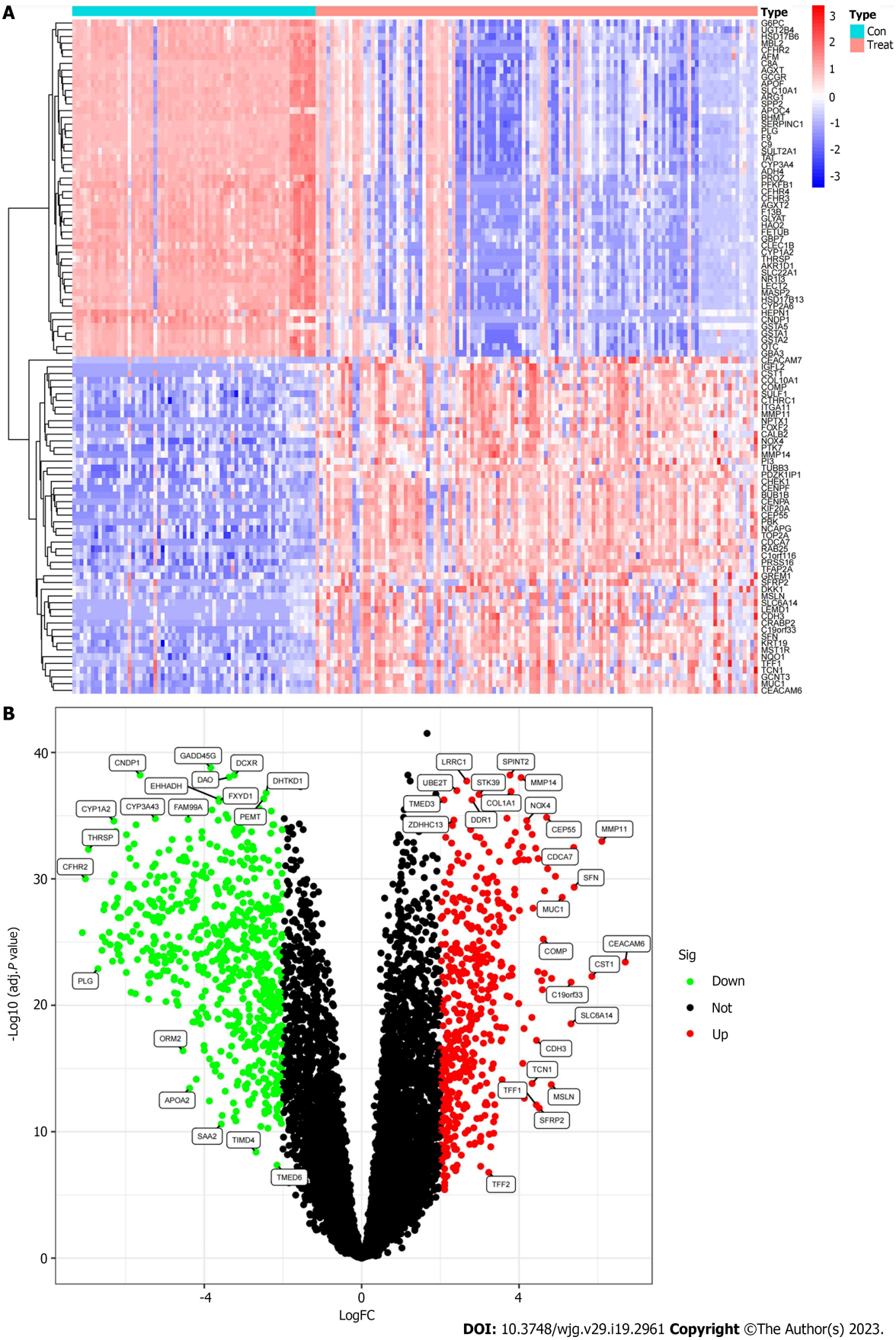
RESULTS

Downloading and sorting of sample data

Table 1 shows the three datasets (GSE26566, GSE32958, and GSE107943) in the GEO database and the ICC-related information obtained from the TCGA database. Two hundred and eighty-four samples were collected, including 120 cancer tissues and 66 paracancerous tissues in the training group. In the two verification groups, cancer tissue samples were from 30 and 33 cases, respectively, and paracancerous tissue samples from 27 and eight cases, respectively.

Screening of differential genes

By the difference analysis of the training group, 1091 differential mRNAs were obtained, including 463 upregulated and 628 downregulated mRNAs (Figure 1A and B). There were many genes with multiple differences in ICC cancer and paracancerous tissues; therefore, it was important to screen characteristic genes that mediated the occurrence and development of ICC, which laid a foundation for the following mechanistic exploration and target gene identification.



DOI: 10.3748/wjg.v29.i19.2961 **Copyright** ©The Author(s) 2023.

Figure 1 The differentially expressed mRNA of intrahepatic cholangiocarcinoma patients was screened based on GEO database training group. A: The heat map of differential gene expression in cancer tissues (Treat) and paracancerous tissues (Con); B: The Volcano map of differential gene expression between cancer and paracancerous tissues.

Biological functions of differential genes

Through GO functional enrichment analysis, we found that in terms of BP, processes such as small molecule catabolic process, response to xenobiotic stimulus, and carboxylic acid catabolic process had the largest number of enrichment genes. In terms of CC, collagen-containing extracellular matrix (ECM), apical part of cell and other CC had the largest number of enriched genes. In terms of MF, sulfur compound binding, glycosaminoglycan binding, serine hydrolase activity and iron ion binding had the largest number of enriched genes (Figure 2A). KEGG pathway enrichment analysis showed that the differential genes were mainly enriched in 56 related regulatory mechanisms, which were mainly involved in complement and coagulation cascades, bile secretion, biosynthesis of cofactors, drug metabolism cytochrome P450, chemical carcinogenesis DNA adducts, retinol metabolism and other pathways (Figure 2B). DO disease enrichment analysis showed that differential genes were closely related to cardiovascular disease, urinary system disease, fatty liver and cholangiocarcinoma (Figure 2C). GSEA enrichment analysis was carried out on the experimental and control groups. GO enrichment analysis showed that acylglycerol homeostasis and alcohol metabolic process were mainly enriched in paracancerous tissues (Figure 3A). In ICC cancer tissues, differential genes were mainly enriched in cell division, chromosome segregation, embryonic organ development and other functions (Figure 3B). KEGG enrichment analysis showed that complement, coagulation cascades and drug metabolism cytochrome P450 were actively expressed in para-cancerous tissues (Figure 3C), while cell cycle, ECM receptor interaction and pathways in cancer were actively expressed in cancer tissues (Figure 3D).

Determination of diagnostic markers for ICC

To identify the specific genes of value in the diagnosis of ICC, we used machine learning to filter the above 1091 differential genes. A total of 25 genes were screened by LASSO regression algorithm, namely: *MMP14*, *CDCA8*, *ZDHHC13*, *NOX4*, *HEPN1*, *LRRC49*, *PDZK1IP1*, *OR1L4*, *FAP*, *NDST3*, *FXN*, *PYCR1*, *PRR11*, *SPAM1*, *MAD2L1*, *APOBEC3G*, *PI3*, *CYP7A1*, *RNF165*, *MT1M*, *GREM1*, *EME1*, *ENAH*, *CDKN2B* and *FOSB* (Figure 4A). After screening by SVM-RFE algorithm, 19 genes were retained, namely: *CFHR2*, *PROC*, *UBE2T*, *HGD*, *AGMAT*, *ACSL1*, *GADD45G*, *DCXR*, *HGFAC*, *DTL*, *MMP14*, *ADHFE1*, *SLC22A1*, *CBS*, *PIPOX*, *SHMT1*, *RDH5*, *F12*, and *F9* (Figure 4B). After screening by RF algorithm, the first 30 genes obtained good diagnostic effect, namely: *SLC10A1*, *CYP3A43*, *COL8A1*, *CDH13*, *ALDH1A1*, *ITPR3*, *MT1H*, *NRCAM*, *TMOD1*, *TNFAIP6*, *SH2D3A*, *OLFML2A*, *WNT10A*, *ACAA2*, *RGN*, *GADD45G*, *CNDP1*, *SPINT2*, *DCXR*, *DAO*, *MMP14*, *LRRC1*, *UBE2T*, *COL1A1*, *DHTKD1*, *STK39*, *PEMT*, *EHHADH*, *TMED3*, and *DDR1* (Figure 4C and D). After the intersection of the genes determined by the above three results, the best disease characteristic gene was obtained: *MMP14* (Figure 4E).

Feasibility analysis of disease characteristic genes as ICC diagnostic markers

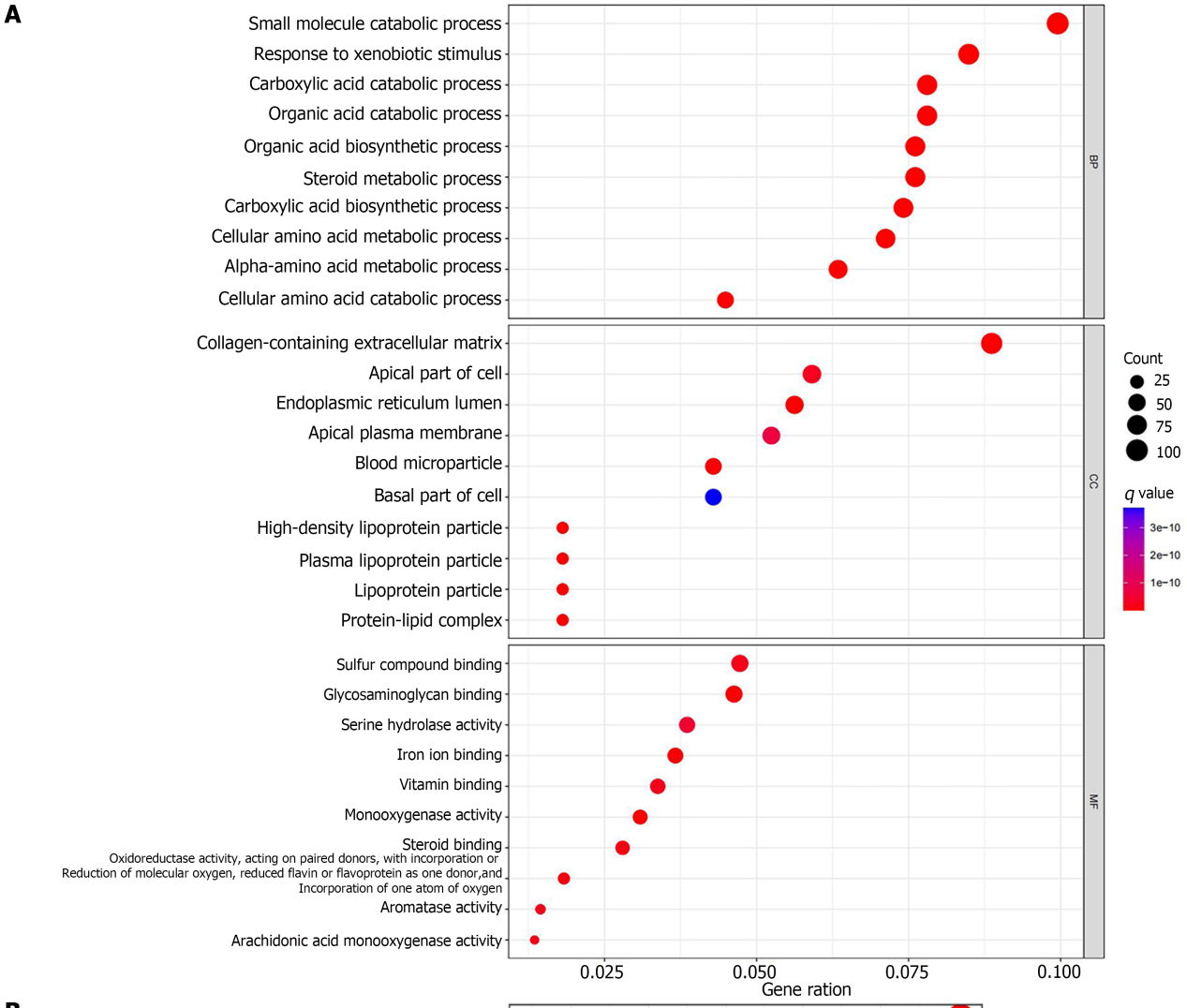
Previous studies had shown that *MMP14* was highly expressed in cancer tissues of ICC patients in the training group, so it was important to clarify its expression in two independent verification groups before evaluating the accuracy of this gene as a disease signature gene. In the GSE107943 dataset, the expression of MMP14 in ICC cancer tissues was apparently higher than that in paracancer tissue (Figure 5A). The same result was obtained by external database verification of *MMP14* in the TCGA database (Figure 5B). ROC curves were drawn for the training and validation groups, which showed that in the training group, AUC was 0.960 (95%CI: 0.932-0.983) (Figure 5C). In the GSE107943 verification group, AUC was 0.999 (95%CI: 0.993-1.000) (Figure 5D), and in the TCGA verification group, AUC was 0.977 (95%CI: 0.924-1.000) (Figure 5E). AUC in the verification group was higher than in the training group, and AUC values were all > 0.9. This showed that *MMP14* had good diagnostic efficiency and could be used as a characteristic gene of ICC, which provided a new reference marker for the selection of gene targets for diagnosis of ICC.

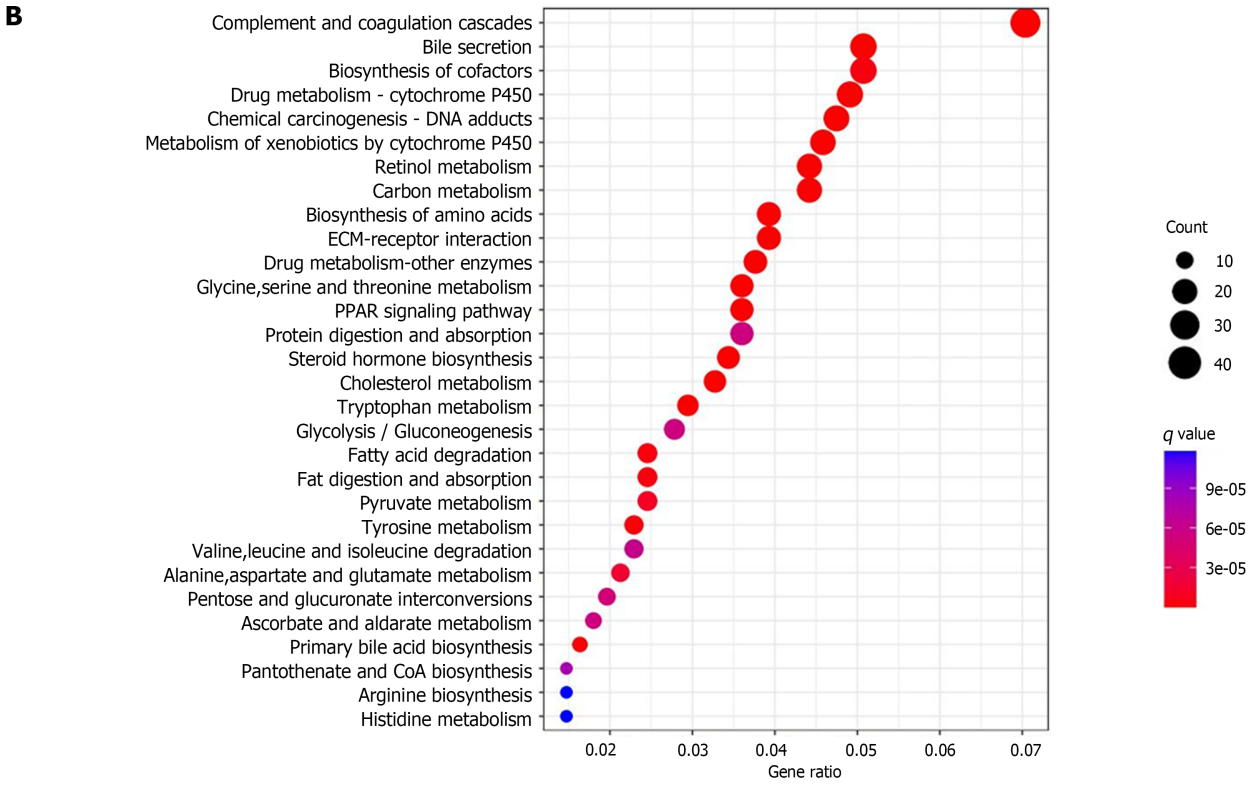
Immune cell infiltration in ICC

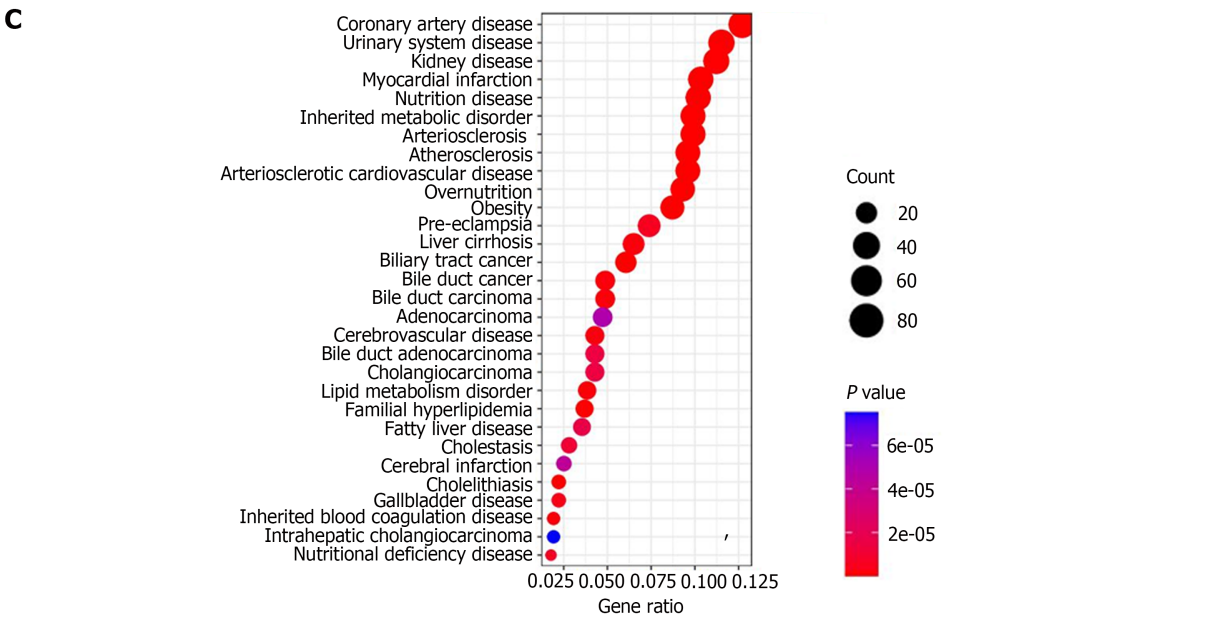
To explore the infiltration of immune cells in the immune microenvironment of ICC, the proportion of 22 types of immune cells in each sample of ICC cancer and paracancerousl tissues was clarified (Figure 6A). The positive correlation between resting dendritic cells resting and resting memory CD4 T cells resting was the strongest (r = 0.45), and the negative correlation between mast cells resting and mast cells activated was the strongest (r = 0.40) (Figure 6B). We then analyzed the infiltration of immune cells in cancer and paracancerous tissues, and was significant for monocytes, M0 macrophages, activated mast cells, and eosinophils. Compared with paracancerous tissues, expression of M0 macrophages in tumor tissues was greatly higher (P = 0.040), while expression of monocytes (P = 0.002) and activated mast cells (P = 0.037) was significantly lower in tumor tissues (Figure 6C).

Correlation analysis of ICC disease signature genes and immune infiltration patterns

There were differences in the distribution of immune infiltrating cells between ICC cancer tissues and paracancerous tissues. To analyze its potential regulatory factors, we explored the correlation between ICC disease signature genes and immune microenvironment. CIBERSORT algorithm analysis showed that among the immune cells, *MMP14* was significantly correlated with the number of seven types of


A
Small molecule catabolic process
Response to xenobiotic stimulus
Carboxylic acid catabolic process
Organic acid catabolic process
Organic acid biosynthetic process
Steroid metabolic process
Carboxylic acid biosynthetic process
Cellular amino acid metabolic process
Alpha-amino acid metabolic process
Cellular amino acid catabolic process
BP
Collagen-containing extracellular matrix
Apical part of cell
Endoplasmic reticulum lumen
Apical plasma membrane
Blood microparticle
Basal part of cell
High-density lipoprotein particle
Plasma lipoprotein particle
Lipoprotein particle
Protein-lipid complex
CC
Sulfur compound binding
Glycosaminoglycan binding
Serine hydrolase activity
Iron ion binding
Vitamin binding
Monooxygenase activity
Steroid binding
Oxidoreductase activity, acting on paired donors, with incorporation or Reduction of molecular oxygen, reduced flavin or flavoprotein as one donor,and Incorporation of one atom of oxygen
Aromatase activity
Arachidonic acid monooxygenase activity
MF
0.025
0.050
0.075
0.100
Gene ration
Count
25
50
75
100
q value
3e-10
2e-10
1e-10


B
Complement and coagulation cascades
Bile secretion
Biosynthesis of cofactors
Drug metabolism - cytochrome P450
Chemical carcinogenesis - DNA adducts
Metabolism of xenobiotics by cytochrome P450
Retinol metabolism
Carbon metabolism
Biosynthesis of amino acids
ECM-receptor interaction
Drug metabolism-other enzymes
Glycine,serine and threonine metabolism
PPAR signaling pathway
Protein digestion and absorption
Steroid hormone biosynthesis
Cholesterol metabolism
Tryptophan metabolism
Glycolysis / Gluconeogenesis
Fatty acid degradation
Fat digestion and absorption
Pyruvate metabolism
Tyrosine metabolism
Valine,leucine and isoleucine degradation
Alanine,aspartate and glutamate metabolism
Pentose and glucuronate interconversions
Ascorbate and aldarate metabolism
Primary bile acid biosynthesis
Pantothenate and CoA biosynthesis
Arginine biosynthesis
Histidine metabolism
0.02
0.03
0.04
0.05
0.06
0.07
Gene ratio
Count
10
20
30
40
q value
9e-05
6e-05
3e-05



DOI: 10.3748/wjg.v29.i19.2961 **Copyright** ©The Author(s) 2023.

Figure 2 Enrichment analysis of differential genes. A: GO functional enrichment analysis; B: KEGG pathway enrichment analysis; C: DO disease enrichment analysis.

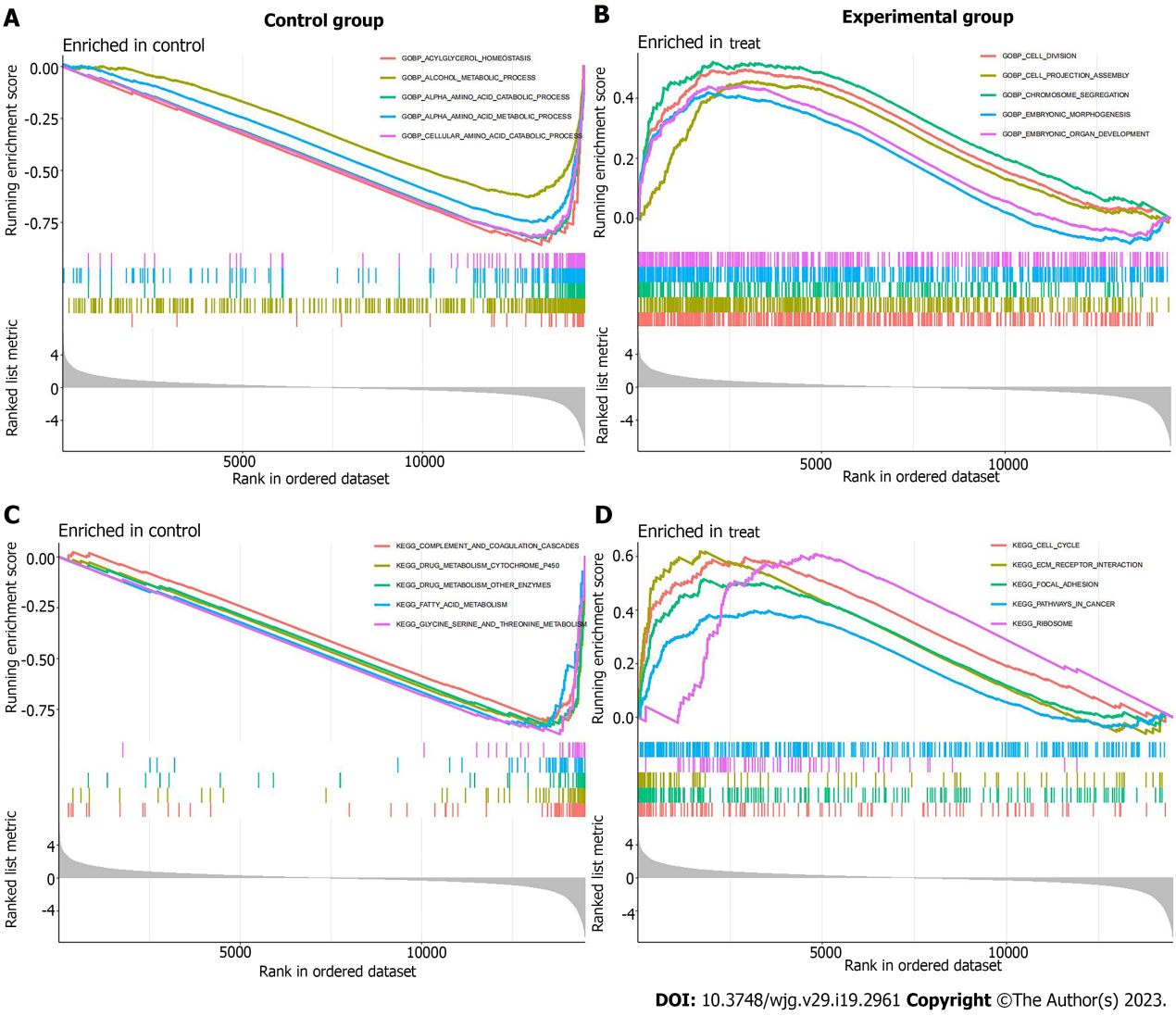
immune cells. Expression of MMP14 was positively related with M0 macrophages M0 (r = 0.40, P = 0.0023), activated dendritic cells (r = 0.32, P = 0.0180) and follicular helper T cells (r = 0.29, P = 0.0300) (Figure 7A-C), and negatively related with activated memory CD4 T cells (r = -0.33, P = 0.0130), monocytes (r = -0.32, P = 0.0190), M1 macrophages (r = -0.28, P = 0.0420) and resting memory CD4 T cells (r = -0.27, P = 0.0440) (Figure 7D-G). The final results of *MMP14* and immune cell infiltration based on the above CIBERSORT algorithm are summarized (Figure 8A). ssGSEA algorithm analysis showed that there was a significant correlation between *MMP14* and the number of four types of immune cells and 28 types of immune cells. It was significantly negatively correlated with the number of neutrophils, monocytes, central memory CD8 T cells and central memory CD4 T cells (Figure 8B). *MMP14* was positively correlated with the expression of *CD200*, *CD40*, *CD44*, *CD70*, *CTLA4*, *HHLA2*, *LGALS9*, *TNFRSF14*, *TNFRSF18*, *TNFRSF25*, *TNFSF4* and *TNFSF9*. However, it was negatively correlated with the expression of *CD14*, *CD160*, *TMIGD2*, and *TNFSF14* (Figure 8C). In summary, *MMP14* regulates the composition of immune infiltrating cells in the tumor microenvironment of ICC and may affect the efficacy of immunotherapy by mediating the expression of immune cell surface markers.

Expression of disease characteristic genes in ICC

HPA database analysis showed that expression of MMP14 protein in ICC cancer tissue was higher than that in paracancerous tissue (Figure 9). It was consistent with the trend in mRNA expression levels in the training and verification groups, which confirmed that *MMP14* could be used as a disease characteristic diagnostic gene of ICC.

DISCUSSION

Although there has been some improvement in the treatment of ICC in recent years, the disease control rate is still low[14]. There is no definite marker for early diagnosis of ICC[15]. Individualized treatment has not yet achieved satisfactory results in ICC patients[16]. At present, immunotherapy is a research hot spot in the field of cancer treatment worldwide, and it has widespread prospects for treatment of cholangiocarcinoma[17]. Therefore, the present study focused on discovering new diagnostic markers and improving immunotherapy and determining synergistic therapeutic targets for ICC. Recently, similar ideas have been developed in the research of a variety of tumors and other diseases. More researchers have begun to identify new disease signature genes and explore their potential links with immune cell infiltration. For example, in chronic obstructive pulmonary disease (COPD), STAU1 and SLC27A3 are considered to be important diagnostic biomarkers. The pathogenesis of COPD is largely affected by the pattern of immune cell infiltration. It has been confirmed that STAU1 and SLC27A3 are important factors in regulating the content of plasma cells, resting NK cells, CD8 T cells, and other immune cells[18]. Studies have pointed out that LTBP2 is a highly effective biomarker for prostate cancer, which may inhibit the proliferation and metastasis of prostate cancer through the PI3K/AKT



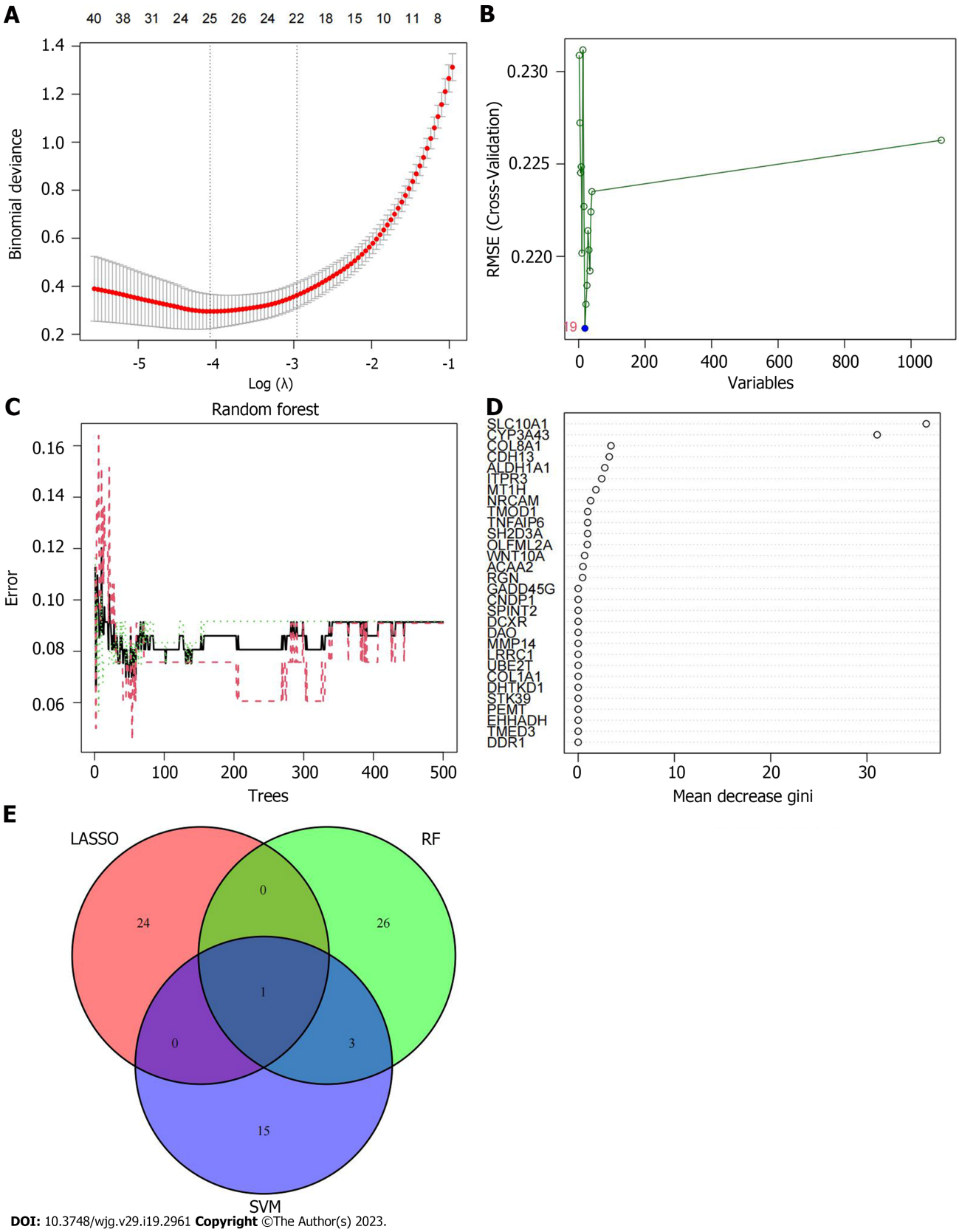
DOI: 10.3748/wjg.v29.i19.2961 **Copyright** ©The Author(s) 2023.

Figure 3 GSEA enrichment analysis of differential genes. A: GO enrichment analysis in the control group; B: GO enrichment analysis in the experimental group; C: KEGG enrichment analysis in the control group; D: KEGG enrichment analysis in the experimental group.

signaling pathway, and is related to CD4 T-cell infiltration and the response to anti-PD-1/PD-L1 immunotherapy[19]. However, for ICC with poor prognosis, there have been few studies on potential diagnostic markers and their correlation with immune cell infiltration. Therefore, we hope to find diagnostic biomarkers for ICC and investigate their relationship with immune cell infiltration.

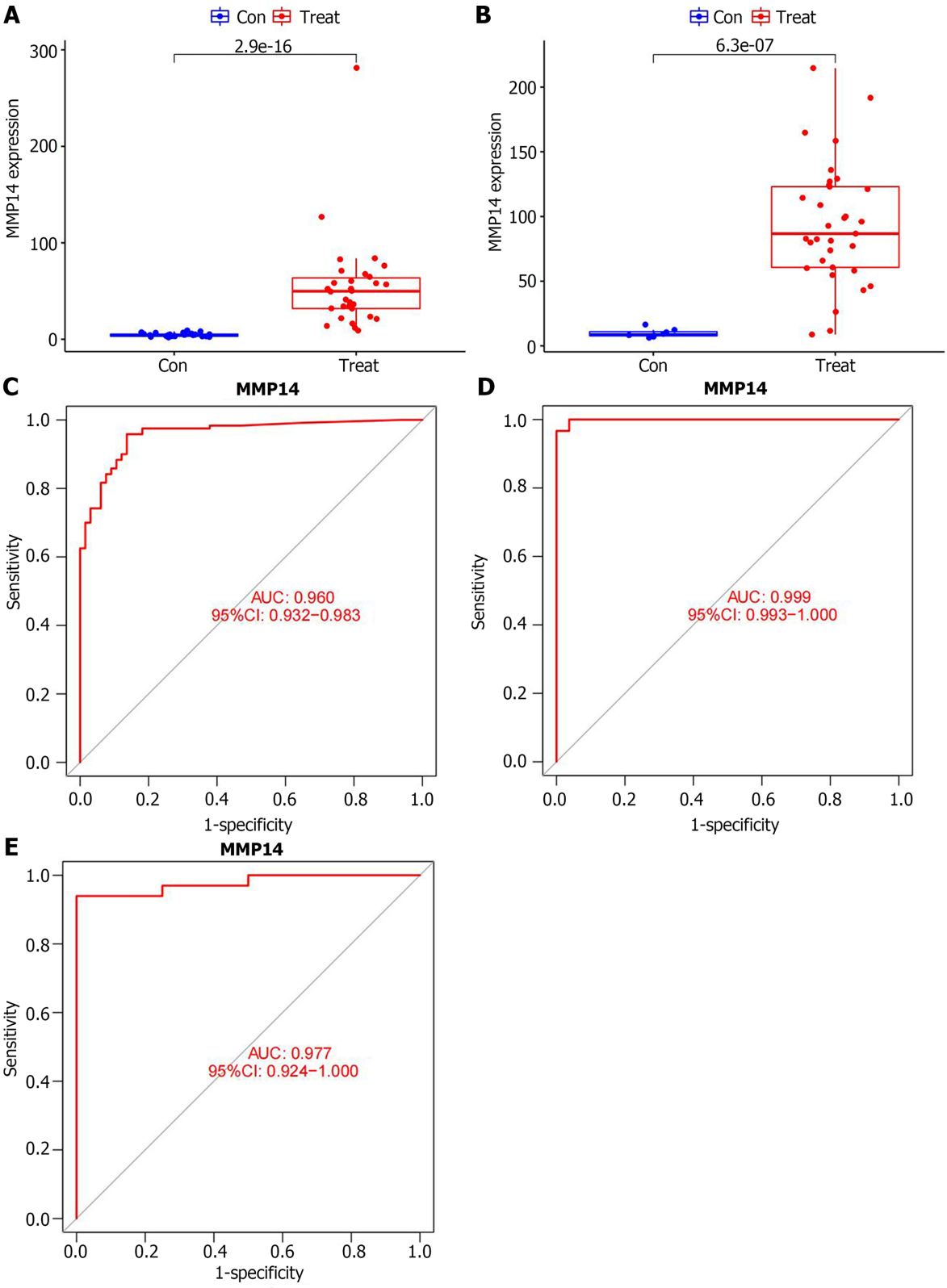
The present study was a series of retrospective studies based on the gene expression matrix of ICC patients in the GEO and TCGA databases, looking for new diagnostic genes for ICC and analyzing the significance of immune cell infiltration. The results obtained are consistent with previous studies that complex metabolic changes occurred in the entire process of cholangiocarcinoma development, and metabolic reprogramming mechanisms such as glucose metabolism, amino acid metabolism, and lipid metabolism all mediate tumor proliferation and invasion are involved[20]. Mechanisms such as ECM-receptor interaction, cell cycle disorder, and stem cell self-renewal have also been confirmed to affect the development of ICC, which is consistent with our enrichment analysis[21-23]. To accurately screen for disease characteristic genes, we used LASSO regression, SVM-RFE, and RF learning algorithms for joint analysis. After the joint verification of another data set in the GEO and TCGA databases, we identified *MMP14* as having high diagnostic accuracy for ICC.

The MMP family are proteolytic enzymes closely related to angiogenesis and tumor progression. MMP14 was the first transmembrane protein found in the family[24]. Previous studies have indicated that MMP14 plays a key role in the malignant transformation of liver cancer, pancreatic cancer, colorectal cancer and other tumors[25-28]. In primary liver cancer, the expression of MMP14 in cancer tissues is significantly higher than that in paracancerous tissues. The expression level of MMP14 is positively correlated with tumor size, Edmondson-Steiner grade and α-fetoprotein level, and mediates the poor prognosis of patients with primary liver cancer[29]. In renal cell carcinoma, MMP14, as a member of the circPTCH1/miR-485-5p/MMP14 endogenous competitive network, participates in promoting metastasis and activating epithelial-mesenchymal transformation of renal cell carcinoma



DOI: 10.3748/wjg.v29.i19.2961 **Copyright** ©The Author(s) 2023.

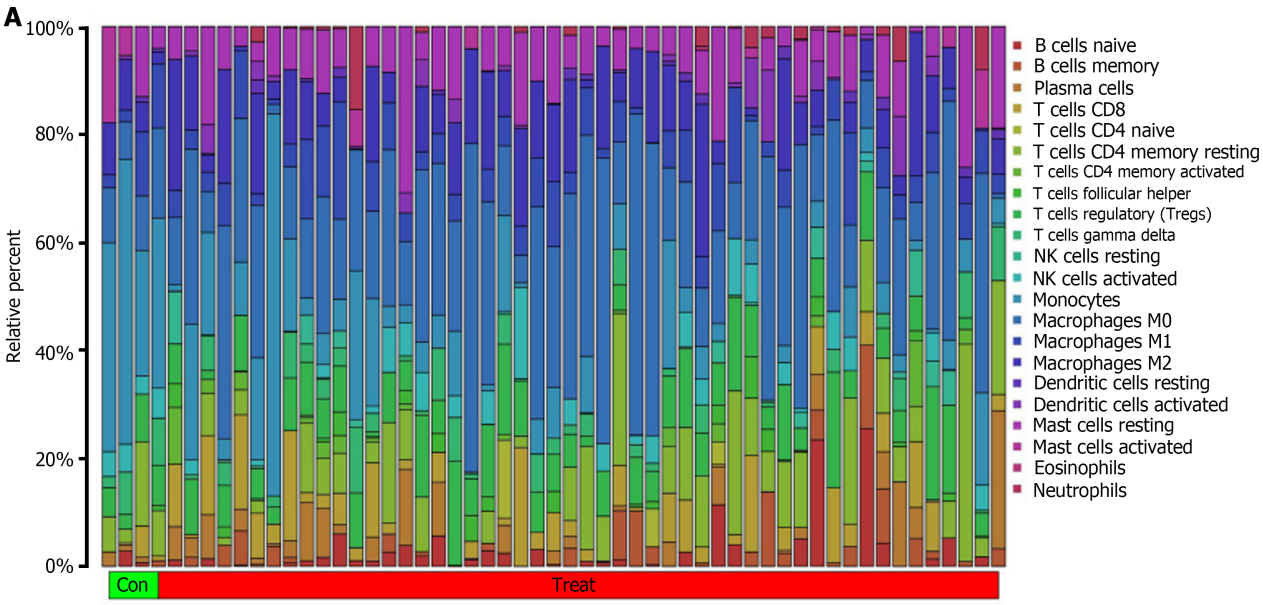
Figure 4 Screening of disease signature genes. A: The process of least absolute shrinkage and selection operator regression screening of characteristic genes; B: The relationship between the error and the number of variables in support vector machine-recursive feature elimination; C: The impact of the amount of decision trees on the error rate; D: The name of the characteristic gene and the score of gene importance obtained by RF screening; E: The Venn diagrams of the intersection eigengenes obtained by the three algorithms. SVM: Support vector machine; LASSO: The least absolute shrinkage and selection operator; RF: Random forest.

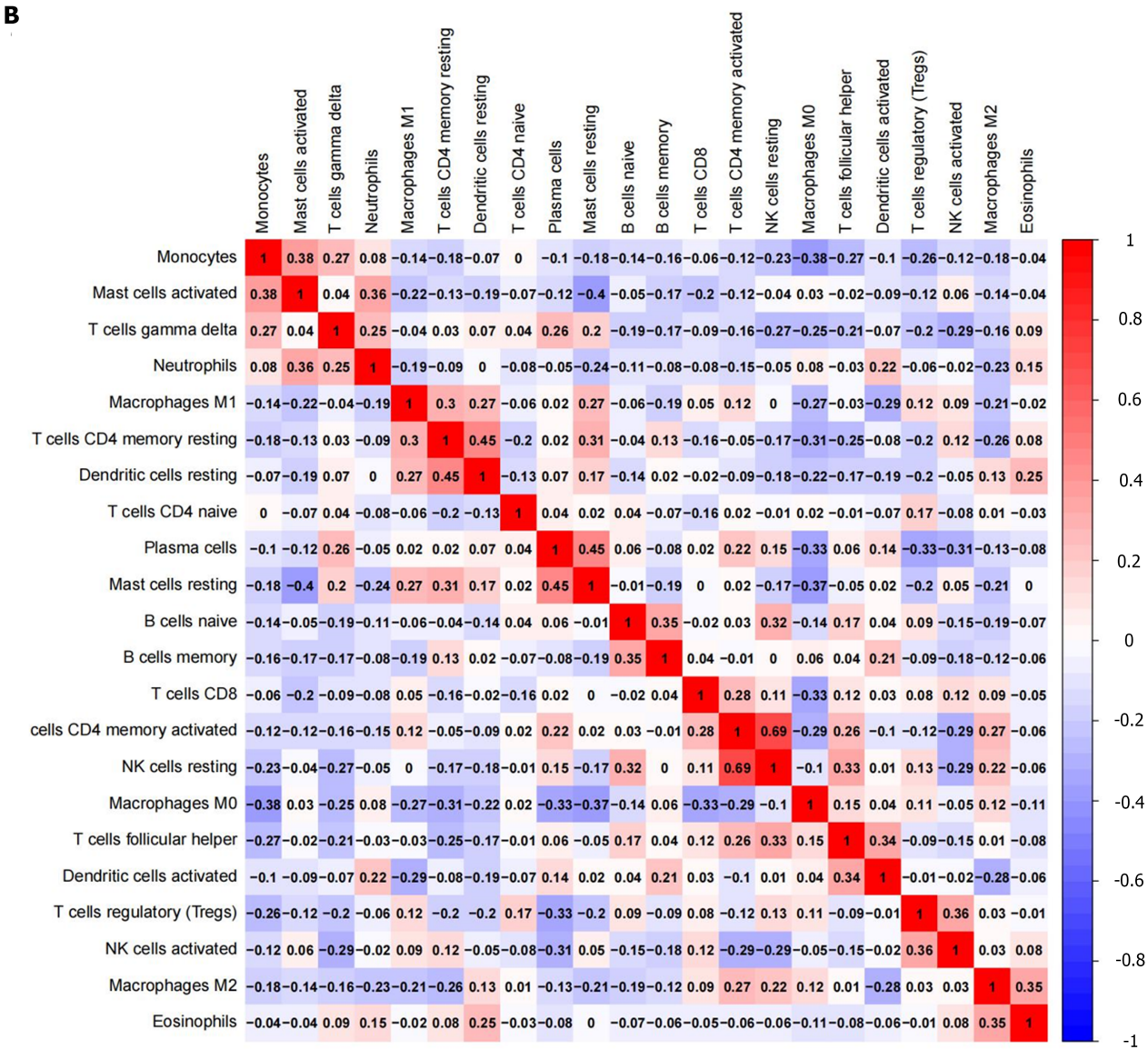


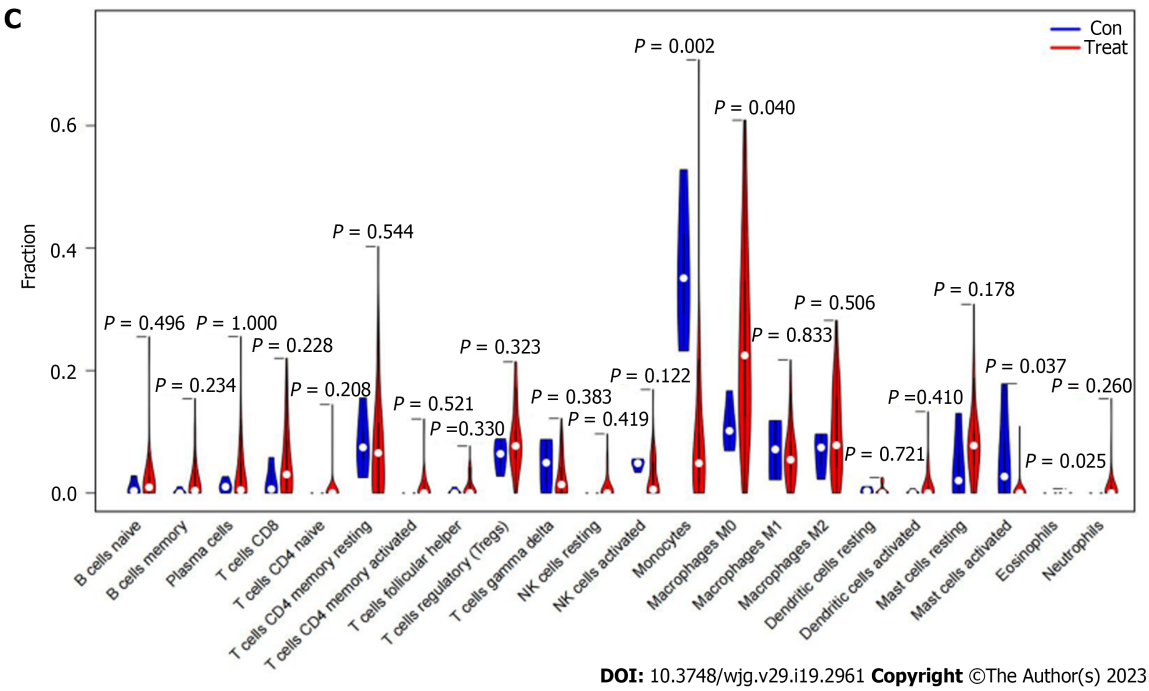
DOI: 10.3748/wjg.v29.i19.2961 **Copyright** ©The Author(s) 2023.

Figure 5 Analysis of the diagnostic value of intrahepatic cholangiocarcinoma characteristic genes. A: The boxplot of the differential expression of MMP14 in the GSE107943 dataset; B: The boxplot of the differential expression of MMP14 in the The Cancer Genome Atlas (TCGA) database; C: In the training group, the receiver operating characteristic (ROC) curve of MMP14 to evaluate the diagnostic efficacy of intrahepatic cholangiocarcinoma (ICC); D: In the GSE107943 dataset of the verification group, the ROC curve of MMP14 to evaluate the diagnostic efficacy of ICC; E: In the TCGA dataset of the verification group, the ROC curve of MMP14 to evaluate the diagnostic efficacy of ICC. AUC: Area under the curve; 95%CI: 95% confidence interval.

[30]. Direct degradation of ECM or indirect activation of MMP2 is also the main way for MMP14 to promote the invasion and metastasis of many types of tumors[31,32]. Ragusa and colleagues found that, in a chemotherapy-resistant, aggressive, matrix-rich colorectal cancer subtype, fluctuations in tumor


A
100%
80%
60%
40%
20%
0%
Relative percent
Con
Treat
B cells naive
B cells memory
Plasma cells
T cells CD8
T cells CD4 naive
T cells CD4 memory resting
T cells CD4 memory activated
T cells follicular helper
T cells regulatory (Tregs)
T cells gamma delta
NK cells resting
NK cells activated
Monocytes
Macrophages M0
Macrophages M1
Macrophages M2
Dendritic cells resting
Dendritic cells activated
Mast cells resting
Mast cells activated
Eosinophils
Neutrophils


B
Monocytes
Mast cells activated
T cells gamma delta
Neutrophils
Macrophages M1
T cells CD4 memory resting
Dendritic cells resting
T cells CD4 naive
Plasma cells
Mast cells resting
B cells naive
B cells memory
T cells CD8
T cells CD4 memory activated
NK cells resting
Macrophages M0
T cells follicular helper
Dendritic cells activated
T cells regulatory (Tregs)
NK cells activated
Macrophages M2
Eosinophils
1
0.8
0.6
0.4
0.2
0
-0.2
-0.4
-0.6
-0.8
-1



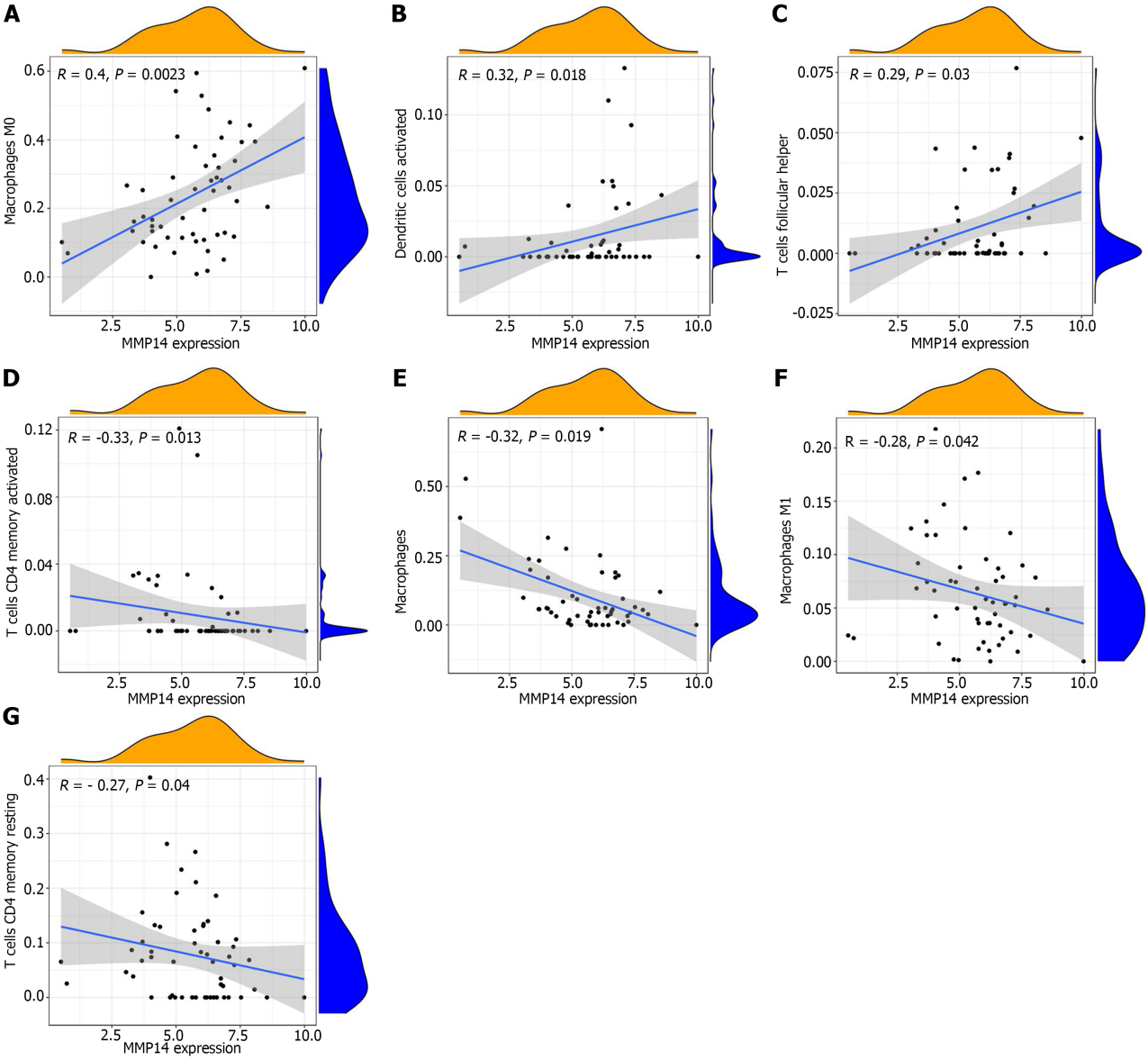
DOI: 10.3748/wjg.v29.i19.2961 **Copyright** ©The Author(s) 2023.

Figure 6 The distribution of immune infiltrating cells in intrahepatic cholangiocarcinoma. A: The relative content of immune infiltrating cells in each sample; B: The correlation heatmap composed of cells in all samples; C: The violin plot of the difference in immune cell infiltration between intrahepatic cholangiocarcinoma cancer and paracancerous tissues.

signals triggered a decrease in PROX1 Levels and upregulation of MMP14 through the WNT and Notch pathways, which promoted a series of adverse tumor microenvironmental changes, including activation of fibroblasts, vascular dysfunction, and inability of cytotoxic T cells to enter the tumor[33]. It can be seen that, as a clear tumor-promoting factor, MMP14 is a key regulator in the tumor microenvironment, tumor immune infiltration and tumorigenesis, but its effect on disease diagnosis and tumor immune microenvironment in ICC has not been reported, so our research is important.

Tumor microenvironment plays an important role in the occurrence, development and prognosis of tumor. As an important part of tumor microenvironment, immune cells are involved in the prognosis of the disease and guidance of clinical treatment[34-36]. We calculated the profiles of immune cell infiltration in ICC cancer and paracancerous tissues, and elucidated ICC-associated immune cell subtypes and their potential relationships. Compared with paracancerous tissues, the infiltration of M0 macrophages in ICC tissues was significantly increased, while the proportion of monocytes and mast cells activated was significantly decreased. The correlation analysis between MMP14 and immune cells showed that it was positively correlated with M0 macrophages, activated dendritic cells and follicular helper T cells, and negatively correlated with activated memory CD4 T cells, monocytes, M1 macrophages and resting memory CD4 T cells. The ssGSEA algorithm showed that MMP14 was closely related to the degree of immune cell infiltration, and the number of central memory CD8 T cells, neutrophils, monocytes and central memory CD4 T cells decreased significantly in ICC patients with high expression of MMP14. We found that MMP14 was positively correlated with expression of 12 molecules, including CTLA4 and CD40, and negatively correlated with expressions of four molecules, including CD14 and CD160. Differential regulatory mechanisms of the tumor microenvironment in ICC patients may help explain individual differences in immunotherapy. The expression of MMP14 was negatively regulated by the distribution of monocytes and CD4 T cells in the analysis of CIBERSORT and ssGSEA algorithms. Coincidentally, in the correlation analysis with immune checkpoints, we found that MMP14 was related to the expression of many important molecules, such as monocyte surface marker CD14 and transmembrane receptor CTLA4 on T cells. As an important part of effective antitumor immunity, CD4 T cells can directly eliminate tumor cells through cytolytic mechanisms, or indirectly target tumor cells by regulating the tumor microenvironment to kill tumor cells[37]. Different subpopulations of monocytes perform exclusive functions for tumor promotion or antitumor immunity [38]. It has been reported that CD14 and CD16 monocyte subsets can induce cancer cell death through antibody-dependent cytotoxicity[24,39]. Therefore, we have the reason to speculate that MMP14 may accelerate the progression of ICC by interfering with the abundance of monocytes and CD4 T cells.

In our study, we found new ICC characteristic gene, *MMP14*, and clarified that it might influence the infiltration pattern of immune cells in complex tumor microenvironments. It could be helpful for the clinical diagnosis and immunotherapy of ICC, and provides new ideas for the future study of the occurrence and molecular mechanism of ICC.



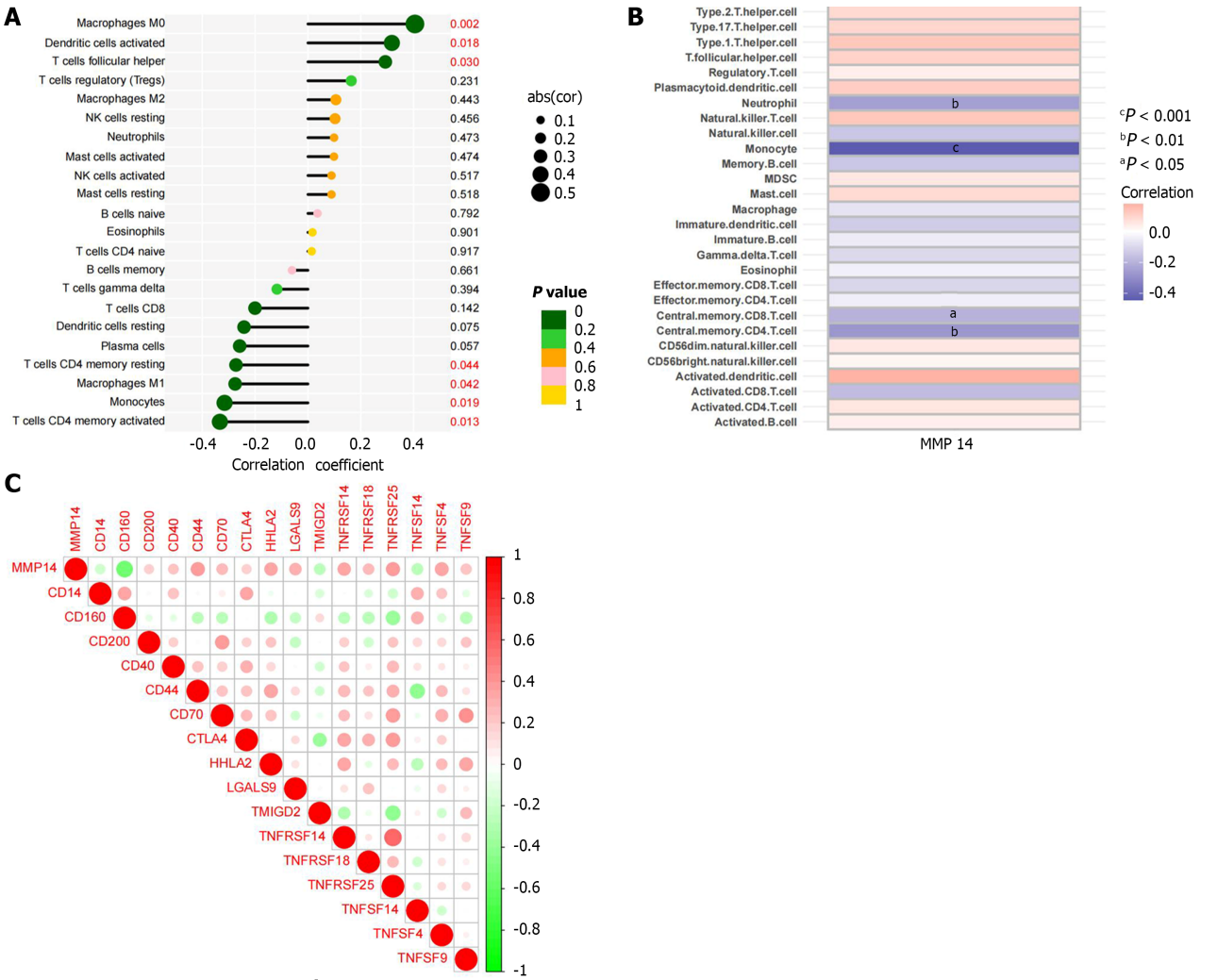
DOI: 10.3748/wjg.v29.i19.2961 **Copyright** ©The Author(s) 2023.

Figure 7 The scatter plot of the correlation between MMP14 expression and immune cells. A: Macrophage M0; B: Dendritic cell activation; C: T cell follicular assisted cell activation; D: T cell CD4 memory activation; E: monocyte; F: Macrophage M1; G: T cell CD4 memory resting.

However, our research still had some limitations. Firstly, all data came from public databases, which could have led to inevitable errors or biases. Secondly, the expression and specific function of disease characteristic genes need to be verified by further experiments. Although bioinformatics and machine learning have been used to evaluate the diagnostic efficacy of ICC feature genes and their relationship with immune infiltration, a larger prospective study is needed to confirm our conclusions.

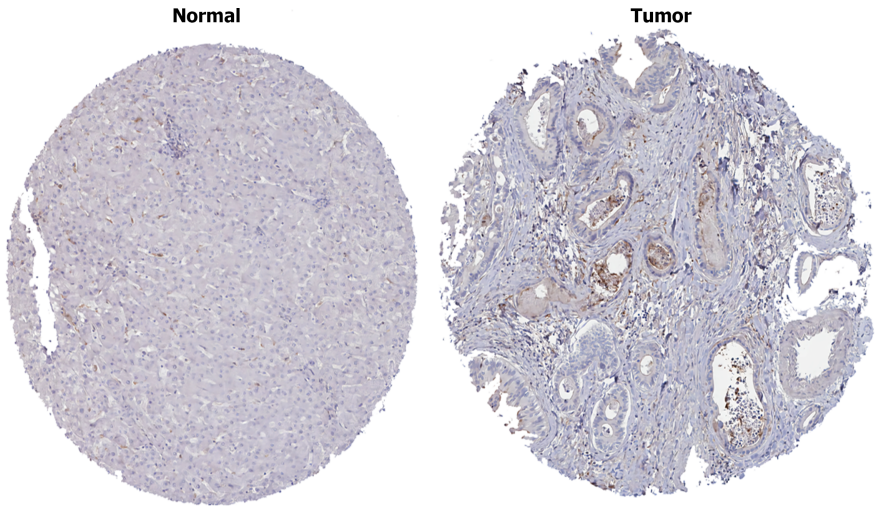
CONCLUSION

Here we investigated new candidate molecular markers that are important for the diagnosis of ICC, which was related to a variety of immune cell components and participated in the occurrence and development of ICC. The findings may have a beneficial impact on the diagnosis of ICC and the provision of precise immunotherapy in future clinical work.



DOI: 10.3748/wjg.v29.i19.2961 **Copyright** ©The Author(s) 2023.

Figure 8 Correlation of MMP14 with immune cell content and immune checkpoint expression. A: Correlation between MMP14 and immune cell infiltration based on CIBERSORT algorithm; B: Correlation between MMP14 and immune cell infiltration based on ssGSEA algorithm; C: The heat map of the correlation between MMP14 and immune checkpoint expression.



DOI: 10.3748/wjg.v29.i19.2961 **Copyright** ©The Author(s) 2023.

Figure 9 Human Protein Atlas analysis of MMP14 protein expression levels in intrahepatic cholangiocarcinoma cancer and paracancerous tissues.

ARTICLE HIGHLIGHTS

Research background

Intrahepatic cholangiocarcinoma (ICC) has a high mortality rate. Its early diagnosis is very important.

Research motivation

At present, there are no diagnostic markers of ICC, and most patients are in the middle and late stage when the tumors are found, and the treatment options for these patients are limited, resulting in a poor prognosis.

Research objectives

It is urgent to find new biomarkers for early screening and diagnosis of ICC.

Research methods

Bioinformatics analysis and machine learning algorithm were used to screen for ICC disease characteristic genes, and the diagnostic performance of characteristic gene *MMP14* was verified by different databases. The relationship between different immune cell infiltration in MMP14 and ICC tumor microenvironment was analyzed.

Research results

We discovered for the first time a new gene *MMP14* for the diagnosis of ICC. We further analyzed the expression of *MMP14* and its significance in immune cell infiltration in ICC tumor microenvironment, indicating that *MMP14* is closely related to a variety of immune cell infiltration, which may provide a new direction for immune-related research.

Research conclusions

In this study, we found that *MMP14* can be used as a disease characteristic gene for ICC diagnosis using a variety of machine learning algorithms. There is a relationship between different immune cell infiltration in *MMP14* and ICC tumor microenvironment, which plays an important role in the occurrence and development of tumor. *MMP14* may be a potential target for ICC immunotherapy.

Research perspectives

Based on bioinformatics analysis and machine learning algorithm, *MMP14* was identified as the characteristic gene of ICC and was associated with ICC immune cell infiltration. In the future research, it will be of great significance to explore the signal pathway mediated by *MMP14* in the occurrence and development of ICC and the mechanism of immune cell infiltration.

FOOTNOTES

Author contributions: Han L conceived and directed the entire study, and should be regarded as corresponding author; Wu J and Guo Y designed the study and prepared the manuscript; Zuo ZF defined the intellectual content of the study and participated in the literature research; Wu J, Guo Y, and Zuo ZF contributed equally to this study; Zhu ZW conducted data analysis; Han L and Wu J revised the manuscript; and all authors approved to submit the manuscript.

Institutional review board statement: This study is not involved any human and animal.

Conflict-of-interest statement: The authors declare no conflict of interest.

Data sharing statement: The bioinformatic data could be downloaded from the public databases, and no additional data are available.

Open-Access: This article is an open-access article that was selected by an in-house editor and fully peer-reviewed by external reviewers. It is distributed in accordance with the Creative Commons Attribution NonCommercial (CC BY-NC 4.0) license, which permits others to distribute, remix, adapt, build upon this work non-commercially, and license their derivative works on different terms, provided the original work is properly cited and the use is non-commercial. See: https://creativecommons.org/Licenses/by-nc/4.0/

Country/Territory of origin: China

ORCID number: Lei Han 0000-0002-9606-7837.

S-Editor: Chen YL
L-Editor: A

P-Editor: Cai YX

REFERENCES

1 **Siegel RL**, Miller KD, Fuchs HE, Jemal A. Cancer statistics, 2022. *CA Cancer J Clin* 2022; **72**: 7-33 [PMID: 35020204 DOI: 10.3322/caac.21708]

2 **Bridgewater J**, Galle PR, Khan SA, Llovet JM, Park JW, Patel T, Pawlik TM, Gores GJ. Guidelines for the diagnosis and management of intrahepatic cholangiocarcinoma. *J Hepatol* 2014; **60**: 1268-1289 [PMID: 24681130 DOI: 10.1016/j.jhep.2014.01.021]

3 **Khan SA**, Tavolari S, Brandi G. Cholangiocarcinoma: Epidemiology and risk factors. *Liver Int* 2019; **39** Suppl 1: 19-31 [PMID: 30851228 DOI: 10.1111/liv.14095]

4 **Clements O**, Eliahoo J, Kim JU, Taylor-Robinson SD, Khan SA. Risk factors for intrahepatic and extrahepatic cholangiocarcinoma: A systematic review and meta-analysis. *J Hepatol* 2020; **72**: 95-103 [PMID: 31536748 DOI: 10.1016/j.jhep.2019.09.007]

5 **Mazzaferro V**, Gorgen A, Roayaie S, Droz Dit Busset M, Sapisochin G. Liver resection and transplantation for intrahepatic cholangiocarcinoma. *J Hepatol* 2020; **72**: 364-377 [PMID: 31954498 DOI: 10.1016/j.jhep.2019.11.020]

6 **Chen Q**, Wang H, Li Z, Li F, Liang L, Zou Y, Shen H, Li J, Xia Y, Cheng Z, Yang T, Wang K, Shen F. Circular RNA ACTN4 promotes intrahepatic cholangiocarcinoma progression by recruiting YBX1 to initiate FZD7 transcription. *J Hepatol* 2022; **76**: 135-147 [PMID: 34509526 DOI: 10.1016/j.jhep.2021.08.027]

7 **Chen C**, Wu YH, Zhang JW, Qiu YH, Wu H, Li Q, Song TQ, He Y, Mao XH, Zhai WL, Cheng ZJ, Li JD, Si SB, Cai ZQ, Geng ZM, Tang ZH. [A prognostic model of intrahepatic cholangiocarcinoma after curative intent resection based on Bayesian network]. *Zhonghua Wai Ke Za Zhi* 2021; **59**: 265-271 [PMID: 33706443 DOI: 10.3760/cma.j.cn112139-20201230-00891]

8 **Moris D**, Palta M, Kim C, Allen PJ, Morse MA, Lidsky ME. Advances in the treatment of intrahepatic cholangiocarcinoma: An overview of the current and future therapeutic landscape for clinicians. *CA Cancer J Clin* 2023; **73**: 198-222 [PMID: 36260350 DOI: 10.3322/caac.21759]

9 **Izquierdo-Sanchez L**, Lamarca A, La Casta A, Buettner S, Utpatel K, Klümpen HJ, Adeva J, Vogel A, Lleo A, Fabris L, Ponz-Sarvise M, Brustia R, Cardinale V, Braconi C, Vidili G, Jamieson NB, Macias RI, Jonas JP, Marzioni M, Hołówko W, Folseraas T, Kupčinskas J, Sparchez Z, Krawczyk M, Krupa Ł, Scripcariu V, Grazi GL, Landa-Magdalena A, Ijzermans JN, Evert K, Erdmann JI, López-López F, Saborowski A, Scheiter A, Santos-Laso A, Carpino G, Andersen JB, Marin JJ, Alvaro D, Bujanda L, Forner A, Valle JW, Koerkamp BG, Banales JM. Cholangiocarcinoma landscape in Europe: Diagnostic, prognostic and therapeutic insights from the ENSCCA Registry. *J Hepatol* 2022; **76**: 1109-1121 [PMID: 35167909 DOI: 10.1016/j.jhep.2021.12.010]

10 **Kam AE**, Masood A, Shroff RT. Current and emerging therapies for advanced biliary tract cancers. *Lancet Gastroenterol Hepatol* 2021; **6**: 956-969 [PMID: 34626563 DOI: 10.1016/S2468-1253(21)00171-0]

11 **Greener JG**, Kandathil SM, Moffat L, Jones DT. A guide to machine learning for biologists. *Nat Rev Mol Cell Biol* 2022; **23**: 40-55 [PMID: 34518686 DOI: 10.1038/s41580-021-00407-0]

12 **Handelman GS**, Kok HK, Chandra RV, Razavi AH, Lee MJ, Asadi H. eDoctor: machine learning and the future of medicine. *J Intern Med* 2018; **284**: 603-619 [PMID: 30102808 DOI: 10.1111/joim.12822]

13 **Mosele F**, Remon J, Mateo J, Westphalen CB, Barlesi F, Lolkema MP, Normanno N, Scarpa A, Robson M, Meric-Bernstam F, Wagle N, Stenzinger A, Bonastre J, Bayle A, Michiels S, Bièche I, Rouleau E, Jezdic S, Douillard JY, Reis-Filho JS, Dienstmann R, André F. Recommendations for the use of next-generation sequencing (NGS) for patients with metastatic cancers: a report from the ESMO Precision Medicine Working Group. *Ann Oncol* 2020; **31**: 1491-1505 [PMID: 32853681 DOI: 10.1016/j.annonc.2020.07.014]

14 **Nault JC**, Villanueva A. Biomarkers for Hepatobiliary Cancers. *Hepatology* 2021; **73** Suppl 1: 115-127 [PMID: 32045030 DOI: 10.1002/hep.31175]

15 **Banales JM**, Cardinale V, Carpino G, Marzioni M, Andersen JB, Invernizzi P, Lind GE, Folseraas T, Forbes SJ, Fouassier L, Geier A, Calvisi DF, Mertens JC, Trauner M, Benedetti A, Maroni L, Vaquero J, Macias RI, Raggi C, Perugorria MJ, Gaudio E, Boberg KM, Marin JJ, Alvaro D. Expert consensus document: Cholangiocarcinoma: current knowledge and future perspectives consensus statement from the European Network for the Study of Cholangiocarcinoma (ENS-CCA). *Nat Rev Gastroenterol Hepatol* 2016; **13**: 261-280 [PMID: 27095655 DOI: 10.1038/nrgastro.2016.51]

16 **Rizvi S**, Khan SA, Hallemeier CL, Kelley RK, Gores GJ. Cholangiocarcinoma - evolving concepts and therapeutic strategies. *Nat Rev Clin Oncol* 2018; **15**: 95-111 [PMID: 28994423 DOI: 10.1038/nrclinonc.2017.157]

17 **Charalampakis N**, Papageorgiou G, Tsakatikas S, Fioretzaki R, Kole C, Kykalos S, Tolia M, Schizas D. Immunotherapy for cholangiocarcinoma: a 2021 update. *Immunotherapy* 2021; **13**: 1113-1134 [PMID: 34190581 DOI: 10.2217/imt-2021-0126]

18 **Zhang Y**, Xia R, Lv M, Li Z, Jin L, Chen X, Han Y, Shi C, Jiang Y, Jin S. Machine-Learning Algorithm-Based Prediction of Diagnostic Gene Biomarkers Related to Immune Infiltration in Patients With Chronic Obstructive Pulmonary Disease. *Front Immunol* 2022; **13**: 740513 [PMID: 35350787 DOI: 10.3389/fimmu.2022.740513]

19 **Zhang X**, Tian C, Cheng J, Mao W, Li M, Chen M. LTBP2 inhibits prostate cancer progression and metastasis *via* the PI3K/AKT signaling pathway. *Exp Ther Med* 2022; **24**: 563 [PMID: 36034756 DOI: 10.3892/etm.2022.11500]

20 **Raggi C**, Taddei ML, Rae C, Braconi C, Marra F. Metabolic reprogramming in cholangiocarcinoma. *J Hepatol* 2022; **77**: 849-864 [PMID: 35594992 DOI: 10.1016/j.jhep.2022.04.038]

21 **Li H**, Long J, Xie F, Kang K, Shi Y, Xu W, Wu X, Lin J, Xu H, Du S, Xu Y, Zhao H, Zheng Y, Gu J. Transcriptomic analysis and identification of prognostic biomarkers in cholangiocarcinoma. *Oncol Rep* 2019; **42**: 1833-1842 [PMID: 31545466 DOI: 10.3892/or.2019.7318]

22 **Fan S**, Ge Y, Liu J, Liu H, Yan R, Gao T, Fan X, Xiao Z, An G. Combination of anlotinib and gemcitabine promotes the G0/G1 cell cycle arrest and apoptosis of intrahepatic cholangiocarcinoma in vitro. *J Clin Lab Anal* 2021; **35**: e23986 [PMID: 34462984 DOI: 10.1002/jcla.23986]

23 **Lin Y**, Cai Q, Chen Y, Shi T, Liu W, Mao L, Deng B, Ying Z, Gao Y, Luo H, Yang X, Huang X, Shi Y, He R. CAFs shape myeloid-derived suppressor cells to promote stemness of intrahepatic cholangiocarcinoma through 5-lipoxygenase. *Hepatology* 2022; **75**: 28-42 [PMID: 34387870 DOI: 10.1002/hep.32099]

24 **Claesson-Welsh L**. How the matrix metalloproteinase MMP14 contributes to the progression of colorectal cancer. *J Clin Invest* 2020; **130**: 1093-1095 [PMID: 32015228 DOI: 10.1172/JCI135239]

25 **Määttä M**, Soini Y, Liakka A, Autio-Harmainen H. Differential expression of matrix metalloproteinase (MMP)-2, MMP-9, and membrane type 1-MMP in hepatocellular and pancreatic adenocarcinoma: implications for tumor progression and clinical prognosis. *Clin Cancer Res* 2000; **6**: 2726-2734 [PMID: 10914717]

26 **Qiang L**, Cao H, Chen J, Weller SG, Krueger EW, Zhang L, Razidlo GL, McNiven MA. Pancreatic tumor cell metastasis is restricted by MT1-MMP binding protein MTCBP-1. *J Cell Biol* 2019; **218**: 317-332 [PMID: 30487181 DOI: 10.1083/jcb.201802032]

27 **Yu J**, He Z, He X, Luo Z, Lian L, Wu B, Lan P, Chen H. Comprehensive Analysis of the Expression and Prognosis for MMPs in Human Colorectal Cancer. *Front Oncol* 2021; **11**: 771099 [PMID: 34804973 DOI: 10.3389/fonc.2021.771099]

28 **Decotret LR**, Wadsworth BJ, Li LV, Lim CJ, Bennewith KL, Pallen CJ. Receptor-type protein tyrosine phosphatase alpha (PTPα) mediates MMP14 Localization and facilitates triple-negative breast cancer cell invasion. *Mol Biol Cell* 2021; **32**: 567-578 [PMID: 33566639 DOI: 10.1091/mbc.E20-01-0060]

29 **Jin Y**, Liang ZY, Zhou WX, Zhou L. High MMP14 expression is predictive of poor prognosis in resectable hepatocellular carcinoma. *Pathology* 2020; **52**: 359-365 [PMID: 32122646 DOI: 10.1016/j.pathol.2020.01.436]

30 **Liu H**, Hu G, Wang Z, Liu Q, Zhang J, Chen Y, Huang Y, Xue W, Xu Y, Zhai W. circPTCH1 promotes invasion and metastasis in renal cell carcinoma *via* regulating miR-485-5p/MMP14 axis. *Theranostics* 2020; **10**: 10791-10807 [PMID: 32929380 DOI: 10.7150/thno.47239]

31 **Poincloux R**, Lizárraga F, Chavrier P. Matrix invasion by tumour cells: a focus on MT1-MMP trafficking to invadopodia. *J Cell Sci* 2009; **122**: 3015-3024 [PMID: 19692588 DOI: 10.1242/jcs.034561]

32 **Gonzalez-Molina J**, Gramolelli S, Liao Z, Carlson JW, Ojala PM, Lehti K. MMP14 in Sarcoma: A Regulator of Tumor Microenvironment Communication in Connective Tissues. *Cells* 2019; **8** [PMID: 31466240 DOI: 10.3390/cells8090991]

33 **DeBerardinis RJ**. Tumor Microenvironment, Metabolism, and Immunotherapy. *N Engl J Med* 2020; **382**: 869-871 [PMID: 32101671 DOI: 10.1056/NEJMcibr1914890]

34 **Vitale I**, Manic G, Coussens LM, Kroemer G, Galluzzi L. Macrophages and Metabolism in the Tumor Microenvironment. *Cell Metab* 2019; **30**: 36-50 [PMID: 31269428 DOI: 10.1016/j.cmet.2019.06.001]

35 **Bader JE**, Voss K, Rathmell JC. Targeting Metabolism to Improve the Tumor Microenvironment for Cancer Immunotherapy. *Mol Cell* 2020; **78**: 1019-1033 [PMID: 32559423 DOI: 10.1016/j.molcel.2020.05.034]

36 **Borst J**, Ahrends T, Bąbała N, Melief CJM, Kastenmüller W. CD4(+) T cell help in cancer immunology and immunotherapy. *Nat Rev Immunol* 2018; **18**: 635-647 [PMID: 30057419 DOI: 10.1038/s41577-018-0044-0]

37 **Olingy CE**, Dinh HQ, Hedrick CC. Monocyte heterogeneity and functions in cancer. *J Leukoc Biol* 2019; **106**: 309-322 [PMID: 30776148 DOI: 10.1002/JLB.4RI0818-311R]

38 **Gordon IO**, Freedman RS. Defective antitumor function of monocyte-derived macrophages from epithelial ovarian cancer patients. *Clin Cancer Res* 2006; **12**: 1515-1524 [PMID: 16533776 DOI: 10.1158/1078-0432.CCR-05-2254]

39 **Yeap WH**, Wong KL, Shimasaki N, Teo EC, Quek JK, Yong HX, Diong CP, Bertoletti A, Linn YC, Wong SC. CD16 is indispensable for antibody-dependent cellular cytotoxicity by human monocytes. *Sci Rep* 2016; **6**: 34310 [PMID: 27670158 DOI: 10.1038/srep34310]

World Journal of Gastroenterology

Submit a Manuscript: https://www.f6publishing.com

World J Gastroenterol 2023 May 21; 29(19): 2979-2991

DOI: 10.3748/wjg.v29.i19.2979

ISSN 1007-9327 (print) ISSN 2219-2840 (online)

ORIGINAL ARTICLE

Case Control Study

Machine learning model for prediction of low anterior resection syndrome following laparoscopic anterior resection of rectal cancer: A multicenter study

Zhang Wang, Sheng-Li Shao, Lu Liu, Qi-Yi Lu, Lei Mu, Ji-Chao Qin

Specialty type: Surgery

Provenance and peer review: Unsolicited article; Externally peer reviewed.

Peer-review model: Single blind

Peer-review report's scientific quality classification

Grade A (Excellent): 0
Grade B (Very good): 0
Grade C (Good): C, C
Grade D (Fair): 0
Grade E (Poor): 0

P-Reviewer: Calabro F, Italy; Muneer A, Malaysia

Received: February 23, 2023
Peer-review started: February 23, 2023
First decision: March 23, 2023
Revised: April 2, 2023
Accepted: April 25, 2023
Article in press: April 25, 2023
Published online: May 21, 2023

Zhang Wang, Sheng-Li Shao, Lu Liu, Qi-Yi Lu, Lei Mu, Ji-Chao Qin, Department of Surgery, Tongji Hospital, Tongji Medical College, Huazhong University of Science and Technology, Wuhan 430030, Hubei Province, China

Zhang Wang, Sheng-Li Shao, Lu Liu, Qi-Yi Lu, Lei Mu, Ji-Chao Qin, Molecular Medicine Center, Tongji Hospital, Tongji Medical College, Huazhong University of Science and Technology, Wuhan 430030, Hubei Province, China

Corresponding author: Ji-Chao Qin, MD, PhD, Professor, Researcher, Surgeon, Department of Surgery, Tongji Hospital, Tongji Medical College, Huazhong University of Science and Technology, No. 1095 Jiefang Avenue, Wuhan 430030, Hubei Province, China.
jcqin@tjh.tjmu.edu.cn

Abstract

BACKGROUND

Low anterior resection syndrome (LARS) severely impairs patient postoperative quality of life, especially major LARS. However, there are few tools that can accurately predict major LARS in clinical practice.

AIM

To develop a machine learning model using preoperative and intraoperative factors for predicting major LARS following laparoscopic surgery of rectal cancer in Chinese populations.

METHODS

Clinical data and follow-up information of patients who received laparoscopic anterior resection for rectal cancer from two medical centers (one discovery cohort and one external validation cohort) were included in this retrospective study. For the discovery cohort, the machine learning prediction algorithms were developed and internally validated. In the external validation cohort, we evaluated the trained model using various performance metrics. Further, the clinical utility of the model was tested by decision curve analysis.

RESULTS

Overall, 1651 patients were included in the present study. Anastomotic height, neoadjuvant therapy, diverting stoma, body mass index, clinical stage, specimen

length, tumor size, and age were the risk factors associated with major LARS. They were used to construct the machine learning model to predict major LARS. The trained random forest (RF) model performed with an area under the curve of 0.852 and a sensitivity of 0.795 (95%CI: 0.681-0.877), a specificity of 0.758 (95%CI: 0.671-0.828), and Brier score of 0.166 in the external validation set. Compared to the previous preoperative LARS score model, the current model exhibited superior predictive performance in predicting major LARS in our cohort (accuracy of 0.772 for the RF model *vs* 0.355 for the preoperative LARS score model).

CONCLUSION

We developed and validated a robust tool for predicting major LARS. This model could potentially be used in the clinic to identify patients with a high risk of developing major LARS and then improve the quality of life.

Key Words: Machine learning; Low anterior resection syndrome; Rectal cancer; Laparoscopy; Prediction

©The Author(s) 2023. Published by Baishideng Publishing Group Inc. All rights reserved.

Core Tip: We developed and externally validated a machine learning-based prediction model that integrated preoperative and intraoperative risk factors as input features and showed satisfactory predictive performance in Chinese patients. According to the decision curve analysis, patients with major low anterior resection syndrome (LARS) would have a net benefit superior to "treat all" or "treat none" with a range of threshold probabilities by using the model. This study provides a new tool for predicting major LARS, which can potentially be used for rectal cancer patients to acquire early postoperative consultation and strengthen self-management to improve their quality of life.

Citation: Wang Z, Shao SL, Liu L, Lu QY, Mu L, Qin JC. Machine learning model for prediction of low anterior resection syndrome following laparoscopic anterior resection of rectal cancer: A multicenter study. *World J Gastroenterol* 2023; 29(19): 2979-2991

URL: https://www.wjgnet.com/1007-9327/full/v29/i19/2979.htm

DOI: https://dx.doi.org/10.3748/wjg.v29.i19.2979

INTRODUCTION

With advances in surgical techniques and the introduction of a multidisciplinary approach, the sphincter-saving procedure for rectal cancer has increased[1], with up to 50%-80% of rectal cancer patients undergoing this procedure[2] compared with only 25% before the circular stapling device was widely used[3]. However, low anterior resection syndrome (LARS), a postoperative complication that seriously impairs patient quality of life, has also increased[4,5], and 70%-90% of these patients undergoing sphincter-saving procedures have developed LARS[2]. The majority of LARS may go into remission within a variable interval of 6-18 mo following surgery[6,7]. However, beyond this point further improvements may be impossible, and the complication may become irreversible. It is reported that approximately 40% of patients with major LARS remain 'toilet dependent,' which results in a low quality of life[8,9].

Early management of major LARS, such as conservative drugs, transanal or transtomal irrigation, pelvic floor rehabilitation, biofeedback, and sacral nerve stimulation, can improve LARS symptoms[10-14]. Therefore, it is important to identify the patients who are at a high risk of developing major LARS after surgery. A recent study established a model based on preoperative risk factors to predict a LARS score for improving patient preoperative education and counseling[15]. However, it failed to achieve an accurate prediction when it was applied to other populations[16]. Furthermore, certain intraoperative factors that were previously reported as important contributors to LARS were not included in this aforementioned model[17,18].

Due to better vision and less surgical trauma[19], laparoscopic surgery has improved the post-operative course in the treatment of rectal cancer and was widely applied in China. In theory, laparoscopic surgery ensures minimal surgical trauma and improves postoperative patient recovery as well as functional bowel outcome. However, there is still no tool to predict LARS in Asian patients who receive laparoscopic surgery.

Artificial intelligence (AI) is an innovative modeling technology and has produced promising results; our previous studies have shown that AI algorithms allow for good discrimination of anastomotic leakage and would be helpful in assisting surgeons' decision-making[20,21]. Therefore, the present study aimed to develop a machine learning model based on AI technology using preoperative and

intraoperative factors for predicting major LARS following laparoscopic surgery of rectal cancer in Chinese populations. This model was created to guide early postoperative management of medical intervention and improve patient postoperative consultation and quality of life.

MATERIALS AND METHODS

Data and participants

The present study included a discovery cohort and an external validation cohort. To develop the machine learning model, clinical data of 2120 patients with rectal cancer who received laparoscopic anterior resection in the Department of Gastrointestinal Surgery, Tongji Hospital, Huazhong University of Science and Technology from January 1, 2012 to December 31, 2020 were reviewed and collected. For external validation, data from 289 patients from the Central Hospital of Enshi Tujia and Miao Autonomous Prefecture affiliated to Wuhan University between January 1, 2012 and December 31, 2020 were collected with the same criteria. The present study was performed according to the guidelines of the Declaration of Helsinki and approved by the ethics committees of Tongji Hospital, Huazhong University of Science and Technology and The Central Hospital of Enshi Tujia and Miao Autonomous Prefecture. The requirement for informed consent was waived due to the retrospective nature of the study.

Inclusion and exclusion criteria

The inclusion criteria were as follows: (1) Age ≥ 18; (2) Primary rectal adenocarcinoma located 0-15 cm from the anal verge; and (3) Patients without communication difficulties. The exclusion criteria were as follows: (1) Patients who had their diverting stoma open; (2) Less than 1 year after laparoscopic anterior resection or after stoma reversal; (3) Patients with a history of abnormal bowel function, including drug-induced diarrhea, a chronic history of constipation, irritable bowel syndrome, and a history of pelvic injury; (4) Patients with local recurrence within 1 year after surgery; and (5) Missing data, death, or lost to follow-up.

Candidate variables

In order to develop the early postoperative major LARS prediction model, only the clinical preoperative and intraoperative variables of each patient were included. The variables were as following: age at surgery; sex; body mass index (BMI); hypertension; diabetes; previous abdominal surgery; neoadjuvant therapy; American Society of Anesthesiologists (ASA) classification; tumor size (cm); clinical stages; anastomotic height (cm); diverting stoma; and specimen length (cm). Two authors independently completed the collection and collation of clinical data, and conflicting data were documented and confirmed by a final discussion. Anastomotic height was defined as the distance between anastomosis and anal verge measured using digital rectal examination, computed tomography, or magnetic resonance imaging. Specimen length was defined as the length of the bowel removed during surgery.

Outcome

The Chinese version of the LARS score system was used to evaluate postoperative intestinal function [22], which is described by five questions concerning intestinal function. Each response was weighted and given a score according to the severity of the patient's symptoms. Scores of 0-20 indicated no LARS, 21-29 indicated minor LARS, and 30-42 indicated major LARS. All the participants were followed up by telephone, short message service, and outpatient or inpatient visits using a LARS score questionnaire from November 1, 2021 to May 1, 2022. LARS scores of each participant at 1 year after anterior resection or after stoma reversal were obtained. To highlight major LARS, patients were classified into two groups according to LARS score, one with major LARS and another with no or minor LARS.

Feature selection

Excessive variables could lead to adverse predictions and be inconvenient in an application. The Boruta algorithm can address the minimal optimization problem of multidimensional clinical features in feature selection[23]. Thus, feature selection was conducted using the Boruta algorithm. The algorithm can screen out all the variables associated with the ground truth. The importance of the features was quantified by repeated iterations based on shadow feature creation, and some weakly correlated features were removed. Finally, the selected features, combined with clinical experience, were used as predictors. R software and Boruta packages (7.0.0) were used for feature selection (R version 4.1.2[2021-11-01]).

Sample size

The one-in-ten rule is a generally accepted rule for estimating the minimum sample size[24]. According to at least ten events per variable, at least 325 to 667 patients were required in the discovery cohort for the 13 predictor variables, with an estimated event (major LARS) rate of 30%-50% and a lost follow-up

rate of 20%-35%.

Machine learning algorithms

In the present study, four prevailing machine learning algorithms, including logistic regression (LR), random forest (RF), support vector machine (SVM), and extreme gradient boosting (XGBoost), were employed to develop the predictive models. Machine learning algorithms based on AI can overcome the limitations of traditional linear models by combining clinical nonlinear features. The participants from Tongji Hospital were randomly divided into a training set and a testing set at a ratio of 8:2. To gain high-performance models, hyperparameter adjustment was adopted using a grid search approach. To balance sensitivity and specificity, the optimal Youden index (cutoff value) was calculated *via* maximizing the value of sensitivity + specificity - 1[25]. The area under the curve (AUC) and Brier scores, which represent the discrimination and calibration power of the prediction model, were calculated. The Brier score measures the difference between the predicted probability and the ground truth[26], and a value of the Brier Score closer to 0 indicates a better calibration. In addition, to assess the clinical utility of the prediction model, decision curve analysis was used, which can determine whether patients benefit from using predictive models in clinical practice[27]. All machine learning algorithms were implemented using Python (version 3.9.7) with the scikit-learn (version 0.24.2) package.

Statistical analyses

The continuous variables were presented as mean ± SD and categorical variables as the count (%). A one-way analysis of variance with post hoc contrasts by the student-Newman-Keuls test was used to compare the differences between the continuous variables. For categorical variables, as appropriate, χ^2 or Fisher's exact test was used. All P values were reported as two-tailed, and $P < 0.05$ was considered as statistical significance. 95%CI for the AUC, sensitivity, specificity, positive predictive value (PPV), negative predictive value (NPV), and accuracy of the four models were calculated using IBM SPSS Statistics 20.0 (IBM Corp, Armonk, NY, United States) or Vassar Stats (online tool, http://vassarstats.net/index.html).

RESULTS

Summary of demographic and clinical characteristics for training, testing, and external validation sets

Figure 1 presents the patient flow chart. A total of 1651 eligible cases were included, with 1163 subjects included in the training set, 291 subjects included in the testing set, and another 197 subjects in the external validation set. Comparisons between the training, testing, and external validation sets are presented in Table 1. The mean age of the 1163 patients in the training set was 57.6 years, and 59.7% were males. For the testing and the external validation sets, the mean age was 57.6 and 59.7 years, and 56.0% and 53.8% were males, respectively. Major LARS was observed in 37.2% of patients in the training set, 35.1% in the testing set, and 37.1% in the external validation set.

Risk factors associated with major LARS

The importance of all the included variables calculated by the Boruta algorithm was shown in Figure 2A. Boruta calculates variables that are both strongly and weakly relevant to provide the best prediction accuracy. The blue boxes were shadow features automatically generated by the algorithm and were not included in the analysis. As the data indicated that anastomotic height, neoadjuvant therapy, diverting stoma, BMI, clinical stage, specimen length, tumor size, and age were selected as significantly relevant to major LARS.

Model development in the training set

The LR, RF, SVM and XGBoost algorithms were trained using the eight strongly related variables, and the AUCs, sensitivities, specificities, PPVs, NPVs, and accuracies were calculated (Figure 2B and C). The RF model exhibited optimal diagnostic performance (AUC = 0.869), and the optimal cutoff was 0.406. Therefore, the RF model was used for subsequent analysis. The details of the predictions generated by the RF model using the optimal threshold were shown in Figure 2D. Additionally, the predicted probabilities for major LARS were significantly relevant to the ground truth in the training set ($P < 0.001$) (Figure 2E).

Performance of the RF model in the testing set

We tested the performance of the RF model in the testing set. The results demonstrated that the RF model performed with a favorable discrimination ability (AUC = 0.870, 95%CI: 0.833-0.901) (Figure 3A). The details of the predicted outcomes were presented in Figure 3B. Subsequently, the comparison of the predicted probabilities between the major LARS and no/minor LARS groups was conducted, and significant differences were observed (Figure 3C). Furthermore, a decision curve was plotted to evaluate

Table 1 Baseline characteristics of the training, testing, and external validation sets, *n* (%)

Variables	Training cohort, *n* = 1163	Testing cohort, *n* = 291	Validation cohort, *n* = 197	*P* value
Age, yr	57.60 ± 10.83	57.56 ± 11.23	59.72 ± 9.58	0.034
Male	694 (59.67)	163 (56.01)	106 (53.81)	0.206
BMI, kg/m^2	22.79 ± 2.92	22.89 ± 2.75	22.61 ± 4.02	0.382
Neoadjuvant	67 (5.76)	19 (6.53)	9 (4.57)	0.659
Hypertension	254 (21.84)	66 (22.68)	43 (21.83)	0.952
Diabetes	83 (7.14)	26 (8.93)	9 (4.57)	0.185
Previous abdominal surgery	141 (12.12)	45 (15.46)	22 (11.17)	0.250
ASA				< 0.001
1	178 (15.31)	42 (14.43)	55 (27.92)	
2	893 (76.78)	218 (74.91)	89 (45.12)	
3	90 (7.74)	30 (10.31)	50 (25.38)	
4	2 (0.17)	1 (0.34)	3 (1.52)	
Anastomotic height, cm	4.82 ± 2.37	4.57 ± 2.14	4.77 ± 2.56	0.298
Specimen length, cm	10.99 ± 3.01	10.88 ± 3.11	15.21 ± 4.49	< 0.001
Diverting ileostomy	315 (27.09)	81 (27.84)	35 (17.77)	0.017
Tumor size, cm	3.60 ± 1.29	3.53 ± 1.25	3.89 ± 1.35	0.546
Stage				< 0.001
1	354 (30.44)	91 (31.27)	31 (15.74)	
2	405 (34.82)	94 (32.30)	108 (54.82)	
3	404 (34.74)	106 (36.43)	58 (29.44)	
LARS				0.800
Minor/no	731 (62.85)	189 (64.95)	124 (62.94)	
Major	432 (37.15)	102 (35.05)	73 (37.06)	

ASA: American Society of Anesthesiologists classification; BMI: Body mass index; LARS: Low anterior resection syndrome.

whether using the RF model in the clinic would do better than harm[28]. According to the decision curve analysis, patients with major LARS would have a net benefit superior to "treat all" or "treat none" with a range of threshold probability in approximately 20%-75% (Figure 3D).

External validation of the RF model

To assess the generalization capability of the RF model, an external validation based on 197 patients from another independent center was performed. The RF model identified patients with major LARS with an AUC of 0.852 (95%CI: 0.820-0.890) (Figure 4A). The confusion matrix presented the classification results generated by the RF model for identifying major LARS in the external validation set (Figure 4B). Figure 4C showed that the probabilities generated by the RF model for major LARS were significantly higher than those of no/minor LARS, suggesting that the predicted probabilities were significantly associated with the ground truth in the external validation set. Decision curve analysis also showed that patients would derive clinical benefits in a range of threshold probabilities (Figure 4D).

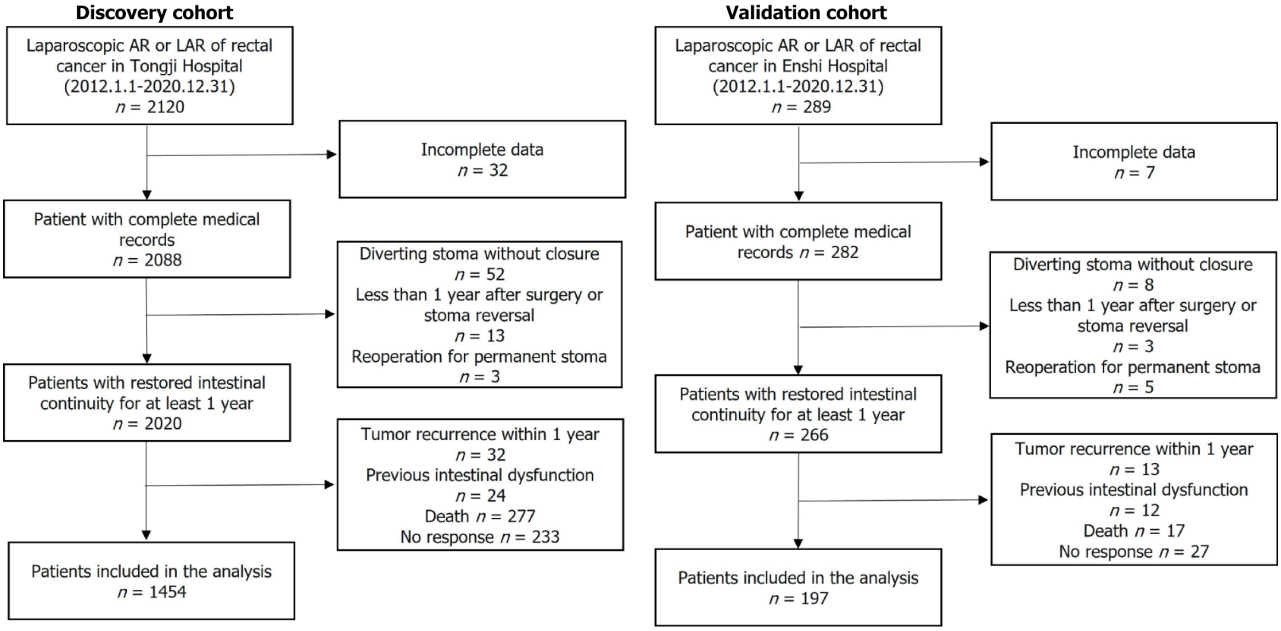
Evaluation of the prediction model

To assess the performance and calibration degree of the RF model in both the testing set and the external validation set, six performance metrics such as sensitivity, specificity, PPV, NPV, accuracy, and Brier score were applied. Their results calculated based on the optimal Youden index (cutoff) were summarized in Table 2. These results suggested that the RF model was determined to be capable and reliable in predicting major LARS, with satisfactory Brier score of 0.152 and 0.166 and accuracy of 0.787 and 0.772, in both the testing set and the external validation set, respectively. In addition, to highlight the advantages of the RF model, the sensitivity, specificity, PPV, NPV, and accuracy of the preoperative LARS score (POLARS) model were calculated in both our testing set and external validation set. Taken

Table 2 Performance of the random forest model in the testing and external validation sets

Indicator (95%CI)	RF	
	Testing set, *n* = 291	Validation set, *n* = 197
Sensitivity	0.843 (0.755-0.905)	0.795 (0.681-0.877)
Specificity	0.757 (0.688-0.815)	0.758 (0.671-0.828)
PPV	0.652 (0.563-0.731)	0.659 (0.549-0.755)
NPV	0.899 (0.839-0.940)	0.862 (0.780-0.918)
Accuracy	0.787 (0.736-0.830)	0.772 (0.708-0.825)
Brier score	0.152	0.166

CI: Confidence interval; NPV: Negative predictive value; PPV: Positive predictive value; RF: Random forest.



DOI: 10.3748/wjg.v29.i19.2979 **Copyright** ©The Author(s) 2023.

Figure 1 Flow chart of the patients from two independent medical centers who were enrolled in the present study. AR: Anterior resection; LAR: Low anterior resection.

together, these values demonstrated that the performance of the RF model surpassed that of the POLARS score model, as shown in Table 3.

DISCUSSION

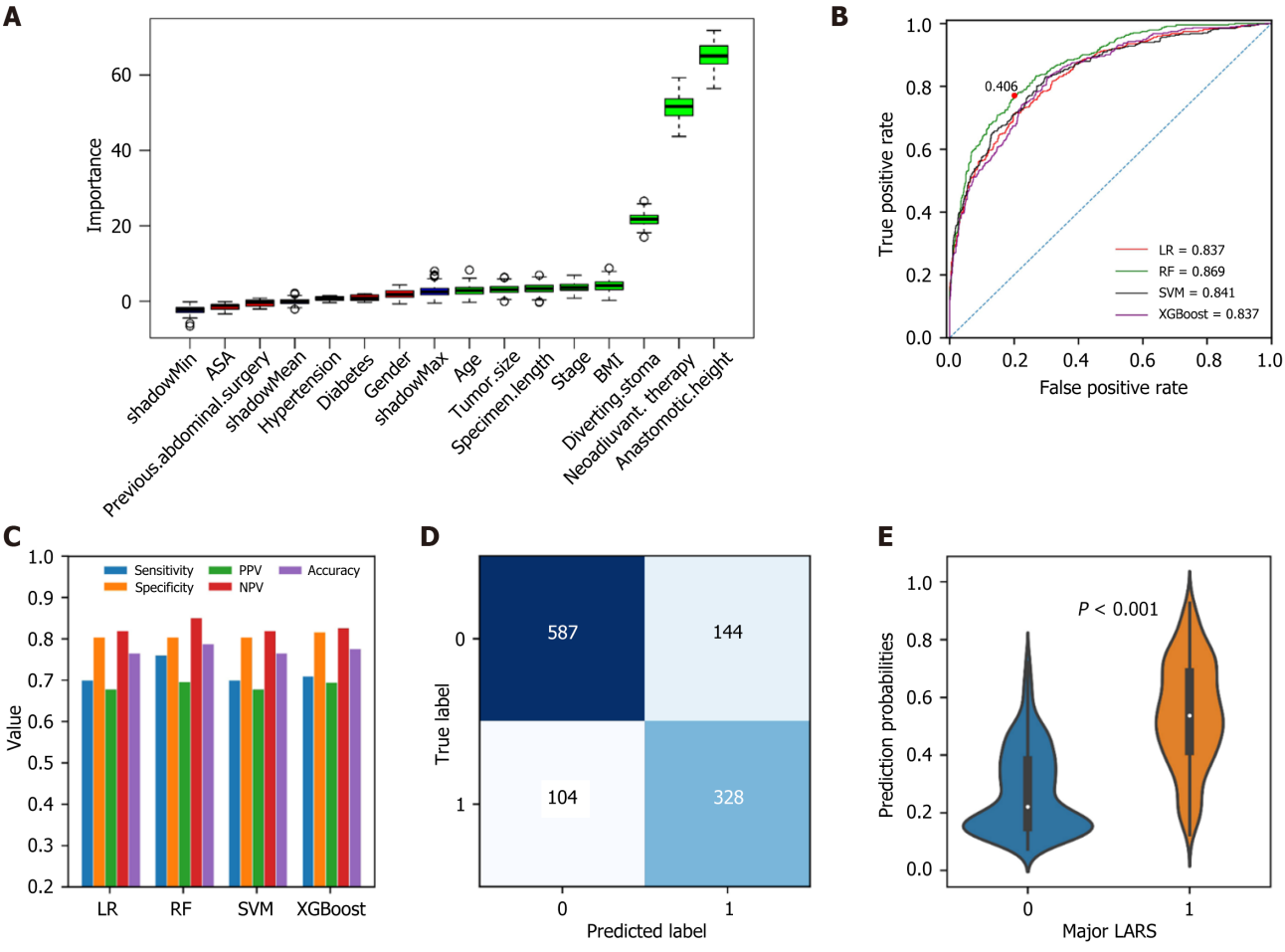
LARS is the most common complication following rectal cancer surgery. It is a severe complication and seriously impairs patient quality of life[1]. A meta-analysis based on 11 studies indicated that the morbidity of major LARS was as high as 41% (95%CI: 34-48)[5]. Fortunately, surgeons are now paying more and more attention to the functional consequences of cancer treatment and the quality of life[1,4]. LARS is a time-dependent syndrome, and the symptoms of some patients with LARS are relieved partly or completely 1 year or more after surgery. However, the symptoms in approximately 40% of patients remain stable and cannot be further improved[6,9,29].

Due to the variable symptom spectrum of LARS, ranging from incontinence for gas and liquid fecal matter to evacuation dysfunctions, the complex etiology, and unknown pathophysiology, there is no standard treatment available at present[30]. However, if patients with a high-risk major LARS can be treated with a conservative method (*e.g.*, pelvic floor rehabilitation, transanal irrigation), minimally invasive therapies (*e.g.*, biofeedback therapy, sacral nerve stimulation), or multimodal treatments during the period of the first year after surgery, their intestinal dysfunction may be significantly improved[9].

Table 3 Performance of the preoperative low anterior resection syndrome score model in the testing and external validation sets

Indicators (95%CI)	Testing set, *n* = 291	*P* value	Validation set, *n* = 197	*P* value
Sensitivity	0.931 (0.859-0.970)	0.046	0.836 (0.727-0.909)	0.522
Specificity	0.079 (0.047-0.130)	< 0.001	0.073 (0.036-0.137)	< 0.001
PPV	0.353 (0.297-0.414)	< 0.001	0.347 (0.278-0.422)	< 0.001
NPV	0.682 (0.451-0.853)	0.004	0.429 (0.226-0.656)	< 0.001
Accuracy	0.378 (0.323-0.437)	< 0.001	0.355 (0.289-0.427)	< 0.001

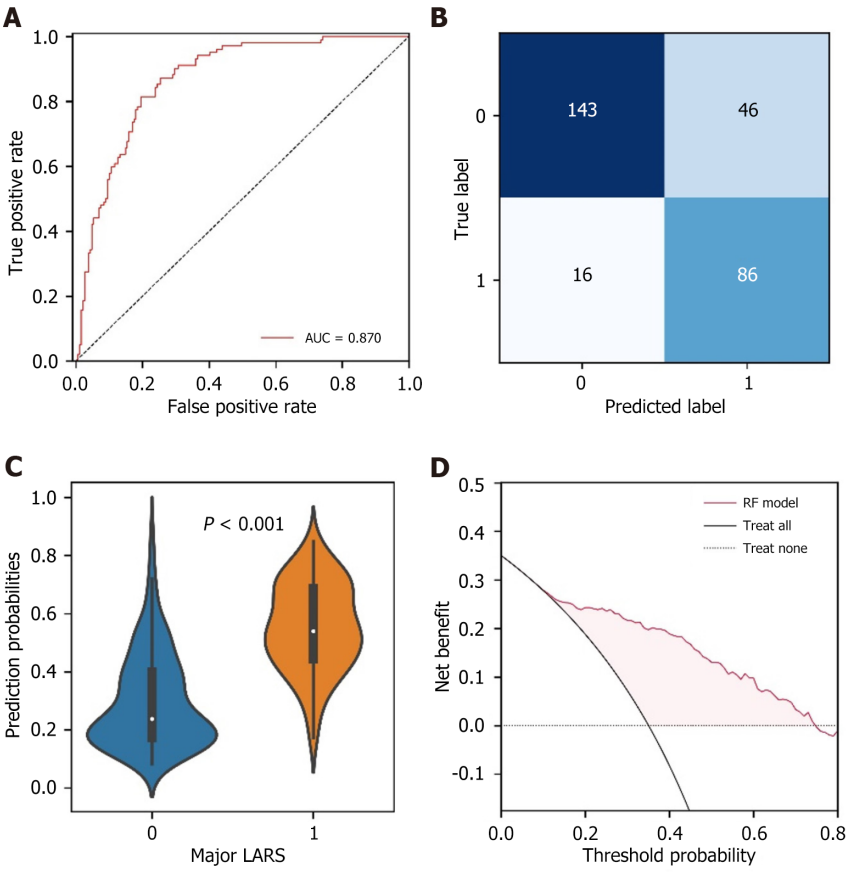
PPV: Positive predictive value; NPV: Negative predictive value.



DOI: 10.3748/wjg.v29.i19.2979 **Copyright** ©The Author(s) 2023.

Figure 2 Variable selection using the Boruta algorithm and overview of development of the models in the training set. A: The importance of all variables. The red boxes indicated the variables weakly relevant to major low anterior resection syndrome (LARS). The blue boxes were random variables automatically generated by the algorithm and were not included in the analysis. The green boxes indicated the variables strongly relevant to major LARS; B: Receiver operating characteristic curves of the four machine learning models in the training set. The red dot denotes the optimal Youden index for the random forest (RF) model; C: Performance measurements of the four machine learning models illustrated by sensitivity, specificity, positive predictive value, negative predictive value and accuracy; D: Confusion matrix of the optimization RF model; E: Comparison of predicted probabilities calculated by the RF model in patients with and without major LARS in the training set. ASA: American Society of Anesthesiologists classification; BMI: Body mass index; LR: Logistic regression; LARS: Low anterior resection syndrome; RF: Random forest; SVM: Support vector machine; XGBoost: Extreme gradient boosting; PPV: Positive predictive value; NPV: Negative predictive value.

Consequently, the negative impact of LARS on their quality of life could be minimized. In addition, since major LARS may counteract the relative benefits of anal sphincter-preserving surgery, the accurate prediction of major LARS may be helpful for patients and surgeons when deciding on temporary ileostomy, permanent colostomy, or sphincter-preserving surgery for low rectal cancer[31-33]. Therefore, it is crucial to perform risk stratification of rectal surgery cases to identify patients with a high risk of major LARS and to highlight patients who may require additional postoperative support.



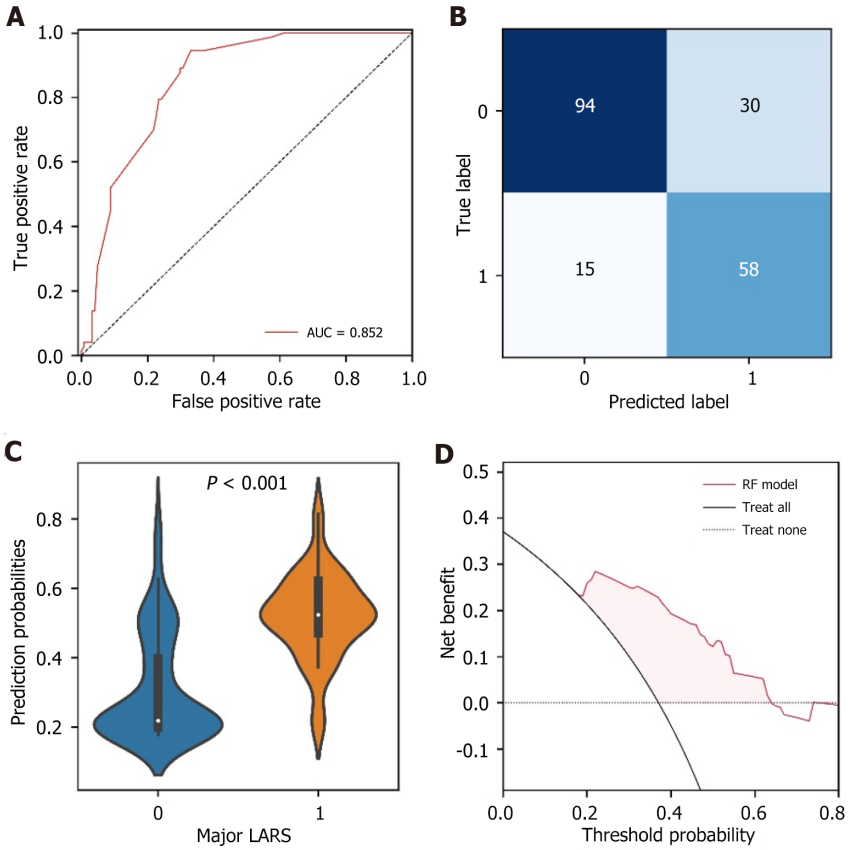
DOI: 10.3748/wjg.v29.i19.2979 **Copyright** ©The Author(s) 2023.

Figure 3 Performance of the random forest model in the testing set. A: Receiver operating characteristic curve of the random forest (RF) model in the testing set; B: Confusion matrices showed the predicted outcomes generated by the RF model in the testing set; C: Comparison of predicted probabilities between patients with and without major low anterior resection syndrome in the testing set; D: Decision curve analysis for the RF model in the testing set. AUC: Area under the curve; LARS: Low anterior resection syndrome; RF: Random forest; ROC: Receiver operating characteristic.

Battersby *et al*[15] developed and validated the POLARS score for restorative sphincter-sparing surgery for rectal cancer to predict intestinal dysfunction. The POLARS score includes six risk factors, such as age at surgery, sex, tumor height, preoperative radiotherapy, total/partial mesorectal excision, and the presence of stoma, as predictors. The model performs with moderate discriminative accuracy with Harrell's C statistic of 0.615 and 0.625 in their two datasets. Essangri *et al*[16] reported that the POLARS score was questionable, and it failed to successfully validate the model in another population. This previous study implied that the model predictions may be dependent on patient background, including treatment strategies and physical, lifestyle, and dietary habit differences. In the present study, all participants were Chinese and underwent laparoscopic sphincter-sparing surgery for rectal cancer without splenic flexure mobilization. Several previous studies have pointed out that routine splenic flexure mobilization is not necessary for anterior resection of rectal cancer[34-36]. Instead, no splenic flexure mobilization would result in a shorter operation time and lower morbidity of postoperative complications associated with intestinal function, such as anastomotic leakage[37]. Moreover, to date, there is no machine learning model for predicting major LARS in Asian patients undergoing laparoscopic anterior resection based on a multicenter study.

In the present study, four machine learning algorithms were used to develop the machine learning model for major LARS prediction. These data suggested that the RF model performed with an optimal AUC in the training set. As expected, the RF model also achieved favorable predictions when it was tested in the testing and external validation sets. To the best of our knowledge, this is the first multicentric study to develop a machine-learning model for predicting major LARS in Asian patients undergoing laparoscopic anterior resection of rectal cancer. More importantly, the model performed with a satisfactory prediction in an independent medical center (AUC = 0.852; 95%CI: 0.820-0.890). Moreover, compared with the POLARS score, the RF model achieved superior performance in predicting major LARS in our cohort (accuracy of 0.772 for the RF model *vs* 0.355 for the POLARS score). In addition, the decision curve analysis demonstrated the net benefit (benefit minus risk) by using the model for patients diagnosed with major LARS within a range of threshold probabilities.

Although the explicit pathophysiological mechanism of LARS is still unclear, numerous studies[38-40] agree that intestinal dysfunction in patients with rectal cancer who received restorative sphincter-



DOI: 10.3748/wjg.v29.i19.2979 **Copyright** ©The Author(s) 2023.

Figure 4 Performance of the random forest model in the external validation set. A: Receiver operating characteristic curve of the random forest (RF) model in the external validation set; B: Confusion matrices showed the predicted outcomes generated by the RF model in the external validation set; C: Comparison of predicted probabilities between patients with and without major low anterior resection syndrome in the external validation set; D: Decision curve analysis for the RF model in the external validation set. AUC: Area under the curve; LARS: Low anterior resection syndrome; RF: Random forest.

sparing surgery is the result of a combination of multiple pathophysiological mechanisms. These include loss of rectal storage function, autonomic denervation, enhanced colonic movement, rectal-anus sensitivity reduction, anal resting pressure reduction, and diverting colitis[38]. Certain factors directly or indirectly related to these pathophysiological changes have been reported as important variables associated with LARS, such as low anastomosis, neoadjuvant therapy, postoperative chemoradiotherapy, anastomotic leakage, diverting stoma, and the time interval from the creation of diverting stoma to closure[5,18,41,42]. In order to identify major LARS in the early postoperative period, some postoperative factors were not included, such as chemoradiotherapy and the time interval from creating diverting stoma to its closure. Among the included factors, low anastomosis and neoadjuvant therapy have been unanimously considered as important predictors for major LARS[5,43]. For example, Filips *et al*[44] reported that LARS was negatively correlated with the distance from anastomosis to the anal verge (OR: -1.145, 95%CI: -2.149 to -1.141, P = 0.026). In the present study, our data also indicated that the anastomotic height was the most important factor in the development of major LARS. In addition, the specimen length was selected as a predictor for major LARS in the present study, and it may be caused by greater surgical trauma.

As with any retrospective observational study, the present study had some uncontrollable limitations. First, the model is based on the Chinese population and does not necessarily reflect the worldwide target population. Its generalizability needs to be further tested. Second, the influence of a patient's socioeconomic and cultural background, self-management ability, and social support are difficult to control. Third, the data reflecting anal sphincter injury and its severity during surgery cannot be evaluated. Finally, the LARS score may be affected by a variety of biases, such as patient selective memory, exaggeration, or understatement. To overcome these limitations, a prospective study is proposed to assess the predictive ability of the model.

CONCLUSION

In the present study, a machine learning model based on preoperative and intraoperative risk factors for

predicting LARS was developed. The model may be helpful for clinical medical staff to identify patients at an early stage with a high risk of developing major LARS within 1 year following laparoscopic surgery for rectal cancer. Moreover, it can potentially be used for patients to acquire early postoperative consultation and strengthen self-management to improve patient quality of life.

ARTICLE HIGHLIGHTS

Research background

Low anterior resection syndrome (LARS) severely impairs patient postoperative quality of life, especially major LARS. However, there are few tools that can accurately predict major LARS in clinical practice.

Research motivation

To stratify patients with LARS and predict patients at high risk of developing major LARS, improve patient counseling, and highlight patients who may need additional support after surgery.

Research objectives

The study aimed to identify the risk factors associated with major LARS and develop a prediction model that helps improve patient counseling and highlight patients who may need additional support after surgery.

Research methods

Clinical data and follow-up information of patients from two medical centers (one discovery cohort and one external validation cohort) were analyzed to identify independent factors associated with major LARS. For the discovery cohort, the machine learning prediction algorithms were developed and internally validated. In the external validation cohort, we evaluated the trained model using various performance metrics. Further, the clinical utility of the model was tested by decision curve analysis.

Research results

Eight factors, such as anastomotic height, neoadjuvant therapy, diverting stoma, body mass index, clinical stage, specimen length, tumor size, and age, were selected as significantly relevant to major LARS. A machine learning-based prediction model that integrated eight risk factors as input features was developed, externally validated, and demonstrated an acceptable predictive performance.

Research conclusions

We have developed and validated a robust tool for predicting major LARS. This model could potentially be used in the clinic to identify patients with a high risk of developing major LARS and then improve their quality of life.

Research perspectives

A prospective study including more medical centers is proposed to assess the model's predictive ability.

ACKNOWLEDGEMENTS

I would like to thank all the medical staff of the Department of Gastrointestinal Surgery in Tongji Hospital and Enshi Central Hospital for providing convenient conditions for implementing this study.

FOOTNOTES

Author contributions: Wang Z and Shao SL contributed equally to this work; Wang Z contributed to methodology, formal analysis, data extraction, follow-up, writing, reviewing, and editing; Shao SL contributed to data extraction, data curation, follow-up, formal analysis, writing, reviewing, and editing; Liu L was involved in supervision and software; Lu QY contributed to follow-up and data curation; Mu L performed data curation; Qin JC contributed to conceptualization, funding acquisition, methodology, writing, reviewing, and editing; All authors contributed to the interpretation of the study and approved the final version to be published.

Supported by the National Natural Science Foundation of China, No. 82173368 and 81903047.

Institutional review board statement: This study was supported by the Ethics Committee of Tongji Hospital, Tongji Medical College, Huazhong University of Science and Technology, and the Central Hospital of Enshi Tujia and Miao

Autonomous Prefecture.

Informed consent statement: The requirement for informed consent was waived due to the retrospective nature of the study.

Conflict-of-interest statement: All the authors report having no relevant conflicts of interest for this article.

Data sharing statement: The dataset used during the current study is available from the corresponding author on reasonable request. E-mail: jcqin@tjh.tjmu.edu.cn.

STROBE statement: The authors have read the STROBE statement-checklist of items, and the manuscript was prepared and revised according to the STROBE statement-checklist of items.

Open-Access: This article is an open-access article that was selected by an in-house editor and fully peer-reviewed by external reviewers. It is distributed in accordance with the Creative Commons Attribution NonCommercial (CC BY-NC 4.0) license, which permits others to distribute, remix, adapt, build upon this work non-commercially, and license their derivative works on different terms, provided the original work is properly cited and the use is non-commercial. See: https://creativecommons.org/Licenses/by-nc/4.0/

Country/Territory of origin: China

ORCID number: Sheng-Li Shao 0000-0001-8786-0051; Ji-Chao Qin 0000-0002-2961-7624.

S-Editor: Zhang H
L-Editor: Filipodia
P-Editor: Chen YX

REFERENCES

1 **Pieniowski EHA**, Palmer GJ, Juul T, Lagergren P, Johar A, Emmertsen KJ, Nordenvall C, Abraham-Nordling M. Low Anterior Resection Syndrome and Quality of Life After Sphincter-Sparing Rectal Cancer Surgery: A Long-term Longitudinal Follow-up. *Dis Colon Rectum* 2019; **62**: 14-20 [PMID: 30394987 DOI: 10.1097/DCR.0000000000001228]
2 **Bryant CL**, Lunniss PJ, Knowles CH, Thaha MA, Chan CL. Anterior resection syndrome. *Lancet Oncol* 2012; **13**: e403-e408 [PMID: 22935240 DOI: 10.1016/S1470-2045(12)70236-X]
3 **Ståhle E**, Påhlman L, Enblad P. Double stapling technique in the management of rectal tumours. *Acta Chir Scand* 1986; **152**: 743-747 [PMID: 3591203]
4 **Pieniowski EHA**, Nordenvall C, Palmer G, Johar A, Tumlin Ekelund S, Lagergren P, Abraham-Nordling M. Prevalence of low anterior resection syndrome and impact on quality of life after rectal cancer surgery: population-based study. *BJS Open* 2020; **4**: 935-942 [PMID: 32530135 DOI: 10.1002/bjs5.50312]
5 **Croese AD**, Lonie JM, Trollope AF, Vangaveti VN, Ho YH. A meta-analysis of the prevalence of Low Anterior Resection Syndrome and systematic review of risk factors. *Int J Surg* 2018; **56**: 234-241 [PMID: 29936195 DOI: 10.1016/j.ijsu.2018.06.031]
6 **Nicotera A**, Falletto E, Arezzo A, Mistrangelo M, Passera R, Morino M. Risk factors for Low Anterior Resection Syndrome (LARS) in patients undergoing laparoscopic surgery for rectal cancer. *Surg Endosc* 2022; **36**: 6059-6066 [PMID: 35137257 DOI: 10.1007/s00464-021-09002-y]
7 **Varghese C**, Wells CI, O'Grady G, Christensen P, Bissett IP, Keane C; on behalf of the Longitudinal LARS Group. The Longitudinal Course of Low-anterior Resection Syndrome: An individual Patient Meta-analysis. *Ann Surg* 2022; **276**: 46-54 [PMID: 35185131 DOI: 10.1097/SLA.0000000000005423]
8 **Juul T**, Ahlberg M, Biondo S, Espin E, Jimenez LM, Matzel KE, Palmer GJ, Sauermann A, Trenti L, Zhang W, Laurberg S, Christensen P. Low anterior resection syndrome and quality of life: an international multicenter study. *Dis Colon Rectum* 2014; **57**: 585-591 [PMID: 24819098 DOI: 10.1097/DCR.0000000000000116]
9 **Sturiale A**, Martellucci J, Zurli L, Vaccaro C, Brusciano L, Limongelli P, Docimo L, Valeri A. Long-term functional follow-up after anterior rectal resection for cancer. *Int J Colorectal Dis* 2017; **32**: 83-88 [PMID: 27695976 DOI: 10.1007/s00384-016-2659-6]
10 **van der Heijden JAG**, Kalkdijk-Dijkstra AJ, Pierie JPEN, van Westreenen HL, Broens PMA, Klarenbeek BR; FORCE trial group. Pelvic Floor Rehabilitation After Rectal Cancer Surgery: A Multicenter Randomized Clinical Trial (FORCE Trial). *Ann Surg* 2022; **276**: 38-45 [PMID: 34966064 DOI: 10.1097/SLA.0000000000005353]
11 **Li H**, Guo C, Gao J, Yao H. Effectiveness of Biofeedback Therapy in Patients with Bowel Dysfunction Following Rectal Cancer Surgery: A Systemic Review with Meta-Analysis. *Ther Clin Risk Manag* 2022; **18**: 71-93 [PMID: 35140468 DOI: 10.2147/TCRM.S344375]
12 **Embleton R**, Henderson M. Using transanal irrigation in the management of low anterior resection syndrome: a service audit. *Br J Nurs* 2021; **30**: 1226-1230 [PMID: 34839681 DOI: 10.12968/bjon.2021.30.21.1226]
13 **Itagaki R**, Koda K, Yamazaki M, Shuto K, Kosugi C, Hirano A, Arimitsu H, Shiragami R, Yoshimura Y, Suzuki M. Serotonin (5-HT3) receptor antagonists for the reduction of symptoms of low anterior resection syndrome. *Clin Exp Gastroenterol* 2014; **7**: 47-52 [PMID: 24648748 DOI: 10.2147/CEG.S55410]

14 **De Meyere C**, Nuytens F, Parmentier I, D'Hondt M. Five-year single center experience of sacral neuromodulation for isolated fecal incontinence or fecal incontinence combined with low anterior resection syndrome. *Tech Coloproctol* 2020; **24**: 947-958 [PMID: 32556866 DOI: 10.1007/s10151-020-02245-2]

15 **Battersby NJ**, Bouliotis G, Emmertsen KJ, Juul T, Glynne-Jones R, Branagan G, Christensen P, Laurberg S, Moran BJ; UK and Danish LARS Study Groups. Development and external validation of a nomogram and online tool to predict bowel dysfunction following restorative rectal cancer resection: the POLARS score. *Gut* 2018; **67**: 688-696 [PMID: 28115491 DOI: 10.1136/gutjnl-2016-312695]

16 **Essangri H**, Majbar MA, Benkabbou A, Belkhadir Z, Amrani L, Mohsine R, Souadka A. Do we have enough Foreknowledge to predict the low anterior resection syndrome (LARS) score preoperatively? *Colorectal Dis* 2020; **22**: 1445 [PMID: 32270539 DOI: 10.1111/codi.15062]

17 **Miacci FLC**, Guetter CR, Moreira PH, Sartor MC, Savio MC, Baldin Júnior A, Nóbrega NL. Predictive factors of low anterior resection syndrome following anterior resection of the rectum. *Rev Col Bras Cir* 2020; **46**: e20192361 [PMID: 32022113 DOI: 10.1590/0100-6991e-20192361]

18 **Ekkarat P**, Boonpipattanapong T, Tantiphlachiva K, Sangkhathat S. Factors determining low anterior resection syndrome after rectal cancer resection: A study in Thai patients. *Asian J Surg* 2016; **39**: 225-231 [PMID: 26340884 DOI: 10.1016/j.asjsur.2015.07.003]

19 **Lourenco T**, Murray A, Grant A, McKinley A, Krukowski Z, Vale L. Laparoscopic surgery for colorectal cancer: safe and effective? *Surg Endosc* 2008; **22**: 1146-1160 [PMID: 18071810 DOI: 10.1007/s00464-007-9686-x]

20 **Shao S**, Liu L, Zhao Y, Mu L, Lu Q, Qin J. Application of Machine Learning for Predicting Anastomotic Leakage in Patients with Gastric Adenocarcinoma Who Received Total or Proximal Gastrectomy. *J Pers Med* 2021; **11** [PMID: 34442391 DOI: 10.3390/jpm11080748]

21 **Shao S**, Zhao Y, Lu Q, Liu L, Mu L, Qin J. Artificial intelligence assists surgeons' decision-making of temporary ileostomy in patients with rectal cancer who have received anterior resection. *Eur J Surg Oncol* 2023; **49**: 433-439 [PMID: 36244844 DOI: 10.1016/j.ejso.2022.09.020]

22 **Hou XT**, Pang D, Lu Q, Yang P, Jin SL, Zhou YJ, Tian SH. Validation of the Chinese version of the low anterior resection syndrome score for measuring bowel dysfunction after sphincter-preserving surgery among rectal cancer patients. *Eur J Oncol Nurs* 2015; **19**: 495-501 [PMID: 25813530 DOI: 10.1016/j.ejon.2015.02.009]

23 **Kursa MB**, Rudnicki WR. Feature selection with the Boruta Package. *J Stat Softw* 2010; **36**: 1-13 [DOI: 10.18637/jss.v036.i11]

24 **Peduzzi P**, Concato J, Kemper E, Holford TR, Feinstein AR. A simulation study of the number of events per variable in logistic regression analysis. *J Clin Epidemiol* 1996; **49**: 1373-1379 [PMID: 8970487 DOI: 10.1016/s0895-4356(96)00236-3]

25 **Fluss R**, Faraggi D, Reiser B. Estimation of the Youden Index and its associated cutoff point. *Biom J* 2005; **47**: 458-472 [PMID: 16161804 DOI: 10.1002/bimj.200410135]

26 **Roulston MS**. Performance targets and the Brier score. *Meteorological Applications* 2007; **14**: 185-194 [DOI: 10.1002/met.21]

27 **Vickers AJ**, Elkin EB. Decision curve analysis: a novel method for evaluating prediction models. *Med Decis Making* 2006; **26**: 565-574 [PMID: 17099194 DOI: 10.1177/0272989X06295361]

28 **Vickers AJ**, van Calster B, Steyerberg EW. A simple, step-by-step guide to interpreting decision curve analysis. *Diagn Progn Res* 2019; **3**: 18 [PMID: 31592444 DOI: 10.1186/s41512-019-0064-7]

29 **Afshari K**, Smedh K, Wagner P, Chabok A, Nikberg M. Risk factors for developing anorectal dysfunction after anterior resection. *Int J Colorectal Dis* 2021; **36**: 2697-2705 [PMID: 34471965 DOI: 10.1007/s00384-021-04024-3]

30 **Dulskas A**, Smolskas E, Kildusiene I, Samalavicius NE. Treatment possibilities for low anterior resection syndrome: a review of the literature. *Int J Colorectal Dis* 2018; **33**: 251-260 [PMID: 29313107 DOI: 10.1007/s00384-017-2954-x]

31 **Pachler J**, Wille-Jørgensen P. Quality of life after rectal resection for cancer, with or without permanent colostomy. *Cochrane Database Syst Rev* 2012; **12**: CD004323 [PMID: 23235607 DOI: 10.1002/14651858.CD004323.pub4]

32 **Cornish JA**, Tilney HS, Heriot AG, Lavery IC, Fazio VW, Tekkis PP. A meta-analysis of quality of life for abdominoperineal excision of rectum versus anterior resection for rectal cancer. *Ann Surg Oncol* 2007; **14**: 2056-2068 [PMID: 17431723 DOI: 10.1245/s10434-007-9402-z]

33 **Trenti L**, Galvez A, Biondo S, Solis A, Vallribera-Valls F, Espin-Basany E, Garcia-Granero A, Kreisler E. Quality of life and anterior resection syndrome after surgery for mid to low rectal cancer: A cross-sectional study. *Eur J Surg Oncol* 2018; **44**: 1031-1039 [PMID: 29665980 DOI: 10.1016/j.ejso.2018.03.025]

34 **Park JS**, Kang SB, Kim DW, Lee KH, Kim YH. Laparoscopic versus open resection without splenic flexure mobilization for the treatment of rectum and sigmoid cancer: a study from a single institution that selectively used splenic flexure mobilization. *Surg Laparosc Endosc Percutan Tech* 2009; **19**: 62-68 [PMID: 19238070 DOI: 10.1097/SLE.0b013e318196cdb0]

35 **Kim J**, Choi DJ, Kim SH. Laparoscopic rectal resection without splenic flexure mobilization: a prospective study assessing anastomotic safety. *Hepatogastroenterology* 2009; **56**: 1354-1358 [PMID: 19950790]

36 **Tian C**, Li H, Meng WJ. Should splenic flexure be routinely mobilized during laparoscopic low anterior resection for rectal cancer? *Surg Laparosc Endosc Percutan Tech* 2014; **24**: 283-284 [PMID: 24887544 DOI: 10.1097/SLE.0b013e3182937c67]

37 **Brennan DJ**, Moynagh M, Brannigan AE, Gleeson F, Rowland M, O'Connell PR. Routine mobilization of the splenic flexure is not necessary during anterior resection for rectal cancer. *Dis Colon Rectum* 2007; **50**: 302-7; discussion 307 [PMID: 17211537 DOI: 10.1007/10350-006-0811-z]

38 **Buzatti KCLR**, Petroianu A. Pathophysiological aspects of the low anterior resection syndrome for treatment of rectal cancer. *Rev Col Bras Cir* 2017; **44**: 397-402 [PMID: 29019544 DOI: 10.1590/0100-69912017004003]

39 **Ziv Y**, Zbar A, Bar-Shavit Y, Igov I. Low anterior resection syndrome (LARS): cause and effect and reconstructive considerations. *Tech Coloproctol* 2013; **17**: 151-162 [PMID: 23076289 DOI: 10.1007/s10151-012-0909-3]

40 **van der Heijden JAG**, van Heinsbergen M, Thomas G, Caers F, Slooter GD, Maaskant-Braat AJG. Implementation of a

Postoperative Screening and Treatment Guidance for the Low Anterior Resection Syndrome: Preliminary Results. *Dis Colon Rectum* 2019; **62**: 1033-1042 [PMID: 31318775 DOI: 10.1097/DCR.0000000000001428]

41 **Hughes DL**, Cornish J, Morris C; LARRIS Trial Management Group. Functional outcome following rectal surgery-predisposing factors for low anterior resection syndrome. *Int J Colorectal Dis* 2017; **32**: 691-697 [PMID: 28130593 DOI: 10.1007/s00384-017-2765-0]

42 **Vogel I**, Reeves N, Tanis PJ, Bemelman WA, Torkington J, Hompes R, Cornish JA. Impact of a defunctioning ileostomy and time to stoma closure on bowel function after low anterior resection for rectal cancer: a systematic review and meta-analysis. *Tech Coloproctol* 2021; **25**: 751-760 [PMID: 33792822 DOI: 10.1007/s10151-021-02436-5]

43 **Battersby NJ**, Juul T, Christensen P, Janjua AZ, Branagan G, Emmertsen KJ, Norton C, Hughes R, Laurberg S, Moran BJ; United Kingdom Low Anterior Resection Syndrome Study Group. Predicting the Risk of Bowel-Related Quality-of-Life Impairment After Restorative Resection for Rectal Cancer: A Multicenter Cross-Sectional Study. *Dis Colon Rectum* 2016; **59**: 270-280 [PMID: 26953985 DOI: 10.1097/DCR.0000000000000552]

44 **Filips A**, Haltmeier T, Kohler A, Candinas D, Brügger L, Studer P. LARS is Associated with Lower Anastomoses, but not with the Transanal Approach in Patients Undergoing Rectal Cancer Resection. *World J Surg* 2021; **45**: 873-879 [PMID: 33301048 DOI: 10.1007/s00268-020-05876-6]

World Journal of Gastroenterology

Submit a Manuscript: https://www.f6publishing.com

World J Gastroenterol 2023 May 21; 29(19): 2992-3002

DOI: 10.3748/wjg.v29.i19.2992

ISSN 1007-9327 (print) ISSN 2219-2840 (online)

ORIGINAL ARTICLE

Retrospective Study

Where is the optimal plane to mobilize the anterior rectal wall in female patients undergoing total mesorectal excision?

Wei Jin, Jun Yang, Xin-Yu Li, Wei-Cheng Wang, Wen-Jian Meng, You Li, Yi-Chao Liang, Yi-Ming Zhou, Xin-Dong Yang, Yang-Yang Li, Shao-Tang Li

Specialty type: Gastroenterology and hepatology

Provenance and peer review: Unsolicited article; Externally peer reviewed.

Peer-review model: Single blind

Peer-review report's scientific quality classification
Grade A (Excellent): 0
Grade B (Very good): B, B, B
Grade C (Good): C, C, C
Grade D (Fair): 0
Grade E (Poor): 0

P-Reviewer: Bae SU, South Korea; Brisinda G, Italy; Luglio G, Italy; Martínez-Pérez A, Spain; M'Koma AE, United States; Tonelli F, Italy

Received: February 6, 2023
Peer-review started: February 6, 2023
First decision: March 20, 2023
Revised: April 3, 2023
Accepted: April 20, 2023
Article in press: April 20, 2023
Published online: May 21, 2023

Wei Jin, Jun Yang, Wei-Cheng Wang, Department of Colorectal and Anal Surgery, The First Affiliated Hospital of Wenzhou Medical University, Wenzhou 325000, Zhejiang Province, China

Xin-Yu Li, Department of Gastrointestinal Surgery, The First Hospital of Quanzhou Affiliated to Fujian Medical University, Quanzhou 362002, Fujian Province, China

Wen-Jian Meng, Department of Gastrointestinal Surgery, West China Hospital. Sichuan University, Chengdu 610041, Sichuan Province, China

You Li, Department of General Surgery, Shanghai Jiao Tong University Medical School Affiliated Ruijin, Shanghai 201800, China

Yi-Chao Liang, Department of General Surgery, Shengjing Hospital of China Medical University, Shenyang 111300, Liaoning Province, China

Yi-Ming Zhou, Department of General Surgery, Huashan Hospital Fudan University, Shanghai 201800, China

Xin-Dong Yang, School of Basic Medicine, Wenzhou Medical University, Wenzhou 325000, Zhejiang Province, China

Yang-Yang Li, Department of Pathology, the First Affiliated Hospital of Wenzhou Medical University, Wenzhou 325000, Zhejiang Province, China

Shao-Tang Li, National Key Clinical Specialty (General Surgery), The First Affiliated Hospital of Wenzhou Medical University, Wenzhou 325000, Zhejiang Province, China

Corresponding author: Shao-Tang Li, MD, PhD, Chief Doctor, Doctor, Instructor, Professor, Surgeon, National Key Clinical Specialty (General Surgery), The First Affiliated Hospital of Wenzhou Medical University, Nanbaixiang Street, Ouhai District, Wenzhou 325000, Zhejiang Province, China. lishaotang163@163.com

Abstract

BACKGROUND

Since Heald proposed the total mesorectal excision (TME) procedure, the prognosis of patients with rectal cancer has been significantly improved. But Heald did not specifically describe the anterior surgical plane in female patients.

And the surgical plane for mobilizing the anterior rectal wall during TME surgery in female patients remains controversial.

AIM

To investigate the anatomy of the female pelvis and identify the optimal plane for mobilizing the anterior rectal wall.

METHODS

We retrospectively collected surgical procedure videos and clinical data of female patients diagnosed with middle or low rectal cancer who underwent the TME procedure between January 2020 and October 2022 across six hospitals. The patients were divided into two groups based on the surgical approach used to mobilize the anterior rectal wall: The experimental group was to open the peritoneum at the lowest point of the peritonea reflection and enter the plane for mobilizing, while the control group was cut at 0.5-1 cm above the peritoneal reflection and enter another plan. Then, we compared the preoperative and postoperative information between the two groups. We also dissected and observed ten adult female pelvises to analyze the anatomic structure and compare the entry plane between the two approaches. Finally, we researched the pathological structure between the rectum and the vagina.

RESULTS

Finally, 77 cases that met the criteria were included in our study. Our observations revealed that the experimental group underwent a smooth procedure, entering the plane amidst the mesorectal fascia and adventitia of the vagina, whereas the control group entered the plane between the vaginal adventitia and muscle layers. Compared to the control group, the experimental group showed a significant decrease in intraoperative bleeding [22.5 (19.5-50) mL *vs* 17 (5-20) mL, P = 0.01], as well as a shorter duration of hospitalization [9 (7-11.25) d *vs* 7 (6-10) d, P = 0.03]. Through the examination of surgical videos and cadaveric studies, we discovered that Denonvilliers' fascia is absent in females. Additionally, pathological sections further revealed the absence of Denonvilliers' fascia in females, with only loose connective tissue present between the mesorectal fascia and adventitia of the vagina.

CONCLUSION

The plane amidst the mesorectal fascia and vaginal adventitia is the optimal surgical plane to mobilize the anterior rectal wall for female patients undergoing the TME procedure.

Key Words: Rectal cancer; Procedure; Female; Rectal surgery specialty; Fascia; Laparoscopic

©The Author(s) 2023. Published by Baishideng Publishing Group Inc. All rights reserved.

Core Tip: In combination with the macroscopic and microscopic perspectives, we discovered that liberating the anterior rectal wall within a certain plane not only guarantees negative perirectal margins but also mitigates the potential for hemorrhage. This plane, situated amidst the mesorectal fascia and vaginal adventitia, proves to be the most advantageous approach for female patients undergoing total mesorectal excision.

Citation: Jin W, Yang J, Li XY, Wang WC, Meng WJ, Li Y, Liang YC, Zhou YM, Yang XD, Li YY, Li ST. Where is the optimal plane to mobilize the anterior rectal wall in female patients undergoing total mesorectal excision? *World J Gastroenterol* 2023; 29(19): 2992-3002

URL: https://www.wjgnet.com/1007-9327/full/v29/i19/2992.htm

DOI: https://dx.doi.org/10.3748/wjg.v29.i19.2992

INTRODUCTION

In 1982, Heald proposed the total mesorectal excision (TME) procedure[1], which significantly improved the prognosis of patients with rectal cancer[2]. The local recurrence of rectal cancer in 5 years decreased from 25% to 5%, as compared to the traditional operation plus radiotherapy group in the TME operation group[3]. TME soon became a classical operation method and was widely accepted by colorectal surgeons. Heald subsequently described the bloodless planes of TME surgery, known as the "holy plane," as follows: “If we cut straight on to the vesicles we find an essentially bloodless plane between

them and the fascia of Denonvilliers and we can proceed down the enemy to this until it comes forward to become somewhat should come to the state, when we must cut through it to liberate the lower third of the correction enemy"[4].

Professor Heald believes that in male patients, the anterior plane of TME should be anterior to Denonvilliers' fascia, and the anterior aspect of the specimen should include the complete Denonvilliers' fascia and peritoneal folds[3]. However, he did not specifically describe the anterior surgical plane in female patients[1], and the presence of Denonvilliers' fascia in females (rectovaginal septum[5]) remains controversial[6,7]. We also haven't found any research describing the plane of TME for female patients when the front rectal wall performs mobilization till now[8-10]. Many colorectal surgeons struggle to find an ideal plane for mobilizing the anterior rectal wall during TME, which can result in intraoperative bleeding or vaginal damage.

Therefore, we conducted this study to explore the optimal plane to mobilize the anterior rectal wall in female patients. We retrospectively analyzed rectal cancer surgery videos collected from different medical centers and studied the anatomy of the female pelvis for the accurate determination of the optimal plane to mobilize the anterior rectal wall in female patients with rectal cancer.

MATERIALS AND METHODS

Clinical data and video review

We retrospectively collected clinical data and surgical videos from six hospitals between January 2020 and October 2022. The surgeries were performed by experienced colorectal surgeons, each of whom performed more than 100 colorectal cancer operations annually. Our study initially included female patients with middle or low rectal cancer who underwent laparoscopic TME. Patients who had preoperative magnetic resonance imaging assessment indicating invasion of the anterior rectal wall, a history of rectal surgery, absence of surgical videos or relevant clinical data, and the presence of distant metastases were excluded. And they were divided into two groups based on the surgical approaches used. In the experimental group, the peritoneum was incised at the lowest point of peritoneal reflection to access the mobilization plane, while in the control group, the peritoneum was incised 0.5-1 cm above the peritoneal reflection, accessing a different plane. The surgical procedures were reviewed by two experienced colorectal surgeons separately.

The patient's pre- and postoperative data were obtained from medical records, while intraoperative bleeding was measured as the total amount of blood loss recorded in surgical records. Postoperative complications were classified into postoperative bleeding, anastomotic leakage, and other complications (such as pleural effusion, fever, *etc.*). Anastomotic leakage was defined as a communication between the intra- and extraluminal compartments due to a defect in the integrity of the intestinal wall at the anastomosis between the colon and rectum or colon and anus[11], diagnosis through computed tomography (CT) imaging. Pleural effusion was confirmed through CT imaging to establish the diagnosis. Complications were graded by the Clavien-Dindo classification[12].

Cadaver specimens

Ten female cadavers were dissected in the anatomy laboratory of Wenzhou Medical University, which had been donated to the Department of Anatomy following ethical guidelines. The cadavers underwent arterial perfusion with 8% formalin and preservation with 30% alcohol. The corpses were well-preserved, without tissue decay and structural damage. All female cadavers were sourced from young adult females without a history of pelvic diseases. After separating the pelvis from the body, the pelvises were cut in the midsagittal position to expose the rectum and vagina. The pelvises were divided into two to show the rectum and vagina. After clearly exposing the rectal and vaginal structures, a skilled colorectal surgeon and anatomist performed the subsequent operations in accordance with the two different operation procedures of TME, on the same pelvis. At first, the peritoneum was cut at the lowest point of peritoneal reflection and entered the plane to mobilize as the procedure of the experimental group. Then, the surgeon incised the peritoneum at approximately 0.5–1 cm above the peritoneal reflection and started the separation as the procedure of the control group. Photos and records were taken during the dissection.

Pathological histochemistry

A pathologist participated in and supervised the pathological research. We separated the rectovaginal tissue from the other half of the complete pelvis and preserved it in 8% formalin. Then, the remaining tissue was used for pathology and immunohistochemistry analysis. Sections were stained with hematoxylin-eosin and observed under an electron microscope with a magnification of ten times. Microscopic examination of the rectal and vaginal structures enabled us to determine the presence of Denonvilliers' fascia. Immunohistochemical and pathological studies were completed by the Pathology Department of Wenzhou Medical University.

Stastical analysis

IBM SPSS Statistics 25 software was used for the analysis of clinical data, Two-sided $P < 0.05$ indicated significance. Continuous variables with normal distribution were summarized as mean (SD) and two independent samples *t*-test was used for the statistics. For continuous variables with non-normal distribution were summarized as median (IQR) and Mann-Whitney U test were used for the statistics. Categorical variables were summarized as numbers (percentages) and analyzed using the chi-square test, while the Mann-Whitney U test was used for the Statistics of ordered classification variables. The statistical review of this study was performed by a biomedical statistician.

RESULTS

Video review and clinical data

Seventy-seven patients who met the criteria were included in our study, with 35 in the experimental group and 42 in the control group. There were no significant differences in the general information between the two groups. The patients' general information is summarized in Table 1.

In the experimental group, the peritoneum was cut at the lowest point of the peritoneal reflection to enter the anterior rectal space (as shown in Figure 1), in which the anterior rectal wall can be easily dissociated from the posterior wall of the vagina. The rectum was light yellow due to the light-yellow adipose tissue surrounded by the mesorectal fascia. Blood vessels could be seen in the mesorectum, and the mesorectum was dissected completely. It can be dissociated through blunt separation combined with sharp separation. In this process, the operation field could remain bloodless, and the vaginal structure and rectal structure were easy to distinguish from each other. The mesorectal fascia and vaginal were complete after dissection, and no Denonvilliers' fascia-like structure was present between them. In contrast, the control group cut the peritoneum at approximately 0.5–1 cm above the peritoneal reflection and freed the rectal wall between the vaginal muscular and the vaginal adventitia (as shown in Figure 2). Although a structure similar to Denonvilliers' fascia was found, it was closely connected to the vaginal muscular and could only be torn off through sharp separation. The muscular structure of the vagina was revealed after the operation, which often caused bleeding. Furthermore, the vaginal structure was no longer intact after dissection since the vaginal adventitia was separated from the muscular layer. After reviewing all the surgical procedures, finding an obvious membrane structure between the mesorectal fascia and vaginal adventitia in females was difficult. The fascial structure that we found during the operation was the vaginal adventitia, while the so-called female Denonvilliers' fascia does not exist.

Compared with the control group, the experimental group had less intraoperative bleeding [22.5 (19.5-50) mL *vs* 17 (5-20) mL; $P = 0.01$], and shorter length of hospitalization [9 (7-11.25) d *vs* 7 (6-10) d; $P = 0.03$]. Although the incidence of postoperative complications was lower than that of the control group, the results were not statistically significant. No deaths occurred in either group in the first 30 d after surgery. All Pathological specimens' Circumferential Resection Margins (CRM) were negative after the operation. Statistical result is summarized in Table 2.

Gross anatomy

As depicted in Figure 3A, the layers of the rectum and vagina were displayed, and the main structures could be distinguished. The vaginal muscular layer was brown, and the mucosal layer was gray. The mucosa of the rectum was yellowish, the submucosa was white, and the muscular layer was brown. However, distinguishing between the vaginal adventitia and the mesorectal fascia with the naked eye was difficult.

The dissociation process of the experimental group proceeded seamlessly. As depicted in Figure 3B, the mobilization plane traversed the interface between the vaginal adventitia and the fascia of the mesorectum. A discernible space between the vaginal adventitia and the mesorectal fascia was observed, which could be adroitly separated through blunt dissection. The vaginal adventitia and the mesorectal fascia were generally white without fascia-like tissues or blood vessels between them. Occasionally, blood vessels were visible beneath the vaginal adventitia. The boundary between the muscular layer and the adventitia was clear, with the muscular layer appearing dark and the adventitia appearing white.

As shown in Figure 3C, the mobilization plane entered the plane between the vaginal adventitia and the muscular layer by the procedure of the control group. When the vaginal adventitia was separated from the muscular layer, we found that the attachment between the vaginal adventitia and the muscular layer was stronger than the attachment between the vaginal adventitia and the mesorectal fascia, which could not be easily mobilized by blunt separation and can only be mobilized by sharp separation. After dissociation, the vaginal adventitia could be seen to be a single-layer fascia-like structure with a white color that was different and easy to distinguish from the dark muscle layer. No distinct or separate Denonvilliers' fascia was identified. At the same time, after the vaginal adventitia was forcibly torn off from the muscular layer, the muscular layer structure was damaged. Some residual muscle fiber tissue could be seen on the vaginal adventitia.

Table 1 General information of the patient

	Control group (*n* = 42)	Experimental group (*n* = 35)	*P* value
Height, mean (SD), cm	157.64 (6.03)	157.17 (5.29)	0.72
Weight, mean (SD), kg	57.02 (8.82)	57.37 (10.22)	0.87
BSA, mean (SD)	1.62 (0.14)	1.67 (0.15)	0.17
Age, mean (SD), y	60.50 (10.94)	63.86 (12.77)	0.22
Preoperative chemoradiotherapy	6 (14.3)	4 (11.4)	0.98

BSA: Body surface area.

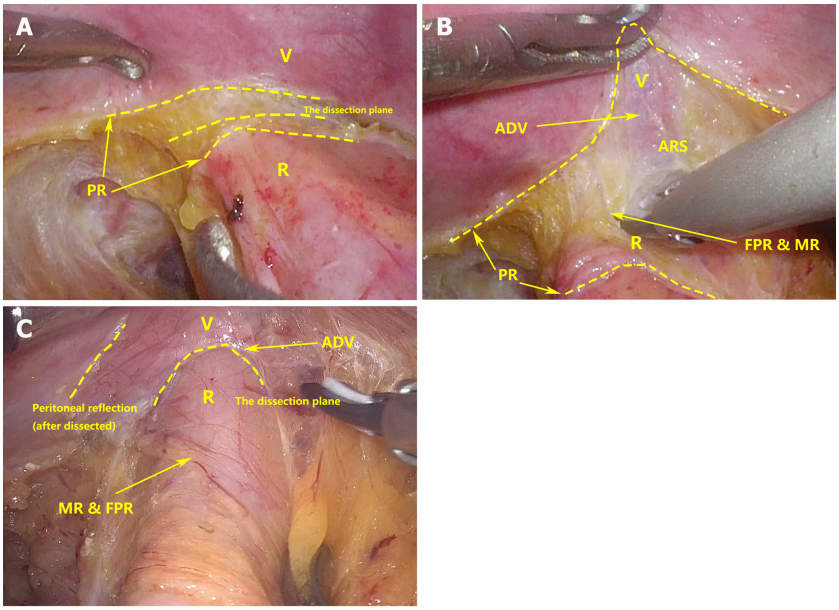
Table 2 Postoperative information of the patient

	Control group (*n* = 42)	Experimental group (*n* = 35)	*P* value
Operation time, mean (SD), min	233.14 (75.12)	228.66 (80.32)	0.8
IB, median (IQR), mL	22.5 (19.5-50)	17 (5-20)	0.01
NRL, median (IQR)	13.5 (10-16.5)	15 (13-19)	0.24
Hospital stays, median (IQR), days	9 (7-11.25)	7 (6-10)	0.03
Pathology stage			0.52
I	21 (50.0)	15 (42.8)	
II	10 (23.8)	9 (25.7)	
III	11 (26.2)	11 (31.5)	
T			0.62
1	12 (28.6)	8 (22.9)	
2	12 (28.6)	12 (34.3)	
3	15 (35.7)	10 (28.6)	
4	3 (7.1)	5 (14.3)	
N			0.75
0	32 (76.2)	24 (68.6)	
1	8 (19.0)	9 (25.7)	
2	2 (4.8)	2 (5.7)	
CDC			0.84
I	8 (19.0)	3 (8.6)	
II	2 (4.8)	1 (2.9)	
Postoperative complications	10 (23.81)	4 (11.43)	0.16
Postoperative bleeding	1	0	
Anastomotic leakage	3	2	
Other complications	8	4	

CDC: Clavien-Dindo classification; IB: Intraoperative bleeding; IQR: Inter-quartile range; NRL: Number of retrieved lymph nodes.

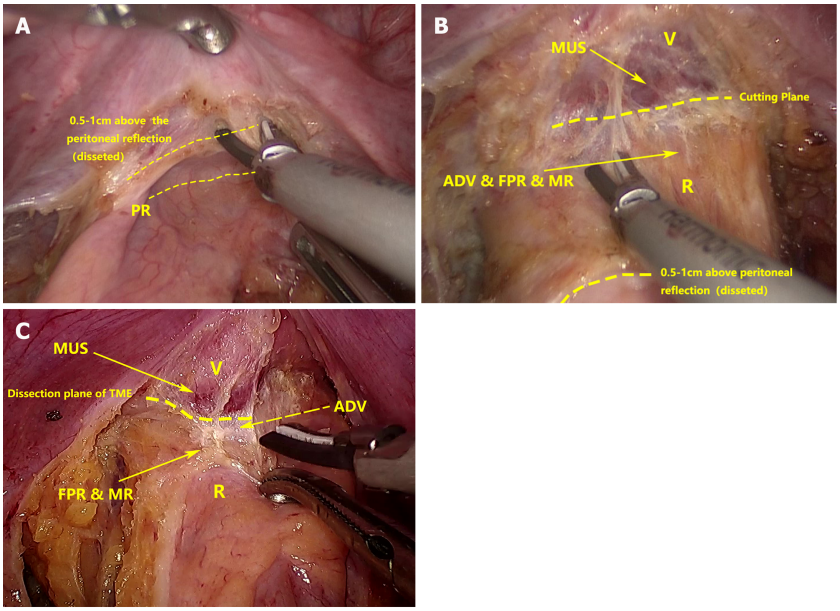
Pathological histochemistry

As shown in Figure 4, the rectal and vaginal tissues showed clear stratification: The rectum was divided into the mucosa, submucosa, inner ring muscle layer, outer longitudinal muscle layer, mesorectum, and the mesorectal fascia surrounding the mesorectum. The vaginal wall was divided into three layers: Mucosa, muscular, and adventitia layers. The adventitia layer was composed of dense connective tissue with scattered loose connective tissue among it. A gap was present between the mesorectal fascia and the vaginal adventitia. Numerous loose connective tissue, but no obvious fascia-like structures, were



DOI: 10.3748/wjg.v29.i19.2992 **Copyright** ©The Author(s) 2023.

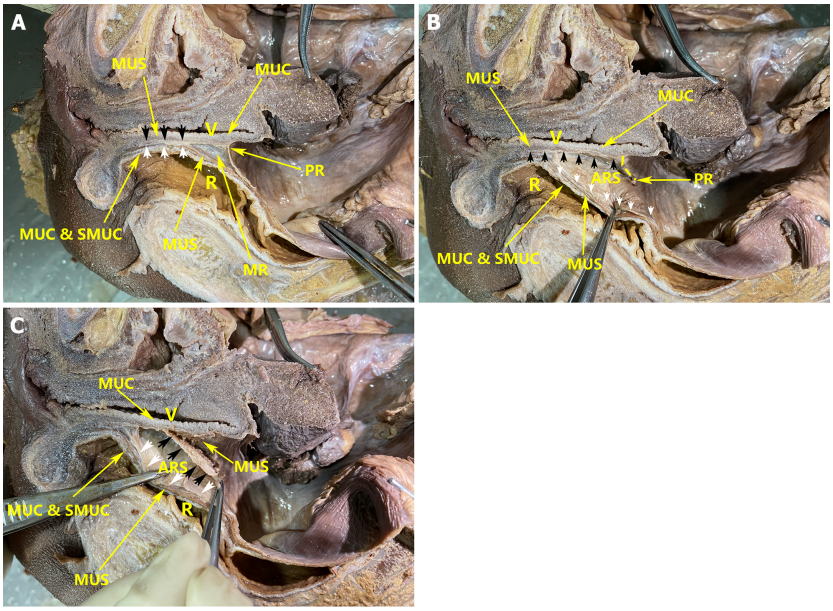
Figure 1 The procedure of the experimental group. A: The peritoneum was cut at the lowest point of the peritoneal reflection to enter the anterior rectal space; B: After the incision of the peritoneal reflection, a space can be seen, in which can we easily free the anterior rectal wall. This space is considered the rectovaginal space; C: No other fascial structure was present between the fascia propria of the rectum and the adventitia of the vagina, and these two fascial structures could be pushed away from each other by an ultrasonic knife through blunt separation. ADV: Adventitia of the vagina; FPR: Fascia propria of the rectum; MR: Mesorectum; PR: Peritoneal reflection; R: Rectum; V: Vagina; ARS: Anterior rectal space.



DOI: 10.3748/wjg.v29.i19.2992 **Copyright** ©The Author(s) 2023.

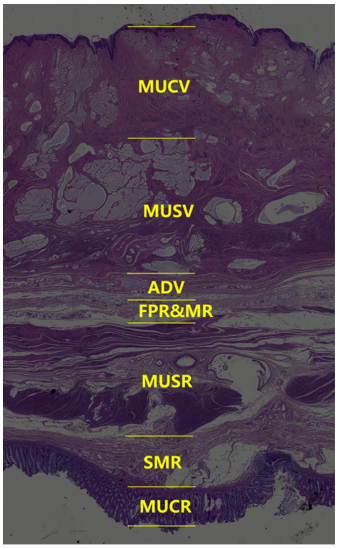
Figure 2 The procedure of the control group. A: The peritoneum was cut 0.5-1 cm above the peritoneal reflection. The peritoneal reflection was slightly white, and its texture was different from the texture of other structures during the operation; B: The cutting plane was between the vaginal muscle layer and the adventitia. The vaginal adventitia was closely adherent to the muscle layer; C: Bleeding occurred after stripping the vaginal adventitia from the muscle, and hemostasis was performed. ADV: Adventitia of the vagina; FPR: Fascia propria of the rectum; MR: Mesorectum; MUS: Muscle; PR: Peritoneal reflection; R: Rectum; V: Vagina.

present inside this gap. Occasionally, some scattered dense connective tissue and fragment-like fascial structure could be seen but were difficult to identify as fascial structures.



DOI: 10.3748/wjg.v29.i19.2992 **Copyright** ©The Author(s) 2023.

Figure 3 Gross anatomy. A: Observation of the female pelvis; B: The procedure of the experimental group; C: The procedure of the control group. Black arrow: Adventitia of the vagina; white arrow: Fascia propria of the rectum. ARS: Anterior rectal space; MR: Mesorectum; MUC: Mucosa; MUS: Muscle; PR: Peritoneal reflection; R: Rectum; SMUC: Submucosa; V: Vagina; FPR: Fascia propria of the rectum; MR: Mesorectum.



DOI: 10.3748/wjg.v29.i19.2992 **Copyright** ©The Author(s) 2023.

Figure 4 Pathological section of the rectovaginal structure. Pathological section showing the absence of an obvious fascia-like structure between the fascia propria of the rectum and the adventitia of the vagina. ADV: Adventitia of the vagina; FPR & MR: Fascia propria of the rectum and mesorectum; MUCV: Mucosa of the vagina; MUSR: Muscle of the rectum; MUSV: Muscle of the vagina; SMR: Submucosa of the rectum; MUCR: Mucosa of the rectum.

DISCUSSION

In 1836, after observing the anatomy of the male pelvis, Denonvillier found a single-layer membrane-like structure between the rectum and prostate that he called the "prostatoperitoneal membrane"[13]. Later, in memory of Denonvillier, people called this fascial structure Denonvilliers' fascia, which is considered a structure that starts from the peritoneal reflection and ends at the perineum. The prostate and seminal vesicle glands are located in front of this structure. The rectum locates behind it, and vascular and nerve bundles are located on both sides of this structure. Undoubtedly, colorectal doctors have reached a consensus on the existence of Denonvilliers' fascia in the male pelvis. However, whether this fascia exists in females remains highly debated. Denonvillier elaborated on this structure by dissecting the male pelvis but did not mention its relevance in females. Later researchers also encountered many contradictions and disputes regarding the description of this structure.

In 1969, after dissecting 143 bodies, Milley and Nichols[14] confirmed the presence of a rectovaginal septum. They found a rectovaginal septum in 23 of 25 adult females and all dissected female infants. Despite the individual differences, the existence of this structure appears to be unaffected by age and hormones. At the same time, a close adhesion existed between this diaphragm and the fascia surrounding the vagina, they believed that this close adhesion may be a major reason why some anatomists deny the existence of the vaginal rectal septum[14].

Zhai *et al*[5] proved the existence of the female rectovaginal septum by studying the whole pelvic viscera embedded in celloidin (25 female pelvic visceral organs). He pointed out that the rectovaginal septum could be divided into two layers: Denonvilliers' fascia and the mesorectal fascia from the traditional point of view. Denonvilliers' fascia tightly surrounds the posterior and lateral walls of the vagina, and the Denonvilliers' fascia and the mesorectal fascia are not attached to the rectouterine pouch. Instead, they extend upward along the peritoneum. In this anatomy, the anterior layer integrates into the uterus, and the posterior layer gradually thins and disappears. The rectovaginal septum plays an important role in preventing the spread of malignant tumors[5].

Bertrand *et al*[6] found that Denonvilliers' fascia is an independent structure of the mesorectal fascia and the cervix as well as the vagina by studying female fetuses' anatomy[6]. However, they were likely to mistake the vaginal adventitia for Denonvilliers' fascia (rectovaginal septum). In our study on adult females, we only found loose connective tissue in the plane between the mesorectal fascia and the adventitia of the vagina. No other fascia-like structures were found between these structures. Due to the absence of other structures in this plane, we were able to easily separate the rectum and vagina without causing damage to the vaginal structure during the complete removal of the mesorectum. And the vaginal adventitia seems like Denonvilliers' fascia if it was separated from the vaginal muscle. Recognizing the adventitia of the vagina as Denonvilliers' fascia and forcefully separating it from the muscular layer could often cause bleeding.

At the same time, some people proposed the opposite opinion. Zhang *et al*[15] found only some membrane-like fascial fragments in the adipose tissue between the rectum and the vagina in the frozen sections of the corpses of three adult females aged 58–86 years old. They believed that previous studies may have regarded these fascial fragments as Denonvilliers' fascia; however, considering the age limit of their samples, their results still need further research[15]. An analysis of surgical and pathological samples from three females showed that the so-called fascia and vaginal wall had the same histological manifestations under pathology and were not distinguishable[16]. Therefore, Farrell *et al*[16] believed that the so-called fascia was an artificial surgical separation from the vagina that occurred when separating the vagina and surrounding organs[16]. In 2005, through the analysis of four female anatomical samples, Kleeman *et al*[17] also obtained a similar conclusion, that is, no fascia exists between the rectum and vagina. The rectovaginal septum used to repair the rectocele is an artificial surgical separation of tears from the vagina[17]. Meanwhile, after dissecting twenty-five female cadavers, García-Gausí *et al*[7] came to the same conclusion as Farrell *et al*[16]: That an independent rectovaginal septum could only be produced by tearing the vaginal adventitia. They found only a layer of loose connective tissue between the vagina and the rectum[7]. This is consistent with the findings of our study.

Based on the anatomy of four cadavers, Fang proposed that for surgery in early rectal cancer, mobilizing the rectum behind Denonvilliers' fascia can not only ensure the integrity of the mesorectum but also control related postoperative complications[18]. Although his viewpoint on whether Denonvilliers' fascia exists in females is different from ours, his conclusion on the female surgical approach is similar to ours. Simultaneously, some researchers have discovered that in the case of early rectal cancer, mobilizing the rectal wall behind Denonvilliers' fascia results in similar 5-year local recurrence rates as the traditional TME approach, while also reducing the incidence of complications [19]. Nevertheless, we believe that these researchers may have misidentified the vaginal adventitia as Denonvilliers' fascia in female patients.

We found that in females, the plane between the vaginal adventitia and the mesorectal fascia is suitable for rectal cancer surgery. By dissecting the rectum along the plane between the mesorectal fascia and the vaginal adventitia, not only can the risk of bleeding and damage to physiological structures be minimized, resulting in a faster recovery and shorter hospitalization, but it can also guarantee complete removal of the mesorectum and negative CRM status. Thus, this plane is the optimal plane in female patients with rectal cancer undergoing TME. Our research focused on the macro- and microlevels, combined with clinical data to explore the anatomy of the rectum and the vagina from multiple angles to obtain a highly scientific conclusion. Not only did we provide stronger evidence supporting the absence of Denonvilliers' fascia as an independent structure in females, but we also discovered that the anterior rectal space is the optimal plane to mobilize the anterior rectal wall for female patients undergoing TME.

However, as this study was retrospective and had a limited sample size, the observed differences in complication rates between the two procedures were not statistically significant. Future studies with larger sample sizes may yield more conclusive results. Additionally, due to the relatively short follow-up period since the patients' surgeries, long-term prognostic and sexual function outcomes have not been thoroughly investigated. Nonetheless, we intend to address this limitation in our subsequent studies.

CONCLUSION

In adult females, Denonvilliers' fascia is absent, we could only find loose connective tissue between the mesorectal fascia and vaginal adventitia. The vaginal adventitia is tightly adherent to the vaginal muscular layer and was difficult to separate from the muscle layer. By incising the peritoneum at the lowest point of peritoneal reflection, a plane between the mesorectal fascia and vaginal adventitia can be accessed. Mobilizing the anterior rectal wall in this plane could not only ensures the integrity of the mesorectum but also reduces intraoperative bleeding and hospital stay. Dissecting in this plane follows a natural avascular space without damaging the vaginal structure and simplifies the surgical procedure. Therefore, this is the optimal plane for mobilizing the anterior rectal wall for female patients undergoing TME procedures.

ARTICLE HIGHLIGHTS

Research background

Currently, there are no comprehensive descriptions available regarding the approach for dissecting the anterior wall of the female rectum. Many surgeons encounter intraoperative bleeding due to the lack of an appropriate dissection plane.

Research motivation

The surgical approach for mobilizing the anterior rectal wall during total mesorectal excision surgery in female patients remains controversial. However, with a more profound comprehension of the pelvic anatomy, we can identify the avascular plane, reducing intraoperative bleeding and preventing harm to physiological structures.

Research objectives

We aim to gain a better understanding of the female pelvic anatomy to identify an optimal approach for dissecting the anterior wall of the rectum. This will facilitate improved surgical outcomes for female patients with middle or low rectal cancer.

Research methods

Firstly, we retrospectively grouped patients based on different approaches after reviewing surgical videos. Clinical information was collected and pre-and post-operative data were compared, along with reviewing surgical videos to understand the anatomy and intraoperative situation. Subsequently, the female pelvic structure was studied through cadaveric dissection and histological sections.

Research results

We discovered that opening the peritoneum at the lowest point of peritoneal reflection allows access to the plane between the vaginal adventitia and mesorectal fascia. Opening the peritoneum 0.5-1 cm above the peritoneal reflection enters another plane located between the vaginal adventitia and vaginal muscle layer. The first approach has lower intraoperative bleeding and shorter hospital stay compared to the second approach. Neither cadaveric dissection nor pathological examination revealed the existence of Denonvilliers' fascia. Only loose connective tissue exists between the rectosacral fascia and the vaginal adventitia.

Research conclusions

Denonvilliers' fascia is absent in females. The plane amidst the mesorectal fascia and vaginal adventitia is the optimal surgical plane to mobilize the anterior rectal wall for female patients.

Research perspectives

In future studies, we will explore the long-term prognosis of the two approaches for women, as well as the impact on postoperative sexual and vaginal function.

ACKNOWLEDGEMENTS

Thanks to Xin-Yu Li, Yang-Yang Li, and Xin-Dong Yang's great contributions to our work.

FOOTNOTES

Author contributions: Li ST contributed to the study conceptualization and completed the dissection of cadavers; Li XY, Li Y, Liang YC, Zhou YM and Li ST provide clinical data; Li XY and Li Y reviewed the surgical videos; Jin W wrote the original draft of the manuscript and made the figures; Wang WC and Jin W finished the analysis of the data; Li XY, Zhou YM, and Yang J directly accessed and verified the underlying data; Li YY finished the pathological research; Yang XD finished the biostatistics jobs; All authors critically revised and approved the final manuscript.

Supported by Huadong Medicine Joint Funds of the Zhejiang Provincial Natura Science Foundation of China, No. LHDMY22H160002.

Institutional review board statement: The study was reviewed and approved by the Ethics Committee in Clinical Research of the First Affiliated Hospital of Wenzhou Medical University Institutional Review Board, No. KY2022-R088.

Informed consent statement: All study participants, or their legal guardian, provided informed written consent prior to study enrollment.

Conflict-of-interest statement: All the authors report no relevant conflicts of interest for this article.

Data sharing statement: Technical appendix, statistical code, and dataset available from the corresponding author at lishaotang163@163.com.

Open-Access: This article is an open-access article that was selected by an in-house editor and fully peer-reviewed by external reviewers. It is distributed in accordance with the Creative Commons Attribution NonCommercial (CC BY-NC 4.0) license, which permits others to distribute, remix, adapt, build upon this work non-commercially, and license their derivative works on different terms, provided the original work is properly cited and the use is non-commercial. See: https://creativecommons.org/Licenses/by-nc/4.0/

Country/Territory of origin: China

ORCID number: Wei Jin 0009-0001-0925-6016; Wen-Jian Meng 0000-0002-4578-0560; You Li 0000-0002-9560-9702; Shao-Tang Li 0000-0002-5385-2472.

S-Editor: Li L
L-Editor: A
P-Editor: Cai YX

REFERENCES

1 **Heald RJ**, Husband EM, Ryall RD. The mesorectum in rectal cancer surgery--the clue to pelvic recurrence? *Br J Surg* 1982; **69**: 613-616 [PMID: 6751457 DOI: 10.1002/bjs.1800691019]
2 **Heald RJ**, Ryall RD. Recurrence and survival after total mesorectal excision for rectal cancer. *Lancet* 1986; **1**: 1479-1482 [PMID: 2425199 DOI: 10.1016/s0140-6736(86)91510-2]
3 **MacFarlane JK**, Ryall RD, Heald RJ. Mesorectal excision for rectal cancer. *Lancet* 1993; **341**: 457-460 [PMID: 8094488 DOI: 10.1016/0140-6736(93)90207-w]
4 **Heald RJ**. The 'Holy Plane' of rectal surgery. *J R Soc Med* 1988; **81**: 503-508 [PMID: 3184105 DOI: 10.1177/014107688808100904]
5 **Zhai LD**, Liu J, Li YS, Yuan W, He L. Denonvilliers' fascia in women and its relationship with the fascia propria of the rectum examined by successive slices of celloidin-embedded pelvic viscera. *Dis Colon Rectum* 2009; **52**: 1564-1571 [PMID: 19690483 DOI: 10.1007/DCR.0b013e3181a8f75c]
6 **Bertrand MM**, Alsaid B, Droupy S, Benoit G, Prudhomme M. Biomechanical origin of the Denonvilliers' fascia. *Surg Radiol Anat* 2014; **36**: 71-78 [PMID: 23732391 DOI: 10.1007/s00276-013-1142-0]
7 **García-Gausí M**, García-Armengol J, Mulas Fernández C, Pellino G, Roig JV, García-Granero A, Pla-Marti V, Martínez-Soriano F. Surgical Anatomy of the Rectovaginal Space: Does a Standalone Rectovaginal Septum or Denonvilliers Fascia Exist in Women? *Dis Colon Rectum* 2021; **64**: 576-582 [PMID: 33939388 DOI: 10.1097/DCR.0000000000001912]
8 **Stevenson AR**, Solomon MJ, Lumley JW, Hewett P, Clouston AD, Gebski VJ, Davies L, Wilson K, Hague W, Simes J; ALaCaRT Investigators. Effect of Laparoscopic-Assisted Resection *vs* Open Resection on Pathological Outcomes in Rectal Cancer: The ALaCaRT Randomized Clinical Trial. *JAMA* 2015; **314**: 1356-1363 [PMID: 26441180 DOI: 10.1001/jama.2015.12009]
9 **Fleshman J**, Branda ME, Sargent DJ, Boller AM, George VV, Abbas MA, Peters WR Jr, Maun DC, Chang GJ, Herline A, Fichera A, Mutch MG, Wexner SD, Whiteford MH, Marks J, Birnbaum E, Margolin DA, Larson DW, Marcello PW, Posner MC, Read TE, Monson JRT, Wren SM, Pisters PWT, Nelson H. Disease-free Survival and Local Recurrence for Laparoscopic Resection Compared With Open Resection of Stage II to III Rectal Cancer: Follow-up Results of the ACOSOG Z6051 Randomized Controlled Trial. *Ann Surg* 2019; **269**: 589-595 [PMID: 30080730 DOI: 10.1097/SLA.0000000000003002]

10 **Fleshman J**, Branda M, Sargent DJ, Boller AM, George V, Abbas M, Peters WR Jr, Maun D, Chang G, Herline A, Fichera A, Mutch M, Wexner S, Whiteford M, Marks J, Birnbaum E, Margolin D, Larson D, Marcello P, Posner M, Read T, Monson J, Wren SM, Pisters PW, Nelson H. Effect of Laparoscopic-Assisted Resection *vs* Open Resection of Stage II or III Rectal Cancer on Pathologic Outcomes: The ACOSOG Z6051 Randomized Clinical Trial. *JAMA* 2015; **314**: 1346-1355 [PMID: 26441179 DOI: 10.1001/jama.2015.10529]

11 **Rahbari NN**, Weitz J, Hohenberger W, Heald RJ, Moran B, Ulrich A, Holm T, Wong WD, Tiret E, Moriya Y, Laurberg S, den Dulk M, van de Velde C, Büchler MW. Definition and grading of anastomotic leakage following anterior resection of the rectum: a proposal by the International Study Group of Rectal Cancer. *Surgery* 2010; **147**: 339-351 [PMID: 20004450 DOI: 10.1016/j.surg.2009.10.012]

12 **Dindo D**, Demartines N, Clavien PA. Classification of surgical complications: a new proposal with evaluation in a cohort of 6336 patients and results of a survey. *Ann Surg* 2004; **240**: 205-213 [PMID: 15273542 DOI: 10.1097/01.sla.0000133083.54934.ae]

13 **Denonvilliers C**. Anatomie du perinee. *Bull Soc Anat Paris* 1836; **10**: 105-107

14 **Milley PS**, Nichols DH. A correlative investigation of the human rectovaginal septum. *Anat Rec* 1969; **163**: 443-451 [PMID: 5774728 DOI: 10.1002/ar.1091630307]

15 **Zhang M**, Kaw A, Chapuis PH, Bokey L. Does Denonvilliers' fascia exist in women? *Am J Obstet Gynecol* 2016; **214**: 663-664 [PMID: 26767795 DOI: 10.1016/j.ajog.2015.12.057]

16 **Farrell SA**, Dempsey T, Geldenhuys L. Histologic examination of "fascia" used in colporrhaphy. *Obstet Gynecol* 2001; **98**: 794-798 [PMID: 11704171 DOI: 10.1016/s0029-7844(01)01533-2]

17 **Kleeman SD**, Westermann C, Karram MM. Rectoceles and the anatomy of the posteriorvaginal wall: revisited. *Am J Obstet Gynecol* 2005; **193**: 2050-2055 [PMID: 16325614 DOI: 10.1016/j.ajog.2005.07.096]

18 **Fang J**, Zheng Z, Wei H. Reconsideration of the Anterior Surgical Plane of Total Mesorectal Excision for Rectal Cancer. *Dis Colon Rectum* 2019; **62**: 639-641 [PMID: 30964796 DOI: 10.1097/DCR.0000000000001358]

19 **Killingback M**, Barron P, Dent OF. Local recurrence after curative resection of cancer of the rectum without total mesorectal excision. *Dis Colon Rectum* 2001; **44**: 473-83; discussion 483 [PMID: 11330574 DOI: 10.1007/BF02234317]

World Journal of Gastroenterology

Submit a Manuscript: https://www.f6publishing.com

World J Gastroenterol 2023 May 21; 29(19): 3003-3012

DOI: 10.3748/wjg.v29.i19.3003

ISSN 1007-9327 (print) ISSN 2219-2840 (online)

ORIGINAL ARTICLE

Retrospective Study

Association of vitamin D and polymorphisms of its receptor with antiviral therapy in pregnant women with hepatitis B

Rui Wang, Xia Zhu, Xuan Zhang, Huan Liu, Yu-Lin Ji, Yong-Hua Chen

Specialty type: Gastroenterology and hepatology

Provenance and peer review: Invited article; Externally peer reviewed.

Peer-review model: Single blind

Peer-review report's scientific quality classification

Grade A (Excellent): 0
Grade B (Very good): B, B
Grade C (Good): 0
Grade D (Fair): 0
Grade E (Poor): 0

P-Reviewer: Dabla PK, India; Shahid M, Pakistan

Received: February 17, 2023
Peer-review started: February 17, 2023
First decision: March 24, 2023
Revised: March 28, 2023
Accepted: April 24, 2023
Article in press: April 24, 2023
Published online: May 21, 2023

Rui Wang, Yong-Hua Chen, Division of Pancreatic Surgery, Department of General Surgery, West China Hospital of Sichuan University, Chengdu 610041, Sichuan Province, China

Xia Zhu, Huan Liu, Center of Infectious Diseases, West China Hospital of Sichuan University, Chengdu 610041, Sichuan Province, China

Xuan Zhang, Yu-Lin Ji, Department of Respiratory and Critical Care Medicine, West China Hospital of Sichuan University, Chengdu 610041, Sichuan Province, China

Corresponding author: Yong-Hua Chen, MD, PhD, Associate Professor, Division of Pancreatic Surgery, Department of General Surgery, West China Hospital of Sichuan University, No. 37 Guoxue Alley, Wuhou District, Chengdu 610041, Sichuan Province, China.
chenyonghua2007@163.com

Abstract

BACKGROUND

The interruption of mother-to-child transmission (MTCT) is considered important to decrease the individual and population morbidity of hepatitis B virus (HBV) infection as well as the global burden of hepatitis B. Serum vitamin D (VD) is associated with hepatitis B.

AIM

To assess whether baseline VD levels and single nucleotide polymorphisms of the VD receptor gene (VDR SNPs) are associated with the efficacy of tenofovir disoproxil fumarate (TDF) in the prevention of MTCT in pregnant women with high HBV viral loads.

METHODS

Thirty-eight pregnant women who were at high risk for MTCT of HBV (those with an HBV DNA level ≥ 2×10^5 IU/mL during 12-24 wk of gestation) receiving antiviral therapy of TDF between June 1, 2019 and June 30, 2021 in Mianyang were included in this retrospective study. The women received 300 mg TDF once daily from gestational weeks 24-28 until 3 mo after delivery. To further characterize the clinical relevance of maternal serum HBV DNA levels, we stratified patients according to HBV DNA level as follows: Those with levels < 2×10^5 (full responder group) *vs* those levels ≥ 2×10^5 IU/mL (partial responder group) at delivery. Serum levels of 25-hydroxyvitamin D [25(OH)D], liver function markers, virological parameters, VDR SNPs and other clinical parameters were collected to

analyze their association with the efficacy of TDF. The Mann-Whitney *U* test or t test was used to analyze the serum levels of 25(OH)D in different groups. Multiple linear regressions were utilized to analyze the determinants of the maternal HBV DNA level at delivery. Univariate and multivariate logistic regression analyses were employed to explore the association of targeted antiviral effects with various characteristics at baseline and delivery.

RESULTS

A total of 38 pregnant women in Mianyang City at high risk for MTCT of HBV were enrolled in the study. The MTCT rate was 0%. No mother achieved hepatitis B e antigen or hepatitis B surface antigen (HBsAg) clearance at delivery. Twenty-three (60.5%) participants were full responders, and 15 (39.5%) participants were partial responders according to antiviral efficacy. The present study showed that a high percentage (76.3%) of pregnant women with high HBV viral loads had deficient (< 20 ng/mL) or insufficient (≥ 20 but < 31 ng/mL) VD levels. Serum 25(OH)D levels in partial responders appeared to be significantly lower than those in full responders both at baseline (25.44 ± 9.42 *vs* 17.66 ± 5.34 ng/mL, $P = 0.006$) and delivery (26.76 ± 8.59 *vs* 21.24 ± 6.88 ng/mL, $P = 0.044$). Serum 25(OH)D levels were negatively correlated with maternal HBV DNA levels [log(10) IU/mL] at delivery after TDF therapy ($r = -0.345$, $P = 0.034$). In a multiple linear regression analysis, maternal HBV DNA levels were associated with baseline maternal serum 25(OH)D levels ($P < 0.0001$, β = -0.446), BMI ($P = 0.03$, β = -0.245), baseline maternal log10 HBsAg levels ($P = 0.05$, β = 0.285) and cholesterol levels at delivery ($P = 0.015$, β = 0.341). Multivariate logistic regression analysis showed that baseline serum 25(OH)D levels (OR = 1.23, 95%CI: 1.04-1.44), maternal VDR Cdx2 TT (OR = 0.09, 95%CI: 0.01-0.88) and cholesterol levels at delivery (OR = 0.39, 95%CI: 0.17-0.87) were associated with targeted antiviral effects (maternal HBV DNA levels < 2×10^5 at delivery).

CONCLUSION

Maternal VD levels and VDR SNPs may be associated with the efficacy of antiviral therapy in pregnant women with high HBV viral loads. Future studies to evaluate the therapeutic value of VD and its analogs in reducing the MTCT of HBV may be justified.

Key Words: Hepatitis B virus; Vitamin D; Vitamin D receptor polymorphism; Antiviral therapy; Pregnancy; Mother-to-child transmission

©The Author(s) 2023. Published by Baishideng Publishing Group Inc. All rights reserved.

Core Tip: This retrospective study investigated the influence of vitamin D (VD) levels and single nucleotide polymorphisms of the VD receptor gene (VDR SNPs) on the efficacy of tenofovir disoproxil fumarate in preventing mother-to-child transmission in 38 pregnant women with high hepatitis B viral loads. We demonstrate a significant association between low serum levels of 25-hydroxyvitamin D and high levels of hepatitis B virus replication in pregnant women with high hepatitis B viral loads, and maternal VD levels as well as VDR SNPs may be associated with the efficacy of antiviral therapy.

Citation: Wang R, Zhu X, Zhang X, Liu H, Ji YL, Chen YH. Association of vitamin D and polymorphisms of its receptor with antiviral therapy in pregnant women with hepatitis B. *World J Gastroenterol* 2023; 29(19): 3003-3012

URL: https://www.wjgnet.com/1007-9327/full/v29/i19/3003.htm

DOI: https://dx.doi.org/10.3748/wjg.v29.i19.3003

INTRODUCTION

Hepatitis B virus (HBV) infection is a serious public health problem that causes a very large medical and economic burden worldwide. Mother-to-child transmission (MTCT) is the main route of HBV transmission, accounting for 30%-50% of chronic infections in China[1]. In particular, China is a major contributor to achieving the global goal of eliminating hepatitis B as a threat to public health by 2030[2]. The interruption of MTCT is considered important to decrease the individual and population morbidity of HBV infection as well as the global burden of hepatitis B. In recent years, Chinese scholars have continuously published and updated the management algorithm for the prevention of the MTCT of HBV, which has achieved good clinical application[3,4]. To date, the use of antiviral drugs in combination with immunoprophylaxis in pregnant women has been shown to be safe and effective in

reducing the MTCT of HBV[4].

Vitamin D (VD) is a fat-soluble steroid hormone that is widely found in systemic organs and tissues, including the brain, bones, cardiac system and immune system, and has multiple effects on human health and many diseases, including infectious diseases. In fact, VD deficiency has been detected in a variety of chronic liver diseases, including chronic viral hepatitis[5-8]. Moreover, VD deficiency is common among patients with chronic hepatitis B infection and is associated with adverse clinical outcomes[9]. Similarly, VD levels are lower in pregnant women with chronic HBV infection than in healthy pregnant women[10]. Clinical and epidemiological studies support the role of VD in inhibiting HBV infection, and this antiviral effect is widely attributed to the VD receptor (VDR)[11].

Different studies have focused on single nucleotide polymorphisms of the VDR gene (VDR SNPs) and HBV. VDR ApaI has been associated with the presence of hepatitis B surface antigen (HBsAg) and viral loads at different times[12]. In addition to its effect on viruses, VD plays an important role for the mother and fetus during pregnancy and has been associated with influencing adverse perinatal events.

However, few data are available with regard to the association of VD levels and VDR SNPs with clinical parameters and treatment outcomes in pregnant women with high HBV viral loads. The aims of our present retrospective study were to study whether baseline VD levels and VDR SNPs were associated with the efficacy of tenofovir disoproxil fumarate (TDF) in the prevention of MTCT in pregnant women with high HBV viral loads.

MATERIALS AND METHODS

Study population

This was a retrospective study. As part of "The National Science & Technology Pillar Program during the 13th Five-year Plan Period", HBsAg-positive pregnant women receiving TDF were included from Mianyang between June 1, 2019 and June 30, 2021. The present study was approved by the Institutional Review Board of the West China Hospital, Sichuan University (No. 2019-151), and informed consent was obtained from all patients before recruitment.

Pregnant women screened for HBV DNA at high risk for MTCT (HBV DNA thresholds ≥ 2×10^5 IU/mL) according to WHO recommendations during 12-24 wk of gestation and completed antiviral therapy as required were included in the study. Women received 300 mg TDF once daily from gestational weeks 24-28 until 3 mo after delivery, in addition to HBV immune globulin and three doses of HBV vaccination, including a birth dose given to the neonate. The main exclusion criteria were as follows: (1) Coinfection of syphilis, *Toxoplasma gondii*, human immunodeficiency viruses, or types of viral hepatitis other than HBV; (2) major systemic disease, including heart disease, malignant neoplasm, or renal insufficiency; (3) evidence of liver cirrhosis, hepatic decompensation and other liver diseases such as drug-induced hepatitis, autoimmune liver disease, or alcoholic liver disease; (4) evidence of congenital anomalies of the fetus; (5) antiviral treatment within a short period of time prior to treatment with TDF or failure to complete TDF antiviral therapy as required; and (6) incomplete data, including basic information, VD levels before and after treatment, VDR SNPs, virological indicators, *etc.*

Data collection and definition

The basic information of the pregnant woman including age, height, weight, season of blood sample collection and other basic information was collected. Meanwhile, maternal virological indicators, including HBsAg, hepatitis B e antigen (HBeAg) and HBV DNA, were recorded before antiviral treatment and at delivery after antiviral treatment. Moreover, common clinical parameters before antiviral treatment and at delivery after antiviral treatment including peripheral blood count, liver function, kidney function and other parameters were also collected. Laboratory tests were performed according to our previous description[13,14].

Previously collected blood samples were used to assess maternal VD levels and VDR SNPs. In particular, VD was assessed at baseline and at the time of delivery by measuring serum 25-hydroxyvitamin D [25(OH)D] levels. Serum 25(OH)D was analyzed by LCMS/MS (Agilent Technologies Inc., LCMS/MS1260-6470, CA, United States) after hexane extraction with deuterated 25(OH)D as a control as previously described[15]. Levels of VD were categorized as follows: < 20 ng/mL = deficient; ≥ 20 but < 31 ng/mL = insufficient; and ≥ 31 ng/mL = normal. Genomic DNA was isolated from blood samples (MagNA Pure Compact, Roche). VDR SNPs were assessed through a real-time PCR allelic discrimination system (LightCycler 96, Roche). We investigated the following gene SNPs: VDR: rs7975232 (ApaI)C>A, rs11568820 (Cdx2)T>C, rs2228570 (FokI)A>G, rs1544410 (BsmI)C>T, rs731236 (TaqI)A>G.

The primary outcomes were the changes in the maternal viral load (HBV DNA level) at baseline and the time of delivery. A sustained virological response was defined as an HBV DNA level lower than 2×10^5 IU/mL at delivery. We aimed to determine whether the levels of VD and VD SNPs were associated with the antiviral effects of TDF in interrupting MTCT during the peripartum period.

Statistical analysis

All statistical analyses were carried out using SPSS Version 26. Categorical variables are represented as frequencies and percentages, and continuous variables are represented as medians (interquartile ranges) or mean ± SD. The outcomes were compared between the two groups using χ^2 tests or Fisher's exact test for categorical variables and the Wilcoxon signed-rank test or Student's *t* test for continuous variables. Associations between VD and each of the baseline demographic and lab values were assessed in univariate analyses using general linear models. Univariate and multivariate logistic regression analyses were employed to explore the association of targeted antiviral effects (HBV DNA levels < 2×10^5 at delivery) with various characteristics at baseline and delivery. Factors with a *P* value < 0.1 in univariate analysis were considered in multivariate analysis. The statistical test was 2-sided, and a *P* value < 0.05 was considered statistically significant.

RESULTS

Patient characteristics

The baseline characteristics, laboratory data, and VDR SNPs of the patients are presented in Table 1. No mother achieved HBeAg or HBsAg clearance at delivery. The decrease in HBV DNA levels from baseline to delivery was significant ($P < 0.001$). A total of 100% of the infants had negative HBsAg and undetectable HBV DNA levels at delivery; thus, the MTCT rate was 0%. To further characterize the clinical relevance of maternal serum HBV DNA levels, we stratified patients according to serum HBV DNA levels as follows: those with levels < 2×10^5 (full responder group) *vs* those with levels ≥ 2×10^5 IU/mL (partial responder group) at delivery. Mothers with serum HBV DNA viral loads below this threshold are generally considered low risk for MTCT. Twenty-three (60.5%) participants were full responders, and 15 (39.5%) participants were partial responders according to antiviral efficacy. Full and partial responders were similar in age (29.09 *vs* 28.73 years) and body mass index (BMI) (23.15 *vs* 21.42 kg/m^2).

In the virological indicators related to HBV, there was no significant difference in the HBsAg log10 and HBeAg log10 values between the two groups both at baseline and delivery. The serum HBV DNA concentration was not significantly different between the two groups at baseline, but the serum HBV DNA concentration of full responders was significantly lower than that of partial responders at delivery after antiviral treatment [log10, 3.61 (2.88, 4.46) *vs* 7.41 (5.79, 7.9), $P < 0.0001$].

For the laboratory test results, there were no significant differences between full and partial responders in most of the main laboratory indices before and after antiviral therapy, including hemoglobin, white blood cell count, platelets, neutrophils, lymphocytes, total bilirubin, albumin, alanine aminotransferase, triglycerides, creatinine, alkaline phosphatase, and gamma-glutamyl transferase. However, cholesterol levels were lower in complete responders than in partial responders at delivery after treatment (4.87 ± 0.79 *vs* 5.56 ± 0.96 mg/dL, $P = 0.001$), but there was no significant difference at baseline.

Serum 25(OH)D levels

There was no VD or multivitamin supplementation between baseline and delivery. The mean baseline serum 25(OH)D level of the entire cohort was similar to the serum 25(OH)D level at delivery, with no significant difference (22.37 ± 8.85 *vs* 24.58 ± 8.32 ng/mL, $P = 0.139$). Of the 38 patients in the entire cohort, 18 (47.4%), 11 (28.9%), and 9 (23.7%) had severe VD deficiency, VD insufficiency or normal serum VD levels, respectively.

In the absence of significant seasonal differences for the collected blood samples, VD deficiency and insufficiency were highly prevalent in partial responders (73.3%, 20% *vs* 30.4%, 34.8%, $P = 0.021$). Overall, the serum 25-hydroxyvitamin D3 [25(OH)D3] level in partial responders appeared to be significantly lower than that in full responders both at baseline (25.44 ± 9.42 *vs* 17.66 ± 5.34 ng/mL, $P = 0.006$) and delivery (26.76 ± 8.59 *vs* 21.24 ± 6.88 ng/mL, $P = 0.044$). In addition, the VDR SNP assay showed no significant difference between full and partial responders based on VDR SNPs, including VDR Cdx2, Bsm1, FokI, Taq1 and Apa1.

Relationship between baseline serum 25(OH)D levels and virological parameters

Maternal HBsAg serum levels were not associated with serum 25(OH)D levels (data not shown). Interestingly, maternal Log10 HBV DNA levels at delivery and baseline serum 25(OH)D levels showed a significant, inverse correlation ($P = 0.034$, Figure 1). Therefore, we performed multiple linear regression analysis of the determinants of maternal HBV DNA levels at delivery. In both univariate and multivariate analyses, baseline maternal serum 25(OH)D levels were the strongest determinant of low maternal HBV DNA levels ($P = 0.034$ and < 0.0001, respectively; Table 2), together with BMI, baseline maternal log10 HBsAg levels and cholesterol levels at delivery.

We further performed univariate and multivariate regression analyses to characterize the relationship between the serum level of 25(OH)D and targeted antiviral effects. The baseline serum 25(OH)D level

Table 1 Baseline characteristics, laboratory data, and single nucleotide polymorphisms of the vitamin D receptor gene of patients included in the study

	Before treatment initiation		*P* value	At delivery after treatment		*P* value
	Full responders (*n* = 23)	Partial responders (*n* = 15)		Full responders (*n* = 23)	Partial responders (*n* = 15)	
Age, yr, mean ± SD	29.09 ± 3.55	28.73 ± 3.01	0.75	NA	NA	
BMI, kg/m^2, mean ± SD	23.15 ± 3.33	21.42 ± 3.61	0.14	NA	NA	
Season of blood draw			0.552			0.311
Winter or spring	10 (43.5%)	8 (53.3%)		16 (69.6%)	8 (53.3%)	
Summer or autumn	13 (56.5%)	7 (46.7%)		7 (30.4%)	7 (46.7%)	
HBsAg log10 IU/mL mean (IQR)	4.33 (3.73, 4.52)	4.36 (4.1, 4.72)	0.663	4.11 (2.56, 5.44)	4.33 (3.95, 4.56)	0.256
HBeAg log10 IU/mL mean (IQR)	3.16 (2.66, 3.2)	3.16 (3.12, 3.19)	0.928	3.18 (2.85, 3.19)	6.75 (6.21, 8.49)	0.510
HBV DNA, log10 mean (IQR)	8.06 (7.61, 8.44)	8.09 (7.53, 8.16)	0.56	3.61 (2.88, 4.46)	7.41 (5.79, 7.9)	< 0.0001
Vitamin D, ng/mL, mean ± SD	25.44 ± 9.42	17.66 ± 5.34	0.006	26.76 ± 8.59	21.24 ± 6.88	0.044
≥ 30	8 (34.8%)	1 (6.7%)	0.021	10 (43.5%)	2 (13.3%)	0.127
20-30	8 (34.8%)	3 (20%)		6 (26.1%)	6 (40%)	
< 20	7 (30.4%)	11 (73.3%)		7 (30.4%)	7 (46.7%)	
Hemoglobin, g/dL, mean ± SD	113.78 ± 9.29	115.47 ± 8.98	0.583	114.3 ± 12.78	118 ± 10.17	0.353
WBC count, × 10^6/μL, mean ± SD	7.83 ± 1.54	8.61 ± 2.26	0.282	7.63 ± 1.77	7.7 ± 2.17	0.918
Platelet, × 10^3/μL, mean ± SD	149.52 ± 56.73	155.6 ± 53.01	0.742	137.17 ± 53.92	149.4 ± 56.21	0.506
Neutrophil, mean ± SD	5.78 ± 1.38	6.51 ± 2.0	0.289	5.33 ± 1.62	5.53 ± 1.96	0.731
Lymphocyte, mean ± SD	1.46 ± 0.4	1.49 ± 0.49	0.823	1.63 ± 1.14	1.61 ± 0.49	0.964
Total bilirubin, mg/dL, mean ± SD	14.73 ± 3.24	13.61 ± 3.09	0.299	14.97 ± 4.15	17.13 ± 4.23	0.128
Albumin, g/dL, mean ± SD	39.21 ± 2.36	39.93 ± 2.28	0.355	26.42 ± 3.19	37.33 ± 3.68	0.698
ALT, U/L, mean (IQR)	22 (19, 28)	21 (15, 32)	0.891	22 (18, 30)	21 (17, 36)	0.893
Triglyceride, mg/dL, mean (IQR)	1.74 (1.59, 2.38)	1.58 (1.34, 1.79)	0.189	3.06 (2.41, 3.67)	2.52 (2.03, 3.21)	0.131
Cholesterol, mg/dL, mean ± SD	5.33 ± 0.85	5.7 ± 1.97	0.347	4.87 ± 0.79	5.56 ± 0.96	0.001
Creatinine, mg/dL, mean (IQR)	43 (38, 49)	43 (39, 45)	0.951	44 (37, 51)	47.5 (39.8, 55)	0.397
Alkaline phosphatase, U/L, mean (IQR)	7 (5, 10)	10 (4, 23)	0.234	48 (19, 72)	52 (47, 111)	0.199
GGT, U/L, mean ± SD	12.91 ± 8.1	13.87 ± 8.4	0.675	14.48 ± 7.57	22 ± 15.19	0.115
VDR SNPs						
Cdx2 TT	9 (39.1%)	2 (13.3%)	0.076	NA		
TC/CC	14 (30.9%)	13 (86.7%)				
Bsm1 CC	20 (87%)	13 (86.7%)	0.979	NA		
CT/TT	3 (13%)	2 (13.3%)				
FokI AA/AG	18 (78.3%)	10 (66.7%)	0.431	NA		
GG	5 (21.7%)	5 (33.3%)				

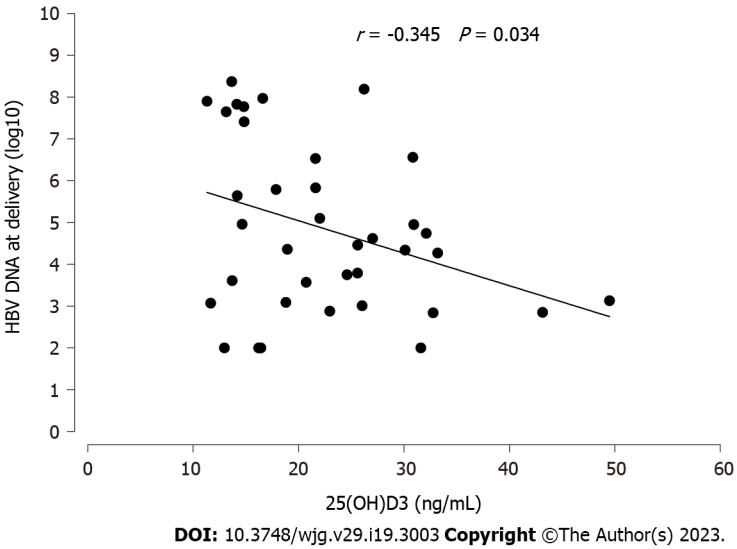
Taq1 AA	15 (65.2%)	9 (60%)	0.744	NA
AG/GG	8 (34.8%)	6 (40%)		
Apa1 CC	10 (43.5%)	7 (46.7%)	0.847	NA
CA/AA	13 (56.5%)	8 (53.3%)		

VDR SNPs: Single nucleotide polymorphisms of the vitamin D receptor gene; BMI: Body mass index; HBsAg: Hepatitis B surface antigen; HBeAg: Hepatitis B e antigen; HBV: Hepatitis B virus; WBC: White blood cell; ALT: Alanine aminotransferase; GGT: Gamma-glutamyl transferase; IQR: Interquartile range; NA: Not available.

Table 2 Factors associated with hepatitis B viral deoxyribonucleic acid serum concentration (log10 IU/mL)

Variable	*P* value, univariate	*P* value, multivariate	Standard beta, multivariate
Age (yr)	0.377		
BMI (kg/m^2)	0.049	0.03	-0.245
25(OH)D3 (ng/mL)	0.034	< 0.0001	-0.446
HBsAg (log10 IU/mL)	0.007		
HBV DNA log10	0.046		
Alkaline phosphatase	0.056		
HBeAg log10	0.025		
WBC count	0.064		
Maternal HBsAg at delivery, log10	0.003	0.05	0.285
Maternal alkaline phosphatase at delivery	0.025		
Maternal cholesterol at delivery	0.001	0.015	0.341

HBV: Hepatitis B virus; BMI: Body mass index; 25(OH)D3: 25-hydroxyvitamin D3; HBsAg: Hepatitis B surface antigen; WBC: White blood cell.



DOI: 10.3748/wjg.v29.i19.3003 **Copyright** ©The Author(s) 2023.

Figure 1 Correlation between maternal hepatitis B virus deoxyribonucleic acid levels at delivery (log10) and baseline serum 25-hydroxyvitamin D3 Levels. HBV: Hepatitis B virus; 25(OH)D3: 25-hydroxyvitamin D3.

was independently associated with targeted antiviral effects (maternal HBV DNA levels < 2 × 10^5 at delivery) in a multivariate regression model [OR 1.23 (1.04-1.44), *P* = 0.026], together with maternal VDR Cdx2 TT and cholesterol levels at delivery (Table 3).

Table 3 Factors associated with the targeted antiviral effects (hepatitis B viral deoxyribonucleic acid at delivery < 2 × 10^5)

Variable	Univariate	*P* value	Multivariate	*P* value
Age (yr, continuous)	1.034 (0.85-1.26)	0.745		0.727
BMI (kg/m^2, continuous)	1.18 (0.95-1.47)	0.146		0.071
25(OH) D3 (ng/mL, continuous)	1.16 (1.03-1.31)	0.014	1.23 (1.04-1.44)	0.026
VDR Cdx2 TT	0.2 (0.036-1.097)	0.064	0.09 (0.01-0.88)	0.039
Maternal GGT at delivery	0.94 (0.86-1.006)	0.075		0.05
Maternal VD at delivery (ng/mL, continuous)	1.1 (0.999-1.21)	0.053		0.385
Maternal alkaline phosphatase at delivery	0.98 (0.96-1.002)	0.081		0.64
Maternal cholesterol at delivery	0.47 (0.26-0.86)	0.015	0.39 (0.17-0.87)	0.021

BMI: Body mass index; 25(OH)D3: 25-hydroxyvitamin D3; VDR: Vitamin D receptor; GGT: Gamma-glutamyl transferase; VD: Vitamin D.

DISCUSSION

The present study showed that a high percentage (76.3%) of pregnant women with high HBV viral loads had deficient (< 20 ng/mL) or insufficient (≥ 20 but < 31 ng/mL) VD levels. There was a profound association between low serum 25(OH)D levels and higher levels of maternal HBV replication at delivery after TDF therapy. In a multiple linear regression analysis, maternal HBV DNA levels were associated with baseline maternal serum 25(OH)D levels, BMI, baseline maternal log10 HBsAg levels and cholesterol levels at delivery. Finally, we observed that baseline serum 25(OH)D levels, maternal VDR Cdx2 TT and cholesterol levels at delivery were associated with targeted antiviral effects (maternal HBV DNA levels < 2 × 10^5 at delivery) in a multivariate regression model.

In the human body, VD and its receptors are widely involved in a variety of life processes, regulating the nervous, immune and endocrine systems through related signaling pathways. Many studies have been conducted to reveal the association effect of VD and its receptors on HBV infection and its development. VD deficiency or declines can be detected in a variety of chronic liver diseases[5,7,16] and is associated with adverse clinical outcomes[9,16]. Abnormally low VD levels are highly prevalent among untreated patients with active chronic hepatitis B infection[6].

For a special group of people, such as pregnant females, VD is a vital nutrient that is important for both the mother and fetus in the perinatal period, and prenatal VD supplementation may reduce the risk of many adverse events and yield potential benefits. A previous study showed that pregnant women with HBV in China had lower VD levels than healthy pregnant women[10]. Our present study also showed that a high percentage (76.3%) of pregnant women with high HBV viral loads had deficient (18/38) or insufficient (11/38) VD levels, while only approximately 25.00% (9/38) had adequate VD levels. Our results suggested that abnormally low VD levels may be a common phenomenon in untreated pregnant women with high HBV viral loads in China.

Based on the evidence provided by a companion systematic review that addressed HBV DNA thresholds for identifying pregnant women at risk of MTCT, the WHO recommends administering TDF to pregnant women infected with HBV with high viral loads (≥ HBV DNA thresholds ≥ 2 × 10^5 IU/mL) from week 28 of pregnancy until at least childbirth to prevent MTCT, in addition to three doses of hepatitis B vaccination, including a birth dose given to the neonate. A recent meta-analysis showed that peripartum antiviral prophylaxis is highly effective at reducing the risk of the MTCT of HBV[17], which supports the 2020 WHO recommendation of administering antivirals during pregnancy, specifically TDF, for the prevention of the MTCT of HBV.

There is growing evidence that VD is associated with infectious diseases and immunity against infection and that VD supplementation has therapeutic potential in the treatment of infectious diseases [18,19]. Low maternal VD levels (< 32 ng/mL) were associated with a higher risk of the MTCT of HIV, and children born to women with low VD levels had a higher risk of death during follow-up[20]. Clinical and epidemiological studies support the role of VD in inhibiting HBV infection, and this antiviral effect is widely attributed to the VDR[11]. Hepatic VDR protein expression was significantly lower in patients with chronic HBV infection, and hepatic VDR expression was inversely correlated with hepatic inflammation and fibrosis[21], which could partly explain the more pronounced decrease in viral DNA in patients with higher VD levels after receiving antiviral therapy in our study.

The present study revealed a profound association between low serum 25(OH)D levels and higher levels of maternal HBV replication at delivery after TDF therapy. Consistent with our previous study, serum 25(OH)D levels were highly negatively correlated with HBV DNA levels[14]. Therefore, for HBV-infected patients, especially pregnant women, monitoring of VD levels is advocated, and increasing VD levels to a normal range in appropriate ways may be beneficial in maintaining low levels of HBV DNA.

It is expected that more in-depth studies will be performed to elucidate the mechanism of the effect of VD on HBV infection and its development, treatment and prognosis, which may offer attractive therapeutic opportunities for the treatment of chronic hepatitis B infection.

A number of studies have recently focused on the association between VDR SNPs and the disease characteristics of HBV infection. Some genotypes in VDR FokI increased the risk of HBV infection in a meta-analysis[22]. In addition, the VDR ApaI SNP was associated with viral load and the presence of HBsAg at different times, and pharmacogenetic data could help physicians identify HBV patients with a higher probability of achieving a good response[12]. In addition, VDR SNPs are correlated with HBV viral load and the severity of liver disease[23] and may be associated with occult hepatitis B infection [9]. Our results revealed that VDR Cdx2 TT was a hindering factor in achieving targeted antiviral therapeutic effects (HBV DNA levels < 2×10^5 at delivery) after TDF therapy. In pregnant women, increasing VD levels to within the normal range may help to achieve targeted antiviral treatment effects, especially in those with VDR Cdx2 TT. More basic and clinical studies are warranted for VD supplementation combined with antiviral therapy and immunoprophylaxis to block MTCT.

VD and cholesterol metabolism overlap significantly in the pathways that promote their biosynthesis and have a complex bidirectional relationship[24]. In our study, there was no significant difference in cholesterol levels between the full and partial responders before antiviral therapy, but cholesterol levels were lower in full responders after treatment. Similarly, in another study, for treatment-naive patients with chronic hepatitis B infection, total cholesterol levels showed a decreasing trend during 42 mo of TDF treatment[25]. Moreover, higher total cholesterol concentrations were associated with lower 25(OH)D concentrations[26], and VD supplementation appeared to have a beneficial effect on reducing total serum cholesterol levels[27]. In addition, VDR SNPs were associated with dyslipidemia in Chinese populations, and some variants may increase susceptibility to dyslipidemia[28]. Together, the difference in cholesterol levels after antiviral therapy may be due to differences in VD levels, VDR SNPs, and reactions to antiviral therapy.

Some limitations of the present study should be acknowledged. Most importantly, due to the type of study, the clinical correlations cannot be interpreted as causal relationships. Therefore, a suggestive functional link between VD metabolism and HBV replication remains elusive. Furthermore, the sample size included in this study was limited. Third, there are still some possible confounding factors that have not been considered. Although factors such as the season of blood collection were taken into account, other factors such as dietary habits, the duration of sunlight exposure and the ultraviolet intensity of pregnant women's living environments may also affect maternal VD levels.

CONCLUSION

In summary, we demonstrate a significant association between low serum levels of 25(OH)D and high levels of HBV replication in pregnant women with high HBV viral loads, and maternal VD levels as well as VDR SNPs may be associated with the efficacy of antiviral therapy. Future studies to evaluate the therapeutic value of VD and its analogs in reducing the MTCT of HBV may be justified.

ARTICLE HIGHLIGHTS

Research background

Mother-to-child transmission (MTCT) is the main route of hepatitis B virus (HBV) transmission, and HBV infection is associated with human vitamin D (VD) levels.

Research motivation

The role of VD and single nucleotide polymorphisms of the VD receptor gene (VDR SNPs) in blocking MTCT in pregnant women with high HBV viral load receiving antiviral therapy is unclear.

Research objectives

This study aimed to assess whether baseline VD levels and VDR SNPs are associated with the efficacy of tenofovir disoproxil fumarate (TDF) in the prevention of MTCT in pregnant women with high HBV viral loads.

Research methods

This retrospective study investigated VD levels, common clinical indicators, and virological parameters before and after antiviral therapy in 38 pregnant women with high HBV viral load, and further analyzed the effect of VD levels and VDR SNPs on the efficacy of TDF for the prevention of MTCT.

Research results

The present study showed that a high percentage (76.3%) of pregnant women with high HBV viral loads had deficient (< 20 ng/mL) or insufficient (≥ 20 but < 31 ng/mL) VD levels. There was a profound association between low serum 25-hydroxyvitamin D [25(OH)D] levels and higher levels of maternal HBV replication at delivery after TDF therapy. Multivariate logistic regression analysis showed that baseline serum 25(OH)D levels (OR = 1.23, 95%CI: 1.04-1.44), maternal VDR Cdx2 TT (OR = 0.09, 95%CI: 0.01-0.88) and cholesterol levels at delivery (OR = 0.39, 95%CI: 0.17-0.87) were associated with targeted antiviral effects (maternal HBV DNA levels < 2×10^5 at delivery).

Research conclusions

We demonstrate a significant association between low serum levels of 25(OH)D and high levels of HBV replication in pregnant women with high HBV viral loads, and maternal VD levels as well as VDR SNPs may be associated with the efficacy of antiviral therapy.

Research perspectives

Future studies to evaluate the therapeutic value of VD and its analogs in reducing the MTCT of HBV may be justified.

FOOTNOTES

Author contributions: Wang R and Zhu X contributed equally to this work; Ji YL, Zhu X and Chen YH participated in design and oversight of the study; Zhu X, Zhang X and Liu H collected and study data; Wang R, Zhu X, Zhang X, Liu H, and Chen YH analyzed the data and wrote the manuscript; Zhu X, Ji YL and Chen YH revised the manuscript for important intellectual content; all authors have read and approved the final manuscript.

Supported by the Key Research and Development Projects in Sichuan Province, No. 2021YFS0168; and the National Scientific and Technological Major Project for Infectious Diseases Control in China, No. 2018ZX10715-003.

Institutional review board statement: The study was reviewed approved by the Institutional Review Board of the West China Hospital, Sichuan University, approval No. 2019-151.

Informed consent statement: All study participants or their legal guardians provided informed written consent about personal and medical data collection prior to study enrollment.

Conflict-of-interest statement: All authors report no relevant conflict of interest for this article.

Data sharing statement: No additional data are available.

Open-Access: This article is an open-access article that was selected by an in-house editor and fully peer-reviewed by external reviewers. It is distributed in accordance with the Creative Commons Attribution NonCommercial (CC BY-NC 4.0) license, which permits others to distribute, remix, adapt, build upon this work non-commercially, and license their derivative works on different terms, provided the original work is properly cited and the use is non-commercial. See: https://creativecommons.org/Licenses/by-nc/4.0/

Country/Territory of origin: China

ORCID number: Rui Wang 0000-0003-0829-152X; Yong-Hua Chen 0000-0001-8485-0755.

S-Editor: Yan JP
L-Editor: A
P-Editor: Yuan YY

REFERENCES

1 **Xu Y**, Liu H, Wang Y, Hao R, Li Z, Song H. The next step in controlling HBV in China. *BMJ* 2013; **347**: f4503 [PMID: 23861426 DOI: 10.1136/bmj.f4503]
2 **Waheed Y**, Siddiq M, Jamil Z, Najmi MH. Hepatitis elimination by 2030: Progress and challenges. *World J Gastroenterol* 2018; **24**: 4959-4961 [PMID: 30510370 DOI: 10.3748/wjg.v24.i44.4959]
3 **Liu Z**, Chen Z, Cui F, Ding Y, Gao Y, Han G, Jia J, Li J, Li Z, Liu Y, Mao Q, Wang A, Wang W, Wei L, Xia J, Xie Q, Yang X, Yin X, Zhang H, Zhang L, Zhang W, Zhuang H, Dou X, Hou J. Management Algorithm for Prevention of Mother-to-child Transmission of Hepatitis B Virus (2022). *J Clin Transl Hepatol* 2022; **10**: 1004-1010 [PMID: 36304493 DOI: 10.14218/JCTH.2022.00047]
4 **Hou J**, Cui F, Ding Y, Dou X, Duan Z, Han G, Jia J, Mao Q, Li J, Li Z, Liu Z, Wei L, Xie Q, Yang X, Zhang H, Zhuang

H. Management Algorithm for Interrupting Mother-to-Child Transmission of Hepatitis B Virus. *Clin Gastroenterol Hepatol* 2019; **17**: 1929-1936.e1 [PMID: 30312789 DOI: 10.1016/j.cgh.2018.10.007]

5 **Pop TL**, Sîrbe C, Benţa G, Mititelu A, Grama A. The Role of Vitamin D and Vitamin D Binding Protein in Chronic Liver Diseases. *Int J Mol Sci* 2022; **23** [PMID: 36142636 DOI: 10.3390/ijms231810705]

6 **Chan HL**, Elkhashab M, Trinh H, Tak WY, Ma X, Chuang WL, Kim YJ, Martins EB, Lin L, Dinh P, Charuworn P, Foster GR, Marcellin P. Association of baseline vitamin D levels with clinical parameters and treatment outcomes in chronic hepatitis B. *J Hepatol* 2015; **63**: 1086-1092 [PMID: 26143444 DOI: 10.1016/j.jhep.2015.06.025]

7 **Farnik H**, Bojunga J, Berger A, Allwinn R, Waidmann O, Kronenberger B, Keppler OT, Zeuzem S, Sarrazin C, Lange CM. Low vitamin D serum concentration is associated with high levels of hepatitis B virus replication in chronically infected patients. *Hepatology* 2013; **58**: 1270-1276 [PMID: 23703797 DOI: 10.1002/hep.26488]

8 **Hoan NX**, Tong HV, Song LH, Meyer CG, Velavan TP. Vitamin D deficiency and hepatitis viruses-associated liver diseases: A literature review. *World J Gastroenterol* 2018; **24**: 445-460 [PMID: 29398866 DOI: 10.3748/wjg.v24.i4.445]

9 **Wong GL**, Chan HL, Chan HY, Tse CH, Chim AM, Lo AO, Wong VW. Adverse effects of vitamin D deficiency on outcomes of patients with chronic hepatitis B. *Clin Gastroenterol Hepatol* 2015; **13**: 783-90.e1 [PMID: 25445773 DOI: 10.1016/j.cgh.2014.09.050]

10 **Gao XR**, Wang CM, Wang WJ, Han GR, Zhang JQ. Serum 25-hydroxyvitamin D status in pregnant women with chronic hepatitis B virus infection. *J Infect Dev Ctries* 2016; **10**: 851-856 [PMID: 27580331 DOI: 10.3855/jidc.6600]

11 **Ahluwalia S**, Choudhary D, Tyagi P, Kumar V, Vivekanandan P. Vitamin D signaling inhibits HBV activity by directly targeting the HBV core promoter. *J Biol Chem* 2021; **297**: 101233 [PMID: 34562448 DOI: 10.1016/j.jbc.2021.101233]

12 **Cusato J**, Boglione L, De Nicolò A, Imbornone R, Cardellino CS, Ghisetti V, Carcieri C, Cariti G, Di Perri G, D'Avolio A. Association of vitamin D pathway SNPs and clinical response to interferon in a cohort of HBeAg-negative patients. *Pharmacogenomics* 2017; **18**: 651-661 [PMID: 28453395 DOI: 10.2217/pgs-2016-0041]

13 **Zhu X**, Wang J, Wang M, Du LY, Ji YL, Zhang X, Tang H. The positive rates of hepatitis B surface antibody in youth after booster vaccination: a 4-year follow-up study with large sample. *Biosci Rep* 2021; **41** [PMID: 34151935 DOI: 10.1042/BSR20210182]

14 **Chen EQ**, Bai L, Zhou TY, Fe M, Zhang DM, Tang H. Sustained suppression of viral replication in improving vitamin D serum concentrations in patients with chronic hepatitis B. *Sci Rep* 2015; **5**: 15441 [PMID: 26486883 DOI: 10.1038/srep15441]

15 **Lankes U**, Elder PA, Lewis JG, George P. Differential extraction of endogenous and exogenous 25-OH-vitamin D from serum makes the accurate quantification in liquid chromatography-tandem mass spectrometry assays challenging. *Ann Clin Biochem* 2015; **52**: 151-160 [PMID: 24714680 DOI: 10.1177/0004563214533316]

16 **Huang CZ**, Zhang J, Zhang L, Yu CH, Mo Y, Mo LY. Serum vitamin D and vitamin-D-binding protein levels in children with chronic hepatitis B. *World J Gastroenterol* 2021; **27**: 255-266 [PMID: 33519140 DOI: 10.3748/wjg.v27.i3.255]

17 **Funk AL**, Lu Y, Yoshida K, Zhao T, Boucheron P, van Holten J, Chou R, Bulterys M, Shimakawa Y. Efficacy and safety of antiviral prophylaxis during pregnancy to prevent mother-to-child transmission of hepatitis B virus: a systematic review and meta-analysis. *Lancet Infect Dis* 2021; **21**: 70-84 [PMID: 32805200 DOI: 10.1016/S1473-3099(20)30586-7]

18 **Ismailova A**, White JH. Vitamin D, infections and immunity. *Rev Endocr Metab Disord* 2022; **23**: 265-277 [PMID: 34322844 DOI: 10.1007/s11154-021-09679-5]

19 **White JH**. Emerging Roles of Vitamin D-Induced Antimicrobial Peptides in Antiviral Innate Immunity. *Nutrients* 2022; **14** [PMID: 35057465 DOI: 10.3390/nu14020284]

20 **Mehta S**, Hunter DJ, Mugusi FM, Spiegelman D, Manji KP, Giovannucci EL, Hertzmark E, Msamanga GI, Fawzi WW. Perinatal outcomes, including mother-to-child transmission of HIV, and child mortality and their association with maternal vitamin D status in Tanzania. *J Infect Dis* 2009; **200**: 1022-1030 [PMID: 19673647 DOI: 10.1086/605699]

21 **Yang K**, Pan Y, Zhang H, Jin L, Wang X. Hepatic vitamin D receptor expression is negatively associated with liver inflammation and fibrosis in patients with chronic HBV infection. *Clin Exp Med* 2022 [PMID: 36289101 DOI: 10.1007/s10238-022-00919-9]

22 **He Q**, Huang Y, Zhang L, Yan Y, Liu J, Song X, Chen W. Association between vitamin D receptor polymorphisms and hepatitis B virus infection susceptibility: A meta-analysis study. *Gene* 2018; **645**: 105-112 [PMID: 29248582 DOI: 10.1016/j.gene.2017.12.027]

23 **Suneetha PV**, Sarin SK, Goyal A, Kumar GT, Shukla DK, Hissar S. Association between vitamin D receptor, CCR5, TNF-alpha and TNF-beta gene polymorphisms and HBV infection and severity of liver disease. *J Hepatol* 2006; **44**: 856-863 [PMID: 16545485 DOI: 10.1016/j.jhep.2006.01.028]

24 **Warren T**, McAllister R, Morgan A, Rai TS, McGilligan V, Ennis M, Page C, Kelly C, Peace A, Corfe BM, Mc Auley M, Watterson S. The Interdependency and Co-Regulation of the Vitamin D and Cholesterol Metabolism. *Cells* 2021; **10** [PMID: 34440777 DOI: 10.3390/cells10082007]

25 **Zhang Q**, Liang J, Yin J, Jiang Y, Yu N, Liao X, Zhao S, Wu L, Fan R. Real-life impact of tenofovir disoproxil fumarate and entecavir therapy on lipid profile, glucose, and uric acid in chronic hepatitis B patients. *J Med Virol* 2022; **94**: 5465-5474 [PMID: 35794065 DOI: 10.1002/jmv.27977]

26 **Vitezova A**, Voortman T, Zillikens MC, Jansen PW, Hofman A, Uitterlinden AG, Franco OH, Kiefte-de Jong JC. Bidirectional associations between circulating vitamin D and cholesterol levels: The Rotterdam Study. *Maturitas* 2015; **82**: 411-417 [PMID: 26358932 DOI: 10.1016/j.maturitas.2015.08.005]

27 **Dibaba DT**. Effect of vitamin D supplementation on serum lipid profiles: a systematic review and meta-analysis. *Nutr Rev* 2019; **77**: 890-902 [PMID: 31407792 DOI: 10.1093/nutrit/nuz037]

28 **Jia J**, Tang Y, Shen C, Zhang N, Ding H, Zhan Y. Vitamin D receptor polymorphism rs2228570 is significantly associated with risk of dyslipidemia and serum LDL levels in Chinese Han population. *Lipids Health Dis* 2018; **17**: 193 [PMID: 30119682 DOI: 10.1186/s12944-018-0819-0]

World Journal of Gastroenterology

Submit a Manuscript: https://www.f6publishing.com

World J Gastroenterol 2023 May 21; 29(19): 3013-3026

DOI: 10.3748/wjg.v29.i19.3013

ISSN 1007-9327 (print) ISSN 2219-2840 (online)

ORIGINAL ARTICLE

Observational Study

Gastrointestinal manifestations of long-term effects after COVID-19 infection in patients with dialysis or kidney transplantation: An observational cohort study

Wiwat Chancharoenthana, Supitcha Kamolratanakul, Asada Leelahavanichkul, Wassawon Ariyanon, Sutatip Chinpraditsuk, Rattanaporn Saelim, Somratai Vadcharavivad, Weerapong Phumratanaprapin, Polrat Wilairatana

Specialty type: Gastroenterology and hepatology

Provenance and peer review: Invited article; Externally peer reviewed.

Peer-review model: Single blind

Peer-review report's scientific quality classification

Grade A (Excellent): 0
Grade B (Very good): B
Grade C (Good): C
Grade D (Fair): 0
Grade E (Poor): 0

P-Reviewer: Awad AK, Egypt; Nooripour R, Iran

Received: January 12, 2023
Peer-review started: January 12, 2023
First decision: February 4, 2023
Revised: February 13, 2023
Accepted: April 21, 2023
Article in press: April 21, 2023
Published online: May 21, 2023

Wiwat Chancharoenthana, Supitcha Kamolratanakul, Weerapong Phumratanaprapin, Polrat Wilairatana, Department of Clinical Tropical Medicine, Faculty of Tropical Medicine, Mahidol University, Bangkok 10400, Thailand

Asada Leelahavanichkul, Department of Microbiology, Faculty of Medicine, Chulalongkorn University, Bangkok 10330, Thailand

Wassawon Ariyanon, Cardiometabolic Centre, Department of Medicine, Bangkok Nursing Hospital, Bangkok 10500, Thailand

Sutatip Chinpraditsuk, Rattanaporn Saelim, Dialysis Center, Hospital for Tropical Diseases, Faculty of Tropical Medicine, Mahidol University, Bangkok 10400, Thailand

Somratai Vadcharavivad, Department of Pharmacy Practice, Faculty of Pharmaceutical Sciences, Chulalongkorn University, Bangkok 10330, Thailand

Corresponding author: Supitcha Kamolratanakul, MD, Assistant Professor, Department of Clinical Tropical Medicine, Faculty of Tropical Medicine, Mahidol University, 420/6 Ratchawithi Rd, Thung Phaya Thai, Ratchathewi, Bangkok 10400, Thailand.
supitcha.kam@mahidol.edu

Abstract

BACKGROUND

Prolonged symptoms after corona virus disease 2019 (Long-COVID) in dialysis-dependent patients and kidney transplant (KT) recipients are important as a possible risk factor for organ dysfunctions, especially gastrointestinal (GI) problems, during immunosuppressive therapy.

AIM

To identify the characteristics of GI manifestations of Long-COVID in patients with dialysis-dependent or KT status.

METHODS

This observational, prospective study included patients with COVID-19 infection,

confirmed by reverse transcription polymerase chain reaction, with the onset of symptoms between 1 January 2022 and 31 July 2022 which was explored at 3 mo after the onset, either through the out-patient follow-up or by telephone interviews.

RESULTS

The 645 eligible participants consisted of 588 cases with hemodialysis (HD), 38 patients with peritoneal dialysis (PD), and 19 KT recipients who were hospitalized with COVID-19 infection during the observation. Of these, 577 (89.5%) cases agreed to the interviews, while 64 (10.9%) patients with HD and 4 (10.5%) cases of PD were excluded. The mean age was 52 ± 11 years with 52% women. The median dialysis duration was 7 ± 3 and 5 ± 1 years for HD and PD groups, respectively, and the median time post-transplantation was 6 ± 2 years. Long-COVID was identified in 293/524 (56%) and 21/34 (62%) in HD and PD, respectively, and 7/19 (37%) KT recipients. Fatigue was the most prevalent (96%) of the non-GI tract symptoms, whereas anorexia (90.9%), loss of taste (64.4%), and abdominal pain (62.5%) were the first three common GI manifestations of Long-COVID. Notably, there were 6 cases of mesenteric panniculitis from 19 patients with GI symptoms in the KT group.

CONCLUSION

Different from patients with non-chronic kidney disease, there was a high prevalence of GI manifestations of Long-COVID in dialysis-dependent patients and KT recipients. An appropriate long-term follow-up in these vulnerable populations after COVID-19 infection is possibly necessary.

Key Words: COVID-19; Kidney transplant; Post-acute COVID-19 syndrome; Long-COVID-19; Gastrointestinal; SARS-CoV-2

©The Author(s) 2023. Published by Baishideng Publishing Group Inc. All rights reserved.

Core Tip: Prolonged symptoms after coronavirus disease 2019 (COVID-19) or prolonged symptoms after COVID-19 (Long-COVID) in dialysis-dependent patients and kidney transplant (KT) recipients are important as a possible risk factor for organ dysfunctions, especially gastrointestinal (GI) problems. In this study, we observed that a GI manifestation of Long-COVID is a frequent condition in patients with dialysis-dependence and kidney-transplant recipients. Long-COVID was significantly more prevalent in peritoneal dialysis patients than in hemodialysis patient or KT cases. We also found that patients who experienced either abdominal pain or diarrhea had a longer duration of other GI manifestations of Long-COVID, suggesting a need for closer observation of these patients during COVID-19 infection.

Citation: Chancharoenthana W, Kamolratanakul S, Leelahavanichkul A, Ariyanon W, Chinpraditsuk S, Saelim R, Vadcharavivad S, Phumratanaprapin W, Wilairatana P. Gastrointestinal manifestations of long-term effects after COVID-19 infection in patients with dialysis or kidney transplantation: An observational cohort study. *World J Gastroenterol* 2023; 29(19): 3013-3026

URL: https://www.wjgnet.com/1007-9327/full/v29/i19/3013.htm

DOI: https://dx.doi.org/10.3748/wjg.v29.i19.3013

INTRODUCTION

The coronavirus disease (COVID-19) pandemic has a significant impact on the management of dialysis-dependent patients and kidney transplant (KT) recipients, while the chronic kidney disease (CKD) condition in these patients is also affecting the clinical manifestation of COVID-19 infection. The persistence of post-COVID-19 syndrome for weeks to months after the infection is a growing public health concern worldwide[1]. Currently, the definition of post-acute COVID-19 syndrome (PACS), also known as the post-acute sequelae of severe acute respiratory syndrome coronavirus 2 (PASC) or prolonged symptoms after COVID-19 (Long-COVID) syndrome, depends on the population being studied, the post-infection timing, and the assessment tools[2,3]. Moreover, the overlap in its pathophysiology between overwhelming pro-inflammatory immune responses and direct viral cytopathic effects remains inconclusive[4]. In general, PACS mainly includes fatigue, pain, headache, neurological and cognitive impairments, cardio-pulmonary symptoms, and anosmia-dysgeusia[5]. The British National Institute for Health and Care Excellence (NICE) defines Long-COVID as any signs and symptoms that develop during or after an infection consistent with COVID-19, continue for over 12 wk,

and cannot be explained by an alternative diagnosis[6]. A clinical case definition of Long-COVID by a Delphi consensus has crystallized the case definition of Long-COVID as clinical symptoms that occur in individuals with a history of probable or confirmed severe acute respiratory syndrome coronavirus 2 (SARS-CoV-2) infection, usually 3 mo from the onset of COVID-19 with symptoms, that last for at least 2 mo without an alternative explainable condition[7].

Both dialysis-dependent patients and KT recipients are classified as vulnerable populations due to their immunosuppressive status derived from their CKD condition and the high number of comorbidities[8]. Thus, a more frequent prevalence of long-term after-effects of COVID-19 infection than in the general population is possible. Accordingly, aggressive approaches, along with prompt management of acute illness, should be used in these populations, making the subject of Long-COVID even more challenging. Recent reports have revealed an incidence of post-COVID-19 syndrome in dialysis patients and KT recipients of approximately 40%-70% of those who experience a COVID-19 infection[9-13]. The Long-COVID symptoms include respiratory-related symptoms, fatigue, peripheral neuropathy, venous thromboembolism, memory impairment, and *de novo* diabetes mellitus[9-11]. Notably, 60% of dialysis patients *vs* 10% of KT recipients had residual symptoms at 6 mo post-COVID-19 infection[11,14].

Even without the gastrointestinal (GI) symptoms, the severity of COVID-19 is associated with the GI tract as the translocation of pathogen molecules from the gut into the blood circulation (leaky gut) is reported[15], possibly from a quiescent the SARS-CoV-2 infection in the intestine[16]. Indeed, the cell entry of SARS-CoV-2 virus through angiotensin-converting enzyme 2 (ACE2) receptors on the squamous and columnar epithelial cells, including enterocytes, is well-known[17]. One large study of hospitalized COVID-19 revealed that 30% of the patients reported GI symptoms, such as abdominal pain, nausea and vomiting, and diarrhea, in addition to their respiratory tract symptoms[18]. Nevertheless, the impacts of COVID-19 infection, and particularly Long-COVID-19, in the GI spectrum is not fully understood in either dialysis patients or KT patients, and data on this topic remains scarce. Of note, data from the most recent report on post-acute SARS-CoV-2 infection sub-phenotype by Zhang *et al*[19] found that GI tract-related symptoms are one of the four most common characteristics in post-acute viral symptoms.

Hence, the aim of the present study was to determine the prevalence and characteristics of Long-COVID in a cohort of these patients. We hypothesize that Long-COVID, especially in the GI symptoms, may be underestimated in these populations and may need more clarification, particularly in the post-pandemic period.

MATERIALS AND METHODS

Study populations

The study is a cohort longitudinal study performed in dialysis-dependent patients and KT recipients with COVID-19 infection under the care of three renal referral tertiary care centers. Eligible participants were those with a diagnosis of COVID-19 confirmed by an RT-PCR test from oro-nasopharyngeal swabs from January 2022 to 31 July 2022. The KT recipients with the following conditions were excluded: (1) Those who died before the follow-up interview, (2) those we were unable to contact, and (3) those without or unable to provide informed consent. The remaining dialysis-dependent patients and KT recipients who had experienced a post-COVID-19 infection for at least 3 mo were included in the study. Purposive sampling was used in order to ensure the representation of a range of characteristics and experiences of analytic relevance. Informed consent for participation in interviews was obtained either written or verbally over the phone from all participants in the study and the study was approved by the Research Ethics Commission of the Faculty of Tropical Medicine, Mahidol University, Thailand (MUTM 2022-081-01) along with adhered to STROBE guideline.

Interview conduct and data collection

An interview consisting of a set of open-ended questions regarding symptoms during COVID-19 and post-COVID-19 infection periods. Then, interviews were designed to explore the specific persistent or emerging symptoms potentially due to GI tract-associated Long COVID-19 syndrome, as previously described[20]. Participants were interviewed either in person or by telephone by trained research nurses. Participants were considered to have GI tract-associated symptoms of Long COVID-19 if they showed one of the following signs: loss of appetite, nausea, weight loss, abdominal pain, heartburn, dysphagia, diarrhea, constipation, altered bowel motility, or irritable bowel syndrome[20]. In addition, the participant's electronic medical records were used to obtain clinical data, including baseline demographics and transplant-related immunological risk, comorbidity, and data about COVID-19 admission. Although abnormal laboratory tests, such as elevated alanine aminotransferase, can present as GI tract-associated Long COVID-19 syndrome[21], only clinical signs and symptoms were explored in the present study.

Statistical analysis

Descriptive characteristics were presented as means and standard deviation (means ± SD) unless otherwise noted. The Kolmogorov-Smirnov and Levene's tests were performed to establish data distribution and homogeneity, respectively. Chi-square tests were performed to compare categorical variables, whereas Tukey-Kramer multiple comparisons were used for continuous variables. Independent risk factors were assessed by applying a backward elimination stepwise binary regression and removing the least significant variables at each step. Odds ratios (ORs) and 95% confidence intervals (CIs) were estimated. $P < 0.05$ was considered statistically significant. Data analysis was performed using the PASW 18.0.0 statistical software package (SPSS Inc., Chicago, IL, United States) and GraphPad Prism 9.3.1 software (GraphPad Software, Inc., La Jolla, CA, United States).

RESULTS

Comparison baseline characteristics among participants of hemodialysis, peritoneal dialysis, and kidney transplantation

This study enrolled 645 eligible participants with COVID-19 infection, including 588 cases with hemodialysis (HD), 38 patients with peritoneal dialysis (PD), and 19 KT recipients. Of these, 577 (89.5%) participants agreed to interviews (Figure 1). All eligible KT recipients were enrolled in the study, and none of the transplant recipients in the KT cohort died or returned to dialysis.

The mean patient age was 52 ± 11 years, 300 (52%) were women, and the median dialysis duration was 7 ± 3 and 5 ± 1 years in the HD and PD groups, respectively. Hypertension (92%) and type 2 diabetes mellitus (77%) were the two most common comorbidities among the three groups of participants. The mean post-transplantation time was 6 ± 2 years (Table 1). Most of the HD patients had three dialysis sessions per week while continuous ambulatory PD (CAPD) was the most treatment modality used in PD patients. The three most common initial symptoms detected in both the dialysis and KT cohorts were fever (98%), coryza (96%), and cough (94%). Of note, the PD patients had a significant predominance of all symptoms compared to the HD and KT groups (P <0.0001); this could be because the highest comorbidities and uttermost severity of COVID-19 were observed in the PD group. For this reason, the combination therapy of Remdesivir (88.2%) and tocilizumab (63.1%) was prescribed significantly more frequently in this group with also correspondent the highest mean levels of both high-sensitivity C-reactive protein and D-dimer compared with HD and KT groups ($P < 0.0001$) (Table 1).

Different prevalence of GI manifestations of Long-COVID among the dialysis-dependent and KT populations

The Thai national guidelines for COVID-19 management in high-risk patients (during this study period) stipulate that all patients with CKD or CKD-equivalent disorders must be hospitalized for intensive care and monitoring during acute COVID-19 infection. As such, all participants in the study were hospitalized. During the early post-COVID-19 infection period, Long-COVID was identified in 293/524 (56%) of the HD, 21/34 (62%) of the PD, and 7/19 (37%) of the KT groups. Fatigue was the most prevalent symptom (96%) of the non-GI tract symptoms and was accompanied by loss of appetite or anorexia (81%), loss of taste (63%), hoarse voice (28%), unusual muscle pains (23%), hair loss (22%), a persistent cough (22%), headache (11%), and impaired cognitive and memory function (9%). Among the GI manifestations of Long-COVID, anorexia was the most prevalent symptom (525 cases, 90.9% from all groups), followed by loss of taste (372 cases, 64% from all groups), and abdominal pain (367 cases, 62.5% from all groups) (Figure 2A). Although anorexia and loss of taste were common in all three groups, they were more predominant in dialysis patients, but most cases showed much improvement by two months after the onset of COVID-19 infection. Abdominal pain and diarrhea were the symptoms that persisted for over 3 mo (Figure 2B).

Notably, our investigation of the causes of abdominal pain, which was reported by 87% of the patients, revealed that non-specific abdominal pain or probably acute gastritis was the main etiology in dialysis-dependent patients, whereas mesenteric panniculitis was the main etiology of abdominal pain (6 from 19 cases) in the KT group with a good response to oral corticosteroids (20 mg prednisolone), which were slowly tapered off in 8 wk. All six cases of mesenteric panniculitis had complete resolution, as indicated by the follow-up abdominal computer tomography.

Figure 2C shows the factors associated with the GI manifestation of Long-COVID. We found that COVID-19 patients who were older than 65 years (ORs 2.00, 95%CIs 1.2-2.8), who had chronic lung disease (ORs 2.10, 95%CIs 1.1-4.2), who were on PD (ORs 1.80, 95%CIs 1.4-2.5), or who had high levels of both C-reactive protein (CRP) and D-dimer at the onset (ORs 4.40, 95%CIs 1.4-8.8) were significantly likely to have GI manifestations of Long-COVID.

Table 1 Baseline characteristics and clinical presentation of corona virus disease 2019 in participants with or without gastrointestinal tract symptoms related to prolonged symptoms after corona virus disease 2019 at enrollment

Variables	Hemodialysis (*n* = 524)	Peritoneal dialysis (*n* = 34)	Kidney Transplantation (*n* = 19)	*P* value
Age, yr, mean ± SD	48 ± 9	71 ± 12	44 ± 12	< 0.001[a,b]
Female sex, *n* (%)	278 (53.1)	14 (41.2)	8 (42.1)	NS
Body mass index, kg/m2, mean ± SD	26 ± 4	23 ± 2	24 ± 4	< 0.001[a]
Comorbidities, *n* (%)				
Hypertension	487 (92.9)	34 (100)	12 (63.2)	< 0.0001[b], 0.0002[c]
Diabetes	408 (77.9)	30 (88.2)	6 (31.6)	< 0.0001[b,c]
Cardiovascular disease	450 (85.9)	28 (82.4)	9 (47.4)	< 0.0001[b], 0.008[c]
Pulmonary disease	52 (9.9)	5 (14.7)	1 (5.3)	NS
Hepatic disease	14 (2.7)	4 (11.8)	0 (0)	0.004[a]
Renal replacement therapy				
Dialysis vintage, years	7 ± 3	5 ± 1	6 ± 2	< 0.001[a]
Frequency, 2× per week, *n* (%)	84 (16.0)	N/A	N/A	
Frequency, 3× per week, *n* (%)	440 (84.0)	N/A	N/A	
CAPD, *n* (%)	N/A	32 (94.1)	N/A	
APD, *n* (%)	N/A	2 (5.9)	N/A	
Deceased donor transplant, *n* (%)	N/A	N/A	11 (57.9)	
Time from transplant, yr, mean ± SD	N/A	N/A	6 ± 2	< 0.001[b,c]
Maintenance immunosuppressive regimen by drug, *n* (%)				
Calcineurin inhibitors				
TAC	N/A	N/A	11 (57.9)	
CsA	N/A	N/A	8 (42.1)	
Prednisolone	N/A	N/A	19 (100)	
Antimetabolites				
MPA	N/A	N/A	16 (84.2)	
Azathioprine	N/A	N/A	0 (0)	
mTOR inhibitors	N/A	N/A	3 (15.8)	
Baseline creatinine, mean ± SD	8 ± 2	11 ± 2	2.5 ± 0.8	< 0.001[a,b,c]
Baseline creatinine > 1.5 mg/dL, *n* (%)[1]	N/A	N/A	7 (36.8)	
Day(s) of illness, mean ± SD	4 ± 2	3 ± 1	3 ± 1	< 0.001[a]
Initial symptoms, *n* (%)				
Fever or chills	511 (97.5)	34 (100)	19 (100)	NS
Cough	488 (93.1)	34 (100)	18 (94.7)	NS
Dyspnea	321 (61.3)	30 (88.2)	16 (84.2)	0.002[a], 0.043[b]
Chest pain	152 (29.0)	11 (32.4)	8 (42.1)	NS
Coryza	501 (95.6)	34 (100)	19 (100)	NS
Headache	161 (30.7)	5 (14.7)	6 (31.6)	0.048[a]
Nasal congestion	359 (68.5)	9 (26.5)	11 (57.9)	< 0.0001[a], 0.025[c]
Fatigue	209 (40.0)	34 (100)	9 (47.4)	< 0.0001[a], < 0.0001[c]
Myalgia	386 (73.7)	31 (91.2)	12 (63.2)	0.023[a], 0.013[c]

Nausea or vomiting	137 (26.1)	30 (88.2)	4 (21.1)	< 0.0001[a,c]
Diarrhea	83 (15.8)	25 (73.5)	3 (15.8)	< 0.0001[a,c]
Anosmia	66 (12.6)	7 (20.6)	1 (5.3)	NS
Ageusia	25 (4.8)	6 (17.6)	2 (10.5)	0.002[a]
Number of symptoms, mean ± SD	7 ± 2	9 ± 1	4 ± 2	< 0.0001[a,b,c]
COVID-19 severity, *n* (%)				
Mild	252 (48.1)	2 (5.9)	0 (0)	< 0.0001[a,b]
Moderate	137 (26.1)	7 (20.6)	4 (21.1)	NS
Severe	135 (25.8)	25 (73.5)	0 (0)	< 0.0001[a,c], 0.011[b]
High-sensitivity C-reactive protein (mg/L)	32 ± 14	59 ± 11	17 ± 9	< 0.0001[a,b,c]
D-dimer (ng/mL)	2749 ± 578	5339 ± 786	1699 ± 175	< 0.0001[a,b,c]
Treatments, *n* (%)				
Remdesivir	352 (67.2)	30 (88.2)	8 (42.1)	0.011[a], 0.023[b], 0.0004[c]
Favipiravir	172 (32.8)	4 (11.8)	11 (57.9)	0.011[a], 0.023[b], < 0.001[c]
Tocilizumab	39 (7.4)	12 (63.1)	0 (0)	< 0.0001[a,c]
Corticosteroids	429 (81.9)	34 (100)	19 (100)	0.007[a], 0.041[b]
Low-molecular weight heparin	482 (92.0)	32 (94.1)	7 (36.8)	< 0.0001[b,c]
Outcomes during the acute phase, *n* (%)				
Hospitalization	524 (100)	34 (100)	19 (100)	-
Intensive care unit	204 (38.9)	27 (79.4)	4 (21.1)	< 0.0001[a,c]
Oxygen therapy	272 (51.9)	32 (94.1)	4 (21.1)	< 0.0001[a,c], 0.008[b]
Invasive mechanical ventilation	104 (19.8)	23 (67.6)	0 (0)	< 0.0001[a,c], 0.031[b]
Increased dialysis frequency	178 (34.0)	0 (0)	N/A	< 0.0001[a]
Immunosuppression suspended except for steroids[1]	N/A	N/A	2 (10.5)	

[1]Only kidney transplant recipient group.

Only the comparisons between following groups with statistical significance are shown.

[a]Hemodialysis *vs* peritoneal dialysis group.

[b]Hemodialysis *vs* kidney transplantation group.

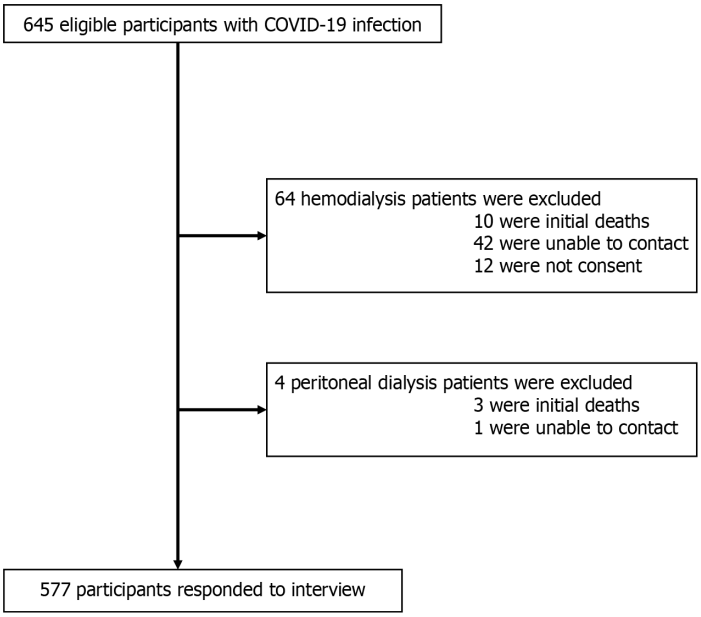
[c]Peritoneal dialysis *vs* kidney transplantation group.

APD: Automated peritoneal dialysis; COVID-19: Coronavirus disease 2019; CAPD: Continuous ambulatory peritoneal dialysis; CsA: Cyclosporin A; MPA: Mycophenolate; mTORi: Mammalian target of rapamycin inhibitors; TAC: Tacrolimus; N/A: Not applicable; NS: Non-significant.

DISCUSSION

In this study, we observed that a GI manifestation of Long-COVID is a frequent condition in patients with dialysis dependence and KT recipients. Long-COVID was significantly more prevalent in PD patients than in HD or KT cases. Notably, patients who experienced either abdominal pain or diarrhea had a longer duration of other GI manifestations of Long-COVID, suggesting a need for closer observation of these patients during COVID-19 infection.

COVID-19 has brought forth a multitude of challenges to healthcare systems across the globe. Apart from the significant morbidity and mortality associated with COVID-19 during its initial phase, recognition and concern are growing regarding the long-term consequences of COVID-19[2,3,22]. Dialysis-dependent patients and KT recipients are clearly high-risk groups associated with higher numbers of comorbidities and immunosuppressive issues and require more aggressive courses of COVID-19 treatment in terms of acute and chronic complications[8,23,24]. Although the most visible manifestation of Long-COVID in the general population is asthenia, or brain fog[22,25], we found that anorexia was the most common GI manifestation of Long-COVID in both dialysis-dependent patients and KT recipients, followed by abdominal pain and loss of taste (Figure 2A).



DOI: 10.3748/wjg.v29.i19.3013 **Copyright** ©The Author(s) 2023.

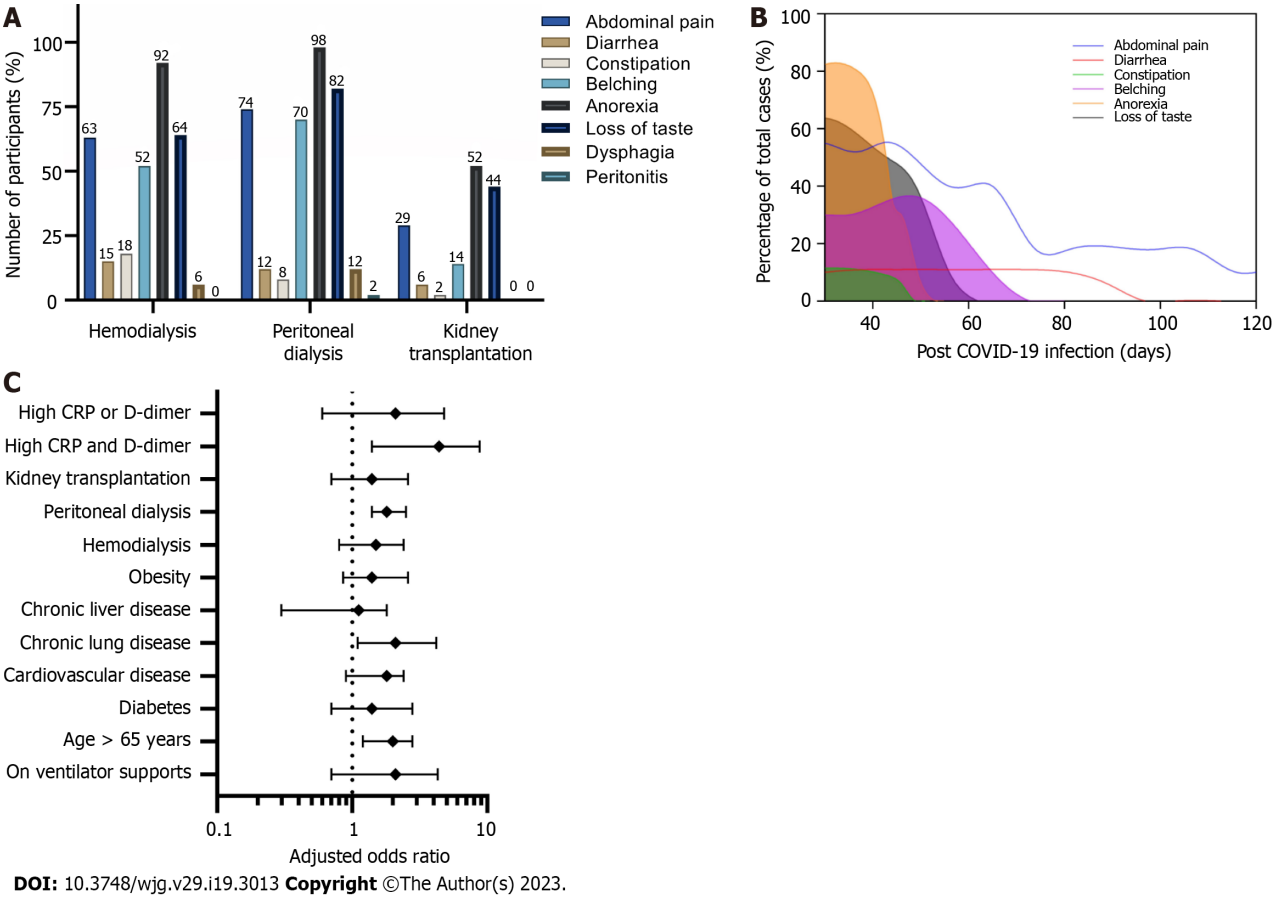
Figure 1 Flow chart showing the number of eligible participants and the final cases enrolled in the study. COVID-19: Coronavirus disease 2019.

The prevalence and characteristics of Long-COVID in the present cohort seem to differ from its manifestations in other populations, in which diarrhea was the most persistently encountered GI symptom[26-31]. This difference could be explained by the combination of pre-existing uremic toxins in dialysis-dependent patients, as well as a delayed clearance of inflammatory cytokines[32] and enhanced oxidative stress associated with end-stage renal disease (ESRD)[33]. As such, restoration of renal function in KT recipients resulted in a decrease in the incidence of GI manifestations of Long-COVID compared with ESRD patients (Figure 2A). However, kidney transplantation does not entirely reverse T cell functions[34], and the underlying mechanisms of epigenetic changes induced by any combination of inflammation and oxidative stress associated with uremia are not easily reversible[35]. For these reasons, KT recipients with COVID-19 infection still have a persistently increased risk for Long-COVID.

As shown in Figure 2B, most of the participants experienced much improvement in the manifestations of Long-COVID after 4 wk and nearly complete resolution by three months. However, the differential diagnosis between the functional limitation during the COVID rehabilitation phase *vs* the Long-COVID syndrome may be difficult. Accordingly, the need for a robust clarification of the sequelae after COVID-19 infection is another concern in the post-pandemic era. The British NICE suggests that the term PASC must refer to any clinical signs and symptoms that develop during or after an infection consistent with COVID-19, that continue for more than 12 wk, and that cannot be explained by any other conditions[6]. Similarly, the World Health Organization (WHO) defines the PASC syndrome as any symptoms without an alternative diagnosis from three months onwards and that last for at least 2 mo[7]. Based on our findings, we found a significant difference in the clinical spectrum between patients with a symptom duration longer than 3 mo *vs* less than 3 mo post-COVID-19 infection (Figure 2B), in agreement with the COVID Symptom Study[36]. One explanation for the persistence of clinical signs and symptoms following COVID-19 infection may involve the underlying biological factors, such as an aberrant immune response[37], diverse functional autoantibodies[38], or gut dysbiosis[39], that drive other virus-initiated chronic syndromes.

We support using the 12-week cut-off duration as recommended by NICE and WHO for the diagnosis of PASC, and we propose an additional revision of the specific nomenclature for early and late Long-COVID syndrome. We propose using the term "post-acute COVID-19 syndrome (PACS)" for the clinical syndrome that develops three months from post-COVID-19 infection and using "chronic COVID-19 syndrome" thereafter (Figure 3). We further recommend reserving the term "Long-COVID syndrome" for the clinical syndrome that develops beyond three months post-COVID-19 infection and lasts for at least six months, because Long-COVID syndrome may be another post-viral illness spectrum, like myalgic encephalomyelitis/chronic fatigue syndrome[40].

The mechanisms underlying the GI manifestations of Long-COVID are not completely understood. One plausible explanation might be that an impairment of gut homeostasis is explained by disruption of gut-lung communication[41]. The manifestations during acute COVID-19 are believed to be related to an increased expression of ACE2 on the small bowel mucosa[17], endotoxemia[16,42], leaky gut[16], and alterations in hepatic blood flow due to sinusoidal thrombi[43], all triggered by an increased proinflammatory state and intestinal dysbiosis. Undoubtedly, the greater severity of COVID-19 infection in the elderly (high C-reactive protein > 5 mg/L, high D-dimer > 500 ng/mL with > 65 years old), as shown in



DOI: 10.3748/wjg.v29.i19.3013 **Copyright** ©The Author(s) 2023.

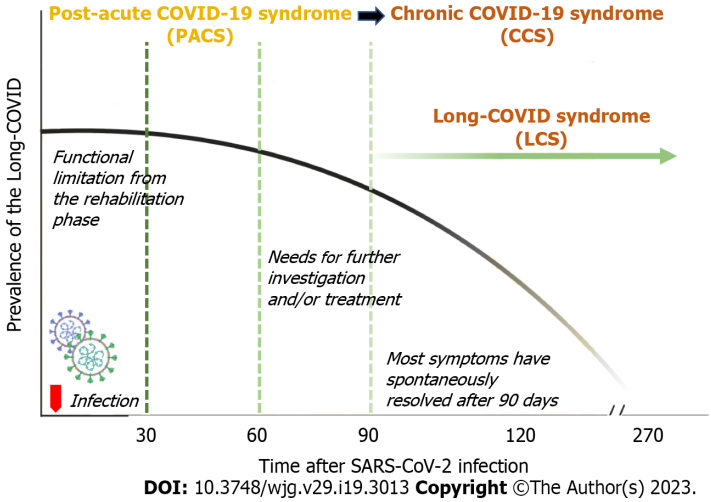
Figure 2 The burden of gastrointestinal manifestations of prolonged symptoms after corona virus disease 2019. Post-acute sequelae were followed from 30 d after infection until the end of follow-up. A: Comparison of the prevalence and characteristics of prolonged symptoms after corona virus disease 2019 (Long-COVID) among dialysis-dependent (HD, *n* = 293; PD, *n* = 21) and kidney transplant recipients (*n* = 7); B: Time course of individual Long-COVID syndrome and resolution of symptoms. The color shading indicates Long-COVID syndrome that resolved within 90 d; C: Risk factors for gastrointestinal manifestations of Long-COVID. Long-COVID: Prolonged symptoms after corona virus disease 2019; CRP: C-reactive protein (high CRP > 5 mg/L, D-dimer > 500 ng/mL).

Figure 2C, also leads to a greater risk of GI manifestations of Long-COVID[44]. Although COVID-19 outcomes are comparable between PD and HD patients[45], the findings of the present study demonstrated that PD patients have a greater risk of developing GI manifestations of Long-COVID. Being elderly and having more symptoms (Table 1) may constitute key risk factors for developing Long-COVID in PD patients[46].

Irritable bowel syndrome, a condition with diverse symptoms, including diarrhea, constipation, and mixed bowel habits according to the Rome criteria[47], has been recently proposed as a possible consequence of COVID-19 infection due to disruption of the diversity and stability of the gut microbiota [48]. For this reason, evaluation of whether diarrhea and indigestion manifestations of Long-COVID alter the gut microbiome would be worth investigating[49]. This possibility also suggests that the use of specific probiotics and prebiotics in COVID-19 clinical treatment may help KT recipients with COVID-19 infections to rebalance their gut and lung microbial ecology, thereby boosting their immune responses against the virus in response to a new metabolic milieu[50].

Moreover, little is known about the pathophysiology of the abdominal pain manifestation of Long-COVID-19. Prolonged shedding of SARS-CoV-2 from the GI tract has been observed and could be responsible for some of the GI manifestations of Long-COVID[51]. Interestingly, we found that over one-third of our KT recipients had been diagnosed with mesenteric panniculitis-related Long-COVID. Although this is a rare condition, concern is growing regarding the conditional pain associated with COVID-19[52,53]. Notably, all of our recipients with mesenteric panniculitis fully recovered after corticosteroid administration, suggesting that systemic inflammation is the process involved here[54]. Although renal allograft dysfunction and graft loss following COVID-19 infection are possibly resulted from direct toxicity of SARS-CoV-2, cytokine storm-induced tubular injury, reduced immunosuppressive drugs during infection and decreased renal allograft blood flow from multiple organ failure[55-57], there was no reported case of acute kidney injury in the cohort.

The strengths of the present study are that we compiled the data available on the prevalence, symptomatology, and specific treatment of the particular GI manifestations of Long-COVID symptoms; this



DOI: 10.3748/wjg.v29.i19.3013 **Copyright** ©The Author(s) 2023.

Figure 3 Illustration of the proposed new nomenclature for clinical syndromes following post-corona virus disease 2019 infection. We propose that the term post-acute-corona virus disease 2019 (COVID-19) syndrome should describe illness occurring within 90 d from the onset of COVID-19 infection. Chronic COVID-19 syndrome (CCS) would then be a modified classification that refers to the clinical syndrome thereafter. By contrast, the term Long-COVID syndrome should be reserved for patients showing CCS lasting for at least six months. In the case of severe symptoms, the investigation and corresponding treatments should be addressed at 60 d to prevent serious CCS. Long-COVID: Prolonged symptoms after corona virus disease 2019.

will help to guide clinicians in dealing with the pandemic. The identification of GI manifestations of Long-COVID in KT recipients could also help to define the contours of this new SARS-CoV-2 virus. Some limitations of the present study should also be acknowledged. This was a renal referral center study with a limited diversity of patient characteristics. No non-COVID-19 patients were included in the study, and the small number of participants made the study underpowered for investigating the risk factors associated with GI symptoms. Thus, the results need confirmation with larger cohorts that can apply the structural equation modeling for analysis, which has greater statistical power in terms of the probability of rejecting of a false null hypothesis than multiple regression analysis does[58]. In addition, the influence of different SARS-CoV-2 variants on GI manifestations of Long-COVID in dialysis-dependent and KT patients was not clarified, nor was the vaccination status against different variants addressed in our cohorts. However, based on the timing of the pandemic, the main strain circulating at the time of our study was the Delta (B.1.617) strain, accompanied by an early wave of the Omicron (B.1.1.529) variants[59,60]. Accordingly, an in-depth analysis of confounders should also be performed in larger, multinational cohorts. It is also challenging to find unrecovered pathophysiology of the long-term GI effects of COVID-19. Future research should not overlook other organ interactions to GI manifestations of Long-COVID, for instance, mental health symptoms (*e.g.*, depression and anxiety symptoms) nor additional post-infectious symptoms that were not assessed in the present study (*e.g.*, cardiovascular disease), as depression[61-63], gut-brain axis[64] or cardiovascular diseases[65] are the main etiology of long-term comorbidity of COVID-19[5], especially in HD patients[66]. In addition to lack of appetite, ESRD is recognized as a high risk of pre-existing undernutrition (malnutrition), including micronutrient deficiencies from malnutrition-inflammation-cachexia complex[67], which has been linked to increased mortality in patients with COVID-19[68]. Thus, nutrition support could be another critical intervention during COVID-19 infection in ESRD that robust research is needed for clarification as, vice versa, reduced long-term GI sequelae is probably part of the overall benefit from nutritional support.

CONCLUSION

In conclusion, at 3 mo after infection with SARS-CoV-2, renal replacement therapy patients and KT recipients with COVID-19 show high rates of GI manifestations of Long-COVID after discharge following their initial episode. These data point to optimized management as a potential line of research for decreasing Long-COVID syndrome in these populations.

ARTICLE HIGHLIGHTS

Research background

The characteristics of persistent coronavirus disease 2019 (COVID-19) symptoms or Long-COVID in

dialysis-dependent patients and kidney transplant (KT) is remain underestimate and urgent needs for investigation to prevent long-term complication in these vulnerable population.

Research motivation

End stage renal disease is a well-known condition for high mortality risk following COVID-19 infection. Thus, it is essential to explore the Long-COVID in these population as an early preventive strategy for preventing further morbidity and mortality.

Research objectives

To identify the characteristics of gastrointestinal (GI) manifestations of Long-COVID in patients with dialysis-dependent or KT status.

Research methods

A prospective, observational study was conducted during January 2022 to July 2022 in patients with COVID-19 infection to explore the Long-COVID symptoms in 3-months after the onset by interviewing.

Research results

As of 577 cases agreed to the interviews, the mean age was 52±11 years with 52% women. Long-COVID was identified in 56%, 62% and 37% in hemodialysis, peritoneal dialysis, and KT respectively. While fatigue was the most prevalent (96%) of the non-GI tract symptoms, anorexia (90.9%), loss of taste (64.4%), and abdominal pain (62.5%) were the first three common GI manifestations of Long-COVID. Of note, there were 6 cases of mesenteric panniculitis from 19 patients with GI symptoms in the KT group.

Research conclusions

Renal replacement therapy patients and KT recipients with COVID-19 show high rates of GI manifestations of Long-COVID after discharge following their initial episode.

Research perspectives

Further study should aim to explore the pathophysiology of the long-term GI effects of COVID-19 in renal replacement therapy and KT patients, which may have different immune response to Long-COVID symptoms compared to those with immunocompetent.

FOOTNOTES

Author contributions: Chancharoenthana W and Kamolratanakul S designed the research study; Chancharoenthana W, Kamolratanakul S, Ariyanon W, Chinpraditsuk S, and Saelim R performed the research and collected data; Chancharoenthana W, Kamolratanakul S, Ariyanon W, and Chinpraditsuk S analysed the data; Chancharoenthana W and Kamolratanakul drafted the manuscript. Chancharoenthana W, Kamolratanakul S, Leelahavanichkul A, Vadcharavivad S, Phumratanaprapin W, and Wilairatana P edited the manuscript; all authors have read and approve the final manuscript.

Institutional review board statement: The study was approved by the Human Research Ethics Committee of Faculty of Tropical Medicine, Mahidol University, Thailand (MUTM 2022-081-01).

Informed consent statement: Informed consent for participation in interviews was obtained either written or verbally over the phone from all participants in the study.

Conflict-of-interest statement: There are no conflicts of interest to disclose.

Data sharing statement: The data underlying this article will be shared on reasonable request to the corresponding author.

STROBE statement: The authors have read the STROBE Statement—checklist of items, and the manuscript was prepared and revised according to the STROBE Statement—checklist of items.

Open-Access: This article is an open-access article that was selected by an in-house editor and fully peer-reviewed by external reviewers. It is distributed in accordance with the Creative Commons Attribution NonCommercial (CC BY-NC 4.0) license, which permits others to distribute, remix, adapt, build upon this work non-commercially, and license their derivative works on different terms, provided the original work is properly cited and the use is non-commercial. See: https://creativecommons.org/Licenses/by-nc/4.0/

Country/Territory of origin: Thailand

ORCID number: Wiwat Chancharoenthana 0000-0002-2965-146X; Supitcha Kamolratanakul 0000-0002-0428-2354; Asada Leelahavanichkul 0000-0002-5566-6403; Somratai Vadcharavivad 0000-0001-5080-7070; Weerapong Phumratanaprapin 0000-

0001-5896-1961.

S-Editor: Chang KL
L-Editor: A
P-Editor: Zhao S

REFERENCES

1 **Marshall M**. The lasting misery of coronavirus long-haulers. *Nature* 2020; **585**: 339-341 [PMID: 32929257 DOI: 10.1038/d41586-020-02598-6]
2 **Nalbandian A**, Sehgal K, Gupta A, Madhavan MV, McGroder C, Stevens JS, Cook JR, Nordvig AS, Shalev D, Sehrawat TS, Ahluwalia N, Bikdeli B, Dietz D, Der-Nigoghossian C, Liyanage-Don N, Rosner GF, Bernstein EJ, Mohan S, Beckley AA, Seres DS, Choueiri TK, Uriel N, Ausiello JC, Accili D, Freedberg DE, Baldwin M, Schwartz A, Brodie D, Garcia CK, Elkind MSV, Connors JM, Bilezikian JP, Landry DW, Wan EY. Post-acute COVID-19 syndrome. *Nat Med* 2021; **27**: 601-615 [PMID: 33753937 DOI: 10.1038/s41591-021-01283-z]
3 **Raveendran AV**, Jayadevan R, Sashidharan S. Long COVID: An overview. *Diabetes Metab Syndr* 2021; **15**: 869-875 [PMID: 33892403 DOI: 10.1016/j.dsx.2021.04.007]
4 **Maltezou HC**, Pavli A, Tsakris A. Post-COVID Syndrome: An Insight on Its Pathogenesis. *Vaccines (Basel)* 2021; **9** [PMID: 34066007 DOI: 10.3390/vaccines9050497]
5 **Visco V**, Vitale C, Rispoli A, Izzo C, Virtuoso N, Ferruzzi GJ, Santopietro M, Melfi A, Rusciano MR, Maglio A, Di Pietro P, Carrizzo A, Galasso G, Vatrella A, Vecchione C, Ciccarelli M. Post-COVID-19 Syndrome: Involvement and Interactions between Respiratory, Cardiovascular and Nervous Systems. *J Clin Med* 2022; **11** [PMID: 35159974 DOI: 10.3390/jcm11030524]
6 National Institute for Health and Care Excellence: Clinical Guidelines. COVID-19 rapid guideline: managing the long-term effects of COVID-19. London: National Institute for Health and Care Excellence (NICE), 2020
7 **Soriano JB**, Murthy S, Marshall JC, Relan P, Diaz JV; WHO Clinical Case Definition Working Group on Post-COVID-19 Condition. A clinical case definition of post-COVID-19 condition by a Delphi consensus. *Lancet Infect Dis* 2022; **22**: e102-e107 [PMID: 34951953 DOI: 10.1016/S1473-3099(21)00703-9]
8 **Modelli de Andrade LG**, de Sandes-Freitas TV, Requião-Moura LR, Viana LA, Cristelli MP, Garcia VD, Alcântara ALC, Esmeraldo RM, Abbud Filho M, Pacheco-Silva A, de Lima Carneiro ECR, Manfro RC, Costa KMAH, Simão DR, de Sousa MV, Santana VBBM, Noronha IL, Romão EA, Zanocco JA, Arimatea GGQ, De Boni Monteiro de Carvalho D, Tedesco-Silva H, Medina-Pestana J; COVID-19-KT Brazil. Development and validation of a simple web-based tool for early prediction of COVID-19-associated death in kidney transplant recipients. *Am J Transplant* 2022; **22**: 610-625 [PMID: 34416075 DOI: 10.1111/ajt.16807]
9 **Basic-Jukic N**, Juric I, Furic-Cunko V, Katalinic L, Radic J, Bosnjak Z, Jelakovic B, Kastelan Z. Follow-up of renal transplant recipients after acute COVID-19-A prospective cohort single-center study. *Immun Inflamm Dis* 2021; **9**: 1563-1572 [PMID: 34414665 DOI: 10.1002/iid3.509]
10 **Malinowska A**, Muchlado M, Ślizień Z, Biedunkiewicz B, Heleniak Z, Dębska-Ślizień A, Tylicki L. Post-COVID-19 Sydrome and Decrease in Health-Related Quality of Life in Kidney Transplant Recipients after SARS-COV-2 Infection-A Cohort Longitudinal Study from the North of Poland. *J Clin Med* 2021; **10** [PMID: 34768725 DOI: 10.3390/jcm10215205]
11 **Chauhan S**, Meshram HS, Kute V, Patel H, Desai S, Dave R. Long-term follow-up of SARS-CoV-2 recovered renal transplant recipients: A single-center experience from India. *Transpl Infect Dis* 2021; **23**: e13735 [PMID: 34547156 DOI: 10.1111/tid.13735]
12 **Amorim CEN**, Gomes VLT, Cristelli MP, Viana LA, de Luca Correa H, Lima GBB, de Sousa Silva FS, de Castro Lima GS, Rosa TDS, Nakamura MR, Quintino PM, Tedesco-Silva H, Medina-Pestana J. High Prevalence of Long-COVID Among Kidney Transplant Recipients: A Longitudinal Cohort Study. *Transplantation* 2022; **106**: 2408-2415 [PMID: 36228200 DOI: 10.1097/TP.0000000000004359]
13 **Och A**, Tylicki P, Polewska K, Puchalska-Reglińska E, Parczewska A, Szabat K, Biedunkiewicz B, Dębska-Ślizień A, Tylicki L. Persistent Post-COVID-19 Syndrome in Hemodialyzed Patients-A Longitudinal Cohort Study from the North of Poland. *J Clin Med* 2021; **10** [PMID: 34640471 DOI: 10.3390/jcm10194451]
14 **Demiray A**, Kanbay A, Kanbay M. Long-term effect of COVID-19 infection on hemodialysis patients: Should we follow hemodialysis patients more closely? *Clin Kidney J* 2022; **15**: 369-371 [PMID: 35198153 DOI: 10.1093/ckj/sfab265]
15 **Zuo T**, Liu Q, Zhang F, Lui GC, Tso EY, Yeoh YK, Chen Z, Boon SS, Chan FK, Chan PK, Ng SC. Depicting SARS-CoV-2 faecal viral activity in association with gut microbiota composition in patients with COVID-19. *Gut* 2021; **70**: 276-284 [PMID: 32690600 DOI: 10.1136/gutjnl-2020-322294]
16 **Saithong S**, Worasilchai N, Saisorn W, Udompornpitak K, Bhunyakarnjanarat T, Chindamporn A, Tovichayathamrong P, Torvorapanit P, Chiewchengchol D, Chancharoenthana W, Leelahavanichkul A. Neutrophil Extracellular Traps in Severe SARS-CoV-2 Infection: A Possible Impact of LPS and (1→3)-β-D-glucan in Blood from Gut Translocation. *Cells* 2022; **11** [PMID: 35406667 DOI: 10.3390/cells11071103]
17 **Hoffmann M**, Kleine-Weber H, Schroeder S, Krüger N, Herrler T, Erichsen S, Schiergens TS, Herrler G, Wu NH, Nitsche A, Müller MA, Drosten C, Pöhlmann S. SARS-CoV-2 Cell Entry Depends on ACE2 and TMPRSS2 and Is Blocked by a Clinically Proven Protease Inhibitor. *Cell* 2020; **181**: 271-280.e8 [PMID: 32142651 DOI: 10.1016/j.cell.2020.02.052]
18 **Docherty AB**, Harrison EM, Green CA, Hardwick HE, Pius R, Norman L, Holden KA, Read JM, Dondelinger F, Carson G, Merson L, Lee J, Plotkin D, Sigfrid L, Halpin S, Jackson C, Gamble C, Horby PW, Nguyen-Van-Tam JS, Ho A, Russell CD, Dunning J, Openshaw PJ, Baillie JK, Semple MG; ISARIC4C investigators. Features of 20 133 UK patients

in hospital with covid-19 using the ISARIC WHO Clinical Characterisation Protocol: prospective observational cohort study. *BMJ* 2020; **369**: m1985 [PMID: 32444460 DOI: 10.1136/bmj.m1985]

19 **Zhang H**, Zang C, Xu Z, Zhang Y, Xu J, Bian J, Morozyuk D, Khullar D, Nordvig AS, Schenck EJ, Shenkman EA, Rothman RL, Block JP, Lyman K, Weiner MG, Carton TW, Wang F, Kaushal R. Data-driven identification of post-acute SARS-CoV-2 infection subphenotypes. *Nat Med* 2023; **29**: 226-235 [PMID: 36456834 DOI: 10.1038/s41591-022-02116-3]

20 **Meringer H**, Mehandru S. Gastrointestinal post-acute COVID-19 syndrome. *Nat Rev Gastroenterol Hepatol* 2022; **19**: 345-346 [PMID: 35383321 DOI: 10.1038/s41575-022-00611-z]

21 **Al-Aly Z**, Xie Y, Bowe B. High-dimensional characterization of post-acute sequelae of COVID-19. *Nature* 2021; **594**: 259-264 [PMID: 33887749 DOI: 10.1038/s41586-021-03553-9]

22 **Burke MJ**, Del Rio C. Long COVID has exposed medicine's blind-spot. *Lancet Infect Dis* 2021; **21**: 1062-1064 [PMID: 34153235 DOI: 10.1016/S1473-3099(21)00333-9]

23 **Requião-Moura LR**, Sandes-Freitas TV, Viana LA, Cristelli MP, Andrade LGM, Garcia VD, Oliveira CMC, Esmeraldo RM, Abbud Filho M, Pacheco-Silva A, Sousa KC, Vicari AR, Costa KMAH, Simão DR, Sousa MV, Campos JB, Almeida RAMB, Deboni LM, Neto MM, Zanocco JA, Tedesco-Silva H, Medina-Pestana J; COVID-19-KT Brazil. High mortality among kidney transplant recipients diagnosed with coronavirus disease 2019: Results from the Brazilian multicenter cohort study. *PLoS One* 2021; **16**: e0254822 [PMID: 34320005 DOI: 10.1371/journal.pone.0254822]

24 **Medina-Pestana J**, Cristelli MP, Foresto RD, Tedesco-Silva H, Requião-Moura LR. The Higher COVID-19 Fatality Rate Among Kidney Transplant Recipients Calls for Further Action. *Transplantation* 2022; **106**: 908-910 [PMID: 35250005 DOI: 10.1097/TP.0000000000004086]

25 **Amin-Chowdhury Z**, Ladhani SN. Causation or confounding: why controls are critical for characterizing long COVID. *Nat Med* 2021; **27**: 1129-1130 [PMID: 34140704 DOI: 10.1038/s41591-021-01402-w]

26 **Romero-Duarte Á**, Rivera-Izquierdo M, Guerrero-Fernández de Alba I, Pérez-Contreras M, Fernández-Martínez NF, Ruiz-Montero R, Serrano-Ortiz Á, González-Serna RO, Salcedo-Leal I, Jiménez-Mejías E, Cárdenas-Cruz A. Sequelae, persistent symptomatology and outcomes after COVID-19 hospitalization: the ANCOHVID multicentre 6-month follow-up study. *BMC Med* 2021; **19**: 129 [PMID: 34011359 DOI: 10.1186/s12916-021-02003-7]

27 **Dennis A**, Wamil M, Alberts J, Oben J, Cuthbertson DJ, Wootton D, Crooks M, Gabbay M, Brady M, Hishmeh L, Attree E, Heightman M, Banerjee R, Banerjee A; COVERSCAN study investigators. Multiorgan impairment in low-risk individuals with post-COVID-19 syndrome: a prospective, community-based study. *BMJ Open* 2021; **11**: e048391 [PMID: 33785495 DOI: 10.1136/bmjopen-2020-048391]

28 **Blackett JW**, Wainberg M, Elkind MSV, Freedberg DE. Potential Long Coronavirus Disease 2019 Gastrointestinal Symptoms 6 Months After Coronavirus Infection Are Associated With Mental Health Symptoms. *Gastroenterology* 2022; **162**: 648-650.e2 [PMID: 34728186 DOI: 10.1053/j.gastro.2021.10.040]

29 **Carfì A**, Bernabei R, Landi F; Gemelli Against COVID-19 Post-Acute Care Study Group. Persistent Symptoms in Patients After Acute COVID-19. *JAMA* 2020; **324**: 603-605 [PMID: 32644129 DOI: 10.1001/jama.2020.12603]

30 **Moreno-Pérez O**, Merino E, Leon-Ramirez JM, Andres M, Ramos JM, Arenas-Jiménez J, Asensio S, Sanchez R, Ruiz-Torregrosa P, Galan I, Scholz A, Amo A, González-delaAleja P, Boix V, Gil J; COVID19-ALC research group. Post-acute COVID-19 syndrome. Incidence and risk factors: A Mediterranean cohort study. *J Infect* 2021; **82**: 378-383 [PMID: 33450302 DOI: 10.1016/j.jinf.2021.01.004]

31 **Carvalho-Schneider C**, Laurent E, Lemaignen A, Beaufils E, Bourbao-Tournois C, Laribi S, Flament T, Ferreira-Maldent N, Bruyère F, Stefic K, Gaudy-Graffin C, Grammatico-Guillon L, Bernard L. Follow-up of adults with noncritical COVID-19 two months after symptom onset. *Clin Microbiol Infect* 2021; **27**: 258-263 [PMID: 33031948 DOI: 10.1016/j.cmi.2020.09.052]

32 **Caso JR**, MacDowell KS, Soto M, Ruiz-Guerrero F, Carrasco-Díaz Á, Leza JC, Carrasco JL, Díaz-Marsá M. Dysfunction of Inflammatory Pathways and Their Relationship With Psychological Factors in Adult Female Patients With Eating Disorders. *Front Pharmacol* 2022; **13**: 846172 [PMID: 35517819 DOI: 10.3389/fphar.2022.846172]

33 **Chancharoenthana W**, Udompronpitak K, Manochantr Y, Kantagowit P, Kaewkanha P, Issara-Amphorn J, Leelahavanichkul A. Repurposing of High-Dose Erythropoietin as a Potential Drug Attenuates Sepsis in Preconditioning Renal Injury. *Cells* 2021; **10** [PMID: 34831360 DOI: 10.3390/cells10113133]

34 **Meijers RW**, Litjens NH, de Wit EA, Langerak AW, Baan CC, Betjes MG. Uremia-associated immunological aging is stably imprinted in the T-cell system and not reversed by kidney transplantation. *Transpl Int* 2014; **27**: 1272-1284 [PMID: 25082296 DOI: 10.1111/tri.12416]

35 **Betjes MG**. Immune cell dysfunction and inflammation in end-stage renal disease. *Nat Rev Nephrol* 2013; **9**: 255-265 [PMID: 23507826 DOI: 10.1038/nrneph.2013.44]

36 **Sudre CH**, Murray B, Varsavsky T, Graham MS, Penfold RS, Bowyer RC, Pujol JC, Klaser K, Antonelli M, Canas LS, Molteni E, Modat M, Jorge Cardoso M, May A, Ganesh S, Davies R, Nguyen LH, Drew DA, Astley CM, Joshi AD, Merino J, Tsereteli N, Fall T, Gomez MF, Duncan EL, Menni C, Williams FMK, Franks PW, Chan AT, Wolf J, Ourselin S, Spector T, Steves CJ. Author Correction: Attributes and predictors of long COVID. *Nat Med* 2021; **27**: 1116 [PMID: 34045738 DOI: 10.1038/s41591-021-01361-2]

37 **Vibholm LK**, Nielsen SSF, Pahus MH, Frattari GS, Olesen R, Andersen R, Monrad I, Andersen AHF, Thomsen MM, Konrad CV, Andersen SD, Højen JF, Gunst JD, Østergaard L, Søgaard OS, Schleimann MH, Tolstrup M. SARS-CoV-2 persistence is associated with antigen-specific CD8 T-cell responses. *EBioMedicine* 2021; **64**: 103230 [PMID: 33530000 DOI: 10.1016/j.ebiom.2021.103230]

38 **Wang EY**, Mao T, Klein J, Dai Y, Huck JD, Liu F, Zheng NS, Zhou T, Israelow B, Wong P, Lucas C, Silva J, Oh JE, Song E, Perotti ES, Fischer S, Campbell M, Fournier JB, Wyllie AL, Vogels CBF, Ott IM, Kalinich CC, Petrone ME, Watkins AE; Yale IMPACT Team, Cruz CD, Farhadian SF, Schulz WL, Grubaugh ND, Ko AI, Iwasaki A, Ring AM. Diverse Functional Autoantibodies in Patients with COVID-19. *medRxiv* 2021 [PMID: 33330894 DOI: 10.1101/2020.12.10.20247205]

39 **Thomas RM**, Jobin C. Microbiota in pancreatic health and disease: the next frontier in microbiome research. *Nat Rev*

Gastroenterol Hepatol 2020; **17**: 53-64 [PMID: 31811279 DOI: 10.1038/s41575-019-0242-7]

40 **Astin R**, Banerjee A, Baker MR, Dani M, Ford E, Hull JH, Lim PB, McNarry M, Morten K, O'Sullivan O, Pretorius E, Raman B, Soteropoulos DS, Taquet M, Hall CN. Long COVID: mechanisms, risk factors and recovery. *Exp Physiol* 2023; **108**: 12-27 [PMID: 36412084 DOI: 10.1113/EP090802]

41 **Enaud R**, Prevel R, Ciarlo E, Beaufils F, Wieërs G, Guery B, Delhaes L. The Gut-Lung Axis in Health and Respiratory Diseases: A Place for Inter-Organ and Inter-Kingdom Crosstalks. *Front Cell Infect Microbiol* 2020; **10**: 9 [PMID: 32140452 DOI: 10.3389/fcimb.2020.00009]

42 **Sirivongrangson P**, Kulvichit W, Payungporn S, Pisitkun T, Chindamporn A, Peerapornratana S, Pisitkun P, Chitcharoen S, Sawaswong V, Worasilchai N, Kampunya S, Putcharoen O, Thawitsri T, Leelayuwatanakul N, Kongpolprom N, Phoophiboon V, Sriprasart T, Samransamruajkit R, Tungsanga S, Tiankanon K, Lumlertgul N, Leelahavanichkul A, Sriphojanart T, Tantawichien T, Thisyakorn U, Chirathaworn C, Praditpornsilpa K, Tungsanga K, Eiam-Ong S, Sitprija V, Kellum JA, Srisawat N. Endotoxemia and circulating bacteriome in severe COVID-19 patients. *Intensive Care Med Exp* 2020; **8**: 72 [PMID: 33284413 DOI: 10.1186/s40635-020-00362-8]

43 **Cichoż-Lach H**, Michalak A. Liver injury in the era of COVID-19. *World J Gastroenterol* 2021; **27**: 377-390 [PMID: 33584070 DOI: 10.3748/wjg.v27.i5.377]

44 **Mandal S**, Barnett J, Brill SE, Brown JS, Denneny EK, Hare SS, Heightman M, Hillman TE, Jacob J, Jarvis HC, Lipman MCI, Naidu SB, Nair A, Porter JC, Tomlinson GS, Hurst JR; ARC Study Group. 'Long-COVID': a cross-sectional study of persisting symptoms, biomarker and imaging abnormalities following hospitalisation for COVID-19. *Thorax* 2021; **76**: 396-398 [PMID: 33172844 DOI: 10.1136/thoraxjnl-2020-215818]

45 **Ghonimi TAL**, Alkad MM, Abuhelaiqa EA, Othman MM, Elgaali MA, Ibrahim RAM, Joseph SM, Al-Malki HA, Hamad AI. Mortality and associated risk factors of COVID-19 infection in dialysis patients in Qatar: A nationwide cohort study. *PLoS One* 2021; **16**: e0254246 [PMID: 34293004 DOI: 10.1371/journal.pone.0254246]

46 **Robineau O**, Zins M, Touvier M, Wiernik E, Lemogne C, de Lamballerie X, Blanché H, Deleuze JF, Saba Villarroel PM, Dorival C, Nicol J, Gomes-Rima R, Correia E, Coeuret-Pellicer M, Druesne-Pecollo N, Esseddik Y, Ribet C, Goldberg M, Severi G, Carrat F; Santé, Pratiques, Relations et Inégalités Sociales en Population Générale Pendant la Crise COVID-19–Sérologie (SAPRIS-SERO) Study Group. Long-lasting Symptoms After an Acute COVID-19 Infection and Factors Associated With Their Resolution. *JAMA Netw Open* 2022; **5**: e2240985 [PMID: 36350653 DOI: 10.1001/jamanetworkopen.2022.40985]

47 **Drossman DA**, Hasler WL. Rome IV-Functional GI Disorders: Disorders of Gut-Brain Interaction. *Gastroenterology* 2016; **150**: 1257-1261 [PMID: 27147121 DOI: 10.1053/j.gastro.2016.03.035]

48 **Settanni CR**, Ianiro G, Ponziani FR, Bibbò S, Segal JP, Cammarota G, Gasbarrini A. COVID-19 as a trigger of irritable bowel syndrome: A review of potential mechanisms. *World J Gastroenterol* 2021; **27**: 7433-7445 [PMID: 34887641 DOI: 10.3748/wjg.v27.i43.7433]

49 **Liu Q**, Mak JWY, Su Q, Yeoh YK, Lui GC, Ng SSS, Zhang F, Li AYL, Lu W, Hui DS, Chan PK, Chan FKL, Ng SC. Gut microbiota dynamics in a prospective cohort of patients with post-acute COVID-19 syndrome. *Gut* 2022; **71**: 544-552 [PMID: 35082169 DOI: 10.1136/gutjnl-2021-325989]

50 **Tungsanga S**, Panpetch W, Bhunyakarnjanarat T, Udompornpitak K, Katavetin P, Chancharoenthana W, Chatthanathon P, Somboonna N, Tungsanga K, Tumwasorn S, Leelahavanichkul A. Uremia-Induced Gut Barrier Defect in 5/6 Nephrectomized Mice Is Worsened by Candida Administration through a Synergy of Uremic Toxin, Lipopolysaccharide, and (1→3)-β-D-Glucan, but Is Attenuated by Lacticaseibacillus rhamnosus L34. *Int J Mol Sci* 2022; **23** [PMID: 35269654 DOI: 10.3390/ijms23052511]

51 **Wu Y**, Guo C, Tang L, Hong Z, Zhou J, Dong X, Yin H, Xiao Q, Tang Y, Qu X, Kuang L, Fang X, Mishra N, Lu J, Shan H, Jiang G, Huang X. Prolonged presence of SARS-CoV-2 viral RNA in faecal samples. *Lancet Gastroenterol Hepatol* 2020; **5**: 434-435 [PMID: 32199469 DOI: 10.1016/S2468-1253(20)30083-2]

52 **Mandala S**, Kodati R, Tadepalli A, Reddy C, Kalyan S. An Unusual Cause of Acute Abdominal Pain in Coronavirus Disease (COVID-19): Report of Two Cases. *Indian J Crit Care Med* 2022; **26**: 1045-1048 [PMID: 36213717 DOI: 10.5005/jp-journals-10071-24310]

53 **Alyousef IA**, Alsaileek ZA, Alabdulsalam MA, Almohanna MA, Alshaqhaa NA, Alqahtani MM, Al Alyany AA, Alzahrani MA, Fallatah HA, Alqadhib JI, Alhawsawi AM, Alsuhaymi AD, Alasmari AM, Alshareef AJ, Al-Hawaj F. Mesenteric Panniculitis and COVID-19: A Rare Association. *Cureus* 2022; **14**: e21314 [PMID: 35186573 DOI: 10.7759/cureus.21314]

54 **Jiang QW**, Wang FD, Wang WZ, Wu X, Shu HJ, Li JN, Yang AM, Qian JM, Wu D. [An analysis of clinical characteristics of twelve cases of mesenteric panniculitis]. *Zhonghua Nei Ke Za Zhi* 2017; **56**: 112-115 [PMID: 28162180 DOI: 10.3760/cma.j.issn.0578-1426.2017.02.006]

55 **Cravedi P**, Mothi SS, Azzi Y, Haverly M, Farouk SS, Pérez-Sáez MJ, Redondo-Pachón MD, Murphy B, Florman S, Cyrino LG, Grafals M, Venkataraman S, Cheng XS, Wang AX, Zaza G, Ranghino A, Furian L, Manrique J, Maggiore U, Gandolfini I, Agrawal N, Patel H, Akalin E, Riella LV. COVID-19 and kidney transplantation: Results from the TANGO International Transplant Consortium. *Am J Transplant* 2020; **20**: 3140-3148 [PMID: 32649791 DOI: 10.1111/ajt.16185]

56 **Mohamed IH**, Chowdary PB, Shetty S, Sammartino C, Sivaprakasam R, Lindsey B, Thuraisingham R, Yaqoob MM, Khurram MA. Outcomes of Renal Transplant Recipients With SARS-CoV-2 Infection in the Eye of the Storm: A Comparative Study With Waitlisted Patients. *Transplantation* 2021; **105**: 115-120 [PMID: 33350626 DOI: 10.1097/TP.0000000000003406]

57 **Hadi YB**, Naqvi SFZ, Kupec JT, Sofka S, Sarwari A. Outcomes of COVID-19 in Solid Organ Transplant Recipients: A Propensity-matched Analysis of a Large Research Network. *Transplantation* 2021; **105**: 1365-1371 [PMID: 33988341 DOI: 10.1097/TP.0000000000003670]

58 **Beran TN**, Violato C. Structural equation modeling in medical research: a primer. *BMC Res Notes* 2010; **3**: 267 [PMID: 20969789 DOI: 10.1186/1756-0500-3-267]

59 **Chantasrisawad N**, Puthanakit T, Kornsitthikul K, Jaru-Ampornpan P, Tawan M, Matapituk P, Sophonphan J, Anugulruengkitt S, Tangsathapornpong A, Katanyutanon A; KIDSBOOST study team. Immunogenicity to SARS-CoV-2

Omicron variant among school-aged children with 2-dose of inactivated SARS-CoV-2 vaccines followed by BNT162b2 booster. *Vaccine X* 2022; **12**: 100221 [PMID: 36213592 DOI: 10.1016/j.jvacx.2022.100221]

60 **Chancharoenthana W**, Leelahavanichkul A, Chinpraditsuk S, Pongpirul K, Kamolratanakul S, Phumratanaprapin W, Wilairatana P, Pitisuttithum P. Social restriction versus herd immunity policies in the early phase of the SARS-CoV-2 pandemic: A mathematical modelling study. *Asian Pac J Allergy Immunol* 2021 [PMID: 33386788 DOI: 10.12932/AP-140720-0914]

61 **Nooripour R**, Ghanbari N, Radwin LE, Hosseinian S, Hassani-Abharian P. Development and validation of COVID-19 Stress Scale (CSS) in an Iranian non-clinical population. *Zahedan J Res Med Sci* 2022; **24**: e118719 [DOI: 10.5812/zjrms-118719]

62 **Nooripour R**, Hosseinian S, Farmani F, Abtahi Foroshani N, Ghanbari N, Farkhojasteh VS. Relationship Between Hardiness and Stress of COVID-19 Through the Mediating Role of Mindfulness in Iranian Students. *PCP* 2022; **10**: 193-202 [DOI: 10.32598/jpcp.10.3.288.7]

63 **Nooripour R**, Hosseinian S, Hussain AJ, Annabestani M, Maadal A, Radwin LE, Hassani-Abharian P, Pirkashani NG, Khoshkonesh A. How Resiliency and Hope Can Predict Stress of Covid-19 by Mediating Role of Spiritual Well-being Based on Machine Learning. *J Relig Health* 2021; **60**: 2306-2321 [PMID: 33398655 DOI: 10.1007/s10943-020-01151-z]

64 **Chen J**, Vitetta L. Gut-brain axis in the neurological comorbidity of COVID-19. *Brain Commun* 2021; **3**: fcab118 [PMID: 34169281 DOI: 10.1093/braincomms/fcab118]

65 **Elseidy SA**, Awad AK, Vorla M, Fatima A, Elbadawy MA, Mandal D, Mohamad T. Cardiovascular complications in the Post-Acute COVID-19 syndrome (PACS). *Int J Cardiol Heart Vasc* 2022; **40**: 101012 [PMID: 35355927 DOI: 10.1016/j.ijcha.2022.101012]

66 **Carriazo S**, Mas-Fontao S, Seghers C, Cano J, Goma E, Avello A, Ortiz A, Gonzalez-Parra E. Increased 1-year mortality in haemodialysis patients with COVID-19: a prospective, observational study. *Clin Kidney J* 2022; **15**: 432-441 [PMID: 35198156 DOI: 10.1093/ckj/sfab248]

67 **Kilpatrick RD**, McAllister CJ, Kovesdy CP, Derose SF, Kopple JD, Kalantar-Zadeh K. Association between serum lipids and survival in hemodialysis patients and impact of race. *J Am Soc Nephrol* 2007; **18**: 293-303 [PMID: 17167113 DOI: 10.1681/ASN.2006070795]

68 **Barazzoni R**, Breda J, Cuerda C, Schneider S, Deutz NE, Wickramasinghe K; COVID-19 Call Editorial Board. COVID-19: Lessons on malnutrition, nutritional care and public health from the ESPEN-WHO Europe call for papers. *Clin Nutr* 2022; **41**: 2858-2868 [PMID: 36075815 DOI: 10.1016/j.clnu.2022.07.033]

World Journal of Gastroenterology

Submit a Manuscript: https://www.f6publishing.com

World J Gastroenterol 2023 May 21; 29(19): 3027-3039

DOI: 10.3748/wjg.v29.i19.3027

ISSN 1007-9327 (print) ISSN 2219-2840 (online)

META-ANALYSIS

Short *vs* long-course antibiotic therapy in adults with acute cholangitis: A systematic review, meta-analysis, and evidence quality assessment

Karampet Kasparian, Chrysanthos D Christou, Konstantinos Petidis, Michail Doumas, Olga Giouleme

Specialty type: Gastroenterology and hepatology

Provenance and peer review: Unsolicited article; Externally peer reviewed.

Peer-review model: Single blind

Peer-review report's scientific quality classification

Grade A (Excellent): A, A
Grade B (Very good): 0
Grade C (Good): 0
Grade D (Fair): 0
Grade E (Poor): 0

P-Reviewer: Jain N, Latvia; Kimura Y, Japan

Received: March 4, 2023
Peer-review started: March 4, 2023
First decision: April 10, 2023
Revised: April 11, 2023
Accepted: April 23, 2023
Article in press: April 23, 2023
Published online: May 21, 2023

Karampet Kasparian, Clinic of Oncology, Gastroenterology and Hematology, Alfried Krupp Hospital, Essen 45131, Germany

Karampet Kasparian, Konstantinos Petidis, Michail Doumas, Olga Giouleme, Second Propedeutic Department of Internal Medicine, Hippokration General Hospital, Aristotle University of Thessaloniki, Thessaloniki 54642, Greece

Chrysanthos D Christou, Department of Transplantation Surgery, Hippokration General Hospital, Aristotle University of Thessaloniki, Thessaloniki 54642, Greece

Corresponding author: Karampet Kasparian, MD, MSc, Doctor, Clinic of Oncology, Gastroenterology and Hematology, Alfried Krupp Hospital, Alfried-Krupp-Strasse 21, Essen 45131, Germany. kar.kasparian@gmail.com

Abstract

BACKGROUND

Acute cholangitis (AC) constitutes an infection with increased mortality rates in the past. Due to new diagnostic tools and therapeutic methods, the mortality of AC has been significantly reduced nowadays. The initial antibiotic treatment of AC has been oriented to the most common pathogens connected to this infection. However, the optimal duration of the antibiotic treatment of AC is still debatable.

AIM

To investigate if shorter-course antibiotic treatments could be similarly effective to long-course treatments in adults with AC.

METHODS

This study constitutes a systematic review and meta-analysis of the existing literature concerning the duration of antibiotic therapy of AC and an assessment of the quality of the evidence. The study was conducted in accordance with the recommendations of the Preferred Reporting Items for Systematic Review and Meta-Analyses. Fifteen studies were included in the systematic review, and eight were eligible for meta-analysis. Due to heterogeneous duration cutoffs, three study-analysis groups were formed, with a cutoff of 2-3, 6-7, and 14 d.

RESULTS

A total of 2763 patients were included in the systematic review, and 1313 were

accounted for the meta-analysis. The mean age was 73.66 ± 14.67 years, and the male and female ratio was 1:08. No significant differences were observed in the mortality rates of antibiotic treatment of 2-3 d, compared to longer treatments (odds ratio = 0.78, 95% confidence interval: 0.23-2.67, $I2$ = 9%) and the recurrence rates and hospitalization length were also not different in all study groups.

CONCLUSION

Short- and long-course antibiotic treatments may be similarly effective concerning the mortality and recurrence rates of AC. Safe conclusions cannot be extracted concerning the hospitalization duration.

Key Words: Acute cholangitis; Antibiotic; Short-course; Long-course; Antimicrobial; Treatment duration

©The Author(s) 2023. Published by Baishideng Publishing Group Inc. All rights reserved.

Core Tip: The exact duration of antibiotic therapy for acute cholangitis in adult patients remains a controversial subject in the field of gastroenterology. A total antibiotic treatment of 4-7 d is recommended by the Tokyo Guidelines of 2018. However, recent studies present that schemata of shorter-course therapies could promise similar efficacy and safety. In our study, we systematically reviewed the existing literature in order to compare the death and recurrence rates and the length of hospitalization between patients with antibiotic treatments of shorter and longer durations. Our findings showed no significant differences between the study groups in all outcomes.

Citation: Kasparian K, Christou CD, Petidis K, Doumas M, Giouleme O. Short *vs* long-course antibiotic therapy in adults with acute cholangitis: A systematic review, meta-analysis, and evidence quality assessment. *World J Gastroenterol* 2023; 29(19): 3027-3039

URL: https://www.wjgnet.com/1007-9327/full/v29/i19/3027.htm

DOI: https://dx.doi.org/10.3748/wjg.v29.i19.3027

INTRODUCTION

The mortality rates of acute cholangitis (AC) have significantly decreased by comparing patients' data before 1980 and after 2000, from 10%-30% to 2.7%-10%[1]. Multiple factors, such as the development of modern diagnostic techniques, therapeutic methods for bile duct decompression, and new antibiotics adapted to microbiological studies, have significantly contributed to this improvement in the prognosis of AC[2].

The bacterial species commonly detected in AC differ in relationship with the severity of AC[1,3]. Because of this fact, the empirical antibiotic therapy provided should be oriented to the severity grade as defined in the Tokyo Guidelines (TG)[4]. Previous operations, the origin of the infection, possible allergies, pharmacodynamics, pharmacokinetics, local antibiogram and liver or renal dysfunction should also determine the choice of antimicrobial therapy in patients with AC[5].

A major issue concerning the therapy of AC is the exact duration of the definite antibiotic treatment. The TG 2018 (TG18) suggest that the antimicrobial therapy should last 4-7 d, and if gram-positive cocci are present, a minimum therapy of two weeks should be administrated[5]. This interval between the recommended treatment days is relatively wide, and the recommendation provided is not based on a high level of evidence (level C). Recent studies suggest that even a therapy of two or three days could be equally effective and safe, and it could reduce the length of in-hospital stay of patients, with a consequent reduction in the economic burden on the health systems[6-8]. A randomized controlled trial also showed similar clinical outcomes for patients with intraabdominal infections who received antibiotic therapy for two days after the resolution of fever, compared to those who received therapy for a maximum of 10 d[9].

Our purpose in conducting this systematic review and meta-analysis is to collect all available data existing in the current bibliography in order to ascertain if short-course antibiotic therapies could promise lower mortality, lower rates of recurrent AC, and shorter hospitalizations in adults with AC, compared to long-course antibiotic therapies and, if possible, to attempt to clarify the optimal duration of the antimicrobial treatment of the AC.

MATERIALS AND METHODS

Review protocol

Our systematic review was conducted according to the guidelines of the Preferred Reporting Items for Systematic reviews and Meta-Analyses (PRISMA)[10]. Two independent reviewers (Kasparian K and Christou CD) performed research in Medline-PubMed and Cochrane databases by applying a predefined research algorithm. The last search date was the 5th of October, 2022. The studies were initially controlled according to their title and abstract and followingly according to their full texts and the extractability of their content. We included studies concerning adults who received antibiotic therapy against AC, and whose therapy duration or mean/median duration was documented. We included only original studies in our systematic review (observational studies and randomized controlled trials). The exclusion criteria for the articles in our review, were studies concerning infantile population, animal studies, non-English studies, case reports or case series, comments or editorials, book chapters, studies with non-extractable data, abstract publications, protocols of incomplete clinical trials, irrelevant articles, surveys, and articles whose full-texts could not be retrieved. Conflicts during the eligibility process were resolved after a discussion between the two reviewers.

From the 1380 articles retrieved from the research, 50 were removed as duplicates and 1150 were excluded according to their titles and abstracts. From the 177 remaining studies, 15 were included in our systematic review[6,8,11-23], and the quantitative analysis of our research question was based on eight studies[8,11,12,16,17,21-23]. Forty-five papers contained data that was not extractable for our review, one study concerned a population of non-adult patients, 49 studies were irrelevant to our research questions, and the remaining excluded papers concerned non-original studies. One of the final papers constitutes a randomized-controlled trial, while the other fourteen concern retrospective observational studies. The details of the reasons for the exclusion of the papers are summarized in the PRISMA flowchart in Figure 1.

Data extraction

The two reviewers (Kasparian K and Christou CD) collected and tabulated independently the data of the final papers chosen for this review. Each reviewer gathered data concerning the study protocol, the baseline characteristics of the participants, and data concerning the outcomes and their definitions. The baseline characteristics to be collected for our review were predefined: Mean age and standard deviations (SD), gender, comorbidities, severity grade of AC, antibiotic therapy, and biliary drainage method. Heterogenous numerical data were transformed into the same predefined measurement units for statistical analysis. The two reviewers compared the data that each one collected, and conflicts were resolved between them.

Outcomes

The primary outcome of our study was the mortality of the patients. Secondary outcomes were the recurrence rate and the length of hospitalization of AC, measured with days. All outcomes were predefined. As mortality, we define the total, all-cause mortality of the participants until the end of the follow-up period of each study. In-hospital mortality due to AC was not examined.

Due to the heterogeneity in the time cutoff points between the intervention groups in each study, our quantitative analysis was divided into three subgroups. More specifically, an analysis was conducted among the studies which compared a therapy of 2-3 d to longer antibiotic treatments[6,8,11,21], studies with a cutoff of 6-7 d were separately analyzed[22,23], and the two papers which assessed clinical outcomes in AC-patients who received antibiotic treatment of for 14 d or less were summarized together [12,16].

Statistical analysis

All continuous variables are presented with the means and SD. For numerical variables which were not normally distributed and for which their medians and interquartile ranges or ranges were provided, we used the Hozo equation to calculate their means and SD[24]. For the data synthesis of the numerical variables, standardized mean differences (SMD) and 95% confidence intervals (95%CI) were calculated, with the use of Hedge´s method, for bias to be minimized[25]. For the categorical variables, we collected the absolute values and calculated the odds ratios (OR) and their 95%CIs. The data synthesis of the qualitative variables was based on the random effects model. In cases where no events were presented concerning a qualitative variable in a study group, the proper changes were conducted, in order for the statistical analysis to be feasible[26]. For the evaluation of the study heterogeneity, the I^2 value was calculated for each outcome. We presume $I^2 > 70\%$ as an indicator of heterogeneity among the studies. For all other measurements, we selected a P value of 0.05 as the cutoff point for the presence of statistical significance. All calculations and Forest plots were conducted through the program R Studio, version 1.4.1103.

Quality assessment

To assess the quality of the observational studies included in our systematic review and meta-analysis,

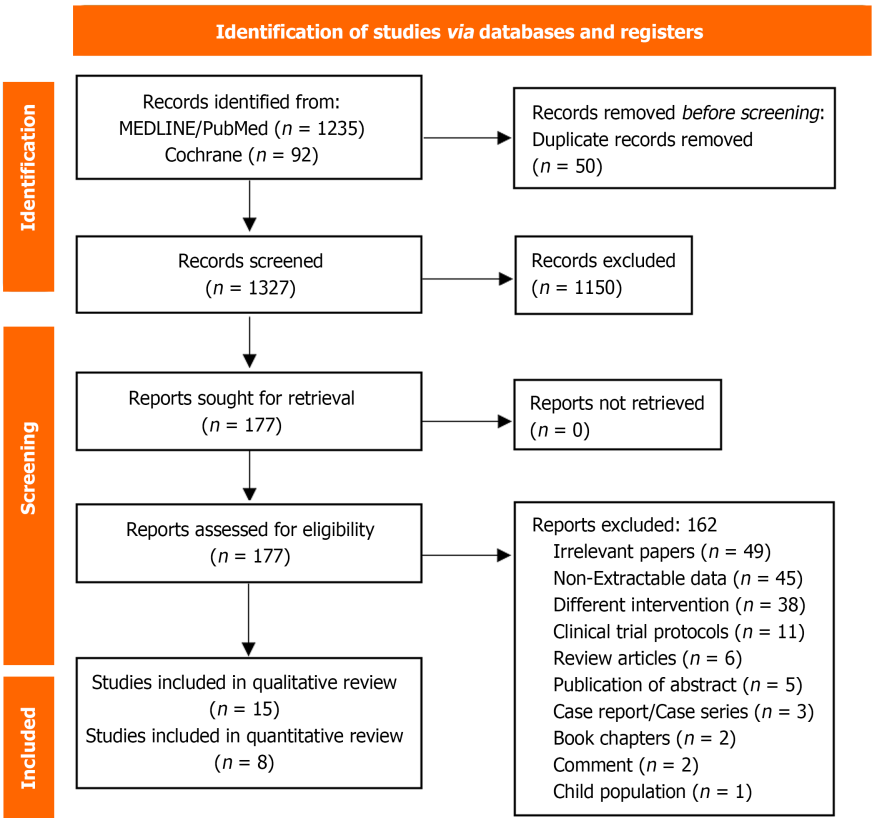


Figure 1 The Preferred Reporting Items for Systematic Review and Meta-Analyses flow chart of the systematic review and meta-analysis.

the Newcastle-Ottawa Scale was used[27]. The randomized clinical trials were evaluated for quality according to the Risk-of-Bias tool version 2 (RoB 2) provided by Cochrane[28]. Two reviewers (Kasparian K and Christou CD) independently assessed the final studies using the methods mentioned above, and possible conflicts were resolved afterward.

RESULTS

Baseline characteristics

As mentioned, 15 studies were included in our systematic review, and eight were considered eligible for the meta-analysis. The included studies were primarily conducted in Japan (8/15), two in the Netherlands, and the remaining studies originated from medical centers in France, Germany, Pakistan, South Korea, and Thailand. In 11/15 studies, the diagnosis of AC was based on the TG18/TG13 guidelines[6,8,12-14,16-18,20,21,23], two studies defined AC, depending on the TG07[15,19], Doi *et al*[22] controlled the presence the proper code of the 10th Edition of the International Classification of Diseases in hospital registries and positive bile or blood cultures for the selection of the patients, while van Lent *et al*[11] based the diagnosis of cholangitis on clinical, laboratory and imaging criteria.

The overall number of patients included in the systematic review was n = 2763, which corresponded to 2812 cases of AC. In the eight studies selected for the quantitative analysis, a total of 1219 patients and 1313 cases received antibiotic treatment against AC. The pooled mean age of the participants in the meta-analysis was 73.66 ± 14.67 years, and 721 (54.9%) of them were males, with a male to female ratio of 1:0.8. According to the TG18 severity grading system, 400/972 (41.1%) patients were classified as grade I, 525/972 (54.1%) as grade II while 45/972 (4.6%) of the patients suffered from grade III AC. Positive blood culture was detected in 383/742 (51.6%) participants. *Escherichia coli* (188/383, 49.1%) and *Klebsiella spp.* (75/383, 19.6%) were the most frequently identified pathogens, while 26/278 (9.3%) patients presented infection with gram-positive bacteria. A total of 244/1155 (21.1%) patients suffered from diabetes mellitus, 126/779 (16.2%) had a history of chronic kidney disease, and 107/779 (13.7%) participants presented a cardiac comorbidity, either chronic heart failure or coronary artery disease. Most patients received Cephalosporines (229/540, 42.4%) as antibiotic treatment and based on the available data, 275/326 (84.3%) patients underwent papillotomy during endoscopic retrograde cholangiopancreatography. For the last characteristic, only two studies included available data. Details for the baseline characteristics of the studies are summarized in Table 1.

Table 1 Baseline characteristics of the studies

Ref.	Country	Study period	Study design	Definition of AC	Population	Intervention	Outcomes
Ferstl *et al* [23], 2022	Germany	2008-2019	Retrospective observational study	TG18/TG13	Grade I and grade II AC after ERCP	Antibiotic therapy of 6 d	Recurrent cholangitis within 28 d
Kihara and Yokomizo [20], 2022	Japan	January 2009 to August 2018	Retrospective observational study	TG18/TG13	Postoperative cholangitis after pancreaticoduodenectomy	Antibiotic therapy and pancreaticoduoedenectomy	Clinical characteristics and outcomes in patients with acute cholangitis
Masuda *et al* [6], 2022	Japan	January 2018 to July 2020	Retrospective observational study	TG18/TG13	Grade I and grade II AC after successful ERCP	Antibiotic therapy of 3 d	30-d-mortality, recurrent cholangitis within 3 mo, length of hospitalization, in-hospital mortality
Sokal *et al*[14], 2022	France	2016-2018	Retrospective observational study	TG18/TG13	Patients with AC with and without malignant etiology	Cancer-associated AC	Duration of antibiotic therapy, 28-d-mortality, liver abscess
Masuda *et al* [17], 2021	Japan	April 2018 to March 2020	Retrospective observational study	TG18/TG13	AC patients with positive blood or bile culture and early ERCP	AC due to antibiotic resistant bacteria	Duration of antibiotic therapy, duration of hospitalization, in-hospital mortality, increased disease severity
Akhtar *et al* [18], 2020	Pakistan	June 2012 to June 2017	Cross-sectional observational study	TG18/TG13	AC patients without liver metastases or other reason for deranged liver function test. 70% of patients received ERCP	3-mo-mortality	Duration of antibiotic therapy, clinical severity, bacteremia
Haal *et al*[21], 2020	Netherlands	January 2012 to January 2017	Retrospective observational study	TG18/TG13	AC only due to stone in the common bile duct, without prior antibiotic therapy after ERCP	Antibiotic therapy of ≤ 3 d	3-mo-mortality, length of hospitalization, recurrent cholangitis, other complications
Satake *et al*[8], 2020	Japan	April 2014 to March 2019	Retrospective observational study	TG18/TG13	Grade I and grade II AC only due to choledocholithiasis who underwent ERCP	Antibiotic therapy of ≤ 3 d	30-d-mortality, length of hospitalization, recurrent cholangitis within 3 mo
Netinatsunton *et al*[16], 2019	Thailand	August 2017 to August 2018	Randomized controlled trial	TG18/TG13	AC only due to choledocholithiasis without presence of the Reynold´s pentad. Time to ERCP same between the study groups	Antibiotic therapy of ≤ 14 d	Recurrent cholangitis, length of hospitalization
Doi *et al*[22], 2018	Japan	January 2012 to February 2017	Retrospective observational study	ICD-10 and positive blood culture	AC and positive blood culture	Antibiotic therapy of ≤ 7 d	30-d-mortality, recurrent cholangitis within 3 mo (recurrence of symptoms)
Tagashira *et al* [13], 2017	Japan	January 2009 to December 2015	Retrospective observational study	TG18/TG13	Bacteriemic AC and ERCP where indicated	Adequate initial antibiotic therapy	Duration of antibiotic treatment, 30-d mortality
Uno *et al*[12], 2017	Japan	July 2012 to March 2014	Retrospective observational study	TG18/TG13	AC patients with gram-negative bacteriemia and after ERCP	Antibiotic therapy of ≤ 14 d	30-d mortality, recurrent cholangitis within 3 mo,

							antimicrobial treatment duration
Park *et al*[15], 2014	South Korea	September 2010 to November 2012	Randomized controlled trial	TG07	AC with bacteremia and ERCP within 24 h after admission	Intravenous antibiotic therapy of 6 d plus 8 d oral antibiotic therapy	30-d mortality, length of hospitalization, eradication of bacteria after 30 d
Kogure *et al* [19], 2011	Japan	September 2007 to August 2009	Retrospective observational study	TG07	Moderate and severe AC with ERCP	Antibiotic therapy of 3 d	Recurrent cholangitis
Van Lent *et al* [11], 2002	Netherlands	February 1999 to September 1999	Retrospective observational study	Fever > 38 °C and elevated bilirubin levels or bile duct dilatation in ultrasound	AC after successful ERCP. Exclusion of patients with primary sclerosing cholangitis, liver transplant recipients, bile duct atresia, inflammatory bowel disease	Antibiotic therapy of ≤ 3 d	6-mo mortality and recurrent cholangitis

AC: Acute cholangitis; TG18: Tokyo Guidelines 2018; TG13: Tokyo Guidelines 2013; TG07: Tokyo Guidelines 2007; ICD-10: The 10th Edition of the International Classification of Diseases; ERCP: Endoscopic retrograde cholangiopancreatography.

Mortality

Among the eight studies which were included in the quantitative analysis, six of them included mortality as an outcome[6,8,11,12,21,22], while five of the studies that were not suitable for the meta-analysis provided information for the participants' death[13-15,17,18]. Six studies calculated a 30-d mortality rate[6,8,12,13,15,22], Sokal *et al*[14] presented data concerning 28-d mortality, and Haal *et al* [21] conducted a follow-up of 3 mo concerning the death rates of the participants. Van Lent *et al*[11] observed the mortality of the patients for the following six months after the intervention.

After summarizing the data of the four studies with a duration of 2-3 of antibiotic treatment as cutoff point[6,8,11,21], no significant difference in the mortality between the two patient groups is present (OR = 0.78, 95%CI: 0.23-2.67, I^2 = 9%) (Figure 2A). No heterogeneity among these studies concerning our primary outcome is noted (I^2 = 9%).

In the study of Doi *et al*[22], patients who received an antibiotic treatment of fewer than seven days presented similar death rates compared to those with longer therapeutic schemata (OR = 0.82, 95%CI: 0.18-2.95, I^2 = 9%). The 30-d mortality rates of AC patients did not seem to differ between antibiotic therapies, of 14 d or shorter, according to Uno *et al*[12] (2 *vs* 0, P = 0.79, Fisher´s exact test).

Similar findings are also observable in the rest of the studies, which were not included in the meta-analysis. Sokal *et al*[14] presented that although patients with cancer-related-AC took an antibiotic treatment of mean duration with no significant difference compared to those that suffered from non-cancer-related-AC (10.6 ± 9.7 *vs* 7.8 ± 7.5 d, P = 0.13), the patients who belonged in the first group had significantly higher mortality rates (17 *vs* 0 deaths, P = 0.0002). In the rest of the studies, no differences concerning mortality were to be noted[13,15,17,18].

Recurrent cholangitis

Five of the included papers calculated a recurrence rate up to a follow-up period of 3 mo[6,8,12,21,22], van Lent *et al*[11] estimated a 28-d recurrence rate, Ferstl *et al*[23] recorded the shortest follow-up period among the studies (28 d) and two studies did not clarify the exact duration of follow-up for this outcome[16,19].

According to the studies retrieved from our review, a two to three-day antibiotic therapy was not associated with a significantly more frequent appearance of recurrent cholangitis (OR = 0.89, 95%CI: 0.49-1.60) (Figure 2B)[6,8,11,21]. No differences were also noted in the rates of recurrent AC neither in the 6-7-d-cutoff (OR = 1.11, 95%CI: 0.45-2.75) nor the 14-d-cutoff study groups (OR = 0.15, 95%CI: 0.02-1.35) (Figures 3 and 4A respectively). In all these comparisons, no significant study heterogeneity was observed (I^2 = 38%, 0%, and 0%, respectively). In the study of Kogure *et al*[19], no recurrent cholangitis was observed in both study groups, with and without withdrawal of the antibiotic therapy on the third day of treatment.

Length of hospitalization

Although in the studies of Masuda *et al*[6] and Haal *et al*[21], the patients who belong to the two-day and three-day antibiotic therapy have a significantly shorter hospitalization duration, the SMD of all three studies with a cutoff of 2-3 d is not significantly lower in the short-term antibiotic group (SMD = -0.53, 95%CI: -1.88 to 0.82, I^2 = 91%) (Figure 2C). Similarly, no difference was found between the short-

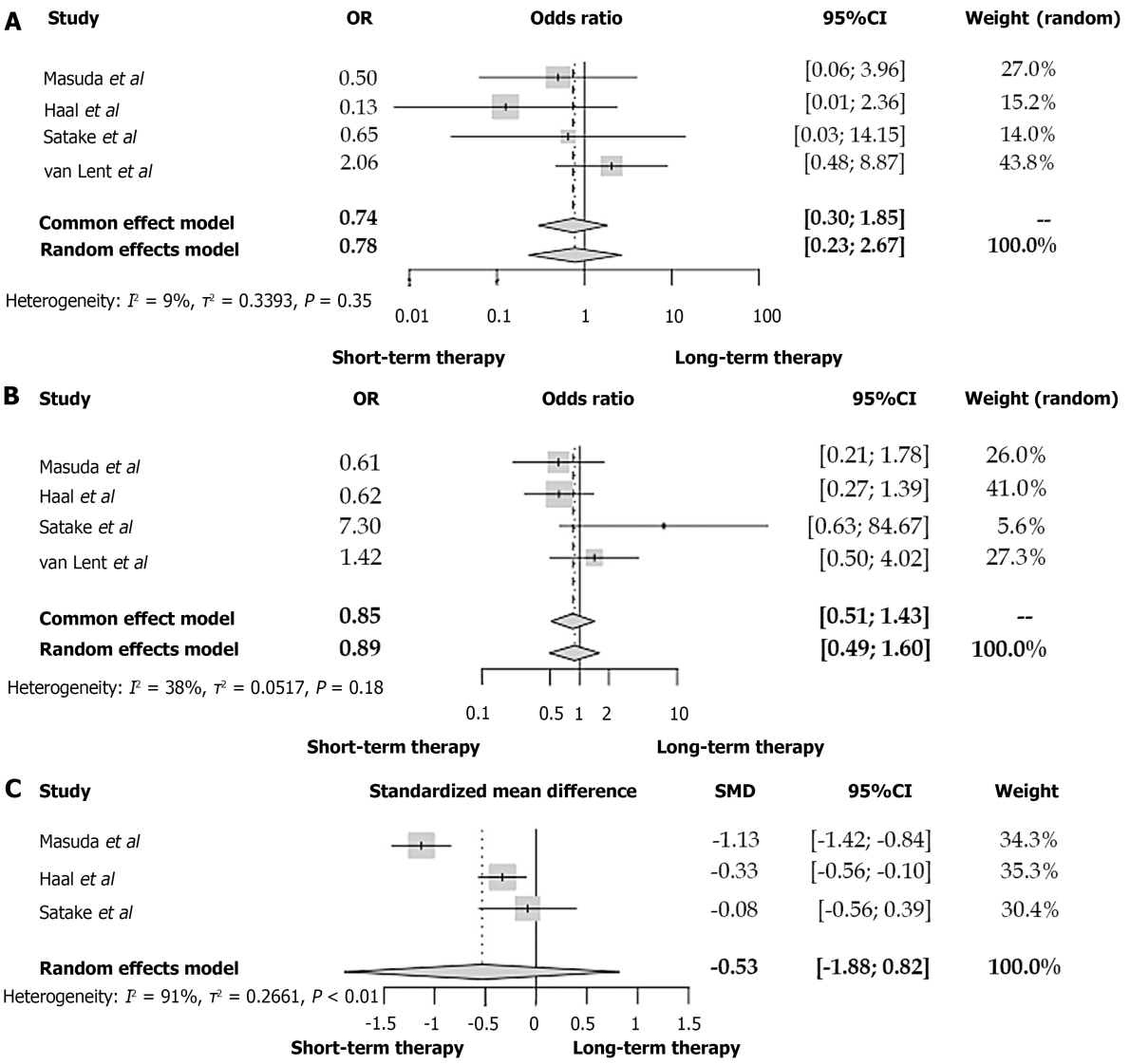


Figure 2 Forest plot between patients with acute cholangitis who received an antibiotic therapy of 2-3 d and acute cholangitis-patients with longer antibiotic treatment. A: Mortality; B: Recurrent cholangitis; C: Duration of hospitalization. OR: Odds ratio; CI: Confidence interval; SMD: Standardized mean difference.

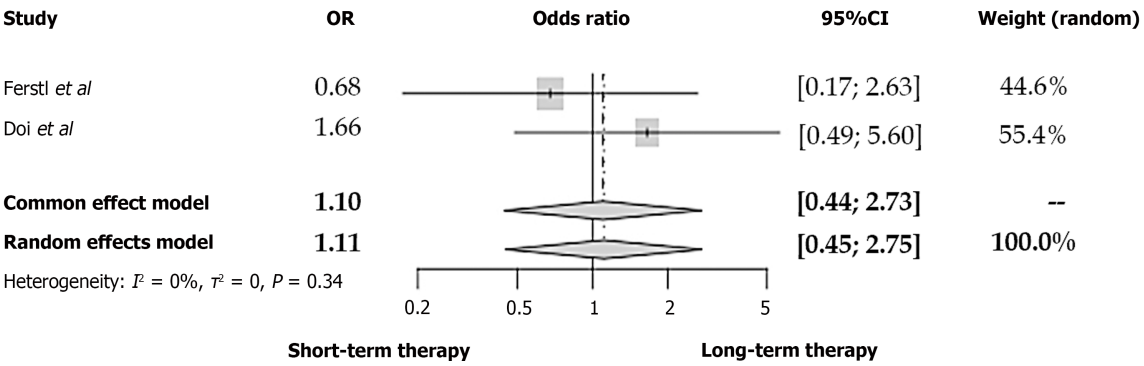


Figure 3 Forest plot of recurrent cholangitis between patients with acute cholangitis who received an antibiotic therapy of 6-7 d and acute cholangitis-patients with longer antibiotic treatment. OR: Odds ratio; CI: Confidence interval.

and long-term treatment groups concerning the length of in-hospital stay (SMD = -1.30, 95%CI: -14.43 to 11.84, I^2 = 95%) (Figure 4B). However, the considerable study heterogeneity (I^2 = 91% and 95%, respectively) does not allow us to extract strong conclusions. On the contrary, Park *et al*[15] estimated that a switch from intravenous to oral antibiotic therapy after six days from the treatment initiation led

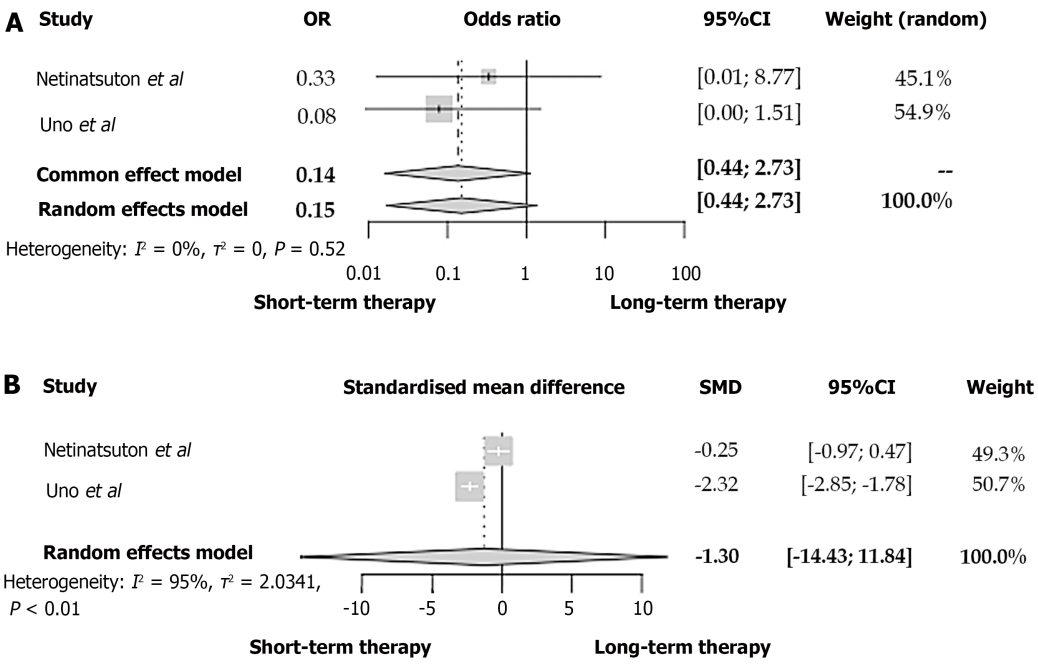


Figure 4 Forest plot between patients with acute cholangitis who received an antibiotic therapy of 14 d and acute cholangitis-patients with shorter antibiotic treatment. A: Recurrent cholangitis; B: Duration of hospitalization. OR: Odds ratio; CI: Confidence interval; SMD: Standardized mean difference.

to a significantly lower length of hospitalization in comparison with a switch at ten days of treatment.

Quality assessment

Based on the Newcastlte-Ottawa Scale, six of the observational studies included in the systematic review were considered of good quality[6,8,13,17,21,23], while the remaining seven were graded as low-quality studies, concerning our outcomes of interest, mostly due to lack of comparability between the cohort participants[11,13,14,18-20,22] (Table 2). In the study of Netinatsunton *et al*[16], as far as the randomization process is concerned, although the patients were randomized with the use of a computer-generated process and the baseline characteristics of the patients did not significantly differ, the results of the randomization were stated to be concealed in envelopes. However, the status and the accessibility of the envelopes are not provided, which raises concerns regarding the absolute transparency of the randomization. Additionally, no information is provided to manage the patients who did not adhere to the trial. Furthermore, the fact that no more information is provided concerning the construction of the study, as the trial protocol is provided neither in the clinicaltrials.gov website nor in the text in its complete form, leads us to the conclusion that the risk of bias in this study is high.

The trial of Park *et al*[15] has been based on a computer-generated block randomization model. However, no allocation concealment was possible due to the different application ways of the different interventions (oral *vs* intravenous). The authors followed an intention-to-treat model, but the lack of blinding may have led to a bias in measuring the outcome. Due to these facts, we conclude that the trial of Park *et al*[15] may also be connected to a high risk of bias.

DISCUSSION

To our knowledge, this is the first complete meta-analysis examining the duration of antibiotic therapy against the AC. In previously conducted systematic reviews with similar thematology, the limited data and the heterogenous outcomes and populations did not allow the authors to perform a meta-analysis [7,29]. Our data synthesis showed that antibiotic treatment of less than 2 or 3 d is not associated with significantly higher mortality rates, according to the random effects model (OR = 0.82, 95%CI: 0.18-2.95, I^2 = 9%). Our findings agree with the conclusions of the systematic review of Haal *et al*[7]. The fact that van Lent *et al*[11] did not base their diagnosis on the TG07 or TG18/13, possibly because the study was conducted before the establishment of the diagnostic criteria, may weaken the weight of this outcome. Although the combination of the diagnostic criteria of van Lent (fever > 38°C + elevated bilirubin levels or dilated bile duct by ultrasound) theoretically covers the criteria needed for the diagnosis of AC[30], the authors did not provide the exact cutoff, above which the bilirubin levels are considered elevated and the sensitivity of ultrasound on the diagnosis of AC is limited[31,32]. This could lead to a false

Table 2 Quality assessment of the observational studies

	Ferstl *et al* [23], *n* = 115	Kihara and Yokomizo [20], *n* = 112	Masuda *et al* [6], *n* = 11	Sokal *et al* [14], *n* = 107	Masuda *et al* [17], *n* = 110	Akhtar *et al* [18], *n* = 55	Haal *et al* [21], *n* = 113	Satake *et al* [8], *n* = 101	Doi *et al* [22], *n* = 114	Tagashira *et al*[13], *n* = 106	Uno *et al* [12], *n* = 105	Kogure *et al* [19], *n* = 111	Van Lent *et al*[11], *n* = 104
Selection													
Representativeness of exposed cohort	*	-	*	-	*	*	*	*	*	*	*	*	*
Selection of non-exposed cohort	*	*	*	*	*	*	*	*	*	*	*	*	*
Ascertainment of exposure	*	*	*	*	*	*	*	*	*	*	*	*	*
Demonstration that outcome of interest was not present at start of study	*	*	*	*	*	*	*	*	*	*	*	*	*
Comparability													
Comparability of the cohorts	**	-	**	-	**	-	**	**	-	-	**	-	-
Outcome													
Assessment of outcome	*	*	*	*	*	*	*	*	*	*	*	*	*
Was follow-up long enough for outcomes to occur?	*	*	*	*	*	*	*	*	*	*	*	*	*
Adequacy of follow-up cohorts	*	*	*	*	*	*	*	*	*	*	*	*	*
Overall	**Good**	**Low**	**Good**	**Low**	**Good**	**Low**	**Good**	**Good**	**Low**	**Low**	**Good**	**Low**	**Low**

*Represents study meets a criterion in each section of the Newcastle-Ottawa scale; -Represents study meets no criterion in each section of the Newcastle-Ottawa scale.

estimation of the actual patients suffering from AC. In the studies of Doi *et al*[22] and Uno *et al*[12], who set higher cutoffs for the definition of short- and long-term treatments, significance in the OR of the mortality rates was also not reached[12,22]. The findings of Sokal *et al*[33] that cancer-related AC patients presented a higher 28-d mortality compared to patients with AC not related to malignancies, in combination with the fact that the patients in the two groups received an antibiotic therapy of no different duration, may imply that the antibiotic therapy in cancer-related AC-patients should be longer. This study alone can provide no evidence for this assumption.

Concerning the rates of recurrent cholangitis, no significant differences were found between the study groups in all three duration cutoffs we set for our analysis. Although Uno *et al*[12] estimated a slightly higher recurrence rate in the group with > 14 d of antibiotic treatment, our synthesis with the study of Netinatsunton *et al*[16] resulted in no significantly different rates compared with the longer-course group. Haal *et al*[7] and Tinusz *et al*[29] enforce our results that the duration of antibiotic treatment of AC does not seem to affect the possibility of the appearance of cholangitis recurrence. The increasing resistance of the usual bacteria causing AC, such as *Escherichia coli*, the higher rates of gram-positive pathogens in recurrent cholangitis, and the possible lack of coverage against those bacteria in the initial empiric scheme provided against AC may constitute the major factors for the appearance of episodes of cholangitis recurrence[3,34,35]. As Tagashira *et al*[13] stated, inadequate initial antibiotic treatment could increase mortality and adverse events in bacteremic patients with AC.

Among the studies with a cutoff of 2-3 d of antibiotic treatment, Masuda *et al*[6] and Haal *et al*[21] presented a significantly shorter in-hospital stay for patients receiving short-term treatment compared to the control group of the study. However, when summarizing those two studies with the observational study of Satake *et al*[8], the SMD in the length of hospitalization was not significant (SMD = -0.6, 95%CI: -2.27 to 1.07, I^2 = 0%). Antibiotic treatment of less than 14 did also not seem to lead to a shorter hospitalization of patients compared to the control group, according to our study (SMD = -1.3, 95%CI: -14.49 to 11.89, I^2 = 96%), even though the short-course antibiotic treatment in Uno *et al*[12], presented a significantly lower hospitalization duration. However, the high heterogeneity of the studies included in these tests concerning this outcome (I^2 = 91% and 96%, respectively) may have affected our results. Park *et al*[15] reinforced the claim that shorter antibiotic treatment may benefit the patients concerning their length of stay in the hospital, as no mortality cases were recorded. In every case, more studies examining the hospitalization length should be conducted, as the extraction of evidence that proves that a short-course antibiotic treatment leads to shorter hospitalizations would protect patients from exposure to several dangers, such as thromboembolic episodes and unwanted infections[36,37].

Our study presents several limitations which should be accounted for. First of all, as many studies were conducted before 2013, the choice of the participants as patients suffering from AC was not based on the updated TG18/13, especially in the study of van Lent *et al*[11]. This may alter the actual population we wish to study. The difference in patients' inclusion and exclusion criteria and the variable severity grades of the patients included in the studies also constitute an important limitation. Additionally, small discrepancies are also noticed in the follow-up periods concerning the mortality and recurrent cholangitis in each study. These inequalities in the follow-up of the patients may lead to lost data which may have altered our results. Finally, significant statistical heterogeneity was detected among the studies selected for the quantitative analysis of the length of hospitalizations, which may lead to invalid conclusions.

CONCLUSION

Depending on our findings, the duration of antibiotic therapy may not significantly affect the mortality rate, the rate of recurrent cholangitis, and the length of hospitalization of patients suffering from AC. More specifically, a 2 to 3-d antibiotic treatment could be similarly effective in preventing mortality and recurrent cholangitis, as the 4 to 7-d therapy proposed by the TG18. However, these results are based on a small number of heterogeneous studies. It is vital that more primary and secondary studies are conducted for new recommendations with high-level evidence to be established.

ARTICLE HIGHLIGHTS

Research background

The mortality rates of acute cholangitis (AC) have significantly decreased in the last decades. The development of new diagnostic and therapeutic tools has contributed to this result.

Research motivation

The Tokyo Guidelines of 2018 suggest an antibiotic treatment of four to seven days in AC cases without gram-positive cocci. This interval between the recommended treatment days is relatively wide, and the recommendation provided is not based on a high level of evidence (level C).

Research objectives

The aim of this study is to investigate if shorter-course antibiotic treatments could be similarly effective to long-course treatments in adults with AC.

Research methods

We conducted a systematic review and meta-analysis of the existing literature based on the recommendations of the Preferred Reporting Items for Systematic Review and Meta-Analyses. Two reviewers (Kasparian K and Christou CD) conducted the literature research, study selection, and data collection. The inclusion and exclusion criteria were predefined. The data synthesis, statistical analysis, and Forest plot creation were conducted through the program R Studio version 1.4.1103.

Research results

Fifteen studies were included in the systematic review and eight in the final meta-analysis. Most of the patients were classified as Grade I (41,1%) or Grade II (54,1%), while only 4,6% of the participants suffered from Grade III AC. No significant differences were observed between patients receiving a 2-3 d antibiotic therapy and those who were treated with longer antibiotic schemata concerning the mortality (odds ratio = 0.78, 95% confidence interval: 0.23-2.67, I^2 = 9%). In all calculations conducted, no differences could be detected among patients receiving shorter and longer antibiotic treatments concerning the rates of recurrent AC and the length of hospitalization.

Research conclusions

Short- and long-course antibiotic treatments may be similarly effective concerning the mortality and recurrence rates of AC.

Research perspectives

This study could constitute the occasion for the conduction of more primary and secondary studies for new robust recommendations with a high level of evidence to be established.

FOOTNOTES

Author contributions: Kasparian K, Christou CD, Petidis K, Doumas M, and Giouleme O designed the research study; Kasparian K and Christou CD performed the research; Kasparian K analyzed the data and wrote the manuscript; and all authors have read and approved the final manuscript.

Conflict-of-interest statement: All the authors report no relevant conflicts of interest for this article.

PRISMA 2009 Checklist statement: The authors have read the PRISMA 2009 Checklist, and the manuscript was prepared and revised according to the PRISMA 2009 Checklist.

Open-Access: This article is an open-access article that was selected by an in-house editor and fully peer-reviewed by external reviewers. It is distributed in accordance with the Creative Commons Attribution NonCommercial (CC BY-NC 4.0) license, which permits others to distribute, remix, adapt, build upon this work non-commercially, and license their derivative works on different terms, provided the original work is properly cited and the use is non-commercial. See: https://creativecommons.org/Licenses/by-nc/4.0/

Country/Territory of origin: Greece

ORCID number: Karampet Kasparian 0000-0002-5443-0749; Chrysanthos D Christou 0000-0002-5417-8686; Olga Giouleme 0000-0003-0176-3598.

S-Editor: Wang JJ
L-Editor: A
P-Editor: Cai YX

REFERENCES

1 **Kimura Y**, Takada T, Strasberg SM, Pitt HA, Gouma DJ, Garden OJ, Büchler MW, Windsor JA, Mayumi T, Yoshida M, Miura F, Higuchi R, Gabata T, Hata J, Gomi H, Dervenis C, Lau WY, Belli G, Kim MH, Hilvano SC, Yamashita Y. TG13 current terminology, etiology, and epidemiology of acute cholangitis and cholecystitis. *J Hepatobiliary Pancreat Sci* 2013; **20**: 8-23 [PMID: 23307004 DOI: 10.1007/s00534-012-0564-0]

2 **Zimmer V**, Lammert F. Acute Bacterial Cholangitis. *Viszeralmedizin* 2015; **31**: 166-172 [PMID: 26468310 DOI: 10.1159/000430965]

3 **Gomi H**, Takada T, Hwang TL, Akazawa K, Mori R, Endo I, Miura F, Kiriyama S, Matsunaga N, Itoi T, Yokoe M, Chen MF, Jan YY, Ker CG, Wang HP, Wada K, Yamaue H, Miyazaki M, Yamamoto M. Updated comprehensive epidemiology, microbiology, and outcomes among patients with acute cholangitis. *J Hepatobiliary Pancreat Sci* 2017; **24**: 310-318 [PMID: 28371094 DOI: 10.1002/jhbp.452]

4 **Kiriyama S**, Kozaka K, Takada T, Strasberg SM, Pitt HA, Gabata T, Hata J, Liau KH, Miura F, Horiguchi A, Liu KH, Su

CH, Wada K, Jagannath P, Itoi T, Gouma DJ, Mori Y, Mukai S, Giménez ME, Huang WS, Kim MH, Okamoto K, Belli G, Dervenis C, Chan ACW, Lau WY, Endo I, Gomi H, Yoshida M, Mayumi T, Baron TH, de Santibañes E, Teoh AYB, Hwang TL, Ker CG, Chen MF, Han HS, Yoon YS, Choi IS, Yoon DS, Higuchi R, Kitano S, Inomata M, Deziel DJ, Jonas E, Hirata K, Sumiyama Y, Inui K, Yamamoto M. Tokyo Guidelines 2018: diagnostic criteria and severity grading of acute cholangitis (with videos). *J Hepatobiliary Pancreat Sci* 2018; **25**: 17-30 [PMID: 29032610 DOI: 10.1002/jhbp.512]

5 **Gomi H**, Solomkin JS, Schlossberg D, Okamoto K, Takada T, Strasberg SM, Ukai T, Endo I, Iwashita Y, Hibi T, Pitt HA, Matsunaga N, Takamori Y, Umezawa A, Asai K, Suzuki K, Han HS, Hwang TL, Mori Y, Yoon YS, Huang WS, Belli G, Dervenis C, Yokoe M, Kiriyama S, Itoi T, Jagannath P, Garden OJ, Miura F, de Santibañes E, Shikata S, Noguchi Y, Wada K, Honda G, Supe AN, Yoshida M, Mayumi T, Gouma DJ, Deziel DJ, Liau KH, Chen MF, Liu KH, Su CH, Chan ACW, Yoon DS, Choi IS, Jonas E, Chen XP, Fan ST, Ker CG, Giménez ME, Kitano S, Inomata M, Mukai S, Higuchi R, Hirata K, Inui K, Sumiyama Y, Yamamoto M. Tokyo Guidelines 2018: antimicrobial therapy for acute cholangitis and cholecystitis. *J Hepatobiliary Pancreat Sci* 2018; **25**: 3-16 [PMID: 29090866 DOI: 10.1002/jhbp.518]

6 **Masuda S**, Koizumi K, Makazu M, Uojima H, Kubota J, Kimura K, Nishino T, Sumida C, Ichita C, Sasaki A, Shionoya K. Antibiotic Administration within Two Days after Successful Endoscopic Retrograde Cholangiopancreatography Is Sufficient for Mild and Moderate Acute Cholangitis. *J Clin Med* 2022; **11** [PMID: 35628824 DOI: 10.3390/jcm11102697]

7 **Haal S**, Wielenga MCB, Fockens P, Leseman CA, Ponsioen CY, van Soest EJ, van Wanrooij RLJ, Sieswerda E, Voermans RP. Antibiotic Therapy of 3 Days May Be Sufficient After Biliary Drainage for Acute Cholangitis: A Systematic Review. *Dig Dis Sci* 2021; **66**: 4128-4139 [PMID: 33462749 DOI: 10.1007/s10620-020-06820-3]

8 **Satake M**, Yamaguchi Y. Three-day antibiotic treatment for acute cholangitis due to choledocholithiasis with successful biliary duct drainage: A single-center retrospective cohort study. *Int J Infect Dis* 2020; **96**: 343-347 [PMID: 32376307 DOI: 10.1016/j.ijid.2020.04.074]

9 **Sawyer RG**, Claridge JA, Nathens AB, Rotstein OD, Duane TM, Evans HL, Cook CH, O'Neill PJ, Mazuski JE, Askari R, Wilson MA, Napolitano LM, Namias N, Miller PR, Dellinger EP, Watson CM, Coimbra R, Dent DL, Lowry SF, Cocanour CS, West MA, Banton KL, Cheadle WG, Lipsett PA, Guidry CA, Popovsky K; STOP-IT Trial Investigators. Trial of short-course antimicrobial therapy for intraabdominal infection. *N Engl J Med* 2015; **372**: 1996-2005 [PMID: 25992746 DOI: 10.1056/NEJMoa1411162]

10 **Page MJ**, McKenzie JE, Bossuyt PM, Boutron I, Hoffmann TC, Mulrow CD, Shamseer L, Tetzlaff JM, Akl EA, Brennan SE, Chou R, Glanville J, Grimshaw JM, Hróbjartsson A, Lalu MM, Li T, Loder EW, Mayo-Wilson E, McDonald S, McGuinness LA, Stewart LA, Thomas J, Tricco AC, Welch VA, Whiting P, Moher D. The PRISMA 2020 statement: an updated guideline for reporting systematic reviews. *BMJ* 2021; **372**: n71 [PMID: 33782057 DOI: 10.1136/bmj.n71]

11 **van Lent AU**, Bartelsman JF, Tytgat GN, Speelman P, Prins JM. Duration of antibiotic therapy for cholangitis after successful endoscopic drainage of the biliary tract. *Gastrointest Endosc* 2002; **55**: 518-522 [PMID: 11923764 DOI: 10.1067/mge.2002.122334]

12 **Uno S**, Hase R, Kobayashi M, Shiratori T, Nakaji S, Hirata N, Hosokawa N. Short-course antimicrobial treatment for acute cholangitis with Gram-negative bacillary bacteremia. *Int J Infect Dis* 2017; **55**: 81-85 [PMID: 28027992 DOI: 10.1016/j.ijid.2016.12.018]

13 **Tagashira Y**, Sakamoto N, Isogai T, Hikone M, Kosaka A, Chino R, Higuchi M, Uehara Y, Honda H. Impact of inadequate initial antimicrobial therapy on mortality in patients with bacteraemic cholangitis: a retrospective cohort study. *Clin Microbiol Infect* 2017; **23**: 740-747 [PMID: 28254686 DOI: 10.1016/j.cmi.2017.02.027]

14 **Sokal A**, Chawki S, Nguyen Y, Sauvanet A, Ponsot P, Maire F, Fantin B, de Lastours V. Specificities of acute cholangitis in patients with cancer: a retrospective comparative study of 130 episodes. *Eur J Clin Microbiol Infect Dis* 2022; **41**: 143-146 [PMID: 34415466 DOI: 10.1007/s10096-021-04289-0]

15 **Park TY**, Choi JS, Song TJ, Do JH, Choi SH, Oh HC. Early oral antibiotic switch compared with conventional intravenous antibiotic therapy for acute cholangitis with bacteremia. *Dig Dis Sci* 2014; **59**: 2790-2796 [PMID: 24898101 DOI: 10.1007/s10620-014-3233-0]

16 **Netinatsunton N**, Limmathurotsakul D, Attasaranya S, Sottisuporn J, Pattarapuntakul T, Ovartlarnporn B. Short Duration versus 14-day Antibiotic Treatment in Acute Cholangitis due to Bile Duct Stone: A randomized study. *J Gastroenterol Hepatol Res* 2019; **8**: 3020-3024

17 **Masuda S**, Koizumi K, Uojima H, Kimura K, Nishino T, Tasaki J, Ichita C, Sasaki A. Effect of Antibiotic Resistance of Pathogens on Initial Antibiotic Therapy for Patients With Cholangitis. *Cureus* 2021; **13**: e18449 [PMID: 34650837 DOI: 10.7759/cureus.18449]

18 **Akhtar F**, Siddique MZ, Raza A, Mehmood S, Yusuf MA, Sultan F. Microbiology and clinical characteristics of acute cholangitis with their impact on mortality; a retrospective cross sectional study. *J Pak Med Assoc* 2020; **70**: 607-612 [PMID: 32296203 DOI: 10.5455/JPMA.29747]

19 **Kogure H**, Tsujino T, Yamamoto K, Mizuno S, Yashima Y, Yagioka H, Kawakubo K, Sasaki T, Nakai Y, Hirano K, Sasahira N, Isayama H, Tada M, Kawabe T, Omata M, Harada S, Ota Y, Koike K. Fever-based antibiotic therapy for acute cholangitis following successful endoscopic biliary drainage. *J Gastroenterol* 2011; **46**: 1411-1417 [PMID: 21842232 DOI: 10.1007/s00535-011-0451-5]

20 **Kihara Y**, Yokomizo H. The clinical features of late postoperative cholangitis following pancreaticoduodenectomy brought on by conditions other than cancer recurrence: a single-center retrospective study. *BMC Surg* 2022; **22**: 301 [PMID: 35932000 DOI: 10.1186/s12893-022-01752-3]

21 **Haal S**, Ten Böhmer B, Balkema S, Depla AC, Fockens P, Jansen JM, Kuiken SD, Liberov BI, van Soest E, van Hooft JE, Sieswerda E, Voermans RP. Antimicrobial therapy of 3 days or less is sufficient after successful ERCP for acute cholangitis. *United European Gastroenterol J* 2020; **8**: 481-488 [PMID: 32213042 DOI: 10.1177/2050640620915016]

22 **Doi A**, Morimoto T, Iwata K. Shorter duration of antibiotic treatment for acute bacteraemic cholangitis with successful biliary drainage: a retrospective cohort study. *Clin Microbiol Infect* 2018; **24**: 1184-1189 [PMID: 29408612 DOI: 10.1016/j.cmi.2018.01.021]

23 **Ferstl PG**, Queck A, Bremer K, Filmann N, Weiler N, Welker MW, Waidmann O, Knabe M, Bechstein WO, Hogardt M, Kempf VAJ, Zeuzem S, Trebicka J, Friedrich-Rust M, Walter D. Comparison of short-course antibiotic therapy of 6 or less

days with a longer treatment in patients with cholangitis after liver transplantation. *Transpl Infect Dis* 2022; **24**: e13868 [PMID: 35598281 DOI: 10.1111/tid.13868]

24 **Hozo SP**, Djulbegovic B, Hozo I. Estimating the mean and variance from the median, range, and the size of a sample. *BMC Med Res Methodol* 2005; **5**: 13 [PMID: 15840177 DOI: 10.1186/1471-2288-5-13]

25 **Lin L**, Aloe AM. Evaluation of various estimators for standardized mean difference in meta-analysis. *Stat Med* 2021; **40**: 403-426 [PMID: 33180373 DOI: 10.1002/sim.8781]

26 **Sweeting MJ**, Sutton AJ, Lambert PC. What to add to nothing? *Stat Med* 2004; **23**: 1351-1375 [PMID: 15116347 DOI: 10.1002/sim.1761]

27 **Cook DA**, Reed DA. Appraising the quality of medical education research methods: the Medical Education Research Study Quality Instrument and the Newcastle-Ottawa Scale-Education. *Acad Med* 2015; **90**: 1067-1076 [PMID: 26107881 DOI: 10.1097/ACM.0000000000000786]

28 **Higgins JPT**, Savović J, Page MJ, Elbers RG, Sterne JAC. Chapter 8: Assessing risk of bias in a randomized trial. In: Cochrane Handbook for Systematic Reviews of Interventions, Version 6.3, 2022. British: Cochrane Collaboration, 2022

29 **Tinusz B**, Szapáry L, Paládi B, Tenk J, Rumbus Z, Pécsi D, Szakács Z, Varga G, Rakonczay Z Jr, Szepes Z, Czimmer J, Vincze Á, Hegyi P, Erőss B. Short-Course Antibiotic Treatment Is Not Inferior to a Long-Course One in Acute Cholangitis: A Systematic Review. *Dig Dis Sci* 2019; **64**: 307-315 [PMID: 30368681 DOI: 10.1007/s10620-018-5327-6]

30 **Kiriyama S**, Takada T, Strasberg SM, Solomkin JS, Mayumi T, Pitt HA, Gouma DJ, Garden OJ, Büchler MW, Yokoe M, Kimura Y, Tsuyuguchi T, Itoi T, Yoshida M, Miura F, Yamashita Y, Okamoto K, Gabata T, Hata J, Higuchi R, Windsor JA, Bornman PC, Fan ST, Singh H, de Santibanes E, Gomi H, Kusachi S, Murata A, Chen XP, Jagannath P, Lee S, Padbury R, Chen MF; Tokyo Guidelines Revision Committee. New diagnostic criteria and severity assessment of acute cholangitis in revised Tokyo Guidelines. *J Hepatobiliary Pancreat Sci* 2012; **19**: 548-556 [PMID: 22825491 DOI: 10.1007/s00534-012-0537-3]

31 **Walas MK**, Skoczylas K, Gierbliński I. Errors and mistakes in the ultrasound diagnostics of the liver, gallbladder and bile ducts. *J Ultrason* 2012; **12**: 446-462 [PMID: 26673428 DOI: 10.15557/JoU.2012.0032]

32 **Majeed AW**, Ross B, Johnson AG, Reed MW. Common duct diameter as an independent predictor of choledocholithiasis: is it useful? *Clin Radiol* 1999; **54**: 170-172 [PMID: 10201865 DOI: 10.1016/s0009-9260(99)91008-5]

33 **Sokal A**, Sauvanet A, Fantin B, de Lastours V. Acute cholangitis: Diagnosis and management. *J Visc Surg* 2019; **156**: 515-525 [PMID: 31248783 DOI: 10.1016/j.jviscsurg.2019.05.007]

34 **Hara T**, Taniguchi M, Hattori C, Sakai H, Oka K, Iwai N, Tsuji T, Harada T, Okuda T, Komaki T, Sakagami J, Kagawa K. Microbiological analysis of patients with first and recurrent episodes of acute cholangitis in a middle-sized hospital: A single-center retrospective study in rural North Kyoto, Japan. *J Infect Chemother* 2022; **28**: 413-419 [PMID: 34973874 DOI: 10.1016/j.jiac.2021.11.025]

35 **van den Hazel SJ**, Speelman P, Tytgat GN, Dankert J, van Leeuwen DJ. Role of antibiotics in the treatment and prevention of acute and recurrent cholangitis. *Clin Infect Dis* 1994; **19**: 279-286 [PMID: 7986900 DOI: 10.1093/clinids/19.2.279]

36 **Welch C**, K Hassan-Smith Z, A Greig C, M Lord J, A Jackson T. Acute Sarcopenia Secondary to Hospitalisation - An Emerging Condition Affecting Older Adults. *Aging Dis* 2018; **9**: 151-164 [PMID: 29392090 DOI: 10.14336/AD.2017.0315]

37 **Heit JA**, Melton LJ 3rd, Lohse CM, Petterson TM, Silverstein MD, Mohr DN, O'Fallon WM. Incidence of venous thromboembolism in hospitalized patients *vs* community residents. *Mayo Clin Proc* 2001; **76**: 1102-1110 [PMID: 11702898 DOI: 10.4065/76.11.1102]

World Journal of Gastroenterology

Submit a Manuscript: https://www.f6publishing.com

World J Gastroenterol 2023 May 21; 29(19): 3040-3047

DOI: 10.3748/wjg.v29.i19.3040

ISSN 1007-9327 (print) ISSN 2219-2840 (online)

CASE REPORT

Pulmonary hypertension, nephrotic syndrome, and polymyositis due to hepatitis C virus infection: A case report

Ya-Nan Zhao, Guo-Hui Liu, Chang Wang, Yi-Xuan Zhang, Ping Yang, Ming Yu

Specialty type: Gastroenterology and hepatology

Provenance and peer review: Unsolicited article; Externally peer reviewed.

Peer-review model: Single blind

Peer-review report's scientific quality classification

Grade A (Excellent): 0
Grade B (Very good): B
Grade C (Good): C, C
Grade D (Fair): 0
Grade E (Poor): 0

P-Reviewer: Beenet L, United States; Rodrigues AT, Brazil; Salvadori M, Italy

Received: March 14, 2023
Peer-review started: March 14, 2023
First decision: April 10, 2023
Revised: April 17, 2023
Accepted: April 25, 2023
Article in press: April 25, 2023
Published online: May 21, 2023

Ya-Nan Zhao, Guo-Hui Liu, Chang Wang, Yi-Xuan Zhang, Ping Yang, Ming Yu, Department of Cardiology, China-Japan Union Hospital of Jilin University, Changchun 130033, Jilin Province, China

Corresponding author: Ming Yu, Doctor, Department of Cardiology, China-Japan Union Hospital of Jilin University, No. 126 Xian-tai Street, Changchun 130033, Jilin Province, China. yuming2019@jlu.edu.cn

Abstract

BACKGROUND

Hepatitis C infection not only damages the liver but also often accompanies many extrahepatic manifestations. Incidences of pulmonary hypertension (PH) caused by hepatitis C are rare, and incidences of concurrent nephrotic syndrome and polymyositis are even rarer.

CASE SUMMARY

Herein we describe the case of a 57-year-old woman who was admitted to our department for intermittent chest tightness upon exertion for 5 years, aggravated with dyspnea for 10 d. After relevant examinations she was diagnosed with PH, nephrotic syndrome, and polymyositis due to chronic hepatitis C infection. A multi-disciplinary recommendation was that the patient should be treated with sildenafil and macitentan in combination and methylprednisolone. During treatment autoimmune symptoms, liver function, hepatitis C RNA levels, and cardiac parameters of right heart catheterization were monitored closely. The patient showed significant improvement in 6-min walking distance from 100 to 300 m at 3-mo follow-up and pulmonary artery pressure drops to 50 mmHg. Long-term follow-up is needed to confirm further efficacy and safety.

CONCLUSION

Increasing evidence supports a relationship between hepatitis C infection and diverse extrahepatic manifestations, but it is very rare to have PH, nephrotic syndrome, and polymyositis in a single patient. We conducted a literature review on the management of several specific extrahepatic manifestations of hepatitis C.

Key Words: Hepatitis C; Nephrotic syndrome; Polymyositis; Pulmonary hypertension; Case report

©The Author(s) 2023. Published by Baishideng Publishing Group Inc. All rights reserved.

Core Tip: Hepatitis C virus (HCV) infection should be considered a systemic disease which is often associated with many extrahepatic manifestations, but it is very rare to have multiple different extrahepatic manifestations in a single patient. In this article, we report a case of pulmonary hypertension (PH), nephrotic syndrome, and polymyositis due to HCV infection. The optimal treatment strategy for hepatitis C-related extrahepatic manifestations remains to be determined. Our case confirms sildenafil and macitentan as effective treatment option for patients suffering from PH due to hepatitis C infection. However, randomized, controlled trials are warranted to confirm the present results.

Citation: Zhao YN, Liu GH, Wang C, Zhang YX, Yang P, Yu M. Pulmonary hypertension, nephrotic syndrome, and polymyositis due to hepatitis C virus infection: A case report. *World J Gastroenterol* 2023; 29(19): 3040-3047
URL: https://www.wjgnet.com/1007-9327/full/v29/i19/3040.htm
DOI: https://dx.doi.org/10.3748/wjg.v29.i19.3040

INTRODUCTION

Hepatitis C virus (HCV) is a sporadic and a common cause of chronic hepatitis after blood transfusion. In recent years various authors have described associations between hepatitis C infection and a heterogeneous group of non-hepatic diseases such as cryoglobulinemia, rheumatoid arthritis, Sjogren's syndrome, and glomerulonephritis, which are seen as extrahepatic manifestations of chronic hepatitis C infection[1].

Pulmonary hypertension (PH) is defined as a mean pulmonary arterial pressure (mPAP) ≥ 20 mmHg at rest with right heart catheterization[2]. PH affects approximately 1% of the global population, up to 10% of individuals aged ≥ 65 years, and at least 50% of patients with heart failure[3]. PH has several different causes with different management and outcomes. However, PH due to hepatitis C has rarely been reported. Herein we describe a case of PH, nephrotic syndrome, and polymyositis following chronic hepatitis C infection in a 57-year-old woman.

CASE PRESENTATION

Chief complaints

A 57-year-old Chinese woman presenting with untreated chest tightness, shortness of breath, and fatigue for 5 years and with dyspnea for 10 d was admitted to the China-Japan Union Hospital of Jilin University.

History of present illness

She had no precordial pain, orthopnea, or palpitation. She had no joint pain, dental ulcers, or rash.

History of past illness

Forty years previously she had received an intravenous blood transfusion for a right ovariectomy. Sixteen years previously she was diagnosed with hepatitis C, nephrotic syndrome, and hypertension, but did not receive standard treatment. Five years previously she developed mild PH with pulmonary arterial pressure of 54 mmHg measured by transthoracic echocardiography, which was not treated further. Three years previously she developed severe myopathy. She was diagnosed with polymyositis and administered methylprednisolone 40 mg once a day (QD) and cyclophosphamide 50 mg QD. She lapsed into intermittent coma due to hyperemic ammonia however, thus cyclophosphamide was discontinued, and methylprednisolone 20 mg QD was initiated and has been maintained to date.

Personal and family history

She had no family history of genetically related diseases, but her daughter had hepatitis C and had been treated with interferon.

Physical examination

Physical examination revealed no fever, heart rate 70 bpm, blood pressure 140/90 mmHg, O_2 saturation 94% on room air, second heart sound accentuation, and moderate edema in both lower limbs.

Laboratory examinations

Primary laboratory data on admission are shown in Table 1. The 6-min walking distance was 100 m.

Table 1 The patient's laboratory data at admission and at 1-mo follow-up

Parameter	Value (admission)	Value (month 1)	References value	Unit
N-terminal-pro B-type natriuretic peptide	590		0-125	pg/mL
Urea	10.02	11.6	2.5-6.1	mmol/L
Creatinine	123.4	124.9	46-92	μmol/L
Troponin	< 0.01		0-0.04	ng/mL
Myoglobin	208.1		0-120	ng/mL
Creatine kinase	576.24	98.6	30-135	U/L
Creatine kinase MB isoenzyme	42.1	50.2	0-16	U/L
Lactic dehydrogenase	378.88	777.2	120-246	U/L
D-dimer	1.28		0-0.5	μg/mL
White blood cell	9.10	14.05	4-10	10^9/L
Platelet	140	111	125-350	10^9/L
Hemoglobin	119	152	110-150	g/L
Alanine aminotransferase	18.28	41.4	5-40	IU/L
Aspartate aminotransferase	15.44	16.1	8-40	IU/L
Total bilirubin	16.48	30.10	5-21	μmol/L
Direct bilirubin	3.36	7.40	0-3.4	μmol/L
Indirect bilirubin	13.12	22.70	1.6-21	μmol/L
Albumin	22.73	25.65	35-52	g/L
Total cholesterol	7.67		3.0-5.7	mmol/L
Low density lipoprotein cholesterol	3.65		< 4.13	mmol/L
High density lipoprotein cholesterol	2.86		1.29-1.55	mmol/L
Fasting blood glucose	4.44		3.9-6.1	Mmol/L
Urinary protein	4+		negative	-
24-h proteinuria	416.01		0-150	mg/d
Hepatitis B surface antigen	0		< 0.05	IU/mL
Antibody to hepatitis C	6.04		< 1	S/CO
Immunodeficiency virus antigen and antibody	0.09		< 1	S/CO
Antibody to treponema pallidum	0.07		< 1	S/CO
Hepatitis C virus RNA	0		0	IU/mL
Anti-nuclear antibodies	negative		negative	-
Anti-cyclic citrullinated peptide antibody	13.89		< 25	RU/mL
Anti-cardiolipin antibody	2.23		0-12	RU/mL
Immunoglobulin G	4.92		7.51-15.60	g/L
Immunoglobulin A	2.82		0.82-4.53	g/L
Immunoglobulin M	1.81		0.46-3.04	g/L
C3	0.58		0.79-1.52	g/L
C4	0.14		0.16-0.38	g/L
Blood ammonia	56		9-30	μmol/L
Erythrocyte sedimentation rate	22	6	0-20	mm/h

Imaging examinations

Muscle biopsy showed striated muscle atrophy with inflammatory cell infiltration (Figure 1A). Electrocardiography indicated a normal sinus rhythm (Figure 1B). Transthoracic echocardiography showed enlargement of the left atrium (43.7 × 45.2 × 60.0), right atrium (59.8 × 39.4), and right ventricle (49.3), normal left ventricular ejection fraction (71.3%), elevated pulmonary artery pressure (61 mmHg), and reduced diastolic function (Figure 1C-F). Chest computed tomography (CT) depicted pulmonary arterial hypertension, right atrium and right ventricle enlargement, and no parenchymal lung disease (Figure 2A-C). Pulmonary ventilation/perfusion scanning indicated no evidence of typical signs of thromboembolic disease (Figure 2D). Abdominal CT suggested normal liver size with a hepato-renal shunt and a spleno-renal shunt (Figure 2E and F). Right heart catheterization showed that mPAP was 55.33, pulmonary artery wedge pressure (PAWP) was 24, and pulmonary vascular resistance (PVR) was 5.13 Woods units (WU) (Table 2).

FINAL DIAGNOSIS

Based on the medical history, symptoms, and auxiliary examinations, a diagnosis of moderate PH, nephrotic syndrome, polymyositis, hypertension, and hepatitis C was determined.

TREATMENT

The patient was treated with sildenafil 20 mg QD, macitentan 10 mg QD, irbesartan and hydrochlorothiazide 150 mg QD, furosemide 20 mg QD, and methylprednisolone 80 mg QD with the dose gradually reduced to 20 mg QD. Due to suspected hepatitis C-induced multiple organ injury the patient was referred to the gastroenterology department for further assessment of liver disease. There was no evidence of a liver tumor. Liver stiffness as evaluated by transient elastography was 8.3 kPa. Hepatitis C antibody was 6.8 S/CO, but serum tests were negative for HCV RNA. Therefore, she was not prescribed antiviral therapy.

OUTCOME AND FOLLOW-UP

At the 3-mo follow up the patient's dyspnea was dramatically improved and the 6-min walking distance was 300 m and pulmonary artery pressure drops to 50 mmHg.

DISCUSSION

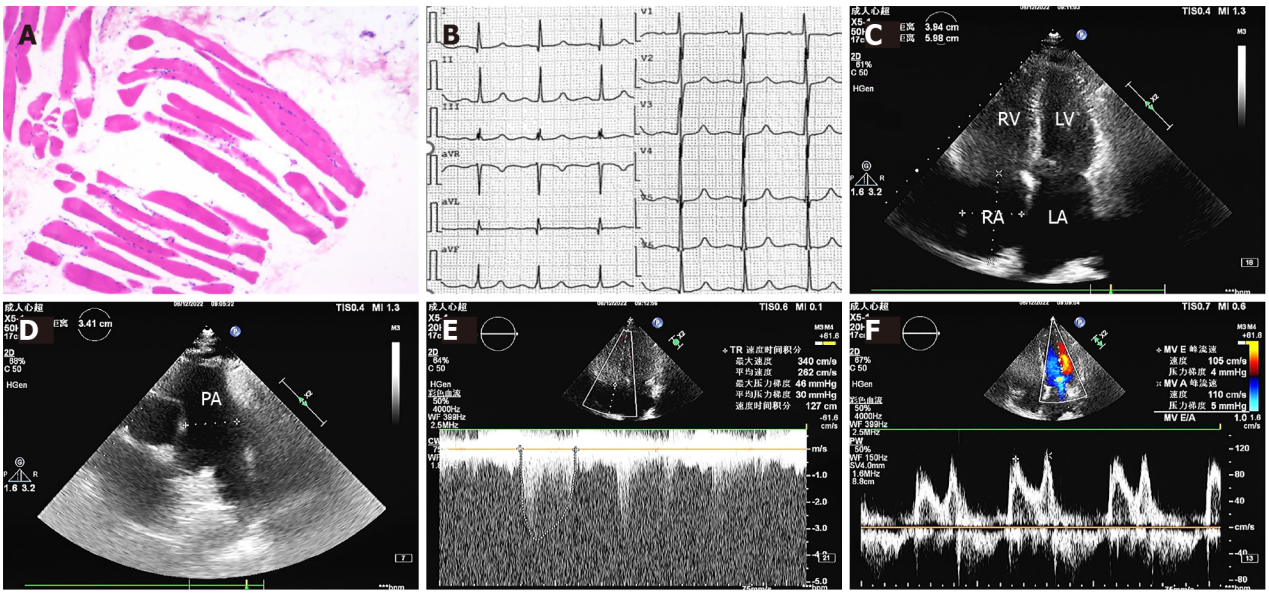
HCV infection should be considered a systemic disease which is often associated with many extrahepatic manifestations. According to different studies, 40%-80% of patients infected with HCV develop at least one extrahepatic manifestation[4]. However, PH associated with HCV is relatively rare.

PH is divided into five clinical subgroups; pulmonary arterial hypertension (PAH), PH associated with left heart disease, PH associated with chronic lung disease and/or hypoxia, chronic thromboembolic, and PH with unclear and/or multifactorial mechanisms. Pre-capillary PH is hemodynamically defined as mPAP > 20 mmHg, PAWP ≤ 15 mmHg, and PVR > 2 WU. PAWP > 15 mmHg is the threshold of post-capillary PH. PVR is used to distinguish patients with post-capillary PH who have significant components of pre-capillary PH (PVR > 2 WU, combined with post-capillary and pre-capillary PH; CpcPH) from those who do not (PVR ≤ 2 WU, isolated post-capillary PH)[5]. The current patient had no relevant family history to support a heritable cause of PH. Valvular/congenital heart diseases, lung diseases, chronic pulmonary artery obstruction, and human immunodeficiency virus infection were systemically eliminated *via* relevant tests. Drugs were also unlikely to have caused her PH. The onset of PH predated the polymyositis, and connective tissue disease could also be excluded as a cause of PH. Thus, the possibility remained that PH associated with portal hypertension was due to chronic hepatitis C.

Portal PH (PoPH) is a well-known serious complication of portal hypertension in chronic liver disease. According to statistics, PoPH occurs in 1%–2% of patients with liver disease and portal hypertension[6]. The incidence of PoPH is higher in patients with HCV-related cirrhosis. In PAH registry studies, PoPH patients accounted for 5%–15% of PAH patients[7-9]. Hemodynamically, patients with PoPH had significantly higher cardiac output and lower systemic and PVR than patients with idiopathic PH[10]. The diagnosis of PoPH is based on the presence of otherwise unexplained pre-capillary PH in patients with portal hypertension or a portosystemic shunt[5]. In patients with an established diagnosis of PoPH, treatment should follow the same general principles as in other patients

Table 2 Results of right heart catheterization

Parameter	Value	Unit
Heart rate	76	bpm
Pulmonary arterial pressure	90/38/55.33	mmHg
Right atrium pressure	12.17	mmHg
Pulmonary artery wedge pressure	34/19/24	mmHg
Pulmonary vascular resistance	5.13	Wood units
Pulmonary vascular resistance	410.23	dyne s/cm
Cardiac output	9.53	L/min
Cardiac index	4.51	L/min/m^2

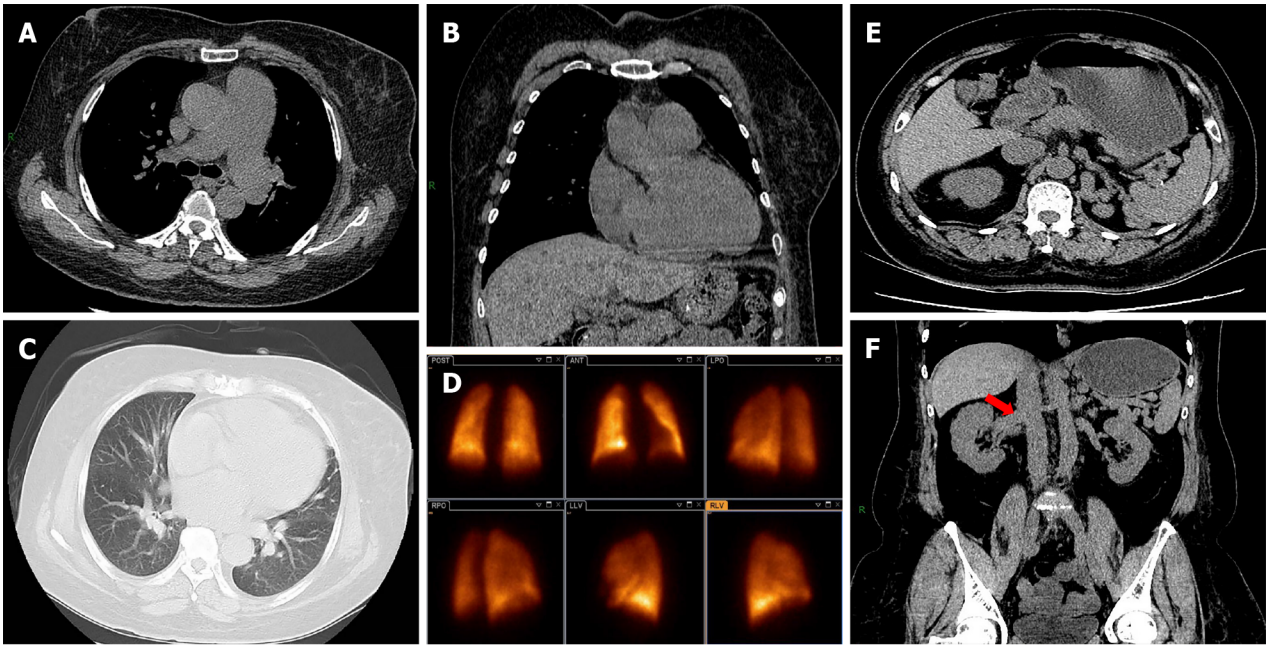


DOI: 10.3748/wjg.v29.i19.3040 **Copyright** ©The Author(s) 2023.

Figure 1 Pathological image of muscle, electrocardiogram, and Echocardiography upon admission. A: Muscle biopsy with hematoxylin and eosin staining (× 100) showed inflammatory cell infiltration; B: Electrocardiography indicated a normal sinus rhythm; C: A four-chamber view showed an enlarged right atrium, right ventricle, and left atrium; D: A long axis view of the pulmonary artery indicated widening of that artery; E: Doppler echocardiography showed that the peak tricuspid regurgitation velocity was 3.4 m/s, and the tricuspid regurgitation pressure gradient was 46 mmHg; F: Bicuspid valve doppler indicated reduced diastolic function. RV: Right ventricular; LV: Left ventricle; RA: Right atrium; LA: Left atrium; PA: Pulmonary artery.

with PAH. PAH medications can affect gas exchange, which may deteriorate with vasodilators in patients with PoPH[11]. Various case series support the use of approved PAH medication in patients with PoPH. The survival and prognostic factors in PoPH remain controversial and are still poorly studied in the current era of PH management[7,12,13]. The current patient had a history of HCV infection, mild liver fibrosis, and hepato-renal shunt, thus the diagnosis of PoPH was considered. The results of right heart catheterization in the present patient were consistent with CpcPH, considering that there may have been other factors involved in PH, not only PoPH. The patient had a history of hypertension with left atrium and right atrium enlargement, and the N-terminal-pro B-type natriuretic peptide was elevated. Therefore, heart failure with preserved ejection fraction was involved in PH. Sildenafil, macitentan, diuretics, and angiotensin receptor blocker were prescribed. Short-term follow-up indicated improvement in respiratory status and increased activity tolerance. Confirmation of further efficacy requires long-term follow-up.

What is intriguing in the current case is the coexistence of PH, nephrotic syndrome, and polymyositis in a chronic hepatitis C patient, which is reported herein for the first time to our knowledge. Increasing epidemiological evidence indicates an association between HCV infection and renal disease, with membranoproliferative glomerulonephritis and membranous nephropathy being the most common [14]. The main clinical manifestations of nephrotic syndrome in HCV-infected patients are proteinuria and hypoalbuminemia, with or without a reduced glomerular filtration rate. Treatments include antiviral and nonspecific immunosuppressive therapy[15], but their efficacy and safety are contro-



DOI: 10.3748/wjg.v29.i19.3040 **Copyright** ©The Author(s) 2023.

Figure 2 Computed tomography images and pulmonary ventilation/perfusion scan. A: Axial chest computed tomography (CT) depicted widening of the pulmonary artery; B: Coronal chest CT depicted right atrial and right ventricle enlargement; C: The pulmonary window showed no significant parenchymal pulmonary disease; D: A pulmonary ventilation/perfusion scan indicated normal perfusion function; E: An axial abdominal CT showed normal liver size, slight spleen enlargement, and multiple venous tortuosity; F: A coronal abdominal CT showed thickened venous shunt between the portal vein, splenic vein and left renal vein (red arrow).

versial. HCV infection is often associated with autoimmune diseases such as cryoglobulinemia, rheumatoid arthritis, Sjogren's syndrome, systemic lupus erythematosus, dermatomyositis, and polymyositis[1,16-18]. Most of these diseases appear to be related to virus-induced non-specific activation of the immune system, including autoantibody production, cryoglobulinemia, autoimmune thyroid disorders, and B cell lymphomas[19]. Although most data are based on small series and case reports, the association between chronic HCV infection and systemic autoimmune disease has received increasing attention. The exact etiology is unknown, but interaction between viral infection and autoimmune responses is thought to be one of the mechanisms involved. Chronic HCV infection should be considered as the cause of polymyositis if no other etiology is found. The diagnosis and treatment of HCV-associated autoimmune features has become a clinical challenge in patients with HCV infection. There are few reports on the outcome of corticosteroid treatment in patients with chronic HCV infection. Several studies have described rapid progression of liver disease after immunosuppression therapy in patients with chronic HCV infection[20]. The current patient's nephrotic syndrome and polymyositis may have been caused by chronic HCV infection *via* an autoimmune mechanism. The patient was initially treated with methylprednisolone and cyclophosphamide at the time of her polymyositis diagnosis. However, cyclophosphamide was discontinued and methylprednisolone was reduced because of her repeated episodes of abnormal behavior and coma due to hyperammonemia.

The optimal treatment strategy for hepatitis C-related extrahepatic manifestations remains to be determined. Due to the limited data available, more information is needed before definitive therapeutic recommendations can be established. The guidelines for treatment of HCV-related extrahepatic manifestations should be based on clinical features rather than underlying pathogenic mechanisms. Because of the poor prognosis and high mortality associated with these manifestations, the establishment of a safe and effective regimen for the therapy of HCV-related extrahepatic features requires further investigation.

CONCLUSION

Herein we have described a case of chronic hepatitis C with coexisting PoPH, nephrotic syndrome, and polymyositis. Increasing evidence supports a relationship between hepatitis C infection and diverse extrahepatic manifestations, but it is very rare to have multiple different extrahepatic manifestations in a single patient. To our knowledge, this is the first reported case. The exact mechanism by which hepatitis C mediated the development of diverse extrahepatic manifestations remains unclear. Further research on the specific mechanism involved is needed, to facilitated the development of safer and more effective

treatment plans.

FOOTNOTES

Author contributions: Zhao YN and Liu GH were the patient's physicians; Yu M reviewed the literature and contributed to manuscript drafting; Wang C and Zhang YX performed the contributed to data collection; Yu M and Yang P were responsible for the revision of the manuscript for important intellectual content; All authors issued final approval for the version to be submitted.

Informed consent statement: Written informed consent was obtained from the patient for publication of this report and any accompanying images.

Conflict-of-interest statement: All the authors report no relevant conflicts of interest for this article.

CARE Checklist (2016) statement: The authors have read CARE Checklist (2016), and the manuscript was prepared and revised according to CARE Checklist (2016).

Open-Access: This article is an open-access article that was selected by an in-house editor and fully peer-reviewed by external reviewers. It is distributed in accordance with the Creative Commons Attribution NonCommercial (CC BY-NC 4.0) license, which permits others to distribute, remix, adapt, build upon this work non-commercially, and license their derivative works on different terms, provided the original work is properly cited and the use is non-commercial. See: https://creativecommons.org/Licenses/by-nc/4.0/

Country/Territory of origin: China

ORCID number: Ya-Nan Zhao 0000-0002-4611-9678; Guo-Hui Liu 0000-0001-5342-1018; Ping Yang 0000-0001-7960-6248; Ming Yu 0000-0003-4264-5811.

S-Editor: Li L
L-Editor: A
P-Editor: Fan JR

REFERENCES

1 **Ramos-Casals M**, Trejo O, García-Carrasco M, Font J. Therapeutic management of extrahepatic manifestations in patients with chronic hepatitis C virus infection. *Rheumatology (Oxford)* 2003; **42**: 818-828 [PMID: 12730523 DOI: 10.1093/rheumatology/keg299]
2 **Simonneau G**, Montani D, Celermajer DS, Denton CP, Gatzoulis MA, Krowka M, Williams PG, Souza R. Haemodynamic definitions and updated clinical classification of pulmonary hypertension. *Eur Respir J* 2019; **53** [PMID: 30545968 DOI: 10.1183/13993003.01913-2018]
3 **Hoeper MM**, Humbert M, Souza R, Idrees M, Kawut SM, Sliwa-Hahnle K, Jing ZC, Gibbs JS. A global view of pulmonary hypertension. *Lancet Respir Med* 2016; **4**: 306-322 [PMID: 26975810 DOI: 10.1016/S2213-2600(15)00543-3]
4 **Böckle BC**, Sepp NT. Hepatitis C virus and autoimmunity. *Auto Immun Highlights* 2010; **1**: 23-35 [PMID: 26000104 DOI: 10.1007/s13317-010-0005-5]
5 **Humbert M**, Kovacs G, Hoeper MM, Badagliacca R, Berger RMF, Brida M, Carlsen J, Coats AJS, Escribano-Subias P, Ferrari P, Ferreira DS, Ghofrani HA, Giannakoulas G, Kiely DG, Mayer E, Meszaros G, Nagavci B, Olsson KM, Pepke-Zaba J, Quint JK, Rådegran G, Simonneau G, Sitbon O, Tonia T, Toshner M, Vachiery JL, Vonk Noordegraaf A, Delcroix M, Rosenkranz S; ESC/ERS Scientific Document Group. 2022 ESC/ERS Guidelines for the diagnosis and treatment of pulmonary hypertension. *Eur Respir J* 2023; **61** [PMID: 36028254 DOI: 10.1183/13993003.00879-2022]
6 **Mancuso L**, Scordato F, Pieri M, Valerio E, Mancuso A. Management of portopulmonary hypertension: new perspectives. *World J Gastroenterol* 2013; **19**: 8252-8257 [PMID: 24363516 DOI: 10.3748/wjg.v19.i45.8252]
7 **Krowka MJ**, Miller DP, Barst RJ, Taichman D, Dweik RA, Badesch DB, McGoon MD. Portopulmonary hypertension: a report from the US-based REVEAL Registry. *Chest* 2012; **141**: 906-915 [PMID: 21778257 DOI: 10.1378/chest.11-0160]
8 **Lazaro Salvador M**, Quezada Loaiza CA, Rodríguez Padial L, Barberá JA, López-Meseguer M, López-Reyes R, Sala-Llinas E, Alcolea S, Blanco I, Escribano-Subías P; REHAP Investigators. Portopulmonary hypertension: prognosis and management in the current treatment era - results from the REHAP registry. *Intern Med J* 2021; **51**: 355-365 [PMID: 31943676 DOI: 10.1111/imj.14751]
9 **Savale L**, Guimas M, Ebstein N, Fertin M, Jevnikar M, Renard S, Horeau-Langlard D, Tromeur C, Chabanne C, Prevot G, Chaouat A, Moceri P, Artaud-Macari É, Degano B, Tresorier R, Boissin C, Bouvaist H, Simon AC, Riou M, Favrolt N, Palat S, Bourlier D, Magro P, Cottin V, Bergot E, Lamblin N, Jaïs X, Coilly A, Durand F, Francoz C, Conti F, Hervé P, Simonneau G, Montani D, Duclos-Vallée JC, Samuel D, Humbert M, De Groote P, Sitbon O. Portopulmonary hypertension in the current era of pulmonary hypertension management. *J Hepatol* 2020; **73**: 130-139 [PMID: 32145258 DOI: 10.1016/j.jhep.2020.02.021]
10 **Galiè N**, Torbicki A, Barst R, Dartevelle P, Haworth S, Higenbottam T, Olschewski H, Peacock A, Pietra G, Rubin LJ, Simonneau G; Grupo de Trabajo sobre el diagnóstico y tratamiento de la Hipertensión Arterial Pulmonar de la Sociedad

Europea de Cardiología. [Guidelines on diagnosis and treatment of pulmonary arterial hypertension]. *Rev Esp Cardiol* 2005; **58**: 523-566 [PMID: 15899198 DOI: 10.1157/13074846]

11 **Olsson KM**, Meyer K, Berliner D, Hoeper MM. Development of hepatopulmonary syndrome during combination therapy for portopulmonary hypertension. *Eur Respir J* 2019; **53** [PMID: 30655448 DOI: 10.1183/13993003.01880-2018]

12 **Le Pavec J**, Souza R, Herve P, Lebrec D, Savale L, Tcherakian C, Jaïs X, Yaïci A, Humbert M, Simonneau G, Sitbon O. Portopulmonary hypertension: survival and prognostic factors. *Am J Respir Crit Care Med* 2008; **178**: 637-643 [PMID: 18617641 DOI: 10.1164/rccm.200804-613OC]

13 **Sithamparanathan S**, Nair A, Thirugnanasothy L, Coghlan JG, Condliffe R, Dimopoulos K, Elliot CA, Fisher AJ, Gaine S, Gibbs JSR, Gatzoulis MA, E Handler C, Howard LS, Johnson M, Kiely DG, Lordan JL, Peacock AJ, Pepke-Zaba J, Schreiber BE, Sheares KKK, Wort SJ, Corris PA; National Pulmonary Hypertension Service Research Collaboration of the United Kingdom and Ireland. Survival in portopulmonary hypertension: Outcomes of the United Kingdom National Pulmonary Arterial Hypertension Registry. *J Heart Lung Transplant* 2017; **36**: 770-779 [PMID: 28190786 DOI: 10.1016/j.healun.2016.12.014]

14 **Sabry AA**, Sobh MA, Sheaashaa HA, Kudesia G, Wild G, Fox S, Wagner BE, Irving WL, Grabowska A, El-Nahas AM. Effect of combination therapy (ribavirin and interferon) in HCV-related glomerulopathy. *Nephrol Dial Transplant* 2002; **17**: 1924-1930 [PMID: 12401848 DOI: 10.1093/ndt/17.11.1924]

15 **Fabrizi F**, Martin P, Cacoub P, Messa P, Donato FM. Treatment of hepatitis C-related kidney disease. *Expert Opin Pharmacother* 2015; **16**: 1815-1827 [PMID: 26161511 DOI: 10.1517/14656566.2015.1066333]

16 **Arrais de Castro R**, Vilas P, Borges-Costa J, Tato Marinho R. Hepatitis C virus infection: 'beyond the liver'. *BMJ Case Rep* 2018; **2018** [PMID: 30049677 DOI: 10.1136/bcr-2018-225817]

17 **Uruha A**, Noguchi S, Hayashi YK, Tsuburaya RS, Yonekawa T, Nonaka I, Nishino I. Hepatitis C virus infection in inclusion body myositis: A case-control study. *Neurology* 2016; **86**: 211-217 [PMID: 26683644 DOI: 10.1212/WNL.0000000000002291]

18 **Aisa Y**, Yokomori H, Kashiwagi K, Nagata S, Yanagisawa R, Takahashi M, Hasegawa H, Tochikubo Y. Polymyositis, pulmonary fibrosis and malignant lymphoma associated with hepatitis C virus infection. *Intern Med* 2001; **40**: 1109-1112 [PMID: 11757765 DOI: 10.2169/internalmedicine.40.1109]

19 **Bianchi FB**, Muratori P, Granito A, Pappas G, Ferri S, Muratori L. Hepatitis C and autoreactivity. *Dig Liver Dis* 2007; **39** Suppl 1: S22-S24 [PMID: 17936218 DOI: 10.1016/s1590-8658(07)80006-5]

20 **Rockstroh JK**, Spengler U, Sudhop T, Ewig S, Theisen A, Hammerstein U, Bierhoff E, Fischer HP, Oldenburg J, Brackmann HH, Sauerbruch T. Immunosuppression may lead to progression of hepatitis C virus-associated liver disease in hemophiliacs coinfected with HIV. *Am J Gastroenterol* 1996; **91**: 2563-2568 [PMID: 8946987]



Published by **Baishideng Publishing Group Inc**
7041 Koll Center Parkway, Suite 160, Pleasanton, CA 94566, USA
Telephone: +1-925-3991568
E-mail: bpgoffice@wjgnet.com
Help Desk: https://www.f6publishing.com/helpdesk
https://www.wjgnet.com



© 2023 Baishideng Publishing Group Inc. All rights reserved.

ISSN 1007-9327 (print)
ISSN 2219-2840 (online)

World Journal of *Gastroenterology*

World J Gastroenterol 2023 May 28; 29(20): 3048-3221



Published by Baishideng Publishing Group Inc

World Journal of Gastroenterology

Contents

Weekly Volume 29 Number 20 May 28, 2023

REVIEW

3048 *Hericium erinaceus*, a medicinal fungus with a centuries-old history: Evidence in gastrointestinal diseases

Gravina AG, Pellegrino R, Auletta S, Palladino G, Brandimarte G, D'Onofrio R, Arboretto G, Imperio G, Ventura A, Cipullo M, Romano M, Federico A

MINIREVIEWS

3066 Machine perfusion and the prevention of ischemic type biliary lesions following liver transplant: What is the evidence?

Durán M, Calleja R, Hann A, Clarke G, Ciria R, Nutu A, Sanabria-Mateos R, Ayllón MD, López-Cillero P, Mergental H, Briceño J, Perera MTPR

ORIGINAL ARTICLE

Basic Study

3084 Metronomic capecitabine inhibits liver transplant rejection in rats by triggering recipients' T cell ferroptosis

Wang H, Wang ZL, Zhang S, Kong DJ, Yang RN, Cao L, Wang JX, Yoshida S, Song ZL, Liu T, Fan SL, Ren JS, Li JH, Shen ZY, Zheng H

3103 Dihydroergotamine ameliorates liver fibrosis by targeting transforming growth factor β type II receptor

Zheng KX, Yuan SL, Dong M, Zhang HL, Jiang XX, Yan CL, Ye RC, Zhou HQ, Chen L, Jiang R, Cheng ZY, Zhang Z, Wang Q, Jin WZ, Xie W

Retrospective Study

3119 Malignancy risk factors and prognostic variables of pancreatic mucinous cystic neoplasms in Chinese patients

Xia Q, Li F, Min R, Sun S, Han YX, Feng ZZ, Li N

Clinical Trials Study

3133 Safety and effectiveness of vonoprazan-based rescue therapy for *Helicobacter pylori* infection

Yu J, Lv YM, Yang P, Jiang YZ, Qin XR, Wang XY

Observational Study

3145 Determination of esophageal squamous cell carcinoma and gastric adenocarcinoma on raw tissue using Raman spectroscopy

Ito H, Uragami N, Miyazaki T, Shimamura Y, Ikeda H, Nishikawa Y, Onimaru M, Matsuo K, Isozaki M, Yang W, Issha K, Kimura S, Kawamura M, Yokoyama N, Kushima M, Inoue H

3157 Real-time continuous image guidance for endoscopic retrograde cholangiopancreatography based on 3D/2D registration and respiratory compensation

Zhang DY, Yang S, Geng HX, Yuan YJ, Ding CJ, Yang J, Li MY

World Journal of Gastroenterology

Weekly Volume 29 Number 20 May 28, 2023

Contents

3168 Inflammation-related nomogram for predicting survival of patients with unresectable hepatocellular carcinoma received conversion therapy

Wu JL, Luo JY, Jiang ZB, Huang SB, Chen GR, Ran HY, Liang QY, Huang MS, Lai LS, Chen JW

META-ANALYSIS

3185 Fecal microbiota transplantation for the treatment of irritable bowel syndrome: A systematic review and meta-analysis

Halkjær SI, Lo B, Cold F, Højer Christensen A, Holster S, König J, Brummer RJ, Aroniadis OC, Lahtinen P, Holvoet T, Gluud LL, Petersen AM

SCIENTOMETRICS

3203 Global research trends on diet and nutrition in Crohn's disease

Shakhshir M, Zyoud SH

CASE REPORT

3216 Inflammatory myofibroblastic tumor of the pancreatic neck misdiagnosed as neuroendocrine tumor: A case report

Liu JB, Gu QB, Liu P

ABOUT COVER

Editorial Board Member of *World Journal of Gastroenterology*, Toshimi Chiba, AGAF, MD, PhD, Professor, Department of Internal Medicine, Iwate Medical University, Morioka 020-8505, Japan. toschiba@iwate-med.ac.jp

AIMS AND SCOPE

The primary aim of *World Journal of Gastroenterology* (*WJG*, *World J Gastroenterol*) is to provide scholars and readers from various fields of gastroenterology and hepatology with a platform to publish high-quality basic and clinical research articles and communicate their research findings online. *WJG* mainly publishes articles reporting research results and findings obtained in the field of gastroenterology and hepatology and covering a wide range of topics including gastroenterology, hepatology, gastrointestinal endoscopy, gastrointestinal surgery, gastrointestinal oncology, and pediatric gastroenterology.

INDEXING/ABSTRACTING

The *WJG* is now abstracted and indexed in Science Citation Index Expanded (SCIE, also known as SciSearch®), Current Contents/Clinical Medicine, Journal Citation Reports, Index Medicus, MEDLINE, PubMed, PubMed Central, Scopus, Reference Citation Analysis, China National Knowledge Infrastructure, China Science and Technology Journal Database, and Superstar Journals Database. The 2022 edition of Journal Citation Reports® cites the 2021 impact factor (IF) for *WJG* as 5.374; IF without journal self cites: 5.187; 5-year IF: 5.715; Journal Citation Indicator: 0.84; Ranking: 31 among 93 journals in gastroenterology and hepatology; and Quartile category: Q2. The *WJG*'s CiteScore for 2021 is 8.1 and Scopus CiteScore rank 2021: Gastroenterology is 18/149.

RESPONSIBLE EDITORS FOR THIS ISSUE

Production Editor: *Yu-Xi Chen*; **Production Department Director:** *Xu Guo*; **Editorial Office Director:** *Jia-Ru Fan*.

NAME OF JOURNAL
World Journal of Gastroenterology

ISSN
ISSN 1007-9327 (print) ISSN 2219-2840 (online)

LAUNCH DATE
October 1, 1995

FREQUENCY
Weekly

EDITORS-IN-CHIEF
Andrzej S Tarnawski

EDITORIAL BOARD MEMBERS
http://www.wjgnet.com/1007-9327/editorialboard.htm

PUBLICATION DATE
May 28, 2023

COPYRIGHT
© 2023 Baishideng Publishing Group Inc

INSTRUCTIONS TO AUTHORS
https://www.wjgnet.com/bpg/gerinfo/204

GUIDELINES FOR ETHICS DOCUMENTS
https://www.wjgnet.com/bpg/GerInfo/287

GUIDELINES FOR NON-NATIVE SPEAKERS OF ENGLISH
https://www.wjgnet.com/bpg/gerinfo/240

PUBLICATION ETHICS
https://www.wjgnet.com/bpg/GerInfo/288

PUBLICATION MISCONDUCT
https://www.wjgnet.com/bpg/gerinfo/208

ARTICLE PROCESSING CHARGE
https://www.wjgnet.com/bpg/gerinfo/242

STEPS FOR SUBMITTING MANUSCRIPTS
https://www.wjgnet.com/bpg/GerInfo/239

ONLINE SUBMISSION
https://www.f6publishing.com

© 2023 Baishideng Publishing Group Inc. All rights reserved. 7041 Koll Center Parkway, Suite 160, Pleasanton, CA 94566, USA

E-mail: bpgoffice@wjgnet.com https://www.wjgnet.com

World Journal of Gastroenterology

Submit a Manuscript: https://www.f6publishing.com

World J Gastroenterol 2023 May 28; 29(20): 3048-3065

DOI: 10.3748/wjg.v29.i20.3048

ISSN 1007-9327 (print) ISSN 2219-2840 (online)

REVIEW

Hericium erinaceus, a medicinal fungus with a centuries-old history: Evidence in gastrointestinal diseases

Antonietta Gerarda Gravina, Raffaele Pellegrino, Salvatore Auletta, Giovanna Palladino, Giovanni Brandimarte, Rossella D'Onofrio, Giusi Arboretto, Giuseppe Imperio, Andrea Ventura, Marina Cipullo, Marco Romano, Alessandro Federico

Specialty type: Gastroenterology and hepatology

Provenance and peer review: Invited article; Externally peer reviewed.

Peer-review model: Single blind

Peer-review report's scientific quality classification

Grade A (Excellent): 0
Grade B (Very good): B
Grade C (Good): C
Grade D (Fair): 0
Grade E (Poor): 0

P-Reviewer: Liu J, China; Sun SY, China

Received: March 3, 2023
Peer-review started: March 3, 2023
First decision: March 21, 2023
Revised: March 22, 2023
Accepted: April 21, 2023
Article in press: April 21, 2023
Published online: May 28, 2023

Antonietta Gerarda Gravina, Raffaele Pellegrino, Salvatore Auletta, Giovanna Palladino, Rossella D'Onofrio, Giusi Arboretto, Giuseppe Imperio, Andrea Ventura, Marina Cipullo, Marco Romano, Alessandro Federico, Department of Precision Medicine, University of Campania "Luigi Vanvitelli", Naples 80138, Italy

Giovanni Brandimarte, Division of Internal Medicine and Gastroenterology, Cristo Re Hospital, Rome 00167, Italy

Corresponding author: Antonietta Gerarda Gravina, MD, MSc, PhD, Assistant Professor, Department of Precision Medicine, University of Campania "Luigi Vanvitelli", Via L. de Crecchio, Naples 80138, Italy. antoniettagerarda.gravina@unicampania.it

Abstract

Hericium erinaceus is an edible and medicinal mushroom commonly used in traditional Chinese medicine for centuries. Several studies have highlighted its therapeutic potential for gastrointestinal disorders such as gastritis and inflammatory bowel diseases. In addition, some components of this mushroom appear to possess strong antineoplastic capabilities against gastric and colorectal cancer. This review aims to analyse all available evidence on the digestive therapeutic potential of this fungus as well as the possible underlying molecular mechanisms.

Key Words: *Hericium erinaceus*; Fungus; Gastritis; Inflammatory bowel diseases; Gastric cancer; Colorectal cancer

©The Author(s) 2023. Published by Baishideng Publishing Group Inc. All rights reserved.

Core Tip: Various natural and non-pharmacological principles have been used to treat gastrointestinal disorders. *Hericium erinaceus* is a Chinese mushroom with a centuries-old medicinal tradition. Several preclinical studies have demonstrated their anti-inflammatory and antineoplastic potential. The therapeutic activity of this mushroom also targets inflammatory bowel diseases, as demonstrated in several animal experiments. However, evidence from *in vivo* studies is not generally available for patients with gastrointestinal disorders. It is also unclear which component of this mushroom has the greatest potency and the best safety profile.

Citation: Gravina AG, Pellegrino R, Auletta S, Palladino G, Brandimarte G, D'Onofrio R, Arboretto G, Imperio G, Ventura A, Cipullo M, Romano M, Federico A. *Hericium erinaceus*, a medicinal fungus with a centuries-old history: Evidence in gastrointestinal diseases. *World J Gastroenterol* 2023; 29(20): 3048-3065
URL: https://www.wjgnet.com/1007-9327/full/v29/i20/3048.htm
DOI: https://dx.doi.org/10.3748/wjg.v29.i20.3048

INTRODUCTION

Gastrointestinal disorders are one of the most prevalent diseases in the general population. They are associated with a significant epidemiological and economic burden, with an estimated annual cost of over a hundred and thirty billion in the United States alone[1]. Many gastrointestinal disorders require a pharmacological approach; however, the possibility of adopting naturally derived complementary therapies whenever possible is emerging[2,3].

Among the abundant natural compounds studied, there is a Chinese mushroom, *Hericium erinaceus* (*H. erinaceus*) that has shown the potential to prevent and treat digestive diseases, such as gastric ulcers [4]. Furthermore, its therapeutic potential has been demonstrated in several conditions, including diabetes, hyperlipidaemia, neurodegenerative disorders, and cancer[5-8]. In addition, mild cognitive impairment is another disorder in which *H. erinaceus* has shown encouraging results in randomised clinical trials[9,10].

Therefore, *H. erinaceus* has traditionally and historically been used as a natural remedy for epigastric pain caused by chronic gastritis, gastric ulcers, or even atrophic gastritis[8].

Despite the strong need for clinical studies, several experiments, mainly preclinical and mouse model-based, have been conducted on the beneficial effects of many *H. erinaceus* extracts and components on gastrointestinal diseases. Therefore, this narrative review aimed to provide overall evidence of the therapeutic potential of *H. erinaceus* in gastrointestinal tract diseases.

H. ERINACEUS: GENERAL CONSIDERATIONS

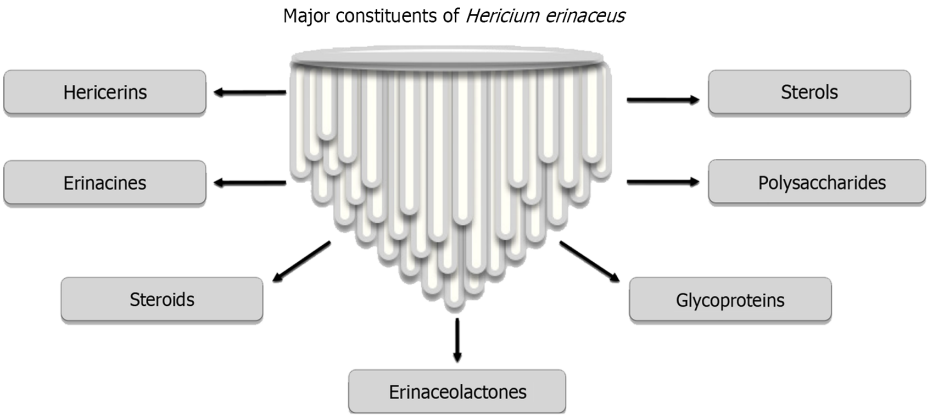
H. erinaceus, also known as Yamabushitake (in the Japanese language), Houtou (in the Chinese language), or also as "lion's mane" is a fungus that belongs to the class *Basidiomycetes*, subclass *Holobasidiomycetidae*, order *Hericiales*, and family *Hericiaceae*[4]. This fungus is mainly distributed in European, Asian, and American regions[11]. It is a saprophytic fungus or weak parasite that typically grows on hardwoods, such as beech, chestnut, and cherry[12].

Many active metabolites of *H. erinaceus* that are structurally different from each other and potentially bioactive have been discovered[13].

The main constituents of *H. erinaceus* are erinacines (cyathane-type diterpenoid aromatic compounds as erinacines A-I), steroids (such as ergosterol, erinarols A-F, and ergostane-type steroids), alkaloids (such as hericirine, 12β-hydroxyverruculogenTR-2, fumitremorgin, methylthioglioto, pseurotin A, and FD-838), and lactones such as vitamin B_{12}-*c*-lactone (Figure 1)[13].

In addition, each 100 g of dried *H. erinaceus* contains approximately 61.3-77.5 g of total sugars, of which β-glucans, α-glucans, and glucan-protein complexes are the most abundant[14,15]. Among these, the β-glucans in the fungal cell wall have known and marked anti-inflammatory and anti-cancer potency and can positively modify the gut microbiota[16].

Much of the research devoted to the chemical characterisation of *H. erinaceus* has focused on its polysaccharide components, which are generally obtained from its fruiting body, and various extraction methods have been developed[17-19].



DOI: 10.3748/wjg.v29.i20.3084 **Copyright** ©The Author(s) 2023.

Figure 1 Several constituents can be obtained from *Hericium erinaceus* by different means of extraction (for example, by alcohol, chloroform, or petroleum). However, fractions such as erinacines and polysaccharides are those most commonly used in studies conducted in the gastrointestinal setting.

H. ERINACEUS IN UPPER GASTROINTESTINAL TRACT DISEASES: THE EVIDENCE

The role of H. erinaceus in non-infectious gastric diseases: Gastroprotective effects and therapeutic potential in repairing gastric mucosal damage

Gastric ulcers are a significant epidemiological burden[20]. Among the most common forms of gastric ulcers, those caused by non-steroidal anti-inflammatory drugs are also included. This is due to the pharmacological inhibition of cyclooxygenases 1 and 2, which are responsible for producing proinflammatory cytokines and prostaglandins, which help maintain the integrity of the gastric mucosal barrier [21]. An adequate balance between proinflammatory and anti-inflammatory cytokines is necessary for maintaining gastric mucosal integrity, such that polymorphisms in genes encoding proinflammatory cytokines can increase the risk of peptic ulcer and gastric cancer[22].

As anticipated, *H. erinaceus* has shown various anti-inflammatory, antioxidative, and gastroprotective properties. Boddy *et al*[23] showed, for example, that the action of several polysaccharides of *H. erinaceus* inhibits the secretion of proinflammatory cytokines interleukin 6 (IL-6), IL-8, and IL-12 and promotes the secretion of the anti-inflammatory cytokine IL-10 in a co-culture system of Cancer coli 2 (Caco-2) cells and Caco-2/RAW264.7 cells under bacterial lipopolysaccharide stimulation. This emphasises how this fungus can intervene in cytokine imbalance in an inflamed environment by shifting the balance toward an anti-inflammatory cytokine pattern.

To evaluate the gastroprotective, antioxidant, and anti-inflammatory activities *in vivo*, Wang *et al*[24] conducted experiments in a mouse model in which ethanol or ligation of the pylorus induced gastric ulcers. The study involved two polysaccharides, namely the crude polysaccharide of *H. erinaceus*, [*i.e.*, crude polysaccharide (HECP)] and the refined polysaccharide of *H. erinaceus* [*i.e.*, refined polysaccharide (HERP)], obtained from the fruiting body using water extraction and ethanol precipitation methods[25]. The mice were divided into several groups, including control groups and those receiving *H. erinaceus* polysaccharides at different dosages (100 mg/kg, 200 mg/kg, and 400 mg/kg). In the ethanol-induced gastric ulcer model, there was a reduction in the severity of the ulcers in a dose-dependent manner in the HERP/HECP-*treated* groups, with a significant reduction when pre-treatment with 400 mg/kg of HERP/HECP was performed. In contrast, in the pylorus-ligation-induced ulcer model, significant ulcer-inhibiting power was achieved when mice were administered HERP or HECP in a 200 mg/kg dosage. Nevertheless, the ulcers appeared to be more mitigated by HECP polysaccharide than HERP.

These results generally indicate a marked gastroprotective effect of HERP/HECP polysaccharides in ethanol-induced and pylorus-ligated gastric ulcers. However, the authors also showed results related to the control of gastric secretions. HERP/HECP administration provided a regulatory advantage over the imbalance in acid secretion induced by pylorus ligation.

Once the gastric mucosa has been damaged, the inflammatory process is activated, thereby increasing the mediators of inflammation, including tumor necrosis factor α (TNF-α), IL-1β, and IL-6[26]. TNF-α stimulates neutrophil infiltration and apoptosis of epithelial cells, reduces gastric microcirculation around the ulcer region, and delays its healing[27]. Leucocyte infarction in the gastric mucosa is generally assessed using myeloperoxidase (MPO) activity[28]. IL-1β significantly promotes ulcer formation[29]. Another defensive element that protects against gastric ulceration is the mucus-bicarbonate barrier. The mucus is a gel that adheres to the mucosa, preventing gastric acid penetration and injury. Mucus typically works in conjunction with nitric oxide (NO), prostaglandin E_2 (PGE_2), and epidermal growth factor (EGF) to maintain mucosal integrity[30]. NO protects the mucosal barrier and integrity of the gastric epithelium by inducing the inactivation of gastric parietal cells that secrete

hydrochloric acid, thereby reducing acidity[31]. PEG_2 increases mucus and bicarbonate production, leading to a decrease in gastric epithelial permeability[32]. EGF induces the proliferation of epithelial cells, thereby promoting tissue healing[30].

Wang *et al*[24] discovered that rats administered with HERP or HECP had lower serum TNF-α and IL-1β levels and lower gastric tissue MPO activity than in the control group, indicating that these polysaccharides reduced the inflammatory response. In addition, the mucus content in the stomach was higher in the *H. erinaceus* polysaccharides-treated group than in the control group, suggesting that polysaccharides may protect the integrity of the gastric mucosa. The latter was also promoted by the increased release of NO, PGE_2, and EGF in the *H. erinaceus* polysaccharides-treated group. HERP/HECP also showed scavenging effects for 2,2-diphenyl-1-picrylhydrazyl, chelating capacity for Fe^{2+} and OH *in vitro*, antioxidant activity, and increased superoxide dismutase (SOD) and glutathione peroxidase (GPx) activities. It is known that SOD can rapidly convert peroxyl radicals into biologically safe and inactive substances[33].

Furthermore, GPx protects the gastric mucosa from reactive oxygen species (ROS)-induced injury and reduces lipid peroxidation[34]. Phenolic compounds appear to be the main contributors to the antioxidant capacity of *H. erinaceus*[35]. The antioxidant and scavenger properties of *H. erinaceus* exerted through its polysaccharide component have also been confirmed by other studies, in which it was shown to prevent H_2O_2-induced apoptotic cell death in gastric epithelial cell lines (*i.e.*, GES-1 cells)[25].

In general, there are several studies on the use of *H. erinaceus* in ethanol-induced ulcers[36-38], with some focusing on acetic acid-induced ulcers[39]. Mao *et al*[36] also highlighted a possible therapeutic mechanism for ethanol-induced ulceration in mice *via* epidermal differentiation by studying the differences in the expression of several keratins, including 16, 6b, and transglutaminase E, in mucosa treated with *H. erinaceus* and untreated mucosa.

In addition to its multidimensional gastroprotective properties, *H. erinaceus* can regulate chaperonins, including HSP70. For example, in a model of ethanol-induced ulcers in Sprague Dawley mice, immunohistochemical studies have demonstrated an increased presence of HSP70 and downregulation of pro-apoptotic Bcl-2-associated X proteins[40]. Heat shock proteins (as, for example, HSP70) have a well-defined role in the pathogenesis of gastric ulcers. They are among the key players in the intracellular defence mechanisms of gastric cells. Some maintain protein integrity under homeostatic and non-stressful conditions, while others are activated after noxious stimuli[41].

However, the literature on this fungus has focused on both the erosive and atrophic patterns of gastric mucosal damage. Wang *et al*[42] examined the EP-1 fraction obtained from *H. erinaceus* mycelium in chronic atrophic gastritis. They found the potential to reduce the proliferation of MC cells (a model of atrophic gastritis) by arresting them in the G_0/G_1 phase of the cell cycle. However, there is a clinical, double-blinded, preliminary Chinese report for atrophic gastritis, although it was conducted in 1985 on 25 patients with atrophic gastritis who were administered *H. erinaceus* orally for three months. Clinical and histological improvements were observed in 63% and 52% of treated patients[43].

Although there is a considerable amount of preclinical experience, there is a substantial lack of clinical trials that have evaluated this mushroom as a pharmacological intervention in erosive gastritis, gastric ulcers, and atrophic gastritis.

H. erinaceus properties against *Helicobacter pylori* infection

Helicobacter pylori (*H. pylori*) is a gram-negative spiral-shaped bacillus that contributes to several gastrointestinal disorders, including chronic gastritis, peptic ulcer, gastric adenocarcinoma, and gastric mucosa-associated lymphoid tissue lymphoma[44]. In addition, it is associated (to varying degrees) with several extra-gastric disorders, including vitamin B_{12} deficiency anemia, primary immune thrombocytopenia, as well as ophthalmic conditions (such as glaucoma and central serous chorioretinopathy), dermatological disorders (such as rosacea and psoriasis), inflammatory bowel diseases (IBD), metabolic and neurological disorders[45]. The International Agency for Research on Cancer has designated *H. pylori* as a Group I carcinogen for gastric cancer[46]. Therefore, eradication is imperative when an infection is diagnosed[47]. However, we frequently encounter this bacterium's substantial antibiotic resistance; therefore, the guidelines suggest an algorithm based on several successive lines of treatment until eradication is achieved[48,49]. In addition to standard drug therapy, probiotics have been proposed to reduce adverse events associated with drug therapy[48]. *H. erinaceus* components (obtained by various extraction techniques) have shown marked antimicrobial properties against *H. pylori*[50-54]; however, the significant available evidence is preclinical. The minimum inhibitory concentrations (MIC) of the various components of *H. erinaceus* against *H. pylori* are shown in Table 1. MIC values fluctuate by varying the extractive, qualitative, and quantitative characteristics of the extracted components while reaching interesting values in some cases, as in the experience of Liu *et al*[52].

Therefore, it would be desirable to determine through clinical trials whether supplementation with *H. erinaceus* can have an additive effect on the anti-*H. pylori* efficacy of available antibiotic therapies, and whether such supplementation can reduce the adverse events associated with these antibiotic therapies.

H. erinaceus antineoplastic properties concerning gastric cancer

Gastric cancer is now the fourth leading cause of cancer-related deaths, based on its incidence and prevalence[55]. Surgical and medical therapy take the lead in managing this neoplasm[56]; however,

Table 1 Preclinical studies evaluating the antimicrobial activity of several *Hericium erinaceus* fraction toward *Helicobacter pylori*

Ref.	*H. erinaceus* fraction employed	Extraction method	Anti-*H. pylori* MIC (μg/mL)
Shang *et al*[50], 2013	Ethyl acetate fractions		62.5-250.0[1]
Zhu *et al*[51], 2014	HEP25 (197 kDa)	Ethanol precipitation (ethanol concentration 25%)	320[2]
	HEP75 (20 kDa)	Ethanol precipitation (ethanol concentration 75%)	160[2]
	Bi^{3+} *plus* HEP25	Complexation of peptides with bismuth[54]	20[2]
	Bi^{3+} *plus* HEP75		20[2]
Liu *et al*[52], 2016	PE2s (4 g)	Petroleum ether extract	250-500[3]
	II-14-18 (311.000 mg)	Methyl alcohol elution from PE2s	12.5-50[3]
	II-19-30 (355.100 mg)		12.5-25[3]
	II-10-13 (306.100 mg)		25-100[3]
	II-54-58 (96.000 mg)		100-400 +[3]
	II-31-45 (363.900 mg)		25-50[3]
	II-46-53 (184.500 mg)		25-100[3]
	II-59-63 (78.100 mg)		50-100[3]
	II-64-78 (425.400 mg)		100-400 +[3]
	II-1-6 (215.700 mg)		50-200[3]
	II-7-9 (319.900 mg)		25-200[3]
	1-(5-chloro-2-hydroxyphenyl)-3-methyl-1-butanone)	Recrystallized from II-10-13 and II-54-58	12.5-50[3]
	2,5-bis(methoxycarbonyl)terephthalic acid	Recrystallized from II-10-13 and II-54-58	6.25-25[3]
Thi My Ngan *et al*[53], 2021	fEtOAc (11.040 g)	Culture filtrate-derived ethyl acetate fraction	1.25[4]
	mEtOAc (0.091 g)	Mycelium-derived Ethyl acetate fraction	1.5[4]
	mHexane (0.162 g)	Mycelium-derived hexane fraction	7.5[4]
	PS (26.400 g)	Culture filtrate-derived polysaccharide	7.5[4]
	fHexane (0.120 g)	Culture filtrate-derived hexane fraction	10[4]
	mWater (0.509 g)	Mycelium-derived water fraction	10 +[4]
	fWater (72.480 g)	Culture filtrate-derived water fraction	10 +[4]

[1]Nine clinical isolates are the employed strain of *Helicobacter pylori* (*H. pylori*).
[2]Colloidal bismuth subcitrate with a minimum inhibitory concentration (MIC) of 20 μg/mL was used as the comparison reference. NTCC11637 is the employed strain of *H. pylori*.
[3]The comparison references were metronidazole (MIC range 0.7800-1.5625 μg/mL) and tetracycline (MIC range 0.780-3.125 μg/mL). In addition, different isolates of *H. pylori* were used (*i.e.*, ATCC 43504, SS1, *H. pylori* $W_2$504, *H. pylori* 9, *H. pylori* 64, *H. pylori* 78, and *H. pylori* 83). Therefore, the results are presented as MIC ranges.
[4]The reference comparison was amoxicillin, with a MIC of 0.032 μg/mL.
ATCC43504 is the employed strain of *H. pylori*. Bi^{3+}: Bismuth; *H. pylori*: *Helicobacter pylori*; MIC: Minimum inhibitory concentration.

while not changing this premise, several natural substances have been studied as complementary treatments[57-59].

Potential applications of *H. erinaceus* also extend in this context with a specific component of this fungus named in connection with these properties (*i.e.*, erinacines). They are diterpenoids with known neuroprotective properties, of which erinacine A is obtained from the ethanol extract of *H. erinaceus* mycelium[13]. With its exact origin, it is possible to obtain another extract, a sesterterpene, erinacine S [60].

Tung *et al*[61] demonstrated a unique mechanism by which erinacine S could intervene in gastric carcinogenesis through epigenetic regulation. This molecule can induce selective apoptosis in gastric cancer cell lines (*i.e.*, AGS) mediated by ROS toxicity while sparing normal cells. A mouse model of AGS-xenografts in which erinacine S suppressed tumour growth also confirmed this phenomenon[61]. In general, erinacine S may promote apoptosis in gastric carcinoma cells by inducing a specific pathway involving several molecules, such as TNF-related apoptosis-inducing ligand T (TRAIL), Fas ligand (Fas-L), and caspases 3,8,9 which are known to be involved in apoptotic death. At the same time, erinacine S suppressed the expression of anti-apoptotic molecules (*i.e.*, Bcl-2 and Bcl-XL). In addition, cell arrest is promoted in the G_1 phase of the cell cycle by the inactivation of specific cyclins and cyclin-dependent kinases[61]. Furthermore, erinacine S promotes the expression of Fas-L and TRAIL in gastric cancer cells undergoing apoptosis by trimethylation of histone H3 in the promoter regions of the Fas-L and TRAIL genes[61].

Erinacine A exhibits characteristics similar to erinacine S with respect to apoptosis induction. Several studies have shown that erinacine S can inhibit the growth of colorectal cancer both *in vitro* and *in vivo*, which could be attributed to the inhibition of proliferation and induction of the apoptosis signalling pathway, such as the generation of ROS *via* the phosphatidylinositol 3-kinase (PI3K)/mechanistic target of rapamycin (mTOR)/ribosomal protein S6 kinase beta-1 (p70S6K) pathway[62,63].

Proteomic analyses have confirmed that erinacine A reduces the growth and invasiveness of TSGH9201 gastric cancer cells *via* ROS-mediated phosphorylation of focal adhesion kinase (FAK)/protein kinase B (also known as AKT)/p70S6K and p21-activated kinase 1 (PAK1)[64]. Previous studies have shown that erinacine A-mediated apoptosis involves the actin depolymerisation pathway[65]. Furthermore, several PAK partners can phosphorylate or activate mitogen-activated protein kinases. The kinases PI3-kinase/AKT and LIM are involved in the regulation of the cytoskeleton[66,67]. In addition, erinacine A is believed to induce upregulation of the onco-suppressive proteins microtubule-associated scaffold protein 2 (MTUS2) and 14-3-3 protein sigma (1433S), associated with antitumour activity in gastric cancer cells[63]. Recent studies have shown that the 1433S protein appears to intervene in gastric cancer by exerting G_2/M checkpoint regulation in the cell cycle[68,69].

Furthermore, the MTUS2 gene plays a central role in controlling microtubule plus-end-tracking proteins (also known as + TIPs) by regulating cell division and migration through its mitotic kinesin-associated centromere, a microtubule depolymerase[70,71]. Moreover, the cytoskeleton depolymerisation pathway has been recognised as a critical cellular response that controls apoptosis and inhibits Rho GTPase-activated cell migration through its effector kinases, Rho-associated coiled-coil containing protein kinases 1 and 2[72]. These findings are significant and imply that phosphorylation of the FAK/AKT/p70S6K and PAK1 pathways determines the downstream expression of the MTUS2 and 1433S genes, the execution of cancer cell apoptosis, and the role of erinacine A as an anti-invasive agent. This effect most likely reflects cytoskeleton rearrangement, reducing erinacine A-dependent cell motility[63,73,74]. Figure 2 summarises the primary antineoplastic mechanisms of erinacines.

An additional polysaccharide protein extracted from the fermented mycelia of *H. erinaceus* (HEG-5) was studied in SGC-7901 gastric cancer lines. Again, positive regulation of apoptosis and the cell cycle appears to be the mechanisms underlying this antineoplastic action. Indeed, it seems that HEG-5 blocks the development of SGC-7901 cells in the S phase of the cell cycle by promoting the opposite regulation of anti- and pro-apoptotic genes. That is, predictably, the downregulation of anti-apoptotic molecules (such as Bcl-2, PI3K, and AKT) and, conversely, by upregulating caspases 3,8, p53, the bcl-2-associated X-protein, and the bcl-2-associated death promoter. Thus, caspase 3,8-dependent, p53-dependent, and PI3K/AKT-mediated apoptotic pathways are activated[75].

A synergy between doxorubicin and *H. erinaceus* was also observed in their pro-apoptotic action toward SGC-7901 cells *via* ROS-induced stress and caspase activation[76].

Moreover, two extracts of *H. erinaceus* (*i.e.*, HTH5 and HTJ5A) have been shown in an experiment conducted in NCI-87 gastric carcinoma cells to possess both *in vitro* and *in vivo* (in xenograft models including severe combined immunodeficient bearing mice) concentration-dependent cytotoxicity toward such cells, lower toxicity, and more efficacy than 5-fluorouracil[77].

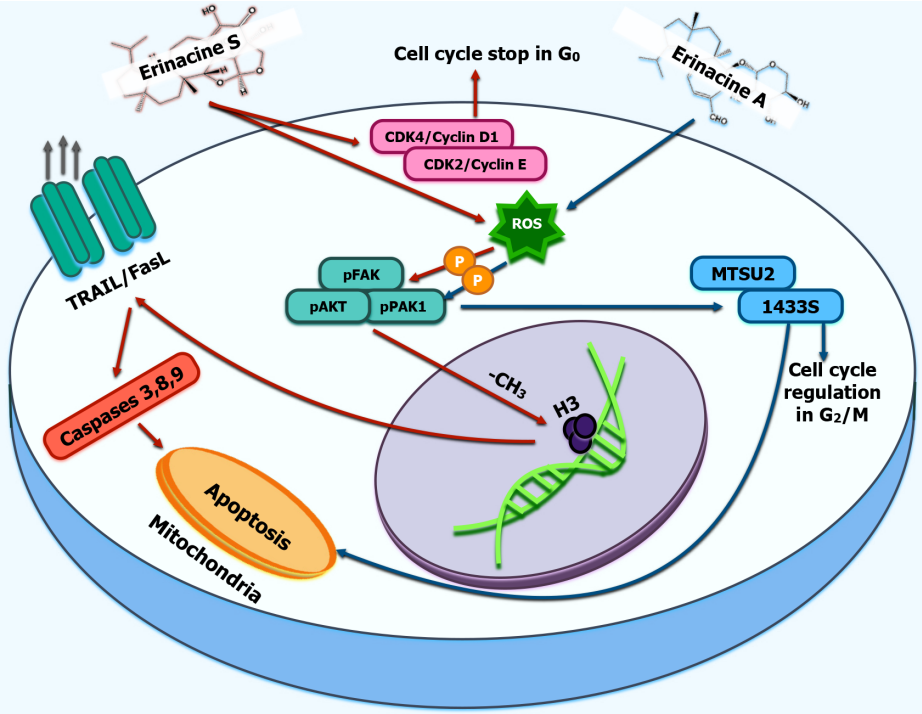
Finally, *H. erinaceus* (via the EP-1 polysaccharide) targets not only cancer cells but also precancerous cell lines by promoting their arrest in the G_0/G_1 phase of the cell cycle[78].

H. ERINACEUS IN LOWER GASTROINTESTINAL TRACT DISEASES: THE EVIDENCE

H. erinaceus and IBD

IBD is a chronic digestive disease that results in sustained gastrointestinal inflammation and consists mainly of ulcerative colitis (UC) and Crohn's disease[79].

Available evidence related to *H. erinaceus* primarily focuses on UC. Wang *et al*[80] evaluated three polysaccharides (*i.e.*, wHEP-1, wHEP-2, and wHEP-3) and proposed the third as the one showing the greatest anti-inflammatory action in a UC-like model in Caco-2 cells inflamed by bacterial lipopolysaccharide.



DOI: 10.3748/wjg.v29.i20.3084 **Copyright** ©The Author(s) 2023.

Figure 2 Main antineoplastic molecular mechanisms of erinacines S and A from *Hericium erinaceus* in gastric cancer cell models. Erinacine S (in AGS gastric cancer cells) can activate a pathway (red arrows) with reactive oxygen species (ROS) mediated phosphorylation of focal adhesion kinase (FAK)/protein kinase B (also known as AKT)/p21-activated kinase 1 (PAK1). Subsequently, by trimethylation of histone H3, the latter pathway can induce the increased expression of TNF-related apoptosis-inducing ligand T and Fas ligand receptors by the cancer cell with the subsequent activation of apoptosis by initiating caspases 3, 8, and 9. Erinacine A (in TSGH9201 gastric cancer cells), once activated (blue arrows), the FAK/AKT/PAK1 pathway, in a similar manner as previously described, upregulates microtubule-associated scaffold protein 2/14-3-3 protein sigma proteins with subsequent activation of caspases-mediated apoptosis. In addition, erinacines can also modulate cell cycle regulation by preventing cell cycle continuation through the blockade at checkpoints, *i.e.*, blocking cyclin-dependent kinases. ROS: Reactive oxygen species; FAK: Focal adhesion kinase; PAK: Activated kinase 1; MTUS2: Microtubule-associated scaffold protein 2; TRAIL: TNF-related apoptosis-inducing ligand T; Fas-L: Fas ligand; CDKs: Cyclin-dependent kinases; 1433S: 14-3-3 protein sigma.

A more complete *in vivo* model has been reported by Diling *et al*[81]. The authors experimentally induced UC-like colitis in mice using trinitrobenzene-sulfonic acid enemas. They were then treated with mixed extracts of *H. erinaceus* (polysaccharide, alcoholic, and cumulative fractions) for 14 d. Significant clinical improvements were observed in the treated mice compared with the untreated control mice. Also, histologically, the treated group had significantly less severe lesions. They recorded reduced MPO levels in the treated mice to verify tissue infiltration of neutrophils. This was accompanied by a modulation of cytokines in the treated group with the restoration of proinflammatory and anti-inflammatory cytokines to pre-treatment levels with trinitro-benzene-sulfonic acid.

Further study has confirmed the anti-UC properties of ethanolic extracts of *H. erinaceus* in C57BL/6 mice exposed to dextran sulphate sodium orally to induce experimental UC-like colitis. The dosage used by the authors was 250/500 mg/kg/d[82]. This study showed as much clinical improvement as histologic (including neutrophil infiltration by MPO dosing) and cytokine improvement. However, these authors also stigmatised antioxidant potential by upregulating NO, malondialdehyde, and SOD. Wang *et al*[83] also focused on the antioxidant potential of *H. erinaceus* polysaccharides as a therapeutic mechanism in UC experimental colitis and discovered the positive regulation of SOD and reduced ROS production. It is no coincidence that combating oxidative stress is part of the therapeutic proposals for IBD[84].

UC pathogenesis remains largely unclear, but bowel inflammation and oxidative stress are considered fundamental mechanisms underlying its pathophysiology. During the active phase of UC, activated leukocytes generate many proinflammatory cytokines and pro-oxidative stress reactions. The joint deterioration caused by inflammation and oxidative stress significantly alters the redox balance within the intestinal mucosa, which accelerates the apoptosis of intestinal epithelial cells[85,86]. Excessive ROS production directly leads to tissue damage and induces an inflammatory cascade[87]. When mitochondria are damaged by oxidative stress, they enter a vicious cycle in which the loss of respiration disrupts redox homeostasis and, in turn, increases intracellular oxygen availability, resulting in increased ROS formation and subsequent oxidative damage to DNA[88]. Several studies have shown that UC onset and course are related to changes in mitochondrial structure and function[89,90].

Finally, in the context of *H. erinaceus* polysaccharides, Ren *et al*[91] confirmed this finding in C57BL/6 mice with experimental UC-like colitis induced by dextran sulphate sodium. Furthermore, the authors recorded (as also done by Diling *et al*[81]) an anti-inflammatory downregulation of nuclear factor kappa B (NF-κB).

NF-κB is part of several pathways (*i.e.*, the canonical and noncanonical pathways) that have been extensively studied in IBD, upon which the mainstay of biological therapy for IBD, namely anti-TNF-α agents, has been built[92].

However, another mechanism by which the anti-IBD effect of *H. erinaceus* has been studied is the modulation of the gut microbiota, as described in the last section of this review.

Colonic diverticulosis and H. erinaceus

Diverticular disease has acquired several modifications of its nomenclature over time, including the concept of symptomatic uncomplicated diverticular disease (SUDD) in its gnoseological entity. SUDD is characterised by colonic diverticulosis associated with chronic abdominal pain without signs, symptoms, or evidence of underlying diverticulitis or colitis[93]. Several pathogenetic mechanisms have been implicated, including visceral hypersensitivity and a reduction in the interstitial Cajal cells, resulting in slowed colonic motility[94]. SUDD therapy includes poorly absorbable antibiotics (such as rifaximin[95]), mesalamine[96], or probiotics[97], as well as modification of habits with increased physical activity[94]. However, definitive medical therapy for SUDD has not yet been defined.

Paradoxically, in the case of diverticular disease, the *H. erinaceus* research trend was reversed with the availability of clinical studies and the absence of preclinical studies.

Brandimarte *et al*[98], in a single study, evaluated a combination nutraceutical compound mainly consisting of polysaccharide extracts of *H. erinaceus* in 305 patients with SUDD. The authors recorded clinical remission rates (defined by them as the disappearance of all symptoms) of 9.34% and 17.64% at three and six months of treatment, respectively. Beyond clinical remission, it is interesting to note that the clinical response rate (defined as symptom reduction) was > 90% at three months and approximately 85% at six months. Furthermore, at three and six months, the authors recorded a significant decrease in faecal calprotectin values from baseline. However, these data should be interpreted within the limitations of a single study and the lack of clarification regarding the actual mechanism underlying this clinical improvement.

Nevertheless, it is clear how the inflammatory process plays a role in the pathogenesis of diverticular disease[99]. In addition, TNF-α levels appear to increase progressively with the severity of diverticular disease in both diverticulitis and SUDD[100]. Therefore, as in the other gastrointestinal disorders already discussed in this review, *H. erinaceus* might potentially intervene in diverticular disease through the regulation of the local inflammatory load; however, as already mentioned, there is currently no evidence.

H. erinaceus and irritable bowel syndrome: A potential ally in this brain-gut interaction disorder?

Unlike IBD, where *H. erinaceus* has been extensively studied in preclinical models, no evidence is available regarding its role in irritable bowel syndrome (IBS). However, it is becoming increasingly clear that IBS is coded within functional gastrointestinal disorders and how ROME IV has now defined these disorders as "disorders of brain-gut interaction", stigmatising the decisive role that the gut-brain axis has acquired in the pathogenesis and clinical features of IBS and other similar functional disorders[101]. Indeed, it is also clear how many brain-derived factors (from neurotransmitters to psychological disorders) are directly involved in IBS pathogenesis[101]. Patients with IBS experience a notably higher prevalence of anxiety-depressive disorders than the healthy population[102]. *H. erinaceus* has been widely studied in clinical settings in patients with anxiety and depression. One randomised controlled trial provided results in favour of positive regulation of psychiatric disorders[103]. Moreover, several pathogenic mechanisms have been suggested in studies on mood disorders. In mice, *H. erinaceus* appears to exert anti-inflammatory effects (negative regulation of proinflammatory cytokines and positive regulation of anti-inflammatory cytokines), stimulate hippocampal neurogenesis, and increase neurotransmitters such as 5-hydroxytryptamine, dopamine, and noradrenaline. However, in humans, it appears to increase salivary levels of free 3-methoxy-4-hydroxyphenethyleneglycol and circulating levels of pro-brain-derived neurotrophic factor. These molecular changes are associated with an improved anxiety-depressive effect[104-107].

Beyond that, the potential of *H. erinaceus* to intervene in the gut-brain axis could also be explored in patients with IBD, where the prevalence and impact on the disease course of anxiety-depressive disorders are not negligible[108,109]. In addition, factors leading to anxiety-depressive disorders can impact therapeutic adherence, as observed during the COVID-19 pandemic[110,111].

IBS therapy is challenging, and much more needs to be added to the research field[112]. In addition, naturally derived substances have repeatedly been considered possible therapies for IBS[113-115]. Ultimately, despite the interesting prospect of the impact of *H. erinaceus* on the dysregulation of the gut-brain axis in IBS, studies evaluating the effects of this fungus on both the gastrointestinal clinical features and the impact of modulation of anxiety and depression on the latter are still awaited.

H. erinaceus and the colorectal cancer

As observed for gastric cancer, even in the case of colorectal cancer, studies have been conducted regarding the antineoplastic potential of *H. erinaceus*. Table 2 summarises the main pathophysiological mechanisms identified.

Liu *et al*[116] focused on two polysaccharides from the fruiting body of *H. erinaceus* extracted by hot water and ferrocyanide-zinc acetate (HEFP-1 and HEFP-2). These polysaccharides showed the ability in their assay to selectively inhibit the growth of colonic cancer cells (*i.e.*, HCT-116) while sparing normal colonic cells. Furthermore, the HEFP polysaccharide 2b fraction (HEFP-2b) was determined to be responsible for this action. In other words, HEFP-2b induced S-phase cell cycle arrest of such cells through the downregulation of CDK1,2 and cyclin A2 and concomitant inhibition of mini-chromosomal maintenance protein 5 (MCM5), a protein essential for the transition from the S-phase to the M-phase [117].

Using the exact extraction mechanism, Hou *et al*[118] obtained and characterised another polysaccharide fraction of the mushroom fruiting body with antineoplastic properties in colonic cancer. The model was similar to the cellular model employing both the same cells as the previous authors (*i.e.*, HCT-116) but with the addition of the DLD1 cell group. They showed an upregulation of cleaved caspase-9 and cleaved caspase-3 without a change in the cleavage of caspase-8, confirming that the apoptotic mechanism was mitochondrial and not extrinsic with relative inhibition of the Bcl-2 protein and stimulation of the pro-apoptotic Bax protein. Confirming this evidence, the authors identified that ROS production might be one of the triggers of this apoptotic phenomenon.

Another study examined fungal extracts obtained by boiling water, microwave extraction in ethanol, and acid or alkaline extracts with hydrochloric acid or sodium hydroxide, respectively[119]. These extracts specifically demonstrated inhibitory effects on implanted tumours in mice (using CT-26 murine cancer cells). Furthermore, intraperitoneal administration of the extracts obtained by boiling water and microwaving in ethanol reduced tumour growth by 38% and 41%, respectively. These extracts increased the cytolytic activity of natural killer cells and phagocytic activity of macrophages and blocked tumour angiogenesis.

In addition, as in gastric cancer, HTJ5 and HTJ5A extracts were shown to block the growth of HT-29 colon cancer cell implants in mice with severe combined immunodeficiency[77]. Another study also confirmed the antineoplastic action of H. erinaceus in HT-29 cells by evaluating its anti-tyrosinase and α -glucosidase activities[120].

As previously described, erinacines are the principal antineoplastic components of *H. erinaceus* in gastric cancer. However, erinacine A showed marked antineoplastic effects against colon cancer. In detail, Lee *et al*[65] highlighted this in HCT-116 and DLD-1 cells by demonstrating how erinacine A was able to exert its cytotoxic action similar to that observed in gastric cancer by increasing ROS production and decreasing cancer cell proliferation through upregulation of the PI3K/mTOR/p70S6K pathway.

H. ERINACEUS AND GUT MICROBIOTA MODULATION

H. erinaceus may promote a shift in the gut microbiota phenotype toward the increased selection of short-chain fatty acids-producing bacteria

The gut microbiota, although not fully detailed and understood, plays a crucial role in the development, progression, and treatment of several gastrointestinal pathological conditions, including IBS and IBD [121].

H. erinaceus is closely related to the modulation of the gut microbiota. In general, it seems to be able to change the gut microbiota's quantitative and qualitative phenotypes in a health-promoting manner. Therefore, it has often been defined as a prebiotic or probiotic[81,122-124]. It appears that *H. erinaceus* selects certain beneficial bacterial strains from the gut microbiota at the expense of pathogenic strains. For example, Xie *et al*[124] studied the fourteen days administration of 1 g of *H. erinaceus* dry powder in submerged cultures in 13 healthy young volunteers and recorded an increase in the alpha diversity of the gut microbiota. They recorded an increase in *Bifidobacterium* and *Bacteroides* and an increase in short-chain fatty acid (SCFAs) production (*i.e.*, *Roseburia faecis*, *Faecalibacterium prausnitzii*, *Eubacterium rectale*, *Fusicatenibacter saccharivorans*, *Kineothrix alysoides*, *Gemmiger formicilis*, and *Dorea longicatena*). Confirming the modulation of the microbiota, in addition to this whole series of beneficial bacterial species, *H. erinaceus* resulted in a reduction in the relative abundance of pathogenic bacteria (*Streptococcus thermophilus*, *Roseburia intestinalis*, *Bacteroides caccae*, and *Anaerostipes hadrus*).

SCFA-producing bacteria may intervene in immune homeostasis through the regulation of lymphocyte chemotaxis and phagocytosis and possess anti-inflammatory and anti-tumourigenic properties[125]. In addition, SCFAs produced mainly in the colon from indigestible polysaccharides are associated with a reduced risk of IBD and IBD-associated dysbiosis[126]. Not surprisingly, they regulate the immune response by suppressing TNF-α production in neutrophils, contributing to intestinal barrier integrity by inducing secretion of IL-18, mucin, and antimicrobial peptides by intestinal epithelial cells and impacting the ability of dendritic cells to bind to T lymphocytes[126].

Table 2 Main studies examining antineoplastic mechanisms of *Hericium erinaceus* against colorectal cancer

Ref.	*H. erinaceus* fraction employed	Colonic cancer model	Identified mechanism
Kim *et al*[119], 2011	Hot water/ microwave ethanol extraction extracts	CT-26 cancer cells graft in mice	NK cells activity ↑; macrophages activity ↑; angiogenesis ↓
Li *et al*[77], 2014	Polysaccharides	HT-29 cancer cells graft in mice	-
Lee *et al*[65], 2017	Erinacine A	Cancer cells (HCT-116, DLD1)	PI3K/AKT/mTOR/; p70S6K pathway; ROS ↑
Sharif *et al*[120], 2018	Ethanolic and methanolic extracts	Cancer cells (HT-29)	α-glucosidase activity ↑; anti-tyrosinase activity ↓
Liu *et al*[116], 2020	Polysaccharides	Cancer cells (HCT-116)	CDK1 ↓; CDK2 ↓; Cyclin A2 ↓; MCM5 ↓
Hou *et al*[118], 2020	Polysaccharides	Cancer cells (HCT-116, DLD1)	Clived caspases 3,9 ↑; ROS ↑; Bax ↑; Bcl-2 ↓

NK: Natural killer; PI3K: Phosphatidylinositol 3-Kinase; AKT: Protein kinase B; mTOR: Mechanistic target of rapamycin; p70S6K: Ribosomal protein S6 kinase beta-1; CDK: Cyclin-dependent kinase; MCM5: Mini-chromosomal maintenance protein 5; ROS: Reactive oxygen species; Bax: Bcl-2-like protein 4; Bcl-2: B-cell lymphoma 2.

Moreover, the authors posited the impact of such changes in the gut microbiota with a shift in several hematochemical parameters by observing a beneficial correlation with several analytes (*i.e.*, alkaline phosphatase, low-density lipoprotein, creatinine, and uric acid). These data suggest a possible clinical impact of *H. erinaceus*-driven modulation of the gut microbiota.

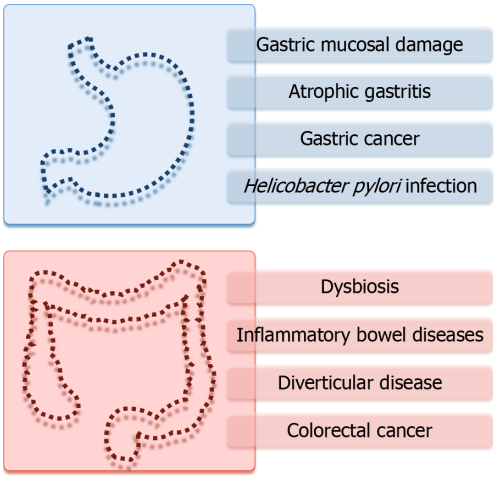
A further study recreated some experimental conditions of digestion to evaluate whether some polysaccharides of *H. erinaceus* could overcome the digestive barrier of the upper digestive tract and influence gut microbiota composition.

Following this experimental model, several *H. erinaceus* polysaccharides obtained by alcohol precipitation (*i.e.*, HEP30, HEP50, and HEP70) increased the relative abundance of SCFA-producing bacteria and reduced pathobiont concentrations (*i.e.*, *Escherichia-Shigella*, *Klebsiella*, and *Enterobacter* in this experience), stigmatised the role of such polysaccharides as possible functional foods[127]. Therefore, they set up an experimental *in vitro* digestion model, as previously described. First, they suggested the likely passage of polysaccharides through the gastrointestinal tract without being digested by the saliva of healthy donors or gastric and small intestinal juices (simulated in the laboratory). Therefore, they may reach the distal tract of the intestine. Second, at that level, the authors demonstrated how the gut microbiota utilised HEP50 for fermentation by increasing the levels of SCFAs and decreasing the pH of the faecal fermentation broth.

Furthermore, Yang *et al*[127] examined the impact of a polysaccharide from the mycelium of *H. erinaceus* on the quality of murine gut microbiota. The authors observed a change in the relative abundance of different bacteria depending on the age of the mice used for the microbiota analysis. In both the control and experimental groups of adult and middle-aged mice, there was an increase in the relative abundance of *Lachnospiraceae*, *Ruminococcaceae,* and *Akkermansiaceae* and a decrease in the relative abundance of *Muribaculaceae*, *Rikenellaceae*, *Lactobacillaceae,* and *Bacteroidaceae*. On the other hand, only the treated adult mice showed an increase in *Erysipelotrichaceae*, *Enterobacteriaceae*, *Christensenellaceae,* and *Coriobacteriaceae* and a decrease in *Bifidobacteriaceae* and *Peptostreptococcaceae*. Finally, in the group of middle-aged and old mice, the increased bacterial species were *Rhizobiaceae*, *Desulfovibrionaceae,* and *Lachnospiraceae,* while the decreased species were *Corynebbacteraceae* and *Rikenellaceae*. Among the many modified families of bacteria, the relevant ones are the butyrate-producing bacteria (*i.e.*, *Lachnospiraceae* and *Ruminococcaceae*). Butyrate is an SCFA used as an energy source by the intestinal mucosa to promote gut health and protect against colorectal cancer[128-130]. These two species of bacteria are among the leading producers of butyrate[131]. Further *in vitro* studies have shown the beneficial effects of *H. erinaceus* in modulating SCFA-producing bacteria[132]. Positive *H. erinaceus*-driven modulation of the gut microbiota has also been confirmed in elderly dogs, with ameliorative effects on immunity and obesity[133].

H. erinaceus in restoring the gut microbiota after dysbiosis induced by antineoplastic drug therapy: The evidence

Cancer therapy is associated with significant adverse events, including gastrointestinal complications. The latter includes dysbiosis induced by antineoplastic treatments[134]. However, while the microbiota may be impacted by antineoplastic therapy, it is also true that several reports suggest an opposite mechanism whereby the gut microbiota may modulate the response to treatment, specifically immunotherapy[135]. In this context, *H. erinaceus* showed some preclinical results, demonstrating its potential in cancer therapy-induced toxicity. For this purpose, an investigation based on polysaccharides was conducted in mice treated with cyclophosphamide[136]. This brought the composition of the gut microbiota of chemotherapy-treated mice closer to that of control and healthy mice through increased



DOI: 10.3748/wjg.v29.i20.3084 **Copyright** ©The Author(s) 2023.

Figure 3 The potential of *Hericium erinaceus* in upper and lower gastrointestinal tract diseases. *Hericium erinaceus* is a promising candidate as a therapeutic modality or functional food in the treatment of various diseases of the gastrointestinal tract. This evidence stems from several experiences, largely preclinical, that have shown that this mushroom possesses anti-inflammatory and antineoplastic capabilities concerning the gastrointestinal tract.

alpha and beta diversity. Similar results were reported in another study[123]. Moreover, these data are also available for 5-fluorouracil toxicity. Wang *et al*[137] examined the proteins of *H. erinaceus* in a xenograft cancer model in mice successfully treated with 5-fluorouracil and revealed an anti-dysbiosis action.

H. erinaceus may intervene in IBD through the gut microbiota

Although a therapy based on the direct modification of the gut microbiota is not yet recommended in the current guidelines for managing IBD, it is clear that the potential of this option has been extensively studied and is currently under investigation[138-141].

Ren *et al*[142] studied whether the administration of *H. erinaceus* to Cynomolgus monkeys affected the clinical features of spontaneous UC by exerting an anti-inflammatory effect through modulation of the gut microbiota. They recorded an increase in the abundance of bacteria, such as *Lactobacillus reuteri* (already implicated in improving the clinical features of IBS, acute gastrointestinal infections, and IBD in children and adults). In contrast, *Streptococcus lutetiensis* is negatively modulated and is known to cause sepsis in newborns[143].

In addition, Diling *et al*[81], in the above cited model of murine colitis induced by trinitro-benzene-sulfonic acid, demonstrated how the administration of extracts (*i.e.*, polysaccharide, alcoholic extracts, and whole extracts) of *H. erinaceus* improved both the clinical and histological picture but, more importantly, the gut microbiota by promoting a switch to a microbial composition similar to that of the controls. In other words, a reduction in proinflammatory strains (*Corynebacterium*, *Staphylococcus*, *Ruminococcus*, *Roseburia*, *Dorea*, and *Sutterella*) and an increase in anti-inflammatory strains (*Bacteroides*, *Bifidobacterium*, *Prevotella*, *Parabacteroides*, *Coprococcus*, *Desulfovibrio*, and *Lactobacillus*) were observed.

In a similar study, in an acetic acid-induced murine colitis model, the mycelium polysaccharide EP-1 drastically improved the gut microbiota of mice by increasing SCFA-producing populations while suppressing the expression of G protein-coupled receptor 41 (GPR41) and GPR43[144]. SCFAs can bind to GPR41 and GPR43 and increase the production of inflammatory cytokines and chemokines in the intestine[145].

Finally, positive microbiota modulation was observed in mice with dextran sulphate sodium-induced colitis[91].

Despite the possibility that *H. erinaceus* may have intervened in the pathogenesis of IBD through the gut microbiota, studies conducted in humans as well as those exploring the clinical impact of such microbiota modification, are still awaited, especially with clinical tools and scores that are widely validated and used in clinical and IBD research practise[146,147].

CONCLUSION

H. erinaceus is a mushroom with a long tradition of use as a medicinal product. Numerous preclinical studies have probed its gastrointestinal anti-inflammatory and antineoplastic properties and its impact on the composition of the intestinal microbiota (Figure 3). In the face of a large body of evidence, there is a strong need for clinical studies conducted on humans, especially considering the promising results of previous studies. Furthermore, it is necessary to determine whether this fungus can represent an

excellent nutritional supplement in gastrointestinal pathologies, the patients who may benefit from it, and whether there is a possible therapeutic role for the compounds extracted from *H. erinaceus*. Finally, various technical processes for such fungi yield many extracts and fractions. Therefore, it is essential to understand which of these presents the best safety and efficacy profiles.

FOOTNOTES

Author contributions: Gravina AG, Pellegrino R, Romano M, and Federico A collected the literature, wrote the initial manuscript, conceptualised the tables and figures, and contributed equally to this work; Gravina AG, Pellegrino R, Auletta S, Palladino G, Brandimarte G, D'Onofrio R, Arboretto G, Imperio G, Ventura A, Cipullo M, Romano M, and Federico A conceptualised the structure of the text, critically revised the manuscript for important intellectual content, and read and approved the final version of the manuscript.

Conflict-of-interest statement: The authors declare no conflicts of interest for this article.

Open-Access: This article is an open-access article that was selected by an in-house editor and fully peer-reviewed by external reviewers. It is distributed in accordance with the Creative Commons Attribution NonCommercial (CC BY-NC 4.0) license, which permits others to distribute, remix, adapt, build upon this work non-commercially, and license their derivative works on different terms, provided the original work is properly cited and the use is non-commercial. See: https://creativecommons.org/Licenses/by-nc/4.0/

Country/Territory of origin: Italy

ORCID number: Antonietta Gerarda Gravina 0000-0001-8049-0115; Raffaele Pellegrino 0000-0001-5074-230X; Salvatore Auletta 0009-0008-8565-0120; Giovanna Palladino 0000-0002-7367-4175; Rossella D'Onofrio 0009-0002-4761-0028; Giusi Arboretto 0009-0000-7938-8949; Giuseppe Imperio 0000-0002-4182-2858; Andrea Ventura 0009-0005-5735-7195; Marina Cipullo 0000-0003-4938-5805; Marco Romano 0000-0002-3271-349X; Alessandro Federico 0000-0002-0885-0793.

S-Editor: Chen YL
L-Editor: A
P-Editor: Zhao S

REFERENCES

1 **Peery AF**, Crockett SD, Murphy CC, Lund JL, Dellon ES, Williams JL, Jensen ET, Shaheen NJ, Barritt AS, Lieber SR, Kochar B, Barnes EL, Fan YC, Pate V, Galanko J, Baron TH, Sandler RS. Burden and Cost of Gastrointestinal, Liver, and Pancreatic Diseases in the United States: Update 2018. *Gastroenterology* 2019; **156**: 254-272.e11 [PMID: 30315778 DOI: 10.1053/j.gastro.2018.08.063]

2 **Deutsch JK**, Levitt J, Hass DJ. Complementary and Alternative Medicine for Functional Gastrointestinal Disorders. *Am J Gastroenterol* 2020; **115**: 350-364 [PMID: 32079860 DOI: 10.14309/ajg.0000000000000539]

3 **Cheifetz AS**, Gianotti R, Luber R, Gibson PR. Complementary and Alternative Medicines Used by Patients With Inflammatory Bowel Diseases. *Gastroenterology* 2017; **152**: 415-429.e15 [PMID: 27743873 DOI: 10.1053/j.gastro.2016.10.004]

4 **Thongbai B**, Rapior S, Hyde KD, Wittstein K, Stadler M. Hericium erinaceus, an amazing medicinal mushroom. *Mycol Progress* 2015; **14**: 91 [DOI: 10.1007/s11557-015-1105-4]

5 **Cheng JH**, Tsai CL, Lien YY, Lee MS, Sheu SC. High molecular weight of polysaccharides from Hericium erinaceus against amyloid beta-induced neurotoxicity. *BMC Complement Altern Med* 2016; **16**: 170 [PMID: 27266872 DOI: 10.1186/s12906-016-1154-5]

6 **Lee JS**, Hong EK. Hericium erinaceus enhances doxorubicin-induced apoptosis in human hepatocellular carcinoma cells. *Cancer Lett* 2010; **297**: 144-154 [PMID: 20554107 DOI: 10.1016/j.canlet.2010.05.006]

7 **Shang HM**, Song H, Xing YL, Niu SL, Ding GD, Jiang YY, Liang F. Effects of dietary fermentation concentrate of Hericium caput-medusae (Bull.:Fr.) Pers. on growth performance, digestibility, and intestinal microbiology and morphology in broiler chickens. *J Sci Food Agric* 2016; **96**: 215-222 [PMID: 25582752 DOI: 10.1002/jsfa.7084]

8 **Zhang Z**, Lv G, Pan H, Pandey A, He W, Fan L. Antioxidant and hepatoprotective potential of endo-polysaccharides from Hericium erinaceus grown on tofu whey. *Int J Biol Macromol* 2012; **51**: 1140-1146 [PMID: 22982810 DOI: 10.1016/j.ijbiomac.2012.09.002]

9 **Saitsu Y**, Nishide A, Kikushima K, Shimizu K, Ohnuki K. Improvement of cognitive functions by oral intake of Hericium erinaceus. *Biomed Res* 2019; **40**: 125-131 [PMID: 31413233 DOI: 10.2220/biomedres.40.125]

10 **Mori K**, Inatomi S, Ouchi K, Azumi Y, Tuchida T. Improving effects of the mushroom Yamabushitake (Hericium erinaceus) on mild cognitive impairment: a double-blind placebo-controlled clinical trial. *Phytother Res* 2009; **23**: 367-372 [PMID: 18844328 DOI: 10.1002/ptr.2634]

11 **Miles PG**, Chang S-T. Mushrooms. 0 ed. CRC Press, Taylor & Francis Group, 2004 [DOI: 10.1201/9780203492086]

12 **Boddy L**, Crockatt ME, Ainsworth AM. Ecology of Hericium cirrhatum, H. coralloides and H. erinaceus in the UK. *Fungal Ecology* 2011; **4**: 163-173 [DOI: 10.1016/j.funeco.2010.10.001]

13 **Friedman M**. Chemistry, Nutrition, and Health-Promoting Properties of Hericium erinaceus (Lion's Mane) Mushroom

Fruiting Bodies and Mycelia and Their Bioactive Compounds. *J Agric Food Chem* 2015; **63**: 7108-7123 [PMID: 26244378 DOI: 10.1021/acs.jafc.5b02914]

14 **Li W**, Gu Z, Yang Y, Zhou S, Liu Y, Zhang J. Non-volatile taste components of several cultivated mushrooms. *Food Chem* 2014; **143**: 427-431 [PMID: 24054262 DOI: 10.1016/j.foodchem.2013.08.006]

15 **Rodrigues DMF**, Freitas AC, Rocha-Santos TAP, Vasconcelos MW, Roriz M, Rodríguez-Alcalá LM, Gomes AMP, Duarte AC. Chemical composition and nutritive value of Pleurotus citrinopileatus var cornucopiae, P. eryngii, P. salmoneo stramineus, Pholiota nameko and Hericium erinaceus. *J Food Sci Technol* 2015; **52**: 6927-6939 [DOI: 10.1007/s13197-015-1826-z]

16 **Jayachandran M**, Chen J, Chung SSM, Xu B. A critical review on the impacts of β-glucans on gut microbiota and human health. *J Nutr Biochem* 2018; **61**: 101-110 [PMID: 30196242 DOI: 10.1016/j.jnutbio.2018.06.010]

17 **Zhu F**, Du B, Xu B. Preparation and Characterization of Polysaccharides from Mushrooms. In: Ramawat KG, Mérillon J-M, editors. Polysaccharides. Cham: Springer International Publishing, 2014: 1-16

18 **Liu J**, Wang W, Hu Q, Wu X, Xu H, Su A, Xie M, Yang W. Bioactivities and molecular mechanisms of polysaccharides from Hericium erinaceus. *J Future Foods* 2022; **2**: 103-111 [DOI: 10.1016/j.jfutfo.2022.03.007]

19 **Łubek-Nguyen A**, Ziemichód W, Olech M. Application of Enzyme-Assisted Extraction for the Recovery of Natural Bioactive Compounds for Nutraceutical and Pharmaceutical Applications. *Appl Sci* 2022; **12**: 3232 [DOI: 10.3390/app12073232]

20 **Lanas A**, Chan FKL. Peptic ulcer disease. *Lancet* 2017; **390**: 613-624 [PMID: 28242110 DOI: 10.1016/S0140-6736(16)32404-7]

21 **Takeuchi K**. Pathogenesis of NSAID-induced gastric damage: importance of cyclooxygenase inhibition and gastric hypermotility. *World J Gastroenterol* 2012; **18**: 2147-2160 [PMID: 22611307 DOI: 10.3748/wjg.v18.i18.2147]

22 **Sugimoto M**, Yamaoka Y, Furuta T. Influence of interleukin polymorphisms on development of gastric cancer and peptic ulcer. *World J Gastroenterol* 2010; **16**: 1188-1200 [PMID: 20222161 DOI: 10.3748/wjg.v16.i10.1188]

23 **Boddy L**, Wald P. Creolophus (Hericium) cirrhatus, Hericium erinaceus and H. coralloides in England (English nature research report 492). *English Nature* 2003; 168-169

24 **Wang XY**, Yin JY, Zhao MM, Liu SY, Nie SP, Xie MY. Gastroprotective activity of polysaccharide from Hericium erinaceus against ethanol-induced gastric mucosal lesion and pylorus ligation-induced gastric ulcer, and its antioxidant activities. *Carbohydr Polym* 2018; **186**: 100-109 [PMID: 29455967 DOI: 10.1016/j.carbpol.2018.01.004]

25 **Wang M**, Kanako N, Zhang Y, Xiao X, Gao Q, Tetsuya K. A unique polysaccharide purified from Hericium erinaceus mycelium prevents oxidative stress induced by H2O2 in human gastric mucosa epithelium cell. *PLoS One* 2017; **12**: e0181546 [PMID: 28742114 DOI: 10.1371/journal.pone.0181546]

26 **Liu J**, Wang F, Luo H, Liu A, Li K, Li C, Jiang Y. Protective effect of butyrate against ethanol-induced gastric ulcers in mice by promoting the anti-inflammatory, anti-oxidant and mucosal defense mechanisms. *Int Immunopharmacol* 2016; **30**: 179-187 [PMID: 26604089 DOI: 10.1016/j.intimp.2015.11.018]

27 **Rozza AL**, Meira de Faria F, Souza Brito AR, Pellizzon CH. The gastroprotective effect of menthol: involvement of anti-apoptotic, antioxidant and anti-inflammatory activities. *PLoS One* 2014; **9**: e86686 [PMID: 24466200 DOI: 10.1371/journal.pone.0086686]

28 **Amirshahrokhi K**, Khalili AR. The effect of thalidomide on ethanol-induced gastric mucosal damage in mice: involvement of inflammatory cytokines and nitric oxide. *Chem Biol Interact* 2015; **225**: 63-69 [PMID: 25478868 DOI: 10.1016/j.cbi.2014.11.019]

29 **Moezi L**, Heidari R, Amirghofran Z, Nekooeian AA, Monabati A, Dehpour AR. Enhanced anti-ulcer effect of pioglitazone on gastric ulcers in cirrhotic rats: the role of nitric oxide and IL-1β. *Pharmacol Rep* 2013; **65**: 134-143 [PMID: 23563031 DOI: 10.1016/s1734-1140(13)70971-x]

30 **Bi WP**, Man HB, Man MQ. Efficacy and safety of herbal medicines in treating gastric ulcer: a review. *World J Gastroenterol* 2014; **20**: 17020-17028 [PMID: 25493014 DOI: 10.3748/wjg.v20.i45.17020]

31 **Yandrapu H**, Sarosiek J. Protective Factors of the Gastric and Duodenal Mucosa: An Overview. *Curr Gastroenterol Rep* 2015; **17**: 24 [PMID: 26109006 DOI: 10.1007/s11894-015-0452-2]

32 **Sofidiya MO**, Orisaremi CO, Sansaliyu I, Adetunde TO. Gastroprotective and antioxidant potentials of ethanolic stem bark extract of Margaritaria discoidea (Euphorbiaceae) in rats. *J Ethnopharmacol* 2015; **171**: 240-246 [PMID: 26068431 DOI: 10.1016/j.jep.2015.05.059]

33 **deFoneska A**, Kaunitz JD. Gastroduodenal mucosal defense. *Curr Opin Gastroenterol* 2010; **26**: 604-610 [PMID: 20948371 DOI: 10.1097/MOG.0b013e32833f1222]

34 **Sidahmed HM**, Hashim NM, Amir J, Abdulla MA, Hadi AH, Abdelwahab SI, Taha MM, Hassandarvish P, Teh X, Loke MF, Vadivelu J, Rahmani M, Mohan S. Pyranocycloartobiloxanthone A, a novel gastroprotective compound from Artocarpus obtusus Jarret, against ethanol-induced acute gastric ulcer in vivo. *Phytomedicine* 2013; **20**: 834-843 [PMID: 23570997 DOI: 10.1016/j.phymed.2013.03.002]

35 **Guo YJ**, Deng GF, Xu XR, Wu S, Li S, Xia EQ, Li F, Chen F, Ling WH, Li HB. Antioxidant capacities, phenolic compounds and polysaccharide contents of 49 edible macro-fungi. *Food Funct* 2012; **3**: 1195-1205 [PMID: 22868715 DOI: 10.1039/c2fo30110e]

36 **Mao X**, Lu ZM, Gong TT, Wang KL, Geng Y, Xu HY, Xu GH, Shi JS, Xu ZH. Therapeutic Effect and Potential Mechanisms of Lion's Mane Medicinal Mushroom, Hericium erinaceus (Agaricomycetes), Mycelia in Submerged Culture on Ethanol-Induced Chronic Gastric Injury. *Int J Med Mushrooms* 2019; **21**: 1137-1150 [PMID: 32450023 DOI: 10.1615/IntJMedMushrooms.2019032885]

37 **Chen W**, Wu D, Jin Y, Li Q, Liu Y, Qiao X, Zhang J, Dong G, Li Z, Li T, Yang Y. Pre-protective effect of polysaccharides purified from Hericium erinaceus against ethanol-induced gastric mucosal injury in rats. *Int J Biol Macromol* 2020; **159**: 948-956 [PMID: 32450327 DOI: 10.1016/j.ijbiomac.2020.05.163]

38 **Hou C**, Liu L, Ren J, Huang M, Yuan E. Structural characterization of two Hericium erinaceus polysaccharides and their protective effects on the alcohol-induced gastric mucosal injury. *Food Chem* 2022; **375**: 131896 [PMID: 34954576 DOI: 10.1016/j.foodchem.2021.131896]

39 **Wang XY**, Wang M, Yin JY, Song YH, Wang YX, Nie SP, Xie MY. Gastroprotective activity of polysaccharide from the fruiting body of Hericium erinaceus against acetic acid-induced gastric ulcer in rats and structure of one bioactive fraction. *Int J Biol Macromol* 2022; **210**: 455-464 [PMID: 35483513 DOI: 10.1016/j.ijbiomac.2022.04.153]

40 **Wong JY**, Abdulla MA, Raman J, Phan CW, Kuppusamy UR, Golbabapour S, Sabaratnam V. Gastroprotective Effects of Lion's Mane Mushroom Hericium erinaceus (Bull.:Fr.) Pers. (Aphyllophoromycetideae) Extract against Ethanol-Induced Ulcer in Rats. *Evid Based Complement Alternat Med* 2013; **2013**: 492976 [PMID: 24302966 DOI: 10.1155/2013/492976]

41 **Choi SR**, Lee SA, Kim YJ, Ok CY, Lee HJ, Hahm KB. Role of heat shock proteins in gastric inflammation and ulcer healing. *J Physiol Pharmacol* 2009; **60** Suppl 7: 5-17 [PMID: 20388941]

42 **Wang M**, Gao Y, Xu D, Gao Q. A polysaccharide from cultured mycelium of Hericium erinaceus and its anti-chronic atrophic gastritis activity. *Int J Biol Macromol* 2015; **81**: 656-661 [PMID: 26314904 DOI: 10.1016/j.ijbiomac.2015.08.043]

43 **Xu CP**, Liu WW, Liu FX, Chen SS, Liao FQ, Xu Z, Jiang LG, Wang CA, Lu XH. A double-blind study of effectiveness of hericium erinaceus pers therapy on chronic atrophic gastritis. A preliminary report. *Chin Med J (Engl)* 1985; **98**: 455-456 [PMID: 3932005]

44 **Gravina AG**, Zagari RM, De Musis C, Romano L, Loguercio C, Romano M. Helicobacter pylori and extragastric diseases: A review. *World J Gastroenterol* 2018; **24**: 3204-3221 [PMID: 30090002 DOI: 10.3748/wjg.v24.i29.3204]

45 **Gravina AG**, Priadko K, Ciamarra P, Granata L, Facchiano A, Miranda A, Dallio M, Federico A, Romano M. Extra-Gastric Manifestations of Helicobacter pylori Infection. *J Clin Med* 2020; **9** [PMID: 33265933 DOI: 10.3390/jcm9123887]

46 **Wang F**, Meng W, Wang B, Qiao L. Helicobacter pylori-induced gastric inflammation and gastric cancer. *Cancer Lett* 2014; **345**: 196-202 [PMID: 23981572 DOI: 10.1016/j.canlet.2013.08.016]

47 **Flores-Treviño S**, Mendoza-Olazarán S, Bocanegra-Ibarias P, Maldonado-Garza HJ, Garza-González E. Helicobacter pylori drug resistance: therapy changes and challenges. *Expert Rev Gastroenterol Hepatol* 2018; **12**: 819-827 [PMID: 29976092 DOI: 10.1080/17474124.2018.1496017]

48 **Romano M**, Gravina AG, Eusebi LH, Pellegrino R, Palladino G, Frazzoni L, Dajti E, Gasbarrini A, Di Mario F, Zagari RM; Members of SIGE; Members of SIED National Council. Management of Helicobacter pylori infection: Guidelines of the Italian Society of Gastroenterology (SIGE) and the Italian Society of Digestive Endoscopy (SIED). *Dig Liver Dis* 2022; **54**: 1153-1161 [PMID: 35831212 DOI: 10.1016/j.dld.2022.06.019]

49 **Malfertheiner P**, Megraud F, Rokkas T, Gisbert JP, Liou JM, Schulz C, Gasbarrini A, Hunt RH, Leja M, O'Morain C, Rugge M, Suerbaum S, Tilg H, Sugano K, El-Omar EM; European Helicobacter and Microbiota Study group. Management of Helicobacter pylori infection: the Maastricht VI/Florence consensus report. *Gut* 2022 [PMID: 35944925 DOI: 10.1136/gutjnl-2022-327745]

50 **Shang X**, Tan Q, Liu R, Yu K, Li P, Zhao GP. In vitro anti-Helicobacter pylori effects of medicinal mushroom extracts, with special emphasis on the Lion's Mane mushroom, Hericium erinaceus (higher Basidiomycetes). *Int J Med Mushrooms* 2013; **15**: 165-174 [PMID: 23557368 DOI: 10.1615/intjmedmushr.v15.i2.50]

51 **Zhu Y**, Chen Y, Li Q, Zhao T, Zhang M, Feng W, Takase M, Wu X, Zhou Z, Yang L. Preparation, characterization, and anti-Helicobacter pylori activity of Bi3+-Hericium erinaceus polysaccharide complex. *Carbohydr Polym* 2014; **110**: 231-237 [PMID: 24906751 DOI: 10.1016/j.carbpol.2014.03.081]

52 **Liu JH**, Li L, Shang XD, Zhang JL, Tan Q. Anti-Helicobacter pylori activity of bioactive components isolated from Hericium erinaceus. *J Ethnopharmacol* 2016; **183**: 54-58 [PMID: 26364939 DOI: 10.1016/j.jep.2015.09.004]

53 **Thi My Ngan L**, Thien Vi N, Thi Mong Tham D, Thi Thanh Loan L, Thanh Ho P, Trung Hieu T. Antioxidant and anti-Helicobacter pylori activities of Hericium erinaceus mycelium and culture filtrate. *Biomed Res Ther* 2021; **8**: 4266-4275 [DOI: 10.15419/bmrat.v8i3.665]

54 **Jin Y**, Ling P, He Y, Chen L, Chen J, Zhang T. Preparation, characterization and anti-Helicobacter pylori activity of Bi3+-hyaluronate complex. *Carbohydr Polym* 2008; **74**: 50-58 [DOI: 10.1016/j.carbpol.2008.01.014]

55 **Machlowska J**, Baj J, Sitarz M, Maciejewski R, Sitarz R. Gastric Cancer: Epidemiology, Risk Factors, Classification, Genomic Characteristics and Treatment Strategies. *Int J Mol Sci* 2020; **21** [PMID: 32512697 DOI: 10.3390/ijms21114012]

56 **Sexton RE**, Al Hallak MN, Diab M, Azmi AS. Gastric cancer: a comprehensive review of current and future treatment strategies. *Cancer Metastasis Rev* 2020; **39**: 1179-1203 [PMID: 32894370 DOI: 10.1007/s10555-020-09925-3]

57 **Ju HM**, Yu KW, Cho SD, Cheong SH, Kwon KH. Anti-cancer effects of traditional Korean wild vegetables in complementary and alternative medicine. *Complement Ther Med* 2016; **24**: 47-54 [PMID: 26860801 DOI: 10.1016/j.ctim.2015.11.004]

58 **Jain A**, Tiwari A, Verma A, Jain SK. Vitamins for Cancer Prevention and Treatment: An Insight. *Curr Mol Med* 2017; **17**: 321-340 [PMID: 29210648 DOI: 10.2174/1566524018666171205113329]

59 **Hassanalilou T**, Ghavamzadeh S, Khalili L. Curcumin and Gastric Cancer: a Review on Mechanisms of Action. *J Gastrointest Cancer* 2019; **50**: 185-192 [PMID: 30725357 DOI: 10.1007/s12029-018-00186-6]

60 **Chen CC**, Tzeng TT, Chen CC, Ni CL, Lee LY, Chen WP, Shiao YJ, Shen CC. Erinacine S, a Rare Sesterterpene from the Mycelia of Hericium erinaceus. *J Nat Prod* 2016; **79**: 438-441 [PMID: 26807743 DOI: 10.1021/acs.jnatprod.5b00474]

61 **Tung SY**, Lee KC, Lee KF, Yang YL, Huang WS, Lee LY, Chen WP, Chen CC, Teng CC, Shen CH, Hsieh MC, Huang CY, Sheen JM, Kuo HC. Apoptotic mechanisms of gastric cancer cells induced by isolated erinacine S through epigenetic histone H3 methylation of FasL and TRAIL. *Food Funct* 2021; **12**: 3455-3468 [PMID: 33900313 DOI: 10.1039/d0fo03089a]

62 **Kallergi G**, Agelaki S, Markomanolaki H, Georgoulias V, Stournaras C. Activation of FAK/PI3K/Rac1 signaling controls actin reorganization and inhibits cell motility in human cancer cells. *Cell Physiol Biochem* 2007; **20**: 977-986 [PMID: 17982280 DOI: 10.1159/000110458]

63 **Kuo HC**, Kuo YR, Lee KF, Hsieh MC, Huang CY, Hsieh YY, Lee KC, Kuo HL, Lee LY, Chen WP, Chen CC, Tung SY. A Comparative Proteomic Analysis of Erinacine A's Inhibition of Gastric Cancer Cell Viability and Invasiveness. *Cell Physiol Biochem* 2017; **43**: 195-208 [PMID: 28854418 DOI: 10.1159/000480338]

64 **Loo G**. Redox-sensitive mechanisms of phytochemical-mediated inhibition of cancer cell proliferation (review). *J Nutr*

Biochem 2003; **14**: 64-73 [PMID: 12667597 DOI: 10.1016/s0955-2863(02)00251-6]
65 **Lee KC**, Kuo HC, Shen CH, Lu CC, Huang WS, Hsieh MC, Huang CY, Kuo YH, Hsieh YY, Teng CC, Lee LY, Tung SY. A proteomics approach to identifying novel protein targets involved in erinacine A-mediated inhibition of colorectal cancer cells' aggressiveness. *J Cell Mol Med* 2017; **21**: 588-599 [PMID: 27709782 DOI: 10.1111/jcmm.13004]
66 **Thomas GM**, Huganir RL. MAPK cascade signalling and synaptic plasticity. *Nat Rev Neurosci* 2004; **5**: 173-183 [PMID: 14976517 DOI: 10.1038/nrn1346]
67 **Johannessen M**, Delghandi MP, Moens U. What turns CREB on? *Cell Signal* 2004; **16**: 1211-1227 [PMID: 15337521 DOI: 10.1016/j.cellsig.2004.05.001]
68 **Luk SC**, Siu SW, Lai CK, Wu YJ, Pang SF. Cell Cycle Arrest by a Natural Product *via* G2/M Checkpoint. *Int J Med Sci* 2005; **2**: 64-69 [PMID: 15968342 DOI: 10.7150/ijms.2.64]
69 **Tsukamoto Y**, Nakada C, Noguchi T, Tanigawa M, Nguyen LT, Uchida T, Hijiya N, Matsuura K, Fujioka T, Seto M, Moriyama M. MicroRNA-375 is downregulated in gastric carcinomas and regulates cell survival by targeting PDK1 and 14-3-3zeta. *Cancer Res* 2010; **70**: 2339-2349 [PMID: 20215506 DOI: 10.1158/0008-5472.CAN-09-2777]
70 **Adams G Jr**, Zhou J, Wang W, Wu H, Quan J, Liu Y, Xia P, Wang Z, Zhou S, Jiang J, Mo F, Zhuang X, Thomas K, Hill DL, Aikhionbare FO, He P, Liu X, Ding X, Yao X. The Microtubule Plus End Tracking Protein TIP150 Interacts with Cortactin to Steer Directional Cell Migration. *J Biol Chem* 2016; **291**: 20692-20706 [PMID: 27451391 DOI: 10.1074/jbc.M116.732719]
71 **Jiang K**, Wang J, Liu J, Ward T, Wordeman L, Davidson A, Wang F, Yao X. TIP150 interacts with and targets MCAK at the microtubule plus ends. *EMBO Rep* 2009; **10**: 857-865 [PMID: 19543227 DOI: 10.1038/embor.2009.94]
72 **Croft DR**, Olson MF. Transcriptional regulation of Rho GTPase signaling. *Transcription* 2011; **2**: 211-215 [PMID: 22231116 DOI: 10.4161/trns.2.5.16904]
73 **Gu S**, Kounenidakis M, Schmidt EM, Deshpande D, Alkahtani S, Alarifi S, Föller M, Alevizopoulos K, Lang F, Stournaras C. Rapid activation of FAK/mTOR/p70S6K/PAK1-signaling controls the early testosterone-induced actin reorganization in colon cancer cells. *Cell Signal* 2013; **25**: 66-73 [PMID: 23316499 DOI: 10.1016/j.cellsig.2012.08.005]
74 **Papakonstanti EA**, Kampa M, Castanas E, Stournaras C. A rapid, nongenomic, signaling pathway regulates the actin reorganization induced by activation of membrane testosterone receptors. *Mol Endocrinol* 2003; **17**: 870-881 [PMID: 12554777 DOI: 10.1210/me.2002-0253]
75 **Zan X**, Cui F, Li Y, Yang Y, Wu D, Sun W, Ping L. Hericium erinaceus polysaccharide-protein HEG-5 inhibits SGC-7901 cell growth *via* cell cycle arrest and apoptosis. *Int J Biol Macromol* 2015; **76**: 242-253 [PMID: 25703932 DOI: 10.1016/j.ijbiomac.2015.01.060]
76 **Yang W**, Han D, Wu L, Huang Y, Li J, Guo H, Liu Y. Hericium erinaceus synergizing with doxorubicin induced SGC7901 cell apoptosis. *Int J Clin Exp Med* 2016; **9**: 1447-1457
77 **Li G**, Yu K, Li F, Xu K, Li J, He S, Cao S, Tan G. Anticancer potential of Hericium erinaceus extracts against human gastrointestinal cancers. *J Ethnopharmacol* 2014; **153**: 521-530 [PMID: 24631140 DOI: 10.1016/j.jep.2014.03.003]
78 **Wang M**, Zhang Y, Xiao X, Xu D, Gao Y, Gao Q. A Polysaccharide Isolated from Mycelia of the Lion's Mane Medicinal Mushroom Hericium erinaceus (Agaricomycetes) Induced Apoptosis in Precancerous Human Gastric Cells. *Int J Med Mushrooms* 2017; **19**: 1053-1060 [PMID: 29431066 DOI: 10.1615/IntJMedMushrooms.2017024975]
79 **Chang JT**. Pathophysiology of Inflammatory Bowel Diseases. *N Engl J Med* 2020; **383**: 2652-2664 [PMID: 33382932 DOI: 10.1056/NEJMra2002697]
80 **Wang D**, Xu D, Zhao D, Wang M. Screening and Comparison of Anti-Intestinal Inflammatory Activities of Three Polysaccharides from the Mycelium of Lion's Mane Culinary-Medicinal Mushroom, Hericium erinaceus (Agaricomycetes). *Int J Med Mushrooms* 2021; **23**: 63-71 [PMID: 34591399 DOI: 10.1615/IntJMedMushrooms.2021039951]
81 **Diling C**, Xin Y, Chaoqun Z, Jian Y, Xiaocui T, Jun C, Ou S, Yizhen X. Extracts from Hericium erinaceus relieve inflammatory bowel disease by regulating immunity and gut microbiota. *Oncotarget* 2017; **8**: 85838-85857 [PMID: 29156761 DOI: 10.18632/oncotarget.20689]
82 **Qin M**, Geng Y, Lu Z, Xu H, Shi JS, Xu X, Xu ZH. Anti-Inflammatory Effects of Ethanol Extract of Lion's Mane Medicinal Mushroom, Hericium erinaceus (Agaricomycetes), in Mice with Ulcerative Colitis. *Int J Med Mushrooms* 2016; **18**: 227-234 [PMID: 27481156 DOI: 10.1615/IntJMedMushrooms.v18.i3.50]
83 **Wang D**, Zhang Y, Yang S, Zhao D, Wang M. A polysaccharide from cultured mycelium of Hericium erinaceus relieves ulcerative colitis by counteracting oxidative stress and improving mitochondrial function. *Int J Biol Macromol* 2019; **125**: 572-579 [PMID: 30543884 DOI: 10.1016/j.ijbiomac.2018.12.092]
84 **Moura FA**, de Andrade KQ, Dos Santos JCF, Araújo ORP, Goulart MOF. Antioxidant therapy for treatment of inflammatory bowel disease: Does it work? *Redox Biol* 2015; **6**: 617-639 [PMID: 26520808 DOI: 10.1016/j.redox.2015.10.006]
85 **Watt DG**, Horgan PG, McMillan DC. Routine clinical markers of the magnitude of the systemic inflammatory response after elective operation: a systematic review. *Surgery* 2015; **157**: 362-380 [PMID: 25616950 DOI: 10.1016/j.surg.2014.09.009]
86 **Biasi F**, Leonarduzzi G, Oteiza PI, Poli G. Inflammatory bowel disease: mechanisms, redox considerations, and therapeutic targets. *Antioxid Redox Signal* 2013; **19**: 1711-1747 [PMID: 23305298 DOI: 10.1089/ars.2012.4530]
87 **Morcillo EJ**, Estrela J, Cortijo J. Oxidative stress and pulmonary inflammation: pharmacological intervention with antioxidants. *Pharmacol Res* 1999; **40**: 393-404 [PMID: 10527653 DOI: 10.1006/phrs.1999.0549]
88 **Sung HJ**, Ma W, Wang PY, Hynes J, O'Riordan TC, Combs CA, McCoy JP Jr, Bunz F, Kang JG, Hwang PM. Mitochondrial respiration protects against oxygen-associated DNA damage. *Nat Commun* 2010; **1**: 5 [PMID: 20975668 DOI: 10.1038/ncomms1003]
89 **Roediger WE**. The colonic epithelium in ulcerative colitis: an energy-deficiency disease? *Lancet* 1980; **2**: 712-715 [PMID: 6106826 DOI: 10.1016/s0140-6736(80)91934-0]
90 **Santhanam S**, Rajamanickam S, Motamarry A, Ramakrishna BS, Amirtharaj JG, Ramachandran A, Pulimood A, Venkatraman A. Mitochondrial electron transport chain complex dysfunction in the colonic mucosa in ulcerative colitis.

Inflamm Bowel Dis 2012; **18**: 2158-2168 [PMID: 22374887 DOI: 10.1002/ibd.22926]

91 **Ren Y**, Geng Y, Du Y, Li W, Lu ZM, Xu HY, Xu GH, Shi JS, Xu ZH. Polysaccharide of Hericium erinaceus attenuates colitis in C57BL/6 mice *via* regulation of oxidative stress, inflammation-related signaling pathways and modulating the composition of the gut microbiota. *J Nutr Biochem* 2018; **57**: 67-76 [PMID: 29677563 DOI: 10.1016/j.jnutbio.2018.03.005]

92 **Wang B**, Shen J. NF-κB Inducing Kinase Regulates Intestinal Immunity and Homeostasis. *Front Immunol* 2022; **13**: 895636 [PMID: 35833111 DOI: 10.3389/fimmu.2022.895636]

93 **Piscopo N**, Ellul P. Diverticular Disease: A Review on Pathophysiology and Recent Evidence. *Ulster Med J* 2020; **89**: 83-88 [PMID: 33093692]

94 **Rezapour M**, Ali S, Stollman N. Diverticular Disease: An Update on Pathogenesis and Management. *Gut Liver* 2018; **12**: 125-132 [PMID: 28494576 DOI: 10.5009/gnl16552]

95 **Colecchia A**, Vestito A, Pasqui F, Mazzella G, Roda E, Pistoia F, Brandimarte G, Festi D. Efficacy of long term cyclic administration of the poorly absorbed antibiotic Rifaximin in symptomatic, uncomplicated colonic diverticular disease. *World J Gastroenterol* 2007; **13**: 264-269 [PMID: 17226906 DOI: 10.3748/wjg.v13.i2.264]

96 **Floch MH**, White JA. Management of diverticular disease is changing. *World J Gastroenterol* 2006; **12**: 3225-3228 [PMID: 16718843 DOI: 10.3748/wjg.v12.i20.3225]

97 **Lahner E**, Esposito G, Zullo A, Hassan C, Cannaviello C, Paolo MC, Pallotta L, Garbagna N, Grossi E, Annibale B. High-fibre diet and Lactobacillus paracasei B21060 in symptomatic uncomplicated diverticular disease. *World J Gastroenterol* 2012; **18**: 5918-5924 [PMID: 23139608 DOI: 10.3748/wjg.v18.i41.5918]

98 **Brandimarte G**, Frajese GV, Bargiggia S, Castellani D, Cocco A, Colucci R, Evangelista E, Gravina AG, Napoletano D, Nardi E, Maisto T, Morabito A, Pianese G, Romano A, Sacco R, Sediari L, Sinnona N, Tifi L, D'Avino A, Elisei W, Tursi A. Performance of a multicompounds nutraceutical formulation in patients with symptomatic uncomplicated diverticular disease. *Minerva Gastroenterol (Torino)* 2022; **68**: 216-222 [PMID: 35262307 DOI: 10.23736/S2724-5985.22.03132-1]

99 **Kupcinskas J**, Strate LL, Bassotti G, Torti G, Herszényi L, Malfertheiner P, Cassieri C, Walker MM, Tursi A. Pathogenesis of Diverticulosis and Diverticular Disease. *J Gastrointestin Liver Dis* 2019; **28**: 7-10 [PMID: 31930230 DOI: 10.15403/jgld-551]

100 **Tursi A**, Elisei W, Brandimarte G, Giorgetti GM, Inchingolo CD, Nenna R, Picchio M, Giorgio F, Ierardi E. Musosal tumour necrosis factor α in diverticular disease of the colon is overexpressed with disease severity. *Colorectal Dis* 2012; **14**: e258-e263 [PMID: 22469482 DOI: 10.1111/j.1463-1318.2012.02926.x]

101 **Fukudo S**, Okumura T, Inamori M, Okuyama Y, Kanazawa M, Kamiya T, Sato K, Shiotani A, Naito Y, Fujikawa Y, Hokari R, Masaoka T, Fujimoto K, Kaneko H, Torii A, Matsueda K, Miwa H, Enomoto N, Shimosegawa T, Koike K. Evidence-based clinical practice guidelines for irritable bowel syndrome 2020. *J Gastroenterol* 2021; **56**: 193-217 [PMID: 33538894 DOI: 10.1007/s00535-020-01746-z]

102 **Fond G**, Loundou A, Hamdani N, Boukouaci W, Dargel A, Oliveira J, Roger M, Tamouza R, Leboyer M, Boyer L. Anxiety and depression comorbidities in irritable bowel syndrome (IBS): a systematic review and meta-analysis. *Eur Arch Psychiatry Clin Neurosci* 2014; **264**: 651-660 [PMID: 24705634 DOI: 10.1007/s00406-014-0502-z]

103 **Nagano M**, Shimizu K, Kondo R, Hayashi C, Sato D, Kitagawa K, Ohnuki K. Reduction of depression and anxiety by 4 weeks Hericium erinaceus intake. *Biomed Res* 2010; **31**: 231-237 [PMID: 20834180 DOI: 10.2220/biomedres.31.231]

104 **Chong PS**, Fung ML, Wong KH, Lim LW. Therapeutic Potential of Hericium erinaceus for Depressive Disorder. *Int J Mol Sci* 2019; **21** [PMID: 31881712 DOI: 10.3390/ijms21010163]

105 **Fijałkowska A**, Jędrejko K, Sułkowska-Ziaja K, Ziaja M, Kała K, Muszyńska B. Edible Mushrooms as a Potential Component of Dietary Interventions for Major Depressive Disorder. *Foods* 2022; **11** [PMID: 35627059 DOI: 10.3390/foods11101489]

106 **Rodriguez MN**, Lippi SLP. Lion's Mane (Hericium erinaceus) Exerts Anxiolytic Effects in the rTg4510 Tau Mouse Model. *Behav Sci (Basel)* 2022; **12** [PMID: 35877305 DOI: 10.3390/bs12070235]

107 **Chou MY**, Ho JH, Huang MJ, Chen YJ, Yang MD, Lin LH, Chi CH, Yeh CH, Tsao TY, Tzeng JK, Hsu RJ, Huang PH, Lu WC, Li PH, Wang MF. Potential antidepressant effects of a dietary supplement from the chlorella and lion's mane mushroom complex in aged SAMP8 mice. *Front Nutr* 2022; **9**: 977287 [PMID: 36118772 DOI: 10.3389/fnut.2022.977287]

108 **Spina A**, Mazzarella C, Dallio M, Romeo M, Pellegrino R, Durante T, Romano M, Loguercio C, Di Mauro M, Federico A, Gravina AG. The Lesson from the First Italian Lockdown: Impacts on Anxiety and Depressive Symptoms and Sleep Quality in Patients with Remission of Inflammatory Bowel Disease. *Rev Recent Clin Trials* 2022; **17**: 109-119 [PMID: 35346015 DOI: 10.2174/1574887117666220328125720]

109 **Barberio B**, Zamani M, Black CJ, Savarino EV, Ford AC. Prevalence of symptoms of anxiety and depression in patients with inflammatory bowel disease: a systematic review and meta-analysis. *Lancet Gastroenterol Hepatol* 2021; **6**: 359-370 [PMID: 33721557 DOI: 10.1016/S2468-1253(21)00014-5]

110 **Ryu JE**, Kang SG, Jung SH, Lee SH, Kang SB. Psychological Effects and Medication Adherence among Korean Patients with Inflammatory Bowel Disease during the Coronavirus Disease 2019 Pandemic: A Single-Center Survey. *J Clin Med* 2022; **11** [PMID: 35683421 DOI: 10.3390/jcm11113034]

111 **Pellegrino R**, Pellino G, Selvaggi F, Federico A, Romano M, Gravina AG. Therapeutic adherence recorded in the outpatient follow-up of inflammatory bowel diseases in a referral center: Damages of COVID-19. *Dig Liver Dis* 2022; **54**: 1449-1451 [PMID: 35973931 DOI: 10.1016/j.dld.2022.07.016]

112 **Barbara G**, Cremon C, Bellini M, Corsetti M, Di Nardo G, Falangone F, Fuccio L, Galeazzi F, Iovino P, Sarnelli G, Savarino EV, Stanghellini V, Staiano A, Stasi C, Tosetti C, Turco R, Ubaldi E, Zagari RM, Zenzeri L, Marasco G. Italian guidelines for the management of irritable bowel syndrome: Joint Consensus from the Italian Societies of: Gastroenterology and Endoscopy (SIGE), Neurogastroenterology and Motility (SINGEM), Hospital Gastroenterologists and Endoscopists (AIGO), Digestive Endoscopy (SIED), General Medicine (SIMG), Gastroenterology, Hepatology and Pediatric Nutrition (SIGENP) and Pediatrics (SIP). *Dig Liver Dis* 2023; **55**: 187-207 [PMID: 36517261 DOI: 10.1016/j.dld.2022.11.015]

113 **Chumpitazi BP**, Kearns GL, Shulman RJ. Review article: the physiological effects and safety of peppermint oil and its efficacy in irritable bowel syndrome and other functional disorders. *Aliment Pharmacol Ther* 2018; **47**: 738-752 [PMID: 29372567 DOI: 10.1111/apt.14519]

114 **Currò D**, Ianiro G, Pecere S, Bibbò S, Cammarota G. Probiotics, fibre and herbal medicinal products for functional and inflammatory bowel disorders. *Br J Pharmacol* 2017; **174**: 1426-1449 [PMID: 27696378 DOI: 10.1111/bph.13632]

115 **Lu Q**, Tan D, Luo J, Ye Y, Zuo M, Wang S, Li C. Potential of natural products in the treatment of irritable bowel syndrome. *Phytomedicine* 2022; **106**: 154419 [PMID: 36087525 DOI: 10.1016/j.phymed.2022.154419]

116 **Liu JY**, Hou XX, Li ZY, Shan SH, Chang MC, Feng CP, Wei Y. Isolation and structural characterization of a novel polysaccharide from Hericium erinaceus fruiting bodies and its arrest of cell cycle at S-phage in colon cancer cells. *Int J Biol Macromol* 2020; **157**: 288-295 [PMID: 32339580 DOI: 10.1016/j.ijbiomac.2020.04.162]

117 **Giaginis C**, Georgiadou M, Dimakopoulou K, Tsourouflis G, Gatzidou E, Kouraklis G, Theocharis S. Clinical significance of MCM-2 and MCM-5 expression in colon cancer: association with clinicopathological parameters and tumor proliferative capacity. *Dig Dis Sci* 2009; **54**: 282-291 [PMID: 18465232 DOI: 10.1007/s10620-008-0305-z]

118 **Hou XX**, Liu JY, Li ZY, Chang MC, Guo M, Feng CP, Shi JY. Fruiting body polysaccharides of Hericium erinaceus induce apoptosis in human colorectal cancer cells *via* ROS generation mediating caspase-9-dependent signaling pathways. *Food Funct* 2020; **11**: 6128-6138 [PMID: 32573644 DOI: 10.1039/d0fo00916d]

119 **Kim SP**, Kang MY, Kim JH, Nam SH, Friedman M. Composition and mechanism of antitumor effects of Hericium erinaceus mushroom extracts in tumor-bearing mice. *J Agric Food Chem* 2011; **59**: 9861-9869 [PMID: 21846141 DOI: 10.1021/jf201944n]

120 **Sharif S**, Atta A, Huma T, Shah AA, Afzal G, Rashid S, Shahid M, Mustafa G. Anticancer, antithrombotic, antityrosinase, and anti-α-glucosidase activities of selected wild and commercial mushrooms from Pakistan. *Food Sci Nutr* 2018; **6**: 2170-2176 [PMID: 30510718 DOI: 10.1002/fsn3.781]

121 **Hills RD Jr**, Pontefract BA, Mishcon HR, Black CA, Sutton SC, Theberge CR. Gut Microbiome: Profound Implications for Diet and Disease. *Nutrients* 2019; **11** [PMID: 31315227 DOI: 10.3390/nu11071613]

122 **Yang Y**, Zhao C, Diao M, Zhong S, Sun M, Sun B, Ye H, Zhang T. The Prebiotic Activity of Simulated Gastric and Intestinal Digesta of Polysaccharides from the Hericium erinaceus. *Molecules* 2018; **23** [PMID: 30513668 DOI: 10.3390/molecules23123158]

123 **Diling C**, Chaoqun Z, Jian Y, Jian L, Jiyan S, Yizhen X, Guoxiao L. Immunomodulatory Activities of a Fungal Protein Extracted from Hericium erinaceus through Regulating the Gut Microbiota. *Front Immunol* 2017; **8**: 666 [PMID: 28713364 DOI: 10.3389/fimmu.2017.00666]

124 **Xie XQ**, Geng Y, Guan Q, Ren Y, Guo L, Lv Q, Lu ZM, Shi JS, Xu ZH. Influence of Short-Term Consumption of Hericium erinaceus on Serum Biochemical Markers and the Changes of the Gut Microbiota: A Pilot Study. *Nutrients* 2021; **13** [PMID: 33800983 DOI: 10.3390/nu13031008]

125 **Tan J**, McKenzie C, Potamitis M, Thorburn AN, Mackay CR, Macia L. The role of short-chain fatty acids in health and disease. *Adv Immunol* 2014; **121**: 91-119 [PMID: 24388214 DOI: 10.1016/B978-0-12-800100-4.00003-9]

126 **Sun M**, Wu W, Liu Z, Cong Y. Microbiota metabolite short chain fatty acids, GPCR, and inflammatory bowel diseases. *J Gastroenterol* 2017; **52**: 1-8 [PMID: 27448578 DOI: 10.1007/s00535-016-1242-9]

127 **Yang Y**, Ye H, Zhao C, Ren L, Wang C, Georgiev MI, Xiao J, Zhang T. Value added immunoregulatory polysaccharides of Hericium erinaceus and their effect on the gut microbiota. *Carbohydr Polym* 2021; **262**: 117668 [PMID: 33838836 DOI: 10.1016/j.carbpol.2021.117668]

128 **Dmitrieva-Posocco O**, Wong AC, Lundgren P, Golos AM, Descamps HC, Dohnalová L, Cramer Z, Tian Y, Yueh B, Eskiocak O, Egervari G, Lan Y, Liu J, Fan J, Kim J, Madhu B, Schneider KM, Khoziainova S, Andreeva N, Wang Q, Li N, Furth EE, Bailis W, Kelsen JR, Hamilton KE, Kaestner KH, Berger SL, Epstein JA, Jain R, Li M, Beyaz S, Lengner CJ, Katona BW, Grivennikov SI, Thaiss CA, Levy M. β-Hydroxybutyrate suppresses colorectal cancer. *Nature* 2022; **605**: 160-165 [PMID: 35477756 DOI: 10.1038/s41586-022-04649-6]

129 **Louis P**, Hold GL, Flint HJ. The gut microbiota, bacterial metabolites and colorectal cancer. *Nat Rev Microbiol* 2014; **12**: 661-672 [PMID: 25198138 DOI: 10.1038/nrmicro3344]

130 **Bultman SJ**. Interplay between diet, gut microbiota, epigenetic events, and colorectal cancer. *Mol Nutr Food Res* 2017; **61** [PMID: 27138454 DOI: 10.1002/mnfr.201500902]

131 **Louis P**, Flint HJ. Formation of propionate and butyrate by the human colonic microbiota. *Environ Microbiol* 2017; **19**: 29-41 [PMID: 27928878 DOI: 10.1111/1462-2920.13589]

132 **Mitsou EK**, Saxami G, Stamoulou E, Kerezoudi E, Terzi E, Koutrotsios G, Bekiaris G, Zervakis GI, Mountzouris KC, Pletsa V, Kyriacou A. Effects of Rich in B-Glucans Edible Mushrooms on Aging Gut Microbiota Characteristics: An In Vitro Study. *Molecules* 2020; **25** [PMID: 32570735 DOI: 10.3390/molecules25122806]

133 **Cho HW**, Choi S, Seo K, Kim KH, Jeon JH, Kim CH, Lim S, Jeong S, Chun JL. Gut microbiota profiling in aged dogs after feeding pet food contained Hericium erinaceus. *J Anim Sci Technol* 2022; **64**: 937-949 [PMID: 36287790 DOI: 10.5187/jast.2022.e66]

134 **Helmink BA**, Khan MAW, Hermann A, Gopalakrishnan V, Wargo JA. The microbiome, cancer, and cancer therapy. *Nat Med* 2019; **25**: 377-388 [PMID: 30842679 DOI: 10.1038/s41591-019-0377-7]

135 **Khan MAW**, Ologun G, Arora R, McQuade JL, Wargo JA. Gut Microbiome Modulates Response to Cancer Immunotherapy. *Dig Dis Sci* 2020; **65**: 885-896 [PMID: 32067144 DOI: 10.1007/s10620-020-06111-x]

136 **Tian B**, Liu R, Xu T, Cai M, Mao R, Huang L, Yang K, Zeng X, Peilong S. Modulating effects of Hericium erinaceus polysaccharides on the immune response by regulating gut microbiota in cyclophosphamide-treated mice. *J Sci Food Agric* 2023; **103**: 3050-3064 [PMID: 36546454 DOI: 10.1002/jsfa.12404]

137 **Wang D**, Zhu X, Tang X, Li H, Yizhen X, Chen D. Auxiliary antitumor effects of fungal proteins from Hericium erinaceus by target on the gut microbiota. *J Food Sci* 2020; **85**: 1872-1890 [PMID: 32460371 DOI: 10.1111/1750-3841.15134]

138 **Larussa T**, Abenavoli L, Fabiano G, Mancuso MA, Polimeni N, Dumitrascu DL, Luzza F. Gut microbiota in inflammatory bowel disease: a target for therapy not to be missed. *Minerva Gastroenterol (Torino)* 2021; **67**: 357-368

[PMID: 35040302 DOI: 10.23736/S2724-5985.21.02907-7]

139 **Wallace KL**, Zheng LB, Kanazawa Y, Shih DQ. Immunopathology of inflammatory bowel disease. *World J Gastroenterol* 2014; **20**: 6-21 [PMID: 24415853 DOI: 10.3748/wjg.v20.i1.6]

140 **Jandhyala SM**, Talukdar R, Subramanyam C, Vuyyuru H, Sasikala M, Nageshwar Reddy D. Role of the normal gut microbiota. *World J Gastroenterol* 2015; **21**: 8787-8803 [PMID: 26269668 DOI: 10.3748/wjg.v21.i29.8787]

141 **Wang WL**, Xu SY, Ren ZG, Tao L, Jiang JW, Zheng SS. Application of metagenomics in the human gut microbiome. *World J Gastroenterol* 2015; **21**: 803-814 [PMID: 25624713 DOI: 10.3748/wjg.v21.i3.803]

142 **Ren Z**, Xu Z, Amakye WK, Liu W, Zhao Z, Gao L, Wang M, Ren J. Hericium erinaceus mycelium-Derived Polysaccharide Alleviates Ulcerative Colitis and Modulates Gut Microbiota in Cynomolgus Monkeys. *Mol Nutr Food Res* 2023; **67**: e2200450 [PMID: 36443636 DOI: 10.1002/mnfr.202200450]

143 **Yu AT**, Shapiro K, Beneri CA, Wilks-Gallo LS. Streptococcus lutetiensis neonatal meningitis with empyema. *Access Microbiol* 2021; **3**: 000264 [PMID: 34712909 DOI: 10.1099/acmi.0.000264]

144 **Shao S**, Wang D, Zheng W, Li X, Zhang H, Zhao D, Wang M. A unique polysaccharide from Hericium erinaceus mycelium ameliorates acetic acid-induced ulcerative colitis rats by modulating the composition of the gut microbiota, short chain fatty acids levels and GPR41/43 respectors. *Int Immunopharmacol* 2019; **71**: 411-422 [PMID: 31059977 DOI: 10.1016/j.intimp.2019.02.038]

145 **Kim MH**, Kang SG, Park JH, Yanagisawa M, Kim CH. Short-chain fatty acids activate GPR41 and GPR43 on intestinal epithelial cells to promote inflammatory responses in mice. *Gastroenterology* 2013; **145**: 396-406.e1 [PMID: 23665276 DOI: 10.1053/j.gastro.2013.04.056]

146 **Kishi M**, Hirai F, Takatsu N, Hisabe T, Takada Y, Beppu T, Takeuchi K, Naganuma M, Ohtsuka K, Watanabe K, Matsumoto T, Esaki M, Koganei K, Sugita A, Hata K, Futami K, Ajioka Y, Tanabe H, Iwashita A, Shimizu H, Arai K, Suzuki Y, Hisamatsu T. A review on the current status and definitions of activity indices in inflammatory bowel disease: how to use indices for precise evaluation. *J Gastroenterol* 2022; **57**: 246-266 [PMID: 35235037 DOI: 10.1007/s00535-022-01862-y]

147 **Lamb CA**, Kennedy NA, Raine T, Hendy PA, Smith PJ, Limdi JK, Hayee B, Lomer MCE, Parkes GC, Selinger C, Barrett KJ, Davies RJ, Bennett C, Gittens S, Dunlop MG, Faiz O, Fraser A, Garrick V, Johnston PD, Parkes M, Sanderson J, Terry H; IBD guidelines eDelphi consensus group, Gaya DR, Iqbal TH, Taylor SA, Smith M, Brookes M, Hansen R, Hawthorne AB. British Society of Gastroenterology consensus guidelines on the management of inflammatory bowel disease in adults. *Gut* 2019; **68**: s1-s106 [PMID: 31562236 DOI: 10.1136/gutjnl-2019-318484]

World Journal of Gastroenterology

Submit a Manuscript: https://www.f6publishing.com

World J Gastroenterol 2023 May 28; 29(20): 3066-3083

DOI: 10.3748/wjg.v29.i20.3066

ISSN 1007-9327 (print) ISSN 2219-2840 (online)

MINIREVIEWS

Machine perfusion and the prevention of ischemic type biliary lesions following liver transplant: What is the evidence?

Manuel Durán, Rafael Calleja, Angus Hann, George Clarke, Ruben Ciria, Anisa Nutu, Rebeca Sanabria-Mateos, María Dolores Ayllón, Pedro López-Cillero, Hynek Mergental, Javier Briceño, M Thamara P R Perera

Specialty type: Gastroenterology and hepatology

Provenance and peer review: Invited article; Externally peer reviewed.

Peer-review model: Single blind

Peer-review report's scientific quality classification

Grade A (Excellent): 0
Grade B (Very good): B, B
Grade C (Good): 0
Grade D (Fair): 0
Grade E (Poor): 0

P-Reviewer: Dabbous H, Egypt; Xu X, China

Received: January 26, 2023
Peer-review started: January 26, 2023
First decision: February 16, 2023
Revised: March 1, 2023
Accepted: April 28, 2023
Article in press: April 28, 2023
Published online: May 28, 2023

Manuel Durán, Rafael Calleja, Ruben Ciria, María Dolores Ayllón, Pedro López-Cillero, Javier Briceño, Department of Liver Transplantation, Reina Sofía University Hospital, Córdoba 14004, Spain

Angus Hann, George Clarke, Anisa Nutu, Rebeca Sanabria-Mateos, Hynek Mergental, M Thamara P R Perera, The Liver Unit, Queen Elizabeth Hospital Birmingham, Birmingham B15 2TH, United Kingdom

Angus Hann, George Clarke, Hynek Mergental, M Thamara P R Perera, Centre for Liver and Gastrointestinal Research, Institute of Immunology and Immunotherapy, University of Birmingham, Birmingham B15 2TH, United Kingdom

Corresponding author: M Thamara P R Perera, FEBS, FRCS, MBBS, MD, MS, Chairman, Professor, Surgeon, The Liver Unit, Queen Elizabeth Hospital Birmingham, Mindelsohn Way, Birmingham B15 2TH, United Kingdom. thamara.perera@uhb.nhs.uk

Abstract

The widespread uptake of different machine perfusion (MP) strategies for liver transplant has been driven by an effort to minimize graft injury. Damage to the cholangiocytes during the liver donation, preservation, or early posttransplant period may result in stricturing of the biliary tree and inadequate biliary drainage. This problem continues to trouble clinicians, and may have catastrophic consequences for the graft and patient. Ischemic injury, as a result of compromised hepatic artery flow, is a well-known cause of biliary strictures, sepsis, and graft failure. However, very similar lesions can appear with a patent hepatic artery and these are known as ischemic type biliary lesions (ITBL) that are attributed to microcirculatory dysfunction rather than main hepatic arterial compromise. Both the warm and cold ischemic period duration appear to influence the onset of ITBL. All of the commonly used MP techniques deliver oxygen to the graft cells, and therefore may minimize the cholangiocyte injury and subsequently reduce the incidence of ITBL. As clinical experience and published evidence grows for these modalities, the impact they have on ITBL rates is important to consider. In this review, the evidence for the three commonly used MP strategies (abdominal normothermic regional perfusion [A-NRP], hypothermic oxygenated perfusion [HOPE], and normothermic machine perfusion [NMP] for ITBL prevention has been critically reviewed. Inconsistencies with ITBL definitions used in trials, coupled with variations in techniques of MP, make interpretation challenging.

Overall, the evidence suggests that both HOPE and A-NRP prevent ITBL in donated after circulatory death grafts compared to cold storage. The evidence for ITBL prevention in donor after brain death grafts with any MP technique is weak.

Key Words: Liver transplant; Ischemic type biliary lesions; Hypothermic oxygenated machine perfusion; Normothermic machine perfusion; Abdominal normothermic regional perfusion; Donation after circulatory death

©The Author(s) 2023. Published by Baishideng Publishing Group Inc. All rights reserved.

Core Tip: In recent years, the development of different machine perfusion (MP) strategies has generated interest in their use for both the assessment of grafts and optimization during the preservation period. The different mechanisms behind the diverse array of MP strategies may reduce the extent of cholangiocyte and may have the subsequent clinical effect of preventing the development of ischemic type biliary lesions (ITBL). This review summarizes the strength and limitations of clinical studies that have been undertaken, their results, and provides a summary of the available literature on MP and the prevention of ITBL.

Citation: Durán M, Calleja R, Hann A, Clarke G, Ciria R, Nutu A, Sanabria-Mateos R, Ayllón MD, López-Cillero P, Mergental H, Briceño J, Perera MTPR. Machine perfusion and the prevention of ischemic type biliary lesions following liver transplant: What is the evidence? *World J Gastroenterol* 2023; 29(20): 3066-3083
URL: https://www.wjgnet.com/1007-9327/full/v29/i20/3066.htm
DOI: https://dx.doi.org/10.3748/wjg.v29.i20.3066

INTRODUCTION

In recent decades, liver transplantation has made several forward strides. These have been in the area of surgical technique, immunosuppressive drug strategies, treatment and prevention of recurrent viral infections, and the increasing use of alternative preservation techniques. Consequently, recipient and graft survival are greater than 90% at 1 year and long-term survival is considered the norm[1]. A longstanding problem that liver transplantation has faced is the mismatch between the number of donors and the higher number of patients listed for transplant. This has led to long waiting lists for a graft, and up to 20% of patients do not survive until transplantation[2,3]. Furthermore, the recent expansion of transplant indications to include certain oncological scenarios may further aggravate this issue[4]. As a response to this shortage in supply, living donor liver transplantation and using more marginal organs, including those donated after circulatory death (DCD) are strategies that have been used to increase the donor pool[5]. Improving long-term graft survival is vital, as the need for retransplantation creates additional demand on a scarce resource.

Adequate biliary drainage is paramount for the success of a liver transplant, and was previously labeled the 'Achilles heel' of this procedure[6]. Although vascular complications have the largest impact on short-term graft outcomes, biliary complications are the main source of long-term morbidity. These conditions often require costly interventions, cause suffering, and adversely affect patients' quality of life[7]. The incidence of these complications is increasing as a result of the growing utilization of extended criteria donor organs, mainly from DCD donors[8].

In recent years, the development of numerous machine perfusion (MP) strategies has generated interest in their use for both the assessment of grafts and optimization during the preservation period [9]. Different techniques of MP have been described and vary in their application, with *in situ* MP occurring during organ procurement while the graft is within the donor and *ex situ* MP which occurs after the donor hepatectomy is completed. Both hepatocytes and cholangiocytes are vulnerable to ischemia-reperfusion injury (IRI), and injury to the latter during organ procurement and preservation lies behind the pathogenesis for biliary dysfunction[10]. Consequently, a current trend of research in the MP field is focused on how these different MP perfusion regimens influence post-transplant biliary complications and more specifically, ischemic type biliary lesions (ITBL).

This narrative literature review describes the strength and limitations of clinical studies that have been undertaken, their results, and provides a summary of the available literature on MP and the prevention of ITBL.

Nonanastomotic biliary strictures and ischemic type biliary lesions

Postliver transplantation biliary complications can comprise one (or both) of the following entities; strictures (anastomotic and non-anastomotic), and biliary leaks[11]. Anastomotic biliary strictures occur

at the site of biliary reconstruction and the surgical technique, and/or local tissue ischemia likely play a role. These strictures are usually managed with endoscopic or radiological procedures, however surgical revision may be required depending on the timing and type of anastomosis[12]. Nonanastomotic strictures (NAS), as the name implies, occur at a site away from the anastomosis and are most common within the initial 12 mo posttransplant. NAS are one of most feared late complications due to it being associated with high rates of graft loss and mortality, and minimal treatment options except re-transplantation[8,13].

NAS is characterized by diffuse fibrotic strictures and dilatation of the biliary tree at any location from the liver periphery to the main extrahepatic ducts (Figure 1). In addition, with the disease evolution, the formation of biliary casts and intrahepatic bilomas may occur in its severest form[14]. The radiological manifestations of NAS are highly variable and range from a peripheral abscess, individual or multiple strictures around the hilum and first order biliary branches, to vanishing ducts seen along the entire biliary tree[15]. NAS can occur as a direct result of ischemia from an identifiable hepatic artery stenosis or thrombosis (HAT). However, very similar lesions can develop in the setting of an entirely patent hepatic artery and this specific situation is termed ITBL, given its similarity to an actual ischemic cholangiopathy (Figure 1).

In a seminal paper by authors from Groningen which excluded patients with HAT, ITBL was classified according to the affected area of the biliary tree[16]. In this study, they demonstrated that the anatomical location of ITBL varied between those that presented early (< 1 year) as opposed to late (> 1 year). In those presenting late, the peripheral liver (zone D) was involved more frequently and there was an association with immunological risk factors. By contrast, patients with an early presentation had lesions around the bifurcation and the common bile duct (zone A). This early group had a longer period of both cold and warm ischemia; therefore, hypoxia is thought to be one of the underlying mechanisms. More recently, a United States group from the Mayo Clinic proposed a radiologic classification of ITBL into four distinct patterns that correlate with a distinct natural evolution and prognosis[17]. In this case, those patients with diffuse necrosis and multifocal progressive patterns experienced more episodes of cholangitis and almost all required stents and eventual retransplant.

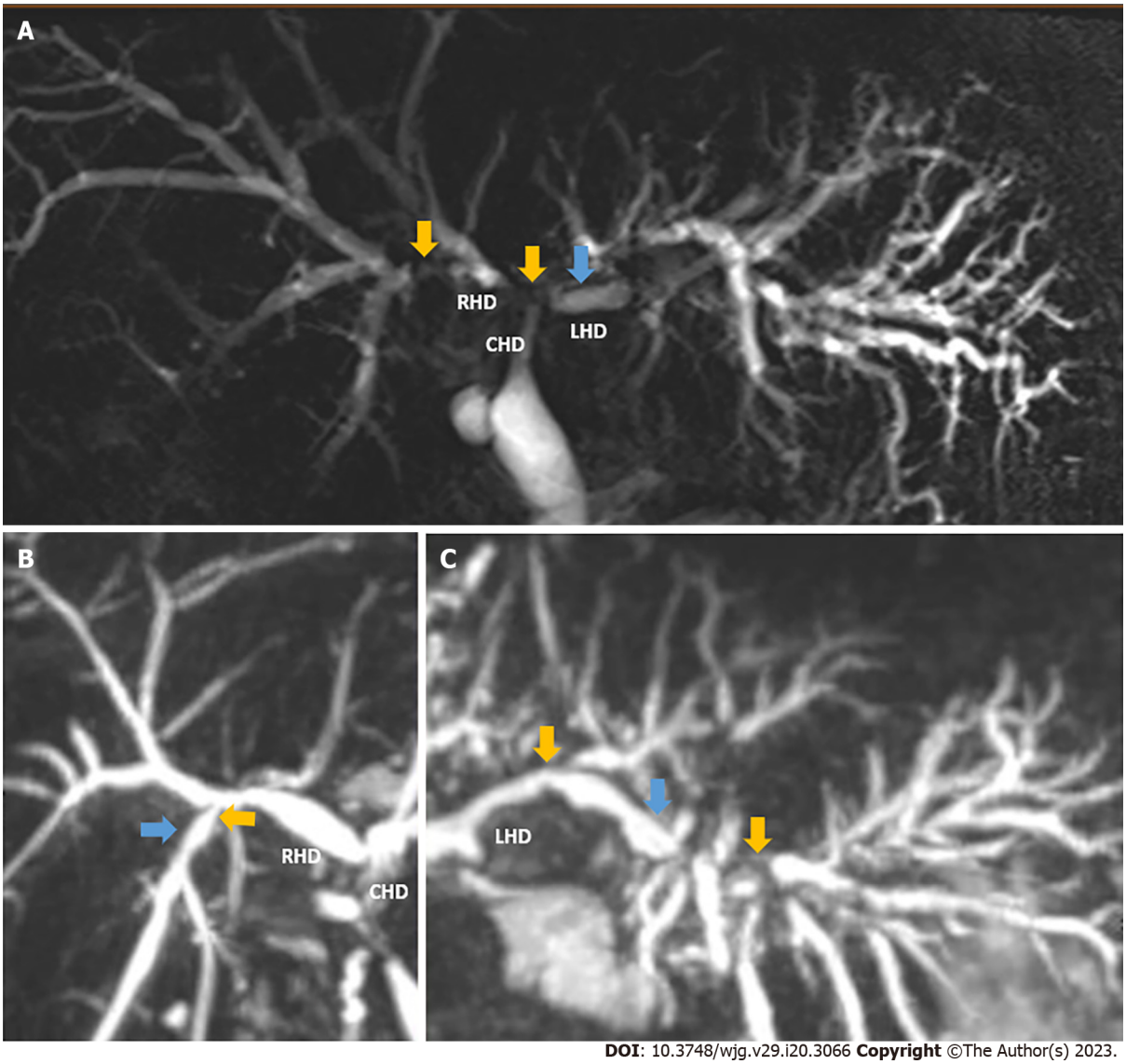
Multiple factors have been associated with ITBL development and are generally divided into three categories: ischemia-related injury; bile salt mediated injury; and immune-mediated injury[18,19]. The cold ischemia time (CIT) and donor warm ischemia time (dWIT), and inadequate microvasculature preservation predispose cholangiocytes to a subsequent IRI[10,18]. The increased incidence of ITBL in DCD grafts, which are characterized by a period of dWIT is well established, with ITBL rates of up to 39% following controlled DCD liver transplantation[13,20,21]. The toxic effect of bile salts on cholangiocytes at low temperatures during preservation is well known. Certain bile acids have been shown to promote the secretion of inflammatory mediators, and others are directly cytotoxic to cholangiocytes [22]. In addition, new bile after implantation and its altered bile salt/phospholipid ratio have detrimental effects on biliary epithelium and induce NAS[23-25]. An immune-mediated component to the cholangiocyte injury has also been proposed due to several clinical associations, but the mechanism remains under investigation. ITBL has been demonstrated in association with ABO incompatibility, recurrence of immune-mediated liver diseases, cytomegalovirus infection, presence of C-C chemokine receptor type 5, polymorphism, and acute or chronic rejection[18].

The pathogenesis of ITBL is multifactorial. Both the cold and warm ischemic periods induce the formation of reactive oxygen species (ROS). These ROS are generated as a result of Kupffer and polymorphonuclear cells activation, mitochondrial permeability transition production, oxidative changes in the structure of the biliary canaliculus and adenosine triphosphate adenosine triphosphate (ATP) depletion. These all lead to the apoptosis and/or necrosis of the cholangiocytes. This mechanism is interrelated with the cytotoxic effect of bile salts, the cholestasis status induced by ischemia-reperfusion and different immune-mediated mechanisms, which all further propagate the biliary injury. Appropriate donor selection, the use of preservation fluids and MP are just some of the strategies which are thought to prevent this condition[26].

The different mechanisms behind the diverse array of MP strategies may reduce the extent of cholangiocyte injury during the transplantation process, in comparison with static cold storage (SCS). This may have the subsequent clinical effect of preventing the development of ITBL. The number of clinical studies on MP strategies continues to increase. With only a few exceptions, the primary outcomes focus mainly on graft and patient survival. In this review, we focus on the available clinical evidence for abdominal normothermic regional perfusion (A-NRP), and *ex situ* hypothermic oxygenated perfusion (HOPE), and normothermic MP (NMP) in relation to the outcome of ITBL.

PREVENTION OF ITBL *VIA* MP

The incidence of ITBL posttransplant varies considerably between institution and nations. These differences likely relate to the type of organ donation permitted, ranging from donor after brain death (DBD) donors only in some parts of the world, to uncontrolled DCD donors in others. Different national laws regarding the donor age and the 'no-touch' period following asystole in DCD donors likely



DOI: 10.3748/wjg.v29.i20.3066 **Copyright** ©The Author(s) 2023.

Figure 1 Magnetic resonance cholangiopancreatography reconstruction images of ischemic type biliary lesions in donated after circulatory death graft recipients. A: Significant structuring and confluence of right and left ducts, in addition to the right posterior duct (yellow arrows). Upstream dilation on left indicated by blue arrow; B: Structuring at a second order duct on the right (yellow arrow) with upstream dilation; C: Strictures in periphery of left biliary system. Figure created with biorender.com, accessed on January 2023. LHD: Left ducts; RHD: Right ducts; CHD: Common hepatic duct.

influences outcome, and these matters also complicate the results and interpretation of clinical trials on MP. In addition, it should be noted that the lack of clear and consistent definitions of ITBL in the currently available literature makes the assessment of the true impact challenging. Many studies either do not differentiate between anastomotic, ischemic NAS and ITBL; furthermore they may include both symptomatic and nonsymptomatic cases[27]. With these limitations in mind, a literature search was performed in October 2022 using PUBMED®, Embase®, and Medline®. Publications were restricted to those in English, however no further search filters were applied. The following search terms were used (in different combinations with Boolean operators): Liver, transplant, biliary stricture, ITBL, MP, machine preservation, normothermic, hypothermic, and NRP. Both prospective and retrospective studies were included if they included outcome data pertaining to biliary strictures. Studies without a control (or comparator) group were excluded. A pooled analysis was not performed due to a significant variation in study methodology, MP application technique, and outcome definitions. Institutional ethical approval was not required.

A-NRP and ITBL

A-NRP is an *in situ* preservation technique using an extracorporeal oxygenated membrane, restoring the perfusion of abdominal organs after the donor is declared deceased. This technique may lead to a reduction in the dWIT depending on the timing of cannulation; however, it provides a period of resuscitation immediately after the cellular injury incurred from the dWIT. The provision of near physiological conditions during A-NRP provides a period in which cells can recover their energy stores,

therefore they tolerate the CIT with minimal additional injury. It can also provide information about graft viability and reduce the effects of the IRI process[28].

In recent years, countries such as Spain, France, United Kingdom, and Italy have developed different A-NRP protocols as a strategy to improve the outcomes of DCD grafts[29-33]. These protocols differ in the liver viability criteria utilized "no-touch" periods required, pre-mortem substance administration, and vessel cannulation. All countries aforementioned have a mandatory no-touch period of 5 min except Italy, which requires 20 min. This inevitably lengthens the dWIT. Sedative analgesia administration is not allowed in the United Kingdom, in contrast to other countries. In Spain, premortem cannulation is allowed while in Italy and France only the identification of femoral vessels to ease cannulation is permitted. The obvious benefit of premortem cannulation is that it minimizes the dWIT and could achieve better outcomes as a result[34]. During A-NRP, certain viability parameters are measured, the most common among the different protocols are transaminase levels. Despite transaminase levels being widely accepted, it only reflects hepatocyte injury and not cholangiocytes. Other viability criteria employed include A-NRP duration[31], lactate clearance[30], and/or the presence of macrosteatosis[30,31]. However, some of these parameters are considered controversial[28].

To date, there has been no randomized controlled trial (RCT) comparing A-NRP to the standard retrieval method, known as the super rapid retrieval (SRR) technique. The clinical studies investigating A-NRP that include a comparator group, and provide data on biliary strictures are summarized in Table 1. The definition of ITBL used in these studies is relatively homogeneous as most authors have considered ITBL to have occurred when NAS developed in the context of a patent hepatic artery. However, two studies did not include an ITBL definition[35,36] and two authors[31,37] considered NAS regardless of the presence of concomitant HAT. Other limitations of these studies include variation in the A-NRP protocols, small sample size, and variability in follow-up periods. These trials can be put into three categories, according to the comparator groups: DCD-A-NRP *vs* DBD-SCS; DCD-A-NRP *vs* DCD-SRR; and DCD-A-NRP *vs* DCD with other MP.

In the first group of studies[31,35,38-40] that compared DCD-NRP-A grafts *vs* DBD-SCS grafts, these authors aimed to demonstrate that DCD grafts after NRP could have similar results of DBD grafts and therefore should not be considered marginal. These studies showed a similar incidence of ITBL between both groups, and the results in regard to early allograft dysfunction were promising. However, they had small sample sizes[35,38,39], differences in follow-up periods[31,35,38,39], and a high proportion of uncontrolled DCD donors[38]. Other authors have assessed the outcomes of DCD NRP grafts *vs* DCDs grafts recovered by *via* the SRR technique and subsequent SCS[33,34,36,41]. Watson *et al*[33] compared two groups, DCD-A-NRP (n = 43) *vs* DCD-SRR (n = 187), and reported both early allograft dysfunction and biliary complication rates. A significantly lower rate of early allograft dysfunction (12% *vs* 32%) and ischemic cholangiopathy (IC) (0% *vs* 27%) occurred in the DCD-A-NRP group. Similar comparisons have been performed by Spanish transplant groups. Muñoz *et al*[36] did not demonstrate significant differences in their cohort, probably due to the short follow-up period in the A-NRP group and the low number of patients. However, Hessheimer *et al*[41] subsequently found an ITBL incidence of 2% in the NRP group (n = 95) *vs* 13% in the SRR group (n = 117). These findings were repeated in a second study [34] with a larger sample size (545 NRP *vs* 258 SRR). In this second study the ITBL incidence was 1% *vs* 9% in favor of A-NRP, and this is at present the largest cohort of patients with A-NRP with premortem cannulation in the literature. Recently, Schurink *et al*[42] have reported the safety of NRP to rescue DCD grafts that were declined by the Eurotransplant region for transplantation, with no differences in primary nonfunction or IC compared to DBD and standard, non-NRP DCD grafts[42].

Finally, other authors[37,43-45] have compared A-NRP with *ex situ* preservation techniques such as NMP or HOPE. However, in many of these trials, accurate data on ITBL are lacking. The only study comparing HOPE *vs* NRP was conducted by Muller *et al*[37]. These authors reported the incidence of NAS regardless of hepatic artery status, rather than ITBL specifically. The rate of NAS was reported to be 6.3% in the NRP group and 12.5% in the HOPE group, but was not significantly different. DCD grafts that underwent A-NRP have been compared to DCD grafts undergoing *ex situ* NMP in a study by Gaurav *et al*[44] This study showed significantly lower rates of ITBL in the NRP group (6.3% *vs* 12.5%) after propensity score matching (PSM)[44]. However, in another study that used PSM analysis[45] (34 NMP *vs* 68 NRP), there were no significant differences in the ITBL rate of both groups (2.9% NRP *vs* 8.8% NMP). In this latter study, NMP was applied at source as opposed to the study by Gaurav *et al* [44], which applied it at the recipient hospital in the majority of cases[44].

A-NRP is a widely used *in situ* perfusion technique that has improved outcomes and graft utilization in DCD grafts. Protocol aspects such as the "no-touch" period or premortem cannulation may impact in these results, due to its association with WIT. Despite the differences between the protocols adopted in different countries, NRP has still achieved superior outcomes in comparison to SRR in regards to ITBL.

HOPE and ITBL

Hypothermic MP (HMP) was first introduced in clinical practice in 2010 by Guarrera *et al*[46], who demonstrate in their pilot case-controlled series that it was a feasible and safe preservation method[46]. Subsequently, in preclinical studies that investigated the active oxygenation of the hypothermic perfusate over a short period, it demonstrated restored mitochondrial integrity. This indicated a reduction of oxygen free radicals and damage-associated molecular patterns after transplantation[47-

Table 1 Clinical studies assessing the impact of abdominal normothermic regional perfusion on ischemic type biliary lesions after liver transplantation

Ref.	Study design	Groups (*n*)	Control group	NRP protocol and viability criteria	Definition of ITBL	Follow up	ITBL in intervention (DCD NRP)	ITBL in control (DCD)	ITBL in control (DBD)
Schurink *et al* [42], 2022	Cohort	NRP[1] (20) *vs* DCD (49) *vs* DBD (81)	DCD/DBD	Dutch protocol[2]	Symptomatic radiologically NAS without the presence of a HAT	Median-NRP 23 mo, DCD25 mo and DBD 26 mo	1/15 (7%); 1/5 (20%)[3]	8/30 (26%)	6/78 (7%)
Mohkam *et al* [45], 2022	Cohort	NRP (157) *vs* NMP (34)	DCD	France protocol[4]	NAS that were unrelated to any hepatic artery complications	Median-NRP 22 mo; NMP 24 mo	2/68 (2.9%)[5]	3/34 (8.8%)[5]	NA
Gaurav *et al* [44], 2022	Cohort	NRP (69) *vs* NMP (67) *vs* SCS (97)	DCD	United Kingdom protocol[6]	Presence of any biliary stricture, dilatation, or irregularity of the intra- or extrahepatic bile ducts and/or cast on MRCP away from the biliary anastomosis in the presence of patent arterial vasculature	Median-54 mo (SCS), 28 mo (NRP) and 24 mo (NMP)	0/69 (0%)[7]	7/67 (11%)[7] NMP and 12/97 (14%)[7] SCS	NA
Hessheimer *et al*[34], 2022	Cohort	NRP (545) *vs* SRR (258)	DCD	Spain protocol[8]	Patient with patent hepatic artery, signs or symptoms of cholestasis, and direct or indirect cholangiographic imaging reflecting strictures of the intra- and/or extrahepatic biliary tree proximal to the transplant anastomosis	Median–31 mo	6/545 (1%)	24/258 (9%)	NA
Ruiz *et al*[40], 2021	Cohort	NRP (100) *vs* DBD (200)	DBD	Spain protocol[8]	Non-anastomotic biliary stricture in the presence of a patent hepatic artery and confirmed based on cholangiographic evidence (T-tube cholangiogram or magnetic resonance)	Mean-36 mo	0/100 (0%)	NA	0/200 (0%)
Muñoz *et al* [36], 2020	Cohort	NRP (23) *vs* SRR (22)	DCD	Spain protocol[8]	NR	Mean-33.9 mo (SRR) and 14.2 mo (NRP)	0/23 (0%)	3/22 (13.6%)	NA
Savier *et al* [31], 2020	Cohort	NRP (50) *vs* DBD (100)	DBD	France protocol[4]	Presence of any disseminated biliary stricture on magnetic resonance and endoscopic retrograde cholangiopancreatography, regardless of the presence or absence of arterial thrombosis or stenosis	Mean-34.8 mo (cDCD NRP) and 51.7 mo (DBD)	1/50 (2%)	NA	1/100 (1%)
Miñambres *et al*[35], 2020	Cohort	NRP (16) *vs* DBD (29)	DBD	Spain protocol[8]	NR	Median-6 mo (cDCD) and 16 mo (DBD)	0/16 (0%)	NA	0/29 (0%)
De carlis *et al* [43], 2021	Cohort	DCD NRP + D-HOPE (37) *vs* DCD SRR SCS (37)	DCD	Italy protocol[9]	Cholangiographic evidence of diffuse intrahepatic, hilar, or extrahepatic biliary strictures in the presence of a patent hepatic artery. Isolated anastomotic strictures were excluded from IC	Median-17 mo (NRP + D-HOPE) and all transplants were followed at least 1 yr	1/37 (3%)	3/37 (8%)	NA
Muller *et al* [37], 2020	Cohort	NRP (132) *vs* HOPE (93)	DCD	France protocol[4]	NAS was defined as either multifocal, unifocal intrahepatic, or hilar strictures with or without the presence of concomitant HAT or arterial complications. NAS was detected clinically and confirmed by magnetic resonance cholangiography	Median-20 mo (NRP) and 28 mo (HOPE)	2/32 (6.3%)[5]	4/32 (12.5%)[5]	NA
Hessheimer *et al*[41], 2019	Cohort	NRP (95) *vs* SRR (117)	DCD	Spain protocol[8]	Cholestasis and confirmed based on cholangiographic evidence (typically coming from magnetic resonance cholangiopancreatography) of diffuse non-anastomotic biliary strictures, with or without prestenotic dilatations, in the presence of a patent hepatic artery	Median-20 mo	2/95 (2%)	15/117 (13%)	NA
Rodríguez-	Cohort	NRP (11) *vs* DBD	DBD	Spain	Diffuse stenosis of the intrahepatic biliary tree–suspected by jaundice,	Ranges between 7-27	2/11 (13.3%)	NA	13/51 (27.7%)

Sanjuán *et al* [39], 2019		(51)		protocol[8]	cholangitis, abnormal biochemical liver test, or abnormal findings on ultrasound or T-tube cholangiography- provided there is no hepatic artery thrombosis	mo. Minimum follow-up of 3 mo			
Watson *et al* [33], 2019	Cohort	NRP (43) *vs* SRR (187)	DCD	United Kingdom protocol[6]	Presence of any non-anastomotic biliary stricture on ERCP or MRCP in the absence of arterial thrombosis or stenosis	Up to 5 yr of follow-up	0/42 (0%)	47/171 (27%)	NA
De Carlis *et al* [38], 2018	Cohort	NRP (20) *vs* DBD ECMO SCS (17) *vs* DBD non-ECMO SCS (52)	DBD-ECMO DBD-non-ECMO	Italy protocol[9]	Strictures, irregularities, or dilatations of the intrahepatic bile duct. Isolated anastomotic biliary strictures were not included in the definition of IC. The diagnosis of IC was confirmed with at least 1 adequate imaging study of the biliary tree, and concomitant hepatic artery thrombosis was excluded by Doppler ultrasound or computed tomography	Median-14 mo (cDCD), 20 mo (DBD-ECMO) and 17 mo (DBD-non-ECMO)	2/20 (10%)	NA	DBD-ECMO 0/17 0%; DBD-non-ECMO 2/52 (4%)

[1]For logistic reasons, 5 patients received additional consecutive dual hypothermic machine perfusion (DHOPE) anticipating a longer cold ischemia time (CIT) due to difficulties in recipient hepatectomy.
[2]Viability criteria used: Assessment 60 min of perfusion, with stable alanine transaminase (ALT) levels < 200 U/L, a plasma glucose peak > 10 mmol/L, and decreasing lactate level, around < 5 mmol/L. Adequate bile quality was defined as a pH > 7.45 and glucose < 3.0 mmol/L. Macroscopy of the liver did not influence. Postmortem cannulation. 5 No touch period. No antemortem interventions are allowed in Netherlands.
[3]Normothermic Regional Perfusion (NRP) + DHOPE patients.
[4]Viability criteria used: (1) serum ALT < 1000 IU/L at the end of NRP; (2) macroscopic appearance; (3) decrease in lactate levels; and (4) presence of macrosteatosis < 30% or fibrosis Ishak score < 2; Ante mortem cannulation not allowed but identification of femoral vessels to facilitate cannulation is permitted; No touch period: 5 min; Ante mortem substances administration allowed.
[5]After propensity score matching.
[6]Viability criteria used: (1) ALT levels stabilized between the first and second hour; and (2) macroscopic appearance. Ante mortem cannulation not allowed; No touch period: 5 min; Ante mortem substances administration not allowed.
[7]Clinically significant nonanastamotic biliary strictures defined as strictures requiring endoscopic or/and surgical intervention.
[8]Viability criteria used: (1) Baseline aspartate aminotransferase (AST) and ALT < 3-4 times normal value and/or AST and ALT < 4-5 times normal value at the end of NRP; and (2) macroscopic appearance; Ante mortem cannulation allowed; No touch period: 5 min; Ante mortem substances administration allowed.
[9]Viability criteria used: (1) AST and ALT > 200 IU/L; (2) macrosteatosis < 20%; and (3) More than 60 min of NRP; Ante mortem cannulation not allowed but identification of femoral vessels to facilitate cannulation is permitted; No touch period: 20 min; Ante mortem substances administration allowed.
BS: Biliary strictures; DBD: Donor after Brain Death; DCD: Donated after circulatory death; ERCP: Endoscopic retrograde cholangiopancreatography; HA: Hepatic artery; HAT: Hepatic artery thrombosis; ITBL: Ischemic type biliary lesions; MRCP: Magnetic resonance cholangiopancreatography; NAS: Nonanastamotic biliary strictures; NR: Not reported; NRP: Normothermic Regional Perfusion; SRR: Super rapid retrieval technique.

49]. Clinical studies have also reported promising results in preventing biliary complication and graft function compared to standard SCS[50,51].

HOPE is employed as an end-ischemic treatment after SRR or standard procurement in the case of DCD and DBD livers respectively, followed by a variable period of SCS. The devices available are not portable and HOPE needs to be applied at the recipient hospital. Its use limits the CIT and extends graft preservation time, avoiding the damage associated with extended periods of preservation. Two main perfusion strategies are currently employed which combine hypothermia with a highly oxygenated perfusate: (1) Single HOPE or 'HOPE', which consists of single perfusion through the portal vein; and (2) dual or 'D-HOPE' consisting of dual perfusion through the portal vein and the hepatic artery[15,52]. Currently, there are no clinical studies comparing the two strategies, although preclinical studies performed on pigs did not find differences regarding the preservation of hepatobiliary or endothelial function when comparing both strategies[53]. Advocates of D-HOPE emphasize that dominant vasculature of the bile ducts comes from arterial supply and single portal perfusion may not provide optimal preservation of the biliary tree. On the other hand, many argue the potential risk of mechanical damage to the hepatic artery intima that may occur during cannulation could cause a higher incidence of acute HAT following liver transplant[51]. Researchers from Zurich have proposed methods for liver

graft assessment during HOPE using real-time quantification of flavin mononucleotide (FMN) in the perfusate[54]. FMN is a molecule part of complex I of the mitochondrial respiratory chain[37]. Its concentration is determined by fluorescence spectroscopy and levels in perfusate correlate with graft function, complications, and graft survival in DCD livers[54].

The available studies on the use of HOPE as a preservation method, with a control group and reporting data on biliary strictures are summarized in Table 2. At present, these include four RCTs and five retrospective cohort studies with an appropriate control group of SCS grafts, and a single study comparing HOPE against NRP. The influence of HOPE on ITBL prevention has been studied only to a limited extent because in the majority, the primary endpoint was not related to biliary complications.

The relationship between ITBL and DCD livers is well established[20]. However, only 4/10 published cohort studies and 1 RCT have studied the influence of HOPE on DCD graft outcomes[51,52,55]. Thus, most published studies included only DBD livers so there is little or no ITBL incidence, and are not powered for this endpoint[56-60]. The most relevant study on ITBL prevention by *ex situ* MP was the multicenter clinical trial led by the Groningen group[52]. This European trial had symptomatic NAS within 6 mo after transplantation as the primary outcome. The study included a clear definition of NAS, which included the presence of a patent hepatic artery and therefore the NAS in this study were all ITBL. The authors demonstrated that two hours of end-ischemic D-HOPE led to a lower risk of symptomatic NAS after liver transplantation of grafts from DCD donors. NAS occurred in 5/78 (6%) of the patients in the HOPE group compared to 14/78 (18%) of SCS grafts with 2 patients from the SCS group requiring a retransplant because of severe NAS. Furthermore, the D-HOPE group showed a reduction by a factor of almost four in treatment interventions required for NAS.

Trials published by Italian and German groups have reported the efficacy of HOPE for the prevention of complications and a shorter intensive care unit stay[56,57]. There was no mention of ITBL in both trials, and grafts studied were from DBD donors so one could assume that most of the biliary complications were from an anastomotic origin. While the primary endpoint in the German[57] study was the peak alanine transaminase within 1 wk after transplantation and demonstrated a 47% reduction in the serum peak of this enzyme in the HOPE group, the authors did not find any difference in biliary complication. rate (4/23, 17% *vs* 26% 6/23). A trial[56] demonstrated benefits of HOPE, with a reduction in EAD and better graft survival rates. This study did provide a clear definition of biliary complications, although reported a rate of biliary complication different from bile leak of 5/55 (9%) in the HOPE group compared to 6/55 (11%). Two patients in each group (4%) had biliary strictures, but it was unclear if these were ITBL. A recent multicenter trial on DBD livers from the Zurich group[61] reported the effects of HOPE on preventing postoperative complications. Although the primary endpoint was not reached, and the proportion of patients with at least one Clavien^3 III complication did not differ, findings suggested that HOPE may decrease the risk of severe liver graft related events. The study did not include a clear definition of NAS and state if hepatic artery patency was required. In this study the NAS incidence was 1/85 (1.2%) in the HOPE group compared to 3/85 (3.5%) in the SCS group.

The only study comparing A-NRP and HOPE for liver grafts from DCD donors included an A-NRP cohort from six high-volume French centers and the HOPE cohort from the Zurich group[37]. In the A-NRP cohort, femoral artery cannulas were introduced post-mortem after a ''no-touch'' period of 5 min. NAS was defined as strictures with or without the presence of concomitant HAT or arterial complications and both groups showed similar rates of HAT, PNF and NAS (6/132 in the A-NRP group *vs* 8/93 in the HOPE group). D-HOPE has an encouraging role in preventing symptomatic ITBL in liver transplants from DCD grafts, due to mitochondrial injury prevention and ATP recovery under the hypothermic aerobic conditions.

NMP and ITBL

NMP provides oxygenated blood at a physiological temperature *via* both the hepatic artery and portal vein, whilst the liver graft is *ex situ*[62]. Several different NMP devices are commercially available, and the majority are transportable even with graft connected. The only major differences between the devices are the nature of the arterial flow (pulsatile or non-pulsatile) and the caval outflow (open or closed). Since the phase 1 first-in-man study that demonstrated safety and feasibility of NMP, there has been a significant uptake in this preservation modality around the world and two large RCTs[63-65]. In contrast to *ex situ* HMP, the more physiological nature of NMP allows cellular function to continue and this can be assessed *via* surrogate parameters[66,67]. Numerous biochemical parameters within the NMP perfusate or bile have been used to predict hepatocellular and cholangiocyte function respectively, in an effort to identify the grafts destined to demonstrate severe EAD or biliary complications[68]. Therefore, an accurate discussion of the impact NMP on ITBL posttransplant needs to consist of two components: (1) The incidence of ITBL in NMP preserved grafts in comparison to other modalities; and (2) the accuracy of NMP parameters to identify livers destined to develop clinically significant ITBL.

Published outcomes for NMP are confounded by the fact that this preservation modality is more frequently applied to organs of marginal quality to facilitate transplantation[69], and it may be applied for the entirety of the preservation period from the donor hospital (“at source”) or following a period of cold storage during transport to the recipient center (“back to base”). The early clinical trials of NMP included both DBD and DCD grafts, with a focus on its feasibility, safety, and impact on the IRI as indicated by markers of early graft function[63,64]. These multicenter trials included standard risk

Table 2 Clinical studies assessing the impact of hypothermic machine perfusion on ischemic type biliary lesions after liver transplantation

Ref.	Study design	Group (*n*)	DBD/DCD	HOPE duration (median)	Definition of ITBL	Follow up	ITBL-intervention		ITBL-control	
							DCD	DBD	DCD	DBD
Schlegel *et al*[61], 2023	RCT	HOPE (85) *vs* SCS (85)	DBD	95.5 min	NR	12 mo	NA	1/85 (1.2%)	NA	3/85 (3.5%)
Ravaioli *et al*[56], 2022	RCT	HOPE (66) *vs* SCS (69)	DBD	145 min	Nonspecifically provided: Biliary strictures; Biliary others	12 mo	NA	5/55 (9%)	NA	6/55 (11%)
van Rijn *et al*[52], 2021	RCT	D-HOPE (78) *vs* SCS (78)	DCD	132 min	Symptomatic NAS diagnosed with the use of 6-mo cholangiography in the presence of a patent HA	6 mo	5/78 (6%)	NA	14/78 (18%)	NA
Czigany *et al*[57], 2021	RCT	HOPE (23) *vs* SCS (23)	DBD	145 min	Biliary complications (clinical; radiological)	12 mo	NA	4/23 (17%)	NA	6/23 (26%)
Patrono *et al*[60], 2022	Cohort	D-HOPE (121) *vs* SCS (723)	DBD	138 min	Biliary complications 3-mo cholangiography if clinically indicated	Median 21.6 (D-HOPE) and 51.1 (SCS) mo	NA	5/121 (4%)	NA	35/723 (5%)
Rayar *et al*[58], 2021	Cohort	HOPE (25) *vs* SCS (69)	DBD	117 min	NR	12 mo	NA	0/25 (0%)	NA	1/69 (1.5%)[1]
Muller *et al*[37], 2020	Cohort	NRP (132) *vs* HOPE (93)	DCD	132 min	NAS was defined as strictures with or without HA thrombosis or arterial complications.	Median 20 (NRP) 28 mo (HOPE) mo	2/32 (6.3%)	NA	4/32 (12.5%)	NA
Ravaioli *et al*[59], 2020	Cohort	HOPE (10) *vs* SCS (30)	DBD	132 min	NR	12 mo	NA	NP	NA	NP
Schlegel *et al*[55], 2019	Cohort	HOPE (50) *vs* SCS DBD (50) *vs* SCS DCD (50)	Both	120 min	Ischemic cholangiopathy defined radiologically, as intrahepatic or hilar BS and dilatations with patent HA	5 yr	4/50 (8%)	NA	11/50 (22%)	1/50 (2%)
van Rijn *et al*[51], 2017	Cohort	D-HOPE (10) *vs* SCS (20)	DCD	126 min	NAS was defined as bile duct stenosis in the biliary tree as detected by ERCP or MRCP with clinical signs of cholestasis and/or cholangitis in the presence of a patent HA	12 mo	1/10 (10%)	NA	9/20 (45%)[2]	NA

[1]Ischemic necrosis.

[2]Biliary necrosis 2/9.

BS: Biliary strictures; DBD: Donor after Brain Death; DCD: Donated after circulatory death; ERCP: Endoscopic retrograde cholangiopancreatography; HA: Hepatic artery; ITBL: Ischemic type biliary lesions; MRCP: Magnetic resonance cholangiopancreatography; NAS: Nonanastamotic biliary strictures; NR: Not reported; NA: Not available.

donors that were accepted for transplant regardless of the preservation modality (NMP or SCS). Subsequently, clinical practice and research shifted to investigate the ability of NMP to resuscitate poor quality grafts that were otherwise deemed untransplantable with SCS[70-72]. Complicating matters further, supposedly untransplantable livers are a heterogenous group with a varying overall risk of ITBL[71,73]. As an example, a DBD graft with severe macrosteatosis has a different risk of ITBL than a DCD graft with 60 min of dWIT, but both will fall into the declined group due to differing clinical concerns. The increased utilization of NMP for livers otherwise deemed to high risk for transplant following SCS has pragmatic consequences for trial design. This loss in equipoise over the safety of randomizing high-risk livers to SCS results in a greater reliance on cohort studies.

The trials that have investigated NMP in the clinical setting, *via* either an RCT or cohort study with a representative control group, are listed in Table 3. Many of these trials unfortunately lacked clear definitions of what was considered ITBL, and whether complete artery patency was required for the diagnosis. To date, three RCTs of NMP have been completed[64,65,74] (Table 3). The first multicenter RCT published by Nasralla *et al*[64] in 2018 included standard risk grafts from both DBD and DCD donors and applied NMP at source. This study included a protocol magnetic resonance cholangiopancreatography at 6 mo to assess for biliary complications of which only a small proportion of subjects

Table 3 Clinical studies assessing the impact of normothermic machine perfusion on ischemic type biliary lesions after liver transplantation

Ref.	Study design	Intervention group (*n*)	Control group (*n*)	DBD, DCD intervention	DBD, DCD control	NMP duration[1]	Viability testing	Definition of ITBL	Follow u	ITBL-intervention		ITBL-control	
										DCD	DBD	DCD	DBD
Markmann *et al*[65], 2022	RCT	NMP at source (153)	SCS (146)	125, 28	133, 13	4.5 h	NR	IBC defined as NAS or bile leaks, confirmed with ERCP or MRCP	12 mo	4/153 (2.6%) (DBD and DCD)		14/146 (9.5%) (DBD and DCD)	
Nasralla *et al* [64], 2018	RCT	NMP at source (121)	SCS (101)	87, 34	80, 21	9.1 h	No viability testing	Protocol MRCP at 6 mo. No distinction between IC and ITBL	6 mo	3/27 (11.1%)[2]	4/54 (7.4%)[2]	5/19 (26.3%)[2]	3/55 (5.5%)[2]
Ghinolfi *et al* [74], 2019	RCT	NMP back-to-base (10)	SCS (10)	All DBD	All DBD	4.2 h	NR	NR	6 mo	NA	1/10 (10%)	NA	0/10
Gaurav *et al* [44], 2022	Cohort	NMP back to base OR at-source (67)	SCS (97); NRP (69)	All DCD	All DCD	7.6 h	Cambridge criteria	NAS defined as any BS, dilatation, or irregularity of the bile ducts and/or cast on MRCP away from the anastomosis with patent HA	6 mo minimum	12/67 (17.9%) [7/67, 10.4%[3]]	NA	NRP-4/69 (5.7%) [0[3]] SCS-22/97 (22.6%) [12/97, 12.3%[3]]	NA
Hann *et al* [82], 2022	Cohort	NMP back to base (26)	SCS (56)	All DBD	All DBD	12 h	Birmingham criteria	Not reported	6 mo minimum	NA	1/26 (3.8%)	NA	6/56 (10.7%)
Fodor *et al* [75], 2021	Cohort	NMP back to base (59)	SCS (59)	49, 9	55, 4	15 h	Certain parameters signs of "good organ function", others considered "warning" signs	ITBL was defined as BS, dilatation or irregularity of the intra- or extrahepatic bile ducts with or without biliary cast formation in the absence of HAS or HAT	3 mo minimum	0/9	2/49 (4%)	1/4 (25%)	7/55 (12.7%)
Mohkam *et al*[45], 2022	Cohort	NMP at source (34)	NRP (68)	All DCDs	All DCD	8.8 h	Not applied	Refers to BS requiring a specific treatment or resulting to graft loss and/or death	23 mo	1/34 (2.9%)	NA	1/68 (1.5%)	NA
Mergental *et al*[71], 2020	Cohort	NMP back-to-base (22)	SCS (44)	12, 10	24, 20[4]	9.8 h	Birmingham criteria	NR	6 mo	7/10 (70%)	0/12	NR	NR
Bral *et al*[83], 2019	Cohort	NMP back-to-base (26)	NMP at source (17)	20, 6	13, 4	7.8 h (back-to-base) 10.3 h (at-source)	Parameters included opening lactate level, lactate clearance, necessity of bicarbonate supplementation, and bile production	IC defined as diffuse BS in the absence of significant arterial stenosis	6 mo	0/6	0/20	0/4	0/13
Ceresa *et al* [62], 2019	Cohort	NMP back-to-base (31)	NMP at-source (104)	23, 8	73, 31	8.4 h (mean)	No viability criteria	NR	12 mo	0/8	0/23	NR	NR
Liu *et al*[84], 2019	Cohort	NMP back to base OR at-source (21)	SCS (84)	13, 8	52, 32	4 h 52	No viability testing	NR	12 mo minimum	0/8	0/13	NR	NR
Bral *et al*[85], 2017	Cohort	NMP at-source (9)	SCS (30)	6, 3	22, 8	11.5 h	No viability testing	NR	6 mo	0/3	0/6	NR	NR

Ravikumar *et al*[63], 2016	Cohort	NMP at-source (20)	SCS (40)	16, 4	32, 8	9.3 h	No viability testing	NR	30 d	0/4	0/16	NR	NR

[1]Median duration unless otherwise stated.
[2]Numerator represents the number of patients that completed the 6 mo protocol magnetic resonance cholangiopancreatography.
[3]Number of clinically significant strictures, defined as those requiring intervention.
[4]Presumed based on propensity matching.
BS: Biliary strictures; DBD: Donor after Brain Death; DCD: Donated after circulatory death; ERCP: Endoscopic retrograde cholangiopancreatography; IC: Ischemic cholangiopathy; HA: Hepatic artery; HAS: Hepatic artery stenosis; HAT: Hepatic artery thrombosis; IBC: Ischemic biliary complication; ITBL: Ischemic type biliary lesions; NAS: Nonanastamotic biliary strictures; NR: Not reported; NRP: Normothermic Regional Perfusion; MRCP: Magnetic resonance cholangiopancreatography; RCT: Randomized controlled trials; NA: Not available.

completed. The difference in stricture incidence was greatest in the DCD subgroup, with a rate of 26.3% in the DCD-SCS group as opposed to 11.1% in the DCD-NMP group. Whether these ischemic strictures were ITBL or the result of a vascular lesion is unclear, as HA patency was not possible to determine from the data provided[64]. The smaller RCT conducted by Ghinolfi *et al*[74] comprised a sample of elderly DBD donors (≥ 70 years) and applied NMP in a back-to-base approach[74]. However, the small sample size and lower overall risk of ITBL in DBD grafts makes the findings of this study less informative. In this study, only one patient developed a biliary stricture, and they were in the NMP group. A recent large RCT from the United States randomized nearly 300 livers (both DBD and DCD) to either at-source NMP or SCS[65]. These authors did provide a definition of what they considered an ischemic biliary complication (Table 3) and this occurred in 4 and 14 of the NMP and SCS livers respectively. Once again, the granularity of the data presented does not allow determination of the proportion of patients with ischemic biliary complications that were truly ITBL. It should be noted that none of these RCTs performed any formal viability testing of the grafts prior to transplant and were not powered appropriately to assess for biliary complications.

Both prospective and retrospective cohort studies have investigated biliary complications following NMP (Table 3). In the VITTAL trial, Mergental *et al*[71] reported the outcomes of a prospective cohort of 22 livers (12 DBD, 10 DCD) destined for discard that were transplanted following back-to-base NMP. After 6 mo follow-up, 3/10 of the DCD livers had developed symptomatic nonanastomotic biliary strictures. Requiring retransplantation[71]. Fodor *et al*[75] subsequently reported a retrospective cohort study of predominantly DBD grafts (49 DBD and 9 DCD) preserved *via* back-to-base NMP and reported both a lower incidence and severity of ITBL in the NMP group in comparison to SCS[75]. This study had a clear definition of ITBL and applied viability testing, which included bile output and pH, however specific parameters for these were not reported. Recently, Gaurav *et al*[44] published a single center retrospective cohort study of DCD grafts preserved by NMP (back-to-base and at-source), NRP and CS with the primary outcome being NAS[44]. These authors also provided a clear definition of NAS and this required hepatic artery patency. In the NMP group, 12/69 developed NAS and in 7/12 it was clinically significant. This was comparable to the SCS group (22/97, 12/22 clinically significant) but higher than the NRP group (4/69, 0/4 clinically significant). It must be noted that this study applied biliary viability testing to NMP preserved livers and 77% of these NMP preserved DCD livers proceeded to transplant.

Utilizing NMP perfusate and bile parameters to predict (and avoid) certain outcomes remains controversial. The risks associated with liberal use of NMP preserved livers is associated morbidity and mortality. The risks associated with being too stringent on the NMP viability criteria, when predictive accuracy is less than perfect, is the discard of a liver that would have resulted in acceptable outcomes. NMP indicators of biliary injury and/or function have been studied by several groups in human livers [76,77]. The early experience of associating bile pH, bicarbonate and glucose with cholangiopathies was reported by Watson *et al*[77] in 2018, from 16 transplanted livers. In this group of livers, a biliary pH < 7.4 occurred in 3/16, and all three of these developed a cholangiopathy. A lower biliary bicarbonate and higher biliary glucose concentration was also associated with subsequent cholangiopathy. Recently, the same group have reported outcomes in a much larger cohort of 144 transplanted livers[78]. Interestingly, 15 of these transplanted livers did not meet their previously reported cholangiocyte viability criteria and in a further three livers no bile was produced which precluded this assessment. Clinically significant NAS developed in 9/144 recipients and all of these had a bile pH > 7.5. Matton *et al* [76] investigated biliary NMP parameters in both the laboratory and a small clinical trial (n = 6)[76]. These authors did not have any cases of ITBL in the recipients within the trial, but demonstrated an inverse correlation between bile pH and bicarbonate concentration with histological evidence of biliary injury in a group of non-transplanted livers. A pH and bicarbonate concentration of < 7.48 and < 18 mmol/L had a positive predictive value of 75% and 91% for significant biliary injury. In summary, the prediction (and avoidance) of ITBL using NMP requires further research. This will undoubtedly be of assistance to the transplant community, however at present the accuracy remains sub-optimal and it must be improved to avoid the unnecessary discard of grafts.

Machine combination approaches

In theory, the different rationale behind the various MP strategies could work synergistically to prevent ITBL. A-NRP abbreviates the dWIT induced damage and provides in-situ resuscitation prior to the cold ischemic period, whereas the *ex situ* techniques may dampen IRI. Conversely, the application of sequential MP strategies may follow the rule of diminishing returns and the resources may not be justified. Despite the report that individual grafts had the combination of A-NRP and NMP, clarity in the ITBL rate with this combination is lacking as they were excluded from the analysis of this study[44,79]. The Groningen group have also reported their experience with sequential *ex-situ* end-ischemic D-HOPE, controlled oxygenated rewarming and NMP for high-risk livers (mostly DCD grafts)[80]. The application of this protocol is proposed to protects these livers against IRI (D-HOPE phase) and enables viability assessment (NMP phase) prior to transplantation, resulting in promising outcomes.

In Italy, as aforementioned circulatory death during DCD procurement is declared after a stand-off period of 20 min. This prolonged dWIT time has been a general reluctance to use such DCD grafts for transplantation due to the probable high risk of graft failure. The combination of A-NRP and D-HOPE has contributed to increase the donor pool in this high-risk donor context. In a retrospective cohort study, this combination has reported satisfactory outcomes in terms of ITBL when compared with relatively low-risk donor control group (A-NRP + D-HOPE 3% *vs* SCS 8%)[43]. Recently, a new procedure called ischemia-free liver transplantation has been proposed, during which liver grafts are procured, preserved and implanted under continuous NMP. Its applicability and clinical impact are yet to be determined[81]. Further studies are required to determine if additional benefits are achieved by combining different techniques.

EVIDENCE SUMMARY

The volume of data on MP and its impact on the development of ITBL following liver transplant is growing. However, with only a few exceptions, ITBL was not the primary outcome under investigation in these studies and therefore were not designed and reported with this entity in mind. It is difficult in many published studies to tease out what biliary complications represent the development of ITBL, as opposed to strictures of another cause. With this considered, the evidence for prevention of ITBL with MP is distinctly different for DCD as opposed to DBD grafts.

The highest quality evidence for ITBL prevention with MP in DCD grafts is D-HOPE, in comparison to SRR and SCS. This is based on finding from a RCT[52]. However, a larger quantity of lower quality evidence supports A-NRP in comparison to both SRR with SCS, and NMP *via* a 'back to base' approach. At present, there is no evidence that D-HOPE is superior to A-NRP or that the combination of these two MP techniques results in a further reduction of ITBL than each one in isolation. Based on the DCD subgroup from one randomized trial[64], there is a suggestion that NMP applied 'at source' reduces ITBL in comparison to SRR and SCS[64]. There is no good quality evidence that NMP applied in a 'back to base' approach for DCD grafts prevents ITBL. In DBD donors, the incidence of ITBL is lower and therefore studies with a large sample size will be required to demonstrate a noticeable effect. The available evidence to suggest that either NMP 'at source' or 'back to base' for DBD grafts is weak, and consists of only one cohort study[75]. There is no trial evidence to support a reduction in ITBL for DBD grafts with HMP strategies.

CONCLUSION

ITBL remains an ongoing issue and the notion that biliary complications are the 'achilles heel' of liver transplantation remains true. However, with the introduction of MP technology, gains are being made in the prevention of this highly morbid condition. The greatest area of improvement is for DCD grafts with RCT evidence for D-HOPE, and large cohort studies supporting A-NRP. Given the demonstrated benefits these modalities have over SCS for DCD grafts, a loss of equipoise within the transplant community is diminishing the opportunity for further RCTs that include a SCS group. As an organ donor often generously gives numerous organs, the impact A-NRP has on other abdominal viscera may influence the decision regarding the most appropriate MP strategies. Multiple factors likely interact to cause ITBL, and a greater understanding of these will undoubtedly help refine both preventative and treatment interventions.

ACKNOWLEDGEMENTS

Angus Hann would like to acknowledge the funding received in the form of the Catherine Marie Enright research scholarship from the Royal Australasian College of Surgeons to support his program of research. Figure created with biorender.com, accessed on January 2023.

FOOTNOTES

Author contributions: Perera MTPR and Hann A contributed to the conceptualization; Durán M, Hann A, Calleja R, and Clarke G performed the literature review; Durán M, Hann A, Clarke G, and Calleja R wrote the original draft; Perera MTPR, Hann A, Briceño J, Calleja R, Nutu A, Ayllón MD, López-Cillero P, Sanabria-Mateos R, and Mergental H wrote the review and performed the editing; All authors have read and agreed to the published version of the manuscript.

Conflict-of-interest statement: The funding provided for normothermic machine perfusion consumables generously donated by the Ann Fox Foundation, under the umbrella of University Hospital Birmingham Charities.

Open-Access: This article is an open-access article that was selected by an in-house editor and fully peer-reviewed by external reviewers. It is distributed in accordance with the Creative Commons Attribution NonCommercial (CC BY-NC 4.0) license, which permits others to distribute, remix, adapt, build upon this work non-commercially, and license their derivative works on different terms, provided the original work is properly cited and the use is non-commercial. See: https://creativecommons.org/Licenses/by-nc/4.0/

Country/Territory of origin: United Kingdom

ORCID number: Manuel Durán 0000-0003-1161-2195; Rafael Calleja 0000-0003-0048-0756; Angus Hann 0000-0003-4431-3642; George Clarke 0000-0002-8913-398X; Ruben Ciria 0000-0002-7839-2329; Anisa Nutu 0000-0003-4699-0970; Rebeca Sanabria-Mateos 0000-0002-1431-6386; María Dolores Ayllón 0000-0003-2493-3756; Pedro López-Cillero 0000-0002-2568-6438; Hynek Mergental 0000-0001-5480-9380; Javier Briceño 0000-0001-7027-7898; M Thamara P R Perera 0000-0002-5417-3850.

S-Editor: Fan JR
L-Editor: Filipodia
P-Editor: Yu HG

REFERENCES

1 **Muller X**, Marcon F, Sapisochin G, Marquez M, Dondero F, Rayar M, Doyle MMB, Callans L, Li J, Nowak G, Allard MA, Jochmans I, Jacskon K, Beltrame MC, van Reeven M, Iesari S, Cucchetti A, Sharma H, Staiger RD, Raptis DA, Petrowsky H, de Oliveira M, Hernandez-Alejandro R, Pinna AD, Lerut J, Polak WG, de Santibañes E, de Santibañes M, Cameron AM, Pirenne J, Cherqui D, Adam RA, Ericzon BG, Nashan B, Olthoff K, Shaked A, Chapman WC, Boudjema K, Soubrane O, Paugam-Burtz C, Greig PD, Grant DR, Carvalheiro A, Muiesan P, Dutkowski P, Puhan M, Clavien PA. Defining Benchmarks in Liver Transplantation: A Multicenter Outcome Analysis Determining Best Achievable Results. *Ann Surg* 2018; **267**: 419-425 [PMID: 28885508 DOI: 10.1097/SLA.0000000000002477]

2 **MacConmara M**, Hanish SI, Hwang CS, De Gregorio L, Desai DM, Feizpour CA, Tanriover B, Markmann JF, Zeh H 3rd, Vagefi PA. Making Every Liver Count: Increased Transplant Yield of Donor Livers Through Normothermic Machine Perfusion. *Ann Surg* 2020; **272**: 397-401 [PMID: 32694447 DOI: 10.1097/SLA.0000000000004198]

3 **Briceño J**, Ciria R, de la Mata M. Donor-recipient matching: myths and realities. *J Hepatol* 2013; **58**: 811-820 [PMID: 23104164 DOI: 10.1016/j.jhep.2012.10.020]

4 **Panayotova G**, Lunsford KE, Latt NL, Paterno F, Guarrera JV, Pyrsopoulos N. Expanding indications for liver transplantation in the era of liver transplant oncology. *World J Gastrointest Surg* 2021; **13**: 392-405 [PMID: 34122730 DOI: 10.4240/wjgs.v13.i5.392]

5 **Kollmann D**, Sapisochin G, Goldaracena N, Hansen BE, Rajakumar R, Selzner N, Bhat M, McCluskey S, Cattral MS, Greig PD, Lilly L, McGilvray ID, Ghanekar A, Grant DR, Selzner M. Expanding the donor pool: Donation after circulatory death and living liver donation do not compromise the results of liver transplantation. *Liver Transpl* 2018; **24**: 779-789 [PMID: 29604237 DOI: 10.1002/lt.25068]

6 **Calne RY**. A new technique for biliary drainage in orthotopic liver transplantation utilizing the gall bladder as a pedicle graft conduit between the donor and recipient common bile ducts. *Ann Surg* 1976; **184**: 605-609 [PMID: 791164 DOI: 10.1097/00000658-197611000-00012]

7 **Boteon YL**, Boteon AP, Attard J, Wallace L, Bhogal RH, Afford SC. Impact of machine perfusion of the liver on post-transplant biliary complications: A systematic review. *World J Transplant* 2018; **8**: 220-231 [PMID: 30370232 DOI: 10.5500/wjt.v8.i6.220]

8 **Hessheimer AJ**, Cárdenas A, García-Valdecasas JC, Fondevila C. Can we prevent ischemic-type biliary lesions in donation after circulatory determination of death liver transplantation? *Liver Transpl* 2016; **22**: 1025-1033 [PMID: 27082839 DOI: 10.1002/lt.24460]

9 **Durán M**, Hann A, Lembach H, Nutu A, Clarke G, Patel I, Sneiders D, Hartog H, Mirza DF, Perera MTPR. Normothermic Machine Perfusion as a Tool for Safe Transplantation of High-Risk Recipients. *Transplantology* 2022; **3**: 169-183 [DOI: 10.3390/transplantology3020018]

10 **Noack K**, Bronk SF, Kato A, Gores GJ. The greater vulnerability of bile duct cells to reoxygenation injury than to anoxia. Implications for the pathogenesis of biliary strictures after liver transplantation. *Transplantation* 1993; **56**: 495-500 [PMID: 8212138 DOI: 10.1097/00007890-199309000-00001]

11 **Kochhar G**, Parungao JM, Hanouneh IA, Parsi MA. Biliary complications following liver transplantation. *World J Gastroenterol* 2013; **19**: 2841-2846 [PMID: 23704818 DOI: 10.3748/wjg.v19.i19.2841]

12 **Verdonk RC**, Buis CI, Porte RJ, van der Jagt EJ, Limburg AJ, van den Berg AP, Slooff MJ, Peeters PM, de Jong KP, Kleibeuker JH, Haagsma EB. Anastomotic biliary strictures after liver transplantation: causes and consequences. *Liver Transpl* 2006; **12**: 726-735 [PMID: 16628689 DOI: 10.1002/Lt.20714]

13 **Jay CL**, Lyuksemburg V, Ladner DP, Wang E, Caicedo JC, Holl JL, Abecassis MM, Skaro AI. Ischemic cholangiopathy after controlled donation after cardiac death liver transplantation: a meta-analysis. *Ann Surg* 2011; **253**: 259-264 [PMID: 21245668 DOI: 10.1097/SLA.0b013e318204e658]

14 **Foley DP**, Fernandez LA, Leverson G, Anderson M, Mezrich J, Sollinger HW, D'Alessandro A. Biliary complications after liver transplantation from donation after cardiac death donors: an analysis of risk factors and long-term outcomes from a single center. *Ann Surg* 2011; **253**: 817-825 [PMID: 21475025 DOI: 10.1097/SLA.0b013e3182104784]

15 **Schlegel A**, Porte R, Dutkowski P. Protective mechanisms and current clinical evidence of hypothermic oxygenated machine perfusion (HOPE) in preventing post-transplant cholangiopathy. *J Hepatol* 2022; **76**: 1330-1347 [PMID: 35589254 DOI: 10.1016/j.jhep.2022.01.024]

16 **Buis CI**, Verdonk RC, Van der Jagt EJ, van der Hilst CS, Slooff MJ, Haagsma EB, Porte RJ. Nonanastomotic biliary strictures after liver transplantation, part 1: Radiological features and risk factors for early vs. late presentation. *Liver Transpl* 2007; **13**: 708-718 [PMID: 17457932 DOI: 10.1002/Lt.21166]

17 **Croome KP**, Mathur AK, Aqel B, Yang L, Taner T, Heimbach JK, Rosen CB, Paz-Fumagalli R, Taner CB. Classification of Distinct Patterns of Ischemic Cholangiopathy Following DCD Liver Transplantation: Distinct Clinical Courses and Long-term Outcomes From a Multicenter Cohort. *Transplantation* 2022; **106**: 1206-1214 [PMID: 34468429 DOI: 10.1097/TP.0000000000003928]

18 **Op den Dries S**, Sutton ME, Lisman T, Porte RJ. Protection of bile ducts in liver transplantation: looking beyond ischemia. *Transplantation* 2011; **92**: 373-379 [PMID: 21629175 DOI: 10.1097/TP.0b013e318223a384]

19 **de Vries Y**, von Meijenfeldt FA, Porte RJ. Post-transplant cholangiopathy: Classification, pathogenesis, and preventive strategies. *Biochim Biophys Acta Mol Basis Dis* 2018; **1864**: 1507-1515 [PMID: 28645651 DOI: 10.1016/j.bbadis.2017.06.013]

20 **O'Neill S**, Roebuck A, Khoo E, Wigmore SJ, Harrison EM. A meta-analysis and meta-regression of outcomes including biliary complications in donation after cardiac death liver transplantation. *Transpl Int* 2014; **27**: 1159-1174 [PMID: 25052036 DOI: 10.1111/tri.12403]

21 **Laing RW**, Scalera I, Isaac J, Mergental H, Mirza DF, Hodson J, Wilkin RJ, Perera MT, Muiesan P. Liver Transplantation Using Grafts From Donors After Circulatory Death: A Propensity Score-Matched Study From a Single Center. *Am J Transplant* 2016; **16**: 1795-1804 [PMID: 26725645 DOI: 10.1111/ajt.13699]

22 **Lamireau T**, Zoltowska M, Levy E, Yousef I, Rosenbaum J, Tuchweber B, Desmoulière A. Effects of bile acids on biliary epithelial cells: proliferation, cytotoxicity, and cytokine secretion. *Life Sci* 2003; **72**: 1401-1411 [PMID: 12527037 DOI: 10.1016/s0024-3205(02)02408-6]

23 **Knoop M**, Schnoy N, Keck H, Neuhaus P. Morphological changes of human common bile ducts after extended cold preservation. *Transplantation* 1993; **56**: 1572-1573 [PMID: 8279043]

24 **Buis CI**, Geuken E, Visser DS, Kuipers F, Haagsma EB, Verkade HJ, Porte RJ. Altered bile composition after liver transplantation is associated with the development of nonanastomotic biliary strictures. *J Hepatol* 2009; **50**: 69-79 [PMID: 19012987 DOI: 10.1016/j.jhep.2008.07.032]

25 **Geuken E**, Visser D, Kuipers F, Blokzijl H, Leuvenink HG, de Jong KP, Peeters PM, Jansen PL, Slooff MJ, Gouw AS, Porte RJ. Rapid increase of bile salt secretion is associated with bile duct injury after human liver transplantation. *J Hepatol* 2004; **41**: 1017-1025 [PMID: 15582136 DOI: 10.1016/j.jhep.2004.08.023]

26 **Cursio R**, Gugenheim J. Ischemia-Reperfusion Injury and Ischemic-Type Biliary Lesions following Liver Transplantation. *J Transplant* 2012; **2012**: 164329 [PMID: 22530107 DOI: 10.1155/2012/164329]

27 **Ramírez-Del Val A**, Guarrera J, Porte RJ, Selzner M, Spiro M, Raptis DA, Friend PJ, Nasralla D; ERAS4OLT. org Working Group. Does machine perfusion improve immediate and short-term outcomes by enhancing graft function and

recipient recovery after liver transplantation? A systematic review of the literature, meta-analysis and expert panel recommendations. *Clin Transplant* 2022; **36**: e14638 [PMID: 35279883 DOI: 10.1111/ctr.14638]

28 **Melandro F**, Basta G, Torri F, Biancofiore G, Del Turco S, Orlando F, Guarracino F, Maremmani P, Lazzeri C, Peris A, De Simone P, Ghinolfi D. Normothermic regional perfusion in liver transplantation from donation after cardiocirculatory death: Technical, biochemical, and regulatory aspects and review of literature. *Artif Organs* 2022; **46**: 1727-1740 [PMID: 35733227 DOI: 10.1111/aor.14330]

29 **Abdel-Misih SR**, Wei L, Benson AB 3rd, Cohen S, Lai L, Skibber J, Wilkinson N, Weiser M, Schrag D, Bekaii-Saab T. Neoadjuvant Therapy for Rectal Cancer Affects Lymph Node Yield and Status Without Clear Implications on Outcome: The Case for Eliminating a Metric and Using Preoperative Staging to Guide Therapy. *J Natl Compr Canc Netw* 2016; **14**: 1528-1534 [PMID: 27956537 DOI: 10.6004/jnccn.2016.0164]

30 **De Carlis L**, De Carlis R, Lauterio A, Di Sandro S, Ferla F, Zanierato M. Sequential Use of Normothermic Regional Perfusion and Hypothermic Machine Perfusion in Donation After Cardiac Death Liver Transplantation With Extended Warm Ischemia Time. *Transplantation* 2016; **100**: e101-e102 [PMID: 27495774 DOI: 10.1097/TP.0000000000001419]

31 **Savier E**, Lim C, Rayar M, Orlando F, Boudjema K, Mohkam K, Lesurtel M, Mabrut JY, Pittau G, Begdadi N, Cherqui D, Adam R, Dondero F, Sepulveda A, Soubrane O, Bucur P, Barbier L, Salame E, Jasseron C, Antoine C, Riou B, Scatton O. Favorable Outcomes of Liver Transplantation from Controlled Circulatory Death Donors Using Normothermic Regional Perfusion Compared to Brain Death Donors. *Transplantation* 2020; **104**: 1943-1951 [PMID: 32639402 DOI: 10.1097/TP.0000000000003372]

32 **Trasplantes ONT**. Protocolo nacional de donación y trasplante hepático en donación en asistolia controlada. 2015. Available from: https://www.enfermeria21.com/revistas/metas/articulo/81185/

33 **Watson CJE**, Hunt F, Messer S, Currie I, Large S, Sutherland A, Crick K, Wigmore SJ, Fear C, Cornateanu S, Randle LV, Terrace JD, Upponi S, Taylor R, Allen E, Butler AJ, Oniscu GC. In situ normothermic perfusion of livers in controlled circulatory death donation may prevent ischemic cholangiopathy and improve graft survival. *Am J Transplant* 2019; **19**: 1745-1758 [PMID: 30589499 DOI: 10.1111/ajt.15241]

34 **Hessheimer AJ**, de la Rosa G, Gastaca M, Ruíz P, Otero A, Gómez M, Alconchel F, Ramírez P, Bosca A, López-Andújar R, Atutxa L, Royo-Villanova M, Sánchez B, Santoyo J, Marín LM, Gómez-Bravo MÁ, Mosteiro F, Villegas Herrera MT, Villar Del Moral J, González-Abos C, Vidal B, López-Domínguez J, Lladó L, Roldán J, Justo I, Jiménez C, López-Monclús J, Sánchez-Turrión V, Rodríguez-Laíz G, Velasco Sánchez E, López-Baena JÁ, Caralt M, Charco R, Tomé S, Varo E, Martí-Cruchaga P, Rotellar F, Varona MA, Barrera M, Rodríguez-Sanjuan JC, Briceño J, López D, Blanco G, Nuño J, Pacheco D, Coll E, Domínguez-Gil B, Fondevila C. Abdominal normothermic regional perfusion in controlled donation after circulatory determination of death liver transplantation: Outcomes and risk factors for graft loss. *Am J Transplant* 2022; **22**: 1169-1181 [PMID: 34856070 DOI: 10.1111/ajt.16899]

35 **Miñambres E**, Ruiz P, Ballesteros MA, Álvarez C, Cifrián JM, Atutxa L, Ventoso A, Castillo F, Gastaca M. Combined lung and liver procurement in controlled donation after circulatory death using normothermic abdominal perfusion. Initial experience in two Spanish centers. *Am J Transplant* 2020; **20**: 231-240 [PMID: 31265753 DOI: 10.1111/ajt.15520]

36 **Muñoz DC**, Pérez BS, Martínez MP, León Díaz FJ, Fernández Aguilar JL, Pérez Daga JA, Santoyo J. Does Normothermic Regional Perfusion Improve the Results of Donation After Circulatory Death Liver Transplantation? *Transplant Proc* 2020; **52**: 1477-1480 [PMID: 32252997 DOI: 10.1016/j.transproceed.2020.01.088]

37 **Muller X**, Mohkam K, Mueller M, Schlegel A, Dondero F, Sepulveda A, Savier E, Scatton O, Bucur P, Salame E, Jeddou H, Sulpice L, Pittau G, Allard MA, Mabrut JY, Dutkowski P, Clavien PA, Lesurtel M. Hypothermic Oxygenated Perfusion Versus Normothermic Regional Perfusion in Liver Transplantation From Controlled Donation After Circulatory Death: First International Comparative Study. *Ann Surg* 2020; **272**: 751-758 [PMID: 32833758 DOI: 10.1097/SLA.0000000000004268]

38 **De Carlis R**, Di Sandro S, Lauterio A, Botta F, Ferla F, Andorno E, Bagnardi V, De Carlis L. Liver Grafts From Donors After Circulatory Death on Regional Perfusion With Extended Warm Ischemia Compared With Donors After Brain Death. *Liver Transpl* 2018; **24**: 1523-1535 [PMID: 30022597 DOI: 10.1002/lt.25312]

39 **Rodríguez-Sanjuán JC**, Ruiz N, Miñambres E, Toledo E, González-Noriega M, Fernández-Santiago R, Castillo F. Liver Transplant From Controlled Cardiac Death Donors Using Normothermic Regional Perfusion: Comparison With Liver Transplants From Brain Dead Donors. *Transplant Proc* 2019; **51**: 12-19 [PMID: 30655135 DOI: 10.1016/j.transproceed.2018.04.067]

40 **Ruiz P**, Valdivieso A, Palomares I, Prieto M, Ventoso A, Salvador P, Senosiain M, Fernandez JR, Testillano M, Bustamante FJ, Gastaca M. Similar Results in Liver Transplantation From Controlled Donation After Circulatory Death Donors With Normothermic Regional Perfusion and Donation After Brain Death Donors: A Case-Matched Single-Center Study. *Liver Transpl* 2021; **27**: 1747-1757 [PMID: 34455694 DOI: 10.1002/lt.26281]

41 **Hessheimer AJ**, Coll E, Torres F, Ruíz P, Gastaca M, Rivas JI, Gómez M, Sánchez B, Santoyo J, Ramírez P, Parrilla P, Marín LM, Gómez-Bravo MÁ, García-Valdecasas JC, López-Monclús J, Boscá A, López-Andújar R, Fundora-Suárez J, Villar J, García-Sesma Á, Jiménez C, Rodríguez-Laíz G, Lladó L, Rodríguez JC, Barrera M, Charco R, López-Baena JÁ, Briceño J, Pardo F, Blanco G, Pacheco D, Domínguez-Gil B, Sánchez Turrión V, Fondevila C. Normothermic regional perfusion vs. super-rapid recovery in controlled donation after circulatory death liver transplantation. *J Hepatol* 2019; **70**: 658-665 [PMID: 30582980 DOI: 10.1016/j.jhep.2018.12.013]

42 **Schurink IJ**, de Goeij FHC, Habets LJM, van de Leemkolk FEM, van Dun CAA, Oniscu GC, Alwayn IPJ, Polak WG, Huurman VAL, de Jonge J. Salvage of Declined Extended-criteria DCD Livers Using In Situ Normothermic Regional Perfusion. *Ann Surg* 2022; **276**: e223-e230 [PMID: 35861530 DOI: 10.1097/SLA.0000000000005611]

43 **De Carlis R**, Schlegel A, Frassoni S, Olivieri T, Ravaioli M, Camagni S, Patrono D, Bassi D, Pagano D, Di Sandro S, Lauterio A, Bagnardi V, Gruttadauria S, Cillo U, Romagnoli R, Colledan M, Cescon M, Di Benedetto F, Muiesan P, De Carlis L. How to Preserve Liver Grafts From Circulatory Death With Long Warm Ischemia? A Retrospective Italian Cohort Study With Normothermic Regional Perfusion and Hypothermic Oxygenated Perfusion. *Transplantation* 2021; **105**: 2385-2396 [PMID: 33617211 DOI: 10.1097/TP.0000000000003595]

44 **Gaurav R**, Butler AJ, Kosmoliaptsis V, Mumford L, Fear C, Swift L, Fedotovs A, Upponi S, Khwaja S, Richards J,

Allison M, Watson CJE. Liver Transplantation Outcomes From Controlled Circulatory Death Donors: SCS vs in situ NRP vs ex situ NMP. *Ann Surg* 2022; **275**: 1156-1164 [PMID: 35258511 DOI: 10.1097/SLA.0000000000005428]

45 **Mohkam K**, Nasralla D, Mergental H, Muller X, Butler A, Jassem W, Imber C, Monbaliu D, Perera MTPR, Laing RW, García-Valdecasas JC, Paul A, Dondero F, Cauchy F, Savier E, Scatton O, Robin F, Sulpice L, Bucur P, Salamé E, Pittau G, Allard MA, Pradat P, Rossignol G, Mabrut JY, Ploeg RJ, Friend PJ, Mirza DF, Lesurtel M; Consortium for Organ Preservation in Europe (COPE). In situ normothermic regional perfusion versus ex situ normothermic machine perfusion in liver transplantation from donation after circulatory death. *Liver Transpl* 2022; **28**: 1716-1725 [PMID: 35662403 DOI: 10.1002/lt.26522]

46 **Guarrera JV**, Henry SD, Samstein B, Odeh-Ramadan R, Kinkhabwala M, Goldstein MJ, Ratner LE, Renz JF, Lee HT, Brown RS Jr, Emond JC. Hypothermic machine preservation in human liver transplantation: the first clinical series. *Am J Transplant* 2010; **10**: 372-381 [PMID: 19958323 DOI: 10.1111/j.1600-6143.2009.02932.x]

47 **Schlegel A**, Kron P, Graf R, Clavien PA, Dutkowski P. Hypothermic Oxygenated Perfusion (HOPE) downregulates the immune response in a rat model of liver transplantation. *Ann Surg* 2014; **260**: 931-7; discussion 937 [PMID: 25243553 DOI: 10.1097/SLA.0000000000000941]

48 **Dutkowski P**, Furrer K, Tian Y, Graf R, Clavien PA. Novel short-term hypothermic oxygenated perfusion (HOPE) system prevents injury in rat liver graft from non-heart beating donor. *Ann Surg* 2006; **244**: 968-76; discussion 976 [PMID: 17122622 DOI: 10.1097/01.sla.0000247056.85590.6b]

49 **de Rougemont O**, Breitenstein S, Leskosek B, Weber A, Graf R, Clavien PA, Dutkowski P. One hour hypothermic oxygenated perfusion (HOPE) protects nonviable liver allografts donated after cardiac death. *Ann Surg* 2009; **250**: 674-683 [PMID: 19806056 DOI: 10.1097/SLA.0b013e3181bcb1ee]

50 **Dutkowski P**, Polak WG, Muiesan P, Schlegel A, Verhoeven CJ, Scalera I, DeOliveira ML, Kron P, Clavien PA. First Comparison of Hypothermic Oxygenated PErfusion Versus Static Cold Storage of Human Donation After Cardiac Death Liver Transplants: An International-matched Case Analysis. *Ann Surg* 2015; **262**: 764-70; discussion 770 [PMID: 26583664 DOI: 10.1097/SLA.0000000000001473]

51 **van Rijn R**, Karimian N, Matton APM, Burlage LC, Westerkamp AC, van den Berg AP, de Kleine RHJ, de Boer MT, Lisman T, Porte RJ. Dual hypothermic oxygenated machine perfusion in liver transplants donated after circulatory death. *Br J Surg* 2017; **104**: 907-917 [PMID: 28394402 DOI: 10.1002/bjs.10515]

52 **van Rijn R**, Schurink IJ, de Vries Y, van den Berg AP, Cortes Cerisuelo M, Darwish Murad S, Erdmann JI, Gilbo N, de Haas RJ, Heaton N, van Hoek B, Huurman VAL, Jochmans I, van Leeuwen OB, de Meijer VE, Monbaliu D, Polak WG, Slangen JJG, Troisi RI, Vanlander A, de Jonge J, Porte RJ; DHOPE-DCD Trial Investigators. Hypothermic Machine Perfusion in Liver Transplantation - A Randomized Trial. *N Engl J Med* 2021; **384**: 1391-1401 [PMID: 33626248 DOI: 10.1056/NEJMoa2031532]

53 **de Vries Y**, Brüggenwirth IMA, Karangwa SA, von Meijenfeldt FA, van Leeuwen OB, Burlage LC, de Jong IEM, Gouw ASH, de Meijer VE, Lisman T, Porte RJ. Dual Versus Single Oxygenated Hypothermic Machine Perfusion of Porcine Livers: Impact on Hepatobiliary and Endothelial Cell Injury. *Transplant Direct* 2021; **7**: e741 [PMID: 34386578 DOI: 10.1097/TXD.0000000000001184]

54 **Muller X**, Schlegel A, Kron P, Eshmuminov D, Würdinger M, Meierhofer D, Clavien PA, Dutkowski P. Novel Real-time Prediction of Liver Graft Function During Hypothermic Oxygenated Machine Perfusion Before Liver Transplantation. *Ann Surg* 2019; **270**: 783-790 [PMID: 31592808 DOI: 10.1097/SLA.0000000000003513]

55 **Schlegel A**, Muller X, Kalisvaart M, Muellhaupt B, Perera MTPR, Isaac JR, Clavien PA, Muiesan P, Dutkowski P. Outcomes of DCD liver transplantation using organs treated by hypothermic oxygenated perfusion before implantation. *J Hepatol* 2019; **70**: 50-57 [PMID: 30342115 DOI: 10.1016/j.jhep.2018.10.005]

56 **Ravaioli M**, Germinario G, Dajti G, Sessa M, Vasuri F, Siniscalchi A, Morelli MC, Serenari M, Del Gaudio M, Zanfi C, Odaldi F, Bertuzzo VR, Maroni L, Laurenzi A, Cescon M. Hypothermic oxygenated perfusion in extended criteria donor liver transplantation-A randomized clinical trial. *Am J Transplant* 2022; **22**: 2401-2408 [PMID: 35671067 DOI: 10.1111/ajt.17115]

57 **Czigany Z**, Pratschke J, Froněk J, Guba M, Schöning W, Raptis DA, Andrassy J, Kramer M, Strnad P, Tolba RH, Liu W, Keller T, Miller H, Pavicevic S, Uluk D, Kocik M, Lurje I, Trautwein C, Mehrabi A, Popescu I, Vondran FWR, Ju C, Tacke F, Neumann UP, Lurje G. Hypothermic Oxygenated Machine Perfusion Reduces Early Allograft Injury and Improves Post-transplant Outcomes in Extended Criteria Donation Liver Transplantation From Donation After Brain Death: Results From a Multicenter Randomized Controlled Trial (HOPE ECD-DBD). *Ann Surg* 2021; **274**: 705-712 [PMID: 34334635 DOI: 10.1097/SLA.0000000000005110]

58 **Rayar M**, Beaurepaire JM, Bajeux E, Hamonic S, Renard T, Locher C, Desfourneaux V, Merdrignac A, Bergeat D, Lakehal M, Sulpice L, Houssel-Debry P, Jezequel C, Camus C, Bardou-Jacquet E, Meunier B. Hypothermic Oxygenated Perfusion Improves Extended Criteria Donor Liver Graft Function and Reduces Duration of Hospitalization Without Extra Cost: The PERPHO Study. *Liver Transpl* 2021; **27**: 349-362 [PMID: 33237618 DOI: 10.1002/lt.25955]

59 **Ravaioli M**, De Pace V, Angeletti A, Comai G, Vasuri F, Baldassarre M, Maroni L, Odaldi F, Fallani G, Caraceni P, Germinario G, Donadei C, Malvi D, Del Gaudio M, Bertuzzo VR, Siniscalchi A, Ranieri VM, D'Errico A, Pasquinelli G, Morelli MC, Pinna AD, Cescon M, La Manna G. Hypothermic Oxygenated New Machine Perfusion System in Liver and Kidney Transplantation of Extended Criteria Donors:First Italian Clinical Trial. *Sci Rep* 2020; **10**: 6063 [PMID: 32269237 DOI: 10.1038/s41598-020-62979-9]

60 **Patrono D**, Cussa D, Sciannameo V, Montanari E, Panconesi R, Berchialla P, Lepore M, Gambella A, Rizza G, Catalano G, Mirabella S, Tandoi F, Lupo F, Balagna R, Salizzoni M, Romagnoli R. Outcome of liver transplantation with grafts from brain-dead donors treated with dual hypothermic oxygenated machine perfusion, with particular reference to elderly donors. *Am J Transplant* 2022; **22**: 1382-1395 [PMID: 35150050 DOI: 10.1111/ajt.16996]

61 **Schlegel A**, Mueller M, Muller X, Eden J, Panconesi R, von Felten S, Steigmiller K, Sousa Da Silva RX, de Rougemont O, Mabrut JY, Lesurtel M, Cerisuelo MC, Heaton ND, Allard MA, Adam R, Monbaliu D, Jochmans I, Haring MPD, Porte RJ, Parente A, Muiesan P, Kron P, Attia M, Kollmann D, Berlakovich G, Rogiers X, Petterson K, Kranich AL, Amberg S, Müllhaupt B, Clavien PA, Dutkowski P. A multicenter randomized-controlled trial of hypothermic oxygenated perfusion

(HOPE) for human liver grafts before transplantation. *J Hepatol* 2023; **78**: 783-793 [PMID: 36681160 DOI: 10.1016/j.jhep.2022.12.030]

62 **Ceresa CDL**, Nasralla D, Coussios CC, Friend PJ. The case for normothermic machine perfusion in liver transplantation. *Liver Transpl* 2018; **24**: 269-275 [PMID: 29272051 DOI: 10.1002/lt.25000]

63 **Ravikumar R**, Jassem W, Mergental H, Heaton N, Mirza D, Perera MT, Quaglia A, Holroyd D, Vogel T, Coussios CC, Friend PJ. Liver Transplantation After Ex Vivo Normothermic Machine Preservation: A Phase 1 (First-in-Man) Clinical Trial. *Am J Transplant* 2016; **16**: 1779-1787 [PMID: 26752191 DOI: 10.1111/ajt.13708]

64 **Nasralla D**, Coussios CC, Mergental H, Akhtar MZ, Butler AJ, Ceresa CDL, Chiocchia V, Dutton SJ, García-Valdecasas JC, Heaton N, Imber C, Jassem W, Jochmans I, Karani J, Knight SR, Kocabayoglu P, Malagò M, Mirza D, Morris PJ, Pallan A, Paul A, Pavel M, Perera MTPR, Pirenne J, Ravikumar R, Russell L, Upponi S, Watson CJE, Weissenbacher A, Ploeg RJ, Friend PJ; Consortium for Organ Preservation in Europe. A randomized trial of normothermic preservation in liver transplantation. *Nature* 2018; **557**: 50-56 [PMID: 29670285 DOI: 10.1038/s41586-018-0047-9]

65 **Markmann JF**, Abouljoud MS, Ghobrial RM, Bhati CS, Pelletier SJ, Lu AD, Ottmann S, Klair T, Eymard C, Roll GR, Magliocca J, Pruett TL, Reyes J, Black SM, Marsh CL, Schnickel G, Kinkhabwala M, Florman SS, Merani S, Demetris AJ, Kimura S, Rizzari M, Saharia A, Levy M, Agarwal A, Cigarroa FG, Eason JD, Syed S, Washburn WK, Parekh J, Moon J, Maskin A, Yeh H, Vagefi PA, MacConmara MP. Impact of Portable Normothermic Blood-Based Machine Perfusion on Outcomes of Liver Transplant: The OCS Liver PROTECT Randomized Clinical Trial. *JAMA Surg* 2022; **157**: 189-198 [PMID: 34985503 DOI: 10.1001/jamasurg.2021.6781]

66 **Hann A**, Lembach H, Nutu A, Mergental H, Isaac JL, Isaac JR, Oo YH, Armstrong MJ, Rajoriya N, Afford S, Bartlett D, Mirza DF, Hartog H, Perera MTPR. Assessment of Deceased Brain Dead Donor Liver Grafts *via* Normothermic Machine Perfusion: Lactate Clearance Time Threshold Can Be Safely Extended to 6 Hours. *Liver Transpl* 2022; **28**: 493-496 [PMID: 34606663 DOI: 10.1002/lt.26317]

67 **Mergental H**, Stephenson BTF, Laing RW, Kirkham AJ, Neil DAH, Wallace LL, Boteon YL, Widmer J, Bhogal RH, Perera MTPR, Smith A, Reynolds GM, Yap C, Hübscher SG, Mirza DF, Afford SC. Development of Clinical Criteria for Functional Assessment to Predict Primary Nonfunction of High-Risk Livers Using Normothermic Machine Perfusion. *Liver Transpl* 2018; **24**: 1453-1469 [PMID: 30359490 DOI: 10.1002/lt.25291]

68 **Hann A**, Nutu A, Clarke G, Patel I, Sneiders D, Oo YH, Hartog H, Perera MTPR. Normothermic Machine Perfusion-Improving the Supply of Transplantable Livers for High-Risk Recipients. *Transpl Int* 2022; **35**: 10460 [PMID: 35711320 DOI: 10.3389/ti.2022.10460]

69 **Hann A**, Raza SS, Sneiders D, Nutu A, Mergental H, Mirza DF, Hartog H, Perera MTP. Comment on: Static cold storage compared with normothermic machine perfusion of the liver and effect on ischaemic-type biliary lesions after transplantation: a propensity-score matched study. *Br J Surg* 2021; **109**: e12-e13 [PMID: 34672319 DOI: 10.1093/bjs/znab349]

70 **Mergental H**, Perera MT, Laing RW, Muiesan P, Isaac JR, Smith A, Stephenson BT, Cilliers H, Neil DA, Hübscher SG, Afford SC, Mirza DF. Transplantation of Declined Liver Allografts Following Normothermic Ex-Situ Evaluation. *Am J Transplant* 2016; **16**: 3235-3245 [PMID: 27192971 DOI: 10.1111/ajt.13875]

71 **Mergental H**, Laing RW, Kirkham AJ, Perera MTPR, Boteon YL, Attard J, Barton D, Curbishley S, Wilkhu M, Neil DAH, Hübscher SG, Muiesan P, Isaac JR, Roberts KJ, Abradelo M, Schlegel A, Ferguson J, Cilliers H, Bion J, Adams DH, Morris C, Friend PJ, Yap C, Afford SC, Mirza DF. Transplantation of discarded livers following viability testing with normothermic machine perfusion. *Nat Commun* 2020; **11**: 2939 [PMID: 32546694 DOI: 10.1038/s41467-020-16251-3]

72 **Reiling J**, Butler N, Simpson A, Hodgkinson P, Campbell C, Lockwood D, Bridle K, Santrampurwala N, Britton L, Crawford D, Dejong CHC, Fawcett J. Assessment and Transplantation of Orphan Donor Livers: A Back-to-Base Approach to Normothermic Machine Perfusion. *Liver Transpl* 2020; **26**: 1618-1628 [PMID: 32682340 DOI: 10.1002/lt.25850]

73 **Marcon F**, Schlegel A, Bartlett DC, Kalisvaart M, Bishop D, Mergental H, Roberts KJ, Mirza DF, Isaac J, Muiesan P, Perera MT. Utilization of Declined Liver Grafts Yields Comparable Transplant Outcomes and Previous Decline Should Not Be a Deterrent to Graft Use. *Transplantation* 2018; **102**: e211-e218 [PMID: 29702538 DOI: 10.1097/TP.0000000000002127]

74 **Ghinolfi D**, Rreka E, De Tata V, Franzini M, Pezzati D, Fierabracci V, Masini M, Cacciatoinsilla A, Bindi ML, Marselli L, Mazzotti V, Morganti R, Marchetti P, Biancofiore G, Campani D, Paolicchi A, De Simone P. Pilot, Open, Randomized, Prospective Trial for Normothermic Machine Perfusion Evaluation in Liver Transplantation From Older Donors. *Liver Transpl* 2019; **25**: 436-449 [PMID: 30362649 DOI: 10.1002/lt.25362]

75 **Fodor M**, Cardini B, Peter W, Weissenbacher A, Oberhuber R, Hautz T, Otarashvili G, Margreiter C, Maglione M, Resch T, Krendl F, Meszaros AT, Bogensperger C, Gasteiger S, Messner F, Henninger B, Zoller H, Tilg H, Öfner D, Schneeberger S. Static cold storage compared with normothermic machine perfusion of the liver and effect on ischaemic-type biliary lesions after transplantation: a propensity score-matched study. *Br J Surg* 2021; **108**: 1082-1089 [PMID: 34027968 DOI: 10.1093/bjs/znab118]

76 **Matton APM**, de Vries Y, Burlage LC, van Rijn R, Fujiyoshi M, de Meijer VE, de Boer MT, de Kleine RHJ, Verkade HJ, Gouw ASH, Lisman T, Porte RJ. Biliary Bicarbonate, pH, and Glucose Are Suitable Biomarkers of Biliary Viability During Ex Situ Normothermic Machine Perfusion of Human Donor Livers. *Transplantation* 2019; **103**: 1405-1413 [PMID: 30395120 DOI: 10.1097/TP.0000000000002500]

77 **Watson CJE**, Kosmoliaptsis V, Pley C, Randle L, Fear C, Crick K, Gimson AE, Allison M, Upponi S, Brais R, Jochmans I, Butler AJ. Observations on the ex situ perfusion of livers for transplantation. *Am J Transplant* 2018; **18**: 2005-2020 [PMID: 29419931 DOI: 10.1111/ajt.14687]

78 **Watson CJE**, Gaurav R, Fear C, Swift L, Selves L, Ceresa CDL, Upponi SS, Brais R, Allison M, Macdonald-Wallis C, Taylor R, Butler AJ. Predicting Early Allograft Function After Normothermic Machine Perfusion. *Transplantation* 2022; **106**: 2391-2398 [PMID: 36044364 DOI: 10.1097/TP.0000000000004263]

79 **Ghinolfi D**, Dondossola D, Rreka E, Lonati C, Pezzati D, Cacciatoinsilla A, Kersik A, Lazzeri C, Zanella A, Peris A, Maggioni M, Biancofiore G, Reggiani P, Morganti R, De Simone P, Rossi G. Sequential Use of Normothermic Regional and Ex Situ Machine Perfusion in Donation After Circulatory Death Liver Transplant. *Liver Transpl* 2021; **27**: 385-402

[PMID: 32949117 DOI: 10.1002/lt.25899]

80 **van Leeuwen OB**, Bodewes SB, Lantinga VA, Haring MPD, Thorne AM, Brüggenwirth IMA, van den Berg AP, de Boer MT, de Jong IEM, de Kleine RHJ, Lascaris B, Nijsten MWN, Reyntjens KMEM, de Meijer VE, Porte RJ. Sequential hypothermic and normothermic machine perfusion enables safe transplantation of high-risk donor livers. *Am J Transplant* 2022; **22**: 1658-1670 [PMID: 35286759 DOI: 10.1111/ajt.17022]

81 **Guo Z**, Zhao Q, Huang S, Huang C, Wang D, Yang L, Zhang J, Chen M, Wu L, Zhang Z, Zhu Z, Wang L, Zhu C, Zhang Y, Tang Y, Sun C, Xiong W, Shen Y, Chen X, Xu J, Wang T, Ma Y, Hu A, Chen Y, Zhu X, Rong J, Cai C, Gong F, Guan X, Huang W, Ko DS, Li X, Tullius SG, Huang J, Ju W, He X. Ischaemia-free liver transplantation in humans: a first-in-human trial. *Lancet Reg Health West Pac* 2021; **16**: 100260 [PMID: 34590063 DOI: 10.1016/j.lanwpc.2021.100260]

82 **Hann A**, Lembach H, Nutu A, Dassanayake B, Tillakaratne S, McKay SC, Boteon APCS, Boteon YL, Mergental H, Murphy N, Bangash MN, Neil DAH, Issac JL, Javed N, Faulkner T, Bennet D, Moore R, Vasanth S, Subash G, Cuell J, Rao R, Cilliers H, Russel S, Haydon G, Mutimer D, Roberts KJ, Mirza DF, Ferguson J, Bartlett D, Isaac JR, Rajoriya N, Armstrong MJ, Hartog H, Perera MTPR. Outcomes of normothermic machine perfusion of liver grafts in repeat liver transplantation (NAPLES initiative). *Br J Surg* 2022; **109**: 372-380 [PMID: 35170730 DOI: 10.1093/bjs/znab475]

83 **Bral M**, Dajani K, Leon Izquierdo D, Bigam D, Kneteman N, Ceresa CDL, Friend PJ, Shapiro AMJ. A Back-to-Base Experience of Human Normothermic Ex Situ Liver Perfusion: Does the Chill Kill? *Liver Transpl* 2019; **25**: 848-858 [PMID: 30938039 DOI: 10.1002/lt.25464]

84 **Liu Q**, Hassan A, Pezzati D, Soliman B, Lomaglio L, Grady P, Del Angel Diaz L, Simioni A, Maikhor S, Etterling J, D'Amico G, Iuppa G, Diago Uso T, Hashimoto K, Aucejo F, Fujiki M, Eghtesad B, Sasaki K, Kwon CHD, Cywinski J, Irefin S, Bennett A, Baldwin W, Miller C, Quintini C. Ex Situ Liver Machine Perfusion: The Impact of Fresh Frozen Plasma. *Liver Transpl* 2020; **26**: 215-226 [PMID: 31642164 DOI: 10.1002/lt.25668]

85 **Bral M**, Gala-Lopez B, Bigam D, Kneteman N, Malcolm A, Livingstone S, Andres A, Emamaullee J, Russell L, Coussios C, West LJ, Friend PJ, Shapiro AM. Preliminary Single-Center Canadian Experience of Human Normothermic Ex Vivo Liver Perfusion: Results of a Clinical Trial. *Am J Transplant* 2017; **17**: 1071-1080 [PMID: 27639262 DOI: 10.1111/ajt.14049]

World Journal of Gastroenterology

Submit a Manuscript: https://www.f6publishing.com

World J Gastroenterol 2023 May 28; 29(20): 3084-3102

DOI: 10.3748/wjg.v29.i20.3084

ISSN 1007-9327 (print) ISSN 2219-2840 (online)

ORIGINAL ARTICLE

Basic Study

Metronomic capecitabine inhibits liver transplant rejection in rats by triggering recipients' T cell ferroptosis

Hao Wang, Zheng-Lu Wang, Sai Zhang, De-Jun Kong, Rui-Ning Yang, Lei Cao, Jian-Xi Wang, Sei Yoshida, Zhuo-Lun Song, Tao Liu, Shun-Li Fan, Jia-Shu Ren, Jiang-Hong Li, Zhong-Yang Shen, Hong Zheng

Specialty type: Gastroenterology and hepatology

Provenance and peer review: Unsolicited article; Externally peer reviewed.

Peer-review model: Single blind

Peer-review report's scientific quality classification

Grade A (Excellent): 0
Grade B (Very good): B
Grade C (Good): C, C
Grade D (Fair): 0
Grade E (Poor): 0

P-Reviewer: Boteon YL, Brazil; Chun JW, Korea

Received: January 21, 2023
Peer-review started: January 21, 2023
First decision: February 7, 2023
Revised: February 19, 2023
Accepted: April 28, 2023
Article in press: April 28, 2023
Published online: May 28, 2023

Hao Wang, Rui-Ning Yang, Jia-Shu Ren, Jiang-Hong Li, The First Central Clinical School, Tianjin Medical University, Tianjin 300190, China

Zheng-Lu Wang, Zhuo-Lun Song, Shun-Li Fan, Zhong-Yang Shen, Hong Zheng, Department of Organ Transplant, Tianjin First Central Hospital, School of Medicine, Nankai University, Tianjin 300190, China

Zheng-Lu Wang, Zhong-Yang Shen, Hong Zheng, Key Laboratory of Transplant Medicine, Chinese Academy of Medical Sciences, Tianjin 300190, China

Sai Zhang, De-Jun Kong, School of Medicine, Nankai University, Tianjin 300190, China

Lei Cao, Jian-Xi Wang, Sei Yoshida, Zhong-Yang Shen, Hong Zheng, Research Institute of Transplant Medicine, Nankai University, Tianjin 300071, China

Lei Cao, Jian-Xi Wang, Zhong-Yang Shen, Hong Zheng, Tianjin Key Laboratory for Organ Transplantation, Tianjin First Central Hospital, School of Medicine, Nankai University, Tianjin 300071, China

Tao Liu, Zhong-Yang Shen, Hong Zheng, National Health Commission's Key Laboratory for Critical Care Medicine, Tianjin First Central Hospital, Tianjin 300071, China

Corresponding author: Hong Zheng, PhD, Professor, Department of Organ Transplant, Tianjin First Central Hospital, School of Medicine, Nankai University, No. 24 Fukang Road, Nankai District, Tianjin 300190, China. zhenghongyx@139.com

Abstract

BACKGROUND

Capecitabine (CAP) is a classic antimetabolic drug and has shown potential antirejection effects after liver transplantation (LT) in clinical studies. Our previous study showed that metronomic CAP can cause the programmed death of T cells by inducing oxidative stress in healthy mice. Ferroptosis, a newly defined non-apoptotic cell death that occurs in response to iron overload and lethal levels of lipid peroxidation, is an important mechanism by which CAP induces cell death. Therefore, ferroptosis may also play an important role in CAP-induced T cell death and play an immunosuppressive role in acute rejection after transplantation.

AIM
To investigate the functions and underlying mechanisms of antirejection effects of metronomic CAP.

METHODS
A rat LT model of acute rejection was established, and the effect of metronomic CAP on splenic hematopoietic function and acute graft rejection was evaluated 7 d after LT. *In vitro*, primary $CD3^+$ T cells were sorted from rat spleens and human peripheral blood, and co-cultured with or without 5-fluorouracil (5-FU) (active agent of CAP). The levels of ferroptosis-related proteins, ferrous ion concentration, and oxidative stress-related indicators were observed. The changes in mitochondrial structure were observed using electron microscopy.

RESULTS
With no significant myelotoxicity, metronomic CAP alleviated graft injury (Banff score 9 *vs* 7.333, $P < 0.001$), prolonged the survival time of the recipient rats (11.5 d *vs* 16 d, $P < 0.01$), and reduced the infiltration rate of $CD3^+$ T cells in peripheral blood (6.859 *vs* 3.735, $P < 0.001$), liver graft (7.459 *vs* 3.432, $P < 0.001$), and spleen (26.92 *vs* 12.9, $P < 0.001$), thereby inhibiting acute rejection after LT. *In vitro*, 5-FU, an end product of CAP metabolism, induced the degradation of the ferritin heavy chain by upregulating nuclear receptor coactivator 4, which caused the accumulation of ferrous ions. It also inhibited nuclear erythroid 2 p45-related factor 2, heme oxygenase-1, and glutathione peroxidase 4, eventually leading to oxidative damage and ferroptosis of T cells.

CONCLUSION
Metronomic CAP can suppress acute allograft rejection in rats by triggering $CD3^+$ T cell ferroptosis, which makes it an effective immunosuppressive agent after LT.

Key Words: Capecitabine; Ferroptosis; T Lymphocytes; Immunosuppressive agents; Graft rejection; Liver transplantation

©The Author(s) 2023. Published by Baishideng Publishing Group Inc. All rights reserved.

Core Tip: Our studies proved that metronomic capecitabine (CAP) alleviated the acute rejection after transplantation in rats without the common side effect of myelosuppression. T cell ferroptosis is the underlying mechanism behind the antirejection effect of CAP, which can induce cell ferrous ions overload and suppress the nuclear erythroid 2 p45-related factor 2, heme oxygenase-1/glutathione peroxidase 4 antioxidant systems, thereby directly increasing the levels of intracellular reactive oxygen species, and leading to severe oxidative damage in T cells. These results revealed a new mechanism of CAP-induced T cell programmed death and suggested the possibility of using CAP as an immunosuppressant after transplantation.

Citation: Wang H, Wang ZL, Zhang S, Kong DJ, Yang RN, Cao L, Wang JX, Yoshida S, Song ZL, Liu T, Fan SL, Ren JS, Li JH, Shen ZY, Zheng H. Metronomic capecitabine inhibits liver transplant rejection in rats by triggering recipients' T cell ferroptosis. *World J Gastroenterol* 2023; 29(20): 3084-3102
URL: https://www.wjgnet.com/1007-9327/full/v29/i20/3084.htm
DOI: https://dx.doi.org/10.3748/wjg.v29.i20.3084

INTRODUCTION

Recurrence of hepatocellular carcinoma (HCC) represents a serious issue after liver transplantation (LT), and is closely related to the usage of immunosuppressant drugs[1-3]. As a classic antimetabolic chemotherapeutic agent, capecitabine (CAP) is widely used in the treatment of cancers and has also shown good effects on HCC[4,5]. Metronomic CAP is suitable for long-term oral administration with low adverse effects and without sacrificing treatment efficacy[6,7]. In patients with recurrent liver cancer after LT, Ravaioli *et al*[8] showed that metronomic CAP achieved similar efficacy to sorafenib, a protein kinase inhibitor approved for HCC but with a high incidence of adverse effects[9]. Interestingly, no acute rejection was seen, suggesting that CAP may have both immunosuppressive and anticarcinogenic effects. CAP is a fluoropyrimidine prodrug that is metabolized in a three-step process to 5-fluorouracil (5-FU)[10]. The last step requires thymidine phosphorylase (TP), the distribution of which determines CAP distribution. This partially explains its different pharmacological characteristics

compared to 5-FU. Because TP is highly expressed in cancer cells and lymphocytes[11,12], the administration of CAP to LT patients with HCC may increase tumor killing while preventing graft rejection. In preliminary work, we found that the differential expression of TP avoided CAP's side effects of myelosuppression and suppressed normal mouse immune responses by inducing T cell apoptosis[13]. However, it is not clear what effect CAP has during the immune activation that follows transplantation, which is key to its use as an immunosuppressant.

Ferroptosis is a newly defined nonapoptotic cell death that occurs with iron overload and lethal levels of lipid peroxidation[14-16]. Ferroptosis is tightly regulated by iron metabolism, while ferritin is the major intracellular iron storage protein complex. Ferritinophagy activation depends on nuclear receptor coactivator 4 (NCOA4) to transport ferritin to the autophagosome and degrade ferritin to increase intracellular iron levels[17,18]. Subsequently, free ferrous ions overload results in oxidative injury by the Fenton reaction. Although the regulatory mechanisms of ferroptosis are poorly understood, some molecules with antioxidant effects may be implicated, such as nuclear erythroid 2 p45-related factor 2 (Nrf2)[19,20], heme oxygenase-1 (HO-1)[21], and glutathione peroxidase 4 (GPX4)[22]. Overall, free ferrous ions result in reactive oxygen species (ROS) generation and oxidative injury, whereas the Nrf2-HO-1/GPX4 antioxidative system protects cells from oxidative damage induced by ferroptosis[23]. In mouse models and *in vitro*, 5-FU mediates injuries in intestinal mucosal cells, such as those occurring during chemotherapy, by reducing Nrf2 expression and increasing ferroptosis[24]. 5-FU also leads to ROS and iron homeostasis-dependent ferroptosis in myocardial cells by reducing the expression of GPX4 and ferritin heavy chain (FTH1) but enhancing the expression of transferrin receptor 1[25]. Thus, mechanistically, ferroptosis plays an important role in the cell-killing effect of 5-FU.

Our previous study indicated that metronomic CAP can increase ROS levels and reduce mitochondrial membrane potential (MMP), thus affecting the immune system of mice[13]. Those results prompted us to further explore whether ferroptosis plays a significant role in 5-FU-induced immunosuppression. In this study, we investigated the effect of metronomic CAP on acute rejection in a rat model of LT, and determined how ferroptosis affects 5-FU-induced immunosuppression. Elucidating the possible mechanism of CAP as an immunosuppressant with anticancer effects is of great relevance to optimize drug regimens for HCC patients after LT in the future.

MATERIALS AND METHODS

Animals

Specific-pathogen-free male Lewis rats (donors) and male Brown Norway rats (recipients) aged 8–10 wk and weighing 250–300 g were obtained from Beijing Vital River Laboratory Animal Technology Co. Ltd. (Beijing, China). The rats were housed in a standard room, and fed filtered clean water and standard laboratory food. To acclimatize, the rats were housed 1 wk before transplantation. According to different postoperative medication regimens, the rats were randomized to untreated control group (CON) (0.9% saline, ig) and metronomic capecitabine-treated (MET) groups (CAP 100 mg/kg/d, ig). A total of 12 recipients (6 rats/group) were used for postoperative specimen collection at 7 d after transplantation, and another 12 recipients (6 rats/group) were used to observe survival. All invasive procedures and specimen collection were performed under isoflurane anesthesia to minimize pain or discomfort.

Orthotopic LT in rats

Anesthesia was induced with isoflurane and orthotopic LT was performed based on Kamada's two-cuff method. The anhepatic phase was controlled within 26 min[26,27]. After transplantation, the rats received 2 mL Ringer's lactate to replenish blood volume and were rewarmed in an incubator at 37 ℃ for 30 min. On day 7 after LT, an overdose of pentobarbital (150 mg/kg) was injected intraperitoneally for euthanasia. Femur, blood, spleen, and the transplanted liver were collected for further examination.

Routine blood tests

Whole blood was used for blood routine tests 7 d after LT. These were performed with an automatic hematology analyzer (BC-2800Vet; Mindray, Shenzhen, China).

Peripheral blood lymphocyte $CD3^+$ T cell count

Peripheral blood lymphocyte $CD3^+$ T cell count was obtained based on peripheral blood lymphocyte count and flow cytometric analysis of the $CD3^+$ T cell ratio.

Liver function assay

Serum levels of aspartate aminotransferase (AST), alanine aminotransferase (ALT), total bilirubin (TBIL), and direct bilirubin (DBIL) were measured using kits (Mindray, Shenzhen, China) and read with an automatic biochemical analyzer (BS-240VET; Mindray, Shenzhen, China).

Flow cytometric analysis

Rat peripheral blood mononuclear cells were isolated by gradient centrifugation with a rat peripheral blood mononuclear cell separation solution (Solarbio, Beijing, China). Anti-CD3 antibodies (APC anti-rat CD3 Antibody, Cat# 201414; RRID: AB_2563366 BioLegend, San Diego, CA, United States) were used for extracellular staining to identify CD3-positive lymphocytes. Flow cytometry was performed using the Accuri C6 Plus flow cytometry (BD Biosciences, Palo Alto, CA, United States), and FlowJo software (TreeStar, Woodburn, OR, United States) was used for data analysis.

The ferrous levels in T cells were measured using FerroOrange (Cat# MX4559, Maokang Biotechnology, Shanghai, China). Cells were incubated with FerroOrange (37 ℃, 20 min) for fluorescence detection. To measure intracellular ROS, cells were resuspended in phosphate-buffered saline (PBS) containing DCFH-DA (Cat# CA1410, Solarbio, Beijing, China) at 37 ℃ for 30 min and washed twice with PBS for fluorescence detection. To measure the lipid ROS of T cells, C11-BODIPY 581/591 (Cat# MX5211, Maokang Biotechnology, Shanghai, China) was added and incubated at 37 ℃ with 5% CO_2 for 30 min. Cells were then washed twice before fluorescence detection. The MMP Assay Kit (Cat# M8650, Solarbio, Beijing, China) was used to measure the MMP in T cells. Cells were incubated with JC-1 working solution at 37 ℃ for 20 min, then washed twice with JC-1 buffer for fluorescence detection. BODIPY emission was recorded on an oxidized C11 signal (FITC channel).

Luminex assay

The rat sera were analyzed for cytokine concentrations [interleukin (IL)-10, IL-2, IL-1α, IL-4, interferon gamma (IFN-γ), tumor necrosis factor alpha (TNF-α), IL-5, IL-6, growth-regulated oncogene (GRO)/keratinocyte chemoattractant (KC), IL-12p70] using the Millipore Luminex 200 instrument (Luminex Corporation, Austin, TX, United States), after incubation of the samples with beads according to the manufacturer's instructions. The quantification was performed with Luminex xPonent version 3.1 software.

Cell culture

Healthy mononuclear cells from the spleen of rats and peripheral blood of humans were collected by gradient centrifugation with respectively, rat tissue mononuclear cell separation solution (Solarbio, Beijing, China) and human peripheral blood mononuclear cell separation solution (Solarbio, Beijing, China). T cells were purified through positive magnetic selection using microbeads (Miltenyi Biotec, Bergisch Gladbac, Germany) and cultivated at 2.0×10^6 cells/well in 6-well plates with RPMI-1640 with 5% fetal bovine serum and 100 IU/mL IL-2. Within the first 72 h, the anti-CD3/CD28 antibody (Cat# 201401, RRID: AB_893302; 2 μg/mL and Cat# 200902, RRID: AB_313891; 1 μg/mL) were used to stimulate the T cells.

Cell proliferation assay

The Cell Counting Kit-8 (CCK-8) assay (Boster, Hubei, China) was used to evaluate T cell proliferation *in vitro*. The CON group (n = 3), 5-FU group (5-FU 15 μmol/L, MCE, Shanghai, China; n = 3); ferrostatin-1 (Fer-1) group (Fer-1 2 μmol/L, MCE, Shanghai, China; n = 3); 5-FU+fer-1 group (5-FU 15 μmol/L + fer-1 2 μmol/L) were included. After 72 h of culture, CCK-8 solution was added to each well of the 96-well plates and allowed to incubate for 2 h at 37 ℃, and the optical density value at 450 nm was recorded.

Histopathology

The femurs and grafts (n = 6 for each group) were removed on postoperative day 7. The femurs were decalcified with EDTA decalcifying solution (Solarbio, Beijing, China). Then both femurs and grafts were fixed in 10% paraformaldehyde, dehydrated, paraffin-embedded, cut into 4 μm slides, and stained with hematoxylin and eosin (H&E; G1120; Solarbio, Beijing, China).

Immunohistochemistry

$CD3^+$ cell infiltration was assessed on spleen and liver graft sections as follows: Tissue sections were heated for 15 min in EDTA (pH 8.0) in a microwave for antigen retrieval, incubated in 3% hydrogen peroxide for 30 min to eliminate endogenous peroxidase activity, and blocked in normal goat serum. Then the sections were incubated overnight at 4 ℃ with a rat anti-CD3 antibody (CD3-12, Cat# ab11089, RRID: AB_2889189; Abcam, Cambridge, MA, United States) and incubated with a secondary antibody (Goat Anti-Rat IgG H&L, Cat# ab97057, RRID: AB_10680316; Abcam, Cambridge, MA, United States) or 30 min at room temperature the next day. Finally, the sections were stained with freshly prepared diaminobenzidine solution and counterstained with hematoxylin. ImageJ software was applied to 200 × images to quantify the CD3-positive fields.

Transmission electron microscopy

Cells were collected after centrifugation and fixed in 2.5% glutaraldehyde. After dehydration through graded ethanol, the cells were embedded in epoxy resins and cut into ultrathin sections. The

morphologic changes in mitochondrial ultrastructure were observed using a transmission electron microscope (HT7800; Hitachi, Tokyo, Japan).

Western blot analysis

Total protein was extracted using RIPA buffer containing protease and phosphatase inhibitors. The mixture was placed on ice for 30 min for cell lysis, and then centrifuged at 12000 g for 15 min at 4 ℃ to discard the cell debris. Total protein concentration was quantified by the BCA Protein Assay Kit (Beyotime Biotechnology, Beijing, China). The proteins were resolved by sodium dodecyl sulfate-polyacrylamide gel electrophoresis, electrotransferred to polyvinylidene fluoride membranes, and blocked in 5% skimmed milk for 1 h. Then the membranes were incubated overnight at 4 ℃ with primary antibodies against FTH1 (EPR18878, Cat# ab183781; Abcam, Cambridge, MA, United States), NCOA4 (Cat# PA5-96398, RRID: AB_2808200; Thermo Fisher Scientific, Waltham, MA, United States), Nrf2 (E5F1A, Cat# 20733S, Cell Signaling Technology, Danvers, MA, United States), HO-1 (EPR1390Y, Cat# ab68477, RRID: AB_11156457; Abcam, Cambridge, MA, United States), and GPX4 (EPNCIR144, Cat# ab125066, RRID: AB_10973901; Abcam, Cambridge, MA, United States). β-actin (SP124, Cat# ab115777, RRID: AB_10899528; Abcam, Cambridge, MA, United States) antibody served as the internal control. The membranes were washed and then incubated with a secondary antibody (Goat anti-Rabbit IgG H+L, Cat# A16110; Thermo Fisher Scientific, Shanghai, China) for 1 h at RT. Proteins were detected with an imaging system (Bio-Rad, Hercules, CA, United States), and band intensities were analyzed with ImageJ software (National Institutes of Health, Bethesda, MD, United States).

Statistical analyses

The statistical analyses were performed with SPSS 23.0 (IBM Analytics) and GraphPad 8.0 (GraphPad Software). The statistical methods of this study were reviewed by Yuan Wang from the Department of Biostatistics and Epidemiology, The First Central Clinical School, Tianjin Medical University. Data are presented as the mean ± standard error of the mean. The unpaired *t*-test was used to assess the differences between the two groups, and a one-way analysis of variance was used to assess the differences among three or more groups. $P < 0.05$ was considered statistically significant.

RESULTS

Metronomic CAP exerts a marginal myelosuppressive effect, compatible with continuous administration

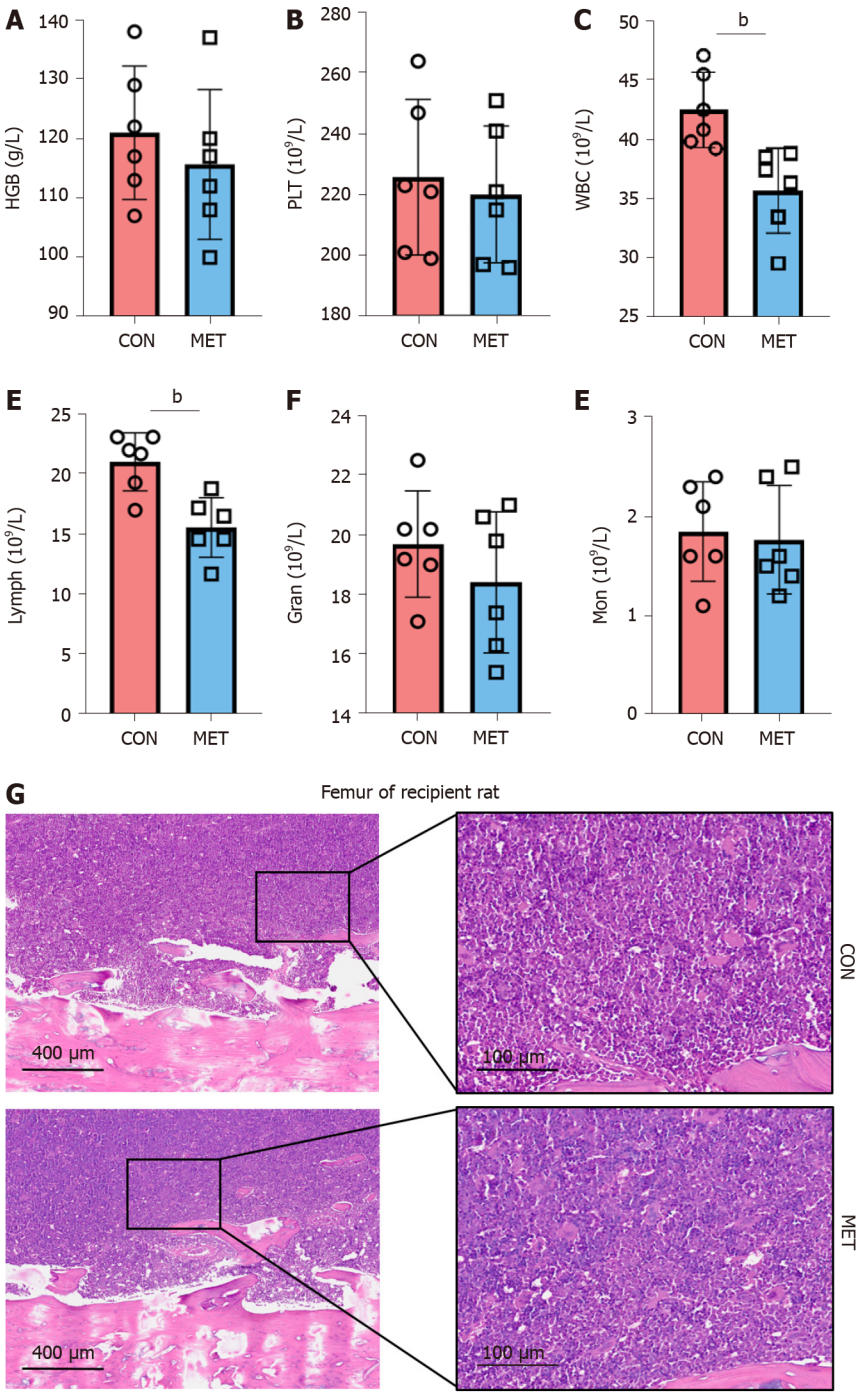
5-FU, the end product of CAP, may induce myelotoxicity. Thus, we first evaluated metronomic CAP's myelotoxicity on peripheral blood hemoglobin (HGB), platelets (PLTs), and leukocytes in a rat model of orthotopic LT, where recipient Brown-Norway rats received the livers from Lewis rats. Seven days after LT, there was no significant difference in the index of HGB and PLTs between the CON group and the MET group (Figure 1A and B). However, leukopenia with a reduced number of lymphocytes was found in the MET group, while the number of other leukocyte subsets (granulocytes and mononuclear cells) was not significantly different (Figure 1C–F). These results suggest that CAP had a relatively targeted killing effect on lymphocytes, but no obvious effect on PLTs, erythrocytes, monocytes, or granulocytes. In the bone marrow, the rats in the MET group had no pathological manifestation of myelosuppression (Figure 1G), suggesting that the lymphocytopenia caused by CAP did not result from myelosuppression.

Metronomic CAP reduces acute rejection and alleviates graft injury

To evaluate the effect of metronomic CAP during acute rejection, the grafted livers were harvested on day 7 after LT for histopathological examination. As shown in Figure 2A, prominent acute rejection with severe bile duct damage, endothelitis, and hepatocyte vacuolation occurred in the grafts of the CON group. Portal areas were infiltrated by inflammatory cells, hepatic sinusoids were greatly expanded, and the sinusoidal endothelial cells were markedly swollen. Compared with the CON group, acute rejection in the MET group was ameliorated, as evidenced by inflammatory cell infiltration being confined to only some of the portal areas and the degeneration of a few bile duct epithelia. The Banff scores[28] decreased in the MET group compared with the CON group (Figure 2B). On day 7 after LT, liver damage was assessed by measuring serum levels of AST and ALT (Figure 2C and D). Compared with the CON group, CAP significantly decreased the serum levels of ALT and AST. However, TBIL and DBIL in both groups showed an increasing trend after the operation, but there was no significant difference between the two groups (Figure 2E and F). In the survival analysis, a log-rank (Mantel Cox) test was conducted. Rats in the MET group had a longer survival time compared with the CON group (Figure 2G, median survival time: 16.5 and 11.5 d; $P < 0.01$).

Metronomic CAP reduces the number of $CD3^+$ T cells in graft recipients

Next, to investigate whether the inhibition of acute rejection by metronomic CAP involved an effect on



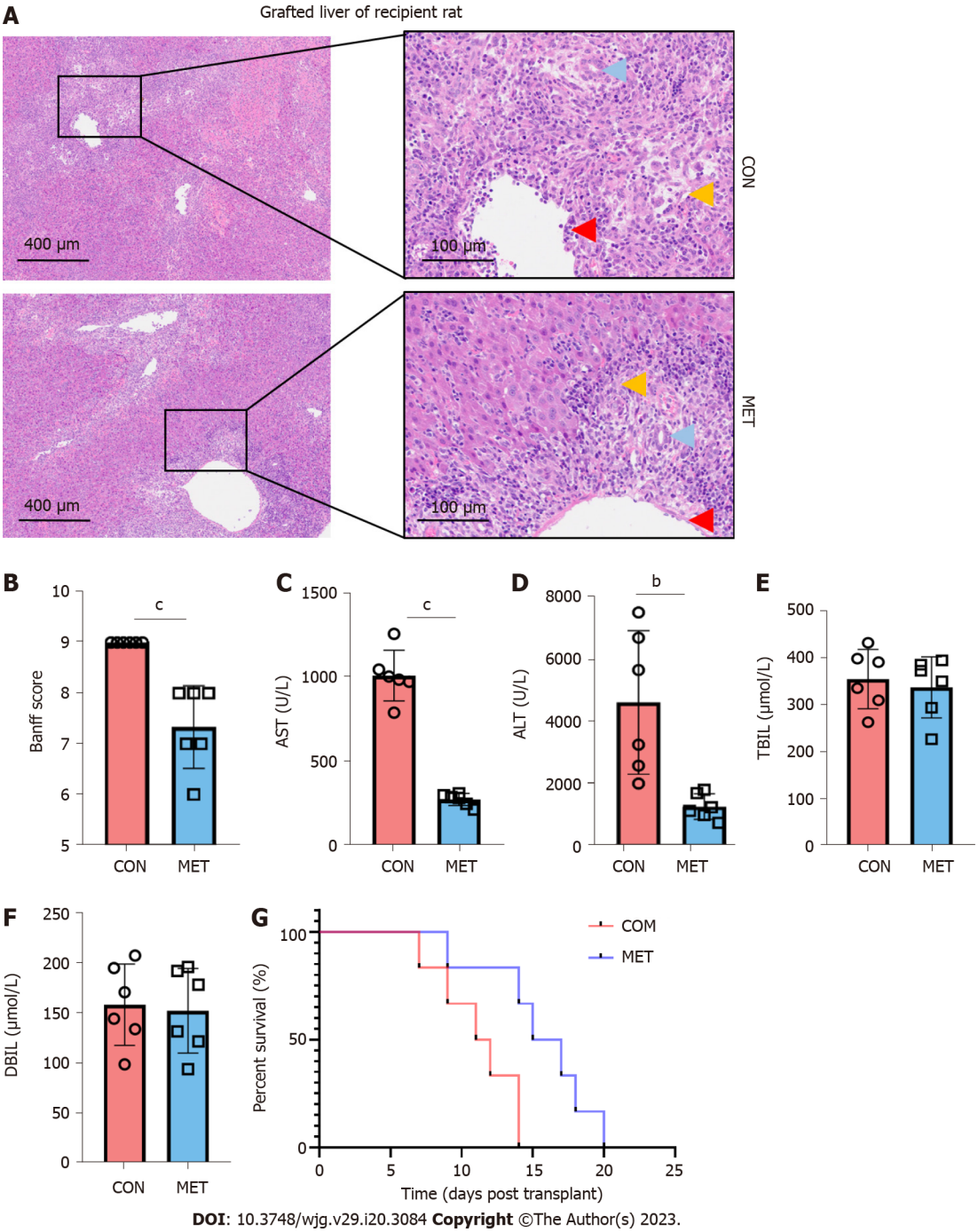
DOI: 10.3748/wjg.v29.i20.3084 **Copyright** ©The Author(s) 2023.

Figure 1 Metronomic capecitabine showed no significant myelosuppression. A and B: Hemoglobin level and platelets count in the peripheral blood; C-F: White blood cells, lymphocytes, granulocytes, and monocytes counts in the peripheral blood; G: Bone marrow tissue was stained with hematoxylin and eosin (50 × and 200 ×). Statistical analysis was done by unpaired *t*-test, $n = 6$. Data are shown as mean ± SD; $^bP < 0.01$ *vs* the control group. CON: Untreated control groups, rats received 0.9% normal saline for 7 d; MET: Metronomic capecitabine (CAP)-treated groups, rats received metronomic CAP (100 mg/kg/d) treated for 7 d; HGB: Hemoglobin; PLT: Platelets; WBC: White blood cells; lymph: Lymphocytes; Gran: Granulocytes; Mon: Monocytes.

T cells, $CD3^+$ T cells in the peripheral blood, grafts, and spleens were analyzed. Compared to the CON group, the $CD3^+$ T cells in the peripheral blood were significantly lower in the MET group (Figure 3A and B). In addition, a large number of $CD3^+$ T cells was localized in the portal canal area of the CON group. Infiltrated $CD3^+$ T cells in both the liver and spleen were significantly reduced in the MET group (Figure 3C and D). These results indicate that metronomic CAP can decrease the number of $CD3^+$ T cells in the peripheral blood, liver, and spleen of the recipient rats.

Metronomic CAP regulates serum cytokine levels

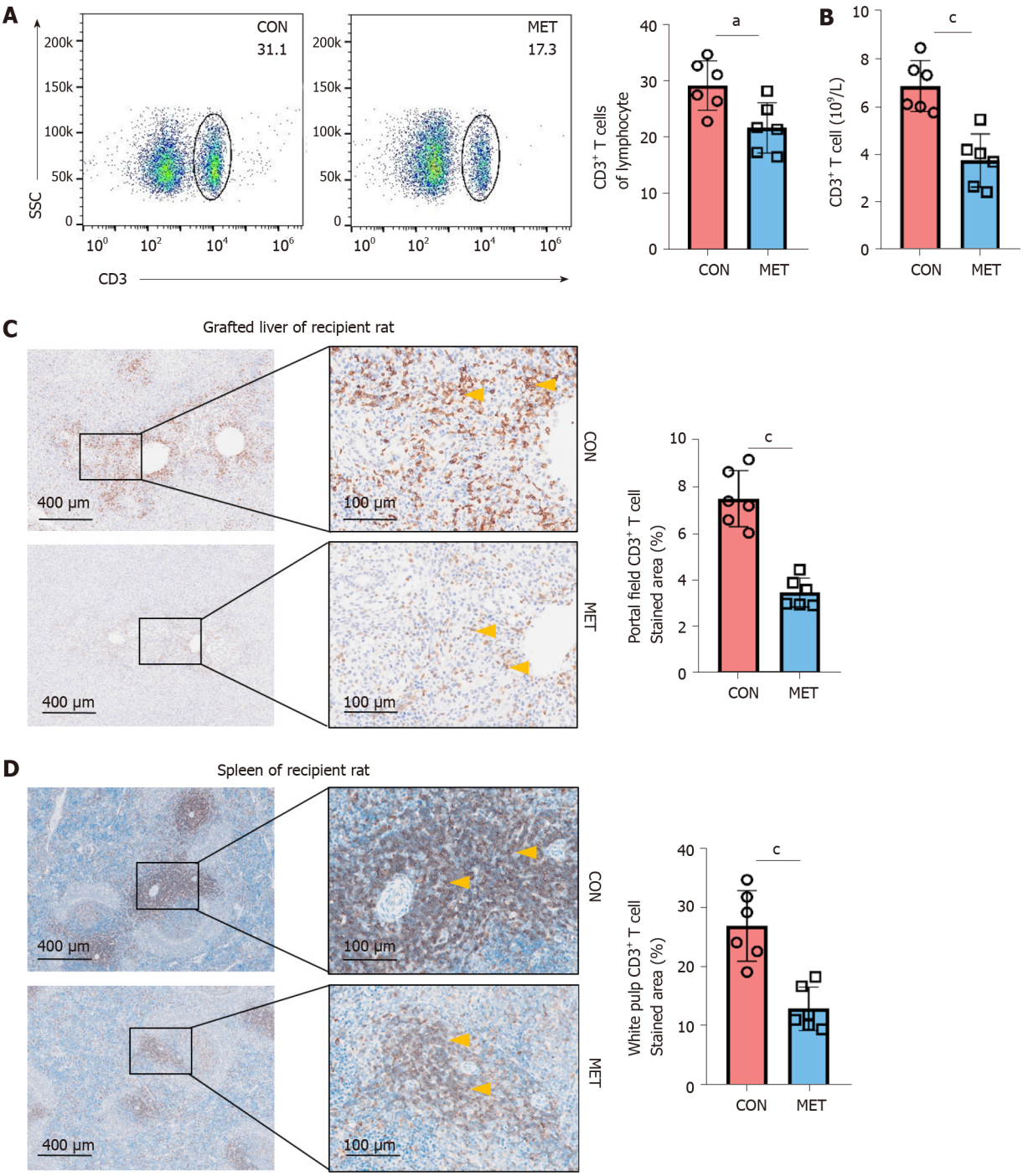
Cytokines are an important reflection of immune cell function and immune status. Thus, the levels of



DOI: 10.3748/wjg.v29.i20.3084 **Copyright** ©The Author(s) 2023.

Figure 2 Metronomic capecitabine improves liver function and ameliorates liver allograft rejection. A: Liver allograft tissue was stained with hematoxylin and eosin (50 × and 200 ×). Liver tissue, portal vein, and bile duct were significantly injured in the untreated control group (CON), with a large number of inflammatory cells infiltrated. In the metronomic capecitabine-treated groups (MET), liver tissue destruction was relatively mild, with limited infiltration of inflammatory cells (yellow arrows), relatively little degeneration of portal vein endothelium (red arrows), and bile duct epithelium (blue arrows); B: The severity of acute rejection was graded according to the Banff liver rejection criteria; C-F: Alanine transaminase, aspartate transaminase, total bilirubin, and direct bilirubin levels in the peripheral blood; G: Survival analysis of rats after liver transplantation. The median survival time of the CON and MET groups were 11.5 d and 16 d, respectively ($P < 0.01$). The survival analysis was done by log-rank (Mantel Cox) test, $n = 6$. Statistical analysis was done by unpaired *t*-test, $n = 6$. Data are shown as mean ± SD; $^{b}P < 0.01$ *vs* the control group, $^{c}P < 0.001$ *vs* the control group. CON: Untreated control groups, rats received 0.9% normal saline for 7 d; MET: Metronomic capecitabine (CAP)-treated groups, rats received metronomic CAP (100 mg/kg/d) treated for 7 d; ALT: Alanine transaminase; AST: Aspartate transaminase; TBIL: Total bilirubin; DBIL: Direct bilirubin.

IFN-γ, TNF-α, human GRO/KC, IL-1β, IL-2, IL-4, IL-5, IL-6, IL-10, and IL-12p70 in peripheral blood and graft were quantified by Luminex assay. As shown in Figure 4, the levels of pro-inflammatory IFN-γ, TNF-α, IL-2, and IL-12p70 in the MET group were significantly lower than those in the CON group. Other cytokines (IL-1β, IL-5, IL-6, IL-4, IL-10, and GRO/KC) did not show significant changes (Supplementary Figure 1). The results showed that metronomic CAP plays an immunosuppressive role by downregulating the concentration of pro-inflammatory cytokines.

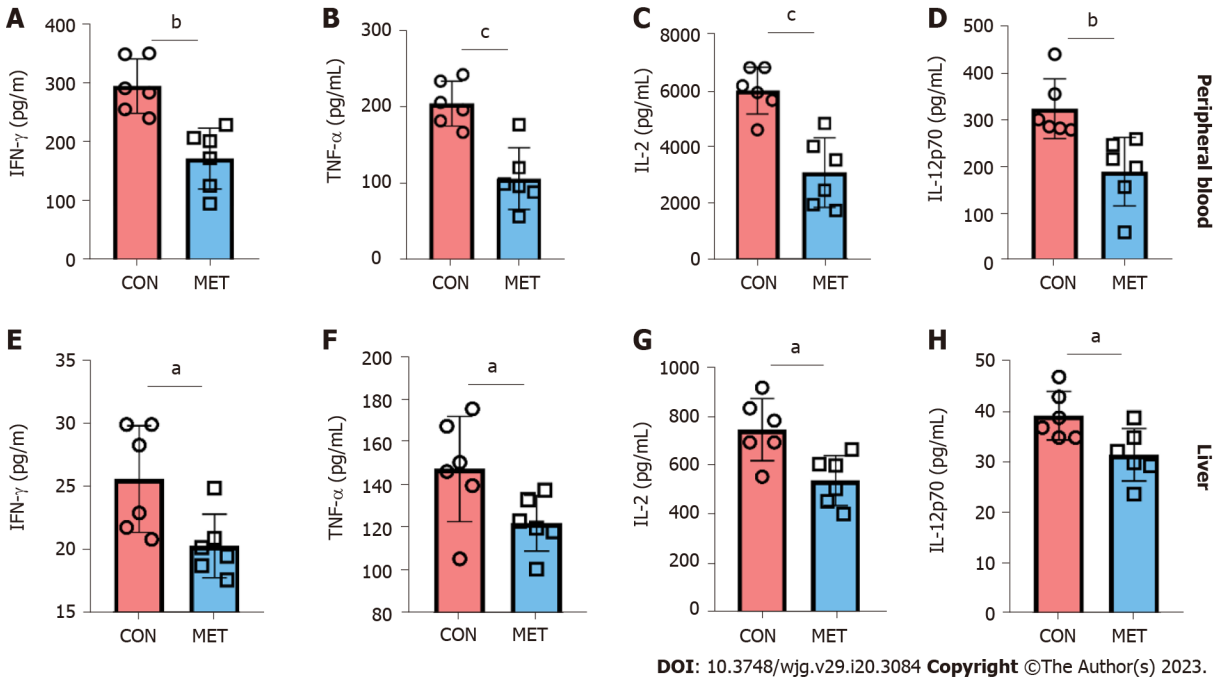


DOI: 10.3748/wjg.v29.i20.3084 **Copyright** ©The Author(s) 2023.

Figure 3 Metronomic capecitabine decreased the infiltration of CD3⁺ T cells in peripheral blood, liver allografts, and spleen. A: The percentage of CD3⁺ T cells among lymphocytes in the peripheral blood at postoperative day 7; B: The number of CD3⁺ T cells in the peripheral blood at postoperative day 7; C and D: Grafted liver (C) and spleen (D) sections were stained for CD3. The samples from each group were collected on postoperative day 7. The arrows show positive staining (50 × and 200 ×). Quantification of the proportion of CD3⁺ positive area within a given section (%). Statistical analysis was done by unpaired *t*-test, $n = 6$. Data are shown as mean ± SD; $^{a}P < 0.05$ *vs* the control group, $^{c}P < 0.001$ *vs* the control group. CON: Untreated control groups, rats received 0.9% normal saline for 7 d; MET: Metronomic capecitabine (CAP)-treated groups, rats received metronomic CAP (100 mg/kg/d) treated for 7 d.

Metronomic CAP increases T cell free ferrous ions and induces lipid peroxidation in vivo

The immune activation of T cells is particularly important in the acute rejection of organ transplants. Similar to many commonly used immunosuppressants, the killing effect of CAP on T cells is also key to its immunosuppressive activity[13]. Therefore, we further explored the mechanism of T cell killing by metronomic CAP. Ferroptosis is a new form of ROS-dependent programmed cell death that may plays an important role in CAP-mediated cytotoxicity. Thus, we measured by flow cytometry the concentration of free ferrous ions, ROS level, and lipid ROS level in peripheral blood CD3⁺ T cells from transplanted rats of both groups at day 7. Compared with the CON group, free ferrous ion concen-



DOI: 10.3748/wjg.v29.i20.3084 **Copyright** ©The Author(s) 2023.

Figure 4 Cytokine concentrations of peripheral blood and liver graft in transplanted rats. Use Luminex assay to detect the concentrations of interferon gamma (IFN-γ), tumor necrosis factor alpha (TNF-α), interleukin (IL)-2 and IL-12 in peripheral blood and graft. A and E: IFN-γ; B and F: TNF-α; C and G: IL-2; D and H: IL-12. Statistical analysis was done by unpaired Students *t*-test, $n = 6$. Data are shown as mean ± SD; $^{a}P < 0.05$ *vs* the control group, $^{b}P < 0.01$ *vs* the control group, $^{c}P < 0.001$ *vs* the control group. CON: Untreated control groups, rats received 0.9% normal saline for 7 d; MET: Metronomic capecitabine (CAP)-treated groups, rats received metronomic CAP (100 mg/kg/d) treated for 7 d; IFN-γ: Interferon gamma; TNF-α: Tumor necrosis factor alpha; IL: Interleukin.

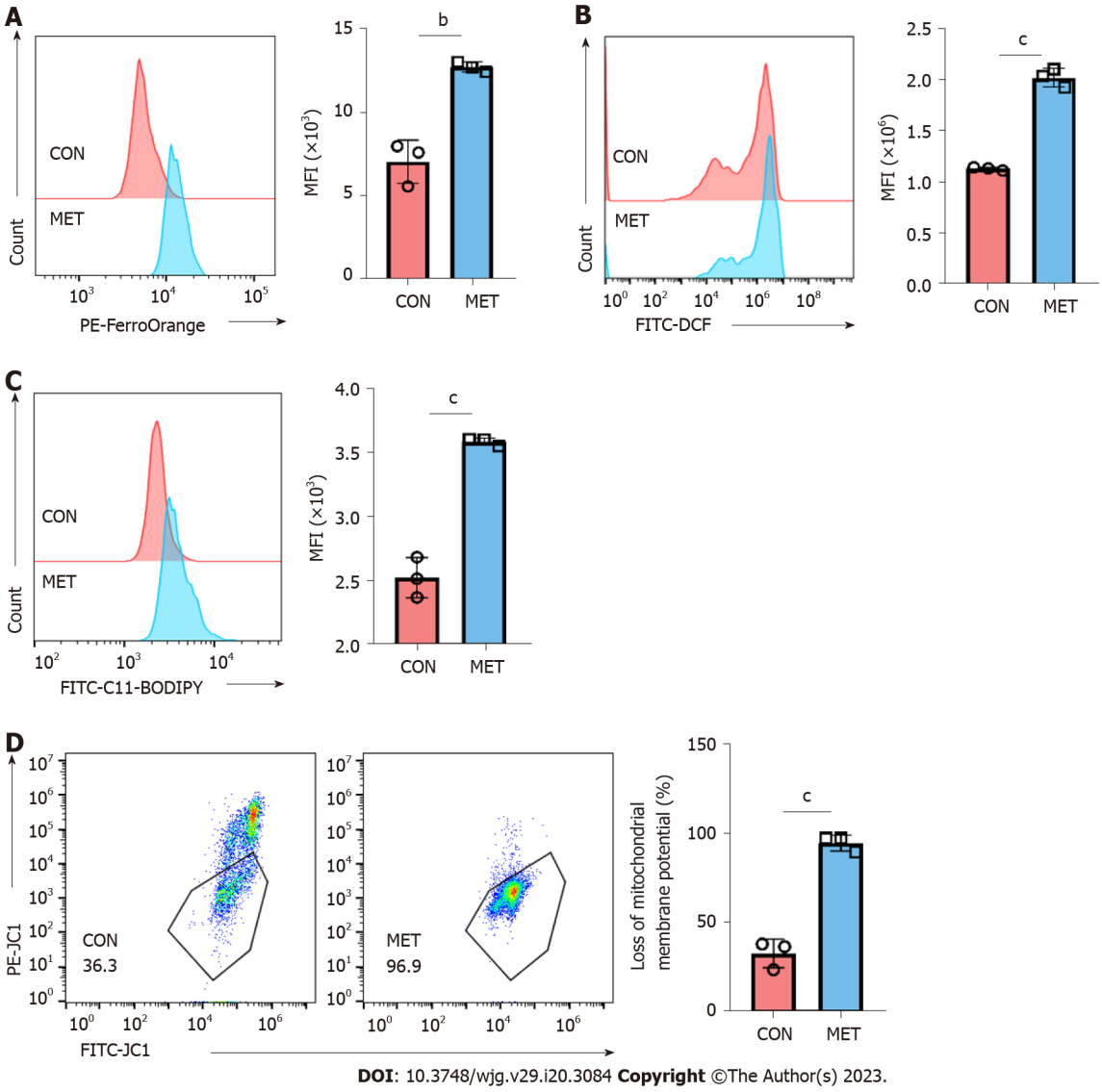
tration (Figure 5A), total ROS (Figure 5B), and lipid ROS (Figure 5C) levels were increased in the MET group. At the same time, the detection of the MMP showed a decreasing trend in the MET group (Figure 5D). These results indicated that metronomic CAP leads to the generation of ferrous ions and results in lipid peroxidation, which conforms to the typical characteristics of ferroptosis.

5-FU triggers ferritinophagy and ferroptosis in T cells in vitro

To further explore *in vitro* the mechanism underlying the CAP-mediated ferroptosis linked to immunosuppression observed *in vivo*, primary $CD3^+$ T cells were sorted from rat spleens and human peripheral blood (Supplementary Figure 2). Both primary $CD3^+$ T cells were treated with 5-FU *in vitro* (Supplementary Figure 3). This treatment significantly inhibited cell viability, which was attenuated by the ferroptosis inhibitor Fer-1 (Figure 6A). Transmission electron microscopy revealed typical characteristics of ferroptosis in 5-FU-treated group, namely, smaller mitochondria with increased membrane density, and diminished mitochondrial cristae (Figure 6B). Free ferrous ions concentration was increased in the 5-FU-treated group, whereas Fer-1 partially reversed the increase of ferrous ions induced by 5-FU (Figure 6C). As a selective cargo receptor, NCOA4 mediates the transport of ferritin into lysosomes, inducing ferroptosis. Western blot analysis revealed that 5-FU treatment induced FTH1 decrease, but a tendency toward increasing NCOA4 expression was observed (Figure 6D), consistent with the *in vivo* studies (Supplementary Figure 4). These results confirmed that the cytotoxicity of 5-FU is at least partly related to the induction of T cell ferroptosis, in which the increase of free ferrous ions caused by NCOA4-mediated ferritinophagy plays an important role.

5-FU-triggered ferroptosis is associated with the inhibition of the Nrf2-HO-1/GPX4 antioxidative pathway

To evaluate the effect of 5-FU on the antioxidant system, antioxidant-related proteins were measured in rat and human primary $CD3^+$ T cells treated with 5-FU. The expression of Nrf-2, HO-1, and GPX4 was evaluated in both groups and compared, and treatment with 5-FU was found to be associated with a marked decrease (Figure 7A), consistent with the *in vivo* studies (Supplementary Figure 4). The results showed that 5-FU treatment increased total ROS and lipid ROS levels and decreased MMP (Figure 7B–D). It also decreased glutathione (GSH) levels and increased the oxidative stress biomarker malondialdehyde (MDA) (Figure 7E and F). Fer-1 inhibits ferroptosis partly by activating Nrf2[29]. Accordingly, it reversed 5-FU-mediated inhibition of Nrf-2, HO-1, and GPX4, increased GSH level, and decreased MDA content, thereby alleviating cell peroxidation induced by 5-FU (Figure 7A–D). These results suggest that 5-FU inhibits the antioxidant system of T cells, inducing the T cells damaged by lipid peroxidation, which results in ferroptosis.



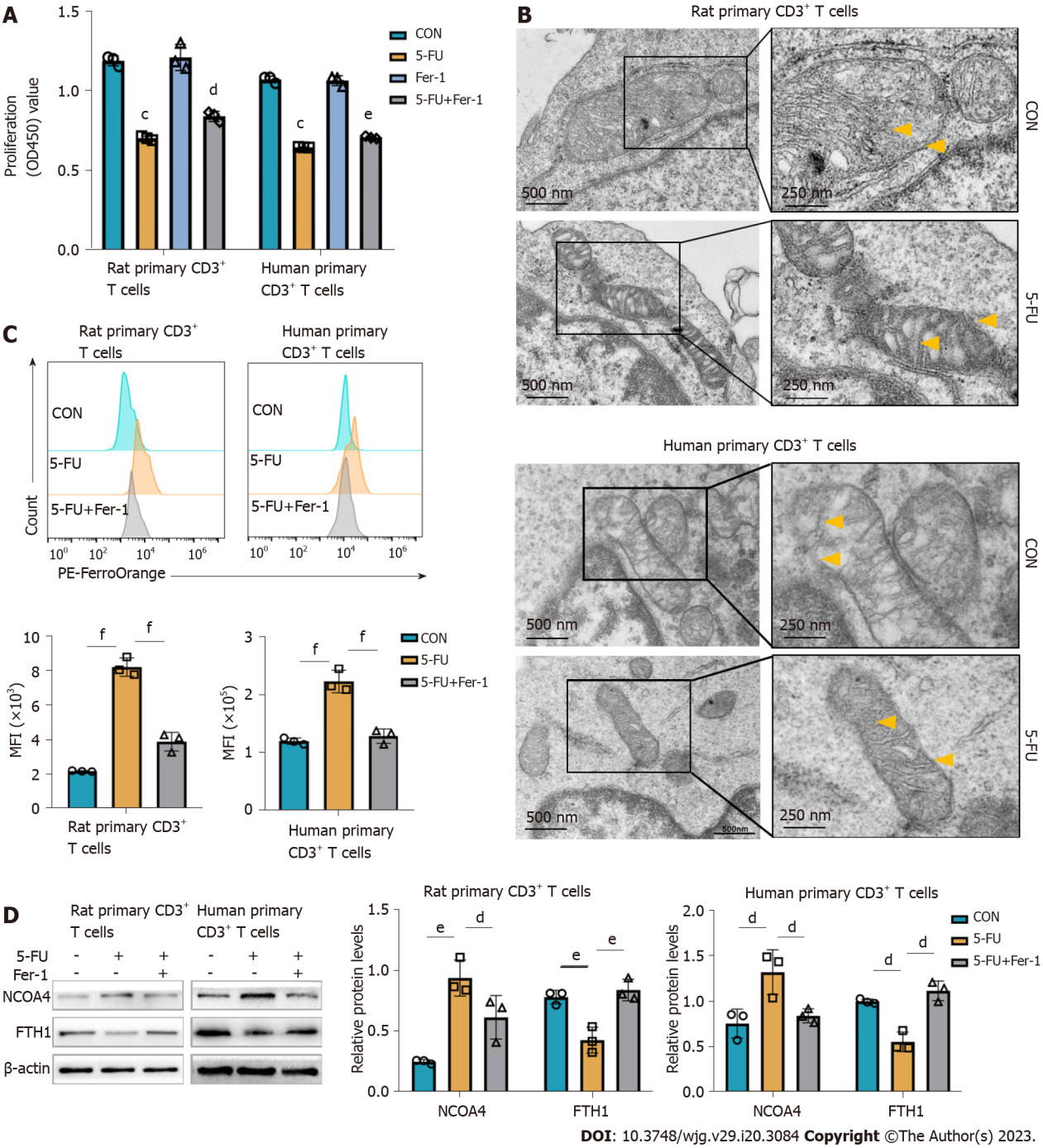
DOI: 10.3748/wjg.v29.i20.3084 **Copyright** ©The Author(s) 2023.

Figure 5 Metronomic capecitabine caused the increase of free ferrous ions and oxidative stress in peripheral blood CD3⁺ T cells of transplanted rats. A: Representative FACS data showing differential FerroOrange staining reflecting different cytoplasmic labile iron concentrations in control groups and metronomic capecitabine-treated rats, followed by statistical analysis of mean fluorescence intensity (MFI); B and C: Reactive oxygen species (ROS) and lipid ROS detected by FACS using DCFH-DA and C11-BODIPY respectively, BODIPY emission was recorded on oxidized C11 (FITC channel) signal. The graph shows the statistical analysis of differential MFIs in the two groups; D: The proportion of cells with reduced mitochondrial membrane potential was assessed by flow cytometry. Statistical analysis was done by unpaired *t*-test, $n = 3$. Data are shown as mean ± SD; $^{b}P < 0.01$ *vs* the control group, $^{c}P < 0.001$ *vs* the control group. CON: Untreated control groups, rats received 0.9% normal saline for 7 d; MET: Metronomic capecitabine (CAP)-treated groups, rats received metronomic CAP (100 mg/kg/d) treated for 7 d; MFI: Mean fluorescence intensity.

DISCUSSION

The conflict between the risk of tumor formation and immune rejection after transplantation has always been a concern. Therefore, it is of great clinical value to identify a drug with both immunosuppressive and anticancer effects. CAP is a classic chemotherapy drug for HCC[4,6], which has been shown to have immunosuppressive effects in a previous study[8], suggesting that metronomic CAP can be used as an immunosuppressant after transplantation and bring long-term benefits to LT patients with HCC. In our previous study, we found that metronomic CAP exerts immunosuppressive effects on normal mice by inducing T cell apoptosis[13]; however, the effect of CAP on the immune system in the context of organ transplantation was unclear. Therefore, we explored the safety, availability, and mechanism of metronomic CAP as an immunosuppressant in a model of rat orthotopic LT. Our results suggest that metronomic CAP can inhibit the acute rejection of LT by inhibiting T cells while avoiding the main side effects of 5-FU. Its mechanism is related to the induction of ferritin degradation and the inhibition of antioxidant-related proteins, which ultimately leads to the death of T cells (Figure 8).

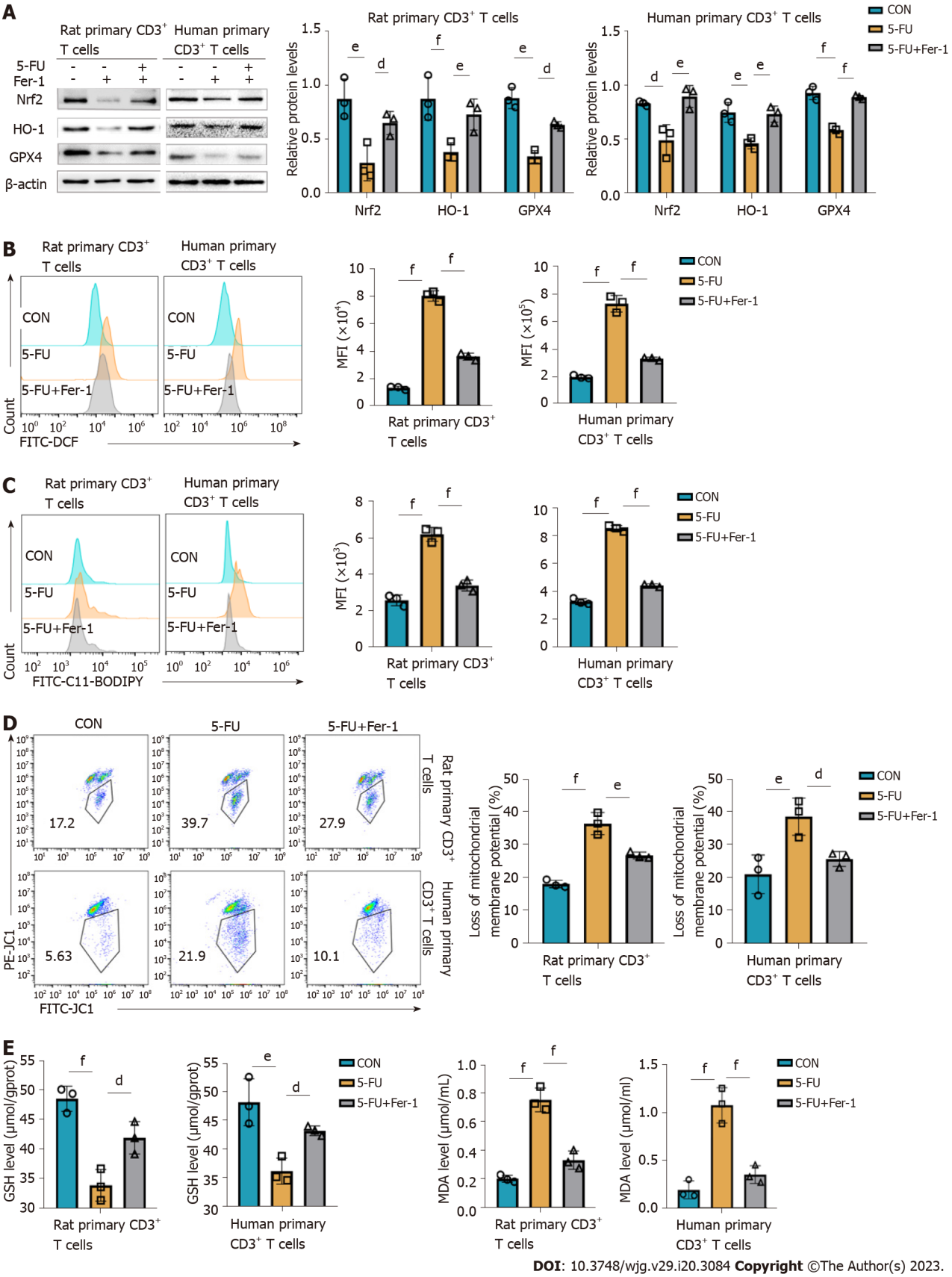
The main effects of 5-FU are on rapidly proliferating tissues, specifically bone marrow. 5-FU suppressed bone marrow hematopoiesis including a significant decrease in the number of erythrocytes,



DOI: 10.3748/wjg.v29.i20.3084 **Copyright** ©The Author(s) 2023.

Figure 6 5-fluorouracil increases the pool of labile iron and contributes to ferroptosis in CD3⁺ T cells. *Vitro* experiments were conducted on rat splenic and human peripheral blood CD3⁺ T cells, which were sorted by immunomagnetic beads. According to predetermined IC50, the rat, and human primary CD3⁺ T cells were treated with 5-fluorouracil (5-FU) (15 μmol/L) and ferrostatin-1 (Fer-1) (2 μmol/L) for 48 h. A: Cell viability was assessed with a Cell Counting Kit-8 kit; the results are expressed as optical density read at 450 nm; B: Transmission electron microscopy images of mitochondria in T cells show increased membrane density (yellow arrows) and a shrunk morphology (Scale bar, 500 nm, and 250 nm); C: Representative FACS data showing FerroOrange staining as the measurement of the level of cytoplasmic labile iron in primary CD3⁺ T cells. The graph shows the statistical analysis of mean fluorescence intensity in the different groups; D: Levels of ferritinophagy-related proteins nuclear receptor coactivator 4 and ferritin heavy chain 1 were assessed by western blot. CON groups: T cells were treated with DMSO for 48 h; 5-FU groups: T cells were treated with 5-FU (15 μmol/L) for 48 h; 5-FU+ Fer-1 groups: T cells were treated with 5-FU (15 μmol/L) and Fer-1 (2 μmol/L) for 48 h. Statistical analysis was done by one-way ANOVA, $n = 3$. Data are shown as mean ± SD. Data are shown as mean ± SD. $^{c}P < 0.001$ *vs* the control group, $^{d}P < 0.05$ *vs* the 5-FU group, $^{e}P < 0.01$ *vs* the 5-FU group, $^{f}P < 0.001$ *vs* the 5-FU group. CON: Untreated control groups; 5-FU: 5-fluorouracil; NCOA4: Nuclear receptor coactivator 4; FTH1: Ferritin heavy chain 1; Fer-1: Ferrostatin-1.

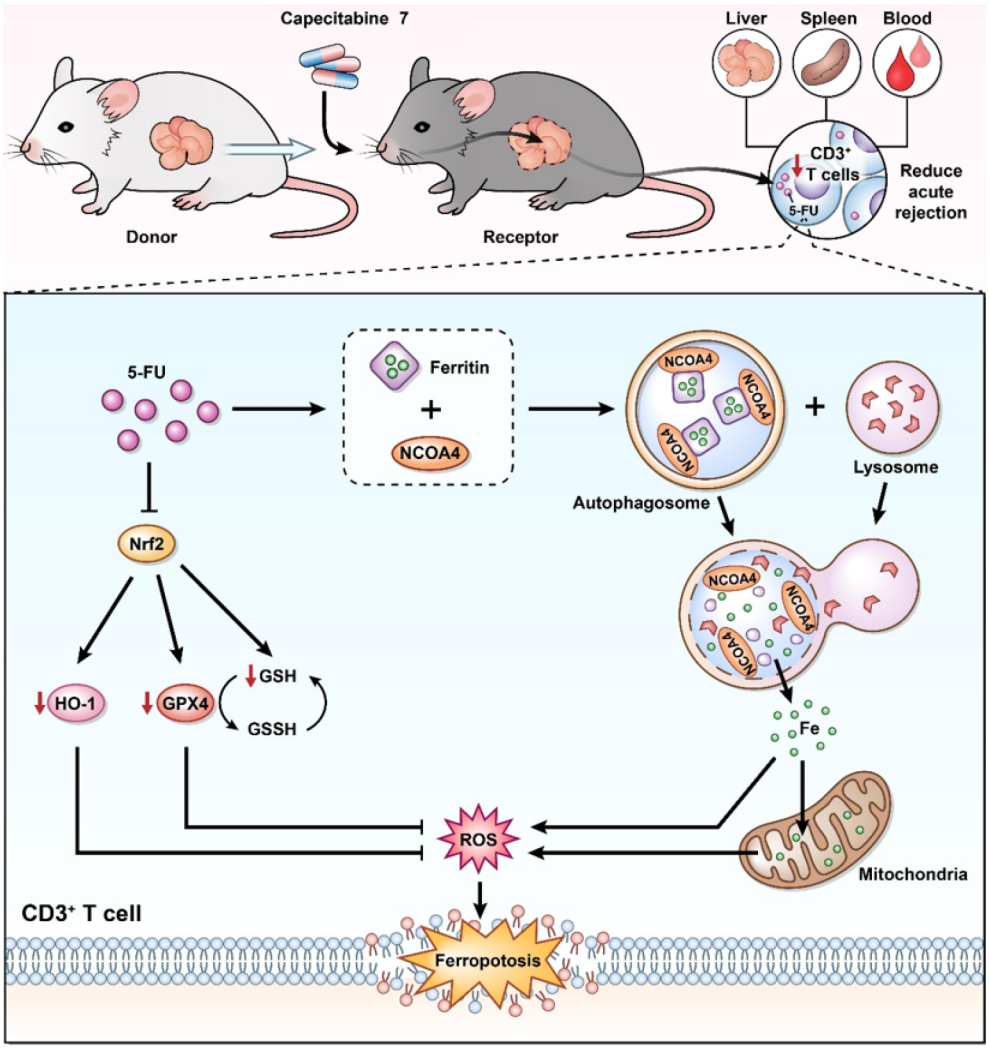
platelet, and leukocyte in the peripheral blood[30,31]. As the prodrug of 5-FU, it is of high clinical relevance to show the safety of the medication of CAP. Overall, metronomic CAP is considered safe, with fewer side effects than traditional chemotherapy regimens. Metronomic CAP is well tolerated and safe in clinical practice, including for patients with HCC or patients after LT[8,32-34]. In mice, there was also no obvious myelosuppression in the MET group 7 d after taking CAP, though the related studies



DOI: 10.3748/wjg.v29.i20.3084 **Copyright** ©The Author(s) 2023.

Figure 7 5-fluorouracil disturbs the antioxidative/oxidative balance, resulting in CD3⁺ T cells ferroptosis. A: Levels of antioxidant proteins nuclear erythroid 2 p45-related factor 2, heme oxygenase-1, and glutathione peroxidase 4 assessed by western blot, and corresponding graphs showing the statistical comparison between groups; B and C: Reactive oxygen species (ROS) and lipid ROS of rat and human CD3⁺ T cells were detected by FACS using DCFH-DA and C11-BODIPY fluorescent conjugates, BODIPY emission was recorded on oxidized C11 (FITC channel) signal; the graphs display the comparison of mean fluorescence intensity levels in the different groups; D: Proportion of cells with reduced mitochondrial membrane potential assessed by flow cytometry; E and F:

Glutathione and malondialdehyde content T cells after treatment for 48 h. CON groups: T cells were treated with DMSO for 48 h; 5-fluorouracil (5-FU) groups: T cells were treated with 5-FU (15 μmol/L) for 48 h; 5-FU+ferrostatin-1 (Fer-1) groups: T cells were treated with 5-FU (15 μmol/L) and Fer-1 (2 μmol/L) for 48 h. Statistical analysis was done by one-way ANOVA, $n = 3$. $^{d}P < 0.05$ *vs* the 5-FU group, $^{e}P < 0.01$ *vs* the 5-FU group, $^{f}P < 0.001$ *vs* the 5-FU group. Nrf2: Nuclear erythroid 2 p45-related factor 2; HO-1: Heme oxygenase-1; GPX4: Glutathione peroxidase 4; GSH: Glutathione; MDA: Malondialdehyde; CON: Untreated control groups; 5-FU: 5-fluorouracil; Fer-1: Ferrostatin-1; MFI: Mean fluorescence intensity.



DOI: 10.3748/wjg.v29.i20.3084 **Copyright** ©The Author(s) 2023.

Figure 8 Possible immunosuppressive mechanisms of metronomic capecitabine on T cells by ferroptosis induction. In the rat model of acute rejection after liver transplantation, metronomic capecitabine (CAP) exerts an immunosuppressive effect by decreasing T cell numbers in peripheral blood, liver graft, and spleen. Metronomic CAP increases the concentration of free ferrous ions by inducing ferritin degradation while inhibiting the expression of antioxidant proteins. Eventually, these effects lead to peroxidation damage and iron toxicity, which induce T cell death. 5-FU: 5-fluorouracil; Nrf2: Nuclear erythroid 2 p45-related factor 2; NCOA4: Nuclear receptor coactivator 4; HO-1: Heme oxygenase-1; GPX4: Glutathione peroxidase 4; GSH: Glutathione; GSSH: Oxidized glutathione; ROS: Reactive oxygen species.

showed that 5-FU could cause severe myelosuppression after 7 d of administration[35]. TP is a key enzyme in the metabolism of CAP[36]. The lack of TP in bone marrow may explain the lack of bone marrow suppression of CAP[11,13]. In a past study, we established the safety of CAP in CAP-fed mice, which did not cause significant myelosuppression after 21 d of administration[13]. However, the depletion of lymphocytes is not related to bone marrow suppression, and the high expression of TP in lymphocytes directly leads to the killing effect of CAP[11]. CAP is safe for long-term use because it can circumvent the inhibitory effect of 5-FU on bone marrow hematopoietic function.

When acute rejection occurs, immune cells mainly infiltrate the hilar region of the grafted liver, inducing pericentral inflammation, damaging the vascular and bile duct endothelium, damaging hepatocytes, and destroying the lobular structure[37,38]. CAP can preserve the function and structure of the transplanted liver by inhibiting acute rejection. Compared with the CON group, the Banff score was significantly lower in the MET group at 7 d after transplantation while the elevation of ALT and AST in

the MET group was significantly less pronounced than that in the CON group. ALT and AST are primarily expressed in liver cells, and liver allograft destruction caused by rejection is positively associated with ALT and AST expression[39,40]. However, TBIL and DBIL in both groups showed an increasing trend after surgery with no significant difference between the two groups. It may be related to biliary tract injury and bilirubin stasis caused by the lack of hepatic artery reconstruction and the use of cannula reconstruction of the bile duct in the traditional rat "two-cuff method" orthotopic LT[41].

Antigen presentation and T cell activation are key steps in rejection. Donor-derived antigen-presenting cells provide immune stimulation to recipient naive $CD4^+$ T cells, known as the direct antigen presentation pathway, which is the main mode of activation in acute rejection[42,43]. Once rejection is initiated, $CD8^+$ T cells mainly differentiate into cytotoxic T cells, which directly cause graft injury. $CD4^+$ T cells can differentiate into many subtypes, mainly helper T cells (Th1, Th2, and Th17) and regulatory T cells (Treg). In acute rejection, T cells differentiate mainly to Th1, driven by pro-inflammatory cytokines such as IL-12 and IFN-γ. Th1 cells secrete IL-2 and IFN-γ, providing a positive feedback loop to stimulate Th1 cells to proliferate further. IFN-γ is usually associated with proinflammatory and immune activation processes while IL-2 is necessary for survival and effects of activated T cells. T cell activation, proliferation, differentiation, and migration are the immune basis of acute rejection after organ transplantation, and are often used as the targets of clinical immunosuppression[42,44,45]. The results of our study showed that IL-2 and IFN-γ were decreased in CAP treated rats. The changes in cytokines suggest that in addition to decreasing the number of T cells, CAP may also target Th0 cells' differentiation. Since IFN-γ has a stimulatory effect on the secretion of TNF-α by M1 macrophages[46], the decrease in TNF-α may be related to the inhibition of IL-2 secretion in T cells by CAP. By inducing the programmed death of T cells, CAP mitigates transplant rejection and protects graft function. Moreover, cytokines associated with rejection were also affected by CAP treatment. Metronomic CAP significantly reduced the levels of pro-inflammatory cytokines (IFN-γ, TNF-α, IL-2, and IL-12p70), which are mainly secreted by immune cells and contributing to rejection[47-50].

The data from our study demonstrated that the selective cytotoxic effect of the T cells of metronomic CAP is crucial for the prevention of acute organ transplant rejection. Next, we further explored the mechanism underlying the immunosuppressive effect of metronomic CAP by studying $CD3^+$ T cells in more details. Mitochondria is a main source of ROS and mitochondria ROS is a critical component of T cell activation, proliferation, and effector function of T cells[51-53]. However, excessive ROS production, inducible by a high level of iron, leads to ROS-mediated membrane phospholipid peroxidation and T cell death upon activation[54]. Thus, we investigated the effect of CAP on the level of $CD3^+$ T cell ferrous ions with a ferrous probe and found that CAP treatment induced ferrous ion accumulation, accompanied by increased ROS and lipid ROS and decreased MMP. Mitochondrial ROS production and MMP reduction are two important parameters of mitochondrial damage, and lipid peroxidation following ROS generation plays an important role in ROS-induced cellular damage[55-57]. These results indicate that metronomic CAP increased ferrous ion accumulation and oxidative damage in the $CD3^+$ T cells of rats after transplantation, which may be the mechanism behind CAP-induced T cell reduction. Next, we used rat and human primary $CD3^+$ T cells to further explore the role of ferroptosis in CAP-induced immunosuppression *in vitro*. Free ferrous iron overload, lipid peroxide accumulation, and specific mitochondrial morphological changes are three key characteristics that distinguish ferroptosis from other programmed cell deaths[14]. In this study, typical mitochondrial changes were observed in T cells of the 5-FU group under transmission electron microscopy. Ferrous ion in rat primary $CD3^+$ T cells of the 5-FU group was increased with the downregulation of FTH1 and upregulation of NCOA4, revealing the occurrence of ferritinophagy. That is, the autophagic degradation of ferritin, contributed to rat T cell ferrous overload, excessive lipid peroxidation, and eventually ferroptosis in the 5-FU group. Nrf2 is a core player in the regulation of antioxidant molecules in cells, which can induce the synthesis of HO-1 and GPX4[20,58]. The Nrf2-HO-1/GPX4 antioxidative system, which participates in the regulation of oxidative damage and inhibits erastin-induced ferroptosis[59], was suppressed by 5-FU *in vitro*. It also reduced GSH levels, indicative of impairment of antioxidant capacity, and improved the levels of MDA, an end-product of lipid peroxidation.

In this study, we showed that metronomic CAP alleviated rat LT rejection without the common side effect (myelosuppression) of antitumor drugs. T cell ferroptosis plays an important role in the antirejection effect of CAP, which can induce cell iron overload and suppress the Nrf2-HO-1/GPX4 antioxidant systems, directly increasing the levels of intracellular ROS, leading to severe mitochondrial damage in T cells. These results revealed a new mechanism of CAP-induced T cell programmed death and suggested the possibility of using CAP as an immunosuppressant after transplantation. As a traditional antitumor drug, CAP has immunosuppressive effects, that may kill tumor cells and induce T cell death at the same time. CAP may have both antirejection and antitumor effects on patients with HCC after LT, thereby having broad clinical application prospects. In light of our findings, CAP alone as an immunosuppressive agent does not achieve satisfactory therapeutic effects. Therefore, the combination and interaction of CAP with other immunosuppressive agents is an important research direction in the future. In addition, we observed interesting effects of CAP on different cytokines, but further observations were lacking. The effects of CAP on T cell subsets and other immune cells are worth further attention. In the future, we plan to establish tumor-bearing animal models for allotransplantation, to clarify the dual antirejection and antitumor effects of CAP. In conclusion, the immunosup-

pressive effect of CAP should be further explored to optimize the drug treatment regimen for LT patients with liver cancer.

CONCLUSION

Metronomic CAP can alleviate liver graft injury and reduce the proliferation and infiltration of $CD3^+$ T cells in peripheral blood, graft, and spleen, thereby inhibiting acute rejection after LT. T cell ferroptosis plays an important role in the antirejection effect of CAP, which can induce cell iron overload and suppress the Nrf2-HO-1/GPX4 antioxidant systems, thereby directly increasing the levels of intracellular ROS and leading to severe oxidative damage in T cells.

ARTICLE HIGHLIGHTS

Research background

As a classical antimetabolite, capecitabine (CAP) has shown potential antirejection effects after liver transplantation (LT) in clinical trials. Our previous study showed that metronomic CAP can cause programmed T cell death in healthy mice by inducing oxidative stress, which is also the key step in ferroptosis. Thus, ferroptosis may play an important role in CAP-induced T cell death and an immunosuppressive role in acute rejection after transplantation.

Research motivation

This study investigated the immunosuppressive effect of metronomic CAP in rat LT and its mechanism, which may be used as an immunosuppressive agent after LT to improve the prognosis of liver transplant patients with hepatocellular carcinoma.

Research objectives

The objective of this study was to investigate the possibility of using CAP as an anti-rejection agent after transplantation. The results showed that metronomic CAP could exert an immunosuppressive effect by inducing T cell ferroptosis, which provided a basis for investigating CAP as part of an immunosuppressive regimen.

Research methods

A rat LT model of acute rejection was established, and the effect of metronomic CAP on splenic hematopoietic function and acute graft rejection was evaluated 7 d after transplantation. *In vitro*, primary $CD3^+$ T cells were sorted and co-cultured with or without 5-fluorouracil (5-FU) (active agent of CAP). The levels of ferroptosis-related proteins, ferrous ion concentration, and oxidative stress-related indicators were observed. The changes in mitochondrial structure were observed using electron microscopy.

Research results

With no significant myelotoxicity, metronomic CAP alleviated graft injury, prolonged the survival time of the recipient rats, and reduced the infiltration rate of $CD3^+$ T cells in peripheral blood, liver graft, and spleen, thereby inhibiting acute rejection after LT. In *vitro*, 5-FU, an end product of CAP metabolism, induced the degradation of the ferritin heavy chain by upregulating nuclear receptor coactivator 4, which caused the accumulation of ferrous ions. It also inhibited nuclear erythroid 2 p45-related factor 2, heme oxygenase-1, and glutathione peroxidase 4, eventually leading to oxidative damage and ferroptosis of T cells.

Research conclusions

Metronomic CAP can alleviate liver graft injury and reduce the proliferation and infiltration of $CD3^+$ T cells in peripheral blood, graft, and spleen by inducing T cell oxidative damage and ferroptosis, thereby inhibiting acute rejection after LT.

Research perspectives

The combination and interaction of CAP with other immunosuppressive agents is an important research direction in the future. In addition, the effects of CAP on T cell subsets and other immune cells are worth further attention. Besides, we plan to establish tumor-bearing animal models for allotransplantation, to clarify the dual antirejection and antitumor effects of CAP.

FOOTNOTES

Author contributions: Wang H conceived the study, performed the experiments, analyzed the data, generated the figures, and wrote the manuscript; Wang ZL, Zhang S, and Kong DJ provided technical help and assisted with the experiments; Zhang S, Kong DJ, Yang RN, Cao L, and Wang JX helped with the data analyses; Wang ZL, Yoshida S, Zhang S, Liu T, Shen ZY, and Zheng H performed critical reading of the manuscript; Fan SL, Ren JS, Li JH, and Zheng H assisted with the editing and writing of the manuscript; Zheng H supervised the study and edited the manuscript.

Supported by National Key Research and Development Program of China, No. 2020YFA0710802; The Youth Science Fund of the Nature Science Foundation of Tianjin, No. 20JCQNJC01370; The Key Projects of Tianjin Science and Technology Project, No. 21JCZDJC00160; and The Science Foundation of Tianjin Health Commission, No. ZC20065 and No. ZC20089.

Institutional review board statement: The studies involving human participants were conducted in accordance with the Declaration of Helsinki (1964) and were reviewed and approved by the Tianjin First Hospital clinical research ethics committee, No. 2022N150KY. The participants provided written informed consent to participate in this study.

Institutional animal care and use committee statement: The animal study was reviewed and approved by the ethics committee of the Institute of Radiation Medicine of the Chinese Academy of Medical Sciences, No. IRM-DWLL-2021184.

Informed consent statement: All study participants or their legal guardian provided informed written consent about personal and medical data collection prior to study enrolment.

Conflict-of-interest statement: All the authors report no relevant conflicts of interest for this article.

Data sharing statement: No additional data are available.

ARRIVE guidelines statement: The authors have read the ARRIVE guidelines, and the manuscript was prepared and revised according to the ARRIVE guidelines.

Open-Access: This article is an open-access article that was selected by an in-house editor and fully peer-reviewed by external reviewers. It is distributed in accordance with the Creative Commons Attribution NonCommercial (CC BY-NC 4.0) license, which permits others to distribute, remix, adapt, build upon this work non-commercially, and license their derivative works on different terms, provided the original work is properly cited and the use is non-commercial. See: https://creativecommons.org/Licenses/by-nc/4.0/

Country/Territory of origin: China

ORCID number: Hao Wang 0000-0002-2841-8834; Zheng-Lu Wang 0000-0003-0463-1080; Sai Zhang 0000-0002-4046-5385; De-Jun Kong 0000-0002-6878-9293; Rui-Ning Yang 0000-0002-3676-733X; Lei Cao 0000-0001-5982-4264; Jian-Xi Wang 0000-0003-3220-9717; Sei Yoshida 0000-0002-4771-3900; Zhuo-Lun Song 0000-0001-5101-3950; Tao Liu 0000-0002-0931-7288; Shun-Li Fan 0000-0002-3848-7905; Jia-Shu Ren 0000-0002-0186-1297; Jiang-Hong Li 0000-0001-5642-2040; Zhong-Yang Shen 0000-0003-0045-4355; Hong Zheng 0000-0001-7386-7084.

S-Editor: Fan JR
L-Editor: A
P-Editor: Liu JH

REFERENCES

1 **Vivarelli M**, Cucchetti A, La Barba G, Ravaioli M, Del Gaudio M, Lauro A, Grazi GL, Pinna AD. Liver transplantation for hepatocellular carcinoma under calcineurin inhibitors: reassessment of risk factors for tumor recurrence. *Ann Surg* 2008; **248**: 857-862 [PMID: 18948815 DOI: 10.1097/SLA.0b013e3181896278]
2 **Gish RG**. Hepatocellular carcinoma: overcoming challenges in disease management. *Clin Gastroenterol Hepatol* 2006; **4**: 252-261 [PMID: 16527686 DOI: 10.1016/j.cgh.2006.01.001]
3 **Kawahara T**, Asthana S, Kneteman NM. m-TOR inhibitors: what role in liver transplantation? *J Hepatol* 2011; **55**: 1441-1451 [PMID: 21781947 DOI: 10.1016/j.jhep.2011.06.015]
4 **Pelizzaro F**, Sammarco A, Dadduzio V, Pastorelli D, Giovanis P, Soldà C, Rizzato MD, Lombardi G, Lonardi S, Peserico G, Imondi A, Sartori A, Maddalo G, Farinati F. Capecitabine in advanced hepatocellular carcinoma: A multicenter experience. *Dig Liver Dis* 2019; **51**: 1713-1719 [PMID: 31320302 DOI: 10.1016/j.dld.2019.06.015]
5 **Changou CA**, Shiah HS, Chen LT, Liu S, Luh F, Liu SH, Cheng YC, Yen Y. A Phase II Clinical Trial on the Combination Therapy of PHY906 Plus Capecitabine in Hepatocellular Carcinoma. *Oncologist* 2021; **26**: e367-e373 [PMID: 33140457 DOI: 10.1002/onco.13582]
6 **Bocci G**, Kerbel RS. Pharmacokinetics of metronomic chemotherapy: a neglected but crucial aspect. *Nat Rev Clin Oncol*

2016; **13**: 659-673 [PMID: 27184418 DOI: 10.1038/nrclinonc.2016.64]
7 **Kerbel RS**, Shaked Y. The potential clinical promise of 'multimodality' metronomic chemotherapy revealed by preclinical studies of metastatic disease. *Cancer Lett* 2017; **400**: 293-304 [PMID: 28202353 DOI: 10.1016/j.canlet.2017.02.005]
8 **Ravaioli M**, Cucchetti A, Pinna AD, De Pace V, Neri F, Barbera MA, Maroni L, Frega G, Palloni A, De Lorenzo S, Ripoli MC, Pantaleo MA, Cescon M, Del Gaudio M, Brandi G. The role of metronomic capecitabine for treatment of recurrent hepatocellular carcinoma after liver transplantation. *Sci Rep* 2017; **7**: 11305 [PMID: 28900245 DOI: 10.1038/s41598-017-11810-z]
9 **Keating GM**, Santoro A. Sorafenib: a review of its use in advanced hepatocellular carcinoma. *Drugs* 2009; **69**: 223-240 [PMID: 19228077 DOI: 10.2165/00003495-200969020-00006]
10 **Ishikawa T**, Utoh M, Sawada N, Nishida M, Fukase Y, Sekiguchi F, Ishitsuka H. Tumor selective delivery of 5-fluorouracil by capecitabine, a new oral fluoropyrimidine carbamate, in human cancer xenografts. *Biochem Pharmacol* 1998; **55**: 1091-1097 [PMID: 9605432 DOI: 10.1016/s0006-2952(97)00682-5]
11 **Yoshimura A**, Kuwazuru Y, Furukawa T, Yoshida H, Yamada K, Akiyama S. Purification and tissue distribution of human thymidine phosphorylase; high expression in lymphocytes, reticulocytes and tumors. *Biochim Biophys Acta* 1990; **1034**: 107-113 [PMID: 2328255 DOI: 10.1016/0304-4165(90)90160-x]
12 **Schüller J**, Cassidy J, Dumont E, Roos B, Durston S, Banken L, Utoh M, Mori K, Weidekamm E, Reigner B. Preferential activation of capecitabine in tumor following oral administration to colorectal cancer patients. *Cancer Chemother Pharmacol* 2000; **45**: 291-297 [PMID: 10755317 DOI: 10.1007/s002800050043]
13 **Zhang S**, Wang Z, Fan S, Liu T, Yoshida S, Yang S, Liu L, Hou W, Cao L, Wang J, Song Z, Li S, Zhang S, Wang H, Li J, Zheng H, Shen Z. Capecitabine Can Induce T Cell Apoptosis: A Potential Immunosuppressive Agent With Anti-Cancer Effect. *Front Immunol* 2021; **12**: 737849 [PMID: 34557199 DOI: 10.3389/fimmu.2021.737849]
14 **Dixon SJ**, Lemberg KM, Lamprecht MR, Skouta R, Zaitsev EM, Gleason CE, Patel DN, Bauer AJ, Cantley AM, Yang WS, Morrison B 3rd, Stockwell BR. Ferroptosis: an iron-dependent form of nonapoptotic cell death. *Cell* 2012; **149**: 1060-1072 [PMID: 22632970 DOI: 10.1016/j.cell.2012.03.042]
15 **Xie Y**, Hou W, Song X, Yu Y, Huang J, Sun X, Kang R, Tang D. Ferroptosis: process and function. *Cell Death Differ* 2016; **23**: 369-379 [PMID: 26794443 DOI: 10.1038/cdd.2015.158]
16 **Li J**, Cao F, Yin HL, Huang ZJ, Lin ZT, Mao N, Sun B, Wang G. Ferroptosis: past, present and future. *Cell Death Dis* 2020; **11**: 88 [PMID: 32015325 DOI: 10.1038/s41419-020-2298-2]
17 **Truman-Rosentsvit M**, Berenbaum D, Spektor L, Cohen LA, Belizowsky-Moshe S, Lifshitz L, Ma J, Li W, Kesselman E, Abutbul-Ionita I, Danino D, Gutierrez L, Li H, Li K, Lou H, Regoni M, Poli M, Glaser F, Rouault TA, Meyron-Holtz EG. Ferritin is secreted *via* 2 distinct nonclassical vesicular pathways. *Blood* 2018; **131**: 342-352 [PMID: 29074498 DOI: 10.1182/blood-2017-02-768580]
18 **Fuhrmann DC**, Mondorf A, Beifuß J, Jung M, Brüne B. Hypoxia inhibits ferritinophagy, increases mitochondrial ferritin, and protects from ferroptosis. *Redox Biol* 2020; **36**: 101670 [PMID: 32810738 DOI: 10.1016/j.redox.2020.101670]
19 **Dodson M**, Castro-Portuguez R, Zhang DD. NRF2 plays a critical role in mitigating lipid peroxidation and ferroptosis. *Redox Biol* 2019; **23**: 101107 [PMID: 30692038 DOI: 10.1016/j.redox.2019.101107]
20 **Song X**, Long D. Nrf2 and Ferroptosis: A New Research Direction for Neurodegenerative Diseases. *Front Neurosci* 2020; **14**: 267 [PMID: 32372896 DOI: 10.3389/fnins.2020.00267]
21 **Kwon MY**, Park E, Lee SJ, Chung SW. Heme oxygenase-1 accelerates erastin-induced ferroptotic cell death. *Oncotarget* 2015; **6**: 24393-24403 [PMID: 26405158 DOI: 10.18632/oncotarget.5162]
22 **Seibt TM**, Proneth B, Conrad M. Role of GPX4 in ferroptosis and its pharmacological implication. *Free Radic Biol Med* 2019; **133**: 144-152 [PMID: 30219704 DOI: 10.1016/j.freeradbiomed.2018.09.014]
23 **Deng HF**, Yue LX, Wang NN, Zhou YQ, Zhou W, Liu X, Ni YH, Huang CS, Qiu LZ, Liu H, Tan HL, Tang XL, Wang YG, Ma ZC, Gao Y. Mitochondrial Iron Overload-Mediated Inhibition of Nrf2-HO-1/GPX4 Assisted ALI-Induced Nephrotoxicity. *Front Pharmacol* 2020; **11**: 624529 [PMID: 33584308 DOI: 10.3389/fphar.2020.624529]
24 **Deng S**, Wu D, Li L, Li J, Xu Y. TBHQ attenuates ferroptosis against 5-fluorouracil-induced intestinal epithelial cell injury and intestinal mucositis *via* activation of Nrf2. *Cell Mol Biol Lett* 2021; **26**: 48 [PMID: 34794379 DOI: 10.1186/s11658-021-00294-5]
25 **Li D**, Song C, Zhang J, Zhao X. ROS and iron homeostasis dependent ferroptosis play a vital role in 5-Fluorouracil induced cardiotoxicity in vitro and in vivo. *Toxicology* 2022; **468**: 153113 [PMID: 35101590 DOI: 10.1016/j.tox.2022.153113]
26 **Xu HS**, Rosenlof LK, Pruett TL, Jones RS. Prostaglandin E1 increases survival with extended anhepatic phase during liver transplantation. *Ann Surg* 1994; **220**: 53-58 [PMID: 8024359 DOI: 10.1097/00000658-199407000-00009]
27 **Kamada N**, Calne RY. Orthotopic liver transplantation in the rat. Technique using cuff for portal vein anastomosis and biliary drainage. *Transplantation* 1979; **28**: 47-50 [PMID: 377595]
28 Banff schema for grading liver allograft rejection: an international consensus document. *Hepatology* 1997; **25**: 658-663 [PMID: 9049215 DOI: 10.1002/hep.510250328]
29 **Li X**, Chen J, Yuan S, Zhuang X, Qiao T. Activation of the P62-Keap1-NRF2 Pathway Protects against Ferroptosis in Radiation-Induced Lung Injury. *Oxid Med Cell Longev* 2022; **2022**: 8973509 [PMID: 35847598 DOI: 10.1155/2022/8973509]
30 **Ishibashi M**, Ishii M, Yamamoto S, Mori Y, Shimizu S. Possible involvement of TRPM2 activation in 5-fluorouracil-induced myelosuppression in mice. *Eur J Pharmacol* 2021; **891**: 173671 [PMID: 33131720 DOI: 10.1016/j.ejphar.2020.173671]
31 **Numazawa S**, Sugihara K, Miyake S, Tomiyama H, Hida A, Hatsuno M, Yamamoto M, Yoshida T. Possible involvement of oxidative stress in 5-fluorouracil-mediated myelosuppression in mice. *Basic Clin Pharmacol Toxicol* 2011; **108**: 40-45 [PMID: 20722640 DOI: 10.1111/j.1742-7843.2010.00621.x]
32 **Brandi G**, de Rosa F, Agostini V, di Girolamo S, Andreone P, Bolondi L, Serra C, Sama C, Golfieri R, Gramenzi A, Cucchetti A, Pinna AD, Trevisani F, Biasco G; Italian Liver Cancer (ITA. LI.CA) Group. Metronomic capecitabine in advanced hepatocellular carcinoma patients: a phase II study. *Oncologist* 2013; **18**: 1256-1257 [PMID: 24232581 DOI:

10.1634/theoncologist.2013-0093]
33 **Granito A**, Marinelli S, Terzi E, Piscaglia F, Renzulli M, Venerandi L, Benevento F, Bolondi L. Metronomic capecitabine as second-line treatment in hepatocellular carcinoma after sorafenib failure. *Dig Liver Dis* 2015; **47**: 518-522 [PMID: 25861840 DOI: 10.1016/j.dld.2015.03.010]
34 **Casadei Gardini A**, Foca F, Scartozzi M, Silvestris N, Tamburini E, Faloppi L, Brunetti O, Rudnas B, Pisconti S, Valgiusti M, Marisi G, Foschi FG, Ercolani G, Tassinari D, Cascinu S, Frassineti GL. Metronomic capecitabine versus best supportive care as second-line treatment in hepatocellular carcinoma: a retrospective study. *Sci Rep* 2017; **7**: 42499 [PMID: 28211921 DOI: 10.1038/srep42499]
35 **Kojima S**, Takaba K, Kimoto N, Takeda T, Kakuni M, Mizutani M, Suzuki K, Sato H, Hara T. Protective effects of glutathione on 5-fluorouracil-induced myelosuppression in mice. *Arch Toxicol* 2003; **77**: 285-290 [PMID: 12734643 DOI: 10.1007/s00204-003-0448-9]
36 **Lam SW**, Guchelaar HJ, Boven E. The role of pharmacogenetics in capecitabine efficacy and toxicity. *Cancer Treat Rev* 2016; **50**: 9-22 [PMID: 27569869 DOI: 10.1016/j.ctrv.2016.08.001]
37 **Fels Elliott DR**, Tavakol M, Lucas CH, Sheahon K, Kakar S, Hameed B, Ferrell LD, Gill RM. Clinicopathological features and outcomes of parenchymal rejection in liver transplant biopsies. *Histopathology* 2020; **76**: 822-831 [PMID: 31894595 DOI: 10.1111/his.14058]
38 **Demirhan B**, Bilezikçi B, Haberal AN, Sevmiş S, Arat Z, Haberal M. Hepatic parenchymal changes and histologic eosinophilia as predictors of subsequent acute liver allograft rejection. *Liver Transpl* 2008; **14**: 214-219 [PMID: 18236397 DOI: 10.1002/lt.21360]
39 **De Lorenzo S**, Tovoli F, Barbera MA, Garuti F, Palloni A, Frega G, Garajovà I, Rizzo A, Trevisani F, Brandi G. Metronomic capecitabine vs. best supportive care in Child-Pugh B hepatocellular carcinoma: a proof of concept. *Sci Rep* 2018; **8**: 9997 [PMID: 29968763 DOI: 10.1038/s41598-018-28337-6]
40 **Vionnet J**, Miquel R, Abraldes JG, Wall J, Kodela E, Lozano JJ, Ruiz P, Navasa M, Marshall A, Nevens F, Gelson W, Leithead J, Masson S, Jaeckel E, Taubert R, Tachtatzis P, Eurich D, Simpson KJ, Bonaccorsi-Riani E, Feng S, Bucuvalas J, Ferguson J, Quaglia A, Sidorova J, Elstad M, Douiri A, Sánchez-Fueyo A. Non-invasive alloimmune risk stratification of long-term liver transplant recipients. *J Hepatol* 2021; **75**: 1409-1419 [PMID: 34437910 DOI: 10.1016/j.jhep.2021.08.007]
41 **Li GL**, Lin HM, Long TZ, Lv LH, Yu JD, Huang YH, Min J, Wan YL. High incidence of biliary complications in rat liver transplantation: can we avoid it? *World J Gastroenterol* 2011; **17**: 3140-3144 [PMID: 21912457 DOI: 10.3748/wjg.v17.i26.3140]
42 **Ronca V**, Wootton G, Milani C, Cain O. The Immunological Basis of Liver Allograft Rejection. *Front Immunol* 2020; **11**: 2155 [PMID: 32983177 DOI: 10.3389/fimmu.2020.02155]
43 **Safinia N**, Vaikunthanathan T, Lechler RI, Sanchez-Fueyo A, Lombardi G. Advances in Liver Transplantation: where are we in the pursuit of transplantation tolerance? *Eur J Immunol* 2021; **51**: 2373-2386 [PMID: 34375446 DOI: 10.1002/eji.202048875]
44 **Kumar BV**, Connors TJ, Farber DL. Human T Cell Development, Localization, and Function throughout Life. *Immunity* 2018; **48**: 202-213 [PMID: 29466753 DOI: 10.1016/j.immuni.2018.01.007]
45 **Wong TC**, Lo CM, Fung JY. Emerging drugs for prevention of T-cell mediated rejection in liver and kidney transplantation. *Expert Opin Emerg Drugs* 2017; **22**: 123-136 [PMID: 28503959 DOI: 10.1080/14728214.2017.1330884]
46 **Sun G**, Yang S, Cao G, Wang Q, Hao J, Wen Q, Li Z, So KF, Liu Z, Zhou S, Zhao Y, Yang H, Zhou L, Yin Z. γδ T cells provide the early source of IFN-γ to aggravate lesions in spinal cord injury. *J Exp Med* 2018; **215**: 521-535 [PMID: 29282251 DOI: 10.1084/jem.20170686]
47 **Li S**, Yu J, Guo C, Jie Y, Pan Z. The Balance of Th1/Th2 and LAP+Tregs/Th17 Cells Is Crucial for Graft Survival in Allogeneic Corneal Transplantation. *J Ophthalmol* 2018; **2018**: 5404989 [PMID: 29576879 DOI: 10.1155/2018/5404989]
48 **Newstead CG**, Lamb WR, Brenchley PE, Short CD. Serum and urine IL-6 and TNF-alpha in renal transplant recipients with graft dysfunction. *Transplantation* 1993; **56**: 831-835 [PMID: 8212202 DOI: 10.1097/00007890-199310000-00010]
49 **Ma L**, Zhang H, Hu K, Lv G, Fu Y, Ayana DA, Zhao P, Jiang Y. The imbalance between Tregs, Th17 cells and inflammatory cytokines among renal transplant recipients. *BMC Immunol* 2015; **16**: 56 [PMID: 26400627 DOI: 10.1186/s12865-015-0118-8]
50 **Assadiasl S**, Mooney N, Nicknam MH. Cytokines in Liver Transplantation. *Cytokine* 2021; **148**: 155705 [PMID: 34564024 DOI: 10.1016/j.cyto.2021.155705]
51 **Sena LA**, Li S, Jairaman A, Prakriya M, Ezponda T, Hildeman DA, Wang CR, Schumacker PT, Licht JD, Perlman H, Bryce PJ, Chandel NS. Mitochondria are required for antigen-specific T cell activation through reactive oxygen species signaling. *Immunity* 2013; **38**: 225-236 [PMID: 23415911 DOI: 10.1016/j.immuni.2012.10.020]
52 **Pearce EL**, Poffenberger MC, Chang CH, Jones RG. Fueling immunity: insights into metabolism and lymphocyte function. *Science* 2013; **342**: 1242454 [PMID: 24115444 DOI: 10.1126/science.1242454]
53 **Gerriets VA**, Kishton RJ, Nichols AG, Macintyre AN, Inoue M, Ilkayeva O, Winter PS, Liu X, Priyadharshini B, Slawinska ME, Haeberli L, Huck C, Turka LA, Wood KC, Hale LP, Smith PA, Schneider MA, MacIver NJ, Locasale JW, Newgard CB, Shinohara ML, Rathmell JC. Metabolic programming and PDHK1 control CD4+ T cell subsets and inflammation. *J Clin Invest* 2015; **125**: 194-207 [PMID: 25437876 DOI: 10.1172/JCI76012]
54 **Matsushita M**, Freigang S, Schneider C, Conrad M, Bornkamm GW, Kopf M. T cell lipid peroxidation induces ferroptosis and prevents immunity to infection. *J Exp Med* 2015; **212**: 555-568 [PMID: 25824823 DOI: 10.1084/jem.20140857]
55 **Ogando DG**, Choi M, Shyam R, Li S, Bonanno JA. Ammonia sensitive SLC4A11 mitochondrial uncoupling reduces glutamine induced oxidative stress. *Redox Biol* 2019; **26**: 101260 [PMID: 31254733 DOI: 10.1016/j.redox.2019.101260]
56 **Zhang J**, Wang X, Vikash V, Ye Q, Wu D, Liu Y, Dong W. ROS and ROS-Mediated Cellular Signaling. *Oxid Med Cell Longev* 2016; **2016**: 4350965 [PMID: 26998193 DOI: 10.1155/2016/4350965]
57 **Zorov DB**, Juhaszova M, Sollott SJ. Mitochondrial reactive oxygen species (ROS) and ROS-induced ROS release. *Physiol Rev* 2014; **94**: 909-950 [PMID: 24987008 DOI: 10.1152/physrev.00026.2013]

58 **Kerins MJ**, Milligan J, Wohlschlegel JA, Ooi A. Fumarate hydratase inactivation in hereditary leiomyomatosis and renal cell cancer is synthetic lethal with ferroptosis induction. *Cancer Sci* 2018; **109**: 2757-2766 [PMID: 29917289 DOI: 10.1111/cas.13701]

59 **Xu C**, Sun S, Johnson T, Qi R, Zhang S, Zhang J, Yang K. The glutathione peroxidase Gpx4 prevents lipid peroxidation and ferroptosis to sustain Treg cell activation and suppression of antitumor immunity. *Cell Rep* 2021; **35**: 109235 [PMID: 34133924 DOI: 10.1016/j.celrep.2021.109235]

World Journal of Gastroenterology

Submit a Manuscript: https://www.f6publishing.com

World J Gastroenterol 2023 May 28; 29(20): 3103-3118

DOI: 10.3748/wjg.v29.i20.3103

ISSN 1007-9327 (print) ISSN 2219-2840 (online)

ORIGINAL ARTICLE

Basic Study

Dihydroergotamine ameliorates liver fibrosis by targeting transforming growth factor β type II receptor

Ke-Xin Zheng, Shou-Li Yuan, Meng Dong, Han-Lin Zhang, Xiao-Xiao Jiang, Chun-Long Yan, Rong-Cai Ye, Hui-Qiao Zhou, Li Chen, Rui Jiang, Zi-Yu Cheng, Zhi Zhang, Qi Wang, Wan-Zhu Jin, Wen Xie

Specialty type: Gastroenterology and hepatology

Provenance and peer review: Unsolicited article; Externally peer reviewed.

Peer-review model: Single blind

Peer-review report's scientific quality classification

Grade A (Excellent): 0
Grade B (Very good): B, B
Grade C (Good): 0
Grade D (Fair): 0
Grade E (Poor): 0

P-Reviewer: Jena MK, India; Shrewsbury SB, United States

Received: February 6, 2023
Peer-review started: February 6, 2023
First decision: March 21, 2023
Revised: April 1, 2023
Accepted: April 24, 2023
Article in press: April 24, 2023
Published online: May 28, 2023

Ke-Xin Zheng, Qi Wang, Wen Xie, Center of Liver Diseases, Beijing Ditan Hospital, Capital Medical University, Beijing 100015, China

Shou-Li Yuan, Meng Dong, Han-Lin Zhang, Xiao-Xiao Jiang, Chun-Long Yan, Rong-Cai Ye, Hui-Qiao Zhou, Li Chen, Rui Jiang, Zi-Yu Cheng, Zhi Zhang, Wan-Zhu Jin, Key Laboratory of Animal Ecology and Conservation Biology, Institute of Zoology, Chinese Academy of Sciences, Beijing 100101, China

Shou-Li Yuan, Han-Lin Zhang, Xiao-Xiao Jiang, Rong-Cai Ye, Hui-Qiao Zhou, Li Chen, Rui Jiang, Zi-Yu Cheng, Zhi Zhang, Graduate School, University of the Chinese Academy of Sciences, Beijing 100049, China

Chun-Long Yan, Graduate School, Agriculture College of Yanbian University, Yanji 133002, Jilin Province, China

Corresponding author: Wen Xie, MD, Doctor, Center of Liver Diseases, Beijing Ditan Hospital, Capital Medical University, No. 8 Jingshun East Street, Chaoyang District, Beijing 100015, China. xiewen6218@163.com

Abstract

BACKGROUND

The transforming growth factor β (TGFβ) signaling pathway plays a crucial role in the development of liver fibrosis by activating TGFβ type II receptor (TGFβR2), followed by the recruitment of TGFβR1 finally triggering downstream signaling pathway.

AIM

To find drugs targeting TGFβR2 that inhibit TGFβR1/TGFβR2 complex formation, theoretically inhibit TGFβ signaling pathway, and thereby ameliorate liver fibrosis.

METHODS

Food and Drug Administration-approved drugs were screened for binding affinity with TGFβR2 by virtual molecular docking. We identified 6 candidates and further explored their potential by Cell Counting Kit-8 (CCK-8) cell cytotoxic experiment to validate toxicity and titrated the best cellular working concentrations. Next, we further demonstrated the detailed molecular working

mechanisms using mutagenesis analysis. Finally, we used a mouse model to investigate its potential anti-liver fibrosis effect.

RESULTS

We identified 6 drug candidates. Among these 6 drugs, dihydroergotamine (DHE) shows great ability in reducing fibrotic gene expressions such as collagen, p-SMAD3, and α-SMA in TGFβ induced cellular model of liver fibrosis in LX-2 cells. Furthermore, we demonstrated that DHE binds to TGFβR2. Moreover, mutation of Leu27, Phe30, Thr51, Ser52, Ile53, and Glu55 of TGFβR2 disrupted the binding of TGFβR2 with DHE. In addition, DHE significantly improved liver fibrosis, as evidenced by Masson's trichrome staining of liver sections. This is further supported by the width and the velocity of the portal vein, and serum markers of liver function. In line with those observations, DHE also decreased macrophages infiltration and extracellular matrix deposition in the liver.

CONCLUSION

DHE alleviates liver fibrosis by binding to TGFβR2 thereby suppressing TGFβ signaling pathway. We show here that as far as drug repurposing, DHE has great potential to treat liver fibrosis.

Key Words: Liver fibrosis; Transforming growth factor β (TGFβ) signaling pathway; TGFβ type II receptor (TGFβR2); Virtual screening; Drug-repurposing; Dihydroergotamine

©The Author(s) 2023. Published by Baishideng Publishing Group Inc. All rights reserved.

Core Tip: An effective and safe drug for treating liver fibrosis is urgently needed in current clinical practice. Here, we investigated and discovered that dihydroergotamine (DHE) could alleviate liver fibrosis by specific binding of transforming growth factor β type II receptor (TGFβR2) to disrupt the binding of TGFβR2 with TGFβ1, and ultimately suppressing its downstream TGFβ signaling pathway. DHE may be an effective anti-liver fibrosis drug, which could be employed in liver cirrhotic patients.

Citation: Zheng KX, Yuan SL, Dong M, Zhang HL, Jiang XX, Yan CL, Ye RC, Zhou HQ, Chen L, Jiang R, Cheng ZY, Zhang Z, Wang Q, Jin WZ, Xie W. Dihydroergotamine ameliorates liver fibrosis by targeting transforming growth factor β type II receptor. *World J Gastroenterol* 2023; 29(20): 3103-3118
URL: https://www.wjgnet.com/1007-9327/full/v29/i20/3103.htm
DOI: https://dx.doi.org/10.3748/wjg.v29.i20.3103

INTRODUCTION

Liver fibrosis is the consequence of various chronic pathogenic factors[1], it is a dynamic process that is characterized by an excessive accumulation of extracellular matrix[2]. Early liver fibrosis can be reversed to a normal architecture by removal of underlying causes[2], but liver fibrosis could further develop into cirrhosis without effective treatment[3]. Liver cirrhosis can be complicated by variceal bleeding, hepatic encephalopathy, ascites, bacterial peritonitis, and hepatocellular carcinoma, which has high mortality[4]. Liver cirrhosis can regress to early stage of disease, but it cannot be reversed to a normal liver[5]. Therefore, it is very important to control the disease progression in the early reversible stage of liver fibrosis.

Etiological treatment of liver fibrosis is most important and effective, such as antivirals, quitting alcohol consumption, and weight loss[1]. However, effects of etiological treatment are limited and insufficient, and difficult to prevent the development of liver fibrosis into cirrhosis. At present, liver transplantation is a radical cure for cirrhosis but is associated with a high cost, organ shortages, and the risk of immune rejection[6]. In addition, almost all current clinical trials targeting fibrosis are focused on non-alcoholic steatohepatitis, specifically focusing on hepatic stellate cell (HSC) activation and/or fibrogenesis[7]. However, there are still no approved antifibrotic therapies for liver fibrosis[7]. Therefore, it is urgent to develop new effective drugs.

Developing new drugs is a difficult, high-cost, and extremely low success rate procedure[8]. A good strategy to address this problem is to investigate new indications of old drugs, a process called "drug repurposing"[9]. Scientists have repurposed many old drugs such as propranolol[10], cimetidine[11], sildenafil[12], and thalidomide[13]. Thus, drug repurposing is an attractive approach and has been widely employed. Drugs that have been approved by Food and Drug Administration (FDA) have passed preliminary clinical trials and are considered extremely safe. Therefore, FDA-approved drugs may be good candidates for developing new indications. Molecular docking, a fast, efficient, and widely

used technique in drug repurposing, is a computational strategy to predict binding sites between ligands and targets based on their structures[9,14].

The activation of HSCs is considered the central effector of liver fibrosis[15]. There are many associated signaling molecules, including transforming growth factor β (TGFβ), platelet-derived growth factor, and connective tissue growth factor[16]. The TGFβ signaling pathway plays a crucial role in the development of liver fibrosis[17]. A review paper illustrated that TGFβ1 activates TGFβ type II receptor (TGFβR2), followed by the recruitment of TGFβR1. Afterward, TGFβR2 phosphorylates TGFβR1 thereby triggering down-stream signaling pathway to regulate the expression of collagens and extracellular matrix (ECM)[18]. Therefore, TGFβR2 is considered an important target for developing drugs against liver fibrosis. Consistently, our group and others demonstrated that both inhibiting the expression of TGFβR2 and exogenous extracellular domain of TGFβR2 supplement effectively alleviated liver fibrosis [19,20].

In the current study, FDA-approved drugs were screened for binding affinity with the TGFβR2 by virtual molecular docking. We used cellular and mouse models to investigate its potential anti-liver fibrosis effect. In addition, by using mutagenesis analysis we further demonstrated detailed molecular working mechanism.

MATERIALS AND METHODS

Molecular docking of FDA-approved drugs and TGFβR2

The structures of FDA-approved drugs were downloaded from the ZINC database (https://zinc12.docking.org/). Then, the files of each small molecular structures were generated using Open Babel GUI (3.1.1). The TGFβR2-TGFβ1 complex (PDB: 3KFD) was downloaded from the Protein Data Bank (https://www.rcsb.org/). The TGFβR2 structure was derived from the TGFβR2-TGFβ1 complex using AutoDock Vina software (https://vina.scripps.edu/). AutoDock Vina software was employed to screen for the lowest energy complex among complexes of the extracellular TGFβR2 domain and the FDA-approved drugs.

Cell culture and viability experiments

The human HSC line LX-2 was purchased from the BeNa Culture Collection (Beijing, China) and cultured in Dulbecco's modified Eagle medium (DMEM, Gibco, United States) with 10% fetal bovine serum (FBS, Gibco, United States) at 37 °C in a 5% CO_2 atmosphere. LX-2 was activated by human recombinant protein TGFβ1 (5 ng/mL) for 24 h, followed by drug treatment for 24 h. The expression of fibrosis-related genes was analyzed.

Cell Counting Kit-8 (CCK-8, Beyotime Biotechnology, Shanghai, China) test was used to test the cytotoxicity of a series of working concentrations of the candidate drugs on LX-2 cell. After 24 h of treatment, the CCK-8 solution was added to each well for an additional 1 h of incubation (37 °C in a 5% CO_2 atmosphere). A microplate analyzer was used to measure the optical density of each well at 450 nm. Cell vitality was expressed as a percentage of optical density between the treatment wells and the negative control cells.

Determination of Kd value between TGFβR2 and dihydroergotamine

The Kd value of the small molecules and the TGFβR2 protein was measured using a microscale thermophoresis (MST)-Nanotemper instrument (Nanotemper, Germany). Micro thermophoresis is the directional movement of particles in the micro temperature gradient. The affinity is determined by measuring the change of micro thermophoresis caused by the change of hydration layer (usually caused by the change of biomolecular structure/conformation). First, 100 μL each of 10 μM TGFβR2 and different concentrations of the small molecules (diluted from 400 μM stock) were prepared. Second, TGFβR2 was labeled with a fluorescent dye and mixed with the small molecules. Third, fluorescence was measured to assess the binding behavior of the small molecule-TGFβR2 complex.

Molecular dynamics simulation

Molecular dynamics simulations were performed using Gromacs 2020.1, in which a charm36-mar2019 force field was chosen. The TGFβR2 or TGFβR2-small molecule complex was solved with TIP3P water and immersed in a dodecahedron box extending to at least 1 nm of the solvent on all sides. The system was neutralized with Na^+ and Cl^- by adding 0.15 M NaCl. It was energy-minimized using the steepest descent algorithm for 5000 steps and creating a maximum force of < 1000 kJ/mol/nm. After energy minimization, the system was equilibrated with a constrained "number of particles, volume, and temperature" (NVT) and "number of particles, pressure, and temperature" (NPT) running for 100 ps. Through NVT and NPT equilibration, the system was well-equilibrated at 300 K and 1 bar. Finally, MD simulations of the TGFβR2 or complex were carried out for 200 ns; trajectories were saved every 10 ps for analysis. The Verlet cut-off scheme and a Leap-frog integrator with a step size of 2 fs were applied. The modified Berendsen thermostat was used for temperature coupling, the Parrinello-Rahman barostat was used for pressure coupling, and the Particle Mesh Ewald method was used to determine long-range

electrostatic interactions.

The root-mean-square displacement (RMSD) and root-mean-square fluctuation (RMSF) of TGFβR2 and the complex were calculated using GROMACS 2020.1. The content of the secondary structure was calculated using DSSP software. The last MD simulation frame of the complex was extracted using GROMACS 2020.1. LigPlot+ software (https://www.ebi.ac.uk/thornton-srv/software/LigPlus/) was used to analyze the detailed interactions between the extracellular TGFβR2 domain and small molecule. PyMOL (http://www.pymol.org/) was used to prepare the structural images.

Production and purification of site-directed mutagenesis of TGFβR2

The binding sites of TGFβR2 and small molecule were established using the molecular docking results. The amino acids at the binding sites were mutated to alanine whose nucleotide sequence was GCG. The sequences of mutated extracellular TGFβR2 and a 6X His-tag were inserted into a pMAL-c5x plasmid that was synthesized by GenScript Biotech Corporation.

The mutated plasmid was transformed into BL21 (DE3) bacteria and induced with 0.8 mmol/L IPTG for 16 h at 28 °C. Then, bacteria were collected and resuspended in phosphate buffered saline (PBS). The mutated TGFβR2 protein was purified by HisTrap FF affinity chromatography and eluted with PBS containing gradient concentrations of imidazole. Finally, the eluted proteins were concentrated and the imidazole was removed by dialysis.

CCl_4 injury mouse model

Six-week-old male C57BL/6N mice were purchased from Vital River Laboratory Animal Technology Co. Ltd. to induce a liver fibrosis model. The animal protocol was designed to minimize pain or discomfort to the animals. The animals were acclimatized to laboratory conditions (23 °C, 12 h/12 h light/dark, 50% humidity, ad libitum access to food and water) for 2 wk prior to experimentation. After being transferred to our institute, the animals were randomly and evenly divided into four groups (eight mice per group) according to their body weight: Corn oil, carbon tetrachloride (CCl_4), low-concentration treatment, and high-concentration treatment groups. The same volume of CCl_4 (0.5 μL/g of body weight, Sigma-Aldrich, St. Louis, MO, United States) and corn oil were intraperitoneally injected three times a week to induce a liver fibrosis model and in control animals for four weeks, respectively. Intragastric gavage administration was carried out with conscious animals, using straight gavage needles appropriate for the animal size. Then, the small molecule aqueous solution and water was administered orally once a day as treatment and control for eight weeks, respectively. All animals were euthanized for tissue collection. All animal studies were performed following the National Institutes of Health's Guide for the Care and Use of Laboratory Animals and conducted with the approval of the Institutional Animal Care and Use Committee of the Institute of Zoology, Chinese Academy of Sciences.

B-mode ultrasonography

Small-animal B-ultrasound was used to inspect the portal veins. A high-resolution ultrasound imaging system (Vevo LAZR, VisualSonics, Canada) was used to measure the width and velocity of the portal vein. Mice were fasted for 12 h and shaved before the ultrasonic examination. Then, the mice were fixed on the platform and examined after being anesthetized with Avertin. After coating the mouse's abdomen with the coupling gel, the probe was used to inspect the mouse's portal vein.

Masson's trichrome staining

Mouse liver tissues were fixed in 4% paraformaldehyde, embedded in paraffin, and sectioned at 5 μm thickness. Then, the liver paraffin-embedded tissue sections were stained with a Masson's trichrome kit (G1281, Solarbio, Beijing, China) and observed under a 10x objective lens. Masson's trichrome staining is used to distinguish collagen fibrosis from muscle fibers. Muscle fibers were stained red and collagen fibrosis was stained green or blue. The collagen area was quantified using ImageJ 1.52a software. And one liver section was taken from each mouse for analysis.

Western blot analysis

Total proteins were extracted from the LX-2 cells or liver tissues using radioimmunoprecipitation assay lysis buffer (50 mmol/L Tris-HCl, pH 7.4; 1% NP-40; 0.25% sodium deoxycholate; 150 mmol/L NaCl; and 1 mmol/L ethylene diamine tetraacetic acid (EDTA)) containing a protease and phosphatase inhibitor mixture (Roche Diagnostics). The proteins were separated on 10% sodium dodecyl sulfate (SDS) polyacrylamide gels and transferred onto polyvinylidene fluoride membranes (Millipore). After blocking with 5% skim milk in Tris-buffered saline-Tween 20 (0.02 M Tris base, 0.1% Tween 20, 0.14 M NaCl, pH 7.4) for 1 h, the membranes were incubated with primary antibodies overnight at 4 °C. The membranes were then incubated with horseradish-peroxidase (HRP)-conjugated secondary antibodies for 1 h at room temperature. Supplementary Table 1 lists the antibodies.

Real-time quantitative PCR (RT-PCR) analysis

Total RNA was extracted from the LX-2 cells or liver tissues using TRIzolTM Reagent (Thermo Fisher Scientific, United States) according to the manufacturer's instructions. Complementary DNA (cDNA)

was obtained from the reverse-transcribed RNA using a high-capacity cDNA reverse-transcription kit (Promega, United States). The relative expression of genes was analyzed by RT-PCR (Light Cycler 480, Roche, Sweden) with SYBR Green Master Mix (Promega, United States). Supplementary Table 2 lists the primer sequences.

Isolation of liver mononuclear cells and flow cytometry analysis

Liver mononuclear cells (MNCs), including Kupffer cells, were isolated from mouse liver tissues. Liver samples were collected from mice under deep anesthesia. The liver samples were cut into pieces, transferred into 5 mL of enzyme mix [RPMI 1640 containing 1 mg/mL collagen IV (Sigma) and 20 U/mL DNase I (Roche, Burgess Hill, United Kingdom)], and digested in a water bath at 37 °C for 30 min. RPMI 1640 containing 10% FBS was added to arrest the digestion. The digested mixture was filtered through a 70 μm strainer, centrifuged at 4 °C for 10 min at 1000 × g, and the pellet was washed in PBS twice. Liver immune cells were subsequently isolated using a 33% Percoll cell separation solution after centrifuging for 25 min at 2200 × g at room temperature. The red blood cells were removed using a red blood cell lysis buffer (YESEN, Shanghai, China). Finally, liver immune cells were counted and stained with anti-F4/80 antibody eFluor® 450 (eBioscience, San Diego, CA), brilliant violet 510™-conjugated anti-CD45 antibody (Biolegend, San Diego, CA), and percp-cyanine5.5-conjugated anti-CD11b antibody (eBioscience, San Diego, CA), which were then filtered into flow tubes through a 0.45 μm strainer. The result of flow cytometry was analyzed using a BD Fortessa instrument (BD, NY, United States).

Plasma biochemical markers

Mouse blood samples were collected from the tail vein, collected into EDTA-containing tubes, and gently shaken. Plasma was collected after centrifuging at 3000 × g for 15 min at 4 °C. Plasma alanine aminotransferase (ALT) and aspartate aminotransferase (AST) levels were measured using a biochemistry analyzer (Cobas c 501, Roche, Sweden).

Statistical analyses

Data are expressed as mean ± standard error of the mean. The statistical significance between groups was analyzed using one-way ANOVA test. Statistical significance was set at $P < 0.05$ and $P < 0.05$, $P < 0.01$, $P < 0.001$, and $P < 0.0001$ were denoted as a, b, c, and d, respectively. GraphPad Prism software was used to perform all statistical analyses.

RESULTS

The docking analysis of FDA-approved small molecule drugs and TGFβR2

AutoDock Vina software was employed to dock drugs with the extracellular domain of TGFβR2 and output the complex structures. The complex and the binding sites of TGFβR2 and TGFβ1 were shown (Figure 1A), and the structure of TGFβR2 was split from the complex (Figure 1B). The binding affinity of each FDA-approved drug was evaluated (Figure 1C). Among those, darifenacin, cyproheptadine, lifitegrast, difenoxin, phenytoin, dihydroergotamine (DHE), naldemedine, and irinotecan showed higher scores out of 1615 drugs (Figure 1C). Darifenacin is a competitive muscarinic M receptor antagonist used to treat urinary frequency, urgency, and incontinence caused by bladder hyperstimulation[21]. Cyproheptadine is an antihistamine used to treat allergies[22]. Lifitegrast is a small molecule integrin inhibitor primarily used to treat symptoms and signs of dry eye[23]. Difenoxin is a human metabolite of diphenoxylate, which is a derivative of pethidine and can be used to treat functional diarrhea and chronic enteritis[24]. Phenytoin is an effective voltage-gated Na^+ channel blocker used to treat epilepsy, neuralgia, and arrhythmia[25]. DHE is an adrenergic receptor antagonist used to treat severe orthostatic hypotension, migraine, and headache[26], which can bind with various receptors. DHE is also an agonist at 5-HT1B, 5-HT1D, and 5-HT1F receptors, but it also binds to 5-HT1A and 5-HT2A receptors. Naldemedine is an opioid receptor antagonist used to treat non-cancerous pain and opioid-induced constipation[27]. Irinotecan is a semi-synthesis of water-soluble camptothecin derivatives used to treat advanced colorectal cancer and postoperative adjuvant chemotherapy[28] (Table 1). All the above drugs were purchased from Selleck Chemicals, except for difenoxin and naldemedine which are banned from purchase as they are under management control. Therefore, we performed the following experiments using the rest 6 small molecule drugs.

Cytotoxicity of candidate drugs

To investigate the cytotoxicity of these drugs, LX-2 cells were treated with 20 μM of each candidate for 24 h. The results demonstrated that irinotecan and cyproheptadine were cytotoxic to LX-2 cells at this concentration (Figure 1D). Therefore, irinotecan and cyproheptadine were regarded as cytotoxic drugs and excluded from subsequent experiments. Next, to identify the best range of concentrations that would not influence the viability of these cells, LX-2 cells were treated with different concentrations of the remaining drugs for 24 h. The results demonstrated that neither lifitegrast nor phenytoin was

Table 1 The drugs with the highest affinity of transforming growth factor β type II receptor

Name	ZINC_ID	Affinity (kcal/mol)	Indications
Darifenacin	ZINC000001996117	-7.6	Urinary frequency, urgency, and incontinence caused by bladder hyperstimulation
Cyproheptadine	ZINC000000968264	-7.4	Allergy
Lifitegrast	ZINC000084668739	-7.4	Symptoms and signs of dry eye
Difenoxin	ZINC000000601317	-7.3	Functional diarrhea and chronic enteritis
Phenytoin	ZINC000002510358	-7.3	Epilepsy, neuralgia, and arrhythmia
DHE	ZINC000003978005	-7.3	Severe orthostatic hypotension, migraine, and headache
Naldemedine	ZINC000100378061	-7.3	Non-cancerous pain and opioid induced constipation
Irinotecan	ZINC000001612996	-7.3	Advanced colorectal cancer and postoperative adjuvant chemotherapy

DHE: Dihydroergotamine.

cytotoxic to LX-2 cells when concentrations were up to 100 μM and 150 μM, respectively (Figure 1E and F). Darifenacin and DHE were cytotoxic to LX-2 cells when concentrations were beyond 50 μM and 20 μM, respectively (Figure 1G and H). Therefore, to avoid interference on fibrosis-related gene expression due to the cytotoxicity of candidate drugs, lifitegrast and phenytoin concentrations below 100 μM and darifenacin and DHE concentrations below 20 μM were used to treat LX-2 cells.

Anti-fibrotic effect of candidate drugs in cellular model

Increased expression of collagen and alpha-smooth muscle actin (α-SMA) are principal markers of HSC activation[29]. LX-2 cells were treated with different concentrations of drugs for 24 h after TGFβ1 stimulation. The results demonstrated that lifitegrast and phenytoin did not decrease the protein levels of collagen III and α-SMA after TGFβ1 stimulation (Figure 2A and B). Moreover, darifenacin did not decrease the protein levels of collagen III, p-SMAD3, and α-SMA as much as DHE (Figure 2C and D). Consistently, DHE significantly decreased the mRNA expression of collagen I alpha 1 (COL1A1), collagen I alpha 2 (COL1A2), collagen III alpha 1 (COL3A1), and α-SMA compared with darifenacin (Figure 2E and F). Taken together, DHE (PubChem CID: 10531) was the most effective small molecule drug that suppressed the TGFβ1 induced LX-2 activation.

The binding affinity of DHE to TGFβR2

We further verified the molecular docking result by MST-Nanotemper. The results demonstrated that the fluorescence intensity of TGFβR2 changed gradually in proportion to the DHE concentration (Figure 3A). The affinity is determined by measuring the change of micro thermophoresis caused by the change of hydration layer, and results showed the binding affinity of DHE to TGFβR2 with a Kd value of 17.64 μM.

Molecular dynamics simulation of DHE and TGFβR2

To identify the specific binding mode of DHE and TGFβR2, we used the complex structure obtained from AutoDock vina to perform the molecular dynamics simulation with GROMACS 2020.1 software for 200 ns. The results demonstrated that the RMSD of the backbone atoms of TGFβR2 and TGFβ R2□DHE in the simulation system reached equilibrium after 100 ns (Figure 3B). The RMSFs of the TGFβ R2 skeleton carbon atoms in the two simulated systems were almost identical (Figure 3C). The secondary structural elements of TGFβR2 in the complex simulation were only slightly changed (Figure 3D and Table 2). The coil and 3-helix components of TGFβR2 decreased in the complex simulation system (Table 2). Finally, we extracted the simulated complex structure and analyzed the amino acid sites of TGFβR2 bound to DHE by Ligplot+ software (Figure 3E and F). In conclusion, our molecular dynamics simulations showed that the binding of DHE to TGFβR2 has little effect on the structure of TGFβR2. We also obtained the binding sites of TGFβR2 to DHE by stimulations.

Leu27, Phe30, Thr51, Ser52, Ile53, and Glu55 of TGFβR2 bind with DHE

Molecule docking demonstrated that Leu27, Phe30, Thr51, Ser52, Ile53, and Glu55 of TGFβR2 were binding sites for DHE (Figure 3F). To verify these binding sites, we mutated the above-mentioned amino acids to alanine. The DNA sequences of mutated extracellular TGFβR2 were synthesized (Table 3) and the binding affinity was measured. The results demonstrated that the mutated TGFβR2 no longer bound to DHE (Figure 3G). Thus, the above-mentioned binding sites of TGFβR2 predicted by molecule docking were the exact binding sites of TGFβR2 and DHE, and this further verified the binding of TGFβR2 and DHE. Therefore, we inferred that the binding of TGFβ1 and TGFβR2 was

Table 2 Content of secondary structural analysis from DSSP method

Structure	Coil	β-Sheet	β-Bridge	Bend	Turn	3-Helix
TGFβR2	0.58	0.3	0.42	0.02	0.12	0.13
TGFβR2-DHE	0.56	0.3	0.42	0.02	0.12	0.12

TGFβR2: Transforming growth factor β type II receptor; DHE: Dihydroergotamine.

Table 3 DNA sequence of extracellular transforming growth factor β type II receptor before and after mutation

	Before mutation	After mutation
DNA sequence of TGFβR2 extracellular domain	ACGATCCCACCGCACGTTCAGAAGTCGGTTAATAACGACA TGATAGTCACTGACAACAACGGTGCAGTCAAGTTTCCACA ACTGTGTAAATTTTGTGATGTGAGATTTTCCACCTGTGACA ACCAGAAATCCTGCATGAGCAACTGCAGCATCACCTCCA TCTGTGAGAAGCCACAGGAAGTCTGTGTGGCTGTATGGA GAAAGAATGACGAGAACATAACACTAGAGACAGTTTGCC ATGACCCCAAGCTCCCCTACCATGACTTTATTCTGGAAGAT GCTGCTTCTCCAAAGTGCATTATGAAGGAAAAAAAAAAGC CTGGTGAGACTTTCTTCATGTGTTCCTGTAGCTCTGATGAG TGCAATGACAACATCATCTTCTCAGAAGAATATAACACCA GCAATCCTGACTTGTTGCTAGTCATATTTCAA	ACGATCCCACCGCACGTTCAGAAGTCGGTTAATAACGACA TGATAGTCACTGACAACAACGGTGCAGTCAAGTTTCCACA AGCGTGTAAAGCGTGTGATGTGAGATTTTCCACCTGTGACA ACCAGAAATCCTGCATGAGCAACTGCAGCATCGCGGCGG CGTGTGCGAAGCCACAGGAAGTCTGTGTGGCTGTATGGA GAAAGAATGACGAGAACATAACACTAGAGACAGTTTGCC ATGACCCCAAGCTCCCCTACCATGACTTTATTCTGGAAGAT GCTGCTTCTCCAAAGTGCATTATGAAGGAAAAAAAAAAGC CTGGTGAGACTTTCTTCATGTGTTCCTGTAGCTCTGATGAG TGCAATGACAACATCATCTTCTCAGAAGAATATAACACCA GCAATCCTGACTTGTTGCTAGTCATATTTCAA

TGFβR2: Transforming growth factor β type II receptor.

blocked by the binding of DHE and TGFβR2, further preventing the TGFβ signaling cascade.

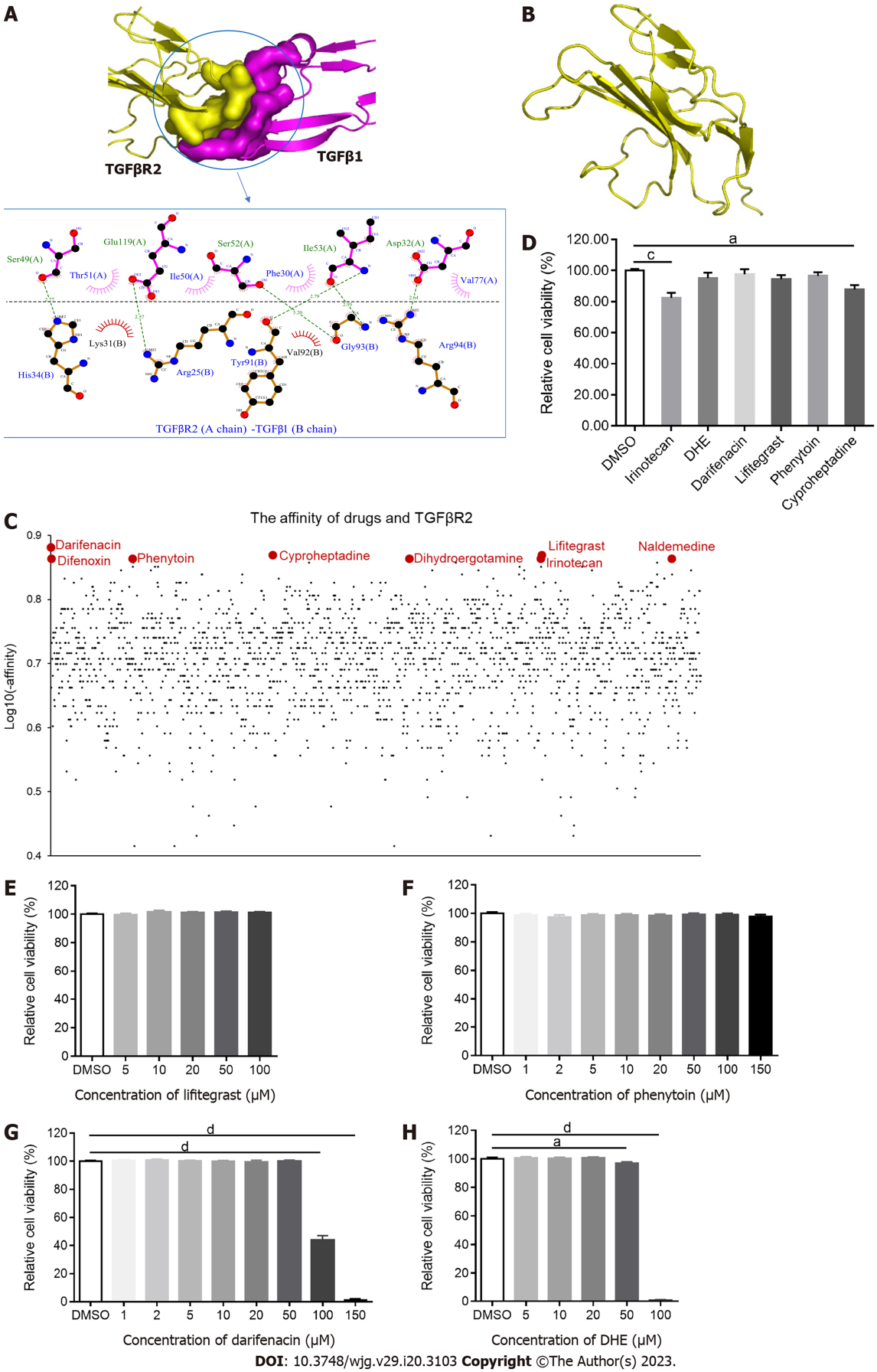
DHE alleviated liver fibrosis in mouse

To explore whether DHE could alleviate fibrosis in vivo, we used two different concentrations of DHE to treat a CCl_4-induced mouse fibrosis model. Six-week-old C57BL/6N mice were intraperitoneally injected three-time per week with CCl_4 and corn oil (control group) during the whole experimental periods (Supplementary Figure 1). After four weeks, the mice intraperitoneally injected with CCl_4 were randomly divided into three groups: CCl_4 and the 2 and 5 mg/kg DHE treatment groups. The aqueous solution of DHE was orally gavaged to the mice in the treatment groups. For vehicle treatment, water was provided by oral gavage to the mice in the corn oil and CCl_4 group (disease group).

It is well known that more serious the degree of liver fibrosis, the wider the portal vein and the slower its velocity. The results demonstrated that the portal vein in the CCl_4 group was significantly wider than that in the corn oil group. Interestingly, the width of the portal vein in the 2 mg/kg DHE treatment group was significantly decreased (Figure 4A). Furthermore, the velocity of the portal vein in the treatment groups was also improved (Figure 4B). After eight weeks of treatment, there were no significant differences in body weight, liver weight, spleen weight, or the ratio of liver weight to body weight among the four groups (Figure 4C and Supplementary Figure 2A). Gross liver specimens of the CCl_4 group were paler and had a rough appearance. However, it was back to normal appearance by DHE treatment compared to the CCl_4 group (Figure 4D). The level of plasma ALT of the CCl_4 group mice was significantly higher than corn oil group. Whereas, DHE treatment significantly decreased the level of ALT compared with CCl_4 group mice. In addition, the level of plasma AST was significantly decreased after 2 mg/kg DHE treatment (Figure 4E). Collagen area were visualized by Masson's trichrome and quantified by using ImageJ 1.52a software. DHE treatment in both dosages significantly reduced collagen accumulation compared with those of the CCl_4 group (Figure 4F and G). Taken together, these results demonstrated that DHE significantly protected from liver fibrosis in CCl_4-induced mouse fibrosis model.

DHE decreased the liver macrophages infiltration and ECM deposition

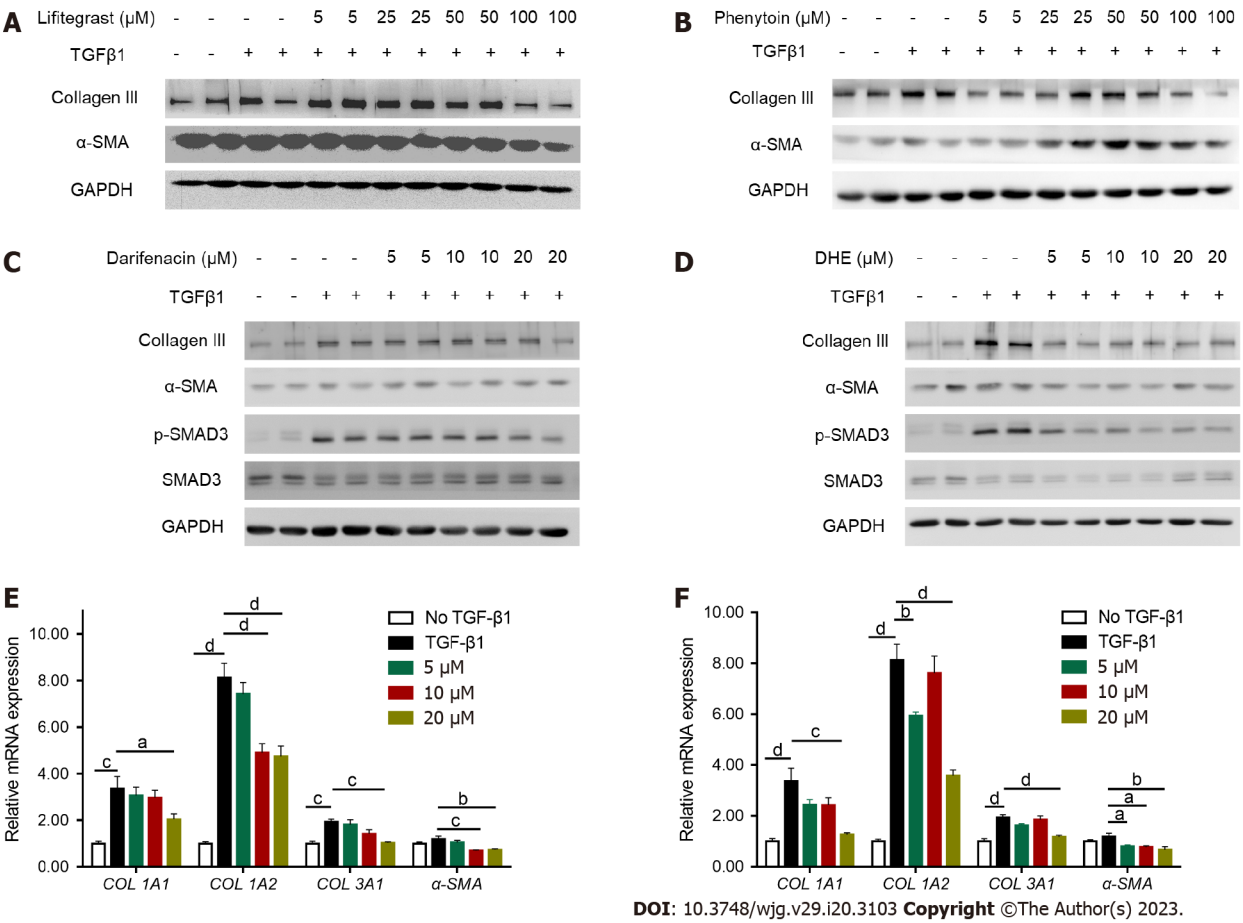
The infiltration of macrophages reflects the severity of liver inflammation. To investigate the degree of macrophages infiltration, the liver immune cells were extracted and labeled with $CD45^+$, $F4/80^+$, and $CD11b^+$ antibodies followed by flow-cytometric analysis. The results demonstrated that the DHE treatment at both dosages significantly reduced proportion of $CD11b^+$ cells (Figure 5A and B, and Supplementary Figure 2B-F). Consistent with the result of flow cytometry, the mRNA levels of tumor necrosis factor alpha (TNFα) and F4/80 which are two important indicators of liver inflammation significantly decreased upon DHE treatment (Figure 5C). On the other hand, the accumulation of ECM is another important sign of liver fibrosis. The results demonstrated that the mRNA levels of COL1A1, COL1A2, and α-SMA significantly decreased in the DHE treatment group more than those of the CCl_4 group (Figure 5D). The mRNA levels of COL3A1 also decreased in the DHE treatment groups



DOI: 10.3748/wjg.v29.i20.3103 **Copyright** ©The Author(s) 2023.

Figure 1 Screening Food and Drug Administration-approved drugs for binding to transforming growth factor β type II receptor. A: The combination of transforming growth factor β type II receptor (TGFβR2) and transforming growth factor β 1 (TGFβ1); B: The structure of TGFβR2; C: The affinity of

each Food and Drug Administration-approved drug and TGFβR2. The affinity of TGFβR2 and darifenacin, cyproheptadine, lifitegrast, difenoxin, phenytoin, dihydroergotamine (DHE), naldemedine, and irinotecan was -7.6, -7.4, -7.4, -7.3, -7.3, -7.3, -7.3, and -7.3 kcal/mol, respectively; D: Cell viability of LX-2 treated with 20 μM of the drugs for 24 h (n = 5); E-H: Cell viability following LX-2 treatment with different concentrations of darifenacin, DHE, lifitegrast, and phenytoin for 24 h (n = 6). All data are presented as mean ± standard error of the mean. One-way ANOVA test was performed. [a]P < 0.05, [b]P < 0.01, [c]P < 0.001, and [d]P < 0.0001. TGFβ: Transforming growth factor β; TGFβR: Transforming growth factor β receptor; DHE: Dihydroergotamine.



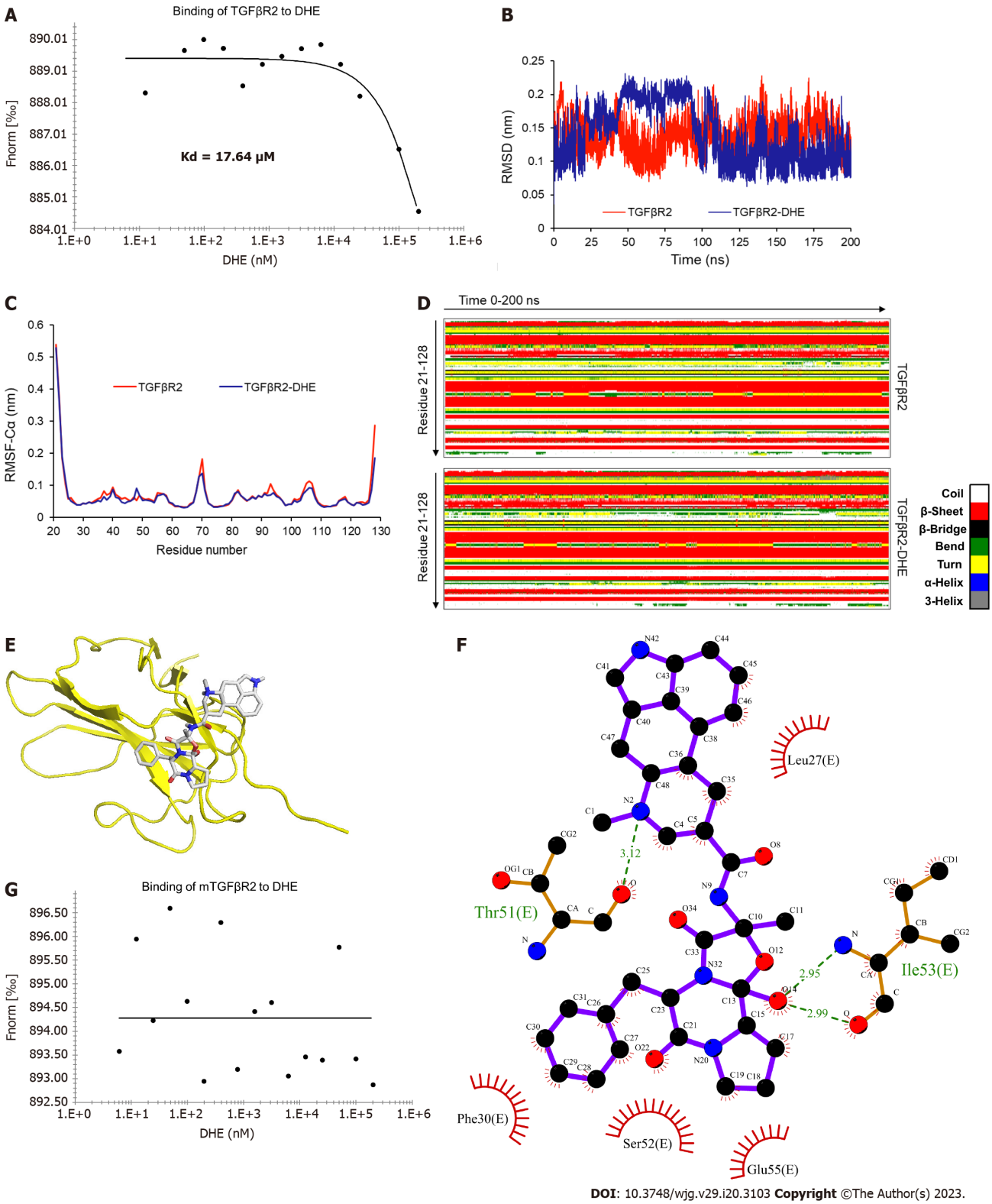
DOI: 10.3748/wjg.v29.i20.3103 **Copyright** ©The Author(s) 2023.

Figure 2 Treatment inhibiting the activation of LX-2 cells. A and B: After LX-2 cell was activated with transforming growth factor β 1 (TGFβ1) (5 ng/mL) for 24 h, different concentrations of lifitegrast and phenytoin were added for 24 h, and the protein levels of collagen III and α-SMA were detected by western blot; C and D: After LX-2 was activated with TGFβ1 (5 ng/mL) for 24 h, different concentrations of darifenacin and dihydroergotamine (DHE) were added for further treatment for 24 h, and the protein levels of collagen III, α-SMA, and p-SMAD3 were detected by western blot; E: Real-time polymerase chain reaction (RT-PCR) was performed to detect the expression of COL1A1, COL1A2, COL3A1, and α-SMA of LX-2 after different concentrations of darifenacin treatment (n = 6); F: RT-PCR was performed to detect the expression of COL1A1, COL1A2, COL3A1, and α-SMA of LX-2 after different concentrations of DHE treatment (n = 5-6). All data are presented as means ± standard error of the mean. One-way ANOVA test was performed. [a]P < 0.05, [b]P < 0.01, [c]P < 0.001, and [d]P < 0.0001. TGFβ: Transforming growth factor β; TGFβR: Transforming growth factor β receptor; DHE: Dihydroergotamine.

(Figure 5D). Meanwhile, the protein levels of α-SMA and p-SMAD3 were significantly decreased in the DHE treatment group compared to those of the CCl_4 group (Figure 5E and F). Thus, we demonstrated here that, DHE significantly decreased the liver macrophages infiltration and ECM deposition.

DISCUSSION

TGFβ1 is regarded as the most potent fibrogenic cytokine, which activates TGFβR2, followed by the recruitment of TGFβR1, therefore triggers HSC activation[30]. In the current study, we aimed to screen drugs targeting TGFβR2 and further blocking TGFβ down-stream signaling pathway from FDA-approved small molecule library. Among these 6 candidate drugs, DHE significantly decreased the protein and mRNA expression of fibrotic-related genes in LX-2 cells. The results of the affinity experiment demonstrated that DHE binds with TGFβR2 at Leu27, Phe30, Thr51, Ser52, Ile53, and Glu55. DHE also significantly alleviated liver fibrosis by decreasing macrophages infiltration and ECM accumulation in CCl_4-induced mouse fibrosis model. Thus, we demonstrate here for the first time that

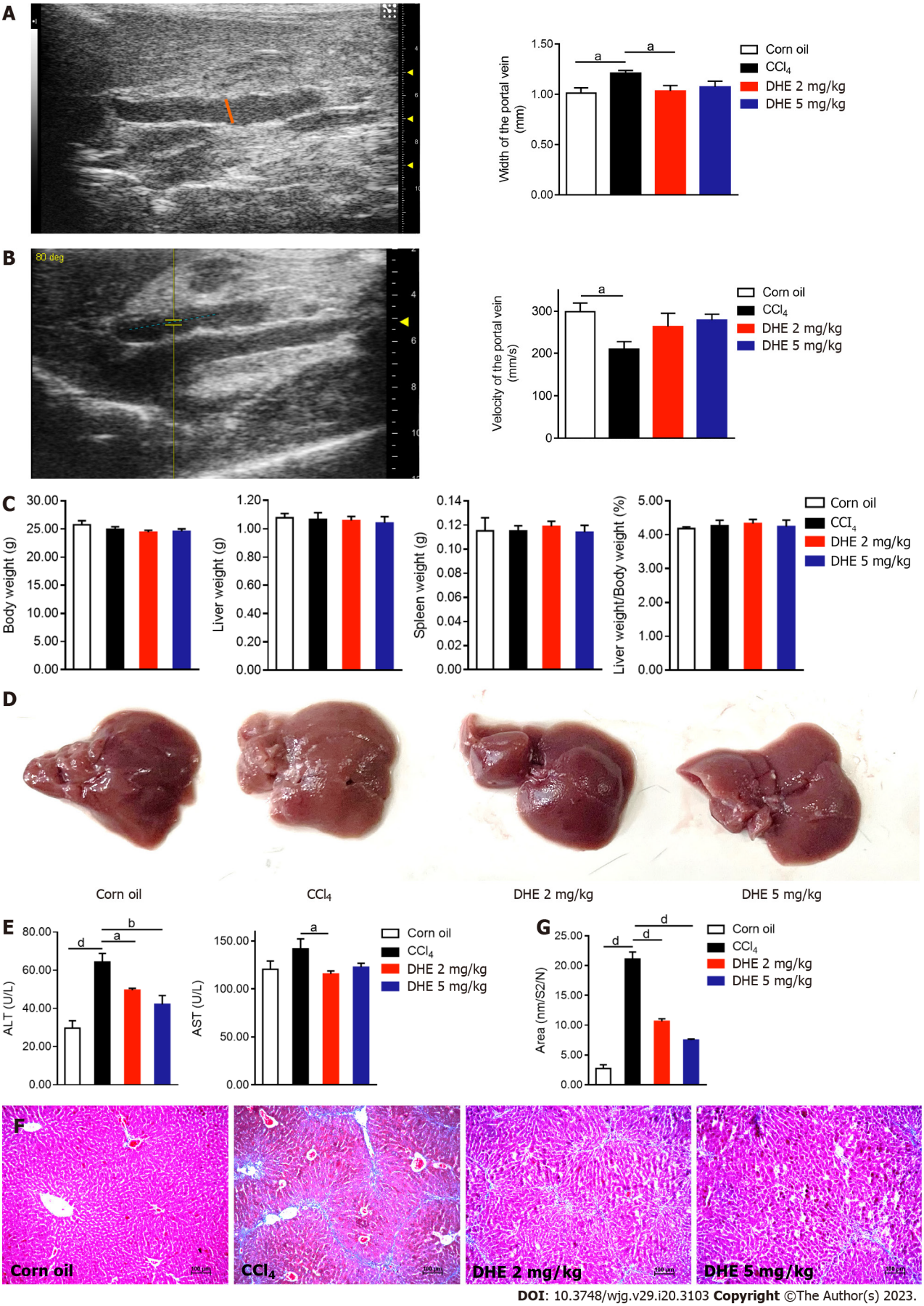


DOI: 10.3748/wjg.v29.i20.3103 **Copyright** ©The Author(s) 2023.

Figure 3 The binding affinity and sites of dihydroergotamine and transforming growth factor β type II receptor. A: Transforming growth factor β type II receptor (TGFβR2) bound to dihydroergotamine (DHE) with a Kd of 17.64 μM; B: Molecular dynamics simulation results of DHE and TGFβR2. Root-mean-square deviation of TGFβR2 skeleton atom; C: Root-mean-square fluctuation of backbone Cα atoms of TGFβR2 skeleton atom; D: The secondary structure components of TGFβR2 and complex simulation systems in 0-200 ns; E and F: The binding sites of DHE and TGFβR2; G: The binding affinity of TGFβR2 mutants with DHE. TGFβ: Transforming growth factor β; TGFβR: Transforming growth factor β receptor; DHE: Dihydroergotamine.

DHE, an anti-headache agent, is used in the treatment of liver fibrosis.

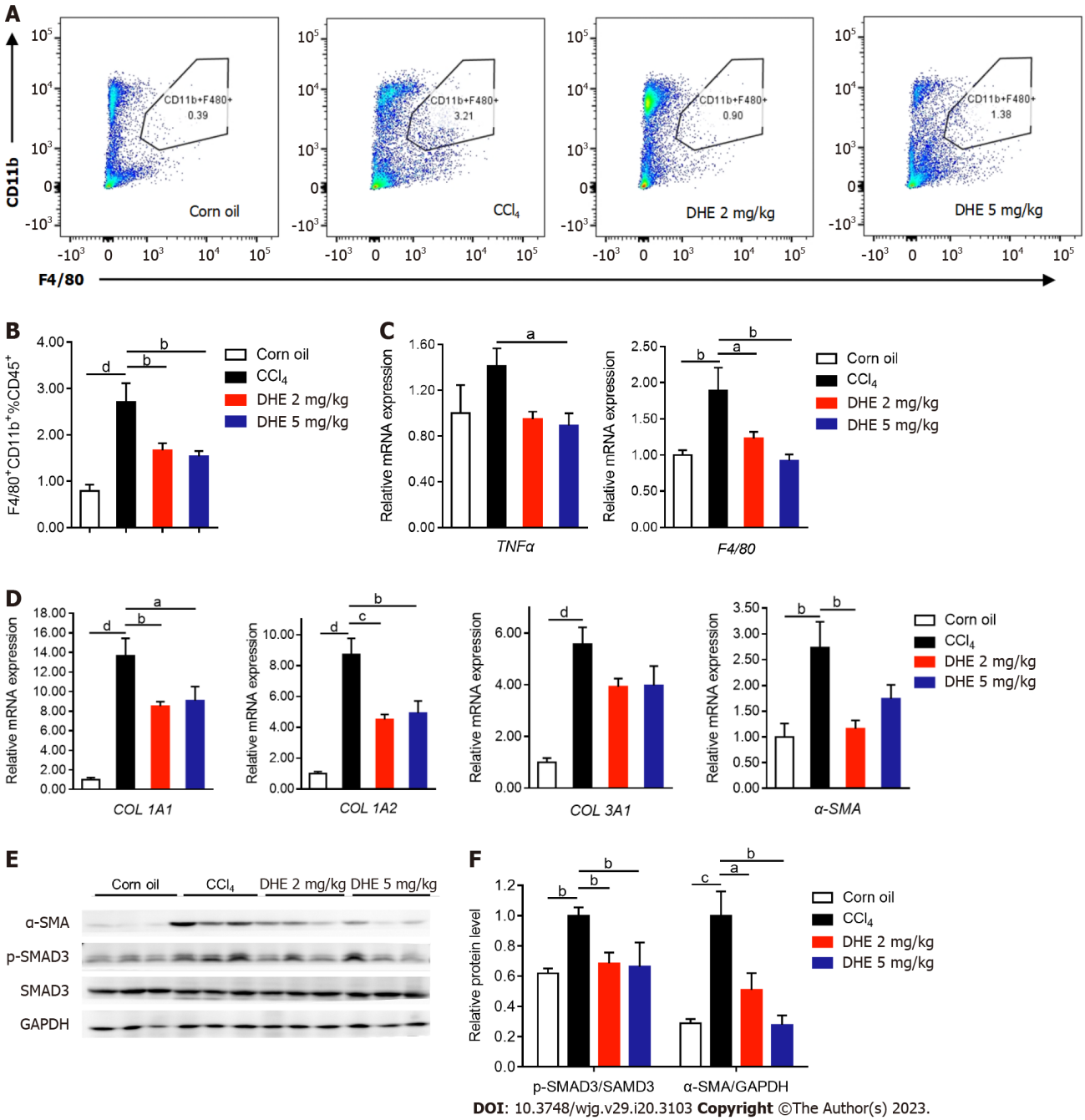
Developing a new drug needs more than a decade and significant investment[8]. Drug repurposing is a potential tool to accelerate the drug discovery process, which has been employed to develop therapies for coronavirus disease 2019[31], antimicrobials[32], and rare diseases[33]. The chemical structure of DHE is similar to that of many natural neurotransmitters, including epinephrine, norepinephrine,



DOI: 10.3748/wjg.v29.i20.3103 **Copyright** ©The Author(s) 2023.

Figure 4 Dihydroergotamine alleviated fibrosis in CCl_4-induced liver fibrosis model mice. A: The width of the portal vein (left panel); portal vein width of mice in each group (right panel, *n* = 7); B: The velocity of the portal vein (left panel); the velocity of mice in each group (right panel, *n* = 7); C: Body weight,

liver weight, spleen weight, and liver weight/body weight of mice in each group (n = 6-8); D: Gross liver specimens of the mice in each group; E: An automated biochemistry analyzer determined the enzymatic activities of serum levels of alanine aminotransferase and aspartate aminotransferase (n = 6-7); F: Masson's trichrome staining was performed on liver sections; G: Collagen area in Masson's trichrome staining (n = 7-8). All data were presented as means ± standard error of the mean. One-way ANOVA test was performed. $^{a}P < 0.05$, $^{b}P < 0.01$, $^{c}P < 0.001$, and $^{d}P < 0.0001$. TGFβ: Transforming growth factor β; TGFβR: Transforming growth factor β receptor; DHE: Dihydroergotamine.



DOI: 10.3748/wjg.v29.i20.3103 **Copyright** ©The Author(s) 2023.

Figure 5 Dihydroergotamine decreased the inflammatory infiltration of macrophages and extracellular matrix deposition in the liver. A and B: The flow cytometric analysis of CD11b^{+} cells (n = 6-8); C: The effects of dihydroergotamine (DHE) treatment on the mRNA expression levels of inflammation-related genes (n = 6-8); D: The effects of DHE treatment on the mRNA expression levels of extracellular matrix-related genes (n = 6-8); E: The protein levels of p-SMAD3 and α-SMA in liver tissues of mice in each group were detected by western blot (n = 3). All data are presented as means ± standard error of the mean. One-way ANOVA test was performed. $^{a}P < 0.05$, $^{b}P < 0.01$, $^{c}P < 0.001$, and $^{d}P < 0.0001$. TGFβ: Transforming growth factor β; TGFβR: Transforming growth factor β receptor; DHE: Dihydroergotamine.

dopamine, and serotonin[26]. It can modulate noradrenergic, serotonergic, and dopaminergic neurotransmission[34]. DHE is an adrenergic receptor antagonist used to treat severe orthostatic hypotension, migraine, and headache[26], which can bind with various receptors. DHE is also an

agonist of 5-HT1B, 5-HT1D, and 5-HT1F receptors, but it also binds to 5-HT1A and 5-HT2A receptors [26]. In the current study, surprisingly, we found that DHE also bind with TGFβR2 at reasonable affinity. Furthermore, we also identified specific binding sites by mutagenesis analysis. These results imply that DHE not only specifically targets 5-HT, but also TGFβR2. It further highlights wide-spread function of DHE in physiology/pathophysiology.

Continuous local and systemic inflammation aggravates liver injury, which is a critical factor in liver fibrosis. The innate immune system plays a pivotal role from the onset to the end stage of chronic liver disease[35]. Hepatic macrophages are considered as the first line of defense against pathogens, are a key cellular determinant in the process of fibrosis[36]. Bone marrow monocyte-derived macrophages and Kupffer cells are two distinct subsets of macrophages in the liver, which have been identified as key regulators of liver inflammation and key to the progression or regression of liver fibrosis. Kupffer cells, which are resident macrophages in liver tissue, exert anti-inflammatory effects[37]. Activated macrophages produce large amounts of TGFβ, which activates HSC into myofibroblast-like cells and synthesizes ECM[38]. This inflammatory response is also evident in the CCl_4-induced mouse model, especially in the increased number of macrophages in liver. Consistent with previous results, we also found that the macrophages infiltration was significantly increased after CCl_4 treatment. We speculate that, upon binding to TGFβR2, DHE prevents recruitment of TGFβR1 to TGFβR2, thereby inhibiting TGF β down-stream signaling pathway. Consistently, F4/80 and TNFα mRNA expression also significantly decreased upon DHE treatment. Taken together, DHE might reduce macrophages infiltration and finally prevent liver inflammation.

Activated HSCs secreting ECM represent a critical event in development of liver fibrosis[37]. In the fibrotic liver, type I and III collagens are deposited instead of laminins, type IV collagen, and proteoglycans in the normal liver[17]. Various mechanisms of HSC activation have been postulated, including TGFβ/SMAD pathway, Notch, Wnt/β-catenin, Hedgehog, and Hippo signaling[16]. In the current study, we revealed that DHE significantly reduced TGFβ induced HSCs activation in LX-2 cellular model through specific blocking of TGFβ signaling pathway. It explained clearly the significant reduction of ECM by DHE treatment. Taken together, our data show that DHE alleviated liver fibrosis by binding to TGFβR2, preventing the binding of TGFβ1 and TGFβR2, and blocking TGFβ1 signaling to reduce liver inflammation.

CONCLUSION

Our study demonstrated that DHE alleviated liver fibrosis while decreasing inflammation-related gene expression and HSC activation. The mechanism of its action is likely to be associated with decreased macrophages infiltration and ECM accumulation. Considering that liver fibrosis can be reversed, DHE might open-up new avenue to treat liver fibrosis in the future.

ARTICLE HIGHLIGHTS

Research background

The transforming growth factor β (TGFβ) signaling pathway plays a crucial role in the development of liver fibrosis by activating TGFβ type II receptor (TGFβR2), followed by the recruitment of TGFβR1 finally triggering downstream signaling pathway.

Research motivation

TGFβR2 is considered an important target for developing drugs against liver fibrosis. Previous studies demonstrated that both inhibiting the expression of TGFβR2 and exogenous extracellular domain of TGFβR2 supplement effectively alleviated liver fibrosis.

Research objectives

To find drugs targeting TGFβR2 that inhibit TGFβR1/TGFβR2 complex formation, theoretically inhibit its downstream TGFβ signaling pathway, and thereby ameliorate liver fibrosis, we screened drugs approved by the Food and Drug Administration (FDA) to identify potential TGFβR2 blockers.

Research methods

FDA-approved drugs were screened for binding affinity with TGFβR2 by virtual molecular docking. We identified 6 candidates and further explored their potential by Cell Counting Kit-8 cell cytotoxic experiment to validate toxicity and titrated the best cellular working concentrations. Next, we further demonstrated the detailed molecular working mechanisms using mutagenesis analysis. Finally, we used a mouse model to investigate its potential anti-liver fibrosis effect.

Research results

Dihydroergotamine (DHE) shows great ability in reducing fibrotic gene expressions such as collagen, p-SMAD3, and α-SMA in TGFβ induced cellular model of liver fibrosis in LX-2 cells. Furthermore, we demonstrated that DHE binds to TGFβR2 with a Kd value of 17.64 μM. In addition, DHE significantly improved liver fibrosis, as evidenced by Masson's trichrome staining of liver sections, the width and the velocity of the portal vein, and serum markers of liver function. In line with those observations, DHE also decreased macrophages infiltration and extracellular matrix deposition in the liver.

Research conclusions

DHE could alleviate liver fibrosis by binding to TGFβR2 thereby suppressing its downstream TGFβ signaling pathway. We show here that as far as drug repurposing, DHE has great potential to treat liver fibrosis.

Research perspectives

Considering that liver fibrosis can be reversed, DHE might open-up new avenue to treat liver fibrosis in the future.

FOOTNOTES

Author contributions: Xie W designed experiments and revised the manuscript; Jin WZ and Wang Q reversed the manuscript; Zheng KX and Yuan SL performed experiments, analyzed data, and wrote the manuscript; Dong M and Zhang HL performed experiments, analyzed data, and revised the manuscript; Other authors helped with the experiments; All authors read and approved the final version of the article.

Supported by the Special Research Project for Capital Health Development, No. 2022-2-2174; and the Beijing Municipal Science and Technology Commission, No. Z191100007619037.

Institutional animal care and use committee statement: All procedures involving animals were reviewed and approved by the Institutional Animal Care and Use Committee the Institute of Zoology, Chinese Academy of Sciences, IACUC protocol No. IOZ-IACUC-2020-114.

Conflict-of-interest statement: Dr. Xie reports in addition, Dr. Xie has a patent Application of dihydroergotamine in the treatment of liver fibrosis issued.

Data sharing statement: No additional data are available.

ARRIVE guidelines statement: The authors have read the ARRIVE guidelines, and the manuscript was prepared and revised according to the ARRIVE guidelines.

Open-Access: This article is an open-access article that was selected by an in-house editor and fully peer-reviewed by external reviewers. It is distributed in accordance with the Creative Commons Attribution NonCommercial (CC BY-NC 4.0) license, which permits others to distribute, remix, adapt, build upon this work non-commercially, and license their derivative works on different terms, provided the original work is properly cited and the use is non-commercial. See: https://creativecommons.org/Licenses/by-nc/4.0/

Country/Territory of origin: China

ORCID number: Ke-Xin Zheng 0000-0002-8252-1170; Shou-Li Yuan 0000-0002-4733-9891; Zhi Zhang 0000-0002-2471-1494; Qi Wang 0000-0002-0269-1568; Wen Xie 0000-0002-7314-8175.

S-Editor: Li L
L-Editor: A
P-Editor: Yuan YY

REFERENCES

1 **Parola M**, Pinzani M. Liver fibrosis: Pathophysiology, pathogenetic targets and clinical issues. *Mol Aspects Med* 2019; **65**: 37-55 [PMID: 30213667 DOI: 10.1016/j.mam.2018.09.002]

2 **Pellicoro A**, Ramachandran P, Iredale JP, Fallowfield JA. Liver fibrosis and repair: immune regulation of wound healing in a solid organ. *Nat Rev Immunol* 2014; **14**: 181-194 [PMID: 24566915 DOI: 10.1038/nri3623]

3 **Karsdal MA**, Nielsen SH, Leeming DJ, Langholm LL, Nielsen MJ, Manon-Jensen T, Siebuhr A, Gudmann NS, Rønnow S, Sand JM, Daniels SJ, Mortensen JH, Schuppan D. The good and the bad collagens of fibrosis - Their role in signaling and organ function. *Adv Drug Deliv Rev* 2017; **121**: 43-56 [PMID: 28736303 DOI: 10.1016/j.addr.2017.07.014]

4 **Ginès P**, Krag A, Abraldes JG, Solà E, Fabrellas N, Kamath PS. Liver cirrhosis. *Lancet* 2021; **398**: 1359-1376 [PMID: 34543610 DOI: 10.1016/S0140-6736(21)01374-X]

5 **Marcellin P**, Gane E, Buti M, Afdhal N, Sievert W, Jacobson IM, Washington MK, Germanidis G, Flaherty JF, Aguilar Schall R, Bornstein JD, Kitrinos KM, Subramanian GM, McHutchison JG, Heathcote EJ. Regression of cirrhosis during treatment with tenofovir disoproxil fumarate for chronic hepatitis B: a 5-year open-label follow-up study. *Lancet* 2013; **381**: 468-475 [PMID: 23234725 DOI: 10.1016/S0140-6736(12)61425-1]

6 **Sapisochin G**, Bruix J. Liver transplantation for hepatocellular carcinoma: outcomes and novel surgical approaches. *Nat Rev Gastroenterol Hepatol* 2017; **14**: 203-217 [PMID: 28053342 DOI: 10.1038/nrgastro.2016.193]

7 **Friedman SL**, Pinzani M. Hepatic fibrosis 2022: Unmet needs and a blueprint for the future. *Hepatology* 2022; **75**: 473-488 [PMID: 34923653 DOI: 10.1002/hep.32285]

8 **Parvathaneni V**, Kulkarni NS, Muth A, Gupta V. Drug repurposing: a promising tool to accelerate the drug discovery process. *Drug Discov Today* 2019; **24**: 2076-2085 [PMID: 31238113 DOI: 10.1016/j.drudis.2019.06.014]

9 **Pushpakom S**, Iorio F, Eyers PA, Escott KJ, Hopper S, Wells A, Doig A, Guilliams T, Latimer J, McNamee C, Norris A, Sanseau P, Cavalla D, Pirmohamed M. Drug repurposing: progress, challenges and recommendations. *Nat Rev Drug Discov* 2019; **18**: 41-58 [PMID: 30310233 DOI: 10.1038/nrd.2018.168]

10 **Knight JM**, Kerswill SA, Hari P, Cole SW, Logan BR, D'Souza A, Shah NN, Horowitz MM, Stolley MR, Sloan EK, Giles KE, Costanzo ES, Hamadani M, Chhabra S, Dhakal B, Rizzo JD. Repurposing existing medications as cancer therapy: design and feasibility of a randomized pilot investigating propranolol administration in patients receiving hematopoietic cell transplantation. *BMC Cancer* 2018; **18**: 593 [PMID: 29793446 DOI: 10.1186/s12885-018-4509-0]

11 **Ramos-Arancibia N**, Varas C, Rozas-Muñoz E. Severe and recalcitrant periungual warts in a child successfully treated with cimetidine. *Dermatol Ther* 2021; **34**: e15154 [PMID: 34623743 DOI: 10.1111/dth.15154]

12 **Galiè N**, Ghofrani HA, Torbicki A, Barst RJ, Rubin LJ, Badesch D, Fleming T, Parpia T, Burgess G, Branzi A, Grimminger F, Kurzyna M, Simonneau G; Sildenafil Use in Pulmonary Arterial Hypertension (SUPER) Study Group. Sildenafil citrate therapy for pulmonary arterial hypertension. *N Engl J Med* 2005; **353**: 2148-2157 [PMID: 16291984 DOI: 10.1056/NEJMoa050010]

13 **Franks ME**, Macpherson GR, Figg WD. Thalidomide. *Lancet* 2004; **363**: 1802-1811 [PMID: 15172781 DOI: 10.1016/S0140-6736(04)16308-3]

14 **Yang J**, Roy A, Zhang Y. Protein-ligand binding site recognition using complementary binding-specific substructure comparison and sequence profile alignment. *Bioinformatics* 2013; **29**: 2588-2595 [PMID: 23975762 DOI: 10.1093/bioinformatics/btt447]

15 **Higashi T**, Friedman SL, Hoshida Y. Hepatic stellate cells as key target in liver fibrosis. *Adv Drug Deliv Rev* 2017; **121**: 27-42 [PMID: 28506744 DOI: 10.1016/j.addr.2017.05.007]

16 **Yan Y**, Zeng J, Xing L, Li C. Extra- and Intra-Cellular Mechanisms of Hepatic Stellate Cell Activation. *Biomedicines* 2021; **9** [PMID: 34440218 DOI: 10.3390/biomedicines9081014]

17 **Tsuchida T**, Friedman SL. Mechanisms of hepatic stellate cell activation. *Nat Rev Gastroenterol Hepatol* 2017; **14**: 397-411 [PMID: 28487545 DOI: 10.1038/nrgastro.2017.38]

18 **Fabregat I**, Moreno-Càceres J, Sánchez A, Dooley S, Dewidar B, Giannelli G, Ten Dijke P; IT-LIVER Consortium. TGF-β signalling and liver disease. *FEBS J* 2016; **283**: 2219-2232 [PMID: 26807763 DOI: 10.1111/febs.13665]

19 **Liu Y**, Wang Z, Wang J, Lam W, Kwong S, Li F, Friedman SL, Zhou S, Ren Q, Xu Z, Wang X, Ji L, Tang S, Zhang H, Lui EL, Ye T. A histone deacetylase inhibitor, largazole, decreases liver fibrosis and angiogenesis by inhibiting transforming growth factor-β and vascular endothelial growth factor signalling. *Liver Int* 2013; **33**: 504-515 [PMID: 23279742 DOI: 10.1111/liv.12034]

20 **Yuan S**, Dong M, Zhang H, Xu H, Wang Q, Yan C, Ye R, Jiang X, Zhou H, Chen L, Cheng J, Xie W, Jin W. Oral delivery of a Lactococcus lactis expressing extracellular TGFβR2 alleviates hepatic fibrosis. *Appl Microbiol Biotechnol* 2021; **105**: 6007-6018 [PMID: 34390354 DOI: 10.1007/s00253-021-11485-7]

21 **Haab F**, Stewart L, Dwyer P. Darifenacin, an M3 selective receptor antagonist, is an effective and well-tolerated once-daily treatment for overactive bladder. *Eur Urol* 2004; **45**: 420-9; discussion 429 [PMID: 15041104 DOI: 10.1016/j.eururo.2004.01.008]

22 **Goudie AJ**, Cooper GD, Cole JC, Sumnall HR. Cyproheptadine resembles clozapine in vivo following both acute and chronic administration in rats. *J Psychopharmacol* 2007; **21**: 179-190 [PMID: 17329298 DOI: 10.1177/0269881107067076]

23 **Haber SL**, Benson V, Buckway CJ, Gonzales JM, Romanet D, Scholes B. Lifitegrast: a novel drug for patients with dry eye disease. *Ther Adv Ophthalmol* 2019; **11**: 2515841419870366 [PMID: 31489402 DOI: 10.1177/2515841419870366]

24 **Scarlett Y**. Medical management of fecal incontinence. *Gastroenterology* 2004; **126**: S55-S63 [PMID: 14978639 DOI: 10.1053/j.gastro.2003.10.007]

25 **Patocka J**, Wu Q, Nepovimova E, Kuca K. Phenytoin - An anti-seizure drug: Overview of its chemistry, pharmacology and toxicology. *Food Chem Toxicol* 2020; **142**: 111393 [PMID: 32376339 DOI: 10.1016/j.fct.2020.111393]

26 **Silberstein SD**, Shrewsbury SB, Hoekman J. Dihydroergotamine (DHE) - Then and Now: A Narrative Review. *Headache* 2020; **60**: 40-57 [PMID: 31737909 DOI: 10.1111/head.13700]

27 **Blair HA**. Naldemedine: A Review in Opioid-Induced Constipation. *Drugs* 2019; **79**: 1241-1247 [PMID: 31267482 DOI: 10.1007/s40265-019-01160-7]

28 **Kciuk M**, Marciniak B, Kontek R. Irinotecan-Still an Important Player in Cancer Chemotherapy: A Comprehensive Overview. *Int J Mol Sci* 2020; **21** [PMID: 32664667 DOI: 10.3390/ijms21144919]

29 **Kisseleva T**, Brenner D. Molecular and cellular mechanisms of liver fibrosis and its regression. *Nat Rev Gastroenterol Hepatol* 2021; **18**: 151-166 [PMID: 33128017 DOI: 10.1038/s41575-020-00372-7]

30 **Dufton NP**, Peghaire CR, Osuna-Almagro L, Raimondi C, Kalna V, Chauhan A, Webb G, Yang Y, Birdsey GM, Lalor P, Mason JC, Adams DH, Randi AM. Dynamic regulation of canonical TGFβ signalling by endothelial transcription factor ERG protects from liver fibrogenesis. *Nat Commun* 2017; **8**: 895 [PMID: 29026072 DOI: 10.1038/s41467-017-01169-0]

31 **Ng YL**, Salim CK, Chu JJH. Drug repurposing for COVID-19: Approaches, challenges and promising candidates.

Pharmacol Ther 2021; **228**: 107930 [PMID: 34174275 DOI: 10.1016/j.pharmthera.2021.107930]

32 **Farha MA**, Brown ED. Drug repurposing for antimicrobial discovery. *Nat Microbiol* 2019; **4**: 565-577 [PMID: 30833727 DOI: 10.1038/s41564-019-0357-1]

33 **Roessler HI**, Knoers NVAM, van Haelst MM, van Haaften G. Drug Repurposing for Rare Diseases. *Trends Pharmacol Sci* 2021; **42**: 255-267 [PMID: 33563480 DOI: 10.1016/j.tips.2021.01.003]

34 **Piechal A**, Blecharz-Klin K, Joniec-Maciejak I, Pyrzanowska J, Krzysztoforska K, Mirowska-Guzel D, Widy-Tyszkiewicz E. Dihydroergotamine affects spatial behavior and neurotransmission in the central nervous system of Wistar rats. *Ann Agric Environ Med* 2021; **28**: 437-445 [PMID: 34558267 DOI: 10.26444/aaem/126020]

35 **Bernsmeier C**, van der Merwe S, Périanin A. Innate immune cells in cirrhosis. *J Hepatol* 2020; **73**: 186-201 [PMID: 32240716 DOI: 10.1016/j.jhep.2020.03.027]

36 **Campana L**, Iredale JP. Regression of Liver Fibrosis. *Semin Liver Dis* 2017; **37**: 1-10 [PMID: 28201843 DOI: 10.1055/s-0036-1597816]

37 **Cheng D**, Chai J, Wang H, Fu L, Peng S, Ni X. Hepatic macrophages: Key players in the development and progression of liver fibrosis. *Liver Int* 2021; **41**: 2279-2294 [PMID: 33966318 DOI: 10.1111/liv.14940]

38 **Binatti E**, Gerussi A, Barisani D, Invernizzi P. The Role of Macrophages in Liver Fibrosis: New Therapeutic Opportunities. *Int J Mol Sci* 2022; **23** [PMID: 35743092 DOI: 10.3390/ijms23126649]

World Journal of Gastroenterology

Submit a Manuscript: https://www.f6publishing.com

World J Gastroenterol 2023 May 28; 29(20): 3119-3132

DOI: 10.3748/wjg.v29.i20.3119

ISSN 1007-9327 (print) ISSN 2219-2840 (online)

ORIGINAL ARTICLE

Retrospective Study

Malignancy risk factors and prognostic variables of pancreatic mucinous cystic neoplasms in Chinese patients

Qing Xia, Fan Li, Rui Min, Shuai Sun, Yue-Xin Han, Zhen-Zhong Feng, Nan Li

Specialty type: Gastroenterology and hepatology

Provenance and peer review: Unsolicited article; Externally peer reviewed.

Peer-review model: Single blind

Peer-review report's scientific quality classification

Grade A (Excellent): 0
Grade B (Very good): B
Grade C (Good): C
Grade D (Fair): 0
Grade E (Poor): 0

P-Reviewer: Tenreiro N, Portugal; Zimmitti G, Italy

Received: March 3, 2023
Peer-review started: March 3, 2023
First decision: April 12, 2023
Revised: April 21, 2023
Accepted: May 4, 2023
Article in press: May 4, 2023
Published online: May 28, 2023

Qing Xia, Rui Min, Nan Li, Department of Pathology, The First Affiliated Hospital of Bengbu Medical College, Bengbu Medical College, Bengbu 233004, Anhui Province, China

Fan Li, Shuai Sun, Department of Pathology, Bengbu Medical College, Bengbu 233030, Anhui Province, China

Yue-Xin Han, School of Clinical Medicine, Bengbu Medical College, Bengbu 233030, Anhui Province, China

Zhen-Zhong Feng, Nan Li, Department of Pathology, The Second Affiliated Hospital of Anhui Medical University, Hefei 230601, Anhui Province, China

Corresponding author: Nan Li, Doctor, MD, PhD, Chief Doctor, Professor, Department of Pathology, The First Affiliated Hospital of Bengbu Medical College, No. 287 Changhuai Road, Bengbu 233004, Anhui Province, China. linanangel100@sina.com

Abstract

BACKGROUND

Pancreatic mucinous cystic neoplasms (MCNs) represent one of the precursor lesions of pancreatic ductal adenocarcinoma, and their detection has been facilitated by advances in preoperative imaging. Due primarily to the rarity of MCNs, however, there is limited knowledge regarding the prognostic variables and high-risk factors for malignant transformation. A more comprehensive and nuanced approach is necessary to fill this gap and provide a basis for improved treatment decisions and patient outcomes.

AIM

To investigate the high-risk factors associated with malignant MCNs and to explore the prognostic factors of MCN with associated invasive carcinoma (MCN-AIC).

METHODS

All cases of resected MCNs from a single high-volume institution between January 2012 and January 2022 were retrospectively reviewed. Only cases with ovarian-type stroma verified by progesterone receptor staining were included. Preoperative features, histological findings and postoperative course were documented. Multivariate logistic regression was employed to investigate variables related to malignancy. Survival analysis was performed using the

Kaplan-Meier curve, and the prognostic factors were assessed to evaluate the postoperative course of patients with MCN-AIC.

RESULTS

Among the 48 patients, 36 had benign MCNs, and 12 had malignant MCNs (1 high-grade atypical hyperplasia and 11 MCN-AIC). Age, tumour size, presence of solid components or mural nodules and pancreatic duct dilatation were identified as independent risk factors associated with malignancy. The follow-up period ranged from 12 mo to 120 mo, with a median overall survival of 58.2 mo. Only three patients with MCN-AIC died, and the 5-year survival rate was 70.1%. All 11 cases of MCN-AIC were stage I, and extracapsular invasion was identified as a prognostic factor for poorer outcomes.

CONCLUSION

The risk factors independently associated with malignant transformation of MCNs included age, tumour size, presence of solid components or mural nodules, and pancreatic duct dilatation. Our study also revealed that encapsulated invasion was a favourable prognostic factor in MCN-AIC patients.

Key Words: Mucinous cystic neoplasms; Pancreatic adenocarcinoma; Invasive carcinoma; Risk of malignancy; Prognostic factor; Retrospective study

©The Author(s) 2023. Published by Baishideng Publishing Group Inc. All rights reserved.

Core Tip: Pancreatic mucinous cystic neoplasms (MCNs) are a rare tumour with a low incidence and one of the precursor lesions of pancreatic ductal adenocarcinoma. The detection of MCN has been increasing by advances in imaging technology. MCNs associated risk factors, clinicopathological manifestations, and prognosis must be explored to improve our understanding of this rare tumour type and optimize clinical treatment.

Citation: Xia Q, Li F, Min R, Sun S, Han YX, Feng ZZ, Li N. Malignancy risk factors and prognostic variables of pancreatic mucinous cystic neoplasms in Chinese patients. *World J Gastroenterol* 2023; 29(20): 3119-3132
URL: https://www.wjgnet.com/1007-9327/full/v29/i20/3119.htm
DOI: https://dx.doi.org/10.3748/wjg.v29.i20.3119

INTRODUCTION

Pancreatic mucinous cystic neoplasm (MCN) is a rare sporadic tumour with a low incidence, accounting for 10%-45% of all resected primary pancreatic cystic neoplasms and 2.5% of exocrine pancreatic tumours[1,2]. With the increasing popularity of imaging evaluation and advances in radiological technology, the rate of MCN identification is on the rise. Pancreatic ductal adenocarcinoma (PDAC) is the leading cause of cancer-related death globally, and its incidence has been consistently increasing[3]. However, the majority of PDAC cases are detected at an advanced stage, highlighting the importance of early diagnosis and treatment of associated precancerous lesions to improve survival rates. MCN is a precancerous lesion of PDAC and evolves from benign adenoma to invasive carcinoma similarly to intraductal papillary mucinous neoplasm (IPMN) and pancreatic intraepithelial neoplasia (Pan IN)[4].

However, MCNs have not been studied in sufficient detail or breadth owing to their infrequency. The risk factors associated with malignancy have not been well characterized, and physicians have not been unanimous in adopting an optimal management profile. Discrepancies in recommendations offered by several medical associations may contribute to further challenges in managing the disease. Moreover, despite PDAC being the most common histopathological type of invasive MCN, notable differences exist in prognosis. However, the precise prognostic determinants of MCNs have yet to be fully elucidated.

Therefore, we conducted a retrospective study of the clinicopathological, radiological and survival data of a sizable cohort of patients. The findings of this study were intended to help identify key risk factors of malignant transformation in MCNs as well as the prognostic determinants of MCN with associated invasive carcinoma (MCN-AIC). The insights gained from this study may be used to inform the development of more effective management strategies for patients with MCNs, ultimately improving their clinical outcomes.

MATERIALS AND METHODS

Patient identification and ethics statement

All cases of MCN identified at the Department of Pathology of the First Affiliated Hospital of Bengbu Medical College from January 2012 to January 2022 were retrospectively retrieved. A total of 48 patients who fit the diagnostic criteria were included in the study. This study was approved by the Ethics Committee of the First Affiliated Hospital of Bengbu Medical College. Written informed consent was obtained from all patients for the use of their clinical data.

Inclusion and exclusion criteria

The inclusion criteria were patients who had been confirmed by surgical pathology to have MCN, underwent imaging examinations, and did not receive preoperative radiotherapy or chemotherapy. The exclusion criteria included poor-quality radiographic images, insufficient pathological diagnostic data, the presence of other pancreatic diseases, and a history of other malignant tumours. These criteria were carefully selected to ensure the accuracy and reliability of the study's findings.

Methods

All patients underwent preoperative imaging examinations, and the imaging data were uploaded to the Picture Archiving and Communication System. After reviewing and interpreting the data, two radiologists evaluated the radiographic tumour size, location, calcification, separation, solid composition or mural nodule status and duct dilatation of the lesion. Clinical information, including patient age and sex, symptoms, and serum tumour marker levels, was obtained through the analysis of medical records. The tumour tissues were paraffin-embedded and stained with haematoxylin-eosin staining (H&E) after being fixed in 10% neutral formaldehyde. MCN is classified by the World Health Organization (2019) as either atypical hyperplasia or MCN-AIC[5]. Low-grade atypical hyperplasia (LGD) and high-grade atypical hyperplasia (HGD, carcinoma in situ) have replaced the former three-tiered classification of atypical hyperplasia in MCN. All slides were reassessed by two senior pathologists who were uninformed of the patients' clinical diagnoses. All tissues were analysed immunohistochemically using the EnVision technique, and the progesterone receptor (PR) primary antibody was purchased from Fuzhou Maixin Biotechnology Co., Ltd., China. Expression of PR was restricted to the subepithelial ovarian-type stroma.

Patient outcomes

From the date of diagnosis to January 31, 2022, 48 patients were followed up by reviewing their medical records, interviewing them *via* phone, or sending emails to acquire follow-up data, including postoperative recurrence, overall survival (OS), and therapy. OS was measured from the date of surgery until the date of death or the end of follow-up.

Statistical analysis

The data were analyzed statistically using IBM SPSS Statistics (version 25.0) and R (version 4.0.0). The χ^2 test or Fisher's exact test was used to compare categorical data. The preoperative risk variables associated with malignant MCNs were evaluated using a multivariate binary logistic regression model. The cumulative survival rate was calculated using the Kaplan-Meier method, and the log rank test was performed to analyse the association between clinicopathological data and survival rate. $P < 0.05$ was regarded as indicating statistical significance.

RESULTS

Clinicopathological and radiological information of patients

A total of 48 patients diagnosed with MCN were included in accordance with strict inclusion and exclusion criteria. MCNs accounted for 2.8% (48/1685) of all pancreatic lesions resected over the same period. The median age of the patients was 47.2 years ± 13.1 years (range, 27-72 years), and 16 patients (33.3%) were more than 50 years old. There were 34 females and 14 males, with a female-to-male ratio of 2.2:1.0. Approximately 41.7% of patients were asymptomatic, including 18 patients whose disease was detected incidentally by imaging evaluation and 2 patients whose disease was identified by elevated preoperative carbohydrate antigen 19-9 (CA19-9) serology. The remaining 28 patients presented with nonspecific clinical symptoms, such as stomach pain, abdominal distension, abdominal discomfort, and jaundice. Serologic CA19-9 Levels were elevated in 16 patients (33.3%).

Imaging revealed oval-shaped, lobulated hypodense masses that were well circumscribed, separated linearly, and surrounded by egg-shell-like foci of calcification. The contents of the cyst were also visible. The average radiological diameter of the tumour was 5.8 cm ± 3.7 cm (1.2-14.5 cm), and in 23 patients (47.9%), the tumour measured more than 4 cm. Thirty-five patients (72.9%) had tumours that were located in the distal pancreas. Solid components or mural nodules were identified in 14 patients (29.2%),

septations in 21 (43.85%), calcification in 13 (27.1%) and duct dilatation in 18 (37.5%) (Figure 1). Detailed data on the imaging findings and clinicopathological information of MCN patients are shown in Table 1.

MCN was correctly diagnosed using preoperative imaging in 35 patients (72.9%). The most common misdiagnoses involved other subtypes of pancreatic cystic lesions (PCLs) and the use of imprecise terms such as pancreatic cystic or solid masses. The preoperative imaging modalities employed in this study comprised computed tomography (CT), magnetic resonance imaging (MRI), and endoscopic ultrasound (EUS). Of the 48 patients, all underwent CT, 33 underwent MRI, and 21 underwent EUS. The corresponding detection accuracy rates were 64.6%, 87.9%, and 71.4%, respectively. Nevertheless, there was no significant difference in diagnostic accuracy among the three methods ($P = 0.64$).

Microscopic and immunohistochemical features

Postoperative pathological diagnosis revealed 36 cases of LGD, 1 case of HGD, and 11 cases of MCN-AIC (the histological type of the invasive component was PDAC in all cases). All cases were solitary without multiple foci. The morphology of the cysts generally manifested as unilocular or multilocular with septa, and the fluid aspirated from the cystic cavity was frequently viscous.

Microscopically, the cyst walls were found to be coated with mucinous columnar epithelium (Figure 2A and B). Subepithelial tissue in the MCN consisted of ovarian-type stroma (OTS) characterized by dense spindle cells expressing PR and possessing round or elongated nuclei with scant cytoplasm. Positive PR staining was observed in all tumours (Figure 2D). The mucin-producing columnar epithelial cells exhibited varying degrees of dysplasia. In cases of LGD, mild to moderate structural and cellular atypia was observed with occasional micropapillae (Figure 2A and B). HGD showed obvious atypia of both structures and cells, including multilayered cell arrangement, nuclear enlargement, loss of alignment polarity, and emergence of aberrant mitotic figures. In cases of MCN-AIC, interstitial infiltration was noted in comparison to HGD, with invasive components growing interspersed in the stroma (Figure 2C). Solid components, mural nodules, or nipple protrusion were also occasionally visible. Notably, 5 cases of MCN-AIC showed atypical hyperplasia adjacent to invasive components.

Risk factors for malignant MCNs and the prediction probability

Based on malignant biological behaviours, LGD was defined as benign MCN in 36 cases (75%), while HGD and MCN-AIC were classified as malignant MCN in 12 cases (25%). Univariate analysis revealed that age ≥ 50 years [8 (66.7%) *vs* 8 (22.2%), $P = 0.013$], tumour size ≥ 4 cm [10 (83.3%) *vs* 13 (36.1%), $P = 0.010$], pancreatic duct dilatation [8 (66.7%) *vs* 10 (27.8%), $P = 0.039$], and presence of a solid component or mural nodule [8 (66.7%) *vs* 10 (27.8%), $P = 0.039$] were associated with malignant MCN. However, sex, clinical symptoms, serum CA19-9 Level, tumour location, septations and calcification did not correlate with malignancy ($P < 0.05$) (Table 1).

Further multivariate analysis demonstrated that all four statistically significant indicators were independent risk factors for the preoperative diagnosis of malignant MCNs ($P < 0.05$) (Figure 3). The prediction probability of each indicator for malignancy risk in a cohort of patients was then explored. The results of the analysis showed that age, tumour size, duct dilatation, and solid component/mural nodule all had good performance in predicting malignancy risk, as evidenced by the area under the curve (AUC) values of 0.722 (95%CI: 0.546-0.898, $P = 0.220$), 0.736 (95%CI: 0.578-0.894, $P = 0.015$), 0.694 (95%CI: 0.517-0.872, $P = 0.046$), and 0.694 (95%CI: 0.517-0.872, $P = 0.046$), respectively. Furthermore, when the four indicators were combined into a total predictor, the AUC value increased to 0.903 (95%CI: 0.814-0.992, $P < 0.010$), improving the accuracy of the prediction model.

Survival analysis and prognostic variables of MCN-AIC

The follow-up period ranged from 12 mo to 120 mo with a mean of 58.2 mo ± 32.7 mo. Of the 36 patients with benign MCNs, 6 were lost to follow-up, and 1 died of an abrupt cerebral infarction. The remaining 29 patients had an excellent prognosis; their 5-year disease-specific survival rate was 100%. Of the 12 patients with malignant MCNs, 3 died at 8, 14, and 46 mo after surgery; the 5-year disease-specific survival rate was 70.1%. All deaths occurred in MCN-AIC patients.

Consequently, the clinicopathological characteristics of the 11 MCN-AIC patients were further explored (Table 2). The tumours examined in this study did not display any signs of lymph node involvement, distant metastasis, or nerve invasion. In addition, all the tumours were successfully resected, and the margins were negative. Based on the AJCC cancer staging system[6], all 11 cases of MAC-AIC were categorized as stage I, with 7 patients having stage IA cancers and 4 having stage IB cancers, depending on the tumour size. The encapsulated invasion of MCN-AIC was defined as infiltrating components not exceeding the outermost layer of the capsule, with or without infiltration into the subepithelial stroma or cystic septa[7]. Using this definition, 9 tumours were encapsulated, while 3 were extracapsular (Cases 1-3). In Case 1 and Case 2, the cancerous tissue extended into the capsule and intersected with the surrounding pancreatic parenchyma. The tumour in Case 3 was located in the head of the pancreas and showed infiltration into the adjacent duodenal muscular layer. There was no significant difference in age ($P = 0.301$), tumour size ($P = 0.109$), sex ($P = 0.402$), postoperative adjuvant therapy ($P = 0.952$) or TNM stage ($P = 0.400$). However, the difference in infiltration of the capsule was

Table 1 Clinicopathologic and radiological features in 48 patients

Variable	Benign group (*n* = 36)	Malignant group (*n* = 12)	*P* value
Sex			0.142
Male	8 (22.2)	6 (50.0)	
Female	28 (77.8)	6 (50.0)	
Age, yr			**0.013**
≥ 50	8 (22.2)	8 (66.7)	
< 50	28 (77.8)	4 (33.3)	
Clinical symptoms			0.499
Yes	20 (55.6)	8 (66.7)	
No	16 (44.4)	4 (33.3)	
Serum CA19-9 level			0.077
Elevate	9 (25)	7 (58.3)	
Normal	27 (75)	5 (41.7)	
Tumor size, cm			**0.005**
≥ 4	13 (36.1)	10 (83.3)	
< 4	23 (63.9)	2 (16.7)	
Location			0.348
Head and neck	8 (22.2)	5 (41.7)	
Body and tail	28 (77.8)	7 (58.3)	
Duct dilatation			**0.039**
Yes	10 (27.8)	8 (66.7)	
No	26 (72.2)	4 (33.3)	
Solid component/mural nodule			**0.039**
Yes	10 (27.8)	8 (66.7)	
No	26 (72.2)	4 (33.3)	
Septations			0.867
Yes	16 (44.4)	5 (41.7)	
No	20 (55.6)	7 (58.3)	
Calcification			0.851
Yes	9 (25)	4 (33.3)	
No	27 (75)	8 (66.7)	

Significant *P* in bold. Data presented in parentheses represent percentages. CA19-9: Carbohydrate antigen 19-9.

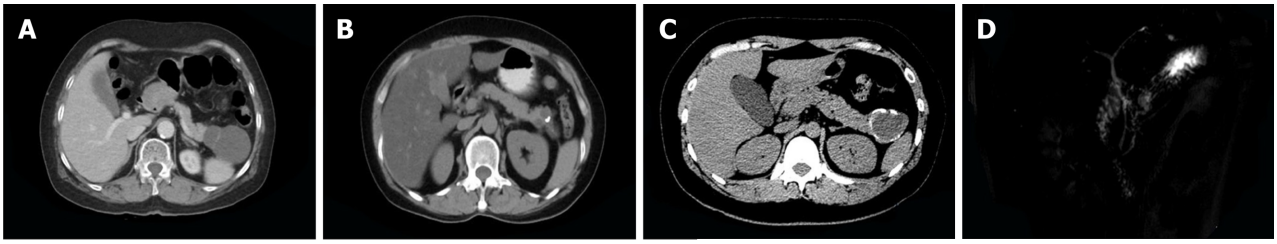
statistically significant ($P < 0.001$) (Figure 4).

DISCUSSION

The advancements and widespread use of imaging technology have led to an apparent rise in the prevalence of PCLs[1]. PCLs encompass both neoplastic and nonneoplastic lesions, with pancreatic cystic neoplasms (PCNs) representing a substantial subset. PCNs comprise serous cystic neoplasms (SCNs), solid pseudopapillary neoplasms (SPNs), IPMNs and mucinous cystic neoplasms. SCNs and SPNs are nearly benign and low-grade malignant tumours, respectively. IPMNs and MCNs, also known as pancreatic mucinous neoplasms, produce viscid mucin and have the potential to progress to PDAC. Notably, they are easier to detect by preoperative imaging than Pan IN due to the particular hypodensity of the cystic tumour.

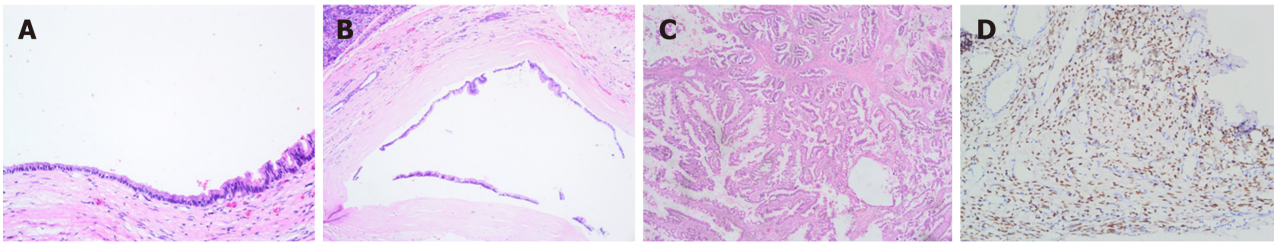
Table 2 Characteristics of 11 patients with mucinous cystic neoplasm associated invasive carcinoma

Case	Age (yr)	Sex	Tumor size (cm)	Largest dimension (cm)	Invasion pattern	pT stage	pTNM stage	Status	Overall survival (mo)	Adjuvant chemotherapy
1	72	Female	8.0	3.0	Extracapsular	T2	IB	Death	8	Yes
2	60	Male	14.0	1.2	Extracapsular	T1	IA	Death	14	Yes
3	57	Male	7.2	4.0	Extracapsular	T2	IB	Death	46	No
4	64	Female	5.0	< 0.1	Encapsulated	T1	IA	Alive	56	Yes
5	56	Male	6.4	2.0	Encapsulated	T1	IA	Alive	53	Yes
6	43	Female	5.0	< 0.1	Encapsulated	T1	IA	Alive	38	No
7	52	Female	4.5	3.0	Encapsulated	T2	IB	Alive	47	No
8	28	Male	11.0	2.0	Encapsulated	T1	IA	Alive	104	Yes
9	34	Female	3.0	< 0.2	Encapsulated	T1	IA	Alive	75	No
10	45	Male	4.0	1.5	Encapsulated	T1	IA	Alive	24	No
11	63	Female	6.0	< 0.2	Encapsulated	T1	IA	Alive	94	Yes



DOI: 10.3748/wjg.v29.i20.3119 **Copyright** ©The Author(s) 2023.

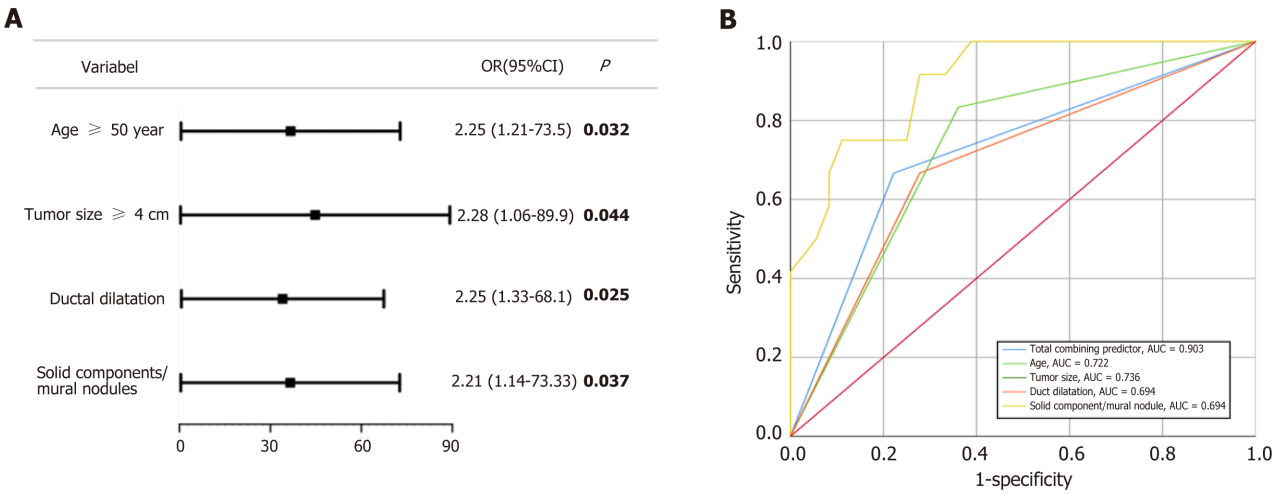
Figure 1 Representative radiographic images showing the mucinous cystic neoplasms. A: Computed tomography (CT) scan showing a cystic neoplasm in the pancreatic tail with a clear boundary and linear separation within the lesion; B: CT scan showing multilocular cysts with a slightly high-density solid component, thickened septa, and punctate calcifications; C: CT scan showing a cyst with a slightly thickened cyst wall and multiple calcification foci; D: Magnetic resonance cholangiopancreatography showing mixed signals of the mass and the dilatation of the nearby pancreatic duct.



DOI: 10.3748/wjg.v29.i20.3119 **Copyright** ©The Author(s) 2023.

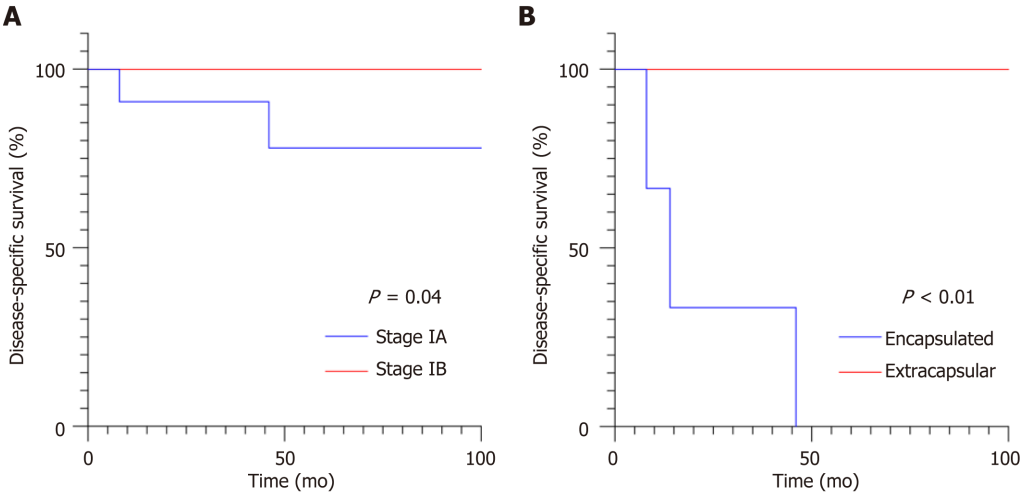
Figure 2 Representative micrographs showing the mucinous cystic neoplasm. A: The epithelium exhibits mild to moderate cellular and structural dysplasia, and there is subepithelial ovarian-type stroma (OTS), haematoxylin-eosin staining (H&E) × 200; B: The epithelium demonstrates papillary hyperplasia with some cells shedding into the lumen, and the stroma is partially replaced by fibrous collagen, H&E × 100; C: MCN-associated invasive carcinoma extended into the adjacent pancreatic tissue, and the epithelium exhibited severe dysplasia, H&E × 100; D: The OTS was positive for PR-staining, EnVision × 200.

Compagno and Oertel[8] initially distinguished MCN from SCN in 1978, citing its higher potential for malignancy. However, confusion between IPMNs and MCNs persisted until the International Association of Pancreatology designated OTS as the diagnostic criterion for MCN in 2006[9]. Earlier reports on MCNs inevitably included IPMN cases, leading to a high reported incidence of malignant transformation ranging from 6% to 39% over the last few decades[10-13]. In our sample, 25% of MCN cases were malignant, a rate nearly consistent with the findings of Höhn *et al*[14]. Loss of OTS was reported after the malignant transformation of MCNs[15]. In our study, although some cases showed this particular phenomenon following malignant transformation, with replacement by interstitial fibrous collagen, the remaining OTS was still visible. Once OTS cannot be recognized, detection of positive PR is recommended for a definitive diagnosis[16]. All cases in our study exhibited positive



DOI: 10.3748/wjg.v29.i20.3119 **Copyright** ©The Author(s) 2023.

Figure 3 Risk factors of malignant mucinous cystic neoplasm. A: Binary logistic regression analysis of preoperative risk factors for malignancy; B: Receiver operating characteristic curve analysis of the combined predictors and individual indicators. 95%CI: 95% confidence interval; AUC: Area under the curve.



DOI: 10.3748/wjg.v29.i20.3119 **Copyright** ©The Author(s) 2023.

Figure 4 Prognostic factors for mucinous cystic neoplasm with associated invasive carcinoma. A: There was no significant difference in prognosis between stage IA and stage IB mucinous cystic neoplasm with associated invasive carcinoma (MCN-AIC) (P = 0.400); B: Encapsulated MCN-AIC is associated with a significantly better prognosis (P < 0.001).

staining, ensuring accurate diagnosis.

Currently, there are no reliable preoperative variables that can be used to accurately predict the malignant potential of PCNs.

As one of the most frequently utilized preoperative assessment modalities, imaging has garnered considerable attention in the field of radiomics research for identifying certain subtypes of PCNs and stratifying the risk of IPMNs[17]. Conversely, MCNs have received far less attention than IPMNs, mainly owing to their less substantial incidence and malignancy rate. The management criteria for MCNs remain ambiguous and differ from those of IPMNs. Due to the inability to accurately predict the malignant potential of MCNs through preoperative inspection, it was formerly recommended that all MCNs amenable to surgery be removed regardless of lesion size[13]. Fortunately, the latest guidelines recommend monitoring for eligible MCNs[4,18], although the inclusion criteria are similar to those for IPMNs. This parallelism with IPMN criteria may warrant further consideration. A substantial proportion of patients diagnosed with pancreatic mucinous cysts prior to surgery are subsequently found to have benign disease and do not need surgery[19], highlighting the need for improved identification of those cases with malignant potential. Therefore, given the limitations of current risk stratification schemes in predicting malignant transformation of MCNs, further investigation regarding potential risk factors is essential. While a variety of clinicopathological features and imaging findings have been proposed as potential risk factors for malignancy, their importance remains controversial across different studies[12,14,20-23]. In addition to the variables included in current guidelines, such as

tumour size, wall nodule, and duct dilation, other factors, including sex, location, wall thickening/enhancement, weight, and serum CA19-9 Level, have also been reported to be relevant. Our own research identified age, tumour size, solid component or mural nodule, and duct dilation as independent risk indicators.

To the best of our knowledge, age has not been widely recognized in the literature as a significant risk factor for malignant transformation of MCNs. The mean ages of patients with benign and malignant MCNs were 45.2 years ± 12.7 years and 52.2 years ± 13.4 years, respectively, which were comparable to those previously described in the literature[24]. Age has been shown to be related to malignancy in a cohort of pancreatic mucinous neoplasms[25]. Crippa *et al*[12] suggested that age was statistically significant in univariate analysis but did not emerge as a significant factor in multivariate analysis for malignant MCNs. Whether age is an independent risk factor for malignant MCNs needs further study. The occurrence of malignant MCNs appears to increase with age and seems to represent a dynamic pathological transition from adenoma to adenocarcinoma over time.

The average diameter of MCN masses in our investigation was found to be 5.8 cm, which is consistent with the previously reported average diameter of 6-11 cm. It has been emphasized that MCNs should be stratified into surveillance and surgery groups based on a diameter threshold of 4.0 cm, as stated in current guidelines[18]. Tumour size ≥ 4 cm was confirmed to be an independent risk for malignant MCNs in our study. In our research, we further identified that the presence of a solid component or mural nodule in MCNs is an independent risk factor for malignancy; it even ranks first in the likelihood of malignancy in certain studies[23]. The combination of solid component or mural nodule and tumour size has been utilized as a tool for identifying malignancy in some studies. In one cohort, it was reported that all malignant MCNs were either larger than 4 cm in diameter or had nodules[12]. Consistent with this, guidelines recommend surgical intervention for MCNs larger than 4 cm in diameter or for those with a mural nodule.

The majority of patients with MCNs are typically asymptomatic. In our analysis, while the percentage of malignant patients with clinical symptoms was higher than that of benign patients, the difference was not statistically significant. The relationship between clinical symptoms and malignancy in MCNs is still debatable[14,25], although surgical excision is advised if symptoms are present[18]. During follow-up, the increase in mass size can often result in nonspecific mass-related clinical complaints. In one case from our cohort, surgical intervention was advised after the tumour became larger than 4 cm and clinical symptoms appeared in the sixth year of imaging surveillance.

Unlike IPMNs, MCNs typically do not communicate with the pancreatic duct, which is one of their distinguishing features. Duct dilatation is a high-risk factor for malignant transformation in IPMNs, with dilatation greater than 10 mm being an unequivocal indication for surgery[18,26]. Similarly, our study found that pancreatic duct dilatation is a concerning imaging finding in MCNs, as verified by other investigations[23].

The management of malignant pancreatic tumours is predominantly centred on postoperative follow-up, whereas the management of MCNs places greater emphasis on the potential risks associated with preoperative monitoring and misdiagnosis. The management plan for IPMN is relatively mature, considering that dedicated management guidelines for IPMN have been published[1]. However, despite MCN being a precursor lesion of pancreatic cancer, similar to IPMN, the management plan for MCN remains unclear, particularly in identifying high-risk factors. Although the risk factors and surgical indications for IPMN and MCN are not differentiated in some guidelines[4], the demographic, cystic, histological and other characteristics of these two tumours differ, so they should be managed differently, particularly with respect to exploring risk factors. Unfortunately, our findings suggest that the risk factors for malignant MCNs are quite similar to those for IPMNs. The size of the lesion and the presence of solid components/wall nodules have been widely recognized as high-risk factors for malignant transformation of MCNs and IPMNs in various guidelines and publications, including our study. While various other malignant risk factors for MCN reported in the literature are statistically significant, they require further confirmation. In the case of IPMNs, the characteristic risk factor is main pancreatic duct dilation, especially when the diameter exceeds 10 mm, given that IPMNs grow within the pancreatic ducts. However, MCNs lack their own characteristic risk factors. Based on their relationship with the pancreatic ducts, IPMNs are classified into the main duct type, mixed duct type, and branch duct type, and direct surgical resection is recommended for the first two types due to a high risk of malignant transformation[18]. However, immediate surgical intervention for MCNs with risk factors remains controversial. Höhn *et al*[14] conducted a retrospective analysis exploring the risk factors for malignant transformation of MCNs, similar to our own analysis. They recommended radical resection surgery for all eligible patients suspected of having MCNs due to concerns about the potential risk of malignant progression and the level of expertise of pancreatic surgeons in low-volume centres. However, this view seems too radical, and the decision for MCN patients to undergo surgery should be more cautious, as the incidence and malignant transformation rate of MCNs are much lower than those of IPMNs[27]. The main argument for surgical resection in all MCN patients based on eliminating the risk of future malignancy seems invalid. It is essential to increase awareness and continuously conduct research on this rare tumour, especially in terms of preoperative malignant risk factors. Based on the above premise, a multidisciplinary team with expertise in pancreatic cysts and surgery can combine various reported risk factors, patient comorbidities, surgery-related complications, and mortality rates

to comprehensively evaluate the potential risks and benefits of surgery and monitoring, thereby making the best treatment decision for the patient.

In addition, preoperative imaging evaluation of various risk indicators for MCNs seems to require the use of different modalities. No single test can accurately diagnose all cases, and in fact, most patients undergo more than one diagnostic procedure[28]. Therefore, the comprehensive use of different detection methods is more conducive to preoperative diagnosis. In our study, this may be attributed to the preference of imaging doctors at our hospital. CT is the preferred initial test for patients undergoing physical examination or with symptoms, and if the CT results are inconclusive or require further confirmation, MRI or EUS will be performed. Unfortunately, there was no significant difference between these three detection methods in our study; nevertheless, combining CT with MRI/EUS increased the preoperative diagnosis rate of our patients from 64.4% to 72.9%. A review of the literature suggests that MRI has slightly higher accuracy in distinguishing between malignant PCNs and benign lesions than CT[29]. MRI was found to be more effective than EUS in distinguishing malignant MCNs [30]. CT combined with MRI was shown to be better than CT alone in the preoperative diagnosis of pancreatic cysts[31]. Moreover, patients with MCNs who have a certain risk of malignant transformation need long-term monitoring or even lifelong monitoring until surgery is no longer a suitable treatment option. For long-term follow-up of MCNs, MRI is the preferred method[18]. This may be because MRI has high contrast resolution and does not involve the use of radiation, which may increase the risk of developing malignant tumours in patients with long-term exposure to CT. EUS is an invasive procedure that highly depends on the operator's skills, especially when combined with aspiration for cyst fluid analysis. EUS is recommended for cysts with significant risk characteristics or when a more accurate diagnosis may change the patient's treatment plan[32].

Complete surgical resection of noninvasive MCNs is a curable treatment, resulting in a 5-year disease-specific survival rate of 100%, as previously reported[33], indicating that postoperative surveillance may not be necessary. As in PDAC patients, prognosis in cases of MCN-AIC was formerly believed to be dismal[34]. However, a series of recent studies have shown that the tumour behaviour and biological characteristics of MCN-AIC are entirely distinct from those of PDAC[23,35,36]. MCN-AIC is often diagnosed at an early stage, and surgical resection is the primary treatment. A study based on SEER research data showed that early-stage MCN-AIC (stage I-II) accounted for 82.9% of cases[37]. All 12 MCN-AIC cases in our study were at stage I, and the 5-year disease-specific survival rate was 70.1%, which was higher than the range of 20%-60% reported in previous literature[12,13,38]. Currently, there is a paucity of studies in which the biological behaviour of invasive MCNs is explored. Previous research indicates that patients with early-stage tumours (stages I and II) have better survival rates than those with high-grade tumours (stages III and IV)[37]. The prognostic variables for patients with MCN-AIC, such as pT grade and capsular invasion, have gained considerable attention. In PDAC, stage I is divided into stages IA and IB, which correspond to stages T1 and T2, respectively, without lymph node metastases and distant metastases[6]. A large cohort study has shown that the survival rate of patients with stage IA PDAC is much higher than that of patients with stage IB PDAC[39]. However, survival disparities between stage IA and IB invasive PDAC derived from MCN-AIC are rarely observed. Our findings, consistent with those of another study[7], demonstrate that there is no significant difference between the two stages. The invasion pattern of the capsule may provide a more accurate prediction of prognosis in MCN-AIC patients than stage classification. The notion of encapsulated invasion is not included in the MCN-AIC classification and guidelines, and the terminology varies somewhat across various research efforts. We adopted the term from the most recent publication[7]. The results of multiple studies have demonstrated that the prognosis is favourable when the invasion is confined to the capsule, and patients with encapsulated invasion exhibit a better survival rate than those with extracapsular invasion. Recurrence has been reported in one of sixteen cases of MCN-AIC confined to the OTS, and the probability of widespread invasion cannot be ruled out because of the minimal quantity of tumour sampled in this case[35]. It has been claimed that encapsulated MCN-AIC has a tumour-free survival rate that is comparable to that of noninvasive MCNs[7]. Our findings revealed that all patients with encapsulated invasion survived, while those with extracapsular invasion died regardless of whether MCN-AIC was stage IA or stage IB. It is recommended that MCN-AIC patients undergo standardized surveillance based on pancreatic cancer guidelines for 5 years after surgery[4]. During monitoring for stage I MCN-AIC, it seems that patients with extracapsular infiltration should be prioritized.

For patients with resected pancreatic cancer, the current standard of care mandates the administration of either a modified FOLFIRINOX (mFOLFIRINOX) or a gemcitabine-based regimen, provided that no contraindications are present[40]. However, limited research has been conducted on the benefits and risks of adjuvant treatment for stage I PDAC, which represents a small proportion of all resectable cases[41]. A study based on the NCDB database indicated that none of the patients with stage IA PDAC had to receive adjuvant treatment following resection, as the side effects and economic costs substantially outweighed the benefits[42]. Despite inadequate data to support this approach, current guidelines advocate adjuvant treatment for MCN-AIC patients comparable to that for patients with PDAC[18]. The role of adjuvant treatment in treating MCN-AIC patients after surgery, particularly for stage I tumours, remains unclear. Two of three patients with stage IA MCN-AIC did not receive adjuvant treatment after surgery, and none of them experienced disease recurrence or death[43]. Of the patients with tumours

who did not receive adjuvant therapy, seven recovered from stage IA and 1 died from stage IB MCN-AIC[7]. These reported cases could be defined as "encapsulated invasion" based on the definition. Patients with stage IA MCN-AIC (T1a and T1b) seem to have the same favourable prognosis as those with LGD or HGD, particularly in the absence of extracapsular invasion. In our research, three IA patients and one IB patient with tumours confined to the capsule did not receive adjuvant treatment and survived, while those with extracapsular infiltration died regardless of whether adjuvant therapy was offered. Diligent monitoring might be preferred over intensive systemic therapy for stage I MCN-AIC with encapsulated invasion.

MCNs are known to harbour gene mutations associated with PDAC, as they are precursor lesions of cancer[17]. However, the genetic pathways underlying IPMNs and MCNs are distinct from one another. The most prevalent and early genetic event in IPMN and MCN carcinogenesis is the KRAS mutation [44], which is present in 30% of MCNs, whereas the GNAS mutation is almost nonexistent[45,46]. In contrast, the combined detection of *KRAS* and *GNAS* mutations exhibits 100% sensitivity for IPMNs [46]. The decreased frequency of genetic mutations in MCNs compared to IPMNs partly explains why MCNs have a lower probability of malignant transformation. Other mutations, including *TP53*, *PIK3CA*, *PTEN*, *CDKN2A*, and *SMAD4*, have also been described in MCNs but only in advanced stages[47,48]. *KRAS* mutation could be detected in all phases of MCNs and increased with the degree of dysplasia. Sawai *et al*[49] discovered *KRAS* mutations in 19% of LGD and 100% of HGD cases, whereas *TP53* and *CDKN2A* mutations were exclusively observed only in HGD cases. Gene sequencing may aid in the early identification and tailored treatment of MCNs.

This study was subject to several limitations. First, it was a retrospective study that only included patients who underwent surgical resection and were pathologically confirmed to have MCNs, which may result in selection bias. Second, the rarity of MCNs limited the sample size, leading to a large confidence interval that may have hindered statistical analysis. Third, the MRI/EUS results were based on previous CT information, potentially affecting the interpretation of imaging results. Therefore, further multicentre and large-scale studies are needed to explore the clinical, pathological, imaging, and biological behaviours of MCNs.

CONCLUSION

In conclusion, this study involved analysing data from 48 patients who underwent complete resection of MCNs. The incidence of malignant MCNs was low, and the specific risk factors for malignancy were age, tumour size, presence of solid components or mural nodules, and duct dilatation. The prognosis of stage I MCN-AIC was closely related to encapsulated invasion, and complete surgical excision alone or in combination with postoperative treatment may be a viable option for invasive masses confined within the capsule.

ARTICLE HIGHLIGHTS

Research background

Mucinous cystic neoplasms (MCNs) are recognized as precursor lesions of pancreatic cancer. Despite their rarity, the detection of MCNs is on the rise due to advancements in preoperative imaging techniques. Thus, there is a pressing need to increase our knowledge of MCNs to ensure that patients receive the most appropriate treatment decisions.

Research motivation

An inadequate understanding of MCNs can hinder the treatment of patients, underscoring the importance of research on MCNs.

Research objectives

To investigate the risk factors for malignancy in MCNs and the prognostic factors associated with MCN-associated invasive carcinoma (MCN-AIC) to advance our comprehension of this uncommon tumour.

Research methods

This study involved a retrospective analysis of clinical and pathological data, imaging records, and outcomes of patients diagnosed with MCNs at our research centre over a 10-year period. We then investigated the risk factors for malignancy in MCNs and the prognostic factors associated with MCN-AIC.

Research results

A total of 48 patients with MCNs, accounting for 2.8% of pancreatic lesions resected during the study

period, were included in this study. Among these patients, 36 had benign MCNs, while 12 had malignant MCNs. We conducted a comparative analysis of clinical and imaging features and discovered that age, tumour size, solid components or wall nodules, and pancreatic duct dilation were significantly associated with malignancy. Subsequently, we performed a prognostic analysis of malignant MCNs and observed that all malignant MCNs in our study were at stage I, and extracapsular invasion was identified as a significant prognostic factor for poor outcomes.

Research conclusions

Age, tumour size, solid components or wall nodules, and pancreatic duct dilation were independent risk factors associated with malignancy in MCN. In addition, extracapsular invasion was indicative of poor prognosis of MCN-AIC.

Research perspectives

The aim of this study was to enhance the management of MCN, a rare disease, by utilizing patient information from our research centre and conducting research from both preoperative and postoperative perspectives. We hope that this study can provide valuable insights into the management of MCNs.

ACKNOWLEDGEMENTS

We would like to thank Dr. Xian-Jie Jia for significant contributions to data analysis.

FOOTNOTES

Author contributions: Xia Q collected the clinical data and prepared the manuscript; Xia Q and Li F designed the study and supervised the statistical data; Xia Q and Min R designed the research and contributed to the analyses; Sun S, Han YX, and Feng ZZ provided clinical advice; Li N made the pathologic diagnosis and supervised the report; and all authors read and approved the final version.

Supported by the Natural Science Key Project in Universities of Anhui Province, No. KJ2021A0701; Natural Science Key Project of Bengbu Medical College, No. 2020byzd030; and Postgraduate Scientific Research Innovation Program of the Bengbu Medical College, No. Byycx22016.

Institutional review board statement: This study was reviewed and approved by the Ethics Committee of the First Affiliated Hospital of Bengbu Medical College (approval No. 2021085).

Informed consent statement: All study participants, or their legal guardian, provided informed written consent prior to study enrollment.

Conflict-of-interest statement: We have no financial relationships to disclose.

Data sharing statement: No additional data are available.

Open-Access: This article is an open-access article that was selected by an in-house editor and fully peer-reviewed by external reviewers. It is distributed in accordance with the Creative Commons Attribution NonCommercial (CC BY-NC 4.0) license, which permits others to distribute, remix, adapt, build upon this work non-commercially, and license their derivative works on different terms, provided the original work is properly cited and the use is non-commercial. See: https://creativecommons.org/Licenses/by-nc/4.0/

Country/Territory of origin: China

ORCID number: Qing Xia 0009-0009-9528-5347; Fan Li 0009-0009-0410-963X; Rui Min 0000-0003-3835-1167; Shuai Sun 0000-0001-5838-9424; Yue-Xin Han 0000-0002-2111-7430; Zhen-Zhong Feng 0000-0002-9610-495X; Nan Li 0000-0002-5622-4252.

S-Editor: Chen YL
L-Editor: A
P-Editor: Zhang YL

REFERENCES

1 **Tanaka M**, Fernández-Del Castillo C, Kamisawa T, Jang JY, Levy P, Ohtsuka T, Salvia R, Shimizu Y, Tada M, Wolfgang CL. Revisions of international consensus Fukuoka guidelines for the management of IPMN of the pancreas. *Pancreatology* 2017; **17**: 738-753 [PMID: 28735806 DOI: 10.1016/j.pan.2017.07.007]

2 **Ketwaroo GA**, Mortele KJ, Sawhney MS. Pancreatic Cystic Neoplasms: An Update. *Gastroenterol Clin North Am* 2016; **45**: 67-81 [PMID: 26895681 DOI: 10.1016/j.gtc.2015.10.006]

3 **Klein AP**. Pancreatic cancer epidemiology: understanding the role of lifestyle and inherited risk factors. *Nat Rev Gastroenterol Hepatol* 2021; **18**: 493-502 [PMID: 34002083 DOI: 10.1038/s41575-021-00457-x]

4 **Elta GH**, Enestvedt BK, Sauer BG, Lennon AM. ACG Clinical Guideline: Diagnosis and Management of Pancreatic Cysts. *Am J Gastroenterol* 2018; **113**: 464-479 [PMID: 29485131 DOI: 10.1038/ajg.2018.14]

5 **Nagtegaal ID**, Odze RD, Klimstra D, Paradis V, Rugge M, Schirmacher P, Washington KM, Carneiro F, Cree IA; WHO Classification of Tumours Editorial Board. The 2019 WHO classification of tumours of the digestive system. *Histopathology* 2020; **76**: 182-188 [PMID: 31433515 DOI: 10.1111/his.13975]

6 **Shi S**, Hua J, Liang C, Meng Q, Liang D, Xu J, Ni Q, Yu X. Proposed Modification of the 8th Edition of the AJCC Staging System for Pancreatic Ductal Adenocarcinoma. *Ann Surg* 2019; **269**: 944-950 [PMID: 29334560 DOI: 10.1097/SLA.0000000000002668]

7 **Liang H**, Xie W, Lin X, Wang T, Xie J, Wang C, Xiao SY, Guo Y. Pathologic T1 and T2 encapsulated invasive carcinomas arising from mucinous cystic neoplasms of the pancreas have favorable prognosis and might be treated conservatively. *J Pathol Clin Res* 2021; **7**: 507-516 [PMID: 34062050 DOI: 10.1002/cjp2.225]

8 **Compagno J**, Oertel JE. Microcystic adenomas of the pancreas (glycogen-rich cystadenomas): a clinicopathologic study of 34 cases. *Am J Clin Pathol* 1978; **69**: 289-298 [PMID: 637043 DOI: 10.1093/ajcp/69.1.289]

9 **Tanaka M**, Chari S, Adsay V, Fernandez-del Castillo C, Falconi M, Shimizu M, Yamaguchi K, Yamao K, Matsuno S; International Association of Pancreatology. International consensus guidelines for management of intraductal papillary mucinous neoplasms and mucinous cystic neoplasms of the pancreas. *Pancreatology* 2006; **6**: 17-32 [PMID: 16327281 DOI: 10.1159/000090023]

10 **Suzuki Y**, Atomi Y, Sugiyama M, Isaji S, Inui K, Kimura W, Sunamura M, Furukawa T, Yanagisawa A, Ariyama J, Takada T, Watanabe H, Suda K; Japanese multiinstitutional study of intraductal papillary mucinous tumor and mucinous cystic tumor. Cystic neoplasm of the pancreas: a Japanese multiinstitutional study of intraductal papillary mucinous tumor and mucinous cystic tumor. *Pancreas* 2004; **28**: 241-246 [PMID: 15084964 DOI: 10.1097/00006676-200404000-00005]

11 **Yamao K**, Yanagisawa A, Takahashi K, Kimura W, Doi R, Fukushima N, Ohike N, Shimizu M, Hatori T, Nobukawa B, Hifumi M, Kobayashi Y, Tobita K, Tanno S, Sugiyama M, Miyasaka Y, Nakagohri T, Yamaguchi T, Hanada K, Abe H, Tada M, Fujita N, Tanaka M. Clinicopathological features and prognosis of mucinous cystic neoplasm with ovarian-type stroma: a multi-institutional study of the Japan pancreas society. *Pancreas* 2011; **40**: 67-71 [PMID: 20924309 DOI: 10.1097/MPA.0b013e3181f749d3]

12 **Crippa S**, Salvia R, Warshaw AL, Domínguez I, Bassi C, Falconi M, Thayer SP, Zamboni G, Lauwers GY, Mino-Kenudson M, Capelli P, Pederzoli P, Castillo CF. Mucinous cystic neoplasm of the pancreas is not an aggressive entity: lessons from 163 resected patients. *Ann Surg* 2008; **247**: 571-579 [PMID: 18362619 DOI: 10.1097/SLA.0b013e31811f4449]

13 **Testini M**, Gurrado A, Lissidini G, Venezia P, Greco L, Piccinni G. Management of mucinous cystic neoplasms of the pancreas. *World J Gastroenterol* 2010; **16**: 5682-5692 [PMID: 21128317 DOI: 10.3748/wjg.v16.i45.5682]

14 **Höhn P**, Soydemir MA, Luu AM, Janot-Matuschek M, Tannapfel A, Uhl W, Belyaev O. It's not all about the size—characteristics and risk factors for malignancy of mucinous cystic neoplasms of the pancreas. *Ann Transl Med* 2020; **8**: 1572-1572 [DOI: 10.21037/atm-20-4774]

15 **Lam MM**, Swanson PE, Upton MP, Yeh MM. Ovarian-type stroma in hepatobiliary cystadenomas and pancreatic mucinous cystic neoplasms: an immunohistochemical study. *Am J Clin Pathol* 2008; **129**: 211-218 [PMID: 18208800 DOI: 10.1309/U2BBP4EMBAHCM6E6]

16 **Izumo A**, Yamaguchi K, Eguchi T, Nishiyama K, Yamamoto H, Yonemasu H, Yao T, Tanaka M, Tsuneyoshi M. Mucinous cystic tumor of the pancreas: immunohistochemical assessment of "ovarian-type stroma". *Oncol Rep* 2003; **10**: 515-525 [PMID: 12684617]

17 **Ardeshna DR**, Cao T, Rodgers B, Onongaya C, Jones D, Chen W, Koay EJ, Krishna SG. Recent advances in the diagnostic evaluation of pancreatic cystic lesions. *World J Gastroenterol* 2022; **28**: 624-634 [PMID: 35317424 DOI: 10.3748/wjg.v28.i6.624]

18 **The European Study Group on Cystic Tumours of the Pancreas**. European evidence-based guidelines on pancreatic cystic neoplasms. *Gut* 2018; **67**: 789-804 [DOI: 10.1136/gutjnl-2018-316027]

19 **Valsangkar NP**, Morales-Oyarvide V, Thayer SP, Ferrone CR, Wargo JA, Warshaw AL, Fernández-del Castillo C. 851 resected cystic tumors of the pancreas: a 33-year experience at the Massachusetts General Hospital. *Surgery* 2012; **152**: S4-12 [PMID: 22770958 DOI: 10.1016/j.surg.2012.05.033]

20 **Chang YT**, Tien YW, Jeng YM, Yang CY, Liang PC, Wong JM, Chang MC. Overweight increases the risk of malignancy in patients with pancreatic mucinous cystic neoplasms. *Medicine (Baltimore)* 2015; **94**: e797 [PMID: 25997051 DOI: 10.1097/MD.0000000000000797]

21 **Jang KT**, Park SM, Basturk O, Bagci P, Bandyopadhyay S, Stelow EB, Walters DM, Choi DW, Choi SH, Heo JS, Sarmiento JM, Reid MD, Adsay V. Clinicopathologic characteristics of 29 invasive carcinomas arising in 178 pancreatic mucinous cystic neoplasms with ovarian-type stroma: implications for management and prognosis. *Am J Surg Pathol* 2015; **39**: 179-187 [PMID: 25517958 DOI: 10.1097/PAS.0000000000000357]

22 **Kim GH**, Choi K, Paik N, Lee KT, Lee JK, Lee KH, Han IW, Kang SH, Heo JS, Park JK. Diagnostic Concordance and Preoperative Risk Factors for Malignancy in Pancreatic Mucinous Cystic Neoplasms. *Gut Liver* 2022; **16**: 637-644 [PMID: 34933278 DOI: 10.5009/gnl210231]

23 **Postlewait LM**, Ethun CG, McInnis MR, Merchant N, Parikh A, Idrees K, Isom CA, Hawkins W, Fields RC, Strand M,

Weber SM, Cho CS, Salem A, Martin RC, Scoggins C, Bentrem D, Kim HJ, Carr J, Ahmad S, Abbott DE, Wilson GC, Kooby DA, Maithel SK. Association of Preoperative Risk Factors With Malignancy in Pancreatic Mucinous Cystic Neoplasms: A Multicenter Study. *JAMA Surg* 2017; **152**: 19-25 [PMID: 27760255 DOI: 10.1001/jamasurg.2016.3598]

24 **Riva G**, Pea A, Pilati C, Fiadone G, Lawlor RT, Scarpa A, Luchini C. Histo-molecular oncogenesis of pancreatic cancer: From precancerous lesions to invasive ductal adenocarcinoma. *World J Gastrointest Oncol* 2018; **10**: 317-327 [PMID: 30364837 DOI: 10.4251/wjgo.v10.i10.317]

25 **Lee CJ**, Scheiman J, Anderson MA, Hines OJ, Reber HA, Farrell J, Kochman ML, Foley PJ, Drebin J, Oh YS, Ginsberg G, Ahmad N, Merchant NB, Isbell J, Parikh AA, Stokes JB, Bauer T, Adams RB, Simeone DM. Risk of malignancy in resected cystic tumors of the pancreas < or =3 cm in size: is it safe to observe asymptomatic patients? A multi-institutional report. *J Gastrointest Surg* 2008; **12**: 234-242 [PMID: 18040749 DOI: 10.1007/s11605-007-0381-y]

26 **Megibow AJ**, Baker ME, Morgan DE, Kamel IR, Sahani DV, Newman E, Brugge WR, Berland LL, Pandharipande PV. Management of Incidental Pancreatic Cysts: A White Paper of the ACR Incidental Findings Committee. *J Am Coll Radiol* 2017; **14**: 911-923 [DOI: 10.1016/j.jacr.2017.03.010]

27 **Stark A**, Donahue TR, Reber HA, Hines OJ. Pancreatic Cyst Disease: A Review. *JAMA* 2016; **315**: 1882-1893 [PMID: 27139061 DOI: 10.1001/jama.2016.4690]

28 **Del Chiaro M**, Segersvärd R, Pozzi Mucelli R, Rangelova E, Kartalis N, Ansorge C, Arnelo U, Blomberg J, Löhr M, Verbeke C. Comparison of preoperative conference-based diagnosis with histology of cystic tumors of the pancreas. *Ann Surg Oncol* 2014; **21**: 1539-1544 [PMID: 24385209 DOI: 10.1245/s10434-013-3465-9]

29 **Mohamed E**, Jackson R, Halloran CM, Ghaneh P. Role of Radiological Imaging in the Diagnosis and Characterization of Pancreatic Cystic Lesions: A Systematic Review. *Pancreas* 2018; **47**: 1055-1064 [PMID: 30199486 DOI: 10.1097/MPA.0000000000001134]

30 **Hwang J**, Kim YK, Min JH, Jeong WK, Hong SS, Kim HJ. Comparison between MRI with MR cholangiopancreatography and endoscopic ultrasonography for differentiating malignant from benign mucinous neoplasms of the pancreas. *Eur Radiol* 2018; **28**: 179-187 [PMID: 28779397 DOI: 10.1007/s00330-017-4926-5]

31 **Jang DK**, Song BJ, Ryu JK, Chung KH, Lee BS, Park JK, Lee SH, Kim YT, Lee JY. Preoperative Diagnosis of Pancreatic Cystic Lesions: The Accuracy of Endoscopic Ultrasound and Cross-Sectional Imaging. *Pancreas* 2015; **44**: 1329-1333 [PMID: 26465956 DOI: 10.1097/MPA.0000000000000396]

32 **van Huijgevoort NCM**, Del Chiaro M, Wolfgang CL, van Hooft JE, Besselink MG. Diagnosis and management of pancreatic cystic neoplasms: current evidence and guidelines. *Nat Rev Gastroenterol Hepatol* 2019; **16**: 676-689 [PMID: 31527862 DOI: 10.1038/s41575-019-0195-x]

33 **Xourafas D**, Tavakkoli A, Clancy TE, Ashley SW. Noninvasive intraductal papillary mucinous neoplasms and mucinous cystic neoplasms: recurrence rates and postoperative imaging follow-up. *Surgery* 2015; **157**: 473-483 [PMID: 25596773 DOI: 10.1016/j.surg.2014.09.028]

34 **Sarr MG**, Carpenter HA, Prabhakar LP, Orchard TF, Hughes S, van Heerden JA, DiMagno EP. Clinical and pathologic correlation of 84 mucinous cystic neoplasms of the pancreas: can one reliably differentiate benign from malignant (or premalignant) neoplasms? *Ann Surg* 2000; **231**: 205-212 [PMID: 10674612 DOI: 10.1097/00000658-200002000-00009]

35 **Lewis GH**, Wang H, Bellizzi AM, Klein AP, Askin FB, Schwartz LE, Schulick RD, Wolfgang CL, Cameron JL, O'Reilly EM, Yu KH, Hruban RH. Prognosis of minimally invasive carcinoma arising in mucinous cystic neoplasms of the pancreas. *Am J Surg Pathol* 2013; **37**: 601-605 [PMID: 23388125 DOI: 10.1097/PAS.0b013e318273f3b0]

36 **Park JW**, Jang JY, Kang MJ, Kwon W, Chang YR, Kim SW. Mucinous cystic neoplasm of the pancreas: is surgical resection recommended for all surgically fit patients? *Pancreatology* 2014; **14**: 131-136 [PMID: 24650968 DOI: 10.1016/j.pan.2013.12.006]

37 **Doulamis IP**, Mylonas KS, Kalfountzos CE, Mou D, Haj-Ibrahim H, Nasioudis D. Pancreatic mucinous cystadenocarcinoma: Epidemiology and outcomes. *Int J Surg* 2016; **35**: 76-82 [PMID: 27638187 DOI: 10.1016/j.ijsu.2016.09.017]

38 **Nilsson LN**, Keane MG, Shamali A, Millastre Bocos J, Marijinissen van Zanten M, Antila A, Verdejo Gil C, Del Chiaro M, Laukkarinen J. Nature and management of pancreatic mucinous cystic neoplasm (MCN): A systematic review of the literature. *Pancreatology* 2016; **16**: 1028-1036 [PMID: 27681503 DOI: 10.1016/j.pan.2016.09.011]

39 **Muralidhar V**, Nipp RD, Mamon HJ, Punglia RS, Hong TS, Ferrone C, Fernandez-Del Castillo C, Parikh A, Nguyen PL, Wo JY. Association Between Very Small Tumor Size and Decreased Overall Survival in Node-Positive Pancreatic Cancer. *Ann Surg Oncol* 2018; **25**: 4027-4034 [PMID: 30298331 DOI: 10.1245/s10434-018-6832-8]

40 **NCCN**. Pancreatic Adenocarcinoma, Version 2. 2022, NCCN Clinical Practice Guidelines in Oncology. [DOI: 10.1111/j.1759-7714.2010.00016.x]

41 **Gong J**, Tuli R, Shinde A, Hendifar AE. Meta-analyses of treatment standards for pancreatic cancer. *Mol Clin Oncol* 2016; **4**: 315-325 [PMID: 26998283 DOI: 10.3892/mco.2015.716]

42 **Shaib WL**, Narayan AS, Switchenko JM, Kane SR, Wu C, Akce M, Alese OB, Patel PR, Maithel SK, Sarmiento JM, Kooby DA, El-Rayes BF. Role of adjuvant therapy in resected stage IA subcentimeter (T1a/T1b) pancreatic cancer. *Cancer* 2019; **125**: 57-67 [PMID: 30457666 DOI: 10.1002/cncr.31787]

43 **Hui L**, Rashid A, Foo WC, Katz MH, Chatterjee D, Wang H, Fleming JB, Tamm EP. Significance of T1a and T1b Carcinoma Arising in Mucinous Cystic Neoplasm of Pancreas. *Am J Surg Pathol* 2018; **42**: 578-586 [PMID: 29462092 DOI: 10.1097/PAS.0000000000001040]

44 **Wu J**, Jiao Y, Dal Molin M, Maitra A, de Wilde RF, Wood LD, Eshleman JR, Goggins MG, Wolfgang CL, Canto MI, Schulick RD, Edil BH, Choti MA, Adsay V, Klimstra DS, Offerhaus GJ, Klein AP, Kopelovich L, Carter H, Karchin R, Allen PJ, Schmidt CM, Naito Y, Diaz LA Jr, Kinzler KW, Papadopoulos N, Hruban RH, Vogelstein B. Whole-exome sequencing of neoplastic cysts of the pancreas reveals recurrent mutations in components of ubiquitin-dependent pathways. *Proc Natl Acad Sci U S A* 2011; **108**: 21188-21193 [PMID: 22158988 DOI: 10.1073/pnas.1118046108]

45 **Reid MD**, Saka B, Balci S, Goldblum AS, Adsay NV. Molecular genetics of pancreatic neoplasms and their morphologic correlates: an update on recent advances and potential diagnostic applications. *Am J Clin Pathol* 2014; **141**: 168-180 [PMID: 24436263 DOI: 10.1309/AJCP0FKDP7ENVKEV]

46 **Singhi AD**, McGrath K, Brand RE, Khalid A, Zeh HJ, Chennat JS, Fasanella KE, Papachristou GI, Slivka A, Bartlett DL, Dasyam AK, Hogg M, Lee KK, Marsh JW, Monaco SE, Ohori NP, Pingpank JF, Tsung A, Zureikat AH, Wald AI, Nikiforova MN. Preoperative next-generation sequencing of pancreatic cyst fluid is highly accurate in cyst classification and detection of advanced neoplasia. *Gut* 2018; **67**: 2131-2141 [PMID: 28970292 DOI: 10.1136/gutjnl-2016-313586]

47 **Singhi AD**, Wood LD. Early detection of pancreatic cancer using DNA-based molecular approaches. *Nat Rev Gastroenterol Hepatol* 2021; **18**: 457-468 [PMID: 34099908 DOI: 10.1038/s41575-021-00470-0]

48 **Theisen BK**, Wald AI, Singhi AD. Molecular Diagnostics in the Evaluation of Pancreatic Cysts. *Surg Pathol Clin* 2016; **9**: 441-456 [PMID: 27523971 DOI: 10.1016/j.path.2016.04.008]

49 **Sawai H**, Kurimoto M, Koide S, Kiriyama Y, Haba S, Matsuo Y, Morimoto M, Koide H, Kamiya A, Yamao K. Invasive Ductal Carcinoma Arising in Mucinous Cystic Neoplasm of Pancreas: A Case Report. *Am J Case Rep* 2019; **20**: 242-247 [PMID: 30798329 DOI: 10.12659/AJCR.914092]

World Journal of Gastroenterology

Submit a Manuscript: https://www.f6publishing.com

World J Gastroenterol 2023 May 28; 29(20): 3133-3144

DOI: 10.3748/wjg.v29.i20.3133

ISSN 1007-9327 (print) ISSN 2219-2840 (online)

ORIGINAL ARTICLE

Clinical Trials Study

Safety and effectiveness of vonoprazan-based rescue therapy for *Helicobacter pylori* infection

Jing Yu, Yi-Ming Lv, Peng Yang, Yi-Zhou Jiang, Xiang-Rong Qin, Xiao-Yong Wang

Specialty type: Gastroenterology and hepatology

Provenance and peer review: Unsolicited article; Externally peer reviewed.

Peer-review model: Single blind

Peer-review report's scientific quality classification

Grade A (Excellent): 0
Grade B (Very good): 0
Grade C (Good): C, C, C
Grade D (Fair): 0
Grade E (Poor): 0

P-Reviewer: Keikha M, Iran; Krzyzek P, Poland; Nishida T, Japan

Received: February 27, 2023
Peer-review started: February 27, 2023
First decision: March 13, 2023
Revised: March 25, 2023
Accepted: April 23, 2023
Article in press: April 23, 2023
Published online: May 28, 2023

Jing Yu, Yi-Ming Lv, Peng Yang, Yi-Zhou Jiang, Xiang-Rong Qin, Xiao-Yong Wang, Department of Gastroenterology, The Affiliated Changzhou No. 2 People's Hospital of Nanjing Medical University, Changzhou 213000, Jiangsu Province, China

Corresponding author: Xiao-Yong Wang, MD, Assistant Professor, Chief Physician, Postdoc, Department of Gastroenterology, The Affiliated Changzhou No. 2 People's Hospital of Nanjing Medical University, No. 29 Xinglong Lane, Tianning District, Changzhou 213000, Jiangsu Province, China. wxy20009@126.com

Abstract

BACKGROUND

Vonoprazan (VPZ)-based regimens are an effective first-line therapy for *Helicobacter pylori* (*H. pylori*) infection. However, their value as a rescue therapy needs to be explored.

AIM

To assess a VPZ-based regimen as *H. pylori* rescue therapy.

METHODS

This prospective, single-center, clinical trial was conducted between January and August 2022. Patients with a history of *H. pylori* treatment failure were administered 20 mg VPZ twice daily, 750 mg amoxicillin 3 times daily, and 250 mg *Saccharomyces boulardii* (*S. boulardii*) twice daily for 14 d (14-d VAS regimen). VPZ and *S. boulardii* were taken before meals, while amoxicillin was taken after meals. Within 3 d after the end of eradication therapy, all patients were asked to fill in a questionnaire to assess any adverse events they may have experienced. At least 4-6 wk after the end of eradication therapy, eradication success was assessed using a ^{13}C-urea breath test, and factors associated with eradication success were explored.

RESULTS

Herein, 103 patients were assessed, and 68 patients were finally included. All included patients had 1-3 previous eradication failures. The overall eradication rates calculated using intention-to-treat and per-protocol analyses were 92.6% (63/68) and 92.3% (60/65), respectively. The eradication rate did not differ with the number of treatment failures (P = 0.433). The rates of clarithromycin, metronidazole, and levofloxacin resistance were 91.3% (21/23), 100.0% (23/23), and 60.9% (14/23), respectively. There were no cases of resistance to tetracycline,

amoxicillin, or furazolidone. In 60.9% (14/23) patients, the *H. pylori* isolate was resistant to all 3 antibiotics (clarithromycin, metronidazole, and levofloxacin); however, eradication was achieved in 92.9% (13/14) patients. All patients showed metronidazole resistance, and had an eradication rate of 91.3% (21/23). The eradication rate was higher among patients without anxiety (96.8%) than among patients with anxiety (60.0%, P = 0.025). No severe adverse events occurred; most adverse events were mild and disappeared without intervention. Good compliance was seen in 95.6% (65/68) patients. Serological examination showed no significant changes in liver and kidney function.

CONCLUSION

VAS is a safe and effective rescue therapy, with an acceptable eradication rate (> 90%), regardless of the number of prior treatment failures. Anxiety may be associated with eradication failure.

Key Words: Vonoprazan; *Saccharomyces boulardii*; Rescue therapy; *Helicobacter pylori*; Eradication; Anxiety

©The Author(s) 2023. Published by Baishideng Publishing Group Inc. All rights reserved.

Core Tip: Vonoprazan (VPZ)-containing triple therapies have been shown to contribute to global antimicrobial resistance, while *Saccharomyces boulardii* (*S. boulardii*) supplementation has significantly improved *Helicobacter pylori* eradication rates and decreased adverse events. This study revealed that the VPZ and amoxicillin dual regimen with *S. boulardii* supplementation is safe and effective H. pylori rescue therapy, regardless of the number of prior treatment failures. Acceptable eradication rates (> 90%) were achieved in patients with resistance to clarithromycin, metronidazole, and levofloxacin. However, the regimen may need to be adjusted for patients with anxiety.

Citation: Yu J, Lv YM, Yang P, Jiang YZ, Qin XR, Wang XY. Safety and effectiveness of vonoprazan-based rescue therapy for *Helicobacter pylori* infection. *World J Gastroenterol* 2023; 29(20): 3133-3144
URL: https://www.wjgnet.com/1007-9327/full/v29/i20/3133.htm
DOI: https://dx.doi.org/10.3748/wjg.v29.i20.3133

INTRODUCTION

Helicobacter pylori (*H. pylori*), which infects over 50% of the global population, is a leading cause of chronic gastritis, peptic ulcer disease, and gastric cancer. The eradication of *H. pylori* can effectively prevent peptic ulcer recurrence and lower gastric cancer incidence[1,2]. In regions with high antibiotic resistance, such as China, 14-d bismuth-containing quadruple therapy (BQT) is the recommended first-line treatment for *H. pylori* infection[3-5]. However, as the rates of resistance to clarithromycin, metronidazole, and levofloxacin have markedly increased worldwide, BQT fails to eradicate *H. pylori* infection in approximately 15%-20% patients[6,7]. Multiple failed attempts at eradication therapy tend to increase the prevalence of multidrug-resistant strains, making rescue treatment more difficult[8,9]. Unlike the above antibiotics, the rates of primary and secondary resistance of *H. pylori* to amoxicillin have remained low and stable[10]. Amoxicillin shows a pH- and time-dependent bactericidal effect. Recently, high-dose, high-frequency dual therapy with amoxicillin and a proton pump inhibitor (PPI) was reported to show promising outcomes when used as a first-line or rescue treatment for the eradication of *H. pylori*[11,12]. The Maastricht VI/Florence Consensus Report recommends high-dose dual therapy with a PPI plus amoxicillin as a rescue therapy for *H. pylori* infection[5].

Vonoprazan (VPZ), the first clinically available potassium-competing acid blocker (P-CAB), produces a more rapid and sustained acid inhibition effect than PPIs[13]. Therefore, VPZ-amoxicillin dual therapy (VA-dual) is expected to be more effective than PPI-amoxicillin dual therapy. In recent years, first-line treatment with VA-dual, consisting of amoxicillin (3 g/d or less) and VPZ (40 mg/d), has been reported to achieve eradication rates of 78.5%-93.5%[14-17]. However, limited reports are available on the success rate of VA-dual as a rescue treatment for *H. pylori* infection; only one retrospective study conducted in China has reported a successful eradication rate of 92.5% after VA-dual[18]. However, the regimens were not consistent, and the frequencies of the amoxicillin and VPZ doses varied. Therefore, further optimization of VA-dual as a rescue treatment is warranted.

Some recent consensus guidelines for the management of *H. pylori* infection have proposed that certain probiotics can effectively decrease the gastrointestinal side effects of *H. pylori* eradication therapies[3-5]. A recent meta-analysis demonstrated that *Saccharomyces boulardii* (*S. boulardii*) supple-

mentation during standard eradication therapy (triple regimen, sequential regimen, or quadruple regimen) significantly improved eradication rates and decreased the overall incidence of adverse events [19]. However, few studies have evaluated the effects of *S. boulardii* as a supplement to the VA-dual regimen in terms of the eradication rate of *H. pylori* and treatment-related adverse events.

Therefore, the aim of this prospective study was to determine the safety and efficacy of VA-dual plus *S. boulardii* supplementation as a rescue treatment for patients with *H. pylori* infection. We additionally explored potential factors influencing eradication rates, and put forward our recommendations to improve *H. pylori* eradication rates in clinical practice.

MATERIALS AND METHODS

Statement of ethics and trial registration

Ethical approval for this pilot study was obtained from Affiliated Changzhou No. 2 People's Hospital of Nanjing Medical University [No. (2021) YLJSD004]. The study adhered to the tenets of the Declaration of Helsinki. Written informed consent was obtained from all patients prior to their enrollment in this study. The study has been registered in the Chinese Clinical Trial Registry (No. ChiCTR2200055125).

Study participants

Patients who attended our center between January and August 2022 were screened for their eligibility to participate in this study. The detailed inclusion criteria were as follows: (1) Patients aged over 18 years; (2) patients with a history of at least one failed *H. pylori* eradication treatment; and (3) a minimum 6-mo interval after the end of the last treatment. The following exclusion criteria were applied: (1) A history of gastric surgery; (2) severe concomitant diseases such as hepatic or renal dysfunction; (3) allergy or contraindication to the drugs used in the study regimen; (4) pregnancy or lactation; (5) treatment with a PPI, bismuth, or an antibiotic within 4 wk before the study treatment; (6) alcohol abuse or drug addiction; and (7) lack of informed consent.

Study design and outcomes

Before enrollment, the patients' demographic data, clinical characteristics, and any concomitant diseases were recorded through medical records and physician interviews. The diagnosis of *H. pylori* infection was based on a positive result of at least one of the following tests: ^{13}C-urea breath test (^{13}C-UBT), rapid urease test, and histological examination. Some patients also underwent gastroscopy, and *H. pylori* culture and antimicrobial susceptibility testing before treatment. Serum chemistry tests were performed before and after treatment.

All patients were administered VPZ (20 mg twice daily; Takeda Pharmaceutical, Tokyo, Japan), amoxicillin (750 mg 3 times daily; Federal Pharmaceutical, Hong Kong, China), and *S. boulardii* (250 mg twice daily; Laboratoires BIOCODEX, France) for 14 d (14-d VAS regimen). VPZ and *S. boulardii* were taken before meals, while amoxicillin was taken after meals. Patients who felt unwell during treatment or forgot to take their medication were advised to contact the investigators immediately.

All patients were asked to keep the remaining drugs after treatment and fill out the relevant questions in the questionnaire within 3 d after the end of eradication therapy. Adverse events and patient compliance were assessed using the questionnaires and the patients' medication diaries. The intensity of the adverse events was graded as follows: None; mild, causing discomfort but not interfering with daily life; moderate, causing discomfort and interfering with daily life; and severe, causing discomfort requiring cessation of treatment. Patient compliance was rated as good if the patient had taken > 80% of all medications prescribed, and as poor, if not[20]. All patients underwent repeat ^{13}C-UBT for the assessment of *H. pylori* infection 4-6 wk after the end of eradication therapy. The *H. pylori* status was interpreted as positive when the δ value was greater than the baseline value of 4, and as negative when the δ value was less than the baseline value of 4. If the δ value exceeded the baseline value, which was between 4 and 6, the test was repeated 1 mo later.

The primary endpoint of this study was the *H. pylori* eradication rate, as confirmed by a negative ^{13}C-UBT. All patients were included in the intention-to-treat (ITT) analysis. Patients who did not undergo a ^{13}C-UBT during follow-up were considered to have treatment failure in the ITT analysis. Patients who failed to attend follow-up assessments and those with poor compliance were excluded from the per protocol (PP) analysis. The secondary endpoints were the rate of adverse events, patient compliance, resistance to antibiotics, and factors related to the eradication rate.

H. pylori culture and antimicrobial susceptibility testing

From patients who underwent gastroscopy, we collected 2 biopsy specimens for *H. pylori* culture, one from the gastric antrum and another from the gastric corpus. Both specimens were stored at -80 °C in brain-heart infusion broth (Oxoid, Basingstoke, United Kingdom) and immediately transported to Zhiyuan Medical Laboratory Institute (Hangzhou, Zhejiang Province, China) for testing. Fully ground specimens were cultured and maintained for 3-7 d in brain-heart infusion agar medium (Oxoid,

Basingstoke, United Kingdom) supplemented with 5% defibrinated sheep blood at 37 °C in a low-oxygen environment (85% N_2, 10% CO_2, and 5% O_2). *H. pylori* isolates were identified on the basis of colony morphology and urease, catalase, and oxidase positivity.

The standard agar plate dilution method was used to assess *H. pylori* susceptibility to commonly used antibiotics. Minimum inhibitory concentrations (MICs) were calculated after 72 h of culture at 37 °C in a low-oxygen environment. We used *H. pylori* ATCC43504 (NCTC11637) for quality control. Antibiotic resistance was defined at the following MIC values: ≥ 1 μg/mL for clarithromycin, ≥ 8 μg/mL for metronidazole, and ≥ 2 μg/mL each for amoxicillin, furazolidone, levofloxacin, and tetracycline. The MIC values for antibiotic resistance were obtained from the fourth edition of the National Guide to Clinical Laboratory Procedures[21].

Sample-size calculation and statistical analysis

We assumed a 93% eradication rate with VPZ-based rescue therapy[22]. The 95% confidence interval was 86.6%-99.4%, and the sample size was 64 patients. Assuming a 5% follow-up loss, at least 68 patients would be required. Continuous variables were expressed as mean ± SD, and compared between groups by using the *t* test or Mann-Whitney *U* test. Categorical variables were expressed as numbers with percentages, and compared between groups by using the Fisher exact test or Pearson χ^2 test. Statistical significance was inferred at *P* values < 0.05. All statistical analyses were conducted using Statistical Package for the Social Sciences *v*23.0 (IBM, Armonk, NY, United States) and Power Analysis and Sample Size software *v*15.0.5 (NCSS LLC, Kaysville, UT, United States).

RESULTS

Patient characteristics

We screened a total of 103 patients for eligibility, and excluded 35 patients who did not meet the inclusion criteria. Thus, finally, 68 patients were enrolled in this study, of whom 62 patients underwent endoscopy, 41 patients underwent serological testing before and after treatment, and 24 patients underwent antimicrobial susceptibility testing. Three patients were excluded from the PP analysis due to poor compliance despite a negative ^{13}C-UBT during follow-up (Figure 1).

Of the 68 patients, 20 were men and 48 were women (Table 1). Prior to the present treatment, 47 patients had undergone treatment once, 15 patients had undergone treatment twice, and 6 patients had undergone treatment 3 times. Most patients were asymptomatic (*n* = 37, 54.4%). The most common concomitant diseases were hypertension (*n* = 14, 20.6%) and diabetes (*n* = 9, 13.2%); 4 patients (5.9%) had anxiety disorder. The most common previous treatment regimen was BQT, and the most commonly used antibiotics were amoxicillin, levofloxacin, clarithromycin, and metronidazole, with a few patients using furazolidone.

H. pylori culture and antimicrobial susceptibility testing

Of the 68 patients, 24 (35.3%) underwent *H. pylori* culture and antimicrobial susceptibility testing. *H. pylori* was successfully isolated in 95.8% (23/24) of patients. The rates of resistance to metronidazole, clarithromycin, and levofloxacin were 100% (23/23), 91.3% (21/23), and 60.0% (14/23), respectively. There were no cases of resistance to tetracycline, amoxicillin, or furazolidone. The triple drug-resistance rate (to metronidazole, levofloxacin, and clarithromycin) was 56.3% (9/16) among patients with one prior treatment failure, which increased to 71.4% (5/7) among patients with 2 or more prior treatment failures.

Eradication rate and factors influencing efficacy

The overall eradication rates of 14-d VAS calculated using the ITT and PP analyses were 92.6% (63/68) and 92.3% (60/65), respectively. In 2 of the 5 patients in whom eradication failed, further treatment with VPZ 20 mg twice daily, amoxicillin 1000 mg 3 times daily, and *S. boulardii* 250 mg twice daily for 14 d successfully eradicated the infection. The remaining 3 patients had not yet received additional rescue therapy at the time of writing as less than 6 mo had passed since the end of the previous treatment.

We stratified the *H. pylori* eradication rate by the number of prior treatment failures (Figure 2). The ITT analysis showed that the eradication rates were 93.6%, 93.3%, and 83.3% (*P* = 0.433) among patients with 1, 2, and 3 prior treatment failures, respectively. The corresponding eradication rates according to the PP analysis were 93.2%, 93.3%, and 83.3% (*P* = 0.585). We found that the eradication rate did not significantly differ with the number of previous treatment failures. In addition, eradication rates did not differ between patients who had previously received amoxicillin and those who had not (85.0% *vs* 95.8%, *P* = 0.433).

Among the 23 patients who successfully underwent *H. pylori* culture and antimicrobial susceptibility testing, the ITT analysis showed that similar eradication rates were achieved in the clarithromycin-resistant (90.4%) and clarithromycin-sensitive groups (100%; *P* = 1.00). PP analysis also showed that the eradication rate did not differ between the clarithromycin-resistant and clarithromycin-sensitive groups

Table 1 Clinicodemographic characteristics of the study patients, *n* (%)

Characteristic	Total No. of patients (*n* = 68)	Number of prior eradication failures		
		1 (*n* = 47)	2 (*n* = 15)	3 (*n* = 6)
Sex (male)	20 (29.4)	10 (21.3)	6 (4.0)	4 (66.7)
Age (yr), mean ± SD	49.60 ± 10.57	49.94 ± 10.00	48.87 ± 12.65	48.83 ± 11.27
Height (m), mean ± SD	1.63 ± 0.07	1.62 ± 0.09	1.64 ± 0.08	1.68 ± 0.10
Weight (kg), mean ± SD	59.52 ± 12.30	56.83 ± 12.19	63.80 ± 9.94	69.92 ± 11.50
BMI (kg/m^2), mean ± SD	22.31 ± 3.64	21.59 ± 3.98	23.63 ± 2.04	24.63 ± 1.80
Lifestyle factors				
Smoking	5 (7.3)	4 (8.5)	0 (0)	1 (16.7)
Drinking	4 (5.9)	0 (0)	1 (6.7)	3 (50.0)
Symptom				
Abdominal pain	7 (10.3)	5 (10.6)	2 (13.3)	0 (0)
Bloating	6 (8.8)	4 (8.5)	2 (13.3)	0 (0)
Diarrhea	1 (1.5)	0 (0)	1 (6.7)	0 (0)
Halitosis	1 (1.5)	1 (2.1)	0 (0)	0 (0)
Belching	13 (19.1)	8 (17.0)	3 (20.0)	2 (33.4)
Nausea	2 (2.9)	2 (4.3)	0 (0)	0 (0)
Bitter taste	1 (1.5)	1 (2.1)	0 (0)	0 (0)
Asymptomatic	37 (54.4)	26 (55.3)	7 (46.7)	4 (66.7)
Concomitant disease				
Diabetes mellitus	9 (13.2)	8 (17.0)	1 (6.7)	0 (0)
Hypertension	14 (20.6)	7 (14.9)	5 (33.3)	2 (33.4)
Anxiety disorder	4 (5.9)	1 (2.1)	2 (13.3)	1 (16.7)
Gastroscopy findings				
Atrophic gastritis	33 (48.6)	27 (57.4)	4 (26.7)	2 (33.4)
Non-atrophic gastritis	24 (35.3)	14 (29.8)	8 (53.3)	2 (33.4)
Peptic ulcer	4 (5.9)	1 (2.1)	1 (6.7)	2 (33.4)
Polyp	1 (1.5)	0 (0)	1 (6.7)	0 (0)
Not applicable (no gastroscopy done)	6 (8.9)	5 (10.6)	1 (13.3)	0 (0)

BMI: Body mass index.

(90.0% *vs* 100%, respectively, P = 1.00). Similarly, we found no significant difference in the *H. pylori* eradication rate between the levofloxacin-resistant and levofloxacin-sensitive groups (ITT: 92.8% *vs* 88.8%, respectively, P = 1.00; PP: 92.3% *vs* 88.8%, respectively, P = 1.00; Figure 3). All patients showed metronidazole resistance, and had an eradication rate of 91.3% (21/23). Notably, eradication was achieved in 92.9% (13/14) patients who showed triple drug resistance (clarithromycin, metronidazole, and levofloxacin).

Anxiety disorder was found to be a risk factor for eradication failure (40.0% *vs* 3.2%, P = 0.025; Table 2). No significant differences in age, sex, height, weight, body mass index, concomitant diseases, gastroscopy findings, and number of prior treatment failures were found between patients with successful and failed rescue therapy.

Adverse events and compliance

A total of 10 patients (14.7%) developed adverse events, including diarrhea (4 patients), skin rash (3 patients), and dry mouth, bloating, and abdominal pain (1 patient each). Most adverse events were mild and disappeared without intervention, except in 2 patients who developed rashes on day 9 and 11, refused continued rescue treatment, and finally recovered after anti-allergy therapy. Another patient

Table 2 Factors potentially influencing *Helicobacter pylori* eradication, *n* (%)

Factor	Eradication failure (*n* = 5)	Successful eradication (*n* = 63)	*P* value
Sex (male)	2 (40.0)	18 (28.6)	0.627
Age (yr), mean ± SD	54.40 ± 5.86	49.22 ± 10.80	0.295
Height (m), mean ± SD	1.62 ± 0.10	1.62 ± 0.07	0.778
Weight (kg), mean ± SD	64.60 ±11.42	59.12 ± 12.37	0.129
BMI (kg/m^2), mean ± SD	24.43 ± 1.88	22.14 ± 3.70	0.112
Concomitant disease			
Diabetes mellitus	1 (20.0)	8 (12.7)	0.520
Hypertension	1 (20.0)	13 (20.6)	1.000
Anxiety disorder	2 (40.0)	2 (3.2)	0.025
Gastroscopy findings			
Atrophic gastritis	2 (40.0)	31 (49.2)	1.000
Non-atrophic gastritis	3 (60.0)	21 (33.3)	0.337
Peptic ulcer	0 (0.0)	4 (6.3)	1.000
Polyp	0 (0.0)	1 (1.6)	1.000
No. of prior treatments			
1	3 (60.0)	44 (69.8)	0.641
≥ 2	2 (40.0)	19 (30.2)	

BMI: body mass index.

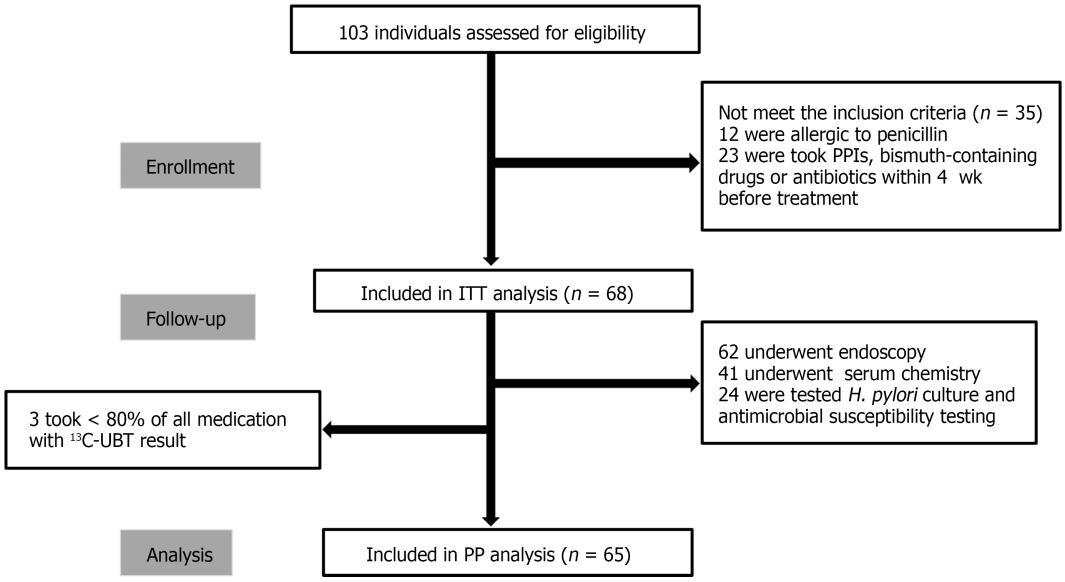


Figure 1 Flow chart of the study. PPI: Proton pump inhibitor; ITT: Intention-to-treat analysis; PP: Per-protocol analysis; UBT: Urea breath test; *H. pylori*: *Helicobacter pylori*.

discontinued treatment on day 7 because of diarrhea, which improved without intervention. The remaining patients took > 80% of all medications prescribed (compliance rate, 95.6%, 65/68; Table 3). Serum chemistry tests revealed no significant differences in liver and kidney function before and after treatment (Table 4). Among the 10 patients who developed adverse events, only 1 patient (with a rash) had eradication failure.

Table 3 Adverse events and patient compliance

Variable	%
Adverse events	
Total adverse events	14.7% (10/68)
Dry mouth	1.5% (1/68)
Skin rash	4.4% (3/68)
Bloating	1.5% (1/68)
Diarrhea	5.9% (4/68)
Abdominal pain	1.5% (1/68)
Grade of adverse event	
Mild	70.0% (7/10)
Moderate	30.0% (3/10)
Severe	0% (0/10)
[1]Compliance	
Good	95.6% (65/68)
Poor	4.4% (3/68)

[1]Compliance was rated as good if the patient had taken > 80% of all medications prescribed, and as poor, if not.

Table 4 Comparison of liver and kidney function before and after treatment

Characteristic	Before (n = 41)	After (n = 41)	P value
Total bilirubin (μmol/L), mean ± SD	13.68 ± 4.82	14.96 ± 5.22	0.252
ALT (U/L), mean ± SD	16.92 ± 8.33	21.46 ± 16.03	0.270
AST (U/L), mean ± SD	18.99 ± 7.61	21.03 ± 10.67	0.670
Creatinine (μmol/L), mean ± SD	60.105 ± 12.060	60.53 ± 11.35	0.974

AST: Aspartate transaminase; ALT: Alanine transaminase.

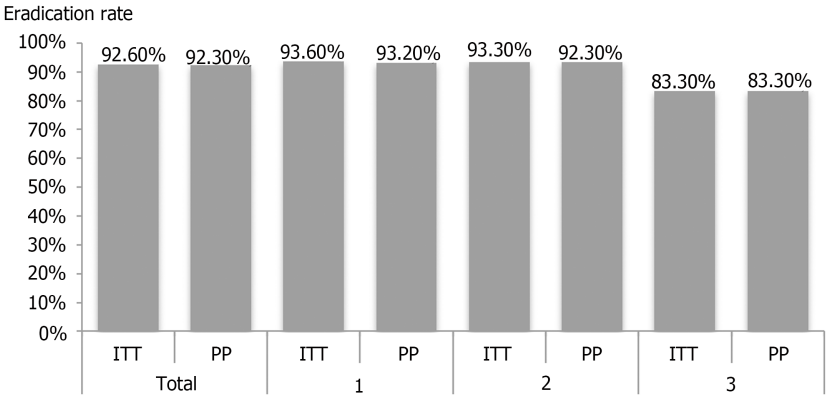


Figure 2 Eradication rates stratified by number of prior treatment failures. ITT: 93.6% *vs* 93.3% *vs* 83.3%, P = 0.433; PP: 93.2% *vs* 93.3% *vs* 83.3%, P = 0.585). ITT: Intention-to-treat analysis; PP: Per-protocol analysis.

DISCUSSION

To our knowledge, this study is the first to determine the safety and efficacy of 14-d VA-dual plus *S. boulardii* supplementation as a rescue therapy for *H. pylori* infection. This VAS regimen achieved an

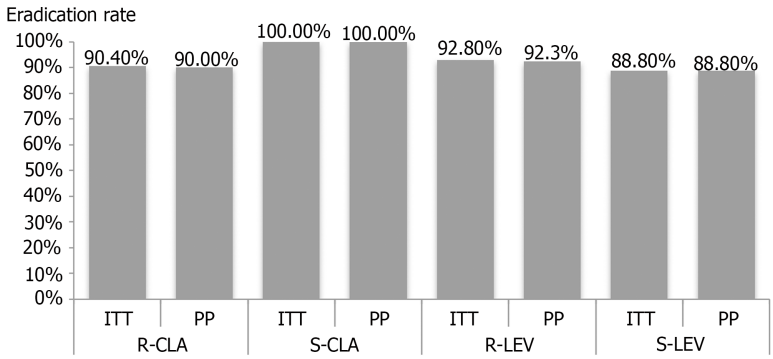


Figure 3 Impact of bacterial antibiotic resistance on eradication rate. ITT: Clarithromycin resistant *vs* clarithromycin sensitive, $P = 1.00$; levofloxacin resistant *vs* levofloxacin sensitive, $P = 1.00$; PP: Clarithromycin resistant *vs* clarithromycin sensitive, $P = 1.00$; levofloxacin resistant *vs* levofloxacin sensitive, $P = 1.00$). R-CLA: Clarithromycin resistant; S-CLA: Clarithromycin sensitive; R-LEV: Levofloxacin resistant; S-LEV: Levofloxacin sensitive; ITT: Intention-to-treat analysis; PP: Per-protocol analysis.

acceptable eradication rate (92.6% by ITT and 92.3% by PP), regardless of the number of prior treatment failures. Most patients could tolerate this regimen, and compliance was good in this Chinese patient population. Except for anxiety disorder, no other factors were observed to be associated with treatment failure. Notably, eradication was successful in 92.9% (13/14) of patients with multiple antibiotic resistance. Therefore, the 14-d VAS regimen is a safe and effective rescue therapy for *H. pylori* infection.

Currently, *H. pylori* culture-guided therapy is recommended by most consensus guidelines as a rescue therapy for *H. pylori* infection. However, culture-guided therapy is not widely used in routine clinical practice[3-5]. Until recently, susceptibility tests still required the microbiological examination of samples obtained through endoscopy, which is invasive and expensive. In addition, many hospitals lack the facilities required to perform *H. pylori* culture and antimicrobial susceptibility testing, which limits the clinical use of culture-guided therapy in many countries[3,5,20]. Furthermore, *H. pylori* culture is technically challenging. Several studies have reported culture success rates of < 80% among patients with failure of at least one prior *H. pylori* eradication treatment[23]. It should be emphasized that in our study, culture was performed in only 35.3% of the patients. This reflects the current state of routine clinical practice in China. Culture-guided therapy has not yet become a routine clinical practice, and rescue therapy is mainly prescribed on an empirical basis in China.

Compared with PPIs, VPZ, the first clinically applied P-CAB, has a faster and stronger acid-inhibition effect[13]. This provides an opportunity to potentially improve *H. pylori* eradication therapy by simplifying complex regimens and possibly helping to develop effective therapies[5]. In one study, a PP analysis showed that a 7-d VPZ-based regimen (VPZ 20 mg twice daily, sitafloxacin 100 mg twice daily, and amoxicillin 750 mg twice daily) as a third-line therapy resulted in a significantly higher eradication rate than a PPI-based regimen (83.3% *vs* 57.1%, $P = 0.043$)[24]. In a small study, a 10-d triple therapy regimen consisting of VPZ 20 mg twice daily, rifabutin 150 mg twice daily, and amoxicillin 750 mg twice daily yielded a 100% eradication rate in 19 patients with ≥ 3 prior treatment attempts[25]. Similarly, in 57 patients administered a 7-d rifabutin-containing triple therapy regimen (VPZ 20 mg twice daily, amoxicillin 500 mg 4 times daily, and 150 mg rifabutin 150 mg once daily) as a third- or later-line *H. pylori* eradication regimen, the eradication rate was 91.2%[26]. It should be emphasized that all the above studies were conducted in Japan, and they all used triple regimens containing VPZ and amoxicillin. Although the use of 2 antibiotics may lead to higher eradication rates, this practice promotes the use of an unnecessary second antibiotic[27]. Hence, optimization of VPZ-based rescue therapy needs to be further explored. However, the relevant research in China is limited. Only one retrospective study has reported that the 14-d VA-dual regimen (VPZ 20 mg/d or 40 mg/d and amoxicillin 3000 mg/d) was safe and effective as a rescue therapy (92.5%, 172/186); however, the frequencies and doses of VA-dual therapy varied among the patients[18].

The 14-d VAS regimen used in this study offers certain advantages over previous rescue therapies. First, it minimizes the use of antibiotics, which is especially important in the light of the global increase in *H. pylori* antibiotic resistance. Indeed, VPZ-containing triple therapies have been shown to contribute to global antimicrobial resistance[27]. The 14-d VAS regimen eliminated the need for a second antibiotic while providing remarkable *H. pylori* eradication efficacy. Second, the optimal amoxicillin dose for dual therapy remains uncertain. Available evidence suggests that a dose of 2 g/d is insufficient, and 3 g or 2.25-3.00 g in split doses (every 6 h or 8 h) may be optimal[27]. Therefore, amoxicillin was administered at a dose of 750 mg 3 times daily in the 14-d VAS regimen. Third, for the first time, we supplemented *S. boulardii* to VA-dual as a rescue therapy for *H. pylori* eradication. Several potential mechanisms by which *S. boulardii* acts as an adjunct to *H. pylori* eradication therapy have been elucidated: (1) It inhibits the growth and proliferation of *H. pylori* by upregulating short-chain fatty acids and other antimicrobial substances[28]; (2) it expresses a neuraminidase that reduces the expression of α(2-3)-linked sialic acid

on the epithelial cell surface, which prevents the adhesion of *H. pylori* to the duodenal epithelium[29]; and (3) it reduces the incidence of adverse events and indirectly improves patient compliance, thereby increasing the eradication rate of *H. pylori*[19].

Poor patient compliance is a main cause of treatment failure, and adverse events are a key factor affecting patient compliance[30]. Our 14-d VAS regimen was well tolerated, and all adverse events were mild or moderate, with diarrhea (5.9%) and rash (4.4%) being the most common. Patient compliance was also good, which may be attributable to the low rate of adverse events and the simplicity of the regimen.

We analyzed the factors potentially influencing the eradication rate of the 14-d VAS regimen. Only anxiety disorder was significantly associated with eradication failure; other factors such as gender, age, smoking, and alcohol consumption were not associated with treatment failure. There is evidence that state anxiety and trait anxiety are related to *H. pylori* infection. Anxiety appears to heighten the intensity and perception of gastrointestinal signals, which gives patients more reasons to worry about their health, leading to a higher anxiety response, and making patients more inclined to seek medical advice [31]. Thus, identifying patients with anxiety prior to the treatment of *H. pylori* infection and management by a professional team including a gastroenterologist and a psychologist to improve anxiety may be necessary to improve eradication rates and reduce the costs associated with frequent medical consultations.

This study has some limitations. First, it is impossible to compare the safety and effectiveness of the VA-dual regimen and the VAS regimen because this study is a single-arm pilot study. Large-scale, multicenter randomized controlled trials in areas with different patterns of antibiotic resistance are needed to confirm our results. Second, the number of patients with anxiety disorder in this study was small, and the relevant conclusions and potential mechanisms need to be further explored in future studies. Third, *H. pylori* culture and antimicrobial susceptibility testing were performed in only 35.3% of our patients, and no resistance was detected to amoxicillin. So, it was impossible to determine whether amoxicillin resistance affected the eradication rate of the 14-d VAS regimen. However, considering that the rates of primary and secondary resistance to amoxicillin are low and stable[10], we believe that the 14-d VAS regimen is an effective rescue therapy. Fourth, this study was underpowered to analyze the association between eradication rate and prior eradication regimens because the study patients had previously been treated with multiple different regimens.

CONCLUSION

In conclusion, the 14-d VAS regimen is safe and effective *H. pylori* rescue therapy, with an acceptable eradication rate (> 90%), regardless of the number of prior treatment failures. This regimen avoids the use of additional antibiotics, but may need to be adjusted for patients with anxiety. Large-scale, multicenter randomized controlled trials are needed to confirm our results.

ARTICLE HIGHLIGHTS

Research background

Vonoprazan (VPZ)-containing triple therapies have been shown to contribute to global antimicrobial resistance. Hence, the value of VPZ-based regimens as rescue therapies needs to be explored.

Research motivation

Saccharomyces boulardii (*S. boulardii*) supplementation significantly improved *H. pylori* eradication rates and decreased the incidence of adverse events. We are the first to combine *S. boulardii* supplementation with VPZ-amoxicillin dual therapy (VAS regimen) as a rescue therapy for *H. pylori* eradication.

Research objectives

To determine the safety and efficacy of the VAS regimen as a rescue treatment for *H. pylori* infection.

Research methods

We performed a prospective, single-center, clinical trial with the VAS regimen.

Research results

The overall eradication rates calculated using intention-to-treat and per-protocol analyses were 92.6% and 92.3%, respectively. The eradication rate did not differ with the number of treatment failures (P = 0.433). Acceptable eradication rates (> 90%) were achieved in patients with resistance to clarithromycin, metronidazole, and levofloxacin. Most adverse events were mild, and 95.6% patients showed good compliance.

Research conclusions

The VAS regimen is a safe and effective rescue therapy, with an acceptable eradication rate (> 90%), regardless of the number of prior treatment failures.

Research perspectives

Large-scale, multicenter randomized controlled trials in areas with different patterns of antibiotic resistance are needed to confirm our results. It will be necessary to compare the safety and effectiveness of the VPZ-amoxicillin dual therapy regimen with the VAS regimen in the future.

ACKNOWLEDGEMENTS

The authors are grateful to Dr. Liu-Lan Qian for her help in the statistical analysis of this paper.

FOOTNOTES

Author contributions: Wang XY contributed to conception and design of the study, critical revision, analysis and interpretation of data, drafting the article, revising the article; Yu J and Lv YM contributed to acquisition of data, analysis and interpretation of data, and drafting the article; Yang P, Jiang YZ, and Qin XR contributed to acquisition of data, analysis and interpretation of data; and all authors approved the final version of the manuscript.

Supported by the Changzhou Special Fund for Introducing Foreign Talents, No. CQ20204037; and the Changzhou High-Level Medical Talents Training Project, No. 2022CZBJ051.

Institutional review board statement: The study was reviewed and approved by the Clinical Medical Technical Ethics Committee of the Affiliated Changzhou No. 2 People's Hospital of Nanjing Medical University [approval. No. (2021) YLJSD004].

Clinical trial registration statement: This study is registered at Chinese Clinical trial Registry. The registration identification number is ChiCTR2200055125.

Informed consent statement: All study participants provided informed written consent prior to the study enrollment and declare that they have no conflict of interest.

Conflict-of-interest statement: The authors declare that they have no conflict of interest.

Data sharing statement: The data that support the findings of this study are available from the corresponding author upon reasonable request.

CONSORT 2010 statement: The authors have read the CONSORT 2010 statement, and the manuscript was prepared and revised according to the CONSORT 2010 statement.

Open-Access: This article is an open-access article that was selected by an in-house editor and fully peer-reviewed by external reviewers. It is distributed in accordance with the Creative Commons Attribution NonCommercial (CC BY-NC 4.0) license, which permits others to distribute, remix, adapt, build upon this work non-commercially, and license their derivative works on different terms, provided the original work is properly cited and the use is non-commercial. See: https://creativecommons.org/Licenses/by-nc/4.0/

Country/Territory of origin: China

ORCID number: Jing Yu 0000-0002-4132-3944; Yi-Ming Lv 0000-0002-1546-0339; Peng Yang 0000-0002-5501-0244; Yi-Zhou Jiang 0000-0002-8274-9327; Xiang-Rong Qin 0000-0001-8135-473X; Xiao-Yong Wang 0000-0001-8401-4888.

S-Editor: Chen YL
L-Editor: A
P-Editor: Cai YX

REFERENCES

1 **Zamani M**, Ebrahimtabar F, Zamani V, Miller WH, Alizadeh-Navaei R, Shokri-Shirvani J, Derakhshan MH. Systematic review with meta-analysis: the worldwide prevalence of Helicobacter pylori infection. *Aliment Pharmacol Ther* 2018; **47**: 868-876 [PMID: 29430669 DOI: 10.1111/apt.14561]

2 **Chiang TH**, Chang WJ, Chen SL, Yen AM, Fann JC, Chiu SY, Chen YR, Chuang SL, Shieh CF, Liu CY, Chiu HM,

Chiang H, Shun CT, Lin MW, Wu MS, Lin JT, Chan CC, Graham DY, Chen HH, Lee YC. Mass eradication of Helicobacter pylori to reduce gastric cancer incidence and mortality: a long-term cohort study on Matsu Islands. *Gut* 2021; **70**: 243-250 [PMID: 32792335 DOI: 10.1136/gutjnl-2020-322200]

3 **Liu WZ**, Xie Y, Lu H, Cheng H, Zeng ZR, Zhou LY, Chen Y, Wang JB, Du YQ, Lu NH; Chinese Society of Gastroenterology, Chinese Study Group on Helicobacter pylori and Peptic Ulcer. Fifth Chinese National Consensus Report on the management of Helicobacter pylori infection. *Helicobacter* 2018; **23**: e12475 [PMID: 29512258 DOI: 10.1111/hel.12475]

4 **Chey WD**, Leontiadis GI, Howden CW, Moss SF. ACG Clinical Guideline: Treatment of Helicobacter pylori Infection. *Am J Gastroenterol* 2017; **112**: 212-239 [PMID: 28071659 DOI: 10.1038/ajg.2016.563]

5 **Malfertheiner P**, Megraud F, Rokkas T, Gisbert JP, Liou JM, Schulz C, Gasbarrini A, Hunt RH, Leja M, O'Morain C, Rugge M, Suerbaum S, Tilg H, Sugano K, El-Omar EM; European Helicobacter and Microbiota Study group. Management of Helicobacter pylori infection: the Maastricht VI/Florence consensus report. *Gut* 2022 [PMID: 35944925 DOI: 10.1136/gutjnl-2022-327745]

6 **Koroglu M**, Ayvaz MA, Ozturk MA. The efficacy of bismuth quadruple therapy, sequential therapy, and hybrid therapy as a first-line regimen for Helicobacter pylori infection compared with standard triple therapy. *Niger J Clin Pract* 2022; **25**: 1535-1541 [PMID: 36149216 DOI: 10.4103/njcp.njcp_89_22]

7 **Song Z**, Suo B, Zhang L, Zhou L. Rabeprazole, Minocycline, Amoxicillin, and Bismuth as First-Line and Second-Line Regimens for Helicobacter pylori Eradication. *Helicobacter* 2016; **21**: 462-470 [PMID: 27060292 DOI: 10.1111/hel.12313]

8 **Cortés P**, Nelson AD, Bi Y, Stancampiano FF, Murray LP, Pujalte GGA, Gomez V, Harris DM. Treatment Approach of Refractory Helicobacter pylori Infection: A Comprehensive Review. *J Prim Care Community Health* 2021; **12**: 21501327211014087 [PMID: 33949229 DOI: 10.1177/21501327211014087]

9 **Graham DY**, Fischbach L. Helicobacter pylori treatment in the era of increasing antibiotic resistance. *Gut* 2010; **59**: 1143-1153 [PMID: 20525969 DOI: 10.1136/gut.2009.192757]

10 **Li SY**, Li J, Dong XH, Teng GG, Zhang W, Cheng H, Gao W, Dai Y, Zhang XH, Wang WH. The effect of previous eradication failure on antibiotic resistance of Helicobacter pylori: A retrospective study over 8 years in Beijing. *Helicobacter* 2021; **26**: e12804 [PMID: 33860967 DOI: 10.1111/hel.12804]

11 **Bi H**, Chen X, Chen Y, Zhao X, Wang S, Wang J, Lyu T, Han S, Lin T, Li M, Yuan D, Liu J, Shi Y. Efficacy and safety of high-dose esomeprazole-amoxicillin dual therapy for Helicobacter pylori rescue treatment: a multicenter, prospective, randomized, controlled trial. *Chin Med J (Engl)* 2022; **135**: 1707-1715 [PMID: 36193978 DOI: 10.1097/CM9.0000000000002289]

12 **Guan JL**, Hu YL, An P, He Q, Long H, Zhou L, Chen ZF, Xiong JG, Wu SS, Ding XW, Luo HS, Li PY. Comparison of high-dose dual therapy with bismuth-containing quadruple therapy in Helicobacter pylori-infected treatment-naive patients: An open-label, multicenter, randomized controlled trial. *Pharmacotherapy* 2022; **42**: 224-232 [PMID: 35075679 DOI: 10.1002/phar.2662]

13 **Sakurai Y**, Mori Y, Okamoto H, Nishimura A, Komura E, Araki T, Shiramoto M. Acid-inhibitory effects of vonoprazan 20 mg compared with esomeprazole 20 mg or rabeprazole 10 mg in healthy adult male subjects--a randomised open-label cross-over study. *Aliment Pharmacol Ther* 2015; **42**: 719-730 [PMID: 26193978 DOI: 10.1111/apt.13325]

14 **Zuberi BF**, Ali FS, Rasheed T, Bader N, Hussain SM, Saleem A. Comparison of Vonoprazan and Amoxicillin Dual Therapy with Standard Triple Therapy with Proton Pump Inhibitor for Helicobacter Pylori eradication: A Randomized Control Trial. *Pak J Med Sci* 2022; **38**: 965-969 [PMID: 35634610 DOI: 10.12669/pjms.38.4.5436]

15 **Chey WD**, Mégraud F, Laine L, López LJ, Hunt BJ, Howden CW. Vonoprazan Triple and Dual Therapy for Helicobacter pylori Infection in the United States and Europe: Randomized Clinical Trial. *Gastroenterology* 2022; **163**: 608-619 [PMID: 35679950 DOI: 10.1053/j.gastro.2022.05.055]

16 **Suzuki S**, Gotoda T, Kusano C, Ikehara H, Ichijima R, Ohyauchi M, Ito H, Kawamura M, Ogata Y, Ohtaka M, Nakahara M, Kawabe K. Seven-day vonoprazan and low-dose amoxicillin dual therapy as first-line Helicobacter pylori treatment: a multicentre randomised trial in Japan. *Gut* 2020; **69**: 1019-1026 [PMID: 31915235 DOI: 10.1136/gutjnl-2019-319954]

17 **Gotoda T**, Kusano C, Suzuki S, Horii T, Ichijima R, Ikehara H. Clinical impact of vonoprazan-based dual therapy with amoxicillin for H. pylori infection in a treatment-naïve cohort of junior high school students in Japan. *J Gastroenterol* 2020; **55**: 969-976 [PMID: 32666199 DOI: 10.1007/s00535-020-01709-4]

18 **Gao W**, Teng G, Wang C, Xu Y, Li Y, Cheng H. Eradication rate and safety of a "simplified rescue therapy": 14-day vonoprazan and amoxicillin dual regimen as rescue therapy on treatment of Helicobacter pylori infection previously failed in eradication: A real-world, retrospective clinical study in China. *Helicobacter* 2022; **27**: e12918 [PMID: 35877765 DOI: 10.1111/hel.12918]

19 **Zhou BG**, Chen LX, Li B, Wan LY, Ai YW. Saccharomyces boulardii as an adjuvant therapy for Helicobacter pylori eradication: A systematic review and meta-analysis with trial sequential analysis. *Helicobacter* 2019; **24**: e12651 [PMID: 31414551 DOI: 10.1111/hel.12651]

20 **Wang JW**, Hsu PI, Lin MH, Kao J, Tsay FW, Wu IT, Shie CB, Wu DC. The efficacy of culture-guided *versus* empirical therapy with high-dose proton pump inhibitor as third-line treatment of Helicobacter pylori infection: A real-world clinical experience. *J Gastroenterol Hepatol* 2022; **37**: 1928-1934 [PMID: 35816187 DOI: 10.1111/jgh.15942]

21 **Shang H**, Wang YS, Shen ZY. National Guide to Clinical Laboratory Procedures. 4th ed. Beijing: People's medical Publishing House, 2014: 574-628

22 **Saito Y**, Konno K, Sato M, Nakano M, Kato Y, Saito H, Serizawa H. Vonoprazan-Based Third-Line Therapy Has a Higher Eradication Rate against Sitafloxacin-Resistant Helicobacter pylori. *Cancers (Basel)* 2019; **11** [PMID: 30669474 DOI: 10.3390/cancers11010116]

23 **Gisbert JP**. Empirical or susceptibility-guided treatment for Helicobacter pylori infection? *Therap Adv Gastroenterol* 2020; **13**: 1756284820968736 [PMID: 33240392 DOI: 10.1177/1756284820968736]

24 **Sue S**, Shibata W, Sasaki T, Kaneko H, Irie K, Kondo M, Maeda S. Randomized trial of vonoprazan-based *versus* proton-pump inhibitor-based third-line triple therapy with sitafloxacin for Helicobacter pylori. *J Gastroenterol Hepatol* 2019; **34**:

686-692 [PMID: 30151994 DOI: 10.1111/jgh.14456]

25 **Hirata Y**, Yamada A, Niikura R, Shichijo S, Hayakawa Y, Koike K. Efficacy and safety of a new rifabutin-based triple therapy with vonoprazan for refractory Helicobacter pylori infection: A prospective single-arm study. *Helicobacter* 2020; **25**: e12719 [PMID: 32602161 DOI: 10.1111/hel.12719]

26 **Inokuchi K**, Mori H, Matsuzaki J, Hirata K, Harada Y, Saito Y, Suzuki H, Kanai T, Masaoka T. Efficacy and safety of low-dose rifabutin-based 7-day triple therapy as a third- or later-line Helicobacter pylori eradication regimen. *Helicobacter* 2022; **27**: e12900 [PMID: 35644041 DOI: 10.1111/hel.12900]

27 **Graham DY**, Lu H, Shiotani A. Vonoprazan-containing Helicobacter pylori triple therapies contribution to global antimicrobial resistance. *J Gastroenterol Hepatol* 2021; **36**: 1159-1163 [PMID: 32918832 DOI: 10.1111/jgh.15252]

28 **McFarland LV**. Systematic review and meta-analysis of Saccharomyces boulardii in adult patients. *World J Gastroenterol* 2010; **16**: 2202-2222 [PMID: 20458757 DOI: 10.3748/wjg.v16.i18.2202]

29 **Sakarya S**, Gunay N. Saccharomyces boulardii expresses neuraminidase activity selective for α2,3-linked sialic acid that decreases Helicobacter pylori adhesion to host cells. *APMIS* 2014; **122**: 941-950 [PMID: 24628732 DOI: 10.1111/apm.12237]

30 **Li H**, Liang X, Chen Q, Zhang W, Lu H. Inappropriate treatment in Helicobacter pylori eradication failure: a retrospective study. *Scand J Gastroenterol* 2018; **53**: 130-133 [PMID: 29214879 DOI: 10.1080/00365521.2017.1413132]

31 **Addolorato G**, Mirijello A, D'Angelo C, Leggio L, Ferrulli A, Abenavoli L, Vonghia L, Cardone S, Leso V, Cossari A, Capristo E, Gasbarrini G. State and trait anxiety and depression in patients affected by gastrointestinal diseases: psychometric evaluation of 1641 patients referred to an internal medicine outpatient setting. *Int J Clin Pract* 2008; **62**: 1063-1069 [PMID: 18422970 DOI: 10.1111/j.1742-1241.2008.01763.x]

World Journal of Gastroenterology

Submit a Manuscript: https://www.f6publishing.com

World J Gastroenterol 2023 May 28; 29(20): 3145-3156

DOI: 10.3748/wjg.v29.i20.3145

ISSN 1007-9327 (print) ISSN 2219-2840 (online)

ORIGINAL ARTICLE

Observational Study

Determination of esophageal squamous cell carcinoma and gastric adenocarcinoma on raw tissue using Raman spectroscopy

Hiroaki Ito, Naoyuki Uragami, Tomokazu Miyazaki, Yuto Shimamura, Haruo Ikeda, Yohei Nishikawa, Manabu Onimaru, Kai Matsuo, Masayuki Isozaki, William Yang, Kenji Issha, Satoshi Kimura, Machiko Kawamura, Noboru Yokoyama, Miki Kushima, Haruhiro Inoue

Specialty type: Gastroenterology and hepatology

Provenance and peer review: Invited article; Externally peer reviewed.

Peer-review model: Single blind

Peer-review report's scientific quality classification
Grade A (Excellent): 0
Grade B (Very good): 0
Grade C (Good): C
Grade D (Fair): 0
Grade E (Poor): 0

P-Reviewer: Gao SG, China

Received: December 12, 2022
Peer-review started: December 12, 2022
First decision: March 9, 2023
Revised: April 10, 2023
Accepted: April 27, 2023
Article in press: April 27, 2023
Published online: May 28, 2023

Hiroaki Ito, Naoyuki Uragami, Yuto Shimamura, Haruo Ikeda, Yohei Nishikawa, Manabu Onimaru, Kai Matsuo, Masayuki Isozaki, Noboru Yokoyama, Haruhiro Inoue, Digestive Disease Center, Showa University Koto Toyosu Hospital, Tokyo 135-8577, Japan

Tomokazu Miyazaki, JSR Corporation, Tokyo 105-0021, Japan

William Yang, Bay Spec Inc., San Jose, CA 95131, United States

Kenji Issha, Fuji Technical Research Inc., Yokohama 220-6215, Japan

Satoshi Kimura, Department of Laboratory Medicine and Central Clinical Laboratory, Showa University Northern Yokohama Hospital, Yokohama 224-8503, Japan

Machiko Kawamura, Department of Hematology, Saitama Cancer Center, Inamachi 362-0806, Japan

Miki Kushima, Department of Pathology, Showa University Koto Toyosu Hospital, Tokyo 135-8577, Japan

Corresponding author: Hiroaki Ito, MD, PhD, Associate Professor, Digestive Disease Center, Showa University Koto Toyosu Hospital, 5-1-38 Toyosu, Koto-ku, Tokyo 135-8577, Japan. h.ito@med.showa-u.ac.jp

Abstract

BACKGROUND

Cancer detection is a global research focus, and novel, rapid, and label-free techniques are being developed for routine clinical practice. This has led to the development of new tools and techniques from the bench side to routine clinical practice. In this study, we present a method that uses Raman spectroscopy (RS) to detect cancer in unstained formalin-fixed, resected specimens of the esophagus and stomach. Our method can record a clear Raman-scattered light spectrum in these specimens, confirming that the Raman-scattered light spectrum changes because of the histological differences in the mucosal tissue.

AIM

To evaluate the use of Raman-scattered light spectrum for detecting endoscop-

ically resected specimens of esophageal squamous cell carcinoma (SCC) and gastric adenocarcinoma (AC).

METHODS

We created a Raman device that is suitable for observing living tissues, and attempted to acquire Raman-scattered light spectra in endoscopically resected specimens of six esophageal tissues and 12 gastric tissues. We evaluated formalin-fixed tissues using this technique and captured shifts at multiple locations based on feasibility, ranging from six to 19 locations 200 microns apart in the vertical and horizontal directions. Furthermore, a correlation between the obtained Raman scattered light spectra and histopathological diagnosis was performed.

RESULTS

We successfully obtained Raman scattered light spectra from all six esophageal and 12 gastric specimens. After data capture, the tissue specimens were sent for histopathological analysis for further processing because RS is a label-free methodology that does not cause tissue destruction or alterations. Based on data analysis of molecular-level substrates, we established cut-off values for the diagnosis of esophageal SCC and gastric AC. By analyzing specific Raman shifts, we developed an algorithm to identify the range of esophageal SCC and gastric AC with an accuracy close to that of histopathological diagnoses.

CONCLUSION

Our technique provides qualitative information for real-time morphological diagnosis. However, further *in vivo* evaluations require an excitation light source with low human toxicity and large amounts of data for validation.

Key Words: Raman spectroscopy; Squamous cell carcinoma; Adenocarcinoma; Esophagus; Stomach; Label-free cancer detection; Real-time diagnosis

©The Author(s) 2023. Published by Baishideng Publishing Group Inc. All rights reserved.

Core Tip: Cancer diagnosis is a critical step in patient management, and involves a combination of diagnostic modalities or a single investigation. Diagnostic techniques that provide comprehensive data on the disease process can be particularly valuable, and Raman spectroscopy (RS) is one such modality that offers detailed molecular-level information. In this study, we utilized RS to rapidly detect cancer in resected esophageal and stomach specimens, providing information beyond morphology. By providing detailed molecular-level data, RS can provide a more comprehensive understanding of disease processes and aid in accurate diagnosis.

Citation: Ito H, Uragami N, Miyazaki T, Shimamura Y, Ikeda H, Nishikawa Y, Onimaru M, Matsuo K, Isozaki M, Yang W, Issha K, Kimura S, Kawamura M, Yokoyama N, Kushima M, Inoue H. Determination of esophageal squamous cell carcinoma and gastric adenocarcinoma on raw tissue using Raman spectroscopy. *World J Gastroenterol* 2023; 29(20): 3145-3156

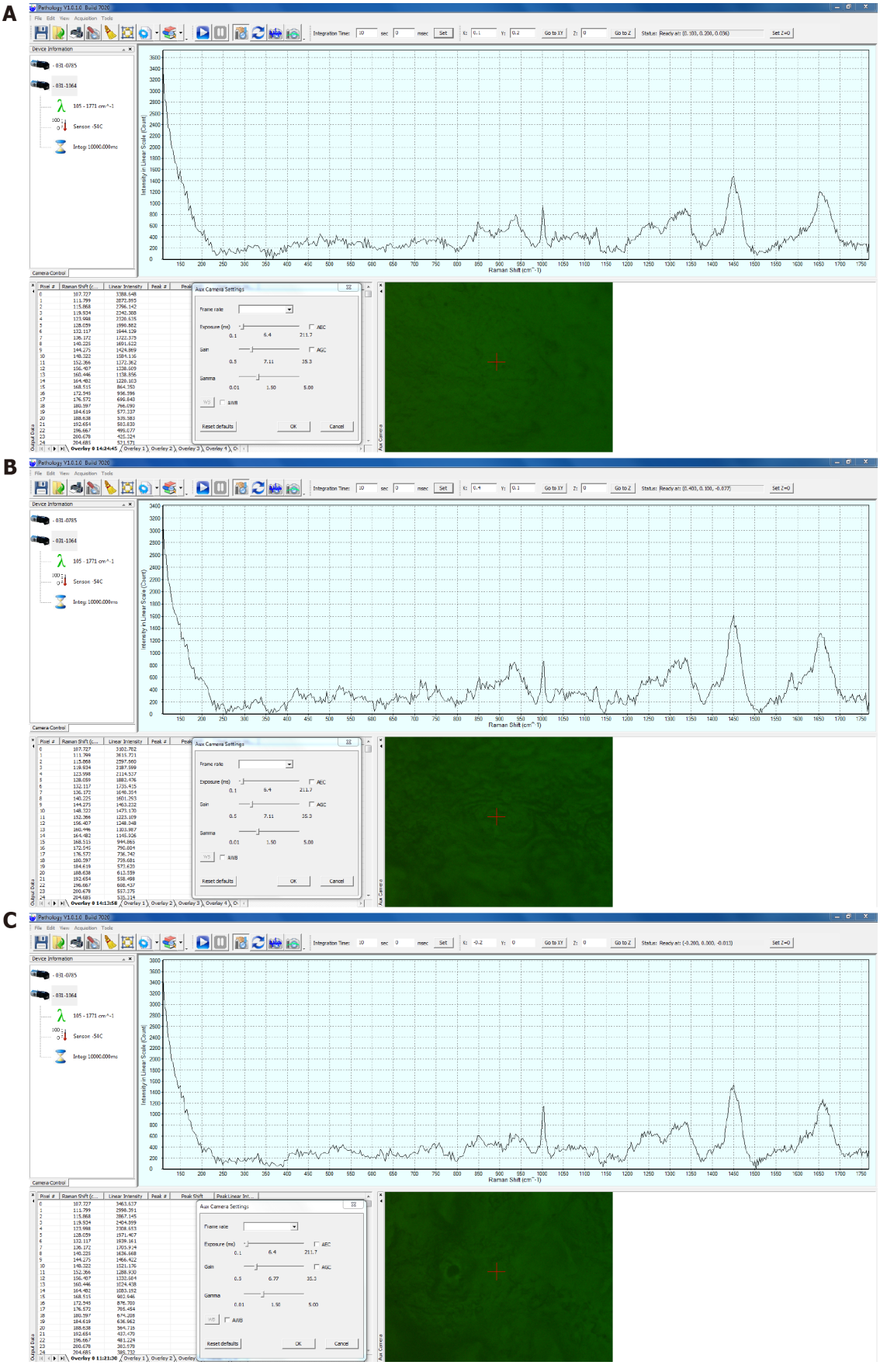
URL: https://www.wjgnet.com/1007-9327/full/v29/i20/3145.htm

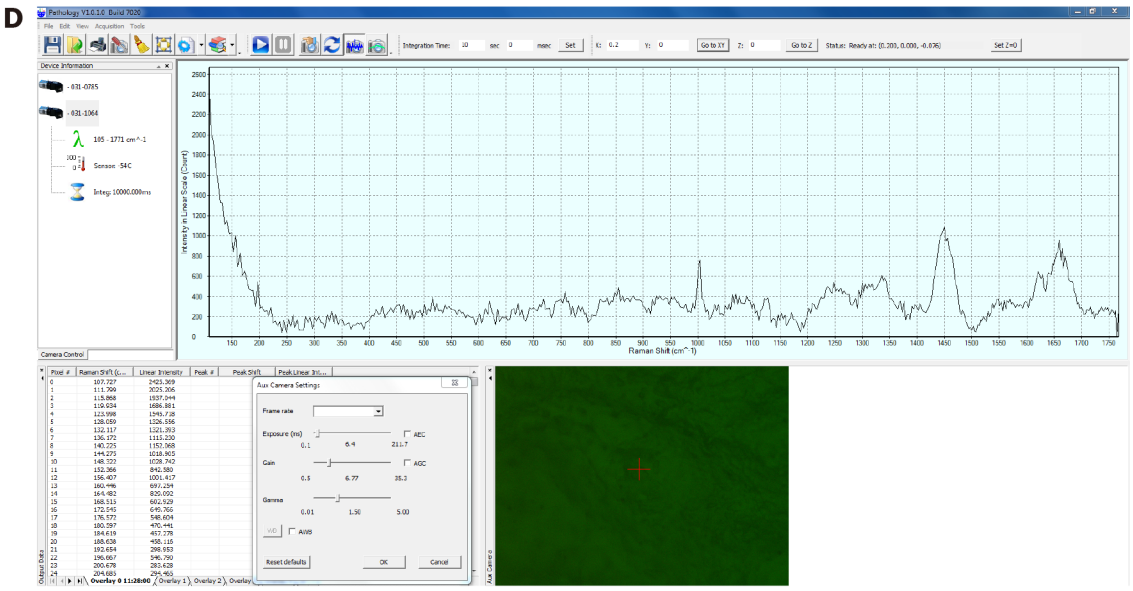
DOI: https://dx.doi.org/10.3748/wjg.v29.i20.3145

INTRODUCTION

Gastrointestinal cancers are typically evaluated using various investigative modalities, like radiological imaging, endoscopy, and histopathology[1,2]. Although tissue diagnosis through histopathological evaluation remains the gold standard for diagnosis, it is primarily based on morphological interpretation, even in current molecular-level evaluation practices[3]. In addition to morphology, many other such modalities are rapidly making inroads into practice[3,4]. Unlike morphology alone, immunohistochemistry, which has become almost synonymous with objective histopathological evaluation, is further aided by fluorescence *in situ* hybridization and sequencing. At the other end of the spectrum lies non-invasive/minimally invasive, non-label-based evaluation options, such as near-infrared spectroscopy and Raman spectroscopy (RS)[5].

Endoscopic biopsy is the preferred diagnostic method for gastrointestinal cancer[6]. Recent technological advances in endoscopy have enabled reliable diagnoses based on endoscopic findings alone, which have been further improved by the incorporation of artificial intelligence[5-7]. However, these


A
B
C
Pathology V1.0.1.0 Build 7020
Device Information
Camera Control
Aux Camera Settings
Frame rate
Exposure (ms)
Gain
Gamma
AEC
AGC
AWB
Reset defaults
OK
Cancel
Raman Shift (cm^-1)



DOI: 10.3748/wjg.v29.i20.3145 **Copyright** ©The Author(s) 2023.

Figure 1 Example of Raman spectra. Screenshots from the software window illustrating the Raman shift plotted against the intensity on a linear scale. A: Normal esophageal mucosa; B: Esophageal squamous cell carcinoma; C: Normal stomach mucosa; D: Stomach adenocarcinoma.

methodologies rely primarily on morphological assessments and do not consider molecular biological information. Tumor tissues contain abnormal molecules and proteins that are absent in normal tissues. The addition of molecular biological information to existing highly evolved morphological diagnostic methods may become an epoch-making technique with higher diagnostic accuracy[5,8,9].

Hence, we evaluated the biological samples using RS to obtain molecular information[8,10]. RS is a nondestructive inspection method that identifies a substance by measuring the type and amount of molecules contained in the substance by analyzing the wavelength of the reflected light obtained by irradiating the target substance with light, such as a laser[11-13]. Furthermore, RS can be used to evaluate substances with all types of properties, including solids[14-16], liquids[9,11], and gases[17], without sample pretreatment. Therefore, RS is an excellent inspection method for evaluating substances within a short time.

Therefore, attempts have been made to evaluate tissue samples using RS. Bergholt *et al*[4] presented a diagnostic technique for esophageal disease in the gastrointestinal tract using RS and published diagnostic techniques for gastric cancer. Moreover, Duraipandian *et al*[3] reported a diagnostic technique for gastric cancer using RS. However, a standard method for biological evaluations using RS has not yet been established.

A major challenge in using RS to evaluate biological samples is interference of autofluorescence[18]. To address this issue, we developed a novel micro-Raman device with unique features that enables effective evaluation of biological samples using RS.

We selected a near-infrared laser, which is not easily affected by autofluorescence, as the excitation light source. Because the Raman-scattered light intensity is inversely proportional to the square of the excitation light wavelength, the scattered light intensity of a long-wavelength near-infrared laser is low [18]. We developed a highly sensitive circuit to detect this weakly scattered light. We attempted to record the Raman-scattered light wavelengths from living esophageal tissues using a micro-Raman device with these characteristics.

MATERIALS AND METHODS

Study population and data collection

Sixteen patients aged 80 years or younger who underwent endoscopic submucosal dissection of the esophagus or stomach at the Digestive Disease Center of Showa University Koto Toyosu Hospital were recruited for this study. Written consent was obtained from all participants. Eleven participants were male and five were female, with an age range of 38-80 years. Eighteen specimens (esophagus, n = 6; stomach, n = 12) were analyzed (Table 1). This study was approved by the in-hospital clinical research review board (approval number: 18T5009) and conducted in accordance with the Declaration of Helsinki.

Table 1 Patients' background

Patient number	Patient	Clinical diagnosis	Number of lesions	Treatment date
1	50-year-old, female	Esophageal cancer	1	December 20, 2018
2	65-year-old, male	Esophageal cancer	1	December 20, 2018
3	61-year-old, male	Esophageal cancer	1	January 11, 2019
4	61-year-old, male	Esophageal cancer	2	January 18, 2019
5	78-year-old, female	Esophageal cancer	1	April 18, 2019
6	72-year-old, female	Stomach cancer	1	January 8, 2019
7	63-year-old, male	Stomach cancer	1	January 18, 2019
8	56-year-old, male	Stomach cancer	1	January 24, 2019
9	58-year-old, male	Stomach cancer	1	February 3, 2019
10	79-year-old, male	Stomach cancer	1	February 4, 2019
11	77-year-old, male	Stomach cancer	1	February 17, 2019
12	80-year-old, male	Stomach cancer	2	February 28, 2019
13	65-year-old, male	Stomach cancer	1	February 28, 2019
14	68-year-old, male	Stomach cancer	1	April 8, 2019
15	66-year-old, female	Stomach adenoma	1	May 19, 2019
16	38-year-old, female	Stomach submucosal tumor	1	April 9, 2019

Measurement protocol and data capture

Esophageal and stomach tissue samples (including mucosal and submucosal tissues) were collected immediately after endoscopic resection. The tissue was attached to a black rubber plate with a metal pin, and a 0.02 mm thick aluminum foil was sandwiched between the rubber plate and the esophageal tissue to prevent Raman scattered light from the rubber plate from being included in the measurements.

A linear or grid-like measurement grid was set up to include endoscopically diagnosed lesions in the mucosa and the surrounding normal mucosa. Multiple measurement points were selected at 5 mm or 10 mm intervals depending on the shape of the clinically determined lesion. Raman scattered light wavelengths were recorded from 19 or 6 locations at intervals of 200 μm in the vertical and horizontal directions for each selected point depending on the feasibility. To prevent the sample from drying out, distilled water was sprayed on the sample as necessary during the measurement.

A RS device (BaySpec Inc., San Jose, CA, United States) was used, with a computer-controlled stage, an objective lens of 20 × magnification, a correction collar for near-infrared microscopy (LCPLN20XIR, Olympus Corporation, Tokyo, Japan), and an excitation laser wavelength of 1064 nm. The measurements were captured with a laser power of 200 mW and an exposure time of 10 s per point. Pathologic System Software Version 1.0.1.0 (BaySpec, Inc., San Jose CA, United States) was used and baseline correction was performed without smoothing the waveform. Examples of the Raman spectra of the esophageal and gastric mucosa are shown in Figure 1.

Analysis

Fifteen types of Raman shifts corresponding to the constituent molecules of living tissues (Table 2) were selected for the analysis. From the recorded Raman-scattered light waveforms, the scattered light intensities of 15 types of Raman shifts were extracted, and the optimum combination matching the range of squamous cell carcinoma (SCC) of the esophagus and gastric adenocarcinoma (AC) by histopathological diagnosis was determined.

RESULTS

The study involved 16 patients, and 18 specimens were resected for histopathological analysis. The results showed that five of the specimens were SCC of the esophagus, 10 were well-differentiated tubular AC of the stomach, one was a gastric adenoma, and one was a gastric carcinoid tumor (NET G1) (Table 3).

Raman spectra were recorded for all six esophageal and 12 gastric specimens. All combinations of the scattered light intensities of the 15 Raman shifts were calculated to determine the combination that best matched the range of cancer by histopathological diagnosis. In esophageal squamous cell cancer, the

Table 2 Fifteen Raman shift parameters obtained from the raw tissues and the range of the shifts[7,9]

Number	Assigned peak	Shift start (cm^{-1})	Shift end (cm^{-1})
RS 1	Phenylalanine C-C twist	611	631
RS 2	Cholesterol	700	720
RS 3	Tryptophane ring breath	751	771
RS 4	Tyrosine ring breath	830	850
RS 5	Phenylalanine ring breath	993	1013
RS 6	Skeletal C-C	1060	1080
RS 7	Nucleotide O-P-O	1091	1111
RS 8	Skeletal C-C stretch	1123	1143
RS 9	Amide III beta-sheet	1244	1264
RS 10	Amide III delta $(CH)_2$	1275	1295
RS 11	Amide III alpha-helix	1322	1342
RS 12	CH_2 stretch	1408	1428
RS 13	CH_3 deformation	1448	1468
RS 14	Phenylalanine C=C	1596	1616
RS 15	Amide I alpha-helix	1647	1667

Table 3 Esophageal and gastric samples and histopathological diagnosis along with TNM classification

Sample number	Patient	Pathological diagnosis (UICC TNM classification)
Eso-1	50-year-old, female	SCC, pT1a (LPM)
Eso-2	65-year-old, male	SCC, pT1a (LPM)
Eso-3	61-year-old, male	SCC, pT1a (MM)
Eso-4	61-year-old, male	SCC, pTis
Eso-5	61-year-old, male	SCC, pTis
Eso-6	78-year-old, female	SCC, pT1b (SM)
Sto-1	72-year-old, female	Tub1, pT1a
Sto-2	63-year-old, male	Tub1>tub2, pT1b2
Sto-3	56-year-old, male	Tub1, pT1b1
Sto-4	58-year-old, male	Tub1, pT1b1
Sto-5	79-year-old, male	Tub1, pT1b1
Sto-6	77-year-old, male	Tub1, pT1a
Sto-7	80-year-old, male	Tub1, pT1b1
Sto-8	80-year-old, male	Tub1, pT1a
Sto-9	65-year-old, male	Tub1, pT1a
Sto-10	68-year-old, male	Tub1, pT1a
Sto-11	66-year-old, female	Tubular adenoma
Sto-12	38-year-old, female	Carcinoid tumor (NET G1), pT1b

Tub1: Well differentiated tubular adenocarcinoma. UICC: Union for International Cancer Control; SCC: Squamous cell carcinoma; TNM: Tumor node metastasis.

Table 4 Raman shift peaks observed in the esophageal and the gastric samples

	Peak 1	Peak 2	Peak 3
Esophagus	RS 8	RS 1	RS 13
Stomach	RS12	RS 5	RS 15

Table 5 Cut-off ratios obtained from the esophagus and stomach samples

	Cut-off 1 (peak 2/peak 1)	Cut-off 2 (peak 3/peak 1)
Esophagus	0.65	2.0
Stomach	1.85	2.0

scattered light intensity of Skeletal C-C stretch was Peak 1, the scattered light intensity of Phenylalanine C-C twist was Peak 2, the scattered light intensity of CH_3 deformation was Peak 3 (Table 4), and Peak 2/Peak 1 was defined as Cut-off 1. Peak 3/Peak 1 was defined as Cut-off 2 (Table 5). The site with more than half of the measurement points having Cut-off 1 greater than 0.65 and Cut-off 2 greater than 2.0 was determined to be the best match for histopathological SCC of the esophagus (Figure 2).

For gastric AC, the scattered light intensity of the CH_2 stretch was Peak 1, Phenylalanine ring breadth was Peak 2, and Amide I alpha helix was Peak 3 (Table 4). The ratio of Peak 2/Peak 1 was defined as Cut-off 1 and Peak 3/Peak 1 was defined as Cut-off 2 (Table 5). The site with more than half of the measurement points with Cut-off 1 greater than 1.85 and Cut-off 2 greater than 2.0 was determined to be the best match for the histopathological diagnosis of gastric AC (Figure 3).

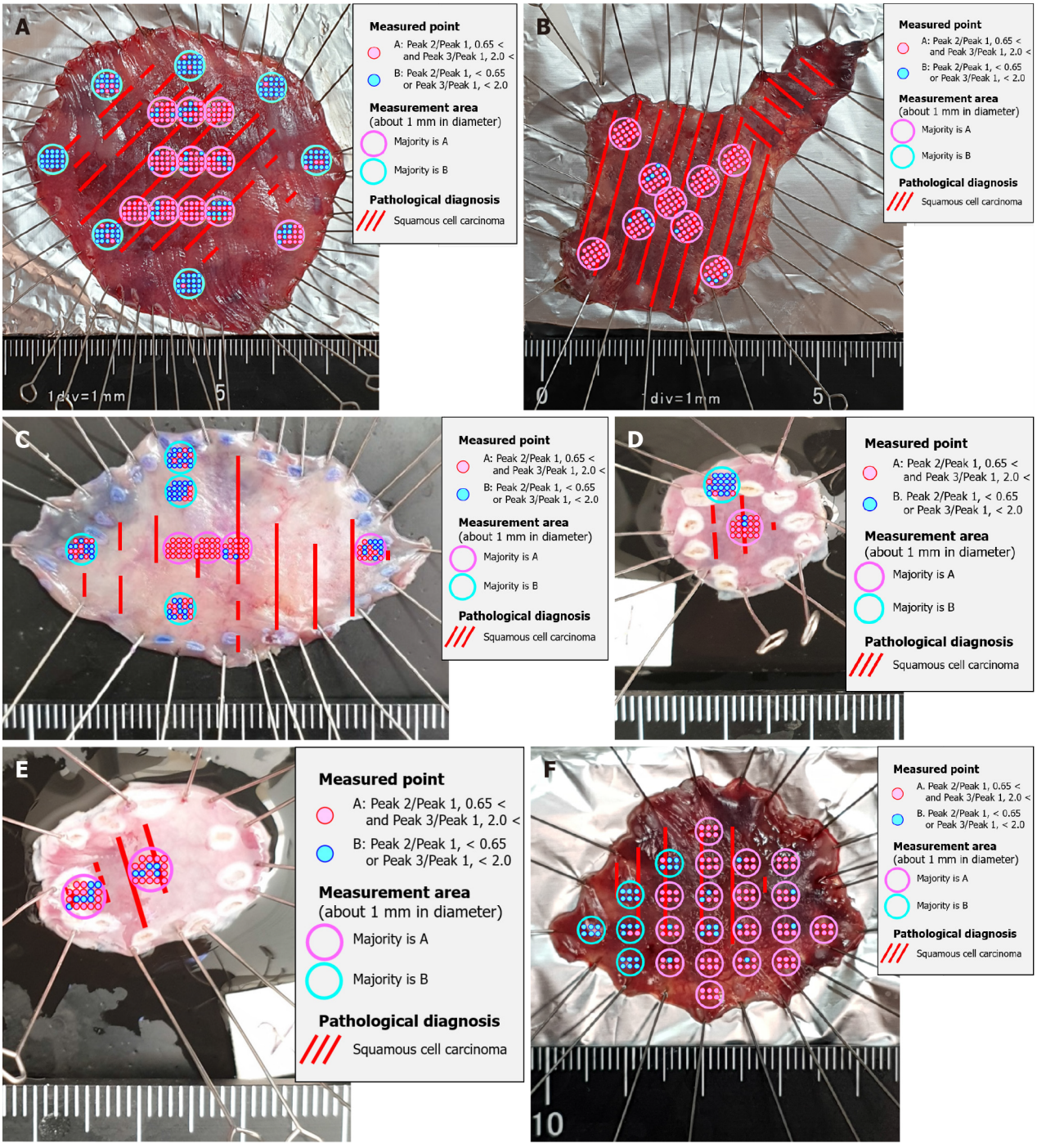
DISCUSSION

Patients with gastrointestinal cancers affecting the esophagus and stomach have symptoms, such as difficulty in swallowing, heartburn, and fullness[6]. Contrast examination or endoscopy is often performed in patients with a clinical evaluation suggestive of esophageal or gastric cancer[6]. Histopathological evaluation of the tissues obtained *via* endoscopic biopsy can be used to confirm the diagnosis[3,4,6]. In recent years, the accuracy of endoscopic finding-based diagnoses has dramatically improved. One of the reasons for this is the better quality of images obtained through high-resolution camera optics[3,6].

It is highly possible that the ability to diagnose cancer will improve further if it is feasible to depict what cannot be delineated using conventional equipment by making the image richer in features. Another reason is the use of image classification algorithms based on artificial intelligence[13,16,19]. By recognizing and patterning endoscopic images using artificial intelligence, the existence of lesions is clarified, and diagnosis by doctors is supported. Since the diagnosis using artificial intelligence evaluates endoscopic images morphologically, it is possible to prevent the lesion from being overlooked [13,16]. However, its diagnostic ability is not higher than that of an experienced doctor. Another drawback is that diagnostic ability is greatly affected by the quality of the endoscopic image[5,9,14].

As mentioned above, the accuracy of endoscopic diagnosis of lesions in the gastrointestinal tract has greatly improved; however, it is still at the morphological interpretation level[6,7]. Histopathological diagnosis, which is the current definitive diagnostic method, is a form of morphological evaluation; moreover, qualitative information that assists in morphological evaluation is required to improve diagnostic accuracy beyond the existing practice. RS can be used to add qualitative information to the morphological information[2,20]. Short *et al*[1] published a technique for diagnosing lung cancer using bronchoscopy combined with RS. Lui *et al*[21] reported a method for diagnosing skin cancer using RS. Krishna *et al*[22] reported a method for diagnosing oral cancer using RS. Jermyn *et al*[20] reported that RS can be used to identify lesion areas during brain surgery. Furthermore, Bergholt *et al*[6] presented a diagnostic technique for esophageal disease in the gastrointestinal tract using RS, and published diagnostic techniques for gastric cancer[4]. Duraipandian *et al*[3] reported a diagnostic technique for gastric cancer using RS. Molckovsky *et al*[2] reported a diagnostic technique for colon cancer using RS. However, a standard method for analyzing living organisms and biological samples using RS is yet to be developed.

In this study, we selected 15 Raman shifts corresponding to constituent molecules in living tissues. The analysis results of the scattered light intensity of Raman shift of Skeletal C-C stretch, Phenylalanine C-C twist, and CH_3 deformation in SCC of the esophagus, and Raman shift of CH_2 stretch, Phenylalanine ring breadth, and Amide I alpha-helix in gastric AC. The results of the analysis of the scattered light intensity of the shift were in good agreement with the range of morphological cancer

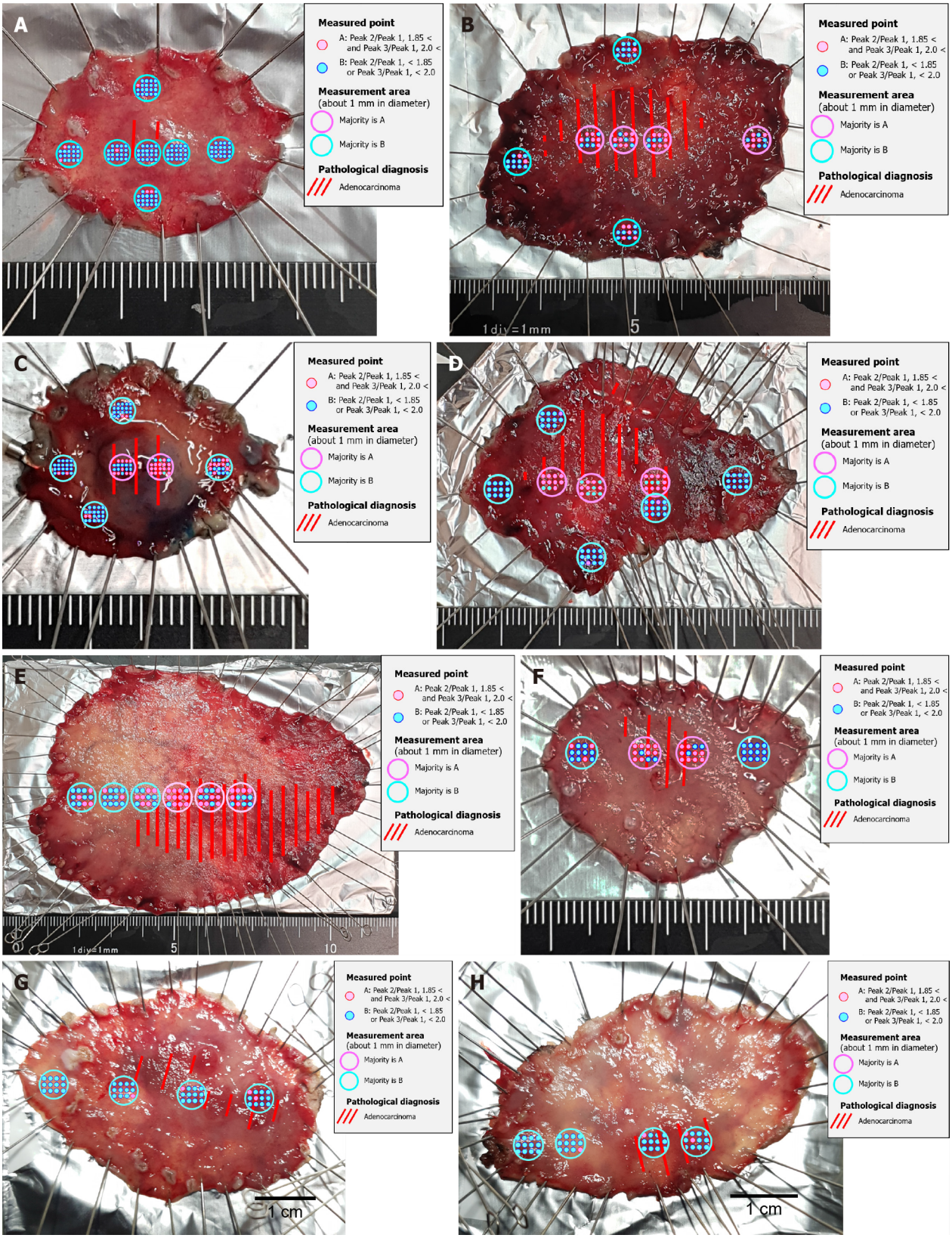


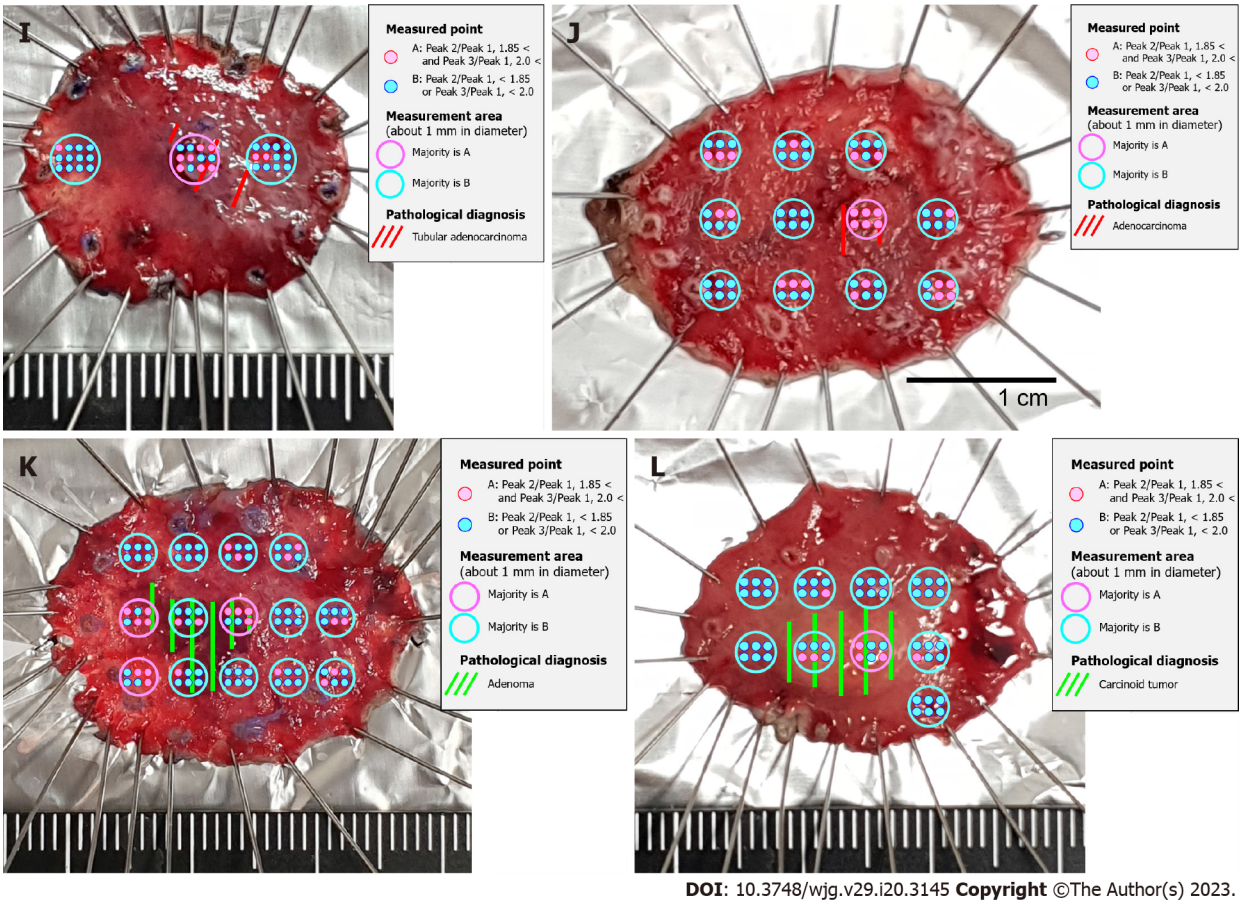
DOI: 10.3748/wjg.v29.i20.3145 **Copyright** ©The Author(s) 2023.

Figure 2 Comparison of Raman spectroscopic analysis and pathological diagnosis of sample Eso [squamous cell carcinoma, pT1a(LPM)-pT1b(SM)]. A: Eso-1; B: Eso-2; C: Eso-3; D: Eso-4; E: Eso-5; F: Eso-6.

diagnoses offered by histopathological evaluation. SCC of the esophagus and gastric AC are distinct types of cancers with different biological characteristics. Therefore, a significant Raman shift is expected to differ in the analysis conducted using RS. The technique presented in this study has the potential to provide qualitative evaluation in addition to the morphological evaluation currently used. In particular, it may offer valuable information regarding lesions that are challenging to assess using endoscopic or histopathological diagnoses alone.

However, at some sites, the results of this technique did not match the histopathological diagnoses. The limitations of this study include the small number of samples analyzed (n = 18), which included both the esophagus and stomach. Hence, there is no doubt that more samples must be analyzed in the future to confirm the accuracy of this technique. Using this technique, molecular information not solely dependent on morphological interpretation can be obtained. Furthermore, it may indicate the degree of mucosal abnormality from normal to cancerous. Evaluation of precancerous tissues may enable highly


A
B
C
D
E
F
G
H
Measured point
A: Peak 2/Peak 1, 1.85 < and Peak 3/Peak 1, 2.0 <
B: Peak 2/Peak 1, < 1.85 or Peak 3/Peak 1, < 2.0
Measurement area
(about 1 mm in diameter)
Majority is A
Majority is B
Pathological diagnosis
Adenocarcinoma
1 div=1mm
1 cm



DOI: 10.3748/wjg.v29.i20.3145 **Copyright** ©The Author(s) 2023.

Figure 3 Comparison of Raman spectroscopic analysis and pathological diagnosis of sample Sto (well-differentiated tubular adenocarcinoma, pT1a-pT1b1; tubular adenoma; carcinoid tumor, NET G1). A: Sto-1; B: Sto-2; C: Sto-3; D: Sto-4; E: Sto-5; F: Sto-6; G: Sto-7; H: Sto-8; I: Sto-9; J: Sto-10; K: Sto-11; L: Sto-12.

accurate preventive medicine. We aim to further advance this research and establish a method for predicting the current and future states of the gastrointestinal mucosa with high accuracy by clarifying the correlation between the Raman-scattered light intensity and the tissue state at each Raman shift.

CONCLUSION

Based on the results, it was concluded that RS could accurately identify esophageal SCC and gastric AC by analyzing the scattered light intensities of the 15 types of Raman shifts. The optimum combinations of Raman shifts were identified as Peak 1, Peak 2, and Peak 3 for both cancer types, with specific cut-off values for each peak. Although it is currently used in endoscopic treatment, the qualitative diagnosis of lesions, risk of residual lesions, *etc.*, can be confirmed in a short time by analyzing excised specimens, and treatment can be provided as necessary.

ARTICLE HIGHLIGHTS

Research background

Cancer diagnosis plays an important role in patient management, many researchers focused on the cancer detection, and novel, rapid, and label-free techniques are being developed for routine clinical practice.

Research motivation

To address the issue of using Raman spectroscopy (RS) to evaluate biological samples is interference of autofluorescence.

Research objectives

Our study is to evaluate the use of Raman-scattered light spectrum for detecting endoscopically resected specimens of esophageal squamous cell carcinoma (SCC) and gastric adenocarcinoma (AC).

Research methods

We created a Raman device, which is suitable for observing living tissues, and we attempted to acquire Raman-scattered light spectra in endoscopically resected specimens of six esophageal tissues and 12 gastric tissues. Furthermore, we performed a correlation between the obtained Raman scattered light spectra and histopathological diagnosis.

Research results

We obtained Raman scattered light spectra from all six esophageal and 12 gastric specimens successfully, and developed an algorithm to identify the range of esophageal SCC and gastric AC with an accuracy close to that of histopathological diagnoses.

Research conclusions

In this study, we utilized RS to rapidly detect cancer in resected esophageal and stomach specimens, providing information beyond morphology.

Research perspectives

By providing detailed molecular level data, RS can provide a more comprehensive understanding of disease processes and aid in accurate diagnosis.

FOOTNOTES

Author contributions: Ito H and Miyazaki T designed the study; Ito H was the guarantor, performed measurement, analysis, and interpretation of the data, and drafted the initial manuscript; Uragami N and Miyazaki T contributed to the acquisition, analysis, and interpretation of the data; Uragami N, Shimamura Y, Ikeda H, Nishikawa Y, Onimaru M, Matsuo K, and Isozaki M participated in the collection of the sample; Yang W designed and produced the Raman spectroscopy; Issha K continued importing the Raman spectroscopy; Kimura S, Kawamura M, Yokoyama N, Kushima M, and Inoue H revised the article critically for important intellectual content; Kushima M performed histopathological diagnosis of samples.

Supported by MEXT KAKENHI, JP17K09022 and JP20K07643.

Institutional review board statement: The study protocol was reviewed and approved (No. 18T5009) by the Institutional Review Board of Showa University Koto Toyosu Hospital.

Informed consent statement: All the participants provided written informed consent to participate in the study.

Conflict-of-interest statement: All the authors report no relevant conflicts of interest for this article.

Data sharing statement: No additional data are available.

STROBE statement: The authors read the STROBE Statement checklist of items and the manuscript was prepared and revised according to the STROBE guidelines.

Open-Access: This article is an open-access article that was selected by an in-house editor and fully peer-reviewed by external reviewers. It is distributed in accordance with the Creative Commons Attribution NonCommercial (CC BY-NC 4.0) license, which permits others to distribute, remix, adapt, build upon this work non-commercially, and license their derivative works on different terms, provided the original work is properly cited and the use is non-commercial. See: https://creativecommons.org/Licenses/by-nc/4.0/

Country/Territory of origin: Japan

ORCID number: Hiroaki Ito 0000-0002-0761-0632; Naoyuki Uragami 0000-0003-2974-8250; Tomokazu Miyazaki 0000-0002-6108-8945; Yuto Shimamura 0000-0002-3831-8327; Haruo Ikeda 0000-0002-1690-8422; Manabu Onimaru 0000-0002-5368-8377; Kai Matsuo 0000-0001-7951-2444; William Yang 0000-0002-8476-3026; Satoshi Kimura 0000-0002-6843-8127; Machiko Kawamura 0000-0002-6138-1690; Noboru Yokoyama 0000-0003-1882-0018; Miki Kushima 0000-0002-1642-0478; Haruhiro Inoue 0000-0002-0551-7274.

S-Editor: Wang JJ
L-Editor: A
P-Editor: Liu JH

REFERENCES

1 **Short MA**, Lam S, McWilliams A, Zhao J, Lui H, Zeng H. Development and preliminary results of an endoscopic Raman probe for potential *in vivo* diagnosis of lung cancers. *Opt Lett* 2008; **33**: 711-713 [PMID: 18382526 DOI: 10.1364/OL.33.000711]

2 **Molckovsky A**, Song LM, Shim MG, Marcon NE, Wilson BC. Diagnostic potential of near-infrared Raman spectroscopy in the colon: differentiating adenomatous from hyperplastic polyps. *Gastrointest Endosc* 2003; **57**: 396-402 [PMID: 12612529 DOI: 10.1067/mge.2003.105]

3 **Duraipandian S**, Sylvest Bergholt M, Zheng W, Yu Ho K, Teh M, Guan Yeoh K, Bok Yan So J, Shabbir A, Huang Z. Real-time Raman spectroscopy for in vivo, online gastric cancer diagnosis during clinical endoscopic examination. *J Biomed Opt* 2012; **17**: 081418 [PMID: 23224179 DOI: 10.1117/1.JBO.17.8.081418]

4 **Bergholt MS**, Zheng W, Lin K, Ho KY, Teh M, Yeoh KG, So JB, Huang Z. Raman endoscopy for *in vivo* differentiation between benign and malignant ulcers in the stomach. *Analyst* 2010; **135**: 3162-3168 [PMID: 20941419 DOI: 10.1039/c0an00336k]

5 **Chakraborty A**, Ghosh A, Barui A. Advances in surface-enhanced Raman spectroscopy for cancer diagnosis and staging. *J Raman Spectrosc* 2020; **51**: 7-36 [DOI: 10.1002/jrs.5726]

6 **Bergholt MS**, Zheng W, Ho KY, Yeoh KG, Teh M, So JBY, Huang Z. Real-time depth-resolved Raman endoscopy for in vivo diagnosis of dysplasia in Barrett's esophagus. Proceedings of the SPIE BiOS; 2013 Mar 20; San Francisco, California, United States: Society of Photo-Optical Instrumentation Engineers, 2003

7 **Ito H**, Uragami N, Miyazaki T, Yang W, Issha K, Matsuo K, Kimura S, Arai Y, Tokunaga H, Okada S, Kawamura M, Yokoyama N, Kushima M, Inoue H, Fukagai T, Kamijo Y. Highly accurate colorectal cancer prediction model based on Raman spectroscopy using patient serum. *World J Gastrointest Oncol* 2020; **12**: 1311-1324 [PMID: 33250963 DOI: 10.4251/wjgo.v12.i11.1311]

8 **Wang K**, Qiu Y, Wu C, Wen ZN, Li Y. Surface-enhanced Raman spectroscopy and multivariate analysis for the diagnosis of oral squamous cell carcinoma. *J Raman Spectrosc* 2023; **54**: 355-362 [DOI: 10.1002/jrs.6495]

9 **Lei J**, Yang D, Li R, Dai Z, Zhang C, Yu Z, Wu S, Pang L, Liang S, Zhang Y. Label-free surface-enhanced Raman spectroscopy for diagnosis and analysis of serum samples with different types lung cancer. *Spectrochim Acta A Mol Biomol Spectrosc* 2021; **261**: 120021 [PMID: 34116414 DOI: 10.1016/j.saa.2021.120021]

10 **Yue X**, Wang Y, Guo D, He G, Sui C, Qu Z, Zhao Y, Liu X. Surface-enhanced Raman spectroscopy is an accurate technique in diagnosis of breast cancer: A meta-analysis. *J Raman Spectrosc* 2022; **53**: 2058-2067 [DOI: 10.1002/jrs.6437]

11 **Falamas A**, Faur CI, Baciut M, Rotaru H, Chirila M, Cinta Pinzaru S, Hedesiu M. Raman spectroscopic characterization of saliva for the discrimination of oral squamous cell carcinoma. *Anal Lett* 2020; **54** [DOI: 10.1080/00032719.2020.1719129]

12 **Zhang H**, Cheng C, Gao R, Yan Z, Zhu Z, Yang B, Chen C, Lv X, Li H, Huang Z. Rapid identification of cervical adenocarcinoma and cervical squamous cell carcinoma tissue based on Raman spectroscopy combined with multiple machine learning algorithms. *Photodiagnosis Photodyn Ther* 2021; **33**: 102104 [PMID: 33212265 DOI: 10.1016/j.pdpdt.2020.102104]

13 **Zhang L**, Wu Y, Zheng B, Su L, Chen Y, Ma S, Hu Q, Zou X, Yao L, Yang Y, Chen L, Mao Y, Ji M. Rapid histology of laryngeal squamous cell carcinoma with deep-learning based stimulated Raman scattering microscopy. *Theranostics* 2019; **9**: 2541-2554 [PMID: 31131052 DOI: 10.7150/thno.32655]

14 **Zhan Q**, Li Y, Yuan Y, Liu J. The accuracy of Raman spectroscopy in the detection and diagnosis of oral cancer: A systematic review and meta-analysis. *J Raman Spectrosc* 2020; **51**: 2377-2397 [DOI: 10.1002/jrs.5940]

15 **Zheng C**, Qing S, Wang J, Lü G, Li H, Lü X, Ma C, Tang J, Yue X. Diagnosis of cervical squamous cell carcinoma and cervical adenocarcinoma based on Raman spectroscopy and support vector machine. *Photodiagnosis Photodyn Ther* 2019; **27**: 156-161 [PMID: 31136828 DOI: 10.1016/j.pdpdt.2019.05.029]

16 **Yu M**, Yan H, Xia J, Zhu L, Zhang T, Zhu Z, Lou X, Sun G, Dong M. Deep convolutional neural networks for tongue squamous cell carcinoma classification using Raman spectroscopy. *Photodiagnosis Photodyn Ther* 2019; **26**: 430-435 [PMID: 31082525 DOI: 10.1016/j.pdpdt.2019.05.008]

17 **Bögözi T**, Popp J, Frosch T. Fiber-enhanced Raman multi-gas spectroscopy: what is the potential of its application to breath analysis? *Bioanalysis* 2015; **7**: 281-284 [PMID: 25697186 DOI: 10.4155/bio.14.299]

18 **Wachsmann-Hogiu S**, Weeks T, Huser T. Chemical analysis *in vivo* and *in vitro* by Raman spectroscopy--from single cells to humans. *Curr Opin Biotechnol* 2009; **20**: 63-73 [PMID: 19268566 DOI: 10.1016/j.copbio.2009.02.006]

19 **Xia J**, Zhu L, Yu M, Zhang T, Zhu Z, Lou X, Sun G. Dong M. Analysis and classification of oral tongue squamous cell carcinoma based on Raman spectroscopy and convolutional neural networks. *J Mod Opt* 2020; **67**: 481-489 [DOI: 10.1080/09500340.2020.1742395]

20 **Jermyn M**, Mok K, Mercier J, Desroches J, Pichette J, Saint-Arnaud K, Bernstein L, Guiot MC, Petrecca K, Leblond F. Intraoperative brain cancer detection with Raman spectroscopy in humans. *Sci Transl Med* 2015; **7**: 274ra19 [PMID: 25673764 DOI: 10.1126/scitranslmed.aaa2384]

21 **Lui H**, Zhao J, McLean D, Zeng H. Real-time Raman spectroscopy for *in vivo* skin cancer diagnosis. *Cancer Res* 2012; **72**: 2491-2500 [PMID: 22434431 DOI: 10.1158/0008-5472.CAN-11-4061]

22 **Krishna H**, Majumder SK, Chaturvedi P, Sidramesh M, Gupta PK. In vivo Raman spectroscopy for detection of oral neoplasia: a pilot clinical study. *J Biophotonics* 2014; **7**: 690-702 [PMID: 23821433 DOI: 10.1002/jbio.201300030]

World Journal of Gastroenterology

Submit a Manuscript: https://www.f6publishing.com

World J Gastroenterol 2023 May 28; 29(20): 3157-3167

DOI: 10.3748/wjg.v29.i20.3157

ISSN 1007-9327 (print) ISSN 2219-2840 (online)

ORIGINAL ARTICLE

Observational Study

Real-time continuous image guidance for endoscopic retrograde cholangiopancreatography based on 3D/2D registration and respiratory compensation

Da-Ya Zhang, Shuo Yang, Hai-Xiao Geng, Yu-Jia Yuan, Chi-Jiao Ding, Jian Yang, Ming-Yang Li

Specialty type: Surgery

Provenance and peer review: Unsolicited article; Externally peer reviewed.

Peer-review model: Single blind

Peer-review report's scientific quality classification

Grade A (Excellent): 0
Grade B (Very good): B, B
Grade C (Good): C
Grade D (Fair): 0
Grade E (Poor): 0

P-Reviewer: Donato G, Italy; Lucke-Wold B, United States

Received: February 27, 2023
Peer-review started: February 27, 2023
First decision: March 28, 2023
Revised: April 7, 2023
Accepted: April 18, 2023
Article in press: April 18, 2023
Published online: May 28, 2023

Da-Ya Zhang, Ming-Yang Li, Department of Gastroenterology, The First Medical Center, Chinese PLA General Hospital, Beijing 100853, China

Shuo Yang, Hai-Xiao Geng, Yu-Jia Yuan, Chi-Jiao Ding, Jian Yang, School of Optics and Photonics, Beijing Institute of Technology, Beijing 100081, China

Corresponding author: Ming-Yang Li, PhD, Chief Physician, Doctor, Department of Gastroenterology, The First Medical Center, Chinese PLA General Hospital, No. 28 Fuxing Road, Haidian District, Beijing 100853, China. mingyangli_pla@163.com

Abstract

BACKGROUND

It has been confirmed that three-dimensional (3D) imaging allows easier identification of bile duct anatomy and intraoperative guidance of endoscopic retrograde cholangiopancreatography (ERCP), which reduces the radiation dose and procedure time with improved safety. However, current 3D biliary imaging does not have good real-time fusion with intraoperative imaging, a process meant to overcome the influence of intraoperative respiratory motion and guide navigation. The present study explored the feasibility of real-time continuous image-guided ERCP.

AIM

To explore the feasibility of real-time continuous image-guided ERCP.

METHODS

We selected 2 3D-printed abdominal biliary tract models with different structures to simulate different patients. The ERCP environment was simulated for the biliary phantom experiment to create a navigation system, which was further tested in patients. In addition, based on the estimation of the patient's respiratory motion, preoperative 3D biliary imaging from computed tomography of 18 patients with cholelithiasis was registered and fused in real-time with 2D fluoroscopic sequence generated by the C-arm unit during ERCP.

RESULTS

Continuous image-guided ERCP was applied in the biliary phantom with a registration error of 0.46 mm ± 0.13 mm and a tracking error of 0.64 mm ± 0.24

mm. After estimating the respiratory motion, 3D/2D registration accurately transformed preoperative 3D biliary images to each image in the X-ray image sequence in real-time in 18 patients, with an average fusion rate of 88%.

CONCLUSION
Continuous image-guided ERCP may be an effective approach to assist the operator and reduce the use of X-ray and contrast agents.

Key Words: Endoscopic retrograde cholangiopancreatography; Three-dimensional images; Registration; Cholelithiasis; Hilar cholangiocarcinoma

©The Author(s) 2023. Published by Baishideng Publishing Group Inc. All rights reserved.

Core Tip: Three-dimensional imaging allows easier identification of bile duct anatomy and intraoperative guidance of endoscopic retrograde cholangiopancreatography (ERCP). Continuous image-guided ERCP may be an effective means to assist the operator and reduce the use of X-ray and contrast agents.

Citation: Zhang DY, Yang S, Geng HX, Yuan YJ, Ding CJ, Yang J, Li MY. Real-time continuous image guidance for endoscopic retrograde cholangiopancreatography based on 3D/2D registration and respiratory compensation. *World J Gastroenterol* 2023; 29(20): 3157-3167
URL: https://www.wjgnet.com/1007-9327/full/v29/i20/3157.htm
DOI: https://dx.doi.org/10.3748/wjg.v29.i20.3157

INTRODUCTION

Endoscopic retrograde cholangiopancreatography (ERCP) was first described by McCune *et al*[1] at George Washington University in 1968. Superselection of difficult bile ducts contributes to a higher incidence of adverse events, as well as increased radiation exposure for patients and endoscopists[2,3]. Recent studies have shown that even low doses of radiation may induce carcinogenic effects[4]. The radiation dose is one of the recommended quality indicators for ERCP[5,6]. Furthermore, injection of a contrast medium is considered a risk factor for post-ERCP pancreatitis and cholangitis[7]. Therefore, developing new technologies to enhance the efficacy and safety of ERCP is urgent.

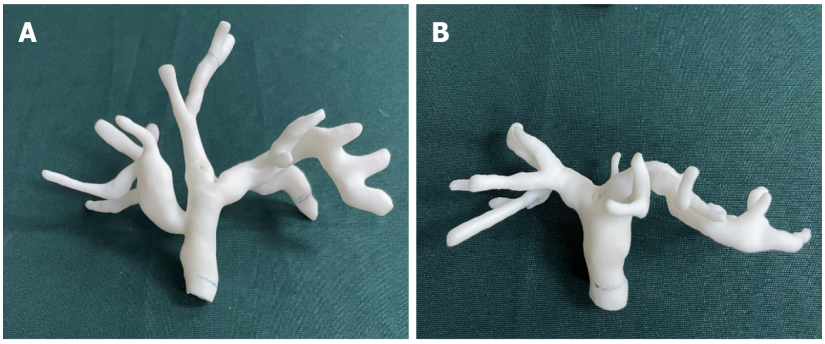
Preoperative three-dimensional (3D) imaging is widely used for planning in interventional radiosurgery. Three-dimensional computed tomography (3D-CT) has been utilized in transcatheter arterial chemoembolization (TACE), and allows for better visualization of small vessels[8,9]. Transjugular intrahepatic portosystemic shunt (TIPS) combines preoperative 3D-CT images with images taken at the time of intervention, and has demonstrated a significant reduction in operation times and radiation doses[10]. Three-dimensional imaging is also beneficial in guiding therapeutic ERCP[11], as it allows easier identification of bile duct anatomy and guides intraoperative navigation, reducing necessary radiation dose and operation time with improved safety[11]. For example, biliary stent placement *via* ERCP in the setting of indeterminate biliary stricture, the X-ray exposure time was reduced from 8.1 min to 35.1 min. However, current 3D biliary imaging does not have good real-time fusion with intraoperative images.

Here, we explored the feasibility of real-time continuous image-guided ERCP, which overcomes the influence of intraoperative respiratory motion and provides an accurate navigation method. Preoperative 3D-CT bile duct sequences were registered and fused with real-time 2D images from the C-arm taken during ERCP; this strategy may improve the quality of ERCP.

MATERIALS AND METHODS

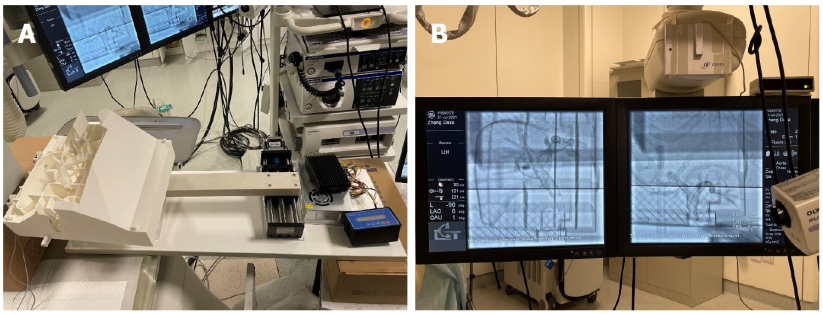
Study population

This was a single-centered prospective observational study of patients receiving ERCP at a tertiary care hospital between July 2021 and March 2022. Twenty patients with cholelithiasis undergoing therapeutic ERCP were recruited. Only patients with a preoperative 3D-CT sequence of the bile duct were eligible. Dynamic 2D images of the bile duct generated by the fluoroscopic C-arm were obtained. Exclusion criteria were: age < 18 y, poor general health, inability to tolerate basic or intravenous anesthesia, uncontrollable coagulation disorder, anticoagulation therapy that could not be discontinued, altered anatomy (*e.g.*, Billroth II gastrectomy or Roux-en-Y anastomosis), pregnancy, and intraoperative



DOI: 10.3748/wjg.v29.i20.3157 **Copyright** ©The Author(s) 2023.

Figure 1 Biliary phantom setup. A: Biliary model based on patient A; B: Biliary model based on patient B.



DOI: 10.3748/wjg.v29.i20.3157 **Copyright** ©The Author(s) 2023.

Figure 2 Surgical environment for endoscopic retrograde cholangiopancreatography phantom. A: Respiratory motion simulator; B: X-ray fluoroscopy guidance in navigation.

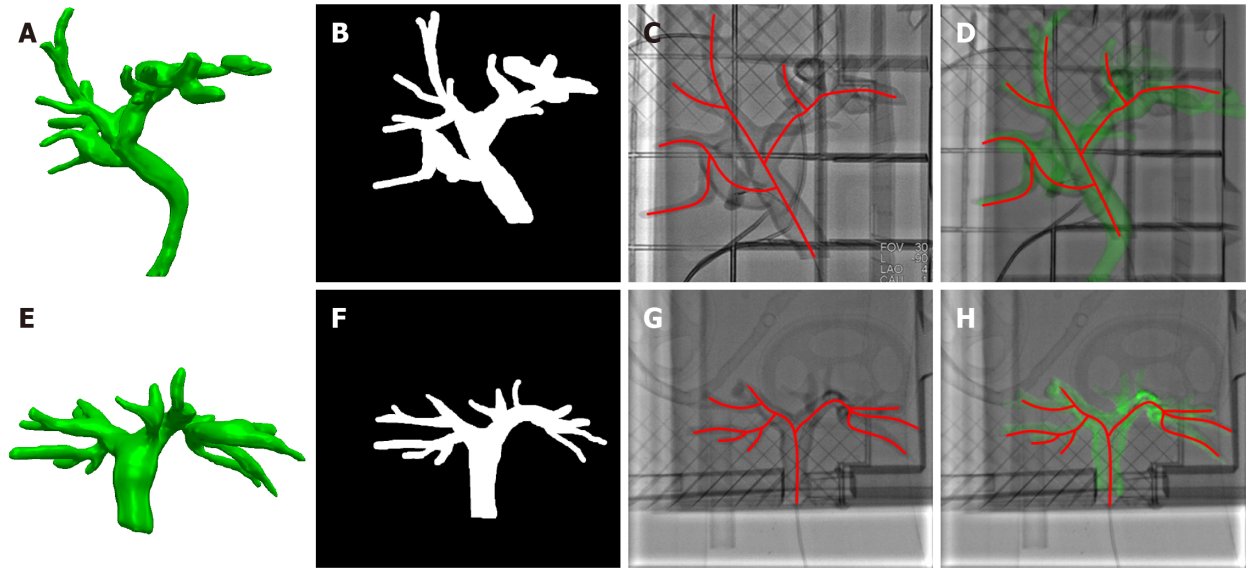
placement of a biliopancreatic stent. Written informed consent was obtained from all patients. The study was approved by the Ethics Committee of the Chinese People's Liberation Army (PLA) General Hospital (No. S2021-415-01) and was conducted per the Declaration of Helsinki.

Human biliary phantom

To verify the accuracy of our 3D/2D registration algorithm, we created 2 3D-printed biliary tract models with different structures to simulate different patients. Enhanced CT scan data of 2 patients with biliary dilatation were inputted into a 3D biomechanics research software tool (Visual 3D, Beijing, China). The operator manually segmented the contours of the biliary tract to acquire surface models. The acquired surface models were inputted into a Stratasys J750 3D printer (Markforged, Watertown, Massachusetts) and printed using resin (Figure 1). The printed phantom was life-sized and hollow, allowing sphincterotomes to enter. The phantom experiment was carried out in the PLA General Hospital operating room (Figure 2). Unlike in clinical experiments, model experiments could be repeated many times to simulate real intraoperative conditions to adjust the algorithm parameters.

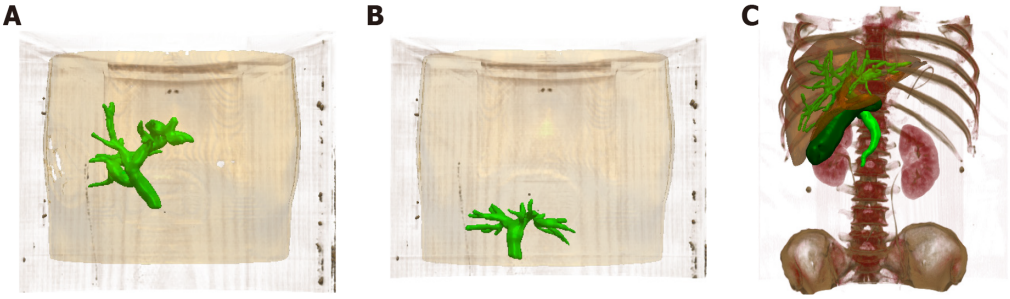
CT and fluoroscopic imaging

An iopromide contrast medium (Ultravist 370; Bayer Healthcare, Leverkusen, Germany) was diluted to visualize the biliary tract. All CT scans were performed in the Imaging Department of PLA General Hospital (uCT 510; United Imaging Healthcare, Shanghai, China) with a slice thickness of 1.25 mm and a tube voltage of 120 kV. Patients were asked to remain in the end-inspiratory state for CT scan. To acquire the best alignment transformation, patients were asked to maintain the same pre-operative state at the beginning of surgery. Then, fluoroscopy was performed and the image was defined as the best matching frame. On the day of the ERCP procedure, the acquired CT scan data were imported into Mimics (Materialise, Belgium) to reconstruct the 3D volume-render models of the biliary tract, liver, gallbladder, and bone. All patients received intraoperative deep sedation. ERCP was performed using a standard endoscope (Olympus Duodenoscope TJF260). When the guidewire was successfully superselected in the bile duct and the contrast agent was injected into the duct, the C-arm system performed 1 consecutive respiratory cycle of fluoroscopy around the patient, producing approximately 20 images which were transmitted in real time to our image navigation system.



DOI: 10.3748/wjg.v29.i20.3157 **Copyright** ©The Author(s) 2023.

Figure 3 Phantom study of registration and fusion. A and E: Biliary phantom segmentation using computed tomography images; B and F: Biliary phantom segmentation using X-ray fluoroscopy; C and G: Biliary lumen centerline extraction; D and H: Three-dimensional biliary model registered with the best matching frame using X-ray fluoroscopy.



DOI: 10.3748/wjg.v29.i20.3157 **Copyright** ©The Author(s) 2023.

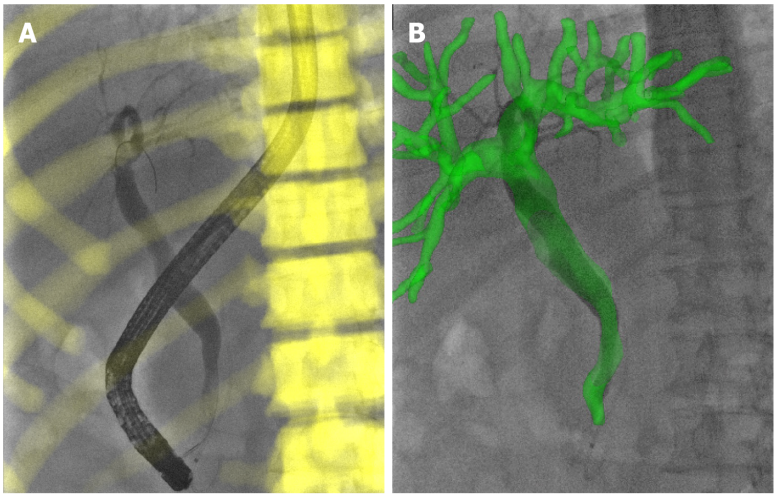
Figure 4 Automatic segmentation of structures based on preoperative computed tomography. A and B: Biliary and skin phantoms of different patients; C: Bone, liver, biliary tract, and gallbladder segmented by a three-dimensional UNet network based on preoperative computed tomography data.

CT co-registration and fusion with the fluoroscopic image

During the registration between CT and X-ray fluoroscopic images, the CT image was aligned with X-ray fluoroscopy through common features. For the biliary phantom, the registration fiducials were extracted from the CT and X-ray images, respectively, to get rigid transformation, by which the 3D biliary model segmented from CT was projected onto the X-ray fluoroscopic image to finish the overlap of biliary roadmapping. The biliary ducts were observed with X-ray images without contrast agents during model experimentation (Figure 3). After the 3D/2D registration was completed, the biliary ducts segmented from CT were projected onto the X-ray image, and the validity of the registration was judged according to the edge blending effect.

The bone, liver, gallbladder, and biliary tract were segmented by a 3D-UNet model based on preoperative CT data (Figure 4). Afterward, the Medical Imaging Interaction Toolkit was used to extract 2D bone structures. Mimics software (Materialise, Leuven, Belgium) was used to extract 3D and 2D biliary centerlines for analysis. Finally, 3D/2D registration based on bone structures was performed to achieve effective fusion of the 3D biliary model and the best matching frame (Figure 3).

The respiratory motion of the patient during the operation affects fusion accuracy. Some researchers have estimated the patient's respiratory state by extracting diaphragm data in real time[12-15]. The diaphragm-based method not only requires manual annotation, but also cannot guarantee real-time performance, thus prolonging the operation time and increasing X-ray radiation exposure. The method based on X-ray image centroid extraction was used in the current study to estimate the respiratory state [9] and monitor the motion change between frames through X-ray image gray distribution. The respiratory motion curve was acquired and used to complete continuous compensation for the fluoroscopy sequence, and real-time biliary roadmapping projected onto X-ray fluoroscopy was completed. This 3D/2D image registration technology is available in the current intraoperative imaging



DOI: 10.3748/wjg.v29.i20.3157 **Copyright** ©The Author(s) 2023.

Figure 5 Registration and fusion on the best matching frame of the patient. A: Three- dimensional/two-dimensional registration based on bone during endoscopic retrograde cholangiopancreatography; B: Overlay the biliary model on X-ray fluoroscopy through the transformation from bone registration.

system takes approximately 60 s. Our method has a fast calculation speed and is convenient to operate, features that aid in real-time navigation.

Data collection

Quantitative data included the registration error and the tracking error (TE). The registration error was calculated as the mean square error (MSE) between the projection of the 3D and 2D centerline. After finishing respiratory compensation and projecting, the mean MSE was set as the TE. Qualitative parameters included image quality and real-time fusion rates for both preoperative and intraoperative images.

Definitions

Image-guided ERCP: Image quality was defined as "good" if the 3D-CT and fluoroscopic images of the bile duct filled by a contrast medium were visible. The outcome of real-time fusion rates was assessed by the degree to which the bile duct in the fluoroscopic mode matched perfectly with the 3D-CT biliary imaging.

Statistical analysis

Data were assessed for normality, and appropriate descriptive statistics were calculated and expressed as mean ± standard deviation (SD) and frequency (percentages). Data were analyzed using SPSS version 22 (IBM Corp., Armonk, NY, United States).

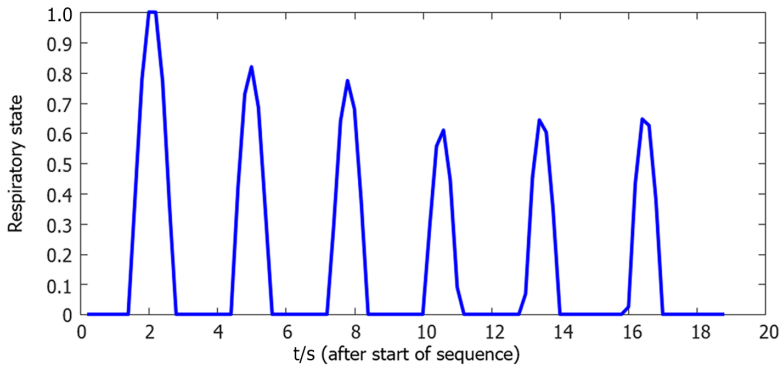
RESULTS

Image-guided ERCP had a mean registration error of 0.46 mm ± 0.13 mm and a TE of 0.64 mm ± 0.24 mm. For patients, the biliary model was projected onto the X-ray based on 3D/2D registration (Figure 5), and the respiratory motion curve was estimated through a continuous X-ray fluoroscopy sequence (Figure 6). Continuous biliary roadmapping guidance was acquired (Figure 7). Our navigation system was performed in the operating room (Figure 8), and it provided image-based guidance in multiple patients (Figure 9). Image quality was good in all 18 cases and CT to X-ray fluoroscopic image registration and fusion were technically feasible, with an average fusion rate of 88% (Supplementary material).

DISCUSSION

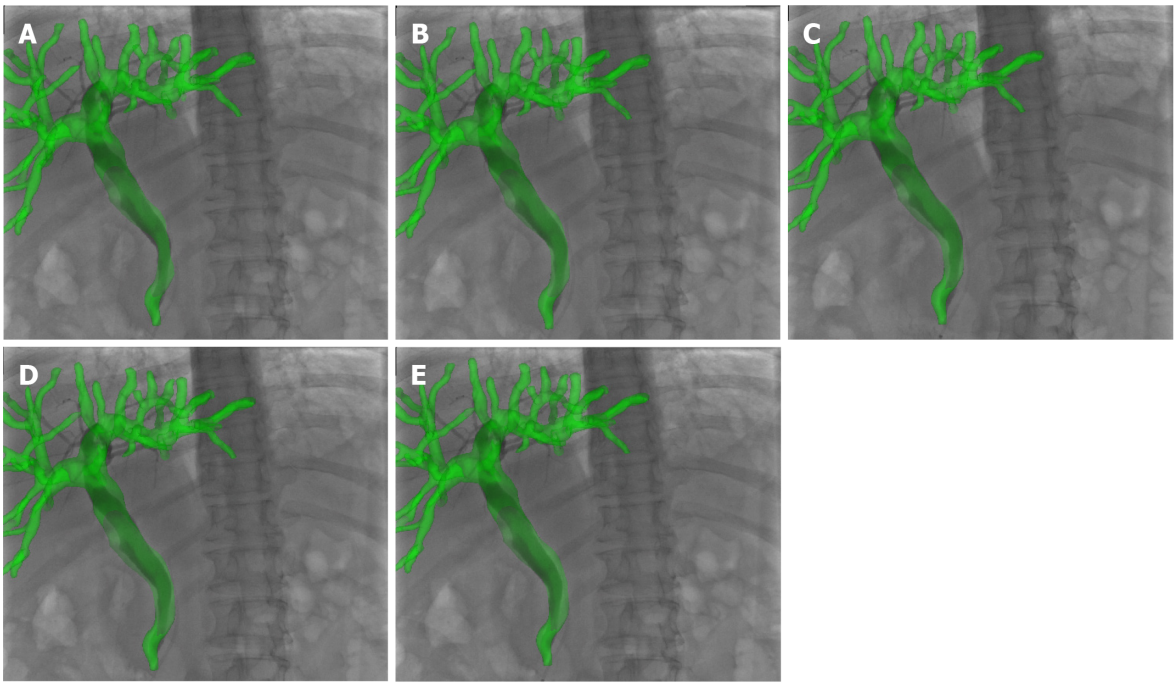
In the current study, continuous image guidance for ERCP based on 3D/2D registration was evaluated, and we found that this strategy may be an effective means of real-time localization of the bile duct.

The prognosis of hilar cholangiocarcinoma (HCCA) is extremely poor, and surgery is the only radical treatment modality. However, most patients present with an unresectable tumor or cholangitis, high bilirubin, and insufficient volume of the residual liver; as such, biliary drainage by ERCP is often best



DOI: 10.3748/wjg.v29.i20.3157 **Copyright** ©The Author(s) 2023.

Figure 6 Example of the estimated respiratory state over an 18.8 s X-ray fluoroscopic image sequence.



DOI: 10.3748/wjg.v29.i20.3157 **Copyright** ©The Author(s) 2023.

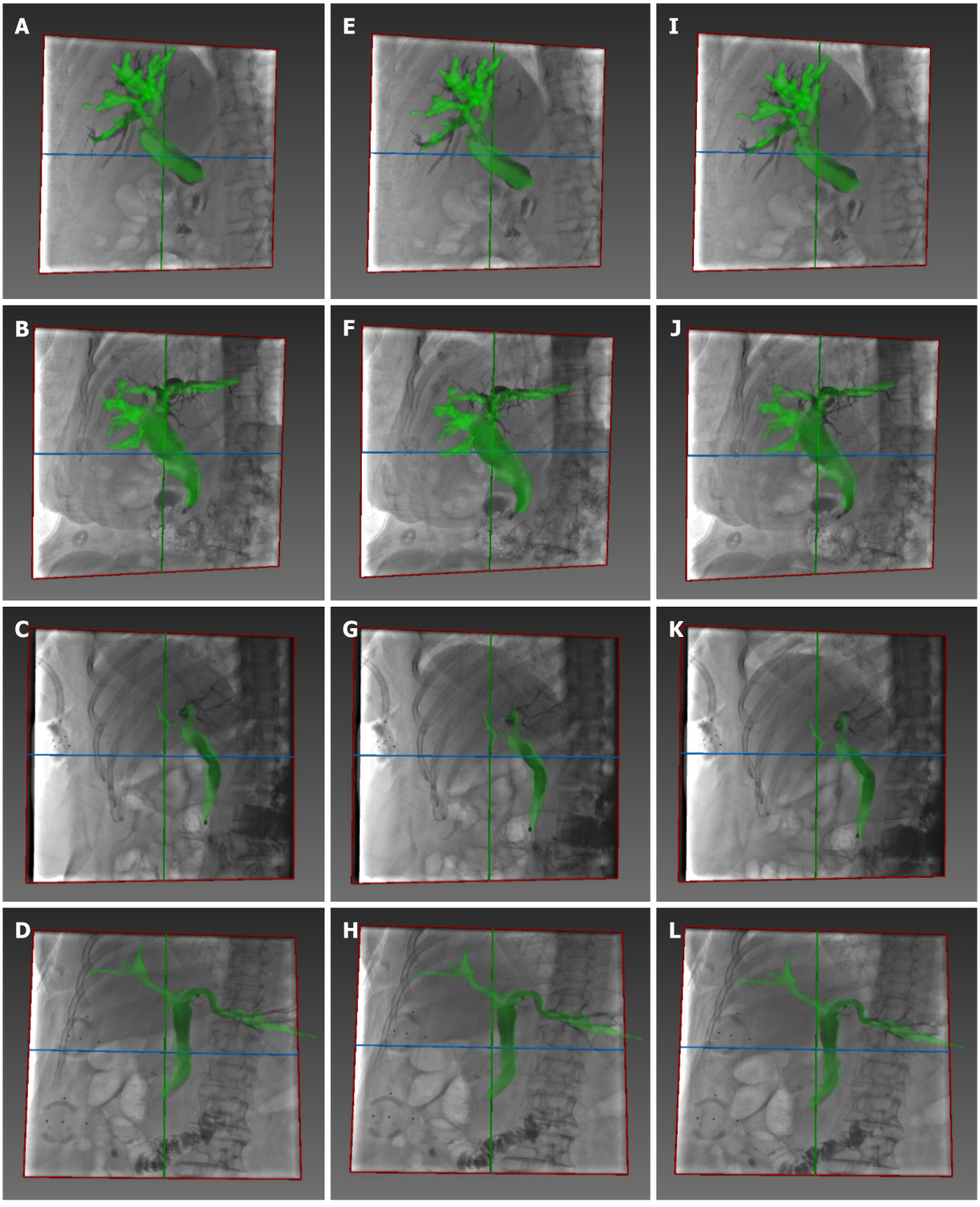
Figure 7 Real-time navigation of image-guided endoscopic retrograde cholangiopancreatography. A: Beginning of inhalation; B: During inhalation; C: End of inhalation; D: During exhalation; E: End of exhalation.



DOI: 10.3748/wjg.v29.i20.3157 **Copyright** ©The Author(s) 2023.

Figure 8 Image-guided endoscopic retrograde cholangiopancreatography navigation system.

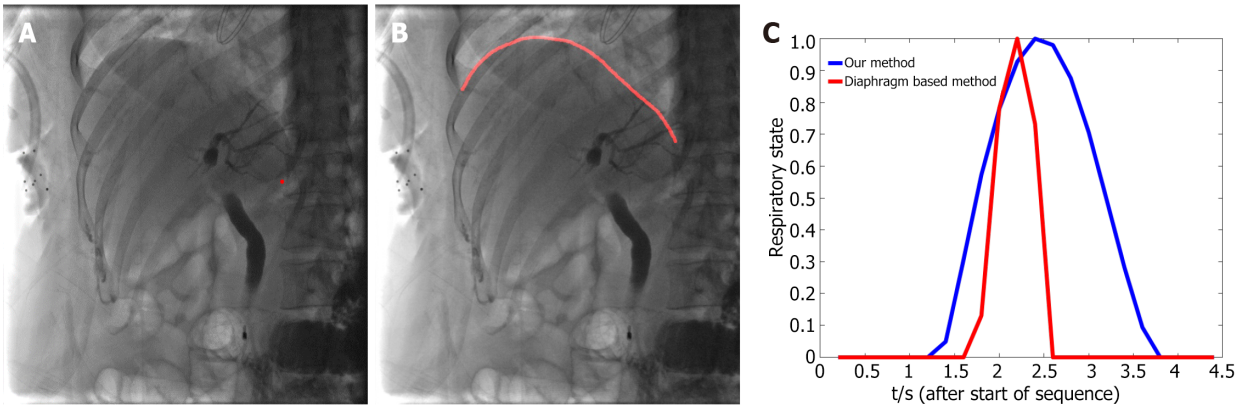
available treatment. Previous studies have shown the benefit of 3D imaging in guiding difficult ERCP procedures[11]. Preoperative 3D-CT, magnetic resonance cholangiopancreatography, magnetic resonance virtual endoscopy, or intraoperative 3D-CT of the cone beam have all provided adequate



DOI: 10.3748/wjg.v29.i20.3157 **Copyright** ©The Author(s) 2023.

Figure 9 Additional examples of real-time image guidance navigation. A-D: Beginning of the inhalation; E-H: During the inhalation; I-L: End of the inhalation.

guidance for biliary stenting in patients with HCCA, but do not achieve real-time fusion of 3D images with 2D fluoroscopic images or display guidewire or sphincterotomes in three dimensions[16-19]. Our technology can obtain 3D models of the biliary duct, tumor, and hilar vessels through preoperative magnetic resonance imaging/CT segmentation. The registration between preoperative 3D models and intraoperative 2D X-ray images was completed based on the centerlines of the biliary ducts, and 3D models were projected onto X-ray images for display. Meanwhile, based on the respiratory compensation method, a continuous fusion between 3D models and the X-ray image sequences was achieved, and real-time guidance was realized through graphics processing unit acceleration. We believe that our method may provide physicians with more visual information during surgery and



DOI: 10.3748/wjg.v29.i20.3157 **Copyright** ©The Author(s) 2023.

Figure 10 Comparison between two methods with respect to respiratory state estimation. A: Centroid of the X-ray image; B: Diaphragm of the X-ray image; C: Example of the estimated respiratory state over a 4.4 s X-ray image sequence.

effectively improve the operability of the intervention.

The present study reports real-time fusion of preoperative 3D-CT images with the 2D fluoroscopic images during ERCP. The radiation dose required for the registration between 3D-CT and fluoroscopic image can be considered negligible compared with the total radiation dose for difficult ERCP procedures. In addition, image registration was completed in an average time of 1 min, with a minimal overall increase in total operation time. Therefore, with the real-time visual aid during ERCP, it is likely that less radiation, contrast medium, and operative time may be required during the navigation.

Furthermore, our methods estimated the respiratory state better than the classical diaphragm extraction method[17]. Since the diaphragm is incomplete or invisible during ERCP in some patients, the applicability and robustness of our method are better based on image gray distribution. Furthermore, this method can achieve a more accurate estimation of the respiratory state of the biliary tract, thus ensuring better fusion of 3D-CT and 2D X-ray images. The main reason for this is that the respiratory motion of the diaphragm can reflect well upon the upper edge of the liver, but cannot directly represent the motion of the biliary tract. Experimental results also proved that our method is more accurate for biliary motion estimation of patients under free breathing. Compared with the TE of the diaphragm-based method, based on our cholangiography image fusion results, TE was relatively low (1.68 mm ± 0.34 mm *vs* 0.64 mm ± 0.24 mm), providing more accurate guidance. As shown in Figure 10, the respiratory state estimation based on our method was smoother and closer to the true breathing curve, which ensures the stability of image-guided navigation. Moreover, our method is simpler and faster to compute and process intraoperative X-ray fluoroscopic image sequences in real-time. Conversely, the diaphragm-based method requires real-time segmentation of the diaphragm whether manual or network methods are used, which represents a complex task and ultimately leads to an increase in operation time and radiation dose.

There are further implications of our technology in the context of other minimally invasive procedures such as TACE, TIPS, and spine surgery[8-10,20]. Coronavirus disease-2019 (COVID-19) had devastating impacts on healthcare system operations. The pandemic disrupted normal workflow of spine surgeries, restricting and postponing elective procedures[20]. This disruption may have resulted in the prolonged impairment of patients who were forced to postpone their procedures. Minimally invasive surgery and perioperative telemedicine are inevitable trends in spine surgery after COVID-19. Spine surgery is usually completed under the guidance of X-ray images, and physicians need to conceive the 3D structure of the patient's spine based on clinical experience. The spine is different from the soft liver and there is no respiratory interference; however, the similarity of the structure between the joints and the overall length makes surgery more difficult to perform only under the guidance of X-ray images. Meanwhile, the increase in operation time has also caused longer waiting periods for treatment. Our method can extract the 3D spine structure from preoperative CT and complete 3D/2D registration through the bone structure line, achieving the fusion of 3D information with intraoperative X-ray images. This technology could help physicians better localize lesions and enhance visual perception of depth. Fusion of 3D/2D imaging could also help physicians, especially those with insufficient clinical experience, to observe the patient's spine structure more intuitively and improve surgical efficiency. In summary, the number of spinal surgeries increased following COVID-19 and has continued to rise; our technology may help the hospital to perform more operations and allow patients to receive timely and effective treatment.

COVID-19 has also been associated with an increased risk for ischemic and hemorrhagic strokes[21], conditions often treated with a vascular intervention procedure very similar to TACE that is achieved by embolizing the vessels connected to the aneurysm. Unlike liver vessels, intracranial vessels are not affected by respiratory motion and remain static with the use of X-ray images for guidance. However,

intracranial vessels are generally thin and have multiple branching structures, and thus the risks associated with intracranial surgery are high. Surgeons require more clinical experience to ensure the accuracy of the surgery; otherwise, they may injure other blood vessels or tissues and cause secondary harm to the patient. Our technology can extract data regarding blood vessels connected to the lesion (*e.g.*, aneurysm) before the surgery and guide the surgeon intraoperatively through high-precision registration and fusion. Given the risk of intracranial vascular intervention procedures, our technology could display the vessels around the catheter and render them in different colors to remind the surgeon to be cautious, thus benefiting the safety of the procedure. We believe that our technology may have potential clinical value in treating cerebrovascular diseases and could precisely treat ischemic and hemorrhagic strokes associated COVID-19.

CONCLUSION

Our image-guided ERCP strategy was fully validated in models that may be useful in cannulating specific biliary ducts in patients with complex biliopancreatic diseases such as HCCA. However, clinical studies are still needed to determine if this new approach could improve technical success while reducing radiation exposure and contrast agent administration during ERCP.

ARTICLE HIGHLIGHTS

Research background

Three-dimensional (3D) imaging is beneficial in guiding therapeutic endoscopic retrograde cholangiopancreatography (ERCP), reducing the radiation dose and procedure time while increasing overall procedure safety. However, current 3D biliary imaging does not have good real-time fusion with intraoperative images.

Research motivation

We explored the feasibility of real-time continuous image-guided ERCP, which was shown to overcome the influence of intraoperative respiratory motion and provides an accurate navigation method.

Research objectives

To explore the feasibility of real-time continuous image-guided ERCP.

Research methods

We simulated an ERCP environment using an experimental biliary phantom with the aim of designing a navigation system; this system was further tested in patients undergoing ERCP.

Research results

Continuous image-guided ERCP was applied in the biliary phantom with low registration and tracking errors. This 3D/2D registration accurately transformed preoperative 3D biliary images to each image in the X-ray sequence in real-time.

Research conclusions

Continuous image-guided ERCP may be an effective approach to assist the operator and reduce the use of X-ray and contrast agents.

Research perspectives

Clinical studies are needed to determine if this image-guided ERCP strategy could improve technical success while reducing radiation exposure and contrast agent administration during ERCP.

FOOTNOTES

Author contributions: Yang S and Zhang DY designed the registration algorithm and finished the manuscript; Geng HX designed the experiment and revised the manuscript; Ding CJ and Yuan YJ collected the data; Yang J and Li MY made corrections to the article. Zhang DY and Yang S contributed equally to this work, and they are co-first authors; Li MY and Yang J contributed equally to this work, and they are co-corresponding authors.

Institutional review board statement: The study was reviewed and approved by the Ethics Committee of the General Hospital of the Chinese People's Liberation Army (approval No. S2021-415-01).

Informed consent statement: All study participants or their legal guardian(s) provided informed written consent prior to study enrollment.

Conflict-of-interest statement: The authors declare that they have no conflicts of interest.

Data sharing statement: All data and materials involved in the manuscript are available upon request.

STROBE statement: The authors have read the STROBE Statement—checklist of items, and the manuscript was prepared and revised according to the STROBE Statement—checklist of items.

Open-Access: This article is an open-access article that was selected by an in-house editor and fully peer-reviewed by external reviewers. It is distributed in accordance with the Creative Commons Attribution NonCommercial (CC BY-NC 4.0) license, which permits others to distribute, remix, adapt, build upon this work non-commercially, and license their derivative works on different terms, provided the original work is properly cited and the use is non-commercial. See: https://creativecommons.org/Licenses/by-nc/4.0/

Country/Territory of origin: China

ORCID number: Da-Ya Zhang 0000-0001-6133-8919; Ming-Yang Li 0000-0003-1567-7121.

S-Editor: Chen YL
L-Editor: Filipodia
P-Editor: Chen YX

REFERENCES

1 **McCune WS**, Shorb PE, Moscovitz H. Endoscopic cannulation of the ampulla of vater: a preliminary report. *Ann Surg* 1968; **167**: 752-756 [PMID: 5646296 DOI: 10.1097/00000658-196805000-00013]
2 **Weiser R**, Pencovich N, Mlynarsky L, Berliner-Senderey A, Lahat G, Santo E, Klausner JM, Nachmany I. Management of endoscopic retrograde cholangiopancreatography-related perforations: Experience of a tertiary center. *Surgery* 2017; **161**: 920-929 [PMID: 28027817 DOI: 10.1016/j.surg.2016.10.029]
3 **Fung BM**, Pitea TC, Tabibian JH. Difficult Biliary Cannulation in Endoscopic Retrograde Cholangiopancreatography: Definitions, Risk Factors, and Implications. *Eur Med J Hepatol* 2021; **9**: 64-72 [PMID: 34621527]
4 **Hong JY**, Han K, Jung JH, Kim JS. Association of Exposure to Diagnostic Low-Dose Ionizing Radiation With Risk of Cancer Among Youths in South Korea. *JAMA Netw Open* 2019; **2**: e1910584 [PMID: 31483470 DOI: 10.1001/jamanetworkopen.2019.10584]
5 **Adler DG**, Lieb JG 2nd, Cohen J, Pike IM, Park WG, Rizk MK, Sawhney MS, Scheiman JM, Shaheen NJ, Sherman S, Wani S. Quality indicators for ERCP. *Gastrointest Endosc* 2015; **81**: 54-66 [PMID: 25480099 DOI: 10.1016/j.gie.2014.07.056]
6 **Hayashi S**, Takenaka M, Hosono M, Nishida T. Radiation exposure during image-guided endoscopic procedures: The next quality indicator for endoscopic retrograde cholangiopancreatography. *World J Clin Cases* 2018; **6**: 1087-1093 [PMID: 30613666 DOI: 10.12998/wjcc.v6.i16.1087]
7 **Dumonceau JM**, Tringali A, Papanikolaou IS, Blero D, Mangiavillano B, Schmidt A, Vanbiervliet G, Costamagna G, Devière J, García-Cano J, Gyökeres T, Hassan C, Prat F, Siersema PD, van Hooft JE. Endoscopic biliary stenting: indications, choice of stents, and results: European Society of Gastrointestinal Endoscopy (ESGE) Clinical Guideline - Updated October 2017. *Endoscopy* 2018; **50**: 910-930 [PMID: 30086596 DOI: 10.1055/a-0659-9864]
8 **Hammami H**, Lalys F, Rolland Y, Petit A, Haigron P. Catheter navigation support for liver radioembolization guidance: feasibility of structure-driven intensity-based registration. *Int J Comput Assist Radiol Surg* 2020; **15**: 1881-1894 [PMID: 32870445 DOI: 10.1007/s11548-020-02250-8]
9 **Wagner MG**, Periyasamy S, Longhurst C, McLachlan MJ, Whitehead JF, Speidel MA, Laeseke PF. Real-time respiratory motion compensated roadmaps for hepatic arterial interventions. *Med Phys* 2021; **48**: 5661-5673 [PMID: 34431111 DOI: 10.1002/mp.15187]
10 **Meine TC**, Dewald CLA, Becker LS, Mähringer-Kunz A, Maasoumy B, Maschke SK, Kirstein MM, Werncke T, Wacker FK, Meyer BC, Hinrichs JB. Correction to: Transjugular intrahepatic portosystemic shunt placement: portal vein puncture guided by 3D/2D image registration of contrast-enhanced multi-detector computed tomography and fluoroscopy. *Abdom Radiol (NY)* 2021; **46**: 398 [PMID: 32642854 DOI: 10.1007/s00261-020-02617-0]
11 **Wang Y**, Cao D, Chen SL, Li YM, Zheng YW, Ohkohchi N. Current trends in three-dimensional visualization and real-time navigation as well as robot-assisted technologies in hepatobiliary surgery. *World J Gastrointest Surg* 2021; **13**: 904-922 [PMID: 34621469 DOI: 10.4240/wjgs.v13.i9.904]
12 **Timinger H**, Krueger S, Dietmayer K, Borgert J. Motion compensated coronary interventional navigation by means of diaphragm tracking and elastic motion models. *Phys Med Biol* 2005; **50**: 491-503 [PMID: 15773725 DOI: 10.1088/0031-9155/50/3/007]
13 **Chen PY**. A novel network module for medical devices. *Annu Int Conf IEEE Eng Med Biol Soc* 2008; **2008**: 1553-1556 [PMID: 19162969 DOI: 10.1109/IEMBS.2008.4649466]
14 **King AP**, Boubertakh R, Rhode KS, Ma YL, Chinchapatnam P, Gao G, Tangcharoen T, Ginks M, Cooklin M, Gill JS, Hawkes DJ, Razavi RS, Schaeffter T. A subject-specific technique for respiratory motion correction in image-guided

cardiac catheterisation procedures. *Med Image Anal* 2009; **13**: 419-431 [PMID: 19223220 DOI: 10.1016/j.media.2009.01.003]

15 **Shahshahani A**, Laverdiere C, Bhadra S, Zilic Z. Ultrasound Sensors for Diaphragm Motion Tracking: An Application in Non-Invasive Respiratory Monitoring. *Sensors (Basel)* 2018; **18** [PMID: 30096945 DOI: 10.3390/s18082617]

16 **Toki M**, Tateishi H, Yoshida T, Gondo K, Watanabe S, Hisamatsu T. Utilization of a new technology of 3D biliary CT for ERCP-related procedures: a case report. *BMC Gastroenterol* 2020; **20**: 158 [PMID: 32448154 DOI: 10.1186/s12876-020-01304-0]

17 **Reuterwall M**, Waldthaler A, Lubbe J, Kadesjö N, Pozzi Mucelli R, Del Chiaro M, Lohr M, Arnelo U. Bimodal ERCP, a new way of seeing things. *Endosc Int Open* 2020; **8**: E368-E376 [PMID: 32118109 DOI: 10.1055/a-1070-8749]

18 **Azuma T**, Yamaguchi K, Iida T, Oouhida J, Suzuki M. MR virtual endoscopy for biliary tract and pancreatic duct. *Magn Reson Med Sci* 2007; **6**: 249-257 [PMID: 18239363 DOI: 10.2463/mrms.6.249]

19 **Weigt J**, Pech M, Kandulski A, Malfertheiner P. Cone-beam computed tomography - adding a new dimension to ERCP. *Endoscopy* 2015; **47**: 654-657 [PMID: 25675173 DOI: 10.1055/s-0034-1391483]

20 **Lucke-Wold B**, Cerillo JL, Becsey AN, Chernicki BP, Root KT. Minimally Invasive Procedures, Perioperative Telemedicine, and Decreased Hospital Stays Following Covid-19 Surgical Restrictions: Spinal Surgery. *Arch Med Case Rep Case Study* 2022; **6** [PMID: 36844926]

21 **Small C**, Mehkri Y, Panther E, Felisma P, Lucke-Wold B. Coronavirus Disease-2019 and Stroke: Pathophysiology and Management. *Can J Neurol Sci* 2022; 1-8 [PMID: 35762309 DOI: 10.1017/cjn.2022.267]

World Journal of Gastroenterology

Submit a Manuscript: https://www.f6publishing.com

World J Gastroenterol 2023 May 28; 29(20): 3168-3184

DOI: 10.3748/wjg.v29.i20.3168

ISSN 1007-9327 (print) ISSN 2219-2840 (online)

ORIGINAL ARTICLE

Observational Study

Inflammation-related nomogram for predicting survival of patients with unresectable hepatocellular carcinoma received conversion therapy

Jia-Lin Wu, Jun-Yang Luo, Zai-Bo Jiang, Si-Bo Huang, Ge-Run Chen, Hui-Ying Ran, Qi-Yue Liang, Ming-Sheng Huang, Li-Sha Lai, Jun-Wei Chen

Specialty type: Oncology

Provenance and peer review: Unsolicited article; Externally peer reviewed.

Peer-review model: Single blind

Peer-review report's scientific quality classification

Grade A (Excellent): 0
Grade B (Very good): B, B
Grade C (Good): 0
Grade D (Fair): 0
Grade E (Poor): 0

P-Reviewer: Li YW, China; Yang M, United States

Received: March 3, 2023
Peer-review started: March 3, 2023
First decision: March 24, 2023
Revised: April 2, 2023
Accepted: April 24, 2023
Article in press: April 24, 2023
Published online: May 28, 2023

Jia-Lin Wu, Jun-Yang Luo, Zai-Bo Jiang, Ming-Sheng Huang, Jun-Wei Chen, Department of Interventional Radiology, The Third Affiliated Hospital of Sun Yat-sen University, Guangzhou 510630, Guangdong Province, China

Si-Bo Huang, Ge-Run Chen, The First Clinical Medical College, Guangdong Medical University, Zhanjiang 524000, Guangdong Province, China

Hui-Ying Ran, Qi-Yue Liang, Zhongshan School of Medicine, Sun Yat-sen University, Guangzhou 510080, Guangdong Province, China

Li-Sha Lai, Department of Radiology, Guangzhou First People's Hospital, School of Medicine, South China University of Technology, Guangzhou 510010, Guangdong Province, China

Corresponding author: Jun-Wei Chen, MD, Professor, Interventional Radiologist, Department of Interventional Radiology, The Third Affiliated Hospital of Sun Yat-sen University, No. 600 Tianhe Road, Guangzhou 510630, Guangdong Province, China. chenjw53@mail.sysu.edu.cn

Abstract

BACKGROUND

The efficacy of conversion therapy for patients with unresectable hepatocellular carcinoma (HCC) is a common clinical concern.

AIM

To analyse the prognostic factors of overall survival (OS) in patients with unresectable HCC who received conversion therapy.

METHODS

One hundred and fifty patients who met the inclusion criteria were enrolled and divided into a training cohort (n = 120) and a validation cohort (n = 30). Using the independent risk factors in the training cohort, a nomogram model was constructed to predict OS for patients treated with transarterial chemoembolization following hepatic resection. The nomogram was internally validated with the bootstrapping method. The predictive performance of nomogram was assessed by Harrell's concordance index (C-index), calibration plot and time-dependent receiver operating characteristic curves and compared with six other

conventional HCC staging systems.

RESULTS

Multivariate Cox analysis identified that albumin, blood urea nitrogen, gamma-glutamyl transpeptidase to platelet ratio, platelet to lymphocyte ratio, macrovascular invasion and tumour number were the six independent prognostic factors correlated with OS in nomogram model. The C-index in the training cohort and validation cohort were 0.752 and 0.807 for predicting OS, which were higher than those of the six conventional HCC staging systems (0.563 to 0.715 for the training cohort and 0.458 to 0.571 for the validation cohort). The calibration plots showed good consistency between the nomogram prediction of OS and the actual observations of OS. Decision curve analyses indicated satisfactory clinical utility. With a total nomogram score of 196, patients were accurately classified into low-risk and high-risk groups. Furthermore, we have deployed the model into online calculators that can be accessed for free at https://ctmodelforunresectablehcc.shinyapps.io/DynNomapp/.

CONCLUSION

The nomogram achieved optimal individualized prognostication of OS in HCC patients who received conversion therapy, which could be a useful clinical tool to help guide postoperative personalized interventions and prognosis judgement.

Key Words: Hepatocellular carcinoma; Conversion therapy; Nomogram; Inflammation; Transarterial chemoembolization

©The Author(s) 2023. Published by Baishideng Publishing Group Inc. All rights reserved.

Core Tip: We developed and validated a prognostic nomogram based on inflammation-related biomarkers for patients with unresectable hepatocellular carcinoma after conversion therapy. The proposed conversion therapy model shows increased accuracy, good clinical utility, and better prognostic performance compared with conventional staging systems. Based on the total predictive risk scores, the patients were classified into two groups: low-risk (score < 196) and high-risk group (score ≥ 196), to guide postoperative adjuvant interventions and follow-ups. Furthermore, we have made this prognostic nomogram online for free use (https://ctmodelforunresectablehcc.shinyapps.io/DynNomapp/).

Citation: Wu JL, Luo JY, Jiang ZB, Huang SB, Chen GR, Ran HY, Liang QY, Huang MS, Lai LS, Chen JW. Inflammation-related nomogram for predicting survival of patients with unresectable hepatocellular carcinoma received conversion therapy. *World J Gastroenterol* 2023; 29(20): 3168-3184
URL: https://www.wjgnet.com/1007-9327/full/v29/i20/3168.htm
DOI: https://dx.doi.org/10.3748/wjg.v29.i20.3168

INTRODUCTION

Hepatocellular carcinoma (HCC), the most common type of primary liver cancer, ranks as the sixth most prevalent malignancy and third leading cause of cancer-related deaths worldwide[1]. More so than other cancers, hepatitis B virus (HBV) infection is a hallmark of HCC, with 70%-90% of diagnoses occurring with a background of cirrhosis in highly prevalent Asian countries[2]. Hepatic resection (HR) is deemed the most efficacious therapeutic option for patients diagnosed with early to intermediate stages of HCC. Unfortunately, the majority of Chinese patients with HCC are diagnosed at intermediate or advanced stages with massive or multifocal lesions. Nevertheless, HR is possible for a minority of carefully selected patients with the help of a "conversion therapy" strategy, which refers to conversion of an unresectable HCC to achieve adequate tumour shrinkage and downstaging to undergo HR. However, only a limited number of meticulously screened patients with intermediate or advanced stage HCC qualify for HR.

As per the Barcelona Clinic Liver Cancer (BCLC) staging system, transarterial chemoembolization (TACE) is recommended as the first-line treatment for intermediate stage HCC and has been extensively investigated and widely acknowledged as an effective approach for conversion therapy[3]. Previous studies have demonstrated that HR after local treatments, such as TACE, hepatic artery infusion chemotherapy and radiotherapy with or without other systemic therapeutic measures, can improve tumour shrinkage as well as downstaging. Moreover, these treatments have been shown to enhance patient survival rates without causing significant complications[4-7]. While TACE could potentially

provide surgical options to previously ineligible HCC patients, its high incidence of short-term recurrence remains a significant challenge for conversion therapy. Meanwhile, active conversion strategies to increase the volume of future liver remnant and planning for patients who cannot achieve R0 resection are worth greater consideration. Thus, the development of a validated clinical risk score based on preoperative indices to assess those at high risk of recurrence and death may help formulate optimal management strategies and prevent disease progression.

Links between inflammation and the development of cancer are well established, and HCC is one of the most classic inflammation-linked tumours. During liver inflammation, inflammatory cells and mediators are present before hepatocarcinogenesis and prompt the malignant activity of cancer cells. Additionally, a persistent cancer-related inflammatory microenvironment leads to immune suppression, which promotes the development of HCC[8]. Recently, numerous previous studies have indicated that preoperative inflammatory biomarkers can be capable of predicting HCC prognosis after HR[9,10]. A previous study by Wang *et al*[9] assessed the prognostic value of inflammation-related markers prior to surgery and demonstrated their high effectiveness in predicting survival after surgical resection of HCC. In addition, the researchers concluded that two inflammation-related markers, gamma-glutamyl transpeptidase (GGT) to platelet ratio (GPR) and neutrophil to lymphocyte ratio (NLR), were independently associated with prognosis. However, it is unclear whether preoperative inflammatory biomarkers have a high efficacy in predicting the overall survival (OS) of unresectable HCC patients following conversion therapy.

Nomograms have recently been used as an easy-to-operate predictive tool in HCC and have compared favorably to traditional tumour staging systems[10,11]. However, studies focusing on inflammatory biomarkers for the prognosis of HCC treated with TACE following HR are rare. Therefore, the aim of this study was to develop a conversion therapy model (CT model) that combined clinical factors, tumour radiologic features, inflammation biomarkers and TACE strategy for prognosis in patients with unresectable HCC successfully treated with conversion therapy. A browser-based calculator was developed to conveniently help guide individualized follow-up. A precise estimation of OS prognosis can assist clinical surgeons in selecting more appropriate therapeutic measures for recurrent patients through risk-benefit analysis.

MATERIALS AND METHODS

Study population and design

This study was conducted in accordance with the Declaration of Helsinki and approved by the Institutional Review Board of Ethical Committee of the Third Affiliated Hospital of Sun Yat-sen University (No. II2023-027). Due to the retrospective design of this study, written informed consent from patients was waived. Consecutive Chinese adult individuals with pathologically confirmed primary unresectable HCC who were treated with TACE following HR in our institution from January 2011 to July 2020 were enrolled. The inclusion criteria were as follows: (1) Age between 18 years and 80 years; (2) pathologically proven HCC; and (3) unresectable HCC according to the Chinese expert consensus and acceptance of TACE as the conventional therapy following HR[3]. The exclusion criteria were as follows: (1) Extrahepatic metastasis; (2) history of other malignancies; (3) previous anticancer therapy; (4) current or recent system infection disease and incomplete clinical data; and (5) death or loss to follow-up within 30 d after resection. One hundred fifty patients from our center were included in this study and randomly assigned to a training cohort (n = 120) and a validation cohort (n = 30). The flow chart of patient selection is shown in Supplementary Figure 1.

Data collection and preoperative examination

For each patient, the following clinical parameters were collected: (1) Preoperative patient characteristics (age, sex, factor of HCC, aetiology of HCC, ascites, and Child-Pugh class); (2) TACE technique [conventional-TACE (cTACE) or drug eluting bead-TACE (DEB-TACE)] and number of TACE treatments; (3) baseline laboratory data, including alpha fetoprotein (AFP) level, white blood cell count, haemoglobin level, platelet count, neutrophil count, lymphocyte ratio, monocyte ratio, neutrophil ratio, aspartate aminotransferase (AST) level, alanine aminotransferase level, GGT level, albumin (ALB) level, total bilirubin level, blood urea nitrogen (BUN) level, serum creatinine level, urea level and prothrombin time (PT); (4) inflammation biomarkers, including GPR, NLR, lymphocyte to monocyte ratio, prognostic nutritional index, platelet to lymphocyte ratio (PLR), systemic immune inflammation index, neutrophil times GGT-to-lymphocyte ratio, AST to platelet ratio index, AST to neutrophil ratio index, and AST (the detailed formulas of inflammation biomarkers are summarized in Supplementary Table 1); (5) baseline tumour radiologic features [tumour number, largest tumour diameter, tumour capsule, macrovascular invasion (MVI)]; and (6) surgical factors (resection margin and blood transfusion).

TACE procedure and HR

The cTACE or DEB-TACE procedure was performed according to our previously reported protocol[12]. Repeated TACE was implemented according to a multidisciplinary treatment board (consisting of

interventional radiologists, liver surgeons, and medical oncologists) during the follow-up periods and after in-depth discussion with the patient. HR was performed according to the liver surgeons' assessment that the unresectable HCC had transformed into radically operable HCC. HR was performed by clinicians who possessed more than ten years of experience in hepatectomy. Under general anesthesia, HR was conducted through an L-shaped laparotomy or bilateral subcostal incision with a midline extension. Intraoperative ultrasound (US) was performed as standard practice to assess tumor burden, liver remnant, and resection margin[13]. Curative resection was defined as complete remove of all tumor nodules with no residual tumor margin (R0 resection), which was confirmed through pathological examination.

Follow-up and assessment

All patients were monitored in the first month post HR, then at three-month intervals for the first two years, and bi-annual assessments thereafter. During each follow-up, routine blood tests, liver function tests, AFP and imaging examinations (abdominal contrast-enhanced magnetic resonance imaging and computed tomography) were performed. Follow-up ended in July 2022. OS was described as the period from the initial TACE treatment to death attributable to any cause, and patients alive at the end of follow-up were recorded as censored.

Statistical analysis

The statistical analyses were conducted using R software (Version 4.2.1, http://www.r-project.org). Categorical variables are presented as *n* (%) and were compared using the chi-square test or Fisher's exact test. Continuous variables are reported as the mean ± SD, compared by Student's *t* test, or median (interquartile range, IQR), compared by the Mann-Whitney *U* test. We determined the optimal cut-off value for continuous variables and inflammation biomarkers, except AFP and tumour diameter, based on the outcome of OS among all patients, using the "surv_cutpoint" function form the "survminer" R package. OS was calculated using the Kaplan-Meier method, and the log-rank test was used to construct survival curves. Univariate and multivariate Cox proportional hazard regression were conducted to select the independent factors of OS. All factors with $P < 0.1$ in univariate Cox regression were selected for multivariate Cox regression. The nomograms were created using multivariate analysis in the training cohort. The final model selection for the nomograms was determined by a backwards step-down process with the Akaike information criterion.

The predictive performance was measured by the concordance index (C-index) and time-dependent area under the curve (AUC). To assess the clinical utility of the nomogram, decision curve analysis (DCA) was performed by quantifying the net benefits relative-e to six other conventional HCC staging systems (including BCLC[14], American Joint Committee on Cancer Tumour-Node-Metastasis eighth edition (AJCC TNM 8th)[15], China liver cancer staging (CNLC)[16], Japan integrated staging (JIS)[17], Cancer of the Liver Italian Program (CLIP)[18] and Okuda staging system[19]). The total score of nomogram was used to categorize patients into low-risk and high-risk groups using X-tile[20]. A 2-sided *P* value of less than 0.05 in multivariate Cox regression was considered statistically significant.

RESULTS

Baseline characteristics

A total of 150 patients were recruited in this study and randomly divided into training (n = 120) and validation (n = 30) cohorts in an 8:2 ratio. The baseline characteristics of patients in the training and validation cohorts are summarized in Table 1. Among all patients, the mean age was 52.1 years (SD: 11.9), 128 (85.3%) patients were male, and 134 (89.3%) patients were HBsAg positive. Regarding TACE techniques, a total of 100 (66.7%) patients received cTACE therapy. In terms of surgical aspects, a resection margin larger than 1 cm was present in 133 patients (88.7%). Fifty-two patients (34.7%) required a blood transfusion during the perioperative period. The median size of the largest intrahepatic tumours was 62.5 mm (range: 10.0-191.0), and 100 (66.7%) were larger than 5.0 cm. More than half of the patients (n = 96, 64.0%) were with solitary tumour. Tumour radiologic features showed that well-defined tumour capsule, satellite nodules, and MVI were observed in 110 (73.3%), 36 (24.0%) and 68 (45.3%) patients, respectively. There were no statistically significant differences in baseline clinicopathological features between the training and validation cohorts.

Overall survival

In this study, the median follow-up was 31.5 (range: 4.0-112.0) months. The median survival of the entire cohort was 54 [95% confidence interval (CI): 42-95] mo (Figure 1A). The 1-, 2-, and 3-year OS rates for the training and validation cohorts were 87.5%, 49.3%, 44.2%, and 83.3%, 66.7%, 53.3%, respectively (Figure 1B and C). There was no significant difference observed in OS between the training and validation cohorts [mean OS 37.9 (range, 4-112) mo *vs* 38.0 (range, 5-93 mo, P = 0.7].

Table 1 Demographics and clinical characteristics of hepatocellular carcinoma patients

Variables	Training cohort (*n* = 120)	Validation cohort (*n* = 30)	Overall cohort (*n* = 150)	*P* value
Patient factors				
Age [yr, mean (SD)]	51.5 (12.1)	54.4 (10.9)	52.1 (11.9)	0.419
Sex, male/female	104/16 (86.7%/13.3%)	24/6 (80.0%/20.0%)	128/22 (85.3%/14.7%)	0.526
Etiology, HBV/other	109/11 (90.8%/9.2%)	25/5 (83.3%/16.7%)	134/16 (89.3%/10.7%)	0.39
Ascites, yes/no	20/100 (16.7%/83.3%)	7/23 (23.3%/76.7%)	27/123 (18.0%/82.0%)	0.559
Child-Pugh, A/B	114/6 (95.0%/5.0%)	29/1 (96.7%/3.3%)	143/7 (95.3%/4.7%)	1
Laboratory parameters				
AFP (ng/mL, ≤ 200/> 200)	68/52 (56.7%/43.3%)	15/15 (50.0%/50.0%)	83/67 (55.3%/44.7%)	0.652
HGB [g/dL, median (min, max)]	139 (72, 838)	139 (100, 162)	139 (72, 838)	0.714
PLT [count, × 10^9 /L, median (min, max)]	197 (70, 950)	189 (97, 370)	192 (70, 950)	0.873
AST [U/L, median (min, max)]	36.0 (2, 471)	33.0 (16, 251)	35.0 (2, 471)	0.925
ALT [U/L, median (min, max)]	34.0 (9, 423)	29.0 (12, 329)	34.0 (9, 423)	0.541
ALB (g/L, ≤ 35/> 35)	18/102 (15.0%/85.0%)	2/28 (6.7%/93.3%)	20/130 (13.3%/86.7%)	0.368
TB [μmol/L, median (min, max)]	12.5 (3.2, 28.2)	12.9 (4.3, 30.9)	12.7 (3.2, 30.9)	0.996
GGT [U/L, median (min, max)]	59.5 (15, 435)	57.0 (22, 375)	59.0 (15, 435)	0.987
BUN (mmol/L, ≤ 6.7/> 6.7(	109/11 (90.8%/9.2%)	26/4 (86.7%/13.3%)	135/15 (90.0%/10.0%)	0.734
Creatinine [μmol/L, median (min, max)]	77.6 (23, 218)	74.0 (43, 110)	77.0 (23, 218)	0.263
UA [μmol/L, median (min, max)]	335 (172, 680)	329 (143, 572)	334 (143, 680)	0.899
PT [s, median (min, max)]	13.6 (11.1, 16.5)	13.6 (12.1, 15.6)	13.6 (11.1, 16.5)	0.212
Tumor factors				
Tumor number (1/2/≥ 3)	80/22/18 (66.7%/18.3%/15.0%)	16/7/7 (53.3%//23.3%/23.3%)	96/29/25 (64.0%/19.3%/16.7%)	
Tumor size (cm, ≤ 5/> 5)	39/81 (32.5%/67.5%)	11/19 (36.7%/63.3%)	50/100 (33.3%/66.7%)	0.829
MVI, yes/no	55/65 (45.8%/54.2%)	13/17 (43.3%/56.7%)	68/82 (45.3%/54.7%)	1
Tumor capsule, ill-defined/well-defined	29/91 (24.2%/75.8%)	11/19 (36.7%/63.3%)	40/110 (26.7%/73.3%)	0.249
Satellite nodules, yes/no	26/94 (21.7%/78.3%)	10/20 (33.3%/66.7%)	36/114 (24.0%/76.0%)	0.272
Surgical factors				

TACE (c-TACE/DEB-TACE)	79/41 (65.8%/34.2%)	21/9 (70.0%/30.0%)	100/50 (66.7%/33.3%)	0.829
Resection Margin (cm, < 1/≥ 1)	13/107 (10.8%/89.2%)	4/26 (13.3%/86.7%)	17/133 (11.3%/88.7%)	0.949
Blood transfusion, yes/no	38/82 (31.7%/68.3%)	14/16 (46.7%/53.3%)	52/98 (34.7%/65.3%)	0.184
Conventional staging system				
AJCC (I/II/III)	42/20/58 (35.0%/16.7%/48.3%)	10/4/16 (33.3%/13.3%/53.3%)	52/24/74 (34.7%/16.0%/49.3%)	0.889
BCLC (A/B/C)	31/35/54 (25.8%/29.2%/45.0%)	10/7/13 (33.3%/23.3%/43.3%)	41/42/67 (27.3%/28.0%/44.7%)	0.678
CNLC (I/II/III)	47/19/54 (39.2%/15.8%/45.0%)	12/5/13 (40.0%/16.7%/43.3%)	59/24/67 (39.3%/16.0%/44.7%)	1
Okuda (I/II/III)	65/54/1 (54.2%/45.0%/0.8%)	15/15/0 (50.0%/50.0%/0%)	80/69/1 (53.3%/46.0%/0.7%)	0.749
JIS (0/1/2/3/4)	1/42/55/21/1 (0.8%/35.0%/45.8%/17.5%/0.8%)	0/10/12/8/0 (0%/33.3%/40.0%/26.7%/0%)	1/52/67/29/1 (0.7%/34.7%/44.7%/19.3%/0.7%)	0.716
CLIP (0/1/2/3/4)	27/28/35/21/9 (22.5%/23.3%/29.2%/17.5%/7.5%)	7/7/9/4/3 (23.3%/23.3%/30.0%/13.3%/10.0%)	34/35/44/25/12 (22.7%/23.3%/29.3%/16.7%/8.0%)	0.962
Inflammation index				
GPR (≤ 0.38/> 0.38)	66/54 (55.0%/45.0%)	18/12 (60.0%/40.0%)	84/66 (56.0%/44.0%)	0.773
LMR (≤ 2.39/> 2.39)	26/94 (21.7%/78.3%)	6/24 (20.0%/80.0%)	32/118 (21.3%/78.7%)	1
NLR (≤ 2.00/> 2.00)	60/60 (50.0%/50.0%)	16/14 (53.3%/46.7%)	76/74 (50.7%/49.3%)	0.903
PLR (≤ 84.38/> 84.38)	35/85 (29.2%/70.8%)	13/17 (43.3%/56.7%)	48/102 (32.0%/68.0%)	0.204
NrLR (≤ 644.61/> 644.61)	106/14 (88.3%/11.7%)	28/2 (93.3%/6.7%)	134/16 (89.3%/10.7%)	0.643
APRI (≤ 0.30/> 0.30)	91/29 (75.8%/24.2%)	20/10 (66.7%/33.3%)	111/39 (74.0%/26.0%)	0.429
ANRI (≤ 4.76/> 4.76)	10/110 (8.3%/91.7%)	4/26 (13.3%/86.7%)	14/136 (9.3%/90.7%)	0.623
ALRI (≤ 41.96/> 41.96)	97/23 (80.8%/19.2%)	24/6 (80.0%/20.0%)	121/29 (80.7%/19.3%)	1
PNI (≤ 52.62/> 52.62)	93/27 (77.5%/22.5%)	22/8 (73.3%/26.7%)	115/35 (76.7%/23.3%)	0.809
SII (≤ 336.22/> 336.22)	48/72 (40.0%/60.0%)	13/17 (43.3%/56.7%)	61/89 (40.7%/59.3%)	0.901

AFP: An alpha fetoprotein; HGB: Hemoglobin; PLT: Platelet; AST: Aspartate aminotransferase; ALT: Alanine aminotransferase; GGT: Gamma-glutamyl transpeptidase; ALB: Albumin; TBIL: Total bilirubin; BUN: Blood urea nitrogen; UA: Uric acid; PT: Prothrombin time; MVI: Microvascular invasion; TACE: Transarterial chemoembolization; cTACE: Conventional TACE; DEB-TACE: Drug-eluting beads TACE; GPR: Gamma-glutamyl transpeptidase to platelet ratio; LMR: Lymphocyte to monocyte ratio; NLR: Neutrophil to lymphocyte ratio; PLR: Platelet to lymphocyte ratio; NrLR: Neutrophil times GGT-to-lymphocyte ratio; APRI: Aspartate aminotransferase to platelet ratio index; ANRI: AST to neutrophil ratio index; ALRI: AST to lymphocyte ratio index; PNI: Prognostic nutritional index; SII: Systemic immune-inflammation index.

Independent risk factors and development of the prognostic nomogram

Univariate and multivariate Cox regression analyses were performed in 120 patients from the training cohort to determine the risk factors associated with OS (Supplementary Table 2). As previously described, the optimal cutoff values for inflammation biomarkers were recorded (Supplementary Table 3). Briefly, multivariate analysis identified that preoperative ALB level, BUN level, GPR, PLR, MVI and tumour number were independent risk factors associated with OS (Figure 2). All of these significant independent factors of OS were incorporated into the nomogram (Figure 3A). In addition, a mobile online tool was built to facilitate clinical application, available at https://ctmodelforunresectablehcc.shinyapps.io/DynNomapp/ (Figure 3B).

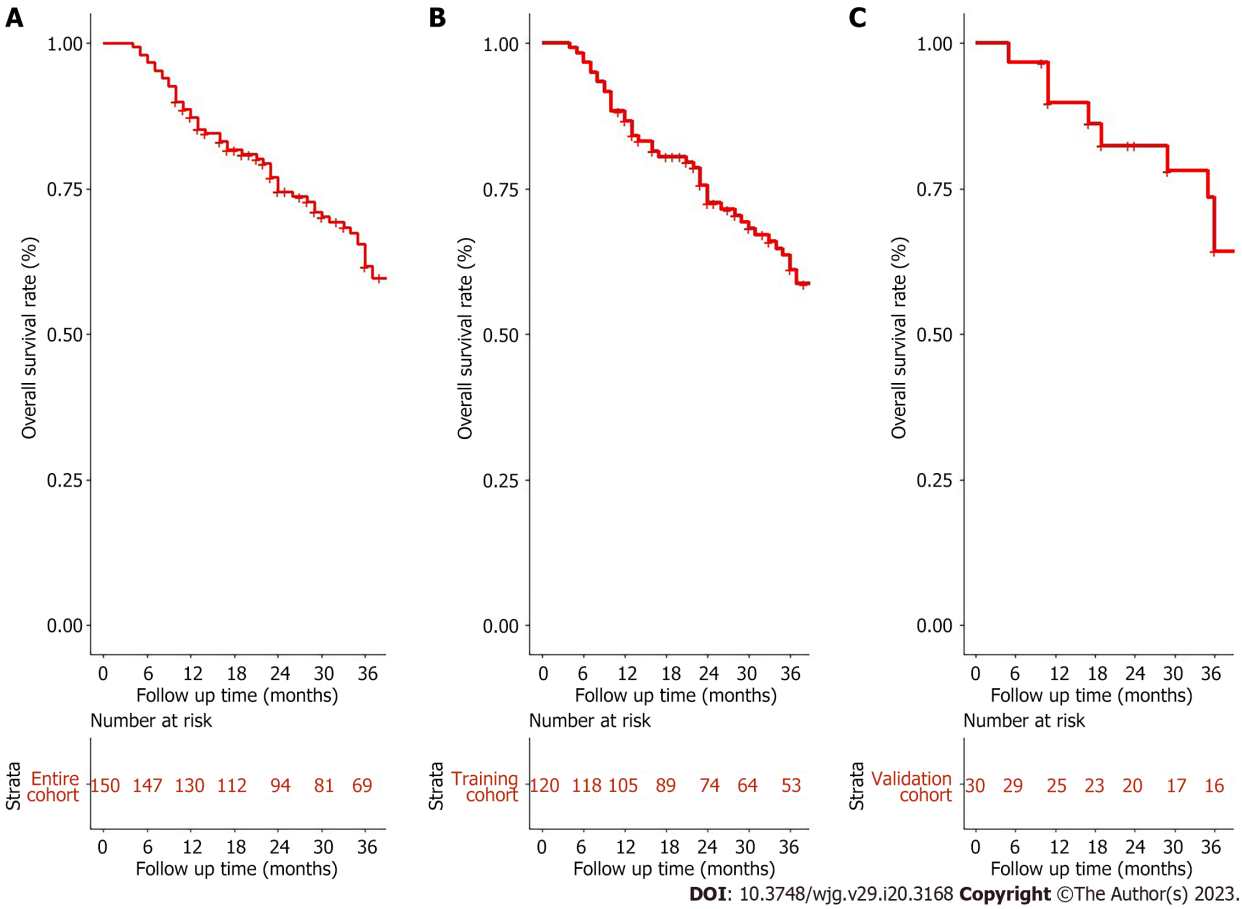


Figure 1 Overall survival for unresectable hepatocellular carcinoma patients accepted conversion therapy. A: Entire cohort; B: Training cohort; C: Validation cohort.

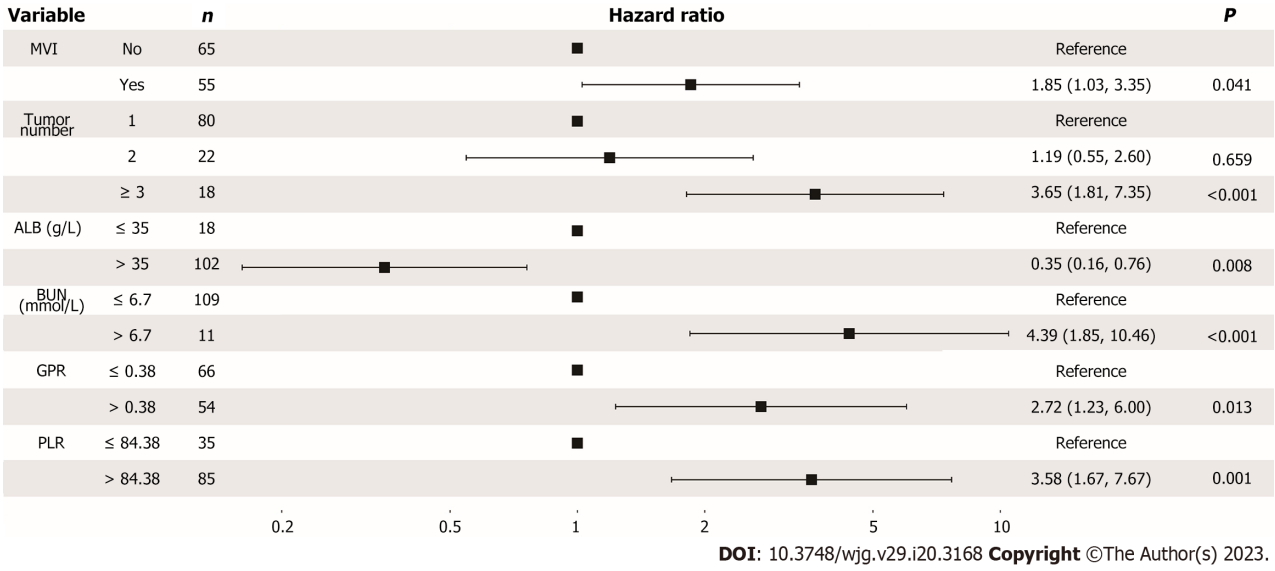
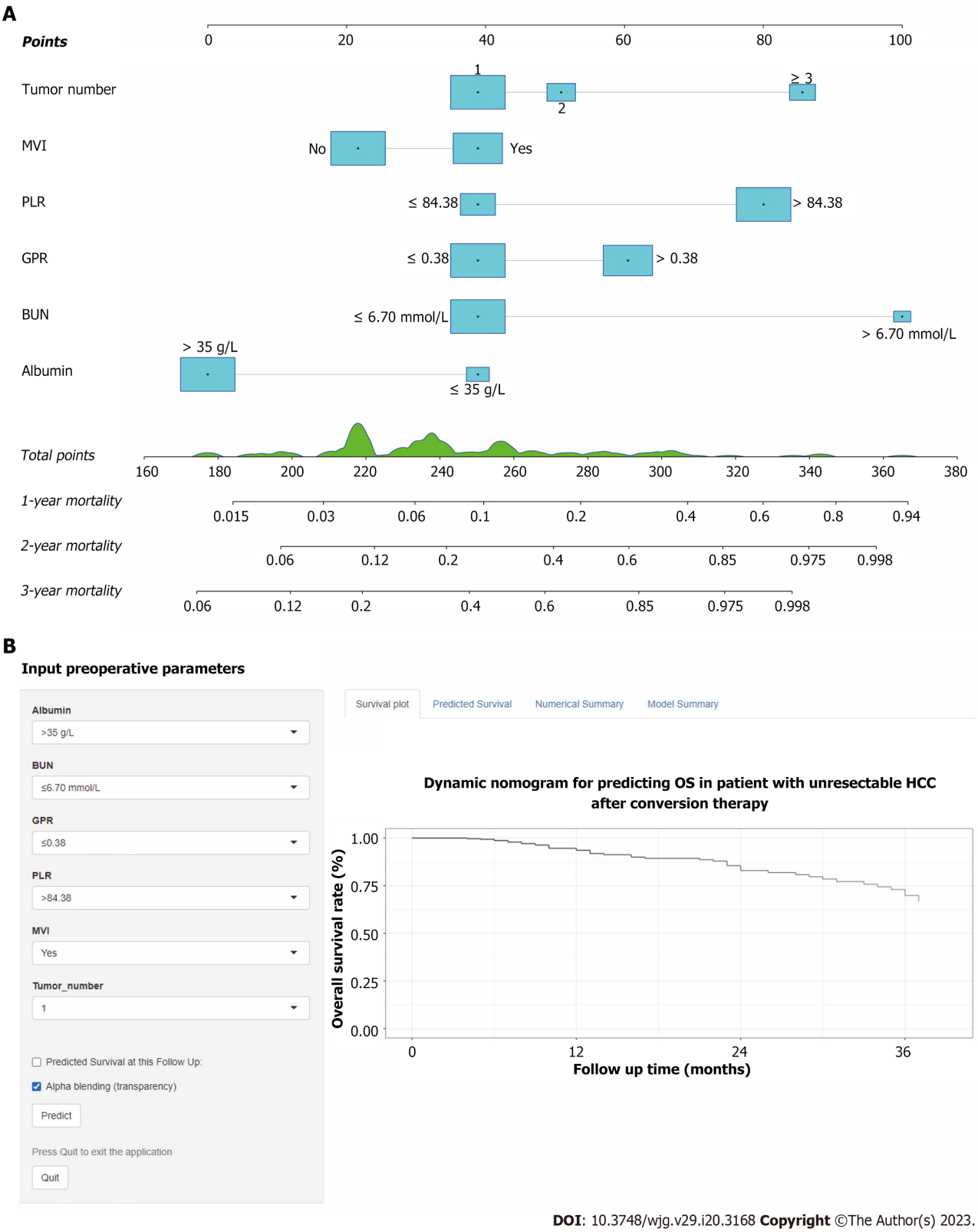


Figure 2 Forest plot for multivariance cox analysis of overall survival in the training cohort. CI: Confident interval; MVI: Macrovascular invasion; ALB: Albumin; BUN: Blood urea nitrogen; GPR: Gamma-glutamyl transpeptidase to platelet ratio; PLR: Platelet to lymphocyte ratio.

Validation of the prediction CT model

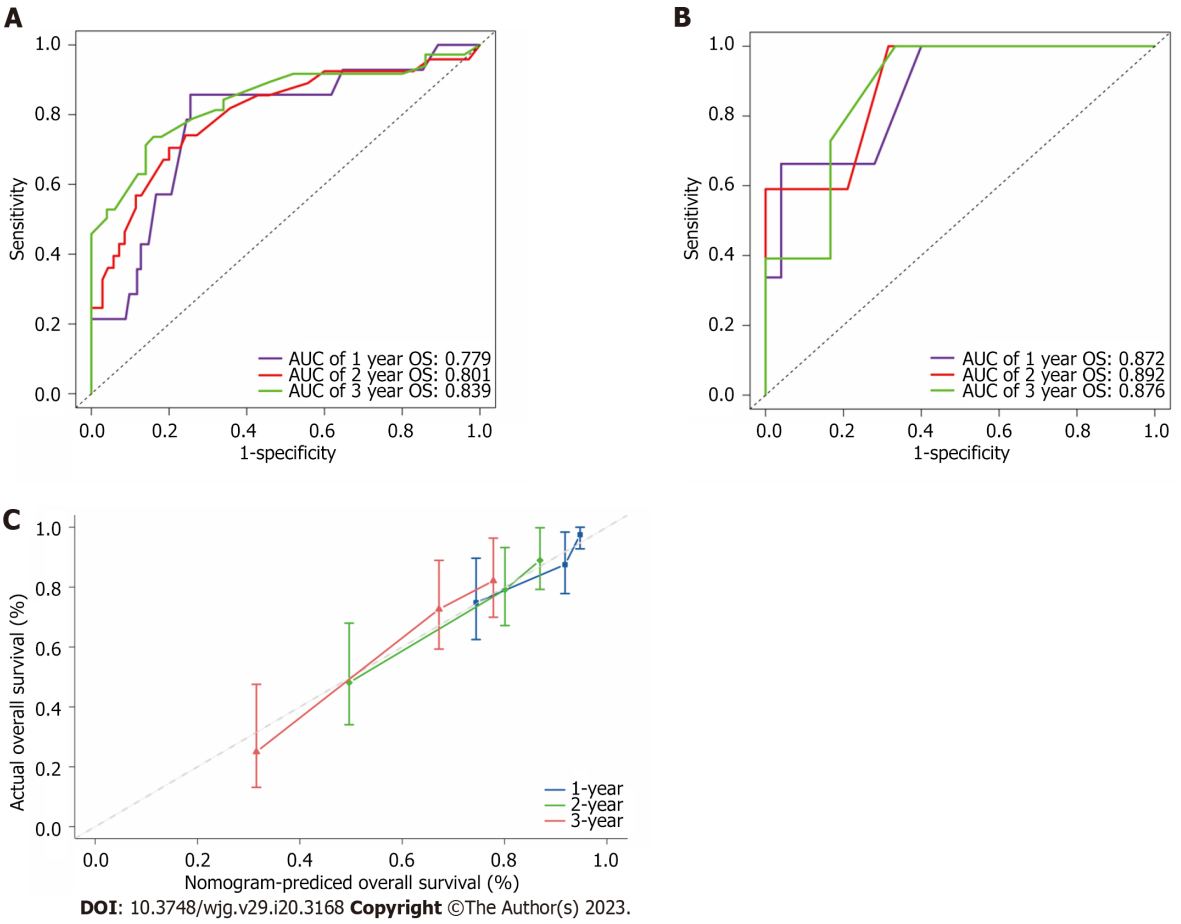
Bootstrapping with 1000 resamples in the primary training cohort revealed good predictive performance for OS, resulting in a C-index of 0.752 (95%CI: 0.688-0.815). The AUC in predicting the 1-, 2-, and 3-year OS rates were 0.779 (95%CI: 0.0.646-0.912), 0.801 (95%CI: 0.693-0.908) and 0.839 (95%CI: 0.748-0.931) in the training cohort and 0.872 (95%CI: 0.682-0.951), 0.892 (95%CI: 0.753-0.974) and 0.876



DOI: 10.3748/wjg.v29.i20.3168 **Copyright** ©The Author(s) 2023.

Figure 3 Conversion therapy model for unresectable hepatocellular carcinoma patients accepted conversion therapy. A: A constructed nomogram for predicting 1-, 2-, 3-year overall survival; B: Screenshot of the online individualized prediction tool based on the overall survival nomogram model. OS: Overall survival; MVI: Macrovascular invasion; BUN: Blood urea nitrogen; GPR: Gamma-glutamyl transpeptidase to platelet ratio; PLR: Platelet to lymphocyte ratio.

(95%CI: 0.727-0.962) in the validation cohort, respectively (Figure 4A and B). Accordingly, the C-index in the validation cohort reached 0.807 (95%CI: 0.705-0.908), while the calibration plot for the probability of OS at 1, 2, and 3 years depicted a favorable concordance between the predicted and actual outcomes (Figure 4C).



DOI: 10.3748/wjg.v29.i20.3168 **Copyright** ©The Author(s) 2023.

Figure 4 The receiver operating characteristic curves, calibration curve and decision curve analysis curves of the model. A and B: Receiver operating characteristic for overall survival in the training (A) and validation cohort (B), respectively; C: Calibration curve plots of nomogram for predicting 1-year, 2-year and 3-year probability of survival in the training cohort. OS: Overall survival; AUC: Area under the curve.

Comparison of model predictive performance

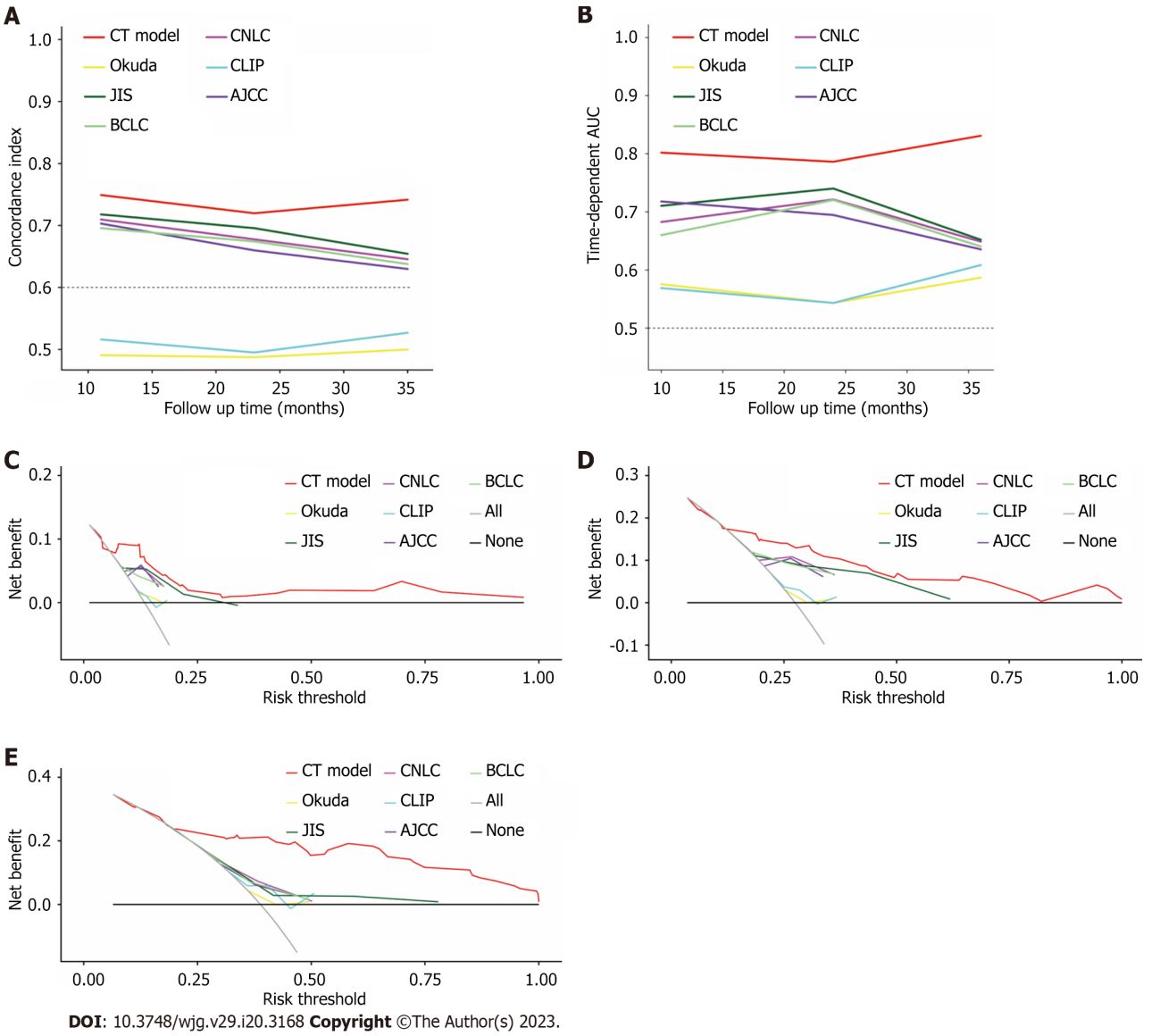
The discrimination power of the nomogram and common staging systems were compared by the C-index and time-dependent AUC (1, 2, and 3 years). In both the training and validation cohorts, the predictive performance of the CT model was superior to that of the other six conventional HCC staging systems ($P < 0.01$, Figure 5A and B, Supplementary Table 4). DCA indicated a good net benefit compared with six other conventional HCC staging systems at 1, 2 and 3 years after conversion therapy in the training cohort (Figure 5C-E).

Risk stratification based on nomogram scores and prognostic assessment

The patients were categorized into two groups based on their overall predictive risk score: Low risk (score < 196) and high risk (score ≥ 196). The distribution of clinical features and corresponding risk scores in each patient are presented in Figure 6A. The OS curves exhibited significant discrimination between the low-risk and high-risk groups among the entire ($P < 0.001$), training ($P < 0.001$) and validation ($P = 0.041$) cohorts (Figure 6B-D). Additionally, given that inflammation biomarkers are associated with postoperative prognosis, we found that high values of both GPR and PLR were significantly correlated with worse prognostic outcomes in patients after conversion therapy. The low-GPR group exhibited higher 1-, 2-, and 3-year OS rates compared to the high-GPR group (0.93, 0.69, and 0.54 *vs* 0.79, 0.55, and 0.36, $P = 0.038$). Similarly, the low-PLR group demonstrated greater 1-, 2-, and 3-year OS rates in contrast to the high-PLR group (0.92, 0.73, and 0.58 *vs* 0.84, 0.58, and 0.40, $P = 0.01$) (Figure 7A and B). Besides, individuals who exhibited MVI demonstrated an inferior prognosis in contrast to those without vascular invasion (Figure 7C).

DISCUSSION

Conversion therapy is a new therapeutic strategy for individuals diagnosed with HCC at an advanced stage and who may not initially be suitable for radical surgery. Several studies have shown that patients with unresectable HCC who underwent conversion following surgical excision have a much longer OS



DOI: 10.3748/wjg.v29.i20.3168 **Copyright** ©The Author(s) 2023.

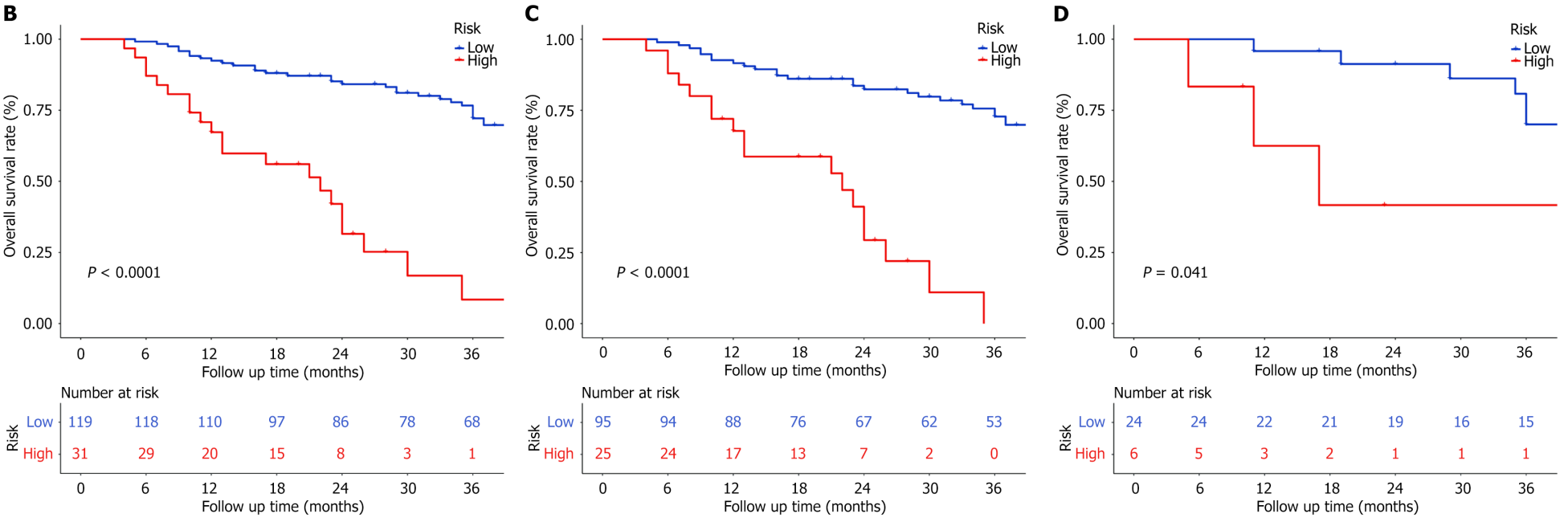
Figure 5 Comparison of model predictive performance in predicting overall survival. A: Comparison of concordance index between conversion therapy (CT) model and traditional staging systems in the training cohort; B: Comparison of time-dependent areas under receiver operating characteristic curve between CT model and other staging systems in the training cohort; the decision curve analysis curve compared the clinical practicability of the CT model and other six conventional hepatocellular carcinoma staging systems; C-E: 1-year (C), 2-year (D) and 3-year (E) survival benefit in the training cohort. AUC: Areas under receiver operating characteristic curve; CT: Conversion therapy; CNLC: China liver cancer staging; CLIP: Cancer of the Liver Italian Program; JIS: Japan integrated staging; BCLC: Barcelona Clinic Liver Cancer; AJCC: American Joint Committee on Cancer.

than those who received palliative treatments such as TACE[3,6,21]. Furthermore, 5-year survival rates for patients with unresectable HCC after conversion therapy (25%-57%) are comparable to those for patients with resectable HCC (30%-60%)[22]. Previous studies have developed prognostic models using preoperative factors to predict postoperative outcomes of early-stage HCC patients after curative resection that achieved good results[9-11], but it remains unclear in the CT model. In this study, we developed and validated a CT model that could accurately predicts prognosis for patients with unresectable HCC treated with TACE following HR.

The nomogram demonstrated great accuracy in predicting conversion therapy outcomes of patients with unresectable HCC. The nomogram developed in our study achieved AUC of 0.779, 0.801, and 0.839 in the training cohort and 0.872, 0.892 and 0.876 in the validation cohort, which were superior to those of the other six conventional HCC staging systems. DCA was also performed and revealed that the nomograms have good clinical utility in patients with unresectable HCC who received the CT model.

Using the nomogram score, clinicians can classify unresectable HCC patients into low- and high-risk groups. Effective postoperative therapeutic management and intensive clinical follow-up can be guided for high-risk individuals following this strategy. Additionally, a web-based dynamic nomogram provides a well-calibrated tool for predicting future clinical outcomes.


A
Low risk
Cut-off = 196
High risk
Risk
OS (months)
0
30
60
90
Risk score
MVI
ALB
Tumor number
BUN
GPR
PLR
Child-Pugh
BCLC
CNLC
AJCC
Okuda
CLIP
JIS
c
b
a
c
c
a
c
c
c
c
c
c
Status
Dead
Alive
Risk score
High
Low
MVI
No
Yes
ALB
≤ 35 g/L
> 35 g/L
Tumor number
1
2
≥ 3
BUN
≤ 6.7 mmol/L
> 6.7 mmol/L
GPR
≤ 0.38
> 0.38
PLR
≤ 84.38
> 84.38
Child-pugh
A
B
BCLC
A stage
B stage
C stage
CNLC
I stage
II stage
III stage
AJCC
A stage
B stage
C stage
Okuda
I
II
III
CLIP
0
1
2
3
4
JIS
0 stage
1 stage
2 stage
3 stage
4 stage

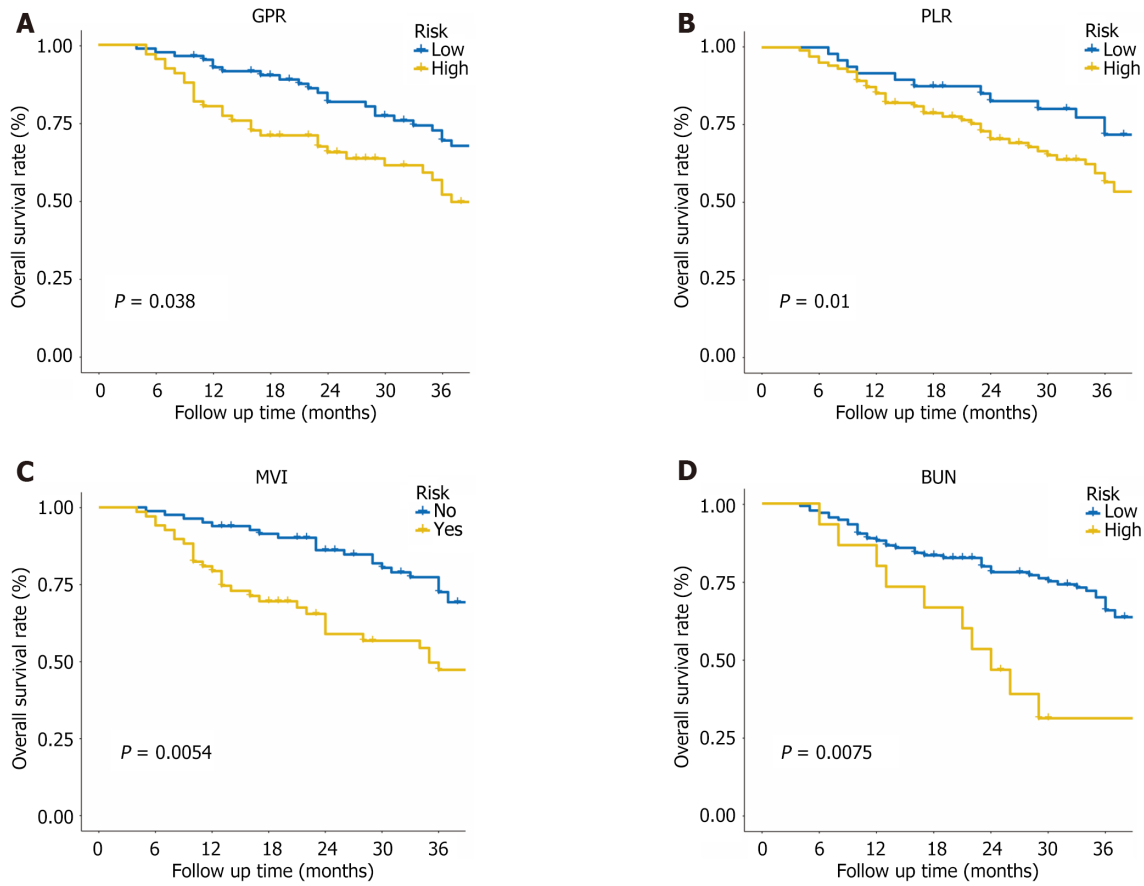


DOI: 10.3748/wjg.v29.i20.3168 **Copyright** ©The Author(s) 2023.

Figure 6 A Heatmap presents the distribution of corresponding risk score and clinical feature in each patient within high and low risk groups. A: It shows that the patients in low-risk group have more favourable prognosis; B-D: Kaplan-Meier survival curves for patients with low and high risk stratified by the total nomogram score in the entire cohort (B), training cohort (C), and validation cohort (D). $^{a}P < 0.05$, $^{b}P < 0.01$, $^{c}P < 0.001$ was considered significant. ALB: Albumin; MVI: Macrovascular invasion; BUN: Blood urea nitrogen; GPR: Gamma-glutamyl transpeptidase to platelet ratio; PLR: Platelet to lymphocyte ratio; CNLC: China liver cancer staging; CLIP: Cancer of the Liver Italian Program; JIS: Japan integrated staging; BCLC: Barcelona Clinic Liver Cancer; AJCC: American Joint Committee on Cancer.

The present study combined liver and renal function factors, tumour burden and inflammation biomarkers (six significantly independent predictors: ALB, BUN, MVI, tumour number, GPR, and PLR) to establish a more comprehensive model and construct a nomogram CT model that could accurately predict the prognosis for patients with unresectable HCC after conversion therapy. Our findings are consistent with research in previous HCC populations that lower ALB level, MVI presence and multiple tumours were risk factors for long-term survival in patients with unresectable HCC with the CT model [10,23-26].

In terms of clinical utility, the prediction ability of the CT model was significantly improved compared with that of six conventional staging systems (AJCC TNM 8th, CNLC, JIS, CLIP, Okuda, and BCLC staging systems) in both the training and validation cohorts (Figure 5). The conventional staging systems mainly contain factors that may only take certain aspects of the tumour into consideration. Previous studies have noted that inflammatory biomarker combination scores have promising prognostic values in predicting patient survival for different HCC stages in various therapeutic



DOI: 10.3748/wjg.v29.i20.3168 **Copyright** ©The Author(s) 2023.

Figure 7 Kaplan-Meier survival curves for patients with different level of gamma-glutamyl transpeptidase to platelet ratio, platelet to lymphocyte ratio, macrovascular invasion, and blood urea nitrogen in the entire cohort. A: Gamma-glutamyl transpeptidase to platelet ratio; B: Platelet to lymphocyte ratio; C: Macrovascular invasion; D: Blood urea nitrogen.

modalities[27,28], indicating that combining these potential indicators would greatly improve the model's predictive abilities. Meanwhile, the AUC for the prediction of the 1-, 2-, and 3-year OS rates reached 0.755, 0.750, and 0.838 in the training cohort when we only used clinical information (MVI, ALB, tumour number and BUN) to develop a model, and they were unable to perform robustly in the validation cohort (Supplementary Figure 2). Hence, we constructed a nomogram CT model with clinical information (ALB, BUN, MVI, tumour number) and inflammation biomarkers (PLR and GPR).

PLR and GPR have been reported to be risk indicators of prognosis for OS in previous studies[10,29]. Meanwhile, high GPR was also proven to be an independent risk factor for HCC development and recurrence[30-32]. Our findings indicate that the high-PLR (> 84.38) and high-GPR (> 0.38) groups had significantly lower 12-, 24-, and 36-mo survival rates. Since inflammatory factors in the tumor microenvironment are crucial for HCC therapies, this information can assist clinicians in devising follow-up regimens and postoperative therapies for HCC patients at high or low risk of tumor recurrence after hepatectomy.

We also found that BUN was an independent prognostic factor in this study. Renal function impairment represents a clinically significant event in cirrhosis patients[33]. Preoperative renal dysfunction with high levels of BUN may lead to the development of major complications such as intractable ascites and spontaneous bacterial peritonitis (SBP). Moreover, the development of hepatorenal impairment is strongly associated with circulatory dysfunction, which can lead to various complications such as complicated or refractory ascites, SBP, hyponatremia and hepatorenal syndrome, and a high risk of mortality[34]. In clinical practice, serum creatinine concentration is generally used to assess kidney function in patients with liver diseases, which is also a major prognostic factor of cirrhosis included in the Model for End-Stage Liver Disease. However, several reports have shown that BUN levels have greater prognostic accuracy than serum creatinine concentrations[35-37]. In this study, our findings also showed that high BUN levels were related to worse liver function stage and poor OS outcomes (Figure 7D). Further research is needed to better understand this factor in advanced HCC and better classify and manage patients after conversion therapy.

While this nomogram CT model performed well, we do acknowledge a few potential limitations to this study. First, the nomogram was formulated based on a relatively small sample size obtained from

our single institution, which unavoidably led to selection bias. Further prospective and multicenter cohorts are required to evaluate its performance. Second, statistical power may be limited because several routine clinical variables were not included in our study. Because our study was retrospective, there were variations in performance score, body mass index, dosage and type of injected drugs during TACE, as well as postoperative treatments, among patients. To further bolster our findings, it is necessary to conduct larger and multicenter prospective cohorts. Hence, we will undertake additional research that incorporates more complete clinicopathological information, treatment details, and postoperative treatment modalities to improve the predictive performance of our model. Third, this study was mainly based on HBV-infected patients. Our results may not be applicable in different geographic regions and aetiologies. Fourth, systematic bioinformatic analyses were not included in this nomogram, which showed excellent predictive ability for early-stage HCC patients[38,39]. We will therefore develop a robust prognostic model that integrates both clinical parameters and multi-omics biomarkers to facilitate an understanding of HCC from a biological perspective and contribute to tailoring therapeutic strategies. Despite these limitations, we believe that our work is meaningful for individualized management in HCC patients following conversion therapy.

CONCLUSION

We developed and validated a prognostic nomogram combined with inflammation biomarkers for patients with unresectable HCC after conversion therapy. The proposed CT model shows increased accuracy, good clinical utility, and better prognostic performance than conventional staging systems. Furthermore, we have uploaded this prognostic nomogram online for free use (https://ctmodelforunresectablehcc.shinyapps.io/DynNomapp/).

ARTICLE HIGHLIGHTS

Research perspectives

Larger and multicentre prospective cohorts were required to further strengthen our results. We will conduct further investigation that incorporates more complete clinicopathological information, treatment details, and postoperative treatment modalities to improve the predictive performance of our model.

Research conclusions

The nomogram achieved optimal individualized prognostication of OS in HCC patients who received conversion therapy. It could be a useful clinical tool to help guide postoperative personalized interventions and prognosis judgement.

Research results

Multivariate Cox analysis identified that albumin, blood urea nitrogen, gamma-glutamyl transpeptidase to platelet ratio, platelet to lymphocyte ratio, macrovascular invasion and tumour number were the six independent prognostic factors correlated with OS in nomogram model. The C-indices in the training cohort and validation cohort were 0.752 and 0.807 for predicting OS, which were higher than those of the six conventional HCC staging systems (0.563 to 0.715 for the training cohort and 0.458 to 0.571 for the validation cohort). We have deployed the model into online calculators that are freely available at https://ctmodelforunresectablehcc.shinyapps.io/DynNomapp/.

Research methods

All patients met the inclusion criteria were enrolled and divided into training and a validation cohort. Using the independent risk factors in the training cohort, nomogram models were constructed to predict OS for patients treated with transarterial chemoembolization following HR. The nomograms were internally validated with the bootstrapping method. The predictive performance of the nomograms was assessed by Harrell's concordance index, calibration plot and time-dependent receiver operating characteristic curves and compared with six other conventional HCC staging systems.

Research objectives

To develop a nomogram to help guide postoperative personalized interventions and prognosis judgement.

Research motivation

To investigate the prognostic factors of overall survival (OS) in patients with unresectable HCC who received conversion therapy.

Research background

Hepatocellular carcinoma (HCC) is the sixth most common malignancy and the third leading cause of cancer-related mortality worldwide. Hepatic resection (HR) is the best therapeutic option for patients with early- and some intermediate-stage HCC. Unfortunately, the majority of Chinese patients with HCC are diagnosed at intermediate or advanced stages with massive or multifocal lesions. HR is possible for a minority of carefully selected patients with the help of a "conversion therapy" strategy, which refers to conversion of an unresectable HCC to achieve adequate tumour shrinkage and downstaging to undergo HR.

FOOTNOTES

Author contributions: Jiang ZB, Chen JW, and Huang MS contributed to conceptualization; Wu JL, Huang SB, Chen GR, Ran HY, and Liang QY contributed to acquisition of data, formal analysis (statistics), and visualization; Wu JL and Luo JY contributed to writing-original draft; Chen JW contributed to writing-review and editing; Huang MS, Jiang ZB, Lai LS, and Chen JW contributed to supervision; and all authors read and approved the final version of the manuscript.

Supported by the National Natural Science Foundation of China, No. 82072035; and Science and Guangzhou Planned Project of Science and Technology, No. 202102010028.

Institutional review board statement: This study was reviewed and approved by the Institutional Review Board of Ethical Committee of the Third Affiliated Hospital of Sun Yat-sen University (approval No. II2023-027-11).

Informed consent statement: Written informed consent of the patients was waived because of the retrospective nature of this study.

Conflict-of-interest statement: The authors declare that they have no known competing financial interests or personal relationships that could have appeared to influence the work reported in this paper.

Data sharing statement: The datasets used and/or analysed during the current study are available from the corresponding author on reasonable request.

STROBE statement: The authors have read the STROBE Statement—checklist of items, and the manuscript was prepared and revised according to the STROBE Statement—checklist of items.

Open-Access: This article is an open-access article that was selected by an in-house editor and fully peer-reviewed by external reviewers. It is distributed in accordance with the Creative Commons Attribution NonCommercial (CC BY-NC 4.0) license, which permits others to distribute, remix, adapt, build upon this work non-commercially, and license their derivative works on different terms, provided the original work is properly cited and the use is non-commercial. See: https://creativecommons.org/Licenses/by-nc/4.0/

Country/Territory of origin: China

ORCID number: Jia-Lin Wu 0000-0002-8877-8348; Jun-Yang Luo 0000-0002-2665-1608; Zai-Bo Jiang 0000-0003-0523-6488; Si-Bo Huang 0000-0002-2366-6599; Ge-Run Chen 0000-0002-0871-6623; Hui-Ying Ran 0000-0003-4022-9937; Qi-Yue Liang 0000-0001-9926-2622; Ming-Sheng Huang 0000-0003-4749-4231; Jun-Wei Chen 0000-0002-4227-0944.

S-Editor: Chen YL
L-Editor: A
P-Editor: Chen YX

REFERENCES

1 **Villanueva A**. Hepatocellular Carcinoma. *N Engl J Med* 2019; **380**: 1450-1462 [PMID: 30970190 DOI: 10.1056/NEJMra1713263]
2 **Lavanchy D**. Hepatitis B virus epidemiology, disease burden, treatment, and current and emerging prevention and control measures. *J Viral Hepat* 2004; **11**: 97-107 [PMID: 14996343 DOI: 10.1046/j.1365-2893.2003.00487.x]
3 **Sun HC**, Zhou J, Wang Z, Liu X, Xie Q, Jia W, Zhao M, Bi X, Li G, Bai X, Ji Y, Xu L, Zhu XD, Bai D, Chen Y, Dai C, Guo R, Guo W, Hao C, Huang T, Huang Z, Li D, Li T, Li X, Liang X, Liu J, Liu F, Lu S, Lu Z, Lv W, Mao Y, Shao G, Shi Y, Song T, Tan G, Tang Y, Tao K, Wan C, Wang G, Wang L, Wang S, Wen T, Xing B, Xiang B, Yan S, Yang D, Yin G, Yin T, Yin Z, Yu Z, Zhang B, Zhang J, Zhang S, Zhang T, Zhang Y, Zhang A, Zhao H, Zhou L, Zhang W, Zhu Z, Qin S, Shen F, Cai X, Teng G, Cai J, Chen M, Li Q, Liu L, Wang W, Liang T, Dong J, Chen X, Wang X, Zheng S, Fan J; Alliance of Liver Cancer Conversion Therapy, Committee of Liver Cancer of the Chinese Anti-Cancer Association. Chinese expert consensus on conversion therapy for hepatocellular carcinoma (2021 edition). *Hepatobiliary Surg Nutr*

2022; **11**: 227-252 [PMID: 35464283 DOI: 10.21037/hbsn-21-328]
4 **Hamaoka M**, Kobayashi T, Kuroda S, Iwako H, Okimoto S, Kimura T, Aikata H, Nagata Y, Chayama K, Ohdan H. Hepatectomy after down-staging of hepatocellular carcinoma with portal vein tumor thrombus using chemoradiotherapy: A retrospective cohort study. *Int J Surg* 2017; **44**: 223-228 [PMID: 28676383 DOI: 10.1016/j.ijsu.2017.06.082]
5 **Zhao HT**, Cai JQ. Chinese expert consensus on neoadjuvant and conversion therapies for hepatocellular carcinoma. *World J Gastroenterol* 2021; **27**: 8069-8080 [PMID: 35068855 DOI: 10.3748/wjg.v27.i47.8069]
6 **Fan J**, Tang ZY, Yu YQ, Wu ZQ, Ma ZC, Zhou XD, Zhou J, Qiu SJ, Lu JZ. Improved survival with resection after transcatheter arterial chemoembolization (TACE) for unresectable hepatocellular carcinoma. *Dig Surg* 1998; **15**: 674-678 [PMID: 9845635 DOI: 10.1159/000018676]
7 **Lau WY**, Lai EC. Salvage surgery following downstaging of unresectable hepatocellular carcinoma--a strategy to increase resectability. *Ann Surg Oncol* 2007; **14**: 3301-3309 [PMID: 17891443 DOI: 10.1245/s10434-007-9549-7]
8 **Mantovani A**, Allavena P, Sica A, Balkwill F. Cancer-related inflammation. *Nature* 2008; **454**: 436-444 [PMID: 18650914 DOI: 10.1038/nature07205]
9 **Wang Y**, Sun K, Shen J, Li B, Kuang M, Cao Q, Peng S. Novel Prognostic Nomograms Based on Inflammation-Related Markers for Patients with Hepatocellular Carcinoma Underwent Hepatectomy. *Cancer Res Treat* 2019; **51**: 1464-1478 [PMID: 30913869 DOI: 10.4143/crt.2018.657]
10 **Zeng J**, Zeng J, Liu J. Development of pre and post-operative nomograms to predict individual survival for ideal liver resection candidates with hepatocellular carcinoma. *Liver Int* 2021; **41**: 2974-2985 [PMID: 34416088 DOI: 10.1111/liv.15042]
11 **Wang JC**, Hou JY, Chen JC, Xiang CL, Mao XH, Yang B, Li Q, Liu QB, Chen J, Ye ZW, Peng W, Sun XQ, Chen MS, Zhou QF, Zhang YJ. Development and validation of prognostic nomograms for single large and huge hepatocellular carcinoma after curative resection. *Eur J Cancer* 2021; **155**: 85-96 [PMID: 34371445 DOI: 10.1016/j.ejca.2021.07.009]
12 **Chen J**, Lai L, Luo J, Wang H, Li M, Huang M. DEM-TACE as the initial treatment could improve the clinical efficacy of the hepatocellular carcinoma with portal vein tumor thrombus: a retrospective controlled study. *BMC Cancer* 2022; **22**: 1242 [PMID: 36451104 DOI: 10.1186/s12885-022-10361-5]
13 **Chen J**, Lai L, Lin Q, Huang W, Cai M, Zhu K, Huang M. Hepatic resection after transarterial chemoembolization increases overall survival in large/multifocal hepatocellular carcinoma: a retrospective cohort study. *Oncotarget* 2017; **8**: 408-417 [PMID: 27880724 DOI: 10.18632/oncotarget.13427]
14 **Llovet JM**, Brú C, Bruix J. Prognosis of hepatocellular carcinoma: the BCLC staging classification. *Semin Liver Dis* 1999; **19**: 329-338 [PMID: 10518312 DOI: 10.1055/s-2007-1007122]
15 **Amin MB**, Greene FL, Edge SB, Compton CC, Gershenwald JE, Brookland RK, Meyer L, Gress DM, Byrd DR, Winchester DP. The Eighth Edition AJCC Cancer Staging Manual: Continuing to build a bridge from a population-based to a more "personalized" approach to cancer staging. *CA Cancer J Clin* 2017; **67**: 93-99 [PMID: 28094848 DOI: 10.3322/caac.21388]
16 **Zhou J**, Sun H, Wang Z, Cong W, Wang J, Zeng M, Zhou W, Bie P, Liu L, Wen T, Han G, Wang M, Liu R, Lu L, Ren Z, Chen M, Zeng Z, Liang P, Liang C, Yan F, Wang W, Ji Y, Yun J, Cai D, Chen Y, Cheng W, Cheng S, Dai C, Guo W, Hua B, Huang X, Jia W, Li Y, Liang J, Liu T, Lv G, Mao Y, Peng T, Ren W, Shi H, Shi G, Tao K, Wang X, Xiang B, Xing B, Xu J, Yang J, Yang Y, Ye S, Yin Z, Zhang B, Zhang L, Zhang S, Zhang T, Zhao Y, Zheng H, Zhu J, Zhu K, Shi Y, Xiao Y, Dai Z, Teng G, Cai J, Cai X, Li Q, Shen F, Qin S, Dong J, Fan J. Guidelines for the Diagnosis and Treatment of Hepatocellular Carcinoma (2019 Edition). *Liver Cancer* 2020; **9**: 682-720 [PMID: 33442540 DOI: 10.1159/000509424]
17 **Kudo M**, Chung H, Osaki Y. Prognostic staging system for hepatocellular carcinoma (CLIP score): its value and limitations, and a proposal for a new staging system, the Japan Integrated Staging Score (JIS score). *J Gastroenterol* 2003; **38**: 207-215 [PMID: 12673442 DOI: 10.1007/s005350300038]
18 A new prognostic system for hepatocellular carcinoma: a retrospective study of 435 patients: the Cancer of the Liver Italian Program (CLIP) investigators. *Hepatology* 1998; **28**: 751-755 [PMID: 9731568 DOI: 10.1002/hep.510280322]
19 **Okuda K**, Ohtsuki T, Obata H, Tomimatsu M, Okazaki N, Hasegawa H, Nakajima Y, Ohnishi K. Natural history of hepatocellular carcinoma and prognosis in relation to treatment. Study of 850 patients. *Cancer* 1985; **56**: 918-928 [PMID: 2990661 DOI: 10.1002/1097-0142(19850815)56:4<918::AID-CNCR2820560437>3.0.CO;2-E]
20 **Camp RL**, Dolled-Filhart M, Rimm DL. X-tile: a new bio-informatics tool for biomarker assessment and outcome-based cut-point optimization. *Clin Cancer Res* 2004; **10**: 7252-7259 [PMID: 15534099 DOI: 10.1158/1078-0432.CCR-04-0713]
21 **Lewandowski RJ**, Kulik LM, Riaz A, Senthilnathan S, Mulcahy MF, Ryu RK, Ibrahim SM, Sato KT, Baker T, Miller FH, Omary R, Abecassis M, Salem R. A comparative analysis of transarterial downstaging for hepatocellular carcinoma: chemoembolization *vs* radioembolization. *Am J Transplant* 2009; **9**: 1920-1928 [PMID: 19552767 DOI: 10.1111/j.1600-6143.2009.02695.x]
22 **Zhang T**, Merle P, Wang H, Zhao H, Kudo M. Combination therapy for advanced hepatocellular carcinoma: do we see the light at the end of the tunnel? *Hepatobiliary Surg Nutr* 2021; **10**: 180-192 [PMID: 33898559 DOI: 10.21037/hbsn-2021-7]
23 **Wang YY**, Xiang BD, Ma L, Zhong JH, Ye JZ, Wang K, Xing BC, Li LQ. Development and Validation of a Nomogram to Preoperatively Estimate Post-hepatectomy Liver Dysfunction Risk and Long-term Survival in Patients With Hepatocellular Carcinoma. *Ann Surg* 2021; **274**: e1209-e1217 [PMID: 32097166 DOI: 10.1097/SLA.0000000000003803]
24 **Zhang B**, Zhang B, Zhang Z, Huang Z, Chen Y, Chen M, Bie P, Peng B, Wu L, Wang Z, Li B, Fan J, Qin L, Chen P, Liu J, Tang Z, Niu J, Yin X, Li D, He S, Jiang B, Mao Y, Zhou W, Chen X. 42,573 cases of hepatectomy in China: a multicenter retrospective investigation. *Sci China Life Sci* 2018; **61**: 660-670 [PMID: 29417360 DOI: 10.1007/s11427-017-9259-9]
25 **Zeng J**, Zeng J, Lin K, Lin H, Wu Q, Guo P, Zhou W, Liu J. Development of a machine learning model to predict early recurrence for hepatocellular carcinoma after curative resection. *Hepatobiliary Surg Nutr* 2022; **11**: 176-187 [PMID: 35464276 DOI: 10.21037/hbsn-20-466]
26 **Wang X**, Mao M, He Z, Zhang L, Li H, Lin J, He Y, Dai S, Hu W, Liu W. Development and Validation of a Prognostic Nomogram in AFP-negative hepatocellular carcinoma. *Int J Biol Sci* 2019; **15**: 221-228 [PMID: 30662361 DOI: 10.7150/ijbs.28720]

27 **Nakano M**, Kuromatsu R, Niizeki T, Okamura S, Iwamoto H, Shimose S, Shirono T, Noda Y, Kamachi N, Koga H, Torimura T; Kurume Liver Cancer Study Group of Japan. Immunological inflammatory biomarkers as prognostic predictors for advanced hepatocellular carcinoma. *ESMO Open* 2021; **6**: 100020 [PMID: 33399083 DOI: 10.1016/j.esmoop.2020.100020]

28 **Wang C**, He W, Yuan Y, Zhang Y, Li K, Zou R, Liao Y, Liu W, Yang Z, Zuo D, Qiu J, Zheng Y, Li B. Comparison of the prognostic value of inflammation-based scores in early recurrent hepatocellular carcinoma after hepatectomy. *Liver Int* 2020; **40**: 229-239 [PMID: 31652394 DOI: 10.1111/liv.14281]

29 **Li J**, Liao Y, Suo L, Zhu P, Chen X, Dang W, Liao M, Qin L, Liao W. A novel prognostic index-neutrophil times γ-glutamyl transpeptidase to lymphocyte ratio (NγLR) predicts outcome for patients with hepatocellular carcinoma. *Sci Rep* 2017; **7**: 9229 [PMID: 28835713 DOI: 10.1038/s41598-017-09696-y]

30 **Zhu YF**, Tan YF, Xu X, Zheng JL, Zhang BH, Tang HR, Yang JY. Gamma-glutamyl transpeptidase-to-platelet ratio and the fibrosis-4 index in predicting hepatitis B virus-related hepatocellular carcinoma development in elderly chronic hepatitis B patients in China: A single-center retrospective study. *Medicine (Baltimore)* 2019; **98**: e18319 [PMID: 31852119]

31 **Lemoine M**, Shimakawa Y, Nayagam S, Khalil M, Suso P, Lloyd J, Goldin R, Njai HF, Ndow G, Taal M, Cooke G, D'Alessandro U, Vray M, Mbaye PS, Njie R, Mallet V, Thursz M. The gamma-glutamyl transpeptidase to platelet ratio (GPR) predicts significant liver fibrosis and cirrhosis in patients with chronic HBV infection in West Africa. *Gut* 2016; **65**: 1369-1376 [PMID: 26109530 DOI: 10.1136/gutjnl-2015-309260]

32 **Wang WL**, Zheng XL, Zhang ZY, Zhou Y, Hao J, Tang G, Li O, Xiang JX, Wu Z, Wang B. Preoperative γ-glutamyl transpeptidase to platelet ratio (GPR) is an independent prognostic factor for HBV-related hepatocellular carcinoma after curative hepatic resection. *Medicine (Baltimore)* 2016; **95**: e4087 [PMID: 27399101 DOI: 10.1097/MD.0000000000004087]

33 **Sort P**, Navasa M, Arroyo V, Aldeguer X, Planas R, Ruiz-del-Arbol L, Castells L, Vargas V, Soriano G, Guevara M, Ginès P, Rodés J. Effect of intravenous albumin on renal impairment and mortality in patients with cirrhosis and spontaneous bacterial peritonitis. *N Engl J Med* 1999; **341**: 403-409 [PMID: 10432325 DOI: 10.1056/NEJM199908053410603]

34 **Piano S**, Tonon M, Angeli P. Management of ascites and hepatorenal syndrome. *Hepatol Int* 2018; **12**: 122-134 [PMID: 28836115 DOI: 10.1007/s12072-017-9815-0]

35 **Shimada M**, Takenaka K, Fujiwara Y, Gion T, Shirabe K, Yanaga K, Sugimachi K. Risk factors linked to postoperative morbidity in patients with hepatocellular carcinoma. *Br J Surg* 1998; **85**: 195-198 [PMID: 9501814 DOI: 10.1046/j.1365-2168.1998.00567.x]

36 **Wang Q**, Ma L, Li J, Yuan C, Sun J, Li K, Qin L, Zang C, Zhao Y, Zhang Y. A Novel Scoring System for Patients with Recurrence of Hepatocellular Carcinoma After Undergoing Minimal Invasive Therapies. *Cancer Manag Res* 2019; **11**: 10641-10649 [PMID: 31908536 DOI: 10.2147/CMAR.S224711]

37 **Yoneyama K**, Taniguchi H, Kiuchi Y, Shibata M, Mitamura K. Prognostic index of liver cirrhosis with ascites with and without hepatocellular carcinoma. *Scand J Gastroenterol* 2004; **39**: 1272-1279 [PMID: 15743006 DOI: 10.1080/00365520410008042]

38 **Liu F**, Liu D, Wang K, Xie X, Su L, Kuang M, Huang G, Peng B, Wang Y, Lin M, Tian J. Deep Learning Radiomics Based on Contrast-Enhanced Ultrasound Might Optimize Curative Treatments for Very-Early or Early-Stage Hepatocellular Carcinoma Patients. *Liver Cancer* 2020; **9**: 397-413 [PMID: 32999867 DOI: 10.1159/000505694]

39 **Wan S**, Lei Y, Li M, Wu B. A prognostic model for hepatocellular carcinoma patients based on signature ferroptosis-related genes. *Hepatol Int* 2022; **16**: 112-124 [PMID: 34449009 DOI: 10.1007/s12072-021-10248-w]

World Journal of Gastroenterology

Submit a Manuscript: https://www.f6publishing.com

World J Gastroenterol 2023 May 28; 29(20): 3185-3202

DOI: 10.3748/wjg.v29.i20.3185

ISSN 1007-9327 (print) ISSN 2219-2840 (online)

META-ANALYSIS

Fecal microbiota transplantation for the treatment of irritable bowel syndrome: A systematic review and meta-analysis

Sofie Ingdam Halkjær, Bobby Lo, Frederik Cold, Alice Højer Christensen, Savanne Holster, Julia König, Robert Jan Brummer, Olga C Aroniadis, Perttu Lahtinen, Tom Holvoet, Lise Lotte Gluud, Andreas Munk Petersen

Specialty type: Gastroenterology and hepatology

Provenance and peer review: Unsolicited article; Externally peer reviewed.

Peer-review model: Single blind

Peer-review report's scientific quality classification
Grade A (Excellent): A
Grade B (Very good): B
Grade C (Good): C, C
Grade D (Fair): 0
Grade E (Poor): 0

P-Reviewer: Bao CH, China; Rahmati M, Iran; Wu LH, China

Received: February 22, 2023
Peer-review started: February 22, 2023
First decision: March 18, 2023
Revised: April 6, 2023
Accepted: April 18, 2023
Article in press: April 18, 2023
Published online: May 28, 2023

Sofie Ingdam Halkjær, Bobby Lo, Frederik Cold, Lise Lotte Gluud, Andreas Munk Petersen, Gastro Unit, Medical Division, Copenhagen University Hospital Hvidovre, Hvidovre 2650, Denmark

Sofie Ingdam Halkjær, Bobby Lo, Frederik Cold, Andreas Munk Petersen, Copenhagen IBD Center, Copenhagen University Hospital Hvidovre, Hvidovre 2650, Denmark

Alice Højer Christensen, Department of Gastroenterology, Aleris-Hamlet Hospitals Copenhagen, Søborg 2860, Denmark

Savanne Holster, Julia König, Robert Jan Brummer, Nutrition-Gut-Brain Interactions Research Centre, Faculty of Medicine and Health, School of Medical Sciences, Örebro University, Örebro 70362, Sweden

Olga C Aroniadis, Department of Internal Medicine, Division of Gastroenterology, Renaissance School of Medicine, Stony Brook University Hospital, New York, NY 11794-8434, United States

Perttu Lahtinen, Department of Internal Medicine, Päijät-Häme Central Hospital, Lahti 15850, Finland

Perttu Lahtinen, Department of Medicine, University of Helsinki, Helsinki 00014, Finland

Tom Holvoet, Department of Gastroenterology, University Hospital Ghent, Ghent 9000, Belgium

Lise Lotte Gluud, Andreas Munk Petersen, Department of Clinical Medicine, University of Copenhagen, Copenhagen 2200, Denmark

Andreas Munk Petersen, Department of Clinical Microbiology, Copenhagen University Hospital Hvidovre, Hvidovre 2650, Denmark

Corresponding author: Sofie Ingdam Halkjær, MSc, PhD, Senior Researcher, Gastro Unit, Medical Division, Copenhagen University Hospital Hvidovre, Kettegård Alle 30, Hvidovre 2650, Denmark. sofie.ingdam.halkjaer@regionh.dk

Abstract

BACKGROUND

Irritable bowel syndrome (IBS) is the most prevalent gastrointestinal disorder in

developed countries and reduces patients' quality of life, hinders their ability to work, and increases health care costs. A growing number of trials have demonstrated an aberrant gut microbiota composition in IBS, also known as 'gut dysbiosis'. Fecal microbiota transplantation (FMT) has been suggested as a treatment for IBS.

AIM

To assess the efficacy and safety of FMT for the treatment of IBS.

METHODS

We searched Cochrane Central, MEDLINE, EMBASE and Web of Science up to 24 October 2022 for randomised controlled trials (RCTs) investigating the effectiveness of FMT compared to placebo (including autologous FMT) in treating IBS. The primary outcome was the number of patients with improvements of symptoms measured using a validated, global IBS symptoms score. Secondary outcomes were changes in quality-of-life scores, non-serious and serious adverse events. Risk ratios (RR) and corresponding 95%CI were calculated for dichotomous outcomes, as were the mean differences (MD) and 95%CI for continuous outcomes. The Cochrane risk of bias tool was used to assess the quality of the trials. GRADE criteria were used to assess the overall quality of the evidence.

RESULTS

Eight RCTs (484 participants) were included in the review. FMT resulted in no significant benefit in IBS symptoms three months after treatment compared to placebo (RR 1.19, 95%CI: 0.68-2.10). Adverse events were reported in 97 participants in the FMT group and in 45 participants in the placebo group (RR 1.17, 95%CI: 0.63-2.15). One serious adverse event occurred in the FMT group and two in the placebo group (RR 0.42, 95%CI: 0.07-2.60). Endoscopic FMT delivery resulted in a significant improvement in symptoms, while capsules did not. FMT did not improve the quality of life of IBS patients but, instead, appeared to reduce it, albeit non significantly (MD -6.30, 95%CI: -13.39-0.79). The overall quality of the evidence was low due to moderate-high inconsistency, the small number of patients in the studies, and imprecision.

CONCLUSION

We found insufficient evidence to support or refute the use of FMT for IBS. Larger trials are needed.

Key Words: Fecal microbiota transplantation; Irritable bowel syndrome; Meta-analysis; Systematic review

©The Author(s) 2023. Published by Baishideng Publishing Group Inc. All rights reserved.

Core Tip: We did not find evidence to support the use of fecal microbiota transplantation (FMT) for irritable bowel syndrome (IBS) patients outside of clinical trials in this systematic review and meta-analysis. We report possible beneficial effects when FMT is delivered by endoscopy (colonoscopy or gastroscopy). FMT appears to be safe compared to placebo in patients with IBS, regardless of route of administration. Further randomised clinical trials are necessary to clarify the effect, if any, of FMT in IBS.

Citation: Halkjær SI, Lo B, Cold F, Højer Christensen A, Holster S, König J, Brummer RJ, Aroniadis OC, Lahtinen P, Holvoet T, Gluud LL, Petersen AM. Fecal microbiota transplantation for the treatment of irritable bowel syndrome: A systematic review and meta-analysis. *World J Gastroenterol* 2023; 29(20): 3185-3202
URL: https://www.wjgnet.com/1007-9327/full/v29/i20/3185.htm
DOI: https://dx.doi.org/10.3748/wjg.v29.i20.3185

INTRODUCTION

Irritable bowel syndrome (IBS) is the most prevalent gastrointestinal disorder in developed countries, affecting around 11% of the adult population[1]. The condition reduces patients' quality of life, hinders their ability to work, and increases health care costs[2,3]. A diagnosis of IBS is based on symptoms, assessed using the Rome criteria, that include abdominal pain and altered bowel habits combined with the absence of organic or structural causes[4]. The criteria have changed over time and the most recent are the Rome IV criteria[5]. IBS can be sub-categorised as diarrhoea-predominant, constipation-predominant, mixed, or unclassified[5]. In most patients, IBS is chronic, with symptoms that fluctuate

over time.

The pathogenic mechanisms underlying IBS remain more or less unknown. Genetics[6,7], dietary habits[8], post-infectious conditions[9] and psychological mechanisms[10] are all suspected to be involved. In recent years an increasing number of trials have demonstrated an aberrant gut microbiota composition in IBS[11-14], although not all trials report this aberration and descriptions of it vary between studies[15]. The microbial pathophysiology of IBS remains unknown.

Treating IBS poses a challenge; the syndrome probably represents a heterogeneity of disease mechanisms, which makes it difficult to develop effective therapeutic strategies[16]. Understanding the causes of gut dysbiosis in IBS is crucial[17]. Some trials indicate that probiotics and prebiotics can reduce the symptoms of IBS[18,19]. Fecal microbiota transplantation (FMT) might be an effective therapeutic intervention in IBS[16,20].

FMT is the transfer of stool from a healthy donor to a patient[21]. FMT has been described as far back as the fourth century in China[22]. In modern times, the first published FMT treatment is from 1958, when it was used successfully in four patients with pseudomembranous colitis[23]. Pseudomembranous colitis is now known to be caused by *Clostridioides difficile* infection (CDI). Based on subsequent placebo-controlled studies, FMT is now accepted in daily clinical practice for the treatment of recurrent CDI[24]. In addition, FMT is being investigated as a treatment option in a range of other diseases, *e.g.*, metabolic syndrome, inflammatory bowel diseases, hepatic encephalopathy and multiple sclerosis[25]. The most promising results with FMT, apart from treating recurrent CDI, are for the treatment of inflammatory bowel disease[26-28].

FMT donors can be healthy relatives or anonymous donors. The advantages of the latter are the possibility of selecting donors with a high microbiota diversity and to store screened donor stool in freezers, to be made use of for multiple patients[29]. A European consensus report recommends that donors are chosen based on detailed information about illnesses with a presumed link to intestinal dysbiosis and rigorous testing of faecal and blood samples to avoid the transfer of infectious diseases [30].

FMT can be delivered in several ways, including through upper or lower endoscopic procedures, or by a gastro-duodenal or a rectal tube[31]. Additionally, capsules can release the stool in the small intestines and have been used successfully for the treatment of CDI[32-34]. In the treatment of recurrent CDI, the highest cure rates have been reported with repeated treatments delivered through lower endoscopy[35]; FMT has proven highly effective and patients are willing to undergo the treatment[36].

The microbial pathophysiology of IBS is not clearly understood, as microbiota alterations in IBS could either be a cause of the disease or a consequence of intestinal secretion and motility altered by IBS[37]. The prevailing hypothesis is that FMT might correct the dysbiosis associated with IBS[38,39], leading to a reversal or improvement of symptoms. Gut dysbiosis in IBS is characterised by a lower diversity of bacteria in the microbiota and abnormal proportions of specific bacteria as compared to the microbiota of healthy individuals[37,40]. In IBS and in other patient groups, FMT has resulted in increased bacterial diversity[41,42] and the coexistence of donor and recipient microbiota strains up to one year after treatment[43-45]. However, this is a new and developing field of study and the long-term effects of FMT on the microbiota remain largely unknown, not least of all because donor stools contain many things other than bacteria.

There is increasing evidence for a connection between gut dysbiosis and IBS[46,47]. The administration of FMT by various methods has been described in published case reports and abstracts, as compiled in an earlier review[48]. A number of smaller trials have examined the effect of FMT on IBS specifically[49-57], and several randomised controlled trials (RCTs), using different methods of administration, have been published with mixed results[43,44,58-63]. The effect of FMT can be difficult to assess due to the absence of reliable outcome measures and high placebo response rates[64]. The short- and long-term safety of FMT in patients with IBS is currently unclear.

The objectives of this systematic review were to examine the benefits and harms of FMT *vs* placebo (including autologous FMT, *i.e.*, a participant's own faecal material) for the treatment of patients with IBS.

MATERIALS AND METHODS

We conducted a systematic review and meta-analysis following the recommendations from the Cochrane Handbook for Systematic Reviews of Interventions[65]. The systematic review was registered a priori as a protocol[66].

We included RCTs comparing FMT to placebo for the treatment of IBS, regardless of publication status and language of publication. For cross-over trials only data from the first intervention were used. For multi-arm trials only the data from intervention groups relevant to the review were used. We excluded trials with quasi-random designs and cluster RCTs. Trials with mixed disease populations were excluded.

Trials were included if their participants were diagnosed with IBS by a physician or according to accepted, symptom-based diagnostic criteria, such as the Rome III or IV criteria[67] (Supple-

mentary Table 1). We only included trials that had follow-up after FMT for one week or more. Participants were included regardless of their gender and age.

FMT could be administered in different ways and at different frequencies as there was no standardised procedure. Therefore, we included trials irrespective of FMT procedure, in terms of the quantity of faeces used, the form of faeces (fresh or frozen), the route of administration, the frequency of treatment (*i.e.*, single *vs* multiple infusions) and donor selection (relatives or not). Only trials that used the whole gut microbiome from the donor were included. Trials that used a placebo, or autologous FMT as a placebo, were included. Trials that used selective microbial communities were excluded.

Primary outcomes

The primary outcome was the proportion of patients experiencing an improvement of symptoms (patient-reported), as measured by a validated, global IBS symptoms score (*e.g.*, IBS severity scoring system), as defined by each trial's organisers.

Secondary outcomes

Secondary outcomes were the change in quality of life, as measured by a validated quality of life assessment, *e.g.*, IBS-specific quality-of-life (IBS-QoL), the proportion of patients with non-serious adverse events and serious adverse events according to International Conference on Harmonization-Good Clinical Practice, and dropouts due to adverse events. Outcomes were measured after three and six months.

Literature search

We searched Cochrane Central, MEDLINE, EMBASE and Web of Science. No language or publication date restrictions were applied to the searches. The detailed search strategy is provided in Supplementary Table 2.

We searched the following sources from the inception of each database up until 24 October 2022 and placed no restrictions on the language of publication (Supplementary Table 2): Cochrane Central (*via* the Ovid Evidence-Based Medicine Reviews Database, from inception); MEDLINE (*via* Ovid from 1946); and EMBASE (*via* Ovid from 1974).

We also searched for ongoing trials on ClinicalTrials.gov (https://clinicaltrials.gov/) and the World Health Organisation International Clinical Trials Registry Platform (https://trialsearch.who.int/).

The reference lists of all trials identified were then scanned for additional relevant trials. We also contacted the first authors of published and ongoing trials to request recent data or additional data, as needed.

Data collection and analysis

Two independent authors performed the study selection (BL, SIH). Disagreements were resolved by consensus using a third author (AMP). The search results were first screened by title and abstract and subsequently excluded if found non-relevant; the remaining results were screened by full text. Data were extracted independently by two investigators (BL, SIH). Any discrepancies were resolved by consensus using a third author (LLG). An attempt to contact the corresponding author by e-mail was made if data were not available.

A data extraction protocol was developed based on the Cochrane Consumers and Communication Review Group's data and results template and refined accordingly[68]. The following information was extracted from each trial: (1) Author, year of publication, trial design, and study site (country); (2) the mean or median (SD or IQR) change in symptoms, as measured by IBS scoring systems, at the end of the trial; (3) the mean or median (SD or IQR) change in quality of life, as measured by IBS quality of life scoring systems; (4) treatment description (including route of administration, mixed or single donor and fresh or frozen transplant); (5) reported non-serious adverse events and serious adverse events; and (6) dropouts due to adverse events.

Assessment of risk of bias in the studies

The risk of bias was independently assessed by two investigators (BL, FC) using the Cochrane risk of bias tool[69] and the following seven domains were assessed: random sequence generation, allocation concealment, blinding of participants and personnel, blinding of outcome assessment, incomplete outcome data, selective reporting, and other sources of bias (Supplementary Table 3).

The risk of bias for each domain was rated as either 'high', 'unclear' or 'low'. We classified the overall risk of bias in the trials as low if all the bias domains were classified as being at low risk of bias; we classified the overall risk as high if one or more of the bias domains were classified as having an unclear or high risk of bias. Any disagreement was solved by consensus using a third author (LLG).

Data synthesis

We compared the fixed-effects and random-effects estimates of the intervention effect. If the estimates were similar, we assumed that any small-study effects had a minimal impact on the intervention effect estimate. If the random-effects estimate showed a larger statistical effect, we re-evaluated whether it

was reasonable to conclude that the intervention was more effective in the smaller trials. If the larger trials appeared to be conducted with greater methodological rigour, or were conducted in circumstances more typical of the use of the intervention in practice, we reported the results of meta-analyses only from the larger trials.

Based on predictable clinical heterogeneity, we expected that several analyses would show, at a minimum, moderate heterogeneity (I^2 > 30%). For random-effects models precision decreases, and confidence intervals widen, with increasing heterogeneity. We therefore expected the random-effects model would provide the most conservative (and thus a more accurate) estimate of the intervention effect. As such, we planned to report the results of our analyses based on meta-analyses of random-effects models.

Subgroup and sensitivity analysis

We conducted a number of subgroup analyses: fresh *vs* frozen FMT; quantity of FMT; route of administration (upper gastrointestinal tract (*e.g.*, capsulated, nasogastric, nasoduodenal, gastric tube) *vs* colonic (*e.g.*, rectal)); type of donor (single *vs* mixed); frequency of administration (single *vs* multiple); IBS subtypes (diarrhoea-predominant, constipation-predominant, or mixed type).

Statistical analyses

We combined data from individual trials for meta-analysis when the interventions, patient groups, and outcomes were sufficiently similar, using the Review Manager version 5.4.1. Risk ratios (RR) were calculated for dichotomous outcomes with 95%CI. For continuous outcomes, we calculated the mean difference (MD) if all studies reported their outcomes using the same scale, and standardised MD with 95%CI if the studies used different scales to report their outcomes. We extracted data for all randomised participants and all participants with missing outcome data. Missing data were described, including dropouts and reasons for dropout, as reported by the authors.

Heterogeneity was assessed through a systematic examination of forest plots and quantified by calculating I^2 values. The classification of heterogeneity levels was established using the subsequent thresholds: 0%-40% (insignificant), 40%-60% (moderate), 60%-80% (substantial), and > 80% (considerable). Additionally, the *P* value for the chi-squared test was included in the evaluation[66].

The outcomes reported in protocols were compared with published trial reports. In addition, for direct meta-analyses with at least 10 randomised clinical trials, we assessed reporting biases through regression analyses and visual inspection of funnel plots from the pairwise meta-analyses.

Assessing the certainty of the evidence

We used the GRADE approach to evaluate the overall certainty of the evidence and we followed the recommendations of the Cochrane Handbook for Systematic Reviews of Interventions[65]. We classified the certainty of evidence as 'high', 'moderate', 'low', or 'very low'.

High certainty: We are very confident that the true effect lies close to that of the estimate of the effect.

Moderate certainty: We are moderately confident in the effect estimate; the true effect is likely to be close to the estimate of the effect, but there is a possibility that it is substantially different.

Low certainty: Our confidence in the effect estimate is limited; the true effect may be substantially different from the estimate of the effect.

Very low certainty: We have very little confidence in the effect estimate; the true effect is likely to be substantially different from the estimate of the effect.

RESULTS

Trial selection

A search conducted on 24 October 2022 identified 2067 records, which were imported for screening into the computer program Covidence (https://www.covidence.org/). Of these records, 840 were removed as duplicates. We screened the titles and abstracts of the remaining 1227. We excluded 1160 reports as non-relevant. In total, 67 records met the criteria for full-text review.

After reading the full texts, we excluded 45 as they did not fulfil our eligibility criteria. The remaining 22 texts, originating from eight different trials, were included in our systematic review (Figure 1)[43,44,58-63].

Supplementary Table 2 contains the complete set of search terms used in each electronic database.

A summary of the trials can be found in Table 1; a full description of them is provided in Supplementary Table 4.

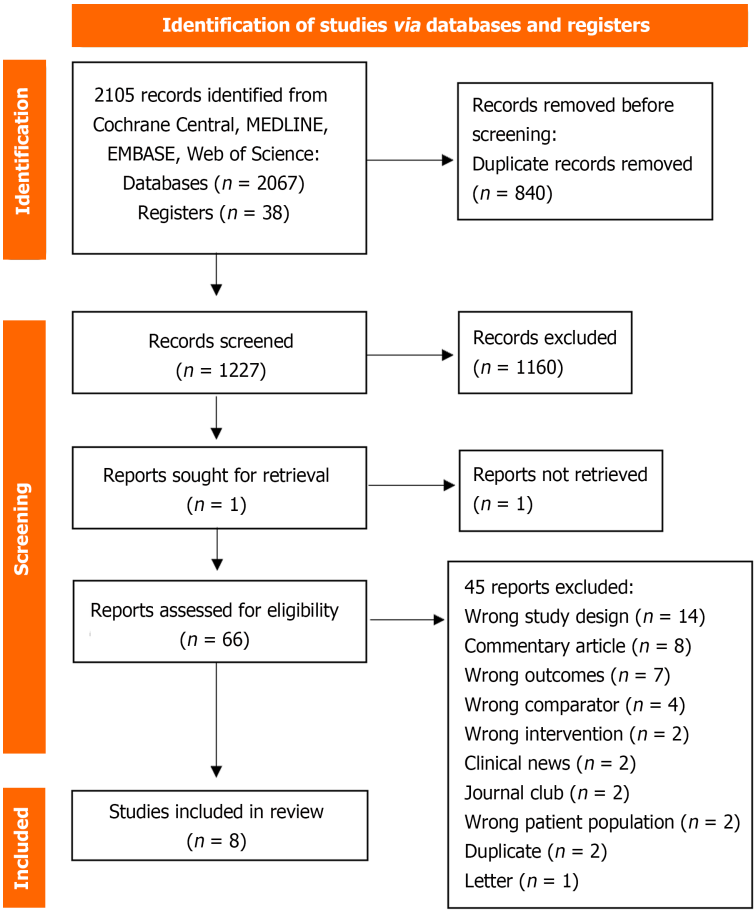
Table 1 Characteristics of randomised controlled trials of faecal microbiota transplantation for treating irritable bowel syndrome

Ref.	Trial design	Country	Sample size	IBS subtypes	Inclusion criteria	Frequency and route of administration	FMT-content	Placebo content	Pretreatment	Number of donors
Aroniadis *et al*[59], 2019	RCT, crossover	United States	48 (25 FMT *vs* 23 placebo)	IBS-D	Moderate-to-severe IBS symptoms (IBS-SSS > 175)	3 d of 25 oral capsules	3 × 25 frozen capsules (0.38 g donor stool/capsule) (Openbiome)	Non-toxic brown pigment	PPI for three days	One donor for one patient (four different donors)
El-Salhy *et al*[60], 2020	RCT, 3 parallel groups	Norway	164 (54/30 gram FMT, 55/60 gram FMT, 55 placebo)	All subtypes	Moderate-to-severe IBS symptoms (IBS-SSS > 175)	Single treatment *via* gastroscope to distal duodenum	Once 30 g or 60 gram of frozen feces in sterile saline solution	Autologous faeces	None	One donor
Halkjær *et al*[43], 2018	RCT, 2 parallel groups	Denmark	51 (25 FMT, 26 placebo)	All subtypes	Moderate-to-severe IBS symptoms (IBS-SSS > 175)	12 d of 25 oral capsules	25 FMT capsules (one daily dose containing approximately 12 g frozen faecal material)	Saline, glycerol and food colouring E150	Bowel cleansing	Donor mix from four donors
Holster *et al*[61], 2019	RCT, 2 parallel groups	Sweden	16 (8 FMT, 8 placebo)	All subtypes	IBS with small amounts of butyrate-producing bacteria	Single treatment *via* colonoscopy to the caecum	30 g frozen stool in sterile saline and glycerol	Autologous feces	Bowel cleansing and 4 mg loperamide	Two donors (three patients received stool from donor 1, the remaining five from donor 2)
Holvoet *et al*[44], 2021	RCT, 2 parallel groups	Belgium	62 (43 FMT, 19 placebo)	IBS-D and IBS-M	Refractory IBS with failure of at least three conventional IBS therapies	Single treatment *via* nasojejunal administration	Fresh feces mixed with saline	Autologous feces	Bowel cleansing	Two donors
Johnsen *et al*[62], 2018	RCT, 3 parallel groups	Norway	83 (26 fresh FMT, 29 frozen FMT, 28 placebo)	IBS-D and IBS-M	Moderate-to-severe IBS symptoms (IBS-SSS > 175)	Single treatment administered into the caecum *via* colonoscopy	50–80 g fresh or frozen feces mixed with saline and glycerol	Autologous feces	Bowel cleansing and 8 mg loperamid	Donor mix from two donors
Lahtinen *et al*[58], 2020	RCT, 2 parallel groups	Finland	51 (25 FMT, 26 placebo)	IBS-D, IBS-M and IBS-U	Patients who remained symptomatic despite receiving conventional treatment	Single treatment administered into the caecum *via* colonoscopy	30 g frozen suspension	Autologous feces	Bowel cleansing	One donor
Singh *et al* [63], 2022	RCT, 4 parallel groups	United States	23 (11 FMT, 12 placebo)	IBS-D	IBS-SSS > 150 or > 175	Single treatment with 19 oral capsules	Capsule contain 0.75 frozen fecal filtrate) (Openbiome)	Glycerol with brown coloring agent	Bowel cleansing	Six donors (unknown if donors were mixed)

FMT: Fecal microbiota transplantation; IBS: Irritable bowel syndrome; IBS-C: Constipation-predominant irritable bowel syndrome; IBS-D: Diarrhoea-predominant irritable bowel syndrome; IBS-M: Mixed irritable bowel syndrome; IBS-U: Unclassified irritable bowel syndrome; RCT: Randomised controlled trials; PPI: Proton pump inhibitors.

Study design and setting

We included eight trials that were published between 2018 and 2022[43,44,58-63]. These were either single-centre trials[44,60-63] or multicentre trials[43,58,59] and were conducted in Belgium[44], Denmark[43], Finland[58], Norway[60,62], Sweden[61] and the United States[59,63].



DOI: 10.3748/wjg.v29.i20.3185 **Copyright** ©The Author(s) 2023.

Figure 1 PRISMA flow diagram for the literature search.

All participants in the trials were diagnosed with IBS by a physician and according to accepted, symptom-based diagnostic criteria (*e.g.*, the Rome criteria)[5]. Participants in the Lahtinen *et al*[58] trial were diagnosed by a gastroenterologist, Aroniadis *et al*[59], Halkjær *et al*[43], Holster *et al*[61], Holvoet *et al*[44], Johnsen *et al*[62] and Singh *et al*[63] all used the Rome III criteria; El-Salhy *et al*[60] used the Rome IV criteria.

Four trials included participants with moderate-to-severe IBS symptoms, indicated by a score of 175 or more on the IBS severity scoring system (IBS-SSS)[43,59,60,62]. We are unsure whether Singh *et al*[63] used a score of 150 or 175 or more on the IBS-SSS, as both are referred to in their article. The remaining three trials used other criteria: Holster *et al*[61] only included participants with small amounts of butyrate-producing bacteria in faecal samples, Holvoet *et al*[44] included participants with refractory IBS who had experienced failure of at least three conventional IBS therapies, and Lahtinen *et al*[58] included participants who remained symptomatic despite receiving conventional treatment.

The trials differed in the IBS subtypes they investigated. All subtypes were included in the trials conducted by El-Salhy *et al*[60], Halkjær *et al*[43] and Holster *et al*[61]. Aroniadis *et al*[59] and Singh *et al*[63] included only diarrhoea-predominant participants. Holvoet *et al*[44] and Johnsen *et al*[62] included diarrhoea-predominant or mixed participants. Lahtinen *et al*[58] included diarrhoea-predominant, mixed or un-subtyped participants.

Characteristics of the interventions

All eight trials used faeces from healthy donors for the FMT. Supplementary Table 5 describes their inclusion and exclusion criteria for donors.

The route of administration varied between the trials. Three trials used colonoscopy[58,61,62], one used gastroscopy[60], one used the nasojejunal route[44] and three used oral capsules[43,59,63].

The frequency of administration varied between trials. El Salhy *et al*[60], Holster *et al*[61], Holvoet *et al*[44], Johnsen *et al*[62], Lahtinen *et al*[58] and Singh *et al*[63] administered FMT just once. Aroniadis *et al*[59] administered a total of three doses across three consecutive days. Halkjær *et al*[43] administered a total of 12 doses across 12 consecutive days.

The volume of FMT administered ranged from approximately 100 mL in the El-Salhy *et al*[60] trial to 300 mL in the Holvoet *et al*[44] trial. The faecal quantity varied from 30 g[58,61] to 50-80 g[62]. The

capsule trials used approximately 28.5 g of minimally processed faecal matter[59], 14.25 frozen faecal filtrate[63] and faecal matter derived from approximately 600 g of faeces[43]. Holvoet *et al*[44] used fresh FMT transplant, Johnsen *et al*[62] used both fresh and frozen FMT transplant, while the remaining trials used frozen FMT transplants[43,58-61,63].

Two trials used a single donor for all FMT treatments[58,60]. Holster *et al*[61], Holvoet *et al*[44] and Johnsen *et al*[62] used two donors. Aroniadis *et al*[59] used four donors, where each participant received a FMT from one donor. Singh *et al*[63] used six donors, where each participant received a FMT from one donor. Halkjær *et al*[43] used a FMT donor mix from four donors.

Six trials included bowel cleansing before transplantation[43,44,58,61-63]. Two trials used loperamide before endoscopy to retain the transplant[61,62]. One trial used proton pump inhibitors (PPI) for the three days prior to the transplantation[59].

Five trials used autologous faeces as an alternative to placebo for the comparison group[44,58,60-62]. In the capsule trials, Aroniadis *et al*[59] and Singh *et al*[63] used placebo capsules with a non-toxic, brown pigment and Halkjær *et al*[43] used placebo capsules made from saline, glycerol and food colouring E150.

Risk of bias in the studies

A summary of the risk of bias assessments is reported in Figure 2 and bias assessments for the individual trials are reported in Supplementary Table 4.

Overall, none of the studies had a high risk of bias in any of the seven dimensions considered. However, five of the eight trials[44,58,60,62,63] had an unclear bias for the blinding of outcomes, and four out of eight[43,58,60,61] had a similarly unclear bias in terms of how they reported the handling of incomplete data. In both cases this unclear bias was primarily due to a lack of information.

Effects of the interventions

A summary of the findings is provided in Table 2 for comparing FMT and placebo in treating IBS. We did not assess publication bias as this review only consisted of eight trials. Furthermore, we chose to report the random-effect models' results despite some of the fixed-effect models being found significant as we did not find any larger trial that was more methodologically rigorous. The significant outcomes of the fixed-effect models were most likely due to the small number of trials available in each analysis and their high heterogeneity.

The GRADE rating for the certainty of the evidence examined was low due to moderate-high inconsistency, small numbers of patients and imprecision.

Primary outcomes

Improvement of symptoms: Eight randomised trials, comprising 484 participants, examined whether IBS symptoms improved after three months. Six trials defined improvement of symptoms as a decrease in IBS-SSS of 50 or more[43,44,59,60,63], while Johnson *et al*[62] defined it as a decrease of more than 75 points. Holster *et al*[61] used the gastrointestinal symptom rating scale-IBS and defined improvement as a change of more than 30%. Sixty-four percent (185/290) of FMT participants experienced an improvement of symptoms after three months compared to 42% (82/194) in the placebo group. A meta-analysis showed there was no significant difference between FMT and placebo (RR 1.19, 95%CI: 0.68-2.10, $P = 0.54$, $I^2 = 82\%$; Figure 3).

Three trials (99 participants) reported on the improvement of symptoms after six months. Thirty per cent (14/47) of FMT participants saw an improvement of their symptoms after six months compared to 38% (20/52) of the placebo group (RR 0.88, 95%CI: 0.33-12.39, $P = 0.8$, $I^2 = 51\%$; Figure 3).

Secondary outcomes

Adverse events: Seven trials, comprising 450 participants, reported on the proportion of participants who experienced adverse events. Thirty-five per cent (97/274) of the FMT group experienced an adverse event compared to 26% (45/176) of the placebo group (RR 1.17, 95%CI: 0.63-2.15, $P = 0.62$, $I^2 = 69\%$; Figure 4).

The most frequent adverse events reported in the trials were mild and transient symptoms of the gastrointestinal system.

Serious adverse events: All eight trials, comprising 501 participants, provided data for serious adverse events. A serious adverse event was reported once in a FMT group and twice in placebo groups. In the FMT group, 0.33 per cent (1/302) reported a serious adverse event, compared to 1% (2/199) in the placebo group (RR 0.42, 95%CI: 0.07-2.60, $P = 0.35$, $I^2 = 0\%$; Supplementary Figure 1).

Holvoet *et al*[44] reported that one participant from the placebo group committed suicide 10 d after the transplantation procedure. Aroniadis *et al*[59] reported one participant from the placebo group was admitted to hospital during week 20 of the trial with acute cholecystitis. Johnsen *et al*[62] reported that one participant from the FMT group was admitted to hospital after the FMT procedure due to transient vertigo and nausea.

Table 2 Summarised findings for comparing fecal microbiota transplantation with placebo for the treatment of irritable bowel syndrome

Outcomes and timeframe	Anticipated absolute effects		Relative effect (95%CI)	Number of participants (trials)	Certainty of the evidence (GRADE)	Comments
	Effect in placebo	Effect difference with FMT (95%CI)				
Improvement of symptoms after three months	42 per 100	8 or more per 100 (from 13 or fewer to 46 or more)	RR 1.19 (0.68-2.10)	484 (8 RCTs)	++--[1] Low	Improvement of symptoms as measured by a validated global IBS symptoms score (*e.g.*, IBS-SSS scale from 0, no symptoms, to 500, maximum symptoms) (as defined by each trial)
Improvement of symptoms after six months	38 per 100	5 or fewer per 100 (from 25 or fewer to 52 or more)	RR 0.88 (0.33-2.39)	99 (3 RCTs)	++--[2] Low	Improvement of symptoms as measured by a validated global IBS symptoms score (*e.g.*, IBS-SSS scale from 0, no symptoms, to 500, maximum symptoms) (as defined by each trial)
Adverse events prior to end of trial	26 per 100	4 or more per 100 (from 10 or fewer to 30 or more)	RR 1.17 (0.63-2.15)	450 (7 RCTs)	++--[3] Low	Common adverse events were mild and self-limiting gastrointestinal symptoms
Serious adverse events prior to end of trial	1 per 100	1 or fewer per 100 (from 1 or fewer to 2 or more)	RR 0.42 (0.07-2.60)	501 (8 RCTs)	++--[4] Low	Serious adverse events included one suicide (placebo), cholecystitis (placebo), and one admission to the hospital due to discomfort after the FMT procedure
Dropouts due to adverse events prior to end of trial	1 per 100	1 or fewer per 100 (from 1 or fewer to 1 or more)	RR 0.24 (0.03-2.17)	502 (8 RCTs)	++--[5] Low	Dropouts due to adverse events include one suicide (placebo) and one for discomfort after the FMT procedure (placebo)
Improvement in QoL scores after three months	NA	NA	MD -6.30 (-13.39 to 0.79)	406 (7 RCTs)	++--[6] Low	Improvement of quality of life as measured by a validated scale IBS-QoL, where 34 items are summed and averaged for a total score and then transformed to a 0-100 scale for interpretation (high scores indicate better IBS-QoL)

[1]Downgraded two levels due to considerable inconsistency (I^2 = 82%) and imprecision (267 events).
[2]Downgraded two levels due to moderate inconsistency (I^2 = 51%) and serious imprecision (34 events).
[3]Downgraded two levels due to substantial inconsistency (I^2 = 69%) and imprecision (142 events).
[4]Downgraded two levels due to serious imprecision (three events) and wide confidence interval.
[5]Downgraded two levels due to serious imprecision (two events) and wide confidence interval.
[6]Downgraded two levels due to moderate inconsistency (I^2 = 45%), heterogeneous method, and a small number of participants.
Patients or population: Participants diagnosed with irritable bowel syndrome according to a physician's opinion or an accepted, symptom-based diagnostic criteria. Settings: Inpatient and outpatient. Intervention: Fecal microbiota transplantation. Comparison: Placebo (or autologous feces). FMT: Fecal microbiota transplantation; IBS: Irritable bowel syndrome; SSS: Symptom severity score; QOL: Quality of life measure; MD: mean difference; NA: Not available; RR: Risk ratio.

Dropouts due to adverse events: Eight trials, comprising 502 participants, reported on dropouts due to adverse events; there were none in the FMT groups, but two instances in the placebo groups. None (0/302) of the FMT groups had dropouts due to adverse events compared to 1% (2/200) in the placebo group (RR 0.24, 95%CI: 0.03-2.17, P = 0.2, I^2 = 0%; Supplementary Figure 2).

Holster *et al*[61] reported that one participant from the placebo group discontinued the trial after the FMT procedure due to discomfort. The dropout due to an adverse event in Holvoet *et al*[44] was the suicide occurring 10 d after the transplantation procedure in the placebo group.

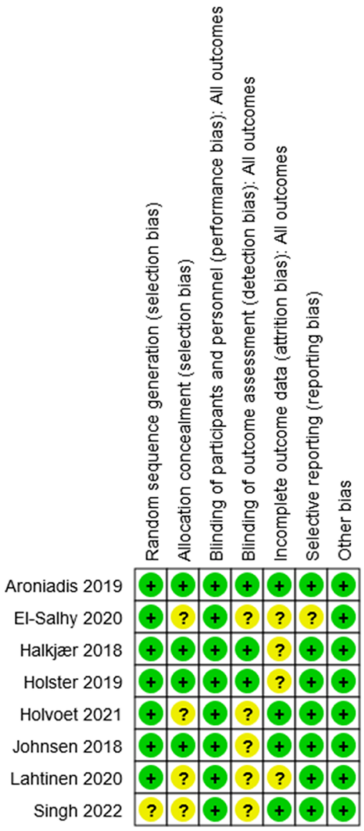
QoL measurements

Seven trials, comprising 406 participants, reported on QoL outcomes. There were no significant differences between the FMT and placebo treatment groups; however, there was a slightly favorable effect seen in the placebo groups (MD -6.30, 95%CI: -13.39 to 0.79, P = 0.08, I^2 = 45%; Figure 5).

Subgroup analyses

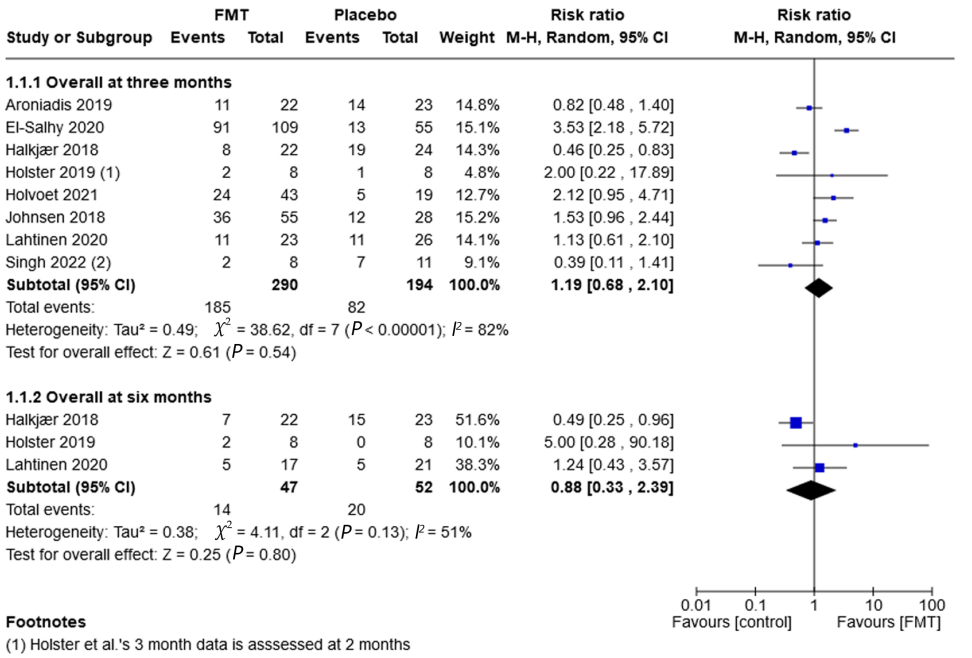
Planned subgroup analyses included fresh *vs* frozen transplant, quantity of transplant, route of administration, type of donor (single *vs* mixed donor), frequency of administration and subtype of IBS (Supplementary Figures 3-8, Figure 6).

Overall, we found that endoscopic delivery (colonoscopy and upper endoscopy) of the FMT improved IBS-SSS after three months (RR 1.56, 95%CI: 1.04-2.34, P = 0.03, I^2 = 0% and RR 3.03, 95%CI: 1.92-4.80, $P \leq 0.00001$, I^2 = 13%; Figure 6). Furthermore, administering a single, large dose of FMT resulted in a greater improvement of the IBS-SSS, while increasing the dose across several treatments was comparable to a placebo (Supplementary Figures 4 and 6). None of the other subgroup analyses



DOI: 10.3748/wjg.v29.i20.3185 **Copyright** ©The Author(s) 2023.

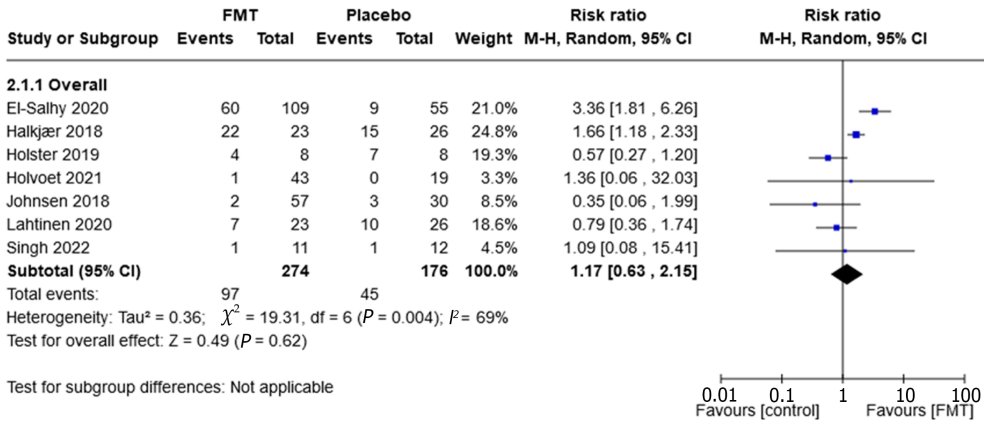
Figure 2 Risk of bias assessments for the trials reviewed.



DOI: 10.3748/wjg.v29.i20.3185 **Copyright** ©The Author(s) 2023.

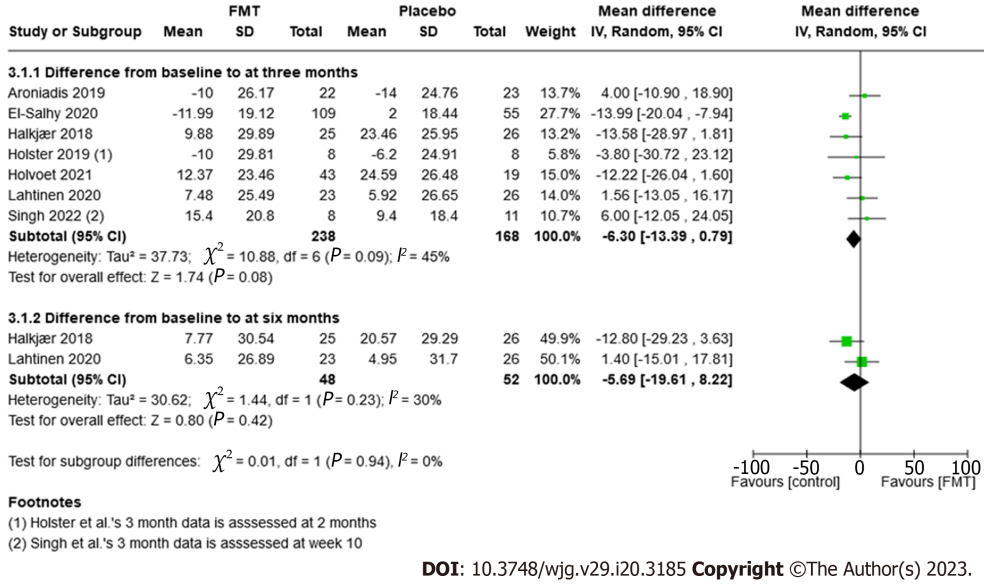
Figure 3 Forest plot of randomised controlled trials of fecal microbiota transplantation for treating irritable bowel syndrome: Improvement of symptoms after three and six months. FMT: Fecal microbiota transplantation.

demonstrated an effect of FMT over placebo.



DOI: 10.3748/wjg.v29.i20.3185 **Copyright** ©The Author(s) 2023.

Figure 4 Forest plot of randomised controlled trials of fecal microbiota transplantation for treating irritable bowel syndrome: Adverse events. FMT: Fecal microbiota transplantation.



DOI: 10.3748/wjg.v29.i20.3185 **Copyright** ©The Author(s) 2023.

Figure 5 Forest plot of randomised controlled trials of fecal microbiota transplantation for treating irritable bowel syndrome: Quality-of-life scores after three and six months.

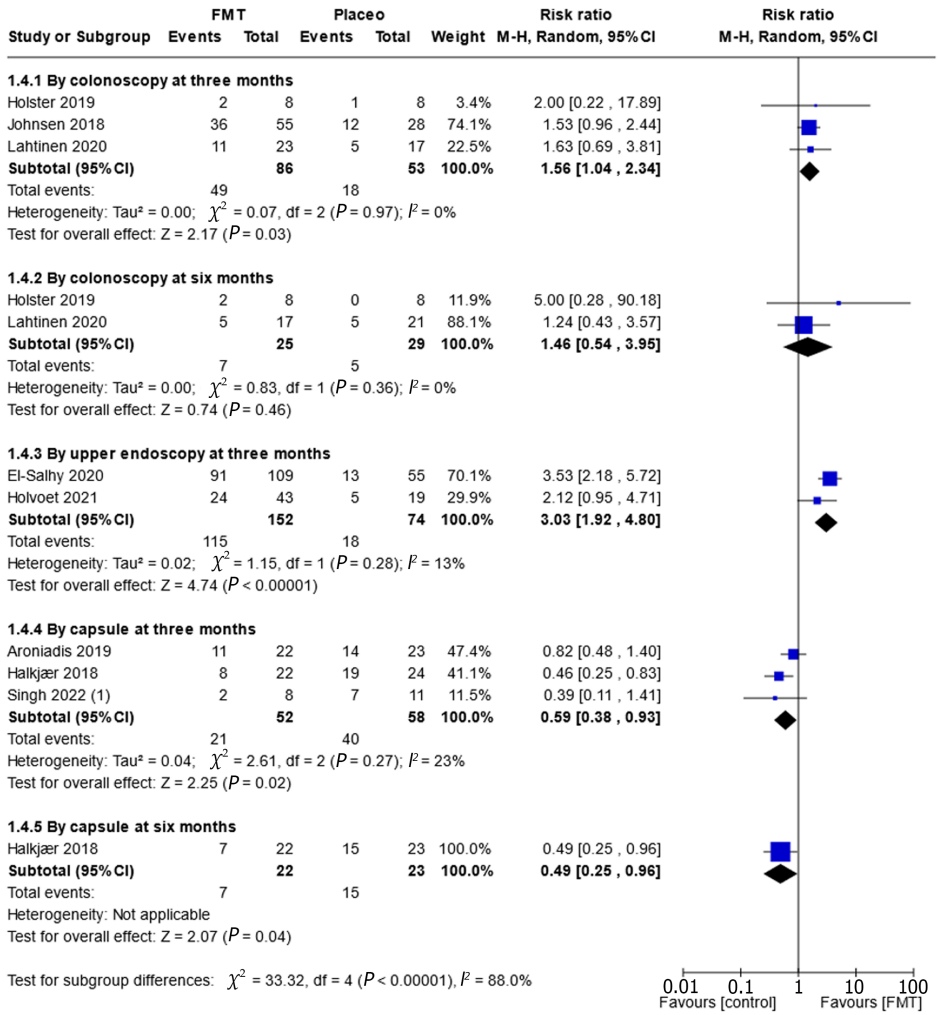
DISCUSSION

This review systematically examined the benefits and harms of FMT *vs* placebo or autologous FMT for the treatment of patients with IBS. Our main objective was to assess the efficacy of FMT for the improvement of symptoms in patients with IBS.

This review combined findings from eight randomised clinical trials that assessed the efficacy of FMT in 465 IBS patients. We found no significant difference in the improvement of symptoms in the FMT groups compared to the placebo groups (P = 0.54). The meta-analysis suggests a favorable, but non-significant, effect on quality of life in patients treated with placebo.

In general, placebo response rates are high in IBS patients. Placebo response estimates in prior meta-analyses range from 16% to 72%[64,70]. Likewise, bowel cleansing might contribute to symptom improvement; however, its effects on the microbiota seem to be transient[71,72].

FMT appears to be safe, with mild and self-limiting gastrointestinal symptoms like nausea, constipation, diarrhoea, and stomach pain - all of which are common IBS symptoms. This conclusion was also reached in a previous review assessing FMT for the treatment of inflammatory bowel disease [73]. FMT was not associated with serious adverse events in the treatment of IBS; three such events were reported in total (two in the placebo group and one in the FMT group) and none were considered to be related to the treatment.



DOI: 10.3748/wjg.v29.i20.3185 **Copyright** ©The Author(s) 2023.

Figure 6 Forest plot of randomised controlled trials of fecal microbiota transplantation for treating irritable bowel syndrome: Improvement of symptoms after three and six months (route of administration subgroup analysis). FMT: Fecal microbiota transplantation.

In general, the results from the trials used for this review were highly heterogeneous. Therefore, it is possible that the absence of a positive overall effect is simply the result of how different the trials were from one another. The trials had pronounced differences in their selection processes for participants and donors, the routes of administration, the transplant quantities, and the frequency of administration. These differences make it difficult to draw conclusions about FMT as a treatment for IBS.

There is scientific evidence to support the hypothesis that FMT may be beneficial for patients with IBS. Observational trials have reported that IBS patients have reduced diversity or aberrant microbiota composition when compared to healthy controls[74]. Altered gut microbiota is also referred to as 'microbiota dysbiosis' and has been connected with disturbances in the microbiota gut-brain axis signaling[75]. Furthermore, other modulating agents targeting the microbiota, such as specific probiotic strains and antibiotics, have had demonstrable effects in IBS patients[76]. However, the underlying causes and mechanisms of dysbiosis in IBS and other diseases remain largely unknown. It has yet to be determined whether dysbiosis is a cause or a consequence of IBS, and even a 'healthy' microbiome has yet to be satisfactorily defined.

All eight trials included in this review reported on changes in gut microbiota after FMT. Aroniadis *et al*[59], El-Salhy *et al*[60], Halkjær *et al*[43], Lahtinen *et al*[58] and Singh *et al*[63] reported that participants receiving FMT saw changes in their gut microbiota that made their profiles more like the donors, when compared to placebo participants. Johnsen *et al*[62] reported these data in a later publication with the same outcome[77]. Holster *et al*[61] reported that microbiota diversity was not significantly affected by either FMT or placebo (autologous FMT). Holvoet *et al*[44] reported that responders to FMT had a higher baseline microbial diversity compared to those whose FMT treatment failed.

The possible effects, both positive and negative, of autologous FMT as placebo should be borne in mind.

In the treatment of recurrent CDI, the highest cure rates have been reported with repeated treatments delivered through lower endoscopy, but delivery through capsules is also highly effective[35,78]. In contrast, in IBS, FMT administered *via* upper or lower endoscopy, rather than capsules, has resulted in significant improvements in IBS-SSS. While much research has focused on FMT capsules[79], it is possible that the engraftment of the donor microbiota is better accomplished through endoscopic methods in IBS patients. Future RCTs in IBS patients that examines the combination of different routes of delivery for strain engraftment could be very interesting. Such studies would also contribute towards a more comprehensive understanding of microbial engraftment dynamics, which is currently lacking. A recent, systematic meta-analysis with shotgun metagenomic results showed that receiving FMT from multiple routes (for example, both *via* colonoscopy and capsules during the same treatment) resulted in increased engraftment[80]. Likewise, El-Salhy *et al*[81] present additional data from their trial and argue for using super donors since the efficacy of FMT appears to be donor-dependent. This argument needs further corroboration. Finally, data about patient and donor diets could prove relevant when determining the optimal patient-donor match[82].

The findings of this review have limited applicability and generalisability. More trials are needed to investigate whether FMT is a beneficial treatment strategy for IBS. Several aspects of the methods used in these trials could have influenced the effect of FMT, such as the route of administration, duration and interval between treatments, and the quantity of faecal microbiota transplanted to the patient. Despite the subgroup analyses we conducted as part of this review, firm conclusions cannot be drawn due to the small number of events and participants in the trials. Nonetheless, the results do suggest a possible beneficial effect in delivering FMT by endoscopy (colonoscopy or gastroscopy) over other routes.

Most of the patients in the trials we reviewed had moderate-to-severe IBS and were diagnosed according to the Rome III criteria. The newest, Rome IV criteria are more rigorous and it is not clear whether the greater homogeneity of IBS study populations they encourage will affect the efficacy of FMT. We recommend that future trials use the Rome IV criteria.

Additional investigations of microbiota, both when selecting patients of interest and after interventions, are needed in order to establish the precise mechanism of action of FMT as a potential treatment for IBS.

CONCLUSION

We did not find evidence to support the use of FMT for IBS patients outside of clinical trials in this systematic review and meta-analysis. We report a possible beneficial effect when delivering FMT by endoscopy (colonoscopy or gastroscopy). FMT appears to be safe, when compared to placebo, in patients with IBS, regardless of route of administration. Further randomised clinical trials are necessary in order to determine the effect of FMT in IBS.

ARTICLE HIGHLIGHTS

Research background

Irritable bowel syndrome (IBS) is a widespread gastrointestinal disorder accompanied by chronic abdominal pain and altered bowel habits. Gut microbiota disturbances have been linked to the pathophysiology of IBS, with fecal microbiota transplantation (FMT) emerging as a potential treatment strategy.

Research motivation

Manipulating gut microbiota composition *via* FMT could offer a promising avenue for IBS treatment, warranting further investigation into its efficacy and safety.

Research objectives

This review and meta-analysis aimed to evaluate the effectiveness and safety of FMT for treating IBS.

Research methods

A comprehensive search of Cochrane Central, MEDLINE, EMBASE, and Web of Science to identify randomised controlled trials (RCT) comparing FMT to placebo or autologous FMT in IBS patients. Primary outcome was improvement of symptoms, while secondary outcomes were quality-of-life scores and adverse events.

Research results

Our analysis incorporated data from eight RCTs with 484 participants. FMT did not result in significant improvement of symptoms when compared to placebo after three months, and no significant

improvement in quality of life was observed. Subgroup analysis indicated that endoscopic FMT delivery led to symptom improvement, whereas FMT capsules did not. FMT was found to be safe.

Research conclusions

This systematic review and meta-analysis do not support FMT as a treatment for IBS outside of clinical trials. Nevertheless, FMT was found to be safe.

Research perspectives

Large-scale, RCTs are needed to confirm or refute these findings. Investigating the potential significance of combining different FMT delivery routes for strain engraftment could provide a more comprehensive understanding of microbial engraftment dynamics in IBS patients.

FOOTNOTES

Author contributions: Halkjær SI, Gluud LL and Petersen AM conceived the review; Halkjær SI, Lo B, Cold F, Højer Christensen A, Gluud LL and Petersen AM wrote the protocol for the review; Halkjær SI and Lo B searched and selected studies for the review; Halkjær SI, Lo B, Holster S, König J, Brummer RJ, Aroniadis OC, Holvoet T and Lahtinen P collected data for the review; Lo B, Cold F and Gluud LL assessed the risk of bias in the studies used; Halkjær SI, Lo B, Gluud LL and Petersen AM assessed the certainty of the evidence; Halkjær SI and Lo B interpreted the data; Halkjær SI and Lo B wrote the review; Halkjær SI, Lo B, Cold F, Højer Christensen A, Petersen AM, Holster S, König J, Brummer RJ, Aroniadis OC, Holvoet T, Lahtinen P and Gluud LL commented on the review. All authors have read and approved the final manuscript. None of the authors have extracted data from, or assessed the risk of bias in, trials they carried out themselves.

Conflict-of-interest statement: None of the authors report relevant conflicts of interest for this article.

PRISMA 2009 Checklist statement: The authors have read the PRISMA 2009 Checklist, and the manuscript was prepared and revised according to the PRISMA 2009 Checklist.

Open-Access: This article is an open-access article that was selected by an in-house editor and fully peer-reviewed by external reviewers. It is distributed in accordance with the Creative Commons Attribution NonCommercial (CC BY-NC 4.0) license, which permits others to distribute, remix, adapt, build upon this work non-commercially, and license their derivative works on different terms, provided the original work is properly cited and the use is non-commercial. See: https://creativecommons.org/Licenses/by-nc/4.0/

Country/Territory of origin: Denmark

ORCID number: Sofie Ingdam Halkjær 0000-0001-7518-4252; Bobby Lo 0000-0002-0252-9341; Julia König 0000-0003-0466-1861; Robert Jan Brummer 0000-0002-0362-0008; Perttu Lahtinen 0000-0001-6430-4642; Tom Holvoet 0000-0002-4540-4012; Lise Lotte Gluud 0000-0002-9462-4468; Andreas Munk Petersen 0000-0003-0531-0553.

S-Editor: Zhang H
L-Editor: A
P-Editor: Cai YX

REFERENCES

1 **Lovell RM**, Ford AC. Global prevalence of and risk factors for irritable bowel syndrome: a meta-analysis. *Clin Gastroenterol Hepatol* 2012; **10**: 712-721.e4 [PMID: 22426087 DOI: 10.1016/j.cgh.2012.02.029]
2 **Spiegel BM**. The burden of IBS: looking at metrics. *Curr Gastroenterol Rep* 2009; **11**: 265-269 [PMID: 19615301 DOI: 10.1007/s11894-009-0039-x]
3 **Canavan C**, West J, Card T. Review article: the economic impact of the irritable bowel syndrome. *Aliment Pharmacol Ther* 2014; **40**: 1023-1034 [PMID: 25199904 DOI: 10.1111/apt.12938]
4 **Saha L**. Irritable bowel syndrome: pathogenesis, diagnosis, treatment, and evidence-based medicine. *World J Gastroenterol* 2014; **20**: 6759-6773 [PMID: 24944467 DOI: 10.3748/wjg.v20.i22.6759]
5 **Drossman DA**. Functional gastrointestinal disorders: what's new for Rome IV? *Lancet Gastroenterol Hepatol* 2016; **1**: 6-8 [PMID: 28404114 DOI: 10.1016/S2468-1253(16)30022-X]
6 **Choi HH**, Cho YS. Fecal Microbiota Transplantation: Current Applications, Effectiveness, and Future Perspectives. *Clin Endosc* 2016; **49**: 257-265 [PMID: 26956193 DOI: 10.5946/ce.2015.117]
7 **Kelly CR**, Kahn S, Kashyap P, Laine L, Rubin D, Atreja A, Moore T, Wu G. Update on Fecal Microbiota Transplantation 2015: Indications, Methodologies, Mechanisms, and Outlook. *Gastroenterology* 2015; **149**: 223-237 [PMID: 25982290 DOI: 10.1053/j.gastro.2015.05.008]
8 **Khanna S**, Tosh PK. A clinician's primer on the role of the microbiome in human health and disease. *Mayo Clin Proc* 2014; **89**: 107-114 [PMID: 24388028 DOI: 10.1016/j.mayocp.2013.10.011]

9 **Spiller R**, Garsed K. Postinfectious irritable bowel syndrome. *Gastroenterology* 2009; **136**: 1979-1988 [PMID: 19457422 DOI: 10.1053/j.gastro.2009.02.074]

10 **Pinn DM**, Aroniadis OC, Brandt LJ. Is fecal microbiota transplantation (FMT) an effective treatment for patients with functional gastrointestinal disorders (FGID)? *Neurogastroenterol Motil* 2015; **27**: 19-29 [PMID: 25424663 DOI: 10.1111/nmo.12479]

11 **Kassinen A**, Krogius-Kurikka L, Mäkivuokko H, Rinttilä T, Paulin L, Corander J, Malinen E, Apajalahti J, Palva A. The fecal microbiota of irritable bowel syndrome patients differs significantly from that of healthy subjects. *Gastroenterology* 2007; **133**: 24-33 [PMID: 17631127 DOI: 10.1053/j.gastro.2007.04.005]

12 **King TS**, Elia M, Hunter JO. Abnormal colonic fermentation in irritable bowel syndrome. *Lancet* 1998; **352**: 1187-1189 [PMID: 9777836 DOI: 10.1016/s0140-6736(98)02146-1]

13 **Malinen E**, Rinttilä T, Kajander K, Mättö J, Kassinen A, Krogius L, Saarela M, Korpela R, Palva A. Analysis of the fecal microbiota of irritable bowel syndrome patients and healthy controls with real-time PCR. *Am J Gastroenterol* 2005; **100**: 373-382 [PMID: 15667495 DOI: 10.1111/j.1572-0241.2005.40312.x]

14 **Mättö J**, Maunuksela L, Kajander K, Palva A, Korpela R, Kassinen A, Saarela M. Composition and temporal stability of gastrointestinal microbiota in irritable bowel syndrome--a longitudinal study in IBS and control subjects. *FEMS Immunol Med Microbiol* 2005; **43**: 213-222 [PMID: 15747442 DOI: 10.1016/j.femsim.2004.08.009]

15 **Hugerth LW**, Andreasson A, Talley NJ, Forsberg AM, Kjellström L, Schmidt PT, Agreus L, Engstrand L. No distinct microbiome signature of irritable bowel syndrome found in a Swedish random population. *Gut* 2020; **69**: 1076-1084 [PMID: 31601615 DOI: 10.1136/gutjnl-2019-318717]

16 **Rodiño-Janeiro BK**, Vicario M, Alonso-Cotoner C, Pascua-García R, Santos J. A Review of Microbiota and Irritable Bowel Syndrome: Future in Therapies. *Adv Ther* 2018; **35**: 289-310 [PMID: 29498019 DOI: 10.1007/s12325-018-0673-5]

17 **Chong PP**, Chin VK, Looi CY, Wong WF, Madhavan P, Yong VC. The Microbiome and Irritable Bowel Syndrome - A Review on the Pathophysiology, Current Research and Future Therapy. *Front Microbiol* 2019; **10**: 1136 [PMID: 31244784 DOI: 10.3389/fmicb.2019.01136]

18 **Didari T**, Mozaffari S, Nikfar S, Abdollahi M. Effectiveness of probiotics in irritable bowel syndrome: Updated systematic review with meta-analysis. *World J Gastroenterol* 2015; **21**: 3072-3084 [PMID: 25780308 DOI: 10.3748/wjg.v21.i10.3072]

19 **Hungin AP**, Mulligan C, Pot B, Whorwell P, Agréus L, Fracasso P, Lionis C, Mendive J, Philippart de Foy JM, Rubin G, Winchester C, de Wit N; European Society for Primary Care Gastroenterology. Systematic review: probiotics in the management of lower gastrointestinal symptoms in clinical practice -- an evidence-based international guide. *Aliment Pharmacol Ther* 2013; **38**: 864-886 [PMID: 23981066 DOI: 10.1111/apt.12460]

20 **El-Salhy M**, Mazzawi T. Fecal microbiota transplantation for managing irritable bowel syndrome. *Expert Rev Gastroenterol Hepatol* 2018; **12**: 439-445 [PMID: 29493330 DOI: 10.1080/17474124.2018.1447380]

21 **Cammarota G**, Ianiro G, Tilg H, Rajilić-Stojanović M, Kump P, Satokari R, Sokol H, Arkkila P, Pintus C, Hart A, Segal J, Aloi M, Masucci L, Molinaro A, Scaldaferri F, Gasbarrini G, Lopez-Sanroman A, Link A, de Groot P, de Vos WM, Högenauer C, Malfertheiner P, Mattila E, Milosavljević T, Nieuwdorp M, Sanguinetti M, Simren M, Gasbarrini A; European FMT Working Group. European consensus conference on faecal microbiota transplantation in clinical practice. *Gut* 2017; **66**: 569-580 [PMID: 28087657 DOI: 10.1136/gutjnl-2016-313017]

22 **Zhang F**, Luo W, Shi Y, Fan Z, Ji G. Should we standardize the 1,700-year-old fecal microbiota transplantation? *Am J Gastroenterol* 2012; **107**: 1755; author reply p.1755-1755; author reply p.1756 [PMID: 23160295 DOI: 10.1038/ajg.2012.251]

23 **Sha S**, Liang J, Chen M, Xu B, Liang C, Wei N, Wu K. Systematic review: faecal microbiota transplantation therapy for digestive and nondigestive disorders in adults and children. *Aliment Pharmacol Ther* 2014; **39**: 1003-1032 [PMID: 24641570 DOI: 10.1111/apt.12699]

24 **van Nood E**, Vrieze A, Nieuwdorp M, Fuentes S, Zoetendal EG, de Vos WM, Visser CE, Kuijper EJ, Bartelsman JF, Tijssen JG, Speelman P, Dijkgraaf MG, Keller JJ. Duodenal infusion of donor feces for recurrent Clostridium difficile. *N Engl J Med* 2013; **368**: 407-415 [PMID: 23323867 DOI: 10.1056/NEJMoa1205037]

25 **Wortelboer K**, Nieuwdorp M, Herrema H. Fecal microbiota transplantation beyond Clostridioides difficile infections. *EBioMedicine* 2019; **44**: 716-729 [PMID: 31201141 DOI: 10.1016/j.ebiom.2019.05.066]

26 **Sokol H**, Landman C, Seksik P, Berard L, Montil M, Nion-Larmurier I, Bourrier A, Le Gall G, Lalande V, De Rougemont A, Kirchgesner J, Daguenel A, Cachanado M, Rousseau A, Drouet É, Rosenzwajg M, Hagege H, Dray X, Klatzman D, Marteau P; Saint-Antoine IBD Network, Beaugerie L, Simon T. Fecal microbiota transplantation to maintain remission in Crohn's disease: a pilot randomized controlled study. *Microbiome* 2020; **8**: 12 [PMID: 32014035 DOI: 10.1186/s40168-020-0792-5]

27 **Stojek M**, Jabłońska A, Adrych K. The Role of Fecal Microbiota Transplantation in the Treatment of Inflammatory Bowel Disease. *J Clin Med* 2021; **10** [PMID: 34575166 DOI: 10.3390/jcm10184055]

28 **Costello SP**, Soo W, Bryant RV, Jairath V, Hart AL, Andrews JM. Systematic review with meta-analysis: faecal microbiota transplantation for the induction of remission for active ulcerative colitis. *Aliment Pharmacol Ther* 2017; **46**: 213-224 [PMID: 28612983 DOI: 10.1111/apt.14173]

29 **Cammarota G**, Ianiro G, Kelly CR, Mullish BH, Allegretti JR, Kassam Z, Putignani L, Fischer M, Keller JJ, Costello SP, Sokol H, Kump P, Satokari R, Kahn SA, Kao D, Arkkila P, Kuijper EJ, Vehreschild MJG, Pintus C, Lopetuso L, Masucci L, Scaldaferri F, Terveer EM, Nieuwdorp M, López-Sanromán A, Kupcinskas J, Hart A, Tilg H, Gasbarrini A. International consensus conference on stool banking for faecal microbiota transplantation in clinical practice. *Gut* 2019; **68**: 2111-2121 [PMID: 31563878 DOI: 10.1136/gutjnl-2019-319548]

30 **Keller JJ**, Ooijevaar RE, Hvas CL, Terveer EM, Lieberknecht SC, Högenauer C, Arkkila P, Sokol H, Gridnyev O, Mégraud F, Kump PK, Nakov R, Goldenberg SD, Satokari R, Tkatch S, Sanguinetti M, Cammarota G, Dorofeev A, Gubska O, Ianiro G, Mattila E, Arasaradnam RP, Sarin SK, Sood A, Putignani L, Alric L, Baunwall SMD, Kupcinskas J, Link A, Goorhuis AG, Verspaget HW, Ponsioen C, Hold GL, Tilg H, Kassam Z, Kuijper EJ, Gasbarrini A, Mulder CJJ, Williams HRT, Vehreschild MJGT. A standardised model for stool banking for faecal microbiota transplantation: a

consensus report from a multidisciplinary UEG working group. *United European Gastroenterol J* 2021; **9**: 229-247 [PMID: 33151137 DOI: 10.1177/2050640620967898]

31 **König J**, Siebenhaar A, Högenauer C, Arkkila P, Nieuwdorp M, Norén T, Ponsioen CY, Rosien U, Rossen NG, Satokari R, Stallmach A, de Vos W, Keller J, Brummer RJ. Consensus report: faecal microbiota transfer - clinical applications and procedures. *Aliment Pharmacol Ther* 2017; **45**: 222-239 [PMID: 27891639 DOI: 10.1111/apt.13868]

32 **Lee CH**, Steiner T, Petrof EO, Smieja M, Roscoe D, Nematallah A, Weese JS, Collins S, Moayyedi P, Crowther M, Ropeleski MJ, Jayaratne P, Higgins D, Li Y, Rau NV, Kim PT. Frozen vs Fresh Fecal Microbiota Transplantation and Clinical Resolution of Diarrhea in Patients With Recurrent Clostridium difficile Infection: A Randomized Clinical Trial. *JAMA* 2016; **315**: 142-149 [PMID: 26757463 DOI: 10.1001/jama.2015.18098]

33 **Youngster I**, Russell GH, Pindar C, Ziv-Baran T, Sauk J, Hohmann EL. Oral, capsulized, frozen fecal microbiota transplantation for relapsing Clostridium difficile infection. *JAMA* 2014; **312**: 1772-1778 [PMID: 25322359 DOI: 10.1001/jama.2014.13875]

34 **Satokari R**, Mattila E, Kainulainen V, Arkkila PE. Simple faecal preparation and efficacy of frozen inoculum in faecal microbiota transplantation for recurrent Clostridium difficile infection--an observational cohort study. *Aliment Pharmacol Ther* 2015; **41**: 46-53 [PMID: 25355279 DOI: 10.1111/apt.13009]

35 **Baunwall SMD**, Lee MM, Eriksen MK, Mullish BH, Marchesi JR, Dahlerup JF, Hvas CL. Faecal microbiota transplantation for recurrent Clostridioides difficile infection: An updated systematic review and meta-analysis. *EClinicalMedicine* 2020; **29-30**: 100642 [PMID: 33437951 DOI: 10.1016/j.eclinm.2020.100642]

36 **Zellmer C**, De Wolfe TJ, Van Hoof S, Blakney R, Safdar N. Patient Perspectives on Fecal Microbiota Transplantation for Clostridium Difficile Infection. *Infect Dis Ther* 2016; **5**: 155-164 [PMID: 27048199 DOI: 10.1007/s40121-016-0106-1]

37 **Lee KN**, Lee OY. Intestinal microbiota in pathophysiology and management of irritable bowel syndrome. *World J Gastroenterol* 2014; **20**: 8886-8897 [PMID: 25083061 DOI: 10.3748/wjg.v20.i27.8886]

38 **Fan WT**, Ding C, Xu NN, Zong S, Ma P, Gu B. Close association between intestinal microbiota and irritable bowel syndrome. *Eur J Clin Microbiol Infect Dis* 2017; **36**: 2303-2317 [PMID: 28785822 DOI: 10.1007/s10096-017-3060-2]

39 **Ringel-Kulka T**, Benson AK, Carroll IM, Kim J, Legge RM, Ringel Y. Molecular characterization of the intestinal microbiota in patients with and without abdominal bloating. *Am J Physiol Gastrointest Liver Physiol* 2016; **310**: G417-G426 [PMID: 26702134 DOI: 10.1152/ajpgi.00044.2015]

40 **Jeffery IB**, O'Toole PW, Öhman L, Claesson MJ, Deane J, Quigley EM, Simrén M. An irritable bowel syndrome subtype defined by species-specific alterations in faecal microbiota. *Gut* 2012; **61**: 997-1006 [PMID: 22180058 DOI: 10.1136/gutjnl-2011-301501]

41 **Mizuno S**, Masaoka T, Naganuma M, Kishimoto T, Kitazawa M, Kurokawa S, Nakashima M, Takeshita K, Suda W, Mimura M, Hattori M, Kanai T. Bifidobacterium-Rich Fecal Donor May Be a Positive Predictor for Successful Fecal Microbiota Transplantation in Patients with Irritable Bowel Syndrome. *Digestion* 2017; **96**: 29-38 [PMID: 28628918 DOI: 10.1159/000471919]

42 **Vaughn BP**, Vatanen T, Allegretti JR, Bai A, Xavier RJ, Korzenik J, Gevers D, Ting A, Robson SC, Moss AC. Increased Intestinal Microbial Diversity Following Fecal Microbiota Transplant for Active Crohn's Disease. *Inflamm Bowel Dis* 2016; **22**: 2182-2190 [PMID: 27542133 DOI: 10.1097/MIB.0000000000000893]

43 **Halkjær SI**, Christensen AH, Lo BZS, Browne PD, Günther S, Hansen LH, Petersen AM. Faecal microbiota transplantation alters gut microbiota in patients with irritable bowel syndrome: results from a randomised, double-blind placebo-controlled study. *Gut* 2018; **67**: 2107-2115 [PMID: 29980607 DOI: 10.1136/gutjnl-2018-316434]

44 **Holvoet T**, Joossens M, Vázquez-Castellanos JF, Christiaens E, Heyerick L, Boelens J, Verhasselt B, van Vlierberghe H, De Vos M, Raes J, De Looze D. Fecal Microbiota Transplantation Reduces Symptoms in Some Patients With Irritable Bowel Syndrome With Predominant Abdominal Bloating: Short- and Long-term Results From a Placebo-Controlled Randomized Trial. *Gastroenterology* 2021; **160**: 145-157.e8 [PMID: 32681922 DOI: 10.1053/j.gastro.2020.07.013]

45 **Li SS**, Zhu A, Benes V, Costea PI, Hercog R, Hildebrand F, Huerta-Cepas J, Nieuwdorp M, Salojärvi J, Voigt AY, Zeller G, Sunagawa S, de Vos WM, Bork P. Durable coexistence of donor and recipient strains after fecal microbiota transplantation. *Science* 2016; **352**: 586-589 [PMID: 27126044 DOI: 10.1126/science.aad8852]

46 **Pimentel M**, Lembo A. Microbiome and Its Role in Irritable Bowel Syndrome. *Dig Dis Sci* 2020; **65**: 829-839 [PMID: 32026278 DOI: 10.1007/s10620-020-06109-5]

47 **Wang L**, Alammar N, Singh R, Nanavati J, Song Y, Chaudhary R, Mullin GE. Gut Microbial Dysbiosis in the Irritable Bowel Syndrome: A Systematic Review and Meta-Analysis of Case-Control Studies. *J Acad Nutr Diet* 2020; **120**: 565-586 [PMID: 31473156 DOI: 10.1016/j.jand.2019.05.015]

48 **Halkjær SI**, Boolsen AW, Günther S, Christensen AH, Petersen AM. Can fecal microbiota transplantation cure irritable bowel syndrome? *World J Gastroenterol* 2017; **23**: 4112-4120 [PMID: 28652664 DOI: 10.3748/wjg.v23.i22.4112]

49 **Andrews P**, Barnes P, Borody T. Chronic constipation reversed by restoration of bowel flora. A case and a hypothesis. *Eur J Gastroenterol Hepatol* 1992; **4**: 245-247

50 **Borody TJ**, George L, Andrews P, Brandl S, Noonan S, Cole P, Hyland L, Morgan A, Maysey J, Moore-Jones D. Bowel-flora alteration: a potential cure for inflammatory bowel disease and irritable bowel syndrome? *Med J Aust* 1989; **150**: 604 [PMID: 2783214 DOI: 10.5694/j.1326-5377.1989.tb136704.x]

51 **Borody TJ**, Warren EF, Leis SM, Surace R, Ashman O, Siarakas S. Bacteriotherapy using fecal flora: toying with human motions. *J Clin Gastroenterol* 2004; **38**: 475-483 [PMID: 15220681 DOI: 10.1097/01.mcg.0000128988.13808.dc]

52 **Cruz Aguilar R**, Buch T, Bajbouj. Fecal microbiota transplantation as a novel therapy for irritable bowel syndrome with predominant diarrhea. *Neurogastroenterol Motil* 2015; 110 [DOI: 10.1111/nmo.14353]

53 **Holvoet T**, Boelens J, Joossens M, Raes J, De Vos M, De Looze D. Fecal Microbiota Transplantation in Irritable Bowel Syndrome With Bloating: Results From a Prospective Pilot Study. *Gastroenterology* 2015; **148**: S963-S964 [DOI: 10.1016/s0016-5085(15)33291-1]

54 **Hong J**, Bang B, Shin Y, Kim H, Kwon K. Treatment of Irritable Bowel Syndrome with Fecal Microbiota Transplantation: A case series of 10 patients. *United European Gastroenterol J* 2016; A102 [DOI: 10.1177/2050640619866990]

55 **Mazzawi T**, El-Salhy M, Lied GA, Hausken T. The Effects of Fecal Microbiota Transplantation on the Symptoms and the Duodenal Neurogenin 3, Musashi 1, and Enteroendocrine Cells in Patients With Diarrhea-Predominant Irritable Bowel Syndrome. *Front Cell Infect Microbiol* 2021; **11**: 524851 [PMID: 34055657 DOI: 10.3389/fcimb.2021.524851]

56 **Pinn D**, Aroniadis O, Brandt L. Follow-up Study of Fecal Microbiota Transplantation (FMT) for the Treatment of Refractory Irritable Bowel Syndrome (IBS) 1862. *Am J Gastroenterol* 2013; **108**: S563 [DOI: 10.14309/00000434-201310001-01862]

57 **Syzenko G**, Budovska L, Puchkov K. P0397 Efficiency of FMT in cases of 'Treatment-resistant' IBS. *United European Gastroenterol J* 2016; **2**: A294

58 **Lahtinen P**, Jalanka J, Hartikainen A, Mattila E, Hillilä M, Punkkinen J, Koskenpato J, Anttila VJ, Tillonen J, Satokari R, Arkkila P. Randomised clinical trial: faecal microbiota transplantation versus autologous placebo administered *via* colonoscopy in irritable bowel syndrome. *Aliment Pharmacol Ther* 2020; **51**: 1321-1331 [PMID: 32343000 DOI: 10.1111/apt.15740]

59 **Aroniadis OC**, Brandt LJ, Oneto C, Feuerstadt P, Sherman A, Wolkoff AW, Kassam Z, Sadovsky RG, Elliott RJ, Budree S, Kim M, Keller MJ. Faecal microbiota transplantation for diarrhoea-predominant irritable bowel syndrome: a double-blind, randomised, placebo-controlled trial. *Lancet Gastroenterol Hepatol* 2019; **4**: 675-685 [PMID: 31326345 DOI: 10.1016/S2468-1253(19)30198-0]

60 **El-Salhy M**, Hatlebakk JG, Gilja OH, Bråthen Kristoffersen A, Hausken T. Efficacy of faecal microbiota transplantation for patients with irritable bowel syndrome in a randomised, double-blind, placebo-controlled study. *Gut* 2020; **69**: 859-867 [PMID: 31852769 DOI: 10.1136/gutjnl-2019-319630]

61 **Holster S**, Lindqvist CM, Repsilber D, Salonen A, de Vos WM, König J, Brummer RJ. The Effect of Allogenic Versus Autologous Fecal Microbiota Transfer on Symptoms, Visceral Perception and Fecal and Mucosal Microbiota in Irritable Bowel Syndrome: A Randomized Controlled Study. *Clin Transl Gastroenterol* 2019; **10**: e00034 [PMID: 31009405 DOI: 10.14309/ctg.0000000000000034]

62 **Johnsen PH**, Hilpüsch F, Cavanagh JP, Leikanger IS, Kolstad C, Valle PC, Goll R. Faecal microbiota transplantation versus placebo for moderate-to-severe irritable bowel syndrome: a double-blind, randomised, placebo-controlled, parallel-group, single-centre trial. *Lancet Gastroenterol Hepatol* 2018; **3**: 17-24 [PMID: 29100842 DOI: 10.1016/S2468-1253(17)30338-2]

63 **Singh P**, Alm EJ, Kelley JM, Cheng V, Smith M, Kassam Z, Nee J, Iturrino J, Lembo A. Effect of antibiotic pretreatment on bacterial engraftment after Fecal Microbiota Transplant (FMT) in IBS-D. *Gut Microbes* 2022; **14**: 2020067 [PMID: 35014601 DOI: 10.1080/19490976.2021.2020067]

64 **Ford AC**, Moayyedi P. Meta-analysis: factors affecting placebo response rate in the irritable bowel syndrome. *Aliment Pharmacol Ther* 2010; **32**: 144-158 [PMID: 20412064 DOI: 10.1111/j.1365-2036.2010.04328.x]

65 **Higgins JPT**, Green S (editors). Cochrane Handbook for Systematic Reviews of Interventions Version 5.1.0 [updated March 2011]. The Cochrane Collaboration, 2011

66 **Halkjær SI**, Lo B, Cold F, Christensen AHH, Gluud LL, Petersen AM. Fecal microbiota transplantation for treatment of irritable bowel syndrome (Protocol). *Cochrane Database Syst Rev* 2020 [DOI: 10.1002/14651858.CD013602]

67 **Simren M**, Palsson OS, Whitehead WE. Update on Rome IV Criteria for Colorectal Disorders: Implications for Clinical Practice. *Curr Gastroenterol Rep* 2017; **19**: 15 [PMID: 28374308 DOI: 10.1007/s11894-017-0554-0]

68 **Cochrane Consumers and Communication La Trobe University**, Ryan R, Synnot A, M P, Hill S. Data extraction template. 2018 [DOI: 10.26181/5b57cfd711743]

69 **Higgins JP**, Altman DG, Gøtzsche PC, Jüni P, Moher D, Oxman AD, Savovic J, Schulz KF, Weeks L, Sterne JA; Cochrane Bias Methods Group; Cochrane Statistical Methods Group. The Cochrane Collaboration's tool for assessing risk of bias in randomised trials. *BMJ* 2011; **343**: d5928 [PMID: 22008217 DOI: 10.1136/bmj.d5928]

70 **Patel SM**, Stason WB, Legedza A, Ock SM, Kaptchuk TJ, Conboy L, Canenguez K, Park JK, Kelly E, Jacobson E, Kerr CE, Lembo AJ. The placebo effect in irritable bowel syndrome trials: a meta-analysis. *Neurogastroenterol Motil* 2005; **17**: 332-340 [PMID: 15916620 DOI: 10.1111/j.1365-2982.2005.00650.x]

71 **Li M**, Qian W, Yu L, Tian F, Zhang H, Chen W, Xue Y, Zhai Q. Multi-Time-Point Fecal Sampling in Human and Mouse Reveals the Formation of New Homeostasis in Gut Microbiota after Bowel Cleansing. *Microorganisms* 2022; **10** [PMID: 36557570 DOI: 10.3390/microorganisms10122317]

72 **Jalanka J**, Hillamaa A, Satokari R, Mattila E, Anttila VJ, Arkkila P. The long-term effects of faecal microbiota transplantation for gastrointestinal symptoms and general health in patients with recurrent Clostridium difficile infection. *Aliment Pharmacol Ther* 2018; **47**: 371-379 [PMID: 29226561 DOI: 10.1111/apt.14443]

73 **Imdad A**, Nicholson MR, Tanner-Smith EE, Zackular JP, Gomez-Duarte OG, Beaulieu DB, Acra S. Fecal transplantation for treatment of inflammatory bowel disease. *Cochrane Database Syst Rev* 2018; **11**: CD012774 [PMID: 30480772 DOI: 10.1002/14651858.CD012774.pub2]

74 **Liu HN**, Wu H, Chen YZ, Chen YJ, Shen XZ, Liu TT. Altered molecular signature of intestinal microbiota in irritable bowel syndrome patients compared with healthy controls: A systematic review and meta-analysis. *Dig Liver Dis* 2017; **49**: 331-337 [PMID: 28179092 DOI: 10.1016/j.dld.2017.01.142]

75 **Mayer EA**, Knight R, Mazmanian SK, Cryan JF, Tillisch K. Gut microbes and the brain: paradigm shift in neuroscience. *J Neurosci* 2014; **34**: 15490-15496 [PMID: 25392516 DOI: 10.1523/JNEUROSCI.3299-14.2014]

76 **Ford AC**, Harris LA, Lacy BE, Quigley EMM, Moayyedi P. Systematic review with meta-analysis: the efficacy of prebiotics, probiotics, synbiotics and antibiotics in irritable bowel syndrome. *Aliment Pharmacol Ther* 2018; **48**: 1044-1060 [PMID: 30294792 DOI: 10.1111/apt.15001]

77 **Goll R**, Johnsen PH, Hjerde E, Diab J, Valle PC, Hilpusch F, Cavanagh JP. Effects of fecal microbiota transplantation in subjects with irritable bowel syndrome are mirrored by changes in gut microbiome. *Gut Microbes* 2020; **12**: 1794263 [PMID: 32991818 DOI: 10.1080/19490976.2020.1794263]

78 **Cold F**, Baunwall SMD, Dahlerup JF, Petersen AM, Hvas CL, Hansen LH. Systematic review with meta-analysis: encapsulated faecal microbiota transplantation - evidence for clinical efficacy. *Therap Adv Gastroenterol* 2021; **14**: 17562848211041004 [PMID: 34484424 DOI: 10.1177/17562848211041004]

79 **Franc A**, Vetchý D, Fülöpová N. Commercially Available Enteric Empty Hard Capsules, Production Technology and Application. *Pharmaceuticals (Basel)* 2022; **15** [PMID: 36422528 DOI: 10.3390/ph15111398]

80 **Ianiro G**, Punčochář M, Karcher N, Porcari S, Armanini F, Asnicar F, Beghini F, Blanco-Míguez A, Cumbo F, Manghi P, Pinto F, Masucci L, Quaranta G, De Giorgi S, Sciumè GD, Bibbò S, Del Chierico F, Putignani L, Sanguinetti M, Gasbarrini A, Valles-Colomer M, Cammarota G, Segata N. Variability of strain engraftment and predictability of microbiome composition after fecal microbiota transplantation across different diseases. *Nat Med* 2022; **28**: 1913-1923 [PMID: 36109637 DOI: 10.1038/s41591-022-01964-3]

81 **El-Salhy M**, Hausken T, Hatlebakk JG. Current status of fecal microbiota transplantation for irritable bowel syndrome. *Neurogastroenterol Motil* 2021; **33**: e14157 [PMID: 34236740 DOI: 10.1111/nmo.14157]

82 **Orr MR**. The biodiversity dose-response curve translates theory and practice from ecological restoration into research and clinical priorities for fecal microbiota transplantation. *Front Med (Lausanne)* 2022; **9**: 1059148 [PMID: 36438048 DOI: 10.3389/fmed.2022.1059148]

World Journal of Gastroenterology

Submit a Manuscript: https://www.f6publishing.com

World J Gastroenterol 2023 May 28; 29(20): 3203-3215

DOI: 10.3748/wjg.v29.i20.3203

ISSN 1007-9327 (print) ISSN 2219-2840 (online)

SCIENTOMETRICS

Global research trends on diet and nutrition in Crohn's disease

Muna Shakhshir, Sa'ed H Zyoud

Specialty type: Nutrition and dietetics

Provenance and peer review: Invited article; Externally peer reviewed.

Peer-review model: Single blind

Peer-review report's scientific quality classification

Grade A (Excellent): 0
Grade B (Very good): B, B
Grade C (Good): C
Grade D (Fair): 0
Grade E (Poor): 0

P-Reviewer: Bukhari SM, Saudi Arabia; Leowattana W, Thailand; Valek V, Czech Republic

Received: January 9, 2023
Peer-review started: January 9, 2023
First decision: March 8, 2023
Revised: March 20, 2023
Accepted: May 4, 2023
Article in press: May 4, 2023
Published online: May 28, 2023

Muna Shakhshir, Department of Nutrition, An-Najah National University Hospital, Nablus 44839, Palestine

Sa'ed H Zyoud, Department of Clinical and Community Pharmacy, College of Medicine and Health Sciences, An-Najah National University, Nablus 44839, Palestine

Sa'ed H Zyoud, Poison Control and Drug Information Center (PCDIC), College of Medicine and Health Sciences, An-Najah National University, Nablus 44839, Palestine

Sa'ed H Zyoud, Clinical Research Centre, An-Najah National University Hospital, Nablus 44839, Palestine

Corresponding author: Sa'ed H Zyoud, PhD, Full Professor, Department of Clinical and Community Pharmacy, College of Medicine and Health Sciences, An-Najah National University, Academic Street, Nablus 44839, Palestine. saedzyoud@yahoo.com

Abstract

BACKGROUND

Crohn's disease represents a challenge for patients concerned with the modified diet regimen as well as practitioners who seek the best nutritional therapy. Crohn's disease can alter the body's ability to digest food and to absorb nutrients, resulting in severe vitamin deficiencies, malnutrition and sometimes life-threatening complications. However, a comprehensive bibliometric analysis is lacking to map the current links between nutrition and Crohn's disease in terms of the number of citations, geographic distribution and growth trends of publications.

AIM

To introduce the current state of research as well as hotspots in the field of nutrition and Crohn's disease from a bibliometric standpoint.

METHODS

We searched the Scopus database and selected the relevant literature on nutrition and Crohn's disease that met the inclusion criteria. We analyzed the publication trends and research hotspots by using video object segmentation viewer software.

RESULTS

We included 1237 publications. The number of documents published each year has increased steadily. The United States and the University of Otago, Christchurch, have had the highest productivity, with 208 (16.81%) and 29 (2.34%) documents, respectively. The "role of exclusive enteral nutrition for complicated Crohn's disease" and "manipulation of the gut microbiota as a key target for

Crohn's disease" were the major research areas in 2016-2021, and they could be extensively investigated in the future. Meanwhile, research on "malnutrition in patients with Crohn's disease" appeared to be an area that attracted more research attention before 2016.

CONCLUSION

This is the first bibliometric analysis to map the knowledge structure and trends regarding nutrition in Crohn's disease research over the past two decades. The results provide a comprehensive summary and identification of the frontiers of nutrition and Crohn's disease-related research, which may be used as a resource by researchers in the field.

Key Words: Nutrition; Diet; Crohn's disease; Bibliometric; Microbiota; Malnutrition

©The Author(s) 2023. Published by Baishideng Publishing Group Inc. All rights reserved.

Core Tip: There is much interest in using nutrition therapy approaches to treat Crohn's disease, while the current state of knowledge is still inadequate to make general recommendations. Therefore, a bibliometric analysis of the global trend in research on nutrition and Crohn's disease was conducted. This study outlines the current state of research themes and hotspots in nutrition and Crohn's disease research because no bibliometric research has been conducted to determine worldwide trends in nutrition and Crohn's disease. This facilitates researchers and healthcare providers in identifying potential future research directions.

Citation: Shakhshir M, Zyoud SH. Global research trends on diet and nutrition in Crohn's disease. *World J Gastroenterol* 2023; 29(20): 3203-3215
URL: https://www.wjgnet.com/1007-9327/full/v29/i20/3203.htm
DOI: https://dx.doi.org/10.3748/wjg.v29.i20.3203

INTRODUCTION

Crohn's disease is a relapsing transmural inflammatory disease of the gut with an unclear etiology; it involves acute attacks followed by periods of remission[1,2]. Crohn's disease can affect the entire gastrointestinal tract, from the mouth to the anus[3]. However, the disease affects the terminal ileum and the colon in most cases, which can result in complications such as stenosis, abscesses and fistula[4]. The prevalence rate of Crohn's disease ranges from 0.6 to 322 per 100000 people[5].

Malnutrition is frequently visible in approximately 65%-75% of patients with Crohn's disease[6]. Malabsorption, gut dysbiosis, small intestinal bacterial overgrowth and symptoms such as weight loss, reduced dietary intake, deficiency of individual nutrients or many nutrients are just a few of the mechanisms that can be related to Crohn's disease-related malnutrition[7,8]. In this case, nutrition, which may take the form of dietary adjustments, parenteral nutrition, or enteral nutrition, plays an important role in treating Crohn's disease[7,9,10]. Parenteral nutrition is a type of nutrition support that is given through an intravenous line. It is used when the digestive tract cannot properly absorb nutrients. In severe cases of Crohn's disease, where the digestive tract is severely damaged, parenteral nutrition may be necessary[7,11]. Furthermore, enteral nutrition is a type of nutrition support that is given through a feeding tube. It can help reduce inflammation and promote healing of the digestive tract. Enteral nutrition may be used as a primary treatment for Crohn's disease or as a supplement to other treatments[7,11].

There is much interest in using nutritional approaches to control and reduce the symptoms of Crohn's disease and to increase the remission time. Nevertheless, there is insufficient scientific support to give health care providers more options regarding dietary therapies. As a result, we performed a bibliometric analysis of the global trends in research on nutrition and Crohn's disease. We summarize the current state of research themes and hotspots in nutrition and Crohn's disease to look for global trends. Our findings will make it easier for researchers and newcomers to understand the current state of the field, to strategize future goals in research and to identify potential future research directions.

MATERIALS AND METHODS

Data sources

We conducted a shortlisted quantitative analysis with an approach based on previously published

scientific outputs to characterize the development of research on nutrition and Crohn's disease over the past two decades. On December 30, 2022, we searched the Scopus database for studies that had been published between 2002 and 2021. The Scopus database is often an essential source of information for bibliometric research and evaluations of scientific publications[12]. Numerous successful bibliometric studies have been performed using the Scopus database as a data source[13-17].

Search strategy

We used relevant publications on nutrition[18,19] and Crohn's disease[20] to choose keywords to search the Scopus database and to identify studies. Each of the chosen keywords relates to nutrition, and we used them as an entry for the "Article Title" field. Due to the possibility that the title/abstract/keyword search would retrieve unnecessary papers, we searched the titles with specific limits to reduce false-positive results[21-24]. When writing the keywords, we used asterisks (*) and quote marks to narrow and broaden the search scope. The keywords we used were nutrt* or nutrient* or diet* or eat* or feeding-pertain to nutrition or diet *per se* rather than other related terminology such as specific names or classes of dietary compounds. Furthermore, we searched all terms related to Crohn's disease in the "Article Title" and/or "Abstract" fields.

Bibliometric indicators

We imported the retrieved data into Microsoft Excel so that we could analyze and tabulate it. We retrieved relevant bibliometric data (such as the number of articles published per year, the types of documents retrieved, countries/regions, institutions, funding agencies, journals and their impact factors (*IF*), citation patterns and the h-index) for research publications related to nutrition and Crohn's disease. We used descriptive statistics to analyze our findings. The *Impact Index Per Article* that is being shown refers to the top 10 papers with the highest number of citations, which were obtained from the *Reference Citation Analysis* (*RCA*, https://referencecitationanalysis.com/). *RCA* is a citation analysis database that is open and covers multiple disciplines. The company is located in Pleasanton, CA 94566, United States [25-27].

Data visualization

We analyzed and visualized the data by using VOSviewer software version 1.6.8, a free online tool[28-30]. The software generated visualization maps that displayed the most commonly occurring keywords in the retrieved publications. The size of the node in each map represented the frequency of a particular keyword, indicating the relevance and popularity of the corresponding topic in the field. Based on these maps, the hot topics in the field were identified, revealing the areas that received the most attention and research focus. This analysis provided valuable insights into the current trends and research directions in the field, which can be used to guide future research and inform the decision-making processes. In addition, visualization maps were used to determine international collaboration. VOSviewer can determine the extent of the collaboration between two countries by considering the width of the connecting line and the total number of publications.

RESULTS

Analysis of publication trends

There were 1237 publications on nutrition and Crohn's disease published between 2002 and 2021. The documents recovered were of 9 types, mainly research articles (n = 791; 63.95%), followed by reviews (n = 285; 23.04%). The total number of publications by year is shown in Figure 1. The number of publications per year increased from 28 in 2002 to 123 in 2021.

Analysis of the country distribution

The publications were from authors representing 108 countries/regions. The top 10 active countries are shown in Table 1. The top 10 countries contributed 905 (73.16%) of the recovered documents. Among the eligible countries, the United States had the highest number of publications (n = 208, 16.81%), followed by the United Kingdom (n = 192, 15.52%), China (n = 109, 8.81%), Japan (n = 98, 7.92%), and Canada (n = 88, 7.11%). Furthermore, we analyzed countries that had more than 20 publications on nutrition and Crohn's disease. Based on our findings from 18 eligible countries, the United States, the United Kingdom, and Canada are the central countries with links to other countries (Figure 2).

Contributions of institutions

Based on the number of publications, Table 2 includes the top 10 institutions that have produced publications on nutrition and Crohn's disease. The University of Otago, Christchurch (New Zealand), has had the highest scientific production (n = 29, 2.34%), followed by Tel Aviv University (Israel), with 25 publications (2.02%). Massachusetts General Hospital (United States) and Jinling Hospital (China) have the third highest production (n = 22, 1.78%).

Table 1 Top 10 productive countries/regions involved in nutrition and Crohn's disease from 2002 to 2021

Ranking	Country	No. of documents	%
1st	United States	208	16.81
2nd	United Kingdom	192	15.52
3rd	China	109	8.81
4th	Japan	98	7.92
5th	Canada	88	7.11
6th	Germany	73	5.90
7th	Spain	71	5.74
8th	Italy	70	5.66
9th	France	67	5.42
10th	Poland	61	4.93

Table 2 Top 10 productive institutions ranked by the number of publications

Ranking	Institute	Country	No. of documents	%
1st	University of Otago, Christchurch	New Zealand	29	2.34
2nd	Tel Aviv University	Israel	25	2.02
3rd	Massachusetts General Hospital	United States	22	1.78
3rd	Jinling Hospital	China	22	1.78
5th	UNSW Sydney	Australia	21	1.70
6th	Harvard Medical School	United States	20	1.62
7th	University of Glasgow	United Kingdom	19	1.54
7th	Sydney Children's Hospital, Randwick	Australia	19	1.54
9th	Medical School of Nanjing University	China	18	1.46
9th	University of Washington	United States	18	1.46

Analysis of funding agencies

We identified 274 (22.15%) articles that were part of financed projects. The United States funding agencies were the most active in this field, with the National Institute of Diabetes and Digestive and Kidney Diseases (n = 34, 2.75%) being the most active. This was followed by the National Institutes of Health (n = 30, 2.43%), the National Natural Science Foundation for China Diseases (n = 30, 2.43%) and the Crohn's and Colitis Foundation (n = 20, 1.62%) (Table 3).

Journal analysis

The top 10 journals that have published the most articles concerning nutrition and Crohn's disease are listed in Table 4 with their *IF* in 2022. Nutrients was the most productive journal, with 57 documents contributing to 4.61% of the total publications, followed by *Inflammatory Bowel Diseases* (n = 55, 4.45%), *Alimentary Pharmacology and Therapeutics* (n = 39, 3.15%), *Clinical Nutrition* (n = 29, 2.34%), and the *Journal of Pediatric Gastroenterology and Nutrition* (n = 29, 2.34%).

Citation analysis

There was an average of 29.46 citations per document, for a total of 36444 citations. The h-index of the retrieved documents was 93. A total of 183 (14.8%) of the retrieved documents did not have citations, but 83 had been cited ≥ 100 times. The top 10 articles were cited 3912 times[31-40]. There was a wide range in the total number of citations for these publications, from 310 to 603 (Table 5). The impact index per article for the top 10 most cited articles varied between 10.4 and 70.6 (Table 5).

Keyword analysis of research hotspots

The co-occurrence network map of author keywords with at least 10 occurrences is displayed in Figure 3. Of the 1589 keywords, 43 met the threshold and were mainly concentrated in three aspects: (1)

Table 3 Top 10 funding agencies involved in nutrition and Crohn's disease from 2002 to 2021

Ranking	Funding agencies	Country	No. of publication	%
1st	National Institute of Diabetes and Digestive and Kidney Diseases	United States	34	2.75
2nd	National Institutes of Health	United States	30	2.43
2nd	The National Natural Science Foundation of China	China	30	2.43
4th	Crohn's and Colitis Foundation	United States	20	1.62
5th	Medical Research Council	United Kingdom	16	1.29
6th	AbbVie	United States	12	0.97
6th	National Cancer Institute	United States	12	0.97
8th	Canadian Institutes of Health Research	Canada	10	0.81
9th	Japan Society for the Promotion of Science	Japan	10	0.81
8th	National Center for Research Resources	United States	10	0.81
8th	Nestlé Health Science	Switzerland	10	0.81
8th	Pfizer	United States	10	0.81

Table 4 Ten most productive journals involved in nutrition and Crohn's disease from 2002 to 2021

Ranking	Journal/source title	No. of documents	%	*IF*[1]
1st	*Nutrients*	57	4.61	6.706
2nd	*Inflammatory Bowel Diseases*	55	4.45	7.290
3rd	*Alimentary Pharmacology and Therapeutics*	39	3.15	9.524
4th	*Clinical Nutrition*	29	2.34	7.643
4th	*Journal of Pediatric Gastroenterology and Nutrition*	29	2.34	3.288
6th	*Digestive Diseases and Sciences*	24	1.94	3.487
7th	*Journal of Crohns and Colitis*	22	1.78	10.020
7th	*World Journal of Gastroenterology*	22	1.78	5.374
9th	*Gastroenterology*	17	1.37	33.883
9th	*Nutrition in Clinical Practice*	17	1.37	3.204

[1]Journal Citation Reports (Clarivate, 2022). IF: Impact index.

The "role of exclusive enteral nutrition (EEN) for complicated Crohn's disease" (red cluster); (2) "manipulation of the gut microbiota as a key target for Crohn's disease" (green cluster); and (3) "malnutrition in patients with Crohn's disease" (blue group).

We then divided the keywords by specific colors based on the average number of times they appeared in all publications (Figure 4). The blue color represents prior research (before 2016), while more recent studies are indicated by the yellow color (after 2018). Keywords in the groups of "role of EEN for complicated Crohn's disease"; and "manipulation of the gut microbiota as a key target for Crohn's disease" were the major areas in 2016-2021, and they could be extensively considered in the future. Meanwhile, research on "malnutrition in patients with Crohn's disease" appeared to be a research area that attracted more attention before 2016.

DISCUSSION

This bibliometric analysis represents a comprehensive shortlisted overview of nutrition and Crohn's disease research. In the last decade, there has been significant growth in worldwide research interest in this topic. The steady scientific progress over time shows that "manipulation of the gut microbiota as a key target for Crohn's disease" and "EEN for complicated Crohn's disease" are promising clinical approaches that should receive more investigation.

Table 5 Top 10 articles on total citations

Ranking	Title	Source title	Cited by	Impact index per article[1]	Ref.
1st	"Dietary intake and risk of developing inflammatory bowel disease: A systematic review of the literature"	*American Journal of Gastroenterology*	603	29.2	Hou *et al*[31], 2011
2nd	"Inflammation, Antibiotics, and Diet as Environmental Stressors of the Gut Microbiome in Pediatric Crohn's Disease"	*Cell Host and Microbe*	449	70.6	Lewis *et al*[37], 2015
3rd	"Diet-induced dysbiosis of the intestinal microbiota and the effects on immunity and disease"	*Nutrients*	425	36.5	Brown *et al*[32], 2012
4th	"Differentiating ulcerative colitis from Crohn disease in children and young adults: Report of a Working Group of the North American Society for Pediatric Gastroenterology, Hepatology, and Nutrition and the Crohn's and Colitis Foundation of America"	*Journal of Pediatric Gastroenterology and Nutrition*	377	21.3	North American Society for Pediatric Gastroenterology, Hepatology, and Nutrition[33], 2007
5th	"Enteral nutritional therapy for induction of remission in Crohn's disease"	*Cochrane Database of Systematic Reviews*	371	10.4	Zachos *et al*[34], 2007
6th	"A prospective study of long-term intake of dietary fiber and risk of Crohn's disease and ulcerative colitis"	*Gastroenterology*	358	38.1	Ananthakrishnan *et al*[39], 2013
7th	"Polymeric Diet Alone Versus Corticosteroids in the Treatment of Active Pediatric Crohn's Disease: A Randomized Controlled Open-Label Trial"	*Clinical Gastroenterology and Hepatology*	342	18.4	Borrelli *et al*[38], 2006
8th	"ESPEN guideline: Clinical nutrition in inflammatory bowel disease"	*Clinical Nutrition*	341	48.9	Forbes *et al*[35], 2017
9th	"Western diet induces dysbiosis with increased e coli in CEABAC10 mice, alters host barrier function favouring AIEC colonization"	*Gut*	336	38.4	Martinez-Medina *et al*[40], 2014
10th	"Fine and ultrafine particles of the diet: Influence on the mucosal immune response and association with Crohn's disease"	*Proceedings of the Nutrition Society*	310	13.3	Lomer *et al*[36], 2002

[1]The impact index per article is presented based on *Reference Citation Analysis* (https://referencecitationanalysis.com/).

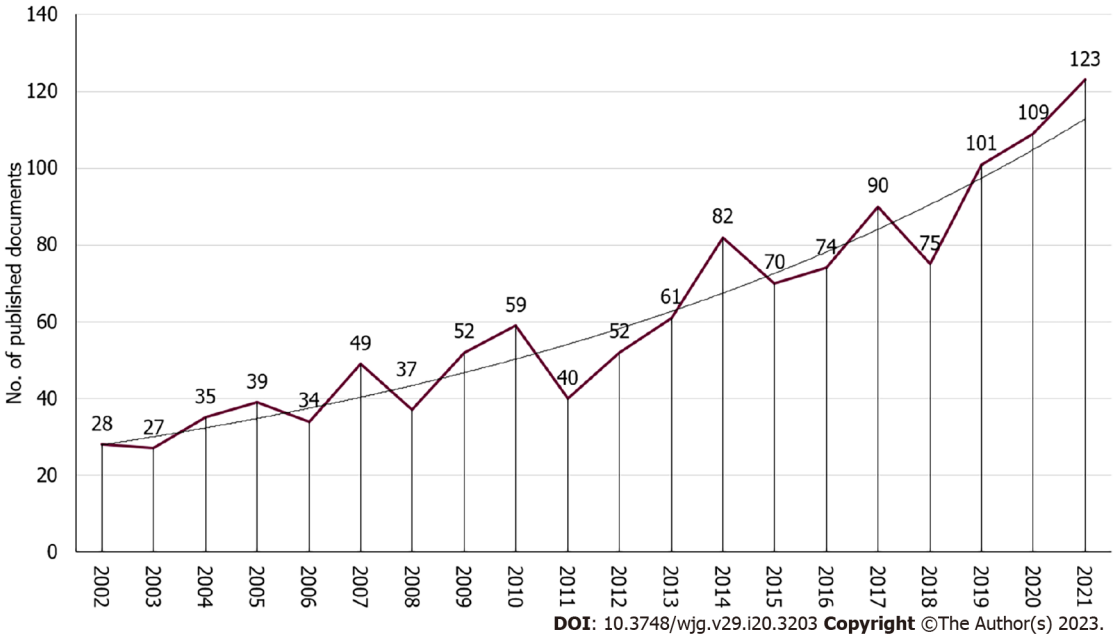
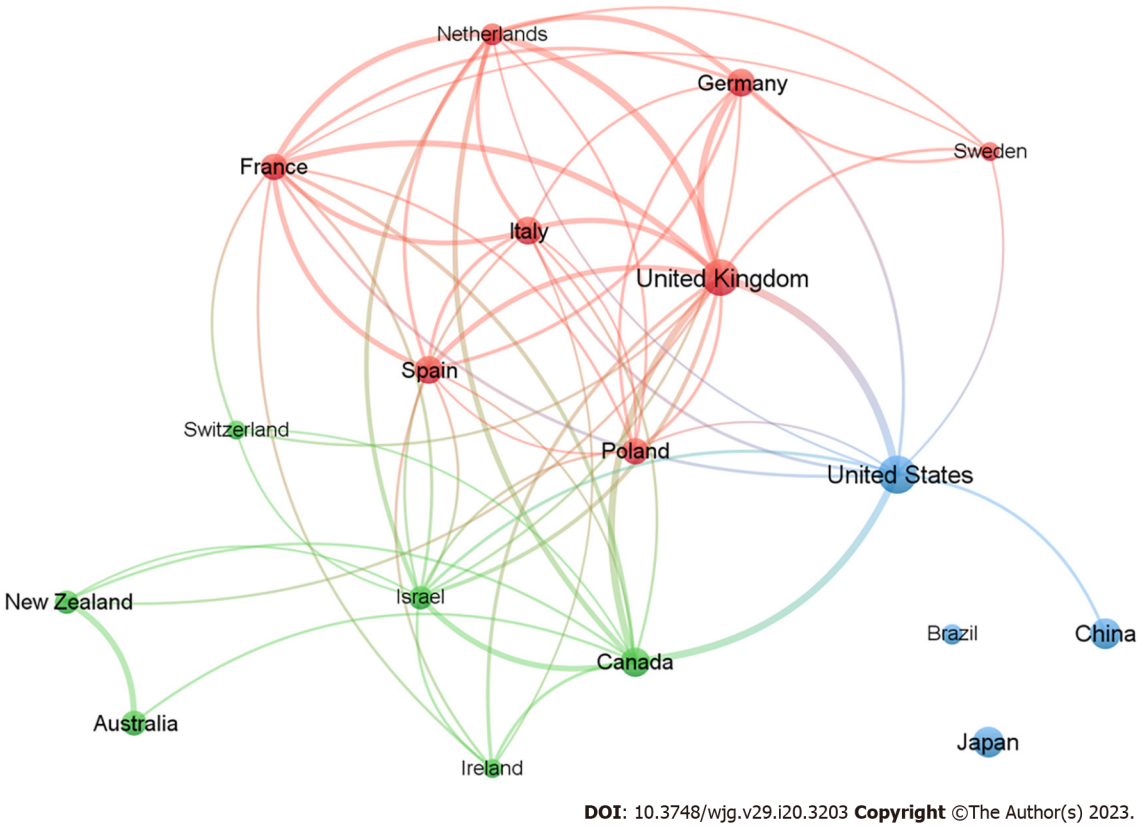


Figure 1 Growth trends of publications on nutrition and Crohn's disease from 2002 to 2021.

The research found that the United States is the dominant country in this field, potentially due to various factors. These factors could include a higher prevalence of Crohn's disease in Western Europe and North America, where the disease affects 100 to 300 per 100000 people[5]. Other reasons may



DOI: 10.3748/wjg.v29.i20.3203 **Copyright** ©The Author(s) 2023.

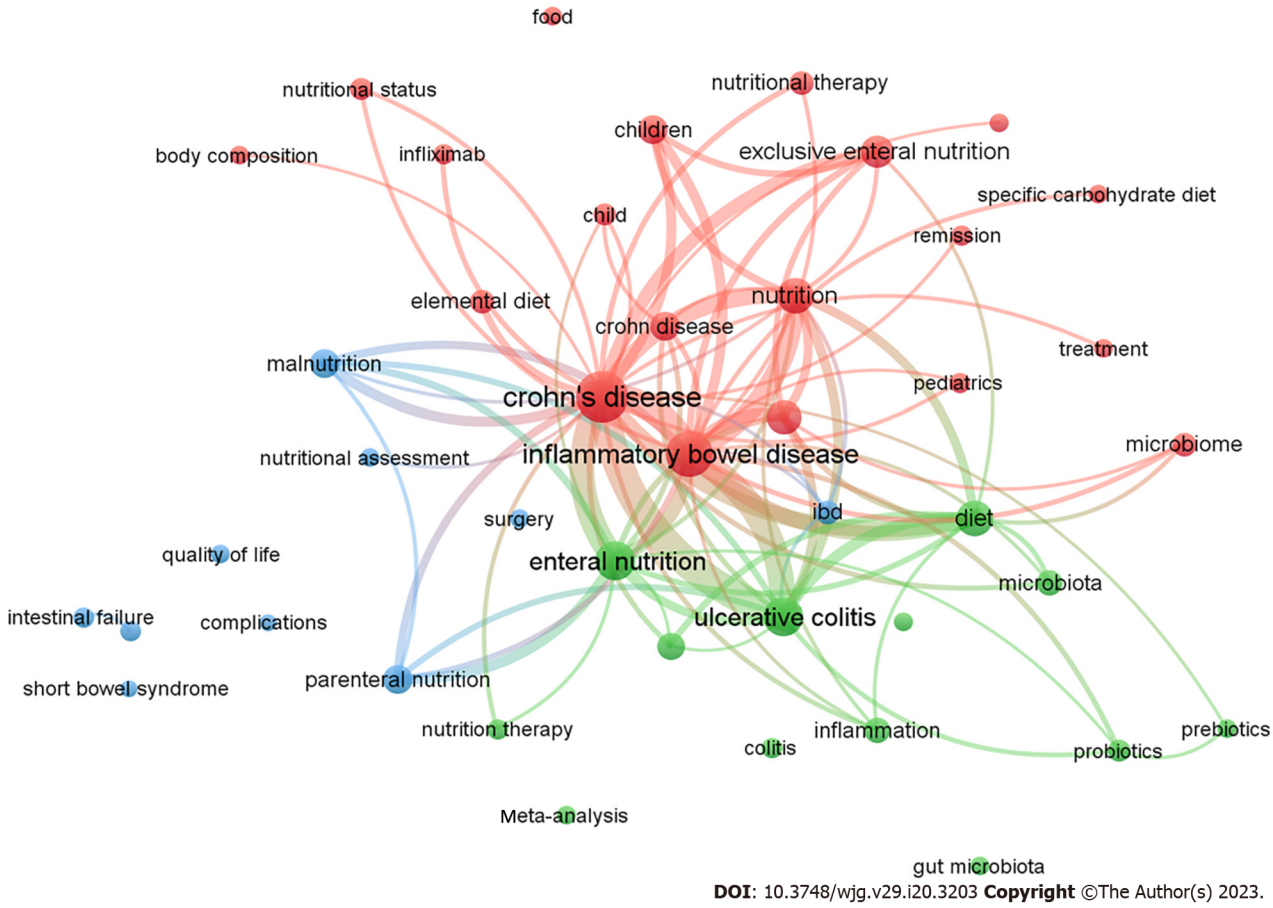
Figure 2 Network visualization map depicting international collaboration in research related to nutrition and Crohn's disease during 2002-2021.

involve the country's investment in research, a diverse range of researchers in the field, access to well-resourced research environments, and a well-trained workforce. Researchers may profit from their country's economic success, which may provide financial assistance and travel chances. This finding is consistent with past studies that have shown the United States to be the top in research productivity[41-43]. Nonetheless, it is critical to remember that research productivity is only one component of scientific research. Other elements, such as research impact and societal ramifications, should be included when assessing the overall success of a research field or country.

Studying collaboration networks can offer useful insights into research partnerships and help pinpoint essential collaborators in a particular field. The United States and the United Kingdom have a distinct advantage in this regard because of their greater economic resources and scientific investments. Both countries have invested significantly in research and development, establishing world-class research institutions and universities. Additionally, they have implemented policies to foster global scientific and technological collaboration, leading to the formation of robust networks of researchers and institutions worldwide. Furthermore, these countries' substantial funding and resources enable them to attract the best talent globally, which has facilitated scientific progress and innovation. The extensive cooperation and collaboration among researchers in these countries have resulted in diverse and strong networks that are crucial in addressing complex scientific challenges[44-47].

We may gain insight into the areas of interest and potential future research directions in this field by analyzing the cooccurrence of the keywords. Its key terms often refer to the most important aspects of a publication; the threshold was met by 43 of the 1589 keywords retrieved from the authors' keywords. Therefore, it is helpful to define important concepts and create a framework for nutrition and Crohn's disease studies by analyzing the associated keywords.

One of the main research hotspots in our study was the role of EEN for complicated Crohn's disease. Enteral nutrition is the preferred feeding route in the induction of remission of active Crohn's disease, as it is a minimally invasive procedure with low risk. On the other hand, enteral nutrition has a beneficial effect on the gut microbiota and intestinal inflammation. Therefore, enteral nutrition has several advantages over parenteral nutrition: It can maintain enterohepatic circulation, reduce the inflammatory response, decrease bacterial overgrowth and translocation and avoid intravenous access complications [4]. EEN was first used in the 1970s and has been established over the last 20 years as an effective nutritional therapy that induces mucosal healing in approximately 80% of patients and provides 100% of daily nutrition requirements from high-energy artificial supplements and modified feeds with probiotics, amino acids, and fatty acids[48]. On the other hand, a prospective study showed that 3 mo of



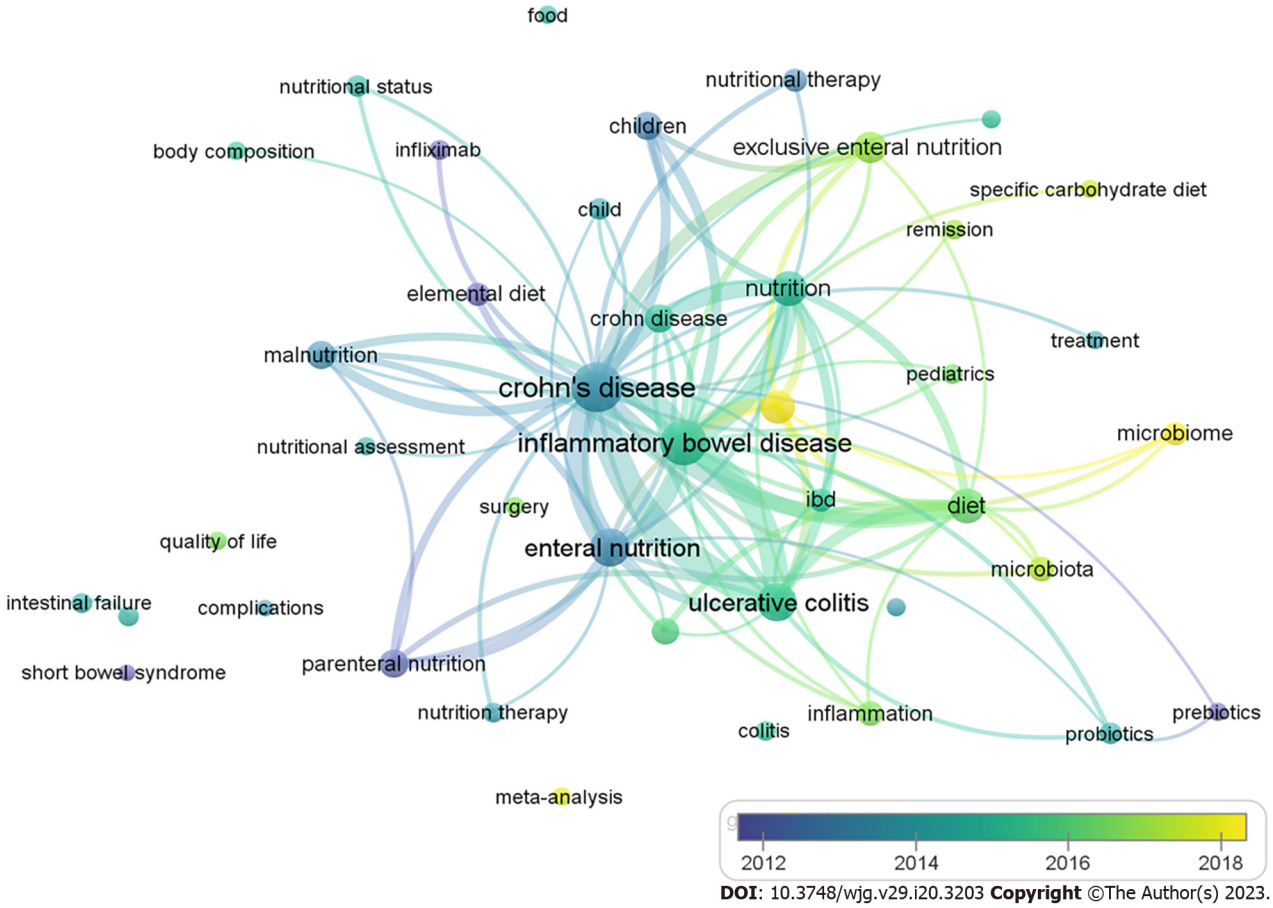
DOI: 10.3748/wjg.v29.i20.3203 **Copyright** ©The Author(s) 2023.

Figure 3 Analysis of the co-occurrence network of authors' keywords. Keywords of the authors with at least 10 occurrences were analyzed.

EEN could effectively relieve stenosis[4,49]. However, there is still variation in the use of EEN in different parts of the world. In addition, enteral nutrition and oral nutrition supplements are rarely recommended by doctors as first-line therapies, so much research is needed to address the uncertainty and barriers around the use of enteral nutrition globally[50,51].

Another research hotspot is the "manipulation of the gut microbiota as a key target of Crohn's disease". The intestinal microbiota is an important factor in developing irritable bowel disease. Long-standing inflammation in Crohn's disease can cause small intestinal bacterial overgrowth due to intestinal stenosis, leading to fibrosis, scarring and contraction in both the transverse and longitudinal directions. Bacterial overgrowth is enabled by reduced intestinal secretion of soluble immunoglobulin A (sIgA), which permits an increase in adherence and pathogenicity of bacteria that form the normal gut microbiome, particularly *Escherichia coli*, *Klebsiella* spp. and *Pseudomonas* spp., and a decrease in protective bacterial strains such as *Lactobacillus* and *Bifidobacterium* spp., resulting in diarrhea, abdominal pain and distension, weight loss and fatigue. Bacterial overgrowth acts as a snare due to the increased risk of mucosal inflammation, bacterial translocation, and sepsis, so many experimental studies are needed to assess the effectiveness of probiotic supplements and palatability in patients to achieve clarity and standardization of therapy[52,53].

Another research hotspot is "malnutrition in patients with Crohn's disease". The prevalence of malnutrition and nutritional deficiencies in patients with Crohn's disease is high because inflammation induces a catabolic response with endogenous proteolysis. Researchers have found weight loss due to decreased fat and muscle mass in 65%-75% of hospitalized patients; anemia due to iron, folic acid and vitamin B12 deficiency in 60%-80% of patients; and negative nitrogen balance in approximately 70% of patients[54]. Protein-energy malnutrition is common due to increased energy and nutrient needs, particularly in acute attacks, in addition to cytokine-induced anorexia, nausea, diarrhea, reduced dietary intake, malabsorption, and food-drug interactions. Protein requirements will depend on the disease phase. An increased requirement will be essential only in the catabolic stage and for septic and severe undernutrition in the active Crohn's disease phase. Screening for malnutrition is essential to select patients with the highest risk and develop the appropriate care plan. In addition, malnutrition is rarely treated as an additional disease, especially in low- and middle-income countries. Therefore, more studies are needed to manage and control this life-threatening issue[55].



DOI: 10.3748/wjg.v29.i20.3203 **Copyright** ©The Author(s) 2023.

Figure 4 Co-occurrence overlay visualization of the authors' keywords. Yellow highlights indicate the most recent keywords.

One of the most important techniques for assessing the impact of an article or demonstrating its recognition is citation analysis[56,57]. It is possible to determine which study areas have received the most attention from the scientific community by analyzing the most cited papers. Those interested in becoming authorities on nutrition-related studies of Crohn's disease should become familiar with the most widely referenced works. We found several articles on the connections between nutrition and Crohn's disease[31-40] that highlighted a number of subtopics that are closely related to the aforementioned hotspots. For example, the article on this subject that has been cited the most has 603 references and was published in the *American Journal of Gastroenterology*. High dietary intakes of total lipids, omega-6 fatty acids, polyunsaturated fatty acids, and meat were associated with an elevated risk of Crohn's disease, according to this systematic analysis[31]. Conversely, fruit and high-fiber diets were linked to a lower risk of developing Crohn's disease[31]. The article by Lewis *et al*[37], published in *Cell Host and Microbe*, was the second most cited. This study established that fungi are involved in the dysbiosis of Crohn's disease in addition to bacteria. Inflammation, exposure to antibiotics, and dietary modifications contribute to dysbiosis in different ways by altering the composition of the gut microbiota [37]. These results shed light on the therapeutic options for Crohn's disease by showing that dysbiosis develops from independent influences of diet, inflammation, and antibiotics[37]. The third most cited paper was published in *Nutrients*[32]. The study presented proof that the microbiota structure in the intestines can influence the likelihood of developing chronic illnesses in the gastrointestinal tract, including celiac disease, Crohn's disease, ulcerative colitis, and irritable bowel syndrome. Nevertheless, the enduring advantages of probiotics and prebiotics are still uncertain, despite their potential as efficacious treatments for inflammatory disease symptoms[32].

Research strengths and limitations

Our study has several strengths. We systematically reviewed the literature on nutrition and Crohn's disease. Our findings offer a comprehensive and quantitative analysis of the most important articles related to nutrition and Crohn's disease. We have also acknowledged the important contributions that have been made to the development and progress of this specialized field. However, our study has several limitations. First, we only searched Scopus and we did not include data from other databases, such as PubMed, Web of Science, and Google Scholar. This approach could have led to the exclusion of papers relevant to the investigated topic. Second, the research strategy has certain errors, even though it has been validated. Consequently, researchers should keep in mind that both false-positive and false-

negative results could have been included. Nevertheless, we believe that the use of title searches significantly reduces research errors. Third, regarding the credibility of the data gathered for our study, the precision and completeness of the keywords we used have a considerable impact. Hence, certain significant and influential articles could have been left off the representative list because the titles of those articles could contain specific types of nutrition or diet.

CONCLUSION

We employed bibliometric techniques to gather 1237 articles on nutrition and Crohn's disease that were published from January 2002 to December 2021. Our findings highlight a network of collaboration among countries, institutions, journals and funding agencies, shedding light on the latest trends and areas of interest in the field of emerging nutrition and Crohn's disease. Research in this area has been increasing steadily over the past decade. The United States and the United Kingdom are the leading contributors to this field, with the highest number of publications and a strong emphasis on international cooperation. The "role of EEN for complicated Crohn's disease" and "manipulation of the gut microbiota as a key target for Crohn's disease" are the current research hotspots. This bibliometric study provides a detailed analysis of nutrition and Crohn's disease research, which can serve as a resource for academics and policymakers in this field.

ARTICLE HIGHLIGHTS

Research background

Crohn's disease symptoms can include abdominal pain, diarrhea, fatigue, and weight loss. While Crohn's disease has no cure, there are techniques to control symptoms, including food and nutrition.

Research motivation

Assessing the current status of research and hotspots in nutrition and Crohn's disease is critical for identifying knowledge gaps and informing future research paths.

Research objectives

Using bibliometric analysis, the purpose of this study is to provide an overview of the current state of nutrition and Crohn's disease research.

Research methods

We conducted a thorough and rigorous analysis utilizing SciVerse Scopus to identify relevant material on nutrition and Crohn's disease. Next, we used VOSviewer software to examine prevalent areas of study and publishing patterns in related domains.

Research results

Over the past 20 years, there has been a rise in cross-border partnerships and interdisciplinary studies concerning the relationship between nutrition and Crohn's disease. Currently, the key areas of research in this field are the use of exclusive enteral nutrition for complicated cases of Crohn's disease and the manipulation of the gastrointestinal microbiome.

Research conclusions

There has been no bibliometric analysis of nutrition and Crohn's disease research in the last two decades. This study provides a complete assessment of the knowledge structure and developments in this topic. As such, the findings are a helpful resource for academics because they provide a detailed assessment and emphasize the frontiers of nutrition and Crohn's disease research.

Research perspectives

The purpose of this research is to identify current trends and focus areas in the field of nutrition and Crohn's disease to guide future research and treatment practice. Using bibliometric analysis, this study provides a comprehensive assessment of the relevant literature, assisting researchers and clinicians in staying up to date on the most recent advances in this field.

ACKNOWLEDGEMENTS

The author thanks An-Najah National University Hospital for all administrative assistance during the

implementation of the project.

FOOTNOTES

Author contributions: Zyoud SH designed the study, collected the data, analyzed the data, made major contributions to the manuscript's literature search and interpretation, and drafted the manuscript; Shakhshir M made major contributions to the manuscript's literature search and interpretation and made revisions to the initial draft; all authors provided a critical review and approved the final manuscript before submission.

Conflict-of-interest statement: The authors have no financial disclosures or conflicts of interest to declare.

PRISMA 2009 Checklist statement: The authors have read the PRISMA 2009 Checklist, and the manuscript was prepared and revised according to the PRISMA 2009 Checklist.

Open-Access: This article is an open-access article that was selected by an in-house editor and fully peer-reviewed by external reviewers. It is distributed in accordance with the Creative Commons Attribution NonCommercial (CC BY-NC 4.0) license, which permits others to distribute, remix, adapt, build upon this work non-commercially, and license their derivative works on different terms, provided the original work is properly cited and the use is non-commercial. See: https://creativecommons.org/Licenses/by-nc/4.0/

Country/Territory of origin: Palestine

ORCID number: Muna Shakhshir 0000-0002-6213-8457; Sa'ed H Zyoud 0000-0002-7369-2058.

S-Editor: Chen YL
L-Editor: Filipodia
P-Editor: Yu HG

REFERENCES

1 **GBD 2017 Inflammatory Bowel Disease Collaborators**. The global, regional, and national burden of inflammatory bowel disease in 195 countries and territories, 1990-2017: a systematic analysis for the Global Burden of Disease Study 2017. *Lancet Gastroenterol Hepatol* 2020; **5**: 17-30 [PMID: 31648971 DOI: 10.1016/S2468-1253(19)30333-4]
2 **Danese S**, Parigi TL, Peyrin-Biroulet L, Ghosh S. Defining difficult-to-treat inflammatory bowel disease: why and how. *Lancet Gastroenterol Hepatol* 2021; **6**: 520-522 [PMID: 34019799 DOI: 10.1016/S2468-1253(21)00141-2]
3 **Jairath V**, Feagan BG. Global burden of inflammatory bowel disease. *Lancet Gastroenterol Hepatol* 2020; **5**: 2-3 [PMID: 31648974 DOI: 10.1016/S2468-1253(19)30358-9]
4 **Adamji M**, Day AS. An overview of the role of exclusive enteral nutrition for complicated Crohn's disease. *Intest Res* 2019; **17**: 171-176 [PMID: 30508476 DOI: 10.5217/ir.2018.00079]
5 **Ng SC**, Shi HY, Hamidi N, Underwood FE, Tang W, Benchimol EI, Panaccione R, Ghosh S, Wu JCY, Chan FKL, Sung JJY, Kaplan GG. Worldwide incidence and prevalence of inflammatory bowel disease in the 21st century: a systematic review of population-based studies. *Lancet* 2017; **390**: 2769-2778 [PMID: 29050646 DOI: 10.1016/S0140-6736(17)32448-0]
6 **Scaldaferri F**, Pizzoferrato M, Lopetuso LR, Musca T, Ingravalle F, Sicignano LL, Mentella M, Miggiano G, Mele MC, Gaetani E, Graziani C, Petito V, Cammarota G, Marzetti E, Martone A, Landi F, Gasbarrini A. Nutrition and IBD: Malnutrition and/or Sarcopenia? A Practical Guide. *Gastroenterol Res Pract* 2017; **2017**: 8646495 [PMID: 28127306 DOI: 10.1155/2017/8646495]
7 **Caio G**, Lungaro L, Caputo F, Zoli E, Giancola F, Chiarioni G, De Giorgio R, Zoli G. Nutritional Treatment in Crohn's Disease. *Nutrients* 2021; **13** [PMID: 34066229 DOI: 10.3390/nu13051628]
8 **Mentella MC**, Scaldaferri F, Pizzoferrato M, Gasbarrini A, Miggiano GAD. Nutrition, IBD and Gut Microbiota: A Review. *Nutrients* 2020; **12** [PMID: 32235316 DOI: 10.3390/nu12040944]
9 **de Castro MM**, Pascoal LB, Steigleder KM, Siqueira BP, Corona LP, Ayrizono MLS, Milanski M, Leal RF. Role of diet and nutrition in inflammatory bowel disease. *World J Exp Med* 2021; **11**: 1-16 [PMID: 33585174 DOI: 10.5493/wjem.v11.i1.1]
10 **Verburgt CM**, Ghiboub M, Benninga MA, de Jonge WJ, Van Limbergen JE. Nutritional Therapy Strategies in Pediatric Crohn's Disease. *Nutrients* 2021; **13** [PMID: 33450982 DOI: 10.3390/nu13010212]
11 **Roncoroni L**, Gori R, Elli L, Tontini GE, Doneda L, Norsa L, Cuomo M, Lombardo V, Scricciolo A, Caprioli F, Costantino A, Scaramella L, Vecchi M. Nutrition in Patients with Inflammatory Bowel Diseases: A Narrative Review. *Nutrients* 2022; **14** [PMID: 35215401 DOI: 10.3390/nu14040751]
12 **Baas J**, Schotten M, Plume A, Cote G, Karimi R. Scopus as a curated, high-quality bibliometric data source for academic research in quantitative science studies. *Quantitative Science Studies* 2020; **1**: 377-386 [DOI: 10.1162/qss_a_00019]
13 **Keighobadi M**, Nakhaei M, Sharifpour A, Khasseh AA, Safanavaei S, Tabaripour R, Aliyali M, Abedi S, Mehravaran H, Banimostafavi ES, Fakhar M. A Bibliometric Analysis of Global Research on Lophomonas Spp. in Scopus (1933-2019). *Infect Disord Drug Targets* 2021; **21**: 230-237 [PMID: 32718299 DOI: 10.2174/1871526520666200727153142]
14 **Beovich B**, Olaussen A, Williams B. A bibliometric analysis of paramedicine publications using the Scopus database:

2010-2019. *Int Emerg Nurs* 2021; **59**: 101077 [PMID: 34571451 DOI: 10.1016/j.ienj.2021.101077]
15 **Morandi G**, Guido D, Tagliabue A. A bibliometric study of scientific literature on the dietary therapies for epilepsy in Scopus. *Nutr Neurosci* 2015; **18**: 201-209 [PMID: 24628043 DOI: 10.1179/1476830514Y.0000000118]
16 **Zahri KNM**, Zulkharnain A, Sabri S, Gomez-Fuentes C, Ahmad SA. Research Trends of Biodegradation of Cooking Oil in Antarctica from 2001 to 2021: A Bibliometric Analysis Based on the Scopus Database. *Int J Environ Res Public Health* 2021; **18** [PMID: 33669826 DOI: 10.3390/ijerph18042050]
17 **Kanmodi KK**, Nwafor JN, Salami AA, Egbedina EA, Nnyanzi LA, Ojo TO, Duckworth RM, Zohoori FV. A Scopus-Based Bibliometric Analysis of Global Research Contributions on Milk Fluoridation. *Int J Environ Res Public Health* 2022; **19** [PMID: 35886086 DOI: 10.3390/ijerph19148233]
18 **Zyoud SH**, Shakhshir M, Abushanab AS, Al-Jabi SW, Koni A, Shahwan M, Jairoun AA, Abu Taha A. Mapping the global research landscape on nutrition and the gut microbiota: Visualization and bibliometric analysis. *World J Gastroenterol* 2022; **28**: 2981-2993 [PMID: 35978868 DOI: 10.3748/wjg.v28.i25.2981]
19 **Zyoud SH**, Al-Jabi SW, Koni A, Shakhshir M, Shahwan M, Jairoun AA. Mapping the landscape and structure of global research on nutrition and COVID-19: visualization analysis. *J Health Popul Nutr* 2022; **41**: 25 [PMID: 35689295 DOI: 10.1186/s41043-022-00304-y]
20 **Shen JL**, Zhou Z, Cao JS, Zhang B, Hu JH, Li JY, Liu XM, Juengpanich S, Li MS, Feng X. Biologic therapy for Crohn's disease over the last 3 decades. *World J Clin Cases* 2022; **10**: 594-606 [PMID: 35097085 DOI: 10.12998/wjcc.v10.i2.594]
21 **Sweileh WM**. Analysis and mapping of global research publications on shift work (2012-2021). *J Occup Med Toxicol* 2022; **17**: 22 [PMID: 36514070 DOI: 10.1186/s12995-022-00364-0]
22 **Sweileh WM**. Global research activity on mathematical modeling of transmission and control of 23 selected infectious disease outbreak. *Global Health* 2022; **18**: 4 [PMID: 35062966 DOI: 10.1186/s12992-022-00803-x]
23 **Sweileh WM**. Global research publications on irrational use of antimicrobials: call for more research to contain antimicrobial resistance. *Global Health* 2021; **17**: 94 [PMID: 34429128 DOI: 10.1186/s12992-021-00754-9]
24 **Sweileh WM**. Substandard and falsified medical products: bibliometric analysis and mapping of scientific research. *Global Health* 2021; **17**: 114 [PMID: 34556126 DOI: 10.1186/s12992-021-00766-5]
25 **Wang JL**, Ma YJ, Ma L, Ma N, Guo DM, Ma LS. Baishideng's Reference Citation Analysis database announces the first Article Influence Index of multidisciplinary scholars. *World J Clin Cases* 2022; **10**: 10391-10398 [PMID: 36312463 DOI: 10.12998/wjcc.v10.i29.10391]
26 **Wang JL**, Ma YJ, Ma L, Ma N, Guo DM, Ma LS. Baishideng's Reference Citation Analysis database announces the first Journal Article Influence Index of 101 core journals and a list of high-quality academic journals in gastroenterology and hepatology. *World J Gastroenterol* 2022; **28**: 5383-5394 [PMID: 36312837 DOI: 10.3748/wjg.v28.i37.5383]
27 **Wang JL**, Ma YJ, Ma L, Ma N, Guo DM, Ma LS. Baishideng's Reference Citation Analysis database announces the first Journal Article Influence Index of 104 core journals and a list of high-quality academic journals in orthopedics. *World J Orthop* 2022; **13**: 891-902 [PMID: 36312521 DOI: 10.5312/wjo.v13.i10.891]
28 **Van Eck NJ**, Waltman L. Text mining and visualization using VOSviewer. 2011. [cited 21 March 2023]. Available from: https://arxiv.org/ftp/arxiv/papers/1109/1109.2058.pdf
29 **van Eck NJ**, Waltman L. VOSviewer manual. 2013. [cited 21 March 2023]. Available from: https://www.researchgate.net/publication/265012369_VOSviewer_Manual
30 **van Eck NJ**, Waltman L. Software survey: VOSviewer, a computer program for bibliometric mapping. *Scientometrics* 2010; **84**: 523-538 [PMID: 20585380 DOI: 10.1007/s11192-009-0146-3]
31 **Hou JK**, Abraham B, El-Serag H. Dietary intake and risk of developing inflammatory bowel disease: a systematic review of the literature. *Am J Gastroenterol* 2011; **106**: 563-573 [PMID: 21468064 DOI: 10.1038/ajg.2011.44]
32 **Brown K**, DeCoffe D, Molcan E, Gibson DL. Diet-induced dysbiosis of the intestinal microbiota and the effects on immunity and disease. *Nutrients* 2012; **4**: 1095-1119 [PMID: 23016134 DOI: 10.3390/nu4081095]
33 **North American Society for Pediatric Gastroenterology Hepatology and Nutrition**; Colitis Foundation of America, Bousvaros A, Antonioli DA, Colletti RB, Dubinsky MC, Glickman JN, Gold BD, Griffiths AM, Jevon GP, Higuchi LM, Hyams JS, Kirschner BS, Kugathasan S, Baldassano RN, Russo PA. Differentiating ulcerative colitis from Crohn disease in children and young adults: report of a working group of the North American Society for Pediatric Gastroenterology, Hepatology, and Nutrition and the Crohn's and Colitis Foundation of America. *J Pediatr Gastroenterol Nutr* 2007; **44**: 653-674 [PMID: 17460505 DOI: 10.1097/MPG.0b013e31805563f3]
34 **Zachos M**, Tondeur M, Griffiths AM. Enteral nutritional therapy for induction of remission in Crohn's disease. *Cochrane Database Syst Rev* 2007; CD000542 [PMID: 17253452 DOI: 10.1002/14651858.CD000542.pub2]
35 **Forbes A**, Escher J, Hébuterne X, Kłęk S, Krznaric Z, Schneider S, Shamir R, Stardelova K, Wierdsma N, Wiskin AE, Bischoff SC. ESPEN guideline: Clinical nutrition in inflammatory bowel disease. *Clin Nutr* 2017; **36**: 321-347 [PMID: 28131521 DOI: 10.1016/j.clnu.2016.12.027]
36 **Lomer MC**, Thompson RP, Powell JJ. Fine and ultrafine particles of the diet: influence on the mucosal immune response and association with Crohn's disease. *Proc Nutr Soc* 2002; **61**: 123-130 [PMID: 12002786 DOI: 10.1079/pns2001134]
37 **Lewis JD**, Chen EZ, Baldassano RN, Otley AR, Griffiths AM, Lee D, Bittinger K, Bailey A, Friedman ES, Hoffmann C, Albenberg L, Sinha R, Compher C, Gilroy E, Nessel L, Grant A, Chehoud C, Li H, Wu GD, Bushman FD. Inflammation, Antibiotics, and Diet as Environmental Stressors of the Gut Microbiome in Pediatric Crohn's Disease. *Cell Host Microbe* 2015; **18**: 489-500 [PMID: 26468751 DOI: 10.1016/j.chom.2015.09.008]
38 **Borrelli O**, Cordischi L, Cirulli M, Paganelli M, Labalestra V, Uccini S, Russo PM, Cucchiara S. Polymeric diet alone *vs* corticosteroids in the treatment of active pediatric Crohn's disease: a randomized controlled open-label trial. *Clin Gastroenterol Hepatol* 2006; **4**: 744-753 [PMID: 16682258 DOI: 10.1016/j.cgh.2006.03.010]
39 **Ananthakrishnan AN**, Khalili H, Konijeti GG, Higuchi LM, de Silva P, Korzenik JR, Fuchs CS, Willett WC, Richter JM, Chan AT. A prospective study of long-term intake of dietary fiber and risk of Crohn's disease and ulcerative colitis. *Gastroenterology* 2013; **145**: 970-977 [PMID: 23912083 DOI: 10.1053/j.gastro.2013.07.050]
40 **Martinez-Medina M**, Denizot J, Dreux N, Robin F, Billard E, Bonnet R, Darfeuille-Michaud A, Barnich N. Western diet

induces dysbiosis with increased E coli in CEABAC10 mice, alters host barrier function favouring AIEC colonisation. *Gut* 2014; **63**: 116-124 [PMID: 23598352 DOI: 10.1136/gutjnl-2012-304119]

41 **Zyoud SeH**, Shakhshir M, Abushanab AS, Koni A, Shahwan M, Jairoun AA, Al-Jabi SW. Global research trends on the links between insulin resistance and obesity: a visualization analysis. *Translational Medicine Communications* 2022; **7**: 18 [DOI: 10.1186/s41231-022-00124-6]

42 **Zyoud SH**, Al-Jabi SW, Amer R, Shakhshir M, Shahwan M, Jairoun AA, Akkawi M, Abu Taha A. Global research trends on the links between the gut microbiome and cancer: a visualization analysis. *J Transl Med* 2022; **20**: 83 [PMID: 35148757 DOI: 10.1186/s12967-022-03293-y]

43 **Yang J**, Deng Y, Cai Y, Liu Y, Peng L, Luo Z, Li D. Mapping trends and hotspot regarding gastrointestinal microbiome and neuroscience: A bibliometric analysis of global research (2002-2022). *Front Neurosci* 2022; **16**: 1048565 [PMID: 36466165 DOI: 10.3389/fnins.2022.1048565]

44 **Dusdal J**, Powell JJW. Benefits, Motivations, and Challenges of International Collaborative Research: A Sociology of Science Case Study. *Science and Public Policy* 2021; **48**: 235-245 [DOI: 10.1093/scipol/scab010]

45 **Widmer RJ**, Widmer JM, Lerman A. International collaboration: promises and challenges. *Rambam Maimonides Med J* 2015; **6**: e0012 [PMID: 25973264 DOI: 10.5041/RMMJ.10196]

46 **Moradi R**, Zargham-Boroujeni A, Soleymani MR. Factors related to the international research collaboration in the health area: A qualitative study. *J Educ Health Promot* 2020; **9**: 267 [PMID: 33282972 DOI: 10.4103/jehp.jehp_497_20]

47 **Meißner F**, Weinmann C, Vowe G. Understanding and Addressing Problems in Research Collaboration: A Qualitative Interview Study From a Self-Governance Perspective. *Front Res Metr Anal* 2021; **6**: 778176 [PMID: 35224422 DOI: 10.3389/frma.2021.778176]

48 **Ashton JJ**, Gavin J, Beattie RM. Exclusive enteral nutrition in Crohn's disease: Evidence and practicalities. *Clin Nutr* 2019; **38**: 80-89 [PMID: 29398336 DOI: 10.1016/j.clnu.2018.01.020]

49 **Fuchigami T**, Ohgushi H, Imamura K, Yao T, Omae T, Watanabe H, Nakano H. Effects of total parenteral nutrition on colonic lesions in Crohn's disease: radiographic and endoscopic study. *Gastroenterol Jpn* 1982; **17**: 521-529 [PMID: 6819178 DOI: 10.1007/BF02779129]

50 **Viani K**. Parenteral and enteral nutrition for pediatric oncology in low- and middle-income countries. *Indian J Cancer* 2015; **52**: 182-184 [PMID: 26853395 DOI: 10.4103/0019-509X.175837]

51 **Di Caro S**, Fragkos KC, Keetarut K, Koo HF, Sebepos-Rogers G, Saravanapavan H, Barragry J, Rogers J, Mehta SJ, Rahman F. Enteral Nutrition in Adult Crohn's Disease: Toward a Paradigm Shift. *Nutrients* 2019; **11** [PMID: 31540038 DOI: 10.3390/nu11092222]

52 **Wu L**, Estrada O, Zaborina O, Bains M, Shen L, Kohler JE, Patel N, Musch MW, Chang EB, Fu YX, Jacobs MA, Nishimura MI, Hancock RE, Turner JR, Alverdy JC. Recognition of host immune activation by Pseudomonas aeruginosa. *Science* 2005; **309**: 774-777 [PMID: 16051797 DOI: 10.1126/science.1112422]

53 **Spitz J**, Hecht G, Taveras M, Aoys E, Alverdy J. The effect of dexamethasone administration on rat intestinal permeability: the role of bacterial adherence. *Gastroenterology* 1994; **106**: 35-41 [PMID: 8276206 DOI: 10.1016/s0016-5085(94)94155-6]

54 **Lochs H**, Dejong C, Hammarqvist F, Hebuterne X, Leon-Sanz M, Schütz T, van Gemert W, van Gossum A, Valentini L; DGEM (German Society for Nutritional Medicine), Lübke H, Bischoff S, Engelmann N, Thul P; ESPEN (European Society for Parenteral and Enteral Nutrition). ESPEN Guidelines on Enteral Nutrition: Gastroenterology. *Clin Nutr* 2006; **25**: 260-274 [PMID: 16698129 DOI: 10.1016/j.clnu.2006.01.007]

55 **Han PD**, Burke A, Baldassano RN, Rombeau JL, Lichtenstein GR. Nutrition and inflammatory bowel disease. *Gastroenterol Clin North Am* 1999; **28**: 423-443, ix [PMID: 10372275 DOI: 10.1016/s0889-8553(05)70063-7]

56 **Moed HF**. Citation analysis in research evaluation. Springer Science & Business Media. 2006. [cited 21 March 2023]. Available from: https://link.springer.com/book/10.1007/1-4020-3714-7#book-header

57 **Aksnes DW**, Langfeldt L, Wouters P. Citations, Citation Indicators, and Research Quality: An Overview of Basic Concepts and Theories. *SAGE Open* 2019; **9**: 21582440198 [DOI: 10.1177/2158244019829575]

World Journal of Gastroenterology

Submit a Manuscript: https://www.f6publishing.com

World J Gastroenterol 2023 May 28; 29(20): 3216-3221

DOI: 10.3748/wjg.v29.i20.3216

ISSN 1007-9327 (print) ISSN 2219-2840 (online)

CASE REPORT

Inflammatory myofibroblastic tumor of the pancreatic neck misdiagnosed as neuroendocrine tumor: A case report

Jia-Bei Liu, Qian-Biao Gu, Peng Liu

Specialty type: Gastroenterology and hepatology

Provenance and peer review: Unsolicited article; Externally peer reviewed.

Peer-review model: Single blind

Peer-review report's scientific quality classification

Grade A (Excellent): 0
Grade B (Very good): B, B
Grade C (Good): C
Grade D (Fair): 0
Grade E (Poor): 0

P-Reviewer: Kamer E, Turkey; Kumar M, India; Yarmahmoodi F, Iran

Received: March 10, 2023
Peer-review started: March 10, 2023
First decision: April 14, 2023
Revised: April 21, 2023
Accepted: May 4, 2023
Article in press: May 4, 2023
Published online: May 28, 2023

Jia-Bei Liu, Department of Radiology, The First Affiliated Hospital of Hunan Normal University, Hunan Provincial People's Hospital, Changsha 410005, Hunan Province, China

Qian-Biao Gu, Peng Liu, Department of Radiology, The First Affiliated Hospital of Hunan Normal University (Hunan Provincial People's Hospital), Changsha 410005, Hunan Province, China

Corresponding author: Peng Liu, MD, Chief Doctor, Department of Radiology, The First Affiliated Hospital of Hunan Normal University (Hunan Provincial People's Hospital), No. 61 Jiefang West Road, Changsha 410005, Hunan Province, China. lpradiology@163.com

Abstract

BACKGROUND

Inflammatory myofibroblastic tumor (IMT) is a relatively rare tumor. The global incidence of IMT is less than 1%. There is no specific clinical manifestation. It usually occurs in the lungs, but the pancreas is not the predilection site.

CASE SUMMARY

We present a case of a male patient, 51 years old, who was diagnosed with a pancreatic neck small mass on ultrasound one year ago during a physical examination. As he had no clinical symptoms and the mass was relatively small, he did not undergo treatment. However, the mass was found to be larger on review, and he was referred to our hospital. Since the primal clinical diagnosis was pancreatic neuroendocrine tumor, the patient underwent surgical treatment. However, the case was confirmed as pancreatic IMT by postoperative pathology.

CONCLUSION

Pancreatic IMT is relatively rare and easily misdiagnosed. We can better understand and correctly diagnose this disease by this case report.

Key Words: Inflammatory myofibroblastic tumor; Diagnosis; Imaging; Pancreas; Case report

©The Author(s) 2023. Published by Baishideng Publishing Group Inc. All rights reserved.

Core Tip: Inflammatory myofibroblastic tumor (IMT) is a rare mesenchymal tumor composed of spindle-shaped myofibroblasts accompanied by a mixed inflammatory infiltrate, and is particularly rare in the pancreas. The diagnosis of pancreatic IMT is made on the basis of histopathology and immunohistochemistry. Different lesions exhibit diverse biological characteristics, and there are several surgical treatment protocols. This case emphasizes the importance of correct preoperative diagnosis of IMT and reminds us to broaden our thinking in relation to the diagnosis of pancreatic lesions.

Citation: Liu JB, Gu QB, Liu P. Inflammatory myofibroblastic tumor of the pancreatic neck misdiagnosed as neuroendocrine tumor: A case report. *World J Gastroenterol* 2023; 29(20): 3216-3221
URL: https://www.wjgnet.com/1007-9327/full/v29/i20/3216.htm
DOI: https://dx.doi.org/10.3748/wjg.v29.i20.3216

INTRODUCTION

Inflammatory myofibroblastic tumor (IMT) is a rare mesenchymal tumor. This concept of IMT was first put forward by Pettinato *et al*[1] in 1990. According to the current World Health Organisation (WHO) guidelines, IMTs are typically low-grade neoplasms with occasional malignant potential[2]. An IMT can occur anywhere at any age. This report describes a case of pancreatic IMT.

CASE PRESENTATION

Chief complaints

A 51-year-old male patient was found to have a pancreatic mass more than one year ago.

History of present illness

The patient found a small pancreatic tumor in a physical examination one year ago. However, two months ago, the follow-up of the physical examination center found that the tumor became bigger, then he was referred to our hospital. There were no clinical symptoms throughout the course of the disease.

History of past illness

The patient had a history of hypertension, hyperglycemia, hyperlipidemia, thyroid nodule, prediabetes, and urticaria.

Personal and family history

The patient had no family history of malignant tumors, psychological, or genetic disorders.

Physical examination

The physical examination did not reveal any obvious abnormalities.

Laboratory examinations

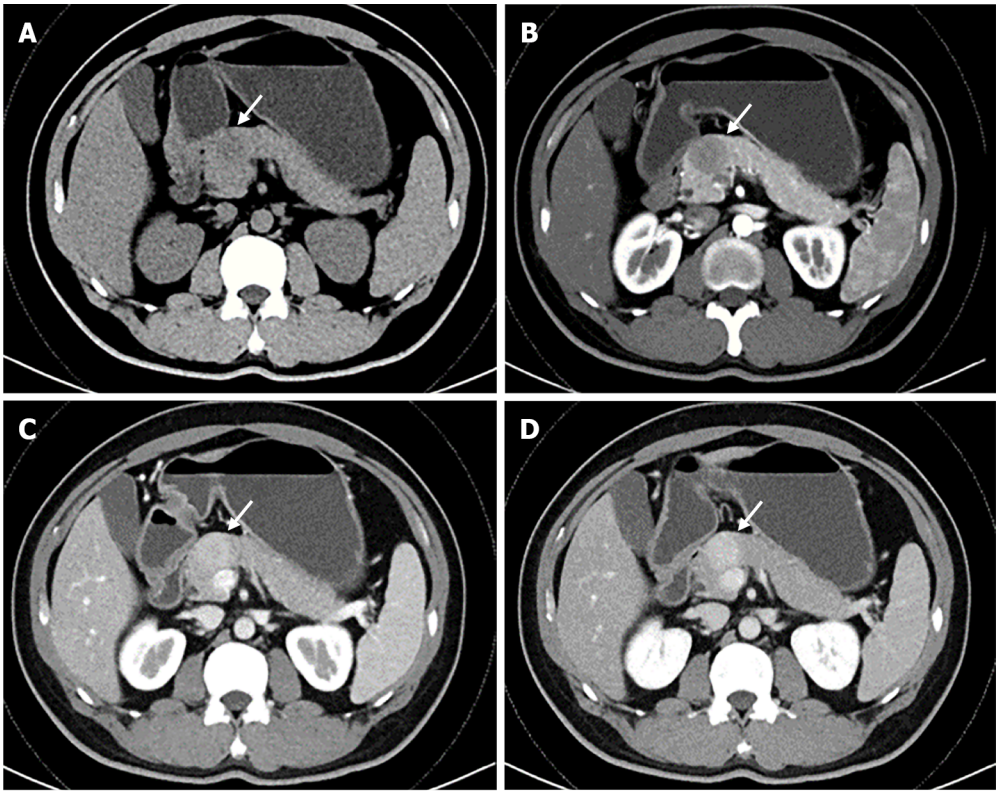
Uric acid and triglyceride levels were elevated. Other blood parameters and tumor markers (carcinoembryonic antigen and cancer antigen 19-9) levels were within the normal range.

Imaging examinations

An abdominal contrast-enhanced computed tomography (CECT) scan showed a round, well-defined, low-density mass 3.5 cm in diameter in the neck of the pancreas. On the CECT scan, the mass showed lower attenuation than the normal pancreatic parenchyma in the pre-contrast phase and arterial phase, and heterogeneous hyperenhancement in the portal venous phase (Figure 1). A pancreatic neuroendocrine tumour was strongly suspected.

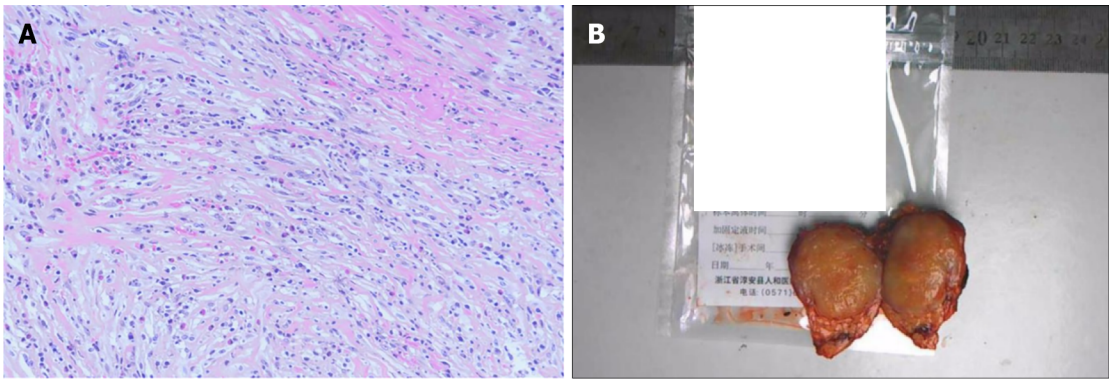
FINAL DIAGNOSIS

The patient was diagnosed with IMT of the pancreas by postoperative pathology (Figure 2).



DOI: 10.3748/wjg.v29.i20.3216 **Copyright** ©The Author(s) 2023.

Figure 1 Abdominal contrast-enhanced computed tomography. A: Axial non-contrast showed a low-density mass in the neck of the pancreas; B: Arterial phase indicated a distinct hypoattenuating mass; C and D: Venous phase revealed persistent hyperenhancement of the mass (magnetic resonance imaging is similar to computed tomography in enhancement mode and characteristics).



DOI: 10.3748/wjg.v29.i20.3216 **Copyright** ©The Author(s) 2023.

Figure 2 Histopathological image and resected tumor specimen. A: Spindle-shaped myofibroblasts accompanied by large amounts of plasma cells. B: The resected specimen showing a well-defined neoplasm (some information has been excluded due to patient privacy).

TREATMENT

After completion of preoperative investigations, a laparoscopic middle pancreatectomy was performed.

OUTCOME AND FOLLOW-UP

Postoperative pancreatic leakage occurred in the patient. However, he was discharged in good clinical condition after 40 d. No apparent events were observed at the 2-mo postoperative follow-up.

DISCUSSION

IMT is a rare mesenchymal tumor. Due to its rarity and the fact that the etiology is unknown, there are only a few cases reported. It has been revealed that IMT may have gene rearrangement with anaplastic lymphoma kinase (ALK)[3], and ALK positivity was also associated with a higher recurrence and less chance of distant metastasis[4]. A recent literature review by Chen *et al*[5] in 2021, included 30 patients with IMT occurring in the pancreas. The reported mean age of the patients was 40 years (range, 0-82 years) with an obvious male preponderance. The tumor was mostly located in the head of the pancreas (21/30 patients). In this series, abdominal pain was the most frequent symptom followed by jaundice. Only five cases of asymptomatic pancreatic IMT have been reported in the medical literature[5-9]. Our patient had no clinical symptoms and the pancreatic mass was found on physical examination. Among the previously reported cases of pancreatic IMT, many were initially misdiagnosed as pancreatic cancer, while the present case was misdiagnosed as pancreatic neuroendocrine tumor. Therefore, it is meaningful to collect more cases and information to obtain reliable diagnosis and treatment methods for IMT.

As the low incidence of pancreatic IMT, there is no specific clinical manifestations has been established. It commonly manifests as abdominal pain or jaundice, and can sometimes be asymptomatic. Although IMT is considered a low-grade tumor, one case of pulmonary metastasis has been reported[10].

At present, pancreatic IMT is mainly diagnosed by histopathology and immunohistochemistry[11]. Under the light microscope, the tumour tissue in this case consisted mainly of spindle-shaped myofibroblasts accompanied by a mixed inflammatory infiltrate. The histopathological findings of this case were consistent with previous reports. Myofibroblasts in IMT stain positive for alpha-smooth muscle antigen (SMA), vimentin, and fibronectin, and stain negative for desmin and caldesmon[12]. In this case, immunohistochemistry report showed positive for IgG4, SMA and actin, and negative for desmin, ALK, CD30, S-100, and Catenin B, similar to those in the literature.

To date, pancreatic IMT is easily misdiagnosed as pancreatic neuroendocrine tumour and pancreatic cancer due to the lack of specific imaging features, and its diagnosis is unclear in clinical practice. A circular low-density mass was observed in the pancreatic IMT reported here. After enhancement, the arterial mass is mildly enhanced, the venous phase is significantly enhanced, and the density is progressively higher than that of the surrounding normal pancreas.

However, in some cases, CECT did not show an enhancing mass and was suspected to be ductal adenocarcinoma, which was ultimately confirmed by pathology to be pancreatic IMT. Hence, the radiologic features of pancreatic IMT require further data.

Pancreatic IMT needs to be differentiated from pancreatic neuroendocrine tumor, pancreatic cancer, and solid-pseudopapillary neoplasm. Pancreatic neuroendocrine tumor is uncommon and has no gender predilection[13]. Additionally, the mass shows high enhancement in the arterial or portal phases due to the rich capillary network in the stroma. Pancreatic cancer is typically seen in patients over 60 years old, with a slight male predominance. It is a hypovascular mass with extensive fibrosis on histopathologic examination[14]. Typical ductal adenocarcinomas appear as poorly defined masses with extensive surrounding desmoplastic reaction and they enhance poorly compared to adjacent normal pancreatic tissue. The presence of abrupt pancreatic duct cutoff, upstream pancreatic duct dilatation, upstream pancreatic parenchymal atrophy, and decreased enhancement in the distal pancreatic parenchyma favors a diagnosis of malignancy[15]. Solid-pseudopapillary neoplasms of the pancreas are cystic-solid masses with a complete capsule. They are prone to bleeding, necrosis and calcification. The solid portion shows enhancement in the arterial phase and can continue to enhance in the delayed phase. However, the imaging features of pancreatic IMT from some pancreatic lesions overlap.

In the present case, a wrong diagnosis was made for several reasons. First, the patient had no clinical manifestations, and the clinical history and laboratory indices are unremarkable. Second, the preoperative imaging findings were difficult to distinguish from a pancreatic neuroendocrine tumour. The border of the lesion was distinct, with persistent hyperenhancement of the mass, and typical double duct sign and vascular involvement were not observed. Accordingly, preliminary diagnosis of imaging was limited to benign mass. In general, IMT of the pancreas is lack of characteristic in terms of clinic-radiological features. Therefore, for more accurate diagnosis and treatment of pancreatic IMT, there is a need to obtain more meaningful information.

CONCLUSION

Given the rarity of pancreatic IMT, this case can contribute to further understanding of the etiology, mechanism, imaging characteristics of this disease. Obtaining a better understanding of all aspects of this disease will help provide a more precise diagnosis.

ACKNOWLEDGEMENTS

We are very grateful to Dr. Liu Yu (Hunan Provincial People's Hospital, First Affiliated Hospital of Hunan Normal University) for providing professional guidance to the pathological analysis.

FOOTNOTES

Author contributions: Liu JB contributed to manuscript writing and editing, and data collection; Liu P and Gu QB contributed to conceptualization and supervision; and all authors have read and approved the final manuscript.

Supported by the Clinical Medical Technology Innovation Guiding Project of Hunan Province, No. 2021SK50911; and Scientific Research Project of Hunan Health Commission, No. 202209010030.

Informed consent statement: Informed written consent was obtained from the patient for publication of this report and any accompanying images.

Conflict-of-interest statement: The authors declare that they have no conflict of interest to disclose.

CARE Checklist (2016) statement: The authors have read the CARE Checklist (2016), and the manuscript was prepared and revised according to the CARE Checklist (2016).

Open-Access: This article is an open-access article that was selected by an in-house editor and fully peer-reviewed by external reviewers. It is distributed in accordance with the Creative Commons Attribution NonCommercial (CC BY-NC 4.0) license, which permits others to distribute, remix, adapt, build upon this work non-commercially, and license their derivative works on different terms, provided the original work is properly cited and the use is non-commercial. See: https://creativecommons.org/Licenses/by-nc/4.0/

Country/Territory of origin: China

ORCID number: Jia-Bei Liu 0009-0007-7049-2484; Qian-Biao Gu 0000-0002-2545-3175; Peng Liu 0000-0002-9023-2344.

S-Editor: Chen YL
L-Editor: A
P-Editor: Chen YL

REFERENCES

1 **Pettinato G**, Manivel JC, De Rosa N, Dehner LP. Inflammatory myofibroblastic tumor (plasma cell granuloma). Clinicopathologic study of 20 cases with immunohistochemical and ultrastructural observations. *Am J Clin Pathol* 1990; **94**: 538-546 [PMID: 2239820 DOI: 10.1093/ajcp/94.5.538]
2 **Choi JH**, Ro JY. The 2020 WHO Classification of Tumors of Soft Tissue: Selected Changes and New Entities. *Adv Anat Pathol* 2021; **28**: 44-58 [PMID: 32960834 DOI: 10.1097/PAP.0000000000000284]
3 **Zhu L**, Li J, Liu C, Ding W, Lin F, Guo C, Liu L. Pulmonary inflammatory myofibroblastic tumor *vs* IgG4-related inflammatory pseudotumor: differential diagnosis based on a case series. *J Thorac Dis* 2017; **9**: 598-609 [PMID: 28449468 DOI: 10.21037/jtd.2017.02.89]
4 **Coffin CM**, Hornick JL, Fletcher CD. Inflammatory myofibroblastic tumor: comparison of clinicopathologic, histologic, and immunohistochemical features including ALK expression in atypical and aggressive cases. *Am J Surg Pathol* 2007; **31**: 509-520 [PMID: 17414097 DOI: 10.1097/01.pas.0000213393.57322.c7]
5 **Chen ZT**, Lin YX, Li MX, Zhang T, Wan DL, Lin SZ. Inflammatory myofibroblastic tumor of the pancreatic neck: A case report and review of literature. *World J Clin Cases* 2021; **9**: 6418-6427 [PMID: 34435007 DOI: 10.12998/wjcc.v9.i22.6418]
6 **Pungpapong S**, Geiger XJ, Raimondo M. Inflammatory myofibroblastic tumor presenting as a pancreatic mass: a case report and review of the literature. *JOP* 2004; **5**: 360-367 [PMID: 15365204]
7 **Yamamoto H**, Watanabe K, Nagata M, Tasaki K, Honda I, Watanabe S, Soda H, Takenouti T. Inflammatory myofibroblastic tumor (IMT) of the pancreas. *J Hepatobiliary Pancreat Surg* 2002; **9**: 116-119 [PMID: 12021906 DOI: 10.1007/s005340200013]
8 **Dulundu E**, Sugawara Y, Makuuchi M. Inflammatory myofibroblastic tumor of the pancreas--a case report. *Biosci Trends* 2007; **1**: 167-169 [PMID: 20103888]
9 **Berhe S**, Goldstein S, Thompson E, Hackam D, Rhee DS, Nasr IW. Challenges in Diagnosis and Management of Pancreatic Inflammatory Myofibroblastic Tumors in Children. *Pancreas* 2019; **48**: e27-e29 [PMID: 30973469 DOI: 10.1097/MPA.0000000000001290]
10 **Walsh SV**, Evangelista F, Khettry U. Inflammatory myofibroblastic tumor of the pancreaticobiliary region: morphologic and immunocytochemical study of three cases. *Am J Surg Pathol* 1998; **22**: 412-418 [PMID: 9537467 DOI: 10.1097/00000478-199804000-00004]
11 **A G H**, Kumar S, Singla S, Kurian N. Aggressive Inflammatory Myofibroblastic Tumor of Distal Pancreas: A Diagnostic

and Surgical Challenge. *Cureus* 2022; **14**: e22820 [PMID: 35399449 DOI: 10.7759/cureus.22820]

12 **Chan JK**, Cheuk W, Shimizu M. Anaplastic lymphoma kinase expression in inflammatory pseudotumors. *Am J Surg Pathol* 2001; **25**: 761-768 [PMID: 11395553 DOI: 10.1097/00000478-200106000-00007]

13 **Lewis RB**, Lattin GE Jr, Paal E. Pancreatic endocrine tumors: radiologic-clinicopathologic correlation. *Radiographics* 2010; **30**: 1445-1464 [PMID: 21071369 DOI: 10.1148/rg.306105523]

14 **Frampas E**, Morla O, Regenet N, Eugène T, Dupas B, Meurette G. A solid pancreatic mass: tumour or inflammation? *Diagn Interv Imaging* 2013; **94**: 741-755 [PMID: 23751230 DOI: 10.1016/j.diii.2013.03.013]

15 **Tamada T**, Ito K, Kanomata N, Sone T, Kanki A, Higaki A, Hayashida M, Yamamoto A. Pancreatic adenocarcinomas without secondary signs on multiphasic multidetector CT: association with clinical and histopathologic features. *Eur Radiol* 2016; **26**: 646-655 [PMID: 26084602 DOI: 10.1007/s00330-015-3880-3]



Published by **Baishideng Publishing Group Inc**
7041 Koll Center Parkway, Suite 160, Pleasanton, CA 94566, USA
Telephone: +1-925-3991568
E-mail: bpgoffice@wjgnet.com
Help Desk: https://www.f6publishing.com/helpdesk
https://www.wjgnet.com



© 2023 Baishideng Publishing Group Inc. All rights reserved.

ISSN 1007-9327 (print)
ISSN 2219-2840 (online)

World Journal of *Gastroenterology*

World J Gastroenterol 2023 June 7; 29(21): 3222-3384



Published by Baishideng Publishing Group Inc

World Journal of Gastroenterology

Contents

Weekly Volume 29 Number 21 June 7, 2023

REVIEW

3222 Crohn's disease: Why the ileum?

Richard N, Savoye G, Leboutte M, Amamou A, Ghosh S, Marion-Letellier R

3241 Emerging role of the gut microbiome in post-infectious irritable bowel syndrome: A literature review

Lupu VV, Ghiciuc CM, Stefanescu G, Mihai CM, Popp A, Sasaran MO, Bozomitu L, Starcea IM, Adam Raileanu A, Lupu A

MINIREVIEWS

3257 Biliary complications after liver transplantation: A computed tomography and magnetic resonance imaging pictorial review

Vernuccio F, Mercante I, Tong XX, Crimì F, Cillo U, Quaia E

ORIGINAL ARTICLE

Basic Study

3269 Effects of ethanol and sex on propionate metabolism evaluated *via* a faster ^{13}C-propionate breath test in rats

Sasaki Y, Kawagoe N, Imai T, Urita Y

3280 Fibroblast growth factor 15, induced by elevated bile acids, mediates the improvement of hepatic glucose metabolism after sleeve gastrectomy

Wei M, Cao WB, Zhao RD, Sun DP, Liang YZ, Huang YD, Cheng ZW, Ouyang J, Yang WS, Yu WB

Retrospective Cohort Study

3292 Ineffective esophageal motility is associated with acute rejection after lung transplantation independent of gastroesophageal reflux

Lo WK, Hiramoto B, Goldberg HJ, Sharma N, Chan WW

Clinical Trials Study

3302 Peutz-Jeghers syndrome without *STK11* mutation may correlate with less severe clinical manifestations in Chinese patients

Jiang LX, Chen YR, Xu ZX, Zhang YH, Zhang Z, Yu PF, Dong ZW, Yang HR, Gu GL

Observational Study

3318 Artifacts in two-dimensional shear wave elastography of liver

Wang HP, Zheng PC, Wang XM, Sang L

3328 Therapeutic anticoagulation for splanchnic vein thrombosis in acute pancreatitis: A national survey and case-vignette study

Sissingh NJ, Groen JV, Timmerhuis HC, Besselink MG, Boekestijn B, Bollen TL, Bonsing BA, Klok FA, van Santvoort HC, Verdonk RC, van Eijck CHJ, van Hooft JE, Mieog JSD

World Journal of Gastroenterology

Weekly Volume 29 Number 21 June 7, 2023

Contents

SYSTEMATIC REVIEWS

3341 Lumen-apposing-metal stent misdeployment in endoscopic ultrasound-guided drainages: A systematic review focusing on issues and rescue management

Armellini E, Metelli F, Anderloni A, Cominardi A, Aragona G, Marini M, Pace F

META-ANALYSIS

3362 Association of non-alcoholic fatty liver and metabolic-associated fatty liver with COVID-19 outcomes: A systematic review and meta-analysis

Jagirdhar GSK, Qasba RK, Pattnaik H, Rama K, Banga A, Reddy ST, Flumignan Bucharles AC, Kashyap R, Elmati PR, Bansal V, Bains Y, DaCosta T, Surani S

ACADEMIC WRITING

3379 How to select a journal for your research

Ramia JM

ABOUT COVER

Editorial Board Member of *World Journal of Gastroenterology*, Wei Jiang, MD, PhD, Chief Doctor, Professor, Department of Gastroenterology, Zhongshan Hospital, Fudan University, Shanghai 200032, China. jiang.wei@zs-hospital.sh.cn

AIMS AND SCOPE

The primary aim of *World Journal of Gastroenterology* (*WJG*, *World J Gastroenterol*) is to provide scholars and readers from various fields of gastroenterology and hepatology with a platform to publish high-quality basic and clinical research articles and communicate their research findings online. *WJG* mainly publishes articles reporting research results and findings obtained in the field of gastroenterology and hepatology and covering a wide range of topics including gastroenterology, hepatology, gastrointestinal endoscopy, gastrointestinal surgery, gastrointestinal oncology, and pediatric gastroenterology.

INDEXING/ABSTRACTING

The *WJG* is now abstracted and indexed in Science Citation Index Expanded (SCIE, also known as SciSearch®), Current Contents/Clinical Medicine, Journal Citation Reports, Index Medicus, MEDLINE, PubMed, PubMed Central, Scopus, Reference Citation Analysis, China National Knowledge Infrastructure, China Science and Technology Journal Database, and Superstar Journals Database. The 2022 edition of Journal Citation Reports® cites the 2021 impact factor (IF) for *WJG* as 5.374; IF without journal self cites: 5.187; 5-year IF: 5.715; Journal Citation Indicator: 0.84; Ranking: 31 among 93 journals in gastroenterology and hepatology; and Quartile category: Q2. The *WJG*'s CiteScore for 2021 is 8.1 and Scopus CiteScore rank 2021: Gastroenterology is 18/149.

RESPONSIBLE EDITORS FOR THIS ISSUE

Production Editor: *Ying-Yi Yuan*; **Production Department Director:** *Xiang Li*; **Editorial Office Director:** *Jia-Ru Fan.*

NAME OF JOURNAL
World Journal of Gastroenterology

ISSN
ISSN 1007-9327 (print) ISSN 2219-2840 (online)

LAUNCH DATE
October 1, 1995

FREQUENCY
Weekly

EDITORS-IN-CHIEF
Andrzej S Tarnawski

EDITORIAL BOARD MEMBERS
http://www.wjgnet.com/1007-9327/editorialboard.htm

PUBLICATION DATE
June 7, 2023

COPYRIGHT
© 2023 Baishideng Publishing Group Inc

INSTRUCTIONS TO AUTHORS
https://www.wjgnet.com/bpg/gerinfo/204

GUIDELINES FOR ETHICS DOCUMENTS
https://www.wjgnet.com/bpg/GerInfo/287

GUIDELINES FOR NON-NATIVE SPEAKERS OF ENGLISH
https://www.wjgnet.com/bpg/gerinfo/240

PUBLICATION ETHICS
https://www.wjgnet.com/bpg/GerInfo/288

PUBLICATION MISCONDUCT
https://www.wjgnet.com/bpg/gerinfo/208

ARTICLE PROCESSING CHARGE
https://www.wjgnet.com/bpg/gerinfo/242

STEPS FOR SUBMITTING MANUSCRIPTS
https://www.wjgnet.com/bpg/GerInfo/239

ONLINE SUBMISSION
https://www.f6publishing.com

© 2023 Baishideng Publishing Group Inc. All rights reserved. 7041 Koll Center Parkway, Suite 160, Pleasanton, CA 94566, USA
E-mail: bpgoffice@wjgnet.com https://www.wjgnet.com

World Journal of Gastroenterology

Submit a Manuscript: https://www.f6publishing.com

World J Gastroenterol 2023 June 7; 29(21): 3222-3240

DOI: 10.3748/wjg.v29.i21.3222

ISSN 1007-9327 (print) ISSN 2219-2840 (online)

REVIEW

Crohn's disease: Why the ileum?

Nicolas Richard, Guillaume Savoye, Mathilde Leboutte, Asma Amamou, Subrata Ghosh, Rachel Marion-Letellier

Specialty type: Gastroenterology and hepatology

Provenance and peer review: Invited article; Externally peer reviewed.

Peer-review model: Single blind

Peer-review report's scientific quality classification

Grade A (Excellent): 0
Grade B (Very good): B, B
Grade C (Good): 0
Grade D (Fair): 0
Grade E (Poor): 0

P-Reviewer: Castelucci P, Brazil; Leal RF, Brazil

Received: December 28, 2022
Peer-review started: December 28, 2022
First decision: January 10, 2023
Revised: January 23, 2023
Accepted: May 8, 2023
Article in press: May 8, 2023
Published online: June 7, 2023

Nicolas Richard, Guillaume Savoye, Mathilde Leboutte, Rachel Marion-Letellier, University of Rouen Normandie, INSERM, ADEN UMR 1073, Nutrition, Inflammation and Microbiota-Gut-Brain Axis, Rouen F-76000, France

Nicolas Richard, Guillaume Savoye, CHU Rouen, Department of Gastroenterology, Rouen University Hospital-Charles Nicolle, Rouen F-76000, France

Nicolas Richard, Guillaume Savoye, Mathilde Leboutte, Rachel Marion-Letellier, Institute for Research and Innovation in Biomedicine, University of Rouen Normandie, Rouen F-76000, France

Asma Amamou, Subrata Ghosh, APC Microbiome Ireland, Biosciences Building, University College Cork, Cork T12 YT20, Ireland

Corresponding author: Rachel Marion-Letellier, PhD, Associate Professor, University of Rouen Normandie, INSERM, ADEN UMR 1073, Nutrition, Inflammation and Microbiota-Gut-Brain Axis, 22 Boulevard Gambetta, Rouen F-76000, France. rachel.letellier@univ-rouen.fr

Abstract

Crohn's disease (CD) is an inflammatory bowel disease characterized by immune-mediated flares affecting any region of the intestine alternating with remission periods. In CD, the ileum is frequently affected and about one third of patients presents with a pure ileal type. Moreover, the ileal type of CD presents epidemiological specificities like a younger age at onset and often a strong link with smoking and genetic susceptibility genes. Most of these genes are associated with Paneth cell dysfunction, a cell type found in the intestinal crypts of the ileum. Besides, a Western-type diet is associated in epidemiological studies with CD onset and increasing evidence shows that diet can modulate the composition of bile acids and gut microbiota, which in turn modulates the susceptibility of the ileum to inflammation. Thus, the interplay between environmental factors and the histological and anatomical features of the ileum is thought to explain the specific transcriptome profile observed in CD ileitis. Indeed, both immune response and cellular healing processes harbour differences between ileal and non-ileal CD. Taken together, these findings advocate for a dedicated therapeutic approach to managing ileal CD. Currently, interventional pharmacological studies have failed to clearly demonstrate distinct response profiles according to disease site. However, the high rate of stricturing disease in ileal CD requires the identification of new therapeutic targets to significantly change the natural history of this debilitating disease.

Key Words: Ileum; Crohn's disease; Bile acids; Paneth cells; Diet; Genetics; Strictures

©The Author(s) 2023. Published by Baishideng Publishing Group Inc. All rights reserved.

Core Tip: The ileum is most frequently affected by Crohn's disease (CD). Ileal CD differs from other CD types in its epidemiology and natural history. Anatomical and histological features of the ileum provide the keys to understanding this distinct phenotype. Moreover, we discuss herein the crosstalk that occurs in the ileum between an individual and her/his environment and the clinical significance.

Citation: Richard N, Savoye G, Leboutte M, Amamou A, Ghosh S, Marion-Letellier R. Crohn's disease: Why the ileum? *World J Gastroenterol* 2023; 29(21): 3222-3240
URL: https://www.wjgnet.com/1007-9327/full/v29/i21/3222.htm
DOI: https://dx.doi.org/10.3748/wjg.v29.i21.3222

INTRODUCTION

Crohn's disease (CD) is an inflammatory bowel disease (IBD) characterized by repetitive inflammatory flares, and often chronicity. Unlike ulcerative colitis (UC), the other main subtype of IBD, CD can affect any part of the digestive tract. The site of the disease is a critical biological aspect of CD whereas inflammatory, stricturing or penetrating behaviour is thought to be a reflection of disease progression[1].

Data on the epidemiology of IBD are provided by population-based studies showing an increasing incidence and prevalence of IBD in the West over the last 50 years[2,3]. In a systematic review pooling all epidemiological studies on IBD worldwide since 1990, the global prevalence of IBD is higher in Western countries (322 per 100000 in Germany) than in newly industrialized countries[4]. In newly industrialized countries like Asia and the Middle East, epidemiological studies report a rising incidence of CD[4,5]. The Montreal classification distinguishes CD involving the ileum, the colon and both the colon and the ileum[6]. About one third of patients with CD presents a disease involvement limited to the ileum and this proportion does not vary between 'Western' and newly industrialized countries[3,5,7]. Once the diagnosis of ileal CD is made, less than one fifth of patients will present colonic lesions over time[3]. In addition, ileal CD occurs in younger patients than colonic CD[1]. These epidemiological observations have led some experts to plead for personalized approaches to therapy based on the disease site.

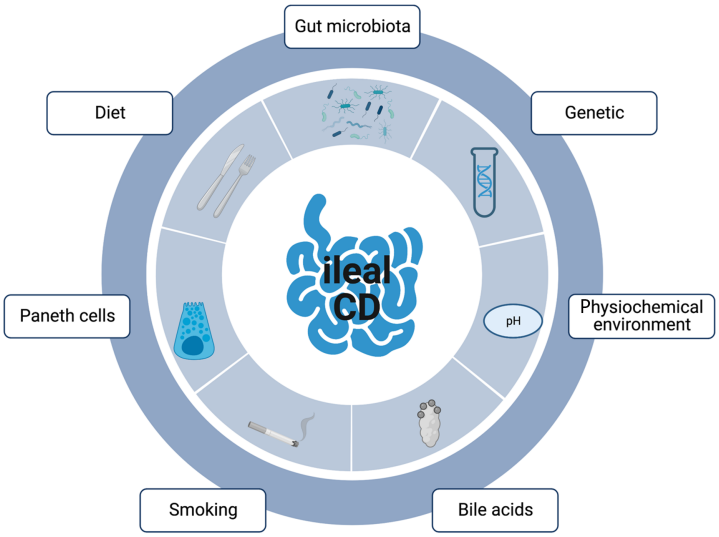
Even though CD pathogenesis remains elusive, current consensus considers CD a result of genetic, immunological and environmental factors[2]. Of relevance, the ileum is the site for the crosstalk of these multiple etiological factors in CD. In this review, we will depict the different physiopathological aspects of ileal CD and their clinical impact (Figure 1).

GENETIC SUSCEPTIBILITY

Genetic factors are involved in IBD physiopathology and genome-wide association studies have linked several genes with the site of the disease. In a large epidemiological study performed in more than 34000 patients with IBD across Europe, North America and Australia, susceptibility genes were determinants of the site of the disease whereas inherited genes showed a loose link with the inflammatory, penetrating or stricturing behaviour of the disease[1]. The genetic variants presented herein sum up the current state-of-the-art but new techniques such as genomic DNA are likely to provide new insights in the next few years.

NOD2

NOD2 is a sensor of the innate immune system, able to detect bacterial fragments, specifically muramyl dipeptide[8]. During *in vitro* differentiation of intestinal epithelial cells into Paneth cells, NOD2 signalling can modulate the expression of enteric antimicrobial peptides[9]. Even though intracellular pattern recognition receptor gene *NOD2* is widely associated with CD risk[2], mutations in the *NOD2* gene are strongly associated with ileal CD and are correlated with a younger age at diagnosis[1,10,11]. The specific association between *NOD2* mutations and ileal CD is partially explained by its distribution along the gastrointestinal tract. Histologically, *NOD2* is overexpressed in ileal crypts compared to colonic crypts[12].



DOI: 10.3748/wjg.v29.i21.3222 **Copyright** ©The Author(s) 2023.

Figure 1 Potential factors involved in ileal Crohn's disease. While Crohn's disease (CD) occurs in any part of the gastrointestinal tract, the ileum is frequently involved. Potential factors involved in ileal CD are genetic susceptibility genes and most of these genes are associated with Paneth cell dysfunction. Environmental factors may also be involved such as diet, gut microbiota and smoking. Diet can modulate the composition of bile acids and gut microbiota, which in turn affect the susceptibility of the ileum to inflammation. Created with BioRender.com. CD: Crohn's disease.

LRRK2

Like *NOD2*, the *LRRK2* gene is expressed in Paneth cells. *LRRK2* gene is implicated in vesicular trafficking, cytoskeleton homeostasis and consequently in inflammation and immune response[13]. More specifically, LRRK2 is overexpressed in Paneth cells and its deficiency causes deprivation of lysozyme in Paneth cells[14]. In a case-control study, mutations of *LRRK2* were associated with ileitis and an early onset of CD[15].

Major histocompatibility complex

The expression of other genes involved in immune response is likewise implicated in ileal CD. The major histocompatibility complex is involved in the presentation of antigen in a large variety of cell types including T-cells. In a recent meta-analysis, several mutations of these genes were associated with CD especially in the Korean population but also in the European population[16]. Of note, single nucleotide polymorphisms of these genes were more common in patients with ileal CD compared to patients with colonic CD[1].

ATG16L1

Among susceptibility genes identified in CD, the allele ATG16L1^{T300A} was associated with impaired autophagy[17,18]. The expression of *ATG16L1* was decreased in CD patients[19]. In 9-10-month-old mice, the specific deletion of *Atg16L1* allele in intestinal epithelium cells (IEC) led to a transmural CD-like ileitis associated with endoplasmic reticulum stress[20]. Interestingly, *NOD2* mutations are also associated with autophagy defects.

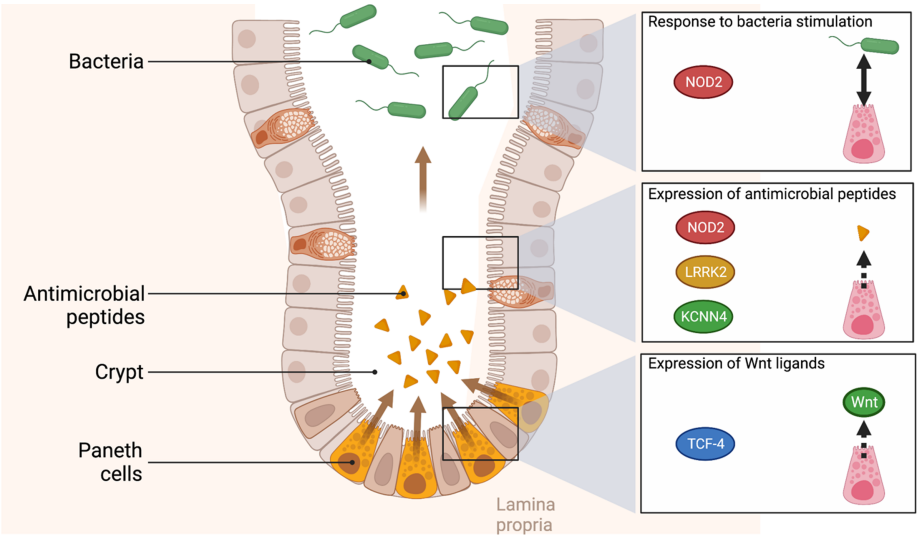
Tcf-4

In IBD patients, the reduction of the Wnt-signalling pathway transcription factor Tcf-4 was associated with a predisposition for ileal CD[21,22]. A reduced expression of Tcf-4 resulted in a reduced expression of Paneth cell defensins[21]. In a murine Tcf-4 knockout model, a decreased expression of alpha-defensin levels and a reduced capacity of bacterial killing were observed[21].

KCNN4

Finally, in the array of genes implicated in the immune response mediated by Paneth cells, the conductance calcium-activated potassium channel protein (KCNN4) is part of the potassium pump in the human intestine[23]. The blocking of this calcium-activated potassium channel protein reduced mouse Paneth cell secretion in response to bacterial stimulation[24]. In human, mutation of the *KCNN4* gene was associated with ileal CD in the Australian and New Zealand population[25].

In the susceptibility genes mentioned above, most genes are associated with Paneth cell dysfunction as illustrated in Figure 2. We will detail below the potential involvement of Paneth cells in ileal CD.



DOI: 10.3748/wjg.v29.i21.3222 **Copyright** ©The Author(s) 2023.

Figure 2 Putative role of gene susceptibility in Paneth cell dysfunction. Paneth cells are secretory epithelial cells located in the intestinal crypts. Paneth cells produce antimicrobial peptides in response to bacterial components and support stem cell function through Wnt signalling. Most of the susceptibility genes associated with ileal Crohn's disease (CD) involve Paneth cell dysfunction. NOD2 and *LRRK2* genes are expressed in Paneth cells and their deficiency in ileal CD modulates the expression of antimicrobial peptides such as alpha-defensins or lysozyme. Similarly, the reduction of the Wnt-signalling pathway transcription factor Tcf-4 is associated with a predisposition for ileal CD and leads to a reduced expression of Paneth cell defensins. The blocking of calcium-activated potassium channel protein (KCNN4) inhibits mouse Paneth cell secretion in response to bacterial stimulation. Created with BioRender.com.

THE ILEUM, A SPECIFIC PART OF THE GASTROINTESTINAL TRACT

Beyond genetic factors, the histological and anatomical features of the ileum itself may partially explain the propensity of this specific part of the gastrointestinal tract to be affected by CD.

Physicochemical environment

The ileum presents a unique chemical microenvironment. The intraluminal pH in the ileum is 7.4, the highest of the human digestive tract as a result of small bowel mucosal bicarbonate secretion[26]. Comparatively, the intraluminal pH in the caecum is lower, 6.5, due to the bacterial production of short fatty acids by colonic bacteria[26,27]. The functional characteristics of the digestive tract microbiota are modulated by pH level. In the environment of the ileum (pH = 7.4), short chain fatty acids increase the growth and the motility of pathobionts whereas, in the colonic environment (pH = 6.5), short chain fatty acids downregulate the virulence of gene expression of these strains[28].

Histological changes in ileal CD

From a clinical point of view, most of histological features encountered in ileal CD were also found in other diseases as backwash ileitis in UC for instance[29]. Although epithelioid granuloma is considered as the histological hallmark for the diagnosis of ileal CD, it is not a mandatory prerequisite[30]. In about one quarter of patients with ileal CD, pyloric gland metaplasia resulting from the expression of mucin genes normally specific to the stomach (*MUC5AC* and *MUC6*) were noted[30,31]. Although numerous other histological features are described in ileal CD, focal crypt irregularities are considered by expert consensus as one of the most reliable signs of CD[30].

From a biological point of view, the most noteworthy change is found in Peyer's patches. Peyer's patches are ileal immune structures characterized by a B-cell germinal centre surrounded by a T-cell interfollicular region. These mucosal-associated lymphoid tissues can act as "gateways" of the intestine. The epithelium and the underlying lymphoid follicle differ from the surrounding villus epithelium of the ileum. Indeed, the function of this follicle-associated epithelium consists in sampling and transporting luminal antigens through M cells and dendritic cells to CD^{4+} cells[32]. Early histological changes in Peyer's patches were reported in ileal CD such as an increase in mast cells or erosive epithelial lesions[33,34]. Further, the increased number of glial cells in the Peyer's patches of patients with ileal CD resulted in an enhanced intestinal permeability[34]. Together these phenomena may explain the increased vulnerability of the ileal mucosa to bacterial invasion in CD patients[35].

Enteric nervous system

As mentioned in the previous section, the histological changes observed in ileal CD include glial cells and the enteric nervous system (ENS). In patients with ileal CD, both the submucous and the myenteric plexus present an overall increase in the number of neuronal cell bodies, enteroglia and interstitial cells

of Cajal associated with an upregulation of apoptosis in enteric neurons and enteric glial cells[36,37]. To that extent, although functional evidence is lacking in the literature to fully support this hypothesis, the increased transit time observed in CD patients could be seen as a consequence of ultrastructural injury to interstitial cells of Cajal in the myenteric plexus[38,39].

Beyond the role of the ENS in intestinal mobility, the density of enteric glial cells conveys a higher risk of ileal CD recurrence after surgery. Thus, after ileocolonic resection for CD, inflammation in or around nerve bundles or enteric ganglia was reported in several clinical studies as a risk factor for CD recurrence[40-43]. In the uninflamed section from ileocolonic samples, the number of S100-positive enteric glial cells was enhanced in patients with relapsing disease unlike vasoactive intestinal polypeptide or substance P positive cells[44]. Furthermore, the ileum of CD patients harbours a different distribution of enteric glial cells with a higher density of these cells around Peyer's patches. In parallel, the mediators of enteric glial cell increased the permeability of the ileal mucosa in CD patients whereas they decreased the permeability of the mucosa in non-IBD patients[34]. The importance of these findings on the natural history of CD remains to be determined. In particular, the effect of the modulation of the ENS in neuro-immune interplay needs to be investigated.

Paneth cells

Paneth cells are mostly located in the ileum and nearly absent from the colon[45]. This cellular type is found between intestinal stem cells in the small intestinal crypts. Paneth cells produce not only antimicrobial peptides that regulate host-microbe interplay but also factors such as Wnt ligands modulating the activity of intestinal stem cells. Many of the ileal CD-associated mutations discussed before involve cellular pathways of Paneth cells.

Paneth cells are rich in mitochondria to sustain their energy-expending secretory functions. In *SAMP1* mice, mice genetically predisposed to CD-like ileitis, the number of Paneth cells was decreased and abnormal Paneth cells were associated with disease progression[46,47]. Likewise, the number of Paneth cells is decreased in the small intestine of CD patients. This observation was made in several ethnic populations and particularly in paediatric cohorts[19,48,49]. Mucosal biopsies from adult CD showed ultrastructural abnormalities in mitochondria, especially in CD patients with inflammation (73.3%) but also in inactive CD patients (20.3%) which was not the case for goblet cells and enterocytes[50]. In patients with ileal CD, the count of abnormal Paneth cells correlated with disease activity and was predictive of recurrence after surgery[51]. Some authors hypothesised that this dysfunction in Paneth cells could result from mitochondrial impairment[50-52]. Besides, in mice, Paneth cell defects triggered by loss of prohibitin 1, a major component protein of the inner mitochondrial membrane implicated in cell respiration, caused ileitis[52]. This effect is mediated by oxidative stress. Furthermore, the use of a specific mitochondrial-targeted antioxidant (Mito-Tempo) ameliorates ileitis in mice. The use of the same mitochondrial-targeted antioxidant (Mito-Tempo) in human ileal biopsies of CD patients normalized the expression of 25% of altered CD genes, including genes implicated in antigen processing, lipid metabolism, apoptosis, and interleukin (IL)-17/IL-23 signalling[50].

Immune response

As highlighted by research in immunological processes, Paneth cells are part of the crosstalk with the immune system to maintain intestinal microbial homeostasis and intestinal barrier[53,54]. When biopsies from CD patients were compared according to the site of inflammation in the gastrointestinal tract, differences in neutrophil activities were observed. For instance, matrix metalloproteinase-9 and myeloperoxidase were relatively less increased in ulcer edges of ileal CD compared to colonic CD, suggesting less neutrophilic degranulation in ileal CD[55].

Likewise, innate lymphoid cells (ILCs) are gaining interest as components of the immune system. Three groups have been individualized according to their properties: ILC1, ILC2 and ILC3. A switch was noted in the inflamed ileal mucosa of CD patients, from an ILC3 phenotype limiting commensal bacteria specific $CD4^+$ T cell response to an ILC1 phenotype associated with interferon (IFN)-γ production[56]. The aryl hydrocarbon receptor (AhR), a ligand-dependent transcription factor, was involved in this process and downregulated in inflamed mucosa of IBD patients[57,58]. Pharmacological or genetic activation of the AhR enhanced ILC3 maintenance conferring a protection against pathogenic bacteria in mice and downregulated ILC2 maintenance implicated in immune response in worm[59]. AhR agonists arise from the environment, commensal flora and tryptophan metabolism[60]. In patients with ileal CD, impaired tryptophan metabolism was observed with decreased levels of kynurenine and expression of kynureninase[61].

Concordantly with a typical cellular immune response, ileal CD instigates a specific cytokine profile. Interferon lambda (IFNL) is secreted in response to microbial stimulation or to T-cell-mediated mucosal inflammation. IFNL was upregulated in the ileal mucosa of patients with CD and triggered ileitis in a murine model and induced Paneth cell depletion independently of tumour necrosis factor (TNF)[62]. The effect of IFNL in the ileum is mediated by the JAK-STAT pathway which represents a promising therapeutic target already being used in the clinic[62].

Besides the role played by IFNL, IL-22 contributes to the pathogenesis of ileal CD. IL-22 is produced by T-cells and ICL3 during IBD flares[63,64]. IL-22 is thought to assume an immunoregulative role as its inhibition by the IL-22 binding protein induced a severe inflammation in a rodent colitis model[64]. In

the ileum, interestingly, the levels of IL-22 binding protein were specifically high in comparison with the colon[65]. This heterogenous distribution along the gastrointestinal tract may result from the infiltration of eosinophils in the ileum and the production of IL-22 binding protein[64,65].

The ileum as an endocrine organ

If a high proportion of eosinophil cells was present in the ileum, an enhanced enteroendocrine cell activity was also found[66]. Additionally, terminal ileal chromogranin A cells and glucagon-like peptide 1 (GLP-1) positive L-cells were increased in ileal CD specifically[66]. However, studies on the serum levels of GLP-1 are rare and include small cohorts (< 20 patients). Data were inconclusive and showed similar serum levels of GLP-1 between patients with ileocolic CD and colonic CD but a higher serum level of GLP-1 in IBD compared to healthy controls[67,68]. Thus, no firm conclusion can be drawn regarding the nutritional and immune impact of this discovery.

Besides harbouring enteroendocrine cells, the ileum harbours oestrogen receptor subtype β, whether the ileum is affected by CD or not. The expression of subtype β was associated with a milder disease course in a cohort of 37 patients with ileal CD. Accordingly, the inflammation score was inversely correlated with the expression of oestrogen receptor β. Similarly, a higher expression of oestrogen receptor β was found in patients with non-stricturing non-penetrating disease[69]. In a chemical colitis model in rats, the activation of oestrogen receptor b reduced inflammation score as well as inflammatory pain and inhibited the ionotropic P2X3 receptor[70]. Notwithstanding this observation, female sex was not independently associated with ileal CD[1,71].

Myofibroblasts

While ileitis is often studied from an inflammation perspective, little is published about cell repair. The gene encoding tumour progression locus-2 kinase, a proinflammatory enzyme, was associated in a genetically invalidated murine model with a surprising homeostatic role, modulating the effect of chemically induced colitis. Mechanistically, this gene does not directly impact the immune response but plays a critical role in intestinal myofibroblasts which contribute to the healing of intestinal epithelium. In response to inflammatory signals from the microenvironment, intestinal myofibroblasts trigger compensatory epithelial proliferation in the intestinal crypts[72].

Transcriptome studies

The integration of the different pathways mentioned above in the pathogenesis of ileal CD is facilitated by multi-omic studies. Thus, differences in pathogenesis between the ileum and the colon are highlighted by these techniques. For instance, in CD patients, the metabolomic study of non-inflamed ileum and non-inflamed colon biopsies distinguish clearly different profiles. It is noteworthy that these differences were blurred in inflamed ileum and colon samples[73].

Although the physiopathology of ileal CD has been studied as a unique phenomenon, emerging evidence advocates for a more heterogeneous process in which physiopathological pathways differ from one patient to the other. Thus, transcriptomic data analysis from CD ileal tissue sample was able to identify subgroups of patients with distinct recurrence rates after surgery[74].

In a recent transcriptomic study of ileal mucosa samples, inflammatory genes (IL-6, IL-8, IL-1β) were upregulated whereas metabolic process genes were downregulated in ileal samples from CD patients compared to controls. Early post-operative recurrence of CD was associated with an overexpression of TNF-α, IFN-γ, IL-23A and IL-17A upregulation. In addition, using a regression model to predict post-operative recurrence of CD, mitochondrial dysfunction and JAK/STAT upregulation in the ileum were independently associated with post-operative recurrence[75]. Transcriptomic studies also provide new insights into cell population specificities in ileal CD. When mapping the cell type of the ileal mucosa of CD patients, tuft and $BEST^{4+}$ cells were the cell types associated with CD, irrespectively of the treatment status[76]. Intestinal tuft cells are a rare cell type implicated in the defence against helminthic and protozoan infections[77]. $BEST^{4+}$ cells represent about 1% of ileal epithelial cells and plausibly contribute to the mucus secretion of goblet cells[78]. Surprisingly in this ileal cell type study, immune compartment was slightly affected by CD despite the fact that treatment status in CD patients modified the epithelial and immune compartment[76].

Among the differentially expressed genes in ileal inflammatory response, activating transcription factor 4 (ATF4) is a transcription factor widely expressed in the human body, including the ileum. ATF4 downregulation in intestinal epithelial cells has been observed in active CD in patients and causes spontaneous enterocolitis in mice while altering ileal Paneth cell function. Furthermore, murine ATF4 deletion impaired the glutamine uptake of the intestinal epithelium and concordantly glutamine supplementation restored Paneth cell function and decreased intestinal inflammation[79]. A few years earlier, the inhibition of the ATF4 pathway demonstrated an altered autophagy in human intestinal epithelium in the presence of adherent-invasive Escherichia coli (AIEC). This pathological response resulted in the intracellular bacterial replication of AIEC and consequently in pro-inflammatory patterns[80].

BILE ACIDS

The role of bile acids is largely reported in liver disease in which bile acids are inflammatory cues and treatment targets[81]. The involvement of the gut in the pathogenesis of inflammatory liver diseases and similarities in etiological factors has led to consideration of the role of bile acids in IBD[82].

Primary bile acids are produced in the liver and secreted through the biliary tree into the gastrointestinal tract. Most primary bile acids are reabsorbed by the ileum and hence recycled several times. A minority of primary bile acids are transformed into secondary bile acids by a narrow range of gut bacteria. The pool of bile acids influenced the composition of gut microbiota which in turn modulated the composition of the bile acid pool[83]. Thus, impaired bile acid pools in relation to impaired microbiota enzymatic activities have been described as contributing to the inflammatory loop of IBD[84]. Bile acid composition in the lumen of the ileum differs between CD and non-CD patients with a relative decrease of primary bile acids in the ileum of CD patients[85]. Nevertheless, this finding should be interpreted with caution as malabsorption of bile acids was documented as a consequence of ileal CD especially in patients with a history of ileal resection[86,87]. Moreover, in a cohort of 166 patients, enhanced primary biliary level in the stool was independently associated with ileitis[88]. In a multi-omics approach based on a stool collection of 200 IBD patients, ileal CD profile was characterized by increased primary and secondary bile acid levels and shifts in taxa in favour of bacteria associated with bile acid-rich environments (*Gammaproteobacteria* and *Blautia sp*.)[89]. Further, the level of secondary bile acids in patients with inflammation limited to the ileum tended to increase after biological treatment reaching a similar level with control subjects[90].

In addition, bile acids exert inflammatory modulating properties through the stimulation of farnesoid X receptor (FXR). In a murine model of chemically induced inflammation, the activation of FXR demonstrated anti-inflammatory effects through a reduction of epithelial hyperpermeability and of proinflammatory cytokine production[91]. Furthermore, the obstruction of bile flow in mice induced mucosal ileal injuries reversed by administration of bile acids. In detail, this result may be explained by the activation of FXR by bile acids which promoted enteroprotective genes and limited ileal bacterial overgrowth[92]. Furthermore, bile acid pool modulation directly affects the ileum and Paneth cells. According to a recent article, Paneth cell number was linked to diet and to microbiota by bile acid in obese CD and non-CD patients irrespectively of other risk alleles (ATG16L1 and NOD2)[93]. In fact, in mice fed with a high fat diet, a similar phenomenon was observed and notably, high fat diet alone in germ-free mice as well as microbiome transfer alone in mice fed with standard diet were unable to induce an alteration in Paneth cells. The reason for this phenomenon was also dependent on FXR activation by the bile acid pool. Thus, the conjunction of a high fat diet and *Clostridium*-mediated production of secondary bile acids may explain the role of both diet and microbiome in this mechanism [93].

Lastly, bile acids promoted the expression of long polar fimbriae favouring the interplay of these strains with Peyer's patches and bacterial translocations[94]. For example, primary bile acid level was inversely correlated with the abundance of *Faecalibacterium prausnitzii* (*F. prausnitzii*) and its acetate and L-methionine producing enzyme[88]. In patients treated by surgery for ileal CD, bile acid metabolism specificities were associated with an ileal recurrence of CD[89].

Nevertheless, there is only limited evidence on the therapeutic role of bile acids in ileal CD. While several authors reported the protective role of ursodeoxycholic acid and of its precursor, the lithocholic acid, against chemically induced colitis in mice[95-97], there is a lack of data about the effect of oral supplementation with ursodeoxycholic acid in patients with IBD. Thus, only one small single-centre trial examined the effect of ursodeoxycholic acid in UC and none was performed in patients with CD [98].

MICROBIOTA

An increasing number of authors have investigated the link between gut microbiota and CD. However, many of these studies focused on the analysis of DNA extracted from stool. This methodology shed light on the colonic microbiota of the colonic lumen but was unable to draw any conclusions on the microbiota associated specifically with the ileum. Moreover, in a systematic review, the study mucosa-associated microbiota was regarded as more relevant in the understanding of CD pathogenesis[99]. In addition, dysbiosis was described in some mice models as a by-stander of ileitis. For example, in genetically predisposed mice Atg16L1$^{\Delta IEC}$, dysbiosis was observed but litter cross-fostering predisposed to colitis but not ileitis[20].

Host/microbiota interplay

Microbiota homeostasis plays a critical role in CD physiopathology[2]. Thus, mucosal immunity regulator molecules such as vitamin D receptors (VDR) have been associated with a susceptibility to bacterial and chemical colitis. The genetic inhibition of VDR in the Paneth cells of VDR$^{\Delta PC}$ mice resulted in a lower expression of lysozymes in Paneth cells[19]. Inhibition of VDR influences the response to

pathogenic bacteria. VDR$^{\Delta IPC}$ mice are not only more sensitive to bacterial infection but also to chemical damage. Conversely, this susceptibility in VDR$^{\Delta IPC}$ mice was reduced in case of co-housing with non-VDR$^{\Delta IPC}$ mice, indirectly suggesting a protective role of the microbiome[19]. In SAMP1/YitFcsJ (SAMP1) mice which develop spontaneous terminal ileitis, dysbiosis occurred during disease progression with a decrease in *Lachnospiraceae* and in *Bacteroides*. In the same animal model, α-defensins misfolding was associated with dysbiosis and even induced dysbiosis in wild-type mice[47].

In this regard, the barrier function of the ileum is also a major feature in the understanding of host-microbiota interplay. Accordingly, human β-defensin 3 peptide was decreased and redistributed to the basolateral surface of the ileal epithelium[100]. In parallel, increased enzyme indoleamine 2,3-dioxygenase 1 (IDO1) was found in patients with active CD. This enzyme is the first enzyme in tryptophan metabolism on the kynurenine pathway and is responsible for mucus layer thickening and mucus-associated modulation of microbiota. In a murine enterocolitis model, IDO1 upregulation reduced the abundance of enteropathogenic *E. coli* in the ileum. Likewise, IDO1 downregulated inflammation in response to chemical colitis in mice and augmented *A. muciniphila* and *M. schaedleri* abundance[101].

AIEC

In the nineties, a French team identified a strain of *Escherichia coli*, AIEC, which was adherent to the ileum without harbouring virulence factor-encoding genes[102]. AIEC was shown to be associated with ileal CD in further studies and to be able to invade epithelial cells[102,103]. Interestingly, AIEC was able to induce granulomas *in vitro*, which is one of the main histologic features of CD[2,104]. AIEC is classically identified on ileal biopsy but a dedicated serology could also be informative and less invasive [105]. The invasive property of AIEC is favoured by the overexpression of the glycoprotein *CEACAM6* in the ileal epithelium. The interaction of this glycoprotein with the bacterial adhesive factor FimH promoted AIEC-enterocyte interplay in the ileum[106]. Using this receptor, AIEC modulated the metabolism of the ileal epithelium and induced strong gut inflammation[107]. AIEC induced the expression of hypoxia inducible factor, overexpressed in the ileum of CD patients and promoted barrier defects in the intestinal epithelium paving the way for the onset of inflammation[108].

The relapse of CD in patients after surgical treatment may be used to understand the early steps in CD onset. In a recent prospective, multicentric cohort of patients with ileal resection, AIEC in the remaining ileum was associated with an early ileal lesion of CD recurrence. The presence of AIEC within the surgical ileal specimen was predictive of the endoscopic recurrence of CD[109].

As highlighted in a recently published article, factors influencing ileal susceptibility to AIEC were numerous and among them epigenetic regulators had a modulating effect on a large range of proteins [110]. For this reason, before considering a clinical application in ileal CD, further studies are needed to prevent possible adverse effects induced by the modulation of these epigenetic targets or to identify more specific genes associated with AIEC colonisation. Another promising approach would be the use of bacteriophages to target specifically AIEC in ileal disease[111]. To date, no bacteriophage has been approved for intestinal therapeutic use in human, either in the European Union or in the United States, despite numerous studies that have reported encouraging results *in vivo*. Therefore, data about the effect of bacteriophages on human microbiota are needed in the future[111].

F. prausnitzii

In a stool based multi-omics analysis of 200 IBD patients, the abundance of a member of Firmicutes, *F. prausnitzii,* was highly discriminant of ileal CD compared to colonic CD[89]. Even in non-inflamed ileal samples of CD patients, the commensal bacterium *F. prausnitzii* was decreased in comparison with healthy controls which suggests a relevant causal link between this bacteria and CD onset[112]. Accordingly, a low level of *F. prausnitzii* in the ileal mucosa-associated microbiota was associated with a higher recurrence rate of CD after ileal resection, corroborating the putative role of *F. prausnitzii* in the pathogenesis of ileal CD[113]. In addition, a recent study confirmed the role of *F. prausnitzii* in ileitis after ileocolectomy, pointing to a possible association with a bile salt profile. Thus, elevated levels of primary bile acids were associated with a decreased abundance of *F. prausnitzii*. These two parameters were the only factors associated with ileitis in this cohort of 166 patients[88]. The administration of *F. prausnitzii* or of its supernatant *in vitro* and *in vivo* counterbalanced gut inflammation by blocking nuclear factor kB activation and IL-8 production[113]. Interestingly, in CD patients, *F. prausnitzii* was associated specifically with ileitis, irrespectively of their genetic background[89,114]. In an original work conducted in twins in whom biopsies were performed in the lower gastrointestinal tract, the abundance of *F. prausnitzii* was specifically decreased in ileal CD, compared to colonic CD or in healthy twins[114].

Mycobiota

The study of microbiota in IBD is not limited to bacteria but also includes fungi. Fungal microbiota was suspected to be strongly involved in CD pathogenesis in particular because of the diagnosis value of anti-Saccharomyces cerevisiae antibodies in CD[2]. In a study of 168 ileal biopsies, mycobiota was modified in CD patients with an increased abundance of *Malassezia* and a decreased abundance of Saccharomyces. The increase of Malassezia was notably associated with a severe evolution of the disease

during follow-up[115].

The fungus *Debaryomyces hansenii* was increased in CD patients with inflamed ileum compared to non-inflamed ileum. Moreover, oral gavage with *Debaryomyces hansenii* impaired crypt regeneration and wound healing after biopsy injury[116].

ENVIRONMENTAL FACTORS

The microbiota bridges the gap between host susceptibility factors and its environment. Most environmental factors are identified by epidemiological studies and associated with the onset of CD or its recurrence after surgery. Few of them though can impede the natural history of CD once the disease is established.

Smoking

Cigarette smoking is a well-established risk factor for developing CD[1-3]. In patients with CD, the relative statistical weight of smoking was larger than the relative weight of the genetic variants presented in the previous section[1]. Besides, cannabis is frequently used as a symptomatic treatment by patients with CD involving the ileum and is associated with tobacco[117]. Regarding cannabis use, in a double-blind, randomized, placebo-controlled trial, cannabis oil induced clinical improvement without any endoscopic change[118].

Regarding tobacco, in mice, cigarette smoke extract induced intestinal inflammation and morphometric changes in the ileal epithelium regardless of the route of administration (intragastric or intraperitoneal), advocating for a systemic effect[119]. Moreover, mice exposed to cigarette smoking were more likely to develop pathological inflammation in response to bacterial inflammation which could be the hallmark of an impaired expression of antimicrobial peptides[119]. Besides, smoking was associated with a reduced number of normal Paneth cells in the ileum, both in patients presenting a CD susceptibility allele ($ATG16L1^{T300A}$) as well as in mice presenting this genetic susceptibility. This defect in the ileum was mediated by the Paneth cell apoptosis driven by the activation of peroxisome proliferator-activated receptor gamma (PPARγ) and prevented in mice by the use of anti-TNF-α drugs[120].

Moreover, smoking is associated with an upregulation of angiogenesis in smokers with CD compared to their non-smoking counterparts. Importantly, mice exposed to cigarette smoke for 8 wk presented mucosal tissue hypoxia associated with an increased expression of pro-inflammatory cytokines and of angiogenic factors whereas smoking cessation reversed this process in the ileal mucosa. In addition, cigarette smoke exposure was associated with an increased sensitivity to chemically induced colitis [121]. Although genes of hypoxia-inducible factor were overexpressed in the inflamed ileum and in the adjacent mesenteric tissue of CD patients, hypoxia in mice did not impact experimental ileitis[122-124]. All together, these results advocate for a specific impact of tobacco smoking in the pathogenesis of ileitis.

Evidence for other environmental factor is rare in the literature. Recently, serum levels of bisphenol A, a component used in the manufacture of various plastics, have been linked to inflammatory status in CD patients. Furthermore, patients with bacterial DNA translocation presented a higher serum level of bisphenol A associated with a reduced expression of tight junction genes[125].

Diet

Western diet is characterized by a low intake of fibres contrasting with a high intake of refined sugar, animal protein and total fat. Numerous links between diet and IBD have been established[126]. To that extent, diet modulates the microbiota associated with the ileal epithelium. Thus, AIEC was associated with hyperacetylated histone H3 in the ileal epithelium and consequently histone deacetylase enzymes controlled the entry of AIEC in IECs in a murine model. Interestingly, a high fat diet enhanced histone acetylation in mice compared to a standard diet[110]. Overweight (body mass index > 25 kg/m^2) in IBD and in non-IBD patients was associated with Paneth cell defects in the ileal epithelium. This defect can be induced by Western diet in mice[93].

Regarding fat intake, the ratio between n-3 and n-6 polyunsaturated fatty acids (PUFAs) is unbalanced in favour of an excessive intake of n-6 PUFAs in Western diet. Oral feeding with n-3 PUFAs in SAMP1/Yit mice ameliorated the histological features of ileitis, and decreased addressin molecule expression (MAdCAM-1) as well as lymphocyte infiltration in the ileum[127]. To that extent, oral supplementation with linseed oil rich in α-linolenic acid (n-3 PUFAs), in a physically active murine model, reduced inflammation after oral challenge with AIEC[128]. However, oral n-3 PUFAs supplementation has not shown definitive results in patients with CD[129]. In all likelihood, n-3 PUFAs alone are unable to stop the inflammatory loop once started but remain putative candidates to prevent the onset of ileal CD.

Fibre intake was identified as a protective factor against CD onset but not UC[130]. Although epidemiological data were based on a 40-year-old population, fibre intake and more accurately inulin supplementation modulated PPARγ signalling pathway in pigs[131].

Vitamin D deficiency in IBD patients has been reported in numerous studies reviewed elsewhere as an explanation of the North-South gradient of IBD prevalence[132]. In mice fed with a vitamin D deficient diet, miR-142-3p expression was upregulated, culminating in a reduction of ATG16L1 and autophagy specifically in ileal Paneth cells. In a paediatric cohort of IBD patients, colonic samples displayed likewise an enhanced expression of miR-142-3p statistically associated with low serum vitamin D levels[133]. As discussed previously, VDR were overexpressed in the ileum and were involved in the adequate response to enteropathogens[19]. When associated with a high fat diet, vitamin D deficiency and genetic VDR inhibition led to defective Paneth cell defensins secretion and gut permeability driving endotoxemia and systemic inflammation[134].

Last, Western diet is also characterized by a high intake of dietary additives related to the consumption of ultra-processed food. To that extent, dietary emulsifiers carboxymethylcellulose and polysorbate-80 were associated with an increased virulence and enrichment of ileal pathobionts[135].

More generally speaking, diet in patients with ileal CD should be based on the guidelines of the European Society of Nutrition. The findings discussed above and others have led to recommendations for a balanced diet rich in fruit, vegetables and n-3 fatty acids, avoiding a restrictive diet[136]. As highlighted in this European consensus, good quality data regarding the effects of experimental diets are rare in the literature. In particular, there is a lack of randomized control trials to recommend a more specific diet in patients with active ileal CD[136].

CLINICAL IMPLICATIONS

The factors summarised in the previous paragraphs give rise to a distinctive natural history of ileal CD with specific clinical consequences and interventions necessary.

Natural history of ileal CD

In CD, the shortest time from diagnosis to first surgery is in ileal CD compared to other disease sites. Thus, the median time to surgery in ileal CD is about 6 years. Thirty years after being diagnosed with ileal CD, almost all patients had undergone at least one surgery according to a broad international study [1]. At 12 mo after surgery, a recurrence was observed on colonoscopy, at and above this anastomosis in 73% of patients in absence of any treatment[137]. These data regarding recurrence rates published 30 years ago led to the development of preventive strategies after surgery.

In terms of behaviour, ileal CD was more likely than colonic CD to be complicated by penetrating or stricturing lesions[3]. These severe manifestations contribute to the high rate of surgery. Accordingly, strictures are challenging complications that are usually unresponsive to medical therapy in the absence of surgery[3]. Strictures result from the accumulation of fibrotic protein in the extracellular matrix produced by fibroblasts which are partially derived from epithelial cells *via* epithelial-mesenchymal transition (EMT)[138]. Accordingly, based on a comparative study of ileal *versus* colonic ulcers, EMT appeared to be a highly noticeable feature in ileal ulcers of CD unlike colonic ulcers of CD[55]. Ileal strictures were likely to present mesenteric fat wrapped around the stricture, known as creeping fat [139], which harbours viable bacterial translocation and leads to a pro-fibrosis M2-type microenvironment[140-143]. Remarkably, creeping fat associated with the ileum presented a 10-fold higher concentration of T-cells than colonic fat[144]. In addition, adipocyte hyperplasia was observed in ileal fat unlike colonic fat[144].

Beyond the ileum

Ileal crypts have been reported in the colon of CD patients[12,45]. Recently, the presence of ectopic ileal crypts discriminated IBD subtype in patients with undetermined (unclassified) colitis. The presence of ileal metaplasia in the colon was strongly associated with a final diagnosis of colonic CD[145]. This interesting discovery could enhance understanding of ileal physiopathology, pivotal to understand CD.

In a specific statistical model based on HLA types and single nucleotide polymorphism, colonic CD appeared to be an intermediate between UC and ileal CD[1]. Consecutively, knowledge of ileal CD may pave the way to understanding other phenotypes of CD.

A dedicated treatment for ileal CD?

Logically, the specificities of ileal CD discussed in this review should lead to a dedicated treatment strategy. Nevertheless, current ECCO guidelines on the medical management of CD do not advocate for a specific treatment in ileal CD[146]. Indeed, studies are controversial. Some studies reported a lower rate of response to infliximab, an anti-TNF treatment[147,148]. Conversely, numerous other studies did not describe such a difference in response rates with anti-TNF[149]. This discrepancy may result from a bias such as the extent of the disease irrespectively of the site of the disease. Interventional trials specifically dedicated to the study of ileal CD treatment are henceforth required. In the literature, colonic CD is more likely to respond to treatment compared to ileocolonic CD and mucosal healing may be more difficult to achieve in ileal disease. Likewise, ileal stricturing CD may have lower response rates [149].

As ileal stricture may develop in spite ofCD treatment, an American team sought to determine the gene pattern associated with ileal stricturing in a paediatric CD cohort. This analysis identified a long-chain fatty acid, the eicosatetranoic acid as a possible antifibrotic tool[150]. In a follow-up study, the same team showed a decrease in fibrosis and an improvement in stiffness in human intestinal organoids exposed to eicosatetraynoic acid[151]. In parallel, butyrate, a short-chain fatty acid, also downregulated fibrosis according to the same protocol[151].

CONCLUSION

The histological and anatomical features of the ileum are direct answers to the question "why the ileum?". Furthermore, the recent works presented in this review highlight the specific interplay between environmental factors, like smoking or diet, and the ileum. Currently, the prevailing requirement for surgery in a significant proportion of patients with ileal CD testifies to the urgent need for a dedicated pharmacological approach according to disease site. As the ileum is the site of interplay between host characteristics and environmental influences, a full understanding of the molecular crosstalk that occurs in the ileum is crucial to identify new therapeutic targets to significantly change the natural history of this debilitating disease.

ACKNOWLEDGEMENTS

Mathilde Leboutte was supported by a PhD from Normandie Region. Authors are grateful to Nikki Sabourin-Gibbs, CHU Rouen, for her help in editing the manuscript.

FOOTNOTES

Author contributions: Richard N wrote the first draft; all authors have read and approve the final manuscript.

Conflict-of-interest statement: All the authors report no relevant conflicts of interest for this article.

Open-Access: This article is an open-access article that was selected by an in-house editor and fully peer-reviewed by external reviewers. It is distributed in accordance with the Creative Commons Attribution NonCommercial (CC BY-NC 4.0) license, which permits others to distribute, remix, adapt, build upon this work non-commercially, and license their derivative works on different terms, provided the original work is properly cited and the use is non-commercial. See: https://creativecommons.org/Licenses/by-nc/4.0/

Country/Territory of origin: France

ORCID number: Guillaume Savoye 0000-0002-9200-2067; Rachel Marion-Letellier 0000-0002-3006-5943.

S-Editor: Fan JR
L-Editor: A
P-Editor: Cai YX

REFERENCES

1 **Cleynen I**, Boucher G, Jostins L, Schumm LP, Zeissig S, Ahmad T, Andersen V, Andrews JM, Annese V, Brand S, Brant SR, Cho JH, Daly MJ, Dubinsky M, Duerr RH, Ferguson LR, Franke A, Gearry RB, Goyette P, Hakonarson H, Halfvarson J, Hov JR, Huang H, Kennedy NA, Kupcinskas L, Lawrance IC, Lee JC, Satsangi J, Schreiber S, Théâtre E, van der Meulen-de Jong AE, Weersma RK, Wilson DC; International Inflammatory Bowel Disease Genetics Consortium, Parkes M, Vermeire S, Rioux JD, Mansfield J, Silverberg MS, Radford-Smith G, McGovern DP, Barrett JC, Lees CW. Inherited determinants of Crohn's disease and ulcerative colitis phenotypes: a genetic association study. *Lancet* 2016; **387**: 156-167 [PMID: 26490195 DOI: 10.1016/S0140-6736(15)00465-1]

2 **Roda G**, Chien Ng S, Kotze PG, Argollo M, Panaccione R, Spinelli A, Kaser A, Peyrin-Biroulet L, Danese S. Crohn's disease. *Nat Rev Dis Primers* 2020; **6**: 22 [PMID: 32242028 DOI: 10.1038/s41572-020-0156-2]

3 **Cosnes J**, Gower-Rousseau C, Seksik P, Cortot A. Epidemiology and natural history of inflammatory bowel diseases. *Gastroenterology* 2011; **140**: 1785-1794 [PMID: 21530745 DOI: 10.1053/j.gastro.2011.01.055]

4 **Ng SC**, Shi HY, Hamidi N, Underwood FE, Tang W, Benchimol EI, Panaccione R, Ghosh S, Wu JCY, Chan FKL, Sung JJY, Kaplan GG. Worldwide incidence and prevalence of inflammatory bowel disease in the 21st century: a systematic review of population-based studies. *Lancet* 2017; **390**: 2769-2778 [PMID: 29050646 DOI: 10.1016/S0140-6736(17)32448-0]

5 **Ng SC**, Tang W, Ching JY, Wong M, Chow CM, Hui AJ, Wong TC, Leung VK, Tsang SW, Yu HH, Li MF, Ng KK, Kamm MA, Studd C, Bell S, Leong R, de Silva HJ, Kasturiratne A, Mufeena MNF, Ling KL, Ooi CJ, Tan PS, Ong D, Goh KL, Hilmi I, Pisespongsa P, Manatsathit S, Rerknimitr R, Aniwan S, Wang YF, Ouyang Q, Zeng Z, Zhu Z, Chen MH, Hu PJ, Wu K, Wang X, Simadibrata M, Abdullah M, Wu JC, Sung JJY, Chan FKL; Asia-Pacific Crohn's and Colitis Epidemiologic Study (ACCESS) Study Group. Incidence and phenotype of inflammatory bowel disease based on results from the Asia-pacific Crohn's and colitis epidemiology study. *Gastroenterology* 2013; **145**: 158-165.e2 [PMID: 23583432 DOI: 10.1053/j.gastro.2013.04.007]

6 **Silverberg MS**, Satsangi J, Ahmad T, Arnott ID, Bernstein CN, Brant SR, Caprilli R, Colombel JF, Gasche C, Geboes K, Jewell DP, Karban A, Loftus EV Jr, Peña AS, Riddell RH, Sachar DB, Schreiber S, Steinhart AH, Targan SR, Vermeire S, Warren BF. Toward an integrated clinical, molecular and serological classification of inflammatory bowel disease: report of a Working Party of the 2005 Montreal World Congress of Gastroenterology. *Can J Gastroenterol* 2005; **19** Suppl A: 5A-36A [PMID: 16151544 DOI: 10.1155/2005/269076]

7 **Park SJ**, Kim WH, Cheon JH. Clinical characteristics and treatment of inflammatory bowel disease: a comparison of Eastern and Western perspectives. *World J Gastroenterol* 2014; **20**: 11525-11537 [PMID: 25206259 DOI: 10.3748/wjg.v20.i33.11525]

8 **Grimes CL**, Ariyananda Lde Z, Melnyk JE, O'Shea EK. The innate immune protein Nod2 binds directly to MDP, a bacterial cell wall fragment. *J Am Chem Soc* 2012; **134**: 13535-13537 [PMID: 22857257 DOI: 10.1021/ja303883c]

9 **Tan G**, Li RH, Li C, Wu F, Zhao XM, Ma JY, Lei S, Zhang WD, Zhi FC. Down-regulation of human enteric antimicrobial peptides by NOD2 during differentiation of the paneth cell lineage. *Sci Rep* 2015; **5**: 8383 [PMID: 25670499 DOI: 10.1038/srep08383]

10 **Cuthbert AP**, Fisher SA, Mirza MM, King K, Hampe J, Croucher PJ, Mascheretti S, Sanderson J, Forbes A, Mansfield J, Schreiber S, Lewis CM, Mathew CG. The contribution of NOD2 gene mutations to the risk and site of disease in inflammatory bowel disease. *Gastroenterology* 2002; **122**: 867-874 [PMID: 11910337 DOI: 10.1053/gast.2002.32415]

11 **Ahmad T**, Armuzzi A, Bunce M, Mulcahy-Hawes K, Marshall SE, Orchard TR, Crawshaw J, Large O, de Silva A, Cook JT, Barnardo M, Cullen S, Welsh KI, Jewell DP. The molecular classification of the clinical manifestations of Crohn's disease. *Gastroenterology* 2002; **122**: 854-866 [PMID: 11910336 DOI: 10.1053/gast.2002.32413]

12 **Ogura Y**, Lala S, Xin W, Smith E, Dowds TA, Chen FF, Zimmermann E, Tretiakova M, Cho JH, Hart J, Greenson JK, Keshav S, Nuñez G. Expression of NOD2 in Paneth cells: a possible link to Crohn's ileitis. *Gut* 2003; **52**: 1591-1597 [PMID: 14570728 DOI: 10.1136/gut.52.11.1591]

13 **Wallings R**, Manzoni C, Bandopadhyay R. Cellular processes associated with LRRK2 function and dysfunction. *FEBS J* 2015; **282**: 2806-2826 [PMID: 25899482 DOI: 10.1111/febs.13305]

14 **Zhang Q**, Pan Y, Yan R, Zeng B, Wang H, Zhang X, Li W, Wei H, Liu Z. Commensal bacteria direct selective cargo sorting to promote symbiosis. *Nat Immunol* 2015; **16**: 918-926 [PMID: 26237551 DOI: 10.1038/ni.3233]

15 **Hui KY**, Fernandez-Hernandez H, Hu J, Schaffner A, Pankratz N, Hsu NY, Chuang LS, Carmi S, Villaverde N, Li X, Rivas M, Levine AP, Bao X, Labrias PR, Haritunians T, Ruane D, Gettler K, Chen E, Li D, Schiff ER, Pontikos N, Barzilai N, Brant SR, Bressman S, Cheifetz AS, Clark LN, Daly MJ, Desnick RJ, Duerr RH, Katz S, Lencz T, Myers RH, Ostrer H, Ozelius L, Payami H, Peter Y, Rioux JD, Segal AW, Scott WK, Silverberg MS, Vance JM, Ubarretxena-Belandia I, Foroud T, Atzmon G, Pe'er I, Ioannou Y, McGovern DPB, Yue Z, Schadt EE, Cho JH, Peter I. Functional variants in the LRRK2 gene confer shared effects on risk for Crohn's disease and Parkinson's disease. *Sci Transl Med* 2018; **10** [PMID: 29321258 DOI: 10.1126/scitranslmed.aai7795]

16 **Jung S**, Ye BD, Lee HS, Baek J, Kim G, Park D, Park SH, Yang SK, Han B, Liu J, Song K. Identification of Three Novel Susceptibility Loci for Inflammatory Bowel Disease in Koreans in an Extended Genome-Wide Association Study. *J Crohns Colitis* 2021; **15**: 1898-1907 [PMID: 33853113 DOI: 10.1093/ecco-jcc/jjab060]

17 **Hampe J**, Franke A, Rosenstiel P, Till A, Teuber M, Huse K, Albrecht M, Mayr G, De La Vega FM, Briggs J, Günther S, Prescott NJ, Onnie CM, Häsler R, Sipos B, Fölsch UR, Lengauer T, Platzer M, Mathew CG, Krawczak M, Schreiber S. A genome-wide association scan of nonsynonymous SNPs identifies a susceptibility variant for Crohn disease in ATG16L1. *Nat Genet* 2007; **39**: 207-211 [PMID: 17200669 DOI: 10.1038/ng1954]

18 **Murthy A**, Li Y, Peng I, Reichelt M, Katakam AK, Noubade R, Roose-Girma M, DeVoss J, Diehl L, Graham RR, van Lookeren Campagne M. A Crohn's disease variant in Atg16 L1 enhances its degradation by caspase 3. *Nature* 2014; **506**: 456-462 [PMID: 24553140 DOI: 10.1038/nature13044]

19 **Lu R**, Zhang YG, Xia Y, Zhang J, Kaser A, Blumberg R, Sun J. Paneth Cell Alertness to Pathogens Maintained by Vitamin D Receptors. *Gastroenterology* 2021; **160**: 1269-1283 [PMID: 33217447 DOI: 10.1053/j.gastro.2020.11.015]

20 **Tschurtschenthaler M**, Adolph TE, Ashcroft JW, Niederreiter L, Bharti R, Saveljeva S, Bhattacharyya J, Flak MB, Shih DQ, Fuhler GM, Parkes M, Kohno K, Iwawaki T, Janneke van der Woude C, Harding HP, Smith AM, Peppelenbosch MP, Targan SR, Ron D, Rosenstiel P, Blumberg RS, Kaser A. Defective ATG16L1-mediated removal of IRE1α drives Crohn's disease-like ileitis. *J Exp Med* 2017; **214**: 401-422 [PMID: 28082357 DOI: 10.1084/jem.20160791]

21 **Wehkamp J**, Wang G, Kübler I, Nuding S, Gregorieff A, Schnabel A, Kays RJ, Fellermann K, Burk O, Schwab M, Clevers H, Bevins CL, Stange EF. The Paneth cell alpha-defensin deficiency of ileal Crohn's disease is linked to Wnt/Tcf-4. *J Immunol* 2007; **179**: 3109-3118 [PMID: 17709525 DOI: 10.4049/jimmunol.179.5.3109]

22 **Koslowski MJ**, Kübler I, Chamaillard M, Schaeffeler E, Reinisch W, Wang G, Beisner J, Teml A, Peyrin-Biroulet L, Winter S, Herrlinger KR, Rutgeerts P, Vermeire S, Cooney R, Fellermann K, Jewell D, Bevins CL, Schwab M, Stange EF, Wehkamp J. Genetic variants of Wnt transcription factor TCF-4 (TCF7L2) putative promoter region are associated with small intestinal Crohn's disease. *PLoS One* 2009; **4**: e4496 [PMID: 19221600 DOI: 10.1371/journal.pone.0004496]

23 **Ishii TM**, Silvia C, Hirschberg B, Bond CT, Adelman JP, Maylie J. A human intermediate conductance calcium-activated potassium channel. *Proc Natl Acad Sci U S A* 1997; **94**: 11651-11656 [PMID: 9326665 DOI: 10.1073/pnas.94.21.11651]

24 **Ayabe T**, Wulff H, Darmoul D, Cahalan MD, Chandy KG, Ouellette AJ. Modulation of mouse Paneth cell alpha-defensin secretion by mIKCa1, a Ca2+-activated, intermediate conductance potassium channel. *J Biol Chem* 2002; **277**: 3793-3800 [PMID: 11724775 DOI: 10.1074/jbc.M107507200]

25 **Simms LA**, Doecke JD, Roberts RL, Fowler EV, Zhao ZZ, McGuckin MA, Huang N, Hayward NK, Webb PM,

Whiteman DC, Cavanaugh JA, McCallum R, Florin TH, Barclay ML, Gearry RB, Merriman TR, Montgomery GW, Radford-Smith GL. KCNN4 gene variant is associated with ileal Crohn's Disease in the Australian and New Zealand population. *Am J Gastroenterol* 2010; **105**: 2209-2217 [PMID: 20407432 DOI: 10.1038/ajg.2010.161]

26 **Chikina A**, Matic Vignjevic D. At the right time in the right place: How do luminal gradients position the microbiota along the gut? *Cells Dev* 2021; **168**: 203712 [PMID: 34174490 DOI: 10.1016/j.cdev.2021.203712]

27 **Nugent SG**, Kumar D, Rampton DS, Evans DF. Intestinal luminal pH in inflammatory bowel disease: possible determinants and implications for therapy with aminosalicylates and other drugs. *Gut* 2001; **48**: 571-577 [PMID: 11247905 DOI: 10.1136/gut.48.4.571]

28 **Zhang S**, Dogan B, Guo C, Herlekar D, Stewart K, Scherl EJ, Simpson KW. Short Chain Fatty Acids Modulate the Growth and Virulence of Pathosymbiont Escherichia coli and Host Response. *Antibiotics (Basel)* 2020; **9** [PMID: 32751519 DOI: 10.3390/antibiotics9080462]

29 **Goldstein N**, Dulai M. Contemporary morphologic definition of backwash ileitis in ulcerative colitis and features that distinguish it from Crohn disease. *Am J Clin Pathol* 2006; **126**: 365-376 [PMID: 16880149 DOI: 10.1309/UAXMW3428PGN9HJ3]

30 **Magro F**, Langner C, Driessen A, Ensari A, Geboes K, Mantzaris GJ, Villanacci V, Becheanu G, Borralho Nunes P, Cathomas G, Fries W, Jouret-Mourin A, Mescoli C, de Petris G, Rubio CA, Shepherd NA, Vieth M, Eliakim R; European Society of Pathology (ESP); European Crohn's and Colitis Organisation (ECCO). European consensus on the histopathology of inflammatory bowel disease. *J Crohns Colitis* 2013; **7**: 827-851 [PMID: 23870728 DOI: 10.1016/j.crohns.2013.06.001]

31 **Buisine MP**, Desreumaux P, Leteurtre E, Copin MC, Colombel JF, Porchet N, Aubert JP. Mucin gene expression in intestinal epithelial cells in Crohn's disease. *Gut* 2001; **49**: 544-551 [PMID: 11559653 DOI: 10.1136/gut.49.4.544]

32 **Kiyono H**, Fukuyama S. NALT- *vs* Peyer's-patch-mediated mucosal immunity. *Nat Rev Immunol* 2004; **4**: 699-710 [PMID: 15343369 DOI: 10.1038/nri1439]

33 **Casado-Bedmar M**, Heil SDS, Myrelid P, Söderholm JD, Keita ÅV. Upregulation of intestinal mucosal mast cells expressing VPAC1 in close proximity to vasoactive intestinal polypeptide in inflammatory bowel disease and murine colitis. *Neurogastroenterol Motil* 2019; **31**: e13503 [PMID: 30407703 DOI: 10.1111/nmo.13503]

34 **Biskou O**, Meira de-Faria F, Walter SM, Winberg ME, Haapaniemi S, Myrelid P, Söderholm JD, Keita ÅV. Increased Numbers of Enteric Glial Cells in the Peyer's Patches and Enhanced Intestinal Permeability by Glial Cell Mediators in Patients with Ileal Crohn's Disease. *Cells* 2022; **11** [PMID: 35159145 DOI: 10.3390/cells11030335]

35 **Keita ÅV**, Alkaissi LY, Holm EB, Heil SDS, Chassaing B, Darfeuille-Michaud A, McKay DM, Söderholm JD. Enhanced E. coli LF82 Translocation through the Follicle-associated Epithelium in Crohn's Disease is Dependent on Long Polar Fimbriae and CEACAM6 expression, and Increases Paracellular Permeability. *J Crohns Colitis* 2020; **14**: 216-229 [PMID: 31393983 DOI: 10.1093/ecco-jcc/jjz144]

36 **Bassotti G**, Villanacci V, Nascimbeni R, Cadei M, Fisogni S, Antonelli E, Corazzi N, Salerni B. Enteric neuroglial apoptosis in inflammatory bowel diseases. *J Crohns Colitis* 2009; **3**: 264-270 [PMID: 21172285 DOI: 10.1016/j.crohns.2009.06.004]

37 **Villanacci V**, Bassotti G, Nascimbeni R, Antonelli E, Cadei M, Fisogni S, Salerni B, Geboes K. Enteric nervous system abnormalities in inflammatory bowel diseases. *Neurogastroenterol Motil* 2008; **20**: 1009-1016 [PMID: 18492026 DOI: 10.1111/j.1365-2982.2008.01146.x]

38 **Tursi A**, Brandimarte G, Giorgetti G, Nasi G. Assessment of orocaecal transit time in different localization of Crohn's disease and its possible influence on clinical response to therapy. *Eur J Gastroenterol Hepatol* 2003; **15**: 69-74 [PMID: 12544697 DOI: 10.1097/00042737-200301000-00012]

39 **Wang XY**, Zarate N, Soderholm JD, Bourgeois JM, Liu LW, Huizinga JD. Ultrastructural injury to interstitial cells of Cajal and communication with mast cells in Crohn's disease. *Neurogastroenterol Motil* 2007; **19**: 349-364 [PMID: 17509017 DOI: 10.1111/j.1365-2982.2006.00894.x]

40 **Decousus S**, Boucher AL, Joubert J, Pereira B, Dubois A, Goutorbe F, Déchelotte PJ, Bommelaer G, Buisson A. Myenteric plexitis is a risk factor for endoscopic and clinical postoperative recurrence after ileocolonic resection in Crohn's disease. *Dig Liver Dis* 2016; **48**: 753-758 [PMID: 27005857 DOI: 10.1016/j.dld.2016.02.023]

41 **Misteli H**, Koh CE, Wang LM, Mortensen NJ, George B, Guy R. Myenteric plexitis at the proximal resection margin is a predictive marker for surgical recurrence of ileocaecal Crohn's disease. *Colorectal Dis* 2015; **17**: 304-310 [PMID: 25581299 DOI: 10.1111/codi.12896]

42 **Lemmens B**, de Buck van Overstraeten A, Arijs I, Sagaert X, Van Assche G, Vermeire S, Tertychnyy A, Geboes K, Wolthuis A, D'Hoore A, De Hertogh G, Ferrante M. Submucosal Plexitis as a Predictive Factor for Postoperative Endoscopic Recurrence in Patients with Crohn's Disease Undergoing a Resection with Ileocolonic Anastomosis: Results from a Prospective Single-centre Study. *J Crohns Colitis* 2017; **11**: 212-220 [PMID: 27466173 DOI: 10.1093/ecco-jcc/jjw135]

43 **Sokol H**, Polin V, Lavergne-Slove A, Panis Y, Treton X, Dray X, Bouhnik Y, Valleur P, Marteau P. Plexitis as a predictive factor of early postoperative clinical recurrence in Crohn's disease. *Gut* 2009; **58**: 1218-1225 [PMID: 19625280 DOI: 10.1136/gut.2009.177782]

44 **Li Y**, Ge Y, Zhu W, Gong J, Cao L, Guo Z, Gu L, Li J. Increased enteric glial cells in proximal margin of resection is associated with postoperative recurrence of Crohn's disease. *J Gastroenterol Hepatol* 2018; **33**: 638-644 [PMID: 28873259 DOI: 10.1111/jgh.13973]

45 **Lala S**, Ogura Y, Osborne C, Hor SY, Bromfield A, Davies S, Ogunbiyi O, Nuñez G, Keshav S. Crohn's disease and the NOD2 gene: a role for paneth cells. *Gastroenterology* 2003; **125**: 47-57 [PMID: 12851870 DOI: 10.1016/s0016-5085(03)00661-9]

46 **Lee C**, Hong SN, Kim ER, Chang DK, Kim YH. Depletion of Intestinal Stem Cell Niche Factors Contributes to the Alteration of Epithelial Differentiation in SAMP1/YitFcsJ Mice With Crohn Disease-Like Ileitis. *Inflamm Bowel Dis* 2021; **27**: 667-676 [PMID: 33274375 DOI: 10.1093/ibd/izaa314]

47 **Shimizu Y**, Nakamura K, Yoshii A, Yokoi Y, Kikuchi M, Shinozaki R, Nakamura S, Ohira S, Sugimoto R, Ayabe T.

Paneth cell α-defensin misfolding correlates with dysbiosis and ileitis in Crohn's disease model mice. *Life Sci Alliance* 2020; **3** [PMID: 32345659 DOI: 10.26508/lsa.201900592]

48 **Liu TC**, Gurram B, Baldridge MT, Head R, Lam V, Luo C, Cao Y, Simpson P, Hayward M, Holtz ML, Bousounis P, Noe J, Lerner D, Cabrera J, Biank V, Stephens M, Huttenhower C, McGovern DP, Xavier RJ, Stappenbeck TS, Salzman NH. Paneth cell defects in Crohn's disease patients promote dysbiosis. *JCI Insight* 2016; **1**: e86907 [PMID: 27699268 DOI: 10.1172/jci.insight.86907]

49 **Liu TC**, Naito T, Liu Z, VanDussen KL, Haritunians T, Li D, Endo K, Kawai Y, Nagasaki M, Kinouchi Y, McGovern DP, Shimosegawa T, Kakuta Y, Stappenbeck TS. LRRK2 but not ATG16L1 is associated with Paneth cell defect in Japanese Crohn's disease patients. *JCI Insight* 2017; **2**: e91917 [PMID: 28352666 DOI: 10.1172/jci.insight.91917]

50 **Alula KM**, Jackson DN, Smith AD, Kim DS, Turner K, Odstrcil E, Kaipparettu BA, Dassopoulos T, Venuprasad K, Feagins LA, Theiss AL. Targeting Mitochondrial Damage as a Therapeutic for Ileal Crohn's Disease. *Cells* 2021; **10** [PMID: 34072441 DOI: 10.3390/cells10061349]

51 **Khaloian S**, Rath E, Hammoudi N, Gleisinger E, Blutke A, Giesbertz P, Berger E, Metwaly A, Waldschmitt N, Allez M, Haller D. Mitochondrial impairment drives intestinal stem cell transition into dysfunctional Paneth cells predicting Crohn's disease recurrence. *Gut* 2020; **69**: 1939-1951 [PMID: 32111634 DOI: 10.1136/gutjnl-2019-319514]

52 **Jackson DN**, Panopoulos M, Neumann WL, Turner K, Cantarel BL, Thompson-Snipes L, Dassopoulos T, Feagins LA, Souza RF, Mills JC, Blumberg RS, Venuprasad K, Thompson WE, Theiss AL. Mitochondrial dysfunction during loss of prohibitin 1 triggers Paneth cell defects and ileitis. *Gut* 2020; **69**: 1928-1938 [PMID: 32111635 DOI: 10.1136/gutjnl-2019-319523]

53 **Walker CR**, Hautefort I, Dalton JE, Overweg K, Egan CE, Bongaerts RJ, Newton DJ, Cruickshank SM, Andrew EM, Carding SR. Intestinal intraepithelial lymphocyte-enterocyte crosstalk regulates production of bactericidal angiogenin 4 by Paneth cells upon microbial challenge. *PLoS One* 2013; **8**: e84553 [PMID: 24358364 DOI: 10.1371/journal.pone.0084553]

54 **Matsuzawa-Ishimoto Y**, Yao X, Koide A, Ueberheide BM, Axelrad JE, Reis BS, Parsa R, Neil JA, Devlin JC, Rudensky E, Dewan MZ, Cammer M, Blumberg RS, Ding Y, Ruggles KV, Mucida D, Koide S, Cadwell K. The γδ IEL effector API5 masks genetic susceptibility to Paneth cell death. *Nature* 2022; **610**: 547-554 [PMID: 36198790 DOI: 10.1038/s41586-022-05259-y]

55 **Pierre N**, Salée C, Massot C, Blétard N, Mazzucchelli G, Smargiasso N, Morsa D, Baiwir D, De Pauw E, Reenaers C, Van Kemseke C, Loly JP, Delvenne P, Meuwis MA, Louis E. Proteomics Highlights Common and Distinct Pathophysiological Processes Associated with Ileal and Colonic Ulcers in Crohn's Disease. *J Crohns Colitis* 2020; **14**: 205-215 [PMID: 31282946 DOI: 10.1093/ecco-jcc/jjz130]

56 **Li J**, Doty AL, Iqbal A, Glover SC. The differential frequency of Lineage(-)CRTH2(-)CD45(+)NKp44(-)CD117(-)CD127(+)ILC subset in the inflamed terminal ileum of patients with Crohn's disease. *Cell Immunol* 2016; **304-305**: 63-68 [PMID: 27215784 DOI: 10.1016/j.cellimm.2016.05.001]

57 **Li J**, Doty A, Glover SC. Aryl hydrocarbon receptor signaling involves in the human intestinal ILC3/ILC1 conversion in the inflamed terminal ileum of Crohn's disease patients. *Inflamm Cell Signal* 2016; **3** [PMID: 28286805 DOI: 10.14800/ics.1404]

58 **Monteleone I**, Rizzo A, Sarra M, Sica G, Sileri P, Biancone L, MacDonald TT, Pallone F, Monteleone G. Aryl hydrocarbon receptor-induced signals up-regulate IL-22 production and inhibit inflammation in the gastrointestinal tract. *Gastroenterology* 2011; **141**: 237-248, 248.e1 [PMID: 21600206 DOI: 10.1053/j.gastro.2011.04.007]

59 **Li S**, Bostick JW, Ye J, Qiu J, Zhang B, Urban JF Jr, Avram D, Zhou L. Aryl Hydrocarbon Receptor Signaling Cell Intrinsically Inhibits Intestinal Group 2 Innate Lymphoid Cell Function. *Immunity* 2018; **49**: 915-928.e5 [PMID: 30446384 DOI: 10.1016/j.immuni.2018.09.015]

60 **Rothhammer V**, Borucki DM, Kenison JE, Hewson P, Wang Z, Bakshi R, Sherr DH, Quintana FJ. Detection of aryl hydrocarbon receptor agonists in human samples. *Sci Rep* 2018; **8**: 4970 [PMID: 29563571 DOI: 10.1038/s41598-018-23323-4]

61 **Huhn M**, Juan MHS, Melcher B, Dreis C, Schmidt KG, Schwiebs A, Collins J, Pfeilschifter JM, Vieth M, Stein J, Radeke HH. Inflammation-Induced Mucosal KYNU Expression Identifies Human Ileal Crohn's Disease. *J Clin Med* 2020; **9** [PMID: 32384670 DOI: 10.3390/jcm9051360]

62 **Günther C**, Ruder B, Stolzer I, Dorner H, He GW, Chiriac MT, Aden K, Strigli A, Bittel M, Zeissig S, Rosenstiel P, Atreya R, Neurath MF, Wirtz S, Becker C. Interferon Lambda Promotes Paneth Cell Death Via STAT1 Signaling in Mice and Is Increased in Inflamed Ileal Tissues of Patients With Crohn's Disease. *Gastroenterology* 2019; **157**: 1310-1322.e13 [PMID: 31352002 DOI: 10.1053/j.gastro.2019.07.031]

63 **Geremia A**, Arancibia-Cárcamo CV, Fleming MP, Rust N, Singh B, Mortensen NJ, Travis SP, Powrie F. IL-23-responsive innate lymphoid cells are increased in inflammatory bowel disease. *J Exp Med* 2011; **208**: 1127-1133 [PMID: 21576383 DOI: 10.1084/jem.20101712]

64 **Martin JC**, Bériou G, Heslan M, Bossard C, Jarry A, Abidi A, Hulin P, Ménoret S, Thinard R, Anegon I, Jacqueline C, Lardeux B, Halary F, Renauld JC, Bourreille A, Josien R. IL-22BP is produced by eosinophils in human gut and blocks IL-22 protective actions during colitis. *Mucosal Immunol* 2016; **9**: 539-549 [PMID: 26329427 DOI: 10.1038/mi.2015.83]

65 **Fantou A**, Lagrue E, Laurent T, Delbos L, Blandin S, Jarry A, Beriou G, Braudeau C, Salabert N, Marin E, Moreau A, Podevin J, Bourreille A, Josien R, Martin JC. IL-22BP production is heterogeneously distributed in Crohn's disease. *Front Immunol* 2022; **13**: 1034570 [PMID: 36311796 DOI: 10.3389/fimmu.2022.1034570]

66 **Moran GW**, Pennock J, McLaughlin JT. Enteroendocrine cells in terminal ileal Crohn's disease. *J Crohns Colitis* 2012; **6**: 871-880 [PMID: 22398079 DOI: 10.1016/j.crohns.2012.01.013]

67 **Keller J**, Beglinger C, Holst JJ, Andresen V, Layer P. Mechanisms of gastric emptying disturbances in chronic and acute inflammation of the distal gastrointestinal tract. *Am J Physiol Gastrointest Liver Physiol* 2009; **297**: G861-G868 [PMID: 20501434 DOI: 10.1152/ajpgi.00145.2009]

68 **Keller J**, Binnewies U, Rösch M, Juul Holst J, Beglinger C, Andresen V, Layer P. Gastric emptying and disease activity in inflammatory bowel disease. *Eur J Clin Invest* 2015; **45**: 1234-1242 [PMID: 26426315 DOI: 10.1111/eci.12542]

69 **Li H**, Chen H, Chen L, Shen D, Xu X. Expression of oestrogen receptor beta was negatively correlated with disease

activity in patients with Crohn's disease involving the terminal ileum. *Steroids* 2019; **141**: 36-40 [PMID: 30278183 DOI: 10.1016/j.steroids.2018.09.013]

70 **Jiang Q**, Li WX, Sun JR, Zhu TT, Fan J, Yu LH, Burnstock G, Yang H, Ma B. Inhibitory effect of estrogen receptor beta on P2X3 receptors during inflammation in rats. *Purinergic Signal* 2017; **13**: 105-117 [PMID: 27817132 DOI: 10.1007/s11302-016-9540-5]

71 **Subramanian S**, Ekbom A, Rhodes JM. Recent advances in clinical practice: a systematic review of isolated colonic Crohn's disease: the third IBD? *Gut* 2017; **66**: 362-381 [PMID: 27802156 DOI: 10.1136/gutjnl-2016-312673]

72 **Roulis M**, Nikolaou C, Kotsaki E, Kaffe E, Karagianni N, Koliaraki V, Salpea K, Ragoussis J, Aidinis V, Martini E, Becker C, Herschman HR, Vetrano S, Danese S, Kollias G. Intestinal myofibroblast-specific Tpl2-Cox-2-PGE2 pathway links innate sensing to epithelial homeostasis. *Proc Natl Acad Sci U S A* 2014; **111**: E4658-E4667 [PMID: 25316791 DOI: 10.1073/pnas.1415762111]

73 **Santoru ML**, Piras C, Murgia F, Leoni VP, Spada M, Murgia A, Liggi S, Lai MA, Usai P, Caboni P, Manzin A, Atzori L. Metabolic Alteration in Plasma and Biopsies From Patients With IBD. *Inflamm Bowel Dis* 2021; **27**: 1335-1345 [PMID: 33512485 DOI: 10.1093/ibd/izab012]

74 **Potdar AA**, Li D, Haritunians T, VanDussen KL, Fiorino MF, Liu TC, Stappenbeck TS, Fleshner P, Targan SR, McGovern DPB, Bilsborough J. Ileal Gene Expression Data from Crohn's Disease Small Bowel Resections Indicate Distinct Clinical Subgroups. *J Crohns Colitis* 2019; **13**: 1055-1066 [PMID: 30877309 DOI: 10.1093/ecco-jcc/jjz021]

75 **Ngollo M**, Perez K, Hammoudi N, Gorelik Y, Delord M, Auzolle C, Bottois H, Cazals-Hatem D, Bezault M, Nancey S, Nachury M, Treton X, Fumery M, Buisson A, Barnich N, Seksik P; REMIND Study Group Investigators, Shen-Orr SS, Le Bourhis L, Allez M. Identification of Gene Expression Profiles Associated with an Increased Risk of Post-Operative Recurrence in Crohn's Disease. *J Crohns Colitis* 2022; **16**: 1269-1280 [PMID: 35143619 DOI: 10.1093/ecco-jcc/jjac021]

76 **Maddipatla SC**, Kolachala VL, Venkateswaran S, Dodd AF, Pelia RS, Geem D, Yin H, Sun Y, Xu C, Mo A, Kosters A, Yang J, Matthews JD, Ghosn E, Kugathasan S, Qiu P. Assessing Cellular and Transcriptional Diversity of Ileal Mucosa Among Treatment-Naïve and Treated Crohn's Disease. *Inflamm Bowel Dis* 2023; **29**: 274-285 [PMID: 36206201 DOI: 10.1093/ibd/izac201]

77 **Hendel SK**, Kellermann L, Hausmann A, Bindslev N, Jensen KB, Nielsen OH. Tuft Cells and Their Role in Intestinal Diseases. *Front Immunol* 2022; **13**: 822867 [PMID: 35237268 DOI: 10.3389/fimmu.2022.822867]

78 **Elmentaite R**, Kumasaka N, Roberts K, Fleming A, Dann E, King HW, Kleshchevnikov V, Dabrowska M, Pritchard S, Bolt L, Vieira SF, Mamanova L, Huang N, Perrone F, Goh Kai'En I, Lisgo SN, Katan M, Leonard S, Oliver TRW, Hook CE, Nayak K, Campos LS, Domínguez Conde C, Stephenson E, Engelbert J, Botting RA, Polanski K, van Dongen S, Patel M, Morgan MD, Marioni JC, Bayraktar OA, Meyer KB, He X, Barker RA, Uhlig HH, Mahbubani KT, Saeb-Parsy K, Zilbauer M, Clatworthy MR, Haniffa M, James KR, Teichmann SA. Cells of the human intestinal tract mapped across space and time. *Nature* 2021; **597**: 250-255 [PMID: 34497389 DOI: 10.1038/s41586-021-03852-1]

79 **Hu X**, Deng J, Yu T, Chen S, Ge Y, Zhou Z, Guo Y, Ying H, Zhai Q, Chen Y, Yuan F, Niu Y, Shu W, Chen H, Ma C, Liu Z, Guo F. ATF4 Deficiency Promotes Intestinal Inflammation in Mice by Reducing Uptake of Glutamine and Expression of Antimicrobial Peptides. *Gastroenterology* 2019; **156**: 1098-1111 [PMID: 30452920 DOI: 10.1053/j.gastro.2018.11.033]

80 **Bretin A**, Carrière J, Dalmasso G, Bergougnoux A, B'chir W, Maurin AC, Müller S, Seibold F, Barnich N, Bruhat A, Darfeuille-Michaud A, Nguyen HT. Activation of the EIF2AK4-EIF2A/eIF2α-ATF4 pathway triggers autophagy response to Crohn disease-associated adherent-invasive Escherichia coli infection. *Autophagy* 2016; **12**: 770-783 [PMID: 26986695 DOI: 10.1080/15548627.2016.1156823]

81 **Shao JW**, Ge TT, Chen SZ, Wang G, Yang Q, Huang CH, Xu LC, Chen Z. Role of bile acids in liver diseases mediated by the gut microbiome. *World J Gastroenterol* 2021; **27**: 3010-3021 [PMID: 34168404 DOI: 10.3748/wjg.v27.i22.3010]

82 **Calzadilla N**, Comiskey SM, Dudeja PK, Saksena S, Gill RK, Alrefai WA. Bile acids as inflammatory mediators and modulators of intestinal permeability. *Front Immunol* 2022; **13**: 1021924 [PMID: 36569849 DOI: 10.3389/fimmu.2022.1021924]

83 **Jia W**, Xie G, Jia W. Bile acid-microbiota crosstalk in gastrointestinal inflammation and carcinogenesis. *Nat Rev Gastroenterol Hepatol* 2018; **15**: 111-128 [PMID: 29018272 DOI: 10.1038/nrgastro.2017.119]

84 **Duboc H**, Rajca S, Rainteau D, Benarous D, Maubert MA, Quervain E, Thomas G, Barbu V, Humbert L, Despras G, Bridonneau C, Dumetz F, Grill JP, Masliah J, Beaugerie L, Cosnes J, Chazouillères O, Poupon R, Wolf C, Mallet JM, Langella P, Trugnan G, Sokol H, Seksik P. Connecting dysbiosis, bile-acid dysmetabolism and gut inflammation in inflammatory bowel diseases. *Gut* 2013; **62**: 531-539 [PMID: 22993202 DOI: 10.1136/gutjnl-2012-302578]

85 **Bamba S**, Inatomi O, Nishida A, Ohno M, Imai T, Takahashi K, Naito Y, Iwamoto J, Honda A, Inohara N, Andoh A. Relationship between the gut microbiota and bile acid composition in the ileal mucosa of Crohn's disease. *Intest Res* 2022; **20**: 370-380 [PMID: 33975420 DOI: 10.5217/ir.2021.00054]

86 **Nyhlin H**, Merrick MV, Eastwood MA. Bile acid malabsorption in Crohn's disease and indications for its assessment using SeHCAT. *Gut* 1994; **35**: 90-93 [PMID: 8307458 DOI: 10.1136/gut.35.1.90]

87 **Skouras T**, Dodd S, Prasad Y, Rassam J, Morley N, Subramanian S. Brief report: length of ileal resection correlates with severity of bile acid malabsorption in Crohn's disease. *Int J Colorectal Dis* 2019; **34**: 185-188 [PMID: 30116880 DOI: 10.1007/s00384-018-3144-1]

88 **Battat R**, Scherl EJ, Lukin D, Charilaou P, Mahtani P, Gerber J, Gandara JA; JRI Live Cell Bank, Dündar F, Zumbo P, Betel D, Guo CJ, Longman RS. Increased Primary Bile Acids with Ileocolonic Resection Impact Ileal Inflammation and Gut Microbiota in Inflammatory Bowel Disease. *J Crohns Colitis* 2022 [PMID: 36322790 DOI: 10.1093/ecco-jcc/jjac173]

89 **Gonzalez CG**, Mills RH, Zhu Q, Sauceda C, Knight R, Dulai PS, Gonzalez DJ. Location-specific signatures of Crohn's disease at a multi-omics scale. *Microbiome* 2022; **10**: 133 [PMID: 35999575 DOI: 10.1186/s40168-022-01331-x]

90 **Roda G**, Porru E, Katsanos K, Skamnelos A, Kyriakidi K, Fiorino G, Christodoulou D, Danese S, Roda A. Serum Bile Acids Profiling in Inflammatory Bowel Disease Patients Treated with Anti-TNFs. *Cells* 2019; **8** [PMID: 31382518 DOI: 10.3390/cells8080817]

91 **Gadaleta RM**, van Erpecum KJ, Oldenburg B, Willemsen EC, Renooij W, Murzilli S, Klomp LW, Siersema PD, Schipper ME, Danese S, Penna G, Laverny G, Adorini L, Moschetta A, van Mil SW. Farnesoid X receptor activation inhibits

inflammation and preserves the intestinal barrier in inflammatory bowel disease. *Gut* 2011; **60**: 463-472 [PMID: 21242261 DOI: 10.1136/gut.2010.212159]

92 **Inagaki T**, Moschetta A, Lee YK, Peng L, Zhao G, Downes M, Yu RT, Shelton JM, Richardson JA, Repa JJ, Mangelsdorf DJ, Kliewer SA. Regulation of antibacterial defense in the small intestine by the nuclear bile acid receptor. *Proc Natl Acad Sci U S A* 2006; **103**: 3920-3925 [PMID: 16473946 DOI: 10.1073/pnas.0509592103]

93 **Liu TC**, Kern JT, Jain U, Sonnek NM, Xiong S, Simpson KF, VanDussen KL, Winkler ES, Haritunians T, Malique A, Lu Q, Sasaki Y, Storer C, Diamond MS, Head RD, McGovern DPB, Stappenbeck TS. Western diet induces Paneth cell defects through microbiome alterations and farnesoid X receptor and type I interferon activation. *Cell Host Microbe* 2021; **29**: 988-1001.e6 [PMID: 34010595 DOI: 10.1016/j.chom.2021.04.004]

94 **Chassaing B**, Etienne-Mesmin L, Bonnet R, Darfeuille-Michaud A. Bile salts induce long polar fimbriae expression favouring Crohn's disease-associated adherent-invasive Escherichia coli interaction with Peyer's patches. *Environ Microbiol* 2013; **15**: 355-371 [PMID: 22789019 DOI: 10.1111/j.1462-2920.2012.02824.x]

95 **Lajczak-McGinley NK**, Porru E, Fallon CM, Smyth J, Curley C, McCarron PA, Tambuwala MM, Roda A, Keely SJ. The secondary bile acids, ursodeoxycholic acid and lithocholic acid, protect against intestinal inflammation by inhibition of epithelial apoptosis. *Physiol Rep* 2020; **8**: e14456 [PMID: 32562381 DOI: 10.14814/phy2.14456]

96 **Ward JBJ**, Lajczak NK, Kelly OB, O'Dwyer AM, Giddam AK, Ní Gabhann J, Franco P, Tambuwala MM, Jefferies CA, Keely S, Roda A, Keely SJ. Ursodeoxycholic acid and lithocholic acid exert anti-inflammatory actions in the colon. *Am J Physiol Gastrointest Liver Physiol* 2017; **312**: G550-G558 [PMID: 28360029 DOI: 10.1152/ajpgi.00256.2016]

97 **Martínez-Moya P**, Romero-Calvo I, Requena P, Hernández-Chirlaque C, Aranda CJ, González R, Zarzuelo A, Suárez MD, Martínez-Augustin O, Marín JJ, de Medina FS. Dose-dependent antiinflammatory effect of ursodeoxycholic acid in experimental colitis. *Int Immunopharmacol* 2013; **15**: 372-380 [PMID: 23246254 DOI: 10.1016/j.intimp.2012.11.017]

98 **Wang Z**, Chen J, Chen Z, Xie L, Wang W. Clinical effects of ursodeoxycholic acid on patients with ulcerative colitis may improve *via* the regulation of IL-23-IL-17 axis and the changes of the proportion of intestinal microflora. *Saudi J Gastroenterol* 2021; **27**: 149-157 [PMID: 33835051 DOI: 10.4103/sjg.SJG_462_20]

99 **Pittayanon R**, Lau JT, Leontiadis GI, Tse F, Yuan Y, Surette M, Moayyedi P. Differences in Gut Microbiota in Patients With *vs* Without Inflammatory Bowel Diseases: A Systematic Review. *Gastroenterology* 2020; **158**: 930-946.e1 [PMID: 31812509 DOI: 10.1053/j.gastro.2019.11.294]

100 **Meisch JP**, Nishimura M, Vogel RM, Sung HC, Bednarchik BA, Ghosh SK, Fu P, McCormick T, Weinberg A, Levine AD. Human β-defensin 3 peptide is increased and redistributed in Crohn's ileitis. *Inflamm Bowel Dis* 2013; **19**: 942-953 [PMID: 23511030 DOI: 10.1097/MIB.0b013e318280b11a]

101 **Alvarado DM**, Chen B, Iticovici M, Thaker AI, Dai N, VanDussen KL, Shaikh N, Lim CK, Guillemin GJ, Tarr PI, Ciorba MA. Epithelial Indoleamine 2,3-Dioxygenase 1 Modulates Aryl Hydrocarbon Receptor and Notch Signaling to Increase Differentiation of Secretory Cells and Alter Mucus-Associated Microbiota. *Gastroenterology* 2019; **157**: 1093-1108.e11 [PMID: 31325428 DOI: 10.1053/j.gastro.2019.07.013]

102 **Darfeuille-Michaud A**, Neut C, Barnich N, Lederman E, Di Martino P, Desreumaux P, Gambiez L, Joly B, Cortot A, Colombel JF. Presence of adherent Escherichia coli strains in ileal mucosa of patients with Crohn's disease. *Gastroenterology* 1998; **115**: 1405-1413 [PMID: 9834268 DOI: 10.1016/s0016-5085(98)70019-8]

103 **Darfeuille-Michaud A**, Boudeau J, Bulois P, Neut C, Glasser AL, Barnich N, Bringer MA, Swidsinski A, Beaugerie L, Colombel JF. High prevalence of adherent-invasive Escherichia coli associated with ileal mucosa in Crohn's disease. *Gastroenterology* 2004; **127**: 412-421 [PMID: 15300573 DOI: 10.1053/j.gastro.2004.04.061]

104 **Meconi S**, Vercellone A, Levillain F, Payré B, Al Saati T, Capilla F, Desreumaux P, Darfeuille-Michaud A, Altare F. Adherent-invasive Escherichia coli isolated from Crohn's disease patients induce granulomas in vitro. *Cell Microbiol* 2007; **9**: 1252-1261 [PMID: 17223928 DOI: 10.1111/j.1462-5822.2006.00868.x]

105 **Buisson A**, Vazeille E, Fumery M, Pariente B, Nancey S, Seksik P, Peyrin-Biroulet L, Allez M, Ballet N, Filippi J, Yzet C, Nachury M, Boschetti G, Billard E, Dubois A, Rodriguez S, Chevarin C, Goutte M, Bommelaer G, Pereira B, Hebuterne X, Barnich N; CEALIVE & REMIND study group. Faster and less invasive tools to identify patients with ileal colonization by adherent-invasive E. coli in Crohn's disease. *United European Gastroenterol J* 2021; **9**: 1007-1018 [PMID: 34791806 DOI: 10.1002/ueg2.12161]

106 **Sivignon A**, Chervy M, Chevarin C, Ragot E, Billard E, Denizot J, Barnich N. An adherent-invasive Escherichia coli-colonized mouse model to evaluate microbiota-targeting strategies in Crohn's disease. *Dis Model Mech* 2022; **15** [PMID: 36172858 DOI: 10.1242/dmm.049707]

107 **Carvalho FA**, Barnich N, Sivignon A, Darcha C, Chan CH, Stanners CP, Darfeuille-Michaud A. Crohn's disease adherent-invasive Escherichia coli colonize and induce strong gut inflammation in transgenic mice expressing human CEACAM. *J Exp Med* 2009; **206**: 2179-2189 [PMID: 19737864 DOI: 10.1084/jem.20090741]

108 **Mimouna S**, Gonçalvès D, Barnich N, Darfeuille-Michaud A, Hofman P, Vouret-Craviari V. Crohn disease-associated Escherichia coli promote gastrointestinal inflammatory disorders by activation of HIF-dependent responses. *Gut Microbes* 2011; **2**: 335-346 [PMID: 22157238 DOI: 10.4161/gmic.18771]

109 **Buisson A**, Sokol H, Hammoudi N, Nancey S, Treton X, Nachury M, Fumery M, Hébuterne X, Rodrigues M, Hugot JP, Boschetti G, Stefanescu C, Wils P, Seksik P, Le Bourhis L, Bezault M, Sauvanet P, Pereira B, Allez M, Barnich N; Remind study group. Role of adherent and invasive Escherichia coli in Crohn's disease: lessons from the postoperative recurrence model. *Gut* 2023; **72**: 39-48 [PMID: 35361684 DOI: 10.1136/gutjnl-2021-325971]

110 **Chervy M**, Sivignon A, Dambrine F, Buisson A, Sauvanet P, Godfraind C, Allez M, Le Bourhis L; The Remind Group, Barnich N, Denizot J. Epigenetic master regulators HDAC1 and HDAC5 control pathobiont Enterobacteria colonization in ileal mucosa of Crohn's disease patients. *Gut Microbes* 2022; **14**: 2127444 [PMID: 36175163 DOI: 10.1080/19490976.2022.2127444]

111 **Boucher D**, Barnich N. Phage Therapy Against Adherent-invasive E. coli: Towards a Promising Treatment of Crohn's Disease Patients? *J Crohns Colitis* 2022; **16**: 1509-1510 [PMID: 35796668 DOI: 10.1093/ecco-jcc/jjac070]

112 **Zakrzewski M**, Simms LA, Brown A, Appleyard M, Irwin J, Waddell N, Radford-Smith GL. IL23R-Protective Coding

Variant Promotes Beneficial Bacteria and Diversity in the Ileal Microbiome in Healthy Individuals Without Inflammatory Bowel Disease. *J Crohns Colitis* 2019; **13**: 451-461 [PMID: 30445599 DOI: 10.1093/ecco-jcc/jjy188]

113 **Sokol H**, Pigneur B, Watterlot L, Lakhdari O, Bermúdez-Humarán LG, Gratadoux JJ, Blugeon S, Bridonneau C, Furet JP, Corthier G, Grangette C, Vasquez N, Pochart P, Trugnan G, Thomas G, Blottière HM, Doré J, Marteau P, Seksik P, Langella P. Faecalibacterium prausnitzii is an anti-inflammatory commensal bacterium identified by gut microbiota analysis of Crohn disease patients. *Proc Natl Acad Sci U S A* 2008; **105**: 16731-16736 [PMID: 18936492 DOI: 10.1073/pnas.0804812105]

114 **Willing B**, Halfvarson J, Dicksved J, Rosenquist M, Järnerot G, Engstrand L, Tysk C, Jansson JK. Twin studies reveal specific imbalances in the mucosa-associated microbiota of patients with ileal Crohn's disease. *Inflamm Bowel Dis* 2009; **15**: 653-660 [PMID: 19023901 DOI: 10.1002/ibd.20783]

115 **Olaisen M**, Richard ML, Beisvåg V, Granlund AVB, Røyset ES, Rué O, Martinsen TC, Sandvik AK, Sokol H, Fossmark R. The ileal fungal microbiota is altered in Crohn's disease and is associated with the disease course. *Front Med (Lausanne)* 2022; **9**: 868812 [PMID: 36237548 DOI: 10.3389/fmed.2022.868812]

116 **Jain U**, Ver Heul AM, Xiong S, Gregory MH, Demers EG, Kern JT, Lai CW, Muegge BD, Barisas DAG, Leal-Ekman JS, Deepak P, Ciorba MA, Liu TC, Hogan DA, Debbas P, Braun J, McGovern DPB, Underhill DM, Stappenbeck TS. Debaryomyces is enriched in Crohn's disease intestinal tissue and impairs healing in mice. *Science* 2021; **371**: 1154-1159 [PMID: 33707263 DOI: 10.1126/science.abd0919]

117 **Martinho-Grueber M**, Kapoglou I, Bravo F, Sarraj R, Benz E, Restellini S, Biedermann L, Rogler G, Vavricka SR, Schoepfer A, Maillard MH, Michetti P, Brunner F, Clair C, Barry MP, Pittet V, von Känel R, Juillerat P. Alcohol and cannabis consumption in patients with inflammatory bowel disease: prevalence, pattern of consumption and impact on the disease. *Eur J Gastroenterol Hepatol* 2023; **35**: 21-30 [PMID: 36317770 DOI: 10.1097/MEG.0000000000002453]

118 **Naftali T**, Bar-Lev Schleider L, Almog S, Meiri D, Konikoff FM. Oral CBD-rich Cannabis Induces Clinical but Not Endoscopic Response in Patients with Crohn's Disease, a Randomised Controlled Trial. *J Crohns Colitis* 2021; **15**: 1799-1806 [PMID: 33858011 DOI: 10.1093/ecco-jcc/jjab069]

119 **Berkowitz L**, Pardo-Roa C, Salazar GA, Salazar-Echegarai F, Miranda JP, Ramírez G, Chávez JL, Kalergis AM, Bueno SM, Álvarez-Lobos M. Mucosal Exposure to Cigarette Components Induces Intestinal Inflammation and Alters Antimicrobial Response in Mice. *Front Immunol* 2019; **10**: 2289 [PMID: 31608070 DOI: 10.3389/fimmu.2019.02289]

120 **Liu TC**, Kern JT, VanDussen KL, Xiong S, Kaiko GE, Wilen CB, Rajala MW, Caruso R, Holtzman MJ, Gao F, McGovern DP, Nunez G, Head RD, Stappenbeck TS. Interaction between smoking and ATG16L1T300A triggers Paneth cell defects in Crohn's disease. *J Clin Invest* 2018; **128**: 5110-5122 [PMID: 30137026 DOI: 10.1172/JCI120453]

121 **Fricker M**, Goggins BJ, Mateer S, Jones B, Kim RY, Gellatly SL, Jarnicki AG, Powell N, Oliver BG, Radford-Smith G, Talley NJ, Walker MM, Keely S, Hansbro PM. Chronic cigarette smoke exposure induces systemic hypoxia that drives intestinal dysfunction. *JCI Insight* 2018; **3** [PMID: 29415878 DOI: 10.1172/jci.insight.94040]

122 **De Galan C**, De Vos M, Hindryckx P, Laukens D, Van Welden S. Long-Term Environmental Hypoxia Exposure and Haematopoietic Prolyl Hydroxylase-1 Deletion Do Not Impact Experimental Crohn's Like Ileitis. *Biology (Basel)* 2021; **10** [PMID: 34571764 DOI: 10.3390/biology10090887]

123 **Knyazev E**, Maltseva D, Raygorodskaya M, Shkurnikov M. HIF-Dependent NFATC1 Activation Upregulates ITGA5 and PLAUR in Intestinal Epithelium in Inflammatory Bowel Disease. *Front Genet* 2021; **12**: 791640 [PMID: 34858489 DOI: 10.3389/fgene.2021.791640]

124 **Zuo L**, Li Y, Zhu W, Shen B, Gong J, Guo Z, Zhang W, Wu R, Gu L, Li N, Li J. Mesenteric Adipocyte Dysfunction in Crohn's Disease is Associated with Hypoxia. *Inflamm Bowel Dis* 2016; **22**: 114-126 [PMID: 26332309 DOI: 10.1097/MIB.0000000000000571]

125 **Linares R**, Fernández MF, Gutiérrez A, García-Villalba R, Suárez B, Zapater P, Martínez-Blázquez JA, Caparrós E, Tomás-Barberán FA, Francés R. Endocrine disruption in Crohn's disease: Bisphenol A enhances systemic inflammatory response in patients with gut barrier translocation of dysbiotic microbiota products. *FASEB J* 2021; **35**: e21697 [PMID: 34085740 DOI: 10.1096/fj.202100481R]

126 **Marion-Letellier R**, Savoye G, Ghosh S. IBD: In Food We Trust. *J Crohns Colitis* 2016; **10**: 1351-1361 [PMID: 27194533 DOI: 10.1093/ecco-jcc/jjw106]

127 **Matsunaga H**, Hokari R, Kurihara C, Okada Y, Takebayashi K, Okudaira K, Watanabe C, Komoto S, Nakamura M, Tsuzuki Y, Kawaguchi A, Nagao S, Miura S. Omega-3 polyunsaturated fatty acids ameliorate the severity of ileitis in the senescence accelerated mice (SAM)P1/Yit mice model. *Clin Exp Immunol* 2009; **158**: 325-333 [PMID: 19793338 DOI: 10.1111/j.1365-2249.2009.04020.x]

128 **Plissonneau C**, Sivignon A, Chassaing B, Capel F, Martin V, Etienne M, Wawrzyniak I, Chausse P, Dutheil F, Mairesse G, Chesneau G, Boisseau N, Barnich N. Beneficial Effects of Linseed Supplementation on Gut Mucosa-Associated Microbiota in a Physically Active Mouse Model of Crohn's Disease. *Int J Mol Sci* 2022; **23** [PMID: 35682570 DOI: 10.3390/ijms23115891]

129 **MacLean CH**, Mojica WA, Newberry SJ, Pencharz J, Garland RH, Tu W, Hilton LG, Gralnek IM, Rhodes S, Khanna P, Morton SC. Systematic review of the effects of n-3 fatty acids in inflammatory bowel disease. *Am J Clin Nutr* 2005; **82**: 611-619 [PMID: 16155275 DOI: 10.1093/ajcn.82.3.611]

130 **Ananthakrishnan AN**, Khalili H, Konijeti GG, Higuchi LM, de Silva P, Korzenik JR, Fuchs CS, Willett WC, Richter JM, Chan AT. A prospective study of long-term intake of dietary fiber and risk of Crohn's disease and ulcerative colitis. *Gastroenterology* 2013; **145**: 970-977 [PMID: 23912083 DOI: 10.1053/j.gastro.2013.07.050]

131 **Schroyen M**, Li B, Arévalo Sureda E, Zhang Y, Leblois J, Deforce D, Van Nieuwerburgh F, Wavreille J, Everaert N. Pre-Weaning Inulin Supplementation Alters the Ileal Transcriptome in Pigs Regarding Lipid Metabolism. *Vet Sci* 2021; **8** [PMID: 34679037 DOI: 10.3390/vetsci8100207]

132 **Fletcher J**, Cooper SC, Ghosh S, Hewison M. The Role of Vitamin D in Inflammatory Bowel Disease: Mechanism to Management. *Nutrients* 2019; **11** [PMID: 31067701 DOI: 10.3390/nu11051019]

133 **McGillis L**, Bronte-Tinkew DM, Dang F, Capurro M, Prashar A, Ricciuto A, Greenfield L, Lozano-Ruf A, Siddiqui I, Hsieh A, Church P, Walters T, Roth DE, Griffiths A, Philpott D, Jones NL. Vitamin D deficiency enhances expression of

autophagy-regulating miR-142-3p in mouse and "involved" IBD patient intestinal tissues. *Am J Physiol Gastrointest Liver Physiol* 2021; **321**: G171-G184 [PMID: 34159811 DOI: 10.1152/ajpgi.00398.2020]

134 **Su D**, Nie Y, Zhu A, Chen Z, Wu P, Zhang L, Luo M, Sun Q, Cai L, Lai Y, Xiao Z, Duan Z, Zheng S, Wu G, Hu R, Tsukamoto H, Lugea A, Liu Z, Pandol SJ, Han YP. Vitamin D Signaling through Induction of Paneth Cell Defensins Maintains Gut Microbiota and Improves Metabolic Disorders and Hepatic Steatosis in Animal Models. *Front Physiol* 2016; **7**: 498 [PMID: 27895587 DOI: 10.3389/fphys.2016.00498]

135 **Viennois E**, Bretin A, Dubé PE, Maue AC, Dauriat CJG, Barnich N, Gewirtz AT, Chassaing B. Dietary Emulsifiers Directly Impact Adherent-Invasive E. coli Gene Expression to Drive Chronic Intestinal Inflammation. *Cell Rep* 2020; **33**: 108229 [PMID: 33027647 DOI: 10.1016/j.celrep.2020.108229]

136 **Bischoff SC**, Escher J, Hébuterne X, Kłęk S, Krznaric Z, Schneider S, Shamir R, Stardelova K, Wierdsma N, Wiskin AE, Forbes A. ESPEN practical guideline: Clinical Nutrition in inflammatory bowel disease. *Clin Nutr* 2020; **39**: 632-653 [PMID: 32029281 DOI: 10.1016/j.clnu.2019.11.002]

137 **Rutgeerts P**, Geboes K, Vantrappen G, Beyls J, Kerremans R, Hiele M. Predictability of the postoperative course of Crohn's disease. *Gastroenterology* 1990; **99**: 956-963 [PMID: 2394349 DOI: 10.1016/0016-5085(90)90613-6]

138 **Rieder F**, Fiocchi C, Rogler G. Mechanisms, Management, and Treatment of Fibrosis in Patients With Inflammatory Bowel Diseases. *Gastroenterology* 2017; **152**: 340-350.e6 [PMID: 27720839 DOI: 10.1053/j.gastro.2016.09.047]

139 **Li XH**, Feng ST, Cao QH, Coffey JC, Baker ME, Huang L, Fang ZN, Qiu Y, Lu BL, Chen ZH, Li Y, Bettenworth D, Iacucci M, Sun CH, Ghosh S, Rieder F, Chen MH, Li ZP, Mao R. Degree of Creeping Fat Assessed by Computed Tomography Enterography is Associated with Intestinal Fibrotic Stricture in Patients with Crohn's Disease: A Potentially Novel Mesenteric Creeping Fat Index. *J Crohns Colitis* 2021; **15**: 1161-1173 [PMID: 33411893 DOI: 10.1093/ecco-jcc/jjab005]

140 **Huang L**, Qian W, Xu Y, Guo Z, Yin Y, Guo F, Zhu W, Li Y. Mesenteric Adipose Tissue Contributes to Intestinal Fibrosis in Crohn's Disease Through the ATX-LPA Axis. *J Crohns Colitis* 2022; **16**: 1124-1139 [PMID: 35104318 DOI: 10.1093/ecco-jcc/jjac017]

141 **Wang J**, Lin S, Brown JM, van Wagoner D, Fiocchi C, Rieder F. Novel mechanisms and clinical trial endpoints in intestinal fibrosis. *Immunol Rev* 2021; **302**: 211-227 [PMID: 33993489 DOI: 10.1111/imr.12974]

142 **Kredel LI**, Batra A, Stroh T, Kühl AA, Zeitz M, Erben U, Siegmund B. Adipokines from local fat cells shape the macrophage compartment of the creeping fat in Crohn's disease. *Gut* 2013; **62**: 852-862 [PMID: 22543156 DOI: 10.1136/gutjnl-2011-301424]

143 **Ha CWY**, Martin A, Sepich-Poore GD, Shi B, Wang Y, Gouin K, Humphrey G, Sanders K, Ratnayake Y, Chan KSL, Hendrick G, Caldera JR, Arias C, Moskowitz JE, Ho Sui SJ, Yang S, Underhill D, Brady MJ, Knott S, Kaihara K, Steinbaugh MJ, Li H, McGovern DPB, Knight R, Fleshner P, Devkota S. Translocation of Viable Gut Microbiota to Mesenteric Adipose Drives Formation of Creeping Fat in Humans. *Cell* 2020; **183**: 666-683.e17 [PMID: 32991841 DOI: 10.1016/j.cell.2020.09.009]

144 **Kredel LI**, Jödicke LJ, Scheffold A, Gröne J, Glauben R, Erben U, Kühl AA, Siegmund B. T-cell Composition in Ileal and Colonic Creeping Fat - Separating Ileal from Colonic Crohn's Disease. *J Crohns Colitis* 2019; **13**: 79-91 [PMID: 30272118 DOI: 10.1093/ecco-jcc/jjy146]

145 **Rana T**, Korolkova OY, Rachakonda G, Williams AD, Hawkins AT, James SD, Sakwe AM, Hui N, Wang L, Yu C, Goodwin JS, Izban MG, Offodile RS, Washington MK, Ballard BR, Smoot DT, Shi XZ, Forbes DS, Shanker A, M'Koma AE. Linking bacterial enterotoxins and alpha defensin 5 expansion in the Crohn's colitis: A new insight into the etiopathogenetic and differentiation triggers driving colonic inflammatory bowel disease. *PLoS One* 2021; **16**: e0246393 [PMID: 33690604 DOI: 10.1371/journal.pone.0246393]

146 **Torres J**, Bonovas S, Doherty G, Kucharzik T, Gisbert JP, Raine T, Adamina M, Armuzzi A, Bachmann O, Bager P, Biancone L, Bokemeyer B, Bossuyt P, Burisch J, Collins P, El-Hussuna A, Ellul P, Frei-Lanter C, Furfaro F, Gingert C, Gionchetti P, Gomollon F, González-Lorenzo M, Gordon H, Hlavaty T, Juillerat P, Katsanos K, Kopylov U, Krustins E, Lytras T, Maaser C, Magro F, Marshall JK, Myrelid P, Pellino G, Rosa I, Sabino J, Savarino E, Spinelli A, Stassen L, Uzzan M, Vavricka S, Verstockt B, Warusavitarne J, Zmora O, Fiorino G. ECCO Guidelines on Therapeutics in Crohn's Disease: Medical Treatment. *J Crohns Colitis* 2020; **14**: 4-22 [PMID: 31711158 DOI: 10.1093/ecco-jcc/jjz180]

147 **Vermeire S**, Louis E, Carbonez A, Van Assche G, Noman M, Belaiche J, De Vos M, Van Gossum A, Pescatore P, Fiasse R, Pelckmans P, Reynaert H, D'Haens G, Rutgeerts P; Belgian Group of Infliximab Expanded Access Program in Crohn's Disease. Demographic and clinical parameters influencing the short-term outcome of anti-tumor necrosis factor (infliximab) treatment in Crohn's disease. *Am J Gastroenterol* 2002; **97**: 2357-2363 [PMID: 12358256 DOI: 10.1111/j.1572-0241.2002.05991.x]

148 **Choi CH**, Song ID, Kim YH, Koo JS, Kim YS, Kim JS, Kim N, Kim ES, Kim JH, Kim JW, Kim TO, Kim HS, Kim HJ, Park YS, Park DI, Park SJ, Song HJ, Shin SJ, Yang SK, Ye BD, Lee KM, Lee BI, Lee SY, Lee CK, Im JP, Jang BI, Jeon TJ, Cho YK, Chang SK, Jeon SR, Jung SA, Jeen YT, Cha JM, Han DS, Kim WH; IBD Study Group of the Korean Association for the Study of the Intestinal Diseases. Efficacy and Safety of Infliximab Therapy and Predictors of Response in Korean Patients with Crohn's Disease: A Nationwide, Multicenter Study. *Yonsei Med J* 2016; **57**: 1376-1385 [PMID: 27593865 DOI: 10.3349/ymj.2016.57.6.1376]

149 **Gisbert JP**, Chaparro M. Predictors of Primary Response to Biologic Treatment [Anti-TNF, Vedolizumab, and Ustekinumab] in Patients With Inflammatory Bowel Disease: From Basic Science to Clinical Practice. *J Crohns Colitis* 2020; **14**: 694-709 [PMID: 31777929 DOI: 10.1093/ecco-jcc/jjz195]

150 **Haberman Y**, Minar P, Karns R, Dexheimer PJ, Ghandikota S, Tegge S, Shapiro D, Shuler B, Venkateswaran S, Braun T, Ta A, Walters TD, Baldassano RN, Noe JD, Rosh J, Markowitz J, Dotson JL, Mack DR, Kellermayer R, Griffiths AM, Heyman MB, Baker SS, Moulton D, Patel AS, Gulati AS, Steiner SJ, LeLeiko N, Otley A, Oliva-Hemker M, Ziring D, Gokhale R, Kim S, Guthery SL, Cohen SA, Snapper S, Aronow BJ, Stephens M, Gibson G, Dillman JR, Dubinsky M, Hyams JS, Kugathasan S, Jegga AG, Denson LA. Mucosal Inflammatory and Wound Healing Gene Programs Reveal Targets for Stricturing Behavior in Pediatric Crohn's Disease. *J Crohns Colitis* 2020; **15**: 273-286 [PMID: 32770196 DOI: 10.1093/ecco-jcc/jjaa166]

151 **Jurickova I**, Bonkowski E, Angerman E, Novak E, Huron A, Akers G, Iwasawa K, Braun T, Hadar R, Hooker M, Han S, Cutler DJ, Okou DT, Kugathasan S, Jegga A, Wells J, Takebe T, Mollen KP, Haberman Y, Denson LA. Eicosatetraynoic Acid and Butyrate Regulate Human Intestinal Organoid Mitochondrial and Extracellular Matrix Pathways Implicated in Crohn's Disease Strictures. *Inflamm Bowel Dis* 2022; **28**: 988-1003 [PMID: 35259271 DOI: 10.1093/ibd/izac037]

World Journal of Gastroenterology

Submit a Manuscript: https://www.f6publishing.com

World J Gastroenterol 2023 June 7; 29(21): 3241-3256

DOI: 10.3748/wjg.v29.i21.3241

ISSN 1007-9327 (print) ISSN 2219-2840 (online)

REVIEW

Emerging role of the gut microbiome in post-infectious irritable bowel syndrome: A literature review

Vasile Valeriu Lupu, Cristina Mihaela Ghiciuc, Gabriela Stefanescu, Cristina Maria Mihai, Alina Popp, Maria Oana Sasaran, Laura Bozomitu, Iuliana Magdalena Starcea, Anca Adam Raileanu, Ancuta Lupu

Specialty type: Gastroenterology and hepatology

Provenance and peer review: Invited article; Externally peer reviewed.

Peer-review model: Single blind

Peer-review report's scientific quality classification

Grade A (Excellent): 0
Grade B (Very good): B
Grade C (Good): C
Grade D (Fair): 0
Grade E (Poor): 0

P-Reviewer: Belkova N, Russia; Zamani M, Iran

Received: February 16, 2023
Peer-review started: February 16, 2023
First decision: April 2, 2023
Revised: April 4, 2023
Accepted: May 8, 2023
Article in press: May 8, 2023
Published online: June 7, 2023

Vasile Valeriu Lupu, Cristina Mihaela Ghiciuc, Gabriela Stefanescu, Laura Bozomitu, Iuliana Magdalena Starcea, Anca Adam Raileanu, Ancuta Lupu, Faculty of General Medicine, "Grigore T. Popa" University of Medicine and Pharmacy, Iasi 700115, Romania

Cristina Maria Mihai, Faculty of General Medicine, Ovidius University, Constanta 900470, Romania

Alina Popp, Faculty of General Medicine, "Carol Davila" University of Medicine and Pharmacy, Bucharest 020021, Romania

Maria Oana Sasaran, Faculty of General Medicine, "George Emil Palade" University of Medicine, Pharmacy, Science and Technology, Targu Mures 540142, Romania

Corresponding author: Anca Adam Raileanu, MD, PhD, Attending Doctor, Faculty of General Medicine, "Grigore T. Popa" University of Medicine and Pharmacy, 16 University Street, Iasi 700115, Romania. anca.adam60@gmail.com

Abstract

Post-infectious irritable bowel syndrome (PI-IBS) is a particular type of IBS, with symptom onset after an acute episode of infectious gastroenteritis. Despite infectious disease resolution and clearance of the inciting pathogen agent, 10% of patients will develop PI-IBS. In susceptible individuals, the exposure to pathogenic organisms leads to a marked shift in the gut microbiota with prolonged changes in host-microbiota interactions. These changes can affect the gut-brain axis and the visceral sensitivity, disrupting the intestinal barrier, altering neuromuscular function, triggering persistent low inflammation, and sustaining the onset of IBS symptoms. There is no specific treatment strategy for PI-IBS. Different drug classes can be used to treat PI-IBS similar to patients with IBS in general, guided by their clinical symptoms. This review summarizes the current evidence for microbial dysbiosis in PI-IBS and analyzes the available data regarding the role of the microbiome in mediating the central and peripheral dysfunctions that lead to IBS symptoms. It also discusses the current state of evidence on therapies targeting the microbiome in the management of PI-IBS. The results of microbial modulation strategies used in relieving IBS symptomatology are encouraging. Several studies on PI-IBS animal models reported promising results. However, published data that describe the efficacy and safety of microbial targeted therapy in PI-IBS patients are scarce. Future research is required.

Key Words: Gut microbiome; Infectious gastroenteritis; Irritable bowel syndrome; Post infection syndrome; Pathophysiology; Inflammation

©The Author(s) 2023. Published by Baishideng Publishing Group Inc. All rights reserved.

Core Tip: Acute infectious gastroenteritis can trigger the onset of irritable bowel syndrome (IBS), leading to the development of post-infectious IBS (PI-IBS). PI-IBS is a clinical entity associated with gut dysbiosis. Alterations in the gut microbiome can affect the gut-brain axis, visceral sensitivity, intestinal barrier, intestinal secretion, gut motility, and immune activation, which in turn can cause IBS symptoms. A better understanding of PI-IBS is necessary to develop more targeted and effective treatments. Therapies targeting the microbiome, such as probiotics, antibiotics, diet, and fecal microbiota transplants, improve IBS symptoms. There is a lack of evidence of their efficiency in PI-IBS.

Citation: Lupu VV, Ghiciuc CM, Stefanescu G, Mihai CM, Popp A, Sasaran MO, Bozomitu L, Starcea IM, Adam Raileanu A, Lupu A. Emerging role of the gut microbiome in post-infectious irritable bowel syndrome: A literature review. *World J Gastroenterol* 2023; 29(21): 3241-3256
URL: https://www.wjgnet.com/1007-9327/full/v29/i21/3241.htm
DOI: https://dx.doi.org/10.3748/wjg.v29.i21.3241

INTRODUCTION

Irritable bowel syndrome (IBS) is the most frequently encountered disorder of gut-brain interactions[1], with a worldwide prevalence ranging between 7% and 15% of the general population[2,3]. According to the Rome IV criteria, it is characterized by mild to severe recurrent abdominal pain and bloating associated with alterations in bowel habits in the absence of organic disease or biochemical abnormalities[4]. Due to its symptoms, IBS is thought to be a disabling disease. It generates significant healthcare costs, reduces work productivity and school attendance, and decreases the health-related quality of life of the affected individuals[5,6]. Despite being a frequent entity in current gastroenterology practice, the physiopathology of IBS is not fully understood. It is considered to be a complex multifactorial disorder affected by several factors such as age, sex, genetics, diet, psychosocial status, altered microbiota, subclinical inflammation, and hypersensitivity of the neural network[7,8]. In recent years, accumulating evidence has suggested that the alteration of the gut microbiota plays an important role in the pathophysiology of IBS, as gut microbes exert effects on the host immune system, on gut barrier function, and on the brain-gut axis[9,10].

Acute infectious gastroenteritis [bacterial-*Campylobacter* species[11], *Salmonella* species[12,13], *Escherichia coli* (*E. coli*)[14], *Shigella*[15], *Clostridium difficile* (*C. difficile*)[16], viral-norovirus[17], rotavirus [18], severe acute respiratory syndrome coronavirus 2 (SARS-CoV-2)[19], and protozoal-*Giardia*[20]] has been shown to be one of the strongest risk factors for the development of post-infectious IBS (PI-IBS), a distinct condition in which IBS diagnostic criteria are met[21,22]. PI-IBS occurs after the resolution of a gastrointestinal-related infection and the clearance of the inciting pathogen, in a patient without a prior history of IBS symptoms[22,23]. IBS clinical features usually develop 6-18 mo after the infectious gastroenteritis episode[24]. PI-IBS management strategies involve nonpharmacologic and pharmacologic therapies. Current guidance relies on IBS treatment experience, as there is a lack of evidence-based recommendations for PI-IBS treatment[1]. The aim of this review is to analyze the current literature and to describe the role of the human gut microbiota on PI-IBS physiopathology. The main questions to be answered include which long-term consequences of acute enteric infections may serve as triggers to PI-IBS and whether the acute enteric infection associated dysbiosis and its recovery can be used to predict PI-IBS development. Additionally, under discussion is whether there is a specific microbial signature associated with PI-IBS, as most studies of PI-IBS combine patients infected by varying pathogens, thus generating a considerable variability of outcomes. The gut microbiota modulation and its potential therapeutic implications in PI-IBS in terms of efficacy and safety continue to be a subject of debate and highlight the need for specific treatment protocols. A better characterization of the relationship between gut-associated dysbiosis and PI-IBS progression will lead the way to personalized medicine and the individualized management of each patient.

PI-IBS GENERAL DATA

A globally accepted definition of PI-IBS is not currently available in the literature. Most authors consider

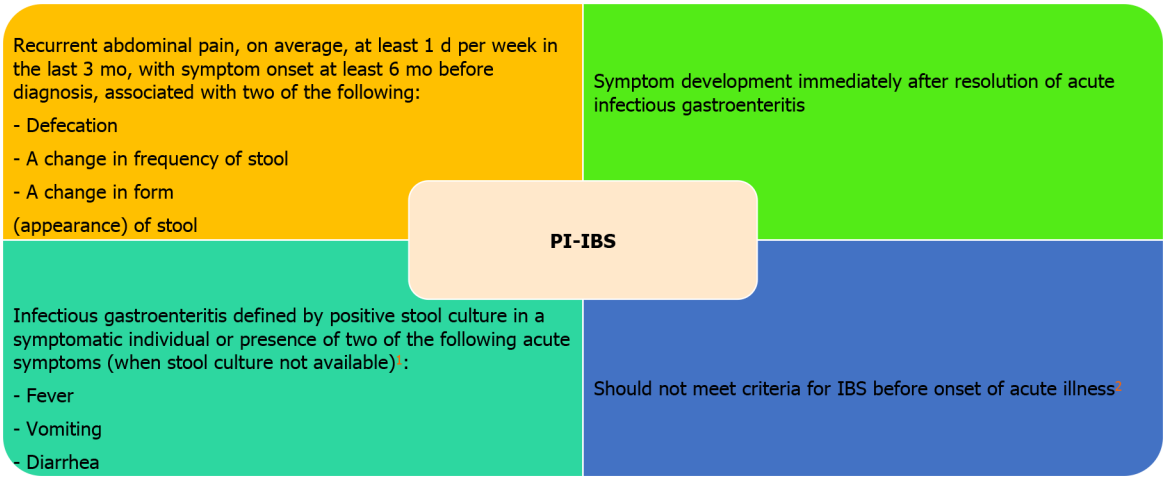
PI-IBS as a form of IBS for which the symptoms, as specified in the Rome IV criteria, appear after the resolution of an acute gastroenteritis episode in patients without any IBS symptomatology before the gastrointestinal infection[1,4]. In 2019, the Rome Foundation Working Group proposed symptomatic diagnostic criteria for PI-IBS based on the Rome IV criteria (Figure 1), as there are no sensitive and specific diagnostic markers available yet[25]. Considering the predominant bowel pattern graded on the Bristol stool scale, PI-IBS can be classified as diarrhea-predominant IBS (IBS-D), constipation-predominant (IBS-C), mixed bowel habits (IBS-M), and unclassified[1,26]. A bowel pattern is considered predominant when it is ≥ 25% of the time as either hard/lumpy (IBS-C), loose/watery (IBS-D), or both (IBS-M)[1]. PI-IBS patients are more likely than sporadic IBS patients to present a diarrhea-predominant phenotype. The association between each patient and a PI-IBS subtype is important for disease management and therapy[22].

While most pathogen agents cause self-limiting acute gastroenteritis, subsequent chronic alteration may persist in some genetically predisposed individuals[27]. According to several studies, about 1 in 10 individuals with an acute episode of gastroenteritis will develop PI-IBS[21,28]. A 2017 meta-analysis reported that the incidence of PI-IBS more than a year after the acute episode of gastroenteritis was 14.5%[29]. Epidemiologic data of the reported incidence and prevalence vary across the literature, in part due to the methodological heterogeneity, including the criteria used to define IBS (Rome criteria I, II, III, or IV)[3,16,22]. Moreover, there is evidence that the data might be underestimated due to the high incidence of infectious gastroenteritis and the poor recall of milder episodes, as the diagnosis relies on self-reported symptom clusters[2,21,30].

Female sex, a young age, certain psychological factors before or during acute infectious gastroenteritis (anxiety, depression, somatization, and/or neuroticism), and genetic predisposition (carriers of the *TLR9*, *CDH1*, and *IL6* genes) seem to increase the risk of developing PI-IBS[29,31]. The severity of the acute infectious episode also seems to increase the probability of developing PI-IBS after the gastroenteritis resolution[29]. The risk of PI-IBS is doubled when diarrhea lasts > 7 d and is tripled when diarrhea lasts > 21 d. Other symptoms such as abdominal cramps, weight loss, and bloody stools are also associated with an elevated risk, with abdominal cramps increasing the PI-IBS risk four times. Fever is not mentioned as a risk factor[32]. Moreover, it might have a protective action, representing the host's response to the infectious injury[33]. The risk of IP-IBS remains high for at least 2 to 3 years post infection[22].

Various pathogens have been reported as related to PI-IBS development. A systematic review evaluating the prevalence and risk factors of PI-IBS after acute gastroenteritis by specific pathogens revealed the fact that the evidence indicated a similar risk for bacterial pathogens, while for viral and parasitic gastroenteritis, the data were limited[34]. However, a recent study found the incidence of PI-IBS to be higher in patients with *Campylobacter jejuni* (*C. jejuni*) gastroenteritis, compared to other etiologic agents such as bacteria, viruses, or protozoa[35]. When comparing different pathogens, protozoal enteritis shows the highest risk for PI-IBS development, followed by bacterial and then viral [33,36]. Bacterial infections seem to generate more PI-IBS cases than viral gastroenteritis probably due to the fact that the mucosal damage and inflammation caused by bacteria is often greater than that caused by viral agents[37].

There is a strong association between travelers' diarrhea and PI-IBS. Self-reports of exposure seem to result in a higher PI-IBS occurrence than laboratory-confirmed cases of travelers' diarrhea, but further studies are needed to confirm this finding[38]. Culture-confirmed infections, either bacterial or viral, seem to present an equally increased risk of PI-IBS as nonspecific gastrointestinal infections[39]. However, viral gastroenteritis is more likely to develop transient forms of PI-IBS than bacterial episodes [40]. The significant decrease in the PI-IBS prevalence from 19% to 4% one year after a viral infection may be due to the less invasive nature of the pathogen, perhaps avoiding a stronger host response[29]. During the recent pandemic, the novel coronavirus SARS-CoV-2 displayed its potential to generate gastrointestinal manifestations[41,42]. It seems that the prevalence of gastrointestinal symptoms in coronavirus disease 2019 (COVID-19) patients is around 10%, and it is following an increasing trend[43, 44]. A multicenter study from 2020 reported that digestive symptoms such as diarrhea, vomiting, and abdominal pain were present in 50.5% of COVID-19 patients, while other studies concluded that the incidence of diarrhea in the same category of patients varied from 2% to 20%[41,45,46]. A recent study found an incidence of 11.6% of IBS, according to the Rome IV criteria, with symptom onset following COVID-19 infection[41]. Another group of researchers reported similar results, with 10% of the included patients with an acute episode of SARS-CoV-2 in their medical history meeting the Rome IV criteria for IBS 6 mo after the viral infection. Three percent of them had gastrointestinal symptoms during COVID-19[47]. Noviello *et al*[48] found an incidence of PI-IBS in 26.2% of patients. The risk of developing *de novo* IBS post-COVID-19 increases in patients with gastrointestinal symptoms present during the active viral infection. Similar to noninfectious IBS, the risk is higher in female patients. The presence of severe disease markers, such as an oxygen requirement and high procalcitonin levels, increases the risk of post-COVID-19 IBS[49]. Another similar study reported that patients with dyspnea at time of admission and a history of allergies and chronic treatment with proton pump inhibitors had an increased risk of developing post-COVID-19 IBS[50].



DOI: 10.3748/wjg.v29.i21.3241 **Copyright** ©The Author(s) 2023.

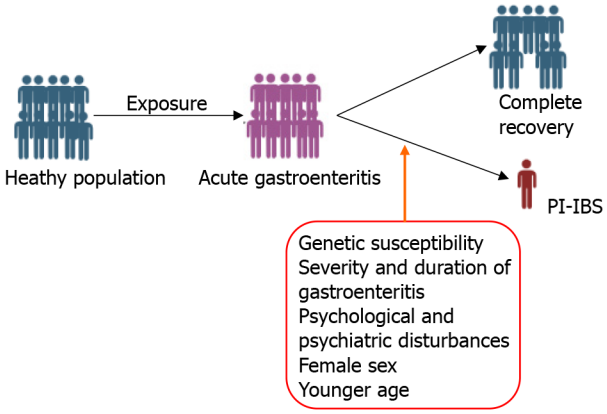
Figure 1 Diagnostic criteria for post-infection irritable bowel syndrome (based on Rome IV criteria). [1]Mentioning the exact date of onset of irritable bowel syndrome (IBS) symptomatology can also be suggestive for post-infectious IBS; [2]Irregular bowel movements can be experienced even before the onset of the acute gastroenteritis episode (but not in association with frequent pain, as an IBS characteristic). IBS: Irritable bowel syndrome; PI-IBS: Post-infectious irritable bowel syndrome.

Compared to sporadic IBS, PI forms of the disease might have a better outcome[2]. The prognosis of PI-IBS appears favorable with the spontaneous and gradual resolution of symptoms in most patients [22]. However, one longitudinal follow-up study showed that 15% of patients with post-infection IBS remained symptomatic 8 years after disease onset[28].

PI-IBS PATHOPHYSIOLOGY

Available studies have failed to give a clear holistic picture on the underlying pathophysiology of PI-IBS. As IBS is a multifactorial disease, it has been hypothesized that the development of PI-IBS could result from the interplay of fecal microbiota, the immune response of the host, and the psychological factors[51], as illustrated in Figure 2. The current conceptual framework regarding the pathophysiologic mechanism for PI-BS suggests that the exposure to pathogenic organisms leads to the alteration of the gut microbiome. PI-IBS is associated with hyperplasia of enterochromaffin (EC) cells and increased counts of neutrophils, mast cells, and T cells in the colonic mucosa. It is believed that gastrointestinal infections stimulate the immune system causing low-grade inflammation leading to PI-IBS[52].

It was reported that patients with PI-IBS often present an increased visceral pain perception known as visceral hypersensitivity (VHS). The incomplete resolution of the immune response to acute infectious injury might facilitate the persistence of a microscopic inflammation of the bowel, activating and sensitizing pain-sensing nerves[53]. A persistent low-grade inflammation of the bowel is thought to trigger PI-IBS symptoms, by aberrant activation of intrinsic and extrinsic nerves. The increased numbers of immune cells and the enhanced cytokine signaling play an important role in the underlying mechanism of PI-IBS pathophysiology[54]. A group of researchers found an increased IL-1β mRNA expression in rectal tissue biopsies after an acute episode of infectious gastroenteritis. Patients with a *Campylobacter* enteritis were found to present increased EC cell numbers, intraepithelial lymphocytes, and intestinal permeability up to one year after the infectious episode[55], while patients with PI-IBS following a *Shigella* gastroenteritis had an increased number of mast cell in the terminal ileum[56]. These cells release mediators such as histamine, IL-1β, IL-6, and TNF-α, mediators that can stimulate or sensitize visceral nociceptors and possibly generate the abdominal pain in PI-IBS[54]. Excessive secretion of IL-8 is a hallmark of *Campylobacter* pathogenesis, being initiated by the host recognition of the pathogen-associated lipooligosaccharide[57,58]. Another study on PI-IBS patients, however, found no evidence of increased inflammatory gene expression or infiltrating inflammatory cells in biopsies and no increase in cytokine levels[54]. Similarly, no difference was reported in the number of T lymphocytes or proinflammatory cytokines between PI-IBS patients and infected healthy volunteers, 3 years after a *Salmonella* infection[59]. Another study on a large cohort found similar results, with no difference in serum cytokines and mucosal cytokine expression between PI-IBS patients and healthy volunteers[60]. γδT cells are a subset of T cells involved in initiating inflammatory responses and can acquire the capacity of inducing various cytokines. A recent study of Dong *et al*[61] found that the Vδ1 γδ T cells subset from PI-IBS patients remarkably proliferated, activated, and produced abundant IL-17. In these patients, the IFN-γ level remained unchanged, as proof of the fact that the local IL-17 could participate in the intestinal pathological disorder during PI-IBS, as the major proinflammatory cytokine



DOI: 10.3748/wjg.v29.i21.3241 **Copyright** ©The Author(s) 2023.

Figure 2 Conceptual model for post-infectious irritable bowel syndrome. PI-IBS: Post-infectious irritable bowel syndrome.

[61]. Furthermore, a rodent study concluded that the upregulation of A2AR increased PI-IBS by promoting the T17 polarization of CD4+ T cells[62]. In their study, Balemans *et al*[54] reported that although initiated by inflammation, the pronociceptive changes seen in PI-IBS patients were mediated by the Hrh1 receptor sensitization of TRPV1 signaling, suggesting that similar to the "standard" IBS12, Hrh1 antagonism may represent an interesting new target for treatment of PI-IBS[54]. In conclusion, the presence of low-grade inflammation is an inconsistent finding in PI-IBS, as it might be an interim event following gastroenteritis that is superseded by another more persistent change in the gut microenvironment[54].

Increased intestinal permeability was shown to be an early event in PI-IBS physiopathology, associated with low-grade inflammation[1]. Patients with PI-IBS and high fecal proteolytic activity presented *in vivo* and *ex vivo* distal gut permeability that depended on the fecal level of proteolytic activity[63]. Following a mixed infection of enterohemorrhagic *E. coli* (EHEC) O157:H7 and *C. jejuni* during a waterborne outbreak of bacterial gastroenteritis, there was reported an increased intestinal permeability[58]. EHEC is known for its deleterious impact on the epithelial barrier[64]. *Giardia duodenalis* (*G. duodenalis*), a protozoan pathogen also implicated in promoting PI-IBS development, is well known to disturb the homeostatic barrier function through several mechanisms[65].

Viral gastroenteritis is a known risk factor for the PI onset of IBS. There are many studies describing the relation between norovirus infection and PI-IBS. As a conclusion to their study, Porter *et al*[66] suggested that dysmotility disorders may follow viral infections. A high incidence of functional gastrointestinal disorders was reported in patients who suffered from a norovirus gastroenteritis[66]. Similarly, another two studies reported an increased prevalence of PI-IBS in patients who experienced an acute episode of gastroenteritis during a confirmed norovirus outbreak[40,67]. It is thought that norovirus infection can cause epithelial barrier dysfunction, increased intestinal permeability, a reduction in the villous surface area and villous height, and a mucosal immune response with an increase in cytotoxic intraepithelial T cells, impairing the gut's sensory-motor function[67].

COVID-19, an immunologic and inflammatory response associated with low-grade inflammation and mucosal injury, caused the development of IBS features in genetically predisposed individuals. Patients with PI-IBS can present high levels of macrophages and T lymphocytes in intestinal samples, increased levels of calproctin and fecal cytokines, such as IL-8; all these were found in COVID-19 patients, as well as the presence of virus-specific IgA, together with increased blood levels of proinflammatory cytokines [68,69]. Similar to IBS, the altered intestinal permeability associated with gut dysbiosis and with an alteration of the neuromuscular function might also be involved in PI-IBS onset[67].

On the other hand, the pandemic led to a stressful situation, anxiety, and depression. These factors resulted in other diseases related to psychological stress and the nervous system similar to IBS[70,71]. Farsi *et al*[41] in their study found that psychological stress had no significant influence on COVID-19-induced IBS symptoms[41]. However, another similar study reported that COVID-19 had adverse effects on both GI and psychological symptoms among individuals with functional dyspepsia-IBS overlap syndrome[70]. Similarly, another study concluded that the COVID-19 pandemic increased psychosocial stress and gastrointestinal symptoms in patients already known to have IBS[72]. The interaction between the gut-brain axis disturbances and genetic and psychosocial factors can contribute to IBS development[41]. Psychological stress acts as a trigger in developing IBS through its adverse effects on intestinal permeability and motility and hypersensitivity to visceral pain. Acute and chronic stressful situations lead to cortico-tropin-releasing hormone secretion, activating the hypothalamic-pituitary-adrenal axis and creating new premises for IBS onset. Stress-induced dysbiosis can modulate the neuro-immune-endocrine systems and interfere with the brain-gut axis[73,74].

PI-IBS MICROBIOME ALTERATION

Due to the bioavailability of nutrients, the human gastrointestinal tract harbors the largest concentration and diversity of microbiota of the human body. Healthy adult gastrointestinal microbiota are represented by five primary bacteria phyla: *Firmicutes* (synonym *Bacillota*) and *Bacteroides* (synonym *Bacteroidota*) phylum predominate the microbiota, while *Actinobacteria* (synonym *Actinomycetota*), *Proteobacteria* (synonym *Pseudomonadota*), and *Verrucomicrobia* phylum are found in modest proportions[75]. The gut microbiota have a dynamic composition, influenced by many intrinsic and extrinsic factors, such as genetic inheritance, birth mode, breastfeeding duration, age, sex, diet, and drugs[75-77]. The alteration of the healthy microbial structure leads to dysbiosis, resulting in various gastrointestinal disorders, systemic metabolic diseases, and neurological impairments[75].

During an acute infectious gastroenteritis, there is a decline in the gut's microbial diversity[78]. There are several mechanisms explaining the disruption of the indigenous microbiota. One would be directly throughout pathogen agent-microbiota interaction. Secondly, the alteration of the microbiota might occur *via* the host's mucosal immune response, or there is the possibility of a combination of the two presented mechanisms[27,79]. In rodents, *Salmonella enterica* serovar typhimurium was shown to induce the loss of 95% of the total bacterial numbers of the intestinal tract, 7 d after the infectious episode[80]. *G. duodenalis* and *C. jejuni* can directly alter the composition of human gut microbiota[81]. Aside from the predominance of the etiologic bacterial pathogen, certain native taxa of the gut microbiome such as *Streptococci, Fusobacteria,* and *Campylobacter*, can also increase their numbers throughout the acute episode but also in the weeks following the bacterial infection[82,83].

Immediately after acute gastroenteritis with *Vibrio cholerae* (*V. cholerae*), increased levels of *V. cholerae, Streptococcus, Fusobacterium,* and *Campylobacter* species were found during a 16S rRNA gene polymerase chain reaction (PCR) analysis of the infected patients' stool samples. Two months after the first assessment, there was a decrease in *V. cholerae*, *Streptococcus, Fusobacterium,* and *Campylobacter* species, while *Ruminococcus obeum, Collinsella aerofasciens, Ruminococcus torques, Eubacterium rectale,* and *Faecalibacterium prausnitzii* increased their levels as a marker of recovery from the infection[82].

As for gastroenteritis triggered by viral agents, the alterations in the microbiota seem to be less consistent. The immune response to the viral injury is usually less harmful, resulting in a decreased diversity and the expansion of *Proteobacteria* species in some patients with viral gastroenteritis[83]. A study including patients with all-cause traveler's diarrhea investigated their gut microbial composition using fecal samples. In diarrheal patients, there was a decreased *Bacteroidota/Bacillota* ratio and changes in β-diversity, compared to healthy travelers who displayed an unexpected increased abundance of *Bacillota* phylum (*Streptococcus* and *Lactococcus* genera). Stool samples of patients with confirmed norovirus infection had an increased diversity of species characterizing their microbiota during the active infection, including *Clostridium XIVb, Bilophilia, Alistipes, Barnesiella,* and *Roseburia* species[84]. When assessing the gut microbiome correlation in symptomatic and asymptomatic patients infected with norovirus, Patin *et al*[85] found no significant difference between the alpha and beta diversity of the two groups studied. The symptomatic subjects presented relatively more species of *Bacillota* phylum, especially in the order *Clostridia,* while *Bacteroidota* phylum displayed fewer species than the asymptomatic subjects, particularly in the *Bacteroidia* order. In asymptomatic patients, three members of the genus *Parasutterella* and one in the *Nitrosomonadaceae* family were found in higher levels. The increased levels of *Bacteroidota* in the asymptomatic individuals suggest that its presence could improve the host's effort of resisting enteric viral infection or neutralizing its pathogenicity and symptoms[85]. Another study on Chinese patients with diarrhea of viral etiology reported a decreased diversity in the gut microbiota at stool sample examination, when compared to healthy individuals. *Bacillota* phylum with species of *Enterococcus, Peptostreptococcaceae, Incertae Sedi, Shigella, Weissella,* and *Clostridium* dominated the microbiota during the acute episode, while beneficial bacteria such as *Bacteroides vulgatus, Bifidobacterium,* and *Lactobacillus* species were found in decreased amounts[83]. Nelson *et al*[86] also tried to characterize the stool microbiota in norovirus-infected human patients. Their research found similarities between infected patients' and uninfected healthy individuals' microbiota. However, in a small number of infected patients there was found a significantly altered microbiome characterized by a reduced relative number of *Bacteriodota* and a corresponding increase in *Pseudomonadota.* Interestingly, the increased level of *Pseudomondota* phylum was due to a single operational taxonomic unit of *E. coli*[86]. This finding raises the concern that the alteration in gut microbiota during an acute viral gastroenteritis exposes the affected patients to some possible long term gastrointestinal complications.

SARS-CoV-2 infected patients seem to present an altered gut microbiota, characterized by the depletion of anti-inflammatory butyrate-producing bacteria and the enrichment of taxa with proinflammatory properties[87,88]. The Alpha and beta diversity index values appear to be significantly lower than in healthy individuals, all through the active infection and the recovery period[87,89]. Furthermore, an important reduction in the major bacterial phylum composition and diversity was also observed[90]. *Ruminococcusm gnavus* and *Bacteroides vulgatus* were found in increase amounts in post-acute COVID-19 patients' microbiomes, while *Faecalibacterium prausnitzii*, known for its anti-inflammatory proprieties, was characterized as decreased, when compared to healthy individuals[70].

Streptococcus, *Enterococcus,* and *Corynebacterium* species, well known as opportunistic pathogens, seem to be found in higher amounts in COVID-19 patients' stools than in healthy individuals[87]. *Fusicatenibacter*, *Romboutsia*, *Intestinibacter*, *Actinomyces,* and *Erysipelatoclostridium* species could actually be used as biomarkers in order to identify COVID-19 positive patients[91]. There is proof that the development of PI-IBS may be predicted by the composition of the salivary microbiome during acute SARS-CoV-2 infection[40,92]. Butyrate-producing bacteria showed an inverse correlation with IBS symptom onset 6 mo post-acute viral infection[93]. The gut microbiota composition was reported to be correlated with proinflammatory cytokine levels, as proof of its contribution to the immune response. The *Faecalibacterium* genus, belonging to the *Clostridia* class, was found to be decreased in COVID-19 patients during the acute episode and was inversely correlated with the IL-8 and IL-12 serum levels. The same study reported an enrichment of the *Actinomycetota* phylum and the *Propionibacteriaceae* family, which was positively correlated with the gp130/sIL-6Rb level[90]. The *Streptococcus* species was also associated with an increased expression of proinflammatory cytokines such as IL-18, TNF-α, and IFN-γ[87]. In contrast, IFN-gamma and IL-28A/IFN-12 levels were found to be negatively correlated to the class *Clostridia*, reduced in abundance in COVID-19 patients[90]. Changes in the microbiome composition were also identified in COVID-19 patients without antibiotic exposure. Depletion of beneficial commensal species and enrichment of opportunistic pathogenic bacteria, such as *Clostridium hathewayi*, *Actinomyces viscosus*, and *Bacteroides nordii,* were found in COVID-19 patients' stool samples. According to Zuo *et al*[94], the disease severity and the baseline abundance of certain genera and strains might be in close relationship, as the gut microbiota might actively influence the immune system response. Moreover, it appears that 50% of COVID-19 patients had an active intestinal infection, even in cases with no gastrointestinal complaints[94]. The deleterious effect of SARS-CoV-2 infection on beneficial gut microbiota seems to persist even after disease resolution, sustaining the possibility of the gut microbiome alteration's role in PI-IBS pathogenesis[95]. The intestinal infection persisted despite respiratory viral clearance[19,94]. There were cases described, where dysbiosis was persistent 30 d after the acute viral episode, suggesting the long-term influence of COVID-19 on gut microbiota[96]. Opportunistic pathogens such as *Collinsella aerofaciens*, *Collinsella tanakaei*, *Streptococcus infantis,* and *Morganella morganii* have been found in large amounts in stool samples with high SARS-CoV-2 infectivity. In stool samples with low-to-no viral infectivity, there were higher amounts of *Parabacteroides merdae*, *Bacteroides stercoris,* and *Lachnospiraceae bacterium 1_1_57FAA*, some of these within important role in augmenting host immunity[19,94]. Current evidence suggests that a high microbial exposure to Gram-negative bacteria could offer protective effects against COVID-19, possibly due to the increased interferon type I levels[43]. These findings sustain the idea that the gut homeostasis may suffer some alterations during the acute COVID-19 episode, independent from the presence of gastrointestinal symptoms, alterations that can persist beyond disease resolution[73]. There is evidence that COVID-19-induced impairment of the gut-lung axis might create predisposing factors for IBS development[43,97].

Moreover, there is evidence that microbiota composition prior to infection may also influence the possibility of developing an acute infection as well as PI-IBS[33]. Dicksved *et al*[98] reported that an increased abundance of *Bacteroidota* in pre-employment stool samples of abattoir workers increased the risk of developing a *C. jejuni* infection during the period of employment[98]. A *Clostridiales*-predominant microbiota type has a protective role, as an individual with such intestinal microbiota is more likely to return to a state of eubiosis after the remission of the infectious episode and pathogen clearance. A *Bacteroidota* predominant community, in contrast, may increase the risk of long-term dysbiosis after the acute episode's resolution[21].

Although the gut microbiota profile of IBS patients has been evaluated in several studies, there is not the same consistency of data regarding PI-IBS patients' gut microbiome alteration. In their study of the real-time PCR assay of rectal epithelium RNA expression, Jalanka-Tuovinen *et al*[51] concluded that the intestinal microbiota of PI-IBS patients were significantly different from healthy individuals but similar to patients with IBS-like symptoms (PI bowel disease, PI-IBS and IBS-D). They identified an "index of microbial dysbiosis" (IMD) that characterized the intestinal microbiota of PI-IBS. The IMD included 27 genus-like microbial groups including a twelvefold increased level of *Bacteroidota* phylum, including as *Bacteroides* and *Prevotella* species. The *Bacillota* phylum was less abundant, with decreased levels of various uncultured *Clostridiales* and *Clostridium* clusters. Moreover, dysbiosis was associated with gastrointestinal symptoms' severity and not with psychological symptoms. Dysbiosis was also associated with biopsy findings, such as increased levels of eotaxins, mast cells, and goblet cells and decreased EC cells[51]. Similar results were obtained by Sundin *et al*[99], when analyzing the mucosal and fecal microbiota of patients with PI-IBS. The fecal microbiota composition of PI-IBS patients was significantly different from the fecal microbiota of IBS patients and healthy individuals. Patients with PI-IBS had a reduced mucosal and fecal microbial diversity, with reduced levels of *Bacillota*, including *Clostridium* clusters IV and XIVa, and increased *Bacteroidota*, including *Bacteroides* species. The reduced diversity of the fecal microbiota was associated with increased activated lymphocytes in the lamina propria. At the level of major butyrate producer bacteria abundance, there was no difference identified between the PI-IBS patients and healthy individuals. Unlike Jalanka-Tuovinen *et al*[51], the reduced diversity of the microbiota was associated with the presence of psychological symptoms[99]. In PI-IBS patients, the *Bacteroidota* phylum seems to have a relatively greater abundance of microbes than in healthy individuals, while *Bacillota* phylum display a relative reduction in representative members in

the gut microbiota[78]. The main findings are summarized in Table 1.

MICROBIOME-DIRECTED THERAPY

Acute gastroenteritis, as mentioned above, can alter the gut microbiota, initiating the underlying mechanisms of PI-IBS. Modulation of the microbiota can be performed using probiotics, symbiotics, prebiotics, and antibiotics or by performing a fecal microbial transplantation, with the purpose of downregulating inflammation, improving barrier function, and reducing visceral sensitivity[100]. To date, there is no specific practice guideline or treatment strategies for PI-IBS. Different drug classes can be used for treating PI-IBS similar to patients with IBS in general[37].

Probiotics are known to be "live microorganisms that, when administered in adequate amounts, confer a health benefit on the host"[101]. *Lactobacillus casei* DG (LC-DG) and its postbiotic were shown to attenuate the inflammatory mucosal response in an *ex vivo* organ culture model of PI-IBS-D[102]. Similarly, Hong *et al*[103] reported that probiotic administration (*Lactobacillus acidophilus* LA5, *Bifidobacterium animalis* subsp. *lactis* BB12, and *Saccharomyces cerevisiae* var. *boulardii*) decreased proinflammatory cytokine levels in both the control and PI-IBS induced mice[103].

Saccharomyces boulardii, given 750 mg/day for a period of 6 wk, was reported to improve the quality of life and the cytokine profile in PI-IBS patients[104]. *Bifidobacterium infantis,* M-63 1 × 109 cfu/sachet/day given daily for 3 mo, restored the normal composition of the gut microbiota and improved mental health in individuals with post-flood acquired IBS[105].

Given the current evidence that serotonin levels are increased in PI-IBS patients, serotonin-based therapy is a treatment option that deserves further study[106]. Cao *et al*[107] proved that an *Lactobacillus rhamnosus* supernatant had a positive effect on serotonin transporter (SERT) expression in colon tissues of rats with PI-IBS. By modulating the microbial composition, the serotonergic imbalance can be restored, followed by the improvement in IBS symptoms[107]. Another similar study on an animal model evaluated the efficacy of a *Bacillus subtilis* (*B. subtilis*), *Enterococcus faecium,* and *Enterococcus faecalis* (*E. faecalis*) supernatant, administrated in PI-IBS rats. The researchers reported that the supernatants could upregulate the expression level of SERT in intestinal cells, mentioning the fact that the combined supernatants of *B. subtilis* and *E. faecalis* had a superior effect to the administration of a single supernatant[108]. Studies regarding prebiotic and symbiotic use in PI-IBS patients are not available.

Fecal microbiota transplantation (FMT) is used in order to restore microbial dysbiosis by transferring a healthy microbiome to an individual with an alteration of microbial composition[109]. FMT has shown benefits in IBS patients. However, there is a lack of data on FMT use in PI-IBS. A recent randomized clinical trial assessed FMT's safety as well as its clinical and microbiological efficacy in patients with PI-IBS. The results demonstrated FMT's effectiveness compared to traditional pharmacotherapy, its safety, and tolerability[110].

However, FMT could be used in reestablishing the microbiota homeostasis following acute gastroenteritis, with the purpose of decreasing the risk of PI-IBS development. It is known that FMT is recommended for recurrent or refractory *C. difficile* enterocolitis, as a proved effective therapy[111]. There is evidence that FMT treatment can improve gut microbiota alteration in recovered COVID-19 patients, particularly in those who presented severe gastrointestinal symptomatology during the acute phase[112].

Jin *et al*[113] assessed the action of rifaximin on the VHS, barrier function, gut inflammation, and microbiota in a PI-IBS mouse model. Rifaximin administration improved the VHS, recovered the intestinal barrier function, and inhibited low-grade inflammation in the colon and ileum, without changing the composition and diversity of the gut microbiota[113]. However, Harris *et al*[114] and Tuteja *et al*[115] reported no benefit of rifaximin therapy on PI-IBS patients.

The results of mesalazine's efficacy in treating PI-IBS patients are contradictory. Lam *et al*[116] reported a significant improvement in symptoms such as abdominal pain, urgency, and stool consistency, when mesalazine was given to a small group of PI-IBS patients[116]. Bafutto *et al*[117] found that mesalazine administration in PI-IBS patients decreased the stool frequency and improved its form and consistency, after 30 d of treatment[117]. In contrast, another double-blind controlled trial including a small number of patients with diarrhea predominant PI-IBS reported no positive effect on clinical symptoms or quality of life[118]. However, mesalazine use during the acute infectious gastroenteritis may have a protective effect on PI-IBS development, as reported by a study on patients affected by hemorrhagic enterocolitis with *Shiga*-like toxin-producing *E. coli*[119]. Dunlop *et al*[120] found a significant reduction in the T- lymphocyte counts in the rectal tissue of PI-IBS patients treated with prednisone, although there was no positive effect on the EC cell count or symptom improvement[120].

Bile acid malabsorption may occur after an episode of acute gastroenteritis. It is confirmed that cholestyramine administration can alleviate symptoms in PI-IBS patients, especially with diarrhea symptoms[121]. The information regarding the therapeutic options in PI-IBS are summarized in Table 2.

Table 1 Alterations of the gut microbiota observed during acute gastroenteritis and during post-infectious irritable bowel syndrome

Ref.	Subjects/methods	Sample and techniques	Microbiota alterations	Other findings
Jalanka-Tuovinen *et al*[51], 2014	11 postinfection IBS, 11 postinfection bowel dysfunction, 12 postinfection without bowel dysfunction, 12 IBS-D, 11 healthy controls adults	16S rRNA gene phylogenetic microarray analysis with HITChip, 16S rRNA gene qPCR with group and species-specific primers of feacal sample	Index of microbial dysbiosis" comprised of 27 genus-like groups including: ↑ *Bacteroidota* including various *Bacteroides and Prevotella* species, ↓*Bacillota* including various uncultured *Clostridiales*, and *Clostridium* clusters	Dysbiosis was associated with bowel, not psychological symptoms; Dysbiosis associated biopsy findings: ↑eotaxin, mast cells, goblet cells, ↓enterochromaffin cells; Dysbiosis associated RNA expression pathways: ↑serotonin transport, condensed chromosome, B cell antigen receptor, ↓caspase
Hsiao *et al* [82], 2014	7 adults with *V. cholerae* AGE history, 50 healthy children, 12 healthy adults	16S rRNA gene PCR, V4 region analysis of faecal sample	One week after AGE: ↑*V. cholerae Streptococcus* spp *Fusobacterium* spp *Campylobacter* spp	Two months after AGE (recovery period): ↓*V. cholerae Streptococcus* spp *Fusobacterium* spp *Campylobacter* spp, ↑ species indicating recovery *Ruminococcus obeum*, *Collinsella aerofasciens Ruminococcus torques*, *Eubacterium rectale Faecalibacterium prausnitzii*
Ma *et al* [83], 2011	13 Adenovirus diarrhea, 13 Rotavirus diarrhea, 13 Astrovirus diarrhea, 13 Norvirus diarrhea, 6 control children	16S rRNA gene PCR, V3 region analysis of faecal sample	↓Diversity in diarrheal patients, ↑*Enterococcus*, *Peptostreptococcaceae*, *Incertae Sedi*, *Shigella*, *Weissella* spp	↓*Bacteroides vulgatus Bifidobacterium*, *Lactobacillus* spp
Youmans *et al*[84], 2015	111 all-cause traveler's diarrhea/12 healthy travelers	16S rRNA gene PCR, V3 and V5 regions analysis of faecal sample	↓*Bacteroidota: Bacillota* ratio in diarrheal patients; ↑Species diversity during norovirus infection; ↑*Clostridium XIVb Bilophilia Alistipes Barnesiella*, *Roseburia* spp during norovirus infection	↑*Bacillota* phylum *Streptococcus Lactococcus* spp in healthy travelers (unexpected)
Patin *et al* [88], 2020	4 symptomatic and 5 asymptomatic norovirus infected adults	16S rRNA gene analysis of faecal sample	Post norovirus challenge: ↑*Bacillota* phylum, particularly *Clostridia*, ↓*Bacteroidota Pseudomonadota*	Prior to norovirus challenge: Asymptomatic patients had ↑*Bacteroidota* phylum and ↓*Clostridia* compared to symptomatic
Nelson *et al*[86], 2012	38 norovirus infection, 22 healthy controls	16S rRNA gene 454 pyrosequencing, V3-V5 regions analysis of faecal sample	A subset (approximately 1/5) patients with norovirus had: ↓diversity, ↑*Pseudomonadota* phylum, *Enterobacteriaceae* family	*Escherichia coli* diversity and virulence was not associated with norovirus infection
Cheng *et al* [87], 2022	COVID-19 acute and recovery phase; Non COVID-19	Meta-analysis of 16S rRNA microbial data	↓Ruminococcus Faecalibacterium Roseburia, Coprococcus genus, ↑ Fusobacterium Streptococcus in recovery/post-recovery COVID-19 compared to non COVID-19	↓Clostridium clostridioforme, ↑ Bifidobacterium breve in COVID-19 compared to recovery/post-recovery COVID-19
Liu *et al* [93], 2022	68 COVID-19 patients, 68 non-COVID-19 patients	Shotgun metagenomic sequencing	At 6 mo follow up 76% developed PACS; Non-PACS showed recovered gut microbiome profile at 6 mo comparable to that of non-COVID-19 controls; ↑ *Ruminococcus gnavus*, *Bacteroides vulgatus* and ↓*Faecalibacterium prausnitzii* in PACS	Butyrate-producing bacteria, including *Bifidobacterium pseudocatenulatum* and *Faecalibacterium prausnitzii* showed the largest inverse correlation with PACS at 6 mo
Zuo *et al* [95], 2020	15 Acute COVID-patients, 6 community acquired pneumonia patients, 15 healthy controls	Shotgun metagenomic sequencing	Antibiotic naïve patients ↑*Clostridium hathewayi*, *Actinomyces viscosus*, and *Bacteroides nordii* compared with controls; COVID-19 with antibiotic use ↓ *Faecalibacterium prausnitzii*, *Lachnospiraceae bacterium 5_1_63FAA*, *Eubacterium rectale*, *Ruminococcus obeum*, and *Dorea formicigenerans* compared with COVID-19 naïve patients	Baseline abundance of *Coprobacillus*, *Clostridium ramosum*, and *Clostridium hathewayi* correlated with COVID-19 severity: There was an inverse correlation between abundance of *Faecalibacterium prausnitzii* and disease severity; Depletion of symbionts and enrichment of opportunistic pathogens persisted after clearance of SARS-CoV-2
Yeoh *et al* [96], 2021	100 COVID-19 patients, 78 non COVID-19 controls	Shotgun sequencing total DNA extraction from stool sample	Patients with COVID-19 were depleted in *Faecalibacterium prausnitzii*, *Eubacterium rectale* and several bifidobacterial species, which remain low up to 30 d from disease resolution	Composition of the gut microbiota in patients with COVID-19 is concordant with disease severity and magnitude of plasma concentrations of several inflammatory cytokines, chemokines and blood markers of tissue damage
Sundin *et al*[99], 2015	13 PI-IBS patients, 19 general IBS patients, 16 healthy controls	HITChip for mucosal and fecal microbiota	↓Mucosal and faecal diversity *Bacillota* phylum including *Clostridium* clusters IV and XIVa, ↑*Bacteroidota* phyum including *Bacteroides* spp	Reduced diversity was associated with psychological symptoms and increased activated lamina propria lymphocytes. Did not find a difference in major butyrate producer abundance

AGE: Acute gastroenteritis; COVID-19: Coronavirus disease 2019; IBS-D: Diarrhea-predominant irritable bowel syndrome; PACS: Post-acute coronavirus disease 2019 syndrome; PI-IBS: Post-infectious irritable bowel syndrome; qPCR: Quantitative polymerase chain reaction; SARS-CoV-2: Severe acute respiratory syndrome coronavirus 2.

Table 2 Post-infectious irritable bowel syndrome therapeutic options

Ref.	Therapeutic intervention	Outcome
Compare *et al* [102], 2017	*Lactobacillus casei* DG + postbiotic	↓The inflammatory mucosal response in an *ex vivo* organ culture model of PI-IBS-D
Hong *et al* [103], 2019	*Lactobacillus acidophilus* LA5, *Bifidobacterium animalis* subsp. *lactis* BB12 and *Saccharomyces cerevisiae* var. *boulardii*)	↓Pro-inflammatory cytokine levels in both the control and PI-IBS induced mice
Abbas *et al* [104], 2014	*Saccharomyces boulardii*	Improved the quality of life and the cytokine profile in PI-IBS patients
Lee *et al*[106], 2017	*Bifidobacterium infantis*	Restored the normal composition of gut microbiota and improved mental health among individuals with post-flood acquired IBS
Cao *et al* [107], 2018	*Lactobacillus rhamnosus* supernatant	Had a positive effect on SERT expression in colon tissues of rats with PI-IBS, improving IBS symptoms in PI-IBS rats
Chen *et al* [108], 2022	*Enterococcus faecium* and *Enterococcus faecalis* supernatant, in PI-IBS rats	The supernatants of B. subtilis, *Enterococcus faecium*, and *Enterococcus faecalis* can upregulate SERT expression in intestinal epithelial cells and the intestinal tissues in the rat model of PI-IBS
Tkach *et al* [110], 2022	RCT, low FODMAP diet + Otilonium Bromide + a multi-strain probiotic *vs* FMT procedure	FMT proved effectiveness in restoring normal gut microbiota and ameliorating PI-IBS symptoms, compared to traditional pharmacotherapy, as well as a high degree of safety and good tolerability
Liu *et al*[111], 2021	FMT procedure	FMT can partially restore the gut dysbiosis in COVID-19 patients by increasing the relative abundance of *Actinobacteria* (15.0%) and reducing *Proteobacteria* (2.8%) at the phylum level. At the genera level, *Bifidobacterium* and *Faecalibacterium* had significantly increased after FMT
Jin *et al*[113], 2017	Rifamixin in PI-IBS rats	Rifaximin alleviated visceral hypersensitivity, recoverd intestinal barrier function and inhibited low-grade inflammation in colon and ileum of PI-IBS rats. Exerts anti-inflammatory effects with only a minimal action on the overall composition and diversity of the gut microbiota
Harris *et al* [114], 2019	Rifamixin *vs* placebo in veterans with IBS	Rifaximin was not associated with signifcant improvement in global symptoms, abdominal pain, stool frequency, urgency, bloating, or stool consistency
Tuteja *et al* [115], 2019	Rifamixin *vs* placebo in veterans with IBS	Rifaximin was not effective in improving IBS symptoms and QOL in GW veterans with non-constipated IBS
Lam *et al* [116], 2016	Mesalazine *vs* placebo	Mesalazine was no better than placebo in relieving symptoms of abdominal discomfort or disturbed bowel habit. Mesalazine did not reduce mast cell percentage area stained. A subgroup of patients with postinfectious IBS may benefit from mesalazine
Bafutto *et al* [117], 2011	Mesalazine in PI-IBS patients compared to non-infective IBS patients	Mesalazine reduced key symptoms of postinfectious irritable bowel syndrome and noninfective irritable bowel syndrome with diarrhea patients, with no statistical difference between IBS and PI-IBS
Tuteja *et al* [118], 2012	Mesalazine *vs* placebo	There was no significant improvement in global symptoms or overall QOL with mesalazine in patients with PI-IBS
Andresen *et al*[119], 2016	Mesalazine during the AGE with STEC	Mesalazine administration during AGE with STEC might be a protective factor for PI-IBS
Dunlop *et al* [120], 2003	Prednisolone *vs* placebo	Prednisolone does not appear to reduce the number of enterochromaffin cells or cause an improvement in symptoms in PI-IBS

AGE: Acute gastroenteritis; FMT: Fecal microbial transplantation; IBS-D: Diarrhea-predominant irritable bowel syndrome; PI-IBS: Post-infectious irritable bowel syndrome; RCT: Randomised controlled trial; QOL: Quality of life; SERT: Serotonin transporter; STEC: Shiga-like toxin-producing *Escherichia coli*.

CONCLUSION

Acute gastroenteritis can significantly increase the risk of developing IBS, a chronic gastrointestinal pathology with high health-care utilization. Current studies in humans as well as animal models describe specific host-pathogen interactions that may lead to the onset of post-infection IBS symptoms. There is no curative treatment option for PI-IBS, and patients rely only on symptomatic therapy. There are numerous studies on IBS treatment options. However, there is a lack of data regarding PI-IBS therapeutic management, and there is a great need for evidence-based recommendations in post-acute

gastroenteritis IBS.

These advancements in understanding will be helpful in elaborating specific biomarkers used to identify patients with a high risk of developing IBS symptoms following an acute infectious gastroenteritis, as well as designing targeted pharmacotherapy. Microbial restoration, augmentation of barrier function, and targeting VHS remain the most promising areas for therapeutic interventions and represent a future research perspective.

FOOTNOTES

Author contributions: Lupu VV, Bozomitu L, Starcea IM, Adam Raileanu A, and Lupu A wrote the initial draft; Ghiciuc CM, Stefanescu G, Mihai CM, Popp A, and Sasaran MO reviewed and edited the article; Ghiciuc CM, Stefanescu G, Mihai CM, Popp A, Sasaran MO, Bozomitu L, Starcea IM, Adam Raileanu A and Lupu A contributed equally with Lupu VV to this article.

Conflict-of-interest statement: Authors declare no conflict of interests for this article.

Open-Access: This article is an open-access article that was selected by an in-house editor and fully peer-reviewed by external reviewers. It is distributed in accordance with the Creative Commons Attribution NonCommercial (CC BY-NC 4.0) license, which permits others to distribute, remix, adapt, build upon this work non-commercially, and license their derivative works on different terms, provided the original work is properly cited and the use is non-commercial. See: https://creativecommons.org/Licenses/by-nc/4.0/

Country/Territory of origin: Romania

ORCID number: Vasile Valeriu Lupu 0000-0003-2640-8795; Cristina Mihaela Ghiciuc 0000-0003-1791-0425; Gabriela Stefanescu 0000-0002-1394-8648; Cristina Maria Mihai 0000-0001-8844-0593; Alina Popp 0000-0002-7809-5762; Maria Oana Sasaran 0000-0001-8156-7460; Iuliana Magdalena Starcea 0000-0002-3937-7425; Anca Adam Raileanu 0000-0003-1979-8174; Ancuta Lupu 0000-0001-8147-3632.

S-Editor: Zhang H
L-Editor: A
P-Editor: Ma YJ

REFERENCES

1 **Drossman DA**, Hasler WL. Rome IV-Functional GI Disorders: Disorders of Gut-Brain Interaction. *Gastroenterology* 2016; **150**: 1257-1261 [PMID: 27147121 DOI: 10.1053/j.gastro.2016.03.035]
2 **Ford AC**, Sperber AD, Corsetti M, Camilleri M. Irritable bowel syndrome. *Lancet* 2020; **396**: 1675-1688 [PMID: 33049223 DOI: 10.1016/S0140-6736(20)31548-8]
3 **Oka P**, Parr H, Barberio B, Black CJ, Savarino EV, Ford AC. Global prevalence of irritable bowel syndrome according to Rome III or IV criteria: a systematic review and meta-analysis. *Lancet Gastroenterol Hepatol* 2020; **5**: 908-917 [PMID: 32702295 DOI: 10.1016/S2468-1253(20)30217-X]
4 **Mearin F**, Lacy BE, Chang L, Chey WD, Lembo AJ, Simren M, Spiller R. Bowel Disorders. *Gastroenterology* 2016 [PMID: 27144627 DOI: 10.1053/j.gastro.2016.02.031]
5 **Canavan C**, West J, Card T. The epidemiology of irritable bowel syndrome. *Clin Epidemiol* 2014; **6**: 71-80 [PMID: 24523597 DOI: 10.2147/CLEP.S40245]
6 **Spiegel BM**. The burden of IBS: looking at metrics. *Curr Gastroenterol Rep* 2009; **11**: 265-269 [PMID: 19615301 DOI: 10.1007/s11894-009-0039-x]
7 **Chen YQ**, Yang X, Xu W, Yan Y, Chen XM, Huang ZQ. Knockdown of lncRNA TTTY15 alleviates myocardial ischemia-reperfusion injury through the miR-374a-5p/FOXO1 axis. *IUBMB Life* 2021; **73**: 273-285 [PMID: 33296140 DOI: 10.1002/iub.2428]
8 **Ansari MH**, Ebrahimi M, Fattahi MR, Gardner MG, Safarpour AR, Faghihi MA, Lankarani KB. Viral metagenomic analysis of fecal samples reveals an enteric virome signature in irritable bowel syndrome. *BMC Microbiol* 2020; **20**: 123 [PMID: 32429898 DOI: 10.1186/s12866-020-01817-4]
9 **Pimentel M**, Lembo A. Microbiome and Its Role in Irritable Bowel Syndrome. *Dig Dis Sci* 2020; **65**: 829-839 [PMID: 32026278 DOI: 10.1007/s10620-020-06109-5]
10 **Singh P**, Lembo A. Emerging Role of the Gut Microbiome in Irritable Bowel Syndrome. *Gastroenterol Clin North Am* 2021; **50**: 523-545 [PMID: 34304786 DOI: 10.1016/j.gtc.2021.03.003]
11 **Takakura W**, Kudaravalli P, Chatterjee C, Pimentel M, Riddle MS. Campylobacter infection and the link with Irritable Bowel Syndrome: on the pathway towards a causal association. *Pathog Dis* 2022; **80** [PMID: 35134916 DOI: 10.1093/femspd/ftac003]
12 **Cambrea SC**, Petcu LC, Mihai CM, Hangan TL, Iliescu DM. Influence of environmental factors about evolution of shigellosis in constanta county of Romania. *J Environ Prot Ecol* 2019; **20**: 986-994
13 **Halichidis S**, Balasa AL, Ionescu EV, Iliescu MG, Cambrea SC, Petcu LC, Mihai CM. Evolution of salmonellosis in Constanta area in correlation with environmental factors. *J Environ Prot Ecol* 2019; 20: 1496-1504

14 **Lashermes A**, Boudieu L, Barbier J, Sion B, Gelot A, Barnich N, Ardid D, Carvalho FA. Adherent-Invasive E. coli enhances colonic hypersensitivity and P2X receptors expression during post-infectious period. *Gut Microbes* 2018; **9**: 26-37 [PMID: 28806140 DOI: 10.1080/19490976.2017.1361091]

15 **Kim HS**, Lim JH, Park H, Lee SI. Increased immunoendocrine cells in intestinal mucosa of postinfectious irritable bowel syndrome patients 3 years after acute Shigella infection--an observation in a small case control study. *Yonsei Med J* 2010; **51**: 45-51 [PMID: 20046513 DOI: 10.3349/ymj.2010.51.1.45]

16 **Saha S**, Sehgal K, Singh S, Grover M, Pardi D, Khanna S. Postinfection Irritable Bowel Syndrome Following Clostridioides difficile Infection: A Systematic-review and Meta-analysis. *J Clin Gastroenterol* 2022; **56**: e84-e93 [PMID: 34049374 DOI: 10.1097/MCG.0000000000001536]

17 **Hassan E**, Baldridge MT. Norovirus encounters in the gut: multifaceted interactions and disease outcomes. *Mucosal Immunol* 2019; **12**: 1259-1267 [PMID: 31501514 DOI: 10.1038/s41385-019-0199-4]

18 **Baaleman DF**, Di Lorenzo C, Benninga MA, Saps M. The Effects of the Rome IV Criteria on Pediatric Gastrointestinal Practice. *Curr Gastroenterol Rep* 2020; **22**: 21 [PMID: 32193635 DOI: 10.1007/s11894-020-00760-8]

19 **Cooney J**, Appiahene P, Findlay R, Al-Hillawi L, Rafique K, Laband W, Shandro B, Poullis A. COVID-19 infection causing residual gastrointestinal symptoms - a single UK centre case series. *Clin Med (Lond)* 2022; **22**: 181-183 [PMID: 35105680 DOI: 10.7861/clinmed.2021-0522]

20 **Litleskare S**, Rortveit G, Eide GE, Hanevik K, Langeland N, Wensaas KA. Prevalence of Irritable Bowel Syndrome and Chronic Fatigue 10 Years After Giardia Infection. *Clin Gastroenterol Hepatol* 2018; **16**: 1064-1072.e4 [PMID: 29378314 DOI: 10.1016/j.cgh.2018.01.022]

21 **Barbara G**, Grover M, Bercik P, Corsetti M, Ghoshal UC, Ohman L, Rajilić-Stojanović M. Rome Foundation Working Team Report on Post-Infection Irritable Bowel Syndrome. *Gastroenterology* 2019; **156**: 46-58.e7 [PMID: 30009817 DOI: 10.1053/j.gastro.2018.07.011]

22 **Thabane M**, Marshall JK. Post-infectious irritable bowel syndrome. *World J Gastroenterol* 2009; **15**: 3591-3596 [PMID: 19653335 DOI: 10.3748/wjg.15.3591]

23 **Moshiree B**, Heidelbaugh JJ, Sayuk GS. A Narrative Review of Irritable Bowel Syndrome with Diarrhea: A Primer for Primary Care Providers. *Adv Ther* 2022; **39**: 4003-4020 [PMID: 35869354 DOI: 10.1007/s12325-022-02224-z]

24 **Ruigómez A**, García Rodríguez LA, Panés J. Risk of irritable bowel syndrome after an episode of bacterial gastroenteritis in general practice: influence of comorbidities. *Clin Gastroenterol Hepatol* 2007; **5**: 465-469 [PMID: 17445753 DOI: 10.1016/j.cgh.2007.02.008]

25 **Ghaffari P**, Shoaie S, Nielsen LK. Irritable bowel syndrome and microbiome; Switching from conventional diagnosis and therapies to personalized interventions. *J Transl Med* 2022; **20**: 173 [PMID: 35410233 DOI: 10.1186/s12967-022-03365-z]

26 **Lewis SJ**, Heaton KW. Stool form scale as a useful guide to intestinal transit time. *Scand J Gastroenterol* 1997; **32**: 920-924 [PMID: 9299672 DOI: 10.3109/00365529709011203]

27 **Beatty JK**, Bhargava A, Buret AG. Post-infectious irritable bowel syndrome: mechanistic insights into chronic disturbances following enteric infection. *World J Gastroenterol* 2014; **20**: 3976-3985 [PMID: 24744587 DOI: 10.3748/wjg.v20.i14.3976]

28 **Marshall JK**, Thabane M, Garg AX, Clark WF, Moayyedi P, Collins SM; Walkerton Health Study Investigators. Eight year prognosis of postinfectious irritable bowel syndrome following waterborne bacterial dysentery. *Gut* 2010; **59**: 605-611 [PMID: 20427395 DOI: 10.1136/gut.2009.202234]

29 **Klem F**, Wadhwa A, Prokop LJ, Sundt WJ, Farrugia G, Camilleri M, Singh S, Grover M. Prevalence, Risk Factors, and Outcomes of Irritable Bowel Syndrome After Infectious Enteritis: A Systematic Review and Meta-analysis. *Gastroenterology* 2017; **152**: 1042-1054.e1 [PMID: 28069350 DOI: 10.1053/j.gastro.2016.12.039]

30 **Borgaonkar MR**, Ford DC, Marshall JK, Churchill E, Collins SM. The incidence of irritable bowel syndrome among community subjects with previous acute enteric infection. *Dig Dis Sci* 2006; **51**: 1026-1032 [PMID: 16758307 DOI: 10.1007/s10620-006-9348-1]

31 **Villani AC**, Lemire M, Thabane M, Belisle A, Geneau G, Garg AX, Clark WF, Moayyedi P, Collins SM, Franchimont D, Marshall JK. Genetic risk factors for post-infectious irritable bowel syndrome following a waterborne outbreak of gastroenteritis. *Gastroenterology* 2010; **138**: 1502-1513 [PMID: 20044998 DOI: 10.1053/j.gastro.2009.12.049]

32 **Kamp KJ**, Cain KC, Utleg A, Burr RL, Raftery D, Luna RA, Shulman RJ, Heitkemper MM. Bile Acids and Microbiome Among Individuals With Irritable Bowel Syndrome and Healthy Volunteers. *Biol Res Nurs* 2021; **23**: 65-74 [PMID: 32666807 DOI: 10.1177/1099800420941255]

33 **Berumen A**, Edwinson AL, Grover M. Post-infection Irritable Bowel Syndrome. *Gastroenterol Clin North Am* 2021; **50**: 445-461 [PMID: 34024451 DOI: 10.1016/j.gtc.2021.02.007]

34 **Svendsen AT**, Bytzer P, Engsbro AL. Systematic review with meta-analyses: does the pathogen matter in post-infectious irritable bowel syndrome? *Scand J Gastroenterol* 2019; **54**: 546-562 [PMID: 31112663 DOI: 10.1080/00365521.2019.1607897]

35 **Iacob T**, Țățulescu DF, Lupșe MS, Dumitrașcu DL. Post-infectious irritable bowel syndrome after a laboratory-proven enteritis. *Exp Ther Med* 2020; **20**: 3517-3522 [PMID: 32905134 DOI: 10.3892/etm.2020.9018]

36 **Shariati A**, Fallah F, Pormohammad A, Taghipour A, Safari H, Chirani AS, Sabour S, Alizadeh-Sani M, Azimi T. The possible role of bacteria, viruses, and parasites in initiation and exacerbation of irritable bowel syndrome. *J Cell Physiol* 2019; **234**: 8550-8569 [PMID: 30480810 DOI: 10.1002/jcp.27828]

37 **Sadeghi A**, Biglari M, Nasseri Moghaddam S. Post-infectious Irritable Bowel Syndrome: A Narrative Review. *Middle East J Dig Dis* 2019; **11**: 69-75 [PMID: 31380002 DOI: 10.15171/mejdd.2019.130]

38 **Schwille-Kiuntke J**, Mazurak N, Enck P. Systematic review with meta-analysis: post-infectious irritable bowel syndrome after travellers' diarrhoea. *Aliment Pharmacol Ther* 2015; **41**: 1029-1037 [PMID: 25871571 DOI: 10.1111/apt.13199]

39 **Donnachie E**, Schneider A, Mehring M, Enck P. Incidence of irritable bowel syndrome and chronic fatigue following GI infection: a population-level study using routinely collected claims data. *Gut* 2018; **67**: 1078-1086 [PMID: 28601847 DOI: 10.1136/gutjnl-2017-313713]

40 **Marshall JK**, Thabane M, Borgaonkar MR, James C. Postinfectious irritable bowel syndrome after a food-borne outbreak of acute gastroenteritis attributed to a viral pathogen. *Clin Gastroenterol Hepatol* 2007; **5**: 457-460 [PMID: 17289440 DOI: 10.1016/j.cgh.2006.11.025]

41 **Farsi F**, Zonooz SR, Ebrahimi Z, Jebraili H, Morvaridi M, Azimi T, Sikaroudi MK, Heshmati J, Khorrami S, Mokhtare M, Faghihi A, Masoodi M. The Incidence of Post-infectious Irritable Bowel Syndrome, Anxiety, and Depression in Iranian Patients with Coronavirus Disease 2019 Pandemic: A Cross-Sectional Study. *Turk J Gastroenterol* 2022; **33**: 1033-1042 [PMID: 36098366 DOI: 10.5152/tjg.2022.21651]

42 **Hussain I**, Cher GLY, Abid MA, Abid MB. Role of Gut Microbiome in COVID-19: An Insight Into Pathogenesis and Therapeutic Potential. *Front Immunol* 2021; **12**: 765965 [PMID: 34721437 DOI: 10.3389/fimmu.2021.765965]

43 **Cheung KS**, Hung IFN, Chan PPY, Lung KC, Tso E, Liu R, Ng YY, Chu MY, Chung TWH, Tam AR, Yip CCY, Leung KH, Fung AY, Zhang RR, Lin Y, Cheng HM, Zhang AJX, To KKW, Chan KH, Yuen KY, Leung WK. Gastrointestinal Manifestations of SARS-CoV-2 Infection and Virus Load in Fecal Samples From a Hong Kong Cohort: Systematic Review and Meta-analysis. *Gastroenterology* 2020; **159**: 81-95 [PMID: 32251668 DOI: 10.1053/j.gastro.2020.03.065]

44 **Sultan S**, Altayar O, Siddique SM, Davitkov P, Feuerstein JD, Lim JK, Falck-Ytter Y, El-Serag HB; AGA Institute. AGA Institute Rapid Review of the Gastrointestinal and Liver Manifestations of COVID-19, Meta-Analysis of International Data, and Recommendations for the Consultative Management of Patients with COVID-19. *Gastroenterology* 2020; **159**: 320-334.e27 [PMID: 32407808 DOI: 10.1053/j.gastro.2020.05.001]

45 **Pan L**, Mu M, Yang P, Sun Y, Wang R, Yan J, Li P, Hu B, Wang J, Hu C, Jin Y, Niu X, Ping R, Du Y, Li T, Xu G, Hu Q, Tu L. Clinical Characteristics of COVID-19 Patients With Digestive Symptoms in Hubei, China: A Descriptive, Cross-Sectional, Multicenter Study. *Am J Gastroenterol* 2020; **115**: 766-773 [PMID: 32287140 DOI: 10.14309/ajg.0000000000000620]

46 **Montazeri M**, Maghbouli N, Jamali R, Sharifi A, Pazoki M, Salimzadeh A, Barzegari B, Rafiei N, Mansouri ES, Hadadi A. Clinical Characteristics of COVID-19 Patients with Gastrointestinal Symptoms. *Arch Iran Med* 2021; **24**: 131-138 [PMID: 33636982 DOI: 10.34172/aim.2021.21]

47 **Austhof E**, Bell ML, Riddle MS, Catalfamo C, McFadden C, Cooper K, Scallan Walter E, Jacobs E, Pogreba-Brown K. Persisting gastrointestinal symptoms and post-infectious irritable bowel syndrome following SARS-CoV-2 infection: results from the Arizona CoVHORT. *Epidemiol Infect* 2022; **150**: e136 [PMID: 35801302 DOI: 10.1017/S0950268822001200]

48 **Noviello D**, Costantino A, Muscatello A, Bandera A, Consonni D, Vecchi M, Basilisco G. Functional gastrointestinal and somatoform symptoms five months after SARS-CoV-2 infection: A controlled cohort study. *Neurogastroenterol Motil* 2022; **34**: e14187 [PMID: 34060710 DOI: 10.1111/nmo.14187]

49 **Siyal M**, Abbas Z, Ashraf J, Ali Qadeer M, Altaf A. Incidence and predisposing factors for de novo post-COVID-19 irritable bowel syndrome. *Eur J Gastroenterol Hepatol* 2023; **35**: 59-63 [PMID: 36468570 DOI: 10.1097/MEG.0000000000002475]

50 **Marasco G**, Cremon C, Barbaro MR, Cacciari G, Falangone F, Kagramanova A, Bordin D, Drug V, Miftode E, Fusaroli P, Mohamed SY, Ricci C, Bellini M, Rahman MM, Melcarne L, Santos J, Lobo B, Bor S, Yapali S, Akyol D, Sapmaz FP, Urun YY, Eskazan T, Celebi A, Kacmaz H, Ebik B, Binicier HC, Bugdayci MS, Yağcı MB, Pullukcu H, Kaya BY, Tureyen A, Hatemi İ, Koc ES, Sirin G, Calıskan AR, Bengi G, Alıs EE, Lukic S, Trajkovska M, Hod K, Dumitrascu D, Pietrangelo A, Corradini E, Simren M, Sjölund J, Tornkvist N, Ghoshal UC, Kolokolnikova O, Colecchia A, Serra J, Maconi G, De Giorgio R, Danese S, Portincasa P, Di Sabatino A, Maggio M, Philippou E, Lee YY, Salvi D, Venturi A, Borghi C, Zoli M, Gionchetti P, Viale P, Stanghellini V, Barbara G; GI-COVID19 study group. Post COVID-19 irritable bowel syndrome. *Gut* 2022 [PMID: 36591612 DOI: 10.1136/gutjnl-2022-328483]

51 **Jalanka-Tuovinen J**, Salojärvi J, Salonen A, Immonen O, Garsed K, Kelly FM, Zaitoun A, Palva A, Spiller RC, de Vos WM. Faecal microbiota composition and host-microbe cross-talk following gastroenteritis and in postinfectious irritable bowel syndrome. *Gut* 2014; **63**: 1737-1745 [PMID: 24310267 DOI: 10.1136/gutjnl-2013-305994]

52 **Devanarayana NM**, Rajindrajith S. Irritable bowel syndrome in children: Current knowledge, challenges and opportunities. *World J Gastroenterol* 2018; **24**: 2211-2235 [PMID: 29881232 DOI: 10.3748/wjg.v24.i21.2211]

53 **Brierley SM**, Linden DR. Neuroplasticity and dysfunction after gastrointestinal inflammation. *Nat Rev Gastroenterol Hepatol* 2014; **11**: 611-627 [PMID: 25001973 DOI: 10.1038/nrgastro.2014.103]

54 **Balemans D**, Mondelaers SU, Cibert-Goton V, Stakenborg N, Aguilera-Lizarraga J, Dooley J, Liston A, Bulmer DC, Vanden Berghe P, Boeckxstaens GE, Wouters MM. Evidence for long-term sensitization of the bowel in patients with post-infectious-IBS. *Sci Rep* 2017; **7**: 13606 [PMID: 29051514 DOI: 10.1038/s41598-017-12618-7]

55 **Spiller RC**, Jenkins D, Thornley JP, Hebden JM, Wright T, Skinner M, Neal KR. Increased rectal mucosal enteroendocrine cells, T lymphocytes, and increased gut permeability following acute Campylobacter enteritis and in post-dysenteric irritable bowel syndrome. *Gut* 2000; **47**: 804-811 [PMID: 11076879 DOI: 10.1136/gut.47.6.804]

56 **Gwee KA**, Collins SM, Read NW, Rajnakova A, Deng Y, Graham JC, McKendrick MW, Moochhala SM. Increased rectal mucosal expression of interleukin 1beta in recently acquired post-infectious irritable bowel syndrome. *Gut* 2003; **52**: 523-526 [PMID: 12631663 DOI: 10.1136/gut.52.4.523]

57 **Rodiño-Janeiro BK**, Vicario M, Alonso-Cotoner C, Pascua-García R, Santos J. A Review of Microbiota and Irritable Bowel Syndrome: Future in Therapies. *Adv Ther* 2018; **35**: 289-310 [PMID: 29498019 DOI: 10.1007/s12325-018-0673-5]

58 **Flynn AN**, Wang A, McKay DM, Buret AG. Apoptosis-inducing factor contributes to epithelial cell apoptosis induced by enteropathogenic Escherichia coli. *Can J Physiol Pharmacol* 2011; **89**: 143-148 [PMID: 21326346 DOI: 10.1139/y11-002]

59 **Mearin F**, Perelló A, Balboa A, Perona M, Sans M, Salas A, Angulo S, Lloreta J, Benasayag R, García-Gonzalez MA, Pérez-Oliveras M, Coderch J. Pathogenic mechanisms of postinfectious functional gastrointestinal disorders: results 3 years after gastroenteritis. *Scand J Gastroenterol* 2009; **44**: 1173-1185 [PMID: 19711225 DOI: 10.1080/00365520903171276]

60 **Bennet SM**, Polster A, Törnblom H, Isaksson S, Capronnier S, Tessier A, Le Nevé B, Simrén M, Öhman L. Global Cytokine Profiles and Association With Clinical Characteristics in Patients With Irritable Bowel Syndrome. *Am J*

Gastroenterol 2016; **111**: 1165-1176 [PMID: 27272011 DOI: 10.1038/ajg.2016.223]

61 **Dong LW**, Sun XN, Ma ZC, Fu J, Liu FJ, Huang BL, Liang DC, Sun DM, Lan C. Increased Vδ1γδT cells predominantly contributed to IL-17 production in the development of adult human post-infectious irritable bowel syndrome. *BMC Gastroenterol* 2021; **21**: 271 [PMID: 34193069 DOI: 10.1186/s12876-021-01722-8]

62 **Dong LW**, Ma ZC, Fu J, Huang BL, Liu FJ, Sun D, Lan C. Upregulated adenosine 2A receptor accelerates post-infectious irritable bowel syndrome by promoting CD4+ T cells' T helper 17 polarization. *World J Gastroenterol* 2022; **28**: 2955-2967 [PMID: 35978875 DOI: 10.3748/wjg.v28.i25.2955]

63 **Edogawa S**, Edwinson AL, Peters SA, Chikkamenahalli LL, Sundt W, Graves S, Gurunathan SV, Breen-Lyles M, Johnson S, Dyer R, Graham R, Chen J, Kashyap P, Farrugia G, Grover M. Serine proteases as luminal mediators of intestinal barrier dysfunction and symptom severity in IBS. *Gut* 2020; **69**: 62-73 [PMID: 30923071 DOI: 10.1136/gutjnl-2018-317416]

64 **Roxas JL**, Koutsouris A, Bellmeyer A, Tesfay S, Royan S, Falzari K, Harris A, Cheng H, Rhee KJ, Hecht G. Enterohemorrhagic E. coli alters murine intestinal epithelial tight junction protein expression and barrier function in a Shiga toxin independent manner. *Lab Invest* 2010; **90**: 1152-1168 [PMID: 20479715 DOI: 10.1038/labinvest.2010.91]

65 **Hanevik K**, Dizdar V, Langeland N, Hausken T. Development of functional gastrointestinal disorders after Giardia lamblia infection. *BMC Gastroenterol* 2009; **9**: 27 [PMID: 19383162 DOI: 10.1186/1471-230X-9-27]

66 **Porter CK**, Faix DJ, Shiau D, Espiritu J, Espinosa BJ, Riddle MS. Postinfectious gastrointestinal disorders following norovirus outbreaks. *Clin Infect Dis* 2012; **55**: 915-922 [PMID: 22715178 DOI: 10.1093/cid/cis576]

67 **Zanini B**, Ricci C, Bandera F, Caselani F, Magni A, Laronga AM, Lanzini A; San Felice del Benaco Study Investigators. Incidence of post-infectious irritable bowel syndrome and functional intestinal disorders following a water-borne viral gastroenteritis outbreak. *Am J Gastroenterol* 2012; **107**: 891-899 [PMID: 22525306 DOI: 10.1038/ajg.2012.102]

68 **Britton GJ**, Chen-Liaw A, Cossarini F, Livanos AE, Spindler MP, Plitt T, Eggers J, Mogno I, Gonzalez-Reiche AS, Siu S, Tankelevich M, Grinspan LT, Dixon RE, Jha D, van de Guchte A, Khan Z, Martinez-Delgado G, Amanat F, Hoagland DA, tenOever BR, Dubinsky MC, Merad M, van Bakel H, Krammer F, Bongers G, Mehandru S, Faith JJ. Limited intestinal inflammation despite diarrhea, fecal viral RNA and SARS-CoV-2-specific IgA in patients with acute COVID-19. *medRxiv* 2020 [PMID: 32909002 DOI: 10.1101/2020.09.03.20183947]

69 **Jena A**, Kumar-M P, Singh AK, Sharma V. Fecal calprotectin levels in COVID-19: Lessons from a systematic review on its use in inflammatory bowel disease during the pandemic. *Dig Liver Dis* 2021; **53**: 295-297 [PMID: 33132062 DOI: 10.1016/j.dld.2020.10.021]

70 **Oshima T**, Siah KTH, Yoshimoto T, Miura K, Tomita T, Fukui H, Miwa H. Impacts of the COVID-19 pandemic on functional dyspepsia and irritable bowel syndrome: A population-based survey. *J Gastroenterol Hepatol* 2021; **36**: 1820-1827 [PMID: 33197076 DOI: 10.1111/jgh.15346]

71 **Chan WW**, Grover M. The COVID-19 Pandemic and Post-Infection Irritable Bowel Syndrome: What Lies Ahead for Gastroenterologists. *Clin Gastroenterol Hepatol* 2022; **20**: 2195-2197 [PMID: 35944588 DOI: 10.1016/j.cgh.2022.05.044]

72 **Kamp KJ**, Levy RL, Munson SA, Heitkemper MM. Impact of COVID-19 on Individuals With Irritable Bowel Syndrome and Comorbid Anxiety and/or Depression. *J Clin Gastroenterol* 2022; **56**: e149-e152 [PMID: 33780216 DOI: 10.1097/MCG.0000000000001515]

73 **Settanni CR**, Ianiro G, Ponziani FR, Bibbò S, Segal JP, Cammarota G, Gasbarrini A. COVID-19 as a trigger of irritable bowel syndrome: A review of potential mechanisms. *World J Gastroenterol* 2021; **27**: 7433-7445 [PMID: 34887641 DOI: 10.3748/wjg.v27.i43.7433]

74 **Oświęcimska J**, Szymlak A, Roczniak W, Girczys-Połedniok K, Kwiecień J. New insights into the pathogenesis and treatment of irritable bowel syndrome. *Adv Med Sci* 2017; **62**: 17-30 [PMID: 28135659 DOI: 10.1016/j.advms.2016.11.001]

75 **Bozomitu L**, Miron I, Adam Raileanu A, Lupu A, Paduraru G, Marcu FM, Buga AML, Rusu DC, Dragan F, Lupu VV. The Gut Microbiome and Its Implication in the Mucosal Digestive Disorders. *Biomedicines* 2022; **10** [PMID: 36551874 DOI: 10.3390/biomedicines10123117]

76 **Lupu VV**, Miron IC, Raileanu AA, Starcea IM, Lupu A, Tarca E, Mocanu A, Buga AML, Lupu V, Fotea S. Difficulties in Adaptation of the Mother and Newborn *via* Cesarean Section versus Natural Birth-A Narrative Review. *Life (Basel)* 2023; **13**: 300 [PMID: 36836657 DOI: 10.3390/life13020300]

77 **Zugravu C**, Nanu MI, Moldovanu F, Arghir OC, Mihai CM, Oţelea MR, Cambrea SC. The influence of perinatal education on breastfeeding decision and duration. *Int J Child Health Nutr* 2018; **7**: 74-81 [DOI: 10.6000/1929-4247.2018.07.02.4]

78 **Downs IA**, Aroniadis OC, Kelly L, Brandt LJ. Postinfection Irritable Bowel Syndrome: The Links Between Gastroenteritis, Inflammation, the Microbiome, and Functional Disease. *J Clin Gastroenterol* 2017; **51**: 869-877 [PMID: 28885302 DOI: 10.1097/MCG.0000000000000924]

79 **Ghoshal UC**. Postinfection Irritable Bowel Syndrome. *Gut Liver* 2022; **16**: 331-340 [PMID: 34789582 DOI: 10.5009/gnl210208]

80 **Barman M**, Unold D, Shifley K, Amir E, Hung K, Bos N, Salzman N. Enteric salmonellosis disrupts the microbial ecology of the murine gastrointestinal tract. *Infect Immun* 2008; **76**: 907-915 [PMID: 18160481 DOI: 10.1128/IAI.01432-07]

81 **Buret AG**, Akierman SV, Feener T, McKnight W, Rioux KP, Beck PL, Wallace JL, Beatty J. Campylobacter Jejuni- or Giardia duodenalis-Mediated Disruptions of Human Intestinal Microbiota Biofilms: Novel Mechanisms Producing Post-Infectious Intestinal Inflammatory Disorders. *Gastroenterology* 2013; **144**: S-309

82 **Hsiao A**, Ahmed AM, Subramanian S, Griffin NW, Drewry LL, Petri WA Jr, Haque R, Ahmed T, Gordon JI. Members of the human gut microbiota involved in recovery from Vibrio cholerae infection. *Nature* 2014; **515**: 423-426 [PMID: 25231861 DOI: 10.1038/nature13738]

83 **Ma C**, Wu X, Nawaz M, Li J, Yu P, Moore JE, Xu J. Molecular characterization of fecal microbiota in patients with viral diarrhea. *Curr Microbiol* 2011; **63**: 259-266 [PMID: 21739252 DOI: 10.1007/s00284-011-9972-7]

84 **Youmans BP**, Ajami NJ, Jiang ZD, Campbell F, Wadsworth WD, Petrosino JF, DuPont HL, Highlander SK. Characterization of the human gut microbiome during travelers' diarrhea. *Gut Microbes* 2015; **6**: 110-119 [PMID: 25695334 DOI: 10.1080/19490976.2015.1019693]

85 **Patin NV**, Peña-Gonzalez A, Hatt JK, Moe C, Kirby A, Konstantinidis KT. The Role of the Gut Microbiome in Resisting Norovirus Infection as Revealed by a Human Challenge Study. *mBio* 2020; **11** [PMID: 33203758 DOI: 10.1128/mBio.02634-20]

86 **Nelson AM**, Walk ST, Taube S, Taniuchi M, Houpt ER, Wobus CE, Young VB. Disruption of the human gut microbiota following Norovirus infection. *PLoS One* 2012; **7**: e48224 [PMID: 23118957 DOI: 10.1371/journal.pone.0048224]

87 **Cheng X**, Zhang Y, Li Y, Wu Q, Wu J, Park SK, Guo C, Lu J. Meta-analysis of 16S rRNA microbial data identified alterations of the gut microbiota in COVID-19 patients during the acute and recovery phases. *BMC Microbiol* 2022; **22**: 274 [PMID: 36376804 DOI: 10.1186/s12866-022-02686-9]

88 **Li S**, Zhou Y, Yan D, Wan Y. An Update on the Mutual Impact between SARS-CoV-2 Infection and Gut Microbiota. *Viruses* 2022; **14** [PMID: 36016396 DOI: 10.3390/v14081774]

89 **Neag MA**, Vulturar DM, Gherman D, Burlacu CC, Todea DA, Buzoianu AD. Gastrointestinal microbiota: A predictor of COVID-19 severity? *World J Gastroenterol* 2022; **28**: 6328-6344 [PMID: 36533107 DOI: 10.3748/wjg.v28.i45.6328]

90 **Mizutani T**, Ishizaka A, Koga M, Ikeuchi K, Saito M, Adachi E, Yamayoshi S, Iwatsuki-Horimoto K, Yasuhara A, Kiyono H, Matano T, Suzuki Y, Tsutsumi T, Kawaoka Y, Yotsuyanagi H. Correlation Analysis between Gut Microbiota Alterations and the Cytokine Response in Patients with Coronavirus Disease during Hospitalization. *Microbiol Spectr* 2022; **10**: e0168921 [PMID: 35254122 DOI: 10.1128/spectrum.01689-21]

91 **Gu S**, Chen Y, Wu Z, Gao H, Lv L, Guo F, Zhang X, Luo R, Huang C, Lu H, Zheng B, Zhang J, Yan R, Zhang H, Jiang H, Xu Q, Guo J, Gong Y, Tang L, Li L. Alterations of the Gut Microbiota in Patients With Coronavirus Disease 2019 or H1N1 Influenza. *Clin Infect Dis* 2020; **71**: 2669-2678 [PMID: 32497191 DOI: 10.1093/cid/ciaa709]

92 **Haran JP**, Bradley E, Zeamer AL, Cincotta L, Salive MC, Dutta P, Mutaawe S, Anya O, Meza-Segura M, Moormann AM, Ward DV, McCormick BA, Bucci V. Inflammation-type dysbiosis of the oral microbiome associates with the duration of COVID-19 symptoms and long COVID. *JCI Insight* 2021; **6** [PMID: 34403368 DOI: 10.1172/jci.insight.152346]

93 **Liu Q**, Mak JWY, Su Q, Yeoh YK, Lui GC, Ng SSS, Zhang F, Li AYL, Lu W, Hui DS, Chan PK, Chan FKL, Ng SC. Gut microbiota dynamics in a prospective cohort of patients with post-acute COVID-19 syndrome. *Gut* 2022; **71**: 544-552 [PMID: 35082169 DOI: 10.1136/gutjnl-2021-325989]

94 **Zuo T**, Liu Q, Zhang F, Lui GC, Tso EY, Yeoh YK, Chen Z, Boon SS, Chan FK, Chan PK, Ng SC. Depicting SARS-CoV-2 faecal viral activity in association with gut microbiota composition in patients with COVID-19. *Gut* 2021; **70**: 276-284 [PMID: 32690600 DOI: 10.1136/gutjnl-2020-322294]

95 **Zuo T**, Zhang F, Lui GCY, Yeoh YK, Li AYL, Zhan H, Wan Y, Chung ACK, Cheung CP, Chen N, Lai CKC, Chen Z, Tso EYK, Fung KSC, Chan V, Ling L, Joynt G, Hui DSC, Chan FKL, Chan PKS, Ng SC. Alterations in Gut Microbiota of Patients With COVID-19 During Time of Hospitalization. *Gastroenterology* 2020; **159**: 944-955.e8 [PMID: 32442562 DOI: 10.1053/j.gastro.2020.05.048]

96 **Yeoh YK**, Zuo T, Lui GC, Zhang F, Liu Q, Li AY, Chung AC, Cheung CP, Tso EY, Fung KS, Chan V, Ling L, Joynt G, Hui DS, Chow KM, Ng SSS, Li TC, Ng RW, Yip TC, Wong GL, Chan FK, Wong CK, Chan PK, Ng SC. Gut microbiota composition reflects disease severity and dysfunctional immune responses in patients with COVID-19. *Gut* 2021; **70**: 698-706 [PMID: 33431578 DOI: 10.1136/gutjnl-2020-323020]

97 **Budden KF**, Gellatly SL, Wood DL, Cooper MA, Morrison M, Hugenholtz P, Hansbro PM. Emerging pathogenic links between microbiota and the gut-lung axis. *Nat Rev Microbiol* 2017; **15**: 55-63 [PMID: 27694885 DOI: 10.1038/nrmicro.2016.142]

98 **Dicksved J**, Ellström P, Engstrand L, Rautelin H. Susceptibility to Campylobacter infection is associated with the species composition of the human fecal microbiota. *mBio* 2014; **5**: e01212-e01214 [PMID: 25227462 DOI: 10.1128/mBio.01212-14]

99 **Sundin J**, Rangel I, Fuentes S, Heikamp-de Jong I, Hultgren-Hörnquist E, de Vos WM, Brummer RJ. Altered faecal and mucosal microbial composition in post-infectious irritable bowel syndrome patients correlates with mucosal lymphocyte phenotypes and psychological distress. *Aliment Pharmacol Ther* 2015; **41**: 342-351 [PMID: 25521822 DOI: 10.1111/apt.13055]

100 **Mari A**, Abu Baker F, Mahamid M, Sbeit W, Khoury T. The Evolving Role of Gut Microbiota in the Management of Irritable Bowel Syndrome: An Overview of the Current Knowledge. *J Clin Med* 2020; **9** [PMID: 32143424 DOI: 10.3390/jcm9030685]

101 **Hill C**, Guarner F, Reid G, Gibson GR, Merenstein DJ, Pot B, Morelli L, Canani RB, Flint HJ, Salminen S, Calder PC, Sanders ME. Expert consensus document. The International Scientific Association for Probiotics and Prebiotics consensus statement on the scope and appropriate use of the term probiotic. *Nat Rev Gastroenterol Hepatol* 2014; **11**: 506-514 [PMID: 24912386 DOI: 10.1038/nrgastro.2014.66]

102 **Compare D**, Rocco A, Coccoli P, Angrisani D, Sgamato C, Iovine B, Salvatore U, Nardone G. Lactobacillus casei DG and its postbiotic reduce the inflammatory mucosal response: an ex-vivo organ culture model of post-infectious irritable bowel syndrome. *BMC Gastroenterol* 2017; **17**: 53 [PMID: 28410580 DOI: 10.1186/s12876-017-0605-x]

103 **Hong KB**, Seo H, Lee JS, Park Y. Effects of probiotic supplementation on post-infectious irritable bowel syndrome in rodent model. *BMC Complement Altern Med* 2019; **19**: 195 [PMID: 31366385 DOI: 10.1186/s12906-019-2610-9]

104 **Abbas Z**, Yakoob J, Jafri W, Ahmad Z, Azam Z, Usman MW, Shamim S, Islam M. Cytokine and clinical response to Saccharomyces boulardii therapy in diarrhea-dominant irritable bowel syndrome: a randomized trial. *Eur J Gastroenterol Hepatol* 2014; **26**: 630-639 [PMID: 24722560 DOI: 10.1097/MEG.0000000000000094]

105 **Lawenko RMA**, Lee YY, Nurfadhilah Y, Yaacob N, Mohammad WMZW, Liong MT. The role of gut dysbiosis and probiotics in persistent abdominal pain following a major flood disaster. *J Gastroenterol Hepatol* 2016; **31**: 131

106 **Lee YY**, Annamalai C, Rao SSC. Post-Infectious Irritable Bowel Syndrome. *Curr Gastroenterol Rep* 2017; **19**: 56 [PMID: 28948467 DOI: 10.1007/s11894-017-0595-4]

107 **Cao YN**, Feng LJ, Liu YY, Jiang K, Zhang MJ, Gu YX, Wang BM, Gao J, Wang ZL, Wang YM. Effect of Lactobacillus rhamnosus GG supernatant on serotonin transporter expression in rats with post-infectious irritable bowel syndrome. *World J Gastroenterol* 2018; **24**: 338-350 [PMID: 29391756 DOI: 10.3748/wjg.v24.i3.338]

108 **Chen YM**, Li Y, Wang X, Wang ZL, Hou JJ, Su S, Zhong WL, Xu X, Zhang J, Wang BM, Wang YM. Effect of Bacillus subtilis, Enterococcus faecium, and Enterococcus faecalis supernatants on serotonin transporter expression in cells and tissues. *World J Gastroenterol* 2022; **28**: 532-546 [PMID: 35316963 DOI: 10.3748/wjg.v28.i5.532]

109 **Zhang F**, Lau RI, Liu Q, Su Q, Chan FKL, Ng SC. Gut microbiota in COVID-19: key microbial changes, potential mechanisms and clinical applications. *Nat Rev Gastroenterol Hepatol* 2023; **20**: 323-337 [PMID: 36271144 DOI: 10.1038/s41575-022-00698-4]

110 **Tkach S**, Dorofeyev A, Kuzenko I, Sulaieva O, Falalyeyeva T, Kobyliak N. Fecal microbiota transplantation in patients with post-infectious irritable bowel syndrome: A randomized, clinical trial. *Front Med (Lausanne)* 2022; **9**: 994911 [PMID: 36341232 DOI: 10.3389/fmed.2022.994911]

111 **Liu X**, Li Y, Wu K, Shi Y, Chen M. Fecal Microbiota Transplantation as Therapy for Treatment of Active Ulcerative Colitis: A Systematic Review and Meta-Analysis. *Gastroenterol Res Pract* 2021; **2021**: 6612970 [PMID: 33981340 DOI: 10.1155/2021/6612970]

112 **Liu F**, Ye S, Zhu X, He X, Wang S, Li Y, Lin J, Wang J, Lin Y, Ren X, Deng Z. Gastrointestinal disturbance and effect of fecal microbiota transplantation in discharged COVID-19 patients. *J Med Case Rep* 2021; **15**: 60 [PMID: 33557941 DOI: 10.1186/s13256-020-02583-7]

113 **Jin Y**, Ren X, Li G, Li Y, Zhang L, Wang H, Qian W, Hou X. Beneficial effects of Rifaximin in post-infectious irritable bowel syndrome mouse model beyond gut microbiota. *J Gastroenterol Hepatol* 2018; **33**: 443-452 [PMID: 28573746 DOI: 10.1111/jgh.13841]

114 **Harris LA**. Rifaximin for Irritable Bowel Syndrome (IBS) in Gulf War Veterans: Losing the Battle but Winning the War? *Dig Dis Sci* 2019; **64**: 609-610 [PMID: 30725300 DOI: 10.1007/s10620-019-05505-w]

115 **Tuteja AK**, Talley NJ, Stoddard GJ, Verne GN. Double-Blind Placebo-Controlled Study of Rifaximin and Lactulose Hydrogen Breath Test in Gulf War Veterans with Irritable Bowel Syndrome. *Dig Dis Sci* 2019; **64**: 838-845 [PMID: 30370492 DOI: 10.1007/s10620-018-5344-5]

116 **Lam C**, Tan W, Leighton M, Hastings M, Lingaya M, Falcone Y, Zhou X, Xu L, Whorwell P, Walls AF, Zaitoun A, Montgomery A, Spiller R. A mechanistic multicentre, parallel group, randomised placebo-controlled trial of mesalazine for the treatment of IBS with diarrhoea (IBS-D). *Gut* 2016; **65**: 91-99 [PMID: 25765462 DOI: 10.1136/gutjnl-2015-309122]

117 **Bafutto M**, Almeida JR, Leite NV, Oliveira EC, Gabriel-Neto S, Rezende-Filho J. Treatment of postinfectious irritable bowel syndrome and noninfective irritable bowel syndrome with mesalazine. *Arq Gastroenterol* 2011; **48**: 36-40 [PMID: 21537540 DOI: 10.1590/s0004-28032011000100008]

118 **Tuteja AK**, Fang JC, Al-Suqi M, Stoddard GJ, Hale DC. Double-blind placebo-controlled study of mesalamine in post-infective irritable bowel syndrome--a pilot study. *Scand J Gastroenterol* 2012; **47**: 1159-1164 [PMID: 22783919 DOI: 10.3109/00365521.2012.694903]

119 **Andresen V**, Löwe B, Broicher W, Riegel B, Fraedrich K, von Wulffen M, Gappmayer K, Wegscheider K, Treszl A, Rose M, Layer P, Lohse AW. Post-infectious irritable bowel syndrome (PI-IBS) after infection with Shiga-like toxin-producing Escherichia coli (STEC) O104:H4: A cohort study with prospective follow-up. *United European Gastroenterol J* 2016; **4**: 121-131 [PMID: 26966532 DOI: 10.1177/2050640615581113]

120 **Dunlop SP**, Jenkins D, Neal KR, Naesdal J, Borgaonker M, Collins SM, Spiller RC. Randomized, double-blind, placebo-controlled trial of prednisolone in post-infectious irritable bowel syndrome. *Aliment Pharmacol Ther* 2003; **18**: 77-84 [PMID: 12848628 DOI: 10.1046/j.1365-2036.2003.01640.x]

121 **Barkun AN**, Love J, Gould M, Pluta H, Steinhart H. Bile acid malabsorption in chronic diarrhea: pathophysiology and treatment. *Can J Gastroenterol* 2013; **27**: 653-659 [PMID: 24199211 DOI: 10.1155/2013/485631]

World Journal of Gastroenterology

Submit a Manuscript: https://www.f6publishing.com

World J Gastroenterol 2023 June 7; 29(21): 3257-3268

DOI: 10.3748/wjg.v29.i21.3257

ISSN 1007-9327 (print) ISSN 2219-2840 (online)

MINIREVIEWS

Biliary complications after liver transplantation: A computed tomography and magnetic resonance imaging pictorial review

Federica Vernuccio, Irene Mercante, Xiao-Xiao Tong, Filippo Crimì, Umberto Cillo, Emilio Quaia

Specialty type: Radiology, nuclear medicine and medical imaging

Provenance and peer review: Invited article; Externally peer reviewed.

Peer-review model: Single blind

Peer-review report's scientific quality classification
Grade A (Excellent): A
Grade B (Very good): 0
Grade C (Good): C
Grade D (Fair): 0
Grade E (Poor): 0

P-Reviewer: Gupta T, India; Oura S, Japan

Received: January 6, 2023
Peer-review started: January 6, 2023
First decision: March 18, 2023
Revised: March 23, 2023
Accepted: April 27, 2023
Article in press: April 27, 2023
Published online: June 7, 2023

Federica Vernuccio, Department of Radiology, University Hospital of Padova, Padova 35128, Italy

Irene Mercante, Xiao-Xiao Tong, Filippo Crimì, Emilio Quaia, Department of Radiology-DIMED, University of Padova, Padova 35128, Italy

Umberto Cillo, Department of Surgery, Hepatobiliary Surgery and Liver Transplant Center, Oncology and Gastroenterology (DISCOG), University of Padova, Padova 35128, Italy

Corresponding author: Federica Vernuccio, MD, PhD, Staff Physician, Department of Radiology, University Hospital of Padova, 2 Via Nicolò Giustiniani, Padova 35128, Italy. federicavernuccio@gmail.com

Abstract

Biliary complications are the most common complications after liver transplantation. Computed tomography (CT) and magnetic resonance imaging (MRI) are cornerstones for timely diagnosis of biliary complications after liver transplantation. The diagnosis of these complications by CT and MRI requires expertise, mainly with respect to identifying subtle early signs to avoid missed or incorrect diagnoses. For example, biliary strictures may be misdiagnosed on MRI due to size mismatch of the common ducts of the donor and recipient, postoperative edema, pneumobilia, or susceptibility artifacts caused by surgical clips. Proper and prompt diagnosis of biliary complications after transplantation allows the timely initiation of appropriate management. The aim of this pictorial review is to illustrate various CT and MRI findings related to biliary complications after liver transplantation, based on time of presentation after surgery and frequency of occurrence.

Key Words: Liver transplantation; Biliary; Complications; Computed tomography; Magnetic resonance imaging; Hepatic imaging; Biliary tract; Cholangiopancreatography; Stricture

©The Author(s) 2023. Published by Baishideng Publishing Group Inc. All rights reserved.

Core Tip: Biliary complications are the most common surgical complications after liver transplantation, and represent a major source of morbidity and mortality in liver transplant recipients. Magnetic resonance cholangiopancreatography is the gold standard for the non-invasive diagnosis of intra- and extrahepatic biliary complications. Computed tomography may also be helpful for the assessment of biliary complications, and it is often used due to its more widespread availability as compared to that of magnetic resonance imaging.

Citation: Vernuccio F, Mercante I, Tong XX, Crimì F, Cillo U, Quaia E. Biliary complications after liver transplantation: A computed tomography and magnetic resonance imaging pictorial review. *World J Gastroenterol* 2023; 29(21): 3257-3268
URL: https://www.wjgnet.com/1007-9327/full/v29/i21/3257.htm
DOI: https://dx.doi.org/10.3748/wjg.v29.i21.3257

INTRODUCTION

Computed tomography (CT) and magnetic resonance imaging (MRI) are cornerstones in the postoperative assessment of patients after liver transplantation[1]. Complications may be categorized by etiology, and include surgical, graft-related, immunologic, infectious, and neoplastic. Complications can also be classified based on their timing: Early (within 6 mo) or late (after 6 mo; Table 1). Surgical complications are typically categorized as vascular, biliary, or parenchymal. Biliary complications are the most common and represent a major source of morbidity and mortality in liver transplant recipients with an incidence of 10%-32%[2-4]. Biliary complications after liver transplantation include anastomotic stricture, non-anastomotic stricture, bile leak, bile cast, biloma, sphincter of Oddi dysfunction, and mucocele of the cystic duct remnant[4-9]. Biliary complications have a significant negative impact on patient survival and may lead to the need for re-transplantation[3,6]. Magnetic resonance cholangiopancreatography (MRCP) is currently the gold standard for the diagnosis of intra- and extrahepatic biliary complications, while invasive cholangiography should be restricted for therapeutic uses or when MRCP is equivocal[10].

The aim of this pictorial review is to illustrate CT and MRI findings of surgery-related biliary complications after liver transplantation, classified based on their usual timing of appearance and their frequency. The knowledge of surgical techniques is of key importance to understand postoperative anatomic changes and imaging evaluation. Therefore, we will first provide a short summary of the main techniques of liver transplantation with focus on biliary anastomosis. Then, we will discuss imaging tips and tricks for the prompt diagnosis of biliary complications on CT and MRI.

SURGICAL TECHNIQUE

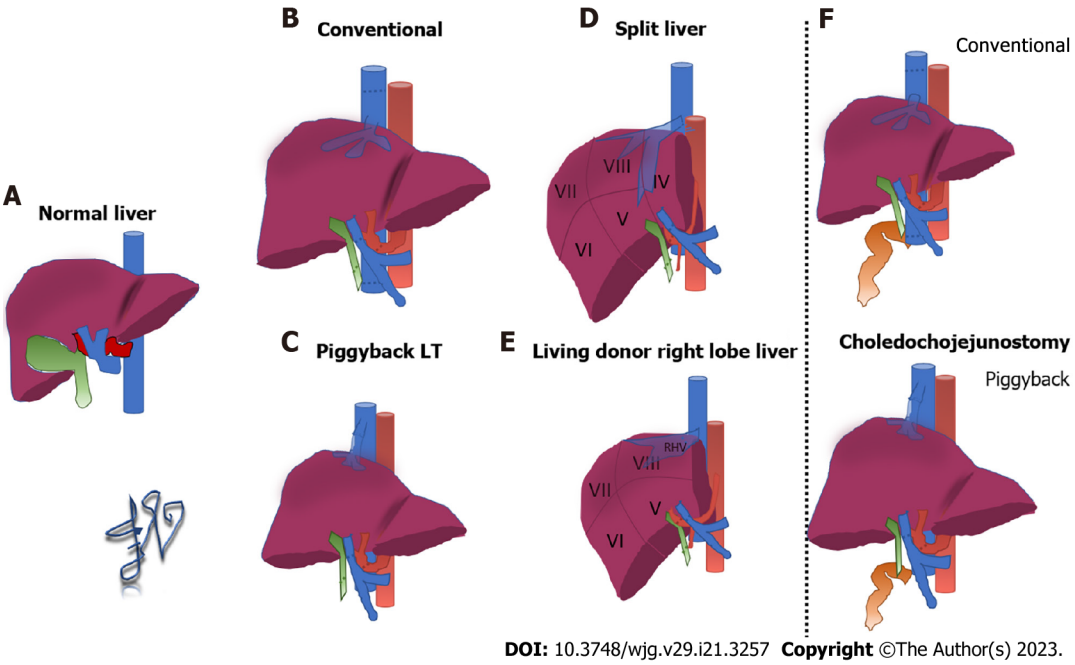
Most liver transplantations are performed with orthotopic implantation of a deceased donor whole liver graft, and may be performed with a conventional or piggyback technique. Other surgical options include split or segmental liver transplantation (Figure 1)[7]. The split liver procedure may be performed by either of 2 approaches: In the most common approach, the liver is divided into a left lateral segment graft (II + III ± IV segments) if the recipient is a child or a right extended liver lobe graft (I + V-VIII ± IV segments) if the recipient is an adult; in the less common and more challenging variant of this procedure, the liver is split into 2 hemigrafts and the left side (I-IV) is transplanted to a small adult or a teenager and the right side (V-VIII) to a medium-sized adult. In patients with prior biliary disease or re-transplantation, a different biliary anastomosis technique may be performed[7]. Liver transplantation is a multi-step surgery. After skin preparation and incision, the surgeon checks if there is any undiagnosed malignancy or anatomic variant and then dissects the recipient's liver and gallbladder. The donor's liver, without the gallbladder, is then implanted into the recipient with the anastomoses between recipient and donor performed in the following order: (1) Systemic venous outflow (inferior cava vein-hepatic veins); (2) portal venous inflow; (3) hepatic arterial inflow; and (4) biliary anastomosis. The types of anastomosis depend on donor and recipient anatomy and surgeon preference. Finally, when the surgical field is dry, the abdomen is closed. Each of the above-mentioned steps is critical, and complications may be directly or indirectly related to failure of any of these steps [11,12].

Biliary anastomosis is known as the "Achilles tendon" of liver transplantation. The most common form of biliary reconstruction is choledochocholedochostomy (duct-to-duct anastomosis)[7], which may be performed in an end-to-end or end-to-side fashion. Choledochocholedochostomy can be performed either with a T-tube, which allows rapid decompression of the biliary tree if needed and reduces the risk of anastomotic stricture formation but may lead to biliary leakage and cholangitis at the time of

Table 1 Post-transplant complications with the relevance of computed tomography and magnetic resonance imaging in diagnosis

Time of onset	Type of complications	Relevance of CT/MRI for diagnosis
Early (< 6 mo)	Surgical	++++
	Graft-related	++
	Immunologic	+
	Infectious	++
Late (> 6 mo)	Surgical	++++
	Graft-related	++
	Immunologic	+
	Infectious	+++
	Neoplastic	++++
	Disease recurrence	++

++++: Highly relevant, often mandatory; +++: Very useful; ++: Useful; + sometimes helpful, but clinical diagnosis is usually very relevant. CT: Computed tomography; MRI: Magnetic resonance imaging.



DOI: 10.3748/wjg.v29.i21.3257 **Copyright** ©The Author(s) 2023.

Figure 1 Schematic representation of surgical techniques for liver transplantation. A: Normal anatomy of the liver; B: Conventional technique for liver transplantation; C: Piggyback technique; D: Split liver technique in adults; E: Living donor right lobe liver transplantation; F: Conventional (top row) and piggyback (bottom row) techniques with choledochojejunostomy.

removal, or without a T-tube[13]. Choledochojejunostomy to a Roux-en-Y defunctionalized intestinal loop (*i.e.* the connection of the bile duct to jejunum loop) (Figure 1F) is the second most common type of biliary reconstruction technique, usually preferred in patients with pre-existing biliary disease and in case of size mismatch between donor and recipient ducts, re-transplantation, or previous biliary surgery [7]. Potential complications of choledochojejunostomy include stricture, leakage, and bleeding at the jejuno-jejunostomy site. Choledochocholedochostomy is preferred over choledochojejunostomy due to shorter operation time, lower risk of septic complication, preserved sphincter of Oddi, better physiologic enteric function, and easier endoscopic access to the biliary tree for any future need.

CT/MRI OF BILIARY COMPLICATIONS

MRI has sensitivity and specificity of 98%-99% and 94%-96%, respectively, for the diagnosis of biliary

complications after liver transplantation[14,15]. MRI protocol includes 2D-MRCP and 3D-MRCP and an unenhanced T1-weighted sequence, while gadoxetate disodium hepatobiliary MRI is performed in selected cases[16]. Ultrasound is usually performed first, and may help identify any features that suggest the presence of complication. Despite not being as comprehensive as MRI, CT may also be helpful for the assessment of biliary complications and is often used due to its more widespread availability. Table 2 summarizes biliary complications related to surgery classified according to frequency, time of occurrence, and treatment[4-10].

Biliary strictures

Biliary strictures are distinguished as anastomotic or non-anastomotic. Anastomotic strictures (Figure 2) account for about 47% of biliary complications, being slightly more frequent after choledochocholedochostomy *vs* choledochojejunostomy, and may also occur after split liver donation[3]. Currently, percutaneous biliary techniques are considered effective treatment options with good outcomes in the setting of liver transplant with anastomotic biliary stricture[17]. Non-anastomotic strictures account for about 23% of all biliary complications, being slightly more frequent after choledochojejunostomy *vs* choledochocholedochostomy[3]. Non-anastomotic strictures (Figure 3) typically comprise ischemic-type biliary lesions in the early period after transplant, and are mostly related to recurrence of the primary biliary disease, chronic rejection, or secondary sclerosing cholangitis if occurring in the late postoperative period.

Biliary strictures are one of the most critical complications in ABO-incompatible living donor liver transplant recipients, and may occur as perihilar or diffuse, with the latter having worse clinical outcomes[18].

MRI demonstrates any stenosis at the level of the stricture as well as upstream irregular dilation of the biliary system; typically, the change in duct caliber at the level of the stricture is abrupt. Anastomotic strictures tend to be single, short in length, and occur at the level of anastomosis, usually in the late postoperative period. Non-anastomotic strictures are frequently multiple, long, hilar in location, and tend to occur early after transplantation and may result in graft loss. Radiologists should report the level of the biliary injury and the length of the obstruction. Although not routinely recommended for the diagnosis of biliary strictures, MRCP with hepatobiliary contrast may allow the assessment of the severity of bile duct obstruction based on the degree of hepatobiliary contrast filling distal to the stricture. Complete obstruction of the biliary tree is demonstrated in the case of absence of contrast distal to the stricture, while the obstruction is partial if there is limited passage of contrast beyond the stricture. In the case of complete obstruction, hepatic function may be impaired as evidenced by elevated bilirubin, which may hamper the excretion of hepatobiliary contrast[19]. Biliary strictures must be differentiated from their mimickers on MRI, which may include size mismatch of the donor and recipient common ducts (appearing as gradual tapering of the bile duct lumen at the anastomosis) and postoperative edema (can cause extrinsic compression at the level of the anastomosis and have a tapered "hour-glass" appearance). Other potential mimickers of biliary strictures on MRI include pneumobilia (which may occur normally if a choledochojejunostomy anastomosis has been performed) and MRI susceptibility artifacts caused by nearby surgical clips. CT may help in identifying the inadvertent placement of metallic surgical clips. In ABO-incompatible living donor liver transplant recipients, imaging and clinical follow-up is recommended if post-transplantation CT at 1 mo demonstrates subtle intrahepatic duct dilatation with perihilar abnormality to assess for the possible occurrence of diffuse intrahepatic duct dilatation stricture[18].

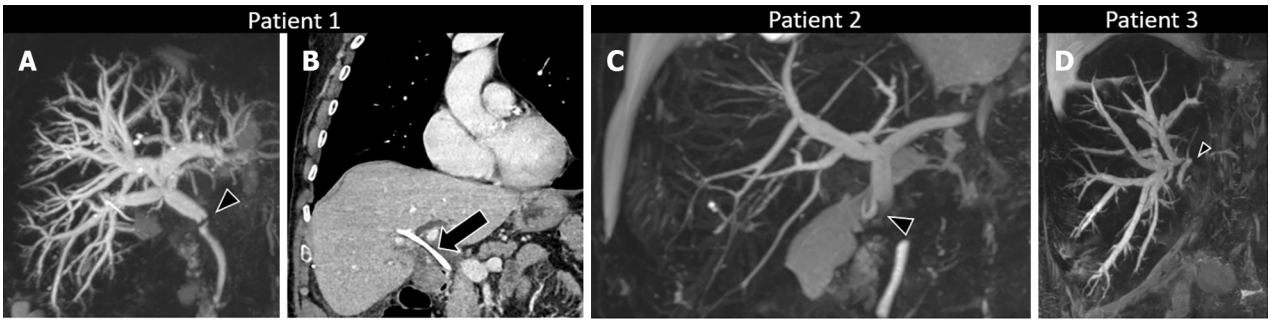
Biliary leak and biloma

Biliary leaks account for approximately 23% of all biliary complications[3]. They may be anastomotic or non-anastomotic (Figure 4) and are more common after choledochocholedochostomy *vs* choledochojejunostomy. Leaks at the biliary anastomosis are most common[20]. Non-anastomotic leaks may occur at the level of T-tube insertion, cystic duct, or the cut surface of a partial liver graft. The use of a T-tube may be a risk factor for biliary leak, most commonly after removal of the tube[21]. However, there are discordant data with respect to the causative mechanism of T-tube-related biliary leaks[22,23]. Non-anastomotic biliary leaks may be cut-surface leaks, such as those originating from small bile ducts that are transected perioperatively during hepatic resection, from the cystic duct stump, or may be caused by bile duct necrosis in patients with hepatic artery occlusion. Biliary leaks may result in the development of bilomas. Bilomas may be intra- or extrahepatic depending on the origin of the leak, although they most commonly occur in the perihepatic space. Bilomas may become infected and can potentially lead to sepsis. Another potential serious complication of biloma is erosion of the adjacent hepatic artery. Ultrasound (US) and CT are most commonly performed as first-line imaging techniques due to their wide availability; biliary leak or biloma are demonstrated as free fluid or fluid collection, usually in the perihepatic and subhepatic spaces, mostly anechoic on US and hypoattenuating with fluid density on CT. On MRI, biliary leaks and biloma are hypointense on T1-weighted sequence and hyperintense on T2-weighted sequence, with the former appearing as free fluid and the latter as a fluid collection (Figure 5). However, these findings are nonspecific, and biliary leaks and bilomas are virtually indistinguishable from other types of fluid collection and ascites. In the case of a biliary leak occurring after bile duct necrosis in the setting of hepatic artery occlusion, intrahepatic bilomas or bile lakes may develop in

Table 2 Post-transplant biliary complications related to surgery based on frequency, onset, and management

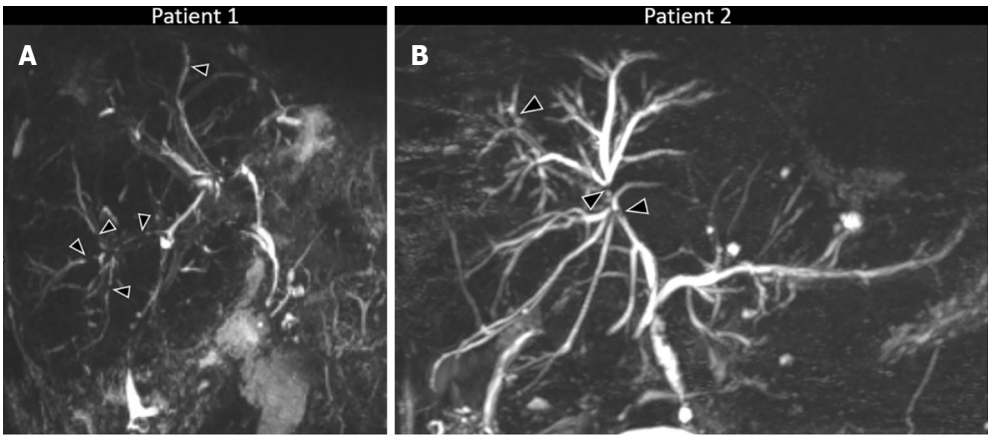
Type of complication	Frequency	Timing of onset	Common treatment
Biliary stricture	5%-15% (up to 30% in LDLT)	Early late	Refashioning after stenting
Biliary leak	2%-25%	Early	ERCP and stenting if anastomotic
Biloma/Biliary lake	2.6%-11.5%	Early	Percutaneous drainage and antibiotics if large
Bile duct filling defect	3%-6%	Early late	ERCP/percutaneous drainage
Sphincter of oddi dysfunction	2%-5%	Late	ERCP with sphincterotomy and consideration of stent placement
Redundant common bile duct	Rare	Late	Stent
Mucocele of bile duct remnant	Rare	Late	Surgery if causing compression

ERCP: Endoscopic retrograde cholangiopancreatography; LDLT: Living donor liver transplantation.



DOI: 10.3748/wjg.v29.i21.3257 **Copyright** ©The Author(s) 2023.

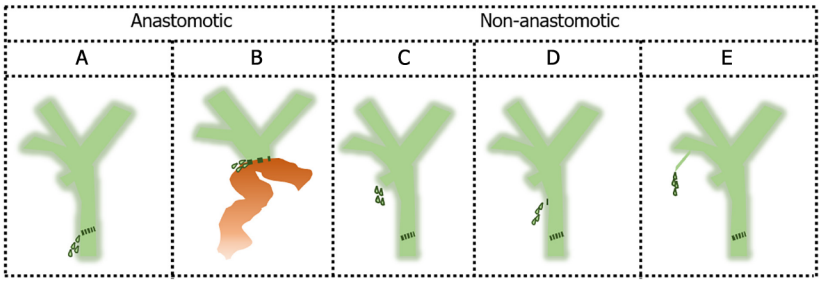
Figure 2 Anastomotic biliary strictures. A: Anastomotic stricture of choledochocholedochostomy 3 mo after liver transplantation. Endoscopic retrograde cholangiopancreatography was performed with balloon dilatation of the stricture and stent positioning. Magnetic resonance cholangiopancreatography (MRCP) maximum intensity projection (MIP) demonstrates anastomotic biliary stricture (arrowhead) with marked upstream biliary dilatation; B: Contrast enhanced computed tomography in the coronal plane shows in the same patient the stent in the biliary tree (arrow) and normal biliary tree caliber; C: Anastomotic stricture of choledochojejunostomy 6 mo after liver transplantation. MRCP MIP demonstrates anastomotic biliary stricture (arrowhead) with marked upstream biliary dilatation; D: Anastomotic stricture of end-to-end biliary anastomosis after split liver transplantation with right split lobe. MRCP MIP demonstrates anastomotic biliary stricture (arrowhead) with marked upstream biliary dilatation of the right split transplanted lobe.



DOI: 10.3748/wjg.v29.i21.3257 **Copyright** ©The Author(s) 2023.

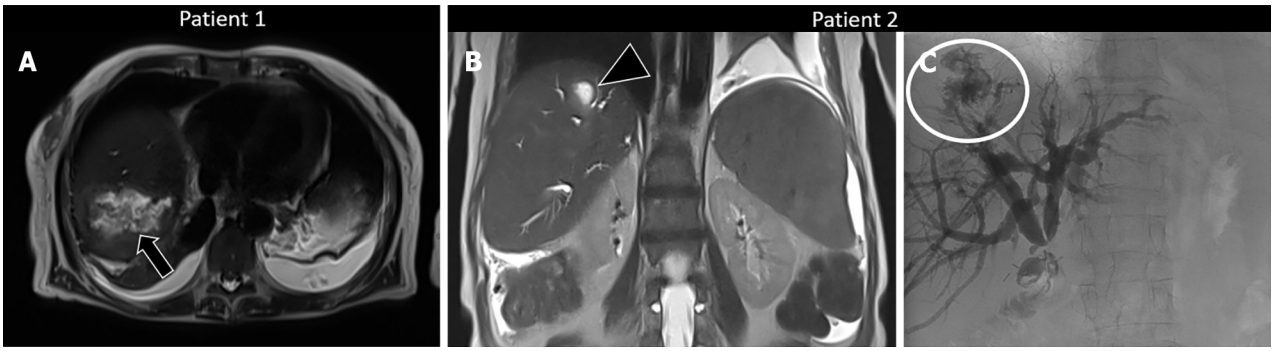
Figure 3 Non-anastomotic biliary strictures. A: Non-anastomotic strictures in a patient with chronic rejection demonstrated at biopsy 11 y after transplant and then re-transplanted. Magnetic resonance cholangiopancreatography (MRCP) maximum intensity projection (MIP) demonstrates multiple non-anastomotic biliary strictures (arrowheads); B: Non-anastomotic strictures in a patient with recurrent secondary cholangitis 4 y after liver transplantation. MRCP MIP demonstrates multiple non-anastomotic biliary strictures (arrowheads) with upstream biliary dilatation.

the early postoperative period, with a characteristic appearance on imaging as cystic or linear dilatations of the intrahepatic bile ducts (Figure 6). MRCP with hepatobiliary contrast has 100% sensitivity and 98% specificity with respect to the diagnosis of bile leaks[24,25]. MRCP with hepatobiliary contrast allows to



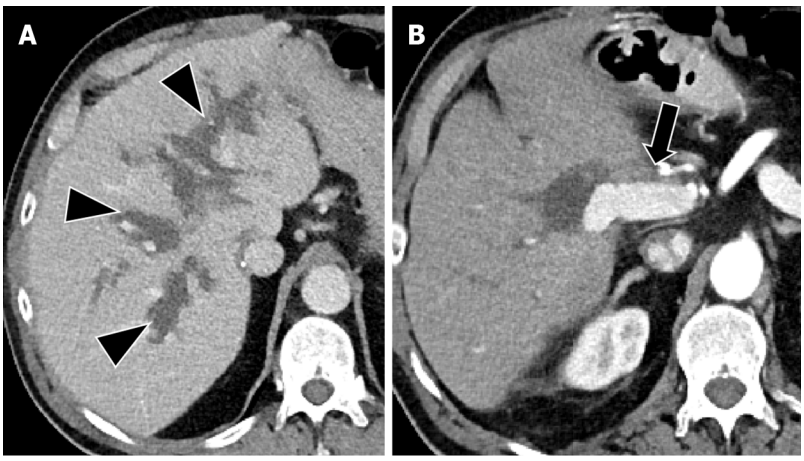
DOI: 10.3748/wjg.v29.i21.3257 **Copyright** ©The Author(s) 2023.

Figure 4 Schematic representation of biliary leaks. A: Anastomotic leak at the level of choledochocholedochostomy; B: Anastomotic leak at the level of choledochojejunostomy; C: Non-anastomotic leak at the level of the cystic duct stump; D: Non-anastomotic leak at the level of T-tube removal; E: Non-anastomotic leak from small bile ducts that are transected perioperatively during hepatic resection.



DOI: 10.3748/wjg.v29.i21.3257 **Copyright** ©The Author(s) 2023.

Figure 5 Biloma and biliary leak after liver transplantation. A: Patient with biloma occurring 9 mo after liver transplantation. T2-weighted axial image shows a collection (arrow) in the right hepatic lobe with internal heterogenous signal intensities. Percutaneous drainage of the collection was performed demonstrating superinfected biloma; B: Patient with biliary leak occurring after liver transplantation. T2-weighted coronal magnetic resonance imaging shows an intrahepatic fluid collection (arrowhead) consistent with biloma; C: Cholangiographic image in the same patient demonstrated the biliary leak (circle) causing an intrahepatic biloma.



DOI: 10.3748/wjg.v29.i21.3257 **Copyright** ©The Author(s) 2023.

Figure 6 Biliary lakes occurring after liver transplantation. A: Contrast-enhanced computed tomography (CT) in the axial plane in the portal venous phase demonstrates biliary lakes (arrowheads) adjacent to the portal vein branches; B: Contrast-enhanced CT in the arterial phase demonstrates lack of enhancement of the hepatic artery (arrow) caused by the adjacent surgical clip.

demonstrate the level and the entity of biliary leakage, showing contrast agent extravasation into bilomas in case of active leakage. However, small bilomas are often self-limiting, and active extravasation may not be demonstrated. The lack of active bile leak into a biloma as evidenced on imaging is highly clinically relevant, as it may help in choosing a conservative management. However, it is important to highlight that the diagnostic accuracy of MRCP with hepatobiliary contrast depends on the timing of acquisition of the hepatobiliary phase. When conventional acquisition at 20 min only is

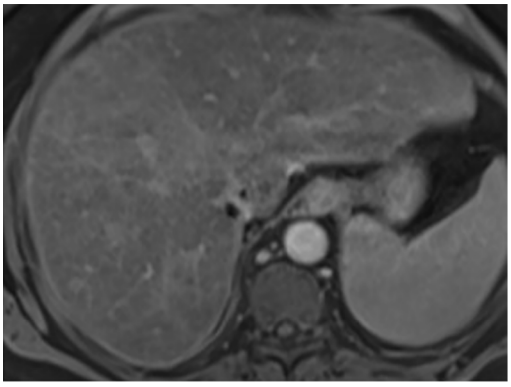
adopted, sensitivity may be as low as 42.9%[26], while the acquisition at 60 min-90 min, 150 min-180 min, or even 210 min-240 min to 390 min increases the sensitivity[26,27]. The reason behind the lower sensitivity of the 20 min hepatobiliary phase compared to acquisitions at later times may be 2-fold. On one hand, the increased bilirubin in these patients may result in low uptake of hepatobiliary contrast by the hepatocytes at 20 min; indeed, bilirubin is taken up at the hepatocyte level by the same family of organic anion transport proteins of gadoxetate disodium (Figure 7). On the other hand, bile duct obstruction may result in the upregulation of a multidrug resistance protein, which could reduce the excretion of gadoxetate disodium, delaying or preventing the visualization of the bile ducts and any bile leak[28,29]. For this reason, based on consensus reports for liver MRI, an elevated bilirubin level is considered a relative contraindication to injection of gadoxetate disodium at some centers, with threshold bilirubin levels from 2.0 mg/dL-5.0 mg/dL. Overall, delayed acquisitions may prove to be helpful for the diagnosis of biliary leaks[29,30].

Biliary casts, stones and sludge

Biliary casts, stones, or sludge account for about 6% of all biliary complications[3], and usually complicate any biliary stricture present. Casts, stones, or sludge may occur at both the intra- and extrahepatic bile ducts as the consequence of bile stasis and may lead to cholangitis, graft failure, or the need for re-transplantation[31]. Biliary concretions after liver transplantation are related to a heterogenous group of lithogenic conditions mostly related to bile tract damage with a multifactorial, complex pathophysiology[32]. Biliary casts complicate up to 4.5% of liver transplantations, may recur, and may lead to biliary strictures in up to 85.0% of patients on follow-up[4]. Morphologically, biliary casts after liver transplantation may have a cordlike, columnar, or dendritic shape within the biliary tree[33]. The prompt identification of biliary casts is of utmost importance, as patients with biliary cast syndrome have lower overall and graft survival rates compared to patients with non-anastomotic and anastomotic strictures only[4]. MRCP has very good sensitivity in the identification of biliary concretions, which appear as filling defects surrounded by a thin film of hyperintense bile (Figure 8). Importantly, the sensitivity for biliary cast detection increases when using T1-weighted imaging compared to T2-weighted MRCP; unenhanced T1-weighted images show hyperintensities in the bile ducts (Figure 8C), leading to the correct diagnosis of biliary cast[34]. As recently pointed out, intraductal hyperintense filling material on T1-weighted MRI is a sensitive sign for biliary casts, and intraductal filling defect on T2-weighted MRI with the duct-in-a-duct feature is a specific sign and likely reflects biliary mucosal detachment[4].

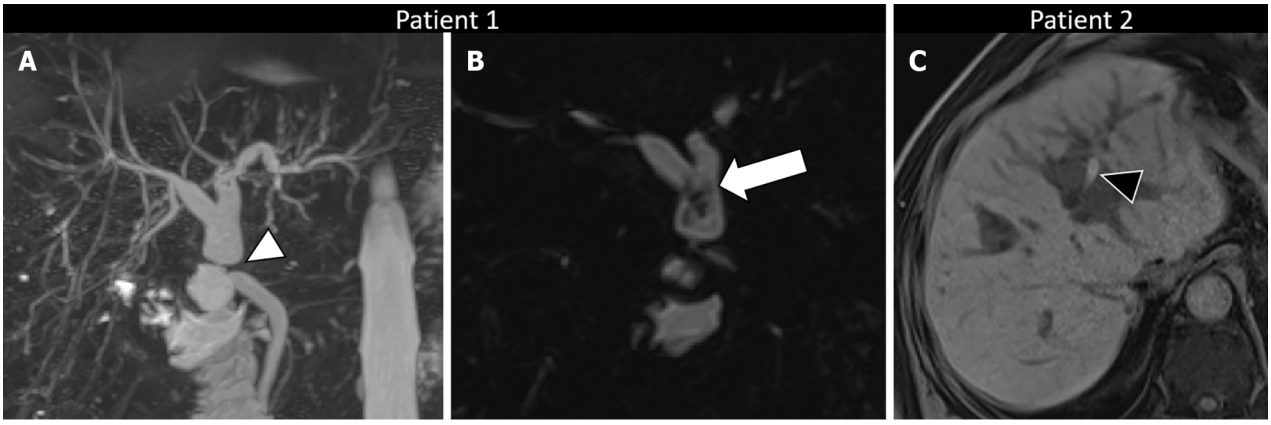
Sphincter of Oddi dysfunction

Sphincter of Oddi dysfunction (SOD) comprises functional or mechanical obstruction of the sphincter of Oddi and involves the biliary sphincter and/or the pancreatic sphincter. Biliary and pancreatic SOD have each been subclassified into 3 types based on related symptoms, laboratory testing, and imaging (common bile duct diameter of at least 12 mm): Type I with biliary pain, abnormal liver enzymes and dilatation of the common bile duct; Type II with biliary pain and either abnormal liver enzymes or dilatation of the common bile duct; and Type III with biliary pain and no objective criteria[35,36]. More recently, the Rome IV consensus has proposed new classification, as most type I patients present with papillary stenosis rather than a functional disorder and have an excellent response after sphincterotomy; type II has now been renamed as suspected functional biliary sphincter disorder; and type III patients have no response to sphincterotomy[37,38]. SOD after liver transplantation has been reported in about 2%-5% of patients, with papillary stenosis (*i.e.* SOD type I) accounting for about 1% of cases and suspected functional biliary sphincter disorder (*i.e.* SOD type II) for about 1% as well[39]. The pathogenesis of biliary sphincter disorder in liver transplantation recipients is poorly understood; possible predisposing factors include the use of a T-tube, the presence of opportunistic infection, and postsurgical edema[40,41]. Patients with functional biliary sphincter disorder after liver transplantation may be asymptomatic due to hepatic denervation after the surgery and immunosuppression, thus making the diagnosis more difficult[41]. Therefore, suspicion of SOD after liver transplantation should be raised when cholestasis or dilation of bile ducts appears in the absence of bile stones or other structural abnormalities. Sphincter of Oddi manometry has been the gold standard for years, although it is invasive, patient- and operator-dependent, and may lead to post-procedure pancreatitis. Due to these factors, it is no longer routinely used in all patients with suspected SOD and its general utility has been questioned[39-41]. Hepatobiliary scintigraphy can demonstrate structural or functional partial biliary obstruction as evidenced by increased time to hepatic peak, delayed biliary visualization, delayed clearance of the radiotracer from the dilated bile ducts, and prolonged biliary to bowel transit[42-44]. MRCP may be used to exclude biliary lithiasis and other structural abnormalities, and may show an enlarged papilla in some cases of papillary stenosis (Figure 9). Secretin-MRCP may suggest the diagnosis of SOD, showing stenosis of the sphincter and lack of relaxation of the main pancreatic duct after secretin injection, increased prominence of pancreatic duct side branches, or acinarization[45]. Secretin-MRCP seems more useful for SOD type II, with a diagnostic accuracy of 73%, rather than for SOD type III for which accuracy drops to only 46%[46]. Given the low accuracy, the cost of secretin, and the acquisition time of at least 15 min, secretin-MRCP for SOD should be considered only in a few selected cases (*i.e.* noninvasive evaluation is preferred or when endoscopic evaluation is not available or



DOI: 10.3748/wjg.v29.i21.3257 **Copyright** ©The Author(s) 2023.

Figure 7 Lack of excretion of hepatobiliary contrast after liver transplantation in a patient with increased serum bilirubin of 2.2 mg/dL. Gadoxetate disodium-enhanced magnetic resonance imaging in the hepatobiliary phase acquired at 20 min is inadequate as demonstrated by hypointensity of the liver parenchyma compared to that of hepatic vessels and lack of contrast in the biliary tree.



DOI: 10.3748/wjg.v29.i21.3257 **Copyright** ©The Author(s) 2023.

Figure 8 Biliary sludge and biliary cast. A: Patient with biliary sludge and anastomotic stricture 3 mo after liver re-transplantation. Magnetic resonance cholangiopancreatography (MRCP) maximum intensity projection image demonstrates anastomotic biliary stricture (arrowhead) with marked upstream biliary dilatation; B: Three-dimensional MRCP in the coronal plane in the same patient demonstrates biliary sludge (arrow) in the dilated hepatic duct extending into the left and right ducts. C: Patient with biliary cast 2 y after liver transplantation. Unenhanced T1-weighted gradient-recalled image shows hyperintense content (arrowhead) in the left biliary duct, consistent with biliary cast.

impractical)[45]. Gadoxetate disodium-enhanced MRCP may help in ruling out SOD in the case of normal passage of hepatobiliary contrast in the duodenum at 20 min-30 min, and in suggesting the diagnosis in the case of delayed or no passage of bile through the ampulla of Vater after 30 min-1 h[47]. Interestingly, the diagnostic accuracy of gadoxetate disodium-enhanced MRCP for SOD has not yet been investigated; this represents an area of interest particularly when invasive evaluation is not indicated.

Mucocele of the cystic duct remnant

Mucocele of the cystic duct remnant, whether recipient or donor in origin, is an extremely rare complication after liver transplantation[48-51]. It is characterized by an abnormally dilated cystic duct remnant with flattening of the walls of the residual cystic duct to form a collection of mucus from cells lining the cystic duct remnant. The causative mechanism of the mucocele is still unclear. Lack of nervous regulation of the biliary tract after liver transplant may affect bile secretion and outflow. The differential diagnosis includes abscess, biloma, hemobilia, tumor, or aneurysm. If left untreated, the enlarged mucocele may cause chronic mechanical compression of the biliary system; however, it may also remain stable in size[50]. Ultrasound and CT demonstrate the presence of a collection at the level of the hepatic hilum. MRCP demonstrates a rounded and well-circumscribed collection adjacent to the common hepatic duct in the absence of other cause of obstruction (Figure 10).

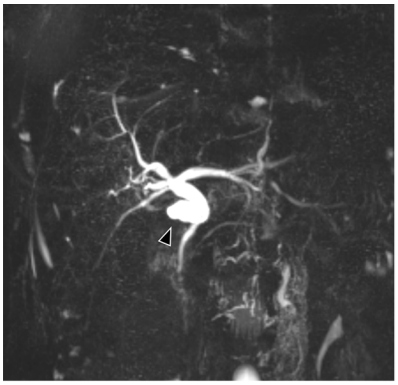
Bile duct redundancy

Bile duct redundancy is described as a surgically reconstructed donor-recipient extrahepatic bile duct that creates a looped, sigmoid-shaped appearance in the absence of any anastomotic stricture[8]. A



DOI: 10.3748/wjg.v29.i21.3257 **Copyright** ©The Author(s) 2023.

Figure 9 Enlarged ampullary papilla occurring years after liver transplantation and causing minimal cholestasis. T2-weighted imaging in the coronal plane demonstrates an enlarged ampullary papilla (arrowhead) protruding in the duodenal lumen (arrow). Ultrasonography-endoscopy confirmed the enlarged ampullary papilla and biopsy was performed, which excluded malignancy and confirmed the diagnosis of papillary stenosis (*i.e.* sphincter of Oddi dysfunction); sphincterotomy was then performed.



DOI: 10.3748/wjg.v29.i21.3257 **Copyright** ©The Author(s) 2023.

Figure 10 Mucocele occurring years after liver transplantation. Magnetic resonance cholangiopancreatography maximum intensity projection shows a fluid collection in communication with biliary tree. Biliary content was confirmed with percutaneous drainage.

redundant bile duct occurs when the donor or the recipient bile duct is too long, and may lead to delayed bile flow into the duodenum, functionally translating into cholestasis, abnormal liver laboratory test results, and cholangitis; it may also predispose to kinking of the redundant bile duct with subsequent obstruction[8,52,53]. Two-dimensional and 3-dimensional MRCP may demonstrate the abnormal long-constructed donor-recipient extrahepatic bile duct shape as well as any kinking, if present.

Vanishing bile duct syndrome

Vanishing bile duct syndrome is a very rare biliary complication occurring after liver transplantation, characterized by progressive destruction and disappearance of the intrahepatic bile ducts in the portal area leading to cholestasis[54,55]. It is caused by an acute or chronic T-cell-mediated rejection of the allograft[54,55]. The diagnosis of vanishing bile duct syndrome is suspected in a patient with liver biochemical abnormalities consistent with cholestasis in the absence of other conditions associated with cholestasis[54-56]. Histologic examination through liver biopsy is needed for the diagnosis, and MRI may help in excluding other causes of cholestasis[54,56].

CONCLUSION

In conclusion, biliary complications represent a clinically relevant problem after liver transplantation and occur in up to 1/3 of liver transplant recipients. Radiologists need to be aware of surgical techniques and post-surgical anatomy as well as clinical information for comprehensive image interpretation. MRCP is an established non-invasive procedure for the diagnosis of post-transplantation biliary complications. In selected cases, gadoxetate disodium-enhanced MRCP is needed for improving diagnostic accuracy of biliary complications and the protocol for this technique must be tailored based

on the clinical suspicion.

FOOTNOTES

Author contributions: Vernuccio F conceptualized the manuscript, wrote the outline of the manuscript, prepared some of the figures, and extensively revised the draft of the manuscript; Mercante I and Tong XX performed the literature search, wrote the first draft of the manuscript, and prepared most of the figures; Crimì F and Cillo U revised the draft of the manuscript and provided input; Quaia E conceptualized the manuscript, provided input, and revised the draft of the manuscript.

Conflict-of-interest statement: The authors report having no relevant conflicts of interest for this article.

Open-Access: This article is an open-access article that was selected by an in-house editor and fully peer-reviewed by external reviewers. It is distributed in accordance with the Creative Commons Attribution NonCommercial (CC BY-NC 4.0) license, which permits others to distribute, remix, adapt, build upon this work non-commercially, and license their derivative works on different terms, provided the original work is properly cited and the use is non-commercial. See: https://creativecommons.org/Licenses/by-nc/4.0/

Country/Territory of origin: Italy

ORCID number: Federica Vernuccio 0000-0003-0350-1794; Umberto Cillo 0000-0002-2310-0245.

S-Editor: Chen YL
L-Editor: Filipodia
P-Editor: Yu HG

REFERENCES

1 **Di Martino M**, Rossi M, Mennini G, Melandro F, Anzidei M, De Vizio S, Koryukova K, Catalano C. Imaging follow-up after liver transplantation. *Br J Radiol* 2016; **89**: 20151025 [PMID: 27188846 DOI: 10.1259/bjr.20151025]
2 **Daniel K**, Said A. Early Biliary complications after liver transplantation. *Clin Liver Dis (Hoboken)* 2017; **10**: 63-67 [PMID: 30992762 DOI: 10.1002/cld.654]
3 **Rönning J**, Berglund E, Arnelo U, Ericzon BG, Nowak G. Long-term Outcome of Endoscopic and Percutaneous Transhepatic Approaches for Biliary Complications in Liver Transplant Recipients. *Transplant Direct* 2019; **5**: e432 [PMID: 30882037 DOI: 10.1097/TXD.0000000000000869]
4 **Lemmers A**, Pezzullo M, Hadefi A, Dept S, Germanova D, Gustot T, Degré D, Boon N, Moreno C, Blero D, Arvanitakis M, Delhaye M, Vandermeeren A, Njimi H, Devière J, Le Moine O, Lucidi V. Biliary cast syndrome after liver transplantation: A cholangiographic evolution study. *J Gastroenterol Hepatol* 2021; **36**: 1366-1377 [PMID: 33150992 DOI: 10.1111/jgh.15318]
5 **Millson C**, Considine A, Cramp ME, Holt A, Hubscher S, Hutchinson J, Jones K, Leithead J, Masson S, Menon K, Mirza D, Neuberger J, Prasad R, Pratt A, Prentice W, Shepherd L, Simpson K, Thorburn D, Westbrook R, Tripathi D. Adult liver transplantation: UK clinical guideline - part 2: surgery and post-operation. *Frontline Gastroenterol* 2020; **11**: 385-396 [PMID: 32879722 DOI: 10.1136/flgastro-2019-101216]
6 **Akamatsu N**, Sugawara Y, Hashimoto D. Biliary reconstruction, its complications and management of biliary complications after adult liver transplantation: a systematic review of the incidence, risk factors and outcome. *Transpl Int* 2011; **24**: 379-392 [PMID: 21143651 DOI: 10.1111/j.1432-2277.2010.01202.x]
7 **Miller C**, Diago Uso T. The liver transplant operation. *Clin Liver Dis (Hoboken)* 2013; **2**: 192-196 [PMID: 30992860 DOI: 10.1002/cld.232]
8 **Torres V**, Martinez N, Lee G, Almeda J, Gross G, Patel S, Rosenkranz L. How do we manage post-OLT redundant bile duct? *World J Gastroenterol* 2013; **19**: 2501-2506 [PMID: 23674851 DOI: 10.3748/wjg.v19.i16.2501]
9 **Lisotti A**, Fusaroli P, Caletti G. Role of endoscopy in the conservative management of biliary complications after deceased donor liver transplantation. *World J Hepatol* 2015; **7**: 2927-2932 [PMID: 26730271 DOI: 10.4254/wjh.v7.i30.2927]
10 **Magro B**, Tacelli M, Mazzola A, Conti F, Celsa C. Biliary complications after liver transplantation: current perspectives and future strategies. *Hepatobiliary Surg Nutr* 2021; **10**: 76-92 [PMID: 33575291 DOI: 10.21037/hbsn.2019.09.01]
11 **McElroy LM**, Daud A, Davis AE, Lapin B, Baker T, Abecassis MM, Levitsky J, Holl JL, Ladner DP. A meta-analysis of complications following deceased donor liver transplant. *Am J Surg* 2014; **208**: 605-618 [PMID: 25118164 DOI: 10.1016/j.amjsurg.2014.06.006]
12 **Polak WG**, Porte RJ. The sequence of revascularization in liver transplantation: it does make a difference. *Liver Transpl* 2006; **12**: 1566-1570 [PMID: 17058245 DOI: 10.1002/Lt.20797]
13 **Scatton O**, Meunier B, Cherqui D, Boillot O, Sauvanet A, Boudjema K, Launois B, Fagniez PL, Belghiti J, Wolff P, Houssin D, Soubrane O. Randomized trial of choledochocholedochostomy with or without a T tube in orthotopic liver transplantation. *Ann Surg* 2001; **233**: 432-437 [PMID: 11224633 DOI: 10.1097/00000658-200103000-00019]
14 **Boraschi P**, Donati F, Gigoni R, Volpi A, Salemi S, Filipponi F, Falaschi F. MR cholangiography in orthotopic liver transplantation: sensitivity and specificity in detecting biliary complications. *Clin Transplant* 2010; **24**: E82-E87 [PMID: 20041910 DOI: 10.1111/j.1399-0012.2009.01190.x]

15 **Boraschi P**, Donati F, Pacciardi F, Ghinolfi D, Falaschi F. Biliary complications after liver transplantation: Assessment with MR cholangiopancreatography and MR imaging at 3T device. *Eur J Radiol* 2018; **106**: 46-55 [PMID: 30150050 DOI: 10.1016/j.ejrad.2018.07.009]

16 **Vernuccio F**, Whitney SA, Ravindra K, Marin D. CT and MR imaging evaluation of living liver donors. *Abdom Radiol (NY)* 2021; **46**: 17-28 [PMID: 31901101 DOI: 10.1007/s00261-019-02385-6]

17 **Kulkarni CB**, Prabhu NK, Kader NP, Rajeshkannan R, Pullara SK, Moorthy S. Percutaneous transhepatic techniques for management of biliary anastomotic strictures in living donor liver transplant recipients. *Indian J Radiol Imaging* 2017; **27**: 92-99 [PMID: 28515595 DOI: 10.4103/0971-3026.202950]

18 **Choi SH**, Kim KW, Kim SY, Kim JS, Kwon JH, Song GW, Lee SG. Computed tomography findings in ABO-incompatible living donor liver transplantation recipients with biliary strictures. *Eur Radiol* 2018; **28**: 2572-2581 [PMID: 29294154 DOI: 10.1007/s00330-017-5226-9]

19 **Khouri Chalouhi C**, Vernuccio F, Rini F, Duca P, Tuscano B, Brancatelli G, Vanzulli A. Hepatobiliary phase in cirrhotic patients with different Model for End-stage Liver Disease score: comparison of the performance of gadoxetic acid to gadobenate dimeglumine. *Eur Radiol* 2019; **29**: 3090-3099 [PMID: 30547205 DOI: 10.1007/s00330-018-5884-2]

20 **Verdonk RC**, Buis CI, Porte RJ, van der Jagt EJ, Limburg AJ, van den Berg AP, Slooff MJ, Peeters PM, de Jong KP, Kleibeuker JH, Haagsma EB. Anastomotic biliary strictures after liver transplantation: causes and consequences. *Liver Transpl* 2006; **12**: 726-735 [PMID: 16628689 DOI: 10.1002/Lt.20714]

21 **Sundaram V**, Jones DT, Shah NH, de Vera ME, Fontes P, Marsh JW, Humar A, Ahmad J. Posttransplant biliary complications in the pre- and post-model for end-stage liver disease era. *Liver Transpl* 2011; **17**: 428-435 [PMID: 21445926 DOI: 10.1002/lt.22251]

22 **Sotiropoulos GC**, Sgourakis G, Radtke A, Molmenti EP, Goumas K, Mylona S, Fouzas I, Karaliotas C, Lang H. Orthotopic liver transplantation: T-tube or not T-tube? Systematic review and meta-analysis of results. *Transplantation* 2009; **87**: 1672-1680 [PMID: 19502959 DOI: 10.1097/TP.0b013e3181a5cf3f]

23 **Huang WD**, Jiang JK, Lu YQ. Value of T-tube in biliary tract reconstruction during orthotopic liver transplantation: a meta-analysis. *J Zhejiang Univ Sci B* 2011; **12**: 357-364 [PMID: 21528489 DOI: 10.1631/jzus.B1100054]

24 **Ratcliffe GE**, Kirkpatrick ID, Anik Sahni V, Greenberg HM, Henderson B, Radulovic D, Mottola JC. Detection and localization of bile duct leaks after cholecystectomy using Gd-EOB-DTPA-enhanced MR cholangiography: retrospective study of 16 patients. *J Comput Assist Tomogr* 2014; **38**: 518-525 [PMID: 24651750 DOI: 10.1097/RCT.0000000000000083]

25 **Alegre Castellanos A**, Molina Granados JF, Escribano Fernandez J, Gallardo Muñoz I, Triviño Tarradas Fde A. Early phase detection of bile leak after hepatobiliary surgery: value of Gd-EOB-DTPA-enhanced MR cholangiography. *Abdom Imaging* 2012; **37**: 795-802 [PMID: 22213118 DOI: 10.1007/s00261-011-9834-6]

26 **Spies CK**, Unglaub F. Comment on "3-T direct MR arthrography of the wrist: value of finger trap distraction to assess intrinsic ligament and triangular fibrocartilage complex tears", Cerny M *et al*. Eur J Radiol (2013). *Eur J Radiol* 2013; **82**: e909 [PMID: 24016831 DOI: 10.1016/j.ejrad.2013.08.022]

27 **Kul M**, Erden A, Düşünceli Atman E. Diagnostic value of Gd-EOB-DTPA-enhanced MR cholangiography in non-invasive detection of postoperative bile leakage. *Br J Radiol* 2017; **90**: 20160847 [PMID: 28181823 DOI: 10.1259/bjr.20160847]

28 **Belinsky MG**, Dawson PA, Shchaveleva I, Bain LJ, Wang R, Ling V, Chen ZS, Grinberg A, Westphal H, Klein-Szanto A, Lerro A, Kruh GD. Analysis of the in vivo functions of Mrp3. *Mol Pharmacol* 2005; **68**: 160-168 [PMID: 15814571 DOI: 10.1124/mol.104.010587]

29 **Merkle EM**, Zech CJ, Bartolozzi C, Bashir MR, Ba-Ssalamah A, Huppertz A, Lee JM, Ricke J, Sakamoto M, Sirlin CB, Ye SL, Zeng M. Consensus report from the 7th International Forum for Liver Magnetic Resonance Imaging. *Eur Radiol* 2016; **26**: 674-682 [PMID: 26070500 DOI: 10.1007/s00330-015-3873-2]

30 **Koh DM**, Ba-Ssalamah A, Brancatelli G, Fananapazir G, Fiel MI, Goshima S, Ju SH, Kartalis N, Kudo M, Lee JM, Murakami T, Seidensticker M, Sirlin CB, Tan CH, Wang J, Yoon JH, Zeng M, Zhou J, Taouli B. Consensus report from the 9(th) International Forum for Liver Magnetic Resonance Imaging: applications of gadoxetic acid-enhanced imaging. *Eur Radiol* 2021; **31**: 5615-5628 [PMID: 33523304 DOI: 10.1007/s00330-020-07637-4]

31 **Gor NV**, Levy RM, Ahn J, Kogan D, Dodson SF, Cohen SM. Biliary cast syndrome following liver transplantation: Predictive factors and clinical outcomes. *Liver Transpl* 2008; **14**: 1466-1472 [PMID: 18825683 DOI: 10.1002/lt.21492]

32 **Cillo U**, Burra P, Norberto L, D'Amico D. Bile duct stones and casts after liver transplantation: Different entities but similar prevention strategy? *Liver Transpl* 2008; **14**: 1400-1403 [PMID: 18825732 DOI: 10.1002/lt.21628]

33 **Yang YL**, Zhang C, Lin MJ, Shi LJ, Zhang HW, Li JY, Yu Q. Biliary casts after liver transplantation: morphology and biochemical analysis. *World J Gastroenterol* 2013; **19**: 7772-7777 [PMID: 24282366 DOI: 10.3748/wjg.v19.i43.7772]

34 **Kinner S**, Umutlu L, Dechêne A, Ladd SC, Barkhausen J, Gerken G, Lauenstein TC, Hunold P. Biliary complications after liver transplantation: addition of T1-weighted images to MR cholangiopancreatography facilitates detection of cast in biliary cast syndrome. *Radiology* 2012; **263**: 429-436 [PMID: 22517958 DOI: 10.1148/radiol.12111625]

35 **Hogan WJ**, Geenen JE. Biliary dyskinesia. *Endoscopy* 1988; **20** Suppl 1: 179-183 [PMID: 3168947 DOI: 10.1055/s-2007-1018172]

36 **Geenen JE**, Hogan WJ, Dodds WJ, Toouli J, Venu RP. The efficacy of endoscopic sphincterotomy after cholecystectomy in patients with sphincter-of-Oddi dysfunction. *N Engl J Med* 1989; **320**: 82-87 [PMID: 2643038 DOI: 10.1056/NEJM198901123200203]

37 **Cotton PB**, Elta GH, Carter CR, Pasricha PJ, Corazziari ES. Rome IV. Gallbladder and Sphincter of Oddi Disorders. *Gastroenterology* 2016 [PMID: 27144629 DOI: 10.1053/j.gastro.2016.02.033]

38 **Cotton PB**, Pauls Q, Keith J, Thornhill A, Drossman D, Williams A, Durkalski-Mauldin V. The EPISOD study: long-term outcomes. *Gastrointest Endosc* 2018; **87**: 205-210 [PMID: 28455162 DOI: 10.1016/j.gie.2017.04.015]

39 **Fernandez-Simon A**, Sendino O, Chavez-Rivera K, Córdova H, Colmenero J, Crespo G, Fundora Y, Samaniego F, Ruiz P, Fondevila C, Navasa M, Cárdenas A. The presence and outcome of biliary sphincter disorders in liver-transplant recipients according to the Rome IV classification. *Gastroenterol Rep (Oxf)* 2021; **9**: 299-305 [PMID: 34567561 DOI:

10.1093/gastro/goab025]
40 **Riediger C**, Müller MW, Michalski CW, Hüser N, Schuster T, Kleeff J, Friess H. T-Tube or no T-tube in the reconstruction of the biliary tract during orthotopic liver transplantation: systematic review and meta-analysis. *Liver Transpl* 2010; **16**: 705-717 [PMID: 20517904 DOI: 10.1002/lt.22070]
41 **Douzdjian V**, Abecassis MM, Johlin FC. Sphincter of Oddi dysfunction following liver transplantation. Screening by bedside manometry and definitive manometric evaluation. *Dig Dis Sci* 1994; **39**: 253-256 [PMID: 8313805 DOI: 10.1007/BF02090194]
42 **Tulchinsky M**, Ciak BW, Delbeke D, Hilson A, Holes-Lewis KA, Stabin MG, Ziessman HA; Society of Nuclear Medicine. SNM practice guideline for hepatobiliary scintigraphy 4.0. *J Nucl Med Technol* 2010; **38**: 210-218 [PMID: 21078782 DOI: 10.2967/jnmt.110.082289]
43 **Sostre S**, Kalloo AN, Spiegler EJ, Camargo EE, Wagner HN Jr. A noninvasive test of sphincter of Oddi dysfunction in postcholecystectomy patients: the scintigraphic score. *J Nucl Med* 1992; **33**: 1216-1222 [PMID: 1597742]
44 **Rosenblatt ML**, Catalano MF, Alcocer E, Geenen JE. Comparison of sphincter of Oddi manometry, fatty meal sonography, and hepatobiliary scintigraphy in the diagnosis of sphincter of Oddi dysfunction. *Gastrointest Endosc* 2001; **54**: 697-704 [PMID: 11726844 DOI: 10.1067/mge.2001.118946]
45 **Swensson J**, Zaheer A, Conwell D, Sandrasegaran K, Manfredi R, Tirkes T. Secretin-Enhanced MRCP: How and Why-AJR Expert Panel Narrative Review. *AJR Am J Roentgenol* 2021; **216**: 1139-1149 [PMID: 33263419 DOI: 10.2214/AJR.20.24857]
46 **Pereira SP**, Gillams A, Sgouros SN, Webster GJ, Hatfield AR. Prospective comparison of secretin-stimulated magnetic resonance cholangiopancreatography with manometry in the diagnosis of sphincter of Oddi dysfunction types II and III. *Gut* 2007; **56**: 809-813 [PMID: 17005767 DOI: 10.1136/gut.2006.099267]
47 **Lee NK**, Kim S, Lee JW, Lee SH, Kang DH, Kim GH, Seo HI. Biliary MR imaging with Gd-EOB-DTPA and its clinical applications. *Radiographics* 2009; **29**: 1707-1724 [PMID: 19959517 DOI: 10.1148/rg.296095501]
48 **Chatterjee S**, Das D, Hudson M, Bassendine MF, Scott J, Oppong KE, Sen G, French JJ. Mucocele of the cystic duct remnant after orthotopic liver transplant: a problem revisited. *Exp Clin Transplant* 2011; **9**: 214-216 [PMID: 21649573]
49 **Caputo M**, Piolanti M, Riccioli LA, Pazienza L, Fabbro E, Gruppioni F, Grazi G, Gavelli G. [Nonobstructive residual mucocele of the cystic duct. Reassessment of complications in our 13 years' experience with liver transplantation]. *Radiol Med* 2000; **100**: 354-356 [PMID: 11213414]
50 **Zajko AB**, Bennett MJ, Campbell WL, Koneru B. Mucocele of the cystic duct remnant in eight liver transplant recipients: findings at cholangiography, CT, and US. *Radiology* 1990; **177**: 691-693 [PMID: 2243970 DOI: 10.1148/radiology.177.3.2243970]
51 **Chaly T**, Campsen J, O'Hara R, Hardman R, Gallegos-Orozco JF, Thiesset H, Kim RD. Mucocele mimicking a gallbladder in a transplanted liver: A case report and review of the literature. *World J Transplant* 2017; **7**: 359-363 [PMID: 29312865 DOI: 10.5500/wjt.v7.i6.359]
52 **Killenberg PG**, Clavien PA, Smith A, M¿llhaupt B. Medical Care of the Liver Transplant Patient: Total Pre-, Intra- and Post-Operative Management. 3rd Edition. Wiley-Blackwell, 2008 [DOI: 10.1016/j.dld.2006.09.014]
53 **Nöldge G**, Otto G, Theilmann L. Cholangiography After Orthotopic Liver Transplantation. Heidelberg: Springer Berlin, 1996 [DOI: 10.1007/978-3-642-61064-6]
54 **Hubscher SG**, Buckels JA, Elias E, McMaster P, Neuberger J. Vanishing bile-duct syndrome following liver transplantation--is it reversible? *Transplantation* 1991; **51**: 1004-1010 [PMID: 1851580 DOI: 10.1097/00007890-199105000-00014]
55 **Inomata Y**, Tanaka K. Pathogenesis and treatment of bile duct loss after liver transplantation. *J Hepatobiliary Pancreat Surg* 2001; **8**: 316-322 [PMID: 11521176 DOI: 10.1007/s005340170003]
56 **Yeh KH**, Hsieh HC, Tang JL, Lin MT, Yang CH, Chen YC. Severe isolated acute hepatic graft-versus-host disease with vanishing bile duct syndrome. *Bone Marrow Transplant* 1994; **14**: 319-321 [PMID: 7994249]

World Journal of Gastroenterology

Submit a Manuscript: https://www.f6publishing.com

World J Gastroenterol 2023 June 7; 29(21): 3269-3279

DOI: 10.3748/wjg.v29.i21.3269

ISSN 1007-9327 (print) ISSN 2219-2840 (online)

ORIGINAL ARTICLE

Basic Study

Effects of ethanol and sex on propionate metabolism evaluated *via* a faster ^{13}C-propionate breath test in rats

Yosuke Sasaki, Naoyuki Kawagoe, Tsunehiko Imai, Yoshihisa Urita

Specialty type: Gastroenterology and hepatology

Provenance and peer review: Unsolicited article; Externally peer reviewed.

Peer-review model: Single blind

Peer-review report's scientific quality classification

Grade A (Excellent): 0
Grade B (Very good): B
Grade C (Good): C
Grade D (Fair): 0
Grade E (Poor): 0

P-Reviewer: Baryshnikova NV, Russia; Wang Z, China

Received: February 2, 2023
Peer-review started: February 2, 2023
First decision: March 8, 2023
Revised: March 13, 2023
Accepted: May 6, 2023
Article in press: May 6, 2023
Published online: June 7, 2023

Yosuke Sasaki, Naoyuki Kawagoe, Tsunehiko Imai, Yoshihisa Urita, Department of General Medicine and Emergency Care, Toho University School of Medicine, Tokyo 143-8541, Japan

Corresponding author: Yosuke Sasaki, MD, PhD, Assistant Professor, Lecturer, Department of General Medicine and Emergency Care, Toho University School of Medicine, 6-11-1 Omori-Nishi, Ota-Ku, Tokyo 143-8541, Japan. yousuke.sasaki@med.toho-u.ac.jp

Abstract

BACKGROUND

Alcoholism is regarded as a risk factor for vitamin B_{12} (VB_{12}) deficiency. Because V B_{12} serves as a coenzyme of methylmalonyl-CoA mutase, a key enzyme in propionate metabolism, the ^{13}C-propionate breath test (PBT) has been studied as a non-invasive diagnostic modality for VB_{12} deficiency. However, the conventional PBT requires 2 h, which is inconvenient in clinical practice. We hypothesized that a faster PBT can be used to evaluate propionate metabolism and is more easily adaptable for clinical practice.

AIM

To evaluate a faster PBT for assessing the effects of long-term ethanol consumption on propionate metabolism in ethanol-fed rats (ERs).

METHODS

ERs were obtained by replacing standard drinking water (for control rats, CRs) with 16% ethanol solution in descendants of F344/DuCrj rats. Faster PBT was performed by administering ^{13}C-propionate aqueous solution to male and female ERs and CRs by inserting a metal tubule from the mouth to the stomach; exhaled gas was collected in a bag to measure its $^{13}CO_2/^{12}CO_2$ isotope ratio *via* infrared isotope spectrometry. Serum VB_{12} and alanine transaminase (ALT) levels were measured *via* chemiluminescence immunoassay and the lactate dehydrogenase-ultraviolet method, respectively. We evaluated statistical differences in mean body weight, change in $^{13}CO_2$ ($\Delta^{13}CO_2$‰), peak $\Delta^{13}CO_2$‰, and serum VB_{12} and ALT, between males and females and between ERs and CRs using the *t*-test and Mann-Whitney U test for normally and non-normally distributed variables, respectively.

RESULTS

Males weighed significantly more than females ($P < 0.001$); CRs weighed significantly more than ERs ($P < 0.008$). $\Delta^{13}CO_2$ reached a peak (C_{max}) at 20 min and

30 min in females and males, respectively, decreasing after 20-30 min without rebound in all groups. Males had significantly higher C_{max} and $\Delta^{13}CO_2$ at 15-45 min than females ($P < 0.05$; for all pairs). Propionate metabolism was enhanced in male ERs relative to male CRs, whereas metabolism did not differ markedly between ERs and CRs for females. Males had higher serum VB_{12} levels than females, without prominent differences between the ER and CR groups. Male CRs had notably higher ALT levels than male ERs. Thus, chronic ethanol consumption may trigger fatty acid production *via* intestinal bacteria and changes in gut microbiome composition.

CONCLUSION

Faster PBT shows that 16% ethanol consumption promotes propionate metabolism without inducing liver injury. This PBT may be used clinically to evaluate gut flora status.

Key Words: Alcoholism; Breath test; Carbon isotope; Gut flora; Propionate; Vitamin B12

©The Author(s) 2023. Published by Baishideng Publishing Group Inc. All rights reserved.

Core Tip: Alcoholism is a risk factor for vitamin B_{12} (VB_{12}) deficiency. The ^{13}C-propionate breath test (PBT) is a diagnostic modality for VB_{12} deficiency, but requires 2 h for completion. We applied a faster PBT to evaluate propionate metabolism using an ethanol-fed rat model. After ^{13}C-propionate administration, the $^{13}CO_2/^{12}CO_2$ isotope ratio of gas collected every 5 min for 60 min was measured using infrared isotope spectrometry. The $\Delta^{13}CO_2$ peak occurred within 30 min. Ethanol-fed males showed marked propionate metabolism without associated liver injury. This study demonstrates the potential of the faster PBT to evaluate propionate metabolism under various clinical conditions.

Citation: Sasaki Y, Kawagoe N, Imai T, Urita Y. Effects of ethanol and sex on propionate metabolism evaluated *via* a faster ^{13}C-propionate breath test in rats. *World J Gastroenterol* 2023; 29(21): 3269-3279
URL: https://www.wjgnet.com/1007-9327/full/v29/i21/3269.htm
DOI: https://dx.doi.org/10.3748/wjg.v29.i21.3269

INTRODUCTION

Chronic alcoholism is a risk factor for vitamin B_{12} (VB_{12}) deficiency[1,2]. Because VB_{12} works as a coenzyme of methylmalonyl-CoA mutase, a key enzyme in propionate metabolism (Figure 1), the ^{13}C-propionate breath test (PBT) has been studied as a non-invasive diagnostic modality for VB_{12} deficiency, with favorable results[3,4]. For instance, Wagner *et al*[3] reported that the conventional PBT could reliably predict VB_{12} deficiency in humans, with an area under the curve of the receiver operating curve value of 0.88. Propionate is a ubiquitous short chain fatty acid produced by intestinal bacteria, such as *Phascolarctobacterium*[5]. Emerging evidence suggests that intestinal microbial flora have a healing influence on alcoholic liver damage[6], and propionate produced by intestinal bacteria has protective effects against alcoholic liver damage[7]. Thus, we believe that PBT may provide important information not only regarding VB_{12}deficiency, but also regarding alcohol metabolism and alcoholic liver damage.

However, the conventional PBT requires 2 h to complete, which can be highly inconvenient for patients in clinical settings. Thus, in the present study, we aimed to evaluate the potential of a faster PBT for assessing the effects of long-term ethanol consumption on propionate metabolism as well as VB_{12} deficiency using ethanol-fed rats (ERs) as an animal model of chronic alcoholism. As the protective effects of estrogen against VB_{12} deficiency have been reported[8], we also evaluated the effect of sex-related differences on propionate metabolism, as detected by the faster PBT.

MATERIALS AND METHODS

Animals and treatments

All animal experiments were performed with approval of the Toho University School of Medicine, No. 21-51-4960. Descendants of F344/DuCrj rats purchased from CLEA Japan Inc. (Tokyo, Japan) for our previous study[9] were used to establish the ER and control rat (CR) groups for this study. All rats used in the present study were 18th-generation descendants of the originally established ER and CR groups, maintaining the lines within treatments (*i.e.*, parents of ERs were ERs, parents of CRs were CRs).

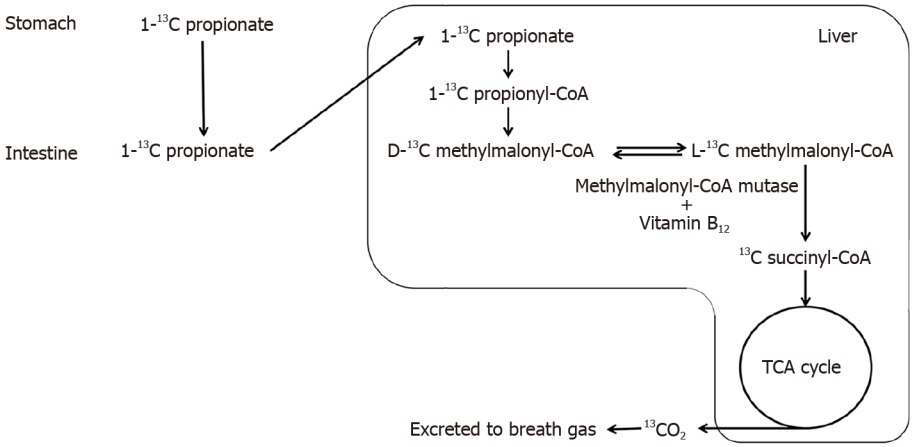


Figure 1 Propionate metabolism and the measuring principle of the propionate breath test. TCA: Tricarboxylic acid. Citation: Sasaki Y, Sato T, Maeda T, Komatsu F, Kawagoe N, Imai T, Shigeta T, Kashima N, Urita Y. [In Press] Evaluation of the One-Hour ^{13}C-Propionate Breath Test in 49 Patients from a Single Center in Japan to Detect Vitamin B_{12} Deficiency. *Med. Sci. Monit.* 2023 [DOI: 10.12659/MSM.940238]. Copyright © The Authors 2023. Published by Medical Science Monitor, International Scientific Information, Inc.

All rats were housed with their mothers until weaning at 4 wk of age. Subsequently, all rats were individually housed in a controlled environment (temperature, 23 ± 2 °C; humidity, 55% ± 5%) and provided a standard diet (CE-7; CLEA Japan Inc., Tokyo, Japan) and drinking liquid *ad libitum*. In the ER group, a 16% ethanol solution (Japanese Sake, Ozeki Corporation, Hyogo, Japan) was provided as a substitute for water by replacing the content of water bottles with ethanol solution in all cages of ERs.

A total of 16 ERs (8 males and 8 females) and 16 CRs (8 males and 8 females) aged 27-30 wk were used in the experiments; ERs continuously consumed alcohol for 23-27 wk. We used available descendants of F344/DuCrj rats that we had utilized in previous studies[9]. Therefore, we did not perform sample size calculation, randomization, or blinding.

Administration of ^{13}C-propionate and collection of exhaled gas

We purchased 1-^{13}C-sodium propionate from Cambridge Isotope Laboratories (Andover, MA, United States) and prepared a ^{13}C-propionate aqueous solution at 1 g/mL using distilled water immediately before administration. Body weight was measured immediately before administration. We performed gastrointestinal intubation in each rat and used a metal tubule, extending from the mouth to the stomach, to administer 0.1 mL/g of the ^{13}C-propionate solution. Immediately after administration, the rats were individually placed in the chambers of a dedicated exhaled-gas collection machine consisting of sealed chambers, pumps, and collecting bags, designed by Uchida *et al*[10]. We collected 100-200 mL of exhaled gas in the collecting bag for 90 s every 5 min for a total of 60 min.

Measurement of the ^{13}C recovery rate

Because ^{13}C-propionate is metabolized in the liver and exhaled as $^{13}CO_2$ (Figure 1), we measured the $^{13}CO_2/^{12}CO_2$ isotope ratio of the collected gas using infrared isotope spectrometry (POCone; Otsuka Electrics Co, Ltd., Hirakata, Japan) and monitored the change in $^{13}CO_2$ ($\Delta^{13}CO_2$‰), as reported previously[11].

Evaluation of serum VB_{12} and alanine transaminase levels

After collecting the exhaled gas for 60 min, the rats were immediately anesthetized *via* sevoflurane inhalation, and 5-10 mL of venous blood was collected from the inferior vena cava and the right atrium under laparotomy. After collecting sufficient blood samples, the animals were euthanized by rapid blood release. The blood was immediately centrifuged (relative centrifugal force: 1700 ×*g*) for 10 min, and the serum was collected. The serum was promptly frozen and submitted to FUJIFILM VET Systems Co. Ltd. (Tokyo, Japan) for measuring serum VB_{12} and ALT levels *via* chemiluminescence immunoassay and the lactate dehydrogenase-ultraviolet method, respectively.

Statistical analyses

We analyzed $\Delta^{13}CO_2$‰ measured every 5 min after ^{13}C-propionate administration for 60 min and serum VB_{12} levels, comparing the sexes and the ER and CR groups. The normality of the distribution of all variables was evaluated using the Kolmogorov-Smirnov test, and differences between groups were compared using the *t*-test and Mann-Whitney U test for normally and non-normally distributed variables, respectively. Statistical significance was set at $P < 0.05$. All statistical analyses were performed using Stata/IC software (version 15.1; Stata Corp., College Station, TX, United States). We used R 4.2.0 for construction of graphics[12]. The statistical methods were reviewed by Yosuke Sasaki from the Toho

University School of Medicine (the first author). As Yosuke Sasaki has completed several certified biostatistics courses, we did not obtain additional biostatical review suggestions by external biomedical statisticians.

RESULTS

Influence of ethanol and sex on body weight

Body weight was significantly higher ($P < 0.0001$) in males (335.8 ± 37.0 g) than in females (176.6 ± 21.9 g). In addition, body weight was significantly higher in CRs than in ERs for both males and females ($P = 0.0082$ and $P = 0.005$, respectively, Table 1).

Sex-related difference in PBT results

The $\Delta^{13}CO_2$ reached its peak (C_{max}) at 20 min and 30 min in females and males, respectively. The $\Delta^{13}CO_2$ decreased after 20-30 min without rebound in both groups (Table 2 and Figure 2). Therefore, the overall trends in $\Delta^{13}CO_2$ over time were similar between males and females, although C_{max} was delayed in males and $\Delta^{13}CO_2$ was significantly higher in males at 30 min and thereafter (Table 2 and Figure 2). The C_{max} and $\Delta^{13}CO_2$ values between 15 and 45 min were significantly higher in males than in females ($P < 0.05$, Table 2). Considering these sex-based differences, we further compared the effects of ethanol in males and females separately.

Effects of ethanol on propionate metabolism

Propionate metabolism was accelerated in the ERs relative to that in the CRs in males (Figure 3), with $\Delta^{13}CO_2$ at 10 and 20 min being markedly higher in male ERs. However, $\Delta^{13}CO_2$ after 40 min was higher in the CR group (Table 3). The $\Delta^{13}CO_2$ reached C_{max} earlier in the ERs (at 20 min) than in the CRs (at 30 min). These findings suggest that ethanol promoted propionate metabolism in male rats. However, propionate metabolism was similar between the ER and CR groups among females, without any significant differences ($P > 0.110$ for all pairs, Table 3, Figure 4).

Effects of ethanol on serum VB_{12} and ALT levels

The serum VB_{12} levels were significantly higher in males than in females ($P = 0.0013$, Table 4); however, no significant differences were observed between the ER and CR groups for either sex ($P > 0.05$ for all pairs, Table 4). In contrast, serum ALT levels were significantly higher in male CRs than in male ERs ($P = 0.0347$, Table 5).

DISCUSSION

In this study, we compared propionate metabolism using a faster PBT in rats and compared serum VB_{12} and ALT levels between males and females and between ER and CR groups. Overall, our study demonstrates that (1) The faster PBT is useful for evaluating differences in propionate metabolism after administration of a ^{13}C-propionate solution; (2) Males show greater propionate metabolism, with higher serum VB_{12} levels, than females; (3) Ethanol consumption promotes propionate metabolism in male rats only; and (4) Ethanol consumption reduces body weight and serum ALT levels.

In the faster PBT, $\Delta^{13}CO_2$ peaked at 30 min, then decreased over time without rebound in all groups. Accordingly, we consider the faster PBT, which is completed within only 60 min after ^{13}C propionate administration, to be sufficiently sensitive to evaluate propionate metabolism, as a substitute for the conventional PBT that requires collecting exhaled gas for 2 h.

Using the PBT, our study showed a higher C_{max} and $\Delta^{13}CO_2$ between 15 and 45 min in male rats than in female rats, which suggests that male rats have stronger propionate metabolism. Suppression of carbohydrate metabolism and promotion of lipid metabolism by estrogen in females have been proposed as mechanisms contributing to lower carbohydrate metabolism in females than in males[13]. Furthermore, a protective effect of estrogen against VB_{12} deficiency in fertile females has been reported, along with higher susceptibility to VB_{12} deficiency in postmenopausal women[8,14]. Considering that VB_{12} works as a coenzyme of methylmalonyl-CoA mutase, and that serum VB_{12} levels were not pathologically low in the rats used in our study, we postulate that the lower propionate metabolism detected by the faster PBT and the lower serum VB_{12} levels in females than in males may reflect underlying physiological sex-related differences in carbohydrate metabolism associated with estrogen.

As we aimed to use the faster PBT to evaluate impaired propionate metabolism due to VB_{12} deficiency and liver disease caused by chronic alcohol consumption, we expected to find lower propionate metabolism and higher serum ALT levels in the ER group than in the CR group. However, we obtained contrasting results, with acceleration of propionate metabolism in the ER group and higher serum ALT levels in the CR group. Changes in the gut flora caused by chronic alcohol consumption may explain the promotion of propionate metabolism in the ER group. Using male marmosets, Zhu *et al*[15] reported

Table 1 Body weight (g) in the ethanol-fed rat and control rat groups

	ER (*n* = 16)	CR (*n* = 16)	*P* value
Male (*n* = 16)	313.0 (18.4)	358.5 (37.5)	0.0082[a]
Female (*n* = 16)	162.5 (14.9)	190.6 (18.7)	0.005[a]

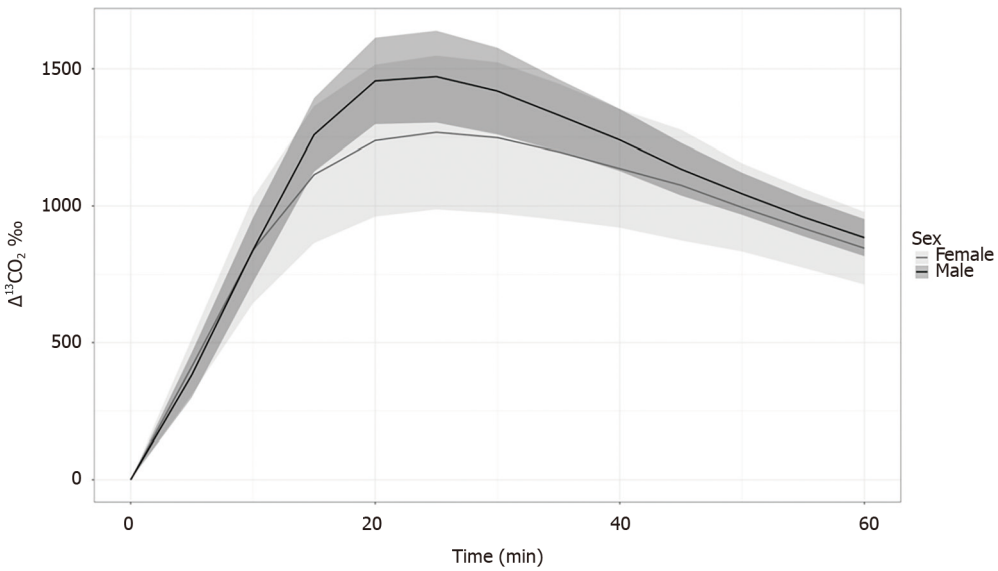
[a]*P* < 0.05.

Data are presented as mean (SD). CR: Control rat; ER: Ethanol-fed rat.

Table 2 Propionate breath test results in male and female rats

	Male (*n* = 16)	Female (*n* = 16)	*P* value
C_{max}	1478.0	1302.3	0.039[a]
5 min	381.8	412.5	0.358
10 min	838.6	837.4	0.983
15 min	1259.2	1114.1	0.049[a]
20 min	1455.7	1238.2	0.011[a]
25 min	1471.3	1267.9	0.007[a]
30 min	1418.5	1248.2	0.008[a]
35 min	1330.6	1197.1	0.010[a]
40 min	1240.3	1136.5	0.013[a]
45 min	1134.5	1075.9	0.035[a]
50 min	1044.7	994.6	0.050
55 min	959.9	918.8	0.083
60 min	884.2	845.6	0.309

[a]*P* < 0.05.



DOI: 10.3748/wjg.v29.i21.3269 **Copyright** ©The Author(s) 2023.

Figure 2 Comparison of faster propionate breath test results between the male and female rats. Note: Tinted area around each line indicates the standard deviation range.

Table 3 Propionate breath test results in the ethanol-fed rat and control rat groups

	Male			Female		
	CR (*n* = 8)	ER (*n* = 8)	*P* value	CR (*n* = 8)	ER (*n* = 8)	*P* value
C_{max}	1422.8	1533.1	0.192	1366.1	1238.5	0.401
5 min	345.8	417.9	0.080	410.8	414.2	0.950
10 min	752.3	924.9	0.0008[a]	867.6	807.3	0.552
15 min	1186.1	1332.5	0.023[a]	1203.2	1025	0.160
20 min	1402.3	1509.1	0.186	1324.7	1151.7	0.223
25 min	1402.1	152.6	0.235	1334.5	1201.4	0.462
30 min	1379.9	1457	0.348	1296.8	1199.7	0.753
35 min	1313.9	46	0.629	1237.2	1157.1	0.753
40 min	1223.2	1257.3	0.565	1179.2	1093.8	0.529
45 min	1126.6	1142.3	0.756	1131.3	1020.6	0.208
50 min	1051.8	1037.5	0.724	1050.4	938.7	0.172
55 min	974.2	945.6	0.436	976.4	861.3	0.142
60 min	904.1	864.4	0.256	898.9	792.3	0.110

[a]$P < 0.05$.
CR: Control rat; ER: Ethanol-fed rat.

Table 4 Effects of ethanol and sex on serum vitamin B_{12} (pg/mL)

	Male (*n* = 16)	Female (*n* = 16)	*P* value[1]	Total (*n* = 32)
All (*n* = 32)	884.0 (124.8)	728.5 (123.3)	0.0013[a]	-
ER (*n* = 16)	878.0 (152.5)	696.3 (152.5)	0.0323[a]	787.1 (175.1)
CR (*n* = 16)	890.0 (100.2)	760.8 (81.7)	0.0134[a]	825.4 (110.7)
P value[2]	0.8551	0.3117	-	0.4658

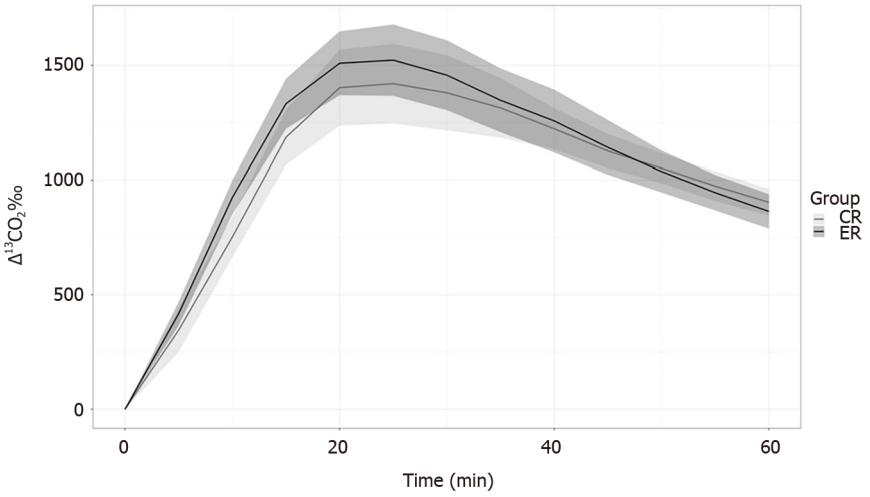
[1]Comparison of males *vs* females.
[2]Comparison of Ethanol-fed rat *vs* Control rat.
[a]$P < 0.05$.
Data are presented as mean (SD). CR: Control rat; ER: Ethanol-fed rat.

Table 5 Serum alanine transaminase (IU/L) levels

	ER (*n* = 16)	CR (*n* = 16)	*P* value
Total (*n* = 32)	55.7 (16.1)	79.3 (39.5)	0.0347[a]
Male (*n* = 16)	65.0 (16.8)	110.3 (32.3)	0.0034[a]
Female (*n* = 16)	46.4 (8.5)	48.3 (9.9)	0.6898

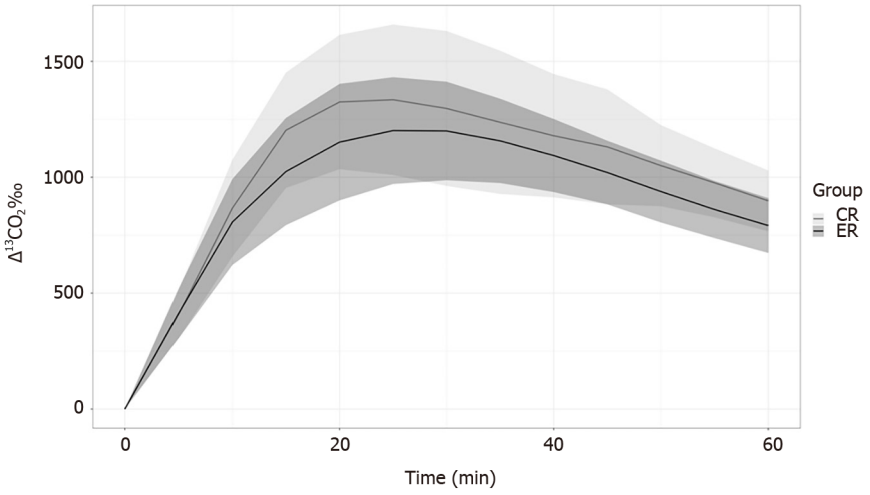
[a]$P < 0.05$.
Data are presented as mean (SD). CR: Control rat; ER: Ethanol-fed rat.

that the concentrations of short-chain fatty acids, including propionate, depend on changes in intestinal bacteria, based on an observed reduction in fecal propionate levels along with a reduction in the relative abundance of *Phascolarctobacterium* in the gut. Moreover, Watanabe *et al*[5] reported that the substrates of short-chain fatty acids, including propionate, produced by intestinal bacteria depend not only on a single bacterial strain, but also on the specific composition of other bacteria present in the gut. According to these reports, ethanol can serve as both a potential substrate of fatty acid production by



DOI: 10.3748/wjg.v29.i21.3269 **Copyright** ©The Author(s) 2023.

Figure 3 Comparison of propionate breath test results between the male ethanol-fed rat and male control rat groups. Note: Tinted area around each line indicates the standard deviation range. CR: Control rat; ER: Ethanol-fed rat.



DOI: 10.3748/wjg.v29.i21.3269 **Copyright** ©The Author(s) 2023.

Figure 4 Comparison of propionate breath test results between the female ethanol-fed rat and female control rat groups. Note: Tinted area around each line indicates the standard deviation range. CR: Control rat; ER: Ethanol-fed rat.

intestinal bacteria, such as *Phascolarctobacterium*, and as a trigger for changes in gut flora. Thus, we hypothesized that chronic alcohol consumption promotes propionate production both as a substrate for various fatty acids and as a trigger for changes in gut flora.

Alternatively, these observations may be due to the well-known difficulties in recapitulating the effects of chronic alcohol consumption in an animal model. We intended to establish a rat model of chronic alcoholism to evaluate the metabolic effect of ethanol consumption by oral administration of a 16% ethanol solution (corresponding to the level of alcohol commonly consumed by Japanese drinkers in the form of sake) for > 20 wk based on a previous study[16]. Therefore, we expected higher serum ALT levels in the ER group. Our contrasting result (lower serum ALT after 16% ethanol consumption) highlights the difficulty in the development of alcoholic animal models. A recent review on the utility of animal models for alcoholic liver disease mentioned that, in contrast to primates, rodent models fail to sufficiently display the full disease spectrum of alcoholic liver disease found in humans, despite many trials under various conditions[17]. The absence of craving in rats, owing to their natural aversion to ethanol[18,19], the faster ethanol catabolism in rodents than in humans[20], and differences in the innate immune systems of the species, have been proposed as the main factors contributing to the difficulty in establishing a useful rat model of human alcoholism[21]. It is therefore possible that our results also reflect failure to generate a chronic alcoholism rat model; thus, studies using primates or other small animals rather than rodents may be more appropriate. Considering the *ad libitum* diet administration, and the higher body weight in the CR group, fatty liver due to excessive dietary intake may explain the higher serum ALT levels in CRs. Because all of the rats consumed the same diet, it is possible that

consumption of 16% ethanol solution had a protective effect against liver damage. Given that propionate itself reportedly has protective effects against steatohepatitis[7], and that improvement of gut flora is an effective way to suppress liver damage[6], enhanced propionate metabolism and favorable changes in the gut flora might suppress liver damage in male ERs. As discussed earlier, the lack of acceleration in propionate metabolism in female ERs can be explained by sex-related differences in carbohydrate metabolism.

In addition to the lack of confirmation of the chronic alcoholism model, our study has other limitations. For instance, the serum methylmalonic acid (MMA) level, rather than the serum VB_{12} level, is required for the precise diagnosis of VB_{12} deficiency in humans[3]. However, we were not able to evaluate MMA levels because major domestic commercial laboratories no longer perform MMA testing of human serum or urine, and we could not find or access domestic laboratories measuring serum MMA in animal samples. Similarly, comparing the PBT results with biomarkers, such as aldehyde dehydrogenase and alcohol dehydrogenase, which sensitively and precisely reflect hepatic alcohol metabolism, may provide more information[22]. We believe that comparing levels of serum MMA and the markers evaluated using the faster PBT may provide further insight into the association between VB_{12} deficiency and alcoholism. Moreover, the present study only focused on the association between propionate metabolism and VB_{12} deficiency based on a previous study on PBT[3]. However, considering the complexity of intestinal propionate production due to the variety of propionate-producing bacteria, including *Clostridium* spp., *Veillonella* spp., *Fusobacterium* spp., *Salmonella ruminantium*, and *Propionibacterium* spp., and the complexity of substrates[23], the findings obtained herein, including the promoted propionate metabolism in male ERs and sex-related difference, may have potential clinical utility and provide a basis for future research into propionate metabolism and intestinal microbiota under various conditions. For instance, comparison of findings between faster PBT and the composition or changes in gut microbiota may provide interesting information on the association between gut microbiota and their products. Despite these limitations and lack of confirmation of VB_{12} deficiency under our experimental conditions, our study highlights the influence of ethanol and sex-related differences in propionate metabolism.

CONCLUSION

We evaluated a faster PBT in which C_{max} peaked within 30 min. This PBT could serve as a substitute for conventional PBT (which takes at least 2 h) for evaluating propionate metabolism and diagnosing VB_{12} deficiency. Although we could not evaluate the usefulness of faster PBT as a diagnostic modality for VB_{12} deficiency as initially intended because we failed to create a rat alcoholism model with VB_{12} deficiency, our study suggests that chronic consumption of 16% ethanol changed the composition of fatty acids produced by the intestinal flora, likely by changing the intestinal flora composition without causing corresponding liver injury. Considering the accumulating evidence of alteration of the gut flora as one of the mechanisms of alcoholism-related health impacts[24], our study demonstrates the potential utility of the faster PBT as a non-invasive and more convenient modality to evaluate changes in the gut flora associated with ethanol consumption and various other conditions.

ARTICLE HIGHLIGHTS

Research background

The ^{13}C-propionate breath test (PBT) has been studied as a non-invasive diagnostic modality for vitamin B_{12} (VB_{12}) deficiency by utilizing the role of VB_{12} as a coenzyme of methylmalonyl-CoA mutase in propionate metabolism. Although alcoholism has been regarded as a risk factor for deficiency, studies on propionate metabolism using the PBT in individuals with alcoholism is limited. Furthermore, conventional PBT requires up to 2 hours of breath collection time, which may undermine its clinical utility.

Research motivation

The scarcity of studies regarding the PBT in alcoholism, and the possibility of improving the clinical utility of the PBT by shortening the breath collection time, motivated us to perform this study.

Research objectives

The aim of this study was to evaluate the change in propionate metabolism due to long-term ethanol consumption in ethanol-fed rats (ERs) as an animal model of chronic alcoholism. We also aimed to evaluate the utility of a faster PBT that requires only 1 hour to collect breath.

Research methods

The ERs were 18th generation descendants of F344/DuCrj rats that had been bred by replacing standard drinking water with a 16% ethanol solution. A faster PBT was performed by injecting the ^{13}C-propionate aqueous solution from the mouth to the stomach of ERs and control rats (CRs); we collected exhaled gas in bags, and measured the $^{13}CO_2/^{12}CO_2$ isotope ratio using infrared isotope spectrometry. We measured serum VB_{12} and alanine transaminase (ALT) levels *via* chemiluminescence immunoassay and the lactate dehydrogenase-ultraviolet method, respectively. We evaluated statistical differences in mean body weight, change in $^{13}CO_2$ ($\Delta^{13}CO_2$‰), peak $\Delta^{13}CO_2$‰, and serum VB_{12} and ALT, between ERs and CRs, and males and females, respectively.

Research results

Besides male dominance of body weight ($P < 0.001$), CRs weighed significantly more than ERs ($P < 0.008$). The $\Delta^{13}CO_2$ reached a peak (C_{max}) within 30 min in both sex groups, while males had a significantly higher C_{max} and $\Delta^{13}CO_2$ at 15-45 min than females ($P < 0.05$; for all pairs). Enhanced propionate metabolism was observed in male ERs relative to male CRs, and although males had higher serum VB_{12} levels than females, no prominent differences were observed between the ER and CR groups. Male CRs had notably higher ALT levels than male ERs. These results suggest that chronic ethanol consumption may trigger fatty acid production *via* intestinal bacteria and changes in gut microbiome composition.

Research conclusions

We believe that a faster (1-h) PBT could serve as a substitute for the conventional PBT, as the $\Delta^{13}CO_2$ reached a peak (C_{max}) within 30 min in both sex groups. We failed to evaluate the usefulness of the faster PBT as a diagnostic modality for VB_{12} deficiency in the chronic alcoholism rat model; however, our study suggests that instead of inducing alcoholism, chronic consumption of 16% ethanol changed the composition of fatty acids produced by the intestinal flora.

Research perspectives

Our study demonstrates the potential utility of the faster PBT as a non-invasive and more convenient modality to evaluate changes in the gut flora associated with ethanol consumption and various other conditions *via* changes in propionate metabolism.

ACKNOWLEDGEMENTS

We thank Ms. Mitsuko Sato for her contributions to this study in a wide variety of areas, including the breeding of rats and the preparation of and participation in experiments.

FOOTNOTES

Author contributions: Sasaki Y and Urita Y coordinated the study; Sasaki Y, Kawagoe N, Imai T, and Urita Y performed the experiments; Sasaki Y and Urita Y acquired and analyzed the data; Sasaki Y and Urita Y interpreted the data; and Sasaki Y and Urita Y wrote the manuscript; All authors approved the final version of the article.

Supported by the Japan Society for the Promotion of Science KAKENHI Grant, No. JP21K18089.

Institutional review board statement: The study was reviewed and approved by the Toho University School of Medicine Institutional Review Board, No. 21-51-496.

Conflict-of-interest statement: All the authors report no relevant conflicts of interest for this article.

Data sharing statement: Technical appendix, statistical code, and dataset available from the corresponding author at yousuke.sasaki@med.toho-u.ac.jp.

ARRIVE guidelines statement: The authors have read the ARRIVE guidelines, and the manuscript was prepared and revised according to the ARRIVE guidelines.

Open-Access: This article is an open-access article that was selected by an in-house editor and fully peer-reviewed by external reviewers. It is distributed in accordance with the Creative Commons Attribution NonCommercial (CC BY-NC 4.0) license, which permits others to distribute, remix, adapt, build upon this work non-commercially, and license their derivative works on different terms, provided the original work is properly cited and the use is non-commercial. See: https://creativecommons.org/Licenses/by-nc/4.0/

Country/Territory of origin: Japan

ORCID number: Yosuke Sasaki 0000-0002-5290-4875; Naoyuki Kawagoe 0000-0001-8644-8583; Tsunehiko Imai 0000-0002-1483-6226; Yoshihisa Urita 0000-0003-1740-0572.

S-Editor: Li L
L-Editor: A
P-Editor: Li L

REFERENCES

1 **Lambert D**, Benhayoun S, Adjalla C, Gélot MM, Renkes P, Gérard P, Felden F, Belleville F, Gaucher P, Guéant JL, Nicolas JP. Alcoholic cirrhosis and cobalamin metabolism. *Digestion* 1997; **58**: 64-71 [PMID: 9018012 DOI: 10.1159/000201425]
2 **Han KM**, Chang HS, Choi IK, Ham BJ, Lee MS. CYP2D6 P34S Polymorphism and Outcomes of Escitalopram Treatment in Koreans with Major Depression. *Psychiatry Investig* 2013; **10**: 286-293 [PMID: 24302953 DOI: 10.4306/pi.2013.10.3.286]
3 **Wagner DA**, Schatz R, Coston R, Curington C, Bolt D, Toskes PP. A new 13C breath test to detect vitamin B12 deficiency: a prevalent and poorly diagnosed health problem. *J Breath Res* 2011; **5**: 046001 [PMID: 21697586 DOI: 10.1088/1752-7155/5/4/046001]
4 **Manoli I**, Pass AR, Harrington EA, Sloan JL, Gagné J, McCoy S, Bell SL, Hattenbach JD, Leitner BP, Duckworth CJ, Fletcher LA, Cassimatis TM, Galarreta CI, Thurm A, Snow J, Van Ryzin C, Ferry S, Mew NA, Shchelochkov OA, Chen KY, Venditti CP. 1-(13)C-propionate breath testing as a surrogate endpoint to assess efficacy of liver-directed therapies in methylmalonic acidemia (MMA). *Genet Med* 2021; **23**: 1522-1533 [PMID: 33820958 DOI: 10.1038/s41436-021-01143-8]
5 **Watanabe Y**, Nagai F, Morotomi M. Characterization of Phascolarctobacterium succinatutens sp. nov., an asaccharolytic, succinate-utilizing bacterium isolated from human feces. *Appl Environ Microbiol* 2012; **78**: 511-518 [PMID: 22081579 DOI: 10.1128/AEM.06035-11]
6 **Meroni M**, Longo M, Dongiovanni P. Alcohol or Gut Microbiota: Who Is the Guilty? *Int J Mol Sci* 2019; **20** [PMID: 31540133 DOI: 10.3390/ijms20184568]
7 **Xu Q**, Zhang R, Mu Y, Song Y, Hao N, Wei Y, Wang Q, Mackay CR. Propionate Ameliorates Alcohol-Induced Liver Injury in Mice *via* the Gut-Liver Axis: Focus on the Improvement of Intestinal Permeability. *J Agric Food Chem* 2022; **70**: 6084-6096 [PMID: 35549256 DOI: 10.1021/acs.jafc.2c00633]
8 **Margalit I**, Cohen E, Goldberg E, Krause I. Vitamin B12 Deficiency and the Role of Gender: A Cross-Sectional Study of a Large Cohort. *Ann Nutr Metab* 2018; **72**: 265-271 [PMID: 29597190 DOI: 10.1159/000488326]
9 **Kawagoe N**, Kijma S, Tanaka H, Takemoto I, Suzuki K, Saito T, Komatsu F, Yamada A, Kumade E, Sasaki Y, Maeda T, Kido H, Ishii T, Watanabe T, Miyazaki T, Hike N, Zai H, Urita Y, Nakajima H, Arai K, Imai T. Alteration of Breath Hydrogen and Methane in Ethanol-Fed Rats. *Nihon Arukoru Yakubutsu Igakkai Zasshi* 2016; **51**: 403-413 [PMID: 30461248]
10 **Uchida M**, Endo N, Shimizu K. Simple and noninvasive breath test using 13C-acetic acid to evaluate gastric emptying in conscious rats and its validation by metoclopramide. *J Pharmacol Sci* 2005; **98**: 388-395 [PMID: 16082175 DOI: 10.1254/jphs.fp0050153]
11 **Kawagoe N**, Kano O, Kijima S, Tanaka H, Takayanagi M, Urita Y. Investigation of Metabolism of Exogenous Glucose at the Early Stage and Onset of Diabetes Mellitus in Otsuka Long-Evans Tokushima Fatty Rats Using [1, 2, 3-13C]Glucose Breath Tests. *PLoS One* 2016; **11**: e0160177 [PMID: 27483133 DOI: 10.1371/journal.pone.0160177]
12 **R Core Team**. R: A language and environment for statistical computing. R Foundation for Statistical Computing, Vienna, Austria. 2022. [cited 14 January 2023]. Available from: https://www.R-project.org/ [DOI: 10.1007/s00607-022-01129-7]
13 **Tarnopolsky MA**, Ruby BC. Sex differences in carbohydrate metabolism. *Curr Opin Clin Nutr Metab Care* 2001; **4**: 521-526 [PMID: 11706287 DOI: 10.1097/00075197-200111000-00010]
14 **Miki A**, Kinno R, Ochiai H, Kubota S, Mori Y, Futamura A, Sugimoto A, Kuroda T, Kasai H, Yano S, Hieda S, Kokaze A, Ono K. Sex Differences in the Relationship of Serum Vitamin B1 and B12 to Dementia Among Memory Clinic Outpatients in Japan. *Front Aging Neurosci* 2021; **13**: 667215 [PMID: 33897411 DOI: 10.3389/fnagi.2021.667215]
15 **Zhu L**, Suhr Van Haute MJ, Hassenstab HR, Smith C, Rose DJ, Mustoe AC, Benson AK, French JA. Fecal Short-Chain Fatty Acid Concentrations Increase in Newly Paired Male Marmosets (Callithrix jacchus). *mSphere* 2020; **5** [PMID: 32938699 DOI: 10.1128/mSphere.00794-20]
16 **Lieber CS**, DeCarli LM, Sorrell MF. Experimental methods of ethanol administration. *Hepatology* 1989; **10**: 501-510 [PMID: 2673971 DOI: 10.1002/hep.1840100417]
17 **Lamas-Paz A**, Hao F, Nelson LJ, Vázquez MT, Canals S, Gómez Del Moral M, Martínez-Naves E, Nevzorova YA, Cubero FJ. Alcoholic liver disease: Utility of animal models. *World J Gastroenterol* 2018; **24**: 5063-5075 [PMID: 30568384 DOI: 10.3748/wjg.v24.i45.5063]
18 **Brandon-Warner E**, Schrum LW, Schmidt CM, McKillop IH. Rodent models of alcoholic liver disease: of mice and men. *Alcohol* 2012; **46**: 715-725 [PMID: 22960051 DOI: 10.1016/j.alcohol.2012.08.004]
19 **Bertola A**, Mathews S, Ki SH, Wang H, Gao B. Mouse model of chronic and binge ethanol feeding (the NIAAA model). *Nat Protoc* 2013; **8**: 627-637 [PMID: 23449255 DOI: 10.1038/nprot.2013.032]
20 **Holmes RS**, Duley JA, Algar EM, Mather PB, Rout UK. Biochemical and genetic studies on enzymes of alcohol metabolism: the mouse as a model organism for human studies. *Alcohol Alcohol* 1986; **21**: 41-56 [PMID: 2937415]
21 **Mestas J**, Hughes CC. Of mice and not men: differences between mouse and human immunology. *J Immunol* 2004; **172**: 2731-2738 [PMID: 14978070 DOI: 10.4049/jimmunol.172.5.2731]

22 **Zakhari S**. Overview: how is alcohol metabolized by the body? *Alcohol Res Health* 2006; **29**: 245-254 [PMID: 17718403]
23 **Eş I**, Khaneghah AM, Hashemi SMB, Koubaa M. Current advances in biological production of propionic acid. *Biotechnol Lett* 2017; **39**: 635-645 [PMID: 28150076 DOI: 10.1007/s10529-017-2293-6]
24 **Engen PA**, Green SJ, Voigt RM, Forsyth CB, Keshavarzian A. The Gastrointestinal Microbiome: Alcohol Effects on the Composition of Intestinal Microbiota. *Alcohol Res* 2015; **37**: 223-236 [PMID: 26695747]

World Journal of Gastroenterology

Submit a Manuscript: https://www.f6publishing.com

World J Gastroenterol 2023 June 7; 29(21): 3280-3291

DOI: 10.3748/wjg.v29.i21.3280

ISSN 1007-9327 (print) ISSN 2219-2840 (online)

ORIGINAL ARTICLE

Basic Study

Fibroblast growth factor 15, induced by elevated bile acids, mediates the improvement of hepatic glucose metabolism after sleeve gastrectomy

Meng Wei, Wei-Bo Cao, Ru-Dong Zhao, Dan-Ping Sun, Yi-Ze Liang, Ya-Di Huang, Ze-Wei Cheng, Jun Ouyang, Wen-Shuo Yang, Wen-Bin Yu

Specialty type: Gastroenterology and hepatology

Provenance and peer review: Unsolicited article; Externally peer reviewed.

Peer-review model: Single blind

Peer-review report's scientific quality classification

Grade A (Excellent): 0
Grade B (Very good): B, B
Grade C (Good): 0
Grade D (Fair): 0
Grade E (Poor): 0

P-Reviewer: Higashi Y, Japan; Pergamo M, United States

Received: March 6, 2023
Peer-review started: March 6, 2023
First decision: March 18, 2023
Revised: March 31, 2023
Accepted: May 8, 2023
Article in press: May 8, 2023
Published online: June 7, 2023

Meng Wei, Wei-Bo Cao, Ru-Dong Zhao, Dan-Ping Sun, Yi-Ze Liang, Ya-Di Huang, Ze-Wei Cheng, Jun Ouyang, Wen-Shuo Yang, Wen-Bin Yu, Department of General Surgery, Qilu Hospital of Shandong University, Jinan 250012, Shandong Province, China

Corresponding author: Wen-Bin Yu, MD, PhD, Chief Doctor, Professor, Department of General Surgery, Qilu Hospital of Shandong University, No. 107 Wenhua Xi Road, Jinan 250012, Shandong Province, China. wenbin_yu2003@163.com

Abstract

BACKGROUND

Fibroblast growth factor (FGF) 15/19, which is expressed in and secreted from the distal ileum, can regulate hepatic glucose metabolism in an endocrine manner. The levels of both bile acids (BAs) and FGF15/19 are elevated after bariatric surgery. However, it is unclear whether the increase in FGF15/19 is induced by BAs. Moreover, it remains to be understood whether FGF15/19 elevations contribute to improvements in hepatic glucose metabolism after bariatric surgery.

AIM

To investigate the mechanism of improvement of hepatic glucose metabolism by elevated BAs after sleeve gastrectomy (SG).

METHODS

By calculating and comparing the changes of body weight after SG with SHAM group, we examined the weight-loss effect of SG. The oral glucose tolerance test (OGTT) test and area under the curve of OGTT curves were used to assess the anti-diabetic effects of SG. By detecting the glycogen content, expression and activity of glycogen synthase as well as the glucose-6-phosphatase (G6Pase) and phosphoenolpyruvate carboxykinase (Pepck), we evaluated the hepatic glycogen content and gluconeogenesis activity. We examined the levels of total BA (TBA) together with the farnesoid X receptor (FXR)-agonistic BA subspecies in systemic serum and portal vein at week 12 post-surgery. Then the histological expression of ileal FXR and FGF15 and hepatic FGF receptor 4 (FGFR4) with its corresponding signal pathways involved in glucose metabolism were detected.

RESULTS

After surgery, food intake and body weight gain of SG group was decreased compare with the SHAM group. The hepatic glycogen content and glycogen synthase activity was significantly stimulated after SG, while the expression of the key enzyme for hepatic gluconeogenesis: G6Pase and Pepck, were depressed. TBA levels in serum and portal vein were both elevated after SG, the FXR-agonistic BA subspecies: Chenodeoxycholic acid (CDCA), lithocholic acid (LCA) in serum and CDCA, DCA, LCA in portal vein were all higher in SG group than that in SHAM group. Consequently, the ileal expression of FXR and FGF15 were also advanced in SG group. Moreover, the hepatic expression of FGFR4 was stimulated in SG-operated rats. As a result, the activity of its corresponding pathway for glycogen synthesis: FGFR4-Ras-extracellular signal regulated kinase pathway was stimulated, while the corresponding pathway for hepatic gluconeogenesis: FGFR4-cAMP regulatory element-binding protein- peroxisome proliferator-activated receptor γ coactivator-1α pathway was suppressed.

CONCLUSION

Elevated BAs after SG induced FGF15 expression in distal ileum by activating their receptor FXR. Furthermore, the promoted FGF15 partly mediated the improving effects on hepatic glucose metabolism of SG.

Key Words: Sleeve gastrectomy; Fibroblast growth factor 15; Bile acids; Hepatic glucose metabolism; Type 2 diabetes mellitus

©The Author(s) 2023. Published by Baishideng Publishing Group Inc. All rights reserved.

Core Tip: Sleeve gastrectomy (SG) improves hepatic glucose metabolism and alleviates type 2 diabetes mellitus through the intestine-liver crosstalk mediated by fibroblast growth factor 15 (FGF15). Following SG, bile acids are elevated, inducing the expression and secretion of FGF15 *via* the activation of farnesoid X receptor in the ileum. FGF15 then acts as an endocrine factor to promote glycogen synthesis and inhibit gluconeogenesis in the liver by specifically stimulating hepatic FGF receptor 4 and its corresponding signaling pathways.

Citation: Wei M, Cao WB, Zhao RD, Sun DP, Liang YZ, Huang YD, Cheng ZW, Ouyang J, Yang WS, Yu WB. Fibroblast growth factor 15, induced by elevated bile acids, mediates the improvement of hepatic glucose metabolism after sleeve gastrectomy. *World J Gastroenterol* 2023; 29(21): 3280-3291
URL: https://www.wjgnet.com/1007-9327/full/v29/i21/3280.htm
DOI: https://dx.doi.org/10.3748/wjg.v29.i21.3280

INTRODUCTION

The incidence of obesity along with the relative metabolic abnormalities[1], especially type 2 diabetes mellitus (T2DM)[2], is on the rise globally. Bariatric surgery becomes the most efficient treatment option for obese patients with diabetes[3] due to its prominent weight reduction and durable metabolic improvement effect[4,5]. Roux-en-Y gastric bypass (RYGB) and sleeve gastrectomy (SG) are the most commonly performed surgical procedures currently[3]. Moreover, SG has now exceeded RYGB as the preferred approach for most surgeons[6,7]. Still, the mechanisms underlying effects of bariatric surgery remain to be fully elucidated.

Bile acid (BA) has been considered as prospective factor for the metabolic actions of bariatric surgery [8] because of the considerable significance of its receptors, Takeda G protein-coupled receptor 5[9] and farnesoid X receptor (FXR)[10]. Through intestinal FXR, BAs could induce the expression and secretion of fibroblast growth factor (FGF) 15/19 in the distal ileum[11,12]. Recent studies illustrate that both BAs and FGF19 -the human ortholog of rodent FGF15[13]- are elevated after bariatric surgery[14-17]. Hence, the elevation of FGF19 after bariatric surgery probably results from the induction of FXR by elevated BAs, which needs further investigation. Moreover, FGF15/19 also plays a role in regulating the metabolic homeostasis, especially the hepatic glucose metabolism[18]. Similar to insulin's actions, FGF15/19 could act to lower the blood glucose level by repressing gluconeogenesis[19] and promoting glycogen synthesis[20] in the liver. Taken together, the ileal FXR-FGF15/19 pathway triggered by BAs might be another potential mechanism underlying the metabolic effects of bariatric surgery. However, to prove this, we need to confirm that the elevation of FGF15/19 results from the induction of FXR by elevated BAs and FGF15/19 participates in the improvement of hepatic glucose metabolism after

bariatric surgery.

As insulin and FGF15/19 can exert comparable metabolic actions on liver, only to detect the activities of glycogen synthesis and gluconeogenesis of liver could not distinguish the action of FGF15/19 from insulin. Previous studies demonstrated that FGF15/19 functions in an insulin-independent manner through activating FGF receptor 4 (FGFR4)[21] and its corresponding signal pathways. FGF15/19 could promote glycogen synthesis by activating the Ras- extracellular signal regulated kinase (ERK) pathway [20] and inhibit hepatic gluconeogenesis by suppressing the cAMP regulatory element-binding protein (CREB)- peroxisome proliferator-activated receptor γ coactivator-1α (PGC-1α) pathway[19]. However, insulin induces these effects through phosphoinositide 3-kinase (PI3K)-Akt pathway. The signaling pathways engaged in regulation of hepatic glucose metabolism by FGF15/19 and insulin permit overlapping, but can distinct the biological effects of these two hormones. Hence, to detect the expression of FGFR4 and the activities of its corresponding signaling pathways after bariatric surgery would help to confirm the action of FGF15/19 on hepatic glucose metabolism.

We conducted SHAM and SG operations on an obese diabetic rat model induced by high-fat diet (HFD) and streptozotocin (STZ) in this study. BAs levels in serum and portal vein, and the ileal expression of FXR and FGF15 were detected to confirm the elevation of the FGF15 as well as the underlying mechanism after surgery. Moreover, we detected the hepatic expression of FGFR4 and the activity of its corresponding signaling pathways involved in glucose metabolism to investigate whether FGF15 mediates the improvement of hepatic glucose metabolic after SG.

MATERIALS AND METHODS

Animals

We used Wistar rats in this study, and the rats (8-wk-old, 200 g on average) were purchased and housed in Laboratory Animal Center of Shandong University (Jinan, Shandong Province, China). The obese diabetic rat model was induced as previously reported[22,23]. The rats received a HFD (40% fat, 42% carbohydrate, 18% protein, Huafukang Biotech, China) for 1 mo, followed by low dose intraperitoneal STZ injection (35 mg/kg, Sigma, United States). The glucose level of peripheral blood obtained from tail vein was tested using a glucometer (Roche Diagnostics, Germany). Diabetes induction was confirmed based on the Oral Glucose Tolerance Test (OGTT) results and blood glucose levels examined at random time-points (≥ 16.7 mmol/L). The diabetic rats then randomly divided into matched SHAM (n = 10) and SG (n = 10) group. All actions and interventions applied on rats were approved and guided by Laboratory Animal Ethical and Welfare Committee of Shandong University Cheeloo College of Medicine.

Before operation, rats were fasted for about 12 h after two-days feeding of 10% Ensure (Abbott, United States). Moreover, anesthesia for rats was induced by 10% chloral hydrate (3 mL/kg).

Surgical procedures

SG: First, the relevant vessels and gastro-epiploic structures were ligated and transected to externalize the greater curvature of the stomach. Then, we conducted gastrectomy of 80% of the whole stomach from greater curvature, including the whole gastric fundus. The residual stomach was closed and continuously sutured with a 5-0 silk suture (Ningbo medical, China). The cardia, pylorus of stomach and continuity of stomach with esophagus and duodenum were all remained unaffected.

SHAM: In order to minimize the concomitant influence and bias triggered by surgical operation and anesthesia, we set SHAM group as previously reported. First, we isolated the greater curvature of stomach similarly as what we did in SG group. Then we clamped the stomach along the greater curvature with a pair of blunt forceps between cardia and pylorus to exert a similar pressure on the stomach. The exposed area and time of surgical field were extended as that of SG group to eliminate the undeserving influence of operation and anesthesia.

Postsurgical care: After surgery, the rats were only supplied with some water during the first 24 h. Then following 3-d feeding of 10% Ensure, the rats resumed the HDF diet till the end of the study. We recorded the body weight and calorie intake of every rat in both groups every day. Antibiotics were unnecessary and all rats in both groups survived and were sacrificed until the end of the study (week 12 post-surgery).

OGTT

We conducted OGTTs preoperatively to confirm diabetes induction and to evaluate the anti-diabetic effects of SG at week 12 post-surgery. After 12-h fasting, the rats received 20% glucose (1 g/kg) chow *via* oral gavage. Blood glucose levels were measured at time point of 0 min, 10 min, 30 min, 60 min, and 120 min after administration.

Detection of BAs

At 12 wk after surgery, total BAs (TBA) levels were examined in both the systemic serum and portal vein. In addition, the specific levels of the following four FXR-agonist BA species were also examined: Chenodeoxycholic acid (CDCA), DCA, lithocholic acid (LCA), and cholic acid (CA). One hour before sacrificed, all rats were gavaged with 10% Ensure after 12-h fasting. When sacrificing the rats, we collected blood samples from the retrobulbar venous plexus and portal vein. Portal and systemic serum levels of TBA were detected on the Roche Cobas 8000 system using the enzyme cycling method. As previously described[22,23], the levels of BA species (CDCA, DCA, LCA, and CA) in these samples were evaluated using high-pressure liquid chromatography coupled with tandem mass spectrometry (HPLC-MS/MS). Standard substrates for these four BA species were purchased from Sigma Aldrich (United States).

Histological analysis of ileum and liver tissues

After sacrificing, ileum and liver tissues in both groups were divided into three parts. Some were fixed in 4% paraformaldehyde and then embedded in paraffin for Periodic Acid-Schiff (PAS) staining and immunohistochemistry staining; some were stored at -80 °C for western blotting and hepatic glycogen content detection; and the others were stored in RNA*later*™ Stabilization Solution (Thermo Fisher Scientific™) for real-time PCR.

Real-time PCR

The levels of FGF15, FXR in ileum and FGFR4, glucose-6-phosphatase (G6Pase), phosphoenolpyruvate carboxykinase (Pepck) in liver were measured using RT-PCR. Total RNA was extracted from the tissue using TRIzol reagent (Invitrogen, United States) and then reversely transcribed to cDNA by the High Capacity cDNA Reverse Transcription Kit (TOYOBO, Japan). Subsequently, the relative level of mRNA amplification was determined through the SYBR Green Real-time PCR Master Mix Kit (TOYOBO, Japan) according to manufacturer's instructions. The following primers were used for analysis: FGF15: 5′-GCCATCAAGGACGTCAGCA-3′(F), 5′-CTTCCTCCGAGTAGCGAATCAG-3′ (R); FXR: 5′-TCCGGACATTCAACCATCAC-3′ (F), 5′-TCACTGCACATCCCAGATCTC-3′ (R); FGFR4: 5′-GGCCAGGTATACGGACATCA-3′ (F), 5′-GAGTCAGGCTGTCACATGTG-3′ (R); G6Pase: 5′-GTGGCAGTGGTCGGAGACT-3′ (F), 5′-ACGGGCGTTGTCCAAAC-3′ (R); Pepck: 5′-CACCATCACCTCCTGGAAGA-3′ (F), 5′-GGGTGCAGAATCTCGAGTTG-3′ (R).

Glycogen detecting and immunohistochemistry staining

We detected the hepatic glycogen content using the Glycogen Assay kit (ab65620, Abcam, United States) according to manufacturer's protocol. Sections of the paraffin-embedded tissues were prepared for PAS and immunohistochemistry staining. We stained the glycogen in hepatocytes with the PAS Stain Kit (Mucin Stain) (ab150680, Abcam, United States) according to the manufacturer's protocol. And we also examined the ileal expression of FGF15 and hepatic expression of FGFR4 by immunohistochemistry staining. The antibody for FGF15 (sc-16816) and FGFR4 (sc-136988) were both purchased from Santa Cruz Biotechnology (United States). Percentage of PAS- positive cells was calculated and quantification of immunoreactive signal was performed using Image J software.

Western blotting

We detected the hepatic expression of ERK1/2, p-ERK1/2, glycogen synthase (GS), p-GS, CREB, p-CREB and PGC-1α by western blotting. Anti-ERK1/2, anti-p-ERK1/2, anti-GS, anti-p-GS, anti-CREB, and anti-p-CREB for western blotting were purchased from Cell Signaling Technology (CST, United States), and anti-PGC-1α, anti-Actin were purchased from Abcam (United States).

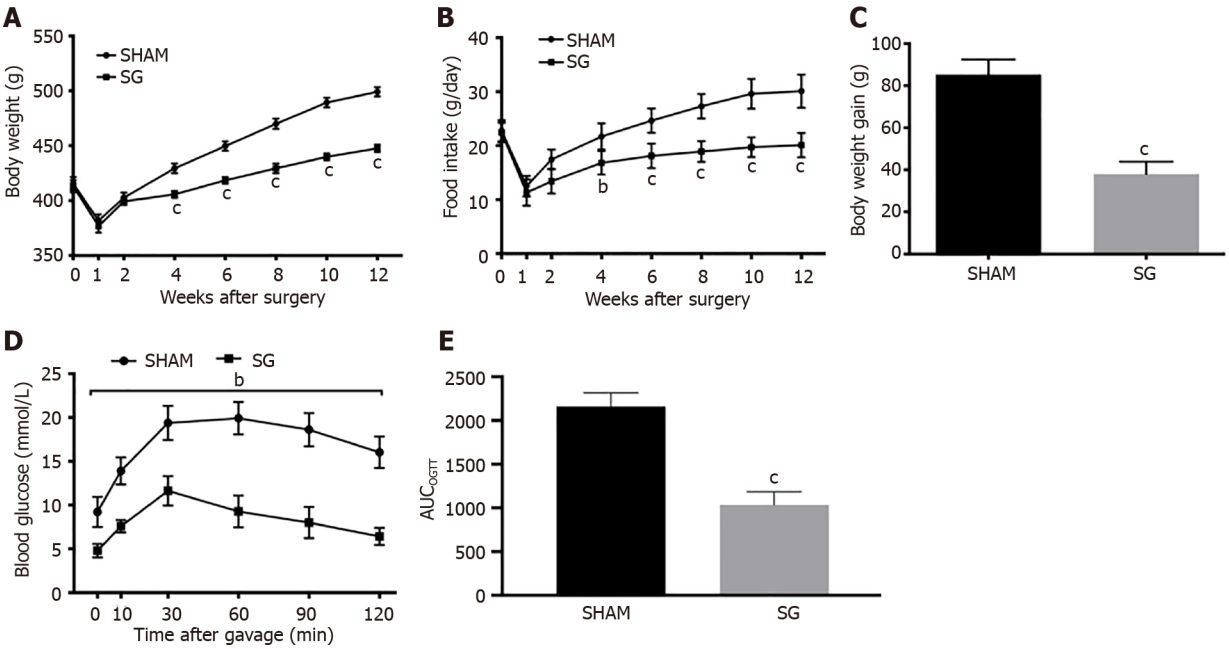
Statistical analysis

All quantitative data are presented in the pattern of mean ± SEM. The area under the curve (AUC) was evaluated using trapezoidal integration. We used unpaired Student's *t* test to analyzed statistical significance, and $P < 0.05$ indicated statistical significance. All statistical analyses were performed by SPSS version 20.0.

RESULTS

Weight loss and anti-diabetic effects of SG

According to our previous studies, we evaluated the weight-loss and anti-diabetic effects of SG postoperatively. First, we assessed the weight-loss action by tracking the body weight and daily food intake of the rats in SHAM and SG group. After a sharp decrease during the first week after surgery, the body weight and food intake gradually increased in both groups. Since week 4 post-surgery, the increase of body weight and food intake in SG group became significantly slower than that in SHAM group (Figure 1A and B). And the body weight gain of SG group was correspondingly lower than that



DOI: 10.3748/wjg.v29.i21.3280 **Copyright** ©The Author(s) 2023.

Figure 1 The weight-loss and anti-diabetic effects of sleeve gastrectomy. A: Body weight; B: Food intake; C: Body weight gain after surgery; D: The oral glucose tolerance test (OGTT) curves; E: Area under the curve for OGTT curves of SHAM and sleeve gastrectomy (SG) group at week 12 postoperation. $^{a}P < 0.05$, $^{b}P < 0.01$, $^{c}P < 0.001$; SG *vs* SHAM group. SG: Sleeve gastrectomy.

in SHAM group till week 12 post-surgery (Figure 1C). Then, we conducted the OGTT in both groups to evaluate the anti-diabetic effects of SG. The OGTT curves and result of AUC$_{OGTT}$ showed much better glucose tolerance in SG group than SHAM group (Figure 1D and E), which indicated a considerable anti-diabetic effect of SG.

Effects of SG on BA levels and ileal FGF15, FXR expressions

We detected the TBA levels both in systemic serum and portal vein at week 12 post-surgery, together with four BA species: CDCA, DCA, LCA, and CA, which are all FXR agonists. TBA levels of SG group in serum and portal vein were significantly higher than that in SHAM group (Figure 2A and B). Both CDCA and LCA levels in these two kinds samples were elevated and the portal vein DCA level was also higher in SG group (Figure 2C and D).

Then, we detected the influence of SG on FGF15 and FXR expressions in distal ileum. Both mRNA and protein expression levels of FGF15 in SG group were significantly higher than that in SHAM group (Figure 3A and D; Figure 4). Also, FXR mRNA level was also considerably elevated after SG (Figure 4).

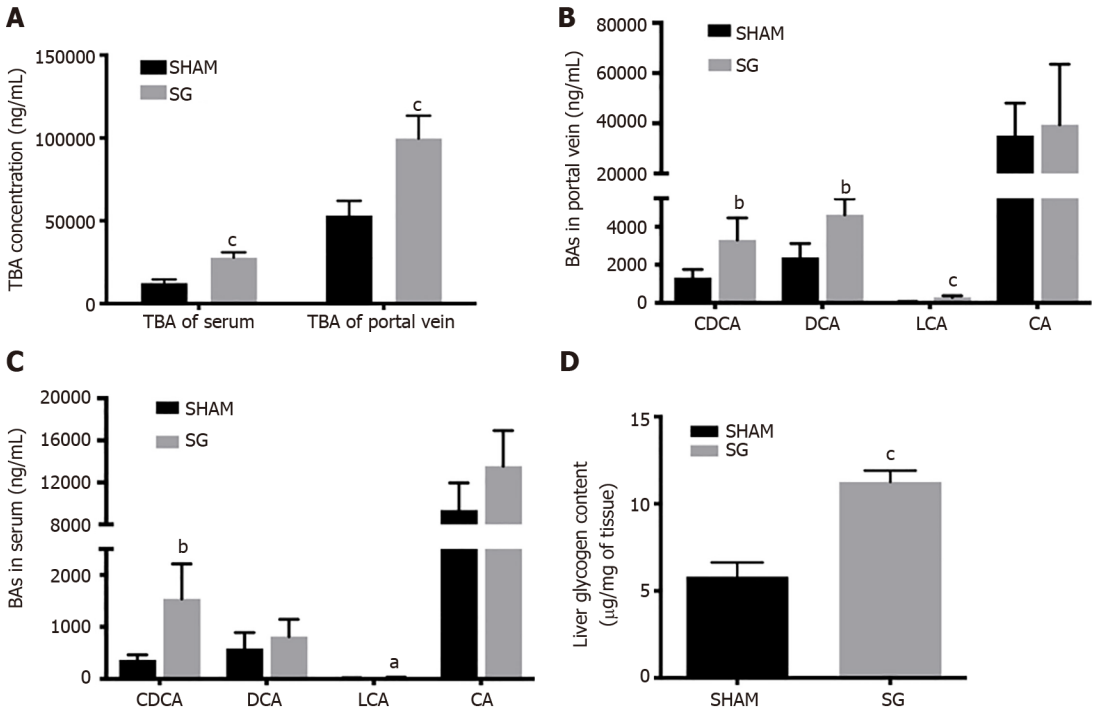
SG significantly improved the hepatic glucose metabolism

To evaluate the hepatic glucose metabolism, we detected the activities of hepatic glycogen synthesis and gluconeogenesis, together with the glycogen content in both groups after SG. The expression of glycogen synthase (GS) was significantly higher in the SG-operated rats, while the phosphorylation degree of GS (p-GS) was declined (Figure 5). In other words, the hepatic glycogen synthetic activity was significantly promoted after SG. Correspondingly, the glycogen content and the percentage of PAS-positive cells in liver were significantly higher in SG-operated rats (Figures 2A, 3B and E).

We then measured two key enzymes within hepatic gluconeogenesis, G6Pase and Pepck mRNA levels of both enzymes were significantly declined in SG group compared with SHAM group, which illustrated an inhibited gluconeogenesis process in SG-operated rats (Figure 4).

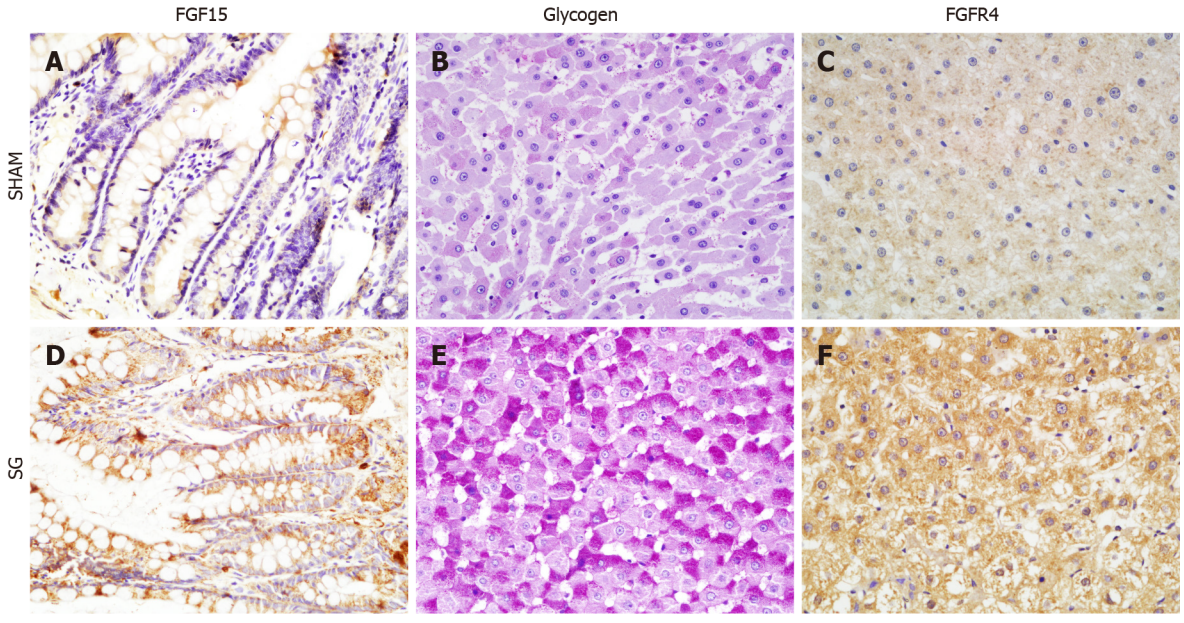
SG activated the receptor and regulated activities of the corresponding signal pathways of FGF15

FGF15/19 can activate its receptor, FGFR4 in the liver with unique specificity[25]. The expression of FGFR4 was significantly promoted at both mRNA and protein levels in SG group (Figure 4). FGF15-FGFR4 regulates hepatic glycogen synthesis and gluconeogenesis through Ras-ERK pathway and CREB-PGC-1α pathway, respectively. ERK1/2 regulates the phosphorylation degree of GS. We detected no difference in the expression of total ERK1/2 protein level. Whereas, the phosphorylation of ERK1/2 was increased in SG-operated rats, which indicates the activation of ERK1/2 pathway (Figure 5). On the contrary, the declined phosphorylation degree of CREB and decreased expression of PGC-1α (Figure 5) together with the inhibition of G6Pase and Pepck (G6Pase and Pepck are two target genes of PGC-1α) illustrated the inhibition of CREB-PGC-1α pathway in SG group.



DOI: 10.3748/wjg.v29.i21.3280 **Copyright** ©The Author(s) 2023.

Figure 2 Sleeve gastrectomy increased the bile acids levels and hepatic glycogen content. A: The concentration of total bile acid; B and C: The levels of chenodeoxycholic acid, DCA, lithocholic acid, and cholic acid in serum and portal vein, respectively; D: The glycogen content in liver at week 12 postoperation in SHAM and SG group. $^{a}P < 0.05$, $^{b}P < 0.01$, $^{c}P < 0.001$; SG *vs* SHAM group. BA: Bile acid; TBA: Total bile acid; SG: Sleeve gastrectomy; CDCA: Chenodeoxycholic acid; LCA: Lithocholic acid; CA: Cholic acid.

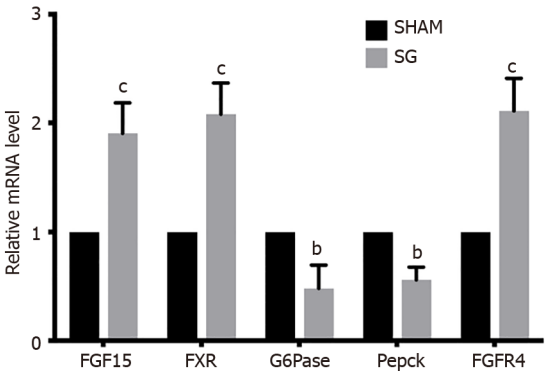


DOI: 10.3748/wjg.v29.i21.3280 **Copyright** ©The Author(s) 2023.

Figure 3 Sleeve gastrectomy promoted fibroblast growth factor 15, fibroblast growth factor receptor 4 expression and hepatic glycogen synthesis. A and D: The result of immune-histochemistry staining for ileal fibroblast growth factor (FGF) 15; B and E: The result of Periodic Acid-Schiff staining for glycogen in hepatocytes; C and F: Immune-histochemistry staining of hepatic FGF receptor 4 in SHAM and sleeve gastrectomy group at week 12 postoperation. Scale bar: 100 μm. SG: Sleeve gastrectomy; FGF: Fibroblast growth factor; FGFR4: Fibroblast growth factor receptor 4.

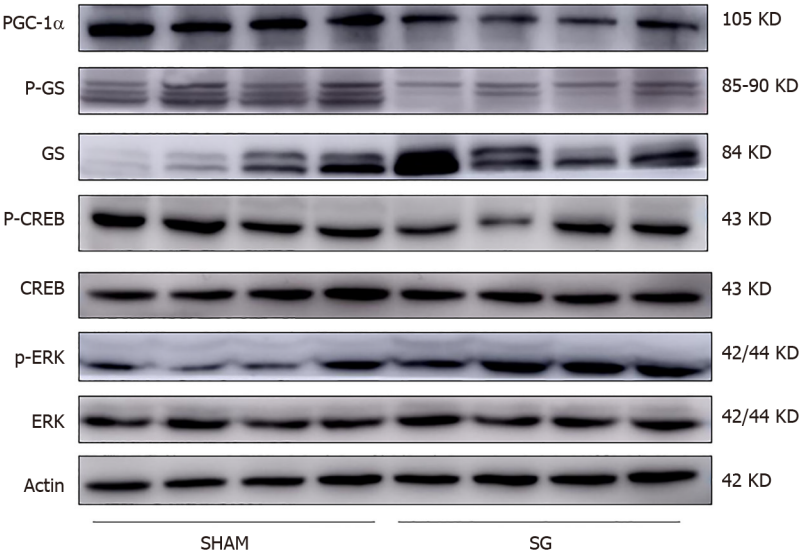
DISCUSSION

In this study, SG induced considerable weight loss and significantly improved the glucose homeostasis, especially the hepatic glucose metabolism in an obese diabetic rat model. Levels of TBA and FXR-



DOI: 10.3748/wjg.v29.i21.3280 **Copyright** ©The Author(s) 2023.

Figure 4 Farnesoid X receptor- fibroblast growth factor 15-fibroblast growth factor receptor 4 were stimulated and hepatic gluconeogenesis were depressed after sleeve gastrectomy. The mRNA relative expression of ileal fibroblast growth factor (FGF) 15, farnesoid X receptor, and hepatic glucose-6-phosphatase, phosphoenolpyruvate carboxykinase and fibroblast growth factor receptor 4 in SHAM and sleeve gastrectomy (SG) group at week 12 postoperation. $^{a}P < 0.05$, $^{b}P < 0.01$, $^{c}P < 0.001$, SG *vs* SHAM group. SG: Sleeve gastrectomy; FXR: Farnesoid X receptor; FGF: Fibroblast growth factor; FGFR4: Fibroblast growth factor receptor 4; Pepck: Phosphoenolpyruvate carboxykinase; G6Pase: Glucose-6-phosphatase.



DOI: 10.3748/wjg.v29.i21.3280 **Copyright** ©The Author(s) 2023.

Figure 5 Sleeve gastrectomy regulated activities of the corresponding pathways of fibroblast growth factor 15. Western blotting for expression of extracellular signal regulated kinase (ERK), p-ERK, cAMP regulatory element-binding protein (CREB), p-CREB, glycogen synthase (GS), p-GS, and proliferator-activated receptor γ coactivator-1α (PGC-1α) in the liver of both SHAM and sleeve gastrectomy group at week 12 postoperation. PGC-1α: Proliferator-activated receptor γ coactivator-1α; ERK: Extracellular signal regulated kinase; CREB: cAMP regulatory element-binding protein; GS: Glycogen synthase; SG: Sleeve gastrectomy.

agonistic BA subspecies were all increased in the serum of both peripheral circulation and portal vein. Besides, the expression of FGF15 which was induced by FXR activation in the ileum was increased after SG. And the FGF15 receptor FGFR4 in the liver together with its corresponding signal pathways involved in hepatic glycogen synthesis and gluconeogenesis were also activated.

Liver plays a key role in the metabolic regulation of the whole body, especially in maintaining homeostasis of blood glucose level through synthesis or breaking down of glycogen and the action of gluconeogenesis. One of the insulin's actions is to promote glycogen synthesis and inhibit hepatic gluconeogenesis which is impaired in diabetic patients. While, we found that SG improved the glucose tolerance of diabetic rats in this study, the hepatic glycogen content was elevated and the expression of two key enzymes[19] (G6pase and Pepck) responsible for hepatic gluconeogenesis were decreased in the SG-operated rats. In other words, SG increased the insulin sensitivity by promoting the synthesis of glycogen and inhibiting the hepatic gluconeogenesis. Moreover, recent studies found that FGF15/19 could also exert the similar effects as insulin on hepatic metabolism in an insulin-independent pattern [19,20]. Furthermore, the serum FGF19 Level of diabetic patients was elevated after bariatric surgery[14-17]. Therefore, except the improvement of insulin sensitivity, the improvement of glucose tolerance post-surgery may also be partly mediated by the elevated FGF15/19.

Consistent with previous findings of FGF 19 in human, the ileal expression of FGF15 was increased in SG-operated rats in our study and the TBA levels in systemic serum and portal vein were also increased after SG. This may inconsistent with previous reports that FGF15 acts as an endocrinal factor to repress BA synthesis in the liver[11]. However, our previous studies have already proved that the elevation of serum BA level was mainly a result of the promoted ileal reabsorption rather than hepatic synthesis[22,23]. According to the process of the enterohepatic circulation, systemic serum BAs is a combinational result of hepatic uptake and ileal reabsorption of BAs and portal vein BAs levels can reflect the ileal reabsorption and the BA concentration of distal ileum[26,27]. Hence, the elevation of TBAs in systemic serum and portal vein in this study must be a result of the promoted ileal reabsorption. Then, we also explored the cause for the elevated expression of FGF15 in our study. FGF15/19 is mainly expressed in distal ileum and can be induced by FXR[28,29]. The increased ileal mRNA level of FXR in our study should be responsible for the elevation of FGF15 after SG. Moreover, FXR can be activated by different BA subspecies, among which CDCA is the most efficacious[30]. Furthermore, oral or intraduodenal infusion of CDCA triggers increase of serum FGF19 Level in humans[31,32]. Consistent with our previous study[22,23], CDCA levels as well as other FXR agonists were elevated after SG both in systemic serum and portal vein. Hence, activation of ileal FXR in this study would result from the elevation of these agonists among the SG-operated rats. Taken together, enhanced reabsorption of BAs after SG activated FXR in the ileum, which then promoted the expression and secretion of FGF15.

Stimulated by ileal FXR, FGF15/19 is promoted and secreted into the enterohepatic circulation. In addition of the regulation of BA homeostasis, FGF15/19 also plays a role in the hepatic glucose metabolism. Evidence have shown that FGF 15 knockout mice showed impaired glucose tolerance with decreased hepatic glycogen storage and advanced hepatic gluconeogenesis[20]. Diet-induced obesity and insulin resistance was failed in FGF19 transgenic mice[33,34]. These effects of FGF15/19 are all mediated through FGFR[35-37], the receptor of FGF15/19 with an unique specificity[21,25]. Moreover, expression of FGFR4 in liver was decreased among STZ-induced diabetes[36]. FGFR4-deficient mice displayed glucose intolerance and insulin resistance as well as increased weight gain[35]. As described above, FGF15/19-FGFR4 plays an important role in hepatic glucose metabolism. Considering the elevation of FGF15, we then examined whether FGF15-FGFR4 functions in the improvement of hepatic glucose metabolism after SG. The hepatic expression of FGFR4 among the HFD and STZ-induced diabetic rats was elevated after SG in this study, which indicates that FGF15-FGFR4 was activated in SG-operated rats. However, we still can't conclude that FGF15-FGFR4 acts in improving the hepatic glucose metabolism because the regulation of BAs synthesis by FGF15 also needs activation of FGFR4.

To further confirm whether FGF15-FGFR4 contributes to the improvement of glucose metabolism in SG-operated rats, we detected the corresponding pathways of FGF15-FGFR4 involved in the hepatic glucose metabolism. Comparable to insulin, FGF15/19 could regulate hepatic glucose metabolism by promoting glycogen synthesis and inhibiting hepatic gluconeogenesis. But unlike the insulin-inducing PI3K-Akt patway, FGF15/19 acts through two different pathways. Moreover, FGF15/19 the inhibiting effect on BA synthesis of FGF15/19 was through a c-Jun N-terminal kinase-dependent pathway[12]. FGF15/19 promotes the hepatic glycogen synthesis by activating Ras-ERK pathway[20]. FGF15/19-FGFR4 triggers the phosphorylation of ERK1/2, which then increase the activity of GS by inhibiting the phosphorylation of this enzyme. Therefore, the increased phosphorylation of ERK1/2 and the declined phosphorylation of GS observed in this study indicated that FGF15-FGFR4-Ras-ERK pathway was activated in SG-operated rats. Together with the elevated glycogen content, we can conclude that the action of FGF15 (and its corresponding pathways) contributed to the glycogen synthesis promoting effect of SG. Moreover, FGF15/19 inhibits hepatic gluconeogenesis by supressing the CREB-PGC-1α pathway[19]. FGF15/19 could induce dephosphorylate and suppress the transcription factor CREB and correspondingly inhibited the expression of PGC-1α. Besides, G6Pase, and Pepck, the two key enzymes for hepatic gluconeogenesis, are two target genes of PGC-1α. So, integrating together the depressed phosphorylation of CREB, reduced expression of PGC-1α and the inhibited expression of G6Pase and Pepck, we could predicate that FGF15 inhibited the CREB-PGC-1α pathway and participated in suppressing the hepatic gluconeogenesis in SG-operated rats. Hence, the activated Ras-ERK1/2 pathway and inhibited CREB-PGC-1α pathway indicated that elevated FGF15 after SG played a role in regulating the hepatic glucose metabolism in parallel to insulin.

In this study, we confirmed the effect of elevated BAs and FGF15 on the hepatic glucose metabolism. FGF15, induced by elevated BAs in ileum, acts as an endocrine factor on the liver through portal vein. By specifically binding and activating the FGFR4 and its corresponding signal pathways, FGF15 improves the hepatic glucose metabolism through the intestine-liver crosstalk. Similarly, human FGF19, which is an ortholog of rodent FGF15, was also elevated after SG together with BAs. Besides, FGF19 can also bind and activate the FGFR 4 specifically. Thus, the results of this study presented basics for the research of human FGF19 after SG, and the FGF19 would be developed to be a target for clinical treatment of T2DM in the future.

Certainly, this study has several limitations. First, we did not directly detect the FGF15 Levels in serum and portal vein because no ELISA kits for FGF15 was available at that time. However, we detected the expression of FGF15 in the ileum at both mRNA and protein levels. As FGF15 is mainly expressed and secreted from the ileum into enterohepatic circulation, the ileal expression could reflect the FGF15 Levels in serum and portal vein. Second, the postprandial FGF15 Level varies with time, it is

better to trace the FGF15 Levels at different time points after gavage. However, we can only sacrifice the rat and detect the expression of FGF15 in the ileum once. And, as previously reported, the expression level of FGF15 mRNA in ileum and the phosphorylation degree of downstream hepatic ERK1/2 reach the peak 1h after feeding in rodent[19]. So, we sacrificed the rats 1h after gavage and the following results then may be more meaningful and advisable. Third, the improvement of hepatic glucose metabolism after SG should surely be mainly mediated by insulin. Though the action of FGF15 underlying the effects of SG was proved in our study, the proportion of these effects accounted by FGF15 still needs further evaluation. Finally, the data presented in this study only show associations, but no causal relationships between the alteration of FGF15 and improvement of hepatic glucose metabolism after SG, which would have to be further investigated by using KO models.

CONCLUSION

BAs levels were elevated in the SG-operated rats and induced FGF15 expression by activating their receptor, FXR in distal ileum. Moreover, the action of FGF15 on hepatic glycogen synthesis and gluconeogenesis further contributes to the anti-diabetic effects of SG.

ARTICLE HIGHLIGHTS

Research background

Bariatric surgery can significantly ameliorate type 2 diabetes mellitus (T2DM) through its rapid and durable weight-loss and hypoglycemic action. Both biles acids (BAs) and fibroblast growth factor (FGF) 15/19 are increased after surgery. Whether BAs and FGF15/19 participates in amelioration of T2DM after bariatric surgery and the underlying mechanism remain incompletely illuminated.

Research motivation

FGF15 which is induced by farnesoid X receptor (FXR) in ileum can improve the hepatic glucose metabolism through entero-hepatic circulation. Our previous study confirms that BA profiles within peripheral circulation and portal vein have changed after SG, with significant increase of FXR- activated BAs levels.

Research objectives

This study aimed to evaluate the effect of FGF15 on improvement of T2DM triggered by elevated BAs after sleeve gastrectomy (SG) and investigate the underlying mechanism.

Research methods

The weight-loss and hypoglycemic action of SG were detected in a diabetic rat model induced by High-fat diet and streptozotocin (STZ), as well as the hepatic glycogen content and gluconeogenesis activity. Total BA (TBA) together with the FXR-agonistic BA subspecies levels in systemic serum and portal vein were examined at week 12 post-surgery. Then the expression and activity of ileal FXR and FGF15 and hepatic FGFR4 with its corresponding signal pathways involved in glucose metabolism were detected.

Research results

Compared with SHAM group, SG induced sustained weight loss and improved the hepatic glucose metabolism by promoting hepatic glycogen synthesis and inhibiting the gluconeogenesis. TBA levels and the FXR-agonistic subspecies in serum and portal vein were elevated after SG. Consequently, the ileal expression of FXR and FGF15 were also advanced. Moreover, the hepatic expression of FGFR4 and the activities of its corresponding pathways were stimulated in SG-operated rats.

Research conclusions

FGF15, triggered by elevated BAs after SG, acts as an endocrine factor to induce the improvement of hepatic glucose metabolism through the intestine-liver crosstalk.

Research perspectives

FXR-agonistic BA subspecies and FGF15 participate in improvement of hepatic glucose metabolism, and may be developed as new targets for the treatment of T2DM.

FOOTNOTES

Author contributions: Wei M and Yu WB contributed to conception and design of research; Wei M, Sun DP, Yang WS, Cao WB, and Zhao RD contributed to performed experiments; Wei M, Liang YZ, and Cheng ZW analyzed data; Wei M, Sun DP, Liang YZ, and Ouyang J prepared figures; Wei M, Huang YD, and Sun DP drafted manuscript; Wei M, Liang YZ, and Yu WB edited and revised manuscript; Wei M, Sun DP, Cao WB, Zhao RD, Liang YZ, Huang YD, Cheng ZW, Ouyang J, Yang WS, and Yu WB approved final version of manuscript.

Supported by the National Natural Science Foundation of China, No. 81600617.

Institutional review board statement: The study was reviewed and approved by the laboratory animal ethical and welfare committee of Shandong University Cheeloo College of Medicine Institutional Review Board (Approval No. 19200).

Conflict-of-interest statement: The authors declare that they have no competing interests.

Data sharing statement: No additional data are available.

ARRIVE guidelines statement: The authors have read the ARRIVE Guidelines, and the manuscript was prepared and revised according to the ARRIVE Guidelines.

Open-Access: This article is an open-access article that was selected by an in-house editor and fully peer-reviewed by external reviewers. It is distributed in accordance with the Creative Commons Attribution NonCommercial (CC BY-NC 4.0) license, which permits others to distribute, remix, adapt, build upon this work non-commercially, and license their derivative works on different terms, provided the original work is properly cited and the use is non-commercial. See: https://creativecommons.org/Licenses/by-nc/4.0/

Country/Territory of origin: China

ORCID number: Meng Wei 0000-0002-0402-5083; Wen-Bin Yu 0000-0001-7111-3780.

S-Editor: Chen YL
L-Editor: A
P-Editor: Ma YJ

REFERENCES

1 **Sun H**, Saeedi P, Karuranga S, Pinkepank M, Ogurtsova K, Duncan BB, Stein C, Basit A, Chan JCN, Mbanya JC, Pavkov ME, Ramachandaran A, Wild SH, James S, Herman WH, Zhang P, Bommer C, Kuo S, Boyko EJ, Magliano DJ. IDF Diabetes Atlas: Global, regional and country-level diabetes prevalence estimates for 2021 and projections for 2045. *Diabetes Res Clin Pract* 2022; **183**: 109119 [PMID: 34879977 DOI: 10.1016/j.diabres.2021.109119]

2 **Magliano DJ**, Chen L, Islam RM, Carstensen B, Gregg EW, Pavkov ME, Andes LJ, Balicer R, Baviera M, Boersma-van Dam E, Booth GL, Chan JCN, Chua YX, Fosse-Edorh S, Fuentes S, Gulseth HL, Gurevicius R, Ha KH, Hird TR, Jermendy G, Khalangot MD, Kim DJ, Kiss Z, Kravchenko VI, Leventer-Roberts M, Lin CY, Luk AOY, Mata-Cases M, Mauricio D, Nichols GA, Nielen MM, Pang D, Paul SK, Pelletier C, Pildava S, Porath A, Read SH, Roncaglioni MC, Lopez-Doriga Ruiz P, Shestakova M, Vikulova O, Wang KL, Wild SH, Yekutiel N, Shaw JE. Trends in the incidence of diagnosed diabetes: a multicountry analysis of aggregate data from 22 million diagnoses in high-income and middle-income settings. *Lancet Diabetes Endocrinol* 2021; **9**: 203-211 [PMID: 33636102 DOI: 10.1016/S2213-8587(20)30402-2]

3 **Madsbad S**, Dirksen C, Holst JJ. Mechanisms of changes in glucose metabolism and bodyweight after bariatric surgery. *Lancet Diabetes Endocrinol* 2014; **2**: 152-164 [PMID: 24622719 DOI: 10.1016/S2213-8587(13)70218-3]

4 **Schauer PR**, Bhatt DL, Kirwan JP, Wolski K, Aminian A, Brethauer SA, Navaneethan SD, Singh RP, Pothier CE, Nissen SE, Kashyap SR; STAMPEDE Investigators. Bariatric Surgery *versus* Intensive Medical Therapy for Diabetes - 5-Year Outcomes. *N Engl J Med* 2017; **376**: 641-651 [PMID: 28199805 DOI: 10.1056/NEJMoa1600869]

5 **Angrisani L**, Santonicola A, Iovino P, Vitiello A, Zundel N, Buchwald H, Scopinaro N. Bariatric Surgery and Endoluminal Procedures: IFSO Worldwide Survey 2014. *Obes Surg* 2017; **27**: 2279-2289 [PMID: 28405878 DOI: 10.1007/s11695-017-2666-x]

6 **Mingrone G**, Panunzi S, De Gaetano A, Guidone C, Iaconelli A, Capristo E, Chamseddine G, Bornstein SR, Rubino F. Metabolic surgery *versus* conventional medical therapy in patients with type 2 diabetes: 10-year follow-up of an open-label, single-centre, randomised controlled trial. *Lancet* 2021; **397**: 293-304 [PMID: 33485454 DOI: 10.1016/S0140-6736(20)32649-0]

7 **Horwitz D**, Padron C, Kelly T, Saunders JK, Ude-Welcome A, Schmidt AM, Parikh M. Long-term outcomes comparing metabolic surgery to no surgery in patients with type 2 diabetes and body mass index 30-35. *Surg Obes Relat Dis* 2020; **16**: 503-508 [PMID: 32088110 DOI: 10.1016/j.soard.2020.01.016]

8 **Cai J**, Rimal B, Jiang C, Chiang JYL, Patterson AD. Bile acid metabolism and signaling, the microbiota, and metabolic disease. *Pharmacol Ther* 2022; **237**: 108238 [PMID: 35792223 DOI: 10.1016/j.pharmthera.2022.108238]

9 **Thomas C**, Gioiello A, Noriega L, Strehle A, Oury J, Rizzo G, Macchiarulo A, Yamamoto H, Mataki C, Pruzanski M, Pellicciari R, Auwerx J, Schoonjans K. TGR5-mediated bile acid sensing controls glucose homeostasis. *Cell Metab* 2009;

10: 167-177 [PMID: 19723493 DOI: 10.1016/j.cmet.2009.08.001]

10 **Ryan KK**, Tremaroli V, Clemmensen C, Kovatcheva-Datchary P, Myronovych A, Karns R, Wilson-Pérez HE, Sandoval DA, Kohli R, Bäckhed F, Seeley RJ. FXR is a molecular target for the effects of vertical sleeve gastrectomy. *Nature* 2014; **509**: 183-188 [PMID: 24670636 DOI: 10.1038/nature13135]

11 **Inagaki T**, Choi M, Moschetta A, Peng L, Cummins CL, McDonald JG, Luo G, Jones SA, Goodwin B, Richardson JA, Gerard RD, Repa JJ, Mangelsdorf DJ, Kliewer SA. Fibroblast growth factor 15 functions as an enterohepatic signal to regulate bile acid homeostasis. *Cell Metab* 2005; **2**: 217-225 [PMID: 16213224 DOI: 10.1016/j.cmet.2005.09.001]

12 **Holt JA**, Luo G, Billin AN, Bisi J, McNeill YY, Kozarsky KF, Donahee M, Wang DY, Mansfield TA, Kliewer SA, Goodwin B, Jones SA. Definition of a novel growth factor-dependent signal cascade for the suppression of bile acid biosynthesis. *Genes Dev* 2003; **17**: 1581-1591 [PMID: 12815072 DOI: 10.1101/gad.1083503]

13 **Wright TJ**, Ladher R, McWhirter J, Murre C, Schoenwolf GC, Mansour SL. Mouse FGF15 is the ortholog of human and chick FGF19, but is not uniquely required for otic induction. *Dev Biol* 2004; **269**: 264-275 [PMID: 15081372 DOI: 10.1016/j.ydbio.2004.02.003]

14 **Docherty NG**, Le Roux CW. Physiological adaptations following Roux-en-Y gastric bypass and the identification of targets for bariatric mimetic pharmacotherapy. *Curr Opin Pharmacol* 2015; **25**: 23-29 [PMID: 26496012 DOI: 10.1016/j.coph.2015.09.012]

15 **Pournaras DJ**, Glicksman C, Vincent RP, Kuganolipava S, Alaghband-Zadeh J, Mahon D, Bekker JH, Ghatei MA, Bloom SR, Walters JR, Welbourn R, le Roux CW. The role of bile after Roux-en-Y gastric bypass in promoting weight loss and improving glycaemic control. *Endocrinology* 2012; **153**: 3613-3619 [PMID: 22673227 DOI: 10.1210/en.2011-2145]

16 **Sachdev S**, Wang Q, Billington C, Connett J, Ahmed L, Inabnet W, Chua S, Ikramuddin S, Korner J. FGF 19 and Bile Acids Increase Following Roux-en-Y Gastric Bypass but Not After Medical Management in Patients with Type 2 Diabetes. *Obes Surg* 2016; **26**: 957-965 [PMID: 26259981 DOI: 10.1007/s11695-015-1834-0]

17 **Thöni V**, Pfister A, Melmer A, Enrich B, Salzmann K, Kaser S, Lamina C, Ebenbichler CF, Hackl H, Tilg H, Moschen AR. Dynamics of Bile Acid Profiles, GLP-1, and FGF19 After Laparoscopic Gastric Banding. *J Clin Endocrinol Metab* 2017; **102**: 2974-2984 [PMID: 28591793 DOI: 10.1210/jc.2017-00235]

18 **Cicione C**, Degirolamo C, Moschetta A. Emerging role of fibroblast growth factors 15/19 and 21 as metabolic integrators in the liver. *Hepatology* 2012; **56**: 2404-2411 [PMID: 22753116 DOI: 10.1002/hep.25929]

19 **Potthoff MJ**, Boney-Montoya J, Choi M, He T, Sunny NE, Satapati S, Suino-Powell K, Xu HE, Gerard RD, Finck BN, Burgess SC, Mangelsdorf DJ, Kliewer SA. FGF15/19 regulates hepatic glucose metabolism by inhibiting the CREB-PGC-1α pathway. *Cell Metab* 2011; **13**: 729-738 [PMID: 21641554 DOI: 10.1016/j.cmet.2011.03.019]

20 **Kir S**, Beddow SA, Samuel VT, Miller P, Previs SF, Suino-Powell K, Xu HE, Shulman GI, Kliewer SA, Mangelsdorf DJ. FGF19 as a postprandial, insulin-independent activator of hepatic protein and glycogen synthesis. *Science* 2011; **331**: 1621-1624 [PMID: 21436455 DOI: 10.1126/science.1198363]

21 **Kurosu H**, Choi M, Ogawa Y, Dickson AS, Goetz R, Eliseenkova AV, Mohammadi M, Rosenblatt KP, Kliewer SA, Kuro-O M. Tissue-specific expression of betaKlotho and fibroblast growth factor (FGF) receptor isoforms determines metabolic activity of FGF19 and FGF21. *J Biol Chem* 2007; **282**: 26687-26695 [PMID: 17623664 DOI: 10.1074/jbc.M704165200]

22 **Zhang X**, Wang Y, Zhong M, Liu T, Han H, Zhang G, Liu S, Wei M, Wu Q, Hu S. Duodenal-Jejunal Bypass Preferentially Elevates Serum Taurine-Conjugated Bile Acids and Alters Gut Microbiota in a Diabetic Rat Model. *Obes Surg* 2016; **26**: 1890-1899 [PMID: 26715331 DOI: 10.1007/s11695-015-2031-x]

23 **Wu Q**, Zhang X, Zhong M, Han H, Liu S, Liu T, Wei M, Guo W, Xie H, Hu S, Zhang G. Effects of Bariatric Surgery on Serum Bile Acid Composition and Conjugation in a Diabetic Rat Model. *Obes Surg* 2016; **26**: 2384-2392 [PMID: 26843082 DOI: 10.1007/s11695-016-2087-2]

24 **Ding L**, Sousa KM, Jin L, Dong B, Kim BW, Ramirez R, Xiao Z, Gu Y, Yang Q, Wang J, Yu D, Pigazzi A, Schones D, Yang L, Moore D, Wang Z, Huang W. Vertical sleeve gastrectomy activates GPBAR-1/TGR5 to sustain weight loss, improve fatty liver, and remit insulin resistance in mice. *Hepatology* 2016; **64**: 760-773 [PMID: 27312543 DOI: 10.1002/hep.28689]

25 **Xie MH**, Holcomb I, Deuel B, Dowd P, Huang A, Vagts A, Foster J, Liang J, Brush J, Gu Q, Hillan K, Goddard A, Gurney AL. FGF-19, a novel fibroblast growth factor with unique specificity for FGFR4. *Cytokine* 1999; **11**: 729-735 [PMID: 10525310 DOI: 10.1006/cyto.1999.0485]

26 **Sayin SI**, Wahlström A, Felin J, Jäntti S, Marschall HU, Bamberg K, Angelin B, Hyötyläinen T, Orešič M, Bäckhed F. Gut microbiota regulates bile acid metabolism by reducing the levels of tauro-beta-muricholic acid, a naturally occurring FXR antagonist. *Cell Metab* 2013; **17**: 225-235 [PMID: 23395169 DOI: 10.1016/j.cmet.2013.01.003]

27 **Li T**, Chiang JY. Bile acid signaling in metabolic disease and drug therapy. *Pharmacol Rev* 2014; **66**: 948-983 [PMID: 25073467 DOI: 10.1124/pr.113.008201]

28 **Fang S**, Suh JM, Reilly SM, Yu E, Osborn O, Lackey D, Yoshihara E, Perino A, Jacinto S, Lukasheva Y, Atkins AR, Khvat A, Schnabl B, Yu RT, Brenner DA, Coulter S, Liddle C, Schoonjans K, Olefsky JM, Saltiel AR, Downes M, Evans RM. Intestinal FXR agonism promotes adipose tissue browning and reduces obesity and insulin resistance. *Nat Med* 2015; **21**: 159-165 [PMID: 25559344 DOI: 10.1038/nm.3760]

29 **Stroeve JH**, Brufau G, Stellaard F, Gonzalez FJ, Staels B, Kuipers F. Intestinal FXR-mediated FGF15 production contributes to diurnal control of hepatic bile acid synthesis in mice. *Lab Invest* 2010; **90**: 1457-1467 [PMID: 20531290 DOI: 10.1038/labinvest.2010.107]

30 **Parks DJ**, Blanchard SG, Bledsoe RK, Chandra G, Consler TG, Kliewer SA, Stimmel JB, Willson TM, Zavacki AM, Moore DD, Lehmann JM. Bile acids: natural ligands for an orphan nuclear receptor. *Science* 1999; **284**: 1365-1368 [PMID: 10334993 DOI: 10.1126/science.284.5418.1365]

31 **Borup C**, Wildt S, Rumessen JJ, Bouchelouche PN, Graff J, Damgaard M, McQuitty C, Rainteau D, Munck LK. Chenodeoxycholic acid stimulated fibroblast growth factor 19 response - a potential biochemical test for bile acid diarrhoea. *Aliment Pharmacol Ther* 2017; **45**: 1433-1442 [PMID: 28378364 DOI: 10.1111/apt.14056]

32 **Meyer-Gerspach AC**, Steinert RE, Keller S, Malarski A, Schulte FH, Beglinger C. Effects of chenodeoxycholic acid on the secretion of gut peptides and fibroblast growth factors in healthy humans. *J Clin Endocrinol Metab* 2013; **98**: 3351-3358 [PMID: 23783097 DOI: 10.1210/jc.2012-4109]

33 **Fu L**, John LM, Adams SH, Yu XX, Tomlinson E, Renz M, Williams PM, Soriano R, Corpuz R, Moffat B, Vandlen R, Simmons L, Foster J, Stephan JP, Tsai SP, Stewart TA. Fibroblast growth factor 19 increases metabolic rate and reverses dietary and leptin-deficient diabetes. *Endocrinology* 2004; **145**: 2594-2603 [PMID: 14976145 DOI: 10.1210/en.2003-1671]

34 **Tomlinson E**, Fu L, John L, Hultgren B, Huang X, Renz M, Stephan JP, Tsai SP, Powell-Braxton L, French D, Stewart TA. Transgenic mice expressing human fibroblast growth factor-19 display increased metabolic rate and decreased adiposity. *Endocrinology* 2002; **143**: 1741-1747 [PMID: 11956156 DOI: 10.1210/endo.143.5.8850]

35 **Huang X**, Yang C, Luo Y, Jin C, Wang F, McKeehan WL. FGFR4 prevents hyperlipidemia and insulin resistance but underlies high-fat diet induced fatty liver. *Diabetes* 2007; **56**: 2501-2510 [PMID: 17664243 DOI: 10.2337/db07-0648]

36 **Shin DJ**, Osborne TF. FGF15/FGFR4 integrates growth factor signaling with hepatic bile acid metabolism and insulin action. *J Biol Chem* 2009; **284**: 11110-11120 [PMID: 19237543 DOI: 10.1074/jbc.M808747200]

37 **Wu X**, Li Y. Role of FGF19 induced FGFR4 activation in the regulation of glucose homeostasis. *Aging (Albany NY)* 2009; **1**: 1023-1027 [PMID: 20157585 DOI: 10.18632/aging.100108]

World Journal of Gastroenterology

Submit a Manuscript: https://www.f6publishing.com

World J Gastroenterol 2023 June 7; 29(21): 3292-3301

DOI: 10.3748/wjg.v29.i21.3292

ISSN 1007-9327 (print) ISSN 2219-2840 (online)

ORIGINAL ARTICLE

Retrospective Cohort Study

Ineffective esophageal motility is associated with acute rejection after lung transplantation independent of gastroesophageal reflux

Wai-Kit Lo, Brent Hiramoto, Hilary J Goldberg, Nirmal Sharma, Walter W Chan

Specialty type: Gastroenterology and hepatology

Provenance and peer review: Invited article; Externally peer reviewed.

Peer-review model: Single blind

Peer-review report's scientific quality classification

Grade A (Excellent): A
Grade B (Very good): B
Grade C (Good): 0
Grade D (Fair): 0
Grade E (Poor): 0

P-Reviewer: Ladic A, Croatia; Morozov S, Russia

Received: March 5, 2023
Peer-review started: March 5, 2023
First decision: April 3, 2023
Revised: April 14, 2023
Accepted: April 28, 2023
Article in press: April 28, 2023
Published online: June 7, 2023

Wai-Kit Lo, Brent Hiramoto, Walter W Chan, Division of Gastroenterology, Hepatology and Endoscopy, Brigham and Women's Hospital, Boston, MA 02115, United States

Hilary J Goldberg, Nirmal Sharma, Division of Pulmonary and Critical Care Medicine, Brigham and Women's Hospital, Boston, MA 02115, United States

Corresponding author: Walter W Chan, AGAF, FACG, MD, Associate Professor, Division of Gastroenterology, Hepatology and Endoscopy, Brigham and Women's Hospital, 75 Francis Street, Boston, MA 02115, United States. wwchan@bwh.harvard.edu

Abstract

BACKGROUND

Gastroesophageal reflux is associated with poorer outcomes after lung transplant, likely through recurrent aspiration and allograft injury. Although prior studies have demonstrated a relationship between impedance-pH results and transplant outcomes, the role of esophageal manometry in the assessment of lung transplant patients remains debated, and the impact of esophageal dysmotility on transplant outcomes is unclear. Of particular interest is ineffective esophageal motility (IEM) and its associated impact on esophageal clearance.

AIM

To assess the relationship between pre-transplant IEM diagnosis and acute rejection after lung transplantation.

METHODS

This was a retrospective cohort study of lung transplant recipients at a tertiary care center between 2007 and 2018. Patients with pre-transplant anti-reflux surgery were excluded. Manometric and reflux diagnoses were recorded from pre-transplant esophageal function testing. Time-to-event analysis using Cox proportional hazards model was applied to evaluate outcome of first episode of acute cellular rejection, defined histologically per International Society of Heart and Lung Transplantation guidelines. Subjects not meeting this endpoint were censored at time of post-transplant anti-reflux surgery, last clinic visit, or death. Fisher's exact test for binary variables and student's *t*-test for continuous variables were performed to assess for differences between groups.

RESULTS

Of 184 subjects (54% men, mean age: 58, follow-up: 443 person-years) met criteria

for inclusion. Interstitial pulmonary fibrosis represented the predominant pulmonary diagnosis (41%). During the follow-up period, 60 subjects (33.5%) developed acute rejection. The all-cause mortality was 16.3%. Time-to-event univariate analyses demonstrated significant association between IEM and acute rejection [hazard ratio (HR): 1.984, 95%CI: 1.03-3.30, P = 0.04], confirmed on Kaplan-Meier curve. On multivariable analysis, IEM remained independently associated with acute rejection, even after controlling for potential confounders such as the presence of acid and nonacid reflux (HR: 2.20, 95%CI: 1.18-4.11, P = 0.01). Nonacid reflux was also independently associated with acute rejection on both univariate (HR: 2.16, 95%CI: 1.26-3.72, P = 0.005) and multivariable analyses (HR: 2.10, 95%CI: 1.21-3.64, P = 0.009), adjusting for the presence of IEM.

CONCLUSION

Pre-transplant IEM was associated with acute rejection after transplantation, even after controlling for acid and nonacid reflux. Esophageal motility testing may be considered in lung transplant to predict outcomes.

Key Words: Ineffective esophageal motility; Esophageal hypomotility; Esophageal manometry; Gastroesophageal reflux disease; Lung transplantation; Acute rejection

©The Author(s) 2023. Published by Baishideng Publishing Group Inc. All rights reserved.

Core Tip: While gastroesophageal reflux (GER) has been associated with poorer outcomes after lung transplant, the impact of esophageal dysmotility remains unclear. Our study found that ineffective esophageal motility identified on pre-transplant esophageal manometry was independently associated with increased acute allograft rejection, even after adjusting for GER. This suggests that esophageal hypomotility may increase the risk of poor lung transplant outcome independent of GER. Routine esophageal function assessment should be considered in the peri-transplant evaluation of lung transplant patients to identify, risk stratify, and more effectively manage esophageal dysfunction in such patients at risk of poorer outcomes.

Citation: Lo WK, Hiramoto B, Goldberg HJ, Sharma N, Chan WW. Ineffective esophageal motility is associated with acute rejection after lung transplantation independent of gastroesophageal reflux. *World J Gastroenterol* 2023; 29(21): 3292-3301

URL: https://www.wjgnet.com/1007-9327/full/v29/i21/3292.htm

DOI: https://dx.doi.org/10.3748/wjg.v29.i21.3292

INTRODUCTION

Lung transplantation survival remains the lowest among solid organ transplants despite small gains over the past decade. Current 5-year survival rates are estimated at 59.2%[1]. Gastroesophageal reflux disease (GERD) and esophageal dysmotility are commonly found in patients undergoing lung transplant evaluation and have been associated with worsened transplant outcomes. For example, GERD has been implicated in the development of acute rejection and chronic lung allograft dysfunction (CLAD). Acute rejection is an early risk factor for CLAD, an important mediator of mortality after the first year post-transplant[2,3]. While esophageal dysmotility may be associated with worsened severity of GERD due to aberrant peristaltic clearance of refluxed gastroduodenal contents, less is known regarding its independent effects on lung transplant outcomes[4-6].

Acute lung rejection is common within the first year post-transplant with rates as high as > 50%[7]. Prior work from our group demonstrated an association between pre-transplant impedance measures of reflux and early allograft injury post-transplant as well as early hospital readmission[8,9]. These measures included prolonged bolus clearance, and increased total proximal and distal reflux episodes [10]. Studies in humans and mouse models have demonstrated that markers of refluxate such as pepsin and bile acids are also associated with allograft dysfunction, and result in impaired innate immune responses[11-14].

Despite the established connection between esophageal motility and reflux clearance, few studies have analyzed transplant outcomes in patients with esophageal dysmotility. Notably, the International Society of Heart and Lung Transplantation (ISHLT) guidelines consider severe esophageal dysmotility to be a risk factor associated with a substantially increased risk of a poor outcome[15]. A few single center studies to date have demonstrated disorders of esophageal motility impacting lung transplant outcomes like CLAD in esophagogastric junction outflow obstruction (EGJOO), as well as 1-, 3-, and 5-

year survival in the more severe phenotype of esophageal aperistalsis[16,17]. Thus far, limited data has impeded our understanding of less severe phenotypes of impaired peristalsis on lung transplant outcomes. The goal of our study is to determine the impact of pre-transplant esophageal dysmotility on lung transplant outcomes of acute rejection, specifically subjects with weak or impaired, but not fully absent, contractility, characterized as ineffective esophageal motility (IEM). We hypothesized that measures of esophageal dysmotility such as IEM are associated with increased rates of acute rejection in lung transplant patients.

MATERIALS AND METHODS

This was a retrospective cohort study of adult patients age > 18 who underwent lung transplantation between 2007 and 2018 at a tertiary care referral center. Patients with pre-transplant high-resolution manometry (HRM) and multichannel intraluminal impedance and pH (MII-pH) testing were included, and patients with a history of pre-transplant antireflux surgery were excluded. Study subjects meeting inclusion and exclusion criteria were reviewed for collection of baseline characteristics and outcomes data.

Baseline demographics included age at time of transplantation, sex, body mass index, primary pulmonary diagnosis, and pre-transplant cardiac ejection fraction. Covariates of interest included IEM on HRM, and presence of acid reflux and non-acid reflux on MII-pH study. The primary outcome of interest was development of first episode of acute cellular rejection. This was defined by clinical and histologic criteria per ISHLT guidelines[18]. Other measured outcomes included all-cause mortality during the study period, use of proton pump inhibitor (PPI) medication post-transplant, and development of pulmonary infection.

Pre-transplant HRM

All patients included in the study underwent HRM (Diversatek Healthcare, Milwaukee, WI, United States) prior to transplant. This system utilized a solid-state catheter with 32 circumferential pressure sensors spaced 1 cm apart. Transnasal catheter placement was performed with distal sensor placement directed into the proximal stomach, ensuring that the catheter is properly positioned across the lower esophageal sphincter (LES). After a brief accommodation period, patients were asked to perform ten 5-mL liquid swallows in the supine position. Results were analyzed utilizing a dedicated software package (BioView 5.6.3.0; Diversatek Healthcare, Milwaukee, WI, United States). IEM was defined by ≥ 50% weak or failed swallows using Chicago Classification v3.0 criteria[19]. Presence of IEM was classified as a dichotomous variable for data analysis.

Pre-transplant MII-pH Monitoring

All patients included in the study also MII-pH monitoring (Diversatek Healthcare, Milwaukee, WI, United States) off PPI prior to transplant. This system includes a portable data collection device, as well as the MII-pH catheter with two pH sensors (0, 15 cm) and eight impedance electrodes (-3, -1, 1, 3, 5, 9, 11, 13 cm). Transnasal catheter placement was performed and positioned with the distal pH sensor localized to 5 cm above the LES. Patients were asked to continue their normal daily activities during the 24-h study and to record meal periods, which were excluded from the analysis. MII-pH tracings were manually reviewed and analyzed utilizing a dedicated software package (BioView 5.6.3.0; Diversatek Healthcare, Milwaukee, WI, United States). Increased acid reflux was defined by acid exposure time (AET) > 4%, while increased non-acid reflux was defined as > 27 weakly acidic or alkaline (pH > 4) episodes per prior publications[20].

Post-transplant management and diagnosis of early allograft injury

Patients were placed on a standard immunosuppressive regimen consisting of azathioprine or mycophenolate, tacrolimus, and methylprednisolone. Surveillance bronchoscopy and biopsies were obtained according to standardized post-transplant protocol at 1, 3, 6, and 12 mo. Additional diagnostic bronchoscopies were triggered by development of clinical symptoms concerning for infection or rejection. Acute rejection was categorized according to ISHLT criteria. Minimal rejection grades of A1B0 were counted as acute rejection if the patient presented with suggestive clinical symptoms and received treatment with pulsed steroids, or had persistent grade A rejection on repeat bronchoscopy.

Statistical analysis

All statistical analyses were performed utilizing SAS 9.3 statistical package (SAS Institute Inc., Cary, NC, United States). Baseline characteristics were compared using student's *t*-test for continuous variables and Fisher's exact test for dichotomous variables. Time-to-event analysis using Cox proportional hazards model was utilized to analyze the primary outcome of first episode of acute rejection. Cox proportional hazards regression was used to adjust for baseline covariates in the final analysis.

RESULTS

Of the 181 patients met inclusion criteria for the study with a total of 439 person-years of follow-up. The mean age of the cohort was 58 with a slight male predominance (54%), and the most common pulmonary diagnosis was idiopathic pulmonary fibrosis which accounted for 41% of patients. Acute rejection was demonstrated in 59 patients (33.5% of those receiving at least one bronchoscopy with biopsy) during the follow-up period for this study. There were 30 deaths during the study period reflecting an all-cause mortality rate of 16.6%.

Pre-transplant HRM revealed normal esophageal motility in 130 patients (71.8%) and IEM in 31 patients (17.1%). The remaining 20 patients had abnormal manometry of other causes (7 distal esophageal spasm, 7 Jackhammer, 6 EGJOO). No patients had achalasia or absent contractility. The IEM group had slightly fewer Caucasian patients, but the remaining demographics were statistically similar compared to the normal group (Table 1). For the primary outcome on univariate analysis, IEM was associated with a decreased time to acute rejection [hazard ratio (HR): 1.984, 95%CI: 1.03-3.30, $P = 0.04$). The Kaplan-Meier survival curve trended toward significance with 40% of the IEM cohort developing acute rejection within approximately 250 d, compared to 500 d for the normal esophageal motility group (Figure 1). On multivariable analysis after adjusting for potential confounders including the presence of acid and nonacid reflux, IEM remained independently associated with acute rejection (HR: 2.20, 95%CI: 1.18-4.11, $P = 0.01$) (Table 2).

The presence of pathologic acid or nonacid reflux per MII-pH testing was also analyzed. Notably, pathologic acid reflux defined by AET > 4.2% was not associated with acute rejection on univariate (HR: 1.06, 95%CI: 0.63-1.76, $P = 0.83$) or multivariable analyses (HR: 0.92, 95%CI: 0.53-1.61, $P = 0.77$). On the other hand, increased non-acid reflux was associated with decreased time to acute rejection in the IEM group on univariate analysis (HR: 2.16, 95%CI: 1.26-3.72, $P = 0.005$) and multivariable analysis (HR: 2.10, 95%CI: 1.21-3.64, $P = 0.009$) (Table 2). This relationship occurred independent of the presence of IEM.

DISCUSSION

GERD and esophageal dysmotility are frequent comorbid conditions in patients with end-stage lung disease. There is increasing recognition of the role these esophageal dysfunctions play in the pathogenesis and clinical progression of specific etiologies of end-stage lung disease, as well as their role in the clinical outcomes of lung transplantation. Our study sought to determine the impact of esophageal hypomotility in the development of acute rejection after lung transplantation. We found that IEM demonstrated on pre-transplant testing was associated with increased risk of acute rejection after lung transplantation. This relationship remained after controlling for covariates including pre-transplant measures of acid and non-acid reflux. The magnitude of association was increased after controlling for these baseline factors on multivariate analysis. This suggests that esophageal motility may play a role in lung transplant outcomes that is independent of reflux-related allograft injury and rejection.

Acute rejection was demonstrated in 33.5% of the cohort in the study follow up. This is consistent with prior estimates which have ranged from 28% in the ISHLT registry to 53.3%[7,21]. Baseline demographics did not differ significantly between the IEM and control groups. Amongst the other covariates of interest, non-acid reflux was independently associated with decreased time to the development of acute rejection, and did not substantially alter the association between IEM and acute rejection.

Abnormal esophageal motility was found in 29.3% of our cohort. Of those with abnormal esophageal motility, 59% of these patients were classified as having IEM (or 17% of the total cohort). Prior studies have demonstrated esophageal dysmotility in as high as 78% of patients undergoing lung transplant evaluation, though it is important to note significant heterogeneity in how esophageal dysmotility has been categorized[22-25]. The prevalence in our cohort was consistent with another study that also categorized HRM diagnoses based on Chicago Classification v3.0, which found IEM in 32.7% of patients undergoing lung transplant evaluation[25], supporting the generalizability of our findings.

Recent studies have begun to characterize the impact of esophageal dysmotility on lung transplant outcomes. In a single center study of 31 patients with pre-transplant esophageal aperistalsis, defined as ≥ 90% failed swallows without any effective peristalsis on HRM, the 1-, 3-, and 5-year post-lung transplant survivals were lower than that of the control group with normal esophageal motility[17]. This study also demonstrated that recovery of peristaltic function post-transplant was associated with improved transplant survival outcomes matching that of the control group. Another study from the same group noted HRM diagnoses of esophageal dysmotility frequently changed post-lung transplant (51.4%) and that peristaltic vigor tends to increase, implicating a dynamic relationship between esophageal motility and pulmonary function[25]. These studies suggest that chronic lung diseases and the resultant altered respiratory mechanics may impact esophageal motility, most commonly associated with hypomotility that may improve with recovery of pulmonary function after transplantation. Two other single center studies utilizing post-lung transplant HRM also demonstrated associations between

Table 1 Baseline demographics between manometric diagnoses, mean ± SD

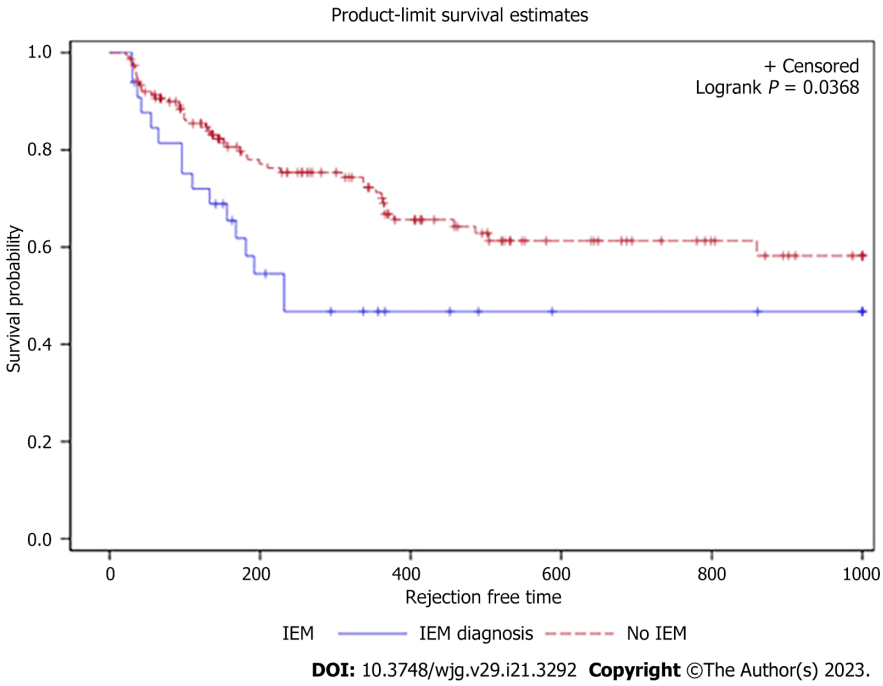
	Total (*n* = 181)	IEM (*n* = 31)	Normal motility (*n* = 130)	Other motility disorder (*n* = 20)
Follow-up (years)	2.43 ± 2.45	2.85 ± 2.77	2.43 ± 2.41	1.76 ± 2.11
Male sex	97 (53.6%)	20 (64.5%)	70 (53.8%)	7 (35.0%)
BMI	26.6 ± 4.37	25.8 ± 3.88	26.6 ± 4.55	28.0 ± 3.66
Age at transplant (years)	58.4 ± 10.2	57.9 ± 12.1	58.1 ± 10.2	61.6 ± 7.17
White race[1]	166 (92.2%)	24 (77.4%)	123 (94.6%)	20 (100%)
Pulmonary diagnosis				
ILD	99 (54.7%)	19 (61.3%)	69 (53.1%)	11 (55.0%)
IPF	74 (40.9%)	14 (45.2%)	51 (39.2%)	9 (45.0%)
COPD	57 (31.5%)	7 (22.6%)	43 (33.1%)	7 (35.0%)
CF	17 (9.39%)	4 (12.9%)	13 (10.0%)	0 (0%)
Cardiac function[2]				
LVEF (%)	61.7 ± 5.73	62.2 ± 5.79	61.4 ± 5.42	62.6 ± 7.55
PaP (mmHg)	27.7 ± 10.3	28.6 ± 11.0	27.3 ± 10.3	29.2 ± 8.91
PCWP (mmHg)	10.8 ± 4.96	9.06 ± 4.01	11.2 ± 5.15	11.5 ± 4.65
PVR (dynes/sec/cm^{-5})	252 ± 194	300 ± 238	233 ± 175	300 ± 217
Pulmonary function, baseline[2]				
FVC	1.93 ± 0.82	1.97 ± 0.92	1.94 ± 0.81	1.77 ± 0.78
FVC, %-pred	50.1 ± 47.0	49.2 ± 18.4	50.1 ± 19.0	51.3 ± 24.4
FEV1	1.24 ± 0.68	1.39 ± 0.74	1.22 ± 0.68	1.15 ± 0.57
FEV1, %-pred	40.5 ± 20.4	44.1 ± 21.1	39.4 ± 20.1	42.6 ± 21.6
FEV1/FVC	0.66 ± 0.25	0.72 ± 0.22	0.64 ± 0.25	0.67 ± 0.26
Manometry results				
Normal	130	0	130	0
IEM	31	31	0	0
DES	7	0	0	7
Jackhammer	7	0	0	7
EGJOO	6	0	0	6
Reflux monitoring				
Acid reflux	69 (38.1%)	13 (41.9%)	50 (38.5%)	6 (30.0%)
Nonacid reflux[2]	42 (26.6%)	11 (39.3%)	30 (26.8%)	1 (5.56%)
Lungs transplanted				
Unilateral	43 (23.8%)	6 (19.3%)	34 (26.1%)	3 (15.0%)
Bilateral	138 (76.2%)	25 (80.6%)	96 (73.8%)	17 (85.0%)
CMV mismatch	53 (29.3%)	7 (22.6%)	42 (32.3%)	4 (20.0%)
High-risk donor	69 (38.1%)	7 (22.6%)	52 (40.0%)	10 (50.0%)
Post-transplant PPI	128 (70.7%)	24 (77.4%)	92 (70.8%)	12 (60.0%)

[1]Indicates statistically significant difference between ineffective esophageal motility and normal, $P < 0.05$.
[2]Indicates subjects with available data.
BMI: Body mass index; ILD: Interstitial lung disease; IPF: Idiopathic pulmonary fibrosis; COPD: Chronic obstructive pulmonary disease; CF: Cystic fibrosis; LVEF: Left ventricular ejection fraction; PaP: Pulmonary arterial pressure; PCWP: Pulmonary capillary wedge pressure; PVR: Pulmonary vascular resistance; FVC: Forced vital capacity; FEV1: Forces expiratory volume in 1 second; IEM: Ineffective esophageal motility; DES: Distal esophageal spasm;

EGJOO: Esophagogastric junction outflow obstruction; CMV: Cytomegalovirus; PPI: Proton pump inhibitor.

Table 2 Cox univariate and multivariable analyses demonstrating the association between manometric diagnosis of ineffective esophageal motility as defined by CCv3.0 and acid reflux based on acid exposure time > 4.2%, and increased risk of acute rejection after lung transplantation

Covariate	Cox univariate analysis	*P* value	Cox multivariable analysis	*P* value
Ineffective esophageal motility	1.84 (1.03-3.30)	0.04	2.20 (1.18-4.11)	0.01
Nonacid reflux	2.16 (1.26-3.72)	0.005	2.10 (1.21-3.64)	0.009
Acid reflux	1.06 (0.63-1.76)	0.83	0.92 (0.53-1.61)	0.77
Body-mass Index	1.01 (0.95-1.06)	0.85	1.02 (0.96-1.09)	0.43
Age at transplant	1.00 (0.98-1.02)	0.94	1.00 (0.97-1.02)	0.93
Male gender	0.85 (0.51-1.41)	0.53	0.75 (0.44-1.29)	0.30



DOI: 10.3748/wjg.v29.i21.3292 **Copyright** ©The Author(s) 2023.

Figure 1 Kaplan-Meier showing trend toward increased acute rejection in the ineffective esophageal motility compared to normal motility group. 40% developed acute rejection in approximately 250 d in the ineffective esophageal motility cohort *vs* 500 d in the normal cohort. IEM: Ineffective esophageal motility.

esophageal dysmotility and outcomes of acute and chronic rejection[16,26].

The mechanism through which esophageal dysmotility may impact lung transplantation outcomes is not completely clear, although it is speculated to largely be related to increased risk of microaspiration due to reduced esophageal clearance. Esophageal hypomotility may result in decreased clearance and increased proximal migration of gastric refluxate, thereby leading to higher risk for exposure to the airway. Reduced esophageal bolus transit and clearance may also be associated with elevated risk of esophago-pharyngeal reflux, with potential resultant injury to the lung allograft. On the other hand, abnormal reflux, which has already been previously linked with worse lung transplant outcomes, may also lead to esophageal hypomotility. However, our results suggested that esophageal hypomotility may be associated with higher risk of allograft rejection independent of reflux burden.

There remains significant heterogeneity in reflux and esophageal motility testing in the pre- and post-lung transplant settings. HRM is standardized within the pre-transplant evaluation at our institution. The results of this study indicate that results of pre-transplant HRM are informative for risk stratification and prognostication for lung transplant outcomes. This information, in turn, may also guide post-transplant care and monitoring for acute rejection.

There are several notable strengths to our study. Pre-transplant evaluation of esophageal motility on HRM and reflux measurements on MII-pH were standardized across all lung transplant candidates. Ascertainment bias for determination of acute rejection was minimized by surveillance bronchoscopy per standard protocol with biopsy at 1, 3, 6, and 12 months, though clinical symptoms in between these intervals could trigger additional diagnostic bronchoscopies. Baseline characteristics of the study cohort were consistent with previously published data for rates of acute rejection, prevalence of esophageal dysmotility during pre-transplant evaluation, and indication for lung transplantation. Lastly, distinct HRM diagnoses were categorized according to established classification criteria for analysis, and we were able to control for potential confounding of specific measures of reflux based on MII-pH monitoring results that were collected on all patients.

There are also several limitations to our study. This is a retrospective cohort study with results that are limited to a single academic institution with high volume of lung transplantation. The sample size is relatively limited within the IEM group, though consistent with prior studies published on the association between esophageal motility and lung transplant outcomes. While a small number of recent studies have suggested dynamic changes in esophageal motility post-transplant, post-transplant motility measurements were not obtained routinely as part of our study. Finally, due to the retrospective nature and inclusion period of our study cohort, Chicago classification v3.0 was used to define IEM. However, the most current Chicago classification v4.0 mainly further restricted the diagnosis of IEM with more stringent criteria than v3.0. Therefore, the use of Chicago classification v3.0 to define IEM would likely have biased our results towards the null, as some patients in our IEM group would have been classified as normal under v4.0. The fact that our results remained significant despite this potential bias would strengthen the observed relationship between IEM and acute allograft rejection.

CONCLUSION

In summary, our study demonstrated that IEM on pre-transplant esophageal motility testing was associated with decreased time to development of acute rejection after lung transplantation. Our study provides additional evidence for the association between esophageal dysmotility and poor lung transplant outcomes. It builds upon prior studies on esophageal aperistalsis and survival outcomes in lung transplantation by providing additional evidence for acute rejection in the less severe phenotype of IEM. It also suggests esophageal dysmotility may mediate long-term lung transplant outcomes through a pathway starting with acute rejection. Further studies are needed in delineating transplant outcomes by underlying pulmonary diagnosis, analyzing longer term outcomes such as chronic rejection and 3- and 5-year survival outcomes in the context of esophageal dysmotility, and comparing pre- and post-transplant esophageal function testing results on lung transplant outcomes.

ARTICLE HIGHLIGHTS

Research background

Gastroesophageal reflux is associated with poor outcomes after lung transplantation. However, the impact of esophageal dysmotility and role of esophageal manometry remains unclear. Ineffective esophageal motility (IEM) is a disorder of esophageal motility associated with decreased esophageal clearance that may worsen transplant outcomes.

Research motivation

Esophageal evaluation remains poorly standardized in lung transplantation, and this work suggests that routine esophageal motility testing to identify IEM may help identify patients at risk for acute rejection.

Research objectives

To evaluate the relationship between IEM and acute rejection after lung transplantation, controlling for confounders including coexisting pathologic acid and nonacid reflux.

Research methods

This was a retrospective cohort study of lung transplant recipients that underwent pre-transplant esophageal testing including manometry and pH at a tertiary referral center.

Research results

IEM on pre-transplant esophageal manometry was associated with higher risk of acute rejection on time-to-event analysis. On multivariable Cox regression analysis, IEM remains independently

associated with increased acute rejection, even after controlling for pathologic reflux. In addition, increased non-acid reflux was also an independent risk factor for acute rejection in the multivariable model.

Research conclusions

Lung transplant candidates with IEM had a greater risk of developing acute rejection, independent of pathologic acid and nonacid reflux. Additionally, nonacid reflux was independently associated with acute rejection. These findings suggest that IEM and other disorders affecting esophageal clearance may contribute to the pathophysiology of allograft injury, independent of a reflux-associated pathway.

Research perspectives

Future research should focus on the implementation of standardized esophageal motility testing in lung transplantation, investigation of the impact of IEM and other disorders of esophageal motility on longer term transplant outcomes including chronic rejection and survival, and assessment of changes in esophageal motility after transplant and its effect on transplant outcomes.

FOOTNOTES

Author contributions: Chan WW and Lo WK initiated study concepts and design; Lo WK, Goldberg HJ, and Chan WW contributed to acquisition of data; Chan WW, Lo WK, Hiramoto B, Goldberg HJ, and Sharma N performed analysis and interpretation of data; Lo WK, Hiramoto B, and Chan WW drafted the manuscript; Chan WW, Lo WK, Hiramoto B, Goldberg HJ, and Sharma N contributed to critical revision of manuscript for important intellectual content; Chan WW and Lo WK performed statistical analyses; Chan WW provided administrative support and overall study supervision.

Institutional review board statement: The study was reviewed and approved by the Mass General Brigham Healthcare Institutional Review Board, No. 2011P001563.

Informed consent statement: All study participants or their legal guardian provided informed written consent about personal and medical data collection prior to study enrolment.

Conflict-of-interest statement: Lo WK, Hiramoto B, and Goldberg HJ, Sharma N-no relevant conflicts of interest for this article; Chan WW-Scientific Advisory Board (Takeda Pharmaceuticals, Phathom Pharmaceuticals, Sanofi Pharmaceuticals).

Data sharing statement: No additional data are available.

STROBE statement: The authors have read the STROBE Statement—checklist of items, and the manuscript was prepared and revised according to the STROBE Statement—checklist of items.

Open-Access: This article is an open-access article that was selected by an in-house editor and fully peer-reviewed by external reviewers. It is distributed in accordance with the Creative Commons Attribution NonCommercial (CC BY-NC 4.0) license, which permits others to distribute, remix, adapt, build upon this work non-commercially, and license their derivative works on different terms, provided the original work is properly cited and the use is non-commercial. See: https://creativecommons.org/Licenses/by-nc/4.0/

Country/Territory of origin: United States

ORCID number: Walter W Chan 0000-0002-1709-8230.

S-Editor: Fan JR
L-Editor: A
P-Editor: Chen YX

REFERENCES

1 **Valapour M**, Lehr CJ, Skeans MA, Smith JM, Miller E, Goff R, Foutz J, Israni AK, Snyder JJ, Kasiske BL. OPTN/SRTR 2019 Annual Data Report: Lung. *Am J Transplant* 2021; **21** Suppl 2: 441-520 [PMID: 33595190 DOI: 10.1111/ajt.16495]
2 **Glanville AR**, Aboyoun CL, Havryk A, Plit M, Rainer S, Malouf MA. Severity of lymphocytic bronchiolitis predicts long-term outcome after lung transplantation. *Am J Respir Crit Care Med* 2008; **177**: 1033-1040 [PMID: 18263803 DOI: 10.1164/rccm.200706-951OC]
3 **Khalifah AP**, Hachem RR, Chakinala MM, Yusen RD, Aloush A, Patterson GA, Mohanakumar T, Trulock EP, Walter MJ. Minimal acute rejection after lung transplantation: a risk for bronchiolitis obliterans syndrome. *Am J Transplant* 2005; **5**: 2022-2030 [PMID: 15996255 DOI: 10.1111/j.1600-6143.2005.00953.x]

4 **Savarino E**, Gemignani L, Pohl D, Zentilin P, Dulbecco P, Assandri L, Marabotto E, Bonfanti D, Inferrera S, Fazio V, Malesci A, Tutuian R, Savarino V. Oesophageal motility and bolus transit abnormalities increase in parallel with the severity of gastro-oesophageal reflux disease. *Aliment Pharmacol Ther* 2011; **34**: 476-486 [PMID: 21671968 DOI: 10.1111/j.1365-2036.2011.04742.x]

5 **Mittal R**, Vaezi MF. Esophageal Motility Disorders and Gastroesophageal Reflux Disease. *N Engl J Med* 2020; **383**: 1961-1972 [PMID: 33176086 DOI: 10.1056/NEJMra2000328]

6 **Ribolsi M**, Balestrieri P, Emerenziani S, Guarino MP, Cicala M. Weak peristalsis with large breaks is associated with higher acid exposure and delayed reflux clearance in the supine position in GERD patients. *Am J Gastroenterol* 2014; **109**: 46-51 [PMID: 24189712 DOI: 10.1038/ajg.2013.373]

7 **Todd JL**, Neely ML, Kopetskie H, Sever ML, Kirchner J, Frankel CW, Snyder LD, Pavlisko EN, Martinu T, Tsuang W, Shino MY, Williams N, Robien MA, Singer LG, Budev M, Shah PD, Reynolds JM, Palmer SM, Belperio JA, Weigt SS. Risk Factors for Acute Rejection in the First Year after Lung Transplant. A Multicenter Study. *Am J Respir Crit Care Med* 2020; **202**: 576-585 [PMID: 32379979 DOI: 10.1164/rccm.201910-1915OC]

8 **Lo WK**, Burakoff R, Goldberg HJ, Feldman N, Chan WW. Pre-lung transplant measures of reflux on impedance are superior to pH testing alone in predicting early allograft injury. *World J Gastroenterol* 2015; **21**: 9111-9117 [PMID: 26290637 DOI: 10.3748/wjg.v21.i30.9111]

9 **Lo WK**, Goldberg HJ, Burakoff R, Feldman N, Chan WW. Increased proximal acid reflux is associated with early readmission following lung transplantation. *Neurogastroenterol Motil* 2016; **28**: 251-259 [PMID: 26568193 DOI: 10.1111/nmo.12720]

10 **Lo WK**, Burakoff R, Goldberg HJ, Feldman N, Chan WW. Pre-transplant impedance measures of reflux are associated with early allograft injury after lung transplantation. *J Heart Lung Transplant* 2015; **34**: 26-35 [PMID: 25444368 DOI: 10.1016/j.healun.2014.09.005]

11 **Hartwig MG**, Appel JZ, Li B, Hsieh CC, Yoon YH, Lin SS, Irish W, Parker W, Davis RD. Chronic aspiration of gastric fluid accelerates pulmonary allograft dysfunction in a rat model of lung transplantation. *J Thorac Cardiovasc Surg* 2006; **131**: 209-217 [PMID: 16399314 DOI: 10.1016/j.jtcvs.2005.06.054]

12 **D'Ovidio F**, Mura M, Ridsdale R, Takahashi H, Waddell TK, Hutcheon M, Hadjiliadis D, Singer LG, Pierre A, Chaparro C, Gutierrez C, Miller L, Darling G, Liu M, Post M, Keshavjee S. The effect of reflux and bile acid aspiration on the lung allograft and its surfactant and innate immunity molecules SP-A and SP-D. *Am J Transplant* 2006; **6**: 1930-1938 [PMID: 16889547 DOI: 10.1111/j.1600-6143.2006.01357.x]

13 **Olson MT**, Liu W, Mohanakumar T, Bremner RM. A potential mechanism by which aspiration of duodenogastric fluid augments the risk for bronchiolitis obliterans syndrome after lung transplantation. *J Thorac Cardiovasc Surg* 2023; **165**: e23-e37 [PMID: 35428458 DOI: 10.1016/j.jtcvs.2022.03.009]

14 **Zhang CYK**, Ahmed M, Huszti E, Levy L, Hunter SE, Boonstra KM, Moshkelgosha S, Sage AT, Azad S, Zamel R, Ghany R, Yeung JC, Crespin OM, Frankel C, Budev M, Shah P, Reynolds JM, Snyder LD, Belperio JA, Singer LG, Weigt SS, Todd JL, Palmer SM, Keshavjee S, Martinu T; CTOT-20 investigators. Bronchoalveolar bile acid and inflammatory markers to identify high-risk lung transplant recipients with reflux and microaspiration. *J Heart Lung Transplant* 2020; **39**: 934-944 [PMID: 32487471 DOI: 10.1016/j.healun.2020.05.006]

15 **Leard LE**, Holm AM, Valapour M, Glanville AR, Attawar S, Aversa M, Campos SV, Christon LM, Cypel M, Dellgren G, Hartwig MG, Kapnadak SG, Kolaitis NA, Kotloff RM, Patterson CM, Shlobin OA, Smith PJ, Solé A, Solomon M, Weill D, Wijsenbeek MS, Willemse BWM, Arcasoy SM, Ramos KJ. Consensus document for the selection of lung transplant candidates: An update from the International Society for Heart and Lung Transplantation. *J Heart Lung Transplant* 2021; **40**: 1349-1379 [PMID: 34419372 DOI: 10.1016/j.healun.2021.07.005]

16 **Tangaroonsanti A**, Lee AS, Crowell MD, Vela MF, Jones DR, Erasmus D, Keller C, Mallea J, Alvarez F, Almansa C, DeVault KR, Houghton LA. Impaired Esophageal Motility and Clearance Post-Lung Transplant: Risk For Chronic Allograft Failure. *Clin Transl Gastroenterol* 2017; **8**: e102 [PMID: 28662022 DOI: 10.1038/ctg.2017.30]

17 **Masuda T**, Mittal SK, Csucska M, Kovacs B, Walia R, Huang JL, Smith MA, Bremner RM. Esophageal aperistalsis and lung transplant: Recovery of peristalsis after transplant is associated with improved long-term outcomes. *J Thorac Cardiovasc Surg* 2020; **160**: 1613-1626 [PMID: 32197903 DOI: 10.1016/j.jtcvs.2019.12.120]

18 **Stewart S**, Fishbein MC, Snell GI, Berry GJ, Boehler A, Burke MM, Glanville A, Gould FK, Magro C, Marboe CC, McNeil KD, Reed EF, Reinsmoen NL, Scott JP, Studer SM, Tazelaar HD, Wallwork JL, Westall G, Zamora MR, Zeevi A, Yousem SA. Revision of the 1996 working formulation for the standardization of nomenclature in the diagnosis of lung rejection. *J Heart Lung Transplant* 2007; **26**: 1229-1242 [PMID: 18096473 DOI: 10.1016/j.healun.2007.10.017]

19 **Kahrilas PJ**, Bredenoord AJ, Fox M, Gyawali CP, Roman S, Smout AJ, Pandolfino JE; International High Resolution Manometry Working Group. The Chicago Classification of esophageal motility disorders, v3.0. *Neurogastroenterol Motil* 2015; **27**: 160-174 [PMID: 25469569 DOI: 10.1111/nmo.12477]

20 **Shay S**, Tutuian R, Sifrim D, Vela M, Wise J, Balaji N, Zhang X, Adhami T, Murray J, Peters J, Castell D. Twenty-four hour ambulatory simultaneous impedance and pH monitoring: a multicenter report of normal values from 60 healthy volunteers. *Am J Gastroenterol* 2004; **99**: 1037-1043 [PMID: 15180722 DOI: 10.1111/j.1572-0241.2004.04172.x]

21 **Chambers DC**, Yusen RD, Cherikh WS, Goldfarb SB, Kucheryavaya AY, Khusch K, Levvey BJ, Lund LH, Meiser B, Rossano JW, Stehlik J; International Society for Heart and Lung Transplantation. The Registry of the International Society for Heart and Lung Transplantation: Thirty-fourth Adult Lung And Heart-Lung Transplantation Report-2017; Focus Theme: Allograft ischemic time. *J Heart Lung Transplant* 2017; **36**: 1047-1059 [PMID: 28784324 DOI: 10.1016/j.healun.2017.07.016]

22 **Sweet MP**, Herbella FA, Leard L, Hoopes C, Golden J, Hays S, Patti MG. The prevalence of distal and proximal gastroesophageal reflux in patients awaiting lung transplantation. *Ann Surg* 2006; **244**: 491-497 [PMID: 16998357 DOI: 10.1097/01.sla.0000237757.49687.03]

23 **Gasper WJ**, Sweet MP, Golden JA, Hoopes C, Leard LE, Kleinhenz ME, Hays SR, Patti MG. Lung transplantation in patients with connective tissue disorders and esophageal dysmotility. *Dis Esophagus* 2008; **21**: 650-655 [PMID: 18459990 DOI: 10.1111/j.1442-2050.2008.00828.x]

24 **Seccombe J**, Mirza F, Hachem R, Gyawali CP. Esophageal motor disease and reflux patterns in patients with advanced pulmonary disease undergoing lung transplant evaluation. *Neurogastroenterol Motil* 2013; **25**: 657-663 [PMID: 23594384 DOI: 10.1111/nmo.12135]

25 **Masuda T**, Mittal SK, Kovács B, Smith MA, Walia R, Huang JL, Bremner RM. Foregut function before and after lung transplant. *J Thorac Cardiovasc Surg* 2019; **158**: 619-629 [PMID: 31084982 DOI: 10.1016/j.jtcvs.2019.02.128]

26 **Burlen J**, Chennubhotla S, Ahmed S, Landes S, Ramirez A, Stocker AM, Abell TL. Investigating Defects of Esophageal Motility in Lung Transplant Recipients. *Gastroenterology Res* 2022; **15**: 120-126 [PMID: 35836705 DOI: 10.14740/gr1501]

World Journal of Gastroenterology

Submit a Manuscript: https://www.f6publishing.com

World J Gastroenterol 2023 June 7; 29(21): 3302-3317

DOI: 10.3748/wjg.v29.i21.3302

ISSN 1007-9327 (print) ISSN 2219-2840 (online)

ORIGINAL ARTICLE

Clinical Trials Study

Peutz-Jeghers syndrome without *STK11* mutation may correlate with less severe clinical manifestations in Chinese patients

Li-Xin Jiang, Yu-Rui Chen, Zu-Xin Xu, Yu-Hui Zhang, Zhi Zhang, Peng-Fei Yu, Zhi-Wei Dong, Hai-Rui Yang, Guo-Li Gu

Specialty type: Gastroenterology and hepatology

Provenance and peer review: Unsolicited article; Externally peer reviewed.

Peer-review model: Single blind

Peer-review report's scientific quality classification

Grade A (Excellent): 0
Grade B (Very good): B, B, B
Grade C (Good): 0
Grade D (Fair): 0
Grade E (Poor): 0

P-Reviewer: Katagiri R, Japan; Lee EW, South Korea; Yashiro M, Japan

Received: January 20, 2023
Peer-review started: January 20, 2023
First decision: February 15, 2023
Revised: April 6, 2023
Accepted: May 4, 2023
Article in press: May 4, 2023
Published online: June 7, 2023

Li-Xin Jiang, Yu-Rui Chen, Air Force Clinical College of China Medical University, Beijing 100142, China

Zu-Xin Xu, Fifth Clinical College (Air Force Clinical College) of Anhui Medical University, Beijing 100142, China

Yu-Hui Zhang, Zhi Zhang, Peng-Fei Yu, Zhi-Wei Dong, Hai-Rui Yang, Guo-Li Gu, Department of General Surgery, Air Force Medical Center, Chinese People's Liberation Army, Fifth Clinical (Air Force Clinical College) of China Medical University, Beijing 100142, China

Corresponding author: Guo-Li Gu, MM, Chief Doctor, Director, Department of General Surgery, Air Force Medical Center, Chinese People's Liberation Army, Air Force Clinical College of China Medical University, No. 30 Fucheng Road, Haidian District, Beijing 100142, China. kzggl@163.com

Abstract

BACKGROUND

Peutz-Jeghers syndrome (PJS) is an autosomal dominant genetic disease with skin mucosal pigment spots and gastrointestinal (GI) multiple hamartoma polyps as clinical characteristics. At present, it is considered that the germline mutation of *STK11* gene is the genetic cause of PJS. However, not all PJS patients can be detected *STK11* germline mutations. The specific clinical characteristics of these PJS patients without *STK11* mutation is an interesting clinical question. Or, like wild type GI stromal tumor, whether these PJS without *STK11* mutation are also called PJS is worth discussing. Therefore, we designed the study to understand the clinical characteristics of these PJS patients without *STK11* mutation.

AIM

To investigates whether PJS patients with known *STK11* mutations have a more severe spectrum of clinical phenotypes compared to those without.

METHODS

A total of 92 patients with PJS admitted to the Air Force Medical Center from 2010 to 2022 were randomly selected for study. Genomic DNA samples were extracted from peripheral blood samples, and pathogenic germline mutations of *STK11* were detected by high-throughput next-generation gene sequencing. Clinical-pathologic manifestations of patients with and without *STK11/LKB1* mutations

were compared.

RESULTS

STK11 germline mutations were observed in 73 patients with PJS. Among 19 patients with no detectable *STK11* mutations, six had no pathogenic germline mutations of other genes, while 13 had other genetic mutations. Compared with PJS patients with *STK11* mutations, those without tended to be older at the age of initial treatment, age of first intussusception and age of initial surgery. They also had a lower number of total hospitalizations relating to intussusception or intestinal obstruction, and a lower load of small intestine polyps.

CONCLUSION

PJS patients without *STK11* mutations might have less severe clinical-pathologic manifestations than those with.

Key Words: Peutz-Jeghers syndrome; *STK11*; Mutant type; Wild type

©The Author(s) 2023. Published by Baishideng Publishing Group Inc. All rights reserved.

Core Tip: Peutz-Jeghers syndrome (PJS) is an autosomal dominant genetic disease with skin mucosal pigment spots and gastrointestinal (GI) multiple hamartoma polyps as clinical characteristics. At present, it is considered that the germline mutation of *STK11* gene is the genetic cause of PJS. However, not all PJS patients can be detected *STK11* germline mutations. The specific clinical characteristics of these PJS patients without *STK11* mutation is an interesting clinical question. Or, like wild type GI stromal tumor, whether these PJS without *STK11* mutation are also called PJS is worth discussing. Therefore, we designed the study to understand the clinical characteristics of these PJS patients without *STK11* mutation. Final results found that PJS patients without *STK11* mutations might have less severe clinical-pathologic manifestations than those with.

Citation: Jiang LX, Chen YR, Xu ZX, Zhang YH, Zhang Z, Yu PF, Dong ZW, Yang HR, Gu GL. Peutz-Jeghers syndrome without *STK11* mutation may correlate with less severe clinical manifestations in Chinese patients. *World J Gastroenterol* 2023; 29(21): 3302-3317
URL: https://www.wjgnet.com/1007-9327/full/v29/i21/3302.htm
DOI: https://dx.doi.org/10.3748/wjg.v29.i21.3302

INTRODUCTION

Peutz-Jeghers syndrome (PJS) is an autosomal dominant disorder which is mainly characterized by mucocutaneous pigmentation and hamartomatous polyps of the gastrointestinal (GI) tract[1,2]. While PJS is rare, with an estimated prevalence of 1:200000 births[3], the continuous growth of multiple GI polyps predisposes patients to serious complications including intussusception, intestinal obstruction, GI bleeding and malignancies. PJS patients also have a markedly increased risk of developing various neoplasms in extraintestinal sites such as the lungs, liver and breast[4].

Germline mutations in the *STK11* gene (also named *LKB1*), which is located on Chromosome 19p13.3 and encodes a serine/threonine protein kinase[5], have been identified as the major cause of PJS[6,7]. *STK11* is a tumor suppressor gene comprised of 433 amino acids with nine coding exons and one non-coding exon[8]. Depending on the screening method, *STK11* variants can be detected in over 80%-90% of PJS cases[8,9]. Previous studies have largely focused on exploring the phenotypic landscape of *STK11* variants based on their type or location. Due to the rare nature of PJS, very few studies have attempted to examine the correlations between *STK11* mutations and overall severity of PJS phenotype in terms of the earlier onset of GI pathology arising from the polyps, such as intussusception or earlier onset malignancy. Understanding the phenotypic differences between PJS patients with and without *STK11* variants could facilitate more personalized care for PJS patients and their families *via* appropriate counseling, risk stratification and targeted cancer screening[10].

A total of 92 PJS patients admitted to the Air Force Medical Center between February 2010 and February 2022 were randomly selected for inclusion in the study, and their peripheral venous blood was collected for high-throughput next-generation gene sequencing (NGS). 73 cases in which *STK11* gene mutations were detected were named mutant-type, and 19 cases in which no *STK11* gene mutations were detected were named wild-type. In this retrospective study, we aimed to investigate the differences in clinical phenotypes between wild-type and mutant-type *STK11* gene, and provide a theoretical basis for a more precise medical monitoring and follow-up strategy for different types of PJS

patients.

MATERIALS AND METHODS

Study participants

A total of 92 patients with PJS admitted to the Air Force Medical Center, PLA between February 2010 and February 2022 were randomly selected for inclusion in the study, and all patients met the diagnostic criteria for PJS recommended by the NCCN guidelines[11]. All enrolled patients and their guardians were aware of the purpose and process of the study, and had signed informed consent agreements. All data and information collection for this study followed the ethical principles of the Universal Declaration on the Human Genome and Human Rights, Declaration of Helsinki and Statement of the Human Genome Organisation Ethics Committee on DNA Sampling, Control and Access.

Inclusion and exclusion criteria

Inclusion criteria: All enrolled patients met the clinical diagnostic criteria of PJS[12-14] (in accordance with any of the following): (1) Two or more histologically confirmed PJS polyps; (2) Any number of PJS polyps in an individual with a family history of PJS in close relative(s); (3) Characteristic mucocutaneous pigmentation in an individual with a family history of PJS in close relative(s); and (4) Any number of PJS polyps in an individual with characteristic mucocutaneous pigmentation. Peripheral venous blood was retained and genomic DNA extracted, and the sequence of the coding region of the *STK11* gene was detected using polymerase chain reaction (PCR) amplification and NGS sequencing.

Exclusion criteria: Patients who could not meet both of the above two inclusion criteria, could not provide experimental specimens or did not agree to participate in this study.

Research methods

Observational index: The general information, diagnosis and treatment history, pathology, times of examination and other clinical data of the 92 enrolled PJS patients were collected for statistical analysis. The observed indices were as follows: (1) General patient information: Origin, gender, personal marital status, family history and ABO/RH blood groups; (2) History of diagnosis and treatment: Age of initial treatment, age of mucocutaneous pigmentation appearance, order of mucocutaneous pigmentation appearance, time interval from mucocutaneous pigmentation appearance to abdominal symptoms (abdominal pain, intestinal obstruction, GI bleeding, *etc.*), location of GI polyps, load and maximum diameter of GI polyps, pathology of polyps, carcinogenesis, total hospitalizations, number of operations and final age of follow-up; (3) Examinations: Endoscopic examinations and times of GI imaging examinations; and (4) Other: Comorbidities.

Genetic sequencing: EDTA anticoagulation tubes were used to extract 8 mL of peripheral venous blood from PJS patients. Leukocytes were isolated and DNA extracted, and the extracted DNA was interrupted by ultrasound using a Covaris M220 instrument to build a DNA library. The DNA library was then purified and hybridised by the probe library, which would bind specifically to the target DNA fragment through the principle of complementary binding of nucleic acid sequences. Magnetic beads conjugated with streptavidin were mixed with the hybridisation solution, and the streptavidin was tightly bound to the biotin. The captured exon target fragment was indirectly bound by the probe to the beads, which were adsorbed by a magnet, and the supernatant was discarded. The unbound DNA fragments were washed off and the desired DNA library eluted from the beads with the eluent. The eluted DNA library was then amplified using a PCR instrument. Lastly, NGS sequencing was used to detect full exons and associated single nucleotide polymorphism (SNP) and microsatellite instability sites for previously reported genes associated with hereditary GI tract tumors, including *STK11* (Table 1).

Statistical analysis: Statistical analysis was carried out using the SPSS 26.0 software package: (1) Cases and proportion of qualitative data were presented as percentages (%), and comparisons between groups were conducted using the *chi-square test* or *Fisher's exact test*; and (2) The *t*-test was used for quantitative data that matched the normal distribution with equal variance, the *t*-test was used for those with unequal variance and the rank sum test was used for skewed data; $P < 0.05$ was considered statistically significant.

RESULTS

Analysis of NGS test results

The 73 of 92 patients with PJS (79.3%) in this group had *STK11* gene mutations, of which 47 had *STK11* gene mutations in combination with other mutations. 19 of the 92 PJS patients (20.7%) had no *STK11*

Table 1 41 digestive tract tumour-associated genes

No.	Genes
1	*AKT1*
2	*BRAF*
3	*CYP2D6*
4	*GALNT12*
5	*MET*
6	*NRAS*
7	*POLD1*
8	*SDHC*
9	*UGT1A1*
10	*APC*
11	*BRCA1*
12	*DPYD*
13	*GREM1*
14	*MLH1*
15	*PDGFRA*
16	*POLE*
17	*SDHD*
18	*ATM*
19	*BRCA2*
20	*EGFR*
21	*HRAS*
22	*MSH2*
23	*PIK3CA*
24	*PTCH1*
25	*SMAD4*
26	*BLM*
27	*CDH1*
28	*EPCAM*
29	*KIT*
30	*MSH6*
31	*PMS1*
32	*PTEN*
33	*STK11*
34	*BMPRA*
35	*CHEK2*
36	*ERBB2*
37	*KRAS*
38	*MUTYH*
39	*PMS2*
40	*SDHB*
41	*TP53*

gene mutations, of which 6 (6.6%) had no other gene mutations and 13 (14.1%) had other gene mutations in the 41 genes group. By comparing the Human Gene Mutation Database (HGMD) (http://www.hgmd.cf.ac.uk/ac/index.php), dbSNP database (https://www.ncbi.nlm.nih.gov/snp/) and COSMIC database (https://cancer.sanger.ac.uk/cosmic/), a total of 582 *STK11* gene mutant sites were included in HGMD as of March 1, 2022. We identified 21 new mutant sites in other genes (Table 2) and 26 new *STK11* gene mutant sites (Table 3).

Gene detection results and pathogenicity analysis of PJS with mutant-type *STK11*: *STK11* gene detection results and pathogenicity analysis. *STK11* gene mutations were detected in 73 PJS patients in our group. By making comparisons with the dbSNP and COSMIC databases, 49 PJS-related gene mutations were included and 26 *STK11* gene mutation sites were newly identified by sequencing in this group (Table 3). Types of *STK11* gene mutations included premature termination codons (24), frame shift mutations (14), splice site variants (13), missense mutations (17), nonsense mutations (4), mutations in the 3' untranslated region (2) and gene fusion (1).

The pathogenicity of *STK11* gene mutations was determined by comparing the HGMD and ClinVar gene mutations in the disease database, and following the corresponding grading criteria (Table 3). By making conservative predictions of amino acid sequences, we made determinations about the pathogenicity of *STK11* gene mutations according to the corresponding grading criteria (Table 3): Premature termination codons, frame shift mutations, splice site variants, missense mutations, nonsense mutations and mutations in the 3' untranslated region were associated with pathogenicity. Premature termination codons accounted for 58.3% (14/24) that were clearly pathogenic and 41.7% (10/24) that were probably pathogenic. Frameshift mutations accounted for 35.7% (5/14) that were clearly pathogenic, 50.0% (7/14) that were probably pathogenic and 14.3% (2/14) that were of uncertain significance. Splice site mutations accounted for 23.1% (3/13) that were clearly pathogenic, 61.5% (8/13) that were probably pathogenic and 15.4% (2/13) that were of uncertain significance. Missense mutations accounted for 17.6% (3/17) that were clearly pathogenic, 41.2% (7/17) that were probably pathogenic and 41.2% (7/17) that were of uncertain significance. 3' untranslated region mutations accounted for 50.0% (1/2) that were clearly pathogenic and 50.0% (1/2) that were probably pathogenic. All four nonsense mutations were clearly pathogenic (100.0%).

Other gene detection results and pathogenicity analysis in PJS patients with mutant-type *STK11*: Among the 73 PJS patients with mutant-type *STK11*, 47 were combined with other gene mutations: Combined with *AKT1* mutation in 3 cases, *APC* mutation in 4 cases, *ATM* mutation in 5 cases, *BLM* mutation in 3 cases, *BRCA2* mutation in 4 cases, *CDH1* mutation in 3 cases, *CHEK2* mutation in 3 cases, *EGFR* mutation in 1 case, *EPCAM* mutation in 1 case, *GALNT12* mutation in 6 cases, *KIT* mutation in 3 cases, *MUTYH* mutation in 5 cases, *MSH6* mutation in 5 cases, *MSH2* mutation in 4 cases, *MLH1* mutation in 1 case, *PDGFRA* mutation in 5 cases, *PIK3CA* mutation in 1 case, *PMS1* mutation in 1 case, *PMS2* mutation in 1 case, *POLD1* mutation in 3 cases, *PTCH1* mutation in 4 cases, *POLE* mutation in 8 cases and *TP53* mutation in 2 cases.

Among the other gene mutations in PJS patients with mutant-type *STK11*, there were 52 missense mutations (68.4%), 5 intron mutations (6.6%), 11 mutations in the 3' untranslated region (14.5%), 3 splice site mutations (4.0%), 1 premature termination codon (1.3%), 1 frameshift deletion (1.3%), 1 mutation in the 5' untranslated region (1.3%), 1 upstream gene mutation (1.3%) and 1 case (1.3%) of stop gain. All mutations were of uncertain significance (100.0%) (Figure 1).

Gene detection results and pathogenicity analysis in PJS patients with wild-type *STK11*: Wild-type PJS gene mutations included *BLM* mutation in 2 cases, *BMPR1A* mutation in 1 case, *POLD1* mutation in 3 cases, *CHEK2* mutation in 4 cases, *MUTYH* mutation in 6 cases, *SDHC* mutation in 1 case, *POLE* mutation in 2 cases, *BRCA* mutation in 3 cases, *APC* mutation in 2 cases, *CDH1* mutation in 1 case, *ATM* mutation in 3 cases, *ERBB2* mutation in 1 case, *SMAD4* mutation in 1 case and *SBDS* mutation in 1 case.

Among the other gene mutations in wild-type PJS patients, there were 23 missense mutations (74.2%), 5 intron mutations (16.1%), 1 splice site mutation (3.2%), 1 frameshift deletion (3.2%) and 1 mutation in the 3' untranslated region (3.2%). All mutations were of uncertain significance (Table 4).

Comparison of general information, diagnosis and treatment, pathology and examinations

Through the comparison of related items between the two groups (Table 5), it can be found that there were significant differences between the two groups in the following items ($P < 0.05$). Such as Age of initial treatment, Total hospitalizations, Age of first intussusception, Frequency of intussusception, Age of initial surgery, Time interval from mucocutaneous pigmentation appearance to abdominal symptoms, Maximum diameter of gastric polyps, Load of duodenal intestine polyps, Distribution of colorectal polyps, Times of endoscopic examinations.

Exploration of PJS genotype-clinical phenotype linkage

Clinical phenotypic variations between PJS with mutant-type and wild-type *STK11*: (1) There were no statistical differences in gender, family history, ABO blood group or Rh blood group between PJS with mutant-type and wild-type *STK11*; (2) There were differences ($P < 0.05$) between wild-type and mutant-type in age of initial treatment, total hospitalizations, age of first intussusception, frequency of intussus-

Table 2 21 new mutant sites in other genes

Sample	Gene	Description	HGVSc	Mutation type
1	*AKT1*	p.E135G	c.404A>G	Missense variant
2	*APC*	p.A41T	c.121G>A	Missense variant
3	*APC*	p.C417G	c.1249T>G	Missense variant
4	*ATM*	p.L2750[1]	c.8249T>G	Stop gained
5	*ATM*	p.A84S	c.250G>T	Missense variant
6	*ATM*	p.I1332M	c.3996T>G	Missense variant
7	*BLM*	p.E1035G	c.3104A>G	Missense variant
8	*BRCA2*	p.D635E	c.1905T>A	Missense variant
9	*BRCA2*	p.T1346N	c.4037C>A	Missense variant
10	*CHEK2*	c.908+16T>G	c.908+16T>G	Intron variants
11	*CDH1*	c.47G>A[1]	c.47G>A[1]	3 prime UTR variant
12	*CDH1*	p.S145Y	c.434C>A	Missense variant
13	*CDH1*	p.883Yext?[1]	c.2649G>C	Stop lost
14	*GALNT12*	c.-6G>T	c.-6G>T	Upstream genetic variant
15	*KIT*	p.M289I	c.867G>C	Missense variant
16	*MLH1*	p.T451R	c.1352C>G	Missense variant
17	*PMS1*	p.D405E	c.1215T>A	Missense variant
18	*POLE*	p.R1556G	c.4666C>G	Missense variant
19	*POLD1*	p.K486del	c.1456_1458del	Conservative inframe deletion
20	*SDHC*	p.L106V	c.316C>G	Missense variant
21	*SMAD4*	p.A309V	c.926C>T	Missense variant

[1]Nonsense mutation leading to protein inactivation.

ception and age of initial surgery, with wild-type PJS having a much higher age of initial treatment, much smaller number of total hospitalizations, higher age of first intussusception and lower frequency of intussusception than mutant-type PJS. There was no statistical difference between wild-type and mutant-type PJS in number of operations; (3) There was no statistical difference between wild-type and mutant-type PJS in age or order of mucocutaneous pigmentation appearance, but there was a difference in time interval from mucocutaneous pigmentation appearance to abdominal symptoms ($P < 0.05$), which was longer in wild-type PJS than in the mutant-type PJS; (4) There was no statistical difference in distribution and load of gastric polyps between wild-type and mutant-type PJS, but the maximum diameter of gastric polyps was significantly lower in wild-type PJS than mutant-type PJS ($P < 0.05$). There was no statistical difference in distribution and maximum diameter of duodenal intestine polyps, but there was a difference in load of duodenal intestine polyps ($P < 0.05$), which was much lower in wild-type PJS than in mutant-type PJS. There was no statistical difference in load and maximum diameter of colorectal polyps, but distribution of colorectal polyps was significantly lower in wild-type PJS than in mutant-type PJS; and (5) There was no statistical difference in pathology or carcinogenesis of polyps between wild-type and mutant-type PJS. There was a difference in endoscopic examination between wild-type and mutant-type PJS ($P < 0.05$), with fewer times of endoscopic examination in wild-type than mutant-type PJS.

Clinical phenotypic differences between mutant-type PJS combined with other mutations and not combined with other mutations: (1) *MUYTH*: There was a difference in ABO blood group between mutant-type PJS with and without *MUYTH* mutations ($P < 0.05$); (2) *CHEK2:* There were differences in ABO blood group, total hospitalizations and number of operations between mutant-type PJS with and without *CHEK2* mutations ($P < 0.05$); (3) *APC:* There were differences in distribution, load and maximum diameter of gastric polyps between mutant-type PJS with and without *APC* mutations ($P < 0.05$); (4) *CDH1*: There were differences in load and maximum diameter of duodenal intestine polyps between mutant-type PJS with and without *CDH1* mutations ($P < 0.05$); (5) *GALNT12:* There were differences in time interval from mucocutaneous pigmentation appearance to abdominal symptoms and

Table 3 Characterization and pathogenicity of *STK11* mutations

Sample	Mutation_type	Description	HGVSc	dbSNP RS	COSM_ID	Classification
1	Stop gained	p.Y60[1]	c.180C>G	/	COSM20874	P
2	Splice acceptor variant	c.921-1G>A	c.921-1G>A	/	COSM49008	LP
3	Splice acceptor variant	c.921-1G>C	c.921-1G>C	rs398123406	/	P
4	Stop gained	p.K84[1]	c.250A>T	rs137853076	COSM3388586; COSM3388585	P
5	Splice acceptor variant	c.921-1G>C	c.921-1G>C	rs398123406	/	P
6	Stop gained	p.Q123[1]	c.367C>T	/	COSM5224269; COSM380443	P
7	Missense variant	p.W239C	c.717G>T	/	COSM333593; COSM4278104	LP
8	Missense variant	p.R297S	c.891G>T	rs730881984	/	P
9	Stop gained	p.Q100[1]	c.298C>T	/	/	LP
10	Stop gained	p.K84[1]	c.250A>T	rs137853076	COSM3388586; COSM3388585	P
11	Missense variant	p.R409W	c.1225C>T	rs368466538	COSM25854	VUS
12	Stop gained	p.Q112[1]	c.334C>T	/	COSM3528680; COSM3528681	LP
13	Missense variant	p.D176N	c.526G>A	rs730881979	COSM4827691; COSM4827690	P
14	Stop gained	p.K84[1]	c.250A>T	rs137853076	COSM3388586; COSM3388585	P
15	Missense variant	p.R304W	c.910C>T	rs786201090	COSM29468	LP
16	Stop gained	p.E120[1]	c.358G>T	rs775595174	COSM20875	P
17	Stop gained	p.K84[1]	c.250A>T	rs137853076	COSM3388586; COSM3388585	P
18	Conservative inframe deletion	p.Y60fs	c.179dup	rs876661012	COSM5219400; COSM1480565	P
19	Stop gained	p.R86[1]	c.256C>T	/	COSM4767773; COSM4767772	P
20	Stop gained	p.Q170[1]	c.508C>T	rs121913323	COSM20943	LP
21	Stop gained	p.Q170[1]	c.508C>T	rs121913323	COSM20943	LP
22	Missense variant	p.S240W	c.719C>G	rs730881976	/	VUS
23	Splice acceptor variant	c.921-2A>G	c.921-2A>G	/	/	LP
24	Splice acceptor variant	c.921-1G>C	c.921-1G>C	rs398123406	/	P
25	Conservative inframe deletion	p.P281fs	c.842del	rs121913321	COSM4336438; COSM20871	P
26	Splice acceptor variant	p.L245F	c.733C>T	/	COSM1523960; COSM4278108	VUS
27	Stop gained	p.Q137[1]	c.409C>T	rs730881970	COSM48901	P
28	Stop gained	p.Q137[1]	c.409C>T	rs730881970	COSM48901	P
29	Stop gained	p.Q123[1]	c.367C>T	/	COSM5224269; COSM380443	P
30	Missense variant	p.D194N	c.580G>A	rs121913315	COSM25847	VUS
31	3_prime_UTR_variant	c.201G>A[1]	c.201G>A[1]	rs528679025	/	P
32	Splice acceptor variant	c.598-2A>G	c.598-2A>G	/	/	LP
33	Stop gained	p.Q159[1]	c.475C>T	/	COSM5002233; COSM27316	LP
34	Gene fusion	STK11-MIDN	/	/	/	LP
35	Conservative inframe deletion	p.D53fs	c.157del	/	COSM27282; COSM6048514	VUS
36	Missense variant	p.D194N	c.580G>A	rs121913315	COSM25847	LP
37	Missense variant	p.P179Q	c.536C>A	/	COSM4822602; COSM4822601	LP
38	Stop gained	p.W308[1]	c.924G>A	/	/	LP
39	Stop gained	p.E65[1]	c.193G>T	/	COSM20876	P

40	Splice acceptor variant	c.920+1G>C	c.920+1G>C	/	COSM4412472; COSM4412473	LP
41	Conservative inframe deletion	p.C134fs	c.402_403del	rs587782424	COSM5508976; COSM5508975	P
42	Nonsense variant	p.Q220X	c.658C>T	/	COSM13480; COSM4278102	P
43	Nonsense variant	p.Y60X	c.180del	/	COSM20874; COSM27322; COSM48900; COSM5490514	P
44	Missense variant	p.D194N	c.580G>A	rs121913315	/	LP
45	Missense variant	p.R297K	c.890G>A	/	COSM401786; COSM6149636	LP
46	Splice acceptor variant	/	c.863-2A>G	/	/	LP
47	Nonsense variant	p.Q137X	c.409C>T	rs730881970	/	P
48	Splice acceptor variant	c.735-6_735-2del	c.735-6_735-2del	rs759090799	/	VUS
	Conservative inframe deletion[2]	p.L183fs	c.548del	/	/	LP
49	3 prime UTR variant	c.201G>A[1]	c.201G>A[1]	rs528679025	/	LP
	Conservative inframe deletion[2]	p.C158fs	c.472del	/	/	VUS
50	Stop gained[2]	p.K81[1]	c.241A>T	/	/	LP
51	Missense variant[2]	p.R304P	c.911G>C	/	/	P
52	Missense variant[2]	p.R297K	c.890G>A	/	/	LP
53	Conservative inframe deletion[2]	p.E145fs	c.426_448del	/	/	LP
54	Stop gained[2]	p.Y272[1]	c.816C>A	/	/	LP
55	Stop gained[2]	p.Q100[1]	c.298C>T	/	/	LP
56	Conservative inframe deletion[2]	p.K64fs	c.190_191del	/	/	LP
57	Splice acceptor variant[2]	c.921-2A>G	c.921-2A>G	/	/	LP
58	Stop gained[2]	p.Y292[1]	c.876C>G	/	/	LP
59	Conservative inframe deletion[2]	p.T212fs	c.634del	/	/	LP
60	Stop gained[2]	p.K97[1]	c.289A>T	/	/	P
61	Missense variant[2]	p.H154P	c.461A>C	/	/	VUS
62	Missense variant[2]	p.A153P	c.457G>C	/	/	VUS
63	Missense variant[2]	p.L140P	c.419T>C	/	/	VUS
64	Conservative inframe deletion[2]	p.F264fs	c.792del	/	/	P
65	Stop gained[2]	p.W308[1]	c.924G>A	/	/	P
66	Splice acceptor variant[2]	c.598-2A>G	c.598-2A>G	/	/	LP
67	Conservative inframe deletion[2]	p.F157fs	c.471_472del	/	/	LP
68	Conservative inframe deletion[2]	p.S193fs	c.577_578del	/	/	LP
69	Splice acceptor variant[2]	c.734+1G>A	c.734+1G>A	/	/	LP
70	Missense variant[2]	p.L290H	c.869T>A	/	COSM20944; COSM25847; COSM4278092	VUS
71	Nonsense variant[2]	p.Y60X	c.179dup	/	/	P
72	Conservative inframe deletion[2]	p.L282Afs	c.842dup	/	/	P
73	Conservative inframe deletion[2]	p.V77Rfs	c.228dup	/	COSM48901	LP

[1]Nonsense mutation leading to protein inactivationy.
[2]The table shows the 26 new *STK11* mutation sites.
P: Pathogenic; LP: Likely pathogenic; VUS: Uncertain significance; SNP: Single nucleotide polymorphism.

Table 4 Characterization and pathogenicity of mutations in wild-type Peutz-Jeghers syndrome patients

Sample	Gene	Description	HGVSc	Mutation_type	dbSNP RS	COSM_ID	Classification
1	*BLM*	p.I947V	c.2839A>G	Missense mutation	rs189925962	NA	VUS
	BMPR1A	p.A13T	c.37G>A	Missense mutation	rs200115604	NA	VUS
	POLD1	p.K486del	c.1456_1458del	Frameshift deletion	NA	NA	VUS
2	*CHEK2*	p.S252N	c.755G>A	Missense mutation	rs587781379	COSM6004987; COSM6004988	VUS
	MUTYH	c.36+11C>T	c.36+11C>T	Intron mutations	rs2275602	COSN17145138	VUS
	SDHC	p.L106V	c.316C>G	Missense mutation	NA	NA	VUS
3	*CHEK2*	p.R181H	c.542G>A	Missense mutation	rs121908701	NA	VUS
	MUTYH	c.37_39del[1]	c.37_39del[1]	Mutation in the 3' untranslated region	rs373507005	NA	VUS
	MUTYH	c.36+11C>T	c.36+11C>T	Intron mutations	rs2275602	COSN17145138	VUS
	MUTYH	p.G25D	c.74G>A	Missense mutation	rs75321043	NA	VUS
	MUTYH	p.P18L	c.53C>T	Missense mutation	rs79777494	NA	VUS
	POLE	c.3378+10A>G	c.3378+10A>G	Intron mutations	rs193075152	NA	VUS
4	*BLM*	p.M348I	c.1044G>A	Missense mutation	rs184657475	COSM1580597	VUS
5	*BRCA1*	p.P1192L	c.3575C>T	Missense mutation	NA	COSM4991001; COSM4991000	VUS
	BRCA2	p.F3328C	c.9983T>G	Missense mutation	rs770826575	NA	VUS
	CHEK2	p.H371Y	c.1111C>T	Missense mutation	rs531398630	COSM4002125	VUS
6	*APC*	p.I1524R	c.4571T>G	Missense mutation	rs200803739	NA	VUS
7	*CDH1*	p.S145Y	c.434C>A	Missense mutation	NA	NA	VUS
	POLE	c.3378+10A>G	c.3378+10A>G	Intron mutations	rs193075152	NA	VUS
8	*ATM*	c.3154-5C>T	c.3154-5C>T	Intron mutations	rs55719759	NA	VUS
	CHEK2	p.S252N	c.755G>A	Missense mutation	rs587781379	COSM6004987; COSM6004988	VUS
	ERBB2	p.V1253M	c.3757G>A	Missense mutation	rs36085723	NA	VUS
9	*ATM*	p.I1332M	c.3996T>G	Missense mutation	NA	NA	VUS
	POLD1	p.A532T	c.1594G>A	Missense mutation	rs765276497	NA	VUS
10	*MUTYH*	c.934-2A>G	c.934-2A>G	Splice receptor mutation	rs77542170	NA	VUS
	SMAD4	p.A309V	c.926C>T	Missense mutation	NA	NA	VUS
11	*APC*	p.A41T	c.121G>A	Missense mutation	NA	NA	VUS
	POLD1	p.R218H	c.653G>A	Missense mutation	rs150010804	NA	VUS
12	*SBDS*	p.K33R	c.98A>G	Missense mutation	rs373730800	COSM4826086	VUS
13	*ATM*	p.V519I	c.1555G>A	Missense mutation	NA	NA	VUS
	BRCA2	p.H523R	c.1568A>G	Missense mutation	rs80358443	NA	VUS

[1]Nonsense mutation leading to protein inactivation.
P: Pathogenic; LP: Likely pathogenic; VUS: Uncertain significance; NA: Not available.

Table 5 Comparison of clinicopathological parameters between two groups

Project	Wild-type (*n* = 19)	Mutant-type (*n* = 73)	*P* value
Gender			
Male	11	44	0.851
Female	8	29	
Family history			
No	13	51	0.903
Yes	6	22	
ABO blood group[1]			
A	7	23	0.964
B	6	21	
AB	4	18	
O	2	9	
Rh blood group[1]			
Negative	0	0	
Positive	19	71	
Age of initial treatment (years)	18.474 ± 8.8089	12.973 ± 8.3881	0.021
Final age of follow-up (years)	30.842 ± 11.3101	27.425 ± 9.7680	0.239
Total hospitalizations	3 (1, 4)	4 (3, 6)	0.003
Age of first intussusception (years)	22 (14, 27)	15 (9.25, 24)	0.025
Frequency of intussusception	1 (1, 2)	2 (1, 3)	0.006
Age of initial surgery (years)	19 (14, 25)	14 (8, 23.75)	0.007
Number of operations	1 (1, 2)	1 (1, 2)	0.924
Age of mucocutaneous pigmentation appearance (years)	3 (0, 5)	3 (0.5, 5)	0.811
Order of mucocutaneous pigmentation appearance			
Lips	2	17	0.213
Lips and limbs	1	46	
Lips to limbs	16	10	
Time interval from mucocutaneous pigmentation appearance to abdominal symptoms (years)	14.5 (8, 25.5)	10 (5, 15)	0.038
Distribution of gastric polyps			
Yes	16 (84.2%)	60 (82.2%)	1
No	3 (15.8%)	13 (17.8%)	
Load of gastric polyps	5 (5, 10)	5 (3.25, 10)	0.111
Maximum diameter of gastric polyps (mm)	7 (4.25, 10)	10 (6, 15)	0.012
Distribution of duodenal intestine polyps			
Yes	18 (94.7%)	71 (97.3%)	1
No	1 (5.3%)	2 (2.7%)	
Load of duodenal intestine polyps	3 (1, 6.5)	7 (4, 15.5)	0.013
Maximum diameter of duodenal intestine polyps (mm)	30 (15, 50)	48 (30, 60)	0.110
Distribution of colorectal polyps			
Yes	6 (31.6%)	52 (71.2%)	0.001
No	13 (68.4%)	21 (28.8%)	
Load of colorectal polyps	4 (1.5, 12)	3 (1, 10)	0.864

Maximum diameter of colorectal polyps (mm)	30 (15, 50)	25 (13.5, 40)	0.664
Carcinogenesis			
Yes	0 (0%)	9 (9.52%)	0.239
No	19 (100%)	64 (90.48%)	
Pathology of polyps			
Hamartoma	12	35	0.344
Adenoma	2	8	
Hamartoma + adenoma	2	4	
Carcinogenesis	0	9	
Deletion	3	17	
Times of endoscopic examinations	2 (1, 2)	2 (2, 4.75)	0.012

[1]A few cases did not undergo relevant laboratory tests.

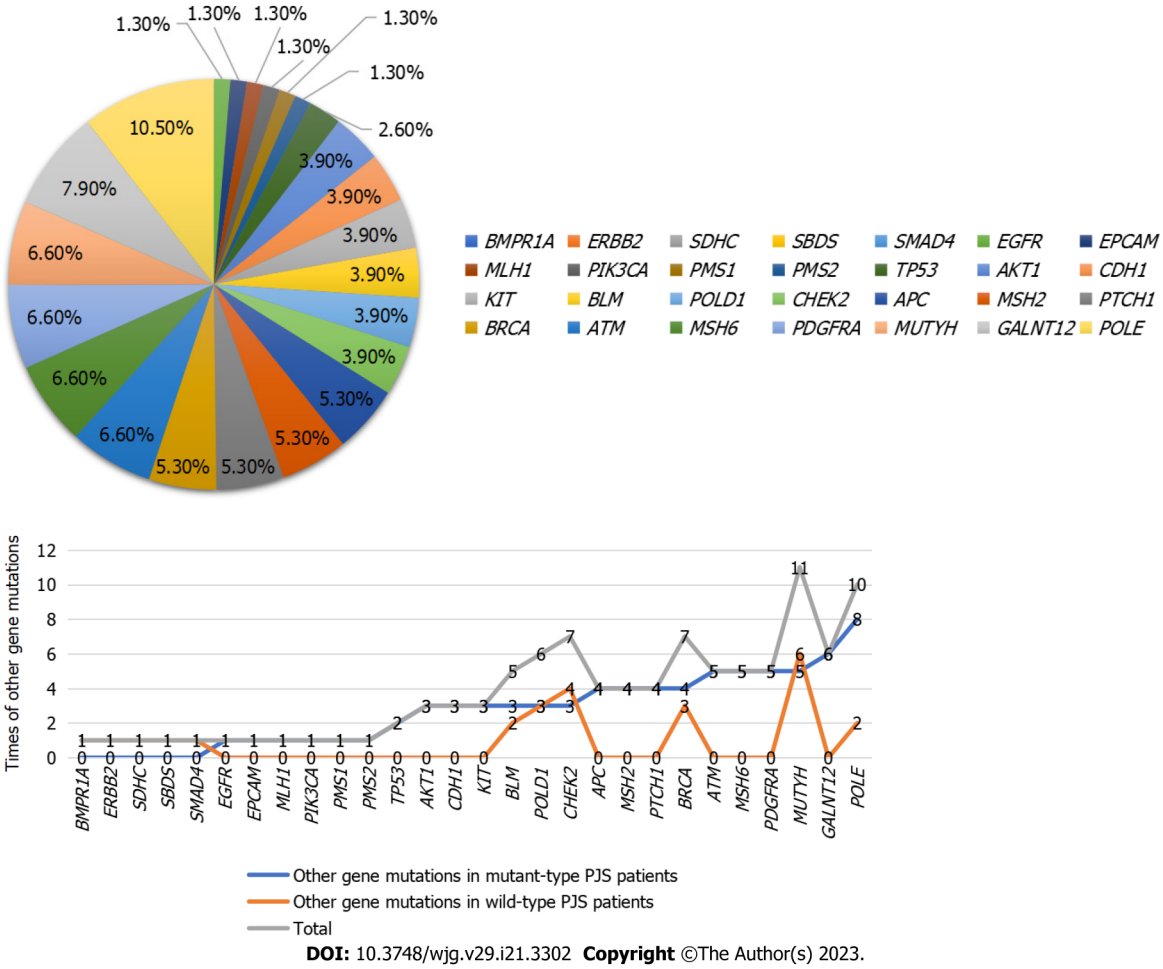


Figure 1 Comparisons of percentage of other gene mutations.

maximum diameter of duodenal intestine polyps between mutant-type PJS with and without *GALNT12* mutations ($P < 0.05$); (6) *BRCA*: There were differences in maximum diameter of duodenal intestine polyps between mutant-type PJS with and without *BRCA* mutations ($P < 0.05$); (7) *KIT:* There were differences in ABO blood group and age of first intussusception between mutant-type PJS with and without *KIT* mutations ($P < 0.05$); (8) *MSH:* There was a difference in distribution of colorectal polyps between mutant-type PJS with and without *MSH* mutations ($P < 0.05$); (9) *PTCH1:* There were differences in load of gastric polyps and maximum diameter of colorectal polyps between mutant-type

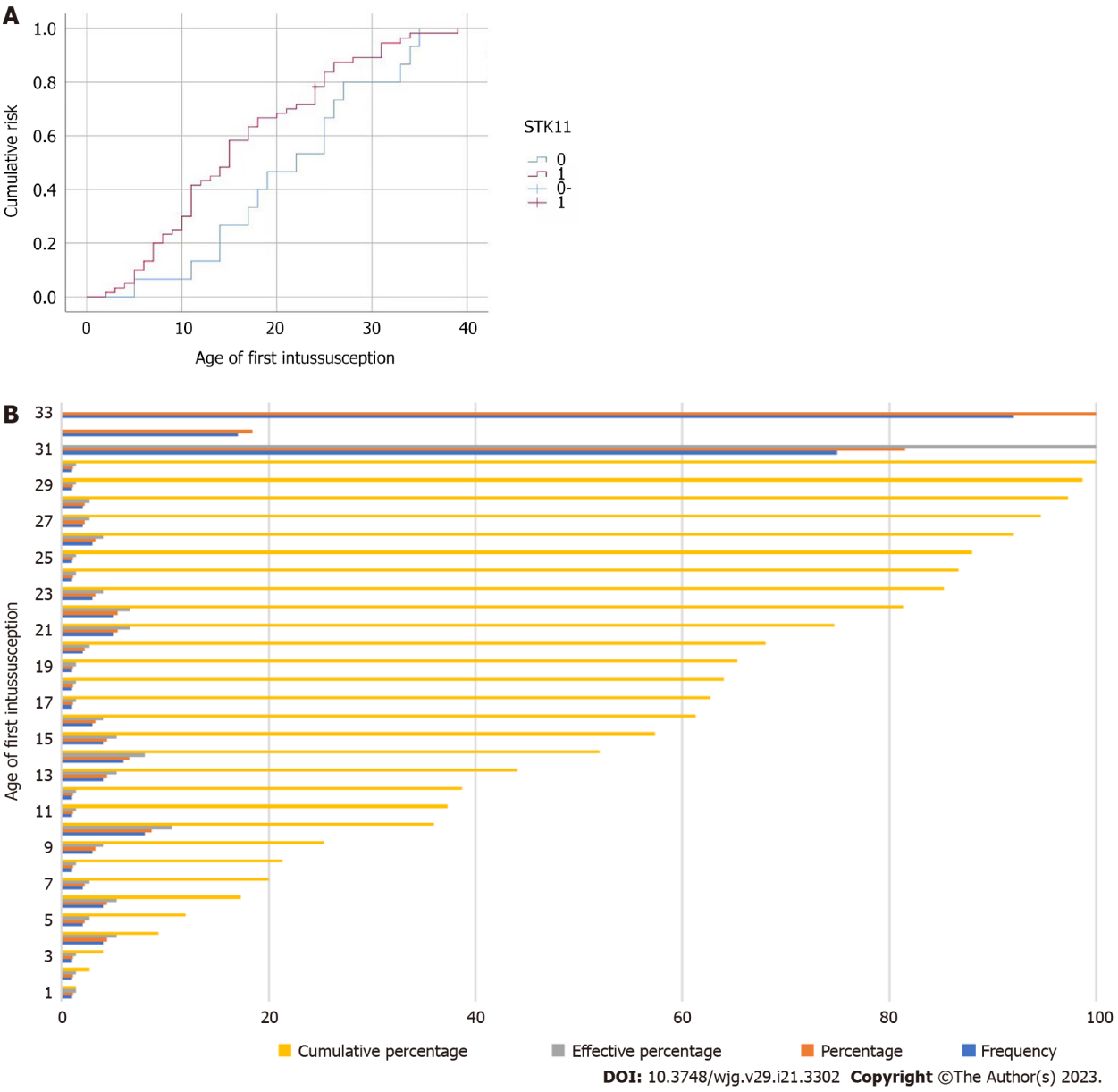


Figure 2 Intussusception. A: Cumulative risk function for intussusception; B: Cumulative percentage at age of first intussusception.

PJS with and without *PTCH1* mutations ($P < 0.05$); (10) *ATM:* There was a difference in age of mucocutaneous pigmentation appearance between mutant-type PJS with and without *ATM* mutations ($P < 0.05$); (11) *PDGFRA*: There was a difference in final age of follow-up between mutant-type PJS with and without *PDGFRA* mutations ($P < 0.05$); and (12) *POLD1:* There was a difference in age of first intussusception between mutant-type PJS with and without *POLD1* mutations ($P < 0.05$).

DISCUSSION

PJS is an autosomal dominant disorder with a prevalence of approximately 1 in 200000[15,16]. Although PJS is a rare disease, the large population of China and the prolonged course of PJS lead to the accumulation of a great number of PJS patients in Chinese society. Germline mutations in the *STK11* gene are recognized as the molecular genetic cause of PJS. The tumor suppressor gene *STK11* is involved in multiple processes such as embryonic development, cell polarity, cell cycle arrest, apoptosis and metabolism, and its mutations have been detected in a variety of disseminated cancers. A related study [17] demonstrated that the lack of the *STK11* gene resulted in a significant increase of intracellular reactive oxygen species levels and enhanced expression of phosphorylated histone γ-H2AX, which resulted in DNA damage, oxidative damage to the genome and an increased mutation rate. The rate of *STK11* germline mutations detected in this group of PJS patients was 79.35%, which is generally

Table 6 Recommended follow-up and intervention strategies for mutant-type and wild-type Peutz-Jeghers syndrome

Age (yr)	Mutant-type		Wild-type	
	Surveillance	Intervention	Surveillance	Intervention
< 7	Routine abdominal ultrasound surveillance is recommended every year	Removal of polyps	Abdominal ultrasound is recommended every 3-5 yr	Follow-up observation
8-11	Routine abdominal ultrasound surveillance is recommended every year. For symptomatic individuals with PJS, an abdominal ultrasound should be performed earlier	Removal of polyps	Abdominal ultrasound is recommended every 3-5 yr. For symptomatic individuals with PJS, an abdominal ultrasound should be performed earlier	Removal of polyps
8-18	Total GI surveillance every year (CT scan of small-bowel or enteroscopy/capsule endoscopy should be offered as options	Polyps > 10 mm should be removed	Total GI surveillance 2-3 yr	Removal of polyps
19-30	Routine total GI polyps surveillance every 2-3 yr and screening for systemic tumors	Removal of polyps and treatment of tumors	Routine total GI polyps surveillance every 2-3 yr	Removal of polyps
> 30	Focus on detection of tumors in digestive tract and other organs	Treatment of tumors	Focus on detection of tumors in digestive tract and other organs	Treatment of tumors

PJS: Peutz-Jeghers syndrome; GI: Gastrointestina; CT: Computed tomography.

consistent with the literature[18].

The target genome covered 41 pathogenic genes associated with digestive tract tumors, including *STK11*, and PJS patients were classified into wild-type or mutant-type based on the presence or absence of *STK11* mutations. The results of the clinical characteristic analysis showed that there were significant differences between wild-type and mutant-types PJS in age of initial treatment, age of first intussusception, frequency of intussusception, age of initial surgery, time interval from mucocutaneous pigmentation appearance to abdominal symptoms, maximum diameter of gastric polyps, load of duodenal intestine polyps, distribution of colorectal polyps, times of hospitalization and times of endoscopic examinations. Mutant-type PJS typically has an earlier age of initial treatment and a shorter time interval from mucocutaneous pigmentation appearance to abdominal symptoms than wild-type PJS. They are often first admitted to hospital for serious complications such as intussusception and intestinal obstruction. Our study found that the age of first intussusception was significantly younger in mutant-type PJS than in wild-type PJS, and its cumulative risk of intussusception at the age of 20 years was 68.3%, which was significantly higher than that of wild-type PJS (Figure 2). This is consistent with the findings of domestic and international studies[19,20]. As a result, complications such as intestinal obstruction and intussusception are more likely to occur in mutant-type PJS than in wild-type, and occur earlier. The earlier intervention of treatment for GI polyps in mutant-type PJS patients would be beneficial in reducing the occurrence of these complications. In addition, mutant-type PJS has a higher distribution of colorectal polyps and a larger maximum diameter of gastric polyps than wild-type PJS, requiring more frequent endoscopic examinations and treatment in hospital.

Overseas studies have shown that PJS patients have an increased risk of cancer at several sites, including the GI tract, breast, ovaries, testes and lungs[21]. PJS malignancy is a serious threat to the life and health of patients; studies have shown[21,22] that the death rate of PJS patients is as high as 32%, and malignancy is the main cause of death. The incidence of malignant tumors in PJS patients is 19%-32%, with an average age of 42-45 years, and a predominance of GI tract tumors (51%-69%), followed by gynecological tumors (22%-26%). The risk of GI malignancy is 50 times higher than that of the general population. The 19 cases of wild-type PJS in this study were not combined with malignant tumors. Among the 73 mutant-type patients, 8 had GI polyps and 4 had cancers of other sites: 1 adnexal cystadenocarcinoma, 1 ovarian mucinous tumor, 1 cervical adenocarcinoma and 1 nasopharyngeal carcinoma. It was found that patients with a detectable *STK11* truncating mutation tend to develop more polyps and cancers, and require more surgical intervention[23]. There was no statistically significant difference in the cancer rate between mutant-type and wild-type in this study, which may be related to the shorter follow-up period of the enrolled patients. Germline mutations of *STK11* are essential factors in GI tumourigenesis, and the cell types and signal pathways that lead to the malignant transformation of polyps are still unclear. A foreign study showed[24] that after the knockout of *STK11* in mice, IL-11 inflammatory mediators mediated the activation of the JAK/STAT3 pathway due to *STK11* deficiency in mouse stromal cells, which eventually resulted in the formation of polyp malignancy in mice, and the treatment of *STK11*-deficient mice with JAK1/2 inhibitors significantly reduced the occurrence of polyps. We can block the development and malignancy of polyps at the root by blocking the associated inflammatory mediators or transduction pathways, which provides a new idea for us in studying the pharmacological treatment of PJS patients. Previous studies have shown that PJS patients have a progression pathway of hamartoma-(adenoma)-carcinoma[25], which is corrob-

orated by the presence in our study of PJS patients with malformation combined with adenomatous polyps and with adenoma combined with polyp carcinoma. Accordingly, the detection of *STK11* mutations can be useful for guiding the assessment of polyp carcinogenesis risk in PJS patients and their relatives.

PJS patients have a prolonged disease course, with GI polyps growing larger with age and recurring more easily, and can result in intestinal obstruction, intussusception or even cancer, but the characteristics and severity of the disease vary significantly among PJS patients. The clinical presentation is distinctly heterogeneous. Clinical data and epidemiological data collected from more than 500 PJS patients at our center suggests that polyps grow fastest in adolescence, leading to serious complications such as intussusception, and the age of first surgery is significantly younger in mutant-type PJS than in wild-type PJS. Meanwhile, the incidence of tumors in the digestive tract and other organs of the body is significantly higher in middle-aged PJS patients.

CONCLUSION

Therefore, in the individualized treatment of PJS patients, we recommend that they should have the *STK11* gene tested, and the genotypes classified into mutant-type and wild-type. Patients with mutant-type PJS should be strictly controlled in terms of treatment and follow-up strategies, while patients with wild-type PJS can be treated with relaxed treatment conditions and follow-up years. For the monitoring and treatment of PJS, we refer to the different follow-up strategies by age group proposed by a domestic study[26], and further refine the treatment and follow-up strategies for PJS based on this treatment strategy as follows (Table 6).

ARTICLE HIGHLIGHTS

Research background

Peutz-Jeghers syndrome (PJS) is an autosomal dominant genetic disease with skin mucosal pigment spots and gastrointestinal multiple hamartoma polyps as clinical characteristics. At present, it is considered that the germline mutation of *STK11* gene is the genetic cause of PJS. However, not all PJS patients can be detected *STK11* germline mutations.

Research motivation

The specific clinical characteristics of these PJS patients without *STK11* mutation is an interesting clinical question. Or, like wild type gastrointestinal stromal tumor (GIST), whether these PJS without *STK11* mutation are also called PJS is worth discussing. Therefore, we designed the study to understand the clinical characteristics of these PJS patients without *STK11* mutation.

Research objectives

To investigates whether PJS patients with known *STK11* mutations have a more severe spectrum of clinical phenotypes compared to those without.

Research methods

The general information, diagnosis and treatment history, pathology, times of examination and other clinical data of the 92 enrolled PJS patients were collected for statistical analysis. Genomic DNA samples were extracted from peripheral blood samples, and pathogenic germline mutations of *STK11* were detected by high-throughput next-generation gene sequencing. Clinical-pathologic manifestations of patients with and without *STK11/LKB1* mutations were compared.

Research results

Compared with PJS patients with *STK11* mutations, those without tended to be older at the age of initial treatment, age of first intussusception and age of initial surgery. They also had a lower number of total hospitalizations relating to intussusception or intestinal obstruction, and a lower load of small intestine polyps. Final results found that PJS patients without *STK11* mutations might have less severe clinical-pathologic manifestations than those with.

Research conclusions

PJS patients without *STK11* mutations might have less severe clinical-pathologic manifestations than those with.

Research perspectives

At present, it is considered that the germline mutation of *STK11* gene is the genetic cause of PJS.

However, not all PJS patients can be detected *STK11* germline mutations. The specific clinical characteristics of these PJS patients without *STK11* mutation is an interesting clinical question. Or, like wild type GIST, whether these PJS without *STK11* mutation are also called PJS is worth discussing.

FOOTNOTES

Author contributions: Jiang LX, Chen YR, Xu ZX and Zhang YH contributed equally to this study; Gu GL designed the research; Jiang LX, Chen YR, Xu ZX, Zhang YH, Zhang Z, Yu PF, Dong ZW and Yang HR collected and analyzed the clinical data; Jiang LX, Chen YR and Xu ZX wrote the manuscript; Gu GL and Dong ZW revised the manuscript.

Supported by Beijing Capital Medical Development Research Fund, No. Shoufa2020-2-5122; Outstanding Young Talents Program of Air Force Medical Center, PLA, No. 22BJQN004; and Clinical Program of Air Force Medical University, No. Xiaoke2022-07.

Institutional review board statement: The study was reviewed and approved by the Air Force Medical Center, PLA, Institutional Review Board, No. 2020-105-PJ01, No. 2020-105-YJ01.

Clinical trial registration statement: This study is a special research project for the development of capital health which approved by the Beijing Municipal Health Commission in 2020. No further clinical trial registration has been conducted. Hereby declare.

Informed consent statement: All study participants, or their legal guardian, provided informed written consent prior to study enrollment.

Conflict-of-interest statement: All the authors report no relevant conflicts of interest for this article.

Data sharing statement: No additional data are available.

CONSORT 2010 statement: The authors have read the CONSORT 2010 statement, and the manuscript was prepared and revised according to the CONSORT 2010 statement.

Open-Access: This article is an open-access article that was selected by an in-house editor and fully peer-reviewed by external reviewers. It is distributed in accordance with the Creative Commons Attribution NonCommercial (CC BY-NC 4.0) license, which permits others to distribute, remix, adapt, build upon this work non-commercially, and license their derivative works on different terms, provided the original work is properly cited and the use is non-commercial. See: https://creativecommons.org/Licenses/by-nc/4.0/

Country/Territory of origin: China

ORCID number: Yu-Hui Zhang 0000-0002-3224-9017; Zhi Zhang 0000-0001-5870-1940; Peng-Fei Yu 0000-0002-0528-1839; Zhi-Wei Dong 0000-0001-7009-9331; Hai-Rui Yang 0000-0003-2768-8493; Guo-Li Gu 0000-0002-9998-047X.

S-Editor: Fan JR
L-Editor: A
P-Editor: Chen YX

REFERENCES

1 **Sato E**, Goto T, Honda H. Peutz-Jeghers Syndrome. *JAMA Dermatol* 2022; **158**: 1316 [PMID: 36197686 DOI: 10.1001/jamadermatol.2022.3979]
2 **Alharbi ES**, Alrumayh JS, Alzaghran RH, Algaith NK, Shaheen AN. A Case of Multiple Polyps Causing Intussusception in an Adult Patient With Peutz-Jeghers Syndrome. *Cureus* 2022; **14**: e30532 [PMID: 36415380 DOI: 10.7759/cureus.30532]
3 **Borun P**, Bartkowiak A, Banasiewicz T, Nedoszytko B, Nowakowska D, Teisseyre M, Limon J, Lubinski J, Kubaszewski L, Walkowiak J, Czkwianianc E, Siolek M, Kedzia A, Krokowicz P, Cichy W, Plawski A. High Resolution Melting analysis as a rapid and efficient method of screening for small mutations in the STK11 gene in patients with Peutz-Jeghers syndrome. *BMC Med Genet* 2013; **14**: 58 [PMID: 23718779 DOI: 10.1186/1471-2350-14-58]
4 **Jelsig AM**. Hamartomatous polyps - a clinical and molecular genetic study. *Dan Med J* 2016; **63** [PMID: 27477802]
5 **Klimkowski S**, Ibrahim M, Ibarra Rovira JJ, Elshikh M, Javadi S, Klekers AR, Abusaif AA, Moawad AW, Ali K, Elsayes KM. Peutz-Jeghers Syndrome and the Role of Imaging: Pathophysiology, Diagnosis, and Associated Cancers. *Cancers (Basel)* 2021; **13** [PMID: 34680270 DOI: 10.3390/cancers13205121]
6 **Altamish M**, Dahiya R, Singh AK, Mishra A, Aljabali AAA, Satija S, Mehta M, Dureja H, Prasher P, Negi P, Kapoor DN, Goyal R, Tambuwala MM, Chellappan DK, Dua K, Gupta G. Role of the Serine/Threonine Kinase 11 (STK11) or Liver Kinase B1 (LKB1) Gene in Peutz-Jeghers Syndrome. *Crit Rev Eukaryot Gene Expr* 2020; **30**: 245-252 [PMID: 32749111

DOI: 10.1615/CritRevEukaryotGeneExpr.2020033451]

7 **Kuroda Y**, Saito T, Nagai J, Ida K, Naruto T, Masuno M, Kurosawa K. Microdeletion of 19p13.3 in a girl with Peutz-Jeghers syndrome, intellectual disability, hypotonia, and distinctive features. *Am J Med Genet A* 2015; **167A**: 389-393 [PMID: 25487640 DOI: 10.1002/ajmg.a.36813]

8 **Duan FX**, Gu GL, Yang HR, Yu PF, Zhang Z. Must Peutz-Jeghers syndrome patients have the LKB1/STK11 gene mutation? A case report and review of the literature. *World J Clin Cases* 2018; **6**: 224-232 [PMID: 30148152 DOI: 10.12998/wjcc.v6.i8.224]

9 **Byrjalsen A**, Roos L, Diemer T, Karstensen JG, Løssl K, Jelsig AM. Preimplantation genetic testing in two Danish couples affected by Peutz-Jeghers syndrome. *Scand J Gastroenterol* 2023; **58**: 314-318 [PMID: 36200740 DOI: 10.1080/00365521.2022.2129031]

10 **Daniell J**, Plazzer JP, Perera A, Macrae F. An exploration of genotype-phenotype link between Peutz-Jeghers syndrome and STK11: a review. *Fam Cancer* 2018; **17**: 421-427 [PMID: 28900777 DOI: 10.1007/s10689-017-0037-3]

11 **Ueki A**, Hirasawa A. Molecular Features and Clinical Management of Hereditary Gynecological Cancers. *Int J Mol Sci* 2020; **21** [PMID: 33327492 DOI: 10.3390/ijms21249504]

12 **Boland CR**, Idos GE, Durno C, Giardiello FM, Anderson JC, Burke CA, Dominitz JA, Gross S, Gupta S, Jacobson BC, Patel SG, Shaukat A, Syngal S, Robertson DJ. Diagnosis and management of cancer risk in the gastrointestinal hamartomatous polyposis syndromes: recommendations from the U.S. Multi-Society Task Force on Colorectal Cancer. *Gastrointest Endosc* 2022; **95**: 1025-1047 [PMID: 35487765 DOI: 10.1016/j.gie.2022.02.044]

13 **Boland CR**, Idos GE, Durno C, Giardiello FM, Anderson JC, Burke CA, Dominitz JA, Gross S, Gupta S, Jacobson BC, Patel SG, Shaukat A, Syngal S, Robertson DJ. Diagnosis and Management of Cancer Risk in the Gastrointestinal Hamartomatous Polyposis Syndromes: Recommendations From the US Multi-Society Task Force on Colorectal Cancer. *Am J Gastroenterol* 2022; **117**: 846-864 [PMID: 35471415 DOI: 10.14309/ajg.0000000000001755]

14 **Shaunak M**, Side L, Afzal N, Davies JH. An atypical presentation of a pathogenic STK11 gene variant in siblings not fulfilling the clinical diagnostic criteria for Peutz-Jeghers Syndrome. *J Pediatr Endocrinol Metab* 2022; **35**: 131-134 [PMID: 34674413 DOI: 10.1515/jpem-2021-0567]

15 **Wang R**, Qi X, Liu X, Guo X. Peutz-Jeghers syndrome: Four cases in one family. *Intractable Rare Dis Res* 2016; **5**: 42-43 [PMID: 26989648 DOI: 10.5582/irdr.2015.01036]

16 **Chae HD**, Jeon CH. Peutz-Jeghers syndrome with germline mutation of STK11. *Ann Surg Treat Res* 2014; **86**: 325-330 [PMID: 24949325 DOI: 10.4174/astr.2014.86.6.325]

17 **Wang YS**, Chen J, Cui F, Wang H, Wang S, Hang W, Zeng Q, Quan CS, Zhai YX, Wang JW, Shen XF, Jian YP, Zhao RX, Werle KD, Cui R, Liang J, Li YL, Xu ZX. LKB1 is a DNA damage response protein that regulates cellular sensitivity to PARP inhibitors. *Oncotarget* 2016; **7**: 73389-73401 [PMID: 27705915 DOI: 10.18632/oncotarget.12334]

18 **Jiang YL**, Zhao ZY, Li BR, Wang H, Yu ED, Ning SB. STK11 gene analysis reveals a significant number of splice mutations in Chinese PJS patients. *Cancer Genet* 2019; **230**: 47-57 [PMID: 30528796 DOI: 10.1016/j.cancergen.2018.11.008]

19 **Rycyk A**, Kasztelan-Szczerbinska B, Cichoz-Lach H. A rare case of a juvenile polyp of patient with Peutz-Jeghers syndrome, complicated with intussusception of the small intestine. *Folia Med (Plovdiv)* 2022; **64**: 693-696 [PMID: 36045464 DOI: 10.3897/folmed.64.e67044]

20 **Kariv R**, Dahary D, Yaron Y, Petel-Galil Y, Malcov M, Rosner G. Whole Genome Sequencing Applied in Familial Hamartomatous Polyposis Identifies Novel Structural Variations. *Genes (Basel)* 2022; **13** [PMID: 36011318 DOI: 10.3390/genes13081408]

21 **Wu M**, Krishnamurthy K. Peutz-Jeghers Syndrome. 2022 Aug 21. In: StatPearls [Internet]. Treasure Island (FL): StatPearls Publishing; 2023 Jan- [PMID: 30570978]

22 **Latchford AR**, Clark SK. Gastrointestinal aspects of Peutz-Jeghers syndrome. *Best Pract Res Clin Gastroenterol* 2022; **58-59**: 101789 [PMID: 35988959 DOI: 10.1016/j.bpg.2022.101789]

23 **Gorji L**, Huish G, Morgan J, Levy P. A case of sporadic Peutz-Jeghers syndrome presenting as multiple intussusceptions. *J Surg Case Rep* 2022; **2022**: rjac070 [PMID: 35280052 DOI: 10.1093/jscr/rjac070]

24 **Ollila S**, Domènech-Moreno E, Laajanen K, Wong IP, Tripathi S, Pentinmikko N, Gao Y, Yan Y, Niemelä EH, Wang TC, Viollet B, Leone G, Katajisto P, Vaahtomeri K, Mäkelä TP. Stromal Lkb1 deficiency leads to gastrointestinal tumorigenesis involving the IL-11-JAK/STAT3 pathway. *J Clin Invest* 2018; **128**: 402-414 [PMID: 29202476 DOI: 10.1172/JCI93597]

25 **Ma H**, Brosens LAA, Offerhaus GJA, Giardiello FM, de Leng WWJ, Montgomery EA. Pathology and genetics of hereditary colorectal cancer. *Pathology* 2018; **50**: 49-59 [PMID: 29169633 DOI: 10.1016/j.pathol.2017.09.004]

26 **Li BR**, Sun T, Li J, Zhang YS, Ning SB, Jin XW, Zhu M, Mao GP. Primary experience of small bowel polypectomy with balloon-assisted enteroscopy in young pediatric Peutz-Jeghers syndrome patients. *Eur J Pediatr* 2020; **179**: 611-617 [PMID: 31863304 DOI: 10.1007/s00431-019-03534-1]

World Journal of Gastroenterology

Submit a Manuscript: https://www.f6publishing.com

World J Gastroenterol 2023 June 7; 29(21): 3318-3327

DOI: 10.3748/wjg.v29.i21.3318

ISSN 1007-9327 (print) ISSN 2219-2840 (online)

ORIGINAL ARTICLE

Observational Study

Artifacts in two-dimensional shear wave elastography of liver

Hui-Peng Wang, Peng-Chao Zheng, Xue-Mei Wang, Liang Sang

Specialty type: Gastroenterology and hepatology

Provenance and peer review: Unsolicited article; Externally peer reviewed.

Peer-review model: Single blind

Peer-review report's scientific quality classification

Grade A (Excellent): 0
Grade B (Very good): B, B, B
Grade C (Good): 0
Grade D (Fair): 0
Grade E (Poor): 0

P-Reviewer: Lattanzi S, Italy; Macias-Rodriguez RU, Mexico; Singh D, India

Received: February 27, 2023
Peer-review started: February 27, 2023
First decision: March 14, 2023
Revised: March 23, 2023
Accepted: May 6, 2023
Article in press: May 6, 2023
Published online: June 7, 2023

Hui-Peng Wang, Peng-Chao Zheng, Xue-Mei Wang, Liang Sang, Department of Ultrasound, The First Hospital of China Medical University, Shenyang 110001, Liaoning Province, China

Corresponding author: Liang Sang, MD, PhD, Associate Professor, Doctor, Department of Ultrasound, The First Hospital of China Medical University, No. 155 Nanjing North Street, Shenyang 110001, Liaoning Province, China. 13889167622@163.com

Abstract

BACKGROUND

Artifacts are common when using two-dimensional shear wave elastography (2-D SWE) to measure liver stiffness (LS), but they are poorly recognized.

AIM

To investigate the presence and influence of artifacts in 2-D SWE of liver.

METHODS

We included 158 patients with chronic liver disease, who underwent 2-D SWE examination by a novice and an expert. A cross line at the center of the elastogram was drawn and was divided it into four locations: top-left, top-right, bottom-left, and bottom-right. The occurrence frequency of artifacts in different locations was compared. The influence of artifacts on the LS measurements was evaluated by comparing the elastogram with the most artifacts (EMA) and the elastogram with the least artifacts (ELA).

RESULTS

The percentage of elastograms with artifacts in the novice (51.7%) was significantly higher than that of the expert (19.6%) ($P < 0.001$). It was found that both operators had the highest frequency of artifacts at bottom-left, followed by top-left and bottom-right, and top-right had the lowest frequency. The LS values (LSVs) and standard deviation values of EMAs were significantly higher than those of ELAs for both operators. An intraclass correlation coefficient value of 0.96 was found in the LSVs of EMAs of the two operators, and it increased to 0.98 when the LSVs of the ELAs were used. Both operators had lower stability index values for EMAs than ELAs, but the difference was only statistically significant for the novice.

CONCLUSION

Artifacts are common when using 2-D SWE to measure LS, especially for the novice. Artifacts may lead to the overestimation of LS and reduce the repeatability and reliability of LS measurements.

Key Words: Ultrasound; Elastography; Artifact; Liver

©The Author(s) 2023. Published by Baishideng Publishing Group Inc. All rights reserved.

Core Tip: Artifacts are common when using two-dimensional shear wave elastography (2-D SWE) to measure liver stiffness (LS), especially for the novice. We investigated the presence and influence of artifacts in 2-D SWE of liver. Our results showed artifacts were more likely to occur in the bottom-left corner of the elastogram. Artifacts may lead to the overestimation of LS and reduce the repeatability and reliability of LS measurements. For the elastograms with artifacts, we should place the Q-Box away from the artifacts.

Citation: Wang HP, Zheng PC, Wang XM, Sang L. Artifacts in two-dimensional shear wave elastography of liver. *World J Gastroenterol* 2023; 29(21): 3318-3327
URL: https://www.wjgnet.com/1007-9327/full/v29/i21/3318.htm
DOI: https://dx.doi.org/10.3748/wjg.v29.i21.3318

INTRODUCTION

Chronic liver disease is a growing problem worldwide. The main causes of chronic liver disease include hepatitis virus infection, alcoholic liver disease, and non-alcoholic fatty liver disease[1]. It mainly causes diffuse liver fibrosis, which in turn leads to liver cirrhosis. Some of them eventually develop hepatocellular carcinoma, portal hypertension, and hepatic encephalopathy[2,3]. Accurate assessment of liver fibrosis is important for treatment prioritization, surveillance, and determination of prognosis[4]. Moreover, liver biopsy allows the assessment of the degree of fibrosis[5]. However, liver biopsy is an expensive and invasive diagnostic tool. Its main complications are bleeding and pain[6,7], which limit its clinical application.

Recently, the application of ultrasound elastography in the diagnosis of non-invasive assessment of liver fibrosis has developed rapidly[8]. US elastography is mainly classified into two major types: Strain elastography and shear wave elastography[9,10]. Two-dimensional shear wave elastography (2-D SWE) is a type of shear wave elastography that uses acoustic radiation force to create shear waves. The velocity of the shear wave can be used to calculate the tissue stiffness by the formula $E = 3\rho c^2$, where E is tissue elasticity (Young's modulus, kPa), ρ is tissue density (kg/m^3), and c is shear wave velocity (m/s). The 2-D SWE is based on the quantification of the propagation speed of shear waves in the liver to create an elastogram. The elastogram is displayed using a color-coded map superimposed on a conventional B-mode image, where different colors represent different stiffness, allowing an assessment of homogeneity[10].

It has been reported that 2-D SWE has shown sufficient accuracy in evaluating the degree of liver fibrosis[11-13]. However, there was significant heterogeneity in the results of these studies. This heterogeneity may be caused by different patient populations, research designs and equipment used[14]. Another important reason may be that the presence of artifacts leads to inaccurate liver stiffness (LS) measurements. Bruce *et al*[15] reported that 2-D SWE artifacts resulted in a significant variability in the assessed LS.

Although 2-D SWE artifacts of the liver are common in clinical practice, they are poorly recognized, and there is even no clear definition. To the best of our knowledge, only a few review articles have been published[15,16]. Therefore, the purpose of this study was to investigate the presence and effects of artifacts in 2-D SWE of the liver. This is important to avoid artifacts and improve diagnostic performance in future operations.

MATERIALS AND METHODS

Patient selection

This prospective study was approved by the institutional ethical review board of our hospital. All patients signed a written informed consent document to participate in the study. We included 158 consecutive patients with chronic liver disease, who underwent 2-D SWE examination in our department. The study was conducted according to the principles reported in the Declaration of Helsinki and approved by the authors' institutional review board. The exclusion criterion was that no valid measurement was obtained by either operator. Seven patients were excluded because the novice operator did not obtain any valid measurements after five consecutive measurements. The baseline

characteristics of the patients were presented in Table 1.

2-D SWE examination

LS measurements were performed with an Aixplorer US system (SuperSonic Imagine, Aix-en-Provence, France) with a convex probe (SC6-1, 1-6 MHz). Patients fasted for more than 6 h and were examined in the supine position with the right arm in maximal abduction. The right anterior lobe of the liver was examined by intercostal scanning, and the SWE mode was started with neutral breathing during breath-holding. The upper limit of the color-coding scale was set to 70 kPa. The sampling frame was approximately 2.5 cm × 3.5 cm, placed at least 1 cm below the liver capsule, avoiding the large vascular structures. Image acquisition was performed after the elastography image was stable for 3-5 s. The quantitative analysis system (Q-Box) was then activated and placed at the center of the sampling frame. The Q-Box was 2 cm in diameter and the measurement depth was 3-5 cm. The LS measurement was considered invalid if there was no color-coding or the coded area was smaller than the Q-Box size[17]. When the area of color-coding is larger than the Q-Box size, the LS measurement was considered valid even if there are artifacts within it.

Each patient was continuously measured five times by an expert and a novice, respectively. The operators performed consecutive LS measurements in a randomized blinded manner. The median value of all valid measurements performed by the two operators represents the LS value (LSV) of the subject and was used for the correlation analysis with artifacts. The expert operator had 9 years of experience in the 2-D SWE examinations and had successfully performed approximately 15000 2D SWE examinations. The novice operator was trained by an expert operator and successfully performed 50 2-D SWE examinations.

Analysis of elastogram for artifacts

Artifacts were defined as the mottled area in the elastograms, and the area of the artifacts was measured using a tracing instrument attached to the device. We can manually trace the edge of the artifacts and automatically display the area and perimeter of the artifacts (Figure 1A). We drew a cross line at the center of the elastogram and divided it into four locations: top-left, top-right, bottom-left, and bottom-right. The location of the artifacts in each elastogram was recorded. The elastogram with the most artifacts (EMA) and the elastogram with the least artifacts (ELA) in each patient measured by the two operators were found by all authors. For the elastograms with artifacts, the Q-Box was placed in the center of the sampling frame (Figure 1B) and away from the artifacts for measurements (Figure 1C). The influence of artifacts on LS measurement was evaluated by comparing the differences in LSVs, standard deviation (SD) values and stability index (SI) values.

Statistical analysis

All quantitative data are expressed as mean ± SD (range), and qualitative variables are expressed as numbers (percentages). The Shapiro-Wilk test was used to test whether the numeric variables were normally distributed. Non-parametric tests with the Kruskal-Wallis method were used to compare the difference in numeric variables with a non-normal distribution. Differences between numeric variables with a normal distribution were assessed using a parametric test (*t*-test). The χ^2-test was used to compare the proportions expressed as percentages. Interobserver repeatability was evaluated using intraclass correlation coefficient (ICC). Relationships between various parameters were examined using Pearson's correlation test. Statistical significance was set at $P < 0.05$, and all P values were two-sided. Statistical analysis was performed using MedCalc software (MedCalc Software, version 17.4, Ostend, Belgium).

RESULTS

Among the 158 patients, 151 patients with valid measurements obtained by both operators were enrolled in this study. In theory, each operator should obtain 755 (151 × 5 = 755) elastography images. However, in the examination of 12 patients by the two operators, 35 elastography images were invalid and excluded. To ensure that the two operators had the same number of valid elastograms for each patient, valid measurements corresponding to the 35 invalid measurements were also excluded. Therefore, 720 elastography images from each operator were included (Figure 2).

The presence of artifacts

For the expert operator, the percentage of elastograms with artifacts was 19.6% (141/720), and the area of artifacts was 0.92 ± 0.68 cm^2. For the novice operator, the percentage of elastograms with artifacts was 51.7% (372/720), and the area of artifacts was 1.36 ± 0.87 cm^2. The percentage of elastograms with artifacts and the area of artifacts in the novice were significantly higher than those in the expert, and the difference were both statistically significant (both $P < 0.001$). We counted all the artifacts according to their locations, and the results are shown in Table 2. There were no significant differences in the frequency of the occurrence of artifacts between the two operators at the same location (all $P > 0.05$).

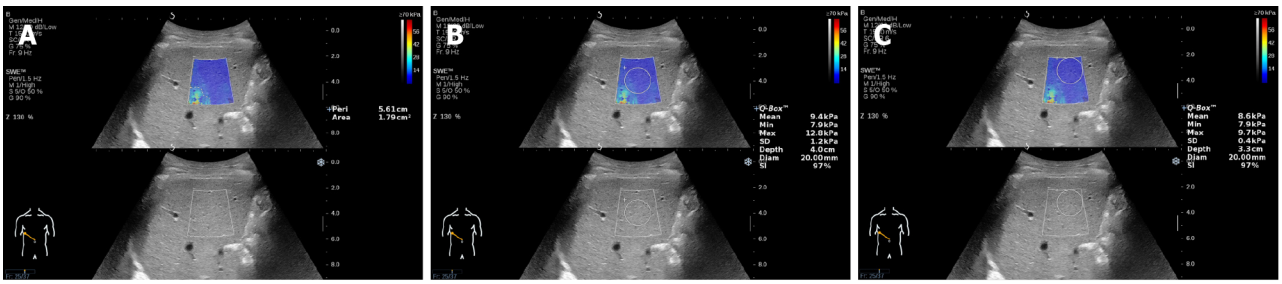
Table 1 Patient characteristics (*n* = 151)

Characteristic	Value
Age (yr)	46.2 ± 13.1 (19-75)
Liver stiffness value (kPa)	9.7 ± 7.8 (3.8-34.9)
Liver cirrhosis, *n* (%)	17 (11.3)
Subcutaneous fat thickness (cm)	0.4 ± 0.3 (0.1-2.4)
Sex, *n* (%)	
Male	72 (47.7)
Female	79 (52.3)
Body mass index (kg/m^2)	23.3 ± 3.4 (17.2-36.3)
Normal (< 25 kg/m^2), *n* (%)	101 (66.9)
Overweight (25-30 kg/m^2), *n* (%)	41 (27.2)
Obese (> 30 kg/m^2), *n* (%)	9 (5.9)
Etiology of chronic liver disease, *n* (%)	
Hepatitis B virus	122 (80.8)
Hepatitis C virus	8 (5.3)
Alcoholic liver disease	10 (6.6)
Nonalcoholic fatty liver disease	6 (4)
Autoimmune disease	5 (3.3)

Table 2 Artifacts at different locations of the two operators

Locations	Expert, *n* (%)	Novice, *n* (%)	*P* value
Top-left	40 (21.5)	120 (20.5)	0.769
Bottom-left	102 (54.8)	309 (52.8)	0.634
Top-right	7 (3.8)	42 (7.2)	0.098
Bottom-right	37 (19.9)	114 (19.5)	0.904

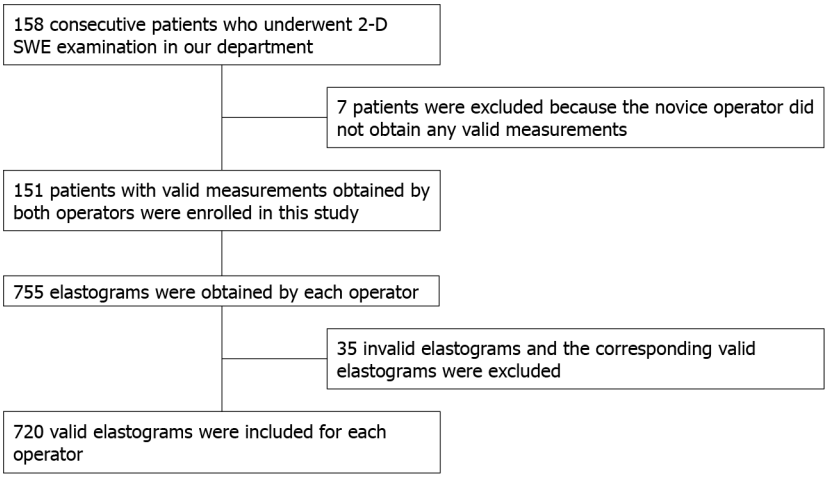
Qualitative data are expressed as *n* (%).



DOI: 10.3748/wjg.v29.i21.3318 **Copyright** ©The Author(s) 2023.

Figure 1 Elastograms of a 60-year-old man with hepatitis B virus. A: Elastogram with artifacts at the bottom-left of the sampling frame, and the area of artifacts was 1.79 square centimeters; B: For the elastogram with artifacts, the Q-Box was placed in the center of the sampling frame [mean liver stiffness: 9.4 kPa, standard deviation (SD): 1.2 kPa, stability index (SI): 97%]; C: For the elastogram with artifacts, the Q-Box was placed away from the artifacts (mean liver stiffness: 8.6 kPa, SD: 0.4 kPa, SI: 97%). SD: Standard deviation; SI: Stability index.

Comparing the occurrence frequency of artifacts in all locations of the two operators, it was found that both operators had the highest frequency of bottom-left, followed by top-left and bottom-right, and top-right had the lowest frequency. No statistical difference was found between the frequency of top-left and bottom-right ($P > 0.05$), but the frequency among other locations was statistically different (all $P <$



DOI: 10.3748/wjg.v29.i21.3318 **Copyright** ©The Author(s) 2023.

Figure 2 Study flow diagram. 2-D SWE: Two-dimensional shear wave elastography.

0.001) (Table 3).

Influence of artifacts on LS measurements

The LSVs of EMAs were higher than those of ELAs for both operators, and the differences were statistically significant (both $P < 0.001$). There was a significant difference in the LSVs of the EMAs between the two operators ($P = 0.006$). However, there was no statistically significant difference in the LSVs of the ELAs between the two operators ($P = 0.051$) (Table 4).

The ICC values and 95%CIs were calculated by comparing the LSVs of the EMAs and ELAs of the two operators. An ICC value of 0.96 (95%CI: 0.94-0.98) was found in the LSVs of EMAs, and it increased to 0.98 (95%CI: 0.97-0.99) when the LSVs of the ELAs were used. The SD values of EMAs were higher than those of ELAs for both operators, and the differences were statistically significant (both $P < 0.001$). The SI values of the EMAs were lower than those of the ELAs for both operators. The difference was only statistically significant for the novice ($P = 0.002$), but not for the expert ($P = 0.135$) (Table 5).

For the elastograms with artifacts, the LSVs and SD values of the Q-Box placed in the center of the sampling frame were higher than those of the Q-Box placed away from the artifacts. The SI values of the Q-Box placed in the center of the sampling frame were lower than those of the Q-Box placed away from the artifacts. There were significant differences in LSVs, SD values and SI values between the Q-Box placed in the center of the sampling frame and away from the artifacts for both operators (all $P < 0.05$) (Table 6).

Patient characteristics and artifacts

The total number of elastograms with artifacts measured by the two operators was 513 (141 by the expert, 372 by the novice). The number of elastograms with artifacts in male subjects was 238 (46.4%), and that in female subjects was 275 (53.6%). There was no significant difference between the male and female subjects ($P = 0.378$). Pearson's correlation test showed that there was no significant linear correlation between age and the number of elastograms with artifacts ($r = 0.21$, $P = 0.126$). In the entire cohort, Pearson's correlation test showed that there was a positive correlation between LSV, body mass index (BMI), subcutaneous fat thickness and the number of elastograms with artifacts ($r = 0.47$, $P = 0.001$; $r = 0.41$, $P = 0.002$; and $r = 0.42$, $P = 0.002$, respectively).

DISCUSSION

When using 2-D SWE to measure LS in clinical practice, artifacts are commonly observed in elastograms [18]. It is difficult for some subjects to obtain satisfactory elastograms, such as obesity, poor acoustic window and inability of the subjects to hold their breath. Despite our best efforts to avoid artifacts, even operators with 9 years of operating experience still have a certain percentage of artifacts. In this study, we compared the difference in the frequency of occurrence artifacts between two different experienced operators. The results showed that the percentage of elastograms with artifacts and the area of artifacts in the novice were significantly higher than that of the expert. This may be because the expert operator can obtain high-quality B-mode imaging, which is required for accurately tracking shear waves[18]. Previous studies have shown that experts have better repeatability and reliability in measuring LS, which may have an important relationship with the fact that there were few artifacts in their elastograms[19,20]. Therefore, some studies have suggested that novices should perform at least 300

Table 3 Compare the percentage of artifacts at different locations

Locations of artifacts	P^1 value	P^2 value
Top-left *vs* bottom-left	< 0.001	< 0.001
Top-left *vs* top-right	< 0.001	< 0.001
Top-left *vs* bottom-right	0.703	0.669
Bottom-left *vs* top-right	< 0.001	< 0.001
Bottom-left *vs* bottom-right	< 0.001	< 0.001
Top-right *vs* bottom-right	< 0.001	< 0.001

[1]Compare the percentage of artifacts at different locations of the expert.
[2]Compare the percentage of artifacts at different locations of the novice.

Table 4 Comparison of liver stiffness values of elastograms with different area artifacts for two operators

	Expert	Novice	P^1 value
LSVs of EMAs (kPa)	10.2 ± 8.3	11.0 ± 8.7	0.006
LSVs of ELAs (kPa)	9.5 ± 7.4	9.8 ± 7.7	0.051
P^2 value	< 0.001	< 0.001	N/A

[1]Compare the liver stiffness values (LSVs) of the two operators.
[2]Compare the LSVs of elastograms with the most artifacts and elastograms with the least artifacts.
LSVs: Liver stiffness values; EMAs: Elastograms with the most artifacts; ELAs: Elastograms with the least artifacts; N/A: Not applicable.

Table 5 Standard deviation and stability index of the elastograms with different area artifacts for two operators

	SD of EMAs (kPa)	SD of ELAs (kPa)	P^1 value	SI of EMAs	SI of ELAs	P^2 value
Expert	1.2 ± 1.2	0.8 ± 0.6	< 0.001	92% ± 12%	95% ± 5%	0.135
Novice	2.1 ± 1.7	1.1 ± 1.1	< 0.001	89% ± 8%	93% ± 6%	0.002

[1]Compare the standard deviation values of elastograms with the most artifacts (EMAs) and elastograms with the least artifacts (ELAs).
[2]Compare the stability index values of EMAs and ELAs.
SD: Standard deviation; SI: Stability index; EMAs: Elastograms with the most artifacts; ELAs: Elastograms with the least artifacts.

Table 6 Comparison of Q-Box parameters measured at different positions of the elastograms with artifacts

	Number	Q-Box in the center of the sampling frame			Q-Box away from the artifacts		
		LSV	SD	SI	LSV	SD	SI
Expert	141	14.6 ± 9.5	1.7 ± 1.1	93% ± 6%	14.1 ± 9.3	0.8 ± 0.6	94% ± 7%
Novice	372	12.1 ± 9.5	1.9 ± 1.3	90% ± 7%	11.6 ± 9.4	0.9 ± 0.7	93% ± 6%

LSV: Liver stiffness value; SD: Standard deviation; SI: Stability index.

abdominal US scans or more than 50 supervised 2-D SWE examinations; however, this may not be sufficient[19,21]. A learning curve has been observed for 2-D SWE, a proportion of operator error would decrease over time[22].

We divided the elastogram into four locations and calculated the frequency of occurrence of artifacts at each location. The occurrence frequency of artifacts is arranged in descending order: bottom-left, top-left, bottom-right, and top-right. The two operators in this study had the same results, indicating that this difference may have certain regularity. The reason for this result may be that the aerated lung leads to a shadowing artifact on the left side of the B-mode image, which makes it impossible to form a well-defined push beam in this area[15,23]. On the other hand, to avoid liver capsule reverberation artifacts,

the depth of the sampling frame has increased, especially in obese or overweight patients. When the depth exceeds the penetration limit, attenuation artifacts and larger vessels may have more pulsatile artifacts at the bottom of the sampling frame[16,23]. We found the same phenomenon on another 2-D SWE ultrasound system (Aplio500, Canon, Tochigi, Japan). We found that artifacts were more likely to occur in the bottom-left corner of the elastogram, where distortion waves were noted in the propagation map of the corresponding site. The distribution of artifacts may also be applicable to other devices of 2-D SWE technology, because they have the same imaging principles.

Usually a color-coding scale of up to 30 kPa is sufficient, but in this study the upper limit of the color-coding scale was set to 70 kPa. The reason is that some patients have an LSV greater than 30 kPa, and a lower color-coding scale setting will make the elastogram appear only in red. At this time, it is impossible to distinguish whether there is an artifact or not. Although the color-coding scale was set to 70 kPa may ignore tiny artifacts, it is easier to show obvious artifacts.

The presence of artifacts affects the assessment of LS, but there is no detailed research report yet. This study showed that the LSVs of the EMAs were higher than those of the ELAs. This indicates that artifacts may lead to the overestimation of LS. This study compared the differences between the two operators in the LSVs of EMAs and ELAs. The results showed that in either the EMAs or ELAs, the LSVs of the novice were higher than that of the expert, which may be due to the higher proportion of artifacts in the elastograms measured by the novice. The ICC value between the two operators calculated with the LSVs of the EMAs was lower than that calculated with the LSVs of ELAs. This shows that artifacts can reduce inter-observer repeatability.

Although the degree of liver fibrosis in chronic liver disease will be slightly different, the color-coded LSmapping image will hardly show obvious mottled area. These mottled areas are considered as artifacts and belong to noise. Some studies use signal-to-noise ratio as the standard to evaluate image quality[24,25]. The new software version of the device provides SD and SI as indicators to evaluate the reliability of LS measurement[26-28]. The SD reflects the homogeneity of LSVs in the measurement area of the Q-Box. The higher the SD values, the greater heterogeneity of the LSVs in the measurement area. Thiele *et al*[29] reported that the diagnostic accuracy for cirrhosis by 2D SWE increased at SD < 1.75 kPa. The SI is an indicator of temporal stability of the measurement area, and the manufacturer recommends that a reliable LS measurement should have a SI greater than 90%. Our study showed that the SD values of the EMAs were much higher than those of the ELAs, which indicated that artifacts made the elastograms heterogeneous. The SI values of the EMAs were lower than those of the ELAs, which showed that artifacts may reduce the temporal stability of the elastograms. In short, artifacts can reduce the reliability of the LS measurements. For the elastograms with artifacts, we found that placing the Q-Box away from the artifacts can obtain more reliable LS measurements than placing it in the center of the sampling frame (generally the default measurement position of the equipment).

Furthermore, we investigated the relationship between patient characteristics and the occurrence of artifacts. We found that the occurrence of artifacts had no significant relationship with sex or age. However, we found that patients' BMI, subcutaneous fat thickness and LSVs were positively correlated with the occurrence of artifacts. Higher BMI and subcutaneous fat thickness usually indicate overweight or obesity with a thicker abdominal wall. Artifacts are prone to occur when measuring LS in overweight or obese subjects due to the combined effects of attenuation artifacts, reverberation artifacts, and vessels [16,30]. Previous studies have also shown that a high BMI is the main reason for measurement failure and unreliable assessment[17,31,32]. Patients with liver cirrhosis usually have higher LSVs, and they often have artifacts because of their shrunken liver volumes and poor sonic window. Other studies have demonstrated that severe liver fibrosis is a risk factor for unreliable LS measurements[17,33].

To the best of our knowledge, this is the first prospective study to analyze artifacts in 2-D SWE of the liver. This study analyzed the predilection sites and people for artifacts, and explored the effects of artifacts on LS measurements. Knowledge of the artifacts is essential to improve operation technology to obtain high-quality images. It is very important to obtain accurate measurements in an attempt to optimize its performance and application value. In addition, knowledge from this and other studies on artifacts can be used to investigate how training and education could reduce the occurrence of artifacts. Hopefully, engineers and researchers can improve the product design, provide quality indicators and other ways to avoid the acquisition of improper data due to artifacts.

Our study had several limitations. First, artifacts may be ignored when the color changes are inconspicuous. Second, only one device was tested in this study. Third, this study did not analyze the causes of artifacts, because it is sometimes difficult to accurately determine. Finally, we analyzed only a small sample of data from two operators. Therefore, a larger sample study involving more operators and devices needs to be conducted in future.

CONCLUSION

In conclusion, artifacts are common when using 2-D SWE to measure LS, especially for the novice. Artifacts may lead to the overestimation of LS and reduce the repeatability and reliability of LS measurements. For the elastograms with artifacts, we should place the Q-Box away from the artifacts.

ARTICLE HIGHLIGHTS

Research background

Chronic liver disease is a growing problem worldwide. Accurate assessment of liver fibrosis is important for treatment prioritization, surveillance, and determination of prognosis. Liver biopsy is still considered as the gold standard for staging liver fibrosis. However, liver biopsy is an expensive and invasive diagnostic tool. Its main complications are bleeding and pain, which limit its clinical application. Recently, the application of two-dimensional shear wave elastography (2-D SWE) in the diagnosis of non-invasive assessment of liver fibrosis has developed rapidly. However, the presence of artifacts leads to inaccurate liver stiffness (LS) measurements.

Research motivation

Although 2-D SWE artifacts of the liver are common in clinical practice, they are poorly recognized, and there is even no clear definition. To the best of our knowledge, only a few review articles have been published. Knowledge of the artifacts is essential to improve operation technology to obtain high-quality images. It is very important to obtain accurate measurements in an attempt to optimize its performance and application value.

Research objectives

We aim to investigate the presence and influence of artifacts in 2-D SWE of liver.

Research methods

In this study, we performed 2-D SWE examination in patients with chronic liver disease by a novice and an expert. The elastogram was divided into four locations: top-left, top-right, bottom-left, and bottom-right. The occurrence frequency of artifacts in different locations was compared. The effect of artifacts on the LS measurements was evaluated by comparing the elastogram with the most artifacts (EMA) and the elastogram with the least artifacts (ELA).

Research results

Each operator had 720 elastography images were included for analysis. The percentage of elastograms with artifacts and the area of artifacts in the novice were significantly higher than those in the expert (both $P < 0.001$). Comparing the occurrence frequency of artifacts in all locations of the two operators, it was found that both operators had the highest frequency of bottom-left, followed by top-left and bottom-right, and top-right had the lowest frequency. This study showed that the LS values and standard deviation values of the EMAs were higher than those of the ELAs. Both operators had lower stability index values and intraclass correlation coefficient values for EMAs than ELAs.

Research conclusions

Artifacts are common when using 2-D SWE to measure LS, especially for the novice. Our results showed artifacts were more likely to occur in the bottom-left corner of the elastogram. Artifacts may lead to the overestimation of LS and reduce the repeatability and reliability of LS measurements.

Research perspectives

In this study, we only analyzed a small sample of data from two operators of one device. Therefore, a larger sample study involving more operators and devices needs to be conducted in future studies.

FOOTNOTES

Author contributions: Wang HP and Sang L designed the research study; Wang HP and Zheng PC performed the research; Wang HP and Wang XM collected and analyzed the data; Wang HP and Sang L wrote the manuscript; all authors reviewed and approved the manuscript.

Institutional review board statement: The study was approved by the Institutional Ethical Review Board of The First Hospital of China Medical University (Approval No. AF-SOP-07-1.1-01).

Informed consent statement: All patients provided written informed consent prior to study enrollment.

Conflict-of-interest statement: The authors of this manuscript having no conflicts of interest to disclose.

Data sharing statement: No additional data are available.

STROBE statement: The authors have read the STROBE Statement—checklist of items, and the manuscript was prepared and revised according to the STROBE Statement—checklist of items.

Open-Access: This article is an open-access article that was selected by an in-house editor and fully peer-reviewed by external reviewers. It is distributed in accordance with the Creative Commons Attribution NonCommercial (CC BY-NC 4.0) license, which permits others to distribute, remix, adapt, build upon this work non-commercially, and license their derivative works on different terms, provided the original work is properly cited and the use is non-commercial. See: https://creativecommons.org/Licenses/by-nc/4.0/

Country/Territory of origin: China

ORCID number: Hui-Peng Wang 0000-0002-9803-1838; Peng-Chao Zheng 0000-0002-1617-2857; Xue-Mei Wang 0000-0002-4477-1865; Liang Sang 0000-0002-9331-0985.

S-Editor: Yan JP
L-Editor: A
P-Editor: Yuan YY

REFERENCES

1 **Paik JM**, Golabi P, Younossi Y, Mishra A, Younossi ZM. Changes in the Global Burden of Chronic Liver Diseases From 2012 to 2017: The Growing Impact of NAFLD. *Hepatology* 2020; **72**: 1605-1616 [PMID: 32043613 DOI: 10.1002/hep.31173]
2 **Aydın MM**, Akçalı KC. Liver fibrosis. *Turk J Gastroenterol* 2018; **29**: 14-21 [PMID: 29391303 DOI: 10.5152/tjg.2018.17330]
3 **Pryke R**, Guha IN. Time to focus on chronic liver diseases in the community: A review of primary care hepatology tools, pathways of care and reimbursement mechanisms. *J Hepatol* 2023; **78**: 663-671 [PMID: 36283499 DOI: 10.1016/j.jhep.2022.10.010]
4 **Soon G**, Wee A. Updates in the quantitative assessment of liver fibrosis for nonalcoholic fatty liver disease: Histological perspective. *Clin Mol Hepatol* 2021; **27**: 44-57 [PMID: 33207115 DOI: 10.3350/cmh.2020.0181]
5 **Younossi ZM**, Golabi P, Paik JM, Henry A, Van Dongen C, Henry L. The global epidemiology of nonalcoholic fatty liver disease (NAFLD) and nonalcoholic steatohepatitis (NASH): a systematic review. *Hepatology* 2023; **77**: 1335-1347 [PMID: 36626630 DOI: 10.1097/HEP.0000000000000004]
6 **Sharma S**, Khalili K, Nguyen GC. Non-invasive diagnosis of advanced fibrosis and cirrhosis. *World J Gastroenterol* 2014; **20**: 16820-16830 [PMID: 25492996 DOI: 10.3748/wjg.v20.i45.16820]
7 **Seeff LB**, Everson GT, Morgan TR, Curto TM, Lee WM, Ghany MG, Shiffman ML, Fontana RJ, Di Bisceglie AM, Bonkovsky HL, Dienstag JL; HALT-C Trial Group. Complication rate of percutaneous liver biopsies among persons with advanced chronic liver disease in the HALT-C trial. *Clin Gastroenterol Hepatol* 2010; **8**: 877-883 [PMID: 20362695 DOI: 10.1016/j.cgh.2010.03.025]
8 **Ferraioli G**, Roccarina D. Update on the role of elastography in liver disease. *Therap Adv Gastroenterol* 2022; **15**: 17562848221140657 [PMID: 36506750 DOI: 10.1177/17562848221140657]
9 **Dietrich CF**, Bamber J, Berzigotti A, Bota S, Cantisani V, Castera L, Cosgrove D, Ferraioli G, Friedrich-Rust M, Gilja OH, Goertz RS, Karlas T, de Knegt R, de Ledinghen V, Piscaglia F, Procopet B, Saftoiu A, Sidhu PS, Sporea I, Thiele M. EFSUMB Guidelines and Recommendations on the Clinical Use of Liver Ultrasound Elastography, Update 2017 (Long Version). *Ultraschall Med* 2017; **38**: e16-e47 [PMID: 28407655 DOI: 10.1055/s-0043-103952]
10 **Ferraioli G**, Wong VW, Castera L, Berzigotti A, Sporea I, Dietrich CF, Choi BI, Wilson SR, Kudo M, Barr RG. Liver Ultrasound Elastography: An Update to the World Federation for Ultrasound in Medicine and Biology Guidelines and Recommendations. *Ultrasound Med Biol* 2018; **44**: 2419-2440 [PMID: 30209008 DOI: 10.1016/j.ultrasmedbio.2018.07.008]
11 **Abe T**, Kuroda H, Fujiwara Y, Yoshida Y, Miyasaka A, Kamiyama N, Takikawa Y. Accuracy of 2D shear wave elastography in the diagnosis of liver fibrosis in patients with chronic hepatitis C. *J Clin Ultrasound* 2018; **46**: 319-327 [PMID: 29624693 DOI: 10.1002/jcu.22592]
12 **Luo QT**, Zhu Q, Zong XD, Li MK, Yu HS, Jiang CY, Liao X. Diagnostic Performance of Transient Elastography Versus Two-Dimensional Shear Wave Elastography for Liver Fibrosis in Chronic Viral Hepatitis: Direct Comparison and a Meta-Analysis. *Biomed Res Int* 2022; **2022**: 1960244 [PMID: 36164448 DOI: 10.1155/2022/1960244]
13 **Villani R**, Cavallone F, Romano AD, Bellanti F, Serviddio G. Two-Dimensional Shear Wave Elastography versus Transient Elastography: A Non-Invasive Comparison for the Assessment of Liver Fibrosis in Patients with Chronic Hepatitis C. *Diagnostics (Basel)* 2020; **10** [PMID: 32429410 DOI: 10.3390/diagnostics10050313]
14 **Xie LT**, Yan CH, Zhao QY, He MN, Jiang TA. Quantitative and noninvasive assessment of chronic liver diseases using two-dimensional shear wave elastography. *World J Gastroenterol* 2018; **24**: 957-970 [PMID: 29531460 DOI: 10.3748/wjg.v24.i9.957]
15 **Bruce M**, Kolokythas O, Ferraioli G, Filice C, O'Donnell M. Limitations and artifacts in shear-wave elastography of the liver. *Biomed Eng Lett* 2017; **7**: 81-89 [PMID: 30603154 DOI: 10.1007/s13534-017-0028-1]
16 **Naganuma H**, Ishida H, Uno A, Nagai H, Kuroda H, Ogawa M. Diagnostic problems in two-dimensional shear wave elastography of the liver. *World J Radiol* 2020; **12**: 76-86 [PMID: 32549956 DOI: 10.4329/wjr.v12.i5.76]
17 **Yoon JH**, Lee JM, Han JK, Choi BI. Shear wave elastography for liver stiffness measurement in clinical sonographic examinations: evaluation of intraobserver reproducibility, technical failure, and unreliable stiffness measurements. *J Ultrasound Med* 2014; **33**: 437-447 [PMID: 24567455 DOI: 10.7863/ultra.33.3.437]
18 **Barr RG**, Wilson SR, Rubens D, Garcia-Tsao G, Ferraioli G. Update to the Society of Radiologists in Ultrasound Liver

Elastography Consensus Statement. *Radiology* 2020; **296**: 263-274 [PMID: 32515681 DOI: 10.1148/radiol.2020192437]
19 **Moga TV**, Stepan AM, Pienar C, Bende F, Popescu A, Şirli R, Dănilă M, Sporea I. Intra- and Inter-Observer Reproducibility of a 2-D Shear Wave Elastography Technique and the Impact of Ultrasound Experience in Achieving Reliable Data. *Ultrasound Med Biol* 2018; **44**: 1627-1637 [PMID: 29801976 DOI: 10.1016/j.ultrasmedbio.2018.03.029]
20 **Wang H**, Zheng P, Sang L, Wang X. Does Operator Experience and the Q-Box Diameter Affect the Repeatability of Liver Stiffness Measurements Obtained by 2-Dimensional Shear Wave Elastography? *J Ultrasound Med* 2020; **39**: 741-747 [PMID: 31626345 DOI: 10.1002/jum.15153]
21 **Fang C**, Konstantatou E, Romanos O, Yusuf GT, Quinlan DJ, Sidhu PS. Reproducibility of 2-Dimensional Shear Wave Elastography Assessment of the Liver: A Direct Comparison With Point Shear Wave Elastography in Healthy Volunteers. *J Ultrasound Med* 2017; **36**: 1563-1569 [PMID: 28370146 DOI: 10.7863/ultra.16.07018]
22 **Woo H**, Lee JY, Yoon JH, Kim W, Cho B, Choi BI. Comparison of the Reliability of Acoustic Radiation Force Impulse Imaging and Supersonic Shear Imaging in Measurement of Liver Stiffness. *Radiology* 2015; **277**: 881-886 [PMID: 26147680 DOI: 10.1148/radiol.2015141975]
23 **Dubinsky TJ**, Shah HU, Erpelding TN, Sannananja B, Sonneborn R, Zhang M. Propagation Imaging in the Demonstration of Common Shear Wave Artifacts. *J Ultrasound Med* 2019; **38**: 1611-1616 [PMID: 30380161 DOI: 10.1002/jum.14840]
24 **Dighe M**, Hippe DS, Thiel J. Artifacts in Shear Wave Elastography Images of Thyroid Nodules. *Ultrasound Med Biol* 2018; **44**: 1170-1176 [PMID: 29573887 DOI: 10.1016/j.ultrasmedbio.2018.02.007]
25 **Wang CZ**, Zheng J, Huang ZP, Xiao Y, Song D, Zeng J, Zheng HR, Zheng RQ. Influence of measurement depth on the stiffness assessment of healthy liver with real-time shear wave elastography. *Ultrasound Med Biol* 2014; **40**: 461-469 [PMID: 24361224 DOI: 10.1016/j.ultrasmedbio.2013.10.021]
26 **O'Hara S**, Zelesco M, Rocke K, Stevenson G, Sun Z. Reliability Indicators for 2-Dimensional Shear Wave Elastography. *J Ultrasound Med* 2019; **38**: 3065-3071 [PMID: 30887548 DOI: 10.1002/jum.14984]
27 **Gatos I**, Tsantis S, Spiliopoulos S, Karnabatidis D, Theotokas I, Zoumpoulis P, Loupas T, Hazle JD, Kagadis GC. Temporal stability assessment in shear wave elasticity images validated by deep learning neural network for chronic liver disease fibrosis stage assessment. *Med Phys* 2019; **46**: 2298-2309 [PMID: 30929260 DOI: 10.1002/mp.13521]
28 **Hong EK**, Choi YH, Cheon JE, Kim WS, Kim IO, Kang SY. Accurate measurements of liver stiffness using shear wave elastography in children and young adults and the role of the stability index. *Ultrasonography* 2018; **37**: 226-232 [PMID: 29096427 DOI: 10.14366/usg.17025]
29 **Thiele M**, Madsen BS, Procopet B, Hansen JF, Møller LMS, Detlefsen S, Berzigotti A, Krag A. Reliability Criteria for Liver Stiffness Measurements with Real-Time 2D Shear Wave Elastography in Different Clinical Scenarios of Chronic Liver Disease. *Ultraschall Med* 2017; **38**: 648-654 [PMID: 27273177 DOI: 10.1055/s-0042-108431]
30 **Bouchet P**, Gennisson JL, Podda A, Alilet M, Carrié M, Aubry S. Artifacts and Technical Restrictions in 2D Shear Wave Elastography. *Ultraschall Med* 2020; **41**: 267-277 [PMID: 30577047 DOI: 10.1055/a-0805-1099]
31 **Cassinotto C**, Boursier J, de Lédinghen V, Lebigot J, Lapuyade B, Cales P, Hiriart JB, Michalak S, Bail BL, Cartier V, Mouries A, Oberti F, Fouchard-Hubert I, Vergniol J, Aubé C. Liver stiffness in nonalcoholic fatty liver disease: A comparison of supersonic shear imaging, FibroScan, and ARFI with liver biopsy. *Hepatology* 2016; **63**: 1817-1827 [PMID: 26659452 DOI: 10.1002/hep.28394]
32 **Guo HY**, Liao M, Zheng J, Huang ZP, Xie SD. Two-dimensional shear wave elastography utilized in patients with ascites: a more reliable method than transient elastography for noninvasively detecting the liver stiffness-an original study with 170 patients. *Ann Transl Med* 2023; **11**: 80 [PMID: 36819487 DOI: 10.21037/atm-22-6454]
33 **Piscaglia F**, Salvatore V, Mulazzani L, Cantisani V, Schiavone C. Ultrasound Shear Wave Elastography for Liver Disease. A Critical Appraisal of the Many Actors on the Stage. *Ultraschall Med* 2016; **37**: 1-5 [PMID: 26871407 DOI: 10.1055/s-0035-1567037]

World Journal of Gastroenterology

Submit a Manuscript: https://www.f6publishing.com

World J Gastroenterol 2023 June 7; 29(21): 3328-3340

DOI: 10.3748/wjg.v29.i21.3328

ISSN 1007-9327 (print) ISSN 2219-2840 (online)

ORIGINAL ARTICLE

Observational Study

Therapeutic anticoagulation for splanchnic vein thrombosis in acute pancreatitis: A national survey and case-vignette study

Noor J Sissingh, Jesse V Groen, Hester C Timmerhuis, Marc G Besselink, Bas Boekestijn, Thomas L Bollen, Bert A Bonsing, Frederikus A Klok, Hjalmar C van Santvoort, Robert C Verdonk, Casper H J van Eijck, Jeanin E van Hooft, Jan Sven D Mieog

Specialty type: Gastroenterology and hepatology

Provenance and peer review: Unsolicited article; Externally peer reviewed.

Peer-review model: Single blind

Peer-review report's scientific quality classification

Grade A (Excellent): A, A, A
Grade B (Very good): 0
Grade C (Good): 0
Grade D (Fair): 0
Grade E (Poor): 0

P-Reviewer: Govindarajan KK, India; Liu C, China; Pécsi D, Hungary

Received: March 3, 2023
Peer-review started: March 3, 2023
First decision: March 24, 2023
Revised: April 3, 2023
Accepted: April 25, 2023
Article in press: April 25, 2023
Published online: June 7, 2023

Noor J Sissingh, Jeanin E van Hooft, Department of Gastroenterology and Hepatology, Leiden University Medical Centre, Leiden 2333 ZA, Netherlands

Noor J Sissingh, Hester C Timmerhuis, Department of Research and Development, St. Antonius Hospital, Nieuwegein 3420 EM, Netherlands

Jesse V Groen, Bert A Bonsing, Jan Sven D Mieog, Department of Surgery, Leiden University Medical Centre, Leiden 2333 ZA, Netherlands

Hester C Timmerhuis, Hjalmar C van Santvoort, Department of Surgery, St. Antonius Hospital, Nieuwegein 3420 EM, Netherlands

Marc G Besselink, Department of Surgery, Amsterdam UMC, Location University of Amsterdam, Amsterdam 1081 HZ, Netherlands

Marc G Besselink, Amsterdam Gastroenterology Endocrinology Metabolism, Amsterdam 1105 AZ, Netherlands

Bas Boekestijn, Department of Radiology, Leiden University Medical Centre, Leiden 2333 ZA, Netherlands

Thomas L Bollen, Department of Radiology, St. Antonius Hospital, Nieuwegein 3420 EM, Netherlands

Frederikus A Klok, Department of Medicine-Thrombosis and Hemostasis, Leiden University Medical Centre, Leiden 2333 ZA, Netherlands

Hjalmar C van Santvoort, Department of Surgery, University Medical Centre Utrecht, Utrecht, Utrecht 3584 CX, Netherlands

Robert C Verdonk, Department of Gastroenterology and Hepatology, St. Antonius Hospital, Nieuwegein 3420 EM, Netherlands

Casper H J van Eijck, Department of Surgery, Erasmus Medical Centre, Rotterdam 3015 GD, Netherlands

Corresponding author: Jan Sven D Mieog, MD, PhD, Department of Surgery, Leiden University Medical Centre, 2 Albinusdreef, Leiden 2333 ZA, Netherlands. j.s.d.mieog@lumc.nl

Abstract

BACKGROUND

Splanchnic vein thrombosis (SVT) is a major complication of moderate and severe acute pancreatitis. There is no consensus on whether therapeutic anticoagulation should be started in patients with acute pancreatitis and SVT.

AIM

To gain insight into current opinions and clinical decision making of pancreatologists regarding SVT in acute pancreatitis.

METHODS

A total of 139 pancreatologists of the Dutch Pancreatitis Study Group and Dutch Pancreatic Cancer Group were approached to complete an online survey and case vignette survey. The threshold to assume group agreement was set at 75%.

RESULTS

The response rate was 67% (n = 93). Seventy-one pancreatologists (77%) regularly prescribed therapeutic anticoagulation in case of SVT, and 12 pancreatologists (13%) for narrowing of splanchnic vein lumen. The most common reason to treat SVT was to avoid complications (87%). Acute thrombosis was the most important factor to prescribe therapeutic anticoagulation (90%). Portal vein thrombosis was chosen as the most preferred location to initiate therapeutic anticoagulation (76%) and splenic vein thrombosis as the least preferred location (86%). The preferred initial agent was low molecular weight heparin (LMWH; 87%). In the case vignettes, therapeutic anticoagulation was prescribed for acute portal vein thrombosis, with or without suspected infected necrosis (82% and 90%), and thrombus progression (88%). Agreement was lacking regarding the selection and duration of long-term anticoagulation, the indication for thrombophilia testing and upper endoscopy, and about whether risk of bleeding is a major barrier for therapeutic anticoagulation.

CONCLUSION

In this national survey, the pancreatologists seemed to agree on the use of therapeutic anticoagulation, using LMWH in the acute phase, for acute portal thrombosis and in the case of thrombus progression, irrespective of the presence of infected necrosis.

Key Words: Acute pancreatitis; Splanchnic vein thrombosis; Therapeutic anticoagulation; Bleeding; Recanalization; Outcomes

©The Author(s) 2023. Published by Baishideng Publishing Group Inc. All rights reserved.

Core Tip: Splanchnic vein thrombosis is a relatively common complication of moderate and severe acute pancreatitis, but there is still much debate about its treatment with therapeutic anticoagulation. This national survey and case vignette study among 93 pancreatologists demonstrates that the majority prescribe therapeutic anticoagulation for acute portal vein thrombosis and thrombus progression in patients with or without infected necrosis, despite the absence of evidence supporting its use. Whether this collective opinion is accurate needs to be confirmed in future (preferably prospective) studies.

Citation: Sissingh NJ, Groen JV, Timmerhuis HC, Besselink MG, Boekestijn B, Bollen TL, Bonsing BA, Klok FA, van Santvoort HC, Verdonk RC, van Eijck CHJ, van Hooft JE, Mieog JSD. Therapeutic anticoagulation for splanchnic vein thrombosis in acute pancreatitis: A national survey and case-vignette study. *World J Gastroenterol* 2023; 29(21): 3328-3340

URL: https://www.wjgnet.com/1007-9327/full/v29/i21/3328.htm

DOI: https://dx.doi.org/10.3748/wjg.v29.i21.3328

INTRODUCTION

Acute pancreatitis is an inflammatory disorder of the pancreas and is self-limiting in the majority of patients[1,2]. However, approximately 20% of patients develop a moderate or severe disease course, with (peri) pancreatic necrosis and collections[3,4]. Due to the combination of local inflammation and

mechanical compression, these complications may cause thrombus formation in the splanchnic circulation, including the portal, splenic and superior mesenteric vein[5,6]. The reported estimates on the incidence of splanchnic vein thrombosis (SVT) in acute pancreatitis range from 17% to 23%, and are even higher in complicated acute pancreatitis[7,8]. The clinical presentation of SVT varies between an asymptomatic thrombus to potential lethal complications, such as portal or left side hypertensive bleeding and small bowel ischemia[9-11]. For this reason, early treatment with therapeutic anticoagulation is recommended in patients with acute SVT[12-14]. However, consistent evidence to drive this decision in acute pancreatitis patients does not exist[15-18]. In fact, a recent meta-analysis from our study group showed that 53% of acute pancreatitis patients do not receive therapeutic anticoagulation [15]. This proportion of untreated patients is substantially higher than previously reported in other SVT populations[19], probably because of the fear of serious bleeding. Variation in clinical practice also became apparent in this meta-analysis[15], as anticoagulation use and the type of agent used were very heterogeneous between studies. Therefore, the aim of this survey was to gain more insight into current opinions of pancreatologists on anticoagulation therapy for SVT following acute pancreatitis.

MATERIALS AND METHODS

We conducted an online national survey and case vignette study among members of the Dutch Pancreatitis Study Group (DPSG) and the Dutch Pancreatic Cancer Group (DPCG). Members were excluded if they were not primary care-takers in the treatment of patients with AP (*e.g.*, radiologists, oncologists, basic scientists). The survey was built in Research Electronic Data Capture, and invitations to participate were sent by e-mail in November 2021, followed by four weekly reminders. Additionally, the survey was promoted through newsletters and during annual study group meetings of the DPSG and DPCG.

Survey design

The survey was developed by a multidisciplinary team of surgeons, gastroenterologists, and radiologists, and included 3 demographical questions, 17 general questions and 3 case vignettes (Supplementary material). Demographic information included the responders' specialty, type of hospital and working experience. The general questions focused on treatment of SVT and potential factors that may influence the responders' decision. The case-vignettes addressed the preferred treatment strategy in different clinical cases at different time points. All cases however, concerned a 50-year-old male patient with acute alcoholic necrotising pancreatitis, and can be summarized as follows.

Case vignette 1: A patient visited the emergency department, 5 d after onset of abdominal pain. Contrast-enhanced CT (CECT) showed necrotising pancreatitis with acute necrotic collection in the head of the pancreas (Figure 1A) and: A1: Luminal narrowing of the portal vein without the presence of collateral circulation (Figure 1B); A2: Intraluminal filling defect in the portal vein without the presence of collateral circulation; A3: Intraluminal filling defect in the portal vein without the presence of collateral circulation + a pseudoaneurysm in the proximal splenic artery (Figure 1C).

Case vignette 2: A patient admitted to the ward, 14 d after onset of abdominal pain. The patient showed signs of clinical detoriation with fever and rising inflammatory parameters. The CECT showed almost fully encapsulated pancreatic necrosis without gas configurations (Figure 1D) and a new intraluminal filling defect in the portal vein without the presence of collateral circulation (Figure 1E). The diagnosis of suspected infected pancreatic necrosis was made.

Case vignette 3: A homeless patient visited the emergency department, 30 d after onset of vague abdominal pain. CECT showed necrotising pancreatitis and: CA: Intraluminal filling defect in the portal vein with the presence of collateral circulation; CB: Thrombus progression and expansion of the collateral circulation (Figure 1F).

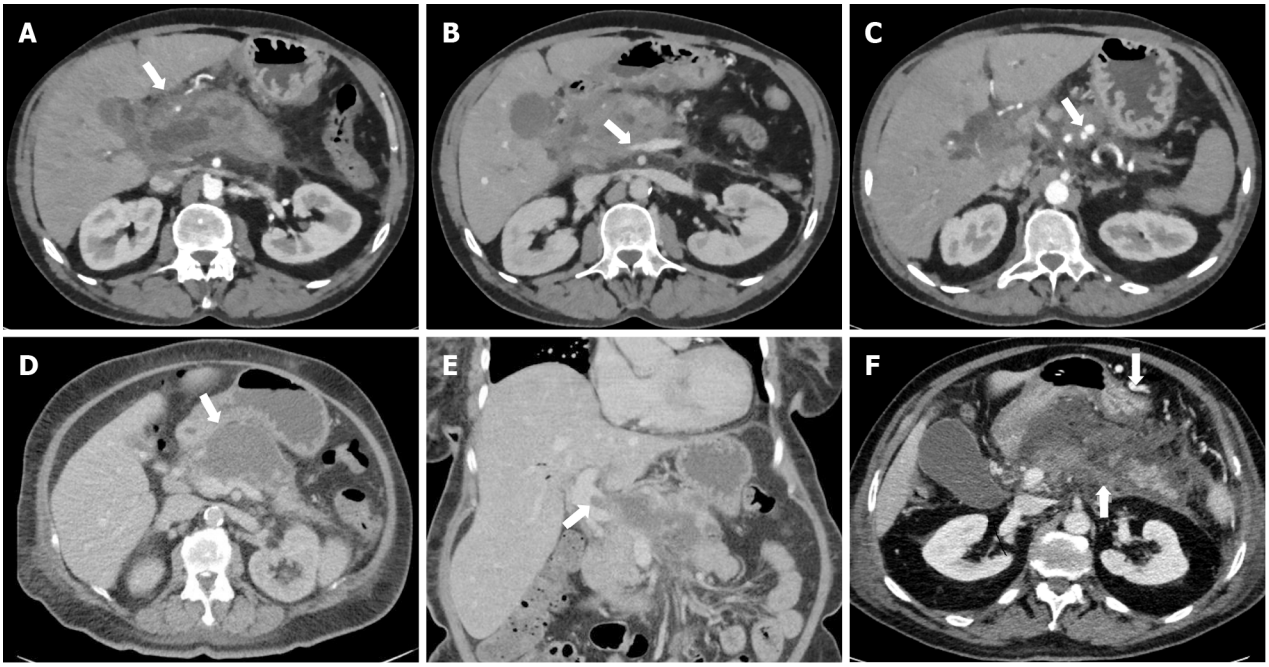
The threshold to assume group agreement was set at 75%. If a question ranged from always, usually, sometimes and never, agreement was defined when 75% of the pancreatologists rated it as always or usually (regularly), or sometimes and never (infrequently).

Definitions

SVT was predefined as an actual intraluminal filling defect on imaging of one or more of the splanchnic veins. The chronicity was divided into (sub)acute thrombosis or chronic thrombosis (with concomitant collaterals), anatomical location into portal, splenic and/or superior mesenteric vein, degree into a total or partial occlusion and extent into an isolated thrombus or a thrombus in several venous segments. Thrombus progression was defined as progression into other splanchnic vein(s), into total occlusion, or both.

Statistical analysis

Descriptive data are presented as counts with proportions for categorical data. All analyses were performed using IBM SPSS (20).



DOI: 10.3748/wjg.v29.i21.3328 **Copyright** ©The Author(s) 2023.

Figure 1 Imaging findings of case vignette. A: Acute necrotic collection in the head of the pancreas in case vignette 1; B: Luminal narrowing of the portal vein without the presence of collateral circulation in case vignette 1; C: Pseudoaneurysm in the proximal splenic artery in case vignette 1; D: Almost fully encapsulated pancreatic necrosis without gas configurations in case vignette 2; E: Luminal filling defect in the portal vein without the presence of collateral circulation in case vignette 2; F: Extension of the thrombus to the splenic vein (arrow pointing upwards) and expansion of the collateral pathway in the gastroepiploic veins along the great curvature of the stomach (arrow pointing downwards) in case vignette 3.

RESULTS

A total of 93 of the 139 invited pancreatologists (67%) responded and participated in this survey and case vignette study; 67 gastroenterologists (72%), 25 surgeons (27%) and 1 intensivist (1%). The majority worked in a non-academic centre (70%) and had more than 10 years of experience in treating AP patients (60%). Demographic characteristics are presented in Table 1.

Indications for and details of treatment with therapeutic anticoagulation

Agreement was reached on whether therapeutic anticoagulation should be prescribed for SVT and luminal narrowing of one or more of the splanchnic veins in acute pancreatitis patients. For SVT, therapeutic anticoagulation was regularly prescribed by 71 (76%) and infrequently by 22 (24%) pancreatologists. In case of luminal narrowing, therapeutic anticoagulation was only regularly prescribed by 12 (13%) pancreatologists. Avoiding complications, such as portal hypertension and bowel ischemia, was the main reason for 81 pancreatologists (87%) to start therapeutic anticoagulation. Screening for an underlying prothrombotic disorder in patients diagnosed with SVT was regularly performed by 14 (15%) pancreatologists, only in patients with a history of one (or more) thrombotic events by 40 (43%), and infrequently by 39 (42%) pancreatologists. There was agreement on the preferred initial type of therapeutic anticoagulation for SVT 81 pancreatologists (87%) preferred subcutaneous low-molecular-weight heparin (LMWH)], but not on the preferred follow-up type. Imaging after the index admission was chosen as follow-up strategy by 79 pancreatologists (85%). Thirteen pancreatologists (13%) indicated that they usually stop anticoagulant therapy in case of achieved radiological recanalization, 35 (38%) after a period of 3 mo, 42 (45%) after 6 mo, and 3 (3%) after 12 mo. All details are provided in Table 2.

Determinants of prescribing therapeutic anticoagulation

Seventy-eight pancreatologists (84%) have chosen the time course of thrombosis as the most important factor supporting anticoagulant therapy; 84 pancreatologists (90%) prescribe therapeutic anticoagulation in case of a (sub)acute thrombosis *vs* 9 (10%) for both (sub)acute and chronic thrombosis. Moreover, 70 pancreatologists (76%) have chosen portal vein thrombosis as the most preferred location to initiate therapeutic anticoagulation, whereas splenic vein thrombosis was chosen as least preferred location by 80 pancreatologists (86%). The majority of pancreatologists (85%) treat both total and partial occlusive thrombosis. There was no agreement whether the risk of different types of bleeding should be considered as a major barrier to prescribe therapeutic anticoagulation. The need for invasive interventions for local complications of acute pancreatitis influenced the decision whether or not to

Table 1 Details of respondents, *n* (%)

Demographics	*n* = 93
Specialty	
Surgeon	25 (27)
Gastroenterologist	67 (72)
Intensivist	1 (1)
Type of hospital	
Academic	28 (30)
Non-academic, teaching hospital	60 (65)
Non-academic, non-teaching hospital	5 (5)
Experience in treating patients with acute pancreatitis	
0-5 years	10 (11)
5-10 years	27 (29)
10-15 years	17 (18)
15-20 years	23 (25)
> 20 years	16 (17)

initiate anticoagulation therapy in about half of pancreatologists (52%). All details are outlined in Table 3.

Statements on prognosis

An association between the presence of SVT and worse clinical outcomes in patients with acute pancreatitis was assumed by 67 pancreatologists (72%) (Figure 2). Moreover, the vast majority (88%) agreed that therapeutic anticoagulation for splanchnic vein thrombosis improves clinical outcomes in these patients. Insufficient evidence was the most frequently quoted reason among pancreatologists who disagreed with this second statement.

Case-vignettes

The results of the case vignettes are summarized in Figure 3. In the first case vignette (patient 1, day 5 of acute necrotising pancreatitis), 11 pancreatologists (12%) would prescribe a therapeutic dose anticoagulation if luminal narrowing without collateral circulation was detected in the portal vein. Of the 82 pancreatologists (88%) who opted for no therapeutic dose anticoagulation, 73 (89%) would change treatment strategy in case an actual filling defect in the portal vein was detected. In total, 84 pancreatologists (90%) would prescribe therapeutic dose anticoagulation to this patient with an actual portal vein thrombosis without collateral circulation. If a pseudoaneurysm was concomitantly present, 43 of those 84 pancreatologists (51%) who favoured a therapeutic dose anticoagulation would switch to a prophylactic dose anticoagulation (*n* = 28, 65%) or no anticoagulation at all (*n* = 15, 35%), leaving 41 pancreatologists (44%) in the therapeutic anticoagulation group.

In the second case vignette (patient 2, day 14 of suspected infected necrotising pancreatitis), 77 pancreatologists (82%) would prescribe therapeutic dose anticoagulation if a portal vein thrombosis without collateral circulation was detected. The presence of (suspected) infected pancreatic necrosis influenced the choice of anticoagulation agent in 49 pancreatologists (52%). Almost all of these pancreatologists pointed out that once infected pancreatic necrosis is suspected, they would choose an agent with a short half-life because of the potentially need of invasive intervention.

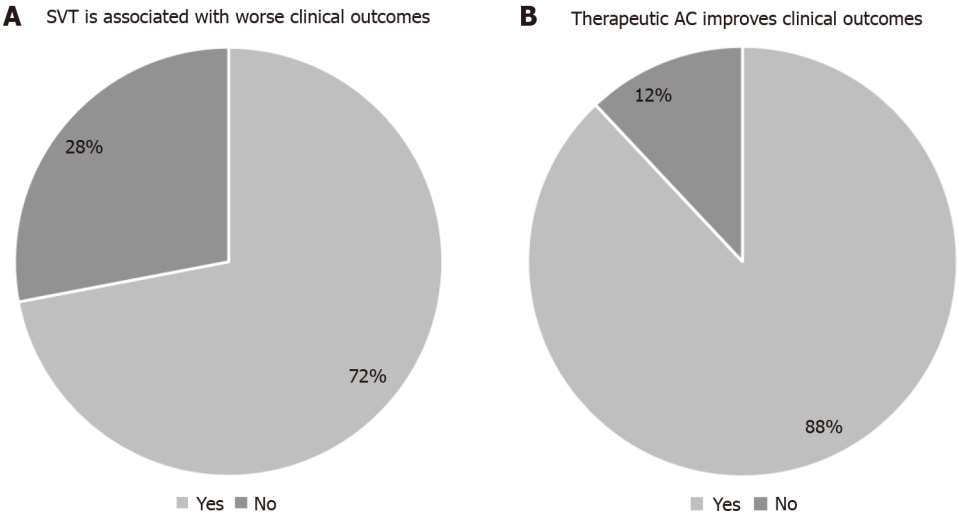
In the third case vignette (patient 3, day 30 of acute necrotising pancreatitis), 44 pancreatologists (47%) would prescribe a therapeutic dose anticoagulation if a portal vein thrombosis with collateral circulation was detected. Of these 44 pancreatologists, 19 (43%) would perform upper endoscopy to screen for and-if present-treat oesophageal varices before starting anticoagulation therapy. In case of thrombus progression (extension of the thrombus to the splenic vein and expansion of the collateral pathway), 11 pancreatologists (12%) would stay conservative (*i.e.*, no therapeutic dose of anticoagulation), 82 (88%) would start or continue a therapeutic dose anticoagulation and none would proceed to an intervention.

Table 2 Survey results: Indication for and details of treatment with therapeutic anticoagulation, *n* (%)

Item	Total (*n* = 93)
Do you prescribe therapeutic AC in case of detected thrombosis in one (or more) of the splanchnic veins?	
Always	23 (25)
Usually	48 (52)
Sometimes	21 (23)
Never	1 (1)
Do you prescribe therapeutic AC in case of detected luminal narrowing of one (or more) of the splanchnic veins?	
Always	3 (3)
Usually	9 (10)
Sometimes	29 (31)
Never	52 (56)
Main reason(s) to start therapeutic AC (multiple answers were possible)	
To achieve vessel recanalization	52 (56)
To avoid complications	81 (87)
To prevent formation of altered venous anatomy	31 (33)
To prevent recurrence of SVT	27 (29)
To prevent another venous thromboembolism	30 (32)
Other reason[1]	1 (1)
Do you screen for an underlying prothrombotic disorder?	
Always	2 (2)
Usually	12 (13)
Sometimes	25 (27)
Only in patients with a history of one (or more) thrombotic events	40 (43)
Never	14 (15)
Which initial type of therapeutic AC do you prefer?	
(Low molecular weight) heparin subcutaneous	81 (87)
Unfractionated heparin intravenous	4 (4)
Direct oral anticoagulation	3 (3)
Vitamin K antagonist	4 (4)
Platelet aggregation inhibitor	1 (1)
Urokinase/recombinant tissue plasminogen activator	0
Which follow-up type of therapeutic AC do you prefer?	
(Low molecular weight) heparin subcutaneous	9 (10)
Unfractionated heparin intravenous	0
Direct oral anticoagulation	53 (57)
Vitamin K antagonist	29 (31)
Platelet aggregation inhibitor	2 (2)
Urokinase/recombinant tissue plasminogen activator	0
Do you generally follow-up SVT after index admission?	
Yes, clinically only	5 (5)
Yes, with imaging	79 (85)
No	9 (10)

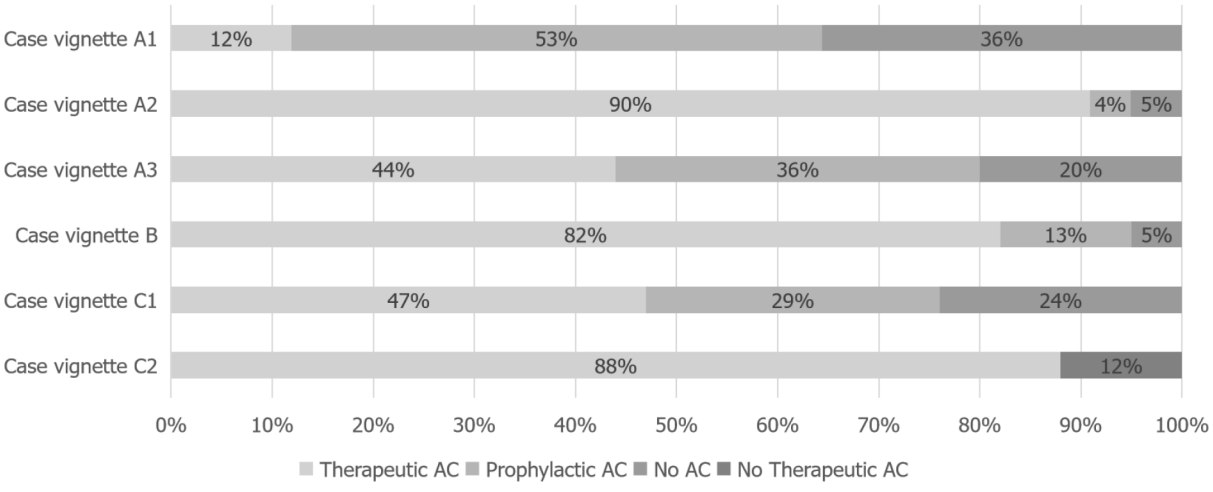
After how long do you usually stop the therapeutic AC?	
In case of achieved radiological recanalization	13 (14)
3 mo	35 (38)
6 mo	42 (45)
12 mo	3 (3)
Never	0

[1]In free text: expansion of thrombosis.
AC: Anticoagulation; SVT: Splanchnic vein thrombosis.



DOI: 10.3748/wjg.v29.i21.3328 **Copyright** ©The Author(s) 2023.

Figure 2 Statements on prognosis. A: Splanchnic vein thrombosis is associated with worse clinical outcomes; B: Therapeutic anticoagulation improves clinical outcomes. AC: Anticoagulation; SVT: Splanchnic vein thrombosis.



DOI: 10.3748/wjg.v29.i21.3328 **Copyright** ©The Author(s) 2023.

Figure 3 Case vignettes results: Choice of treatment. AC: Anticoagulation.

DISCUSSION

This first nationwide survey and case vignette study gives insight into the clinical scenarios in which therapeutic anticoagulation is currently used, and not used to treat or prevent splanchnic vein thrombosis in acute pancreatitis patients. In an earlier study[15], we found 7 retrospective cohort studies evaluating therapeutic anticoagulation in this patient category with conflicting results in clinical

Table 3 Survey results: Determinants of prescribing therapeutic anticoagulation, *n* (%)

Item	Total (*n* = 93)
Do you consider of ... the thrombosis as an important factor to prescribe therapeutic AC? (multiple answers were possible)	
Age (acute or chronic)	78 (84)
Anatomical location (portal, splenic or superior mesenteric vein)	42 (45)
Degree (total or partial)	45 (48)
Extent (isolated thrombosis or thrombosis in several segments)	49 (53)
Progression (over time)	40 (43)
When do you prescribe therapeutic AC? In case of:	
(Sub)acute thrombosis	84 (90)
Chronic thrombosis	0
Both	9 (10)
Rank the anatomical location of the thrombosis from most likely to less likely to start therapeutic AC:	
Portal vein-splenic vein-superior mesenteric vein	9 (10)
Portal vein-superior mesenteric vein-splenic vein	61 (66)
Splenic vein-portal vein-superior mesenteric vein	0
Splenic vein-superior mesenteric vein-portal vein	1 (1)
Superior mesenteric vein-portal vein-splenic vein	19 (20)
Superior mesenteric vein-splenic vein-portal vein	3 (3)
When do you prescribe therapeutic AC? In case of:	
Total thrombosis	9 (10)
Partial thrombosis	5 (5)
Both	79 (85)
Do you consider the risk of ... as a major barrier to prescribe therapeutic AC? (multiple answers were possible)	
Bleeding in general	52 (56)
Bleeding related to portal hypertension	17 (18)
Bleeding related to pseudoaneurysm	49 (53)
Other risk[1]	1 (1)
Does the need for invasive interventions for local complications of acute pancreatitis influence your decision regarding AC therapy?	
Yes	48 (52)
No	45 (48)

[1]In free text: CVA bleeding history.
AC: Anticoagulation; SVT: Splanchnic vein thrombosis.

outcome[20-27]. These studies were of moderate quality and therefore the pancreatologist' preference and belief predominate in current decision making rather than scientific evidence.

An important finding of the current study was that more than 75% of pancreatologists regularly prescribe therapeutic anticoagulation for SVT, particularly for a thrombus that acutely developed. This is in line with recommendations from general guidelines for SVT management[12-14]. In the absence of a visualized thrombus, most pancreatologists indicated not to treat compressed veins with anticoagulation. Although wall shear stress in a compressed vessel may promote platelet activation, and subsequently thrombus formation[28], there is no data yet to question the opinion of the pancreatologists.

In this study, the most important reason to administer therapeutic anticoagulation was to avoid complications including bowel ischemia and portal hypertension. Bowel ischemia has been reported in up to 33% of acute pancreatitis patients treated with therapeutic anticoagulation *vs* 16% of untreated patients[22,24,25]. A potential explanation for this discrepancy could be that bowel ischemia was already present prior to the start of therapy, therefore being an indication for therapeutic anticoagu-

lation rather than a consequence. In addition, the presence of varices and other collaterals have been equally reported[15], and only one of the aforementioned studies described one case of bleeding from oesophageal varices in an anticoagulated patient[24]. Again, it is likely that a perceived bleeding risk influenced the decision whether or not to prescribe therapeutic anticoagulation. This confounding by indication clearly limits the interpretation of these retrospective studies.

Achieving vessel recanalization was chosen as the second goal. A recent meta-analysis showed that the pooled rate of recanalization of SVT was similar between treated (36%) and untreated patients (31%) [15]. However, there is reason to believe that the benefit of anticoagulation therapy may alter when considering the anatomical location of the thrombosis[21,29]. Patients with portal vein or superior mesenteric vein thrombosis may have an increased risk of complications, while having lower spontaneous recanalization rates. In particular, mortality rates of patients with superior mesenteric vein thrombosis are reported up to 50%[30,31]. On the other hand, splenic vein thrombosis, which is by far the most common site of thrombosis in acute pancreatitis patients, forms a less serious concern for gastrointestinal bleeding and insufficient recanalization[8,26,32]. A selective anticoagulation policy, in which therapeutic anticoagulation was reserved for portal- and superior mesenteric vein thrombosis, was recently assessed in a retrospective study[33]. This study showed a recanalization rate of 67% in portal- and superior mesenteric vein thrombosis, which is substantially higher than previously reported [15]. In addition, a recent practice guideline from the Pancreas study group, Chinese Society of Gastroenterology, recommends a selective anticoagulation policy[34]. In this survey, portal vein thrombosis, followed by superior mesenteric vein thrombosis, was also the pancreatologists' preferred location for prescribing therapeutic anticoagulation, while splenic vein was the least preferred location.

With respect to chronic SVT, the current guidelines do not recommend therapeutic anticoagulation [10]. This is in line with the reported use in case vignette 3, with the exception of the case of the patient with thrombus progression and expansion of the collateral circulation. In this scenario, 88% of pancreatologists would treat such patient with therapeutic anticoagulation. A recent multicentre randomised controlled trial comparing daily rivaroxaban 15 mg/d to no anticoagulation in patients with noncirrhotic chronic portal vein thrombosis[35], formally challenged the guideline recommendations. This study showed that rivaroxaban, even in prophylactic dose, reduced the incidence of venous thromboembolism; therefore, this study may initiate a shift towards a more frequent use of anticoagulation in chronic SVT. On that note, primary prophylaxis of portal hypertensive bleeding should be performed, as laid out by the BAVENO IV guideline[13]. In this survey, however, the minority of pancreatologists followed this recommendation. Improvements should also be made to distinguish acute from chronic SVT. Currently, no clear definition for chronic SVT exists other than a presumed time course of more than 6 mo or the presence of multiple small collaterals around the obstructed veins [10,36], which is not useful to diagnose a nonocclusive chronic thrombosis (*i.e.*, absence of collateral pathways). A promising invention to overcome this problem is magnetic resonance noncontrast thrombus imaging, though validation is still needed[37].

According to our survey, subcutaneous LMWH was the favoured initial type of therapeutic anticoagulation, while no agreement regarding the choice of long-term anticoagulation and its duration was found. In current guidelines, switching LMWH to a vitamin K antagonist once reaching the target range is the reported strategy for patients with SVT[12-14,38]. The use of direct oral anticoagulation (*i.e.*, apixaban) in acute pancreatitis patients with SVT is reported in two studies and showed comparable results[21,33]. However, in the case of (suspected) infected pancreatic necrosis, LMWH seems to be preferred by more than half of the pancreatologists, due to its short half-life and reversibility. Besides, many acute pancreatitis patients have reduced caloric intake limiting the absorption of DOACS. Therefore, it seems fair to advise LWMH, especially in the acute phase. Looking at the duration of anticoagulation therapy for provoked SVT in patients with a transient risk factor, such as acute pancreatitis, the suggested duration is 3 mo to 6 mo[12-14,38]. Consistently, 38% and 45% of the pancreatologists in our survey preferred 3 mo and 6 mo treatment duration, respectively.

Based on the available literature, it remains unclear whether therapeutic anticoagulation is associated with higher rates of bleeding. An increased bleeding risk with therapeutic anticoagulation has been reported up to 33% of patients[21,25,26], but there are also studies showing lower rates of bleeding[24]. The theory for this latter finding is that therapeutic anticoagulation prevents thrombus progression, therefore reducing the portal pressure and consequently the risk of bleeding[19]. In this study, the risk of bleeding was not identified as a significant discouraging factor, as only about half of the pancreatologists considered bleeding in general and bleeding related to pseudoaneurysm as a major barrier to prescribe therapeutic anticoagulation. Also, the possible need for invasive intervention, due to suspected infected necrosis, did not significantly influence the treatment strategy. Another critical question is whether SVT influences the disease course of acute pancreatitis patients, but again this remains unanswered[15]. In this survey, the majority of pancreatologists assumed that the occurrence of SVT is associated with worse clinical outcomes, and interestingly, even more pancreatologists were convinced that the use of therapeutic anticoagulation leads to improved patient outcomes.

A strength of this study is the response rate of 67%, which is relatively high compared to previous surveys among pancreatologists[39-41]. Furthermore, the ratio of 30:70 between academic and non-academic pancreatologists attributed to a valuable insight into the pancreatologists' opinions on the use of therapeutic anticoagulation. This study also has several limitations. First, the results may not directly

reflect the actual practice in other countries as only members of two Dutch associations of pancreatology were invited. This decision was made to avoid selection based on publication record, and consequently include pancreatologists who are not actively involved in the treatment of acute pancreatitis[40]. Another advantage of our method is that it allowed us to calculate the survey's response rate by bypassing the confidentiality of membership lists of international pancreatic associations. Second, the clinical presentation of SVT is very heterogeneous, as well as the patient characteristics and clinical disease course among acute pancreatitis patients, which influences current decision making. For this reason, it might have been difficult for pancreatologists to answer some of the general questions. Therefore, case vignettes were used to explore what considerations underpin their decisions. As the descriptions throughout the case vignettes were consistently formulated and only one clinical detail was changed at a time, treatment of patients with superior mesenteric vein and splenic vein thrombosis was not assessed in the case vignettes. Consequently, the pancreatologists' preference on this manifestation of SVT in acute pancreatitis remained unknown. Finally, the rationale behind the "nonprescribing trend" was not assessed adequately, which could be a focus for future research.

CONCLUSION

In conclusion, this national survey demonstrates the tendency of pancreatologists to prescribe therapeutic anticoagulation for acute thrombosis, in particular for acute portal vein thrombosis and in case of thrombus progression, irrespective of the presence of infected necrosis. With therapeutic anticoagulation, the majority of pancreatologists believed that the clinical outcomes of acute pancreatitis patients with splanchnic vein thrombosis will improve. Furthermore, this study reflects on several knowledge gaps in literature, and sets out clear points for future research. Specifically, a deeper understanding of the pathophysiology and natural course of splanchnic vein thrombosis secondary to acute pancreatitis would allow us to clarify the therapeutic role of anticoagulation.

ARTICLE HIGHLIGHTS

Research background

Splanchnic vein thrombosis (SVT) is a severe complication of acute pancreatitis that may cause portal hypertensive complications and bowel ischemia. To prevent such complications, therapeutic anticoagulation is recommended in the general population of patients with an acute SVT.

Research motivation

Evidence to support this recommendation in acute pancreatitis patients does however not exist and as a result, clinical decision-making is mostly based on the preferences and beliefs of the pancreatologists.

Research objectives

To gain insight into current opinions on the use of therapeutic anticoagulation for SVT in acute pancreatitis.

Research methods

An online survey was sent to 139 Dutch pancreatologists. The threshold to assume agreement was set at 75%.

Research results

The response rate was 67% (n = 93). Seventy-one pancreatologists (77%) regularly prescribed therapeutic anticoagulation for SVT, using LMWH in the acute phase (87%). The majority favored therapeutic anticoagulation for acute thrombosis (90%), portal vein thrombosis in patients with or without infected necrosis (82% and 90%) and in case of thrombus progression (88%). There was no agreement whether the risk of bleeding is a barrier for initiation of therapeutic anticoagulation.

Research conclusions

The pancreatologists reached agreement regarding the use of therapeutic anticoagulation for SVT, particularly in cases of acute thrombosis, portal vein thrombosis and thrombus progression.

Research perspectives

To get a better understanding of the therapeutic role of anticoagulation, it is crucial to conduct prospective studies targeting the pathophysiology and natural course of SVT in acute pancreatitis patients.

ACKNOWLEDGEMENTS

We are very grateful to all 93 pancreatologists who participated in this study, 54 of whom agreed to be included in the acknowledgement: M Anten; A Bhalla; M Boermeester; K Bosscha; S Bouwense; H Braat; M Bruno; F van Delft; W Derksen; L van Driel; P van Duijvendijk; P Dura; R Eichhorn; P Fockens; E van Geenen; M Hadithi; M van der Have; J Haveman; M Hemmink; I de Hingh; H Hofker; L Holl; A Inderson; J Jansen; M Liem; D Lips; L Kager; V de Meijer; M Meijssen; H Moeniralam; V Nieuwenhuijs; M van de Poll; R Quispel; T Romkens; J Schreinemakers; M Schwartz; M Spanier; J Sprakel; M Stommel; J Straathof; J Tenthof van Noorden; W Thijs; M Tielemans; N Venneman; R Verbeek; F Vleggaar; R Voermans; J Vrolijk; L van der Waaij; R van Wanrooij; M Wielenga; R de Wilde; R Zoutendijk.

FOOTNOTES

Author contributions: Sissingh NJ, Groen JV, and Mieog JSD designed the study; all authors critically assessed the study design; Boekestijn B and Bollen TL provided the radiological images; Sissingh NJ, van Hooft JE, Mieog JSD, and van Eijck CHJ sent or promoted the study; Sissingh NJ did the statistical analysis and wrote the initial draft of the manuscript; Groen JV, Timmerhuis HC, Besselink MG, Boekestijn B, Bollen TL, Bonsing BA, Klok FA, van Santvoort HC, Verdonk RC, van Eijck CHJ, van Hooft JE, and Mieog JSD critically assessed and edited the manuscript; Sissingh NJ coordinated the writing process and revised the manuscript; and all authors read and approved the final manuscript.

Institutional review board statement: This survey research is not subject to the Dutch Medical Research involving Human Subjects Acts (WMO) as participants are not subject to procedures or are required to follow rules of behavior. Consequently, this study does not need a full review by an accredited MREC or the CCMO.

Conflict-of-interest statement: All authors declare no conflict of interest.

Data sharing statement: Requests for data can be made to the corresponding author and will be discussed during a meeting of the Dutch Pancreatitis Study Group. After approval by the Dutch Pancreatitis Study Group, data that underlie the results reported in this study, will be shared.

STROBE statement: The authors have read the STROBE Statement—checklist of items, and the manuscript was prepared and revised according to the STROBE Statement—checklist of items.

Open-Access: This article is an open-access article that was selected by an in-house editor and fully peer-reviewed by external reviewers. It is distributed in accordance with the Creative Commons Attribution NonCommercial (CC BY-NC 4.0) license, which permits others to distribute, remix, adapt, build upon this work non-commercially, and license their derivative works on different terms, provided the original work is properly cited and the use is non-commercial. See: https://creativecommons.org/Licenses/by-nc/4.0/

Country/Territory of origin: Netherlands

ORCID number: Noor J Sissingh 0000-0002-6728-949X; Jesse V Groen 0000-0002-2438-4665; Hester C Timmerhuis 0000-0001-5714-4951; Marc G Besselink 0000-0003-2650-9350; Bas Boekestijn 0000-0003-3682-6560; Thomas L Bollen 0000-0002-5734-9823; Bert A Bonsing 0000-0003-4513-5737; Frederikus A Klok 0000-0001-9961-0754; Hjalmar C van Santvoort 0009-0007-1218-2883; Robert C Verdonk 0000-0001-5591-0499; Casper H J van Eijck 0000-0002-9511-2157; Jeanin E van Hooft 0000-0002-4424-0079; Jan Sven D Mieog 0000-0002-3649-8504.

S-Editor: Chen YL
L-Editor: A
P-Editor: Fan JR

REFERENCES

1 **Boxhoorn L**, Voermans RP, Bouwense SA, Bruno MJ, Verdonk RC, Boermeester MA, van Santvoort HC, Besselink MG. Acute pancreatitis. *Lancet* 2020; **396**: 726-734 [PMID: 32891214 DOI: 10.1016/S0140-6736(20)31310-6]
2 **Lankisch PG**, Apte M, Banks PA. Acute pancreatitis. *Lancet* 2015; **386**: 85-96 [PMID: 25616312 DOI: 10.1016/S0140-6736(14)60649-8]
3 **Schepers NJ**, Bakker OJ, Besselink MG, Ahmed Ali U, Bollen TL, Gooszen HG, van Santvoort HC, Bruno MJ; Dutch Pancreatitis Study Group. Impact of characteristics of organ failure and infected necrosis on mortality in necrotising pancreatitis. *Gut* 2019; **68**: 1044-1051 [PMID: 29950344 DOI: 10.1136/gutjnl-2017-314657]
4 **van Santvoort HC**, Bakker OJ, Bollen TL, Besselink MG, Ahmed Ali U, Schrijver AM, Boermeester MA, van Goor H, Dejong CH, van Eijck CH, van Ramshorst B, Schaapherder AF, van der Harst E, Hofker S, Nieuwenhuijs VB, Brink MA, Kruyt PM, Manusama ER, van der Schelling GP, Karsten T, Hesselink EJ, van Laarhoven CJ, Rosman C, Bosscha K, de

Wit RJ, Houdijk AP, Cuesta MA, Wahab PJ, Gooszen HG; Dutch Pancreatitis Study Group. A conservative and minimally invasive approach to necrotizing pancreatitis improves outcome. *Gastroenterology* 2011; **141**: 1254-1263 [PMID: 21741922 DOI: 10.1053/j.gastro.2011.06.073]

5 **Nadkarni NA**, Khanna S, Vege SS. Splanchnic venous thrombosis and pancreatitis. *Pancreas* 2013; **42**: 924-931 [PMID: 23587854 DOI: 10.1097/MPA.0b013e318287cd3d]

6 **Mendelson RM**, Anderson J, Marshall M, Ramsay D. Vascular complications of pancreatitis. *ANZ J Surg* 2005; **75**: 1073-1079 [PMID: 16398814 DOI: 10.1111/j.1445-2197.2005.03607.x]

7 **Anis FS**, Adiamah A, Lobo DN, Sanyal S. Incidence and treatment of splanchnic vein thrombosis in patients with acute pancreatitis: A systematic review and meta-analysis. *J Gastroenterol Hepatol* 2022; **37**: 446-454 [PMID: 34657310 DOI: 10.1111/jgh.15711]

8 **Butler JR**, Eckert GJ, Zyromski NJ, Leonardi MJ, Lillemoe KD, Howard TJ. Natural history of pancreatitis-induced splenic vein thrombosis: a systematic review and meta-analysis of its incidence and rate of gastrointestinal bleeding. *HPB (Oxford)* 2011; **13**: 839-845 [PMID: 22081918 DOI: 10.1111/j.1477-2574.2011.00375.x]

9 **Spaander MC**, Hoekstra J, Hansen BE, Van Buuren HR, Leebeek FW, Janssen HL. Anticoagulant therapy in patients with non-cirrhotic portal vein thrombosis: effect on new thrombotic events and gastrointestinal bleeding. *J Thromb Haemost* 2013; **11**: 452-459 [PMID: 23289370 DOI: 10.1111/jth.12121]

10 **Valeriani E**, Riva N, Di Nisio M, Ageno W. Splanchnic Vein Thrombosis: Current Perspectives. *Vasc Health Risk Manag* 2019; **15**: 449-461 [PMID: 31695400 DOI: 10.2147/VHRM.S197732]

11 **Nawacki Ł**, Matykiewicz J, Stochmal E, Głuszek S. Splanchnic Vein Thrombosis in Acute Pancreatitis and Its Consequences. *Clin Appl Thromb Hemost* 2021; **27**: 10760296211010260 [PMID: 33887991 DOI: 10.1177/10760296211010260]

12 **Kearon C**, Akl EA, Ornelas J, Blaivas A, Jimenez D, Bounameaux H, Huisman M, King CS, Morris TA, Sood N, Stevens SM, Vintch JRE, Wells P, Woller SC, Moores L. Antithrombotic Therapy for VTE Disease: CHEST Guideline and Expert Panel Report. *Chest* 2016; **149**: 315-352 [PMID: 26867832 DOI: 10.1016/j.chest.2015.11.026]

13 **de Franchis R**; Baveno VI Faculty. Expanding consensus in portal hypertension: Report of the Baveno VI Consensus Workshop: Stratifying risk and individualizing care for portal hypertension. *J Hepatol* 2015; **63**: 743-752 [PMID: 26047908 DOI: 10.1016/j.jhep.2015.05.022]

14 **European Association for the Study of the Liver**. EASL Clinical Practice Guidelines: Vascular diseases of the liver. *J Hepatol* 2016; **64**: 179-202 [PMID: 26516032 DOI: 10.1016/j.jhep.2015.07.040]

15 **Sissingh NJ**, Groen JV, Koole D, Klok FA, Boekestijn B, Bollen TL, van Santvoort HC, Verdonk RC, Bonsing BA, van Eijck CHJ, van Hooft JE, Mieog JSD; Dutch Pancreatitis Study Group. Therapeutic anticoagulation for splanchnic vein thrombosis in acute pancreatitis: A systematic review and meta-analysis. *Pancreatology* 2022; **22**: 235-243 [PMID: 35012902 DOI: 10.1016/j.pan.2021.12.008]

16 **Hajibandeh S**, Hajibandeh S, Agrawal S, Irwin C, Obeidallah R, Subar D. Anticoagulation Versus No Anticoagulation for Splanchnic Venous Thrombosis Secondary to Acute Pancreatitis: Do We Really Need to Treat the Incidental Findings? *Pancreas* 2020; **49**: e84-e85 [PMID: 33003093 DOI: 10.1097/MPA.0000000000001644]

17 **Norton W**, Lazaraviciute G, Ramsay G, Kreis I, Ahmed I, Bekheit M. Current practice of anticoagulant in the treatment of splanchnic vein thrombosis secondary to acute pancreatitis. *Hepatobiliary Pancreat Dis Int* 2020; **19**: 116-121 [PMID: 31954635 DOI: 10.1016/j.hbpd.2019.12.007]

18 **Chandan S**, Buddam A, Khan SR, Mohan BP, Ramai D, Bilal M, Dhindsa B, Bhogal N, Kassab LL, Goyal H, Perisetti A, Facciorusso A, Adler DG. Use of therapeutic anticoagulation in splanchnic vein thrombosis associated with acute pancreatitis: a systematic review and meta-analysis. *Ann Gastroenterol* 2021; **34**: 862-871 [PMID: 34815653 DOI: 10.20524/aog.2021.0661]

19 **Valeriani E**, Di Nisio M, Riva N, Cohen O, Garcia-Pagan JC, Magaz M, Porreca E, Ageno W. Anticoagulant therapy for splanchnic vein thrombosis: a systematic review and meta-analysis. *Blood* 2021; **137**: 1233-1240 [PMID: 32911539 DOI: 10.1182/blood.2020006827]

20 **IBM Corp**. IBM SPSS Statistics for Windows, version 26.0. Armonk, NY: IBM Corp. 2019. [cited 20 March 2023]. Available from: https://www.ibm.com/products/spss-statistics

21 **Pagliari D**, Cianci R, Brizi MG, Mancarella FA, Musso M, Cintoni M, Franza L, Flore RA, Gasbarrini A, Tondi P. Anticoagulant therapy in the treatment of splanchnic vein thrombosis associated to acute pancreatitis: a 3-year single-centre experience. *Intern Emerg Med* 2020; **15**: 1021-1029 [PMID: 31916010 DOI: 10.1007/s11739-019-02271-5]

22 **Junare PR**, Udgirkar S, Nair S, Debnath P, Jain S, Modi A, Rathi P, Rane S, Contractor Q. Splanchnic Venous Thrombosis in Acute Pancreatitis: Does Anticoagulation Affect Outcome? *Gastroenterology Res* 2020; **13**: 25-31 [PMID: 32095170 DOI: 10.14740/gr1223]

23 **Toqué L**, Hamy A, Hamel JF, Cesbron E, Hulo P, Robert S, Aube C, Lermite E, Venara A. Predictive factors of splanchnic vein thrombosis in acute pancreatitis: A 6-year single-center experience. *J Dig Dis* 2015; **16**: 734-740 [PMID: 26513113 DOI: 10.1111/1751-2980.12298]

24 **Harris S**, Nadkarni NA, Naina HV, Vege SS. Splanchnic vein thrombosis in acute pancreatitis: a single-center experience. *Pancreas* 2013; **42**: 1251-1254 [PMID: 24152951 DOI: 10.1097/MPA.0b013e3182968ff5]

25 **Easler J**, Muddana V, Furlan A, Dasyam A, Vipperla K, Slivka A, Whitcomb DC, Papachristou GI, Yadav D. Portosplenomesenteric venous thrombosis in patients with acute pancreatitis is associated with pancreatic necrosis and usually has a benign course. *Clin Gastroenterol Hepatol* 2014; **12**: 854-862 [PMID: 24161350 DOI: 10.1016/j.cgh.2013.09.068]

26 **Gonzelez HJ**, Sahay SJ, Samadi B, Davidson BR, Rahman SH. Splanchnic vein thrombosis in severe acute pancreatitis: a 2-year, single-institution experience. *HPB (Oxford)* 2011; **13**: 860-864 [PMID: 22081920 DOI: 10.1111/j.1477-2574.2011.00392.x]

27 **Garret C**, Péron M, Reignier J, Le Thuaut A, Lascarrou JB, Douane F, Lerhun M, Archambeaud I, Brulé N, Bretonnière C, Zambon O, Nicolet L, Regenet N, Guitton C, Coron E. Risk factors and outcomes of infected pancreatic necrosis: Retrospective cohort of 148 patients admitted to the ICU for acute pancreatitis. *United European Gastroenterol J* 2018; **6**:

910-918 [PMID: 30023069 DOI: 10.1177/2050640618764049]
28 **Casa LD**, Deaton DH, Ku DN. Role of high shear rate in thrombosis. *J Vasc Surg* 2015; **61**: 1068-1080 [PMID: 25704412 DOI: 10.1016/j.jvs.2014.12.050]
29 **Plessier A**, Darwish-Murad S, Hernandez-Guerra M, Consigny Y, Fabris F, Trebicka J, Heller J, Morard I, Lasser L, Langlet P, Denninger MH, Vidaud D, Condat B, Hadengue A, Primignani M, Garcia-Pagan JC, Janssen HL, Valla D; European Network for Vascular Disorders of the Liver (EN-Vie). Acute portal vein thrombosis unrelated to cirrhosis: a prospective multicenter follow-up study. *Hepatology* 2010; **51**: 210-218 [PMID: 19821530 DOI: 10.1002/hep.23259]
30 **Kumar S**, Sarr MG, Kamath PS. Mesenteric venous thrombosis. *N Engl J Med* 2001; **345**: 1683-1688 [PMID: 11759648 DOI: 10.1056/NEJMra010076]
31 **Kumar S**, Kamath PS. Acute superior mesenteric venous thrombosis: one disease or two? *Am J Gastroenterol* 2003; **98**: 1299-1304 [PMID: 12818273 DOI: 10.1111/j.1572-0241.2003.07338.x]
32 **Besselink MG**. Splanchnic vein thrombosis complicating severe acute pancreatitis. *HPB (Oxford)* 2011; **13**: 831-832 [PMID: 22081916 DOI: 10.1111/j.1477-2574.2011.00411.x]
33 **K T**, Chan SJ, Varghese C, Lim WB, Cheemungtoo GM, Akter N, Nayar M, Pandanaboyana S. A selective anticoagulation policy for splanchnic vein thrombosis in acute pancreatitis is associated with favourable outcomes: experience from a UK tertiary referral centre. *HPB (Oxford)* 2022; **24**: 1937-1943 [PMID: 35786365 DOI: 10.1016/j.hpb.2022.06.003]
34 **Pancreas Study Group**, Chinese Society of Gastroenterology; Chinese Medical Association. Practice guidance for diagnosis and treatment of pancreatitis-related splanchnic vein thrombosis (Shenyang, 2020). *J Dig Dis* 2021; **22**: 2-8 [PMID: 33215862 DOI: 10.1111/1751-2980.12962]
35 **Plessier A**, Goria O, Cervoni JP, Ollivier I, Bureau C, Poujol-Robert A, Minello A, Houssel-Debry P, Rautou PE, Payancé A, Scoazec G, Bruno O, Corbic M, Durand F, Vilgrain V, Paradis V, Boudaoud L, de Raucourt E, Roy C, Gault N, Valla D. Rivaroxaban Prophylaxis in Noncirrhotic Portal Vein Thrombosis. *NEJM Evid* 2022; **1** [DOI: 10.1056/EVIDoa2200104]
36 **de Franchis R**, Bosch J, Garcia-Tsao G, Reiberger T, Ripoll C; Baveno VII Faculty. Baveno VII - Renewing consensus in portal hypertension. *J Hepatol* 2022; **76**: 959-974 [PMID: 35120736 DOI: 10.1016/j.jhep.2021.12.022]
37 **van Dam LF**, Dronkers CEA, Gautam G, Eckerbom Å, Ghanima W, Gleditsch J, von Heijne A, Hofstee HMA, Hovens MMC, Huisman MV, Kolman S, Mairuhu ATA, Nijkeuter M, van de Ree MA, van Rooden CJ, Westerbeek RE, Westerink J, Westerlund E, Kroft LJM, Klok FA; Theia Study Group. Magnetic resonance imaging for diagnosis of recurrent ipsilateral deep vein thrombosis. *Blood* 2020; **135**: 1377-1385 [PMID: 32016390 DOI: 10.1182/blood.2019004114]
38 **DeLeve LD**, Valla DC, Garcia-Tsao G; American Association for the Study Liver Diseases. Vascular disorders of the liver. *Hepatology* 2009; **49**: 1729-1764 [PMID: 19399912 DOI: 10.1002/hep.22772]
39 **Boxhoorn L**, Timmerhuis HC, Verdonk RC, Besselink MG, Bollen TL, Bruno MJ, Elmunzer BJ, Fockens P, Horvath KD, van Santvoort HC, Voermans RP; Dutch Pancreatitis Study Group. Diagnosis and treatment of pancreatic duct disruption or disconnection: an international expert survey and case vignette study. *HPB (Oxford)* 2021; **23**: 1201-1208 [PMID: 33541807 DOI: 10.1016/j.hpb.2020.11.1148]
40 **de Rijk FEM**, van Veldhuisen CL, Besselink MG, van Hooft JE, van Santvoort HC, van Geenen EJM, Hegyi P, Löhr JM, Dominguez-Munoz JE, de Jonge PJF, Bruno MJ, Verdonk RC; Dutch Pancreatitis Study Group. Diagnosis and treatment of exocrine pancreatic insufficiency in chronic pancreatitis: An international expert survey and case vignette study. *Pancreatology* 2022; **22**: 457-465 [PMID: 35346599 DOI: 10.1016/j.pan.2022.03.013]
41 **Sperna Weiland CJ**, Engels MML, Poen AC, Bhalla A, Venneman NG, van Hooft JE, Bruno MJ, Verdonk RC, Fockens P, Drenth JPH, van Geenen EJM; Dutch Pancreatitis Study Group. Increased Use of Prophylactic Measures in Preventing Post-Endoscopic Retrograde Cholangiopancreatography Pancreatitis. *Dig Dis Sci* 2021; **66**: 4457-4466 [PMID: 33630216 DOI: 10.1007/s10620-020-06796-0]

World Journal of Gastroenterology

Submit a Manuscript: https://www.f6publishing.com

World J Gastroenterol 2023 June 7; 29(21): 3341-3361

DOI: 10.3748/wjg.v29.i21.3341

ISSN 1007-9327 (print) ISSN 2219-2840 (online)

SYSTEMATIC REVIEWS

Lumen-apposing-metal stent misdeployment in endoscopic ultrasound-guided drainages: A systematic review focusing on issues and rescue management

Elia Armellini, Flavio Metelli, Andrea Anderloni, Anna Cominardi, Giovanni Aragona, Michele Marini, Fabio Pace

Specialty type: Gastroenterology and hepatology

Provenance and peer review: Invited article; Externally peer reviewed.

Peer-review model: Single blind

Peer-review report's scientific quality classification

Grade A (Excellent): 0
Grade B (Very good): B, B
Grade C (Good): 0
Grade D (Fair): 0
Grade E (Poor): 0

P-Reviewer: Mestrovic A, Croatia; Nakamura K, Japan

Received: December 29, 2022
Peer-review started: January 1, 2023
First decision: January 10, 2023
Revised: February 1, 2023
Accepted: May 6, 2023
Article in press: May 6, 2023
Published online: June 7, 2023

Elia Armellini, Flavio Metelli, Fabio Pace, Department of Gastroenterology, ASST-Bergamoest, Seriate 24068, Bergamo, Italy

Andrea Anderloni, Gastroenterology and Digestive Endoscopy Unit, Fondazione IRCCS Policlinico San Matteo, Pavia 27100, Italy

Anna Cominardi, Giovanni Aragona, Department of Gastroenterology, "Guglielmo da Saliceto" Hospital, Piacenza 29121, Italy

Michele Marini, Department of General Surgery, ASST-Bergamoest, Seriate 24068, Italy

Corresponding author: Elia Armellini, MD, Department of Gastroenterology, ASST-Bergamoest, Via Paderno 21, Seriate 24068, Bergamo, Italy. elia_armellini@hotmail.com

Abstract

BACKGROUND

The introduction of lumen-apposing metal stents (LAMS) for endoscopic ultrasound (EUS)-guided drainages has marked a turning point in the field of interventional ultrasound and it is gathering worldwide diffusion in different clinical settings. Nevertheless, the procedure may conceal unexpected pitfalls. LAMS misdeployment is the most frequent cause of technical failure and it can be considered a procedure-related adverse event when it hampers the conclusion of the planned procedure or results in significant clinical consequences. Stent misdeployment can be managed successfully by endoscopic rescue maneuvers to allow the completion of the procedure. To date, no standardized indication is available to guide an appropriate rescue strategy depending on the type of procedure or of misdeployment.

AIM

To evaluate the incidence of LAMS misdeployment during EUS-guided choledochoduodenostomy (EUS-CDS), gallbladder drainage (EUS-GBD) and pancreatic fluid collections drainage (EUS-PFC) and to describe the endoscopic rescue strategies adopted under the circumstance.

METHODS

We conducted a systematic review of the literature on PubMed by searching for

studies published up to October 2022. The search was carried out using the exploded medical subject heading terms "lumen apposing metal stent", "LAMS", "endoscopic ultrasound" and "choledochoduodenostomy" or "gallbladder" or "pancreatic fluid collections". We included in the review on-label EUS-guided procedures namely EUS-CDS, EUS-GBD and EUS-PFC. Only those publications reporting EUS-guided LAMS positioning were considered. The studies reporting a technical success rate of 100% and other procedure-related adverse events were considered to calculate the overall rate of LAMS misdeployment, while studies not reporting the causes of technical failure were excluded. Case reports were considered only for the extraction of data regarding the issues of misdeployment and rescue techniques. The following data were collected from each study: Author, year of publication, study design, study population, clinical indication, technical success, reported number of misdeployment, stent type and size, flange misdeployed and type of rescue strategy.

RESULTS

The overall technical success rate of EUS-CDS, EUS-GBD and EUS-PFC was 93.7%, 96.1%, and 98.1% respectively. Significant rates of LAMS misdeployment have been reported for EUS-CDS, EUS-GBD and EUS-PFC drainage, respectively 5.8%, 3.4%, and 2.0%. Endoscopic rescue treatment was feasible in 86.8%, 80%, and 96.8% of cases. Non endoscopic rescue strategies were required only in 10.3%, 16% and 3.2% for EUS-CDS, EUS-GBD, and EUS-PFC. The endoscopic rescue techniques described were over-the-wire deployment of a new stent through the created fistula tract in 44.1%, 8% and 64.5% and stent-in-stent in 23.5%, 60%, and 12.9%, respectively for EUS-CDS, EUS-GBD, and EUS-PFC. Further therapeutic option were endoscopic rendezvous in 11.8% of EUS-CDS and repeated procedure of EUS-guided drainage in 16.1% of EUS-PFC.

CONCLUSION

LAMS misdeployment is a relatively common adverse event in EUS-guided drainages. There is no consensus on the best rescue approach in these cases and the choice is often made by the endoscopist relying upon the clinical scenario, anatomical characteristics, and local expertise. In this review, we investigated the misdeployment of LAMS for each of the on-label indications focusing on the rescue therapies used, with the aim of providing useful data for endoscopists and to improve patient outcomes.

Key Words: Lams misdeployment; Endoscopic ultrasound-guided drainage; Lams maldeployment; Biliary drainage; Gallbladder drainage; Pancreatic fluid collections; Lumen-apposing metal stents

©The Author(s) 2023. Published by Baishideng Publishing Group Inc. All rights reserved.

Core Tip: Scant data are available about rescue techniques in cases of lumen-apposing metal stents (LAMS) misdeployment which is the main cause of technical failure in endoscopic ultrasound-guided drainage procedures. We performed a systematic review of the literature about LAMS misdeployment and rescue techniques in the biliopancreatic setting, focusing on technical aspects and success rate of endoscopic maneuvers. In accordance with our results endoscopic rescue techniques are feasible in most cases (up to 96.8%). Three endoscopic rescue strategies have been identified. The choice of the endoscopic rescue maneuver is based on the clinical scenario, type of misdeployment and expertise of the endoscopic team.

Citation: Armellini E, Metelli F, Anderloni A, Cominardi A, Aragona G, Marini M, Pace F. Lumen-apposing-metal stent misdeployment in endoscopic ultrasound-guided drainages: A systematic review focusing on issues and rescue management. *World J Gastroenterol* 2023; 29(21): 3341-3361
URL: https://www.wjgnet.com/1007-9327/full/v29/i21/3341.htm
DOI: https://dx.doi.org/10.3748/wjg.v29.i21.3341

INTRODUCTION

The progress in interventional endoscopy, particularly in the field of endoscopic ultrasound (EUS), has changed the treatment algorithms for digestive and pancreaticobiliary diseases. The evolution of devices combined with improvements in endoscopic techniques, have allowed access to mini-invasive therapeutic solutions for complex diseases that affect areas beyond the gastrointestinal tract.

Nowadays, interventional EUS can manage local complications of acute pancreatitis[1], drain the biliary tree and gallbladder[2], establish gastrointestinal anastomoses[3], and treat tumors by radiofrequency ablation or injection of substances[4,5]. A paradigmatic example of this evolution is the approach to biliopancreatic drainage. The first EUS-guided transluminal drainage of the biliary tree was performed in 2001. Giovannini *et al*[6] used a 10-Fr plastic stent to achieve trans-duodenal biliary drainage (BD) under EUS guidance in a patient with a pancreatic head mass after failed endoscopic retrograde cholangiopancreatography (ERCP). Since then, the evolution of EUS-guided drainage has led to the continuous improvement of available devices and of endoscopic techniques. The introduction of self-expanding metal stents (SEMS) and lumen-apposing metal stents (LAMS) for EUS-guided drainage is a turning point in the field of endoscopic drainage. The first transluminal stenting between two nonadherent lumens of the digestive tract using a bi-flanged covered metal stent with lumen-to-lumen apposition property was described by Binmoeller and Shah[7] in an *ex vivo* model. Itoi *et al*[8] reported the first use of LAMS in humans, describing the successful treatment of 15 symptomatic pancreatic pseudocysts and five acute cholecystitis cases in patients unfit for surgery.

Itoi and Binmoeller[9] successfully performed the first EUS-guided choledochoduodenostomy (EUS-CDS) with LAMS in a patient with unresectable pancreatic cancer and obstructive jaundice. Prior to that, the technique of LAMS deployment was the same as that of tubular stents (plastic or metal stents), which is a multi-step procedure with device exchanges that are exposed to the risk of adverse events (*i.e.*, loss of the wire and/or scope position, biliary leak). To address this issue, a new LAMS delivery system with an electrocautery tip [electrocautery-enhanced (EC)-LAMS-Hot-Axios, Boston Scientific Corp., Marlborough, Massachusetts, United States] was developed, giving rise to a single-stage technique[10,11]. Presently, two LAMS in different diameters and lengths are commercially available: The Hot Axios stent (Boston Scientific, Marlborough, Mass, United States) and the Hot Spaxus stent (Taewoong Medical Co. Gimpo, Korea), and new LAMS types are on the way. Other fully covered (FC) metal stents are available for similar indications: Aixstent (Leufen Medical, Aachen, Germany), Hanarostent (Mi-TECH-Medical Co, Seoul, South Korea), and NAGI stents (Taewoong Medical Co., Ltd., Ilsan, Korea)[11,12]. These stents are non-cautery and require a multi-step procedure for their insertion. Anyway, LAMS loaded on an EC delivery system require precise execution of some sequential steps (puncture of the target lumen, opening and retraction of the distal flange to the adjacent cavity wall, deployment, and release of the proximal flange) to achieve technical success, which is defined as the correct placement of the stent across the newly created tract.

There are various issues that may occur during LAMS deployment, resulting in stent misdeployment. Unfavorable conditions range from unfamiliarity with the stent to patient movement, angled scope tip or confined space within the gastrointestinal cavity, small diameter of the target lumen[13], and target structure located at a distance of more than 15-20 mm[14]. Stent misdeployment usually results in a full-thickness defect of the gastrointestinal wall, possibly associated with the perforation of the target organ. Prompt identification of this complication is crucial to managing the perforation, possibly completing the procedure, and avoiding major consequences. This paper reviews EUS-guided drainage procedures using LAMS, with a focus on misdeployment and endoscopic rescue therapies.

MATERIALS AND METHODS

Data collection

This systematic review was performed in agreement with PRISMA guidelines. Two independent investigators (Cominardi A and Metelli F) performed a review on PubMed by searching for studies published up to October 2022. The search was limited to English-language articles and human studies, and it was carried out using the exploded medical subject heading terms "lumen apposing metal stent", "LAMS", "endoscopic ultrasound" and "choledochoduodenostomy" or "gallbladder" or "pancreatic fluid collections". We included in the review on-label EUS-guided procedures namely EUS-CDS, EUS-guided gallbladder drainage (EUS-GBD) and EUS-guided pancreatic fluid collections drainage (EUS-PFC). Boolean operators (NOT, AND, OR) were also used in succession to narrow and widen the search.

Both investigators used a standardized data collection form to increase uniformity and reduce bias in reporting. In the case of discrepancy, the investigators resolved the disagreement by discussion with a senior investigator (Armellini E). Only publications on EUS-guided LAMS positioning were considered, whereas studies on drainage with other metallic or plastic stents were excluded. Meta-analysis, review and drainage performed in non-human models were also excluded.

The studies reporting a technical success rate of 100% and other procedure-related adverse events were considered to calculate the overall rate of LAMS misdeployment, while studies not reporting the causes of technical failure were excluded. Case reports were considered only for the extraction of data regarding the issues of misdeployment and rescue techniques.

The full paper of each identified article was retrieved, and references were evaluated to search for potentially missed articles. Data were extracted independently and entered standardized Excel spreadsheet (Microsoft Inc. Redmond, Washington, United States). For EUS-CDS and EUS-PFC drainage the following data were extracted from each study: Year of publication, study design, study

population, clinical indication, technical success, reported number of misdeployment, LAMS type and size, flange misdeployed, and type of rescue strategy. For EUS-GBD the following data were collected from each study: Author, year of publication, study design, study population, clinical indication, access to GB (stomach or duodenum), technical success, reported number of misdeployment, LAMS type and size, flange misdeployed, and type of rescue strategy.

Data analysis

Baseline characteristics of study population, EUS-guided procedures, technical details, and procedure outcomes were summarized as means (SD) or medians (with interquartile range and range) for continuous data, and as frequencies and proportions for categorical data. Data were analyzed using the Statistical Package for Social Sciences (SPSS software v. 15.0, Chicago, Illinois, United States) for Windows.

RESULTS

EUS-CDS

Literature research identified 82 studies that were fully assessed for eligibility in this review. We excluded 57 studies since they did not meet our inclusion criteria. A total of 25 studies were included in our review[15-39]; in 20 studies LAMS misdeployment occurred[20-39] (study flow chart was shown in Figure 1).

A total of 1081 patients underwent EUS-CDS for malignant biliary obstruction (MBO), almost all after failed ERCP. The overall technical success rate of EUS-CDS was 93.7%. Excluding 5 case reports, a total of 63 LAMS misdeployments were reported, with a rate of 5.8%; the study detailed characteristics were summarized in Table 1. Including case reports, an Axios stent was employed in 61 (89.7%) cases of EUS-CDS. Spaxus stent was used in 3 (4.4%) cases. In 4 cases (5.9%) type of stent was not declared. The procedures were performed with a pre-loaded guidewire in 23 (33.8%) cases, without a pre-loaded guidewire in 12 (17.6%) cases, whereas this data was not available in most of cases (48.6%).

In 28 (41.2%) cases the misdeployment of the distal flange was reported, in 4 (5.9%) cases the misdeployment involved the proximal flange, in 3 (4.7%) EUS-CDS LAMS was entirely misdeployed inside the common bile duct (CBD) and in 2 (2.9%) patients no bile flow was observed after LAMS deployment despite no evidence of LAMS misdeployment. The type of misdeployment was not properly described in 31 (45.6%) EUS-CDS. Seven other causes of technical failure were reported in four studies[15,22,24,38]: 1 massive bleeding, 1 inability to puncture the bile duct, 2 duodenal perforations, 1 failure of fistula creation, 1 mechanical failure and 1 patient intolerance. In three studies[31,33,37], the effective rescue therapy after LAMS misdeployment was considered a technical success by the authors and in one study[15] duodenal perforation during dilation of the fistulous tract was the cause of technical failure.

LAMS misdeployment was managed by endoscopy in 86.8% (n = 59/68) cases, while 4.4% (n = 3/68) misdeployment cases were treated by percutaneous transhepatic BD (PTBD), 2.9% (n = 2/68) by rendezvous *via* PTBD and during surgery, and 2.9% (n = 2/68) by surgery. In 2 cases the procedure was abandoned in favor of supportive therapy. In 44.1% (n = 30/68) cases of LAMS misdeployment, the rescue strategy was LAMS removal followed by over-the-wire deployment of a new stent; in 7 (23.3%) cases a new LAMS was deployed and in 23 (76.7%) cases a SEMS was used.

The stent-in-stent technique was the treatment of choice in 16 (23.5%) cases of misdeployment; in 7 (43.7%) cases SEMS was used, in 1 (6.3%) a plastic stent and in 8 (50%) the stent type was not specified. In 8 (11.8%) cases rendezvous procedure was performed by EUS/endoscopic technique. EUS-CDS was repeated in 4 (5.9%) cases. In 1 (1.5%) case EUS-GBD was used as a rescue strategy (see Table 2).

EUS-GBD

We identified 213 studies using our search strategy; 185 studies were excluded since they did not meet inclusion criteria. A total of 28 studies reported cases of EUS-GBD[8,22,29,37,40-63] including 16 studies in which LAMS misdeployment occurred[22,29,50-63]. The study flow chart is shown in Figure 2.

A total of 667 patients underwent EUS-GBD for acute cholecystitis since they were unfit for surgery. Only in one study patients were treated by EUS-GBD for unsuccessful BD with ERCP[60]. Studies characteristics are summarized in Table 3. The overall technical success of EUS-GBD was 96.1%. Excluding two case reports, we identified 23 LAMS misdeployments among patients who underwent EUS-GBD, with a rate of 3.4%. In 19/25 (76%) cases an Axios stent was employed for EUS-GBD, while a Spaxus stent was used in the remaining 6/25 (24%) cases.

Only 8 studies reported if the GB was accessed from the stomach (n = 7/11, 63.6%) or duodenum (n = 4/11, 36.4%)[22,51-55,59,61]. The misdeployment of the proximal flange occurred in 9/25 (36%) cases, while the distal flange was misdeployed in 16/25 (64%) cases. The use of a guidewire was reported in 16/25 (64%) cases of misdeployment. Endoscopic management was the treatment of choice in 21/25 (84%) cases of LAMS misdeployment during EUS-CDS. In 15 of these 25 (60%) complicated EUS-GBD collected in our study, the initial failed LAMS deployment was overcome by reinsertion of a FC-SEMS

Table 1 Characteristics of studies reporting lumen-apposing metal stents misdeployment during endoscopic ultrasound-guided choledochoduodenostomy

Ref.	Study design	Study population (*n*)	Clinical indication	Technical success (%)	LAMS misdeployment (*n*)	LAMS type	Size of LAMS (mm)	Use of guidewire	LAMS flange misdeployed	Rescue therapy
Anderloni *et al*[20], 2019	Retrospective single center	46	MBO	93.5	3	Hot Axios	-	No	Distal (1/3), not specified (2/3)	Rendezvous technique with transpapillary placement of 10 mm × 40 mm FCSEMS after advancing a guidewire through the existing fistula into the bile duct and then across the papilla (1/3); 10 mm × 10 mm LAMS placement through the existing fistula (1/3); double-pigtail plastic stent placement across the LAMS (1/3)
Di Mitri R *et al*[21], 2022	Retrospective single center	31	MBO	80.6	7	Hot Axios	8 mm × 8 mm (6/7) 10 mm × 10 mm (1/7)	Yes	Distal	Over-the-wire FCSEMS placement (5/7); transpapillary percutaneous-transhepatic-endoscopic rendezvous (1/7); transpapillary laparoscopic-endoscopic rendezvous (1/7)
Rajadurai *et al* [22], 2022	Retrospective multicenter	66	MBO	90.9	6	Hot Axios	-	No (4/6). Yes (2/6)	Distal	Over-the-wire FCSEMS placement (2/6); laparotomy (2/6); EUS-GBD (1/6); palliation due to rapid deterioration (1/6)
Jacques *et al* [23], 2019	Retrospective multicenter	52	MBO	88.5	4	Hot Axios	-	-	Distal (1/4), proximal (1/4 intraperitoneal, 2/4 intraparietal)	Stent-in-stent strategy with SEMS (1/4); ERCP rendezvous (1/4); repeat classic EUS-CDS with SEMS (2/4)
Jacques *et al* [24], 2020	Retrospective multicenter	70	MBO	98.6	1	Hot Axios	-	-	No evidence of bile flow even if stent was correctly in situ	Stent-in-stent strategy
El Chafic *et al* [25], 2019	Retrospective multicenter	67	MBO	95.5	2	Hot Axios	-	Yes	-	Over the same guidewire FCSEMS placement (all)
Fugazza *et al* [26], 2022	Retrospective multicenter	256	MBO	93.3	17	Hot Axios	-	-	-	Over the guidewire SEMS placement (10/17); deployment of a second LAMS (4/17); EUS-guided rendezvous with subsequent placement of a transpapillary stent (3/17)
Hindryckx and Degroote [27], 2021	Retrospective single center	13	-	92.3	1	Hot Axios	8 mm × 6 mm	Yes	Distal	Clip closure of duodenal defect and new EUS-CDS with 8 mm × 6 mm LAMS
Armellini *et al* [28], 2023	Case report	1	Difficult biliary lithiasis	-	1	Hot Axios	8 mm × 8 mm	Yes	Distal	Rendezvous technique with transpapillary placement of FCSEMS after advancing a guidewire directly through the LAMS and choledochal breach into the bile duct and then across the papilla
Teoh *et al* [29], 2021	Prospective multicenter	26	MBO	88.5	3	Cold spaxus	-	Yes	Entirely into the bile duct	Over the guidewire SEMS placement
Fugazza *et al* [30], 2020	Case report	1	Pancreatic adenocarcinoma	-	1	Axios	6 mm × 8 mm	Yes	Proximal	Stent-in-stent strategy using SEMS
Brückner *et al*	Case series	5	MBO	80	1	Cold	6 mm × 8	Yes	Distal	Over the guidewire stent placement

[31], 2015						Axios	mm			
Vanella *et al* [32], 2023	Retrospective study of prospectively maintained databases	93	MBO	97.8	4	Hot Axios	-	No	Distal (2/4); misdeployments after both flanges release (2/4)	Repeat EUS-CDS (1/4); inserting a guidewire through the LAMS catheter followed by over the guidewire LAMS placement (1/4) (the effective rescue therapies were counted as technical success); PTBD (2/4)
de Benito Sanz *et al*[33], 2021	Retrospective single center	37	MBO	100	4	-	-	-	Distal (2/4); not specified (2/4)	Stent-in-stent strategy (the effective rescue therapies were counted as technical success)
Garcia-Sumalla *et al* [34], 2021	Retrospective multicenter	41	MBO	95.1	2	Hot Axios	-	-	No evidence of bile flow even if stent was correctly in situ; distal flange	Stent-in-stent strategy using SEMS; rendezvous technique with placement of a transpapillary FCSEMS
Sanchez-Ocana *et al* [35], 2022	Case report	1	Pancreatic adenocarcinoma	-	1	Axios	8 mm × 8 mm	Yes	Distal	EUS-guided gallbladder drainage as a portal for antegrade transcystic guidewire passage, followed by rendezvous ERCP with placement of a biliary metal stent and clips to seal the perforation
Graves *et al* [36], 2021	Case report	1	Pancreatic metastasis of renal cell carcinoma	-	1	Axios	10 mm × 10 mm	No	Distal	A bridging 10 mm × 8 mm FCSEMS was deployed over the guidewire and through theccessing LAMS
Chin *et al*[37], 2020	Retrospective analysis of a prospectively maintained database	56	MBO	100	1	Axios	-	-	-	Over the guidewire tubular biliary stent placement (the effective rescue therapy was counted as technical success)
On *et al*[38], 2022	Retrospective multicenter	120	MBO	90.8	7	Hot Axios	-	No (4/7). Yes (3/7)	-	Bridging stents (5/7), PTBD (1/7), conservative management (1/7)
Ligresti *et al* [39], 2018	Case report	1	Pancreatic adenocarcinoma	-	1	Axios	8 mm × 8 mm	Yes	Distal	Reinsertion of the delivery system over the guide wire and second deployment of distal flange into common bile duct under EUS guidance

MBO: Malignant biliary obstruction; FCSEMS: Fully covered self-expanding metal stent; SEMS: Self-expanding metal stent; LAMS: Lumen-apposing metal stent; EUS-GBD: Endoscopic ultrasound-guided gallbladder drainage; ERCP: Endoscopic retrograde cholangiopancreatography; EUS-CDS: Endoscopic ultrasound-guided choledochoduodenostomy; PTBD: Percutaneous transhepatic biliary drainage.

through the LAMS lumen, the so-called "stent-in-stent" strategy; only in 1/15 a double pigtail stent was inserted. In 2/25 (8%) cases, the misdeployed stent was removed and a new LAMS was re-deployed over the guidewire across the fistula created during the first attempt for EUS-GBD.

In 3/25 (12%) cases, the LAMS was endoscopically removed, and the gastrointestinal wall perforation was closed by endoscopic clipping followed by transpapillary stent placement in 1 case. No further endoscopic maneuvers were attempted in the remaining 2 cases in favour of supportive care. Surgical management was the therapeutic option in 3/25 (12%) cases of misdeployment. In 1 (4%) case, emergent percutaneous cholecystostomy was performed after unsuccessful stent-in-stent placement attempt. In 1 (4%) case, palliation was the preferred strategy (see Table 2).

Table 2 Summary of rescue strategies for lumen-apposing metal stent misdeployment

EUS-CDS	
Deployment of a new stent through the created fistula tract	44.1%
Stent-in-stent strategy	23.5%
Endoscopic rendezvous	11.8%
Non-endoscopic rescue strategies	10.3%
EUS-GBD	
Stent-in-stent strategy	60%
Clip closure of gastrointestinal wall defect	13%
Deployment of a new stent through the created fistula tract	8%
Non-endoscopic rescue strategies	16%
EUS-PFC	
Deployment of a new stent through the created fistula tract	64.5%
Repeated EUS-guided drainage	16.1%
Stent-in-stent strategy	12.9%
Non-endoscopic rescue strategies	3.2%

LAMS: Lumen-apposing metal stent; EUS-CDS: Endoscopic ultrasound-guided choledochoduodenostomy; EUS-GBD: Endoscopic ultrasound-guided gallbladder drainage; EUS-PFC: Endoscopic ultrasound-guided pancreatic fluid collections drainage.

EUS-PFC

We collected 48 studies from the literature that were fully assessed for eligibility in this review; 20 studies were excluded since they did not meet our inclusion criteria. A total of 28 studies were included in our review[10,12,57,64-88] including 15 studies in which LAMS misdeployment occurred[10,12,70,77-88] (Figure 3). The overall technical success of EUS-PFC drainage was 98.1%. The cause of technical failure corresponded to LAMS misdeployment in all the studies except in one reporting two cases of technical failure due to a difficult scope position that prevented the advancement of the EC-LAMS device outside the operative channel of the echoendoscope[57]. In 3 cases, the effective rescue therapy by re-insertion of the same LAMS after misdeployment was considered a technical success by the authors[78,79].

Excluding two case reports, we collected 1684 patients who underwent EUS-PFC drainage in which 34 LAMS misdeployments occurred, with a rate of 2.0%. All study characteristics were reported in Table 4. In 13 (36.1%) cases misdeployment of the distal flange occurred, in 2 (5.5%) cases the proximal flange was deployed and then migrated entirely into the PFC. In most cases included in our study (20/36; 55.5%), the issue of misdeployment was not clearly described. A case report described the misdeployment of the stent in a non-target organ. In 4 cases data regarding rescue strategy were not available and the procedure was abandoned in one case.

The LAMS misdeployment in EUS-PFC drainage was managed as following: In 20/31 (64.5%) cases an over-the-wire deployment of a new stent was performed (10/20 with LAMS, 2/20 with SEMS, 8/20 with plastic stents), in 5/31 (16.1%) cases the EUS-PFC drainage was repeated, in 1/31 (3.2%) case surgical drainage was performed. The stent-in-stent strategy was the rescue treatment in 4/31 (12.9%) cases of LAMS misdeployment; in 3 (75%) cases a LAMS-in-LAMS technique was performed and in 1 (25%) case a SEMS was deployed inside the misdeployed LAMS (see Table 2).

DISCUSSION

Technical success of EUS-drainage is defined as the correct deployment of the stent between the gastrointestinal wall and target organ with evidence of bile flow in patients who underwent EUS-BD[24,25,32] or content flow/established access to the cavity in EUS-PFC or EUS-GBD cases[52,57].

Actually, stent misdeployment emerges as the primary cause of technical failure in the procedure of EUS-guided drainage. Among the studies we collected, different terms were used to define this complication, including misdeployment, dislodgement, and flange migration. We adopted the term ‘misdeployment’, as reported in the European Society of Gastrointestinal Endoscopy guidelines for therapeutic EUS[14].

Table 3 Characteristics of studies reporting lumen-apposing metal stents misdeployment during endoscopic ultrasound-guided gallbladder drainage

Ref.	Study design	Study population (*n*)	Clinical indication	Access to GB	Technical success (%)	LAMS maldeployment (*n*)	LAMS type	Size of LAMS (mm)	LAMS flange misdeployed	Rescue therapy
Ngamruengphong *et al* [50], 2015	Case report	1	Cholecysto-choledocal lithiasis	Duodenum	-	1	Hot Axios	-	Proximal	Stent-in-stent strategy using SEMS
Rajadurai *et al*[22], 2022	Retrospective multicenter	49	-	Duodenum	95.7	2	Hot Axios	10 mm × 10 mm; 15 mm × 10 mm	Distal	Closure of the defect with clip; palliation (no further endoscopic treatment)
Cho *et al*[51], 2019	Prospective single center	22	Acute cholecystitis unfit for surgery	-	95.5	1	Spaxus	10 mm × 20 mm	Proximal	Stent-in-stent strategy using SEMS
Walter *et al*[52], 2016	Prospective multicenter	30	Acute cholecystitis unfit for surgery	Stomach	90	3	Hot Axios			Stent-in-stent strategy using SEMS
Irani *et al*[53], 2015	Retrospective multicenter	15	Acute cholecystitis unfit for surgery	Duodenum	93	1	Axios	10 mm × 10 mm	Distal	Stent-in-stent strategy using SEMS
de la Serna-Higuera *et al*[54], 2013	Prospective single center	13	Acute cholecystitis unfit for surgery	Stomach	84.6	1	Axios	10 mm × 10 mm	Distal	Closure of the defect with clip (no further endoscopic treatment)
Dollhopf *et al*[55], 2017	Retrospective multicenter	75	Acute cholecystitis unfit for surgery	Stomach	98.7	1	Hot-Axios	10 mm × 10 mm	Proximal	Surgery
Teoh *et al*[56], 2017	Retrospective multicenter	59	Acute cholecystitis unfit for surgery	-	96.6	1	Axios	10 mm × 10 mm	Distal	Surgery
Mangiavillano *et al* [57], 2021	Retrospective multicenter	18	Acute cholecystitis unfit for surgery	-	83.3	1	Spaxus		Distal	Closure of the defect with clip followed by transpapillary stent placment
Teoh *et al*[29], 2021	Retrospective multicenter	27	Acute cholecystitis unfit for surgery	-	88.9	2	Spaxus	10 mm × 10 mm; 16	Proximal	Stent-in-stent strategy using SEMS
Higa *et al*[58], 2019	Retrospective single center	40	Acute cholecystitis unfit for surgery	-	97.5	2	Hot Axios	10 mm × 10 mm; 15 mm × 10 mm	Distal	Redeployment of a new LAMS
Garg *et al*[59], 2018	Case report	1	Acute cholecystitis unfit for surgery	Stomach	-	1	Hot Axios	10 mm × 10 mm	Distal	Stent-in-stent strategy using SEMS
Torres Yuste *et al*[60], 2020	Retrospective single center	34	Acute cholecystitis unfit for surgery	-	97.1	3	Axios	10 mm × 10 mm; 15 mm × 10 mm	Distal	Stent-in-stent strategy using SEMS (2/3); double pig-tail plastic stent in LAMS (1/3)
		37		-	97.3	1	Axios	10 mm × 10 mm; 15 mm × 10 mm	Proximal	Stent-in-stent strategy using SEMS

James *et al*[61], 2019	Retrospective multicenter	15	Acute cholecystitis unfit for surgery	Stomach	93.3	1	Axios	10 mm × 10 mm; 15 mm × 10 mm	Proximal	Surgery
Irani *et al*[62],2017	Retrospective multicenter	45	Acute cholecystitis unfit for surgery	-	97.8	1	Axios	-	Distal	Stent-in-stent strategy using SEMS
Cho *et al*[63], 2020	Retrospective multicenter	36	Acute cholecystitis, advanced malignancy unfit for surgery	-	94.4	2	Spaxus	-	Proximal	Stent-in-stent strategy using SEMS, emergent PTC

SEMS: Self-expanding metal stent; LAMS: Lumen-apposing metal stent; PTC: Percutaneous cholecystostomy; GB: Gallbladder.

According to the American Society for Gastrointestinal Endoscopy lexicon for endoscopic adverse events, LAMS misdeployment can be considered a procedure-related adverse event when it hampers the completion of the planned procedure and/or results in significant clinical consequences (*i.e.*, prolongation of existing hospital stay and elicitation of the need for another procedure)[89]. Misdeployment can be defined as an incident if it does not interfere with the completion of the planned procedure or change the plan of care. Therefore, stent misdeployment can be managed successfully by endoscopic rescue maneuvers to allow the completion of the procedure; however, complications with different levels of severity can occur in some cases. In EUS-BD, stent misdeployment may be associated with spillage of bile and secretions into the peritoneal cavity or retroperitoneal space, resulting in peritonitis and pneumoretroperitoneum[90]. Recently Fabbri *et al*[91] proposed a classification of misdeployment types during EUS-guided gastroenterostomy as follows: Proximal flange misdeployment, distal flange misdeployment, stent misdeployment perforating other organs, and stent misdeployment into the peritoneum. This model considers which flange is misdeployed and the anatomical localization of the stent after misdeployment and can be supposedly adopted for all EUS-guided procedures involving the use of LAMS.

EUS-CDS

The rate of ERCP failure is 2%-10% and it is due to surgically altered anatomy, gastric outlet obstruction, duodenal and/or bile duct tumor infiltration, indwelling enteral stent, periampullary diverticula, impacted stones, and technical difficulties[92]. European guidelines suggest EUS-BD as the second-line treatment for patients with MBO. The optimal drainage strategy depends on the underlying disease (benign/malignant) and location of the obstruction (distal/hilar)[15].

EUS-BD proved to be equally effective with fewer adverse events and re-intervention compared to PTBD especially in gastric outlet obstructions[93]. In addition, EUS-BD is less invasive, leads to better nutrition, prevents electrolyte imbalances, and provides better quality of life[94]. As experience in EUS-BD continues to grow, comparative studies of EUS-CDS and ERCP have reported encouraging data in support of EUS-CDS as the primary treatment for distal MBO, challenging the role of ERCP[95].

In a meta-analysis, the technical and clinical success rates of EUS-CDS using LAMS were 93.6% and 94.8%, respectively, with pooled rate of overall adverse events of 17.1% and procedure-related adverse events of 6.2%[96]. In our research, LAMS misdeployment rate was 5.8%, and LAMS misdeployment represented the main cause of technical failure in EUS-CDS. Notably, technical failure was due to other

Table 4 Characteristics of studies reporting lumen-apposing metal stent misdeployment during endoscopic ultrasound-guided pancreatic fluid collections drainage

Ref.	Study design	Study population (*n*)	Clinical indication	Technical success (%)	LAMS misdeployment (*n*)	LAMS type	Size of LAMS (mm)	Use of guidewire	LAMS flange misdeployed	Rescue therapy
Venkatachalapathy *et al*[77], 2018	Retrospective multicenter	116	WON, PFC	99	1	Hot Axios	-	No	Distal	LAMS removal followed by over-the-wire deployment of a new LAMS
Khan *et al*[78], 2021	Retrospective multicenter	208	PFC	97.1	7	-	-	-	Distal	LAMS re-insertion (not counted as technical failure) (1/7); immediate repeat drainage (5/7); procedure abandoned (1/7)
Law *et al*[79], 2018	Retrospective single center	46	WON	93.5	5	Cold Axios/hot Axios	-	-	-	LAMS removal followed by over-the-wire deployment of a new LAMS (4/5; 2 LAMS re-insertion, not counted as technical failure) and of a FCSEMS 10 × 60 mm (1/5)
Walter *et al*[10], 2015	Prospective multicenter	61	PFC	98	1	Axios	-	Yes	Entirely inside the PFC	Placement of double pigtail stents
Siddiqui *et al*[80], 2016	Retrospective multicenter	82	PFC	97.5	2	Cold Axios	-	Yes	Distal	LAMS removal followed by over-the-wire deployment of a SEMS; surgical cystogastrostomy (difficulty to re-advance the guidewire into the PFC to perform an endoscopic rescue therapy)
Mendoza *et al*[81], 2020	Retrospective single center	21	WON	95	1	Hot Axios	-	Yes	Entirely inside the PFC	LAMS misdeployed was left inside the collection and a new one was then successfully placed through the original puncture site (both stents were removed 4 wk later)
Shah *et al*[82], 2015	Prospective multicenter	33	PFC	91	3	Cold Axios	-	Yes	-	Placement of double pigtail stents
Despott *et al*[83], 2020	Case report	1	WON	-	1	Hot Axios	20x10	-	Deployment in a non-target organ (colon)	LAMS removal and closure of both colonic and gastric defects with over-the-scope-clips
Rinninella *et al*[84], 2015	Retrospective multicenter	93	PFC	98.9	1	Hot Axios	-	Yes	Distal	Placement of double pigtail stents
Song *et al*[85], 2019	Prospective multicenter	34	PFC	97.1	1	Hot spaxus	-	Yes	Distal	LAMS in LAMS technique
Fugazza *et al*[86], 2020	Retrospective multicenter	328	PFC, WON	97.9	7	Hot Axios	-	-	-	New LAMS placement (4/7); placement of plastic stents (3/7)
Zhang *et al*[12], 2022	Retrospective multicenter	35	PFC	97	1	Hot Axios	15 mm × 15 mm	Yes	-	SEMS in LAMS technique
Yang *et al*[87], 2019	Retrospective multicenter	80	PFC	97.5	3	Cold Axios/hot Axios	-	-	-	-

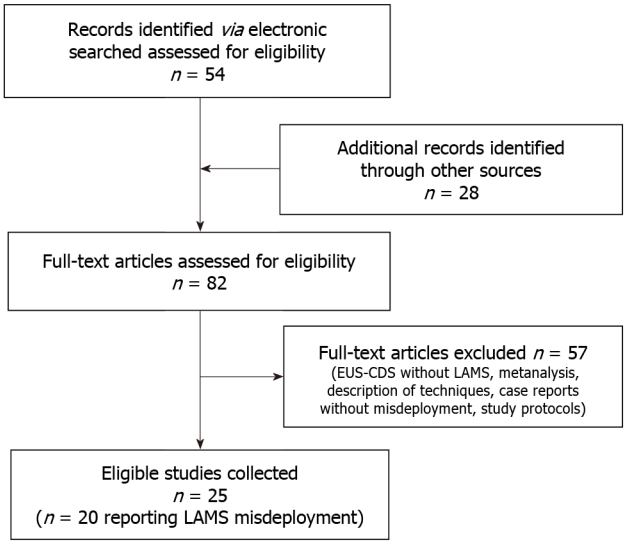
Adler *et al*[70], 2018	Retrospective multicenter	80	WON	98.7	1	Cold Axios	-	-	-	-
Curieses Luengo *et al* [88], 2019	Case report	1	WON	-	1	Hot Axios	10 mm × 10 mm	-	Distal	LAMS in LAMS technique

WON: Walled of necrosis; PFC: Pancreatic fluid collections; FCSEMS: Fully covered self-expanding metal stent; SEMS: Self-expanding metal stent; LAMS: Lumen-apposing metal stent.

causes in only seven cases (0.6%). In up to 86.8% of cases, the endoscopist managed LAMS misdeployment with an endoscopic rescue strategy during the index procedure.

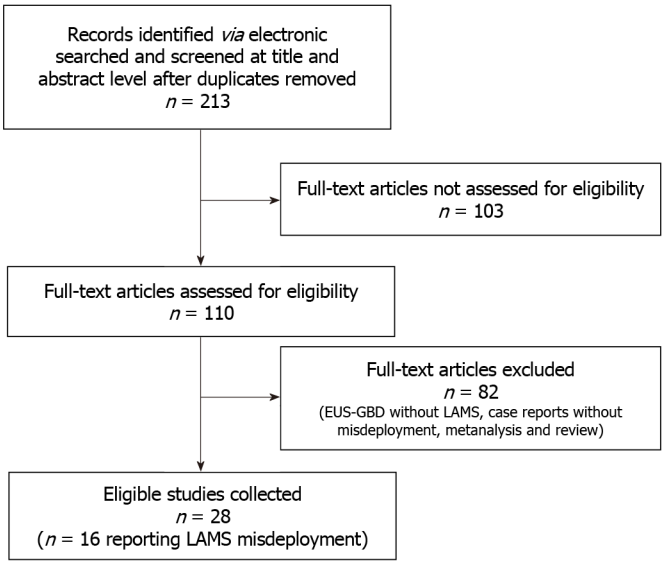
The most common endoscopic rescue technique involved misdeployed LAMS removal and over-the-wire deployment of a new stent through the same fistula tract (44.1%). SEMS were employed in most cases (76.7%). Other rescue strategies used include stent-in-stent (23.5%), EUS-guided/endoscopic rendezvous with transpapillary placement of a biliary SEMS (11.8%), and repeated EUS-drainage procedure (5.9%).

As reported in literature, the most common causes of LAMS misdeployment are related to difficult scope position[17,28,39] and small CBD diameter (< 15 mm)[21,27,34]. In a retrospective analysis by Jacques *et al*[23] involving 52 patients who underwent LAMS placement using various techniques, the technical and clinical success rates were 88.5% and 100%, respectively. In univariate analysis, CBD diameter > 15 mm, use of a 6-mm LAMS, and use of a one-step technique (direct puncture using the electrocautery system without needle puncture) were predictors of technical success in EUS-CDS. In another study, the authors performed EUS-CDS using a one-step technique in 97.1% (n = 68/70) of patients and achieved 98.6% of technical success[24]. The more frequent use of a pre-loaded guidewire in the group of patients with CBD < 15 mm compared to those with CBD ≥ 15 mm (33% *vs* 3.6%, P = 0.036) might have contributed to the comparable technical success, clinical success, and adverse event rates between the two groups. On the other hand, Di Mitri *et al*[21] reported seven cases of LAMS misdeployment in 31 patients with distal MBO who underwent EUS-CDS. CBD was ≤ 15 mm in six of the seven patients. In five cases, rescue therapies involved placing a fully covered self-expanding metal stent (FCSEMS) over the previously inserted guidewire, restoring the connection through the iatrogenic fistulous tract. In the remaining two cases, bile duct decompression after the puncture prevented the correct visualization of the CBD on EUS imaging and the possibility of approaching the CBD again; these cases were managed successfully by percutaneous- and laparoscopic-endoscopic rendezvous techniques. The authors assumed that the small caliber of the CBD forced the tip of the LAMS delivery catheter to be too close to the facing wall of the CBD and in an oblique direction, increasing the risk of misdeployment, even with the use of a small-size LAMS. In the largest study (256 patients enrolled) included in our review, Fugazza *et al*[26] reported that significantly higher technical success was achieved in patients with a larger CBD diameter compared to those with a smaller CBD diameter. The authors demonstrated that larger CBD size, use of a needle with a guidewire, fluoroscopy guidance, and LAMS placement in the proximal CBD were more likely in the non-expert group than in the expert group; however, technical [101 (94.4%) *vs* 138 (92.6%); P = 0.574] and clinical success [96 (95.0%) *vs* 134 (97.1%); P = 0.415] did not statistically differ between these two groups.



DOI: 10.3748/wjg.v29.i21.3341 **Copyright** ©The Author(s) 2023.

Figure 1 Study flow-chart of endoscopic ultrasound-choledochoduodenostomy. EUS-CDS: Endoscopic ultrasound-choledochoduodenostomy; LAMS: Lumen-apposing metal stents.



DOI: 10.3748/wjg.v29.i21.3341 **Copyright** ©The Author(s) 2023.

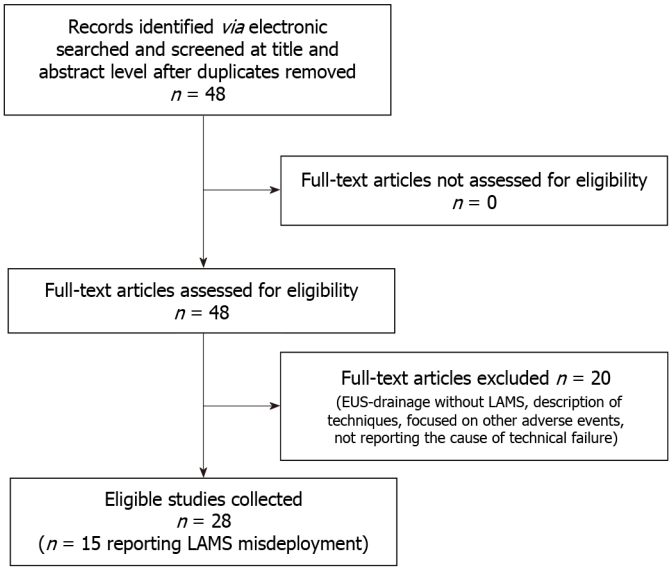
Figure 2 Study flow-chart of endoscopic ultrasound-gallbladder drainage. EUS-GBD: Endoscopic ultrasound-gallbladder drainage; LAMS: Lumen-apposing metal stents.

The use of a delivery system pre-loaded with a guidewire in complex cases (*i.e.*, endoscope instability in the duodenal bulb or smaller CBD diameter) was emphasized by Anderloni *et al*[97] because it allowed rescue using an over-the-wire stent placement in cases of LAMS misdeployment, and the single-step technique was preferred in cases of dilated CBD > 15 mm.

Wire access into the CBD could be regained in some cases, allowing endoscopic rescue maneuvers to be performed, even in cases of non-identifiable CBD on EUS imaging[28,35]. Our data show that over-the-wire deployment of a tubular stent, particularly a biliary SEMS, was the preferred rescue procedure for LAMS misdeployment during EUS-CDS (44.1%). We suppose that this technique was preferred since EUS-BD with SEMS has long been a consolidated technique for BD and that SEMS placement can be performed without EUS guidance, which may be lost in these circumstances.

EUS-GBD

Laparoscopic cholecystectomy is the standard approach for acute calculus cholecystitis. In cases of severe inflammation, adhesive disease, bleeding in the surgical area, or suspected bile duct injury, open cholecystectomy may be required to achieve safe dissection and gallbladder resection. In recent years, EUS-GBD has emerged as the preferred alternative to surgical treatment over percutaneous GBD



DOI: 10.3748/wjg.v29.i21.3341 **Copyright** ©The Author(s) 2023.

Figure 3 Study flow-chart of endoscopic ultrasound-pancreatic fluid collections. EUS: Endoscopic ultrasound; LAMS: Lumen-apposing metal stents.

(PGBD) or endoscopic transpapillary GBD (ETP-GBD) and is included in the international guidelines for grade II cholecystitis and recommended for grade 3 cholecystitis in patients with American Society of Anesthesiologists scores ≥ 3 or Charlson Comorbidity Index ≥ 6[98,99]. It has a technical and clinical success rate of 94.65% [95% confidence interval (CI): 91.54-96.67; I^2 = 0.00] and 92.06% (95%CI: 88.65-94.51; I^2 = 0.00), respectively. The rates of adverse events associated with EUS-GBD, including perforations, misdeployment, bile leakage, stent migration into the gallbladder or peritoneum, bleeding, gastroduodenal perforation, pneumoperitoneum, and recurrent acute cholecystitis due to stent occlusion, varies between 8% and 17%[100-102]. EUS-GBD showed higher technical and clinical success rates and lower recurrence rates than those of ETP-GBD[103].

Moreover, several studies have compared EUS-GBD with PGBD, demonstrating similar technical and clinical success rates for both procedures[43,104-106]; however, EUS-GBD was associated with significantly fewer adverse events, including lower mortality, lower post-procedure pain, shorter hospital stay, and fewer readmissions and reinterventions. According to our data, LAMS misdeployment occurred in 3.4% of the patients who underwent EUS-GBD. In almost 63% of cases, LAMS misdeployment occurred when EUS-GBD was performed through the stomach.

Although studies comparing gastric and duodenal LAMS access for EUS-GBD did not find any significant differences in technical or clinical success or adverse event rates[107], the duodenum is a less mobile organ and is closer to the gallbladder than the stomach. Therefore, there is a lower risk of LAMS migration when gallbladder access is *via* the duodenum.

In 68% of cases, LAMS misdeployment involved the distal flange. This suggests that a careful choice of the position and proper advancement of the LAMS inside the GB are critical to avoiding misdeployment. The use of guidewire, reported in 68% of cases of misdeployment, helped to maintain secure access to the newly created fistula between the gastrointestinal system and GB. The most frequently performed rescue maneuver was the placement of LAMS or a longer SEMS through the lumen of the misdeployed stent (stent-in-stent strategy). The stent-in-LAMS was particularly the rescue strategy of choice in up to 60% of LAMS misdeployment cases.

Surgery or PTBD after endoscopic closure of the luminal perforation was required after the failure of endoscopic therapies[55,56,61]. LAMS removal and clip closure of digestive tract wall defect was the treatment of choice in 3 patients (one of them was treated by ETP-GBD while no further endoscopic maneuver was performed in the remaining two patients). This strategy allows a second drainage attempt during the index procedure or later in selected patients. According to our data, two patients died after LAMS misdeployment, one for surgical complications and one left to supportive care[22,56].

EUS-PFC drainage

EUS-guided transmural drainage is considered the first-line treatment option for PFC, including walled-off necrosis (WON) and pancreatic pseudocysts[108]. Transluminal drainage in the "before-LAMS age" was achieved by the placement of double-pigtail plastic stents and afterward, by biliary/esophageal FC SEMS, which were associated with risks of migration, leakage, ulceration, and bleeding[109]. The LAMS design has the advantage of supporting drainage, preventing migration, and allowing direct access inside the WON cavity for endoscopic necrosectomy because it has a larger diameter, shorter length, and stent-anchoring flanges[110].

In our study, LAMS misdeployment during EUS-guided PFC drainage occurred in 34/1684 (2.0%) patients. This result is in accordance with the high technical success rate of these procedures reported in the literature (97.6%)[111]. Distal flange misdeployment in the peritoneal cavity, external to the cystic wall, was reported in up to 36.1% of cases[77,78,80,81,85]. Over-the-wire placement of a new stent (LAMS, SEMS, or double pigtail stents/plastic) through the novel fistula tract was the rescue therapy of choice in 64.5% of misdeployments. In 50% of cases, LAMS were deployed over the guidewire to complete the procedure as initially planned. The re-insertion of the same LAMS was performed in 15% of cases[78,79], resulting in a lower cost; these cases were counted as technical successes. In a study by Khan *et al*[78] involving 208 patients who underwent EUS-PFC drainage, 5/7 cases of LAMS misdeployment were managed by repeated EUS-guided drainage during index endoscopy.

There were two cases (5.5%) of complete LAMS misdeployment inside the PFC. In such cases, Mendoza Ladd *et al*[81] decided to leave the LAMS inside the PFC, and they deployed a new one through the fistula. After LAMS dilation, direct endoscopic necrosectomy was performed. Both stents were successfully removed four weeks later. The deployment of LAMS into an adjacent organ (the splenic flexure of the colon), described as WON, was reported by Despott *et al*[83], who identified the misdeployment only at the post-procedure scan (computerized tomography). After bowel preparation through a naso-jejunal tube to bypass the gastrocolic fistula, simultaneous upper and lower gastrointestinal endoscopies were performed, and the LAMS was removed. Both the colonic and gastric perforations were closed using over-the-scope clips. Although data regarding predictive factors related to LAMS misdeployment were lacking in the studies included in our review, Curieses Luengo *et al*[88] identified excessive flexion of the echoendoscope tip due to severe inflammatory duodenal stenosis as an unfavorable condition for correct LAMS deployment.

CONCLUSION

The use of LAMS has been demonstrated to have high technical and clinical success rates in EUS-CDS, EUS-GBD and EUS-PFC drainage, however significant rates of LAMS misdeployment are reported in 5.8%, 3.4%, and 2.0% of procedures, respectively. In a relevant rate of LAMS misdeployment, endoscopic rescue management has been shown to be technically feasible and effective in completing the procedure and avoiding major clinical consequences.

Although no algorithm is available to guide the appropriate rescue strategy for each case, three endoscopic techniques have been identified: (1) Gaining wire access to the target through the newly created tract and completing the procedure; (2) "Stent-in-stent" over the wire; and (3) Repeated procedures (*ex novo* or rendezvous). When endoscopic rescue procedures are not feasible, non-endoscopic options include percutaneous drainage or surgery.

In our analysis, the preferred strategy for LAMS misdeployment in EUS-CDS was LAMS removal and over-the-wire deployment of a new stent (44.1%), frequently SEMS (76.7% of cases), followed by stent-in-stent strategy (23.5%) and endoscopic rendezvous (11.8%). In EUS-GBD, the preferred technique was the stent-in-stent strategy (60%) using a SEMS in 93.3% of cases.

In EUS-PFC, the procedure of choice was LAMS removal followed by over-the-wire deployment of a new stent (64.5%), which was a LAMS or a plastic stent, in 50% and 40% of cases respectively. In conclusion, LAMS misdeployment is a relatively common adverse event, especially in EUS-BD. Endoscopic rescue strategies are feasible, and they vary depending on type of procedure, endoscopic technique used, and experience of the operators.

ARTICLE HIGHLIGHTS

Research background

Scant data are available about rescue techniques in cases of lumen-apposing metal stents (LAMS) misdeployment which is the main cause of technical failure in endoscopic ultrasound (EUS)-guided drainage procedures. We performed a systematic review of the literature about LAMS misdeployment and rescue techniques in the biliopancreatic setting, focusing on technical aspects and success rate of endoscopic maneuvers.

Research motivation

LAMS misdeployment is a relatively common adverse event in EUS-guided drainages. There is no consensus on the best rescue approach in these cases and the choice is often made by the endoscopist relying upon the clinical scenario, anatomical characteristics, and local expertise.

Research objectives

The overall technical success rate of EUS-guided choledochoduodenostomy (EUS-CDS), gallbladder drainage (EUS-GBD) and pancreatic fluid collections drainage (EUS-PFC) was 93.7%, 96.1%, and 98.1%

respectively. Significant rates of LAMS misdeployment have been reported for EUS-CDS, EUS-GBD and EUS-PFC drainage, respectively 5.8%, 3.4%, and 2.0%. Endoscopic rescue treatment was feasible in 86.8%, 80%, and 96.8% of cases. Non endoscopic rescue strategies were required only in 10.3%, 16% and 3.2% for EUS-CDS, EUS-GBD, and EUS-PFC.

Research methods

We conducted a systematic review of the literature on PubMed searching for studies published up to October 2022 about on-label EUS-guided procedures namely EUS-CDS, EUS-GBD and EUS-PFC. The search was carried out using the exploded medical subject heading terms 'lumen apposing metal stent', 'LAMS', 'endoscopic ultrasound' and "choledochoduodenostomy" or "gallbladder" or "pancreatic fluid collections".

Research results

The overall technical success rate of EUS-CDS, EUS-GBD and EUS-PFC was 93.7%, 96.1%, and 98.1% respectively. Significant rates of LAMS misdeployment have been reported for EUS-CDS, EUS-GBD and EUS-PFC drainage, 5.8%, 3.4%, and 2.0%, respectively. Endoscopic rescue treatment was feasible in 86.8%, 80%, and 96.8% of cases. Non endoscopic rescue strategies were required only in 10.3%, 16% and 3.2% for EUS-CDS, EUS-GBD, and EUS-PFC. The endoscopic rescue techniques described were over-the-wire deployment of a new stent through the created fistula tract in 44.1%, 8% and 64.5% and stent-in-stent in 23.5%, 60%, and 12.9%, respectively for EUS-CDS, EUS-GBD, and EUS-PFC. Further therapeutic option were endoscopic rendezvous in 11.8% of EUS-CDS and repeated procedure of EUS-guided drainage in 16.1% of EUS-PFC.

Research conclusions

Stent misdeployment can be managed successfully by endoscopic rescue maneuvers to allow the completion of the procedure. In accordance with our results endoscopic rescue techniques are feasible in most cases (up to 96.8%). Three endoscopic rescue strategies have been identified: Gaining wire access to the target through the created fistula and completing the procedure; placement of a new stent through the misdeployed LAMS to the target ("stent-in-stent") and repeated drainage procedures (*ex novo* or rendezvous).

Research perspectives

LAMS misdeployment is the main cause of technical failure of EUS-drainages and it is potentially harmful to the patient. Knowledge of risk factors, classification of misdeployment and of endoscopic rescue techniques is useful to improve patient outcome and the safety of the procedure. Further prospective studies describing these issues are expected.

FOOTNOTES

Author contributions: Armellini E contributed to the concept, design, drafting of the article, and approved final revision; Metelli F and Marini M involved in the acquisition, statistical analysis, or interpretation of data for biliary duct and pancreatic fluid collection section, and contribution to drafting the article; Cominardi A and Aragona G contributed to the acquisition and statistical analysis, or interpretation of data for gallbladder section; Anderloni A and Pace F revised the manuscript critically for intellectual content; and all the authors approved the version to be published.

Conflict-of-interest statement: All the authors report no relevant conflicts of interest for this article. Andrea Anderloni is consultant for BSCI, Olympus.

PRISMA 2009 Checklist statement: The authors have read the PRISMA 2009 Checklist, and the manuscript was prepared and revised according to the PRISMA 2009 Checklist.

Open-Access: This article is an open-access article that was selected by an in-house editor and fully peer-reviewed by external reviewers. It is distributed in accordance with the Creative Commons Attribution NonCommercial (CC BY-NC 4.0) license, which permits others to distribute, remix, adapt, build upon this work non-commercially, and license their derivative works on different terms, provided the original work is properly cited and the use is non-commercial. See: https://creativecommons.org/Licenses/by-nc/4.0/

Country/Territory of origin: Italy

ORCID number: Elia Armellini 0000-0001-8810-3597; Andrea Anderloni 0000-0002-1021-0031; Anna Cominardi 0000-0002-7003-2855.

S-Editor: Wang JJ
L-Editor: A

P-Editor: Yuan YY

REFERENCES

1 **Yasuda I**, Takahashi K. Endoscopic management of walled-off pancreatic necrosis. *Dig Endosc* 2021; **33**: 335-341 [PMID: 32306430 DOI: 10.1111/den.13699]

2 **Dhindsa BS**, Mashiana HS, Dhaliwal A, Mohan BP, Jayaraj M, Sayles H, Singh S, Ohning G, Bhat I, Adler DG. EUS-guided biliary drainage: A systematic review and meta-analysis. *Endosc Ultrasound* 2020; **9**: 101-109 [PMID: 32295967 DOI: 10.4103/eus.eus_80_19]

3 **Vanella G**, Bronswijk M, Arcidiacono PG, Larghi A, Wanrooij RLJV, de Boer YS, Rimbas M, Khashab M, van der Merwe SW. Current landscape of therapeutic EUS: Changing paradigms in gastroenterology practice. *Endosc Ultrasound* 2023; **12**: 16-28 [PMID: 36124531 DOI: 10.4103/EUS-D-21-00177]

4 **Armellini E**, Crinò SF, Ballarè M, Occhipinti P. Endoscopic ultrasound-guided radiofrequency ablation of a pancreatic neuroendocrine tumor. *Endoscopy* 2015; **47** Suppl 1 UCTN: E600-E601 [PMID: 26671543 DOI: 10.1055/s-0034-1393677]

5 **Melita G**, Pallio S, Tortora A, Crinò SF, Macrì A, Dionigi G. Diagnostic and Interventional Role of Endoscopic Ultrasonography for the Management of Pancreatic Neuroendocrine Neoplasms. *J Clin Med* 2021; **10** [PMID: 34203922 DOI: 10.3390/jcm10122638]

6 **Giovannini M**, Moutardier V, Pesenti C, Bories E, Lelong B, Delpero JR. Endoscopic ultrasound-guided bilioduodenal anastomosis: a new technique for biliary drainage. *Endoscopy* 2001; **33**: 898-900 [PMID: 11571690 DOI: 10.1055/s-2001-17324]

7 **Binmoeller KF**, Shah J. A novel lumen-apposing stent for transluminal drainage of nonadherent extraintestinal fluid collections. *Endoscopy* 2011; **43**: 337-342 [PMID: 21264800 DOI: 10.1055/s-0030-1256127]

8 **Itoi T**, Binmoeller KF, Shah J, Sofuni A, Itokawa F, Kurihara T, Tsuchiya T, Ishii K, Tsuji S, Ikeuchi N, Moriyasu F. Clinical evaluation of a novel lumen-apposing metal stent for endosonography-guided pancreatic pseudocyst and gallbladder drainage (with videos). *Gastrointest Endosc* 2012; **75**: 870-876 [PMID: 22301347 DOI: 10.1016/j.gie.2011.10.020]

9 **Itoi T**, Binmoeller KF. EUS-guided choledochoduodenostomy by using a biflanged lumen-apposing metal stent. *Gastrointest Endosc* 2014; **79**: 715 [PMID: 24424399 DOI: 10.1016/j.gie.2013.11.021]

10 **Walter D**, Will U, Sanchez-Yague A, Brenke D, Hampe J, Wollny H, López-Jamar JM, Jechart G, Vilmann P, Gornals JB, Ullrich S, Fähndrich M, de Tejada AH, Junquera F, Gonzalez-Huix F, Siersema PD, Vleggaar FP. A novel lumen-apposing metal stent for endoscopic ultrasound-guided drainage of pancreatic fluid collections: a prospective cohort study. *Endoscopy* 2015; **47**: 63-67 [PMID: 25268308 DOI: 10.1055/s-0034-1378113]

11 **Stier MW**, Waxman I. Lumen-Apposing Metal Stents: Which One and Why? *Gastrointest Endosc Clin N Am* 2018; **28**: 207-217 [PMID: 29519333 DOI: 10.1016/j.giec.2017.11.008]

12 **Zhang LY**, Kunda R, Aerts M, Messaoudi N, Pawa R, Pawa S, Robles-Medranda C, Oleas R, Al-Haddad MA, Obaitan I, Muniraj T, Fabbri C, Binda C, Anderloni A, Tarantino I, Bejjani M, Ghandour B, Singh V, Khashab MA. Novel 15-mm-long lumen-apposing metal stent for endoscopic ultrasound-guided drainage of pancreatic fluid collections located ≥10 mm from the luminal wall. *Endoscopy* 2022; **54**: 706-711 [PMID: 34905796 DOI: 10.1055/a-1682-7095]

13 **Rimbaş M**, Anderloni A, Napoléon B, Seicean A, Forti E, Crinò SF, Tarantino I, Arcidiacono PG, Fabbri C, Rizzatti G, Amato A, Voiosu T, Fugazza A, Moşteanu O, Ginès À, de Nucci G, Fusaroli P, Nguyen NQ, Di Mitri R, Minelli Grazioli L, Mutignani M, Archibugi L, Binda C, Cominardi A, Barbera C, Fernández-Esparrach G, Palazzo L, Palazzo M, Poley JW, Spada C, Valerii G, Itoi T, Matsunami Y, Mateescu RB, Băicuş C, Costamagna G, Larghi A. Common bile duct size in malignant distal obstruction and lumen-apposing metal stents: a multicenter prospective study. *Endosc Int Open* 2021; **9**: E1801-E1810 [PMID: 34790548 DOI: 10.1055/a-1526-1208]

14 **van der Merwe SW**, van Wanrooij RLJ, Bronswijk M, Everett S, Lakhtakia S, Rimbas M, Hucl T, Kunda R, Badaoui A, Law R, Arcidiacono PG, Larghi A, Giovannini M, Khashab MA, Binmoeller KF, Barthet M, Perez-Miranda M, van Hooft JE. Therapeutic endoscopic ultrasound: European Society of Gastrointestinal Endoscopy (ESGE) Guideline. *Endoscopy* 2022; **54**: 185-205 [PMID: 34937098 DOI: 10.1055/a-1717-1391]

15 **Kunda R**, Pérez-Miranda M, Will U, Ullrich S, Brenke D, Dollhopf M, Meier M, Larghi A. EUS-guided choledochoduodenostomy for malignant distal biliary obstruction using a lumen-apposing fully covered metal stent after failed ERCP. *Surg Endosc* 2016; **30**: 5002-5008 [PMID: 26969661 DOI: 10.1007/s00464-016-4845-6]

16 **Tsuchiya T**, Teoh AYB, Itoi T, Yamao K, Hara K, Nakai Y, Isayama H, Kitano M. Long-term outcomes of EUS-guided choledochoduodenostomy using a lumen-apposing metal stent for malignant distal biliary obstruction: a prospective multicenter study. *Gastrointest Endosc* 2018; **87**: 1138-1146 [PMID: 28843583 DOI: 10.1016/j.gie.2017.08.017]

17 **Anderloni A**, Buda A, Carrara S, Di Leo M, Fugazza A, Maselli R, Repici A. Single-session double-stent placement in concomitant malignant biliary and duodenal obstruction with a cautery-tipped lumen apposing metal stent. *Endoscopy* 2016; **48**: E321-E322 [PMID: 27706541 DOI: 10.1055/s-0042-117425]

18 **Yoo HW**, Moon JH, Jo SJ, Lee YN, Park JK, Lee TH, Cha SW, Cho YD, Park SH, Park SI, Jeong S, Lee DH. A novel electrocautery-enhanced delivery system for one-step endoscopic ultrasound-guided drainage of the gallbladder and bile duct using a lumen-apposing metal stent: a feasibility study. *Endoscopy* 2021; **53**: 922-926 [PMID: 33336343 DOI: 10.1055/a-1301-1526]

19 **Sawas T**, Bailey NJ, Yeung KYKA, James TW, Reddy S, Fleming CJ, Marya NB, Storm AC, Abu Dayyeh BK, Petersen BT, Martin JA, Levy MJ, Baron TH, Bun Teoh AY, Chandrasekhara V. Comparison of EUS-guided choledochoduodenostomy and percutaneous drainage for distal biliary obstruction: A multicenter cohort study. *Endosc Ultrasound* 2022; **11**: 223-230 [PMID: 35102902 DOI: 10.4103/EUS-D-21-00031]

20 **Anderloni A**, Fugazza A, Troncone E, Auriemma F, Carrara S, Semeraro R, Maselli R, Di Leo M, D'Amico F, Sethi A, Repici A. Single-stage EUS-guided choledochoduodenostomy using a lumen-apposing metal stent for malignant distal biliary obstruction. *Gastrointest Endosc* 2019; **89**: 69-76 [PMID: 30189198 DOI: 10.1016/j.gie.2018.08.047]

21 **Di Mitri R**, Amata M, Mocciaro F, Conte E, Bonaccorso A, Scrivo B, Scimeca D. EUS-guided biliary drainage with LAMS for distal malignant biliary obstruction when ERCP fails: single-center retrospective study and maldeployment management. *Surg Endosc* 2022; **36**: 4553-4569 [PMID: 34724586 DOI: 10.1007/s00464-021-08808-0]

22 **Rajadurai A**, Zorron Cheng Tao Pu L, Cameron R, Tagkalidis P, Holt B, Bassan M, Gupta S, Croagh D, Swan M, Saxena P, Efthymiou M, Vaughan R, Chandran S; ANZEC. Endoscopic ultrasound-guided gallbladder and bile duct drainage with lumen apposing metal stent: A large multicenter cohort (with videos). *J Gastroenterol Hepatol* 2022; **37**: 179-189 [PMID: 34562319 DOI: 10.1111/jgh.15688]

23 **Jacques J**, Privat J, Pinard F, Fumex F, Valats JC, Chaoui A, Cholet F, Godard B, Grandval P, Legros R, Kerever S, Napoleon B. Endoscopic ultrasound-guided choledochoduodenostomy with electrocautery-enhanced lumen-apposing stents: a retrospective analysis. *Endoscopy* 2019; **51**: 540-547 [PMID: 30347424 DOI: 10.1055/a-0735-9137]

24 **Jacques J**, Privat J, Pinard F, Fumex F, Chaput U, Valats JC, Cholet F, Jezequel J, Grandval P, Legros R, Lepetit H, Albouys J, Napoleon B. EUS-guided choledochoduodenostomy by use of electrocautery-enhanced lumen-apposing metal stents: a French multicenter study after implementation of the technique (with video). *Gastrointest Endosc* 2020; **92**: 134-141 [PMID: 32084411 DOI: 10.1016/j.gie.2020.01.055]

25 **El Chafic AH**, Shah JN, Hamerski C, Binmoeller KF, Irani S, James TW, Baron TH, Nieto J, Romero RV, Evans JA, Kahaleh M. EUS-Guided Choledochoduodenostomy for Distal Malignant Biliary Obstruction Using Electrocautery-Enhanced Lumen-Apposing Metal Stents: First US, Multicenter Experience. *Dig Dis Sci* 2019; **64**: 3321-3327 [PMID: 31175495 DOI: 10.1007/s10620-019-05688-2]

26 **Fugazza A**, Fabbri C, Di Mitri R, Petrone MC, Colombo M, Cugia L, Amato A, Forti E, Binda C, Maida M, Sinagra E, Repici A, Tarantino I, Anderloni A; i-EUS Group. EUS-guided choledochoduodenostomy for malignant distal biliary obstruction after failed ERCP: a retrospective nationwide analysis. *Gastrointest Endosc* 2022; **95**: 896-904.e1 [PMID: 34995640 DOI: 10.1016/j.gie.2021.12.032]

27 **Hindryckx P**, Degroote H. Lumen-apposing metal stents for approved and off-label indications: a single-centre experience. *Surg Endosc* 2021; **35**: 6013-6020 [PMID: 33051767 DOI: 10.1007/s00464-020-08090-6]

28 **Armellini E**, Metelli F, Piazzini Albani A, Vescovi L, Spinelli L, Pace F. Fast endoscopic rendezvous to the rescue after maldeployment of lumen-apposing metal stent during endoscopic ultrasound-guided choledochoduodenostomy. *Endoscopy* 2023; **55**: E37-E38 [PMID: 36138522 DOI: 10.1055/a-1929-9148]

29 **Teoh AYB**, Kongkam P, Bapaye A, Ratanachu T, Reknimitr R, Lakthakia S, Chan SM, Gadhikar HP, Korrapati SK, Lee YN, Medarapalem J, Ridtitid W, Moon JH. Use of a novel lumen apposing metallic stent for drainage of the bile duct and gallbladder: Long term outcomes of a prospective international trial. *Dig Endosc* 2021; **33**: 1139-1145 [PMID: 33284467 DOI: 10.1111/den.13911]

30 **Fugazza A**, Gabbiadini R, Colombo M, Carrara S, Maselli R, Repici A, Anderloni A. Self-expandable metal stent placement as a rescue procedure for lumen-apposing metal stent misdeployment in biliary drainage. *Endoscopy* 2020; **52**: E430-E431 [PMID: 32375187 DOI: 10.1055/a-1158-8749]

31 **Brückner S**, Arlt A, Hampe J. Endoscopic ultrasound-guided biliary drainage using a lumen-apposing self-expanding metal stent: a case series. *Endoscopy* 2015; **47**: 858-861 [PMID: 26021309 DOI: 10.1055/s-0034-1392104]

32 **Vanella G**, Bronswijk M, Dell'Anna G, Voermans RP, Laleman W, Petrone MC, van Malenstein H, Fockens P, Arcidiacono PG, van der Merwe S, van Wanrooij RLJ. Classification, risk factors, and management of lumen apposing metal stent dysfunction during follow-up of endoscopic ultrasound-guided choledochoduodenostomy: Multicenter evaluation from the Leuven-Amsterdam-Milan Study Group. *Dig Endosc* 2023; **35**: 377-388 [PMID: 36177532 DOI: 10.1111/den.14445]

33 **de Benito Sanz M**, Nájera-Muñoz R, de la Serna-Higuera C, Fuentes-Valenzuela E, Fanjul I, Chavarría C, García-Alonso FJ, Sanchez-Ocana R, Carbajo AY, Bazaga S, Perez-Miranda M. Lumen apposing metal stents versus tubular self-expandable metal stents for endoscopic ultrasound-guided choledochoduodenostomy in malignant biliary obstruction. *Surg Endosc* 2021; **35**: 6754-6762 [PMID: 33258038 DOI: 10.1007/s00464-020-08179-y]

34 **Garcia-Sumalla A**, Loras C, Guarner-Argente C, Velasquez-Rodriguez JG, Andujar X, Salord S, Busquets J, Tebe C, Laquente B, Gornals JB. Is a coaxial plastic stent within a lumen-apposing metal stent useful for the management of distal malignant biliary obstruction? *Surg Endosc* 2021; **35**: 4873-4881 [PMID: 33721090 DOI: 10.1007/s00464-021-08435-9]

35 **Sanchez-Ocana R**, de Benito Sanz M, Nájera-Muñoz R, Chavarria C, de la Serna-Higuera C, Perez-Miranda M. Rendezvous ERCP *via* endoscopic ultrasound-guided gallbladder drainage to salvage a dislodged lumen-apposing metal stent during choledochoduodenostomy. *Endoscopy* 2022; **54**: E65-E67 [PMID: 33682904 DOI: 10.1055/a-1368-3985]

36 **Graves M**, Krafft M, Nasr J. EUS-guided choledochoduodenostomy creation using a biliary fully covered self-expanding metal stent after maldeployment of lumen-apposing metal stent. *VideoGIE* 2021; **6**: 234-235 [PMID: 34027257 DOI: 10.1016/j.vgie.2021.01.010]

37 **Chin JY**, Seleq S, Weilert F. Safety and outcomes of endoscopic ultrasound-guided drainage for malignant biliary obstruction using cautery-enabled lumen-apposing metal stent. *Endosc Int Open* 2020; **8**: E1633-E1638 [PMID: 33140019 DOI: 10.1055/a-1236-3217]

38 **On W**, Paranandi B, Smith AM, Venkatachalapathy SV, James MW, Aithal GP, Varbobitis I, Cheriyan D, McDonald C, Leeds JS, Nayar MK, Oppong KW, Geraghty J, Devlin J, Ahmed W, Scott R, Wong T, Huggett MT. EUS-guided choledochoduodenostomy with electrocautery-enhanced lumen-apposing metal stents in patients with malignant distal biliary obstruction: multicenter collaboration from the United Kingdom and Ireland. *Gastrointest Endosc* 2022; **95**: 432-442 [PMID: 34637805 DOI: 10.1016/j.gie.2021.09.040]

39 **Ligresti D**, Amata M, Granata A, Cipolletta F, Barresi L, Traina M, Tarantino I. Salvage procedure following lumen-apposing metal stent maldeployment during endoscopic ultrasound-guided biliary drainage. *Endoscopy* 2018; **50**: E190-E191 [PMID: 29895062 DOI: 10.1055/a-0605-3198]

40 **Sharaiha RZ**, Tyberg A, Desai AP. Novel applications for lumen apposing metal stents: how far can we go? *Gastrointest*

Endosc 2015; **81**: AB425-AB426 [DOI: 10.1016/j.gie.2015.03.1618]
41 **Moon JH**, Choi HJ, Kim DC, Lee YN, Kim HK, Jeong SA, Lee TH, Cha SW, Cho YD, Park SH, Jeong S, Lee DH, Isayama H, Itoi T. A newly designed fully covered metal stent for lumen apposition in EUS-guided drainage and access: a feasibility study (with videos). *Gastrointest Endosc* 2014; **79**: 990-995 [PMID: 24721518 DOI: 10.1016/j.gie.2014.02.015]
42 **Law R**, Grimm IS, Stavas JM, Baron TH. Conversion of Percutaneous Cholecystostomy to Internal Transmural Gallbladder Drainage Using an Endoscopic Ultrasound-Guided, Lumen-Apposing Metal Stent. *Clin Gastroenterol Hepatol* 2016; **14**: 476-480 [PMID: 26528802 DOI: 10.1016/j.cgh.2015.10.026]
43 **Teoh AYB**, Kitano M, Itoi T, Pérez-Miranda M, Ogura T, Chan SM, Serna-Higuera C, Omoto S, Torres-Yuste R, Tsuichiya T, Wong KT, Leung CH, Chiu PWY, Ng EKW, Lau JYW. Endosonography-guided gallbladder drainage versus percutaneous cholecystostomy in very high-risk surgical patients with acute cholecystitis: an international randomised multicentre controlled superiority trial (DRAC 1). *Gut* 2020; **69**: 1085-1091 [PMID: 32165407 DOI: 10.1136/gutjnl-2019-319996]
44 **Anderloni A**, Leo MD, Carrara S, Fugazza A, Maselli R, Buda A, Amato A, Auriemma F, Repici A. Endoscopic ultrasound-guided transmural drainage by cautery-tipped lumen-apposing metal stent: exploring the possible indications. *Ann Gastroenterol* 2018; **31**: 735-741 [PMID: 30386125 DOI: 10.20524/aog.2018.0299]
45 **Issa D**, Irani S, Law R, Shah S, Bhalla S, Mahadev S, Hajifathalian K, Sampath K, Mukewar S, Carr-Locke DL, Khashab MA, Sharaiha RZ. Endoscopic ultrasound-guided gallbladder drainage as a rescue therapy for unresectable malignant biliary obstruction: a multicenter experience. *Endoscopy* 2021; **53**: 827-831 [PMID: 32898918 DOI: 10.1055/a-1259-0349]
46 **Nishiguchi K**, Ogura T, Okuda A, Ueno S, Nishioka N, Yamada M, Matsuno J, Ueshima K, Yamamoto Y, Higuchi K. Endoscopic gallbladder drainage for acute cholecystitis with high-risk surgical patients between transduodenal and transpapillary stenting. *Endosc Ultrasound* 2021; **10**: 448-454 [PMID: 34782492 DOI: 10.4103/EUS-D-20-00130]
47 **Chang JI**, Dong E, Kwok KK. Endoscopic ultrasound-guided transmural gallbladder drainage in malignant obstruction using a novel lumen-apposing stent: a case series (with video). *Endosc Int Open* 2019; **7**: E655-E661 [PMID: 31058208 DOI: 10.1055/a-0826-4309]
48 **Saumoy M**, Tyberg A, Brown E, Eachempati SR, Lieberman M, Afaneh C, Kunda R, Cosgrove N, Siddiqui A, Gaidhane M, Kahaleh M. Successful Cholecystectomy After Endoscopic Ultrasound Gallbladder Drainage Compared With Percutaneous Cholecystostomy, Can it Be Done? *J Clin Gastroenterol* 2019; **53**: 231-235 [PMID: 29697498 DOI: 10.1097/MCG.0000000000001036]
49 **Anderloni A**, Attili F, Sferrazza A, Rimbaș M, Costamagna G, Repici A, Larghi A. EUS-guided gallbladder drainage using a lumen-apposing self-expandable metal stent in patients with coagulopathy or anticoagulation therapy: a case series. *Endosc Int Open* 2017; **5**: E1100-E1103 [PMID: 29250587 DOI: 10.1055/s-0043-118828]
50 **Ngamruengphong S**, Kumbhari V, Tieu AH, Haito-Chavez Y, El-Zein MH, Aguila G, Khashab MA. EUS-guided rescue of early dislodgement of a lumen-apposing stent. *Gastrointest Endosc* 2015; **82**: 1124 [PMID: 26175334 DOI: 10.1016/j.gie.2015.06.009]
51 **Cho DH**, Jo SJ, Lee JH, Song TJ, Park DH, Lee SK, Kim MH, Lee SS. Feasibility and safety of endoscopic ultrasound-guided gallbladder drainage using a newly designed lumen-apposing metal stent. *Surg Endosc* 2019; **33**: 2135-2141 [PMID: 30334155 DOI: 10.1007/s00464-018-6485-5]
52 **Walter D**, Teoh AY, Itoi T, Pérez-Miranda M, Larghi A, Sanchez-Yague A, Siersema PD, Vleggaar FP. EUS-guided gall bladder drainage with a lumen-apposing metal stent: a prospective long-term evaluation. *Gut* 2016; **65**: 6-8 [PMID: 26041748 DOI: 10.1136/gutjnl-2015-309925]
53 **Irani S**, Baron TH, Grimm IS, Khashab MA. EUS-guided gallbladder drainage with a lumen-apposing metal stent (with video). *Gastrointest Endosc* 2015; **82**: 1110-1115 [PMID: 26142558 DOI: 10.1016/j.gie.2015.05.045]
54 **de la Serna-Higuera C**, Pérez-Miranda M, Gil-Simón P, Ruiz-Zorrilla R, Diez-Redondo P, Alcaide N, Sancho-del Val L, Nuñez-Rodriguez H. EUS-guided transenteric gallbladder drainage with a new fistula-forming, lumen-apposing metal stent. *Gastrointest Endosc* 2013; **77**: 303-308 [PMID: 23206813 DOI: 10.1016/j.gie.2012.09.021]
55 **Dollhopf M**, Larghi A, Will U, Rimbaș M, Anderloni A, Sanchez-Yague A, Teoh AYB, Kunda R. EUS-guided gallbladder drainage in patients with acute cholecystitis and high surgical risk using an electrocautery-enhanced lumen-apposing metal stent device. *Gastrointest Endosc* 2017; **86**: 636-643 [PMID: 28259594 DOI: 10.1016/j.gie.2017.02.027]
56 **Teoh AYB**, Serna C, Penas I, Chong CCN, Perez-Miranda M, Ng EKW, Lau JYW. Endoscopic ultrasound-guided gallbladder drainage reduces adverse events compared with percutaneous cholecystostomy in patients who are unfit for cholecystectomy. *Endoscopy* 2017; **49**: 130-138 [PMID: 27875855 DOI: 10.1055/s-0042-119036]
57 **Mangiavillano B**, Moon JH, Crinò SF, Larghi A, Pham KD, Teoh AYB, Paduano D, Lee YN, Yoo HW, Shin IS, Rizzatti G, Robles-Medranda C, Oleas R, Conti Bellocchi MC, Auriemma F, Lamonaca L, Spatola F, Conigliaro R, Facciorusso A, Gabbrielli A, Repici A. Safety and efficacy of a novel electrocautery-enhanced lumen-apposing metal stent in interventional EUS procedures (with video). *Gastrointest Endosc* 2022; **95**: 115-122 [PMID: 34339667 DOI: 10.1016/j.gie.2021.07.021]
58 **Higa JT**, Sahar N, Kozarek RA, La Selva D, Larsen MC, Gan SI, Ross AS, Irani SS. EUS-guided gallbladder drainage with a lumen-apposing metal stent versus endoscopic transpapillary gallbladder drainage for the treatment of acute cholecystitis (with videos). *Gastrointest Endosc* 2019; **90**: 483-492 [PMID: 31054909 DOI: 10.1016/j.gie.2019.04.238]
59 **Garg R**, Barawi M. A Guidewire May Save the Day. *Korean J Gastroenterol* 2018; **72**: 83-85 [PMID: 30145860 DOI: 10.4166/kjg.2018.72.2.83]
60 **Torres Yuste R**, Garcia-Alonso FJ, Sanchez-Ocana R, Cimavilla Roman M, Peñas Herrero I, Carbajo AY, De Benito Sanz M, Mora Cuadrado N, De la Serna Higuera C, Perez-Miranda M. Safety and efficacy of endoscopic ultrasound-guided gallbladder drainage combined with endoscopic retrograde cholangiopancreatography in the same session. *Dig Endosc* 2020; **32**: 608-615 [PMID: 31608503 DOI: 10.1111/den.13562]
61 **James TW**, Krafft M, Croglio M, Nasr J, Baron T. EUS-guided gallbladder drainage in patients with cirrhosis: results of a multicenter retrospective study. *Endosc Int Open* 2019; **7**: E1099-E1104 [PMID: 31475226 DOI: 10.1055/a-0965-6662]
62 **Irani S**, Ngamruengphong S, Teoh A, Will U, Nieto J, Abu Dayyeh BK, Gan SI, Larsen M, Yip HC, Topazian MD, Levy

MJ, Thompson CC, Storm AC, Hajiyeva G, Ismail A, Chen YI, Bukhari M, Chavez YH, Kumbhari V, Khashab MA. Similar Efficacies of Endoscopic Ultrasound Gallbladder Drainage With a Lumen-Apposing Metal Stent Versus Percutaneous Transhepatic Gallbladder Drainage for Acute Cholecystitis. *Clin Gastroenterol Hepatol* 2017; **15**: 738-745 [PMID: 28043931 DOI: 10.1016/j.cgh.2016.12.021]

63 **Cho SH**, Oh D, Song TJ, Park DH, Seo DW, Lee SK, Kim MH, Lee YN, Moon JH, Lee SS. Comparison of the effectiveness and safety of lumen-apposing metal stents and anti-migrating tubular self-expandable metal stents for EUS-guided gallbladder drainage in high surgical risk patients with acute cholecystitis. *Gastrointest Endosc* 2020; **91**: 543-550 [PMID: 31629721 DOI: 10.1016/j.gie.2019.09.042]

64 **Larghi A**, Crinò SF, Vanella G, Rizzatti G, Bernardoni L, Arcidiacono PG. Preliminary experience of EUS-guided pancreatic fluid collections drainage using a new lumen-apposing metal stent mounted on a cautery device. *Endosc Ultrasound* 2022; **11**: 84-85 [PMID: 34755703 DOI: 10.4103/EUS-D-21-00033]

65 **Garg R**, Chaar A, Szpunar S, Mohan BP, Barawi M. Efficacy and Safety of Lumen-Apposing Stents for Management of Pancreatic Fluid Collections in a Community Hospital Setting. *Clin Endosc* 2020; **53**: 480-486 [PMID: 31615198 DOI: 10.5946/ce.2019.116]

66 **Anderloni A**, Fabbri C, Nieto J, Uwe W, Dollhopf M, Aparicio JR, Perez-Miranda M, Tarantino I, Arlt A, Vleggaar F, Vanbiervliet G, Hampe J, Kahaleh M, Vila JJ, Dayyeh BKA, Storm AC, Fugazza A, Binda C, Charachon A, Sevilla-Ribota S, Tyberg A, Robert M, Wani S, Repici A, Sethi A, Khashab MA, Kunda R. The safety and efficacy of a new 20-mm lumen apposing metal stent (lams) for the endoscopic treatment of pancreatic and peripancreatic fluid collections: a large international, multicenter study. *Surg Endosc* 2021; **35**: 1741-1748 [PMID: 32323015 DOI: 10.1007/s00464-020-07567-8]

67 **Olaiya B**, Mekaroonkamol P, Li BW, Massaad J, Vachaparambil CT, Xu J, Lamm V, Luo H, Shen SS, Chen HM, Keilin S, Willingham FF, Cai Q. Outcomes of a single-step endoscopic ultrasound-guided drainage of pancreatic-fluid collections using an electrocautery-enhanced coaxial lumen-apposing, self-expanding metal stent with and without fluoroscopy. *Gastroenterol Rep (Oxf)* 2020; **8**: 425-430 [PMID: 33442474 DOI: 10.1093/gastro/goaa020]

68 **Li J**, Zhang Q, Zhou A, Zhao G, Li P. Comparative outcomes of endoscopic ultrasound-guided lumen-apposing mental stents drainage for pancreatic pseudocysts and walled-off necrosis: Case series and meta-analysis. *Chronic Dis Transl Med* 2021; **7**: 157-168 [PMID: 34505016 DOI: 10.1016/j.cdtm.2021.07.001]

69 **Garcia Garcia de Paredes A**, Gonzalez Martin JA, Foruny Olcina JR, Juzgado Lucas D, Gonzalez Panizo F, Lopez Duran S, Martinez Sanchez A, Sanjuanbenito A, Caminoa A, Albillos A, Vazquez-Sequeiros E. Lumen-apposing metal stents versus biliary fully-covered metal stents for EUS-guided drainage of pancreatic fluid collections: a case control study: Meeting presentations: European Society of Gastrointestinal Endoscopy ESGE Days 2018. *Endosc Int Open* 2020; **8**: E6-E12 [PMID: 31921978 DOI: 10.1055/a-1031-9295]

70 **Adler DG**. Single-operator experience with a 20-mm diameter lumen apposing metal stent to treat patients with large pancreatic fluid collections from pancreatic necrosis. *Endosc Ultrasound* 2018; **7**: 422-423 [PMID: 30531025 DOI: 10.4103/eus.eus_39_18]

71 **Adler DG**, Shah J, Nieto J, Binmoeller K, Bhat Y, Taylor LJ, Siddiqui AA. Placement of lumen-apposing metal stents to drain pseudocysts and walled-off pancreatic necrosis can be safely performed on an outpatient basis: A multicenter study. *Endosc Ultrasound* 2019; **8**: 36-42 [PMID: 29770780 DOI: 10.4103/eus.eus_30_17]

72 **Sharaiha RZ**, Tyberg A, Khashab MA, Kumta NA, Karia K, Nieto J, Siddiqui UD, Waxman I, Joshi V, Benias PC, Darwin P, DiMaio CJ, Mulder CJ, Friedland S, Forcione DG, Sejpal DV, Gonda TA, Gress FG, Gaidhane M, Koons A, DeFilippis EM, Salgado S, Weaver KR, Poneros JM, Sethi A, Ho S, Kumbhari V, Singh VK, Tieu AH, Parra V, Likhitsup A, Womeldorph C, Casey B, Jonnalagadda SS, Desai AP, Carr-Locke DL, Kahaleh M, Siddiqui AA. Endoscopic Therapy With Lumen-apposing Metal Stents Is Safe and Effective for Patients With Pancreatic Walled-off Necrosis. *Clin Gastroenterol Hepatol* 2016; **14**: 1797-1803 [PMID: 27189914 DOI: 10.1016/j.cgh.2016.05.011]

73 **Teoh AYB**, Bapaye A, Lakhtakia S, Ratanachu T, Reknimitr R, Chan SM, Choi HJ, Gadhikar HP, Kongkam P, Korrapati SK, Lee YN, Medarapalem J, Ridtitid W, Moon JH. Prospective multicenter international study on the outcomes of a newly developed self-approximating lumen-apposing metallic stent for drainage of pancreatic fluid collections and endoscopic necrosectomy. *Dig Endosc* 2020; **32**: 391-398 [PMID: 31343773 DOI: 10.1111/den.13494]

74 **Yoo J**, Yan L, Hasan R, Somalya S, Nieto J, Siddiqui AA. Feasibility, safety, and outcomes of a single-step endoscopic ultrasonography-guided drainage of pancreatic fluid collections without fluoroscopy using a novel electrocautery-enhanced lumen-apposing, self-expanding metal stent. *Endosc Ultrasound* 2017; **6**: 131-135 [PMID: 28440239 DOI: 10.4103/2303-9027.204814]

75 **Adler DG**, Mallery S, Amateau S, Nieto J, Taylor LJ, Siddiqui A. A pilot study of a 20-mm lumen-apposing metal stent to treat pancreatic fluid collections: First reported multicenter use of a new device. *Endosc Ultrasound* 2019; **8**: 136-138 [PMID: 31006708 DOI: 10.4103/eus.eus_58_18]

76 **Nieto J**, Mekaroonkamol P, Shah R, Khashab MA, Loren DE, Waxman I, Edmundowicz SA, Willingham FF. Electrocautery-enhanced Lumen-apposing Metal Stents in the Management of Symptomatic Pancreatic Fluid Collections: Results From the Multicenter Prospective Pivotal Trial. *J Clin Gastroenterol* 2023; **57**: 218-226 [PMID: 33899781 DOI: 10.1097/MCG.0000000000001545]

77 **Venkatachalapathy SV**, Bekkali N, Pereira S, Johnson G, Oppong K, Nayar M, Leeds J, Paranandi B, Penman I, Carroll N, Godfrey E, James M, Aithal G, McKay C, Devlin J, Wong T, Makin A, Ryan B, Huggett M. Multicenter experience from the UK and Ireland of use of lumen-apposing metal stent for transluminal drainage of pancreatic fluid collections. *Endosc Int Open* 2018; **6**: E259-E265 [PMID: 29497684 DOI: 10.1055/s-0043-125362]

78 **Khan S**, Chandran S, Chin J, Karim S, Mangira D, Nasr M, Ermerak G, Trinh A, Kia CYH, Mules T, Zad M, Ang TL, Johns E, Tee D, Kaul A, Ratanachu-Ek T, Jirathan-Opas J, Fisher L, Cameron R, Welch C, Lim G, Metz AJ, Moss A, Bassan M, Saxena P, Kaffes A, St John A, Hourigan LF, Tagkalidis P, Weilert F, Vaughan R, Devereaux B. Drainage of pancreatic fluid collections using a lumen-apposing metal stent with an electrocautery-enhanced delivery system. *J Gastroenterol Hepatol* 2021; **36**: 3395-3401 [PMID: 34370869 DOI: 10.1111/jgh.15658]

79 **Law ST**, De La SernaHiguera C, Simón PG, Pérez-MirandaCastillo M. Comparison of clinical efficacies and safeties of

lumen-apposing metal stent and conventional-type metal stent-assisted EUS-guided pancreatic wall-off necrosis drainage: a real-life experience in a tertiary hospital. *Surg Endosc* 2018; **32**: 2448-2453 [PMID: 29101565 DOI: 10.1007/s00464-017-5946-6]

80 **Siddiqui AA**, Adler DG, Nieto J, Shah JN, Binmoeller KF, Kane S, Yan L, Laique SN, Kowalski T, Loren DE, Taylor LJ, Munigala S, Bhat YM. EUS-guided drainage of peripancreatic fluid collections and necrosis by using a novel lumen-apposing stent: a large retrospective, multicenter U.S. experience (with videos). *Gastrointest Endosc* 2016; **83**: 699-707 [PMID: 26515956 DOI: 10.1016/j.gie.2015.10.020]

81 **Mendoza Ladd A**, Bashashati M, Contreras A, Umeanaeto O, Robles A. Endoscopic pancreatic necrosectomy in the United States-Mexico border: A cross sectional study. *World J Gastrointest Endosc* 2020; **12**: 149-158 [PMID: 32477449 DOI: 10.4253/wjge.v12.i5.149]

82 **Shah RJ**, Shah JN, Waxman I, Kowalski TE, Sanchez-Yague A, Nieto J, Brauer BC, Gaidhane M, Kahaleh M. Safety and efficacy of endoscopic ultrasound-guided drainage of pancreatic fluid collections with lumen-apposing covered self-expanding metal stents. *Clin Gastroenterol Hepatol* 2015; **13**: 747-752 [PMID: 25290534 DOI: 10.1016/j.cgh.2014.09.047]

83 **Despott EJ**, Lazaridis N, Johnson G, Yano T, Murino A. Over-the-scope clip closure of an iatrogenic gastro-colic fistula following maldeployment of a lumen-apposing metal stent. *Endoscopy* 2020; **52**: E300-E302 [PMID: 32084668 DOI: 10.1055/a-1085-9343]

84 **Rinninella E**, Kunda R, Dollhopf M, Sanchez-Yague A, Will U, Tarantino I, Gornals Soler J, Ullrich S, Meining A, Esteban JM, Enz T, Vanbiervliet G, Vleggaar F, Attili F, Larghi A. EUS-guided drainage of pancreatic fluid collections using a novel lumen-apposing metal stent on an electrocautery-enhanced delivery system: a large retrospective study (with video). *Gastrointest Endosc* 2015; **82**: 1039-1046 [PMID: 26014960 DOI: 10.1016/j.gie.2015.04.006]

85 **Song TJ**, Lee SS, Moon JH, Choi HJ, Cho CM, Lee KH, Park SW, Kim SH, Lee SO, Lee YN, Lee JK. Efficacy of a novel lumen-apposing metal stent for the treatment of symptomatic pancreatic pseudocysts (with video). *Gastrointest Endosc* 2019; **90**: 507-513 [PMID: 31152738 DOI: 10.1016/j.gie.2019.05.033]

86 **Fugazza A**, Sethi A, Trindade AJ, Troncone E, Devlin J, Khashab MA, Vleggaar FP, Bogte A, Tarantino I, Deprez PH, Fabbri C, Aparicio JR, Fockens P, Voermans RP, Uwe W, Vanbiervliet G, Charachon A, Packey CD, Benias PC, El-Sherif Y, Paiji C, Ligresti D, Binda C, Martínez B, Correale L, Adler DG, Repici A, Anderloni A. International multicenter comprehensive analysis of adverse events associated with lumen-apposing metal stent placement for pancreatic fluid collection drainage. *Gastrointest Endosc* 2020; **91**: 574-583 [PMID: 31759037 DOI: 10.1016/j.gie.2019.11.021]

87 **Yang J**, Chen YI, Friedland S, Holmes I, Paiji C, Law R, Hosmer A, Stevens T, Matheus F, Pawa R, Mathur N, Sejpal D, Inamdar S, Berzin TM, DiMaio CJ, Gupta S, Yachimski PS, Anderloni A, Repici A, James T, Jamil LH, Ona M, Lo SK, Gaddam S, Dollhopf M, Alammar N, Shieh E, Bukhari M, Kumbhari V, Singh V, Brewer O, Sanaei O, Fayad L, Ngamruengphong S, Shin EJ, Baron TH, Khashab MA. Lumen-apposing stents versus plastic stents in the management of pancreatic pseudocysts: a large, comparative, international, multicenter study. *Endoscopy* 2019; **51**: 1035-1043 [PMID: 30536255 DOI: 10.1055/a-0759-1353]

88 **Curieses Luengo M**, Consiglieri CF, Puga M, Gornals JB. A novel rescue maneuver for a distal dislodged lumen-apposing metal stent (LAMS): "LAMS-in-LAMS" technique. *Rev Esp Enferm Dig* 2019; **111**: 243-245 [PMID: 30746951 DOI: 10.17235/reed.2019.5924/2018]

89 **Cotton PB**, Eisen GM, Aabakken L, Baron TH, Hutter MM, Jacobson BC, Mergener K, Nemcek A Jr, Petersen BT, Petrini JL, Pike IM, Rabeneck L, Romagnuolo J, Vargo JJ. A lexicon for endoscopic adverse events: report of an ASGE workshop. *Gastrointest Endosc* 2010; **71**: 446-454 [PMID: 20189503 DOI: 10.1016/j.gie.2009.10.027]

90 **Han SY**, Kim SO, So H, Shin E, Kim DU, Park DH. EUS-guided biliary drainage versus ERCP for first-line palliation of malignant distal biliary obstruction: A systematic review and meta-analysis. *Sci Rep* 2019; **9**: 16551 [PMID: 31719562 DOI: 10.1038/s41598-019-52993-x]

91 **Fabbri C**, Binda C, Fugazzola P, Sbrancia M, Tomasoni M, Coluccio C, Jung CFM, Prosperi E, Agnoletti V, Ansaloni L. Hybrid gastroenterostomy using a lumen-apposing metal stent: a case report focusing on misdeployment and systematic review of the current literature. *World J Emerg Surg* 2022; **17**: 6 [PMID: 35065661 DOI: 10.1186/s13017-022-00409-z]

92 **Sarkaria S**, Sundararajan S, Kahaleh M. Endoscopic ultrasonographic access and drainage of the common bile duct. *Gastrointest Endosc Clin N Am* 2013; **23**: 435-452 [PMID: 23540968 DOI: 10.1016/j.giec.2012.12.013]

93 **Sharaiha RZ**, Khan MA, Kamal F, Tyberg A, Tombazzi CR, Ali B, Tombazzi C, Kahaleh M. Efficacy and safety of EUS-guided biliary drainage in comparison with percutaneous biliary drainage when ERCP fails: a systematic review and meta-analysis. *Gastrointest Endosc* 2017; **85**: 904-914 [PMID: 28063840 DOI: 10.1016/j.gie.2016.12.023]

94 **Holt BA**, Hawes R, Hasan M, Canipe A, Tharian B, Navaneethan U, Varadarajulu S. Biliary drainage: role of EUS guidance. *Gastrointest Endosc* 2016; **83**: 160-165 [PMID: 26215648 DOI: 10.1016/j.gie.2015.06.019]

95 **Hathorn KE**, Bazarbashi AN, Sack JS, McCarty TR, Wang TJ, Chan WW, Thompson CC, Ryou M. EUS-guided biliary drainage is equivalent to ERCP for primary treatment of malignant distal biliary obstruction: a systematic review and meta-analysis. *Endosc Int Open* 2019; **7**: E1432-E1441 [PMID: 31673615 DOI: 10.1055/a-0990-9488]

96 **Amato A**, Sinagra E, Celsa C, Enea M, Buda A, Vieceli F, Scaramella L, Belletrutti P, Fugazza A, Cammà C, Radaelli F, Repici A, Anderloni A. Efficacy of lumen-apposing metal stents or self-expandable metal stents for endoscopic ultrasound-guided choledochoduodenostomy: a systematic review and meta-analysis. *Endoscopy* 2021; **53**: 1037-1047 [PMID: 33246343 DOI: 10.1055/a-1324-7919]

97 **Anderloni A**, Troncone E, Fugazza A, Cappello A, Del Vecchio Blanco G, Monteleone G, Repici A. Lumen-apposing metal stents for malignant biliary obstruction: Is this the ultimate horizon of our experience? *World J Gastroenterol* 2019; **25**: 3857-3869 [PMID: 31413524 DOI: 10.3748/wjg.v25.i29.3857]

98 **Mayumi T**, Okamoto K, Takada T, Strasberg SM, Solomkin JS, Schlossberg D, Pitt HA, Yoshida M, Gomi H, Miura F, Garden OJ, Kiriyama S, Yokoe M, Endo I, Asbun HJ, Iwashita Y, Hibi T, Umezawa A, Suzuki K, Itoi T, Hata J, Han HS, Hwang TL, Dervenis C, Asai K, Mori Y, Huang WS, Belli G, Mukai S, Jagannath P, Cherqui D, Kozaka K, Baron TH, de Santibañes E, Higuchi R, Wada K, Gouma DJ, Deziel DJ, Liau KH, Wakabayashi G, Padbury R, Jonas E, Supe AN, Singh H, Gabata T, Chan ACW, Lau WY, Fan ST, Chen MF, Ker CG, Yoon YS, Choi IS, Kim MH, Yoon DS, Kitano S,

Inomata M, Hirata K, Inui K, Sumiyama Y, Yamamoto M. Tokyo Guidelines 2018: management bundles for acute cholangitis and cholecystitis. *J Hepatobiliary Pancreat Sci* 2018; **25**: 96-100 [PMID: 29090868 DOI: 10.1002/jhbp.519]

99 **Pisano M**, Allievi N, Gurusamy K, Borzellino G, Cimbanassi S, Boerna D, Coccolini F, Tufo A, Di Martino M, Leung J, Sartelli M, Ceresoli M, Maier RV, Poiasina E, De Angelis N, Magnone S, Fugazzola P, Paolillo C, Coimbra R, Di Saverio S, De Simone B, Weber DG, Sakakushev BE, Lucianetti A, Kirkpatrick AW, Fraga GP, Wani I, Biffl WL, Chiara O, Abu-Zidan F, Moore EE, Leppäniemi A, Kluger Y, Catena F, Ansaloni L. 2020 World Society of Emergency Surgery updated guidelines for the diagnosis and treatment of acute calculus cholecystitis. *World J Emerg Surg* 2020; **15**: 61 [PMID: 33153472 DOI: 10.1186/s13017-020-00336-x]

100 **Chan JHY**, Teoh AYB. Current Status of Endoscopic Gallbladder Drainage. *Clin Endosc* 2018; **51**: 150-155 [PMID: 29145349 DOI: 10.5946/ce.2017.125]

101 **Jain D**, Bhandari BS, Agrawal N, Singhal S. Endoscopic Ultrasound-Guided Gallbladder Drainage Using a Lumen-Apposing Metal Stent for Acute Cholecystitis: A Systematic Review. *Clin Endosc* 2018; **51**: 450-462 [PMID: 29852730 DOI: 10.5946/ce.2018.024]

102 **Mohan BP**, Asokkumar R, Shakhatreh M, Garg R, Ponnada S, Navaneethan U, Adler DG. Adverse events with lumen-apposing metal stents in endoscopic gallbladder drainage: A systematic review and meta-analysis. *Endosc Ultrasound* 2019; **8**: 241-248 [PMID: 31115387 DOI: 10.4103/eus.eus_63_18]

103 **McCarty TR**, Hathorn KE, Bazarbashi AN, Jajoo K, Ryou M, Thompson CC. Endoscopic gallbladder drainage for symptomatic gallbladder disease: a cumulative systematic review meta-analysis. *Surg Endosc* 2021; **35**: 4964-4985 [PMID: 34231061 DOI: 10.1007/s00464-020-07758-3]

104 **Luk SW**, Irani S, Krishnamoorthi R, Wong Lau JY, Wai Ng EK, Teoh AY. Endoscopic ultrasound-guided gallbladder drainage versus percutaneous cholecystostomy for high risk surgical patients with acute cholecystitis: a systematic review and meta-analysis. *Endoscopy* 2019; **51**: 722-732 [PMID: 31238375 DOI: 10.1055/a-0929-6603]

105 **Teoh AY**, Perez-Miranda M, Kunda R, Lee SS, Irani S, Yeaton P, Sun S, Baron TH, Moon JH, Holt B, Khor CJL, Rerknimitr R, Bapaye A, Chan SM, Choi HJ, James TW, Kongkam P, Lee YN, Parekh P, Ridtitid W, Serna-Higuera C, Tan DMY, Torres-Yuste R. Outcomes of an international multicenter registry on EUS-guided gallbladder drainage in patients at high risk for cholecystectomy. *Endosc Int Open* 2019; **7**: E964-E973 [PMID: 31367676 DOI: 10.1055/a-0915-2098]

106 **Rana SS**. Endoscopic ultrasound-guided gallbladder drainage: a technical review. *Ann Gastroenterol* 2021; **34**: 142-148 [PMID: 33654351 DOI: 10.20524/aog.2020.0568]

107 **Sobani ZA**, Ling C, Rustagi T. Endoscopic Ultrasound-Guided Gallbladder Drainage. *Dig Dis Sci* 2021; **66**: 2154-2161 [PMID: 32749635 DOI: 10.1007/s10620-020-06520-y]

108 **Arvanitakis M**, Dumonceau JM, Albert J, Badaoui A, Bali MA, Barthet M, Besselink M, Deviere J, Oliveira Ferreira A, Gyökeres T, Hritz I, Hucl T, Milashka M, Papanikolaou IS, Poley JW, Seewald S, Vanbiervliet G, van Lienden K, van Santvoort H, Voermans R, Delhaye M, van Hooft J. Endoscopic management of acute necrotizing pancreatitis: European Society of Gastrointestinal Endoscopy (ESGE) evidence-based multidisciplinary guidelines. *Endoscopy* 2018; **50**: 524-546 [PMID: 29631305 DOI: 10.1055/a-0588-5365]

109 **Kawakami H**, Itoi T, Sakamoto N. Endoscopic ultrasound-guided transluminal drainage for peripancreatic fluid collections: where are we now? *Gut Liver* 2014; **8**: 341-355 [PMID: 25071899 DOI: 10.5009/gnl.2014.8.4.341]

110 **Mussetto A**, Fugazza A, Fuccio L, Triossi O, Repici A, Anderloni A. Current uses and outcomes of lumen-apposing metal stents. *Ann Gastroenterol* 2018; **31**: 535-540 [PMID: 30174389 DOI: 10.20524/aog.2018.0287]

111 **Guzmán-Calderón E**, Chacaltana A, Díaz R, Li B, Martinez-Moreno B, Aparicio JR. Head-to-head comparison between endoscopic ultrasound guided lumen apposing metal stent and plastic stents for the treatment of pancreatic fluid collections: A systematic review and meta-analysis. *J Hepatobiliary Pancreat Sci* 2022; **29**: 198-211 [PMID: 34107170 DOI: 10.1002/jhbp.1008]

World Journal of Gastroenterology

Submit a Manuscript: https://www.f6publishing.com

World J Gastroenterol 2023 June 7; 29(21): 3362-3378

DOI: 10.3748/wjg.v29.i21.3362

ISSN 1007-9327 (print) ISSN 2219-2840 (online)

META-ANALYSIS

Association of non-alcoholic fatty liver and metabolic-associated fatty liver with COVID-19 outcomes: A systematic review and meta-analysis

Gowthami Sai Kogilathota Jagirdhar, Rakhtan K Qasba, Harsha Pattnaik, Kaanthi Rama, Akshat Banga, Shiva Teja Reddy, Anna Carolina Flumignan Bucharles, Rahul Kashyap, Praveen Reddy Elmati, Vikas Bansal, Yatinder Bains, Theodore DaCosta, Salim Surani

Specialty type: Gastroenterology and hepatology

Provenance and peer review: Invited article; Externally peer reviewed.

Peer-review model: Single blind

Peer-review report's scientific quality classification

Grade A (Excellent): 0
Grade B (Very good): B
Grade C (Good): C, C
Grade D (Fair): 0
Grade E (Poor): 0

P-Reviewer: Pham TTT, Viet Nam; Protopapas AA, Greece; Silva LD, Brazil

Received: December 29, 2022
Peer-review started: December 29, 2022
First decision: February 15, 2023
Revised: February 25, 2023
Accepted: April 28, 2023
Article in press: April 28, 2023
Published online: June 7, 2023

Gowthami Sai Kogilathota Jagirdhar, Department of Medicine, Saint Michaels Medical Center, Newark, NJ 07102, United States

Rakhtan K Qasba, Department of Medicine, Green Life Medical College and Hospital, Dhaka 1205, Bangladesh

Harsha Pattnaik, Department of Medicine, Lady Hardinge Medical College, New Delhi 110001, India

Kaanthi Rama, Shiva Teja Reddy, Department of Medicine, Gandhi Medical College, Telangana 500003, India

Akshat Banga, Department of Medicine, Sawai Man Singh Medical College, Jaipur 302004, Rajistan, India

Anna Carolina Flumignan Bucharles, Department of Medicine, Universidade Positivo, Curitiba 81290-000, PR, Brazil

Rahul Kashyap, Research, WellSpan Health, York, PA 17403, United States

Praveen Reddy Elmati, Department of Interventional Pain Medicine, University of Louisville, Louisville, KY 40292, United States

Vikas Bansal, Department of Internal Medicine, Mayo Clinic, Rochester, MN 55902, United States

Yatinder Bains, Theodore DaCosta, Department of Gastroenterology, Saint Michaels Medical Center, Newark, NJ 07102, United States

Salim Surani, Department of Medicine, Texas A&M University, College Station, TX 77843, United States

Corresponding author: Salim Surani, FCCP, MD, MHSc, Professor, Department of Medicine, Texas A&M University, Administration Building, 400 Bizzell St, College Station, TX 77843, United States. srsurani@hotmail.com

Abstract

BACKGROUND

Non-alcoholic fatty liver disease (NAFLD) and metabolic-associated fatty liver disease (MAFLD) are on the rise like any other liver disease, and tend to affect 25% of the United States population. The impact of NAFLD and MAFLD on patients with coronavirus disease 2019 (COVID-19) remains unclear.

AIM

To identify the association of NAFLD and MAFLD with mortality, hospitalization, hospital length of stay, and supplemental oxygen utilization in COVID-19 patients.

METHODS

A systematic review of literature on Cochrane, Embase, PubMed, ScienceDirect, and Web of Science databases was conducted from January 2019 to July 2022. Studies that evaluated NAFLD/MAFLD using laboratory methods, noninvasive imaging, or liver biopsy were included. The study protocol was registered in PROSPERO (ID CRD42022313259) and PRISMA guidelines were followed. The National Institutes of Health quality assessment tool was used to assess the quality of the studies. Pooled analysis was conducted using software Rev Man version 5.3. The stability of the results was assessed using sensitivity analysis.

RESULTS

Thirty-two studies with 43388 patients were included in the meta-analysis of whom 8538 (20%) patients were observed to have NAFLD. There were 42254 patients from 28 studies included in the mortality analysis. A total of 2008 patients died from COVID-19; 837 (10.52%) in the NAFLD group and 1171 (3.41%) in the non-NAFLD group. The odds ratio (OR) was 1.38 for mortality with a 95% confidence interval (95%CI) = 0.97-1.95 and P = 0.07. A total of 5043 patients from eight studies were included in the hospital length of stay analysis. There were 1318 patients in the NAFLD group and 3725 patients in the non-NAFLD group. A qualitative synthesis showed that the mean difference in hospital length of stay was about 2 d between the NAFLD and non-NAFLD groups with a 95%CI = 0.71-3.27 and P = 0.002. For hospitalization rates, the OR was 3.25 with a 95%CI of 1.73-6.10 and P = 0.0002. For supplemental oxygen utilization, the OR was 2.04 with a 95%CI of 1.17-3.53 and P = 0.01.

CONCLUSION

Our meta-analysis suggests that there are increased odds of hospitalization, longer hospital length of stay, and increased use of supplemental oxygen in NAFLD/MAFLD patients.

Key Words: Non-alcoholic fatty liver; Fatty liver; Coronavirus; COVID-19; Metabolic-associated fatty liver

©The Author(s) 2023. Published by Baishideng Publishing Group Inc. All rights reserved.

Core Tip: Metabolic-associated fatty liver disease (MAFLD) is like non-alcoholic fatty liver disease (NAFLD) and is a hepatic presentation of metabolic syndrome. They are widely prevalent. It is estimated that 25% of the United States population have this condition. The association and effect size between fatty liver disease and coronavirus disease 2019 (COVID-19) infection is still unconfirmed. The discrepancies in the available literature may be due to study design, confounding, small study population, and heterogeneity. We performed a systematic review and meta-analysis to study the impact of NAFLD/MAFLD on mortality, hospitalization, hospital length of stay, and supplemental oxygen utilization in COVID-19 patients.

Citation: Jagirdhar GSK, Qasba RK, Pattnaik H, Rama K, Banga A, Reddy ST, Flumignan Bucharles AC, Kashyap R, Elmati PR, Bansal V, Bains Y, DaCosta T, Surani S. Association of non-alcoholic fatty liver and metabolic-associated fatty liver with COVID-19 outcomes: A systematic review and meta-analysis. *World J Gastroenterol* 2023; 29(21): 3362-3378

URL: https://www.wjgnet.com/1007-9327/full/v29/i21/3362.htm

DOI: https://dx.doi.org/10.3748/wjg.v29.i21.3362

INTRODUCTION

Severe acute respiratory syndrome coronavirus 2 (SARS-CoV-2) is one of the subspecies of coronavirus that is responsible for causing coronavirus disease 2019 (COVID-19), the respiratory illness responsible for the ongoing COVID-19 pandemic. The first detected case was reported back in December of 2019 from Wuhan, China[1]. Since then, it has spread worldwide leading to a global pandemic. As of 12 December 2022, over 650 million confirmed cases have been reported with more than 6 million deaths [2]. Most COVID-19 cases are mild to moderate with usual signs and symptoms varying from general fatigue, fever, and dry cough to some very unusual ones like loss of smell and taste. In the severe form, it is associated with several comorbidities such as diabetes, hypertension, obesity, chronic obstructive pulmonary disease, and other cardiovascular diseases[3,4]. Patients with metabolic syndrome (MS) having obesity, hyperglycemia, dyslipidemia, and hypertension had worse outcomes in COVID-19[5,6]. A retrospective study from Cleveland Clinic, United States concluded that patients with MS were 77% more likely to be hospitalized, 56% more likely to be admitted to the intensive care unit, and 81% more likely to die from COVID-19[6]. A recent consensus of experts proposed redefining non-alcoholic fatty liver disease (NAFLD) as metabolic-associated fatty liver disease (MAFLD)[7-9]. It is now considered the hepatic form of MS[10] and is one of the most common etiologies of chronic liver diseases (CLDs). It has an estimated global prevalence rate of about 24%[11]. These patients may have a higher risk of hospitalization and severity of COVID-19 according to recently published reports. A cohort of Chinese patients indicated a higher risk of respiratory disease progression in MAFLD patients[12]. In another subsequent study, there was an increased risk for COVID-19 progression in younger patients with MAFLD[13]. However, there is still conflicting evidence addressing the severity of COVID-19 in MAFLD and NAFLD patients. Prior meta-analysis of a small number of studies did not detect worse outcomes in NAFLD/MAFLD patients with COVID-19[14-16].

Therefore, we conducted this systematic review and meta-analysis to assess the effects of NAFLD or MAFLD on mortality, hospitalization, length of hospital stay, and supplemental oxygen utilization among patients with COVID-19.

MATERIALS AND METHODS

This review is reported following the Preferred Reporting Items for Systematic Reviews and Meta-Analysis (PRISMA) statement[17] as indicated in the PRISMA checklist and was registered with PROSPERO (ID CRD42022313259; www.crd.york.ac.uk/prospero).

Search and selection

A literature search was performed in six bibliographic databases PubMed, Cochrane, Embase, Science Direct, and Web of Science from January 2020 to July 2022. Using a combination of keywords and medical subject headings, we used vocabulary related to "COVID-19" OR "SARS-CoV-2" AND "NASH" OR "NAFLD" OR "non-alcoholic fatty liver disease" OR "fatty liver" OR "metabolic syndrome" (Supplementary Table 1 shows the search strategy for the study).

Six authors (Jagirdhar GSK, Qasba RK, Kashyap R, Flumignan Bucharles AC, Banga A, and Reddy ST) were involved in the study selection. After removing duplicates using Endnote reference manager software, two authors did the title and abstract screening independently using the Rayyan software (https://rayyan.ai/). Studies satisfying the inclusion criteria were retrieved and screened for full-text eligibility. Conflicts between two authors on study selection were resolved among the authors or were solved by an additional third arbiter in case a consensus could not be reached. We included observational studies that studied mortality, hospitalization, hospital length of stay, and supplemental oxygen utilization outcomes in COVID-19 patients. We included studies that assessed NAFLD/MAFLD using lab assessment (fibrosis-4 [FIB-4], aminotransferase/platelet ratio index, fibrosis score, hepatic steatosis index [HIS]), non-invasive imaging (elastography, liver ultrasound or computed tomography [CT] scan, magnetic resonance elastography, liver stiffness measurement), or liver biopsy. For studies that diagnosed NAFLD using biomarkers/lab diagnosis, we only included studies that measured NAFLD prior to index admission since acute COVID infection can increase biomarker/lab values leading to misdiagnosis as NAFLD. We excluded studies that were: (1) Systematic reviews; (2) meta-analyses; (3) literature reviews; (4) survey studies; (5) case reports; (6) animal studies; (7) single-arm studies; (8) studies that do not measure NAFLD/MAFLD/fatty liver; (9) not a retrospective or prospective study; (10) randomized controlled trials; (11) studies not related to COVID-19 patients; (12) not in English language; and (13) abstract only studies. We studied NAFLD/MAFLD patients together since recent studies are emerging that NAFLD is related to MS both mutually and bi-directionally. We included studies that compared no or mild NAFLD/MAFLD patient outcomes to moderate or severe NAFLD/MAFLD patient outcomes. We also searched systematic reviews and meta-analyses obtained from our search for eligible articles and added studies meeting our inclusion criteria. When multiple publications used overlapping study populations, we included the study with greater sample size. We grouped studies for the meta-analysis based on mortality, hospitalization, hospital length of stay, and supple-

mental oxygen utilization outcomes.

Data extraction

Three independent authors (Qasba RK, Banga A, Flumignan Bucharles AC) performed data extraction from all of the included studies into a prepiloted data extraction form in Microsoft Excel. A fourth author (Jagirdhar GSK) independently assessed the extracted data for validation. The following was extracted from each study: (1) General information: First author, title, digital object identifier, and year of publication; (2) study characteristics: Study site/country, study period, number of centers, journal, study design; (3) participant characteristics: Number of NAFLD/MAFLD and non-NAFLD/MAFLD patients and their demographic characteristics, method of assessment of NAFLD; and (4) outcomes: Number of patients with the events (mortality, hospital length of stay, hospitalization, and supplemental oxygen utilization) in NAFLD/MAFLD and non-NAFLD/MAFLD populations.

Statistical analyses

The Review Manager (RevMan) [Computer application] Version 5.4.1, the Cochrane Collaboration, 2020 was used to assess all results[18]. Using a random-effects model, crude odds ratios (ORs) for each study with corresponding 95% confidence intervals (CIs) were calculated from raw data for events and non-events from each research[19]. $P < 0.05$ was considered statistically significant for the analysis. Forest plots were generated to present the results of the meta-analyses. A previously proven technique was used to transform the median to mean to examine continuous outcomes[20]. The estimates for mean differences were then produced using the random effects model[19]. To measure study heterogeneity, the Cochrane Q and the I^2 statistics were used[19]. Low-level heterogeneity was defined as I^2 20%[19]. The stability of the results was assessed using sensitivity analysis. Egger's test and funnel plots were used to determine the likelihood of publication bias[21].

Quality assessment

The National Institutes of Health scale was used to assess case control, cohort, and randomized controlled trials for appraisal of study quality. As per the scale, studies were classified into three categories: good, fair, or poor. Five authors (Jagirdhar GSK, Qasba RK, Banga A, Rama K, Pattnaik H) independently performed the quality assessment of the included studies, and any discrepancies were resolved through discussion.

RESULTS

Search and selection

A total of 1084 records were identified from the initial search, of which 242 were excluded as duplicates and 842 articles were selected for the screening of title and abstract. Eighty-seven were chosen for full-text screening and a total of thirty-two studies met the inclusion criteria. These papers were eligible for qualitative and quantitative.

Figure 1 shows the PRISMA diagram for the study selection process. Since we included studies that compared mortality, hospitalization, hospital length of stay, and supplemental oxygen utilization in mild or no NAFLD/MAFLD to moderate to severe NAFLD/MAFLD. We excluded studies that did not present these outcomes or those that did not mention the method of NAFLD assessment[22-28].

Characteristics of included studies

We analyzed data for a total of 43388 patients from 32 studies in the meta-analysis of which 8538 (20%) patients were observed to have NAFLD and 34850 did not have NAFLD. The studies observed the outcomes of patients infected with COVID-19 with and without NAFLD/MAFLD. The outcomes recorded were the rate of hospitalization, length of stay in the hospital, supplemental oxygen requirement, and mortality of patients in both groups.

All 29 of 32 studies reported mortality data for COVID-19 infection. Ten studies reported hospital length of stay, four studies reported need for hospitalization, and four reported supplemental oxygen utilization. The main characteristics of the included studies are summarized in Table 1.

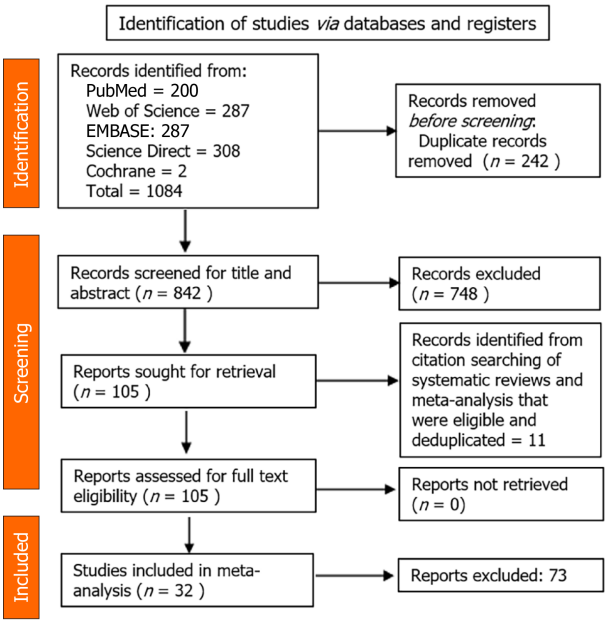
NAFLD/MAFLD and mortality outcomes in COVID-19: A total of 42254 patients from 28 studies were included in the qualitative analysis. A total of 2008 patients died from COVID-19: 837 (10.52%) in the NAFLD group and 1171 (3.41%) in the non-NAFLD group. The OR was 1.38 for mortality with a 95%CI = 0.97-1.95, I^2 = 84%, and P = 0.07. Figure 2A shows the forest plot and meta-analysis of mortality outcomes in COVID-19 patients. Figure 2B shows the sensitivity analysis of the studies. We failed to observe an association between NAFLD/MAFLD and in-hospital mortality in COVID-19 patients. Visual inspection of the standard error plots for the mortality meta-analysis (Supplementary Figure 1) suggests symmetry without an underrepresentation of studies of any precision. No publication bias was found on Egger's test, P = 0.466.

Table 1 Main characteristics of the included studies in the systematic review and meta-analysis

Serial No.	Ref.	Country	Study design	NAFLD, *n*	No NAFLD, *n*	mean ± SD	Male, *n*	Measure of NAFLD	Measure of NAFLD
1	Calapod *et al* [27]	Romania	Prospective descriptive study	47	79	66.32 ± 13.72	57.20%	Imaging evidence (ultrasound or computer tomography)	Biochemical enzymes (liver function test) within the past 12 mo
2	Campos-Varela *et al*[28]	Spain	Prospective observational (cohort) study	271	29	55.25 ± 11.69	49%	Liver steatosis by hepatic steatosis index	Transient elastography by controlled attenuation parameter
3	Chang *et al*[29]	South Korea	Retrospective cohort study	2082	1040	-	30.72%	FLI index	
4	Chen *et al*[30]	United States	Retrospective single-center cohort study	178	164	62.6 ± 15.6	53.50%	Liver steatosis	Imaging evidence of steatosis > 30 d before COVID-19 diagnosis, or hepatic steatosis index
5	Çoraplı *et al* [31]	Turkey	Retrospective cohort study	106	308	-	56.04%	Hepatic-to-splenic attenuation ratio	
6	Davidov-Derevynko *et al*[32]	Israel	Single center retrospective cohort study	47	335	58.6 ± 18.6	61%	Imaging, previous medical records, admission fibrosis-4	Prior liver enzymes
7	Demir *et al*[33]	Turkey	Retrospective cohort study	349	270	51.6 ± 9.65	58.60%	Fibrosis-4 index	
8	Ji *et al*[34]	China	Cohort	19	35	43.6 ± 14.1	58.6	Fibrosis-4 index, APRI, ultrasound	
9	Effenberger *et al*[35]	Austria	Prospective study	12	20	-	40.62%	Liver stiffness measurements and controlled attenuation parameter with a fibro scan	Liver and spleen sonography and elastography
10	Elfeki *et al*[36]	United States	Retrospective cohort study	88	285	63.3 ± 14.8	52%	Prior data lab values	
11	Forlano *et al* [14]	United Kingdom	Retrospective cohort study	61	132	-	60%	Fibrosis-4 index	Imaging (either ultrasound or computerized tomography) or past medical history
12	Hashemi *et al* [37]	United States	Retrospective cohort	55	294	63.4 ± 16.5	55.4%	Hepatic steatosis on any prior imaging studies or liver histology	
13	Huang *et al*[38]	China	Retrospective cohort study	86	194	43.6 ± 17.8	52.10%	Hepatic steatosis index	
14	Hussain *et al* [39]	Pakistan	Cross sectional study	87	63	59.73 ± 11.35	56%	Clinical parameters like hepatomegaly and lab parameters like AST, ALT	
15	Kim *et al*[40]	United States	Observational cohort study	456	411	56.9 ± 14.5	54.70%	Fibrosis by magnetic resonance elastography	Fibro scan, fibrosis-4, or biopsy
16	Madan *et al*[41]	India	Case control study	289	157	-	64.5%	Liver attenuation index	
17	Marjot *et al*[42]	United States	Cohort study	322	367	58 ± 15.6	62.40%	Reported by clinician	
18	Mushtaq *et al* [13]	Qatar	Prospective study	320	269	-	84.71%	Hepatic steatosis index	
19	Romero-Cristóbal *et al*[43]	Spain	Prospective observational (cohort) study	81	96	59.58 ± 13.79	71.96	Fibrosis-4 index	
20	Rentsch *et al* [44]	United States	Retrospective cohort study	377	139	65.8 ± 7.8	95.4	Fibrosis-4 index	
21	Shao *et al*[45]	China	Observational	37	84	60.6 ±	64.46%	Liver enzyme/GGT	

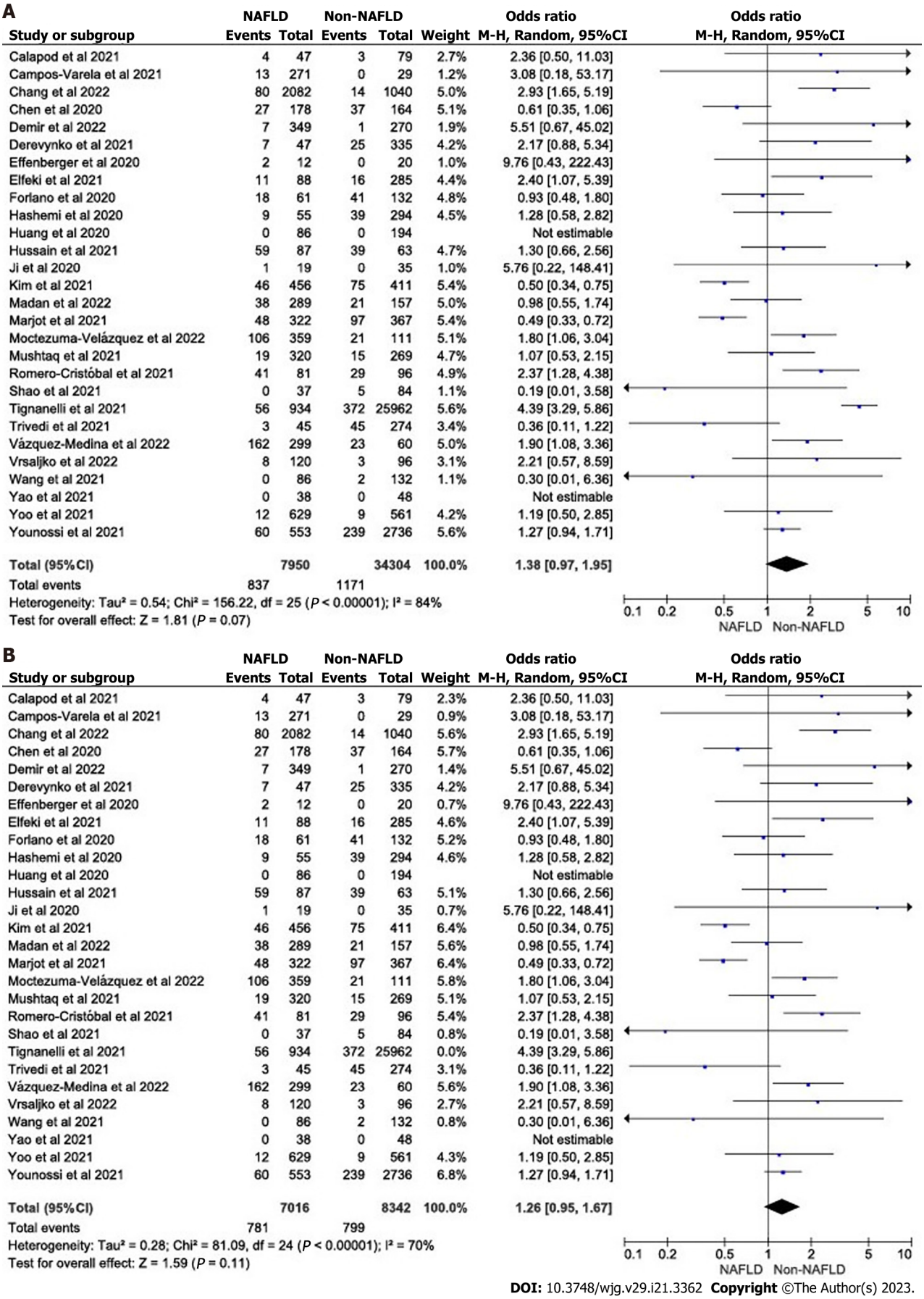
			cohort study			13.5		twice upper limit of normal	
22	Targher *et al* [46]	China	Cohort study	50	43	-	48%	Fibrosis-4	NAFLD fibrosis score
23	Tignanelli *et al* [47]	United States	Retrospective cohort study	934	25962	51 ± 23.7	56%	Elevated ALT level on 3 separate dates	
24	Trivedi *et al* [48]	United States	Case control study	45	274	65 (median)	50%	Abdominal imaging (computed tomography, magnetic resonance imaging, or ultrasound)	
25	Vázquez-Medina *et al* [49]	Mexico	Retrospective case control study	299	60	54.3 ± 14.69	22.01%	Fibrosis-4 index	
26	Moctezuma-Velázquez *et al* [50]	Mexico	Retrospective cohort study	359	111	51.6 ± 14.8	63%	Computed tomography scans	
27	Vrsaljko *et al* [51]	Republic of Croatia	Prospective observational (cohort) study	120	96	59.3 ± 12.6	63.43%	Ultrasound	Difference between liver and spleen computed tomography attenuation
28	Wang *et al*[52]	China	Retrospective cohort study	86	132	-	50.40%	Ultrasound parameters	
29	Yao *et al*[53]	China	Retrospective cohort study	38	48	43.2 ± 15.45	58.10%	Hepatic steatosis index	NAFLD fibrosis score
30	Yoo *et al*[54]	South Korea	Retrospective cohort study	629	561	-	-	Hepatic steatosis index, FLI, claims based NAFLD	
31	Younossi *et al* [55]	United States	Observational cohort study	553	2736	-	49.55%	Abdominal imaging, magnetic resonance imaging, computer tomography, ultra-sound	
32	Zhou *et al*[56]	China	Cohort study	55	55	42.1 ± 11.4	74.50%	Computed tomography	

Non-alcoholic fatty liver disease is used synonymously with metabolic-associated fatty liver disease in this table.
ALT: Alanine aminotransferase; APRI: Aminotransferase/platelet ratio index; AST: Aspartate aminotransferase; COVID-19: Coronavirus disease 2019; FLI: Fatty liver index; GGT: Gamma-glutamyl transferase; NAFLD: Non-alcoholic fatty liver disease.



DOI: 10.3748/wjg.v29.i21.3362 **Copyright** ©The Author(s) 2023.

Figure 1 PRISMA flowchart outlining the study search.



DOI: 10.3748/wjg.v29.i21.3362 **Copyright** ©The Author(s) 2023.

Figure 2 Forest plot for mortality outcomes in coronavirus disease 2019 patients. A: In coronavirus disease 2019 (COVID-19) patients with and without non-alcoholic fatty liver disease/metabolic-associated fatty liver disease (NAFLD/MAFLD); B: In COVID-19 patients with and without NAFLD/MAFLD

sensitivity analysis after excluding Tignanelli *et al*[47]. CI: Confidence interval.

NAFLD/MAFLD and hospitalization in COVID-19: Four studies were taken for the quantitative analysis with 28199 patients to assess the need for hospitalization in NAFLD and non-NAFLD groups with COVID-19. A total of 4302 patients were hospitalized for COVID-19: 765 (50.83%) patients from the NAFLD group and 3537 (13.25%) patients from the non-NAFLD group. The OR was 3.25 with a 95%CI of 1.73-6.10, I^2 = 92%, and a P = 0.0002. Figure 3A shows the forest plot for hospitalization in COVID-19 patients with and without NAFLD/MAFLD. Figure 3B shows the sensitivity analysis of the studies. Visual inspection of the standard error plots for the need for hospital admission meta-analysis showed (Supplementary Figure 2) symmetry without an underrepresentation of studies of any precision. No publication bias was found (Egger's test, P = 0.254). However, as there were < 10 studies included in the analysis, publication bias cannot be completely excluded.

NAFLD/ MAFLD and hospital length of stay in COVID-19: A total of 5043 patients from 10 studies were included in the qualitative analysis. A total of 1318 patients were in the NAFLD group and 3725 patients were in the non-NAFLD group. A qualitative synthesis showed that the mean difference in hospital length of stay was 1.99 d between the NAFLD and non-NAFLD groups with a 95%CI = 0.71-3.27, I^2 = 70%, and P = 0.002. This denotes an average of about 2 d of additional hospital stays among NAFLD/MAFLD patients with COVID-19. Figure 4A shows a forest plot and meta-analysis of hospital length of stay in COVID-19 patients with and without NAFLD/MAFLD. Figure 4B shows the sensitivity analysis of the studies. Visual inspection of the standard error plots for the hospital length of stay meta-analysis (Supplementary Figure 3) suggests symmetry without an underrepresentation of studies of any precision. Publication bias was found on Egger's test, P = 0.013.

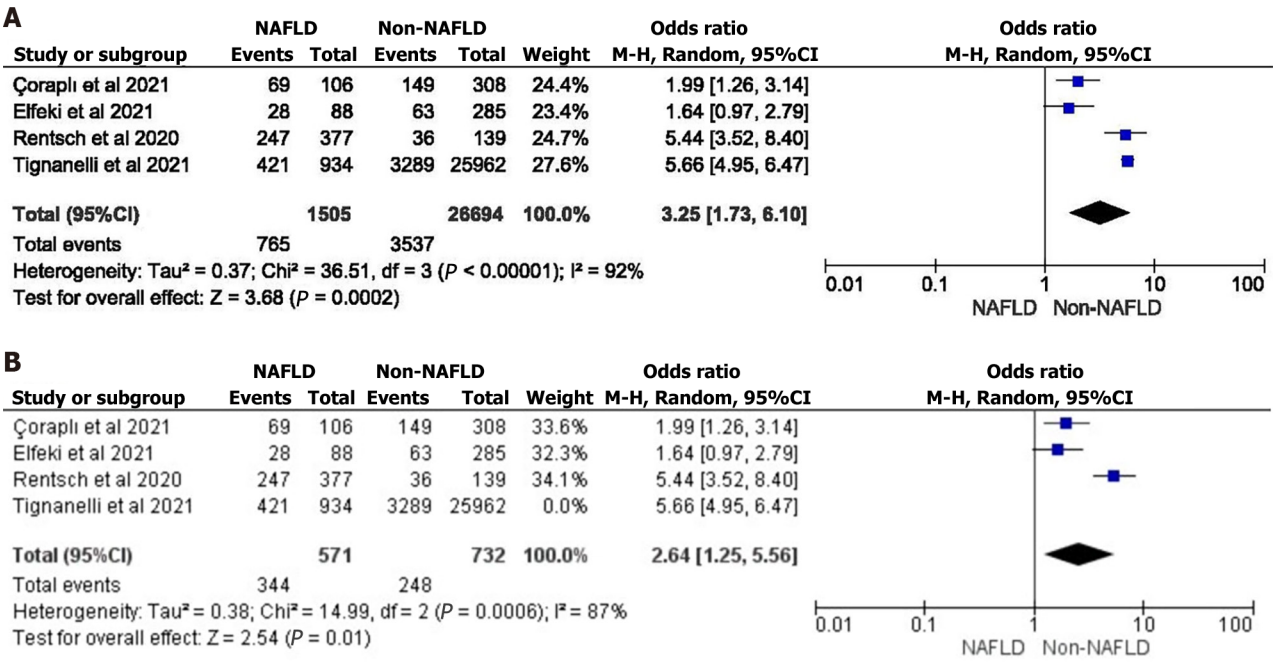
NAFLD/MAFLD and supplemental oxygen utilization in COVID-19: A total of 3609 patients from four studies were included in the qualitative analysis to assess the requirement for supplemental oxygen in COVID-19 patients during their in-hospital stay. A total of 170 (7.30%) patients in the NAFLD group and 96 (7.48 %) in the non-NAFLD group required supplemental oxygen. The OR was 2.04 with a 95%CI of 1.17-3.53, I^2 = 56%, and P = 0.01. Figure 5A shows a forest plot and meta-analysis of supplemental oxygen utilization in COVID-19 patients with and without NAFLD/MAFLD. Figure 5B shows the sensitivity analysis of the studies. Visual inspection of the standard error plots for the need for supplemental oxygen requirement meta-analysis (Supplementary Figure 4) suggests symmetry without an underrepresentation of studies of any precision. No publication bias was found on Egger's test, P = 0.500. However, as there were < 10 studies included in the analysis, publication bias cannot be completely excluded.

Quality assessment

Figures for quality assessment of case-control, cross-sectional, and cohort studies included in our study are attached with Supplementary material. For case-control studies, the quality assessment of included studies identified three as good quality, one as fair, and no poor rated studies. None of the studies were able to recruit a concurrent control or blind the outcome assessors. Only Madan *et al*[41] discussed reasons for selecting included participants, providing a sample size justification additionally, Trivedi *et al*[48] were the only ones to include a random selection of participants. For included cohorts, 19 were identified as good and 10 as fair with no poor rated studies. Only Kim *et al*[40], Yoo *et al*[54], and Zhou *et al*[56] could provide a sample size justification additionally studies scored poorly on blinding of outcome assessors with only Marjot *et al*[42] and Zhou *et al*[56] being able to do so, Furthermore Ji *et al*[34] and Huang *et al*[38] were the only ones to measure exposure more than once for each person during the study period (Supplementary Tables 2 and 3 show the Quality assessment of the studies included based on the National Institutes of Health quality appraisal tool for case control, cohort, and cross-sectional studies).

DISCUSSION

Our systematic review and meta-analysis of 32 studies and 43388 COVID-19 patients, of which 8538 (20%) patients were observed to have NAFLD/MAFLD, provided a comprehensive assessment of mortality, need for hospitalization, hospital length of stay, and need for supplemental oxygen in COVID-19-afflicted patients with fatty liver disease. In the current meta-analysis, there was no relation between pre-existing NAFLD/MAFLD and COVID-19-related mortality. The results for the unadjusted analysis showed an increased risk of mortality, but the results were not statistically significant. Similar results were seen in a prior meta-analysis[57]. Meta-analysis of seven studies by Hayat *et al*[58] on MAFLD and COVID-19 mortality found an OR of 1.45 and a non-significant 95%CI = 0.74-2.84 (P < 0.01).



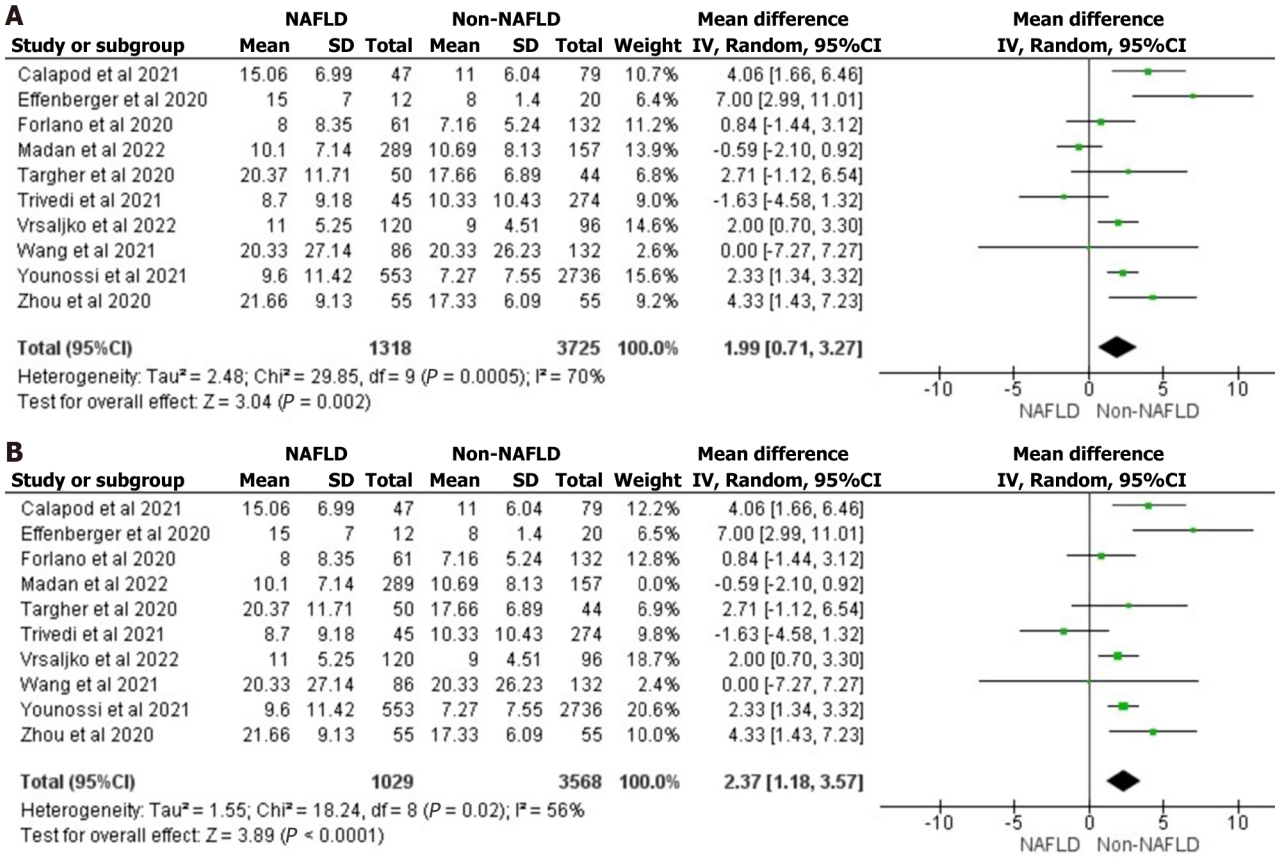
DOI: 10.3748/wjg.v29.i21.3362 **Copyright** ©The Author(s) 2023.

Figure 3 Forest plot for hospitalization and need for hospitalization in coronavirus disease 2019 patients. A: Forest plot for hospitalization in coronavirus disease 2019 (COVID-19) patients with and without non-alcoholic fatty liver disease/metabolic-associated fatty liver disease (NAFLD/MAFLD); B: Forest plot for need for hospitalization in COVID-19 patients with and without NAFLD/MAFLD sensitivity analysis after excluding Tignanelli *et al*[47]. CI: Confidence interval.

As per our meta-analysis, patients with NAFLD/MAFLD had higher hospitalization rates compared to non-NAFLD/MAFLD patients (OR = 2.71, 95%CI: 1.10-6.70; P = 0.03). COVID-19 is associated with increased inflammation and thrombosis, while NAFLD/MAFLD are states of chronic inflammation. When occurring together, these may worsen disease status causing increased hospitalization rates. Contrarily, some studies have reported no increase in disease severity or need for hospitalization in NAFLD patients with COVID compared to controls. This could be due to the small study population and the retrospective nature of the study results[39,54]. Since our meta-analysis may be one of the largest to date, the results provided are expected to be closer to the true value. Our meta-analysis found that patients with NAFLD/MAFLD had a statistically significant longer hospital length of stay compared to those without. An unadjusted assessment of eight studies found that patients with pre-existing NAFLD, on average, spent an additional 2 d in the hospital compared to COVID-19 patients without NAFLD. Patients with NAFLD have ongoing inflammation processes which compound the disease process of COVID-19, thus leading to a more severe course of illness. This could explain the higher hospitalization rates and longer duration of hospital stay. Previous studies have reported similar results with longer hospital stays for NAFLD patients afflicted with COVID-19[32,58,59]. On the contrary, some studies reported no difference in the duration of hospital stay in those with or without NAFLD[52,60].

Our meta-analysis of four studies revealed that NAFLD patients had a greater need for supplemental oxygen as compared to controls. NAFLD patients may have a more severe disease course and therefore, require supplemental oxygen during their hospital stay. One previous study reported that NAFLD patients had a more frequent need for oxygen support[51].

CLD due to NAFLD has seen a rising trend over the years. Over 83 million Americans suffered from NAFLD with a prevalence rate of 26% according to data from 2015. This value is said to rise by 21% to over 100 million patients by the year 2030. The growing epidemics of obesity and diabetes mellitus II have played a major role in increasing the prevalence of NAFLD worldwide, including the progression of NAFLD to non-alcoholic steatohepatitis (NASH), cirrhosis, and even hepatocellular malignancy[61,62]. NAFLD is found in more than 50% of individuals suffering from obesity or type 2 diabetes mellitus. In their study, Estes *et al*[61] reported the median age of NAFLD patients to be about 50 years. They also found that more males suffered from NAFLD as compared to females. These results are similar to our study. The absence of an established screening method and global health policies focusing on NAFLD, and primary care interventions lead to a substantial increase in patients with NAFLD going undetected [55]. It also means that it is up to the clinician's preference and choice of the screening tool to measure NAFLD, thus creating a selection bias amongst various studies. This discrepancy could be observed in the studies included in our meta-analysis as multiple screening modalities were used in different clinical settings, including HSI, FIB-4 scoring, CT scan of the liver, liver function tests, and liver biopsy among others.

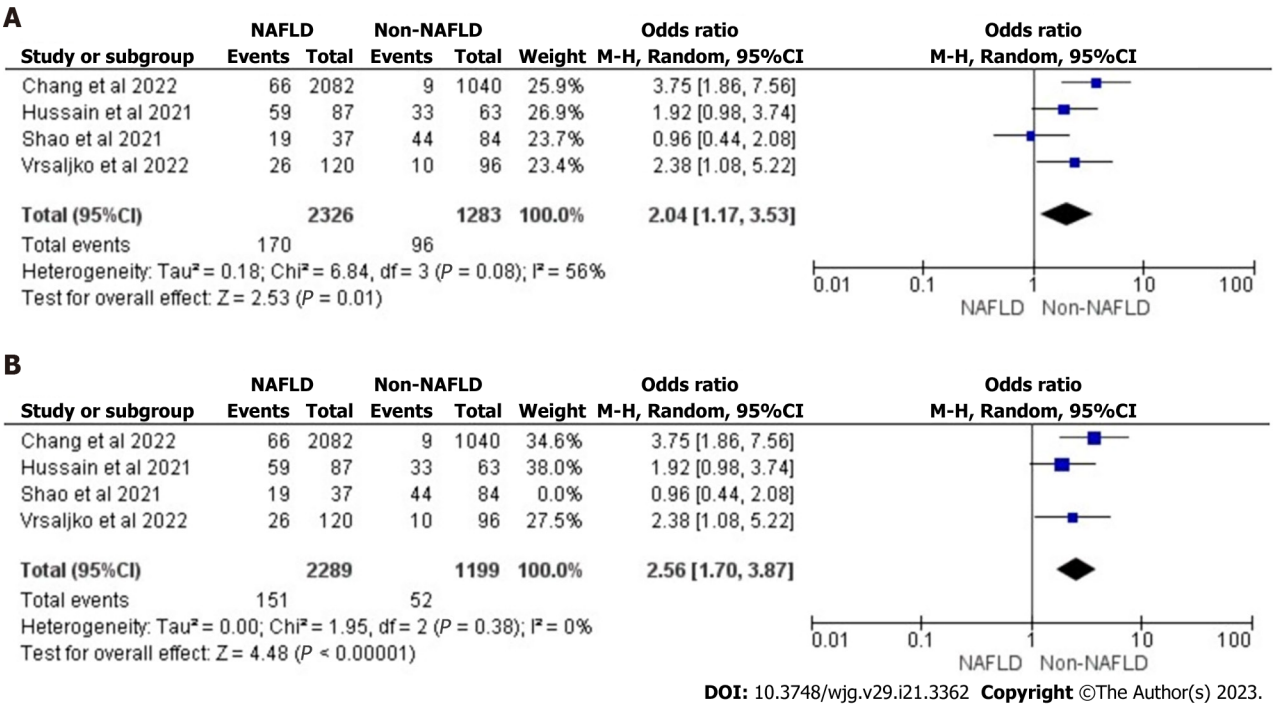


DOI: 10.3748/wjg.v29.i21.3362 **Copyright** ©The Author(s) 2023.

Figure 4 Forest plot for hospital length of stay in coronavirus disease 2019 patients. A: In coronavirus disease 2019 (COVID-19) patients with and without non-alcoholic fatty liver disease/metabolic-associated fatty liver disease (NAFLD/MAFLD); B: In COVID-19 patients with and without NAFLD/MAFLD sensitivity analysis after excluding Madan *et al*[41]. CI: Confidence interval.

The presence of NAFLD confers additional susceptibility to COVID-19 infection in individuals exposed to SARS-CoV-2[63]. Pre-existing NAFLD at the time of COVID-19 diagnosis can be an indicator of increased severity of infection and utilization of health care services. As mentioned earlier, more than half of the individuals with type 2 diabetes mellitus (2nd most common comorbidity in COVID-19) have comorbid NAFLD to a certain degree[60]. Similarly, NAFLD is associated with multiple risk factors like cardiovascular diseases, obesity, and coexisting chronic lung disease which independently influences COVID-19 susceptibility and severity[61,64-68]. The impact of NAFLD on disease severity is seen through a blunted immune response to SARS-CoV-2 infection in COVID-19, leading to an increased risk of severe disease[30,13,47,55]. A retrospective observational study observed that ongoing inflammation in NAFLD puts patients with active COVID-19 infection at an increased risk of thromboembolism and associated mortality[51]. Various SARS-CoV-2 entry factors like angiotensin-converting enzyme (ACE), a disintegrin and metalloprotease 17, dipeptidyl peptidase 4, and transmembrane protease, serine 2 and NAFLD-related genes such as ACE, dipeptidyl peptidase 4, interleukin 10 (IL-10), tumor necrosis factor (TNF), and AKT1 as well as cytokine-mediated signaling, phosphoinositide 3 kinase-Akt, AMP-activated protein kinase, and mechanistic target of rapamycin signaling pathways have been identified which sheds light on the propensity for increased severity of illness in SARS-CoV-2 infected NAFLD patients. The spike protein of coronavirus has a high affinity for the receptor of ACE, which is found in the lung and the hepatobiliary cells. Furthermore, COVID-19 infection upregulates the expression of ACE receptors[69]. This leads to the hyperactivation of an immune cascade that damages the hepatocytes[70,71]. Chronic low-grade inflammatory state in individuals with NAFLD/MS creates a hypoxic environment for adipocytes leading to their dysfunction. This promotes the increased release of pro-inflammatory cytokines IL-6, IL-8, C-reactive protein, and TNF-α, and the recruitment of macrophages, B cells, and T cells. This effect is compounded by the systemic hyperactivation of the inflammatory cascade in active COVID-19 infection, which aggravates the ongoing inflammation of the hepatocytes, leading to decompensation of NAFLD and extensive hepatocyte damage[72]. Additionally, patients with NAFLD have insulin resistance, which further serves as a conducive ground for widespread inflammation[73,74].

Bramante *et al*[75] conducted a retrospective study that showed that with each additional year of having NAFLD/NASH the risk of hospitalization for COVID-19 increased. An assessment of the association between liver fibrosis scores and the clinical outcomes in patients with COVID-19 reported



DOI: 10.3748/wjg.v29.i21.3362 **Copyright** ©The Author(s) 2023.

Figure 5 Forest plot for need for supplemental oxygen utilization in coronavirus disease 2019 patients. A: In coronavirus disease 2019 (COVID-19) patients with and without non-alcoholic fatty liver disease/metabolic-associated fatty liver disease (NAFLD/MAFLD); B: In COVID-19 patients with and without NAFLD/MAFLD sensitivity analysis after excluding Shao *et al*[45]. CI: Confidence interval.

that a one-point score increase in FIB-4 was significantly associated with increased death, but not hospitalization. The authors also found that for every unit elevation in aspartate aminotransferase/alanine aminotransferase ratio, the risk of death increased by 178%[76]. Patients with higher FIB-4 > 2.67 scores had a higher risk of developing COVID-19[77]. Therefore, primary prevention is essential to control NAFLD during its development. Bramante *et al*[75] also showed that patients on prior treatments for NAFLD such as metformin and glucagon-like-peptide 1 receptor agonists had a reduced risk of hospitalization with the most significantly decreased risk from recent bariatric surgery. This highlights the importance of obesity as a cofactor to worse outcomes in COVID-19 patients and weight loss as the most significant contributing factor to improved outcomes in NAFLD[60]. Several studies found a higher incidence of obesity and NAFLD in patients hospitalized for COVID, which can also worsen disease severity[53,59,75]. This association may be confounded by the presence of obesity, which is an independent risk factor for COVID-19 severity. Previous studies reported odds ratios after adjusting for obesity and found statistically significant results in the association between NAFLD and COVID-19[77,78]. However, in a regression analysis, Li *et al*[79] observed that NAFLD independently does not affect the prognosis of severe COVID-19. Any association between NAFLD and COVID-19 is likely attributed to the confounding effect of obesity, measured in terms of body mass index, waist circumference, and hip circumference. Further studies with a larger sample size are needed to explain the varied results observed in these studies. Roca-Fernández *et al*[63] reported that higher liver fat percentages or evidence of liver fibro-inflammation, and features of NAFLD, increased the likelihood of symptomatic COVID-19. Interestingly, they found that obese patients with higher liver fat had a higher probability of having symptomatic COVID-19 compared to obese patients with normal liver fat. This is in favor of NAFLD being an independent risk factor for COVID-19 irrespective of obesity.

Strengths and limitations

We followed rigorous methodology, adhered to PRISMA guidelines, and registered our study in PROSPERO. Most of the studies were retrospective case-control and cohort studies which can be associated with the risk of bias, particularly in the absence of adjusting for confounders. NAFLD/MAFLD patients underlying medical conditions and co-morbidities that are components of MS can interfere with the outcomes studied. We excluded studies on NAFLD/MAFLD patients with other underlying causes for liver diseases including alcoholic liver disease. We understand there may be additional etiology for liver disease in patients that are underdiagnosed and may impact our study findings. The retrospective nature of most of the studies in our analysis does not imply a causal relationship between NAFLD/MAFLD and measured outcomes. We included studies that measured NAFLD/MAFLD using non-invasive procedures such as imaging and biomarker/lab diagnosis. Since they are not the gold standard for diagnosis, there may be misclassification of patients with and without NAFLD/MAFLD. The method of diagnosis of NAFLD/MAFLD varied across studies so, there may be

some misdiagnoses that can influence the results of the study. However, we included studies that compared absent or mild NAFLD/MAFLD to moderate or severe NAFLD/MAFLD to maintain homogeneity. We considered NAFLD/MAFLD patients in the same group, however, there may be important differences between these two groups that may alter the outcomes. We observed the per-study protocol in our meta-analysis. We detected significant differences in our study population for the various outcomes measured. However, there was statistical heterogeneity in our results that should be taken into consideration. We also excluded studies in a language other than English due to difficulty with translation and interpretation of results. This can introduce bias in our study results. The studies included in our meta-analysis were from 12 different countries with more studies from China and the United States, but we consider the results to be generalizable globally. However, since the studies were from different countries the level of care at each health institution may be different, which can lead to different levels of disease severity, disease progression, and death. Our study aims for hypothesis generation and further research in NAFLD/MAFLD patients to better understand the disease pathophysiology and patient risk profiles.

CONCLUSION

Our meta-analysis suggests that NAFLD/MAFLD patients appear to have higher rates of hospital admissions and longer in-hospital stays without any increase in mortality compared to non-NAFLD/MAFLD patients. Further research is needed to explore if fatty liver disease may be a risk factor that can lead to severe COVID-19 infection.

Implications for clinical practice

NAFLD/MAFLD are chronic pandemics rapidly on the rise. There is a lack of awareness and education among healthcare professionals and patients about its health impact, morbidity, and economic impact as they progress. There is a lack of systems/protocols in place to enforce the diagnosis of NAFLD globally and as a part of regular screening in primary care clinics, diabetic clinics, and routine health care visits. Propagation of information on NAFLD and involvement of international organizations, scientific societies, and the pharmaceutical industry to improve public health policies related to NAFLD. Patient education on NAFLD/MAFLD as a co-morbid risk factor for infectious diseases such as COVID-19 like other known risk factors such as hypertension, obesity, and diabetes, and measures to diagnose and treat NAFLD actively are needed.

Implication for research

Futures research on longitudinal prospective studies with larger numbers on NAFLD/MAFLD as a risk factor for COVID-19. Future studies should focus on genetics, immunology, and molecular epidemiology to better understand the mechanisms for poor outcomes in the NAFLD population.

ARTICLE HIGHLIGHTS

Research background

Non-alcoholic fatty liver disease (NAFLD) and its hepatic manifestation metabolic-associated fatty liver disease (MAFLD) have a rising prevalence worldwide. It is a co-morbidity like obesity, hypertension, and chronic kidney disease. NAFLD/MAFLD like obesity is considered chronic inflammatory states according to recent literature. Therefore, patients with NAFLD/MAFLD are hypothesized to have worse outcomes with coronavirus disease 2019 (COVID-19).

Research motivation

Existing literature shows conflicting information on the association of NAFLD/MAFLD in COVID-19 patients. Some studies show worse outcomes with NAFLD/MAFLD and COVID-19 infection. Some studies state it is not a risk factor for severe COVID-19. Understanding the pathophysiology and pathogenesis between fatty liver disease and COVID-19 is necessary for prevention, and management of NAFLD/MAFLD patients. Insight into this relationship will help further research and better preventative and nutritional management of these patients. It is imperative to explore the relationship of NAFLD/MAFLD with COVID-19 to improve patient care and treatment protocols for better outcomes.

Research objectives

In this meta-analysis, we investigated the association between NAFLD/MAFLD with the mortality and severity of COVID-19 infection.

Research methods

A systematic review of literature across five databases was done from January 2019 to June 2022. Observational studies were included. Studies that evaluated NAFLD/MAFLD using lab assessment/biomarker assessment, non-invasive imaging, or liver biopsy were included. We registered our study protocol in Prospero and followed the "PRISMA" guidelines (Figure 1). Meta-analysis was conducted on studies with outcomes for hospitalization, hospital length of stay, supplemental oxygen utilization, and mortality of COVID-19 infection outcomes using Rev Man version 5.3. To evaluate the validity of our studies the National Institutes of Health quality assessment tool was used. The stability of the results was assessed using sensitivity analysis.

Research results

A total of 43388 patients from thirty-two studies were included in the final analysis. There were 8538 (20%) with NAFLD/MAFLD. A total of 42475 patients from twenty-nine studies were included in the mortality analysis. There was an odds ratio of 1.36, a *P* value = 0.07 for mortality with COVID-19. A total of 5043 patients from eight studies were included in the hospital length of stay analysis. NAFLD patients spent a mean hospital stay of an additional about 2 d when compared to non-NAFLD. For hospitalization rates, the odds ratio is 3.25 and a *P* value = 0.0002. For supplemental oxygen utilization, the odds ratio was 2.04 with a *P* value = 0.01. Our meta-analysis was able to show that there is an association between NAFLD/MAFLD and COVID-19. Our study aims to increase awareness that NAFLD/MAFLD may be a potential risk factor for severe outcomes in infections. More research is needed to better explain the relationship and the pathophysiology behind it.

Research conclusions

This systematic review and meta-analysis of observational studies suggests that NAFLD/MAFLD patients had higher odds of developing severe forms of COVID-19 in comparison to non-NAFLD patients. Further research to understand the causality and strength of this relationship is needed.

Research perspectives

This review was not able to clarify why the association between NAFLD/MAFLD and COVID-19 was seen. Large size prospective studies with balanced confounding factors are necessary. Since the global burden of NAFLD/MAFLD is rapidly rising, understanding genetics and immunological mechanisms will help advance treatment and prevention strategies.

FOOTNOTES

Author contributions: Jagirdhar GSK conceived and designed the study; Jagirdhar GSK, Qasba RK, Rama K, Banga A, Reddy ST, and Flumignan Bucharles AC included studies and data extraction; Jagirdhar GSK, Qasba RK, Pattnaik H, Rama K, Banga A, Elmati PR, and Bansal V contributed to the data processing; Jagirdhar GSK, Qasba RK, Pattnaik H, Rama K, Banga A, Reddy ST, Flumignan Bucharles AC, Kashyap R, Elmati PR, Bansal V, Bains Y, and DaCosta T wrote the original manuscript; Jagirdhar GSK, Kashyap R, Bains Y, DaCosta T, and Surani S revised the paper and approved the final version.

Conflict-of-interest statement: The authors have no conflicts of interest to declare.

PRISMA 2009 Checklist statement: The authors have read the PRISMA 2009 Checklist, and the manuscript was prepared and revised according to the PRISMA 2009 Checklist.

Open-Access: This article is an open-access article that was selected by an in-house editor and fully peer-reviewed by external reviewers. It is distributed in accordance with the Creative Commons Attribution NonCommercial (CC BY-NC 4.0) license, which permits others to distribute, remix, adapt, build upon this work non-commercially, and license their derivative works on different terms, provided the original work is properly cited and the use is non-commercial. See: https://creativecommons.org/Licenses/by-nc/4.0/

Country/Territory of origin: United States

ORCID number: Gowthami Sai Kogilathota Jagirdhar 0000-0003-1855-0863; Rakhtan K Qasba 0000-0001-5051-9319; Harsha Pattnaik 0000-0002-6316-7006; Kaanthi Rama 0000-0002-1691-7812; Akshat Banga 0000-0003-2626-8219; Anna Carolina Flumignan Bucharles 0000-0002-8431-2495; Rahul Kashyap 0000-0002-4383-3411; Praveen Reddy Elmati 0000-0003-1283-2368; Vikas Bansal 0000-0001-6047-5559; Yatinder Bains 0000-0002-6331-1194; Theodore DaCosta 0000-0002-1805-6323; Salim Surani 0000-0001-7105-4266.

S-Editor: Wang JJ
L-Editor: Filipodia
P-Editor: Yu HG

REFERENCES

1 **Zhou Y**, Yang Q, Chi J, Dong B, Lv W, Shen L, Wang Y. Comorbidities and the risk of severe or fatal outcomes associated with coronavirus disease 2019: A systematic review and meta-analysis. *Int J Infect Dis* 2020; **99**: 47-56 [PMID: 32721533 DOI: 10.1016/j.ijid.2020.07.029]

2 **Zádori N**, Váncsa S, Farkas N, Hegyi P, Erőss B; KETLAK Study Group. The negative impact of comorbidities on the disease course of COVID-19. *Intensive Care Med* 2020; **46**: 1784-1786 [PMID: 32601834 DOI: 10.1007/s00134-020-06161-9]

3 **Földi M**, Farkas N, Kiss S, Zádori N, Váncsa S, Szakó L, Dembrovszky F, Solymár M, Bartalis E, Szakács Z, Hartmann P, Pár G, Erőss B, Molnár Z, Hegyi P, Szentesi A; KETLAK Study Group. Obesity is a risk factor for developing critical condition in COVID-19 patients: A systematic review and meta-analysis. *Obes Rev* 2020; **21**: e13095 [PMID: 32686331 DOI: 10.1111/obr.13095]

4 **Wu S**, Zhou K, Misra-Hebert A, Bena J, Kashyap SR. Impact of Metabolic Syndrome on Severity of COVID-19 Illness. *Metab Syndr Relat Disord* 2022; **20**: 191-198 [PMID: 34995147 DOI: 10.1089/met.2021.0102]

5 **Eslam M**, Sanyal AJ, George J; International Consensus Panel. MAFLD: A Consensus-Driven Proposed Nomenclature for Metabolic Associated Fatty Liver Disease. *Gastroenterology* 2020; **158**: 1999-2014.e1 [PMID: 32044314 DOI: 10.1053/j.gastro.2019.11.312]

6 **Eslam M**, Newsome PN, Sarin SK, Anstee QM, Targher G, Romero-Gomez M, Zelber-Sagi S, Wai-Sun Wong V, Dufour JF, Schattenberg JM, Kawaguchi T, Arrese M, Valenti L, Shiha G, Tiribelli C, Yki-Järvinen H, Fan JG, Grønbæk H, Yilmaz Y, Cortez-Pinto H, Oliveira CP, Bedossa P, Adams LA, Zheng MH, Fouad Y, Chan WK, Mendez-Sanchez N, Ahn SH, Castera L, Bugianesi E, Ratziu V, George J. A new definition for metabolic dysfunction-associated fatty liver disease: An international expert consensus statement. *J Hepatol* 2020; **73**: 202-209 [PMID: 32278004 DOI: 10.1016/j.jhep.2020.03.039]

7 **Tilg H**, Effenberger M. From NAFLD to MAFLD: when pathophysiology succeeds. *Nat Rev Gastroenterol Hepatol* 2020; **17**: 387-388 [PMID: 32461575 DOI: 10.1038/s41575-020-0316-6]

8 **Kim CH**, Younossi ZM. Nonalcoholic fatty liver disease: a manifestation of the metabolic syndrome. *Cleve Clin J Med* 2008; **75**: 721-728 [PMID: 18939388 DOI: 10.3949/ccjm.75.10.721]

9 **Cheemerla S**, Balakrishnan M. Global Epidemiology of Chronic Liver Disease. *Clin Liver Dis (Hoboken)* 2021; **17**: 365-370 [PMID: 34136143 DOI: 10.1002/cld.1061]

10 **Ji D**, Qin E, Xu J, Zhang D, Cheng G, Wang Y, Lau G. Non-alcoholic fatty liver diseases in patients with COVID-19: A retrospective study. *J Hepatol* 2020; **73**: 451-453 [PMID: 32278005 DOI: 10.1016/j.jhep.2020.03.044]

11 **Zhou YJ**, Zheng KI, Wang XB, Yan HD, Sun QF, Pan KH, Wang TY, Ma HL, Chen YP, George J, Zheng MH. Younger patients with MAFLD are at increased risk of severe COVID-19 illness: A multicenter preliminary analysis. *J Hepatol* 2020; **73**: 719-721 [PMID: 32348790 DOI: 10.1016/j.jhep.2020.04.027]

12 **Lopez-Mendez I**, Aquino-Matus J, Gall SM, Prieto-Nava JD, Juarez-Hernandez E, Uribe M, Castro-Narro G. Association of liver steatosis and fibrosis with clinical outcomes in patients with SARS-CoV-2 infection (COVID-19). *Ann Hepatol* 2021; **20**: 100271 [PMID: 33099028 DOI: 10.1016/j.aohep.2020.09.015]

13 **Mushtaq K**, Khan MU, Iqbal F, Alsoub DH, Chaudhry HS, Ata F, Iqbal P, Elfert K, Balaraju G, Almaslamani M, Al-Ejji K, AlKaabi S, Kamel YM. NAFLD is a predictor of liver injury in COVID-19 hospitalized patients but not of mortality, disease severity on the presentation or progression - The debate continues. *J Hepatol* 2021; **74**: 482-484 [PMID: 33223215 DOI: 10.1016/j.jhep.2020.09.006]

14 **Forlano R**, Mullish BH, Mukherjee SK, Nathwani R, Harlow C, Crook P, Judge R, Soubieres A, Middleton P, Daunt A, Perez-Guzman P, Selvapatt N, Lemoine M, Dhar A, Thursz MR, Nayagam S, Manousou P. In-hospital mortality is associated with inflammatory response in NAFLD patients admitted for COVID-19. *PLoS One* 2020; **15**: e0240400 [PMID: 33031439 DOI: 10.1371/journal.pone.0240400]

15 **Liberati A**, Altman DG, Tetzlaff J, Mulrow C, Gøtzsche PC, Ioannidis JP, Clarke M, Devereaux PJ, Kleijnen J, Moher D. The PRISMA statement for reporting systematic reviews and meta-analyses of studies that evaluate healthcare interventions: explanation and elaboration. *BMJ* 2009; **339**: b2700 [PMID: 19622552 DOI: 10.1136/bmj.b2700]

16 **Cochrane Training**. Cochrane RevMan. [cited 15 November 2022]. Available from: https://training.cochrane.org/online-learning/core-software/revman

17 **Deeks JJ**, Higgins JP, Altman DG; group on behalf of the Cochrane Statistical Methods Group. Analysing data and undertaking meta-analyses. In: Cochrane Handbook for Systematic Reviews of Interventions. United States: John Wiley & Sons, Ltd, 2019

18 **Wan X**, Wang W, Liu J, Tong T. Estimating the sample mean and standard deviation from the sample size, median, range and/or interquartile range. *BMC Med Res Methodol* 2014; **14**: 135 [PMID: 25524443 DOI: 10.1186/1471-2288-14-135]

19 **Boutron I**, Page MJ, Higgins JP, Altman DG, Lundh A, Hróbjartsson A; group on behalf of the Cochrane Statistical Methods Group. Considering bias and conflicts of interest among the included studies. In: Cochrane Handbook for Systematic Reviews of Interventions. United States: John Wiley & Sons, Ltd, 2019

20 **Demirtas CO**, Keklikkiran C, Ergenc I, Erturk Sengel B, Eskidemir G, Cinel I, Odabasi Z, Korten V, Yilmaz Y. Liver stiffness is associated with disease severity and worse clinical scenarios in coronavirus disease 2019: A prospective transient elastography study. *Int J Clin Pract* 2021; **75**: e14363 [PMID: 33993597 DOI: 10.1111/ijcp.14363]

21 **Ma Y**, Zhu DS, Chen RB, Shi NN, Liu SH, Fan YP, Wu GH, Yang PY, Bai JF, Chen H, Chen LY, Feng Q, Guo TM, Hou Y, Hu GF, Hu XM, Hu YH, Huang J, Huang QH, Huang SZ, Ji L, Jin HH, Lei X, Li CY, Li MQ, Li QT, Li XY, Liu H, Liu JP, Liu Z, Ma YT, Mao Y, Mo LF, Na H, Wang JW, Song FL, Sun S, Wang DT, Wang MX, Wang XY, Wang YZ, Wang YD, Wu W, Wu LP, Xiao YH, Xie HJ, Xu HM, Xu SF, Xue RX, Yang C, Yang KJ, Yuan SL, Zhang GQ, Zhang JB, Zhang LS, Zhao SS, Zhao WY, Zheng K, Zhou YC, Zhu JT, Zhu TQ, Zhang HM, Wang YP, Wang YY; 'lung cleansing & detoxifying decoction' emergency project expert group for covid-19. Association of Overlapped and Un-overlapped Comorbidities with COVID-19 Severity and Treatment Outcomes: A Retrospective Cohort Study from Nine Provinces in China. *Biomed Environ Sci* 2020; **33**: 893-905 [PMID: 33472729 DOI: 10.3967/bes2020.123]

22 **Campos-Murguía A**, Román-Calleja BM, Toledo-Coronado IV, González-Regueiro JA, Solís-Ortega AA, Kúsulas-Delint D, Cruz-Contreras M, Cruz-Yedra N, Cubero FJ, Nevzorova YA, Martínez-Cabrera CF, Moreno-Guillén P, Lozano-Cruz OA, Chapa-Ibargüengoitia M, Gulías-Herrero A, Aguilar-Salinas CA, Ruiz-Margáin A, Macías-Rodríguez RU. Liver fibrosis in patients with MAFLD is a risk factor for adverse outcomes in COVID-19. *Dig Liver Dis* 2021; **53**: 525-533 [PMID: 33551355 DOI: 10.1016/j.dld.2021.01.019]

23 **Ge J**, Pletcher MJ, Lai JC; N3C Consortium. Outcomes of SARS-CoV-2 Infection in Patients With Chronic Liver Disease and Cirrhosis: A National COVID Cohort Collaborative Study. *Gastroenterology* 2021; **161**: 1487-1501.e5 [PMID: 34284037 DOI: 10.1053/j.gastro.2021.07.010]

24 **Kim SW**, Jeon JH, Moon JS, Kim MK. High Fibrosis-4 Index Is Related with Worse Clinical Outcome in Patients with Coronavirus Disease 2019 and Diabetes Mellitus: A Multicenter Observational Study. *Endocrinol Metab (Seoul)* 2021; **36**: 800-809 [PMID: 34418914 DOI: 10.3803/EnM.2021.1040]

25 **Park JG**, Kang MK, Lee YR, Song JE, Kim NY, Kweon YO, Tak WY, Jang SY, Lee C, Kim BS, Hwang JS, Jang BK, Bae J, Lee JY, Suh JI, Park SY, Chung WJ; Daegu-Gyeongbuk Liver Study Group (DGLSG). Fibrosis-4 index as a predictor for mortality in hospitalised patients with COVID-19: a retrospective multicentre cohort study. *BMJ Open* 2020; **10**: e041989 [PMID: 33184086 DOI: 10.1136/bmjopen-2020-041989]

26 **Gao F**, Zheng KI, Wang XB, Yan HD, Sun QF, Pan KH, Wang TY, Chen YP, George J, Zheng MH. Metabolic associated fatty liver disease increases coronavirus disease 2019 disease severity in nondiabetic patients. *J Gastroenterol Hepatol* 2021; **36**: 204-207 [PMID: 32436622 DOI: 10.1111/jgh.15112]

27 **Calapod OP**, Marin AM, Onisai M, Tribus LC, Pop CS, Fierbinteanu-Braticevici C. The Impact of Increased Fib-4 Score in Patients with Type II Diabetes Mellitus on Covid-19 Disease Prognosis. *Medicina (Kaunas)* 2021; **57** [PMID: 33946377 DOI: 10.3390/medicina57050434]

28 **Campos-Varela I**, Villagrasa A, Simon-Talero M, Riveiro-Barciela M, Ventura-Cots M, Aguilera-Castro L, Alvarez-Lopez P, Nordahl EA, Anton A, Bañares J, Barber C, Barreira-Diaz A, Biagetti B, Camps-Relats L, Ciudin A, Cocera R, Dopazo C, Fernandez A, Jimenez C, Jimenez MM, Jofra M, Gil C, Gomez-Gavara C, Guanozzi D, Guevara JA, Lobo B, Malagelada C, Martinez-Camprecios J, Mayorga L, Miret E, Pando E, Pérez-Lopez A, Pigrau M, Prio A, Rivera-Esteban JM, Romero A, Tasayco S, Vidal-Gonzalez J, Vidal L, Minguez B, Augustin S, Genesca J. The role of liver steatosis as measured with transient elastography and transaminases on hard clinical outcomes in patients with COVID-19. *Therap Adv Gastroenterol* 2021; **14**: 17562848211016567 [PMID: 34104210 DOI: 10.1177/17562848211016567]

29 **Chang Y**, Jeon J, Song TJ, Kim J. Association between the fatty liver index and the risk of severe complications in COVID-19 patients: a nationwide retrospective cohort study. *BMC Infect Dis* 2022; **22**: 384 [PMID: 35430797 DOI: 10.1186/s12879-022-07370-x]

30 **Chen VL**, Hawa F, Berinstein JA, Reddy CA, Kassab I, Platt KD, Hsu CY, Steiner CA, Louissaint J, Gunaratnam NT, Sharma P. Hepatic Steatosis Is Associated with Increased Disease Severity and Liver Injury in Coronavirus Disease-19. *Dig Dis Sci* 2021; **66**: 3192-3198 [PMID: 32980956 DOI: 10.1007/s10620-020-06618-3]

31 **Çoraplı M**, Çil E, Oktay C, Kaçmaz H, Çoraplı G, Bulut HT. Role of hepatosteatosis in the prognosis of COVID 19 disease. *Clin Imaging* 2021; **80**: 1-5 [PMID: 34214871 DOI: 10.1016/j.clinimag.2021.06.034]

32 **Davidov-Derevynko Y**, Ben Yakov G, Wieder A, Segal G, Naveh L, Orlova N, Gringauz I, Amit S, Mor O, Klempfner R, Rahav G, Ben Ari Z. The liver in severe acute respiratory syndrome coronavirus 2 (SARS-CoV-2) infection. *Eur J Gastroenterol Hepatol* 2021; **33**: e313-e319 [PMID: 33653988 DOI: 10.1097/MEG.0000000000002048]

33 **Demir N**, Yüzbasıoglu B, Calhan T, Ozturk S. Prevalence and Prognostic Importance of High Fibrosis-4 Index in COVID-19 Patients. *Int J Clin Pract* 2022; **2022**: 1734896 [PMID: 35685537 DOI: 10.1155/2022/1734896]

34 **Ji D**, Zhang D, Yang T, Mu J, Zhao P, Xu J, Li C, Cheng G, Wang Y, Chen Z, Qin E, Lau G. Effect of COVID-19 on patients with compensated chronic liver diseases. *Hepatol Int* 2020; **14**: 701-710 [PMID: 32734407 DOI: 10.1007/s12072-020-10058-6]

35 **Effenberger M**, Grander C, Fritsche G, Bellmann-Weiler R, Hartig F, Wildner S, Seiwald S, Adolph TE, Zoller H, Weiss G, Tilg H. Liver stiffness by transient elastography accompanies illness severity in COVID-19. *BMJ Open Gastroenterol* 2020; **7** [PMID: 32665398 DOI: 10.1136/bmjgast-2020-000445]

36 **Elfeki MA**, Robles J, Akhtar Z, Ullah F, Ganapathiraju I, Tran C, Inman C, Collin SM, Rosa R. Impact of Fibrosis-4 Index Prior to COVID-19 on Outcomes in Patients at Risk of Non-alcoholic Fatty Liver Disease. *Dig Dis Sci* 2022; **67**: 3333-3339 [PMID: 34173917 DOI: 10.1007/s10620-021-07120-0]

37 **Hashemi N**, Viveiros K, Redd WD, Zhou JC, McCarty TR, Bazarbashi AN, Hathorn KE, Wong D, Njie C, Shen L, Chan WW. Impact of chronic liver disease on outcomes of hospitalized patients with COVID-19: A multicentre United States experience. *Liver Int* 2020; **40**: 2515-2521 [PMID: 32585065 DOI: 10.1111/liv.14583]

38 **Huang R**, Zhu L, Wang J, Xue L, Liu L, Yan X, Huang S, Li Y, Zhang B, Xu T, Li C, Ji F, Ming F, Zhao Y, Cheng J, Wang Y, Zhao H, Hong S, Chen K, Zhao XA, Zou L, Sang D, Shao H, Guan X, Chen X, Chen Y, Wei J, Zhu C, Wu C. Clinical Features of Patients With COVID-19 With Nonalcoholic Fatty Liver Disease. *Hepatol Commun* 2020; **4**: 1758-1768 [PMID: 32838108 DOI: 10.1002/hep4.1592]

39 **Hussain A**, Iftikhar M, Rizvi A, Latif M, Javed Ahmed M, Zartash S, Laique T. Outcomes of Nonalcoholic Fatty Liver Disease In Covid Positive Diabetic Patients: Cross Sectional Study. *Pakistan J Med Health Sci* 2021; **15**: 3241-3243 [DOI: 10.53350/pjmhs2115123241]

40 **Kim D**, Adeniji N, Latt N, Kumar S, Bloom PP, Aby ES, Perumalswami P, Roytman M, Li M, Vogel AS, Catana AM, Wegermann K, Carr RM, Aloman C, Chen VL, Rabiee A, Sadowski B, Nguyen V, Dunn W, Chavin KD, Zhou K, Lizaola-Mayo B, Moghe A, Debes J, Lee TH, Branch AD, Viveiros K, Chan W, Chascsa DM, Kwo P, Dhanasekaran R. Predictors of Outcomes of COVID-19 in Patients With Chronic Liver Disease: US Multi-center Study. *Clin Gastroenterol Hepatol* 2021; **19**: 1469-1479.e19 [PMID: 32950749 DOI: 10.1016/j.cgh.2020.09.027]

41 **Madan K**, Rastogi R, Bhargava R, Dagar V, Singla V, Sahu A, Singh P, Garg P, Aggarwal B, Singh RK. Is Fatty Liver Associated with Increased Mortality and Morbidity in Coronavirus Disease 2019 (COVID-19) Pneumonia? *J Clin Exp Hepatol* 2022; **12**: 1320-1327 [PMID: 35469129 DOI: 10.1016/j.jceh.2022.04.013]

42 **Marjot T**, Moon AM, Cook JA, Abd-Elsalam S, Aloman C, Armstrong MJ, Pose E, Brenner EJ, Cargill T, Catana MA,

Dhanasekaran R, Eshraghian A, García-Juárez I, Gill US, Jones PD, Kennedy J, Marshall A, Matthews C, Mells G, Mercer C, Perumalswami PV, Avitabile E, Qi X, Su F, Ufere NN, Wong YJ, Zheng MH, Barnes E, Barritt AS 4th, Webb GJ. Outcomes following SARS-CoV-2 infection in patients with chronic liver disease: An international registry study. *J Hepatol* 2021; **74**: 567-577 [PMID: 33035628 DOI: 10.1016/j.jhep.2020.09.024]

43 **Romero-Cristóbal M**, Clemente-Sánchez A, Piñeiro P, Cedeño J, Rayón L, Del Río J, Ramos C, Hernández DA, Cova M, Caballero A, Garutti I, García-Olivares P, Hortal J, Guerrero JE, García R, Bañares R, Rincón D. Possible unrecognised liver injury is associated with mortality in critically ill COVID-19 patients. *Therap Adv Gastroenterol* 2021; **14**: 17562848211023410 [PMID: 34178116 DOI: 10.1177/17562848211023410]

44 **Rentsch CT**, Kidwai-Khan F, Tate JP, Park LS, King JT Jr, Skanderson M, Hauser RG, Schultze A, Jarvis CI, Holodniy M, Re VL 3rd, Akgün KM, Crothers K, Taddei TH, Freiberg MS, Justice AC. Covid-19 Testing, Hospital Admission, and Intensive Care Among 2,026,227 United States Veterans Aged 54-75 Years. medRxiv 2020 [PMID: 32511595 DOI: 10.1101/2020.04.09.20059964]

45 **Shao J**, Liang Y, Li Y, Ding R, Zhu M, You W, Wang Z, Huang B, Wu M, Zhang T, Li K, Wu W, Wu L, Wang Q, Xia X, Wang S, Lu L. Implications of liver injury in risk-stratification and management of patients with COVID-19. *Hepatol Int* 2021; **15**: 202-212 [PMID: 33548030 DOI: 10.1007/s12072-020-10123-0]

46 **Targher G**, Mantovani A, Byrne CD, Wang XB, Yan HD, Sun QF, Pan KH, Zheng KI, Chen YP, Eslam M, George J, Zheng MH. Risk of severe illness from COVID-19 in patients with metabolic dysfunction-associated fatty liver disease and increased fibrosis scores. *Gut* 2020; **69**: 1545-1547 [PMID: 32414813 DOI: 10.1136/gutjnl-2020-321611]

47 **Tignanelli CJ**, Bramante CT, Dutta N, Tamariz L, Usher MG, Ikramuddin S. Metabolic surgery may protect against admission for COVID-19 in persons with nonalcoholic fatty liver disease. *Surg Obes Relat Dis* 2021; **17**: 1780-1786 [PMID: 34326020 DOI: 10.1016/j.soard.2021.05.029]

48 **Trivedi HD**, Wilechansky R, Goyes D, Vieira Barbosa J, Canakis A, Lai M, Long MT, Fricker Z. Radiographic Hepatic Steatosis Is Not Associated With Key Clinical Outcomes Among Patients Hospitalized With COVID-19. *Gastroenterology Res* 2021; **14**: 179-183 [PMID: 34267833 DOI: 10.14740/gr1389]

49 **Vázquez-Medina MU**, Cerda-Reyes E, Galeana-Pavón A, López-Luna CE, Ramírez-Portillo PM, Ibañez-Cervantes G, Torres-Vázquez J, Vargas-De-León C. Interaction of metabolic dysfunction-associated fatty liver disease and nonalcoholic fatty liver disease with advanced fibrosis in the death and intubation of patients hospitalized with coronavirus disease 2019. *Hepatol Commun* 2022; **6**: 2000-2010 [PMID: 35438253 DOI: 10.1002/hep4.1957]

50 **Moctezuma-Velázquez P**, Miranda-Zazueta G, Ortiz-Brizuela E, Garay-Mora JA, González-Lara MF, Tamez-Torres KM, Román-Montes CM, Díaz-Mejía BA, Pérez-García E, Villanueva-Reza M, Chapa-Ibargüengoitia M, Uscanga-Domínguez L, Sifuentes-Osornio J, Ponce-de-León A, Kershenobich-Stalnikowitz D, Mota-Ayala B, Moctezuma-Velázquez C. NAFLD determined by Dallas Steatosis Index is associated with poor outcomes in COVID-19 pneumonia: a cohort study. *Intern Emerg Med* 2022; **17**: 1355-1362 [PMID: 35138548 DOI: 10.1007/s11739-022-02933-x]

51 **Vrsaljko N**, Samadan L, Viskovic K, Mehmedović A, Budimir J, Vince A, Papic N. Association of Nonalcoholic Fatty Liver Disease With COVID-19 Severity and Pulmonary Thrombosis: CovidFAT, a Prospective, Observational Cohort Study. *Open Forum Infect Dis* 2022; **9**: ofac073 [PMID: 35287335 DOI: 10.1093/ofid/ofac073]

52 **Wang G**, Wu S, Wu C, Zhang Q, Wu F, Yu B, Zhang S, Wu G, Zhong Y. Association between non-alcoholic fatty liver disease with the susceptibility and outcome of COVID-19: A retrospective study. *J Cell Mol Med* 2021; **25**: 11212-11220 [PMID: 34761514 DOI: 10.1111/jcmm.17042]

53 **Yao R**, Zhu L, Wang J, Liu J, Xue R, Xue L, Liu L, Li C, Zhao H, Cheng J, Huang S, Li Y, Zhao XA, Zhu C, Li M, Huang R, Wu C. Risk of severe illness of COVID-19 patients with NAFLD and increased NAFLD fibrosis scores. *J Clin Lab Anal* 2021; **35**: e23880 [PMID: 34213039 DOI: 10.1002/jcla.23880]

54 **Yoo HW**, Jin HY, Yon DK, Effenberger M, Shin YH, Kim SY, Yang JM, Kim MS, Koyanagi A, Jacob L, Smith L, Yoo IK, Shin JI, Lee SW. Non-alcoholic Fatty Liver Disease and COVID-19 Susceptibility and Outcomes: a Korean Nationwide Cohort. *J Korean Med Sci* 2021; **36**: e291 [PMID: 34697932 DOI: 10.3346/jkms.2021.36.e291]

55 **Younossi ZM**, Stepanova M, Lam B, Cable R, Felix S, Jeffers T, Younossi E, Pham H, Srishord M, Austin P, Estep M, Terra K, Escheik C, de Avila L, Golabi P, Kolacevski A, Racila A, Henry L, Gerber L. Independent Predictors of Mortality Among Patients With NAFLD Hospitalized With COVID-19 Infection. *Hepatol Commun* 2022; **6**: 3062-3072 [PMID: 34558853 DOI: 10.1002/hep4.1802]

56 **Zhou YJ**, Zheng KI, Wang XB, Sun QF, Pan KH, Wang TY, Ma HL, Chen YP, George J, Zheng MH. Metabolic-associated fatty liver disease is associated with severity of COVID-19. *Liver Int* 2020; **40**: 2160-2163 [PMID: 32573883 DOI: 10.1111/liv.14575]

57 **Singh A**, Hussain S, Antony B. Non-alcoholic fatty liver disease and clinical outcomes in patients with COVID-19: A comprehensive systematic review and meta-analysis. *Diabetes Metab Syndr* 2021; **15**: 813-822 [PMID: 33862417 DOI: 10.1016/j.dsx.2021.03.019]

58 **Hayat U**, Ashfaq MZ, Johnson L, Ford R, Wuthnow C, Kadado K, El Jurdi K, Okut H, Kilgore WR, Assi M, Siddiqui AA. The Association of Metabolic-Associated Fatty Liver Disease with Clinical Outcomes of COVID-19: A Systematic Review and Meta-Analysis. *Kans J Med* 2022; **15**: 241-246 [PMID: 35899064 DOI: 10.17161/kjm.vol15.16522]

59 **Ziaee A**, Azarkar G, Ziaee M. Role of fatty liver in coronavirus disease 2019 patients' disease severity and hospitalization length: a case-control study. *Eur J Med Res* 2021; **26**: 115 [PMID: 34565475 DOI: 10.1186/s40001-021-00590-y]

60 **Nath P**, Kumar R, Mallick B, Das S, Anand A, Panigrahi SC, Duseja A, Acharya SK, Chawla YK, Praharaj DL. Effect of Nonalcoholic Fatty Liver Disease (NAFLD) on COVID-19: A Single-Center Study of 3983 Patients With Review of Literature. *Cureus* 2022; **14**: e26683 [PMID: 35949776 DOI: 10.7759/cureus.26683]

61 **Estes C**, Razavi H, Loomba R, Younossi Z, Sanyal AJ. Modeling the epidemic of nonalcoholic fatty liver disease demonstrates an exponential increase in burden of disease. *Hepatology* 2018; **67**: 123-133 [PMID: 28802062 DOI: 10.1002/hep.29466]

62 **Mitra S**, De A, Chowdhury A. Epidemiology of non-alcoholic and alcoholic fatty liver diseases. *Transl Gastroenterol Hepatol* 2020; **5**: 16 [PMID: 32258520 DOI: 10.21037/tgh.2019.09.08]

63 **Roca-Fernández A**, Dennis A, Nicolls R, McGonigle J, Kelly M, Banerjee R. High Liver Fat Associates with Higher

Risk of Developing Symptomatic COVID-19 Infection - Initial UK Biobank Observations. 2020 Preprint. Available from: medRxiv:2020.06.04.20122457 [DOI: 10.1101/2020.06.04.20122457]

64 **Singh R**, Rathore SS, Khan H, Karale S, Chawla Y, Iqbal K, Bhurwal A, Tekin A, Jain N, Mehra I, Anand S, Reddy S, Sharma N, Sidhu GS, Panagopoulos A, Pattan V, Kashyap R, Bansal V. Association of Obesity With COVID-19 Severity and Mortality: An Updated Systemic Review, Meta-Analysis, and Meta-Regression. *Front Endocrinol (Lausanne)* 2022; **13**: 780872 [PMID: 35721716 DOI: 10.3389/fendo.2022.780872]

65 **Bae S**, Kim SR, Kim MN, Shim WJ, Park SM. Impact of cardiovascular disease and risk factors on fatal outcomes in patients with COVID-19 according to age: a systematic review and meta-analysis. *Heart* 2021; **107**: 373-380 [PMID: 33334865 DOI: 10.1136/heartjnl-2020-317901]

66 **He ZF**, Zhong NS, Guan WJ. Impact of Chronic Respiratory Diseases on the Outcomes of COVID-19. *Arch Bronconeumol* 2022; **58**: 5-7 [PMID: 34075267 DOI: 10.1016/j.arbres.2021.05.009]

67 **Apicella M**, Campopiano MC, Mantuano M, Mazoni L, Coppelli A, Del Prato S. COVID-19 in people with diabetes: understanding the reasons for worse outcomes. *Lancet Diabetes Endocrinol* 2020; **8**: 782-792 [PMID: 32687793 DOI: 10.1016/S2213-8587(20)30238-2]

68 **Lighter J**, Phillips M, Hochman S, Sterling S, Johnson D, Francois F, Stachel A. Obesity in Patients Younger Than 60 Years Is a Risk Factor for COVID-19 Hospital Admission. *Clin Infect Dis* 2020; **71**: 896-897 [PMID: 32271368 DOI: 10.1093/cid/ciaa415]

69 **Zou X**, Chen K, Zou J, Han P, Hao J, Han Z. Single-cell RNA-seq data analysis on the receptor ACE2 expression reveals the potential risk of different human organs vulnerable to 2019-nCoV infection. *Front Med* 2020; **14**: 185-192 [PMID: 32170560 DOI: 10.1007/s11684-020-0754-0]

70 **Xu Z**, Shi L, Wang Y, Zhang J, Huang L, Zhang C, Liu S, Zhao P, Liu H, Zhu L, Tai Y, Bai C, Gao T, Song J, Xia P, Dong J, Zhao J, Wang FS. Pathological findings of COVID-19 associated with acute respiratory distress syndrome. *Lancet Respir Med* 2020; **8**: 420-422 [PMID: 32085846 DOI: 10.1016/S2213-2600(20)30076-X]

71 **Polakos NK**, Cornejo JC, Murray DA, Wright KO, Treanor JJ, Crispe IN, Topham DJ, Pierce RH. Kupffer cell-dependent hepatitis occurs during influenza infection. *Am J Pathol* 2006; **168**: 1169-78; quiz 1404 [PMID: 16565492 DOI: 10.2353/ajpath.2006.050875]

72 **Muscogiuri G**, Pugliese G, Barrea L, Savastano S, Colao A. Commentary: Obesity: The "Achilles heel" for COVID-19? *Metabolism* 2020; **108**: 154251 [PMID: 32353356 DOI: 10.1016/j.metabol.2020.154251]

73 **Chen Z**, Yu R, Xiong Y, Du F, Zhu S. A vicious circle between insulin resistance and inflammation in nonalcoholic fatty liver disease. *Lipids Health Dis* 2017; **16**: 203 [PMID: 29037210 DOI: 10.1186/s12944-017-0572-9]

74 **de Luca C**, Olefsky JM. Inflammation and insulin resistance. *FEBS Lett* 2008; **582**: 97-105 [PMID: 18053812 DOI: 10.1016/j.febslet.2007.11.057]

75 **Bramante C**, Tignanelli CJ, Dutta N, Jones E, Tamariz L, Clark JM, Usher M, Metlon-Meaux G, Ikramuddin S. Non-alcoholic fatty liver disease (NAFLD) and risk of hospitalization for Covid-19. medRxiv 2020 [PMID: 32909011 DOI: 10.1101/2020.09.01.20185850]

76 **Liu M**, Mei K, Tan Z, Huang S, Liu F, Deng C, Ma J, Yu P, Liu X. Liver Fibrosis Scores and Hospitalization, Mechanical Ventilation, Severity, and Death in Patients with COVID-19: A Systematic Review and Dose-Response Meta-Analysis. *Can J Gastroenterol Hepatol* 2022; **2022**: 7235860 [PMID: 35369116 DOI: 10.1155/2022/7235860]

77 **Targher G**, Mantovani A, Byrne CD, Wang XB, Yan HD, Sun QF, Pan KH, Zheng KI, Chen YP, Eslam M, George J, Zheng MH. Detrimental effects of metabolic dysfunction-associated fatty liver disease and increased neutrophil-to-lymphocyte ratio on severity of COVID-19. *Diabetes Metab* 2020; **46**: 505-507 [PMID: 32505652 DOI: 10.1016/j.diabet.2020.06.001]

78 **Sachdeva S**, Khandait H, Kopel J, Aloysius MM, Desai R, Goyal H. NAFLD and COVID-19: a Pooled Analysis. *SN Compr Clin Med* 2020; **2**: 2726-2729 [PMID: 33173850 DOI: 10.1007/s42399-020-00631-3]

79 **Li J**, Tian A, Zhu H, Chen L, Wen J, Liu W, Chen P. Mendelian Randomization Analysis Reveals No Causal Relationship Between Nonalcoholic Fatty Liver Disease and Severe COVID-19. *Clin Gastroenterol Hepatol* 2022; **20**: 1553-1560.e78 [PMID: 35124268 DOI: 10.1016/j.cgh.2022.01.045]

World Journal of Gastroenterology

Submit a Manuscript: https://www.f6publishing.com

World J Gastroenterol 2023 June 7; 29(21): 3379-3384

DOI: 10.3748/wjg.v29.i21.3379

ISSN 1007-9327 (print) ISSN 2219-2840 (online)

ACADEMIC WRITING

How to select a journal for your research

José M Ramia

Specialty type: Gastroenterology and hepatology

Provenance and peer review: Invited articles; Externally peer reviewed.

Peer-review model: Single blind

Peer-review report's scientific quality classification

Grade A (Excellent): A
Grade B (Very good): B
Grade C (Good): 0
Grade D (Fair): 0
Grade E (Poor): 0

P-Reviewer: Osawa S, Japan; Tai XT, China

Received: January 14, 2023
Peer-review started: January 14, 2023
First decision: January 31, 2023
Revised: February 19, 2023
Accepted: May 8, 2023
Article in press: May 8, 2023
Published online: June 7, 2023

José M Ramia, Department of Surgery, Hospital General Universitario Dr. Balmis, Alicante 03010, Spain

Corresponding author: José M Ramia, FACS, FRCS, FRCS (Ed), Assistant Professor, Department of Surgery, Hospital General Universitario Dr. Balmis, 11 Pintor Baeza, Alicante 03010, Spain. jose_ramia@hotmail.com

Abstract

Publication in a peer-reviewed journal is the goal of any research project. One of the most important (and possibly the least understood) aspects of the publication process is the choice of a suitable journal that is likely to accept your work. Detailed information and tips and tricks to success are given in this editorial.

Key Words: Research; Journal; Altmetrics; Publication

©The Author(s) 2023. Published by Baishideng Publishing Group Inc. All rights reserved.

Core Tip: Knowing the tips and tricks to choose the best journal for publishing your research is crucial. A narrative check list including all these tricks has been performed.

Citation: Ramia JM. How to select a journal for your research. *World J Gastroenterol* 2023; 29(21): 3379-3384
URL: https://www.wjgnet.com/1007-9327/full/v29/i21/3379.htm
DOI: https://dx.doi.org/10.3748/wjg.v29.i21.3379

INTRODUCTION

Publication in a peer-reviewed journal is the goal of any research project. It is through publication that your research reaches your colleagues in the field, advancing knowledge and encouraging communication between groups[1]. Although peer review can be a time-consuming and often tiring process, the publication of your manuscript validates your work and can help to advance your career, attract students and experienced staff, and obtain funding for future studies[1]. One of the most important (and possibly the least understood) aspects of the publication process is the choice of a suitable journal that is likely to accept your work[2,3]. Submitting your paper to the wrong journal may result in a series of rejections, stalling both your

research and your career[1,2,4].

Realistic assessment of your work is crucial. Both novice and well-known researchers can make the error of submitting their work to an inappropriate journal[1]. First-time authors or those who are branching out into broader areas of research may be unfamiliar with the journals in the field. In these cases, seeking out mentorship could be crucial[5]. For their part, experienced authors may be tempted to publish in the same journals as always, and thus ignore the new publication opportunities that are constantly arising. Even rigorous, high-impact work may be rejected when the topic of the research does not align with the scope of the journal and making this mistake wastes time and money and affects motivation[1] (Table 1).

EVALUATE YOUR RESEARCH

The three key features of your work to consider are its novelty, relevance, and appeal[2]. "Novelty" refers to how new your findings are compared with those previously published in your field. If your findings only offer a small step forward in what is already known, your paper is suitable for a journal with a low-to-medium impact factor (IF). However, if you feel your findings might change the way researchers in your field think about a specific topic, you should aim at a high impact factor journal[2]. "Relevance" refers to the applicability of your findings. Relevance may be geographical[2]: That is to say, if your findings with only a regional focus, choose a regional journal, but if they have worldwide implications, choose an international journal. Or relevance might be disciplinary: If your findings are highly specific for your field, choose a specialized journal, but if they have implications for researchers in other fields, choose a more general or interdisciplinary journal[2,5]. Finally, "appeal" refers to the topical interest of your study: journal editors are keen on manuscripts on current hot topics or with real-world applications[2].

You should also narrow your focus with regard to your expected readership[2,6]. The main questions to answer are the following. Is your study clinical or basic? Are the findings relevant to a broad cross-section of the scientific community, or to researchers in a specialist field? Are the findings preliminary or definitive? And finally, if you collect more data, could you try a journal with a higher IF[2]?

IDENTIFYING THE RIGHT JOURNAL

It is best to choose your journal before you start writing[2,3]. The reasons are that journals have specific criteria related to the manuscript structure, word limits, and reference style; they have specific focuses, or scopes; and editors will often look at your references to see whether you have cited articles published in their journal[2]. So, once you have chosen a journal, identify articles published there that have a bearing on your manuscript and include them among your references.

A tip for how choosing the journal is to perform a search with the keywords (or title) of your manuscript in literature databases such as Medline and PubMed. This search can identify similar or related studies and the journals where they were published[6]. Try to find between three and five manuscripts published in the last five years and decide whether they resemble yours in terms of quality and scope[7]. Identifying previously published papers in your specific subject area is an excellent way to be sure that your research topic is of interest to the readership of a particular journal, and this will obviously increase your chances of review.

There are also a variety of online resources that suggest target journals based on keywords, abstract content and so on: Journal/Author Name Estimator (Jane)®, Manuscript Matcher®, and JournalGuide® (Clarivate), *etc*. But remember that journals that have not previously published in the same area of research might also be interested in your findings.

FACTORS TO CONSIDER IN SELECTING THE BEST JOURNAL

Impact factor

IF is still the default method to assess the quality and reputation of a journal[7]. It displays the total citations made of the journal's articles[7]. IF is the most important factor that researchers consider when they submit a paper, and it is often used as a measure of a researcher's success in his/her field[2,6]. Funding agencies, Institutions, employers, and university committees also consider IF the best method to evaluate a paper[2,6,7]. Journals with higher IF often have a higher profile, and this obviously will increase your article's visibility[4,6].

Nonetheless, the validity of the Journal IF as a metric for journal quality is controversial due to the many factors that can influence the rating achieved, and to the fact that not all these factors are directly related to the quality of the publications within the journal[3]. Although it is tempting to submit a manuscript to the journal with the highest IF factor, it is important to evaluate your research objectively

Table 1 Tips and tricks for selecting best journal

Item	Description
Evaluate your research	Novelty, relevance, and appeal
Identifying the right journal	
Factors to consider in selecting the best journal	Impact factor
	Aims and scope
	Publication types
	Publication mode and rights: Type of publication; supplementary materials/media and relevant links; type of subscription; open access; and copyright
	Publication charges
	Publication frequency
	Time from acceptance to publication
	Rejection rates
	Readership
	Indexing
	Editor's preferences
	Peer-review
	Transfer cascades
	Journal reputation

and decide whether it is truly suitable for a high IF journal. Otherwise, you will risk wasting valuable time and effort as you submit your manuscript time and again to multiple journals[1].

Other scores are: Scimago Journal Rank, Eigenfactor, SNIP, Cited Halflife, Altmetric Attention Score, and Cited Score, *etc*[3,5,8].

Aims and scope

Even remarkable research may be rejected if the topic is not in line with the scope of the journal[2,6,7]. This information is usually readily available on the journal's homepage[3,6,7]. Check to see whether the journal is publishing research like yours[5,7,9]. The topics, the focus and the novelty and potential impact are all important factors[7].

Publication types

Find out which article types (*e.g.*, originals, reviews, systematic reviews, metanalysis, case reports, images, and so on) are accepted and which are not; limits on length (word count) or number of illustrations or references; whether supplementary files are allowed, or the prior inclusion of a preprint (unsubmitted draft) in a preprint server such as arXiv or bioRxiv[1-3,7,9]. Submission to a journal that does not accept the type of article you have written is a sure way of guaranteeing immediate rejection. Please read the guide to authors carefully and follow the instructions closely[1,7,9]. The abstract and cover letter are your way of presenting yourself to the Editor: Take your time over them.

To avoid initial rejection, the registration of research in international databases (ClinicalTrials, Research Registry, PROSPERO, *etc*) is often mandatory. The inclusion of a reporting Checklist, depending on the type of manuscript (*e.g.*, STROBE, PRISMA, and so on) is normally required. You should check this before sending your manuscript.

Publication mode and rights

You should be familiar with the journal's characteristics: Type of publication: print only, print plus online version (PDF), which may be a longer version, with or without early view ("early online", "online first", or "ahead of print") version, or only online version, which is becoming the most usual type[9].

Supplementary materials/media and relevant links: Many journals have links to supplementary materials in an online repository[2].

Type of subscription: Membership-based, pay per view, site license, subscription, or open access.

Open access

Open access means that the entire content of the paper is freely available to all readers, with no need to subscribe to a journal or pay to access the paper[6]. Many researchers prefer this publication model because it can help disseminate their research to a wider audience[2,6]. There is no doubt that increasing the accessibility of your article will ensure that your target audience will have access to your article worldwide, but expenses are high. There are three formats:

Green open access: which means free access to preprint or accepted manuscript (final draft) on a personal website, institutional website, or nonprofit repository such as Pubmed®, with or without a time delay before uploading; in most cases the copyright will be retained by the publisher[6].

Gold open access: free access to the final published version (typically on the publisher's website), and authors retain copyright[6]. Gold open access gives you ownership of your work after publication and ensures that the most accurate, final form of the paper is available to all readers[6].

Hybrid open access: (some content is open access, and some is subscription-based; this can depend on authors' choice or on journal policy, which may include "delayed open access".

Copyright

It may be owned by the author or the journal publisher. Another important issue is whether a Creative Commons license is available.

Publication charges

Publication charges are the fees that you will be charged to publish in a journal[6]. It is essential to read the section about charges very carefully[2]. If you are on a tight Article budget, you may need to rule out open access journals or journals with high publication charges. There are several types of charge: Submission fee, production fee and charges for color figures (usually black and white images do not incur charges)[2]. Find out whether there are free batches of reprints or online copies, and free online access for authors to published articles. Some editorials waive article processing charges to authors from developing countries for open access publication.

Find out whether the following services are provided free or included in the publication charge: Editing/illustration service; news release service; marketing; social media promotion; post-publication commenting and altmetrics (article-level metrics) tracking.

Publication frequency

Check the journal's table of contents for the number of monthly/weekly articles, articles per issue and issues per year, and how often articles appear in the journal's Online First section[2,7].

Time from acceptance to publication

There are several publication times: From submission to first/final decision, first online publication, final (online) publication. If you need rapid publication, you should specifically look for journals that offer fast response times and short periods from acceptance to publication[2].

The normal time taken for a good manuscript to be published in a reputed journal is around 9 mo to 12 mo. The optimum time limit for rejection is 4-6 wk[7]. The best time is to wait for the special editions from reputed journals and then submit a relevant paper: due to the smaller number of research papers submitted at that time, your research stands a better chance of being published[7].

Rejection rates

It is important to know the selectivity (% acceptance rate) of the journal[2]. The acceptance rate in poor journals is over 90%, while predatory journals publish almost everything, they can lay their hands on. In good journals the acceptance rate is 10%-20%[7,9].

Readership

Identify the interests of the readers[2,3] Be sure that the target audience you are trying to reach is part of the readership of the journal. Your goal is not just to be published, but also to be widely read in your field. Review the "Most Downloaded" or "Most Cited" lists from your potential journals. If you find that your manuscript is similar in scope to articles in this list from one of your potential journals, this suggests that if you publish in this journal your article will be widely read as well.

Indexing

To increase the online visibility of your article, be sure that the journal is indexed in the online databases that your target audience will use to find articles. PubMed® and Scopus® are the main indexing services used by researchers in the biomedical sciences[2,6].

Editor's preferences

It is also very useful to identify the interests of the journal's editor. Just because your manuscript may be similar in scope to the journal, this does not mean that the Editor is currently interested in your topic. Check when similar articles were published in the journal. If similar articles have been published within the last two or three years, this suggests that the Editor is probably interested in your topic. Look at recently published Editorials, Review Articles, and Special Issues, because these usually focus on topics the Editor feels are currently important for the field. If you find that your manuscript is similar in scope to others published by one of your potential journals, this suggests that the Editor may regard your research topic as important.

Peer-review

Articles published in peer-reviewed journals enjoy high esteem among the academic and scientific community[6,7,9]. The quality of the reviewers is also a crucial factor[9]. There are several types of peer-review: The most common is a closed (single- or double-blind) review, but open peer-review is also performed. Other types of review are collaborative (in which reviewers may discuss issues with each other, or reviewers/editors may discuss specific points with the authors) and transparent (in which reviews are published with or without reviewers' names). As for the speed of peer review, you should find out whether fast-track review and pre-submission inquiries are allowed. Journals with very short review times (1-2 wk) are often poor quality (though bear in mind that there are also some top journals with very short review times).

Transfer cascades

One feature of scientific publishing that many researchers are unaware of is the existence of "families" or portfolios of journals inside the same publishing house. Many portfolios with prestigious journals that receive a high volume of submissions also contain less competitive journals that publish papers on the same or similar topics. In many cases, if a publisher with this type of portfolio rejects your paper from a high IF journal, they may offer to transfer it to a lower IF journal inside the same "family". This can help accelerate the overall publication process by avoiding the need to identify a new journal, reformat the paper and prepare a new submission[6]. Bear in mind that some transfer cascades direct you to journals with publication charges.

Journal reputation

Remember that publishing in poor quality journals does not count as scientific contribution to knowledge. Avoid sending work to predatory journals, as this is a waste of time and effort[3,7]. There are many points to check in order to ensure the quality of the journal before sending your manuscript [2]: Are the journal/publisher, editor and editorial board well known? Is the journal affiliated to a professional society? Is the journal recommended by your library/society? Do your colleagues read the journal, or have they been cited there, or have they published there? Is the journal known for ethics, quality content, language, and production? Is the journal included in respected general or specific indexes, with a long history and a permanent online archive[7]? What are the journal's bibliometric scores (IF)? How old is the journal (those aged 10 years or more are often good)?

CONCLUSION

After all the hard work that goes into performing successful research, the final crucial step is choosing the right journal in which to publish. With almost 10000 journals in the Directory of Open Access Journals alone, choosing the best journal can be a daunting prospect even for experienced researchers, and making the wrong decision can cost valuable time, money, and effort. Key factors are being aware of the aims and scope of the journal; identifying papers that are similar in quality and scope; assessing the journal's restrictions; and considering the impact factor and potential reach. Despite the existence of support platforms, the development of artificial intelligence platforms may help us to decide the best journal for our research. Items like specific area, number of patients included, clinical relevance and innovation may well be able to identify the most interesting journal.

FOOTNOTES

Author contributions: Ramia JM wrote the manuscript.

Conflict-of-interest statement: The authors declare that they have no conflict of interest.

Open-Access: This article is an open-access article that was selected by an in-house editor and fully peer-reviewed by external reviewers. It is distributed in accordance with the Creative Commons Attribution NonCommercial (CC BY-

NC 4.0) license, which permits others to distribute, remix, adapt, build upon this work non-commercially, and license their derivative works on different terms, provided the original work is properly cited and the use is non-commercial. See: https://creativecommons.org/Licenses/by-nc/4.0/

Country/Territory of origin: Spain

ORCID number: José M Ramia 0000-0003-1186-953X.

S-Editor: Chen YL
L-Editor: A
P-Editor: Ma YJ

REFERENCES

1 **AJE**. [cited 3 March 2023]. Available from: https://www.aje.com/arc/choosing-right-journal-your-research/
2 **Edanz Learning Lab**. How to Choose the Best Journal for Publishing Your Scientific Research. [cited 3 March 2023]. Available from: https://Learning.edanz.com/choosing-the-right-journal/
3 **Taylor Francis Groups**. Choosing the right journal for your research. [cited 3 March 2023]. Available from: https://authorservices.taylorandfrancis.com/wp-content/uploads/2021/03/Choosing_a_journal_ebook.pdf
4 **Clarivate**. How to find the right journal for your research (using actual data). [cited 3 March 2023]. Available from: https://clarivate.com/blog/how-to-find-the-right-journal-for-your-research-using-actual-data/
5 **Wiley**. Infographic: 6 Steps for Writing a Literature Review. [cited 3 March 2023]. Available from: https://www.wiley.com/network/researchers/preparing-your-article/6-steps-to-choosing-the-right-journal-for-your-research-infographic
6 **Charlesworth Editing Logo**. How do you select the best journal for your research? [cited 3 March 2023]. Available from: https://www.cwauthors.com/article/How-do-I-select-the-best-Journal-for-my-research
7 **Pubrica Knowledge Works**. How to select the right journal for publication? July 26, 2019. [cited 3 March 2023]. Available from: https://pubrica.com/academy/publication-ethics/how-to-select-the-right-journal-for-publication/
8 **Elsevier**. How to Choose a Journal to Submit an Article. [cited 3 March 2023]. Available from: https://scientific-publishing.webshop.elsevier.com/research-process/how-to-choose-a-journal-to-submit-an-article/
9 **Enago Academy**. Selecting The Right Journal: A Quick Guide (Part 3). [cited 3 March 2023]. Available from: https://www.enago.com/academy/how-to-select-the-right-journal-for-publication/



Published by **Baishideng Publishing Group Inc**
7041 Koll Center Parkway, Suite 160, Pleasanton, CA 94566, USA
Telephone: +1-925-3991568
E-mail: bpgoffice@wjgnet.com
Help Desk: https://www.f6publishing.com/helpdesk
https://www.wjgnet.com



© 2023 Baishideng Publishing Group Inc. All rights reserved.

ISSN 1007-9327 (print)
ISSN 2219-2840 (online)

World Journal of *Gastroenterology*

World J Gastroenterol 2023 June 14; 29(22): 3385-3573



Published by Baishideng Publishing Group Inc

World Journal of Gastroenterology

Contents

Weekly Volume 29 Number 22 June 14, 2023

REVIEW

3385 Overview of current detection methods and microRNA potential in *Clostridioides difficile* infection screening

Bocchetti M, Ferraro MG, Melisi F, Grisolia P, Scrima M, Cossu AM, Yau TO

3400 Epidemiology of small intestinal bacterial overgrowth

Efremova I, Maslennikov R, Poluektova E, Vasilieva E, Zharikov Y, Suslov A, Letyagina Y, Kozlov E, Levshina A, Ivashkin V

ORIGINAL ARTICLE

Basic Study

3422 Mechanism of annexin A1/N-formylpeptide receptor regulation of macrophage function to inhibit hepatic stellate cell activation through Wnt/β-catenin pathway

Fan JH, Luo N, Liu GF, Xu XF, Li SQ, Lv XP

3440 Study of the roles of caspase-3 and nuclear factor kappa B in myenteric neurons in a P2X7 receptor knockout mouse model of ulcerative colitis

Magalhães HIR, Machado FA, Souza RF, Caetano MAF, Figliuolo VR, Coutinho-Silva R, Castelucci P

3469 Comparative analysis of the gut microbiota of wild adult rats from nine district areas in Hainan, China

Niu LN, Zhang GN, Xuan DD, Lin C, Lu Z, Cao PP, Chen SW, Zhang Y, Cui XJ, Hu SK

Case Control Study

3482 Plasma exosomal hsa_circ_0079439 as a novel biomarker for early detection of gastric cancer

Li X, Lin YL, Shao JK, Wu XJ, Li X, Yao H, Shi FL, Li LS, Zhang WG, Chang ZY, Chai NL, Wang YL, Linghu EQ

Retrospective Cohort Study

3497 Per-oral endoscopic myotomy is safe and effective for pediatric patients with achalasia: A long-term follow-up study

Bi YW, Lei X, Ru N, Li LS, Wang NJ, Zhang B, Yao Y, Linghu EQ, Chai NL

Retrospective Study

3508 Efficacy and safety of modified tetracycline dosing in a quadruple therapy for *Helicobacter pylori*: A retrospective single center study

Sun YC, Zhu MJ, Chen XQ, Yue L, Zhao YR, Wang XJ, Kim JJ, Du Q, Hu WL

Observational Study

3519 Pre-transjugular-intrahepatic-portosystemic-shunt measurement of hepatic venous pressure gradient and its clinical application: A comparison study

Wang XX, Yin XC, Gu LH, Guo HW, Cheng Y, Liu Y, Xiao JQ, Wang Y, Zhang W, Zou XP, Wang L, Zhang M, Zhu-Ge YZ, Zhang F

3534 Difference and clinical value of metabolites in plasma and feces of patients with alcohol-related liver cirrhosis

Xu YF, Hao YX, Ma L, Zhang MH, Niu XX, Li Y, Zhang YY, Liu TT, Han M, Yuan XX, Wan G, Xing HC

Prospective Study

3548 Prospective study comparing hepatic steatosis assessment by magnetic resonance imaging and four ultrasound methods in 105 successive patients

Collin R, Magnin B, Gaillard C, Nicolas C, Abergel A, Buchard B

SCIENTOMETRICS

3561 Research trends on artificial intelligence and endoscopy in digestive diseases: A bibliometric analysis from 1990 to 2022

Du RC, Ouyang YB, Hu Y

World Journal of Gastroenterology

Weekly Volume 29 Number 22 June 14, 2023

Contents

ABOUT COVER

Editorial Board Member of *World Journal of Gastroenterology*, Wolfgang Kreisel,MD, Emeritus Professor, Department of Medicine II, Gastroenterology, Hepatology, Endocrinology, and Infectious Diseases, Faculty of Medicine, Medical Center-University of Freiburg, Hugstetter Str. 55, Freiburg 79106, Germany.Wolfgang.Kreisel@uniklinik-freiburg.de

AIMS AND SCOPE

The primary aim of *World Journal of Gastroenterology* (*WJG*, *World J Gastroenterol*) is to provide scholars and readers from various fields of gastroenterology and hepatology with a platform to publish high-quality basic and clinical research articles and communicate their research findings online. *WJG* mainly publishes articles reporting research results and findings obtained in the field of gastroenterology and hepatology and covering a wide range of topics including gastroenterology, hepatology, gastrointestinal endoscopy, gastrointestinal surgery, gastrointestinal oncology, and pediatric gastroenterology.

INDEXING/ABSTRACTING

The *WJG* is now abstracted and indexed in Science Citation Index Expanded (SCIE, also known as SciSearch®), Current Contents/Clinical Medicine, Journal Citation Reports, Index Medicus, MEDLINE, PubMed, PubMed Central, Scopus, Reference Citation Analysis, China National Knowledge Infrastructure, China Science and Technology Journal Database, and Superstar Journals Database. The 2022 edition of Journal Citation Reports® cites the 2021 impact factor (IF) for *WJG* as 5.374; IF without journal self cites: 5.187; 5-year IF: 5.715; Journal Citation Indicator: 0.84; Ranking: 31 among 93 journals in gastroenterology and hepatology; and Quartile category: Q2. The *WJG*'s CiteScore for 2021 is 8.1 and Scopus CiteScore rank 2021: Gastroenterology is 18/149.

RESPONSIBLE EDITORS FOR THIS ISSUE

Production Editor: *Hua-Ge Yu*; **Production Department Director:** *Xu Guo*; **Editorial Office Director:** *Jia-Ru Fan.*

NAME OF JOURNAL
World Journal of Gastroenterology

ISSN
ISSN 1007-9327 (print) ISSN 2219-2840 (online)

LAUNCH DATE
October 1, 1995

FREQUENCY
Weekly

EDITORS-IN-CHIEF
Andrzej S Tarnawski

EDITORIAL BOARD MEMBERS
http://www.wjgnet.com/1007-9327/editorialboard.htm

PUBLICATION DATE
June 14, 2023

COPYRIGHT
© 2023 Baishideng Publishing Group Inc

INSTRUCTIONS TO AUTHORS
https://www.wjgnet.com/bpg/gerinfo/204

GUIDELINES FOR ETHICS DOCUMENTS
https://www.wjgnet.com/bpg/GerInfo/287

GUIDELINES FOR NON-NATIVE SPEAKERS OF ENGLISH
https://www.wjgnet.com/bpg/gerinfo/240

PUBLICATION ETHICS
https://www.wjgnet.com/bpg/GerInfo/288

PUBLICATION MISCONDUCT
https://www.wjgnet.com/bpg/gerinfo/208

ARTICLE PROCESSING CHARGE
https://www.wjgnet.com/bpg/gerinfo/242

STEPS FOR SUBMITTING MANUSCRIPTS
https://www.wjgnet.com/bpg/GerInfo/239

ONLINE SUBMISSION
https://www.f6publishing.com

© 2023 Baishideng Publishing Group Inc. All rights reserved. 7041 Koll Center Parkway, Suite 160, Pleasanton, CA 94566, USA
E-mail: bpgoffice@wjgnet.com https://www.wjgnet.com

World Journal of Gastroenterology

Submit a Manuscript: https://www.f6publishing.com

World J Gastroenterol 2023 June 14; 29(22): 3385-3399

DOI: 10.3748/wjg.v29.i22.3385

ISSN 1007-9327 (print) ISSN 2219-2840 (online)

REVIEW

Overview of current detection methods and microRNA potential in *Clostridioides difficile* infection screening

Marco Bocchetti, Maria Grazia Ferraro, Federica Melisi, Piera Grisolia, Marianna Scrima, Alessia Maria Cossu, Tung On Yau

Specialty type: Gastroenterology and hepatology

Provenance and peer review: Invited article; Externally peer reviewed.

Peer-review model: Single blind

Peer-review report's scientific quality classification

Grade A (Excellent): 0
Grade B (Very good): B, B
Grade C (Good): 0
Grade D (Fair): 0
Grade E (Poor): 0

P-Reviewer: Lopitz-Otsoa F, Spain; Zhou B, China

Received: January 25, 2023
Peer-review started: January 25, 2023
First decision: March 15, 2023
Revised: March 23, 2023
Accepted: May 4, 2023
Article in press: May 4, 2023
Published online: June 14, 2023

Marco Bocchetti, Federica Melisi, Piera Grisolia, Alessia Maria Cossu, Department of Precision Medicine, University of Campania "Luigi Vanvitelli," Naples 80138, Italy

Marco Bocchetti, Federica Melisi, Piera Grisolia, Marianna Scrima, Alessia Maria Cossu, Department of Molecular Oncology, Precision Medicine Laboratory and COVID19 Laboratory, Biogem Scarl, Ariano Irpino 83031, Italy

Maria Grazia Ferraro, School of Infection and Immunity, College of Medical Veterinary and Life Sciences, University of Glasgow, Glasgow G12 8QQ, United Kingdom

Maria Grazia Ferraro, Department of Pharmacy, School of Medicine and Surgery, University of Naples "Federico II," Naples 80131, Italy

Tung On Yau, School of Science and Technology, Nottingham Trent University, Nottingham NG11 8NS, United Kingdom

Tung On Yau, Department of Rural Land Use, Scotland's Rural College, Aberdeen AB21 9YA, Scotland, United Kingdom

Tung On Yau, Department of Health Science, University of the People, Pasadena, CA 9110112, United States

Corresponding author: Tung On Yau, BSc, MSc, PhD, Instructor, Lecturer, Researcher, School of Science and Technology, Nottingham Trent University, Clifton Lane, Clifton, Nottingham NG11 8NS, United Kingdom. payton.yau@ntu.ac.uk

Abstract

Clostridioides difficile (formerly called *Clostridium difficile*, *C. difficile*) infection (CDI) is listed as an urgent threat on the 2019 antibiotic resistance threats report in the United States by the Centers for Disease Control and Prevention. Early detection and appropriate disease management appear to be essential. Meanwhile, although the majority of cases are hospital-acquired CDI, community-acquired CDI cases are also on the rise, and this vulnerability is not limited to immunocompromised patients. Gastrointestinal treatments and/or gastrointestinal tract surgeries may be required for patients diagnosed with digestive diseases. Such treatments could suppress or interfere with the patient's immune system and disrupt gut flora homeostasis, creating a suitable microecosystem for *C. difficile* overgrowth. Currently, stool-based non-invasive screening is the first-line approach to CDI

diagnosis, but the accuracy is varied due to different clinical microbiology detection methods; therefore, improving reliability is clearly required. In this review, we briefly summarised the life cycle and toxicity of *C. difficile*, and we examined existing diagnostic approaches with an emphasis on novel biomarkers such as microRNAs. These biomarkers can be easily detected through non-invasive liquid biopsy and can yield crucial information about ongoing pathological phenomena, particularly in CDI.

Key Words: *Clostridioides difficile*; microRNA; Diagnostic; Prognostic; Biomarker

©The Author(s) 2023. Published by Baishideng Publishing Group Inc. All rights reserved.

Core Tip: *Clostridioides difficile* infection (CDI) is listed as an urgent threat, and early detection and appropriate disease management from hospital-acquired or community-acquired CDI appear to be essential. Currently, stool-based non-invasive screening is the first-line approach to CDI diagnosis, but the accuracy is varied due to different clinical microbiology detection methods. Therefore, improving reliability is clearly required. This review summarised the life cycle and toxicity of *Clostridioides difficile* and examined existing diagnostic potentials on microRNA as novel biomarkers. MicroRNAs can be easily detected through non-invasive liquid biopsy and can yield crucial information about ongoing pathological phenomena, particularly in CDI.

Citation: Bocchetti M, Ferraro MG, Melisi F, Grisolia P, Scrima M, Cossu AM, Yau TO. Overview of current detection methods and microRNA potential in *Clostridioides difficile* infection screening. *World J Gastroenterol* 2023; 29(22): 3385-3399
URL: https://www.wjgnet.com/1007-9327/full/v29/i22/3385.htm
DOI: https://dx.doi.org/10.3748/wjg.v29.i22.3385

INTRODUCTION

Clostridioides difficile (formerly called *Clostridium difficile*, *C. difficile*) infection (CDI) was classified as an urgent threat in the 2019 antibiotic resistance report in the United States by the Centers for Disease Control and Prevention. Early detection and disease management are urgently needed to reduce public health spending[1]. In addition, of those infected with a medically-related CDI, 1 in 11 people over the age of 65 dies within a month[2]. The acute inflammation caused by the bacteria triggers cytokine production, neutrophil recruitment, mucosal permeability and fluid secretion, leading to colonic tissue damage, nasal diarrhoea and colitis[3,4], which is similar to inflammatory bowel disease[5].

Presently, although most cases are hospital-acquired CDI, community-acquired CDI cases are rising in frequency[6]. Exposure to *C. difficile* in the community might come from various factors, including pets, water, soil, livestock, farms, food processing and production[7]. Previous studies focused on the hospitalisation length and indicated that environmental exposure to animals would be associated with a greater possibility of *C. difficile* colonisation[8]. A population-based study in India found that the composition of the gut microbiota was primarily associated with several geographical factors rather than body mass index and that these changes extended to circulating immunometabolic profiles such as serum N-glycans, immunoglobulins and short-chain fatty acid profiles[9]. These factors may also affect the infection rate.

Once patients have been diagnosed with digestive diseases, gastrointestinal treatments, including gastric-acid suppressing agents, broad-spectrum antibiotics, chemotherapy and/or gastrointestinal tract surgery may be required[10,11]. Such therapies could suppress or interfere with the patient's immune system and disrupt gut flora homeostasis, creating a suitable microecosystem for *C. difficile* overgrowth [12]. Antibiotics such as metronidazole, vancomycin and fidaxomicin have been approved for treatment of patients with CDI, while *C. difficile* strains resistant to various antibiotics have been reported that do not respond to the treatments[13-15]. Faecal microbiota transplantation (FMT) is an alternative treatment strategy for CDI patients; however, it is still in clinical trials because of the treatment safety concern[16].

To date, there are several diagnostic methods for CDI in medical laboratories. However, due to technical limitations and the difficulty of distinguishing symptomatic infections from asymptomatic *C. difficile* colonisation, the accuracy and turnaround time of the test varies[17]. As a result, searching for better tools may increase the accuracy of the detection. In this light, microRNA (miRNA) expression profiling can be helpful for prognosis and diagnosis.

This article reviewed this proposition by briefly presenting the *C. difficile* life cycle and describing the toxins produced. We then described the current laboratory-based diagnostic tools for CDI patient screening. We discussed the potential use of miRNA to monitor and improve the management of CDI patients.

C. DIFFICILE LIFE CYCLE AND TOXINS

C. difficile is a Gram-positive, anaerobic bacterium belonging to the phylum Firmicutes. There are three main stages that define the *C. difficile* life cycle: spore formation; germination; and growth (vegetative). At the spore stage (dormant phase), it is typically harmless in a balanced gut flora microenvironment. *C. difficile* can resist oxygen, heat and many other environmental insults, including ethanol-based disinfectants (Figure 1)[18].

Once set in a stable environment, spores germinate rapidly and produce two major toxins, toxin A and toxin B encoded by *TcdA* and *TcdB*, which are located at the 19.6 kbp long pathogenicity locus region (Figure 2)[19]. Toxin A and toxin B trigger cytosol translocation of target host cells and inactivate small GTP-binding proteins (such as CDC42, Rho and Rac) through monoglucosylation, leading to actin condensation, cytoskeleton disintegration, cell rounding and apoptosis[20]. tcdR is an RNA polymerase sigma factor that initiates tcdA and tcdB translation *via* its two tandem promoters[21,22] and is involved in the final stages of flagellar assembly[23]. Some *C. difficile* strains, such as ribotype 027 and ribotype 078 are able to produce *C. difficile* transferase toxin, an actin-specific ADP-ribosyltransferase homologous to iota-toxin from *Clostridium perfringens* and *Clostridium spiroforme* toxin, and potentially enhances *C. difficile* virulence and disease severity[24,25].

CURRENT DIAGNOSTIC TOOLS FOR IDENTIFYING PATIENTS WITH *C. DIFFICILE* INFECTION

Similar to colorectal cancer screening, CDI can be detected by examining the colon through flexible sigmoidoscopy or colonoscopy to look for pseudomembranes and inflamed areas. X-ray abdominal imaging or computerised tomography scan can also be applied on a case-by-case basis. In addition to the invasive approaches, the cost effective, non-invasive faecal-based screening is the first-line approach for CDI diagnosis. Still, it varies widely due to different clinical microbiology methods and their different accuracy and variance[26,27]. These methods include cell cytotoxicity neutralisation assay, toxigenic culture (TC), enzyme immunoassay (EIAs) [including toxins and glutamate dehydrogenase (GDH)] and nucleic acid amplification test (NAAT) and each of the methods has advantages and disadvantages in terms of turn-around time and the screening performance (Table 1).

Cell cytotoxicity neutralisation assay and C. difficile culture

The cell cytotoxicity neutralisation assay is the first-line faecal-based diagnostic test for CDI[28,29]. It requires multiple steps in order to isolate *C. difficile* toxins from faeces and at least 24 h of cell culture (mainly human fibroblasts). The cytopathic effect is characterised by rounding and morphologic changes of the cultured cells[29,30], and the phenomena must also be reverted by *C. difficile* or *Clostridium sordellii* anti-toxin used as a control to prove that the cytopathic effect is not related to nonspecific substances in the faeces. In contrast, toxigenic culture requires faeces inoculation to selective cycloserine-cefoxitin-fructose, chromogenic or similar agar plates for a specific incubation period; suspicious colonies are selected for further bacteria culture and/or *C. difficile* toxin test to confirm the finding (Figure 3)[31-33]. It is important to remember that there is no standard to eliminate or reduce nonspecific bacteria colonisation from *C. difficile* culture. Heat shock and alcohol shock are the traditional preculture approaches, while a culture media containing bacteria "suppressors" such as antibiotics may also be applied[34-38]. Both culture-based assays are time-consuming, labour-intensive and require a certain level of laboratory skill. As such, it is unlikely to be used for first-line clinical screening and is commonly used as the reference method for research and outbreak investigations, even though it is considered the gold standard[31,32,38].

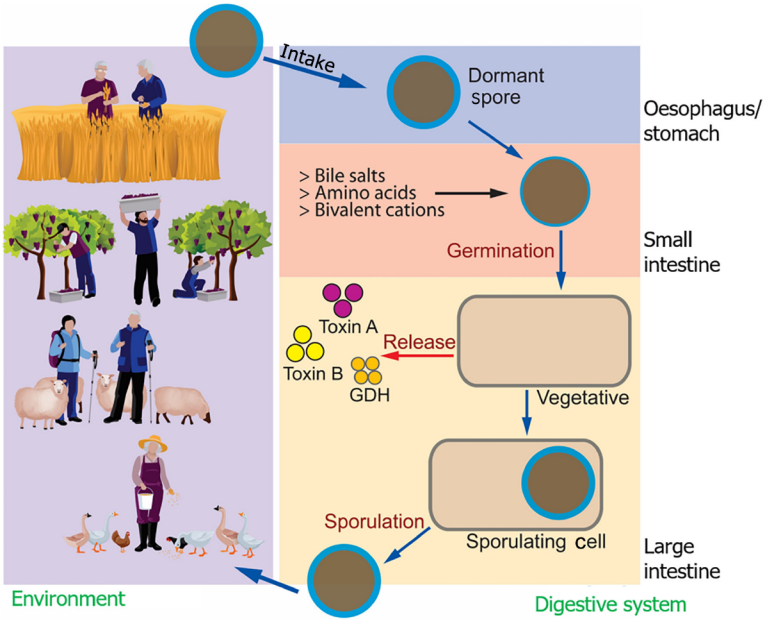
Nucleic acid-based detection assays

The nucleic acid amplification test is a quantitative real-time (qRT)-PCR-based diagnostic assay able to rapidly detect *C. difficile* toxin genes such as *tcdA, tcdB, tcdBv, cdt* and/or *tcdC*Δ117 at the DNA level. There is a wide range of United States Food and Drug Administration-approved detection assays, from *C. difficile* specific point-of-care testing to high-volume, high-throughput multiple gastrointestinal pathogens laboratory tests. The majority of PCR detection approaches for *C. difficile* screening are probe-based qRT-PCR (Table 2). The use of probes increases amplification specificity during the PCR cycle since the additional sequence of the probe is specific for and binds to the *C. difficile* DNA sequence. Additionally, it is possible to perform multiplex qRT-PCR by using different fluorescent dyes[39]. The

Table 1 Summary of *Clostridioides difficile* diagnostic tests

Test	Abbreviation	Sensitivity	Specificity	Turn-around time	Target substance
Culture-based					
Cell cytotoxicity neutralisation assay	CCTN	High	High	< 24 h	Toxins
Toxigenic culture	TC	High	Low[1]	> 3 d	*C. difficile* vegetative cells or spores
DNA-based					
Nucleic acid amplification test[2]	NAAT	High	Low/moderate	< 4 h	Toxin genes
Protein-based					
Glutamate dehydrogenase	GDH-EIA	High	Low[1]	< 2 h	*C. difficile* antigens
Toxin A and B enzyme immunoassays	EIA	Low	Moderate	< 2 h	Toxins

[1]Nucleic acid amplification test, mainly using the PCR technique.
[2]Must be combined with a toxin test.
C. difficile: *Clostridioides difficile*; TC: Toxigenic culture; NAAT: Nucleic acid amplification test; CCTN: Cell cytotoxicity neutralisation assay; GDH: Glutamate dehydrogenase; EIA: Enzyme immunoassay.



DOI: 10.3748/wjg.v29.i22.3385 **Copyright** ©The Author(s) 2023.

Figure 1 *Clostridioides difficile* life cycle. *Clostridioides difficile* (*C. difficile*) can be found in soil and is transmitted to humans (as well as animals) through different daily activities. Besides hospital-acquired *C. difficile* infections, community-acquired *C. difficile* infections are also known, with agriculture being one of the main sources, from the spore stage into the human digestive system. Once stable, *C. difficile* may repopulate and release toxins that can affect intestinal health. *C. difficile* may go back to the environment and repeat the life cycle. GDH: Glutamate dehydrogenase.

nucleic acid-based *C. difficile* toxin screening has over ten times higher sensitivity than a cytotoxin assay [40,41], but the screening specificity is relatively low due to high false positive cases from asymptomatic infection. As a result, optimisation is required, especially on PCR threshold cycle settings[42,43]. In addition, patient preselection based on clinical symptoms and intestinal inflammation biomarkers (*i.e.* faecal calprotectin, lactoferrin and cytokines) appears to be necessary to reduce the risk of a false positive[27,43-47].

Toxins and GDH EIA

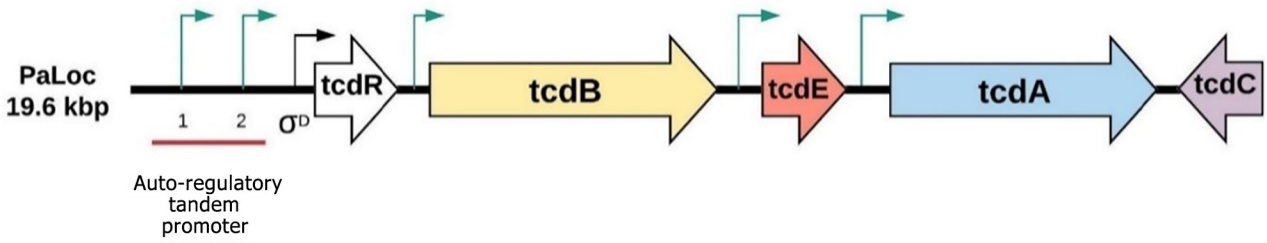
EIAs utilise antibodies to detect the presence of antigens. It is still relatively common to detect toxin A, toxin B and/or GDH in faeces for CDI. There are several types of EIAs available for CDI, including microplates (enzyme-linked immunosorbent assay), membrane EIA, chemiluminescence immunoassay, enzyme-linked fluorescent assay and chromatographic immunoassay (Table 3). A meta-analysis

Table 2 Selected Food and Drug Administration-approved molecular assays

Assay name	Developer	Target	Method	Sensitivity/specificity (%)
AmpliVue *C. difficile* assay[70]	Quidel	*tcdA*	Isothermal nucleic acid amplification	93.6/94.1
ARIES *C. difficile* assay[71,72]	Luminex	*tcdA* and *tcdB*	qRT-PCR	90-98/92-98
ARTUS *C. difficile* QS-RGQ MDX Kit [73]	QIAGEN, GMBH	*tcdA* and *tcdB* (+ *tcdBv*)	qRT-PCR	100/90-100
BD Diagnostics BD MAX *C. diff* assay[71,74-77]	GeneOhm Sciences	*tcdB*	TaqMan probe-based qRT-PCR	86-98/89-100
BD GeneOhm *C. diff* assay[78-82]	BD Diagnostics/GeneOhm Sciences	*tcdB*	Beacon probe-based PCR	91-95/96-100
Cobas *C. diff* Nucleic Acid Test For Use On The Cobas Liat System[83, 84]	Roche	*tcdB*	TaqMan probe-based qRT-PCR	93/99
GenePOC *C. diff*[85]	GenePOC	*tcdB* of toxigenic C	TaqMan probe-based qRT-PCR	81/97
ICEPlex *C. diff* Kit[1][86]	PrimeraDx	*tcdB*	qRT-PCR + capillary electrophoresis-based detection	90/97
Illumigene *C. diff* DNA Amplification assay[77]	Meridian Bioscience	*tcdA*	Loop-mediated isothermal DNA amplification	82-100/94-100
IMDx *C. difficile* for Abbott m2000 [76,77]	Intelligent Medical Devices	*tcdA* and *tcdB* (+ *tcdBv*)	Probe-based qRT-PCR	62-84/94-99
Portrait Toxigenic *C. difficile* assay [87,88]	Great Basin Scientific	*tcdB*	Primer-mediated helicase-dependent amplification + chip-based detection	98.2/92.8
ProGastro Cd assay[81,89]	Prodesse	*tcdB*	Probe-based qRT-PCR	77-100/94-99
Quidel Molecular Direct *C. difficile* assay[70,90]	Quidel	tcdA and tcdB	TaqMan probe-based qRT-PCR	82-96/97-100
Simplexa *C. difficile* Universal Direct assay[70,91]	Focus Diagnostics	*tcdB*	qRT-PCR + bifunctional fluorescent primer-probes	87-98/99-100
Solana *C. difficile* assay[1][92]	Quidel	*tcdA*	Helicase-dependent amplification	93/99
Verigene *C. difficile* Nucleic acid Test [91,93,94]	Nanosphere	tcdA, tcdB, *cdt* and *tcdC*Δ117	PCR + nanoparticle-based array	94-96/96-98
X/Pert *C. difficile*/Epi[71,77,95,96]	Cepheid	tcdA, tcdB, *cdt* and *tcdC*Δ117	TaqMan probe-based qRT-PCR	90-100/93-99

[1]The sensitivity and specificity were provided by the manufacturer.

*tcdC*Δ117: The *tcdC* deletion nt 117; *tcdBv*: tcdB variant; *cdt*: Binary toxin; *C. difficile* or *C. diff*: *Clostridioides difficile*; qRT: Quantitative real-time.



DOI: 10.3748/wjg.v29.i22.3385 **Copyright** ©The Author(s) 2023.

Figure 2 Pathogenicity loci of toxicogenic *Clostridioides difficile*. The 19.6 kbp long pathogenicity loci in toxicogenic *Clostridioides difficile*, including *tcdC*, *tcdA*, *tcdE*, *tcdB* and *tcdR* coding genes. *tcdR* codes for an RNA polymerase sigma factor that controls the expression of the *tcdB* and *tcdA* genes and possibly *tcdE*. The transcription of *tcdR* can be regulated by three promoters. One is under the control of σ^0, and the other two are autoregulatory tandem promoters. Figure adopted and modified from Isidro *et al*[19].

published in 2016 evaluated the major commercially available *C. difficile* diagnosis assays compared to the gold standards. The pooled sensitivities were 83% [95% confidence interval (CI): 76%-88%] and 57% (95%CI: 51%-63%) compared to cell culture cytotoxicity assay and toxigenic bacterial culture,

Table 3 Major immunochromatographic membrane assays

Methods/assays	Target(s)	Developer	Cell cytotoxicity assay		Toxigenic culture	
			Sen, %	Spe, %	Sen, %	Spe, %
Microwell enzyme immunoassay (enzyme-linked immunosorbent assay)						
GA *C. diff* Antigen[97]	Toxin A + B	The Binding Site	76.8	90.0	68.8	91.4
Premier toxin A+B[97-106]	Toxin A + B	Meridian Bioscience	58-99	94-100	40-86	91-100
Ridascreen toxin A/B[97,107,108]	Toxin A + B	Ridascreen	57-67	95-97	52-60	96-98
ProSpecT toxin A/B[97,109]	Toxin A + B	Remel/Oxoid (Thermo Scientific)	90-91	93-97	82	93
Techlab *C. diff* Chek-60 (GDH)[53,97,110]	GDH	Techlab	92.0-93.5	94.0-98.0	88.0-93.0	94.0-97.0
TechLab toxin A/B II[81,97,100,109-111]	Toxin A + B	TechLab	72-91	87-100	58-85	96-99
Membrane enzyme immunoassay						
ImmunoCard toxins A/B[41,97,109,112,113]	Toxin A + B	Meridian Bioscience	85-96	97-99	41-69	93-99
Quick Chek Complete[40,105,112,114-117]	Toxin A + B	TechLab	50-73	100	29-79	89-100
Remel X/pect *C. diff* toxin A/B[97,113,118]	Toxin A + B	Remel	44-83	99-100	48-69	95-99
Tox A/B Quick Check[97,115,119-121]	Toxin A + B	TechLab	61-84	99	40-74	94-100
Chemiluminescence immunoassay						
Liaison *C. difficile* toxins A and B[122,123]	Toxin A + B	DiaSorin	88	95	69-88	95-99
Enzyme-linked fluorescent assay						
Vidas toxin A and B[97,116,123-128]	Toxin A + B	Vidas	53-98	99-100	44-80	95-99
Vidas GDH[40,129]	GDH	Vidas	97	87	56	100

Sen: Sensitivity; Sep: Specificity; GDH: Glutamate dehydrogenase; *C. difficile* or *C. diff*: *Clostridioides difficile*.

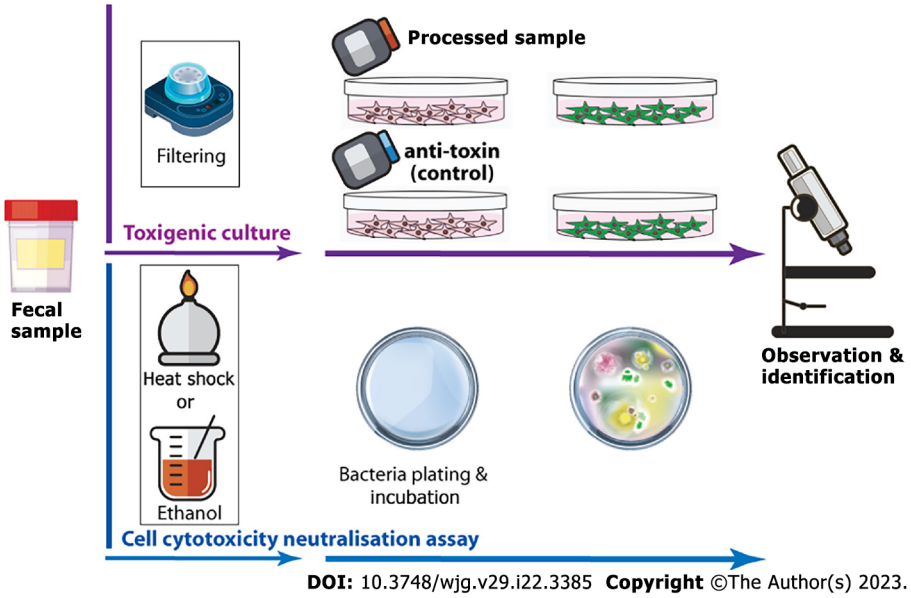


Figure 3 Idealised summary of toxigenic culture and cell cytotoxicity neutralisation assay for *Clostridioides difficile* infection identification. In toxigenic culture, the faecal sample is first exposed to heat shock or alcohol shock to kill *Clostridioides difficile* (*C. difficile*) and other microorganisms, and heat/alcohol resistant spores of *C. difficile* survive. The sample is then plated on selective agar and incubated anaerobically at 37 °C for at least 48 h to observe and confirm the colonisation of *C. difficile*. For the cell cytotoxicity neutralisation assay, the faecal sample is filtered and added to a toxin-sensitive cell line with/without antiserum. After 24-48 h of incubation, the cytopathological effect is then examined microscopically.

respectively, at a specificity of 99%[48]. This may be because these EIAs were developed in the early 21st century and are less sensitive to low toxin(s) levels, and immunocompromised CDI patients have a lower concentration trigger point[49]. This meta-analysis also indicated that GDH detection had a range

of 94% (95%CI: 86%-97%) for sensitivity and 96% (95%CI: 92%-98%) for specificity compared to toxigenic bacterial culture and cell culture cytotoxicity assay together[48]. However, a few studies reported sensitivities below 90% for GDH assays[38,50,51]. Due to the known limitations and relatively poor accuracy, stand-alone toxin or GDH EIA tests are not recommended by professional medical societies, including the European Society of Clinical Microbiology and Infectious Diseases and the Infectious Diseases Society of America[27,48,52].

As a result, several multiple-step diagnostic algorithms have been proposed to improve assay performance and detection accuracy. For example, a two-step algorithm initially detects GDH, and positive GDH cases are followed up with a toxin A and/or toxin B immunoassay. If the toxin immunoassay result is negative, a bacterial culture will be performed[53]. In addition, new protein-based assays such as lateral flow assay are under development and may potentially yield a result in 15 min[54].

MIRNA DYSREGULATION AND *C. DIFFICILE* INFECTION DETECTION AND MONITORING POTENTIAL

miRNAs are small single-stranded endogenous RNA molecules that are key regulators of gene expression and silencing at the post-transcriptional level. miRNA complex biosynthesis begins in the nucleus where primary miRNAs are produced by transcription of miRNAs from DNA sequences or miRNA genes. Precursor miRNAs are transcripts of approximately 60-110 nucleotides in length with a shorter stem-loop structure, produced from primary miRNAs by RNase type III enzymes (DROSHA) and undergo several maturation processes inside and outside the nucleus to form mature miRNAs, which are transported into the cytoplasm[55].

The stability of miRNA-specific target mRNAs is disturbed when RNA-induced silencing complexes possess loaded miRNAs. A portion of the miRNA, the seed sequence, which is two to eight nucleotides long, pairs with a specific sequence on the target mRNA and is referred to as an miRNA response element that results in translational repression and degradation of the target mRNA due to the binding of miRNAs in the 3′ untranslated region. miRNAs primarily repress genes by inhibiting protein synthesis, preventing elongation and ribosome decline and disrupting mRNAs through the processes of demethylation and decap, resulting in their degradation[56].

miRNAs have the potential to act *via* molecular mechanisms at every step of CDI, inhibiting specific transcripts or inflammatory molecule transcription, thereby influencing the pathology grade. The imbalance of these biomarkers can be measured and exploited for diagnosis, coupled with standard methods to strengthen the results. In particular, miRNAs are easily detectable (through sequencing, RT-qPCR, *etc*) in body fluids such as saliva, blood and even faecal material, and their levels correlate with target transcript alterations or non-physiological events[57]. These biomarkers are contributing increasingly to the establishment of less invasive "liquid biopsies," which is important and appealing for patient compliance compared to normal, invasive biopsies that require a long time for results. Although, it cannot fully substitute canonical diagnosis methods in most cases currently, it will undoubtedly happen in the near future.

Numerous studies have shown that miRNAs can be used to detect diseases and for their management. This may apply to patients with CDI. However, studies of the relationship between CDI and host miRNA are limited. To the best of our knowledge, the first reported study utilised C57BL/6J wild-type mice with a CDI model and identified the induction of mmu-miR-146b, mmu-miR-1940 and mmu-miR-1298 expression and upregulated proinflammatory cytokine expression, such as monocyte chemoattractant protein-1, interleukin (IL)-6, IL-17 and IL-1β in colonic tissues[58]. The authors also showed that the miR-146b potentially targets nuclear receptor co-activator 4 (NCOA4), *CD36* and *GLUT4* mRNA expression levels were downregulated. *In silico* simulation predicts upregulation of mmu-miR-146b and IL-17 resulting in the downregulation of *NCOA4* and peroxisome proliferator-activated receptor gamma (*PPAR-γ*) in the CDI mice model. Null mice silenced for *PPAR-γ* in T cells following CDI presented more severe colonic disease activity, inflammatory lesions and inflammatory cytokine expression[58]. There is also a filed patent claiming that miR-27a-5p could modulate the inflammatory response induced by CDI[59]. The inventors claim that miR-27a-5p can be linked to a matrix and delivered by vectors and/or incorporated into particles. The miR-27a-5p-linked particle could be administered to infected subjects for the treatment[59]. In faeces, a small-scale study with only 8 CDI participants demonstrated that a higher level of faecal hsa-miR-1246 was found in human CDI patients compared to the control group[60].

FMT has been proven in the treatment of recurrent CDI[61,62]. It is intended to restore colonic microbiota through introducing "healthy" bacteria *via* colonoscopy, enema or oral capsules that contain bacteria in a powder form. However, the safety concerns of FMT could be an obstacle to extending the application as a regular treatment strategy[63,64]. To monitor treatment conditions, detecting a panel of miRNA markers in circulation could help physicians make a more accurate decision[65,66]. Another study showed that 71 different circulating miRNAs were found to be expressed in 126 sera from 42 patients at 4 wk and 12 wk after FMT treatment[65]. The authors used qRT-PCR and 3′ untranslated

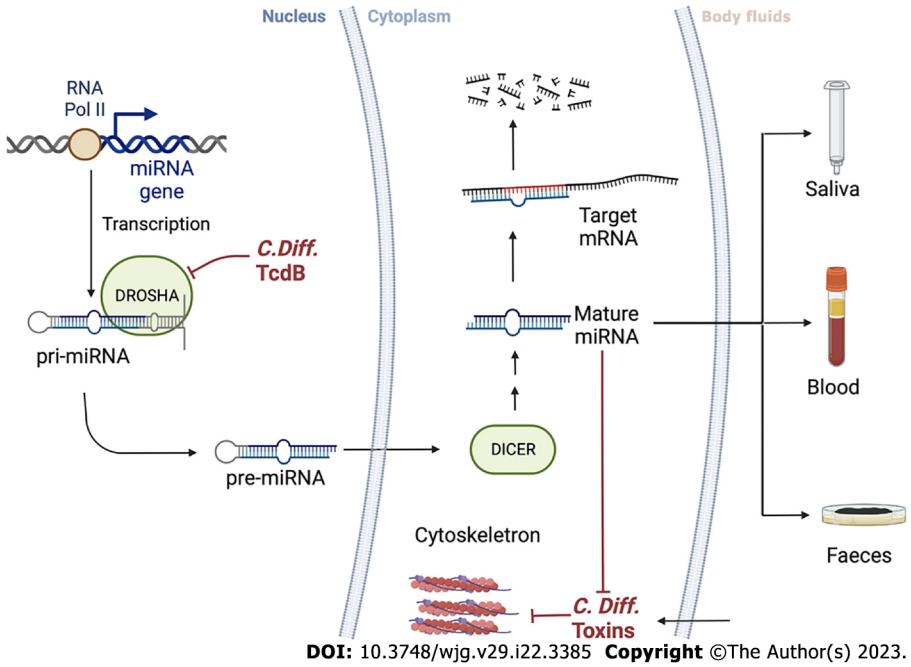


Figure 4 *Clostridioides difficile* and microRNAs cross-interact inside the cells. microRNA (miRNA) is a small single-stranded RNA that plays a key role in gene expression regulation. It starts in the cell nucleus, where primary miRNAs are produced by RNA Pol II through miRNA transcription from DNA sequences or miRNA genes. Precursor miRNA, around 60-110 nucleotides long transcripts with a shorter stem-loop structure, are produced from primary miRNAs by RNase type III (DROSHA) enzyme with several maturation processes and is then transported to the cytoplasm *via* DICER. Toxin B from *Clostridioides difficile* may interfere with DROSHA function. A fraction of miRNA binding specific sequences (2-8 nucleotides long) can pair with miRNA response elements in the 3' untranslated region of the target mRNA, causing translational repression and degradation of the target mRNA. Thus, miRNA expression patterns can indicate non-physiological events such as *Clostridioides difficile* infection. By detecting changes in miRNA patterns in body fluids, such as saliva, blood, and stool, the screening accuracy can be improved. miRNA: microRNA; pri-miRNA: Primary miRNA; pre-miRNA: Precursor miRNA; *C. difficile*: *Clostridioides difficile*.

region luciferase reporter assays to validate the top miRNA candidates and confirmed that hsa-miR-23a-3p, hsa-miR-150-5p, hsa-miR-26b-5p and hsa-miR-28-5p expression levels inversely correlated with the sera protein and cell-free circulating mRNA on several inflammation-related biomarkers, such as IL-12B, IL-18, FGF21 and TNFRSF9[65].

In a mouse model of relapsing CDI, qRT-PCR analyses of faecal and sera RNA extracts revealed inhibition of these miRNAs, while the FMT treatment enabled the recovery of their inhibitory effect. This study also showed that toxin B (TcdB) mediates the inhibitory effect of CDI on miRNA *via* DROSHA, based on the human colonoids and the mice colon models, where miR-23a and miR-150 were used to demonstrate the cytoprotective effects against TcdB[65]. A small, in-depth phenomics study of four adults treated with sequential FMT for severe or fulminant CDI found that miR-451a and miR-16 from the serum samples were upregulated in the responders *vs* the non-responders on average across all timepoints[66].

Using miRNAs as a diagnostic tool for CDI presents both opportunities and challenges. On one hand, as miRNAs play a role in controlling and influencing gene expression, changes in their activity and expression levels can be associated with different pathological events. This makes miRNA expression patterns a potentially powerful diagnostic tool, with the potential for use in therapeutic applications. Monitoring the response to FMT with miRNA can be an additional indicator for personalised treatment, and miRNA detection from non-invasive sources, such as blood, faeces, urine and saliva, can provide convenient and longitudinal measurements of miRNA levels for CDI. On the other hand, the fact that miRNA can be derived from blood cells released by different pathological events makes detecting CDI specifically a challenging task. Therefore, the use of miRNAs as a diagnostic tool for CDI requires further research and validation. Figure 4 provides a schematic summary of the intracellular mechanisms discussed and the potential use of miRNA profiling from a variety of body fluids, such as liquid biopsies, for diagnostic purposes as demonstrated in various research studies related to colorectal cancer screening[67-69].

CONCLUSION

To date, current laboratory-based CDI assays have varied in their detection accuracy. The expression of miRNAs has become increasingly important as novel biomarkers for assessment. The different signature profiles obtained through the differential expression of these small non-coding RNAs are essential for

early diagnosis and prediction of therapeutic response and disease management, these are also including cancer and infection. Notably, this can be accomplished by using liquid biopsy, enabling a non-invasive and low-cost screening approach. This approach may also be used to detect *C. difficile* infections, while further research and validation are clearly needed. These reported miRNA studies can be used in conjunction with current diagnostic tools to improve diagnostic accuracy aiding in patient management for both symptomatic and asymptomatic CDI patients.

FOOTNOTES

Author contributions: Yau TO and Bocchetti M contributed to conceptualisation; Yau TO, Bocchetti M and Ferraro MG wrote the original draft; Yau TO, Bocchetti M, Ferraro MG, Melisi F, Grisolia P, Scrima M and Cossu AM wrote the review and contributed to editing; Yau TO and Bocchetti M contributed to visualisation; Yau TO performed the project administration and funding acquisition; All authors read and agreed to the published version of the manuscript.

Conflict-of-interest statement: All the authors report no relevant conflicts of interest for this article.

Open-Access: This article is an open-access article that was selected by an in-house editor and fully peer-reviewed by external reviewers. It is distributed in accordance with the Creative Commons Attribution NonCommercial (CC BY-NC 4.0) license, which permits others to distribute, remix, adapt, build upon this work non-commercially, and license their derivative works on different terms, provided the original work is properly cited and the use is non-commercial. See: https://creativecommons.org/Licenses/by-nc/4.0/

Country/Territory of origin: United Kingdom

ORCID number: Marco Bocchetti 0000-0002-2143-6669; Tung On Yau 0000-0002-3283-0370.

S-Editor: Fan JR
L-Editor: Filipodia
P-Editor: Yu HG

REFERENCES

1 **U. S. Centers for Disease Control and Prevention**. Antibiotic resistance threats in the United States, 2019. Atlanta, Georgia. Available from: https://stacks.cdc.gov/view/cdc/82532
2 **Lessa FC**, Mu Y, Bamberg WM, Beldavs ZG, Dumyati GK, Dunn JR, Farley MM, Holzbauer SM, Meek JI, Phipps EC, Wilson LE, Winston LG, Cohen JA, Limbago BM, Fridkin SK, Gerding DN, McDonald LC. Burden of Clostridium difficile infection in the United States. *N Engl J Med* 2015; **372**: 825-834 [PMID: 25714160 DOI: 10.1056/NEJMoa1408913]
3 **Karlsson S**, Dupuy B, Mukherjee K, Norin E, Burman LG, Akerlund T. Expression of Clostridium difficile toxins A and B and their sigma factor TcdD is controlled by temperature. *Infect Immun* 2003; **71**: 1784-1793 [PMID: 12654792 DOI: 10.1128/iai.71.4.1784-1793.2003]
4 **Adams SD**, Mercer DW. Fulminant Clostridium difficile colitis. *Curr Opin Crit Care* 2007; **13**: 450-455 [PMID: 17599017 DOI: 10.1097/MCC.0b013e3282638879]
5 **Yau TO**, Vadakekolathu J, Foulds GA, Du G, Dickins B, Polytarchou C, Rutella S. Hyperactive neutrophil chemotaxis contributes to anti-tumor necrosis factor-α treatment resistance in inflammatory bowel disease. *J Gastroenterol Hepatol* 2022; **37**: 531-541 [PMID: 34931384 DOI: 10.1111/jgh.15764]
6 **Fu Y**, Luo Y, Grinspan AM. Epidemiology of community-acquired and recurrent Clostridioides difficile infection. *Therap Adv Gastroenterol* 2021; **14**: 17562848211016248 [PMID: 34093740 DOI: 10.1177/17562848211016248]
7 **Kachrimanidou M**, Tzika E, Filioussis G. Clostridioides (Clostridium) Difficile in Food-Producing Animals, Horses and Household Pets: A Comprehensive Review. *Microorganisms* 2019; **7** [PMID: 31835413 DOI: 10.3390/microorganisms7120667]
8 **Muñoz-Price LS**, Hanson R, Singh S, Nattinger AB, Penlesky A, Buchan BW, Ledeboer NA, Beyer K, Namin S, Zhou Y, Pezzin LE. Association Between Environmental Factors and Toxigenic Clostridioides difficile Carriage at Hospital Admission. *JAMA Netw Open* 2020; **3**: e1919132 [PMID: 31922563 DOI: 10.1001/jamanetworkopen.2019.19132]
9 **Monaghan TM**, Biswas RN, Nashine RR, Joshi SS, Mullish BH, Seekatz AM, Blanco JM, McDonald JAK, Marchesi JR, Yau TO, Christodoulou N, Hatziapostolou M, Pucic-Bakovic M, Vuckovic F, Klicek F, Lauc G, Xue N, Dottorini T, Ambalkar S, Satav A, Polytarchou C, Acharjee A, Kashyap RS. Multiomics Profiling Reveals Signatures of Dysmetabolism in Urban Populations in Central India. *Microorganisms* 2021; **9** [PMID: 34361920 DOI: 10.3390/microorganisms9071485]
10 **Janarthanan S**, Ditah I, Adler DG, Ehrinpreis MN. Clostridium difficile-associated diarrhea and proton pump inhibitor therapy: a meta-analysis. *Am J Gastroenterol* 2012; **107**: 1001-1010 [PMID: 22710578 DOI: 10.1038/ajg.2012.179]
11 **Roughead EE**, Chan EW, Choi NK, Griffiths J, Jin XM, Lee J, Kimura M, Kimura T, Kubota K, Lai EC, Man KK, Nguyen TA, Ooba N, Park BJ, Sato T, Shin JY, Wang T, Wong IC, Yang YK, Pratt NL. Proton pump inhibitors and risk of Clostridium difficile infection: a multi-country study using sequence symmetry analysis. *Expert Opin Drug Saf* 2016;

15: 1589-1595 [PMID: 27645304 DOI: 10.1080/14740338.2016.1238071]
12 **Rineh A**, Kelso MJ, Vatansever F, Tegos GP, Hamblin MR. Clostridium difficile infection: molecular pathogenesis and novel therapeutics. *Expert Rev Anti Infect Ther* 2014; **12**: 131-150 [PMID: 24410618 DOI: 10.1586/14787210.2014.866515]
13 **Lyras D**, Adams V, Lucet I, Rood JI. The large resolvase TnpX is the only transposon-encoded protein required for transposition of the Tn4451/3 family of integrative mobilizable elements. *Mol Microbiol* 2004; **51**: 1787-1800 [PMID: 15009902 DOI: 10.1111/j.1365-2958.2003.03950.x]
14 **Sebaihia M**, Wren BW, Mullany P, Fairweather NF, Minton N, Stabler R, Thomson NR, Roberts AP, Cerdeño-Tárraga AM, Wang H, Holden MT, Wright A, Churcher C, Quail MA, Baker S, Bason N, Brooks K, Chillingworth T, Cronin A, Davis P, Dowd L, Fraser A, Feltwell T, Hance Z, Holroyd S, Jagels K, Moule S, Mungall K, Price C, Rabbinowitsch E, Sharp S, Simmonds M, Stevens K, Unwin L, Whithead S, Dupuy B, Dougan G, Barrell B, Parkhill J. The multidrug-resistant human pathogen Clostridium difficile has a highly mobile, mosaic genome. *Nat Genet* 2006; **38**: 779-786 [PMID: 16804543 DOI: 10.1038/ng1830]
15 **Maxwell-Scott HG**, Goldenberg SD. Existing and investigational therapies for the treatment of Clostridium difficile infection: A focus on narrow spectrum, microbiota-sparing agents. *Med Mal Infect* 2018; **48**: 1-9 [PMID: 29169816 DOI: 10.1016/j.medmal.2017.10.008]
16 **Hensgens MP**, Goorhuis A, Dekkers OM, Kuijper EJ. Time interval of increased risk for Clostridium difficile infection after exposure to antibiotics. *J Antimicrob Chemother* 2012; **67**: 742-748 [PMID: 22146873 DOI: 10.1093/jac/dkr508]
17 **Bagdasarian N**, Rao K, Malani PN. Diagnosis and treatment of Clostridium difficile in adults: a systematic review. *JAMA* 2015; **313**: 398-408 [PMID: 25626036 DOI: 10.1001/jama.2014.17103]
18 **Wilcox MH**. Gastrointestinal disorders and the critically ill. Clostridium difficile infection and pseudomembranous colitis. *Best Pract Res Clin Gastroenterol* 2003; **17**: 475-493 [PMID: 12763508 DOI: 10.1016/s1521-6918(03)00017-9]
19 **Isidro J**, Mendes AL, Serrano M, Henriques AO, Oleastro M. Overview of Clostridium difficile Infection: Life Cycle, Epidemiology, Antimicrobial Resistance and Treatment. In: Clostridium Difficile-A Comprehensive Overview. *InTech* 2017 [DOI: 10.5772/intechopen.69053]
20 **Voth DE**, Ballard JD. Clostridium difficile toxins: mechanism of action and role in disease. *Clin Microbiol Rev* 2005; **18**: 247-263 [PMID: 15831824 DOI: 10.1128/CMR.18.2.247-263.2005]
21 **Mani N**, Dupuy B. Regulation of toxin synthesis in Clostridium difficile by an alternative RNA polymerase sigma factor. *Proc Natl Acad Sci U S A* 2001; **98**: 5844-5849 [PMID: 11320220 DOI: 10.1073/pnas.101126598]
22 **Mani N**, Lyras D, Barroso L, Howarth P, Wilkins T, Rood JI, Sonenshein AL, Dupuy B. Environmental response and autoregulation of Clostridium difficile TxeR, a sigma factor for toxin gene expression. *J Bacteriol* 2002; **184**: 5971-5978 [PMID: 12374831 DOI: 10.1128/jb.184.21.5971-5978.2002]
23 **El Meouche I**, Peltier J, Monot M, Soutourina O, Pestel-Caron M, Dupuy B, Pons JL. Characterization of the SigD regulon of C. difficile and its positive control of toxin production through the regulation of tcdR. *PloS One* 2013; **8**: e83748 [PMID: 24358307 DOI: 10.1371/journal.pone.0083748]
24 **Perelle S**, Gibert M, Bourlioux P, Corthier G, Popoff MR. Production of a complete binary toxin (actin-specific ADP-ribosyltransferase) by Clostridium difficile CD196. *Infect Immun* 1997; **65**: 1402-1407 [PMID: 9119480 DOI: 10.1128/IAI.65.4.1402-1407.1997]
25 **Barth H**, Aktories K, Popoff MR, Stiles BG. Binary bacterial toxins: biochemistry, biology, and applications of common Clostridium and Bacillus proteins. *Microbiol Mol Biol Rev* 2004; **68**: 373-402, table of contents [PMID: 15353562 DOI: 10.1128/MMBR.68.3.373-402.2004]
26 **Lübbert C**, John E, von Müller L. Clostridium difficile infection: guideline-based diagnosis and treatment. *Dtsch Arztebl Int* 2014; **111**: 723-731 [PMID: 25404529 DOI: 10.3238/arztebl.2014.0723]
27 **McDonald LC**, Gerding DN, Johnson S, Bakken JS, Carroll KC, Coffin SE, Dubberke ER, Garey KW, Gould CV, Kelly C, Loo V, Shaklee Sammons J, Sandora TJ, Wilcox MH. Clinical Practice Guidelines for Clostridium difficile Infection in Adults and Children: 2017 Update by the Infectious Diseases Society of America (IDSA) and Society for Healthcare Epidemiology of America (SHEA). *Clin Infect Dis* 2018; **66**: e1-e48 [PMID: 29462280 DOI: 10.1093/cid/cix1085]
28 **Bartlett JG**, Chang TW, Gurwith M, Gorbach SL, Onderdonk AB. Antibiotic-associated pseudomembranous colitis due to toxin-producing clostridia. *N Engl J Med* 1978; **298**: 531-534 [PMID: 625309 DOI: 10.1056/NEJM197803092981003]
29 **Chang TW**, Lauermann M, Bartlett JG. Cytotoxicity assay in antibiotic-associated colitis. *J Infect Dis* 1979; **140**: 765-770 [PMID: 231071 DOI: 10.1093/infdis/140.5.765]
30 **Tichota-Lee J**, Jaqua-Stewart MJ, Benfield D, Simmons JL, Jaqua RA. Effect of age on the sensitivity of cell cultures to Clostridium difficile toxin. *Diagn Microbiol Infect Dis* 1987; **8**: 203-214 [PMID: 3449315 DOI: 10.1016/0732-8893(87)90051-4]
31 **Perry JD**. A Decade of Development of Chromogenic Culture Media for Clinical Microbiology in an Era of Molecular Diagnostics. *Clin Microbiol Rev* 2017; **30**: 449-479 [PMID: 28122803 DOI: 10.1128/CMR.00097-16]
32 **Housman ST**, Banevicius MA, Lamb LM, Nicolau DP. Isolation and quantitation of Clostridium difficile in aqueous and fecal matter using two types of selective media. *J Microbiol Immunol Infect* 2016; **49**: 445-447 [PMID: 26198865 DOI: 10.1016/j.jmii.2015.05.012]
33 **Binning M**, John MA, Schieven BC, Austin TW, Lannigan R, Hussain Z. Comparison of culture, cytotoxin assay and two EIA tests with clinical diagnosis of Clostridium difficile-associated diarrhea. *Can J Infect Dis* 1994; **5**: 163-167 [PMID: 22346495 DOI: 10.1155/1994/804205]
34 **Tyrrell KL**, Citron DM, Leoncio ES, Merriam CV, Goldstein EJ. Evaluation of cycloserine-cefoxitin fructose agar (CCFA), CCFA with horse blood and taurocholate, and cycloserine-cefoxitin mannitol broth with taurocholate and lysozyme for recovery of Clostridium difficile isolates from fecal samples. *J Clin Microbiol* 2013; **51**: 3094-3096 [PMID: 23804392 DOI: 10.1128/JCM.00879-13]
35 **Hink T**, Burnham CA, Dubberke ER. A systematic evaluation of methods to optimize culture-based recovery of Clostridium difficile from stool specimens. *Anaerobe* 2013; **19**: 39-43 [PMID: 23247066 DOI: 10.1016/j.anaerobe.2012.12.001]

36 **Mundy LS**, Shanholtzer CJ, Willard KE, Gerding DN, Peterson LR. Laboratory detection of Clostridium difficile. A comparison of media and incubation systems. *Am J Clin Pathol* 1995; **103**: 52-56 [PMID: 7817945 DOI: 10.1093/ajcp/103.1.52]

37 **Bliss DZ**, Johnson S, Clabots CR, Savik K, Gerding DN. Comparison of cycloserine-cefoxitin-fructose agar (CCFA) and taurocholate-CCFA for recovery of Clostridium difficile during surveillance of hospitalized patients. *Diagn Microbiol Infect Dis* 1997; **29**: 1-4 [PMID: 9350408 DOI: 10.1016/s0732-8893(97)00113-2]

38 **Burnham CA**, Carroll KC. Diagnosis of Clostridium difficile infection: an ongoing conundrum for clinicians and for clinical laboratories. *Clin Microbiol Rev* 2013; **26**: 604-630 [PMID: 23824374 DOI: 10.1128/CMR.00016-13]

39 **Angione SL**, Sarma AA, Novikov A, Seward L, Fieber JH, Mermel LA, Tripathi A. A novel subtyping assay for detection of Clostridium difficile virulence genes. *J Mol Diagn* 2014; **16**: 244-252 [PMID: 24434086 DOI: 10.1016/j.jmoldx.2013.11.006]

40 **Xiao Y**, Liu Y, Qin X. Comparative Study of Clostridium difficile Clinical Detection Methods in Patients with Diarrhoea. *Can J Infect Dis Med Microbiol* 2020; **2020**: 8753284 [PMID: 32064010 DOI: 10.1155/2020/8753284]

41 **van den Berg RJ**, Bruijnesteijn van Coppenraet LS, Gerritsen HJ, Endtz HP, van der Vorm ER, Kuijper EJ. Prospective multicenter evaluation of a new immunoassay and real-time PCR for rapid diagnosis of Clostridium difficile-associated diarrhea in hospitalized patients. *J Clin Microbiol* 2005; **43**: 5338-5340 [PMID: 16208012 DOI: 10.1128/JCM.43.10.5338-5340.2005]

42 **Crobach MJT**, Duszenko N, Terveer EM, Verduin CM, Kuijper EJ. Nucleic Acid Amplification Test Quantitation as Predictor of Toxin Presence in Clostridium difficile Infection. *J Clin Microbiol* 2018; **56** [PMID: 29237788 DOI: 10.1128/JCM.01316-17]

43 **Anikst VE**, Gaur RL, Schroeder LF, Banaei N. Organism burden, toxin concentration, and lactoferrin concentration do not distinguish between clinically significant and nonsignificant diarrhea in patients with Clostridium difficile. *Diagn Microbiol Infect Dis* 2016; **84**: 343-346 [PMID: 26778484 DOI: 10.1016/j.diagmicrobio.2015.11.022]

44 **Dubberke ER**, Han Z, Bobo L, Hink T, Lawrence B, Copper S, Hoppe-Bauer J, Burnham CA, Dunne WM Jr. Impact of clinical symptoms on interpretation of diagnostic assays for Clostridium difficile infections. *J Clin Microbiol* 2011; **49**: 2887-2893 [PMID: 21697328 DOI: 10.1128/JCM.00891-11]

45 **Buckel WR**, Avdic E, Carroll KC, Gunaseelan V, Hadhazy E, Cosgrove SE. Gut check: Clostridium difficile testing and treatment in the molecular testing era. *Infect Control Hosp Epidemiol* 2015; **36**: 217-221 [PMID: 25633006 DOI: 10.1017/ice.2014.19]

46 **Popiel KY**, Gheorghe R, Eastmond J, Miller MA. Usefulness of Adjunctive Fecal Calprotectin and Serum Procalcitonin in Individuals Positive for Clostridium difficile Toxin Gene by PCR Assay. *J Clin Microbiol* 2015; **53**: 3667-3669 [PMID: 26354814 DOI: 10.1128/JCM.02230-15]

47 **Crobach MJT**, Baktash A, Duszenko N, Kuijper EJ. Diagnostic Guidance for C. difficile Infections. *Adv Exp Med Biol* 2018; **1050**: 27-44 [PMID: 29383662 DOI: 10.1007/978-3-319-72799-8_3]

48 **Crobach MJ**, Planche T, Eckert C, Barbut F, Terveer EM, Dekkers OM, Wilcox MH, Kuijper EJ. European Society of Clinical Microbiology and Infectious Diseases: update of the diagnostic guidance document for Clostridium difficile infection. *Clin Microbiol Infect* 2016; **22** Suppl 4: S63-S81 [PMID: 27460910 DOI: 10.1016/j.cmi.2016.03.010]

49 **Erb S**, Frei R, Strandén AM, Dangel M, Tschudin-Sutter S, Widmer AF. Low sensitivity of fecal toxin A/B enzyme immunoassay for diagnosis of Clostridium difficile infection in immunocompromised patients. *Clin Microbiol Infect* 2015; **21**: 998.e9-998.e15 [PMID: 26232535 DOI: 10.1016/j.cmi.2015.07.016]

50 **Terveer EM**, Crobach MJ, Sanders IM, Vos MC, Verduin CM, Kuijper EJ. Detection of Clostridium difficile in Feces of Asymptomatic Patients Admitted to the Hospital. *J Clin Microbiol* 2017; **55**: 403-411 [PMID: 27852676 DOI: 10.1128/JCM.01858-16]

51 **Walkty A**, Lagacé-Wiens PR, Manickam K, Adam H, Pieroni P, Hoban D, Karlowsky JA, Alfa M. Evaluation of an algorithmic approach in comparison with the Illumigene assay for laboratory diagnosis of Clostridium difficile infection. *J Clin Microbiol* 2013; **51**: 1152-1157 [PMID: 23363829 DOI: 10.1128/JCM.03203-12]

52 **Bouza E**, Aguado JM, Alcalá L, Almirante B, Alonso-Fernández P, Borges M, Cobo J, Guardiola J, Horcajada JP, Maseda E, Mensa J, Merchante N, Muñoz P, Pérez Sáenz JL, Pujol M, Reigadas E, Salavert M, Barberán J. Recommendations for the diagnosis and treatment of Clostridioides difficile infection: An official clinical practice guideline of the Spanish Society of Chemotherapy (SEQ), Spanish Society of Internal Medicine (SEMI) and the working group of Postoperative Infection of the Spanish Society of Anesthesia and Reanimation (SEDAR). *Rev Esp Quimioter* 2020; **33**: 151-175 [PMID: 32080996 DOI: 10.37201/req/2065.2020]

53 **Fenner L**, Widmer AF, Goy G, Rudin S, Frei R. Rapid and reliable diagnostic algorithm for detection of Clostridium difficile. *J Clin Microbiol* 2008; **46**: 328-330 [PMID: 18032627 DOI: 10.1128/JCM.01503-07]

54 **Qi H**, Sun Q, Ma Y, Wu P, Wang J. Advantages of Lateral Flow Assays Based on Fluorescent Submicrospheres and Quantum Dots for Clostridium difficile Toxin B Detection. *Toxins (Basel)* 2020; **12** [PMID: 33227925 DOI: 10.3390/toxins12110722]

55 **Han J**, Lee Y, Yeom KH, Kim YK, Jin H, Kim VN. The Drosha-DGCR8 complex in primary microRNA processing. *Genes Dev* 2004; **18**: 3016-3027 [PMID: 15574589 DOI: 10.1101/gad.1262504]

56 **Jonas S**, Izaurralde E. Towards a molecular understanding of microRNA-mediated gene silencing. *Nat Rev Genet* 2015; **16**: 421-433 [PMID: 26077373 DOI: 10.1038/nrg3965]

57 **Cossu AM**, Scrima M, Lombardi A, Grimaldi A, Russo M, Ottaiano A, Caraglia M, Bocchetti M. Future directions and management of liquid biopsy in non-small cell lung cancer. *Explor Target Antitumor Ther* 2020; **1**: 239-252 [PMID: 36046776 DOI: 10.37349/etat.2020.00015]

58 **Viladomiu M**, Hontecillas R, Pedragosa M, Carbo A, Hoops S, Michalak P, Michalak K, Guerrant RL, Roche JK, Warren CA, Bassaganya-Riera J. Modeling the role of peroxisome proliferator-activated receptor γ and microRNA-146 in mucosal immune responses to Clostridium difficile. *PloS One* 2012; **7**: e47525 [PMID: 23071818 DOI: 10.1371/journal.pone.0047525]

59 **Imad K**, Hussein K, Cécile L, Jean-christophe M. Use of the mir-27a-5p microRNA for treating Clostridium difficile-

induced bowel inflammation. France patent EP3876948A1. September 15, 2021

60 **Verdier J**, Breunig IR, Ohse MC, Roubrocks S, Kleinfeld S, Roy S, Streetz K, Trautwein C, Roderburg C, Sellge G. Faecal Micro-RNAs in Inflammatory Bowel Diseases. *J Crohns Colitis* 2020; **14**: 110-117 [PMID: 31209454 DOI: 10.1093/ecco-jcc/jjz120]

61 **Drekonja D**, Reich J, Gezahegn S, Greer N, Shaukat A, MacDonald R, Rutks I, Wilt TJ. Fecal Microbiota Transplantation for Clostridium difficile Infection: A Systematic Review. *Ann Intern Med* 2015; **162**: 630-638 [PMID: 25938992 DOI: 10.7326/M14-2693]

62 **Hensley-McBain T**, Zevin AS, Manuzak J, Smith E, Gile J, Miller C, Agricola B, Katze M, Reeves RK, Kraft CS, Langevin S, Klatt NR. Effects of Fecal Microbial Transplantation on Microbiome and Immunity in Simian Immunodeficiency Virus-Infected Macaques. *J Virol* 2016; **90**: 4981-4989 [PMID: 26937040 DOI: 10.1128/JVI.00099-16]

63 **Xu Y**, Li X, Zhu B, Liang H, Fang C, Gong Y, Guo Q, Sun X, Zhao D, Shen J, Zhang H, Liu H, Xia H, Tang J, Zhang K, Gong S. Characteristics of pediatric SARS-CoV-2 infection and potential evidence for persistent fecal viral shedding. *Nat Med* 2020; **26**: 502-505 [PMID: 32284613 DOI: 10.1038/s41591-020-0817-4]

64 **Alang N**, Kelly CR. Weight gain after fecal microbiota transplantation. *Open Forum Infect Dis* 2015; **2**: ofv004 [PMID: 26034755 DOI: 10.1093/ofid/ofv004]

65 **Monaghan TM**, Seekatz AM, Markham NO, Yau TO, Hatziapostolou M, Jilani T, Christodoulou N, Roach B, Birli E, Pomenya O, Louie T, Lacy DB, Kim P, Lee C, Kao D, Polytarchou C. Fecal Microbiota Transplantation for Recurrent Clostridioides difficile Infection Associates With Functional Alterations in Circulating microRNAs. *Gastroenterology* 2021; **161**: 255-270.e4 [PMID: 33844988 DOI: 10.1053/j.gastro.2021.03.050]

66 **Monaghan TM**, Duggal NA, Rosati E, Griffin R, Hughes J, Roach B, Yang DY, Wang C, Wong K, Saxinger L, Pučić-Baković M, Vučković F, Klicek F, Lauc G, Tighe P, Mullish BH, Blanco JM, McDonald JAK, Marchesi JR, Xue N, Dottorini T, Acharjee A, Franke A, Li Y, Wong GK, Polytarchou C, Yau TO, Christodoulou N, Hatziapostolou M, Wang M, Russell LA, Kao DH. A Multi-Factorial Observational Study on Sequential Fecal Microbiota Transplant in Patients with Medically Refractory Clostridioides difficile Infection. *Cells* 2021; **10** [PMID: 34831456 DOI: 10.3390/cells10113234]

67 **Yau TO**, Wu CW, Dong Y, Tang CM, Ng SS, Chan FK, Sung JJ, Yu J. microRNA-221 and microRNA-18a identification in stool as potential biomarkers for the non-invasive diagnosis of colorectal carcinoma. *Br J Cancer* 2014; **111**: 1765-1771 [PMID: 25233396 DOI: 10.1038/bjc.2014.484]

68 **Yau TO**, Wu CW, Tang CM, Chen Y, Fang J, Dong Y, Liang Q, Ng SS, Chan FK, Sung JJ, Yu J. MicroRNA-20a in human faeces as a non-invasive biomarker for colorectal cancer. *Oncotarget* 2016; **7**: 1559-1568 [PMID: 26621842 DOI: 10.18632/oncotarget.6403]

69 **Yau TO**, Tang CM, Harriss EK, Dickins B, Polytarchou C. Faecal microRNAs as a non-invasive tool in the diagnosis of colonic adenomas and colorectal cancer: A meta-analysis. *Sci Rep* 2019; **9**: 9491 [PMID: 31263200 DOI: 10.1038/s41598-019-45570-9]

70 **Deak E**, Miller SA, Humphries RM. Comparison of Illumigene, Simplexa, and AmpliVue Clostridium difficile molecular assays for diagnosis of C. difficile infection. *J Clin Microbiol* 2014; **52**: 960-963 [PMID: 24352999 DOI: 10.1128/JCM.02354-13]

71 **Juretschko S**, Manji R, Khare R, Das S, Dunbar S. Performance Evaluation of the Luminex Aries C. difficile Assay in Comparison to Two Other Molecular Assays within a Multihospital Health Care Center. *J Clin Microbiol* 2019; **57** [PMID: 31413082 DOI: 10.1128/JCM.01092-19]

72 **Pancholi P**, Young S, Widen R, Silbert S, Schmitt B, Dunn R, Drain A, Weissfeld SA. A multicenter evaluation of a sample to answer real-time PCR assay for toxigenic C. difficile in symptomatic subjects. *Diagn Microbiol Infect Dis* 2020; **96**: 114920 [PMID: 31699545 DOI: 10.1016/j.diagmicrobio.2019.114920]

73 **Jazmati N**, Wiegel P, Ličanin B, Plum G. Evaluation of the Qiagen artus C. difficile QS-RGQ Kit for Detection of Clostridium difficile Toxins A and B in Clinical Stool Specimens. *J Clin Microbiol* 2015; **53**: 1942-1944 [PMID: 25809977 DOI: 10.1128/JCM.00613-15]

74 **Hirvonen JJ**, Kaukoranta SS. Comparison of BD Max Cdiff and GenomEra C. difficile molecular assays for detection of toxigenic Clostridium difficile from stools in conventional sample containers and in FecalSwabs. *Eur J Clin Microbiol Infect Dis* 2015; **34**: 1005-1009 [PMID: 25616552 DOI: 10.1007/s10096-015-2320-2]

75 **Dalpke AH**, Hofko M, Zorn M, Zimmermann S. Evaluation of the fully automated BD MAX Cdiff and Xpert C. difficile assays for direct detection of Clostridium difficile in stool specimens. *J Clin Microbiol* 2013; **51**: 1906-1908 [PMID: 23515539 DOI: 10.1128/JCM.00344-13]

76 **Stellrecht KA**, Espino AA, Maceira VP, Nattanmai SM, Butt SA, Wroblewski D, Hannett GE, Musser KA. Premarket evaluations of the IMDx C. difficile for Abbott m2000 Assay and the BD Max Cdiff Assay. *J Clin Microbiol* 2014; **52**: 1423-1428 [PMID: 24554744 DOI: 10.1128/JCM.03293-13]

77 **Shin BM**, Yoo SM, Shin WC. Evaluation of Xpert C. difficile, BD MAX Cdiff, IMDx C. difficile for Abbott m2000, and Illumigene C. difficile Assays for Direct Detection of Toxigenic Clostridium difficile in Stool Specimens. *Ann Lab Med* 2016; **36**: 131-137 [PMID: 26709260 DOI: 10.3343/alm.2016.36.2.131]

78 **Terhes G**, Urbán E, Sóki J, Nacsa E, Nagy E. Comparison of a rapid molecular method, the BD GeneOhm Cdiff assay, to the most frequently used laboratory tests for detection of toxin-producing Clostridium difficile in diarrheal feces. *J Clin Microbiol* 2009; **47**: 3478-3481 [PMID: 19794052 DOI: 10.1128/JCM.01133-09]

79 **Stamper PD**, Alcabasa R, Aird D, Babiker W, Wehrlin J, Ikpeama I, Carroll KC. Comparison of a commercial real-time PCR assay for tcdB detection to a cell culture cytotoxicity assay and toxigenic culture for direct detection of toxin-producing Clostridium difficile in clinical samples. *J Clin Microbiol* 2009; **47**: 373-378 [PMID: 19073875 DOI: 10.1128/JCM.01613-08]

80 **Kvach EJ**, Ferguson D, Riska PF, Landry ML. Comparison of BD GeneOhm Cdiff real-time PCR assay with a two-step algorithm and a toxin A/B enzyme-linked immunosorbent assay for diagnosis of toxigenic Clostridium difficile infection. *J Clin Microbiol* 2010; **48**: 109-114 [PMID: 19864479 DOI: 10.1128/JCM.01630-09]

81 **Karre T**, Sloan L, Patel R, Mandrekar J, Rosenblatt J. Comparison of two commercial molecular assays to a laboratory-developed molecular assay for diagnosis of Clostridium difficile infection. *J Clin Microbiol* 2011; **49**: 725-727 [PMID: 21123537 DOI: 10.1128/JCM.01028-10]

82 **Shin BM**, Mun SJ, Yoo SJ, Kuak EY. Comparison of BD GeneOhm Cdiff and Seegene Seeplex ACE PCR assays using toxigenic Clostridium difficile culture for direct detection of tcdB from stool specimens. *J Clin Microbiol* 2012; **50**: 3765-3767 [PMID: 22952270 DOI: 10.1128/JCM.01440-12]

83 **Garg SK**, Lu K, Duncan J, Peterson LR, Liesenfeld O. Equivalent Performance of the Cobas(®) Cdiff Test for Use on the Cobas(®) Liat(®) System and the Cobas(®) 4800 System. *Eur J Microbiol Immunol (Bp)* 2017; **7**: 310-318 [PMID: 29403660 DOI: 10.1556/1886.2017.00034]

84 **Peterson LR**, Young SA, Davis TE Jr, Wang ZX, Duncan J, Noutsios C, Liesenfeld O, Osiecki JC, Lewinski MA. Evaluation of the cobas Cdiff Test for Detection of Toxigenic Clostridium difficile in Stool Samples. *J Clin Microbiol* 2017; **55**: 3426-3436 [PMID: 28954901 DOI: 10.1128/JCM.01135-17]

85 **Mashock MJ**, Faron ML, Carroll KC, Dang C, Lewis S, Salimnia H, Lephart P, Loo VG, Schmitt BH, Young S, Buchan BW, Ledeboer NA. A Multicenter Study of the Revogene C. difficile System for Detection of the Toxin B Gene from Unformed Stool Specimens. *J Clin Microbiol* 2020; **58** [PMID: 31776191 DOI: 10.1128/JCM.01510-19]

86 **U. S. Food and Drug Administration**. 510(k) Summary ICEPlex C. difficile Kit on the ICEPlex System 2013. Available from: https://www.fda.gov/

87 **Buchan BW**, Mackey TL, Daly JA, Alger G, Denys GA, Peterson LR, Kehl SC, Ledeboer NA. Multicenter clinical evaluation of the portrait toxigenic C. difficile assay for detection of toxigenic Clostridium difficile strains in clinical stool specimens. *J Clin Microbiol* 2012; **50**: 3932-3936 [PMID: 23015667 DOI: 10.1128/JCM.02083-12]

88 **Denys GA**. Portrait Toxigenic Clostridium difficile assay, an isothermal amplification assay detects toxigenic C. difficile in clinical stool specimens. *Expert Rev Mol Diagn* 2014; **14**: 17-26 [PMID: 24308336 DOI: 10.1586/14737159.2014.864239]

89 **Stamper PD**, Babiker W, Alcabasa R, Aird D, Wehrlin J, Ikpeama I, Gluck L, Carroll KC. Evaluation of a new commercial TaqMan PCR assay for direct detection of the clostridium difficile toxin B gene in clinical stool specimens. *J Clin Microbiol* 2009; **47**: 3846-3850 [PMID: 19846637 DOI: 10.1128/JCM.01490-09]

90 **Beck ET**, Buchan BW, Riebe KM, Alkins BR, Pancholi P, Granato PA, Ledeboer NA. Multicenter evaluation of the Quidel Lyra Direct C. difficile nucleic acid amplification assay. *J Clin Microbiol* 2014; **52**: 1998-2002 [PMID: 24671790 DOI: 10.1128/JCM.03089-13]

91 **Gilbreath JJ**, Verma P, Abbott AN, Butler-Wu SM. Comparison of the Verigene Clostridium difficile, Simplexa C. difficile Universal Direct, BD MAX Cdiff, and Xpert C. difficile assays for the detection of toxigenic C. difficile. *Diagn Microbiol Infect Dis* 2014; **80**: 13-18 [PMID: 25027069 DOI: 10.1016/j.diagmicrobio.2014.06.001]

92 **U. S. Food and Drug Administration**. 510(K) Substantial Equivalence Determination Decision Summary Assay and Instrument Combination Template 2018. Available from: https://www.baidu.com/link?url=bxZ2qu2ujOxmV4JObs_gYXHE5P8RRA1m4gfponKdX2KcgYUD6hwTI2h16v_7mP6lA3faJYql3jOpwCrN7NcpQPR98wNFSfu76enVjhfex2a&wd=&eqid=ae7ede620006e9e8000000066447ba8e

93 **Carroll KC**, Buchan BW, Tan S, Stamper PD, Riebe KM, Pancholi P, Kelly C, Rao A, Fader R, Cavagnolo R, Watson W, Goering RV, Trevino EA, Weissfeld AS, Ledeboer NA. Multicenter evaluation of the Verigene Clostridium difficile nucleic acid assay. *J Clin Microbiol* 2013; **51**: 4120-4125 [PMID: 24088862 DOI: 10.1128/JCM.01690-13]

94 **Kosai K**, Iwanaga Y, Akamatsu N, Okada Y, Kaku N, Uno N, Morinaga Y, Hasegawa H, Miyazaki T, Izumikawa K, Mukae H, Yanagihara K. Performance evaluation of the Verigene(®)Clostridium difficile nucleic acid test, an automated multiplex molecular testing system for detection of C. difficile toxin. *J Infect Chemother* 2017; **23**: 674-677 [PMID: 28751156 DOI: 10.1016/j.jiac.2017.07.002]

95 **Bai Y**, Sun X, Jin Y, Wang Y, Li J. Accuracy of Xpert Clostridium difficile assay for the diagnosis of Clostridium difficile infection: A meta analysis. *PloS One* 2017; **12**: e0185891 [PMID: 29016644 DOI: 10.1371/journal.pone.0185891]

96 **Moon HW**, Kim HN, Hur M, Shim HS, Kim H, Yun YM. Comparison of Diagnostic Algorithms for Detecting Toxigenic Clostridium difficile in Routine Practice at a Tertiary Referral Hospital in Korea. *PloS One* 2016; **11**: e0161139 [PMID: 27532104 DOI: 10.1371/journal.pone.0161139]

97 **Eastwood K**, Else P, Charlett A, Wilcox M. Comparison of nine commercially available Clostridium difficile toxin detection assays, a real-time PCR assay for C. difficile tcdB, and a glutamate dehydrogenase detection assay to cytotoxin testing and cytotoxigenic culture methods. *J Clin Microbiol* 2009; **47**: 3211-3217 [PMID: 19710274 DOI: 10.1128/JCM.01082-09]

98 **O'Connor D**, Hynes P, Cormican M, Collins E, Corbett-Feeney G, Cassidy M. Evaluation of methods for detection of toxins in specimens of feces submitted for diagnosis of Clostridium difficile-associated diarrhea. *J Clin Microbiol* 2001; **39**: 2846-2849 [PMID: 11474001 DOI: 10.1128/JCM.39.8.2846-2849.2001]

99 **Drudy D**, Harnedy N, Fanning S, O'Mahony R, Kyne L. Isolation and characterisation of toxin A-negative, toxin B-positive Clostridium difficile in Dublin, Ireland. *Clin Microbiol Infect* 2007; **13**: 298-304 [PMID: 17391385 DOI: 10.1111/j.1469-0691.2006.01634.x]

100 **Planche TD**, Davies KA, Coen PG, Finney JM, Monahan IM, Morris KA, O'Connor L, Oakley SJ, Pope CF, Wren MW, Shetty NP, Crook DW, Wilcox MH. Differences in outcome according to Clostridium difficile testing method: a prospective multicentre diagnostic validation study of C difficile infection. *Lancet Infect Dis* 2013; **13**: 936-945 [PMID: 24007915 DOI: 10.1016/S1473-3099(13)70200-7]

101 **Novak-Weekley SM**, Marlowe EM, Miller JM, Cumpio J, Nomura JH, Vance PH, Weissfeld A. Clostridium difficile testing in the clinical laboratory by use of multiple testing algorithms. *J Clin Microbiol* 2010; **48**: 889-893 [PMID: 20071552 DOI: 10.1128/JCM.01801-09]

102 **Barkin JA**, Nandi N, Miller N, Grace A, Barkin JS, Sussman DA. Superiority of the DNA amplification assay for the diagnosis of C. difficile infection: a clinical comparison of fecal tests. *Dig Dis Sci* 2012; **57**: 2592-2599 [PMID: 22576711 DOI: 10.1007/s10620-012-2200-x]

103 **Babady NE**, Stiles J, Ruggiero P, Khosa P, Huang D, Shuptar S, Kamboj M, Kiehn TE. Evaluation of the Cepheid Xpert

Clostridium difficile Epi assay for diagnosis of Clostridium difficile infection and typing of the NAP1 strain at a cancer hospital. *J Clin Microbiol* 2010; **48**: 4519-4524 [PMID: 20943860 DOI: 10.1128/JCM.01648-10]

104 **Leitner E**, Einetter M, Grisold AJ, Marth E, Feierl G. Evaluation of the BD MAX Cdiff assay for the detection of the toxin B gene of Clostridium difficile out of faecal specimens. *Diagn Microbiol Infect Dis* 2013; **76**: 390-391 [PMID: 23602785 DOI: 10.1016/j.diagmicrobio.2013.03.007]

105 **Ota KV**, McGowan KL. Clostridium difficile testing algorithms using glutamate dehydrogenase antigen and C. difficile toxin enzyme immunoassays with C. difficile nucleic acid amplification testing increase diagnostic yield in a tertiary pediatric population. *J Clin Microbiol* 2012; **50**: 1185-1188 [PMID: 22259201 DOI: 10.1128/JCM.05620-11]

106 **van den Berg RJ**, Vaessen N, Endtz HP, Schülin T, van der Vorm ER, Kuijper EJ. Evaluation of real-time PCR and conventional diagnostic methods for the detection of Clostridium difficile-associated diarrhoea in a prospective multicentre study. *J Med Microbiol* 2007; **56**: 36-42 [PMID: 17172514 DOI: 10.1099/jmm.0.46680-0]

107 **Vanpoucke H**, De Baere T, Claeys G, Vaneechoutte M, Verschraegen G. Evaluation of six commercial assays for the rapid detection of Clostridium difficile toxin and/or antigen in stool specimens. *Clin Microbiol Infect* 2001; **7**: 55-64 [PMID: 11298143 DOI: 10.1046/j.1469-0691.2001.00141.x]

108 **Mattner F**, Winterfeld I, Mattner L. Diagnosing toxigenic Clostridium difficile: new confidence bounds show culturing increases sensitivity of the toxin A/B enzyme immunoassay and refute gold standards. *Scand J Infect Dis* 2012; **44**: 578-585 [PMID: 22404319 DOI: 10.3109/00365548.2012.655772]

109 **Musher DM**, Manhas A, Jain P, Nuila F, Waqar A, Logan N, Marino B, Graviss EA. Detection of Clostridium difficile toxin: comparison of enzyme immunoassay results with results obtained by cytotoxicity assay. *J Clin Microbiol* 2007; **45**: 2737-2739 [PMID: 17567791 DOI: 10.1128/JCM.00686-07]

110 **Snell H**, Ramos M, Longo S, John M, Hussain Z. Performance of the TechLab C. DIFF CHEK-60 enzyme immunoassay (EIA) in combination with the C. difficile Tox A/B II EIA kit, the Triage C. difficile panel immunoassay, and a cytotoxin assay for diagnosis of Clostridium difficile-associated diarrhea. *J Clin Microbiol* 2004; **42**: 4863-4865 [PMID: 15472364 DOI: 10.1128/JCM.42.10.4863-4865.2004]

111 **Massey V**, Gregson DB, Chagla AH, Storey M, John MA, Hussain Z. Clinical usefulness of components of the Triage immunoassay, enzyme immunoassay for toxins A and B, and cytotoxin B tissue culture assay for the diagnosis of Clostridium difficile diarrhea. *Am J Clin Pathol* 2003; **119**: 45-49 [PMID: 12520696 DOI: 10.1309/U8AT-L52Q-60XY-AVX6]

112 **Bruins MJ**, Verbeek E, Wallinga JA, Bruijnesteijn van Coppenraet LE, Kuijper EJ, Bloembergen P. Evaluation of three enzyme immunoassays and a loop-mediated isothermal amplification test for the laboratory diagnosis of Clostridium difficile infection. *Eur J Clin Microbiol Infect Dis* 2012; **31**: 3035-3039 [PMID: 22706512 DOI: 10.1007/s10096-012-1658-y]

113 **Sloan LM**, Duresko BJ, Gustafson DR, Rosenblatt JE. Comparison of real-time PCR for detection of the tcdC gene with four toxin immunoassays and culture in diagnosis of Clostridium difficile infection. *J Clin Microbiol* 2008; **46**: 1996-2001 [PMID: 18434563 DOI: 10.1128/JCM.00032-08]

114 **Hart J**, Putsathit P, Knight DR, Sammels L, Riley TV, Keil A. Clostridium difficile infection diagnosis in a paediatric population: comparison of methodologies. *Eur J Clin Microbiol Infect Dis* 2014; **33**: 1555-1564 [PMID: 24781004 DOI: 10.1007/s10096-014-2108-9]

115 **Kawada M**, Annaka M, Kato H, Shibasaki S, Hikosaka K, Mizuno H, Masuda Y, Inamatsu T. Evaluation of a simultaneous detection kit for the glutamate dehydrogenase antigen and toxin A/B in feces for diagnosis of Clostridium difficile infection. *J Infect Chemother* 2011; **17**: 807-811 [PMID: 21725661 DOI: 10.1007/s10156-011-0267-5]

116 **Swindells J**, Brenwald N, Reading N, Oppenheim B. Evaluation of diagnostic tests for Clostridium difficile infection. *J Clin Microbiol* 2010; **48**: 606-608 [PMID: 20032256 DOI: 10.1128/JCM.01579-09]

117 **Kim H**, Kim WH, Kim M, Jeong SH, Lee K. Evaluation of a rapid membrane enzyme immunoassay for the simultaneous detection of glutamate dehydrogenase and toxin for the diagnosis of Clostridium difficile infection. *Ann Lab Med* 2014; **34**: 235-239 [PMID: 24790912 DOI: 10.3343/alm.2014.34.3.235]

118 **de Boer RF**, Wijma JJ, Schuurman T, Moedt J, Dijk-Alberts BG, Ott A, Kooistra-Smid AM, van Duynhoven YT. Evaluation of a rapid molecular screening approach for the detection of toxigenic Clostridium difficile in general and subsequent identification of the tcdC Δ117 mutation in human stools. *J Microbiol Methods* 2010; **83**: 59-65 [PMID: 20674616 DOI: 10.1016/j.mimet.2010.07.017]

119 **Yoldaş Ö**, Altındiş M, Cufalı D, Aşık G, Keşli R. A Diagnostic Algorithm for the Detection of Clostridium difficile-Associated Diarrhea. *Balkan Med J* 2016; **33**: 80-86 [PMID: 26966622 DOI: 10.5152/balkanmedj.2015.15159]

120 **Le Guern R**, Herwegh S, Grandbastien B, Courcol R, Wallet F. Evaluation of a new molecular test, the BD Max Cdiff, for detection of toxigenic Clostridium difficile in fecal samples. *J Clin Microbiol* 2012; **50**: 3089-3090 [PMID: 22760042 DOI: 10.1128/JCM.01250-12]

121 **Reller ME**, Alcabasa RC, Lema CA, Carroll KC. Comparison of two rapid assays for Clostridium difficile Common antigen and a C difficile toxin A/B assay with the cell culture neutralization assay. *Am J Clin Pathol* 2010; **133**: 107-109 [PMID: 20023265 DOI: 10.1309/AJCPO3QWOU8CYGEU]

122 **Benedek O**, Podbielski A, Warnke P. Laboratory Experience with the Liaison Analyzer in the Diagnosis of Clostridium Difficile-Associated Diarrhea. *Eur J Microbiol Immunol (Bp)* 2016; **6**: 215-218 [PMID: 27766170 DOI: 10.1556/1886.2016.00017]

123 **Makristathis A**, Zeller I, Mitteregger D, Kundi M, Hirschl AM. Comprehensive evaluation of chemiluminescent immunoassays for the laboratory diagnosis of Clostridium difficile infection. *Eur J Clin Microbiol Infect Dis* 2017; **36**: 1253-1259 [PMID: 28181032 DOI: 10.1007/s10096-017-2916-9]

124 **Shin BM**, Kuak EY, Lee EJ, Songer JG. Algorithm combining toxin immunoassay and stool culture for diagnosis of Clostridium difficile infection. *J Clin Microbiol* 2009; **47**: 2952-2956 [PMID: 19625481 DOI: 10.1128/JCM.00609-09]

125 **Shin BM**, Lee EJ, Kuak EY, Yoo SJ. Comparison of VIDAS CDAB and CDA immunoassay for the detection of Clostridium difficile in a tcdA- tcdB+ C. difficile prevalent area. *Anaerobe* 2009; **15**: 266-269 [PMID: 19772927 DOI: 10.1016/j.anaerobe.2009.09.008]

126 **Kim H**, Jeong SH, Kim M, Lee Y, Lee K. Detection of Clostridium difficile toxin A/B genes by multiplex real-time PCR for the diagnosis of C. difficile infection. *J Med Microbiol* 2012; **61**: 274-277 [PMID: 21959205 DOI: 10.1099/jmm.0.035618-0]

127 **Shin S**, Kim M, Lim H, Kim H, Lee K, Chong Y. Evaluation of the Xpert Clostridium difficile assay for the diagnosis of Clostridium difficile infection. *Ann Lab Med* 2012; **32**: 355-358 [PMID: 22950071 DOI: 10.3343/alm.2012.32.5.355]

128 **de Jong E**, de Jong AS, Bartels CJ, van der Rijt-van den Biggelaar C, Melchers WJ, Sturm PD. Clinical and laboratory evaluation of a real-time PCR for Clostridium difficile toxin A and B genes. *Eur J Clin Microbiol Infect Dis* 2012; **31**: 2219-2225 [PMID: 22327373 DOI: 10.1007/s10096-012-1558-1]

129 **Shin BM**, Lee EJ, Moon JW, Lee SY. Evaluation of the VIDAS glutamate dehydrogenase assay for the detection of Clostridium difficile. *Anaerobe* 2016; **40**: 68-72 [PMID: 27282799 DOI: 10.1016/j.anaerobe.2016.06.001]

World Journal of Gastroenterology

Submit a Manuscript: https://www.f6publishing.com

World J Gastroenterol 2023 June 14; 29(22): 3400-3421

DOI: 10.3748/wjg.v29.i22.3400

ISSN 1007-9327 (print) ISSN 2219-2840 (online)

REVIEW

Epidemiology of small intestinal bacterial overgrowth

Irina Efremova, Roman Maslennikov, Elena Poluektova, Ekaterina Vasilieva, Yury Zharikov, Andrey Suslov, Yana Letyagina, Evgenii Kozlov, Anna Levshina, Vladimir Ivashkin

Specialty type: Gastroenterology and hepatology

Provenance and peer review: Invited article; Externally peer reviewed.

Peer-review model: Single blind

Peer-review report's scientific quality classification

Grade A (Excellent): 0
Grade B (Very good): 0
Grade C (Good): C, C, C
Grade D (Fair): D
Grade E (Poor): 0

P-Reviewer: Duan SL, China; Ji G, China; Wen XL, China; Zhang XL, China

Received: March 16, 2023
Peer-review started: March 16, 2023
First decision: March 24, 2023
Revised: March 31, 2023
Accepted: May 11, 2023
Article in press: May 11, 2023
Published online: June 14, 2023

Irina Efremova, Roman Maslennikov, Elena Poluektova, Ekaterina Vasilieva, Anna Levshina, Vladimir Ivashkin, Department of Internal Medicine, Gastroenterology and Hepatology, Sechenov University, Moscow 119435, Russia

Roman Maslennikov, Elena Poluektova, Vladimir Ivashkin, The Scientific Community for Human Microbiome Research, Moscow 119435, Russia

Yury Zharikov, Andrey Suslov, Department of Human Anatomy and Histology, Sechenov University, Moscow 125009, Russia

Yana Letyagina, N.V. Sklifosovsky Institute of Clinical Medicine, Sechenov University, Moscow 119991, Russia

Evgenii Kozlov, Anna Levshina, Department of Clinical Immunology and Allergy, Sechenov University, Moscow 119991, Russia

Corresponding author: Roman Maslennikov, MD, PhD, Academic Editor, Assistant Professor, Doctor, Professor, Department of Internal Medicine, Gastroenterology and Hepatology, Sechenov University, Pogodinskaya str., 1, bld. 1, Moscow 119435, Russia.
mmmm00@yandex.ru

Abstract

Small intestinal bacterial overgrowth (SIBO) is defined as an increase in the bacterial content of the small intestine above normal values. The presence of SIBO is detected in 33.8% of patients with gastroenterological complaints who underwent a breath test, and is significantly associated with smoking, bloating, abdominal pain, and anemia. Proton pump inhibitor therapy is a significant risk factor for SIBO. The risk of SIBO increases with age and does not depend on gender or race. SIBO complicates the course of a number of diseases and may be of pathogenetic significance in the development of their symptoms. SIBO is significantly associated with functional dyspepsia, irritable bowel syndrome, functional abdominal bloating, functional constipation, functional diarrhea, short bowel syndrome, chronic intestinal pseudo-obstruction, lactase deficiency, diverticular and celiac diseases, ulcerative colitis, Crohn's disease, cirrhosis, metabolic-associated fatty liver disease (MAFLD), primary biliary cholangitis, gastroparesis, pancreatitis, cystic fibrosis, gallstone disease, diabetes, hypothyroidism, hyperlipidemia, acromegaly, multiple sclerosis, autism, Parkinson's disease, systemic sclerosis, spondylarthropathy, fibromyalgia, asthma, heart failure, and other diseases. The development of SIBO is often associated with a slowdown in orocecal transit time that decreases the normal clearance of bacteria

from the small intestine. The slowdown of this transit may be due to motor dysfunction of the intestine in diseases of the gut, autonomic diabetic polyneuropathy, and portal hypertension, or a decrease in the motor-stimulating influence of thyroid hormones. In a number of diseases, including cirrhosis, MAFLD, diabetes, and pancreatitis, an association was found between disease severity and the presence of SIBO. Further work on the effect of SIBO eradication on the condition and prognosis of patients with various diseases is required.

Key Words: Gut microbiota; Gut-liver axis; Breath test; Lactulose; Methane; Hydrogen

©The Author(s) 2023. Published by Baishideng Publishing Group Inc. All rights reserved.

Core Tip: Small intestinal bacterial overgrowth (SIBO) is common in functional and organic bowel diseases, liver diseases, other diseases of digestive organs, a number of endocrine, nervous, and rheumatic diseases, asthma, heart failure, and certain other diseases. In a number of diseases, including cirrhosis, metabolic-associated fatty liver disease, diabetes mellitus, pancreatitis, and cystic fibrosis, an association was found between disease severity and the presence of SIBO. Further work on the effect of SIBO eradication on the condition and prognosis of patients in various diseases is required.

Citation: Efremova I, Maslennikov R, Poluektova E, Vasilieva E, Zharikov Y, Suslov A, Letyagina Y, Kozlov E, Levshina A, Ivashkin V. Epidemiology of small intestinal bacterial overgrowth. *World J Gastroenterol* 2023; 29(22): 3400-3421
URL: https://www.wjgnet.com/1007-9327/full/v29/i22/3400.htm
DOI: https://dx.doi.org/10.3748/wjg.v29.i22.3400

INTRODUCTION

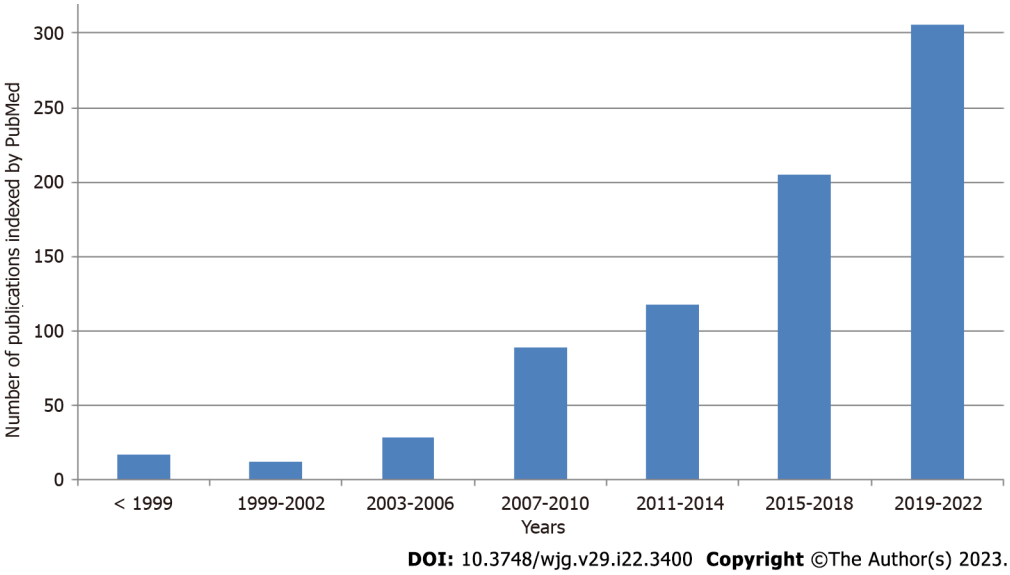
Small intestinal bacterial overgrowth (SIBO) is defined as an increase in the bacterial content of the small intestine above normal values (100000 cells per mL)[1-4]. This leads to excessive gas formation in the small intestine, bloating, and pain in the umbilical region, which may be accompanied by malabsorption, malnutrition, and osmotic diarrhea. The main causes of SIBO are dysfunctional movement of contents through the small intestine [delayed orocecal transit time (OCTT)], reduced gastric acid secretion [for example, due to the use of proton pump inhibitors (PPI) or after gastric surgery], and reflux of the colon contents into the small intestine due to ileocecal valve dysfunction[1-4].

Interest in SIBO is increasing, as evidenced by the continuous growth in publications on this topic indexed in PubMed (Figure 1). An important issue is the standardization of SIBO diagnosis. The main diagnostic methods are lactulose and glucose breath tests (LBT and GBT, respectively), as well as jejunal bacterial culture quantification[5-7]. Unfortunately, the results obtained using these different methods do not always correspond with each other, which may explain the variation in results between different studies that use different tests. In addition, while SIBO was initially associated with hydrogen release, it is now accepted that SIBO can also accompany the formation of methane. Methane SIBO and hydrogen SIBO are not only detected with different frequencies, but can also have different effects. It is important that the test for hydrogen SIBO does not detect methane SIBO and vice versa[8,9].

SIBO complicates the course of a number of diseases and may be of pathogenetic significance in the development of their symptoms[1-4]. The aim of this review is to provide up-to-date information on the association of SIBO with various diseases and their manifestations.

PATIENTS WITH GASTROENTEROLOGICAL COMPLAINTS

The presence of SIBO was detected in 33.8% of patients with gastroenterological complaints who underwent a breath test, and was significantly associated with smoking [odds ratio (OR) = 6.66], bloating (OR = 5.39), abdominal pain (OR = 4.78), and anemia (OR = 4.08)[10]. The risk of SIBO increased with age [OR = 1.04, 95% confidence interval (CI): 1.01-1.07][11] and did not depend on gender or race[11,12]. Ileocecal junction pressure was lower, small bowel, colonic, and whole gut transit times were longer, and gastric and small bowel pH was higher in patients with SIBO than in those without[13,14]. There were no significant differences in gastric emptying time and other small intestinal motility parameters (small intestinal motility index, contractions per minute, and peak amplitudes)[13,15], or in fecal calprotectin levels[16]. SIBO was more frequent in patients who consumed a moderate amount of alcohol than in abstainers (58% *vs* 39%)[17]. SIBO was identified in 63% of children with



DOI: 10.3748/wjg.v29.i22.3400 **Copyright** ©The Author(s) 2023.

Figure 1 Number of publications indexed by PubMed on small intestinal bacterial overgrowth by year.

abdominal pain[18].

DIET

Patients with SIBO consumed lower amounts of dietary fiber and red meat than SIBO-negative individuals. Those with methane SIBO consumed more fruits, vegetables, and fish compared with those with other variants of SIBO and the control group, while individuals with hydrogen SIBO ate more poultry than those with other SIBO types and controls[19]. SIBO was detected more frequently in preschool children who were on a long-term dairy-free diet than in children on a regular diet (55.0% *vs* 20.0%)[20].

PPI THERAPY

A meta-analysis of 19 studies revealed that PPI therapy is a significant risk factor for SIBO (OR = 1.71, 95%CI: 1.20-2.43)[21]. The prevalence of SIBO increased after 1 year of continuous PPI use[22]. Interestingly, SIBO following PPI therapy is associated with decreased OCTT, and the concomitant use of prokinetics in patients receiving PPI reduces the risk of SIBO by increasing OCTT[23]. In older patients undergoing long-term PPI therapy, the prevalence of SIBO was higher than that in patients not receiving PPI (77.1% *vs* 58.3%) and increased significantly when the administration time was longer than 6 mo[24]. The prevalence of SIBO was also higher in older patients undergoing continuous PPI therapy (88.6%) than in those receiving on-demand PPI therapy (65.7%); no significant difference was found in the incidence of SIBO between the on-demand PPI and control groups[24].

FUNCTIONAL DIGESTIVE DISEASES

Breath tests revealed that 68.1% of patients with functional bowel diseases also had SIBO[25].

Functional dyspepsia

A meta-analysis of seven studies found that the prevalence of SIBO in functional dyspepsia is 34.7% (95%CI: 24.8%-45.4%)[26]. Another meta-analysis found SIBO prevalence in functional dyspepsia to be significantly higher using the LBT (53.4%, 95%CI: 33.9%-71.9%) compared with the GBT (17.2%, 95%CI: 8.6%-31.6%). There was no significant difference in SIBO prevalence between patients with different subtypes of functional dyspepsia. The risk of SIBO in patients with functional dyspepsia was significantly higher than that in controls (OR = 4.3, 95%CI: 1.1-17.5)[27].

Irritable bowel syndrome

A meta-analysis of 37 studies revealed that the prevalence of SIBO in irritable bowel syndrome (IBS)

was 36.7% (95%CI: 24.2%-44.6%). The lactulose hydrogen breath test (LHBT) for SIBO was positive in patients with IBS no more often than in the control group [risk ratio (RR) = 1.6, 95%CI: 0.9-2.8], while SIBO was detected in patients with IBS significantly more often than in controls using the glucose hydrogen breath test (RR = 4.2, 95%CI: 3.0-5.9) and upper gut aspirate culture (RR = 3.2, 95%CI: 1.4-7.3). Patients with diarrhea-predominant IBS (IBS-D) were more likely to have SIBO than patients with other subtypes (OR = 1.4, 95%CI: 1.02-1.63)[28].

Another meta-analysis of 25 studies showed that SIBO prevalence in patients with IBS was significantly higher than that in controls [31.0% (95%CI: 29.4%-32.6%) *vs* 20.9% (95%CI: 19.5%-22.2%); OR = 3.7 (95%CI: 2.3-6.0) for all studies, OR = 4.9 (95%CI: 2.8-8.6) for studies using only healthy controls, and OR = 1.3 (95%CI: 0.6-3.3) for studies using non-IBS disease controls]. Using breath testing, SIBO prevalence in patients with IBS was 35.5% (95%CI: 33.6%-37.4%) *vs* 29.7% (95%CI: 27.6%-31.8%) in controls. Culture-based studies found an SIBO incidence of 13.9% (95%CI: 11.5%-16.4%) in patients with IBS and 5.0% (95%CI: 3.9%-6.2%) in controls. SIBO prevalence as diagnosed by the LBT was much greater in patients with IBS (3.6-fold) and controls (7.6-fold) than that diagnosed by the GBT. Similar differences were observed when LBT was compared with the bacterial culture method of diagnosis. SIBO prevalence was greater in patients with IBS-D (35.5%, 95%CI: 32.7%-40.3%) compared with patients with constipation-predominant IBS [IBS-C; 22.5% (95%CI: 18.1%-26.9%); OR = 1.8 (95%CI: 1.2-2.8) *vs* IBS-D] and mixed IBS (25.2%, 95%CI: 22.2%-28.4%). PPI use by patients with IBS was not associated with SIBO (OR = 0.8, 95%CI: 0.5-1.5). The prevalence of SIBO both in patients with IBS and controls was greatest in the United States [(54.6%, 95%CI: 51.2%-58.0%) and 37.2% (95%CI: 34.7%-39.7%), respectively], followed by Europe [23.4% (95%CI: 21.1%-26.0%) and 8.1% (95%CI: 6.6%-9.6%), respectively], and lowest in India [14.1% (95%CI: 11.5%-16.7%) and 1.1% (95%CI: 0%-2.2%), respectively][29].

The third meta-analysis revealed that among patients with IBS, female sex (OR = 1.5, 95%CI: 1.0-2.1), older age [standardized mean difference = 3.1 years (95%CI: 0.9-5.4)], and IBS-D (OR = 1.7, 95%CI: 1.3-2.3) compared with other IBS subtypes increased the odds of SIBO[30].

Separately, a meta-analysis of studies investigating methane SIBO in IBS was performed. It showed that the incidence of methane SIBO in patients with IBS was 25.0% (95%CI: 18.8%-32.4%), not significantly different from that in the control group (OR = 1.2, 95%CI: 0.8-1.7). In patients with IBS, the LBT provided positive results for methane SIBO almost three times as often as the GBT [29.0% (95%CI: 20.9%-38.6%) *vs* 11.5% (95%CI: 5.0%-24.3%)]. In contrast with hydrogen SIBO, the prevalence of methane SIBO in patients with IBS-C was higher than that in patients with IBS-D [37.7% (95%CI: 33.5%-42.1%) *vs* 12.4% (95%CI: 10.2%-14.9%); OR = 3.1 (95%CI: 1.7-5.6)][31].

Serum interleukin (IL)-1β levels were higher and serum IL-10 levels were lower in SIBO-positive patients with IBS than in the SIBO-negative group[32]. Another study also showed that increased IL-1α and IL-1β levels were associated with SIBO[33]. A third study reported that IL-10 levels were reduced in IBS patients with SIBO compared with those without, but found no significant differences in serum tumor necrosis factor (TNF)-α, IL-6, and IL-8 concentrations[34].

The body mass index (BMI) of patients with IBS-D and SIBO was significantly lower than that of patients without SIBO. IBS-D patients with SIBO had higher scores of abdominal pain than those without SIBO in this study. The proportion of dietary fat was significantly higher in IBS patients with SIBO than in those without. Breath methane peak value was positively correlated with the proportion of fat in the diet[35]. Another study also showed that in non-constipation IBS, patients with SIBO had lower BMI and waist circumference than patients without SIBO. Moreover, multivariate analysis revealed that the OR of SIBO was 0.396 for obesity and 0.482 for abdominal obesity[36].

The presence of SIBO did not affect IBS symptoms in another study[37], although OCTT was significantly increased in SIBO-positive compared with SIBO-negative patients[37]. Intestinal permeability did not differ significantly between IBS patients with and without SIBO[38]. The severity of anxiety, depression, and other psychological disorders was not different between patients with IBS who were positive and negative for hydrogen SIBO[34]. Another study confirmed that the severity of IBS symptoms and associated psychological disorders did not differ between SIBO-positive and -negative patients[39]. However, it has been shown that IBS patients with SIBO who are predominant methane producers have higher urge thresholds for colon contraction and higher baseline levels of colon phasic contractions than SIBO-negative IBS patients, and report more 'hard or lumpy stools' compared with patients who are predominant hydrogen producers and those who are SIBO-negative[39]. This is consistent with the findings that hydrogen SIBO is more prevalent in IBS-D, whereas methane SIBO is more prevalent in IBS-C[30,31]. In children with IBS, the prevalence of SIBO was significantly higher than that in control subjects [65% *vs* 7%; OR = 3.9 (95%CI: 7.3-80.1)]. Among abdominal symptoms, significant differences were observed only in bloating[40].

Other functional digestive diseases

Tests for SIBO were positive in 43% of patients with functional abdominal bloating/distention[41] (although this proportion reached 68% in another study[42]), 73% of those with functional constipation [42], and 69% of those with functional diarrhea[42].

ORGANIC GUT DISEASES

Non-steroidal anti-inflammatory drug-induced small intestinal damage

The LHBT was positive in 59% of patients with and 24% of patients without severe non-steroidal anti-inflammatory drug (NSAID)-induced small intestinal damage. Multiple regression analysis showed that SIBO was significantly associated with severe NSAID-induced small intestinal damage (OR = 6.54, 95%CI: 1.40-30.50). However, there was no significant difference in symptoms between patients with severe small intestinal damage with and without SIBO[43].

Short bowel syndrome

SIBO was found in 50% of children with short bowel syndrome and predisposed these patients to ambulatory central line-associated bloodstream infection (RR = 1.87, 95%CI: 1.1-3.17)[44].

Chronic intestinal pseudo-obstruction

Methane SIBO was detected more frequently in patients with chronic intestinal pseudo-obstruction than in patients with other diseases (52.6% *vs* 11.8%), while no significant difference was found in the prevalence of hydrogen SIBO between these groups (23.7% *vs* 25.7)[45].

Lactase deficiency and lactose malabsorption

SIBO was detected at a significantly higher rate in patients with lactase deficiency than in healthy controls (27.6% *vs* 6.7%)[46]. SIBO was found in 90% of asymptomatic well-nourished older people with lactose malabsorption compared with 20% of those without it[47].

Symptomatic uncomplicated diverticular disease

SIBO was found in 58.9% of patients with symptomatic uncomplicated diverticular disease (SUDD), more specifically in 93.1% of patients with diarrhea-prevalent disease and 42.6% of patients with constipation-prevalent disease[48]. OCTT was delayed in 92.5% of SUDD patients with SIBO and 48.6% of patients without SIBO (OR = 12.9). Lactose malabsorption was identified in 92.5% of SUDD patients with SIBO and 27.0% of patients without (OR = 33.0)[48].

Celiac disease

A meta-analysis of 14 studies showed that SIBO was more prevalent in patients with celiac disease than in controls [18.3% (95%CI: 11.4-28.1)[1]; OR = 5.1, 95%CI: 2.1-12.4]. The prevalence of SIBO as diagnosed by breath tests was 20.8% (95%CI: 11.9%-33.7%), while that of SIBO identified by culture-based methods was 12.6% (95%CI: 5.1%-28.0%). The prevalence of SIBO in patients with celiac disease was lower in the United States [8.7% (95%CI: 6.1%-11.9%)] than in Asia [22.1 (95%CI: 15.4%-30.2%)] and Europe [23.3% (95%CI: 17.5%-29.9%)]. SIBO prevalence in non-responders to a gluten-free diet was similar to that in responders. Antibiotic therapy for SIBO in patients with celiac disease resulted in an improvement in gastrointestinal symptoms in 95.6% (95%CI: 78.0%-99.9%) of cases. There were no significant differences in the degree of intestinal damage as measured by histology or celiac serology between patients with celiac disease with and without SIBO. Patients with celiac disease and SIBO tended to be older and have more severe signs of malabsorption (lower hemoglobin, serum beta-carotene, albumin levels, and higher fecal fat level), compared with those without SIBO[49]. SIBO was present in 67% of celiac patients with persistence of gastrointestinal symptoms who had histological response to a gluten-free diet[50].

Environmental enteric dysfunction

Environmental enteric dysfunction is an incompletely defined syndrome of inflammation, reduced absorptive capacity, and barrier dysfunction in the small intestine. It is widespread in low- and middle-income countries[51]. The prevalence of SIBO is 85.3% in children with stunted growth due to this disease[52].

Inflammatory bowel disease

A meta-analysis of 11 studies revealed that the proportion of SIBO in patients with inflammatory bowel disease (IBD) was greater than that in controls [22.3% (95%CI: 19.92%-24.68%); OR = 9.51 (95%CI: 3.39-26.68)]. The severity of abdominal symptoms (bloating, flatus, satiety, and loose stools) was also greater in patients with SIBO than in those without. Patients with SIBO had increased stool frequency, lower body weight, and prolonged OCTT compared with SIBO-negative patients[53]. The prevalence of methane SIBO was assessed in a meta-analysis of six studies, which did not reveal a significant difference between patients with IBD and healthy individuals[31]. The incidence of SIBO was significantly higher in patients with Crohn's disease (CD) compared with patients with ulcerative colitis (UC)[54].

CD

A meta-analysis showed that the prevalence of SIBO in CD was higher than that in controls [25.4%

(95%CI: 22.5%-28.3%); OR = 10.9 (95%CI: 2.8-42.69)]. CD patients who had undergone prior surgery were more likely to test positive for SIBO than those who had not [31.8% (95%CI: 26.7%-36.9%) *vs* 19.2% (95%CI: 15.4%-23.0%); OR = 2.4 (95%CI: 1.7-3.4)]. The prevalence of SIBO in CD was highest [33% (95%CI: 19.2%-50.6%)] in patients following ileocecal valve surgery. Among different forms of the disease, fibrostenosing CD was associated with an increased risk of SIBO compared to others [OR = 7.5 (95%CI: 2.5-22.2)]. No association was found between the prevalence of SIBO and CD activity index score, or thiopurine or biologic treatment[53].

OCTT was significantly longer in patients with CD with SIBO than in those without[54]. SIBO also occurred more frequently in patients who had CD recurrence within 18 mo than in those who remained in remission (63.0% *vs* 37.0%; OR = 2.79). Relapses were more frequent in patients with SIBO than in those without (26.5% *vs* 7.7% at the 6-mo follow-up, and 50.0% *vs* 25.6% at the 18-mo follow-up)[55].

CD patients with and without SIBO were comparable with regard to demographics, systemic inflammatory biomarkers, and disease characteristics, except for the fibrostenosing phenotype that was more common in patients with SIBO than in those without [43.3% *vs* 19.3%; OR = 3.8 (95%CI: 1.5-6.8)]. Fecal calprotectin levels were significantly higher in SIBO-positive than in SIBO-negative patients (OR = 9.4, 95%CI: 3.0-11.3)[56].

Another study reported that CD patients with SIBO had increased stool frequency and significant reduction of stool solidity, were older, reported a longer history of CD, and were significantly more likely to have had prior surgery than CD patients without SIBO. An association was identified between the number of surgical procedures and the presence of SIBO (OR = 2.83, 95%CI: 1.15-6.96)[57].

In CD patients in remission, the prevalence of SIBO was 16.8%. No associations were observed between SIBO in these remission patients and the use of thiopurine or biological drugs. Multivariate analysis revealed that the presence of meteorism and a fistulizing phenotype were associated with the presence of SIBO in patients with CD in remission[58].

UC

A meta-analysis showed that the prevalence of SIBO in patients with UC was greater than in controls [14.3% (95%CI: 10.52%-18.1%); OR = 8.0 (95%CI: 1.67-38.4)][31]; OCTT has also been shown to be significantly longer in these patients than in controls[54]. Serum levels of lipopolysaccharide (LPS), and the expression levels of Toll-like receptor (TLR)2 and TLR4 on the surface of peripheral blood mononuclear cells were higher in UC patients with SIBO than in those without. LPS levels were positively correlated with the expression levels of TLR2 and TLR4[59]. Serum levels of pro-inflammatory cytokines (IL-6, IL-8, and TNF-α), anti-inflammatory cytokines (IL-10), and lipid peroxidates (a marker of oxidative stress) were significantly higher, and levels of reduced glutathione (antioxidant) were lower in UC patients with SIBO than in those without[60].

LIVER DISEASES

In a mixed cohort of patients with various liver diseases, SIBO prevalence was significantly higher in patients with cirrhosis than in those without (41.2% *vs* 13.1%). Moreover, both cirrhotic and non-cirrhotic patients had a greater SIBO prevalence than healthy controls[61].

Cirrhosis

A meta-analysis of 21 studies revealed that the prevalence of SIBO in patients with cirrhosis was greater than that in healthy controls [(40.8%, 95%CI: 34.8%-47.1%) and OR = 6.83 (95%CI: 4.16-11.21) for all studies; 48.0% (95%CI: 27.5%-69.1%) and OR = 5.32 (95%CI: 1.02-27.82) for studies using culture-based methods; 52.7% (95%CI: 43.9%-61.4%) and OR = 3.24 (95%CI: 1.34-7.84) for studies using the LBT; and 35.9% (95%CI: 30.6%-41.6%) and OR = 8.65 (95%CI: 4.30-14.42) for studies using the GBT]. The prevalence of SIBO in patients with decompensated cirrhosis (classes B and C) was higher than that in those with compensated cirrhosis class A [50.5% (95%CI: 40.3%-60.7%) *vs* 31.2% (95%CI: 19.9%-45.1%); OR = 2.56 (95%CI: 1.60-4.09)]. The prevalence of SIBO was higher in patients with cirrhosis class C than in patients with cirrhosis class B [59.2% (95%CI: 45.0%-71.7%) *vs* 47.6% (95%CI: 35.9%-59.5%); OR = 1.79 (95%CI: 1.18-2.71)][62].

Patients with cirrhosis and SIBO were more likely to have ascites, minimal hepatic encephalopathy, and spontaneous bacterial peritonitis than those without SIBO. The relationship of SIBO with hypocoagulation, alanine aminotransferase and glutamyl transpeptidase activity, white blood cell and platelet counts, hemoglobin and ascitic fluid albumin levels, or esophageal varices was not found[62]. Recent meta-analyses have shown that SIBO in cirrhosis is associated with hepatic encephalopathy (OR = 4.43, 95%CI: 1.73-11.32)[63]. Short-term treatment with rifaximin effectively reduced blood ammonia levels, improved psychometric test scores, and reduced the rate of SIBO as determined by breath testing[64]. No significant association was found between SIBO and hepatic venous pressure gradient[65]. SIBO in patients with cirrhosis was associated with the presence of bacterial DNA in peripheral blood[66], higher plasma LPS levels[67], a shift to alkaline pH in gastric juices[68], malnutrition[69], prolonged OCTT[70,71], lower systolic blood pressure and systemic vascular resistance, higher cardiac output and

serum C-reactive protein levels[72], splanchnic vasodilation, and abdominal hyperdynamic circulation [73].

In patients with cirrhosis, gut microbiota changes with SIBO (a higher abundance of *Firmicutes* and *Fusobacteria*, and a lower abundance of *Bacteroidetes*) did not correspond to cirrhosis-associated gut dysbiosis; therefore, it can be assumed that gut dysbiosis and SIBO are most likely independent disorders of gut microbiota in patients with cirrhosis[74].

Hepatocellular carcinoma

The incidence of SIBO in patients with hepatocellular carcinoma (HCC) was higher than that in cirrhosis patients without HCC (71.8% *vs* 41.1%; OR = 3.7) and healthy controls (71.8% *vs* 3.0%; OR = 81.5). The expression levels of TLR2 and TLR4 on the surface of peripheral blood mononuclear cells in patients with HCC and SIBO were higher than those in patients without SIBO[75].

Extra-hepatic portal vein obstruction

Patients with extra-hepatic portal vein obstruction had similar rates of SIBO compared with healthy controls (7.14% *vs* 1.97%)[76].

Metabolic-associated fatty liver disease

A meta-analysis of 18 studies revealed that, among patients with metabolic-associated fatty liver disease (MAFLD), the rate of SIBO was 35.0% (95%CI: 24.4%-47.2%); in patients with metabolic-associated steatohepatitis (MASH), the rate of SIBO was 41.1% (95%CI: 21.9%-63.4%)[77]. The prevalence of SIBO in MAFLD was higher than that in controls (OR = 3.82, 95%CI: 1.93-7.59) in another meta-analysis that included ten studies[78].

Patients with MAFLD and SIBO had increased OCTT; echomarkers of liver steatosis and fibrosis; severity of liver steatosis, fibrosis, lobular and portal inflammation, and ballooning by liver biopsy; levels of hepatic *CD14* mRNA, nuclear factor kappa beta mRNA, and TLR4 protein expression; homeostatic model assessment for insulin resistance scores; and serum LPS levels compared with patients without SIBO. However, there was no significant difference in BMI, or in serum levels of TNF-α , adiponectin, glutamyl transpeptidase, triglycerides, or low-density lipoprotein between MAFLD patients with and without SIBO. SIBO was associated with significant fibrosis and MASH in MAFLD [79-81]. However, the presence of abdominal obesity was significantly associated with the absence of SIBO (RR = 0.38; 95%CI: 0.02-0.48)[82]. There was no significant difference in the incidence of SIBO in MASH patients with and without signs of metabolic syndrome[83].

A meta-analysis of three studies showed that children with SIBO were more likely to have MAFLD (OR = 5.27; 95%CI: 1.66-16.68) and children with MAFLD were at an increased risk of developing SIBO (RR = 2.17; 95%CI: 1.54-2.81)[84]. Metabolic syndrome and MAFLD were risk factors for SIBO development in obese children[85].

Primary biliary cholangitis

The prevalence of SIBO was higher in patients with primary biliary cholangitis (PBC) than in controls (32.8% *vs* 2.5%; OR = 18.9). Patients with PBC and SIBO were significantly more likely to have diarrhea (78.9% *vs* 35.9%) than those without SIBO. Age, sex, BMI, comorbidities, severity of disease, signs of portal hypertension, and the prevalence of abdominal pain and bloating were similar in PBC patients with and without SIBO[86].

ABDOMINAL SURGERY

Bariatric surgery

SIBO was detected in 43% of patients who had undergone bariatric Roux-en-Y gastric bypass or one-anastomosis gastric bypass and was associated with a higher frequency of defecation in these patients than in those without SIBO[87]. In a separate study, SIBO was detected in 73.4% of patients who received a Roux-en-Y gastric bypass[88]. A third study reported that SIBO testing was negative in all pre-surgery patients and positive in 37.0% of patients 6 mo after one-anastomosis gastric bypass. SIBO in this study was associated with lower reported dietary intake and folate levels and higher vitamin A deficiency rates. No significant differences in alpha and beta diversities of gut microbiota were observed between patients with and without SIBO at 6 mo post-surgery[89]. Among patients that underwent Roux-en-Y gastric bypass at least 1 year before, the SIBO-positive group had a higher BMI than the SIBO-negative group[90]. SIBO prevalence does not increase after adjustable gastric banding (before, 15%; after, 10%), whereas it increased from 15% before Roux-en-Y gastric bypass to up to 40% afterwards. This study also found an association between SIBO and lower weight loss[91].

Gastrectomy

SIBO was found in 61.6% of patients who had undergone gastrectomy. No correlation was found with

any malnutrition parameter[92]. Another study reported significant differences in SIBO prevalence between postgastrectomy patients and controls (77.6% *vs* 6.7%)[93]. Abdominal fullness or borborygmus during oral glucose load was more common in patients with SIBO than in those without. The prevalence of dumping syndrome and postprandial hypoglycemia, pulse rate, and hematocrit levels were not different between patients following gastrectomy with and without SIBO[93]. A third study also revealed that SIBO was more frequent in patients after gastrectomy than in controls (71.4% *vs* 13.3%; OR = 16.3). Specifically, 75% of patients that had undergone a Billroth I or II operation and 50% of patients that had undergone total gastrectomy were positive for SIBO[94].

Colectomy

Patients who had undergone colectomy had a greater incidence of SIBO than healthy controls (62% *vs* 32%; OR = 3.47). There was a higher prevalence of aerobic organisms and a lower prevalence of anaerobic organisms in the duodenal contents in the colectomy group compared with controls[95]. SIBO was detected in 74% of patients after right-sided hemicolectomy for colorectal cancer; no association between SIBO and bile acid malabsorption, delayed OCTT, or loose stools was found in these patients [96].

Cholecystectomy

Patients that had undergone cholecystectomy were more likely to have SIBO than controls (46.8% *vs* 13.3%; OR = 5.7)[97]. Another study reported similar results (41.1% *vs* 13.3%; OR = 4.5)[94]. Cholecystectomy patients with SIBO had more severe abdominal and chest discomfort, bloating, early satiety, nausea, and tenesmus than those without SIBO[97].

Other abdominal surgery

The presence of asymptomatic chronic pouchitis after ileoanal anastomosis was not associated with SIBO[98].

OTHER DIGESTIVE DISEASES

Erosive esophagitis

Patients with erosive esophagitis had SIBO more frequently than controls (65% *vs* 31%; OR = 4.0)[99].

Helicobacter pylori infection

Among patients with abdominal symptoms, SIBO was detected more frequently in *Helicobacter pylori* (*H. pylori*)-infected patients than in uninfected ones (60.4% *vs* 30.6%; OR = 3.45). The incidence of SIBO after *H. pylori* eradication decreased to 20.8%. The remission rate of SIBO after eradication was 66.7%[100].

Gastroparesis

SIBO was present in 60% of patients with gastroparesis, 43.8% of whom had hydrogen SIBO and 22.2% of whom had methane SIBO (6% of patients produced both gases). SIBO was associated with greater disease duration. No significant differences were noted in age, sex, gastric emptying parameters, and etiology of gastroparesis between patients with and without SIBO[101].

Chronic pancreatitis

A meta-analysis of 13 studies showed that the prevalence of SIBO in patients with chronic pancreatitis (CP) was higher than that in controls in all patients [38.6% (95%CI: 25.5%-53.5%); OR = 5.58 (95%CI: 2.26-13.75)], nonsurgical cases [34.6% (95%CI: 20.7%-51.8%); OR = 4.61 (95%CI: 1.67-12.73)], and cases that needed surgical intervention [54.2% (95%CI: 23.3%-82.2%); OR = 10.86 (95%CI: 0.90-131.72)]. Diabetes mellitus (OR = 2.1; 95%CI: 1.2-3.5) and pancreatic exocrine insufficiency (OR = 2.5; 95%CI: 1.3-4.8), but not narcotic drug or PPI use, were associated with SIBO in patients with CP[102]. SIBO was more prevalent in patients with alcohol-induced CP than in patients with other forms of this disease [103]. A separate study showed no association between the severity of CP symptoms and the presence of SIBO[104].

Acute pancreatitis

SIBO was found in 17.8% of patients with acute pancreatitis (AP) and was associated with disease severity, as it was detected in 8.42%, 25.58%, and 25.92% of patients with mild, moderate, and severe AP, respectively. The production of hydrogen by gut microbiota was significantly lower in the late than in the early stage, and SIBO mainly developed within 72 h of AP onset. The incidence of organ failure was significantly higher in patients with SIBO than in those without. However, the incidence of infectious or local complications was not associated with SIBO, and neither was systemic inflammatory response syndrome[105]. Another study reported that SIBO incidence in AP was 12.0%, similar to the results of historic healthy controls, and that glucose tolerance was lower in AP patients with SIBO than

in those without[106].

Cystic fibrosis

The prevalence of SIBO in cystic fibrosis was 31.6%. SIBO was associated with pancreas insufficiency, and independently associated with lower BMI and serum albumin levels[107]. Another study reported the prevalence of SIBO in cystic fibrosis as 40.0%; fecal calprotectin levels did not differ between patients with and without SIBO[108].

Gallstone disease

SIBO prevalence in patients with gallstones was higher than that in controls and those who had undergone cholecystectomy (40.5% *vs* 20.5% and 24.6%; OR = 2.23)[109]. Another study also reported that SIBO was more frequent in patients with gallstones than in controls (14.8% *vs* 0.7%; OR = 26.9)[110]. OCTT and serum bile acid levels were increased in patients with SIBO compared with patients without SIBO, and there was a positive correlation between OCTT and serum bile acid levels in SIBO-positive patients[110].

Children with encopresis

Hydrogen SIBO was detected in 42% of children with encopresis and 23% of controls (OR = 2.4). Methane was produced in 56% of children with encopresis and 23.1% of controls[111].

ENDOCRINE AND METABOLIC DISEASES

Obesity and metabolic syndrome

A meta-analysis of five studies reveled that the increased risk of SIBO in obese individuals did not reach statistical significance (OR = 2.08; 95%CI: 0.82-5.31) but was significant when including only studies from Western countries (OR = 3.41; 95%CI: 1.21-9.59)[112]. However, SIBO was not related to BMI. Small intestinal manometry showed a marked increase of clustered contractions in obese individuals with SIBO compared with those without; no other differences were observed in parameters of fasting cyclic activity[113]. Patients with SIBO have higher visceral to subcutaneous fat ratios than the general population. Metabolic syndrome (OR = 2.5; 95%CI: 1.1-5.7) and higher visceral to subcutaneous fat ratio (OR = 3.3; 95%CI: 1.6-7.2) were independently associated with SIBO in the general population[114]. Obese individuals with SIBO ingested more carbohydrates and refined sugars and less total and insoluble fibers than those without SIBO. There were no significant differences in lipid and protein intake between the two groups[115].

The prevalence of SIBO in obese children was greater than that in controls (37.6% *vs* 3.3%; OR = 17.5). Obese children with SIBO had higher rates of MAFLD, hypertension, and metabolic syndrome, and higher alanine transaminase and aspartate transaminase levels than those without SIBO[116].

Diabetes mellitus

A meta-analysis of 14 studies showed that SIBO is detected in patients with diabetes mellitus more frequently than in controls [29% (95%CI: 20%-39%); OR = 4.18 (95%CI: 1.34-13.05)]. The rate of SIBO was 35% (95%CI: 21%-49%) in Western countries and 24% (95%CI: 14%-34%) in Eastern countries. The prevalence of SIBO in type 2 diabetes was similar to that in type 1 diabetes [30% (95%CI: 13%-47%) *vs* 25% (95%CI: 14%-36%)][117].

Serum levels of biomarkers of oxidative stress (lipid peroxidates, catalase, and superoxide dismutase) and systemic inflammation (TNF-α, IL-6, and IL-10) were higher and serum levels of the antioxidant glutathione were lower in type 2 diabetic patients with SIBO than in those without[118]. SIBO was associated with lower fasting insulin levels, lower insulin release after glucose load, and poorer glucose tolerance and long-term glycemic control (higher glycated hemoglobin) in patients with type 2 diabetes. At the same time, insulin resistance and BMI were lower in patients with SIBO than in those without [119]. In type 2 diabetics, OCTT was more delayed, urinary D-xylose levels were more reduced, and lactose intolerance was more severe in patients with SIBO than in those without[120].

In type 1 diabetes mellitus, OCTT was more delayed and a history of uncontrolled diabetes was more likely in patients with SIBO than in those without. SIBO was significantly higher in patients who had had type 1 diabetes for ≥ 5 years than in those who were diagnosed < 5 years previously[121]. Patients with autonomic neuropathy in type 1 diabetes have a higher prevalence of SIBO, which was associated with higher daily insulin requirements[122].

The rate of SIBO in patients with gestational diabetes mellitus was greater than that in those patients without (54.6% *vs* 27.5%; OR = 3.16). Patients with SIBO had higher levels of fasting blood glucose, glycated hemoglobin, and C-reactive protein, and lower levels vitamin D than those without; neonates from these patients with SIBO had higher weights and lower levels of blood glucose than those from patients without SIBO[123].

Hypothyroidism

SIBO prevalence in patients with hypothyroidism was higher than that in controls [54% *vs* 5%; OR = 22.3 (95%CI: 4.8-102.7)]. Abdominal discomfort, flatulence, and bloating were more prevalent in the patients with SIBO[124].

The positive rates of SIBO were 56.7% and 31.6% in pregnant women with and without subclinical hypothyroidism, respectively (OR = 2.83). The incidence of abdominal distension and constipation, presence of thyroid peroxidase antibody, levels of thyroid-stimulating hormone, and BMI were higher, and the levels of thyroxine were lower in women with SIBO compared with those without[125].

Acromegaly

Patients with acromegaly showed an increased prevalence of SIBO compared with controls (43.9% *vs* 3.3%; OR = 22.7)[126].

Atherosclerosis and hyperlipidemia

SIBO was found in 78.9% of patients with hyperlipidemia and 40% of controls. The level of exhaled hydrogen at 120 min was positively correlated with serum triglyceride and low- and very-low-density lipoprotein levels, and negatively correlated with serum high-density lipoprotein levels[127]. Among patients who did not have previous cardiovascular events and presented with gastrointestinal discomfort, asymptomatic atherosclerotic plaques were detected more often in patients with SIBO than in those without. This was true for the abdominal aorta (OR = 4.18; 95%CI: 2.56-6.80), carotid arteries (OR = 1.93; 95%CI: 1.23-3.02), lower extremity arteries (OR = 1.81; 95%CI: 1.14-2.88), and any-territory plaque presence (OR = 5.42; 95%CI: 2.78-10.58)[128]. Arterial stiffness was elevated in patients with SIBO compared with those without, but carotid intima-media thickness and arterial calcifications did not differ between the two groups[129].

NERVOUS DISEASES

Multiple sclerosis

SIBO was detected in patients with multiple sclerosis more frequently than in controls [38.1% (95%CI: 29.4%-46.9%); OR = 4.50 (95%CI: 2.38-8.50)]. SIBO was associated with more severe disease according to the Expanded Disability Status Scale and Multiple Sclerosis Severity Score[130].

Restless legs syndrome

Patients with restless legs syndrome were more likely to have SIBO than healthy controls (69% *vs* 10%; OR = 19.8)[131].

Alzheimer's disease

SIBO was detected in 49% of patients with Alzheimer's disease, a higher level than that in controls (OR = 3.35). SIBO was not associated with fecal calprotectin and zonulin levels, degree of cognitive impairment, comorbidities, or drug treatment[132].

Autism

Children with autism had an SIBO incidence of 31.0% (95%CI: 25.8%-36.1%), which was higher than that in controls (OR = 4.35). Autistic children with SIBO had higher Autism Treatment Evaluation Checklist scores than those without[133].

Spinal cord injury

SIBO was detected in 21% of patients after spinal cord injury. SIBO was observed more frequently in the subacute than in the chronic phase (37.5% *vs* 0%), and in tetraplegia more frequently than in paraplegia (55.6% *vs* 0.5%)[134]. Another study reported that the SIBO rate after spinal cord injury was 38.5% (95%CI: 29.9%-59.0%) and that SIBO was associated with deep vein thrombosis in these patients (OR = 3.72; 95%CI: 1.97-6.62)[135].

Parkinson's disease

A meta-analysis of 11 studies showed that the prevalence of SIBO in patients with Parkinson's disease was 46% (95%CI: 36%-56%), which was higher than that in controls (OR = 5.22; 95%CI: 3.33-8.19). This incidence was greater in Western countries than in Eastern ones [52% (95%CI: 40%-64%) *vs* 33% (95%CI: 22%-43%)][136]. Patients with SIBO used smaller doses of dopaminergic drugs and had lower serum triglyceride and total bilirubin levels. SIBO was not associated with motor or abdominal symptoms[137] or weight loss[138]. However, another study reported that disease duration, Hoehn and Yahr stage, unified Parkinson's disease rating-III and -IV scores, and Non-Motor Symptoms Scale score were associated with SIBO in these patients[139].

RHEUMATIC DISEASES

Systemic sclerosis

A meta-analysis of 14 studies reported that the prevalence of SIBO in patients with systemic sclerosis was 34% (95%CI: 27%-42%), which was higher than that in controls (OR = 12.51; 95%CI: 6.51-24.03). SIBO prevalence was greater in Western countries than in Asian countries [38% (95%CI: 31%-47%) *vs* 15% (95%CI: 10%-23%)]. Systemic sclerosis patients with SIBO were more likely to have diarrhea (OR = 8.82; 95%CI: 4.09-19) than those without. Sex, diffuse or limited disease, digital ulcer, pulmonary fibrosis, and the presence of anticentromere or Scl-70 antibodies were not associated with SIBO in these patients[140,141]. Fecal calprotectin levels were higher in patients with SIBO than in those without[141]. The average disease duration was longer in patients with SIBO, and these patients had lower levels of hemoglobin, ferritin, total serum protein, phosphorus, calcium, and triglycerides and an elevated erythrocyte sedimentation rate compared with patients without SIBO[142]. The duration of disease (> 5 years) was significantly associated with the presence of SIBO in systemic sclerosis (OR = 9.38; 95%CI: 1.09-80.47)[143].

Behçet's disease

SIBO was diagnosed in 36% of patients with Behçet's disease. No significant differences in disease activity, patient age, severity of abdominal symptoms, frequency of drug use, surgery, smoking status, serum total protein, albumin, and C-reactive protein levels, and erythrocyte sedimentation rate were found between patients with and without SIBO[144].

Spondylarthropathy

The prevalence of SIBO in patients with spondylarthropathy was higher than that in the control group (63% *vs* 5%; OR = 32.9) and did not depend on the presence of HLA-B27, or treatment with NSAID, salazopyrin, or PPI[145].

Fibromyalgia

SIBO was diagnosed in 100% of patients with fibromyalgia, compared with 20% of controls. The degree of somatic pain correlated significantly with hydrogen level as measured by the breath test[146].

ASTHMA

SIBO was detected in 67% and 43% of patients with allergic and non-allergic asthma, respectively. Patients with SIBO had higher levels of immunoglobulin E in serum and eosinophils in sputum, and more severe impairment of respiratory function[147].

HEART FAILURE

Among patients with heart failure (HF), 45% were positive for SIBO, including 41% of patients with reduced ejection fraction (EF) and 51% of patients with preserved EF. SIBO was associated with an increased risk of rehospitalization in patients with reduced EF and cardiovascular death in patients with preserved EF. Patients with SIBO showed higher rates of New York Heart Association functional class III–IV, atrial fibrillation, peripheral edema, spironolactone and intravenous diuretic use, lower use of beta-blockers, and increased left atrial diameter and pulmonary artery systolic pressure than patients without SIBO. Among patients with reduced EF, those with SIBO had higher serum levels of N-terminal pro-B-type natriuretic peptide (a biomarker of HF) than those without[148]. Another study also reported higher SIBO incidence in HF than in controls (41.7% *vs* 9.1%; OR = 7.14) but found that SIBO in HF was not associated with the New York Heart Association functional class, echocardiographic data, number of supraventricular and ventricular extrasystoles, or indicators of complete blood count or biochemical blood analysis. However, patients with SIBO had higher C-reactive protein levels and ventricular tachycardia incidence (OR = 6.8; 95%CI: 1.5-30.2) compared with those without[149].

CANCER

SIBO was found in 63.3% of patients with pancreatic cancer and 46.7% of patients with cholangiocarcinoma, which was greater than that in the healthy controls (OR = 11.2 and 5.7, respectively). TLR4 protein expression in pancreatic carcinoma and cholangiocarcinoma patients was significantly higher in patients with SIBO than in those without[150].

OTHER DISEASES

Obstructive sleep apnea

Among patients with obstructive sleep apnea, 30.8% tested positive for SIBO. The incidence of flatulence was significantly greater in patients with SIBO than in those without. Waist-to-hip ratio was independently associated with SIBO in these patients (OR = 12.9; 95%CI: 1.3-132.2)[151].

Post coronavirus disease 2019 syndrome

SIBO was detected more frequently in patients with post coronavirus disease 2019 IBS than in those with typical IBS (93.3% *vs* 60.0%; OR = 9.3)[152].

Deep vein thrombosis

The prevalence of SIBO in patients with deep vein thrombosis was higher than in controls (69.8% *vs* 39.9%; OR = 3.5) and SIBO was independently associated with this disease (OR = 3.27; 95%CI: 1.70-6.32)[153].

Rosacea and psoriasis

SIBO was detected in patients with rosacea more frequently than in controls in one study (46.0% *vs* 5.0 %; OR = 16.2)[154] and was not more common in these patients than in controls in the other (10.0% *vs* 7.8%)[155]. The prevalence of SIBO in psoriatic patients did not differ from that in the controls (10% *vs* 5%)[156].

SIBO AND OTHER DISEASES: COMMON PATTERNS

As shown above, SIBO is often detected in functional and organic bowel diseases, liver diseases, other diseases of the digestive organs, a number of endocrine, nervous and rheumatic diseases, asthma, HF, and certain other diseases. We have summarized all the reported information on the incidence and OR for SIBO in various diseases in Table 1. An important issue in comparing data is that the presence of SIBO was determined by different tests in different studies, giving different results. In addition, we have observed pronounced heterogeneity in the frequency of SIBO detection in healthy individuals within the control groups, which ranged from fractions of a percent to several tens of percent. The reason for this is yet to be established. However, the detection of SIBO in such a large number of clinically healthy individuals shows that this disorder can be relatively harmless and often asymptomatic.

For many diseases, the development of SIBO is associated with an increased OCTT that decreases the normal clearance of bacteria from the small intestine and is one of the mechanisms underlying the development of SIBO. The slowdown of this transit may be associated with motor dysfunction of the intestine in diseases of the gut, autonomic diabetic polyneuropathy, and portal hypertension, or a decrease in the motor-stimulating influence of thyroid hormones.

Bariatric surgery and gastrectomy lead to a decrease in the barrier function of the stomach which prevents the colonization of the small intestine by oral microbiota. Colectomy leads to a decrease in the barrier function of the ileocecal valve, which prevents the colonization of the small intestine by the colon microbiota. This may explain the increased risk of SIBO following these surgeries.

Interestingly, the frequency of SIBO is increased in a number of nervous and rheumatic diseases, which may support the existence of the gut-brain[157-159] and gut-joint[160-162] axes, suggesting that the products of gut microbiota metabolism can directly or indirectly affect emotional-cognitive and immune function[163], predisposing individuals to the development of these diseases, which is well illustrated by the example of hepatic encephalopathy[164,165] and reactive arthritis[166,167].

The presence of SIBO affects the course of various diseases in different ways. Some diseases, such as IBS, functional diarrhea, and functional constipation, can be mimicked by SIBO with the same symptoms. In these cases, it is not clear what disease is present: SIBO, which manifests itself as IBS and other functional bowel diseases, or these diseases, which are aggravated by the development of SIBO.

In a number of diseases, including cirrhosis, MAFLD, diabetes mellitus, pancreatitis, and cystic fibrosis, an association was found between disease severity and the presence of SIBO. This may be due to the fact that intestinal motility is more severely disturbed in more severe diseases (in cirrhosis or autonomic diabetic polyneuropathy) or that the digestive capabilities of the gut are more affected (in severe pancreatitis and cystic fibrosis) in these cases, which increases the nutrients available for bacteria of the small intestine, leading to their excess growth. However, in SIBO, the overgrown bacteria themselves can, through their metabolic products, affect the metabolism of lipids and carbohydrates, aggravating the course of diabetes[168] and MAFLD[169], and also, through bacterial translocation and systemic inflammation, aggravate the course of portal hypertension in cirrhosis[170-172].

Since SIBO is associated with many diseases, even those not related to the intestines, it seems useful to continue studying the association of SIBO with other diseases and their manifestations. It is also important to clarify the pathogenetic ways in which the underlying disease can contribute to the development of SIBO, and SIBO, in turn, can have a negative effect on the course of the underlying

Table 1 Association of small intestinal bacterial overgrowth with various diseases

Disease	Prevalence of SIBO	OR
Functional digestive diseases		
Functional dyspepsia	17.2%-53.4%	4.3
Irritable bowel syndrome	31.0%-36.7%	3.7
Functional abdominal bloating/distention	43%-68%	
Functional constipation	78%	
Functional diarrhea	69%	
Organic (non-functional) digestive diseases		
Short bowel syndrome	50%	
Chronic intestinal pseudo-obstruction	23.7%-52.6%	
Lactase deficiency	27.6%	5.3
Lactose malabsorption in elderly persons	90%	36
Symptomatic uncomplicated diverticular disease	58.9%	8.7
Celiac disease	18.3%	5.1
Environmental enteric dysfunction	85.3%	
Crohn's disease	25.4%	10.9
Ulcerative colitis	14.3%	8.0
Liver diseases		
Cirrhosis	40.8%	6.8
Hepatocellular carcinoma	71.8%	81.5
Metabolic associated fatty liver disease	35.0%	3.8
Primary biliary cholangitis	32.8%	18.9
Abdominal surgery		
Bariatric surgery	37.0%-73.4%	
Gastrectomy	61.6%-77.6%	16.3
Colectomy	62%-74%	3.47
Cholecystectomy	24.6%-46.8%	4.5-5.7
Other digestive diseases		
Erosive esophagitis	65%	4.0
Helicobacter pylori infection	60.4%	3.45
Gastroparesis	60%	
Chronic pancreatitis	38.6%	5.58
Acute pancreatitis	12.0%-17.8%	
Cystic fibroris	31.6%-40.0%	
Gallstone disease	14.8%-40.5%	2.2-26.9
Encopresis	42%	2.4
Endocrine and metabolic diseases		
Diabetes mellitus	29%	4.18
Hypothyroidism	54%	22.3
Acromegaly	43.9%	22.7
Hyperlipidemia	78.9%	
Nervous diseases		

Multiple sclerosis	38.1%	4.5
Restless legs syndrome	69%	19.8
Azheimer's disease	49%	3.35
Autism	31.0%	4.35
Spinal cord injuries	37.5%-38.5%	
Parkinson's disease	46%	5.22
Rheumatic diseases		
Systemic sclerosis	34%	12.51
Behçet's disease	36%	
Spondylarthropathy	63%	32.9
Fibromyalgia	100%	
Other diseases		
Allergic asthma	67%	
Non-allergic asthma	43%	
Heart failure	41.7%-45.0%	7.14
Pancreatic cancer	63.3%	11.2
Cholangiocarcinoma	46.7%	5.7
Obstructive sleep apnea	30.8%	
Post-COVID-19 irritable bowel syndrome	93.3%	9.3
Deep vein thrombosis	69.8%	3.5
Rosacea	10%-46%	16.2

SIBO: Small intestinal bacterial overgrowth; OR: Odds ratio; COVID-19: Coronavirus disease 2019.

disease. Currently, such studies are being conducted in cirrhosis[72], MAFLD[79-81], diabetes[118,119], and other diseases. An important question is how the course of the underlying disease will respond to SIBO treatment. These results have already been obtained for some diseases[49,154], but their presentation is the aim for the next review.

CONCLUSION

In conclusion, we have summarized almost all published information on the association of SIBO with various diseases and their manifestations. Almost one third of cited studies were published within the last 2 years, highlighting the recent interest in the field and the importance of our review. However, further study on SIBO in various diseases, and particularly on the effect of its eradication on the condition and prognosis of patients, is required.

FOOTNOTES

Author contributions: Ivashkin V reviewed the idea; all authors contributed to the draft editing; Maslennikov R is the guarantor.

Conflict-of-interest statement: All the authors report no relevant conflicts of interest for this article.

Open-Access: This article is an open-access article that was selected by an in-house editor and fully peer-reviewed by external reviewers. It is distributed in accordance with the Creative Commons Attribution NonCommercial (CC BY-NC 4.0) license, which permits others to distribute, remix, adapt, build upon this work non-commercially, and license their derivative works on different terms, provided the original work is properly cited and the use is non-commercial. See: https://creativecommons.org/Licenses/by-nc/4.0/

Country/Territory of origin: Russia

ORCID number: Irina Efremova 0000-0002-4112-0426; Roman Maslennikov 0000-0001-7513-1636; Elena Poluektova 0000-0002-9038-3732; Yury Zharikov 0000-0001-9636-3807; Andrey Suslov 0000-0003-0613-8556; Yana Letyagina 0009-0003-0491-5179; Evgenii Kozlov 0000-0001-6244-1088; Vladimir Ivashkin 0000-0002-6815-6015.

S-Editor: Wang JJ
L-Editor: Wang TQ
P-Editor: Wang JJ

REFERENCES

1 **Bushyhead D**, Quigley EMM. Small Intestinal Bacterial Overgrowth-Pathophysiology and Its Implications for Definition and Management. *Gastroenterology* 2022; **163**: 593-607 [PMID: 35398346 DOI: 10.1053/j.gastro.2022.04.002]
2 **Ghoshal UC**, Sachdeva S, Ghoshal U, Misra A, Puri AS, Pratap N, Shah A, Rahman MM, Gwee KA, Tan VPY, Ahmed T, Lee YY, Ramakrishna BS, Talukdar R, Rana SV, Sinha SK, Chen M, Kim N, Holtmann G. Asian-Pacific consensus on small intestinal bacterial overgrowth in gastrointestinal disorders: An initiative of the Indian Neurogastroenterology and Motility Association. *Indian J Gastroenterol* 2022; **41**: 483-507 [PMID: 36214973 DOI: 10.1007/s12664-022-01292-x]
3 **Skrzydło-Radomańska B**, Cukrowska B. How to Recognize and Treat Small Intestinal Bacterial Overgrowth? *J Clin Med* 2022; **11** [PMID: 36294338 DOI: 10.3390/jcm11206017]
4 **Ivashkin VT**, Maev IV, Abdulganieva DI, Alekseeva OP, Alekseenko SA, Zolnikova OY, Korochanskaya NV, Medvedev OS, Poluektova EA, Simanenkov VI, Trukhmanov AS, Khlynov IB, Tsukanov VV, Shifrin OS, Ivashkin KV, Lapina TL, Maslennikov RV, Fadeeva MV, Ulyanin AI. Practical Recommendation of the Scientific Community for Human Microbiome Research (CHMR) and the Russian Gastroenterological Association (RGA) on Small Intestinal Bacterial Overgrowth in Adults. *Russ J Gastroenterol Hepatol Coloproctol* 2022; **32**: 68-85 [DOI: 10.22416/1382-4376-2022-32-3-68-85]
5 **Broekaert IJ**, Borrelli O, Dolinsek J, Martin-de-Carpi J, Mas E, Miele E, Pienar C, Ribes-Koninckx C, Thomassen R, Thomson M, Tzivinikos C, Benninga M. An ESPGHAN Position Paper on the Use of Breath Testing in Paediatric Gastroenterology. *J Pediatr Gastroenterol Nutr* 2022; **74**: 123-137 [PMID: 34292218 DOI: 10.1097/MPG.0000000000003245]
6 **Baker JR**, Chey WD, Watts L, Armstrong M, Collins K, Lee AA, Dupati A, Menees S, Saad RJ, Harer K, Hasler WL. How the North American Consensus Protocol Affects the Performance of Glucose Breath Testing for Bacterial Overgrowth Versus a Traditional Method. *Am J Gastroenterol* 2021; **116**: 780-787 [PMID: 33982948 DOI: 10.14309/ajg.0000000000001110]
7 **Losurdo G**, Leandro G, Ierardi E, Perri F, Barone M, Principi M, Leo AD. Breath Tests for the Non-invasive Diagnosis of Small Intestinal Bacterial Overgrowth: A Systematic Review With Meta-analysis. *J Neurogastroenterol Motil* 2020; **26**: 16-28 [PMID: 31743632 DOI: 10.5056/jnm19113]
8 **Madigan KE**, Bundy R, Weinberg RB. Distinctive Clinical Correlates of Small Intestinal Bacterial Overgrowth with Methanogens. *Clin Gastroenterol Hepatol* 2022; **20**: 1598-1605.e2 [PMID: 34597730 DOI: 10.1016/j.cgh.2021.09.035]
9 **de Lacy Costello BP**, Ledochowski M, Ratcliffe NM. The importance of methane breath testing: a review. *J Breath Res* 2013; **7**: 024001 [PMID: 23470880 DOI: 10.1088/1752-7155/7/2/024001]
10 **Liu Chen Kiow J**, Bellila R, Therrien A, Sidani S, Bouin M. Predictors of Small Intestinal Bacterial Overgrowth in Symptomatic Patients Referred for Breath Testing. *J Clin Med Res* 2020; **12**: 655-661 [PMID: 33029272 DOI: 10.14740/jocmr4320]
11 **Erdogan A**, Rao SS, Gulley D, Jacobs C, Lee YY, Badger C. Small intestinal bacterial overgrowth: duodenal aspiration vs glucose breath test. *Neurogastroenterol Motil* 2015; **27**: 481-489 [PMID: 25600077 DOI: 10.1111/nmo.12516]
12 **Choung RS**, Ruff KC, Malhotra A, Herrick L, Locke GR 3rd, Harmsen WS, Zinsmeister AR, Talley NJ, Saito YA. Clinical predictors of small intestinal bacterial overgrowth by duodenal aspirate culture. *Aliment Pharmacol Ther* 2011; **33**: 1059-1067 [PMID: 21395630 DOI: 10.1111/j.1365-2036.2011.04625.x]
13 **Roland BC**, Ciarleglio MM, Clarke JO, Semler JR, Tomakin E, Mullin GE, Pasricha PJ. Small Intestinal Transit Time Is Delayed in Small Intestinal Bacterial Overgrowth. *J Clin Gastroenterol* 2015; **49**: 571-576 [PMID: 25319735 DOI: 10.1097/MCG.0000000000000257]
14 **Chander Roland B**, Mullin GE, Passi M, Zheng X, Salem A, Yolken R, Pasricha PJ. A Prospective Evaluation of Ileocecal Valve Dysfunction and Intestinal Motility Derangements in Small Intestinal Bacterial Overgrowth. *Dig Dis Sci* 2017; **62**: 3525-3535 [PMID: 28871499 DOI: 10.1007/s10620-017-4726-4]
15 **Calderon G**, Siwiec RM, Bohm ME, Nowak TV, Wo JM, Gupta A, Xu H, Shin A. Delayed Gastric Emptying Is Not Associated with a Microbiological Diagnosis of Small Intestinal Bacterial Overgrowth. *Dig Dis Sci* 2021; **66**: 160-166 [PMID: 32124195 DOI: 10.1007/s10620-020-06153-1]
16 **Montalto M**, Santoro L, Dalvai S, Curigliano V, D'Onofrio F, Scarpellini E, Cammarota G, Panunzi S, Gallo A, Gasbarrini A, Gasbarrini G. Fecal calprotectin concentrations in patients with small intestinal bacterial overgrowth. *Dig Dis* 2008; **26**: 183-186 [PMID: 18431069 DOI: 10.1159/000116777]
17 **Gabbard SL**, Lacy BE, Levine GM, Crowell MD. The impact of alcohol consumption and cholecystectomy on small intestinal bacterial overgrowth. *Dig Dis Sci* 2014; **59**: 638-644 [PMID: 24323179 DOI: 10.1007/s10620-013-2960-y]
18 **Siniewicz-Luzeńczyk K**, Bik-Gawin A, Zeman K, Bąk-Romaniszyn L. Small intestinal bacterial overgrowth syndrome in children. *Prz Gastroenterol* 2015; **10**: 28-32 [PMID: 25960812 DOI: 10.5114/pg.2014.47494]
19 **Pilipenko VI**, Isakov VA, Morozov SV, Vlasova AV, Naydenova MA. [Association of food patterns with different forms of small intestinal bacterial overgroth syndrome and treatment efficacy]. *Ter Arkh* 2019; **91**: 82-90 [PMID: 32598636 DOI: 10.26442/00403660.2019.10.000496]

20 **Nalyotov AV**, Svistunova NA. [Assessment of the state of the small intestine microbiota in children on a long-term dairy-free diet]. *Vopr Pitan* 2022; **91**: 15-20 [PMID: 35596631 DOI: 10.33029/0042-8833-2022-91-2-15-20]

21 **Su T**, Lai S, Lee A, He X, Chen S. Meta-analysis: proton pump inhibitors moderately increase the risk of small intestinal bacterial overgrowth. *J Gastroenterol* 2018; **53**: 27-36 [PMID: 28770351 DOI: 10.1007/s00535-017-1371-9]

22 **Lombardo L**, Foti M, Ruggia O, Chiecchio A. Increased incidence of small intestinal bacterial overgrowth during proton pump inhibitor therapy. *Clin Gastroenterol Hepatol* 2010; **8**: 504-508 [PMID: 20060064 DOI: 10.1016/j.cgh.2009.12.022]

23 **Revaiah PC**, Kochhar R, Rana SV, Berry N, Ashat M, Dhaka N, Rami Reddy Y, Sinha SK. Risk of small intestinal bacterial overgrowth in patients receiving proton pump inhibitors versus proton pump inhibitors plus prokinetics. *JGH Open* 2018; **2**: 47-53 [PMID: 30483563 DOI: 10.1002/jgh3.12045]

24 **Zhang R**, Li Y, Ma JX, Tang S, Li CM, Wan J. [The effects of continuous proton pump inhibitor therapy on small intestinal bacterial overgrowth in elderly]. *Zhonghua Nei Ke Za Zhi* 2020; **59**: 706-710 [PMID: 32838502 DOI: 10.3760/cma.j.cn112138-20191218-00823]

25 **Plauzolles A**, Uras S, Pénaranda G, Bonnet M, Dukan P, Retornaz F, Halfon P. Small Intestinal Bacterial Overgrowths and Intestinal Methanogen Overgrowths Breath Testing in a Real-Life French Cohort. *Clin Transl Gastroenterol* 2023; **14**: e00556 [PMID: 36515897 DOI: 10.14309/ctg.0000000000000556]

26 **Kucheryavyy YA**, Andreev DN, Maev IV. [Prevalence of small bowel bacterial overgrowth in patients with functional dyspepsia: a meta-analysis]. *Ter Arkh* 2020; **92**: 53-58 [PMID: 33720574 DOI: 10.26442/00403660.2020.12.200433]

27 **Gurusamy SR**, Shah A, Talley NJ, Koloski N, Jones MP, Walker MM, Morrison M, Holtmann G. Small Intestinal Bacterial Overgrowth in Functional Dyspepsia: A Systematic Review and Meta-Analysis. *Am J Gastroenterol* 2021; **116**: 935-942 [PMID: 33734110 DOI: 10.14309/ajg.0000000000001197]

28 **Ghoshal UC**, Nehra A, Mathur A, Rai S. A meta-analysis on small intestinal bacterial overgrowth in patients with different subtypes of irritable bowel syndrome. *J Gastroenterol Hepatol* 2020; **35**: 922-931 [PMID: 31750966 DOI: 10.1111/jgh.14938]

29 **Shah A**, Talley NJ, Jones M, Kendall BJ, Koloski N, Walker MM, Morrison M, Holtmann GJ. Small Intestinal Bacterial Overgrowth in Irritable Bowel Syndrome: A Systematic Review and Meta-Analysis of Case-Control Studies. *Am J Gastroenterol* 2020; **115**: 190-201 [PMID: 31913194 DOI: 10.14309/ajg.0000000000000504]

30 **Chen B**, Kim JJ, Zhang Y, Du L, Dai N. Prevalence and predictors of small intestinal bacterial overgrowth in irritable bowel syndrome: a systematic review and meta-analysis. *J Gastroenterol* 2018; **53**: 807-818 [PMID: 29761234 DOI: 10.1007/s00535-018-1476-9]

31 **Gandhi A**, Shah A, Jones MP, Koloski N, Talley NJ, Morrison M, Holtmann G. Methane positive small intestinal bacterial overgrowth in inflammatory bowel disease and irritable bowel syndrome: A systematic review and meta-analysis. *Gut Microbes* 2021; **13**: 1933313 [PMID: 34190027 DOI: 10.1080/19490976.2021.1933313]

32 **Yu X**, Li Y, Xiang F, Feng J. Correlation between small intestinal bacterial overgrowth and irritable bowel syndrome and the prognosis of treatment. *Ann Palliat Med* 2021; **10**: 3364-3370 [PMID: 33849121 DOI: 10.21037/apm-21-427]

33 **Srivastava D**, Ghoshal U, Mittal RD, Ghoshal UC. Associations between IL-1RA polymorphisms and small intestinal bacterial overgrowth among patients with irritable bowel syndrome from India. *Neurogastroenterol Motil* 2014; **26**: 1408-1416 [PMID: 25073651 DOI: 10.1111/nmo.12399]

34 **Chu H**, Fox M, Zheng X, Deng Y, Long Y, Huang Z, Du L, Xu F, Dai N. Small Intestinal Bacterial Overgrowth in Patients with Irritable Bowel Syndrome: Clinical Characteristics, Psychological Factors, and Peripheral Cytokines. *Gastroenterol Res Pract* 2016; **2016**: 3230859 [PMID: 27379166 DOI: 10.1155/2016/3230859]

35 **Wei H**, Liu ZJ, Wang K, Zheng W, Duan LP. [The dietary features of diarrhea predominant irritable bowel syndrome patients with small intestinal bowel overgrowth]. *Zhonghua Nei Ke Za Zhi* 2017; **56**: 567-571 [PMID: 28789488 DOI: 10.3760/cma.j.issn.0578-1426.2017.08.003]

36 **Jung SE**, Joo NS, Han KS, Kim KN. Obesity Is Inversely Related to Hydrogen-Producing Small Intestinal Bacterial Overgrowth in Non-Constipation Irritable Bowel Syndrome. *J Korean Med Sci* 2017; **32**: 948-953 [PMID: 28480652 DOI: 10.3346/jkms.2017.32.6.948]

37 **Ding XW**, Liu YX, Fang XC, Liu K, Wei YY, Shan MH. The relationship between small intestinal bacterial overgrowth and irritable bowel syndrome. *Eur Rev Med Pharmacol Sci* 2017; **21**: 5191-5196 [PMID: 29228433 DOI: 10.26355/eurrev_201711_13839]

38 **Park JH**, Park DI, Kim HJ, Cho YK, Sohn CI, Jeon WK, Kim BI, Won KH, Park SM. The Relationship between Small-Intestinal Bacterial Overgrowth and Intestinal Permeability in Patients with Irritable Bowel Syndrome. *Gut Liver* 2009; **3**: 174-179 [PMID: 20431742 DOI: 10.5009/gnl.2009.3.3.174]

39 **Grover M**, Kanazawa M, Palsson OS, Chitkara DK, Gangarosa LM, Drossman DA, Whitehead WE. Small intestinal bacterial overgrowth in irritable bowel syndrome: association with colon motility, bowel symptoms, and psychological distress. *Neurogastroenterol Motil* 2008; **20**: 998-1008 [PMID: 18482250 DOI: 10.1111/j.1365-2982.2008.01142.x]

40 **Scarpellini E**, Giorgio V, Gabrielli M, Lauritano EC, Pantanella A, Fundarò C, Gasbarrini A. Prevalence of small intestinal bacterial overgrowth in children with irritable bowel syndrome: a case-control study. *J Pediatr* 2009; **155**: 416-420 [PMID: 19535093 DOI: 10.1016/j.jpeds.2009.03.033]

41 **Noh CK**, Lee KJ. Fecal Microbiota Alterations and Small Intestinal Bacterial Overgrowth in Functional Abdominal Bloating/Distention. *J Neurogastroenterol Motil* 2020; **26**: 539-549 [PMID: 32989189 DOI: 10.5056/jnm20080]

42 **Madrid AM**, Defilippi C C, Defilippi G C, Slimming A J, Quera P R. [Small intestinal bacterial overgrowth in patients with functional gastrointestinal diseases]. *Rev Med Chil* 2007; **135**: 1245-1252 [PMID: 18180830]

43 **Muraki M**, Fujiwara Y, Machida H, Okazaki H, Sogawa M, Yamagami H, Tanigawa T, Shiba M, Watanabe K, Tominaga K, Watanabe T, Arakawa T. Role of small intestinal bacterial overgrowth in severe small intestinal damage in chronic non-steroidal anti-inflammatory drug users. *Scand J Gastroenterol* 2014; **49**: 267-273 [PMID: 24417613 DOI: 10.3109/00365521.2014.880182]

44 **Seddik TB**, Tian L, Nespor C, Kerner J, Maldonado Y, Gans H. Risk Factors of Ambulatory Central Line-Associated Bloodstream Infection in Pediatric Short Bowel Syndrome. *JPEN J Parenter Enteral Nutr* 2020; **44**: 500-506 [PMID: 31179578 DOI: 10.1002/jpen.1667]

45 **Khan MZ**, Lyu R, McMichael J, Gabbard S. Chronic Intestinal Pseudo-Obstruction Is Associated with Intestinal Methanogen Overgrowth. *Dig Dis Sci* 2022; **67**: 4834-4840 [PMID: 35001241 DOI: 10.1007/s10620-021-07343-1]

46 **Jo IH**, Paik CN, Kim YJ, Lee JM, Choi SY, Hong KP. Lactase Deficiency Diagnosed by Endoscopic Biopsy-based Method is Associated With Positivity to Glucose Breath Test. *J Neurogastroenterol Motil* 2023; **29**: 85-93 [PMID: 36606439 DOI: 10.5056/jnm22023]

47 **Almeida JA**, Kim R, Stoita A, McIver CJ, Kurtovic J, Riordan SM. Lactose malabsorption in the elderly: role of small intestinal bacterial overgrowth. *Scand J Gastroenterol* 2008; **43**: 146-154 [PMID: 18224561 DOI: 10.1080/00365520701676617]

48 **Tursi A**, Brandimarte G, Giorgetti GM, Elisei W. Transient lactose malabsorption in patients affected by symptomatic uncomplicated diverticular disease of the colon. *Dig Dis Sci* 2006; **51**: 461-465 [PMID: 16614952 DOI: 10.1007/s10620-006-3155-6]

49 **Shah A**, Thite P, Hansen T, Kendall BJ, Sanders DS, Morrison M, Jones MP, Holtmann G. Links between celiac disease and small intestinal bacterial overgrowth: A systematic review and meta-analysis. *J Gastroenterol Hepatol* 2022; **37**: 1844-1852 [PMID: 35734803 DOI: 10.1111/jgh.15920]

50 **Tursi A**, Brandimarte G, Giorgetti G. High prevalence of small intestinal bacterial overgrowth in celiac patients with persistence of gastrointestinal symptoms after gluten withdrawal. *Am J Gastroenterol* 2003; **98**: 839-843 [PMID: 12738465 DOI: 10.1111/j.1572-0241.2003.07379.x]

51 **Keusch GT**, Denno DM, Black RE, Duggan C, Guerrant RL, Lavery JV, Nataro JP, Rosenberg IH, Ryan ET, Tarr PI, Ward H, Bhutta ZA, Coovadia H, Lima A, Ramakrishna B, Zaidi AK, Hay Burgess DC, Brewer T. Environmental enteric dysfunction: pathogenesis, diagnosis, and clinical consequences. *Clin Infect Dis* 2014; **59** Suppl 4: S207-S212 [PMID: 25305288 DOI: 10.1093/cid/ciu485]

52 **Collard JM**, Andrianonimiadana L, Habib A, Rakotondrainipiana M, Andriantsalama P, Randriamparany R, Rabenandrasana MAN, Weill FX, Sauvonnet N, Randremanana RV, Guillemot V, Vonaesch P, Sansonetti PJ; Afribiota Investigators. High prevalence of small intestine bacteria overgrowth and asymptomatic carriage of enteric pathogens in stunted children in Antananarivo, Madagascar. *PLoS Negl Trop Dis* 2022; **16**: e0009849 [PMID: 35533199 DOI: 10.1371/journal.pntd.0009849]

53 **Shah A**, Morrison M, Burger D, Martin N, Rich J, Jones M, Koloski N, Walker MM, Talley NJ, Holtmann GJ. Systematic review with meta-analysis: the prevalence of small intestinal bacterial overgrowth in inflammatory bowel disease. *Aliment Pharmacol Ther* 2019; **49**: 624-635 [PMID: 30735254 DOI: 10.1111/apt.15133]

54 **Rana SV**, Sharma S, Malik A, Kaur J, Prasad KK, Sinha SK, Singh K. Small intestinal bacterial overgrowth and orocecal transit time in patients of inflammatory bowel disease. *Dig Dis Sci* 2013; **58**: 2594-2598 [PMID: 23649377 DOI: 10.1007/s10620-013-2694-x]

55 **Wei J**, Feng J, Chen L, Yang Z, Tao H, Li L, Xuan J, Wang F. Small intestinal bacterial overgrowth is associated with clinical relapse in patients with quiescent Crohn's disease: a retrospective cohort study. *Ann Transl Med* 2022; **10**: 784 [PMID: 35965806 DOI: 10.21037/atm-22-3335]

56 **Ricci JER Júnior**, Chebli LA, Ribeiro TCDR, Castro ACS, Gaburri PD, Pace FHDL, Barbosa KVBD, Ferreira LEVVDC, Passos MDCF, Malaguti C, Delgado ÁHDA, Campos JD, Coelho AR, Chebli JMF. Small-Intestinal Bacterial Overgrowth is Associated With Concurrent Intestinal Inflammation But Not With Systemic Inflammation in Crohn's Disease Patients. *J Clin Gastroenterol* 2018; **52**: 530-536 [PMID: 28134633 DOI: 10.1097/MCG.0000000000000803]

57 **Greco A**, Caviglia GP, Brignolo P, Ribaldone DG, Reggiani S, Sguazzini C, Smedile A, Pellicano R, Resegotti A, Astegiano M, Bresso F. Glucose breath test and Crohn's disease: Diagnosis of small intestinal bacterial overgrowth and evaluation of therapeutic response. *Scand J Gastroenterol* 2015; **50**: 1376-1381 [PMID: 25990116 DOI: 10.3109/00365521.2015.1050691]

58 **Sánchez-Montes C**, Ortiz V, Bastida G, Rodríguez E, Yago M, Beltrán B, Aguas M, Iborra M, Garrigues V, Ponce J, Nos P. Small intestinal bacterial overgrowth in inactive Crohn's disease: influence of thiopurine and biological treatment. *World J Gastroenterol* 2014; **20**: 13999-14003 [PMID: 25320539 DOI: 10.3748/wjg.v20.i38.13999]

59 **Yang C**, Guo X, Wang J, Fan H, Huo X, Dong L, Duan Z. Relationship between Small Intestinal Bacterial Overgrowth and Peripheral Blood ET, TLR2 and TLR4 in Ulcerative Colitis. *J Coll Physicians Surg Pak* 2020; **30**: 245-249 [PMID: 32169129 DOI: 10.29271/jcpsp.2020.03.245]

60 **Rana SV**, Sharma S, Kaur J, Prasad KK, Sinha SK, Kochhar R, Malik A, Morya RK. Relationship of cytokines, oxidative stress and GI motility with bacterial overgrowth in ulcerative colitis patients. *J Crohns Colitis* 2014; **8**: 859-865 [PMID: 24456736 DOI: 10.1016/j.crohns.2014.01.007]

61 **Scarpellini E**, Abenavoli L, Cassano V, Rinninella E, Sorge M, Capretti F, Rasetti C, Svegliati Baroni G, Luzza F, Santori P, Sciacqua A. The Apparent Asymmetrical Relationship Between Small Bowel Bacterial Overgrowth, Endotoxemia, and Liver Steatosis and Fibrosis in Cirrhotic and Non-Cirrhotic Patients: A Single-Center Pilot Study. *Front Med (Lausanne)* 2022; **9**: 872428 [PMID: 35559337 DOI: 10.3389/fmed.2022.872428]

62 **Maslennikov R**, Pavlov C, Ivashkin V. Small intestinal bacterial overgrowth in cirrhosis: systematic review and meta-analysis. *Hepatol Int* 2018; **12**: 567-576 [PMID: 30284684 DOI: 10.1007/s12072-018-9898-2]

63 **Feng X**, Li X, Zhang X, Chen W, Tian Y, Yang Q, Yang Y, Pan H, Jiang Z. Hepatic Encephalopathy in Cirrhotic Patients and Risk of Small Intestinal Bacterial Overgrowth: A Systematic Review and Meta-Analysis. *Biomed Res Int* 2022; **2022**: 2469513 [PMID: 36303585 DOI: 10.1155/2022/2469513]

64 **Zhang Y**, Feng Y, Cao B, Tian Q. Effects of SIBO and rifaximin therapy on MHE caused by hepatic cirrhosis. *Int J Clin Exp Med* 2015; **8**: 2954-2957 [PMID: 25932262]

65 **Pande C**, Kumar A, Sarin SK. Small-intestinal bacterial overgrowth in cirrhosis is related to the severity of liver disease. *Aliment Pharmacol Ther* 2009; **29**: 1273-1281 [PMID: 19302262 DOI: 10.1111/j.1365-2036.2009.03994.x]

66 **Jun DW**, Kim KT, Lee OY, Chae JD, Son BK, Kim SH, Jo YJ, Park YS. Association between small intestinal bacterial overgrowth and peripheral bacterial DNA in cirrhotic patients. *Dig Dis Sci* 2010; **55**: 1465-1471 [PMID: 19517230 DOI: 10.1007/s10620-009-0870-9]

67 **Wang J**, Chen M, Sun G. Small bowel bacterial overgrowth and endotoxemia in cirrhosis. *Zhonghua Nei Ke Za Zhi* 2002;

41: 459-461 [PMID: 12189115]

68 **Shindo K**, Machida M, Miyakawa K, Fukumura M. A syndrome of cirrhosis, achlorhydria, small intestinal bacterial overgrowth, and fat malabsorption. *Am J Gastroenterol* 1993; **88**: 2084-2091 [PMID: 8249977]

69 **Yao J**, Chang L, Yuan L, Duan Z. Nutrition status and small intestinal bacterial overgrowth in patients with virus-related cirrhosis. *Asia Pac J Clin Nutr* 2016; **25**: 283-291 [PMID: 27222411 DOI: 10.6133/apjcn.2016.25.2.06]

70 **Lunia MK**, Sharma BC, Sachdeva S. Small intestinal bacterial overgrowth and delayed orocecal transit time in patients with cirrhosis and low-grade hepatic encephalopathy. *Hepatol Int* 2013; **7**: 268-273 [PMID: 26201641 DOI: 10.1007/s12072-012-9360-9]

71 **Gupta A**, Dhiman RK, Kumari S, Rana S, Agarwal R, Duseja A, Chawla Y. Role of small intestinal bacterial overgrowth and delayed gastrointestinal transit time in cirrhotic patients with minimal hepatic encephalopathy. *J Hepatol* 2010; **53**: 849-855 [PMID: 20675008 DOI: 10.1016/j.jhep.2010.05.017]

72 **Maslennikov R**, Pavlov C, Ivashkin V. Is small intestinal bacterial overgrowth a cause of hyperdynamic circulation in cirrhosis? *Turk J Gastroenterol* 2019; **30**: 964-975 [PMID: 31767551 DOI: 10.5152/tjg.2019.18551]

73 **Maslennikov RV**, Tatarkina MA, Mayevskaya MV, Pavlov CS, Zharkova MS, Ivashkin VT. The impact of bacterial overgrowth syndrome and systemic inflammation on abdominal hemodynamics in liver cirrhosis. *Russ J Gastroenterol Hepatol Coloproctol* 2017; **27**: 52-61

74 **Maslennikov R**, Ivashkin V, Efremova I, Poluektova E, Kudryavtseva A, Krasnov G. Gut dysbiosis and small intestinal bacterial overgrowth as independent forms of gut microbiota disorders in cirrhosis. *World J Gastroenterol* 2022; **28**: 1067-1077 [PMID: 35431497 DOI: 10.3748/wjg.v28.i10.1067]

75 **Zhou DX**, Ma YJ, Chen GY, Gao X, Yang L. [Relationship of TLR2 and TLR4 expressions on the surface of peripheral blood mononuclear cells to small intestinal bacteria overgrowth in patients with hepatocellular carcinoma]. *Zhonghua Gan Zang Bing Za Zhi* 2019; **27**: 286-290 [PMID: 31082340 DOI: 10.3760/cma.j.issn.1007-3418.2019.04.009]

76 **Lakshmi CP**, Ghoshal UC, Kumar S, Goel A, Misra A, Mohindra S, Choudhuri G. Frequency and factors associated with small intestinal bacterial overgrowth in patients with cirrhosis of the liver and extra hepatic portal venous obstruction. *Dig Dis Sci* 2010; **55**: 1142-1148 [PMID: 19424796 DOI: 10.1007/s10620-009-0826-0]

77 **Gudan A**, Jamioł-Milc D, Hawryłkowicz V, Skonieczna-Żydecka K, Stachowska E. The Prevalence of Small Intestinal Bacterial Overgrowth in Patients with Non-Alcoholic Liver Diseases: NAFLD, NASH, Fibrosis, Cirrhosis-A Systematic Review, Meta-Analysis and Meta-Regression. *Nutrients* 2022; **14** [PMID: 36558421 DOI: 10.3390/nu14245261]

78 **Wijarnpreecha K**, Lou S, Watthanasuntorn K, Kroner PT, Cheungpasitporn W, Lukens FJ, Pungpapong S, Keaveny AP, Ungprasert P. Small intestinal bacterial overgrowth and nonalcoholic fatty liver disease: a systematic review and meta-analysis. *Eur J Gastroenterol Hepatol* 2020; **32**: 601-608 [PMID: 31567712 DOI: 10.1097/MEG.0000000000001541]

79 **Shi H**, Mao L, Wang L, Quan X, Xu X, Cheng Y, Zhu S, Dai F. Small intestinal bacterial overgrowth and orocecal transit time in patients of nonalcoholic fatty liver disease. *Eur J Gastroenterol Hepatol* 2021; **33**: e535-e539 [PMID: 33867442 DOI: 10.1097/MEG.0000000000002157]

80 **Mikolasevic I**, Delija B, Mijic A, Stevanovic T, Skenderevic N, Sosa I, Krznaric-Zrnic I, Abram M, Krznaric Z, Domislovic V, Filipec Kanizaj T, Radic-Kristo D, Cubranic A, Grubesic A, Nakov R, Skrobonja I, Stimac D, Hauser G. Small intestinal bacterial overgrowth and non-alcoholic fatty liver disease diagnosed by transient elastography and liver biopsy. *Int J Clin Pract* 2021; **75**: e13947 [PMID: 33406286 DOI: 10.1111/ijcp.13947]

81 **Kapil S**, Duseja A, Sharma BK, Singla B, Chakraborti A, Das A, Ray P, Dhiman RK, Chawla Y. Small intestinal bacterial overgrowth and toll-like receptor signaling in patients with non-alcoholic fatty liver disease. *J Gastroenterol Hepatol* 2016; **31**: 213-221 [PMID: 26212089 DOI: 10.1111/jgh.13058]

82 **Fitriakusumah Y**, Lesmana CRA, Bastian WP, Jasirwan COM, Hasan I, Simadibrata M, Kurniawan J, Sulaiman AS, Gani RA. The role of Small Intestinal Bacterial Overgrowth (SIBO) in Non-alcoholic Fatty Liver Disease (NAFLD) patients evaluated using Controlled Attenuation Parameter (CAP) Transient Elastography (TE): a tertiary referral center experience. *BMC Gastroenterol* 2019; **19**: 43 [PMID: 30894137 DOI: 10.1186/s12876-019-0960-x]

83 **De Oliveira JM**, Pace FL, Ghetti FF, Barbosa KVBD, Cesar DE, Chebli JMF, Ferreira LEVVC. Non-alcoholic Steatohepatitis: Comparison of Intestinal Microbiota between Different Metabolic Profiles. A Pilot Study. *J Gastrointestin Liver Dis* 2020; **29**: 369-376 [PMID: 32830817 DOI: 10.15403/jgld-497]

84 **Kuang L**, Zhou W, Jiang Y. Association of small intestinal bacterial overgrowth with nonalcoholic fatty liver disease in children: A meta-analysis. *PLoS One* 2021; **16**: e0260479 [PMID: 34855819 DOI: 10.1371/journal.pone.0260479]

85 **Stepanov YM**, Zavhorodnia NY, Yagmur VB, Lukianenko OY, Zygalo EV. Association of nonalcoholic fatty liver disease with small intestine bacterial overgrowth in obese children. *Wiad Lek* 2019; **72**: 350-356 [PMID: 31050979]

86 **Liu Chen Kiow J**, Vincent C, Sidani S, Bouin M. High occurrence of small intestinal bacterial overgrowth in primary biliary cholangitis. *Neurogastroenterol Motil* 2019; **31**: e13691 [PMID: 31373141 DOI: 10.1111/nmo.13691]

87 **Novljan U**, Pintar T. Small Intestinal Bacterial Overgrowth in Patients with Roux-en-Y Gastric Bypass and One-Anastomosis Gastric Bypass. *Obes Surg* 2022; **32**: 4102-4109 [PMID: 36197573 DOI: 10.1007/s11695-022-06299-z]

88 **Dolan RD**, Baker J, Harer K, Lee A, Hasler W, Saad R, Schulman AR. Small Intestinal Bacterial Overgrowth: Clinical Presentation in Patients with Roux-en-Y Gastric Bypass. *Obes Surg* 2021; **31**: 564-569 [PMID: 33047289 DOI: 10.1007/s11695-020-05032-y]

89 **Kaniel O**, Sherf-Dagan S, Szold A, Langer P, Khalfin B, Kessler Y, Raziel A, Sakran N, Motro Y, Goitein D, Moran-Gilad J. The Effects of One Anastomosis Gastric Bypass Surgery on the Gastrointestinal Tract. *Nutrients* 2022; **14** [PMID: 35057486 DOI: 10.3390/nu14020304]

90 **Coelho LK**, Carvalho NS, Navarro-Rodriguez T, Marson FAL, Carvalho PJPC. Lactulose Breath Testing Can Be a Positive Predictor Before Weight Gain in Participants with Obesity Submitted to Roux-en-Y Gastric Bypass. *Obes Surg* 2019; **29**: 3457-3464 [PMID: 31187458 DOI: 10.1007/s11695-019-04006-z]

91 **Sabate JM**, Coupaye M, Ledoux S, Castel B, Msika S, Coffin B, Jouet P. Consequences of Small Intestinal Bacterial Overgrowth in Obese Patients Before and After Bariatric Surgery. *Obes Surg* 2017; **27**: 599-605 [PMID: 27576576 DOI: 10.1007/s11695-016-2343-5]

92 **Pérez Aisa A**, García Gavilán MC, Alcaide García J, Méndez Sánchez IM, Rivera Irigoin R, Fernández Cano F, Pereda Salguero T, Rivas Ruiz F. Small intestinal bacterial overgrowth is common after gastrectomy but with little impact on nutritional status. *Gastroenterol Hepatol* 2019; **42**: 1-10 [PMID: 30197248 DOI: 10.1016/j.gastrohep.2018.07.001]

93 **Paik CN**, Choi MG, Lim CH, Park JM, Chung WC, Lee KM, Jun KH, Song KY, Jeon HM, Chin HM, Park CH, Chung IS. The role of small intestinal bacterial overgrowth in postgastrectomy patients. *Neurogastroenterol Motil* 2011; **23**: e191-e196 [PMID: 21324050 DOI: 10.1111/j.1365-2982.2011.01686.x]

94 **Kim DB**, Paik CN, Kim YJ, Lee JM, Jun KH, Chung WC, Lee KM, Yang JM, Choi MG. Positive Glucose Breath Tests in Patients with Hysterectomy, Gastrectomy, and Cholecystectomy. *Gut Liver* 2017; **11**: 237-242 [PMID: 27965476 DOI: 10.5009/gnl16132]

95 **Rao SSC**, Tan G, Abdulla H, Yu S, Larion S, Leelasinjaroen P. Does colectomy predispose to small intestinal bacterial (SIBO) and fungal overgrowth (SIFO)? *Clin Transl Gastroenterol* 2018; **9**: 146 [PMID: 29691369 DOI: 10.1038/s41424-018-0011-x]

96 **Larsen HM**, Krogh K, Borre M, Gregersen T, Mejlby Hansen M, Arveschoug AK, Christensen P, Drewes AM, Emmertsen KJ, Laurberg S, Ladefoged Fassov J. Chronic loose stools following right-sided hemicolectomy for colon cancer and the association with bile acid malabsorption and small intestinal bacterial overgrowth. *Colorectal Dis* 2023; **25**: 600-607 [PMID: 36347822 DOI: 10.1111/codi.16409]

97 **Sung HJ**, Paik CN, Chung WC, Lee KM, Yang JM, Choi MG. Small Intestinal Bacterial Overgrowth Diagnosed by Glucose Hydrogen Breath Test in Post-cholecystectomy Patients. *J Neurogastroenterol Motil* 2015; **21**: 545-551 [PMID: 26351251 DOI: 10.5056/jnm15020]

98 **Lisowska A**, Banasiewicz T, Marciniak R, Drews M, Majewski P, Herzig KH, Walkowiak J. Chronic pouchitis is not related to small intestine bacterial overgrowth. *Inflamm Bowel Dis* 2008; **14**: 1102-1104 [PMID: 18452204 DOI: 10.1002/ibd.20432]

99 **Kim KM**, Kim BT, Lee DJ, Park SB, Joo NS, Kim YS, Kim KN. Erosive esophagitis may be related to small intestinal bacterial overgrowth. *Scand J Gastroenterol* 2012; **47**: 493-498 [PMID: 22416969 DOI: 10.3109/00365521.2012.668932]

100 **Zhu D**, Wang XL, Dai Y, Li SY, Wang WH. [Influence of Helicobacter pylori infection and its eradication treatment on small intestinal bacterial overgrowth]. *Zhonghua Yi Xue Za Zhi* 2022; **102**: 3382-3387 [PMID: 36372768 DOI: 10.3760/cma.j.cn112137-20220316-00551]

101 **Reddymasu SC**, McCallum RW. Small intestinal bacterial overgrowth in gastroparesis: are there any predictors? *J Clin Gastroenterol* 2010; **44**: e8-13 [PMID: 20027008 DOI: 10.1097/MCG.0b013e3181aec746]

102 **El Kurdi B**, Babar S, El Iskandarani M, Bataineh A, Lerch MM, Young M, Singh VP. Factors That Affect Prevalence of Small Intestinal Bacterial Overgrowth in Chronic Pancreatitis: A Systematic Review, Meta-Analysis, and Meta-Regression. *Clin Transl Gastroenterol* 2019; **10**: e00072 [PMID: 31517648 DOI: 10.14309/ctg.0000000000000072]

103 **Ní Chonchubhair HM**, Bashir Y, Dobson M, Ryan BM, Duggan SN, Conlon KC. The prevalence of small intestinal bacterial overgrowth in non-surgical patients with chronic pancreatitis and pancreatic exocrine insufficiency (PEI). *Pancreatology* 2018; **18**: 379-385 [PMID: 29502987 DOI: 10.1016/j.pan.2018.02.010]

104 **Therrien A**, Bouchard S, Sidani S, Bouin M. Prevalence of Small Intestinal Bacterial Overgrowth among Chronic Pancreatitis Patients: A Case-Control Study. *Can J Gastroenterol Hepatol* 2016; **2016**: 7424831 [PMID: 27446865 DOI: 10.1155/2016/7424831]

105 **Zhang M**, Zhu HM, He F, Li BY, Li XC. Association between acute pancreatitis and small intestinal bacterial overgrowth assessed by hydrogen breath test. *World J Gastroenterol* 2017; **23**: 8591-8596 [PMID: 29358867 DOI: 10.3748/wjg.v23.i48.8591]

106 **Kim DB**, Paik CN, Lee JM, Kim YJ. Association between increased breath hydrogen methane concentration and prevalence of glucose intolerance in acute pancreatitis. *J Breath Res* 2020; **14**: 026006 [PMID: 31689699 DOI: 10.1088/1752-7163/ab5460]

107 **Furnari M**, De Alessandri A, Cresta F, Haupt M, Bassi M, Calvi A, Haupt R, Bodini G, Ahmed I, Bagnasco F, Giannini EG, Casciaro R. The role of small intestinal bacterial overgrowth in cystic fibrosis: a randomized case-controlled clinical trial with rifaximin. *J Gastroenterol* 2019; **54**: 261-270 [PMID: 30232597 DOI: 10.1007/s00535-018-1509-4]

108 **Lisowska A**, Madry E, Pogorzelski A, Szydłowski J, Radzikowski A, Walkowiak J. Small intestine bacterial overgrowth does not correspond to intestinal inflammation in cystic fibrosis. *Scand J Clin Lab Invest* 2010; **70**: 322-326 [PMID: 20560844 DOI: 10.3109/00365513.2010.486869]

109 **Kim DB**, Paik CN, Song DS, Kim YJ, Lee JM. The characteristics of small intestinal bacterial overgrowth in patients with gallstone diseases. *J Gastroenterol Hepatol* 2018; **33**: 1477-1484 [PMID: 29392773 DOI: 10.1111/jgh.14113]

110 **Kaur J**, Rana SV, Gupta R, Gupta V, Sharma SK, Dhawan DK. Prolonged orocecal transit time enhances serum bile acids through bacterial overgrowth, contributing factor to gallstone disease. *J Clin Gastroenterol* 2014; **48**: 365-369 [PMID: 24598592 DOI: 10.1097/MCG.0b013e3182a14fba]

111 **Leiby A**, Mehta D, Gopalareddy V, Jackson-Walker S, Horvath K. Bacterial overgrowth and methane production in children with encopresis. *J Pediatr* 2010; **156**: 766-770, 770.e1 [PMID: 20036380 DOI: 10.1016/j.jpeds.2009.10.043]

112 **Wijarnpreecha K**, Werlang ME, Watthanasuntorn K, Panjawatanan P, Cheungpasitporn W, Gomez V, Lukens FJ, Ungprasert P. Obesity and Risk of Small Intestine Bacterial Overgrowth: A Systematic Review and Meta-Analysis. *Dig Dis Sci* 2020; **65**: 1414-1422 [PMID: 31605277 DOI: 10.1007/s10620-019-05887-x]

113 **Madrid AM**, Poniachik J, Quera R, Defilippi C. Small intestinal clustered contractions and bacterial overgrowth: a frequent finding in obese patients. *Dig Dis Sci* 2011; **56**: 155-160 [PMID: 20431947 DOI: 10.1007/s10620-010-1239-9]

114 **Fialho A**, Fialho A, Thota P, McCullough A, Shen B. Higher visceral to subcutaneous fat ratio is associated with small intestinal bacterial overgrowth. *Nutr Metab Cardiovasc Dis* 2016; **26**: 773-777 [PMID: 27282099 DOI: 10.1016/j.numecd.2016.04.007]

115 **Ierardi E**, Losurdo G, Sorrentino C, Giorgio F, Rossi G, Marinaro A, Romagno KR, Di Leo A, Principi M. Macronutrient intakes in obese subjects with or without small intestinal bacterial overgrowth: an alimentary survey. *Scand J Gastroenterol* 2016; **51**: 277-280 [PMID: 26375876 DOI: 10.3109/00365521.2015.1086020]

116 **Belei O**, Olariu L, Dobrescu A, Marcovici T, Marginean O. The relationship between non-alcoholic fatty liver disease and

small intestinal bacterial overgrowth among overweight and obese children and adolescents. *J Pediatr Endocrinol Metab* 2017; **30**: 1161-1168 [PMID: 28988228 DOI: 10.1515/jpem-2017-0252]

117 **Feng X**, Li XQ. The prevalence of small intestinal bacterial overgrowth in diabetes mellitus: a systematic review and meta-analysis. *Aging (Albany NY)* 2022; **14**: 975-988 [PMID: 35086065 DOI: 10.18632/aging.203854]

118 **Malik A**, Morya RK, Saha S, Singh PK, Bhadada SK, Rana SV. Oxidative stress and inflammatory markers in type 2 diabetic patients. *Eur J Clin Invest* 2020; **50**: e13238 [PMID: 32298466 DOI: 10.1111/eci.13238]

119 **Yan LH**, Mu B, Pan D, Shi YN, Yuan JH, Guan Y, Li W, Zhu XY, Guo L. Association between small intestinal bacterial overgrowth and beta-cell function of type 2 diabetes. *J Int Med Res* 2020; **48**: 300060520937866 [PMID: 32691685 DOI: 10.1177/0300060520937866]

120 **Rana SV**, Malik A, Bhadada SK, Sachdeva N, Morya RK, Sharma G. Malabsorption, Orocecal Transit Time and Small Intestinal Bacterial Overgrowth in Type 2 Diabetic Patients: A Connection. *Indian J Clin Biochem* 2017; **32**: 84-89 [PMID: 28149017 DOI: 10.1007/s12291-016-0569-6]

121 **Malik A**, Morya RK, Bhadada SK, Rana S. Type 1 diabetes mellitus: Complex interplay of oxidative stress, cytokines, gastrointestinal motility and small intestinal bacterial overgrowth. *Eur J Clin Invest* 2018; **48**: e13021 [PMID: 30155878 DOI: 10.1111/eci.13021]

122 **Ojetti V**, Pitocco D, Scarpellini E, Zaccardi F, Scaldaferri F, Gigante G, Gasbarrini G, Ghirlanda G, Gasbarrini A. Small bowel bacterial overgrowth and type 1 diabetes. *Eur Rev Med Pharmacol Sci* 2009; **13**: 419-423 [PMID: 20085122]

123 **Zhang M**, Xu Y, Zhang J, Sun Z, Ban Y, Wang B, Hou X, Cai Y, Li J, Wang M, Wang W. Application of methane and hydrogen-based breath test in the study of gestational diabetes mellitus and intestinal microbes. *Diabetes Res Clin Pract* 2021; **176**: 108818 [PMID: 33932493 DOI: 10.1016/j.diabres.2021.108818]

124 **Lauritano EC**, Bilotta AL, Gabrielli M, Scarpellini E, Lupascu A, Laginestra A, Novi M, Sottili S, Serricchio M, Cammarota G, Gasbarrini G, Pontecorvi A, Gasbarrini A. Association between hypothyroidism and small intestinal bacterial overgrowth. *J Clin Endocrinol Metab* 2007; **92**: 4180-4184 [PMID: 17698907 DOI: 10.1210/jc.2007-0606]

125 **Wang B**, Xu Y, Hou X, Li J, Cai Y, Hao Y, Ouyang Q, Wu B, Sun Z, Zhang M, Ban Y. Small Intestinal Bacterial Overgrowth in Subclinical Hypothyroidism of Pregnant Women. *Front Endocrinol (Lausanne)* 2021; **12**: 604070 [PMID: 34108932 DOI: 10.3389/fendo.2021.604070]

126 **Resmini E**, Parodi A, Savarino V, Greco A, Rebora A, Minuto F, Ferone D. Evidence of prolonged orocecal transit time and small intestinal bacterial overgrowth in acromegalic patients. *J Clin Endocrinol Metab* 2007; **92**: 2119-2124 [PMID: 17405840 DOI: 10.1210/jc.2006-2509]

127 **Kvit KB**, Kharchenko NV, Kharchenko VV, Chornenka OI, Chornovus RI, Dorofeeva US, Draganchuk OB, Slaba OM. The role of small intestinal bacterial overgrowth in the pathogenesis of hyperlipidemia. *Wiad Lek* 2019; **72**: 645-649 [PMID: 31055549]

128 **Dong C**, Wang G, Xian R, Li C, Wang S, Cui L. Association between Small Intestinal Bacterial Overgrowth and Subclinical Atheromatous Plaques. *J Clin Med* 2022; **12** [PMID: 36615114 DOI: 10.3390/jcm12010314]

129 **Ponziani FR**, Pompili M, Di Stasio E, Zocco MA, Gasbarrini A, Flore R. Subclinical atherosclerosis is linked to small intestinal bacterial overgrowth *via* vitamin K2-dependent mechanisms. *World J Gastroenterol* 2017; **23**: 1241-1249 [PMID: 28275304 DOI: 10.3748/wjg.v23.i7.1241]

130 **Zhang Y**, Liu G, Duan Y, Han X, Dong H, Geng J. Prevalence of Small Intestinal Bacterial Overgrowth in Multiple Sclerosis: a Case-Control Study from China. *J Neuroimmunol* 2016; **301**: 83-87 [PMID: 27890460 DOI: 10.1016/j.jneuroim.2016.11.004]

131 **Weinstock LB**, Walters AS. Restless legs syndrome is associated with irritable bowel syndrome and small intestinal bacterial overgrowth. *Sleep Med* 2011; **12**: 610-613 [PMID: 21570907 DOI: 10.1016/j.sleep.2011.03.007]

132 **Kowalski K**, Mulak A. Small intestinal bacterial overgrowth in Alzheimer's disease. *J Neural Transm (Vienna)* 2022; **129**: 75-83 [PMID: 34797427 DOI: 10.1007/s00702-021-02440-x]

133 **Wang L**, Yu YM, Zhang YQ, Zhang J, Lu N, Liu N. Hydrogen breath test to detect small intestinal bacterial overgrowth: a prevalence case-control study in autism. *Eur Child Adolesc Psychiatry* 2018; **27**: 233-240 [PMID: 28799094 DOI: 10.1007/s00787-017-1039-2]

134 **Vallès M**, Antuori A, Mearin F, Serra J. Small intestinal bacterial overgrowth in spinal cord injury patients. *Gastroenterol Hepatol* 2021; **44**: 539-545 [PMID: 33640466 DOI: 10.1016/j.gastrohep.2021.01.010]

135 **Cheng X**, Zhang L, Xie NC, Xu HL, Lian YJ. Association between small-intestinal bacterial overgrowth and deep vein thrombosis in patients with spinal cord injuries. *J Thromb Haemost* 2017; **15**: 304-311 [PMID: 27930853 DOI: 10.1111/jth.13583]

136 **Li X**, Feng X, Jiang Z. Association of small intestinal bacterial overgrowth with Parkinson's disease: a systematic review and meta-analysis. *Gut Pathog* 2021; **13**: 25 [PMID: 33863370 DOI: 10.1186/s13099-021-00420-w]

137 **Hasuike Y**, Endo T, Koroyasu M, Matsui M, Mori C, Yamadera M, Fujimura H, Sakoda S. Bile acid abnormality induced by intestinal dysbiosis might explain lipid metabolism in Parkinson's disease. *Med Hypotheses* 2020; **134**: 109436 [PMID: 31678900 DOI: 10.1016/j.mehy.2019.109436]

138 **DiBaise JK**, Crowell MD, Driver-Dunckley E, Mehta SH, Hoffman-Snyder C, Lin T, Adler CH. Weight Loss in Parkinson's Disease: No Evidence for Role of Small Intestinal Bacterial Overgrowth. *J Parkinsons Dis* 2018; **8**: 571-581 [PMID: 30149465 DOI: 10.3233/JPD-181386]

139 **Niu XL**, Liu L, Song ZX, Li Q, Wang ZH, Zhang JL, Li HH. Prevalence of small intestinal bacterial overgrowth in Chinese patients with Parkinson's disease. *J Neural Transm (Vienna)* 2016; **123**: 1381-1386 [PMID: 27589873 DOI: 10.1007/s00702-016-1612-8]

140 **Feng X**, Li XQ, Jiang Z. Prevalence and predictors of small intestinal bacterial overgrowth in systemic sclerosis: a systematic review and meta-analysis. *Clin Rheumatol* 2021; **40**: 3039-3051 [PMID: 33426631 DOI: 10.1007/s10067-020-05549-8]

141 **Polkowska-Pruszyńska B**, Gerkowicz A, Rawicz-Pruszyński K, Krasowska D. The Role of Fecal Calprotectin in Patients with Systemic Sclerosis and Small Intestinal Bacterial Overgrowth (SIBO). *Diagnostics (Basel)* 2020; **10** [PMID: 32823752 DOI: 10.3390/diagnostics10080587]

142 **Polkowska-Pruszyńska B**, Gerkowicz A, Szczepanik-Kułak P, Krasowska D. Small intestinal bacterial overgrowth in systemic sclerosis: a review of the literature. *Arch Dermatol Res* 2019; **311**: 1-8 [PMID: 30382339 DOI: 10.1007/s00403-018-1874-0]

143 **Sawadpanich K**, Soison P, Chunlertrith K, Mairiang P, Sukeepaisarnjaroen W, Sangchan A, Suttichaimongkol T, Foocharoen C. Prevalence and associated factors of small intestinal bacterial overgrowth among systemic sclerosis patients. *Int J Rheum Dis* 2019; **22**: 695-699 [PMID: 30729669 DOI: 10.1111/1756-185X.13495]

144 **Jo JH**, Park SJ, Cheon JH, Kim TI, Kim WH. Rediscover the clinical value of small intestinal bacterial overgrowth in patients with intestinal Behçet's disease. *J Gastroenterol Hepatol* 2018; **33**: 375-379 [PMID: 28666309 DOI: 10.1111/jgh.13855]

145 **Laroche JM**, Kapel N, Benahmed N, Claudepierre P, Chevalier X, Barbot-Trystram L. High prevalence of small intestinal bacterial overgrowth (SIBO) in spondylarthropathy. *Clin Exp Rheumatol* 2021; **39**: 703 [PMID: 33427609 DOI: 10.55563/clinexprheumatol/nyanfu]

146 **Pimentel M**, Wallace D, Hallegua D, Chow E, Kong Y, Park S, Lin HC. A link between irritable bowel syndrome and fibromyalgia may be related to findings on lactulose breath testing. *Ann Rheum Dis* 2004; **63**: 450-452 [PMID: 15020342 DOI: 10.1136/ard.2003.011502]

147 **Potskhverashvili ND**, Zolnikova OY, Kokina NI, Dzhakhaya NL, Sedova AV, Bueverova EL, Trukhmanov AS. Small Bowel Bacterial Overgrowth Syndrome in Patients with Bronchial Asthma. *Russ J Gastroenterol Hepatol Coloproctol* 2018; **28**: 47-54 [DOI: 10.22416/1382-4376-2018-28-4-47-54]

148 **Song Y**, Liu Y, Qi B, Cui X, Dong X, Wang Y, Han X, Li F, Shen D, Zhang X, Hu K, Chen S, Zhou J, Ge J. Association of Small Intestinal Bacterial Overgrowth With Heart Failure and Its Prediction for Short-Term Outcomes. *J Am Heart Assoc* 2021; **10**: e015292 [PMID: 33728933 DOI: 10.1161/JAHA.119.015292]

149 **Fadeeva MV**, Skhirtladze MR, Ivashkin VT. Small Intestinal Bacterial Overgrowth Syndrome as a Risk Factor for Ventricular Tachycardia in Chronic Heart Failure with Left Ventricular Systolic Dysfunction. *Russ J Gastroenterol Hepatol Coloproctol* 2019; **29**: 38-48 [DOI: 10.22416/1382-4376-2019-29-3-38-48]

150 **Ma X**, Wang H, Zhang P, Xu L, Tian Z. Association between small intestinal bacterial overgrowth and toll-like receptor 4 in patients with pancreatic carcinoma and cholangiocarcinoma. *Turk J Gastroenterol* 2019; **30**: 177-183 [PMID: 30457560 DOI: 10.5152/tjg.2018.17512]

151 **Kim DB**, Park CS, Paik CN, Kang YJ, Jo IH, Lee JM. Relationship between untreated obstructive sleep apnea and breath hydrogen and methane after glucose load. *Saudi J Gastroenterol* 2022; **28**: 355-361 [PMID: 35848702 DOI: 10.4103/sjg.sjg_134_22]

152 **Nalyotov AV**, Guz NP. Prevalence of Small Intestinal Bacterial Overgrowth Syndrome in Patients with Irritable Bowel Syndrome who Have Suffered COVID-19. *Russ J Gastroenterol Hepatol Coloproctol* 2022; **32**: 35-39 [DOI: 10.22416/1382-4376-2022-32-3-35-39]

153 **Fialho A**, Fialho A, Schenone A, Thota P, McCullough A, Shen B. Association between small intestinal bacterial overgrowth and deep vein thrombosis. *Gastroenterol Rep (Oxf)* 2016; **4**: 299-303 [PMID: 27044499 DOI: 10.1093/gastro/gow004]

154 **Parodi A**, Paolino S, Greco A, Drago F, Mansi C, Rebora A, Parodi A, Savarino V. Small intestinal bacterial overgrowth in rosacea: clinical effectiveness of its eradication. *Clin Gastroenterol Hepatol* 2008; **6**: 759-764 [PMID: 18456568 DOI: 10.1016/j.cgh.2008.02.054]

155 **Gravina A**, Federico A, Ruocco E, Lo Schiavo A, Masarone M, Tuccillo C, Peccerillo F, Miranda A, Romano L, de Sio C, de Sio I, Persico M, Ruocco V, Riegler G, Loguercio C, Romano M. Helicobacter pylori infection but not small intestinal bacterial overgrowth may play a pathogenic role in rosacea. *United European Gastroenterol J* 2015; **3**: 17-24 [PMID: 25653855 DOI: 10.1177/2050640614559262]

156 **Drago F**, Ciccarese G, Indemini E, Savarino V, Parodi A. Psoriasis and small intestine bacterial overgrowth. *Int J Dermatol* 2018; **57**: 112-113 [PMID: 29057460 DOI: 10.1111/ijd.13797]

157 **Majumdar A**, Siva Venkatesh IP, Basu A. Short-Chain Fatty Acids in the Microbiota-Gut-Brain Axis: Role in Neurodegenerative Disorders and Viral Infections. *ACS Chem Neurosci* 2023; **14**: 1045-1062 [PMID: 36868874 DOI: 10.1021/acschemneuro.2c00803]

158 **Anand N**, Gorantla VR, Chidambaram SB. The Role of Gut Dysbiosis in the Pathophysiology of Neuropsychiatric Disorders. *Cells* 2022; **12** [PMID: 36611848 DOI: 10.3390/cells12010054]

159 **Lewandowska-Pietruszka Z**, Figlerowicz M, Mazur-Melewska K. The History of the Intestinal Microbiota and the Gut-Brain Axis. *Pathogens* 2022; **11** [PMID: 36558874 DOI: 10.3390/pathogens11121540]

160 **Romero-Figueroa MDS**, Ramírez-Durán N, Montiel-Jarquín AJ, Horta-Baas G. Gut-joint axis: Gut dysbiosis can contribute to the onset of rheumatoid arthritis *via* multiple pathways. *Front Cell Infect Microbiol* 2023; **13**: 1092118 [PMID: 36779190 DOI: 10.3389/fcimb.2023.1092118]

161 **Qaiyum Z**, Lim M, Inman RD. The gut-joint axis in spondyloarthritis: immunological, microbial, and clinical insights. *Semin Immunopathol* 2021; **43**: 173-192 [PMID: 33625549 DOI: 10.1007/s00281-021-00845-0]

162 **Gracey E**, Vereecke L, McGovern D, Fröhling M, Schett G, Danese S, De Vos M, Van den Bosch F, Elewaut D. Revisiting the gut-joint axis: links between gut inflammation and spondyloarthritis. *Nat Rev Rheumatol* 2020; **16**: 415-433 [PMID: 32661321 DOI: 10.1038/s41584-020-0454-9]

163 **Campbell C**, Kandalgaonkar MR, Golonka RM, Yeoh BS, Vijay-Kumar M, Saha P. Crosstalk between Gut Microbiota and Host Immunity: Impact on Inflammation and Immunotherapy. *Biomedicines* 2023; **11** [PMID: 36830830 DOI: 10.3390/biomedicines11020294]

164 **Luo M**, Xin RJ, Hu FR, Yao L, Hu SJ, Bai FH. Role of gut microbiota in the pathogenesis and therapeutics of minimal hepatic encephalopathy *via* the gut-liver-brain axis. *World J Gastroenterol* 2023; **29**: 144-156 [PMID: 36683714 DOI: 10.3748/wjg.v29.i1.144]

165 **Won SM**, Oh KK, Gupta H, Ganesan R, Sharma SP, Jeong JJ, Yoon SJ, Jeong MK, Min BH, Hyun JY, Park HJ, Eom JA, Lee SB, Cha MG, Kwon GH, Choi MR, Kim DJ, Suk KT. The Link between Gut Microbiota and Hepatic Encephalopathy. *Int J Mol Sci* 2022; **23** [PMID: 36012266 DOI: 10.3390/ijms23168999]

166 **Berthelot JM**, Claudepierre P. Trafficking of antigens from gut to sacroiliac joints and spine in reactive arthritis and spondyloarthropathies: Mainly through lymphatics? *Joint Bone Spine* 2016; **83**: 485-490 [PMID: 26968111 DOI: 10.1016/j.jbspin.2015.10.015]

167 **García-Kutzbach A**, Chacón-Súchite J, García-Ferrer H, Iraheta I. Reactive arthritis: update 2018. *Clin Rheumatol* 2018; **37**: 869-874 [PMID: 29455267 DOI: 10.1007/s10067-018-4022-5]

168 **Bajinka O**, Tan Y, Darboe A, Ighaede-Edwards IG, Abdelhalim KA. The gut microbiota pathway mechanisms of diabetes. *AMB Express* 2023; **13**: 16 [PMID: 36754883 DOI: 10.1186/s13568-023-01520-3]

169 **Maestri M**, Santopaolo F, Pompili M, Gasbarrini A, Ponziani FR. Gut microbiota modulation in patients with non-alcoholic fatty liver disease: Effects of current treatments and future strategies. *Front Nutr* 2023; **10**: 1110536 [PMID: 36875849 DOI: 10.3389/fnut.2023.1110536]

170 **Maslennikov R**, Ivashkin V, Efremova I, Poluektova E, Shirokova E. Gut-liver axis in cirrhosis: Are hemodynamic changes a missing link? *World J Clin Cases* 2021; **9**: 9320-9332 [PMID: 34877269 DOI: 10.12998/wjcc.v9.i31.9320]

171 **Tilg H**, Adolph TE, Trauner M. Gut-liver axis: Pathophysiological concepts and clinical implications. *Cell Metab* 2022; **34**: 1700-1718 [PMID: 36208625 DOI: 10.1016/j.cmet.2022.09.017]

172 **Albillos A**, de Gottardi A, Rescigno M. The gut-liver axis in liver disease: Pathophysiological basis for therapy. *J Hepatol* 2020; **72**: 558-577 [PMID: 31622696 DOI: 10.1016/j.jhep.2019.10.003]

World Journal of Gastroenterology

Submit a Manuscript: https://www.f6publishing.com

World J Gastroenterol 2023 June 14; 29(22): 3422-3439

DOI: 10.3748/wjg.v29.i22.3422

ISSN 1007-9327 (print) ISSN 2219-2840 (online)

ORIGINAL ARTICLE

Basic Study

Mechanism of annexin A1/N-formylpeptide receptor regulation of macrophage function to inhibit hepatic stellate cell activation through Wnt/β-catenin pathway

Jun-Hua Fan, Na Luo, Geng-Feng Liu, Xiao-Fang Xu, Shi-Quan Li, Xiao-Ping Lv

Specialty type: Gastroenterology and hepatology

Provenance and peer review: Unsolicited article; Externally peer reviewed.

Peer-review model: Single blind

Peer-review report's scientific quality classification

Grade A (Excellent): 0
Grade B (Very good): B
Grade C (Good): C, C
Grade D (Fair): 0
Grade E (Poor): 0

P-Reviewer: Dauyey K, Kazakhstan; Mohamed GA, Egypt; Nakade Y, Japan

Received: February 15, 2023
Peer-review started: February 15, 2023
First decision: March 28, 2023
Revised: April 10, 2023
Accepted: May 11, 2023
Article in press: May 11, 2023
Published online: June 14, 2023

Jun-Hua Fan, Na Luo, Geng-Feng Liu, Xiao-Fang Xu, Shi-Quan Li, Xiao-Ping Lv, Department of Gastroenterology, The First Affiliated Hospital of Guangxi Medical University, Nanning 530021, Guangxi Zhuang Autonomous Region, China

Corresponding author: Jun-Hua Fan, Doctor, MD, PhD, Associate Professor, Doctor, Department of Gastroenterology, The First Affiliated Hospital of Guangxi Medical University, No. 6 Shuangyong Road, Nanning 530021, Guangxi Zhuang Autonomous Region, China. fanjunhuaxiaoshe@hotmail.com

Abstract

BACKGROUND

Hepatic fibrosis is a common pathological process of chronic liver diseases with various causes, which can progress to cirrhosis.

AIM

To evaluate the effect and mechanism of action annexin (Anx)A1 in liver fibrosis and how this could be targeted therapeutically.

METHODS

CCl_4 (20%) and active N-terminal peptide of AnxA1 (Ac2-26) and N-formylpeptide receptor antagonist N-Boc-Phe-Leu-Phe-Leu-Phe (Boc2) were injected intraperitoneally to induce liver fibrosis in eight wild-type mice/Anxa1 knockout mice, and to detect expression of inflammatory factors, collagen deposition, and the role of the Wnt/β-catenin pathway in hepatic fibrosis.

RESULTS

Compared with the control group, AnxA1, transforming growth factor (TGF)-β1, interleukin (IL)-1β and IL-6 expression in the liver of mice with hepatic fibrosis induced by CCl_4 was significantly increased, which promoted collagen deposition and expression of α-smooth muscle actin (α-SMA), collagen type I and connective tissue growth factor (CTGF), and increased progressively with time. CCl_4 induced an increase in TGF-β1, IL-1β and IL-6 in liver tissue of AnxA1 knockout mice, and the degree of liver inflammation and fibrosis and expression of α-SMA, collagen I and CTGF were significantly increased compared with in wild-type mice. After treatment with Ac2-26, expression of liver inflammatory factors, degree of collagen deposition and expression of a-SMA, collagen I and CTGF were decrea-

sed compared with before treatment. Boc2 inhibited the anti-inflammatory and antifibrotic effects of Ac2-26. AnxA1 downregulated expression of the Wnt/β-catenin pathway in CCl_4-induced hepatic fibrosis. *In vitro*, lipopolysaccharide (LPS) induced hepatocyte and hepatic stellate cell (HSC) expression of AnxA1. Ac2-26 inhibited LPS-induced RAW264.7 cell activation and HSC proliferation, decreased expression of α-SMA, collagen I and CTGF in HSCs, and inhibited expression of the Wnt/β-catenin pathway after HSC activation. These therapeutic effects were inhibited by Boc2.

CONCLUSION

AnxA1 inhibited liver fibrosis in mice, and its mechanism may be related to inhibition of HSC Wnt/β-catenin pathway activation by targeting formylpeptide receptors to regulate macrophage function.

Key Words: Annexin A1; Active N-terminal peptide of annexin A1; Macrophage; Hepatic stellate cell; Wnt/β-catenin; Liver fibrosis

©The Author(s) 2023. Published by Baishideng Publishing Group Inc. All rights reserved.

Core Tip: Hepatic stellate cells (HSCs) are the main receiver of inflammatory signals and the main promoter of fibrosis. Kupffer cells are activated by damage-associated molecular patterns or lipopolysaccharide, and other pathogen-associated molecular patterns, producing and releasing cytokines to activate HSCs, causing secretion and deposition of extracellular matrix and liver fibrosis. Annexin (Anx)A1 is a glucocorticoid regulatory protein that enhances efferocytosis in macrophages, inhibits activation of phospholipase A2, downregulates expression of inflammatory arachidonic acid, and negatively regulates inflammatory cells and factors. Whether AnxA1 is involved in the formation of liver fibrosis and its mechanism of action were the focus of this study.

Citation: Fan JH, Luo N, Liu GF, Xu XF, Li SQ, Lv XP. Mechanism of annexin A1/N-formylpeptide receptor regulation of macrophage function to inhibit hepatic stellate cell activation through Wnt/β-catenin pathway. *World J Gastroenterol* 2023; 29(22): 3422-3439

URL: https://www.wjgnet.com/1007-9327/full/v29/i22/3422.htm

DOI: https://dx.doi.org/10.3748/wjg.v29.i22.3422

INTRODUCTION

Various chronic liver diseases cause inflammation and necrosis of liver cells, and abnormal hyperplasia of fibrous connective tissue, leading to fibrosis, which is the early reversible stage of cirrhosis and one of the most important threats to human health worldwide[1,2]. When liver parenchyma is damaged, extracellular matrix (ECM) synthesis increases due to liver repair. When the cause is not removed, the continuously damaged liver leads to the failure of timely degradation of a large amount of synthetic ECM and excessive deposition in the liver tissue, which eventually develops into fibrosis[1-4]. The process involves a variety of fibrosis-promoting cells, including vascular smooth muscle cells, portal fibroblasts, and hepatic stellate cells (HSCs), and the activation and proliferation of HSCs is the main cell source of ECM[5-10]. Liver injury leads to necrosis or apoptosis of liver cells, and immune cells, mainly Kupffer cells are activated. Transforming growth factor (TGF)-β1, interleukin (IL)-1β, IL-6 and other cytokines are released, which promote the activation and proliferation of HSCs and secretion of inflammatory and fibrogenic factors. The activated HSCs express α-smooth muscle actin (α-SMA) and cytokines induce HSCs to differentiate into myofibroblasts, which secrete ECM components and cause liver fibrosis[5-11]. These changes may become an important target for the treatment of liver fibrosis.

Annexin (Anx)A1 is a member of the structurally related calcium-dependent phospholipid binding protein superfamily, which is widely distributed in all human tissues and cells, and involved in cell proliferation, differentiation, signal transduction, apoptosis, immunity and other physiological processes[12]. The proteins of the AnxA1 superfamily are homologous in structure, and each member has its unique N-terminal structure, which is related to its different functions and physiological effects [12]. After hydrolysis of full-length AnxA1, the N terminus is disconnected, and 26 amino acids in the N segment form a peptide chain fragment N-terminal peptide of AnxA1 (Ac2-26)[13]. AnxA1 and Ac2-26 both activate and bind to a specific G-protein-coupled receptor known as N-formylpeptide receptor (FPR)2[13], and Ac2-26 binds to FPR1[14]. AnxA1 inhibits expression of α-SMA and collagen I genes in TGF-β1-induced renal cortical fibroblasts[15] and regulates cigarette-smoke-induced pulmonary fibrosis

[16]. However, whether AnxA1 regulates cell proliferation and collagen deposition in liver tissue remains unclear. The purpose of this study was to investigate the effects of AnxA1 on CCl_4-induced inflammation, proliferation and collagen deposition in liver injury.

The Wnt/β-catenin signaling pathway is highly evolutionarily conserved and widespread in multicellular organisms. It is essential for cell growth, differentiation, ontogeny, genetic stability, apoptosis, self-renewal of stem cells, and homeostatic maintenance of adult tissues[17,18]. In normal liver tissue, the Wnt/β-catenin signaling pathway is almost inactive, but its abnormal activation plays an important role in the physiological and pathological processes of the liver. Increasing evidence has shown that abnormal expression of the Wnt/β-catenin signaling pathway is involved in the incidence of liver tumors, and the occurrence of liver inflammation, cirrhosis, and focal nodular hyperplasia[19]. AnxA1 has been reported as an important regulator of Wnt/β-catenin signaling[20], but whether AnxA1 contributes to the formation of liver fibrosis was the focus of this study.

MATERIALS AND METHODS

Animal treatment

Six-to-eight-week-old C57BL/6 mice (weighing 18-25 g; SLC, Guangxi, China) and C57BL/6JGpt Anxa1-KO mice (B6/JGptAnxa1em4Cd9634/Gpt, Strain NO. T016864; weighing 18-25 g; SLC, Jiangsu, China) were maintained in climate-controlled rooms under a 12-h light-dark cycle. All experiments were conducted in accordance with the institutional guidelines of Guangxi Medical University for the care and use of laboratory animals.

Thirty-two wild-type mice and 32 *Anxa1*$^{-/-}$ mice were each randomized into four subgroups of eight: Control, CCl_4-induced liver fibrosis, liver fibrosis + Ac2-26, and liver fibrosis + Ac2-26 + FPR antagonist N-Boc-Phe-Leu-Phe-Leu-Phe (Boc-2). Mice in the control group received olive oil for intraperitoneal injection, while mice in the other three subgroups received 20% CCl_4 (500 mL; Shanghai Acmec Biochemical Co., Ltd, China), and CCl_4 + Ac2-26 1 mg/kg (500 mg; MedChemExpress, CAT: HY-P1098A/CS-0093919) with or without N-Boc2 1 mg/kg (500 mL; MedChemExpress, CAT: HY-103473A) for intraperitoneal injection twice weekly. Eight mice were used for each time point. At 4 and 8 wk after injection, animals were anesthetized with pentobarbital sodium (50 mg/kg intravenous injection), and blood samples were collected from the inferior vena cava. The livers were removed, and a small portion of liver tissue was fixed with 4% formaldehyde solution, and the remaining liver tissue was immediately frozen and stored in liquid nitrogen for RNA and protein extraction.

Histopathological examination of liver

Hematoxylin-eosin (HE) staining and modified Masson three-color staining (Modified Masson's Trichrome Staining Kit; Beijing Solarbio Science & Technology,) were performed after liver tissue fixation, dehydration, paraffin embedding, sectioning, dewaxing and hydration (bar: 50 mm).

In situ expression of AnxA1 in liver tissue determined by immunohistochemistry

The sections were dewaxed and hydrated according to AnxA1 monoclonal antibody instructions and SP-9000 Histostain™ - SP Kits (6 mL, Beijing Zhongshan Jinqiao Biotechnology, cat: K197712D/K196915F) requirements, antigenic alkaline repair, endogenous peroxidase blocking, goat serum blocking, and AnxA1 monoclonal antibody dilution 1: 1000 (Abcam, United Kingdom, cat: ab214486) were incubated overnight at 4 °C, the biotin-labeled goat anti-mouse/rabbit immunoglobulin G (IgG) (Invitrogen, United States, cat: TJ26211) was incubated for 15 min, and the horseradish-labeled Streptomyces vitellin was incubated for 15 min. Diaminobenzidine staining, counterstaining, dehydration, transparency, sealing, and microscopic examination. For each sample, five high-power fields (bar: 100 mm) were randomly selected, each containing an average of 400 cells, and the number of positive cells was counted for each field.

Preparation of HSCs, hepatocytes and Kupffer cells

JS1 HSCs and AML1 hepatocytes were separately cultivated in Williams' E medium containing 10% calf serum, 2 mmol/L L-glutamate and antibiotics (100 U/mL penicillin G and 100 μg/mL streptomycin). RAW246.7 cells were cultured in RPMI 1640 medium containing 10% calf serum and antibiotics. Cells were plated at (2×10^6)-(3×10^6)/mL and preincubated for 24 h at 37 °C in a humidified atmosphere containing 5% CO_2. The purity and viability of cells ranged from 87% to 95%. RAW246.7 cells HSCs and hepatocytes were incubated with 100 ng/mL lipopolysaccharide (LPS) (Sigma, St. Louis, MO, United States), LPS + 100 ng/mL Ac2-26, or LPS + Ac2-26 + 100 ng/mL Boc2 for 1, 3, 6, 12 and 24 h to activate expression of AnxA1, α-SMA, TGF-β1, connective tissue growth factor (CTGF), collagen I, IL-1β and IL-6. Ac2-26 or Ac2-26 + Boc2 dissolved in medium was added to the incubation medium 1 h prior to the addition of LPS.

Quantitative real-time polymerase chain reaction

Total RNA (1 μg) was extracted from liver or primary cells using TRIzol reagent (Takara Bio, Beijing, China) and reverse transcribed using a ReverTra Ace qPCR RT kit (Takara Bio). Target mRNA expression was quantified using quantitative real-time polymerase chain reaction (qPCR) as described previously[21]. TaqMan Gene Expression Assays for AnxA1 (forward primer 5′-AGCAGATCAAGGCCGCGTA-3′, reverse primer 5′-CATGGCACCACGGAGTTCA-3′), IL-6 (forward primer 5′-AGGATACCACTCCCAACAGACC-3′, reverse primer 5′-GCACAACTCTTTTCTCATTTCCAC-3′), TGF-β1 (forward primer 5′-TACGGCAGTGGCTGAACCAA-3′, reverse primer 5′-CGGTTCATGTCATGGATGGTG-3′), IL-1β (forward primer 5′-CACTACAGGCTCCGAGATGAACAAC-3′, reverse primer 5′-TGTCGTTGCTTGGTTCTCCTTGTAC-3′), α-SMA (forward primer 5′-CTGACAGAGGCACCACTGAA-3′, reverse primer 5′-CATCTCCAGAGTCCAGCACA-3′), collagen I (forward primer 5′-AAGAGGCGAGAGGTTTCC-3′, reverse primer 5′-AGAACCATCAGCACCTTTGG-3′), CTGF (forward primer 5′-CAAAGCAGCAAATACCA-3′, reverse primer 5′-GGCCAAATGTGTCTTCCAGT-3′), and GAPDH (forward primer 5′-TGTGTCCGTCGTGGATCTGA-3′, reverse primer 5′-TTGCTGTTGAAGTCGCAGGAG-3′) were purchased from Takara Bio.

Western blotting

Protein samples (30-50 μg) were prepared from livers and cells and separated by SDS-PAGE, followed by transfer to polyvinylidene difluoride membranes as reported previously[21]. Blots were incubated with antibodies (1:1000) against AnxA1 (Abcam, cat: ab214486), α-SMA (50 μL, Affinity Biosciences, Jiangsu, cat: AF1032), β-catenin (50 mL, MedChemExpress, cat: 51067-2-AP) and GAPDH (Abcam, cat: ab181602), followed by incubation with a peroxidase-conjugated goat anti-mouse/rabbit IgG(H + L) (1:5000; Invitrogen, cat: TJ26211). Proteins were visualized using fluorescence scanner imaging system (Odyssey; Bio-Rad, Hercules, CA, United States).

Statistical analysis

Results are expressed as mean ± SE (n = 8), unless otherwise indicated. Statistical analyses were performed using Kruskal-Wallis one-way analysis of variance. $P < 0.05$ was considered significant.

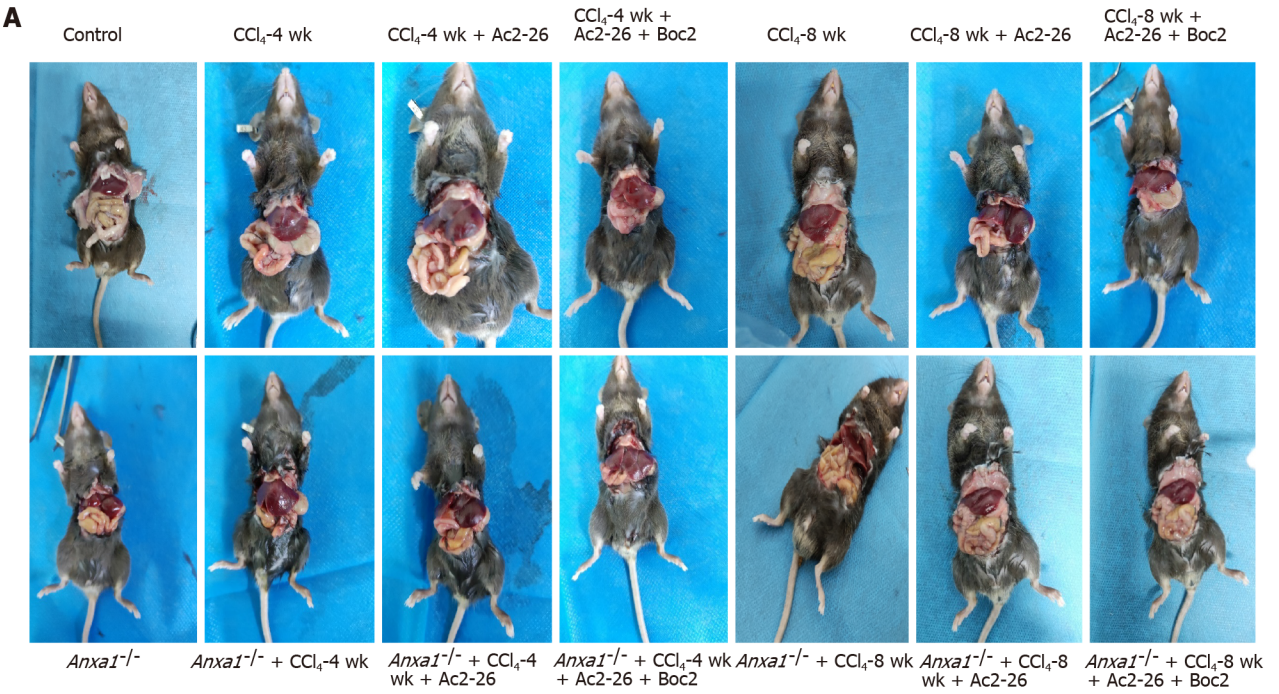
RESULTS

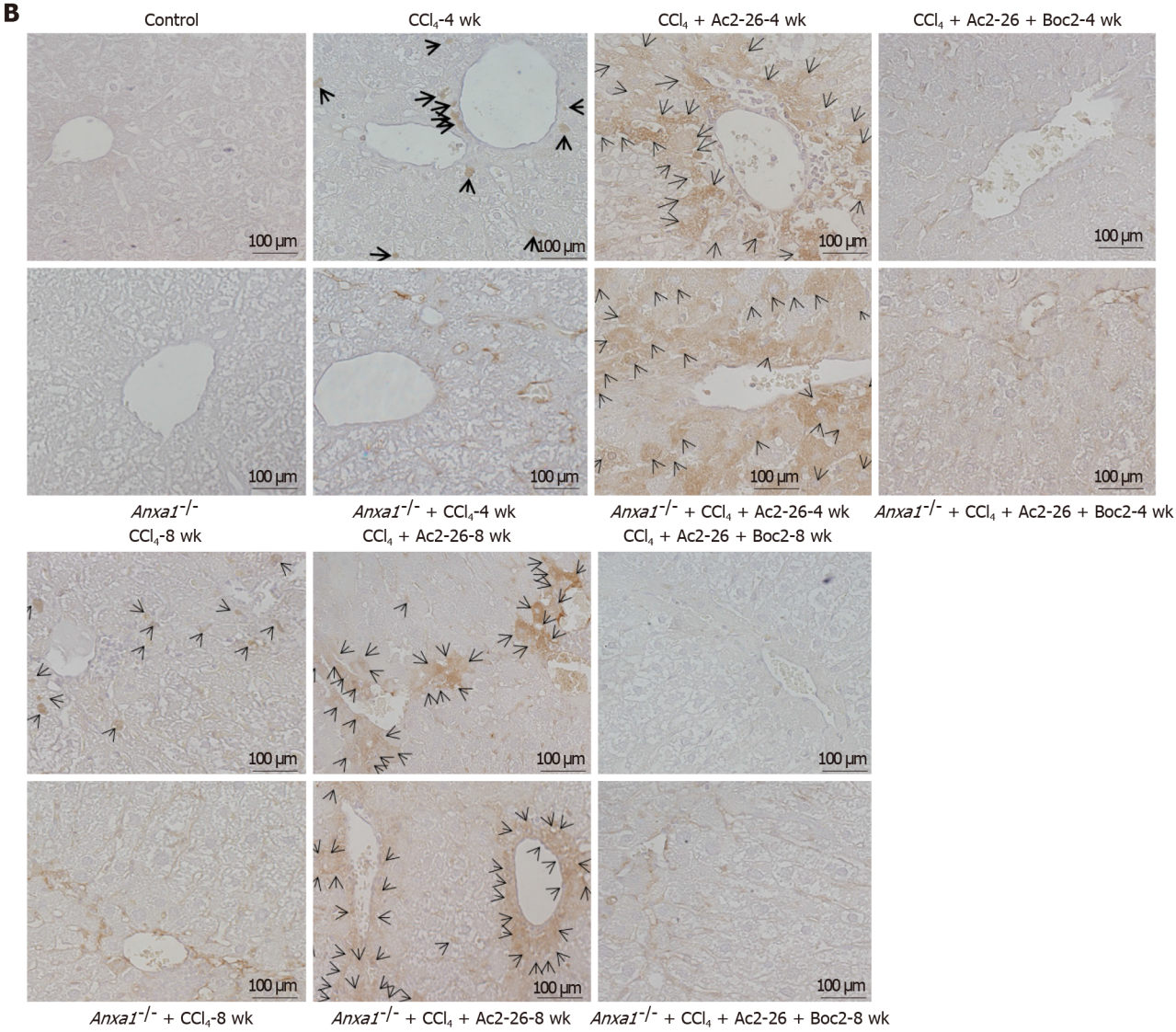
Effects of AnxA1 on liver appearance

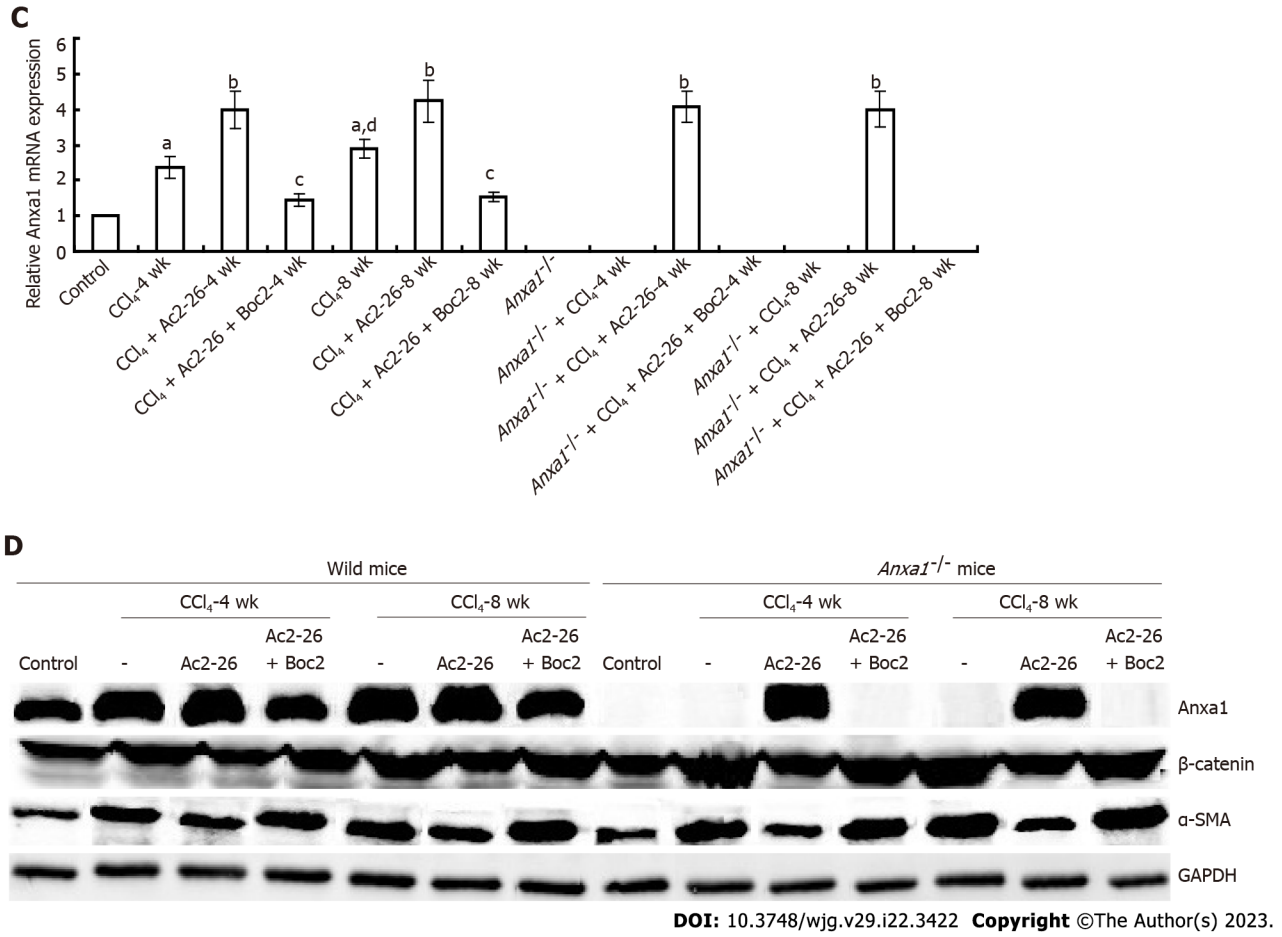
The liver of the control mice was red with bright color and smooth surface. In the CCl_4-induced wild-type mice group, the liver tissue became light in color, rough on the surface, dull around the edge, and hard in texture, and nodules or even cellulose-like changes appeared over time. The lesions in the *AnxA1*$^{-/-}$ group were more severe than in the wild-type mice. After treatment with Ac2-26, the appearance of the liver in the CCl_4-induced mice was significantly improved with dark red color, and the surface roughness and nodulation were significantly reduced, the effects of Ac2-26 were inhibited by Boc2 (Figure 1A). Compared with the control group, AnxA1 expression was significantly increased in the CCl_4 model group, and was higher at 8 wk than 4 wk, suggesting that AnxA1 was related to the development of liver fibrosis. AnxA1 expression was higher in liver tissues of the CCl_4 model group after Ac2-26 treatment, while Boc2 inhibited AnxA1 expression (Figures 1B and C), and the difference was significant ($P < 0.05$). Western blotting and qPCR results were consistent with immunohistochemical results (Figure 1D).

AnxA1 inhibits CCl_4-induced liver injury and inflammatory cell infiltration in mice

HE staining showed that the structure of hepatic lobules in the control group was clear, and there was no vacuole formation or obvious inflammatory cell infiltration. In the CCl_4-induced wild model group, HE staining for 4 wk showed that the hepatocytes were swollen and enlarged, with scattered degeneration and necrosis, as well as infiltration of monocytes and lymphocyte cells. Degeneration and necrosis of hepatocytes were observed at 8 wk. In the *AnxA1*$^{-/-}$ model group with fibrosis induced by CCl_4, liver tissue destruction was accompanied by a large number of inflammatory cell infiltration and steatosis. At 4 wk, there was massive necrosis of liver cells, massive infiltration of inflammatory cells, and disorder of hepatic lobular structure. At 8 wk, there was obvious structural destruction that became more severe over time. The infiltration of liver inflammatory cells and destruction of liver lobular structure in the *AnxA1*$^{-/-}$ mice were more obvious than those in the wild-type mice. After treatment with Ac2-26, the damage to the hepatic lobular structure and inflammatory cell infiltration in the CCl_4-induced mice was reduced compared with that before treatment. AnxA1 mimics the peptide Ac2-26, which largely controls inflammation and is protective against hepatic fibrosis. In the model group treated with Ac2-26 and Boc2, Boc2 almost completely eliminated the effects of Ac2-26 at 4 wk (Figure 2A), suggesting that AnxA1 inhibited CCl_4-induced liver tissue injury and reduced inflammatory cell infiltration. AnxA1 works by targeting mainly FPR receptors.


A
Control
CCl4-4 wk
CCl4-4 wk + Ac2-26
CCl4-4 wk + Ac2-26 + Boc2
CCl4-8 wk
CCl4-8 wk + Ac2-26
CCl4-8 wk + Ac2-26 + Boc2
Anxa1-/-
Anxa1-/- + CCl4-4 wk
Anxa1-/- + CCl4-4 wk + Ac2-26
Anxa1-/- + CCl4-4 wk + Ac2-26 + Boc2
Anxa1-/- + CCl4-8 wk
Anxa1-/- + CCl4-8 wk + Ac2-26
Anxa1-/- + CCl4-8 wk + Ac2-26 + Boc2


B
Control
CCl4-4 wk
CCl4 + Ac2-26-4 wk
CCl4 + Ac2-26 + Boc2-4 wk
100 μm
Anxa1-/- CCl4-8 wk
Anxa1-/- + CCl4-4 wk
Anxa1-/- + CCl4 + Ac2-26-4 wk
Anxa1-/- + CCl4 + Ac2-26 + Boc2-4 wk
CCl4 + Ac2-26-8 wk
CCl4 + Ac2-26 + Boc2-8 wk
Anxa1-/- + CCl4-8 wk
Anxa1-/- + CCl4 + Ac2-26-8 wk
Anxa1-/- + CCl4 + Ac2-26 + Boc2-8 wk

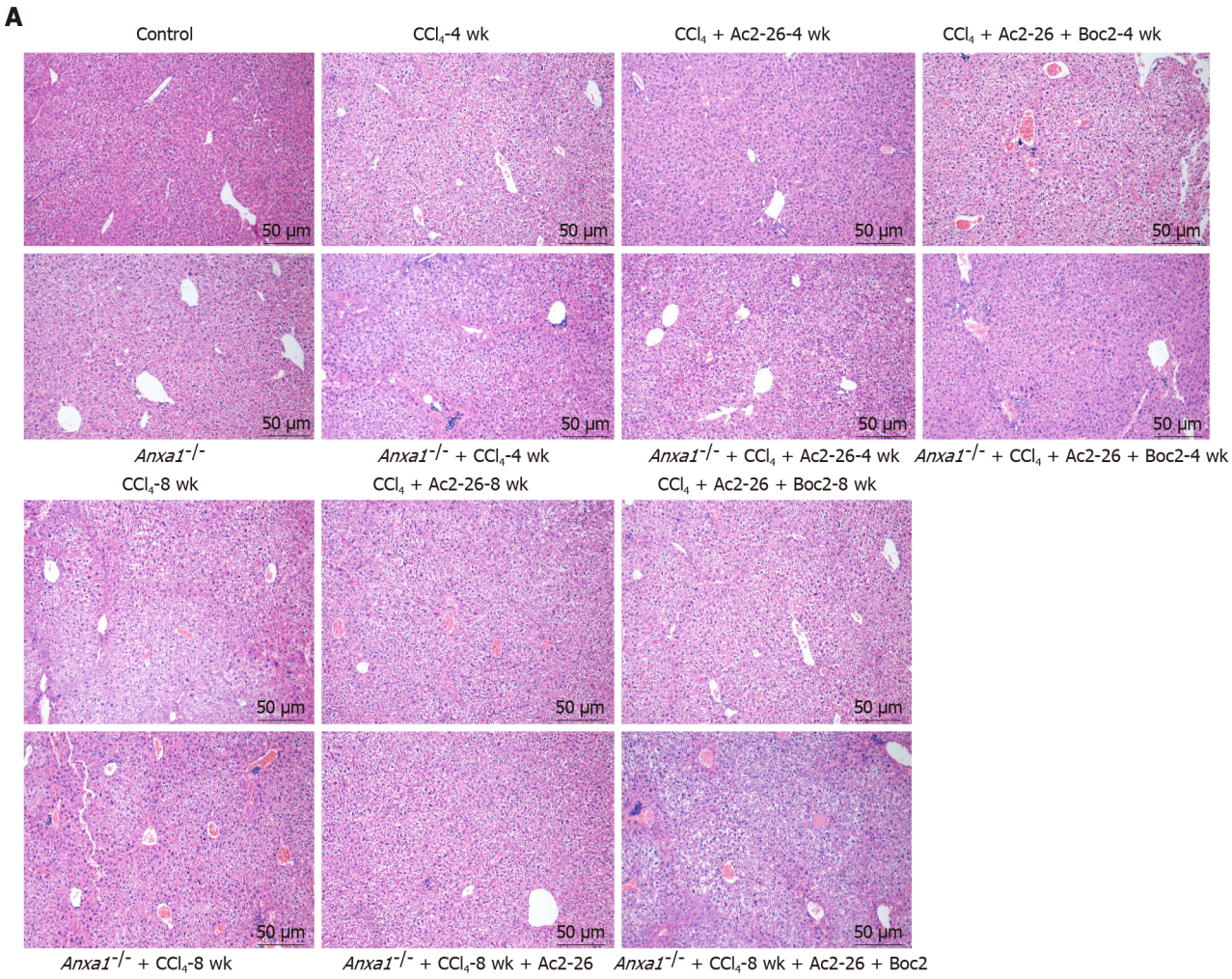


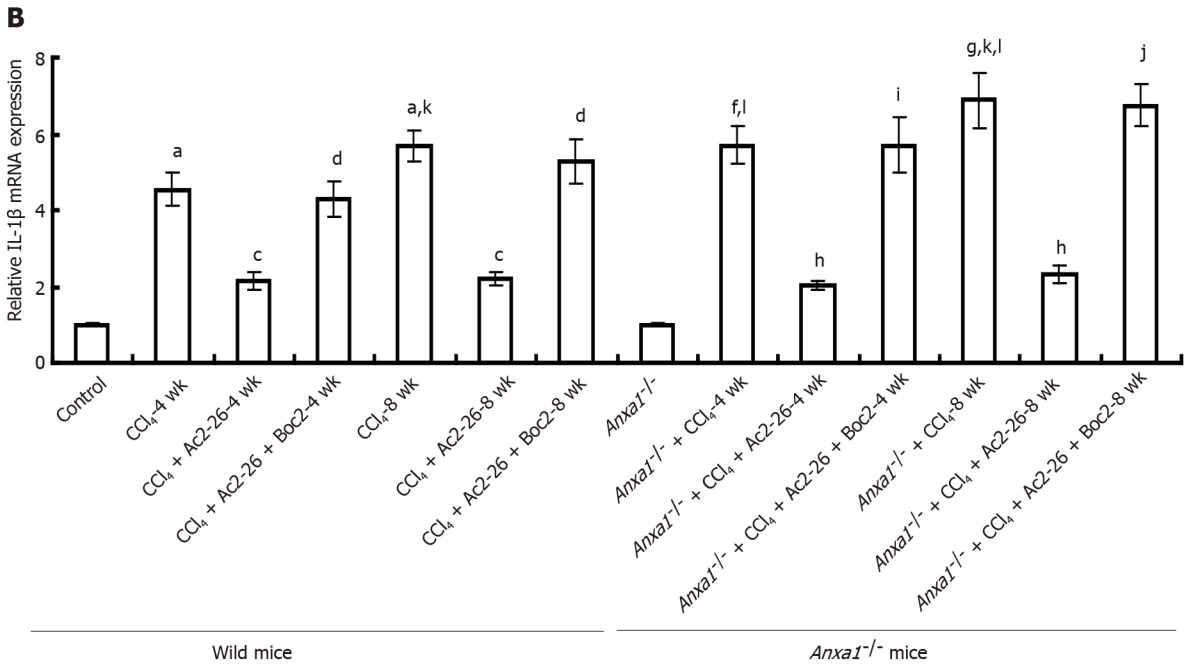
DOI: 10.3748/wjg.v29.i22.3422 **Copyright** ©The Author(s) 2023.

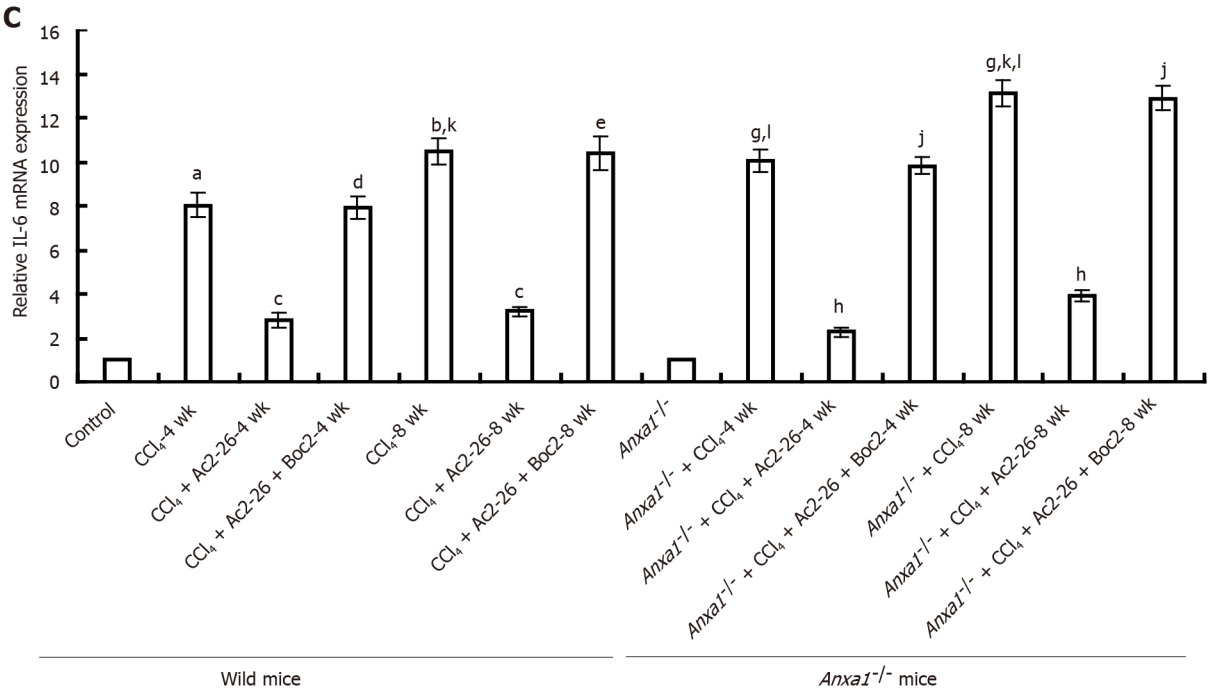
Figure 1 Annexin A1 inhibited CCl_4-induced liver injury. A: Gross view of liver tissue. The liver of mice in the control group was red with bright color and smooth surface. In the CCl_4-induced model group, the liver was light in color, rough and grainy on the surface. Liver tissue nodules appeared at 8 wk, and fibrosis appeared at 8 wk in *Anxa1*$^{-/-}$ mice. After Ac2-26 treatment, the liver was mostly dark red, and the surface roughness was reduced. The effect of Ac2-26 was reversed by Boc2, and the liver color became lighter, the surface was grainy, the edge was blunt, and the texture was hard; B: Annexin (Anx)A1 was expressed in liver tissue. Anxa1 was stained brown. Compared with the control group, the liver tissue in mice treated with CCl_4 showed obvious AnxA1 staining. More liver tissue was stained at 8 wk than at 4 wk. The *AnxA1*$^{-/-}$ model groups were hardly stained. More tissue staining was observed in the CCl_4-induced model group after Ac2-26 treatment, while staining was almost absent after Boc2 intervention; C: *AnxA1* mRNA expression; D: Protein expression of AnxA1, α-smooth muscle actin, β-catenin, and GAPDH (n = 8). Results are presented as ratios of target mRNA or protein normalized to internal GAPDH. $^{a}P < 0.05$ *vs* control; $^{b}P < 0.01$ *vs* CCl_4; $^{c}P < 0.05$ *vs* CCl_4 + Ac2-26; $^{d}P < 0.05$ *vs* intra-group. Ac2-26: Active N-terminal peptide of annexin A1; AnxA1: Annexin A1; Boc2: N-formyl peptide receptor antagonist N-Boc-Phe-Leu-Phe-Leu-Phe; α-SMA: α-smooth muscle actin.

AnxA1 inhibits CCl_4-induced collagen deposition in mouse liver tissue

Collagen deposition is an important indicator of the degree of liver fibrosis, and can be visualized by Masson staining. Staining clearly showed that there was no collagen staining in the control group of wild-type and *AnxA1*$^{-/-}$ mice. In the CCl_4-induced wild model group, blue collagen fibers proliferated in the portal area at 4 wk, but the degree of collagen fibrosis was mild. Similarly, the proliferation of blue-stained collagen fibers in the portal area was observed in the wild model group at 8 wk, but the collagen fibers were further increased, widened and extended to the surrounding hepatic lobular space than at 4 wk, suggesting that the liver fibers were gradually aggravated with the extension of modeling time. Compared with wild model mice, CCl_4 induced more significant collagen deposition in the liver tissue of *AnxA1*$^{-/-}$ mice. At 4 wk, blue collagen fibers proliferated obviously in hepatic portal area and began to extend to liver parenchyma, and collagen fibers began to segment liver parenchyma. At 8 wk, a large amount of collagen surrounded the liver cells to form pseudolobules, which seriously damaged the normal structure of the liver tissue, indicating formation of fibrosis. The collagen deposition in the liver of *AnxA1*$^{-/-}$ mice was significantly aggravated by CCl_4, and the degree of liver fibrosis was even more severe. The collagen deposition and wrapping in the liver of mice in the CCl_4-induced mice was significantly weakened after Ac2-26 treatment, and the severity of liver fibrosis was relieved. In the model group, the damage to the liver tissue structure and collagen deposition after treatment with Ac2-26 and Boc2 were similar to those before treatment (Figure 3A).


A
Control
CCl4-4 wk
CCl4 + Ac2-26-4 wk
CCl4 + Ac2-26 + Boc2-4 wk
50 μm
Anxa1-/-
Anxa1-/- + CCl4-4 wk
Anxa1-/- + CCl4 + Ac2-26-4 wk
Anxa1-/- + CCl4 + Ac2-26 + Boc2-4 wk
CCl4-8 wk
CCl4 + Ac2-26-8 wk
CCl4 + Ac2-26 + Boc2-8 wk
Anxa1-/- + CCl4-8 wk
Anxa1-/- + CCl4-8 wk + Ac2-26
Anxa1-/- + CCl4-8 wk + Ac2-26 + Boc2


B
Relative IL-1β mRNA expression
0
2
4
6
8
a
c
d
a,k
c
d
f,l
h
i
g,k,l
h
j
Control
CCl4-4 wk
CCl4 + Ac2-26-4 wk
CCl4 + Ac2-26 + Boc2-4 wk
CCl4-8 wk
CCl4 + Ac2-26-8 wk
CCl4 + Ac2-26 + Boc2-8 wk
Anxa1-/-
Anxa1-/- + CCl4-4 wk
Anxa1-/- + CCl4 + Ac2-26-4 wk
Anxa1-/- + CCl4 + Ac2-26 + Boc2-4 wk
Anxa1-/- + CCl4-8 wk
Anxa1-/- + CCl4 + Ac2-26-8 wk
Anxa1-/- + CCl4 + Ac2-26 + Boc2-8 wk
Wild mice
Anxa1-/- mice



DOI: 10.3748/wjg.v29.i22.3422 **Copyright** ©The Author(s) 2023.

Figure 2 Annexin A1 inhibits CCl_4-induced hepatic inflammatory cytokines release. A: Annexin A1 (AnxA1) inhibited CCl_4-induced liver injury and inflammatory cell infiltration in mice. Normal mouse liver lobule structure was clear, with no obvious vacuole formation or inflammatory cell infiltration. In the wild-type model group, hepatic lobules were severely damaged; a large number of hepatic nuclei were shrunken, hepatocytes were vacuolated, and inflammatory cells infiltrated. *AnxA1*$^{-/-}$ mice had more severe vacuolation and extensive inflammatory cell infiltration than wild-type mice had. After treatment with active N-terminal peptide of AnxA1 (Ac2-26), the damage to hepatic lobules was reduced, hepatocyte vacuolation was reduced but necrosis was observed, clusters of regenerated hepatocytes were observed in some tissues, and inflammatory cell infiltration was also reduced. N-formylpeptide receptor antagonist N-Boc-Phe-Leu-Phe-Leu-Phe almost reversed the therapeutic effect of Ac2-26, but the inflammatory infiltration and damage to hepatic lobule structure were not significantly improved. Initial magnification: 200 ×; B: Effect of Ac2-26 on interleukin (IL)-1β mRNA expression; C: Effect of Ac2-26 on IL-6 mRNA expression; total RNA was extracted using TRIzol reagent and relative concentration of mRNA was quantified using quantitative real-time polymerase chain reaction (n = 8). Results are presented as ratios of target mRNA or protein normalized to internal GAPDH. $^{a}P < 0.05$ and $^{b}P < 0.01$ *vs* control; $^{c}P < 0.05$ *vs* CCl_4; $^{d}P < 0.05$ and $^{e}P < 0.01$ *vs* CCl_4 + Ac2-26; $^{f}P < 0.05$ and $^{g}P < 0.01$ *vs AnxA1-/-* + control; $^{h}P < 0.05$ *vs AnxA1-/-* + CCl_4; $^{i}P < 0.05$ and $^{j}P < 0.01$ *vs AnxA1-/-* + CCl_4 + Ac2-26; $^{k}P < 0.05$ *vs* intra-group; $^{l}P < 0.05$ *vs* inter-group. Ac2-26: Active N-terminal peptide of AnxA1; AnxA1: Annexin A1; Boc2: N-formyl peptide receptor antagonist N-Boc-Phe-Leu-Phe-Leu-Phe; IL: Interleukin.

AnxA1 inhibits CCl_4-induced HSC activation in liver tissue

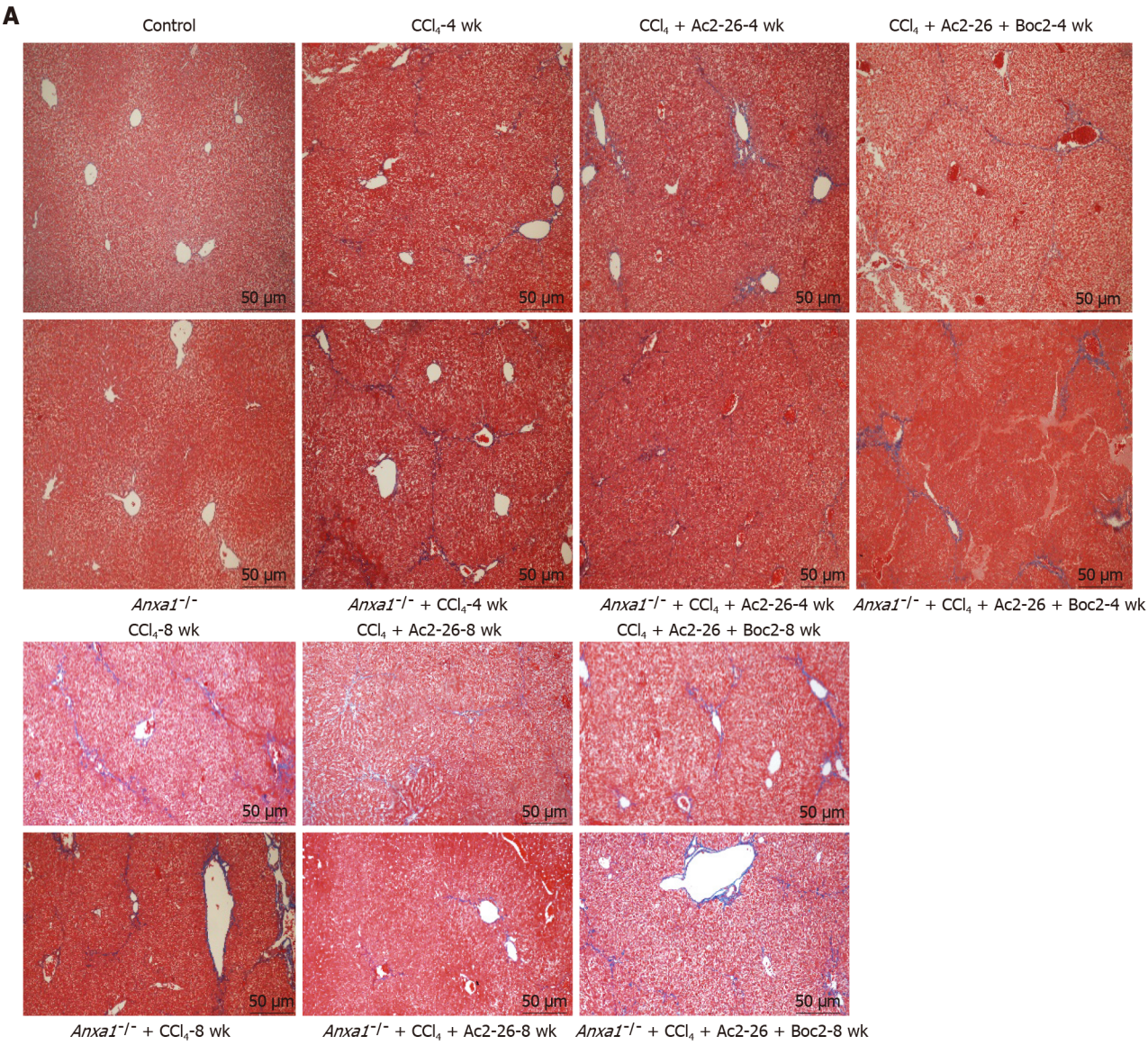
α-SMA is a marker of HSC activation and transformation into fibroblasts. HSC activation generates and secretes ECM, and type I collagen is the ECM marker of HSCs. In this study, qPCR and western blotting were used to detect the expression levels of α-SMA and collagen I in liver tissue, and to evaluate the activation status of HSCs. Expression of α-SMA and type I collagen in the liver of wild-type mice was significantly increased by CCl_4, while expression of α-SMA and collagen I in the liver of mice in the *AnxA1*$^{-/-}$ group was higher and increased with time, which was in accordance with the progression of liver fibrosis in the CCl_4-induced mice. All of the above effects were inhibited by Ac2-26, suggesting that AnxA1 inhibited HSC activation and collagen deposition. In contrast, Boc2 reversed the therapeutic effect of Ac2-26 (Figures 3B and C), and the difference was significant ($P < 0.05$). Western blotting and qPCR results were consistent with immunohistochemical results (Figure 1D).

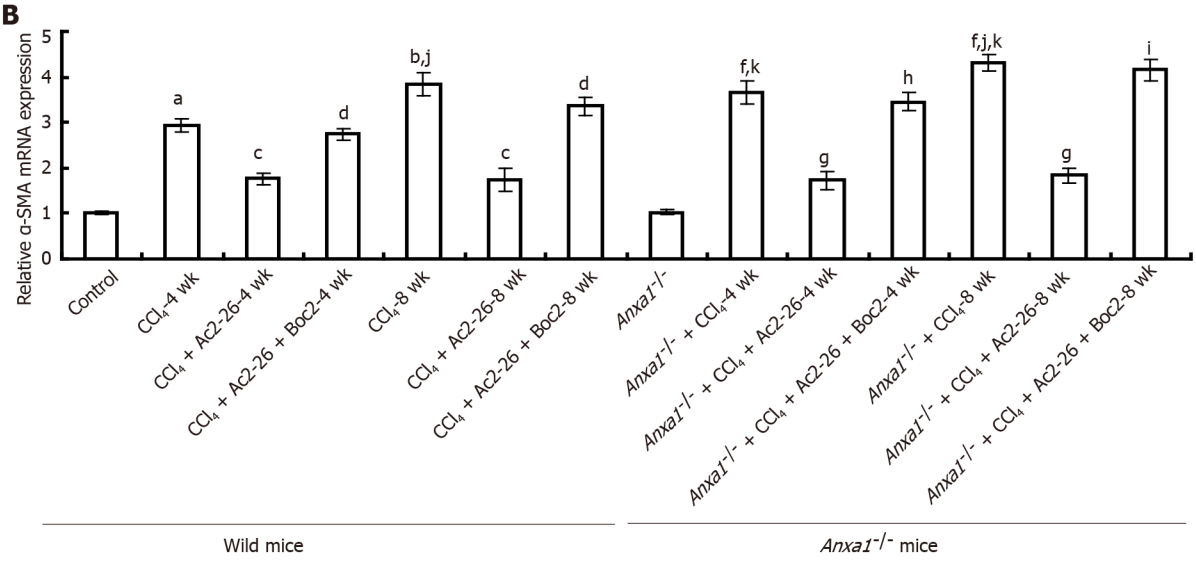
AnxA1 inhibits CCl_4-induced release of hepatic inflammatory cytokines

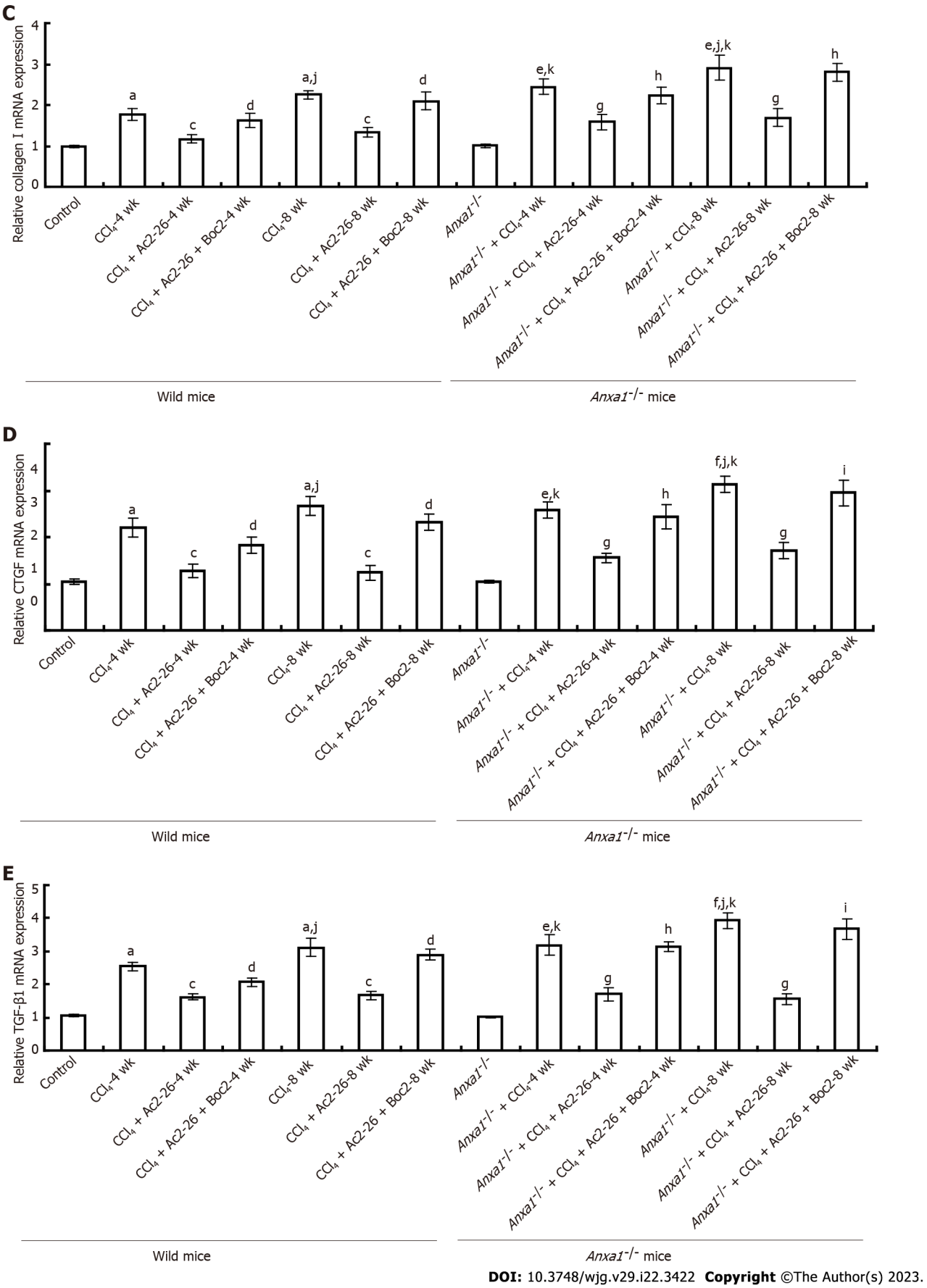
CCl_4 induces expression of various cytokines in liver tissues, among which IL-1β, IL-6 and TGF-β1 are important factors leading to the formation of fibrosis. Expression of IL-1β, IL-6 and TGF-β1 in the liver of the CCl_4-induced wild model group was increased simultaneously, and upregulation of inflammatory cytokines was more obvious and increased with time in the *AnxA1*$^{-/-}$ model group, while the Ac2-26 significantly inhibited expression of IL-1β, IL-6 and TGF-β1. Boc2 inhibited the anti-inflammatory effect of Ac2-26 (Figures 2B, 2C and 3E), and the difference was significant ($P < 0.05$). This suggested that AnxA1 exerted its anti-inflammatory and antifibrotic effects by inhibiting expression of TGF-β1, IL-1β and IL-6 through FPR.

AnxA1 reduces the level of CTGF in the liver

CTGF mediates TGF-β1 promotion of ECM production and accumulation. CTGF regulates the growth of fibroblasts and epidermal cells, promoting cell adhesion, proliferation and ECM synthesis. Compared with the control group, the concentration of CTGF in the liver tissue of the CCl_4-induced wild model


A
Control
CCl4-4 wk
CCl4 + Ac2-26-4 wk
CCl4 + Ac2-26 + Boc2-4 wk
50 μm
Anxa1-/-
Anxa1-/- + CCl4-4 wk
Anxa1-/- + CCl4 + Ac2-26-4 wk
Anxa1-/- + CCl4 + Ac2-26 + Boc2-4 wk
CCl4-8 wk
CCl4 + Ac2-26-8 wk
CCl4 + Ac2-26 + Boc2-8 wk
Anxa1-/- + CCl4-8 wk
Anxa1-/- + CCl4 + Ac2-26-8 wk
Anxa1-/- + CCl4 + Ac2-26 + Boc2-8 wk


B
Relative α-SMA mRNA expression
0
1
2
3
4
5
a
c
d
b,j
c
d
f,k
g
h
f,j,k
g
i
Control
CCl4-4 wk
CCl4 + Ac2-26-4 wk
CCl4 + Ac2-26 + Boc2-4 wk
CCl4-8 wk
CCl4 + Ac2-26-8 wk
CCl4 + Ac2-26 + Boc2-8 wk
Anxa1-/-
Anxa1-/- + CCl4-4 wk
Anxa1-/- + CCl4 + Ac2-26-4 wk
Anxa1-/- + CCl4 + Ac2-26 + Boc2-4 wk
Anxa1-/- + CCl4-8 wk
Anxa1-/- + CCl4 + Ac2-26-8 wk
Anxa1-/- + CCl4 + Ac2-26 + Boc2-8 wk
Wild mice
Anxa1-/- mice



DOI: 10.3748/wjg.v29.i22.3422 **Copyright** ©The Author(s) 2023.

Figure 3 Annexin A1 inhibits CCl_4 induced hepatic stellate cell activation in liver tissue. A: Annexin A1 (AnxA1) inhibited collagen deposition induced by CCl_4 in mouse liver tissue. Collagen was stained blue by Masson staining. The collagen content in the liver tissues in the control group was low, while collagen deposition in the liver of the CCl_4-induced model group was high. Collagen deposition in the liver of the *AnxA1*$^{-/-}$ model group was significantly aggravated

compared with that in the wild-type model group. Active N-terminal peptide of AnxA1 (Ac2-26) significantly reduced collagen deposition in the CCl_4-induced model group, and the collagen deposition in the mice after the intervention of Ac2-26 + N-formylpeptide receptor antagonist N-Boc-Phe-Leu-Phe-Leu-Phe was similar to that in the CCl_4-induced model group. Initial magnification: 100 ×; B: Effect of Ac2-26 on α-smooth muscle actin mRNA expression; C: Effect of Ac2-26 on collagen I mRNA expression; D: Effect of Ac2-26 on connective tissue growth factor mRNA expression; E: Effect of Ac2-26 on transforming growth factor-β1 mRNA expression; total RNA was extracted using TRIzol reagent and relative mRNA concentration was quantified using quantitative real-time polymerase chain reaction (n = 8). Results are presented as ratios of target mRNA or protein normalized to internal GAPDH. [a]P < 0.05 and [b]P < 0.01 *vs* control; [c]P < 0.05 *vs* CCl_4; [d]P < 0.05 *vs* CCl_4 + Ac2-26; [e]P < 0.05 and [f]P < 0.01 *vs AnxA1-/-* + control; [g]P < 0.05 *vs AnxA1-/-* + CCl_4; [h]P < 0.05 and [i]P < 0.01 *vs AnxA1-/-* + CCl_4 + Ac2-26; [j]P < 0.05 *vs* intra-group; [k]P < 0.05 *vs* inter-group. Ac2-26: Active N-terminal peptide of AnxA1; AnxA1: Annexin A1; Boc2: N-formyl peptide receptor antagonist N-Boc-Phe-Leu-Phe-Leu-Phe; CTGF: Connective tissue growth factor; TGF-β1: Transforming growth factor β1.

group and *AnxA1*$^{-/-}$ model group was higher, and paralleled the progression of liver fibrosis. The more severe the fibrosis, the higher the expression of CTGF, suggesting that CTGF was closely related to the occurrence and development of liver fibrosis. After Ac2-26 treatment, expression of CTGF in liver tissues of mice in the CCl_4-induced mice was significantly decreased. AnxA1 inhibited expression of CTGF in liver tissue and alleviated the occurrence of liver fibrosis, while Boc2 almost reversed the therapeutic effect of Ac2-26 (Figure 3D), and the difference was significant (P < 0.05).

AnxA1 inhibits activation of RAW264.7 cells and HSCs

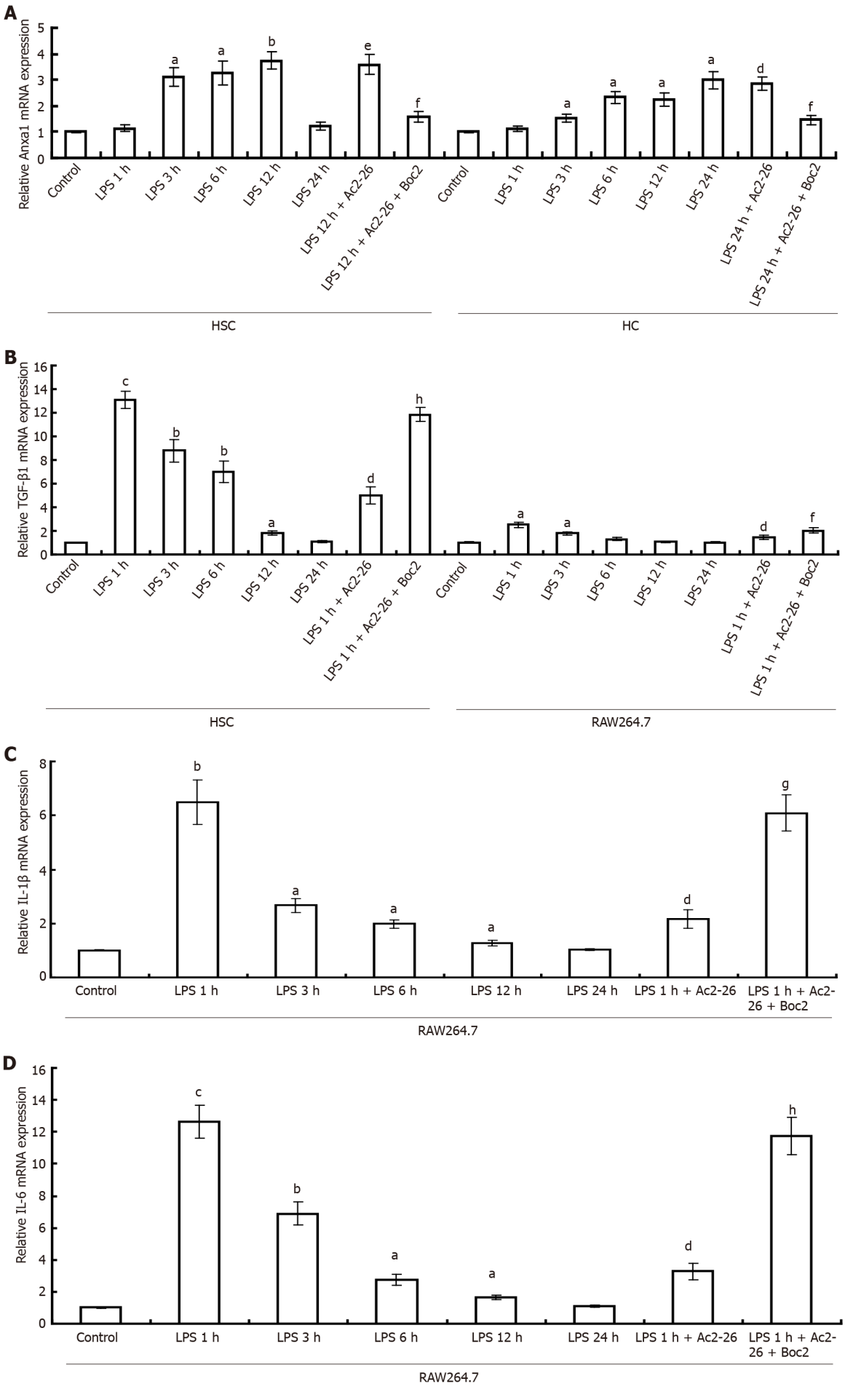
LPS induced activation of RAW264.7 cells and the release of inflammatory cytokines. Compared with the control group, expression of TGF-β1, IL-1β and IL-6 in RAW264.7 cells was significantly induced by LPS, and reached a peak within 1 h, then gradually decreased to the normal level. After activation of RAW264.7 cells, AnxA1 was not significantly increased, but Ac2-26 inhibited TGFβ1, and IL-6 expression in RAW264.7 cells, while Boc2 blocked the inhibitory effect of Ac2-26 on RAW264.7 cells (Figures 4B-D), and the difference was significant (P < 0.05). LPS induced activation of HSCs, which expressed TGFβ1, α-SMA, CTGF, and collagen I simultaneously (Figures 4B and 5A-C). Expression of TGF-β1 and CTGF began to increase at 1 h and peaked at 3 and 6 h, respectively. AnxA1 expression began to increase at 3 h and peaked at 12 h. Expression of α-SMA and collagen I began to increase significantly at 12 h and peaked at 24 h. Ac2-26 treatment significantly decreased LPS-induced expression of TGF-β1, α-SMA, CTGF and collagen I, and Boc2 significantly inhibited this effect (Figures 4B and 5A-C and the difference was significant (P < 0.05). LPS induced activation of hepatocytes. Compared with the control group, AnxA1 was highly expressed after hepatocyte (HC) activation, which was time-dependent and increased from 4 to 24 h (Figure 4A). Ac2-26 significantly upregulated HSC AnxA1 expression, while Boc2 inhibited AnxA1 expression (Figure 4A), and the difference was significant (P < 0.05). The results of western blotting and qPCR were consistent (Figures 4E and F).

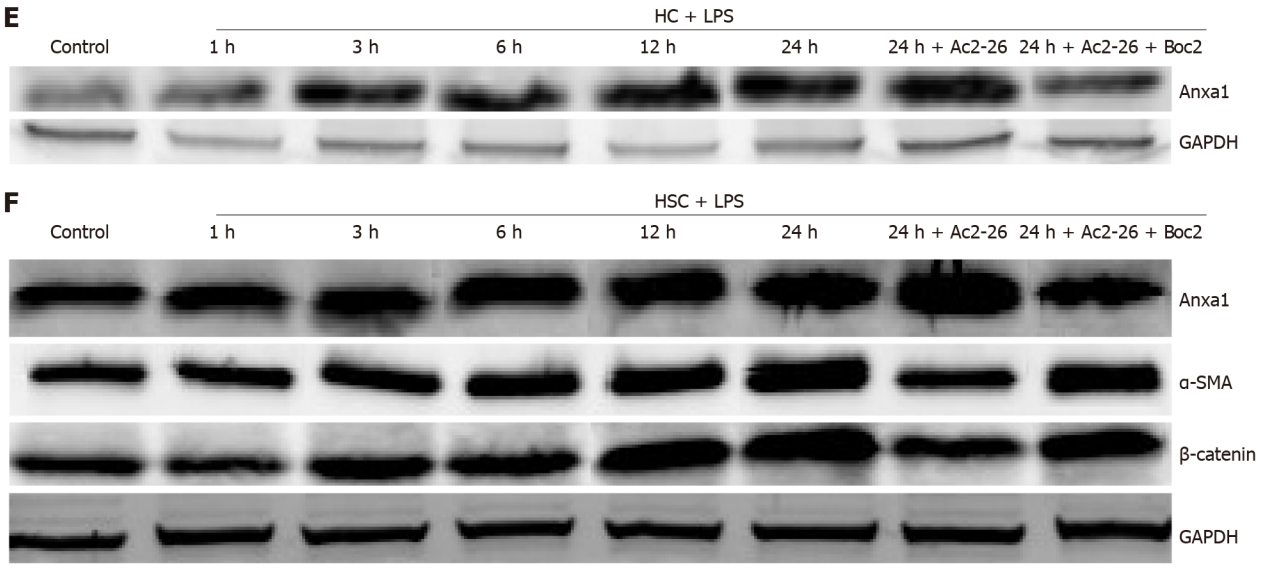
AnxA1 inhibits Wnt/β-catenin activation in liver tissue

The Wnt/β-catenin pathway plays an important role in the formation of liver fibrosis. We used western blotting to detect β-catenin expression, which was associated with inflammation and fibrosis. Compared with the low expression of β-catenin in control mice, expression of β-catenin was upregulated in the model group and higher in the *AnxA1*$^{-/-}$ group, and expression was higher at 8 wk than at 4 wk. After Ac2-26 treatment, expression of β-catenin protein in the CCl_4-induced model group was significantly decreased compared with that before treatment, while Boc2 inhibited the effect of Ac2-26 (Figure 1D). The results of the animal experiments were verified by *in vitro* cell experiments. β-catenin was highly expressed in LPS-induced HSC activation, and increased progressively with time, starting at 3 h and reaching a peak at 24 h. Ac2-26 inhibited expression of β-catenin protein in LPS-induced HSCs, while Boc2 inhibition blocked this effect, β-catenin protein expression was maintained at a high level in LPS-induced HSCs (Figure 4F).

DISCUSSION

Hepatic fibrosis is a self-repair response of the liver to sustained injury. It is the abnormal structure and function of the liver caused by the excessive accumulation of ECM in the intercellular spaces caused by activation of HSCs and imbalance of synthesis and degradation of ECM. Chronic inflammation caused by sustained injury is the initiating factor of hepatic fibrosis[15]. When the pathogenic factors act on the body, a variety of injurious changes occur, but they also stimulate the body to produce defense, adaptation, compensation and other anti-injury responses. AnxA1 is a glucocorticoid regulatory protein that inhibits neutrophil apoptosis, enhances efferocytosis in macrophages, inhibits activation of phospholipase A2, downregulates expression of inflammatory arachidonic acid, and has a significant negative regulatory effect on several inflammatory cells and factors[22]. In this study, a mouse model of experimental liver fibrosis was established by intraperitoneal injection of 20%CCl_4, and treatment or intervention was performed by knockout of *AnxA1* gene, intraperitoneal injection of AnxA1-simulated peptide Ac2-26 and AnxA1 receptor inhibitor Boc2, to observe the effects of AnxA1 on liver fibrosis and


A
Relative Anxa1 mRNA expression
Control
LPS 1 h
LPS 3 h
LPS 6 h
LPS 12 h
LPS 24 h
LPS 12 h + Ac2-26
LPS 12 h + Ac2-26 + Boc2
LPS 24 h + Ac2-26
LPS 24 h + Ac2-26 + Boc2
HSC
HC
B
Relative TGF-β1 mRNA expression
LPS 1 h + Ac2-26
LPS 1 h + Ac2-26 + Boc2
RAW264.7
C
Relative IL-1β mRNA expression
LPS 1 h + Ac2-26
LPS 1 h + Ac2-26 + Boc2
D
Relative IL-6 mRNA expression

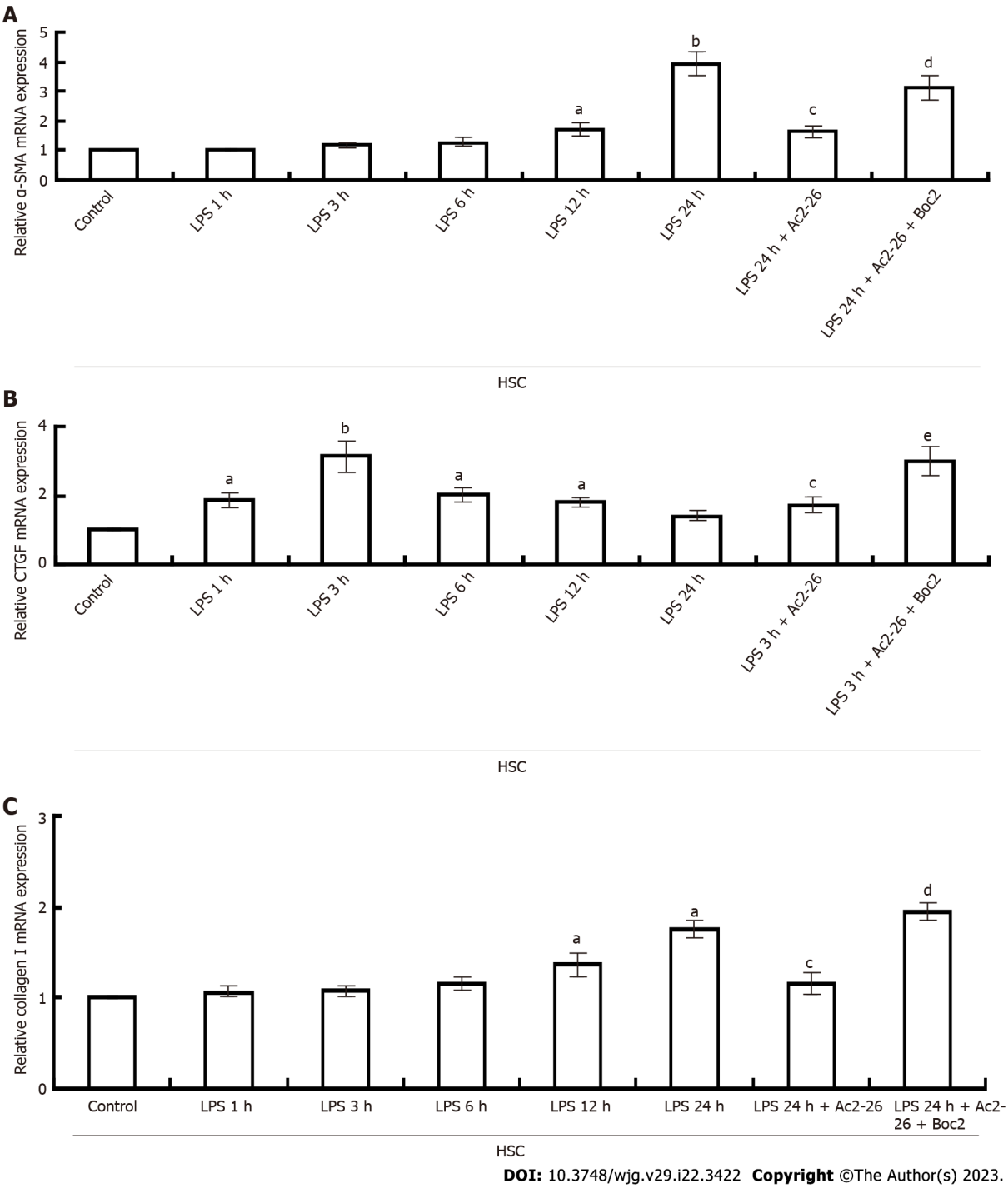


DOI: 10.3748/wjg.v29.i22.3422 **Copyright** ©The Author(s) 2023.

Figure 4 Annexin A1 inhibits activation of RAW264.7 cells and hepatic stellate cells. A: Changes in annexin A1 (AnxA1) expression in hepatocyte and hepatic stellate cells; B: Transforming growth factor-β1 mRNA expression; C: Interleukin (IL)-1β mRNA was quantified using quantitative real-time polymerase chain reaction; D: Changes in IL-6 mRNA in RAW264.7; E: Immunoblotting assay for the detection of AnxA1 in hepatocytes; F: Immunoblotting assay for AnxA1, α-smooth muscle actin (α-SMA) and β-catenin, lysates were analyzed with AnxA1, α-SMA or β-catenin antibody. GAPDH was used as an internal control. $^{a}P < 0.05$, $^{b}P < 0.01$ and $^{c}P < 0.001$ *vs* controls; $^{d}P < 0.05$ and $^{e}P < 0.01$ *vs* lipopolysaccharide; $^{f}P < 0.05$, $^{g}P < 0.01$ and $^{h}P < 0.001$ *vs* lipopolysaccharide + Ac2-26 ($n = 8$). AnxA1: Annexin A1; α-SMA: α-smooth muscle actin; HSC: Hepatic stellate cell; LPS: Lipopolysaccharide; TGF-β1: Transforming growth factor β1; HCs: Hepatocyte; IL: Interleukin; Ac2-26: Active N-terminal peptide of AnxA1; Boc2: N-formyl peptide receptor antagonist N-Boc-Phe-Leu-Phe-Leu-Phe.

explore its main targets. We found that AnxA1 protein and mRNA levels in the liver fibrosis model group were higher than those in the normal control group, and were time-dependent. AnxA1 began to increase at 4 wk, peaked at 8 wk, and then began to decline, consistent with the severity of liver fibrosis in mice, suggesting that AnxA1 is associated with the onset of liver fibrosis. Further studies showed that AnxA1 inhibited fibrosis. Firstly, gross liver specimens revealed that the liver surface roughness and nodulation of mice in the *AnxA1*$^{-/-}$ model group were more severe than those in the wild-type model group, while the lesions in the Ac2-26 group were significantly reduced after treatment, suggesting that Ac2-26 alleviated liver damage. Secondly, HE staining showed that compared with the wild-type model group, liver damage and inflammatory cell infiltration were further aggravated in the *AnxA1*$^{-/-}$ model group, suggesting serious liver damage, which was significantly reduced after treatment with Ac2-26. In addition, Masson staining indicated collagen deposition in the portal area in the wild-type model group, CCl_4 induced more significant collagen deposition in the liver tissue of the *AnxA1*$^{-/-}$ model group, with a wide area, especially at 8 wk, when large amounts of collagen surrounded the liver tissue to form pseudolobules rather than concentrating in the portal area. Collagen deposition in liver tissue of the *AnxA1*$^{-/-}$ model group progressed significantly, and was significantly improved in the group treated with Ac2-26. AnxA1 inhibited liver inflammation and collagen deposition, and relieved liver fibrosis. AnxA1 may play an important role in the occurrence and development of liver fibrosis. While Boc2 blocked the anti-inflammatory and antifibrotic effects of Ac2-26, AnxA1 may have participated in the pathogenesis of liver fibrosis by targeting FPR. Chronic liver disease is progressive, in which inflammation and fibrosis form a vicious cycle, and eventually the excess deposition of ECM, especially type I collagen, makes the lesions difficult to reverse[19,20]. The results of our study showed that the collagen I concentration in liver tissues of mice in the CCl_4-induced model group was significantly increased, and collagen I content in the *AnxA1*$^{-/-}$ model group was higher than that in the wild-type model group, and Boc2 reversed the therapeutic effect of Ac2-26 by reducing the collagen I concentration in liver tissues. High collagen I expression was maintained in the CCl_4-induced model group. It was verified that AnxA1 inhibited liver collagen deposition and relieved liver fibrosis through FPR. Therefore, AnxA1 has a protective effect on hepatic fibrosis.

There have been few studies on the effects of AnxA1 on liver fibrosis. The possible protective mechanism of AnxA1 on liver fibrosis is discussed. HSCs play an important role in the formation of liver fibrosis[19,20], and activation of HSCs is the main cause of deposition of fibrous collagen (types I, III and IV) and other stroma-like proteins in chronic liver disease[23,24], and α-SMA is an activation marker of HSCs. The activation and development of HSCs into fibroblasts is accompanied by increased expression of α-SMA[25], and the degree of HSC activation can be determined by detecting the expression level of α-SMA. In this study, the expression of α-SMA was detected by western blotting and qPCR. The expression of α-SMA in liver tissue of mice in the CCl_4-induced model group was higher than that in the control group, and the activation of HSCs induced by CCl_4 in *AnxA1*$^{-/-}$ mice was higher



DOI: 10.3748/wjg.v29.i22.3422 **Copyright** ©The Author(s) 2023.

Figure 5 Annexin A1 inhibits hepatic stellate cell activation. A: Changes in α-smooth muscle actin expression in hepatic stellate cell; B: Connective tissue growth factor mRNA was quantified using quantitative real-time polymerase chain reaction; C: Collagen I mRNA expression. GAPDH was used as an internal control. $^{a}P < 0.05$ and $^{b}P < 0.01$ *vs* controls; $^{c}P < 0.05$ *vs* lipopolysaccharide; $^{d}P < 0.05$ and $^{e}P < 0.01$ *vs* lipopolysaccharide + Ac2-26 ($n = 8$). AnxA1: Annexin A1; α-SMA: α-smooth muscle actin; HSC: Hepatic stellate cell; CTGF: Connective tissue growth factor; LPS: Lipopolysaccharide; Ac2-26: Active N-terminal peptide of AnxA1; Boc2: N-formyl peptide receptor antagonist N-Boc-Phe-Leu-Phe-Leu-Phe.

than that in wild-type mice. Supplementation of exogenous Ac2-26 significantly inhibited the expression of α-SMA, and Boc2 blocked the inhibitory effect of Ac2-26. It is suggested that Ac2-26 inhibits HSC activation, which may be one of the key factors in inhibiting liver fibrosis by AnxA1, in which FPR receptors are involved.

HSCs are the main receivers of inflammatory signals and the main promoters of liver fibrosis. Hepatocyte injury triggers an inflammatory response, releases various cytokines and inflammatory factors, activates HSCs, and causes secretion and deposition of ECM, leading to liver fibrosis[26,27]. Immune cells, especially Kupffer cells and macrophages in the liver, are key regulators of inflammation [28]. Kupffer cells are intrinsic macrophages in the liver, which play an important role in the elimination of and defense against bacteria and pathogenic substances from the gastrointestinal tract[29]. In the case

of liver injury, Kupffer cells are activated by damage-associated pathogenic patterns or LPS, viral DNA, and other pathogen-associated molecular patterns, producing and releasing TGF-β1, IL-1β and IL-6 to activate HSCs, causing the secretion and deposition of ECM and leading to liver fibrosis[30-32]. Our results showed that hepatic fibrosis was accompanied by inflammatory infiltration and secretion of inflammatory cytokines TGF-β1, IL-1β and IL-6, which increased with time, suggesting that hepatic inflammation is related to the severity of fibrosis. Exogenous Ac2-26 significantly reduced hepatic inflammatory cell infiltration and inflammatory factor expression in the CCl_4-induced model group, while alleviating the formation of liver fibrosis, and Boc2 inhibited the anti-inflammatory effect of Ac2-26. AnxA1 may reduce fibrosis by inhibiting the inflammatory response in the liver, and its mechanism may be related to inhibition of HSC activation by targeting FPR to regulate macrophage function.

TGF-β1 is a key regulatory factor in the process of liver fibrosis[32], and CTGF, as its downstream factor, mediates TGF-β1, promoting ECM production and accumulation[33]. HSCs are the main source of CTGF, and blocking CTGF can significantly inhibit HSC activation and proliferation, and reduce tissue inhibitors of metalloproteinase, matrix metalloproteinase (MMP)2, MMP9 and type I collagen. Our results showed that increased expression of CTGF in the liver tissue of mice in the CCl_4-induced model group was also inhibited by Ac2-26, suggesting that the inhibitory effect of AnxA1 on liver fibrosis is closely related to the expression of TGF-β1 and its downstream factor CTGF.

In order to verify the results of the animal experiments and to better investigate the mechanism of AnxA1 in liver fibrosis, we conducted *in vitro* cell experiments. Ac2-26 significantly inhibited LPS-induced activation of RAW264.7 cells and downregulated TGF-β1 and other inflammatory factors expressed in RAW264.7 cells after activation, and Boc2 reversed the above results. LPS induced HCs and HSCs to increase Anxa1 expression, but LPS induced RAW264.7 cells did not upregulate AnxA1 expression, and the activated HSCs that overexpressed SMA, collagen, and CTGF were inhibited by exogenous Ac2-26. AnxA1 mediated by FPR may affect the function of macrophages through HC paracrine or HSC autocrine effects, control inflammatory responses, inhibit HSC activation, and reduce ECM deposition by negative feedback, so as to prevent liver fibrosis formation.

Recent studies have shown that the Wnt/β-catenin signaling pathway can promote liver fibrosis and play an important role in HSC proliferation, metastasis and ECM formation[34]. Inhibition of Wnt/β-catenin signaling can inhibit the proliferation of HSCs and induce their apoptosis, thus alleviating CCl_4-induced liver fibrosis[34-36]. In addition, TGF-β1 activates the Wnt/β-catenin pathway by inhibiting the expression of Wnt/β-catenin inhibitors[36]. Our results suggest that Ac2-26 downregulates the expression of β-catenin in the Wnt signaling pathway in mouse liver fibrosis, and inhibits the expression of activated HSC β-catenin. Combined with previous findings, the therapeutic effects of AnxA1 may alleviate the development of liver fibrosis by inhibiting the Wnt/β-catenin pathway of HSCs.

CONCLUSION

AnxA1 may play an important role in the formation of liver fibrosis, including regulating macrophage function, reducing inflammation, inhibiting HSC activation, and improving collagen deposition. AnxA1 mediated by FPR receptors may regulate the activity of macrophages through HSC autocrine or paracrine functions, inhibit the Wnt/β-catenin pathway, and inhibit HSC activity. Although its further mechanism of action has not been clearly elucidated, our results suggest that AnxA1 has potential activity against hepatic fibrosis and can block the occurrence of fibrosis at multiple targets, which may provide a new option for liver fibrosis treatment.

ARTICLE HIGHLIGHTS

Research background

Liver fibrosis is a pathological change caused by chronic liver injury, and is a key link in the progression of chronic liver diseases to cirrhosis or liver cancer. How to prevent and reverse liver fibrosis is currently a hot and difficult research topic, and fully understanding and elucidating the pathogenesis of liver fibrosis is the foundation of prevention and treatment. At present, there is still a lack of safe and effective treatment for liver cirrhosis clinically. It is of great significance to deeply study the pathogenesis of liver fiber and prevent and treat it in order to reduce the incidence rate and mortality of liver cirrhosis.

Research motivation

Studies have shown that liver fibrosis is closely related to inflammation in chronic liver disease, and annexin (Anx)A1 has strong anti-inflammatory effects. Therefore, this study focuses on the pathogenesis of liver fibrosis and investigates the role of AnxA1 in liver fibrosis. Provide valuable information for antifibrosis therapy.

Research objectives
To investigate molecular and cellular mechanisms of liver fibrosis and evaluate the effect of AnxA1 in hepatic fibrosis.

Research methods
Biomarkers as drug development tools, biomarker discovery and validation using a combination of *in vitro* and *in vivo* studies. A large and wide range of animal models and cell experiments can be used, and experiments can be repeated multiple times.

Research results
AnxA1/formylpeptide receptor (FPR) inhibits the activation of hepatic stellate cells by regulating macrophage function through the Wnt/β-catenin pathway in the CCl_4-induced hepatic fibrosis mice.

Research conclusions
AnxA1 may involve in the pathogenesis of liver fibrosis and as a potential therapeutic target.

Research perspectives
This study investigates the mechanism of Anxa1 in liver fibrosis by using wild mice/Anxa1 knockout mice in combination with Anxa1 mimetic peptide and FPR receptor inhibitor to provide an experimental basis for the possible use of Anxa1 in the treatment of liver fibrosis.

FOOTNOTES

Author contributions: Fan JH, Luo N and Liu GF performed most of the experiments; Luo N, Xu XF and Li SQ analyzed the data; Fan JH and Lv XP designed the study and wrote the paper.

Supported by a Grant-in-Aid for Scientific Research from National Natural Science Foundation of China, No. 81860120 and 81860104; Guangxi Natural Science Foundation, No. 2017GXNSFBA198134, 2017GXNSFAA198299 and 2015GXNSFCA139024.

Institutional animal care and use committee statement: All experiments were conducted in accordance with the institutional guidelines of Guangxi Medical University for the care and use of laboratory animals.

Conflict-of-interest statement: All the authors report no relevant conflicts of interest for this article.

Data sharing statement: No additional data are available.

ARRIVE guidelines statement: The authors have read the ARRIVE guidelines, and the manuscript was prepared and revised according to the ARRIVE guidelines.

Open-Access: This article is an open-access article that was selected by an in-house editor and fully peer-reviewed by external reviewers. It is distributed in accordance with the Creative Commons Attribution NonCommercial (CC BY-NC 4.0) license, which permits others to distribute, remix, adapt, build upon this work non-commercially, and license their derivative works on different terms, provided the original work is properly cited and the use is non-commercial. See: https://creativecommons.org/Licenses/by-nc/4.0/

Country/Territory of origin: China

ORCID number: Jun-Hua Fan 0000-0002-7292-7484; Na Luo 0000-0001-7269-4476; Geng-Feng Liu 0000-0002-2414-7707; Xiao-Fang Xu 0000-0001-7986-1740; Shi-Quan Li 0000-0003-3744-2737; Xiao-Ping Lv 0000-0001-7144-9508.

S-Editor: Wang JJ
L-Editor: A
P-Editor: Wang JJ

REFERENCES

1 **Caligiuri A**, Gentilini A, Pastore M, Gitto S, Marra F. Cellular and Molecular Mechanisms Underlying Liver Fibrosis Regression. *Cells* 2021; **10** [PMID: 34685739 DOI: 10.3390/cells10102759]
2 **Liu X**, Mi X, Wang Z, Zhang M, Hou J, Jiang S, Wang Y, Chen C, Li W. Ginsenoside Rg3 promotes regression from hepatic fibrosis through reducing inflammation-mediated autophagy signaling pathway. *Cell Death Dis* 2020; **11**: 454 [PMID: 32532964 DOI: 10.1038/s41419-020-2597-7]
3 **Seki E**, Brenner DA. Recent advancement of molecular mechanisms of liver fibrosis. *J Hepatobiliary Pancreat Sci* 2015;

22: 512-518 [PMID: 25869468 DOI: 10.1002/jhbp.245]
4 **Ezhilarasan D**, Sokal E, Najimi M. Hepatic fibrosis: It is time to go with hepatic stellate cell-specific therapeutic targets. *Hepatobiliary Pancreat Dis Int* 2018; **17**: 192-197 [PMID: 29709350 DOI: 10.1016/j.hbpd.2018.04.003]
5 **Koo JH**, Lee HJ, Kim W, Kim SG. Endoplasmic Reticulum Stress in Hepatic Stellate Cells Promotes Liver Fibrosis *via* PERK-Mediated Degradation of HNRNPA1 and Up-regulation of SMAD2. *Gastroenterology* 2016; **150**: 181-193.e8 [PMID: 26435271 DOI: 10.1053/j.gastro.2015.09.039]
6 **Parola M**, Pinzani M. Liver fibrosis: Pathophysiology, pathogenetic targets and clinical issues. *Mol Aspects Med* 2019; **65**: 37-55 [PMID: 30213667 DOI: 10.1016/j.mam.2018.09.002]
7 **Lan T**, Li C, Yang G, Sun Y, Zhuang L, Ou Y, Li H, Wang G, Kisseleva T, Brenner D, Guo J. Sphingosine kinase 1 promotes liver fibrosis by preventing miR-19b-3p-mediated inhibition of CCR2. *Hepatology* 2018; **68**: 1070-1086 [PMID: 29572892 DOI: 10.1002/hep.29885]
8 **Cheng D**, Chai J, Wang H, Fu L, Peng S, Ni X. Hepatic macrophages: Key players in the development and progression of liver fibrosis. *Liver Int* 2021; **41**: 2279-2294 [PMID: 33966318 DOI: 10.1111/liv.14940]
9 **Li P**, He K, Li J, Liu Z, Gong J. The role of Kupffer cells in hepatic diseases. *Mol Immunol* 2017; **85**: 222-229 [PMID: 28314211 DOI: 10.1016/j.molimm.2017.02.018]
10 **Alegre F**, Pelegrin P, Feldstein AE. Inflammasomes in Liver Fibrosis. *Semin Liver Dis* 2017; **37**: 119-127 [PMID: 28564720 DOI: 10.1055/s-0037-1601350]
11 **Gan C**, Cai Q, Tang C, Gao J. Inflammasomes and Pyroptosis of Liver Cells in Liver Fibrosis. *Front Immunol* 2022; **13**: 896473 [PMID: 35707547 DOI: 10.3389/fimmu.2022.896473]
12 **Senchenkova EY**, Ansari J, Becker F, Vital SA, Al-Yafeai Z, Sparkenbaugh EM, Pawlinski R, Stokes KY, Carroll JL, Dragoi AM, Qin CX, Ritchie RH, Sun H, Cuellar-Saenz HH, Rubinstein MR, Han YW, Orr AW, Perretti M, Granger DN, Gavins FNE. Novel Role for the AnxA1-Fpr2/ALX Signaling Axis as a Key Regulator of Platelet Function to Promote Resolution of Inflammation. *Circulation* 2019; **140**: 319-335 [PMID: 31154815 DOI: 10.1161/CIRCULATIONAHA.118.039345]
13 **Xu X**, Gao W, Li L, Hao J, Yang B, Wang T, Bai X, Li F, Ren H, Zhang M, Zhang L, Wang J, Wang D, Zhang J, Jiao L. Annexin A1 protects against cerebral ischemia-reperfusion injury by modulating microglia/macrophage polarization *via* FPR2/ALX-dependent AMPK-mTOR pathway. *J Neuroinflammation* 2021; **18**: 119 [PMID: 34022892 DOI: 10.1186/s12974-021-02174-3]
14 **Vecchi L**, Alves Pereira Zóia M, Goss Santos T, de Oliveira Beserra A, Colaço Ramos CM, França Matias Colombo B, Paiva Maia YC, Piana de Andrade V, Teixeira Soares Mota S, Gonçalves de Araújo T, Van Petten de Vasconcelos Azevedo F, Soares FA, Oliani SM, Goulart LR. Inhibition of the AnxA1/FPR1 autocrine axis reduces MDA-MB-231 breast cancer cell growth and aggressiveness *in vitro* and in vivo. *Biochim Biophys Acta Mol Cell Res* 2018; **1865**: 1368-1382 [PMID: 29932988 DOI: 10.1016/j.bbamcr.2018.06.010]
15 **Neymeyer H**, Labes R, Reverte V, Saez F, Stroh T, Dathe C, Hohberger S, Zeisberg M, Müller GA, Salazar J, Bachmann S, Paliege A. Activation of annexin A1 signalling in renal fibroblasts exerts antifibrotic effects. *Acta Physiol (Oxf)* 2015; **215**: 144-158 [PMID: 26332853 DOI: 10.1111/apha.12586]
16 **Lai T**, Li Y, Mai Z, Wen X, Lv Y, Xie Z, Lv Q, Chen M, Wu D, Wu B. Annexin A1 is elevated in patients with COPD and affects lung fibroblast function. *Int J Chron Obstruct Pulmon Dis* 2018; **13**: 473-486 [PMID: 29440885 DOI: 10.2147/COPD.S149766]
17 **Vallée A**, Lecarpentier Y, Guillevin R, Vallée JN. Interactions between TGF-β1, canonical WNT/β-catenin pathway and PPAR γ in radiation-induced fibrosis. *Oncotarget* 2017; **8**: 90579-90604 [PMID: 29163854 DOI: 10.18632/oncotarget.21234]
18 **Yu FJ**, Dong PH, Fan XF, Lin Z, Chen YP, Li J. Down-regulation of angiotensin II by shRNA reduces collagen synthesis in hepatic stellate cells. *Int J Mol Med* 2010; **25**: 801-806 [PMID: 20372825 DOI: 10.3892/ijmm_00000407]
19 **Katoh M**. Multilayered prevention and treatment of chronic inflammation, organ fibrosis and cancer associated with canonical WNT/βcatenin signaling activation (Review). *Int J Mol Med* 2018; **42**: 713-725 [PMID: 29786110 DOI: 10.3892/ijmm.2018.3689]
20 **Zhang C**, Zhang Y, Zhang W, Tong H, Li S, Yan Y. WISP1 promotes bovine MDSC differentiation *via* recruitment of ANXA1 for the regulation of the TGF-β signalling pathway. *Mol Cell Biochem* 2020; **470**: 215-227 [PMID: 32458119 DOI: 10.1007/s11010-020-03763-1]
21 **Fan JH**, Feng GG, Huang L, Tang GD, Jiang HX, Xu J. Naofen promotes TNF-α-mediated apoptosis of hepatocytes by activating caspase-3 in lipopolysaccharide-treated rats. *World J Gastroenterol* 2014; **20**: 4963-4971 [PMID: 24803807 DOI: 10.3748/wjg.v20.i17.4963]
22 **Zharkova O**, Salamah MF, Babak MV, Rajan E, Lim LHK, Andrade F, Gil CD, Oliani SM, Moraes LA, Vaiyapuri S. Deletion of Annexin A1 in Mice Upregulates the Expression of Its Receptor, Fpr2/3, and Reactivity to the AnxA1 Mimetic Peptide in Platelets. *Int J Mol Sci* 2023; **24** [PMID: 36834844 DOI: 10.3390/ijms24043424]
23 **Hall A**, Cotoi C, Luong TV, Watkins J, Bhathal P, Quaglia A. Collagen and elastic fibres in acute and chronic liver injury. *Sci Rep* 2021; **11**: 14569 [PMID: 34267266 DOI: 10.1038/s41598-021-93566-1]
24 **Rong X**, Yang Y, Zhang G, Zhang H, Li C, Wang Y. Antler stem cells as a novel stem cell source for reducing liver fibrosis. *Cell Tissue Res* 2020; **379**: 195-206 [PMID: 31428875 DOI: 10.1007/s00441-019-03081-z]
25 **Wang R**, Zhang D, Tang D, Sun K, Peng J, Zhu W, Yin S, Wu Y. Amygdalin inhibits TGFβ1-induced activation of hepatic stellate cells (HSCs) *in vitro* and CCl(4)-induced hepatic fibrosis in rats in vivo. *Int Immunopharmacol* 2021; **90**: 107151 [PMID: 33296784 DOI: 10.1016/j.intimp.2020.107151]
26 **Delgado ME**, Cárdenas BI, Farran N, Fernandez M. Metabolic Reprogramming of Liver Fibrosis. *Cells* 2021; **10** [PMID: 34944111 DOI: 10.3390/cells10123604]
27 **Papachristoforou E**, Ramachandran P. Macrophages as key regulators of liver health and disease. *Int Rev Cell Mol Biol* 2022; **368**: 143-212 [PMID: 35636927 DOI: 10.1016/bs.ircmb.2022.04.006]
28 **Seo HY**, Lee SH, Han E, Hwang JS, Han S, Kim MK, Jang BK. Evogliptin Directly Inhibits Inflammatory and Fibrotic Signaling in Isolated Liver Cells. *Int J Mol Sci* 2022; **23** [PMID: 36232933 DOI: 10.3390/ijms231911636]

29 **Wu J**, Zern MA. Hepatic stellate cells: a target for the treatment of liver fibrosis. *J Gastroenterol* 2000; **35**: 665-672 [PMID: 11023037 DOI: 10.1007/s005350070045]

30 **Ohara M**, Ohnishi S, Hosono H, Yamamoto K, Yuyama K, Nakamura H, Fu Q, Maehara O, Suda G, Sakamoto N. Extracellular Vesicles from Amnion-Derived Mesenchymal Stem Cells Ameliorate Hepatic Inflammation and Fibrosis in Rats. *Stem Cells Int* 2018; **2018**: 3212643 [PMID: 30675167 DOI: 10.1155/2018/3212643]

31 **Xiang DM**, Sun W, Ning BF, Zhou TF, Li XF, Zhong W, Cheng Z, Xia MY, Wang X, Deng X, Wang W, Li HY, Cui XL, Li SC, Wu B, Xie WF, Wang HY, Ding J. The HLF/IL-6/STAT3 feedforward circuit drives hepatic stellate cell activation to promote liver fibrosis. *Gut* 2018; **67**: 1704-1715 [PMID: 28754776 DOI: 10.1136/gutjnl-2016-313392]

32 **Zigmond E**, Samia-Grinberg S, Pasmanik-Chor M, Brazowski E, Shibolet O, Halpern Z, Varol C. Infiltrating monocyte-derived macrophages and resident kupffer cells display different ontogeny and functions in acute liver injury. *J Immunol* 2014; **193**: 344-353 [PMID: 24890723 DOI: 10.4049/jimmunol.1400574]

33 **Trampuž SR**, van Riet S, Nordling Å, Ingelman-Sundberg M. The Role of CTGF in Liver Fibrosis Induced in 3D Human Liver Spheroids. *Cells* 2023; **12** [PMID: 36672237 DOI: 10.3390/cells12020302]

34 **Rong X**, Liu J, Yao X, Jiang T, Wang Y, Xie F. Human bone marrow mesenchymal stem cells-derived exosomes alleviate liver fibrosis through the Wnt/β-catenin pathway. *Stem Cell Res Ther* 2019; **10**: 98 [PMID: 30885249 DOI: 10.1186/s13287-019-1204-2]

35 **Lee IH**, Im E, Lee HJ, Sim DY, Lee JH, Jung JH, Park JE, Shim BS, Kim SH. Apoptotic and antihepatofibrotic effect of honokiol *via* activation of GSK3β and suppression of Wnt/β-catenin pathway in hepatic stellate cells. *Phytother Res* 2021; **35**: 452-462 [PMID: 32776713 DOI: 10.1002/ptr.6824]

36 **El-Fadaly AA**, Afifi NA, El-Eraky W, Salama A, Abdelhameed MF, El-Rahman SSA, Ramadan A. Fisetin alleviates thioacetamide-induced hepatic fibrosis in rats by inhibiting Wnt/β-catenin signaling pathway. *Immunopharmacol Immunotoxicol* 2022; **44**: 355-366 [PMID: 35255766 DOI: 10.1080/08923973.2022.2047198]

World Journal of Gastroenterology

Submit a Manuscript: https://www.f6publishing.com

World J Gastroenterol 2023 June 14; 29(22): 3440-3468

DOI: 10.3748/wjg.v29.i22.3440

ISSN 1007-9327 (print) ISSN 2219-2840 (online)

ORIGINAL ARTICLE

Basic Study

Study of the roles of caspase-3 and nuclear factor kappa B in myenteric neurons in a P2X7 receptor knockout mouse model of ulcerative colitis

Henrique Inhauser Riceti Magalhães, Felipe Alexandre Machado, Roberta Figueiroa Souza, Marcos Antônio Ferreira Caetano, Vanessa Ribeiro Figliuolo, Robson Coutinho-Silva, Patricia Castelucci

Specialty type: Anatomy and morphology

Provenance and peer review: Invited article; Externally peer reviewed.

Peer-review model: Single blind

Peer-review report's scientific quality classification

Grade A (Excellent): 0
Grade B (Very good): B, B
Grade C (Good): 0
Grade D (Fair): 0
Grade E (Poor): 0

P-Reviewer: Arslan M, Turkey; Pisani LF, Italy

Received: February 27, 2023
Peer-review started: February 27, 2023
First decision: April 3, 2023
Revised: April 25, 2023
Accepted: May 12, 2023
Article in press: May 12, 2023
Published online: June 14, 2023

Henrique Inhauser Riceti Magalhães, Department of Surgery, School of Veterinary Medicine and Animal Sciences, University of São Paulo, São Paulo 05508-270, Brazil

Felipe Alexandre Machado, Roberta Figueiroa Souza, Marcos Antônio Ferreira Caetano, Patricia Castelucci, Department of Anatomy, University of São Paulo, São Paulo 05508-000, Brazil

Vanessa Ribeiro Figliuolo, Robson Coutinho-Silva, Biophysics Institute Carlos Chagas Filho, Federal University of Rio de Janeiro, Rio de Janeiro 21941-902, Brazil

Corresponding author: Patricia Castelucci, MHSc, PhD, Associate Professor, Associate Research Scientist, Lecturer, Department of Anatomy, University of São Paulo, 2415, Av. Dr Lineu Prestes, São Paulo 05508-000, Brazil. pcastel@usp.br

Abstract

BACKGROUND

The literature indicates that the enteric nervous system is affected in inflammatory bowel diseases (IBDs) and that the P2X7 receptor triggers neuronal death. However, the mechanism by which enteric neurons are lost in IBDs is unknown.

AIM

To study the role of the caspase-3 and nuclear factor kappa B (NF-κB) pathways in myenteric neurons in a P2X7 receptor knockout (KO) mouse model of IBDs.

METHODS

Forty male wild-type (WT) C57BL/6 and P2X7 receptor KO mice were euthanized 24 h or 4 d after colitis induction by 2,4,6-trinitrobenzene sulfonic acid (colitis group). Mice in the sham groups were injected with vehicle. The mice were divided into eight groups (n = 5): The WT sham 24 h and 4 d groups, the WT colitis 24 h and 4 d groups, the KO sham 24 h and 4 d groups, and the KO colitis 24 h and 4 d groups. The disease activity index (DAI) was analyzed, the distal colon was collected for immunohistochemistry analyses, and immunofluorescence was performed to identify neurons immunoreactive (ir) for calretinin, P2X7 receptor, cleaved caspase-3, total caspase-3, phospho-NF-κB, and total NF-κB. We analyzed the number of calretinin-ir and P2X7 receptor-ir neurons per ganglion, the neuronal profile area (μm²), and corrected total cell fluorescence (CTCF).

RESULTS

Cells double labeled for calretinin and P2X7 receptor, cleaved caspase-3, total caspase-3, phospho-NF-κB, or total NF-κB were observed in the WT colitis 24 h and 4 d groups. The number of calretinin-ir neurons per ganglion was decreased in the WT colitis 24 h and 4 d groups compared to the WT sham 24 h and 4 d groups, respectively (2.10 ± 0.13 *vs* 3.33 ± 0.17, $P < 0.001$; 2.92 ± 0.12 *vs* 3.70 ± 0.11, $P < 0.05$), but was not significantly different between the KO groups. The calretinin-ir neuronal profile area was increased in the WT colitis 24 h group compared to the WT sham 24 h group (312.60 ± 7.85 *vs* 278.41 ± 6.65, $P < 0.05$), and the nuclear profile area was decreased in the WT colitis 4 d group compared to the WT sham 4 d group (104.63 ± 2.49 *vs* 117.41 ± 1.14, $P < 0.01$). The number of P2X7 receptor-ir neurons per ganglion was decreased in the WT colitis 24 h and 4 d groups compared to the WT sham 24 h and 4 d groups, respectively (19.49 ± 0.35 *vs* 22.21 ± 0.18, $P < 0.001$; 20.35 ± 0.14 *vs* 22.75 ± 0.51, $P < 0.001$), and no P2X7 receptor-ir neurons were observed in the KO groups. Myenteric neurons showed ultrastructural changes in the WT colitis 24 h and 4 d groups and in the KO colitis 24 h group. The cleaved caspase-3 CTCF was increased in the WT colitis 24 h and 4 d groups compared to the WT sham 24 h and 4 d groups, respectively (485949 ± 14140 *vs* 371371 ± 16426, $P < 0.001$; 480381 ± 11336 *vs* 378365 ± 4053, $P < 0.001$), but was not significantly different between the KO groups. The total caspase-3 CTCF, phospho-NF-κB CTCF, and total NF-κB CTCF were not significantly different among the groups. The DAI was recovered in the KO groups. Furthermore, we demonstrated that the absence of the P2X7 receptor attenuated inflammatory infiltration, tissue damage, collagen deposition, and the decrease in the number of goblet cells in the distal colon.

CONCLUSION

Ulcerative colitis affects myenteric neurons in WT mice but has a weaker effect in P2X7 receptor KO mice, and neuronal death may be associated with P2X7 receptor-mediated caspase-3 activation. The P2X7 receptor can be a therapeutic target for IBDs.

Key Words: Cell death; Enteric nervous system; Gastroenterology; Inflammatory bowel diseases; P2X7 receptor; Purinergic signaling

©The Author(s) 2023. Published by Baishideng Publishing Group Inc. All rights reserved.

Core Tip: In the present study, we compared pathological changes resulting from 2,4,6-trinitrobenzene sulfonic acid (TNBS)-induced colitis at two different time points after colitis induction. At both 24 h and four days post-inflammatory induction, there was a decrease in the number of myenteric neurons in the wild-type groups but not in the knockout groups. Morphometric and ultrastructural changes were also observed. In addition, our results confirm that neuronal death mediated by caspase-3 activation is related to purinergic signaling *via* the P2X7 receptor in the myenteric plexus of mice with TNBS-induced colitis.

Citation: Magalhães HIR, Machado FA, Souza RF, Caetano MAF, Figliuolo VR, Coutinho-Silva R, Castelucci P. Study of the roles of caspase-3 and nuclear factor kappa B in myenteric neurons in a P2X7 receptor knockout mouse model of ulcerative colitis. *World J Gastroenterol* 2023; 29(22): 3440-3468
URL: https://www.wjgnet.com/1007-9327/full/v29/i22/3440.htm
DOI: https://dx.doi.org/10.3748/wjg.v29.i22.3440

INTRODUCTION

According to Martin[1] and Kanduc *et al*[2], cells usually die by apoptosis or necrosis, each of which has distinct microscopic and biochemical characteristics. In the process of apoptosis, the death stimulus activates a cascade of events that orchestrate the destruction of the cell under both physiological and pathological conditions[3,4]. Apoptosis is a programmed, dynamic, and energy-demanding process[5] and can occur in areas not severely affected by acute injury[4]. The cell volume decreases, the cytoplasm and nucleus become condensed, cytoskeletal proteins are cleaved, and apoptotic bodies form[3-10]. On the other hand, in necrosis, an unintentional, passive, and pathological process, the death stimulus itself causes the death of the cell[3-5] and affects groups of cells across tissues[8]. Cells and their organelles swell, and disruption of cytoplasmic membranes and degradation of deoxyribonucleic acid (DNA) occur[1,5,6,8,11,12]. Nuclear dissolution results from autolysis[5]. Activation of caspases is the main mechanism underlying cell death[3,7,8,13-15].

Studies of the central nervous system have shown that degeneration of neurons can occur through different pathways, including apoptotic pathways[4,8,16,17]. In acute neurological diseases, cell loss can occur either through necrosis or apoptosis[18-23], whereas in chronic neurodegenerative diseases, caspase-mediated pathways play dominant roles in mediating neuronal dysfunction and death[4,8,21,24-28]. In addition, loss of enteric nervous system (ENS) neurons has been demonstrated to occur after intestinal ischemia and reperfusion[29-34] and in experimental colitis[35-40].

The unexpected ability of certain cells to survive the activation of caspases[41-43] demonstrates the remarkable plasticity of cell death programs and suggests that the action of these proteases alone is not sufficient to cause cell loss[3]. Cell death, including that of enteric neurons, can occur through several caspase-independent pathways[3,44-47], and the signals that result in nonapoptotic cell death can come from numerous membrane receptors associated, directly or indirectly, or not with the activation of caspases themselves[3]. The P2X7 receptor is an important inducer of cell death[37,47-55] and is strongly associated with both the activation of caspases and the release and regulation of proinflammatory cytokines and transcription factors such as nuclear factor kappa B (NF-κB)[47,50,52,56-59].

Thus, improving the understanding of the cellular and molecular basis of neuronal death can aid in the identification and development of specific therapeutic strategies[8]. However, studies on the mechanisms underlying the death of enteric neurons, especially the role of the P2X7 receptor as an inducer of the death of these neurons in inflammatory bowel diseases (IBDs), are still lacking[37-40,51,52,60-63].

We aimed to study the roles of the caspase-3 and NF-κB pathways in myenteric neurons of the distal colon in a P2X7 receptor knockout (KO) mouse model of ulcerative colitis. The effects of colitis on calretinin neurons and intestinal tissue were analyzed by immunohistochemistry and histology, respectively.

MATERIALS AND METHODS

The animal experiments were conducted in accordance with the current regulations of the Ethics Committee on Animal Use of the Institute of Biomedical Sciences of the University of São Paulo. In addition, all procedures were approved by the Ethics Committee on Animal Use of the School of Veterinary Medicine and Animal Science of the University of São Paulo (No. 2841270120) and by the Ethics Committee on Animal Use of the Institute of Biomedical Sciences of the University of São Paulo (No. 2372300921).

Forty eight-week-old male C57BL/6 mice weighing 20 g to 30 g, *i.e.*, 20 wild-type (WT) and 20 P2X7 receptor KO (P2X7$^{-/-}$, P2X7 KO) animals, were used. The animal protocol was designed to minimize pain and discomfort in the animals. The mice were provided water and food *ad libitum* in ventilated cages on a 12 h light/dark cycle at a controlled temperature (21 °C). The animals were divided into eight groups of five animals each (n = 5): The WT sham 24 h and 4 days (d) groups, the WT colitis 24 h and 4 d groups, the KO sham 24 h and 4 d groups, and the KO colitis 24 h and 4 d groups.

Ulcerative colitis model

Mice were anesthetized *via* subcutaneous administration of an anesthetic solution of 2% xylazine (5 mg/kg) and 10% ketamine (80 mg/kg). Then, the animals in the colitis groups (WT colitis 24 h, KO colitis 24 h, WT colitis 4 d, and KO colitis 4 d groups) were given an intrarectal injection of 100 μL of 2,4,6-trinitrobenzene sulfonic acid (TNBS, Sigma, United States of America) diluted to 1.5% in 35.0% ethanol (Synth, Brazil). The solution was deposited directly in the lumen of the large intestine with a four-centimeter-long polypropylene cannula. The animals in the sham groups (WT sham 24 h, KO sham 24 h, WT sham 4 d, and KO sham 4 d groups) received 100 μL of 35% ethanol (vehicle) by the same method. The animals were euthanized by administration of an overdose of anesthetic solution 24 h or four days after the procedures. After the abdominal cavity of each animal was opened, the large intestine was identified, dissected, collected, and measured. The tissue was then sectioned along the mesenteric margin, and its contents were flushed with 0.01 M phosphate buffered saline (PBS) (pH 7.1-7.2). Only the distal colon was used for the analyses.

Disease activity index: Changes in weight, stool consistency, and the presence of blood in the stools were scored daily, and these scores were summed to calculate the Disease activity index (DAI). These parameters were scored according to a scale adapted from Cooper *et al*[64] and Hoffman *et al*[65] (Table 1).

Macroscopic and microscopic evaluation of intestinal lesions: The macroscopic features of intestinal lesions, *i.e.*, the presence of hyperemia and ulcers and the severity of intestinal inflammation, were scored according to the scale proposed by Wallace *et al*[66]. The microscopic features of the intestinal lesions, *i.e.*, the presence of ulcers, the severity of edema in the submucosal layer, and the degree of inflammatory cell infiltration, were scored according to the scale proposal by Fabia *et al*[67] following hematoxylin and eosin staining (Table 2).

Table 1 Changes in weight, stool consistency, and the presence of blood in the stool were scored for the ulcerative colitis model mice and mice that received intrarectal injection of 35% ethanol according to the following scale

Disease activity index		Score
A	Weight change (< 1%)	0
	Weight change (1%-2%)	1
	Weight change (2%-4%)	2
	Weight change (4%-6%)	3
	Weight change (> 6%)	4
B	Stool consistency (normal)	0
	Stool consistency (normal and well-formed)	1
	Stool consistency (pasty that did not stick to the anus)	2
	Stool consistency (loose stool)	3
	Stool consistency (diarrhea)	4
C	Rectal bleeding (absent)	0
	Rectal bleeding (+)	1
	Rectal bleeding (++)	2
	Rectal bleeding (+++)	3
	Rectal bleeding (gross bleeding)	4

A: Weight; B: Stool consistency; C: Presence of blood in the stool.

Immunohistochemistry

The large intestines of all mice were washed in PBS, stretched, fixed with the mucosa facing down on wooden platforms, and submerged in 4% paraformaldehyde in 0.1 M PBS (pH 7.3) for 24 h at 4 °C. Subsequently, the tissues were bleached by three 10-min washes in 100% dimethyl sulfoxide (Synth, Brazil) and then washed three more 10-min washes in PBS for 10 min each. Finally, the samples were stored at 4 °C in PBS containing sodium azide (0.1%).

To prepare whole mounts, the mucosal and submucosal layers and the circular muscle layer were removed from segments of the distal colon, leaving only the longitudinal muscle layer and the myenteric plexus. The whole mounts were preincubated for 45 min at room temperature with 10% normal horse serum in PBS containing 1.5% Triton X-100. The tissues were incubated for 48 h at 4 °C with the primary antibodies (Table 3). After 48 h of primary antibody incubation, the preparations were washed three times in PBS for 10 min each and then incubated for one hour at room temperature with the secondary antibodies (Table 3). Finally, they were washed three times for 10 min each in PBS, incubated in 4′,6′-diamino-2-phenyl-indol (DAPI) for three minutes, and washed three times in PBS for five minutes each. Whole mounts were mounted on slides in glycerol buffered with 0.5 M sodium carbonate (pH 8.6).

Qualitative analysis of the myenteric neurons was performed on a Nikon 80i fluorescence microscope and an Olympus FluoView 1000 confocal laser microscope. The captured images were processed with CorelDRAW software.

Quantitative analyses

The neuronal density (number of neurons per ganglion) was obtained by counting calretinin-immunoreactive (ir) and P2X7 receptor-ir neurons in 50 myenteric ganglia of the distal colon of each animal at 40 × magnification under a Nikon 80i microscope. The slides were analyzed in a zigzag pattern, and the ganglia were chosen randomly. In total, 2000 myenteric ganglia were analyzed for each protein of interest.

For analysis of the neuronal profile area, 125 calretinin-ir neurons in the distal colon myenteric plexus of each animal were randomly photographed at 40 × magnification under a Nikon 80i microscope *via* NIS-elements AR 3.1 software. For analysis of the nuclear profile area, the DAPI-labeled nuclei of these same 125 neurons were photographed. Neuronal and nuclear morphometry was performed by manually delimiting each of the structures individually in Image Pro-Plus 5.0 software. The cytoplasmic profile area was obtained by subtracting the nuclear area from the neuronal area. The results are presented in μm[2]. In total, 5000 neurons and 5000 nuclei were analyzed.

Table 2 Scale used to score the severity of macroscopic and microscopic lesions in the distal colon of ulcerative colitis model mice and mice that received intrarectal injection of 35% ethanol

Macroscopic injury	Score
Normal	0
Hyperemia without ulcers	1
Ulcerations without hyperemia	2
Ulcerations at one site	3
Ulcerations at two or more sites	4
Sites of damage extending > 1 cm	5
Sites of damage extending > 2 cm; the score increases by 1 for each additional cm	6-10
A	
No ulcer	0
Single ulceration not exceeding the lamina muscularis mucosa	1
Ulcerations not exceeding the mucosa	2
Ulcerations exceeding the submucosa	3
B	
No submucosal edema	0
Mild edema	1
Moderate edema	2
Severe edema	3
C	
No inflammatory cell infiltration	0
Mild infiltration	1
Moderate infiltration	2
Dense infiltration	3

The presence of ulcers (A), the severity of edema in the submucosal layer (B), and the degree of inflammatory cell infiltration (C) were assessed by histological analysis.

Table 3 Characteristics of primary and secondary antibodies

Antigen	Host	Dilution	Source
Calretinin	Goat	1:300	Swant
P2X7 receptor	Rabbit	1:200	Merck Millipore
Cleaved caspase-3	Rabbit	1:100	Cell Signaling
Total caspase-3	Rabbit	1:100	Cell Signaling
Phospho- NF-κB	Rabbit	1:100	Cell Signaling
Total NF-κB (p65)	Rabbit	1:100	Cell Signaling
Secondary antibodies			
Alexa Fluor 488-conjugated donkey anti-rabbit IgG	Donkey	1:500	Molecular Probes
Alexa Fluor 594-conjugated donkey anti-sheep IgG	Donkey	1:100	Molecular Probes

NF-κB: Nuclear factor kappa B.

For corrected total cell fluorescence (CTCF) analysis, 20 calretinin-ir, P2X7 receptor-ir, cleaved caspase-3-ir, total caspase-3-ir, phospho- NF-κB-ir, and total NF-κB-ir ganglia of the myenteric plexus of the distal colon of each animal were photographed at 40 × magnification under a Nikon 80i microscope *via* NIS-elements AR 3.1 software. The ganglia were individually manually delineated in ImageJ software (v1.45, NIH). The area, integrated density, and average gray value of each ganglion were systematically measured. The areas, integrated densities, and average gray values of five regions adjacent to the myenteric ganglion that were not positive for the protein of interest were measured as background values. The CTCF was calculated by the following formula: CTCF = integrated density-(area of the selected ganglion × average background fluorescence)[68,69]. In total, 800 myenteric ganglia were analyzed for each protein of interest.

Transmission electron microscopy

An approximately 0.5 cm piece of the distal colon of each mouse was collected for ultrastructural analysis of the myenteric plexus by transmission electron microscopy. Immediately after collection, the samples were cut into three-millimeter pieces. The samples were fixed for three hours at 4 °C in modified Karnovsky solution (4.0% formaldehyde, 0.2 M phosphate buffer and 25% glutaraldehyde) and postfixed for two hours at 4 °C in 1% osmium tetroxide. Then, the tissues were placed in 0.5% uranyl acetate for 12 h at room temperature, dehydrated by sequential incubations in alcohol solutions of increasing concentrations, and immersed in propylene oxide twice for 15 min each. Finally, the tissues were incubated in a 1:1 mixture of Spurr resin and propylene oxide for one hour, a 3:1 mixture of Spurr resin and propylene oxide for one and a half hours, and pure resin for 12 h. The tissues were then embedded in pure Spurr resin for three days in an oven at 60 °C. Semifine 250 nanometer (nm)-thick semithin sections were made with a Leica Ultracut UCT ultramicrotome, and the sections were stained with 1% toluidine blue for one and a half minutes and then washed with distilled water. Then, the sections were cut into 60 nm thick ultrathin sections, collected on 200 mesh copper screens and contrasted with uranyl acetate for five minutes and lead citrate 1% for three minutes. The prepared screens were analyzed with a Morgagni 268D transmission electron microscope, and the captured images were processed with CorelDRAW software.

Tissue preparation and histological analysis

An approximately 0.5 cm piece of the distal colon of each mouse was collected for histological analysis. After being washed in PBS, the samples were fixed with the mucosa facing up on wooden platforms and immersed in 4% paraformaldehyde in 0.1 M PBS (pH 7.3) for 48 h at 4 °C. Then, the tissues were dehydrated by sequential incubation in alcohol solutions of increasing concentrations, diaphanized in xylol, and embedded in paraffin. The samples were cut into five μm thick transverse sections with a specialized microtome and subjected to hematoxylin and eosin staining. Picrosirius red and Masson's trichrome were used to visualize collagen fibers, and periodic acid-Schiff staining was used to identify neutral mucin-secreting goblet cells. The slides were analyzed under light and polarized light microscopy with a Nikon 80i microscope. Images were captured *via* NIS-elements AR 3.1 software and processed with CorelDRAW software.

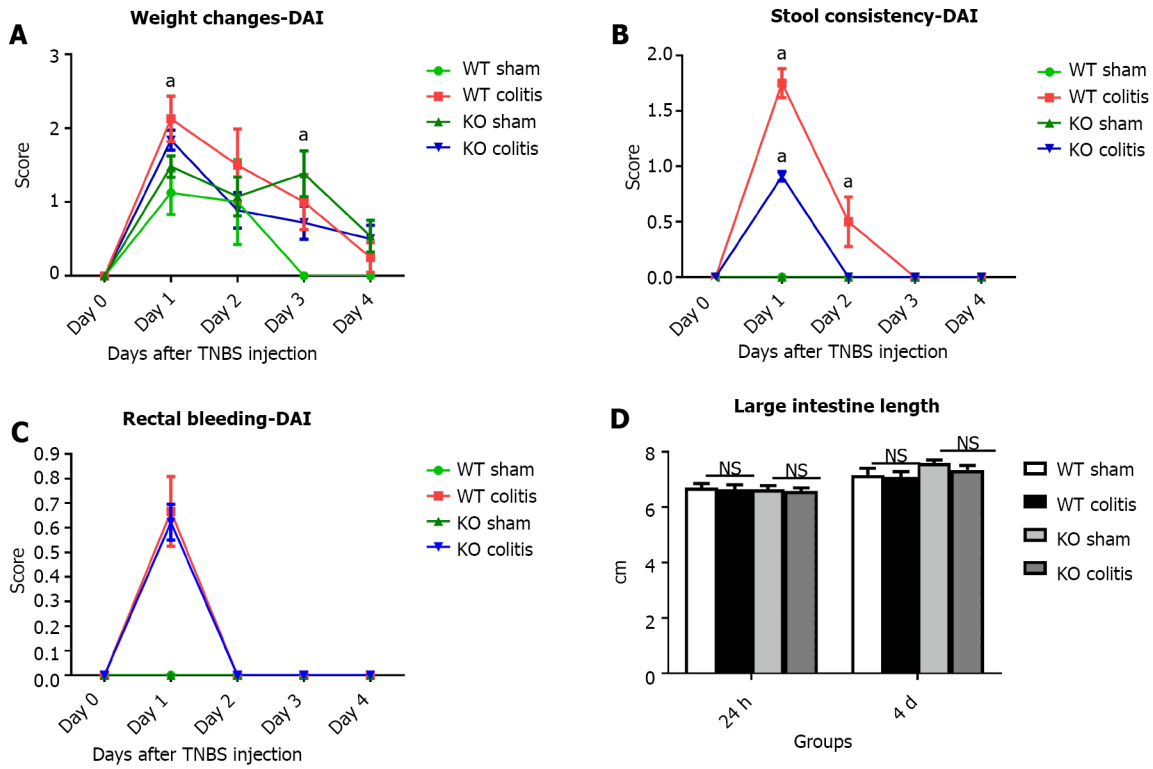
Analysis of the number of goblet cells per intestinal crypt of the distal colon: The density of goblet cells (number of goblet cells per intestinal crypt) was determined by counting goblet cells in 40 intestinal crypts of the distal colon *via* periodic acid Schiff staining. Four histological sections per animal were analyzed with a Nikon 80i microscope with a 40 × objective[70-73]. Sections separated by an interval of 10 μm were analyzed, and crypts were chosen randomly. In total, 1600 crypts of the distal colon were analyzed.

Statistical analysis

Quantitative data were analyzed, and the results are expressed as the mean ± SE. Comparisons between groups were performed by two-way ANOVA followed by Bonferroni correction with GraphPad Prism 5.0 software. Statistical significance is displayed as $P < 0.05$.

RESULTS

At 24 h, the average reduction in weight was 1.5% in the WT sham group, 3.5% in the WT colitis group, 2.4% in the KO sham group, and 2.7% in the KO colitis group. By four days, the animals in all groups recovered weight. Regarding the DAI, scores for weight change, stool consistency, and the presence of blood in stool were higher in the WT colitis group than in the WT sham group and in the KO colitis group than in the KO sham group. There was no statistically significant difference in large intestine length between the WT colitis (24 h and 4 d) and WT sham (24 h and 4 d) groups or between the KO colitis (24 h and 4 d) and KO sham (24 h and 4 d) groups (Figure 1). According to macroscopic analysis, tissue hyperemia without ulcers was observed in the 24 h and 4 d WT colitis and 24 h KO colitis groups. Microscopic analysis was performed after hematoxylin and eosin staining. No ulceration was observed



DOI: 10.3748/wjg.v29.i22.3440 **Copyright** ©The Author(s) 2023.

Figure 1 The disease activity index of wild-type and knockout mice was determined beginning the day of ulcerative colitis induction or intrarectal injection of 35% ethanol. A: Changes in weight; B: Stool consistency; C: The presence of blood in the stool; D: Large intestine length was analyzed. DAI: Disease activity index; WT: Wild-type; KO: Knockout; TNBS: 2,4,6-trinitrobenzene sulfonic acid. The data are presented as the arithmetic mean ± SE. $^{a}P < 0.05$ *vs* sham groups; NS: Not significant.

in the analyzed tissues. Edema of the submucosal layer was observed in all groups, but with the mean score, edema was higher in the WT colitis 24 h group. Finally, inflammatory cell infiltration in the mucosa and lamina propria was severe in the WT colitis 24 h group but was mild in the other groups (Table 4).

Qualitative analysis

Indirect immunofluorescence analysis revealed that neurons in the myenteric plexus of the distal colon were positive for calretinin, P2X7 receptor, cleaved caspase-3, total caspase-3, phospho-NF-κB, and total NF-κB.

Calretinin-ir neurons showed a Dogiel type II morphology, and calretinin was localized in the nucleus and cytoplasm. In the WT colitis 24 h and 4 d groups, there was an apparent reduction in fluorescence intensity, and in the WT colitis 24 h and KO colitis 24 h groups, the neurons appeared swollen. There was also an apparent reduction in the number of neurons in the WT colitis 24 h and 4 d and KO colitis 24 h groups (Figures 2-6).

The P2X7 receptor was expressed in the plasma membrane and cytoplasm. The P2X7 receptor staining intensity appeared to be stronger in the WT colitis 24 h group and weaker in the WT colitis 4 d group. There was an apparent reduction in the number of P2X7 receptor-ir cells in both groups, and the P2X7 receptor-ir cells colocalized with calretinin-ir neurons. P2X7 receptor staining was not observed in the KO sham 24 h, KO sham 4 d, KO colitis 24 h or KO colitis 4 d groups (Figure 2).

Cleaved caspase-3 was localized in the cytoplasm, and the cleaved caspase-3 fluorescence intensity was apparently higher in the WT colitis 24 h and 4 d groups and KO colitis 24 h group. Cleaved caspase-3 colocalized with calretinin-ir neurons in all groups, especially the colitis groups (WT colitis 24 h and 4 d and KO colitis 24 h and 4 d groups) (Figure 3). Total caspase-3, on the other hand, was expressed in the nucleus and cytoplasm, and the total caspase-3 fluorescence intensity was apparently similar among all groups. Total caspase-3 colocalized with calretinin-ir neurons, and nuclear staining of total caspase-3 was the lowest in the WT colitis 24 h group (Figure 4).

Phospho-NF-κB and total NF-κB were expressed in the cytoplasm. Phospho-NF-κB staining appeared to be more intense in the WT colitis 24 h group (Figure 5). Phospho- NF-κB and total NF-κB colocalized with calretinin-ir neurons in all groups (Figure 6).

Table 4 Macroscopic and microscopic lesions in the distal colon of ulcerative colitis model mice and mice that received intrarectal injection of 35% ethanol

Groups	Macroscopic injury	Microscopic injury		
		Ulcer	Submucosal edema	Inflammatory cell infiltration
WT sham 24 h	0.0 ± 0.0^{NS}	0.0 ± 0.0^{NS}	0.8 ± 0.2^{NS}	1.2 ± 0.2^{NS}
WT colitis 24 h	1.0 ± 0.0^{NS}	0.0 ± 0.0^{NS}	1.6 ± 0.2^{NS}	2.0 ± 0.2^{NS}
KO sham 24 h	0.0 ± 0.0^{NS}	0.0 ± 0.0^{NS}	0.8 ± 0.2^{NS}	1.0 ± 0.0^{NS}
KO colitis 24 h	0.4 ± 0.1^{NS}	0.0 ± 0.0^{NS}	0.8 ± 0.4^{NS}	1.2 ± 0.2^{NS}
WT sham 4 d	0.0 ± 0.0^{NS}	0.0 ± 0.0^{NS}	1.0 ± 0.2^{NS}	1.0 ± 0.0^{NS}
WT colitis 4 d	0.5 ± 0.2^{NS}	0.0 ± 0.0^{NS}	1.0 ± 0.0^{NS}	1.2 ± 0.2^{NS}
KO sham 4 d	0.0 ± 0.0^{NS}	0.0 ± 0.0^{NS}	0.6 ± 0.2^{NS}	0.4 ± 0.2^{NS}
KO colitis 4 d	0.0 ± 0.0^{NS}	0.0 ± 0.0^{NS}	0.8 ± 0.2^{NS}	0.4 ± 0.2^{NS}

The presence of ulcers, severity of edema in the submucosal layer, and degree of inflammatory cell infiltration were assessed by histological analysis. NS: Not significant; WT: Wild-type; KO: Knockout.

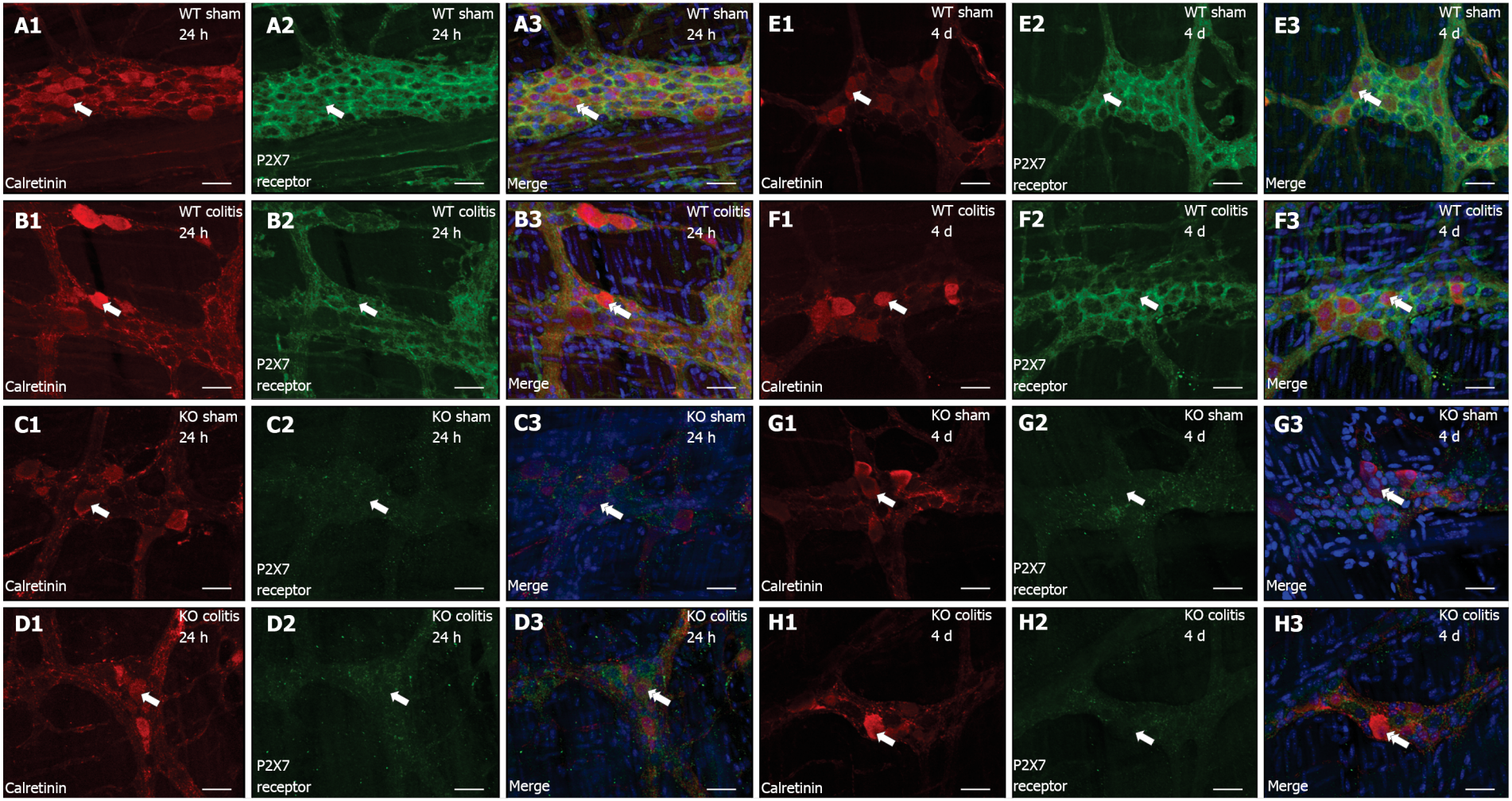
Quantitative analyses

The number of calretinin-ir neurons per myenteric ganglion of the distal colon was decreased by 36.9% in the WT colitis 24 h group compared to the WT sham 24 h group (2.1 ± 0.13 *vs* 3.33 ± 0.17, $P < 0.001$) and decreased by 21.1% in the WT colitis 4 d group compared to the WT sham 4 d group (2.92 ± 0.12 *vs* 3.7 ± 0.11, $P < 0.05$). No statistically significant differences in calretinin-ir neuron density were observed between the KO colitis (24 h and 4 d) groups and the KO sham (24 h and 4 d) groups (Figure 7A).

The number of P2X7-ir receptor neurons per myenteric ganglion of the distal colon was decreased by 12.2% in the WT colitis 24 h group compared to the WT sham 24 h group (19.49 ± 0.35 *vs* 22.21 ± 0.18, $P < 0.001$) and decreased by 10.5% in the WT colitis 4 d group compared to the WT sham 4 d group (20.35 ± 0.14 *vs* 22.75 ± 0.51, $P < 0.001$). No P2X7 receptor-ir neurons were observed in the myenteric ganglia in the KO sham (24 h and 4 d) or KO colitis (24 h and 4 d) groups (Figure 7B).

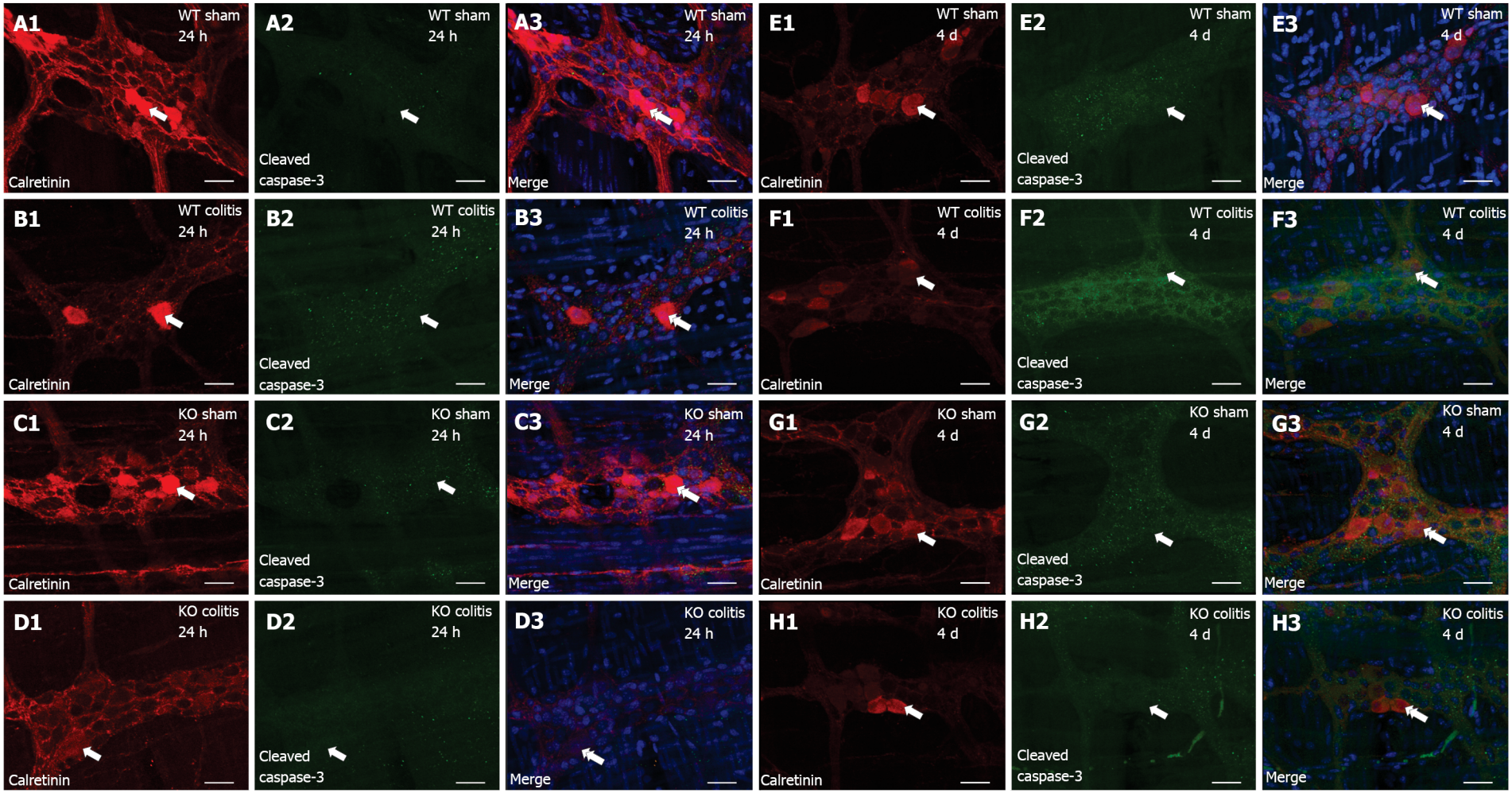
The profile area of calretinin-ir neurons in the myenteric plexus of the distal colon was increased by 10.9% in the WT colitis 24 h group compared to the WT sham 24 h group (312.6 ± 7.85 *vs* 278.41 ± 6.65, $P < 0.05$) and increased by 14.6% in the KO colitis 24 h group compared to the KO sham 24 h group (302.99 ± 16.78 *vs* 258.67 ± 9.49, $P < 0.01$). The neuronal profile area was decreased by 16.4% in the WT colitis 4 d group compared to the WT sham 4 d group (277.23 ± 9.94 *vs* 331.54 ± 7.63, $P < 0.001$), and there was no difference in this measure between the KO colitis 4 d and KO sham 4 d groups (Figure 8A). The nuclear profile area in the WT colitis 4 d group was decreased by 10.9% compared to that in the WT sham 4 d group (104.63 ± 2.49 *vs* 117.41 ± 1.14, $P < 0.01$). No statistically significant differences in nuclear profile area were observed between the KO colitis (24 h and 4 d) groups and the KO sham (24 h and 4 d) groups (Figure 8B). The cytoplasmic profile area of calretinin-ir neurons in the myenteric plexus of the distal colon was increased by 15% in the WT colitis 24 h group compared to the WT sham 24 h group (195.86 ± 6.88 *vs* 166.37 ± 5.98, $P < 0.05$) and increased by 20.4% in the KO colitis 24 h group compared to the KO sham 24 h group (178.88 ± 15.52 *vs* 142.41 ± 8.62, $P < 0.05$). The cytoplasmic profile area in the WT colitis 4 d group was decreased by 19.4% compared with that in the WT sham 4 d group (172.61 ± 10.4 *vs* 214.13 ± 6.73, $P < 0.01$). No statistically significant difference in the cytoplasmic profile area was observed between the KO colitis 4 d group and the KO sham 4 d group (Figure 8C).

The profile area of calretinin-ir neurons in the myenteric plexus of the distal colon ranged from 50 μm^2 to 1050 μm^2. In the WT sham 24 h, WT colitis 24 h and KO colitis 24 h groups, 54.4%, 48.0%, and 59.5% of calretinin-ir neurons, respectively, had an area between 200 μm^2 and 300 μm^2. In the KO sham 24 h group, 58.5% of neurons had an area between 100 μm^2 and 200 μm^2 (Figure 9A). In the WT sham 4 d, WT colitis 4 d, KO sham 4 d and KO colitis 4 d groups, 58.1%, 65.6%, 62.7% and 60.6% of calretinin-ir neurons, respectively, had an area between 200 μm^2 and 300 μm^2 (Figure 9B). The nuclear profile area of these same calretinin-ir neurons ranged from 50 μm^2 to 230 μm^2. In the WT sham 24 h and KO sham 24 h groups, 57.9% and 52.6% of calretinin-ir neurons, respectively, had a nuclear area between 90 μm^2 and 110 μm^2. In the WT colitis 24 h and KO colitis 24 h groups, 62.4% and 55.5% of calretinin-ir neurons, respectively, had a nuclear area between 110 μm^2 and 130 μm^2 (Figure 9C). In the WT colitis 4 d group, 63.5% of calretinin-ir neurons had a nuclear area between 90 μm^2 and 110 μm^2, and in the WT sham 4 d, KO sham 4 d and KO colitis 4 d groups, 62.4%, 52.6% and 55% of calretinin-ir neurons, respectively, had a nuclear area between 110 μm^2 and 130 μm^2 (Figure 9D). Finally, the cytoplasmic profile area of these same calretinin-ir neurons ranged from 0 μm^2 to 840 μm^2. In the WT sham 24 h and WT colitis 24 h groups, 55.3% and 50.2% of calretinin-ir neurons, respectively, had a cytoplasmic area between 130 μm^2



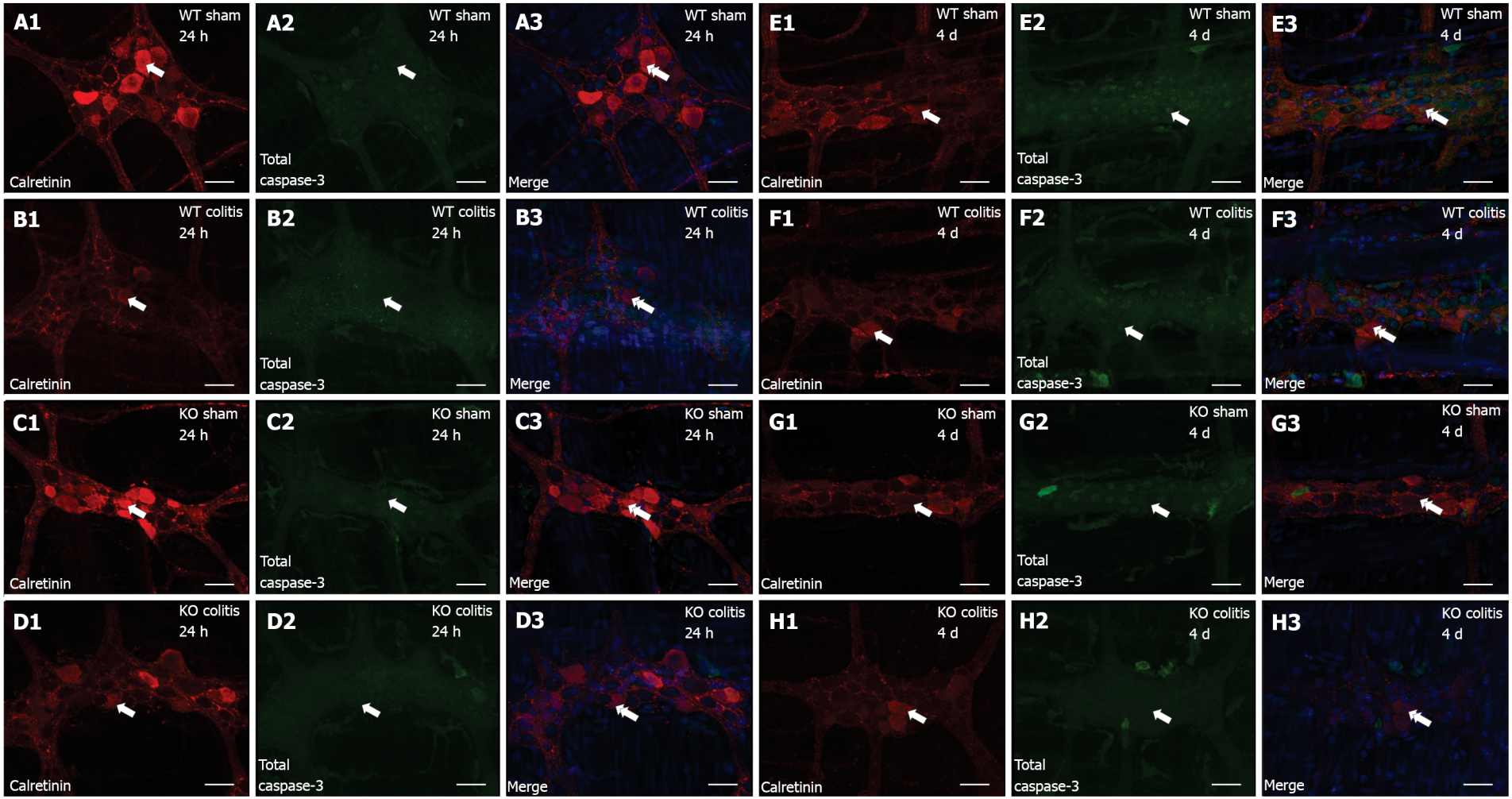
DOI: 10.3748/wjg.v29.i22.3440 **Copyright** ©The Author(s) 2023.

Figure 2 Colocalization of calretinin (red) with the P2X7 receptor (green) and DAPI (blue) in neurons in the myenteric plexus of the distal colon in mice. A1-A3: Wild-type (WT) sham 24 h; B1-B3: WT colitis 24 h; C1-C3: Knockout (KO) sham 24 h; D1-D3: KO colitis 24 h; E1-E3: WT sham 4 d; F1-F3: WT colitis 4 d; G1-G3: KO sham 4 d; H1-H3: KO colitis 4 d groups. The single arrows indicate calretinin-ir (A1-H1) and P2X7 receptor-ir (A2-H2) neurons, and the double arrows indicate the colocalization of calretinin with the P2X7 receptor and DAPI (A3-H3). Scale bar = 30 μm. WT: Wild-type; KO: Knockout.



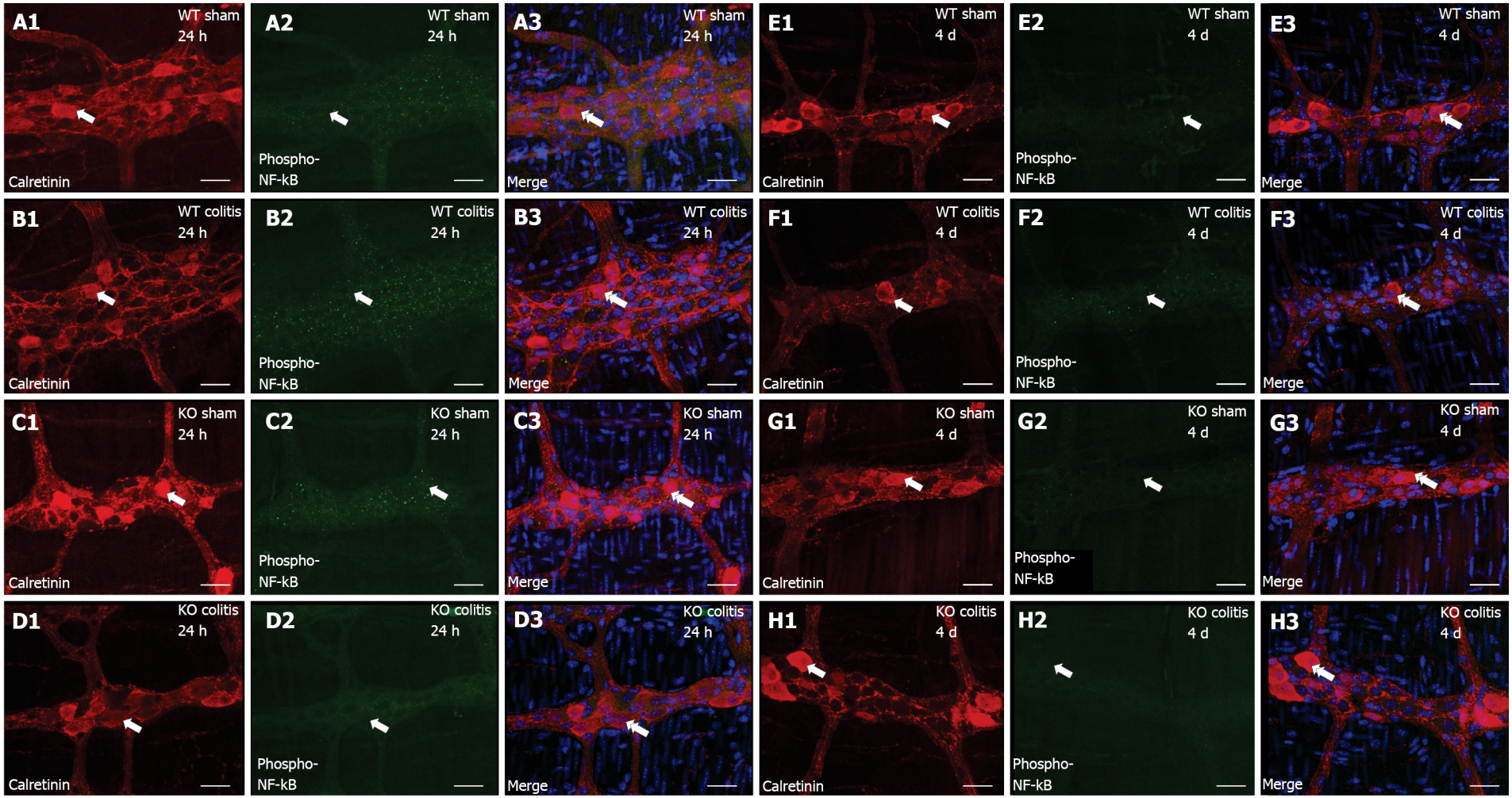
DOI: 10.3748/wjg.v29.i22.3440 **Copyright** ©The Author(s) 2023.

Figure 3 Colocalization of calretinin (red) with cleaved caspase-3 (green) and DAPI (blue) in neurons in the myenteric plexus of the distal colon in mice of different groups. A1-A3: Wild-type (WT) sham 24 h; B1-B3: WT colitis 24 h; C1-C3: Knockout (KO) sham 24 h; D1-D3: KO colitis 24 h; E1-E3: WT sham 4 d; F1-F3: WT colitis 4 d; G1-G3: KO sham 4 d; and H1-H3: KO colitis 4 d groups. The single arrows indicate calretinin-ir (A1-H1) and cleaved caspase-3-ir (A2-H2) neurons, and the double arrows indicate the colocalization of calretinin with cleaved caspase-3 and DAPI (A3-H3). Scale bar = 30 μm. WT: Wild-type; KO: Knockout.



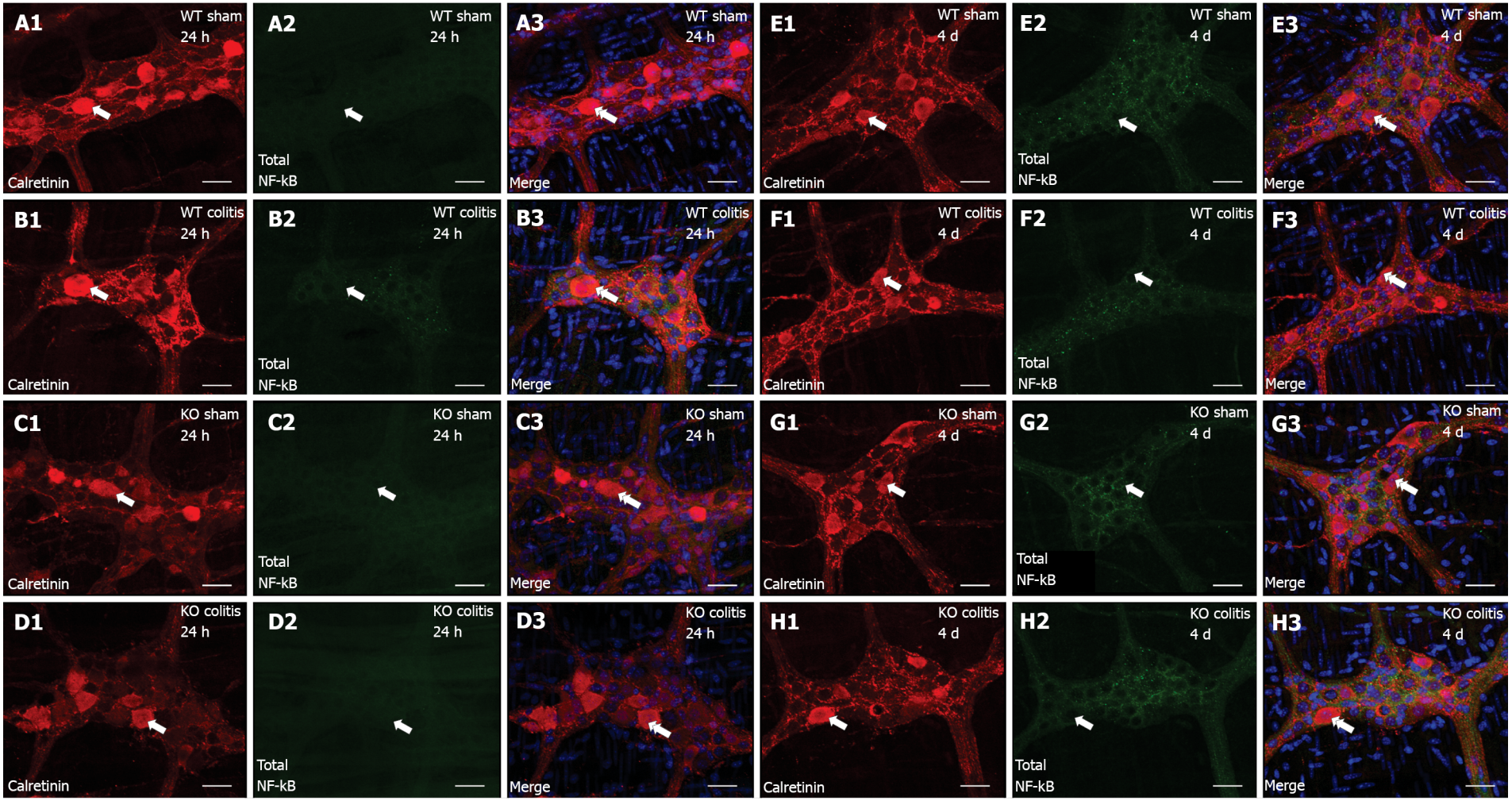
DOI: 10.3748/wjg.v29.i22.3440 **Copyright** ©The Author(s) 2023.

Figure 4 Colocalization of calretinin (red) with total caspase-3 (green) and DAPI (blue) in neurons in the myenteric plexus of the distal colon in mice of different groups. A1-A3: Wild-type (WT) sham 24 h; B1-B3: WT colitis 24 h; C1-C3: Knockout (KO) sham 24 h; D1-D3: KO colitis 24 h; E1-E3: WT sham 4 d; F1-F3: WT colitis 4 d; G1-G3: KO sham 4 d; and H1-H3: KO colitis 4 d groups. The single arrows indicate calretinin-ir (A1-H1) and total caspase-3-ir (A2-H2) neurons, and the double arrows indicate the colocalization of calretinin with total caspase-3 and DAPI (A3-H3). Scale bar = 30 μm. WT: Wild-type; KO: Knockout.



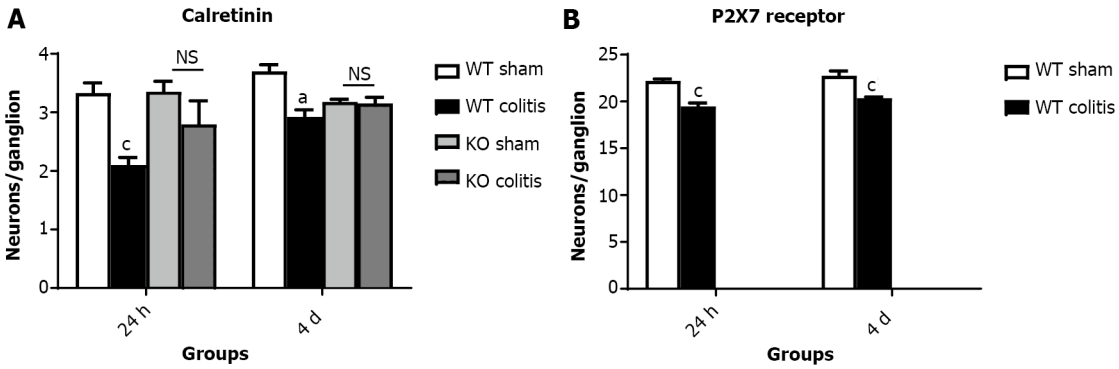
DOI: 10.3748/wjg.v29.i22.3440 **Copyright** ©The Author(s) 2023.

Figure 5 Colocalization of calretinin (red) with phospho-nuclear factor kappa B (green) and DAPI (blue) in neurons in the myenteric plexus of the distal colon in mice of different groups. A1-A3: Wild-type (WT) sham 24 h; B1-B3: WT colitis 24 h; C1-C3: Knockout (KO) sham 24 h; D1-D3: KO colitis 24 h; E1-E3: WT sham 4 d; F1-F3: WT colitis 4 d; G1-G3: KO sham 4 d; and H1-H3: KO colitis 4 d groups. The single arrows indicate calretinin-ir (A1-H1) and phospho-nuclear factor kappa B (NF-κB)-ir (A2-H2) neurons, and the double arrows indicate the colocalization of calretinin with phospho- NF-κB and DAPI (A3-H3). Scale bar = 30 μm. WT: Wild-type; KO: Knockout.



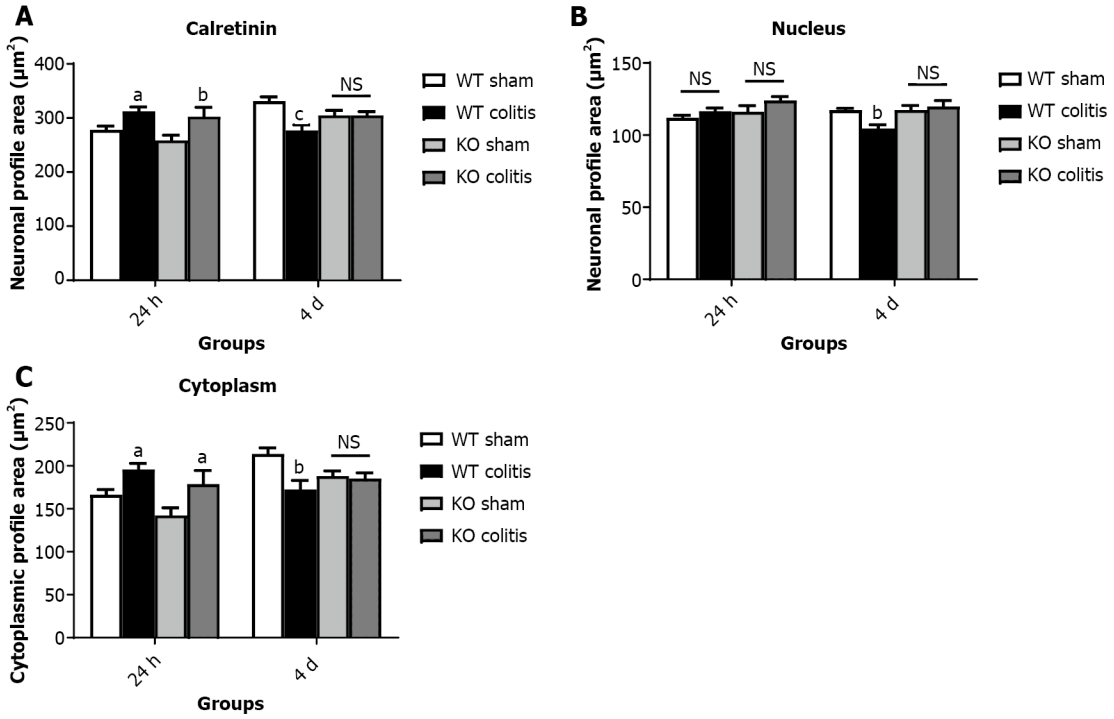
DOI: 10.3748/wjg.v29.i22.3440 **Copyright** ©The Author(s) 2023.

Figure 6 Colocalization of calretinin (red) with total nuclear factor kappa B (green) and DAPI (blue) in neurons in the myenteric plexus of the distal colon in mice of different groups. A1-A3: Wild-type (WT) sham 24 h; B1-B3: WT colitis 24 h; C1-C3: Knockout (KO) sham 24 h; D1-D3: KO colitis 24 h; E1-E3: WT sham 4 d; F1-F3: WT colitis 4 d; G1-G3: KO sham 4 d; and H1-H3: KO colitis 4 d groups. The single arrows indicate calretinin-ir (A1-H1) and total nuclear factor kappa B (NF-κB)-ir (A2-H2) neurons, and the double arrows indicate the colocalization of calretinin with total NF-κB and DAPI (A3-H3). Scale bar = 30 μm. WT: Wild-type; KO: Knockout.



DOI: 10.3748/wjg.v29.i22.3440 **Copyright** ©The Author(s) 2023.

Figure 7 Number of calretinin-ir and P2X7 receptor-ir neurons per myenteric ganglion in the distal colon in mice from the wild-type sham 24 h and 4 d, wild-type colitis 24 h and 4 d, knockout sham 24 h and 4 d, and knockout colitis 24 h and 4 d groups. A: Calretinin-ir; B: P2X7 receptor-ir. The data are presented as the arithmetic mean ± SE. [a]*P* < 0.05 *vs* sham groups; [c]*P* < 0.001 *vs* sham groups; NS: Not significant. WT: Wild-type; KO: Knockout.

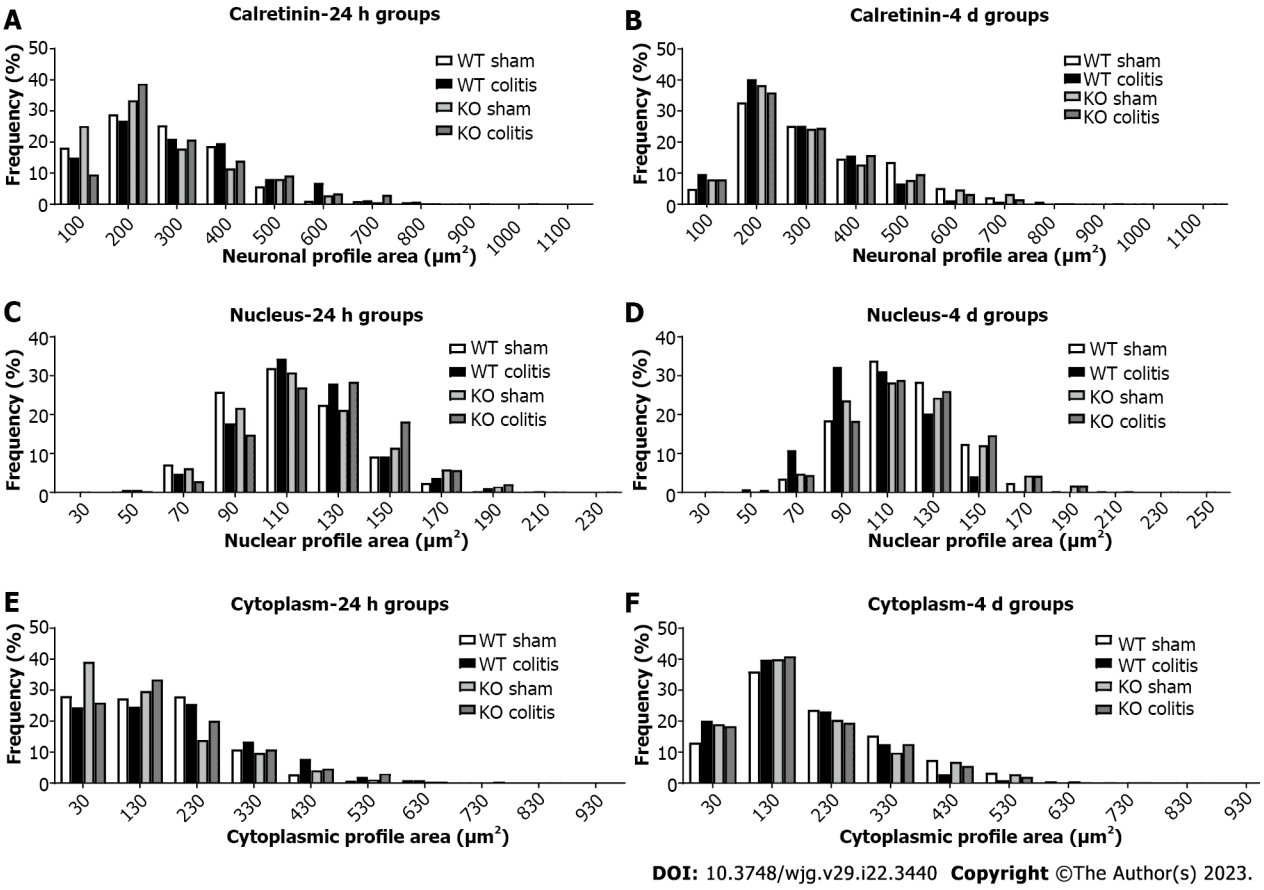


DOI: 10.3748/wjg.v29.i22.3440 **Copyright** ©The Author(s) 2023.

Figure 8 Neuronal, nuclear, and cytoplasmic profile areas of calretinin-ir neurons in the myenteric plexus of the distal colon in mice from the wild-type sham 24 h and 4 d, wild-type colitis 24 h and 4 d, knockout sham 24 h and 4 d, and knockout colitis 24 h and 4 d groups. A: Neuronal; B: Nuclear; C: Cytoplasmic. The data are presented as the arithmetic mean ± SE. [a]*P* < 0.05 *vs* sham groups; [b]*P* < 0.01 *vs* sham groups; [c]*P* < 0.001 *vs* sham groups; NS: Not significant. WT: Wild-type; KO: Knockout.

and 230 μm². In the KO sham 24 h and KO colitis 24 h groups, 69% and 59.3% of calretinin-ir neurons, respectively, had a cytoplasmic area between 30 μm² and 130 μm² (Figure 9E). In the WT sham 4 d, WT colitis 4 d, KO sham 4 d and KO colitis 4 d groups, 59.7%, 63%, 60.5% and 60.5% of calretinin-ir neurons, respectively, had a cytoplasmic area between 130 μm² and 230 μm² (Figure 9F).

The CTCF of calretinin-ir ganglia in the myenteric plexus of the distal colon was decreased by 24.5% in the WT colitis 24 h group compared to the WT sham 24 h group (2322102 ± 154255 *vs* 3076921 ± 104235, $P < 0.001$) and was decreased by 13.7% in the WT colitis 4 d group compared to the WT sham 4 d group (2976603 ± 52989 *vs* 3452123 ± 30894, $P < 0.01$). No statistically significant differences in the CTCF of calretinin-ir myenteric ganglia were observed between the KO colitis (24 h and 4 d) groups and the KO sham (24 h and 4 d) groups (Figure 10A).



DOI: 10.3748/wjg.v29.i22.3440 **Copyright** ©The Author(s) 2023.

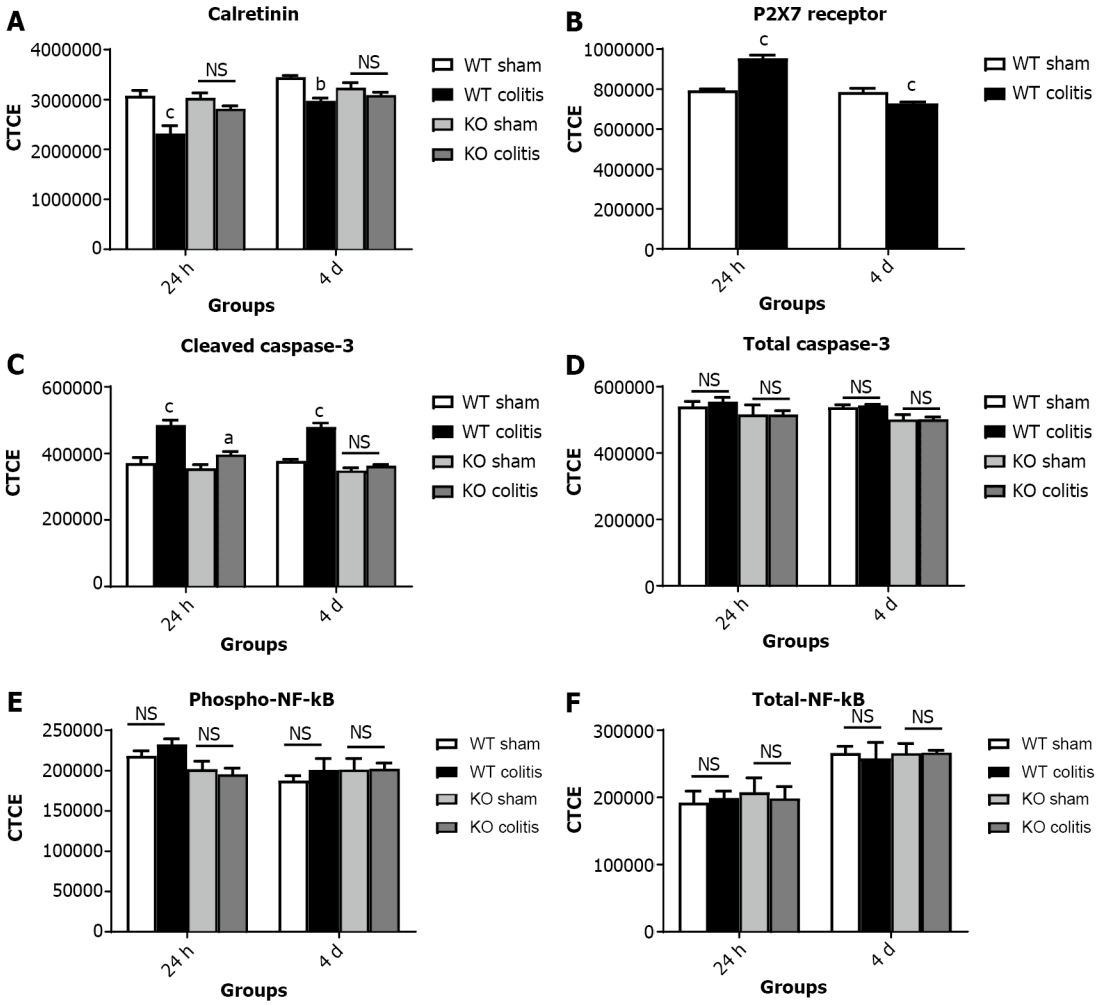
Figure 9 Distribution frequency (%) of the profile areas. A and B: Calretinin-ir neurons; C and D: Calretinin-ir nucleus; E and F: Calretinin-ir cytoplasm in the myenteric plexus of the distal colon in mice from the wild-type (WT) sham 24 h and 4 d, WT colitis 24 h and 4 d, knockout (KO) sham 24 h and 4 d, and KO colitis 24 h and 4 d groups. WT: Wild-type; KO: Knockout.

The CTCF of P2X7 receptor-ir ganglia in the myenteric plexus of the distal colon was increased by 16.8% in the WT colitis 24 h group compared to the WT sham 24 h group (953784 ± 15825 *vs* 793451 ± 6809, $P < 0.001$) and decreased by 7.2% in the WT colitis 4 d group compared to the WT sham 4 d group (728412 ± 6295 *vs* 785419 ± 18143, $P < 0.01$). P2X7 receptor expression was not observed in the myenteric ganglia in the KO sham (24 h and 4 d) and KO colitis (24 h and 4 d) groups (Figure 10B).

The CTCF of cleaved caspase-3-ir ganglia in the myenteric plexus of the distal colon was increased by 23.6% in the WT colitis 24 h group compared to the WT sham 24 h group (485949 ± 14140 *vs* 371371 ± 16426, $P < 0.001$) and increased by 10.5% in the KO colitis 24 h group compared to the KO sham 24 h group (396888 ± 8737 *vs* 355154 ± 11060, $P < 0.05$). The CTCF of cleaved caspase-3-ir myenteric ganglia was increased by 21.2% in the WT colitis 4 d group compared to the WT sham 4 d group (480381 ± 11336 *vs* 378365 ± 4053, $P < 0.001$). No statistically significant difference in the CTCF of cleaved caspase-3-ir myenteric ganglia was observed between the KO colitis 4 d group and the KO sham 4 d group (Figure 10C). In addition, no statistically significant difference in the CTCF of total caspase-3-ir (Figure 10D), phospho-NF-κB-ir (Figure 10E) and total NF-κB-ir (Figure 10F) ganglia was observed between the WT colitis (24 h and 4 d) and WT sham (24 h and 4 d) groups or between the KO colitis (24 h and 4 d) and KO sham (24 h and 4 d) groups.

Transmission electron microscopy

Transmission electron microscopy was used to assess the ultrastructural morphology of the myenteric plexus of the distal colon in mice from all groups. Myenteric neurons, neuronal nuclei and organelles, and the interaction between neurons and enteric glial cells were visualized. In the WT colitis 24 h and KO colitis 24 h groups, neurons with a necrotic phenotype characterized mainly by nuclear disruption and apparent nuclear autolysis, chromatin fragmentation and condensation, and cytoplasmic disorganization were observed. Enteric glial cells also showed morphological changes similar to those of neurons. In the WT colitis 4 d group and less frequently in the KO colitis 4 d group, neurons showed irregular nuclei and nuclear membrane invaginations. The cell membrane remained intact, and apoptotic bodies were sometimes observed. Enteric glial cells also showed features consistent with apoptosis. In the WT sham (24 h and 4 d) and KO sham (24 h and 4 d) groups, neurons showed large and round/oval nuclei and no sign of structural disruption in the cytoplasm (Figure 11).



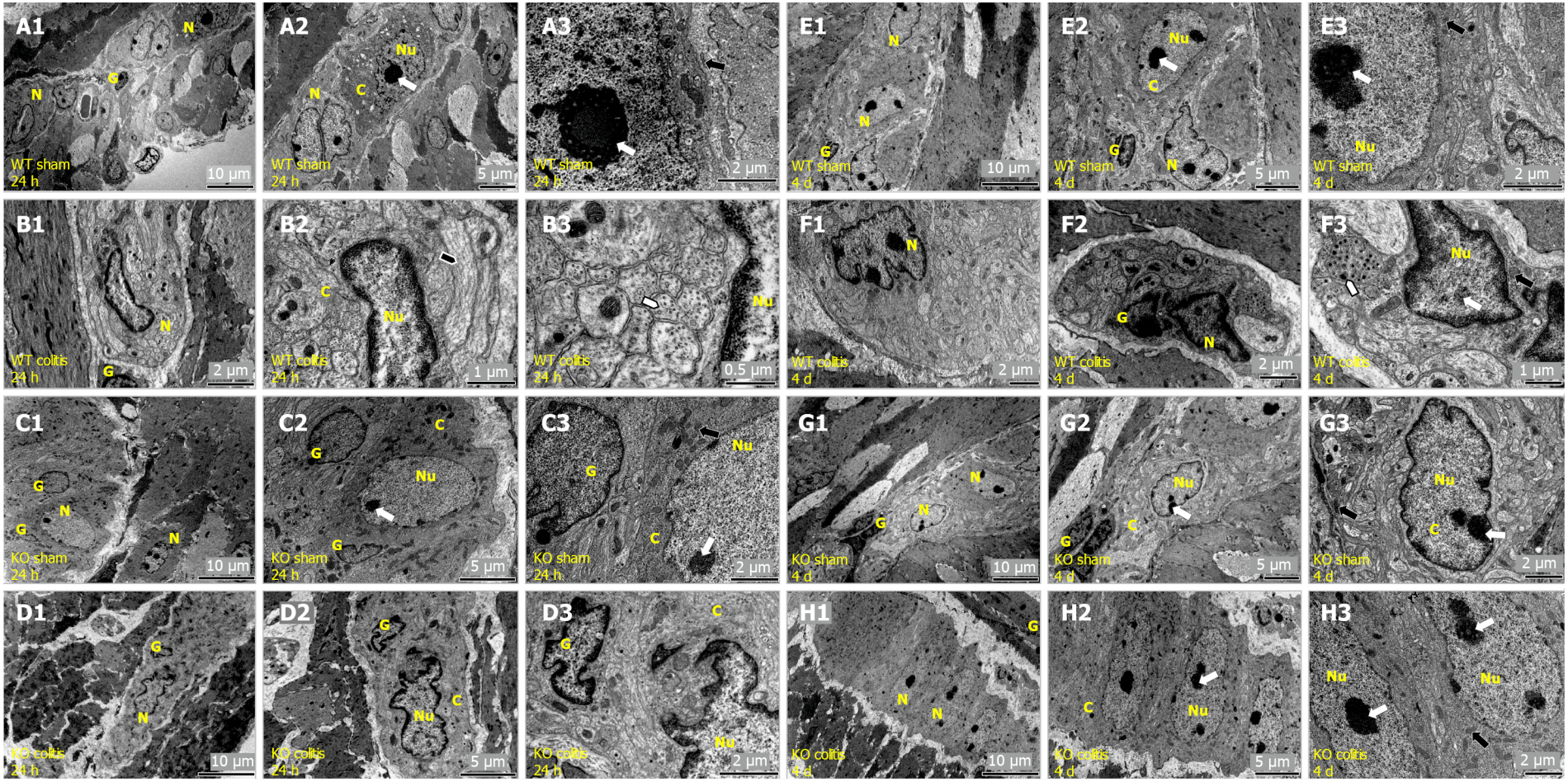
DOI: 10.3748/wjg.v29.i22.3440 **Copyright** ©The Author(s) 2023.

Figure 10 Corrected total cell fluorescence of myenteric neurons. A: calretinin; B: P2X7 receptor; C: Cleaved caspase-3; D: Total caspase-3; E: Phospho-nuclear factor kappa B (NF-κB); F: Total NF-κB in the myenteric plexus of the distal colon in mice from the WT sham 24 h and 4 d, wild-type (WT) colitis 24 h and 4 d, knockout (KO) sham 24 h and 4 d, and KO colitis 24 h and 4 d groups. The data are presented as the arithmetic mean ± SE. [a]*P* < 0.05 *vs* sham groups; [b]*P* < 0.01 *vs* sham groups; [c]*P* < 0.001 *vs* sham groups; NS: Not significant. WT: Wild-type; KO: Knockout; NF-κB: Nuclear factor kappa B.

Histology

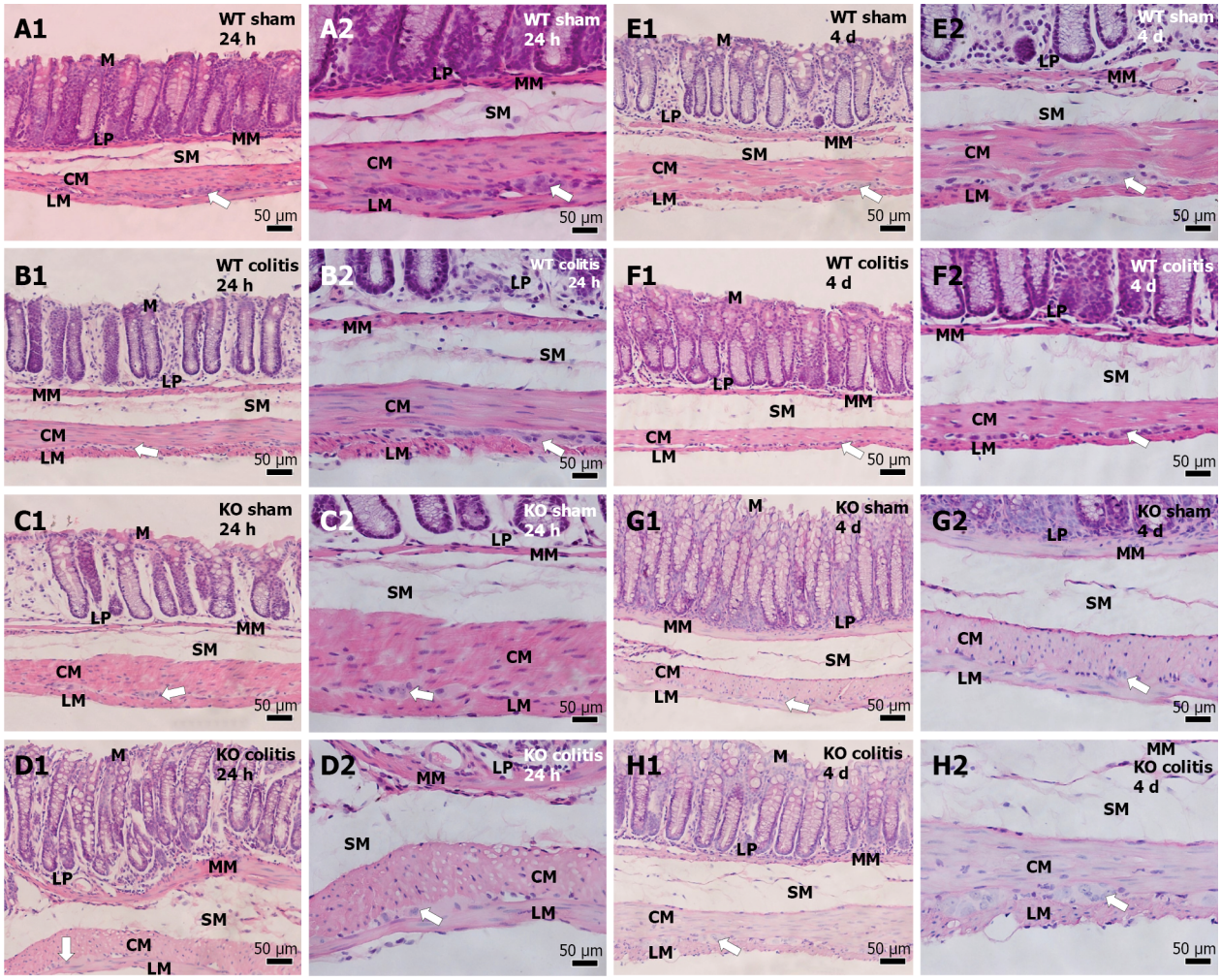
Distal colon morphology was evaluated by hematoxylin and eosin staining. In the WT sham 24 h, KO sham 24 h, WT sham 4 d, and KO sham 4 d groups, the mucosa and submucosal layers, the intestinal crypts, the lamina propria, and the longitudinal and circular muscles were intact. In the WT colitis 24 h group, tissue damage characterized by cellular disruption in the mucosal layer and thickening of the lamina propria was noted. Increased infiltration of inflammatory cells in the lamina propria and evident edema in the submucosal layer were also observed. Furthermore, the distal colon architecture was better preserved, and there were fewer inflammatory cells and less severe submucosal edema in the KO colitis 24 h, WT colitis 4 d, and KO colitis 4 d groups than in the WT colitis 24 h group (Figure 12).

Picrosirius red staining revealed the presence of thick fibers (red) in the lamina propria, in the submucosal layer, intermingled with and surrounding the muscle layer, and circumscribing the myenteric ganglia, the presence of fine fibers (green under polarized light microscopy) in the lamina propria and submucosal layer, and the presence of mixed fibers (yellow under polarized light microscopy) in all regions of the intestinal tissue in the WT sham 24 h and WT sham 4 d groups. In contrast, in the WT colitis 24 h group, the number of thick collagen fibers in the submucosal layer and around the myenteric ganglia was increased, and collagen fibers were increased in number and disorganized in the lamina propria and accumulated in the subepithelial region. In the KO sham 24 h group, greater integrity and organization of collagen fibers was visualized in the submucosal layer. In the KO colitis 24 h group, there were fewer thick collagen fibers in the lamina propria and involving the myenteric ganglia and more disordered fibers in the submucosa and subepithelial region than in the corresponding sham group. The tissue in the WT colitis 4 d group was very similar to that in the WT colitis 24 h group. However, there were more thick collagen fibers around the myenteric ganglia, and they were better organized in the submucosal layer due to more discrete local edema. Tissue



DOI: 10.3748/wjg.v29.i22.3440 **Copyright** ©The Author(s) 2023.

Figure 11 Transmission electron microscopy photomicrograph showing the ultrastructural organization of the myenteric plexus of the distal colon in mice. A1-A3: Wild-type (WT) sham 24 h; B1-B3: WT colitis 24 h; C: Knockout (KO) sham 24 h; D1-D3: KO colitis 24 h; E1-E3: WT sham 4 d; F1-F3: WT colitis 4 d; G1-G3: KO sham 4 d; H1-H3: KO colitis 4 d groups. In the WT colitis 24 h and KO colitis 24 h groups, neurons with a necrotic phenotype characterized by nuclear disruption and apparent nuclear autolysis, chromatin fragmentation and condensation, and cytoplasmic disorganization were observed. Enteric glial cells also showed morphological changes. In the WT colitis 4 d group and less frequently in the KO colitis 4 d group, neurons showed irregular nuclei and nuclear membrane invaginations. The cell membrane remained intact, and apoptotic bodies were sometimes observed. Enteric glial cells also showed features consistent with cell apoptosis. In the WT sham 24 h, KO sham 24 h, WT sham 4 d and KO sham 4 d groups, neurons exhibited large and rounded/oval nuclei, and there were no signs of structural changes in the cytoplasm. N: Myenteric neuron; G: Enteric glial cells; C: Myenteric neuron cytoplasm; Nu: Myenteric neuron nucleus. Nucleolus (white arrow), mitochondria (black arrow), nuclear membrane invaginations (black arrowhead), and vesicles and microtubules (white arrowhead). WT: Wild-type; KO: Knockout.



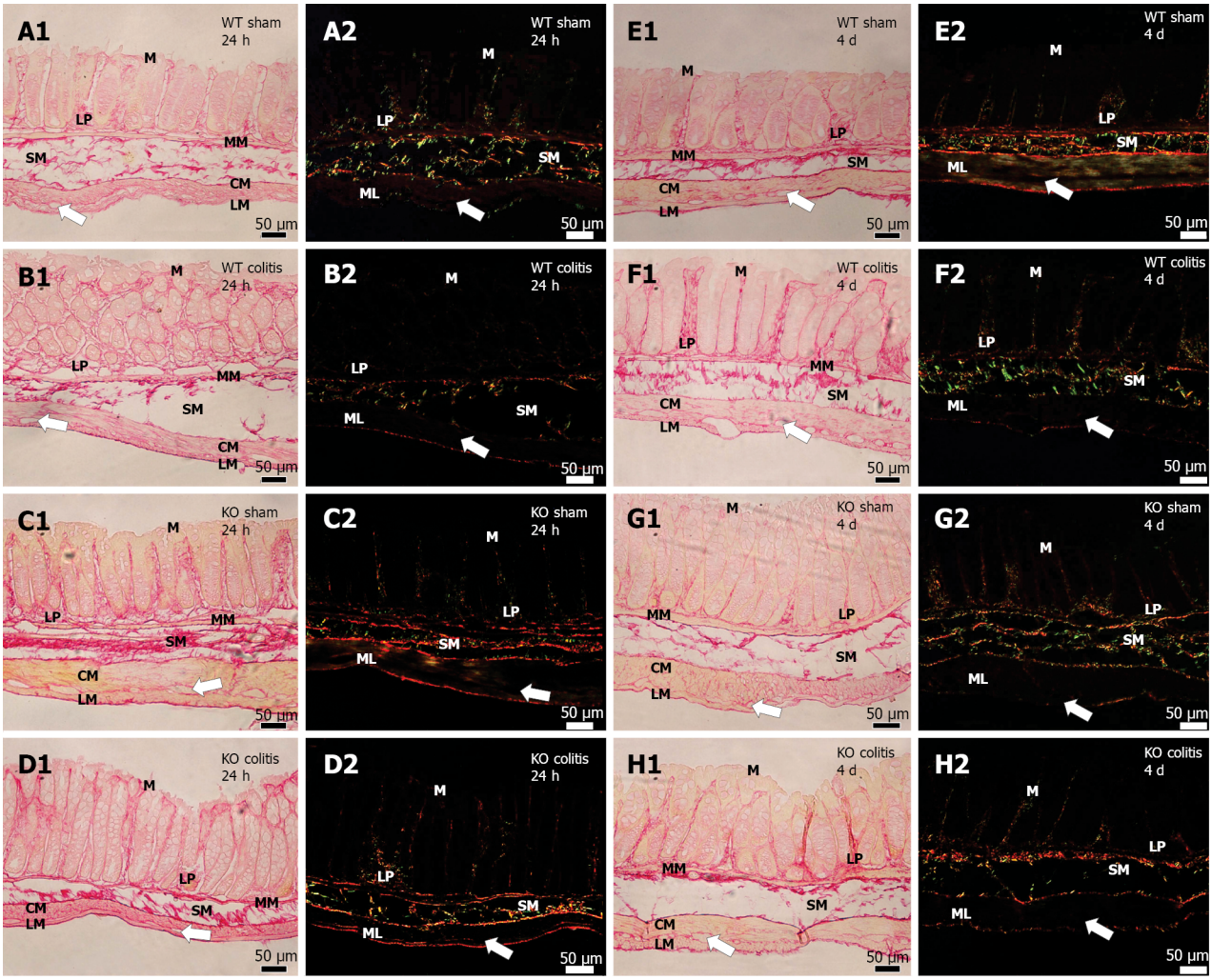
DOI: 10.3748/wjg.v29.i22.3440 **Copyright** ©The Author(s) 2023.

Figure 12 Photomicrographs of hematoxylin-eosin-stained transverse sections of the distal colons of mice of different groups. A1 and A2: Wild-type (WT) sham 24 h; B1 and B2: WT colitis 24 h; C1 and C2: Knockout (KO) sham 24 h; D1 and D2: KO colitis 24 h; E1 and E2: WT sham 4 d; F1 and F2: WT colitis 4 d; G1 and G2: KO sham 4 d; H1 and H2: KO colitis 4 d groups. Tissue integrity was maintained in the sham groups, and cellular disruption and thickening of the lamina propria and submucosal layer were observed in the WT colitis group. Tissue was better preserved, and there were fewer inflammatory cells in the KO colitis group than in the WT colitis group. M: Mucosal layer; LP: Lamina propria; MM: Mucosal muscle; SM: Submucosal layer; ML: Muscle layer; CM: Circular musculature; LM: Longitudinal musculature; WT: Wild-type; KO: Knockout. White arrows mean myenteric ganglion.

architecture was similar between the KO sham 4 d and KO colitis 4 d groups and the KO sham 24 h and KO colitis 24 h groups (Figure 13).

Masson's trichome staining demonstrated that in the WT sham 24 h, KO sham 24 h, and WT sham 4 d groups, collagen fibers (blue) were present in the lamina propria and between the mucosal muscle and muscle layer (muscle fibers and cell nuclei shown in red) and enveloped the myenteric ganglia, and there were more collagen fibers throughout the submucosal layer. In the WT colitis 24 h and WT colitis 4 d groups, a greater number of collagen fibers was observed in the lamina propria, and collagen fibers were interspersed in the muscle layer. There were fewer collagen fibers in the submucosal layer, and the collagen fibers in this layer were hyperplastic and disorganized. The tissue structure in the KO colitis 24 h group was similar to that in the KO sham 24 h group, but there were fewer collagen fibers in the submucosal layer. Tissue architecture was similar between the KO sham 4 d and KO colitis 4 d groups and the WT sham 4 d and WT colitis 4 d groups; however, in both the KO sham and KO colitis groups, the collagen fibers in the submucosal layer were more organized (Figure 14).

Periodic acid-Schiff staining was performed to evaluate the presence and morphology of goblet cells in the distal colon. In the WT sham 24 h and WT sham 4 d groups, goblet cells in the distal colon were present throughout the epithelium, typically showed a columnar or oval shape and were circular when filled with mucus. In the WT colitis 24 h group, these cells were present in smaller quantities, were reduced in size, and presented a more rounded shape with an intumescent appearance. On the other hand, in the KO sham 24 h and KO colitis 24 h groups, the number of goblet cells was apparently increased. In the KO sham 24 h group, the cells were similar in size to those in the WT sham group, and in the KO colitis 24 h group, there was a more heterogeneous cell population. In the WT colitis 4 d group, goblet cells were apparently increased in number but still reduced in size. However, larger cells



DOI: 10.3748/wjg.v29.i22.3440 **Copyright** ©The Author(s) 2023.

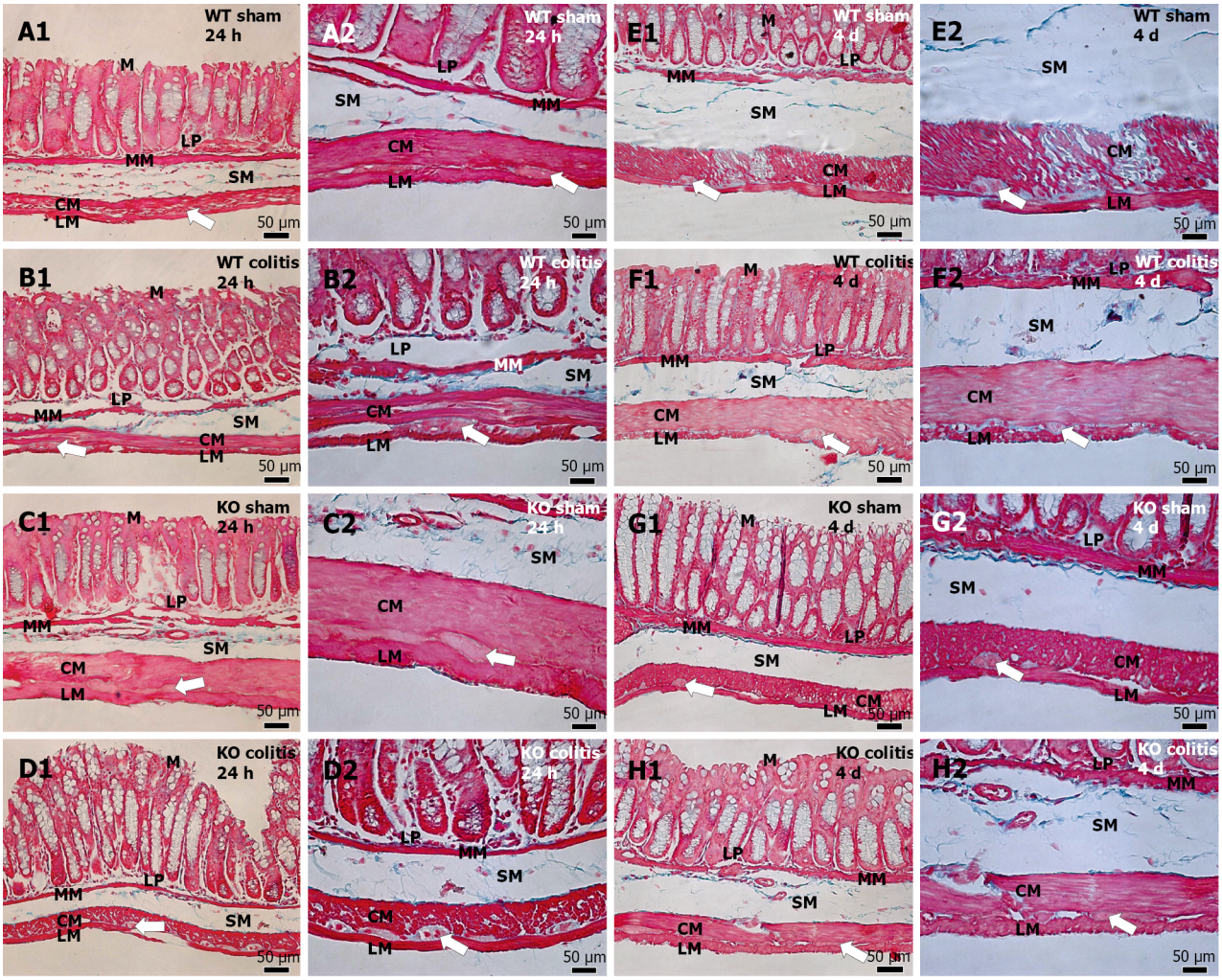
Figure 13 Photomicrograph of picrosirius red-stained transverse sections of the distal colons of mice of different groups. A1 and A2: Wild-type (WT) sham 24 h; B1 and B2: WT colitis 24 h; C1 and C2: Knockout (KO) sham 24 h; D1 and D2: KO colitis 24 h; E1 and E2: WT sham 4 d; F1 and F2: WT colitis 4 d; G1 and G2: KO sham 4 d; H1 and H2: KO colitis 4 d groups taken under an optical light (red) or polarized light (green) microscope. Thick collagen fibers (red) in the lamina propria and submucosal layer, intermingled with and involving the muscle layer, and circumscribing the myenteric ganglia were observed in the sham groups. In the WT colitis group, there was a decrease in the number of these fibers in the submucosal layer and around the myenteric ganglia, an increase in the number and disorganization of these fibers in the lamina propria and accumulation of these fibers in the subepithelial region. Tissue was better preserved in the KO colitis group. M: Mucosal layer; LP: Lamina propria; MM: Mucosal muscle; SM: Submucosal layer; ML: Muscle layer; CM: Circular musculature; LM: Longitudinal musculature; WT: Wild-type; KO: Knockout. White arrows mean myenteric ganglion.

were also observed near the surface of the intestinal crypts. Finally, there was a notable increase in the number of goblet cells in the distal colon in the KO sham 4 d and KO colitis 4 d groups (Figure 15).

Number of goblet cells per intestinal crypt: The number of goblet cells per intestinal crypt in the distal colon was decreased by 37.6% in the WT colitis 24 h group compared to the WT sham 24 h group (8.63 ± 0.43 *vs* 13.84 ± 1.00, $P < 0.01$). No statistically significant differences in the goblet cell density were observed between the KO colitis (24 h and 4 d) groups and the KO sham (24 h and 4 d) groups, but the goblet cell density was significantly different between the WT and KO groups ($P < 0.001$). In the KO groups, there was a greater number of goblet cells per intestinal crypt (Figure 16).

DISCUSSION

Despite the large amount of research on IBDs, the pathogenesis of these diseases is still unclear[74,75]. However, it is known that changes in the interaction between immune cells and the gut microbiota may contribute to the clinical progression of IBDs[76-80] and that nonimmune components may alter cellular structure and function in response to inflammation[81]. Indeed, recent evidence has indicated that colitis affects not only the intestinal mucosa but also the muscle layer and components of the ENS. Hence, gastrointestinal symptoms result from degenerative changes and a reduction in the number of



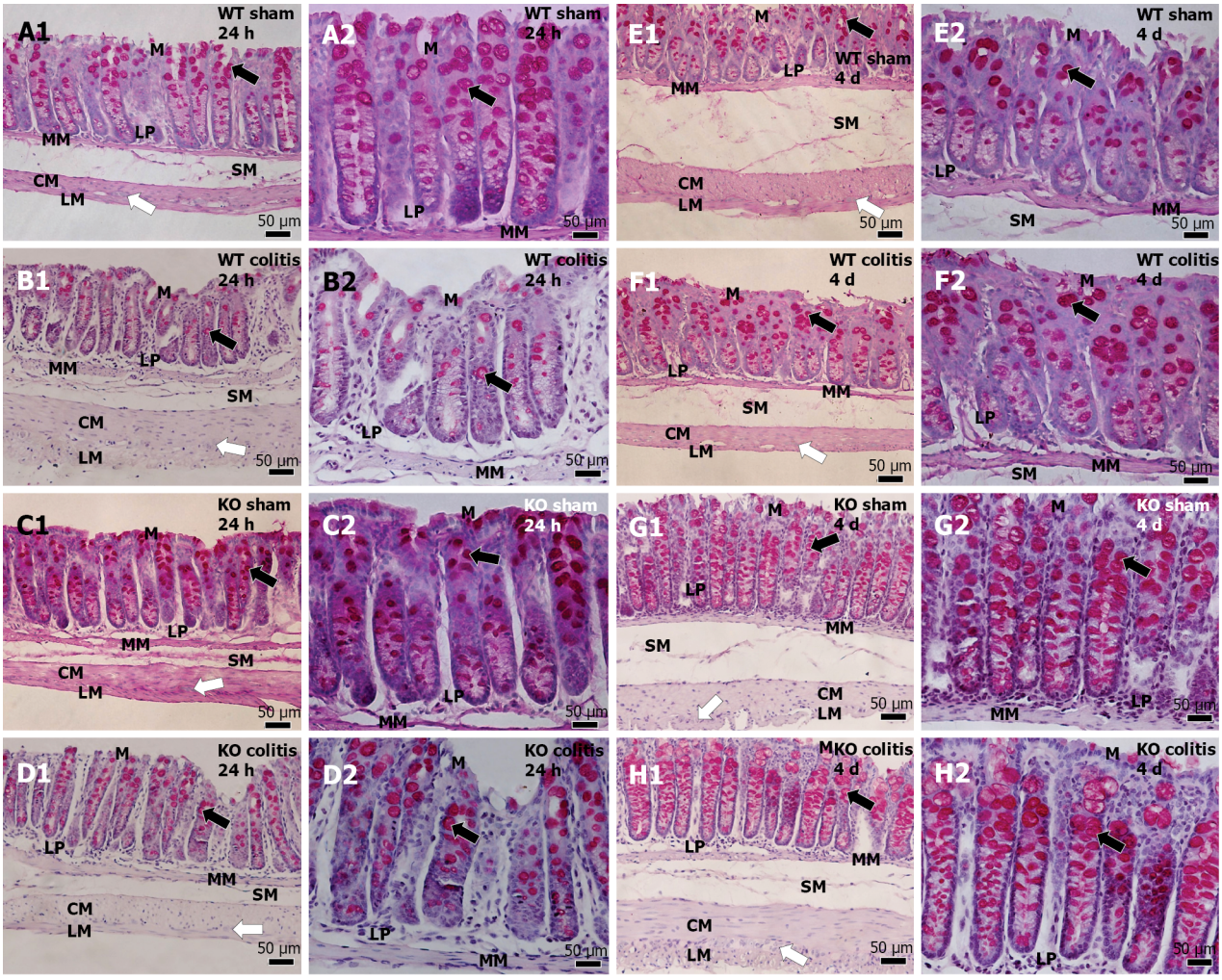
DOI: 10.3748/wjg.v29.i22.3440 **Copyright** ©The Author(s) 2023.

Figure 14 Photomicrographs of Masson's trichrome-stained transverse sections of the distal colons of mice in different groups. A1 and A2: Wild-type (WT) sham 24 h; B1 and B2: WT colitis 24 h; C1 and C2: Knockout (KO) sham 24 h; D1 and D2: KO colitis 24 h; E1 and E2: WT sham 4 d; F1 and F2: WT colitis 4 d; G1 and G2: KO sham 4 d; H1 and H2: KO colitis 4 d groups. Collagen fibers (blue) in the lamina propria and submucosal layer, intermingled with and involving the muscle layer, and circumscribing the myenteric ganglia were observed in the sham groups. In the WT colitis group, there was a decrease in the number of these fibers in the submucosal layer, and the collagen fibers in this layer were hyperplastic and disorganized. Moreover, the number of collagen fibers was increased in the lamina propria, and collagen fibers were intermingled in the muscular layer. Tissue was better preserved in the KO colitis group. WT: Wild-type; KO: Knockout; M: Mucosal layer; LP: Lamina propria; MM: Mucosal muscle; SM: Submucosal layer; ML: Muscle layer; CM: Circular musculature; LM: Longitudinal musculature; White arrows: Myenteric ganglion.

enteric neurons and glial cells, sometimes induced by the P2X7 receptor[35-40,48,50,62,63,82-84]. However, little is known about the cellular signaling mechanisms responsible for the loss of enteric innervation in IBDs[85].

In the present study, we hypothesized that the loss of myenteric neurons resulting from TNBS-induced colitis is related to cell death pathways mediated by caspase-3 and NF-κB-mediated transcription. In addition, we hypothesized that KO animals would be less affected by administration of an inflammatory stimulus. We compared pathological changes at two different time points after colitis induction. At both 24 h and four days post-inflammatory stimulus administration, there was a significant reduction in the number of myenteric neurons in the WT groups but not in the KO groups. In addition, the neuronal area was increased in the WT colitis 24 h and KO colitis 24 h groups, and this change was due to an increase in the cytoplasmic area; however, a decrease in the cytoplasmic area along with nuclear shrinkage was observed in the WT colitis 4 d group. We also demonstrated that when the P2X7 receptor was knocked out and at four days after colitis induction, the infiltration of inflammatory cells and microscopic tissue damage were attenuated, indicating that disease symptoms evolved during the experimental period.

According to Brenna *et al*[86], the TNBS-induced colitis model is a suitable model for studying biological processes associated with IBDs and can provide clinically relevant data; moreover, there are well-established protocols for constructing this model in both rats and mice[38-40,86-92]. Furthermore, KO animals have been used to study the onset and development of these disorders[83,86,93,94];



DOI: 10.3748/wjg.v29.i22.3440 **Copyright** ©The Author(s) 2023.

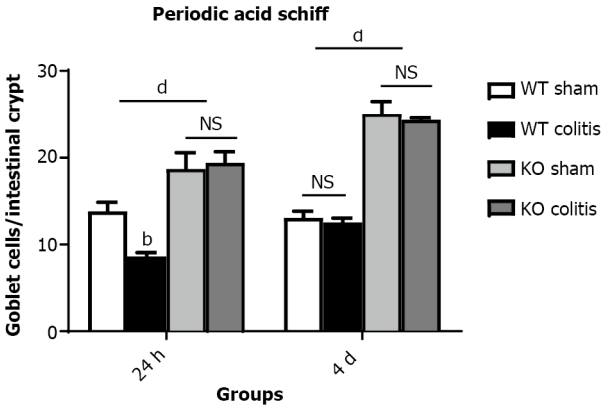
Figure 15 Photomicrograph of periodic acid Schiff-stained transverse sections of the distal colons of mice. A1 and A2: Wild-type (WT) sham 24 h; B1 and B2: WT colitis 24 h; C1 and C2: Knockout (KO) sham 24 h; D1 and D2: KO colitis 24 h; E1 and E2: WT sham 4 d; F1 and F2: WT colitis 4 d; G1 and G2: KO sham 4 d; H1 and H2: KO colitis 4 d groups. Goblet cells were observed throughout the epithelium in the sham groups, and there was an apparent reduction in goblet cell number and size in the WT colitis group. In addition, goblet cells showed a more rounded shape and an intumescent appearance in the WT colitis group. In the KO groups, an apparent increase in the number of goblet cells was noted. WT: Wild-type; KO: Knockout; M: Mucosal layer; LP: Lamina propria; MM: Mucosal muscle; SM: Submucosal layer; ML: Muscle layer; CM: Circular musculature; LM: Longitudinal musculature; white arrows: Myenteric ganglion; black arrows: Goblet cells.

however, the degree of similarity between experimentally induced colitis and spontaneous colitis in humans is still unclear[86].

In the present study, we recorded body weight and the change in DAI daily. After euthanasia, the macro- and microscopic lesions in the distal colon were characterized[64-67]. The colitis model animals lost more weight on the first day but recovered on the subsequent days. It is worth noting that in the colitis model groups, there were also greater changes in stool consistency and the presence of blood in the stool. Similarly, tissue hyperemia was noted only in the colitis groups, and the WT colitis 24 h group exhibited more severe microscopic damage. The absence of statistically significant differences in phenotype between the KO sham and KO colitis groups is consistent with previous literature showing that KO of the P2X7 receptor provides greater protection against inflammation[52,56,83,93,94].

It was previously demonstrated that intestinal inflammation induces changes in the density of neurons expressing different chemical codes in the ENS and that these changes vary between animal models and human patients. It is known that the number of neurons is reduced 24 h to seven days after the induction of colitis[35-40,62,81,89,95]. It has been reported that this decrease in the number of neurons occurs as early as six hours after colitis induction[35,81] and that, as observed in the present study, this decrease is already significant at 24 h.

According to Sanovic *et al*[81], the number of enteric neurons continues to decrease from the second to the fourth day and remains constant until day 35, suggesting that enteric neuron loss is long lasting and irreversible. Similarly, Linden *et al*[95] also reported that the number of neurons is not yet recovered at 56 d after colitis induction. In contrast, Poli *et al*[96] observed that at 30 d after inflammation



DOI: 10.3748/wjg.v29.i22.3440 **Copyright** ©The Author(s) 2023.

Figure 16 Number of goblet cells per intestinal crypt of the distal colon in mice from the wild-type sham 24 h and 4 d, wild-type colitis 24 h and 4 d, knockout sham 24 h and 4 d, and knockout colitis 24 h and 4 d groups. The data are presented as the arithmetic mean ± SE. $^{b}P < 0.01$ *vs* sham groups; $^{d}P < 0.001$ *vs* wild-type groups; NS: Not significant. WT: Wild-type; KO: Knockout.

induction, the myenteric plexus showed similar labeling to that in the control group. In our study, there was a slight increase in the number of calretinin-ir neurons in the WT colitis 4 d and KO colitis 4 d groups compared with the WT sham 24 h and KO sham 24 h groups, which may indicate that neurons exhibit some degree of plasticity in response to inflammatory injury. Despite this apparent alleviation of pathological changes after the inflammatory stimulus is removed, neuronal damage and activation of signaling pathways that potentially lead to cell death have already occurred.

The neuronal area was significantly increased in the WT colitis 24 h and KO colitis 24 h groups compared to the WT sham 24 h and KO sham 24 h groups, and this change was due to an increase in the cytoplasmic area. On the other hand, a significant reduction in neuronal area accompanied by a reduction in nuclear area was observed in the WT colitis 4 d group. In addition, ultrastructural analysis of myenteric neurons revealed nuclear disruption and cytoplasmic disorganization in the 24 h WT colitis and 24 h KO colitis groups and nuclear membrane folding associated with the formation of apoptotic bodies in the 4 d WT colitis group. Thus, neurons first underwent necrosis characterized by massive cell death and then, after four days, underwent apoptosis characterized by cytoplasmic condensation and nuclear shrinkage[4,6-8,10,14,35,82,97].

As reported by Martin[1] and Kanduc *et al*[2], cell death can occur either through necrosis or apoptosis and results from the activation of intrinsic death programs or passive disruption of the cell membrane resulting from damaging environmental stimuli[10]. In necrosis, the death stimulus alone causes the loss of the cell[4], whereas in apoptosis, a cascade of events that orchestrate destruction of the cell in a controlled manner is activated. The main effector of both processes is caspase-3[4,8,10,45,98], a protease that when activated fragments DNA and disrupts cellular organization and leads to cell death [4,7,98-101].

From the CTCF analysis, a greater intensity of cleaved caspase-3 was observed in the 24 h WT colitis, 24 h KO colitis and 4 d WT colitis groups, indicating a higher activation of myenteric neuron pathway death. Indeed, these results are in line with the decrease in enteric neuronal density arising from colitis. In addition, we observed a higher fluorescence of the P2X7 receptor in the WT colitis 24 h group, suggesting its greater activation during the inflammatory process[52,54,60,93,102-104].

According to North[105], Burnstock[106], and Dubyak[107], constant stimulation of the P2X7 receptor *via* ATP results in the efflux of K^+ and the influx of Ca^{2+} and Na^+ and triggers the formation of a nonselective membrane pore that makes the cell permeable to molecules of up to 900 daltons. Because of this imbalance, specific phospholipases and kinases that, in addition to exerting other effects, can trigger the caspase cascade are activated. As a result, the activation of the transcription factor NF-κB leads to the expression of proinflammatory genes and stimulates both inflammation and cell death. It has also been found that ATP is released *via* the panexin-1 channel[37,49,50], and the extracellular increase in ATP indicates exacerbation of inflammation[56,60], increased P2X7 receptor activation and severe neuronal death[37,51,52,56,103].

Consistent with the findings presented above, our results showed that in KO mice, myenteric calretinin-ir neurons were protected to a greater extent, and the loss of this receptor obviously prevented its activation, inhibiting the subsequent cascade of events culminating in cell death. Despite this, a decrease in the number of myenteric neurons was observed in the KO colitis 24 h group compared to the KO sham 24 h group, which suggests that neuronal protection and cell death also involve pathways not linked to the P2X7 receptor[4,7,8,45,47].

Our results are in line with what has been reported in the literature and confirm that neuronal death mediated by caspase-3 activation is related to purinergic signaling *via* the P2X7 receptor in the

myenteric plexus of mice with TNBS-induced colitis. However, it is worth noting that NF-κB plays a role in IBDs[108-111], but its activation is minimal during the inflammatory process[112].

Histologically, inflammatory infiltration, tissue damage, and loss of goblet cells in intestinal tissue were attenuated at four days compared with 24 h after colitis induction. This finding is consistent with the alleviation of symptoms observed in the colitis groups since the inflammatory stimulus was removed and corroborates the findings reported in the literature demonstrating that tissue recovery indicates better clinical outcomes[113,114]. Nevertheless, in the WT colitis 4 d group, collagen fibers in the lamina propria were increased in number and disorganized, indicating that the fibrosis in the mucosal layer[38,52,115,116] observed at 24 h did not decrease. On the other hand, KO animals always showed milder tissue injury and better recovery than WT animals.

It is possible that the reduction in the number of goblet cells observed in the colitis groups aggravated acute intestinal inflammation; this phenomenon has already been reported both in experimental animals and in human patients[38,52,83,117-120]. However, even though these cells play a critical role in maintaining a physical barrier by producing mucus in the gut[117,121-123], it is unclear whether the loss of their function contributes to the onset of inflammation or is a consequence of it[117]. The results of our study indicated that colitis induced the loss of these cells, and tissue recovery was observed at four days, as indicated by an increased number of goblet cells that grew as they emerged from the basal lamina and moved toward the epithelial surface. The increase in cell proliferation in the KO groups[94], which resulted in the increase in the number of goblet cells, may have also protected the mucosa by leading to increased mucus production. As reported by Van der Sluis *et al*[121], Niv[124], and Grondin *et al*[123], deficiencies in the production of diverse types of mucins favor the onset and progression of intestinal inflammation.

CONCLUSION

In conclusion, we demonstrate that although the distal colons of mice with colitis showed good histological recovery, neuronal injury occurred in the myenteric plexus and probably impaired intestinal function. Studies in which animals are maintained for a longer period of time seem to be needed to elucidate the effects of P2X7 signaling on long-term neuronal survival. Moreover, it was confirmed that the P2X7 receptor is closely associated with neuronal necrosis and apoptosis dependent on the caspase-3 pathway but not on NF-κB. KO animals were less affected by ulcerative colitis. Thus, the P2X7 receptor may be a potential therapeutic target for IBDs.

ARTICLE HIGHLIGHTS

Research background

Inflammation affects enteric neurons and has P2X7 receptor signaling.

Research motivation

The motivation of the work was to study the mechanisms of nuclear factor kappa B (NF-κB) and caspase-3.

Research objectives

To study calretinin-positive neurons and caspase-3 and NF-κB pathways in intestinal inflammation.

Research methods

Research methods of immunohistochemistry, morphometry, conventional histology and transmission electron microscopy were used.

Research results

There was a decrease in calretinin neurons in wild type colitis (WT) animals and recovery of neurons in mice deficient for the P2X7 receptor (KO). There was an increase in caspase-3 and NF-κB pathways in the WT colitis and recovery animals in the KO groups.

Research conclusions

The P2X7 receptor is involved in the decrease of neurons in the WT colitis group, and this receptor could be a therapeutic target.

Research perspectives

The perspective of the work is to use other techniques to explain other pathways of action mechanisms.

FOOTNOTES

Author contributions: Magalhães HIR was responsible for the literature review and analysis and wrote the manuscript; Machado FA, Souza RF, Caetano MAF, Figliuolo VR, and Coutinho-Silva R helped with acquisition, analysis and interpretation of data and made critical suggestions about the writing; Castelucci P designed the study, helped with acquisition, analysis and interpretation of data, performed the critical interpretation and revised the manuscript for intellectual content; and all authors approved the final version of the manuscript.

Supported by the National Council for Scientific and Technological Development, No. 168015/2018-8; and the São Paulo Research Foundation, No. 2014/25927-2 and No. 2018/07862-1.

Institutional review board statement: The study was reviewed and approved by the pela Comissão de Ética no Uso de Animais da Instituto de Ciências Biomédicas Universidade de São Paulo (Approval No. CEUA 2372300921).

Institutional animal care and use committee statement: All procedures involving animals were reviewed and approved by the Ethic Committee on Animal Use of the School of Veterinary Medicine and Animal Science University of São Paulo (Approval No. CEUA 2841270120).

Conflict-of-interest statement: The authors have no conflicts of interest.

Data sharing statement: Technical appendix, statistical code, and dataset available from the corresponding author at pcastel@usp.br. Participants gave informed consent for data sharing.

ARRIVE guidelines statement: The authors have read the ARRIVE Guidelines, and the manuscript was prepared and revised according to the ARRIVE Guidelines.

Open-Access: This article is an open-access article that was selected by an in-house editor and fully peer-reviewed by external reviewers. It is distributed in accordance with the Creative Commons Attribution NonCommercial (CC BY-NC 4.0) license, which permits others to distribute, remix, adapt, build upon this work non-commercially, and license their derivative works on different terms, provided the original work is properly cited and the use is non-commercial. See: https://creativecommons.org/Licenses/by-nc/4.0/

Country/Territory of origin: Brazil

ORCID number: Henrique Inhauser Riceti Magalhães 0000-0001-9151-8160; Roberta Figueiroa Souza 0000-0003-4380-6373; Marcos Antônio Ferreira Caetano 0000-0002-9981-3241; Patricia Castelucci 0000-0002-7475-5962.

Corresponding Author's Membership in Professional Societies: American Gastroenterological Association, No. C-1029455.

S-Editor: Chen YL
L-Editor: A
P-Editor: Chen YL

REFERENCES

1 **Martin LJ**. Neuronal cell death in nervous system development, disease, and injury (Review). *Int J Mol Med* 2001; **7**: 455-478 [PMID: 11295106 DOI: 10.3892/ijmm.7.5.455]
2 **Kanduc D**, Mittelman A, Serpico R, Sinigaglia E, Sinha AA, Natale C, Santacroce R, Di Corcia MG, Lucchese A, Dini L, Pani P, Santacroce S, Simone S, Bucci R, Farber E. Cell death: apoptosis versus necrosis (review). *Int J Oncol* 2002; **21**: 165-170 [PMID: 12063564 DOI: 10.3892/ijo.21.1.165]
3 **Leist M**, Jäättelä M. Four deaths and a funeral: from caspases to alternative mechanisms. *Nat Rev Mol Cell Biol* 2001; **2**: 589-598 [PMID: 11483992 DOI: 10.1038/35085008]
4 **Friedlander RM**. Apoptosis and caspases in neurodegenerative diseases. *N Engl J Med* 2003; **348**: 1365-1375 [PMID: 12672865 DOI: 10.1056/NEJMra022366]
5 **Dong Z**, Saikumar P, Weinberg JM, Venkatachalam MA. Calcium in cell injury and death. *Annu Rev Pathol* 2006; **1**: 405-434 [PMID: 18039121 DOI: 10.1146/annurev.pathol.1.110304.100218]
6 **Kerr JF**, Wyllie AH, Currie AR. Apoptosis: a basic biological phenomenon with wide-ranging implications in tissue kinetics. *Br J Cancer* 1972; **26**: 239-257 [PMID: 4561027 DOI: 10.1038/bjc.1972.33]
7 **Hengartner MO**. The biochemistry of apoptosis. *Nature* 2000; **407**: 770-776 [PMID: 11048727 DOI: 10.1038/35037710]
8 **Mattson MP**. Apoptosis in neurodegenerative disorders. *Nat Rev Mol Cell Biol* 2000; **1**: 120-129 [PMID: 11253364 DOI: 10.1038/35040009]
9 **Hotchkiss RS**, Strasser A, McDunn JE, Swanson PE. Cell death. *N Engl J Med* 2009; **361**: 1570-1583 [PMID: 19828534 DOI: 10.1056/NEJMra0901217]
10 **Zhang Y**, Chen X, Gueydan C, Han J. Plasma membrane changes during programmed cell deaths. *Cell Res* 2018; **28**: 9-21 [PMID: 29076500 DOI: 10.1038/cr.2017.133]

11 **Zong WX**, Thompson CB. Necrotic death as a cell fate. *Genes Dev* 2006; **20**: 1-15 [PMID: 16391229 DOI: 10.1101/gad.1376506]

12 **Golstein P**, Kroemer G. Cell death by necrosis: towards a molecular definition. *Trends Biochem Sci* 2007; **32**: 37-43 [PMID: 17141506 DOI: 10.1016/j.tibs.2006.11.001]

13 **D'Amelio M**, Cavallucci V, Cecconi F. Neuronal caspase-3 signaling: not only cell death. *Cell Death Differ* 2010; **17**: 1104-1114 [PMID: 19960023 DOI: 10.1038/cdd.2009.180]

14 **Yuan J**, Najafov A, Py BF. Roles of Caspases in Necrotic Cell Death. *Cell* 2016; **167**: 1693-1704 [PMID: 27984721 DOI: 10.1016/j.cell.2016.11.047]

15 **D'Arcy MS**. Cell death: a review of the major forms of apoptosis, necrosis and autophagy. *Cell Biol Int* 2019; **43**: 582-592 [PMID: 30958602 DOI: 10.1002/cbin.11137]

16 **Gorman AM**. Neuronal cell death in neurodegenerative diseases: recurring themes around protein handling. *J Cell Mol Med* 2008; **12**: 2263-2280 [PMID: 18624755 DOI: 10.1111/j.1582-4934.2008.00402.x]

17 **Nixon RA**, Yang DS. Autophagy and neuronal cell death in neurological disorders. *Cold Spring Harb Perspect Biol* 2012; **4** [PMID: 22983160 DOI: 10.1101/cshperspect.a008839]

18 **Emery E**, Aldana P, Bunge MB, Puckett W, Srinivasan A, Keane RW, Bethea J, Levi AD. Apoptosis after traumatic human spinal cord injury. *J Neurosurg* 1998; **89**: 911-920 [PMID: 9833815 DOI: 10.3171/jns.1998.89.6.0911]

19 **Fink KB**, Andrews LJ, Butler WE, Ona VO, Li M, Bogdanov M, Endres M, Khan SQ, Namura S, Stieg PE, Beal MF, Moskowitz MA, Yuan J, Friedlander RM. Reduction of post-traumatic brain injury and free radical production by inhibition of the caspase-1 cascade. *Neuroscience* 1999; **94**: 1213-1218 [PMID: 10625061 DOI: 10.1016/s0306-4522(99)00345-0]

20 **Beattie MS**, Hermann GE, Rogers RC, Bresnahan JC. Cell death in models of spinal cord injury. *Prog Brain Res* 2002; **137**: 37-47 [PMID: 12440358 DOI: 10.1016/s0079-6123(02)37006-7]

21 **Ekshyyan O**, Aw TY. Apoptosis in acute and chronic neurological disorders. *Front Biosci* 2004; **9**: 1567-1576 [PMID: 14977568 DOI: 10.2741/1357]

22 **Che Mohd Nassir CMN**, Zolkefley MKI, Ramli MD, Norman HH, Abdul Hamid H, Mustapha M. Neuroinflammation and COVID-19 Ischemic Stroke Recovery-Evolving Evidence for the Mediating Roles of the ACE2/Angiotensin-(1-7)/Mas Receptor Axis and NLRP3 Inflammasome. *Int J Mol Sci* 2022; **23** [PMID: 35328506 DOI: 10.3390/ijms23063085]

23 **Xu Y**, Hu Y, Xu S, Liu F, Gao Y. Exosomal microRNAs as Potential Biomarkers and Therapeutic Agents for Acute Ischemic Stroke: New Expectations. *Front Neurol* 2021; **12**: 747380 [PMID: 35173663 DOI: 10.3389/fneur.2021.747380]

24 **Friedlander RM**, Brown RH, Gagliardini V, Wang J, Yuan J. Inhibition of ICE slows ALS in mice. *Nature* 1997; **388**: 31 [PMID: 9214497 DOI: 10.1038/40299]

25 **Gervais FG**, Xu D, Robertson GS, Vaillancourt JP, Zhu Y, Huang J, LeBlanc A, Smith D, Rigby M, Shearman MS, Clarke EE, Zheng H, Van Der Ploeg LH, Ruffolo SC, Thornberry NA, Xanthoudakis S, Zamboni RJ, Roy S, Nicholson DW. Involvement of caspases in proteolytic cleavage of Alzheimer's amyloid-beta precursor protein and amyloidogenic A beta peptide formation. *Cell* 1999; **97**: 395-406 [PMID: 10319819 DOI: 10.1016/s0092-8674(00)80748-5]

26 **Li M**, Ona VO, Guégan C, Chen M, Jackson-Lewis V, Andrews LJ, Olszewski AJ, Stieg PE, Lee JP, Przedborski S, Friedlander RM. Functional role of caspase-1 and caspase-3 in an ALS transgenic mouse model. *Science* 2000; **288**: 335-339 [PMID: 10764647 DOI: 10.1126/science.288.5464.335]

27 **Okouchi M**, Ekshyyan O, Maracine M, Aw TY. Neuronal apoptosis in neurodegeneration. *Antioxid Redox Signal* 2007; **9**: 1059-1096 [PMID: 17571960 DOI: 10.1089/ars.2007.1511]

28 **Verma M**, Lizama BN, Chu CT. Excitotoxicity, calcium and mitochondria: a triad in synaptic neurodegeneration. *Transl Neurodegener* 2022; **11**: 3 [PMID: 35078537 DOI: 10.1186/s40035-021-00278-7]

29 **Palombit K**, Mendes CE, Tavares-de-Lima W, Silveira MP, Castelucci P. Effects of ischemia and reperfusion on subpopulations of rat enteric neurons expressing the P2X7 receptor. *Dig Dis Sci* 2013; **58**: 3429-3439 [PMID: 23990036 DOI: 10.1007/s10620-013-2847-y]

30 **Marosti AR**, da Silva MV, Palombit K, Mendes CE, Tavares-de-Lima W, Castelucci P. Differential effects of intestinal ischemia and reperfusion in rat enteric neurons and glial cells expressing P2X2 receptors. *Histol Histopathol* 2015; **30**: 489-501 [PMID: 25400134 DOI: 10.14670/HH-30.489]

31 **Mendes CE**, Palombit K, Vieira C, Silva I, Correia-de-Sá P, Castelucci P. The Effect of Ischemia and Reperfusion on Enteric Glial Cells and Contractile Activity in the Ileum. *Dig Dis Sci* 2015; **60**: 2677-2689 [PMID: 25917048 DOI: 10.1007/s10620-015-3663-3]

32 **Mendes CE**, Palombit K, Tavares-de-Lima W, Castelucci P. Enteric glial cells immunoreactive for P2X7 receptor are affected in the ileum following ischemia and reperfusion. *Acta Histochem* 2019; **121**: 665-679 [PMID: 31202513 DOI: 10.1016/j.acthis.2019.06.001]

33 **Palombit K**, Mendes CE, Tavares-de-Lima W, Barreto-Chaves ML, Castelucci P. Blockage of the P2X7 Receptor Attenuates Harmful Changes Produced by Ischemia and Reperfusion in the Myenteric Plexus. *Dig Dis Sci* 2019; **64**: 1815-1829 [PMID: 30734238 DOI: 10.1007/s10620-019-05496-8]

34 **Mendes CE**, Palombit K, Alves Pereira TT, Riceti Magalhães HI, Ferreira Caetano MA, Castelucci P. Effects of probenecid and brilliant blue G on rat enteric glial cells following intestinal ischemia and reperfusion. *Acta Histochem* 2023; **125**: 151985 [PMID: 36495673 DOI: 10.1016/j.acthis.2022.151985]

35 **Boyer L**, Ghoreishi M, Templeman V, Vallance BA, Buchan AM, Jevon G, Jacobson K. Myenteric plexus injury and apoptosis in experimental colitis. *Auton Neurosci* 2005; **117**: 41-53 [PMID: 15620569 DOI: 10.1016/j.autneu.2004.10.006]

36 **Sarnelli G**, De Giorgio R, Gentile F, Calì G, Grandone I, Rocco A, Cosenza V, Cuomo R, D'Argenio G. Myenteric neuronal loss in rats with experimental colitis: role of tissue transglutaminase-induced apoptosis. *Dig Liver Dis* 2009; **41**: 185-193 [PMID: 18635410 DOI: 10.1016/j.dld.2008.06.004]

37 **Gulbransen BD**, Bashashati M, Hirota SA, Gui X, Roberts JA, MacDonald JA, Muruve DA, McKay DM, Beck PL, Mawe GM, Thompson RJ, Sharkey KA. Activation of neuronal P2X7 receptor-pannexin-1 mediates death of enteric neurons during colitis. *Nat Med* 2012; **18**: 600-604 [PMID: 22426419 DOI: 10.1038/nm.2679]

38 **da Silva MV**, Marosti AR, Mendes CE, Palombit K, Castelucci P. Differential effects of experimental ulcerative colitis on

P2X7 receptor expression in enteric neurons. *Histochem Cell Biol* 2015; **143**: 171-184 [PMID: 25201348 DOI: 10.1007/s00418-014-1270-6]

39 **da Silva MV**, Marosti AR, Mendes CE, Palombit K, Castelucci P. Submucosal neurons and enteric glial cells expressing the P2X7 receptor in rat experimental colitis. *Acta Histochem* 2017; **119**: 481-494 [PMID: 28501138 DOI: 10.1016/j.acthis.2017.05.001]

40 **Evangelinellis MM**, Souza RF, Mendes CE, Castelucci P. Effects of a P2X7 receptor antagonist on myenteric neurons in the distal colon of an experimental rat model of ulcerative colitis. *Histochem Cell Biol* 2022; **157**: 65-81 [PMID: 34626216 DOI: 10.1007/s00418-021-02039-z]

41 **Wright SC**, Schellenberger U, Wang H, Kinder DH, Talhouk JW, Larrick JW. Activation of CPP32-like proteases is not sufficient to trigger apoptosis: inhibition of apoptosis by agents that suppress activation of AP24, but not CPP32-like activity. *J Exp Med* 1997; **186**: 1107-1117 [PMID: 9314559 DOI: 10.1084/jem.186.7.1107]

42 **Jäättelä M**, Wissing D, Kokholm K, Kallunki T, Egeblad M. Hsp70 exerts its anti-apoptotic function downstream of caspase-3-like proteases. *EMBO J* 1998; **17**: 6124-6134 [PMID: 9799222 DOI: 10.1093/emboj/17.21.6124]

43 **Harvey KJ**, Lukovic D, Ucker DS. Caspase-dependent Cdk activity is a requisite effector of apoptotic death events. *J Cell Biol* 2000; **148**: 59-72 [PMID: 10629218 DOI: 10.1083/jcb.148.1.59]

44 **Uesaka T**, Jain S, Yonemura S, Uchiyama Y, Milbrandt J, Enomoto H. Conditional ablation of GFRalpha1 in postmigratory enteric neurons triggers unconventional neuronal death in the colon and causes a Hirschsprung's disease phenotype. *Development* 2007; **134**: 2171-2181 [PMID: 17507417 DOI: 10.1242/dev.001388]

45 **Fricker M**, Tolkovsky AM, Borutaite V, Coleman M, Brown GC. Neuronal Cell Death. *Physiol Rev* 2018; **98**: 813-880 [PMID: 29488822 DOI: 10.1152/physrev.00011.2017]

46 **Galluzzi L**, Vitale I, Aaronson SA, Abrams JM, Adam D, Agostinis P, Alnemri ES, Altucci L, Amelio I, Andrews DW, Annicchiarico-Petruzzelli M, Antonov AV, Arama E, Baehrecke EH, Barlev NA, Bazan NG, Bernassola F, Bertrand MJM, Bianchi K, Blagosklonny MV, Blomgren K, Borner C, Boya P, Brenner C, Campanella M, Candi E, Carmona-Gutierrez D, Cecconi F, Chan FK, Chandel NS, Cheng EH, Chipuk JE, Cidlowski JA, Ciechanover A, Cohen GM, Conrad M, Cubillos-Ruiz JR, Czabotar PE, D'Angiolella V, Dawson TM, Dawson VL, De Laurenzi V, De Maria R, Debatin KM, DeBerardinis RJ, Deshmukh M, Di Daniele N, Di Virgilio F, Dixit VM, Dixon SJ, Duckett CS, Dynlacht BD, El-Deiry WS, Elrod JW, Fimia GM, Fulda S, García-Sáez AJ, Garg AD, Garrido C, Gavathiotis E, Golstein P, Gottlieb E, Green DR, Greene LA, Gronemeyer H, Gross A, Hajnoczky G, Hardwick JM, Harris IS, Hengartner MO, Hetz C, Ichijo H, Jäättelä M, Joseph B, Jost PJ, Juin PP, Kaiser WJ, Karin M, Kaufmann T, Kepp O, Kimchi A, Kitsis RN, Klionsky DJ, Knight RA, Kumar S, Lee SW, Lemasters JJ, Levine B, Linkermann A, Lipton SA, Lockshin RA, López-Otín C, Lowe SW, Luedde T, Lugli E, MacFarlane M, Madeo F, Malewicz M, Malorni W, Manic G, Marine JC, Martin SJ, Martinou JC, Medema JP, Mehlen P, Meier P, Melino S, Miao EA, Molkentin JD, Moll UM, Muñoz-Pinedo C, Nagata S, Nuñez G, Oberst A, Oren M, Overholtzer M, Pagano M, Panaretakis T, Pasparakis M, Penninger JM, Pereira DM, Pervaiz S, Peter ME, Piacentini M, Pinton P, Prehn JHM, Puthalakath H, Rabinovich GA, Rehm M, Rizzuto R, Rodrigues CMP, Rubinsztein DC, Rudel T, Ryan KM, Sayan E, Scorrano L, Shao F, Shi Y, Silke J, Simon HU, Sistigu A, Stockwell BR, Strasser A, Szabadkai G, Tait SWG, Tang D, Tavernarakis N, Thorburn A, Tsujimoto Y, Turk B, Vanden Berghe T, Vandenabeele P, Vander Heiden MG, Villunger A, Virgin HW, Vousden KH, Vucic D, Wagner EF, Walczak H, Wallach D, Wang Y, Wells JA, Wood W, Yuan J, Zakeri Z, Zhivotovsky B, Zitvogel L, Melino G, Kroemer G. Molecular mechanisms of cell death: recommendations of the Nomenclature Committee on Cell Death 2018. *Cell Death Differ* 2018; **25**: 486-541 [PMID: 29362479 DOI: 10.1038/s41418-017-0012-4]

47 **Kopp R**, Krautloher A, Ramírez-Fernández A, Nicke A. P2X7 Interactions and Signaling - Making Head or Tail of It. *Front Mol Neurosci* 2019; **12**: 183 [PMID: 31440138 DOI: 10.3389/fnmol.2019.00183]

48 **Volonté C**, Amadio S, Cavaliere F, D'Ambrosi N, Vacca F, Bernardi G. Extracellular ATP and neurodegeneration. *Curr Drug Targets CNS Neurol Disord* 2003; **2**: 403-412 [PMID: 14683468 DOI: 10.2174/1568007033482643]

49 **Franke H**, Illes P. Involvement of P2 receptors in the growth and survival of neurons in the CNS. *Pharmacol Ther* 2006; **109**: 297-324 [PMID: 16102837 DOI: 10.1016/j.pharmthera.2005.06.002]

50 **Franke H**, Verkhratsky A, Burnstock G, Illes P. Pathophysiology of astroglial purinergic signalling. *Purinergic Signal* 2012; **8**: 629-657 [PMID: 22544529 DOI: 10.1007/s11302-012-9300-0]

51 **Roberts JA**, Lukewich MK, Sharkey KA, Furness JB, Mawe GM, Lomax AE. The roles of purinergic signaling during gastrointestinal inflammation. *Curr Opin Pharmacol* 2012; **12**: 659-666 [PMID: 23063457 DOI: 10.1016/j.coph.2012.09.011]

52 **Marques CC**, Castelo-Branco MT, Pacheco RG, Buongusto F, do Rosário A Jr, Schanaider A, Coutinho-Silva R, de Souza HS. Prophylactic systemic P2X7 receptor blockade prevents experimental colitis. *Biochim Biophys Acta* 2014; **1842**: 65-78 [PMID: 24184714 DOI: 10.1016/j.bbadis.2013.10.012]

53 **Ohishi A**, Keno Y, Marumiya A, Sudo Y, Uda Y, Matsuda K, Morita Y, Furuta T, Nishida K, Nagasawa K. Expression level of P2X7 receptor is a determinant of ATP-induced death of mouse cultured neurons. *Neuroscience* 2016; **319**: 35-45 [PMID: 26812038 DOI: 10.1016/j.neuroscience.2016.01.048]

54 **Di Virgilio F**, Dal Ben D, Sarti AC, Giuliani AL, Falzoni S. The P2X7 Receptor in Infection and Inflammation. *Immunity* 2017; **47**: 15-31 [PMID: 28723547 DOI: 10.1016/j.immuni.2017.06.020]

55 **Zhang WJ**, Zhu ZM, Liu ZX. The role and pharmacological properties of the P2X7 receptor in neuropathic pain. *Brain Res Bull* 2020; **155**: 19-28 [PMID: 31778766 DOI: 10.1016/j.brainresbull.2019.11.006]

56 **Wan P**, Liu X, Xiong Y, Ren Y, Chen J, Lu N, Guo Y, Bai A. Extracellular ATP mediates inflammatory responses in colitis *via* P2 × 7 receptor signaling. *Sci Rep* 2016; **6**: 19108 [PMID: 26739809 DOI: 10.1038/srep19108]

57 **Burnstock G**, Jacobson KA, Christofi FL. Purinergic drug targets for gastrointestinal disorders. *Curr Opin Pharmacol* 2017; **37**: 131-141 [PMID: 29149731 DOI: 10.1016/j.coph.2017.10.011]

58 **Cheng N**, Zhang L, Liu L. Understanding the Role of Purinergic P2X7 Receptors in the Gastrointestinal System: A Systematic Review. *Front Pharmacol* 2021; **12**: 786579 [PMID: 34987401 DOI: 10.3389/fphar.2021.786579]

59 **Mishra A**, Behura A, Kumar A, Naik L, Swain A, Das M, Sarangi SS, Dokania P, Dirisala VR, Bhutia SK, Mishra A, Singh R, Dhiman R. P2X7 receptor in multifaceted cellular signalling and its relevance as a potential therapeutic target in

different diseases. *Eur J Pharmacol* 2021; **906**: 174235 [PMID: 34097884 DOI: 10.1016/j.ejphar.2021.174235]

60 **Antonioli L**, Giron MC, Colucci R, Pellegrini C, Sacco D, Caputi V, Orso G, Tuccori M, Scarpignato C, Blandizzi C, Fornai M. Involvement of the P2X7 purinergic receptor in colonic motor dysfunction associated with bowel inflammation in rats. *PLoS One* 2014; **9**: e116253 [PMID: 25549098 DOI: 10.1371/journal.pone.0116253]

61 **Liu Y**, Liu X. Research progress of P2X7 receptor in inflammatory bowel disease. *Scand J Gastroenterol* 2019; **54**: 521-527 [PMID: 31056977 DOI: 10.1080/00365521.2019.1609077]

62 **Souza RF**, Evangelinellis MM, Mendes CE, Righetti M, Lourenço MCS, Castelucci P. P2X7 receptor antagonist recovers ileum myenteric neurons after experimental ulcerative colitis. *World J Gastrointest Pathophysiol* 2020; **11**: 84-103 [PMID: 32587788 DOI: 10.4291/wjgp.v11.i4.84]

63 **Magalhães HIR**, Castelucci P. Enteric nervous system and inflammatory bowel diseases: Correlated impacts and therapeutic approaches through the P2X7 receptor. *World J Gastroenterol* 2021; **27**: 7909-7924 [PMID: 35046620 DOI: 10.3748/wjg.v27.i46.7909]

64 **Cooper HS**, Murthy SN, Shah RS, Sedergran DJ. Clinicopathologic study of dextran sulfate sodium experimental murine colitis. *Lab Invest* 1993; **69**: 238-249 [PMID: 8350599]

65 **Hoffmann M**, Schwertassek U, Seydel A, Weber K, Falk W, Hauschildt S, Lehmann J. A refined and translationally relevant model of chronic DSS colitis in BALB/c mice. *Lab Anim* 2018; **52**: 240-252 [PMID: 29192559 DOI: 10.1177/0023677217742681]

66 **Wallace JL**, Keenan CM. An orally active inhibitor of leukotriene synthesis accelerates healing in a rat model of colitis. *Am J Physiol* 1990; **258**: G527-G534 [PMID: 1970708 DOI: 10.1152/ajpgi.1990.258.4.G527]

67 **Fabia R**, Ar'Rajab A, Johansson ML, Willén R, Andersson R, Molin G, Bengmark S. The effect of exogenous administration of Lactobacillus reuteri R2LC and oat fiber on acetic acid-induced colitis in the rat. *Scand J Gastroenterol* 1993; **28**: 155-162 [PMID: 8382837 DOI: 10.3109/00365529309096063]

68 **Vieira C**, Ferreirinha F, Magalhães-Cardoso MT, Silva I, Marques P, Correia-de-Sá P. Post-inflammatory Ileitis Induces Non-neuronal Purinergic Signaling Adjustments of Cholinergic Neurotransmission in the Myenteric Plexus. *Front Pharmacol* 2017; **8**: 811 [PMID: 29167643 DOI: 10.3389/fphar.2017.00811]

69 **Orechio D**, Andrade Aguiar B, Baroni Diniz G, Cioni Bittencourt J, Haemmerle CAS, Watanabe IS, Miglino MA, Castelucci P. Morphological and Cellular Characterization of the Fetal Canine (Canis lupus familiaris) Subventricular Zone, Rostral Migratory Stream, and Olfactory Bulb. *Anat Rec (Hoboken)* 2018; **301**: 1570-1584 [PMID: 29752870 DOI: 10.1002/ar.23855]

70 **Sant'Ana DM**, Góis MB, Zanoni JN, da Silva AV, da Silva CJ, Araújo EJ. Intraepithelial lymphocytes, goblet cells and VIP-IR submucosal neurons of jejunum rats infected with Toxoplasma gondii. *Int J Exp Pathol* 2012; **93**: 279-286 [PMID: 22804764 DOI: 10.1111/j.1365-2613.2012.00824.x]

71 **Góis MB**, Hermes-Uliana C, Barreto Zago MC, Zanoni JN, da Silva AV, de Miranda-Neto MH, de Almeida Araújo EJ, Sant'Ana Dde M. Chronic infection with Toxoplasma gondii induces death of submucosal enteric neurons and damage in the colonic mucosa of rats. *Exp Parasitol* 2016; **164**: 56-63 [PMID: 26902605 DOI: 10.1016/j.exppara.2016.02.009]

72 **Pavanelli MF**, Colli CM, Gomes ML, Góis MB, de Alcântara Nogueira de Melo G, de Almeida Araújo EJ, de Mello Gonçales Sant'Ana D. Comparative study of effects of assemblages AII and BIV of Giardia duodenalis on mucosa and microbiota of the small intestine in mice. *Biomed Pharmacother* 2018; **101**: 563-571 [PMID: 29514129 DOI: 10.1016/j.biopha.2018.02.141]

73 **Furlan-Murari PJ**, de Lima ECS, de Souza FP, Urrea-Rojas AM, Eugenio Pupim AC, de Almeida Araújo EJ, Meletti PC, Seino Leal CN, Fernandes LL, Lopera-Barrero NM. Inclusion of β-1,3/1,6-glucan in the ornamental fish, Jewel tetra (Hyphessobrycon eques), and its effects on growth, blood glucose, and intestinal histology. *Aquacult Int* 2022; **30**: 501-515 [DOI: 10.1007/s10499-021-00815-1]

74 **Ke P**, Shao BZ, Xu ZQ, Chen XW, Liu C. Intestinal Autophagy and Its Pharmacological Control in Inflammatory Bowel Disease. *Front Immunol* 2016; **7**: 695 [PMID: 28119697 DOI: 10.3389/fimmu.2016.00695]

75 **Ishisono K**, Mano T, Yabe T, Kitaguchi K. Dietary Fiber Pectin Ameliorates Experimental Colitis in a Neutral Sugar Side Chain-Dependent Manner. *Front Immunol* 2019; **10**: 2979 [PMID: 31921214 DOI: 10.3389/fimmu.2019.02979]

76 **Arseneau KO**, Tamagawa H, Pizarro TT, Cominelli F. Innate and adaptive immune responses related to IBD pathogenesis. *Curr Gastroenterol Rep* 2007; **9**: 508-512 [PMID: 18377804 DOI: 10.1007/s11894-007-0067-3]

77 **Frank DN**, St Amand AL, Feldman RA, Boedeker EC, Harpaz N, Pace NR. Molecular-phylogenetic characterization of microbial community imbalances in human inflammatory bowel diseases. *Proc Natl Acad Sci U S A* 2007; **104**: 13780-13785 [PMID: 17699621 DOI: 10.1073/pnas.0706625104]

78 **Neurath MF**. Host-microbiota interactions in inflammatory bowel disease. *Nat Rev Gastroenterol Hepatol* 2020; **17**: 76-77 [PMID: 31848474 DOI: 10.1038/s41575-019-0248-1]

79 **Tavakoli P**, Vollmer-Conna U, Hadzi-Pavlovic D, Grimm MC. A Review of Inflammatory Bowel Disease: A Model of Microbial, Immune and Neuropsychological Integration. *Public Health Rev* 2021; **42**: 1603990 [PMID: 34692176 DOI: 10.3389/phrs.2021.1603990]

80 **Caetano MAF**, Castelucci P. Role of short chain fatty acids in gut health and possible therapeutic approaches in inflammatory bowel diseases. *World J Clin Cases* 2022; **10**: 9985-10003 [PMID: 36246826 DOI: 10.12998/wjcc.v10.i28.9985]

81 **Sanovic S**, Lamb DP, Blennerhassett MG. Damage to the enteric nervous system in experimental colitis. *Am J Pathol* 1999; **155**: 1051-1057 [PMID: 10514387 DOI: 10.1016/S0002-9440(10)65207-8]

82 **Cirillo C**, Sarnelli G, Cuomo R. Enteric nervous system abnormalities in ulcerative colitis. In: O'Connor MB. Ulcerative Colitis-Epidemiology, Pathogenesis and Complications. 2011. [cited 20 March 2023]. Available from: https://cdn.intechopen.com/pdfs/24837/InTech-Enteric_nervous_system_abnormalities_in_ulcerative_colitis.pdf

83 **Figliuolo VR**, Savio LEB, Safya H, Nanini H, Bernardazzi C, Abalo A, de Souza HSP, Kanellopoulos J, Bobé P, Coutinho CMLM, Coutinho-Silva R. P2X7 receptor promotes intestinal inflammation in chemically induced colitis and triggers death of mucosal regulatory T cells. *Biochim Biophys Acta Mol Basis Dis* 2017; **1863**: 1183-1194 [PMID: 28286160 DOI: 10.1016/j.bbadis.2017.03.004]

84 **Spear ET**, Mawe GM. Enteric neuroplasticity and dysmotility in inflammatory disease: key players and possible therapeutic targets. *Am J Physiol Gastrointest Liver Physiol* 2019; **317**: G853-G861 [PMID: 31604034 DOI: 10.1152/ajpgi.00206.2019]

85 **Stavely R**, Abalo R, Nurgali K. Targeting Enteric Neurons and Plexitis for the Management of Inflammatory Bowel Disease. *Curr Drug Targets* 2020; **21**: 1428-1439 [PMID: 32416686 DOI: 10.2174/1389450121666200516173242]

86 **Brenna Ø**, Furnes MW, Drozdov I, van Beelen Granlund A, Flatberg A, Sandvik AK, Zwiggelaar RT, Mårvik R, Nordrum IS, Kidd M, Gustafsson BI. Relevance of TNBS-colitis in rats: a methodological study with endoscopic, histologic and Transcriptomic [corrected] characterization and correlation to IBD. *PLoS One* 2013; **8**: e54543 [PMID: 23382912 DOI: 10.1371/journal.pone.0054543]

87 **Morris GP**, Beck PL, Herridge MS, Depew WT, Szewczuk MR, Wallace JL. Hapten-induced model of chronic inflammation and ulceration in the rat colon. *Gastroenterology* 1989; **96**: 795-803 [PMID: 2914642]

88 **Kawada M**, Arihiro A, Mizoguchi E. Insights from advances in research of chemically induced experimental models of human inflammatory bowel disease. *World J Gastroenterol* 2007; **13**: 5581-5593 [PMID: 17948932 DOI: 10.3748/wjg.v13.i42.5581]

89 **Sigalet DL**, Wallace L, De Heuval E, Sharkey KA. The effects of glucagon-like peptide 2 on enteric neurons in intestinal inflammation. *Neurogastroenterol Motil* 2010; **22**: 1318-e350 [PMID: 20718942 DOI: 10.1111/j.1365-2982.2010.01585.x]

90 **Chassaing B**, Aitken JD, Malleshappa M, Vijay-Kumar M. Dextran sulfate sodium (DSS)-induced colitis in mice. *Curr Protoc Immunol* 2014; **104**: 15.25.1-15.25.14 [PMID: 24510619 DOI: 10.1002/0471142735.im1525s104]

91 **Wirtz S**, Neufert C, Weigmann B, Neurath MF. Chemically induced mouse models of intestinal inflammation. *Nat Protoc* 2007; **2**: 541-546 [PMID: 17406617 DOI: 10.1038/nprot.2007.41]

92 **Silva I**, Pinto R, Mateus V. Preclinical Study in Vivo for New Pharmacological Approaches in Inflammatory Bowel Disease: A Systematic Review of Chronic Model of TNBS-Induced Colitis. *J Clin Med* 2019; **8** [PMID: 31581545 DOI: 10.3390/jcm8101574]

93 **Neves AR**, Castelo-Branco MT, Figliuolo VR, Bernardazzi C, Buongusto F, Yoshimoto A, Nanini HF, Coutinho CM, Carneiro AJ, Coutinho-Silva R, de Souza HS. Overexpression of ATP-activated P2X7 receptors in the intestinal mucosa is implicated in the pathogenesis of Crohn's disease. *Inflamm Bowel Dis* 2014; **20**: 444-457 [PMID: 24412990 DOI: 10.1097/01.MIB.0000441201.10454.06]

94 **Hofman P**, Cherfils-Vicini J, Bazin M, Ilie M, Juhel T, Hébuterne X, Gilson E, Schmid-Alliana A, Boyer O, Adriouch S, Vouret-Craviari V. Genetic and pharmacological inactivation of the purinergic P2RX7 receptor dampens inflammation but increases tumor incidence in a mouse model of colitis-associated cancer. *Cancer Res* 2015; **75**: 835-845 [PMID: 25564520 DOI: 10.1158/0008-5472.CAN-14-1778]

95 **Linden DR**, Couvrette JM, Ciolino A, McQuoid C, Blaszyk H, Sharkey KA, Mawe GM. Indiscriminate loss of myenteric neurones in the TNBS-inflamed guinea-pig distal colon. *Neurogastroenterol Motil* 2005; **17**: 751-760 [PMID: 16185315 DOI: 10.1111/j.1365-2982.2005.00703.x]

96 **Poli E**, Lazzaretti M, Grandi D, Pozzoli C, Coruzzi G. Morphological and functional alterations of the myenteric plexus in rats with TNBS-induced colitis. *Neurochem Res* 2001; **26**: 1085-1093 [PMID: 11699935 DOI: 10.1023/a:1012313424144]

97 **Ziegler U**, Groscurth P. Morphological features of cell death. *News Physiol Sci* 2004; **19**: 124-128 [PMID: 15143207 DOI: 10.1152/nips.01519.2004]

98 **Elmore S**. Apoptosis: a review of programmed cell death. *Toxicol Pathol* 2007; **35**: 495-516 [PMID: 17562483 DOI: 10.1080/01926230701320337]

99 **Degterev A**, Yuan J. Expansion and evolution of cell death programmes. *Nat Rev Mol Cell Biol* 2008; **9**: 378-390 [PMID: 18414491 DOI: 10.1038/nrm2393]

100 **Poon IK**, Lucas CD, Rossi AG, Ravichandran KS. Apoptotic cell clearance: basic biology and therapeutic potential. *Nat Rev Immunol* 2014; **14**: 166-180 [PMID: 24481336 DOI: 10.1038/nri3607]

101 **Ponder KG**, Boise LH. The prodomain of caspase-3 regulates its own removal and caspase activation. *Cell Death Discov* 2019; **5**: 56 [PMID: 30701088 DOI: 10.1038/s41420-019-0142-1]

102 **Lister MF**, Sharkey J, Sawatzky DA, Hodgkiss JP, Davidson DJ, Rossi AG, Finlayson K. The role of the purinergic P2X7 receptor in inflammation. *J Inflamm (Lond)* 2007; **4**: 5 [PMID: 17367517 DOI: 10.1186/1476-9255-4-5]

103 **Antonioli L**, Colucci R, Pellegrini C, Giustarini G, Tuccori M, Blandizzi C, Fornai M. The role of purinergic pathways in the pathophysiology of gut diseases: pharmacological modulation and potential therapeutic applications. *Pharmacol Ther* 2013; **139**: 157-188 [PMID: 23588157 DOI: 10.1016/j.pharmthera.2013.04.002]

104 **Rotondo JC**, Mazziotta C, Lanzillotti C, Stefani C, Badiale G, Campione G, Martini F, Tognon M. The Role of Purinergic P2X7 Receptor in Inflammation and Cancer: Novel Molecular Insights and Clinical Applications. *Cancers (Basel)* 2022; **14** [PMID: 35267424 DOI: 10.3390/cancers14051116]

105 **North RA**. Molecular physiology of P2X receptors. *Physiol Rev* 2002; **82**: 1013-1067 [PMID: 12270951 DOI: 10.1152/physrev.00015.2002]

106 **Burnstock G**. Purine and pyrimidine receptors. *Cell Mol Life Sci* 2007; **64**: 1471-1483 [PMID: 17375261 DOI: 10.1007/s00018-007-6497-0]

107 **Dubyak GR**. P2X7 receptor regulation of non-classical secretion from immune effector cells. *Cell Microbiol* 2012; **14**: 1697-1706 [PMID: 22882764 DOI: 10.1111/cmi.12001]

108 **Neurath MF**, Pettersson S, Meyer zum Büschenfelde KH, Strober W. Local administration of antisense phosphorothioate oligonucleotides to the p65 subunit of NF-kappa B abrogates established experimental colitis in mice. *Nat Med* 1996; **2**: 998-1004 [PMID: 8782457 DOI: 10.1038/nm0996-998]

109 **Schreiber S**, Nikolaus S, Hampe J. Activation of nuclear factor kappa B inflammatory bowel disease. *Gut* 1998; **42**: 477-484 [PMID: 9616307 DOI: 10.1136/gut.42.4.477]

110 **Lawrance IC**, Wu F, Leite AZ, Willis J, West GA, Fiocchi C, Chakravarti S. A murine model of chronic inflammation-induced intestinal fibrosis down-regulated by antisense NF-kappa B. *Gastroenterology* 2003; **125**: 1750-1761 [PMID: 14724828 DOI: 10.1053/j.gastro.2003.08.027]

111 **Atreya I**, Atreya R, Neurath MF. NF-kappaB in inflammatory bowel disease. *J Intern Med* 2008; **263**: 591-596 [PMID: 18479258 DOI: 10.1111/j.1365-2796.2008.01953.x]

112 **Listwak SJ**, Rathore P, Herkenham M. Minimal NF-κB activity in neurons. *Neuroscience* 2013; **250**: 282-299 [PMID: 23872390 DOI: 10.1016/j.neuroscience.2013.07.013]

113 **Peyrin-Biroulet L**, Bressenot A, Kampman W. Histologic remission: the ultimate therapeutic goal in ulcerative colitis? *Clin Gastroenterol Hepatol* 2014; **12**: 929-34.e2 [PMID: 23911875 DOI: 10.1016/j.cgh.2013.07.022]

114 **Chateau T**, Feakins R, Marchal-Bressenot A, Magro F, Danese S, Peyrin-Biroulet L. Histological Remission in Ulcerative Colitis: Under the Microscope Is the Cure. *Am J Gastroenterol* 2020; **115**: 179-189 [PMID: 31809296 DOI: 10.14309/ajg.0000000000000437]

115 **Udawat H**, Nunia V, Mathur P, Udawat HP, Gaur KL, Saxena AK, Mohan MK. Histopathological and Immunohistochemical Findings in Congenital Pouch Colon: A Prospective Study. *Pathobiology* 2017; **84**: 202-209 [PMID: 28605747 DOI: 10.1159/000460821]

116 **Xu X**, Lin S, Yang Y, Gong X, Tong J, Li K, Li Y. Histological and ultrastructural changes of the colon in dextran sodium sulfate-induced mouse colitis. *Exp Ther Med* 2020; **20**: 1987-1994 [PMID: 32782508 DOI: 10.3892/etm.2020.8946]

117 **Kim YS**, Ho SB. Intestinal goblet cells and mucins in health and disease: recent insights and progress. *Curr Gastroenterol Rep* 2010; **12**: 319-330 [PMID: 20703838 DOI: 10.1007/s11894-010-0131-2]

118 **McCauley HA**, Guasch G. Three cheers for the goblet cell: maintaining homeostasis in mucosal epithelia. *Trends Mol Med* 2015; **21**: 492-503 [PMID: 26144290 DOI: 10.1016/j.molmed.2015.06.003]

119 **Parikh K**, Antanaviciute A, Fawkner-Corbett D, Jagielowicz M, Aulicino A, Lagerholm C, Davis S, Kinchen J, Chen HH, Alham NK, Ashley N, Johnson E, Hublitz P, Bao L, Lukomska J, Andev RS, Björklund E, Kessler BM, Fischer R, Goldin R, Koohy H, Simmons A. Colonic epithelial cell diversity in health and inflammatory bowel disease. *Nature* 2019; **567**: 49-55 [PMID: 30814735 DOI: 10.1038/s41586-019-0992-y]

120 **Pu Z**, Che Y, Zhang W, Sun H, Meng T, Xie H, Cao L, Hao H. Dual roles of IL-18 in colitis through regulation of the function and quantity of goblet cells. *Int J Mol Med* 2019; **43**: 2291-2302 [PMID: 31017261 DOI: 10.3892/ijmm.2019.4156]

121 **Van der Sluis M**, De Koning BA, De Bruijn AC, Velcich A, Meijerink JP, Van Goudoever JB, Büller HA, Dekker J, Van Seuningen I, Renes IB, Einerhand AW. Muc2-deficient mice spontaneously develop colitis, indicating that MUC2 is critical for colonic protection. *Gastroenterology* 2006; **131**: 117-129 [PMID: 16831596 DOI: 10.1053/j.gastro.2006.04.020]

122 **Vergnolle N**, Cirillo C. Neurons and Glia in the Enteric Nervous System and Epithelial Barrier Function. *Physiology (Bethesda)* 2018; **33**: 269-280 [PMID: 29897300 DOI: 10.1152/physiol.00009.2018]

123 **Grondin JA**, Kwon YH, Far PM, Haq S, Khan WI. Mucins in Intestinal Mucosal Defense and Inflammation: Learning From Clinical and Experimental Studies. *Front Immunol* 2020; **11**: 2054 [PMID: 33013869 DOI: 10.3389/fimmu.2020.02054]

124 **Niv Y**. Mucin gene expression in the intestine of ulcerative colitis patients: a systematic review and meta-analysis. *Eur J Gastroenterol Hepatol* 2016; **28**: 1241-1245 [PMID: 27442499 DOI: 10.1097/MEG.0000000000000707]

World Journal of Gastroenterology

Submit a Manuscript: https://www.f6publishing.com

World J Gastroenterol 2023 June 14; 29(22): 3469-3481

DOI: 10.3748/wjg.v29.i22.3469

ISSN 1007-9327 (print) ISSN 2219-2840 (online)

ORIGINAL ARTICLE

Basic Study

Comparative analysis of the gut microbiota of wild adult rats from nine district areas in Hainan, China

Li-Na Niu, Guan-Nan Zhang, Duan-Duan Xuan, Chong Lin, Zi Lu, Pei-Pei Cao, Shao-Wen Chen, Yong Zhang, Xiu-Ji Cui, Shou-Kui Hu

Specialty type: Gastroenterology and hepatology

Provenance and peer review: Unsolicited article; Externally peer reviewed.

Peer-review model: Single blind

Peer-review report's scientific quality classification

Grade A (Excellent): 0
Grade B (Very good): B, B
Grade C (Good): 0
Grade D (Fair): 0
Grade E (Poor): 0

P-Reviewer: Calinescu AM, Switzerland; Landberg G, Sweden

Received: March 28, 2023
Peer-review started: March 28, 2023
First decision: April 10, 2023
Revised: April 19, 2023
Accepted: May 16, 2023
Article in press: May 16, 2023
Published online: June 14, 2023

Li-Na Niu, Guan-Nan Zhang, Pei-Pei Cao, Yong Zhang, Xiu-Ji Cui, Key Laboratory of Tropical Translational Medicine of Ministry of Education, Hainan Medical University, Haikou 571199, Hainan Province, China

Li-Na Niu, Guan-Nan Zhang, Pei-Pei Cao, Yong Zhang, Xiu-Ji Cui, The University of Hong Kong Joint Laboratory of Tropical Infectious Diseases, Hainan Medical University, Haikou 571199, Hainan Province, China

Li-Na Niu, Guan-Nan Zhang, Pei-Pei Cao, Yong Zhang, Xiu-Ji Cui, Department of Pathogen Biology, Hainan Medical University, Haikou 571199, Hainan Province, China

Duan-Duan Xuan, Department of Laboratory, Xinxiang First People's Hospital, Xinxiang 453000, Henan Province, China

Chong Lin, Zi Lu, Shao-Wen Chen, Department of Laboratory, The Second Affiliated Hospital of Hainan Medical University, Haikou 570311, Hainan Province, China

Shou-Kui Hu, Department of Clinical Laboratory, Peking University Shougang Hospital, Beijing 100144, China

Corresponding author: Shou-Kui Hu, MD, Professor, Department of Clinical Laboratory, Peking University Shougang Hospital, No. 9 Jinyuanzhuang Road, Shijingshan District, Beijing 100144, China. shoukuihu@163.com

Abstract

BACKGROUND

Wild rats have the potential to hold zoonotic infectious agents that can spread to humans and cause disease.

AIM

To better understand the composition of gut bacterial communities in rats is essential for preventing and treating such diseases. As a tropical island located in the south of China, Hainan province has abundant rat species. Here, we examined the gut bacterial composition in wild adult rats from Hainan province.

METHODS

Fresh fecal samples were collected from 162 wild adult rats, including three

species (*Rattus norvegicus*, *Leopoldamys edwardsi*, and *Rattus losea*), from nine regions of Hainan province between 2017-2018.

RESULTS

We analyzed the composition of gut microbiota using the 16S rRNA gene amplicon sequencing. We identified 4903 bacterial operational taxonomic units (30 phyla, 175 families, and 498 genera), which vary between samples of different rat species in various habitats at various times of the year. In general, Firmicutes were the most abundant phyla, followed by Bacteroidetes (15.55%), Proteobacteria (6.13%), and Actinobacteria (4.02%). The genus *Lactobacillus* (20.08%), unidentified_*Clostridiales* (5.16%), *Romboutsia* (4.33%), unidentified_*Ruminococcaceae* (3.83%), *Bacteroides* (3.66%), *Helicobacter* (2.40%) and *Streptococcus* (2.37%) were dominant.

CONCLUSION

The composition and abundance of the gut microbial communities varied between rat species and locations. This work provides fundamental information to identify microbial communities useful for disease control in Hainan province.

Key Words: Hainan; Rat; Fecal microbiome; Microbial community; 16S rRNA

©The Author(s) 2023. Published by Baishideng Publishing Group Inc. All rights reserved.

Core Tip: Several researches have investigated the microbial communities in arthropods but few researches have investigated microbial diversity in wild rats' gut in Hainan province. Here, by 16S rRNA gene amplicon sequencing we compared the gut bacterial communities in fecal samples from 162 wild rats of three species and nine geographic locations in Hainan.

Citation: Niu LN, Zhang GN, Xuan DD, Lin C, Lu Z, Cao PP, Chen SW, Zhang Y, Cui XJ, Hu SK. Comparative analysis of the gut microbiota of wild adult rats from nine district areas in Hainan, China. *World J Gastroenterol* 2023; 29(22): 3469-3481

URL: https://www.wjgnet.com/1007-9327/full/v29/i22/3469.htm

DOI: https://dx.doi.org/10.3748/wjg.v29.i22.3469

INTRODUCTION

The laboratory rat has been used as a useful experimental model for biomedical sciences since the last century. Rats were domesticated as early as the Edo period[1]. Gut microbiota is composed of myriad microbes (archaea, bacteria, fungi, and viruses) that interact with each other and with their host, playing important roles in the host's metabolism, physiology, homeostasis, health, and disease development[2]. There is an increase in studies of the laboratory rat gut microbiota[3-9], but very few on wild rats[10].

Wild rats pose a serious threat to public health because they are reservoirs for a number of zoonotic pathogens[11-13] and frequently and closely interact with people, domestic animals, and other animals.

Only a small number of researchers have looked into the microbial diversity in the guts of wild rats in the province of Hainan, compared to the number of researchers who have looked into the microbial communities in arthropods. Here, by 16S rRNA gene amplicon sequencing we compared the gut bacterial communities in fecal samples from 162 wild rats of three species and nine geographic locations in Hainan.

MATERIALS AND METHODS

Rat collection and morphology identification

Between December 2017 and November 2018, wild adult rats were collected using mousetraps in rat cages from nine geographic locations in Hainan province (L1-L9: L1 = Yinggeling; L2 = Huangjingjiaoling; L3 = Danzhou; L4 = Dongfang; L5 = Haikou; L6 = Jianfengling; L7 = Baisha; L8 = Sanya; L9 = Lingao) (Figure 1 and Supplementary Table 1). The trap sites we selected included mountains, residential areas, and farmland. When the team got back to the lab, they based their determination of gender on the morphology of the external reproductive organs. Based on DNA barcode analysis, a polymerase chain reaction (PCR) assay was used to confirm the identification of the species of rats. The characteristics of all rats are recorded, including acquisition time, location, sex, weight, and adult or

immaturity (Supplementary Table 1).

Molecular identification of rats

The SDS method was used for DNA extraction. The PCR assay was performed to identify rat species using the primer 5′-TACCATGAGGACAAATATCATTCTG-3′ and 5′-CCTCCTAGTTTGTTAGGGATTGATCG-3′[14]. Amplification was performed in 25 μL total volume, including DNA template (2 μL), each primer (0.5 μL), 10 × Gene Amp PCR Buffer (2.5 μL), dNTP (1.25 mmol/L) (2 μL), rTaq DNA polymerase (5 U/μL) (0.5 μL) and double distilled water (17 μL). The PCR procedure was as follows: (1) Initial denaturation 95 ℃ (5 min); (2) 35 cycles each of denaturation 94 ℃ (30 s); (3) primer annealing 51 ℃ (30 s); and (4) extension 72 ℃ (30 s). It took 5 min to complete the extension step's 35th cycle. The mouse species was determined through a blast to the NCBI nucleotide database, and the amplification products were identified using Sanger sequencing.

Tissue and fecal sampling

CO_2 was used for euthanizing rats. Intestinal tissue was dissected for each rat species, rinsing three times in sterile normal saline. In the meantime, samples of feces were taken from the intestinal tissues. Then, samples were immediately collected in a brain heart infusion medium with glycerol and subsequently stored at -80 ℃ until analysis.

16S rRNA microbial profiling preparation

Fecal samples weighing about 50 mg were used for 16S rRNA microbial profiling analyses. Following the manufacturer's instructions, microbial DNA was extracted from the fecal samples using a QIAamp Fast DNA Stool Mini Kit (Qiagen, Germany). The PCR products were examined using electrophoresis. Thermo GeneJET Gel Extraction Kit was used to recover the PCR products after running them on 2% agarose gels in TAE buffer. Until analyses, all of the extracted DNA was kept at -20 ℃.

The hypervariable regions V3-V4 of the bacterial 16S rRNA were amplified with primers 5′-CCTAYGGGRBGCASCAG-3′ and 5′-GGACTACNNGGGTATCTAAT-3′. PCR reactions were performed in a 30 μL volume consisting of Phusion® High-Fidelity PCR Master Mix with GC buffer (New England Biolabs) (15 μL), forward and reverse primers (0.2 μM), and template DNA (10 ng). The PCR reaction was done with the following conditions: (1) Initial denaturation at 98 ℃ for 1 min; (2) 30 cycles of denaturation at 98 ℃ for 10 s; (3) annealing at 50 ℃ for 30 s; (4) elongation at 72 ℃ for 30 s; and (5) final extension 72 ℃ for 5 min. Sequencing libraries were made with an Ion Plus Fragment Library Kit (48 rxns) (Thermo Scientific) according to the manufacturer's protocols. The Qubit 2.0 Fluorometer (Thermo Scientific) was used to evaluate the library's quality. Sequencing was done on the Ion S5TM XL platform last.

16S rRNA microbial profiling analysis

Based on the unique barcode, single-end reads were assigned to samples and truncated by cutting off the barcode and primer sequence. The Cutadapt quality control process involved treating the raw reads with quality filtering under specific filtering conditions in order to produce high-quality clean reads [15]. Then, we compared the reads with the Silva database, and reference database[16] using UCHIME Algorithm[17] to detect and remove chimera sequences[18] to obtain clean reads.

Uparse software performed analyses of microbial profiling[19]. Sequences with a 97% or higher similarity to one another were found to the same Operational taxonomic unit (OTU). We screened the representative sequence of each OTU for further annotation. Taxonomic data was annotated at various taxonomic levels using the Silva Database, which uses the Mothur algorithm[16]. We used the MUSCLE software to conduct multiple sequence alignment to study the difference between the dominant species in different groups[20]. We normalized OTUs abundance using the standard sequence number of the sample with the least sequences and summarized the OTU abundance in a table. Subsequently, we analyzed the alpha diversity (α-diversity) and beta diversity (β-diversity) based on this normalized data.

Bacterial diversity analysis

In the complexity of species diversity, we applied α-diversity through 6 indices (Observed-species, Chao1, ACE, Shannon, Simpson, Good's coverage). Chao1 and ACE were selected as the Chao1 and ACE estimators to determine richness. The Shannon index and Simpson index were used to calculating Shannon diversity and Simpson diversity. Using Good's coverage, Coverage was chosen to describe the depth of the Sequencing.

We applied β-diversity for evaluating the similarity of different samples rather than describing within-sample diversity like α-diversity. We calculated β-diversity on both Weighted and Unweighted unifrac. The dimension of the original variables was reduced using principal component analysis. Principal coordinate analysis (PCoA) was performed to visualize complex, multidimensional data and was displayed to visualize microbial community structure relationships. Firstly, we obtained a distance matrix among samples in weighted or unweighted unifrac. Secondly, we transformed the distance matrix to a new set of orthogonal axes. Finally, the first principal coordinate demonstrated the maximum variation factor, and the second principal coordinate demonstrated the second maximum

one, and so on. We performed Adonis analysis to know to what extent location explained variation in microbial composition. For significant difference analysis, either the USEARCH software (https://www.drive5.com/usearch) or R software (version 4.0.3) was used.

RESULTS

Rat species from different sampling areas

Among the 162 wild rats collected by traps from nine district areas which covered almost half of Hainan province (Figure 1), three rat species (*Rattus norvegicus*, *Leopoldamys edwardsi*, and *Rattus losea*) were predominant (Table 1 and Supplementary Table 1). These rat species showed distinct geographic distributions. *Rattus norvegicus* (brown rat) was mainly found in farmland (Danzhou, Dongfang, Baisha, and Sanya) and residential areas (Haikou); *Leopoldamys edwardsi* (Edward's long-tailed rat) was exclusively found in mountain areas in Yinggeling, Huangjingjiaoling, and Jianfengling; *Rattus losea* (Lesser rice-field rat) was only found from mountains in Lingao area (Table 1).

Gut bacterial species composition among rat species

A total of 162 fecal samples (one from each rat) were collected from the field-collected wild adult rats and subjected to bacterial profiling analyses, and estimating the bacterial community composition of these samples involved 16S rRNA gene amplicon sequencing. A total of 13326753 raw reads (mean ± SE = 82263.91 ± 8277.45 per sample) were obtained from the 162 samples that were sequenced (Supplementary Table 2). Among them, 12537453 clean reads (mean ± SE = 77391.69 ± 7604.97 per sample) remained for subsequent analyses after quality control processing. These sequences were divided into 4903 OTUs that belonged to 30 phyla, 175 families, and 498 genera (Supplementary Table 3). Among those OTUs that were defined to species level (Supplementary Table 3), some notoriously famous bacteria were found, such as *Bacillus anthracis* (OUT_426), *Bacteroides pyogenes* (OUT_3846), *Clostridium perfringens* (OUT_8), *Streptococcus suis* (OUT_410), and *Vibrio cholerae* (OUT_3092).

As shown in Figure 2A, sequences originating from Firmicutes (average 65.76%, Supplementary Table 4) were dominant, followed by Bacteroidetes (15.55%), Proteobacteria (6.13%), Actinobacteria (4.02%), Unclassified bacteria (3.68%), Tenericutes (1.93%), Fusobacteria (1.00%), Spirochaetes (0.88%), Chlamydiae (0.27%), Melainabacteria (0.17%), and so on (detailed in Supplementary Table 4, those < 0.15% were pooled together as "Others" in Figure 2A). Although Bacteroidetes were the second most abundant on average, this was not the case for samples from Danzhou, Haikou, Baisha, and Lingao (Supplementary Table 4).

Following a similar trend, Clostridia (averaged 32.72%) and Bacilli (averaged 26.48%) were the top two classes of bacteria in most samples (Figure 2B), but Clostridia only ranked fourth in samples from the Jianfengling area, and Bacteroidia was the 2nd most abundant in samples from Yinggeling, Huangjingjiaoling and Sanya (Supplementary Table 5).

According to the average value, the most abundant family was Lactobacillaceae (20.08%), followed by Ruminococcaceae (12.03%), Lachnospiraceae (8.11%), Muribaculaceae (6.33%), Peptostreptococcaceae (5.61%), unidentified_Clostridiales (5.58%), Erysipelotrichaceae (5.50%), Bacteroidaceae (3.66%), Enterobacteriaceae (3.25%), and Streptococcaceae (2.71%) (detailed in Supplementary Table 6, those < 2.5% were pooled together as "Others" in Figure 2C). Compared to the profiles for the bacterial phylum and class, the profiles for the actual values were more complex. Lactobacillaceae was the most abundant in samples from five areas (Danzhou, Dongfang, Jianfengling, Baisha, and Lingao), Ruminococcaceae was most abundant in samples from Yinggeling and Huangjingjiaoling, and Peptostreptococcaceae and Bacteroidaceae were the richest in samples from Haikou and Sanya, respectively (Supplementary Table 6).

As illustrated in Figure 2D and detailed in Supplementary Table 7, the genus with the highest OTU abundance in the feces of rats was those (with relative abundance less than 0.5%) designated as 'others' (average 26.80%), followed by *Lactobacillus* (20.08%), unidentified_*Clostridiales* (5.16%), *Romboutsia* (4.33%), and so on. In samples from eight different areas, "Others" or *Lactobacillus* ranked first and second, but not in samples from the Haikou area, which had the highest concentrations of unidentified *Clostridiales* and *Romboutsia*.

As shown in Figure 3, the heatmap color-coded the different OUT compositions in samples of the nine groups (Figure 3A); all of the samples contained unique bacterial OTUs, according to the upset plot (Figure 3B), but those from the Jianfengling region had the highest numbers of both (618 for unique and 153 for common with the Lingao area).

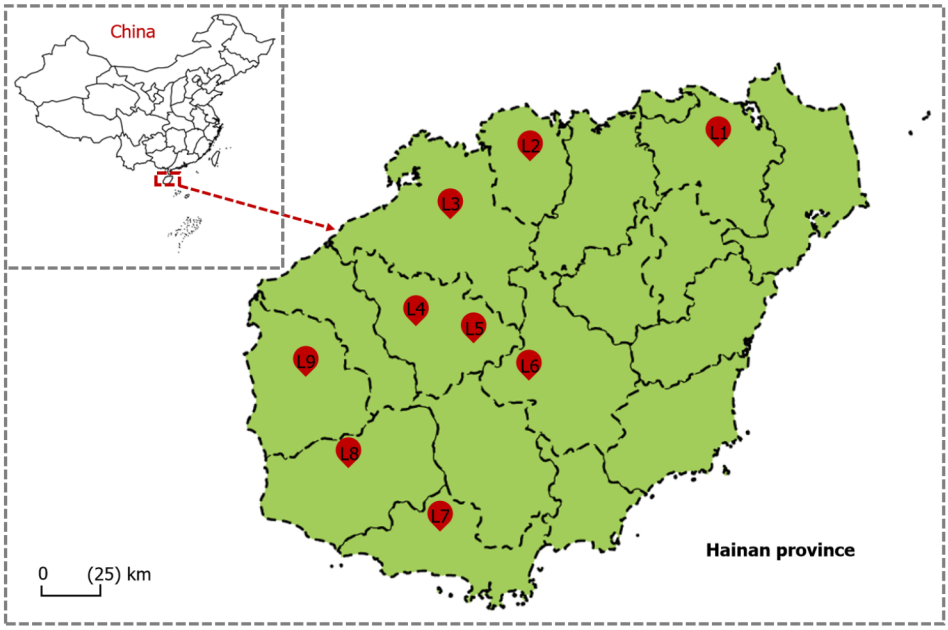
Gut bacterial diversity of rat

Alpha diversity indices were performed to detect whether bacterial diversity and richness significantly varied among samples of different rat species and geographic locations. The bacterial species richness, represented by Chao1 and ace denoting the number of species rather than the abundance of each species was highest for samples from the Yinggeling area (Table 2). Statistics were conducted for the Chao1 values because the values of both indices (Chao1 and ace) changed in a remarkably similar way across

Table 1 Location, species, number, season, and habitat of trapped rats

Site	Rat species	Number of midgut samples	Sampling season	Trap sites
YGL	LE	32	2018.11	Mountains
HJJL	LE	25	2018.11	Mountains
DZ	RN	12	2017.12	Farmland
DF	RN	12	2018.01	Farmland
HK	RN	13	2017.12	Residential areas
JFL	LE	13	2018.06	Mountains
BS	RN	12	2018.01	Farmland
SY	RN	23	2018.05	Farmland
LG	RL	20	2018.11	Mountains

YGL: Yinggeling; HJJL: Huangjingjiaoling; DZ: Danzhou; DF: Dongfang; HK: Haikou; JFL: Jianfengling; BS: Baisha; SY: Sanya; LG: Lingao; LE: Leopoldamys edwardsi; RN: Rattus norvegicus; RL: Rattus losea.



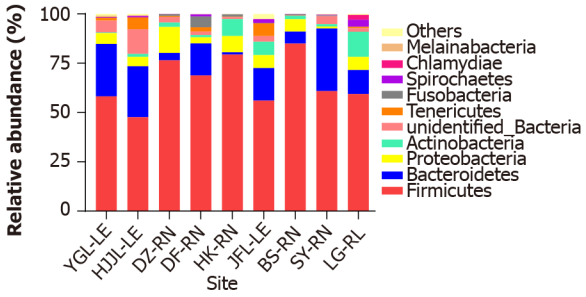
DOI: 10.3748/wjg.v29.i22.3469 **Copyright** ©The Author(s) 2023.

Figure 1 Sketch map of Hainan province. The map shows the locations of the nine collection study sites. L1 = Yinggeling, mountain; L2 = Huangjingjiaoling, mountain; L3 = Danzhou, residential areas; L4 = Dongfang, residential areas; L5 = Haikou, residential areas; L6 = Jianfengling, mountain; L7 = Baisha, residential areas; L8 = Sanya, residential areas; L9 = Lingao, farmland.

the nine groups. Except for Lingao and Jianfengling, samples from Yinggeling and Huangjingjiaoling, the two highest among all, had significantly more bacteria than the other five samples (Figure 4A). Taking Yinggeling as an example, it was most significantly higher ($P < 0.0001$) than those from Danzhou, Dongfang, Haikou, Sanya and Baisha, and significant ($P < 0.05$) compared to Lingao and Jianfengling (Figure 4A). In addition, samples from the Jianfengling area had higher bacterial richness compared to those from Danzhou and Sanya, and those from the Lingao area had higher richness than those from Danzhou and Sanya. There was no significant difference between other groups if not mentioned above.

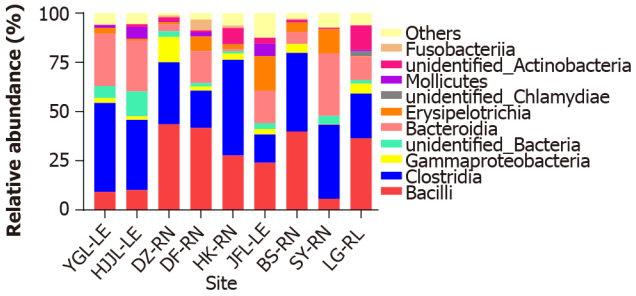
Species diversity, represented by Shannon diversity and Simpson diversity, indicates species richness and evenness in the community. As the two indices changed accordingly (Table 2), values of the Shannon diversity were used to do the statistics. In comparison to samples from Danzhou ($P < 0.0001$), Dongfang ($P < 0.01$), Haikou ($P < 0.001$), and Sanya ($P < 0.05$), samples from the Yinggeling area showed significant differences. Although similar in its bacterial composition pattern to those from the Yinggeling area, the species diversity of samples from the Huangjingjiaoling area was less significant with samples from Danzhou ($P < 0.001$) and Haikou ($P < 0.05$). In contrast to the insignificant results

A



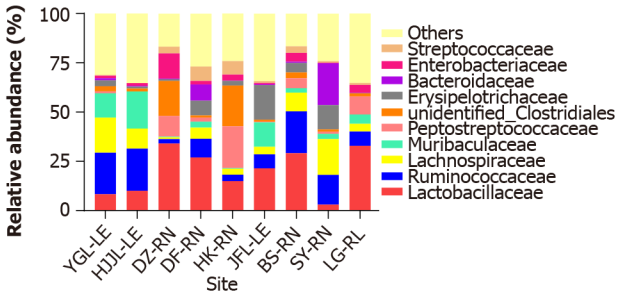
Taxonomy	YGL	HJJL	DZ	DF	HK	JFL	BS	SY	LG
Firmicutes	58.24%	47.63%	76.45%	68.80%	79.36%	56.07%	84.96%	60.89%	59.41%
Bacteroidetes	26.57%	25.85%	3.72%	16.23%	1.15%	16.48%	6.12%	31.77%	12.10%
Proteobacteria	5.41%	4.69%	13.20%	3.09%	8.31%	6.61%	6.23%	0.99%	6.68%
Actinobacteria	0.32%	1.55%	2.22%	1.13%	8.53%	6.70%	1.77%	1.18%	12.78%
unidentified_Bacteria	6.10%	12.52%	2.86%	1.76%	1.04%	2.97%	0.08%	4.02%	1.80%
Tenericutes	1.39%	5.96%	0.46%	2.20%	0.19%	6.35%	0.07%	0.05%	0.71%
Fusobacteria	0.07%	0.02%	0.95%	5.50%	1.22%	0.19%	0.60%	0.39%	0.04%
Spirochaetes	0.25%	0.67%	0.13%	1.07%	0.01%	1.88%	0.06%	0.34%	3.51%
Chlamydiae	0.00%	0.00%	0.00%	0.01%	0.01%	0.00%	0.00%	0.02%	2.43%
Melainabacteria	0.74%	0.38%	0.01%	0.11%	0.07%	0.09%	0.02%	0.05%	0.05%

B

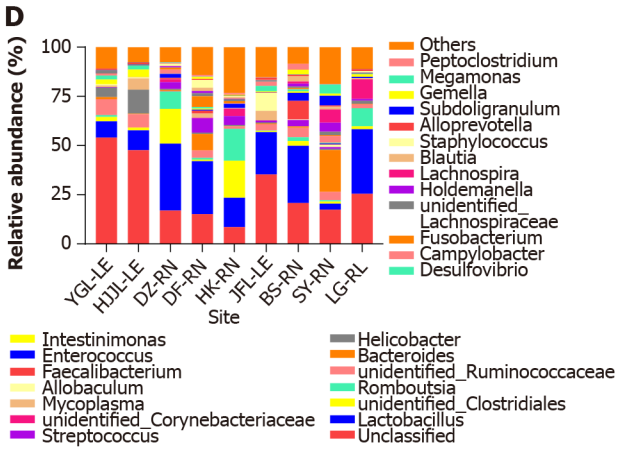


Taxonomy	YGL	HJJL	DZ	DF	HK	JFL	BS	SY	LG
Lactobacillaceae	8.27%	10.02%	34.03%	26.94%	14.94%	21.44%	29.09%	3.08%	32.91%
Ruminococcaceae	21.12 %	21.43%	2.30%	9.52%	3.23%	7.09%	21.31%	15.04%	7.21%
Lachnospiraceae	17.80%	10.17%	0.84%	5.66%	3.06%	3.87%	9.50%	18.17%	3.94%
Muribaculaceae	12.39 %	18.82%	0.39%	3.04%	0.34%	12.41%	2.22%	2.67%	4.70%
Peptostreptococcaceae	0.96%	0.04%	10.46%	2.08%	21.22%	0.31%	5.08%	1.09%	9.23%
unidentified_Clostridiales	2.55%	1.51%	17.77%	1.07%	20.65%	1.00%	2.95%	1.19%	1.53%
Erysipelotrichaceae	3.06%	1.00%	0.88%	7.44%	2.42%	17.58%	4.77%	12.27%	0.11%
Bacteroidaceae	1.10%	0.38%	0.40%	8.28%	0.17%	0.39%	0.69%	21.30%	0.25%
Enterobacteriaceae	1.24%	1.33%	12.68%	1.74%	2.98%	0.71%	4.43%	0.21%	3.89%
Streptococcaceae	0.37%	0.03%	3.49%	7.38%	6.86%	0.93%	3.36%	0.88%	1.04%

C



Taxonomy	YGL	HJJL	DZ	DF	HK	JFL	BS	SY	LG
Bacilli	9.24%	10.09%	43.51%	41.70%	27.73%	24.06%	39.85%	5.75%	36.39%
Clostridia	45.17%	35.68%	31.53%	18.95%	48.56%	14.30%	39.92%	37.65%	22.69%
Gammaproteobacteria	2.43%	1.89%	12.87%	2.03%	3.28%	2.76%	4.52%	0.35%	5.09%
unidentified_Bacteria	6.10%	12.52%	2.86%	1.76%	1.04%	2.97%	0.08%	4.02%	1.80%
Bacteroidia	26.57%	25.85%	3.72%	16.23%	1.15%	16.48%	6.12%	31.77%	12.10%
Erysipelotrichia	3.06%	1.00%	0.88%	7.44%	2.42%	17.58%	4.77%	12.27%	0.11%
unidentified_Chlamydiae	0.00%	0.00%	0.00%	0.01%	0.01%	0.00%	0.00%	0.02%	2.43%
Mollicutes	1.39%	5.96%	0.46%	2.20%	0.19%	6.35%	0.07%	0.05%	0.71%
unidentified_Actinobacteria	0.12%	1.42%	2.07%	0.85%	8.12%	2.92%	1.28%	0.62%	12.47%
Fusobacteriia	0.07%	0.02%	0.95%	5.50%	1.22%	0.19%	0.60%	0.39%	0.04%



Taxonomy	YGL	HJJL	DZ	DF	HK	JFL	BS	SY	LG
Others	54.03%	47.66%	16.93%	15.13%	8.51%	35.32%	20.79%	17.39%	25.42%
Lactobacillus	8.27%	10.02%	34.03%	26.94%	14.92%	21.44%	29.08%	3.08%	32.91%
unidentified_Clostridiales	2.23%	1.43%	17.63%	0.68%	18.88%	0.59%	2.45%	1.08%	1.46%
Romboutsia	0.96%	0.03%	8.87%	0.97%	16.15%	0.29%	1.91%	0.67%	9.13%
unidentified_Ruminococcaceae	8.06%	6.70%	0.32%	3.85%	1.26%	3.19%	4.81%	4.21%	2.06%
Bacteroides	1.10%	0.38%	0.40%	8.28%	0.17%	0.39%	0.69%	21.30%	0.25%
Helicobacter	4.79%	12.13%	0.61%	0.72%	0.58%	0.58%	0.02%	0.59%	1.59%
Streptococcus	0.26%	0.02%	3.45%	7.29%	4.46%	0.91%	3.19%	0.86%	0.90%
unidentified_Corynebacteriaceae	0.01%	0.00%	1.47%	0.30%	3.83%	0.00%	0.07%	0.01%	9.93%
Mycoplasma	0.86%	5.78%	0.06%	1.98%	0.04%	4.88%	0.02%	0.02%	0.55%

DOI: 10.3748/wjg.v29.i22.3469 **Copyright** ©The Author(s) 2023.

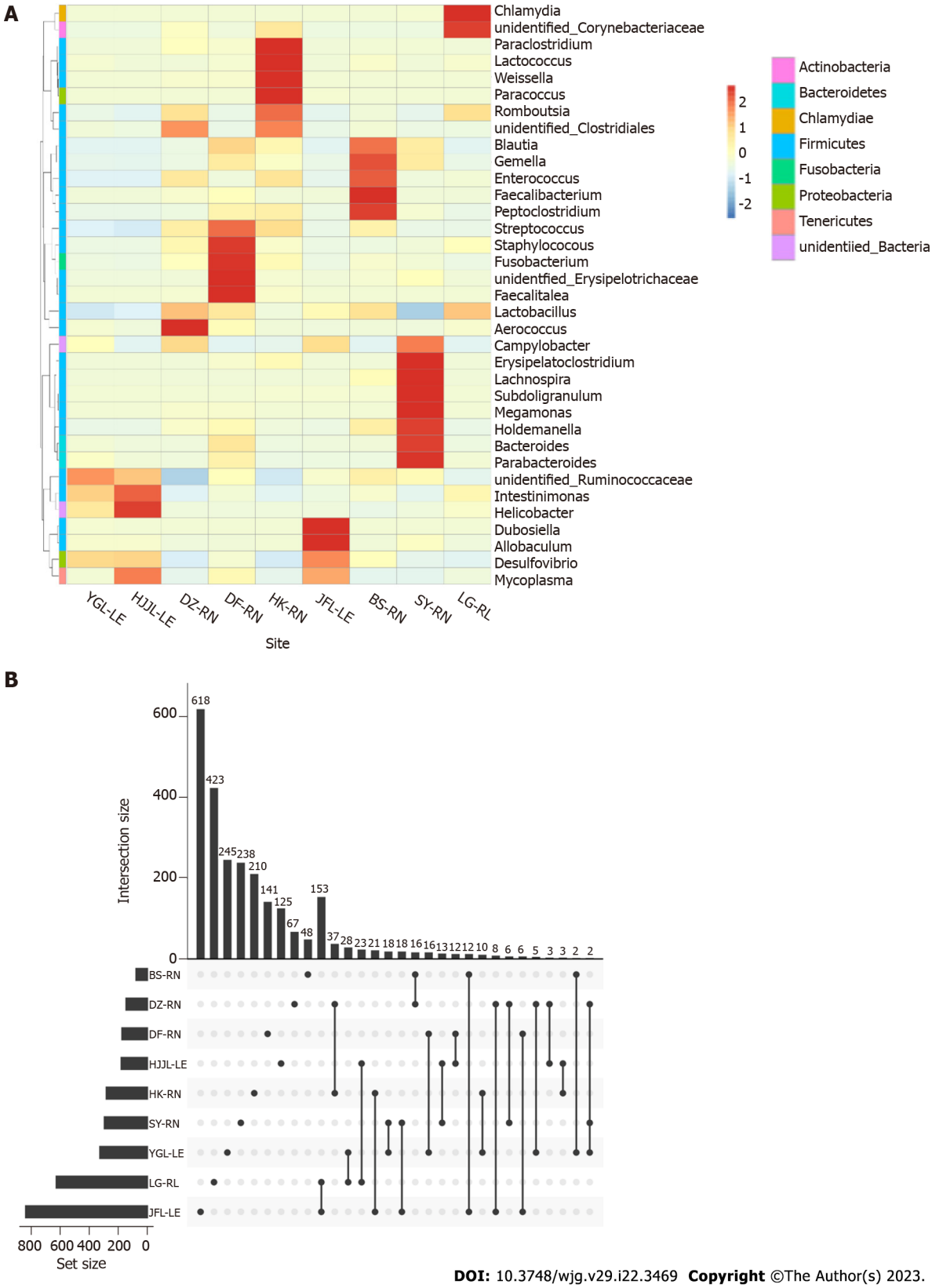
Figure 2 Mean relative abundances of bacterial phylum, class, family, and genus associated with three rat species at different sites. A: Phylum; B: Class; C: Family; D: Genus. Families with an abundance of less than 2.50% and Phyla with an abundance of less than 0.15% were combined to form the category "Others." YGL: Yinggeling; HJJL: Huangjingjiaoling; DZ: Danzhou; DF: Dongfang; HK: Haikou; JFL: Jianfengling; BS: Baisha; SY: Sanya; LG: Lingao; LE: Leopoldamys edwardsi; RN: Rattus norvegicus; RL: Rattus losea.

among sample groups not mentioned above, the species diversity of samples from the Danzhou area was significantly different ($P < 0.05$) from those from the Lingao area (Figure 4B).

Variation of gut bacterial communities among study locations

Distance metrics were used to estimate differences between rat species and geographical locations in bacterial community profiles. The results showed a significant difference in microbiota among the three rat species and nine locations based on unweighted unifrac and weighted unifrac distances. When analyzing the fecal microbiota from various study sites, we used PCoA plots to visualize its composition. Using Unweighted Unifrac distance, two PCoA coordinates percent variation explained PCo1 (21.33%) and PCo2 (6.98%) of the total variation, respectively. We observed significant differences in fecal microbial β-diversity among communities from different locations, including *Leopoldamys edwardsi* from Yinggeling, Huangjingjiaoling, and Jianfengling; *Rattus norvegicus* from Danzhou, Baisha, and Sanya. *Rattus norvegicus* from the Dongfang area does not cluster tightly. There were no observable differences between Rattus norvegicus from Danzhou and Haikou (Figure 5A). Two PCoA coordinates based on Weighted Unifrac distance percent variation revealed PCo1 (44.41%) and PCo2 (10.69%), respectively (Figure 5B). These differences were mainly due to the geographical location, which included a plethora of variables (rat species, habitat, season, diet, *etc.*).

Heatmaps based on Bray-Curtis distances and Weighted unifrac distances, respectively, showed the diversity and similarity of microbial communities (Figure 5C and D). As shown in Figure 5C, the most similar (0.508, the lowest in Supplementary Table 8) intestinal bacterial community structure was between samples from Jianfengling and Huangjingjiaoling (highlighted with blue triangles in



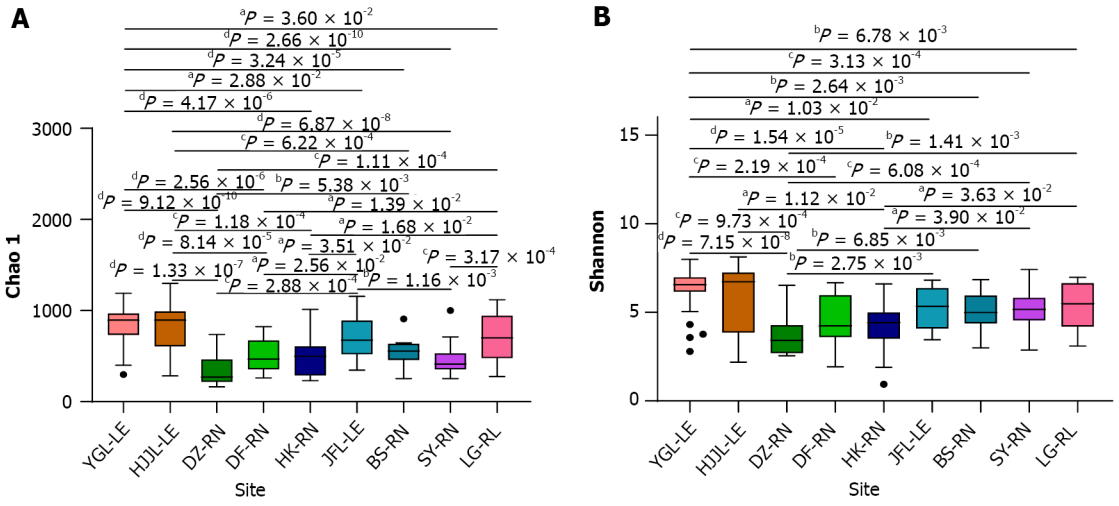
DOI: 10.3748/wjg.v29.i22.3469 **Copyright** ©The Author(s) 2023.

Figure 3 Heatmap and upset plot featuring the rat gut bacterial community. A: The heatmap in log scale depicting the gut bacterial community of rat feces obtained with open reference operational taxonomic unit (OTU) picking methods. Blue colors represent high abundance, and red colors represent low abundance; white indicates absence; B: Visualizing the relationships between OTUs in all rat species across all sites using an upset plot. The Sangerbox tools, a free online platform for data analysis, were used to create the plot (http://www.sangerbox.com/tool). YGL: Yinggeling; HJJL: Huangjingjiaoling; DZ: Danzhou; DF: Dongfang; HK: Haikou; JFL: Jianfengling; BS: Baisha; SY: Sanya; LG: Lingao; LE: Leopoldamys edwardsi; RN: Rattus norvegicus; RL: Rattus losea.

Table 2 Richness and diversity (mean ± SD) of the rat intestinal content bacterial community

Group	Observed_species	Chao1	Ace	Shannon	Simpson
YGL-LE	662.16 ± 185.6	853.76 ± 201.05	862.86 ± 191.94	6.30 ± 1.19	0.95 ± 0.05
HJJL-LE	654.16 ± 207.22	827.96 ± 227.51	835.31 ± 217.91	5.83 ± 1.88	0.88 ± 0.15
DZ-RN	213.42 ± 128.99	340.60 ± 168.92	348.04 ± 161.47	3.70 ± 1.14	0.82 ± 0.10
DF-RN	369.50 ± 177.23	490.55 ± 186.68	511.53 ± 179.36	4.59 ± 1.39	0.87 ± 0.12
HK-RN	346.85 ± 188.71	492.23 ± 226.98	511.22 ± 234.13	4.19 ± 1.59	0.80 ± 0.21
JFL-LE	533.77 ± 209.11	696.02 ± 238.19	700.85 ± 227.48	5.25 ± 1.17	0.89 ± 0.07
BS-RN	424.17 ± 126.51	550.92 ± 164.77	574.32 ± 159.53	5.04 ± 1.07	0.89 ± 0.09
SY-RN	342.91 ± 129.91	458.86 ± 162.56	466.06 ± 153.41	5.12 ± 1.01	0.92 ± 0.06
LG-RL	532.85 ± 221.85	715.35 ± 259.97	747.67 ± 259.51	5.30 ± 1.31	0.90 ± 0.09

YGL: Yinggeling; HJJL: Huangjingjiaoling; DZ: Danzhou; DF: Dongfang; HK: Haikou; JFL: Jianfengling; BS: Baisha; SY: Sanya; LG: Lingao; LE: Leopoldamys edwardsi; RN: Rattus norvegicus; RL: Rattus losea.



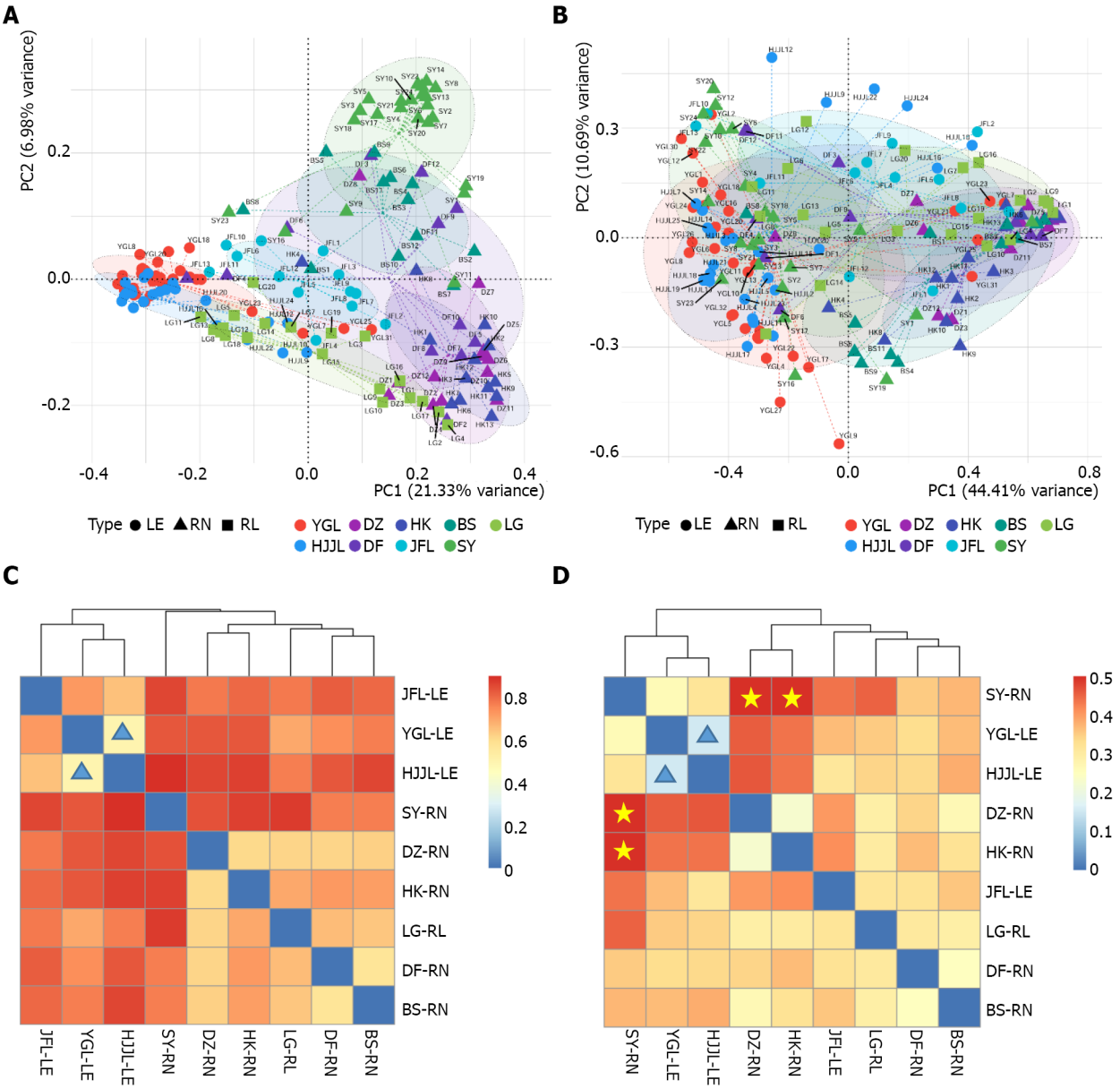
DOI: 10.3748/wjg.v29.i22.3469 **Copyright** ©The Author(s) 2023.

Figure 4 Boxplot representation of observed species. Boxplots show the distribution of bacteria between rat samples categorized under different locations and rat species. A: Boxplot representation of chao1; B: Boxplot representation of Shannon diversity. Values from all statistical tests are available in additional Table 2. YGL: Yinggeling; HJJL: Huangjingjiaoling; DZ: Danzhou; DF: Dongfang; HK: Haikou; JFL: Jianfengling; BS: Baisha; SY: Sanya; LG: Lingao; LE: Leopoldamys edwardsi; RN: Rattus norvegicus; RL: Rattus losea. $^{a}P < 0.05$; $^{b}P < 0.01$; $^{c}P < 0.001$; $^{d}P < 0.0001$.

Figure 5C), followed by that between Baisha and Dongfang (0.57), and those of Danzhou area (0.61-0.63, Supplementary Table 8) with Baisha, Dongfang, Haikou, and Lingao (Figure 5C). Conversely, samples from the Sanya area were most dissimilar to those from Huangjingjiaoling (0.91), Lingao (0.89), and Haikou (0.88). As shown in Figure 5D, the lowest difference (0.16, Supplementary Table 9) was observed between samples from Yinggeling and Huangjingjiaoling (highlighted by the blue triangles), suggesting the bacteria in these two groups of samples were evolutionary more similar. Conversely, the bacteria in the samples from the Sanya area were evolutionary most distant (highlighted by the stars in Figure 5D) to those from Danzhou and Haikou (0.51 and 0.57, respectively; Supplementary Table 9).

DISCUSSION

Through the same procedure from sample collection and processing to sequencing, the gut bacterial communities differed at all levels (phylum, class, family, and genus) among fecal samples of wild rats from nine geographical locations, three different habitats, and rat species, and two seasons (winter *vs* summer). According to scant research, diet uncontrollable for wild rats is a significant determinant of gut bacterial composition[21-23], which differs for rats living in diverse habitats in every location at all



DOI: 10.3748/wjg.v29.i22.3469 **Copyright** ©The Author(s) 2023.

Figure 5 Principal coordinate analysis plot based on unweighted Unifrac distance and weighted Unifrac distance matrix depicting differences in the composition of the gut microbiota from different rat species and locations. A: unweighted Unifrac distance; B: Weighted Unifrac distance; C and D: Colors represent community profiles of location. Matrix heatmap of the Bray-Curtis distances (C) and the weighted unifrac beta diversity (D) between the microbial communities of rats from nine different areas. YGL: Yinggeling; HJJL: Huangjingjiaoling; DZ: Danzhou; DF: Dongfang; HK: Haikou; JFL: Jianfengling; BS: Baisha; SY: Sanya; LG: Lingao; LE: Leopoldamys edwardsi; RN: Rattus norvegicus; RL: Rattus losea.

seasons. There were quite a few striking findings from our study. As the only representative samples of residential area (Haikou) rats, their gut bacterial composition was different at the family and genus level, richest with *Peptostreptococcaceae* and unidentified_*Clostridiales* at the family level, and with unidentified_*Clostridiales* and *Romboutsia* at the genus level. Although collected from the same rat species (*Rattus norvegicus*) during the same winter season, the bacterial profiles of the four groups of samples from different areas (Baisha, Dongfang, Danzhou, and Haikou) were distinctly different at the class, family, and genus level, revealing the complexity of factors (*e.g.*, habitat, farmland *vs* residential area) behind the bacterial community. The general bacterial profile of samples taken from the same species of rat (*Leopoldamys edwardsi*) in the summer in one mountain area (Yinggeling) varied from samples taken in the winter from the other two mountain areas (Huangjingjiaoling and Jianfengling), indicating that season (and thus a variety of factors) played a significant role in determining their gut bacterial composition.

Several studies report that Firmicutes, Bacteroidetes, and Proteobacteria are the most abundant phyla, and *Lactobacillus* is the predominant genus in fecal samples from both wild (*Rattus norvegicus*) and laboratory (Sprague-Dawley) rats[7,9], a pattern similar to our results. Fusobacteria was interestingly

the fourth most prevalent phylum in[10], which is most consistent with findings from one of our nine groups (Dongfang) (Figure 2B). Although of the same species (*Rattus norvegicus*), sample size (12), and similar climate, rats from the Dongfang area of this study were trapped in January from farmland on an isolated island contrasting to all year round (one mouse per month) from a residential area in an inland metropolitan city[10].

Although we identified some potential bacterial pathogens by their species names and reputation in the samples (Supplementary Table 3), a profile distinct from the results of other studies[11,12], they still need to be tested for virulence and pathogenesis. Because wild rats carry some bacteria (*Bacillus anthracis*, *Vibrio cholerae,* and *Yersinia pestis*)[11,12] and this study] can cause a serious outbreak or even a pandemic, it would be prudent to start a regular survey program at some strategic points to monitor the distribution of sentinel rodents and the target pathogens the animals may transmit.

The ideal comparison should only have one factor, but this seems like an impossible task for our current research. Admittedly our study had some limitations, to name a few: (1) As some variables, like sex, age, and so on, were difficult, if not impossible, to control as a baseline investigation; (2) despite the interesting findings (having the highest *Corynebacteriaceae* in all samples) of the gut bacterial composition in *Rattus losea*, it was from only one area (Lingao); (3) the summer samples were collected from two different rat species (*Rattus norvegicus vs Leopoldamys edwardsi*,) in two different habitats (farmland *vs* mountain) from only one area each, making the results less conclusive and comparable; and (4) samples from residential rats were only from Haikou area, making some of the results less comparable.

CONCLUSION

The study revealed the structure of gut bacterial communities by sampling wild rats' feces. In general, the gut microbiota was different in both composition and abundance in samples from the nine areas of Hainan of three wild rat species, three habitats (mountain, farmland, and residential area), and two seasons (summer and winter). This study provides fundamental information for identifying microbial communities that will be useful for disease control in Hainan Province.

ARTICLE HIGHLIGHTS

Research background

Wild rats are potential reservoirs for zoonotic infectious agents which can be transmitted to and cause diseases in humans.

Research motivation

As a tropical island locating in the south of China, Hainan province has abundant rat species.

Research objectives

To better understand the composition of gut bacterial communities in rats is essential for preventing and treating such diseases. Here, we examined the gut bacterial composition in wild adult rats from Hainan province.

Research methods

Fresh faecal samples were collected from 162 wild adult rats, including three species (*Rattus norvegicus*, *Leopoldamys edwardsi*, and *Rattus losea*), from nine regions of Hainan province between 2017-2018.

Research results

We analyzed the composition of gut microbiota using the 16S rRNA gene amplicon sequencing. We identified 4,903 bacterial operational taxonomic units (30 phyla, 175 families, and 498 genera), which is different among samples of different rat species in different habitat during different season. In general, Firmicutes were the most abundant phyla, followed by Bacteroidetes (15.55%), Proteobacteria (6.13%) and Actinobacteria (4.02%). The genus *Lactobacillus* (20.08%), unidentified_*Clostridiales* (5.16%), *Romboutsia* (4.33%), unidentified_*Ruminococcaceae* (3.83%), *Bacteroides* (3.66%), *Helicobacter* (2.40%) and *Streptococcus* (2.37%) were dominant.

Research conclusions

Among locations for rat species, the gut microbial communities were different in composition and abundance. This work provides fundamental information to identify microbial communities useful for disease control in Hainan province.

Research perspectives

The study revealed the structure of gut bacterial communities by sampling wild rats' feces. In general, the gut microbiota was different in both composition and abundance in samples from the nine areas of Hainan of three wild rat species, three habitats (mountain, farmland and residential area), and of two seasons (summer and winter). This work provides fundamental information to identify microbial communities which will be useful for disease control in Hainan province.

FOOTNOTES

Author contributions: Niu LN, Zhang GN, Xuan DD, Lin C and Lu Z contributed equally; Niu LN contributed to the conceptualization; Zhang GN, Xuan DD, and Cao PP performed the data curation; Lu Z, Chen SW, and Zhang Y contributed to the formal analysis; Cao PP, Cui XJ, and Lu Z performed the investigation; Niu LN, and Lin C performed the methodology; Hu SK, and Lin C contributed to the supervision; Niu LN, Zhang GN, Xuan DD, and Hu SK wrote the original draft; All authors contributed to the article and approved the submitted version.

Supported by Hainan Province Science and Technology Special Fund, No. ZDYF2022SHFZ114; Hainan Provincial Natural Science Foundation of China, No. 820RC650; National Natural Science Foundation of China, No. 82060377; Innovative Research Project for Graduate Students of Hainan Medical University, No. HYYS2020-18, No. HYYS2021A09, and No. HYYS2021A22.

Institutional animal care and use committee statement: The study was approved by the Animal Ethics Committee of Hainan Medical University, China. We confirmed that all methods were performed under the relevant guidelines and regulations.

Conflict-of-interest statement: All the authors report no relevant conflicts of interest for this article.

Data sharing statement: The study's datasets have been added to the Sequence Read Archive repository (SRA). This item has accession number PRJNA767903.

ARRIVE guidelines statement: The authors have read the ARRIVE guidelines, and the manuscript was prepared and revised according to the ARRIVE guidelines.

Open-Access: This article is an open-access article that was selected by an in-house editor and fully peer-reviewed by external reviewers. It is distributed in accordance with the Creative Commons Attribution NonCommercial (CC BY-NC 4.0) license, which permits others to distribute, remix, adapt, build upon this work non-commercially, and license their derivative works on different terms, provided the original work is properly cited and the use is non-commercial. See: https://creativecommons.org/Licenses/by-nc/4.0/

Country/Territory of origin: China

ORCID number: Shou-Kui Hu 0000-0001-6339-3954.

S-Editor: Fan JR
L-Editor: A
P-Editor: Fan JR

REFERENCES

1 **Hulme-Beaman A**, Orton D, Cucchi T. The origins of the domesticate brown rat (Rattus norvegicus) and its pathways to domestication. *Anim Front* 2021; **11**: 78-86 [PMID: 34158992 DOI: 10.1093/af/vfab020]
2 **Chen Y**, Zhou J, Wang L. Role and Mechanism of Gut Microbiota in Human Disease. *Front Cell Infect Microbiol* 2021; **11**: 625913 [PMID: 33816335 DOI: 10.3389/fcimb.2021.625913]
3 **Brooks SP**, McAllister M, Sandoz M, Kalmokoff ML. Culture-independent phylogenetic analysis of the faecal flora of the rat. *Can J Microbiol* 2003; **49**: 589-601 [PMID: 14663493 DOI: 10.1139/w03-075]
4 **Manichanh C**, Reeder J, Gibert P, Varela E, Llopis M, Antolin M, Guigo R, Knight R, Guarner F. Reshaping the gut microbiome with bacterial transplantation and antibiotic intake. *Genome Res* 2010; **20**: 1411-1419 [PMID: 20736229 DOI: 10.1101/gr.107987.110]
5 **Ferrario C**, Statello R, Carnevali L, Mancabelli L, Milani C, Mangifesta M, Duranti S, Lugli GA, Jimenez B, Lodge S, Viappiani A, Alessandri G, Dall'Asta M, Del Rio D, Sgoifo A, van Sinderen D, Ventura M, Turroni F. How to Feed the Mammalian Gut Microbiota: Bacterial and Metabolic Modulation by Dietary Fibers. *Front Microbiol* 2017; **8**: 1749 [PMID: 28955319 DOI: 10.3389/fmicb.2017.01749]
6 **Flemer B**, Gaci N, Borrel G, Sanderson IR, Chaudhary PP, Tottey W, O'Toole PW, Brugère JF. Fecal microbiota variation across the lifespan of the healthy laboratory rat. *Gut Microbes* 2017; **8**: 428-439 [PMID: 28586297 DOI: 10.1080/19490976.2017.1334033]

7 **Li D**, Chen H, Mao B, Yang Q, Zhao J, Gu Z, Zhang H, Chen YQ, Chen W. Microbial Biogeography and Core Microbiota of the Rat Digestive Tract. *Sci Rep* 2017; **8**: 45840 [PMID: 28374781 DOI: 10.1038/srep45840]

8 **Nagpal R**, Wang S, Solberg Woods LC, Seshie O, Chung ST, Shively CA, Register TC, Craft S, McClain DA, Yadav H. Comparative Microbiome Signatures and Short-Chain Fatty Acids in Mouse, Rat, Non-human Primate, and Human Feces. *Front Microbiol* 2018; **9**: 2897 [PMID: 30555441 DOI: 10.3389/fmicb.2018.02897]

9 **Pan H**, Guo R, Zhu J, Wang Q, Ju Y, Xie Y, Zheng Y, Wang Z, Li T, Liu Z, Lu L, Li F, Tong B, Xiao L, Xu X, Li R, Yuan Z, Yang H, Wang J, Kristiansen K, Jia H, Liu L. A gene catalogue of the Sprague-Dawley rat gut metagenome. *Gigascience* 2018; **7** [PMID: 29762673 DOI: 10.1093/gigascience/giy055]

10 **He WQ**, Xiong YQ, Ge J, Chen YX, Chen XJ, Zhong XS, Ou ZJ, Gao YH, Cheng MJ, Mo Y, Wen YQ, Qiu M, Huo ST, Chen SW, Zheng XY, He H, Li YZ, You FF, Zhang MY, Chen Q. Composition of gut and oropharynx bacterial communities in Rattus norvegicus and Suncus murinus in China. *BMC Vet Res* 2020; **16**: 413 [PMID: 33129337 DOI: 10.1186/s12917-020-02619-6]

11 **Himsworth CG**, Parsons KL, Jardine C, Patrick DM. Rats, cities, people, and pathogens: a systematic review and narrative synthesis of literature regarding the ecology of rat-associated zoonoses in urban centers. *Vector Borne Zoonotic Dis* 2013; **13**: 349-359 [PMID: 23590323 DOI: 10.1089/vbz.2012.1195]

12 **Easterbrook JD**, Kaplan JB, Vanasco NB, Reeves WK, Purcell RH, Kosoy MY, Glass GE, Watson J, Klein SL. A survey of zoonotic pathogens carried by Norway rats in Baltimore, Maryland, USA. *Epidemiol Infect* 2007; **135**: 1192-1199 [PMID: 17224086 DOI: 10.1017/S0950268806007746]

13 **Zhao W**, Zhou H, Yang L, Ma T, Zhou J, Liu H, Lu G, Huang H. Prevalence, genetic diversity and implications for public health of Enterocytozoon bieneusi in various rodents from Hainan Province, China. *Parasit Vectors* 2020; **13**: 438 [PMID: 32878633 DOI: 10.1186/s13071-020-04314-9]

14 **Verma SK**, Singh L, Novel universal primers establish identity of an enormous number of animal species for forensic application.
Molecular Ecology Notes 2010; 3: 28-31 [DOI: 10.1046/j.1471-8286.2003.00340.x]

15 **Martin M**. Cutadapt removes adapter sequences from high-throughput sequencing reads. *EMBnet J* 2011; **17** [DOI: 10.14806/ej.17.1.200]

16 **Quast C**, Pruesse E, Yilmaz P, Gerken J, Schweer T, Yarza P, Peplies J, Glöckner FO. The SILVA ribosomal RNA gene database project: improved data processing and web-based tools. *Nucleic Acids Res* 2013; **41**: D590-D596 [PMID: 23193283 DOI: 10.1093/nar/gks1219]

17 **Edgar RC**, Haas BJ, Clemente JC, Quince C, Knight R. UCHIME improves sensitivity and speed of chimera detection. *Bioinformatics* 2011; **27**: 2194-2200 [PMID: 21700674 DOI: 10.1093/bioinformatics/btr381]

18 **Haas BJ**, Gevers D, Earl AM, Feldgarden M, Ward DV, Giannoukos G, Ciulla D, Tabbaa D, Highlander SK, Sodergren E, Methé B, DeSantis TZ; Human Microbiome Consortium, Petrosino JF, Knight R, Birren BW. Chimeric 16S rRNA sequence formation and detection in Sanger and 454-pyrosequenced PCR amplicons. *Genome Res* 2011; **21**: 494-504 [PMID: 21212162 DOI: 10.1101/gr.112730.110]

19 **Edgar RC**. UPARSE: highly accurate OTU sequences from microbial amplicon reads. *Nat Methods* 2013; **10**: 996-998 [PMID: 23955772 DOI: 10.1038/nmeth.2604]

20 **Edgar RC**. MUSCLE: multiple sequence alignment with high accuracy and high throughput. *Nucleic Acids Res* 2004; **32**: 1792-1797 [PMID: 15034147 DOI: 10.1093/nar/gkh340]

21 **Queipo-Ortuño MI**, Seoane LM, Murri M, Pardo M, Gomez-Zumaquero JM, Cardona F, Casanueva F, Tinahones FJ. Gut microbiota composition in male rat models under different nutritional status and physical activity and its association with serum leptin and ghrelin levels. *PLoS One* 2013; **8**: e65465 [PMID: 23724144 DOI: 10.1371/journal.pone.0065465]

22 **Liu X**, Blouin JM, Santacruz A, Lan A, Andriamihaja M, Wilkanowicz S, Benetti PH, Tomé D, Sanz Y, Blachier F, Davila AM. High-protein diet modifies colonic microbiota and luminal environment but not colonocyte metabolism in the rat model: the increased luminal bulk connection. *Am J Physiol Gastrointest Liver Physiol* 2014; **307**: G459-G470 [PMID: 24970777 DOI: 10.1152/ajpgi.00400.2013]

23 **Qi X**, Xu W, Guo M, Chen S, Liu Y, He X, Huang K. Rice- or pork-based diets with similar calorie and content result in different rat gut microbiota. *Int J Food Sci Nutr* 2017; **68**: 829-839 [PMID: 28320221 DOI: 10.1080/09637486.2017.1301889]

World Journal of Gastroenterology

Submit a Manuscript: https://www.f6publishing.com

World J Gastroenterol 2023 June 14; 29(22): 3482-3496

DOI: 10.3748/wjg.v29.i22.3482

ISSN 1007-9327 (print) ISSN 2219-2840 (online)

ORIGINAL ARTICLE

Case Control Study

Plasma exosomal hsa_circ_0079439 as a novel biomarker for early detection of gastric cancer

Xiao Li, Yan-Li Lin, Jia-Kang Shao, Xiao-Jie Wu, Xiang Li, He Yao, Fa-Liang Shi, Long-Song Li, Wen-Gang Zhang, Zheng-Yao Chang, Ning-Li Chai, You-Liang Wang, En-Qiang Linghu

Specialty type: Gastroenterology and hepatology

Provenance and peer review: Unsolicited article; Externally peer reviewed.

Peer-review model: Single blind

Peer-review report's scientific quality classification

Grade A (Excellent): 0
Grade B (Very good): B
Grade C (Good): C
Grade D (Fair): 0
Grade E (Poor): 0

P-Reviewer: Liu L, China; Schmidt T, Germany

Received: April 16, 2023
Peer-review started: April 16, 2023
First decision: April 28, 2023
Revised: May 4, 2023
Accepted: May 11, 2023
Article in press: May 11, 2023
Published online: June 14, 2023

Xiao Li, Long-Song Li, Wen-Gang Zhang, Ning-Li Chai, En-Qiang Linghu, Department of Gastroenterology, The First Medical Center of Chinese PLA General Hospital, Beijing 100853, China

Xiao Li, Jia-Kang Shao, Long-Song Li, Wen-Gang Zhang, Zheng-Yao Chang, Medical School of Chinese PLA, Beijing 100853, China

Xiao Li, Yan-Li Lin, Xiao-Jie Wu, Xiang Li, He Yao, Fa-Liang Shi, You-Liang Wang, Beijing Institute of Biotechnology, Beijing 100071, China

Corresponding author: En-Qiang Linghu, PhD, Chief Physician, Professor, Department of Gastroenterology, The First Medical Center of Chinese PLA General Hospital, No. 28 Fuxing Road, Haidian District, Beijing 100853, China. linghuenqiang@vip.sina.com

Abstract

BACKGROUND

Due to the poor prognosis of gastric cancer (GC), early detection methods are urgently needed. Plasma exosomal circular RNAs (circRNAs) have been suggested as novel biomarkers for GC.

AIM

To identify a novel biomarker for early detection of GC.

METHODS

Healthy donors (HDs) and GC patients diagnosed by pathology were recruited. Nine GC patients and three HDs were selected for exosomal whole-transcriptome RNA sequencing. The expression profiles of circRNAs were analyzed by bioinformatics methods and validated by droplet digital polymerase chain reaction. The expression levels and area under receiver operating characteristic curve values of plasma exosomal circRNAs and standard serum biomarkers were used to compare their diagnostic efficiency.

RESULTS

There were 303 participants, including 240 GC patients and 63 HDs, involved in the study. The expression levels of exosomal hsa_circ_0079439 were significantly higher in GC patients than in HDs ($P < 0.0001$). However, the levels of standard serum biomarkers were similar between the two groups. The area under the curve

value of exosomal hsa_circ_0079439 was higher than those of standard biomarkers, including carcinoembryonic antigen, carbohydrate antigen (CA)19-9, CA72-4, alpha-fetoprotein, and CA125 (0.8595 *vs* 0.5862, 0.5660, 0.5360, 0.5082, and 0.5018, respectively). The expression levels of exosomal hsa_circ_0079439 were significantly decreased after treatment ($P < 0.05$). Moreover, the expression levels of exosomal hsa_circ_0079439 were obviously higher in early GC (EGC) patients than in HDs ($P < 0.0001$).

CONCLUSION

Our results suggest that plasma exosomal hsa_circ_0079439 is upregulated in GC patients. Moreover, the levels of exosomal hsa_circ_0079439 could distinguish EGC and advanced GC patients from HDs. Therefore, plasma exosomal hsa_circ_0079439 might be a potential biomarker for the diagnosis of GC during both the early and late stages.

Key Words: Gastric cancer; Exosomes; Circular RNA; Droplet digital polymerase chain reaction; Biomarker

©The Author(s) 2023. Published by Baishideng Publishing Group Inc. All rights reserved.

Core Tip: Gastric cancer (GC) remains a prevalent disease worldwide. Due to its atypical clinical manifestations, GC is usually diagnosed at late stages in most patients and has a poor prognosis. Therefore, early detection of GC is of great importance. Based on the results of exosomal whole-transcriptome RNA sequencing, we performed bioinformatic analysis and droplet digital polymerase chain reaction (dd-PCR) tests. As validated by dd-PCR, exosomal hsa_circ_0079439 had a higher area under the curve value than standard biomarkers. Therefore, plasma exosomal hsa_circ_0079439 could serve as a novel biomarker for the early detection of GC.

Citation: Li X, Lin YL, Shao JK, Wu XJ, Li X, Yao H, Shi FL, Li LS, Zhang WG, Chang ZY, Chai NL, Wang YL, Linghu EQ. Plasma exosomal hsa_circ_0079439 as a novel biomarker for early detection of gastric cancer. *World J Gastroenterol* 2023; 29(22): 3482-3496

URL: https://www.wjgnet.com/1007-9327/full/v29/i22/3482.htm

DOI: https://dx.doi.org/10.3748/wjg.v29.i22.3482

INTRODUCTION

Gastric cancer (GC) is the fifth most commonly diagnosed cancer and the fourth leading cause of cancer-related death; it accounted for 1089103 new cases and 768793 deaths in 2020 globally[1]. The prognosis of advanced GC (AGC) patients is poor[2]. Early detection of GC and identification of individuals who might benefit from a given treatment are of great importance. Unfortunately, the most common symptoms associated with GC are nonspecific, such as weight loss, poor appetite, and abdominal pain [2]. Based on the abovementioned conditions, the diagnosis of GC is often at a late stage[2]. Therefore, accurate early detection of GC is one of the most urgent issues in its management.

A previous study showed that carcinoembryonic antigen (CEA), carbohydrate antigen (CA)19-9, and CA72-4 levels are significantly associated with tumor stage and patient survival[3]. In addition, some studies have shown that CA125 and alpha-fetoprotein (AFP) are linked to GC[4,5]. However, the widespread use of less invasive detection methods has resulted in a number of inaccurate diagnoses due to their low sensitivity and specificity[6-8]. Therefore, it is necessary to identify novel biomarkers with higher accuracy for the early detection of GC.

Exosomes, a subset of nanometer-sized (50-150 nm) extracellular vesicles, can be secreted by almost all kinds of cells[9,10]. In addition, exosomes comprise diverse components, including proteins, DNAs, circular RNAs (circRNAs), long noncoding RNAs (lncRNAs), microRNAs (miRNAs), messenger RNAs (mRNAs), and lipids[10-13]. An increasing number of studies have shown that exosomes are involved in mediating intercellular communication and many pathological processes[9,10,14]. Therefore, they have great potential to become novel biomarkers in liquid biopsy. CircRNAs, a class of lncRNAs, were first discovered by electron microscopy more than 40 years ago[15-17]. Because of the exosomal phospholipid bilayer membrane structure, circRNAs are stable within exosomes.

Furthermore, a number of studies have demonstrated that circRNAs play an important role in GC progression, invasion, and metastasis. However, the utility of exosomal circRNAs for early detection of GC is largely unknown. Profiling circRNAs in exosomes could be useful for identifying molecular markers for early detection and prognosis prediction for various types of cancers[14,18-20].

In this study, we analyzed the expression levels of plasma exosomal circRNAs from GC patients in different clinical stages. The findings of this study support the notion that plasma exosomal circRNAs could serve as biomarkers for the diagnosis of early GC (EGC). Moreover, they might be considered as new therapeutic targets as well as effective prognostic markers for GC.

MATERIALS AND METHODS

Definitions

EGC is defined as GC confined to the mucosal and submucosal layers. Locally AGC (LAGC) was defined as stages T2-4aN0-3M0 GC, corresponding to stages Ib to IIIc and excluding T1 or T4b tumors [21-23]. Metastatic GC (MGC) refers to the invasion of GC cells into other tissues or organs. AGC includes LAGC and MGC[24].

Patients and plasma sample collection

A total of 240 GC patients (including 177 EGC patients and 63 AGC patients) and 63 healthy donors (HDs) were enrolled in our study from April 2018 to October 2022 (Figure 1). All of the GC patients had been diagnosed with adenocarcinoma after surgery. Patients who had been treated by chemoradiotherapy, targeted therapy, or cytotoxic therapy were excluded. HDs had undergone gastric endoscopy, and they did not have GC or any other gastric disease. We selected plasma exosomal samples obtained from nine GC patients (3 EGC, 3 LAGC, and 3 MGC) and three HDs for whole transcriptome RNA sequencing (nine GC patients were included in the validation cohort, and the expression levels of circRNA were verified). None of these GC patients had received any previous treatment before their first blood samples were obtained.

All participants were divided into a test cohort and a validation cohort. There were 69 GC patients and 22 HDs in the test cohort from April 2018 to December 2018. Another 171 GC patients and 41 HDs were included in the validation cohort from January 2019 to October 2022. According to the American Joint Committee on Cancer 8th edition[22,23], the clinical stage and TNM classification of GC in all patients were assessed and analyzed. All patients underwent endoscopic submucosal dissection or minimally invasive surgery to remove the lesions, which meant that accurate pathology results could be confirmed. In addition, plasma samples were acquired from GC patients 7 d after treatment.

Blood samples were collected from GC patients or HDs in K2-EDTA Blood Collection Tubes (Becton, Dickinson and Company). Blood samples were centrifuged at 500 × *g* for 15 min, and the supernatant collected was plasma. Plasma was transferred to a new tube and a unique classification number was written on the tube, which was then stored at -80 °C.

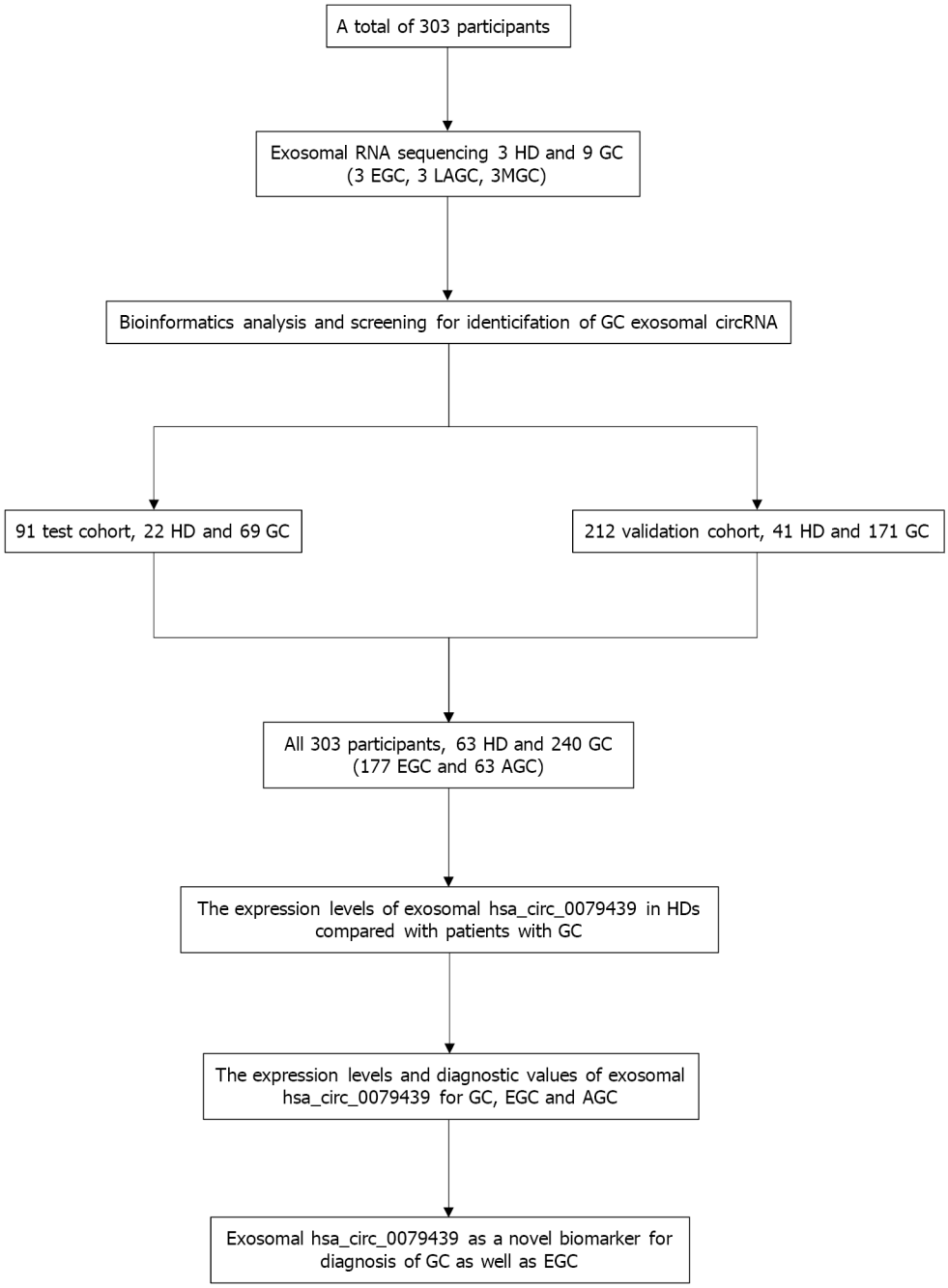
Cell culture

GC cells (GCCs) (AGS and HGC-27) were obtained from Shanghai Gaining Biological Technology Company (http://www.shgnsw.com). KATO III was obtained from the American Type Culture Collection (ATCC, http://www.atcc.org). Other GCCs (SNU-1, SGC-7901, MGC-803, and BGC-823) were obtained from the BeNa Culture Collection (BNCC, http://www.bncc.org.cn). Normal gastric epithelial cells (NGECs) were obtained from the Shanghai Qincheng Biological Technology Company (http://www.shqcsw.com). The culture methods used for the cell lines are shown in Supplementary Table 1.

Isolation and purification of exosomes

For whole-transcriptome RNA sequencing, exosomes were isolated by size-exclusion chromatography. We used a procedure described in a previous study with a few minor modifications[25]. PBS was used to perform a 1.5-fold dilution of 1 mL of each plasma sample (0.8 μm filtered). Then, the mixture was purified using Exosupur® columns (Echobiotech, China) and more PBS was used to perform elution, which resulted in a total of 2 mL of eluate. Finally, by using 100 kDa molecular weight cutoff Amicon® Ultra spin filters (Merck, Germany), the fractions obtained during the previous step were concentrated to 200 μL.

For droplet digital polymerase chain reaction (dd-PCR) test, plasma exosomes were isolated according to the manufacturer's instructions for the ExoQuick™ Exosome Precipitation Solution (SBI). Briefly, 16 μL of thrombin was added to 1000 μL of plasma at a final concentration of 5 U/mL. The mixture was incubated at room temperature for 5 min and centrifuged at 10000 rpm for 5 min, and a visible pellet was observed at the bottom of the tube. The supernatant was transferred to a new tube and centrifuged at 3000 × *g* for 5 min to remove cells and other debris. The supernatant was transferred to a new tube; 63 μL of ExoQuick Exosome Precipitation Solution was added, and the mixture was incubated at 4 °C for 30 min. After centrifuging the mixture at 1500 × *g* for 30 min, the fluid was removed. The pellet at the bottom of the tube, which contained exosomes, was collected.



DOI: 10.3748/wjg.v29.i22.3482 **Copyright** ©The Author(s) 2023.

Figure 1 Study design. HD: Healthy donor; GC: Gastric cancer; EGC: Early gastric cancer; LAGC: Locally advanced gastric cancer; MGC: Metastatic gastric cancer; circRNA: Circular RNA; AGC: Advanced gastric cancer.

Transmission electron microscopy

Exosomes isolated from plasma were diluted. Ten microliters of exosome solution was added to a copper mesh and incubated for 10 min. After cleaning the mesh with sterile distilled water, filter paper was used to absorb the liquid. Ten microliters of 2% phosphotungstic acid was added to the copper mesh and incubated for 1 min. Then, the copper mesh was dried with filter paper. The copper mesh was kept dry for several minutes at room temperature. And transmission electron microscopy (TEM) was performed.

Nanoparticle tracking analysis

After the instrument qualification test, the diameter and quantity of the exosomes isolated from plasma were measured by ZetaView PMX 110 (Particle Metrix, Meerbusch). The movement of particles was analyzed by nanoparticle tracking analysis (NTA) software (ZetaView 8.02.28) by taking 60 s of video at a rate of 30 frames/s.

Western blot analysis

After total protein extraction from exosomes, the protein concentration was measured with the Pierce BCA Protein Assay kit (Thermo). Western blot (WB) analysis was performed to measure protein expression in the extracts. The positive markers of exosomes that were used included CD9 (Abcam), TSG101 (Abcam), and CD81 (Abcam). The negative marker was calnexin (Abcam).

Total RNA extraction of exosomes and RNA analysis

Total RNA was extracted from plasma exosomes and purified with the miRNeasy Serum/Plasma Advanced Kit (Qiagen). The concentration and purity were evaluated with the RNA Nano 6000 Assay Kit and an Agilent Bioanalyzer 2100 System (Agilent Technologies).

Whole-transcriptome RNA library preparation and sequencing

According to the instructions of the SMARTer Stranded Total RNA-Seq Kit V2 (Takara), a total amount of 250 pg-10 ng RNA per sample was used as input material for RNA-seq library preparation. For small RNA libraries, a total amount of 1 ng-500 ng RNA per sample was used as input material for the QIAseq miRNA Library Kit (Qiagen). The quality of RNA-seq libraries and small RNA libraries was assessed with an Agilent Bioanalyzer 2100 (Agilent Technologies). Based on the acBot Cluster Generation System, the index-coded samples were clustered using TruSeq PE Cluster Kitv3-cBot-HS (Illumina). Then, the prepared libraries were sequenced on an Illumina NovaSeq 6000 platform. Paired-end reads were generated at EchoBiotech Co. Ltd., Beijing, P. R. China.

Bioinformatics analysis

The R package DESeq2 was used for the differential expression analysis of circRNAs, lncRNAs, miRNAs, and mRNAs between HDs and GC patients. The criteria were set as $|\log_2 FC| > 1$ and $P < 0.01$. The R package pheatmap was used for clustering analysis of these differentially expressed circRNAs, lncRNAs, miRNAs, and mRNAs. The Cancer-Specific CircRNA Database (CSCD) and CircInteractome databases were used to predict the target miRNAs of circRNAs. The TargetScan, miRDB, and miRTarBase databases were used to predict the target genes of miRNAs. Kyoto Encyclopedia of Genes and Genomes (KEGG) pathway enrichment analysis and Gene Ontology (GO) functional enrichment analysis were performed with R 4.1.1 software to identify the enriched genes.

Verification of circRNA expression by dd-PCR

Dd-PCR was performed on a QX200 Droplet System using dd-PCR EvaGreen Supermix (Bio-Rad). The divergent primers overlapping the splice junction of hsa_circ_0079439 were designed by Primer-BLAST (Supplementary Table 2).

Statistical analysis

Statistical analyses were performed with SPSS 26.0 and GraphPad Prism 8.0. The expression levels of plasma exosomal hsa_circ_0079439 and standard serum biomarkers, including CEA, CA19-9, CA72-4, AFP, and CA125, were compared between the test cohort and validation cohort, and the differences were analyzed by the *t* test. The data are shown as the mean (SD). The expression levels and area under the receiver operating characteristic (ROC) curve (AUC) values of plasma exosomal hsa_circ_0079439 and standard serum biomarkers were used to assess their diagnostic efficiency for GC, EGC, and AGC. The results with $P < 0.05$ were considered significant.

RESULTS

Clinical characteristics of patients

There were 303 participants, including 63 HDs and 240 GC patients, enrolled in our study (Table 1). There were 177 patients (73.75%) with GC at T1 stage, 7 (2.92%) with GC at T2 stage, 37 (15.42%) with GC at T3 stage, and 19 (7.91%) with GC at T4 stage. Among these GC patients, 47 (19.58%) had lymph node metastasis, and 9 (3.75%) had distant metastasis. Most GC cases were in stage I (180, 75.00%), and others were in stage II (16, 6.67%), stage III (35, 14.58%), and stage IV (9, 3.75%). The median age (range) of the HD group was 53 years (24-81 years) and that of the GC group was 64 years (34-94 years). The ratio of males to females was 43/20 in the HD group, and 187/53 in the GC group.

Isolation and identification of exosomes

To characterize exosomes and confirm their isolation from GC patients and HDs, TEM, NTA, and WB analysis were performed. The exosomes appeared to be almost round in shape according to electron microscopy images (Figure 2A). NTA indicated that the diameter of exosomes ranged from 40 nm to 200 nm, which was consistent with previous research results[26] (Figure 2B). WB results showed that exosomes expressed typical markers, including CD9, TSG101, and CD81. The negative marker calnexin was not expressed (Figure 2C).

Table 1 Clinical characteristics of individuals in test cohort and validation cohort, and total participants, *n* (%)

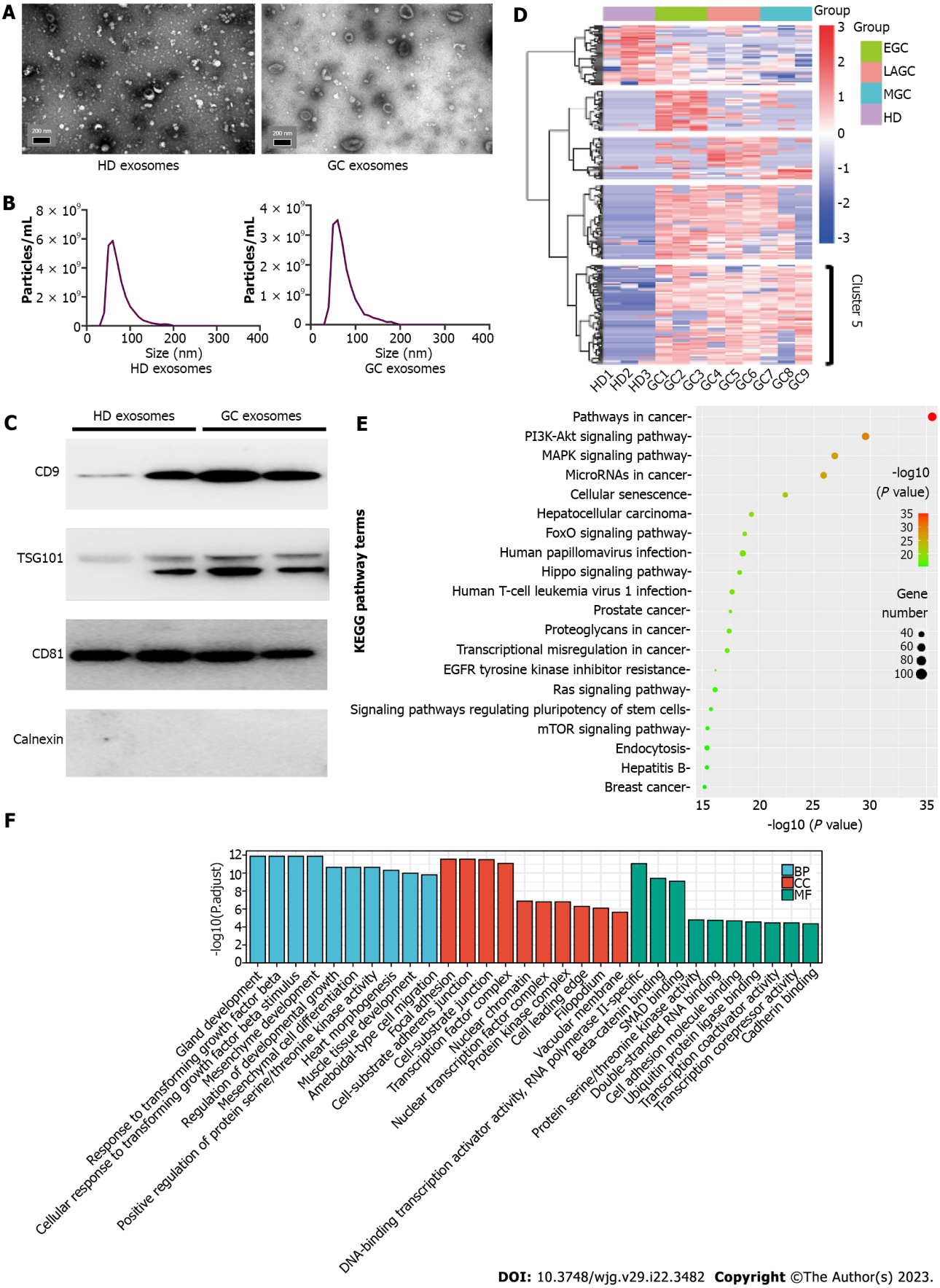
Characteristic	Test cohort (*n* = 91)		Validation cohort (*n* = 212)		Total participants (*n* = 303)	
	HD (*n* = 22)	GC (*n* = 69)	HD (*n* = 41)	GC (*n* = 171)	HD (*n* = 63)	GC (*n* = 240)
Gender						
Male	12 (54.55)	51 (73.91)	31 (75.61)	136 (79.53)	43 (68.25)	187 (77.92)
Female	10 (45.45)	18 (26.09)	10 (24.39)	35 (20.47)	20 (31.75)	53 (22.08)
Age (yr), median (range)	54 (32-77)	66 (35-84)	53 (24-81)	64 (34-94)	53 (24-81)	64 (34-94)
T stage	/		/		/	
T1		69 (100.00)		108 (63.16)		177 (73.75)
T2		0		7 (4.09)		7 (2.92)
T3		0		37 (21.64)		37 (15.42)
T4		0		19 (11.11)		19 (7.91)
N stage	/		/		/	
N0		69 (100.00)		124 (72.51)		193 (80.42)
N1		0		11 (6.43)		11 (4.58)
N2		0		14 (8.19)		14 (5.83)
N3		0		22 (12.87)		22 (9.17)
M stage	/		/		/	
M0		69 (100.00)		162 (94.74)		231 (96.25)
M1		0		9 (5.26)		9 (3.75)
Clinical stage	/		/		/	
I		69 (100.00)		111 (64.91)		180 (75.00)
II		0		16 (9.36)		16 (6.67)
III		0		35 (20.47)		35 (14.58)
IV		0		9 (5.26)		9 (3.75)

HD: Healthy donor; GC: Gastric cancer.

Bioinformatic analysis of whole-transcriptome RNA sequencing results

There were 14976 circRNAs, 3061 lncRNAs, 1629 miRNAs, and 12830 mRNAs identified by whole transcriptome RNA sequencing of exosomes. Clustering analysis was performed to reveal the differentially expressed circRNAs, lncRNAs, miRNAs, and mRNAs between HDs and GC patients. Unlike the relatively ambiguous clusters observed for the latter three RNA types (Supplementary Figure 1A-C), circRNAs were clearly clustered into five groups (Figure 2D). Based on data obtained from CSCD and CircInteractome, 2262 miRNA response elements were predicted. By intersecting the results obtained from TargetScan, miRDB, and miRTarBase, 8145 common potential target genes were identified. Then, we performed differential expression analyses of GC patient samples *vs* HD samples by using The Cancer Genome Atlas (TCGA) and identified 2512 genes (1072 upregulated, 1440 downregulated); 998 of these genes were also identified as potential targets in the abovementioned analysis. KEGG pathway analysis demonstrated that these genes were enriched in pathways in cancer, the cell cycle, and the PI3K-Akt signaling pathway (Supplementary Figure 2A). GO enrichment analysis indicated that these genes were associated with nuclear division, organelle fission, and cell cycle G1/S phase transition (Supplementary Figure 2B).

To further investigate the function of cluster 5 (68 circRNAs, marked in Figure 2D), similar analysis methods were used. These circRNAs were significantly upregulated in all GC samples, and 1731 target miRNAs were predicted. To identify potential miRNAs related to GC, we performed differential expression analyses based on TCGA and identified 64 miRNAs that were downregulated in GC samples *vs* HD samples. Thirty-one miRNAs were selected by taking the intersection of the two groups of results. These miRNAs were predicted to bind 1578 target genes. KEGG pathway analysis demonstrated that these genes were enriched in five pathways, including pathways in cancer, the PI3K-Akt signaling pathway, the MAPK signaling pathway, miRNAs in cancer, and cellular senescence (Figure 2E). GO enrichment analysis indicated that these genes were associated with nuclear division, organelle fission



DOI: 10.3748/wjg.v29.i22.3482 **Copyright** ©The Author(s) 2023.

Figure 2 Identification of exosomes and bioinformatic analysis of exosomal circular RNAs. A: Exosomes were observed by transmission electron microscopy. The scale bar is 200 nm; B: Diameter and quantity of the exosomes; C: The positive markers of exosomes (CD9, TSG101, and CD81) and the negative marker (Calnexin) were tested by Western blot; D: Clustering analysis of circular RNAs (circRNAs); E: Kyoto Encyclopedia of Genes and Genomes pathway analysis

of cluster 5 of differently expressed circRNAs; F: Gene Ontology enrichment analysis of cluster 5 of differently expressed circRNAs. HD: Healthy donor; GC: Gastric cancer; EGC: Early gastric cancer; LAGC: Locally advanced gastric cancer; MGC: Metastatic gastric cancer; AGC: Advanced gastric cancer; BP: Biological process; CC: Cell component; MF: Molecular function.

and cell cycle G1/S phase transition (Figure 2F).

We generated a circRNA-miRNA-mRNA regulatory network related to the genes enriched in the top 5 KEGG pathways. Ultimately, we found that six circRNAs (hsa_circ_0113953, hsa_circ_0076179, hsa_circ_0007353, hsa_circ_0012823, hsa_circ_0001470, and hsa_circ_0079439) were included in all the networks (Supplementary Figure 3A-E).

Similar to a previous study, the expression levels of ncRNAs in exosomes were consistent with those in GCCs or tissues[27]. Then, we assessed the expression levels of the six circRNAs in NGECs and GCCs (AGS, MGC-803, SGC-7901, HGC-27, SNU-1, KATO III, and BGC-823) (Supplementary Figure 4A-F). The results showed that the expression levels of hsa_circ_0079439 in the GCCs were obviously higher than those in NGECs. Thus, hsa_circ_0079439 was selected for further validation by dd-PCR. The primers used to measure the levels of the six circRNAs are shown in Supplementary Table 1.

Expression levels of exosomal hsa_circ_0079439 in test and validation cohorts

In the test cohort, the expression levels of exosomal hsa_circ_0079439 were significantly higher in GC patients than in HDs ($P < 0.0001$) (Figure 3A). In addition, the levels of serum CEA in GC patients were higher than those in HDs ($P < 0.001$) (Figure 3B). However, the expression levels of CA19-9, CA72-4, AFP, and CA125 were not significantly different between GC patients and HDs (Figure 3C-F).

Furthermore, in the validation cohort, we again found that the expression levels of exosomal hsa_circ_0079439 were significantly higher in GC patients than in HDs ($P < 0.0001$) (Figure 4A). However, the expression levels of standard serum biomarkers between GC patients and HDs were not significantly different (Figure 4B-F).

Expression of exosomal hsa_circ_0079439 and its value in diagnosing GC, EGC, and AGC

To evaluate the diagnostic value of exosomal hsa_circ_0079439 for GC, EGC, and AGC, we combined the data obtained from the test cohort and validation cohort. We compared the expression levels and analyzed the ROC curves of exosomal hsa_circ_0079439, CEA, CA19-9, CA72-4, AFP, and CA125. The expression levels of exosomal hsa_circ_0079439 were significantly higher in GC patients than in HDs ($P < 0.0001$) (Figure 5A). However, the levels of standard serum biomarkers showed no significant difference between GC patients and HDs (Figure 5B-F). The AUC value of exosomal hsa_circ_0079439 was higher than those of CEA, CA19-9, CA72-4, AFP, and CA125 (0.8595 *vs* 0.5862, 0.5660, 0.5360, 0.5082, and 0.5018, respectively) (Figure 5G). To investigate the changes in the expression levels of exosomal hsa_circ_0079439 before and after treatment, we analyzed 30 paired plasma samples obtained from GC patients. The expression levels of exosomal hsa_circ_0079439 were significantly decreased after treatment (Figure 5H) ($P < 0.05$).

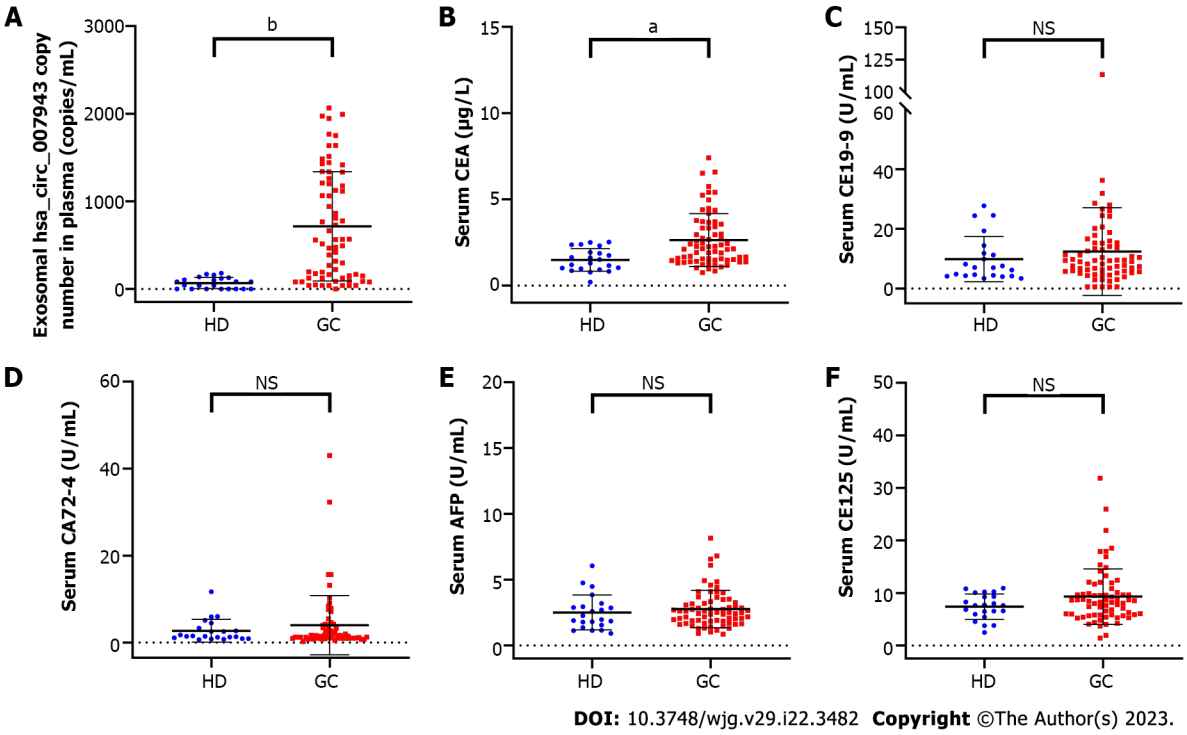
To determine whether the results were similar in EGC patients, all GC patients were divided into two groups (EGC patients and AGC patients). The expression levels of exosomal hsa_circ_0079439 were obviously higher in EGC patients ($P < 0.0001$) and AGC patients ($P < 0.0001$) than in HDs (Figure 6A). However, the serum levels of CEA, CA19-9, CA72-4, AFP, and CA125 could not be used to distinguish EGC patients from HDs (Figure 6B-F). The AUC value of exosomal hsa_circ_0079439 was obviously higher than those of CEA, CA19-9, CA72-4, AFP, and CA125 (0.8433 *vs* 0.5732, 0.5362, 0.5203, 0.5024, and 0.5352, respectively) (Figure 6G).

In addition, the serum levels of CEA, CA19-9, and CA125 were apparently higher in AGC patients than in HDs ($P < 0.05$) (Figure 6B, C and F). However, when comparing the levels of CA72-4 and AFP, there was no significant difference between AGC patients and HDs (Figure 6D and E). The AUC value of exosomal hsa_circ_0079439 was obviously higher than those of CEA, CA19-9, CA72-4, AFP, and CA125 (0.9050 *vs* 0.6228, 0.6497, 0.5801, 0.5379, and 0.6058, respectively) (Figure 6H).

DISCUSSION

Although the incidence and mortality rates of GC have declined over the past century, GC is still a major health problem worldwide, especially in East Asian countries[2,28]. GC has a poor prognosis in most patients due to late detection. Currently, the overall survival rate of EGC patients treated by endoscopy can exceed 90%[28,29]. Nonetheless, the 5-year survival rate of AGC patients with distant metastases is lower than 5%[30]. However, a screening program carried out by the Shanghai Research Institute in ten medical centers showed that the rate of EGC diagnosis is only 9.61%[28].

The clinical symptoms of EGC are atypical in most patients, and these symptoms include anorexia, malnutrition, and stomachache[2]. The methods of early diagnosis of GC include detection of standard serum biomarkers, barium radiography, computerized tomography, and endoscopic biopsy[31]. Over



DOI: 10.3748/wjg.v29.i22.3482 **Copyright** ©The Author(s) 2023.

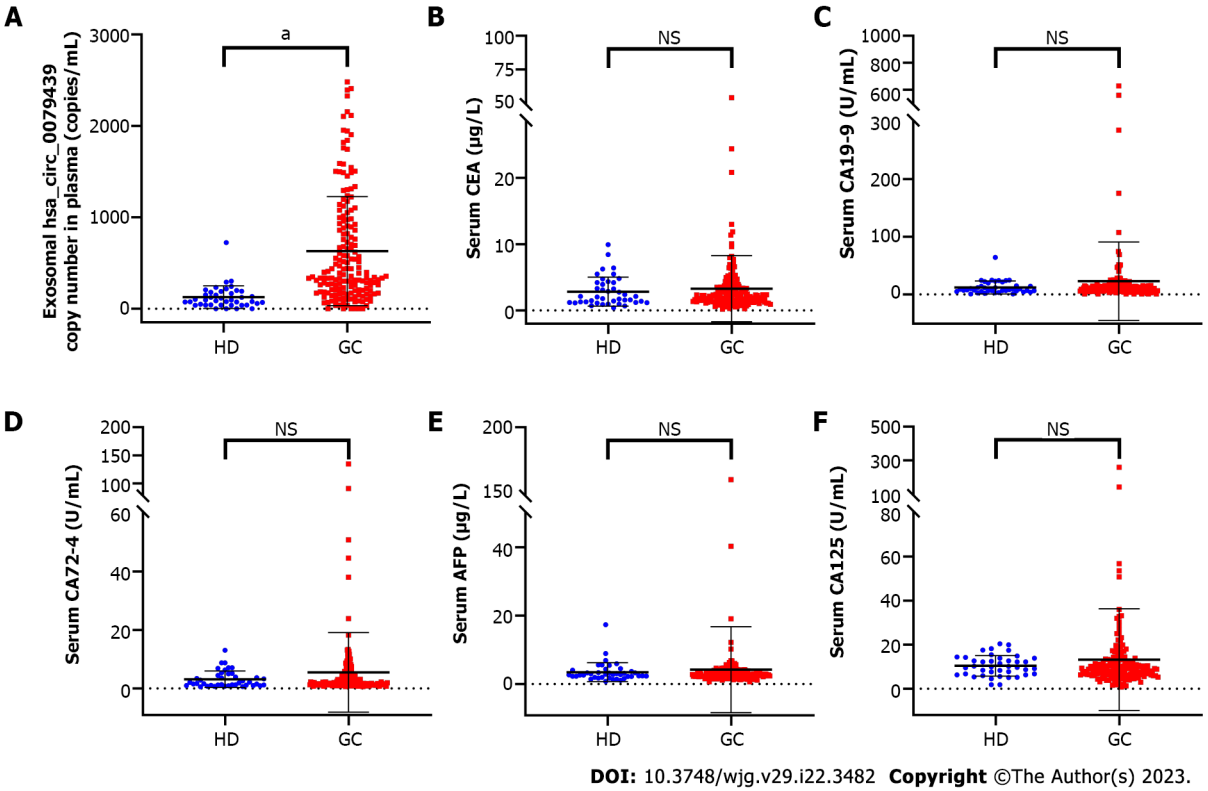
Figure 3 Expression levels of exosomal hsa_circ_0079439, carcinoembryonic antigen, carbohydrate antigen 19-9, carbohydrate antigen 72-4, alpha-fetoprotein, and carbohydrate antigen 125 in the test cohort. A: Absolutely quantitative detection of exosomal hsa_circ_0079439 copy number in plasma between healthy donors (HDs) (n = 22) and gastric cancer (GC) patients (n = 69) by droplet digital polymerase chain reaction; B-F: Expression levels of standard serum biomarkers in HDs and GC patients, including carcinoembryonic antigen (B), carbohydrate antigen (CA)19-9 (C), CA72-4 (D), alpha-fetoprotein (E), and CA125 (F). And all the results are shown as the mean (SD). $^{a}P < 0.001$, $^{b}P < 0.0001$, NS: Not significant. HD: Healthy donor; GC: Gastric cancer; CEA: Carcinoembryonic antigen; CA19-9: Carbohydrate antigen 19-9; CA72-4: Carbohydrate antigen 72-4; CA 125: Carbohydrate antigen 125; AFP: Alpha-fetoprotein.

time, the role of liquid biopsy in GC has received close attention. Furthermore, liquid biopsy has emerged as a revolutionary strategy for the early diagnosis of cancers, detection of therapeutic targets, prediction of prognosis, monitoring of therapeutic efficacy, and analysis of drug resistance; it also has the advantage of being minimally invasive[14,32-34]. Although numerous studies have investigated biomarkers for the early detection of GC, there are still many limitations regarding the use of these biomarkers for the early diagnosis of GC. For example, CEA and CA72-4 are standard clinical biomarkers, but both lack sensitivity and specificity.

In recent years, exosomes have been found in nearly all types of human body fluids, such as blood, urine, breast milk, saliva, ascites, and cerebrospinal fluid. Because of their phospholipid bilayer membrane structure, they can protect bioactive cargos from degradation. There are many metabolites and products in exosomes produced by all kinds of cells. These cargoes include nucleic acids, proteins, lipids, and metabolites[35].

CircRNAs are a class of single-stranded noncoding RNAs[36]. Initially, circRNAs were considered to be the result of splicing errors. However, with the development of bioinformatics and high-throughput sequencing technologies, more circRNAs have been identified, and they have been found to be involved in the occurrence and development of many human diseases. Many studies have demonstrated that circRNAs are abundant, stable and conserved rather than random products of RNA splicing[36]. Due to their high stability, circRNAs have many important biological functions, including noncoding and coding functions. The most widely studied function is their role in the regulation of miRNA target genes as miRNA sponges or decoys. They can protect target mRNAs from miRNA-dependent degradation. Moreover, it has been found that circRNAs may function as protein sponges or decoys, enhancers of protein function, protein scaffolds, protein recruiters, and templates for translation[17,37].

For instance, Zhang *et al*[38] reported that exosomal circNRIP1, as a tumor promoter, sponges miR-149-5p to regulate the expression level of AKT1 in GC. Similarly, exosomal circSHKBP1 may be a promising circulating biomarker for GC diagnosis and prognosis[39]. Exosomal circSHKBP1 regulates the miR-582-3p/HUR/vascular endothelial growth factor pathway and suppresses HSP90 degradation to promote GC progression[39]. In addition, Lu *et al*[40] found that exosomal circ-RanGAP1 facilitates GC invasion and metastasis by targeting miR-877-3p to regulate vascular endothelial growth factor-A expression, suggesting that circ-RanGAP1 may act as a tumor promoter in GC.



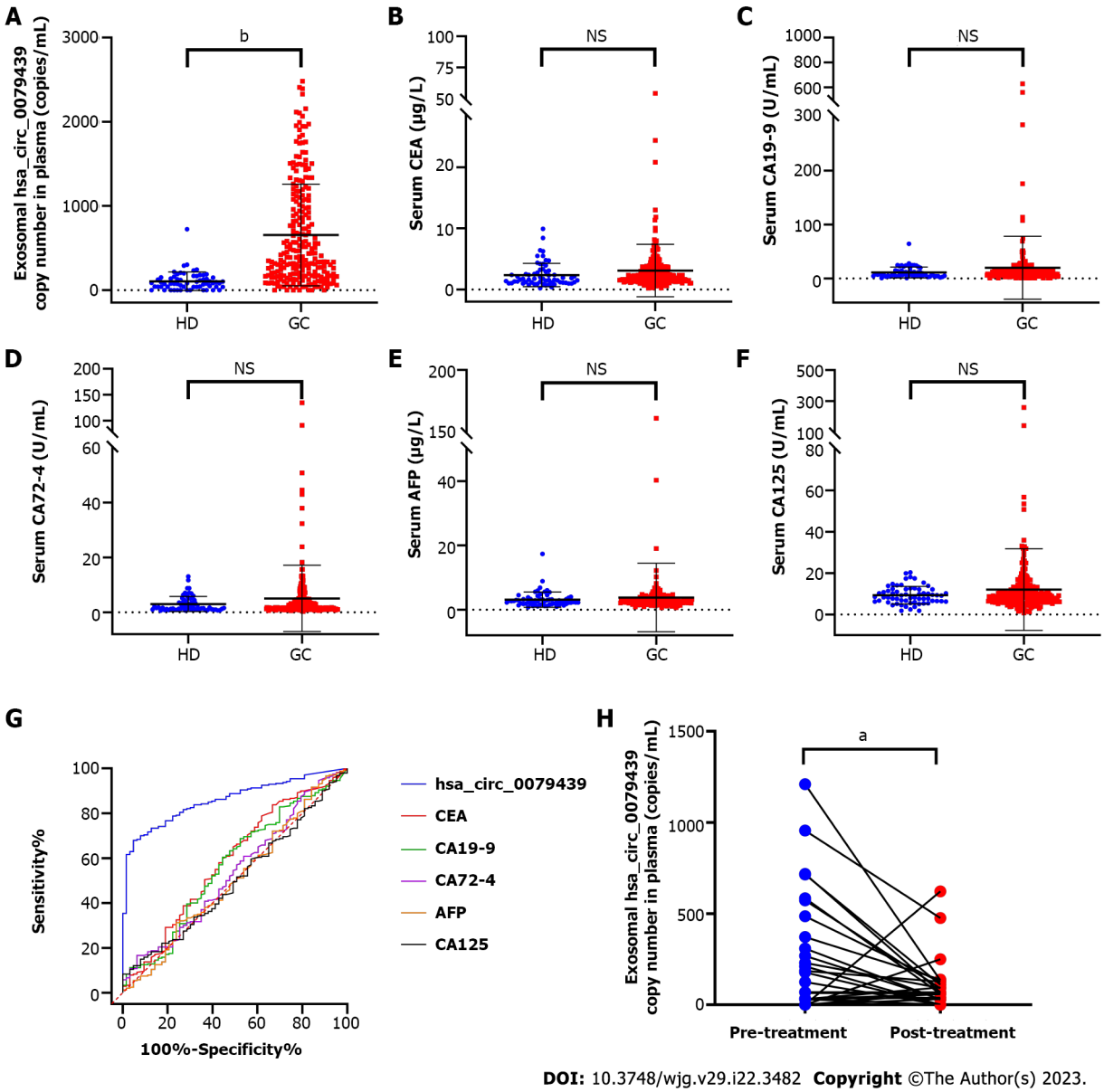
DOI: 10.3748/wjg.v29.i22.3482 **Copyright** ©The Author(s) 2023.

Figure 4 Expression levels of exosomal hsa_circ_0079439, carcinoembryonic antigen, carbohydrate antigen 19-9, carbohydrate antigen 72-4, alpha-fetoprotein, and carbohydrate antigen 125 in the validation cohort. A: Absolutely quantitative detection of exosomal hsa_circ_0079439 copy number in plasma from healthy donors (HDs) (n = 41) and gastric cancer (GC) patients (n = 171) by droplet digital polymerase chain reaction; B-F: Expression levels of standard serum biomarkers in GC patients and HDs, including carcinoembryonic antigen (B), carbohydrate antigen (CA)19-9 (C), CA72-4 (D), alpha-fetoprotein (E), and CA125 (F). And all the results are shown as mean (SD). [a]P < 0.0001, NS: Not significant. HD: Healthy donor; GC: Gastric cancer; CEA: Carcinoembryonic antigen; CA19-9: Carbohydrate antigen 19-9; CA72-4: Carbohydrate antigen 72-4; CA 125: Carbohydrate antigen 125; AFP: Alpha-fetoprotein.

In this study, we performed cluster analysis of exosomal circRNAs, lncRNAs, miRNAs, and mRNAs based on the results of whole-transcriptome RNA sequencing. The results showed that circRNAs could be used to distinguish GC patients from HDs better than lncRNAs, miRNAs, and mRNAs. Then, we investigated the expression of exosomal hsa_circ_0079439 in HDs and GC patients, including EGC and AGC, by dd-PCR. The expression levels of exosomal hsa_circ_0079439 were significantly higher in GC patients.

In recent years, dd-PCR has become the latest technology used for DNA quantification. The reaction volume containing the nucleic acids is divided into thousands of nanosized droplets, each of which either contains the gene of interest or does not. After PCR amplification, each droplet is detected one by one. A droplet with a fluorescence signal is interpreted as a 1, and a droplet without a fluorescence signal is interpreted as a 0. According to the Poisson distribution principle and the number and proportion of positive droplets, the initial copy number or concentration of the gene of interest can be obtained. There is no suitable reference gene in exosomes for normalization of the expression levels of circRNAs in real-time PCR (RT-PCR) experiments. Previous studies have shown that dd-PCR can be used to accurately quantify the copy numbers of specific nucleotides in plasma without external calibrators and has higher sensitivity than RT-PCR[41-44]. Therefore, we compared the diagnostic efficiency of exosomal hsa_circ_0079439 in GC patients, especially EGC patients, with standard clinical biomarkers, by dd-PCR. We found that exosomal hsa_circ_0079439 had higher sensitivity and specificity than standard clinical biomarkers. The findings of this study support the notion that plasma exosomal circRNAs could serve as biomarkers for the diagnosis of EGC and might be new therapeutic targets as well as effective prognostic markers for GC.

However, there are still some limitations to our study. First, the main limitation of this study is that since it was conducted at a single center, selection bias may have affected the results. This may indicate that this method is suitable for the early diagnosis of GC in Asians but not necessarily in other populations. Second, some groups had relatively few samples, so the generalizability of our study results may be affected. Third, since there is no standard isolation method for exosomes, the use of different isolation methods may result in differences in detection efficiency for the early diagnosis of GC [45-47]. Fourth, although circulating exosomal circRNAs serve as good candidates for blood-based biomarkers, it will take some time before they can be applied in the clinic. Therefore, multicenter studies with larger sample sizes are encouraged to obtain more accurate results for the early diagnosis of GC.

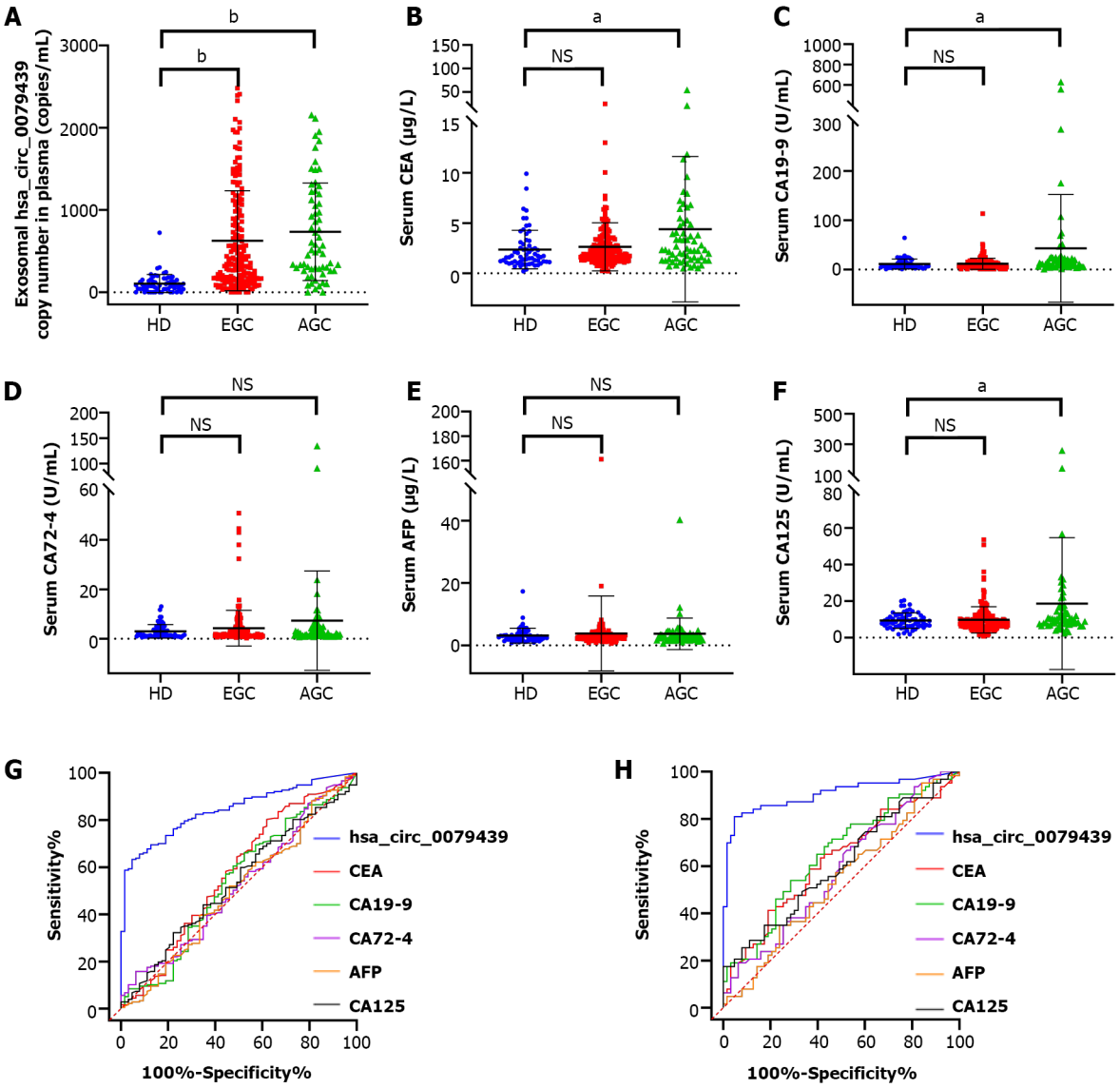


DOI: 10.3748/wjg.v29.i22.3482 **Copyright** ©The Author(s) 2023.

Figure 5 Diagnostic value and expression levels of exosomal hsa_circ_0079439, carcinoembryonic antigen, carbohydrate antigen 19-9, carbohydrate antigen 72-4, alpha-fetoprotein, and carbohydrate antigen 125 in total participants for gastric cancer. A: Absolutely quantitative detection of exosomal hsa_circ_0079439 copy number in plasma from healthy donors (HDs) (n = 63) and gastric cancer (GC) patients (n = 240) by droplet digital polymerase chain reaction; B-F: Expression levels of standard serum biomarkers in GC patients and HDs, including carcinoembryonic antigen (B), carbohydrate antigen (CA)19-9 (C), CA72-4 (D), alpha-fetoprotein (E), and CA125 (F); G: Receiver operating characteristic curves of hsa_circ_0079439, carcinoembryonic antigen, CA19-9, CA72-4, alpha-fetoprotein, and CA125 in distinguish GC patients (n = 240) from HDs (n = 63); H: Changes of expression levels of exosomal hsa_circ_0079439 before and after treatment. And all the results are shown as the mean (SD). $^{a}P < 0.05$, $^{b}P < 0.0001$, NS: Not significant. HD: Healthy donor; GC: Gastric cancer; CEA: Carcinoembryonic antigen; CA19-9: Carbohydrate antigen 19-9; CA72-4: Carbohydrate antigen 72-4; CA 125: Carbohydrate antigen 125; AFP: Alpha-fetoprotein.

CONCLUSION

Based on whole-transcriptome RNA resequencing data, we found that circRNAs have greater potential than other RNA types as novel biomarkers for the detection of GC, especially EGC. To our knowledge, this study is the first to discover and verify that the levels of exosomal hsa_circ_0079439 are higher in GC patients than in HDs. In addition, exosomal hsa_circ_0079439 performs better in distinguishing EGC patients from HDs than standard clinical biomarkers. Overall, exosomal hsa_circ_0079439 is a prospective biomarker for the diagnosis of GC, including EGC and AGC.



DOI: 10.3748/wjg.v29.i22.3482 **Copyright** ©The Author(s) 2023.

Figure 6 Diagnostic value and expression levels of exosomal hsa_circ_0079439, carcinoembryonic antigen, carbohydrate antigen 19-9, carbohydrate antigen 72-4, alpha-fetoprotein, and carbohydrate antigen 125 among healthy donors, early gastric cancer patients, and advanced gastric cancer patients. A: Absolutely quantitative detection of exosomal hsa_circ_0079439 copy number in plasma from early gastric cancer (EGC) patients (n = 177), advanced GC (AGC) patients (n = 63), and healthy donors (HDs) (n = 63) by droplet digital polymerase chain reaction; B-F: Expression levels of standard serum biomarkers in EGC patients, AGC patients, and HDs, including carcinoembryonic antigen (CEA) (B), carbohydrate antigen (CA)19-9 (C), CA72-4 (D), alpha-fetoprotein (E), and CA125 (F); G: Receiver operating characteristic (ROC) curves of hsa_circ_0079439, CEA, CA19-9, CA72-4, alpha-fetoprotein, and CA125 in distinguish EGC patients from HDs; H: ROC curves of hsa_circ_0079439, CEA, CA19-9, CA72-4, alpha-fetoprotein, and CA125 in distinguish AGC patients from HDs. All the results are shown as the mean (SD). $^{a}P < 0.05$, $^{b}P < 0.0001$, NS: Not significant. HD: Healthy donor; CEA: Carcinoembryonic antigen; CA19-9: Carbohydrate antigen 19-9; CA72-4: Carbohydrate antigen 72-4; CA 125: Carbohydrate antigen 125; AFP: Alpha-fetoprotein; EGC: Early gastric cancer; AGC: Advanced gastric cancer.

ARTICLE HIGHLIGHTS

Research background

Gastric cancer (GC) is a major health problem worldwide, especially in East Asian countries, and GC has a poor prognosis in most patients due to late detection. Therefore, accurate early detection of GC is one of the most urgent issues in its management.

Research motivation

A number of studies have demonstrated that circular RNAs (circRNAs) play an important role in GC progression, invasion, and metastasis. However, the utility of exosomal circRNAs for early detection of GC is largely unknown.

Research objectives
To analyze the expression levels of plasma exosomal circRNAs from GC patients in different clinical stages to identify a novel biomarker for early detection of GC.

Research methods
Healthy donors (HDs) and GC patients diagnosed by pathology were recruited. Based on the results of whole-transcriptome RNA sequencing, the expression profiles of circRNAs were analyzed by bioinformatics methods and validated by droplet digital polymerase chain reaction. Then we compared the diagnostic efficiency of plasma exosomal circRNAs and standard serum biomarkers.

Research results
The expression levels of exosomal hsa_circ_0079439 were obviously higher in GC patients than in HDs ($P < 0.0001$). And the area under the curve value of exosomal hsa_circ_0079439 was obviously higher than those of carcinoembryonic antigen, carbohydrate antigen (CA)19-9, CA72-4, alpha-fetoprotein, and CA125 (0.8433 *vs* 0.5732, 0.5362, 0.5203, 0.5024, and 0.5352, respectively).

Research conclusions
Plasma exosomal hsa_circ_0079439 is a prospective biomarker for the diagnosis of GC.

Research perspectives
Multicenter studies with larger sample sizes are encouraged to obtain more accurate results for the early diagnosis of GC.

FOOTNOTES

Author contributions: Chai NL, Wang YL, and Linghu EQ designed the study; Li X, Shao JK, Li LS, Zhang WG, and Chang ZY collected the plasma samples; Li X, Lin YL, Wu XJ, Yao H, Shi FL, and Li X performed the dd-PCR test and data analysis; Li X, Lin YL, and Shao JK contributed equally to this work, and they should be considered as co-first authors; Chai NL, Wang YL, and Linghu EQ were co-corresponding authors; and all authors approved the final manuscript.

Supported by the National Key Research and Development Program, No. 2019YFA0903802, 2022YFC2503600, and 2016YFC1303601.

Institutional review board statement: This study was approved by the ethics committee of Chinese PLA General Hospital.

Informed consent statement: Informed consent was obtained from all participants in this study.

Conflict-of-interest statement: All the authors report no relevant conflicts of interest for this article.

Data sharing statement: The data that support the findings of this study are available from the corresponding author upon reasonable request.

STROBE statement: The authors have read the STROBE Statement-checklist of items, and the manuscript was prepared and revised according to the STROBE Statement-checklist of items.

Open-Access: This article is an open-access article that was selected by an in-house editor and fully peer-reviewed by external reviewers. It is distributed in accordance with the Creative Commons Attribution NonCommercial (CC BY-NC 4.0) license, which permits others to distribute, remix, adapt, build upon this work non-commercially, and license their derivative works on different terms, provided the original work is properly cited and the use is non-commercial. See: https://creativecommons.org/Licenses/by-nc/4.0/

Country/Territory of origin: China

ORCID number: Xiao Li 0000-0003-0254-6675; Yan-Li Lin 0000-0002-7711-9355; Jia-Kang Shao 0000-0002-8630-6777; Xiao-Jie Wu 0000-0001-7307-5503; Xiang Li 0009-0006-2559-7992; He Yao 0009-0005-4152-6425; Fa-Liang Shi 0009-0005-7294-8401; Long-Song Li 0000-0002-4000-7501; Wen-Gang Zhang 0000-0002-3314-0283; Zheng-Yao Chang 0000-0003-2836-7862; Ning-Li Chai 0000-0002-6791-5817; You-Liang Wang 0000-0003-1319-0344; En-Qiang Linghu 0000-0003-4506-7877.

S-Editor: Wang JJ
L-Editor: Wang TQ
P-Editor: Chen YL

REFERENCES

1 **Sung H**, Ferlay J, Siegel RL, Laversanne M, Soerjomataram I, Jemal A, Bray F. Global Cancer Statistics 2020: GLOBOCAN Estimates of Incidence and Mortality Worldwide for 36 Cancers in 185 Countries. *CA Cancer J Clin* 2021; **71**: 209-249 [PMID: 33538338 DOI: 10.3322/caac.21660]

2 **Smyth EC**, Nilsson M, Grabsch HI, van Grieken NC, Lordick F. Gastric cancer. *Lancet* 2020; **396**: 635-648 [PMID: 32861308 DOI: 10.1016/S0140-6736(20)31288-5]

3 **Shimada H**, Noie T, Ohashi M, Oba K, Takahashi Y. Clinical significance of serum tumor markers for gastric cancer: a systematic review of literature by the Task Force of the Japanese Gastric Cancer Association. *Gastric Cancer* 2014; **17**: 26-33 [PMID: 23572188 DOI: 10.1007/s10120-013-0259-5]

4 **Feng F**, Tian Y, Xu G, Liu Z, Liu S, Zheng G, Guo M, Lian X, Fan D, Zhang H. Diagnostic and prognostic value of CEA, CA19-9, AFP and CA125 for early gastric cancer. *BMC Cancer* 2017; **17**: 737 [PMID: 29121872 DOI: 10.1186/s12885-017-3738-y]

5 **Liu X**, Cheng Y, Sheng W, Lu H, Xu Y, Long Z, Zhu H, Wang Y. Clinicopathologic features and prognostic factors in alpha-fetoprotein-producing gastric cancers: analysis of 104 cases. *J Surg Oncol* 2010; **102**: 249-255 [PMID: 20740583 DOI: 10.1002/jso.21624]

6 **Guo X**, Lv X, Ru Y, Zhou F, Wang N, Xi H, Zhang K, Li J, Chang R, Xie T, Wang X, Li B, Chen Y, Yang Y, Chen L. Circulating Exosomal Gastric Cancer-Associated Long Noncoding RNA1 as a Biomarker for Early Detection and Monitoring Progression of Gastric Cancer: A Multiphase Study. *JAMA Surg* 2020; **155**: 572-579 [PMID: 32520332 DOI: 10.1001/jamasurg.2020.1133]

7 **Xu Y**, Zhang P, Zhang K, Huang C. The application of CA72-4 in the diagnosis, prognosis, and treatment of gastric cancer. *Biochim Biophys Acta Rev Cancer* 2021; **1876**: 188634 [PMID: 34656687 DOI: 10.1016/j.bbcan.2021.188634]

8 **Thanh Huong P**, Gurshaney S, Thanh Binh N, Gia Pham A, Hoang Nguyen H, Thanh Nguyen X, Pham-The H, Tran PT, Truong Vu K, Xuan Duong N, Pelucchi C, La Vecchia C, Boffetta P, Nguyen HD, Luu HN. Emerging Role of Circulating Tumor Cells in Gastric Cancer. *Cancers (Basel)* 2020; **12** [PMID: 32183503 DOI: 10.3390/cancers12030695]

9 **Zhou R**, Chen KK, Zhang J, Xiao B, Huang Z, Ju C, Sun J, Zhang F, Lv XB, Huang G. The decade of exosomal long RNA species: an emerging cancer antagonist. *Mol Cancer* 2018; **17**: 75 [PMID: 29558960 DOI: 10.1186/s12943-018-0823-z]

10 **Kok VC**, Yu CC. Cancer-Derived Exosomes: Their Role in Cancer Biology and Biomarker Development. *Int J Nanomedicine* 2020; **15**: 8019-8036 [PMID: 33116515 DOI: 10.2147/IJN.S272378]

11 **Hannafon BN**, Trigoso YD, Calloway CL, Zhao YD, Lum DH, Welm AL, Zhao ZJ, Blick KE, Dooley WC, Ding WQ. Plasma exosome microRNAs are indicative of breast cancer. *Breast Cancer Res* 2016; **18**: 90 [PMID: 27608715 DOI: 10.1186/s13058-016-0753-x]

12 **Xu H**, Zhou J, Tang J, Min X, Yi T, Zhao J, Ren Y. Identification of serum exosomal lncRNA MIAT as a novel diagnostic and prognostic biomarker for gastric cancer. *J Clin Lab Anal* 2020; **34**: e23323 [PMID: 32274858 DOI: 10.1002/jcla.23323]

13 **Kim KU**, Kim WH, Jeong CH, Yi DY, Min H. More than Nutrition: Therapeutic Potential of Breast Milk-Derived Exosomes in Cancer. *Int J Mol Sci* 2020; **21** [PMID: 33023062 DOI: 10.3390/ijms21197327]

14 **Yu D**, Li Y, Wang M, Gu J, Xu W, Cai H, Fang X, Zhang X. Exosomes as a new frontier of cancer liquid biopsy. *Mol Cancer* 2022; **21**: 56 [PMID: 35180868 DOI: 10.1186/s12943-022-01509-9]

15 **Memczak S**, Jens M, Elefsinioti A, Torti F, Krueger J, Rybak A, Maier L, Mackowiak SD, Gregersen LH, Munschauer M, Loewer A, Ziebold U, Landthaler M, Kocks C, le Noble F, Rajewsky N. Circular RNAs are a large class of animal RNAs with regulatory potency. *Nature* 2013; **495**: 333-338 [PMID: 23446348 DOI: 10.1038/nature11928]

16 **Shan C**, Zhang Y, Hao X, Gao J, Chen X, Wang K. Biogenesis, functions and clinical significance of circRNAs in gastric cancer. *Mol Cancer* 2019; **18**: 136 [PMID: 31519189 DOI: 10.1186/s12943-019-1069-0]

17 **Kristensen LS**, Andersen MS, Stagsted LVW, Ebbesen KK, Hansen TB, Kjems J. The biogenesis, biology and characterization of circular RNAs. *Nat Rev Genet* 2019; **20**: 675-691 [PMID: 31395983 DOI: 10.1038/s41576-019-0158-7]

18 **Yu W**, Hurley J, Roberts D, Chakrabortty SK, Enderle D, Noerholm M, Breakefield XO, Skog JK. Exosome-based liquid biopsies in cancer: opportunities and challenges. *Ann Oncol* 2021; **32**: 466-477 [PMID: 33548389 DOI: 10.1016/j.annonc.2021.01.074]

19 **Baassiri A**, Nassar F, Mukherji D, Shamseddine A, Nasr R, Temraz S. Exosomal Non Coding RNA in LIQUID Biopsies as a Promising Biomarker for Colorectal Cancer. *Int J Mol Sci* 2020; **21** [PMID: 32092975 DOI: 10.3390/ijms21041398]

20 **Poulet C**, Njock MS, Moermans C, Louis E, Louis R, Malaise M, Guiot J. Exosomal Long Non-Coding RNAs in Lung Diseases. *Int J Mol Sci* 2020; **21** [PMID: 32438606 DOI: 10.3390/ijms21103580]

21 **Yu J**, Huang C, Sun Y, Su X, Cao H, Hu J, Wang K, Suo J, Tao K, He X, Wei H, Ying M, Hu W, Du X, Hu Y, Liu H, Zheng C, Li P, Xie J, Liu F, Li Z, Zhao G, Yang K, Liu C, Li H, Chen P, Ji J, Li G; Chinese Laparoscopic Gastrointestinal Surgery Study (CLASS) Group. Effect of Laparoscopic *vs* Open Distal Gastrectomy on 3-Year Disease-Free Survival in Patients With Locally Advanced Gastric Cancer: The CLASS-01 Randomized Clinical Trial. *JAMA* 2019; **321**: 1983-1992 [PMID: 31135850 DOI: 10.1001/jama.2019.5359]

22 **Marano L**, D'Ignazio A, Cammillini F, Angotti R, Messina M, Marrelli D, Roviello F. Comparison between 7th and 8th edition of AJCC TNM staging system for gastric cancer: old problems and new perspectives. *Transl Gastroenterol Hepatol* 2019; **4**: 22 [PMID: 31143843 DOI: 10.21037/tgh.2019.03.09]

23 **He X**, Wu W, Lin Z, Ding Y, Si J, Sun LM. Validation of the American Joint Committee on Cancer (AJCC) 8th edition stage system for gastric cancer patients: a population-based analysis. *Gastric Cancer* 2018; **21**: 391-400 [PMID: 29052053 DOI: 10.1007/s10120-017-0770-1]

24 **Digklia A**, Wagner AD. Advanced gastric cancer: Current treatment landscape and future perspectives. *World J Gastroenterol* 2016; **22**: 2403-2414 [PMID: 26937129 DOI: 10.3748/wjg.v22.i8.2403]

25 **Böing AN**, van der Pol E, Grootemaat AE, Coumans FA, Sturk A, Nieuwland R. Single-step isolation of extracellular

vesicles by size-exclusion chromatography. *J Extracell Vesicles* 2014; **3** [PMID: 25279113 DOI: 10.3402/jev.v3.23430]
26 **Pegtel DM**, Gould SJ. Exosomes. *Annu Rev Biochem* 2019; **88**: 487-514 [PMID: 31220978 DOI: 10.1146/annurev-biochem-013118-111902]
27 **Li W**, Gao YQ. MiR-217 is involved in the carcinogenesis of gastric cancer by down-regulating CDH1 expression. *Kaohsiung J Med Sci* 2018; **34**: 377-384 [PMID: 30063010 DOI: 10.1016/j.kjms.2018.02.003]
28 **Hu Y**, Fang JY, Xiao SD. Can the incidence of gastric cancer be reduced in the new century? *J Dig Dis* 2013; **14**: 11-15 [PMID: 23134264 DOI: 10.1111/j.1751-2980.2012.00647.x]
29 **Hatta W**, Gotoda T, Oyama T, Kawata N, Takahashi A, Yoshifuku Y, Hoteya S, Nakagawa M, Hirano M, Esaki M, Matsuda M, Ohnita K, Yamanouchi K, Yoshida M, Dohi O, Takada J, Tanaka K, Yamada S, Tsuji T, Ito H, Hayashi Y, Nakaya N, Nakamura T, Shimosegawa T. A Scoring System to Stratify Curability after Endoscopic Submucosal Dissection for Early Gastric Cancer: "eCura system". *Am J Gastroenterol* 2017; **112**: 874-881 [PMID: 28397873 DOI: 10.1038/ajg.2017.95]
30 **Mattiuzzi C**, Lippi G. Current Cancer Epidemiology. *J Epidemiol Glob Health* 2019; **9**: 217-222 [PMID: 31854162 DOI: 10.2991/jegh.k.191008.001]
31 **Karimi P**, Islami F, Anandasabapathy S, Freedman ND, Kamangar F. Gastric cancer: descriptive epidemiology, risk factors, screening, and prevention. *Cancer Epidemiol Biomarkers Prev* 2014; **23**: 700-713 [PMID: 24618998 DOI: 10.1158/1055-9965.EPI-13-1057]
32 **Vaidyanathan R**, Soon RH, Zhang P, Jiang K, Lim CT. Cancer diagnosis: from tumor to liquid biopsy and beyond. *Lab Chip* 2018; **19**: 11-34 [PMID: 30480287 DOI: 10.1039/c8lc00684a]
33 **Ignatiadis M**, Sledge GW, Jeffrey SS. Liquid biopsy enters the clinic - implementation issues and future challenges. *Nat Rev Clin Oncol* 2021; **18**: 297-312 [PMID: 33473219 DOI: 10.1038/s41571-020-00457-x]
34 **Alix-Panabières C**, Pantel K. Liquid Biopsy: From Discovery to Clinical Application. *Cancer Discov* 2021; **11**: 858-873 [PMID: 33811121 DOI: 10.1158/2159-8290.CD-20-1311]
35 **Dai J**, Su Y, Zhong S, Cong L, Liu B, Yang J, Tao Y, He Z, Chen C, Jiang Y. Exosomes: key players in cancer and potential therapeutic strategy. *Signal Transduct Target Ther* 2020; **5**: 145 [PMID: 32759948 DOI: 10.1038/s41392-020-00261-0]
36 **Chen L**, Shan G. CircRNA in cancer: Fundamental mechanism and clinical potential. *Cancer Lett* 2021; **505**: 49-57 [PMID: 33609610 DOI: 10.1016/j.canlet.2021.02.004]
37 **Li R**, Jiang J, Shi H, Qian H, Zhang X, Xu W. CircRNA: a rising star in gastric cancer. *Cell Mol Life Sci* 2020; **77**: 1661-1680 [PMID: 31659415 DOI: 10.1007/s00018-019-03345-5]
38 **Zhang X**, Wang S, Wang H, Cao J, Huang X, Chen Z, Xu P, Sun G, Xu J, Lv J, Xu Z. Circular RNA circNRIP1 acts as a microRNA-149-5p sponge to promote gastric cancer progression *via* the AKT1/mTOR pathway. *Mol Cancer* 2019; **18**: 20 [PMID: 30717751 DOI: 10.1186/s12943-018-0935-5]
39 **Xie M**, Yu T, Jing X, Ma L, Fan Y, Yang F, Ma P, Jiang H, Wu X, Shu Y, Xu T. Exosomal circSHKBP1 promotes gastric cancer progression *via* regulating the miR-582-3p/HUR/VEGF axis and suppressing HSP90 degradation. *Mol Cancer* 2020; **19**: 112 [PMID: 32600329 DOI: 10.1186/s12943-020-01208-3]
40 **Lu J**, Wang YH, Yoon C, Huang XY, Xu Y, Xie JW, Wang JB, Lin JX, Chen QY, Cao LL, Zheng CH, Li P, Huang CM. Circular RNA circ-RanGAP1 regulates VEGFA expression by targeting miR-877-3p to facilitate gastric cancer invasion and metastasis. *Cancer Lett* 2020; **471**: 38-48 [PMID: 31811909 DOI: 10.1016/j.canlet.2019.11.038]
41 **Pinheiro LB**, Coleman VA, Hindson CM, Herrmann J, Hindson BJ, Bhat S, Emslie KR. Evaluation of a droplet digital polymerase chain reaction format for DNA copy number quantification. *Anal Chem* 2012; **84**: 1003-1011 [PMID: 22122760 DOI: 10.1021/ac202578x]
42 **Li T**, Shao Y, Fu L, Xie Y, Zhu L, Sun W, Yu R, Xiao B, Guo J. Plasma circular RNA profiling of patients with gastric cancer and their droplet digital RT-PCR detection. *J Mol Med (Berl)* 2018; **96**: 85-96 [PMID: 29098316 DOI: 10.1007/s00109-017-1600-y]
43 **Sillence KA**, Roberts LA, Hollands HJ, Thompson HP, Kiernan M, Madgett TE, Welch CR, Avent ND. Fetal Sex and RHD Genotyping with Digital PCR Demonstrates Greater Sensitivity than Real-time PCR. *Clin Chem* 2015; **61**: 1399-1407 [PMID: 26354802 DOI: 10.1373/clinchem.2015.239137]
44 **Huggett JF**, Cowen S, Foy CA. Considerations for digital PCR as an accurate molecular diagnostic tool. *Clin Chem* 2015; **61**: 79-88 [PMID: 25338683 DOI: 10.1373/clinchem.2014.221366]
45 **Nordin JZ**, Lee Y, Vader P, Mäger I, Johansson HJ, Heusermann W, Wiklander OP, Hällbrink M, Seow Y, Bultema JJ, Gilthorpe J, Davies T, Fairchild PJ, Gabrielsson S, Meisner-Kober NC, Lehtiö J, Smith CI, Wood MJ, El Andaloussi S. Ultrafiltration with size-exclusion liquid chromatography for high yield isolation of extracellular vesicles preserving intact biophysical and functional properties. *Nanomedicine* 2015; **11**: 879-883 [PMID: 25659648 DOI: 10.1016/j.nano.2015.01.003]
46 **Van Deun J**, Mestdagh P, Sormunen R, Cocquyt V, Vermaelen K, Vandesompele J, Bracke M, De Wever O, Hendrix A. The impact of disparate isolation methods for extracellular vesicles on downstream RNA profiling. *J Extracell Vesicles* 2014; **3** [PMID: 25317274 DOI: 10.3402/jev.v3.24858]
47 **Tang XH**, Guo T, Gao XY, Wu XL, Xing XF, Ji JF, Li ZY. Exosome-derived noncoding RNAs in gastric cancer: functions and clinical applications. *Mol Cancer* 2021; **20**: 99 [PMID: 34330299 DOI: 10.1186/s12943-021-01396-6]

World Journal of Gastroenterology

Submit a Manuscript: https://www.f6publishing.com

World J Gastroenterol 2023 June 14; 29(22): 3497-3507

DOI: 10.3748/wjg.v29.i22.3497

ISSN 1007-9327 (print) ISSN 2219-2840 (online)

ORIGINAL ARTICLE

Retrospective Cohort Study

Per-oral endoscopic myotomy is safe and effective for pediatric patients with achalasia: A long-term follow-up study

Ya-Wei Bi, Xiao Lei, Nan Ru, Long-Song Li, Nan-Jun Wang, Bo Zhang, Yi Yao, En-Qiang Linghu, Ning-Li Chai

Specialty type: Gastroenterology and hepatology

Provenance and peer review: Unsolicited article; Externally peer reviewed.

Peer-review model: Single blind

Peer-review report's scientific quality classification

Grade A (Excellent): 0
Grade B (Very good): B, B
Grade C (Good): 0
Grade D (Fair): 0
Grade E (Poor): 0

P-Reviewer: Lee HS, South Korea; Topi S, Italy

Received: May 8, 2023
Peer-review started: May 8, 2023
First decision: May 11, 2023
Revised: May 12, 2023
Accepted: May 19, 2023
Article in press: May 19, 2023
Published online: June 14, 2023

Ya-Wei Bi, Nan Ru, Long-Song Li, Nan-Jun Wang, Bo Zhang, Yi Yao, En-Qiang Linghu, Ning-Li Chai, Department of Gastroenterology, The First Medical Center of Chinese PLA General Hospital, Beijing 100853, China

Xiao Lei, Senior Department of Oncology, The Fifth Medical Center of PLA General Hospital, Beijing 100859, China

Corresponding author: Ning-Li Chai, MD, Chief Physician, Professor, Department of Gastroenterology, The First Medical Center of Chinese PLA General Hospital, No. 28 Fuxing Road, Haidian District, Beijing 100853, China. chainingli@vip.163.com

Abstract

BACKGROUND

Per-oral endoscopic myotomy (POEM) is emerging as a prefer treatment option for pediatric achalasia. However, data are limited on the long-term efficacy of POEM in children and adolescents with achalasia.

AIM

To evaluate the safety and long-term efficacy of POEM for pediatric patients with achalasia and compare those outcomes with adult patients.

METHODS

This retrospective cohort study was conducted in patients with achalasia who underwent POEM. Patients aged under 18 years were included in the pediatric group; patients aged between 18 to 65 years who underwent POEM in the same period were assigned to the control group. For investigation of long-term follow-up, the pediatric group were matched with patients from the control group in a 1:1 ratio. The procedure-related parameters, adverse events, clinical success, gastroesophageal reflux disease (GERD) after POEM, and quality of life (QoL) were evaluated.

RESULTS

From January 2012 to March 2020, POEM was performed in 1025 patients aged under 65 years old (48 in the pediatric group, 1025 in the control group). No significant differences were observed in the occurrence of POEM complications between the two groups (14.6% *vs* 14.6%; P = 0.99). Among the 34 pediatric patients (70.8%) who underwent follow-up for 5.7 years (range 2.6-10.6 years), clinical success was achieved in 35 patients (35/36; 97.2%). No differences were

observed in post-POEM GERD occurrence (17.6% *vs* 35.3%; P = 0.10). QoL was significantly improved in both groups after POEM.

CONCLUSION

POEM is safe and effective for pediatric patients with achalasia. It can achieve significant symptoms relief and improve QoL.

Key Words: Achalasia; Pediatric; Per-oral endoscopic myotomy; Long-term outcomes

©The Author(s) 2023. Published by Baishideng Publishing Group Inc. All rights reserved.

Core Tip: Per-oral endoscopic myotomy (POEM) is widely accepted in adult patients with achalasia. However, there is limited data on the application of POEM in pediatric patients, particularly regarding the long-term outcomes. In this study, we evaluated the safety and long-term efficacy of POEM in pediatric patients and compared those results with adult patients. The results show that POEM is safe and effective for pediatric patients with achalasia.

Citation: Bi YW, Lei X, Ru N, Li LS, Wang NJ, Zhang B, Yao Y, Linghu EQ, Chai NL. Per-oral endoscopic myotomy is safe and effective for pediatric patients with achalasia: A long-term follow-up study. *World J Gastroenterol* 2023; 29(22): 3497-3507

URL: https://www.wjgnet.com/1007-9327/full/v29/i22/3497.htm

DOI: https://dx.doi.org/10.3748/wjg.v29.i22.3497

INTRODUCTION

Achalasia is a rare disorder of the esophageal smooth muscle characterized by impaired relaxation of the lower esophageal sphincter (LES) and absent or spastic contractions in the esophageal body[1]. Recent studies have estimated that the annul incidence of achalasia in pediatric population is approximately 0.02-0.31 per 100000 individuals[2-4]. Despite this modest incidence rate, the disease burden of achalasia in pediatric patients is substantial owing to the extreme disruption caused to the patients' childhood and education. Children with achalasia suffer from dysphagia, regurgitation, vomiting, chest pain, weight loss, and respiratory symptoms (nocturnal cough, aspiration), with frequent emergency department visits, hospitalizations, and malnutrition caused by decreased dietary intake of these children[5].

The traditional management of achalasia includes medication, endoscopy, and laparoscopic Heller myotomy (LHM)[6]. Per-oral endoscopic myotomy (POEM) is a minimally invasive method of myotomy first applied in clinical since 2010[7]. Since then, numerous large scales, retrospective and prospective with long-term follow-up studies have shown that POEM is safe and effective in the treatment of achalasia in adult patients[8,9]. However, studies on the safety and long-term effectiveness of POEM in the treatment of pediatric population are limited[10-13]. Owning to the low incidence of achalasia in pediatric population, the sample sizes that can be included in studies are usually small which may affect the credibility of the results. POEM has been proved to be safe and effective in adult patients, comparing the results in pediatric patients with adult patients may further validated the effectiveness of POEM in pediatric patients. Furthermore, the long-term outcome of POEM is needed to be studied as children have a long-life expectancy. Therefore, the aim of this study was to comprehensively evaluate and analyze the safety and long-term outcomes of POEM in pediatric patients and compare with those in adults.

MATERIALS AND METHODS

Study design

We performed a retrospective cohort study to evaluate the outcome of pediatric patients with achalasia who underwent POEM in comparison to the outcome of all adult patients who underwent POEM within the same period. Written informed consent was obtained from each patient, and the study was approved by the Medical Ethics Committee of The First Medical Center of Chinese PLA General Hospital. Informed consent for patients aged less than 18 years was provided by their guardian.

Patients and data collection

The inclusion criteria in this study included: (1) Achalasia diagnosed by Eckardt score ≥ 4 and further confirmed by esophagogastroduodenoscopy (EGD), barium esophagram, and/or esophageal manometry; and excluding others secondary to tumor, autoimmune diseases, *etc.*; and (2) Patients with age ≤ 65 when performing POEM. Those patients with severe cardiopulmonary disease, blood coagulation disorders, or other underlying diseases were excluded from this study.

Patients aged less than 18 years who underwent POEM in The First Medical Center of Chinese PLA General Hospital, Beijing, China from January 2012 to March 2020 were included in the pediatric group, whereas patients between the ages of 18-65 who underwent POEM in the same period were assigned to the control group. Demographic data and the disease course of the achalasia, including the manifestations, diagnosis, and prior treatments, were recorded in detail upon admission to the hospital. In addition, the Urbach scale questionaries were completed to assess the quality of life (QoL) of achalasia patients[14].

To evaluate the long-term outcomes of POEM in pediatric patients, we matched the pediatric group with patients from the control group in a 1:1 ratio. The matching principles were based on identical gender, the same type of Chicago classification and Ling classification, a surgery date that did not differ by more than three months, and the involvement of the same operating physician.

Patients were scheduled for follow-up visits at 3 mo, 6 mo, and 1 year after POEM, then yearly. EGD was performed to assess wound healing and to determine whether or not post-POEM reflux esophagitis existed. Moreover, esophageal high-resolution manometry, an X-ray barium meal, and 24-h esophageal pH monitoring were performed if possible. Patients were also contacted *via* telephone and the post-POEM complications, Eckardt score and the Urbach questionaries were recorded.

POEM procedure

POEM was performed after the patients fasted for 48 h and underwent EGD to ensure that no food residue remained in the esophageal lumen. The standard POEM procedure was performed as previously described and generally consisted of the following major steps: First, a submucosal injection of methylene blue saline solution (1:10000) was administered, then a mucosal incision was made approximately 6–10 cm above the gastroesophageal junction (GEJ); second, a submucosal tunnel was established, passing over the GEJ and 2–3 cm into the proximal stomach; third, a myotomy started 2 cm distal to the incision and extended 2–3 cm into the stomach; and finally, after assuring hemostasis and verifying that the endoscope could easily pass the cardia, the mucosal incision was closed with clips (Figure 1). Adequate extension of the submucosal tunnel across the GEJ was confirmed by visualizing blanched gastric mucosa and a vascular pattern. Carbon dioxide gas was used for insufflation with a CO_2 insufflator (UCR; Olympus) during procedures.

All patients were kept fasting for 3 d after the procedure. A liquid diet was started for an additional day. Antibiotics and proton pump inhibitor (PPI) were administered intravenously during the fasting period. An oral PPI was required for at least 4 wk subsequently. X-ray or chest and abdominal computed tomography was performed to evaluate gas-related adverse events.

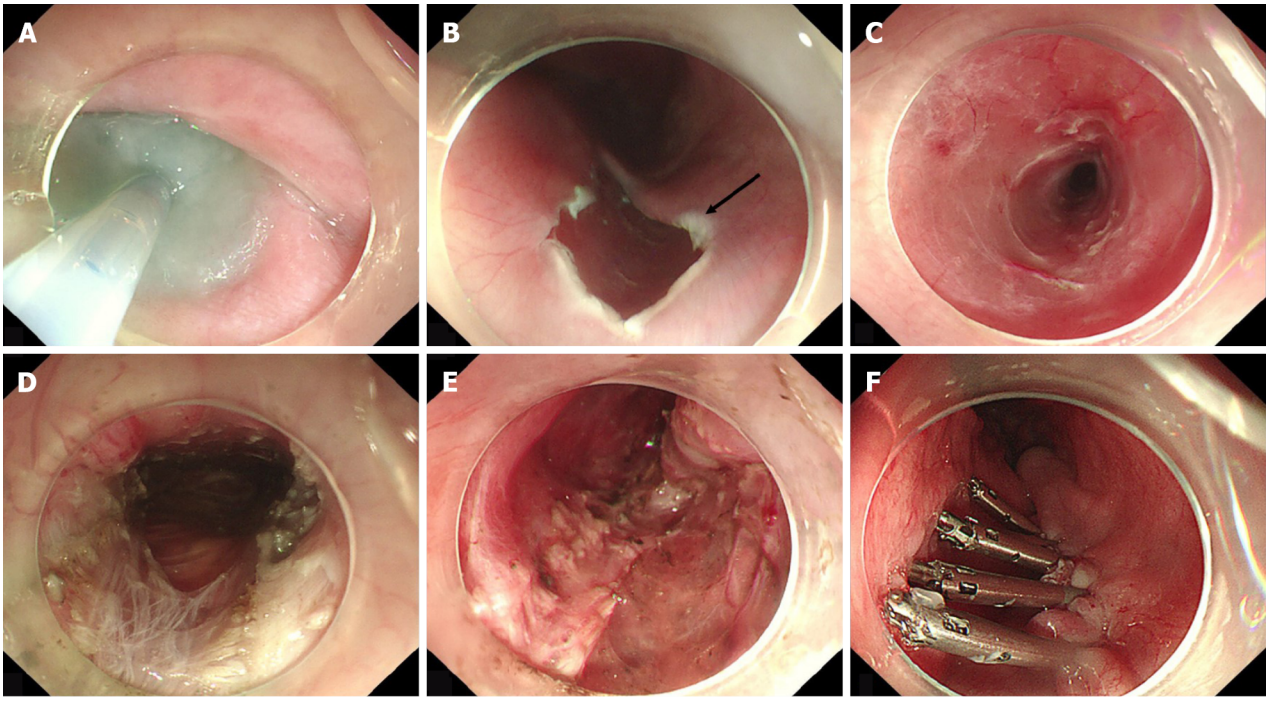
Endoscopic classifications and definitions

The Ling classification was based on the endoscopic morphology of the esophageal lumen[15]. According to multiring structures, crescent-like structures, and diverticula, the Ling classification was recorded as Ling I, Ling IIa, Ling Ib, Ling IIc, and Ling III.

Perioperative outcomes and clinical follow-up were evaluated. Perioperative outcomes included technical success, and perioperative adverse events. Technical success was defined as the successful completion of the entire POEM procedure; if the procedure was not completed, it was defined as technical failure. Perioperative adverse events include mucosa injury, gas-related adverse events (pneumothorax, pneumoperitoneum and subcutaneous emphysema), pleural effusion, and bleeding. Procedure time was defined as the time from submucosal injection to the end of incision closure with clips. Clinical success was defined as a post-POEM Eckardt score ≤ 3. QoL was accessed by Urbach questionaries.

Statistical analysis

Depending on the distributional properties, outcome measures were expressed as the mean ± SD or as median values with ranges. For normally distributed continuous data, statistical significance was assessed by the Student's *t*-test; for categorical data, significance was assessed by the χ^2 test with Yates' correction when appropriate or by the Fisher's exact test; and for non-normally distributed continuous data, statistical significance was assessed by the Wilcoxon test. A P value of < 0.05 was established as the significance level.



DOI: 10.3748/wjg.v29.i22.3497 **Copyright** ©The Author(s) 2023.

Figure 1 The procedure of per-oral endoscopic myotomy. A: Submucosal injection of methylene blue saline solution; B: Mucosal incision. The black arrow points to the inversed T-shaped incision; C: The submucosal tunnel establishment; D and E: Myotomy in the submucosal tunnel; F: Mucosal incision was closed with clips.

RESULTS

From January 2012 to March 2020, POEM was performed in 1073 patients aged under 65 years old (48 in the pediatric group and 1025 in the control group).

Baseline characters

The demographic and clinical characteristics of the patients in the two groups are shown in Table 1. There was no significant difference in gender distribution between the two groups. The median age of the pediatric patients who underwent POEM in our hospital was 16 years (range 7-18 years). Compared with control group, body weight index of pediatric group was significantly lower (17.7 *vs* 20.9, $P < 0.001$). Although the median disease course was significantly shorter in the pediatric group (median 17.5 mo *vs* 48 mo, $P < 0.001$), no significant differences were observed between the two groups regarding the type of Chicago classification, type of Ling classification and residual LES pressure. Twelve pediatric patients and 183 adult patients had undergone prior treatments, including botulinum toxin injection, pneumatic balloon dilation, endoscopic stent placement, POEM and LHM. In terms of prior treatment history, there were 4 (8.3%) patients received botulinum toxin injection, 5 (10.4%) patients received pneumatic balloon dilation, 1 (2.1%) patient had POEM and 2 (4.2%) patients had more than one treatment method in pediatric group. While 46 (4.5%) patients had botulinum toxin injection, 92 (9.0%) patients had pneumatic balloon dilation, 9 (0.9%) patients had POEM, 10 (1.0%) had LHM, 14 (1.4%) patients had endoscopic stent placement, and 12 (1.2%) had more than one treatment method in control group.

Procedure-related characteristics and safety

The procedure results in the two groups are shown in Table 2. All pediatric patients successfully underwent POEM. Of the 1025 patients in control group, 1016 (99.1%) had technique success; nine patients could not complete the POEM procedure because of serious submucosal adhesions. No significant differences were observed between the pediatric and control groups regarding the length of tunnel, length of esophageal myotomy, length of gastric myotomy, types of myotomy and procedure time. The mean lengths of the tunnel were 10.8 cm (range, 7–14 cm) and 11.2 cm (range, 5-20 cm), respectively, whereas the length of the esophageal and gastric tunnels were 5.3 cm (range, 1-9 cm) and 1.9 cm (range, 0-4 cm) in pediatric group and were 5.2 cm (range, 3-15 cm) and 1.9 cm (range, 0-4 cm) in control group. A progressive full-thickness myotomy was the most common type of myotomy in both group (87.5% in pediatric group and 78.0% in control group). The types of myotomy in the remaining pediatric patients involved full thickness muscle myotomy (6.3%), circular muscle myotomy (2.1%), and other types (4.2%). In the control group, full-thickness myotomy accounted for 9.6%, circular myotomy

Table 1 General characteristics of the pediatric group and the control group

	Pediatric group (*n* = 48)	Control group (*n* = 1025)	*P* value
Sex, *n* (%)			
Male	26 (54.2)	469 (45.8)	0.253
Female	22 (45.8)	556 (54.2)	
Age, median (range), years	16 (7-18)	43 (19-65)	< 0.001
BMI, median (range), kg/m^2	17.7 (11.2-26.8)	20.9 (12.9-40.4)	< 0.001
Chicago classification, *n* (%)	*n* = 42, 87.5	*n* = 1003, 97.8	0.928
Type I	7 (16.7)	156 (15.5)	
Type II	32 (76.2)	787 (78.5)	
Type III	3 (7.1)	60 (6.0)	
Ling classification, *n* (%)			0.076
Ling I	9 (18.8)	189 (17.0)	
Ling IIa	17 (35.4)	340 (30.6)	
Ling IIb	18 (37.5)	249 (22.4)	
Ling IIc	4 (8.3)	206 (18.5)	
Ling III	0 (0.0)	41 (1.35)	
Disease course, median (range), month	17.5 (2-120)	48 (1-540)	< 0.001
LES pressure, median (range), mmHg	*n* = 42, 87.5	*n* = 1003, 97.8	0.214
	25.8 (8.4-65.9)	24.5 (1-83.2)	
Prior treatment			0.210
Patients without prior treatment, *n* (%)	36 (75.0)	842 (82.1)	
Patients with prior treatment, *n* (%)	12 (25.0)	183 (17.9)	
BTI	4 (8.3)	46 (4.5)	
PBD	5 (10.4)	92 (9.0)	
POEM	1 (2.1)	9 (0.9)	
LHM	0 (0.0)	10 (1.0)	
ESP	0 (0.0)	14 (1.4)	
PBD + BTI	1 (2.1)	3 (0.3)	
ESP + BTI	1 (2.1)	1 (0.1)	
POEM + PBD	0 (0.0)	2 (0.2)	
PBD + ESP	0 (0.0)	3 (0.3)	
PBD + LHM	0 (0.0)	1 (0.1)	
BTI + LHM	0 (0.0)	1 (0.1)	
ESP + LHM	0 (0.0)	1 (0.1)	

BTI: Botulinum toxin injection; BMI: Body mass index; PBD: Pneumatic balloon dilation; POEM: Per-oral endoscopic myotomy; LHM: Laparoscopic Heller myotomy; ESP: Endoscopic stent placement; LES: Lower esophageal sphincter.

accounted for 5.5%, and other incision types accounted for 6.9%. The mean procedure time was 43.9 min (range, 24-116 min) and 47.1 min (14-160 min) respectively.

No significant differences were observed between the pediatric and control groups regarding the overall complications of POEM (14.6 % *vs* 14.6 %; *P* = 0.997). All of the mucosa injuries were closed with titanium clips and porcine fibrin glue. Patients with pneumoperitoneum treated by puncture with a 10-mL syringe intra-operatively and patients with subcutaneous emphysema gradually absorbed the gas without special intervention. In the pediatric group, three complications of POEM occurred in seven patients (7/48; 14.6%), with three of these patients presenting with mucosa injury, two presenting with

Table 2 Procedure-related characteristics and complications of pediatric group and control group, *n* (%)

	Pediatric group	Control group	*P* value
Technique success	48 (100.0)	1016 (99.1)	> 0.999
Length of tunnel, mean (range), cm	10.8 (7-14)	11.2 (5-20)	0.206
Length of esophageal myotomy, mean (range), cm	5.3 (1-9)	5.2 (3-15)	0.529
Length of gastric myotomy, mean (range), cm	1.9 (0-4)	1.9 (0-4)	0.648
Types of myotomy			0.458
Progressive full-thickness myotomy	42 (87.5)	792 (78.0)	
Full-thickness muscle myotomy	3 (6.3)	98 (9.6)	
Circular muscle myotomy	1 (2.1)	56 (5.5)	
Others[1]	2 (4.2)	70 (6.9)	
Procedure time, mean (range), min	43.9 (24-116)	47.1 (14-160)	0.394
Complications	7 (14.6)	148 (14.6)	0.997
Mucosa injury	3 (6.2)	84 (8.3)	
Gas-related adverse event			
Pneumothorax	0 (0.0)	3 (0.3)	
Pneumoperitoneum	2 (4.2)	27 (2.7)	
Subcutaneous emphysema	2 (4.2)	32 (3.2)	
Pleural effusion	0 (0.0)	1 (0.1)	
Bleeding	0 (0.0)	1 (0.1)	

[1]Other types of myotomy include circular muscle incision plus balloon plasty and glass-style anti-reflux myotomy.

pneumoperitoneum, and two presenting with subcutaneous emphysema. In control group, in addition to mucosa injury and gas-related complications, a 27-year-old male patient had delayed bleeding with hematemesis 11 d after the POEM and he underwent gastroscopic hemostasis. The patient with pleural effusion was treated with closed thoracic drainage. None of the patients with complications required surgical intervention or intensive care unit (ICU) transfer.

Efficacy

The median follow-up period was 5.7 years (range 2.6-10.6 years) for the pediatric group and 14 patients were lost for long-term follow-up. Significant differences were shown in the Eckardt score, QoL, height, weight, residual LES pressure and numbers of months absent from school of the pediatric patients before and after POEM (Table 3). The Eckardt score after median 5.7 years of follow-up was significantly declined compared with the score before POEM (8.0 *vs* 1.1, $P < 0.001$) and all symptom component of the Eckardt score decreased significantly. QoL was assessed by Urbach scale questionaries, which is a 10-item measure of disease-specific health-related QoL that sampled the concepts of food tolerance, dysphagiarelated behavior modifications, pain, heartburn, distress, lifestyle limitation, and satisfaction. Scores on the Urbach scale questionaries range from 10-33, and lower scores indicate better QoL. Urbach scores were significantly lower in pediatric patients at long-term follow-up after POEM treatment compared with pre-treatment scores (24.7 *vs* 12.8, $P < 0.001$). The height and weight of pediatric patients also improved significantly at follow-up (163.7 cm *vs* 170.5 cm and 49.9 kg *vs* 64.3 kg, $P < 0.001$). Moreover, the absences from school decreased significantly (median 3.3 mo *vs* 0.1 mo, $P < 0.001$).

To compare the long-term outcomes of POEM in pediatric patients and adult patients, we matched the pediatric group with patients from the control group in a 1:1 ratio. The matching principles were based on identical gender, the same type of Chicago classification and Ling classification, a surgery date that did not differ by more than three months, and the involvement of the same operating physician. The long-term outcomes of POEM in pediatric patients and matched adult patients were shown in Table 4. The median follow-up time in pediatric group and matched adult group was 5.7years (range 2.6-10.6 years) and 6.0 years (range 2.7-10.7 years) respectively. Patients in both groups had clinical symptoms relief and QoL improvement after POEM. No significant differences were observed between the two groups regarding the Eckardt scores, Urbach scores, clinical failure and clinical reflux evaluation. Before POEM treatment and at post-operative follow-up, the body mass index (BMI) of matched control group was significantly greater than that of pediatric group (17.7 *vs* 20.0; 20.8 *vs* 24.0).

Table 3 The long-term outcomes of per-oral endoscopic myotomy in pediatric patients

	Pre-POEM	Post-POEM	*P* value
Eckardt score, mean (range)	8.0 (4-11)	1.1 (0-4)	< 0.001
Dysphagia, mean ± SD	2.8 ± 0.7	0.6 ± 0.7	< 0.001
Regurgitation, mean ± SD	1.7 ± 0.8	0.1 ± 0.2	< 0.001
Chest pain, mean ± SD	1.0 ± 0.9	0.4 ± 0.6	< 0.001
Weight loss, mean ± SD	1.5 ± 1.2	0.0 ± 0.0	< 0.001
Urbach score, mean (range)	12.8 (10-20)	24.7 (18-30)	< 0.001
Height, mean (range), cm	163.7 (120-184)	170.5 (159-185)	< 0.001
Weight, mean (range), kg	49.9 (22.2-82)	64.3 (47-100)	< 0.001
Number of months absent from school, mean (range), months	3.3 (0.5-24)	0.1 (0-1)	< 0.001

POEM: Per-oral endoscopic myotomy.

Table 4 The long-term outcomes of per-oral endoscopic myotomy in pediatric group and matched control group

	Pediatric group (*n* = 34)	Matched control group (*n* = 34)	*P* value
Follow-up time, median (range), years	5.7 (2.6-10.6)	6.0 (2.7-10.7)	0.954
Pre-POEM, Eckardt score, mean (range)	8.0 (4-11)	7.9 (4-12)	0.975
Post-POEM (3 mo), Eckardt score, mean (range)	0.3 (0-3)	0.3 (0-2)	0.978
Post-POEM, Eckardt score, mean (range)	1.1 (0-4)	1.4 (0-3)	0.088
Eckardt score[1] (pre-post), mean (range)	6.9 (2-10)	6.4 (0-12)	0.578
Pre-POEM BMI, median (range), kg/m^2	17.7 (11.2-26.8)	20.0 (16.4-28.7)	< 0.001
Post-POEM BMI, median (range), kg/m^2	20.8 (15.8-29.5)	24.0 (19.5-29.4)	< 0.001
BMI (Post-pre)[2], median (range), kg/m^2	3.7 (-1.7-13)	3.5 (0.7-12.9)	0.502
Pre-POEM, Urbach score, mean (range)	12.8 (10-20)	12.7 (10-20)	0.842
Post-POEM, Urbach score, mean (range)	24.7 (18-30)	25.7 (17-33)	0.221
Urbach score[3] (pre-post), mean (range)	11.9 (1-18)	13.0 (4-23)	0.254
Clinical success, *n* (%)	33 (97.1)	34 (100.0)	> 0.999
Clinical reflux evaluation	6 (17.6)	12 (35.3)	0.099
Reflux esophagitis by gastroscopy	2 (5.9)	2 (5.9)	
Symptomatic reflux	4 (11.8)	10 (29.4)	

[1]Eckardt score: The Eckardt score before per-oral endoscopic myotomy (POEM) minus the Eckardt score at last follow-up.
[2]Body mass index (BMI): The BMI value at the last follow-up minus the BMI value before POEM.
[3]Urbach score: The Urbach score before POEM minus the Urbach score at last follow-up.
POEM: Per-oral endoscopic myotomy; BMI: Body mass index.

However, the difference in BMI before and after POEM was similar in both groups (3.7 *vs* 3.5, $P = 0.502$).

All adult patients in matched group received clinical success. One pediatric patient was considered clinical failure because his Eckardt score was 4. The patient mainly has substernal pain and need to drink water to when eating dry food without weight loss and chest pain.

Gastroesophageal reflux disease (GERD) is the most common adverse event after POEM treatment [16]. Reflux esophagitis identified by EGD and assessed by the Los Angeles classification. A GerdQ score of GERD with a score of > 7 was defined as symptomatic reflux[11,13]. At median 5.7 years follow-up, 6 patients (6/34, 17.6%) were suffered from symptomatic reflux, with 2 patients (5.9%) showed reflux esophagitis (1 Los Angeles type A, 1 Los Angeles type B) on endoscopy and 4 patients (11.8%) were suffered from clinical reflux. In matched control group, 2 patients (5.9%) showed reflux esophagitis (1 Los Angeles type A, 1 Los Angeles type C) on endoscopy, 10 patients (29.4%) were suffered from clinical reflux. All patients were well controlled with medical therapy.

DISCUSSION

In this study, we included 48 pediatric patients and 1025 adult patients with achalasia and patients had a median 5.7 years followed-up. The risk of complications relating to POEM was not increased in pediatric patients, and the long-term efficacy of POEM in pediatric patients were similar to the results of adult group. Our results indicated that POEM is a safe and effective procedure for the management of pediatric achalasia.

Achalasia is a primary esophageal motility disorder with unknown etiology. While adults and children both present with progressive dysphagia initially to solids and in some cases to liquids, the manifestations can be more protean and challenging to diagnose in children. A majority of pediatric patients, especially those under 6-7 years of age, are often misdiagnosed as GERD and given acid-suppressive therapy[17]. Patients have dysphagia due to esophageal motility disorder, and some children may show reluctance to eat and be misdiagnosed as anorexia[18]. Up to 50% of children are treated with antacids or prokinetics before the diagnosis of achalasia is identified[19]. Dysphagia and regurgitation are the main symptoms of achalasia, and patients often suffer from malnutrition due to insufficient intake[20]. Upon majority of patients present normal BMI or even obese, there are almost 50% of patients to be at moderate or high risk for malnutrition at presentation[21]. Compared with adult patients, malnutrition in a pediatric patient may negatively affect long-term growth and development. Furthermore, psychology of children is immature, and the decline in QoL caused by achalasia can lead to a series of mental illnesses in pediatric patients such as low self-esteem, depression, anxiety, school stress or decreased performance[22]. Therefore, it is urgent to find an effective treatment method to relieve the symptoms of achalasia in pediatric patients. POEM is a is a less invasive therapy with promising treatment effect. Since the clinical application of POEM in 2010, a large number of studies have been conducted and shown that POEM is a safe and effective method for the treatment of achalasia in adult patients[7,23,24]. However, data of POEM for pediatric patients are limited. Due to the low incidence of achalasia in children and adolescents, the sample size is small in most studies which is difficult to systematically evaluate and avoid statistical bias. Therefore, comparing its outcomes with those in adults seems particularly necessary. In addition, pediatric patients have a long-life expectancy and the long-term outcomes of POEM should be investigated. To our best knowledge, this is the first study evaluated the safety and long-term efficacy of POEM in children and compared those with adults with the median follow-up time over 5 years.

In our study, we compare 48 pediatric patients with 1025 adults with a median follow-up over 5 years. The technique success achieved 100% in pediatric group and 99.1% in control group. Standard tunnel and the length of myotomy were applied during POEM procedure in both groups. According to the previous studies, pediatric patients were all received standard tunnel and myotomy length[11,13,25]. POEM-related parameters such as length of tunnel, length of myotomy, types of myotomy and operation time were similar to those of adult patients.

Our results showed that there are no significant differences between the pediatric and control groups regarding the overall complications of POEM. All pediatric patients who developed complications recovered with conservative management. While one adult patient had delayed bleeding with hematemesis need another endoscopic invention and one pleural effusion which treated with closed thoracic drainage. Liu *et al*[13] showed only five children (3.8%) experienced major adverse events, which were resolved by conservative treatment[13]. Peng *et al*[11] found two children (8.3%) developed perioperative subcutaneous emphysema during the procedure and were spontaneously absorbed without any intervention[11]. Wood *et al*[25] showed that among 21 pediatric patients who received POEM, one had mucosa injury and one had pneumoperitoneum. None of them need for reintervention [25]. Choné *et al*[26] indicated that 1 case (1%) of significant per-procedure bleeding, 7 cases (6%) had postoperative adverse events. None of them need surgery or transfer to ICU[26]. All these results indicate that POEM is a safe treatment method for pediatric patients.

In our study, all the pediatric patients with preoperative dysphagia and regurgitation reported improved or resolved symptoms at the median 5.7 years follow-up. All of them were free from the further intervention for achalasia after POEM. Compared with adult patients, POEM also achieved satisfactory long-term outcomes in pediatric patients. One pediatric patient was considered clinical failure at last time follow-up as his Eckardt score was 4. The patient began to experience intermittent dysphagia symptoms again in the second year after POEM and at last time follow-up the patient mainly has substernal pain and need to drink water to when eating dry food every day. In this patient, a submucosal tunnel of standard length was established, but the end of the tunnel was located at the EGJ, and only esophagomyotomy was performed. Studies had showed that in order to ensure the curative effect of POEM, the length of myotomy is routinely 8-10 cm, at least 2 cm below the EGJ[27]. Therefore, symptom recurrence of the patient may be related to insufficient myotomy and we suggested him could receive a re-POEM.

Several factors could limit the extent to which the results can be generalized in our study. First, we did not analysis the risk factors for complications of POEM in pediatric patients due to the small sample size. Second, the mean age was slightly older in pediatric group (median age was 16). This shortage is due to younger children tend to receive treatment in children's hospitals in China. Third, the study was retrospective and a single-center analysis.

CONCLUSION

In summary, POEM is safe treatment method and could achieve satisfactory long-term outcomes in pediatric patients. Furthermore, prospective, multicenter, and large sample studies are warranted to validate our conclusions.

ARTICLE HIGHLIGHTS

Research background

Achalasia is a rare disorder of the esophageal smooth muscle which cause dysphagia, regurgitation, chest pain and weight loss. In recent years, per-oral endoscopic myotomy (POEM) is emerging as a prefer treatment option for patients achalasia.

Research motivation

Although POEM was proved to be safe and efficacy for adult patients with achalasia, data of POEM in pediatric patients are limited.

Research objectives

To evaluate the safety and long-term efficacy of POEM for pediatric patients with achalasia.

Research methods

We performed a retrospective cohort study to evaluate the outcome of pediatric patients with achalasia who underwent POEM in comparison to the outcome of all adult patients who underwent POEM within the same period. To evaluate the safety of POEM, we compare the operation-related parameters and complications in the two groups. To evaluate the long-term efficacy of POEM, we compare the body mass index, clinical symptoms, quality of life in pediatric group before and after POEM; and we also compare those outcomes in pediatric group and matched adult group.

Research results

The risk of complications relating to POEM was not increased in pediatric patients, and the long-term efficacy of POEM in pediatric patients were similar to the results of adult group.

Research conclusions

POEM is safe treatment method and could achieve satisfactory long-term outcomes in pediatric patients.

Research perspectives

POEM can be an an effective treatment option for achalasia in pediatric patients.

FOOTNOTES

Author contributions: Bi YW, Lei X and Ru N contributed equally to this article; Bi YW, Lei X, Linghu EQ and Chai NL contributed to this paper with conception and design of the study; Bi YW, Lei X, Ru N, Li LS, Wang NJ, Zhang B and Yao Y did the data collection, literature review and analysis; Bi YW, Lei X and Ru N wrote the paper; all authors made the critical revision and editing of the article for important intellectual content, and approved the final version.

Supported by National Natural Science Foundation of China, No. 82070682.

Institutional review board statement: The study was reviewed and approved by the First Medical Center of Chinese PLA General Hospital Institutional Review Board, No. 20230301.

Informed consent statement: All study participants or their legal guardian provided informed written consent about personal and medical data collection prior to study enrolment.

Conflict-of-interest statement: All the authors report no relevant conflicts of interest for this article.

Data sharing statement: No additional data are available.

STROBE statement: The authors have read the STROBE Statement—checklist of items, and the manuscript was prepared and revised according to the STROBE Statement—checklist of items.

Open-Access: This article is an open-access article that was selected by an in-house editor and fully peer-reviewed by external reviewers. It is distributed in accordance with the Creative Commons Attribution NonCommercial (CC BY-

NC 4.0) license, which permits others to distribute, remix, adapt, build upon this work non-commercially, and license their derivative works on different terms, provided the original work is properly cited and the use is non-commercial. See: https://creativecommons.org/Licenses/by-nc/4.0/

Country/Territory of origin: China

ORCID number: Ya-Wei Bi 0000-0003-3762-5920; Xiao Lei 0000-0002-0428-1749; Nan Ru 0009-0008-6212-6385; Long-Song Li 0000-0002-4000-7501; Nan-Jun Wang 0000-0002-6061-4798; Bo Zhang 0000-0002-4333-0750; Yi Yao 0000-0001-6976-3418; En-Qiang Linghu 0000-0003-4506-7877; Ning-Li Chai 0000-0002-6791-5817.

S-Editor: Fan JR
L-Editor: A
P-Editor: Fan JR

REFERENCES

1 **Savarino E**, Bhatia S, Roman S, Sifrim D, Tack J, Thompson SK, Gyawali CP. Achalasia. *Nat Rev Dis Primers* 2022; **8**: 28 [PMID: 35513420 DOI: 10.1038/s41572-022-00356-8]
2 **Sato H**, Yokomichi H, Takahashi K, Tominaga K, Mizusawa T, Kimura N, Kawata Y, Terai S. Epidemiological analysis of achalasia in Japan using a large-scale claims database. *J Gastroenterol* 2019; **54**: 621-627 [PMID: 30607612 DOI: 10.1007/s00535-018-01544-8]
3 **Miller J**, Khlevner J, Rodriguez L. Upper Gastrointestinal Functional and Motility Disorders in Children. *Pediatr Clin North Am* 2021; **68**: 1237-1253 [PMID: 34736587 DOI: 10.1016/j.pcl.2021.07.009]
4 **Smits M**, van Lennep M, Vrijlandt R, Benninga M, Oors J, Houwen R, Kokke F, van der Zee D, Escher J, van den Neucker A, de Meij T, Bodewes F, Schweizer J, Damen G, Busch O, van Wijk M. Pediatric Achalasia in the Netherlands: Incidence, Clinical Course, and Quality of Life. *J Pediatr* 2016; **169**: 110-5.e3 [PMID: 26616251 DOI: 10.1016/j.jpeds.2015.10.057]
5 **Meyer A**, Catto-Smith A, Crameri J, Simpson D, Alex G, Hardikar W, Cameron D, Oliver M. Achalasia: Outcome in children. *J Gastroenterol Hepatol* 2017; **32**: 395-400 [PMID: 27411173 DOI: 10.1111/jgh.13484]
6 **Vaezi MF**, Pandolfino JE, Yadlapati RH, Greer KB, Kavitt RT. ACG Clinical Guidelines: Diagnosis and Management of Achalasia. *Am J Gastroenterol* 2020; **115**: 1393-1411 [PMID: 32773454 DOI: 10.14309/ajg.0000000000000731]
7 **Werner YB**, Hakanson B, Martinek J, Repici A, von Rahden BHA, Bredenoord AJ, Bisschops R, Messmann H, Vollberg MC, Noder T, Kersten JF, Mann O, Izbicki J, Pazdro A, Fumagalli U, Rosati R, Germer CT, Schijven MP, Emmermann A, von Renteln D, Fockens P, Boeckxstaens G, Rösch T. Endoscopic or Surgical Myotomy in Patients with Idiopathic Achalasia. *N Engl J Med* 2019; **381**: 2219-2229 [PMID: 31800987 DOI: 10.1056/NEJMoa1905380]
8 **de Moura ETH**, Jukemura J, Ribeiro IB, Farias GFA, de Almeida Delgado AA, Coutinho LMA, de Moura DTH, Aissar Sallum RA, Nasi A, Sánchez-Luna SA, Sakai P, de Moura EGH. Peroral endoscopic myotomy vs laparoscopic myotomy and partial fundoplication for esophageal achalasia: A single-center randomized controlled trial. *World J Gastroenterol* 2022; **28**: 4875-4889 [PMID: 36156932 DOI: 10.3748/wjg.v28.i33.4875]
9 **Shiwaku H**, Inoue H, Sato H, Onimaru M, Minami H, Tanaka S, Sato C, Ogawa R, Okushima N, Yokomichi H. Peroral endoscopic myotomy for achalasia: a prospective multicenter study in Japan. *Gastrointest Endosc* 2020; **91**: 1037-1044.e2 [PMID: 31759035 DOI: 10.1016/j.gie.2019.11.020]
10 **Nabi Z**, Ramchandani M, Basha J, Goud R, Darisetty S, Reddy DN. POEM Is a Durable Treatment in Children and Adolescents With Achalasia Cardia. *Front Pediatr* 2022; **10**: 812201 [PMID: 35281245 DOI: 10.3389/fped.2022.812201]
11 **Peng D**, Tan Y, Li C, Lv L, Zhu H, Liang C, Li R, Liu D. Peroral Endoscopic Myotomy for Pediatric Achalasia: A Retrospective Analysis of 21 Cases With a Minimum Follow-Up of 5 Years. *Front Pediatr* 2022; **10**: 845103 [PMID: 35444970 DOI: 10.3389/fped.2022.845103]
12 **Miao S**, Wu J, Lu J, Wang Y, Tang Z, Zhou Y, Huang Z, Ying H, Zhou P. Peroral Endoscopic Myotomy in Children With Achalasia: A Relatively Long-term Single-center Study. *J Pediatr Gastroenterol Nutr* 2018; **66**: 257-262 [PMID: 28691974 DOI: 10.1097/MPG.0000000000001675]
13 **Liu Z**, Wang Y, Fang Y, Huang Y, Yang H, Ren X, Xu M, Chen S, Chen W, Zhong Y, Zhang Y, Qin W, Hu J, Cai M, Yao L, Li Q, Zhou P. Short-term safety and efficacy of peroral endoscopic myotomy for the treatment of achalasia in children. *J Gastroenterol* 2020; **55**: 159-168 [PMID: 31679066 DOI: 10.1007/s00535-019-01607-4]
14 **Urbach DR**, Tomlinson GA, Harnish JL, Martino R, Diamant NE. A measure of disease-specific health-related quality of life for achalasia. *Am J Gastroenterol* 2005; **100**: 1668-1676 [PMID: 16144120 DOI: 10.1111/j.1572-0241.2005.50141.x]
15 **Li HK**, Linghu EQ. New endoscopic classification of achalasia for selection of candidates for peroral endoscopic myotomy. *World J Gastroenterol* 2013; **19**: 556-560 [PMID: 23382636 DOI: 10.3748/wjg.v19.i4.556]
16 **Familiari P**, Greco S, Gigante G, Calì A, Boškoski I, Onder G, Perri V, Costamagna G. Gastroesophageal reflux disease after peroral endoscopic myotomy: Analysis of clinical, procedural and functional factors, associated with gastroesophageal reflux disease and esophagitis. *Dig Endosc* 2016; **28**: 33-41 [PMID: 26173511 DOI: 10.1111/den.12511]
17 **Hallal C**, Kieling CO, Nunes DL, Ferreira CT, Peterson G, Barros SG, Arruda CA, Fraga JC, Goldani HA. Diagnosis, misdiagnosis, and associated diseases of achalasia in children and adolescents: a twelve-year single center experience. *Pediatr Surg Int* 2012; **28**: 1211-1217 [PMID: 23135808 DOI: 10.1007/s00383-012-3214-3]
18 **Franklin AL**, Petrosyan M, Kane TD. Childhood achalasia: A comprehensive review of disease, diagnosis and therapeutic management. *World J Gastrointest Endosc* 2014; **6**: 105-111 [PMID: 24748917 DOI: 10.4253/wjge.v6.i4.105]
19 **Lee CW**, Kays DW, Chen MK, Islam S. Outcomes of treatment of childhood achalasia. *J Pediatr Surg* 2010; **45**: 1173-

1177 [PMID: 20620315 DOI: 10.1016/j.jpedsurg.2010.02.086]

20 **Mari A**, Sweis R. Assessment and management of dysphagia and achalasia. *Clin Med (Lond)* 2021; **21**: 119-123 [PMID: 33762370 DOI: 10.7861/clinmed.2021-0069]

21 **Newberry C**, Vajravelu RK, Pickett-Blakely O, Falk G, Yang YX, Lynch KL. Achalasia Patients Are at Nutritional Risk Regardless of Presenting Weight Category. *Dig Dis Sci* 2018; **63**: 1243-1249 [PMID: 29468378 DOI: 10.1007/s10620-018-4985-8]

22 **Frankhuisen R**, van Herwaarden MA, Heijkoop R, Smout AJ, Baron A, Vermeijden JR, Gooszen HG, Samsom M. Persisting symptoms and decreased health-related quality-of-life in a cross-sectional study of treated achalasia patients. *Aliment Pharmacol Ther* 2007; **26**: 899-904 [PMID: 17767474 DOI: 10.1111/j.1365-2036.2007.03423.x]

23 **Bechara R**, Ikeda H, Inoue H. Peroral endoscopic myotomy: an evolving treatment for achalasia. *Nat Rev Gastroenterol Hepatol* 2015; **12**: 410-426 [PMID: 26035678 DOI: 10.1038/nrgastro.2015.87]

24 **Xu S**, Chai N, Tang X, Linghu E, Li L, Wang S, Zhang X. Outcomes of peroral endoscopic myotomy in challenging achalasia patients: a long-term follow-up study. *Surg Endosc* 2021; **35**: 3732-3743 [PMID: 32794046 DOI: 10.1007/s00464-020-07864-2]

25 **Wood LS**, Chandler JM, Portelli KE, Taylor JS, Kethman WC, Wall JK. Treating children with achalasia using per-oral endoscopic myotomy (POEM): Twenty-one cases in review. *J Pediatr Surg* 2020; **55**: 1006-1012 [PMID: 32197825 DOI: 10.1016/j.jpedsurg.2020.02.028]

26 **Choné A**, Familiari P, von Rahden B, Desai P, Inoue H, Shimamura Y, Eleftheriadis N, Yamashita K, Khashab MA, Shiwaku H, Seewald S, Draganov PV, Alvarez LBM, Chaussade S, Tantau M, Abraham M, Marks J, Arevalo G, Albéniz E, Mion F, Roman S, Rivory J, Dubois R, Lachaux A, Benech N, Subtil F, Ponchon T, Barret M, Pioche M. Multicenter Evaluation of Clinical Efficacy and Safety of Per-oral Endoscopic Myotomy in Children. *J Pediatr Gastroenterol Nutr* 2019; **69**: 523-527 [PMID: 31259787 DOI: 10.1097/MPG.0000000000002432]

27 **Li L**, Chai N, Linghu E, Li Z, Du C, Zhang W, Zou J, Xiong Y, Zhang X, Tang P. Safety and efficacy of using a short tunnel versus a standard tunnel for peroral endoscopic myotomy for Ling type IIc and III achalasia: a retrospective study. *Surg Endosc* 2019; **33**: 1394-1402 [PMID: 30187204 DOI: 10.1007/s00464-018-6414-7]

World Journal of Gastroenterology

Submit a Manuscript: https://www.f6publishing.com

World J Gastroenterol 2023 June 14; 29(22): 3508-3518

DOI: 10.3748/wjg.v29.i22.3508

ISSN 1007-9327 (print) ISSN 2219-2840 (online)

ORIGINAL ARTICLE

Retrospective Study

Efficacy and safety of modified tetracycline dosing in a quadruple therapy for *Helicobacter pylori*: A retrospective single center study

Ying-Chao Sun, Meng-Jia Zhu, Xue-Qin Chen, Lei Yue, Yi-Ru Zhao, Xin-Jie Wang, John J Kim, Qin Du, Wei-Ling Hu

Specialty type: Gastroenterology and hepatology

Provenance and peer review: Unsolicited article; Externally peer reviewed.

Peer-review model: Single blind

Peer-review report's scientific quality classification

Grade A (Excellent): A
Grade B (Very good): 0
Grade C (Good): C
Grade D (Fair): 0
Grade E (Poor): 0

P-Reviewer: Nikolić M, Croatia; Ulasoglu C, Turkey

Received: March 28, 2023
Peer-review started: March 28, 2023
First decision: April 26, 2023
Revised: May 9, 2023
Accepted: May 15, 2023
Article in press: May 15, 2023
Published online: June 14, 2023

Ying-Chao Sun, Meng-Jia Zhu, Xue-Qin Chen, Lei Yue, Yi-Ru Zhao, Xin-Jie Wang, Wei-Ling Hu, Department of Gastroenterology, Sir Run Run Shaw Hospital, Medical School, Zhejiang University, Hangzhou 310016, Zhejiang Province, China

John J Kim, Division of Gastroenterology, Loma Linda University Health, Loma Linda, CA 92354, United States

Qin Du, Department of Gastroenterology, Zhejiang University School of Medicine Second Affiliated Hospital, Hangzhou 310009, Zhejiang Province, China

Wei-Ling Hu, Institute of Gastroenterology, Zhejiang University, Hangzhou 310016, Zhejiang Province, China

Corresponding author: Wei-Ling Hu, MD, Doctor, Department of Gastroenterology, Sir Run Run Shaw Hospital, Medical School, Zhejiang University, No. 3 East Qingchun Road, Hangzhou 310016, Zhejiang Province, China. huweiling@zju.edu.cn

Abstract

BACKGROUND

Although highly effective as a component of *Helicobacter pylori* (*H. pylori*) treatment regimen, tetracycline is associated with a high incidence of medication-related adverse events. Modified dosing of tetracycline as part of quadruple therapy may improve safety while providing comparable eradication rates.

AIM

To evaluate the efficacy and safety of modified dosing of tetracycline in patients receiving tetracycline and furazolidone-containing quadruple therapy in patients with *H. pylori* infection.

METHODS

Consecutive patients (10/2020-12/2021) who received tetracycline and furazolidone quadruple therapy for *H. pylori* infection at Sir Run Run Shaw Hospital were identified. All patients received tetracycline, furazolidone, proton pump inhibitor, and bismuth for 14 d as primary or rescue therapy. Modified tetracycline dose group received tetracycline 500 mg twice daily while standard group received 750 mg twice daily or 500 mg three times daily.

RESULTS

Three hundred and ninety-four patients [mean age = 46.3 ± 13.9, male = 137 (34.8%), and 309 (78.4%) primary therapy] completed tetracycline and furazolidone quadruple therapy for *H. pylori* infection including those who received modified tetracycline dose in 157 and standard doses in 118 (750 mg twice daily) and 119 (500 mg three times daily). Eradication rates in the modified tetracycline dose group were 92.40% and in the standard groups, eradication rates were 93.20% for 750 mg twice daily group and 92.43% for 500 mg three times daily group, respectively, without statistical difference (P = 0.959). The incidence of adverse events was lower in the modified tetracycline dose (15.3% *vs* 32.3% and 29.4%; P = 0.002) compared to the standard dose group.

CONCLUSION

In a real-world experience, modified tetracycline dosing as part of tetracycline and furazolidone quadruple therapy for 14 d demonstrated high efficacy, comparable to standard tetracycline dose regimens, with a favorable safety profile.

Key Words: *Helicobacter pylori*; Tetracycline; Furazolidone; Eradication; Penicillin allergy; Bismuth quadruple therapy

©The Author(s) 2023. Published by Baishideng Publishing Group Inc. All rights reserved.

Core Tip: To our knowledge, this is the first real-world study to evaluate the efficacy and safety of modified dosing of tetracycline as part of tetracycline and furazolidone-containing bismuth quadruple therapy in patients with *Helicobacter pylori* infection.

Citation: Sun YC, Zhu MJ, Chen XQ, Yue L, Zhao YR, Wang XJ, Kim JJ, Du Q, Hu WL. Efficacy and safety of modified tetracycline dosing in a quadruple therapy for *Helicobacter pylori*: A retrospective single center study. *World J Gastroenterol* 2023; 29(22): 3508-3518
URL: https://www.wjgnet.com/1007-9327/full/v29/i22/3508.htm
DOI: https://dx.doi.org/10.3748/wjg.v29.i22.3508

INTRODUCTION

Helicobacter pylori (*H. pylori*) infection is associated with the development of chronic gastritis, peptic ulcer, and gastric cancer. Approximately 75% of gastric cancers worldwide can be attributed to *H. pylori*-induced inflammation and injury[1]. China is in a geographic area with high prevalence of *H. pylori* infection which parallels to high incidence of gastric cancer. Prevalence of *H. pylori* infection is estimated to be as high as 50%, and the number of incident cases of gastric cancer accounts for about 44% all patients newly diagnosed with gastric cancer globally[2,3]. Following the recognition of *H. pylori* gastritis as an infectious disease in 2015, guideline recommend that all patients diagnosed with infection should receive eradication therapy. Unless there are competing considerations such as comorbidities, re-infection rates in their communities, competing health priorities of society and financial cost[4].

With the alarming rise in the prevalence of clarithromycin-resistant *H. pylori* infection, increased incidence of treatment failure has been observed[5,6]. In addition, other proposed causes of treatment failure of *H. pylori* eradication therapy include poor patient adherence, host genetics (low gastric pH and metabolism-enhancing phenotypes of CYP2C19), and high bacterial load[7,8]. A systematic review and meta-analysis that included data from 45 countries, found that secondary resistance rates by regions ranged from 15% to 67% for clarithromycin, 19% to 30% for levofloxacin, and 30% to 65% for metronidazole[9]. However, resistance rate remains low for tetracycline, generally occurring in less than 5%. The proportion of strains with dual resistance to tetracycline and furazolidone was 0.5%[10]. Given high efficacy, tetracycline-based bismuth quadruple therapy is the preferred first-line therapy in China [3]. All major society guidelines including Maastricht VI/Florence Consensus Report[11], Toronto Consensus[12], and American College of Gastroenterology guidelines[9] recommend tetracycline-based quadruple therapy as first-line therapy in areas with high (> 15%) prevalence of clarithromycin resistance or in patients with previous macrolide exposure.

Tetracycline exhibits activity against *H. pylori* by binding reversibly to a pocket in the 30S subunit of bacterial ribosomes containing 16S rRNA, causing bacteriostatic and bactericidal effects by inhibiting protein synthesis and bacterial growth[13]. Furazolidone is a nitrofuran antibiotic with activity against *H. pylori* with a high absorption and distribution profile[14]. Tetracycline and furazolidone-based quadruple therapies have achieved high eradication rates in China of 91.7% and 95.2% on intention-to-

treat (ITT) and per-protocol (PP) analyses[15]. However frequent dosing requirements (three to four times daily) and high incidence of antibiotic related adverse events have resulted in reduced adherence and treatment failure[15,16], limiting effectiveness in clinical practice.

The aim of the study is to compare the efficacy and safety of modified twice daily dosing of tetracycline compared to standard tetracycline, furazolidone-containing bismuth quadruple therapy in *H. pylori* infection patients. Our goal is to determine whether lower and simplified dosing of tetracycline can achieve similar eradication rate as standard tetracycline, furazolidone quadruple therapy in a real-world setting.

MATERIALS AND METHODS

Study design and participants

Consecutive patients age > 18 years of age who were diagnosed with *H. pylori* infection and received tetracycline, furazolidone-containing quadruple therapy for 14 d at Sir Run Run Shaw Hospital (Hangzhou, China) between October 2020 to December 2021 were identified. This study was approved by the Institutional Review Board of Sir Run Run Shaw Hospital, Medical School, Zhejiang University, Hangzhou (SRRSH: 2022-431).

All patients were diagnosed as *H. pylori* infection by positive ^{13}C-urea breath test (UBT) and ^{13}C-UBT was performed again one month after completion of the planned treatment. Patients who had prior use of PPI, bismuth, or antibiotics one month prior to initiation of tetracycline, furazolidone-containing quadruple therapy were excluded. Furthermore, patients who had previous surgical history of upper gastrointestinal diseases; pregnant, severe medical comorbidities, allergies to any component of the tetracycline, furazolidone-containing quadruple regimen, or incomplete information were excluded for the analysis.

Diagnosis of H. pylori infection and treatment regimen

H. pylori infection was diagnosed by positive 13C-UBT (75 mg 13C-urea, Shenzhen Zhonghe Headway Bio-Sci & Tech Co., Ltd.) and 13C collection time was 30 min. Eradication was defined as negative urea breath test (< 0.4%; 0.4% as the cutoff value) according to previous Chinese studies[17-19]. Three treatment groups consisting of tetracycline-furazolidone-PPI and bismuth for 14 d with differing doses and frequency of tetracycline administration were examined. Tetracycline was given as 500 mg twice daily in the modified tetracycline dose group, and 750 mg twice daily or 500 mg three times daily in the standard tetracycline dose group[3]. Tetracycline and furazolidone were prescribed half an hour after meals; proton pump inhibitors (PPIs) included esomeprazole, rabeprazole, lansoprazole, and pantoprazole, were given 30 min before morning and evening meals; colloidal bismuth pectin capsules and bismuth potassium citrate capsules were also prescribed 30 min before morning and evening meals. Specific drugs dosage information is as follows: Furazolidone 100 mg twice daily, colloidal bismuth pectin capsules 400 mg twice daily, bismuth potassium citrate capsules 600 mg twice daily, esomeprazole 20 mg twice daily, rabeprazole 10 mg twice daily, lansoprazole 30 mg twice daily, pantoprazole 20 mg twice daily.

Medication adherence and adverse events

13C-UBT result medication adherence and adverse events were obtained by reviewing electronic medical records and telephone surveys when patients were at completion of 14-d *H. pylori* therapy and 4 wk after completion of the treatment. Medication adherence was defined as poor when they had taken < 80% of the total medication.

Endpoint

The primary outcome was the eradication rate of *H. pylori* infection in each treatment group, the secondary endpoint was the incidence of adverse events and medication adherence rate.

Statistical analysis

Continuous variables were expressed as the mean ± SD, and categorical variables were expressed as numbers and percentages. Continuous variables were evaluated using one-way ANOVA and categorical variables using Pearson χ^2 or Fisher's exact test. Furthermore, adjusted for age, gender, education, smoking, alcohol drinking, hypertension, hyperlipidemia, diabetes, treatment line, bismuth type, PPI type, and treatment regimen into multivariate logistic regression model to identify independent risk factors associated with eradication failure. Two-sided $P < 0.05$ was considered significant. IBM SPSS Statistics SPSS 26.0 software (IBM Corp.,) was used for all analysis.

RESULTS

Patients enrolled and baseline characteristics

During the study period, 394 patients received tetracycline, furazolidone-containing quadruple therapy for *H. pylori* infection met study criteria. The mean age was 46.3 ± 13.9, male = 137 (34.8%), and 309 (78.4%) received treatment as primary therapy for *H. pylori* infection. Of the 85 patient who had prior *H. pylori* therapy, 72 (18.3%) had one and 13 (3.3%) had two or more previous therapies. Most common failed *H. pylori* regimens among those with available data included amoxicillin-furazolidone in 25 (34.7%) and furazolidone-clarithromycin in 8 (11.1%) (Supplementary Table 1).

In this study, eradication of *H. pylori* infection was successful in 365 patients and failed in 29 patients. Patients with successful or failed eradication did not differ between groups in demographic characteristics such as age, sex, smoking history, drinking history, educational background, and family history of gastric cancer. A total of 316 patients completed gastroscopy, of which 67.7% and 12.3% were endoscopy diagnosed with gastritis or peptic ulcer in the successful eradication group, respectively, with no difference between the two groups (P = 0.597). Pathological diagnosis of intestinal metaplasia was present in 30.9% and 24.1% of patients between the two groups, respectively, with no difference between groups (P = 0.557). A total of 157 patients received low-dose tetracycline and 237 patients received standard-dose tetracycline, including 118 and 119 patients in the 750 mg twice daily and 500 mg three times daily groups, respectively. There was no difference in the distribution of treatment regimens between eradication success or failure groups (P = 0.959). Initial treatment was achieved in 79.7% of patients in the eradication success group and 66.7% of patients in the failure group. Specific patient demographics and clinical data are presented in Table 1.

When stratified by tetracycline dose, 157 (39.8%) patients received modified tetracycline dose and 237 (60.2%) received standard tetracycline dose including 118 (49.8%) and 119 (50.2%) who received 750 mg b.i.d. and 500 mg t.i.d. dosing, respectively (Supplementary Table 2). Demographic data including age, gender, education, and alcohol/tobacco use were similar among the three groups (Supplementary Table 2). However, a higher proportion of patients who received modified tetracycline dose (87% *vs* 57% and 79%, P = 0.003) compared to standard tetracycline dose received primary therapy for *H. pylori.*

Eradication of H. pylori infection

The eradication rates in the modified tetracycline dose group were 92.4% compared to 93.2% in the 750 mg b.i.d. group and 92.4% in the 500 mg t.i.d. group without difference (P = 0.959).

Eradication of *H. pylori* infection as primary or rescue therapy: Of the 309 patients naïve to prior *H. pylori* treatment, eradication rates for those receiving 500 mg b.i.d., 750 mg b.i.d., and 500 mg t.i.d. dosing were 93.4%, 97.5%, and 92.6%, respectively, without difference P = 0.338) (Table 2).

Of the 85 patients who had prior *H. pylori* treatment as rescue therapy, eradication rates for those receiving 500 mg b.i.d., 750 mg b.i.d., and 500 mg t.i.d. dosing were 85.7%, 84.6%, and 92.0%, respectively, with difference P < 0.0001).

Among subgroup of patients who previously received amoxicillin-furazolidone regimen, eradication rates for those receiving 500 mg b.i.d., 750 mg b.i.d., and 500 mg t.i.d. dosing were 83.3%, 88.2%, and 83.3%, respectively, without difference (P = 0.918) (Supplementary Table 1).

Eradication of *H. pylori* infection with penicillin allergy: Of the 76 (19.3%) patients with penicillin allergy, eradication rates for those receiving 500 mg b.i.d., 750 mg b.i.d., and 500 mg t.i.d. dosing were 91.7%, 95.5%, and 93.1% by ITT analysis, respectively, without difference (P = 0.770) (Table 3).

Of the 63 patients with penicillin allergy naïve to *H. pylori* therapy, eradication rates for those receiving 500 mg b.i.d., 750 mg b.i.d., and 500 mg t.i.d. dosing were 95.0%, 100%, and 90.0%, respectively, without difference (P = 0.372) (Supplementary Table 3).

Eradication rates of removing the discontinued treatment population: Of all 394 patients, a total of 14 discontinued treatment due to serious adverse events or arbitrarily, including 5, 3, and 6 in the three treatment groups, respectively. Five patients in the 500 mg twice daily group and six patients in the 500 mg three times daily group discontinued treatment due to adverse reactions, but eradication of *H. pylori* infection was eventually successful. Three patients in the 750 mg twice daily group discontinued treatment, and eventually two patients failed eradication therapy. After removing these 14 patients, the eradication efficacy of the population was re-counted. The eradication rates in the three treatment groups were 92.10% (140/152), 95.65% (109/115), and 92.04% (104/113), respectively, with no statistically significant difference (P = 0.447).

Of the 298 patients naïve to prior *H. pylori* treatment, eradication rates among those 500 mg b.i.d., 750 mg b.i.d., and 500 mg t.i.d. dosing were 93.1%, 97.4%, and 92.1%, respectively, without difference (P = 0.310). Of the 82 patients who had prior *H. pylori* treatment as rescue therapy, eradication rates those receiving 500 mg b.i.d., 750 mg b.i.d., and 500 mg t.i.d. dosing were 85.7%, 89.2%, and 91.7%, respectively, with difference P < 0.0001). Of the 75 patients with penicillin allergy, eradication rates those receiving 500 mg b.i.d., 750 mg b.i.d., and 500 mg t.i.d. dosing were 91.7%, 95.5%, and 93.1%, respectively, without difference (P = 0.870).

Table 1 Demographic and clinical data of patients according to eradication outcome

Outcome	Successful	Failed	*P*
N	365	29	
Age (mean ± SD)	45.90 ± 13.95	52.5 ± 12.2	0.319
Age range	(20-77)	(27-68)	
Age (≤ 50)	221	15	0.046
Gender (M/F)	122/243	44/74	0.685
Smoking (Yes/No)	31/334	5/29	0.168
Drinking (Yes/No)	61/304	8/29	0.138
Education			0.099
Primary school	61	19	
Middle school	138	40	
College	158	57	
GC family history			0.361
Yes/No	15/350	2/27	
Endoscopy diagnosis			0.597
Gastritis	247	22	
Ulcer	45	2	
Unknown	73	5	
Intestinal metaplasia			0.557
No	176	17	
Yes	113	7	
Unknown	76	5	
Treatment			0.959
500 mg b.i.d.	145	12	
750 mg b.i.d.	110	8	
500 mg t.i.d.	110	9	
Treatment line[1]			0.026
First line	291	18	
Rescue therapy	74	11	
PPI			0.762
Pantoprazole	151	14	
Esomeprazole	69	4	
Rabeprazole	139	11	
Lansoprazole	6	0	
Bismuth			0.351
Bismuth potassium citrate	302	22	
Colloidal bismuth pectin	63	7	
Type 2 diabetes	18	6	0.020
Hypertension	48	15	< 0.0001
Hyperlipidemia	19	7	< 0.0001
Penicillin allergy	70	6	0.843

[1]Recording this treatment as start of frequency. Rescue therapy was defined as patients who had eradicated therapy once or more but failed.
P values were from two-side comparisons the differences between two groups. M: male; F: female; 500 mg b.i.d.: Tetracycline twice daily; 750 mg b.i.d.: Tetracycline twice daily; 500 mg t.i.d.: Tetracycline three times daily.

Table 2 Treatment times previously of the enrolled patients and its eradication rates

Treatment times	500 mg b.i.d.	750 mg b.i.d.	500 mg t.i.d.
1	93.4% (127/136)	97.5% (77/79)	92.6% (87/94)
2	83.3% (15/18)	87.5% (28/32)	90.9% (20/22)
≥ 3	100% (3/3)	71.4% (5/7)	100% (3/3)
Rescue therapy[1]	85.7% (18/21)	84.6% (33/39)	92.0% (23/25)

[1]Rescue therapy was defined as patients who had eradicated therapy once or more but failed.
500 mg b.i.d.: Tetracycline twice daily; 750 mg b.i.d.: Tetracycline twice daily; 500 mg t.i.d.: Tetracycline three times daily.

Table 3 Penicillin allergy of the enrolled patients and its intention-to-treat eradication rates

Penicillin allergy	500 mg b.i.d.	750 mg b.i.d.	500 mg t.i.d.
Yes	91.7% (22/24)	95.5% (21/22)	90.0% (27/30)
No	92.5% (123/133)	92.7% (89/96)	93.3% (83/89)

500mg b.i.d.: Tetracycline twice daily; 750 mg b.i.d.: Tetracycline twice daily; 500 mg t.i.d.: Tetracycline three times daily.

Medication adherence and adverse events

Of 394 patients, 380 (96.4%) demonstrated good adherence to prescribed therapy. Furthermore, 79 patients (20.1%) experienced at least one adverse event with a cumulative number of 98 adverse events during the treatment period (Table 4). Subsequently, 14 (3.6%) patients discontinued the treatment.

The rates of adverse events among those receiving 500 mg b.i.d., 750 mg b.i.d., and 500 mg t.i.d. dosing was 5.3%, 32.3%, and 30.3%, respectively. The incidence of adverse events in the modified dose group was lower than the standard dose group ($P = 0.002$). The most frequent adverse event was fever in 18 (4.7%), bitter taste in 16 (4.1%), nausea in 12 (3.0%), and rash in 10 (2.5%) (Table 4).

Predictors of failed H. pylori eradication

On univariate analysis, age > 50 years (OR = 1.821, 95%CI: 0.841-3.943, $P = 0.128$), male gender (OR = 2.314, 95%CI: 0.998-4.564, $P = 0.051$), smoking status (OR = 2.245, 95%CI: 0.800-6.296, $P = 0.124$), alcohol use (OR = 1.899, 95%CI: 0.804-4.484, $P = 0.144$), rescue therapy (OR = 2.403, 95%CI: 1.088-5.307, $P = 0.03$), type 2 diabetes (OR = 4.016, 95%CI: 1.373-11.752, $P = 0.011$), hyperlipidemia (OR = 6.937, 95%CI: 2.720-17.691, $P < 0.0001$), and hypertension (OR = 6.964, 95%CI: 3.163-15.333, $P < 0.0001$) were associated failed *H. pylori* eradication. On multivariate analysis model, hyperlipidemia (aOR = 3.697, 95%CI: 1.149-11.899, $P = 0.028$) and hypertension aOR = 7.885, 95%CI: 2.582-24.081, $P < 0.0001$) were associated with failed *H. pylori* eradication (Supplementary Table 4).

DISCUSSION

To our knowledge, this is the first real-world study to evaluate the effectiveness and safety of modified dosing of tetracycline as part of tetracycline and furazolidone-containing bismuth quadruple therapy in patients with *H. pylori* infection. Our study demonstrated high *H. pylori* eradication rates of in the modified tetracycline dose of utilizing tetracycline 500 mg twice daily were 92.4%, similar to standard dosing utilizing tetracycline 750 mg twice daily or 500 mg three times daily regimens. Furthermore, the incidence of adverse events was lower in the modified tetracycline dosing (15.3% *vs* 32.3% and 29.4%; $P = 0.002$) compared to the regimen with standard tetracycline dosing.

Previous studies demonstrated that tetracycline and furazolidone quadruple therapy provide high eradication rates of 91.7% and 95.2% per ITT and PP analysis[15]. A randomized trial performed China demonstrated robust eradication rates of tetracycline and furazolidone quadruple therapy, even as rescue therapy of 77.5% and 85.0% per ITT and PP analysis[16]. Lower eradication rates may be

Table 4 Drug adverse events in different treatment groups (n/N)

Group	500 mg b.i.d.	750 mg b.i.d.	500 mg t.i.d.	All	*P*
Taste distortion	2	6	8	16	0.060
Nausea	2	6	4	12	0.190
Abdominal pain	1	2	0	3	0.320
Vomiting	0	1	0	1	0.310
Bloating	3	0	1	4	0.290
Diarrhea	4	2	1	7	0.570
Dizziness	1	2	1	4	0.670
Skin rash	3	4	3	10	0.740
Fatigue	1	4	1	6	0.140
Fever	4	6	8	18	0.250
Constipation	1	1	0	2	0.630
Decreased appetite	0	3	7	10	0.009
Chills	0	1	0	1	0.310
Melena	0	0	1	1	0.310
Abdominal discomfort[1]	2	0	1	3	0.480
All[2]	15.3% (24/157)	32.3% (38/118)	30.3% (36/119)	98/394	0.002

[1]Abdominal discomfort, but not of specified.

[2]The symptoms of a single adverse reaction are counted as 1, and a patient may have multiple adverse events.

P values were from two-side comparisons the differences among three treatment group. N: Total patient number; n: Patient number with side effects; 500 mg b.i.d.: Tetracycline twice daily; 750 mg b.i.d.: Tetracycline twice daily; 500 mg t.i.d.: Tetracycline three times daily.

attributed to clinical or agricultural overuse of antibiotics in northwest China where the primary resistance rates of *H. pylori* for furazolidone and tetracycline reached 21.0% and 19.3%[10]. Another study using Lactobacillus acidophilus (1 g t.i.d.) for 2 wk followed by bismuth-containing quadruple regimen (tetracycline 750 mg b.i.d. + furazolidone 100 mg b.i.d.) for 10 d as rescue therapy in patients showed eradication rates of 92.0% and 91.8% in ITT and PP analysis, respectively, suggesting that patients with refractory infection may benefit from tetracycline-containing bismuth quadruple regimen therapy[20].

Tetracycline exert bacteriostatic activity by binding bacterial ribosome and inhibit protein synthesis [13]. Pharmacokinetic properties including time over MIC (T > MIC) and maximum concentration (Cmax/MIC) are vital to antimicrobial activity of tetracycline leading to recommendations for frequent dosing regimens[21]. Interestingly our results demonstrated that tetracycline twice a day dosing was comparable to three times a day dosing. Our findings are consistent with a previous Korean study[22] that demonstrated that comparable high eradication rates of 93.9% with twice a day dosing of tetracycline comparable to four times a day dosing of 92.9% when maintaining a total tetracycline dose of 2 g a day utilizing tetracycline and metronidazole quadruple therapy. Furthermore, tetracycline concentrations in blood follow a plateau-shaped course with a slow rise and a slower drop, the serum half-life (t1/2) being in the range 6 h to 10 h. Although sparse data, previous study demonstrated that tetracycline dose of 300 mg produced a consistent and robust areas under the serum time curves of 26.9 mg × h/L ± 6.0 mg × h/L[23]. Our study demonstrated no appreciable difference in *H. pylori* eradication with tetracycline 750 mg and 500 mg twice daily dosing regimens. However, studies evaluating pharmacokinetics and pharmacodynamics of tetracyclines in *H. pylori* infection is limited and are mainly derived from treatment of primary or secondary syphilis[21].

Previously studied explored the optimal dose and interval of tetracycline as a component of tetracycline and furazolidone triple therapy for *H. pylori* infection. For example, an Iranian study of 52 patients receiving tetracycline 500 mg twice a day combined with furazolidone and PPI for 14 d resulted in an eradication rate of 96.3% with only occasional serious side effects[24]. Furthermore, a Chinese study of 60 patients evaluating 7-d therapy tetracycline 500 mg twice daily with furazolidone, ranitidine, and bismuth citrate demonstrated eradication rate of 85% in the ITT analysis and 91% in the PP analysis[25]. Studies evaluating tetracycline twice a day dosing as a component of tetracycline and metronidazole quadruple therapy resulted in high eradication rates of over 90%[22,26,27]. However, they were not comparative studies[22,27] or agents at doses different from that of standard BQT[26]. A

Korean study comparing tetracycline twice a day compared to four times a day as part of tetracycline and metronidazole quadruple therapy demonstrated eradication rate of 90.1%, similar to four times a day dosing but also similar adherence and incidence of adverse events (32.4% and 43.1%, $P = 0.254$)[28]. This study raised the possibility that dose reduction of tetracycline to improve adherence and reduce adverse events is possible while maintaining high eradication rates.

The minority (22.6%) of patients in our study population received tetracycline and furazolidone quadruple therapy for previous failed treatment. As expected, eradications appeared reduced among patients receiving rescue therapy. This may be related to development of resistance to furazolidone with recent study in China demonstrating alarming prevalence of 63.1% (736/1167) of furazolidone-resistance *H. pylori* strains among those who experienced prior treatment failure[29].

Safety of tetracycline-containing regimen have raised concern given high incidence of adverse events including gastrointestinal symptoms, allergies, asthma, and hemolytic anemia, loss of appetite, and severe liver injury. Early studies have reported impaired bone growth and maturation as well as deposition in teeth with tetracycline leading to avoidance of use in the pediatric population[30]. In previous studies evaluating tetracycline-containing bismuth quadruple regimens used as rescue therapy in penicillin-allergic patients, approximately one-third developed adverse events leading to discontinuation on therapy in tenth despite high (> 90%) eradication rates[15]. Standard dose of tetracycline in tetracycline and metronidazole regimens are generally lower than the doses utilize in tetracycline and furazolidone regimens given concern for compounded risk of adverse events associated with furazolidone. Our study confirmed that modified dosing and frequency of tetracycline as part of tetracycline and furazolidone therapy had a lower incidence of adverse events (15.3%) compared to the groups that received standard dosing (750 mg twice a day) or frequency (500 mg three times a day) of tetracycline of 32.3% and 29.4%, respectively. Previous studies showed similar incidence of overall adverse events (26%-32%) with *H. pylori* therapy containing standard dosing of 500 mg three times a day [15,16]. Furthermore, 14 (3.6%) patients discontinued therapy due to adverse reactions including 5 in the 500 mg twice a day group (3.2%). Previous studies have suggested as development of serious adverse effects of furazolidone (*i.e.*, fever, fatigue, and dizziness) led to discontinuation of the therapy related to high dose (*i.e.*, 200 mg twice a day) or longer duration (> 7 d) of therapy[31-33]. A recent randomized trial demonstrated that furazolidone had higher incidence of adverse events (37.6% *vs* 20.2%; $P = 0.003$) compared to tetracycline containing amoxicillin quadruple therapy[34]. Although unclear, some of the adverse events in the study are likely driven by the use of furazolidone rather than tetracycline.

There were limitations in our study mostly related to retrospective study design. Although categorized tetracycline and furazolidone doses were consistent across groups, variation in bismuth and PPI types and dose were observed. The differences in pharmacodynamic effects of different PPIs driven by CYP2C19 genetic polymorphism and higher proportion of patients receiving standard compared to modified dosing of tetracycline among those receiving rescue therapy may have introduced bias in the results. The treatment and eradication testing time taken in this study was 4 wk apart, but many previous studies have suggested that more accurate results can be obtained with a duration of 6-8 wk [35], and shorter testing intervals may have an impact on the results. Furthermore, lack of *H. pylori* culture and antibiotic sensitivity testing precluded determine for reasons for failed therapy.

CONCLUSION

Modified tetracycline dosing as a component of tetracycline and furazolidone quadruple therapy for 14 d demonstrated high and comparable *H. pylori* eradication rate while reducing the incidence of adverse events compared to standard tetracycline dose regimen. Randomized controlled studies comparing difference doses of tetracycline as a component of tetracycline and furazolidone quadruple therapy are needed to confirm our findings in patients with *H. pylori* infection.

ARTICLE HIGHLIGHTS

Research background

Although highly effective as a component of *Helicobacter pylori* (*H. pylori*) treatment regimen, tetracycline is associated with a high incidence of medication-related adverse events. Modified dosing of tetracycline as part of quadruple therapy may improve safety while providing comparable eradication rates.

Research motivation

To evaluate the efficacy and safety of modified dosing of tetracycline in a quadruple therapy in patients with *H. pylori* infection.

Research objectives
To compare the efficacy and safety of modified twice daily dosing of tetracycline compared to standard tetracycline, furazolidone-containing bismuth quadruple therapy in *H. pylori* infection patients. Our goal is to determine whether lower and simplified dosing of tetracycline can achieve similar eradication rate as standard tetracycline, furazolidone quadruple therapy in a real-world setting.

Research methods
Consecutive patients (10/2020-12/2021) who received tetracycline and furazolidone quadruple therapy for *H. pylori* infection at Sir Run Run Shaw Hospital were identified. All patients received tetracycline, furazolidone, proton pump inhibitor, and bismuth for 14 d as primary or rescue therapy. Statistical analysis was applied to analyze the eradication rate and the occurrence of adverse events in this population.

Research results
Eradication rates in the modified tetracycline dose group were 92.40% and in the standard groups, eradication rates were 93.20% for 750 mg twice daily group and 92.43% for 500 mg three times daily group, respectively, without statistical difference (P = 0.959). The incidence of adverse events was lower in the modified tetracycline dose (15.3% *vs* 32.3% and 29.4%; P = 0.002) compared to the standard dose group.

Research conclusions
In a real-world experience, modified tetracycline dosing as part of tetracycline and furazolidone quadruple therapy for 14 d demonstrated high efficacy, comparable to standard tetracycline dose regimens, with a favorable safety profile.

Research perspectives
Randomized controlled studies comparing difference doses of tetracycline as a component of tetracycline and furazolidone quadruple therapy are needed to confirm our findings in patients with *H. pylori* infection.

FOOTNOTES

Author contributions: Yingchao Sun, Mengjia Zhu and Xueqin Chen have contributed equally to this work. Sun YC and Hu WL contributed to conceptualization; Sun YC and Wang XJ contributed to writing-original draft preparation; Zhu MJ and Yue L contributed to writing; Chen XQ, Zhao YR, and Zhu MJ contributed to review and editing; Kim JJ contributed to manuscript polishing; Hu WL contributed to supervision; and all authors have read and agreed to the published version of the manuscript.

Supported by the Zhejiang Provincial Natural Science Foundation, No. LY23H160016; and Zhejiang Medical Association, No. 2019ZYC-A88.

Institutional review board statement: This study was reviewed and approved by the Institutional Review Board of Sir Run Run Shaw Hospital, Medical School, Zhejiang University, Hangzhou (Approval No. SRRSH: 2022-431).

Informed consent statement: Patient consent was waived due the impossibility of identifying patients and the retrospective design of the investigation.

Conflict-of-interest statement: The authors declare no conflict of interest.

Data sharing statement: The datasets generated and/or analyzed during the current study are not publicly available but are available from the corresponding author upon reasonable request.

Open-Access: This article is an open-access article that was selected by an in-house editor and fully peer-reviewed by external reviewers. It is distributed in accordance with the Creative Commons Attribution NonCommercial (CC BY-NC 4.0) license, which permits others to distribute, remix, adapt, build upon this work non-commercially, and license their derivative works on different terms, provided the original work is properly cited and the use is non-commercial. See: https://creativecommons.org/Licenses/by-nc/4.0/

Country/Territory of origin: China

ORCID number: Ying-Chao Sun 0000-0002-2514-7848; John J Kim 0000-0003-4341-8661; Qin Du 0000-0002-6840-8358; Wei-Ling Hu 0000-0002-9145-7027.

S-Editor: Chen YL
L-Editor: A

P-Editor: Chen YX

REFERENCES

1 **Amieva M**, Peek RM Jr. Pathobiology of Helicobacter pylori-Induced Gastric Cancer. *Gastroenterology* 2016; **150**: 64-78 [PMID: 26385073 DOI: 10.1053/j.gastro.2015.09.004]

2 **Li WQ**, Zhang JY, Ma JL, Li ZX, Zhang L, Zhang Y, Guo Y, Zhou T, Li JY, Shen L, Liu WD, Han ZX, Blot WJ, Gail MH, Pan KF, You WC. Effects of Helicobacter pylori treatment and vitamin and garlic supplementation on gastric cancer incidence and mortality: follow-up of a randomized intervention trial. *BMJ* 2019; **366**: l5016 [PMID: 31511230 DOI: 10.1136/bmj.l5016]

3 **Liu WZ**, Xie Y, Lu H, Cheng H, Zeng ZR, Zhou LY, Chen Y, Wang JB, Du YQ, Lu NH; Chinese Society of Gastroenterology, Chinese Study Group on Helicobacter pylori and Peptic Ulcer. Fifth Chinese National Consensus Report on the management of Helicobacter pylori infection. *Helicobacter* 2018; **23**: e12475 [PMID: 29512258]

4 **Sugano K**, Tack J, Kuipers EJ, Graham DY, El-Omar EM, Miura S, Haruma K, Asaka M, Uemura N, Malfertheiner P; faculty members of Kyoto Global Consensus Conference. Kyoto global consensus report on Helicobacter pylori gastritis. *Gut* 2015; **64**: 1353-1367 [PMID: 26187502 DOI: 10.1136/gutjnl-2015-309252]

5 **Megraud F**, Coenen S, Versporten A, Kist M, Lopez-Brea M, Hirschl AM, Andersen LP, Goossens H, Glupczynski Y; Study Group participants. Helicobacter pylori resistance to antibiotics in Europe and its relationship to antibiotic consumption. *Gut* 2013; **62**: 34-42 [PMID: 22580412 DOI: 10.1136/gutjnl-2012-302254]

6 **Thung I**, Aramin H, Vavinskaya V, Gupta S, Park JY, Crowe SE, Valasek MA. Review article: the global emergence of Helicobacter pylori antibiotic resistance. *Aliment Pharmacol Ther* 2016; **43**: 514-533 [PMID: 26694080 DOI: 10.1111/apt.13497]

7 **Lin TF**, Hsu PI. Second-line rescue treatment of Helicobacter pylori infection: Where are we now? *World J Gastroenterol* 2018; **24**: 4548-4553 [PMID: 30386104 DOI: 10.3748/wjg.v24.i40.4548]

8 **Shah SC**, Iyer PG, Moss SF. AGA Clinical Practice Update on the Management of Refractory Helicobacter pylori Infection: Expert Review. *Gastroenterology* 2021; **160**: 1831-1841 [PMID: 33524402 DOI: 10.1053/j.gastro.2020.11.059]

9 **Chey WD**, Leontiadis GI, Howden CW, Moss SF. ACG Clinical Guideline: Treatment of Helicobacter pylori Infection. *Am J Gastroenterol* 2017; **112**: 212-239 [PMID: 28071659 DOI: 10.1038/ajg.2016.563]

10 **Zhong Z**, Zhang Z, Wang J, Hu Y, Mi Y, He B, Zhang Y, Zhang X, Xia X, Huang H, Lai Y, Lin M, Su C, Wu Z, Lu L, Zhang B, Huang S, Zhong C, Zeng X, Peng Y, Chen G, Zhang H, Zhou G, Liu S, Yang C, Yan L, Chen A, Zhang G, Xu P, Wang S, Zheng P, Xu S, Gao H. A retrospective study of the antibiotic-resistant phenotypes and genotypes of Helicobacter pylori strains in China. *Am J Cancer Res* 2021; **11**: 5027-5037 [PMID: 34765309]

11 **Malfertheiner P**, Megraud F, Rokkas T, Gisbert JP, Liou JM, Schulz C, Gasbarrini A, Hunt RH, Leja M, O'Morain C, Rugge M, Suerbaum S, Tilg H, Sugano K, El-Omar EM; European Helicobacter and Microbiota Study group. Management of Helicobacter pylori infection: the Maastricht VI/Florence consensus report. *Gut* 2022 [PMID: 35944925 DOI: 10.1136/gutjnl-2022-327745]

12 **Fallone CA**, Chiba N, van Zanten SV, Fischbach L, Gisbert JP, Hunt RH, Jones NL, Render C, Leontiadis GI, Moayyedi P, Marshall JK. The Toronto Consensus for the Treatment of Helicobacter pylori Infection in Adults. *Gastroenterology* 2016; **151**: 51-69.e14 [PMID: 27102658 DOI: 10.1053/j.gastro.2016.04.006]

13 **Chopra I**, Roberts M. Tetracycline antibiotics: mode of action, applications, molecular biology, and epidemiology of bacterial resistance. *Microbiol Mol Biol Rev* 2001; **65**: 232-60 ; second page, table of contents [PMID: 11381101 DOI: 10.1128/MMBR.65.2.232-260.2001]

14 **White AH**. Absorption, distribution, metabolism, and excretion of furazolidone. A review of the literature. *Scand J Gastroenterol Suppl* 1989; **169**: 4-10 [PMID: 2694342 DOI: 10.3109/00365528909091325]

15 **Zhang Y**, Gao W, Cheng H, Zhang X, Hu F. Tetracycline- and furazolidone-containing quadruple regimen as rescue treatment for Helicobacter pylori infection: a single center retrospective study. *Helicobacter* 2014; **19**: 382-386 [PMID: 24849129 DOI: 10.1111/hel.12143]

16 **Zhang J**, Han C, Lu WQ, Wang N, Wu SR, Wang YX, Ma JP, Wang JH, Hao C, Yuan DH, Liu N, Shi YQ. A randomized, multicenter and noninferiority study of amoxicillin plus berberine *vs* tetracycline plus furazolidone in quadruple therapy for Helicobacter pylori rescue treatment. *J Dig Dis* 2020; **21**: 256-263 [PMID: 32348007 DOI: 10.1111/1751-2980.12870]

17 **Chen Q**, Zhang W, Fu Q, Liang X, Liu W, Xiao S, Lu H. Rescue Therapy for Helicobacter pylori Eradication: A Randomized Non-Inferiority Trial of Amoxicillin or Tetracycline in Bismuth Quadruple Therapy. *Am J Gastroenterol* 2016; **111**: 1736-1742 [PMID: 27670603 DOI: 10.1038/ajg.2016.443]

18 **Liang X**, Xu X, Zheng Q, Zhang W, Sun Q, Liu W, Xiao S, Lu H. Efficacy of bismuth-containing quadruple therapies for clarithromycin-, metronidazole-, and fluoroquinolone-resistant Helicobacter pylori infections in a prospective study. *Clin Gastroenterol Hepatol* 2013; **11**: 802-7.e1 [PMID: 23376004 DOI: 10.1016/j.cgh.2013.01.008]

19 **National Clinical Medical Research Center for Digestive Diseases**; Health Management Branch of Chinese Medical Association; Nuclear Medicine Branch of Chinese Medical Association. Chinese Society of Health Management CSoGHPG: Consensus on technical specification of 13C urea breath test in health examination population. *Zhonghua Xiaohua Zazhi* 2020; **40**: 797-802 [DOI: 10.3760/cma.j.cn311367-20200916-00555]

20 **Liu A**, Wang Y, Song Y, Du Y. Treatment with compound Lactobacillus acidophilus followed by a tetracycline- and furazolidone-containing quadruple regimen as a rescue therapy for Helicobacter pylori infection. *Saudi J Gastroenterol* 2020; **26**: 78-83 [PMID: 32295932 DOI: 10.4103/sjg.SJG_589_19]

21 **Agwuh KN**, MacGowan A. Pharmacokinetics and pharmacodynamics of the tetracyclines including glycylcyclines. *J Antimicrob Chemother* 2006; **58**: 256-265 [PMID: 16816396 DOI: 10.1093/jac/dkl224]

22 **Kim JY**, Lee SY, Kim JH, Sung IK, Park HS. Efficacy and safety of twice a day, bismuth-containing quadruple therapy using high-dose tetracycline and metronidazole for second-line Helicobacter pylori eradication. *Helicobacter* 2020; **25**: e12683 [PMID: 32074663 DOI: 10.1111/hel.12683]

23 **Sjölin-Forsberg G**, Hermansson J. Comparative bioavailability of tetracycline and lymecycline. *Br J Clin Pharmacol* 1984; **18**: 529-533 [PMID: 6487493 DOI: 10.1111/j.1365-2125.1984.tb02500.x]

24 **Mansour-Ghanaei F**, Fallah MS, Shafaghi A. Eradication of Helicobacter pylori in duodenal ulcer disease tetracycline & furazolidone vs. metronidazole & amoxicillin in omeprazole based triple therapy. *Med Sci Monit* 2002; **8**: PI27-PI30 [PMID: 11889461]

25 **Lu H**, Zhang DZ, Hu PJ, Li ZS, Lu XH, Fang XC, Xiao SD. One-week regimens containing ranitidine bismuth citrate, furazolidone and either amoxicillin or tetracycline effectively eradicate Helicobacter pylori: a multicentre, randomized, double-blind study. *Aliment Pharmacol Ther* 2001; **15**: 1975-1979 [PMID: 11736729 DOI: 10.1046/j.1365-2036.2001.01122.x]

26 **Dore MP**, Graham DY, Mele R, Marras L, Nieddu S, Manca A, Realdi G. Colloidal bismuth subcitrate-based twice-a-day quadruple therapy as primary or salvage therapy for Helicobacter pylori infection. *Am J Gastroenterol* 2002; **97**: 857-860 [PMID: 12003419 DOI: 10.1111/j.1572-0241.2002.05600.x]

27 **Dore MP**, Marras L, Maragkoudakis E, Nieddu S, Manca A, Graham DY, Realdi G. Salvage therapy after two or more prior Helicobacter pylori treatment failures: the super salvage regimen. *Helicobacter* 2003; **8**: 307-309 [PMID: 12950603 DOI: 10.1046/j.1523-5378.2003.00150.x]

28 **Kim J**, Gong EJ, Seo M, Seo HI, Park JK, Lee SJ, Han KH, Jeong WJ, Kim YD, Cheon GJ. Efficacy of Twice a Day Bismuth Quadruple Therapy for Second-Line Treatment of Helicobacter pylori Infection. *J Pers Med* 2022; **12** [PMID: 35055371 DOI: 10.3390/jpm12010056]

29 **Wen JF**, Wang BJ, Ding Y, Guo LH, Qin LJ, Ye GL, Zhao HM. Drug resistance analysis and sensitive antibiotic screening of Helicobacter pylori in Ningbo area. *Zhejiang Zhongxiyi Jiehe Zazhi* 2018; **28**: 516-521

30 **Oudenhoven MD**, Kinney MA, McShane DB, Burkhart CN, Morrell DS. Adverse effects of acne medications: recognition and management. *Am J Clin Dermatol* 2015; **16**: 231-242 [PMID: 25896771 DOI: 10.1007/s40257-015-0127-7]

31 **Fakheri H**, Malekzadeh R, Merat S, Khatibian M, Fazel A, Alizadeh BZ, Massarrat S. Clarithromycin vs. furazolidone in quadruple therapy regimens for the treatment of Helicobacter pylori in a population with a high metronidazole resistance rate. *Aliment Pharmacol Ther* 2001; **15**: 411-416 [PMID: 11207517 DOI: 10.1046/j.1365-2036.2001.00931.x]

32 **Roghani HS**, Massarrat S, Shirekhoda M, Butorab Z. Effect of different doses of furazolidone with amoxicillin and omeprazole on eradication of Helicobacter pylori. *J Gastroenterol Hepatol* 2003; **18**: 778-782 [PMID: 12795748 DOI: 10.1046/j.1440-1746.2003.03058.x]

33 **Felga GE**, Silva FM, Barbuti RC, Navarro-Rodriguez T, Zaterka S, Eisig JN. Quadruple therapy with furazolidone for retreatment in patients with peptic ulcer disease. *World J Gastroenterol* 2008; **14**: 6224-6227 [PMID: 18985815 DOI: 10.3748/wjg.14.6224]

34 **Wang J**, Cao Y, He W, Li X. Efficacy and safety of bismuth quadruple regimens containing tetracycline or furazolidone for initial eradication of Helicobacter pylori. *Medicine (Baltimore)* 2021; **100**: e28323 [PMID: 34941132 DOI: 10.1097/MD.0000000000028323]

35 **Gisbert JP**, Pajares JM. Stool antigen test for the diagnosis of Helicobacter pylori infection: a systematic review. *Helicobacter* 2004; **9**: 347-368 [PMID: 15270750 DOI: 10.1111/j.1083-4389.2004.00235.x]

World Journal of Gastroenterology

Submit a Manuscript: https://www.f6publishing.com

World J Gastroenterol 2023 June 14; 29(22): 3519-3533

DOI: 10.3748/wjg.v29.i22.3519

ISSN 1007-9327 (print) ISSN 2219-2840 (online)

ORIGINAL ARTICLE

Observational Study

Pre-transjugular-intrahepatic-portosystemic-shunt measurement of hepatic venous pressure gradient and its clinical application: A comparison study

Xi-Xuan Wang, Xiao-Chun Yin, Li-Hong Gu, Hui-Wen Guo, Yang Cheng, Yan Liu, Jiang-Qiang Xiao, Yi Wang, Wei Zhang, Xiao-Ping Zou, Lei Wang, Ming Zhang, Yu-Zheng Zhu-Ge, Feng Zhang

Specialty type: Gastroenterology and hepatology

Provenance and peer review: Unsolicited article; Externally peer reviewed.

Peer-review model: Single blind

Peer-review report's scientific quality classification

Grade A (Excellent): 0
Grade B (Very good): B, B
Grade C (Good): C, C
Grade D (Fair): 0
Grade E (Poor): 0

P-Reviewer: Papadopoulos VP, Greece; Shalimar, India; Torres US, Brazil

Received: January 3, 2023
Peer-review started: January 3, 2023
First decision: March 8, 2023
Revised: March 15, 2023
Accepted: May 17, 2023
Article in press: May 17, 2023
Published online: June 14, 2023

Xi-Xuan Wang, Xiao-Chun Yin, Li-Hong Gu, Yang Cheng, Yan Liu, Jiang-Qiang Xiao, Yi Wang, Wei Zhang, Xiao-Ping Zou, Lei Wang, Ming Zhang, Yu-Zheng Zhu-Ge, Feng Zhang, Department of Gastroenterology, Affiliated Drum Tower Hospital of Nanjing University Medical School, Nanjing 210000, Jiangsu Province, China

Xi-Xuan Wang, Yu-Zheng Zhu-Ge, Medical School, Southeast University, Nanjing 210000, Jiangsu Province, China

Hui-Wen Guo, Department of Gastroenterology, The Affiliated Jiangning Hospital of Nanjing Medical University, Nanjing 210000, Jiangsu Province, China

Corresponding author: Feng Zhang, MD, Doctor, Professor, Department of Gastroenterology, Affiliated Drum Tower Hospital of Nanjing University Medical School, No. 321 Zhongshan Road, Nanjing 210000, Jiangsu Province, China. fzdndx@126.com

Abstract

BACKGROUND

It is controversial whether transjugular intrahepatic portosystemic shunt (TIPS) placement can improve long-term survival.

AIM

To assess whether TIPS placement improves survival in patients with hepatic-venous-pressure-gradient (HVPG) ≥ 16 mmHg, based on HVPG-related risk stratification.

METHODS

Consecutive variceal bleeding patients treated with endoscopic therapy + nonselective β-blockers (NSBBs) or covered TIPS placement were retrospectively enrolled between January 2013 and December 2019. HVPG measurements were performed before therapy. The primary outcome was transplant-free survival; secondary endpoints were rebleeding and overt hepatic ence-phalopathy (OHE).

RESULTS

A total of 184 patients were analyzed (mean age, 55.27 years ± 13.86, 107 males; 102 in the EVL+NSBB group, 82 in the covered TIPS group). Based on the HVPG-

guided risk stratification, 70 patients had HVPG < 16 mmHg, and 114 patients had HVPG ≥ 16 mmHg. The median follow-up time of the cohort was 49.5 mo. There was no significant difference in transplant-free survival between the two treatment groups overall (hazard ratio [HR], 0.61; 95% confidence interval [CI]: 0.35-1.05; P = 0.07). In the high-HVPG tier, transplant-free survival was higher in the TIPS group (HR, 0.44; 95%CI: 0.23-0.85; P = 0.004). In the low-HVPG tier, transplant-free survival after the two treatments was similar (HR, 0.86; 95%CI: 0.33-0.23; P = 0.74). Covered TIPS placement decreased the rate of rebleeding independent of the HVPG tier (P < 0.001). The difference in OHE between the two groups was not statistically significant (P = 0.09; P = 0.48).

CONCLUSION

TIPS placement can effectively improve transplant-free survival when the HVPG is greater than 16 mmHg.

Key Words: Hepatic venous pressure gradient; Transjugular intrahepatic portosystemic shunts; Cirrhosis; Variceal rebleeding; Survival

©The Author(s) 2023. Published by Baishideng Publishing Group Inc. All rights reserved.

Core Tip: Hepatic venous pressure gradient helps clinicians to assess the prognosis of decompensated cirrhotic patients. The study included 184 patients showed that hepatic-venous-pressure-gradient (HVPG) before therapy as a risk stratification provides prognostic value. Treatment can be given with greater confidence with the management of patients by HVPG.

Citation: Wang XX, Yin XC, Gu LH, Guo HW, Cheng Y, Liu Y, Xiao JQ, Wang Y, Zhang W, Zou XP, Wang L, Zhang M, Zhu-Ge YZ, Zhang F. Pre-transjugular-intrahepatic-portosystemic-shunt measurement of hepatic venous pressure gradient and its clinical application: A comparison study. *World J Gastroenterol* 2023; 29(22): 3519-3533
URL: https://www.wjgnet.com/1007-9327/full/v29/i22/3519.htm
DOI: https://dx.doi.org/10.3748/wjg.v29.i22.3519

INTRODUCTION

As a result of portal hypertension related to cirrhosis, variceal bleeding (VB) has been the leading cause of death in cirrhotic patients[1]. More than 50% of cirrhotic patients who undergo the recommended hemostatic treatments are readmitted due to rebleeding within a year. Among them, the mortality rate is nearly 33%[2]. In view of the high rebleeding rate, further therapy to prevent rebleeding, which is defined as secondary prophylaxis, should be performed for patients surviving acute VB. Nonselective beta-blockers (NSBBs) can decrease the portal venous pressure by reducing the cardiac output and splanchnic vasodilation. In addition, to render varices ischemic and necrotic, some endoscopic treatments for VB have been developed. It is advocated that endoscopic variceal ligation (EVL), combined with NSBBs, should be the first line of therapy for the secondary prevention of VB, while transjugular intrahepatic portosystemic shunt (TIPS) placement should be performed in rebleeding patients and preemptive TIPS placement should only be performed for high-risk patients[3,4]. TIPS placement is a fluoroscopy-guided procedure in which a conduit is built between the systemic and portal venous systems with the intent of decreasing the portal pressure[5]. A study with a median follow-up of 16 mo concluded that early TIPS placement could reduce treatment failure and mortality among high-risk patients[6]. Preemptive treatment could also improve the survival of patients with acute-on-chronic liver failure and acute VB, as suggested in a European observational study[7]. However, diversion of the portal flow could also lead to hepatic encephalopathy (HE) resulting from hepatic hypoperfusion and liver failure[6,8]. Holster *et al*[5] noted that TIPS placement was associated with higher rates of early HE (within one year). Thus, it is not clear whether TIPS placement offers a survival benefit.

The hepatic venous pressure gradient (HVPG) has been shown to have prognostic value in both compensated and decompensated cirrhosis[3,4,9]. In patients with HVPG ≥ 16 mmHg, the mortality rate of acute variceal hemorrhage is increased[10]. Moreover, HVPG ≥ 20 mmHg has been a clinically effective predictor of early rebleeding[11]. In our previous study[12], which had a 1-year follow-up period, we concluded that covered TIPS placement was more effective than standard therapy in preventing rebleeding but that it did not improve survival.

On the basis of our earlier findings, we compared TIPS placement with EVL+NSBBs to assess whether TIPS placement improves survival in cirrhotic patients with VB based on HVPG-related risk stratification over a long-term period to obtain more precise individual treatments and better treatment

effects.

MATERIALS AND METHODS

Study design and patients

The study protocol was approved by the ethics committees of the Nanjing Drum Tower Hospital (Nanjing, Jiangsu Province, China). We retrospectively screened clinically stable cirrhotic patients with VB who were admitted to the Department of Gastroenterology of Nanjing Drum Tower Hospital from January 2013 to December 2019 in the prospectively maintained database (Figure 1). The included patients were diagnosed with liver cirrhosis by clinical, radiologic, and endoscopic examinations[13], and signed the informed consent form. The HVPG measurement was performed before therapy. Based on the HVPG-guided risk stratification (with the HVPG as a scale variable), patients with HVPG ≥ 16 mmHg were considered high-HVPG patients, and those with 10 mmHg ≤ HVPG < 16 mmHg were considered low-HVPG patients. The exclusion criteria of the study were as follows: (1) Non-standardized sequential endoscopic therapy; (2) previous secondary preventive intervention; (3) concomitant malignant tumors; (4) failure of sequential endoscopic therapy, *i.e.*, rebleeding before the eradication of varices; (5) severe heart failure (New York Heart Association stage IV), respiratory failure (PaO_2 < 60 mmHg) or severe kidney dysfunction (stage 5 chronic kidney disease); (6) pregnancy or lactation; and (7) missing follow-up data.

Finally, we included 184 patients in our study. All patients signed the informed consent form. Data for 83 of the 184 patients have been previously reported[12]. The prior article examined the effect of covered TIPS placement *vs* EVL+β-blockers in patients with HVPG ≥ 16 mmHg after 1 year, whereas in this study, which included all patients with HVPG ≥ 10 mmHg, we report the long-term outcomes after covered TIPS placement.

HVPG measurement

All included patients underwent preoperative examinations to rule out contraindications followed by HVPG measurements, which were performed under local anesthesia after 6-8 h of fasting (Figure 2). Briefly, the external zero reference point was set at the midaxillary line of the patient. Puncture through the right internal jugular vein was performed. In the TIPS group, a Cobra catheter (RUPS-100, COOK, Bloomington, IN, United States) was introduced into the right or middle hepatic vein, and hepatic venography was performed first to confirm whether stenosis or an obvious lateral shunt was present in the surrounding area. Measurements indicating large shunts were considered meaningless, while measurements indicating small or no shunts were considered meaningful. A 5.5-7 F balloon-tipped catheter (Edwards Lifesciences, Irvine, CA, United States) was guided into the hepatic vein. The free hepatic venous pressure (FHVP) was read after the pressure value stabilized. Air was injected to dilate the balloon to fully block hepatic vein blood flow. The wedged hepatic venous pressure (WHVP) was read after the pressure value stabilized for at least 40 s. The WHVP, FHVP, and inferior vena cava pressure were measured three times. Differences among the WHVP or FHVP measurements should not exceed 1 mmHg. The average of the 3 measurements was taken. After the pressure measurements were completed, a contrast agent was injected to confirm whether the obstruction was complete and whether hepatic vein-to-vein communications were present. The HVPG was calculated according to the following formula: HVPG=WHVP-FHVP.

Therapy

After the HVPG measurements were acquired, the details of the two therapies were explained to the patients, including the procedures, adverse reactions, cost, and so on. Doctors provided professional medical advice based on the patient's performance status, past bleeding history, vascular conditions, and HVPG, among other factors. The final treatment was selected by the patients.

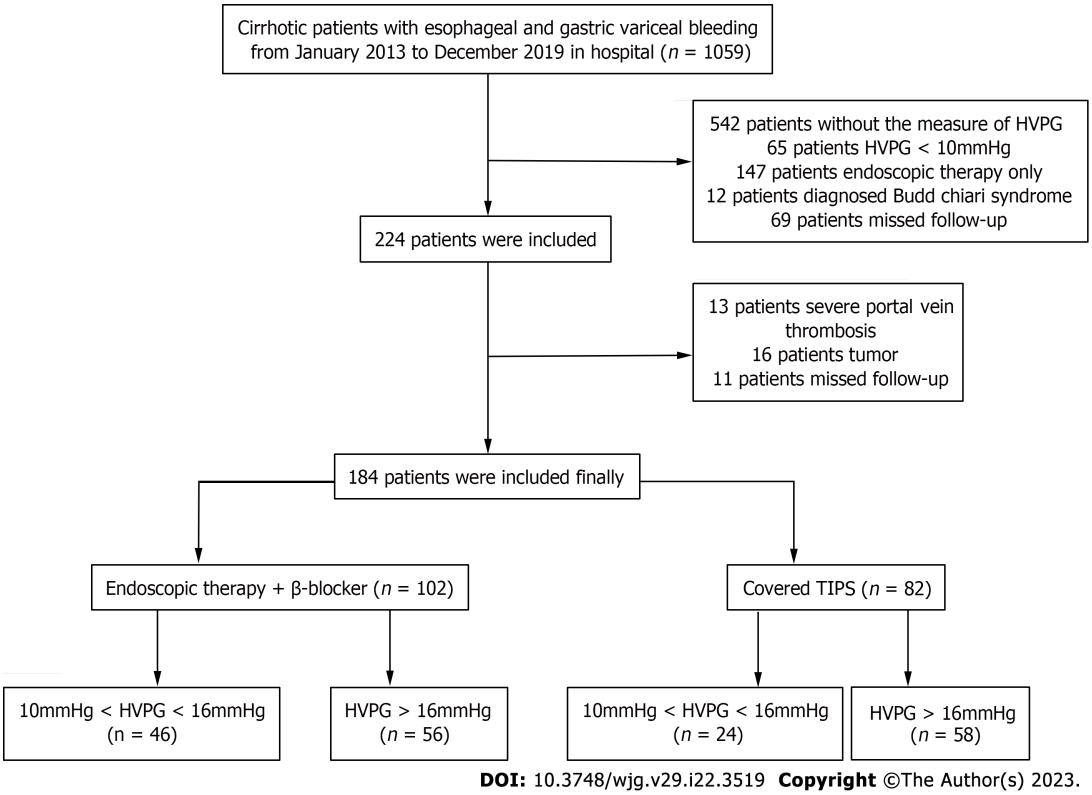
Endoscopic therapy and NSBB usage were the same as described in our previous article[12]; specific details are provided in the Supplementary Methods.

Eighty-two patients underwent covered TIPS placement (Figure 2). Briefly, the process of TIPS placement was the same as described in our previous article[12]; specific details are provided in the Supplementary Methods. All operations were completed by a professional gastroenterology interventional therapy team to avoid surgical complications as much as possible.

Etiological treatment was followed throughout the study.

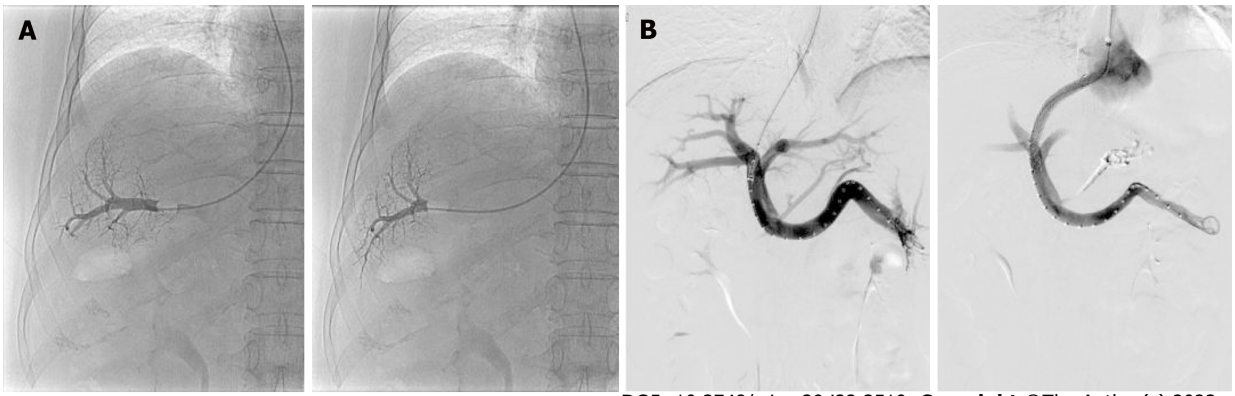
Follow-up and endpoints

Outpatient follow-up was performed 1, 3, 6 and 12 mo after treatment and once a year thereafter. Follow-up examinations included postoperative history collection, routine blood tests and abdominal ultrasound. Any patients with complications during the follow-up period were admitted to the hospital for active treatment.



DOI: 10.3748/wjg.v29.i22.3519 **Copyright** ©The Author(s) 2023.

Figure 1 Flow chart of the patients involved. HVPG: Hepatic venous pressure gradient; TIPS: Transjugular intrahepatic portosystemic shunt.



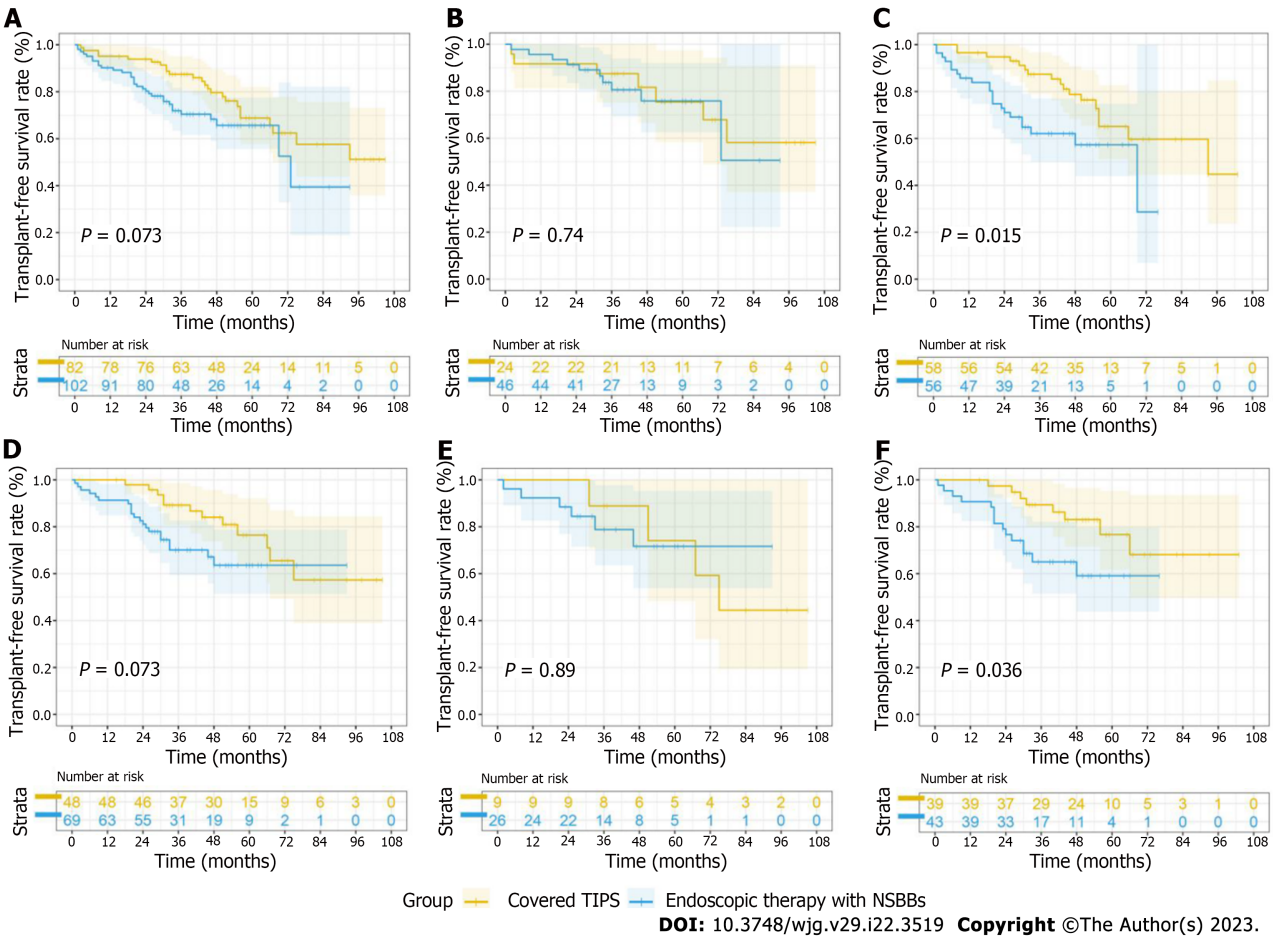
DOI: 10.3748/wjg.v29.i22.3519 **Copyright** ©The Author(s) 2023.

Figure 2 Images taken in hepatic venous pressure gradient measurement and transjugular intrahepatic portosystemic shunts. A: A 68-year-old male received endoscopic therapy with non-selective β-blockers, whose hepatic venous pressure gradient (HVPG) is 16mmHg; B: A 57-year-old female received covered transjugular intrahepatic portosystemic shunts, whose HVPG is 19.6 mmHg.

The primary endpoint of the study was the transplant-free survival time. The secondary endpoints were: (1) Rebleeding; and (2) the development of overt HE (OHE) diagnosed according to the American Association for the Study of Liver Diseases guidelines[14]. The patients were followed up until November 2021 or until death or liver transplantation. Two physicians regularly reviewed the data to detect errors. Two physicians assessed the accuracy of the data. After verification of the collected clinical variables in our study, statistical analysis was performed.

Statistical analysis

Our long-term observational study followed the Strengthening the Reporting of Observational Studies in Epidemiology guidelines[15]. Data are described as frequencies and percentages, means and standard deviations, or medians and interquartile ranges, as appropriate. Baseline characteristics were compared using Fisher's exact test for categorical variables, *t* test for continuous variables, and the Wilcoxon rank-sum test for ordinal and continuous variables. Survival was estimated using the cumulative incidence function. Kaplan–Meier curves were used to illustrate the cumulative rates of survival and variceal



DOI: 10.3748/wjg.v29.i22.3519 **Copyright** ©The Author(s) 2023.

Figure 3 Comparison of transplant-free survival rates between the patients with endoscopic therapy+non-selective β-blockers and covered transjugular intrahepatic portosystemic shunts during the whole follow-up period. A: The total cohort; B: Patients on low-hepatic venous pressure gradient (HVPG) tier; C: Patients on high-HVPG tier; D: Patients with viral cirrhosis or alcoholic cirrhosis; E: Patients with viral cirrhosis or alcoholic cirrhosis on low-HVPG tier; F: Patients with viral cirrhosis or alcoholic cirrhosis on high-HVPG tier; TIPS: Transjugular intrahepatic portosystemic shunt; NSBBs: Non-selective β-blockers.

rebleeding, and differences were assessed by the log-rank test. Associations of the risk factors with mortality were assessed by univariate and multivariate Cox proportional hazards regression models, and forward regression analysis was used to select the variables included in the multivariate model. All analyses were performed using GraphPad software (version 9.0), Statistical Package for Social Sciences (version 22.0) and R studio (version 4.0.1), and a level of significance was established at the two-sided 5% level.

RESULTS

According to the inclusion and exclusion criteria, 184 patients were analyzed. Based on the HVPG-guided risk stratification, 70 patients were in the low-HVPG tier, and 114 were in the high-HVPG tier. The patient characteristics are shown in Table 1. The median follow-up time was 49.5 mo. Patients who were lost to follow-up were excluded. The average time from registering to the end of research was not significantly different between the two groups. There were some differences in the baseline characteristics, which reflected the more severe conditions of the patients undergoing covered TIPS placement.

Transplant-free survival

In general, the mortality rate was not significantly different between the two therapies in the whole cohort of patients who were admitted with VB (P = 0.07) (Figure 3A). In the low-HVPG tier, few differences were observed between the two groups (P = 0.74) (Figure 3B). Interestingly, in the high-HVPG tier, covered TIPS placement markedly improved survival. In patients with HVPG ≥ 16 mmHg, 14 (24.1%) patients in the TIPS group and 19 (33.9%) in the EVL+NSBB group died during the follow-up period; 3 (5.4%) patients in the TIPS group and 3 (5.2%) in the EVL+NSBB group underwent liver transplantation. The transplant-free survival rate was higher in the TIPS group (hazard ratio [HR], 0.44;

Table 1 Baseline characteristics

Parameter	10 mmHg ≤ HVPG < 16 mmHg (*n* = 70)				HVPG ≥ 16 mmHg (*n* = 114)			
	Total	Endoscopic therapy + NSBBs (*n* = 46)	Covered TIPS (*n* = 24)	*P* value	Total	Endoscopic therapy + NSBBs (*n* = 56)	Covered TIPS (*n* = 58)	*P* value
Mean age (yr)	55.27 ± 13.86	55.74 ± 13.44	54.38 ± 14.87	0.7	58.12 ± 11.22	57.30 ± 10.89	58.91 ± 11.57	0.45
Sex								
Male/female	39/31	28/18	11/13	0.31	68/46	34/22	34/24	0.85
Previous bleeding history								
0/1-2/> 3	41/26/3	31/15/0	10/11/3	0.02	77/26/11	41/10/5	36/16/6	0.41
Virus/alcoholic/immune/others	29/6/16/19	23/3/10/10	6/3/6/9	0.21	74/8/15/17	40/3/4/9	34/5/11/8	0.23
PLT (× 10^9/L)	69.80 ± 41.48	67.56 ± 34.80	74.00 ± 52.37	0.54	73.3 ± 52.60	67.71 ± 38.00	78.6 ± 63.32	0.27
ALT (U/L)	28.24 ± 20.56	30.10 ± 22.65	23.94 ± 14.22	0.28	29.97 ± 21.50	30.5 ± 21.56	29.47 ± 21.63	0.80
AST (U/L)	33.09 ± 19.42	34.87 ± 21.50	29.11 ± 13.27	0.27	36.26 ± 23.93	34.72 ± 17.89	37.75 ± 28.67	0.51
Tbil (μmol/L)	21.60 ± 13.80	21.76 ± 18.16	21.28 ± 12.20	0.94	20.69 ± 13.19	18.61 ± 11.60	22.6 9± 14.37	0.10
Creatinine (μmol/L)	64.79 ± 29.51	62.23 ± 18.36	70.91 ± 46.74	0.30	62.78 ± 17.31	62.89 ± 17.31	62.67 ± 17.48	0.95
Albumin (g/L)	35.05 ± 4.31	36.27 ± 3.89	32.71 ± 4.18	< 0.01	34.06 ± 5.11	34.98 ± 4.71	33.16 ± 5.37	0.06
Prothrombin time (s)	14.24 ± 2.33	14.05 ± 2.16	14.67 ± 2.69	0.35	14.89 ± 2.24	14.14 ± 1.84	15.59 ± 2.37	< 0.001
INR	1.24 ± 0.20	1.22 ± 0.19	1.27 ± 0.23	0.4	1.28 ± 0.19	1.23 ± 0.16	1.34 ± 0.21	< 0.001
Child–Pugh scores	6.26 ± 1.15	6.02 ± 1.13	6.71 ± 1.08	0.02	6.89 ± 1.37	6.46 ± 1.21	7.31 ± 1.40	< 0.001
Child–Pugh stage (A/B/C)	46/23/1	35/10/1	11/13/0	0.02	50/59/5	31/24/1	19/35/4	0.03
MELD score	16 ± 5.82	15 ± 5.83	17 ± 5.59	0.12	16 ± 4.95	16 ± 4.37	17 ± 5.44	0.27
Ascites (yes/no)	35/35	27/19	8/16	0.12	24/90	19/36	5/54	< 0.001
Shunt (yes/no)	10/60	6/40	4/20	0.73	9/105	6/50	3/55	0.27
Baseline HVPG (mmHg)	13.04 ± 1.75	12.88 ± 1.78	13.35 ± 1.69	0.30	21.17 ± 4.40	18.82 ± 2.45	23.44 ± 4.68	< 0.001
Baseline WHVP (mmHg)	21.32 ± 3.98	21.37 ± 3.96	21.23 ± 4.13	0.90	29.14 ± 5.24	26.79 ± 4.01	31.41 ± 5.31	< 0.001
Baseline FHVP (mmHg)	8.42 ± 3.11	8.71 ± 3.05	7.88 ± 3.24	0.30	7.98 ± 3.26	7.96 ± 3.07	8.01 ± 3.47	0.93
Baseline IVCP (mmHg)	7.58 ± 3.15	7.75 ± 3.10	7.25 ± 3.30	0.53	7.12 ± 3.18	7.20 ± 3.07	7.05 ± 3.30	0.81
Baseline RAP (mmHg)	6.24 ± 3.05	6.34 ± 3.05	6.06 ± 3.11	0.72	5.68 ± 3.10	5.70 ± 3.10	5.66 ± 3.12	0.94
Severity of varicosity								
(Mild/Moderate/Severe)	11/23/36	7/13/26	4/10/10	0.46	17/30/67	11/13/32	6/17/35	0.35
EV/GOV1/GOV2 /or IGV (no/yes)	47/25/16/3	31/16/9/1	16/9/7/2	0.66	63/31/29/9	31/12/14/4	32/19/15/5	0.80
Numbers of endoscopic therapy (times)	-	2.21 ± 1.32	-	-	-	2.36 ± 1.19	-	-
Pre-TIPS PPG (mmHg)	-	-	28.69 ± 5.67	-	-	-	32.18 ± 5.90	-
post-TIPS PPG (mmHg)	-	-	18.79 ± 5.23	-	-	-	21.69 ± 5.99	-
Interventions required due to stent dysfunction	-	-	3	-	-	-	9	-
Registration time to research ending (mo)	65.14 ± 19.83	62.47 ± 15.82	70.29 ± 25.46	0.18	55.94 ± 19.90	52.91 ± 17.33	58.86 ± 21.86	0.11

Median follow-up time (mo)	56	56	58.5	-	49.5	45	51.5	-

HVPG: Hepatic venous pressure gradient; NSBBs: Non-selective β-blockers; TIPS: Transjugular intrahepatic portosystemic shunts; PLT: Platelets; ALT: Alanine aminotransferase; AST: Aspartate aminotransferase; Tbil: Total bilirubin; INR: International normalized ratio; MELD: The model for end-stage liver disease; WHVP: Wedged hepatic venous pressure; FHVP: Free hepatic venous pressure; IVCP: Inferior vena cava pressure; RAP: Right atrium pressure; EV: Esophageal varices; GOV: Gastroesophageal varices; IGV: Isolated gastric varices; PPG: Portal pressure gradient.

95% confidence interval [CI]: 0.23-0.85; P = 0.004) (Figure 3C). Similar trends were found among patients without a shunt in the hepatic vein (Supplementary Figure 1).

A subgroup analysis was performed according to etiology. For cirrhotic patients with viral hepatitis and alcoholic hepatitis, the difference in transplant-free survival was negligible (HR, 0.53; 95%CI: 0.26-1.06; P = 0.07) (Figure 3D). Among these patients, TIPS placement did not improve transplant-free survival in the low-HVPG tier (HR, 0.91; 95%CI: 0.23-3.61; P = 0.89) (Figure 3E) but did improve transplant-free survival in the high-HVPG tier (HR, 0.41; 95%CI: 0.18-0.94; P = 0.04) (Figure 3F). For cirrhotic patients who had etiologies unrelated to viral and alcoholic hepatitis, TIPS placement did not confer a significant transplant-free survival benefit, as shown in Supplementary Figure 1.

Subgroup analysis was performed according to the endoscopic appearance of varices, whether there were cardiofundal varices or type 2 isolated gastric varices (IGV)[16]. Among patients suffering only from esophagogastric varices and/or type 1 gastroesophageal varices (GOV1), during the follow-up period, TIPS placement showed a significant transplant-free survival advantage in the high-HVPG tier (HR, 0.29; 95%CI: 0.11-0.71; P = 0.007) (Supplementary Figure 1), while there was no significant difference between the two groups (HR, 0.75; 95%CI: 0.22-2.54; P = 0.64) (Supplementary Figure 1). Among 57 patients with GOV2 and/or IGV, TIPS placement did not improve survival, as shown in Supplementary Figure 1.

In the univariate analysis, baseline age, total bilirubin (Tbil), aspartate aminotransferase, HVPG tier and therapy were included as candidate variables for the multivariate model. The final multivariate Cox regression model showed that age (HR, 1.03 per year of age; 95%CI: 1.02-1.07), Tbil (HR, 1.03 per mol/L of Tbil; 95%CI: 1.00-1.06), HVPG tier (HR, 2.01 compared with low-HVPG tier; 95%CI: 1.04-3.89), and therapy (HR, 0.45 compared with EVL+NSBBs; 95%CI: 0.25-0.81) were independent risk factors for mortality (Table 2).

Uncontrolled rebleeding, HE and multiple organ dysfunction syndrome were the most common causes of death (Table 3).

Rebleeding

In the whole cohort, covered TIPS placement significantly reduced rebleeding, as previous studies[17] have reported (P < 0.001) in both the low-HVPG and high-HVPG tiers (Figure 4). The same trends were found for the patients without stents and in the subgroup analyses (Supplementary Figure 2). TIPS placement definitely reduced rebleeding, even when ignoring the etiology and endoscopic appearance. The causes of rebleeding are shown in Table 4.

OHE

Thirteen patients (16.30%) experienced OHE, including 12 (13.33%) patients in the EVL+NSBB group and 18 (28.12%) in the covered TIPS group (Table 5). The occurrence of OHE was consistently similar between the two groups over the long term, while a significant difference was observed in the occurrence of OHE at 1 year (2.90% *vs* 10.98%, P = 0.02).

Jaundice and hyperbilirubinemia

Changes in Tbil after therapy occurred in 184 patients (EVL+NSBB group *vs* covered TIPS group, 102 *vs* 82) at baseline, 156 patients at the 1-year follow-up (92 *vs* 74), and 141 patients at the 2-year follow-up (77 *vs* 64). The TBIL values for 181 patients were registered at the end of follow-up.

Among the included patients (n = 184), excluding those without complete follow-up examinations (n = 43), the changes in the actual values and in the P values after Bonferroni correction at each point are shown in Figure 5A and B. TIPS placement did not induce hyperbilirubinemia (Tbil > 34 μmol/L[18]) in the low-HVPG tier (Figure 5C and D), while in the high-HVPG tier, more patients who underwent TIPS placement experienced hyperbilirubinemia (Figure 5E and F), as shown in Table 5.

Ascites

Changes in the depth of ascites after therapy were obtained, as described for Tbil.

The average of the actual values and the P values after Bonferroni correction at each point are shown in Figure 6 and Table 5. In our research, the depth of ascites in the patients after covered TIPS placement decreased, while after endoscopy therapy with NSBBs, it did not, which agreed with the previously reported findings[19].

Table 2 Cox regression evaluation of factors associated with mortality

Univariate analysis		Multivariate analysis	
Hazard ratio	***P* value**	**Hazard ratio**	***P* value**
1.03 (1.01, 1.06)	0.04	1.03 (1.01, 1.06)	0.02
1.01 (1.01, 1.02)	0.01	-	-
1.01 (1.00, 1.02)	0.03	1.03 (1.00, 1.06)	0.01
1.63 (0.92, 2.89)	0.09	2.01 (1.04, 3.89)	0.04
0.610 (0.35, 1.05)	0.07	0.447 (0.25, 0.81)	0.01

Table 3 Distribution of the causes of endpoint

		Uncontrolled rebleeding	OHE	MODS	Liver transplantation	Nonliver related death
HVPG ≥ 16 mmHg (*n* = 114)	Endoscopic therapy + NSBBs (*n* = 56)	10	6	3	3	0
	Covered TIPS (*n* = 58)	0	10	2	3	2
10 mmHg ≤ HVPG < 16 mmHg (*n* = 70)	Endoscopic therapy + NSBBs (*n* = 46)	5	0	1	2	2
	Covered TIPS (*n* = 24)	0	3	0	4	0

HVPG: Hepatic venous pressure gradient; NSBBs: Non-selective β-blockers; TIPS: Transjugular intrahepatic portosystemic shunts; OHE: Overt hepatic encephalopathy; MODS: Multiple organ dysfunction syndrome.

Table 4 Distribution of the causes of rebleeding

		EGVB	Ectopic variceal bleeding	Ulcer bleeding	Portal hypertensive gastropathy	Venous invasion of HCC	Hematobilia
HVPG ≥ 16 mmHg (*n* = 114)	Endoscopic therapy + NSBBs (*n* = 56)	24	0	3	1	1	0
	Covered TIPS (*n* = 58)	9	0	1	0	0	1
10 mmHg ≤ HVPG < 16 mmHg (*n* = 70)	Endoscopic therapy + NSBBs (*n* = 46)	16	1	3	1	0	1
	Covered TIPS (*n* = 24)	3	0	0	0	0	0

HVPG: Hepatic venous pressure gradient; NSBBs: Non-selective β-blockers; TIPS: Transjugular intrahepatic portosystemic shunts; EGVB: Esophageal and gastric varices bleeding; HCC: Hepatocellular carcinoma.

Hypercreatinemia, hyponatremia and hepatorenal syndrome

The changes in serum creatine and Na^+ after therapy were the same as the changes in Tbil.

TIPS placement had no effects on hypercreatinemia (creatine > 110 μmol/L for males, > 100 μmol/L for females) or hyponatremia (Na^+ < 135 mmol/L) compared with EVL+NSBBs (Supplemental Figure 3), ignoring the HVPG.

Changes in the model for end-stage liver disease score

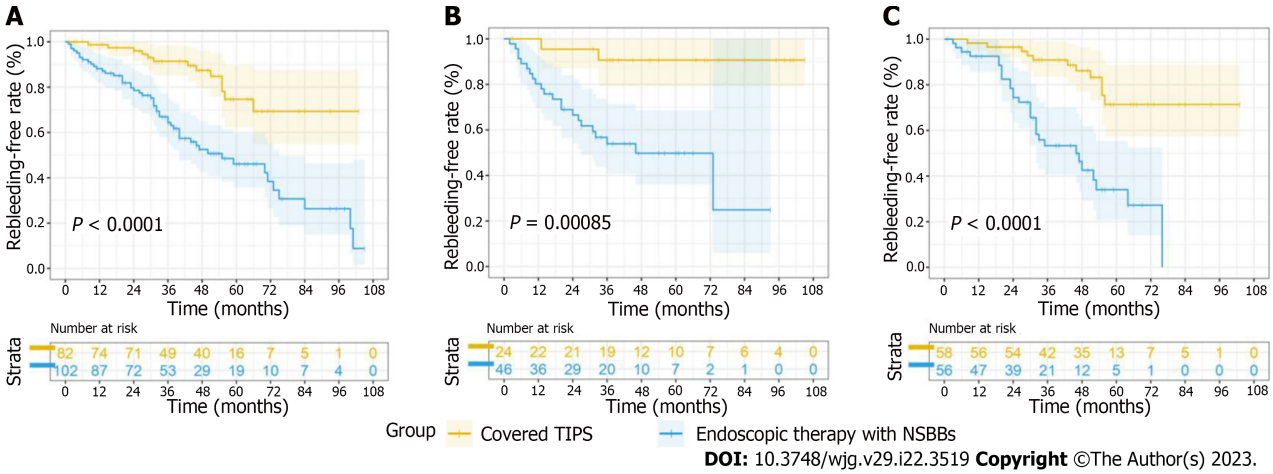
Changes in the model for end-stage liver disease score after therapy were determined the same as described for changes in the Tbil level[20].

In the whole cohort, the scores gradually increased over follow-up after both of the therapies (Figure 7A and B). The patients treated with EVL+NSBBs in the low-HVPG tier showed increased scores after the second year (Figure 7C), while those treated with covered TIPS placement did not. the scores of patients in the high-HVPG tier increased earlier (Figure 7E and F).

Table 5 Rates of complications in the endoscopic therapy+nonselective β-blockers and covered transjugular intrahepatic portosystemic shunt groups

Complications	10 mmHg ≤ HVPG < 16 mmHg (*n* = 70)				HVPG ≥ 16 mmHg (*n* = 114)			
	Total	Endoscopic therapy + NSBBs (*n* = 46)	Covered TIPS (*n* = 24)	*P* value	Total	Endoscopic therapy + NSBBs (*n* = 56)	Covered TIPS (*n* = 58)	*P* value
OHE during follow-up (yes/no)	2/68	0/46	2/22	0.11	10/104	3/53	9/49	0.049
Jaundice during follow-up (yes/no)	22/48	14/32	8/16	0.79	46/68	17/39	29/29	0.04
Ascites during follow-up (yes/no)	29/41	18/28	11/13	0.62	75/39	38/18	37/21	0.70
Hypercreatinemia during follow-up(yes/no)	10/60	5/41	5/19	0.29	13/101	6/50	7/51	1.00
Hyponatremia during follow-up (yes/no)	11/59	9/37	2/22	0.31	8/106	4/52	4/54	1.00
OHE in 1 year (yes/no)	8/62	3/43	5/19	0.09	22/92	9/47	13/45	0.48
Jaundice in 1 year(yes/no)	11/59	5/41	6/18	0.17	29/85	8/48	21/37	0.01
Ascites in 1 year (yes/no)	34/36	23/23	11/13	0.80	74/40	35/21	39/19	0.70
Hypercreatinemia in 1 year (yes/no)	5/65	2/44	3/21	0.33	4/110	3/53	1/57	0.36
Hyponatremia in 1 year (yes/no)	7/63	5/41	2/22	1.00	20/94	12/44	8/50	0.33

HVPG: Hepatic venous pressure gradient; NSBBs: Non-selective β-blockers; TIPS: Transjugular intrahepatic portosystemic shunts; OHE: Overt hepatic encephalopathy.



DOI: 10.3748/wjg.v29.i22.3519 **Copyright** ©The Author(s) 2023.

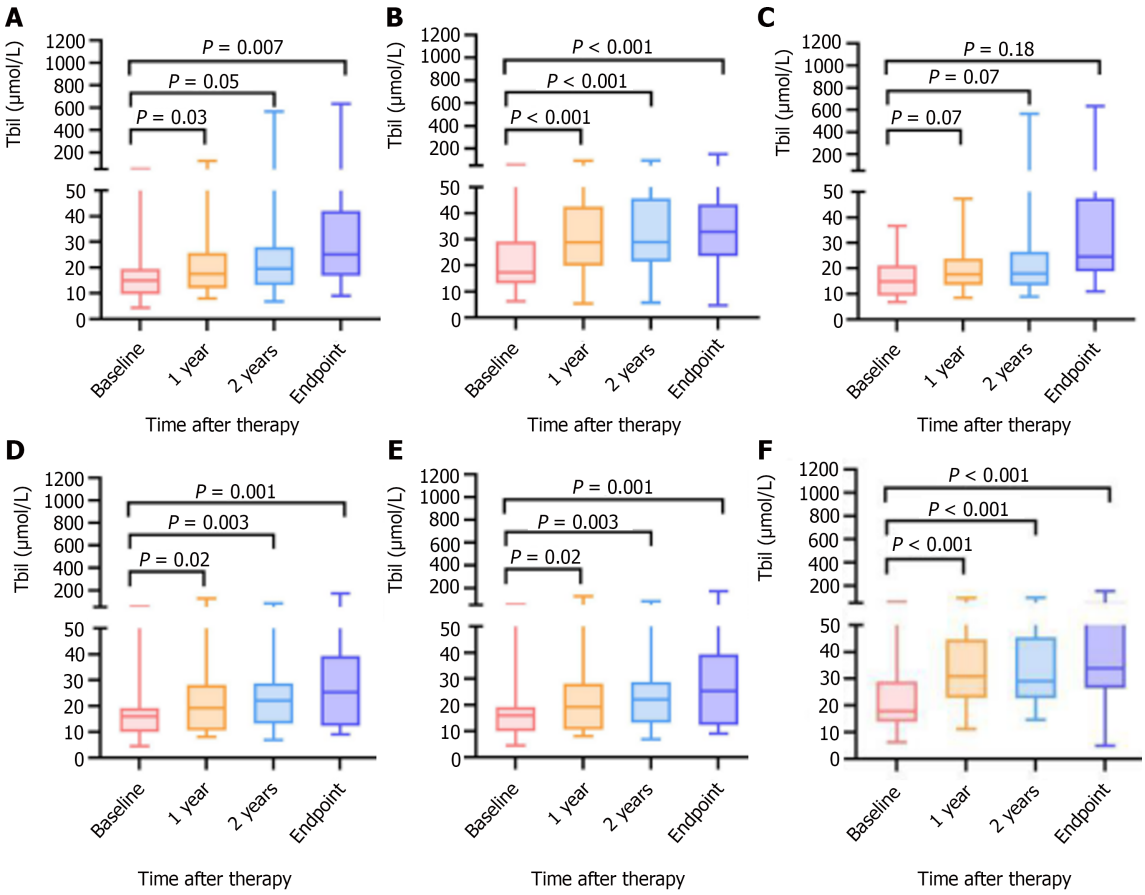
Figure 4 Comparison of the rebleeding-free rate between the patients with endoscopic therapy+non-selective β-blockers and covered transjugular intrahepatic portosystemic shunts. A: The total cohort; B: Patients on low-hepatic venous pressure gradient (HVPG) tier; C: Patients on high-HVPG tier; TIPS: Transjugular intrahepatic portosystemic shunt; NSBBs: Non-selective β-blockers.

Shunt dysfunction

In our study, stent loss occurred in 12 of 82 patients, including 3 (12.50%) in the low-HVPG tier and 9 (16.07%) in the high-HVPG tier. Stent dysfunction was discovered in 6 (66.67%) patients in the high-HVPG tier due to rebleeding or ascites, while stent dysfunction was discovered in patients in the low-HVPG tier during regular follow-up.

DISCUSSION

It would be extremely helpful to be able to distinguish patients with a high risk of uncontrolled



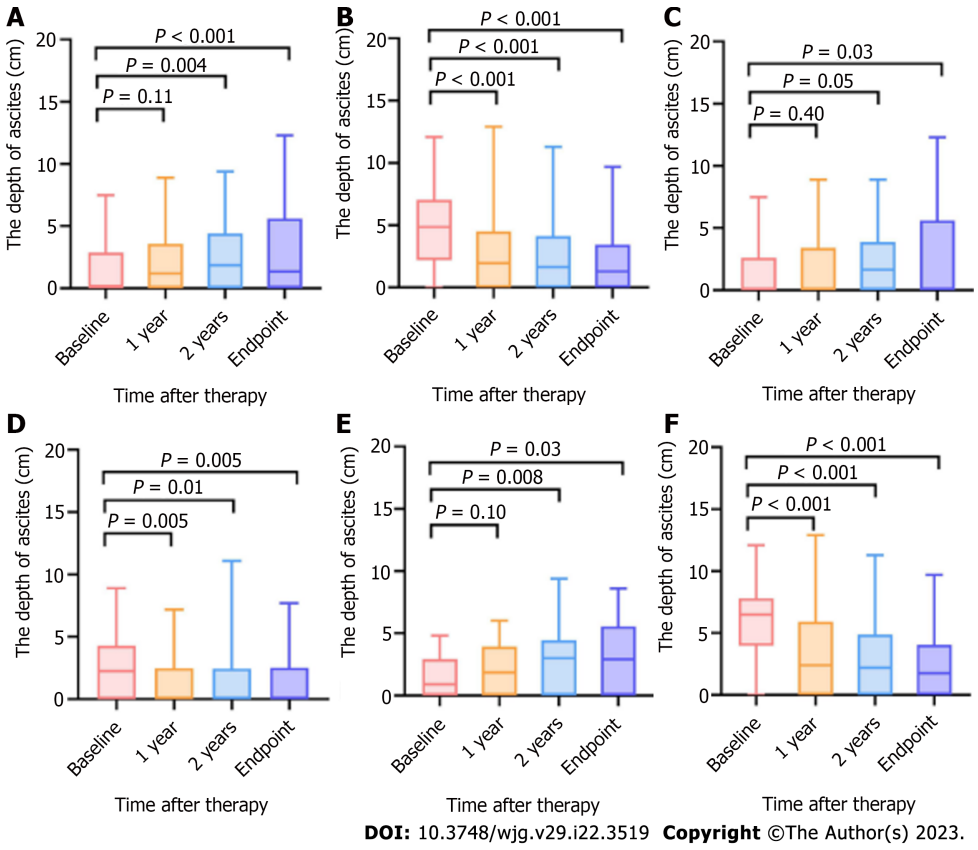
DOI: 10.3748/wjg.v29.i22.3519 **Copyright** ©The Author(s) 2023.

Figure 5 Changes in total bilirubin after therapy at baseline, 1-year follow-up, 2-year follow-up and the endpoint of follow-up. A: Patients received endoscopy therapy + non-selective β-blockers (NSBBs); B: Patients received covered transjugular intrahepatic portosystemic shunt (TIPS); C: Patients received endoscopy therapy + NSBBs in the low-hepatic venous pressure gradient (HVPG) tier; D: Patients received covered TIPS in the low-HVPG tier; E: Patients received endoscopy therapy+NSBBs in the high-HVPG tier; F: Patients received covered TIPS in the high-HVPG tier.

rebleeding. Risk stratification is pivotal for secondary prophylaxis in VB. A recent expert consensus has suggested that HVPG-guided treatment is a reasonable clinical strategy[4]. A study in 2015 concluded that HVPG measurement was useful for making decisions in selecting therapies for secondary prophylaxis[21]. However, the HVPG cutoff for risk stratification has not been clearly demonstrated. In 1991, a study demonstrated that the lowest pressure associated with continued bleeding or rebleeding was 16 mmHg[22]. Furthermore, Villanueva *et al*[23] pointed out that HVPG > 16 mmHg was a predictor of treatment failure. The latest expert consensus is that early TIPS placement reduces treatment failure in patients with HVPG ≥ 20 mmHg[4]. There is established evidence for an HVPG-stratified approach to treatment among compensated cirrhotic patients but very limited data for decompensated patients. On the basis of earlier findings[12], at the beginning of our study and according to the present guidelines, the included patients were divided into 2 groups: the high-HVPG (≥ 16 mmHg) and low-HVPG (10 mmHg ≤ HVPG < 16 mmHg) groups. Consequently, if there were no contraindications, TIPS placement improved survival in patients with HVPG ≥ 16 mmHg (HR, 0.4385; 95%CI: 0.2255-0.8525; P = 0.0037), even though patients who underwent TIPS placement had worse baseline clinical indicators.

A previous study could not conclude whether there were any beneficial effects of TIPS placement on transplant-free survival in all patients. Notably, the median follow-up in all previous studies was shorter than 24 mo, while our median follow-up was 49.5 mo. In our study, the survival benefit can be viewed in the long term. Moreover, the main causes of death were significantly different. Rebleeding in patients treated with covered TIPS placement, which was generally due to stent dysfunction, was controlled in most patients, providing an opportunity for further therapy, while rebleeding in some patients treated with EVL+NSBBs was turbulent.

Our study of HVPG-guided treatment indicated that patients with high HVPG values have a high risk of rebleeding despite treatment with EVL+NSBBs, and in patients with HVPG ≥ 16 mmHg, percutaneous transhepatic variceal embolization or TIPS placement may be a favorable alternative to EVL+NSBBs.



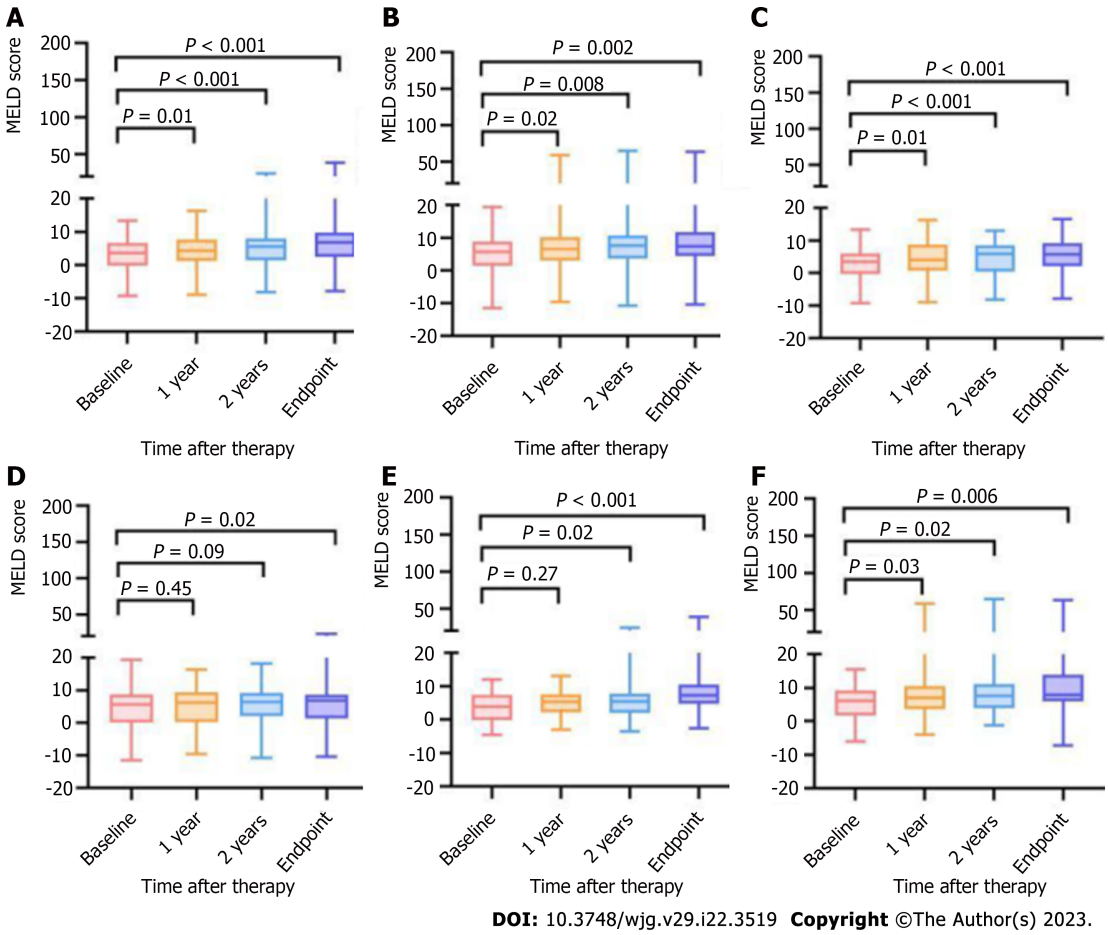
DOI: 10.3748/wjg.v29.i22.3519 **Copyright** ©The Author(s) 2023.

Figure 6 Changes in the depths of ascites after therapy at baseline, 1-year follow-up, 2-year follow-up and the endpoint of follow-up. A: Patients received endoscopy therapy + non-selective β-blockers (NSBBs); B: Patients received covered transjugular intrahepatic portosystemic shunt (TIPS); C: Patients received endoscopy therapy + NSBBs in the low-hepatic venous pressure gradient (HVPG) tier; D: Patients received covered TIPS in the low-HVPG tier; E: Patients received endoscopy therapy + NSBBs in the high-HVPG tier; F: Patients received covered TIPS in the high-HVPG tier.

Considering the high rate of OHE in patients treated with covered TIPS placement mentioned in previous research[8,24], we opted for the placement of small-diameter (8 mm) stents, which can provide adequate bleeding prophylaxis and decrease the OHE rate. Regarding the patients in the low-HVPG tier, there was a trend of growth in the rate of OHE among patients treated with covered TIPS placement, and these results are in accordance with earlier findings. Covered TIPS placement did not increase the rate of OHE among patients in the high-HVPG tier. The differences in encephalopathy between the two treatment groups were the largest in the first year, and this result is in accordance with that of a previous study[6]. A Chinese study proposed that the HVPG is a risk factor for liver failure after TIPS placement[24]. Therefore, we assessed hyperbilirubinemia after therapy. Our results were in accordance with those of a previous study[24].

Based on the HVPG-guided risk stratification, patients with a high HVPG were more likely to benefit from TIPS placement in our study. For patients with a low HVPG, the significant reduction in rebleeding did not improve survival outcomes due to the complications of TIPS placement. Furthermore, HVPG-guided risk stratification may be applied in the evaluation of OHE and hyperbilirubinemia syndrome after TIPS: Patients with a high HVPG have a higher probability of OHE and hyperbilirubinemia than those with a low HVPG. Rebleeding and ascites might occur earlier in patients with a high HVPG who underwent TIPS placement and developed stent dysfunction, but this needs further study. Further research is needed to evaluate whether HVPG-guided risk stratification should be performed before splenectomy.

Notably, our results cannot be extrapolated to older patients or patients with occlusive portal vein thrombosis or hepatocellular carcinoma, as these populations were not included in our study. Additionally, in our study, the numbers of patients with IGV and/or GOV2 were not sufficient, which contributed to the fact that the differences between the two therapies were not significant; as such, the findings could not confirm previous research[25]. Due to the nature of single-center observational studies, an inherent risk of selection bias is inevitable. Another potential bias may be the lower-than-expected attention to the clinical symptoms in patients. Furthermore, selection bias could not be ignored because the therapy was ultimately chosen by the patient. Even with these limitations, this study produced robust data. Further randomized controlled trials need to be performed to prove the benefit of covered TIPS placement in the secondary prevention of VB.



DOI: 10.3748/wjg.v29.i22.3519 **Copyright** ©The Author(s) 2023.

Figure 7 Changes in the model for end-stage liver disease scores after therapy at baseline, 1-year follow-up, 2-year follow-up and the endpoint of follow-up. A: Patients received endoscopy therapy + non-selective β-blockers (NSBBs); B: Patients received covered transjugular intrahepatic portosystemic shunt (TIPS); C: Patients received endoscopy therapy + NSBBs in the low-hepatic venous pressure gradient (HVPG) tier; D: Patients received covered TIPS in the low-HVPG tier; E: Patients received endoscopy therapy + NSBBs in the high-HVPG tier; F: Patients received covered TIPS in the high-HVPG tier.

CONCLUSION

In conclusion, covered TIPS placement increases long-term transplant-free survival in patients with HVPG ≥ 16 mmHg who are admitted with VB, but this advantage may not be observed in patients with 10 mmHg ≤ HVPG < 16 mmHg. More appropriate management and treatment of cirrhotic patients may be achieved by stratification according to HVPG measurements obtained before therapy.

ARTICLE HIGHLIGHTS

Research background

It is controversial whether transjugular intrahepatic portosystemic shunt (TIPS) placement can improve long-term survival.

Research motivation

To clarify the feasibility of hepatic venous pressure gradient (HVPG) as a risk stratification strategy for patients with decompensated cirrhosis.

Research objectives

To assess whether TIPS placement improves survival in patients with HVPG ≥ 16 mmHg based on HVPG-related risk stratification.

Research methods

Consecutive variceal bleeding patients treated with endoscopic variceal ligation (EVL) + nonselective β-blockers (NSBBs) or covered TIPS placement were retrospectively enrolled between January 2013 and

December 2019. HVPG measurements were performed before therapy. The primary outcome was transplant-free survival; secondary endpoints were rebleeding and overt hepatic encephalopathy (OHE).

Research results

A total of 184 patients were analyzed (mean age, 55.27 years ± 13.86, 107 males; 102 in the EVL+NSBB group, 82 in the covered TIPS group). Based on the HVPG-guided risk stratification, 70 patients had HVPG < 16 mmHg, and 114 patients had HVPG ≥ 16 mmHg. The median follow-up time of the cohort was 49.5 mo. There was no significant difference in transplant-free survival between the two treatment groups overall (hazard ratio [HR], 0.61; 95% confidence interval [CI]: 0.35-1.05; P = 0.07). In the high-HVPG tier, transplant-free survival was higher in the TIPS group (HR, 0.44; 95%CI: 0.23, 0.85; P = 0.004). In the low-HVPG tier, transplant-free survival after the two treatments was similar (HR, 0.86; 95%CI: 0.33, 0.23; P = 0.74). Covered TIPS placement decreased the rate of rebleeding independent of the HVPG tier (P < 0.001). The difference in OHE between the two groups was not statistically significant (P = 0.09; P = 0.48).

Research conclusions

TIPS placement can effectively improve transplant-free survival when the HVPG is greater.

Research perspectives

Further randomized controlled trials need to be performed to prove the benefit of covered TIPS placement in the secondary prevention of decompensated cirrhosis.

ACKNOWLEDGEMENTS

The authors would like to thank several researchers from Nanjing Medical University, Nanjing University, Jiangsu University and Southeast University for their help in data collection for the *DCDT COHORT STUDY* since 2012, Nurse Qin Yin from the Department of Gastroenterology of Nanjing Drum Tower Hospital for help in patient follow-up, Dr. Hao Han and Prof. Jian Yang from the Department of Ultrasound Imaging of Nanjing Drum Tower Hospital for their help in collecting abdominal ultrasound images, Dr. Hao Zhang from the Department of Internal Medicine of Nanjing Drum Tower Hospital for his guidance on visualization, and Dr. Taishun Li from the Department of Biomedicine Statistics of Nanjing Drum Tower Hospital for providing statistical suggestions.

FOOTNOTES

Author contributions: Wang XX and Yin XC contributed equally to this work; Zhang F, Zhu-Ge YZ, Wang XX contributed to the conceptualization; Wang XX, Yin XC, Gu LH, Guo HW, Cheng Y, Liu Y contributed to the data curation; Zhang F, Zhu-Ge YZ, Wang XX contributed to the formal analysis; Zhang F acquired the funding; Wang XX, Yin XC, Gu LH, Guo HW, Cheng Y, Liu Y contributed to the investigation; Zhang F, Zhu-Ge YZ, Zhang M, Xiao JQ, Wang Y, Zhang W contributed to the methodology; Zhang F, Zhu-Ge YZ, Zhang M administered the project; Wang L, Zou XP contributed to the resources; Wang L, Zou XP utilized the software; Zhang F, Zhu-Ge YZ, Zhang M contributed to the supervision; Wang XX, Yin XC, Gu LH, Guo HW contributed to the validation; Wang XX, Yin XC contributed to the visualization; Wang XX wrote the original draft; Zhang F, Zhu-Ge YZ reviewed and edited the draft; all authors have read and approve the final manuscript.

Supported by the National Natural Science Foundation of China, No. 81900552; Nanjing Health Science, Technology Development Special Fund Project-Key project, No. ZKX19015; Outstanding Youth Fund project, No. JQX20005; Funding for Clinical Trials from the Affiliated Drum Tower Hospital, Medical School of Nanjing University, No. 2022-LCYJ-MS-13.

Institutional review board statement: The study was reviewed and approved for publication by our institutional (Nanjing Drum Tower Hospital) reviewer.

Informed consent statement: All study participants or their legal guardian provided informed written consent for personal and medical data collection prior to study enrollment.

Conflict-of-interest statement: No authors have conflicts of interest related to the manuscript.

Data sharing statement: The original anonymous dataset is available upon request from the corresponding author at fzdndx@126.com.

STROBE statement: The authors have read the STROBE Statement—checklist of items, and the manuscript was prepared and revised according to the STROBE Statement—checklist of items.

Open-Access: This article is an open-access article that was selected by an in-house editor and fully peer-reviewed by external reviewers. It is distributed in accordance with the Creative Commons Attribution NonCommercial (CC BY-NC 4.0) license, which permits others to distribute, remix, adapt, build upon this work non-commercially, and license their derivative works on different terms, provided the original work is properly cited and the use is non-commercial. See: https://creativecommons.org/Licenses/by-nc/4.0/

Country/Territory of origin: China

ORCID number: Yi Wang 0000-0001-8689-2828; Xiao-Ping Zou 0000-0002-7274-3626; Yu-Zheng Zhu-Ge 0000-0002-3829-5831; Feng Zhang 0000-0002-3653-5977.

S-Editor: Chang KL
L-Editor: A
P-Editor: Cai YX

REFERENCES

1 **Carbonell N**, Pauwels A, Serfaty L, Fourdan O, Lévy VG, Poupon R. Improved survival after variceal bleeding in patients with cirrhosis over the past two decades. *Hepatology* 2004; **40**: 652-659 [PMID: 15349904 DOI: 10.1002/hep.20339]
2 **Garcia-Tsao G**, Bosch J. Management of varices and variceal hemorrhage in cirrhosis. *N Engl J Med* 2010; **362**: 823-832 [PMID: 20200386 DOI: 10.1056/NEJMra0901512]
3 **Garcia-Tsao G**, Abraldes JG, Berzigotti A, Bosch J. Portal hypertensive bleeding in cirrhosis: Risk stratification, diagnosis, and management: 2016 practice guidance by the American Association for the study of liver diseases. *Hepatology* 2017; **65**: 310-335 [PMID: 27786365 DOI: 10.1002/hep.28906]
4 **de Franchis R**, Bosch J, Garcia-Tsao G, Reiberger T, Ripoll C; Baveno VII Faculty. Baveno VII - Renewing consensus in portal hypertension. *J Hepatol* 2022; **76**: 959-974 [PMID: 35120736 DOI: 10.1016/j.jhep.2021.12.022]
5 **Holster IL**, Tjwa ET, Moelker A, Wils A, Hansen BE, Vermeijden JR, Scholten P, van Hoek B, Nicolai JJ, Kuipers EJ, Pattynama PM, van Buuren HR. Covered transjugular intrahepatic portosystemic shunt *vs* endoscopic therapy + β-blocker for prevention of variceal rebleeding. *Hepatology* 2016; **63**: 581-589 [PMID: 26517576 DOI: 10.1002/hep.28318]
6 **García-Pagán JC**, Caca K, Bureau C, Laleman W, Appenrodt B, Luca A, Abraldes JG, Nevens F, Vinel JP, Mössner J, Bosch J; Early TIPS (Transjugular Intrahepatic Portosystemic Shunt) Cooperative Study Group. Early use of TIPS in patients with cirrhosis and variceal bleeding. *N Engl J Med* 2010; **362**: 2370-2379 [PMID: 20573925 DOI: 10.1056/NEJMoa0910102]
7 **Trebicka J**, Gu W, Ibáñez-Samaniego L, Hernández-Gea V, Pitarch C, Garcia E, Procopet B, Giráldez Á, Amitrano L, Villanueva C, Thabut D, Silva-Junior G, Martinez J, Genescà J, Bureau C, Llop E, Laleman W, Palazon JM, Castellote J, Rodrigues S, Gluud L, Ferreira CN, Barcelo R, Cañete N, Rodríguez M, Ferlitsch A, Mundi JL, Gronbaek H, Hernández-Guerra M, Sassatelli R, Dell'Era A, Senzolo M, Abraldes JG, Romero-Gómez M, Zipprich A, Casas M, Masnou H, Primignani M, Weiss E, Catalina MV, Erasmus HP, Uschner FE, Schulz M, Brol MJ, Praktiknjo M, Chang J, Krag A, Nevens F, Calleja JL, Robic MA, Conejo I, Albillos A, Rudler M, Alvarado E, Guardascione MA, Tantau M, Bosch J, Torres F, Pavesi M, Garcia-Pagán JC, Jansen C, Bañares R; International Variceal Bleeding Observational Study Group and Baveno Cooperation. Rebleeding and mortality risk are increased by ACLF but reduced by pre-emptive TIPS. *J Hepatol* 2020; **73**: 1082-1091 [PMID: 32339602 DOI: 10.1016/j.jhep.2020.04.024]
8 **Sauerbruch T**, Mengel M, Dollinger M, Zipprich A, Rössle M, Panther E, Wiest R, Caca K, Hoffmeister A, Lutz H, Schoo R, Lorenzen H, Trebicka J, Appenrodt B, Schepke M, Fimmers R; German Study Group for Prophylaxis of Variceal Rebleeding. Prevention of Rebleeding From Esophageal Varices in Patients With Cirrhosis Receiving Small-Diameter Stents Versus Hemodynamically Controlled Medical Therapy. *Gastroenterology* 2015; **149**: 660-8.e1 [PMID: 25989386 DOI: 10.1053/j.gastro.2015.05.011]
9 **Merkel C**, Bolognesi M, Sacerdoti D, Bombonato G, Bellini B, Bighin R, Gatta A. The hemodynamic response to medical treatment of portal hypertension as a predictor of clinical effectiveness in the primary prophylaxis of variceal bleeding in cirrhosis. *Hepatology* 2000; **32**: 930-934 [PMID: 11050041 DOI: 10.1053/jhep.2000.19322]
10 **Lesmana CRA**, Raharjo M, Gani RA. Managing liver cirrhotic complications: Overview of esophageal and gastric varices. *Clin Mol Hepatol* 2020; **26**: 444-460 [PMID: 33053928 DOI: 10.3350/cmh.2020.0022]
11 **Monescillo A**, Martínez-Lagares F, Ruiz-del-Arbol L, Sierra A, Guevara C, Jiménez E, Marrero JM, Buceta E, Sánchez J, Castellot A, Peñate M, Cruz A, Peña E. Influence of portal hypertension and its early decompression by TIPS placement on the outcome of variceal bleeding. *Hepatology* 2004; **40**: 793-801 [PMID: 15382120 DOI: 10.1002/hep.20386]
12 **Guo H**, Zhang F, Yin X, Zhang M, Xiao J, Wang Y, Zhang B, Zhang W, Zou X, Zhuge Y. Endoscopic therapy + β-blocker vs. covered transjugular intrahepatic portosystemic shunt for prevention of variceal rebleeding in cirrhotic patients with hepatic venous pressure gradient ≥16 mmHg. *Eur J Gastroenterol Hepatol* 2021; **33**: 1427-1435 [PMID: 32868650 DOI: 10.1097/MEG.0000000000001872]
13 **Tajiri T**, Yoshida H, Obara K, Onji M, Kage M, Kitano S, Kokudo N, Kokubu S, Sakaida I, Sata M, Tajiri H, Tsukada K, Nonami T, Hashizume M, Hirota S, Murashima N, Moriyasu F, Saigenji K, Makuuchi H, Oho K, Yoshida T, Suzuki H, Hasumi A, Okita K, Futagawa S, Idezuki Y. General rules for recording endoscopic findings of esophagogastric varices (2nd edition). *Dig Endosc* 2010; **22**: 1-9 [PMID: 20078657 DOI: 10.1111/j.1443-1661.2009.00929.x]
14 **Vilstrup H**, Amodio P, Bajaj J, Cordoba J, Ferenci P, Mullen KD, Weissenborn K, Wong P. Hepatic encephalopathy in chronic liver disease: 2014 Practice Guideline by the American Association for the Study of Liver Diseases and the

European Association for the Study of the Liver. *Hepatology* 2014; **60**: 715-735 [PMID: 25042402 DOI: 10.1002/hep.27210]

15 **von Elm E**, Altman DG, Egger M, Pocock SJ, Gøtzsche PC, Vandenbroucke JP; STROBE Initiative. The Strengthening the Reporting of Observational Studies in Epidemiology (STROBE) Statement: guidelines for reporting observational studies. *Int J Surg* 2014; **12**: 1495-1499 [PMID: 25046131 DOI: 10.1016/j.ijsu.2014.07.013]

16 **Sarin SK**, Lahoti D. Management of gastric varices. *Baillieres Clin Gastroenterol* 1992; **6**: 527-548 [PMID: 1421599 DOI: 10.1016/0950-3528(92)90037-f]

17 **Jalan R**, Forrest EH, Stanley AJ, Redhead DN, Forbes J, Dillon JF, MacGilchrist AJ, Finlayson ND, Hayes PC. A randomized trial comparing transjugular intrahepatic portosystemic stent-shunt with variceal band ligation in the prevention of rebleeding from esophageal varices. *Hepatology* 1997; **26**: 1115-1122 [PMID: 9362350 DOI: 10.1002/hep.510260505]

18 **Sullivan JI**, Rockey DC. Diagnosis and evaluation of hyperbilirubinemia. *Curr Opin Gastroenterol* 2017; **33**: 164-170 [PMID: 28333690 DOI: 10.1097/MOG.0000000000000354]

19 **Inadomi J**, Cello JP, Koch J. Ultrasonographic determination of ascitic volume. *Hepatology* 1996; **24**: 549-551 [PMID: 8781322 DOI: 10.1002/hep.510240314]

20 **Kamath PS**, Wiesner RH, Malinchoc M, Kremers W, Therneau TM, Kosberg CL, D'Amico G, Dickson ER, Kim WR. A model to predict survival in patients with end-stage liver disease. *Hepatology* 2001; **33**: 464-470 [PMID: 11172350 DOI: 10.1053/jhep.2001.22172]

21 **Zhang M**, Wang G, Zhao L, Wu Z, Zhang W, Zhang C. Second prophylaxis of variceal bleeding in cirrhotic patients with a high HVPG. *Scand J Gastroenterol* 2016; **51**: 1502-1506 [PMID: 27379704 DOI: 10.1080/00365521.2016.1193218]

22 **Ready JB**, Robertson AD, Goff JS, Rector WG Jr. Assessment of the risk of bleeding from esophageal varices by continuous monitoring of portal pressure. *Gastroenterology* 1991; **100**: 1403-1410 [PMID: 2013385]

23 **Villanueva C**, Piqueras M, Aracil C, Gómez C, López-Balaguer JM, Gonzalez B, Gallego A, Torras X, Soriano G, Sáinz S, Benito S, Balanzó J. A randomized controlled trial comparing ligation and sclerotherapy as emergency endoscopic treatment added to somatostatin in acute variceal bleeding. *J Hepatol* 2006; **45**: 560-567 [PMID: 16904224 DOI: 10.1016/j.jhep.2006.05.016]

24 **Yao Y**, Satapathy SK, Fernandes ESM, Ramírez-Fernández O, Vitale A, Chen Z. Hepatic venous pressure gradient (HVPG) predicts liver failure after transjugular intrahepatic portal shunt: a retrospective cohort study. *Ann Transl Med* 2022; **10**: 1122 [PMID: 36388791 DOI: 10.21037/atm-22-4737]

25 **Stanley AJ**, Jalan R, Ireland HM, Redhead DN, Bouchier IA, Hayes PC. A comparison between gastric and oesophageal variceal haemorrhage treated with transjugular intrahepatic portosystemic stent shunt (TIPSS). *Aliment Pharmacol Ther* 1997; **11**: 171-176 [PMID: 9042990 DOI: 10.1046/j.1365-2036.1997.106277000.x]

World Journal of Gastroenterology

Submit a Manuscript: https://www.f6publishing.com

World J Gastroenterol 2023 June 14; 29(22): 3534-3547

DOI: 10.3748/wjg.v29.i22.3534

ISSN 1007-9327 (print) ISSN 2219-2840 (online)

ORIGINAL ARTICLE

Observational Study

Difference and clinical value of metabolites in plasma and feces of patients with alcohol-related liver cirrhosis

Yi-Fan Xu, Yan-Xu Hao, Lei Ma, Meng-Han Zhang, Xuan-Xuan Niu, Yan Li, Yuan-Yuan Zhang, Ting-Ting Liu, Ming Han, Xiao-Xue Yuan, Gang Wan, Hui-Chun Xing

Specialty type: Gastroenterology and hepatology

Provenance and peer review: Unsolicited article; Externally peer reviewed.

Peer-review model: Single blind

Peer-review report's scientific quality classification

Grade A (Excellent): 0
Grade B (Very good): B
Grade C (Good): C, C, C
Grade D (Fair): 0
Grade E (Poor): 0

P-Reviewer: Kotlyarov S, Russia; Manautou JE, United States

Received: February 26, 2023
Peer-review started: February 26, 2023
First decision: March 10, 2023
Revised: March 15, 2023
Accepted: May 4, 2023
Article in press: May 4, 2023
Published online: June 14, 2023

Yi-Fan Xu, Yan-Xu Hao, Lei Ma, Meng-Han Zhang, Xuan-Xuan Niu, Yan Li, Hui-Chun Xing, Center of Liver Diseases Division 3, Beijing Ditan Hospital, Capital Medical University, Beijing 100015, China

Yuan-Yuan Zhang, Ting-Ting Liu, Ming Han, Xiao-Xue Yuan, Beijing Key Laboratory of Emerging Infectious Diseases, Institute of Infectious Diseases, Beijing Ditan Hospital, Capital Medical University, Beijing 100015, China

Yuan-Yuan Zhang, Ting-Ting Liu, Ming Han, Xiao-Xue Yuan, Beijing Institute of Infectious Diseases, Beijing Institute of Infectious Diseases, Beijing 100015, China

Yuan-Yuan Zhang, Ting-Ting Liu, Ming Han, Xiao-Xue Yuan, National Center for Infectious Diseases, Beijing Ditan Hospital, Capital Medical University, Beijing 100015, China

Gang Wan, Department of Statistic, Beijing Ditan Hospital, Capital Medical University, Beijing 100015, China

Hui-Chun Xing, Center of Liver Diseases Division 3, Beijing Ditan Hospital, Peking University Ditan Teaching Hospital, Beijing 100015, China

Corresponding author: Hui-Chun Xing, Doctor, MD, Chief Doctor, Professor, Center of Liver Diseases Division 3, Beijing Ditan Hospital, Capital Medical University, No. 8 Jingshun East Street, Chaoyang District, Beijing 100015, China. huichunxing@126.com

Abstract

BACKGROUND

Alterations in plasma and intestinal metabolites contribute to the pathogenesis and progression of alcohol-related liver cirrhosis (ALC).

AIM

To explore the common and different metabolites in the plasma and feces of patients with ALC and evaluate their clinical implications.

METHODS

According to the inclusion and exclusion criteria, 27 patients with ALC and 24 healthy controls (HCs) were selected, and plasma and feces samples were collected. Liver function, blood routine, and other indicators were detected with

automatic biochemical and blood routine analyzers. Liquid chromatography-mass spectrometry was used to detect the plasma and feces metabolites of the two groups and the metabolomics of plasma and feces. Also, the correlation between metabolites and clinical features was analyzed.

RESULTS

More than 300 common metabolites were identified in the plasma and feces of patients with ALC. Pathway analysis showed that these metabolites are enriched in bile acid and amino acid metabolic pathways. Compared to HCs, patients with ALC had a higher level of glycocholic acid (GCA) and taurocholic acid (TCA) in plasma and a lower level of deoxycholic acid (DCA) in the feces, while L-threonine, L-phenylalanine, and L-tyrosine increased simultaneously in plasma and feces. GCA, TCA, L-methionine, L-phenylalanine, and L-tyrosine in plasma were positively correlated with total bilirubin (TBil), prothrombin time (PT), and maddrey discriminant function score (MDF) and negatively correlated with cholinesterase (CHE) and albumin (ALB). The DCA in feces was negatively correlated with TBil, MDF, and PT and positively correlated with CHE and ALB. Moreover, we established a P/S BA ratio of plasma primary bile acid (GCA and TCA) to fecal secondary bile acid (DCA), which was relevant to TBil, PT, and MDF score.

CONCLUSION

The enrichment of GCA, TCA, L-phenylalanine, L-tyrosine, and L-methionine in the plasma of patients with ALC and the reduction of DCA in feces were related to the severity of ALC. These metabolites may be used as indicators to evaluate the progression of alcohol-related liver cirrhosis.

Key Words: Alcohol-related liver cirrhosis; Plasma; Feces; Metabolites; Deoxycholic acid; Amino acids

©The Author(s) 2023. Published by Baishideng Publishing Group Inc. All rights reserved.

Core Tip: Metabolites in enterohepatic circulation play an important role in cross-talk between liver and gut. More than 300 common metabolites were identified in the plasma and feces of patients with alcohol-related liver cirrhosis (ALC) by liquid chromatography-mass spectrometry. And we found bile acid and amino acid were distributed differently in plasma and feces. More importantly, increased glycocholic acid, taurocholic acid, L-phenylalanine, L-tyrosine, and L-methionine in plasma and decreased deoxycholic acid in feces of patients with ALC were related to the severity of ALC. These metabolites have the potential to evaluate the progression of ALC.

Citation: Xu YF, Hao YX, Ma L, Zhang MH, Niu XX, Li Y, Zhang YY, Liu TT, Han M, Yuan XX, Wan G, Xing HC. Difference and clinical value of metabolites in plasma and feces of patients with alcohol-related liver cirrhosis. *World J Gastroenterol* 2023; 29(22): 3534-3547
URL: https://www.wjgnet.com/1007-9327/full/v29/i22/3534.htm
DOI: https://dx.doi.org/10.3748/wjg.v29.i22.3534

INTRODUCTION

Alcohol abuse is one of the major factors causing cirrhosis. According to the research data on global disease burden in 2017, 25% of deaths from liver cirrhosis were caused by alcohol-related liver diseases (ALD)[1]. Several clinical studies have found altered plasma or serum metabolites in patients with alcohol-related liver cirrhosis (ALC)[2]. Previous studies have focused on serum or plasma metabolomics in patients with ALC and demonstrated that alcohol alters the levels of amino acids and bile acids in the plasma or serum[3]. The common changes in plasma or serum include decreased levels of glutamine and increased levels of tyrosine and alanine[4,5]. A few studies on fecal metabolomics showed that fecal metabolomics in patients with alcoholic cirrhosis was changed, while some studies revealed that the fecal amino acids, such as glutamine, isoleucine, phenylalanine, and serine, are reduced[6]. In addition, the production of secondary bile acid, such as deoxycholic acid (DCA), was reduced[6]. Also, intestinal microbiota can metabolize bile acids, aromatic amino acids, carbohydrates, and polysaccharides to produce secondary bile acids, indoles, phenol derivatives, short-chain fatty acids, and polysaccharides[7]. These metabolites can also influence other organs through the gut-liver axis[8]. Therefore, the metabolites in the blood can be either from other organs' metabolites outside the intestine or from intestinal[9]. The metabolites in the blood or the feces may have homogeneity but may also have specific characteristics related to their respective environments. These products participate in the metabolism of glycogen, amino acid, and exogenous substances and exert anti-inflammatory effects

directly in the intestine[10]. However, the correlation between intestinal metabolites and metabolites in plasma for patients with ALC, which might be helpful for the diagnosis and treatment of ALC, has not yet been elucidated. Therefore, the present study aimed to investigate the common and different characteristics of the metabolites in the plasma and feces of patients with ALC, their clinical correlation between plasma metabolomics and fecal metabolomics, and their value in the evaluation of the severity of ALC. This might provide a new direction for understanding the progression of ALC and the diagnosis and treatment of ALD.

MATERIALS AND METHODS

Study design and patients

This was a case-controlled observation study. We prospectively enrolled two groups of subjects: individuals with ALC and healthy controls (HCs). ALC subjects were selected from male inpatients admitted to the Liver Disease Center of Ditan Hospital (Beijing, China) from September 30, 2020 to December 31, 2021. The flow-chart demonstrates the selection of study participants (Figure 1). According to the International Clinical Guidelines[11], individuals with ALC were diagnosed if they met the following criteria: (1) Regular drinking and have a prior or ongoing heavy alcohol intake of > 5 years (males >36 g alcohol/day); and (2) ultrasonography, computed tomography, or magnetic resonance imaging should exhibit liver cirrhosis. Additionally, we recruited age-matched healthy males as controls through recruitment advertisements. These controls met the following criteria after clinical assessment and blood and imaging examinations: (1) Normal physical examination (heart rate, blood pressure, and respiratory rate) and body mass index (BMI) < 30 kg/m^2; (2) no history of alcohol intake; (3) blood routine, liver function, kidney function, tumor maker, and abdominal ultrasound with normal limits; and (4) no sign of any disease, including liver and heart diseases. The following criteria were excluded for all participants: (1) Liver diseases except for alcohol etiologies, such as hepatitis B virus or hepatitis C virus infection, drug-induced liver diseases, and autoimmune hepatitis; (2) Complications except for ascites, such as hepatic encephalopathy, hepatorenal syndrome, hepatopulmonary syndrome, and esophageal and gastric variceal bleeding; (3) human immunodeficiency virus infection; (4) other digestive diseases (colitis, pancreatitis, and cholecystitis); (5) kidney, heart, lung, neurological, and metabolic diseases (diabetes, thyroid, and adrenal diseases); (6) all types of cancers; and (7) systematically using antibiotics, probiotics, and proton pump inhibitors within 1 mo before enrollment.

Clinical information, including demographic indicators, was collected. Moreover, the plasma and feces of all participants were collected and frozen at -80 °C for subsequent biochemical and hematological indexes tests and untargeted metabolomics detection.

This research scheme was approved by the Ethics Committee of Ditan hospital based on the ethical principles of the Declaration of Helsinki and registered at http://www.chictr.org.cn/ (ChiCTR-2000038216). Written informed consent was obtained from all the participants.

Biochemical and hematological indexes examination

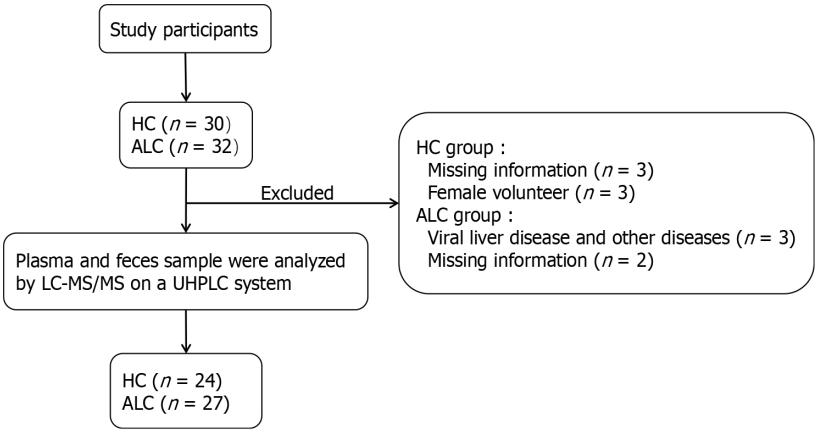
White blood cell, neutrophilic granulocyte percentage, red blood cell (RBC), hemoglobin (HGB), hematocrit (HCT), mean corpuscular volume (MCV), and platelet (PLT) levels were detected on automatic blood routine analyzers (Sysmex, Kobe, Japan). Alanine aminotransferase (ALT), aspartate transaminase (AST), total bilirubin (TBil), albumin (ALB), albumin/globulin (A/G), g-glutamyl transpeptidase (GGT), alkaline phosphatase (ALP), cholinesterase (CHE), total bile acid (TBA), total cholesterol, urea nitrogen, and creatinine (Cr) were detected on automatic biochemical analyzers (Hitachi, Tokyo, Japan). Prothrombin time (PT) was detected by automatic coagulation analyzers (Werfan, Barcelona, Spain), and alpha-fetoprotein (AFP) was detected by chemiluminescence immunoassay analyzer (Abbott, Chicago, IL, United States).

Untargeted metabolomics detection

Plasma or feces sample was mixed with an extract buffer and homogenized in an ice-water bath. The homogenization and sonication cycle was repeated three times. The supernatant was collected by centrifugation of the homogenates and analyzed by liquid chromatography-mass spectrometry (LC-MS/MS) on a UHPLC system (Thermo Fisher Scientific, Waltham, MA, United States) with a UPLC BEH Amide column coupled to Q Exactive HFX mass spectrometer from Thermo Fisher Scientific. The QE HFX mass spectrometer was used for its ability to acquire MS/MS spectra in information-dependent acquisition (IDA) mode using the acquisition software (Thermo Fisher Scientific, Waltham, MA, United States). The acquisition software continuously evaluates the full scan MS spectrum in this mode. The quality control (QC) sample was prepared by mixing an equal aliquot of the supernatants from all the samples.

Statistical analysis

The raw data were converted to the mzXML format using ProteoWizard and processed with an in-house program developed using R and based on XCMS for peak detection, extraction, alignment, and



DOI: 10.3748/wjg.v29.i22.3534 **Copyright** ©The Author(s) 2023.

Figure 1 Flow chart demonstrating the selection of study participants. HC: Healthy control group; ALC: Alcohol-related liver cirrhosis group; LC-MS/MS: Liquid chromatography-mass spectrometry.

integration. Then, an in-house MS2 database (Biotree DB, Shanghai, China) was applied to metabolite annotation. The cutoff for the annotation was set at 0.3. All variables were normalized in MetaboAnalyst 5.0 (https://www.metaboan-alyst.ca) after preprocessing using the Masshunter Profinder software. R script can view details and download them from the website of MetaboAnalyst (https://www.metaboanalyst.ca/MetaboAnalyst/docs/RTutorial.xhtml). The results of the patients' clinical and biochemical characteristics for continuous variables are expressed as median (upper quartile, lower quartile), and categorical variables are expressed as numbers and percentages. The between-group comparisons were made with Kruskal-Wallis *H* test. All statistical analyses were performed using SPSS 26.0 software. The significance level for all statistical tests was set at 0.05. Based on the metabolome profile, the phenotype-associated fingerprint metabolites were projected to one eigen metabolite by the first principal component in the unsupervised principal component analysis (PCA). Fold change (FC): the quantitative ratio of the two groups of experimental substances by comparing the ALC group to the HC group. Furthermore, we analyzed significant differences ($P < 0.05$ and FC > 2 or $P < 0.05$ and FC < 0.5) by comparing the ALC and HC groups and marked them as ALC/HC. We also detected the metabolic pathways of phenotype-associated fingerprint metabolites. PCA was conducted on the MetaboAnalyst website based on R. Furthermore, the *P*- and FC values were obtained from the MetaboAnalyst website. Then, the original variables were narrowed down to fingerprint based on *P*-value and FC.

RESULTS

Clinical characteristics of the study cohort

The clinical characteristics and laboratory tests of participants are shown in Table 1. A total of 51 subjects were included in this study, including 24 HCs and 27 patients with ALC, and all subjects were males. No significant differences were detected in age and BMI between the two groups. The levels of ALT, AST, TBil, GGT, ALP, TBA, and PT were higher in the ALC group than in the HC group, while the number of RBCs and the levels of HGB, HCT, ALB, CHE, PLT, and T-CHO were lower in ALC than in HCs. Compared to HCs, there were no significant differences in UREA, CREA, AFP, and GLU in ALC patients.

Amino acids and derivatives were the most common metabolites in the plasma and feces of patients with ALC

More than 8000 plasma metabolites and more than 10,000 fecal metabolites were detected in this study. HMDB identified > 300 types of co-metabolites in plasma and feces. Amino acids and their derivatives accounted for the largest proportion of co-metabolites in plasma and feces. The remaining metabolites included bile acids, dicarboxylic acids, hydroxy fatty acids, saturated fatty acids, and unsaturated fatty acids (Figure 2A). Principal component analysis on the plasma and feces of patients with ALC showed (Figure 2B and C) that the metabolites in the plasma were clearly distinguished between the two groups based on the first and second principal component scores, while the metabolites in the feces were discretely distributed within the two groups, rendering difficulty in distinguish them between the groups. These findings indicated obvious individual differences in the types and content of fecal metabolites in ALC or HCs.

Table 1 Clinical characteristics of the study cohort

Characteristic	HC (*n* = 24)	ALC (*n* = 27)	*P* value
Age (yr)	53 (48, 57.75)	51 (43, 60)	0.527
BMI (kg/m^2)	22.92 (22.04, 24.09)	24.22 (22.94, 24.94)	0.101
Clinical lab index			
WBC (10^9/L)	5.82 (5.30, 6.76)	4.57 (3.60, 6.62)	0.023
NEU (%)	56.20 (52.1, 60.55)	56.60 (46.60, 67.90)	0.678
RBC (10^{12}/L)	4.83 (4.52, 5.02)	3.66 (2.90, 4.58)	< 0.01
HGB (g/L)	148.00 (144.00, 156.00)	117.00 (100.00, 147.00)	< 0.01
HCT (%)	43.25(41.85, 46.8)	33.60 (29.50, 42.50)	< 0.01
MCV (fl)	91.50 (88.35, 94.68)	97.00 (92.2, 104.00)	0.001
PLT (10^9/L)	246 (223.25, 268.00)	86.00 (46.00, 123.00)	< 0.01
ALT (U/L)	17.35 (12.75, 22.5)	25.7 (15.1, 36.9)	< 0.01
AST (U/L)	19.7 (17.78, 21.73)	36.7 (24.90, 74.20)	< 0.01
TBil (μmol/L)	13.95 (11.75, 15.20)	47.3 (28.70, 115.70)	< 0.01
ALB (g/L)	46.48 (45.68, 47.68)	34.27 (28.4, 39.5)	< 0.01
A/G	1.80 (1.63, 1.80)	1.10 (0.80, 1.60)	< 0.01
GGT (U/L)	14.7 (10.28, 17.50)	94.3 (25.00, 243.80)	< 0.01
ALP (U/L)	58.7 (53.05,70.05)	97.9 (68.40, 137.50)	< 0.01
CHE (U/L)	8326.00 (7251.50, 9304.25)	3547 (1700.00, 5735.00)	< 0.01
TBA (μmol/L)	1.90 (1.45, 2.50)	66.1 (29.30, 174.20)	< 0.01
T-CHO (mmol/L)	4.40(3.72, 4.86)	3.27 (2.54, 4.78)	< 0.05
UREA (mmol/L)	5.04 (4.12, 5.87)	5.05 (4.29, 6.21)	0.734
CREA (mmol/L)	75.5 (72.18, 84.93)	68.8 (60.5, 75.50)	0.051
GLU (mmol/L)	5.27 (4.94, 5.76)	5.24 (4.57, 6.08)	0.977
PT(s)	11.45 (11.20, 11.8)	17.1 (12.10, 22.80)	< 0.01
AFP (ng/mL)	2.37 (1.97, 3.34)	4.01 (2.70, 6.97)	0.002

All clinical information in the table indicates data collected at the time closest to blood collection. Median and quartile values are provided as Median (upper quartile, lower quartile), unless otherwise noted as *n* (%). ALC: Alcohol-related liver cirrhosis; HC: Healthy control; CA: Cholic acid; TCA: Taurocholic acid; WBC: White blood cell; NEU: Neutrophilic granulocyte percentage; RBC: Red blood cell; HGB: Hemoglobin; HCT: Hematocrit; MCV: Mean corpuscular volume; PLT: Platelet; ALT: Alanine aminotransferase; AST: Aspartate transaminase; TBil: Total bilirubin; ALB: Albumin; A/G: Albumin/glubumin; GGT: γ-glutamyl transpeptidase; ALP: Alkaline phosphatase; CHE: Cholinesterase; TBA: Total bile acid; T-CHO: Total cholesterol; UREA: Urea nitrogen; CREA: Creatinine; PT: Prothrombin time; AFP: Alpha-fetoprotein.

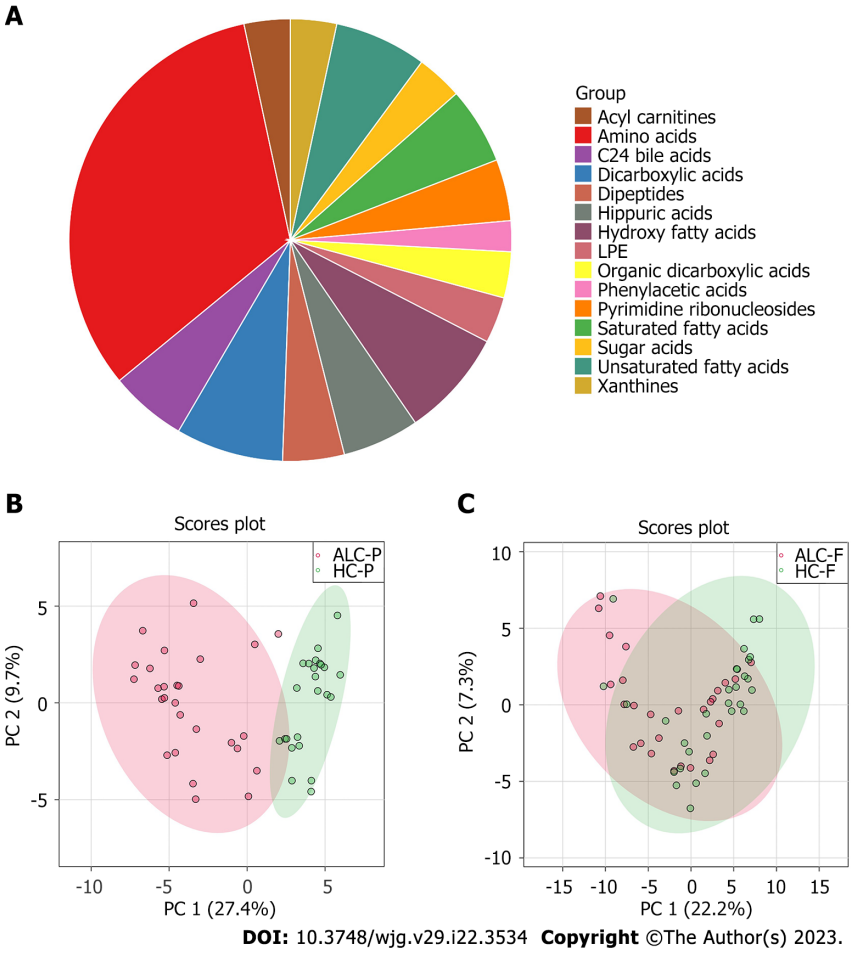
Differences in bile acid and amino acid metabolism pathways in plasma and feces of patients with ALC

The common metabolites were analyzed in plasma and feces, respectively, and compared to HCs after *t*-test and difference analysis. A total of 150 differential metabolites in plasma and 106 differential metabolites in the feces of patients with ALC were screened based on FC > 2 or FC < 0.5. The results showed that 46 metabolites were upregulated and 16 were downregulated in plasma, while 38 metabolites were upregulated and 14 were downregulated in feces (Table 2, Supplementary Tables 1 and 2). Similarly, metabolic pathway analysis showed that the metabolites in plasma and feces of patients with ALC were involved in porphyrin metabolism, phospholipid biosynthesis, inositol metabolism, sugar and starch metabolism, catecholamine biosynthesis, thyroid hormone synthesis, estrone metabolism, betaine metabolism, beta-oxidation of very long chain fatty acids, fatty acid metabolism, caffeine metabolism, and phosphatidylcholine synthesis. The bile acid metabolism pathway was significantly enriched in plasma, while the porphyrin metabolism pathway was significantly enriched in feces (Figures 3A and B). Strikingly, the amino acid metabolism was significantly enriched in both plasma and feces. However, the types of amino acids involved in plasma and feces were

Table 2 Number of altered metabolites

ALC/HC	*P* < 0.05	Up (FC > 2)	Down (FC < 0.5)
Plasma	150	46	16
Feces	106	38	14

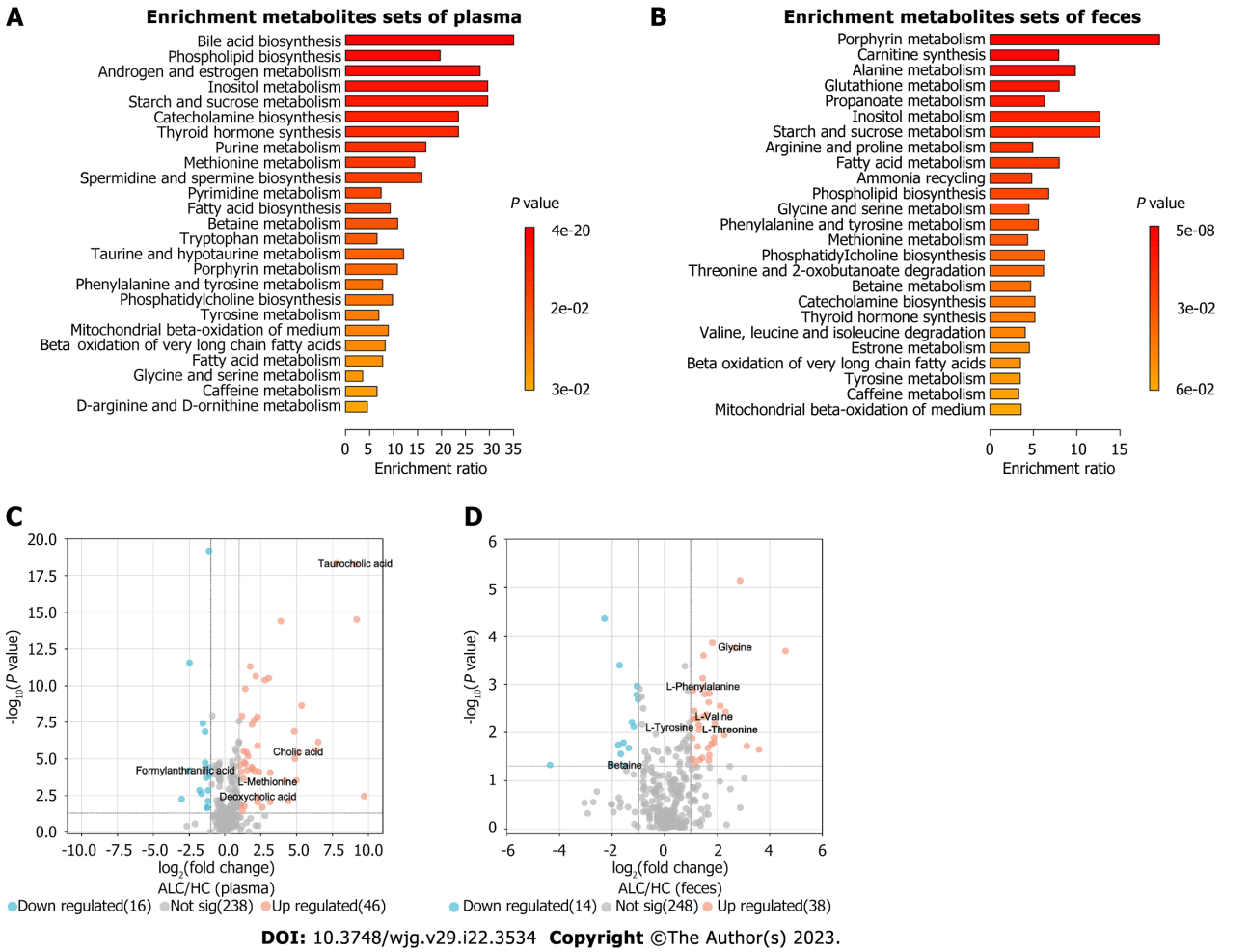
Compared to healthy controls, there were different number of differential metabolites in plasma or feces of patients with alcohol-related liver cirrhosis (ALC) by *t*-test. Fold change: The quantitative ratio of the two groups of experimental substances by comparing ALC group with healthy control (HC) group, and marked them as ALC/HC. ALC: Alcohol-related liver cirrhosis; HC: Healthy control; FC: Fold change.



DOI: 10.3748/wjg.v29.i22.3534 **Copyright** ©The Author(s) 2023.

Figure 2 Subclass and distribution of common metabolites in the plasma and feces of patients with alcohol-related liver cirrhosis. A: Subclass of common metabolites in plasma and feces of patients with alcohol-related liver cirrhosis (ALC); B: Principal component analysis (PCA) of plasma metabolites in two groups; C: PCA of fecal metabolites in two groups. Green dots represent healthy control group, and red dots represented patients with ALC group. Abscissa PC 1 and ordinate PC 2 represent the scores of the first and second principal components respectively, each scatter point represented a sample, the closer the distribution of sample points, it indicates that the types and contents of metabolites in the samples are more similar. On the contrary, the farther the sample is, the greater the difference in its overall metabolic level. The sample is basically within the 95% confidence interval (Hotelling's T-squared ellipse). HC: Healthy control group; ALC: Alcohol-related liver cirrhosis group.

different. The metabolic pathways of methionine, phenylalanine, tyrosine, glycine, and serine were significantly enriched in both plasma and feces; however, the metabolic pathways of tryptophan, taurine, hypotaurine, D-arginine, and D-ornithine were enriched in the plasma, while alanine, valine, leucine, isoleucine, arginine, and proline metabolic pathways were significantly enriched in feces. Various substances were involved in the above-mentioned enrichment pathways (Supplementary Tables 3 and 4). Differential analysis and screening of FC > 2 or FC < 0.5 with $P < 0.05$ showed that nine substances, such as cholic acid (CA), taurocholic acid (TCA), DCA (DCA), and L-methionine were upregulated in plasma, and three metabolites, such as formylanthranilic acid, were down-regulated in ALC. Thirteen metabolites, such as glycine, L-threonine, L-phenylalanine, L-valine, L-tyrosine were upregulated, and betaine was downregulated in feces (Figure 3C and D, Supplementary Table 5).



DOI: 10.3748/wjg.v29.i22.3534 **Copyright** ©The Author(s) 2023.

Figure 3 Enrichment metabolic pathway and volcano map of metabolites. A: Enrichment metabolic pathway in plasma; B: Enrichment metabolic pathway in feces. Enrichment Ratio was computed by Hits/Expected, where hits = observed hits; expected = expected hits (details in Supplementary Tables 3 and 4); C: Volcano map of metabolites in plasma; D: Volcano map of metabolites in feces. All metabolites were screened by fold change (FC) > 2, $P < 0.05$ or FC < 0.5, $P < 0.05$. FC: The quantitative ratio of alcohol-related liver cirrhosis to healthy control group. HC: Healthy control group; ALC: Alcohol-related liver cirrhosis group.

Common and differential bile acids, amino acids, and related metabolites in the plasma and feces of patients with ALC

Compared to HCs, metabolites involved in the above metabolic pathways differed in the plasma and stool of ALC (Table 3). In the bile acid metabolism pathway, primary bile acids, including CA, TCA, and glycocholic acid (GCA), increased in the plasma of patients with ALC, while CA, TCA, and GCA did not change significantly in feces. Additionally, secondary bile acid DCA decreased in feces but did not differ in plasma. In the amino acid metabolism pathway, L-threonine, L-phenylalanine, L-tyrosine, and choline increased in both plasma and feces, while betaine decreased concomitantly. GCA, L-methionine, and taurine increased, while sarcosine decreased only in plasma. Glycine elevated only in feces, while L-valine decreased in plasma but increased in feces.

For patients with ALC, the differential enrichment analysis of bile acid and amino acid metabolites in plasma and feces revealed that the distribution of the above-mentioned metabolites differed in the plasma and feces. In the plasma of patients with ALC, betaine, TCA, GCA, sarcosine, and taurine were significantly enriched, while CA, DCA, and formylanthranilic acid, L-threonine, L-phenylalanine, L-tyrosine, L-methionine, and glycine were markedly enriched in feces (Figure 4).

Association of amino acid or bile acid in plasma or feces with clinical features

Spearman's correlation analysis revealed that plasma amino acids L-methionine, L-phenylalanine, and L-tyrosine in patients with ALC were positively correlated to TBA, MDF, TBil, and PT and negatively correlated with CHE and ALB. L-methionine had the highest correlation with TBA, and L-phenylalanine had the highest correlation with MDF, TBil, and PT. Nonetheless, no correlation was established between L-methionine, L-phenylalanine, L-tyrosine and TBA, MDF, TBil, PT in feces (Figure 5).

Primary bile acids GCA and TCA in plasma exhibited a positive correlation with TBil in clinical practice to varying degrees, with GCA having the strongest correlation with a coefficient of 0.86. However, no correlation was established between DCA in feces and clinical TBil. The levels of both

Table 3 Differential metabolites in plasma and feces

Metabolites	Metabolic pathway	Plasma (ALC/HC)	Feces (ALC/HC)
Cholic acid	Bile acid biosynthesis	↑	NS
Glycocholic acid		↑	NS
Taurocholic acid		↑	NS
Deoxycholic acid		↑	↓
Glycine	Alanine metabolism	NS	↑
	Arginine and proline metabolism		
	Glutathione metabolism		
	Bile acid biosynthesis		
Taurine	Taurine and hypotaurine metabolism	↑	NS
	Bile acid biosynthesis		
Betaine	Glycine and serine metabolism	↓	↓
	Methionine metabolism		
L-Methionine	Glycine and serine metabolism	↑	NS
	Methionine metabolism		
L-Threonine	Glycine and serine metabolism	↑	↑
Choline	Methionine metabolism	↑	↑
Sarcosine	Methionine metabolism	↓	NS
L-Phenylalanine	Phenylalanine and tyrosine metabolism	↑	↑
L-Tyrosine	Phenylalanine and tyrosine metabolism	↑	↑
Formylanthranilic acid	Tryptophan metabolism	↓	NS
L-Valine	Valine, leucine and isoleucine degradation	↓	↑

Compared to healthy controls, variation trend of bile acid and amino acid in plasma or feces of patients with alcohol-related liver cirrhosis. NS: Not significant; ALC: Alcohol-related liver cirrhosis; HC: Healthy control.

GCA and TCA in plasma showed a positive correlation with TBil, MDF, and PT and a negative correlation with CHE and ALB. Conversely, DCA in feces demonstrated a negative correlation with TBil, MDF, and PT but a positive correlation with CHE and ALB. Compared to a single index, the ratio of all primary bile acids in the blood, including GCA and TCA to DCA in the feces (recorded as P/S BA ratio) showed a higher correlation with MDF, TBil, CHE, PT, and ALB (Figure 5).

DISCUSSION

In patients with ALC, the stability of the intestinal microbiota and the integrity of the intestinal barrier were compromised, altering the intestinal microbiota and their metabolites. Both exogenous molecules, such as amino acids, and endogenously produced molecules from intestinal microorganisms can be transported to the liver *via* the portal vein. The liver secretes bile acids and other biologically active mediators into the biliary tract and bloodstream, affecting the intestinal microbiota and their metabolites [12]. This raises questions about the similarities and differences between plasma and intestinal metabolites and their implications in the progression of ALD. In order to gain an in-depth understanding of the primary metabolic pathways involved in enterohepatic circulation and their correlation with ALD, we conducted a metabolomics study that analyzed both plasma and feces metabolites. The current comparative analysis was based on the Human Metabolome Database and identified > 300 metabolites, although their distribution varied between plasma and feces. Notably, bile acid and amino acid metabolism pathways were significantly concentrated in both plasma and feces, which might participate in the progression of the disease.

Bile acid is a critical metabolic substance for maintaining the homeostasis of the gut-liver axis[13]. Primary and secondary bile acids (synthesized by the liver and produced by bacterial metabolism, respectively) performed various functions in the small intestine and played critical roles in lipid

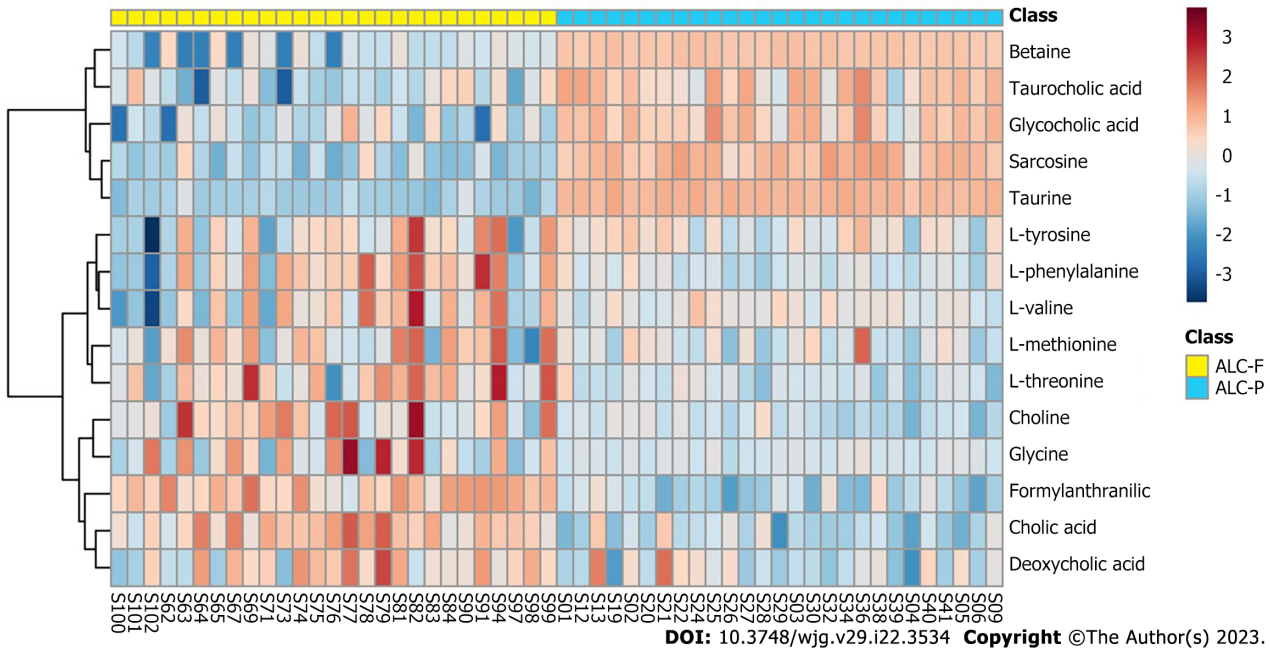


Figure 4 Distribution of bile acids and amino acid and related metabolites in plasma and feces of patients with alcohol-related liver cirrhosis**.** Numerous data basically conformed to the normal distribution after normalizing and scaling. The darker the color, the higher the relative content. ALC-P: Mean metabolites in the plasma of patients with alcohol-related liver cirrhosis; ALC-F: Mean metabolites in the feces of patients with alcohol-related liver cirrhosis.

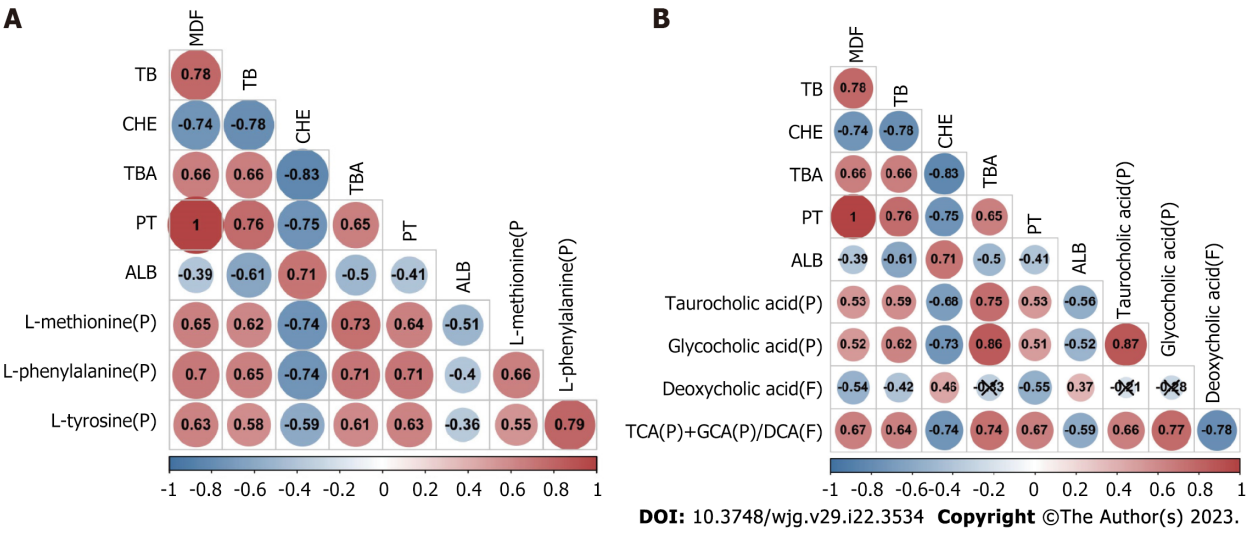


Figure 5 Correlation heatmap of amino acid or bile acid with clinical index. A: Correlation of amino acid with clinical index; B: Correlation of bile acid with clinical index. Relative coefficient in circle were calculated by spearman correlation analysis ($P < 0.05$). "×" in the circle mean no statistical difference ($P > 0.05$). TCA(P)+GCA(P)/DCA(F) also marked as P/S BA ratio represented sum of glycocholic acid and taurocholic acid in plasma divided by deoxycholic acid in feces. MDF: Maddrey discriminant function score; TB: Total bilirubin; CHF: Cholinesterase; TBA: Total bile acid; PT: Prothrombin time; ALB: Albumin.

absorption, cholesterol homeostasis, and hormonal effects *via* their steroid structure[14]. Firstly, pathway enrichment analysis in patients with ALC showed substantial enrichment of bile acid metabolism in plasma. Next, we found that primary bile acids, including CA, TCA, and GCA of patients with ALC increased in plasma but showed no apparent differences in feces, while secondary bile acid DCA decreased in feces but increased in plasma. Ethanol stimulates bile acid formation in primary human hepatocytes[15]. Moreover, liver cirrhosis affects bile acid secretion, and patients suffer from cholestasis. This phenomenon might be the reason for the increase of CA, TCA, and GCA in the plasma of patients with ALC. Kakiyama *et al*[16] reported different levels of serum DCA in ALC with varied amounts of alcohol consumption, and the volume of serum binding DCA in ALC was higher than in HCs. These findings indicated that plasma DCA increased in patients with ALC; this phenomenon was associated with alcohol consumption status. However, several studies have demonstrated that fecal DCA and other secondary bile acids in patients with ALD decreased[17,18], which was in agreement

with our findings. DCA is the most common bile acid in human feces and cecum samples[19]. Most of the DCA in the intestine is only produced by cholic acid transformed by 7α-dehydroxylation-producing bacteria, and the currently known DCA-producing bacteria include very few *Clostridia* and closely related bacteria of other genera[20]. Previous studies demonstrated that *Clostridiales* XIV decreased in the feces of ALC patients[21], which might be related to alcohol-induced dysbiosis and inflammation of the intestine, and *Clostridiales* XIV was predictive of 90-d hospitalizations. This could be one of the mechanisms for the decrease in fecal DCA, which is presented to the colon[6]. On the other hand, due to the impact of DCA on the stability of intestinal epithelial cell membrane, intestinal permeability increased, which might result in the resorption of DCA in the blood[22]. This further suggested that intestinal microbiota play a significant role in bile acid metabolism and disease progression.

Moreover, our analysis of the correlation between bile acids with clinical indicators showed that GCA and TCA in plasma were positively correlated with TBil, PT, and MDF and negatively correlated with ALB and CHE, while fecal DCA was negatively correlated with TBil, PT, and MDF and positively correlated with ALB and CHE. The ratio of primary bile acids in the plasma to secondary bile acids in the feces was correlated with MDF, TBil, CHE, ALB, and PT. Additionally, a positive correlation was established between fecal DCA and T-CHO in blood, suggesting that secondary bile acids in feces might be closely related to cholesterol homeostasis in the blood. TBil, PT, ALB, and MDF reflect the severity of diseases, while CHE reflects the liver's composition function. The current results suggested that plasma GCA and TCA and fecal DCA might be related to the severity of diseases. Furthermore, we calculated the ratio of primary bile acids in the plasma to secondary bile acids in feces (P/S BA ratio) and found that the P/S BA ratio is correlated with MDF, TBil, CHE, ALB, and PT, which might be an alternative indicator of the severity of the diseases. In addition, we found a positive correlation between DCA in feces and T-CHO in the blood, which further suggested that secondary bile acids in feces might be closely related to cholesterol homeostasis in the blood. In conclusion, bile acid metabolism plays a significant role in enterohepatic circulation, and a combined analysis of primary bile acids in the plasma and secondary bile acids in feces might provide valuable insights into the progression of ALD.

The current study also revealed that both plasma and feces exhibit a substantial concentration of amino acid metabolism, yet the specific types of amino acids involved in each vary significantly. Branched-chain amino acids and aromatic amino acids partake in the progression of cirrhosis, as shown previously[23,24]. These findings showed a decrease in the plasma concentration of the branched-chain amino acid L-valine and an increase in its concentration in feces. Some studies have shown that the concentration of L-valine in the plasma of ALC patients decreased[25], and supplementing with L-valine could improve the survival rate of cirrhosis patients[26]. The decrease in *Faecalibacterium prausnitzii* in the feces of cirrhosis patients, which coded for branched-chain amino acid translocators [27], can obstruct the transport of branched-chain amino acids and increase L-valine in feces but decrease it in the plasma. The content of valine in feces is also affected by the dietary intake of branched-chain amino acids. The amino acids with simultaneous changes in plasma and feces are L-phenylalanine, L-tyrosine, and L-threonine, of which L-phenylalanine and L-tyrosine are aromatic amino acids. The elevated levels of aromatic amino acids in cirrhotic patients are linked to the progression of liver disease and the development of hepatic encephalopathy[28]. Previous studies have demonstrated that hydroxylation of L-phenylalanine and L-tyrosine flux is increased in the blood of patients with liver cirrhosis[29]. Phenylalanine is decomposed and hydroxylated to tyrosine, which might explain the elevated levels of L-phenylalanine and L-tyrosine in the plasma. Also, L-phenylalanine and L-tyrosine were raised in feces through enterohepatic circulation, while L-methionine was increased in the plasma but not feces in ALC patients. A previous study by Marchesini *et al*[30] suggested that the increase of plasma methionine in patients with cirrhosis could be attributed to the damage of liver cells and the decrease in methionine's metabolic function. In addition, the NMR-based metabolomics analysis by Kumar *et al*[31] showed increased serum methionine in patients with acute-on-chronic liver failure. Moreover, our study found that plasma L-phenylalanine, L-tyrosine, and L-methionine were positively correlated with TBil and MDF, suggesting that these three amino acids may be related to the severity of diseases, and are designated as markers of disease progression in the blood.

Furthermore, our analysis detected the presence of betaine, a crucial component in the metabolism of amino acids, such as glycine, serine, and methionine, in the enterohepatic circulation. In patients with ALC, betaine decreased in both plasma and feces. It plays a vital role in methylating homocysteine into methionine, a process that is crucial for maintaining liver function stability, cell replication, and detoxification. The reduction in betaine levels in patients with ALC could be due to its depletion or insufficient supply during the disease process. A study by Schofield *et al*[32] showed that changes in betaine were associated with the development of ALC. Previous studies have shown that supplementing betaine can prevent acute alcoholic liver injury[33], and measuring fecal or plasma betaine levels in patients with ALC can assess its insufficiency and is expected to serve as an indicator for evaluating the severity of disease or a therapeutic target for treatment.

In addition, glycine and taurine play crucial roles in both amino acid metabolism and bile acid metabolism. Alcohol consumption may increase in the proportion of secondary bile acids, the total concentration of bile acids, and the proportion of bile acids bound to glycine rather than taurine[10,13]. Bajaj *et al*[6] found that the conjugated bile acids in the duodenal fluid and feces turned into toxic

glycine-conjugated bile acids from harmless taurine-conjugated bile acids in ALC patients. Our study also observed that taurine was concentrated in the plasma of patients with ALC, while glycine was concentrated in their feces. Taurine/glycine ratio was decreased in the serum and feces of patients with ALC. The imbalance in the taurine/glycine ratio may be due to dysbiosis caused by liver cirrhosis, the subsequent reduction of taurine bioavailability, and an increase in the intestine-liver circulation rate[10, 14]. This phenomenon suggested that regulating taurine/glycine ratio might improve the intestinal microecology of ALC patients and alleviate liver diseases.

Taken together, understanding the similarities and differences between plasma and feces metabolites holds significant potential in advancing molecular diagnosis in disease progression. The detection of these metabolites highlights the diversity of substances that can be detected in both plasma and feces. Fecal metabolites are more complex than those in plasma, which might be influenced by several factors, such as race, environment, diet, and medicine. Additionally, changes in intestinal and colon microbiota and their metabolism can alter the fecal metabolites, with secondary metabolites produced by the intestinal microbiota potentially playing a role in disease progression. Thus, further studies with larger samples are required to validate and evaluate bile acid and amino acids as potential markers for disease progression in cirrhosis. Moreover, integrating intestinal microbiome omics and metabonomics analysis is essential to decipher the molecular mechanisms underlying ALC. Since LC-MS analysis used in this study has limitations, further comparisons with other detection methods and complementary studies are required. The analysis of metabolites in plasma and feces provides an in-depth insight into ALC.

CONCLUSION

Bile acid and amino acid metabolism play a very important role in the progression of ALC. The enrichment of GCA, TCA, L-phenylalanine, L-tyrosine, and L-methionine in the plasma of patients with ALC and the reduction of DCA in feces was related to the severity of ALC. These metabolites may be used as indicators to evaluate the progression of ALC.

ARTICLE HIGHLIGHTS

Research background

Alterations in plasma and intestinal metabolites contribute to the pathogenesis and progression of alcohol-related liver cirrhosis (ALC).

Research motivation

Metabolites in enterohepatic circulation play an important role in cross-talk between liver and gut. The metabolites in the blood or the feces may have homogeneity but may also have specific characteristics related to their respective environments. The correlation between intestinal and plasma metabolites in patients with ALC, which might be helpful for the diagnosis and treatment of ALC, has not yet been elucidated.

Research objectives

To explore the common and different metabolites in the plasma and feces of patients with ALC and evaluate their clinical implications.

Research methods

This was a case-controlled observation study. We prospectively enrolled two groups of subjects: individuals with ALC and healthy controls (HCs). We recruited age-matched healthy males as controls through recruitment advertisements. According to the inclusion and exclusion criteria, 27 patients with ALC and 24 HCs were selected. The plasma and feces samples were collected. Liver function, blood routine, and other indicators were detected with automatic biochemical and blood routine analyzers. Liquid chromatography-mass spectrometry was used to detect the plasma and feces metabolites. Also, the association of metabolites with clinical features was analyzed.

Research results

More than 8000 plasma and more than 10000 fecal metabolites of patients with ALC were detected. Among them, More than 300 metabolites were found both in the plasma and feces. Enrichment analysis showed that these common metabolites are enriched in bile and amino acid metabolic pathways. Moreover, patients with ALC had a higher level of glycocholic acid (GCA) and taurocholic acid (TCA) in plasma and a lower level of deoxycholic acid (DCA) in the feces, while L-threonine, L-phenylalanine, and L-tyrosine increased simultaneously in plasma and feces. These results was consistent with previous studies and have indeed confirmed the disorder of bile acid and amino acid metabolism in

patients with ALC. Besides, GCA, TCA, L-methionine, L-phenylalanine, and L-tyrosine in plasma were positively correlated with total bilirubin (TBil), prothrombin time (PT), and maddrey discriminant function score (MDF) and negatively correlated with cholinesterase (CHE) and albumin (ALB). The DCA in feces was negatively correlated with TBil, MDF, and PT and positively correlated with CHE and ALB. AP/S BA ratio of plasma primary bile acid (GCA and TCA) to fecal secondary bile acid (DCA), which was relevant to TBil, PT, and MDF score was established, which may be used as a biomarker of the severity of ALC.

Research conclusions

Bile acid and amino acid metabolism play a very important role in the progression of ALC. The enrichment of GCA, TCA, L-phenylalanine, L-tyrosine, and L-methionine in the plasma of patients with ALC and the reduction of DCA in feces was related to the severity of ALC. The P/S BA ratio of plasma primary bile acids (GCA and TCA) to fecal secondary bile acid (DCA), was relevant to TBil, PT, and MDF score.

Research perspectives

Integrating intestinal microbiomics and metabolomics analysis is essential to decipher the molecular mechanisms underlying ALC. Since LC-MS analysis used in this study has limitations, further comparisons with other detection methods and complementary studies are required.

ACKNOWLEDGEMENTS

The authors would like to thank all patients and healthy volunteers for their participation in this study.

FOOTNOTES

Author contributions: Xing HC had designed the article; Xu YF, Hao YX, Ma L, Zhang MH, Niu XX, and Li Y had enrolled patients and collected data; Han M and Yuan XX had collected samples; Zhang YY, Liu TT, Xu YF, and Wan G had analyzed the data; Xu YF had drafted the manuscript; Xing HC had revised the manuscript for critical content.

Supported by National Key R&D Program of China, No. 21YFC2301801; and Capital's Funds for Health Improvement and Research of China, No. 2020-1-2171.

Institutional review board statement: This research scheme was reviewed and approved by the Ethics Committee of Ditan hospital (Beijing, China) and registered at http://www.chictr.org.cn/ (ChiCTR2000038216).

Informed consent statement: Written informed consent was obtained from all study participants or their legal guardian prior to study enrollment.

Conflict-of-interest statement: There are no conflicts of interest to report.

Data sharing statement: No additional data are available.

STROBE statement: The authors have read the STROBE Statement—checklist of items, and the manuscript was prepared and revised according to the STROBE Statement—checklist of items.

Open-Access: This article is an open-access article that was selected by an in-house editor and fully peer-reviewed by external reviewers. It is distributed in accordance with the Creative Commons Attribution NonCommercial (CC BY-NC 4.0) license, which permits others to distribute, remix, adapt, build upon this work non-commercially, and license their derivative works on different terms, provided the original work is properly cited and the use is non-commercial. See: https://creativecommons.org/Licenses/by-nc/4.0/

Country/Territory of origin: China

ORCID number: Yi-Fan Xu 0000-0003-2188-0804; Yan-Xu Hao 0000-0002-3317-2875; Lei Ma 0009-0009-1098-3948; Meng-Han Zhang 0000-0002-2983-2033; Xuan-Xuan Niu 0000-0002-7418-2076; Yan Li 0009-0003-9313-4840; Yuan-Yuan Zhang 0000-0002-4142-3216; Ting-Ting Liu 0009-0009-3462-6216; Ming Han 0000-0002-8788-1554; Xiao-Xue Yuan 0000-0002-2886-4703; Gang Wan 0009-0001-3103-986X; Hui-Chun Xing 0000-0002-9111-9669.

Corresponding Author's Membership in Professional Societies: Society of Hepatology, Chinese Association of Integrative Medicine; the Microecology Professional Committee of Beijing Association of Preventive Medicine; the Infectious Disease Branch of Chinese Preventive Medicine Association; Chinese Society of Hepatology, Chinese Medical Association; the Microecology Branch of Chinese Preventive Medicine Association; the Hepatology Branch of the Beijing Medical Association.

S-Editor: Yan JP
L-Editor: A
P-Editor: Chen YX

REFERENCES

1 **GBD 2017 Cirrhosis Collaborators**. The global, regional, and national burden of cirrhosis by cause in 195 countries and territories, 1990-2017: a systematic analysis for the Global Burden of Disease Study 2017. *Lancet Gastroenterol Hepatol* 2020; **5**: 245-266 [PMID: 31981519 DOI: 10.1016/S2468-1253(19)30349-8]
2 **Voutilainen T**, Kärkkäinen O. Changes in the Human Metabolome Associated With Alcohol Use: A Review. *Alcohol Alcohol* 2019; **54**: 225-234 [PMID: 31087088 DOI: 10.1093/alcalc/agz030]
3 **Chen Y**, Yang F, Lu H, Wang B, Chen Y, Lei D, Wang Y, Zhu B, Li L. Characterization of fecal microbial communities in patients with liver cirrhosis. *Hepatology* 2011; **54**: 562-572 [PMID: 21574172 DOI: 10.1002/hep.24423]
4 **Lian JS**, Liu W, Hao SR, Guo YZ, Huang HJ, Chen DY, Xie Q, Pan XP, Xu W, Yuan WX, Li LJ, Huang JR. A serum metabonomic study on the difference between alcohol- and HBV-induced liver cirrhosis by ultraperformance liquid chromatography coupled to mass spectrometry plus quadrupole time-of-flight mass spectrometry. *Chin Med J (Engl)* 2011; **124**: 1367-1373 [PMID: 21740750]
5 **Harada S**, Takebayashi T, Kurihara A, Akiyama M, Suzuki A, Hatakeyama Y, Sugiyama D, Kuwabara K, Takeuchi A, Okamura T, Nishiwaki Y, Tanaka T, Hirayama A, Sugimoto M, Soga T, Tomita M. Metabolomic profiling reveals novel biomarkers of alcohol intake and alcohol-induced liver injury in community-dwelling men. *Environ Health Prev Med* 2016; **21**: 18-26 [PMID: 26459263 DOI: 10.1007/s12199-015-0494-y]
6 **Bajaj JS**, Kakiyama G, Zhao D, Takei H, Fagan A, Hylemon P, Zhou H, Pandak WM, Nittono H, Fiehn O, Salzman N, Holtz M, Simpson P, Gavis EA, Heuman DM, Liu R, Kang DJ, Sikaroodi M, Gillevet PM. Continued Alcohol Misuse in Human Cirrhosis is Associated with an Impaired Gut-Liver Axis. *Alcohol Clin Exp Res* 2017; **41**: 1857-1865 [PMID: 28925102 DOI: 10.1111/acer.13498]
7 **Sutherland VL**, McQueen CA, Mendrick D, Gulezian D, Cerniglia C, Foley S, Forry S, Khare S, Liang X, Manautou JE, Tweedie D, Young H, Alekseyenko AV, Burns F, Dietert R, Wilson A, Chen C. The Gut Microbiome and Xenobiotics: Identifying Knowledge Gaps. *Toxicol Sci* 2020; **176**: 1-10 [PMID: 32658296 DOI: 10.1093/toxsci/kfaa060]
8 **Bajaj JS**. Alcohol, liver disease and the gut microbiota. *Nat Rev Gastroenterol Hepatol* 2019; **16**: 235-246 [PMID: 30643227 DOI: 10.1038/s41575-018-0099-1]
9 **Ventura-Cots M**, Argemi J, Jones PD, Lackner C, El Hag M, Abraldes JG, Alvarado E, Clemente A, Ravi S, Alves A, Alboraie M, Altamirano J, Barace S, Bosques F, Brown R, Caballeria J, Cabezas J, Carvalhana S, Cortez-Pinto H, Costa A, Degré D, Fernandez-Carrillo C, Ganne-Carrie N, Garcia-Tsao G, Genesca J, Koskinas J, Lanthier N, Louvet A, Lozano JJ, Lucey MR, Masson S, Mathurin P, Mendez-Sanchez N, Miquel R, Moreno C, Mounajjed T, Odena G, Kim W, Sancho-Bru P, Warren Sands R, Szafranska J, Verset L, Schnabl B, Sempoux C, Shah V, Shawcross DL, Stauber RE, Straub BK, Verna E, Tiniakos D, Trépo E, Vargas V, Villanueva C, Woosley JT, Ziol M, Mueller S, Stärkel P, Bataller R. Clinical, histological and molecular profiling of different stages of alcohol-related liver disease. *Gut* 2022; **71**: 1856-1866 [PMID: 34992134 DOI: 10.1136/gutjnl-2021-324295]
10 **Zafari N**, Velayati M, Fahim M, Maftouh M, Pourali G, Khazaei M, Nassiri M, Hassanian SM, Ghayour-Mobarhan M, Ferns GA, Kiani MA, Avan A. Role of gut bacterial and non-bacterial microbiota in alcohol-associated liver disease: Molecular mechanisms, biomarkers, and therapeutic prospective. *Life Sci* 2022; **305**: 120760 [PMID: 35787997 DOI: 10.1016/j.lfs.2022.120760]
11 **Crabb DW**, Im GY, Szabo G, Mellinger JL, Lucey MR. Diagnosis and Treatment of Alcohol-Associated Liver Diseases: 2019 Practice Guidance From the American Association for the Study of Liver Diseases. *Hepatology* 2020; **71**: 306-333 [PMID: 31314133 DOI: 10.1002/hep.30866]
12 **Hartmann P**, Seebauer CT, Schnabl B. Alcoholic liver disease: the gut microbiome and liver cross talk. *Alcohol Clin Exp Res* 2015; **39**: 763-775 [PMID: 25872593 DOI: 10.1111/acer.12704]
13 **Liu Y**, Liu T, Zhao X, Gao Y. New insights into the bile acid-based regulatory mechanisms and therapeutic perspectives in alcohol-related liver disease. *Cell Mol Life Sci* 2022; **79**: 486 [PMID: 35978227 DOI: 10.1007/s00018-022-04509-6]
14 **Zhong W**, Zhou Z. Alterations of the gut microbiome and metabolome in alcoholic liver disease. *World J Gastrointest Pathophysiol* 2014; **5**: 514-522 [PMID: 25400995 DOI: 10.4291/wjgp.v5.i4.514]
15 **Nilsson LM**, Sjövall J, Strom S, Bodin K, Nowak G, Einarsson C, Ellis E. Ethanol stimulates bile acid formation in primary human hepatocytes. *Biochem Biophys Res Commun* 2007; **364**: 743-747 [PMID: 17976534 DOI: 10.1016/j.bbrc.2007.10.039]
16 **Kakiyama G**, Hylemon PB, Zhou H, Pandak WM, Heuman DM, Kang DJ, Takei H, Nittono H, Ridlon JM, Fuchs M, Gurley EC, Wang Y, Liu R, Sanyal AJ, Gillevet PM, Bajaj JS. Colonic inflammation and secondary bile acids in alcoholic cirrhosis. *Am J Physiol Gastrointest Liver Physiol* 2014; **306**: G929-G937 [PMID: 24699327 DOI: 10.1152/ajpgi.00315.2013]
17 **Muthiah MD**, Smirnova E, Puri P, Chalasani N, Shah VH, Kiani C, Taylor S, Mirshahi F, Sanyal AJ. Development of Alcohol-Associated Hepatitis Is Associated With Specific Changes in Gut-Modified Bile Acids. *Hepatol Commun* 2022; **6**: 1073-1089 [PMID: 34984859 DOI: 10.1002/hep4.1885]
18 **Kakiyama G**, Pandak WM, Gillevet PM, Hylemon PB, Heuman DM, Daita K, Takei H, Muto A, Nittono H, Ridlon JM, White MB, Noble NA, Monteith P, Fuchs M, Thacker LR, Sikaroodi M, Bajaj JS. Modulation of the fecal bile acid profile by gut microbiota in cirrhosis. *J Hepatol* 2013; **58**: 949-955 [PMID: 23333527 DOI: 10.1016/j.jhep.2013.01.003]
19 **Ridlon JM**, Kang DJ, Hylemon PB. Bile salt biotransformations by human intestinal bacteria. *J Lipid Res* 2006; **47**: 241-259 [PMID: 16299351 DOI: 10.1194/jlr.R500013-JLR200]

20 **Streidl T**, Karkossa I, Segura Muñoz RR, Eberl C, Zaufel A, Plagge J, Schmaltz R, Schubert K, Basic M, Schneider KM, Afify M, Trautwein C, Tolba R, Stecher B, Doden HL, Ridlon JM, Ecker J, Moustafa T, von Bergen M, Ramer-Tait AE, Clavel T. The gut bacterium Extibacter muris produces secondary bile acids and influences liver physiology in gnotobiotic mice. *Gut Microbes* 2021; **13**: 1-21 [PMID: 33382950 DOI: 10.1080/19490976.2020.1854008]

21 **Acharya C**, Bajaj JS. Altered Microbiome in Patients With Cirrhosis and Complications. *Clin Gastroenterol Hepatol* 2019; **17**: 307-321 [PMID: 30099098 DOI: 10.1016/j.cgh.2018.08.008]

22 **Ridlon JM**, Alves JM, Hylemon PB, Bajaj JS. Cirrhosis, bile acids and gut microbiota: unraveling a complex relationship. *Gut Microbes* 2013; **4**: 382-387 [PMID: 23851335 DOI: 10.4161/gmic.25723]

23 **Fukui A**, Kawabe N, Hashimoto S, Kamei H, Yoshioka K. Switching from branched-chain amino acid granules to branched-chain amino acid-enriched nutrient improves the branched-chain amino acid-to-tyrosine ratio in patients with cirrhosis with hypoalbuminemia: a prospective study. *Eur J Gastroenterol Hepatol* 2020; **32**: 501-506 [PMID: 31524770 DOI: 10.1097/MEG.0000000000001544]

24 **Lo EKK**, Felicianna, Xu JH, Zhan Q, Zeng Z, El-Nezami H. The Emerging Role of Branched-Chain Amino Acids in Liver Diseases. *Biomedicines* 2022; **10** [PMID: 35740464 DOI: 10.3390/biomedicines10061444]

25 **Konstantis G**, Pourzitaki C, Chourdakis M, Kitsikidou E, Germanidis G. Efficacy of branched chain amino acids supplementation in liver cirrhosis: A systematic review and meta-analysis. *Clin Nutr* 2022; **41**: 1171-1190 [PMID: 35500317 DOI: 10.1016/j.clnu.2022.03.027]

26 **Holeček M**. Branched-chain amino acid supplementation in treatment of liver cirrhosis: Updated views on how to attenuate their harmful effects on cataplerosis and ammonia formation. *Nutrition* 2017; **41**: 80-85 [PMID: 28760433 DOI: 10.1016/j.nut.2017.04.003]

27 **Moran-Ramos S**, Macias-Kauffer L, López-Contreras BE, Villamil-Ramírez H, Ocampo-Medina E, León-Mimila P, Del Rio-Navarro BE, Granados-Portillo O, Ibarra-Gonzalez I, Vela-Amieva M, Tovar AR, Torres N, Gomez-Perez FJ, Aguilar-Salinas C, Canizales-Quinteros S. A higher bacterial inward BCAA transport driven by Faecalibacterium prausnitzii is associated with lower serum levels of BCAA in early adolescents. *Mol Med* 2021; **27**: 108 [PMID: 34525937 DOI: 10.1186/s10020-021-00371-7]

28 **Parés A**, Deulofeu R, Cisneros L, Escorsell A, Salmerón JM, Caballería J, Mas A. Albumin dialysis improves hepatic encephalopathy and decreases circulating phenolic aromatic amino acids in patients with alcoholic hepatitis and severe liver failure. *Crit Care* 2009; **13**: R8 [PMID: 19175915 DOI: 10.1186/cc7697]

29 **Tessari P**, Vettore M, Millioni R, Puricelli L, Orlando R. Effect of liver cirrhosis on phenylalanine and tyrosine metabolism. *Curr Opin Clin Nutr Metab Care* 2010; **13**: 81-86 [PMID: 19898234 DOI: 10.1097/MCO.0b013e32833383af]

30 **Marchesini G**, Bugianesi E, Bianchi G, Fabbri A, Marchi E, Zoli M, Pisi E. Defective methionine metabolism in cirrhosis: relation to severity of liver disease. *Hepatology* 1992; **16**: 149-155 [PMID: 1377658 DOI: 10.1002/hep.1840160125]

31 **Kumar U**, Sharma S, Durgappa M, Gupta N, Raj R, Kumar A, Sharma PN, Krishna VP, Kumar RV, Guleria A, Saraswat VA, Pande G, Kumar D. Serum Metabolic Disturbances Associated with Acute-on-chronic Liver Failure in Patients with Underlying Alcoholic Liver Diseases: An Elaborative NMR-based Metabolomics Study. *J Pharm Bioallied Sci* 2021; **13**: 276-282 [PMID: 34349490 DOI: 10.4103/JPBS.JPBS_333_20]

32 **Schofield Z**, Reed MA, Newsome PN, Adams DH, Günther UL, Lalor PF. Changes in human hepatic metabolism in steatosis and cirrhosis. *World J Gastroenterol* 2017; **23**: 2685-2695 [PMID: 28487605 DOI: 10.3748/wjg.v23.i15.2685]

33 **Arumugam MK**, Chava S, Perumal SK, Paal MC, Rasineni K, Ganesan M, Donohue TM Jr, Osna NA, Kharbanda KK. Acute ethanol-induced liver injury is prevented by betaine administration. *Front Physiol* 2022; **13**: 940148 [PMID: 36267591 DOI: 10.3389/fphys.2022.940148]

World Journal of Gastroenterology

Submit a Manuscript: https://www.f6publishing.com

World J Gastroenterol 2023 June 14; 29(22): 3548-3560

DOI: 10.3748/wjg.v29.i22.3548

ISSN 1007-9327 (print) ISSN 2219-2840 (online)

ORIGINAL ARTICLE

Prospective Study

Prospective study comparing hepatic steatosis assessment by magnetic resonance imaging and four ultrasound methods in 105 successive patients

Remi Collin, Benoit Magnin, Constance Gaillard, Carine Nicolas, Armand Abergel, Benjamin Buchard

Specialty type: Gastroenterology and hepatology

Provenance and peer review: Unsolicited article; Externally peer reviewed.

Peer-review model: Single blind

Peer-review report's scientific quality classification

Grade A (Excellent): 0
Grade B (Very good): B, B, B
Grade C (Good): C, C, C, C
Grade D (Fair): 0
Grade E (Poor): 0

P-Reviewer: Gupta T, India; Liu M, China; Ma L, China; Mu C, Canada; Shariati MBH, Iran

Received: February 8, 2023
Peer-review started: February 8, 2023
First decision: March 21, 2023
Revised: April 4, 2023
Accepted: May 12, 2023
Article in press: May 12, 2023
Published online: June 14, 2023

Remi Collin, Gastroenterology and Endoscopy Unit, Dupuytren University Hospital, Limoges 87000, France

Remi Collin, Carine Nicolas, Armand Abergel, Benjamin Buchard, Department of Hepatology and Gastroenterology, Clermont-Ferrand University Hospital, Clermont-Ferrand 63000, France

Benoit Magnin, Constance Gaillard, Department of Radiology, Clermont-Ferrand University Hospital, Clermont-Ferrand 63000, France

Corresponding author: Remi Collin, MD, Doctor, Gastroenterology and Endoscopy Unit, Dupuytren University Hospital, 2 Avenue Martin Luther King, Limoges 87000, France. remi.collin@chu-limoges.fr

Abstract

BACKGROUND

Non-alcoholic fatty liver disease (NAFLD) is becoming a major health problem, resulting in hepatic, metabolic and cardio-vascular morbidity.

AIM

To evaluate new ultrasonographic tools to detect and measure hepatic steatosis.

METHODS

We prospectively included 105 patients referred to our liver unit for NAFLD suspicion or follow-up. They underwent ultrasonographic measurement of liver sound speed estimation (SSE) and attenuation coefficient (AC) using Aixplorer MACH 30 (Supersonic Imagine, France), continuous controlled attenuation parameter (cCAP) using Fibroscan (Echosens, France) and standard liver ultrasound with hepato-renal index (HRI) calculation. Hepatic steatosis was then classified according to magnetic resonance imaging proton density fat fraction (PDFF). Receiver operating curve (ROC) analysis was performed to evaluate the diagnostic performance in the diagnosis of steatosis.

RESULTS

Most patients were overweight or obese (90%) and had metabolic syndrome (70%). One third suffered from diabetes. Steatosis was identified in 85 patients (81%) according to PDFF. Twenty-one patients (20%) had advanced liver disease.

SSE, AC, cCAP and HRI correlated with PDFF, with respective Spearman correlation coefficient of -0.39, 0.42, 0.54 and 0.59 (P < 0.01). Area under the receiver operating characteristic curve (AUROC) for detection of steatosis with HRI was 0.91 (0.83-0.99), with the best cut-off value being 1.3 (Se = 83%, Sp = 98%). The optimal cCAP threshold of 275 dB/m, corresponding to the recent EASL-suggested threshold, had a sensitivity of 72% and a specificity of 80%. Corresponding AUROC was 0.79 (0.66-0.92). The diagnostic accuracy of cCAP was more reliable when standard deviation was < 15 dB/m with an AUC of 0.91 (0.83-0.98). An AC threshold of 0.42 dB/cm/MHz had an AUROC was 0.82 (0.70-0.93). SSE performed moderately with an AUROC of 0.73 (0.62-0.84).

CONCLUSION

Among all ultrasonographic tools evaluated in this study, including new-generation tools such as cCAP and SSE, HRI had the best performance. It is also the simplest and most available method as most ultrasound scans are equipped with this module.

Key Words: Non-alcoholic fatty liver disease; Ultrasonography; Steatosis assessment; Magnetic resonance imaging; Controlled attenuation parameter

©The Author(s) 2023. Published by Baishideng Publishing Group Inc. All rights reserved.

Core Tip: Among all ultrasonographic tools evaluated in this study, including new-generation systems such as continuous controlled attenuation parameter and sound speed examination, hepato-renal index had the best performance. It is also the simplest and most available method as most ultrasound (US) scans are equipped with this module. The presence of an hyperechogenic liver on US also performed well, confirming that US should remain the first-line screening tool for steatosis.

Citation: Collin R, Magnin B, Gaillard C, Nicolas C, Abergel A, Buchard B. Prospective study comparing hepatic steatosis assessment by magnetic resonance imaging and four ultrasound methods in 105 successive patients. *World J Gastroenterol* 2023; 29(22): 3548-3560

URL: https://www.wjgnet.com/1007-9327/full/v29/i22/3548.htm

DOI: https://dx.doi.org/10.3748/wjg.v29.i22.3548

INTRODUCTION

Non-alcoholic fatty liver disease (NAFLD), considered as the liver manifestation of the metabolic syndrome, has become a major public health issue, affecting around 25% of people in western societies. Its presence has been associated with an increased risk of both cardiovascular, hepatic and cancer-related morbidity[1]. Therefore, identifying steatosis among individuals with increased metabolic risk is crucial for primary care.

Hepatic steatosis is the key manifestation of NAFLD and refers to the excess of fat within the hepatocytes, histologically defined by the presence of at least 5% of hepatocytes containing fat. Histological assessment of steatosis is the gold standard for the diagnosis of liver steatosis but is an invasive procedure and cannot be performed for all patients with metabolic risk factors[2].

Ultrasound (US) is currently the first-line screening test, but several studies have shown that US is lacking the necessary sensitivity to assess mild steatosis < 20%, particularly in obese patients with body mass index (BMI) > 35 kg/m^2[3-7]. It is also subject to inter-observer and intra-observer variabilities[8].

Magnetic resonance imaging (MRI) has demonstrated excellent performances for the diagnosis and grading of steatosis using either spectroscopy, in-phase and opposed-phase technique or multiecho gradient sequences but this process is expensive, with limited access[9-11].

Controlled attenuation parameter (CAP) is a promising technique for steatosis assessment and grading. The interpretation of CAP values remains difficult in practice for several reasons: many cutoffs have been published, the influence of the chosen probe is still debated and solid quality criteria of measures are unavailable[12-17]. A new CAP method called continuous CAP (cCAP) is emerging. The major difference with the alternative method is that it uses ultrasound data continuously acquired during the imaging phase examination[18].

Other non-invasive techniques including B-mode image-guided US attenuation parameter or hepato-renal index (HRI) have been developed in the past years[19-23].

Recently, a new US technique based on sound speed estimation (SSE) demonstrated accurate performances for the detection of steatosis. The speed of sound decreased as the fat content in liver

increased. SSE could be used to detect, quantify and grade liver steatosis. However, the evaluation of steatosis was not specifically done in overweighted/obese patients suffering from NAFLD and SSE needs further investigations in this indication[24-26].

In a monocentric prospective study, we aimed at evaluating diagnosis performances of various US tools compared to MRI proton density fat fraction assessment (PDFF).

MATERIALS AND METHODS

Participants

Study participants were consecutively and prospectively recruited from the University Hospital of Clermont-Ferrand, France, from January 2021 to October 2021 by physicians of the hepatology department. Inclusion criteria were: Age over 18 years, patients with known or suspected NAFLD, referred for non-invasive fibrosis evaluation using impulse elastography, with willingness and ability to participate. Exclusion criteria were clinical, laboratory, or histologic evidence of a liver disease other than NAFLD (chronic hepatitis B or C, autoimmune liver disease, excessive alcohol consumption defined by WHO criteria, Wilson's disease or other), hepatocellular carcinoma and all other liver tumors, secondary causes of liver steatosis (genetic disease, steatogenic or hepatoxic medication use) and contraindications to MRI.

Demographic and anthropometric data were recorded. Biological data collected included platelets, prothrombin time (PT), international normalized ratio (INR), albumin, bilirubin, transaminases (aspartate aminotransferase, AST and alanine aminotransferase, ALT), gamma-glutamyltransferase (GGT), alkaline phosphatase (ALP), total cholesterol, high density lipoprotein (HDL) cholesterol, low density lipoprotein (LDL) cholesterol, triglycerides, fasting glucose, fasting insulinemia.

The study design was approved by local ethic committee (study M210401, Clermont-Ferrand University Hospital) and informed consent was obtained for all participants.

US examinations

All participants underwent US liver examinations using the Aixplorer MACH 30® US system (Supersonic Imagine, Aix-en-Provence, France). Participants were asked to fast for at least 3 h prior to US examinations. They were positioned in the dorsal decubitus position with the right arm at maximum abduction for intercostal stretching. A 3.5 MHz abdominal curved transducer (C6-1X probe) was used. Acquisitions were performed during neutral respiratory apnea as follows: (1) Right intercostal (between the 7th and 9th intercostal space) and subcostal view was considered for every patient; (2) US transducer was placed so that the hepatic capsule was parallel to the US transducer; and (3) Care was taken to avoid the presence of large hepatic vessels or artifacts in the image (ultrasound reflection caused by abdominal gas or by rib interposition). For HRI, the probe was placed to obtain an adequate visualization of the liver and the right kidney in a sagittal or oblique image with minimal artifacts. HRI was calculated using the region of interest (ROI) measure tool, with average brightness ratio between two ROI at least 3 mm wide placed at the same depth in hepatic parenchyma and in renal cortex (Figure 1).

For each patient, 5 measures of sound speed, 5 of attenuation coefficient (AC) and 3 of HRI acquisitions were performed by the same physician. The mean values were used for statistical analysis.

Simultaneously, liver stiffness and cCAP measurements were performed using FibroScan SmartExam® (Echosens, Paris, France) by experienced operators. All patients were measured using either an M- or an XL-probe, according to the device automatically-selected probe.

A liver US was also performed by a radiologist at patient's discretion, in any radiological center, unaware of the study, in the standard clinical care of NAFLD. The presence of a hyperechogenic liver described on the US report was noted (steatosis vs. no steatosis or not mentioned).

MRI PDFF technique

Within the month following US examinations, all participants underwent a chemical shift-encoded liver MRI using a 3.0 Tesla MAGNETOM Vida® system (Siemens Medical Solutions, Erlangen, Germany). A gradient echo dedicated sequence developed by the manufacturer to measure hepatic PDFF was systematically included in MRI acquisition protocols. This sequence is characterized by a low flip angle to reduce T1 bias and six echoes to correct for T2* effect. Images were acquired during a single breath hold. In and out-phases imaging was used prior to fat quantification to assess homogeneity of fat distribution. PDFF (%) estimation was obtained by placing three large regions of interest in the liver parenchyma. Steatosis was regarded as fat fraction ≥ 5.6 %, as defined by EASL. Steatosis grading was not evaluated because correspondence between the steatosis histologic grading and PDFF value has not yet been standardized in the literature[27]. Iron content was also measured using this technique.

Statistical analysis

Patients data were recorded in e-case report form *via* a secure web platform (REDCap® version 9.3.7, Vanderbilt University, United States) where these data were monitored and a database extraction was



DOI: 10.3748/wjg.v29.i22.3548 **Copyright** ©The Author(s) 2023.

Figure 1 Hepato-renal index measurement with 6 mm wide regions of interest, at a depth of 9.4 cm in liver right lobe and right kidney, University Hospital of Clermont-Ferrand.

performed.

Data were expressed as descriptive statistics (mean ± SD, median with IQR or number with corresponding percentage as appropriate). The normality assumption was assessed using the Shapiro-Wilk's test. Chi-Square and Student *t*-test were used to compare categorical and continuous variables. If normality was not ascertained, the Mann-Whitney test was used for continuous variables. Receiver operating curve (ROC) analysis was performed to evaluate the diagnostic performance of US tools compared to MRI PDFF. Optimal cutoff values were identified by maximizing the Youden index, and corresponding sensitivities, specificities, likelihood ratios (LR) were derived. Comparison of areas under receiver operating characteristic curves was made according to Hanley and McNeil. Pearson and Spearman linear correlation coefficients were used to evaluate the relationship between continuous variables, respectively when normality was assessed or not. A non-linear regression analysis was also conducted to assess the relationship between SSE AC, cCAP, HRI and PDFF. All tests were considered statistically significant in the case of $P < 0.05$. Statistical analysis were performed and graphs were designed using GraphPad Prism® (v8, GraphPad Software, La Jolla, California, United States). Multivariable linear regression was used to evaluate the influence of anthropometric parameters and fibrosis severity on US measures (R Software, R Foundation for Statistical Computing, Vienna, Austria).

RESULTS

Clinical, biological and radiological characteristics of the study population

One hundred and five patients were included in this study. Main characteristics are presented in Table 1. Median BMI was 31 kg/m². Most patients were overweight or obese (90%) and had metabolic syndrome (70%). One third suffered from diabetes. Steatosis was identified in 85 patients (81%) according to PDFF. Twenty-five patients (20%) were suspected to have advanced liver disease according to shear-wave elastography.

Mean AST and ALT were respectively 35 (± 28) U/L and 65 (± 49) U/L. Mean GGT was 120 (± 125) U/mL. Only ALT levels correlated significantly but moderately with PDFF (Spearman's ρ = 0.4, $P < 0.001$). One patient failed to receive Fibroscan® and HRI measurement due to poor US signal.

Patients characteristics according to the presence of steatosis are shown in Table 2. Steatotic patients had significantly higher BMI and waist circumference. As expected, metabolic syndrome was more prevalent in patients with steatosis. Mean SSE, AC and cCAP values significantly differed between non-steatotic and steatotic patients, but not liver stiffness.

Relationship between SSE, AC, HRI and cCAP with MRI PDFF

SSE, AC, HRI and cCAP correlated with PDFF, with respective Spearman correlation coefficient of -0.39, 0.42, 0.59 and 0.54 ($P < 0.01$) (Figure 2). SSE, AC, cCAP and HRI specifically displayed a significant non-linear relationship with PDFF as previously demonstrated (Supplementary Figure 1)[28].

Table 1 Characteristics of the 105 patients, *n* (%)

Characteristics of the 105 patients	
Demographic and anthropometric data	
Sex (male)	51 (49)
Age (yr)	56 ± 14
BMI (kg/m^2)	31 ± 6
Overweight	94 (90)
Obesity	50 (48)
Waist circumference (cm)[1]	107 ± 15
Diabetes	38 (36)
Hypertension	42 (40)
Metabolic syndrome	73 (70)
Biological data	
Platelets count (G/L)[1]	231 ± 72
AST (U/L)[1]	35 ± 28
ALT (U/L)[1]	65 ± 49
GGT (U/L)[1]	120 ± 125
Triglycerides (g/L)[1]	1.7 ± 0.93
HDL cholesterol (g/L)[1]	1.3 ± 0.4
Ferritin (ng/mL)[1]	232 ± 283
Steatosis assessment	
PDFF (%)[1]	15 ± 10
Steatosis on MRI	85 (81)
Fibroscan®	
Technical success	104 (99)
cCAP (dB/m)	283 ± 58
Liver stiffness (KPa)[1]	8 ± 7
Liver stiffness > 10 KPa	21 (20)
Use of M probe	83 (80)
Use of XL probe	21 (20)
Aixplorer MACH 30®	
Technical success	105 (100)
SSE (m/s)[1]	1519 ± 22
AC (dB/cm/MHz)[1]	0.48 ± 0.1
HRI[1]	1.43 ± 0.28
Technical success	104 (99)

[1]Data are mean ± SD.

BMI: Body mass index; AST: Aspartate aminotransferase; ALT: Alanine aminotransferase; GGT: Gamma glutamyl transferase; PDFF: Proton density fat fraction; cCAP: Continuous controlled attenuation parameter; SSE: Sound speed estimation; AC: Attenuation coefficient; HRI: Hepato-renal index.

Performances of SSE and AC

Intercostal SSE performed moderately for the diagnosis of steatosis with an area under curve (AUC) of 0.73 [0.62-0.84] (P = 0.001) (Figure 3A). Using the manufacturer cutoff of 1537 m/s resulted in a sensitivity and specificity of 80% and 45%. The best cutoff identified in our work was 1518 m/s but performances remained modest with sensitivity and specificity of 60% and 80% respectively. Of note,

Table 2 Characteristics of steatotic and non-steatotic patients, *n* (%)

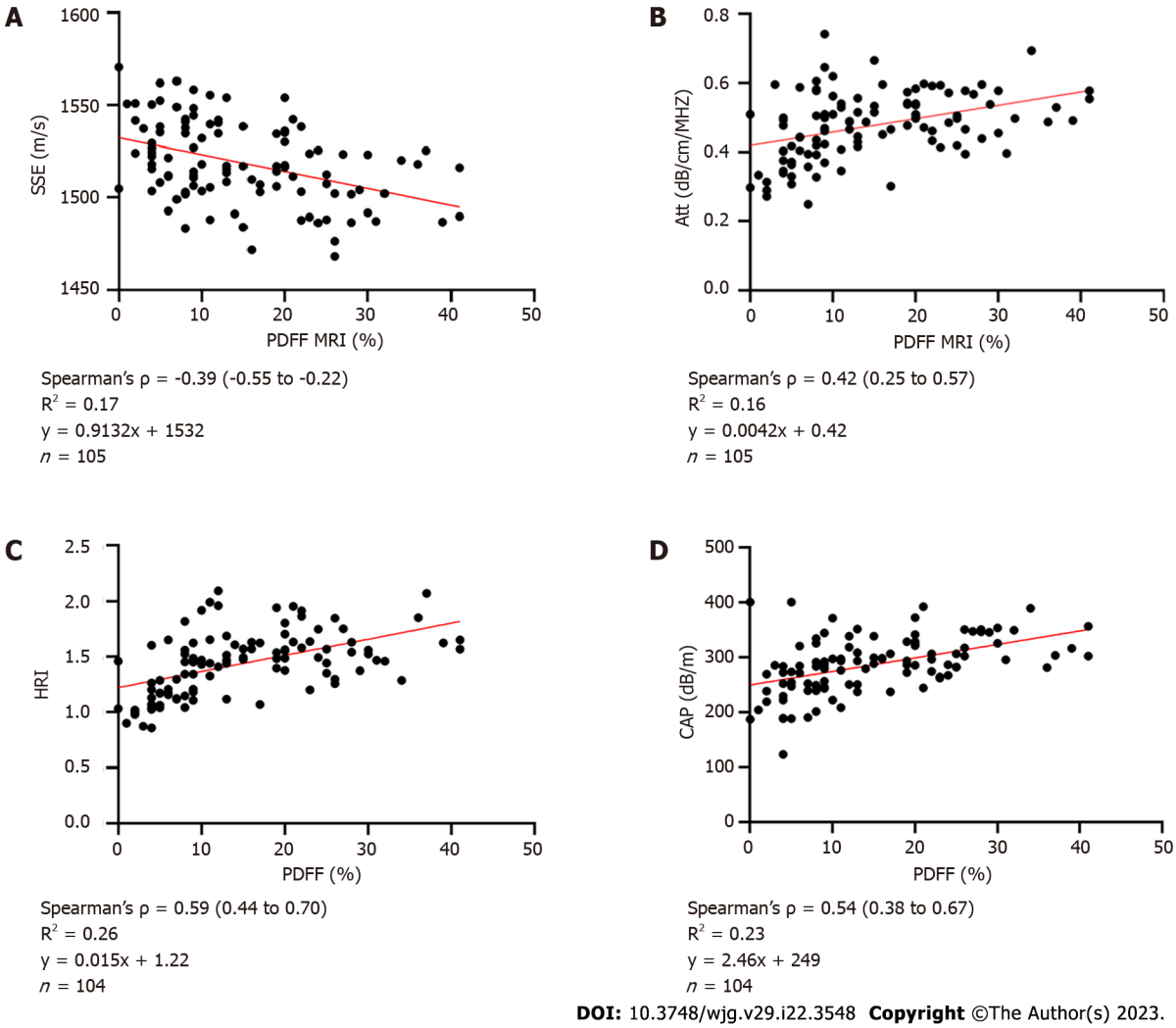
	Patients with steatosis (*n* = 85)	Patients without steatosis (*n* = 20)	*P* value
Demographic and anthropometric data			
Sex (male)	40 (47)	11 (55)	0.62
Age (yr)	56 ± 14	53 ± 14	0.5
BMI (kg/m^2)	31 ± 5	28 ± 6	**0.0004**
Normal BMI	7 (8)	4 (20)	
Overweight	31 (37)	13 (65)	
Obesity	47 (55)	3 (15)	
Waist circumference (cm)[1]	108 ± 14	99 ± 15	**0.004**
Diabetes	33 (39)	5 (25)	0.3
Hypertension	37 (44)	5 (25)	0.2
Metabolic syndrome	65 (76)	8 (40)	**0.0026**
Biological data			
Platelets count (G/L)[1]	236 ± 71	213 ± 78	0.2
AST (U/L)[1]	37 ± 30	27 ± 10	0.13
ALT (U/L)[1]	37 ± 30	49 ± 29	**0.044**
GGT (U/L)[1]	68 ± 53	116 ± 85	0.68
Triglycerides (g/L)[1]	1.8 ± 0.9	1.3 ± 0.9	**0.0058**
HDL cholesterol (g/L)[1]	1.3 ± 0.4	1.3 ± 0.3	0.1
Ferritin (ng/mL)[1]	121 ± 134	172 ± 127	0.45
Steatosis assessment			
PDFF (%)[1]	18 ± 9	2 ± 3	**< 0.0001**
Fibroscan®			
Technical success	84 (99)	20 (100)	
cCAP (dB/m)	296 ± 42	246 ± 67	**< 0.0001**
Liver stiffness (KPa)[1]	8 ± 8	7 ± 5	NS
Liver stiffness > 10 KPa	19 (22)	2 (10)	
Use of M probe	65 (76)	18 (90)	
Use of XL probe	20 (24)	2 (10)	
Aixplorer MACH 30®			
Technical success	85 (100)	20 (100)	
SSE (m/s)[1]	1515 ± 22	1533 ± 19	**0.0009**
AC (dB/cm/MHz)[1]	0.5 ± 0.1	0.39 ± 0.1	**< 0.0001**
HRI	1.52 ± 0.24	1.1 ± 0.18	**< 0.0001**
Technical success	84 (99)	20 (100)	

[1]Data are mean ± SD.

BMI: Body mass index; AST: Aspartate aminotransferase; ALT: Alanine aminotransferase; GGT: Gamma glutamyl transferase; PDFF: Proton density fat fraction; cCAP: Continuous controlled attenuation parameter; SSE: Sound speed estimation; AC: Attenuation coefficient; HRI: Hepato-renal index; NS: Non-significant.

using 5 measures of SSE compared to 3 measures did not improve performances (data not shown).

Intercostal AC performed well for the diagnosis of steatosis with an AUC of 0.82 (0.70-0.93) (P = 0.001) (Figure 3B). The best cutoff identified in our work was 0.42 dB/cm/MHz with sensitivity and specificity of 84 % and 75 % respectively.



DOI: 10.3748/wjg.v29.i22.3548 **Copyright** ©The Author(s) 2023.

Figure 2 Scatterplots. A-D: Scatterplots showing linear relationship between sound speed estimation (A), attenuation coefficient (B), hepato-renal index (C) and continuous controlled attenuation parameter (D) with magnetic resonance imaging-proton density fat fraction using 6-echo gradient ($P < 0.001$). PDFF: Proton density fat fraction; cCAP: Continuous controlled attenuation parameter; SSE: Sound speed estimation; AC: Attenuation coefficient; HRI: Hepato-renal index.

Performances of cCAP

cCAP was accurate for the diagnosis of steatosis with AUC of 0.79 (0.66-0.92) but did not perform better than AC. The best cutoff identified in our work was 275 dB/m but lacked sensitivity and specificity (respectively 72% and 80%) (Figure 3C).

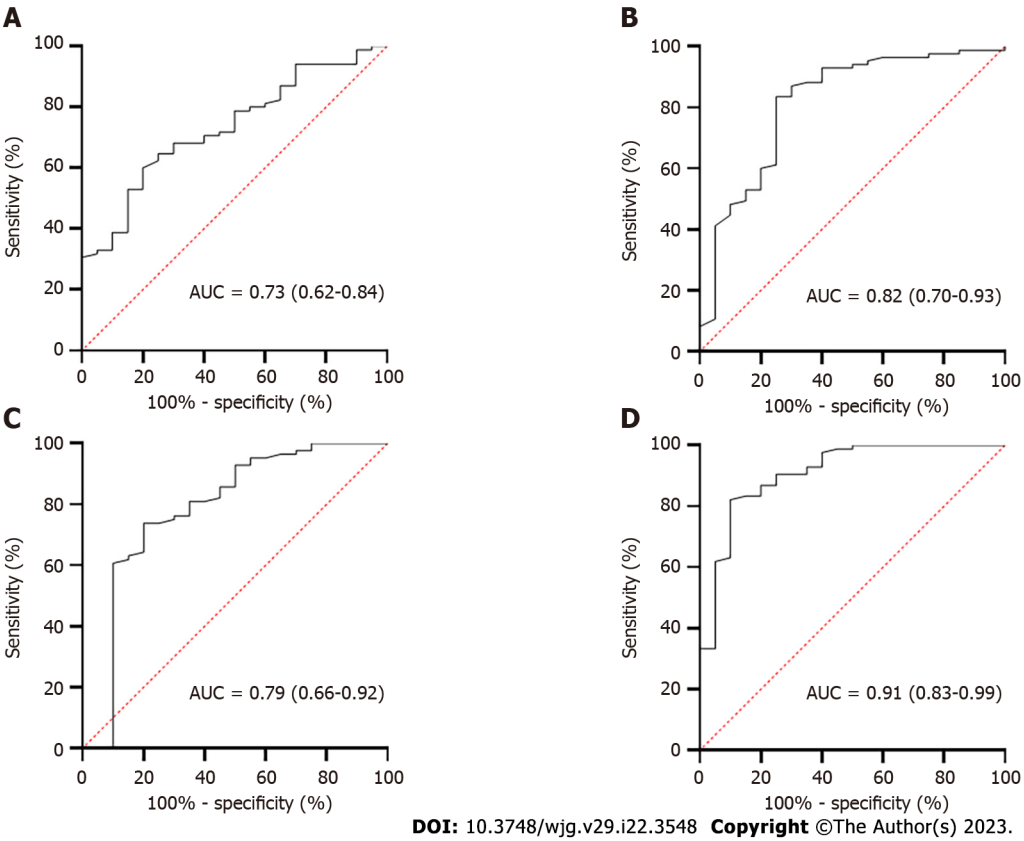
As expected, using cCAP resulted in low coefficient variation with 96% of patients having a coefficient of less than 10%. The diagnostic accuracy of cCAP was significantly improved when SD of cCAP was < 15 dB/m with an AUC of 0.91 (95% confidence interval: 0.83-0.98, $P < 0.01$) resulting in a sensitivity and specificity of 74% and 92%. In this work, one third of patients had an SD > 15 dB/m (Figure 4).

Performances of HRI

HRI performed the best with an AUC of 0.91 (0.83-0.99) ($P < 0.0001$) (Figure 3D). Using a cutoff set at 1.3 resulted in a sensitivity of 82% and specificity of 98%. In other words, only 2 patients had an increased hepatorenal gradient without having liver steatosis. The first patient had borderline steatosis (4% on MRI) and severe fibrosis on elastography (19 KPa) which could explain the increased HRI. For the other patient, moderate iron overload may have increased hepatorenal gradient. Among the 15 false negative patients, two third had mild steatosis on MRI (defined as PDFF < 10%).

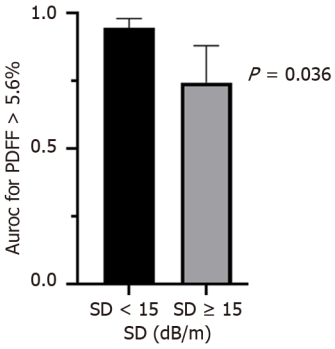
Performances of standard ultrasound

Hyperechogenic liver was described in 73/85 steatotic patients (Figure 5). It showed a sensitivity of 86% and specificity of 70%. Among the 6 patients presenting a hyperechogenic liver on US but no steatosis on MRI, none had severe fibrosis (assessed using Fibroscan) or iron overload. Among the 12 patients with no hyperechogenic liver but steatosis on MRI, 7/12 (58%) had mild steatosis based on PDFF. No other steatosis sign was described by radiologists.



DOI: 10.3748/wjg.v29.i22.3548 **Copyright** ©The Author(s) 2023.

Figure 3 Receiver operating curve. A-D: Receiver operating curve for sound speed estimation (A), attenuation coefficient (B), continuous controlled attenuation parameter (C) and hepato-renal index (D). PDFF: Proton density fat fraction; cCAP: Continuous controlled attenuation parameter; SSE: Sound speed estimation; AC: Attenuation coefficient; HRI: Hepato-renal index.



DOI: 10.3748/wjg.v29.i22.3548 **Copyright** ©The Author(s) 2023.

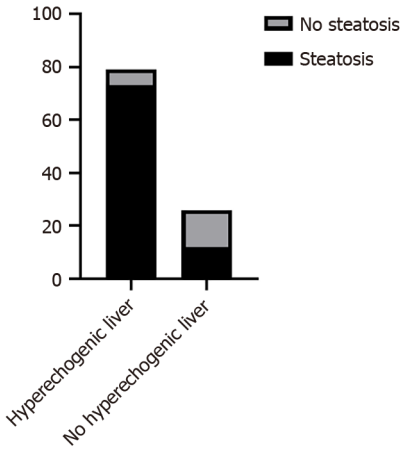
Figure 4 Continuous controlled attenuation parameter area under the receiver operating characteristic curve for the diagnosis of steatosis according to SD. PDFF: Proton density fat fraction; AUROC: Area under the receiver operating characteristic curve.

Intercostal or subcostal access

SSE and AC measurements were made for every patient using intercostal and subcostal view. However, if intercostal access was successful in every patient (success rate: 100% for SSE and AC), subcostal access showed a lower success rate (94% for SSE, 92% for AC) and lower performances (data not shown).

Influence of BMI and severity of fibrosis

Using multivariable linear regression, we demonstrated that both HRI, cCAP, AC and SSE were associated with the presence of steatosis on MRI, independently from BMI, waist circumference elastography, iron overload and the presence of diabetes or metabolic syndrome.



DOI: 10.3748/wjg.v29.i22.3548 **Copyright** ©The Author(s) 2023.

Figure 5 Ultrasound finding according to liver steatosis based on proton density fat fraction.

DISCUSSION

Standard ultrasound is widely used as first diagnostic exam for NAFLD. Our results confirmed past studies reporting poor sensitivity for mild steatosis[3,5]. Furthermore, BMI and fibrosis negatively influence US performances[6,7], and it suffers from inter- and intra-observer variability[8]. Our study collected US report from various radiologists, unaware of the study, chosen at patient's discretion. Steatosis was only described according to parenchyma hyperechogenicity. No other steatosis sign, like vessels blurring, gallbladder blurring or inability to visualize the diaphragm, nor steatosis scoring system, was used by radiologist, even if it proved to improve its diagnostic performance.

HRI calculation is a simple way to improve capabilities, as most US devices or radiology systems propose a dedicated module[21,29,30]. It can be easily performed by someone already familiar with US scan evaluation. Webb *et al*[31] proved that the known limitation of sonography to detect high grade steatosis of more than 30% of hepatocytes is resolved by HRI. In our study, HRI performed the best with a cut-off of 1.30. Previously described cut-off for the detection of any grade steatosis may vary in the literature from 1.22 to 1.49, influenced by system settings and different gold standards, and thus limiting HRI reproducibility and applicability[21,28,30-32].

It was the most reliable technique in our work, permitting an objective and quantitative assessment of steatosis better than cCAP and SSE. Furthermore, B-mode guidance permits to suspect heterogenous steatosis and adapt the location of measurement, which cannot be done with cCAP.

cCAP demonstrated promising performances for diagnosis of steatosis. This confirms a pilot study, which showed that cCAP outperformed significantly conventional CAP for the diagnostic of steatosis [33]. Indeed, the continuous method allows for larger volume sampling, reducing intraindividual variability and increasing correlation with MRI-PDFF. Caussy *et al*[34] described an IQR-based validity criteria significantly improving CAP performances. CAP results were generally expressed as the median and interquartile range of several manually triggered sequential attenuation measurements. Individual measurements collected with the cCAP method being much numerous, its results are expressed as the mean and SD. Thus, we proposed a quality criteria based on SD. In our work, cCAP proved to be perform significantly better for the diagnosis of steatosis when SD < 15 dB/m, reaching HRI measurement performances.

One main advantage of cCAP is to be combined with simultaneous fibrosis measurement, rapidly and without additional capabilities. This is of particular interest considering that the degree of fibrosis is the main prognosis factor in patients suffering from NAFLD[35]. However, on a practical level, not all medical structures have access to this device. This a major issue knowing that the growing prevalence of NAFLD worldwide cannot be fully handled by tertiary-care centers.

SSE and AC measurement on Aixplorer MACH 30 system are new non-invasive tools to quantify liver fat content, which may be useful in patient follow-up or therapeutic studies[36]. Using MRI-PDFF as reference, our study proved mixed performances for detection or exclusion of steatosis, with AUC ranging from 0.73 to 0.82.

SSE is a novel, understudied technique, based on the decrease of US speed as liver fat increases. Dioguardi Burgio *et al*[25] showed that SSE could be used for the detection and quantification of liver steatosis. However, in this study, SSE was acquired during US exam but calculated off-site. This resulted in invalid measurements in almost one quarter of patients due to poor signal quality. Moreover, this study included patients presenting liver diseases of various etiologies, and NAFLD-patients are not the only one known to present a poor echogenicity.

AC uses the same physical principles as cCAP but is performed under B-mode visual control. Several studies demonstrated promising performances, using various devices[19,37]. Nevertheless, optimal thresholds values slightly differ among different published studies, probably due to the use of different US scans and different reference standards (biopsy or MRI). A recent meta-analysis explored performances of AC for the detection of any grade steatosis, compiling 11 studies and more than 1400 patients: AUC was 0.83, close to what was assessed in our work[38].

SSE and AC intra-individual variability with 5 measures per patient was too low to suggest any validity criteria assessing better correlation to PDFF. Using three instead of five measures did not result in significant lower performances. To be noted, even if technical success was high (99% to 100%) with both cCAP and SSE/AC, these last tools were the most difficult to tame as they require a stable position, the strict absence of large hepatic vessels or artifacts in the image.

We found no influence of BMI, waist circumference elastography, iron overload or presence of diabetes or metabolic syndrome on the correlation between MRI-PDFF and both HRI, cCAP, AC and SSE. Previous studies reported unsure influence[37,39].

Several scores have also been developed to detect steatosis: fatty liver index, hepatic steatosis index and NAFLD liver fat score, which combine various clinical and biological parameters[40-42]. These algorithms demonstrated modest performances for the detection of steatosis and were inaccurate for the staging of steatosis[43]. They do not provide add-on features compared to standard clinical and biological data and are mainly used as epidemiological tools.

One limit of this study is that AC, SSE and HRI were assessed by two different examinators. As both examinators did not perform US liver examinations for all patients, we are unable to report an interobserver comparison or concordance.

Although our sample size is quite small, this work is the first one to prospectively evaluate diagnosis performances of various new generations US tools using MRI as gold standard on an exclusively-NAFLD population. Our study population contained patients with high BMI and weight, with a low fibrosis prevalence and moderate hepatic biological abnormalities, representing NAFLD-patients in real life situations.

These results should be validated in a population with a different prevalence of steatosis and in a multicenter study.

CONCLUSION

Among all ultrasonographic tools evaluated in this study, including new-generation systems such as cCAP and SSE, HRI had the best performance. It is also the simplest and most available method as most US scans are equipped with this module.

The presence of an hyperechogenic liver on US also performed well, confirming that US should remain the first-line screening tool for steatosis.

ARTICLE HIGHLIGHTS

Research background

Non-alcoholic fatty liver disease (NAFLD) is the most common liver disease worldwide, ranging from simple steatosis to aggressive hepatitis leading to liver fibrosis, cirrhosis and hepatocellular carcinoma.

Research motivation

Diagnose fatty liver disease and assess its severity during follow-up and after treatment is a key in clinical practice. Liver biopsy can deliver this information, but it is an invasive procedure with potentially severe. Therefore, non-invasive techniques were developed to stage steatosis. Ultrasound is the primary imaging modality in the assessment of patients with confirmed or suspected NAFLD.

Research objectives

We wanted to evaluate new ultrasonographic tools to detect and measure hepatic steatosis.

Research methods

One hundred and five patients underwent ultrasonographic measurement of liver sound speed estimation (SSE) and attenuation coefficient (AC) using Aixplorer MACH 30 (Supersonic Imagine, France), continuous Controlled Attenuation Parameter (cCAP) using Fibroscan (Echosens, France) and standard liver ultrasound with hepato-renal index (HRI) calculation. Hepatic steatosis was then classified according to MRI proton density fat fraction (PDFF) as gold standard.

Research results

SSE, AC, cCAP and HRI correlated with PDFF, with respective Spearman correlation coefficient of -0.39, 0.42, 0.54 and 0.59 ($P < 0.01$). Area under the receiver operating characteristic curve (AUROC) for detection of steatosis with HRI was 0.91 (0.83-0.99), with the best cut-off value being 1.3 (Se = 83%, Sp = 98%). The optimal cCAP threshold of 275 dB/m, corresponding to the recent EASL-suggested threshold, had a sensitivity of 72% and a specificity of 80%. Corresponding AUROC was 0.79 (0.66-0.92). The diagnostic accuracy of cCAP was more reliable when standard deviation was < 15 dB/m with an AUC of 0.91 (0.83-0.98). An AC threshold of 0.42 dB/cm/MHz had an AUROC was 0.82 (0.70-0.93). SSE performed moderately with an AUROC of 0.73 (0.62-0.84).

Research conclusions

HRI had the best performance. It is also the simplest and most available method as most US scans are equipped with this module.

Research perspectives

Measurement quality criteria need to be defined and validated for a wider use of theses techniques. Their improvement could open the way to efficient and easily accessible non-invasive steatosis grading.

FOOTNOTES

Author contributions: Collin R, Nicolas C, Abergel A and Buchard B conceived and designed the analysis; Collin R, Magnin B, Gaillard C, Nicolas C and Buchard B collected the data; Collin R, Magnin B, Gaillard C, Nicolas C, Abergel A and Buchard B contributed data or analysis tools; Collin R, Magnin B and Buchard B performed the analysis; Collin R and Buchard B wrote the paper.

Institutional review board statement: The study was reviewed and approved by the Clermont-Ferrand University Hospital Institutional Review Board.

Clinical trial registration statement: This study is registered at Clermont-Ferrand University Hospital. The registration identification number is M210401.

Informed consent statement: All study participants, or their legal guardian, provided informed written consent prior to study enrollment.

Conflict-of-interest statement: All the authors report no relevant conflicts of interest for this article.

Data sharing statement: No additional data are available.

CONSORT 2010 statement: The authors have read the CONSORT 2010 statement, and the manuscript was prepared and revised according to the CONSORT 2010 statement.

Open-Access: This article is an open-access article that was selected by an in-house editor and fully peer-reviewed by external reviewers. It is distributed in accordance with the Creative Commons Attribution NonCommercial (CC BY-NC 4.0) license, which permits others to distribute, remix, adapt, build upon this work non-commercially, and license their derivative works on different terms, provided the original work is properly cited and the use is non-commercial. See: https://creativecommons.org/Licenses/by-nc/4.0/

Country/Territory of origin: France

ORCID number: Remi Collin 0000-0002-3674-9641; Benoit Magnin 0000-0002-4246-5688; Armand Abergel 0000-0001-7480-1052.

Corresponding Author's Membership in Professional Societies: Société Nationale Française de Gastro-Entérologie, No. 2019021; Société Française d'Endoscopie Digestive; European Association for the Study of the Liver, No. 64959.

S-Editor: Gao CC
L-Editor: A
P-Editor: Yu HG

REFERENCES

1 **Huang DQ**, El-Serag HB, Loomba R. Global epidemiology of NAFLD-related HCC: trends, predictions, risk factors and prevention. *Nat Rev Gastroenterol Hepatol* 2021; **18**: 223-238 [PMID: 33349658 DOI: 10.1038/s41575-020-00381-6]
2 **Diehl AM**, Day C. Cause, Pathogenesis, and Treatment of Nonalcoholic Steatohepatitis. *N Engl J Med* 2017; **377**: 2063-

2072 [PMID: 29166236 DOI: 10.1056/NEJMra1503519]
3 **Charatcharoenwitthaya P**, Lindor KD. Role of radiologic modalities in the management of non-alcoholic steatohepatitis. *Clin Liver Dis* 2007; **11**: 37-54, viii [PMID: 17544971 DOI: 10.1016/j.cld.2007.02.014]
4 **Bril F**, Ortiz-Lopez C, Lomonaco R, Orsak B, Freckleton M, Chintapalli K, Hardies J, Lai S, Solano F, Tio F, Cusi K. Clinical value of liver ultrasound for the diagnosis of nonalcoholic fatty liver disease in overweight and obese patients. *Liver Int* 2015; **35**: 2139-2146 [PMID: 25847730 DOI: 10.1111/liv.12840]
5 **Hernaez R**, Lazo M, Bonekamp S, Kamel I, Brancati FL, Guallar E, Clark JM. Diagnostic accuracy and reliability of ultrasonography for the detection of fatty liver: a meta-analysis. *Hepatology* 2011; **54**: 1082-1090 [PMID: 21618575 DOI: 10.1002/hep.24452]
6 **Hannah WN Jr**, Harrison SA. Noninvasive imaging methods to determine severity of nonalcoholic fatty liver disease and nonalcoholic steatohepatitis. *Hepatology* 2016; **64**: 2234-2243 [PMID: 27338123 DOI: 10.1002/hep.28699]
7 **de Moura Almeida A**, Cotrim HP, Barbosa DB, de Athayde LG, Santos AS, Bitencourt AG, de Freitas LA, Rios A, Alves E. Fatty liver disease in severe obese patients: diagnostic value of abdominal ultrasound. *World J Gastroenterol* 2008; **14**: 1415-1418 [PMID: 18322958 DOI: 10.3748/wjg.14.1415]
8 **Strauss S**, Gavish E, Gottlieb P, Katsnelson L. Interobserver and intraobserver variability in the sonographic assessment of fatty liver. *AJR Am J Roentgenol* 2007; **189**: W320-W323 [PMID: 18029843 DOI: 10.2214/AJR.07.2123]
9 **Cassidy FH**, Yokoo T, Aganovic L, Hanna RF, Bydder M, Middleton MS, Hamilton G, Chavez AD, Schwimmer JB, Sirlin CB. Fatty liver disease: MR imaging techniques for the detection and quantification of liver steatosis. *Radiographics* 2009; **29**: 231-260 [PMID: 19168847 DOI: 10.1148/rg.291075123]
10 **Cowin GJ**, Jonsson JR, Bauer JD, Ash S, Ali A, Osland EJ, Purdie DM, Clouston AD, Powell EE, Galloway GJ. Magnetic resonance imaging and spectroscopy for monitoring liver steatosis. *J Magn Reson Imaging* 2008; **28**: 937-945 [PMID: 18821619 DOI: 10.1002/jmri.21542]
11 **Boudinaud C**, Abergel A, Joubert-Zakeyh J, Fontarensky M, Pereira B, Chauveau B, Garcier JM, Chabrot P, Boyer L, Magnin B. Quantification of steatosis in alcoholic and nonalcoholic fatty liver disease: Evaluation of four MR techniques *vs* biopsy. *Eur J Radiol* 2019; **118**: 169-174 [PMID: 31439237 DOI: 10.1016/j.ejrad.2019.07.025]
12 **Sasso M**, Beaugrand M, de Ledinghen V, Douvin C, Marcellin P, Poupon R, Sandrin L, Miette V. Controlled attenuation parameter (CAP): a novel VCTE™ guided ultrasonic attenuation measurement for the evaluation of hepatic steatosis: preliminary study and validation in a cohort of patients with chronic liver disease from various causes. *Ultrasound Med Biol* 2010; **36**: 1825-1835 [PMID: 20870345 DOI: 10.1016/j.ultrasmedbio.2010.07.005]
13 **Karlas T**, Petroff D, Sasso M, Fan JG, Mi YQ, de Lédinghen V, Kumar M, Lupsor-Platon M, Han KH, Cardoso AC, Ferraioli G, Chan WK, Wong VW, Myers RP, Chayama K, Friedrich-Rust M, Beaugrand M, Shen F, Hiriart JB, Sarin SK, Badea R, Jung KS, Marcellin P, Filice C, Mahadeva S, Wong GL, Crotty P, Masaki K, Bojunga J, Bedossa P, Keim V, Wiegand J. Individual patient data meta-analysis of controlled attenuation parameter (CAP) technology for assessing steatosis. *J Hepatol* 2017; **66**: 1022-1030 [PMID: 28039099 DOI: 10.1016/j.jhep.2016.12.022]
14 **Caussy C**, Reeder SB, Sirlin CB, Loomba R. Noninvasive, Quantitative Assessment of Liver Fat by MRI-PDFF as an Endpoint in NASH Trials. *Hepatology* 2018; **68**: 763-772 [PMID: 29356032 DOI: 10.1002/hep.29797]
15 **de Lédinghen V**, Vergniol J, Foucher J, Merrouche W, le Bail B. Non-invasive diagnosis of liver steatosis using controlled attenuation parameter (CAP) and transient elastography. *Liver Int* 2012; **32**: 911-918 [PMID: 22672642 DOI: 10.1111/j.1478-3231.2012.02820.x]
16 **Petroff D**, Blank V, Newsome PN, Shalimar, Voican CS, Thiele M, de Lédinghen V, Baumeler S, Chan WK, Perlemuter G, Cardoso AC, Aggarwal S, Sasso M, Eddowes PJ, Allison M, Tsochatzis E, Anstee QM, Sheridan D, Cobbold JF, Naveau S, Lupsor-Platon M, Mueller S, Krag A, Irles-Depe M, Semela D, Wong GL, Wong VW, Villela-Nogueira CA, Garg H, Chazouillères O, Wiegand J, Karlas T. Assessment of hepatic steatosis by controlled attenuation parameter using the M and XL probes: an individual patient data meta-analysis. *Lancet Gastroenterol Hepatol* 2021; **6**: 185-198 [PMID: 33460567 DOI: 10.1016/S2468-1253(20)30357-5]
17 **European Association for the Study of the Liver**; Clinical Practice Guideline Panel; Chair; EASL Governing Board representative; Panel members. EASL Clinical Practice Guidelines on non-invasive tests for evaluation of liver disease severity and prognosis - 2021 update. *J Hepatol* 2021; **75**: 659-689 [PMID: 34166721 DOI: 10.1016/j.jhep.2021.05.025]
18 **Audière S**, Miette V, Fournier C, Whitehead J, Paredes AH, Sandrin L, Harrison SA. Continuous CAP method: reduced variability in a prospective cohort of 113 patients. *J Hepatol* 2020; **73**: S436 [DOI: 10.1016/S0168-8278(20)31354-4]
19 **Ferraioli G**, Maiocchi L, Savietto G, Tinelli C, Nichetti M, Rondanelli M, Calliada F, Preda L, Filice C. Performance of the Attenuation Imaging Technology in the Detection of Liver Steatosis. *J Ultrasound Med* 2021; **40**: 1325-1332 [PMID: 32960457 DOI: 10.1002/jum.15512]
20 **Fujiwara Y**, Kuroda H, Abe T, Ishida K, Oguri T, Noguchi S, Sugai T, Kamiyama N, Takikawa Y. The B-Mode Image-Guided Ultrasound Attenuation Parameter Accurately Detects Hepatic Steatosis in Chronic Liver Disease. *Ultrasound Med Biol* 2018; **44**: 2223-2232 [PMID: 30077415 DOI: 10.1016/j.ultrasmedbio.2018.06.017]
21 **Marshall RH**, Eissa M, Bluth EI, Gulotta PM, Davis NK. Hepatorenal index as an accurate, simple, and effective tool in screening for steatosis. *AJR Am J Roentgenol* 2012; **199**: 997-1002 [PMID: 23096171 DOI: 10.2214/AJR.11.6677]
22 **Martín-Rodríguez JL**, Arrebola JP, Jiménez-Moleón JJ, Olea N, González-Calvin JL. Sonographic quantification of a hepato-renal index for the assessment of hepatic steatosis in comparison with 3T proton magnetic resonance spectroscopy. *Eur J Gastroenterol Hepatol* 2014; **26**: 88-94 [PMID: 23921844 DOI: 10.1097/MEG.0b013e3283650650]
23 **Ballestri S**, Lonardo A, Romagnoli D, Carulli L, Losi L, Day CP, Loria P. Ultrasonographic fatty liver indicator, a novel score which rules out NASH and is correlated with metabolic parameters in NAFLD. *Liver Int* 2012; **32**: 1242-1252 [PMID: 22520641 DOI: 10.1111/j.1478-3231.2012.02804.x]
24 **Imbault M**, Faccinetto A, Osmanski BF, Tissier A, Deffieux T, Gennisson JL, Vilgrain V, Tanter M. Robust sound speed estimation for ultrasound-based hepatic steatosis assessment. *Phys Med Biol* 2017; **62**: 3582-3598 [PMID: 28225357 DOI: 10.1088/1361-6560/aa6226]
25 **Dioguardi Burgio M**, Imbault M, Ronot M, Faccinetto A, Van Beers BE, Rautou PE, Castera L, Gennisson JL, Tanter M, Vilgrain V. Ultrasonic Adaptive Sound Speed Estimation for the Diagnosis and Quantification of Hepatic Steatosis: A

Pilot Study. *Ultraschall Med* 2019; **40**: 722-733 [PMID: 30396216 DOI: 10.1055/a-0660-9465]
26 **Popa A**, Bende F, Șirli R, Popescu A, Bâldea V, Lupușoru R, Cotrău R, Fofiu R, Foncea C, Sporea I. Quantification of Liver Fibrosis, Steatosis, and Viscosity Using Multiparametric Ultrasound in Patients with Non-Alcoholic Liver Disease: A "Real-Life" Cohort Study. *Diagnostics (Basel)* 2021; **11** [PMID: 33926073 DOI: 10.3390/diagnostics11050783]
27 **Gu J**, Liu S, Du S, Zhang Q, Xiao J, Dong Q, Xin Y. Diagnostic value of MRI-PDFF for hepatic steatosis in patients with non-alcoholic fatty liver disease: a meta-analysis. *Eur Radiol* 2019; **29**: 3564-3573 [PMID: 30899974 DOI: 10.1007/s00330-019-06072-4]
28 **Moret A**, Boursier J, Houssel Debry P, Riou J, Crouan A, Dubois M, Michalak Provost S, Aubé C, Paisant A. Evaluation of the Hepatorenal B-Mode Ratio and the "Controlled Attenuation Parameter" for the Detection and Grading of Steatosis. *Ultraschall Med* 2022; **43**: 479-487 [PMID: 32992377 DOI: 10.1055/a-1233-2290]
29 **Shiralkar K**, Johnson S, Bluth EI, Marshall RH, Dornelles A, Gulotta PM. Improved method for calculating hepatic steatosis using the hepatorenal index. *J Ultrasound Med* 2015; **34**: 1051-1059 [PMID: 26014325 DOI: 10.7863/ultra.34.6.1051]
30 **Johnson SI**, Fort D, Shortt KJ, Therapondos G, Galliano GE, Nguyen T, Bluth EI. Ultrasound Stratification of Hepatic Steatosis Using Hepatorenal Index. *Diagnostics (Basel)* 2021; **11** [PMID: 34441377 DOI: 10.3390/diagnostics11081443]
31 **Webb M**, Yeshua H, Zelber-Sagi S, Santo E, Brazowski E, Halpern Z, Oren R. Diagnostic value of a computerized hepatorenal index for sonographic quantification of liver steatosis. *AJR Am J Roentgenol* 2009; **192**: 909-914 [PMID: 19304694 DOI: 10.2214/AJR.07.4016]
32 **Kjaergaard M**, Lindvig KP, Hansen CD, Detlefsen S, Krag A, Thiele M. Hepatorenal Index by B-Mode Ratio Versus Imaging and Fatty Liver Index to Diagnose Steatosis in Alcohol-Related and Nonalcoholic Fatty Liver Disease. *J Ultrasound Med* 2023; **42**: 487-496 [PMID: 35475550 DOI: 10.1002/jum.15991]
33 **Audière S**, Labourdette A, Miette V, Fournier C, Ternifi R, Boussida S, Pouletaut P, Charleux F, Bensamoun SF, Harrison SA, Sandrin L. Improved Ultrasound Attenuation Measurement Method for the Non-invasive Evaluation of Hepatic Steatosis Using FibroScan. *Ultrasound Med Biol* 2021; **47**: 3181-3195 [PMID: 34373137 DOI: 10.1016/j.ultrasmedbio.2021.07.007]
34 **Caussy C**, Alquiraish MH, Nguyen P, Hernandez C, Cepin S, Fortney LE, Ajmera V, Bettencourt R, Collier S, Hooker J, Sy E, Rizo E, Richards L, Sirlin CB, Loomba R. Optimal threshold of controlled attenuation parameter with MRI-PDFF as the gold standard for the detection of hepatic steatosis. *Hepatology* 2018; **67**: 1348-1359 [PMID: 29108123 DOI: 10.1002/hep.29639]
35 **Ekstedt M**, Hagström H, Nasr P, Fredrikson M, Stål P, Kechagias S, Hultcrantz R. Fibrosis stage is the strongest predictor for disease-specific mortality in NAFLD after up to 33 years of follow-up. *Hepatology* 2015; **61**: 1547-1554 [PMID: 25125077 DOI: 10.1002/hep.27368]
36 **European Association for the Study of the Liver (EASL)**; European Association for the Study of Diabetes (EASD); European Association for the Study of Obesity (EASO). EASL-EASD-EASO Clinical Practice Guidelines for the management of non-alcoholic fatty liver disease. *J Hepatol* 2016; **64**: 1388-1402 [PMID: 27062661 DOI: 10.1016/j.jhep.2015.11.004]
37 **Tada T**, Kumada T, Toyoda H, Yasuda S, Sone Y, Hashinokuchi S, Ogawa S, Oguri T, Kamiyama N, Chuma M, Akita T, Tanaka J. Liver stiffness does not affect ultrasound-guided attenuation coefficient measurement in the evaluation of hepatic steatosis. *Hepatol Res* 2020; **50**: 190-198 [PMID: 31661724 DOI: 10.1111/hepr.13442]
38 **Jang JK**, Choi SH, Lee JS, Kim SY, Lee SS, Kim KW. Accuracy of the ultrasound attenuation coefficient for the evaluation of hepatic steatosis: a systematic review and meta-analysis of prospective studies. *Ultrasonography* 2022; **41**: 83-92 [PMID: 34399043 DOI: 10.14366/usg.21076]
39 **Cassinotto C**, Jacq T, Anselme S, Ursic-Bedoya J, Blanc P, Faure S, Belgour A, Guiu B. Diagnostic Performance of Attenuation to Stage Liver Steatosis with MRI Proton Density Fat Fraction as Reference: A Prospective Comparison of Three US Machines. *Radiology* 2022; **305**: 353-361 [PMID: 35819322 DOI: 10.1148/radiol.212846]
40 **Bedogni G**, Bellentani S, Miglioli L, Masutti F, Passalacqua M, Castiglione A, Tiribelli C. The Fatty Liver Index: a simple and accurate predictor of hepatic steatosis in the general population. *BMC Gastroenterol* 2006; **6**: 33 [PMID: 17081293 DOI: 10.1186/1471-230X-6-33]
41 **Lee JH**, Kim D, Kim HJ, Lee CH, Yang JI, Kim W, Kim YJ, Yoon JH, Cho SH, Sung MW, Lee HS. Hepatic steatosis index: a simple screening tool reflecting nonalcoholic fatty liver disease. *Dig Liver Dis* 2010; **42**: 503-508 [PMID: 19766548 DOI: 10.1016/j.dld.2009.08.002]
42 **Kotronen A**, Peltonen M, Hakkarainen A, Sevastianova K, Bergholm R, Johansson LM, Lundbom N, Rissanen A, Ridderstråle M, Groop L, Orho-Melander M, Yki-Järvinen H. Prediction of non-alcoholic fatty liver disease and liver fat using metabolic and genetic factors. *Gastroenterology* 2009; **137**: 865-872 [PMID: 19524579 DOI: 10.1053/j.gastro.2009.06.005]
43 **Fedchuk L**, Nascimbeni F, Pais R, Charlotte F, Housset C, Ratziu V; LIDO Study Group. Performance and limitations of steatosis biomarkers in patients with nonalcoholic fatty liver disease. *Aliment Pharmacol Ther* 2014; **40**: 1209-1222 [PMID: 25267215 DOI: 10.1111/apt.12963]

World Journal of Gastroenterology

Submit a Manuscript: https://www.f6publishing.com

World J Gastroenterol 2023 June 14; 29(22): 3561-3573

DOI: 10.3748/wjg.v29.i22.3561

ISSN 1007-9327 (print) ISSN 2219-2840 (online)

SCIENTOMETRICS

Research trends on artificial intelligence and endoscopy in digestive diseases: A bibliometric analysis from 1990 to 2022

Ren-Chun Du, Yao-Bin Ouyang, Yi Hu

Specialty type: Oncology

Provenance and peer review: Unsolicited article; Externally peer reviewed.

Peer-review model: Single blind

Peer-review report's scientific quality classification

Grade A (Excellent): 0
Grade B (Very good): B, B
Grade C (Good): 0
Grade D (Fair): 0
Grade E (Poor): 0

P-Reviewer: Tsoulfas G, Greece; Xie C, China

Received: March 4, 2023
Peer-review started: March 4, 2023
First decision: March 28, 2023
Revised: April 3, 2023
Accepted: May 4, 2023
Article in press: May 4, 2023
Published online: June 14, 2023

Ren-Chun Du, Yao-Bin Ouyang, Yi Hu, Department of Gastroenterology, The First Affiliated Hospital of Nanchang University, Nanchang 330006, Jiangxi Province, China

Yao-Bin Ouyang, Department of Oncology, Mayo Clinic, Rochester, MN 55905, United States

Yi Hu, Department of Surgery, The Chinese University of Hong Kong, Hong Kong 999077, China

Corresponding author: Yi Hu, MD, Doctor, Department of Gastroenterology, The First Affiliated Hospital of Nanchang University, No. 17 Yong Waizheng Street, Donghu District, Nanchang 330006, Jiangxi Province, China. ndyfy06202@ncu.edu.cn

Abstract

BACKGROUND

Recently, artificial intelligence (AI) has been widely used in gastrointestinal endoscopy examinations.

AIM

To comprehensively evaluate the application of AI-assisted endoscopy in detecting different digestive diseases using bibliometric analysis.

METHODS

Relevant publications from the Web of Science published from 1990 to 2022 were extracted using a combination of the search terms "AI" and "endoscopy". The following information was recorded from the included publications: Title, author, institution, country, endoscopy type, disease type, performance of AI, publication, citation, journal and H-index.

RESULTS

A total of 446 studies were included. The number of articles reached its peak in 2021, and the annual citation numbers increased after 2006. China, the United States and Japan were dominant countries in this field, accounting for 28.7%, 16.8%, and 15.7% of publications, respectively. The Tada Tomohiro Institute of Gastroenterology and Proctology was the most influential institution. "Cancer" and "polyps" were the hotspots in this field. Colorectal polyps were the most concerning and researched disease, followed by gastric cancer and gastrointestinal bleeding. Conventional endoscopy was the most common type of examination. The accuracy of AI in detecting Barrett's esophagus, colorectal polyps and gastric cancer from 2018 to 2022 is 87.6%, 93.7% and 88.3%, respectively. The detection

rates of adenoma and gastrointestinal bleeding from 2018 to 2022 are 31.3% and 96.2%, respectively.

CONCLUSION
AI could improve the detection rate of digestive tract diseases and a convolutional neural network-based diagnosis program for endoscopic images shows promising results.

Key Words: Bibliometric analysis; Artificial intelligence; Endoscopy; Publications; Research trends

©The Author(s) 2023. Published by Baishideng Publishing Group Inc. All rights reserved.

Core Tip: Gastrointestinal tumors diagnosed at an early stage had a better prognosis than those diagnosed at a late stage, and performing endoscopy is the most effective approach to detect gastrointestinal tumors. In recent years, artificial intelligence (AI) has been widely used in gastrointestinal endoscopy examinations and it represents a fundamental breakthrough in the field of diagnostic endoscopy by assisting endoscopists with the detection of gastrointestinal tumors. This study aimed to provide a comprehensive analysis of AI applied in diagnostic endoscopy. A basic literature analysis was performed, as well as a subgroup analysis of AI-assisted digestive endoscopy in diagnosing various diseases.

Citation: Du RC, Ouyang YB, Hu Y. Research trends on artificial intelligence and endoscopy in digestive diseases: A bibliometric analysis from 1990 to 2022. *World J Gastroenterol* 2023; 29(22): 3561-3573
URL: https://www.wjgnet.com/1007-9327/full/v29/i22/3561.htm
DOI: https://dx.doi.org/10.3748/wjg.v29.i22.3561

INTRODUCTION

Gastrointestinal cancers (esophageal cancer, gastric cancer, colorectal cancer, *etc*.) account for 26% of global cancer incidence and 35% of all cancer-related deaths, which seriously threaten the health of global populations[1]. Gastrointestinal tumors diagnosed at an early stage had a better prognosis than those diagnosed at a late stage. For example, the 5-year survival rates of early gastric cancer and advanced gastric cancer were > 90% and < 30%, respectively. Performing endoscopy is the most effective approach to detect gastrointestinal tumors. More than 100 million subjects receive gastrointestinal endoscopy examinations each year. However, the current challenge is that the early diagnosis rate of tumors is low, and many lesions cannot be found in routine digestive endoscopy because of the large area of gastrointestinal mucosa, unobvious characteristics of early lesions, the existence of blind zones and uniform quality of examinations conducted by different endoscopists[2]. It is of great importance to improve the quality of endoscopy examinations to discover the lesions.

Artificial intelligence (AI) is intelligence processed by machines, as opposed to intelligence of humans and other animals, which emerged as a powerful and novel technology influencing many aspects of health care. In recent years, image recognition technology of AI has been dramatically improved and widely used in the medical field of diagnostic imaging[3-6]. AI represents a fundamental breakthrough in the field of diagnostic endoscopy by assisting endoscopists with the detection of gastrointestinal tumors[7]. Deep learning networks represented by convolutional neural network (CNN) systems are a hot research topic at present and have been widely applied in the fields of pathology, radiology and endoscopy[8]. The first study focusing on gastrointestinal endoscopy and computer simulation was reported in 1990, which showed that computer simulation was used as a tool to train endoscopists by constructing a model describing the three-dimensional structure of the appropriate parts of the gastrointestinal tract[9]. With the development of AI, it has been extensively used in gastrointestinal endoscopy examinations, such as upper gastrointestinal endoscopy, colonoscopy, wireless capsule and ultrasonic endoscopy.

Bibliometric analysis refers to a statistical approach that helps to comprehensively analyze the hotspots, trends and each unit and scholar's cooperation of published articles in this field[10,11]. In this study, we aimed to analyze the research hot spots and trends in the field of AI and endoscopy from 1990 to 2022 using a quantitative method. We also explored the application of AI-assisted endoscopy in detecting different digestive diseases to provide assistance for the research and clinical application of AI and endoscopy.

MATERIALS AND METHODS

Search strategy

All relevant and qualified data were collected from the Web of Science database. The search strategy was a combination of the following keywords and terms: ("artificial intelligence" OR "AI" OR "deep learning" OR "machine learning" OR "machine intelligence" OR "computer" OR "computational intelligence" OR "neural network" OR "knowledge acquisition" OR "automatic" OR "automated" OR "feature extraction" OR "image segmentation" OR "neural learning" OR "artificial neural network" OR "data mining" OR "data clustering" OR "big data") AND ("endoscopy" OR "endoscope"). Moreover, only publications written in English between 01 January 1990 and 01 November 2022 were considered.

Study selection

Two authors (Ren-Chun Du and Yao-Bin Ouyang) independently evaluated all relevant articles in two stages, and a full discussion was held to resolve any differences and conflicts (the inclusion of literature, classification of disease and endoscopy, and weight of different studies, *etc*) with the third author (Yi Hu). At the first stage of evaluation, basic research, reviews, case reports and meta-analysis were excluded. In the second stage, the contents of the remaining articles were carefully assessed according to the patient, intervention, comparison, outcomes (PICOs) criteria. "P" (patient): Patients with digestive diseases or health care; "I" (intervention): AI-assisted endoscopic examination; "C" (comparison): Routine endoscopic examination; "O" (outcome): The accuracy of AI and routine endoscopic examination in detecting digestive diseases; and "S" (study design): Retrospective studies, prospective randomized controlled trials (RCTs) and non-RCTs.

Data extraction

The included articles were assessed and downloaded into various file formats for analysis by the two investigators. The following data were extracted: Author, institution, country, endoscopy type, disease type, performance of AI (including sensitivity, specificity, and accuracy), citations, year of publications, and H-index. Each study was weighted according to the number of test samples and the weighted average of the performance data of AI in diagnosing diseases was calculated. Any discrepancy was evaluated by the kappa value to assess the agreement between two investigators.

Data analysis

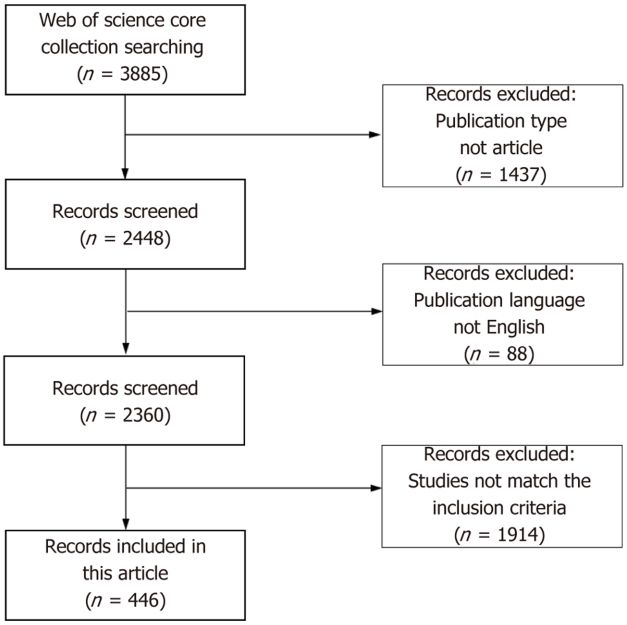
The data were imported into VOSviewer software (version 1.6.18), GraphPad Prism (version 8) and CiteSpace (version 6.1.R3) to generate the visual graphs. CiteSpace and VOSviewer were used to perform the quantitative and qualitative analyses. The cluster network was generated by VOSviewer to assess the most productive and cooperative authors, countries and institutions. Each dot of the visual graphs represents an author, institution and country, and these dots were clustered into various groups based on their cooperations. The size of the dots corresponded to the number of articles, while the strength of the connection was based on the frequency of cooperations. The options used in CiteSpace included a time slice set to "1990-2022," with 1 year per slice and the selection criteria set to "g-index." The scale factor k was set to "25", and "pathfinder" was selected to preserve the optimal structure while reducing the total links[12]. Keywords were used to label clusters and show cluster labels by a latent semantic indexing algorithm.

RESULTS

Study selection and characteristics

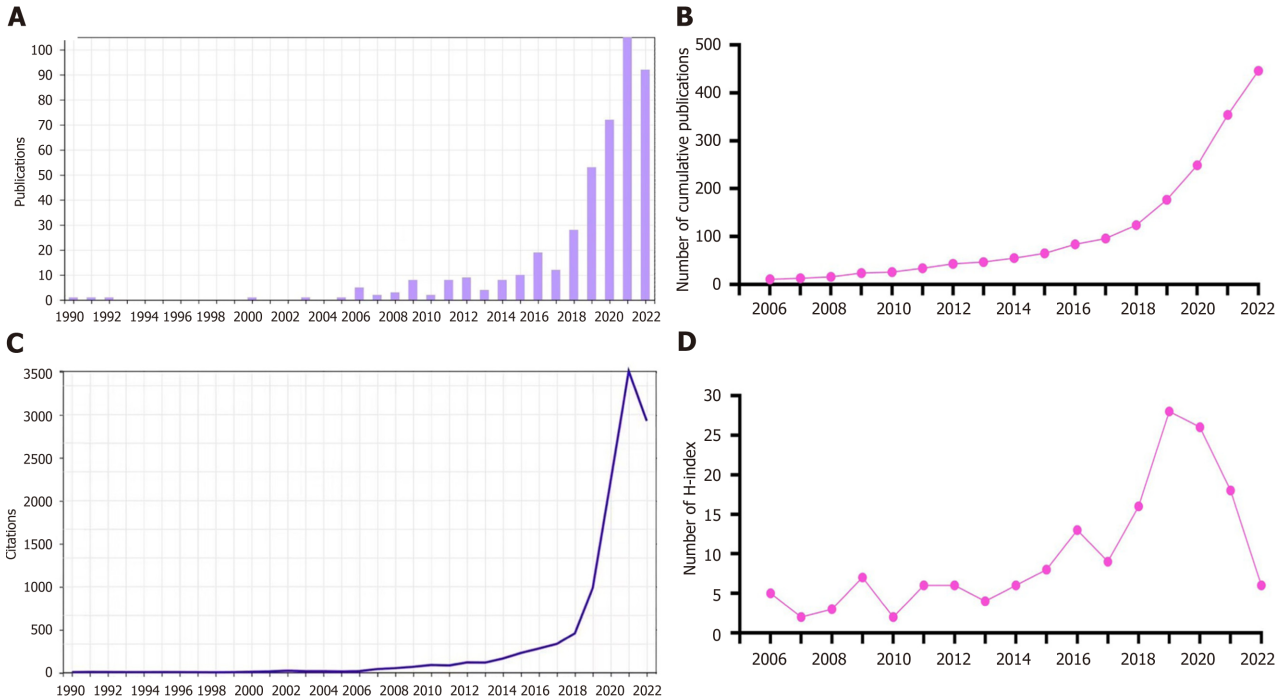
As shown in Figure 1, 3885 papers were enrolled from the Web of Science through our search strategy. At the first stage of selection, 1437 publications were excluded because of publication type, and 88 publications were excluded because of language. The contents of the remaining 2360 articles were carefully assessed. Ultimately, 446 articles meeting the inclusion criteria of this study were included.

Next, we summarized the characteristics of the included articles. The chronological distribution of annual publication numbers from 1990 to 2022 is shown in Figure 2A. The first study we obtained was published in 1990[9]. Less than 10 annual publications were reported in this field before 2015. As depicted in the diagram, the number of publications rapidly increased after 2015, and peaked in 2021, accounting for 23.5% of all publications. Figure 2B displays the cumulative number of publications. The number of annual publications gradually increased after 2013 except for a decrease in 2017. The number of annual citations is shown in Figure 2C, which was relatively low from 1990 to 2010 (below 100 citations for each year). It increased slowly after 2006 and quickly after 2018, remaining at a high number after 2020 (over 2000 citations). The annual H-index is shown in Figure 2D, which was relatively low (< 10) before 2016, but then increased rapidly and peaked at 28 in 2019, followed by a slight decrease from 2020 to 2022.



DOI: 10.3748/wjg.v29.i22.3561 **Copyright** ©The Author(s) 2023.

Figure 1 Flowchart of study enrollment.

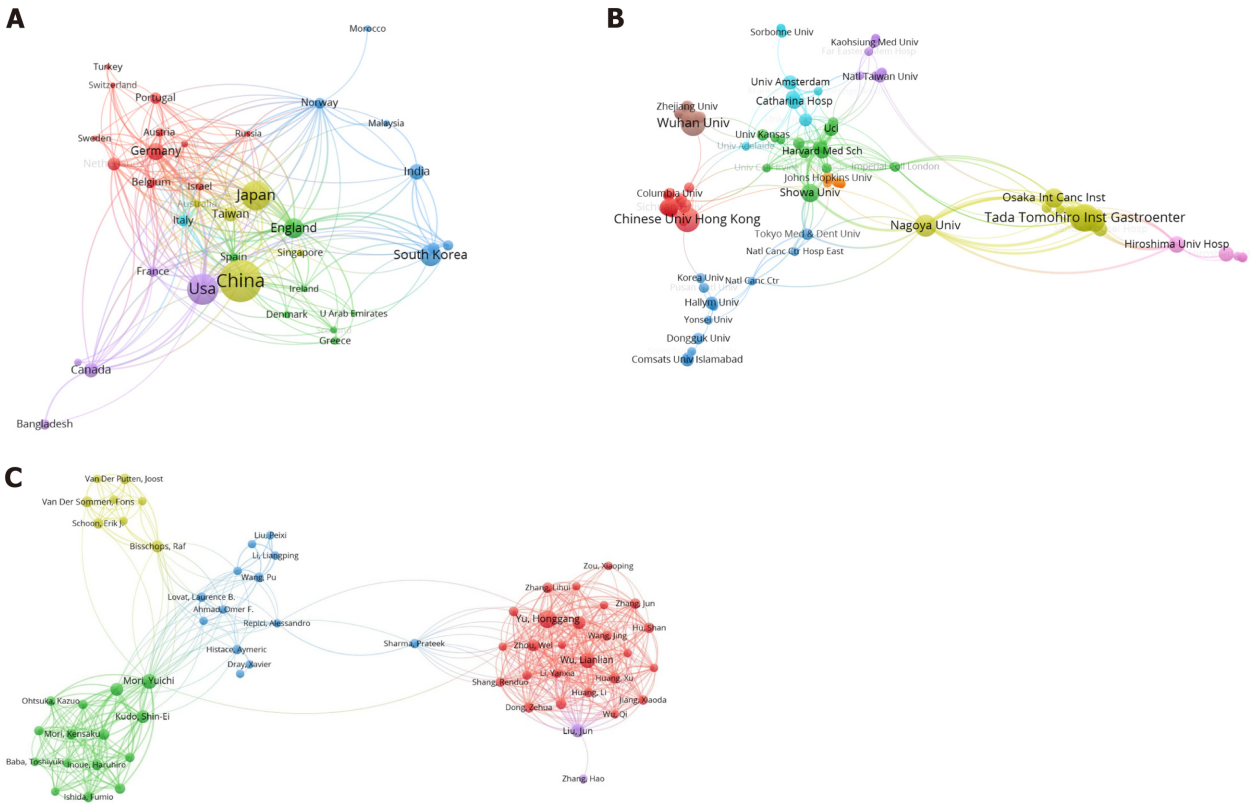


DOI: 10.3748/wjg.v29.i22.3561 **Copyright** ©The Author(s) 2023.

Figure 2 The annual number and H-index values. A: Annual number of published articles; B: Number of annual cumulative articles; C: Global annual number of the publications; D: Annual H-index values of the publications.

Analysis of country, institution and authors

The cooperation network of publication countries is displayed in Figure 3A, including a total of 50 countries and 524 co-operations. Next, the H-index, total citations and publications of the top 10 most productive countries were analyzed and presented in Supplementary Table 1. China emerged as the most productive country with 128 publications, 4089 citations and an H-index of 36. Figure 3B shows the cooperation cluster network of institutions, with a total of 106 institutions and 708 cooperations displayed. These institutions were clustered into different groups according to their cooperations. The top 10 most productive institutions were further analyzed for their publications, citations and H-index, and the results are presented in Supplementary Table 2. The Tada Tomohiro Institute of Gastroenterology and Proctology had the highest number of publications (22), citations (1454), and H-index (17).



DOI: 10.3748/wjg.v29.i22.3561 **Copyright** ©The Author(s) 2023.

Figure 3 Cooperation network. A-C: Cooperation network of countries (A), institutions (B), and authors (C) in the field of artificial intelligence and endoscopy from 1990-2022.

Next, the publications, citations, H-index and co-operations of the 10 most productive authors were also analyzed. A total of 63 authors and 996 co-operations are shown in Figure 3C. As shown in Supplementary Table 3, Tada Tomohiro was the most productive author with 23 publications, an H-index of 17 and 1456 citations, followed by Yu HG, Wu LL, and Ishihara S.

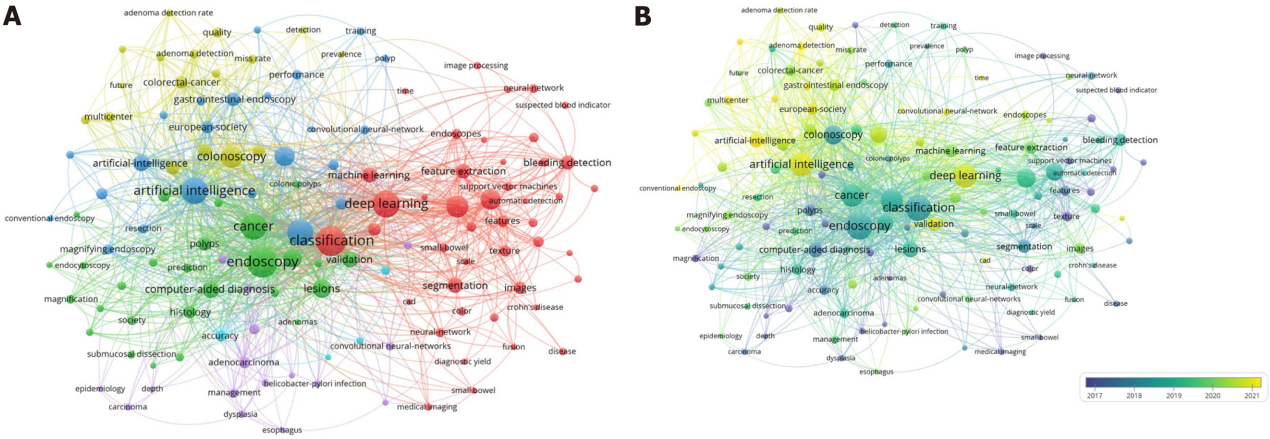
Analysis of keywords and burst detection of publications

To obtain a comprehensive understanding of the popular topics in the realm of AI and endoscopy, a study is conducted utilizing keyword co-occurrence analysis. The analysis involves examining the relevant keywords associated with each paper, based on their titles and abstracts. A total of 131 keywords, appearing at least 5 times, are identified and represented using a bubble graph to visualize citation data. VOSviewer is employed to generate a comprehensive keyword co-occurrence visualization map, where the keywords are grouped into a distinct clusters market with a unique color code. Three categories were identified: AI, deep learning and endoscopy (Figure 4A). The co-occurrence visualization map based on the average year of publication is shown in Figure 4B. "Magnification" and "adenomas" mainly appeared before 2017. The keywords "classification", "endoscopy", and "cancer" became more common after 2017. Keywords colored in yellow are the latest, such as "AI", "deep learning", and "CNN".

Burst detection is a method employed for detecting a sudden surge in the occurrence of novel concepts during a specific period. As shown in Figure 4C, wireless capsule endoscopy ranked first in terms of outbreak intensity (4.83) over the past three decades, followed by color (3.82) and texture (3.82). Computer-assisted diagnosis became the focus of research after 1993. It is worth noting that AI, neoplasia, upper gastrointestinal endoscopy, society, and endoscopic imagine were the strongest bursts since 2022.

Analysis of cocited reference cluster

A network of references that are cocited by publications is referred to as a cocited network. When a group of references are repeatedly cited, it could generate a cluster network diagram (Figure 5A) and a literature cocitation diagram (Figure 5B). The "Pathfinder" and "Pruning Networks" options were utilized to conduct the optimal network. Each node on the network signifies a cited article and the size of it is based on the total cited frequency of pertinent articles. The literature that was cocited was then categorized into 10 major labels: Wireless capsule endoscopy, deep learning, AI, machine learning, CNN, response evaluation, capsule endoscopy, endoscopy imagine, gastrointestinal tract, and small



C

Top 25 keywords with the strongest citation bursts

Key words	Year	Strength	Begin	End	1990-2022
Computer-assisted diagnosis	1992	1.88	1992	2009	
Adenoma	2000	2.01	2000	2016	
Color	2006	3.82	2006	2015	
Ct colonography	2006	3.47	2006	2018	
Support vector machine	2009	3.25	2009	2012	
Capsule endoscopy image	2009	2.44	2009	2011	
Feature selection	2009	2.41	2009	2015	
Magnification	2012	2.74	2012	2016	
Wireless capsule endoscopy	2014	4.83	2014	2019	
Endoscopy	2006	2.04	2015	2017	
Feature	2003	1.95	2015	2020	
Texture	2016	3.82	2016	2019	
Classification	2006	3.76	2016	2018	
System	2008	2.04	2016	2018	
Capsule endoscopy	2008	1.86	2017	2019	
Feature extraction	2011	2.93	2018	2020	
Recognition	2018	2.13	2018	2020	
Impact	2019	1.89	2019	2020	
Artificial intelligence	2017	3.4	2021	2022	
European society	2020	2.1	2021	2022	
Neoplasia	2021	2.09	2021	2022	
Upper gastrointestinal endoscopy	2021	2.09	2021	2022	
Gastrointestinal endoscopy	2008	2.01	2021	2022	
Society	2021	1.83	2021	2022	
Endoscopy image	2021	1.83	2021	2022	

DOI: 10.3748/wjg.v29.i22.3561 **Copyright** ©The Author(s) 2023.

Figure 4 Co-occurrence map. A and B: Co-occurrence map based on keywords; C: Top 25 keywords with the strongest citation bursts.

bowel (Figure 5A). Figure 5B shows a timeline view of distinct cocitations. Deep learning, CNN and response evaluation have always been popular research topics. Wireless capsule endoscopy, AI, and machine learning have been popular research topics since 2000.

Analysis of the most cited studies

Table 1 shows the specifics of the 10 most cited studies from 1990 to 2022. Each study was cited between 145 and 323 times. Three of these studies were published in *Gastroenterology*, and the remaining 7 studies were published in *Gastric Cancer*, *GUT*, *Gastrointestinal Endoscopy*, *IEEE Journal of Biomedical, Health Informatics*, *Lancet Gastroenterology*, and *Hepatology*. The most cited article was the application of AI using a CNN for detecting gastric cancer in endoscopic images. Five articles focused on AI applied in the detection of polyps. Another 5 articles focused on AI applied in cancer detection.

Research trends in AI applied in disease diagnosis

The proportion of the number of diseases in the field of AI and endoscopy was counted. As shown in Figure 5C, gastrointestinal polyps accounted for the largest proportion of disease in this area (14.6%), followed by gastric cancer (13.5%). The proportion of the endoscopy type was also counted. As shown in Figure 5D, conventional endoscopy accounted for the largest proportion in this area (42.3%), followed

Table 1 Top 10 most cited articles in the field of AI and endoscopy from 1990-2022

Rank	Journal	Title	Citations of Web of Science	Affiliations	Ref.
1	*Gastric Cancer* 2018; 21: 653-660	Application of artificial intelligence using a convolutional neural network for detecting gastric cancer in endoscopic images	323	Tada Tomohiro Inst Gastroenterol and Proctol, Saitama, Japan	Hirasawa *et al* [26], 2018
2	*GUT* 2019; 68: 1813-1819	Real-time automatic detection system increases colonoscopic polyp and adenoma detection rates: A prospective randomised controlled study	307	Sichuan Provincial People's Hospital, China	Wang *et al* [23], 2019
3	*Annals of Internal Medicine* 2018; 169: 357-366	Real-Time Use of Artificial Intelligence in Identification of Diminutive Polyps During Colonoscopy A Prospective Study	227	Showa University, Japan	Mori *et al*[39], 2018
4	*Gastroenterology* 2018; 154: 568-575	Accurate Classification of Diminutive Colorectal Polyps Using Computer-Aided Analysis	208	Triservice General Hospital, National Defense Medical Center, Taiwan	Chen *et al*[40], 2018
5	*Gastrointestinal Endoscopy* 2019; 89: 25-32	Diagnostic outcomes of esophageal cancer by artificial intelligence using convolutional neural networks	194	Japanese Foundation for Cancer Research, Japan	Horie *et al* [28], 2019
6	*IEEE Journal of Biomedical and Health Informatics* 2017; 21: 41-47	Automatic Detection and Classification of Colorectal Polyps by Transferring Low-Level CNN Features From Nonmedical Domain	191	Chinese University of Hong Kong, China	Zhang *et al* [35], 2017
7	*Gastroenterology* 2013; 144: 81-91	Real-Time Optical Biopsy of Colon Polyps With Narrow Band Imaging in Community Practice Does Not Yet Meet Key Thresholds for Clinical Decisions	169	Stanford University, United States	Ladabaum *et al*[41], 2013
8	*Gastroenterology* 2020; 159: 512-520	Efficacy of Real-Time Computer-Aided Detection of Colorectal Neoplasia in a Randomized Trial	155	Humanitas University, IRCCS Humanitas Research Hospital, Italy	Repici *et al* [42], 2020
9	*Gastrointestinal Endoscopy* 2019; 89: 806-815	Application of convolutional neural network in the diagnosis of the invasion depth of gastric cancer based on conventional endoscopy	150	Fudan University, China	Zhu *et al*[43], 2019
10	*Lancet Gastroenterology and Hepatology* 2020; 5: 343-351	Effect of a deep-learning computer-aided detection system on adenoma detection during colonoscopy (CADe-DB trial): a double-blind randomised study	145	Sichuan Provincial People's Hospital, China	Wang *et al* [44], 2020

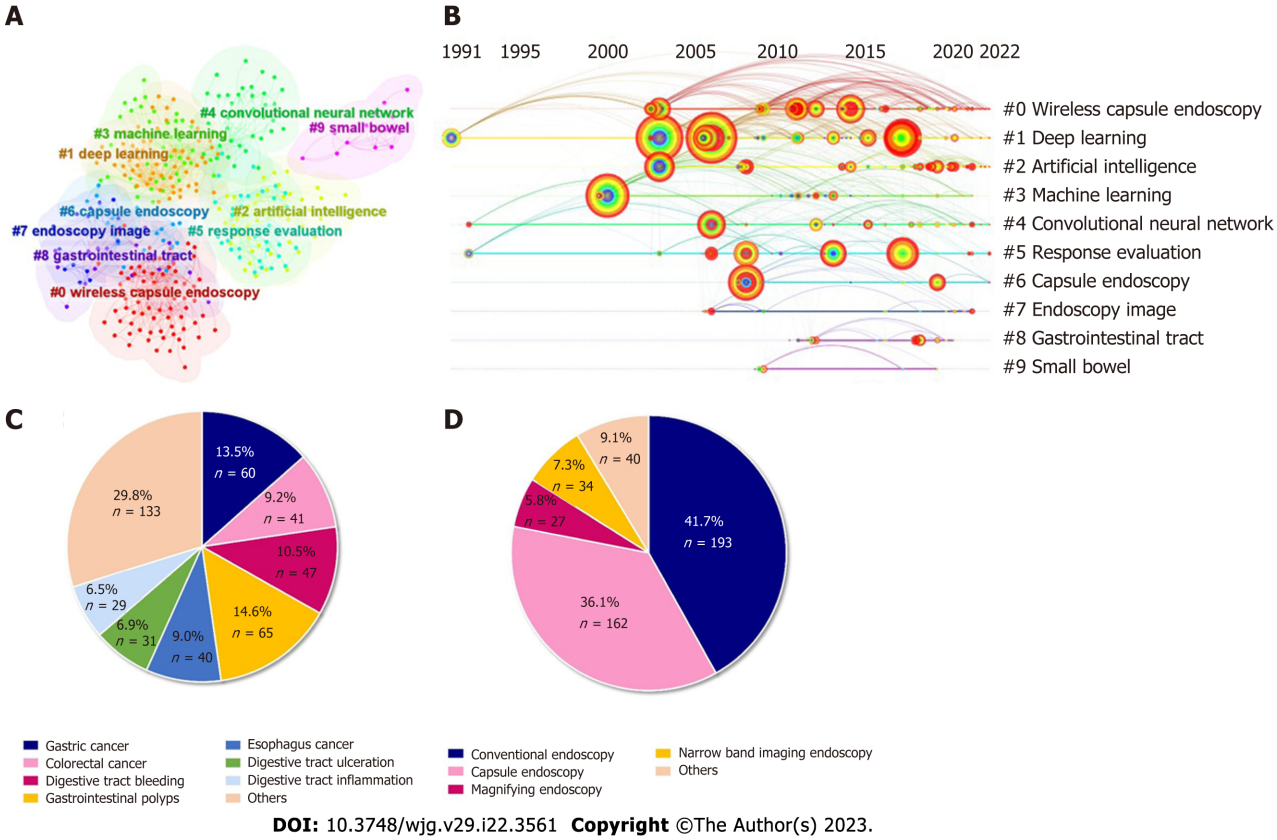
by capsule endoscopy (35.5%).

We further analyzed the temporal variation in the diagnostic performance of AI-assisted endoscopy for digestive diseases. The sensitivity, specificity and accuracy of AI-assisted endoscopy in Barrett's esophagus, gastric cancer and polyps are shown in Figure 6A-C. For Barrett's esophagus, the studies published in 2018 showed the highest sensitivity (97.0%), specificity (88.0%) and accuracy (92.0%). The weighted average sensitivity, specificity and accuracy of AI in detecting Barrett's esophagus from 2018 to 2021 were 90.4%, 84.0%, and 87.6%, respectively. In terms of gastric cancer, the studies in 2019 showed the highest accuracy (90.8%) and specificity (93.3%), and the studies in 2020 showed the highest sensitivity (92.3%). The weighted average sensitivity, specificity and accuracy of AI in detecting gastric cancer from 2019 to 2022 are 82.8%, 89.8%, and 88.3%, respectively. For detecting colorectal polyps, the studies in 2019 showed the highest sensitivity (97.1%), the studies in 2022 showed the highest specificity (97.7%), and 2021 showed the highest accuracy (96.9%). The weighted average sensitivity, specificity and accuracy of AI in detecting polyps from 2019 to 2022 are 89.6%, 82.1% and 93.7%, respectively. As shown in Figure 6D-E, the detection rate of gastrointestinal bleeding remained stable above 95% from 2018 to 2021 (weighted average: 96.2%). The adenoma detection rate remained stable at approximately 29% from 2018 to 2020. A higher detection rate (46.2%) was achieved in 2022 (weighted average: 31.3%).

DISCUSSION

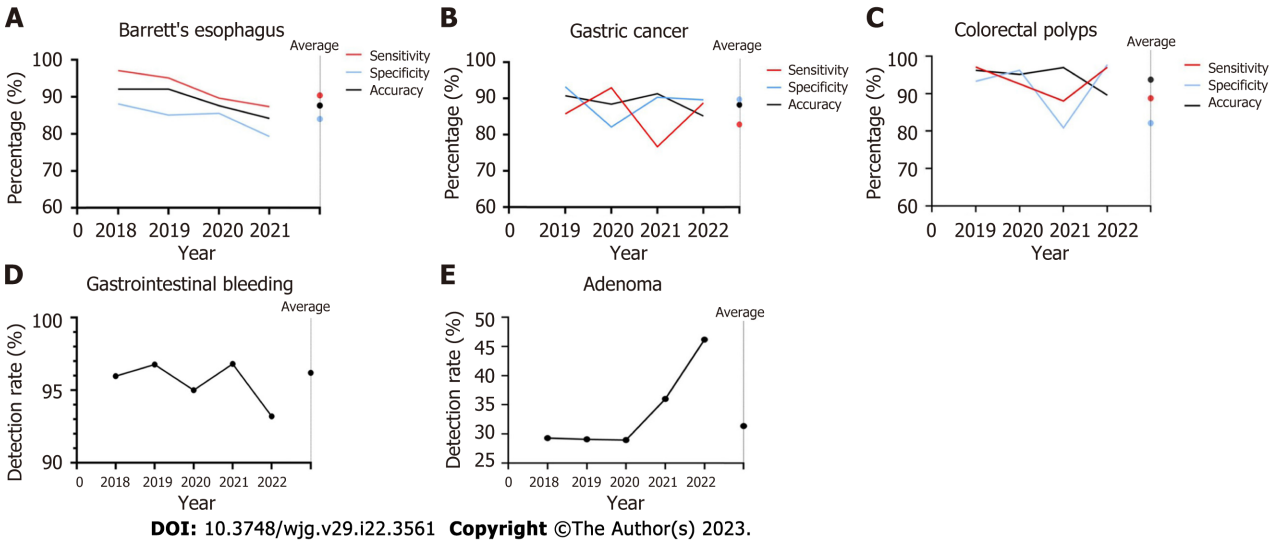
To the best of our knowledge, this is the first bibliometric analysis to comprehensively illustrate the application of AI-assisted digestive endoscopy in digestive diseases. A basic literature analysis was performed, as well as a subgroup analysis of AI-assisted digestive endoscopy in diagnosing various diseases.

The term "AI" was first proposed in 1956[13]. Cortes *et al*[14] suggested the first algorithm for pattern recognition 60 years ago. In 2006, a fast-learning algorithm for deep belief networks was proposed[15].



DOI: 10.3748/wjg.v29.i22.3561 **Copyright** ©The Author(s) 2023.

Figure 5 Diagrams. A: Cluster network diagrams; B: Literature cocitation diagrams; C and D: Proportion of the number of diseases (C) and endoscopy type (D) in the field of AI and endoscopy.



DOI: 10.3748/wjg.v29.i22.3561 **Copyright** ©The Author(s) 2023.

Figure 6 Temporal variation in the diagnostic performance of artificial intelligence-assisted endoscopy for digestive diseases. A-C: Temporal variation in the sensitivity, specificity and accuracy of artificial intelligence (AI)-assisted endoscopy in Barrett's esophagus (A), gastric cancer (B), and polyps (C); D and E: Temporal variation in the detection rate of AI-assisted endoscopy in bleeding (D) and adenoma (E).

Since then, the number of publications and citations in this field has risen steadily. Machine learning is one of the fastest growing areas of technology[16]. Deep learning is an important branch of machine learning and is further divided into deep neural networks, recurrent neural networks and CNNs[17]. The best results were achieved by CNN in the field of image analysis[18]. In this study, we analyzed the most influential authors, institutions and countries regarding AI and endoscopy. Among these countries, China had the largest number of publications, citations and H-index. Moreover, China, United States, and Japan are the centers of the co-occurrence map. Wireless capsule endoscopy is one of

the most effective endoscopic techniques used in the examination of gastrointestinal diseases such as polyps and ulcers[19] and has been a research hot spot and topic since 2014.

AI-assisted endoscopy for disease detection covers almost all endoscopy in the field of digestive endoscopy. Colorectal cancer is the world's fourth most deadly cancer, with almost 900000 deaths annually[20]. AI-assisted colonoscopy has broad prospects in the screening and diagnosis of colorectal cancer. In our study, colorectal cancer accounted for 9.19% of the total disease. Urban *et al*[21] showed excellent performance in AI-assisted colonoscopy studies using CNN based on the deep learning method. The CNN identified polyps with an accuracy of 96.4%. Similarly, Shin *et al*[22] compared two different approaches named the hand-crafted feature method and CNN based on the deep learning method, and the results demonstrated that the CNN-based deep learning framework had better performance for detecting polyps, achieving over 90% accuracy, sensitivity, and specificity. The detection rate of adenoma reflects the quality of colonoscopy. A prospective cohort study was conducted to develop an automatic polyp detection system based on deep learning, and the detection rate of polyps and adenomas could be improved from 29% to 45% and 20% to 29%, respectively[23]. Wang *et al*[24] also studied the development and validation of a deep-learning algorithm for the detection of polyps during colonoscopy, which proved that AI could assist endoscopists efficiently in discovering colorectal adenomas and polyps with high accuracy (per-image sensitivity: 94.4%, per-image specificity: 95.5%). Moreover, Pfeifer *et al*[25] evaluated a newly developed deep CNN with a large sample size (15534 test images), and the deep CNN's sensitivity and specificity for detecting polyps were 90% and 80%, respectively.

Gastric cancer, Barrett's esophagus and *Helicobacter pylori* (*H. pylori*) infection are common upper gastrointestinal diseases. Hirasawa *et al*[26] first reported that AI using a CNN applied in conventional endoscopic images could achieve a diagnostic sensitivity of 92% for gastric cancer in 2018. It is worth noting that the CNN system only required 47 s to analyze 2296 images, which is faster than analyses completed by endoscopists. Ikenoyama *et al*[27] constructed a CNN to detect early gastric cancer with 2940 test samples, and the sensitivity was 58.4%. The prognosis of esophageal cancer is relatively poor. The first report of AI-assisted endoscopy applied in the diagnosis of esophageal cancer was conducted by Horie *et al*[28]. A CNN was trained to diagnose esophageal cancer using 8284 conventional endoscopic images, and eventually, high sensitivity and accuracy were achieved. The weighted average specificity of AI in detecting Barrett's esophagus from 2018 to 2021 was 84.0%. In 2020, a study with 20 samples achieved a specificity of 85.5%[29]. Another study in the same year with a sample size of 100 achieved a specificity of 78%[30]. *H. pylori* is the main pathogenic factor of gastric diseases. Shichijo *et al*[31] reported 89% sensitivity and 87% specificity for the diagnosis of *H. pylori* infection using CNN, and the diagnostic accuracy was significantly higher than that achieved by endoscopists. A consistent result was also achieved by another study[32].

Many studies have shown that cooperation between AI and endoscopists could improve the diagnostic ability to diagnose gastrointestinal diseases. Ikenoyama *et al*[27] compared the performance of endoscopists with an AI classifier based on CNN in detecting early gastric cancer through 2940 test images. Eventually, the results showed that AI had a significantly higher sensitivity than endoscopists. Niikura *et al*[33] obtained similar results in another study, and the diagnostic rate of gastric cancer per image in the AI group was higher than that in the group of experts. Yen *et al*[34] showed a higher accuracy of AI than experts in detecting peptic ulcer bleeding. Zhang *et al*[35] compared a CNN-based image recognition system with visual inspection by endoscopists in identifying polyps. The results showed a significant improvement in accuracy with the application of AI.

Certain limitations existed regarding the use of AI. First, algorithm performance could be different when using endoscopy equipment manufactured by different companies[23,24]. Second, as AI algorithms are highly dependent on the integrity of the database, the number of training images might result in a different diagnostic ability of AI[26]. Third, data privacy and security considerations are also critical, which could be of great concern to endoscopists[36,37]. The potential ethical and legal issues of this technology in clinical application should not be underestimated.

A bibliometric analysis was previously conducted to examine AI applied in digestive endoscopy[38]. A basic analysis of bibliometric indicators was performed. Our study recorded the data of each article in detail. We also analyze the effectiveness of AI-assisted endoscopy in disease detection, specific analysis of digestive endoscopy, and gastrointestinal diseases and evaluate the accuracy of AI.

Our study aimed to provide a comprehensive analysis of AI applied in diagnostic endoscopy: (1) The emergence of deep belief networks contributed to an increase in research in this field; (2) the intelligent detection and recognition of colorectal polyps is the most concerning and researched area at present; (3) capsule endoscopy is one of the most influential keywords; (4) the accuracy of AI in detecting Barrett's esophagus, colorectal polyps and gastric cancer from 2018 to 2022 is 88.08%, 93.71%, and 88.29%, respectively, and the detection rates of adenoma and gastrointestinal bleeding from 2018 to 2022 are 31.38% and 96.20%, respectively; and (5) AI-assisted digestive endoscopy could improve the diagnosis rate of endoscopists in disease detection, and CNN-based diagnosis programs for endoscopic images showed promising results. However, there are some limitations which existed in this study. First, the search for publications was limited to the Web of Science core collection database, which may result in incomplete literature searches of other databases. Second, a number of studies that were not in English might be missed. Third, several bias may affect the results, such as publication bias.

CONCLUSION

In conclusion, AI could improve the detection rate of digestive tract diseases and has been applied widely in the field of endoscopy. Multicenter prospective studies with larger samples should be conducted in the future to further explore the accuracy of AI based on different methods.

ARTICLE HIGHLIGHTS

Research background

Recently, artificial intelligence (AI) has been widely used in gastrointestinal endoscopy examinations.

Research motivation

More than 100 million subjects receive gastrointestinal endoscopy examinations each year. It is of great importance to improve the quality of endoscopy examinations to discover the lesions. With the development of AI, it has been extensively used in gastrointestinal endoscopy examinations.

Research objectives

To provide a comprehensive analysis of AI applied in diagnostic endoscopy.

Research methods

Relevant publications from the Web of Science published from 1990 to 2022 were extracted using a combination of the search terms "AI" and "endoscopy".

Research results

AI-assisted digestive endoscopy could improve the diagnosis rate of endoscopists in disease detection, and convolutional neural network-based diagnosis programs for endoscopic images showed promising results.

Research conclusions

AI could improve the detection rate of digestive tract diseases and has been applied widely in the field of endoscopy. Multicenter prospective studies with larger samples should be conducted in the future to further explore the accuracy of AI based on different methods.

Research perspectives

Gastrointestinal cancers seriously threaten the health of global populations. Gastrointestinal tumors diagnosed at an early stage had a better prognosis than those diagnosed at a late stage. AI represents a fundamental breakthrough in the field of diagnostic endoscopy by assisting endoscopists with the detection of gastrointestinal tumors and it has been extensively used in gastrointestinal endoscopy examinations.

FOOTNOTES

Author contributions: Du RC and Ouyang YB performed the literature search and collected the data; Du RC performed the statistical analysis and wrote the manuscript; Hu Y designed the study, conceived and revised the manuscript; and all authors contributed to the article and approved the final manuscript.

Supported by the National Natural Science Foundation of China, No. 82000531; Project for Academic and Technical Leaders of Major Disciplines in Jiangxi Province, No. 20212BCJL23065; Key Research and Development Program of Jiangxi Province, No. 20212BBG73018; and Youth Project of the Jiangxi Natural Science Foundation, No. 20202BABL216006.

Conflict-of-interest statement: The authors declare having no conflicts of interest.

PRISMA 2009 Checklist statement: The authors have read the PRISMA 2009 Checklist, and the manuscript was prepared and revised according to the PRISMA 2009 Checklist.

Open-Access: This article is an open-access article that was selected by an in-house editor and fully peer-reviewed by external reviewers. It is distributed in accordance with the Creative Commons Attribution NonCommercial (CC BY-NC 4.0) license, which permits others to distribute, remix, adapt, build upon this work non-commercially, and license their derivative works on different terms, provided the original work is properly cited and the use is non-commercial. See: https://creativecommons.org/Licenses/by-nc/4.0/

Country/Territory of origin: China

ORCID number: Ren-Chun Du 0009-0008-8337-9031; Yao-Bin Ouyang 0000-0002-0248-1907; Yi Hu 0000-0003-2708-7612.

S-Editor: Chen YL
L-Editor: Filipodia
P-Editor: Zhang YL

REFERENCES

1 **Arnold M**, Abnet CC, Neale RE, Vignat J, Giovannucci EL, McGlynn KA, Bray F. Global Burden of 5 Major Types of Gastrointestinal Cancer. *Gastroenterology* 2020; **159**: 335-349.e15 [PMID: 32247694 DOI: 10.1053/j.gastro.2020.02.068]
2 **Hassan C**, Spadaccini M, Iannone A, Maselli R, Jovani M, Chandrasekar VT, Antonelli G, Yu H, Areia M, Dinis-Ribeiro M, Bhandari P, Sharma P, Rex DK, Rösch T, Wallace M, Repici A. Performance of artificial intelligence in colonoscopy for adenoma and polyp detection: a systematic review and meta-analysis. *Gastrointest Endosc* 2021; **93**: 77-85.e6 [PMID: 32598963 DOI: 10.1016/j.gie.2020.06.059]
3 **Esteva A**, Kuprel B, Novoa RA, Ko J, Swetter SM, Blau HM, Thrun S. Dermatologist-level classification of skin cancer with deep neural networks. *Nature* 2017; **542**: 115-118 [PMID: 28117445 DOI: 10.1038/nature21056]
4 **Bibault JE**, Giraud P, Burgun A. Big Data and machine learning in radiation oncology: State of the art and future prospects. *Cancer Lett* 2016; **382**: 110-117 [PMID: 27241666 DOI: 10.1016/j.canlet.2016.05.033]
5 **Gulshan V**, Peng L, Coram M, Stumpe MC, Wu D, Narayanaswamy A, Venugopalan S, Widner K, Madams T, Cuadros J, Kim R, Raman R, Nelson PC, Mega JL, Webster DR. Development and Validation of a Deep Learning Algorithm for Detection of Diabetic Retinopathy in Retinal Fundus Photographs. *JAMA* 2016; **316**: 2402-2410 [PMID: 27898976 DOI: 10.1001/jama.2016.17216]
6 **Misawa M**, Kudo SE, Mori Y, Takeda K, Maeda Y, Kataoka S, Nakamura H, Kudo T, Wakamura K, Hayashi T, Katagiri A, Baba T, Ishida F, Inoue H, Nimura Y, Oda M, Mori K. Accuracy of computer-aided diagnosis based on narrow-band imaging endocytoscopy for diagnosing colorectal lesions: comparison with experts. *Int J Comput Assist Radiol Surg* 2017; **12**: 757-766 [PMID: 28247214 DOI: 10.1007/s11548-017-1542-4]
7 **Messmann H**, Bisschops R, Antonelli G, Libânio D, Sinonquel P, Abdelrahim M, Ahmad OF, Areia M, Bergman JJGHM, Bhandari P, Boskoski I, Dekker E, Domagk D, Ebigbo A, Eelbode T, Eliakim R, Häfner M, Haidry RJ, Jover R, Kaminski MF, Kuvaev R, Mori Y, Palazzo M, Repici A, Rondonotti E, Rutter MD, Saito Y, Sharma P, Spada C, Spadaccini M, Veitch A, Gralnek IM, Hassan C, Dinis-Ribeiro M. Expected value of artificial intelligence in gastrointestinal endoscopy: European Society of Gastrointestinal Endoscopy (ESGE) Position Statement. *Endoscopy* 2022; **54**: 1211-1231 [PMID: 36270318 DOI: 10.1055/a-1950-5694]
8 **Min JK**, Kwak MS, Cha JM. Overview of Deep Learning in Gastrointestinal Endoscopy. *Gut Liver* 2019; **13**: 388-393 [PMID: 30630221 DOI: 10.5009/gnl18384]
9 **Williams CB**, Baillie J, Gillies DF, Borislow D, Cotton PB. Teaching gastrointestinal endoscopy by computer simulation: a prototype for colonoscopy and ERCP. *Gastrointest Endosc* 1990; **36**: 49-54 [PMID: 2311883 DOI: 10.1016/s0016-5107(90)70923-6]
10 **Ouyang Y**, Zhu Z, Huang L, Zeng C, Zhang L, Wu WK, Lu N, Xie C. Research Trends on Clinical Helicobacter pylori Eradication: A Bibliometric Analysis from 1983 to 2020. *Helicobacter* 2021; **26**: e12835 [PMID: 34258827 DOI: 10.1111/hel.12835]
11 **Palacios-Marqués AM**, Carratala-Munuera C, Martínez-Escoriza JC, Gil-Guillen VF, Lopez-Pineda A, Quesada JA, Orozco-Beltrán D. Worldwide scientific production in obstetrics: a bibliometric analysis. *Ir J Med Sci* 2019; **188**: 913-919 [PMID: 30627959 DOI: 10.1007/s11845-018-1954-3]
12 **Chen C**, Dubin R, Kim MC. Emerging trends and new developments in regenerative medicine: a scientometric update (2000 - 2014). *Expert Opin Biol Ther* 2014; **14**: 1295-1317 [PMID: 25077605 DOI: 10.1517/14712598.2014.920813]
13 **McCarthy J**, Minsky ML, Shannon CE. A proposal for the Dartmouth summer research project on artificial intelligence-August 31, 1955. *Ai Magazine* 2006; **27**: 12-14 [DOI: 10.1609/aimag.v27i4.1904]
14 **Cortes C**, Vapnik V. Support-vector networks. *Machine Learning* 1995; **20**: 273-297 [DOI: 10.1023/A:1022627411411]
15 **Hinton GE**, Osindero S, Teh YW. A fast learning algorithm for deep belief nets. *Neural Comput* 2006; **18**: 1527-1554 [PMID: 16764513 DOI: 10.1162/neco.2006.18.7.1527]
16 **Jordan MI**, Mitchell TM. Machine learning: Trends, perspectives, and prospects. *Science* 2015; **349**: 255-260 [PMID: 26185243 DOI: 10.1126/science.aaa8415]
17 **Yang YJ**, Bang CS. Application of artificial intelligence in gastroenterology. *World J Gastroenterol* 2019; **25**: 1666-1683 [PMID: 31011253 DOI: 10.3748/wjg.v25.i14.1666]
18 **Ahmad OF**, Soares AS, Mazomenos E, Brandao P, Vega R, Seward E, Stoyanov D, Chand M, Lovat LB. Artificial intelligence and computer-aided diagnosis in colonoscopy: current evidence and future directions. *Lancet Gastroenterol Hepatol* 2019; **4**: 71-80 [PMID: 30527583 DOI: 10.1016/S2468-1253(18)30282-6]
19 **Iddan G**, Meron G, Glukhovsky A, Swain P. Wireless capsule endoscopy. *Nature* 2000; **405**: 417 [PMID: 10839527 DOI: 10.1038/35013140]
20 **Dekker E**, Tanis PJ, Vleugels JLA, Kasi PM, Wallace MB. Colorectal cancer. *Lancet* 2019; **394**: 1467-1480 [PMID: 31631858 DOI: 10.1016/S0140-6736(19)32319-0]
21 **Urban G**, Tripathi P, Alkayali T, Mittal M, Jalali F, Karnes W, Baldi P. Deep Learning Localizes and Identifies Polyps in Real Time With 96% Accuracy in Screening Colonoscopy. *Gastroenterology* 2018; **155**: 1069-1078.e8 [PMID: 29928897 DOI: 10.1053/j.gastro.2018.06.037]

22 **Shin Y**, Balasingham I, Ieee. Comparison of Hand-craft Feature based SVM and CNN based Deep Learning Framework for Automatic Polyp Classification. In: 39th Annual International Conference of the IEEE-Engineering-in-Medicine-and-Biology-Society (EMBC). South Korea, 2017: 3277-3280 [DOI: 10.1109/EMBC.2017.8037556]

23 **Wang P**, Berzin TM, Glissen Brown JR, Bharadwaj S, Becq A, Xiao X, Liu P, Li L, Song Y, Zhang D, Li Y, Xu G, Tu M, Liu X. Real-time automatic detection system increases colonoscopic polyp and adenoma detection rates: a prospective randomised controlled study. *Gut* 2019; **68**: 1813-1819 [PMID: 30814121 DOI: 10.1136/gutjnl-2018-317500]

24 **Wang P**, Xiao X, Glissen Brown JR, Berzin TM, Tu M, Xiong F, Hu X, Liu P, Song Y, Zhang D, Yang X, Li L, He J, Yi X, Liu J, Liu X. Development and validation of a deep-learning algorithm for the detection of polyps during colonoscopy. *Nat Biomed Eng* 2018; **2**: 741-748 [PMID: 31015647 DOI: 10.1038/s41551-018-0301-3]

25 **Pfeifer L**, Neufert C, Leppkes M, Waldner MJ, Häfner M, Beyer A, Hoffman A, Siersema PD, Neurath MF, Rath T. Computer-aided detection of colorectal polyps using a newly generated deep convolutional neural network: from development to first clinical experience. *Eur J Gastroenterol Hepatol* 2021; **33**: e662-e669 [PMID: 34034272 DOI: 10.1097/MEG.0000000000002209]

26 **Hirasawa T**, Aoyama K, Tanimoto T, Ishihara S, Shichijo S, Ozawa T, Ohnishi T, Fujishiro M, Matsuo K, Fujisaki J, Tada T. Application of artificial intelligence using a convolutional neural network for detecting gastric cancer in endoscopic images. *Gastric Cancer* 2018; **21**: 653-660 [PMID: 29335825 DOI: 10.1007/s10120-018-0793-2]

27 **Ikenoyama Y**, Hirasawa T, Ishioka M, Namikawa K, Yoshimizu S, Horiuchi Y, Ishiyama A, Yoshio T, Tsuchida T, Takeuchi Y, Shichijo S, Katayama N, Fujisaki J, Tada T. Detecting early gastric cancer: Comparison between the diagnostic ability of convolutional neural networks and endoscopists. *Dig Endosc* 2021; **33**: 141-150 [PMID: 32282110 DOI: 10.1111/den.13688]

28 **Horie Y**, Yoshio T, Aoyama K, Yoshimizu S, Horiuchi Y, Ishiyama A, Hirasawa T, Tsuchida T, Ozawa T, Ishihara S, Kumagai Y, Fujishiro M, Maetani I, Fujisaki J, Tada T. Diagnostic outcomes of esophageal cancer by artificial intelligence using convolutional neural networks. *Gastrointest Endosc* 2019; **89**: 25-32 [PMID: 30120958 DOI: 10.1016/j.gie.2018.07.037]

29 **Waterhouse DJ**, Januszewicz W, Ali S, Fitzgerald RC, di Pietro M, Bohndiek SE. Spectral Endoscopy Enhances Contrast for Neoplasia in Surveillance of Barrett's Esophagus. *Cancer Res* 2021; **81**: 3415-3425 [PMID: 34039635 DOI: 10.1158/0008-5472.CAN-21-0474]

30 **Struyvenberg MR**, de Groof AJ, van der Putten J, van der Sommen F, Baldaque-Silva F, Omae M, Pouw R, Bisschops R, Vieth M, Schoon EJ, Curvers WL, de With PH, Bergman JJ. A computer-assisted algorithm for narrow-band imaging-based tissue characterization in Barrett's esophagus. *Gastrointest Endosc* 2021; **93**: 89-98 [PMID: 32504696 DOI: 10.1016/j.gie.2020.05.050]

31 **Shichijo S**, Nomura S, Aoyama K, Nishikawa Y, Miura M, Shinagawa T, Takiyama H, Tanimoto T, Ishihara S, Matsuo K, Tada T. Application of Convolutional Neural Networks in the Diagnosis of Helicobacter pylori Infection Based on Endoscopic Images. *EBioMedicine* 2017; **25**: 106-111 [PMID: 29056541 DOI: 10.1016/j.ebiom.2017.10.014]

32 **Itoh T**, Kawahira H, Nakashima H, Yata N. Deep learning analyzes Helicobacter pylori infection by upper gastrointestinal endoscopy images. *Endosc Int Open* 2018; **6**: E139-E144 [PMID: 29399610 DOI: 10.1055/s-0043-120830]

33 **Niikura R**, Aoki T, Shichijo S, Yamada A, Kawahara T, Kato Y, Hirata Y, Hayakawa Y, Suzuki N, Ochi M, Hirasawa T, Tada T, Kawai T, Koike K. Artificial intelligence versus expert endoscopists for diagnosis of gastric cancer in patients who have undergone upper gastrointestinal endoscopy. *Endoscopy* 2022; **54**: 780-784 [PMID: 34607377 DOI: 10.1055/a-1660-6500]

34 **Yen HH**, Wu PY, Su PY, Yang CW, Chen YY, Chen MF, Lin WC, Tsai CL, Lin KP. Performance Comparison of the Deep Learning and the Human Endoscopist for Bleeding Peptic Ulcer Disease. *J Med Biol Eng* 2021; **41**: 504-513 [DOI: 10.1007/s40846-021-00608-0]

35 **Zhang R**, Zheng Y, Mak TW, Yu R, Wong SH, Lau JY, Poon CC. Automatic Detection and Classification of Colorectal Polyps by Transferring Low-Level CNN Features From Nonmedical Domain. *IEEE J Biomed Health Inform* 2017; **21**: 41-47 [PMID: 28114040 DOI: 10.1109/JBHI.2016.2635662]

36 **Hickman SE**, Baxter GC, Gilbert FJ. Adoption of artificial intelligence in breast imaging: evaluation, ethical constraints and limitations. *Br J Cancer* 2021; **125**: 15-22 [PMID: 33772149 DOI: 10.1038/s41416-021-01333-w]

37 **Ngiam KY**, Khor IW. Big data and machine learning algorithms for health-care delivery. *Lancet Oncol* 2019; **20**: e262-e273 [PMID: 31044724 DOI: 10.1016/S1470-2045(19)30149-4]

38 **Gan PL**, Huang S, Pan X, Xia HF, Lü MH, Zhou X, Tang XW. The scientific progress and prospects of artificial intelligence in digestive endoscopy: A comprehensive bibliometric analysis. *Medicine (Baltimore)* 2022; **101**: e31931 [PMID: 36451438 DOI: 10.1097/MD.0000000000031931]

39 **Mori Y**, Kudo SE, Misawa M, Saito Y, Ikematsu H, Hotta K, Ohtsuka K, Urushibara F, Kataoka S, Ogawa Y, Maeda Y, Takeda K, Nakamura H, Ichimasa K, Kudo T, Hayashi T, Wakamura K, Ishida F, Inoue H, Itoh H, Oda M, Mori K. Real-Time Use of Artificial Intelligence in Identification of Diminutive Polyps During Colonoscopy: A Prospective Study. *Ann Intern Med* 2018; **169**: 357-366 [PMID: 30105375 DOI: 10.7326/M18-0249]

40 **Chen PJ**, Lin MC, Lai MJ, Lin JC, Lu HH, Tseng VS. Accurate Classification of Diminutive Colorectal Polyps Using Computer-Aided Analysis. *Gastroenterology* 2018; **154**: 568-575 [PMID: 29042219 DOI: 10.1053/j.gastro.2017.10.010]

41 **Ladabaum U**, Fioritto A, Mitani A, Desai M, Kim JP, Rex DK, Imperiale T, Gunaratnam N. Real-time optical biopsy of colon polyps with narrow band imaging in community practice does not yet meet key thresholds for clinical decisions. *Gastroenterology* 2013; **144**: 81-91 [PMID: 23041328 DOI: 10.1053/j.gastro.2012.09.054]

42 **Repici A**, Badalamenti M, Maselli R, Correale L, Radaelli F, Rondonotti E, Ferrara E, Spadaccini M, Alkandari A, Fugazza A, Anderloni A, Galtieri PA, Pellegatta G, Carrara S, Di Leo M, Craviotto V, Lamonaca L, Lorenzetti R, Andrealli A, Antonelli G, Wallace M, Sharma P, Rosch T, Hassan C. Efficacy of Real-Time Computer-Aided Detection of Colorectal Neoplasia in a Randomized Trial. *Gastroenterology* 2020; **159**: 512-520.e7 [PMID: 32371116 DOI: 10.1053/j.gastro.2020.04.062]

43 **Zhu Y**, Wang QC, Xu MD, Zhang Z, Cheng J, Zhong YS, Zhang YQ, Chen WF, Yao LQ, Zhou PH, Li QL. Application of convolutional neural network in the diagnosis of the invasion depth of gastric cancer based on conventional endoscopy.

Gastrointest Endosc 2019; **89**: 806-815.e1 [PMID: 30452913 DOI: 10.1016/j.gie.2018.11.011]

44 **Wang P**, Liu X, Berzin TM, Glissen Brown JR, Liu P, Zhou C, Lei L, Li L, Guo Z, Lei S, Xiong F, Wang H, Song Y, Pan Y, Zhou G. Effect of a deep-learning computer-aided detection system on adenoma detection during colonoscopy (CADe-DB trial): a double-blind randomised study. *Lancet Gastroenterol Hepatol* 2020; **5**: 343-351 [PMID: 31981517 DOI: 10.1016/S2468-1253(19)30411-X]



Published by **Baishideng Publishing Group Inc**
7041 Koll Center Parkway, Suite 160, Pleasanton, CA 94566, USA
Telephone: +1-925-3991568
E-mail: bpgoffice@wjgnet.com
Help Desk: https://www.f6publishing.com/helpdesk
https://www.wjgnet.com



© 2023 Baishideng Publishing Group Inc. All rights reserved.

ISSN 1007-9327 (print)
ISSN 2219-2840 (online)

World Journal of *Gastroenterology*

World J Gastroenterol 2023 June 21; 29(23): 3574-3747



Published by Baishideng Publishing Group Inc

World Journal of Gastroenterology

Contents

Weekly Volume 29 Number 23 June 21, 2023

EDITORIAL

3574 Recent advances in treatment of nodal and gastrointestinal follicular lymphoma

Watanabe T

MINIREVIEWS

3595 Prognostic role of intestinal ultrasound in Crohn's disease

Manzotti C, Colombo F, Zurleni T, Danelli P, Maconi G

ORIGINAL ARTICLE

Basic Study

3606 BMI-1 activates hepatic stellate cells to promote the epithelial-mesenchymal transition of colorectal cancer cells

Jiang ZY, Ma XM, Luan XH, Liuyang ZY, Hong YY, Dai Y, Dong QH, Wang GY

3622 18β-glycyrrhetinic acid inhibits proliferation of gastric cancer cells through regulating the miR-345-5p/TGM2 signaling pathway

Li X, Ma XL, Nan Y, Du YH, Yang Y, Lu DD, Zhang JF, Chen Y, Zhang L, Niu Y, Yuan L

Retrospective Study

3645 High expression of the circadian clock gene NPAS2 is associated with progression and poor prognosis of gastric cancer: A single-center study

Cao XM, Kang WD, Xia TH, Yuan SB, Guo CA, Wang WJ, Liu HB

3658 SGK3 overexpression correlates with a poor prognosis in endoscopically resected superficial esophageal squamous cell neoplasia: A long-term study

Xu N, Li LS, Li H, Zhang LH, Zhang N, Wang PJ, Cheng YX, Xiang JY, Linghu EQ, Chai NL

3668 Hot snare polypectomy *vs* endoscopic mucosal resection using bipolar snare for intermediate size colorectal lesions: Propensity score matching

Minakata N, Murano T, Wakabayashi M, Sasabe M, Watanabe T, Mitsui T, Yamashita H, Inaba A, Sunakawa H, Nakajo K, Kadota T, Shinmura K, Ikematsu H, Yano T

3678 Lymphocyte-to-white blood cell ratio is associated with outcome in patients with hepatitis B virus-related acute-on-chronic liver failure

Zhang Y, Chen P, Zhu X

Observational Study

3688 Spatial cluster mapping and environmental modeling in pediatric inflammatory bowel disease

Michaux M, Chan JM, Bergmann L, Chaves LF, Klinkenberg B, Jacobson K

World Journal of Gastroenterology

Weekly Volume 29 Number 23 June 21, 2023

Contents

Prospective Study

3703 Novel multi-parametric diagnosis of non-alcoholic fatty liver disease using ultrasonography, body mass index, and Fib-4 index

Funada K, Kusano Y, Gyotoku Y, Shirahashi R, Suda T, Tamano M

3715 Robotic-assisted proctosigmoidectomy for Hirschsprung's disease: A multicenter prospective study

Zhang MX, Zhang X, Chang XP, Zeng JX, Bian HQ, Cao GQ, Li S, Chi SQ, Zhou Y, Rong LY, Wan L, Tang ST

SYSTEMATIC REVIEWS

3733 Paradoxical association between dyspepsia and autoimmune chronic atrophic gastritis: Insights into mechanisms, pathophysiology, and treatment options

Rossi RE, Elvevi A, Sciola V, Mandarino FV, Danese S, Invernizzi P, Massironi S

ABOUT COVER

Editorial Board Member of *World Journal of Gastroenterology*, Kamran Rostami, FRACP, MD, PhD, Department of Gastroenterology, MidCentral District Health Board Palmerston Hospital, Palmerston North 4472, New Zealand. kamran.rostami@midcentraldhb.govt.nz

AIMS AND SCOPE

The primary aim of *World Journal of Gastroenterology* (*WJG*, *World J Gastroenterol*) is to provide scholars and readers from various fields of gastroenterology and hepatology with a platform to publish high-quality basic and clinical research articles and communicate their research findings online. *WJG* mainly publishes articles reporting research results and findings obtained in the field of gastroenterology and hepatology and covering a wide range of topics including gastroenterology, hepatology, gastrointestinal endoscopy, gastrointestinal surgery, gastrointestinal oncology, and pediatric gastroenterology.

INDEXING/ABSTRACTING

The *WJG* is now abstracted and indexed in Science Citation Index Expanded (SCIE, also known as SciSearch®), Current Contents/Clinical Medicine, Journal Citation Reports, Index Medicus, MEDLINE, PubMed, PubMed Central, Scopus, Reference Citation Analysis, China National Knowledge Infrastructure, China Science and Technology Journal Database, and Superstar Journals Database. The 2023 edition of Journal Citation Reports® cites the 2022 impact factor (IF) for *WJG* as 4.3; IF without journal self cites: 4.1; 5-year IF: 5.3; Journal Citation Indicator: 0.82; Ranking: 32 among 93 journals in gastroenterology and hepatology; and Quartile category: Q2. The *WJG*'s CiteScore for 2021 is 8.3 and Scopus CiteScore rank 2022: Gastroenterology is 22/149.

RESPONSIBLE EDITORS FOR THIS ISSUE

Production Editor: *Yi-Xuan Cai*; **Production Department Director:** *Xiang Li*; **Editorial Office Director:** *Jia-Ru Fan*.

NAME OF JOURNAL
World Journal of Gastroenterology

ISSN
ISSN 1007-9327 (print) ISSN 2219-2840 (online)

LAUNCH DATE
October 1, 1995

FREQUENCY
Weekly

EDITORS-IN-CHIEF
Andrzej S Tarnawski

EDITORIAL BOARD MEMBERS
http://www.wjgnet.com/1007-9327/editorialboard.htm

PUBLICATION DATE
June 21, 2023

COPYRIGHT
© 2023 Baishideng Publishing Group Inc

INSTRUCTIONS TO AUTHORS
https://www.wjgnet.com/bpg/gerinfo/204

GUIDELINES FOR ETHICS DOCUMENTS
https://www.wjgnet.com/bpg/GerInfo/287

GUIDELINES FOR NON-NATIVE SPEAKERS OF ENGLISH
https://www.wjgnet.com/bpg/gerinfo/240

PUBLICATION ETHICS
https://www.wjgnet.com/bpg/GerInfo/288

PUBLICATION MISCONDUCT
https://www.wjgnet.com/bpg/gerinfo/208

ARTICLE PROCESSING CHARGE
https://www.wjgnet.com/bpg/gerinfo/242

STEPS FOR SUBMITTING MANUSCRIPTS
https://www.wjgnet.com/bpg/GerInfo/239

ONLINE SUBMISSION
https://www.f6publishing.com

© 2023 Baishideng Publishing Group Inc. All rights reserved. 7041 Koll Center Parkway, Suite 160, Pleasanton, CA 94566, USA
E-mail: bpgoffice@wjgnet.com https://www.wjgnet.com

World Journal of Gastroenterology

Submit a Manuscript: https://www.f6publishing.com

World J Gastroenterol 2023 June 21; 29(23): 3574-3594

DOI: 10.3748/wjg.v29.i23.3574

ISSN 1007-9327 (print) ISSN 2219-2840 (online)

EDITORIAL

Recent advances in treatment of nodal and gastrointestinal follicular lymphoma

Takuya Watanabe

Specialty type: Gastroenterology and hepatology

Provenance and peer review: Invited article; Externally peer reviewed.

Peer-review model: Single blind

Peer-review report's scientific quality classification

Grade A (Excellent): 0
Grade B (Very good): 0
Grade C (Good): C, C
Grade D (Fair): 0
Grade E (Poor): 0

P-Reviewer: Long X, China; Seledtsov V, United States

Received: April 13, 2023
Peer-review started: April 13, 2023
First decision: May 12, 2023
Revised: May 14, 2023
Accepted: May 22, 2023
Article in press: May 22, 2023
Published online: June 21, 2023

Takuya Watanabe, Department of Internal Medicine and Gastroenterology, Watanabe Internal Medicine Aoyama Clinic, Niigata-city 9502002, Japan

Corresponding author: Takuya Watanabe, MD, PhD, Director, Doctor, Department of Internal Medicine and Gastroenterology, Watanabe Internal Medicine Aoyama Clinic, 1-2-21 Aoyama, Nishi-ku, Niigata-city 9502002, Japan. nabetaku@dia-net.ne.jp

Abstract

Follicular lymphoma (FL) is the most common low-grade lymphoma, and although nodal FL is highly responsive to treatment, the majority of patients relapse repeatedly, and the disease has been incurable with a poor prognosis. However, primary FL of the gastrointestinal tract has been increasingly detected in Japan, especially due to recent advances in small bowel endoscopy and increased opportunities for endoscopic examinations and endoscopic diagnosis. However, many cases are detected at an early stage, and the prognosis is good in many cases. In contrast, in Europe and the United States, gastrointestinal FL has long been considered to be present in 12%-24% of Stage-IV patients, and the number of advanced gastrointestinal cases is expected to increase. This editorial provides an overview of the recent therapeutic advances in nodal FL, including antibody-targeted therapy, bispecific antibody therapy, epigenetic modulation, and chimeric antigen receptor T-cell therapy, and reviews the latest therapeutic manuscripts published in the past year. Based on an understanding of the therapeutic advances in nodal FL, we also discuss future possibilities for gastroenterologists to treat gastrointestinal FL, especially in advanced cases.

Key Words: Nodal and gastrointestinal follicular lymphoma; Antibody-based therapy; Bispecific antibody therapy; Phosphatidylinositol-3 kinase inhibitor; Epigenetic modulator; Chimeric antigen receptor-T cell therapy

©The Author(s) 2023. Published by Baishideng Publishing Group Inc. All rights reserved.

Core Tip: Primary gastrointestinal follicular lymphomas (FLs) have been increasingly detected in Japan, especially due to recent advances in small bowel endoscopy and increased opportunities for endoscopic examination and endoscopic diagnosis. Previously, many gastrolienal FL cases are detected at an early stage, however, the number of advanced cases is expected to increase in the future. This editorial provides an overview of the recent therapeutic advances in nodal FL, including antibody-targeted therapy, bispecific antibody therapy, epigenetic mutations, and chimeric antigen receptor T-cell therapy, and we also discuss future possibilities for gastroenterologists to treat gastrointestinal FL, especially in advanced cases.

Citation: Watanabe T. Recent advances in treatment of nodal and gastrointestinal follicular lymphoma. *World J Gastroenterol* 2023; 29(23): 3574-3594
URL: https://www.wjgnet.com/1007-9327/full/v29/i23/3574.htm
DOI: https://dx.doi.org/10.3748/wjg.v29.i23.3574

INTRODUCTION

Follicular lymphoma (FL) is a typical indolent B-cell lymphoma that accounts for 10%-20% of all non-Hodgkin lymphomas (NHLs)[1]. Its incidence is increasing rapidly in Western and Asian countries[2]. In particular, the number of FL cases in Japan has recently increased[3]. FL is histopathologically classified as grades 1, 2, 3a, or 3b, with grade 3b usually treated as aggressive (intermediate/high-grade) lymphoma. Most patients present with enlarged lymph nodes, and 70%-85% of patients have advanced clinical stage III or IV disease at diagnosis, with a high rate of bone marrow involvement. The gastrointestinal tract is the most common site of extranodal NHL, accounting for 30-40% of primary extranodal NHL cases[4,5]; however, gastrointestinal FL (GI-FL) is rare, with a frequency of approximately 2% of GI-NHL[6-8]. However, in recent years, the number of patients with primary GI-FL has increased because capsule and double-balloon endoscopies of the small intestine have become common in Japan. Most GI-FL cases are stage I, but there are 3.4%-40.0% with metastasis or invasion to intra-abdominal lymph nodes (stage II), extensive extranodal organ (stage IV) to extensive extranodal organs or beyond the diaphragm (12%-24%) have been reported[9], and the number of advanced cases of GI-FL (stage III, IV) is expected to increase in the future. Hiddemann *et al*[10] reported the efficacy and prolonged overall survival (OS) of rituximab, an anti-CD20 monoclonal antibody, in combination with cyclophosphamide, doxorubicin, vincristine, and prednisolone (CHOP) in patients with advanced FL. Prior to the introduction of rituximab, the 50% survival period for FL patients was 7-10 years, recent reports have indicated that the 50% survival period exceeds 20 years for patients under 40 years of age at diagnosis[11]. Furthermore, progress has been made in the studies and clinical trials of combination therapies using other monoclonal antibodies and conventional chemotherapy combinations. In the last decade, new therapeutic agents for nodal FL have been developed, including antibody-targeted therapy, bispecific antibody therapy, epigenetic mutation, and chimeric antigen receptor (CAR)-T cell therapy, and many clinical trials of monotherapy and various combinations of two or three of these agents have been conducted, showing high response rates, progression-free survival (PFS). Many clinical trials have been conducted to evaluate the efficacy of single agents and combinations of two or three of these drugs, and have shown high response rates, PFS, and OS. However, the large number of new drugs has led to the creation of many combinations of these drugs, so there is still no definitive conclusion as to which combination is the best in terms of efficacy and safety, and what the optimal order of these therapies should be. We reviewed and summarized the recently reported therapeutic advances in nodal FL, especially the most recent therapeutic publications during the past year. We then discuss the possibilities and directions in which gastroenterologists should utilize and reflect on recent advances in the treatment of nodal FL in primary GI-FL.

Recent advances in the treatment of nodal FL

Radiation therapy used to be the first choice for the treatment of nodal FL when the lesions were localized or multiple but few in number, however, the choice of radiation therapy has been greatly reduced in recent years due to its strong adverse reactions, and chemotherapy, which has advanced significantly in the past 20 years, immunotherapy, which has fewer side effects, or their combination therapies have emerged.

This editorial describes recent advances in the treatment of advanced FL, primarily stage III or IV, with reference to tables summarizing them.

ANTIBODY-BASED THERAPY

Monoclonal antibody-based therapy

Immunotherapy with rituximab and other anti-CD antibodies is highly effective in the treatment of FL and is superior and still central to current FL therapy. The objective response rate (ORR) with single-agent rituximab was 67% in untreated FL patients and 46% in previously treated relapsed FL patients [12].

A German Low-Grade Lymphoma Study Group conducted a randomized trial of CHOP alone *vs* rituximab plus CHOP (R-CHOP) in untreated advanced FLs. In a randomized comparison of CHOP monotherapy and R-CHOP combination therapy, the R-CHOP group significantly outperformed the CHOP group not only in time to failure but also in OS[13]. This evidence is important because it heralds the subsequent progress of combination therapy using anti-CD monoclonal antibody immunotherapy and other novel agents, in addition to conventional chemotherapy. Following rituximab administration, new antibody-based agents have been developed, including tafasitamab, an anti-CD19 antibody; polatuzumab vedotin, an anti-CD79b antibody-drug conjugate (ADC); loncastyximab tesirine, an ADC composed of a humanized antibody targeting the protein CD19; magrolimab, an anti-CD47 antibody; and obinutumab, a humanized anti-CD20 monoclonal antibody. Obinutumab, a humanized anti-CD20 monoclonal antibody, has been developed (Table 1).

Tafasitamab plus lenalidomide, which enhances NK cell activity and antibody-dependent cytotoxicity (ADCC), has been shown to be superior to the monotherapy[14].

Polatuzumab vedotin is a CD79b-directed ADC. In the phase II ROMULUS trial of relapsed and refractory (r/r) FL and diffuse large B-cell lymphoma (DLBCL), patients with FL were treated with rituximab plus polatuzumab (CD79-directed ADC) or rituximab plus pinatuzumab (CD22-directed ADC), and their efficacy was compared[15].

Loncastuximab tesirineis (ADCT-402) is a noble antibody-drug conjugated to a cytotoxic dimer. After bindig to the tumor cells the antibody is internalized, the cytotoxic drug is released, and the cancer cells are killed. The ORR in patients with FL in a phase I study was 78.6%; phase II findings (LOTIS-2 study) of loncastaximab tecilin in r/r DLBCL patients showed a good and sustained antitumor effect with an ORR of 48.3% and complete response rate (CRR) of 24.2%[16]. Clinical trials are currently underway for other carcinomas; a phase II study in combination with rituximab for r/r FL patients is ongoing in Florida, United States.

Magrolimab is a CD47-directed antibody, and a phase I study of its combination with rituximab in r/r lymphoma has been reported[17].

Obinutumab is a humanized anti-CD20 monoclonal antibody with low fucose content in the Fc region through glycosylation technology and the unique properties of a type-2 antibody. Phase 3 trials have shown improved efficacy in indolent non-NHL (iNHL) and chronic lymphocytic leukemia (CLL), and phase 2 trials of these therapeutic regimens have shown promising results in CLL, FL, and mantle cell lymphoma (MCL)[18].

Results of a phase I study of the combination of venetoclax plus obinutumab in previously untreated FL patients ORR and CRR were 87.5% and 25.0%, respectively, by CT evaluation; 84.2% and 68.4%, respectively, by PET/CT evaluation; 1-year PFS was 77.8% and 79%, respectively; 30-mo PFS was 73.2% and 79.0%, respectively and showed efficacy of the combination of venetoclax plus obinutumab[19]. However, in the GALLIUM trial, obinutuzumab had a better PFS than rituximab when combined with conventional chemotherapy as frontline therapy in previously untreated advanced FL patients[20]. Furthermore, transformed-FL (t-FL) patients with more aggressively transformed, more malignant potential had worse survival than r/r FL patients (2-year rate: 55.9% *vs* 83.1%). t-FL relapsed earlier than FL (median observation time: 0.8 years *vs* 2.3 years)[21].

Finally, we discuss the key points regarding recent rituximab biosimilars. In recent years, four rituximab biosimilars have been approved to date in Europe and the United States. CT-P10 is the first Rituximab biosimilar approved CT-P10 is as effective and safe as Rituximab in untreated FL with small tumor volume[22]. They also reported no statistically significant differences in efficacy and serious adverse events between the Rituximab biosimilar group and the reference drug, Mabusera[23]. The Japanese government's policy for 2022 also states that biosimilar will be steadily promoted with a target value set by the end of 2022 based on the effect of medical cost optimization. It is expected that the use of rituximb biosimulators will be recommended and increased worldwide from the viewpoint of cost benefit in reducing the enormous medical costs in the future.

Antibody therapies against novel targets, such as CD19, CD79b, and CD47, as well as rituximab, an anti-CD20 monoclonal antibody and obinutumab, a humanized anti-CD20 monoclonal antibody, have been developed and have demonstrated efficacy in FL. Antibody targeted therapies to FL are innovative immunotherapy medication that offers great efficacy and safety for FL treatment. We have high expectations for improved outcomes in the near future.

Bispecific T cell binding antibody = bispecific antibody therapy

Bispecific T-cell binding antibodies (BTEs) = bispecific antibodies are molecules designed to bind to two or more different antigens, a powerful therapy that allows T cells to more precisely target specific tissues and cells. Summary of clinical trials of BTE treatment for FL is shown in Table 2.

Table 1 Summary of clinical trial results of monoclonal antibody-based therapies

Study	Target disease	No. of patients	Objective response rate	Complete response rate	Median progression-free survival	Overall survival	Adverse events or other subjects	Ref.
Tafasitamab plus lenalidomide phase-II L-MID	r/r DLBCL (no FL) > 35 mo follow up	*n* = 80	57.5% (*n* = 46/80)	40.0% (*n* = 32/80)	11.6 mo	33.5 mo	No unexpected toxicity	[14]
Phase-II ROMULUS, rituximab-polatuzumab *vs* rituximab-pinatuzumab	r/r FL	*n* = 42, *n* = 20, *n* = 21	70% (*n* = 14/20); 62% (*n* = 13/21)	45% (*n* = 9/20); 5% (*n* = 1/21)	Unknown	Unknown		[15]
Loncastuximab tesirine (ADTC-402) frontline therapy	Untreated FL	Total, DLBCL, MZL, FL	45.6%, 42.3%, 46.7%, 78.6%	26.7%	Unknown	Unknown	Median duration response: 5.4 mo	[16]
Magrolimab plus rituximab phase-Ib	r/r DLBCL; r/r FL	*n* = 22; DLBCL:15; FL: 7	50% (CR or PR); 40%, 71% (*n* = 5/7)	33%, 43% (*n* = 3/7)	Unknown	Unknown	90% response were on going, a median follow-up of 6.2 (DLBCL)/8.1 (FL) mo	[17]
Venetoclax plus obinutumab phase-I	Untreated FL	CT, PET/CT	87.5%, 84.2%	25.0%, 68.4%	77.8% (at one yr); 79.0% (at one yr); 73.2% (at 30 mo); 79.0% (at 30 mo)	Unknown; unknown		[19]
GALLIUM trial obinutuzumab + CTx rituximab + CTx	Untreated FL	*n* = 1202, *n* = 601, *n* = 601	88.5%, 86.9%	Unknown, unknown	80.0% (at 3 yr); 73.3% (at 3 yr)	Unknown, unknown	Obinutuzumab is better	[20, 21]

"Unknown" means data not shown, unknown information or not reached. r/r: Refractory and relapsed; FL: Follicular lymphoma; DLBCL: Diffuse large B-cell lymphoma; MZL: Marginal zone lymphoma; (R-)CHOP: (Rituximab plus) cyclophosphamide, doxorubicin, vincristine, and prednisolone; CT: Computed tomography; PET/CT: Positron emission tomography/computed tomography; CTx: Traditional chemotherapy.

The BTEs most commonly used for FL treatment are CD3 and CD20, with Mosunetuzumab and Glofitamab being pioneering representative novel BTEs.

A phase I trial of single-agent mosunetuzumab in patients with r/r iNHL (including FL and t-FL) showed an ORR of 66% and a CRR of 49%, with grade 3 or higher adverse events in 71% of patients with low-grade lymphoma (r/r and t-FL, 96%)[24]. Mosnetuzumab, a CD20 × CD3 bispecific monoclonal antibody, showed a significantly higher CRR of 60% than that of the control group with copanlisib of 14%, when administered to patients with r/r FL, indicating high efficacy[25]. Mosunetuzumab was also studied in combination with lenaridomide; a phase I study of combination therapy in r/r FL patients showed an ORR of 92%, CR of 77%, and grade 3 or higher adverse events in 30% of patients in the abstruct.

Glofitamab was observed to have a better response rate at higher dose levels in the r/r B-NHL (including indolent lymphoma of 25.7%) phase I trial, with an ORR of 65.7% and a CRR of 57.1%. CRS occurred in 50.3% of cases[26]. The results of a study comparing glofitamab with or without obinutuzumab in r/r FL showed an ORR of 81% and a CRR of 70% for glofitamab alone and 100% and 74% for the combination group in the Abstruct.

The results of a phase I/II trial of epcoritamab, an anti-CD3 and anti-CD20 BTE, in r/r NHL patients showed an ORR of 90% and a CRR of 50% in FL patients[27]. The results of a phase I/II study of epcoritamab in combination with lenaridomide and rituximab in patients with r/r FL showed high efficacy, with an ORR of 100% and a CRR of 93%[28].

Odronextamab is a hinge-stabilized fully human IgG4-based CD20 × CD3 bispecificity antibody that binds to CD3 on T cells and CD20 on B cells. In the Odronextamab ELM-1 phase I study, patients with r/r FL who received 5 mg or more of odronextamab had an ORR of 91% and a CRR of 72%; Odronextamab monotherapy showed promising preliminary activity, especially in patients with long-standing previously treated BCL with sustained response[29,30].

BTE is a novel immunotherapy agent that shows high efficacy and safety for FL treatment. We would like to greatly anticipate further improvements in outcomes through future clinical trials.

Anti-programmed death ligand 1 antibody

Programmed death ligand 1 (PD-1) blockade enhances anti-tumor T cell function and ADCC in NK cells. Recntly, the efficacy of the anti-PD-1 ligand (PD-L1) antibodies, atezolitumab and pembrolizumab, in FL has also attracted attention (Table 3).

Table 2 Summary of clinical trial results of bispecific T cell binding antibody therapies

Study	Target disease	No.of patients	Objective response rate	Complete response rate	Median progression-free survival	Overall survival	Adverse events or other subjects	Ref.
Mosunetuzumab alone, phase-I	r/r NHL (including FL and t-FL)	*n* = 157	66.2% (i B-NHL)	48.5% (i B-NHL)	Median duration of response 20.4 mo (i B-NHL	Unknown	G3 and higher in 71% of iNHL patients	[24]
Mosunetuzumab alone, phase-II	r/r FL (Grade 1-3a)	*n* = 90 (median follow-up was 18.3 mo)	Unknown	60% (*n* = 54/90) (14% higher than CRR with copanlisib), high efficacy	Unknown	Unknown	High efficacy	[25]
Mosunetuzumab with lenaridomide, phase-I	r/r FL	Unknown	92%	77%	Unknown	Unknown	G3 and higher in 30% of patients	In abstruct
Glofitamab alone, phase-I	r/r B-NHL (including r/r FL)	*n* = 155	65.7% (at the recommended phase-II dose)	57.1% (at the recommended phase-II dose)	Unknown	Unknown	CRS occurred in 50.3% of patients	[26]
Glofitamab alone *vs* glofitamab with obinutuzumab	r/r FL	Unknown	81%, 100%	70%, 74%	Unknown	Unknown	Combination has a better response rate	In Abstruct
Epcoritamab, phase-I/II	r/r B-NHL	*n* = 68	90% (full dose)	50% (full dose)	Unknown	Unknown	Pyrexia 69%, CRS 59%	[27]
Epcoritamab with lenaridomide and rituximab	r/r FL	Unknown	100%	93%	Unknown	Unknown	High efficacy is revealed	[28]
Odronextamab alone phase-I ELM-1 trial	r/r B-NHL (including r/r FL)	*n* = 145	91% (r/r FL)	72% (r/r FL)	Unknown	Unknown	CRS 28%	[29]

"Unknown" means data not shown, unknown information or not reached. r/r: Refractory and relapsed; (i)NHL: (Indolent) non-Hodgkin lymphoma; i B-NHL: Indolent B-cell non-Hodgkin lymphoma; FL: Follicular lymphoma; t-FL: Transformed follicular lymphoma; G: Grade; CRS: Cytokine release syndrome.

Table 3 Summary of clinical trial results of anti-programmed death ligand 1 antibody-based therapies

Study	Target disease	No. of patients	Objective response rate	Complete response rate	Median progression-free survival	Overall survival	Adverse events or other subjects	Ref.
Atezolitumab (anti-PD-1 antibody) plus obinutumab	Total	*n* = 49				Unknown		[31]
phase-I	r/r FL	*n* = 26	54%	23%	9 mo			
	r/r DLBCL	*n* = 23	17%	4%	3 mo			
Pembrolizumab(anti-PD-1antibody) plus rituximab	r/r FL (one or more prior therapy)	*n* = 30	67%	50%	12.6 mo	97% (at 3 yr)	23% in remission at medianfollow-up of 35 mo	[32]

"Unknown" means data not shown, unknown information or not reached. r/r: Refractory and relapsed; FL: Follicular lymphoma; DLBCL: Diffuse large B-cell lymphoma; PD-1: Programmed death ligand 1.

The results of a phase I study of the combination of atezolizumab, an anti-PD-L1 antibody, and obinutumab showed an ORR of 54% (CRR: 23%) for r/r FL and r/r DLBCL and 17% (CRR: 4%) for DLBCL; PFS was 9 mo in the FL group and 3 mo in the DLBCL group[31]. In addition, a clinical trial of pembrolizumab, an anti-PD-1 monoclonal antibody, in combination with rituximab, an anti-CD20 monoclonal antibody, in r/r FL patients showed an ORR of 67% and CRR of 50%; median PFS was 12.6 mo, 3-year OS was 97%, and at a median follow-up of 35 mo 23% of patients were in remission[32]. Pembrolizumab in combination with rituximab as a novel therapeutic agent for r/r FL showed high efficacy and remission maintenance.

PD-1 blockade enhances anti-tumor T cell function and ADCC in NK cells, and its mechanism of action is more fundamental and makes more sense. We expect further improvement of the therapeutic effect of anti-PD-1 antibody therapy for FL patients.

IMMUNOMODULATORS

Lenaridomide is a typical oral immunomodulatory drug (IMiD) used to treat FL. Lenaridomide is a derivative of thalidomide with a similar structure. Lenaridomide is a derivative of thalidomide with a similar structure. It has both a "tumor-killing" effect by inhibiting the growth of hematological malignancies and inducing apoptosis, and an "immunomodulatory" effect by acting on immune cells and activating their immunity[33]. The combination of lenaridomide and CD20 antibody was initially tested as a salvage therapy for r/r FL in combination with an anti-CD20 antibody; however, owing to its high efficacy, it was recently tested as a frontline therapy for patients with advanced, untreated FL, with good results. Table 4 lists clinical trials in which lenaridomide was administered.

A phase II study comparing lenaridomide alone with R2 (lenaridomide plus rituximab) in patients with r/r FL showed an ORR favoring the R2 group (35% *vs* 24%), with a median follow-up of 2.5 years. The time to progression (median) was also superior in the R2 group (2.0 years *vs* 1.1 years), but there was no significant difference in OS[34].

The results of the phase III AUGMENT study evaluating R2 (lenaridomide plus rituximab) in r/r FL and marginal zone lymphoma (MZL) showed a median PFS of 39 mo in the R2 group compared to 14 mo in the rituximab group, with no difference in OS[35].

The phase IIIb MAGNIFY trial investigated extended R2 treatment in patients with r/r FL and MZL. After 12 cycles of R2 treatment, patients were randomized to receive an additional 18 mo of R2 treatment or rituximab maintenance therapy. The R2 cohort had ORR of 69% and CRR of 40%. The median PFS was 40 mo, similar to that observed in the AUGMENT trial[36].

In a single-arm phase II GALEN trial of patients with r/r FL, Obinutuzumab and lenaridomide were studied[37]. The patients received lenaridomide and obinutuzumab for 18 mo, followed by 1 year of obinutuzumab maintenance therapy[37]. After a median follow-up of 2.6 years, the ORR was 95%, 2-year PFS was 65%, and OS was 87%. No clinical trials have directly compared rituximab and obinutuzumab in combination with lenaridomide, and it is unclear which combination is superior in efficacy.

The phase III RELEVANCE trial of R2 as frontline therapy for advanced FL was conducted[38]. Patients were randomized to receive 18 cycles of R2 therapy plus 6 cycles of rituximab maintenance therapy or a chemoimmunotherapy regimen including rituximab [R-CHOP, bendamustine plus rituximab (BR), or rituximab plus cyclophosphamide, vincristine, and prednisone (R-CVP)]. The primary endpoints of the CR rate (48%-53%) and 3-year PFS (77%-78%) at 120 wk were similar; no superiority of R2 over chemoimmunotherapy in the front-line treatment of FL has been demonstrated [38].

The phase II E2408 trial randomized untreated FL patients into BR induction and R2 maintenance, BR induction and rituximab maintenance, or BR and the proteasome inhibitor boltezomib plus rituximab maintenance, and compared the efficacy among the three groups[39]. The three groups had similar (approximately 90%) and high CRRs, and the 1-year disease-free survival was higher in the rituximab maintenance group (85%) than in the R2 group (67%), possibly due to a higher discontinuation rate due to adverse events in the R2 group.

A clinical trial of lenaridomide plus obinutuzumab as frontline therapy for patients with advanced untreated FL showed very good results, with an ORR of 98%, CR of 92%, and 2-year PFS of 96% after a median follow-up of 22 mo[40]. In the future, the combination of lenalidomide and CD20 antibodies is expected to be the mainstay of front-line therapy for FL.

With the introduction of bendamustine, obinutuzumab, and lenalidomide, which have shown high efficacy in maintenance therapy, front-line treatment of FL has improved and developed. However, how they can be combined to provide the best treatment has recently been studied by network meta-analysis of randomized controlled trials to compare treatment efficacy[41].

With lenaridomide, a further improvement in the therapeutic effect in FL patients was obtained when used in combination with other main agents. As one of the important combination drugs, it is expected to improve treatment outcomes in the future.

MOLECULAR TARGETED THERAPIES (SMALL MOLECULE CONPOUNDS)

Bruton's tyrosine kinase inhibitor

Bruton's tyrosine kinase (BTK) is a type of protein kinase that exists in immune cells and regulates B cell differentiation and activation upon stimulation from the B cell receptor (BCR). Since BCR signaling plays an important role in blood cancers such as B-cell NHL and CLL, BTK inhibitors have been expected to have therapeutic effects in these blood cancers including FL. The results of the clinical trials

Table 4 Summary of clinical trial results of immunomodulator-based therapies

Study	Target disease	No.of patients	Objective response rate	Complete response rate	Progression-free survival	Overall survival	Adverse events or other subjects	Ref.
Randomized phase-II; lenaridomide alone (L) lenaridomide + rituximab (LR)	r/r FL	*n* = 91, *n* = 45 (L); *n* = 46 (LR)	53%, 76%	20%, 39%	Median time to progression: 1.1 yr (at 2.5 yr); 2.0 yr (at 2.5 yr)	Unknown		[34]
Phase-III AUGMENT lenaridomide + R (R2) *vs* lenaridomide + placebo	r/r FL; r/r MZL	*n* = 358; *n* = 180; *n* = 178	Unknown	Unknown	Median duration: 39.4 mo; 14.1 mo	Unknown	Grade 3 neutropenia of R2 is higher than L	[35]
Phase-IIIb MAGNIFY trial; R maintain after R2 additional lenarimide + rituximab (R2) 18 mo after R2	r/r FL; r/r MZL	*n* = 393	69% (R2)	40% (R2)	40 mo (similar to AUGMENT trial)	Unknown		[36]
Phase-II GALEN study; lenarimide + obinutuzumab (R2) 18 mo followed by obinutuzumab alone maintenance therapy 1 year	r/r FL	*n* = 68; evaluable	95% (at 2.6 yr)	38% (*n* = 33/86)	65% (at 2 yr)	87% (at 2 yr); 81% (*n* = 70/86); 84% (*n* = 72/86)		[37]
Phase-III RELEVANCE study, lenaridomide + rituximab (R2) + Rituximab maintenance therapy *vs* CTx (R-CHOP, BR, or R-CVP)	Untreated advanced FL	*n* = 1030; R-maintenance, *n* = 513; CTx, *n* = 517	Unknown	48%-53%, about the same	3 years-PFS 77%-78%, almost equal to superiority of R2 in F2 frontline not proven	Unknown		[38]
	Untreated advanced FL		Unknown	All 3 groups approximately 90%, about the same	3 yr PFS (5 yr median follow-up); -R 77%, BVR-R 82%, BR-LR 76% (higher in the R-maintenance group than in the R2 group) because of more discontinuations in the R2 group)	3 yr PFS (5 yr median follow-up), BR-R 87%, BVR-R 90%, BR-LR 84%		[39]
Single center phase-II frontline therapy; lenaridomide plus obinutuzumab	Untreated advanced FL	*n* = 90	98% (after a median follow-up of 22 mo)	92% (after a median follow-up of 22 mo)	2 yr-PFS 96 (after a median follow-up of 22 mo)	Unknown		[40]

"Unknown" means data not shown, unknown information or not reached. r/r: Refractory and relapsed; FL: Follicular lymphoma; MZL: Marginal zone lymphoma; L: Lenaridomide; R: Rituximab; LR: Lenaridomide plus rituximab; R2: Lenaridomide plus rituximab; (R-)CHOP: (Rituximab plus) cyclophosphamide, doxorubicin, vincristine, and prednisolone; BR: Bendamustine plus rituximab; (R-)CVP: (Rituximab plus) cyclophosphamide, vincristine and prednisolone; BR-R: BR induction followed by 2-year rituximab maintenance; BVR-R: BR with bortezomib and rituximab maintenance; BB-LR: BR followed by lenalidomide (1 year) with rituximab maintenance; CTx: Traditional chemotherapy.

of BTKi treatments for FL are listed in Table 5.

Representative BTKi include, in order of oldest to youngest, first-generation ibrutinib, second-generation acalabrutinib and zanubrutinib, and third-generation piltobrutinib. These BTKi have shown high efficacy in B-cell NHL and CLL[42-46].

The efficacy of zanurutinib monotherapy in patients with r/r FL was sluggish, with an ORR of 36.4% and CR of 18.2%. After a median follow-up of 33.9 mo, the median PFS was 10.4 mo[42]. On the other hand, a phase II study in r/r MCL showed that after a median follow-up of 35.3 mo, the ORR was 83.7%, the CRR was 79.9%, and the median PFS was 33.0 mo[43]. Zanurutinib alone was highly effective in r/r MCL, however, limited in r/r FL.

The phase II DAWN trial evaluated the therapeutic efficacy of single-agent ibrutinib in patients with r/r FL; the ORR was 21% and did not meet the primary endpoint[47]. Frontline therapy was administered to investigate a combination of Ibrutinib and Rituximab. This phase II trial included two arms, both with ibrutinib 560 mg/d, with Rituximab in arm-1 starting at week 1 for four cycles per

Table 5 Summary of Clinical Trial Results of Bruton's Tyrosine Kinase inhibitors

Study	Target disease	No. of patients	Objective response rate	Complete response rate	Progression-free survival	Overall survival	Adverse events or others	Ref.
Zanubrutinib (other BTKi) alone	r/r FL		36.4%	18.2%	Median PFS 10.4 mo (median follow-up 33.9 mo)	Unknown		[42]
Zanubrutinib phase-II	r/r MCL	83.7%	77.9%	Unknown	33.0 mo	Unknown		[43]
	r/r FL	n = 100	21.0% (poor)	Unknown	Unknown	Unknown		[47]
Ibrutinib with rituximab phase-II trial	Untreated FL, r/r FL	n = 13, n = 27	85% (arm-1), 75% (arm-2)	Unknown	62% of untreated FL, 26% of r/r FL, continued treatment	Unknown		[48]

"Unknown" means data not shown, unknown information or not reached. r/r: Refractory and relapsed; FL: Follicular lymphoma; MCL: Mantle cell lymphoma; PFS: Progression-free survival.

week, and Rituximab in arm-2 starting at week 9. The ORR was 85% in arm-1 and 75% in arm-2[48].

Acalabrutinib is an effective BTKi for r/r MCL Results of a phase I trial comparing acalabrutinib with or without rituximab as frontline therapy for untreated FL and salvage therapy for r/r FL, after a median follow-up of 22 mo, 62% of untreated FL patients and 26% of r/r FL patients remained on therapy and showed high tolerability[49].

Results of the randomized phase II ROSEWOOD trial in patients with r/r FL showed that combination therapy with zanubrutinib had better PFS than obinutuzumab alone. Zanubrutinib suggested to be more effective against r/r FL when used in combination with Obinutuzumab[50].

Although the single-agent activity of BTKis in FL is modest, their activity may be demonstrated when used in combination, and there is hope for their efficacy. We will keep a close eye on the future improvements in combination therapy with various combinations of new BTKs and other drugs in patients with FL.

Pro-apoptotic pathway inhibitors (BCL2 inhibitor)

Venetoclax selectively binds with strong affinity to BCL2, an anti-apoptotic protein involved in many blood cancers, and liberates apoptosis-promoting proteins, thus rapidly and irreversibly promoting apoptosis of blood cancer cells because BCL2 is overexpressed in FL, Venetoclax, a BCL2 inhibitor, has shown great promise. A phase I trial of venetoclax monotherapy was conducted in patients with FL, with an ORR of 38% and a median PFS of 11 mo[51]. The phase II CONTRALTO trial compared three groups of patients with r/r FL: Venetoclax plus rituximab, venetoclax plus BR, and BR in combination with venetoclax[52]. The CRR were 17%, 75%, and 69%, respectively; grade 3 or higher adverse events were extremely common in the venetoclax plus BR group (94%). r/r FL was included. In addition, combination therapy with ibrutinib was tested in a phase I/II study of venetolax plus ibrutinib with an ORR of 69% and a CRR of 25%[53].

Since BCL2 is overexpressed in FL, BCL2 inhibitors are expected to have a fundamental antitumor effect on FL tumor cells in terms of their mechanism of action. We look forward to improving the therapeutic outcome of BCL2 inhibitors for FL patients in the near future.

Epigenetic regulator

Progress has been made in drug development that is active against blood cancers through the epigenetic regulation of gene expression, such as DNA methylation. The results of clinical trials of EZH2 treatments in patients with FL are listed in Table 6.

Tazemetostat is a small molecule that inhibits the activity of enhancer of zeste homolog 2 (EZH2), a methyltransferase of histones, *etc.* Tazemetostat inhibits the methylation activity of mutant EZH2, thereby inhibiting the methylation of lysine residue 27 of histone H3 and other methyltransferases. A phase II study of tazemetostat in EZH2-mutant and wild-type r/r FL patients showed a higher ORR in the EZH2-mutant cohort (69% *vs* 35%)[54]. It is important to note that higher activity was observed in patients with FL with high-risk characteristics. Currently, combination therapy for r/r FL with tazemetostat is under investigation in the phase II SYMPHONY-2 trial in combination with rituximab and in the phase Ib/III trial in combination with R2. Tazemetostat as a third, fourth, and subsequent treatment for FL and DLBCL patients, especially r/r FL, has a reduced risk of adverse events compared to the PI3K inhibitors ideralisib, duvelisib, copanlisib, and umbralisib, while the therapeutic efficacy and benefit were comparable[55-57].

More than 10 EZH2 inhibitors have recently entered clinical trials, including tazemetostat[56], and we look forward to improved outcomes in the future.

Table 6 Summary of clinical trial results of epigenetic regulators

Study	Targeted disease	No. of patients	Objective response rate	Complete response rate	Progression-free survival	Overall survival	Adverse events or others	Ref.
Tazemetostat alone, phase-II	r/r FL, EZH2-mut; FL, EZH2-wt. FL	*n* = 99, mut FL *n* = 45; wt FL *n* = 54	69% (EZH2 mut); 35% (EZH2 wt)	Unknown; unknown	Median PFS: 13.8 mo (EZH2 mut); 13.1 mo (EZH2 wt)	Unknown	G3 or higher 27%+, treatment discontinued at 8%	[54]
Tazemetostat (first EZH2 inhibitor) *vs* inderalisib, duvelisib, copanlishib, umbralisib	r/r FL, systematic literature review		Tazemetostat *vs* inderalisib 43% *vs* 56; duvelisib 48% *vs* 47; Kopanlisib 49% *vs* 61; umbralisib 57% *vs* 47; no significant difference in either case	Unknown	Unknown	Unknown	Predominantly reduced risk of adverse events compared to PI3Ki	[57]
Vorinostat (HDACi), phase-II	r/r Inhl + MCL, median with one or more prior treatment	*n* = 39 (r/r FL)	49%	Unknown	Median PFS, 20 mo	Unknown	G3 or higher 8%	[58]
Vorinostat + rituximab, phase-II	Untreated and r/r FL (4 or less prior treatment)	*n* = 22	46% (all patients); 67% (untreated pts); 41% (r/r FL)	Unknown	Median PFS, 29.2 mo (all patients); not reached (untreated pts); 18.8 mo (r/r FL)	Unknown		[59]
Mocetinostat, phase-II	r/r DLBCL, r/r FL	*n* = 41, *n* = 31	18.9% (r/r DLBCL), 11.5% (r/r FL)	Unknown	1.8-22.8 mo (DLBCL); 11.8-26.3 mo (FL)	Unknown	Fatigue (75.0%); nausea (69.4%); diarrhea (61.1%)	[60]

"Unknown" means data not shown, unknown information or not reached. r/r: Refractory and relapsed; FL: Follicular lymphoma; EZH2: Enhancer of zeste homolog 2; mt: Mutant; wt: Wild type; (i)NHL: (Indolent) non-Hodgkin lymphoma; DLBCL: Diffuse large B-cell lymphoma; MZL: Marginal zone lymphoma; MCL: Mantle cell lymphoma; G: Grade; PI3Ki: Phosphoinositide 3 kinase inhibitor.

Vorinostat is a histone deacetylase inhibitor (HDACi). A phase II study of vorinostat in patients with r/r FL reported an ORR of 49%, with a median PFS of 20 mo. Grade 3 or greater adverse events were observed in 80% of the patients, mostly cytopenia[58]. Vorinostat was also evaluated in combination with rituximab, with an ORR of 50% and a CR of 41% in a phase II study of 22 untreated and r/r FL patients[59]. Another HDACi, mocetinostat, has shown poor efficacy, with an ORR of only 12% in patients with FL (*n* = 31) evaluated in a phase II trial of patients with r/r FL[60].

EZH2 inhibitors demonstrate effectiveness as an epigenetic regulator by the mechanism that inhibits the activity of methyltransferase of histones, *etc*. These agents are expected to further improve their therapeutic outcomes in the future, especially as a treatment for t-FL.

Phosphatidylinositol-3 kinase inhibitor

The BCR-mediated signaling pathway has been found to be permanently activated in B cell tumor cells, and inhibitors targeting molecules in the BCR signaling pathway are being developed.

Phosphatidylinositol-3 kinaseb (PI3K) is a lipid kinase that mediates the phosphorylation of the inositol ring 3 of inositol phospholipids, a membrane component[61]. Class I PI3Ks are heterologous. Class I PI3Ks are heterodimers that play important roles in signal transduction. Class 1 kinases are further divided into α, β, ϒ, and δ isoforms. For example, p110α and β are expressed in all cells, their knock out mouse is embryonic lethal[62]. p110γ is involved in neutrophil and macrophage migration [63] and mast cell degranulation[64]. This pathway is important in cancer, including B cell malignancies, and several small-molecule PI3K inhibitors (PI3Ki) have been developed for its treatment. The results of clinical trials of PI3K inhibitors in patients with r/r FL are listed in Table 7.

Idelalisib, a selective inhibitor of the delta isoform, was the first PI3Ki developed for the treatment of FL. In the European phase II DELTA study, idelalisib demonstrated the highest efficacy to date in r/r/ FL patients, with a median treatment duration of 10 mo (range 1-43) and an overall response rate of 73% [65].

In addition, a phase II open-label study of idelalisib in r/r iNHL, including FL, in the United.States. confirmed a response rate of 57% and a median PFS of 11 mo[66]. While idelalisib showed high efficacy against r/r FL, grade 3 or higher adverse events were observed in most participants (54%). Higher rates of adverse events have been observed in relatively young patients with less severe prior therapy, fewer complications, and stronger immune responses[67,68]. Fatal adverse events complicate the use of PI3K inhibitors.

Table 7 Summary of Clinical Trial Results of phosphoinositide 3 kinase inhibitors

Study	Target disease	No. of patients	Objective response rate	Complete response rate	Progression-free survival	Overall survival	Adverse events or others	Ref.
Indelalisib, phase-II DELTA trial	r/r FL	*n* = 55	73% (highest ever reported)	Unknown	72% disease-free after 12 mo	80% alive after 12 months	54% of G3 or higher	[65]
Indelalisib phase-II open-labeled trial	r/r NHL (including FL), median of 4 lines prior therapy	iNHL, *n* = 72; FL, *n* = 42)	57%	Unknown	11 mo	Unknown	54% of G3 or higher	[66]
Duvelisib	iNHL (including FL)	*n* = 187	70% good	Unknown	Unknown	Unknown	63% of G3 or higher	[63, 69]
Conpalisib, phase-II CHRONOS-1 trial	r/r FL, median 3-lines of prior therapy	*n* = 142	59%	12%	11 mo (median)	43 mo (median)	G3 84%, 6 cases of G5 events	[70, 71]
Umbralisib, phase-II trial	iNHL (including FL) median 3-lines or more of prior therapy	*n* = 208 (FL = 117)	47.1% of (after a median follow-up of 27.7 mo)	Unknown	10.6 mo (median PFS)	Unknown		[74]
Parsaclisib, phase-Ib, CITADEL-111 trial	Japanease: r/r FL; r/r MZL; r/r DLBCL	*n* = 9; *n* = 2; *n* = 6	9 cases (= 100%); 2 cases (= 100%); 1 case (= 16.7%)	22.2% (*n* = 2/9); 100% (*n* = 2/2); 16.7% (*n* = 1/6)	Unknown	High incidence of adverse events-need to carefully select target patients	Neutropenia above G3 interrupted in 58.8% and reduced in 29.4%	[75]
Parsaclisib, phase-I/II (phase-II trial is ongoing)	r/r B-NHL	*n* = 72	71% (r/r FL); 78% (r/r MZL); 67% (r/r MCL); 30% (r/r DLBCL)	Unknown	Unknown	Unknown	G3/4 neutropenia occurred in 19%	[76]
Zandelisib (ME-401), phase-I trial	Japanese, r/r iNHL	*n* = 9	100% (*n* = 9/9)	22% (*n* = 2/9), median duration of response 7.9 mo; median time to response 1.9 mo		Unknown	G3 or higher neutropenia 6/9 (55.6%) diarrhea 3/9 (33.3%) and many events	[77]
Zandelisib alone *vs* zandelisib + rituximab	r/r FL	*n* = 12	92% (*n* = 11/12) in the 60 mg group; 83% (*n* = 5/6) in the 180 mg group	Unknown	Unknown	Unknown		[78]
	r/r iNHL, median 3-lines of prior therapy	*n* = 30 + BR (*n* = 19) *vs* + R-CHOP (*n* = 11)	90% (+ BR) *vs* 100% (+ R-CHOP)	Unknown	Unknown	Unknown	G3 or higher, high rate of 70% (BR), 91% (R-CHOP)	[79]

"Unknown" means data not shown, unknown information or not reached. r/r: Refractory and relapsed; FL: Follicular Lymphoma; B-NHL: B-cell non-Hodgkin lymphoma; (i)NHL: (Indolent) non-Hodgkin lymphoma; DLBCL: Diffuse large B-cell lymphoma; MZL: Marginal zone lymphoma; MCL: Mantle cell lymphoma.

Duvelisib is the first FDA-approved oral dual inhibitor of PI3K-δ and PI3K-γ. Wang *et al*[69] reported on the safety and efficacy of duvelisib, a dual PI3K-δ and γ inhibitor, in patients with relapsed and refractory lymphoid neoplasms in a systematic prospective clinical trial reviews and meta-analyses have been reported[63,69]. Although the ORR of 187 patients with iNHL including FL showed a good efficacy of 70%, the relatively high rate of grade 3 or higher adverse events (63%) is still a safety concern[63,69].

The high rate of adverse events associated with these two drugs has made it difficult to gain general acceptance for FL treatment. In such a situation, only conpalisib has been approved for r/r FL after more than two lines of therapy. The phase II CHRONOS-1 study[70,71] of copanlisib in patients with r/r iNHL showed an ORR of 59%, CR of 12%, median PFS of 11 mo, and median OS of 43 mo. There was no increase in serious adverse events during the long-term follow-up period, although the rate of grade 3 or higher adverse events was as high as 84%, including 6 grade 5 events[70,71].

Umbralisib (TGR-1202) is an orally available, effective, potent and selective PI3-K δ and casein kinase-1-ε (CK1ε) inhibitor[72]. Umbralisib is a fourth-generation, late-stage PI3Ki that may play an important role in therapeutic algorithms[73]. The results of a phase II trial of r/r iNHL showed an ORR of 45% and

median PFS of 10.6 mo in a cohort of patients with FL after a median follow-up period of 27 mo[74]. Most recently, a phase II trial of Frontline with umbralisib and ubrituximab in untreated advanced FL patients was completed in Florida, the United States.

Parsaclisib is a potent δ isoform of the PI3Ki. The results of CITADEL-111, a phase Ib study in Japanese patients with relapsed/refractory B-cell lymphoma, showed an ORR of 100% in r/r FL and CR in two patients (22.2%), indicating efficacy. The results for MZL and DLBCL are shown in Table 7. Although potent, adverse events were frequent, requiring careful patient selection and implementation [75]. The Phase I/II trial of parsaclisib in patients with r/r FL showed an ORR of 71%. Grade 3 or higher adverse events were observed in 19% of all participants, and phase II trial is ongoing[76].

Zandelisib (ME-401) is a novel PI3-Kδ inhibitor, and phase I trials have recently been reported in Japanese patients with r/r iNHL. ORR was 100% and CR was 22% in 9 Japanese patients with r/r iNHL, and the median duration of response, progression-free survival, and time to response were 7.9 mo, 11.1 mo, and 1.9 mo, respectively. Neutropenia was the most common adverse event, with 55.6% (6/9) of the patients having neutropenia, and thrombocytopenia was the most common adverse event. In Japanese patients with r/r iNHL, zandelisib showed good antitumor efficacy[77]. The results of a study comparing zandelisib monotherapy with zandelisib plus rituximab combination therapy for r/r FL showed an ORR of 92% in the 60 mg group and 83% in the 180 mg group. Serious adverse events occurred in 21% and 8% of patients in the continuous- and intermittent-dose groups, respectively. There were no treatment-related deaths. The 60 mg once-daily intermittent dose was safe, with a low incidence of grade 3 or higher adverse events[78].

PI3Ki has also been considered in combination with conventional chemotherapy, immunotherapy, and other targeted therapies to achieve more potent therapeutic effects. Results of the phase III CHRONOS-4 trial comparing the efficacy and safety of Conpalisib in combination with BR or R-CHOP in patients with r/riNHL showed an ORR of 90% in the BR group and 100% in the R-CHOP group, with grade 3 or higher adverse events occurring in 70% of the BR group and 91% of the R-CHOP group[79]. Early clinical trials of PI3Ki in combination with other immune checkpoint inhibitors and IMiDs are currently underway.

Inderalisib-induced acute liver injury has also been reported and has been noted to be severe and potentially fatal[80]. In a phase I trial in patients with FL or MCL, the triple combination of inderalisib with lenaridomide and rituximab was discontinued early because of the excessive toxicity of all three drugs[81]. Combination therapy with other drugs, including inderalisib, is complicated for future treatment because of significant safety concerns owing to overtoxicity.

PI3K inhibitors were initially expected to have therapeutic effects, and various types of agents were developed, but due to the large number of adverse reactions, only zandelisib remains in Japan, for example, and clinical trials are continuing. We hope that the treatment effect for FL patients will improve in the future.

PI3K/mechanistic target of rapamycin inhibitor

Numerous studies have shown that somatic mutations in PI3K/Akt/mechanistic target of rapamycin (mTOR)-related genes may induce homeostatic activation of various types of cancer pathways, leading to dysregulation of tumor cell growth, growth, differentiation, metabolism, apoptosis, and other functions supporting tumor cell survival It has been shown[82].

Recently, dual inhibitors targeting two targets of the PI3K/PKB/mTOR signaling pathway have been developed and investigated for their therapeutic effects; PI3K/mTOR inhibitors not only inhibit cell proliferation but also promote cell apoptosis. They are also expected to be promising anticancer agents because of their high efficacy at low doses and low drug resistance[83].

The TOR inhibitors, temisirolimusm (TEM) and lenaridomide (LEN) combination therapy, overlapped within the PAM axis and were expected to have synergistic effects. the FL cohort was discontinued early due to low case numbers. the ORR and CRR of the DLBCL and exploratory cohorts were 26% and 13%, 64% and 18%, respectively. The ORR and CRR of the exploratory cohort for classical Hodgkin lymphoma (CHL) patients were 80% and 35%, respectively. Forty percent of CHL patients could be transferred to allogeneic transplant after TEM/LEN therapy. Grade 3 or higher hematologic adverse events were common, and three grade 5 adverse events occurred; TEM/LEN combination therapy was highly effective in advanced untreated lymphomas and especially in r/r CHL[84].

We look forward to the further development of new PI3K/Akt/mTOR dual inhibitors, and to the improvement of therapeutic results and progress as FL treatment agents through the accumulation of clinical trials.

CELL THERAPY

CAR-T cell therapy uses autologous T cells genetically engineered to attack cancer and other cells by introducing CARs.

CAR-T cell therapy is a highly effective, innovative, and revolutionary treatment for patients with r/r hematologic malignancies and shows great promise. When reinjected into the same patient, these CAR-

T cells trigger a T-cell-mediated immune response against the antigen-expressing malignancy and induce cell death. CAR-T cell therapy has recently been used in the treatment of iNHL such as FL and MCL. However, CAR T-cell therapy has a unique hematological toxicity, and post-treatment cytopenia is a major side effect[85,86].

Recent clinical trials have compared the efficacy and safety of three cell therapy modalities (autologous transplantation, allogeneic transplantation, and CAR-T with respect to their validity and rationale as therapeutic modalities[87]. In addition, there are various issues and barriers to the realization of CAR-T therapy, including complex logistics, manufacturing limitations, toxicity concerns, and economic burdens, which must be addressed and remedy[88]. The results of clinical trials on CAR-T cell therapy are summarized in Table 8.

Clinical trials of the autologous anti-CD19 CART agents axicabtagene ciloleucel (Axi-cell), tisagenlecleucel (Tisa-cell), and lisocabtagene maraleucel (Liso-cell) for r/r DLBCL containing approximately 20% transformed FL (Liso-cell) have shown high efficacy, with ORRs ranging from 52% to 82%[89-91]. Long-term follow-up has shown sustained remission in approximately 40% of the patients and high remission maintenance against t-FL[92]. The results of the Phase II ZUMA-5 trial showed that Axi-cells in r/r FL had a median follow-up of 18 mo, with an ORR of 94%, a CRR of 79%, and an estimated PFS of 66% at 18 mo, although the median PFS and OS were not reached. Grade 3 or higher adverse events were observed in 86%, with Grade-5 adverse events in 3%[93,94].

The results of the phase II ELARA trial showed an ORR of 86% and a CR of 69% after a median follow-up of 17 mo for Tisa-cell r/r FL. The results of the Phase II ELARA trial of Tisa-cell therapy for r/r FL showed an ORR of 86% and CR of 69% at a median follow-up of 17 mo[95-97]. It is important to note that the results of these trials showed that Tisa-cells had a higher sustained response in higher-risk patients with refractory, relapsed, and heavily pretreated FL[98].

Liso-cells are autologous anti-CD19 CAR-T cells. The results of a clinical trial as a second-line therapy for patients with r/r DLBCL not scheduled for hematopoietic stem cell transplantation showed high efficacy, with a median follow-up of 12.3 mo and an ORR of 80%. Grade 3 or higher adverse events ranged from 20%-48% for thrombocytopenia and 21% for serious adverse events[99]. Based on these results, Liso cells have the potential for future use in patients with r/r FL.

The TRANSFORM and PILOT trials demonstrated the high efficacy of Liso-cell in the second-line treatment of r/r large B-cell lymphoma. As a result, Liso-cell was approved as a third-line agent for aggresive B-cell lymphoma[100].

Expectations are high for the future development of CAR-T cell therapy as a fundamental therapeutic tool for FL.

MOLECULAR RESPONSE ADAPTIVE THERAPY RESPONSE-ADOPTED POST-INDUCTION STRATEGY

The FOLL12 study compared a standard 2-year rituximab maintain therapy arm with an experimental post-remission induction arm in patients with FL who responded to induction immunochemotherapy. In the experimental arm, post-induction treatment consisted of observation for patients with complete metabolic response (CMR) and minimal residual disease (MRD)-negative disease, four doses of rituximab for patients with CMR and MRD-positive disease until MRD-negative, and one dose of ibritumomab tixetan for non-CMR patients, followed by three standard treatments with RM. Results showed that After a median follow-up of 53 mo, patients in the standard arm had significantly better PFS than those in the experimental arm (3-year PFS, 86% *vs* 72%; $P < 0.001$). All subgroups except non-CMR patients confirmed the superior PFS of the standard group *vs* the experimental group, with 3-year OS rates of 98% and 97% (95%CI, 95-99) in the reference and experimental groups, respectively[101]. In FL patients who benefited from induction therapy, standard 2-year rituximab maintenance therapy prolonged PFS after the induction of remission.

Future prospects for nodal FL treatment

Although FL progresses slowly and can be effective if treated, it is prone to recurrence and has been considered an incurable disease. Recently, however, research and progress in various new treatment modalities have been remarkable, and improvements in treatment outcomes have been confirmed. In addition, the direction of research is beginning to turn toward how to combine two or more of these anticancer agents, immune agents, immunomodulators, and CAR-T cell therapy, which have different mechanisms of action, and how to arrange the order of treatment in such combinations to obtain the best results. After discussing this important topic, I will conclude this section with the hope that the era of complete cure of FL will arrive in the future.

Prospects for GI-FL treatment

Based on an understanding of the recent advances in the treatment of nodal FL that have been discussed, the current status and future of GI-FL treatment and how gastroenterologists should treat

Table 8 Summary of clinical trials results of chimeric antigen receptor T-cell therapies

Study	Target disease	No. of patients	Objective response rate	Complete response rate	Progression-free survival	Overall survival	Adverse events and others	Ref.
Axicabtagene ciloleucel (Axi-cell), phase-II	r/r DLBCL, t-FL	*n* = 101	82%	40%	Unknown	52% (overall survival rate at 18.8 mo)	Neutropenia 78%; anemia 43%; thrombocytopenia 38%	[90]
Tisagenlecleucel (Tisa-cell), phase-II JULIET trial	r/r DLBCL	*n* = 93	52%	40%	65% (relapse-free survival rate)	Unknown	CRS 22%; neurologic events 12%; infections 20%	[91]
Axicabtagene ciloleucel (Axi-cell), phase-II	r/r iNHL (FL and MZL) after 2 or more treatment	*n* = 148, *n* = 124 (FL), *n* = 24 (MZL)	92%	74%	Unknown	Unknown	Serious adverse events (any grade) occurred in 50% of all	[93]
Tisagenlecleucel (Tisa-cell), phase-II ELARA trial	r/r FL (with 2 and more prior treatments)	*n* = 97	86.2%	69.1%	Unknown	Unknown	CRS 48.5% (> G3) neurological events 37.1% (> G3)	[96]
Lisocabtagene maraleucel (Liso-cell), phase-II	r/r large BCL	*n* = 61	80% (median follow-up 12.3 mo)	Unknown	Unknown	Unknown	Neutropenia 48%, thrombocytopenia 20%, CRS 38%	[99]

"Unknown" means data not shown, unknown information or not reached. r/r: Refractory and relapsed; FL: Follicular lymphoma; t-FL: Transformed follicular lymphoma; (i)NHL: (Indolent) non-Hodgkin lymphoma; DLBCL: Diffuse large B-cell lymphoma; BCL: B-cell lymphoma; MZL: Marginal zone lymphoma; CRS: Cytokine release syndrome.

gastrointestinal FL in the future will be discussed.

FL is the most common low-grade lymphoma, and although nodal FL is highly responsive to treatment, the majority of patients relapse repeatedly, and the disease has been said to be incurable with a poor prognosis. In contrast, primary GI-FL has been detected and treated in a larger number of cases in Japan, especially due to recent advances in small bowel endoscopy and increased opportunities for endoscopic examinations, such as health checkups, diagnostic imaging equipment, endoscopist examination techniques, and endoscopic diagnostic procedures. However, many cases are detected at an early stage, and many of them are at a later stage than those detected at an early stage, owing to the bias of reported cases, and the prognosis is excellent. Therefore, there is still a mainstream view that "watch and wait" is preferable, taking into account the adverse effects of treatment and the decline in patient quality of life. Schmatz *et al*[102] compared the progression of 63 stage I GI-FLs in the treatment, watch, and wait groups and reported no significant difference in PFS or OS. Tari *et al*[103] also reported no difference in prognosis in a study of GI-FL patients with low tumor volume divided between the "watch and wait" groups and the rituximab combination chemotherapy group. GI-FL is considered a potential candidate for "watch and wait" in many cases because of its pathological characteristics: The lesions are widely distributed and not amenable to local therapy, many patients are asymptomatic in the localized stage, and the degree of tumor extension and invasion is lower than that of nodal FL. The number of patients with nodal FL was high, and the degree of tumor progression and invasiveness was low. Yamamoto *et al*[104] have reported that 128 (66.3%) of 193 cases of GI-FL in Japan were stage I and 52 (26.9%) were stage II. The authors attribute this to the higher frequency of grade 1 lymphoma. However, we think that the reported cases may not necessarily represent the overall picture of GI-FL cases in Japan due to a large bias arising when they selected. In a Japanese multicenter study by Takata *et al*[105] in 125 patients with localized GI-FL, CR was observed in 61 (49%) out of 125 patients treated with Watch and Wait (33 patients), combination chemotherapy including rituximab (42 patients), rituximab alone (29 patients), surgical resection (4 patients), radiation therapy (1 patient), and *Helicobacter pylori (H. pylori)* eradication therapy (3 patients). pylori eradication therapy in three cases, 61 cases (49%) achieved CR, and by treatment method, 39/42 cases (93%) were treated with multi-agent chemotherapy including rituximab, 20/29 (69%) with rituximab alone, 1/4 (25%) with surgical resection, 0/1 case (0%) with radiation therapy, *H. pylori* eradication in 1/3 (33%), and Watch and Wait 1/33 (3%). The median follow-up was 40 mo (6-148 mo), with no primary deaths, a 5-year survival rate of 100%, a progression-free survival rate of 93 %, and very good results[105]. It should be noted that the Watch and Wait group had a CR rate of 3%, which was lower than the CR rate in the treatment group, excluding radiotherapy. Damaj *et al*[9] reported that most GI-FL are Stage I, but metastasis or invasion of intra-abdominal lymph nodes (Stage II) is 3.4%-40.0%, and extensive extranodal dissemination or transdiaphragmatic invasion (Stage IV) is reported in 12%-24% of GI-FL cases. The number of reports of advanced GI-FL cases (stages III and IV) is expected to increase further in the future. To understand the recent advances in the treatment of nodal FL, how should gastroenterologists treat gastrointestinal FL in the future? In early stage I cases, endoscopic resection of the gastrointestinal tract or surgical resection plus R-CHOP is the

standard of care. The prognosis was good and the PFS and OS were excellent. The number of refractory and advanced GI-FL cases, grade 3b or higher at the cellular level, and stage II or higher are expected to increase in the future. These cases will likely be treated with the same advanced and recent therapeutic modalities for nodal FL, such as antibody-targeted therapy, bispecific antibody therapy, epigenetic mutation, and CAR T-cell therapy, as described previously. The importance of nodal and Gastrointestinal-FL treatments is expected to increase. The difference is that when GI-FL is treated, the risk of perforation of the gastrointestinal tract must always be considered because if perforation develops due to a decrease in tumor volume, subsequent peritonitis may develop, making the disease more severe, and subsequent treatment impossible to continue. After careful consideration of the risk of gastrointestinal perforation, surgical resection of the gastrointestinal lesion should be performed first, followed by adjuvant therapy. For postoperative recurrence, lymph node metastases outside the gastrointestinal tract, and other distant metastases, it is necessary to collaborate with hematology and gastrointestinal surgery departments to predict possible complications and changes in disease status due to treatment, such as in the treatment of nodal and r/r-FL, and to discuss a royal policy in collaboration with these departments. We look forward to the future development and progress of GI-FL treatment.

Differences in treatment strategies between nodal FL and GI-FL

Staging of nodal FL is determined using the Ann-Arbor clinical staging classification, while GI-FL is classified according to the Lugano staging classification[106], a modified version of the Ann-Arbor staging classification. Basically, the Lugano staging classification[106] should be followed to determine a treatment strategy similar to that for nodal FL. However, due to the characteristics of the gastrointestinal tract, a treatment strategy specific to gastrointestinal FL may be considered in the following cases, which differ from nodal FL.

First, and most importantly, one must be very mindful of gastrointestinal perforation due to the loss of tumor tissue associated with the mass reduction effect of treatment. Careful consideration should be given to the risk of gastrointestinal tract perforation before initiating any type of treatment.

In GI-FL cases, whether the distribution of lesions is unifocal or multifocal is important in the choice of treatment; Yamamoto *et al*[104] reported that in more than 70% of GI-FL patients with lesions in the gastrointestinal tract other than the small bowel, new secondary lesions were found in the small bowel. If the disease is found to be multifocal, immunochemotherapy may be the treatment of choice.

Primary FL in the gastrointestinal tract should be treated with surgical resection first, followed by postoperative chemotherapy (or combination chemotherapy and immunotherapy), depending on the extent of extension and invasion, if the lesions arise from deep submucosal layers and are localized within the wall, lumen, or regional lymph nodes. However, if the disease has invaded or spread beyond the gastrointestinal tract or has distant metastasis beyond the diaphragm, it is stage-4 according to the Lugano classification, and if there is no or little deterioration in quality of life due to gastrointestinal obstruction, local surgical resection is of course not indicated, and combination chemotherapy plus immunotherapy or immunomodulators is the chemotherapy plus immunotherapy or immunomodulators is the first choice.

In cases of extra-gastrointestinal primary disease with gastrointestinal involvement, surgical resection or radiotherapy should be considered if the disease is localized. If there are metastases in multiple organs or bone marrow, the disease is basically stage-4, and chemotherapy (plus immunotherapy) is the first choice.

In addition, other factors such as age, gender, site of disease, and extent of spread should determine the best overall treatment for each case of gastrointestinal FL that is most appropriate for the patient and that offers a better prognosis, especially longer treatment-free period and improved patient quality of life. Because gastrointestinal FL is an organ with "gastrointestinal" characteristics, the treatment strategy is often more controversial than that for nodal FL, and in a sense, the range of treatment options is wider.

In addition, the underlying nature of FL itself, which as a tumor is indolent in its extension, growth, and invasion, responds well to chemotherapy, but is prone to relapse and is currently incurable, further complicates and complicates the treatment options for gastrointestinal FL. The differences in treatment strategy between nodal FL and gastrointestinal FL are described in the author's previous review[107], which should also be consulted.

In the future, the number of advanced-stage, multifocal GI-FL cases will increase more and more, and the treatment strategy should be carefully determined by cooperating multiple physicians in each department, including gastroenterology, surgery, hematology, and radiology.

CONCLUSION

Treatment with Nodal-FL improved the ORR, CRR, PFS, and OS with the addition of rituximab, an anti-CD20 monoclonal antibody, to CHOP therapy, which was the standard chemotherapy regimen for malignant lymphomas 20 years ago. Maintenance therapy with an anti-CD20 antibody prolongs

remission. The last decade has seen remarkable progress with the addition of new therapeutic modalities such as antibody-targeted therapy, bispecific antibody therapy, epigenetic modulator therapy, CAR-T cell therapy, and conventional chemotherapy. The combination of lenaridomide and anti-CD20 antibodies was effective in r/r FL treatment. In contrast, lenaridomide shows good results as frontline therapy for untreated patients with advanced FL and may become a mainstay treatment modality. Antibody therapies against novel targets, such as CD19, CD79b, and CD47, as well as obinutumab, a humanized anti-CD20 monoclonal antibody, have been developed and have demonstrated efficacy in FL. More recently, anti-PD-L1 antibodies such as atezolitumab and pembrolizumab have also demonstrated efficacy in relapsed FL. PI3Kinase inhibitors are effective for treating FL and multiple relapsed lesions. However, the high number of adverse events associated with its toxicity complicates its future use as a combination therapy. As an epigenetic modulator treatment, tazemetostat showed more activity in r/r FL patients with higher risk characteristics. Vorinostat, a histone deacetylase inhibitor HDACi, is also a potential treatment for r/r FL patients. CAR-T cell therapy for FL and T-cell immune attack with bispecific antibodies have shown remarkable efficacy and are expected to become a fundamental therapy, as evidenced by the current approval of CAR-T cell therapy for relapsed and refractory FL in the United States. In Europe and the United States, Damaj *et al*[9] have reported that most GI-FL cases are stage I, but metastasis or invasion of intra-abdominal lymph nodes (stage-II) is present in 3.4%-40.0% and extensive extranodal organ dissemination or involvement beyond the diaphragm (stage-IV) in 12%-24%. The number of advanced GI-FL cases (stages III and IV) is expected to increase further in the future. The number of refractory and advanced GI-FL cases, grade 3b or higher at the cellular level, and stage II or higher are expected to increase in the future. For these cases, recent advances in nodal FL, such as antibody-targeted therapy, bispecific antibody therapy, epigenetic mutation, and CAR-T cell therapy, as described above, should be considered as treatment options, but with careful attention to gastrointestinal perforation and cooperation among the departments of gastroenterology, hematology, and gastroenterological surgery need to work together.

FOOTNOTES

Author contributions: Takuya Watanabe solely contributes to this manuscript.

Conflict-of-interest statement: The authors declare that they have no conflict of interest.

Open-Access: This article is an open-access article that was selected by an in-house editor and fully peer-reviewed by external reviewers. It is distributed in accordance with the Creative Commons Attribution NonCommercial (CC BY-NC 4.0) license, which permits others to distribute, remix, adapt, build upon this work non-commercially, and license their derivative works on different terms, provided the original work is properly cited and the use is non-commercial. See: https://creativecommons.org/Licenses/by-nc/4.0/

Country/Territory of origin: Japan

ORCID number: Takuya Watanabe 0000-0003-3820-0262.

S-Editor: Chen YL
L-Editor: A
P-Editor: Cai YX

REFERENCES

1 The world health organization classification of malignant lymphomas in japan: incidence of recently recognized entities. Lymphoma Study Group of Japanese Pathologists. *Pathol Int* 2000; **50**: 696-702 [PMID: 11012982 DOI: 10.1046/j.1440-1827.2000.01108.x]

2 **Jaffe ES**, Harris NL, Stein H, Vardiman J. World Health Organization Classification of Tumors: Tumors of the Hematopoietic and Lymphoid Tissues. 2001. [cited 20 April 2023]. Avaliable from: https://tumourclassification.iarc.who.int/welcome/

3 **Chihara D**, Ito H, Matsuda T, Shibata A, Katsumi A, Nakamura S, Tomotaka S, Morton LM, Weisenburger DD, Matsuo K. Differences in incidence and trends of haematological malignancies in Japan and the United States. *Br J Haematol* 2014; **164**: 536-545 [PMID: 24245986 DOI: 10.1111/bjh.12659]

4 **d'Amore F**, Christensen BE, Brincker H, Pedersen NT, Thorling K, Hastrup J, Pedersen M, Jensen MK, Johansen P, Andersen E. Clinicopathological features and prognostic factors in extranodal non-Hodgkin lymphomas. Danish LYFO Study Group. *Eur J Cancer* 1991; **27**: 1201-1208 [PMID: 1835586 DOI: 10.1016/0277-5379(91)90081-n]

5 **Cirillo M**, Federico M, Curci G, Tamborrino E, Piccinini L, Silingardi V. Primary gastrointestinal lymphoma: a clinicopathological study of 58 cases. *Haematologica* 1992; **77**: 156-161 [PMID: 1398301]

6 **Yoshino T**, Miyake K, Ichimura K, Mannami T, Ohara N, Hamazaki S, Akagi T. Increased incidence of follicular lymphoma in the duodenum. *Am J Surg Pathol* 2000; **24**: 688-693 [PMID: 10800987 DOI:

10.1097/00000478-200005000-00007]
7 **Lewin KJ**, Ranchod M, Dorfman RF. Lymphomas of the gastrointestinal tract: a study of 117 cases presenting with gastrointestinal disease. *Cancer* 1978; **42**: 693-707 [PMID: 354774 DOI: 10.1002/1097-0142(197808)42:2<693::aid-cncr2820420241>3.0.co;2-j]
8 **Filippa DA**, Lieberman PH, Weingrad DN, Decosse JJ, Bretsky SS. Primary lymphomas of the gastrointestinal tract. Analysis of prognostic factors with emphasis on histological type. *Am J Surg Pathol* 1983; **7**: 363-372 [PMID: 6869665 DOI: 10.1097/00000478-198306000-00008]
9 **Damaj G**, Verkarre V, Delmer A, Solal-Celigny P, Yakoub-Agha I, Cellier C, Maurschhauser F, Bouabdallah R, Leblond V, Lefrère F, Bouscary D, Audouin J, Coiffier B, Varet B, Molina T, Brousse N, Hermine O. Primary follicular lymphoma of the gastrointestinal tract: a study of 25 cases and a literature review. *Ann Oncol* 2003; **14**: 623-629 [PMID: 12649111 DOI: 10.1093/annonc/mdg168]
10 **Hiddemann W**, Buske C, Dreyling M, Weigert O, Lenz G, Forstpointner R, Nickenig C, Unterhalt M. Treatment strategies in follicular lymphomas: current status and future perspectives. *J Clin Oncol* 2005; **23**: 6394-6399 [PMID: 16155025 DOI: 10.1200/JCO.2005.07.019]
11 **Conconi A**, Lobetti-Bodoni C, Montoto S, Lopez-Guillermo A, Coutinho R, Matthews J, Franceschetti S, Bertoni F, Moccia A, Rancoita PM, Gribben J, Cavalli F, Gaidano G, Lister TA, Montserrat E, Ghielmini M, Zucca E. Life expectancy of young adults with follicular lymphoma. *Ann Oncol* 2015; **26**: 2317-2322 [PMID: 26362567 DOI: 10.1093/annonc/mdv376]
12 **Ghielmini M**, Schmitz SF, Cogliatti SB, Pichert G, Hummerjohann J, Waltzer U, Fey MF, Betticher DC, Martinelli G, Peccatori F, Hess U, Zucca E, Stupp R, Kovacsovics T, Helg C, Lohri A, Bargetzi M, Vorobiof D, Cerny T. Prolonged treatment with rituximab in patients with follicular lymphoma significantly increases event-free survival and response duration compared with the standard weekly x 4 schedule. *Blood* 2004; **103**: 4416-4423 [PMID: 14976046 DOI: 10.1182/blood-2003-10-3411]
13 **Hiddemann W**, Kneba M, Dreyling M, Schmitz N, Lengfelder E, Schmits R, Reiser M, Metzner B, Harder H, Hegewisch-Becker S, Fischer T, Kropff M, Reis HE, Freund M, Wörmann B, Fuchs R, Planker M, Schimke J, Eimermacher H, Trümper L, Aldaoud A, Parwaresch R, Unterhalt M. Frontline therapy with rituximab added to the combination of cyclophosphamide, doxorubicin, vincristine, and prednisone (CHOP) significantly improves the outcome for patients with advanced-stage follicular lymphoma compared with therapy with CHOP alone: results of a prospective randomized study of the German Low-Grade Lymphoma Study Group. *Blood* 2005; **106**: 3725-3732 [PMID: 16123223 DOI: 10.1182/blood-2005-01-0016]
14 **Duell J**, Maddocks KJ, González-Barca E, Jurczak W, Liberati AM, De Vos S, Nagy Z, Obr A, Gaidano G, Abrisqueta P, Kalakonda N, André M, Dreyling M, Menne T, Tournilhac O, Augustin M, Rosenwald A, Dirnberger-Hertweck M, Weirather J, Ambarkhane S, Salles G. Long-term outcomes from the Phase II L-MIND study of tafasitamab (MOR208) plus lenalidomide in patients with relapsed or refractory diffuse large B-cell lymphoma. *Haematologica* 2021; **106**: 2417-2426 [PMID: 34196165 DOI: 10.3324/haematol.2020.275958]
15 **Morschhauser F**, Flinn IW, Advani R, Sehn LH, Diefenbach C, Kolibaba K, Press OW, Salles G, Tilly H, Chen AI, Assouline S, Cheson BD, Dreyling M, Hagenbeek A, Zinzani PL, Jones S, Cheng J, Lu D, Penuel E, Hirata J, Wenger M, Chu YW, Sharman J. Polatuzumab vedotin or pinatuzumab vedotin plus rituximab in patients with relapsed or refractory non-Hodgkin lymphoma: final results from a phase 2 randomised study (ROMULUS). *Lancet Haematol* 2019; **6**: e254-e265 [PMID: 30935953 DOI: 10.1016/S2352-3026(19)30026-2]
16 **Hamadani M**, Radford J, Carlo-Stella C, Caimi PF, Reid E, O'Connor OA, Feingold JM, Ardeshna KM, Townsend W, Solh M, Heffner LT, Ungar D, Wang L, Boni J, Havenith K, Qin Y, Kahl BS. Final results of a phase 1 study of loncastuximab tesirine in relapsed/refractory B-cell non-Hodgkin lymphoma. *Blood* 2021; **137**: 2634-2645 [PMID: 33211842 DOI: 10.1182/blood.2020007512]
17 **Advani R**, Flinn I, Popplewell L, Forero A, Bartlett NL, Ghosh N, Kline J, Roschewski M, LaCasce A, Collins GP, Tran T, Lynn J, Chen JY, Volkmer JP, Agoram B, Huang J, Majeti R, Weissman IL, Takimoto CH, Chao MP, Smith SM. CD47 Blockade by Hu5F9-G4 and Rituximab in Non-Hodgkin's Lymphoma. *N Engl J Med* 2018; **379**: 1711-1721 [PMID: 30380386 DOI: 10.1056/NEJMoa1807315]
18 **Davies A**, Kater AP, Sharman JP, Stilgenbauer S, Vitolo U, Klein C, Parreira J, Salles G. Obinutuzumab in the treatment of B-cell malignancies: a comprehensive review. *Future Oncol* 2022; **18**: 2943-2966 [PMID: 35856239 DOI: 10.2217/fon-2022-0112]
19 **Stathis A**, Mey U, Schär S, Hitz F, Pott C, Mach N, Krasniqi F, Novak U, Schmidt C, Hohloch K, Kienle DL, Hess D, Moccia AA, Unterhalt M, Eckhardt K, Hayoz S, Forestieri G, Rossi D, Dirnhofer S, Ceriani L, Sartori G, Bertoni F, Buske C, Zucca E, Hiddemann W. SAKK 35/15: a phase 1 trial of obinutuzumab in combination with venetoclax in patients with previously untreated follicular lymphoma. *Blood Adv* 2022; **6**: 3911-3920 [PMID: 35537101 DOI: 10.1182/bloodadvances.2021006520]
20 **Marcus R**, Davies A, Ando K, Klapper W, Opat S, Owen C, Phillips E, Sangha R, Schlag R, Seymour JF, Townsend W, Trněný M, Wenger M, Fingerle-Rowson G, Rufibach K, Moore T, Herold M, Hiddemann W. Obinutuzumab for the First-Line Treatment of Follicular Lymphoma. *N Engl J Med* 2017; **377**: 1331-1344 [PMID: 28976863 DOI: 10.1056/NEJMoa1614598]
21 **Casulo C**, Herold M, Hiddemann W, Iyengar S, Marcus RE, Seymour JF, Launonen A, Knapp A, Nielsen TG, Mir F. Risk Factors for and Outcomes of Follicular Lymphoma Histological Transformation at First Progression in the GALLIUM Study. *Clin Lymphoma Myeloma Leuk* 2023; **23**: 40-48 [PMID: 36379880 DOI: 10.1016/j.clml.2022.09.003]
22 **Gmoshinskiĭ IV**, Mazo VK, Shaternikov VA. [Breakdown of the soluble soybean antigen in the digestive tract of adult rats]. *Vopr Pitan* 1986; 43-46 [PMID: 3532538]
23 **Yang L**, Zheng Z, Li N, Zheng B, Liu M, Cai H. Efficacy and safety of rituximab biosimilars or reference product as first-line treatment in patients with low-tumour-burden follicular lymphoma: A systematic review and meta-analysis. *J Clin Pharm Ther* 2022; **47**: 1923-1931 [PMID: 36345167 DOI: 10.1111/jcpt.13799]
24 **Budde LE**, Assouline S, Sehn LH, Schuster SJ, Yoon SS, Yoon DH, Matasar MJ, Bosch F, Kim WS, Nastoupil LJ, Flinn

IW, Shadman M, Diefenbach C, O'Hear C, Huang H, Kwan A, Li CC, Piccione EC, Wei MC, Yin S, Bartlett NL. Single-Agent Mosunetuzumab Shows Durable Complete Responses in Patients With Relapsed or Refractory B-Cell Lymphomas: Phase I Dose-Escalation Study. *J Clin Oncol* 2022; **40**: 481-491 [PMID: 34914545 DOI: 10.1200/JCO.21.00931]

25 **Budde LE**, Sehn LH, Matasar M, Schuster SJ, Assouline S, Giri P, Kuruvilla J, Canales M, Dietrich S, Fay K, Ku M, Nastoupil L, Cheah CY, Wei MC, Yin S, Li CC, Huang H, Kwan A, Penuel E, Bartlett NL. Safety and efficacy of mosunetuzumab, a bispecific antibody, in patients with relapsed or refractory follicular lymphoma: a single-arm, multicentre, phase 2 study. *Lancet Oncol* 2022; **23**: 1055-1065 [PMID: 35803286 DOI: 10.1016/S1470-2045(22)00335-7]

26 **Hutchings M**, Morschhauser F, Iacoboni G, Carlo-Stella C, Offner FC, Sureda A, Salles G, Martínez-Lopez J, Crump M, Thomas DN, Morcos PN, Ferlini C, Bröske AE, Belousov A, Bacac M, Dimier N, Carlile DJ, Lundberg L, Perez-Callejo D, Umaña P, Moore T, Weisser M, Dickinson MJ. Glofitamab, a Novel, Bivalent CD20-Targeting T-Cell-Engaging Bispecific Antibody, Induces Durable Complete Remissions in Relapsed or Refractory B-Cell Lymphoma: A Phase I Trial. *J Clin Oncol* 2021; **39**: 1959-1970 [PMID: 33739857 DOI: 10.1200/JCO.20.03175]

27 **Hutchings M**, Mous R, Clausen MR, Johnson P, Linton KM, Chamuleau MED, Lewis DJ, Sureda Balari A, Cunningham D, Oliveri RS, Elliott B, DeMarco D, Azaryan A, Chiu C, Li T, Chen KM, Ahmadi T, Lugtenburg PJ. Dose escalation of subcutaneous epcoritamab in patients with relapsed or refractory B-cell non-Hodgkin lymphoma: an open-label, phase 1/2 study. *Lancet* 2021; **398**: 1157-1169 [PMID: 34508654 DOI: 10.1016/S0140-6736(21)00889-8]

28 **Falchi L**, Lepp¨ AS, Wahlin BE, Nijland M, Christensen JH, De Vos S, Holte H, Linton KM, Abbas A, Wang LW, Dinh M, Elliott B, Belada D. Subcutaneous epcoritamab with rituximab + lenalidomide (R2) in patients (pts) with relapsed or refractory (R/R) follicular lymphoma (FL): Update from a phase 1/2 trial. *J Clin Oncol* 2022; **40** Suppl 16: 7524 [DOI: 10.1200/jco.2022.40.16_suppl.7524]

29 **Bannerji R**, Arnason JE, Advani RH, Brown JR, Allan JN, Ansell SM, Barnes JA, O'Brien SM, Chávez JC, Duell J, Rosenwald A, Crombie JL, Ufkin M, Li J, Zhu M, Ambati SR, Chaudhry A, Lowy I, Topp MS. Odronextamab, a human CD20×CD3 bispecific antibody in patients with CD20-positive B-cell malignancies (ELM-1): results from the relapsed or refractory non-Hodgkin lymphoma cohort in a single-arm, multicentre, phase 1 trial. *Lancet Haematol* 2022; **9**: e327-e339 [PMID: 35366963 DOI: 10.1016/S2352-3026(22)00072-2]

30 **Dickinson M**. Challenges in the development of bispecific antibodies for non-Hodgkin lymphoma. *Lancet Haematol* 2022; **9**: e314-e315 [PMID: 35366964 DOI: 10.1016/S2352-3026(22)00104-1]

31 **Palomba ML**, Till BG, Park SI, Morschhauser F, Cartron G, Marks R, Shivhare M, Hong WJ, Raval A, Chang AC, Penuel E, Popplewell LL. Combination of Atezolizumab and Obinutuzumab in Patients with Relapsed/Refractory Follicular Lymphoma and Diffuse Large B-Cell Lymphoma: Results from a Phase 1b Study. *Clin Lymphoma Myeloma Leuk* 2022; **22**: e443-e451 [PMID: 35031227 DOI: 10.1016/j.clml.2021.12.010]

32 **Nastoupil LJ**, Chin CK, Westin JR, Fowler NH, Samaniego F, Cheng X, Ma MCJ, Wang Z, Chu F, Dsouza L, Obi C, Mims J, Feng L, Zhou S, Green M, Davis RE, Neelapu SS. Safety and activity of pembrolizumab in combination with rituximab in relapsed or refractory follicular lymphoma. *Blood Adv* 2022; **6**: 1143-1151 [PMID: 35015819 DOI: 10.1182/bloodadvances.2021006240]

33 **Gandhi AK**, Kang J, Havens CG, Conklin T, Ning Y, Wu L, Ito T, Ando H, Waldman MF, Thakurta A, Klippel A, Handa H, Daniel TO, Schafer PH, Chopra R. Immunomodulatory agents lenalidomide and pomalidomide co-stimulate T cells by inducing degradation of T cell repressors Ikaros and Aiolos *via* modulation of the E3 ubiquitin ligase complex CRL4(CRBN.). *Br J Haematol* 2014; **164**: 811-821 [PMID: 24328678 DOI: 10.1111/bjh.12708]

34 **Leonard JP**, Jung SH, Johnson J, Pitcher BN, Bartlett NL, Blum KA, Czuczman M, Giguere JK, Cheson BD. Randomized Trial of Lenalidomide Alone Versus Lenalidomide Plus Rituximab in Patients With Recurrent Follicular Lymphoma: CALGB 50401 (Alliance). *J Clin Oncol* 2015; **33**: 3635-3640 [PMID: 26304886 DOI: 10.1200/JCO.2014.59.9258]

35 **Leonard JP**, Trneny M, Izutsu K, Fowler NH, Hong X, Zhu J, Zhang H, Offner F, Scheliga A, Nowakowski GS, Pinto A, Re F, Fogliatto LM, Scheinberg P, Flinn IW, Moreira C, Cabeçadas J, Liu D, Kalambakas S, Fustier P, Wu C, Gribben JG; AUGMENT Trial Investigators. AUGMENT: A Phase III Study of Lenalidomide Plus Rituximab Versus Placebo Plus Rituximab in Relapsed or Refractory Indolent Lymphoma. *J Clin Oncol* 2019; **37**: 1188-1199 [PMID: 30897038 DOI: 10.1200/JCO.19.00010]

36 **Coleman M**, Andorsky DJ, Yacoub A, Melear JM, Fanning SR, Kolibaba KS, Jason M, Lansigan F, Reynolds CM, Nowakowski GS, Gharibo M, Ahn E, Li J, Rummel MJ, Sharman JP. Patients with relapsed/refractory marginal zone lymphoma in the MAGNIFY phase IIIb interim analysis of induction R2 followed by maintenance. *Blood* 2020; **136** Suppl 1: 24-25 [DOI: 10.1016/j.htct.2021.10.167]

37 **Morschhauser F**, Le Gouill S, Feugier P, Bailly S, Nicolas-Virelizier E, Bijou F, Salles GA, Tilly H, Fruchart C, Van Eygen K, Snauwaert S, Bonnet C, Haioun C, Thieblemont C, Bouabdallah R, Wu KL, Canioni D, Meignin V, Cartron G, Houot R. Obinutuzumab combined with lenalidomide for relapsed or refractory follicular B-cell lymphoma (GALEN): a multicentre, single-arm, phase 2 study. *Lancet Haematol* 2019; **6**: e429-e437 [PMID: 31296423 DOI: 10.1016/S2352-3026(19)30089-4]

38 **Morschhauser F**, Fowler NH, Feugier P, Bouabdallah R, Tilly H, Palomba ML, Fruchart C, Libby EN, Casasnovas RO, Flinn IW, Haioun C, Maisonneuve H, Ysebaert L, Bartlett NL, Bouabdallah K, Brice P, Ribrag V, Daguindau N, Le Gouill S, Pica GM, Martin Garcia-Sancho A, López-Guillermo A, Larouche JF, Ando K, Gomes da Silva M, André M, Zachée P, Sehn LH, Tobinai K, Cartron G, Liu D, Wang J, Xerri L, Salles GA; RELEVANCE Trial Investigators. Rituximab plus Lenalidomide in Advanced Untreated Follicular Lymphoma. *N Engl J Med* 2018; **379**: 934-947 [PMID: 30184451 DOI: 10.1056/NEJMoa1805104]

39 **Evens AM**, Hong F, Habermann TM, Advani RH, Gascoyne RD, Witzig TE, Quon A, Ranheim EA, Ansell SM, Cheema PS, Dy PA, O'Brien TE, Winter JN, Cescon TP, Chang JE, Kahl BS. A Three-Arm Randomized Phase II Study of Bendamustine/Rituximab with Bortezomib Induction or Lenalidomide Continuation in Untreated Follicular Lymphoma: ECOG-ACRIN E2408. *Clin Cancer Res* 2020; **26**: 4468-4477 [PMID: 32532790 DOI: 10.1158/1078-0432.CCR-20-1345]

40 **Nastoupil LJ**, Westin JR, Hagemeister FB, Lee HJ, Fayad L, Samaniego F, Ahmed S, Claret L, Steiner RE, Nair R, Parmar S, Rodriguez MA, Wang ML, Green MR, Neelapu SS, Fowler NH. Results of a Phase II study of obinutuzumab in

combination with lenalidomide in previously untreated, high tumor burden follicular lymphoma (FL). *Blood* 2019; **134** Suppl 1: 125 [DOI: 10.1182/blood-2019-129422]

41 **Wang Y**, Zhou S, Qi X, Yang F, Maurer MJ, Habermann TM, Witzig TE, Wang ML, Nowakowski GS. Efficacy of front-line immunochemotherapy for follicular lymphoma: a network meta-analysis of randomized controlled trials. *Blood Cancer J* 2022; **12**: 1 [PMID: 34987165 DOI: 10.1038/s41408-021-00598-x]

42 **Phillips T**, Chan H, Tam CS, Tedeschi A, Johnston P, Oh SY, Opat S, Eom HS, Allewelt H, Stern JC, Tan Z, Novotny W, Huang J, Trotman J. Zanubrutinib monotherapy in relapsed/refractory indolent non-Hodgkin lymphoma. *Blood Adv* 2022; **6**: 3472-3479 [PMID: 35390135 DOI: 10.1182/bloodadvances.2021006083]

43 **Song Y**, Zhou K, Zou D, Zhou J, Hu J, Yang H, Zhang H, Ji J, Xu W, Jin J, Lv F, Feng R, Gao S, Guo H, Zhou L, Huang J, Novotny W, Kim P, Yu Y, Wu B, Zhu J. Zanubrutinib in relapsed/refractory mantle cell lymphoma: long-term efficacy and safety results from a phase 2 study. *Blood* 2022; **139**: 3148-3158 [PMID: 35303070 DOI: 10.1182/blood.2021014162]

44 **Byrd JC**, Brown JR, O'Brien S, Barrientos JC, Kay NE, Reddy NM, Coutre S, Tam CS, Mulligan SP, Jaeger U, Devereux S, Barr PM, Furman RR, Kipps TJ, Cymbalista F, Pocock C, Thornton P, Caligaris-Cappio F, Robak T, Delgado J, Schuster SJ, Montillo M, Schuh A, de Vos S, Gill D, Bloor A, Dearden C, Moreno C, Jones JJ, Chu AD, Fardis M, McGreivy J, Clow F, James DF, Hillmen P; RESONATE Investigators. Ibrutinib versus ofatumumab in previously treated chronic lymphoid leukemia. *N Engl J Med* 2014; **371**: 213-223 [PMID: 24881631 DOI: 10.1056/NEJMoa1400376]

45 **Sharman JP**, Egyed M, Jurczak W, Skarbnik A, Pagel JM, Flinn IW, Kamdar M, Munir T, Walewska R, Corbett G, Fogliatto LM, Herishanu Y, Banerji V, Coutre S, Follows G, Walker P, Karlsson K, Ghia P, Janssens A, Cymbalista F, Woyach JA, Salles G, Wierda WG, Izumi R, Munugalavadla V, Patel P, Wang MH, Wong S, Byrd JC. Acalabrutinib with or without obinutuzumab versus chlorambucil and obinutuzmab for treatment-naive chronic lymphocytic leukaemia (ELEVATE TN): a randomised, controlled, phase 3 trial. *Lancet* 2020; **395**: 1278-1291 [PMID: 32305093 DOI: 10.1016/S0140-6736(20)30262-2]

46 **Mato AR**, Shah NN, Jurczak W, Cheah CY, Pagel JM, Woyach JA, Fakhri B, Eyre TA, Lamanna N, Patel MR, Alencar A, Lech-Maranda E, Wierda WG, Coombs CC, Gerson JN, Ghia P, Le Gouill S, Lewis DJ, Sundaram S, Cohen JB, Flinn IW, Tam CS, Barve MA, Kuss B, Taylor J, Abdel-Wahab O, Schuster SJ, Palomba ML, Lewis KL, Roeker LE, Davids MS, Tan XN, Fenske TS, Wallin J, Tsai DE, Ku NC, Zhu E, Chen J, Yin M, Nair B, Ebata K, Marella N, Brown JR, Wang M. Pirtobrutinib in relapsed or refractory B-cell malignancies (BRUIN): a phase 1/2 study. *Lancet* 2021; **397**: 892-901 [PMID: 33676628 DOI: 10.1016/S0140-6736(21)00224-5]

47 **Gopal AK**, Schuster SJ, Fowler NH, Trotman J, Hess G, Hou JZ, Yacoub A, Lill M, Martin P, Vitolo U, Spencer A, Radford J, Jurczak W, Morton J, Caballero D, Deshpande S, Gartenberg GJ, Wang SS, Damle RN, Schaffer M, Balasubramanian S, Vermeulen J, Cheson BD, Salles G. Ibrutinib as Treatment for Patients With Relapsed/Refractory Follicular Lymphoma: Results From the Open-Label, Multicenter, Phase II DAWN Study. *J Clin Oncol* 2018; **36**: 2405-2412 [PMID: 29851546 DOI: 10.1200/JCO.2017.76.8853]

48 **Fowler NH**, Nastoupil L, De Vos S, Knapp M, Flinn IW, Chen R, Advani RH, Bhatia S, Martin P, Mena R, Davis RE, Neelapu SS, Eckert K, Ping J, Co M, Beaupre DM, Neuenburg JK, Palomba ML. The combination of ibrutinib and rituximab demonstrates activity in first-line follicular lymphoma. *Br J Haematol* 2020; **189**: 650-660 [PMID: 32180219 DOI: 10.1111/bjh.16424]

49 **Fowler NH**, Coleman M, Stevens DA, Smith SM, Venugopal P, Martin P, Phillips TJ, Agajanian R, Stephens DM, Izumi R, Cheung J, Slatter JG, Yin M, Hiremath M, Hunder NNH. Acalabrutinib alone or in combination with rituximab (R) in follicular lymphoma (FL). *J Clin Oncol* 2018; **36** Suppl 15: 7549

50 **Zinzani PL**, Mayer J, Auer R, Bijou F, de Oliverira AC, Flowers C, Merli M, Bouabdallah K, Ganly PS, Johnson R, Yuen S, Kingsley E, Tumyan G, Assouline SE, Ivanova E, Kim P, Huang J, Delarue R, Trotman J. Zanubrutinib plus Obinutuzumab (ZO) vs Obinutuzumab (O) monotherapy in patients (pts) with relapsed or refractory (R/R) follicular ltmphoma (FL): Primary analysis of the phase 2 randomized ROSEWOOD trial. *J Clin Oncol* 2022; **40** Suppl 16: 7510 [DOI: 10.1200/jco.2022.40.16_suppl.7510]

51 **Parikh A**, Gopalakrishnan S, Freise KJ, Verdugo ME, Menon RM, Mensing S, Salem AH. Exposure-response evaluations of venetoclax efficacy and safety in patients with non-Hodgkin lymphoma. *Leuk Lymphoma* 2018; **59**: 871-879 [PMID: 28797193 DOI: 10.1080/10428194.2017.1361024]

52 **Zinzani PL**, Flinn IW, Yuen SLS, Topp MS, Rusconi C, Fleury I, Le Dû K, Arthur C, Pro B, Gritti G, Crump M, Petrich A, Samineni D, Sinha A, Punnoose EA, Szafer-Glusman E, Spielewoy N, Mobasher M, Humphrey K, Kornacker M, Hiddemann W. Venetoclax-rituximab with or without bendamustine vs bendamustine-rituximab in relapsed/refractory follicular lymphoma. *Blood* 2020; **136**: 2628-2637 [PMID: 32785666 DOI: 10.1182/blood.2020005588]

53 **Ujjani CS**, Lai C, Leslie LA, Ramzi P, Tan M, Wang S, Wang HK, Shim E, Swanson N, Broome CM, Gopal AK, Smith SD, Warren EH, Blue K, Kdiry S, Till BG, Lynch RC, Shadman M, Johnson M, Coye H, Shelby M, Tseng YD, Shustov A, Maloney DG, Cheson BD. Ibrutinib and venetoclax in relapsed and refractory follicular lymphoma. *Blood* 2020; **136** Suppl 1: 46-47 [DOI: 10.1182/blood-2020-136219]

54 **Morschhauser F**, Tilly H, Chaidos A, McKay P, Phillips T, Assouline S, Batlevi CL, Campbell P, Ribrag V, Damaj GL, Dickinson M, Jurczak W, Kazmierczak M, Opat S, Radford J, Schmitt A, Yang J, Whalen J, Agarwal S, Adib D, Salles G. Tazemetostat for patients with relapsed or refractory follicular lymphoma: an open-label, single-arm, multicentre, phase 2 trial. *Lancet Oncol* 2020; **21**: 1433-1442 [PMID: 33035457 DOI: 10.1016/S1470-2045(20)30441-1]

55 **Chung C**. A Promising Future for Precision Epigenetic Therapy for Follicular and Diffuse Large B-Cell Lymphoma? *Blood Lymphat Cancer* 2022; **12**: 99-106 [PMID: 35959380 DOI: 10.2147/BLCTT.S282247]

56 **Barghout SH**, Machado RAC, Barsyte-Lovejoy D. Chemical biology and pharmacology of histone lysine methylation inhibitors. *Biochim Biophys Acta Gene Regul Mech* 2022; **1865**: 194840 [PMID: 35753676 DOI: 10.1016/j.bbagrm.2022.194840]

57 **Proudman D**, Nellesen D, Gupta D, Adib D, Yang J, Mamlouk K. A Matching-Adjusted Indirect Comparison of Single-Arm Trials in Patients with Relapsed or Refractory Follicular Lymphoma Who Received at Least Two Prior Systemic Treatments: Tazemetostat was Associated with a Lower Risk for Safety Outcomes Versus the PI3-Kinase Inhibitors Idelalisib, Duvelisib, Copanlisib, and Umbralisib. *Adv Ther* 2022; **39**: 1678-1696 [PMID: 35157216 DOI:

10.1007/s12325-022-02054-z]
58 **Ogura M**, Ando K, Suzuki T, Ishizawa K, Oh SY, Itoh K, Yamamoto K, Au WY, Tien HF, Matsuno Y, Terauchi T, Mori M, Tanaka Y, Shimamoto T, Tobinai K, Kim WS. A multicentre phase II study of vorinostat in patients with relapsed or refractory indolent B-cell non-Hodgkin lymphoma and mantle cell lymphoma. *Br J Haematol* 2014; **165**: 768-776 [PMID: 24617454 DOI: 10.1111/bjh.12819]
59 **Chen R**, Frankel P, Popplewell L, Siddiqi T, Ruel N, Rotter A, Thomas SH, Mott M, Nathwani N, Htut M, Nademanee A, Forman SJ, Kirschbaum M. A phase II study of vorinostat and rituximab for treatment of newly diagnosed and relapsed/refractory indolent non-Hodgkin lymphoma. *Haematologica* 2015; **100**: 357-362 [PMID: 25596263 DOI: 10.3324/haematol.2014.117473]
60 **Batlevi CL**, Crump M, Andreadis C, Rizzieri D, Assouline SE, Fox S, van der Jagt RHC, Copeland A, Potvin D, Chao R, Younes A. A phase 2 study of mocetinostat, a histone deacetylase inhibitor, in relapsed or refractory lymphoma. *Br J Haematol* 2017; **178**: 434-441 [PMID: 28440559 DOI: 10.1111/bjh.14698]
61 **Vanhaesebroeck B**, Leevers SJ, Ahmadi K, Timms J, Katso R, Driscoll PC, Woscholski R, Parker PJ, Waterfield MD. Synthesis and function of 3-phosphorylated inositol lipids. *Annu Rev Biochem* 2001; **70**: 535-602 [PMID: 11395417 DOI: 10.1146/annurev.biochem.70.1.535]
62 **Bi L**, Okabe I, Bernard DJ, Nussbaum RL. Early embryonic lethality in mice deficient in the p110beta catalytic subunit of PI 3-kinase. *Mamm Genome* 2002; **13**: 169-172 [PMID: 11919689 DOI: 10.1007/BF02684023]
63 **Sasaki T**, Irie-Sasaki J, Jones RG, Oliveira-dos-Santos AJ, Stanford WL, Bolon B, Wakeham A, Itie A, Bouchard D, Kozieradzki I, Joza N, Mak TW, Ohashi PS, Suzuki A, Penninger JM. Function of PI3Kgamma in thymocyte development, T cell activation, and neutrophil migration. *Science* 2000; **287**: 1040-1046 [PMID: 10669416 DOI: 10.1126/science.287.5455.1040]
64 **Laffargue M**, Calvez R, Finan P, Trifilieff A, Barbier M, Altruda F, Hirsch E, Wymann MP. Phosphoinositide 3-kinase gamma is an essential amplifier of mast cell function. *Immunity* 2002; **16**: 441-451 [PMID: 11911828 DOI: 10.1016/s1074-7613(02)00282-0]
65 **Isidori A**, Loscocco F, Visani G, Paolasini S, Scalzulli P, Musto P, Perrone T, Guarini A, Pastore D, Mazza P, Tonialini L, Pavone V, De Santis G, Tarantini G. Real-life efficacy and safety of idelalisib in 55 double-refractory follicular lymphoma patients. *Br J Haematol* 2022; **199**: 339-343 [PMID: 36002151 DOI: 10.1111/bjh.18426]
66 **Gopal AK**, Kahl BS, de Vos S, Wagner-Johnston ND, Schuster SJ, Jurczak WJ, Flinn IW, Flowers CR, Martin P, Viardot A, Blum KA, Goy AH, Davies AJ, Zinzani PL, Dreyling M, Johnson D, Miller LL, Holes L, Li D, Dansey RD, Godfrey WR, Salles GA. PI3Kδ inhibition by idelalisib in patients with relapsed indolent lymphoma. *N Engl J Med* 2014; **370**: 1008-1018 [PMID: 24450858 DOI: 10.1056/NEJMoa1314583]
67 **Gordon MJ**, Huang J, Chan RJ, Bhargava P, Danilov AV. Medical comorbidities in patients with chronic lymphocytic leukaemia treated with idelalisib: analysis of two large randomised clinical trials. *Br J Haematol* 2021; **192**: 720-728 [PMID: 32599655 DOI: 10.1111/bjh.16879]
68 **Coutré SE**, Barrientos JC, Brown JR, de Vos S, Furman RR, Keating MJ, Li D, O'Brien SM, Pagel JM, Poleski MH, Sharman JP, Yao NS, Zelenetz AD. Management of adverse events associated with idelalisib treatment: expert panel opinion. *Leuk Lymphoma* 2015; **56**: 2779-2786 [PMID: 25726955 DOI: 10.3109/10428194.2015.1022770]
69 **Wang Z**, Zhou H, Xu J, Wang J, Niu T. Safety and efficacy of dual PI3K-δ, γ inhibitor, duvelisib in patients with relapsed or refractory lymphoid neoplasms: A systematic review and meta-analysis of prospective clinical trials. *Front Immunol* 2022; **13**: 1070660 [PMID: 36685572 DOI: 10.3389/fimmu.2022.1070660]
70 **Dreyling M**, Santoro A, Mollica L, Leppä S, Follows G, Lenz G, Kim WS, Nagler A, Dimou M, Demeter J, Özcan M, Kosinova M, Bouabdallah K, Morschhauser F, Stevens DA, Trevarthen D, Munoz J, Rodrigues L, Hiemeyer F, Miriyala A, Garcia-Vargas J, Childs BH, Zinzani PL. Long-term safety and efficacy of the PI3K inhibitor copanlisib in patients with relapsed or refractory indolent lymphoma: 2-year follow-up of the CHRONOS-1 study. *Am J Hematol* 2020; **95**: 362-371 [PMID: 31868245 DOI: 10.1002/ajh.25711]
71 **Dreyling M**, Santoro A, Mollica L, Leppä S, Follows GA, Lenz G, Kim WS, Nagler A, Panayiotidis P, Demeter J, Özcan M, Kosinova M, Bouabdallah K, Morschhauser F, Stevens DA, Trevarthen D, Giurescu M, Cupit L, Liu L, Köchert K, Seidel H, Peña C, Yin S, Hiemeyer F, Garcia-Vargas J, Childs BH, Zinzani PL. Phosphatidylinositol 3-Kinase Inhibition by Copanlisib in Relapsed or Refractory Indolent Lymphoma. *J Clin Oncol* 2017; **35**: 3898-3905 [PMID: 28976790 DOI: 10.1200/JCO.2017.75.4648]
72 **Maharaj K**, Powers JJ, Achille A, Mediavilla-Varela M, Gamal W, Burger KL, Fonseca R, Jiang K, Miskin HP, Maryanski D, Monastyrskyi A, Duckett DR, Roush WR, Cleveland JL, Sahakian E, Pinilla-Ibarz J. The dual PI3Kδ/CK1ε inhibitor umbralisib exhibits unique immunomodulatory effects on CLL T cells. *Blood Adv* 2020; **4**: 3072-3084 [PMID: 32634240 DOI: 10.1182/bloodadvances.2020001800]
73 **Schweitzer J**, Hoffman M, Graf SA. The evidence to date on umbralisib for the treatment of refractory marginal zone lymphoma and follicular lymphoma. *Expert Opin Pharmacother* 2022; **23**: 535-541 [PMID: 35209784 DOI: 10.1080/14656566.2022.2043273]
74 **Fowler NH**, Samaniego F, Jurczak W, Ghosh N, Derenzini E, Reeves JA, Knopińska-Posłuszny W, Cheah CY, Phillips T, Lech-Maranda E, Cheson BD, Caimi PF, Grosicki S, Leslie LA, Chavez JC, Fonseca G, Babu S, Hodson DJ, Shao SH, Burke JM, Sharman JP, Law JY, Pagel JM, Miskin HP, Sportelli P, O'Connor OA, Weiss MS, Zinzani PL. Umbralisib, a Dual PI3Kδ/CK1ε Inhibitor in Patients With Relapsed or Refractory Indolent Lymphoma. *J Clin Oncol* 2021; **39**: 1609-1618 [PMID: 33683917 DOI: 10.1200/JCO.20.03433]
75 **Fukuhara N**, Suehiro Y, Kato H, Kusumoto S, Coronado C, Rappold E, Zhao W, Li J, Gilmartin A, Izutsu K. Parsaclisib in Japanese patients with relapsed or refractory B-cell lymphoma (CITADEL-111): A phase Ib study. *Cancer Sci* 2022; **113**: 1702-1711 [PMID: 35201656 DOI: 10.1111/cas.15308]
76 **Forero-Torres A**, Ramchandren R, Yacoub A, Wertheim MS, Edenfield WJ, Caimi P, Gutierrez M, Akard L, Escobar C, Call J, Persky D, Iyer S, DeMarini DJ, Zhou L, Chen X, Dawkins F, Phillips TJ. Parsaclisib, a potent and highly selective PI3Kδ inhibitor, in patients with relapsed or refractory B-cell malignancies. *Blood* 2019; **133**: 1742-1752 [PMID: 30803990 DOI: 10.1182/blood-2018-08-867499]

77 **Goto H**, Izutsu K, Ennishi D, Mishima Y, Makita S, Kato K, Hanaya M, Hirano S, Narushima K, Teshima T, Nagai H, Ishizawa K. Zandelisib (ME-401) in Japanese patients with relapsed or refractory indolent non-Hodgkin's lymphoma: an open-label, multicenter, dose-escalation phase 1 study. *Int J Hematol* 2022; **116**: 911-921 [PMID: 36107394 DOI: 10.1007/s12185-022-03450-5]

78 **Pagel JM**, Soumerai JD, Reddy N, Jagadeesh D, Stathis A, Asch A, Salman H, Kenkre VP, Iasonos A, Llorin-Sangalang J, Li J, Zelenetz AD. Zandelisib with continuous or intermittent dosing as monotherapy or in combination with rituximab in patients with relapsed or refractory B-cell malignancy: a multicentre, first-in-patient, dose-escalation and dose-expansion, phase 1b trial. *Lancet Oncol* 2022; **23**: 1021-1030 [PMID: 35835137 DOI: 10.1016/S1470-2045(22)00333-3]

79 **Matasar MJ**, Dreyling M, Leppä S, Santoro A, Pedersen M, Buvaylo V, Fletcher M, Childs BH, Zinzani PL. Feasibility of Combining the Phosphatidylinositol 3-Kinase Inhibitor Copanlisib With Rituximab-Based Immunochemotherapy in Patients With Relapsed Indolent B-cell Lymphoma. *Clin Lymphoma Myeloma Leuk* 2021; **21**: e886-e894 [PMID: 34389273 DOI: 10.1016/j.clml.2021.06.021]

80 LiverTox: Clinical and Research Information on Drug-Induced Liver Injury [Internet]. Bethesda (MD): National Institute of Diabetes and Digestive and Kidney Diseases; 2012- [PMID: 31643176]

81 **Smith SM**, Pitcher BN, Jung SH, Bartlett NL, Wagner-Johnston N, Park SI, Richards KL, Cashen AF, Jaslowski A, Smith SE, Cheson BD, Hsi E, Leonard JP. Safety and tolerability of idelalisib, lenalidomide, and rituximab in relapsed and refractory lymphoma: the Alliance for Clinical Trials in Oncology A051201 and A051202 phase 1 trials. *Lancet Haematol* 2017; **4**: e176-e182 [PMID: 28314699 DOI: 10.1016/S2352-3026(17)30028-5]

82 **Wu X**, Xu Y, Liang Q, Yang X, Huang J, Wang J, Zhang H, Shi J. Recent Advances in Dual PI3K/mTOR Inhibitors for Tumour Treatment. *Front Pharmacol* 2022; **13**: 875372 [PMID: 35614940 DOI: 10.3389/fphar.2022.875372]

83 **McCurdy A**, Visram A. The Role of Belantamab Mafodotin, Selinexor, and Melflufen in Multiple Myeloma. *Curr Hematol Malig Rep* 2022; **17**: 306-318 [PMID: 36417082 DOI: 10.1007/s11899-022-00682-4]

84 **Major A**, Kline J, Karrison TG, Fishkin PAS, Kimball AS, Petrich AM, Nattam S, Rao K, Sleckman BG, Cohen K, Besien KV, Rapoport AP, Smith SM. Phase I/II clinical trial of temsirolimus and lenalidomide in patients with relapsed and refractory lymphomas. *Haematologica* 2022; **107**: 1608-1618 [PMID: 34320785 DOI: 10.3324/haematol.2021.278853]

85 **Sharma N**, Reagan PM, Liesveld JL. Cytopenia after CAR-T Cell Therapy-A Brief Review of a Complex Problem. *Cancers (Basel)* 2022; **14** [PMID: 35326654 DOI: 10.3390/cancers14061501]

86 **Yassine F**, Murthy H, Ghabashi E, Kharfan-Dabaja MA, Iqbal M. Understanding the Etiology of Pancytopenias in the CAR T-Cell Therapy Setting: What We Know and What We Don't? *Hematol Oncol Stem Cell Ther* 2022; **15**: 122-130 [PMID: 36633964 DOI: 10.56875/2589-0646.1047]

87 **Goldsmith SR**, Ghobadi A, Dipersio JF, Hill B, Shadman M, Jain T. Chimeric Antigen Receptor T Cell Therapy versus Hematopoietic Stem Cell Transplantation: An Evolving Perspective. *Transplant Cell Ther* 2022; **28**: 727-736 [PMID: 35878743 DOI: 10.1016/j.jtct.2022.07.015]

88 **Gajra A**, Zalenski A, Sannareddy A, Jeune-Smith Y, Kapinos K, Kansagra A. Barriers to Chimeric Antigen Receptor T-Cell (CAR-T) Therapies in Clinical Practice. *Pharmaceut Med* 2022; **36**: 163-171 [PMID: 35672571 DOI: 10.1007/s40290-022-00428-w]

89 **Abramson JS**, Palomba ML, Gordon LI, Lunning MA, Wang M, Arnason J, Mehta A, Purev E, Maloney DG, Andreadis C, Sehgal A, Solomon SR, Ghosh N, Albertson TM, Garcia J, Kostic A, Mallaney M, Ogasawara K, Newhall K, Kim Y, Li D, Siddiqi T. Lisocabtagene maraleucel for patients with relapsed or refractory large B-cell lymphomas (TRANSCEND NHL 001): a multicentre seamless design study. *Lancet* 2020; **396**: 839-852 [PMID: 32888407 DOI: 10.1016/S0140-6736(20)31366-0]

90 **Neelapu SS**, Locke FL, Bartlett NL, Lekakis LJ, Miklos DB, Jacobson CA, Braunschweig I, Oluwole OO, Siddiqi T, Lin Y, Timmerman JM, Stiff PJ, Friedberg JW, Flinn IW, Goy A, Hill BT, Smith MR, Deol A, Farooq U, McSweeney P, Munoz J, Avivi I, Castro JE, Westin JR, Chavez JC, Ghobadi A, Komanduri KV, Levy R, Jacobsen ED, Witzig TE, Reagan P, Bot A, Rossi J, Navale L, Jiang Y, Aycock J, Elias M, Chang D, Wiezorek J, Go WY. Axicabtagene Ciloleucel CAR T-Cell Therapy in Refractory Large B-Cell Lymphoma. *N Engl J Med* 2017; **377**: 2531-2544 [PMID: 29226797 DOI: 10.1056/NEJMoa1707447]

91 **Schuster SJ**, Bishop MR, Tam CS, Waller EK, Borchmann P, McGuirk JP, Jäger U, Jaglowski S, Andreadis C, Westin JR, Fleury I, Bachanova V, Foley SR, Ho PJ, Mielke S, Magenau JM, Holte H, Pantano S, Pacaud LB, Awasthi R, Chu J, Anak Ö, Salles G, Maziarz RT; JULIET Investigators. Tisagenlecleucel in Adult Relapsed or Refractory Diffuse Large B-Cell Lymphoma. *N Engl J Med* 2019; **380**: 45-56 [PMID: 30501490 DOI: 10.1056/NEJMoa1804980]

92 **Chong EA**, Ruella M, Schuster SJ; Lymphoma Program Investigators at the University of Pennsylvania. Five-Year Outcomes for Refractory B-Cell Lymphomas with CAR T-Cell Therapy. *N Engl J Med* 2021; **384**: 673-674 [PMID: 33596362 DOI: 10.1056/NEJMc2030164]

93 **Jacobson CA**, Chavez JC, Sehgal AR, William BM, Munoz J, Salles G, Munshi PN, Casulo C, Maloney DG, de Vos S, Reshef R, Leslie LA, Yakoub-Agha I, Oluwole OO, Fung HCH, Rosenblatt J, Rossi JM, Goyal L, Plaks V, Yang Y, Vezan R, Avanzi MP, Neelapu SS. Axicabtagene ciloleucel in relapsed or refractory indolent non-Hodgkin lymphoma (ZUMA-5): a single-arm, multicentre, phase 2 trial. *Lancet Oncol* 2022; **23**: 91-103 [PMID: 34895487 DOI: 10.1016/S1470-2045(21)00591-X]

94 **Mohty R**, Kharfan-Dabaja MA. CAR T-cell therapy for follicular lymphoma and mantle cell lymphoma. *Ther Adv Hematol* 2022; **13**: 20406207221142133 [PMID: 36544864 DOI: 10.1177/20406207221142133]

95 **Jacobson CA**, Chavez JC, Sehgal A, William BM, Munoz J, Salles GA. Outcomes in ZUMA-5 with axicabtagene ciloleucel (axi-cel) in patients (pts) Outcomes in ZUMA-5 with axicabtagene ciloleucel (axi-cel) in patients (pts) with relapsed/refractory (R/R) indolent non-Hodgkin lymphoma (iNHL) who had the high-risk feature of progression within 24 mo from initiation of first anti-CD20-containing chemoimmunotherapy (POD24). *J Clin Oncol* 2021; **39** Suppl 15: 7515 [DOI: 10.1200/jco.2021.39.15_suppl.7515]

96 **Fowler NH**, Dickinson M, Dreyling M, Martinez-Lopez J, Kolstad A, Butler J, Ghosh M, Popplewell L, Chavez JC, Bachy E, Kato K, Harigae H, Kersten MJ, Andreadis C, Riedell PA, Ho PJ, Pérez-Simón JA, Chen AI, Nastoupil LJ, von

Tresckow B, Ferreri AJM, Teshima T, Patten PEM, McGuirk JP, Petzer AL, Offner F, Viardot A, Zinzani PL, Malladi R, Zia A, Awasthi R, Masood A, Anak O, Schuster SJ, Thieblemont C. Tisagenlecleucel in adult relapsed or refractory follicular lymphoma: the phase 2 ELARA trial. *Nat Med* 2022; **28**: 325-332 [PMID: 34921238 DOI: 10.1038/s41591-021-01622-0]

97 **Salles G**, Schuster SJ, Dreyling M, Fischer L, Kuruvilla J, Patten PEM, von Tresckow B, Smith SM, Jiménez-Ubieto A, Davis KL, Anjos C, Chu J, Zhang J, Lobetti Bodoni C, Thieblemont C, Fowler NH, Dickinson M, Martínez-López J, Wang Y, Link BK. Efficacy comparison of tisagenlecleucel vs usual care in patients with relapsed or refractory follicular lymphoma. *Blood Adv* 2022; **6**: 5835-5843 [PMID: 35973192 DOI: 10.1182/bloodadvances.2022008150]

98 **Sarkozy C**, Maurer MJ, Link BK, Ghesquieres H, Nicolas E, Thompson CA, Traverse-Glehen A, Feldman AL, Allmer C, Slager SL, Ansell SM, Habermann TM, Bachy E, Cerhan JR, Salles G. Cause of Death in Follicular Lymphoma in the First Decade of the Rituximab Era: A Pooled Analysis of French and US Cohorts. *J Clin Oncol* 2019; **37**: 144-152 [PMID: 30481079 DOI: 10.1200/JCO.18.00400]

99 **Sehgal A**, Hoda D, Riedell PA, Ghosh N, Hamadani M, Hildebrandt GC, Godwin JE, Reagan PM, Wagner-Johnston N, Essell J, Nath R, Solomon SR, Champion R, Licitra E, Fanning S, Gupta N, Dubowy R, D'Andrea A, Wang L, Ogasawara K, Thorpe J, Gordon LI. Lisocabtagene maraleucel as second-line therapy in adults with relapsed or refractory large B-cell lymphoma who were not intended for haematopoietic stem cell transplantation (PILOT): an open-label, phase 2 study. *Lancet Oncol* 2022; **23**: 1066-1077 [PMID: 35839786 DOI: 10.1016/S1470-2045(22)00339-4]

100 **St-Pierre F**, Gordon LI. Lisocabtagene maraleucel in the treatment of relapsed/refractory large B-cell lymphoma. *Future Oncol* 2023; **19**: 19-28 [PMID: 36651471 DOI: 10.2217/fon-2022-0774]

101 **Luminari S**, Manni M, Galimberti S, Versari A, Tucci A, Boccomini C, Farina L, Olivieri J, Marcheselli L, Guerra L, Ferrero S, Arcaini L, Cavallo F, Kovalchuk S, Skrypets T, Del Giudice I, Chauvie S, Patti C, Stelitano C, Ricci F, Pinto A, Margiotta Casaluci G, Zilioli VR, Merli A, Ladetto M, Bolis S, Pavone V, Chiarenza A, Arcari A, Anastasia A, Dondi A, Mannina D, Federico M; Fondazione Italiana Linfomi. Response-Adapted Postinduction Strategy in Patients With Advanced-Stage Follicular Lymphoma: The FOLL12 Study. *J Clin Oncol* 2022; **40**: 729-739 [PMID: 34709880 DOI: 10.1200/JCO.21.01234]

102 **Schmatz AI**, Streubel B, Kretschmer-Chott E, Püspök A, Jäger U, Mannhalter C, Tiemann M, Ott G, Fischbach W, Herzog P, Seitz G, Stolte M, Raderer M, Chott A. Primary follicular lymphoma of the duodenum is a distinct mucosal/submucosal variant of follicular lymphoma: a retrospective study of 63 cases. *J Clin Oncol* 2011; **29**: 1445-1451 [PMID: 21383289 DOI: 10.1200/JCO.2010.32.9193]

103 **Tari A**, Kitadai Y, Mouri R, Takigawa H, Asaoku H, Mihara K, Takata K, Fujihara M, Yoshino T, Koga T, Fujimori S, Tanaka S, Chayama K. Watch-and-wait policy versus rituximab-combined chemotherapy in Japanese patients with intestinal follicular lymphoma. *J Gastroenterol Hepatol* 2018; **33**: 1461-1468 [PMID: 29377265 DOI: 10.1111/jgh.14100]

104 **Yamamoto S**, Nakase H, Yamashita K, Matsuura M, Takada M, Kawanami C, Chiba T. Gastrointestinal follicular lymphoma: review of the literature. *J Gastroenterol* 2010; **45**: 370-388 [PMID: 20084529 DOI: 10.1007/s00535-009-0182-z]

105 **Takata K**, Okada H, Ohmiya N, Nakamura S, Kitadai Y, Tari A, Akamatsu T, Kawai H, Tanaka S, Araki H, Yoshida T, Okumura H, Nishisaki H, Sagawa T, Watanabe N, Arima N, Takatsu N, Nakamura M, Yanai S, Kaya H, Morito T, Sato Y, Moriwaki H, Sakamoto C, Niwa Y, Goto H, Chiba T, Matsumoto T, Ennishi D, Kinoshita T, Yoshino T. Primary gastrointestinal follicular lymphoma involving the duodenal second portion is a distinct entity: a multicenter, retrospective analysis in Japan. *Cancer Sci* 2011; **102**: 1532-1536 [PMID: 21561531 DOI: 10.1111/j.1349-7006.2011.01980.x]

106 **Rohatiner A**, d'Amore F, Coiffier B, Crowther D, Gospodarowicz M, Isaacson P, Lister TA, Norton A, Salem P, Shipp M. Report on a workshop convened to discuss the pathological and staging classifications of gastrointestinal tract lymphoma. *Ann Oncol* 1994; **5**: 397-400 [PMID: 8075046 DOI: 10.1093/oxfordjournals.annonc.a058869]

107 **Watanabe T**. Treatment strategies for nodal and gastrointestinal follicular lymphoma: current status and future development. *World J Gastroenterol* 2010; **16**: 5543-5554 [PMID: 21105187 DOI: 10.3748/wjg.v16.i44.5543]

World Journal of Gastroenterology

Submit a Manuscript: https://www.f6publishing.com

World J Gastroenterol 2023 June 21; 29(23): 3595-3605

DOI: 10.3748/wjg.v29.i23.3595

ISSN 1007-9327 (print) ISSN 2219-2840 (online)

MINIREVIEWS

Prognostic role of intestinal ultrasound in Crohn's disease

Cristina Manzotti, Francesco Colombo, Tommaso Zurleni, Piergiorgio Danelli, Giovanni Maconi

Specialty type: Gastroenterology and hepatology

Provenance and peer review: Invited article; Externally peer reviewed.

Peer-review model: Single blind

Peer-review report's scientific quality classification

Grade A (Excellent): 0
Grade B (Very good): 0
Grade C (Good): C, C
Grade D (Fair): 0
Grade E (Poor): 0

P-Reviewer: Iizuka M, Japan; Miyoshi E, Japan

Received: March 9, 2023
Peer-review started: March 9, 2023
First decision: March 20, 2023
Revised: April 5, 2023
Accepted: May 23, 2023
Article in press: May 23, 2023
Published online: June 21, 2023

Cristina Manzotti, Giovanni Maconi, Gastroenterology Unit, Department of Biomedical and Clinical Sciences, University of Milan, L.Sacco University Hospital, Milano 20157, Italy

Francesco Colombo, Tommaso Zurleni, Piergiorgio Danelli, Division of General Surgery, Department of Biomedical and Clinical Sciences, University of Milan, L.Sacco University Hospital, Milano 20157, Italy

Corresponding author: Francesco Colombo, MD, Assistant Professor, Division of General Surgery, Department of Biomedical and Clinical Sciences, University of Milan, L.Sacco University Hospital, Via Giovanni Battista Grassi 74, Milano 20157, Italy.
colombo.francesco@asst-fbf-sacco.it

Abstract

The majority of patients affected by Crohn's disease (CD) develop a chronic condition with persistent inflammation and relapses that may cause progressive and irreversible damage to the bowel, resulting in stricturing or penetrating complications in around 50% of patients during the natural history of the disease. Surgery is frequently needed to treat complicated disease when pharmacological therapy failes, with a high risk of repeated operations in time. Intestinal ultrasound (IUS), a non-invasive, cost-effective, radiation free and reproducible method for the diagnosis and follow-up of CD, in expert hands, allow a precise assessment of all the disease manifestations: Bowel characteristics, retrodilation, wrapping fat, fistulas and abscesses. Moreover, IUS is able to assess bowel wall thickness, bowel wall stratification (echo-pattern), vascularization and elasticity, as well as mesenteric hypertrophy, lymph-nodes and mesenteric blood flow. Its role in the disease evaluation and behaviour description is well assessed in literature, but less is known about the potential space of IUS as predictor of prognostic factors suggesting response to a medical treatment or postoperative recurrence. The availability of a low cost exam as IUS, able to recognize which patients are more likely to respond to a specific therapy and which patients are at high risk of surgery or complications, could be a very useful instrument in the hands of IBD physician. The aim of this review is to present current evidence about the prognostic role that IUS can show in predicting response to treatment, disease progression, risk of surgery and risk of post-surgical recurrence in CD.

Key Words: Intestinal ultrasound; Crohn's disease; Postoperative recurrence; Bowel wall thickness; Remission; Intestinal surgery

©The Author(s) 2023. Published by Baishideng Publishing Group Inc. All rights reserved.

Core Tip: Intestinal ultrasound (IUS) and magnetic resonance enterography are better tolerated and safer than endoscopy, with IUS more easily available and less expensive than magnetic resonance imaging. Moreover, IUS allows complete visualization of the small-bowel even in patients with stenoses and/or severe inflammation, and can assess for extraintestinal disease. In addition, IUS may predict outcomes better than endoscopic mucosal assessment, possibly identifying more relevant therapeutic targets. This review discusses the role of IUS in Crohn's disease not only as first line investigation but as an extremely useful instrument in predicting response to medical treatment, disease evolution and risk of recurrence before and after surgery.

Citation: Manzotti C, Colombo F, Zurleni T, Danelli P, Maconi G. Prognostic role of intestinal ultrasound in Crohn's disease. *World J Gastroenterol* 2023; 29(23): 3595-3605
URL: https://www.wjgnet.com/1007-9327/full/v29/i23/3595.htm
DOI: https://dx.doi.org/10.3748/wjg.v29.i23.3595

INTRODUCTION

Crohn's disease (CD) is a chronic inflammatory condition that can affect the whole gastrointestinal tract, more frequently involving the ileum and colon, usually presenting in its active phases with abdominal pain, diarrhoea (bloody or non-bloody), urgency, fatigue and weight loss[1]. The majority of patients affected by CD show chronic relapsing disease with potential chronic continuous abdominal symptoms after diagnosis[2].

The available treatments often fail to achieve disease remission or lose their efficacy over time. Moreover, in CD, chronic inflammation and relapses may cause progressive and irreversible damage to the bowel[3], which results in stricturing or penetrating complications in approximately 50% of patients during the natural history of the disease, with a high risk of surgery or repeated surgery[4].

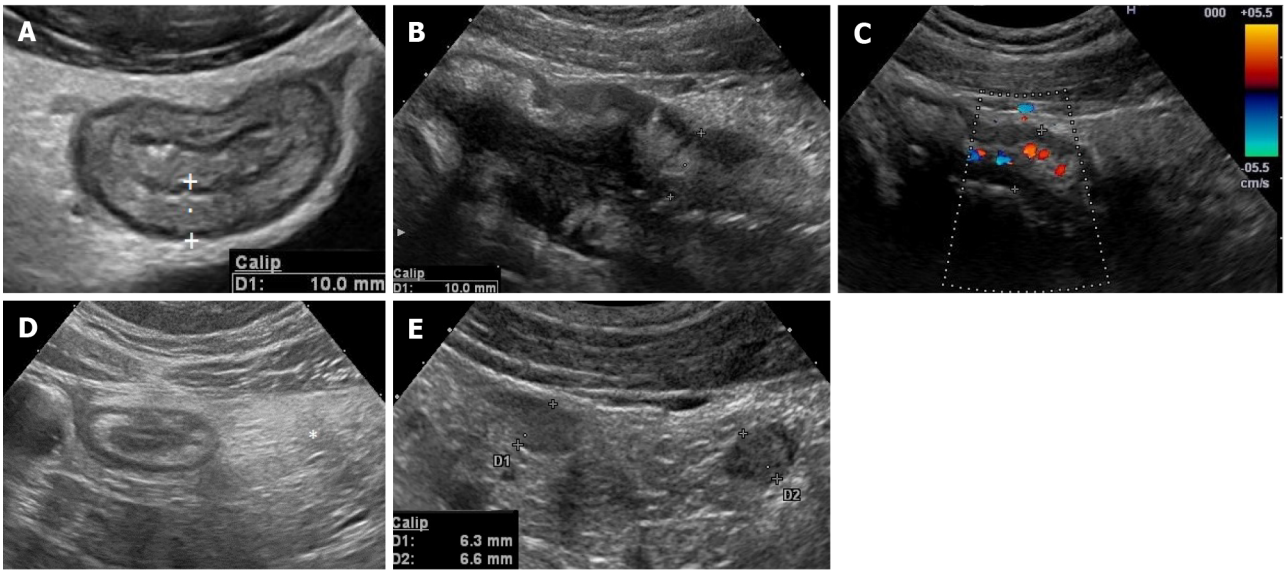
It has been realized that patients' symptoms in CD do not necessarily reflect the underlying inflammatory burden of the disease and that, independent of clinical symptoms, patients can have different rates of disease progression and outcomes[2]. Most CD patients at the time of diagnosis have a disease with inflammatory features, but in some patients, it can evolve to a stenosing or penetrating pattern during follow-up[5]. Therefore, the possibility of identifying which patients are nonresponsive to medical treatment and prone to develop stricturing and penetrating CD would be very important to properly address the treatment. Prognostic factors for favourable or unfavourable outcomes of CD have been extensively researched and assessed with both invasive and noninvasive methods.

Intestinal ultrasound (IUS) is a non-invasive, cost-effective, radiation free and reproducible method for the diagnosis and follow-up of CD, with an accuracy comparable to magnetic resonance imaging and computed tomography[6,7]. IUS can assess several features of the bowel wall and surrounding tissue: Bowel wall thickness (BWT) (Figure 1A), bowel wall stratification (echo-pattern) (Figure 1B), vascularization (Figure 1C) and elasticity, as well as mesenteric hypertrophy (Figure 1D), lymph-nodes (Figure 1E) and mesenteric blood flow. IUS is also able to assess complications such as stenosis, dilations, fistulas and abscesses[8]. During the follow-up of CD patients undergoing biological therapy, IUS features have been correlated with clinical activity, endoscopic activity, laboratory markers (faecal calprotectin and C-reactive protein) and drug serum levels[9-13]. However, IUS specific features have also been suggested as predictive factors for evaluating the response to medical treatment, the risk of clinical relapse or surgery, and the risk of postoperative recurrence[14-17]. We present the current evidence on the prognostic value of IUS and especially the IUS features of the bowel wall in predicting response to treatment and risk of relapse in CD.

LITERATURE REVIEW

Search strategy and selection criteria

Two authors (Manzotti C and Maconi G) searched the literature using the PubMed database from January 2000 to January 2022. The search used the following terms in different combinations: "intestinal ultrasound", "bowel ultrasound", "transabdominal ultrasound", "IUS", "bowel wall thickness", "Doppler", "CEUS", "transmural healing", "Crohn", "Crohn's disease", "IBD", "inflammatory bowel disease", "surgery", "clinical remission", "remission", "predictive value", "outcome", and "post-surgical recurrence". In particular, the following string was used: [(ultrasound OR sonography) AND (bowel OR intestinal) AND (Crohn's disease OR IBD) AND (remission OR response OR transmural OR outcome OR predictive)].



DOI: 10.3748/wjg.v29.i23.3595 **Copyright** ©The Author(s) 2023.

Figure 1 Intestinal ultrasound assess several features of the bowel wall and surrounding tissue. A: Bowel wall thickness should be measured perpendicular to the anterior wall of the bowel (or where it is better visible) avoiding haustrations and mucosal folds. The cursor/calipers should be placed at the end of the interface echo between the serosa and the proper muscle to the start of the interface echo between the lumen and the mucosa; B: Bowel wall stratification. The wall layers in case of active disease may appear focally or extensively disrupted (disrupted or hypoechoic echo pattern); C: Bowel wall vascularity. Bowel wall vascularity can be determined both by colour Doppler or power Doppler signal at the level of the most thickened segments, using special presets optimized for slow flow detection; D: Mesenteric hypertrophy. Mesenteric hypertrophy also called fat wrapping or creeping fat appears on ultrasound (US) as hyperechoic tissue or "mass effect" encircling the diseased bowel; E: Lymphnodes. Enlarged inflammatory mesenteric lymph nodes related to Crohn's disease are usually described at US as oval or elongated with lesser diameter > 5 mm and seem to be correlated with young age, early disease, or disease with shorter duration, and with the presence of fistulae and abscesses.

Additional potentially eligible articles were manually searched through the bibliography of relevant articles. Eligible articles were randomized controlled trials, prospective or retrospective cohort studies, reviews, and systematic reviews with a meta-analysis; duplications and studies in languages other than English were excluded. In each eligible paper, we searched for information on the predictive value of IUS for patients affected by active or quiescent CD in terms of response to treatment, disease course, transmural healing, risk of surgery, and risk of postsurgical recurrence. Two authors (Manzotti C and Maconi G) screened the title and abstract of potentially eligible papers, followed by a full-text analysis of relevant articles. Starting from a total of 1040 articles, 49 were considered suitable and were included in this review.

DISCUSSION

Active disease

Intestinal US, before and early after the start of biologic treatment, showed high accuracy in predicting long-term clinical and endoscopic remission and response[17,18]. Although few data have shown that pretreatment IUS features may predict the outcome and somewhat drive the choice of treatment, much more data have shown that sonographic improvement of BWT, echopattern and vascularization as early as weeks 2-4 of biologic treatment may predict a better long-term response compared to those of patients without an early treatment response[19]. Studies considering predictive value of IUS parameters for response to treatment and course of CD are shown in Table 1.

Intestinal US to predict response to treatment and disease course

Increased BWT and bowel wall vascularity assessed by colour Doppler or IV contrast-enhanced ultrasound (CEUS), variably powered in bowel US scores, was identified as an independent predictor of a negative disease course, namely, the need for steroids, change of therapy, treatment intensification, hospitalization, or need for surgery through 6-12 mo[20,14]. In addition, increased echopatterns coupled with disrupted echopatterns of the bowel wall or lack of bowel wall stratification were independent predictors for the need for subsequent therapeutic optimization[20].

Sonographic response and clinical response

It seems that sonographic response after 12 or 14 wk of therapy with anti-tumor necrosis factor (TNF)

Table 1 Predictive value of intestinal ultrasound parameters for response to treatment and course of Crohn's disease

Ref.	Treatment	Timing of IUS after start of treatment	IUS parameter	Predictive value for
Albshesh *et al*[18], 2020	Anti-TNF	> 14 wk	BWT > 4 mm	Treatment failure
			BWT < 4 mm	Duration of failure-free response
Calabrese *et al*[52], 2022	Anti-TNF, vedolizumab, ustekinumab	Baseline	"Higher BWT"	Low risk of TR
			Colonic localization	High risk of TR
Chen *et al* [19], 2022	Anti-TNF	Baseline-2 wk	Reduction in BWT, vascularization, SWE	Response to treatment
De Voogd *et al*[17], 2022	Anti-TNF	Baseline-4/8 wk	BWT reduction > 18%	Endoscopic response and remission at 12-34 wk
Helwig *et al* [32], 2022	All available biological therapies	Baseline-12 wk	BWT reduction > 25%	Clinical remission and no therapy change at 52 wk
Les *et al*[20], 2021	5-ASA, budesonide, AZA, anti TNF		Worsened BWT, echopattern, vascularization	Need for treatment escalation, negative disease course
Orlando *et al* [29], 2018	Anti-TNF	Baseline	SWE strain ratio > 2	Surgery
Paredes *et al* [53], 2019	Anti-TNF	12 wk	BWT ≤ 3 mm	"Good outcome" (no treatment intensification, no surgery) at 1 yr
Ripollés *et al* [21], 2016	Anti-TNF	Baseline-12 wk	Sonographic response (BWT decrease > 2 mm, diminution of one grade of ECD, decrease > 20% of mural enhancement, disappearance of transmural complications or stenosi	1-yr sonographic response and further 1-yr clinical response and treatment efficacy
Smith *et al* [22], 2022	All available biological therapies and thiopurines	Baseline-14 wk	Sonographic response (BWT decreasing > 0.5 mm and vascularity improvement by ≥ one grade)	Treatment response at 46 wk
Zorzi *et al* [23], 2020	Anti-TNF, budesonide, thiopurines	Baseline-18 mo	Normalization of SICUS (BWT, disease extension, complications)	Long term lower cumulative probability of need for surgery, hospitalization, and need for steroids
Laterza *et al* [54], 2021	Anti-TNF	12 wk	CEUS increased PI and Pw	Clinical relapse within 6 mo
Ungar *et al* [55], 2020	Adalimumab	NA	Terminal ileum BWT < 4 mm	Therapy retention
Quaia *et al* [56], 2019	Anti-TNF	Baseline-6 wk	CEUS pretreatment values and % variations of peak enhancement, AUC, AUC during wash-in, AUC during wash-out	Long term response to therapy

IUS: Intestinal ultrasound; BWT: Bowel wall thickness; ECD: Eco-color-doppler; SWE: Shear wave elastography; UEI: Ultrasound elastography imaging; TR: Transmural remission; CEUS: Contrast enhanced ultrasound; AUC: Area under the curve; TNF: Tumor necrosis factor; NA: Not available; 5-ASA: 5-aminosalicylic acid; AZA: Azacitidine.

drugs predicts the 1-year sonographic response, which in turn correlates with the 1-year clinical response, predicts efficacy of further treatment and inversely correlated with the need for surgery. Stricturing behaviour, namely, the detection of strictures with prestenotic dilatation, seems to be the only sonographic feature associated with a long-term negative predictive value of clinical response[21, 22].

Similar results were demonstrated by using small intestinal contrast US (SICUS), which is used to monitor patients undergoing anti-TNF therapy. An improvement in BWT, a reduction of disease extension, or the absence of intestinal complications as detected by SICUS predicted a better response after 1 year of therapy, as well as a reduction in steroid therapy and hospital admissions[23].

Monitoring BWT with IUS also showed predictive value for patients starting therapy with ustekinumab. A decrease in BWT > 1 mm at week 8 after the start of therapy was a helpful parameter for selecting patients with an early response to ustekinumab and for providing assistance in terms of further treatment intervals[24]. The thickening of each single layer of the bowel wall and its clinical significance in CD have been poorly investigated thusfar. It seems that the thickening of the proper muscle layer in active CD patients is correlated with poor clinical and sonographic responses to vedolizumab treatment[25]. In this regard, smooth muscle hyperplasia has been underlined as a central

contributor to the stricturing phenotype, whereas fibrosis is less significant, and the 'inflammation-smooth muscle hyperplasia axis' seems to be the most important step in the pathogenesis of Crohn's strictures[26].

Additionally, the assessment of bowel wall vascularity by CEUS seems to provide relevant prognostic information regarding treatment efficacy in patients with CD. The improvement of several perfusion parameters, such as peak contrast enhancement, rate of wash-in and wash-out and the area under the time intensity curve of the intestinal wall 4-6 wk after starting anti-inflammatory treatment (anti-TNF-alpha), were correlated with a favourable response[25,27,28]. Finally, the evaluation of ultrasound elasticity of the bowel wall may have a predictive role as well, correlating with therapeutic outcomes for CD patients treated with anti-TNF[29].

With regard to extra bowel findings, especially mesenteric lymphadenopathy and mesenteric fat hypertrophy, their prognostic role in response to treatment remains controversial. Regional mesenteric lymphadenopathy detected by IUS is a common but nonspecific sonographic finding in early CD and could be linked to young age, early disease, and the presence of abscesses or fistulae[30]. However, its prognostic significance remains poorly investigated. Mesenteric fat hypertrophy is associated with clinical and biochemical disease activity, and it may disappear or improve in patients who have responded to medical treatment[31]. However, its prognostic value in predicting response to therapy and risk of relapse is debatable[16,31].

IUS to predict transmural remission

Transmural remission (TR) or transmural healing with different definitions in literature, is now considered as an objective and relevant target in CD. It may be assessed by IUS taking into account BWT normalization (≤ 3 mm) with or without normalization of Doppler vascular signs and peri-intestinal inflammatory signs[32]. It is correlated with improved clinical outcome, such as a reduced demand of medication escalation, corticosteroid use, hospitalization and CD-related surgery.

The rate of TR, with more or less extensive definitions, in patients undergoing biological therapy was obtained from 12% to 46.2% of patients after 12 wk to 2 years of therapy (see Table 2). TR was strictly correlated with time, being higher at later assessments compared with early assessments. Moreover, it is more prevalent in colic CD than in ileal CD and it is associated with lower BWT and lower shear wave elastography strain ratio at baseline (see Table 2). However, a few studies have evaluated baseline or early IUS factors predictive of TR. Further prospective trials are needed to reach more consistent evidence on IUS predictive value, to help in properly selecting the right treatment for the right CD patient and plain maintenance therapy.

IUS to predict the risk of surgery

The ileal localization and stricturing and perforating behaviour of CD are well-known risk factors for surgery both in children and in adults. Children with ileal CD requiring surgical resection may have more severe IUS manifestations (such as loss of mural stratification and severe fibrofatty proliferation) associated with both active inflammation and chronic fibrosis than those managed medically[33].

Even in adults, the routine use of IUS in CD patients may identify a subgroup at high risk of surgery, taking into account that nearly half of patients with CD may require surgery within 10 years of diagnosis[1]. Irrespective of the treatment performed, BWT > 7 mm at IUS, altered bowel wall echopattern, and the presence of complications such as fistulas or stenosis are risk factors for intestinal resection over a short period of time[34-36]. In particular, the presence of strictures, fistulae, and abscesses at baseline bowel US seems to predict the need for surgery through 12 mo[14].

The assessment of fibrosis by means of strain elastography may identify patients who are nonresponsive to anti-TNF and need surgery. Orlando *et al*[29] in a small series of patients, showed that the strain ratio of the thickened bowel wall may predict surgery much better than the degree of its thickening and vascularization and that a strain ratio ≥ 2 before starting anti-TNF was the cut-off value correlated with poor lack of improvement, surgery and worst outcome. Likewise, the lack of improvement or the increase in BWT after the start of treatment is correlated with a high risk of surgery[21,34]. It is debatable whether in selected populations at high risk of surgery, such as CD patients with well-known strictures and fistulas, the features of BWT may suggest the response to treatment and ultimately surgery. In the STRIDENT study, 77 CD patients with a *de novo* or postoperative anastomotic intestinal stricture with symptoms consistent with chronic or subacute intestinal obstruction were randomly assigned to receive adalimumab alone or combined with thiopurines. IUS at 12 mo showed improvement (> 25%) in BWT in 45% of patients, with no significant difference between the two groups of patients and an overall low risk of surgery, but no predictors of improvement were given[10].

IUS to predict post-surgical recurrence

Several studies and systematic reviews have assessed the role of IUS in postoperative follow-up, showing that a BWT > 3 mm of the anastomosis or neoterminal ileum is an accurate indicator for recurrence[11]. In this regard, prospective studies have shown that the use of PEG solution (SICUS)[37] and colour Doppler or CEUS[38] can increase the sensitivity, albeit with a decrease in specificity in detecting postoperative recurrence at 1 year after surgery. Moreover, both IUS and SICUS, adopting

Table 2 Rate of transmural remission and intestinal ultrasound parameters predictive of transmural remission in Crohn's disease patients treated with biologics

Ref.	Patients, *n*	TR definition	Study drug	Treatment duration	Rate of TR	IUS parameters predictive of TR
Calabrese *et al*[52], 2022	188	Normalization of BWT, no ECD, no extra bowel signs of inflammation	Adalimumab, infliximab, vedolizumab, ustekinumab	52 wk	27.5% (26.8% adalimumab; 37% infliximab; 27.2% vedolizumab; 20% ustekinumab	Colonic localization, lower BWT at baseline
Castiglione *et al*[57], 2013	66	NA	Anti-TNF	2 yr	25%	
	67		Thiopurines		4%	
Castiglione *et al*[58], 2017	40	BWT ≤ 3 mm	Anti-TNF	2 yr	25%	
Castiglione *et al*[59], 2019	218	BWT ≤ 3 mm	Anti-TNF	12 wk	31.2%	
Helwig *et al* [32], 2022	180	BWT ≤ 2 mm terminal ileum or ≤ 3 mm colon; BWT ≤ 2 mm terminal ileum or ≤ 3 mm colon + two factors among no ECD, no fibrofatty proliferation, normal stratification; normalization of all parameters	All available biologics	12 wk	33.3%; 38.5%; 24.4% (18.4% I; 29% C)	
	78			46 wk	46.2%; NA; NA	
Kucharzik *et al*[60], 2023	77	Normalization of all IUS parameters	Ustekinumab	48 wk	24.1% (13.2% I; 50.0% C)	
Miranda *et al* [61], 2021	35	BWT ≤ 3 mm	Ustekinumab	52 wk	31.4%	
Orlando *et al* [29], 2018	30	BWT ≤ 3 mm	Anti-TNF	14 wk	29%	UEI strain ratio
				52 wk	30%	
Paredes *et al* [53], 2019	36	BWT ≤ 3 mm	Anti-TNF	52 wk	39%	
Ripollés *et al* [21], 2016	51	BWT ≤ 3 mm, no ECD, absence of complications	Anti-TNF	12 wk	14%	
				52 wk	29.5%	
Civitelli *et al* [62], 2016	32	BWT < 3 mm, no ECD, normal stratification, absence of strictures and dilatation	Anti-TNF	9-12 mo	14%	
Paredes *et al* [63], 2010	24	BWT < 3 mm, no increased ECD	Anti-TNF	2 wk	20.8%	
Vaughan *et al*[64], 2022	79	BWT ≤ 3 mm, no increased ECD	Infliximab	12 wk	41%	
Han *et al* [65], 2022	92	BWT ≤ 3 mm, no increased ECD	Anti-TNF	14 wk	12%	
				52 wk (only 22 patients)	22.7%	
Dolinger *et al* [66], 2021	13	BWT ≤ 3 mm	Infliximab	14 wk	23%	
Zorzi *et al* [23], 2020	80	SICUS normal value for BWT, absence of any length of disease, and absence of perienteric inflammation, fistulas, phlegmon, or abscess)	Anti-TNF, budesonide, thiopurines	18 mo	41%	

TR: Transmural remission; BWT: Bowel wall thickness; ECD: Eco-color-doppler vascular signal; I: Ileal Crohn's disease; C: Colonic Crohn's disease; UEI: Ultrasound elastography imaging; SICUS: Small intestine contrast ultrasonography; IUS: Intestinal ultrasound; TNF: Tumor necrosis factor; NA: Not available.

different cut-off levels for bowel thickness (> 5 mm for conventional sonography and > 4 mm for SICUS), can suggest severe endoscopic postoperative recurrence and could accordingly replace endoscopy in postsurgical follow-up[37] (for detection of recurrence).

IUS is accurate not only in detecting postoperative clinical recurrence but also in predicting endoscopic and surgical recurrence. IUS assessment 3 mo after surgery showed high sensitivity in predicting postoperative recurrence at 12 mo, with lower sensitivity[38] but higher specificity than calprotectin[39]. A retrospective study showed that in postoperative CD patients, independent of the

time elapsed from earlier surgery, patients with BWT > 3 mm had a doubled risk of surgical recurrence compared with patients with BWT < 3 mm, and that the absolute incidence of new surgical interventions positively correlated with increased BWT[40]. In this respect, the prognostic value of increased BWT, as assessed by IUS several years after surgery, needs further confirmation, and in particular, the usefulness of therapy escalation for these patients remains unconfirmed[12].

Additionally, in CD patients treated with conservative surgery (*e.g.*, strictureplasty or minimal bowel resections), IUS is useful for monitoring the postoperative behaviour of BWT and can provide prognostic information: US detection of unchanged or worsened wall thickness 6 mo after surgery or the postoperative persistence of wall thickness > 6 mm is predictive of a high risk of recurrence[41].

In this subset of patients, the estimated 5-year survival probability of symptomatic CD recurrence was 90% and 33%, respectively, for unchanged/worsened BWT *vs* improved BWT at 12 mo after surgery. A BWT > 6.0 mm at 12 mo after surgery was directly associated with the risk of CD recurrence. Hence, systematic IUS follow-up of diseased bowel walls after conservative surgery seems to allow the early identification of patients at high risk of clinical/surgical recurrence[42].

Clinical remission

In CD patients, bowel wall changes such as increased BWT and vascularization may persist after therapy and despite clinical remission. The meaning and prognostic significance of these IUS findings have been widely investigated. In quiescent CD, increased vascularity, detected either by colour Doppler or CEUS, after treatment may suggest an increased risk of relapse[21,43,44].

Vascularization and BWT currently represent the main features of sonographic activity scores, and the investigation on prognostic significance of these scores in clinical studies is still ongoing. However, it is clear that normalization of the bowel wall (the so-called TR), namely, a BWT < 3 mm[45] or a more stringent definition such as the combination of BWT < 3 mm, normalization of vascularity and wall stratification, absence of mesenteric fat hypertrophy, node enlargement, or disease complications (*i.e.*, strictures, fistulas)[46,47], is associated with favourable prognostic long-term outcomes[40,43,46,48,49].

Indeed, it has been demonstrated that sonographic remission evaluated after one year of anti-TNF therapy is associated with a longer remission without the need for a therapy change and a reduced need for surgery[21]. In patients with CD in clinical remission, achieving TR is associated with reduced clinical complications, including medication escalation, corticosteroid use, hospitalization, and surgery. When examining clinical complications occurring more than 90 d following IUS, sonographic inflammation remains associated with an increased risk of clinical complications such asmedication escalation, hospitalization, and surgery[46,50,51].

CONCLUSION

IUS is a useful imaging method to assess CD disease activity and can have a prognostic role in predicting response to treatment, disease progression, risk of surgery and risk of postsurgical recurrence. Response to treatment may be predicted by increased BWT and vascularization, reduced elasticity and absence of CD complications. Disease progression or risk of surgery may be predicted by increased BWT, loss of bowel stratification and the presence of CD complications. Postoperative clinical and surgical relapse may be predicted by increased BWT. As more biological therapies become available in the coming years, further prospective trials will be needed to reach definite evidence on IUS predictive value at baseline, to recognize which patients are more likely to respond to a specific therapy and which patients are at high risk of surgery or complications, needing early intensive treatment.

FOOTNOTES

Author contributions: Manzotti C and Maconi G gave substantial contributions to conception and design of the review, and literature review; Manzotti C drafted and edited the article; Colombo F and Maconi G revised the manuscript critically for important intellectual content; Colombo F, Zurleni T, and Danelli P worked together for the final approval of the version to be published.

Conflict-of-interest statement: All the authors report no relevant conflicts of interest for this article.

Open-Access: This article is an open-access article that was selected by an in-house editor and fully peer-reviewed by external reviewers. It is distributed in accordance with the Creative Commons Attribution NonCommercial (CC BY-NC 4.0) license, which permits others to distribute, remix, adapt, build upon this work non-commercially, and license their derivative works on different terms, provided the original work is properly cited and the use is non-commercial. See: https://creativecommons.org/Licenses/by-nc/4.0/

Country/Territory of origin: Italy

ORCID number: Cristina Manzotti 0000-0003-2836-3068; Francesco Colombo 0000-0002-6478-7055; Tommaso Zurleni 0000-0002-3971-2297; Piergiorgio Danelli 0000-0003-1461-9835; Giovanni Maconi 0000-0003-0810-4026.

S-Editor: Wang JJ
L-Editor: A
P-Editor: Wang JJ

REFERENCES

1 **Torres J**, Mehandru S, Colombel JF, Peyrin-Biroulet L. Crohn's disease. *Lancet* 2017; **389**: 1741-1755 [PMID: 27914655 DOI: 10.1016/S0140-6736(16)31711-1]
2 **Peyrin-Biroulet L**, Reinisch W, Colombel JF, Mantzaris GJ, Kornbluth A, Diamond R, Rutgeerts P, Tang LK, Cornillie FJ, Sandborn WJ. Clinical disease activity, C-reactive protein normalisation and mucosal healing in Crohn's disease in the SONIC trial. *Gut* 2014; **63**: 88-95 [PMID: 23974954 DOI: 10.1136/gutjnl-2013-304984]
3 **Pariente B**, Cosnes J, Danese S, Sandborn WJ, Lewin M, Fletcher JG, Chowers Y, D'Haens G, Feagan BG, Hibi T, Hommes DW, Irvine EJ, Kamm MA, Loftus EV Jr, Louis E, Michetti P, Munkholm P, Oresland T, Panés J, Peyrin-Biroulet L, Reinisch W, Sands BE, Schoelmerich J, Schreiber S, Tilg H, Travis S, van Assche G, Vecchi M, Mary JY, Colombel JF, Lémann M. Development of the Crohn's disease digestive damage score, the Lémann score. *Inflamm Bowel Dis* 2011; **17**: 1415-1422 [PMID: 21560202 DOI: 10.1002/ibd.21506]
4 **Farmer RG**, Whelan G, Fazio VW. Long-term follow-up of patients with Crohn's disease. Relationship between the clinical pattern and prognosis. *Gastroenterology* 1985; **88**: 1818-1825 [PMID: 3922845 DOI: 10.1016/0016-5085(85)90006-x]
5 **Solberg IC**, Vatn MH, Høie O, Stray N, Sauar J, Jahnsen J, Moum B, Lygren I; IBSEN Study Group. Clinical course in Crohn's disease: results of a Norwegian population-based ten-year follow-up study. *Clin Gastroenterol Hepatol* 2007; **5**: 1430-1438 [PMID: 18054751 DOI: 10.1016/j.cgh.2007.09.002]
6 **Gonzalez-Montpetit E**, Ripollés T, Martinez-Pérez MJ, Vizuete J, Martín G, Blanc E. Ultrasound findings of Crohn's disease: correlation with MR enterography. *Abdom Radiol (NY)* 2021; **46**: 156-167 [PMID: 32607648 DOI: 10.1007/s00261-020-02622-3]
7 **Rimola J**, Torres J, Kumar S, Taylor SA, Kucharzik T. Recent advances in clinical practice: advances in cross-sectional imaging in inflammatory bowel disease. *Gut* 2022; **71**: 2587-2597 [PMID: 35927032 DOI: 10.1136/gutjnl-2021-326562]
8 **Maconi G**, Nylund K, Ripolles T, Calabrese E, Dirks K, Dietrich CF, Hollerweger A, Sporea I, Saftoiu A, Maaser C, Hausken T, Higginson AP, Nürnberg D, Pallotta N, Romanini L, Serra C, Gilja OH. EFSUMB Recommendations and Clinical Guidelines for Intestinal Ultrasound (GIUS) in Inflammatory Bowel Diseases. *Ultraschall Med* 2018; **39**: 304-317 [PMID: 29566419 DOI: 10.1055/s-0043-125329]
9 **Dillman JR**, Dehkordy SF, Smith EA, DiPietro MA, Sanchez R, DeMatos-Maillard V, Adler J, Zhang B, Trout AT. Defining the ultrasound longitudinal natural history of newly diagnosed pediatric small bowel Crohn disease treated with infliximab and infliximab-azathioprine combination therapy. *Pediatr Radiol* 2017; **47**: 924-934 [PMID: 28421251 DOI: 10.1007/s00247-017-3848-3]
10 **Schulberg JD**, Wright EK, Holt BA, Hamilton AL, Sutherland TR, Ross AL, Vogrin S, Miller AM, Connell WC, Lust M, Ding NS, Moore GT, Bell SJ, Shelton E, Christensen B, De Cruz P, Rong YJ, Kamm MA. Intensive drug therapy versus standard drug therapy for symptomatic intestinal Crohn's disease strictures (STRIDENT): an open-label, single-centre, randomised controlled trial. *Lancet Gastroenterol Hepatol* 2022; **7**: 318-331 [PMID: 34890567 DOI: 10.1016/S2468-1253(21)00393-9]
11 **Calabrese E**, Maaser C, Zorzi F, Kannengiesser K, Hanauer SB, Bruining DH, Iacucci M, Maconi G, Novak KL, Panaccione R, Strobel D, Wilson SR, Watanabe M, Pallone F, Ghosh S. Bowel Ultrasonography in the Management of Crohn's Disease. A Review with Recommendations of an International Panel of Experts. *Inflamm Bowel Dis* 2016; **22**: 1168-1183 [PMID: 26958988 DOI: 10.1097/MIB.0000000000000706]
12 **Fraquelli M**, Castiglione F, Calabrese E, Maconi G. Impact of intestinal ultrasound on the management of patients with inflammatory bowel disease: how to apply scientific evidence to clinical practice. *Dig Liver Dis* 2020; **52**: 9-18 [PMID: 31732443 DOI: 10.1016/j.dld.2019.10.004]
13 **Puca P**, Del Vecchio LE, Ainora ME, Gasbarrini A, Scaldaferri F, Zocco MA. Role of Multiparametric Intestinal Ultrasound in the Evaluation of Response to Biologic Therapy in Adults with Crohn's Disease. *Diagnostics (Basel)* 2022; **12** [PMID: 36010341 DOI: 10.3390/diagnostics12081991]
14 **Allocca M**, Craviotto V, Bonovas S, Furfaro F, Zilli A, Peyrin-Biroulet L, Fiorino G, Danese S. Predictive Value of Bowel Ultrasound in Crohn's Disease: A 12-Month Prospective Study. *Clin Gastroenterol Hepatol* 2022; **20**: e723-e740 [PMID: 33895360 DOI: 10.1016/j.cgh.2021.04.029]
15 **Huang X**, Li X. Predictive Value of Bowel Ultrasound in Crohn's Disease. *Clin Gastroenterol Hepatol* 2022; **20**: e345-e346 [PMID: 33940228 DOI: 10.1016/j.cgh.2021.04.040]
16 **Maconi G**, Sampietro GM, Sartani A, Bianchi Porro G. Bowel ultrasound in Crohn's disease: surgical perspective. *Int J Colorectal Dis* 2008; **23**: 339-347 [PMID: 18188575 DOI: 10.1007/s00384-007-0418-4]
17 **de Voogd F**, Bots S, Gecse K, Gilja OH, D'Haens G, Nylund K. Intestinal Ultrasound Early on in Treatment Follow-up Predicts Endoscopic Response to Anti-TNFα Treatment in Crohn's Disease. *J Crohns Colitis* 2022; **16**: 1598-1608 [PMID: 35639823 DOI: 10.1093/ecco-jcc/jjac072]
18 **Albshesh A**, Ungar B, Ben-Horin S, Eliakim R, Kopylov U, Carter D. Terminal Ileum Thickness During Maintenance Therapy Is a Predictive Marker of the Outcome of Infliximab Therapy in Crohn Disease. *Inflamm Bowel Dis* 2020; **26**: 1619-1625 [PMID: 32860057 DOI: 10.1093/ibd/izaa219]

19 **Chen YJ**, Chen BL, Liang MJ, Chen SL, Li XH, Qiu Y, Pang LL, Xia QQ, He Y, Zeng ZR, Chen MH, Mao R, Xie XY. Longitudinal Bowel Behavior Assessed by Bowel Ultrasound to Predict Early Response to Anti-TNF Therapy in Patients With Crohn's Disease: A Pilot Study. *Inflamm Bowel Dis* 2022; **28**: S67-S75 [PMID: 34984455 DOI: 10.1093/ibd/izab353]

20 **Les A**, Iacob R, Saizu R, Cotruta B, Saizu AI, Iacob S, Gheorghe L, Gheorghe C. Bowel Ultrasound: a Non-invasive, Easy to Use Method to Predict the Need to Intensify Therapy in Inflammatory Bowel Disease Patients. *J Gastrointestin Liver Dis* 2021; **30**: 462-469 [PMID: 34752586 DOI: 10.15403/jgld-3726]

21 **Ripollés T**, Paredes JM, Martínez-Pérez MJ, Rimola J, Jauregui-Amezaga A, Bouzas R, Martin G, Moreno-Osset E. Ultrasonographic Changes at 12 Weeks of Anti-TNF Drugs Predict 1-year Sonographic Response and Clinical Outcome in Crohn's Disease: A Multicenter Study. *Inflamm Bowel Dis* 2016; **22**: 2465-2473 [PMID: 27580385 DOI: 10.1097/MIB.0000000000000882]

22 **Smith RL**, Taylor KM, Friedman AB, Gibson DJ, Con D, Gibson PR. Early sonographic response to a new medical therapy is associated with future treatment response or failure in patients with inflammatory bowel disease. *Eur J Gastroenterol Hepatol* 2022; **34**: 613-621 [PMID: 35352696 DOI: 10.1097/MEG.0000000000002367]

23 **Zorzi F**, Ghosh S, Chiaramonte C, Lolli E, Ventura M, Onali S, De Cristofaro E, Fantini MC, Biancone L, Monteleone G, Calabrese E. Response Assessed by Ultrasonography as Target of Biological Treatment for Crohn's Disease. *Clin Gastroenterol Hepatol* 2020; **18**: 2030-2037 [PMID: 31866561 DOI: 10.1016/j.cgh.2019.10.042]

24 **Hoffmann T**, Fusco S, Blumenstock G, Sadik S, Malek NP, Froehlich E. Evaluation of bowel wall thickness by ultrasound as early diagnostic tool for therapeutic response in Crohn's disease patients treated with ustekinumab. *Z Gastroenterol* 2022; **60**: 1212-1220 [PMID: 33233006 DOI: 10.1055/a-1283-6550]

25 **Saevik F**, Nylund K, Hausken T, Ødegaard S, Gilja OH. Bowel perfusion measured with dynamic contrast-enhanced ultrasound predicts treatment outcome in patients with Crohn's disease. *Inflamm Bowel Dis* 2014; **20**: 2029-2037 [PMID: 25185684 DOI: 10.1097/MIB.0000000000000159]

26 **Chen W**, Lu C, Hirota C, Iacucci M, Ghosh S, Gui X. Smooth Muscle Hyperplasia/Hypertrophy is the Most Prominent Histological Change in Crohn's Fibrostenosing Bowel Strictures: A Semiquantitative Analysis by Using a Novel Histological Grading Scheme. *J Crohns Colitis* 2017; **11**: 92-104 [PMID: 27364949 DOI: 10.1093/ecco-jcc/jjw126]

27 **Quaia E**, Sozzi M, Angileri R, Gennari AG, Cova MA. Time-Intensity Curves Obtained after Microbubble Injection Can Be Used to Differentiate Responders from Nonresponders among Patients with Clinically Active Crohn Disease after 6 Weeks of Pharmacologic Treatment. *Radiology* 2016; **281**: 606-616 [PMID: 27192460 DOI: 10.1148/radiol.2016152461]

28 **Pecere S**, Holleran G, Ainora ME, Garcovich M, Scaldaferri F, Gasbarrini A, Zocco MA. Usefulness of contrast-enhanced ultrasound (CEUS) in Inflammatory Bowel Disease (IBD). *Dig Liver Dis* 2018; **50**: 761-767 [PMID: 29705029 DOI: 10.1016/j.dld.2018.03.023]

29 **Orlando S**, Fraquelli M, Coletta M, Branchi F, Magarotto A, Conti CB, Mazza S, Conte D, Basilisco G, Caprioli F. Ultrasound Elasticity Imaging Predicts Therapeutic Outcomes of Patients With Crohn's Disease Treated With Anti-Tumour Necrosis Factor Antibodies. *J Crohns Colitis* 2018; **12**: 63-70 [PMID: 28961950 DOI: 10.1093/ecco-jcc/jjx116]

30 **Maconi G**, Di Sabatino A, Ardizzone S, Greco S, Colombo E, Russo A, Cassinotti A, Casini V, Corazza GR, Bianchi Porro G. Prevalence and clinical significance of sonographic detection of enlarged regional lymph nodes in Crohn's disease. *Scand J Gastroenterol* 2005; **40**: 1328-1333 [PMID: 16243717 DOI: 10.1080/00365510510025746]

31 **Kucharzik T**, Wittig BM, Helwig U, Börner N, Rössler A, Rath S, Maaser C; TRUST study group. Use of Intestinal Ultrasound to Monitor Crohn's Disease Activity. *Clin Gastroenterol Hepatol* 2017; **15**: 535-542.e2 [PMID: 27856365 DOI: 10.1016/j.cgh.2016.10.040]

32 **Helwig U**, Fischer I, Hammer L, Kolterer S, Rath S, Maaser C, Kucharzik T. Transmural Response and Transmural Healing Defined by Intestinal Ultrasound: New Potential Therapeutic Targets? *J Crohns Colitis* 2022; **16**: 57-67 [PMID: 34185843 DOI: 10.1093/ecco-jcc/jjab106]

33 **Rosenbaum DG**, Conrad MA, Biko DM, Ruchelli ED, Kelsen JR, Anupindi SA. Ultrasound and MRI predictors of surgical bowel resection in pediatric Crohn disease. *Pediatr Radiol* 2017; **47**: 55-64 [PMID: 27687769 DOI: 10.1007/s00247-016-3704-x]

34 **Castiglione F**, de Sio I, Cozzolino A, Rispo A, Manguso F, Del Vecchio Blanco G, Di Girolamo E, Castellano L, Ciacci C, Mazzacca G. Bowel wall thickness at abdominal ultrasound and the one-year-risk of surgery in patients with Crohn's disease. *Am J Gastroenterol* 2004; **99**: 1977-1983 [PMID: 15447760 DOI: 10.1111/j.1572-0241.2004.40267.x]

35 **Rigazio C**, Ercole E, Laudi C, Daperno M, Lavagna A, Crocella L, Bertolino F, Viganò L, Sostegni R, Pera A, Rocca R. Abdominal bowel ultrasound can predict the risk of surgery in Crohn's disease: proposal of an ultrasonographic score. *Scand J Gastroenterol* 2009; **44**: 585-593 [PMID: 19148846 DOI: 10.1080/00365520802705992]

36 **Kunihiro K**, Hata J, Manabe N, Mitsuoka Y, Tanaka S, Haruma K, Chayama K. Predicting the need for surgery in Crohn's disease with contrast harmonic ultrasound. *Scand J Gastroenterol* 2007; **42**: 577-585 [PMID: 17454878 DOI: 10.1080/00365520601002716]

37 **Castiglione F**, Bucci L, Pesce G, De Palma GD, Camera L, Cipolletta F, Testa A, Diaferia M, Rispo A. Oral contrast-enhanced sonography for the diagnosis and grading of postsurgical recurrence of Crohn's disease. *Inflamm Bowel Dis* 2008; **14**: 1240-1245 [PMID: 18398896 DOI: 10.1002/ibd.20469]

38 **Paredes JM**, Ripollés T, Cortés X, Moreno N, Martínez MJ, Bustamante-Balén M, Delgado F, Moreno-Osset E. Contrast-enhanced ultrasonography: usefulness in the assessment of postoperative recurrence of Crohn's disease. *J Crohns Colitis* 2013; **7**: 192-201 [PMID: 22542055 DOI: 10.1016/j.crohns.2012.03.017]

39 **Orlando A**, Modesto I, Castiglione F, Scala L, Scimeca D, Rispo A, Teresi S, Mocciaro F, Criscuoli V, Marrone C, Platania P, De Falco T, Maisano S, Nicoli N, Cottone M. The role of calprotectin in predicting endoscopic post-surgical recurrence in asymptomatic Crohn's disease: a comparison with ultrasound. *Eur Rev Med Pharmacol Sci* 2006; **10**: 17-22 [PMID: 16494106]

40 **Cammarota T**, Sarno A, Robotti D, Bonenti G, Debani P, Versace K, Astegiano M, Pera A. US evaluation of patients affected by IBD: how to do it, methods and findings. *Eur J Radiol* 2009; **69**: 429-437 [PMID: 19121906 DOI: 10.1016/j.ejrad.2008.11.008]

41 **Maconi G**, Sampietro GM, Cristaldi M, Danelli PG, Russo A, Bianchi Porro G, Taschieri AM. Preoperative characteristics and postoperative behavior of bowel wall on risk of recurrence after conservative surgery in Crohn's disease: a prospective study. *Ann Surg* 2001; **233**: 345-352 [PMID: 11224621 DOI: 10.1097/00000658-200103000-00007]

42 **Parente F**, Sampietro GM, Molteni M, Greco S, Anderloni A, Sposito C, Danelli PG, Taschieri AM, Gallus S, Bianchi Porro G. Behaviour of the bowel wall during the first year after surgery is a strong predictor of symptomatic recurrence of Crohn's disease: a prospective study. *Aliment Pharmacol Ther* 2004; **20**: 959-968 [PMID: 15521843 DOI: 10.1111/j.1365-2036.2004.02245.x]

43 **Ripollés T**, Martínez MJ, Barrachina MM. Crohn's disease and color Doppler sonography: response to treatment and its relationship with long-term prognosis. *J Clin Ultrasound* 2008; **36**: 267-272 [PMID: 18067121 DOI: 10.1002/jcu.20423]

44 **Di Sabatino A**, Fulle I, Ciccocioppo R, Ricevuti L, Tinozzi FP, Tinozzi S, Campani R, Corazza GR. Doppler enhancement after intravenous levovist injection in Crohn's disease. *Inflamm Bowel Dis* 2002; **8**: 251-257 [PMID: 12131608 DOI: 10.1097/00054725-200207000-00003]

45 **Zacharopoulou E**, Craviotto V, Fiorino G, Furfaro F, Zilli A, Gilardi D, Peyrin-Biroulet L, Danese S, Allocca M. Targeting the gut layers in Crohn's disease: mucosal or transmural healing? *Expert Rev Gastroenterol Hepatol* 2020; **14**: 775-787 [PMID: 32515627 DOI: 10.1080/17474124.2020.1780914]

46 **Nardone OM**, Calabrese G, Testa A, Caiazzo A, Fierro G, Rispo A, Castiglione F. The Impact of Intestinal Ultrasound on the Management of Inflammatory Bowel Disease: From Established Facts Toward New Horizons. *Front Med (Lausanne)* 2022; **9**: 898092 [PMID: 35677820 DOI: 10.3389/fmed.2022.898092]

47 **Kucharzik T**, Tielbeek J, Carter D, Taylor SA, Tolan D, Wilkens R, Bryant RV, Hoeffel C, De Kock I, Maaser C, Maconi G, Novak K, Rafaelsen SR, Scharitzer M, Spinelli A, Rimola J. ECCO-ESGAR Topical Review on Optimizing Reporting for Cross-Sectional Imaging in Inflammatory Bowel Disease. *J Crohns Colitis* 2022; **16**: 523-543 [PMID: 34628504 DOI: 10.1093/ecco-jcc/jjab180]

48 **Ma L**, Li W, Zhuang N, Yang H, Liu W, Zhou W, Jiang Y, Li J, Zhu Q, Qian J. Comparison of transmural healing and mucosal healing as predictors of positive long-term outcomes in Crohn's disease. *Therap Adv Gastroenterol* 2021; **14**: 17562848211016259 [PMID: 34178114 DOI: 10.1177/17562848211016259]

49 **Geyl S**, Guillo L, Laurent V, D'Amico F, Danese S, Peyrin-Biroulet L. Transmural healing as a therapeutic goal in Crohn's disease: a systematic review. *Lancet Gastroenterol Hepatol* 2021; **6**: 659-667 [PMID: 34090579 DOI: 10.1016/S2468-1253(21)00096-0]

50 **Vaughan R**, Tjandra D, Patwardhan A, Mingos N, Gibson R, Boussioutas A, Ardalan Z, Al-Ani A, Gibson PR, Christensen B. Toward transmural healing: Sonographic healing is associated with improved long-term outcomes in patients with Crohn's disease. *Aliment Pharmacol Ther* 2022; **56**: 84-94 [PMID: 35343603 DOI: 10.1111/apt.16892]

51 **Wilkens R**, Novak KL, Maaser C, Panaccione R, Kucharzik T. Relevance of monitoring transmural disease activity in patients with Crohn's disease: current status and future perspectives. *Therap Adv Gastroenterol* 2021; **14**: 17562848211006672 [PMID: 33948115 DOI: 10.1177/17562848211006672]

52 **Calabrese E**, Rispo A, Zorzi F, De Cristofaro E, Testa A, Costantino G, Viola A, Bezzio C, Ricci C, Prencipe S, Racchini C, Stefanelli G, Allocca M, Scotto di Santolo S, D'Auria MV, Balestrieri P, Ricchiuti A, Cappello M, Cavallaro F, Guarino AD, Maconi G, Spagnoli A, Monteleone G, Castiglione F. Ultrasonography Tight Control and Monitoring in Crohn's Disease During Different Biological Therapies: A Multicenter Study. *Clin Gastroenterol Hepatol* 2022; **20**: e711-e722 [PMID: 33775896 DOI: 10.1016/j.cgh.2021.03.030]

53 **Paredes JM**, Moreno N, Latorre P, Ripollés T, Martinez MJ, Vizuete J, Moreno-Osset E. Clinical Impact of Sonographic Transmural Healing After Anti-TNF Antibody Treatment in Patients with Crohn's Disease. *Dig Dis Sci* 2019; **64**: 2600-2606 [PMID: 30874986 DOI: 10.1007/s10620-019-05567-w]

54 **Laterza L**, Ainora ME, Garcovich M, Galasso L, Poscia A, Di Stasio E, Lupascu A, Riccardi L, Scaldaferri F, Armuzzi A, Rapaccini GL, Gasbarrini A, Pompili M, Zocco MA. Bowel contrast-enhanced ultrasound perfusion imaging in the evaluation of Crohn's disease patients undergoing anti-TNFα therapy. *Dig Liver Dis* 2021; **53**: 729-737 [PMID: 32900648 DOI: 10.1016/j.dld.2020.08.005]

55 **Ungar B**, Ben-Shatach Z, Selinger L, Malik A, Albshesh A, Ben-Horin S, Eliakim R, Kopylov U, Carter D. Lower adalimumab trough levels are associated with higher bowel wall thickness in Crohn's disease. *United European Gastroenterol J* 2020; **8**: 167-174 [PMID: 32213067 DOI: 10.1177/2050640619878974]

56 **Quaia E**, Gennari AG, Cova MA. Early Predictors of the Long-term Response to Therapy in Patients With Crohn Disease Derived From a Time-Intensity Curve Analysis After Microbubble Contrast Agent Injection. *J Ultrasound Med* 2019; **38**: 947-958 [PMID: 30208230 DOI: 10.1002/jum.14778]

57 **Castiglione F**, Testa A, Rea M, De Palma GD, Diaferia M, Musto D, Sasso F, Caporaso N, Rispo A. Transmural healing evaluated by bowel sonography in patients with Crohn's disease on maintenance treatment with biologics. *Inflamm Bowel Dis* 2013; **19**: 1928-1934 [PMID: 23835441 DOI: 10.1097/MIB.0b013e31829053ce]

58 **Castiglione F**, Mainenti P, Testa A, Imperatore N, De Palma GD, Maurea S, Rea M, Nardone OM, Sanges M, Caporaso N, Rispo A. Cross-sectional evaluation of transmural healing in patients with Crohn's disease on maintenance treatment with anti-TNF alpha agents. *Dig Liver Dis* 2017; **49**: 484-489 [PMID: 28292640 DOI: 10.1016/j.dld.2017.02.014]

59 **Castiglione F**, Imperatore N, Testa A, De Palma GD, Nardone OM, Pellegrini L, Caporaso N, Rispo A. One-year clinical outcomes with biologics in Crohn's disease: transmural healing compared with mucosal or no healing. *Aliment Pharmacol Ther* 2019; **49**: 1026-1039 [PMID: 30854708 DOI: 10.1111/apt.15190]

60 **Kucharzik T**, Wilkens R, D'Agostino MA, Maconi G, Le Bars M, Lahaye M, Bravatà I, Nazar M, Ni L, Ercole E, Allocca M, Machková N, de Voogd FAE, Palmela C, Vaughan R, Maaser C; STARDUST Intestinal Ultrasound study group. Early Ultrasound Response and Progressive Transmural Remission After Treatment With Ustekinumab in Crohn's Disease. *Clin Gastroenterol Hepatol* 2023; **21**: 153-163.e12 [PMID: 35842121 DOI: 10.1016/j.cgh.2022.05.055]

61 **Miranda A**, Gravina AG, Cuomo A, Mucherino C, Sgambato D, Facchiano A, Granata L, Priadko K, Pellegrino R, de Filippo FR, Camera S, Cuomo R, Melina R, D'Onofrio V, Manguso F, Ciacci C, Romano M. Efficacy of ustekinumab in the treatment of patients with Crohn's disease with failure to previous conventional or biologic therapy: a prospective observational real-life study. *J Physiol Pharmacol* 2021; **72** [PMID: 34987127 DOI: 10.26402/jpp.2021.4.05]

62 **Civitelli F**, Nuti F, Oliva S, Messina L, La Torre G, Viola F, Cucchiara S, Aloi M. Looking Beyond Mucosal Healing: Effect of Biologic Therapy on Transmural Healing in Pediatric Crohn's Disease. *Inflamm Bowel Dis* 2016; **22**: 2418-2424 [PMID: 27598739 DOI: 10.1097/MIB.0000000000000897]

63 **Paredes JM**, Ripollés T, Cortés X, Martínez MJ, Barrachina M, Gómez F, Moreno-Osset E. Abdominal sonographic changes after antibody to tumor necrosis factor (anti-TNF) alpha therapy in Crohn's Disease. *Dig Dis Sci* 2010; **55**: 404-410 [PMID: 19267199 DOI: 10.1007/s10620-009-0759-7]

64 **Vaughan R**, Murphy E, Nalder M, Gibson RN, Ardalan Z, Boussioutas A, Christensen B. Infliximab Trough Levels Are Associated With Transmural Sonographic Healing in Inflammatory Bowel Disease. *Inflamm Bowel Dis* 2022 [PMID: 36094156 DOI: 10.1093/ibd/izac186]

65 **Han ZM**, Elodie WH, Yan LH, Xu PC, Zhao XM, Zhi FC. Correlation Between Ultrasonographic Response and Anti-Tumor Necrosis Factor Drug Levels in Crohn's disease. *Ther Drug Monit* 2022; **44**: 659-664 [PMID: 35427284 DOI: 10.1097/FTD.0000000000000988]

66 **Dolinger MT**, Choi JJ, Phan BL, Rosenberg HK, Rowland J, Dubinsky MC. Use of Small Bowel Ultrasound to Predict Response to Infliximab Induction in Pediatric Crohn's Disease. *J Clin Gastroenterol* 2021; **55**: 429-432 [PMID: 32453126 DOI: 10.1097/MCG.0000000000001367]

World Journal of Gastroenterology

Submit a Manuscript: https://www.f6publishing.com

World J Gastroenterol 2023 June 21; 29(23): 3606-3621

DOI: 10.3748/wjg.v29.i23.3606

ISSN 1007-9327 (print) ISSN 2219-2840 (online)

ORIGINAL ARTICLE

Basic Study

BMI-1 activates hepatic stellate cells to promote the epithelial-mesenchymal transition of colorectal cancer cells

Zhong-Yang Jiang, Xi-Mei Ma, Xiao-Hui Luan, Zhen-Yu Liuyang, Yi-Yang Hong, Yuan Dai, Qing-Hua Dong, Guan-Yu Wang

Specialty type: Gastroenterology and hepatology

Provenance and peer review: Unsolicited article; Externally peer reviewed.

Peer-review model: Single blind

Peer-review report's scientific quality classification
Grade A (Excellent): 0
Grade B (Very good): B
Grade C (Good): C, C
Grade D (Fair): 0
Grade E (Poor): 0

P-Reviewer: Emran TB, Bangladesh; Wu C, China

Received: February 1, 2023
Peer-review started: February 1, 2023
First decision: February 12, 2023
Revised: February 25, 2023
Accepted: May 4, 2023
Article in press: May 4, 2023
Published online: June 21, 2023

Zhong-Yang Jiang, Xiao-Hui Luan, Zhen-Yu Liuyang, Guan-Yu Wang, Department of General Surgery, Sir Run Run Shaw Hospital, School of Medicine, Zhejiang University, Hangzhou 310016, Zhejiang Province, China

Xi-Mei Ma, Department of Emergency, The Second Affiliated Hospital of Zhejing University, Hangzhou 310016, Zhejiang Province, China

Yi-Yang Hong, Yuan Dai, Qing-Hua Dong, Biomedical Research Center, Sir Run Run Shaw Hospital, School of Medicine, Zhejiang University, Hangzhou 310016, Zhejiang Province, China

Qing-Hua Dong, Key Laboratory of Cancer Prevention and Intervention, China National Ministry of Education, Hangzhou 310009, Zhejiang Province, China

Corresponding author: Guan-Yu Wang, MD, PhD, Surgeon, Department of General Surgery, Sir Run Run Shaw Hospital, School of Medicine, Zhejiang University, No. 3 East Qingchun Road, Hangzhou 310016, Zhejiang Province, China. wangguanyu@zju.edu.cn

Abstract

BACKGROUND

Activated hepatic stellate cells (aHSCs) are the major source of cancer-associated fibroblasts in the liver. Although the crosstalk between aHSCs and colorectal cancer (CRC) cells supports liver metastasis (LM), the mechanisms are largely unknown.

AIM

To explore the role of BMI-1, a polycomb group protein family member, which is highly expressed in LM, and the interaction between aHSCs and CRC cells in promoting CRC liver metastasis (CRLM).

METHODS

Immunohistochemistry was carried out to examine BMI-1 expression in LM and matched liver specimens of CRC. The expression levels of BMI-1 in mouse liver during CRLM (0, 7, 14, 21, and 28 d) were detected by Western blotting (WB) and the quantitative polymerase chain reaction (qPCR) assay. We overexpressed BMI-1 in HSCs (LX2) by lentivirus infection and tested the molecular markers of aHSCs by WB, qPCR, and the immunofluorescence assay. CRC cells (HCT116 and DLD1)

were cultured in HSC-conditioned medium (LX2 NC CM or LX2 BMI-1 CM). CM-induced CRC cell proliferation, migration, epithelial-mesenchymal transition (EMT) phenotype, and transforming growth factor beta (TGF-β)/SMAD pathway changes were investigated *in vitro*. A mouse subcutaneous xenotransplantation tumor model was established by co-implantation of HSCs (LX2 NC or LX2 BMI-1) and CRC cells to investigate the effects of HSCs on tumor growth and the EMT phenotype *in vivo*.

RESULTS

Positive of BMI-1 expression in the liver of CRLM patients was 77.8%. The expression level of BMI-1 continued to increase during CRLM in mouse liver cells. LX2 overexpressed BMI-1 was activated, accompanied by increased expression level of alpha smooth muscle actin, fibronectin, TGF-β1, matrix metalloproteinases, and interleukin 6. CRC cells cultured in BMI-1 CM exhibited enhanced proliferation and migration ability, EMT phenotype and activation of the TGF-β/SMAD pathway. In addition, the TGF-βR inhibitor SB-505124 diminished the effect of BMI-1 CM on SMAD2/3 phosphorylation in CRC cells. Furthermore, BMI-1 overexpressed LX2 HSCs promoted tumor growth and the EMT phenotype *in vivo*.

CONCLUSION

High expression of BMI-1 in liver cells is associated with CRLM progression. BMI-1 activates HSCs to secrete factors to form a prometastatic environment in the liver, and aHSCs promote proliferation, migration, and the EMT in CRC cells partially through the TGF-β/SMAD pathway.

Key Words: BMI-1; Hepatic stellate cells; Colorectal cancer; Liver metastasis; Epithelial-mesenchymal transition

©The Author(s) 2023. Published by Baishideng Publishing Group Inc. All rights reserved.

Core Tip: This study revealed that BMI-1 was upregulated in liver cells during colorectal cancer (CRC) liver metastasis. BMI-1-activated LX2 hepatic stellate cells (HSCs) promoted CRC cell proliferation, migration, and the epithelial-mesenchymal transition both *in vitro* and *in vivo*. Mechanistically, transforming growth factor beta 1 was increased in BMI-1 overexpressed LX2 HSCs, and triggered the phosphorylation of downstream SMAD2/3 in CRC cells and the interaction of activated HSCs and CRC cells, thereby further promoting CRC progression.

Citation: Jiang ZY, Ma XM, Luan XH, Liuyang ZY, Hong YY, Dai Y, Dong QH, Wang GY. BMI-1 activates hepatic stellate cells to promote the epithelial-mesenchymal transition of colorectal cancer cells. *World J Gastroenterol* 2023; 29(23): 3606-3621
URL: https://www.wjgnet.com/1007-9327/full/v29/i23/3606.htm
DOI: https://dx.doi.org/10.3748/wjg.v29.i23.3606

INTRODUCTION

Colorectal cancer (CRC) is the third most common cancer and ranks second in terms of cancer mortality worldwide[1,2]. Liver metastasis (LM) is the primary cause of death in CRC patients, and the liver plays a major role in survival as it is often the only site of metastasis. In CRC patients, approximately 14%-35% have LM at diagnosis, and about 70% have LM in the late stage of the disease[3]. In colorectal cancer (CRC) liver metastasis (CRLM) patients, liver resection is the primary curative treatment option, with a 5-year survival rate of 20%-50%[4]. Although treatments have advanced in recent years, the rate of intrahepatic recurrence is still high.

During CRLM, CRC cells can orchestrate a premetastatic niche by changing the tumor microenvironment[5,6]. For example, tumor cells secrete cytokines and extracellular vesicles containing microRNAs (miRNAs), integrins, and cytokines, which can modulate distant niches[7]. Zhao *et al*[8] found that CRC-derived miRNA-181a-5p-rich extracellular vesicles induced the activation of hepatic stellate cells (HSCs)[8]. The hepatic microenvironment has numerous signaling factors in liver cells, which consist of parenchymal and nonparenchymal cells, and the interaction between cancer cells and stromal cells facilitates the development of LM[9,10]. Cancer-associated fibroblasts (CAFs), comprising the major stromal cell type, are fibroblast populations found in primary and metastatic cancers and are related to tumor initiation, progression, and metastasis by regulating extracellular matrix (ECM) remodeling and the immune response[11-13]. HSCs are the major nonparenchymal liver cells, which store retinol and

play a role in liver repair, liver fibrosis, and hepatocellular carcinoma (HCC)[14-17]. HSCs contribute 85%–95% of fibroblasts in the liver[18]. HSCs are activated to CAFs by cancer cells to support tumor growth and metastasis[8,19]. Hepatic CAFs are thought to come primarily from HSCs and to a lesser extent from bone marrow-derived precursors, portal fibroblasts, and endothelial cells[20]. In intrahepatic cholangiocarcinoma, HSC-derived CAFs are the main tumor-interacting population[21]. Although CRC is the most common primary cancer that metastasizes to the liver, the mechanisms by which HSCs interact with CRC cells to promote LM are largely unclear.

BMI-1, one of the polycomb group protein family members, plays a critical role in negatively regulating the Ink4a/Arf locus which encodes $p16^{INK4a}$ and $p19^{ARF}$[22]. BMI-1 regulates self-renewal of stem cells and participates in the carcinogenesis of human cancers including CRC[23-25]. We previously reported that BMI-1 was overexpressed in CRLM and contributes to LM by regulating the epithelial-mesenchymal transition (EMT) of CRC cells *in vitro* and *in vivo*[26]. Interestingly, we observed BMI-1-positive staining in liver cells both in human and mouse specimens of CRLM. Studies have shown that quiescent HSCs can be activated by cancer cells and transformed into CAFs, and in turn activated HSCs (aHSCs) promote cancer cell invasion and the EMT[8,19]. Thus, we speculated that BMI-1 plays a role in the crosstalk between HSCs and CRC cells during LM.

In this study, both CRLM patients and mice showed increased BMI-1 expression in liver cells. BMI-1 overexpressed HSCs were activated and transformed into CAFs. CRC cells cultured in conditioned medium (CM) from BMI-1 overexpressed HSCs showed enhanced proliferation, migration, and EMT ability. The experimental *in vivo* subcutaneous xenotransplantation tumor model also showed increased tumor proliferation and EMT of CRC cells cocultured with BMI-1 overexpressed HSCs. These findings may provide a potential new target for the treatment of CRLM.

MATERIALS AND METHODS

Immunohistochemistry analysis of CRLM patients

LM and adjacent normal liver tissues from 18 clinically diagnosed patients with CRLM were collected from the Pathology Department (from 2013 to 2020), Sir Run Run Shaw Hospital, Hangzhou, China. The expression of BMI-1 was investigated by immunohistochemistry (IHC) staining. Anti-BMI-1 (1:100; Cell Signaling Technology, Danvers, MA, United States) was used as the primary antibody before secondary antibody incubation.

Cell culture and treatment

The high metastatic human CRC cell line (HCT116), low metastatic human CRC cell line (DLD1), mouse CRC cell line (CT26), and human HSC line (LX2) were purchased from the American Type Culture Collection (Manassas, VA, United States). Cells were cultured in Dulbecco's Modified Eagle's Medium (Gibco, Waltham, MA, United States) with 10% fetal bovine serum and 1% penicillin/streptomycin in a 5% carbon dioxide humidified incubator at 37 °C. The BMI-1 overexpressed lentiviral construct (pGC-FU-GFP-*BMI-1*) and negative control (pGC-FU-GFP) were obtained from Genechem (Shanghai, China). The control (LX2 NC) and stable BMI-1 overexpressed LX2 (LX2 BMI-1) cells were established by lentivirus transfection following the manufacturer's instructions. In addition, to prepare the CM, we first cultured transfected LX2 cells in a 10 cm plate at a density of 1×10^6 cells. We then used 6 mL serum-free DMEM to culture the cells for 24 h. The supernatants were collected, centrifuged at 1000 × *g* for 10 min, and filtered through a 0.22 mm filter unit (Millex, Duluth, GA, United States). CM from NC LX2 (NC CM) and BMI-1 LX2 (BMI-1 CM) was prepared by mixing the different supernatant with complete medium (1:1). Then the CRC cells were cultured in CM for 24 h. All CM was used within 2 d. CRC cells were pretreated with SB-505124 (0.05 μM) for 1 h to inhibit SMAD2 phosphorylation, and then the cells were incubated with BMI-1 CM for 24 h.

Western blotting

Whole proteins from the tissue and cell samples were extracted using RIPA buffer with a 1% protease/phosphatase inhibitor. After centrifugation of the extraction solutions, the BCA Protein Concentration Assay Kit (Solarbio, Beijing, China) was used to quantify the proteins. Following sodium dodecyl sulfate-polyacrylamide gel electrophoresis, the proteins were electrotransferred to polyvinylidene fluoride membranes. Antibodies against BMI-1, glyceraldehyde-3-phosphate dehydrogenase, β-actin, vimentin, SMAD2/3, phosphorylated SMAD3 (1:1000; Cell Signaling Technology), alpha smooth muscle actin (α-SMA), transforming growth factor beta 1 (TGF-β1), phosphorylated SMAD2 (1:1000; Abcam, Cambridge, MA, United States), fibronectin (1:1000; BD Biosciences, San Jose, CA, United States), E-cadherin, zinc finger E-box-binding homeobox 1 (ZEB-1), Twist-1 (1:1000; Novus Biologicals, Centennial, CO, United States), and Snail (1:1000; Proteintech Group, Rosemont, IL, United States) were used as primary antibodies. After washing with Tris-buffered saline with 0.1% Tween 20 three times every 10 min, goat anti-rabbit/mouse immunoglobulin G (Abcam) was used as the secondary antibody. The Bio-Rad CD Touch Detection System (Hercules, CA, United States) with enhanced chemiluminescence detection reagents was used to detect protein bands.

Quantitative polymerase chain reaction

Whole RNAs from the tissue and cell samples were extracted using Trizol reagent (Cwbio, Dalian, China). HiScript II Q RT SuperMix (Vazyme Biotech, Nanjing, China) was subsequently used for reverse transcription. ChamQ Universal SYBR quantitative polymerase chain reaction (qPCR) Master Mix (Vazyme Biotech) was used for qPCR. The Bio-Rad CFX-96 Real-Time PCR System was utilized to analyze the results. The sequences of all primers are listed in Supplementary Table 1.

Immunofluorescence staining

Immunofluorescence staining was performed in 96-well plates. Cells were fixed in paraformaldehyde and permeabilized with Triton X-100. Before incubation with secondary antibody, antibodies against vimentin (1:100; Cell Signaling Technology) and Snail (1:100; Proteintech Group) were used as primary antibodies. The Zeiss AXIO Observer A1 inverted fluorescence microscope system (Jena, Germany) was used to obtain images.

Cell viability assay

Cells were cultured in CM separately for 24, 48, 72, and 96 h. After treatment, Cell Counting Kit-8 (CCK-8) reagent (Yeasen Biotechnology, Shanghai, China) was added and incubated for 2 h. A spectrophotometer (Thermo Fisher Scientific, Waltham, MA, United States) was used to detect the optical density value (450 nm).

Colony formation assay

CRC cells were cultured in CM for 2 wk. Cells were fixed in paraformaldehyde and stained with crystal violet. Colonies were viewed with the Olympus CKK53 microscope (Tokyo, Japan), and photos were taken. ImageJ software was utilized to measure the number of colonies.

Wound healing assay

CRC cells were cultured until they reached 90% confluence. Following the creation of a linear wound, cells were cultured in CM for 48 h. Wounds were viewed with the Olympus CKK53 microscope, and photos were taken at 0, 24, and 48 h. ImageJ software was used to measure the migration rate.

Transwell migration assay

Transwell chambers were purchased from Corning Inc. (Corning, NY, United States). CRC cells were plated in the upper chambers with serum-free DMEM, while CM was placed in the lower chambers. After 48 h, cells in the upper chambers were removed, and cells on the lower membrane surface were fixed and stained. The migrated cells were viewed with the Olympus CKK53 microscope, and photos were taken. ImageJ software was used to measure the number of cells.

IHC

Tissue samples were fixed, dehydrated, paraffin-embedded, and sectioned. After deparaffinization, the sections were blocked in goat serum and incubated with primary antibodies for 24 h. The sections were incubated with secondary antibody for 30 min, followed by counterstaining with Mayer's hematoxylin. The Olympus CKK53 microscope was used to view and photograph the stained sections.

Animal experiments

All animal experimental procedures were approved by the Committee on the Ethics of Animal Experiments of Zhejiang University (No. ZJU20220447; Hangzhou, China).

Treatment protocol 1

Five-week-old male BALB/c mice (19-20 g) were randomly divided into five groups (n = 3). Isoflurane (inhalation) was utilized to anesthetize the mice. The spleen was then exteriorized through a left flank incision. CT26 cells (2×10^6) were injected intrasplenically to establish the tumor, and then the injection site was pressed for 5 min. Surgical thread was used to close the peritoneum and skin. The mice were sacrificed at 0, 7, 14, 21, and 28 d after inoculation of CT26 cells. Resected liver tissues were collected for qPCR, Western blotting (WB), and the IHC assay.

Treatment protocol 2

Five-week-old male BALB/c nude mice (17-18 g) were randomly divided into four groups (n = 5): (1) HCT116 cells (5×10^6) were mixed with LX2 NC cells (1×10^6); (2) HCT116 cells (5×10^6) were mixed with LX2 BMI-1 cells (1×10^6); (3) DLD1 cells (5×10^6) were mixed with LX2 NC cells (1×10^6); and (4) DLD1 cells (5×10^6) were mixed with LX2 BMI-1 cells (1×10^6). The mixed cells were subcutaneously injected into mouse flanks to establish the tumors. When measurable, tumor sizes were estimated every 2 d. The mice were killed 28 d after cell inoculation. Resected tumor tissues were collected for qPCR, WB, and the IHC assay. Total tumor volume (mm^3) = $L \times W^2/2$ (L = length and W = width).

Table 1 Correlation between clinicopathological characteristics of colorectal cancer patients and *BMI-1* expression in the liver

Characteristics	Cases, *n* = 18	*BMI-1* expression		*P* value
		Negative, *n* = 4	Positive, *n* = 14	
Age in yr				0.051
< 60	12	4	8	
≥ 60	6	0	6	
Sex				0.509
Male	11	3	8	
Female	7	1	6	
Primary tumor site				0.018[a]
Colon	10	4	6	
Rectum	8	0	8	
Tumor size in the liver in mm				0.278
< 30	8	3	5	
30-50	3	0	3	
≥ 50	5	1	5	
Tumor numbers in the liver				0.432
1-2	12	2	10	
≥ 3	6	2	4	
Differentiation degree				0.881
Low	4	1	3	
Middle-high	14	3	11	
T stage				1
III	18	4	14	
N stage				0.248
N0	9	3	6	
N1 + N2	7	1	8	

[a]$P < 0.05$.

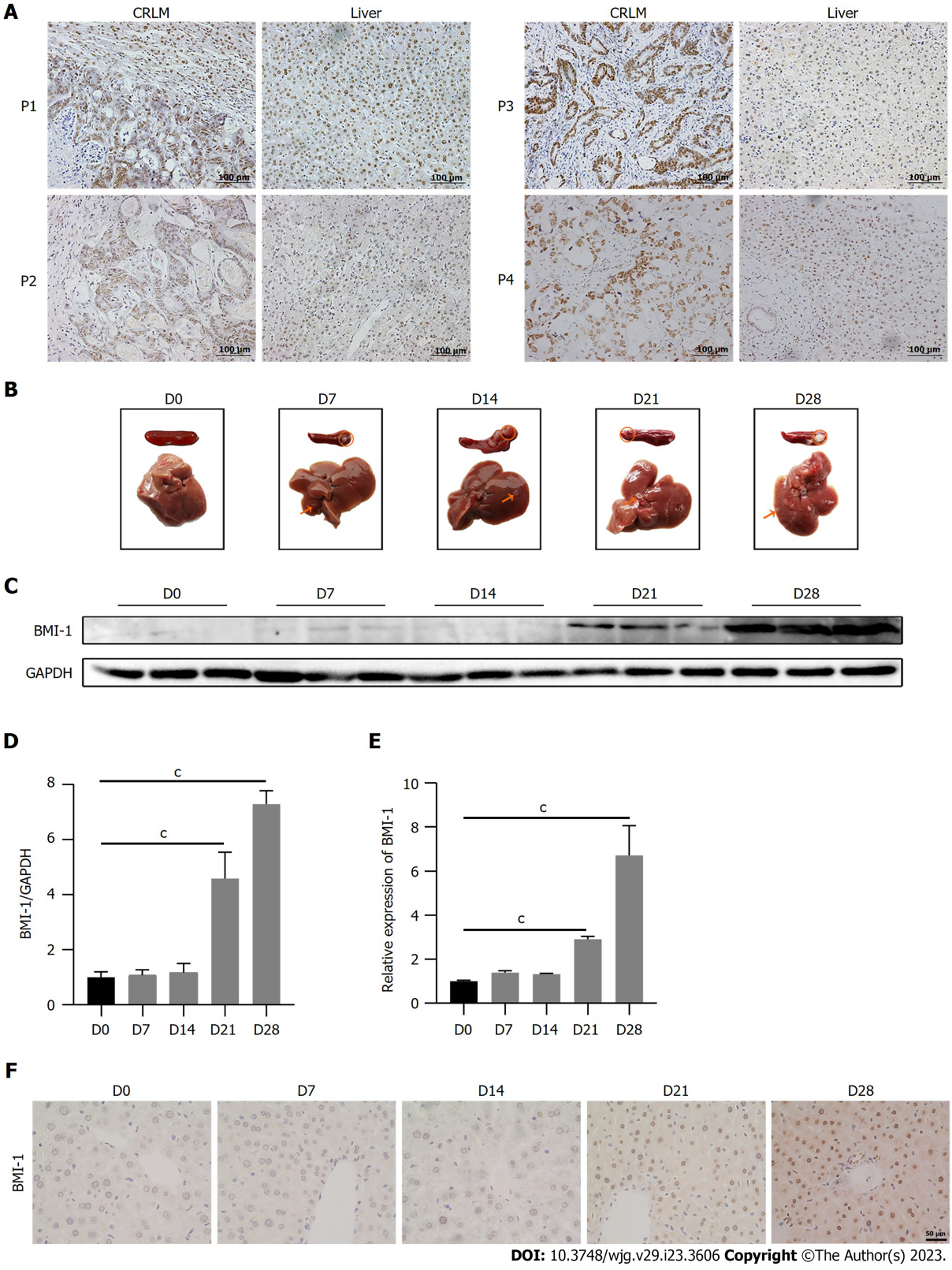
Statistical analyses

In all experiments, the data are shown as the mean ± standard deviation based on three independent experiments. The difference between the groups was analyzed by the χ^2 test, Fisher's exact probability, Student's *t*-test, or one-way analysis of variance using GraphPad Prism 8 software or SPSS 25.0. $P < 0.05$ was considered statistically significant.

RESULTS

BMI-1 expression is upregulated in liver cells during CRLM

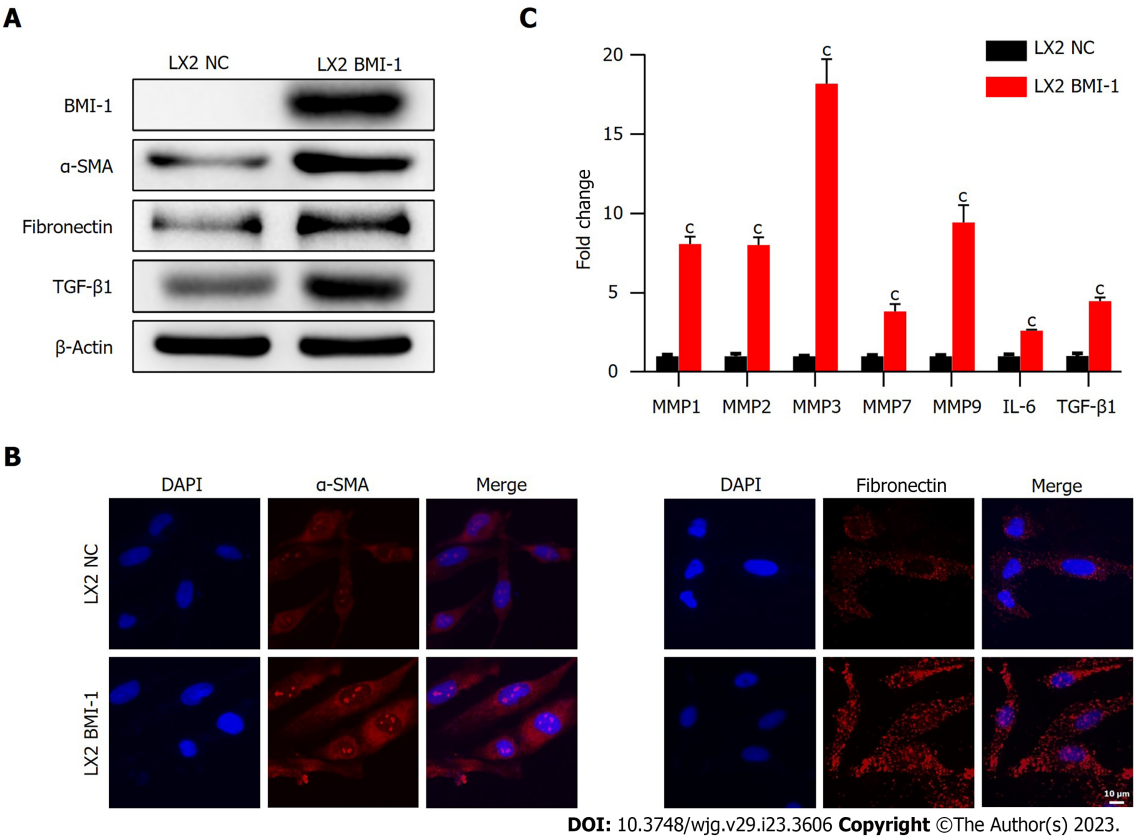
In our previous research, it was found that BMI-1 was overexpressed in LM of human CRC[26]. Interestingly, although normal liver cells were BMI-1-negative, 77.8% of liver cells from CRLM patients (14 of 18 samples; Figure 1A) were BMI-1-positive. The positive expression of BMI-1 was not strongly related to the clinical pathological characteristics (including tumor size and tumor number in the liver, differentiation degree, T stage, N stage) except the tumor site (Table 1). Positive BMI-1 expression in the liver cells of patients with rectal cancer LM was significantly higher (100%) than in patients with CRLM (60%). To investigate BMI-1 expression level in liver cells during CRLM, we measured BMI-1 expression at 0, 7, 14, 21, and 28 d following intrasplenic injection of CT26 cells in mice (Figure 1B). As shown in Figure 1C, small LM had formed by day 7. Compared with healthy control mice, the protein expression level of BMI-1 did not significantly change at 7 and 14 d, but markedly increased 4.58-fold at 21 d and



DOI: 10.3748/wjg.v29.i23.3606 **Copyright** ©The Author(s) 2023.

Figure 1 BMI-1 expression increases in liver cells during colorectal cancer liver metastasis. A: Immunohistochemistry analysis of BMI-1 in liver metastasis and paired liver tissues of colorectal cancer liver metastasis (CRLM) patients; B: Spleens and livers of mice were photographed after intrasplenic injection of CT26 cells at the indicated times; C: Western blot analysis of BMI-1 expression in mouse livers (n = 3); D: Quantitative protein expression of BMI-1 normalized to glyceraldehyde-3-phosphate dehydrogenase (GAPDH) in mouse livers (n = 3); E: Quantitative polymerase chain reaction detection of BMI-1 expression in mouse livers (n = 3); $^cP < 0.001$ *vs* D0; F: Immunohistochemistry confirmed that BMI-1 expression was increased in mouse livers during CRLM.

continued increasing up to 7.29-fold at 28 d (Figure 1D). The mRNA expression level of BMI-1 accordingly increased 2.92-fold at 21 d and 6.71-fold at 28 d (Figure 1E). The IHC results also showed that few nuclei in liver cells were BMI-1-positive in CRLM mice from 14 d, but the BMI-1-positive rate and intensity increased markedly at 21 and 28 d (Figure 1F). These results suggest that BMI-1 was



DOI: 10.3748/wjg.v29.i23.3606 **Copyright** ©The Author(s) 2023.

Figure 2 BMI-1 activates LX2 hepatic stellate cells. A: Western blot analysis of BMI-1 and activated hepatic stellate cell (aHSC)-related markers (alpha smooth muscle actin [α-SMA], fibronectin and transforming growth factor beta 1) in control (LX2 NC) and LX2 BMI-1 HSCs; B: Quantitative polymerase chain reaction detection of matrix metalloproteinases (MMPs) and cytokines in LX2 HSCs, $^{c}P < 0.001$; C: Immunofluorescence analysis showed that α-SMA and fibronectin expression levels were increased in LX2 BMI-1 HSCs. DAPI: 4',6-diamidino-2-phenylindole; IL: Interleukin; NC: Negative control.

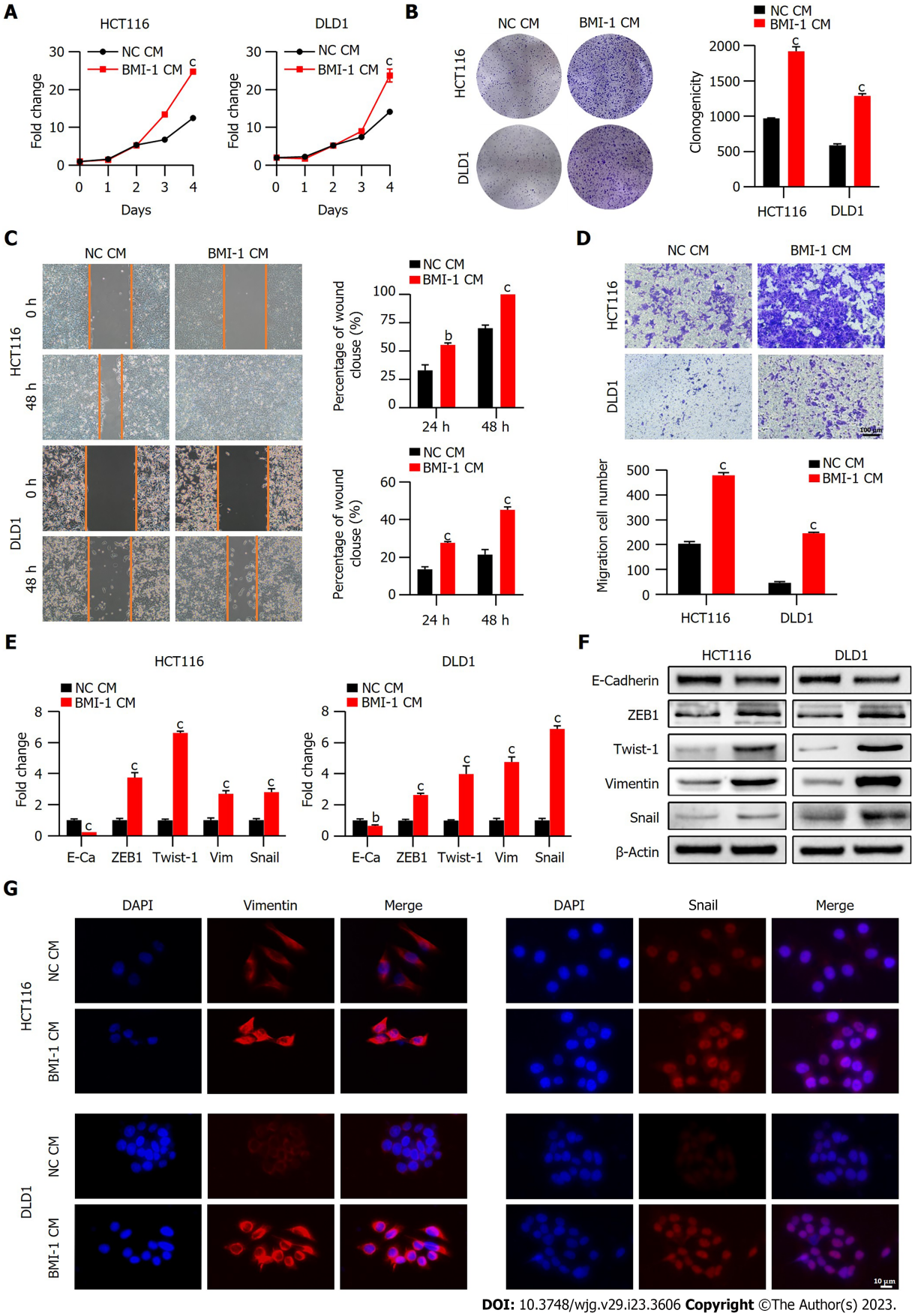
upregulated in liver cells after CRC cells metastasized to the liver, and may play a role in CRLM.

BMI-1 activates HSCs

To investigate the effects of BMI-1 on liver cells, we overexpressed BMI-1 in LX2 HSCs and confirmed the overexpression by WB (Figure 2A). High expression of α-SMA, a myofibroblast marker, is a key marker of aHSCs. aHSCs highly secrete the key cytokine TGF-β1 and promote hepatic fibrosis with fibronectin expression[27]. Compared with control quiescent HSCs, BMI-1 overexpressed LX2 HSCs showed a significant increase in α-SMA expression. Fibronectin and TGF-β1 expression were also markedly increased in BMI-1 overexpressed LX2 HSCs. Immunofluorescence staining also confirmed that the expression of α-SMA and fibronectin was significantly increased in LX2 cells overexpressing BMI-1 (Figure 2B). It was also observed that the transcript levels of matrix metalloproteinases (MMP1, MMP2, MMP3, MMP7, MMP9) and inflammatory cytokines (TGF-β1 and interleukin 6 [IL-6]) were markedly increased (Figure 2C). Thus, LX2 HSCs were activated by the overexpression of BMI-1.

BMI-1 overexpressed HSC CM enhances CRC cell proliferation and migration

To examine the effect of BMI-1 on the interaction between HSCs and CRC cells, CRC cells (HCT116 and DLD1) were cultured in control LX2 CM (NC CM) or BMI-1 overexpressed LX2 CM (BMI-1 CM). We first measured cell proliferation using the CCK-8 assay. Compared with cells cultured in NC CM, the proliferation of CRC cells cultured in BMI-1 CM was markedly enhanced on day 4 (Figure 3A), and the colony formation ability of CRC cells cultured in BMI-1 CM also significantly increased (Figure 3B). In addition, CRC cells cultured in BMI-1 CM showed higher wound healing rates (Figure 3C). Transwell migration assays showed the same results (Figure 3D). Then we investigated EMT-related molecular changes. Consistent with the above results, the mRNA and protein expression levels of ZEB-1, Twist-1, vimentin, and Snail in CRC cells cultured in BMI-1 CM were significantly increased while E-cadherin was decreased (Figure 3E and F). Immunofluorescence staining further demonstrated that Snail and vimentin expression was obviously increased in CRC cells cultured in BMI-1 CM (Figure 3G). Therefore, BMI-1 may be an important regulator in aHSCs, which promoted the malignant phenotype of CRC cells.



DOI: 10.3748/wjg.v29.i23.3606 **Copyright** ©The Author(s) 2023.

Figure 3 Effects of BMI-1 overexpressed hepatic stellate cell conditioned medium on cell proliferation and migration of colorectal cancer cells. A: Viability of HCT116 and DLD-1 cells cultured in conditioned medium (CM) from negative control (NC) LX2 (NC CM) or CM from BMI-1 overexpressed LX2 (BMI-1 CM) was confirmed by the Cell Counting Kit-8 assay; B: Colony formation assay of colorectal cancer (CRC) cells cultured in NC CM or BMI-1 CM; C: Wound healing assay of CRC cells cultured in NC CM or BMI-1 CM, the healing percentages were calculated at 24 h and 48 h; D: Transwell migration assay of CRC cells

cultured in NC CM or BMI-1 CM, the numbers of cells which migrated were counted; E: Quantitative polymerase chain reaction assay of the expression of epithelial-mesenchymal transition (EMT)-related markers in CRC cells cultured in NC CM or BMI-1 CM; F: Western blot assays of the expression of EMT-related markers in CRC cells cultured in NC CM or BMI-1 CM; G: Immunofluorescence analysis showed that vimentin and Snail expression levels were increased in CRC cells cultured in BMI-1 CM. $^{b}P < 0.01$, $^{c}P < 0.001$ *vs* NC CM. DAPI: 4',6-diamidino-2-phenylindole.

BMI-1 overexpressed HSC CM promotes CRC cell EMT by activating the Smad2/3 pathway

As previously mentioned, TGF-β1 was upregulated in BMI-1 overexpressed LX2 HSCs (Figure 2A). The TGF-β/SMAD signal pathway plays an important role in metastasis by modulating the EMT process[28,29]; therefore, we hypothesized that BMI-1 CM induces EMT in CRC cells by activating SMADs. We first determined the expression levels of SMAD2/3. As shown in Figure 4A and B, although the mRNA and protein expression levels of SMAD2 and SMAD3 showed no changes in CRC cells cultured in BMI-1 CM, SMAD2 and SMAD3 phosphorylation was significantly increased compared with CRC cells cultured in NC CM. We then used SB-505124 (a TGF-β receptor [TGF-βR] inhibitor, which inhibits SMAD2 phosphorylation) to further confirm the involvement of SMADs in the pro-EMT effects of BMI-1 CM. SB-505124 markedly decreased BMI-1 CM-induced SMAD2 and SMAD3 phosphorylation in CRC cells (Figure 4C and D). In addition, the downstream target proteins (Snail and vimentin) of the TGF-β/SMAD pathway accordingly decreased in SB-505124-treated CRC cells cultured in BMI-1 CM (Figure 4C and D). These results confirmed that BMI-1 CM induces EMT in CRC cells partially by activating SMAD2/3.

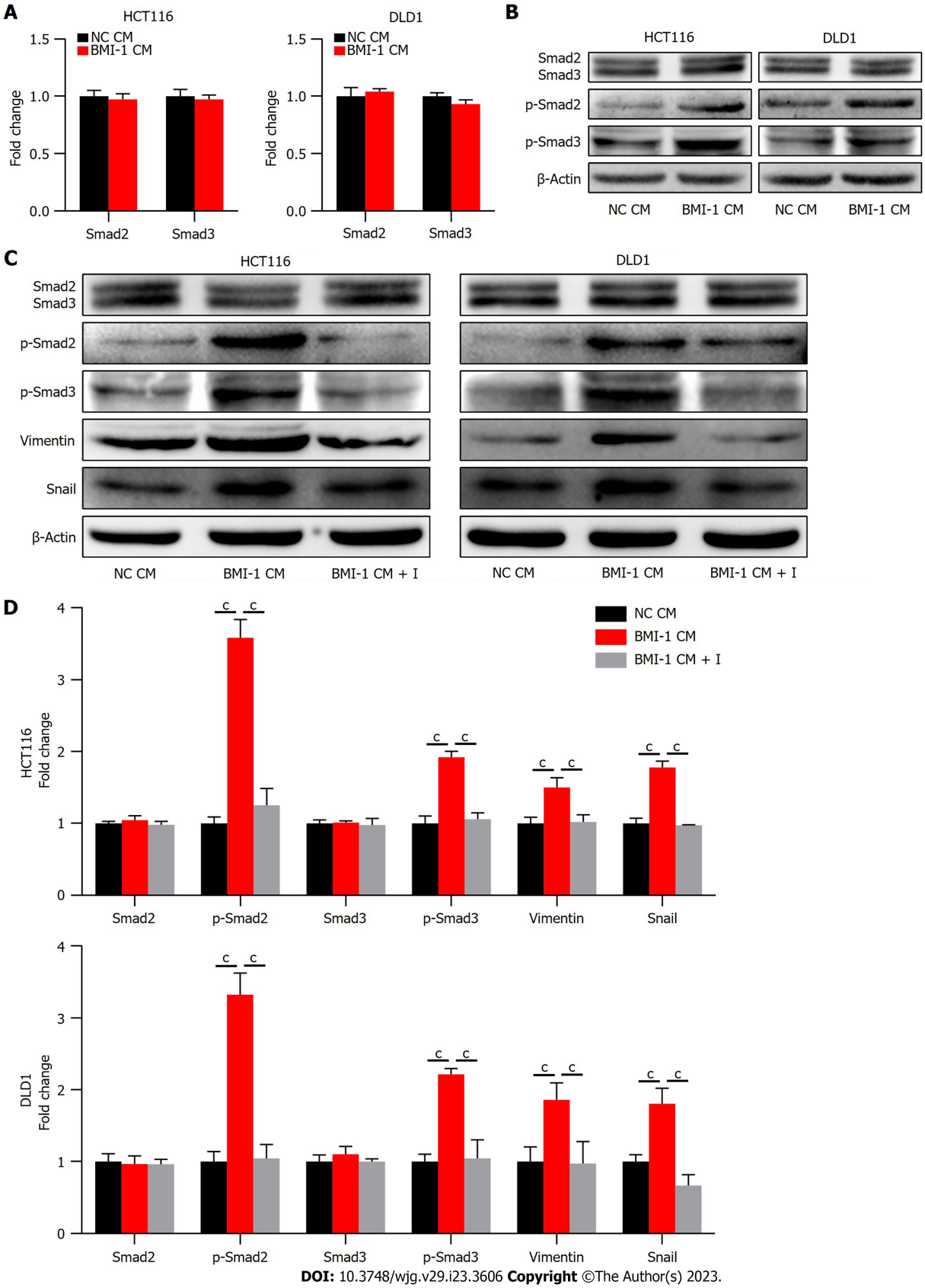
BMI-1 overexpressed HSCs promotes tumor growth in vivo

We further evaluated the effects of BMI-1 overexpressed LX2 HSCs on CRC cell growth *in vivo*. A subcutaneous xenotransplantation tumor model was established by co-implantation of HSCs (LX2 NC or LX2 BMI-1) and CRC cells (Figure 5A). Compared with mice co-implanted with LX2 NC, tumors grew faster and larger in mice co-implanted with LX2 BMI-1 HSCs and CRC cells as shown by increased tumor volume and weight (Figure 5B and C). Moreover, consistent with the *in vitro* results, we found that Snail and vimentin were upregulated in mice co-implanted with LX2 BMI-1 HSCs and CRC cells as shown by the qPCR and WB results (Figure 5D and E). Furthermore, the increased expression of Snail and vimentin in mouse liver co-implanted with LX2 BMI-1 HSCs and CRC cells was confirmed by IHC (Figure 5F). These results showed that LX2 BMI-1 HSCs promoted CRC tumor growth and EMT in the mouse model.

DISCUSSION

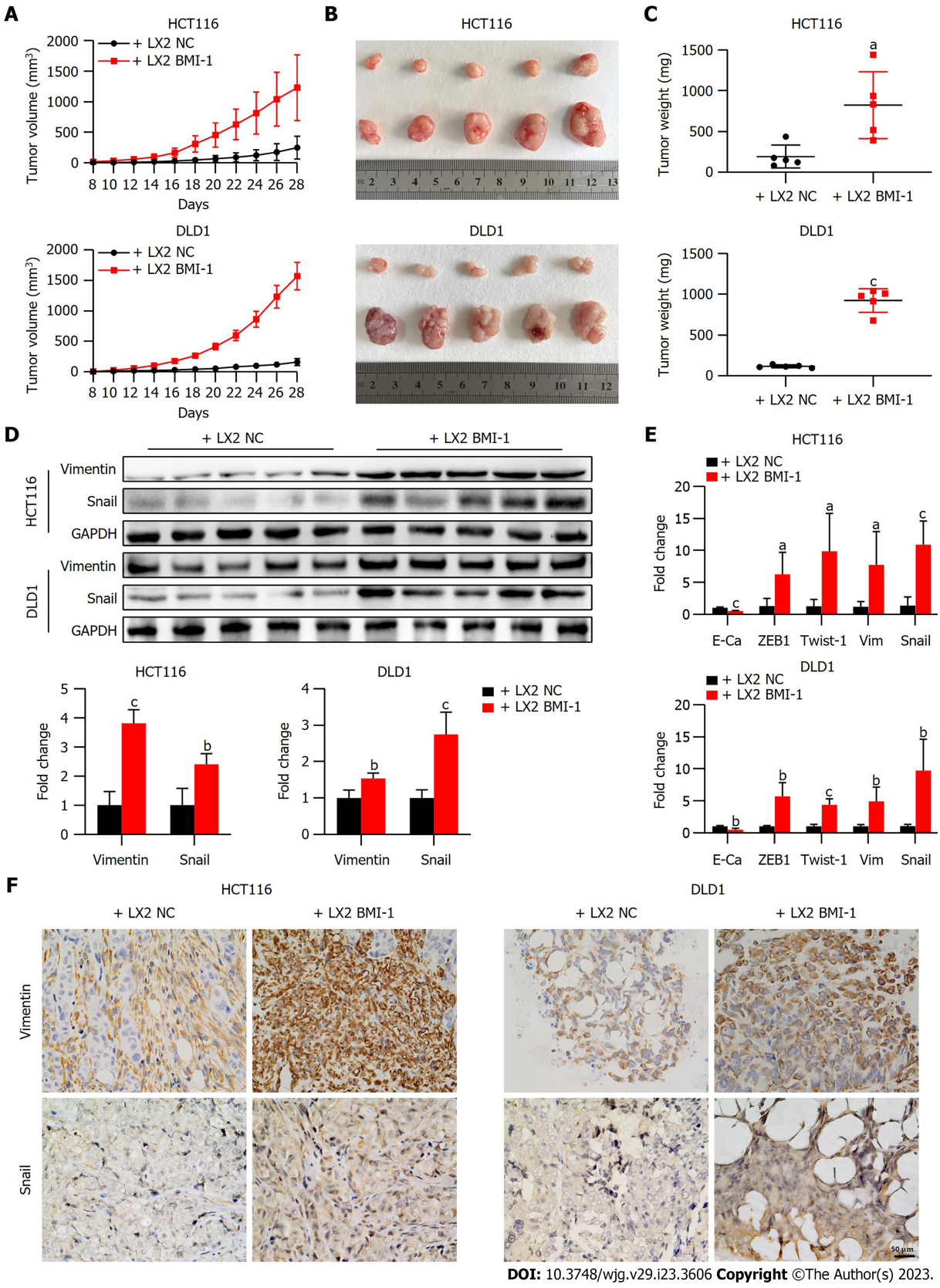
The liver is the most common target organ in terms of CRC metastases. Accumulating evidence suggests that the interactions between cancer cells and the liver microenvironment promote the progression of LM. In the liver microenvironment, HSC-derived CAFs are the main tumor-interacting population and play a vital role in cancer cell metastasis[8,30]. During the development of CRLM, HSC activation was found to be the most common biological process. Tumor-derived factors such as TGF-β and platelet-derived growth factor can activate HSCs[31]. BMI-1 has been proved to promote tumorigenesis and tumor progression in different types of cancers including CRC and HCC[24,26,32-34]. We previously reported that BMI-1 was abnormally highly expressed in CRLM and inhibition of BMI-1 in CRC cells dramatically reduced LM *in vivo*[26]. Normal liver cells were BMI-1-negative, and we observed that BMI-1-positive liver cells were common in CRLM samples from humans and mice. In particular, the mRNA and protein expression levels of BMI-1 in liver cells gradually increased during the development of CRLM in mice, suggesting that BMI-1 also participates in regulating liver cells during the course of CRLM. In this study, we found that BMI-1 had a novel function as a regulator in activating HSCs and plays an important role in the crosstalk between HSCs and CRC cells.

Quiescent HSCs normally resident in the space of Disse become activated with a myofibroblast-like phenotype (α-SMA^{+}) in response to inflammatory stimuli and liver damage[27]. Studies have shown that cancer cells can also activate HSCs to release cytokines and chemokines to promote LM[8,35]. aHSCs reportedly orchestrate a premetastatic and prometastatic niche, which accelerate CRLM[5,6,36]. In this study, we found that BMI-1-positive liver cells appeared on day 14 and increased on days 21 and 28 after injection of CT26 cells, while small LM had formed on day 7. We further confirmed that BMI-1 overexpressed HSCs were activated to α-SMA^{+} myofibroblasts with increased expression of fibronectin, TGF-β1, MMPs, and IL-6. These secreted components can maintain the activated status of HSCs by enhancing the autocrine signaling loop[37]. aHSCs are the major source of ECM, and aHSC-secreted factors play a pivotal role in remodeling the ECM during tumor invasion and metastasis[38]. TGF-β1 is the most potent fibrogenic cytokine and is a fibrotic marker[39,40]. Fibronectin and MMPs are important ECM regulators in the liver fibrosis process[41]. ECM deposition by aHSCs provides a prometastatic environment. Thus, BMI-1 activates HSCs to secrete factors to form a prometastatic environment in the liver.



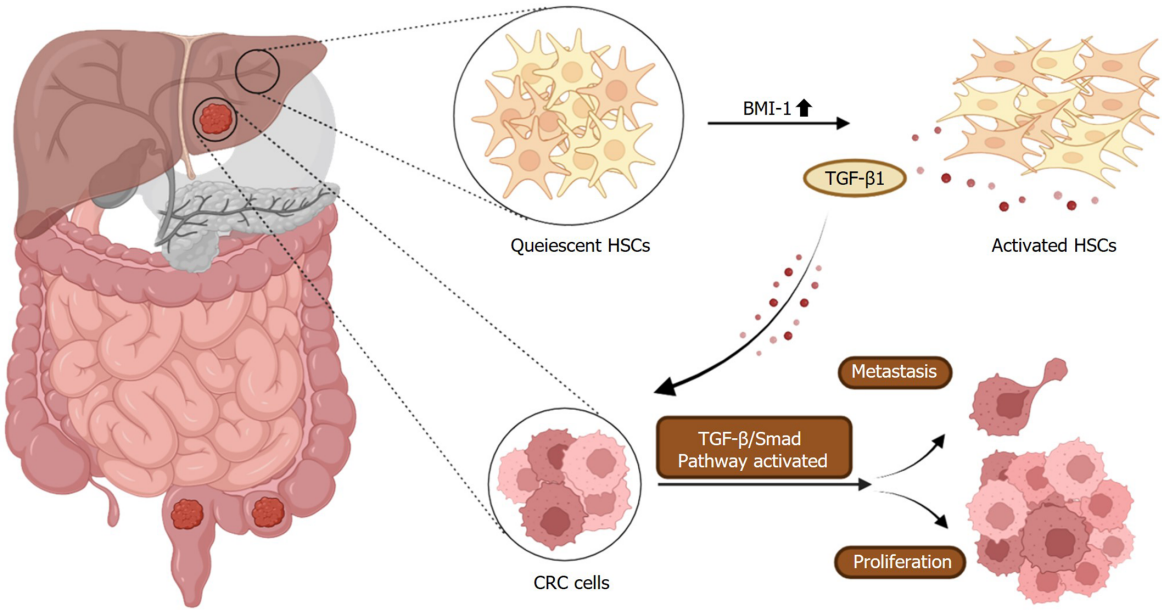
DOI: 10.3748/wjg.v29.i23.3606 **Copyright** ©The Author(s) 2023.

Figure 4 BMI-1 conditioned medium induces activation of the transforming growth factor beta/SMAD pathway in colorectal cancer cells. A: Quantitative polymerase chain reaction analysis showed no difference in the expression of SMAD2 and SMAD3 in colorectal cancer (CRC) cells cultured in conditioned medium (CM) from negative control NC) (NC CM) or CM from BMI-1 overexpressed LX2 (BMI-1 CM); B: Western blot assays of SMAD2, SMAD3, phosphorylated (p)-SMAD2, and p-SMAD3 expression levels in CRC cells cultured in NC CM or BMI-1 CM; C and D: Western blot analysis of the expression of SMAD pathway members and epithelial-mesenchymal transition-related proteins (Snail and vimentin) in CRC cells cultured in NC CM or BMI-1 CM with/without 0.5 μM SB-505124 treatment, the relative expression levels of the proteins were calculated and are shown in D. °$P < 0.001$.



DOI: 10.3748/wjg.v29.i23.3606 **Copyright** ©The Author(s) 2023.

Figure 5 BMI-1 overexpressed LX2 promotes tumor growth of colorectal cancer *in vivo*. A: Colorectal cancer cells (HCT116 or DLD-1) and LX2 cells (negative control [NC] or BMI-1 overexpressed) were co-implanted subcutaneously into the flanks of nude mice. After 7 d, tumor volume was measured every 2 d from 8 d to 28 d; B: Tumors were photographed at 28 d; C: Tumors were weighed (n = 5); D: Western blot assay of vimentin and Snail expression in mouse tumors in the different groups, and the fold changes were calculated; E: Quantitative polymerase chain reaction assay of the expression of epithelial-mesenchymal transition-related markers in mouse tumors in the different groups; F: Immunohistochemistry analysis of vimentin and Snail expression in mouse tumors. $^{a}P < 0.05$, $^{b}P < 0.01$, $^{c}P < 0.001$ *vs* LX2 NC. GAPDH: Glyceraldehyde-3-phosphate dehydrogenase.



DOI: 10.3748/wjg.v29.i23.3606 **Copyright** ©The Author(s) 2023.

Figure 6 Schematic summary of BMI-1-activated hepatic stellate cells, which promote colorectal cancer cell epithelial-mesenchymal transition and liver metastasis. CRC: Colorectal cancer; HSC: Hepatic stellate cell; TGF-β1: Transforming growth factor beta 1.

The interactions between cancer cells and aHSCs promote tumor growth and metastasis. CRC cells can stimulate aHSCs to release cytokines and chemokines, which in turn promote CRC growth and invasion[8,35]. In addition, aHSCs can secrete ECM components, induce angiogenesis, and modulate immunity to facilitate tumor growth and metastasis[31]. We found that high-metastatic HCT116 and low-metastatic DLD1 CRC cells cultured in CM from BMI-1 overexpressed HSCs showed the same enhanced proliferation and migration ability, and both HCT116 and DLD1 cells co-implanted with BMI-1 overexpressed HSCs showed increased tumor growth *in vivo*. These results demonstrated that BMI-1 aHSCs promote CRC cell proliferation and migration regardless of their ability to metastasize.

TGF-β signaling is important in tumor-stroma crosstalk. The TGF-β/SMAD pathway can act as both a tumor suppressor and promoter in CRLM[42,43]. The effect of the TGF-β/SMAD pathway in most malignant tumors is toward migration, the EMT or stemness, thereby promoting LM[44-46]. CRC cells are able to recruit and activate HSCs into CAFs by secreting TGF-β, and aHSCs lead to secretion of TGF-β which influences CRC cells[7]. LM has been found to be dependent on TGF-β signaling in liver stroma [47-50]. TGF-β1 is a key inducer of EMT transcription factors, which can promote EMT through the TGF-β/SMAD pathway[28,29]. The markers of EMT, including vimentin, Snail, ZEB-1, and Twist-1, were upregulated in CRC cells cultured in CM from BMI-1 overexpressed HSCs. The TGF-β/SMAD signaling pathway was activated and the phosphorylation of SMAD2/3 was induced in CRC cells cultured in CM from BMI-1 overexpressed HSCs, and treatment with the TGF-βR inhibitor SB-505124 attenuated the effect of BMI-1. Moreover, CRC cells co-implanted with BMI-1 overexpressed HSCs showed increased expression of EMT markers *in vivo*. Taken together, these findings indicate that BMI-1 overexpressed HSCs promote CRC cell growth and migration partly by activating the TGF-β/SMAD pathway and enhancing the EMT.

CONCLUSION

We propose a novel mechanism for BMI-1 involvement in promoting CRLM. BMI-1 was upregulated in liver cells during CRLM. BMI-1 aHSCs released cytokines and chemokines (fibronectin, TGF-β, MMPs, *etc*) to form a prometastatic environment in the liver, and promoted CRC cell proliferation, migration, and the EMT partially by activating the TGF-β/SMAD pathway (Figure 6). These findings provide a potential target for the treatment of CRLM.

ARTICLE HIGHLIGHTS

Research background

Hepatic stellate cells (HSCs) are an important component of liver tissue and are a major source of

cancer-associated fibroblasts. Cancer cells can activate HSCs, and in turn activated HSCs (aHSCs) promote tumor growth and metastasis. However, the mechanisms by which HSCs interact with colorectal cancer (CRC) cells to promote liver metastases (LM) are largely unknown.

Research motivation

We previously discovered that the expression of BMI-1 was abnormally high in LM of CRC. We speculated that BMI-1 plays an important role in the interaction between HSCs and CRC cells.

Research objectives

To examine the role of BMI-1 in HSC activation, and investigate the potential mechanisms of BMI-1 in the interaction between HSCs and CRC cells.

Research methods

The expression of BMI-1 in liver tissue of patients with CRC liver metastasis (CRLM) was determined by immunohistochemistry analysis. We established a mouse LM model to assess the expression of BMI-1 during CRLM. We used lentiviral vectors to overexpress BMI-1 in LX2 HSCs (LX2 BMI-1) and evaluated the molecular markers of aHSCs. The proliferation and mobility of CRC cells in LX2 BMI-1 conditioned medium (CM) was detected. The epithelial-mesenchymal transition (EMT) and transforming growth factor beta (TGF-β)/SMAD pathway in CRC cells treated with LX2 BMI-1 CM were investigated by Western blot analysis and quantitative polymerase chain reaction. A mouse xenograft model was established to investigate the effects of co-implantation of LX2 BMI-1 and CRC cells on tumor growth, and the EMT phenotype of CRC.

Research results

BMI-1 expression was upregulated in liver cells during CRLM. Overexpression of BMI-1 induced the activation of LX2 HSCs. CRC cells cultured in LX2 BMI-1 CM showed higher proliferation, migration, and EMT ability compared with cells cultured in NC CM. LX2 BMI-1 CM induced activation of the TGF-β/SMAD pathway in CRC cells, and the TGF-βR inhibitor SB-505124 diminished the effect of BMI-1 CM. In addition, LX2 BMI-1 HSCs promoted CRC tumor growth and EMT in the mouse model.

Research conclusions

BMI-1 aHSCs promoted the proliferation and migration of CRC partly *via* the TGF-β/SMAD pathway.

Research perspectives

Targeting BMI-1 in liver tissues may have potential therapeutic implications for the treatment of CRLM.

ACKNOWLEDGEMENTS

We thank Xiao-Li Hong and Chao Bi from the Core Facilities of Zhejiang University School of Medicine for their technical support.

FOOTNOTES

Author contributions: Jiang ZY, Dong QH, and Wang GY conceived and designed the study; Jiang ZY, Ma XM, Luan XH, Liuyang ZY, Hong YY, and Dai Y performed the research, and collected and analyzed the data; Jiang ZY, Dong QH, and Wang GY wrote the manuscript; All authors read and approved the final manuscript.

Supported by National Natural Science Foundation of China, No. 81472213; the Health Commission of Zhejiang Province, No. 2019ZD010 and No. 2019ZD029; the Science Technology Department of Zhejiang Province, No. LGF20H220001; and the Zhejiang Provincial Administration of Traditional Chinese Medicine, No. 2021ZA088.

Institutional review board statement: This study was reviewed and approved by the Ethics Committee of Sir Run Run Shaw Hospital affiliated with the Zhejiang University School of Medicine, No. 2023-404-01.

Institutional animal care and use committee statement: All animal experiments were performed in accordance with the guidelines of the Committee on the Ethics of Animal Experiments of Zhejiang University, No. ZJU20220447.

Informed consent statement: All study participants or their legal guardian provided informed written consent about personal and medical data collection prior to study enrolment.

Conflict-of-interest statement: All the authors report no relevant conflicts of interest for this article.

Data sharing statement: No additional data are available.

ARRIVE guidelines statement: The authors have read the ARRIVE guidelines, and the manuscript was prepared and revised according to the ARRIVE guidelines.

Open-Access: This article is an open-access article that was selected by an in-house editor and fully peer-reviewed by external reviewers. It is distributed in accordance with the Creative Commons Attribution NonCommercial (CC BY-NC 4.0) license, which permits others to distribute, remix, adapt, build upon this work non-commercially, and license their derivative works on different terms, provided the original work is properly cited and the use is non-commercial. See: https://creativecommons.org/Licenses/by-nc/4.0/

Country/Territory of origin: China

ORCID number: Qing-Hua Dong 0000-0002-7543-7528; Guan-Yu Wang 0000-0003-0849-7114.

S-Editor: Fan JR
L-Editor: Filipodia
P-Editor: Chen YX

REFERENCES

1 **Bray F**, Ferlay J, Soerjomataram I, Siegel RL, Torre LA, Jemal A. Global cancer statistics 2018: GLOBOCAN estimates of incidence and mortality worldwide for 36 cancers in 185 countries. *CA Cancer J Clin* 2018; **68**: 394-424 [PMID: 30207593 DOI: 10.3322/caac.21492]
2 **Siegel RL**, Miller KD, Goding Sauer A, Fedewa SA, Butterly LF, Anderson JC, Cercek A, Smith RA, Jemal A. Colorectal cancer statistics, 2020. *CA Cancer J Clin* 2020; **70**: 145-164 [PMID: 32133645 DOI: 10.3322/caac.21601]
3 **Valderrama-Treviño AI**, Barrera-Mera B, Ceballos-Villalva JC, Montalvo-Javé EE. Hepatic Metastasis from Colorectal Cancer. *Euroasian J Hepatogastroenterol* 2017; **7**: 166-175 [PMID: 29201802 DOI: 10.5005/jp-journals-10018-1241]
4 **Tsilimigras DI**, Brodt P, Clavien PA, Muschel RJ, D'Angelica MI, Endo I, Parks RW, Doyle M, de Santibañes E, Pawlik TM. Liver metastases. *Nat Rev Dis Primers* 2021; **7**: 27 [PMID: 33859205 DOI: 10.1038/s41572-021-00261-6]
5 **Illemann M**, Eefsen RH, Bird NC, Majeed A, Osterlind K, Laerum OD, Alpízar-Alpízar W, Lund IK, Høyer-Hansen G. Tissue inhibitor of matrix metalloproteinase-1 expression in colorectal cancer liver metastases is associated with vascular structures. *Mol Carcinog* 2016; **55**: 193-208 [PMID: 25594187 DOI: 10.1002/mc.22269]
6 **Schütte M**, Risch T, Abdavi-Azar N, Boehnke K, Schumacher D, Keil M, Yildiriman R, Jandrasits C, Borodina T, Amstislavskiy V, Worth CL, Schweiger C, Liebs S, Lange M, Warnatz HJ, Butcher LM, Barrett JE, Sultan M, Wierling C, Golob-Schwarzl N, Lax S, Uranitsch S, Becker M, Welte Y, Regan JL, Silvestrov M, Kehler I, Fusi A, Kessler T, Herwig R, Landegren U, Wienke D, Nilsson M, Velasco JA, Garin-Chesa P, Reinhard C, Beck S, Schäfer R, Regenbrecht CR, Henderson D, Lange B, Haybaeck J, Keilholz U, Hoffmann J, Lehrach H, Yaspo ML. Molecular dissection of colorectal cancer in pre-clinical models identifies biomarkers predicting sensitivity to EGFR inhibitors. *Nat Commun* 2017; **8**: 14262 [PMID: 28186126 DOI: 10.1038/ncomms14262]
7 **Marvin DL**, Heijboer R, Ten Dijke P, Ritsma L. TGF-β signaling in liver metastasis. *Clin Transl Med* 2020; **10**: e160 [PMID: 33252863 DOI: 10.1002/ctm2.160]
8 **Zhao S**, Mi Y, Zheng B, Wei P, Gu Y, Zhang Z, Xu Y, Cai S, Li X, Li D. Highly-metastatic colorectal cancer cell released miR-181a-5p-rich extracellular vesicles promote liver metastasis by activating hepatic stellate cells and remodelling the tumour microenvironment. *J Extracell Vesicles* 2022; **11**: e12186 [PMID: 35041299 DOI: 10.1002/jev2.12186]
9 **Milette S**, Sicklick JK, Lowy AM, Brodt P. Molecular Pathways: Targeting the Microenvironment of Liver Metastases. *Clin Cancer Res* 2017; **23**: 6390-6399 [PMID: 28615370 DOI: 10.1158/1078-0432.CCR-15-1636]
10 **Brodt P**. Role of the Microenvironment in Liver Metastasis: From Pre- to Prometastatic Niches. *Clin Cancer Res* 2016; **22**: 5971-5982 [PMID: 27797969]
11 **Mao X**, Xu J, Wang W, Liang C, Hua J, Liu J, Zhang B, Meng Q, Yu X, Shi S. Crosstalk between cancer-associated fibroblasts and immune cells in the tumor microenvironment: new findings and future perspectives. *Mol Cancer* 2021; **20**: 131 [PMID: 34635121 DOI: 10.1186/s12943-021-01428-1]
12 **Kalluri R**. The biology and function of fibroblasts in cancer. *Nat Rev Cancer* 2016; **16**: 582-598 [PMID: 27550820 DOI: 10.1038/nrc.2016.73]
13 **Sahai E**, Astsaturov I, Cukierman E, DeNardo DG, Egeblad M, Evans RM, Fearon D, Greten FR, Hingorani SR, Hunter T, Hynes RO, Jain RK, Janowitz T, Jorgensen C, Kimmelman AC, Kolonin MG, Maki RG, Powers RS, Puré E, Ramirez DC, Scherz-Shouval R, Sherman MH, Stewart S, Tlsty TD, Tuveson DA, Watt FM, Weaver V, Weeraratna AT, Werb Z. A framework for advancing our understanding of cancer-associated fibroblasts. *Nat Rev Cancer* 2020; **20**: 174-186 [PMID: 31980749 DOI: 10.1038/s41568-019-0238-1]
14 **Higashi T**, Friedman SL, Hoshida Y. Hepatic stellate cells as key target in liver fibrosis. *Adv Drug Deliv Rev* 2017; **121**: 27-42 [PMID: 28506744 DOI: 10.1016/j.addr.2017.05.007]
15 **Friedman SL**. Hepatic stellate cells: protean, multifunctional, and enigmatic cells of the liver. *Physiol Rev* 2008; **88**: 125-172 [PMID: 18195085 DOI: 10.1152/physrev.00013.2007]
16 **Barry AE**, Baldeosingh R, Lamm R, Patel K, Zhang K, Dominguez DA, Kirton KJ, Shah AP, Dang H. Hepatic Stellate Cells and Hepatocarcinogenesis. *Front Cell Dev Biol* 2020; **8**: 709 [PMID: 32850829 DOI: 10.3389/fcell.2020.00709]

17 **Shiraha H**, Iwamuro M, Okada H. Hepatic Stellate Cells in Liver Tumor. *Adv Exp Med Biol* 2020; **1234**: 43-56 [PMID: 32040854 DOI: 10.1007/978-3-030-37184-5_4]

18 **Mederacke I**, Hsu CC, Troeger JS, Huebener P, Mu X, Dapito DH, Pradere JP, Schwabe RF. Fate tracing reveals hepatic stellate cells as dominant contributors to liver fibrosis independent of its aetiology. *Nat Commun* 2013; **4**: 2823 [PMID: 24264436 DOI: 10.1038/ncomms3823]

19 **Makino Y**, Hikita H, Kodama T, Shigekawa M, Yamada R, Sakamori R, Eguchi H, Morii E, Yokoi H, Mukoyama M, Hiroshi S, Tatsumi T, Takehara T. CTGF Mediates Tumor-Stroma Interactions between Hepatoma Cells and Hepatic Stellate Cells to Accelerate HCC Progression. *Cancer Res* 2018; **78**: 4902-4914 [PMID: 29967264 DOI: 10.1158/0008-5472.CAN-17-3844]

20 **Biffi G**, Tuveson DA. Diversity and Biology of Cancer-Associated Fibroblasts. *Physiol Rev* 2021; **101**: 147-176 [PMID: 32466724 DOI: 10.1152/physrev.00048.2019]

21 **Affo S**, Nair A, Brundu F, Ravichandra A, Bhattacharjee S, Matsuda M, Chin L, Filliol A, Wen W, Song X, Decker A, Worley J, Caviglia JM, Yu L, Yin D, Saito Y, Savage T, Wells RG, Mack M, Zender L, Arpaia N, Remotti HE, Rabadan R, Sims P, Leblond AL, Weber A, Riener MO, Stockwell BR, Gaublomme J, Llovet JM, Kalluri R, Michalopoulos GK, Seki E, Sia D, Chen X, Califano A, Schwabe RF. Promotion of cholangiocarcinoma growth by diverse cancer-associated fibroblast subpopulations. *Cancer Cell* 2021; **39**: 866-882.e11 [PMID: 33930309 DOI: 10.1016/j.ccell.2021.03.012]

22 **Jacobs JJ**, Kieboom K, Marino S, DePinho RA, van Lohuizen M. The oncogene and Polycomb-group gene bmi-1 regulates cell proliferation and senescence through the ink4a locus. *Nature* 1999; **397**: 164-168 [PMID: 9923679]

23 **Jiang L**, Li J, Song L. Bmi-1, stem cells and cancer. *Acta Biochim Biophys Sin (Shanghai)* 2009; **41**: 527-534 [PMID: 19578716]

24 **Tateishi K**, Ohta M, Kanai F, Guleng B, Tanaka Y, Asaoka Y, Tada M, Seto M, Jazag A, Lianjie L, Okamoto M, Isayama H, Yoshida H, Kawabe T, Omata M. Dysregulated expression of stem cell factor Bmi1 in precancerous lesions of the gastrointestinal tract. *Clin Cancer Res* 2006; **12**: 6960-6966 [PMID: 17145814]

25 **Gil J**, Bernard D, Peters G. Role of polycomb group proteins in stem cell self-renewal and cancer. *DNA Cell Biol* 2005; **24**: 117-125 [PMID: 15699631]

26 **Xu Z**, Zhou Z, Zhang J, Xuan F, Fan M, Zhou D, Liuyang Z, Ma X, Hong Y, Wang Y, Sharma S, Dong Q, Wang G. Targeting BMI-1-mediated epithelial-mesenchymal transition to inhibit colorectal cancer liver metastasis. *Acta Pharm Sin B* 2021; **11**: 1274-1285 [PMID: 34094833 DOI: 10.1016/j.apsb.2020.11.018]

27 **Tsuchida T**, Friedman SL. Mechanisms of hepatic stellate cell activation. *Nat Rev Gastroenterol Hepatol* 2017; **14**: 397-411 [PMID: 28487545 DOI: 10.1038/nrgastro.2017.38]

28 **Xu J**, Lamouille S, Derynck R. TGF-beta-induced epithelial to mesenchymal transition. *Cell Res* 2009; **19**: 156-172 [PMID: 19153598 DOI: 10.1038/cr.2009.5]

29 **Hao Y**, Baker D, Ten Dijke P. TGF-β-Mediated Epithelial-Mesenchymal Transition and Cancer Metastasis. *Int J Mol Sci* 2019; **20** [PMID: 31195692 DOI: 10.3390/ijms20112767]

30 **Kubo N**, Araki K, Kuwano H, Shirabe K. Cancer-associated fibroblasts in hepatocellular carcinoma. *World J Gastroenterol* 2016; **22**: 6841-6850 [PMID: 27570421 DOI: 10.3748/wjg.v22.i30.6841]

31 **Kang N**, Gores GJ, Shah VH. Hepatic stellate cells: partners in crime for liver metastases? *Hepatology* 2011; **54**: 707-713 [PMID: 21520207 DOI: 10.1002/hep.24384]

32 **Effendi K**, Mori T, Komuta M, Masugi Y, Du W, Sakamoto M. Bmi-1 gene is upregulated in early-stage hepatocellular carcinoma and correlates with ATP-binding cassette transporter B1 expression. *Cancer Sci* 2010; **101**: 666-672 [PMID: 20085590 DOI: 10.1111/j.1349-7006.2009.01431.x]

33 **Li X**, Yang Z, Song W, Zhou L, Li Q, Tao K, Zhou J, Wang X, Zheng Z, You N, Dou K, Li H. Overexpression of Bmi-1 contributes to the invasion and metastasis of hepatocellular carcinoma by increasing the expression of matrix metalloproteinase (MMP)2, MMP-9 and vascular endothelial growth factor *via* the PTEN/PI3K/Akt pathway. *Int J Oncol* 2013; **43**: 793-802 [PMID: 23807724 DOI: 10.3892/ijo.2013.1992]

34 **Xu Z**, Tao J, Chen P, Chen L, Sharma S, Wang G, Dong Q. Sodium Butyrate Inhibits Colorectal Cancer Cell Migration by Downregulating Bmi-1 Through Enhanced miR-200c Expression. *Mol Nutr Food Res* 2018; **62**: e1700844 [PMID: 29418071 DOI: 10.1002/mnfr.201700844]

35 **Huang WH**, Zhou MW, Zhu YF, Xiang JB, Li ZY, Wang ZH, Zhou YM, Yang Y, Chen ZY, Gu XD. The Role Of Hepatic Stellate Cells In Promoting Liver Metastasis Of Colorectal Carcinoma. *Onco Targets Ther* 2019; **12**: 7573-7580 [PMID: 31571908 DOI: 10.2147/OTT.S214409]

36 **Eveno C**, Hainaud P, Rampanou A, Bonnin P, Bakhouche S, Dupuy E, Contreres JO, Pocard M. Proof of prometastatic niche induction by hepatic stellate cells. *J Surg Res* 2015; **194**: 496-504 [PMID: 25528682 DOI: 10.1016/j.jss.2014.11.005]

37 **Watanabe T**, Tajima H, Hironori H, Nakagawara H, Ohnishi I, Takamura H, Ninomiya I, Kitagawa H, Fushida S, Tani T, Fujimura T, Ota T, Wakayama T, Iseki S, Harada S. Sodium valproate blocks the transforming growth factor (TGF)-β1 autocrine loop and attenuates the TGF-β1-induced collagen synthesis in a human hepatic stellate cell line. *Int J Mol Med* 2011; **28**: 919-925 [PMID: 21822535 DOI: 10.3892/ijmm.2011.768]

38 **Ahmad SA**, Berman RS, Ellis LM. Biology of colorectal liver metastases. *Surg Oncol Clin N Am* 2003; **12**: 135-150 [PMID: 12735135]

39 **Xu F**, Liu C, Zhou D, Zhang L. TGF-β/SMAD Pathway and Its Regulation in Hepatic Fibrosis. *J Histochem Cytochem* 2016; **64**: 157-167 [PMID: 26747705 DOI: 10.1369/0022155415627681]

40 **Hellerbrand C**, Stefanovic B, Giordano F, Burchardt ER, Brenner DA. The role of TGFbeta1 in initiating hepatic stellate cell activation in vivo. *J Hepatol* 1999; **30**: 77-87 [PMID: 9927153]

41 **Klingberg F**, Hinz B, White ES. The myofibroblast matrix: implications for tissue repair and fibrosis. *J Pathol* 2013; **229**: 298-309 [PMID: 22996908 DOI: 10.1002/path.4104]

42 **Are C**, Simms N, Rajput A, Brattain M. The role of transforming growth factor-beta in suppression of hepatic metastasis from colon cancer. *HPB (Oxford)* 2010; **12**: 498-506 [PMID: 20815859 DOI: 10.1111/j.1477-2574.2010.00219.x]

43 **Korkut A**, Zaidi S, Kanchi RS, Rao S, Gough NR, Schultz A, Li X, Lorenzi PL, Berger AC, Robertson G, Kwong LN, Datto M, Roszik J, Ling S, Ravikumar V, Manyam G, Rao A, Shelley S, Liu Y, Ju Z, Hansel D, de Velasco G, Pennathur A, Andersen JB, O'Rourke CJ, Ohshiro K, Jogunoori W, Nguyen BN, Li S, Osmanbeyoglu HU, Ajani JA, Mani SA, Houseman A, Wiznerowicz M, Chen J, Gu S, Ma W, Zhang J, Tong P, Cherniack AD, Deng C, Resar L; Cancer Genome Atlas Research Network, Weinstein JN, Mishra L, Akbani R. A Pan-Cancer Analysis Reveals High-Frequency Genetic Alterations in Mediators of Signaling by the TGF-β Superfamily. *Cell Syst* 2018; **7**: 422-437.e7 [PMID: 30268436 DOI: 10.1016/j.cels.2018.08.010]

44 **Zhang B**, Halder SK, Kashikar ND, Cho YJ, Datta A, Gorden DL, Datta PK. Antimetastatic role of Smad4 signaling in colorectal cancer. *Gastroenterology* 2010; **138**: 969-80.e1 [PMID: 19909744 DOI: 10.1053/j.gastro.2009.11.004]

45 **Tsushima H**, Ito N, Tamura S, Matsuda Y, Inada M, Yabuuchi I, Imai Y, Nagashima R, Misawa H, Takeda H, Matsuzawa Y, Kawata S. Circulating transforming growth factor beta 1 as a predictor of liver metastasis after resection in colorectal cancer. *Clin Cancer Res* 2001; **7**: 1258-1262 [PMID: 11350892]

46 **Zhang C**, Gao H, Li C, Tu J, Chen Z, Su W, Geng X, Chen X, Wang J, Pan W. TGFβ1 Promotes Breast Cancer Local Invasion and Liver Metastasis by Increasing the CD44(high)/CD24(-) Subpopulation. *Technol Cancer Res Treat* 2018; **17**: 1533033818764497 [PMID: 29658391 DOI: 10.1177/1533033818764497]

47 **Calon A**, Espinet E, Palomo-Ponce S, Tauriello DV, Iglesias M, Céspedes MV, Sevillano M, Nadal C, Jung P, Zhang XH, Byrom D, Riera A, Rossell D, Mangues R, Massagué J, Sancho E, Batlle E. Dependency of colorectal cancer on a TGF-β-driven program in stromal cells for metastasis initiation. *Cancer Cell* 2012; **22**: 571-584 [PMID: 23153532 DOI: 10.1016/j.ccr.2012.08.013]

48 **Tauriello DVF**, Palomo-Ponce S, Stork D, Berenguer-Llergo A, Badia-Ramentol J, Iglesias M, Sevillano M, Ibiza S, Cañellas A, Hernando-Momblona X, Byrom D, Matarin JA, Calon A, Rivas EI, Nebreda AR, Riera A, Attolini CS, Batlle E. TGFβ drives immune evasion in genetically reconstituted colon cancer metastasis. *Nature* 2018; **554**: 538-543 [PMID: 29443964 DOI: 10.1038/nature25492]

49 **Zubeldia IG**, Bleau AM, Redrado M, Serrano D, Agliano A, Gil-Puig C, Vidal-Vanaclocha F, Lecanda J, Calvo A. Epithelial to mesenchymal transition and cancer stem cell phenotypes leading to liver metastasis are abrogated by the novel TGFβ1-targeting peptides P17 and P144. *Exp Cell Res* 2013; **319**: 12-22 [PMID: 23153552 DOI: 10.1016/j.yexcr.2012.11.004]

50 **Zhang B**, Halder SK, Zhang S, Datta PK. Targeting transforming growth factor-beta signaling in liver metastasis of colon cancer. *Cancer Lett* 2009; **277**: 114-120 [PMID: 19147275 DOI: 10.1016/j.canlet.2008.11.035]

World Journal of Gastroenterology

Submit a Manuscript: https://www.f6publishing.com

World J Gastroenterol 2023 June 21; 29(23): 3622-3644

DOI: 10.3748/wjg.v29.i23.3622

ISSN 1007-9327 (print) ISSN 2219-2840 (online)

ORIGINAL ARTICLE

Basic Study

18β-glycyrrhetinic acid inhibits proliferation of gastric cancer cells through regulating the miR-345-5p/TGM2 signaling pathway

Xia Li, Xiao-Ling Ma, Yi Nan, Yu-Hua Du, Yi Yang, Dou-Dou Lu, Jun-Fei Zhang, Yan Chen, Lei Zhang, Yang Niu, Ling Yuan

Specialty type: Gastroenterology and hepatology

Provenance and peer review: Unsolicited article; Externally peer reviewed.

Peer-review model: Single blind

Peer-review report's scientific quality classification

Grade A (Excellent): 0
Grade B (Very good): B, B
Grade C (Good): 0
Grade D (Fair): 0
Grade E (Poor): 0

P-Reviewer: Kotelevets SM, Russia; Liu YQ, United States

Received: March 20, 2023
Peer-review started: March 20, 2023
First decision: April 10, 2023
Revised: April 24, 2023
Accepted: May 17, 2023
Article in press: May 17, 2023
Published online: June 21, 2023

Xia Li, Yu-Hua Du, Ling Yuan, College of Pharmacy, Ningxia Medical University, Yinchuan 750004, Ningxia Hui Autonomous Region, China

Xiao-Ling Ma, Yi Nan, Yan Chen, Yang Niu, Traditional Chinese Medicine College, Ningxia Medical University, Yinchuan 750004, Ningxia Hui Autonomous Region, China

Yi Nan, Lei Zhang, Yang Niu, Key Laboratory of Hui Ethnic Medicine Modernization of Ministry of Education, Ningxia Medical University, Yinchuan 750004, Ningxia Hui Autonomous Region, China

Yi Yang, College of Basic Medicine, Ningxia Medical University, Yinchuan 750004, Ningxia Hui Autonomous Region, China

Dou-Dou Lu, Jun-Fei Zhang, College of Clinical Medicine, Ningxia Medical University, Yinchuan 750004, Ningxia Hui Autonomous Region, China

Corresponding author: Ling Yuan, MD, PhD, Assistant Professor, College of Pharmacy, Ningxia Medical University, No. 1160 Shengli Street, Yinchuan 750004, Ningxia Hui Autonomous Region, China. 20080017@nxmu.edu.cn

Abstract

BACKGROUND

Gastric cancer (GC) is a common gastrointestinal malignancy worldwide. Based on cancer-related mortality, the current prevention and treatment strategies for GC still show poor clinical results. Therefore, it is important to find effective drug treatment targets.

AIM

To explore the molecular mechanism of 18β-glycyrrhetinic acid (18β-GRA) regulating the miR-345-5p/TGM2 signaling pathway to inhibit the proliferation of GC cells.

METHODS

CCK-8 assay was used to determine the effect of 18β-GRA on the survival rate of GES-1 cells and AGS and HGC-27 cells. Cell cycle and apoptosis were detected by flow cytometry, cell migration was detected by a wound healing assay, the effect of 18β-GRA on subcutaneous tumor growth in BALB/c nude mice was inves-

tigated, and the cell autophagy level was determined by MDC staining. TMT proteomic analysis was used to detect the differentially expressed autophagy-related proteins in GC cells after 18β-GRA intervention, and then the protein-protein interaction was predicted using STRING (https://string-db.org/). MicroRNAs (miRNAs) transcriptome analysis was used to detect the miRNA differential expression profile, and use miRBase (https://www.mirbase/) and TargetScan (https://www.targetscan.org/) to predict the miRNA and complementary binding sites. Quantitative real-time polymerase chain reaction was used to detect the expression level of miRNA in 18β-GRA treated cells, and western blot was used to detect the expression of autophagy related proteins. Finally, the effect of miR-345-5p on GC cells was verified by mir-345-5p overexpression.

RESULTS

18β-GRA could inhibit GC cells viability, promote cell apoptosis, block cell cycle, reduce cell wound healing ability, and inhibit the GC cells growth *in vivo*. MDC staining results showed that 18β-GRA could promote autophagy in GC cells. By TMT proteomic analysis and miRNAs transcriptome analysis, it was concluded that 18β-GRA could down-regulate TGM2 expression and up-regulate miR-345-5p expression in GC cells. Subsequently, we verified that TGM2 is the target of miR-345-5p, and that overexpression of miR-345-5p significantly inhibited the protein expression level of TGM2. Western blot showed that the expression of autophagy-related proteins of TGM2 and p62 was significantly reduced, and LC3II, ULK1 and AMPK expression was significantly increased in GC cells treated with 18β-GRA. Overexpression of miR-345-5p not only inhibited the expression of TGM2, but also inhibited the proliferation of GC cells by promoting cell apoptosis and arresting cell cycle.

CONCLUSION

18β-GRA inhibits the proliferation of GC cells and promotes autophagy by regulating the miR-345-5p/TGM2 signaling pathway.

Key Words: 18β-glycyrrhetinic acid; Gastric cancer; MiR-345-5p; TGM2; Proliferation; Autophagy

©The Author(s) 2023. Published by Baishideng Publishing Group Inc. All rights reserved.

Core Tip: Gastric cancer (GC) is a global health problem that seriously endangers human life, so it is urgent to find drugs to treat it. 18β-glycyrrhetinic acid (18β-GRA), as one of the main components of glycyrrhiza, has a strong antitumor effect. In this paper, the inhibitory effect of 18β-GRA on GC was verified by *in vitro* and *in vivo* experiments. In addition, it was found that 18β-GRA promoted autophagy and inhibited the proliferation of GC cells through the miR-345-5p/TGM2 signaling pathway. These findings provide the theoretical basis for the GC clinical treatment of 18β-GRA.

Citation: Li X, Ma XL, Nan Y, Du YH, Yang Y, Lu DD, Zhang JF, Chen Y, Zhang L, Niu Y, Yuan L. 18β-glycyrrhetinic acid inhibits proliferation of gastric cancer cells through regulating the miR-345-5p/TGM2 signaling pathway. *World J Gastroenterol* 2023; 29(23): 3622-3644
URL: https://www.wjgnet.com/1007-9327/full/v29/i23/3622.htm
DOI: https://dx.doi.org/10.3748/wjg.v29.i23.3622

INTRODUCTION

The fourth most common cause of cancer-related death worldwide is gastric cancer (GC)[1]. Environment, diet, genetic factors, and *Helicobacter pylori* infection are the main causes of GC. Because there are no specific diagnostic indicators, the majority of patients ignore their early symptoms because they are inconspicuous. By the time the body shows obvious discomfort, the disease has progressed to intermediate or advanced cancer, and the disease has worsened significantly, allowing the best opportunity for treatment to pass. The existing treatment methods for GC are mainly drug therapy, chemotherapy and surgery[2,3]. But the drug resistance and toxic side effects of anticancer drugs, the low compliance of patients during chemotherapy and the low survival rate after surgery all suggest that we can find a natural, effective and low-toxic active ingredient to treat GC.

18β-glycyrrhetinic acid (18β-GRA) is a compound extracted from licorice[4]. Studies have revealed that 18β-GRA has multiple pharmacological effects, like anti-inflammatory, anti-viral, anti-tumor, liver protection and so on[5-9]. In recent years, the therapeutic effect of 18β-GRA on lung cancer[7], breast

cancer[10], ovarian cancer[11], prostate cancer[12] and other cancers has been confirmed. Cao *et al*[13] revealed that 18β-GRA inhibited GC cells proliferation, energy metabolism and carcinogenesis by down-regulating toll-like receptor 2. Through reactive oxygen species/protein kinase C-α/extracellular signal-regulated kinase pathway, as well as matrix metalloproteinase MMP2 and MMP9 activity, 18β-GRA inhibited GC cells migration and invasion[14]. And our previous study found that 18β-GRA inhibited GC cells proliferation by regulating MRPL35[15]. These results indicated that 18β-GRA may be a useful drug for the prevention and treatment of GC.

MicroRNAs (miRNAs) are highly conserved non-coding RNA molecules, that take part in the occurrence and development of cancer[16]. Many sequences of human miRNAs associated with cancer mechanisms have been identified. They regulate protein expression levels by their target mRNA, and participate in vital cellular processes and pathways[17]. There is growing evidence that the difference in miRNAs expression exists not only between normal and cancer tissues and between different cancer types and subtypes, but also between early and advanced cancers[18,19]. Komatsu *et al*[20] found that up-regulation of miR-148a inhibited the GC cells proliferation, invasion and EMT. The researchers revealed that *Helicobacter pylori* infection reduced miR-1298-5p expression in GC cells, while low-expressed miR-1298-5p could promote GC cells proliferation, migration and invasion[21].

Autophagy is a biological process that occurs in cells[22]. A lot of research has found that it plays a key role in physiological processes and disease occurrences, including development, metabolism, inflammation and cancer[23]. Dysfunctional autophagy results in incorrect organelles and protein breakdown, which kill autophagic cells and affect tumor cell survival. Wei *et al*[24] revealed that miR-183 induced GC cells autophagy and inhibited proliferation *via* targeted inhibition of mechanistic target of rapamycin (mTOR) expression.

In our study, we revealed 18β-GRA's effect on GC cells phenotype and tumor formation in nude mice, and 18β-GRA's effect on GC cells autophagy. We used TMT proteomic analysis and the STRING database to predict the differentially expressed autophagy-related proteins and their interactions. The differentially expressed miRNAs were analyzed using miRNAs transcriptome analysis, and the corresponding miRNAs and complementary binding sites of autophagy-related proteins were predicted using the miRBase and TargetScan databases. Later, we verified the link between miR-345-5p and TGM2 using a dual-luciferase reporter assay. Quantitative real-time polymerase chain reaction (qRT-PCR) was used to detect expression of miR-345-5p, western blot was used to detect autophagy-related proteins, and lentivirus transfection technique verified the effect of miR-345-5p on TGM2. We concluded that 18β-GRA can inhibit GC cells proliferation and promote autophagy *via* regulating the miR-345-5p/TGM2 signaling pathway, which may afford a theoretical basis for GC treatment with 18β-GRA. The research idea is shown in Figure 1.

MATERIALS AND METHODS

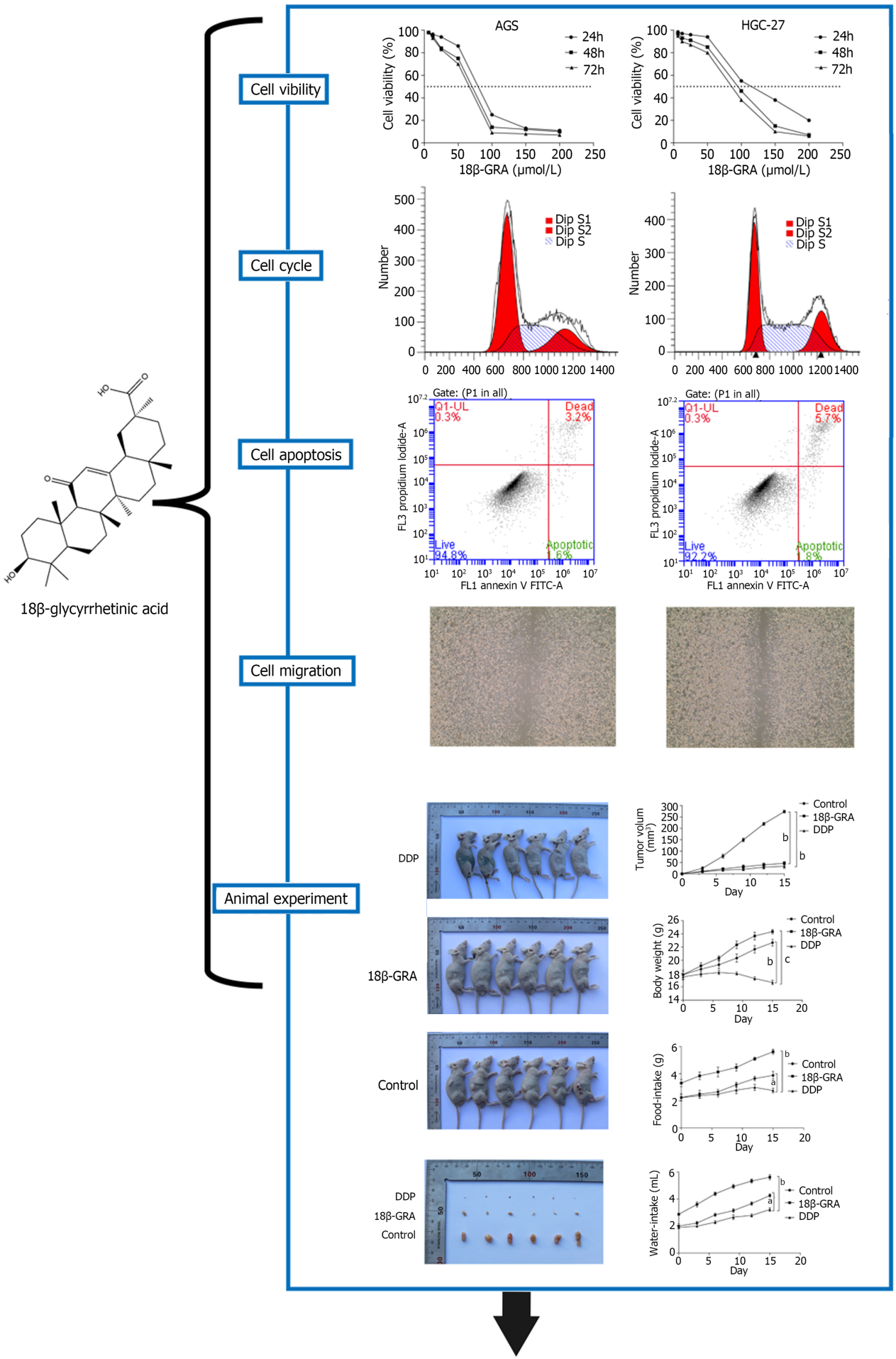
Experimental materials

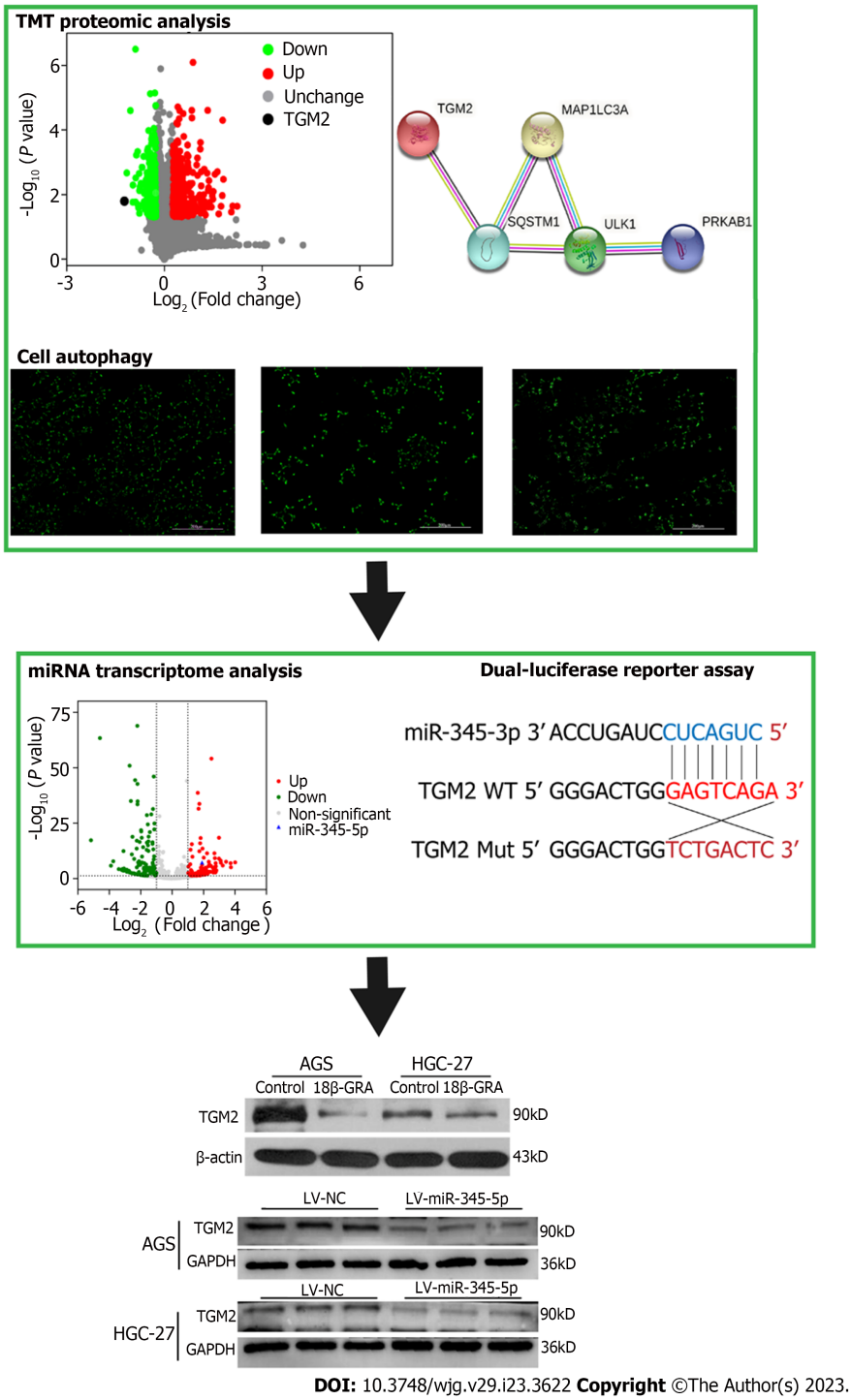
Human gastric epithelial cell GES-1 was purchased from BNCC (Cat. No. BNCC353464, Beijing, China). Human GC cell lines AGS, HGC-27 and MKN-45 were purchased from Procell (Cat. No. CL-0022/CL-0107/CL-0292, Wuhan, China). Fetal bovine serum (FBS) was purchased from Corning (Cat. No. 35-076-CV, United States). DMEM, DMEM/F-12 and RPIM-1640 mediums were purchased from Gibco. The dual-luciferase reporter assay system was purchased from Promega (United States). Shanghai Gene Biotechnology Co., Ltd. (China) provided the plasmid and lentiviral expression vector. The MDC kit, cell apoptosis kit and cell cycle kit (Cat. No. KGATG001/KGA1026/KGA512, Jiangsu, China) were purchased from Jiangsu KeyGEN Bio TECH Corp., Ltd. TaKaRa provided the PrimeScript™ RT reagent kit and TB Green Premix Ex Taq II (Cat. No. RR047A/RR82LR, Japan). Thermofisher provided Trizol. MedChemExpress provided cisplatin (DDP) and 18β-GRA (Cat. No. HY17394/HY-N0180, United States). Immunoway provided TGM2, AMPK, p62, ULK1, LC3I/II, GAPDH and β-actin antibodies, while CST provided anti-mouse/rabbit immunoglobulin G antibodies.

BABL/c nude mice (male, 18-22g, SPF) were provided by the Animal Laboratory Center of Ningxia Medical University. All animals were fed standard laboratory feed and water in 12 h light/dark cycle environment. The animal protocols (IACUC-NYLAC-2022-108) were approved by the Institutional Animal Care and Use Committee of Ningxia Medical University. All animals were euthanized by CO_2.

Cell culture and cell transfection

GES-1 cells were cultured in DMEM medium, HGC-27 cells were cultured in RPIM-1640 medium, and AGS and MKN-45 cells were cultured in DMEM/F-12 medium, and 10% FBS and 1% penicillin-streptomycin liquid were added into all mediums to. The cell culture flask was placed in an incubator with a constant temperature of 37 °C and 5% CO_2. The GFP-labeled miR-345-5p overexpression lentiviral vector (LV-miR-345-5p) and empty lentiviral vector (LV-NC) were then transfected into HGC-27 and AGS cells using the tool virus user manual as a guide.


18β-glycyrrhetinic acid
Cell vibility
Cell cycle
Cell apoptosis
Cell migration
Animal experiment
AGS
HGC-27
Cell viability (%)
18β-GRA (μmol/L)
24h
48h
72h
Dip S1
Dip S2
Dip S
Number
Gate: (P1 in all)
Q1-UL 0.3%
Dead 3.2%
Dead 5.7%
Live 94.8%
Live 92.2%
Apoptotic 1.6%
Apoptotic 1.8%
FL3 propidium Iodide-A
FL1 annexin V FITC-A
DDP
18β-GRA
Control
Tumor volum (mm³)
Body weight (g)
Food-intake (g)
Water-intake (mL)
Day



DOI: 10.3748/wjg.v29.i23.3622 **Copyright** ©The Author(s) 2023.

Figure 1 Flow chart. In this study, we revealed 18β-glycyrrhetinic acid (18β-GRA)'s effect on gastric cancer (GC) cells phenotype and tumor formation in nude mice, and 18β-GRA's effect on GC cells autophagy. We used TMT proteomic analysis and the STRING database to predict the differentially expressed autophagy-related proteins and their interactions. Later, we verified the link between miR-345-5p and TGM2 using a dual-luciferase reporter assay. Quantitative real-time polymerase chain reaction was used to detect expression of miR-345-5p, western blot was used to detect autophagy-related proteins, and lentivirus transfection technique verified the effect of miR-345-5p on TGM2. LV-NC: Empty lentiviral vector.

Cell viability assay

The cells were inoculated into 96-well plates at 4000 cells per well and treated with 18β-GRA (12.5 μmol/L-200 μmol/L) for 24 h, 48 h and 72 h. Next, 10 μL CCK-8 was added to each well, and the absorbance was detected at 450 nm.

Cell cycle and cell apoptosis assay

The cells were treated with 18β-GRA at concentrations of 30, 60 and 120 μmol/L or 45, 90 and 135 μmol/L for 48 h, respectively. Next, the cells were collected and fixed with 70% pre-cooled ethanol. The fixative solution was washed off with PBS. 500 μL pre-configured working solution (RNase A:PI = 1:9)

was added. The percentage of cell cycle was determined by flow cytometry after 30 min. The cells in each group were collected, 500 μL binding buffer, 5 μL Annexin V-FITC and 5 μL PI or 500 μL binding buffer, 5 μL Annexin V-APC and 5 μL 7-AAD were added and mixed. Cell apoptosis was determined after 15 min using flow cytometry.

Wound healing assay

The cells were inoculated into the 6-well plates at the appropriate concentration and cultured for 24 h. Next, we made a scratch in the central part of each hole, and 18β-GRA at concentrations of 30, 60, 120 μmol/L or 45, 90, 135 μmol/L was added for 48 h. Finally, the cells were washed and photographed with a microscope. Cell migration area was calculated by Image J.

MDC staining assay

The cells were treated with 18β-GRA at concentrations of 30, 60 and 120 μmol/L or 45, 90 and 135 μmol/L for 48 h, respectively. Next, the cells were gently washed twice with a wash buffer, stained with MDC and incubated away from light for 15-45 min. Photographs were taken under a fluorescence microscope after washing twice with 1 × wash buffer.

Tumor formation experiment in BALB/c nude mice

The BALB/c nude mice were fed for 1 wk, then 200 μL MKN-45 cells suspension containing 4×10^6 cells were inoculated subcutaneously into nude mice using a microsyringe. The experiment was divided into three groups: Control, cisplatin group (DDP) and 18β-GRA groups. After 5 d of subcutaneous inoculation, the 18β-GRA group was intraperitoneally injected with 50 mg/kg[13,25], the DDP group with 2 mg/kg[26], and the control group was given normal saline. $V = (L \times W^2)/2$ was used to calculate tumor volumes (V, volume; W, width; L, length). After 14 d of continuous administration, all nude mice were killed by CO_2 inhalation and photographed.

TMT proteomic analysis

GC cells were treated with 18β-GRA, and differentially expressed proteins were detected and analyzed by China Gene Biotechnology Co., Ltd. All the obtained original data files were processed by Proteome Discoverer 2.2 (Thermo Fisher, United States) software. Proteins with expression ratio > 1.2 and $P < 0.05$ were considered as differentially expressed proteins.

Cellular processes, biological processes, and molecular functions of differentially expressed proteins were analyzed using Metascape (https://metascape.org/gp/index.html#/main/step1). Gene Ontology annotation, Kyoto Encyclopedia of Genes and Genomes pathway, and InterPro domain enrichment analysis were performed using Fisher accuracy test. WoLFPSOR was used to locate and predict the differentially expressed proteins. The protein expression levels are classified by Matplotlib to form hierarchical clustering heatmaps.

miRNAs transcriptome analysis

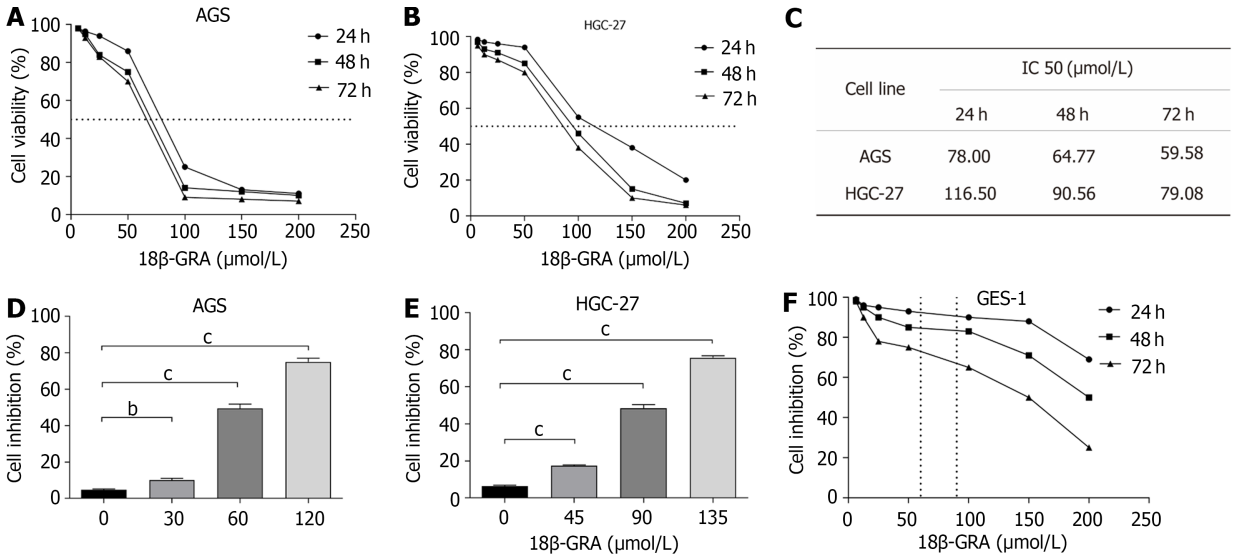
GC cells were treated with 18β-GRA at concentrations of 60 μmol/L and total RNA was extracted from it. Agarose gel electrophoresis, Nanodrop, Qubit 2.0, and Agilent 2100 were used to ensure that the quality of the collected RNA met the requirements of subsequent experiments. A small RNA Sample Pre kit was used to construct the library, and specific enzymes were used to connect the PCR primer connectors at the 3′ and 5′ ends. Then the cDNA synthesis can be completed efficiently and rapidly by reverse transcription. The single strand of DNA is combined with the primer and the PCR amplification stage begins. After PAGE electrophoresis, a cDNA library (effective concentration > 2 nM) was obtained. Qubit 2.0 and Agilent 2100 were combined with qPCR to ensure the quality of the library. The optical signal was transformed into a sequence by computer analysis. The original sequencing data was further assessed for quality with $P < 0.05$ and $|\text{Log}_2 \text{(fold change)}| > 1$ as a filter condition, with a certain number of differential expressions of miRNAs eventually selected.

Target prediction analysis

We predicted protein-protein interaction (PPI) networks from the STRING database (https://string-db.org/). The miRBase website (http://www.mirbase.org/) was used to predict the corresponding miRNAs of autophagy-related proteins and the TargetScan database (https://www.targetscan.org/) was used to predict the binding sites of miRNA and mRNA.

Dual-luciferase reporter assay

TargetScan predicted the binding sites for miR-345-5p and TGM2. The fragments, including the wild 3′UTR regions or mutant 3′UTR regions of TGM2, were inserted into GV716 with a firefly and renilla luciferase reporter gene. The overexpressed miR-345-5p plasmid was then individually transfected into AGS cells. After 48 h of transfection, the relative luciferase activity was detected using a dual-luciferase reporter assay system.



DOI: 10.3748/wjg.v29.i23.3622 **Copyright** ©The Author(s) 2023.

Figure 2 Effect of 18β-glycyrrhetinic acid on cell viability of GES-1, AGS and HGC-27 cells were detected by CCK-8 assay. A: Effect of 18β-glycyrrhetinic acid (18β-GRA) on cell viability of AGS cells; B: Effect of 18β-GRA on cell viability of HGC-27 cells; C: IC_{50} value of AGS and HGC-27 cells were treated with 18β-GRA for 24, 48 and 72 h; D: Effect of low, medium and high doses of 18β-GRA on cell viability of AGS cells; E: Effect of low, medium and high doses of 18β-GRA on cell viability of HGC-27 cells; F: Effect of 18β-GRA on cell viability of GES-1 cells. All data are from three independent samples. The data is represented as the mean ± SD. $^{a}P < 0.05$, $^{b}P < 0.01$, $^{c}P < 0.001$. 18β-GRA: 18β-glycyrrhetinic acid.

qRT-PCR

The cells were cultured and treated 18β-GRA at concentrations of 30, 60 and 120 μmol/L or 45, 90 and 135 μmol/L for 48 h, respectively. Total RNA was extracted using Trizol, and cDNA was synthesized using PrimeScript™ RT reagent kit. The expression level was detected with TB Green Premix Ex Taq II. The primer sequences are as follows: miR-345-5p, forward, 5′-GCTGACTCCTAGTCCAGGGCTC-3′ and reverse, 5′-GGCCAACCGCGAGAAGATG-3′; U6, forward, 5′-CTGCGCAAGGATGACACGCAAATT-3′ and reverse, 5′-GGCCAACCGCGAGAAGATG-3′. U6 as a housekeeping gene. The relative expression was calculated by the $2^{-\Delta\Delta Ct}$ method.

Western blot

The cells were cultured and treated 18β-GRA at concentrations of 60 μmol/L or 90 μmol/L for 48 h, respectively. The cells were collected and the total protein was extracted, the protein content was detected with BCA method. The protein was isolated and transferred onto a PVDF membrane, which is then sealed with 5% skim milk powder, soaked in primary antibodies and incubated overnight. The next day, the PVDF membrane was cleaned with TBST and soaked in secondary antibodies for 2 h. The protein was detected using an ECL solution, and ultimately the grey values were measured using ImageJ.

Statistical analysis

The statistical methods of this study were reviewed by Li-Qun Wang, Department of Epidemiology and Medical Statistics, Institute of Public Health and Management, Ningxia Medical University. All data were statistically analyzed using GraphPad Prism 7. All data were shown as mean ± SD, and the differences between different groups were analyzed using a one-way ANOVA or *t*-test. The significance level was set at $P < 0.05$.

RESULTS

18β-GRA reduced the GC cells viability

The results demonstrated that when the 18β-GRA concentration was 12.5 μmol/L-200 μmol/L, the inhibitory effect of 18β-GRA on AGS and HGC-27 cells viability was enhanced as the 18β-GRA dose was increased (Figures 2A and B). Next, 18β-GRA treated AGS and HGC-27 cells for 24 h, 48 h and 72 h, IC_{50} value was shown in Figure 2C. Therefore, we determined that the low, medium and high concentrations of 18β-GRA treated AGS cells for 48 h were 30, 60 and 120 μmol /L, and the low, medium and high concentrations of 18β-GRA treated HGC-27 cells for 48 h were 45, 90 and 135 μmol/L. AGS and HGC-27 cells viability was inhibited at low, medium and high doses of 18β-GRA when compared with the

control group (0 μmol/L) ($P < 0.01$) (Figures 2D and E).

18β-GRA had slight effect on normal gastric epithelial GES-1 cells

Subsequently, we investigated 18β-GRA's effect on GES-1 cells viability. The results demonstrated that GES-1 cells viability was slightly affected when 18β-GRA concentration was 12.5 μmol/L-100 μmol/L (Figure 2F). When the 18β-GRA concentration was less than 150 μmol/L, the GES-1 cells viability remained above 71% at 48 h.

18β-GRA arrested GC cells cycle

18β-GRA's effect on GC cells cycle results demonstrated that the percentage of G0/G1 phase (49.15%, 56.23% and 73.07%) in AGS cells treated with low, medium and high doses of 18β-GRA was higher than the control group (33.71%) (Figures 3A and B). The percentage of G0/G1 phase (46.58%, 51.69% and 77.11%) in HGC-27 cells treated with low, medium and high doses of 18β-GRA was higher than the control group (41.67%) (Figures 3C and D).

18β-GRA promoted GC cells apoptosis

18β-GRA's effect on GC cells apoptosis results demonstrated that the apoptosis rates of AGS cells treated with low, medium and high doses of 18β-GRA were 7.50%, 19.80% and 72. 00%, which were obviously higher than the control group (4. 80%) ($P < 0.01$) (Figures 3E and F). The apoptosis rates of HGC-27 cells treated with low, medium and high doses of 18β-GRA were 6.50%, 8.10% and 15.40%, which were obviously higher than the control group (6.40%) ($P < 0.05$) (Figures 3G-H).

18β-GRA inhibited the GC cells wound healing

The wound healing assay revealed that both high and medium doses of 18β-GRA can inhibit AGS and HGC-27 cells' wound healing abilities ($P < 0.001$) (Figures 4A-D). The inhibitory effect of 18β-GRA on wound healing ability was gradually enhanced as the 18β-GRA dose was increased in AGS and HGC-27 cells.

18β-GRA inhibited subcutaneous tumor growth in BALB/c nude mice

Through the subcutaneous tumor formation experiment in BALB/c nude mice, we observed that the back tumors in the control group were larger than those in the DDP and 18β-GRA groups ($P < 0.01$) (Figures 5A and B). The tumor volume was measured every 3 d and the tumor growth curve was plotted. In comparison to the control group, tumor size and growth rate were slower in the 18β-GRA and DDP groups ($P < 0.001$) (Figure 5C). Additionally, the body weight of DDP group was lower than the control and 18β-GRA groups. Diet and water intake were lower in the 18β-GRA and DDP groups when compared with the control group ($P < 0.05$) (Figures 5D-F).

Identification of autophagy-related proteins by TMT proteomic analysis and MDC staining assay

Part of the data of TMT proteomics analysis comes from the previous research of our team (Figures 6A-F)[15]. Cluster analysis was performed for differential proteins and heat map was drawn (Figure 6G), and the expression of TGM2 was down-regulated ($P = 0.01593178$). We used the STRING database to construct the PPI network, and the interaction diagram between the differentially expressed autophagy-related protein TGM2 and the autophagy marker proteins ULK1, p62 (SQSTM1), LC3I/II (MAPILC3) and AMPK (PRKAB1) was shown in Figure 6H, which indicated TGM2 was closely related to autophagy marker proteins. The results of MDC staining showed that AGS and HGC-27 cells displayed various degrees of autophagy after 18β-GRA intervention, and the number of autophagy cells increased as the dose of 18β-GRA was increased ($P < 0.05$) (Figures 6I-L).

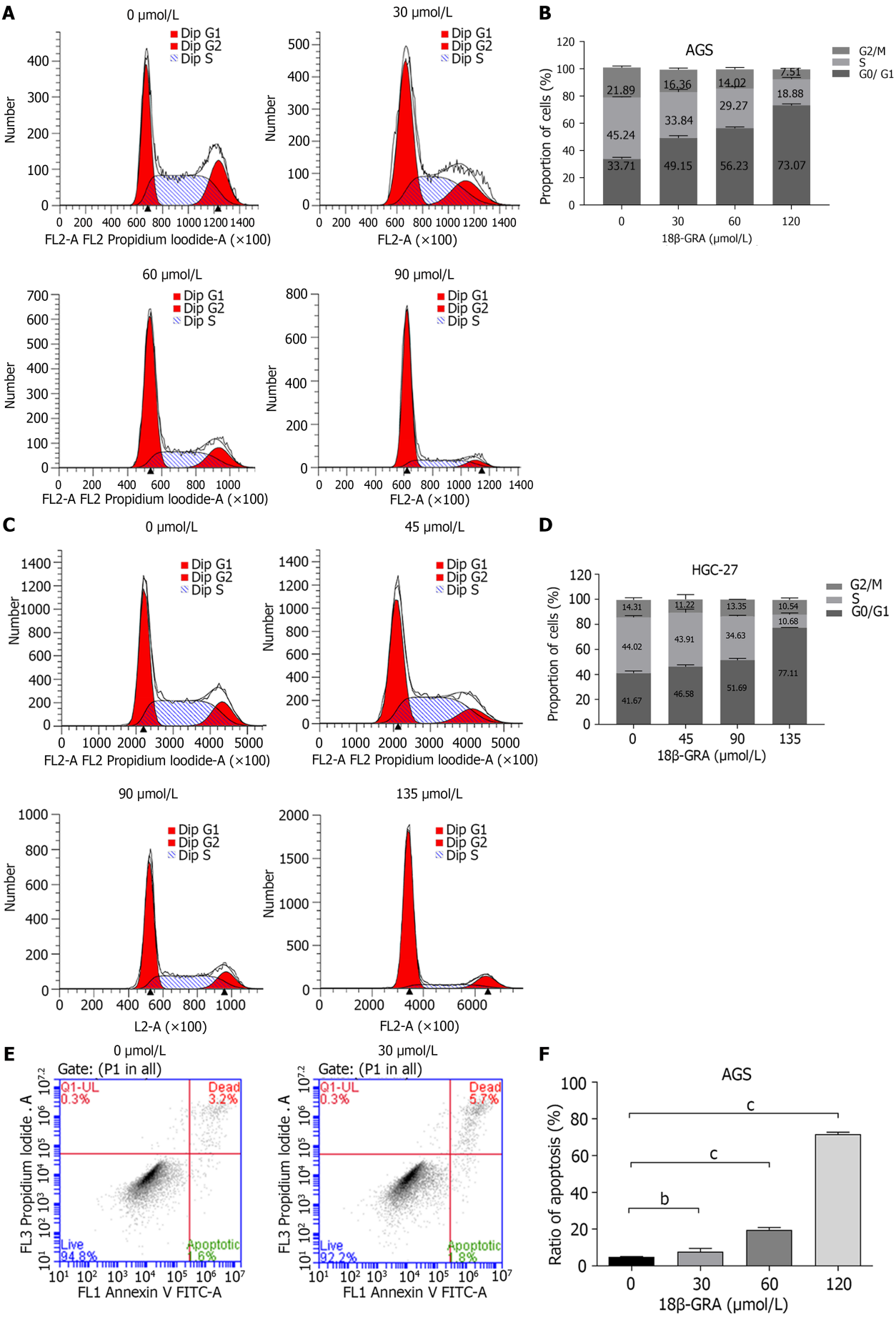
Effect of 18β-GRA on the expression of autophagy-related proteins

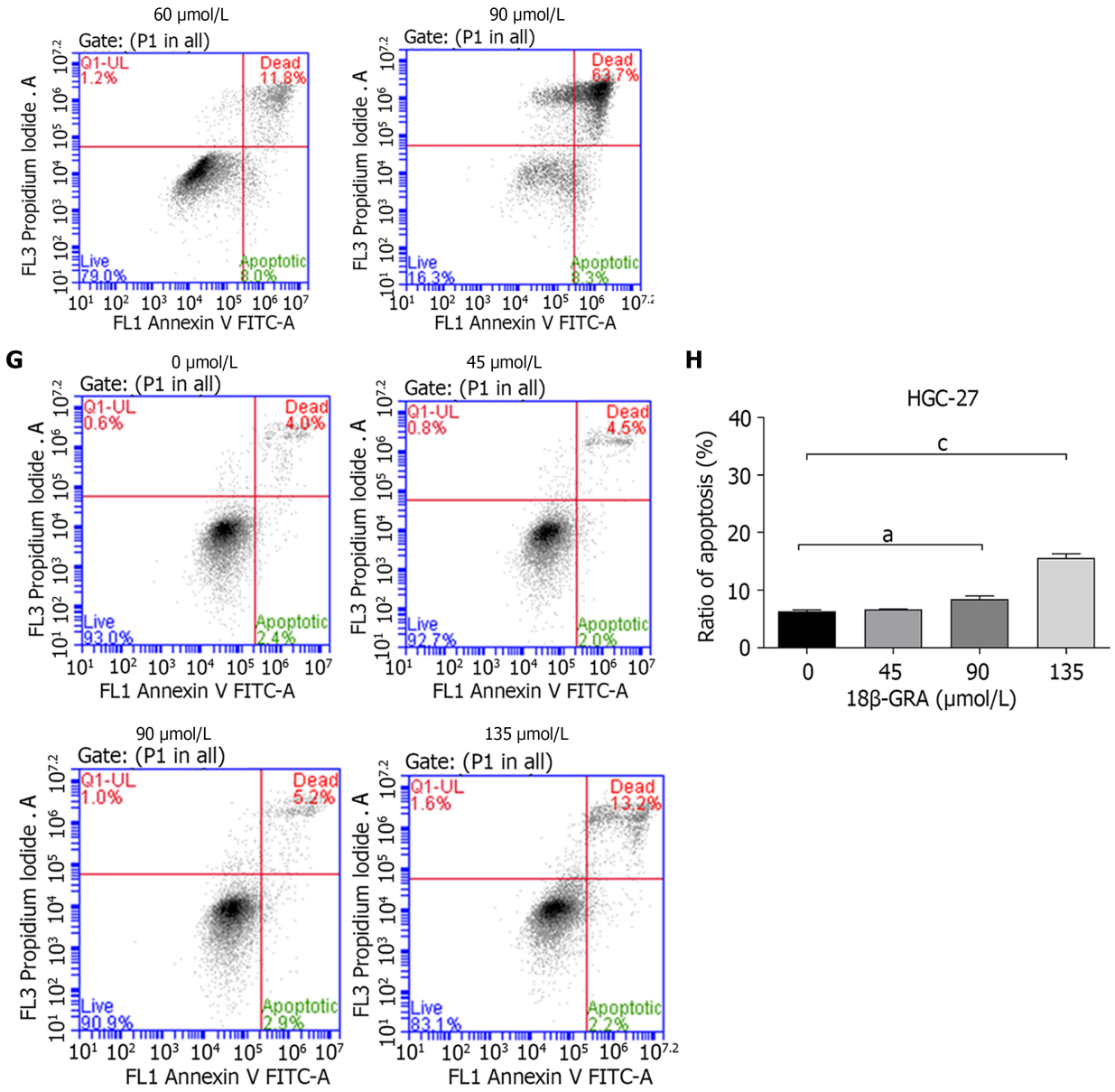
Western blot analysis was used to determine 18β-GRA's influence on autophagy-related proteins in the AGS and HGC-27 cells. The findings demonstrated that, in contrast to the control group, the 18β-GRA group's protein expressions of TGM2 and p62 were lowered, whereas LC3II, ULK1 and AMPK were elevated ($P < 0.01$) (Figures 7A-E).

MiR-345-5p is a drug target of 18β-GRA

283 miRNAs were identified as differentially expressed by miRNAs transcriptome analysis, of which 163 miRNAs were down-regulated and 120 miRNAs were up-regulated, and the selection criteria for $|\text{Log}_2(\text{fold change})| > 1$, $P < 0.05$. Among them, the expression of miR-345-5p was up-regulated ($P =$ 5.68E-08) (Figure 8A). The miRBase website was used to predict the corresponding miRNAs of autophagy-related proteins, and then we intersected the miRNAs corresponding to autophagy-related proteins with the differentially expressed miRNAs screened by miRNA transcriptome. Among the obtained miRNAs, miR-345-5p was expressed most significantly.

We used qRT-PCR to determine the expression changes of miR-345-5p in AGS and HGC-27 cells treated with 18β-GRA. The outcomes demonstrated that miR-345-5p was highly up-regulated in AGS


A
0 μmol/L
30 μmol/L
60 μmol/L
90 μmol/L
Dip G1
Dip G2
Dip S
Number
FL2-A FL2 Propidium loodide-A (×100)
FL2-A (×100)
B
AGS
G2/M
S
G0/ G1
Proportion of cells (%)
18β-GRA (μmol/L)
21.89
45.24
33.71
16.36
33.84
49.15
14.02
29.27
56.23
7.51
18.88
73.07
C
0 μmol/L
45 μmol/L
90 μmol/L
135 μmol/L
L2-A (×100)
D
HGC-27
G2/M
S
G0/G1
14.31
44.02
41.67
11.22
43.91
46.58
13.35
34.63
51.69
10.54
10.68
77.11
E
0 μmol/L
30 μmol/L
Gate: (P1 in all)
Q1-UL
0.3%
Dead
3.2%
5.7%
Live
94.8%
92.2%
Apoptotic
4.6%
8%
FL3 Propidium Iodide . A
FL1 Annexin V FITC-A
F
AGS
Ratio of apoptosis (%)
18β-GRA (μmol/L)
b
c
c



DOI: 10.3748/wjg.v29.i23.3622 **Copyright** ©The Author(s) 2023.

Figure 3 Effect of 18β-glycyrrhetinic acid on cell cycle and cell apoptosis of AGS and HGC-27 cells. A: Effect of 18β-glycyrrhetinic acid (18β-GRA) on AGS cells cycle; B: Statistical results of AGS cell cycle; C: Effect of 18β-GRA on HGC-27 cells cycle; D: Statistical results of HGC-27 cells cycle; E: Effect of 18β-GRA on AGS cells apoptosis; F: Statistical results of AGS cells apoptosis; G: Effect of 18β-GRA on HGC-27 cells apoptosis; H: Statistical results of HGC-27 cells apoptosis. All data are from three independent samples. The data is represented as the mean ± SD. $^{a}P < 0.05$, $^{b}P < 0.01$, $^{c}P < 0.001$. 18β-GRA: 18β-glycyrrhetinic acid.

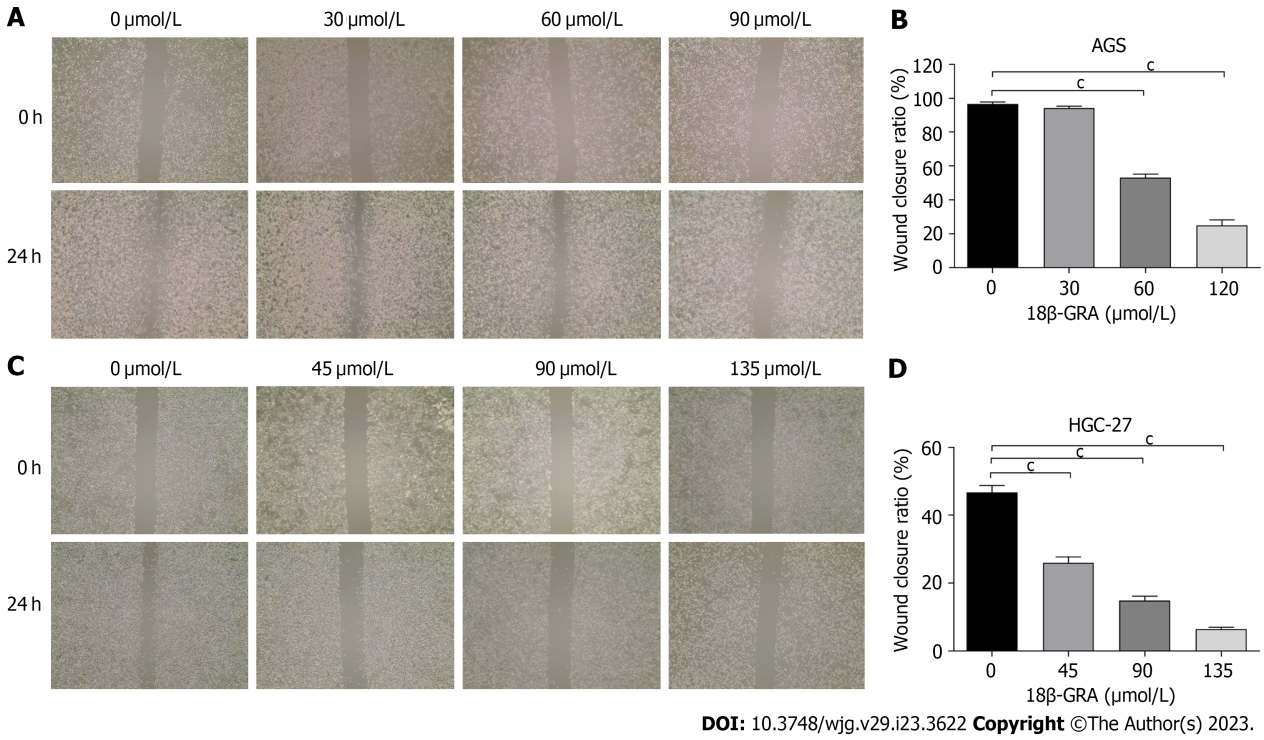
and HGC-27 cells after 18β-GRA treatment ($P < 0.01$) (Figures B and 8C). This verified the results of miRNAs transcriptome.

MiR-345-5p could target TGM2 directly

We utilized TargetScan database to identify complementary binding sites between miR-345-5p and TGM2 (Figure 8D). According to dual-luciferase reporter analyses, overexpression of miR-345-5p reduced luciferase expression in the TGM2-wild-type reporter but not in the mutant reporter ($P < 0.05$) (Figure 8E). These results suggest that miR-345-5p can regulate the expression of TGM2.

Overexpression of miR-345-5p can inhibit TGM2

Lentivirus transfection technique caused miR-345-5p overexpression on AGS and HGC-27 cells, and the transfection rate reached about 90% after 72 h (Figure 9A). Then, qRT-PCR discovered that miR-345-5p expression in the LV-miR-345-5p group was higher compared to the LV-NC group on AGS and HGC-27 cells ($P < 0.001$) (Figure 9B). Meanwhile, overexpression of miR-345-5p inhibited the protein expression of TGM2 ($P < 0.01$) (Figures 9C and D).



DOI: 10.3748/wjg.v29.i23.3622 **Copyright** ©The Author(s) 2023.

Figure 4 Effect of 18β-glycyrrhetinic acid on cell wound healing of AGS and HGC-27 cells. A: Effect of 18β-glycyrrhetinic acid (18β-GRA) on the wound healing of AGS cells; B: Statistical results of the wound healing in AGS cells; C: Effect of 18β-GRA on wound healing of HGC-27 cells; D: Statistical results of the wound healing in HGC-27 cells. All data are from three independent samples. The data is represented as the mean ± SD. °P < 0.001. 18β-GRA: 18β-glycyrrhetinic acid.

Overexpression of miR-345-5p inhibit GC cells proliferation by promoting cell apoptosis and arresting cell cycle

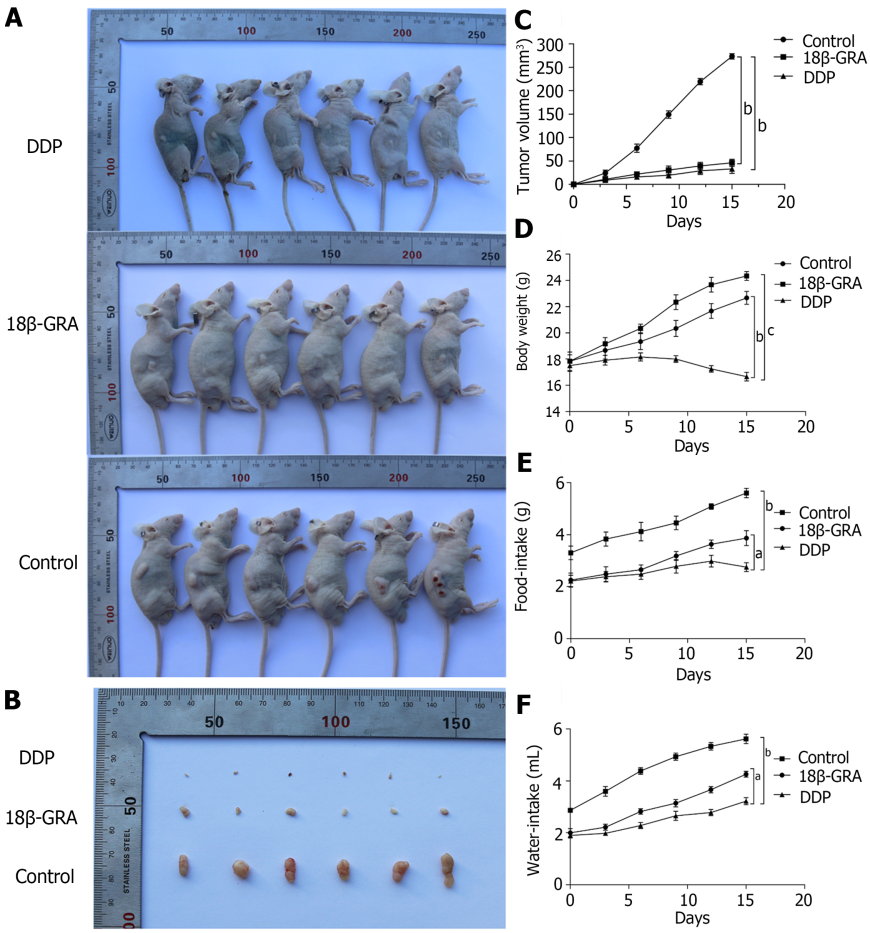
Some researchers found that the expression of miR-345-5p in GC tissues was significantly lower than that in para-carcinoma tissue. which was correlated with aggressive stage and grade[27]. We evaluated the impact of miR-345-5p overexpression on cell viability in GC cells through CCK-8 assay. Our findings indicated that miR-345-5p overexpression resulted in a significant inhibition of the cell viability on AGS and HGC-27 cells (P < 0.01) (Figures 10A and B).

In order to further investigate the impart of miR-345-5p overexpression on GC cells, we conducted flow cytometry analysis to examine its effect on cell apoptosis and cell cycle. Our results showed the cell apoptosis rates in the miR-345-5p overexpression group were significantly higher than that in the LV-NC group on AGS and HGC-27 cells (P < 0.001) (Figures 10C and D). Moreover, the cell cycle experiment revealed that miR-345-5p overexpression caused cell cycle arrest in the G0/G1 phase on AGS and HGC-27 cells (P < 0.001) (Figures 10E and F). These results suggested that miR-345-5p overexpression could inhibit GC cells proliferation by promoting cell apoptosis and arresting cell cycle.

DISCUSSION

In this study, 18β-GRA treated GC cells phenotypic alterations were identified *in vitro*. The findings demonstrated that 18β-GRA had a minimal effect on the survival rate of normal gastric epithelial GES-1 cells, but dramatically reduced the AGS and HGC-27 cells viability. Next, we found that 18β-GRA could block the AGS and HGC-27 cells in G0/G1 phase and promote cell apoptosis. Both DNA replication and mitosis crucially depend on the G0/G1 phase. According to studies, after drug intervention, cells can either irreversibly end the cell cycle through senescence or apoptosis[28], or they can reversibly exit the cell cycle by beginning immobilization. We looked at how 18β-GRA affected the GC cells apoptosis and verified the results of cell cycle, which led us to conclude that 18β-GRA made GC cells exit the cell cycle selectively. It has been demonstrated that cells can exit the cell cycle reversibly by initiating immobilization, or irreversibly by senescence or apoptosis. Our findings confirmed the conclusion that 18β-GRA can induce GC cells to exit the cell cycle selectively.

18β-GRA decreased the migration ability of AGS and HGC-27 cells, according to a wound healing assay. At the same time, we also performed cell invasion experiments, but the results were not statistically significant. Studies have shown that TGM2 could promote GC cells' proliferation, migration and invasion by activating extracellular signal-regulated kinase 1/2[29]. In addition, TGM2 was thought to



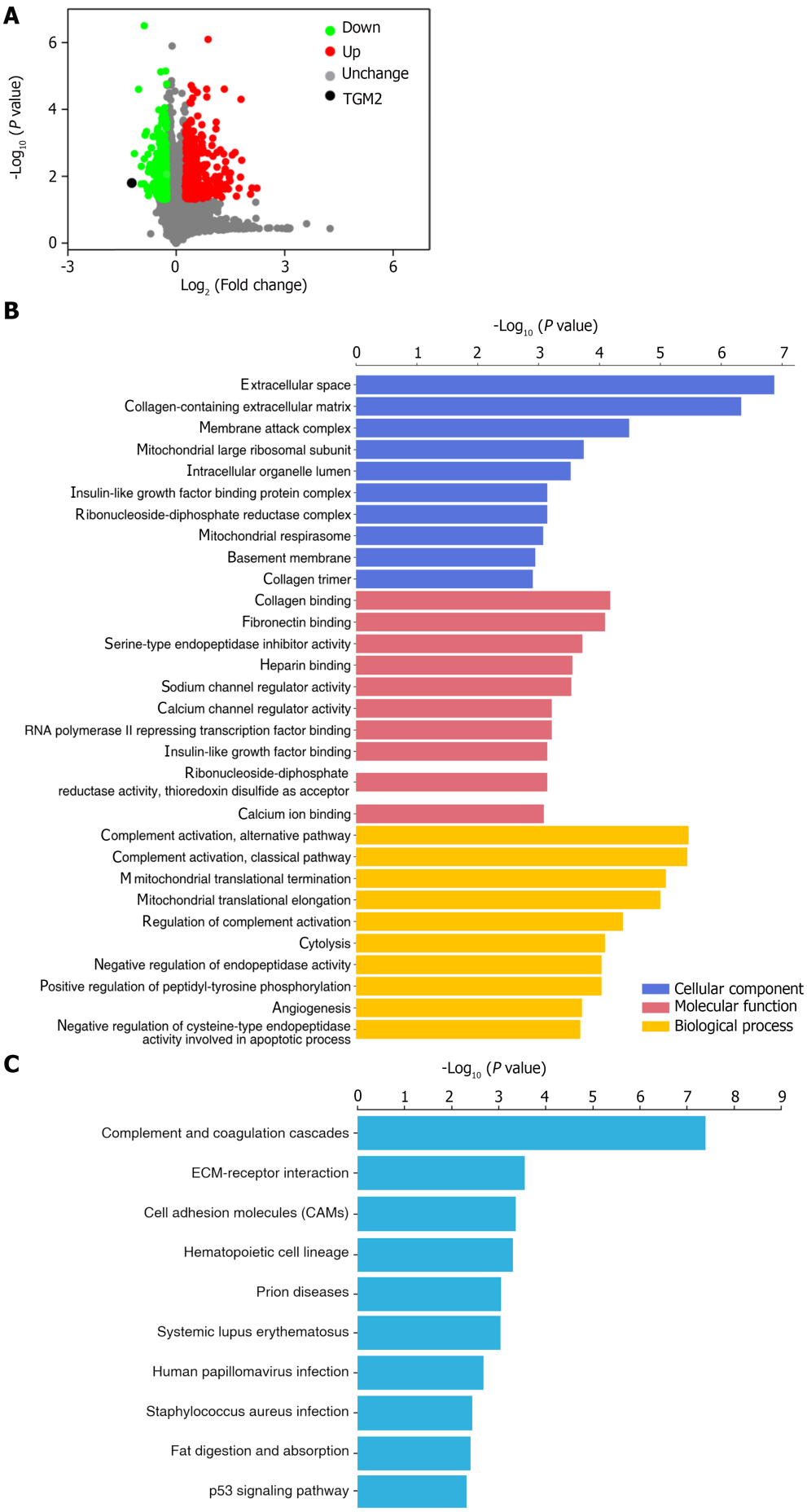
DOI: 10.3748/wjg.v29.i23.3622 **Copyright** ©The Author(s) 2023.

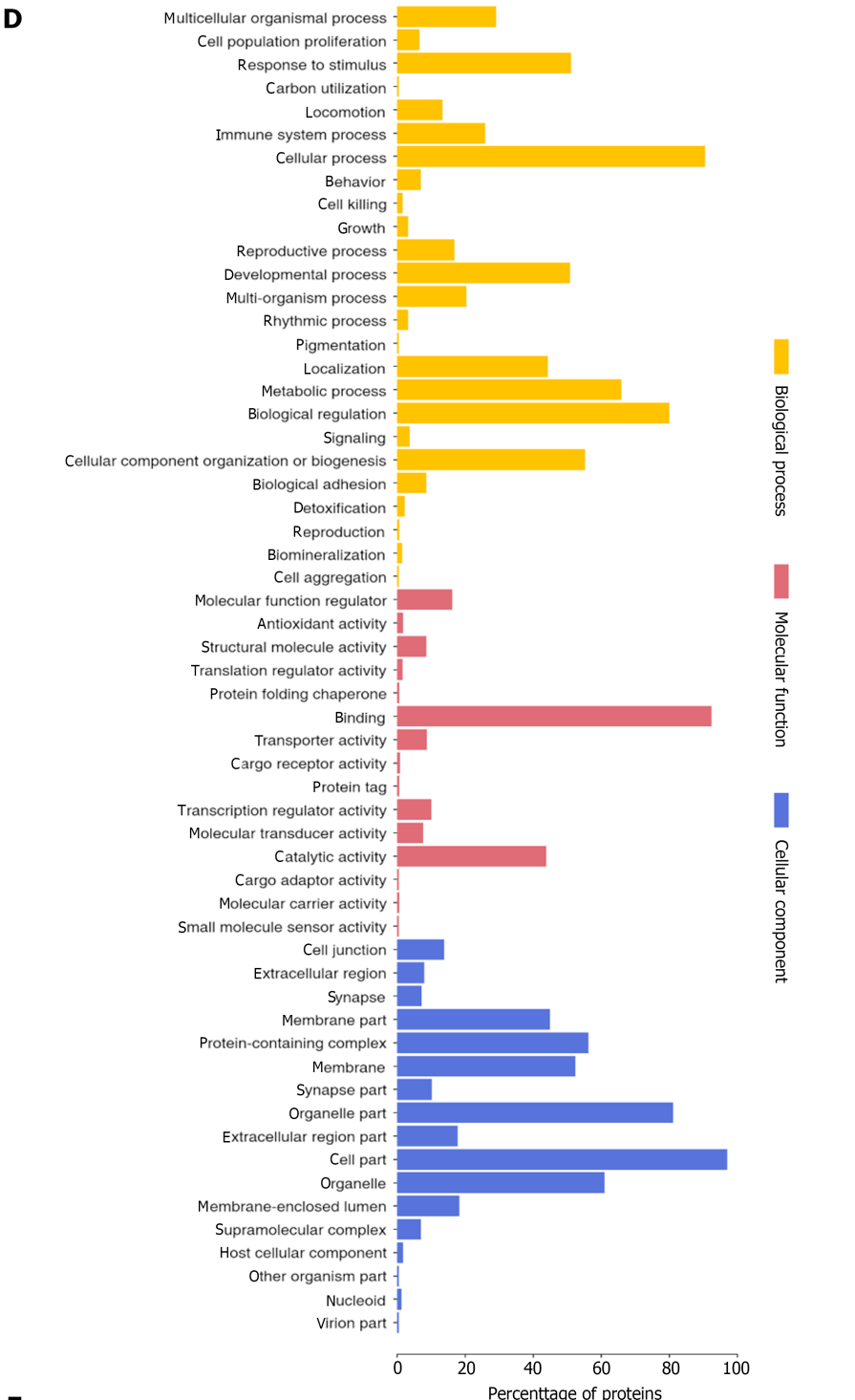
Figure 5 Effect of 18β-glycyrrhetinic acid on subcutaneous tumor growth in BALB/c nude mice. A: Comparison of back tumor in the cisplatin (DDP), 18β-glycyrrhetinic acid (18β-GRA) and control groups; B: Comparison of back tumor volume in the DDP, 18β-GRA and control groups; C: Effect of tumor volume growth in the DDP, 18β-GRA and control groups; D: Effect of body weight in the DDP, 18β-GRA and control groups; E: Effect of water-intake in the DDP, 18β-GRA and control groups; F: Effect of food-intake in the DDP, 18β-GRA and control groups. The data is represented as the mean ± SD. $^{a}P < 0.05$, $^{b}P < 0.01$, $^{c}P < 0.001$. 18β-GRA: 18β-glycyrrhetinic acid; DDP: Cisplatin.

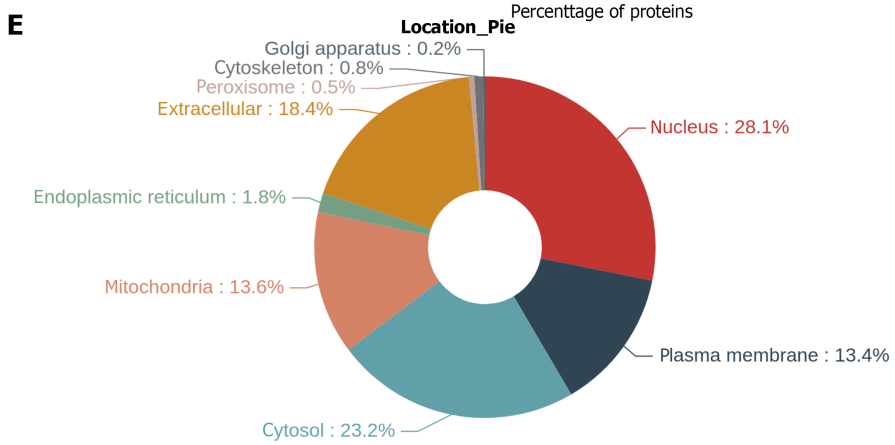
be involved in EMT processes in breast cancer[30], colorectal cancer[31], and hepatocellular carcinoma [32], which are highly correlated with invasion phenotypes. These findings imply that TGM2 is involved in cancer cell invasion. In contrast, 18β-GRA had no impact on AGS and HGC-27 cells invasion during our studies.

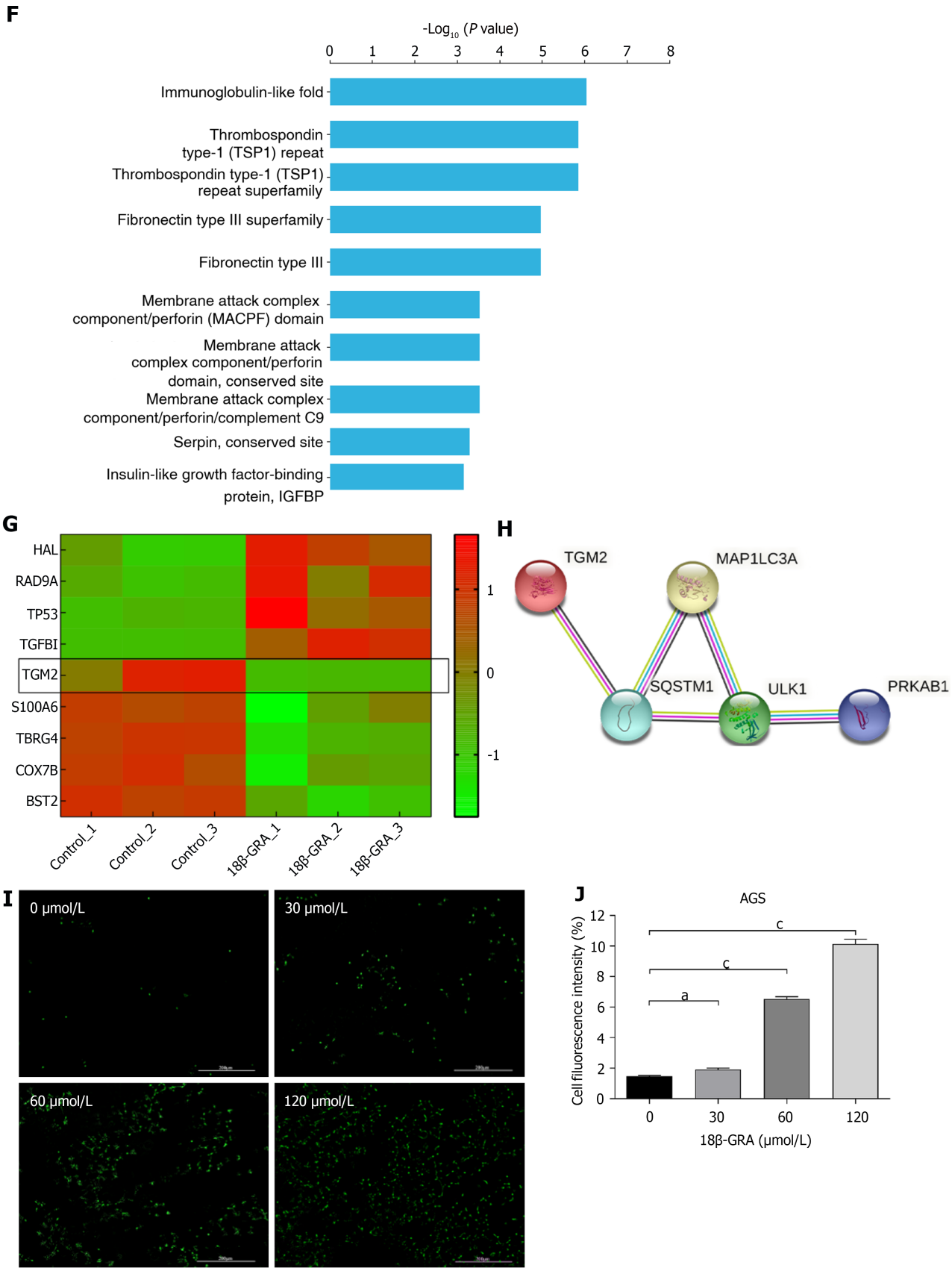
In vivo tumorigenesis experiment was performed on immunodeficient nude mice. The results showed that 18β-GRA and DDP significantly inhibited the subcutaneous tumor volume in nude mice. At the same time, we monitored the body weight, diet and water intake of nude mice during the experiment. It was found that the body weight of nude mice in the DDP group was lighter than that in 18β-GRA and control groups, showing obvious adverse reactions. On the contrary, the body weight of nude mice in 18 β-GRA group was slightly higher than that in the control group and the nude mice were in good health during the experiment. In terms of diet and water intake, nude mice administered with 18β-GRA and DDP had reduced diet and water intake. Overall, the experimental results demonstrated 18β-GRA had fewer side effects.

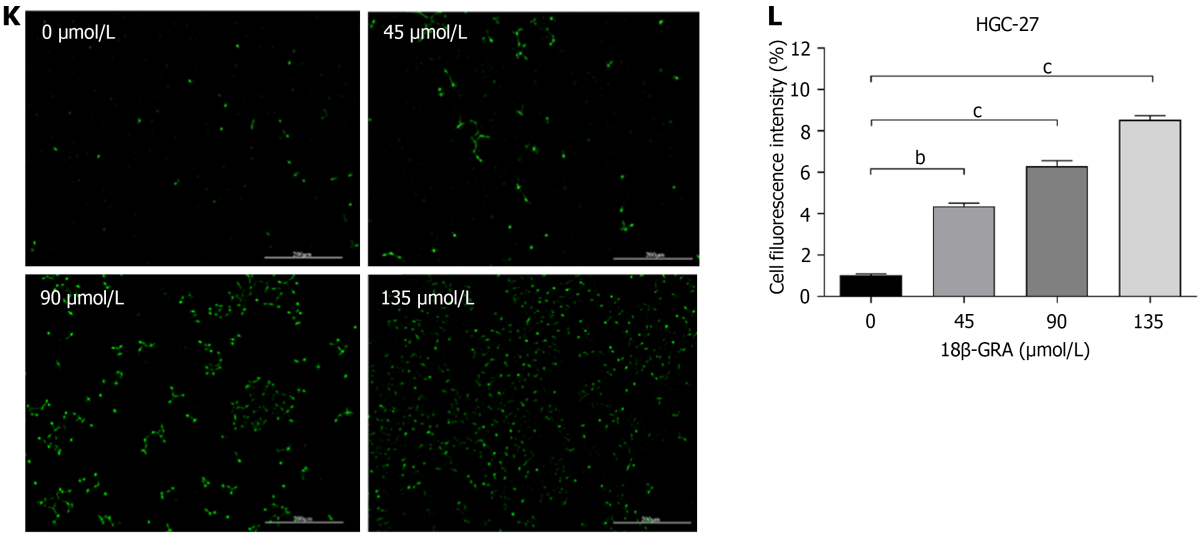
We further investigated the mechanism of GC treatment with 18β-GRA. MDC staining results showed that 18β-GRA can promote autophagy of AGS and HGC-27 cells. TMT proteomic analysis and miRNAs transcriptome analysis revealed that TGM2 was the target of miR-345-5p, which was verified by a dual-luciferase reporter assay. The STRING database was used to build the PPI network, and it was found that TGM2 was closely related to autophagy marker proteins ULK1, p62, LC3I/II and AMPK. TGM2 induces autophagy, differentiation and inhibition of angiogenesis, and its role in cancer is very complex. In fact, it has been proven that TGM2 participates in all aspects of cancer progression by activating mTOR[33]. At the beginning phase of autophagy, AMPK promotes autophagy occurrence by directly activating ULK1 or by negatively regulating mTOR to block its inhibition of ULK1[34,35]. After the formation of pre-autophage, it enters the second stage, which is the stage of autophagy extending into nucleus. ULK1 activates p62 and promotes the binding of p62 mediated substrate proteins to autophagic bodies[36]. At the same time, the substrate protein passes through the LC3 domain of p62


A
Down
Up
Unchange
TGM2
-Log10 (P value)
Log2 (Fold change)
B
-Log10 (P value)
Extracellular space
Collagen-containing extracellular matrix
Membrane attack complex
Mitochondrial large ribosomal subunit
Intracellular organelle lumen
Insulin-like growth factor binding protein complex
Ribonucleoside-diphosphate reductase complex
Mitochondrial respirasome
Basement membrane
Collagen trimer
Collagen binding
Fibronectin binding
Serine-type endopeptidase inhibitor activity
Heparin binding
Sodium channel regulator activity
Calcium channel regulator activity
RNA polymerase II repressing transcription factor binding
Insulin-like growth factor binding
Ribonucleoside-diphosphate reductase activity, thioredoxin disulfide as acceptor
Calcium ion binding
Complement activation, alternative pathway
Complement activation, classical pathway
M mitochondrial translational termination
Mitochondrial translational elongation
Regulation of complement activation
Cytolysis
Negative regulation of endopeptidase activity
Positive regulation of peptidyl-tyrosine phosphorylation
Angiogenesis
Negative regulation of cysteine-type endopeptidase activity involved in apoptotic process
Cellular component
Molecular function
Biological process
C
-Log10 (P value)
Complement and coagulation cascades
ECM-receptor interaction
Cell adhesion molecules (CAMs)
Hematopoietic cell lineage
Prion diseases
Systemic lupus erythematosus
Human papillomavirus infection
Staphylococcus aureus infection
Fat digestion and absorption
p53 signaling pathway


D
Multicellular organismal process
Cell population proliferation
Response to stimulus
Carbon utilization
Locomotion
Immune system process
Cellular process
Behavior
Cell killing
Growth
Reproductive process
Developmental process
Multi-organism process
Rhythmic process
Pigmentation
Localization
Metabolic process
Biological regulation
Signaling
Cellular component organization or biogenesis
Biological adhesion
Detoxification
Reproduction
Biomineralization
Cell aggregation
Molecular function regulator
Antioxidant activity
Structural molecule activity
Translation regulator activity
Protein folding chaperone
Binding
Transporter activity
Cargo receptor activity
Protein tag
Transcription regulator activity
Molecular transducer activity
Catalytic activity
Cargo adaptor activity
Molecular carrier activity
Small molecule sensor activity
Cell junction
Extracellular region
Synapse
Membrane part
Protein-containing complex
Membrane
Synapse part
Organelle part
Extracellular region part
Cell part
Organelle
Membrane-enclosed lumen
Supramolecular complex
Host cellular component
Other organism part
Nucleoid
Virion part
Biological process
Molecular function
Cellular component
0
20
40
60
80
100
Percenttage of proteins


E
Location_Pie
Golgi apparatus : 0.2%
Cytoskeleton : 0.8%
Peroxisome : 0.5%
Extracellular : 18.4%
Nucleus : 28.1%
Endoplasmic reticulum : 1.8%
Mitochondria : 13.6%
Plasma membrane : 13.4%
Cytosol : 23.2%


F
-Log10 (P value)
0 1 2 3 4 5 6 7 8
Immunoglobulin-like fold
Thrombospondin type-1 (TSP1) repeat
Thrombospondin type-1 (TSP1) repeat superfamily
Fibronectin type III superfamily
Fibronectin type III
Membrane attack complex component/perforin (MACPF) domain
Membrane attack complex component/perforin domain, conserved site
Membrane attack complex component/perforin/complement C9
Serpin, conserved site
Insulin-like growth factor-binding protein, IGFBP
G
HAL
RAD9A
TP53
TGFBI
TGM2
S100A6
TBRG4
COX7B
BST2
1
0
-1
Control_1
Control_2
Control_3
18β-GRA_1
18β-GRA_2
18β-GRA_3
H
TGM2
MAP1LC3A
SQSTM1
ULK1
PRKAB1
I
0 μmol/L
30 μmol/L
60 μmol/L
120 μmol/L
J
AGS
Cell filuorescence intensity (%)
0 2 4 6 8 10 12
a
c
c
0 30 60 120
18β-GRA (μmol/L)



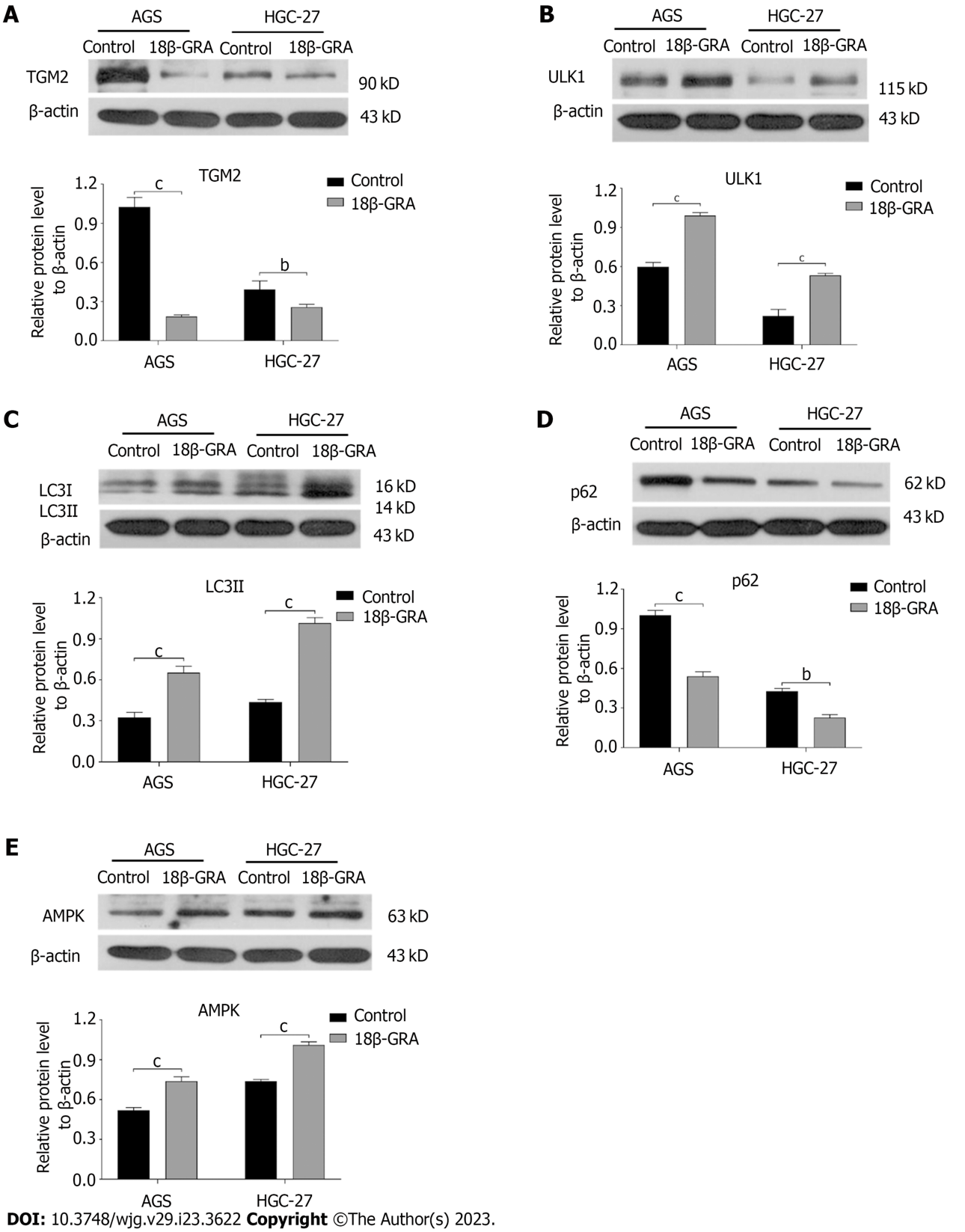
DOI: 10.3748/wjg.v29.i23.3622 **Copyright** ©The Author(s) 2023.

Figure 6 The results of TMT proteomic analysis and MDC staining assay. A: TMT proteomic analysis of differentially expressed proteins (DEPs) volcano map; B: Gene Ontology (GO) enrichment analysis of DEPs. The Y axis denotes the GO functional classification enriched of DEPs, and the X axis denotes the -Log10 of the *P* value of Fisher's exact test of the significance of the enrichment; C: Kyoto Encyclopedia of Genes and Genomes (KEGG) pathway enrichment analysis. The Y axis denotes the categories of KEGG pathways. The X axis is the -Log_{10} of the p value of Fisher's exact test of the significance of enrichment; D: GO annotation analysis of DEPs; E: Subcellular localization analysis; F: Protein domain enrichment analysis; G: Proteins cluster analysis; H: Protein-protein interaction network diagram of TGM2 and autophagy marker proteins; I: The MDC staining results of AGS cells treated with different concentrations of 18β-glycyrrhetinic acid (18β-GRA); J: Statistical results of the MDC staining in AGS cells; K: The MDC staining results of HGC-27 cells treated with different concentrations of 18β-GRA; L: Statistical results of the MDC staining in HGC-27 cells. All data are from three independent samples. The data is represented as the mean ± SD. $^{a}P < 0.05$, $^{b}P < 0.01$, $^{c}P < 0.001$. DEPs: Differentially expressed proteins; GO: Gene Ontology; KEGG: Kyoto Encyclopedia of Genes and Genomes; 18β-GRA: 18β-glycyrrhetinic acid.

into the degradation phase of the autophagic vesicle, where it interacts with LC3, which is the third stage of autophagy. Thus, when the p62 content decreases, it indicates that autophagic lysosomal degradation is inhibited[37,38]. Therefore, when the content of p62 decreases, it indicates that autophagic lysosome degradation is inhibited. LC3I/II, one of the homologues of ATG8, is located in the cytoplasm. LC3I is formed after exposure to glycine at the carboxyl terminal, which is catalyzed to combine with phosphatidyl ethanolamine to form LC3II. The increased amount of LC3II can reflect the increased number of autophagosomes caused by enhanced autophagy activity[39] (Figure 11). Western blot results proved that TGM2 and p62 were reduced, while AMPK, ULK1, and LC3II were increased in AGS and HGC-27 cells treated with 18β-GRA. Additionally, we employed a lentiviral vector to miR-345-5p overexpress in GC cells and observed the expression of TGM2. Our findings indicate that miR-345-5p overexpression significantly reduced the protein expression of TGM2. At the same time, we also found that miR-345-5p overexpression could inhibit GC cells proliferation by promoting cell apoptosis and arresting cell cycle. Based on the aforementioned findings, we draw the conclusion that 18β-GRA may play a role in the occurrence and progression of GC *via* the miR-345-5p/TGM2 signaling pathway.

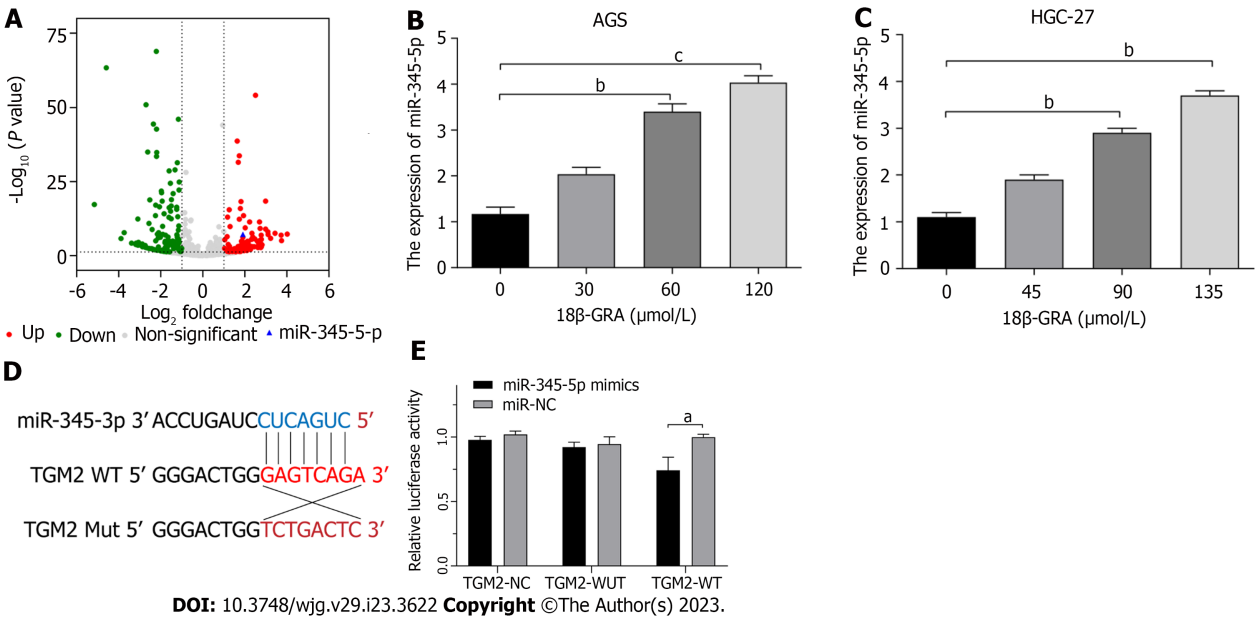
CONCLUSION

To sum up, this study proved that 18β-GRA can inhibit GC cells viability, induce cells apoptosis, block cell cycle, inhibit cell wound healing ability, and induce cell autophagy by regulating the miR-345-5p/TGM2 signaling pathway, thereby inhibiting the GC cells proliferation, which could provide theoretical basis for the research of 18β-GRA in GC treatment. However, our study has some limitations and more experiments are needed to support our future research. Hence, we will carry on exploring the relationship between 18β-GRA and GC in the future. First, GC cells were infected with RFP-GFP-LC3 double-labeled adenoviruses to research 18β-GRA's effect on the autophagic. Secondly, 18β-GRA's effect when combined with chemotherapeutic drugs on chemotherapeutic drug sensitivity will be investigated. Thirdly, the molecular mechanism of 18β-GRA treatment for GC was further studied by gene overexpression, CO-IP and other methods.



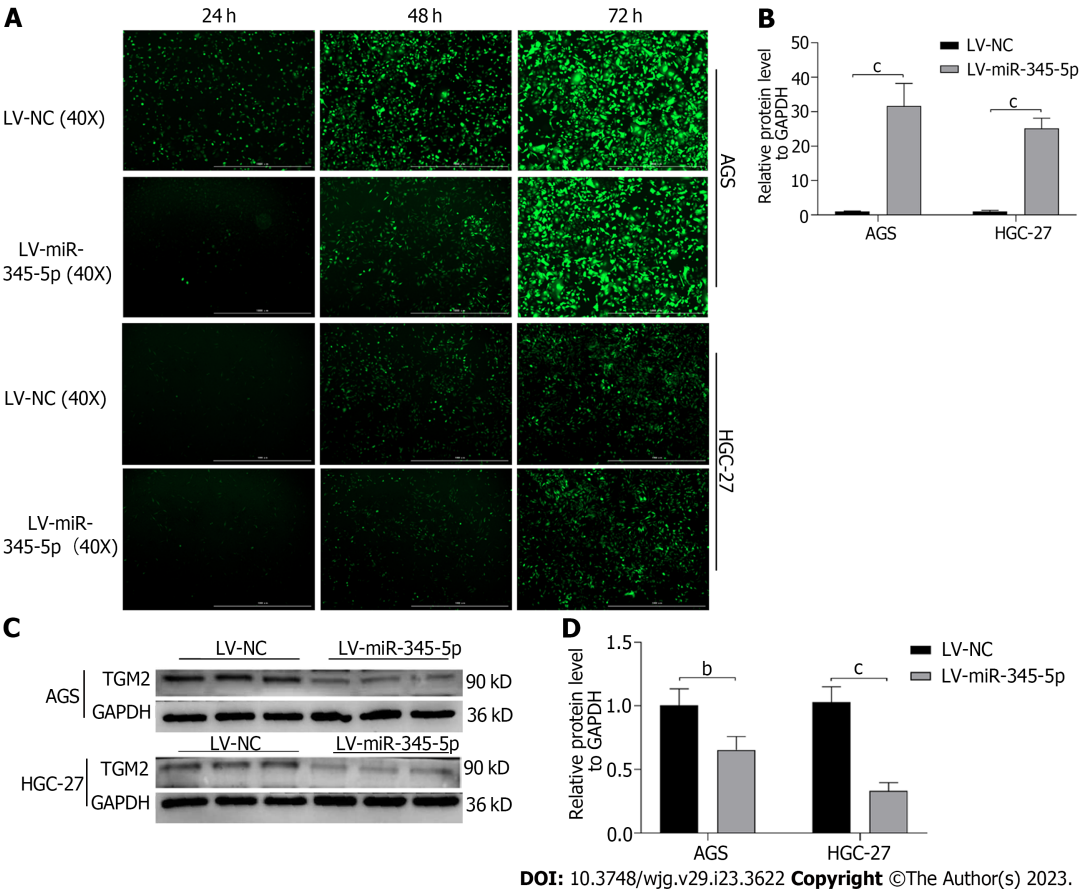
DOI: 10.3748/wjg.v29.i23.3622 **Copyright** ©The Author(s) 2023.

Figure 7 Effect of 18β-glycyrrhetinic acid on the protein expression levels of TGM2, p62, LC3II, ULK1 and AMPK in AGS and HGC-27 cells. All data are from three independent samples. The data is represented as the mean ± SD. $^{b}P < 0.01$ $^{c}P < 0.001$. 18β-GRA: 18β-glycyrrhetinic acid.



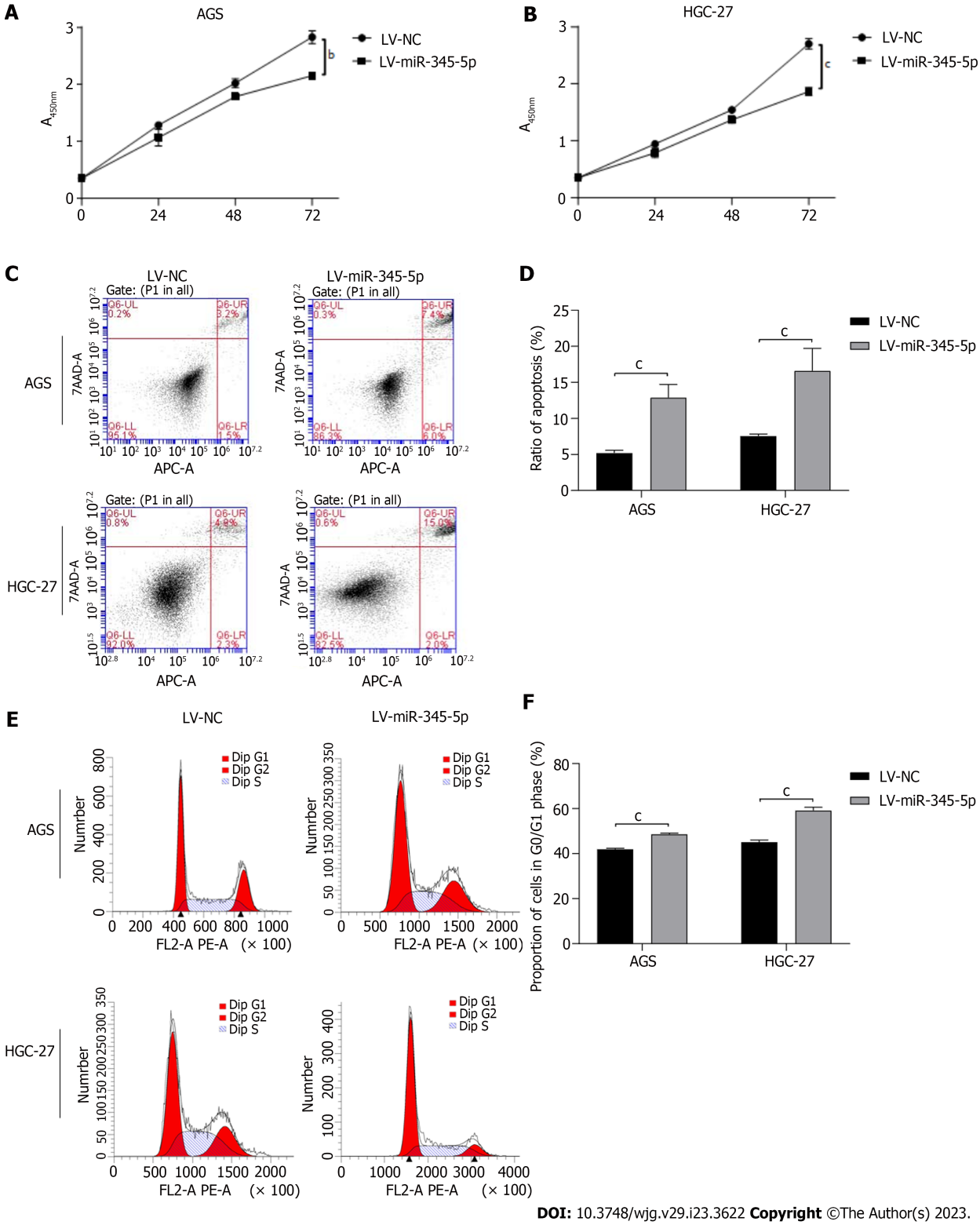
DOI: 10.3748/wjg.v29.i23.3622 **Copyright** ©The Author(s) 2023.

Figure 8 MicroRNAs transcriptomic analysis and dual-luciferase reporter assay. A: MicroRNAs (miRNAs) transcriptomics analysis of differentially expressed miRNAs; B: Effect of 18β-glycyrrhetinic acid (18β-GRA) with different concentrations of miR-345-5p expression level in AGS cells; C: Effect of 18β-GRA with different concentrations of miR-345-5p expression level in HGC-27 cells; D: Complementary binding sites of miR-345-5p and TGM2; E: Elevated expression of miR-345-5p suppressed the luciferase value of the TGM2-wild-type reporter but not that under the mutant reporter. All data are from three independent samples. The data is represented as the mean ± SD. $^{a}P < 0.05$, $^{b}P < 0.01$, $^{c}P < 0.001$. 18β-GRA: 18β-glycyrrhetinic acid; WUT: Mutant; WT: Wild type; NC: Empty lentiviral vector.



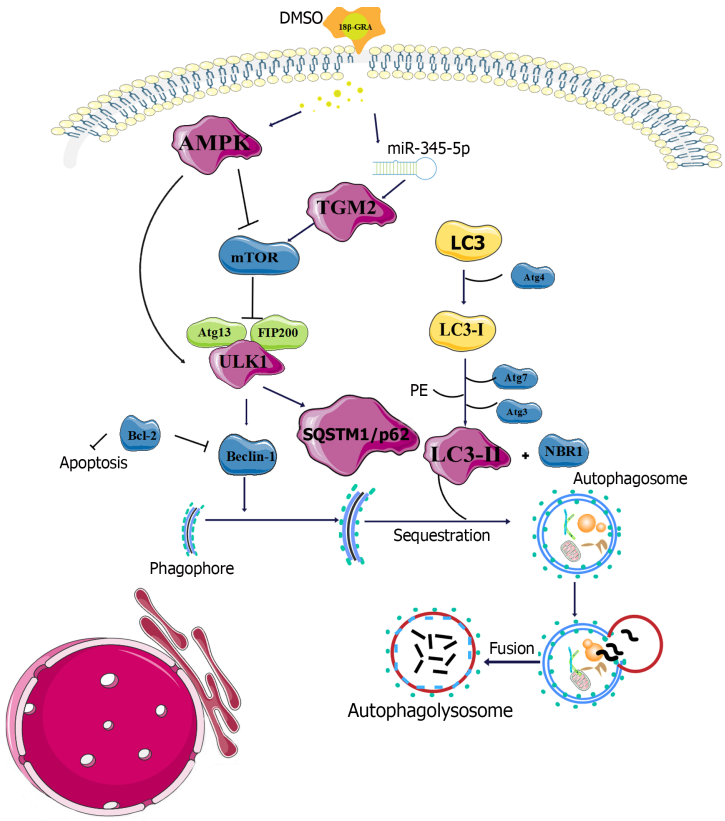
DOI: 10.3748/wjg.v29.i23.3622 **Copyright** ©The Author(s) 2023.

Figure 9 Overexpression of miR-345-5p can inhibit TGM2. A: Transfection efficiency of lentiviral vector; B: The expression level of miR-345-5p in lentivirus transfected AGS and HGC-27 cells; C: Effect of miR-345-5p overexpression on TGM2; D: Statistical results of the effect of miR-345-5p overexpression on TGM2. All data are from three independent samples. The data is represented as the mean ± SD. $^{b}P < 0.01$, $^{c}P < 0.001$. LV-NC: Empty lentiviral vector.



DOI: 10.3748/wjg.v29.i23.3622 **Copyright** ©The Author(s) 2023.

Figure 10 Effect of miR-345-5p overexpression on AGS and HGC-27 cells. A: Effect of miR-345-5p overexpression on AGS cells viability; B: Effect of miR-345-5p overexpression on HGC-27 cells viability; C: Effect of miR-345-5p overexpression on cell apoptosis in AGS and HGC-27 cells; D: Statistical results of cell apoptosis; E: Effect of miR-345-5p overexpression on cell cycle in AGS and HGC-27 cells; F: Statistical results of cell cycle. All data are from three independent samples. The data is represented as the mean ± SD. $^{a}P < 0.05$, $^{b}P < 0.01$, $^{c}P < 0.001$. LV-NC: Empty lentiviral vector.



DOI: 10.3748/wjg.v29.i23.3622 **Copyright** ©The Author(s) 2023.

Figure 11 Diagram of the mechanism of 18β-glycyrrhetinic acid therapy for gastric cancer cells. 18β-GRA: 18β-glycyrrhetinic acid; mTOR: Mammalian target of rapamycin; Bcl-2: B-cell lymphoma 2; NBR1: Neighbor of BRCA1 gene 1; PE: Phosphatidylethanolamine.

ARTICLE HIGHLIGHTS

Research background

Gastric cancer (GC) is a common gastrointestinal malignancy worldwide. Based on the cancer-related mortality, the current prevention and treatment strategies for GC still show poor clinical results. Therefore, it is important to find effective drug treatment targets.

Research motivation

At present, the treatment of GC is mainly surgery, chemotherapy and radiotherapy, and the first-line treatment drugs are harmful to side effects.

Research objectives

The purpose of this study was to explore the molecular mechanism of 18β-glycyrrhetinic acid (18β-GRA) regulating the miR-345-5p/TGM2 signaling pathway to inhibit the proliferation of GC cells.

Research methods

The effects of 18β-GRA on GC cell phenotype and tumor growth *in vivo* were studied. TMT proteomic analysis and microRNAs (miRNAs) transcriptome analysis were used to screen for targets, and targeted connections were validated using a dual-luciferase report assay. Finally, the prediction was confirmed by experiment *in vitro*.

Research results

Our experiment confirmed that 18β-GRA inhibited GC cells growth both *in vitro* and *in vivo*, and MDC staining showed that 18β-GRA promoted GC cell autophagy. By TMT proteomic analysis and miRNAs transcriptomic analysis, we found that 18β-GRA down-regulates TGM2 expression and up-regulates miR-345-5p expression in GC cells. Subsequently, TGM2 was verified as the target of miR-345-5p by a dual-luciferase report assay. In 18β-GRA treated GC cells, the expressions of autophagy-related proteins TGM2 and p62 were significantly decreased, while the expressions of LC3II, ULK1 and AMPK were significantly increased. In addition, overexpression of miR-345-5p not only inhibited TGM2 expression, but also inhibited GC cell proliferation by promoting apoptosis and blocking cell cycle.

Research conclusions

These observations indicate that 18β-GRA can promote autophagy and inhibit GC cells proliferation *via* regulating the miR-345-5p/TGM2 signaling pathway.

Research perspectives

MiR-345-5p can be used for targeted therapy of GC, and can also be used as a new biomarker for GC.

ACKNOWLEDGEMENTS

The authors would like to acknowledge Li-Qun Wang for statistical analysis assistance. Thanks to Joanna Tibenda for revising the article.

FOOTNOTES

Author contributions: Li X carried out most of the studies, and analyzed the data; Li X, Ma XL, and Du YH wrote the manuscript; Ma XL and Du YH carried out the chart-making work; Yang Y, Lu DD, and Zhang JF were responsible for network pharmacology analysis; Chen Y and Niu Y designed the study and revised the manuscript; Yuan L provided the conceptual and technical guidance as well as revised the manuscript critically for important intellectual content; and all authors have read and approved the manuscript.

Supported by the Ningxia Natural Science Foundation, No. 2022AAC03144.

Institutional review board statement: The study was reviewed and approved by the Institutional Review Board of Ningxia Medical University (No.2021-N0063).

Institutional animal care and use committee statement: The animal protocol was approved by the Institutional Animal Care and Use Committee of Ningxia Medical University (IACUC-NYLAC-2022-108).

Conflict-of-interest statement: All the authors report no relevant conflicts of interest for this article.

Data sharing statement: All data generated or analyzed during this study are included in this paper, and further inquiries can be directed to the corresponding author (20080017@nxmu.edu.cn).

ARRIVE guidelines statement: The authors have read the ARRIVE guidelines, and the manuscript was prepared and revised according to the ARRIVE guidelines.

Open-Access: This article is an open-access article that was selected by an in-house editor and fully peer-reviewed by external reviewers. It is distributed in accordance with the Creative Commons Attribution NonCommercial (CC BY-NC 4.0) license, which permits others to distribute, remix, adapt, build upon this work non-commercially, and license their derivative works on different terms, provided the original work is properly cited and the use is non-commercial. See: https://creativecommons.org/Licenses/by-nc/4.0/

Country/Territory of origin: China

ORCID number: Xia Li 0000-0002-4981-9768; Yi Nan 0000-0002-5511-9266; Yu-Hua Du 0000-0002-9669-8065; Yi Yang 0000-0002-8466-5717; Yan Chen 0000-0002-8673-398X; Ling Yuan 0000-0003-2838-0976.

S-Editor: Wang JJ
L-Editor: A
P-Editor: Cai YX

REFERENCES

1 **Sung H**, Ferlay J, Siegel RL, Laversanne M, Soerjomataram I, Jemal A, Bray F. Global Cancer Statistics 2020: GLOBOCAN Estimates of Incidence and Mortality Worldwide for 36 Cancers in 185 Countries. *CA Cancer J Clin* 2021; **71**: 209-249 [PMID: 33538338 DOI: 10.3322/caac.21660]

2 **Abbas M**, Habib M, Naveed M, Karthik K, Dhama K, Shi M, Dingding C. The relevance of gastric cancer biomarkers in prognosis and pre- and post- chemotherapy in clinical practice. *Biomed Pharmacother* 2017; **95**: 1082-1090 [PMID: 28922727 DOI: 10.1016/j.biopha.2017.09.032]

3 **Duan R**, Li X, Zeng D, Chen X, Shen B, Zhu D, Zhu L, Yu Y, Wang D. Tumor Microenvironment Status Predicts the Efficacy of Postoperative Chemotherapy or Radiochemotherapy in Resected Gastric Cancer. *Front Immunol* 2020; **11**: 609337 [PMID: 33569057 DOI: 10.3389/fimmu.2020.609337]

4 **Yang T**, Zhou J, Fang L, Wang M, Dilinuer M, Ainiwaer A. Protection function of 18β-glycyrrhetinic acid on rats with high-altitude pulmonary hypertension based on (1)H NMR metabonomics technology. *Anal Biochem* 2021; **631**: 114342 [PMID: 34419454 DOI: 10.1016/j.ab.2021.114342]

5 **Yang Y**, Zhu Q, Zhong Y, Cui X, Jiang Z, Wu P, Zheng X, Zhang K, Zhao S. Synthesis, anti-microbial and anti-inflammatory activities of 18β-glycyrrhetinic acid derivatives. *Bioorg Chem* 2020; **101**: 103985 [PMID: 32544739 DOI: 10.1016/j.bioorg.2020.103985]

6 **Wang LJ**, Geng CA, Ma YB, Huang XY, Luo J, Chen H, Zhang XM, Chen JJ. Synthesis, biological evaluation and structure-activity relationships of glycyrrhetinic acid derivatives as novel anti-hepatitis B virus agents. *Bioorg Med Chem Lett* 2012; **22**: 3473-3479 [PMID: 22520261 DOI: 10.1016/j.bmcl.2012.03.081]

7 **Stecanella LA**, Bitencourt APR, Vaz GR, Quarta E, Silva Júnior JOC, Rossi A. Glycyrrhizic Acid and Its Hydrolyzed Metabolite 18β-Glycyrrhetinic Acid as Specific Ligands for Targeting Nanosystems in the Treatment of Liver Cancer. *Pharmaceutics* 2021; **13** [PMID: 34834206 DOI: 10.3390/pharmaceutics13111792]

8 **Wang Z**, Ma J, He Y, Miu KK, Yao S, Tang C, Ye Y, Lin G. Nrf2-mediated liver protection by 18β-glycyrrhetinic acid against pyrrolizidine alkaloid-induced toxicity through PI3K/Akt/GSK3β pathway. *Phytomedicine* 2022; **102**: 154162 [PMID: 35598524 DOI: 10.1016/j.phymed.2022.154162]

9 **Liu J**, Xu Y, Yan M, Yu Y, Guo Y. 18β-Glycyrrhetinic acid suppresses allergic airway inflammation through NF-κB and Nrf2/HO-1 signaling pathways in asthma mice. *Sci Rep* 2022; **12**: 3121 [PMID: 35210449 DOI: 10.1038/s41598-022-06455-6]

10 **Yadav DK**, Kalani K, Singh AK, Khan F, Srivastava SK, Pant AB. Design, synthesis and *in vitro* evaluation of 18β-glycyrrhetinic acid derivatives for anticancer activity against human breast cancer cell line MCF-7. *Curr Med Chem* 2014; **21**: 1160-1170 [PMID: 24180274 DOI: 10.2174/09298673113206660330]

11 **Li X**, Liu Y, Wang N, Wang S, Wang H, Li A, Ren S. Synthesis and discovery of 18β-glycyrrhetinic acid derivatives inhibiting cancer stem cell properties in ovarian cancer cells. *RSC Adv* 2019; **9**: 27294-27304 [PMID: 35529208 DOI: 10.1039/c9ra04961d]

12 **Sun Y**, Jiang M, Park PH, Song K. Transcriptional suppression of androgen receptor by 18β-glycyrrhetinic acid in LNCaP human prostate cancer cells. *Arch Pharm Res* 2020; **43**: 433-448 [PMID: 32219716 DOI: 10.1007/s12272-020-01228-z]

13 **Cao D**, Wu Y, Jia Z, Zhao D, Zhang Y, Zhou T, Wu M, Zhang H, Tsukamoto T, Oshima M, Jiang J, Cao X. 18β-glycyrrhetinic acid inhibited mitochondrial energy metabolism and gastric carcinogenesis through methylation-regulated TLR2 signaling pathway. *Carcinogenesis* 2019; **40**: 234-245 [PMID: 30364936 DOI: 10.1093/carcin/bgy150]

14 **Cai H**, Chen X, Zhang J, Wang J. 18β-glycyrrhetinic acid inhibits migration and invasion of human gastric cancer cells *via* the ROS/PKC-α/ERK pathway. *J Nat Med* 2018; **72**: 252-259 [PMID: 29098529 DOI: 10.1007/s11418-017-1145-y]

15 **Yuan L**, Yang Y, Li X, Zhou X, Du YH, Liu WJ, Zhang L, Yu L, Ma TT, Li JX, Chen Y, Nan Y. 18β-glycyrrhetinic acid regulates mitochondrial ribosomal protein L35-associated apoptosis signaling pathways to inhibit proliferation of gastric carcinoma cells. *World J Gastroenterol* 2022; **28**: 2437-2456 [PMID: 35979263 DOI: 10.3748/wjg.v28.i22.2437]

16 **Peng Y**, Croce CM. The role of MicroRNAs in human cancer. *Signal Transduct Target Ther* 2016; **1**: 15004 [PMID: 29263891 DOI: 10.1038/sigtrans.2015.4]

17 **Coradduzza D**, Cruciani S, Arru C, Garroni G, Pashchenko A, Jedea M, Zappavigna S, Caraglia M, Amler E, Carru C, Maioli M. Role of miRNA-145, 148, and 185 and Stem Cells in Prostate Cancer. *Int J Mol Sci* 2022; **23** [PMID: 35163550 DOI: 10.3390/ijms23031626]

18 **Vo JN**, Cieslik M, Zhang Y, Shukla S, Xiao L, Wu YM, Dhanasekaran SM, Engelke CG, Cao X, Robinson DR, Nesvizhskii AI, Chinnaiyan AM. The Landscape of Circular RNA in Cancer. *Cell* 2019; **176**: 869-881.e13 [PMID: 30735636 DOI: 10.1016/j.cell.2018.12.021]

19 **Di Leva G**, Croce CM. miRNA profiling of cancer. *Curr Opin Genet Dev* 2013; **23**: 3-11 [PMID: 23465882 DOI: 10.1016/j.gde.2013.01.004]

20 **Komatsu S**, Imamura T, Kiuchi J, Takashima Y, Kamiya H, Ohashi T, Konishi H, Shiozaki A, Kubota T, Okamoto K, Otsuji E. Depletion of tumor suppressor miRNA-148a in plasma relates to tumor progression and poor outcomes in gastric cancer. *Am J Cancer Res* 2021; **11**: 6133-6146 [PMID: 35018247]

21 **Li X**, Zhu M, Zhao G, Zhou A, Min L, Liu S, Zhang N, Zhu S, Guo Q, Zhang S, Li P. MiR-1298-5p level downregulation induced by Helicobacter pylori infection inhibits autophagy and promotes gastric cancer development by targeting MAP2K6. *Cell Signal* 2022; **93**: 110286 [PMID: 35192930 DOI: 10.1016/j.cellsig.2022.110286]

22 **Itakura E**, Mizushima N. Characterization of autophagosome formation site by a hierarchical analysis of mammalian Atg proteins. *Autophagy* 2010; **6**: 764-776 [PMID: 20639694 DOI: 10.4161/auto.6.6.12709]

23 **Wen X**, Klionsky DJ. At a glance: A history of autophagy and cancer. *Semin Cancer Biol* 2020; **66**: 3-11 [PMID: 31707087 DOI: 10.1016/j.semcancer.2019.11.005]

24 **Wei Y**, Hong D, Zang A, Wang Z, Yang H, Zhang P, Wang Y. miR-183 Enhances Autophagy of GC Cells by Targeted Inhibition of mTOR. *Ann Clin Lab Sci* 2021; **51**: 837-843 [PMID: 34921037]

25 **Lin D**, Zhong W, Li J, Zhang B, Song G, Hu T. Involvement of BID translocation in glycyrrhetinic acid and 11-deoxy glycyrrhetinic acid-induced attenuation of gastric cancer growth. *Nutr Cancer* 2014; **66**: 463-473 [PMID: 24547973 DOI: 10.1080/01635581.2013.877498]

26 **Zhu Y**, Zhou B, Hu X, Ying S, Zhou Q, Xu W, Feng L, Hou T, Wang X, Zhu L, Jin H. LncRNA LINC00942 promotes chemoresistance in gastric cancer by suppressing MSI2 degradation to enhance c-Myc mRNA stability. *Clin Transl Med* 2022; **12**: e703 [PMID: 35073459 DOI: 10.1002/ctm2.703]

27 **Zhang J**, Wang C, Yan S, Yang Y, Zhang X, Guo W. miR-345 inhibits migration and stem-like cell phenotype in gastric cancer *via* inactivation of Rac1 by targeting EPS8. *Acta Biochim Biophys Sin (Shanghai)* 2020; **52**: 259-267 [PMID: 32147678 DOI: 10.1093/abbs/gmz166]

28 **Xiang SS**, Wang XA, Li HF, Shu YJ, Bao RF, Zhang F, Cao Y, Ye YY, Weng H, Wu WG, Mu JS, Wu XS, Li ML, Hu YP, Jiang L, Tan ZJ, Lu W, Liu F, Liu YB. Schisandrin B induces apoptosis and cell cycle arrest of gallbladder cancer cells. *Molecules* 2014; **19**: 13235-13250 [PMID: 25165862 DOI: 10.3390/molecules190913235]

29 **Wang X**, Yu Z, Zhou Q, Wu X, Chen X, Li J, Zhu Z, Liu B, Su L. Tissue transglutaminase-2 promotes gastric cancer

progression *via* the ERK1/2 pathway. *Oncotarget* 2016; **7**: 7066-7079 [PMID: 26771235 DOI: 10.18632/oncotarget.6883]

30 **He W**, Sun Z, Liu Z. Silencing of TGM2 reverses epithelial to mesenchymal transition and modulates the chemosensitivity of breast cancer to docetaxel. *Exp Ther Med* 2015; **10**: 1413-1418 [PMID: 26622499 DOI: 10.3892/etm.2015.2679]

31 **Shan H**, Zhou X, Chen C. MicroRNA214 suppresses the viability, migration and invasion of human colorectal carcinoma cells *via* targeting transglutaminase 2. *Mol Med Rep* 2019; **20**: 1459-1467 [PMID: 31173203 DOI: 10.3892/mmr.2019.10325]

32 **Ma H**, Xie L, Zhang L, Yin X, Jiang H, Xie X, Chen R, Lu H, Ren Z. Activated hepatic stellate cells promote epithelial-to-mesenchymal transition in hepatocellular carcinoma through transglutaminase 2-induced pseudohypoxia. *Commun Biol* 2018; **1**: 168 [PMID: 30393774 DOI: 10.1038/s42003-018-0177-5]

33 **Wang F**, Wang L, Qu C, Chen L, Geng Y, Cheng C, Yu S, Wang D, Yang L, Meng Z, Chen Z. Kaempferol induces ROS-dependent apoptosis in pancreatic cancer cells *via* TGM2-mediated Akt/mTOR signaling. *BMC Cancer* 2021; **21**: 396 [PMID: 33845796 DOI: 10.1186/s12885-021-08158-z]

34 **Mack HI**, Zheng B, Asara JM, Thomas SM. AMPK-dependent phosphorylation of ULK1 regulates ATG9 localization. *Autophagy* 2012; **8**: 1197-1214 [PMID: 22932492 DOI: 10.4161/auto.20586]

35 **Zibrova D**, Vandermoere F, Göransson O, Peggie M, Mariño KV, Knierim A, Spengler K, Weigert C, Viollet B, Morrice NA, Sakamoto K, Heller R. GFAT1 phosphorylation by AMPK promotes VEGF-induced angiogenesis. *Biochem J* 2017; **474**: 983-1001 [PMID: 28008135 DOI: 10.1042/BCJ20160980]

36 **Lim J**, Lachenmayer ML, Wu S, Liu W, Kundu M, Wang R, Komatsu M, Oh YJ, Zhao Y, Yue Z. Proteotoxic stress induces phosphorylation of p62/SQSTM1 by ULK1 to regulate selective autophagic clearance of protein aggregates. *PLoS Genet* 2015; **11**: e1004987 [PMID: 25723488 DOI: 10.1371/journal.pgen.1004987]

37 **Bjørkøy G**, Lamark T, Pankiv S, Øvervatn A, Brech A, Johansen T. Monitoring autophagic degradation of p62/SQSTM1. *Methods Enzymol* 2009; **452**: 181-197 [PMID: 19200883 DOI: 10.1016/S0076-6879(08)03612-4]

38 **Zhang H**, Zhang Y, Zhu X, Chen C, Zhang C, Xia Y, Zhao Y, Andrisani O, Kong L. DEAD Box Protein 5 Inhibits Liver Tumorigenesis by Stimulating Autophagy *via* Interaction with p62/SQSTM1. *Hepatology* 2019; **69**: 1046-1063 [PMID: 30281815 DOI: 10.1002/hep.30300]

39 **Yoshii SR**, Mizushima N. Monitoring and Measuring Autophagy. *Int J Mol Sci* 2017; **18** [PMID: 28846632 DOI: 10.3390/ijms18091865]

World Journal of Gastroenterology

Submit a Manuscript: https://www.f6publishing.com

World J Gastroenterol 2023 June 21; 29(23): 3645-3657

DOI: 10.3748/wjg.v29.i23.3645

ISSN 1007-9327 (print) ISSN 2219-2840 (online)

ORIGINAL ARTICLE

Retrospective Study

High expression of the circadian clock gene NPAS2 is associated with progression and poor prognosis of gastric cancer: A single-center study

Xiao-Meng Cao, Wen-Di Kang, Tian-Hong Xia, Shao-Bin Yuan, Chang-An Guo, Wen-Jie Wang, Hong-Bin Liu

Specialty type: Gastroenterology and hepatology

Provenance and peer review: Unsolicited article; Externally peer reviewed.

Peer-review model: Single blind

Peer-review report's scientific quality classification

Grade A (Excellent): 0
Grade B (Very good): 0
Grade C (Good): C, C, C, C
Grade D (Fair): D
Grade E (Poor): 0

P-Reviewer: Benna C, Italy; Papadia C, United Kingdom; Qin SS, China

Received: February 9, 2023
Peer-review started: February 9, 2023
First decision: March 9, 2023
Revised: March 16, 2023
Accepted: May 4, 2023
Article in press: May 4, 2023
Published online: June 21, 2023

Xiao-Meng Cao, Department of General Surgery, Gansu Provincial Hospital of TCM, Lanzhou 730050, Gansu Province, China

Xiao-Meng Cao, Shao-Bin Yuan, The First Clinical Medical College, Gansu University of Chinese Medicine, Lanzhou 730030, Gansu Province, China

Wen-Di Kang, Department of Interventional Therapy, National Cancer Center/National Clinical Research Center for Cancer/Cancer Hospital, Chinese Academy of Medical Sciences and Peking Union Medical College, Beijing 100021, China

Tian-Hong Xia, Clinical Medicine College, Ningxia Medical University, Clinical Medicine college, Ningxia Medical University, Yinchuan 750004, Ningxia Hui Autonomous Region, China

Chang-An Guo, Department of Emergency, Lanzhou University Second Hospital, Lanzhou 730030, Gansu Province, China

Wen-Jie Wang, Department of General Surgery, Lanzhou University Second Hospital, Lanzhou 730030, Gansu Province, China

Hong-Bin Liu, Department of General Surgery, The 940th Hospital of Joint Logistics Support Force of Chinese People's Liberation Army, Lanzhou 730050, Gansu Province, China. 1554153823@qq.com

Corresponding author: Hong-Bin Liu, MD, Professor, Department of General Surgery, The 940th Hospital of Joint Logistics Support Force of Chinese People's Liberation Army, No. 333 Nanbinhe Road, Qilihe District, Lanzhou 730050, Gansu Province, China. 1554153823@qq.com

Abstract

BACKGROUND

The prognostic assessment of patients after surgical resection of gastric cancer (GC) patients is critical. However, the role of the circadian clock gene NPAS2 expression in GC remains unknown.

AIM

To explore the relationship between NPAS2 and the survival prognosis of GC

patients and clarify its role in evaluating GC prognosis.

METHODS

The tumor tissues and clinical data of 101 patients with GC were collected retrospectively. Immunohistochemical staining (IHC) was used to detect the expression of NPAS2 protein in GC and adjacent tissues. Univariate and multivariate Cox regression analysis was used to determine the independent prognostic factors of GC, and a nomogram prediction model was established. The receiver operating characteristic (ROC) curve, the ROC area under the curve, the calibration curve, and C-index were used to evaluate the predictive effectiveness of the model. Kaplan Meier analysis was used to compare the risk stratification of subgroups according to the median score in the nomogram model of each patient.

RESULTS

Microarray IHC analysis showed that the positive rate of NPAS2 protein expression in GC tissues was 65.35%, which was significantly higher than 30.69% in adjacent tissues. The high expression of NPAS2 was correlated with tumor-node-metastasis (TNM) stage ($P < 0.05$), pN stage ($P < 0.05$), metastasis ($P < 0.05$), venous invasion ($P < 0.05$), lymphatic invasion ($P < 0.05$), and lymph node positive ($P < 0.05$) of GC. Kaplan Meier survival analysis showed that the 3-year overall survival (OS) of patients with high NPAS2 expression was significantly shortened ($P < 0.0001$). Univariate and multivariate COX regression analysis showed that TNM stage ($P = 0.009$), metastasis ($P = 0.009$), and NPAS2 expression ($P = 0.020$) were independent prognostic factors of OS in GC patients for 3 years. The nomogram prediction model based on independent prognostic factors has a C-Index of 0.740 (95%CI: 0.713-0.767). Furthermore, subgroup analysis showed that the 3-year OS time of the high-risk group was significantly lower than that of the low-risk group ($P < 0.0001$).

CONCLUSION

NPAS2 is highly expressed in GC tissues and is closely related to worse OS in patients. Therefore, the evaluation of NPAS2 expression may be a potential marker for GC prognosis evaluation. Notably, the nomogram model based on NPAS2 can improve the accuracy of GC prognosis prediction and assist clinicians in postoperative patient management and decision-making.

Key Words: NPAS2; Gastric cancer; Tissue microarray; Survival analysis; Prediction model; Nomogram

©The Author(s) 2023. Published by Baishideng Publishing Group Inc. All rights reserved.

Core Tip: The prognostic assessment of patients after surgical resection of gastric cancer (GC) is critical. However, the role of NPAS2 expression in GC remains unknown. Our study identified for the first time that high NPAS2 protein expression was associated with poor overall survival prognosis in GC patients and was an independent risk factor for patients after radical resection of GC. We constructed a nomogram prediction model by combining NPAS2 and other clinically independent risk factors, thus improving the predictive accuracy of GC prognosis.

Citation: Cao XM, Kang WD, Xia TH, Yuan SB, Guo CA, Wang WJ, Liu HB. High expression of the circadian clock gene NPAS2 is associated with progression and poor prognosis of gastric cancer: A single-center study. *World J Gastroenterol* 2023; 29(23): 3645-3657

URL: https://www.wjgnet.com/1007-9327/full/v29/i23/3645.htm

DOI: https://dx.doi.org/10.3748/wjg.v29.i23.3645

INTRODUCTION

Gastric cancer (GC) ranks fifth and fourth in the incidence and mortality of global cancer, respectively, and is more likely to occur in men[1,2]. The etiology of GC remains unclear, involving multiple cell types and complex molecular mechanisms[3]. Despite recent improvements in the diagnosis and treatment of GC, the overall treatment outcome remains poor[4]. Notably, radical gastrectomy is the primary treatment method for GC. However, postoperative recurrence rates and mortality remain high, and their mortality rates are closely associated with peritoneal, hematologic, and lymph node metastases in GC[5]. Therefore, there is an urgent need to identify new markers to predict the malignant biological behavior and prognosis of GC to guide the treatment strategy and improve the clinical outcome of GC.

Biological rhythm is a regulatory system in almost all living things. It produces 24-h periodic rhythm changes in many essential behaviors and physiological processes[6], including the sleep-wake cycle, body temperature cycle, hormone secretion, heart rate, blood pressure, excretion, *etc.*[7,8]. The destruction of normal biological rhythm adversely affects mammalian physiology[9]. The role and mechanism of biological rhythm-related genes in tumors, and the design of tumor treatment methods targeting biological rhythm genes, are one of the hot spots in the current cancer research field[10]. NPAS2, also known as MOP4, is the largest core circadian gene found so far, with a length of about 176.68Kb, located on human chromosome 2 (2q11.2), encoding proteins belonging to the basic helix loop helix PAS domain of transcription factors[11]. NPAS2 is mainly present in the forebrain of mammals and is also expressed in some peripheral organs such as the liver and skin[12]. Additionally, it is an important part of the positive circadian rhythm feedback circuit[8]. Furthermore, Studies have confirmed that NPAS2 is associated with various rhythm-related diseases, such as cancer, diabetes, depression, sleep disorders, obesity, *etc.*[13].

Recent studies have shown that low expression of NPAS2 accelerates cell growth and tumor cell cycle progression and plays a unique and critical role in cancer progression[14]. The low expression of NPAS2 promotes the proliferation and invasion of colorectal cancer cells. Additionally, it increases the wound-healing ability of colorectal cancer cells, indicating that NPAS2 has a key tumor inhibitory effect. Additionally, its high expression is positively correlated with overall survival (OS)[15]. However, some studies have found that NPAS2, as an oncogene, promotes the proliferation of hepatocellular carcinoma (HCC) cells and participates in the critical process of hepatocellular carcinogenesis. Its high expression is related to the invasive clinical characteristics and low OS of HCC patients[16]. It promotes the survival of HCC cells by up-regulating the expression of mitotic cycle 25A and inhibiting mitochondrial-dependent intrinsic apoptosis[16]. These results have also been observed in acute myeloid leukemia [17]. In contrast, there are few studies on the expression and role of NPAS2 in GC at home and abroad, and there is a significant lack of experimental research. Therefore, the expression level of NPAS2 in GC and its role in the occurrence and development of GC in different signal pathways are controversial and need to be further studied.

This study intends to detect the expression level of NPAS2 in GC and paraneoplastic tissues by using tissue microarray immunohistochemical staining to establish a nomogram prediction model based on NPAS2 and other clinicopathologically independent risk factors. Furthermore, we aim to investigate the effect of NPAS2 on the prognosis of GC and its value in the prognosis prediction of GC patients.

MATERIALS AND METHODS

This study was approved by the Medical Ethics Committee of the Second Hospital of Lanzhou University. Informed consent was obtained from all patients, and all specimens were pseudonymous. The tumor tissues, precancerous tissues, and clinical data of 101 patients with primary GC resected by surgery from July to October 2019 in the second Hospital of Lanzhou University were collected and followed up by standard outpatient clinic and telephone. The inclusion criteria of the study were as follows: (1) Histopathological diagnosis of gastric adenocarcinoma; (2) age ≥ 18 years old; (3) patients with primary GC underwent surgical resection; (4) complete pathological, treatment, surgical and follow-up data; and (5) the patient gave written informed consent. Exclusion criteria: (1) Death before discharge; (2) preoperative radiotherapy and chemotherapy or neoadjuvant chemotherapy; (3) multiple cancers; and (4) gastric stump cancer. 10% neutral formalin fixation and routine paraffin-embedded GC and paraffin-embedded tissues were confirmed by pathology, and all pathology was independently reviewed by two pathologists. The patients were followed up every 3 mo in the first 2 years and every 6 mo in the third year. Follow-up included laboratory examination, chest X-ray examination, and abdominal computed tomography (CT) examination. The follow-up period was 36 mo, and OS was defined as from the date of the first operation to the end of follow-up or the time of death.

Construction of tissue microarray and immunohistochemical staining

One hundred one paraffin-embedded primary GC tissues and adjacent tissues were fixed with formalin and then serially sectioned on a microtome with a thickness of 4 μm. After drying, hematoxylin and eosin staining (HE) were performed. A professional pathologist selected and marked the representative positions of HE-stained pathological sections and corresponding wax blocks according to the view under the light microscope. The tissue chip wax blocks were made by a drilling mechanism and sliced with a thickness of 4μm. After being dewaxed in xylene and washed in gradient ethanol, the slices were immersed in a pressure tank containing 800 mL of 0.1% sodium citrate buffer solution (pH 6.0) and boiled for 3 min, followed by cooling. Following the manufacturer's instructions, we then conducted a streptavidin-Biotin Complex assay (Fuzhou Maxin Biotechnology Development Company). The slides were then incubated overnight with the primary antibody against NPAS2 at 4 ℃ (diluted, 1:200, rabbit anti-human NPAS2 polyclonal antibody, Biossantibodies, China). Color development, hematoxylin re-staining, differentiation, blueing, and dehydration were performed prior to sealing.

Evaluation of immunostaining

The complete immunohistochemical sections of 101 cases were observed under the microscope. NPAS2 was mainly expressed in the cytoplasm and nucleus, and the positive cells were yellow and brown granular. Two professional pathologists scored the section staining and did not know the clinicopathological factors and clinical outcome of the patient. The positive results were judged by the semi-quantitative integration method. Five high-power visual fields (400 ×) were selected for each chip on each slide under the microscope, and cells' positive rate and staining intensity were observed. (1) The score of cell positive rate: 0 indicates that the proportion of positive cells is less than 5%. The score of 5%-25% is 1, 26%-50% is 2, 51%-75% is 3, and more than 75% is 4; and (2) Staining intensity score: 0 = no coloring, 1 = light yellow, 2 = brown, 3 = brown. The immunostaining score was obtained by multiplying the positive rate of cells with the result of staining intensity. 0 was negative, 1 to 4 was weakly positive, 5 to 8 was moderately positive, and 9 to 12 was strongly positive. In this study, negative and weak positive was defined as low expression of NPAS2, while medium positive and strong positive was defined as high expression.

Statistical analysis

All data were analyzed using R software (Version 4.1.1, http://www.r-project.org) and SPSS (Version 26). Classification variables are represented by percentage (%), chi-square test, and continuity correction. Pearson's chi-squared test was used to evaluate the correlation between NPAS2 expression and clinicopathological factors. Survival analysis was performed by Kaplan-Meier curve and log-rank test. Univariate and multivariate Cox analysis determined the independent prognostic factors of OS and established the Cox proportional hazards model, and the hazard ratios (HRs) and 95% confidence intervals (CIs) were subsequently calculated. "Survival" and "surminer" R package were used for survival and Cox analysis. The "rms" package drew a nomogram model based on independent risk factors to predict OS. Furthermore, the receiver operating characteristic (ROC) curve, aera under the curve (AUC), calibration curve, and C-index were used to evaluate its prediction performance. In this study, $P < 0.05$ was considered to be statistically significant.

RESULTS

High expression of NPAS2 in human GC tissues

To explore the prognostic value of NPAS2 in GC, we performed immunohistochemical staining on 101 GC tissues collected. Strong or moderate positive immunostaining of NPAS2 protein was observed in the nucleus and cytoplasm of tumor cells in GC tissues. In contrast, weak positive or negative immunostaining was mainly detected in adjacent tissues. Representative positive staining results of NPAS2 showed that the positive rate of NPAS2 expression in GC tissues was 65.35% (66/101) (Figure 1), while the positive rate in corresponding adjacent tissues was 30.69% (31/101).

High expression of NPAS2 correlates with clinicopathological factors in GC patients

Of the 101 patients with GC, 65 (64.36%) died during follow-up. Table 1 summarizes the correlation between clinicopathological characteristics and NPAS2, showing that high expression of NPAS2 is associated with clinical progression in GC patients. The high expression of NPAS2 was significantly correlated with tumor-node-metastasis (TNM) stage ($P = 0.001$), pN stage ($P = 0.009$), metastasis ($P = 0.032$), venous invasion ($P = 0.012$), lymphatic invasion ($P = 0.001$) and lymph node positivity ($P = 0.001$).

The high expression of NPAS2 is associated with the prognosis of GC patients

The prognostic value of NPAS2 expression in GC was further investigated by Kaplan-Meier analysis and log-rank test. The results demonstrated that GC patients with high NPAS2 expression were significantly associated with shorter OS ($P < 0.001$) (Figure 2). Univariate Cox regression analysis showed that the TNM stage of GC patients (HR = 7.07, 95%CI: 3.47-14.41, $P < 0.001$), pN stage (HR = 1.72, 95%CI: 1.38-2.15, $P < 0.001$), metastasis (HR = 4.85, 95%CI: 2.24-10.46, $P < 0.001$), venous invasion (HR = 5.01, 95%CI: 1.57-15.98, $P = 0.007$), neural invasion (HR = 1.73, 95%CI: 1.03-2.9, $P = 0.037$), lymphatic invasion (HR = 3.53, 95%CI: 1.88-6.64, $P < 0.001$), lymph node positivity (HR = 3.35, 95%CI: 1.82-6.18, $P < 0.001$), and high expression of NPAS2 (HR = 5.13, 95%CI: 2.6-10.13, $P < 0.001$) were significantly correlated with OS. Multivariate Cox regression analysis showed that the TNM stage (HR = 3.61, 95%CI: 1.37-9.49, $P = 0.009$), metastasis (HR = 3.07, 95%CI: 1.33-7.1, $P = 0.009$), and high expression of NPAS2 (HR = 2.43, 95%CI: 1.15-5.13, $P = 0.020$) were independent risk factors for predicting OS (Table 2). Therefore, these collective data suggest that the expression level of NPAS2 has a good predictive value in the prognosis of GC patients.

Construction and evaluation of the prediction model

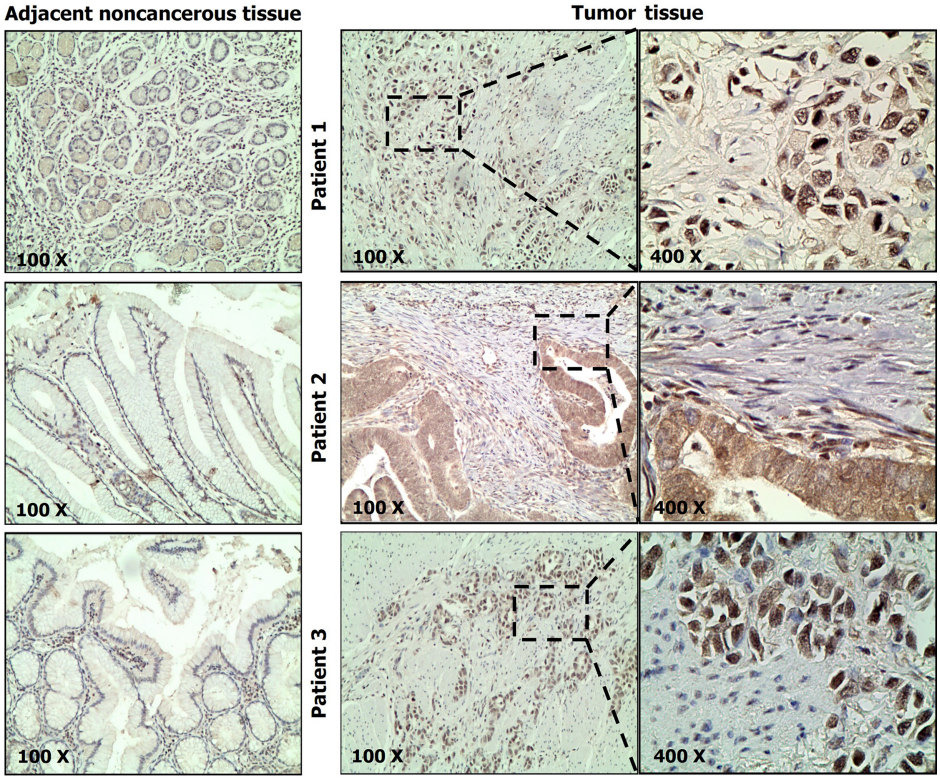
To obtain the best prediction model, TNM stage and metastasis were determined as independent

Table 1 Correlation between clinicopathological characteristic and NPAS2 in gastric cancer

Characteristic	Low expression of NPAS2	High expression of NPAS2	*P* value
Number	35	66	
Age, *n* (%)			0.599
< 60	21 (60.0)	36 (54.5)	
≥ 60	14 (40.0)	30 (45.5)	
Sex, *n* (%)			0.626
Female	7 (20.0)	16 (24.2)	
Male	28 (80.0)	51 (75.8)	
TNM stage, *n* (%)			0.001
I-II	25 (71.4)	11 (16.7)	
III-IV	10 (28.6)	55 (83.3)	
pT stage, *n* (%)			0.351
T1-T2	6 (17.1)	29 (82.9)	
T3-T4	7 (10.6)	59 (89.4)	
pN stage, *n* (%)			0.009
N0	16 (45.7)	12 (18.2)	
N1-N3	19 (54.3)	54 (81.8)	
Metastasis, *n* (%)			0.032
M0	35 (100.0)	58 (87.9)	
M1	0 (0.0)	8 (12.1)	
Tumor size, *n* (%)			0.626
< 5	15 (42.9)	25 (37.9)	
≥ 5	20 (57.1)	41 (62.1)	
Tumor location, *n* (%)			0.611
Antrum	14 (40.0)	33 (50.0)	
Body	9 (25.7)	13 (19.7)	
Cardia	12 (34.3)	20 (30.3)	
Venous invasion, *n* (%)			0.012
Negative	9 (25.7)	5 (7.6)	
Positive	26 (74.3)	61 (92.4)	
Neural invasion, *n* (%)			0.736
Negative	15 (42.9)	26 (39.4)	
Positive	20 (57.1)	40 (60.6)	
Lymphatic invasion, *n* (%)			0.001
Negative	22 (62.9)	12 (18.2)	
Positive	13 (37.1)	54 (81.8)	
Positive lymph node, *n* (%)			0.001
Negative	22 (62.9)	14 (21.2)	
Positive	13 (37.1)	52 (78.8)	
Differentiated degree, *n* (%)			0.16
Poorly	27 (77.1)	58 (87.9)	
Moderately and highly	8 (22.9)	8 (12.1)	

Lauren's Classification, *n* (%)			0.569
Intestinal	23 (65.7)	47 (71.2)	
Diffuse	12 (34.3)	19 (28.8)	

pT stage: Pathological assessment of primary tumor; pN stage: Pathological assessment of regional lymph nodes; TNM: Tumor-node-metastasis.



DOI: 10.3748/wjg.v29.i23.3645 **Copyright** ©The Author(s) 2023.

Figure 1 Expression of NPAS2 in gastric cancer. The expression of NPAS2 in tumor tissues of gastric cancer was detected by immunohistochemical staining and compared with adjacent normal tissues. High expression of NPAS2 in gastric cancer and low expression in adjacent non-cancerous tissue.

prognostic factors for GC according to multivariate Cox regression analysis and combined with NAPS2 high expression. Together, these were used as a combined prediction model for predicting OS at 1, 2, and 3 years after GC resection was constructed. The prediction model was visualized by nomogram (Figure 3). The 1-year, 2-year, and 3-year ROC curves of the Nomogram prediction model and other independent factors (Figure 4A) and the Time-dependent ROC curve were used to show the model's prediction performance (Figure 4C). The AUC of the nomogram prediction model for 1, 2, and 3 years is 0.763, 0.800, and 0.848, respectively (Figure 4B). Additionally, the C-index of each model shows the prediction performance of different models (Figure 4D), and the nomogram has the best prediction performance with a C-index of 0.740 (95%CI: 0.713-0.767). Finally, the prediction accuracy of the nomogram was verified by calibration curves, and the results showed that the combined nomogram model's 1-year, 2-year, and 3-year survival rates based on NPAS2 were in good agreement with the actual survival probability (Figure 5).

Risk stratification of OS by the nomogram model

To evaluate the positive effect of the nomogram prediction model in different subgroups, we divided all patients into a low-risk subgroup (score < 158) and a high-risk subgroup (score ≥ 158) according to the median nomogram score. Our results showed that patients in the high-risk group had significantly lower OS than those in the low-risk group ($P < 0.0001$) (Figure 6).

DISCUSSION

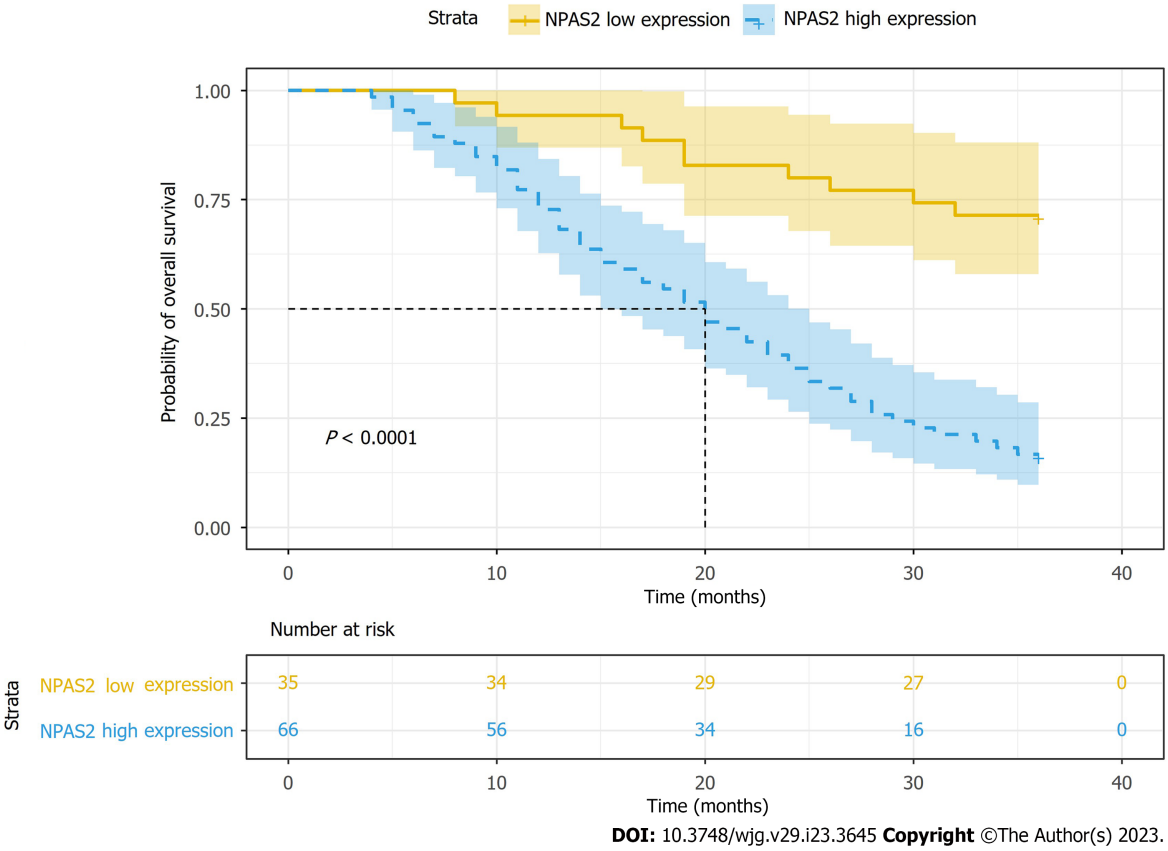
Epidemiological studies have shown that the disruption of normal circadian rhythm may increase the

Table 2 Univariate and multivariate Cox analysis of clinicopathological factors associated with the overall survival of gastric cancers

Characteristics	Univariate analysis		Multivariate analysis	
	Hazard ratio (95%CI)	*P* value	Hazard ratio (95%CI)	*P* value
Age				
< 60	1			
≥ 60	1.33 (0.82-2.17)	0.25		
Gender				
Female	1			
Male	1.13 (0.63-2.05)	0.679		
TNM stage				
I-II	1			
III-IV	7.07 (3.47-14.41)	< 0.001	3.61 (1.37-9.49)	0.009
pT stage				
T1-T2	1			
T3-T4	1.87 (0.81-4.35)	0.143		
pN stage				
N0	1			
N1-N3	1.72 (1.38-2.15)	< 0.001	1.66 (0.68-4.07)	0.265
Metastasis				
M0	1			
M1	4.85 (2.24-10.46)	< 0.001	3.07 (1.33-7.1)	0.009
Tumor size				
< 5	1			
≥ 5	1.63 (0.97-2.72)	0.063		
Tumor location				
Antrum	1			
Body	0.92 (0.53-1.60)	0.76		
Cardia	1.13 (0.58-2.23)	0.72		
Venous invasion				
Negative	1			
Positive	5.01 (1.57-15.98)	0.007	1.69 (0.49-5.84)	0.409
Neural invasion				
Negative	1			
Positive	1.73 (1.03-2.9)	0.037	1.71 (0.98-3)	0.06
Lymphatic invasion				
Negative	1			
Positive	3.53 (1.88-6.64)	< 0.001	0.39 (0.09-1.77)	0.225
Positive lymph node				
Negative				
Positive	3.35 (1.82-6.18)	< 0.001	2.23 (0.58-8.49)	0.241
Differentiated degree				
Moderately and highly	1			
Poorly	0.62 (0.29-1.30)	0.203		

Lauren's Classification				
Diffuse type	1			
Intestinal type	0.97 (0.57-1.64)	0.908		
	0.97 (0.57-1.64)			
NPAS2 expression				
Low	1			
High	5.13 (2.6-10.13)	< 0.001	2.43 (1.15-5.13)	0.020

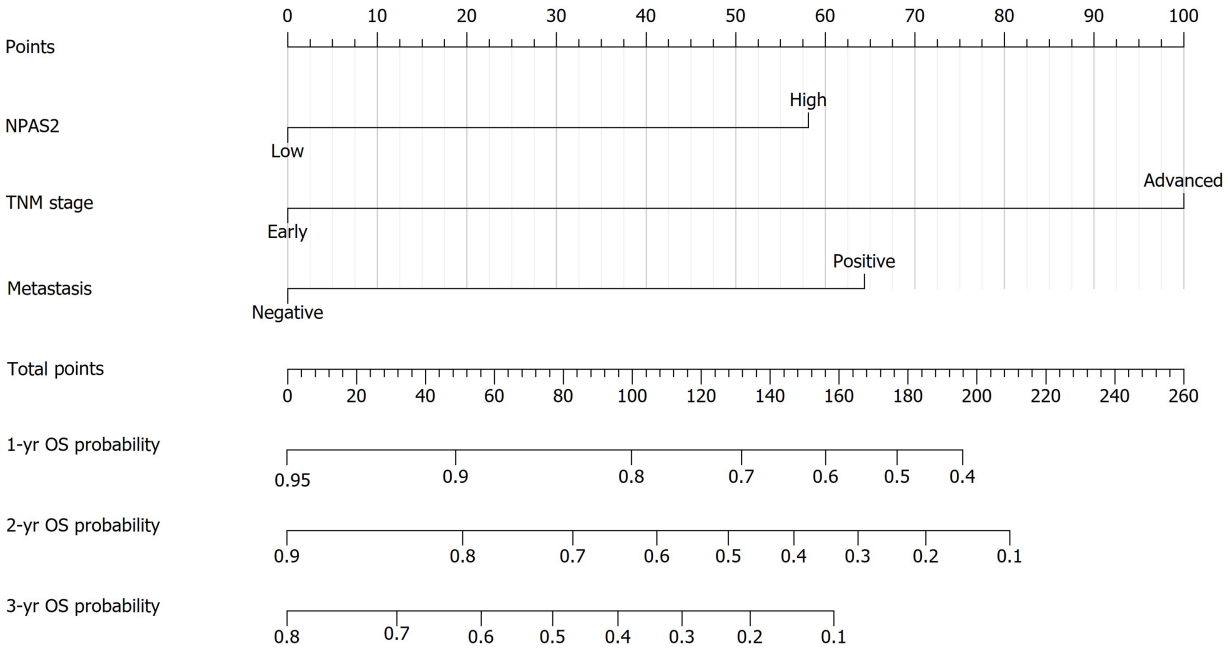
pT stage: Pathological assessment of primary tumor; pN stage: Pathological assessment of regional lymph nodes; TNM: Tumor-node-metastasis.



DOI: 10.3748/wjg.v29.i23.3645 **Copyright** ©The Author(s) 2023.

Figure 2 Kaplan–Meier curves for NPAS2 expression in gastric cancer. Gastric cancer patients with high NPAS2 expression were significantly associated with shorter overall survival.

risk of a variety of cancers[18], such as breast cancer[19], lung cancer[20], bladder cancer[21], prostate cancer[22], and liver cancer[23]. Notably, women on night shifts have a higher risk of breast cancer[19]. Likewise, breast cancer patients with irregular circadian rhythms have a worse prognosis because of changes in the expression of NPAS2 in breast cancer tissues[19]. Additionally, the disruption of biorhythm can promote the occurrence of lung cancer, which is a promising diagnostic marker for patients with lung adenocarcinoma and an independent prognostic marker for non-small cell lung cancer[24]. Notably, NPAS2 regulates the expression of several genes as markers of bladder cancer and further reduces the migration ability of bladder cancer cells[21]. The development of prostate cancer depends on androgen levels, and NPAS2 may interact with dihydrotestosterone, thus affecting the androgen receptor-dependent signaling pathway leading to prostate cancer[25]. Importantly, NPAS2 plays a role in reprogramming glucose metabolism and the progression of liver cancer, suggesting that NPAS2 may be an important therapeutic target to normalize the abnormal glucose metabolism that leads to the advancement of HCC[23]. Furthermore, NPAS2 plays different roles in different tumors, which can be understood that the expression level and function of NPAS2 are tumor-specific. The exact molecular mechanism of the change of NPAS2 expression in GC remains unclear. Moreso, there are no reports on the correlation between NPAS2 expression and clinicopathological data of GC patients.



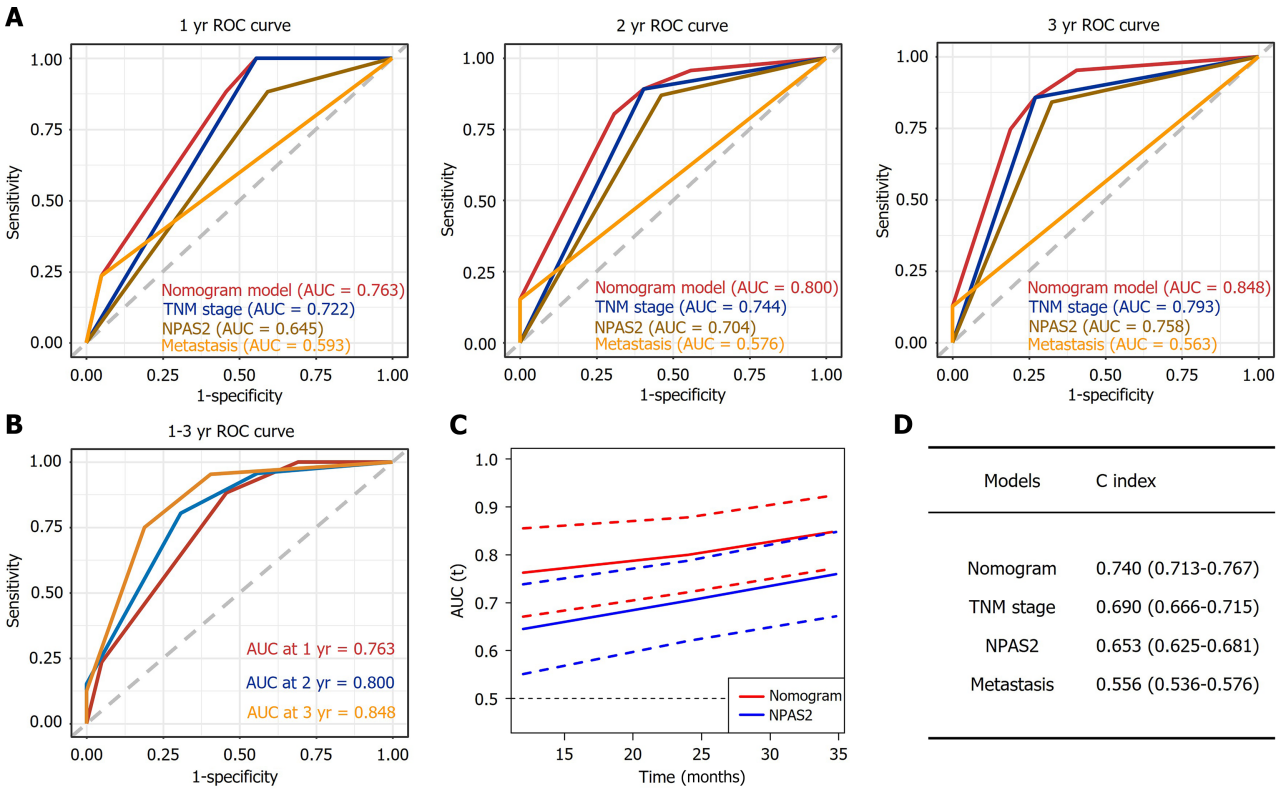
DOI: 10.3748/wjg.v29.i23.3645 **Copyright** ©The Author(s) 2023.

Figure 3 Nomogram prediction of 1-, 2-and 3-year overall survival rate in patients with gastric cancer. The total points is calculated by adding up the points of each factor. The total points corresponds to the 1-year, 2-year and 3-year survival probability of the patients. OS: Overall survival; TNM: Tumor-node-metastasis.

The tissue microarray results in this study showed that NPAS2 was expressed in GC and precancerous tissues and was primarily located in the nucleus and cytoplasm. The results showed that the expression was high in 65.35% of GC tissues and low in 34.65% of GC tissues. To the best of our knowledge, our experimental data demonstrate the role of NPAS2 in the diagnosis and prognosis of GC for the first time. The survival analysis showed that the high expression of NPAS2 in GC was significantly correlated with the shorter OS ($P < 0.001$). Univariate and multivariate Cox analysis also showed that the high expression of NPAS2 was an independent risk factor for GC. Furthermore, the ROC curve shows that NPAS2 is valuable in predicting the prognosis of GC. Therefore, the expression level of NPAS2 in GC tissue directly affects the OS of GC patients and may be used as a tumor-promoting factor to affect the occurrence and development of GC, which is a new prognostic biomarker. Various animal and *in vitro* studies have found that NPAS2 can regulate the expression of oncogenes (such as c-myc), tumor suppressor genes (such as P53 and P21), and transcription factors[26], thereby regulating cell cycle, apoptosis, DNA damage and repair systems, invasion, metastasis, carcinogen metabolism, and detoxification[27]. Notably, DNA repair maintains genetic stability and protects DNA from internal and external stimuli. Once human biorhythm genes are mutated (due to spontaneous mutations, prolonged late nights, or other environmental factors), it may lead to irreversible disorders and loss of DNA repair capacity[27].

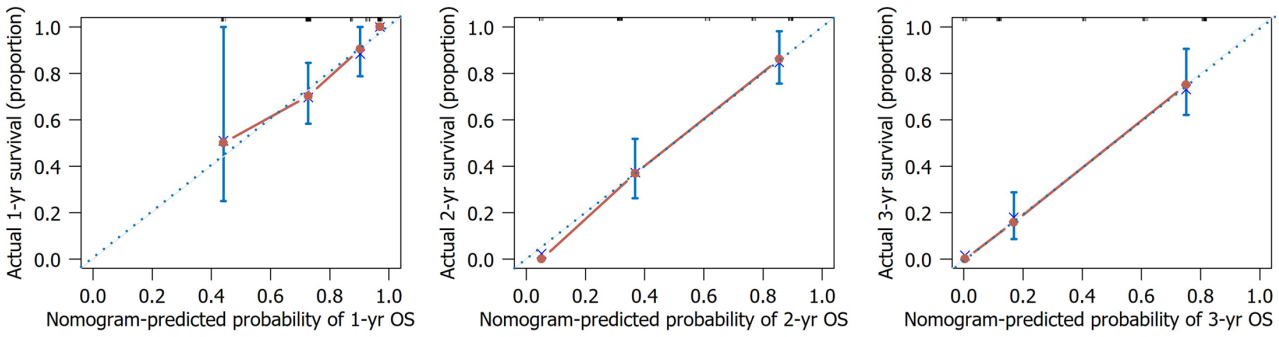
The American Joint Commission on the Cancer TNM staging system is widely used to monitor the prognosis of patients with GC[28]. Our study analyzed the clinicopathological factors affecting OS in patients with GC, and our results showed that TNM stage and metastasis were independent risk factors for poor survival outcomes. Although the TNM stage and metastasis of GC patients have been widely used in the formulation of the treatment plan and the evaluation of prognosis, with the increasing number of GC patients, more studies and related factors are needed to evaluate the survival and prognosis of these patients more accurately and individually. Our study combined three independent risk factors of NPAS2 and TNM stage and metastasis to establish a Cox regression model for predicting 3-year OS in patients with GC. Compared with the TNM stage alone, it has more predictive power and can be used as a more convenient and accurate tool to predict the prognosis of patients with GC following gastrectomy. Therefore, the accurate prognosis prediction by nomogram score is of great significance for postoperative management and diagnosis and treatment of patients.

However, we can not solve the causal relationship in this study. Therefore, further basic and clinical research is needed to explore these aspects. Our advantage is that this is the first study to show that the increased expression of NPAS2 may be related to the malignant biological behavior and poor prognosis of patients with GC. Of course, our research has the following noted limitations. First, the sample size of our study is small, and there may be selection bias. Secondly, this study is a single-center retrospective study, so it is necessary to conduct a multicenter prospective study to verify it further. Finally, we used immunohistochemical staining to detect the expression of NPAS2 in the center and periphery of each



DOI: 10.3748/wjg.v29.i23.3645 **Copyright** ©The Author(s) 2023.

Figure 4 Construction of prognostic nomogram in gastric cancer. A: NPAS2, tumor-node-metastasis (TNM) stage, metastasis, and nomogram predict the receiver operating characteristic (ROC) curves of 1-year, 2-year and 3-year overall survival (OS) in gastric cancer patients; B: Nomogram predict the ROC curve of 1-year, 2-year and 3-year OS in gastric cancer patients; C: Comparison of time-dependent ROC curves between nomogram and NPAS2; D: C-index for nomogram, NPAS2, TNM stage, metastasis. ROC: Receiver operating characteristic; OS: Overall survival; TNM: Tumor-node-metastasis; AUC: Area under the curve.



DOI: 10.3748/wjg.v29.i23.3645 **Copyright** ©The Author(s) 2023.

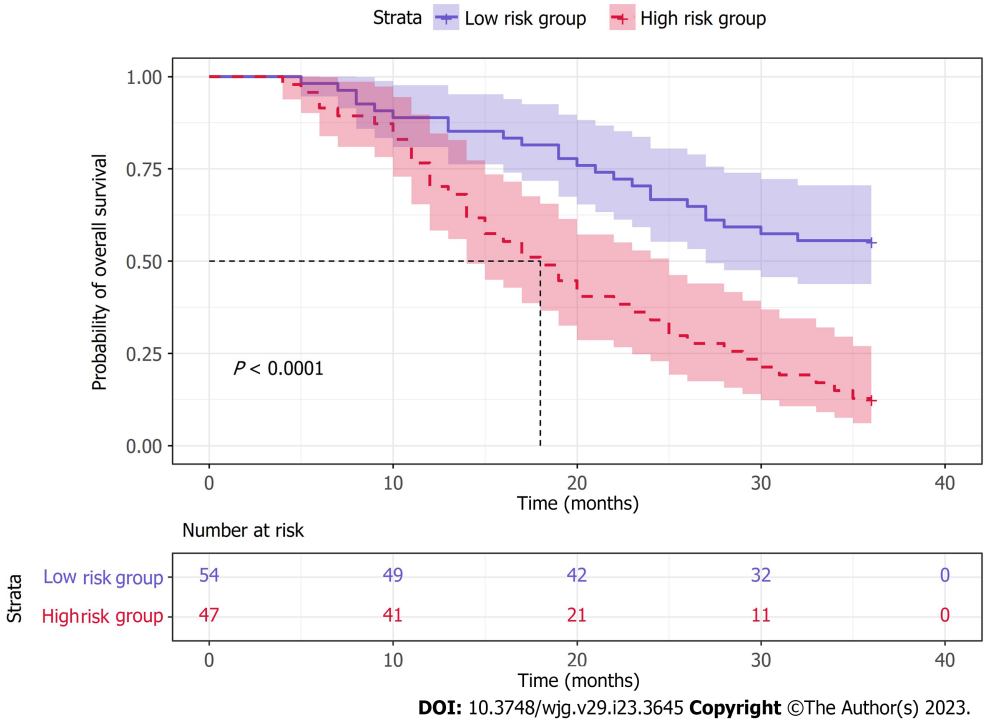
Figure 5 Nomogram calibration plots to predict 1-, 2-, and 3-year overall survival in gastric cancer patients. OS: Overall survival.

GC tissue. However, considering the heterogeneity, the expression level of NPAS2 in the sampling site may not represent whole tumor regions.

Based on these investigations, further exploration of the molecular mechanism and influence of NPAS2 in the occurrence and development of GC will help to promote its clinical application. The established nomogram prediction model provides a potential objective clinical prediction tool to assist clinicians in predicting the prognosis of GC patients and making postoperative management and clinical decisions.

CONCLUSION

In conclusion, our study found that high expression of NAPS2 is associated with poor prognosis of OS in patients with GC and is an independent risk factor for patients after radical resection of GC. We



DOI: 10.3748/wjg.v29.i23.3645 **Copyright** ©The Author(s) 2023.

Figure 6 Overall survival Kaplan-Meier curves for patients in the low- and high-risk groups.

further constructed a nomogram model by combining NAPS2 and other independent risk factors, thus improving the accuracy of predicting the prognosis of GC.

ARTICLE HIGHLIGHTS

Research background

The circadian clock gene NPAS2 expression is associated with multiple tumor prognosis, its role in gastric cancer (GC) is unknown.

Research motivation

NPAS2 can improve the accuracy of GC prognosis prediction and assist clinicians in postoperative patient management and decision-making.

Research objectives

This study aimed to explore the relationship between the circadian clock gene NPAS2 and the survival prognosis of GC patients and clarify its role in evaluating GC prognosis.

Research methods

Immunohistochemical staining was used to detect the expression of NPAS2 protein in GC and adjacent tissues. Univariate and multivariate Cox regression analysis was used to determine the independent prognostic factors of GC, and a nomogram prediction model was established. The receiver operating characteristic curve and area under the curve, the calibration curve, and C-index were used to evaluate the predictive effectiveness of the model.

Research results

The NPAS2 expression were independent prognostic factors of overall survival in GC patients for 3 years.

Research conclusions

NPAS2 is highly expressed in GC and is closely related to worse overall survival in patients. Therefore, the evaluation of NPAS2 expression may be a potential marker for GC prognosis evaluation.

Research perspectives

Based on NPAS2 expression, clinicians can predict patient prognosis and guide clinical decision making and follow up.

FOOTNOTES

Author contributions: Cao XM and Kang WD contributed equally to this work and share first authorship; Cao XM, Kang WD, and Liu HB designed the project and reviewed and edited the manuscript; Cao XM and Kang WD analyzed the data and wrote the main manuscripts; Xia TH and Yuan SB carried out research selection and data collection; Guo CA, Wang WJ and Liu HB participated in the discussion of classification criteria.

Institutional review board statement: The studies involving human participants were reviewed and approved by Medical Ethics Committee of the Second Hospital of Lanzhou University, approval No. 2021A-561. The patients/participants provided written informed consent to participate in this study.

Informed consent statement: The Medical Ethics Committee of the Second Hospital of Lanzhou University waived the need for informed consent due to the retrospective nature of the study.

Conflict-of-interest statement: The authors declare no conflict of interest.

Country/Territory of origin: China

ORCID number: Hong-Bin Liu 0000-0003-3668-6166.

S-Editor: Yan JP
L-Editor: A
P-Editor: Chen YX

REFERENCES

1 **Ferlay J**, Colombet M, Soerjomataram I, Parkin DM, Piñeros M, Znaor A, Bray F. Cancer statistics for the year 2020: An overview. *Int J Cancer* 2021 [PMID: 33818764 DOI: 10.1002/ijc.33588]
2 **Sung H**, Ferlay J, Siegel RL, Laversanne M, Soerjomataram I, Jemal A, Bray F. Global Cancer Statistics 2020: GLOBOCAN Estimates of Incidence and Mortality Worldwide for 36 Cancers in 185 Countries. *CA Cancer J Clin* 2021; **71**: 209-249 [PMID: 33538338 DOI: 10.3322/caac.21660]
3 **Lei ZN**, Teng QX, Tian Q, Chen W, Xie Y, Wu K, Zeng Q, Zeng L, Pan Y, Chen ZS, He Y. Signaling pathways and therapeutic interventions in gastric cancer. *Signal Transduct Target Ther* 2022; **7**: 358 [PMID: 36209270 DOI: 10.1038/s41392-022-01190-w]
4 **Ugai T**, Sasamoto N, Lee HY, Ando M, Song M, Tamimi RM, Kawachi I, Campbell PT, Giovannucci EL, Weiderpass E, Rebbeck TR, Ogino S. Is early-onset cancer an emerging global epidemic? Current evidence and future implications. *Nat Rev Clin Oncol* 2022; **19**: 656-673 [PMID: 36068272 DOI: 10.1038/s41571-022-00672-8]
5 **Gwee YX**, Chia DKA, So J, Ceelen W, Yong WP, Tan P, Ong CJ, Sundar R. Integration of Genomic Biology Into Therapeutic Strategies of Gastric Cancer Peritoneal Metastasis. *J Clin Oncol* 2022; **40**: 2830 [PMID: 35649219 DOI: 10.1200/JCO.21.02745]
6 **Shostak A**. Circadian Clock, Cell Division, and Cancer: From Molecules to Organism. *Int J Mol Sci* 2017; **18** [PMID: 28425940 DOI: 10.3390/ijms18040873]
7 **Milev NB**, Reddy AB. Circadian redox oscillations and metabolism. *Trends Endocrinol Metab* 2015; **26**: 430-437 [PMID: 26113283 DOI: 10.1016/j.tem.2015.05.012]
8 **Franzoni A**, Markova-Car E, Dević-Pavlić S, Jurišić D, Puppin C, Mio C, De Luca M, Petruz G, Damante G, Pavelić SK. A polymorphic GGC repeat in the NPAS2 gene and its association with melanoma. *Exp Biol Med (Maywood)* 2017; **242**: 1553-1558 [PMID: 28799406 DOI: 10.1177/1535370217724093]
9 **Liu H**, Gao Y, Hu S, Fan Z, Wang X, Li S. Bioinformatics Analysis of Differentially Expressed Rhythm Genes in Liver Hepatocellular Carcinoma. *Front Genet* 2021; **12**: 680528 [PMID: 34149816 DOI: 10.3389/fgene.2021.680528]
10 **Sancar A**, Van Gelder RN. Clocks, cancer, and chronochemotherapy. *Science* 2021; **371** [PMID: 33384351 DOI: 10.1126/science.abb0738]
11 **Chen W**, Zheng R, Baade PD, Zhang S, Zeng H, Bray F, Jemal A, Yu XQ, He J. Cancer statistics in China, 2015. *CA Cancer J Clin* 2016; **66**: 115-132 [PMID: 26808342 DOI: 10.3322/caac.21338]
12 **Renthlei Z**, Gurumayum T, Borah BK, Trivedi AK. Daily expression of clock genes in central and peripheral tissues of tree sparrow (Passer montanus). *Chronobiol Int* 2019; **36**: 110-121 [PMID: 30365349 DOI: 10.1080/07420528.2018.1523185]
13 **Roenneberg T**, Merrow M. The Circadian Clock and Human Health. *Curr Biol* 2016; **26**: R432-R443 [PMID: 27218855 DOI: 10.1016/j.cub.2016.04.011]
14 **Zhang J**, Lv H, Ji M, Wang Z, Wu W. Low circadian clock genes expression in cancers: A meta-analysis of its association with clinicopathological features and prognosis. *PLoS One* 2020; **15**: e0233508 [PMID: 32437452 DOI: 10.1371/journal.pone.0233508]

15 **Qiu MJ**, Liu LP, Jin S, Fang XF, He XX, Xiong ZF, Yang SL. Research on circadian clock genes in common abdominal malignant tumors. *Chronobiol Int* 2019; **36**: 906-918 [PMID: 31014126 DOI: 10.1080/07420528.2018.1477792]

16 **Yuan P**, Li J, Zhou F, Huang Q, Zhang J, Guo X, Lyu Z, Zhang H, Xing J. NPAS2 promotes cell survival of hepatocellular carcinoma by transactivating CDC25A. *Cell Death Dis* 2017; **8**: e2704 [PMID: 28333141 DOI: 10.1038/cddis.2017.131]

17 **Song B**, Chen Y, Liu Y, Wan C, Zhang L, Zhang W. NPAS2 regulates proliferation of acute myeloid leukemia cells *via* CDC25A-mediated cell cycle progression and apoptosis. *J Cell Biochem* 2019; **120**: 8731-8741 [PMID: 30536616 DOI: 10.1002/jcb.28160]

18 **Kiessling S**, Beaulieu-Laroche L, Blum ID, Landgraf D, Welsh DK, Storch KF, Labrecque N, Cermakian N. Enhancing circadian clock function in cancer cells inhibits tumor growth. *BMC Biol* 2017; **15**: 13 [PMID: 28196531 DOI: 10.1186/s12915-017-0349-7]

19 **Nagata C**, Tamura T, Wada K, Konishi K, Goto Y, Nagao Y, Ishihara K, Yamamoto S. Sleep duration, nightshift work, and the timing of meals and urinary levels of 8-isoprostane and 6-sulfatoxymelatonin in Japanese women. *Chronobiol Int* 2017; **34**: 1187-1196 [PMID: 28933565 DOI: 10.1080/07420528.2017.1355313]

20 **Gao LW**, Wang GL. Comprehensive bioinformatics analysis identifies several potential diagnostic markers and potential roles of cyclin family members in lung adenocarcinoma. *Onco Targets Ther* 2018; **11**: 7407-7415 [PMID: 30425528 DOI: 10.2147/OTT.S171705]

21 **Iyyanki T**, Zhang B, Wang Q, Hou Y, Jin Q, Xu J, Yang H, Liu T, Wang X, Song F, Luan Y, Yamashita H, Chien R, Lyu H, Zhang L, Wang L, Warrick J, Raman JD, Meeks JJ, DeGraff DJ, Yue F. Subtype-associated epigenomic landscape and 3D genome structure in bladder cancer. *Genome Biol* 2021; **22**: 105 [PMID: 33858483 DOI: 10.1186/s13059-021-02325-y]

22 **Yu CC**, Chen LC, Chiou CY, Chang YJ, Lin VC, Huang CY, Lin IL, Chang TY, Lu TL, Lee CH, Huang SP, Bao BY. Genetic variants in the circadian rhythm pathway as indicators of prostate cancer progression. *Cancer Cell Int* 2019; **19**: 87 [PMID: 30996687 DOI: 10.1186/s12935-019-0811-4]

23 **Yuan P**, Yang T, Mu J, Zhao J, Yang Y, Yan Z, Hou Y, Chen C, Xing J, Zhang H, Li J. Circadian clock gene NPAS2 promotes reprogramming of glucose metabolism in hepatocellular carcinoma cells. *Cancer Lett* 2020; **469**: 498-509 [PMID: 31765736 DOI: 10.1016/j.canlet.2019.11.024]

24 **He Y**, Wang G, Wang Q, Zhao Z, Gan L, Yang S, Wang Y, Guo S, An J, Zhang J, Zhang Z, Zhou F. Genetic variants in NPAS2 gene and clinical outcomes of resectable non-small-cell lung cancer. *Future Oncol* 2021; **17**: 795-805 [PMID: 33541123 DOI: 10.2217/fon-2020-0211]

25 **Mukhopadhyay NK**, Ferdinand AS, Mukhopadhyay L, Cinar B, Lutchman M, Richie JP, Freeman MR, Liu BC. Unraveling androgen receptor interactomes by an array-based method: discovery of proto-oncoprotein c-Rel as a negative regulator of androgen receptor. *Exp Cell Res* 2006; **312**: 3782-3795 [PMID: 17011549 DOI: 10.1016/j.yexcr.2006.07.017]

26 **Yang SL**, Ren QG, Wen L, Hu JL, Wang HY. Research progress on circadian clock genes in common abdominal malignant tumors. *Oncol Lett* 2017; **14**: 5091-5098 [PMID: 29113149 DOI: 10.3892/ol.2017.6856]

27 **LeVan TD**, Xiao P, Kumar G, Kupzyk K, Qiu F, Klinkebiel D, Eudy J, Cowan K, Berger AM. Genetic Variants in Circadian Rhythm Genes and Self-Reported Sleep Quality in Women with Breast Cancer. *J Circadian Rhythms* 2019; **17**: 6 [PMID: 31303884 DOI: 10.5334/jcr.184]

28 **Lu J**, Zheng ZF, Xie JW, Wang JB, Lin JX, Chen QY, Cao LL, Lin M, Tu RH, Huang CM, Zheng CH, Li P. Is the 8th Edition of the AJCC TNM Staging System Sufficiently Reasonable for All Patients with Noncardia Gastric Cancer? A 12,549-Patient International Database Study. *Ann Surg Oncol* 2018; **25**: 2002-2011 [PMID: 29725896 DOI: 10.1245/s10434-018-6447-0]

World Journal of Gastroenterology

Submit a Manuscript: https://www.f6publishing.com

World J Gastroenterol 2023 June 21; 29(23): 3658-3667

DOI: 10.3748/wjg.v29.i23.3658

ISSN 1007-9327 (print) ISSN 2219-2840 (online)

ORIGINAL ARTICLE

Retrospective Study

SGK3 overexpression correlates with a poor prognosis in endoscopically resected superficial esophageal squamous cell neoplasia: A long-term study

Ning Xu, Long-Song Li, Hui Li, Li-Hua Zhang, Nan Zhang, Peng-Ju Wang, Ya-Xuan Cheng, Jing-Yuan Xiang, En-Qiang Linghu, Ning-Li Chai

Specialty type: Gastroenterology and hepatology

Provenance and peer review: Unsolicited article; Externally peer reviewed.

Peer-review model: Single blind

Peer-review report's scientific quality classification

Grade A (Excellent): 0
Grade B (Very good): B, B
Grade C (Good): 0
Grade D (Fair): 0
Grade E (Poor): 0

P-Reviewer: Hwang GS, South Korea; Tsai NM, Taiwan

Received: February 24, 2023
Peer-review started: February 24, 2023
First decision: March 14, 2023
Revised: March 20, 2023
Accepted: May 23, 2023
Article in press: May 23, 2023
Published online: June 21, 2023

Ning Xu, Long-Song Li, Nan Zhang, Peng-Ju Wang, Ya-Xuan Cheng, Jing-Yuan Xiang, En-Qiang Linghu, Ning-Li Chai, Senior Department of Gastroenterology, The First Medical Center of PLA General Hospital, Beijing 100853, China

Hui Li, Department of Gastroenterology, Air Force Medical Center, Beijing 100142, China

Li-Hua Zhang, Department of Pathology, The Fourth Medical Center of PLA General Hospital, Beijing 100142, China

Corresponding author: Ning-Li Chai, MD, PhD, Chief Doctor, Senior Department of Gastroenterology, The First Medical Center of PLA General Hospital, No. 28 Fuxing Road, Haidian District, Beijing 100853, China. chainingli@vip.163.com

Abstract

BACKGROUND

The expression status of serum and glucocorticoid-induced protein kinase 3 (SGK3) in superficial esophageal squamous cell neoplasia (ESCN) remains unknown.

AIM

To evaluate the SGK3 overexpression rate in ESCN and its influence on the prognosis and outcomes of patients with endoscopic resection.

METHODS

A total of 92 patients who had undergone endoscopic resection for ESCN with more than 8 years of follow-up were enrolled. Immunohistochemistry was used to evaluate SGK3 expression.

RESULTS

SGK3 was overexpressed in 55 (59.8%) patients with ESCN. SGK3 overexpression showed a significant correlation with death (P = 0.031). Overall survival and disease-free survival rates were higher in the normal SGK3 expression group than in the SGK3 overexpression group (P = 0.013 and P = 0.004, respectively). Cox regression analysis models demonstrated that SGK3 overexpression was an independent predictor of poor prognosis in ESCN patients (hazard ratio 4.729;

95% confidence interval: 1.042-21.458).

CONCLUSION
SGK3 overexpression was detected in the majority of patients with endoscopically resected ESCN and was significantly associated with shortened survival. Thus, it might be a new prognostic factor for ESCN.

Key Words: Superficial esophageal squamous cell neoplasia; Serum and glucocorticoid-induced protein kinase; Endoscopic submucosal dissection; Immunohistochemistry; Overall survival

©The Author(s) 2023. Published by Baishideng Publishing Group Inc. All rights reserved.

Core Tip: This study demonstrated that the expression status of serum and glucocorticoid-induced protein kinase 3 (SGK3) was high in the majority of patients with superficial esophageal squamous cell neoplasia (ESCN) and that high expression of SGK3 predicts a poor prognosis. These findings provide a new prognostic factor for ESCN.

Citation: Xu N, Li LS, Li H, Zhang LH, Zhang N, Wang PJ, Cheng YX, Xiang JY, Linghu EQ, Chai NL. SGK3 overexpression correlates with a poor prognosis in endoscopically resected superficial esophageal squamous cell neoplasia: A long-term study. *World J Gastroenterol* 2023; 29(23): 3658-3667
URL: https://www.wjgnet.com/1007-9327/full/v29/i23/3658.htm
DOI: https://dx.doi.org/10.3748/wjg.v29.i23.3658

INTRODUCTION

Esophageal cancer remains a leading cause of cancer-related death, and the incidence rates of esophageal cancer worldwide are increasing[1]. Esophageal squamous cell carcinoma (ESCC) accounts for the majority of esophageal cancer cases[2]. It is usually detected at an advanced stage after the symptoms of dysphagia appear[3]. Thus, its prognosis is the worst among digestive carcinomas[4]. Early detection of the malignant epithelium at an early stage followed by endoscopic resection has become the most effective way to improve clinical outcomes[5]. However, the prognosis of patients with superficial esophageal squamous cell neoplasia (ESCN) remains poor[6,7].

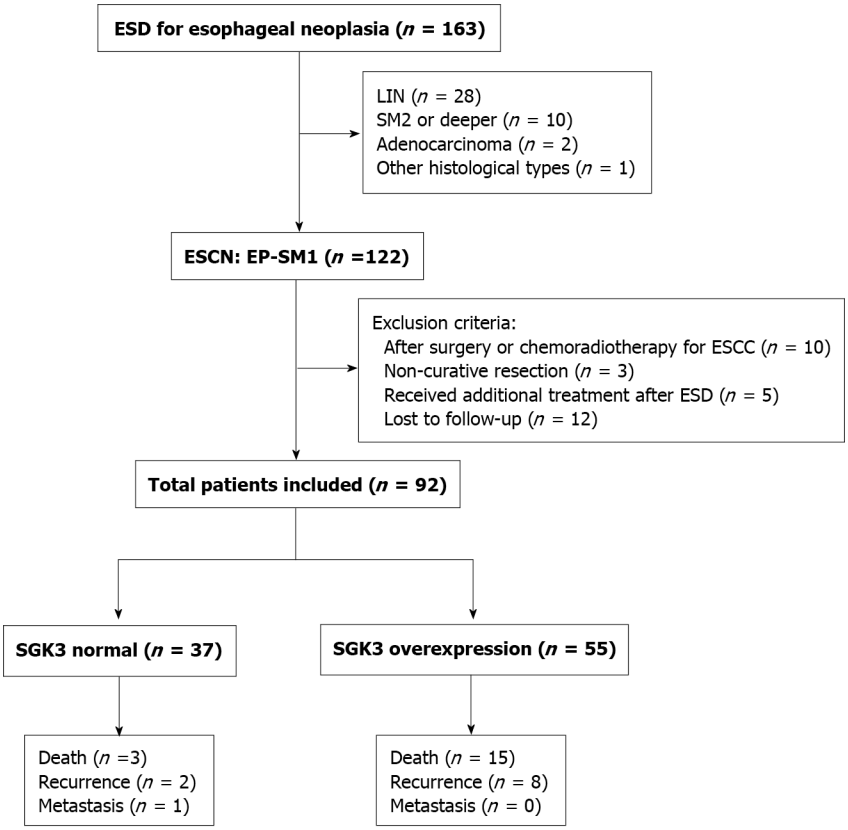
The serum and glucocorticoid-induced protein kinase (SGK) family consists of three isoforms (SGK1, SGK2 and SGK3), and they regulate a range of fundamental cellular processes, such as tumor growth, metastasis, autophagy and survival[8]. SGK is a ubiquitously expressed serine/threonine kinase and plays an active role in a multitude of pathophysiological conditions[9]. It is activated by insulin and growth factors *via* phosphatidylinositol 3-kinase (PI3K) and is frequently altered in human cancers, including breast cancer and hepatocellular carcinoma[10,11]. Although SGK1, SGK2 and SGK3 share a highly similar domain, the lack of a plasma membrane-targeting domain indicates nonoverlapping functions[12].

Previous studies have shown that SGK3 is expressed in all tissues tested thus far and is especially highly expressed in the heart and spleen[13]. Encoded by chromosome 8q12.2, SGK3 is known as a downstream factor of PI3K signaling and has been reported to play a pivotal role in the development and progression of diverse cancers[14]. Therefore, it has been regarded as a potential target for cancer intervention[15]. However, a minority of studies have evaluated the impact of SGK3 expression on clinical outcomes, and the expression of SGK3 in ESCN has not been investigated[16]. Whether SGK3 is associated with the prognosis of ESCN remains unknown. Herein, we assessed the SGK3 expression levels of patients with ESCN *via* immunohistochemistry (IHC) to investigate the possible role of SGK3 as a prognostic factor.

MATERIALS AND METHODS

Patients

Patients who underwent gastrointestinal endoscopy followed by endoscopic submucosal dissection (ESD) between November 2009 and July 2011 at the First Medical Center of PLA General Hospital were included. The inclusion criteria were as follows: (1) Patients were diagnosed with primary ESCN; (2) the histological type of tumor was ESCN; and (3) the tumor penetrated the submucosal layer < 200 μm or 200 μm from the muscularis mucosa. The exclusion criteria were as follows: (1) ESCN was previously



DOI: 10.3748/wjg.v29.i23.3658 **Copyright** ©The Author(s) 2023.

Figure 1 Study flow chart. ESD: Endoscopic submucosal dissection; LIN: Low-grade intraepithelial neoplasia; SM2: Penetration of the submucosal layer > 200 μm from the muscularis mucosa; ESCN: Esophageal squamous cell neoplasia; ESCC: Esophageal squamous cell carcinoma; EP: Epithelium; SM1: Penetration of the submucosal layer < 200 μm or 200 μm from the muscularis mucosa; SGK3: Serum and glucocorticoid-induced protein kinase 3.

treated with surgery or chemoradiotherapy ESCN; (2) pathological evaluation post-ESD indicated noncurative resection; (3) patients received additional treatment immediately after ESD; and (4) incomplete follow-up. All follow-up data were obtained at least 8 years after the first detection of the tumor. Eventually, 92 patients with complete follow-up data were included in the analysis (Figure 1). This study was approved by the Ethics Board of the First Medical Center of PLA General Hospital (approval No. S2020-251-01).

ESD procedure

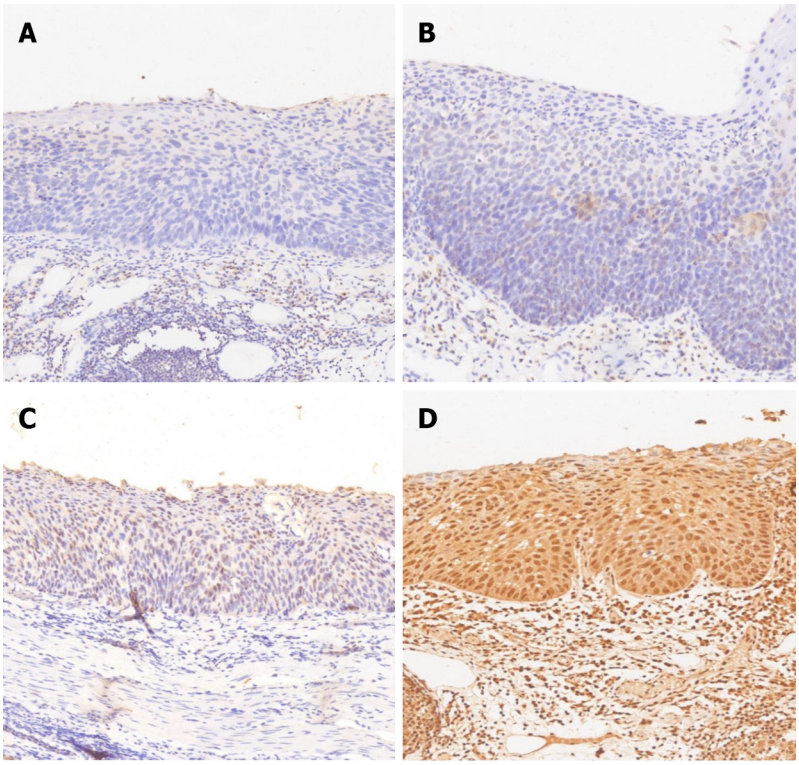
All procedures were performed under general anesthesia by experienced endoscopists. A single-channel upper gastrointestinal endoscope (GIF-Q230; Olympus, Tokyo, Japan) was used during the procedure. The standard ESD is described as follows: the lesions were detected on endoscopy under white light or narrow band imaging, lesion margins were shown by iodine staining, argon plasma coagulation (ERBE Elektromedizin GmbH) was used to mark 5 mm outside the boundary of the lesion, submucosal circumferential injection was performed to lift the lesions, and submucosal dissection followed by a circumferential mucosal incision was performed to remove the lesion.

Pathological examination

Tissue specimens were fixed in formalin. All samples were subjected to histological analysis of differentiation type, depth of invasion, and lymphovascular invasion. Lymphovascular invasion was recognized as any invasion using hematoxylin and eosin staining. Curative resection was defined as complete resection of a mucosal lesion with no lymphovascular invasion, and noncurative resection implied a pathologically positive margin or clinically incomplete resection.

IHC

For IHC, we used a rabbit anti-human SGK3 antibody (Roche Diagnostics Japan. Tokyo, Japan) and 4-μm-thick sections. All sections were deparaffinized in xylene 3 times and rehydrated in a graded series of ethanol with decreasing concentrations. Then, we used Tris-buffered saline (pH 7.4) for rinsing. Heat-induced epitope retrieval was conducted by immersing the slides in Coplin jars filled with 10 mmol/L citrate buffer (pH 6.0) and microwaving the buffer for 25 min. The jars were then cooled for 20 min. The reaction products were visualized with diaminobenzidine and counterstained with hematoxylin. Two



DOI: 10.3748/wjg.v29.i23.3658 **Copyright** ©The Author(s) 2023.

Figure 2 Serum and glucocorticoid-induced protein kinase 3 protein expression in superficial esophageal squamous cell neoplasia (magnification: × 400). A: No serum and glucocorticoid-induced protein kinase 3 (SGK3) expression in esophageal squamous cell neoplasia (ESCN) samples (normal for SGK3 overexpression; 0); B: Weak SGK3 expression in ESCN samples (normal for SGK3 overexpression; 1+); C: Moderate SGK3 expression in ESCN samples (positive for SGK3 overexpression; 2+); D: Strong SGK3 expression in ESCN samples (positive for SGK3 overexpression; 3+).

experienced pathologists independently judged the immunostaining intensity. The staining intensity was graded based on the American Society of Clinical Oncology/College of American Pathology guidelines[17]. The criteria were as follows: 0 = no nuclear staining in tumor cells; 1+ = weak (staining in less than 10% of cells); 2+ = intense complete staining (up to 30% of tumor cells); and 3+ = uniform intense staining (more than 30% of tumor cells). The expression status of SGK3 was classified into 2 groups: normal (0 and 1+) and overexpression (2+ and 3+) (Figure 2).

Clinicopathologic parameters and definitions

In each case, clinicopathologic parameters were retrospectively obtained from the pathological results of our hospital. Basic clinical parameters included age, sex, smoking history and family history of cancer. The longest diameter of the lesion in the specimen was defined as the tumor size. Tumor location was categorized as upper thoracic, middle thoracic and lower thoracic. Based on the histological outcome, tumors were characterized into low-grade intraepithelial neoplasia, high-grade intraepithelial neoplasia, well-differentiated squamous cell carcinoma, intermediate differentiated squamous cell carcinoma, and poorly differentiated squamous cell carcinoma. The T stage of the tumor was categorized based on the 11th Japanese classification of esophageal cancer[18]. Tumors limited to the epithelium and tumors that invaded into the submucosa ≤ 200 or > 200 μm from the muscularis mucosae were classified as EP, submucosa 1 (SM1) or submucosa 2 (SM2), respectively. The two recurrence patterns, metachronous recurrence and metastatic recurrence, were both included in this study, and tumor recurrence was identified using endoscopy and histological biopsy. Tumor recurrence was defined as an ESCN or cancerous lesion detected on the esophagus during the follow-up period. Lymph node or distant metastasis was evaluated by contrast-enhanced computed tomography scan or magnetic resonance imaging and verified *via* histological examination of the biopsy.

Prognostic outcomes

The follow-up of patient survival status and cancer recurrence was completed in July 2022. Prognostic outcomes were obtained by calling patients themselves or asking the family members for the recorded death certificate of the patients. Two main variables were assessed: Overall survival (OS) and disease-free survival (DFS). OS was defined as the time that elapsed from the date of endoscopic treatment to the date of death from any cause. DFS was defined as the duration between the endoscopic treatment and any disease recurrence or any cause of death, whichever occurred first.

Statistical analysis

Continuous variables are expressed as the mean ± SD or median (interquartile range) and were compared using Student's *t* test. Categorical variables are expressed as percentages and were compared using the chi-square test or Fisher's exact test. Multivariate Cox regression was used to further analyze the relationship between SGK3 overexpression and clinical outcomes, and the covariates were screened using stepwise regression. The extended-model method was used to conduct covariate correction: Model 1 was corrected based on SGK3 expression status; Model 2 = model 1 + (age and gender); Model 3 = model 2 + (smoking history + family history of cancer); and Model 4 = model 3 + (tumor location + tumor size + T stage + differentiated types). Multicollinearity was tested using the variance inflation factor (VIF) method, and a VIF ≥ 10 was considered to indicate severe multicollinearity. Kaplan-Meier analysis was used to establish the survival curves based on each prognostic outcome. Survival curves were graphed using GraphPad Prism 8. A P value < 0.05 in the two-tailed tests was considered to indicate statistical significance. All statistical analyses were performed using SPSS 26.0 (SPSS, Inc., Chicago, IL, United States).

RESULTS

Baseline characteristics of patients with ESCN

A total of 92 patients aged 43 to 80 years were finally included in our study. Table 1 lists the baseline characteristics of the normal SGK3 expression group and the SGK3 overexpression group. The normal SGK3 expression group included 37 patients and consisted of 27 males and 10 females. There were 55 patients (36 males and 19 females) in the SGK3 overexpression group. No significant differences were observed in the baseline indicators (age, sex, tumor location, tumor size, T stage, differentiated types, smoking history, lymphovascular infiltration and family history of cancer) between the normal expression and overexpression groups.

Prognostic outcomes

Table 2 summarizes the prognostic outcomes in each group. Tumor recurrence occurred in 10 patients. Of these patients, 2 (5.4%) were in the normal SGK3 expression group, and 8 (14.5%) were in the SGK3 overexpression group. Metastasis was detected in only 1 patient in the normal SGK3 expression group during the follow-up period. No significant associations were observed between SGK3 expression and tumor recurrence and metastasis. Death occurred in 3 (8.1%) patients in the normal SGK3 expression group and 15 (27.3%) patients in the SGK3 overexpression group. A significant correlation was observed between SGK3 expression status and death (P = 0.031).

SGK3 expression is related to prognostic outcomes

To evaluate the association between SGK3 overexpression and OS, a multivariate Cox regression model was performed (Table 3): Model 1 [hazard ratio (HR) 4.243; 95% confidence interval (CI): 1.219-14.773], Model 2 (HR 3.648; 95%CI: 1.030-12.917), Model 3 (HR 3.637; 95%CI: 1.028-12.866), and Model 4 (HR 4.729; 95%CI: 1.042-21.458). The P value of all four models was less than 0.05. The results of the multicollinearity test showed an average VIF of 1.525 (all VIF < 10). Figure 3 show the Kaplan-Meier curves of the relationship between SGK3 expression status and OS and DFS, respectively. The OS and DFS rates of patients were higher in the normal SGK3 expression group than in the SGK3 overexpression group during the follow-up period (P = 0.013 and P = 0.004, respectively).

DISCUSSION

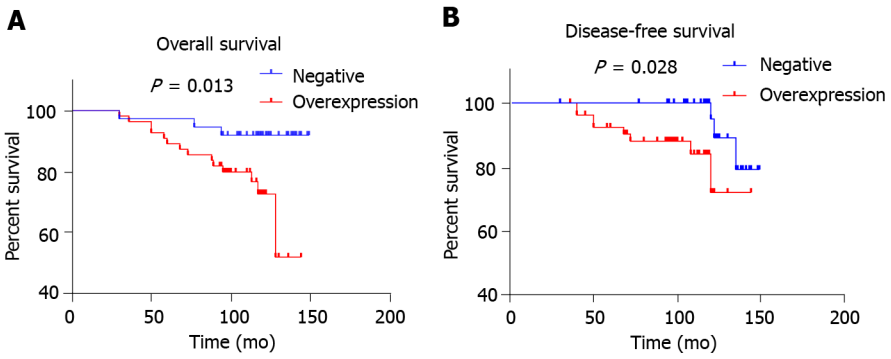
The SGK family is widely dysregulated in numerous human cancers and plays a vital role in tumor development and progression[19]. Among the three members of this family, SGK1 has been well researched, and its correlation with clinical outcomes has been reported in some cancers[20]. It has been suggested that low SGK1 expression in some tumors might induce feedback inhibition by activating the AKT pathway and might result in high SGK3 expression[21]. However, due to the later detection of SGK3, its relationship with tumors or other diseases has been revealed in only a few studies[22,23]. For instance, SGK3, as a novel regulator of renal phosphate transport, is associated with autosomal dominant hypophosphatemic rickets[24,25]. Its relationship with the clinical prognosis of tumors has rarely been reported thus far.

SGK3 exhibits structural and sequence similarity to the AKT family[26]. Its activation is mediated by the PI3K pathway and requires phosphorylation at two regulatory sites, Thr-320 and Ser-486[27]. Deletion of Thr-320 of SGK3 or disruption of the SGK3 protein tertiary structure yields nonfunctional proteins. To our knowledge, the SGK3 expression status of ESCN has not been illustrated. Our analysis of the expression of SGK3 in 92 ESCN tissues identified the expression status of SGK3 in ESCN tissues. Among the 92 tissue samples, the overexpression rate of SGK3 was close to 60%, confirming its high

Table 1 Basic characteristics according to serum and glucocorticoid-induced protein kinase 3 expression status

Characteristics	SGK3 normal, *n* = 37	SGK3 overexpression, *n* = 55	*P* value
Age (yr, mean ± SD)	58.73 ± 6.81	61.21 ± 8.05	0.118
Sex (male), *n* (%)	27 (73.0)	36 (65.5)	0.447
Tumor location, *n* (%)[1]			0.560
Upper esophagus	4 (10.8)	7 (12.7)	
Middle esophagus	14 (37.8)	26 (47.)	
Lower esophagus	19 (51.4)	22 (40.0)	
Tumor size (cm, mean ± SD)	3.16 ± 1.94	3.30 ± 1.89	0.742
Tumor stage, *n* (%)			0.720
Tis	25 (67.6)	38 (69.1)	
T1a	6 (16.2)	11 (20.0)	
T1b	6 (16.2)	6 (10.9)	
Differentiated types[1], *n* (%)			0.487
HIN	25 (67.6)	39 (70.9)	
Well-differentiation	7 (18.9)	13 (23.6)	
Intermediate differentiation	2 (5.4)	2 (3.6)	
Poor differentiation	3 (8.1)	1 (1.8)	
Smoking history, *n* (%)			0.313
Yes	10 (27.0)	10 (18.2)	
No	27 (73.0)	45 (81.8)	
Lymphovascular infiltration, *n* (%)[1]			0.402
Present	1 (2.7)	0 (0)	
Absent	36 (97.3)	55 (100)	
Family history of cancer[1], *n* (%)			0.698
Yes	2 (5.4)	5 (9.1)	
No	35 (94.6)	50 (90.9)	

[1]Tested by Fisher exact test.
SGK3: Serum and glucocorticoid-induced protein kinase 3; HIN: High-grade intraepithelial neoplasia.



DOI: 10.3748/wjg.v29.i23.3668 **Copyright** ©The Author(s) 2023.

Figure 3 Kaplan-Meier curves for overall survival and disease-free survival. A: Overall survival; B: Disease-free survival.

Table 2 Prognosis outcomes in the serum and glucocorticoid-induced protein kinase 3 normal and overexpression groups

Prognosis factors, *n* (%)	SGK3 normal, *n* = 37	SGK3 overexpression, *n* = 55	*P* value
Tumor recurrence[1], *n* (%)			0.306
Present	2 (5.4)	8 (14.5)	
Absent	35 (94.6)	47 (85.5)	
Metastasis[1], *n* (%)			0.402
Present	1 (2.7)	0 (0)	
Absent	36 (97.3)	55 (100)	
Death[1], *n* (%)			0.031
Yes	3 (8.1)	15 (27.3)	
No	34 (91.9)	40 (72.7)	

[1]Tested by Fisher exact test.
SGK3: Serum and glucocorticoid-induced protein kinase 3.

Table 3 Hazard ratio (95% confidence interval) for all-cause mortality between serum and glucocorticoid-induced protein kinase 3 normal and serum and glucocorticoid-induced protein kinase 3 overexpression

Model	HR (95%CI)	*P* value
Model 1	4.243 (1.219-14.773)	0.023
Model 2	3.648 (1.030-12.917)	0.045
Model 3	3.637 (1.028-12.866)	0.045
Model 4	4.729 (1.042-21.458)	0.044

Adjusted covariates: Model 1 = serum and glucocorticoid-induced protein kinase 3; Model 2 = model 1 + (age + sex); Model 3 = model 2 + (smoking history + family history of cancer); Model 4 = model 3 + (tumor location + tumor size + T stage + differentiated types). HR: Hazard ratio; CI: Confidence interval.

expression in esophageal neoplasia tissues. However, the defined functions of SGK3 in the growth or progression of ESCN have not been clarified.

ESCC is the most common pathological type of esophageal cancer and has a high incidence in some districts of China. It is difficult to detect at the early stage because its symptoms are insidious, and the majority of patients seek medical help when advanced symptoms of significant dysphagia occur. As a consequence, the traditional treatment of ESCN is mainly based on a combination of open surgery and chemotherapy/radiotherapy. Progress in imaging modalities and multidisciplinary comprehensive treatment has improved early diagnosis and clinical outcomes, respectively. However, the 5-year survival rate for ESCC is still lower than 30% because of its invasiveness and metastatic ability[28,29]. Recently, the development of endoscopy techniques has transformed the early diagnosis and treatment of diseases of the entire digestive system. In particular, the introduction of amplification techniques and narrow band imaging enables endoscopists to detect neoplasia at an early stage or in an asymptomatic period. In addition, the minimally invasive removal of lesions by ESD improves the clinical prognosis and even the quality of life. Although the 5-year survival rate of patients who undergo ESD is higher than that of patients who undergo open surgery, death caused by tumor recurrence or other reasons still occurs in some patients during the follow-up period[30]. This research focused on further exploration of ways to improve the survival rates of these patients.

The integration of small datasets in the present study demonstrated the high expression level of SGK3 in ESCN, as well as a significant relationship between its overexpression and OS. Furthermore, the 4 regression models showed that after adjusting for confounding factors, only the expression status of SGK3 was significantly associated with increased mortality. All these results indicate that the overexpression of SGK3 is correlated with the occurrence of death in ESCN patients. However, the influence of SGK3 on the occurrence and development of ESCN or cell cycle pathways has not yet been determined. Based on the results of our study, we speculate that SGK3 can be used as a prognostic indicator to assist in the outcome assessment of ESCN patients.

At present, follow-up of post-ESD patients with ESCN is generally performed *via* endoscopy as well as biopsy. The application of a standard follow-up method might aid endoscopists in identifying tumor recurrence in time, but this is only effective when endoscopists can detect the recurrence of cancerous

lesions followed by accurate biopsy sampling. Otherwise, no further action could be taken to intervene. As the overexpression of SGK3 is an independent factor in prognosis, IHC staining of SGK3 could be used to identify the population with a high mortality risk. Thus, active measures, including shortening the follow-up intervals and using moderate radiotherapy or chemotherapy, can be taken to improve survival.

However, our current study has several limitations. First, the sample size of our study was small, and all the included patients came from one hospital. Thus, these results need to be validated by expanding the sample size and performing a multicenter study. Second, this was a retrospective study. Therefore, we could not collect information without data bias. Thus, a prospective study, similar to this study, is needed in the future to verify the relationship between SGK3 overexpression and mortality.

CONCLUSION

In conclusion, SGK3 overexpression is significantly correlated with shortened survival in patients with endoscopic resection of superficial ESCN, and SGK3 might be a useful indicator for prognosis evaluation. Further studies are warranted to determine its mechanisms of action in the growth or progression of ESCN.

ARTICLE HIGHLIGHTS

Research background

Serum and glucocorticoid-induced protein kinase 3 (SGK3) regulate a range of fundamental cellular processes, such as tumor growth, metastasis, autophagy and survival, but SGK3 expression levels in patients with esophageal squamous cell neoplasia (ESCN) and their relationship with the prognosis of ESCN remain unknown.

Research motivation

SGK3 expression levels in patients with ESCN were assessed by immunohistochemistry to investigate the possible role of SGK3 as a prognostic factor.

Research objectives

Ninety-two patients who underwent gastrointestinal endoscopy followed by endoscopic submucosal dissection with complete follow-up data between November 2009 and July 2011 were included.

Research methods

A total of 92 patients who had undergone endoscopic resection for ESCN with more than 8 years of follow-up were enrolled. Immunohistochemistry was used to evaluate SGK3 expression.

Research results

Death occurred in 3 (8.1%) patients in the normal SGK3 expression group and 15 (27.3%) patients in the SGK3 overexpression group. A significant correlation was observed between SGK3 status and death (P = 0.031). The overall survival and disease-free survival rates of patients were higher in the normal SGK3 expression group than in the SGK3 overexpression group during the follow-up period.

Research conclusions

All these results indicate that the overexpression of SGK3 is correlated with the occurrence of death in ESCN patients and that SGK3 might be a useful indicator for prognosis evaluation.

Research perspectives

The sample size of this study was small, and the subjects both came from one hospital. Thus, the results need to be validated by expanding the sample size and performing a multicenter study. A prospective study, similar to this study, is needed in the future to verify the relationship between SGK3 overexpression and mortality.

FOOTNOTES

Author contributions: Xu N and Li LS contributed equally to this manuscript; Chai NL and Xu N contributed to manuscript drafting; Xu N and Li LS wrote the manuscript; Li H, Zhang LH collected the pathological data; Xiang JY, Zhang N, Wang PJ and Cheng YX were responsible for the revision of the manuscript for significant content; Chai NL and Linghu EQ reviewed the literature; all authors issued final approval for the version to be submitted.

Supported by National Natural Science Foundation of China, No. 82070682; and Beijing Municipal Science and Technology Commission, China, No. Z181100001718177.

Institutional review board statement: This study was approved by the Ethics Board of the First Medical Center of PLA General Hospital (approval No. S2020-251-01).

Informed consent statement: Patients were not required to give informed consent to the study because the analysis used anonymous clinical data that were obtained after each patient agreed to treatment by written consent.

Conflict-of-interest statement: There are no conflicts of interest to declare.

Data sharing statement: No additional data are available.

Open-Access: This article is an open-access article that was selected by an in-house editor and fully peer-reviewed by external reviewers. It is distributed in accordance with the Creative Commons Attribution NonCommercial (CC BY-NC 4.0) license, which permits others to distribute, remix, adapt, build upon this work non-commercially, and license their derivative works on different terms, provided the original work is properly cited and the use is non-commercial. See: https://creativecommons.org/Licenses/by-nc/4.0/

Country/Territory of origin: China

ORCID number: Ning Xu 0000-0002-7770-8731; Long-Song Li 0000-0002-4000-7501; Hui Li 0000-0002-2786-9844; Nan Zhang 0000-0001-9979-539X; Jing-Yuan Xiang 0000-0002-1755-7978; En-Qiang Linghu 0000-0003-4506-7877; Ning-Li Chai 0000-0002-6791-5817.

S-Editor: Yan JP
L-Editor: A
P-Editor: Yan JP

REFERENCES

1 **Wu Y**, Huang F, Zhou X, Yu S, Tang Q, Li S, Wang J, Chen L. Hypoxic Preconditioning Enhances Dental Pulp Stem Cell Therapy for Infection-Caused Bone Destruction. *Tissue Eng Part A* 2016; **22**: 1191-1203 [PMID: 27586636 DOI: 10.1089/ten.tea.2016.0086]
2 **Sánchez-Danés A**, Blanpain C. Deciphering the cells of origin of squamous cell carcinomas. *Nat Rev Cancer* 2018; **18**: 549-561 [PMID: 29849070 DOI: 10.1038/s41568-018-0024-5]
3 **van Rossum PSN**, Mohammad NH, Vleggaar FP, van Hillegersberg R. Treatment for unresectable or metastatic oesophageal cancer: current evidence and trends. *Nat Rev Gastroenterol Hepatol* 2018; **15**: 235-249 [PMID: 29235549 DOI: 10.1038/nrgastro.2017.162]
4 **Cui Y**, Chen H, Xi R, Cui H, Zhao Y, Xu E, Yan T, Lu X, Huang F, Kong P, Li Y, Zhu X, Wang J, Zhu W, Ma Y, Zhou Y, Guo S, Zhang L, Liu Y, Wang B, Xi Y, Sun R, Yu X, Zhai Y, Wang F, Yang J, Yang B, Cheng C, Liu J, Song B, Li H, Wang Y, Zhang Y, Cheng X, Zhan Q, Liu Z. Author Correction: Whole-genome sequencing of 508 patients identifies key molecular features associated with poor prognosis in esophageal squamous cell carcinoma. *Cell Res* 2022; **32**: 415-416 [PMID: 35177820 DOI: 10.1038/s41422-022-00625-x]
5 **Pimentel-Nunes P**, Libânio D, Bastiaansen BAJ, Bhandari P, Bisschops R, Bourke MJ, Esposito G, Lemmers A, Maselli R, Messmann H, Pech O, Pioche M, Vieth M, Weusten BLAM, van Hooft JE, Deprez PH, Dinis-Ribeiro M. Endoscopic submucosal dissection for superficial gastrointestinal lesions: European Society of Gastrointestinal Endoscopy (ESGE) Guideline - Update 2022. *Endoscopy* 2022; **54**: 591-622 [PMID: 35523224 DOI: 10.1055/a-1811-7025]
6 **Feng Y**, Wei W, Guo S, Li BQ. Associated risk factor analysis and the prognostic impact of positive resection margins after endoscopic resection in early esophageal squamous cell carcinoma. *Exp Ther Med* 2022; **24**: 457 [PMID: 35747151 DOI: 10.3892/etm.2022.11384]
7 **Yang X**, Men Y, Wang J, Kang J, Sun X, Zhao M, Sun S, Yuan M, Bao Y, Ma Z, Wang G, Hui Z. Additional Radiotherapy With or Without Chemotherapy Following Endoscopic Resection for Stage I Esophageal Carcinoma: A Pilot Study. *Technol Cancer Res Treat* 2021; **20**: 15330338211048051 [PMID: 34657505 DOI: 10.1177/15330338211048051]
8 **Kim J**, Kim D, Jung H, Lee J, Hong VS. Identification and Kinetic Characterization of Serum- and Glucocorticoid-Regulated Kinase Inhibitors Using a Fluorescence Polarization-Based Assay. *SLAS Discov* 2021; **26**: 655-662 [PMID: 33783250 DOI: 10.1177/24725552211002465]
9 **Lang F**, Böhmer C, Palmada M, Seebohm G, Strutz-Seebohm N, Vallon V. (Patho)physiological significance of the serum- and glucocorticoid-inducible kinase isoforms. *Physiol Rev* 2006; **86**: 1151-1178 [PMID: 17015487 DOI: 10.1152/physrev.00050.2005]
10 **Cao H**, Xu Z, Wang J, Cigliano A, Pilo MG, Ribback S, Zhang S, Qiao Y, Che L, Pascale RM, Calvisi DF, Chen X. Functional role of SGK3 in PI3K/Pten driven liver tumor development. *BMC Cancer* 2019; **19**: 343 [PMID: 30975125 DOI: 10.1186/s12885-019-5551-2]
11 **Xu J**, Wan M, He Q, Bassett RL Jr, Fu X, Chen AC, Shi F, Creighton CJ, Schiff R, Huo L, Liu D. SGK3 is associated with estrogen receptor expression in breast cancer. *Breast Cancer Res Treat* 2012; **134**: 531-541 [PMID: 22576469 DOI: 10.1007/s10549-012-2081-x]

12 **Alonso L**, Okada H, Pasolli HA, Wakeham A, You-Ten AI, Mak TW, Fuchs E. Sgk3 links growth factor signaling to maintenance of progenitor cells in the hair follicle. *J Cell Biol* 2005; **170**: 559-570 [PMID: 16103225 DOI: 10.1083/jcb.200504131]

13 **Kobayashi T**, Deak M, Morrice N, Cohen P. Characterization of the structure and regulation of two novel isoforms of serum- and glucocorticoid-induced protein kinase. *Biochem J* 1999; **344** Pt 1: 189-197 [PMID: 10548550 DOI: 10.1042/bj3440189]

14 **Hou M**, Lai Y, He S, He W, Shen H, Ke Z. SGK3 (CISK) may induce tumor angiogenesis (Hypothesis). *Oncol Lett* 2015; **10**: 23-26 [PMID: 26170971 DOI: 10.3892/ol.2015.3182]

15 **Basnet R**, Gong GQ, Li C, Wang MW. Serum and glucocorticoid inducible protein kinases (SGKs): a potential target for cancer intervention. *Acta Pharm Sin B* 2018; **8**: 767-771 [PMID: 30245963 DOI: 10.1016/j.apsb.2018.07.001]

16 **Wang Y**, Zhou D, Phung S, Warden C, Rashid R, Chan N, Chen S. SGK3 sustains ERα signaling and drives acquired aromatase inhibitor resistance through maintaining endoplasmic reticulum homeostasis. *Proc Natl Acad Sci U S A* 2017; **114**: E1500-E1508 [PMID: 28174265 DOI: 10.1073/pnas.1612991114]

17 **Vergara-Lluri ME**, Moatamed NA, Hong E, Apple SK. High concordance between HercepTest immunohistochemistry and ERBB2 fluorescence in situ hybridization before and after implementation of American Society of Clinical Oncology/ College of American Pathology 2007 guidelines. *Mod Pathol* 2012; **25**: 1326-1332 [PMID: 22699517 DOI: 10.1038/modpathol.2012.93]

18 **Japan Esophageal Society**. Japanese Classification of Esophageal Cancer, 11th Edition: part II and III. *Esophagus* 2017; **14**: 37-65 [PMID: 28111536 DOI: 10.1007/s10388-016-0556-2]

19 **Shanmugam I**, Cheng G, Terranova PF, Thrasher JB, Thomas CP, Li B. Serum/glucocorticoid-induced protein kinase-1 facilitates androgen receptor-dependent cell survival. *Cell Death Differ* 2007; **14**: 2085-2094 [PMID: 17932503 DOI: 10.1038/sj.cdd.4402227]

20 **Talarico C**, Dattilo V, D'Antona L, Menniti M, Bianco C, Ortuso F, Alcaro S, Schenone S, Perrotti N, Amato R. SGK1, the New Player in the Game of Resistance: Chemo-Radio Molecular Target and Strategy for Inhibition. *Cell Physiol Biochem* 2016; **39**: 1863-1876 [PMID: 27771704 DOI: 10.1159/000447885]

21 **Lang F**, Perrotti N, Stournaras C. Colorectal carcinoma cells--regulation of survival and growth by SGK1. *Int J Biochem Cell Biol* 2010; **42**: 1571-1575 [PMID: 20541034 DOI: 10.1016/j.biocel.2010.05.016]

22 **Gasser JA**, Inuzuka H, Lau AW, Wei W, Beroukhim R, Toker A. SGK3 mediates INPP4B-dependent PI3K signaling in breast cancer. *Mol Cell* 2014; **56**: 595-607 [PMID: 25458846 DOI: 10.1016/j.molcel.2014.09.023]

23 **Vasudevan KM**, Barbie DA, Davies MA, Rabinovsky R, McNear CJ, Kim JJ, Hennessy BT, Tseng H, Pochanard P, Kim SY, Dunn IF, Schinzel AC, Sandy P, Hoersch S, Sheng Q, Gupta PB, Boehm JS, Reiling JH, Silver S, Lu Y, Stemke-Hale K, Dutta B, Joy C, Sahin AA, Gonzalez-Angulo AM, Lluch A, Rameh LE, Jacks T, Root DE, Lander ES, Mills GB, Hahn WC, Sellers WR, Garraway LA. AKT-independent signaling downstream of oncogenic PIK3CA mutations in human cancer. *Cancer Cell* 2009; **16**: 21-32 [PMID: 19573809 DOI: 10.1016/j.ccr.2009.04.012]

24 **Cebeci AN**, Zou M, BinEssa HA, Alzahrani AS, Al-Rijjal RA, Al-Enezi AF, Al-Mohanna FA, Cavalier E, Meyer BF, Shi Y. Mutation of SGK3, a Novel Regulator of Renal Phosphate Transport, Causes Autosomal Dominant Hypophosphatemic Rickets. *J Clin Endocrinol Metab* 2020; **105** [PMID: 31821448 DOI: 10.1530/ey.18.5.3]

25 **Trepiccione F**, Capasso G. SGK3: a novel regulator of renal phosphate transport? *Kidney Int* 2011; **80**: 13-15 [PMID: 21673735 DOI: 10.1038/ki.2011.60]

26 **Gong GQ**, Wang K, Dai XC, Zhou Y, Basnet R, Chen Y, Yang DH, Lee WJ, Buchanan CM, Flanagan JU, Shepherd PR, Wang MW. Identification, structure modification, and characterization of potential small-molecule SGK3 inhibitors with novel scaffolds. *Acta Pharmacol Sin* 2018; **39**: 1902-1912 [PMID: 30038340 DOI: 10.1038/s41401-018-0087-6]

27 **Pearce LR**, Komander D, Alessi DR. The nuts and bolts of AGC protein kinases. *Nat Rev Mol Cell Biol* 2010; **11**: 9-22 [PMID: 20027184 DOI: 10.1038/nrm2822]

28 **Ohashi S**, Miyamoto S, Kikuchi O, Goto T, Amanuma Y, Muto M. Recent Advances From Basic and Clinical Studies of Esophageal Squamous Cell Carcinoma. *Gastroenterology* 2015; **149**: 1700-1715 [PMID: 26376349 DOI: 10.1053/j.gastro.2015.08.054]

29 **Liang H**, Fan JH, Qiao YL. Epidemiology, etiology, and prevention of esophageal squamous cell carcinoma in China. *Cancer Biol Med* 2017; **14**: 33-41 [PMID: 28443201 DOI: 10.20892/j.issn.2095-3941.2016.0093]

30 **Hirano S**, Nagami Y, Yamamura M, Tanoue K, Sakai T, Maruyama H, Ominami M, Nadatani Y, Fukunaga S, Otani K, Hosomi S, Tanaka F, Kamata N, Taira K, Shiba M, Watanabe T, Fujiwara Y. Evaluation of long-term survival in patients with severe comorbidities after endoscopic submucosal dissection for esophageal squamous cell carcinoma. *Surg Endosc* 2022; **36**: 5011-5022 [PMID: 34748088 DOI: 10.1007/s00464-021-08859-3]

World Journal of Gastroenterology

Submit a Manuscript: https://www.f6publishing.com

World J Gastroenterol 2023 June 21; 29(23): 3668-3677

DOI: 10.3748/wjg.v29.i23.3668

ISSN 1007-9327 (print) ISSN 2219-2840 (online)

ORIGINAL ARTICLE

Retrospective Study

Hot snare polypectomy *vs* endoscopic mucosal resection using bipolar snare for intermediate size colorectal lesions: Propensity score matching

Nobuhisa Minakata, Tatsuro Murano, Masashi Wakabayashi, Maasa Sasabe, Takashi Watanabe, Tomohiro Mitsui, Hiroki Yamashita, Atsushi Inaba, Hironori Sunakawa, Keiichiro Nakajo, Tomohiro Kadota, Kensuke Shinmura, Hiroaki Ikematsu, Tomonori Yano

Specialty type: Gastroenterology and hepatology

Provenance and peer review: Unsolicited article; Externally peer reviewed.

Peer-review model: Single blind

Peer-review report's scientific quality classification

Grade A (Excellent): 0
Grade B (Very good): B, B
Grade C (Good): C
Grade D (Fair): 0
Grade E (Poor): 0

P-Reviewer: Martino A, Italy; Nagami Y, Japan

Received: March 2, 2023
Peer-review started: March 2, 2023
First decision: April 8, 2023
Revised: April 21, 2023
Accepted: May 23, 2023
Article in press: May 23, 2023
Published online: June 21, 2023

Nobuhisa Minakata, Tatsuro Murano, Maasa Sasabe, Takashi Watanabe, Tomohiro Mitsui, Hiroki Yamashita, Atsushi Inaba, Hironori Sunakawa, Keiichiro Nakajo, Tomohiro Kadota, Kensuke Shinmura, Hiroaki Ikematsu, Tomonori Yano, Department of Gastroenterology and Endoscopy, National Cancer Center Hospital East, Kashiwa 2778577, Chiba, Japan

Masashi Wakabayashi, Department of Biostatistics Division, Center for Research Administration and Support, National Cancer Center, Kashiwa 2778577, Chiba, Japan

Corresponding author: Tatsuro Murano, MD, PhD, Doctor, Department of Gastroenterology and Endoscopy, National Cancer Center Hospital East, 6-5-1, Kashiwanoha, Kashiwa 2778577, Chiba, Japan. tatmuran@east.ncc.go.jp

Abstract

BACKGROUND

Endoscopic resection (ER) with bipolar snare, in which the electric current only passes through the tissue between the device's two electrodes, is a prominent method used to prevent perforation due to electricity potentially. ER using bipolar snare with or without submucosal injection enabled safe resection of colorectal lesions measuring 10–15 mm in an *ex vivo* porcine model. ER with bipolar snare is expected to have good treatment outcomes in 10–15 mm colorectal lesions, with high safety even without submucosal injection. However, no clinical reports have compared treatment outcomes with and without submucosal injection.

AIM

To compare the treatment outcomes of bipolar polypectomy with hot snare polypectomy (HSP) to those with endoscopic mucosal resection (EMR).

METHODS

In this single-centre retrospective study, we enrolled 10–15 mm nonpedunculated colorectal lesions (565 Lesions in 463 patients) diagnosed as type 2A based on the Japan Narrow-band Imaging Expert Team classification, resected by either HSP or EMR between January 2018 and June 2021 at the National Cancer Center Hospital East. Lesions were divided into HSP and EMR groups, and propensity score

matching was performed. In the matched cohort, *en bloc* and R0 resection rates and adverse events were compared between the two groups.

RESULTS

Of the 565 lesions in 463 patients, 117 lesions each in the HSP and EMR groups were selected after propensity score matching. In the original cohort, there was a significant difference in antithrombotic drug use ($P < 0.05$), lesion size ($P < 0.01$), location ($P < 0.01$), and macroscopic type ($P < 0.05$) between the HSP and EMR groups. In the matched cohort, the *en bloc* resection rates were comparable between both groups [93.2% (109/117) *vs* 92.3% (108/117), $P = 0.81$], and there was no significant difference in the R0 resection rate [77.8% (91/117) *vs* 80.3% (94/117), $P = 0.64$]. The incidence of delayed bleeding was similar in both groups [1.7% (2/117)]. Perforation occurred in the EMR group [0.9% (1/117)] but not in the HSP group.

CONCLUSION

Using bipolar snare, ER of nonpedunculated 10–15 mm colorectal lesions may be performed safely and effectively, even without submucosal injection.

Key Words: Adenoma; Cohort studies; Colonoscopy; Colorectal cancer; Endoscopic mucosal resection; Treatment outcome

©The Author(s) 2023. Published by Baishideng Publishing Group Inc. All rights reserved.

Core Tip: This study is the first to compare treatment outcomes between hot snare polypectomy (HSP) and endoscopic mucosal resection (EMR) using a bipolar snare for nonpedunculated colorectal lesions measuring 10–15 mm. First, there was no significant difference in *en bloc* and R0 resection rates between the HSP and EMR groups. Second, the incidence of adverse events was similar in both groups, but perforation occurred only in the EMR group. These results suggest that comparable treatment efficiency and safety may be obtained even without submucosal injection when resecting nonpedunculated colorectal lesions measuring 10–15 mm using a bipolar snare.

Citation: Minakata N, Murano T, Wakabayashi M, Sasabe M, Watanabe T, Mitsui T, Yamashita H, Inaba A, Sunakawa H, Nakajo K, Kadota T, Shinmura K, Ikematsu H, Yano T. Hot snare polypectomy *vs* endoscopic mucosal resection using bipolar snare for intermediate size colorectal lesions: Propensity score matching. *World J Gastroenterol* 2023; 29(23): 3668-3677

URL: https://www.wjgnet.com/1007-9327/full/v29/i23/3668.htm

DOI: https://dx.doi.org/10.3748/wjg.v29.i23.3668

INTRODUCTION

Colorectal cancer (CRC) is the leading cause of morbidity and mortality worldwide[1]. Detection and resection of colorectal lesions *via* colonoscopy reduce CRC-related mortality[2,3]. However, complications associated with endoscopic resection (ER), such as post-procedural bleeding and perforation, are concerning[4,5]. Perforation, although infrequent, is the most serious complication that may result in hospitalization, stoma formation, and mortality[6]. Various devices and techniques related to ER have been developed to reduce the risk of complications.

ER using a bipolar snare, wherein the electric current only passes through the tissue between the two electrodes of the device, may potentially prevent perforation due to electricity. Apart from reducing electric damage to tissues, using a bipolar snare does not require a counter electrode, carries a lower risk of burns, and can be used even when a metal, such as a pacemaker, is present inside the patient's body [7]. In an *ex vivo* porcine model, using a bipolar snare for intramucosal lesions measuring 10–15 mm did not cause thermal damage to the muscularis propria. However, perforation occurred with a monopolar snare. Furthermore, thermal damage to the muscularis propria was not observed in bipolar polypectomy, regardless of whether a submucosal injection was performed before resection[8].

An ER with a bipolar snare for 10–15 mm colorectal lesions could result in favourable outcomes even without submucosal injection. However, no reports have compared bipolar polypectomy with and without submucosal injection in clinical practice. Hence, using a bipolar snare for colorectal lesions measuring 10–15 mm, this study aimed to compare the safety and efficiency of hot snare polypectomy (HSP), which involves resection without submucosal injection, to those of endoscopic mucosal resection (EMR), which involves resection with submucosal injection.

MATERIALS AND METHODS

Patients

We retrospectively enrolled 10–15-mm nonpedunculated colorectal lesions diagnosed as type 2A based on the Japan Narrow-band Imaging Expert Team (JNET) classification, resected by either HSP or EMR using a bipolar snare between January 2018 and June 2021 at the National Cancer Center Hospital East. The exclusion criteria were: (1) History of inflammatory bowel disease and familial adenomatous polyposis; (2) Pedunculated type lesions; (3) Residual lesions after previous ER; and (4) Lesions pathologically diagnosed as inflammatory or hyperplastic polyps.

HSP and EMR

Before the colonoscopy, a polyethylene glycol electrolyte solution with ascorbic acid (MobiPrep, EA Pharma, Tokyo, Japan) or magnesium citrate (Magcorol P, Horii Pharmaceutical Industries, Osaka, Japan) was administered to all patients according to the manufacturer's instructions. The examinations were performed using a magnifying endoscope (PCF-H290ZI, CF-HQ290, CF-H290ECI, CF-EZ1500DI, CF-XZ1200I colonoscope, Olympus, Tokyo, Japan; EC-L590ZP, EC-L600ZP, Fujifilm Co., Tokyo, Japan), light source, and video processor (EVIS LUCERAELITE, EVIS X1, Olympus; LASEREO, Fujifilm Co.).

All procedures were performed by either four experts (≥ 2000 colonoscopies performed) or 18 nonexperts (< 2000 colonoscopies performed) endoscopists. The treatment choice (HSP or EMR) was at the endoscopist's discretion. For EMR, a submucosal injection was performed using saline solution alone or combined with sodium hyaluronate acid. A bipolar snare (Dragonare® Xemex Co. Ltd., Tokyo, Japan) was used in both HSP and EMR. An electrosurgery generator unit (ICC200, VIO300D, VIO3; ERBE Elektromedizin GmbH Co. Ltd., Tubingen, Germany; ESG100, Olympus) was used for all ERs. The cutting mode in the forced coagulation mode was used for resection. Subsequently, resection margins were evaluated endoscopically to confirm the absence of remnants. Prophylactic clipping after resection was performed at the endoscopist's discretion. Resected lesions were retrieved by suctioning through the endoscope into a trap, using pentapod-type grasping forceps or a retrieval net. The endocopists recorded the size, location, and macroscopic type of the lesions, diagnosis according to the JNET classification, and *en bloc* or piecemeal resection. The location was recorded as right colon if the lesion was in the caecum, ascending, or transverse colon, and as left colon if it was in the descending or sigmoid colon. Once removed, the lesions were fixed in formalin, embedded in paraffin, sectioned into 2–3 mm slices, stained with hematoxylin-eosin, and evaluated by two experienced pathologists blinded to the patient's clinical information. Pathological results were described according to World Health Organization criteria[9].

Outcomes

Study outcomes were *en bloc* and R0 resection rates, and adverse events, including delayed bleeding and perforation. *En bloc* resection was defined as ER with the entire lesion resected in a single piece. Upon histological evaluation of the horizontal and vertical margins of specimens, R0 resection was defined as negative margins both horizontally and vertically; RX resection, as unclear resection margins either horizontally or vertically; and R1 resection, as positive resection margins either horizontally or vertically [10]. Delayed bleeding was defined as haemorrhage requiring endoscopic intervention within 2 wk after polypectomy. Perforation was defined as any organ or fat outside the muscularis layer visualized on endoscopy during the procedure or free air observed on computed tomography after the procedure. For subgroup analysis, the R0 resection rate according to each clinical characteristic related to lesions was assessed.

Ethical considerations

This was a single-centre retrospective study, and the protocol was approved by the Institutional Review Board of the National Cancer Center (2017-434). All data were collected from the medical records. All procedures were performed after written informed consent was obtained.

Statistical analysis

Propensity score matching was applied at a 1:1 HSP-to-EMR ratio using greedy matching with a calliper width of 0.20 of the standard deviation of the logit transformation for the estimated propensity score[11, 12]. The propensity score was estimated using the multivariate logistic regression model, which included the following: age (continuous), sex (male/female), antithrombotic drug use (no/yes), size (continuous), location (right-sided colon/Left-sided colon/rectum), macroscopic type (0-Is/0-Isp/0-IIa), and endoscopist experience (expert/nonexpert) as explanatory variables without considering outcome variables. To evaluate the balance of patient characteristics between the HSP and EMR groups, we calculated standardized differences and created histograms and box plots. The chi-square and Mann–Whitney U tests were used to compare patient characteristics between groups. For treatment outcomes, univariable analyses were performed using the χ^2 test in all enrolled lesions and the McNemar test in pair-matched lesions. All *P* values were two-sided with a significance level of 0.05. All statistical analyses were performed using EZR (Saitama Medical Center, Jichi Medical University,

Saitama, Japan) and SAS (version 9.4) graphical user interface for R 4.1.0 (R Foundation for Statistical Computing, Vienna, Austria). EZR is a modified version of R commander (version 2.7-0), designed to add statistical functions frequently used in biostatistics[13]. The statistical methods of this study were reviewed by Masashi Wakabayashi from the Biostatistics Division of Center for Research Administration and Support at National Cancer Center.

RESULTS

Background characteristics of patients

Of the 711 consecutive lesions in 602 patients, 463 patients were enrolled, and 565 Lesions in them were analysed in the present study. Of the 565 Lesions, 440 in 346 patients were resected *via* HSP; 125 in 117 patients were resected *via* EMR. A flowchart of patient enrolment is shown in Figure 1. Patient characteristics before and after propensity score matching are shown in Table 1. There was a significant difference in antithrombotic drug use ($P < 0.05$), lesion size ($P < 0.01$), location ($P < 0.01$), and macroscopic type ($P < 0.05$) between the HSP and EMR groups in the original cohort. After propensity score matching, 117/440 Lesions in the HSP group and 117/125 in the EMR group were selected. Nearly all baseline characteristics were balanced (Table 1; standardized differences < 0.1 between HSP and EMR).

En bloc and R0 resection rates

In the original cohort, the *en bloc* and R0 resection rates between the HSP and EMR groups were similar [94.8% (417/440) *vs* 92.8% (116/125), $P = 0.40$; 81.6% (359/440) *vs* 80.8% (101/125), $P = 0.84$, respectively] (Table 2). In the propensity score-matched cohort, the *en bloc* resection rate remained similar between the HSP and EMR groups [93.2% (109/117) *vs* 92.3% (108/117), $P = 0.81$]. Furthermore, there was no significant difference between the HSP and EMR groups in the R0 resection rate [77.8% (91/117) *vs* 80.3% (94/117), $P = 0.64$] (Table 2). All patients who underwent RX/R1 resection were classified as HMX/HM1, and there were no patients with VMX/VM1. There was no significant difference in the R0 resection rate between the HSP and EMR groups according to size, macroscopic type, and endoscopist experience. However, in terms of rectal location, the R0 resection rate was significantly higher in the EMR group than in the HSP group [75.0% (18/24) *vs* 100% (22/22), $P = 0.022$] (Table 3).

Adverse events

In the original cohort, there was no significant difference in the incidence of delayed bleeding between the HSP and EMR groups [1.1% (5/440) *vs* 1.7% (2/125), $P = 0.68$]. Perforation occurred in the EMR group [0.9% (1/125); $P = 0.060$] but not in the HSP group (Table 2). In the propensity score-matched cohort, the incidence of delayed bleeding was similar in both groups [1.7% (2/117)]. Perforation occurred in the EMR group [0.9% (1/117)] but not in the HSP group. One case of perforation in the EMR group occurred intraoperatively.

DISCUSSION

This study is the first to compare treatment outcomes between HSP and EMR using a bipolar snare for nonpedunculated colorectal lesions measuring 10–15 mm in clinical practice. Two important results were obtained in this study. First, there was no significant difference in *en bloc* and R0 resection rates between the HSP and EMR groups. Second, the incidence of adverse events was similar in both groups; however, perforation occurred only in the EMR group. These results suggest that comparable treatment efficiency and safety may be obtained when resecting nonpedunculated colorectal lesions measuring 10–15 mm using a bipolar snare and even without submucosal injection.

Several ER methods have been widely adopted for colorectal lesions, including cold snare polypectomy (CSP), HSP, and EMR. The European Society of Gastrointestinal Endoscopy clinical guidelines proposed selecting ER methods according to the size and macroscopic type of lesions. For nonpedunculated lesions, CSP is recommended for lesions ≤ 9 mm, HSP or EMR for lesions 10–19 mm, and EMR or piecemeal EMR for lesions ≥ 20 mm[14,15]. For HSP and EMR, electrosurgical resection with a monopolar snare is generally performed. However, there is a risk of thermal damage because high-frequency current derived from the monopolar snare flows to the patient's plate through the deep part of the patient's living tissue[7]. In fact, in treatment outcomes of ER using a monopolar snare, perforation occurs in approximately 1.3%–2.8% of cases[16,17]. Therefore, when using a monopolar snare during ER for 10–19 mm colorectal lesions, EMR is recommended instead of HSP as it can reduce the risk of deep thermal damage[14].

We recently reported on endoscopic procedures using either a monopolar or bipolar snare in an *ex vivo* porcine model[8]. When 10–15-mm lesions were resected by HSP, the muscularis propria was thermally damaged when a monopolar snare was used but not when a bipolar snare was used.

Table 1 Patient and lesion characteristics

	Original cohort				Propensity score-matched cohort			
	HSP	EMR	*P* value	Standardized difference	HSP	EMR	*P* value	Standardized difference
No. of lesions	440	125			117	117		
Age (yr), mean ± SD (range)	69.7 ± 9.47 (36–90)	69.8 ± 8.36 (46–89)	0.53	0.013	69.5 ± 8.34 (43–85)	70.1 ± 8.78 (46–89)	0.67	0.072
Sex, *n* (%)			0.83	0.022			1.00	0
Male	328 (74.6)	92 (73.6)			87 (74.4)	87 (74.4)		
Female	112 (25.5)	33 (26.4)			30 (25.6)	30 (25.6)		
Antithrombotic drugs use, *n* (%)			0.031	0.21			0.87	0.021
Yes	66 (15.0)	29 (23.2)			25 (21.4)	26 (22.2)		
No	374 (85.0)	96 (76.8)			92 (78.6)	91 (77.8)		
Size (mm), mean ± SD (range)	11.2 ± 1.76 (10–15)	12.7 ± 2.02 (10–15)	< 0.01	0.77	12.4 ± 2.08 (10–15)	12.5 ± 2.01 (10–15)	0.72	0.054
Location, *n* (%)			< 0.01	0.38			0.94	0.054
Right-sided colon	240 (54.6)	63 (50.4)			61 (52.1)	63 (53.9)		
Left-sided colon	155 (35.2)	36 (28.8)			32 (27.4)	32 (27.4)		
Rectum	45 (10.2)	26 (20.8)			24 (20.5)	22 (18.8)		
Histological findings, *n* (%)			0.087	0.26			0.081	0.23
SSL	5 (1.1)	0 (0)			3 (2.6)	0 (0)		
LGD/HGD	434 (98.6)	123 (98.4)			114 (97.4)	117 (100)		
T1a/T1b	1 (0.2)	2 (1.6)			0 (0)	0 (0)		
Macroscopic type, *n* (%)			0.011	0.3			0.79	0.034
Type 0–Is, 0–Isp	176 (40.0)	66 (52.8)			62 (53.0)	60 (51.3)		
Type 0–IIa	264 (60.0)	59 (47.2)			55 (47.0)	57 (48.7)		
Endoscopist, *n* (%)			0.053	0.2			0.51	0.086
Expert	186 (42.3)	65 (52.0)			63 (53.9)	58 (49.6)		
Non-expert	254 (57.7)	60 (48.0)			54 (46.2)	59 (50.4)		

HSP: Hot snare polypectomy; EMR: Endoscopic mucosal resection; right-sided colon: Caecum to transverse colon; left-sided colon: Descending colon to sigmoid colon; SSL: Sessile serrated lesion; LGD: Low-grade dysplasia; HGD: High-grade dysplasia; T1a: Shallow submucosal invasive cancer; T1b: Deep submucosal invasive cancer; SD: Standard deviation.

Therefore, greater safety can be expected even without submucosal injection when a bipolar snare is used. However, no studies compared the safety and effectivity between HSP and EMR using a bipolar snare in clinical practice. This study revealed that HSP had a similar complication rate as EMR when a bipolar snare was used for 10–15-mm nonpedunculated colorectal lesions. Notably, perforation did not occur following HSP, suggesting a better safety profile when using a bipolar snare over a monopolar snare. The delayed bleeding rate was also reported to be 1.4%–3.1% for EMR[16,17] and 5.3% for HSP [18] when a monopolar snare was used. However, in this study, the delayed bleeding rate for both HSP and EMR when a bipolar snare was used was 1.7%, which is relatively lower than previously reported values. Saraya *et al*[19] also reported that HSP and EMR using a bipolar snare had a similar or lower risk of delayed bleeding and perforation than EMR using a monopolar snare[19]. Although the present study had a small number of cases, HSP did not cause perforation and resulted in less delayed bleeding, suggesting that HSP using a bipolar snare might be an option that results in fewer complications than EMR using a monopolar or bipolar snare.

For ER of medium-sized lesions ≥ 10 mm, determining whether *en bloc* or R0 resection is possible is important for ER method selection. Piecemeal ER and RX/R1 resection are known risk factors for local

Table 2 Comparison of outcomes between the hot snare polypectomy and endoscopic mucosal resection groups

	Original cohort			Propensity score-matched cohort		
	HSP	EMR	*P* value	HSP	EMR	*P* value
No. of lesions	440	125		117	117	
En bloc resection, *n*, % (95%CI)	417, 94.8 (92.3-96.7)	116, 92.8 (86.8-96.7)	0.4	109, 93.2 (87.0-97.0)	108, 92.3 (85.9-96.4)	0.81
Piecemeal resection, *n*, % (95%CI)	23, 5.2 (3.3-7.7)	9, 7.2 (3.3-13.2)		8, 6.8 (3.0-13.0)	9, 7.7 (3.6-14.1)	
R0 resection, *n*, % (95%CI)	359, 81.6 (77.6-85.1)	101, 80.8 (72.8-87.3)	0.84	91, 77.8 (69.2-84.9)	94, 80.3 (72.0-87.1)	0.64
RX/R1 resection, *n*, % (95%CI)	81, 18.4 (14.9-22.4)	24, 19.2 (12.7-27.2)		26, 22.2 (15.1-30.8)	23, 19.7 (12.9-28.0)	
Delayed bleeding, *n*, % (95%CI)	5, 1.1 (0.4-2.6)	2, 1.6 (0.2-5.7)	0.68	2, 1.7 (0.2-6.0)	2, 1.7 (0.2-6.0)	1.00
Perforation, *n*, % (95%CI)	0, 0 (0-0.8)	1, 0.8 (0.0-4.4)	0.06	0, 0 (0-3.1)	1, 0.9 (0-4.7)	N/A

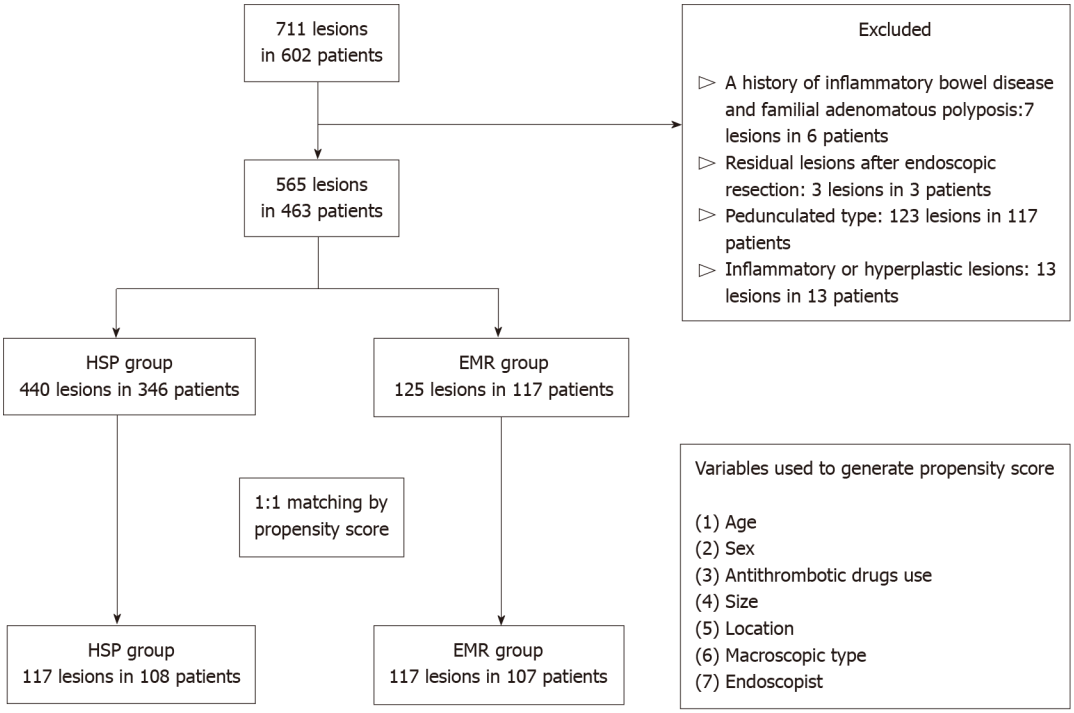
HSP: Hot snare polypectomy; EMR: Endoscopic mucosal resection; R0: Negative margin both horizontally and vertically; RX: Unclear resection margin either horizontally or vertically; R1: Positive resection margin either horizontally or vertically; CI: Confidence interval; N/A: Not applicable.

Table 3 Comparison of negative margin both horizontally and vertically resection rates between the hot snare polypectomy group and endoscopic mucosal resection groups

	R0 resection rate, %, *n/n* (95%CI)		
	HSP	EMR	*P* value
Total	77.8, 91/117 (69.2-84.9)	80.3, 94/117 (72.0-87.1)	
Size			
10–12 mm	77.9, 53/68 (66.2-87.1)	82.9, 58/70 (72.0-90.8)	0.52
13–15 mm	77.6, 38/49 (63.4-88.2)	76.6, 36/47 (62.0-87.7)	1.00
Macroscopic type			
Type 0-Is, 0-Isp	77.4, 48/62 (65.0-87.1)	86.7, 52/60 (75.4-94.1)	0.24
Type 0-IIa	78.2, 43/55 (65.0-88.2)	73.7, 42/57 (60.3-84.5)	0.66
Location			
Right-sided colon	75.4, 46/61 (62.7-85.5)	74.6, 47/63 (62.1-84.7)	1.00
Left-sided colon	84.4, 27/32 (67.2-94.7)	78.1, 25/32 (60.0-90.7)	0.75
Rectum	75.0, 18/24 (53.3-90.2)	100, 22/22 (84.6-100)	0.022
Endoscopist			
Expert	81.0, 51/63 (69.1-89.8)	82.8, 48/58 (70.6-91.4)	0.82
Non-expert	74.1, 40/54 (60.3-85.0)	78.0, 46/59 (65.3-87.7)	0.66

HSP: Hot snare polypectomy; EMR: Endoscopic mucosal resection; R0: Negative margin both horizontally and vertically.

recurrence after ER[20,21]. As the lesion grows, piecemeal endoscopic and RX/R1 resection rates increase, leading to an increased risk of local recurrence. However, the R0 resection rate is equivalent between HSP and EMR using a monopolar snare for colorectal lesions measuring 10–14 mm[22]. Therefore, the *en bloc* and R0 resection rates are equivalent between HSP and EMR with a bipolar snare, although no studies have been conducted to confirm this. In this study, for nonpedunculated colorectal lesions measuring 10–15 mm, HSP resulted in *en bloc* and R0 resection rates equivalent to those of EMR with a bipolar snare. Meanwhile, the *en bloc* resection rate was as high as ≥ 90% in both groups, and the R0 resection rate was approximately 80%, lower than previously reported values[22]. This could be because resection at our hospital is performed under the coagulation mode. Also, given the characteristics of ER using a bipolar snare, it is difficult to horizontally evaluate the pathological specimen due to crushing by cauterization in lesions where the resection margin is close to the lesion edge. However,



DOI: 10.3748/wjg.v29.i23.3668 **Copyright** ©The Author(s) 2023.

Figure 1 Flowchart of patient enrollment. Of the 711 consecutive lesions in 602 patients, 565 lesions in 463 patients were enrolled for the analysis. Of the 565 lesions, 440 in 346 patients were resected *via* hot snare polypectomy (HSP); 125 in 117 patients were resected *via* endoscopic mucosal resection (EMR). After propensity score matching, 117 lesions in the HSP group and 117 lesions in the EMR group were selected. HSP: Hot snare polypectomy; EMR: Endoscopic mucosal resection.

resection in coagulation mode may have contributed to a lower rate of delayed bleeding than previously reported because of the ability to coagulate the vessel[16-18].

The following points contributed to this innovative study design. First, patient and lesion backgrounds were matched using property score matching. The size, location, and macroscopic type of the lesions and endoscopic experience are known factors related to *en bloc* and R0 resection, and oral intake of antithrombotic agents is related to delayed bleeding[23-26]. This is the only study to balance the many confounding factors that may affect the estimation of results by property score matching and to compare treatment outcomes between HSP and EMR with a bipolar snare.

Second, only lesions diagnosed as JNET type 2A using magnifying observation combined with narrow-band imaging were included. In the qualitative diagnosis of colorectal lesions, those diagnosed as JNET type 2A can be diagnosed as adenomas or intramucosal cancers with high accuracy[27]. On the other hand, lesions diagnosed as JNET type 2B or 3 are generally known to develop into T1 cancer more frequently, resulting in bias wherein endoscopists who perform therapeutic endoscopy more carefully select ER methods that secure lesion margins. In this study, only JNET type 2A lesions potentially avoided bias due to differences in ER methods based on the preoperative diagnosis. Therefore, although the results of this study can be applied to adenomas and intramucosal cancers, it is unclear whether ER for T1 cancers will provide similar results. Third, we analysed the R0 resection rate as a factor between HSP and EMR. There was no difference in the R0 resection rate between HSP and EMR for most of the factors. However, the R0 resection rate for lesions in the rectum was better for EMR. No study has reported a change in the R0 resection rate with or without submucosal injection for rectal lesions. However, the R0 resection rate was reportedly significantly better in EMR than in HSP for the left colon [22]. Additionally, it can be difficult to diagnose a range of lesions due to factors such as 'skirt' in the rectum compared to the colon[28]. In rectal lesions of a difficult-to-identify extent with 'skirt', EMR provides wider margins, which may lead to fewer leftovers and improved R0 resection rates.

This study had some limitations. First, this was a single-centre retrospective study. In particular, the sample size was not large enough to prove the non-inferiority of HSP to EMR for any of the outcomes. Furthermore, since the treatment choices for HSP and EMR were left to the discretion of each endoscopist, the present results may be strongly influenced by the skill of a specific endoscopist. They may have been affected by imbalanced confounding factors that were not included in the analysis between the two groups. Second, there was no clear standard for measuring lesion size. Each endoscopist judged the size of the lesion by comparing it with the size of the snare, suggesting inaccurate lesion measurements. Third, the size of the bipolar snare used for resection was not specified, and the effects on the results cannot be denied. To eliminate these biases, conducting a large-cohort, multicentre, prospective, randomized controlled trial after clarifying ER methods, size of the snare, and

lesion measurement methods is desirable.

CONCLUSION

When using a bipolar snare, HSP has comparable treatment outcomes to EMR for nonpedunculated colorectal lesions measuring 10–15 mm. This suggests that the use of a bipolar snare may replace submucosal injection and may enable a more accessible ER while maintaining efficiency and safety.

ARTICLE HIGHLIGHTS

Research background

In endoscopic resection (ER) of colorectal lesions, it is important to develop resection methods that enable efficient and safe resection. Most recently, we have reported in *ex vivo* porcine model that endoscopic resection using bipolar snare for intermediate size lesions didn't lead to thermal injury for the intrinsic muscle layer even without submucosal injection. Therefore, the bipolar ER for intermediate size colorectal lesions of 10-15 mm has the potential to provide prominent outcomes in an efficient and highly safe manner even without submucosal injection.

Research motivation

We would like to assess the treatment outcomes of the bipolar resection with and without submucosal injection.

Research objectives

The present study aims to compare the resection results of endoscopic mucosal resection (EMR), which refers to the resection following submucosal injection, and hot snare polypectomy (HSP), which refers to the resection with no submucosal injection, to evaluate the efficacy and safety of HSP with bipolar snare for 10-15 mm lesions.

Research methods

We conducted the single-centre retrospective analysis of all 10-15 mm size colorectal lesions with a diagnosis of JNET Type 2A and resected by either EMR or HSP from January 2018 to June 2021. The target lesions were divided into two groups, HSP group and EMR group, and treatment outcomes and the adverse events were compared by conducting propensity score matching analysis.

Research results

Of the 565 lesions in 463 patients, 117 lesions each in the HSP and EMR groups were selected after propensity score matching. In the original cohort, there was a significant difference in antithrombotic drug use ($P < 0.05$), lesion size ($P < 0.01$), location ($P < 0.01$), and macroscopic type ($P < 0.05$) between the HSP and EMR groups. In the matched cohort, the *en bloc* resection rates were 93.2% (109/117) in the HSP group and 92.3% (108/117) in the EMR group, in which there was no significant difference ($P = 0.81$). Moreover, no significant difference was observed in the R0 resection rate [77.8% (91/117) *vs* 80.3% (94/117), $P = 0.64$]. The rates of delayed bleeding were comparable between the groups [1.7% (2/117)]. Perforation occurred in the EMR group [0.9% (1/117)] but not in the HSP group.

Research conclusions

Using bipolar snare, ER of nonpedunculated 10–15 mm colorectal lesions may be performed safely and effectively, even without submucosal injection.

Research perspectives

A large-cohort, multicentre, prospective, randomized controlled trial is warranted to prove the non-inferiority of bipolar HSP to bipolar EMR in treatment outcomes with ER of nonpedunculated 10–15 mm colorectal lesions.

FOOTNOTES

Author contributions: Minakata N, Murano T and Ikematsu H contributed to conceptualization; Minakata N and Murano T contributed to methodology; Minakata N and Wakabayashi M contributed to statistical analysis; Minakata N and Murano T contributed to writing - original draft preparation; Wakabayashi M, Sasabe M, Watanabe T, Mitsui T, Yamashita H, Inaba A, Sunakawa H, Nakajo K, Kadota T, Shinmura K, Ikematsu H, and Yano T contributed to writing - review and editing.

Institutional review board statement: The study protocol was approved by the Institutional Review Board of our hospital, No. 2017-434.

Informed consent statement: Patients were not required to provide informed consent for the study because the analysis used anonymous clinical data obtained after each patient agreed to treatment by written consent.

Conflict-of-interest statement: All the authors report no relevant conflicts of interest for this article.

Data sharing statement: The data supporting this study's findings are available from the corresponding author, Murano T, upon reasonable request at tatmuran@east.ncc.go.jp.

Open-Access: This article is an open-access article that was selected by an in-house editor and fully peer-reviewed by external reviewers. It is distributed in accordance with the Creative Commons Attribution NonCommercial (CC BY-NC 4.0) license, which permits others to distribute, remix, adapt, build upon this work non-commercially, and license their derivative works on different terms, provided the original work is properly cited and the use is non-commercial. See: https://creativecommons.org/Licenses/by-nc/4.0/

Country/Territory of origin: Japan

ORCID number: Nobuhisa Minakata 0000-0003-4540-4036; Tatsuro Murano 0000-0003-0423-2151; Masashi Wakabayashi 0009-0001-6368-5671; Maasa Sasabe 0000-0001-5219-4706; Takashi Watanabe 0009-0003-0294-3889; Tomohiro Mitsui 0000-0003-3518-1350; Hiroki Yamashita 0000-0002-6190-7904; Atsushi Inaba 0000-0001-7036-9485; Hironori Sunakawa 0000-0003-0792-9560; Keiichiro Nakajo 0000-0002-7138-9848; Tomohiro Kadota 0000-0002-0408-3494; Kensuke Shinmura 0000-0001-8786-4634; Hiroaki Ikematsu 0000-0001-9840-4588; Tomonori Yano 0000-0002-8030-1449.

S-Editor: Li L
L-Editor: A
P-Editor: Li L

REFERENCES

1 **Siegel RL**, Miller KD, Jemal A. Cancer statistics, 2016. *CA Cancer J Clin* 2016; **66**: 7-30 [PMID: 26742998 DOI: 10.3322/caac.21332]
2 **Winawer SJ**, Zauber AG, Ho MN, O'Brien MJ, Gottlieb LS, Sternberg SS, Waye JD, Schapiro M, Bond JH, Panish JF. Prevention of colorectal cancer by colonoscopic polypectomy. The National Polyp Study Workgroup. *N Engl J Med* 1993; **329**: 1977-1981 [PMID: 8247072 DOI: 10.1056/NEJM199312303292701]
3 **Zauber AG**, Winawer SJ, O'Brien MJ, Lansdorp-Vogelaar I, van Ballegooijen M, Hankey BF, Shi W, Bond JH, Schapiro M, Panish JF, Stewart ET, Waye JD. Colonoscopic polypectomy and long-term prevention of colorectal-cancer deaths. *N Engl J Med* 2012; **366**: 687-696 [PMID: 22356322 DOI: 10.1056/NEJMoa1100370]
4 **Kim SY**, Kim HS, Park HJ. Adverse events related to colonoscopy: Global trends and future challenges. *World J Gastroenterol* 2019; **25**: 190-204 [PMID: 30670909 DOI: 10.3748/wjg.v25.i2.190]
5 **Paszat LF**, Sutradhar R, Luo J, Rabeneck L, Tinmouth J. Perforation and post-polypectomy bleeding complicating colonoscopy in a population-based screening program. *Endosc Int Open* 2021; **9**: E637-E645 [PMID: 33880399 DOI: 10.1055/a-1381-7149]
6 **Derbyshire E**, Hungin P, Nickerson C, Rutter MD. Colonoscopic perforations in the English National Health Service Bowel Cancer Screening Programme. *Endoscopy* 2018; **50**: 861-870 [PMID: 29590669 DOI: 10.1055/a-0584-7138]
7 **Rey JF**, Beilenhoff U, Neumann CS, Dumonceau JM; European Society of Gastrointestinal Endoscopy (ESGE). European Society of Gastrointestinal Endoscopy (ESGE) guideline: the use of electrosurgical units. *Endoscopy* 2010; **42**: 764-772 [PMID: 20635311 DOI: 10.1055/s-0030-1255594]
8 **Shinmura K**, Ikematsu H, Kojima M, Nakamura H, Osera S, Yoda Y, Hori K, Oono Y, Ochiai A, Yano T. Safety of endoscopic procedures with monopolar *vs* bipolar instruments in an *ex vivo* porcine model. *BMC Gastroenterol* 2020; **20**: 27 [PMID: 32005163 DOI: 10.1186/s12876-020-1176-9]
9 **WHO Classification of Tumours Editorial Board**. WHO Classification of Tumors: Digestive System Tumours. 5th ed. Lyon, France: International Agency for Research on Cancer; 2019
10 **Japanese Society for Cancer of the Colon and Rectum**. Japanese Classification of Colorectal, Appendiceal, and Anal Carcinoma: the 3d English Edition [Secondary Publication]. *J Anus Rectum Colon* 2019; **3**: 175-195 [PMID: 31768468 DOI: 10.23922/jarc.2019-018]
11 **Austin PC**. Some methods of propensity-score matching had superior performance to others: results of an empirical investigation and Monte Carlo simulations. *Biom J* 2009; **51**: 171-184 [PMID: 19197955 DOI: 10.1002/bimj.200810488]
12 **Austin PC**. An Introduction to Propensity Score Methods for Reducing the Effects of Confounding in Observational Studies. *Multivariate Behav Res* 2011; **46**: 399-424 [PMID: 21818162 DOI: 10.1080/00273171.2011.568786]
13 **Kanda Y**. Investigation of the freely available easy-to-use software 'EZR' for medical statistics. *Bone Marrow Transplant* 2013; **48**: 452-458 [PMID: 23208313 DOI: 10.1038/bmt.2012.244]
14 **Ferlitsch M**, Moss A, Hassan C, Bhandari P, Dumonceau JM, Paspatis G, Jover R, Langner C, Bronzwaer M, Nalankilli K, Fockens P, Hazzan R, Gralnek IM, Gschwantler M, Waldmann E, Jeschek P, Penz D, Heresbach D, Moons L, Lemmers

A, Paraskeva K, Pohl J, Ponchon T, Regula J, Repici A, Rutter MD, Burgess NG, Bourke MJ. Colorectal polypectomy and endoscopic mucosal resection (EMR): European Society of Gastrointestinal Endoscopy (ESGE) Clinical Guideline. *Endoscopy* 2017; **49**: 270-297 [PMID: 28212588 DOI: 10.1055/s-0043-102569]

15 **Kawamura T**, Takeuchi Y, Asai S, Yokota I, Akamine E, Kato M, Akamatsu T, Tada K, Komeda Y, Iwatate M, Kawakami K, Nishikawa M, Watanabe D, Yamauchi A, Fukata N, Shimatani M, Ooi M, Fujita K, Sano Y, Kashida H, Hirose S, Iwagami H, Uedo N, Teramukai S, Tanaka K. A comparison of the resection rate for cold and hot snare polypectomy for 4-9 mm colorectal polyps: a multicentre randomised controlled trial (CRESCENT study). *Gut* 2018; **67**: 1950-1957 [PMID: 28970290 DOI: 10.1136/gutjnl-2017-314215]

16 **van Hattem WA**, Shahidi N, Vosko S, Hartley I, Britto K, Sidhu M, Bar-Yishay I, Schoeman S, Tate DJ, Byth K, Hewett DG, Pellisé M, Hourigan LF, Moss A, Tutticci N, Bourke MJ. Piecemeal cold snare polypectomy *vs* conventional endoscopic mucosal resection for large sessile serrated lesions: a retrospective comparison across two successive periods. *Gut* 2021; **70**: 1691-1697 [PMID: 33172927 DOI: 10.1136/gutjnl-2020-321753]

17 **Saito Y**, Fukuzawa M, Matsuda T, Fukunaga S, Sakamoto T, Uraoka T, Nakajima T, Ikehara H, Fu KI, Itoi T, Fujii T. Clinical outcome of endoscopic submucosal dissection *vs* endoscopic mucosal resection of large colorectal tumors as determined by curative resection. *Surg Endosc* 2010; **24**: 343-352 [PMID: 19517168 DOI: 10.1007/s00464-009-0562-8]

18 **Ket SN**, Mangira D, Ng A, Tjandra D, Koo JH, La Nauze R, Metz A, Moss A, Brown G. Complications of cold *vs* hot snare polypectomy of 10-20 mm polyps: A retrospective cohort study. *JGH Open* 2020; **4**: 172-177 [PMID: 32280761 DOI: 10.1002/jgh3.12243]

19 **Saraya T**, Ikematsu H, Fu KI, Tsunoda C, Yoda Y, Oono Y, Kojima T, Yano T, Horimatsu T, Sano Y, Kaneko K. Evaluation of complications related to therapeutic colonoscopy using the bipolar snare. *Surg Endosc* 2012; **26**: 533-540 [PMID: 21938574 DOI: 10.1007/s00464-011-1914-8]

20 **Buchner AM**, Guarner-Argente C, Ginsberg GG. Outcomes of EMR of defiant colorectal lesions directed to an endoscopy referral center. *Gastrointest Endosc* 2012; **76**: 255-263 [PMID: 22657404 DOI: 10.1016/j.gie.2012.02.060]

21 **Yoshida N**, Fukumoto K, Hasegawa D, Inagaki Y, Inoue K, Hirose R, Dohi O, Ogiso K, Murakami T, Tomie A, Okuda K, Inada Y, Okuda T, Rani RA, Morinaga Y, Kishimoto M, Itoh Y. Recurrence rate and lesions characteristics after cold snare polypectomy of high-grade dysplasia and T1 Lesions: A multicenter analysis. *J Gastroenterol Hepatol* 2021; **36**: 3337-3344 [PMID: 34260116 DOI: 10.1111/jgh.15625]

22 **Horiuchi A**, Makino T, Kajiyama M, Tanaka N, Sano K, Graham DY. Comparison between endoscopic mucosal resection and hot snare resection of large nonpedunculated colorectal polyps: a randomized trial. *Endoscopy* 2016; **48**: 646-651 [PMID: 27100717 DOI: 10.1055/s-0042-105557]

23 **Ito A**, Suga T, Ota H, Tateiwa N, Matsumoto A, Tanaka E. Resection depth and layer of cold snare polypectomy *vs* endoscopic mucosal resection. *J Gastroenterol* 2018; **53**: 1171-1178 [PMID: 29516270 DOI: 10.1007/s00535-018-1446-2]

24 **Pohl H**, Srivastava A, Bensen SP, Anderson P, Rothstein RI, Gordon SR, Levy LC, Toor A, Mackenzie TA, Rosch T, Robertson DJ. Incomplete polyp resection during colonoscopy-results of the complete adenoma resection (CARE) study. *Gastroenterology* 2013; **144**: 74-80.e1 [PMID: 23022496 DOI: 10.1053/j.gastro.2012.09.043]

25 **Tavakkoli A**, Law RJ, Bedi AO, Prabhu A, Hiatt T, Anderson MA, Wamsteker EJ, Elmunzer BJ, Piraka CR, Scheiman JM, Elta GH, Kwon RS. Specialist Endoscopists Are Associated with a Decreased Risk of Incomplete Polyp Resection During Endoscopic Mucosal Resection in the Colon. *Dig Dis Sci* 2017; **62**: 2464-2471 [PMID: 28600656 DOI: 10.1007/s10620-017-4643-6]

26 **Kishida Y**, Hotta K, Imai K, Ito S, Yoshida M, Kawata N, Tanaka M, Kakushima N, Takizawa K, Ishiwatari H, Matsubayashi H, Ono H. Risk Analysis of Colorectal Post-Polypectomy Bleeding Due to Antithrombotic Agent. *Digestion* 2019; **99**: 148-156 [PMID: 30179871 DOI: 10.1159/000490791]

27 **Hirata D**, Kashida H, Iwatate M, Tochio T, Teramoto A, Sano Y, Kudo M. Effective use of the Japan Narrow Band Imaging Expert Team classification based on diagnostic performance and confidence level. *World J Clin Cases* 2019; **7**: 2658-2665 [PMID: 31616682 DOI: 10.12998/wjcc.v7.i18.2658]

28 **Miyamoto H**, Ikematsu H, Fujii S, Osera S, Odagaki T, Oono Y, Yano T, Ochiai A, Sasaki Y, Kaneko K. Clinicopathological differences of laterally spreading tumors arising in the colon and rectum. *Int J Colorectal Dis* 2014; **29**: 1069-1075 [PMID: 24986136 DOI: 10.1007/s00384-014-1931-x]

World Journal of Gastroenterology

Submit a Manuscript: https://www.f6publishing.com

World J Gastroenterol 2023 June 21; 29(23): 3678-3687

DOI: 10.3748/wjg.v29.i23.3678

ISSN 1007-9327 (print) ISSN 2219-2840 (online)

ORIGINAL ARTICLE

Retrospective Study

Lymphocyte-to-white blood cell ratio is associated with outcome in patients with hepatitis B virus-related acute-on-chronic liver failure

Yue Zhang, Peng Chen, Xuan Zhu

Specialty type: Gastroenterology and hepatology

Provenance and peer review: Unsolicited article; Externally peer reviewed.

Peer-review model: Single blind

Peer-review report's scientific quality classification

Grade A (Excellent): 0
Grade B (Very good): B, B, B
Grade C (Good): 0
Grade D (Fair): 0
Grade E (Poor): 0

P-Reviewer: Desai GS, India; Kao JT, Taiwan; Papazafiropoulou A, Greece

Received: March 22, 2023
Peer-review started: March 22, 2023
First decision: April 14, 2023
Revised: April 28, 2023
Accepted: May 22, 2023
Article in press: June 21, 2023
Published online: June 21, 2023

Yue Zhang, Peng Chen, Xuan Zhu, Department of Gastroenterology, Jiangxi Clinical Research Center for Gastroenterology, The First Affiliated Hospital of Nanchang University, Nanchang 330006, Jiangxi Province, China

Corresponding author: Xuan Zhu, PhD, Professor, Department of Gastroenterology, Jiangxi Clinical Research Center for Gastroenterology, The First Affiliated Hospital of Nanchang University, Yongwaizhengjie Road, Donghu District, Nanchang 330006, Jiangxi Province, China. waiyongtg@163.com

Abstract

BACKGROUND

The lymphocyte-to-white blood cell ratio (LWR) is a blood marker of the systemic inflammatory response. The prognostic value of LWR in patients with hepatitis B virus-associated acute-on-chronic liver failure (HBV-ACLF) remains unclear.

AIM

To explore whether LWR could stratify the risk of poor outcomes in HBV-ACLF patients.

METHODS

This study was conducted by recruiting 330 patients with HBV-ACLF at the Department of Gastroenterology in a large tertiary hospital. Patients were divided into survivor and non-survivor groups according to their 28-d prognosis. The independent risk factors for 28-d mortality were calculated by univariate and multivariate Cox regression analyses. Patients were divided into low- and high-LWR groups according to the cutoff values. Kaplan-Meier analysis was performed according to the level of LWR.

RESULTS

During the 28-d follow-up time, 135 patients died, and the mortality rate was 40.90%. The LWR level in non-surviving patients was significantly decreased compared to that in surviving patients. A lower LWR level was an independent risk factor for poor 28-d outcomes (hazard ratio = 0.052, 95% confidence interval: 0.005-0.535). The LWR level was significantly negatively correlated with the Child-Turcotte-Pugh, model for end-stage liver disease, and Chinese Group on the Study of Severe Hepatitis B-ACLF II scores. In addition, the 28-d mortality was higher for patients with LWR < 0.11 than for those with LWR ≥ 0.11.

CONCLUSION
LWR may serve as a simple and useful tool for stratifying the risk of poor 28-d outcomes in HBV-ACLF patients.

Key Words: Lymphocyte-to-white blood cell ratio; Hepatitis B virus; Acute-on-chronic liver failure; Child-Turcotte-Pugh score; Model for end-stage liver disease score; Chinese Group on the Study of Severe Hepatitis B-Acute-on-chronic liver failure II score

©The Author(s) 2023. Published by Baishideng Publishing Group Inc. All rights reserved.

Core Tip: This manuscript introduced a simple and effective inflammatory marker, the lymphocyte-to-white blood cell ratio (LWR). Our study found that a lower LWR level was associated with poor 28-d outcomes in hepatitis B virus-associated acute-on-chronic liver failure (HBV-ACLF) patients. It may serve as a simple and useful tool for stratifying the risk of poor 28-d outcomes in HBV-ACLF patients, and it may be helpful in guiding a clinician to treatment allocation and assist in the prediction of prognosis.

Citation: Zhang Y, Chen P, Zhu X. Lymphocyte-to-white blood cell ratio is associated with outcome in patients with hepatitis B virus-related acute-on-chronic liver failure. *World J Gastroenterol* 2023; 29(23): 3678-3687
URL: https://www.wjgnet.com/1007-9327/full/v29/i23/3678.htm
DOI: https://dx.doi.org/10.3748/wjg.v29.i23.3678

INTRODUCTION

Acute-on-chronic liver failure (ACLF) is a life-threatening clinically complex syndrome characterized by high short-term mortality due to different combinations of multiorgan failures[1-3]. The main etiology of ACLF is hepatitis B virus (HBV) infection, with HBV-associated ACLF (HBV-ACLF) accounting for more than 70% of ACLF cases in most Asian countries[4]. The clinical characteristics of HBV-ACLF patients differ from those of alcoholic-related ACLF patients in Western countries, wherein coagulation and liver failure are the most common types of organ failure[5]. Early prediction of the prognosis of HBV-ACLF is important for clinical management and diminishing mortality. However, current score models are based on complicated assessments of organ failure. Therefore, it is necessary to identify an accurate and simple indicator to detect high-risk patients.

A growing body of research evidence suggests that HBV-ACLF is associated with systemic inflammation and immune paralysis[6,7]. In many recent studies, inflammation-related markers such as the platelet (PLT) to white blood cell ratio, neutrophil-to-lymphocyte ratio, and monocyte-to-lymphocyte ratio have received increasing attention in clinical settings and are used in predicting the prognosis of HBV-ACLF[8-10]. The lymphocyte-to-white blood cell ratio (LWR) is a blood marker of the systemic inflammatory response. Studies have suggested that LWR has good prognostic value for patients with cancer, infective endocarditis and COVID-19[11-13]. However, the prognostic role of LWR in HBV-ACLF patients remains unclear. Therefore, our study aims to reveal whether LWR can risk-stratify poor prognosis in HBV-ACLF patients.

MATERIALS AND METHODS

Subjects

A total of 330 patients diagnosed with HBV-ACLF were retrospectively included from May 2014 to February 2021 at the Department of Gastroenterology, the First Affiliated Hospital of Nanchang University. The inclusion criteria were as follows: (1) Age ≥ 18 years; (2) Chronic liver disease due to HBV infection; and (3) HBV-ACLF diagnosed based on the diagnostic guidelines for liver failure established in 2019[14]. The exclusion criteria were as follows: (1) Coinfection with hepatitis A/C/D/E virus; (2) Other etiologies such as drugs, autoimmunity, alcohol, or toxins that may contribute to HBV-ACLF; (3) Complicated with hepatocellular carcinoma; (4) Human immunodeficiency virus infection; and (5) Loss to follow-up. The study was approved by the Institutional Review Board of the First Affiliated Hospital of Nanchang University.

Data collection

Demographic information and clinical data were comprehensively collected by searching medical

records. Laboratory blood tests were measured in the first 24-h period on admission. LWR was computed as the lymphocyte count (× 10^9/L) divided by the white blood cell count (× 10^9/L)[12]. The Child-Turcotte-Pugh (CTP), model for end-stage liver disease (MELD) and Chinese Group on the Study of Severe Hepatitis B-ACLF II (COSSHACLFII) scores were calculated as previously described[15-17]. All patients were followed from their diagnosis until either their death or the end of the 28-d follow-up period. The survival rates at 28 d were obtained from patients' medical records or by telephone calls with the patients or their kinsfolks.

Definitions

Chronic HBV infection was defined by the presence of hepatitis B surface antigen for > 6 mo[18]. HBV-ACLF was defined according to the Asian Pacific Association for the Study of the Liver criteria in 2019: (1) Serum bilirubin ≥ 5 mg/dL; (2) International normalized ratio (INR) ≥ 1.5 or prothrombin activity < 40%; (3) Complicated within 4 wk by clinical ascites and/or encephalopathy in patients with pre-existing chronic liver diseases (diagnosed or undiagnosed); and (4) High 28-d mortality[14].

Statistical analysis

Statistical analysis was performed using the SPSS 24.0 statistical package (SPSS Inc., Chicago, IL), R software version 4.1.0 (http://www.r-project.org/), and X-tile software (Version 3.6.1, Yale University, New Haven, CT, United States). Continuous variables were compared using the *t* test or the Mann-Whitney *U* test, whereas categorical variables were compared using the chi-square test or Fisher's exact test. Univariate analysis and multivariate Cox proportional hazards models were performed to identify whether LWR was related to poor outcomes. The optimal cutoff value of LWR was determined by using X-tile. The Kaplan-Meier survival curve was generated by the "survival" and "survminer" packages in R software. All statistical tests were two-sided with a statistical significance level set at *P* values < 0.05.

RESULTS

Baseline characteristics

The baseline characteristics of the patients are summarized in Table 1. A total of 330 patients with HBV-ACLF were recruited. In the cohort, the average age of patients was 49.68 ± 12.39 years, and approximately 83.9% of patients were male. The HBV-ACLF patients were divided into survivor and non-survivor groups according to the prognosis at 28 d. At follow-up, the age, prothrombin time (PT), INR, bilirubin, CTP score (CTPs), MELD score (MELDs), and COSSHACLFII score (COSSHACLFIIs) of the non-survivors were significantly higher than those of the survivors (*P* < 0.05). However, the PLT count and LWR level of the non-survivors were significantly lower than those of the survivors (*P* < 0.05). In addition, there were no significant differences in sex, costs, hemoglobin, albumin, creatinine, blood urea nitrogen (BUN), or serum Na between the non-survivor group and survivor group (*P* > 0.05).

Low LWR as an independent risk factor for mortality in patients with HBV-ACLF

The association between the LWR level and 28-d mortality is shown in Table 2. In univariate analysis, age, PLT, PT, hemoglobin, bilirubin, BUN, and LWR were significant factors for 28-d mortality (all *P* < 0.05). In multivariable analysis, the results showed that age, PT, bilirubin, and LWR were associated with short-term mortality [hazard ratio (HR) = 1.015, 95% confidence interval (CI): 1.001-1.030; HR = 1.028, 95%CI: 1.015-1.042; HR = 1.001, 95%CI: 1.000-1.003; HR = 0.052, 95%CI: 0.005-0.535, respectively].

Correlation between LWR levels and other score models

Next, we investigated the correlation between LWR levels and other score models, including CTPs, MELDs and COSSHACLFIIs. As shown in Figures 1A-C, LWR levels were significantly correlated with the CTPs, MELDs and COSSHACLFIIs (*r* = -0.29, *P* < 0.001; *r* = -0.31, *P* < 0.001; *r* = -0.49, *P* < 0.001, respectively).

Comparison of clinical data with different LWR levels

The median LMR of HBV-ACLF patients was 0.17 (0.11-0.23), and X-tile software was used to determine the optimal cutoff values for LWR for 28-d mortality. Consequently, the threshold of 0.11 enabled us to distinguish favorable and poor outcomes that were most significant in HBV-ACLF patients (Figure 2). HBV-ACLF patients were stratified into low LWR (LWR < 0.11) and high LWR (LWR ≥ 0.11) groups according to the cutoff values. As shown in Table 3, the patients in the group with LWR < 0.11 had an older age, lower PLT count, higher PT, higher INR, lower hemoglobin, lower albumin, higher creatinine, higher BUN, higher CTPs, higher MELDs, higher COSSHACLFIIs, and significantly shorter survival rate than those in the group with LWR ≥ 0.11.

Impact of LWR on the mortality of HBV-ACLF patients

As shown above, the patients with LWR < 0.11 had higher 28-d mortality than the high LWR group (*P* <

Table 1 Baseline characteristics of hepatitis B virus-acute on chronic liver failure patients

	All patients (*n* = 330)	Survivor patients (*n* = 195)	Non-survivor patients (*n* = 135)	*P* value
Age (yr)	49.68 ± 12.39	47.91 ± 12.12	52.23 ± 12.39	0.002
Male, *n* (%)	277 (83.9)	162 (83.1)	115 (85.2)	0.068
Costs (dollars)	10133.88 (5886.57-15955.07)	10734.72 (5958.59-16913.77)	9107.89 (5727.32-14945.14)	0.065
Ascites, *n* (%)				0.016
Mild	158 (47.9)	104 (53.3)	54 (40.0)	
Medium	102 (30.9)	59 (30.3)	43 (31.9)	
Severe	70 (21.2)	32 (16.4)	38 (28.1)	
PLT (10^9/L)	108.00 (72.75-144.25)	115.00 (82.00-148.00)	89.00 (57.00-138.00)	0.004
PT (s)	22.70 (19.30-29.25)	21.10 (18.90-25.20)	25.40 (21.80-32.80)	< 0.001
INR	2.01 (1.74-2.64)	1.88 (1.69-2.30)	2.4 (1.94-3.07)	< 0.001
Hemoglobin (g/L)	122.00 (102.00-136.00)	123.00 (107.00-137.00)	121.00 (94.00-135.00)	0.166
Bilirubin (μmol/L)	312.91 ± 135.85	299.15 ± 126.15	332.79 ± 146.96	0.027
Albumin (g/L)	31.40 (28.20-34.25)	31.50 (28.20-34.60)	31.10 (28.20-33.30)	0.151
Creatinine (μmol/L)	66.60 (57.08-84.73)	65.60 (57.00-81.00)	68.30 (57.50-91.90)	0.294
BUN (mmol/L)	4.00 (2.80-6.10)	4.00 (2.80-5.50)	4.10 (3.00-7.60)	0.074
Serum Na (mmol/L)	137.00 (133.30-139.10)	137.00 (133.20-139.00)	136.90 (133.30-139.10)	0.882
LWR	0.17 (0.11-0.23)	0.19 (0.12-0.25)	0.13 (0.08-0.20)	< 0.001
CTPs	11.00 (10.00-12.00)	11.00 (10.00-12.00)	12.00 (11.00-13.00)	< 0.001
MELDs	23.17 (20.03-27.27)	21.59 (18.86-25.46)	25.04 (21.78-29.10)	< 0.001
COSSHACLFIIs	7.18 (6.54-8.12)	6.80 (6.30-7.37)	7.95 (7.20-8.70)	< 0.001

PLT: Platelet; PT: Prothrombin time; INR: International normalized ratio; BUN: Blood urea nitrogen; LWR: Lymphocyte-to-white blood cell ratio; CTPs: Child-Turcotte-Pugh score; MELDs: Model for end-stage liver disease score; COSSHACLFIIs: Chinese group on the study of severe Hepatitis B-Acute-on-chronic liver failure II score.

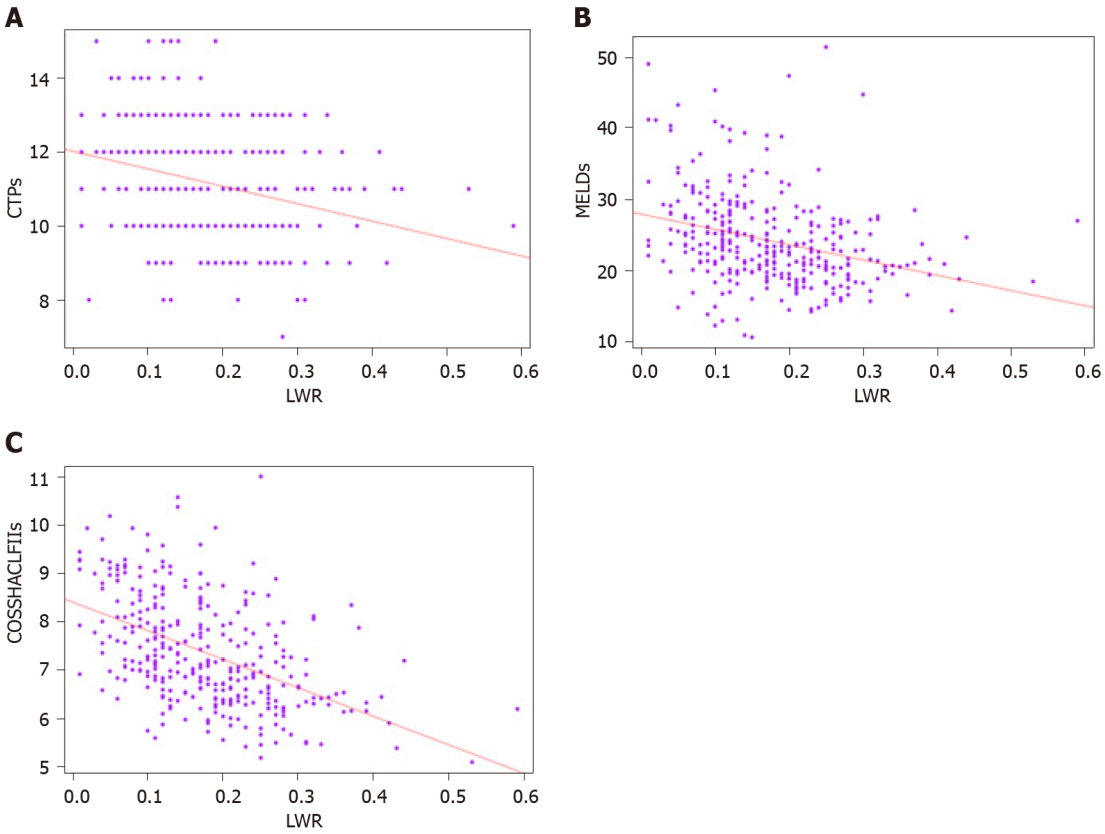
0.05). To confirm the association of the LWR level and 28-d outcomes in detail, Kaplan-Meier analysis was performed to assess LWR in HBV-ACLF patients, and patients with low LWR levels had a worse outcome than those with high LWR levels (Figure 3).

DISCUSSION

In our study, we found that a low LWR level was an independent prognostic factor related to poor 28-d outcomes in patients with HBV-ACLF. Patients with LWR < 0.11 had higher 28-d mortality than those with high LWR levels.

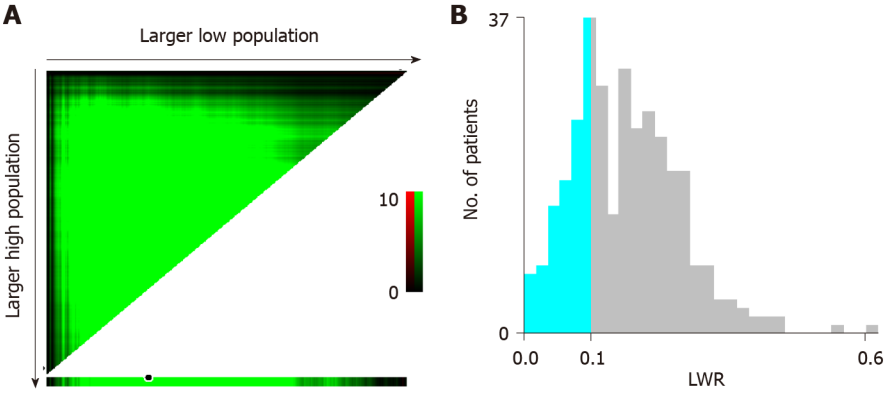
Systemic inflammation plays an important role in the development of HBV-ACLF[19]. The activation of inflammatory cytokines causes organ hypoperfusion and systemic circulatory dysfunction, which increase the activation of coagulation, tissue microthrombosis, and the development of organ failure [20]. Many studies have indicated that the inflammatory response can be reflected by inflammatory markers such as lymphocytes, white blood cells, PLTs, and neutrophils[21,22]. The combination of these inflammatory markers, such as the neutrophil-lymphocyte ratio (NLR), platelet-to-white blood cell ratio (PWR), and LWR, has been confirmed as a prognostic marker in a variety of liver diseases. Bernsmeier *et al*[23] reported that the NLR was an independent risk factor in patients with acute decompensation (AD) cirrhosis. Kim *et al*[22] included 1670 AD patients from a prospective cohort and found that patients with a PWR ≤ 12.1 had a higher 28-d mortality than those with a PWR > 12.1, and a lower PWR level was a prognostic factor for 28-d adverse outcomes. Overall, these inflammation-based markers could be useful for stratifying the severity of liver disease.

Our study found that LWR levels were significantly decreased in non-survivor HBV-ACLF patients, and low LWR levels were an independent risk factor for 28-d mortality in HBV-ACLF patients. The decreased LWR levels may reflect an enhanced inflammatory response and/or impaired immune



DOI: 10.3748/wjg.v29.i23.3678 **Copyright** ©The Author(s) 2023.

Figure 1 Scatter plot illustrating the correlation. A: Scatter plot illustrating the correlation between lymphocyte-to-white blood cell ratio (LWR) and Child-Turcotte-Pugh scores; B: Scatter plot illustrating the correlation between LWR and model for end-stage liver disease scores; C: Scatter plot illustrating the correlation between LWR and Chinese group on the study of severe Hepatitis B-Acute-on-chronic liver failure II scores. CTPs: Child-Turcotte-Pugh score; MELDs: Model for end-stage liver disease score; COSSHACLFIIs: Chinese group on the study of severe Hepatitis B-Acute-on-chronic liver failure II score; LWR: Lymphocyte-to-white blood cell ratio.



DOI: 10.3748/wjg.v29.i23.3678 **Copyright** ©The Author(s) 2023.

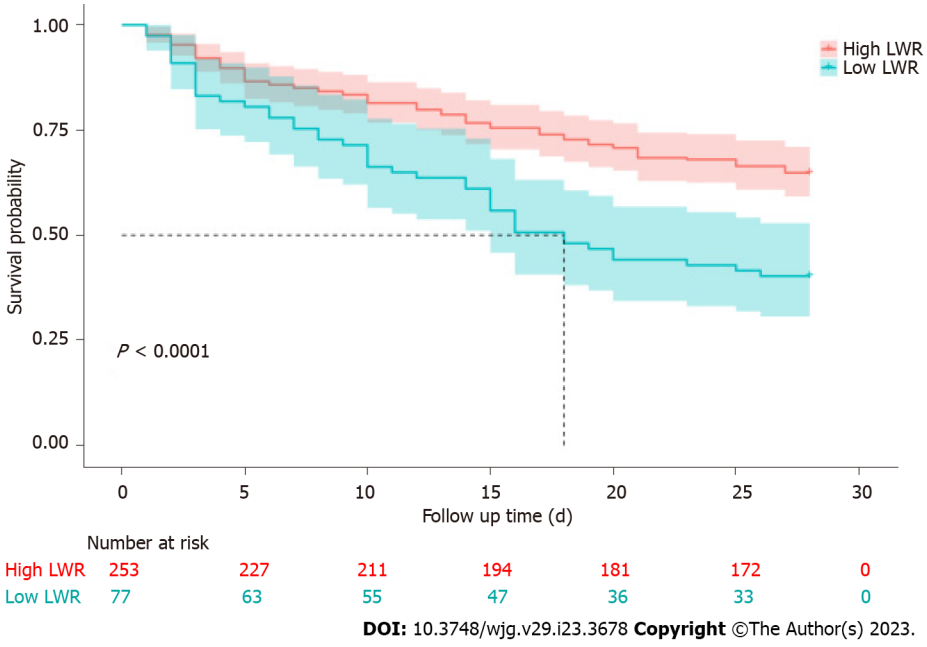
Figure 2 Analysis of lymphocyte-to-white blood cell ratio by using X-tile. A: The data on the horizontal ordinate increase from the left to the right, defined as the larger low population. The data on the vertical ordinate decrease from the top to the bottom, defined as the larger high population; B: The prognostic significance of lymphocyte-to-white blood cell ratio for hepatitis B virus-acute on chronic liver failure patients was determined by using a statistical algorithm in X-tile to calculate the most efficient cutoff point. LWR: Lymphocyte-to-white blood cell ratio.

response, which may explain the results. A previous study confirmed that lymphocytes play a critical role in the body's immune defense functions, immune response, and immune surveillance[12]. The elevated white blood cell count showed severe systemic inflammation, which was related to the prognosis of HBV-ACLF patients[24]. In addition, a recent study indicated that a low LWR level was an independent factor for poor outcomes in patients with decompensated liver cirrhosis, and the cut off value of LWR for 1 mo was 0.163. Patients with LWR < 0.163 had higher mortality than patients with LWR > 0.163[25]. Similar to this study, our research found that the cutoff value of LWR was 0.11, and

Table 2 Univariate and multivariate Cox regression analyses in hepatitis B virus-acute on chronic liver failure patients (*n* = 330)

	Univariate analysis		Multivariate analysis	
	HR (95%CI)	*P* value	HR (95%CI)	*P* value
Age	1.021 (1.007-1.035)	0.002	1.015 (1.001-1.030)	0.037
Male sex	1.202 (0.747-1.932)	0.448		
PLT (10^9/L)	0.997 (0.994-0.999)	0.046		
PT (s)	1.020 (1.011-1.030)	< 0.001	1.028 (1.015-1.042)	< 0.001
INR	1.042 (0.993-1.094)	0.093		
Hemoglobin (g/L)	0.993 (0.987-0.999)	0.027		
Bilirubin (μmol/L)	1.001 (1.000-1.003)	0.025	1.001 (1.000-1.003)	0.041
Albumin (g/L)	0.968 (0.933-1.005)	0.091		
Creatinine (μmol/L)	1.001 (1.000-1.001)	0.179		
BUN (mmol/L)	1.036 (1.014-1.058)	0.001		
Serum Na (mmol/L)	1.001 (0.999-1.003)	0.249		
LWR	0.011 (0.001-0.088)	< 0.001	0.052 (0.005-0.535)	0.013

In univariate analysis, $P < 0.1$ were subjected to multivariate analysis and was indicated in bold; in multivariate analysis, $P < 0.05$ was considered significant and was indicated in bold. CI: Confidence interval; HR: Hazard ratio; PLT: Platelet; PT: Prothrombin time; INR: International normalized ratio; BUN: Blood urea nitrogen; LWR: Lymphocyte-to-white blood cell ratio.



DOI: 10.3748/wjg.v29.i23.3678 **Copyright** ©The Author(s) 2023.

Figure 3 Kaplan-Meier analysis of 28-d overall survival. The mortality rate was higher in patients with lymphocyte-to-white blood cell ratio (LWR) < 0.11 than in patients with LWR ≥ 0.11. LWR: Lymphocyte-to-white blood cell ratio.

patients with LWR < 0.11 had higher mortality than patients with LWR ≥ 0.11, and the results showed a significant negative correlation between LWR and CTPs, MELDs and COSSHACLFIIs. There are several limitations in our study. First, this is a single-center and retrospective study, which may cause selection biases. Second, lymphocytes and white blood cells were not tested dynamically during follow-up.

CONCLUSION

In conclusion, LWR is easily accessible and conveniently calculated, and it might be a good marker for

Table 3 Clinical characteristics between low and high lymphocyte-to-white blood cell ratio groups in hepatitis B virus-acute on chronic liver failure patients

	Low LWR level (*n* = 77)	High LWR level (*n* = 253)	*P* value
Age (yr)	52.99 ± 12.57	48.67 ± 12.19	0.007
Male, *n* (%)	59 (76.6)	218 (86.2)	0.046
Costs (dollars)	7625.18 (3899.37-12070.55)	10984.59 (6639.92-16693.10)	< 0.001
Ascites, *n* (%)			0.007
Mild	25 (32.5)	133 (52.6)	
Medium	29 (37.7)	73 (28.9)	
Severe	23 (29.9)	47 (18.6)	
PLT (10^9/L)	86.00 (55.50-138.50)	110.00 (79.50-145.50)	0.039
PT (s)	23.20 (19.70-33.50)	22.40 (19.20-28.00)	0.016
INR	2.13 (1.76-3.11)	1.99 (1.73-2.54)	0.018
Hemoglobin (g/L)	109.00 (89.50-125.50)	125.00 (108.00-139.00)	< 0.001
Bilirubin (μmol/L)	331.52 ± 153.46	307.25 ± 129.82	0.170
Albumin (g/L)	30.10 (26.30-32.50)	31.80 (28.85-34.55)	< 0.001
Creatinine (μmol/L)	82.40 (58.40-126.10)	64.80 (56.85-77.95)	< 0.001
BUN (mmol/L)	7.00 (4.00-11.10)	3.70 (2.70-5.20)	< 0.001
Serum Na (mmol/L)	135.30 (131.50-139.05)	137.20 (133.90-139.10)	0.086
CTPs	12.00 (11.00-13.00)	11.00 (10.00-12.00)	< 0.001
MELDs	25.79 (22.52-30.91)	22.44 (19.55-26.13)	< 0.001
COSSHACLFIIs	8.11 (7.26-9.06)	6.94 (6.40-7.79)	< 0.001
28-d mortality, *n* (%)	46 (59.7)	89 (35.2)	< 0.001

PLT: Platelet; PT: Prothrombin time; INR: International normalized ratio; BUN: Blood urea nitrogen; LWR: Lymphocyte-to-white blood cell ratio; CTPs: Child-Turcotte-Pugh score; MELDs: Model for end-stage liver disease score; COSSHACLFIIs: Chinese group on the study of severe Hepatitis B-Acute-on-chronic liver failure II score.

identifying the risk of poor outcomes in HBV-ACLF patients. Therefore, our findings can help clinicians intervene in high-risk patients as early as possible.

ARTICLE HIGHLIGHTS

Research background

The lymphocyte-to-white blood cell ratio (LWR) is a blood marker that reflects the systemic inflammatory response. The prognostic value of the LWR remains unclear in hepatitis B virus-associated acute-on-chronic liver failure (HBV-ACLF) patients.

Research motivation

It is necessary to find an easy and effective marker that can reflect the prognosis in HBV-ACLF patients, so we explored whether LWR can risk-stratify poor prognosis in HBV-ACLF patients.

Research objectives

This study aimed to investigate whether LWR could be an easy and useful marker that can identify the risk of poor outcomes in HBV-ACLF patients.

Research methods

A total of 330 HBV-ACLF patients were included in this study, and patients were divided into survivor and non-survivor groups according to 28-d outcome. Univariate and multivariate Cox regression analyses were performed to select independent risk factors for 28-d mortality. The correlation test was

performed to evaluate the correlation between LWR and Child-Turcotte-Pugh score (CTPs), model for end-stage liver disease score (MELDs), and Chinese Group on the Study of Severe Hepatitis B-ACLF II score (COSSHACLFIIs). The cutoff value of LWR was calculated by X-tile software, and Kaplan-Meier analysis was performed to assess the association of the LWR level and 28-d outcomes in HBV-ACLF patients.

Research results

Low LWR was an independent risk factor for 28-d mortality in patients with HBV-ACLF (hazard ratio = 0.052, 95% confidence interval: 0.005-0.535), and LWR levels were significantly negatively correlated with CTPs, MELDs and COSSHACLFIIs. Moreover, the patients with low LWR levels had a higher 28-d mortality than those with high LWR levels.

Research conclusions

LWR is a simple, useful, and effective marker that could stratify the risk of 28-d adverse outcomes in HBV-ACLF patients.

Research perspectives

Further large-sample and multicenter prospective studies should be conducted to verify and confirm the prognostic value of the LWR.

FOOTNOTES

Author contributions: Zhang Y and Chen P contributed equally to this study, and they wrote the original draft; Zhang Y designed this study; Chen P analyzed the data; Zhu X critically revised the manuscript; and all authors have read and approved the final manuscript.

Supported by the National Natural Science Foundation of China, No. 81960120 and 81660110; the Postgraduate Innovation Special Foundation of Jiangxi Province, No. YC2022-B052; and "Gan-Po Talent 555" Project of Jiangxi Province, No. GCZ (2012)-1.

Institutional review board statement: The study was reviewed and approved by the First Affiliated Hospital of Nanchang University Institutional Review Board (Approval No. IIT2021009).

Informed consent statement: All study participants, or their legal guardian, provided informed written consent prior to study enrollment.

Conflict-of-interest statement: All the authors report no relevant conflicts of interest for this article.

Data sharing statement: Data can be acquired from the corresponding author.

Open-Access: This article is an open-access article that was selected by an in-house editor and fully peer-reviewed by external reviewers. It is distributed in accordance with the Creative Commons Attribution NonCommercial (CC BY-NC 4.0) license, which permits others to distribute, remix, adapt, build upon this work non-commercially, and license their derivative works on different terms, provided the original work is properly cited and the use is non-commercial. See: https://creativecommons.org/Licenses/by-nc/4.0/

Country/Territory of origin: China

ORCID number: Yue Zhang 0000-0003-1514-2303; Peng Chen 0000-0002-2215-214X; Xuan Zhu 0000-0002-1240-0947.

S-Editor: Wang JJ
L-Editor: A
P-Editor: Wang JJ

REFERENCES

1 **Zaccherini G**, Weiss E, Moreau R. Acute-on-chronic liver failure: Definitions, pathophysiology and principles of treatment. *JHEP Rep* 2021; **3**: 100176 [PMID: 33205036 DOI: 10.1016/j.jhepr.2020.100176]

2 **Moreau R**, Jalan R, Gines P, Pavesi M, Angeli P, Cordoba J, Durand F, Gustot T, Saliba F, Domenicali M, Gerbes A, Wendon J, Alessandria C, Laleman W, Zeuzem S, Trebicka J, Bernardi M, Arroyo V; CANONIC Study Investigators of the EASL–CLIF Consortium. Acute-on-chronic liver failure is a distinct syndrome that develops in patients with acute decompensation of cirrhosis. *Gastroenterology* 2013; **144**: 1426-1437, 1437.e1 [PMID: 23474284 DOI: 10.1053/j.gastro.2013.02.042]

3 **Trebicka J**, Fernandez J, Papp M, Caraceni P, Laleman W, Gambino C, Giovo I, Uschner FE, Jimenez C, Mookerjee R, Gustot T, Albillos A, Bañares R, Janicko M, Steib C, Reiberger T, Acevedo J, Gatti P, Bernal W, Zeuzem S, Zipprich A, Piano S, Berg T, Bruns T, Bendtsen F, Coenraad M, Merli M, Stauber R, Zoller H, Ramos JP, Solè C, Soriano G, de Gottardi A, Gronbaek H, Saliba F, Trautwein C, Özdogan OC, Francque S, Ryder S, Nahon P, Romero-Gomez M, Van Vlierberghe H, Francoz C, Manns M, Garcia E, Tufoni M, Amoros A, Pavesi M, Sanchez C, Curto A, Pitarch C, Putignano A, Moreno E, Shawcross D, Aguilar F, Clària J, Ponzo P, Jansen C, Vitalis Z, Zaccherini G, Balogh B, Vargas V, Montagnese S, Alessandria C, Bernardi M, Ginès P, Jalan R, Moreau R, Angeli P, Arroyo V; PREDICT STUDY group of the EASL-CLIF Consortium. The PREDICT study uncovers three clinical courses of acutely decompensated cirrhosis that have distinct pathophysiology. *J Hepatol* 2020; **73**: 842-854 [PMID: 32673741 DOI: 10.1016/j.jhep.2020.06.013]

4 **Zheng MH**, Shi KQ, Fan YC, Li H, Ye C, Chen QQ, Chen YP. A model to determine 3-month mortality risk in patients with acute-on-chronic hepatitis B liver failure. *Clin Gastroenterol Hepatol* 2011; **9**: 351-356.e3 [PMID: 21195790 DOI: 10.1016/j.cgh.2010.12.027]

5 **Wu T**, Li J, Shao L, Xin J, Jiang L, Zhou Q, Shi D, Jiang J, Sun S, Jin L, Ye P, Yang L, Lu Y, Li T, Huang J, Xu X, Chen J, Hao S, Chen Y, Xin S, Gao Z, Duan Z, Han T, Wang Y, Gan J, Feng T, Pan C, Li H, Huang Y, Xie Q, Lin S, Li L; Chinese Group on the Study of Severe Hepatitis B (COSSH). Development of diagnostic criteria and a prognostic score for hepatitis B virus-related acute-on-chronic liver failure. *Gut* 2018; **67**: 2181-2191 [PMID: 28928275 DOI: 10.1136/gutjnl-2017-314641]

6 **Clària J**, Stauber RE, Coenraad MJ, Moreau R, Jalan R, Pavesi M, Amorós À, Titos E, Alcaraz-Quiles J, Oettl K, Morales-Ruiz M, Angeli P, Domenicali M, Alessandria C, Gerbes A, Wendon J, Nevens F, Trebicka J, Laleman W, Saliba F, Welzel TM, Albillos A, Gustot T, Benten D, Durand F, Ginès P, Bernardi M, Arroyo V; CANONIC Study Investigators of the EASL-CLIF Consortium and the European Foundation for the Study of Chronic Liver Failure (EF-CLIF). Systemic inflammation in decompensated cirrhosis: Characterization and role in acute-on-chronic liver failure. *Hepatology* 2016; **64**: 1249-1264 [PMID: 27483394 DOI: 10.1002/hep.28740]

7 **Bernsmeier C**, van der Merwe S, Périanin A. Innate immune cells in cirrhosis. *J Hepatol* 2020; **73**: 186-201 [PMID: 32240716 DOI: 10.1016/j.jhep.2020.03.027]

8 **Jie Y**, Gong J, Xiao C, Zhu S, Zhou W, Luo J, Chong Y, Hu B. Low Platelet to White Blood Cell Ratio Indicates Poor Prognosis for Acute-On-Chronic Liver Failure. *Biomed Res Int* 2018; **2018**: 7394904 [PMID: 29854786 DOI: 10.1155/2018/7394904]

9 **Sun J**, Guo H, Yu X, Zhu H, Zhang X, Yang J, Wang J, Qian Z, Shen Z, Mao R, Zhang J. A neutrophil-to-lymphocyte ratio-based prognostic model to predict mortality in patients with HBV-related acute-on-chronic liver failure. *BMC Gastroenterol* 2021; **21**: 422 [PMID: 34758747 DOI: 10.1186/s12876-021-02007-w]

10 **Liu XY**, He X, Cai M, Peng SQ. Prognostic Value of Complete Blood Cell Count-Derived Inflammatory Markers in Hepatitis B Virus-Related Acute-on-Chronic Liver Failure. *Clin Lab* 2021; **67** [PMID: 34655197 DOI: 10.7754/Clin.Lab.2021.210217]

11 **Zhao W**, Wang P, Jia H, Chen M, Gu X, Liu M, Zhang Z, Cheng W, Wu Z. Lymphocyte count or percentage: which can better predict the prognosis of advanced cancer patients following palliative care? *BMC Cancer* 2017; **17**: 514 [PMID: 28768490 DOI: 10.1186/s12885-017-3498-8]

12 **Pitre T**, Jones A, Su J, Helmeczi W, Xu G, Lee C, Shamsuddin A, Mir A, MacGregor S, Duong M, Ho T, Beauchamp MK, Costa AP, Kruisselbrink R; COREG Investigators. Inflammatory biomarkers as independent prognosticators of 28-day mortality for COVID-19 patients admitted to general medicine or ICU wards: a retrospective cohort study. *Intern Emerg Med* 2021; **16**: 1573-1582 [PMID: 33496923 DOI: 10.1007/s11739-021-02637-8]

13 **Zhang M**, Ge Q, Qiao T, Wang Y, Xia X, Zhang X, Zhou J. Prognostic Value of Lymphocyte-to-White Blood Cell Ratio for In-Hospital Mortality in Infective Endocarditis Patients. *Int J Clin Pract* 2022; **2022**: 8667054 [PMID: 35685545 DOI: 10.1155/2022/8667054]

14 **Sarin SK**, Choudhury A, Sharma MK, Maiwall R, Al Mahtab M, Rahman S, Saigal S, Saraf N, Soin AS, Devarbhavi H, Kim DJ, Dhiman RK, Duseja A, Taneja S, Eapen CE, Goel A, Ning Q, Chen T, Ma K, Duan Z, Yu C, Treeprasertsuk S, Hamid SS, Butt AS, Jafri W, Shukla A, Saraswat V, Tan SS, Sood A, Midha V, Goyal O, Ghazinyan H, Arora A, Hu J, Sahu M, Rao PN, Lee GH, Lim SG, Lesmana LA, Lesmana CR, Shah S, Prasad VGM, Payawal DA, Abbas Z, Dokmeci AK, Sollano JD, Carpio G, Shresta A, Lau GK, Fazal Karim M, Shiha G, Gani R, Kalista KF, Yuen MF, Alam S, Khanna R, Sood V, Lal BB, Pamecha V, Jindal A, Rajan V, Arora V, Yokosuka O, Niriella MA, Li H, Qi X, Tanaka A, Mochida S, Chaudhuri DR, Gane E, Win KM, Chen WT, Rela M, Kapoor D, Rastogi A, Kale P, Sharma CB, Bajpai M, Singh V, Premkumar M, Maharashi S, Olithselvan A, Philips CA, Srivastava A, Yachha SK, Wani ZA, Thapa BR, Saraya A, Shalimar, Kumar A, Wadhawan M, Gupta S, Madan K, Sakhuja P, Vij V, Sharma BC, Garg H, Garg V, Kalal C, Anand L, Vyas T, Mathur RP, Kumar G, Jain P, Pasupuleti SSR, Chawla YK, Chowdhury A, Song DS, Yang JM, Yoon EL; APASL ACLF Research Consortium (AARC) for APASL ACLF working Party. Acute-on-chronic liver failure: consensus recommendations of the Asian Pacific association for the study of the liver (APASL): an update. *Hepatol Int* 2019; **13**: 353-390 [PMID: 31172417 DOI: 10.1007/s12072-019-09946-3]

15 **Pugh RN**, Murray-Lyon IM, Dawson JL, Pietroni MC, Williams R. Transection of the oesophagus for bleeding oesophageal varices. *Br J Surg* 1973; **60**: 646-649 [PMID: 4541913 DOI: 10.1002/bjs.1800600817]

16 **Li J**, Liang X, You S, Feng T, Zhou X, Zhu B, Luo J, Xin J, Jiang J, Shi D, Lu Y, Ren K, Wu T, Yang L, Li J, Li T, Cai Q, Sun S, Guo B, Chen J, He L, Li P, Yang H, Hu W, An Z, Jin X, Tian J, Wang B, Chen X, Xin S; Chinese Group on the Study of Severe Hepatitis B (COSSH). Development and validation of a new prognostic score for hepatitis B virus-related acute-on-chronic liver failure. *J Hepatol* 2021; **75**: 1104-1115 [PMID: 34090929 DOI: 10.1016/j.jhep.2021.05.026]

17 **Kamath PS**, Wiesner RH, Malinchoc M, Kremers W, Therneau TM, Kosberg CL, D'Amico G, Dickson ER, Kim WR. A model to predict survival in patients with end-stage liver disease. *Hepatology* 2001; **33**: 464-470 [PMID: 11172350 DOI: 10.1053/jhep.2001.22172]

18 **Liaw YF**, Kao JH, Piratvisuth T, Chan HL, Chien RN, Liu CJ, Gane E, Locarnini S, Lim SG, Han KH, Amarapurkar D, Cooksley G, Jafri W, Mohamed R, Hou JL, Chuang WL, Lesmana LA, Sollano JD, Suh DJ, Omata M. Asian-Pacific consensus statement on the management of chronic hepatitis B: a 2012 update. *Hepatol Int* 2012; **6**: 531-561 [PMID:

26201469 DOI: 10.1007/s12072-012-9365-4]

19 **Premkumar M**, Saxena P, Rangegowda D, Baweja S, Mirza R, Jain P, Bhatia P, Kumar G, Bihari C, Kalal C, Vyas T, Choudhury A, Sarin SK. Coagulation failure is associated with bleeding events and clinical outcome during systemic inflammatory response and sepsis in acute-on-chronic liver failure: An observational cohort study. *Liver Int* 2019; **39**: 694-704 [PMID: 30589495 DOI: 10.1111/liv.14034]

20 **Lisman T**, Luyendyk JP. Systemic inflammation and disorders of hemostasis in the AD-ACLF syndrome. *J Hepatol* 2021; **74**: 1264-1265 [PMID: 33347950 DOI: 10.1016/j.jhep.2020.12.017]

21 **Cai YJ**, Dong JJ, Dong JZ, Chen Y, Lin Z, Song M, Wang YQ, Chen YP, Shi KQ, Zhou MT. A nomogram for predicting prognostic value of inflammatory response biomarkers in decompensated cirrhotic patients without acute-on-chronic liver failure. *Aliment Pharmacol Ther* 2017; **45**: 1413-1426 [PMID: 28345155 DOI: 10.1111/apt.14046]

22 **Kim JH**, Kim SE, Song DS, Kim HY, Yoon EL, Kim TH, Jung YK, Suk KT, Jun BG, Yim HJ, Kwon JH, Lee SW, Kang SH, Kim MY, Jeong SW, Jang JY, Yoo JJ, Kim SG, Jin YJ, Cheon GJ, Kim BS, Seo YS, Kim HS, Sinn DH, Chung WJ, Lee HA, Nam SW, Kim IH, Suh JI, Kim JH, Chae HB, Sohn JH, Cho JY, Kim YJ, Yang JM, Park JG, Kim W, Cho HC, Kim DJ. Platelet-to-White Blood Cell Ratio Is Associated with Adverse Outcomes in Cirrhotic Patients with Acute Deterioration. *J Clin Med* 2022; **11** [PMID: 35566588 DOI: 10.3390/jcm11092463]

23 **Bernsmeier C**, Cavazza A, Fatourou EM, Theocharidou E, Akintimehin A, Baumgartner B, Dhar A, Auzinger G, Thursz M, Bernal W, Wendon JA, Karvellas CJ, Antoniades CG, McPhail MJW. Leucocyte ratios are biomarkers of mortality in patients with acute decompensation of cirrhosis and acute-on-chronic liver failure. *Aliment Pharmacol Ther* 2020; **52**: 855-865 [PMID: 32683724 DOI: 10.1111/apt.15932]

24 **Chen L**, Zhang J, Lu T, Cai J, Zheng J, Yao J, Yi S, Li H, Chen G, Zhao H, Zhang Y, Yang Y. A nomogram to predict survival in patients with acute-on-chronic hepatitis B liver failure after liver transplantation. *Ann Transl Med* 2021; **9**: 555 [PMID: 33987253 DOI: 10.21037/atm-20-6180]

25 **Xie Y**, He C, Wang W. A potential novel inflammation biomarker for predicting the prognosis of decompensated liver cirrhosis. *Ann Med* 2022; **54**: 3201-3210 [PMID: 36369931 DOI: 10.1080/07853890.2022.2142277]

World Journal of Gastroenterology

Submit a Manuscript: https://www.f6publishing.com

World J Gastroenterol 2023 June 21; 29(23): 3688-3702

DOI: 10.3748/wjg.v29.i23.3688

ISSN 1007-9327 (print) ISSN 2219-2840 (online)

ORIGINAL ARTICLE

Observational Study

Spatial cluster mapping and environmental modeling in pediatric inflammatory bowel disease

Mielle Michaux, Justin M Chan, Luke Bergmann, Luis F Chaves, Brian Klinkenberg, Kevan Jacobson

Specialty type: Gastroenterology and hepatology

Provenance and peer review: Unsolicited article; Externally peer reviewed.

Peer-review model: Single blind

Peer-review report's scientific quality classification

Grade A (Excellent): 0
Grade B (Very good): 0
Grade C (Good): C, C
Grade D (Fair): 0
Grade E (Poor): 0

P-Reviewer: Maric I, Croatia; Wang LH, China

Received: February 7, 2023
Peer-review started: February 7, 2023
First decision: March 20, 2023
Revised: March 31, 2023
Accepted: April 23, 2023
Article in press: April 23, 2023
Published online: June 21, 2023

Mielle Michaux, Justin M Chan, Kevan Jacobson, Department of Pediatrics, Division of Gastroenterology, Hepatology and Nutrition, Faculty of Medicine, British Columbia Children's Hospital, University of British Columbia, Vancouver V6H 3V4, British Columbia, Canada

Mielle Michaux, Justin M Chan, Kevan Jacobson, British Columbia Children's Hospital Research Institute, British Columbia Children's Hospital, Vancouver V5Z 4H4, British Columbia, Canada

Luke Bergmann, Brian Klinkenberg, Department of Geography, University of British Columbia, Vancouver V6T 1Z2, British Columbia, Canada

Luis F Chaves, Department of Environmental and Occupational Health, School of Public Health, Indiana University, Bloomington, IN 47405, United States

Kevan Jacobson, Department of Cellular and Physiological Sciences, University of British Columbia, Vancouver V6T 1Z3, British Columbia, Canada

Corresponding author: Kevan Jacobson, AGAF, FRCPC, MBChB, Professor, Senior Scientist, Department of Pediatrics, Division of Gastroenterology, Hepatology and Nutrition, Faculty of Medicine, British Columbia Children's Hospital, University of British Columbia, 4480 Oak Street, Room K4-184, Vancouver V6H 3V4, British Columbia, Canada. kjacobson@cw.bc.ca

Abstract

BACKGROUND

Geographical (geospatial) clusters have been observed in inflammatory bowel disease (IBD) incidence and linked to environmental determinants of disease, but pediatric spatial patterns in North America are unknown. We hypothesized that we would identify geospatial clusters in the pediatric IBD (PIBD) population of British Columbia (BC), Canada and associate incidence with ethnicity and environmental exposures.

AIM

To identify PIBD clusters and model how spatial patterns are associated with population ethnicity and environmental exposures.

METHODS

One thousand one hundred eighty-three patients were included from a BC Children's Hospital clinical registry who met the criteria of diagnosis with IBD ≤

age 16.9 from 2001–2016 with a valid postal code on file. A spatial cluster detection routine was used to identify areas with similar incidence. An ecological analysis employed Poisson rate models of IBD, Crohn's disease (CD), and ulcerative colitis (UC) cases as functions of areal population ethnicity, rurality, average family size and income, average population exposure to green space, air pollution, and vitamin-D weighted ultraviolet light from the Canadian Environmental Health Research Consortium, and pesticide applications.

RESULTS

Hot spots (high incidence) were identified in Metro Vancouver (IBD, CD, UC), southern Okanagan regions (IBD, CD), and Vancouver Island (CD). Cold spots (low incidence) were identified in Southeastern BC (IBD, CD, UC), Northern BC (IBD, CD), and on BC's coast (UC). No high incidence hot spots were detected in the densest urban areas. Modeling results were represented as incidence rate ratios (IRR) with 95%CI. Novel risk factors for PIBD included fine particulate matter ($PM_{2.5}$) pollution (IRR = 1.294, CI = 1.113-1.507, $P < 0.001$) and agricultural application of petroleum oil to orchards and grapes (IRR = 1.135, CI = 1.007-1.270, $P = 0.033$). South Asian population (IRR = 1.020, CI = 1.011-1.028, $P < 0.001$) was a risk factor and Indigenous population (IRR = 0.956, CI = 0.941-0.971, $P < 0.001$), family size (IRR = 0.467, CI = 0.268-0.816, $P = 0.007$), and summer ultraviolet (IBD = 0.9993, CI = 0.9990–0.9996, $P < 0.001$) were protective factors as previously established. Novel risk factors for CD, as for PIBD, included: $PM_{2.5}$ air pollution (IRR = 1.230, CI = 1 .056-1.435, $P = 0.008$) and agricultural petroleum oil (IRR = 1.159, CI = 1.002-1.326, $P = 0.038$). Indigenous population (IRR = 0.923, CI = 0.895–0.951, $P < 0.001$), as previously established, was a protective factor. For UC, rural population (UC IRR = 0.990, CI = 0.983-0.996, $P = 0.004$) was a protective factor and South Asian population (IRR = 1.054, CI = 1.030–1.079, $P < 0.001$) a risk factor as previously established.

CONCLUSION

PIBD spatial clusters were identified and associated with known and novel environmental determinants. The identification of agricultural pesticides and $PM_{2.5}$ air pollution needs further study to validate these observations.

Key Words: Inflammatory bowel diseases; Crohn disease; Ulcerative colitis; Pesticides; Air pollution; South Asian people

©The Author(s) 2023. Published by Baishideng Publishing Group Inc. All rights reserved.

Core Tip: Utilizing spatial mapping methodology, high and low incidence clusters of pediatric inflammatory bowel disease (IBD) were identified in British Columbia, Canada. Associating geographical location with IBD, rurality was negatively associated with ulcerative colitis. Notably, no high incidence hot spots were detected in the densest urban areas, suggesting unexplored urban protective factors. Novel risk factors for PIBD and specifically Crohn's disease included fine particulate matter pollution and agricultural applications of petroleum oil to orchards and grapes. Spatial distribution was partially explained by rurality, population ethnicity, family size, pesticide applications, air pollution, ultraviolet exposure, and residential greenness.

Citation: Michaux M, Chan JM, Bergmann L, Chaves LF, Klinkenberg B, Jacobson K. Spatial cluster mapping and environmental modeling in pediatric inflammatory bowel disease. *World J Gastroenterol* 2023; 29(23): 3688-3702
URL: https://www.wjgnet.com/1007-9327/full/v29/i23/3688.htm
DOI: https://dx.doi.org/10.3748/wjg.v29.i23.3688

INTRODUCTION

Canada has one of the world's highest rates of pediatric inflammatory bowel disease (IBD), which includes Crohn's disease (CD) and ulcerative colitis (UC)[1]. Incidence within countries can be quite varied, but local patterns of IBD incidence are unknown for most countries[1]. Results from studies in Finland, Norway, Northern France, and Manitoba, Canada suggest that IBD may have a clustered spatial distribution, but more research is necessary for understanding local spatial patterns[2-5]. To date, no study has focused on empirically detecting and evaluating disease clusters in Canadian or North American pediatric IBD (PIBD) populations. Notably, detecting local spatial clusters of IBD would allow for a better understanding of clinical populations and identify areas where services are needed.

Moreover, spatial epidemiology can be used to identify novel environmental risk and protective factors. Although it is evident that environmental factors are important determinants for disease development, additional study is necessary.

A variety of population and environmental factors are thought to influence IBD risk. High incidence has been observed in Canadian populations of Jewish ethnicity and South Asian pediatric populations in British Columbia (BC), and low incidence has been reported in Canadian Indigenous communities[4,6,7]. Higher socioeconomic status has been associated with IBD[4,8]. A variety of environmental exposures, including rural residence, green space, ultraviolet (UV) radiation, and air pollution have also been studied[9-13]. No study known to us has examined pesticides as a potential determinant of PIBD. Pesticides can be present in food and the environment, and a variety of pesticides have been linked with changes to the gut microbiota which could have implications for IBD development[14]. Based on Canadian immigration and rural residence studies of IBD, exposures during early life appear to be important[9,15].

The aims of this exploratory study were (1) To determine spatial patterning of PIBD and identify location of disease hot and cold spots in the Canadian province of BC; and (2) to model the association between IBD case counts and population-level ethnicity, average income, rural residence, and known as well as novel environmental determinants. We hypothesized that we would identify IBD clusters that would be associated with ethnicity and environmental exposures. Modeling potential population risk factors provided context to the spatial analysis and helped identify areas where additional novel environmental risk or protective factors might have meaningfully affected disease incidence.

MATERIALS AND METHODS

Study area

BC is Canada's westernmost province. It is divided into five Regional Health Authorities, which can be further subdivided into 89 Local Health Areas (LHAs) (see Figure 1 and Supplementary Figure 1). The majority of BC's population live in urban areas located in the Vancouver Coastal and Fraser Health Authorities near the United States border[16]. Northern, Interior, and Vancouver Island Health serve largely more rural populations.

Participants

Patients for this study were selected from a clinical registry of IBD patients maintained by the BC Children's Hospital (BCCH) Division of Gastroenterology, Hepatology and Nutrition who were diagnosed with or received care for IBD at BCCH in Vancouver[17]. Author Jacobson K is data steward for this registry. As BCCH is the only tertiary care pediatric institution with academic pediatric gastroenterologists in the province, it is where most children with IBD are diagnosed. Our recent study comparing PIBD incidence derived from the BCCH registry with incidence derived from population-wide provincial health administrative data between 1996 and 2008 found similar overall rates, particularly from 2001 onwards, reaffirming the validity of the registry as a reflection of population-based cases[18]. Notably, a small number of cases are diagnosed in the community, use health services from a different province or, in the case of older patients (> 16.9 years), are diagnosed by adult gastroenterology physicians. Registry patients were excluded from the study if they were diagnosed outside the study period (2001 to 2016) or over age 16.9 years, did not have a valid postal code on file, or had a postal code associated with BCCH as this was likely not their permanent address. Postal codes were cleaned to provide consistent formatting. See Table 1 for BC pediatric incidence, and Supplementary Table 1 for incidence by patient age. Patient six-digit postal code point location at diagnosis was associated with latitude and longitude coordinates from DMTI Spatial Inc. obtained from the Canadian Urban Environmental Health Research Consortium (CANUE)[19]. Incidence was pooled for the full study period to maximize the number of cases in each analysis.

This study was approved by the University of British Columbia Children's and Women's Research Ethics Board, No. H19-00739.

Methods

Guidelines from the REporting of studies Conducted using Observational Routinely-collected health Data statement were adapted for this ecological study. The statistical methods of this study were reviewed by biostatistician Jeffrey Bone from the BCCH Research Institute. Data is summarized in Table 2, with additional details on environmental exposures presented in the Supplementary materials. Ethnicity and family size (married or common-law spouses, single parents, and at least one child) data from the Canadian census were obtained at the Dissemination Area level and resampled to LHAs by population-weighted overlay[16,20,21]. Average family income for 2005 and 2015 was available for LHAs[22]. To approximate average environmental exposures for each LHA, census population age 0-19 was used to population-weight postal code exposure data in a process that captured 92.6% of BC's youth population (excluded population resided in areas not covered by single link postal codes). Environmental data provided by CANUE for six digit postal codes included Normalized Difference

Table 1 British Columbia average pediatric incidence for inflammatory bowel disease, Crohn's disease, ulcerative colitis, and inflammatory bowel disease-unclassified from 2001–2016

Diagnosis	Health authority	Cases	Incidence per 100000	95%CI for incidence	
All IBD	All British Columbia	1183	9.22	8.7	9.76
	Fraser	558	10.95	10.06	11.9
	Interior	143	7.15	6.03	8.43
	Northern	64	6.17	4.75	7.88
	Vancouver Coastal	254	9.28	8.17	10.49
	Vancouver Island	164	8.36	7.13	9.74
CD	All British Columbia	780	6.08	5.66	6.52
	Fraser	356	6.99	6.28	7.74
	Interior	96	4.8	3.89	5.85
	Northern	40	3.86	2.76	5.24
	Vancouver Coastal	166	6.06	5.18	7.06
	Vancouver Island	122	6.22	5.17	7.43
UC	All British Columbia	288	2.24	1.99	2.52
	Fraser	151	2.96	2.51	3.48
	Interior	32	1.6	1.09	2.26
	Northern	16	1.54	0.88	2.51
	Vancouver Coastal	62	2.27	1.74	2.9
	Vancouver Island	27	1.38	0.91	2
IBD-U	All British Columbia	115	0.9	0.74	1.08
	Fraser	51	1	0.75	1.32
	Interior	15	0.75	0.42	1.24
	Northern	8	0.77	0.33	1.52
	Vancouver Coastal	26	0.95	0.62	1.39
	Vancouver Island	15	0.76	0.43	1.26

IBD: Inflammatory bowel disease; CD: Crohn's disease, UC: Ulcerative colitis; IBD-U: Inflammatory bowel disease-unclassified.

Vegetation Index (NDVI)[19,23-26] greenness[27,28], vitamin D UV[19,29,30], nitrogen dioxide (NO_2)[19,31,32], ozone (O_3)[33-37], and fine particulate matter ($PM_{2.5}$)[19,38]. Data on metam, petroleum oil, and glyphosate pesticides was resampled from Global Pesticide Grids[39,40]. The least populous LHA was excluded from regression modeling due to missing data.

Spatial cluster analysis

Standardized incidence ratios (SIRs) for each of BC's LHAs were calculated from incident registry cases using BC incidence as the reference rate[41]. DataBC provided geographic data[42]. To reduce the instability in disease rates caused by low case counts and populations, rates were averaged for the study period. In addition, spatial linear empirical Bayes estimation was used to smooth SIRs in areas with average pediatric populations under 10000[43]. The smoothing process calculated averages between a LHA's SIR and the average SIR value of adjacent LHAs. Spatial relationships for smoothing and clustering were defined by direct adjacency (queen contiguity) to approximately model geographic connectivity.

Two forms of spatial analysis were used to identify spatial patterns in PIBD. The Global Moran's I statistic measured the degree to which spatial patterning of IBD, CD, and UC in BC was clustered, dispersed, or had no detectable spatial pattern. The Local Moran's I statistic was used as a Local Indicator of Spatial Association (LISA) to identify the location of hot spots (clusters of comparatively high SIRs) and cold spots (clusters of comparatively low SIRs) among LHAs[44]. To approximate the likelihood that a cluster would arise by chance, we used 999 Monte Carlo simulations to compute a pseudo-*P* value[44], which was then adjusted with a Holm correction for multiple comparisons. We

Table 2 Data used in environmental exposure modeling

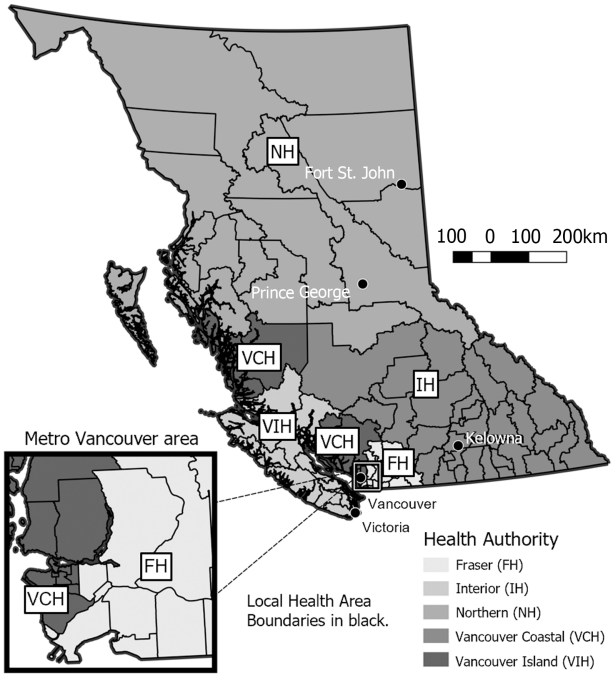
Variable	Description	Data source and database
Income	Mean of 2005 (adjusted to 2015 dollars) and 2015 census average family income for Local Health Areas	Statistics Canada, BC Community Health Atlas
Ethnicity	Census percent of the population of South Asian, Indigenous, Chinese, Jewish, and Non-Jewish European ethnic origin	Statistics Canada, University of Toronto Computing in the Humanities and Social Sciences Data Centre
Family size	Census average family size	Statistics Canada, University of Toronto Computing in the Humanities and Social Sciences Data Centre
Rurality	Percent of residents in each Local Health Area who lived outside a census metropolitan area or census agglomeration	Statistics Canada
NDVI greenness	Green vegetation cover calculated from land satellite imagery of surface reflection. Maximum and average growing season (May – August) NDVI within 250 m from postal code location. Multiplied by 100 so changes could be assessed as percentages	United States Geological Survey, Canadian Urban Environmental Health Research Consortium
UV vitamin D	Long-term stable monthly mean daily vitamin D dose from solar UV radiation adjusted for postal code elevation (J/m^{-2}) which was averaged for winter (December through February) and summer (June through August)	Environment Canada and Cancer Care Ontario, Canadian Urban Environmental Health Research Consortium
NO_2 air pollution	Annual average NO_2 concentration in parts per billion	Canadian Urban Environmental Health Research Consortium
O_3 air pollution	Average of O_3 taken from the highest rolling 8-hour daily average concentration (parts per billion)	Environment and Climate Change Canada, Canadian Urban Environmental Health Research Consortium
$PM_{2.5}$ air pollution	Annual average surface $PM_{2.5}$ ($\mu g/m^3$) concentration	Atmospheric Composition Analysis Group, Canadian Urban Environmental Health Research Consortium
Metam pesticide	2015 metam pesticide applied to fruits and vegetables (kg/ha/yr)	Global Pesticide Grids, Version 1.01, based on the United States Geological Survey's Pesticide National Synthesis Project and the Food and Agriculture Organization Corporate Statistical Database pesticide databases
Petroleum oil pesticide	2015 petroleum oil employed for grapes and orchards (kg/ha/yr)	Global Pesticide Grids, Version 1.01, based on the United States Geological Survey's Pesticide National Synthesis Project and the Food and Agriculture Organization Corporate Statistical Database pesticide databases
Glyphosate pesticide	2015 total glyphosate employed in major crops (wheat, corn, alfalfa, and others) in (kg/ha/yr)	Global Pesticide Grids, Version 1.01, based on the United States Geological Survey's Pesticide National Synthesis Project and the Food and Agriculture Organization Corporate Statistical Database pesticide databases
Population age 0-16.9	Yearly estimates of population age 0-16.9 for Local Health Areas averaged for 2001–2016	Statistics Canada, BC Stats

BC: British Columbia; NDVI: Normalized difference vegetation index; NO_2: Nitrogen dioxide; O_3: Ozone; $PM_{2.5}$: Fine particulate matter; UV: Ultraviolet.

chose LISA statistics over spatial and spatiotemporal SCAN methods given the irregular nature of the spatial areal units under analysis and the relative rarity of the disease, conditions under which LISA statistics have offered high sensitivity and specificity in cluster detection[45,46]. Data was aggregated over time (*i.e.* no spatio-temporal cluster analyses) given the aforementioned relative rarity of PIBD cases in BC.

Count regression modeling

Poisson Rate generalized linear models (PR-GLM) were used in an ecological analysis of LHAs to quantify the impact of population ethnicity, income, family size, rurality, air pollution, greenness, UV, and pesticide exposure on raw (unsmoothed) IBD, CD, and UC case counts. These models adjust for the population of each LHA and have an equal mean and variance. Model selection was based on the minimization of the Akaike Information Criterion using a stepwise algorithm combining backward elimination and forward addition[47]. PR-GLMs performed better than Negative Binomial, zero-inflated Poisson, and hurdle Poisson models. Considerations for reducing collinearity, conducting model selection, testing spatial independence of residuals, examining best model diagnostics, and considerations around the mapping of Incidence Rate Ratios (IRRs) are presented in the Supplementary materials. Multivariate models and high-quality Canadian census and exposure data were used to minimize sources of potential bias.



DOI: 10.3748/wjg.v29.i23.3688 **Copyright** ©The Author(s) 2023.

Figure 1 British Columbia's five Health Authorities and 89 Local Health Areas (black boundaries).

RESULTS

Spatial clustering results

The registry consisted of 1232 eligible patients diagnosed at or before age 16.9. Of these, 49 were associated with invalid or BCCH postal codes. In the spatial cluster modeling of the remaining 1183 PIBD patients, we observed a statistically significant (pseudo-$P < 0.05$) clustered distribution with a Moran's I statistic of 0.65 ($P = 0.001$). For the 780 CD patients we observed a Moran's I of 0.56 ($P = 0.001$) and for the 288 UC patients a Moran's I of 0.28 ($P = 0.001$). See Figure 2 for local cluster locations. Hot spots were observed in the lower mainland, the main urban centre of BC, for IBD ($P \leq 0.031$), CD ($P \leq 0.031$), and UC ($P \leq 0.007$), in the Okanagan region for IBD ($P \leq 0.029$) and CD ($P = 0.030$), and on Vancouver Island for CD ($P = 0.034$). A cold spot cluster was detected in southeastern BC for IBD (P values < 0.001), CD ($P \leq 0.0499$), and UC ($P \leq 0.040$), in Northern BC for IBD ($P = 0.026$) and CD ($P = 0.038$), and on BC's coast for UC ($P = 0.036$). We observed no LHA which had a significantly different trend in incidence than neighboring LHAs (spatial outliers) for IBD, CD, or UC.

Environmental modeling results

Summary statistics for variables are presented in Table 3 for BC and Supplementary Table 2 by Health Authority (see Figure 1 for reference and Table 1 for incidence). Variables (Table 3) were modeled individually and combined in a multivariate model. Lack of spatial clustering observed in the residuals indicates that the model assumption of spatial independence was met, and suggests that within the parameters of the analysis there were either no important missing variables with spatial patterning or that the existing predictors capture similar spatial variability of important unmeasured variables. The final models included variables shown in Table 4 and logged average population as an offset variable.

For the whole PIBD population, Indigenous ethnic origin, average family size, summer UV radiation, and metam pesticide application were identified as significant protective factors. In contrast, South Asian origin, greenness, $PM_{2.5}$, and petroleum oil application were significant risk factors. When broken down by disease subtype, Indigenous ethnic origin, NO_2, and O_3 were statistically significantly negatively correlated with CD, while maximum growing season greenness, $PM_{2.5}$, and petroleum oil application were significant risk factors. Rurality, and alfalfa and corn glyphosate were statistically significant protective factors for UC, while significant risk factors included South Asian origin, mean growing season greenness, O_3 pollution, and wheat glyphosate.

A 1% increase in the Indigenous population of a LHA was associated with a 4.4% decrease in the number of IBD cases (IRR = 0.956, $P < 0.001$) and a 7.7% decrease in CD (IRR = 0.923, $P < 0.001$), while a 20% increase in Indigenous population was associated with a 59% decrease in IBD. Each additional family member added to family size was associated with a 53.3% decrease in IBD cases (IRR = 0.467, $P = 0.007$). An increase of 1 J/m^{-2} in summer UV was associated with 0.001% decrease in IBD cases (IRR = 0.999, $P < 0.001$) while an increase of 500 J/m^{-2} was associated with a 29.4% decrease. A 1% increase in

Table 3 Summary statistics for variables of interest for the 88 local health areas used for modeling

Explanatory variable	Minimum LHA value	Maximum LHA value	Mean of LHA values
Chinese ethnic origin (%)	0.00	47.21	4.35
Indigenous ethnic origin (%)	1.07	93.22	14.38
Jewish ethnic origin (%)	0.00	2.82	0.45
Non-Jewish European ethnic origin (%)	10.67	90.98	70.91
South Asian ethnic origin (%)	0.00	31.19	2.71
Average family income ($)	60265.01	216769.60	91884.26
Family size	2.25	3.13	2.76
Population density (per square km)	0.01	9443.44	553.95
Rural population (%)	0.00	100.00	53.05
NDVI maximum	0.59	0.80	0.70
NDVI mean	0.23	0.62	0.45
NO_2 (ppb)	0.10	23.61	7.71
O_3 (ppb)	17.49	39.54	30.14
$PM_{2.5}$ (μg m^3)	2.73	8.32	6.02
UV vitamin D summer (J/m^{-2})	4488.80	7272.52	6053.15
UV vitamin D winter (J/m^{-2})	102.02	449.6	274.98
Glyphosate used in common crops (kg/ha/yr)	0.00	6.71	0.61
Glyphosate used in alfalfa crops (kg/ha/yr)	0.00	0.17	0.02
Glyphosate used in corn crops (kg/ha/yr)	0.00	6.06	0.49
Glyphosate used in wheat crops (kg/ha/yr)	0.00	0.21	0.02
Metam used in fruits and vegetables (kg/ha/yr)	0.00	8.82	0.60
Petroleum oil used in orchards and grapes (kg/ha/yr)	0.00	4.75	0.28

LHA: Local Health Area; NDVI: Normalized difference vegetation index; UV: Ultraviolet; NO_2: Nitrogen dioxide; O_3: Ozone; $PM_{2.5}$: Fine particulate matter.

rural population was associated with a 1% decrease in UC (IRR = 0.990, P = 0.004). Each unit increase of metam pesticide was associated with a 6.9% decrease in IBD cases (IRR = 0.931, P = 0.001 for 1 kg/ha). Each ppb increase in O_3 was associated with a 9.5% increase in UC (IRR = 1.095, P = 0.001) and a 5.3% decrease in CD (IRR = 9.47, P = 0.010). Each ppb increase in NO_2 was associated with a 4.8% decrease in CD cases (IRR = 0.952, P = 0.006). Each unit increase of glyphosate applied to wheat was associated with an increase in UC (IRR = 121.196, P = 0.019 for 1 kg/ha), while the same pesticide applied to corn (IRR = 0.828, P = 0.021 for 1 kg/ha) and alfalfa (IRR = 0.001, P = 0.024 for 1 kg/ha) was a significant protective factor. It is important to note that glyphosate applications to corn (range 0.00–6.06, mean 0.49 kg/ha) were much higher than those to alfalfa (range 0.00–0.17, mean 0.02 kg/ha) and wheat (range 0.00–0.21, mean 0.02 kg/ha), and the extremely high and low IRRs for glyphosate are more reflective of the small data values than actual effect size.

A 1% increase in the percent of South Asian residents was associated with a 2% increase in IBD (IRR = 1.020, P < 0.001) and a 5.4% increase in UC (IRR = 1.054, P < 0.001), while a 20% increase in South Asian residents was associated with a 47.5% increase in IBD. A 1% increase in maximum growing season greenness was associated with a 6% increase in IBD and a 3.8% increase in CD (IRR = 1.060, P < 0.001, and IRR = 1.038, P = 0.002, respectively). A 1% increase in mean growing season greenness was associated with a 4.3% increase in UC (IRR = 1.043, P = 0.006). Each 1 μg/m^3 concentration increase in $PM_{2.5}$ air pollution was associated with a 29.4% increase in IBD cases (IRR = 1.294, P = 0.001) and a 23% increase in CD cases (IRR = 1.230, P = 0.008). Finally, a 1 kg/ha increase in the application of petroleum oil in grapes and orchards was associated with a 13.5% increase in IBD (IRR = 1.135, P = 0.033) and a 15.9% increase in CD (IRR = 1.159, P = 0.038).

Table 4 Incidence rate ratios and 95%CIs for the best model explaining inflammatory bowel disease, Crohn's disease, and ulcerative colitis rates in local health areas of British Columbia, Canada (*n* = 88)

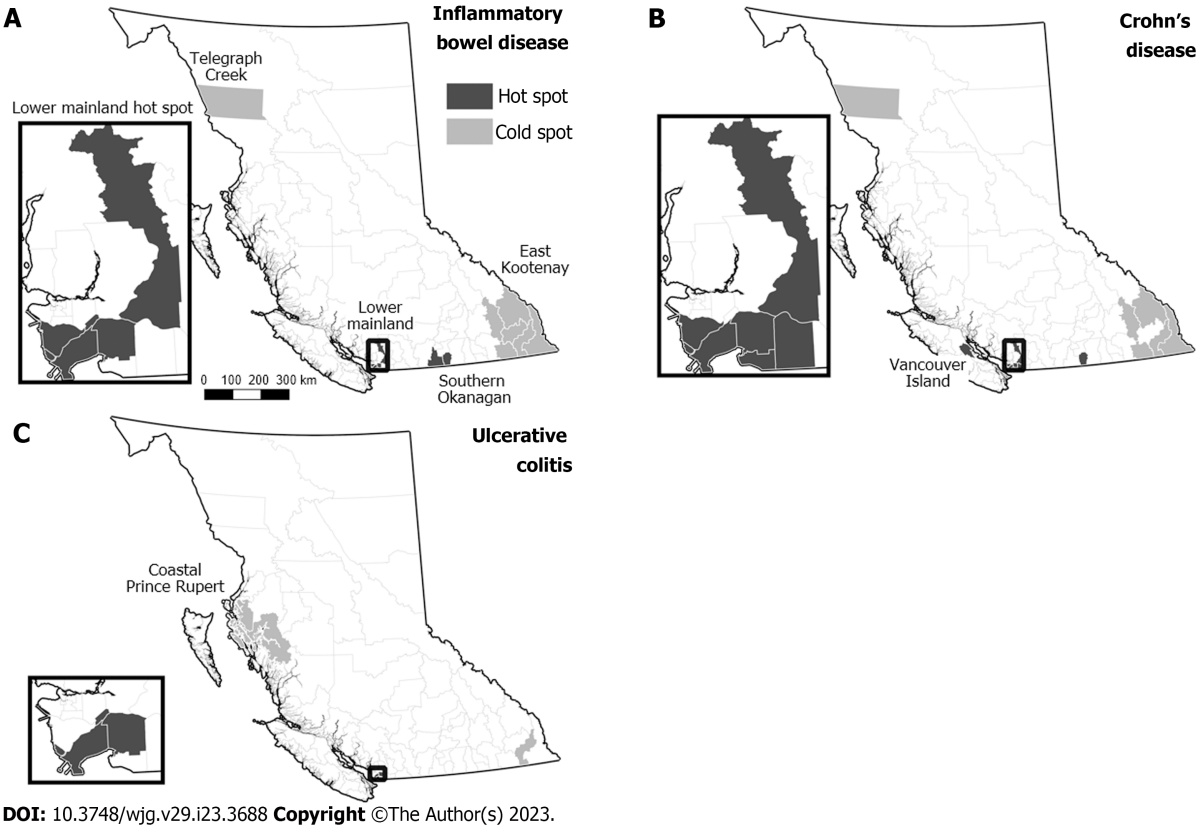
Variable	Inflammatory bowel disease		Crohn's disease		Ulcerative colitis	
	IRR and 95%CI	*P* value	IRR and 95%CI	*P* value	IRR and 95%CI	*P* value
Average family size	0.467 (0.268–0.816)	0.007[b]				
Average family income			0.912 (0.827–1.006)	0.064		
Glyphosate used in alfalfa crops					0.001 (0.000–0.253)	0.024[a]
Glyphosate used in corn crops					0.828 (0.707–0.974)	0.021[a]
Glyphosate used in wheat crops					121.196 (2.252–6671.461)	0.019[a]
Indigenous ethnic origin	0.956 (0.941–0.971)	< 0.001[c]	0.923 (0.895–0.951)	< 0.001[c]		
Metam used in fruits and vegetables	0.931 (0.892–0.970)	0.001[b]				
NDVI Maximum at 250 m (× 100)	1.060 (1.040–1.082)	< 0.001[c]	1.038 (1.014–1.062)	0.002[b]		
NDVI Mean at 250 m (× 100)					1.043 (1.013–1.075)	0.006[b]
NO_2			0.952 (0.919–0.986)	0.006[b]		
O_3			0.947 (0.909–0.987)	0.010[a]	1.095 (1.039–1.154)	0.001[b]
Petroleum oil used in orchards and grapes	1.135 (1.007–1.270)	0.033[a]	1.159 (1.002–1.326)	0.038[a]		
$PM_{2.5}$	1.294 (1.113–1.507)	0.001[b]	1.230 (1.056–1.435)	0.008[b]		
Rural population					0.990 (0.983–0.996)	0.004[b]
South Asian ethnic origin	1.020 (1.011–1.028)	< 0.001[c]			1.054 (1.030–1.079)	< 0.001[c]
UV Summer	0.9993 (0.9990–0.9996)	< 0.001[c]	0.9997 (0.9993–1.0001)	0.091		
UV Winter					0.996 (0.992–1.000)	0.067

[a]$P < 0.05$.
[b]$P < 0.01$.
[c]$P < 0.001$.
IRR: Incidence rate ratio; NDVI: Normalized difference vegetation index; NO_2: Nitrogen dioxide; O_3: Ozone; $PM_{2.5}$: Fine particulate matter; UV: Ultraviolet.

DISCUSSION

Based on our exploratory analysis describing spatial patterning of PIBD in BC, incidence varied substantially across the province in both rural and urban areas, likely reflective of BC's diverse population and environments. The spatial distribution of IBD, CD, and UC was significantly clustered during the period of 2001 to 2016, with substantial overlap between cluster locations for each of the three. The lower mainland hotspot and southeastern BC cold spot were consistent across the study period in the IBD population. As previously reported in PIBD, UC represented a lower percentage of IBD cases than CD and in addition, displayed a less clustered distribution with fewer shared clusters. It is unlikely that these observed clusters resulted from chance. Notably, patients living near the eastern border (Alberta) may receive care in that province, potentially explaining the cold spot in southeastern BC.

In our modeling of the association between IBD case counts and population and environment variables, higher proportions of South Asians tended to be associated with higher IBD and UC case counts. In Ontario, Canada, similar incidence of IBD has been observed for children of immigrants of South Asian origin born in Canada and children of non-immigrants[15]. However, higher rates of IBD have been documented in South Asian populations in BC, the United States, the United Kingdom, New Zealand, and Singapore and Malaysia[7,48-51]. Our observation of lower IBD and CD cases associated with higher proportions of Indigenous residents is consistent with previous Canadian studies[4,52]. When interpreting modeling results, locations where IBD rates were well predicted by population ethnicity should still be considered places where environmental risk or protective factors were also present. Larger family size has been associated with a protective effect on CD, which is consistent with our results for IBD but not CD[6]. Higher socioeconomic status is an established risk factor[4,8], but average income quantile was not a significant predictor in any model (though it improved CD model



DOI: 10.3748/wjg.v29.i23.3688 **Copyright** ©The Author(s) 2023.

Figure 2 Statistically significant standardized incidence ratio spatial clusters, 2001–2016. A: Inflammatory bowel disease; B: Crohn's disease; C: Ulcerative colitis.

fit). While several identified hot spots were located in the highest income areas of BC and cold spots in the lowest income areas, there were also hot spots with low income and cold spots with high income. It may be that average household income is less relevant than other socioeconomic indicators in BC, or that an effect was not observable for aggregated populations.

Our results suggest that at the LHA level, residential environmental exposures at diagnosis may also be significant potential determinants. Links with vitamin D and sunlight have been inconsistent, due in part to variability in study design and exposure assessment[12]. Our findings indicate that summer vitamin D UV radiation may confer a protective effect on IBD development. An individual unit of UV (1 J/m^{-2}) is quite small which resulted in a low measured IRR. Mean UV in BC is significantly higher in summer (6053.15 J/m^{-2}) than winter (274.98 J/m^{-2}) and varies within the province (summer maximum of 7272.52 and minimum of 4488.80 J/m^{-2}). An increase in UV of 500 J/m^{-2}, which is more representative of actual geographic and seasonal UV variation, was associated with a 29.4% decrease in IBD cases. In the analysis stratified by disease type, summer and winter UV vitamin D were nonsignificant protective factors that improved model fit for CD and UC, respectively. Smaller sample size in stratified analysis may have contributed to nonsignificant results. Low winter UV across BC could be particularly relevant for people of South Asian descent who have a higher level of skin melanin and require substantially more UV exposure to synthesize sufficient vitamin D[30]. $PM_{2.5}$ air pollution was a significant risk factor for PIBD and CD. Italian (IBD) and Chinese (UC but not CD) studies of middle and older aged adults have identified $PM_{2.5}$ as a risk factor for incident cases as well as IBD and UC hospitalizations in China [53-55]. In contrast, an Ontario pediatric study found no association and a European adult study found a negative association with $PM_{2.5}$[13,56]. Though population exposure for most LHAs met 2020 national and provincial air quality objectives, BC experiences seasonal wildfire events which can cause short-term high $PM_{2.5}$ concentrations that would be obscured in the yearly average values used in this study [57]. Regular high exposure events should be investigated further, especially as climate change is projected to increase wildfire potential[58]. O_3 air pollution was a significant risk factor for UC which is consistent with a Chinese study which measured an association between O_3 and IBD and UC hospital visits[54]. We observed statistically significant negative associations with CD for NO_2 and O_3. This is in contrast to the lack of association observed for IBD in Ontario and Europe, a United Kingdom study which found a positive association between NO_2 pollution and CD onset before age 23, and a Chinese study which found a positive association between NO_2 and UC incidence in middle and older aged adults[13,55,56,59]. Differential effects on CD and UC have been observed for environmental exposures such as smoking and appendectomy[60].

BC had few areas of low residential greenness and high incidence (Supplementary Figures 3–5), and we observed statistically significant positive associations between IBD, CD, UC, and greenness. Our findings contrast with a pediatric cohort study in Ontario, which found a protective effect for maximum growing season NDVI at 250 m[11]. This inconsistency could be due to methodological differences between the two studies. NDVI is a measure of vegetation greenness only and may not capture other elements of green spaces, such as vegetation composition, environmental microbiome, or pesticide and herbicide applications, which may differ in BC. Measures of greenness in BC are highly dependent on specific indicators, as a Metro Vancouver study comparing green space metrics found that NDVI at 250 m from postal codes diverged significantly from other measures such as street tree density, total percentage of green space, and park quality[61].

A previous Canadian study found a protective effect of rurality on pediatric CD and UC, while our study only observed an effect for UC[9]. BC may have more diverse environments than other provinces; for example, the largely rural Interior Health Authority had many of the highest average $PM_{2.5}$ and O_3 exposures while the majority-urban lower mainland region included significant sections of Agricultural Land Reserve. A hot spot near Vancouver included mostly suburban LHAs rather than the main urban center, which is similar to results observed in Oslo, Norway[62]. Perhaps some suburban and rural areas lack protective effects conferred by other rural regions while also missing potential health-promoting features of dense urban areas (*e.g.* public transportation, public parks, and access to amenities). Some rural and peri-urban areas can also be associated with potential risk factors such as petroleum pesticides.

A novel result in this study is the measured associations between pesticides and PIBD. Petroleum oil applied to grapes and orchards was a significant risk factor for IBD and CD. Indeed, exposure to agricultural petroleum oil has been previously associated with systemic autoimmunity (measured with antinuclear antibodies) and rhinitis in a prospective cohort of pesticide applicators in the United States, suggesting that petroleum pesticide products may have inflammatory properties[63,64]. As numerous other pesticides have been linked with dysbiosis, and petroleum is used as a fungicide, agricultural applications of petroleum oil should be investigated for potential impacts on the gut microbiome which could induce CD[14,39]. Interestingly, glyphosate application appeared to have a different effect on UC depending on which crop it was applied to. Wheat crop glyphosate was a significant risk factor, while alfalfa and corn crop glyphosate were significant protective factors. Differences in agricultural practices between alfalfa, corn, and wheat may be responsible for the negative or both associations observed for UC. The unexpected negative association between IBD and metam pesticide also warrants further investigation. This association could have resulted from an unmeasured confounder such as diet. For example, proximity to fruit and vegetable crops where metam is applied could be correlated with access to these food groups which are known to lower IBD risk[65].

A key strength of this study is the use of high resolution national environmental exposure metrics which increased the quality of the study and will facilitate comparisons between our results and future research. In addition, the clinical registry only contained patients with a confirmed IBD diagnosis, confirmed diagnosis of CD or UC, and accurate date of diagnosis which minimizes risk of misclassification. Moreover, we have demonstrated that our registry data is representative of the BC IBD population[18]. The use of aggregate case counts and reliable population data in both analyses and areal geographic analysis combined with spatial smoothing in the cluster analysis reduced the instability of disease rates caused by low cases numbers. The use of Monte Carlo simulation and a multiple comparison correction for statistical significance increased confidence in the spatial results. Finally, future healthcare service planning in BC would be implemented for health administrative units such as LHAs, so our scale of analysis would allow this research to be directly integrated into planning and intervention efforts.

Despite these strengths, there are several limitations which warrant discussion. Some patients were excluded due to missing data and it is possible that cases were missing from our clinical registry, either of which may have altered spatial clustering or biased modeling results. However, the registry likely included the vast majority of PIBD patients diagnosed in BC during the study period[18]. Patient data was not initially collected for research purposes, which may have affected available variables and may have contributed to missing data. Small numbers of cases could have produced large variation in incidence in sparsely populated areas. In addition, missing early environmental exposure data for several LHAs may have impacted the results, though all but one of the modeled LHAs included environment data from the majority of the study period. An important unmeasured variable in this analysis is diet, and missing potential confounding variables may have biased the results. This was not a birth cohort study, so there is uncertainty about exposures at gestation or early life. However, specific critical periods for many environmental exposures have not been established; consequently, further prospective studies are required. Previous environmental studies have used average childhood exposure[11,13] or did not have a standardized lookback period dating from diagnosis[56,59]. Accordingly, we used broad metrics of average population-level exposure during the study period. This was an ecological analysis and our findings should not be used to make claims about individual risk.

CONCLUSION

To our knowledge, this is the first spatial hot spot analysis focused on PIBD in North America and the first study identifying an association with pesticides. Spatial cluster detection was a valuable method for exploring patterns of IBD, and we identified $PM_{2.5}$ air pollution, petroleum oil, glyphosate, and metam pesticides as novel determinants of PIBD. Given the inconsistency of IBD incidence in urban areas and relatively high incidence in some suburban and rural areas, future research should move beyond binary urban-rural classifications and use specific characteristics such as built environment and pollutant exposures to characterize environments. Expanded regional and global studies are needed to validate these results and to determine the relationship between timing of exposure and clinical onset of disease. Furthermore, the inclusion of other immune-mediated inflammatory diseases will likely uncover potential shared disease clusters and environmental determinants.

ARTICLE HIGHLIGHTS

Research background

Geospatial patterning has been observed in inflammatory bowel disease (IBD) incidence and linked to environmental determinants of disease. However, knowledge of North American IBD spatial patterns is limited, and unknown in pediatric IBD (PIBD). A further understanding of geospatial patterns of IBD will help guide distribution of healthcare services and aid in identifying potential environmental risk and protective factors and populations at risk.

Research motivation

There is a lack of knowledge of the spatial distribution and environmental exposures relevant to PIBD in Canada and specifically in the Canadian province of British Columbia (BC).

Research objectives

The main objectives of this study were (1) To determine spatial patterning of PIBD and identify location of disease hot and cold spots in the Canadian province of BC during the period of 2001–2016; and (2) to model the association between IBD case counts and population-level ethnicity, average income, rural residence, and known as well as novel environmental determinants. Both objectives were addressed using the methods described below.

Research methods

The Moran's I statistic was used as a Local Indicator of Spatial Association to measure the degree, location, and type of geographic clustering of PIBD incidence, a method which improves on visual analysis of mapped incidence by empirically quantifying clustering. Statistical significance of observed clusters was approximated using Monte Carlo simulation. Case counts of IBD, Crohn's disease (CD), and ulcerative colitis (UC) were modeled in Poisson rate models as a function of average population characteristics and average population environmental exposures to assess associations between IBD and rurality, ethnicity, income, family size, and air pollution, green space, ultraviolet (UV) light, and pesticide exposures. Data sources included a BCCH clinical registry of patients diagnosed with IBD ≤ age 16.9, high-quality national environmental exposure datasets developed for health research, and Canadian census data.

Research results

No high incidence hot spots were detected in the densest urban areas, suggesting unexplored urban protective factors. Rurality was negatively associated with UC. Novel risk factors for PIBD and specifically CD included fine particulate matter ($PM_{2.5}$) pollution and agricultural applications of petroleum oil to orchards and grapes. Spatial distribution was partially explained by rurality, population ethnicity, family size, pesticide applications, air pollution, UV exposure, and residential greenness.

Research conclusions

Pesticide and $PM_{2.5}$ exposure are linked to the development of PIBD. Suburban and low-density urban areas of BC appear to lack protective exposures conferred by rural and dense urban areas.

Research perspectives

Exploring geographic patterns of PIBD facilitated the identification of novel environmental determinants, which has prompted followup studies of environmental exposures and IBD onset.

ACKNOWLEDGEMENTS

Mielle Michaux was supported as a MSc student by the University of British Columbia Graduate Support Initiative and International Tuition Award and is currently a research assistant supported by the Moffat Foundation. Justin M Chan is a PhD candidate supported by the BCCH Research Institute Studentship and the Lutsky Foundation. Luke Bergmann acknowledges support by the Canada Research Chairs Program and the Canada Foundation for Innovation. Luis F Chaves acknowledges funding from Indiana University. Kevan Jacobson is a Senior Clinician Scientist supported by the Children with Intestinal and Liver Disorders (CHILD) Foundation and the BCCH Research Institute Clinician Scientists Award Program, University of British Columbia. NDVI metrics, nitrogen dioxide data, calculated ozone metrics, and $PM_{2.5}$ metrics were indexed to DMTI Spatial Inc. postal codes and provided by CANUE (Canadian Urban Environmental Health Research Consortium). Long-term monthly UV data were accessed *via* the CANUE data portal (https://canuedata.ca). Portions of this methodology were developed for Mielle Michaux's MSc thesis.

FOOTNOTES

Author contributions: Michaux M participated in designing the study, acquisition, analysis, and interpretation of the data, and drafted the initial manuscript; Chan JM participated in designing the study, acquisition, analysis, and interpretation of the data, and revised the article critically for important intellectual content; Bergmann L and Chaves LF participated in the acquisition, analysis, and interpretation of the data, and revised the article critically for important intellectual content; Klinkenberg B participated in designing the study and revised the article critically for important intellectual content; Jacobson K was the guarantor and participated in designing the study, analysis, and interpretation of the data, and revised the article critically for important intellectual content.

Institutional review board statement: The study was reviewed and approved by the University of British Columbia Children's and Women's Research Ethics Board (Vancouver), No. H19-00739.

Conflict-of-interest statement: Dr. Jacobson reports other from BC Children's Hospital Research Institute Clinician Scientist Awards Program Award, grants from Janssen, non-financial support from adMare Bioinnovations, other from Engene, outside the submitted work; and has served on the advisory boards of Janssen, AbbVie, Merck, Amgen, Mylan Inc, and McKesson.

Data sharing statement: Data is available upon reasonable request to the corresponding author subject to research ethics board approval, at kjacobson@cw.bc.ca.

STROBE statement: The authors have read the STROBE Statement—checklist of items, and the manuscript was prepared and revised according to the STROBE Statement—checklist of items.

Open-Access: This article is an open-access article that was selected by an in-house editor and fully peer-reviewed by external reviewers. It is distributed in accordance with the Creative Commons Attribution NonCommercial (CC BY-NC 4.0) license, which permits others to distribute, remix, adapt, build upon this work non-commercially, and license their derivative works on different terms, provided the original work is properly cited and the use is non-commercial. See: https://creativecommons.org/Licenses/by-nc/4.0/

Country/Territory of origin: Canada

ORCID number: Mielle Michaux 0000-0003-4742-3126; Justin M Chan 0000-0002-8298-3594; Luis F Chaves 0000-0002-5301-2764; Brian Klinkenberg 0000-0002-3357-1446; Kevan Jacobson 0000-0001-7269-8557.

Corresponding Author's Membership in Professional Societies: Canadian Association of Gastroenterology.

S-Editor: Li L
L-Editor: A
P-Editor: Cai YX

REFERENCES

1 **Benchimol EI**, Fortinsky KJ, Gozdyra P, Van den Heuvel M, Van Limbergen J, Griffiths AM. Epidemiology of pediatric inflammatory bowel disease: a systematic review of international trends. *Inflamm Bowel Dis* 2011; **17**: 423-439 [PMID: 20564651 DOI: 10.1002/ibd.21349]

2 **Aamodt G**, Jahnsen J, Bengtson MB, Moum B, Vatn MH; IBSEN Study Group. Geographic distribution and ecological studies of inflammatory bowel disease in southeastern Norway in 1990-1993. *Inflamm Bowel Dis* 2008; **14**: 984-991 [PMID: 18338775 DOI: 10.1002/ibd.20417]

3 **Declercq C**, Gower-Rousseau C, Vernier-Massouille G, Salleron J, Baldé M, Poirier G, Lerebours E, Dupas JL, Merle V, Marti R, Duhamel A, Cortot A, Salomez JL, Colombel JF. Mapping of inflammatory bowel disease in northern France: spatial variations and relation to affluence. *Inflamm Bowel Dis* 2010; **16**: 807-812 [PMID: 19774647 DOI: 10.1002/ibd.21111]

4 **Green C**, Elliott L, Beaudoin C, Bernstein CN. A population-based ecologic study of inflammatory bowel disease: searching for etiologic clues. *Am J Epidemiol* 2006; **164**: 615-23; discussion 624 [PMID: 16920784 DOI: 10.1093/aje/kwj260]

5 **Nikkilä A**, Auvinen A, Kolho KL. Clustering of pediatric onset inflammatory bowel disease in Finland: a nationwide register-based study. *BMC Gastroenterol* 2022; **22**: 512 [PMID: 36503475 DOI: 10.1186/s12876-022-02579-1]

6 **Bernstein CN**, Rawsthorne P, Cheang M, Blanchard JF. A population-based case control study of potential risk factors for IBD. *Am J Gastroenterol* 2006; **101**: 993-1002 [PMID: 16696783 DOI: 10.1111/j.1572-0241.2006.00381.x]

7 **Pinsk V**, Lemberg DA, Grewal K, Barker CC, Schreiber RA, Jacobson K. Inflammatory bowel disease in the South Asian pediatric population of British Columbia. *Am J Gastroenterol* 2007; **102**: 1077-1083 [PMID: 17378907 DOI: 10.1111/j.1572-0241.2007.01124.x]

8 **Bernstein CN**, Burchill C, Targownik LE, Singh H, Roos LL. Events Within the First Year of Life, but Not the Neonatal Period, Affect Risk for Later Development of Inflammatory Bowel Diseases. *Gastroenterology* 2019; **156**: 2190-2197.e10 [PMID: 30772341 DOI: 10.1053/j.gastro.2019.02.004]

9 **Benchimol EI**, Kaplan GG, Otley AR, Nguyen GC, Underwood FE, Guttmann A, Jones JL, Potter BK, Catley CA, Nugent ZJ, Cui Y, Tanyingoh D, Mojaverian N, Bitton A, Carroll MW, deBruyn J, Dummer TJB, El-Matary W, Griffiths AM, Jacobson K, Kuenzig ME, Leddin D, Lix LM, Mack DR, Murthy SK, Sánchez JNP, Singh H, Targownik LE, Vutcovici M, Bernstein CN. Rural and Urban Residence During Early Life is Associated with Risk of Inflammatory Bowel Disease: A Population-Based Inception and Birth Cohort Study. *Am J Gastroenterol* 2017; **112**: 1412-1422 [PMID: 28741616 DOI: 10.1038/ajg.2017.208]

10 **Soon IS**, Molodecky NA, Rabi DM, Ghali WA, Barkema HW, Kaplan GG. The relationship between urban environment and the inflammatory bowel diseases: a systematic review and meta-analysis. *BMC Gastroenterol* 2012; **12**: 51 [PMID: 22624994 DOI: 10.1186/1471-230X-12-51]

11 **Elten M**, Benchimol EI, Fell DB, Kuenzig ME, Smith G, Kaplan GG, Chen H, Crouse D, Lavigne E. Residential Greenspace in Childhood Reduces Risk of Pediatric Inflammatory Bowel Disease: A Population-Based Cohort Study. *Am J Gastroenterol* 2021; **116**: 347-353 [PMID: 33038129 DOI: 10.14309/ajg.0000000000000990]

12 **Holmes EA**, Rodney Harris RM, Lucas RM. Low Sun Exposure and Vitamin D Deficiency as Risk Factors for Inflammatory Bowel Disease, With a Focus on Childhood Onset. *Photochem Photobiol* 2019; **95**: 105-118 [PMID: 30155900 DOI: 10.1111/php.13007]

13 **Elten M**, Benchimol EI, Fell DB, Kuenzig ME, Smith G, Chen H, Kaplan GG, Lavigne E. Ambient air pollution and the risk of pediatric-onset inflammatory bowel disease: A population-based cohort study. *Environ Int* 2020; **138**: 105676 [PMID: 32217428 DOI: 10.1016/j.envint.2020.105676]

14 **Jin Y**, Wu S, Zeng Z, Fu Z. Effects of environmental pollutants on gut microbiota. *Environ Pollut* 2017; **222**: 1-9 [PMID: 28086130 DOI: 10.1016/j.envpol.2016.11.045]

15 **Benchimol EI**, Mack DR, Guttmann A, Nguyen GC, To T, Mojaverian N, Quach P, Manuel DG. Inflammatory bowel disease in immigrants to Canada and their children: a population-based cohort study. *Am J Gastroenterol* 2015; **110**: 553-563 [PMID: 25756238 DOI: 10.1038/ajg.2015.52]

16 **Statistics Canada**. 2011 census profiles files / 2016 census profiles files / Profile of census dissemination areas; n.d. Database: Canadian Census Analyser. 2011. [cited 1 December 2020]. Available from: http://dc1.chass.utoronto.ca/cgi-bin/census/2011/displayCensus.cgi?year=2011&geo=da

17 **Michaux M**. Exploring spatio-temporal patterns and environmental determinants of pediatric inflammatory bowel disease in British Columbia. M.Sc. Thesis, University of British Columbia. 2020. Available from: https://open.library.ubc.ca/collections/ubctheses/24/items/1.0394067

18 **Chan JM**, Carroll MW, Smyth M, Hamilton Z, Evans D, McGrail K, Benchimol EI, Jacobson K. Comparing Health Administrative and Clinical Registry Data: Trends in Incidence and Prevalence of Pediatric Inflammatory Bowel Disease in British Columbia. *Clin Epidemiol* 2021; **13**: 81-90 [PMID: 33603489 DOI: 10.2147/CLEP.S292546]

19 DMTI Spatial Inc. CanMap postal code suite; n.d. [cited 24 March 2021]. Available from: https://canue.ca/wp-content/uploads/2019/09/CANUE-Browser-Metadata-PostalCodes.pdf

20 **Statistics Canada**. 2011 National Household Survey (NHS) profiles files / Profile of census dissemination areas; n.d. Database: Canadian Census Analyser. 2011. [cited 1 December 2020]. Available from: http://dc1.chass.utoronto.ca/cgi-bin/census/2011nhs/displayCensus.cgi?year=2011&geo=da

21 **Statistics Canada**. Profile of dissemination areas: 2001 census / 2006 census / Cumulative profiles; n.d. 2011. [cited 1 December 2020]. Available from: Database: Canadian Census Analyser. Available from: http://dc1.chass.utoronto.ca/cgi-bin/census/2001/displayCensusDA.cgi

22 **Statistics Canada**. Average family income (dollars), 2005, 2015 n.d. Database: BC Community Health Atlas. [cited 1 December 2020]. Available from: http://maps.gov.bc.ca/ess/hm/cha/

23 **Google Earth Engine**. Landsat 5 TM annual greenest-pixel TOA reflectance composite, 1984 to 2012; n.d. Database: Google Earth Engine. [cited 20 July 2017]. Available from: https://explorer.earthengine.google.com/#detail/LANDSAT%2FLT5_L1T_ANNUAL_GREENEST_TOA

24 **Google Earth Engine**. Landsat 8 annual greenest-pixel TOA reflectance composite, 2013 to 2015; n.d. Database: Google Earth Engine. [cited 20 July 2017]. Available from: https://explorer.earthengine.google.com/#detail/LANDSAT%2FLC8_L1T_ANNUAL_GREENEST_TOA

25 **Google Earth Engine**. USGS Landsat 5 TM TOA reflectance (orthorectified), 1984 to 2011; n.d. Database: Google Earth Engine. [cited 20 July 2007]. Available from: https://explorer.earthengine.google.com/#detail/LANDSAT%2FLT5_L1T_TOA

26 **Google Earth Engine**. USGS Landsat 8 TOA reflectance (orthorectified), 2013 to 2017; n.d. Database: Google Earth

Engine. [cited 20 July 2007]. Available from: https://explorer.earthengine.google.com/#detail/LANDSAT%2FLC8_L1T_TOA

27 **Gorelick N**, Hancher M, Dixon M, Ilyushchenko S, Thau D, Moore R. Google Earth Engine: Planetary-scale geospatial analysis for everyone. *Remote Sens Environ* 2017; **202**: 18-27 [DOI: 10.1016/j.rse.2017.06.031]

28 **Robinson N**, Allred B, Jones M, Moreno A, Kimball J, Naugle D, Erickson T, Richardson A. A dynamic landsat derived normalized difference vegetation index (NDVI) product for the conterminous United States. *Remote Sens* 2017; **9**: 863 [DOI: 10.3390/rs9080863]

29 **Fioletov VE**, Kimlin MG, Krotkov N, McArthur LJB, Kerr JB, Wardle DI, Herman JR, Meltzer R, Mathews TW, Kaurola J. UV index climatology over the United States and Canada from ground-based and satellite estimates. *J Geophys Res Atmospheres* 2004; **109**: 1-13 [DOI: 10.1029/2004JD004820]

30 **Fioletov VE**, McArthur LJ, Mathews TW, Marrett L. Estimated ultraviolet exposure levels for a sufficient vitamin D status in North America. *J Photochem Photobiol B* 2010; **100**: 57-66 [PMID: 20554218 DOI: 10.1016/j.jphotobiol.2010.05.002]

31 **Hystad P**, Setton E, Cervantes A, Poplawski K, Deschenes S, Brauer M, van Donkelaar A, Lamsal L, Martin R, Jerrett M, Demers P. Creating national air pollution models for population exposure assessment in Canada. *Environ Health Perspect* 2011; **119**: 1123-1129 [PMID: 21454147 DOI: 10.1289/ehp.1002976]

32 **Weichenthal S**, Pinault LL, Burnett RT. Impact of Oxidant Gases on the Relationship between Outdoor Fine Particulate Air Pollution and Nonaccidental, Cardiovascular, and Respiratory Mortality. *Sci Rep* 2017; **7**: 16401 [PMID: 29180643 DOI: 10.1038/s41598-017-16770-y]

33 **Environment and Climate Change Canada**. CHRONOS_Ground-Level_O3_NA_2002.nc to CHRONOS_Ground-Level_O3_NA_2009.nc inclusive, generated. July 2017. [cited 18 April 2023]. Available from: https://www.canuedata.ca/tmp/CANUE_METADATA_O3CHG_A_YY.pdf

34 **Environment and Climate Change Canada**. GEMMACH_Ground Level_O3_NA_2010.nc to GEMMACH_Ground-Level_O3_NA_2015.nc inclusive, generated. Jul 2017. [cited 18 April 2023]. Available from: https://www.canuedata.ca/tmp/CANUE_METADATA_O3CHG_A_YY.pdf

35 **Robichaud A**, Ménard R, Zaïtseva Y, Anselmo D. Multi-pollutant surface objective analyses and mapping of air quality health index over North America. *Air Qual Atmos Health* 2016; **9**: 743-759 [PMID: 27785157 DOI: 10.1007/s11869-015-0385-9]

36 **Robichaud A**, Ménard R. Multi-year objective analyses of warm season ground-level ozone and PM 2.5 over North America using real-time observations and Canadian operational air quality models. *Atmospheric Chem Phys* 2014; **14**: 1769-800 [DOI: 10.5194/acp-14-1769-2014]

37 **Canadian Urban Environmental Health Research Consortium**. Canue Metadata - Air Quality Ozone (O3). 2021. [cited 18 April 2023]. Available from: https://www.canuedata.ca/tmp/CANUE_METADATA_O3CHG_A_YY.pdf

38 **Hammer MS**, van Donkelaar A, Li C, Lyapustin A, Sayer AM, Hsu NC, Levy RC, Garay MJ, Kalashnikova OV, Kahn RA, Brauer M, Apte JS, Henze DK, Zhang L, Zhang Q, Ford B, Pierce JR, Martin RV. Global Estimates and Long-Term Trends of Fine Particulate Matter Concentrations (1998-2018). *Environ Sci Technol* 2020; **54**: 7879-7890 [PMID: 32491847 DOI: 10.1021/acs.est.0c01764]

39 **Maggi F**, Tang FHM, la Cecilia D, McBratney A. PEST-CHEMGRIDS, global gridded maps of the top 20 crop-specific pesticide application rates from 2015 to 2025. *Sci Data* 2019; **6**: 170 [PMID: 31515508 DOI: 10.1038/s41597-019-0169-4]

40 **Maggi F**, Tang FHM, la Cecilia D, McBratney A. Global Pesticide Grids (PEST-CHEMGRIDS); Database: NASA Socioeconomic Data and Applications Center (SEDAC) 2020 [DOI: 10.7927/weq9-pv30]

41 **BC Stats**. British Columbia - Population estimates; 2020. [cited 1 December2020]. Available from: https://bcstats.shinyapps.io/popApp/

42 **Ministry of Health**. Local health area boundaries; Database: BC Data Catalogue. 2019. [cited 26 May 2020]. Available from: https://catalogue.data.gov.bc.ca/dataset/Local-health-area-boundaries

43 **Marshall RJ**. Mapping disease and mortality rates using empirical Bayes estimators. *J R Stat Soc Ser C Appl Stat* 1991; **40**: 283-294 [DOI: 10.2307/2347593]

44 **Anselin L**. Local indicators of spatial association-LISA. *Geogr Anal* 1995; **27**: 93-115 [DOI: 10.1111/j.1538-4632.1995.tb00338.x]

45 **Kulldorff M**, Nagarwalla N. Spatial disease clusters: detection and inference. *Stat Med* 1995; **14**: 799-810 [PMID: 7644860 DOI: 10.1002/sim.4780140809]

46 **Moraga P**, Montes F. Detection of spatial disease clusters with LISA functions. *Stat Med* 2011; **30**: 1057-1071 [PMID: 21484847 DOI: 10.1002/sim.4160]

47 **Venables WN**, Ripley BD. Modern Applied Statistics with S. 4th ed. New York: Springer, 2002: 1-498 [DOI: 10.1007/978-0-387-21706-2_1]

48 **Malhotra R**, Turner K, Sonnenberg A, Genta RM. High prevalence of inflammatory bowel disease in United States residents of Indian ancestry. *Clin Gastroenterol Hepatol* 2015; **13**: 683-689 [PMID: 25083563 DOI: 10.1016/j.cgh.2014.06.035]

49 **Misra R**, Faiz O, Munkholm P, Burisch J, Arebi N. Epidemiology of inflammatory bowel disease in racial and ethnic migrant groups. *World J Gastroenterol* 2018; **24**: 424-437 [PMID: 29391765 DOI: 10.3748/wjg.v24.i3.424]

50 **Rajasekaran V**, Evans HM, Andrews A, Bishop JR, Lopez RN, Mouat S, Han DY, Alsweiler J, Roberts AJ. Rising Incidence of Inflammatory Bowel Disease in South Asian children in New Zealand - A Retrospective Population-Based Study. *J Pediatr Gastroenterol Nutr* 2023 [PMID: 36800276 DOI: 10.1097/MPG.0000000000003735]

51 **Huang JG**, Wong YKY, Chew KS, Tanpowpong P, Calixto Mercado KS, Reodica A, Rajindrajith S, Chang KC, Ni YH, Treepongkaruna S, Lee WS, Aw MM. Epidemiological characteristics of Asian children with inflammatory bowel disease at diagnosis: Insights from an Asian-Pacific multi-centre registry network. *World J Gastroenterol* 2022; **28**: 1830-1844 [PMID: 35633913 DOI: 10.3748/wjg.v28.i17.1830]

52 **Torabi M**, Bernstein CN, Yu BN, Wickramasinghe L, Blanchard JF, Singh H. Geographical Variation and Factors Associated With Inflammatory Bowel Disease in a Central Canadian Province. *Inflamm Bowel Dis* 2020; **26**: 581-590

[PMID: 31504519 DOI: 10.1093/ibd/izz168]

53 **Adami G**, Pontalti M, Cattani G, Rossini M, Viapiana O, Orsolini G, Benini C, Bertoldo E, Fracassi E, Gatti D, Fassio A. Association between long-term exposure to air pollution and immune-mediated diseases: a population-based cohort study. *RMD Open* 2022; **8** [PMID: 35292563 DOI: 10.1136/rmdopen-2021-002055]

54 **Ding S**, Sun S, Ding R, Song S, Cao Y, Zhang L. Association between exposure to air pollutants and the risk of inflammatory bowel diseases visits. *Environ Sci Pollut Res Int* 2022; **29**: 17645-17654 [PMID: 34669131 DOI: 10.1007/s11356-021-17009-0]

55 **Li FR**, Wu KY, Fan WD, Chen GC, Tian H, Wu XB. Long-term exposure to air pollution and risk of incident inflammatory bowel disease among middle and old aged adults. *Ecotoxicol Environ Saf* 2022; **242**: 113835 [PMID: 35816845 DOI: 10.1016/j.ecoenv.2022.113835]

56 **Opstelten JL**, Beelen RMJ, Leenders M, Hoek G, Brunekreef B, van Schaik FDM, Siersema PD, Eriksen KT, Raaschou-Nielsen O, Tjønneland A, Overvad K, Boutron-Ruault MC, Carbonnel F, de Hoogh K, Key TJ, Luben R, Chan SSM, Hart AR, Bueno-de-Mesquita HB, Oldenburg B. Exposure to Ambient Air Pollution and the Risk of Inflammatory Bowel Disease: A European Nested Case-Control Study. *Dig Dis Sci* 2016; **61**: 2963-2971 [PMID: 27461060 DOI: 10.1007/s10620-016-4249-4]

57 **Matz CJ**, Egyed M, Xi G, Racine J, Pavlovic R, Rittmaster R, Henderson SB, Stieb DM. Health impact analysis of PM(2.5) from wildfire smoke in Canada (2013-2015, 2017-2018). *Sci Total Environ* 2020; **725**: 138506 [PMID: 32302851 DOI: 10.1016/j.scitotenv.2020.138506]

58 **Wang X**, Thompson DK, Marshall GA, Tymstra C, Carr R, Flannigan MD. Increasing frequency of extreme fire weather in Canada with climate change. Clim Change 2015; 130: 573-586 [DOI: 10.1007/s10584-015-1375-5]

59 **Kaplan GG**, Hubbard J, Korzenik J, Sands BE, Panaccione R, Ghosh S, Wheeler AJ, Villeneuve PJ. The inflammatory bowel diseases and ambient air pollution: a novel association. *Am J Gastroenterol* 2010; **105**: 2412-2419 [PMID: 20588264 DOI: 10.1038/ajg.2010.252]

60 **Piovani D**, Danese S, Peyrin-Biroulet L, Nikolopoulos GK, Lytras T, Bonovas S. Environmental Risk Factors for Inflammatory Bowel Diseases: An Umbrella Review of Meta-analyses. *Gastroenterology* 2019; **157**: 647-659.e4 [PMID: 31014995 DOI: 10.1053/j.gastro.2019.04.016]

61 **Rugel EJ**, Henderson SB, Carpiano RM, Brauer M. Beyond the Normalized Difference Vegetation Index (NDVI): Developing a Natural Space Index for population-level health research. *Environ Res* 2017; **159**: 474-483 [PMID: 28863302 DOI: 10.1016/j.envres.2017.08.033]

62 **Moum B**, Vatn MH, Ekbom A, Aadland E, Fausa O, Lygren I, Stray N, Sauar J, Schulz T. Incidence of Crohn's disease in four counties in southeastern Norway, 1990-93. A prospective population-based study. The Inflammatory Bowel South-Eastern Norway (IBSEN) Study Group of Gastroenterologists. *Scand J Gastroenterol* 1996; **31**: 355-361 [PMID: 8726303 DOI: 10.3109/00365529609006410]

63 **Slager RE**, Poole JA, LeVan TD, Sandler DP, Alavanja MC, Hoppin JA. Rhinitis associated with pesticide exposure among commercial pesticide applicators in the Agricultural Health Study. *Occup Environ Med* 2009; **66**: 718-724 [PMID: 19289390 DOI: 10.1136/oem.2008.041798]

64 **Parks CG**, Santos ASE, Lerro CC, DellaValle CT, Ward MH, Alavanja MC, Berndt SI, Beane Freeman LE, Sandler DP, Hofmann JN. Lifetime Pesticide Use and Antinuclear Antibodies in Male Farmers From the Agricultural Health Study. *Front Immunol* 2019; **10**: 1476 [PMID: 31354699 DOI: 10.3389/fimmu.2019.01476]

65 **Milajerdi A**, Ebrahimi-Daryani N, Dieleman LA, Larijani B, Esmaillzadeh A. Association of Dietary Fiber, Fruit, and Vegetable Consumption with Risk of Inflammatory Bowel Disease: A Systematic Review and Meta-Analysis. *Adv Nutr* 2021; **12**: 735-743 [PMID: 33186988 DOI: 10.1093/advances/nmaa145]

World Journal of Gastroenterology

Submit a Manuscript: https://www.f6publishing.com

World J Gastroenterol 2023 June 21; 29(23): 3703-3714

DOI: 10.3748/wjg.v29.i23.3703

ISSN 1007-9327 (print) ISSN 2219-2840 (online)

ORIGINAL ARTICLE

Prospective Study

Novel multi-parametric diagnosis of non-alcoholic fatty liver disease using ultrasonography, body mass index, and Fib-4 index

Kei Funada, Yumi Kusano, Yoshinori Gyotoku, Ryosaku Shirahashi, Toshikuni Suda, Masaya Tamano

Specialty type: Gastroenterology and hepatology

Provenance and peer review: Unsolicited article; Externally peer reviewed.

Peer-review model: Single blind

Peer-review report's scientific quality classification

Grade A (Excellent): 0
Grade B (Very good): B
Grade C (Good): C
Grade D (Fair): 0
Grade E (Poor): 0

P-Reviewer: Pécsi D, Hungary; Sempokuya T, United States

Received: February 8, 2023
Peer-review started: February 8, 2023
First decision: March 7, 2023
Revised: March 14, 2023
Accepted: May 22, 2023
Article in press: May 22, 2023
Published online: June 21, 2023

Kei Funada, Yumi Kusano, Yoshinori Gyotoku, Ryosaku Shirahashi, Toshikuni Suda, Masaya Tamano, Department of Gastroenterology, Dokkyo Medical University Saitama Medical Center, Koshigaya-shi 343-8555, Saitama, Japan

Corresponding author: Masaya Tamano, PhD, Professor, Department of Gastroenterology, Dokkyo Medical University Saitama Medical Center, 2-1-50 Minami-Koshigaya, Koshigaya-shi 343-8555, Saitama, Japan. mstamano@dokkyomed.ac.jp

Abstract

BACKGROUND

Shear wave speed (SWS), shear wave dispersion (SWD), and attenuation imaging (ATI) are new diagnostic parameters for non-alcoholic fatty liver disease. To differentiate between non-alcoholic steatohepatitis (NASH) and non-alcoholic fatty liver (NAFL), we developed a clinical index we refer to as the "NASH pentagon" consisting of the 3 abovementioned parameters, body mass index (BMI), and Fib-4 index.

AIM

To investigate whether the area of the NASH pentagon we propose is useful in discriminating between NASH and NAFL.

METHODS

This non-invasive, prospective, observational study included patients diagnosed with fatty liver by abdominal ultrasound between September 2021 and August 2022 in whom shear wave elastography, SWD, and ATI were measured. Histological diagnosis based on liver biopsy was performed in 31 patients. The large pentagon group (LP group) and the small pentagon group (SP group), using an area of 100 as the cutoff, were compared; the NASH diagnosis rate was also investigated. In patients with a histologically confirmed diagnosis, receiver-operating characteristic (ROC) curve analyses were performed.

RESULTS

One hundred-seven patients (61 men, 46 women; mean age 55.1 years; mean BMI 26.8 kg/m^2) were assessed. The LP group was significantly older (mean age: 60.8 ± 15.2 years *vs* 46.4 ± 13.2 years; $P < 0.0001$). Twenty-five patients who underwent liver biopsies were diagnosed with NASH, and 6 were diagnosed with NAFL. On ROC curve analyses, the areas under the ROC curves for SWS, dispersion slope, ATI value, BMI, Fib-4 index, and the area of the NASH pentagon were 0.88000,

0.82000, 0.58730, 0.63000, 0.59333, and 0.93651, respectively; the largest was that for the area of the NASH pentagon.

CONCLUSION

The NASH pentagon area appears useful for discriminating between patients with NASH and those with NAFL.

Key Words: Non-alcoholic fatty liver disease; Non-alcoholic steatohepatitis; Attenuation imaging; Shear wave elastography; Shear wave dispersion; Diagnosis

©The Author(s) 2023. Published by Baishideng Publishing Group Inc. All rights reserved.

Core Tip: The non-alcoholic steatohepatitis (NASH) pentagon is a novel clinical index consisting of the five parameters of shear wave speed, dispersion slope, attenuation imaging value, Fib-4 index, and body mass index. It is simple and the calculation of its area is easy. The area of the NASH pentagon is useful for discriminating between patients with NASH and those with non-alcoholic fatty liver.

Citation: Funada K, Kusano Y, Gyotoku Y, Shirahashi R, Suda T, Tamano M. Novel multi-parametric diagnosis of non-alcoholic fatty liver disease using ultrasonography, body mass index, and Fib-4 index. *World J Gastroenterol* 2023; 29(23): 3703-3714

URL: https://www.wjgnet.com/1007-9327/full/v29/i23/3703.htm

DOI: https://dx.doi.org/10.3748/wjg.v29.i23.3703

INTRODUCTION

Non-alcoholic fatty liver disease (NAFLD) is a global public health problem[1,2]. It is a grouping of diseases consisting of either non-alcoholic fatty liver (NAFL) or non-alcoholic steatohepatitis (NASH) [3]. If NASH progresses, it can lead to liver cirrhosis and hepatocellular carcinoma; thus, a clinical index needs to be developed that can efficiently discriminate NASH patients from NAFL patients[4,5]. Assessments based on multiple parameters using ultrasound, including shear wave elastography (SWE), are reported to be useful in stratifying the risk of advanced NASH[6].

SWE measures the speed of shear waves (shear wave speed; SWS) generated by push pulses. SWS is slow in soft objects and fast in hard objects. Measurements of SWS by SWE are considered useful in assessing liver fibrosis in viral hepatitis and NAFLD[7-11].

The shear wave dispersion (SWD) developed in recent years obtains the "frequency dependence" (dispersion slope; DS), which is the extent of the changes in the speed of shear waves, from changes in their frequency. Some preliminary evidence has been reported that DS measurements with SWD are an index of necroinflammation of the liver[12,13].

Attenuation imaging (ATI) was developed as a new testing method for evaluation of hepatic steatosis with ultrasound technology. ATI is a technique that uses the principle of attenuation due to phenomena such as absorption and diffusion of ultrasonic pulses emitted within the body when they pass through body tissue, and it produces a value referred to as the attenuation coefficient. Magnetic resonance imaging (MRI)-determined proton density fat fraction (PDFF) values have been reportedly used for assessing histological hepatic steatosis grades[14], and Tada *et al*[15] reported a good correlation between ATI values and MRI-determined PDFF values.

On the other hand, it is important to have parameters that do not require special equipment to measure. The prevalence of NAFLD in Japanese non-obese patients is 15%[16]. In other words, 85% of NAFLD patients are obese. Therefore, the body mass index (BMI), which can be easily used to determine obesity, is one such parameter of importance.

Similarly, the scoring system for liver fibrosis by the biochemical examination of blood is also relevant. The Fib-4 index, calculated by aspartate aminotransferase (AST), alanine aminotransferase (ALT), platelets (Plts), and age, is simple and easy to use[17].

In this study, a pentagon consisting of five parameters was prepared with the addition of the BMI and the Fib-4 index to the three parameters of SWS, SWD, and ATI. Whether the area of this pentagon is useful in discriminating NASH from NAFL was then investigated.

MATERIALS AND METHODS

Patients

This was a non-invasive, prospective, observational study that conformed with the ethical guidelines of the Declaration of Helsinki in its 2008 revision and was approved by the ethics review board of the hospital with which the authors are affiliated (No. 21057). The study was conducted after complete information disclosure on the website of the authors' hospital.

Of the patients diagnosed with fatty liver by abdominal ultrasound between September 2021 and August 2022, the subjects were patients in whom SWE, SWD, and ATI were measured. Patients with a history of alcohol intake of ethanol ≥ 20 g/d, who had hepatitis B, hepatitis C, or autoimmune liver disease, and patients with concurrent drug-induced liver injury or cholangitis were excluded.

Diagnosis of fatty liver with ultrasonography

The ultrasound scanner used was an Aplio i800 from Canon Medical Systems Corp. (Otawara, Tochigi, Japan). Fatty liver was diagnosed if the following were seen on B-mode ultrasound examination: (1) Bright liver[18]; (2) Positive hepatorenal echo contrast[19]; (3) Deep ultrasound attenuation in the liver [20]; and (4) Vascular blurring in the liver[21]. Specialists with ten or more years of ultrasonographic experience (Suda T and Tamano M) performed the B-mode ultrasound examination and measured SWE, SWD, and ATI.

Measurements of shear wave elastography and SWD

All SWE measurements were done following B-mode scans, using the same diagnostic equipment and transducers. The measurement results are shown as SWS (m/s). A 1-cm-diameter, circular region of interest was placed on the sample box.

SWD was measured at the same time as SWE. Simultaneous measurements could be taken by switching to quad view mode including a SWS map and a SWD slope map. This test was also performed using five or more measurement values, and the measurement results are shown as DS [(m/s)/KHz].

Measurements of attenuation imaging

After SWE and SWD were measured, the same physician performed the ATI test. The measurement result is shown as the ATI value [(dB/cm)/MHz]. A sample box with the default settings was used to acquire the data, set at least 1.5 cm below the liver capsule to avoid reverberation artifacts. The reliability of the results is displayed with R^2 values, categorized as poor ($R^2 < 0.80$), good ($R^2 = 0.81$-0.89), or excellent ($R^2 > 0.90$). According to information provided by the manufacturer, measurements are considered to be valid when $R^2 \geq 0.80$. Attenuation imaging examinations were performed until five valid measurements were obtained, and the mean value of the five measurements was used in the analysis.

Structure of the NASH pentagon

AST, ALT, and Plts were measured on the same day as the abdominal ultrasound. The Fib-4 index was calculated from these values and age. The BMI was calculated from height and weight on the day on which abdominal ultrasound was performed.

A pentagon consisting of these five parameters (SWS, DS, ATI value, BMI, and Fib-4 index) was created. This was defined as the NASH pentagon. The area of the NASH pentagon was calculated automatically by inputting a calculation formula into an Aplio i800 work station.

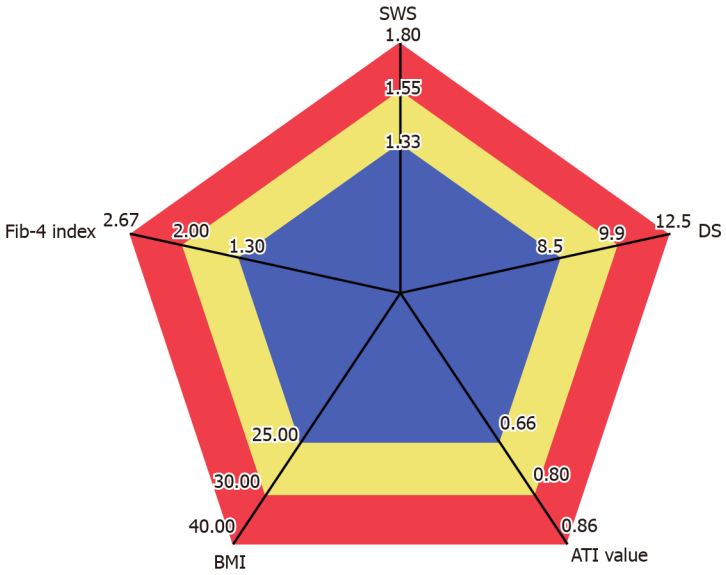
The standard value for each item was set according to previous studies as follows. The standard value of SWS was set as 1.33 m/s (cutoff value of fibrosis stage 1), that of DS was set to 8.5 (m/s)/KHz (cutoff value of lobular inflammation grade 1)[22]. Similarly, the standard value of ATI was set to 0.66 (dB/cm)/MHz, defining steatosis grade 1[16,22]. The standard value for BMI was set at 25.0 kg/m^2 based on the index of the Japanese Society for the Study of Obesity[1]. The standard value for the Fib-4 index was set to 1.30, which is the low cutoff value for advanced fibrosis (stage 3-4), based on a report by Shah *et al*[24] The investigation was done taking the area of this pentagon as 100 (Figure 1).

Diagnosis of NASH

Histological diagnosis based on liver biopsy was performed within three months from SWE measurement in those patients who provided consent. NASH diagnosis was made by an experienced pathologist certified by the Japanese Society of Pathology, based on comprehensive findings including macrovesicular steatosis, ballooning degeneration of hepatocytes, scattered inflammation and apoptotic bodies in the lobules, Mallory-Denk bodies, and fibrosis[25-27]. In this study, all patients without liver biopsy were judged to have NAFL, even if NASH was suspected clinically.

Comparison of two groups classified by the area of the NASH pentagon

Patient characteristics and individual parameters were compared between a large pentagon group (LP group), in which the area of the NASH pentagon was 100 or greater, and a small pentagon group (SP



DOI: 10.3748/wjg.v29.i23.3703 **Copyright** ©The Author(s) 2023.

Figure 1 Non-alcoholic steatohepatitis pentagon. The non-alcoholic steatohepatitis pentagon consists of the five parameters of shear wave speed (SWS), dispersion slope (DS), attenuation imaging value (ATI value), Fib-4 index, and the body mass index (BMI). Based on past reports, the reference values were set as SWS 1.33 m/s, DS 8.5 (m/s)/KHz, ATI value 0.66 (dB/cm)/MHz, BMI 25.0 kg/m^2, and Fib-4 index 1.3. SWS: Shear wave speed; DS: Dispersion slope; BMI: Body mass index; ATI: Attenuation imaging.

group), in which the area was less than 100. In addition, the NASH diagnosis rate was investigated when the NASH pentagon area of 100 was taken as the reference.

Diagnostic accuracy for NASH using the area of the NASH pentagon

In patients for whom liver biopsies were performed during the study period and a histologically confirm-ed diagnosis was made, a receiver-operating characteristic (ROC) curve was drawn for SWS, DS, ATI value, BMI, Fib-4 index, and area of the NASH pentagon.

Statistical analysis

Continuous data for SWS, DS, ATI value, and other clinical parameters are expressed as mean ± SD. A Spearman rank-order correlation coefficient test was used to test the independency of these clinical parameters. A non-paired Wilcoxon test was used in comparisons of each parameter between the two groups divided by NASH pentagon area, with $P < 0.05$ taken to indicate a significant difference.

The NASH diagnostic performance of SWS, DS, ATI value, BMI, Fib-4 index, and the area of the pentagon was investigated using the ROC curve. The area under the ROC curve (AUROC) was used to evaluate NASH diagnostic performance.

RESULTS

Patients' characteristics

The number of patients who were diagnosed with fatty liver based on abdominal ultrasound and in whom SWE, SWD, and ATI were measured was 126. After excluding 7 patients with an alcohol intake history of ≥ 20 g ethanol/d, 10 patients with concurrent hepatitis B, hepatitis C, or autoimmune liver injury, and 2 patients for other reasons, the investigation was conducted with the remaining 107 patients (Figure 2).

The characteristics for these 107 patients are shown in Table 1. There were 61 men and 46 women, with a mean age of 55.1 years. The mean BMI was 26.8 kg/m^2. Of the 107 patients, diabetes mellitus was seen in 25, dyslipidemia in 35, and hypertension in 37. Mean AST, ALT, and γ-glutamyltransferase concentrations were all mildly elevated at 44.9 U/L, 70.6 U/L, and 99.6 U/L, respectively. The mean Fib-4 index was 1.53. Twenty-five of the 107 patients were diagnosed with NASH, and the remaining 82 were diagnosed with NAFL.

The Spearman rank correlation coefficient between SWS and the Fib-4 index was 0.3486; no strong correlation was found. Similarly, the rank correlation coefficient between ATI and BMI was 0.1955, showing no correlation.

Table 1 Patients' characteristics

Patients' characteristics	*n* = 107
M/F	61/46
Age (yr)	55.1 ± 15.9
BMI (kg/m^2)	26.8 ± 4.1
Metabolic diseases	
Diabetes mellitus (yes/no)	25/82
Dyslipidemia (yes/no)	35/72
Hypertension (yes/no)	37/70
Concomitant drugs	
SGLT2 inhibitor	12
DPP-4 inhibitor	13
Thiazolidinedione	2
GLP-1 agonist	2
Statin	19
Bezafibrate	0
Pemafibrate	8
EPA and DHA preparation	1
AST (U/L)	44.9 ± 38.0
ALT (U/L)	70.6 ± 57.7
GGT (U/L)	99.6 ± 139.7
T-B (mg/dL)	0.9 ± 0.5
Alb (mg/dL)	4.5 ± 0.4
eGFR (mL/min)	73.0 ± 15.0
HbA1c (%)	6.5 ± 1.2
T-chol (mg/dL)	202.1 ± 52.6
TG (mg/dL)	180.0 ± 119.0
WBC (10^3/μL)	6731.8 ± 1882.5
Hb (g/dL)	14.7 ± 1.3
Plts (10^4/μL)	23.9 ± 7.6
Fib-4 index	1.53 ± 1.90

M: Male; F: Female; AST: Aspartate aminotransferase; ALT: Alanine aminotransferase; GGT: γ-glutamyltransferase; T-Bil: Total bilirubin; Alb: Albumin; eGFR: Estimated glomerular filtration rate; HbA1c: Glycated hemoglobin A1c; T-chol: Total cholesterol; TG: Triglycerides; WBC: White blood cells; Hb: Hemoglobin; Plts: Platelets.

Comparison of two groups classified by the area of the NASH pentagon

The LP group with a NASH pentagon area ≥ 100 had 64 patients, and the SP group with an area < 100 had 43 patients. A comparison of the two groups is shown in Table 2.

There was no difference in sex between the two groups, but mean age was 60.8 ± 15.2 years in the LP group and 46.4 ± 13.2 years in the SP group, with the LP group significantly older ($P < 0.0001$).

Concurrent diabetes mellitus was seen in 18/64 patients (28.1%) in the LP group and 6/43 patients (13.9%) in the SP group. While this represents a higher tendency in the LP group, no significant difference was seen ($P = 0.0849$). Concurrent dyslipidemia was seen in 27/64 patients (42.2%) in the LP group and 8/43 patients (18.6%) in the SP group, and concurrent hypertension was seen in 29/64 patients (45.3%) and 7/43 patients (16.3%), respectively; both were significantly higher in the LP group ($P = 0.0108$, $P = 0.0183$).

Table 2 Comparison of the two groups classified by area of non-alcoholic steatohepatitis pentagon

	Large pentagon group (*n* = 64)	Small pentagon group (*n* = 43)	*P* value
M/F	33/31	28/15	0.165
Age (yr)	60.8 ± 15.2	46.4 ± 13.2	< 0.0001
Metabolic diseases			
Diabetes mellitus (yes/no)	18/46	6/37	0.0849
Dyslipidemia (yes/no)	27/37	8/35	0.0108
Hypertension (yes/no)	29/35	7/36	0.0183
AST (U/L)	52.6 ± 44.2	40.3 ± 24.4	0.0521
ALT (U/L)	61.1 ± 45.2	83.0 ± 71.6	0.1699
GGT (U/L)	97.3 ± 123.2	102.9 ± 162.0	0.7238
T-B (mg/dL)	1.01 ± 0.6	0.77 ± 0.3	0.0044
Alb (mg/dL)	4.5 ± 0.4	4.6 ± 0.4	0.2843
eGFR (mL/min)	71.8 ± 16.4	74.7 ± 12.1	0.1639
HbA1c (%)	6.5 ± 1.1	6.3 ± 1.2	0.2847
T-chol (mg/dL)	188.5 ± 59.4	221.3 ± 33.8	0.008
TG (mg/dL)	172.9 ± 126.5	189.9 ± 108.8	0.1278
WBC (10^3/μL)	6225.0 ± 1586.9	7463.9 ± 2050.9	0.008
Hb (g/dL)	14.7 ± 1.3	14.7 ± 1.5	0.6836
Plts (10^4/μL)	21.0 ± 6.5	28.8 ± 6.6	< 0.0001
SWS (m/s)	1.78 ± 0.36	1.39 ± 0.14	< 0.0001
DS [(m/s)/kHz]	13.3 ± 3.7	10.8 ± 2.0	< 0.0001
ATI value [(dB/cm)/MHz]	0.78 ± 0.13	0.74 ± 0.13	0.1047
Fib-4 index	2.2 ± 2.3	0.7 ± 0.4	< 0.0001
BMI (kg/m^2)	27.8 ± 4.4	25.6 ± 3.2	0.0249
NASH/NAFL	22/42	3/40	0.0042

M: Male; F: Female; AST: Aspartate aminotransferase; ALT: Alanine aminotransferase; GGT: γ-glutamyltransferase; T-chol: Total cholesterol; TG: Triglycerides; WBC: White blood cells; Hb: Hemoglobin; Plts: Platelets; SWS: Shear wave speed; DS: Dispersion slope; ATI value: Attenuation imaging value; BMI: Body mass index; Alb: Albumin; eGFR: Estimated glomerular filtration rate; NASH: Non-alcoholic steatohepatitis; NAFL: Non-alcoholic fatty liver.

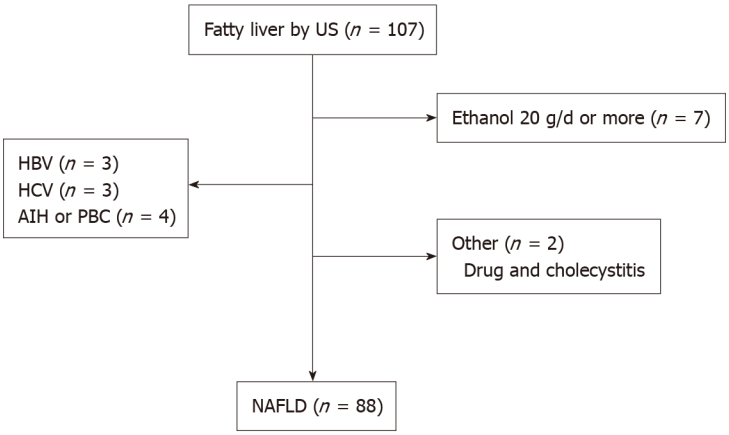
On blood biochemistry tests, total bilirubin was significantly higher in the LP group (P = 0.0044), whereas total cholesterol, white blood cells, and Plts were significantly lower in the LP group (P = 0.0080, P = 0.0080, P < 0.0001). There were no significant differences between the two groups in any of the other test results.

Comparisons of the five parameters that make up the NASH pentagon showed no significant difference between the groups in the ATI value (P = 0.1407), and significantly higher values in the LP group for SWS, DS, Fib-4 index, and BMI (P < 0.0001, P = 0.0004, P < 0.0001, P = 0.0249).

The number of patients diagnosed with NASH was 22 (34.3%) of 64 in the LP group and 3 (7.0%) of 43 in the SP group. The LP group had a significantly higher percentage of NASH patients (P = 0.0042).

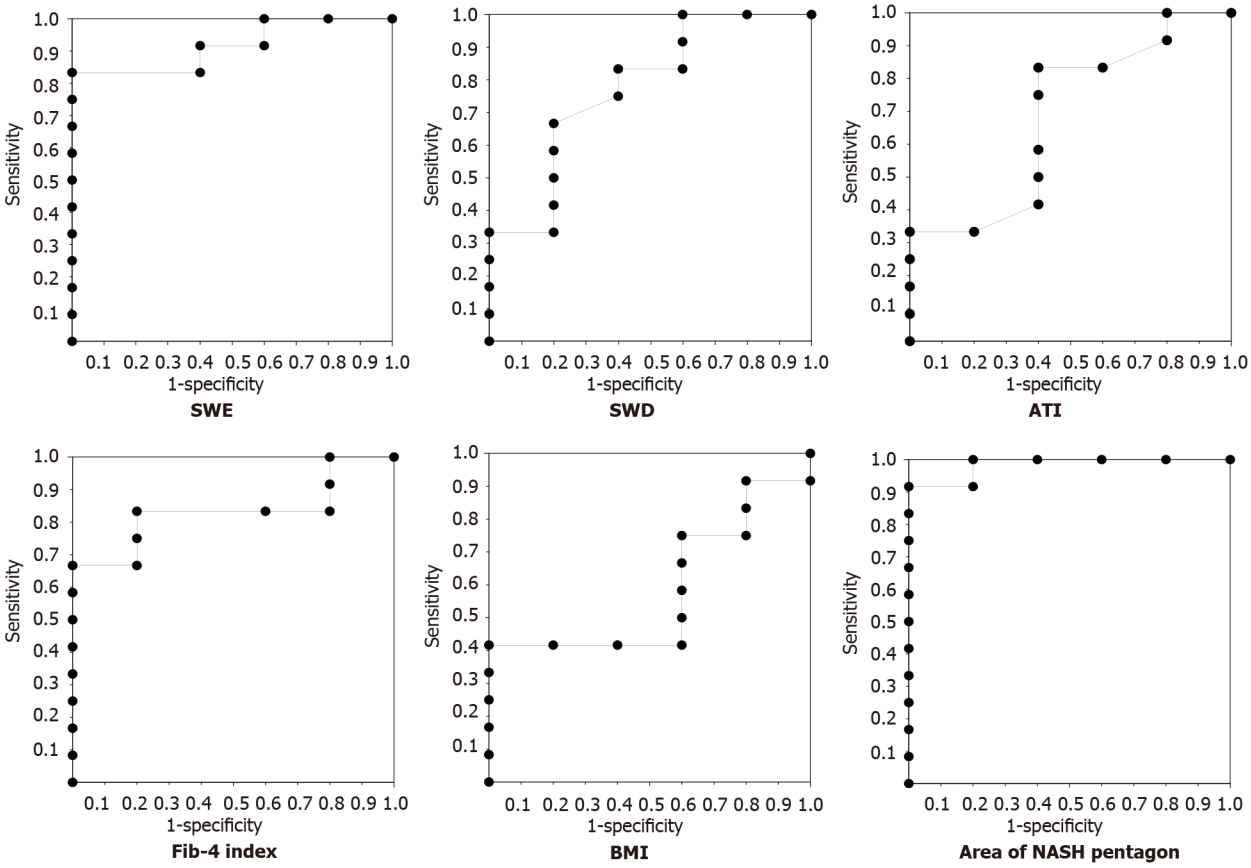
Diagnostic accuracy of histological NAFLD using the area of the NASH pentagon

Liver biopsy was performed during the period of this study in 31 patients. Twenty-five of these 31 patients were diagnosed with NASH, and six were diagnosed with NAFL. The ROC curves indicating the NASH diagnostic performance in these 31 patients are shown in Figure 3. The AUROCs for SWS, DS, ATI value, BMI, Fib-4 index, and the area of the NASH pentagon were 0.88000, 0.82000, 0.58730, 0.63000, 0.59333, and 0.93651, respectively. Of these six items, the largest AUROC was that for the area of the NASH pentagon.



DOI: 10.3748/wjg.v29.i23.3703 **Copyright** ©The Author(s) 2023.

Figure 2 Flowchart of the study. A total of 126 patients who were diagnosed with fatty liver based on abdominal ultrasound and in whom shear wave elastography, shear wave dispersion, and attenuation imaging were measured during the period of this study were entered in the study. Of them, 7 patients with an alcohol intake history of 20 g ethanol/d or more, 3 with hepatitis B, 3 with hepatitis C, and 4 with autoimmune hepatitis or primary biliary cholangitis were excluded. In addition, 1 patient with drug-induced liver injury and 1 patient with cholangitis were excluded, bringing the final number of subjects in this investigation to 107. HBV: Hepatitis B virus; HCV: Hepatitis C virus; AIH: Autoimmune hepatitis; PBC: Primary biliary cholangitis; NAFLD: Non-alcoholic fatty liver disease.



DOI: 10.3748/wjg.v29.i23.3703 **Copyright** ©The Author(s) 2023.

Figure 3 Receiver-operating characteristic curve for each parameter. This shows the receiver-operating characteristic (ROC) curve of the 17 patients who underwent liver biopsy during the period of this study. The areas under the ROC curves (AUROCs) of shear wave speed, dispersion slope, attenuation imaging value, body mass index, Fib-4 index, and the area of the non-alcoholic steatohepatitis (NASH) pentagon are 0.88000, 0.82000, 0.58730, 0.63000, 0.59333, and 0.93651, respectively. Of these six parameters, the largest AUROC is that for the area of the NASH pentagon. SWE: Shear wave elastography; SWD: Shear wave dispersion; ATI: Attenuation imaging; BMI: Body mass index; NASH: Non-alcoholic steatohepatitis.

DISCUSSION

Ultrasound elastography has been used to evaluate fibrosis noninvasively. SWE, one type of ultrasound

elastography, includes transient elastography, point SWE, and other techniques[28-30]. The Aplio i800 used in the present study can measure SWE, SWD, and ATI with the same transducer. This machine is also equipped with a function that automatically creates radar charts from these measured values. The radar charts are created using five parameters. The three parameters of SWS, DS, and ATI value are set in the initial settings, and the remaining two can be freely set by the user. In the present study, these two were set as BMI and Fib-4 index, and it was thought that the area of this pentagon (NASH pentagon) may be useful for the diagnosis of NASH.

There are various reports about the cutoff values of SWE and DS[31]. In the present study, the cutoff values of SWE and DS were set from the report of Sugimoto *et al*[22] based on 120 liver biopsies. The cutoff values for steatosis grade 1 of ATI are reported to be 0.62-0.79[32-34]. In the present study, it was set to 0.66 from the report of Tada *et al*[35] based on 148 liver biopsies.

Obesity is the most important factor in the development of NAFLD. In NASH patients, there is a positive correlation between visceral fat and the amount of fat in hepatocytes[36]. Thus, obesity can lead to a diagnosis of NASH. In the present study, the reference value for BMI was set at 25.0 kg/m^2 based on the index of the Japanese Society for the Study of Obesity and a WHO recommendation[23,37].

The Fib-4 index calculated from age, AST, ALT, and platelet count is regularly used as a noninvasive parameter of hepatic fibrosis[38]. In this study, a value of 1.30, which is the low cutoff value for advanced fibrosis (stage 3-4), based on a report by Shah *et al*[24], was set as the reference value.

SWE and the Fib-4 index are indices of liver fibrosis. However, SWE makes use of ultrasound technology and predicts fibrosis. The Fib-4 index is calculated from biochemical evaluation and age. The correlation of the factors was examined, and no strong correlation was found. ATI is an index of hepatic steatosis assessed using ultrasound technology. BMI is an index of obesity of patients calculated from height and weight. In the present statistical analysis, there was no correlation between these two factors. Due to the above-mentioned reasons, the Fib-4 index and BMI were adopted as constituent factors of the NASH pentagon.

In a comparison of the LP group with a NASH pentagon area of 100 or more and the SP group with an area of less than 100, the LP group was older and had a lower platelet count. This is thought to be a result of the strong involvement of the Fib-4 index among the constituent elements of the pentagon. In fact, a very large difference was seen in the Fib-4 index between the groups, which was 2.2 in the LP group and 0.7 in the SP group ($P < 0.0001$).

The mean BMI, on the other hand, was 27.8 kg/m^2 in the LP group and 25.6 kg/m^2 in the SP group, tending to be higher in the SP group. Obesity is an important element of NAFLD, but as NAFL progresses to NASH, there is a tendency for weight loss. Moreover, even in the SP group, the mean BMI of 25.6 kg/m^2 was only slightly above the reference of 25.0 kg/m^2. This result is also consistent with reports that nonobese NAFLD is more common in Asia than in western countries[39,40].

The onset and progression of NAFLD/NASH are related to metabolic syndrome, and they have an especially strong relationship with diabetes mellitus[41]. In the present study, no difference was seen in concurrent diabetes mellitus by differences in the NASH pentagon area, but concurrent dyslipidemia and hypertension were significantly higher in the LP group.

The NASH pentagon consists of five parameters: Fibrosis based on SWS, inflammation as assessed by DS, steatosis as assessed by ATI value, obesity assessed by BMI, and the level of serological and clinical progression based on the Fib-4 index. Once this pentagon is programmed in the ultrasound machine, it can be automatically created and its area subsequently calculated, making it very simple to use. We thus consider it to be a useful method for identifying NASH among NAFLD patients.

In fact, when ROC curves were made for the six parameters of SWS, DS, ATI value, BMI, Fib-4 index, and the area of the NASH pentagon in 31 patients who underwent liver biopsy during the study period, the largest AUROC was the one for the area of the NASH pentagon.

In the early stage of NASH, liver fibrosis is mild, and in these patients, SWS is expected to be either normal or only mildly elevated. In young patients, the Fib-4 index also tends to be low. Even in these patients, however, DS, ATI value, and BMI are expected to be high, so it may be possible to identify them using the NASH pentagon.

Conversely, BMI tends to decrease when NASH progresses to cirrhosis, and even histologically, a state is present in which reduced fat deposition is seen (so-called "burned-out NASH")[42,43]. Such patients are expected to have low BMI and ATI values in conjunction with high SWS and Fib-4 index values. DS may have different values depending on the individual case, but the NASH pentagon is thought to be useful even in these patients.

Limitations

This was a prospective study, but only 107 patients were included, and only 31 underwent liver biopsy during the study period. These numbers are too small to obtain sufficient results. Additional studies with a larger number of patients will be needed to confirm our results. It may also be necessary to conduct a more detailed pathological investigation and a review of the reference values for the five parameters.

CONCLUSION

The preparation of a NASH pentagon consisting of five parameters, SWS, DS, ATI value, Fib-4 index, and BMI, is simple and the calculation of its area is easy. The authors believe that this multi-parametric index will be useful for identifying NASH patients among NAFLD patients.

ARTICLE HIGHLIGHTS

Research background

Non-alcoholic fatty liver disease (NAFLD) is a major problem throughout the world. If non-alcoholic steatohepatitis (NASH) progresses, it can lead to hepatocellular carcinoma. Novel clinical index needs to be developed that can efficiently discriminate NASH patients from non-alcoholic fatty liver (NAFL) patients.

Research motivation

Shear wave speed (SWS), shear wave dispersion (SWD), and attenuation imaging (ATI) are new ultrasound diagnostic parameters for NAFLD. We developed a novel clinical index as the "NASH pentagon" consisting of the 3 abovementioned parameters, body mass index (BMI), and Fib-4 index.

Research objectives

Objective of this study is to prove the utility of NASH pentagon area in the differentiation of NASH and NAFL.

Research methods

Patients diagnosed with fatty liver by abdominal ultrasound between September 2021 and August 2022 were enrolled. Histological diagnosis based on liver biopsy was performed in 31 patients. The large pentagon group (LP group) and the small pentagon group (SP group), using an area of 100 as the cutoff, were compared; the NASH diagnosis rate was also investigated. In patients with a histologically confirmed diagnosis, receiver-operating characteristic curve analyses were performed.

Research results

The preparation of a NASH pentagon consisting of five parameters, SWS, DS, ATI value, Fib-4 index, and BMI, is simple and the calculation of its area is easy. The LP group with a NASH pentagon area ≥ 100 had 64 patients, and the SP group with an area < 100 had 43 patients. The number of patients diagnosed with NASH was 22 (34.3%) of 64 in the LP group and 3 (7.0%) of 43 in the SP group. The LP group had a significantly higher percentage of NASH patients (P = 0.0042).

Research conclusions

The NASH pentagon is a novel multi-parametric index, and will be useful for identifying NASH patients among NAFLD patients.

Research perspectives

NASH pentagon should be tried in more patients. Besides, the area of NASH pentagon and the details of the histologic diagnosis should be considered.

ACKNOWLEDGEMENTS

The authors would like to thank the institutions that participated in the working group and everyone who helped collect clinical data.

FOOTNOTES

Author contributions: Funada K, Kusano Y, Gyotoku Y and Shirahashi R conceptualized and designed the study, collected data, carried out the initial analysis, and drafted the initial manuscript; Suda T and Tamano M coordinated and supervised data collection and critically reviewed the manuscript for important intellectual content; and all authors approved the final manuscript as submitted and agree to be accountable for all aspects of the work.

Institutional review board statement: The study was reviewed and approved by the Dokkyo Medical University Saitama Medical Center Institutional Review Board (approval No. 21057).

Clinical trial registration statement: This study is registered at clinical research support office, Dokkyo Medical University Saitama Medical Center. The registration identification number is 21057.

Informed consent statement: Patients were not required to give informed consent for participation in the present study because the analysis used anonymous clinical data that were obtained after each patient gave informed consent to treatment. For full disclosure, the details of this prospective, observational study were published on the home page of the medical center.

Conflict-of-interest statement: All the authors report no relevant conflicts of interest for this article.

Data sharing statement: No additional data are available.

CONSORT 2010 statement: The authors have read the CONSORT 2010 statement, and the manuscript was prepared and revised according to the CONSORT 2010 statement.

Open-Access: This article is an open-access article that was selected by an in-house editor and fully peer-reviewed by external reviewers. It is distributed in accordance with the Creative Commons Attribution NonCommercial (CC BY-NC 4.0) license, which permits others to distribute, remix, adapt, build upon this work non-commercially, and license their derivative works on different terms, provided the original work is properly cited and the use is non-commercial. See: https://creativecommons.org/Licenses/by-nc/4.0/

Country/Territory of origin: Japan

ORCID number: Kei Funada 0000-0003-1190-5588; Yumi Kusano 0000-0001-8000-0884; Yoshinori Gyotoku 0000-0003-2395-3421; Ryosaku Shirahashi 0000-0001-7843-3138; Toshikuni Suda 0000-0003-1017-3725; Masaya Tamano 0000-0001-5595-2330.

S-Editor: Gao CC
L-Editor: A
P-Editor: Wang JJ

REFERENCES

1 **Sayiner M**, Koenig A, Henry L, Younossi ZM. Epidemiology of Nonalcoholic Fatty Liver Disease and Nonalcoholic Steatohepatitis in the United States and the Rest of the World. *Clin Liver Dis* 2016; **20**: 205-214 [PMID: 27063264 DOI: 10.1016/j.cld.2015.10.001]
2 **Asrani SK**, Devarbhavi H, Eaton J, Kamath PS. Burden of liver diseases in the world. *J Hepatol* 2019; **70**: 151-171 [PMID: 30266282 DOI: 10.1016/j.jhep.2018.09.014]
3 **Yeh MM**, Brunt EM. Pathological features of fatty liver disease. *Gastroenterology* 2014; **147**: 754-764 [PMID: 25109884 DOI: 10.1053/j.gastro.2014.07.056]
4 **Tsochatzis EA**, Newsome PN. Non-alcoholic fatty liver disease and the interface between primary and secondary care. *Lancet Gastroenterol Hepatol* 2018; **3**: 509-517 [PMID: 29893235 DOI: 10.1016/S2468-1253(18)30077-3]
5 **Younossi ZM**. Non-alcoholic fatty liver disease - A global public health perspective. *J Hepatol* 2019; **70**: 531-544 [PMID: 30414863 DOI: 10.1016/j.jhep.2018.10.033]
6 **Kuroda H**, Fujiwara Y, Abe T, Nagasawa T, Oguri T, Noguchi S, Kamiyama N, Takikawa Y. Two-dimensional shear wave elastography and ultrasound-guided attenuation parameter for progressive non-alcoholic steatohepatitis. *PLoS One* 2021; **16**: e0249493 [PMID: 33826669 DOI: 10.1371/journal.pone.0249493]
7 **Suda T**, Okawa O, Masaoka R, Gyotoku Y, Tokutomi N, Katayama Y, Tamano M. Shear wave elastography in hepatitis C patients before and after antiviral therapy. *World J Hepatol* 2017; **9**: 64-68 [PMID: 28105260 DOI: 10.4254/wjh.v9.i1.64]
8 **Tada T**, Kumada T, Toyoda H, Ito T, Sone Y, Okuda S, Tsuji N, Imayoshi Y, Yasuda E. Utility of real-time shear wave elastography for assessing liver fibrosis in patients with chronic hepatitis C infection without cirrhosis: Comparison of liver fibrosis indices. *Hepatol Res* 2015; **45**: E122-E129 [PMID: 25580959 DOI: 10.1111/hepr.12476]
9 **Meyer G**, Dauth N, Grimm M, Herrmann E, Bojunga J, Friedrich-Rust M. Shear Wave Elastography Reveals a High Prevalence of NAFLD-related Fibrosis even in Type 1 Diabetes. *Exp Clin Endocrinol Diabetes* 2022; **130**: 532-538 [PMID: 34784620 DOI: 10.1055/a-1666-0431]
10 **Bâldea V**, Bende F, Popescu A, Şirli R, Sporea I. Comparative study between two 2D-Shear Waves Elastography techniques for the non-invasive assessment of liver fibrosis in patients with chronic hepatitis C virus (HCV) infection. *Med Ultrason* 2021; **23**: 257-264 [PMID: 33657193 DOI: 10.11152/mu-2863]
11 **Podrug K**, Sporea I, Lupusoru R, Pastrovic F, Mustapic S, Bâldea V, Bozin T, Bokun T, Salkic N, Şirli R, Popescu A, Puljiz Z, Grgurevic I. Diagnostic Performance of 2-D Shear-Wave Elastography with Propagation Maps and Attenuation Imaging in Patients with Non-Alcoholic Fatty Liver Disease. *Ultrasound Med Biol* 2021; **47**: 2128-2137 [PMID: 33985827 DOI: 10.1016/j.ultrasmedbio.2021.03.025]
12 **Sugimoto K**, Moriyasu F, Oshiro H, Takeuchi H, Yoshimasu Y, Kasai Y, Furuichi Y, Itoi T. Viscoelasticity Measurement in Rat Livers Using Shear-Wave US Elastography. *Ultrasound Med Biol* 2018; **44**: 2018-2024 [PMID: 29936025 DOI: 10.1016/j.ultrasmedbio.2018.05.008]

13 **Lee DH**, Lee JY, Bae JS, Yi NJ, Lee KW, Suh KS, Kim H, Lee KB, Han JK. Shear-Wave Dispersion Slope from US Shear-Wave Elastography: Detection of Allograft Damage after Liver Transplantation. *Radiology* 2019; **293**: 327-333 [PMID: 31502939 DOI: 10.1148/radiol.2019190064]

14 **Jeon SK**, Lee JM, Joo I, Yoon JH, Lee DH, Lee JY, Han JK. Prospective Evaluation of Hepatic Steatosis Using Ultrasound Attenuation Imaging in Patients with Chronic Liver Disease with Magnetic Resonance Imaging Proton Density Fat Fraction as the Reference Standard. *Ultrasound Med Biol* 2019; **45**: 1407-1416 [PMID: 30975533 DOI: 10.1016/j.ultrasmedbio.2019.02.008]

15 **Tada T**, Kumada T, Toyoda H, Nakamura S, Shibata Y, Yasuda S, Watanuki Y, Tsujii K, Fukuda N, Fujioka M, Takeshima K, Niwa F, Ogawa S, Hashinokuchi S, Kataoka S, Ichikawa H, Iijima H. Attenuation imaging based on ultrasound technology for assessment of hepatic steatosis: A comparison with magnetic resonance imaging-determined proton density fat fraction. *Hepatol Res* 2020; **50**: 1319-1327 [PMID: 32876367 DOI: 10.1111/hepr.13563]

16 **Nishioji K**, Sumida Y, Kamaguchi M, Mochizuki N, Kobayashi M, Nishimura T, Yamaguchi K, Itoh Y. Prevalence of and risk factors for non-alcoholic fatty liver disease in a non-obese Japanese population, 2011-2012. *J Gastroenterol* 2015; **50**: 95-108 [PMID: 24619537 DOI: 10.1007/s00535-014-0948-9]

17 **Vilar-Gomez E**, Chalasani N. Non-invasive assessment of non-alcoholic fatty liver disease: Clinical prediction rules and blood-based biomarkers. *J Hepatol* 2018; **68**: 305-315 [PMID: 29154965 DOI: 10.1016/j.jhep.2017.11.013]

18 **Joseph AE**, Dewbury KC, McGuire PG. Ultrasound in the detection of chronic liver disease (the "bright liver"). *Br J Radiol* 1979; **52**: 184-188 [PMID: 435696 DOI: 10.1259/0007-1285-52-615-184]

19 **Yajima Y**, Ohta K, Narui T, Abe R, Suzuki H, Ohtsuki M. Ultrasonographical diagnosis of fatty liver: significance of the liver-kidney contrast. *Tohoku J Exp Med* 1983; **139**: 43-50 [PMID: 6220488 DOI: 10.1620/tjem.139.43]

20 **Hamaguchi M**, Kojima T, Itoh Y, Harano Y, Fujii K, Nakajima T, Kato T, Takeda N, Okuda J, Ida K, Kawahito Y, Yoshikawa T, Okanoue T. The severity of ultrasonographic findings in nonalcoholic fatty liver disease reflects the metabolic syndrome and visceral fat accumulation. *Am J Gastroenterol* 2007; **102**: 2708-2715 [PMID: 17894848 DOI: 10.1111/j.1572-0241.2007.01526.x]

21 **Saadeh S**, Younossi ZM, Remer EM, Gramlich T, Ong JP, Hurley M, Mullen KD, Cooper JN, Sheridan MJ. The utility of radiological imaging in nonalcoholic fatty liver disease. *Gastroenterology* 2002; **123**: 745-750 [PMID: 12198701 DOI: 10.1053/gast.2002.35354]

22 **Sugimoto K**, Moriyasu F, Oshiro H, Takeuchi H, Abe M, Yoshimasu Y, Kasai Y, Sakamaki K, Hara T, Itoi T. The Role of Multiparametric US of the Liver for the Evaluation of Nonalcoholic Steatohepatitis. *Radiology* 2020; **296**: 532-540 [PMID: 32573385 DOI: 10.1148/radiol.2020192665]

23 **Examination Committee of Criteria for 'Obesity Disease' in Japan**; Japan Society for the Study of Obesity. New criteria for 'obesity disease' in Japan. *Circ J* 2002; **66**: 987-992 [PMID: 12419927 DOI: 10.1253/circj.66.987]

24 **Shah AG**, Lydecker A, Murray K, Tetri BN, Contos MJ, Sanyal AJ; Nash Clinical Research Network. Comparison of noninvasive markers of fibrosis in patients with nonalcoholic fatty liver disease. *Clin Gastroenterol Hepatol* 2009; **7**: 1104-1112 [PMID: 19523535 DOI: 10.1016/j.cgh.2009.05.033]

25 **Angulo P**. Nonalcoholic fatty liver disease. *N Engl J Med* 2002; **346**: 1221-1231 [PMID: 11961152 DOI: 10.1056/NEJMra011775]

26 **Matteoni CA**, Younossi ZM, Gramlich T, Boparai N, Liu YC, McCullough AJ. Nonalcoholic fatty liver disease: a spectrum of clinical and pathological severity. *Gastroenterology* 1999; **116**: 1413-1419 [PMID: 10348825 DOI: 10.1016/s0016-5085(99)70506-8]

27 **Kleiner DE**, Brunt EM, Van Natta M, Behling C, Contos MJ, Cummings OW, Ferrell LD, Liu YC, Torbenson MS, Unalp-Arida A, Yeh M, McCullough AJ, Sanyal AJ; Nonalcoholic Steatohepatitis Clinical Research Network. Design and validation of a histological scoring system for nonalcoholic fatty liver disease. *Hepatology* 2005; **41**: 1313-1321 [PMID: 15915461 DOI: 10.1002/hep.20701]

28 **Tamano M**, Kojima K, Akima T, Murohisa T, Hashimoto T, Uetake C, Sugaya T, Nakano M, Hiraishi H, Yoneda M. The usefulness of measuring liver stiffness by transient elastography for assessing hepatic fibrosis in patients with various chronic liver diseases. *Hepatogastroenterology* 2012; **59**: 826-830 [PMID: 22469726 DOI: 10.5754/hge11255]

29 **Yoneda M**, Yoneda M, Fujita K, Inamori M, Tamano M, Hiriishi H, Nakajima A. Transient elastography in patients with non-alcoholic fatty liver disease (NAFLD). *Gut* 2007; **56**: 1330-1331 [PMID: 17470477 DOI: 10.1136/gut.2007.126417]

30 **Fang C**, Konstantatou E, Romanos O, Yusuf GT, Quinlan DJ, Sidhu PS. Reproducibility of 2-Dimensional Shear Wave Elastography Assessment of the Liver: A Direct Comparison With Point Shear Wave Elastography in Healthy Volunteers. *J Ultrasound Med* 2017; **36**: 1563-1569 [PMID: 28370146 DOI: 10.7863/ultra.16.07018]

31 **Suda T**, Kanefuji T, Abe A, Nagayama I, Hoshi T, Morita S, Yagi K, Hatakeyama S, Hayatsu M, Hasegawa N, Terai S. A cut-off value of shear wave speed to distinguish nonalcoholic steatohepatitis candidates. *Medicine (Baltimore)* 2019; **98**: e13958 [PMID: 30633176 DOI: 10.1097/MD.0000000000013958]

32 **Sporea I**, Bâldea V, Lupușoru R, Bende F, Mare R, Lazăr A, Popescu A, Șirli R. Quantification of Steatosis and Fibrosis using a new system implemented in an ultrasound machine. *Med Ultrason* 2020; **22**: 265-271 [PMID: 32399537 DOI: 10.11152/mu-2495]

33 **Hsu PK**, Wu LS, Yen HH, Huang HP, Chen YY, Su PY, Su WW. Attenuation Imaging with Ultrasound as a Novel Evaluation Method for Liver Steatosis. *J Clin Med* 2021; **10** [PMID: 33801163 DOI: 10.3390/jcm10050965]

34 **Jang JK**, Lee ES, Seo JW, Kim YR, Kim SY, Cho YY, Lee DH. Two-dimensional Shear-Wave Elastography and US Attenuation Imaging for Nonalcoholic Steatohepatitis Diagnosis: A Cross-sectional, Multicenter Study. *Radiology* 2022; **305**: 118-126 [PMID: 35727151 DOI: 10.1148/radiol.220220]

35 **Tada T**, Iijima H, Kobayashi N, Yoshida M, Nishimura T, Kumada T, Kondo R, Yano H, Kage M, Nakano C, Aoki T, Aizawa N, Ikeda N, Takashima T, Yuri Y, Ishii N, Hasegawa K, Takata R, Yoh K, Sakai Y, Nishikawa H, Iwata Y, Enomoto H, Hirota S, Fujimoto J, Nishiguchi S. Usefulness of Attenuation Imaging with an Ultrasound Scanner for the Evaluation of Hepatic Steatosis. *Ultrasound Med Biol* 2019; **45**: 2679-2687 [PMID: 31277922 DOI: 10.1016/j.ultrasmedbio.2019.05.033]

36 **Koda M**, Kawakami M, Murawaki Y, Senda M. The impact of visceral fat in nonalcoholic fatty liver disease: cross-

sectional and longitudinal studies. *J Gastroenterol* 2007; **42**: 897-903 [PMID: 18008034 DOI: 10.1007/s00535-007-2107-z]

37 **WHO Expert Consultation**. Appropriate body-mass index for Asian populations and its implications for policy and intervention strategies. *Lancet* 2004; **363**: 157-163 [PMID: 14726171 DOI: 10.1016/S0140-6736(03)15268-3]

38 **Sumida Y**, Yoneda M, Hyogo H, Itoh Y, Ono M, Fujii H, Eguchi Y, Suzuki Y, Aoki N, Kanemasa K, Fujita K, Chayama K, Saibara T, Kawada N, Fujimoto K, Kohgo Y, Yoshikawa T, Okanoue T; Japan Study Group of Nonalcoholic Fatty Liver Disease (JSG-NAFLD). Validation of the FIB4 index in a Japanese nonalcoholic fatty liver disease population. *BMC Gastroenterol* 2012; **12**: 2 [PMID: 22221544 DOI: 10.1186/1471-230X-12-2]

39 **Fan JG**, Kim SU, Wong VW. New trends on obesity and NAFLD in Asia. *J Hepatol* 2017; **67**: 862-873 [PMID: 28642059 DOI: 10.1016/j.jhep.2017.06.003]

40 **Wei JL**, Leung JC, Loong TC, Wong GL, Yeung DK, Chan RS, Chan HL, Chim AM, Woo J, Chu WC, Wong VW. Prevalence and Severity of Nonalcoholic Fatty Liver Disease in Non-Obese Patients: A Population Study Using Proton-Magnetic Resonance Spectroscopy. *Am J Gastroenterol* 2015; **110**: 1306-14; quiz 1315 [PMID: 26215532 DOI: 10.1038/ajg.2015.235]

41 **El-Serag HB**, Tran T, Everhart JE. Diabetes increases the risk of chronic liver disease and hepatocellular carcinoma. *Gastroenterology* 2004; **126**: 460-468 [PMID: 14762783 DOI: 10.1053/j.gastro.2003.10.065]

42 **Tokushige K**, Ikejima K, Ono M, Eguchi Y, Kamada Y, Itoh Y, Akuta N, Yoneda M, Iwasa M, Otsuka M, Tamaki N, Kogiso T, Miwa H, Chayama K, Enomoto N, Shimosegawa T, Takehara T, Koike K. Evidence-based clinical practice guidelines for nonalcoholic fatty liver disease/nonalcoholic steatohepatitis 2020. *J Gastroenterol* 2021; **56**: 951-963 [PMID: 34533632 DOI: 10.1007/s00535-021-01796-x]

43 **Tokushige K**, Ikejima K, Ono M, Eguchi Y, Kamada Y, Itoh Y, Akuta N, Yoneda M, Iwasa M, Otsuka M, Tamaki N, Kogiso T, Miwa H, Chayama K, Enomoto N, Shimosegawa T, Takehara T, Koike K. Evidence-based clinical practice guidelines for nonalcoholic fatty liver disease/nonalcoholic steatohepatitis 2020. *Hepatol Res* 2021; **51**: 1013-1025 [PMID: 34533266 DOI: 10.1111/hepr.13688]

World Journal of Gastroenterology

Submit a Manuscript: https://www.f6publishing.com

World J Gastroenterol 2023 June 21; 29(23): 3715-3732

DOI: 10.3748/wjg.v29.i23.3715

ISSN 1007-9327 (print) ISSN 2219-2840 (online)

ORIGINAL ARTICLE

Prospective Study

Robotic-assisted proctosigmoidectomy for Hirschsprung's disease: A multicenter prospective study

Meng-Xin Zhang, Xi Zhang, Xiao-Pan Chang, Ji-Xiao Zeng, Hong-Qiang Bian, Guo-Qing Cao, Shuai Li, Shui-Qing Chi, Ying Zhou, Li-Ying Rong, Li Wan, Shao-Tao Tang

Specialty type: Gastroenterology and hepatology

Provenance and peer review: Unsolicited article; Externally peer reviewed.

Peer-review model: Single blind

Peer-review report's scientific quality classification

Grade A (Excellent): 0
Grade B (Very good): B, B
Grade C (Good): 0
Grade D (Fair): 0
Grade E (Poor): 0

P-Reviewer: Grawish ME, Egypt; Trébol J, Spain

Received: March 16, 2023
Peer-review started: March 16, 2023
First decision: April 21, 2023
Revised: April 29, 2023
Accepted: May 22, 2023
Article in press: May 22, 2023
Published online: June 21, 2023

Meng-Xin Zhang, Xi Zhang, Guo-Qing Cao, Shuai Li, Shui-Qing Chi, Ying Zhou, Li-Ying Rong, Li Wan, Shao-Tao Tang, Department of Pediatric Surgery, Union Hospital, Tongji Medical College, Huazhong University of Science and Technology, Wuhan 430022, Hubei Province, China

Xiao-Pan Chang, Ji-Xiao Zeng, Department of Pediatric Surgery, Guangzhou Women and Children's Medical Center, Guangzhou Medical University, Guangzhou 510623, Guangdong Province, China

Hong-Qiang Bian, Department of General Surgery, Wuhan Children's Hospital, Tongji Medical College, Huazhong University of Science and Technology, Wuhan 430019, Hubei Province, China

Corresponding author: Shao-Tao Tang, Doctor, MD, PhD, Chief Doctor, Professor, Surgeon, Department of Pediatric Surgery, Union Hospital, Tongji Medical College, Huazhong University of Science and Technology, No. 1277 Jiefang Avenue, Wuhan 430022, Hubei Province, China. tshaotao83@hust.edu.cn

Abstract

BACKGROUND

Robotic surgery is a cutting-edge minimally invasive technique that overcomes many shortcomings of laparoscopic techniques, yet few studies have evaluated the use of robotic surgery to treat Hirschsprung's disease (HSCR).

AIM

To analyze the feasibility and medium-term outcomes of robotic-assisted proctosigmoidectomy (RAPS) with sphincter- and nerve-sparing surgery in HSCR patients.

METHODS

From July 2015 to January 2022, 156 rectosigmoid HSCR patients were enrolled in this multicenter prospective study. Their sphincters and nerves were spared by dissecting the rectum completely from the pelvic cavity outside the longitudinal muscle of the rectum and then performing transanal Soave pull-through procedures. Surgical outcomes and continence function were analyzed.

RESULTS

No conversions or intraoperative complications occurred. The median age at surgery was 9.50 months, and the length of the removed bowel was 15.50 ± 5.23 cm. The total operation time, console time, and anal traction time were 155.22 ± 16.77, 58.01 ± 7.71, and 45.28 ± 8.15 min. There were 25 complications within 30 d and 48 post-30-d complications. For children aged ≥ 4 years, the bowel function score (BFS) was 17.32 ± 2.63, and 90.91% of patients showed moderate-to-good bowel function. The postoperative fecal continence (POFC) score was 10.95 ± 1.04 at 4 years of age, 11.48 ± 0.72 at 5 years of age, and 11.94 ± 0.81 at 6 years of age, showing a promising annual trend. There were no significant differences in postoperative complications, BFS, and POFC scores related to age at surgery being ≤ 3 mo or > 3 mo.

CONCLUSION

RAPS is a safe and effective alternative for treating HSCR in children of all ages; it offers the advantage of further minimizing damage to sphincters and perirectal nerves and thus providing better continence function.

Key Words: Robotic-assisted; Hirschsprung's disease; Continence function; Sphincter; Nerve

©The Author(s) 2023. Published by Baishideng Publishing Group Inc. All rights reserved.

Core Tip: We present the largest series of patients with Hirschsprung's disease treated with robotic-assisted proctosigmoidectomy (RAPS). RAPS is a safe and effective alternative for treating Hirschsprung's disease in children of all ages. It offers the advantage of further minimizing damage to sphincters and perirectal nerves and thus providing better fecal function.

Citation: Zhang MX, Zhang X, Chang XP, Zeng JX, Bian HQ, Cao GQ, Li S, Chi SQ, Zhou Y, Rong LY, Wan L, Tang ST. Robotic-assisted proctosigmoidectomy for Hirschsprung's disease: A multicenter prospective study. *World J Gastroenterol* 2023; 29(23): 3715-3732
URL: https://www.wjgnet.com/1007-9327/full/v29/i23/3715.htm
DOI: https://dx.doi.org/10.3748/wjg.v29.i23.3715

INTRODUCTION

Although beneficial for children with Hirschsprung's disease (HSCR), laparoscopic operation is more challenging than open operation, especially in newborns and infants. To address the drawbacks of laparoscopic surgery, a robotic system may be considered. Robotic-assisted surgery is utilized in various areas due to its numerous advantages, particularly in complex operations, such as anorectal malformations in children[1] and prostate and rectal cancer in adults[2,3].

Recently, laparoscopic techniques have developed into an effective treatment for HSCR. As previously shown, these minimally invasive surgical techniques result in better early postoperative outcomes than the open procedure[4,5], and the long-term results are similar between laparoscopic and open procedures[6]. Nevertheless, laparoscopic surgery for HSCR is still considered to be one of the most difficult operations in anorectal surgery. With the introduction and application of robotic surgical platforms, this technology is gradually being adopted for the treatment of HSCR. However, the safety and efficacy of the technology in treating pediatric HSCR patients have been evaluated in only a few studies.

In this paper, we present our initial experience with robotic-assisted proctosigmoidectomy (RAPS) with sphincter- and nerve-sparing surgery (SNS) for treating HSCR. To our knowledge, this represents the largest series of SNS-RAPS in children reported to date. The SNS-RAPS procedure is thoroughly detailed.

MATERIALS AND METHODS

Study design

From July 2015 to January 2022, a multicenter prospective study of consecutive children with rectosigmoid HSCR who underwent uniform SNS-RAPS was carried out at three centers (Union Hospital, Tongji Medical College, Huazhong University of Science and Technology; Guangzhou Women and Children's Medical Center, Guangzhou Medical University; Wuhan Children's Hospital, Tongji Medical College, Huazhong University of Science and Technology). A total of 156 patients were

enrolled, and all operations were performed by experienced surgical teams from three centers. Since the time the da Vinci Surgical System Si (Intuitive Surgical, Sunnyvale, CA) was introduced at the three centers to treat HSCR, all HSCR cases have been recorded in a prospectively designed database. Patient demographics, surgical parameters, and postoperative data were recorded.

This study was approved by the ethics committee at each participating center and registered in the Chinese Clinical Trial Registry (Registration ID: ChiCTR2000035220). Written informed consent was obtained from the legal guardians of each patient. The study has been reported in accordance with the Declaration of Helsinki.

Patients

Patients diagnosed with rectosigmoid HSCR preoperatively were candidates for SNS-RAPS. The diagnosis was based on clinical symptoms and signs, barium enema results, rectal aspiration biopsy, anorectal manometry, and intraoperative biopsy. Patients with trisomy 21, total colonic aganglionosis, long-segment HSCR, HSCR combined with preoperative enterostomy, and surgical contraindications were excluded. The patient selection process is detailed in Figure 1. All patients received a unified preoperative preparation and postoperative treatment plan at all centers.

Colonic irrigation with warm saline (100-200 mL/kg) was used to prepare the colon for 3-7 d. Metronidazole (25 mg/kg, bid) was given orally for 3 d (1-2 d for neonates) preoperatively, and one dose of cefoperazone was provided during anesthesia induction.

Operative procedure

Under general anesthesia, the patient was placed in the supine position, and three trocars were placed. The CO_2 insufflation pressure was set at 8-10 mmHg, and the flow rate at 2.5-4.5 L/min. The operation was performed using three ports, including a straight-cut umbilical trocar accommodating a 12 mm 30° telescope and two working trocars with 8 mm robotic devices on either side (Figure 2). The robotic arms were oriented from the caudal direction. The aganglionic segment range was assessed by seromuscular biopsy using robotic monopolar scissors and interrupted 5-0 sutures were placed in cases of bleeding or mucosal rupture. The needle and suction were alternately inserted for operation through the 8 mm port on one side, which required the process of removing and reinserting the operative instrument. A Maryland dissector and a robotic hook were used to perform the dissection. After creating a window on the sigmoid mesentery, we clipped and divided the sigmoid artery trunk and then mobilized the mesentery up to the level of the inferior mesenteric artery. SNS robotic endorectal dissection was performed circumferentially down to the pelvis, which was the most unique and crucial part of the operation. Dissection was begun circumferentially at 1.0 cm above the peritoneal reflection. The rectum was mobilized outside the longitudinal muscle layer (that is, under its serosa or proper rectal fascia extended serous layer below the peritoneal reflection), with the anatomical plane farther away from Denonvillier's fascia and the nerve plexus anterior or lateral to the rectum (Figure 3A). When we pulled the rectum cranially, intestinal wall muscle layers provided greater tensile strength than the mucosa, allowing the pelvis to be shallower (Figure 4) and avoiding intraoperative intestinal mucosal tearing with peritoneal contamination. Since the robotic platform allowed for dissection in a narrow field, we were able to dissect the rectum to a lower level, nearly up to the dentate line. The mobilization of the rectum reached 4-7 cm into the pelvis (Figure 3B).

After the robot was unlocked, a circular incision was made 0.5-1 cm from the dentate line (Figure 5A), dividing the mucosa upward by 0.2-0.4 cm, breaking through the muscular cuff, and exposing the robotic dissection plane in the pelvis. The diseased colon was then gently pulled out through the anus. The posterior wall was partially resected in a V-shape, and the pointed end of the "V" reached the level of the dentate line to release internal anal sphincter achalasia. To avoid residual dysfunctional bowel, we uniformly excised the dilated and thickened bowel; we then performed Soave's anastomosis with interrupted 5-0 or 4-0 absorbable sutures above the biopsy site. After the diseased bowel was removed, the specimen was measured for its overall length and the pelvic dissection length (Figure 5B).

Postoperative management

Intravenous antibiotics (cefoperazone, 50 mg/kg, bid) were given for the first 3 d, and a urinary catheter was left for 24-48 h after surgery. No nasogastric tube or drains were left in place, but a rectal tube was left for 5 d postoperatively to help the passage of intestinal contents and gas through the anus. Instead of sutures, we used butterfly shaped tape to fixate the tube and reduce postoperative discomfort. The patient was discharged after being confirmed to be clinically stable and tolerant of a full oral diet. A routine digital rectal examination was performed postoperatively at 2 wk, and an anal dilatation plan was formulated.

Postoperative variables and definitions

The bowel function score (BFS) was used to evaluate overall bowel function[7], while the postoperative fecal continence (POFC) score focused on SNS-related incontinence[8]. Children aged ≥ 4 years were assessed twice for each score as shown in Tables 1 and 2. A BFS ≥ 17 was represented as the lower limit of good/normal functional outcomes as more than 90% of people aged ≥ 4 years in the normal

Table 1 Scale for bowel function score

Evaluation on fecal continence	Score
Feels the urge to defecate	
Always	3
Most of the time	2
Uncertain	1
Absent	0
Ability to hold back defecation	
Always	3
Problems less than once a week	2
Weekly problems	1
No voluntary control	0
Frequency of defecation	
Every other day-twice a day	2
More often	1
Less often	1
Soiling	
Never	3
Staining less than once a week, no change of underwear required	2
Frequent staining/soiling, change of underwear required	1
Daily soiling, requires protective aids	0
Accidents	
Never	3
Less than once a week	2
Weekly accidents, often requires protective aids	1
Daily, protective aids required day and night	0
Constipation	
No constipation	3
Manageable with diet	2
Manageable with laxatives	1
Manageable with enemas	0
Social problems	
No social problems	3
Sometimes (fouls odors)	2
Problems causing restrictions in social life	1
Major social/psychosocial problems	0

population met this criterion[9]. Soiling referred to the actual presence of feces in the underwear without the patient's awareness, while fecal marks on the underwear were regarded as staining. We briefly defined the normal stool frequency as 1-3 times daily or once every 1-3 d. The diagnosis of HSCR-associated enterocolitis was based on the definitions by Teitelbaum and Coran[10]. Post-30-d complications were defined as complications occurring 30 d to 1 year after surgery.

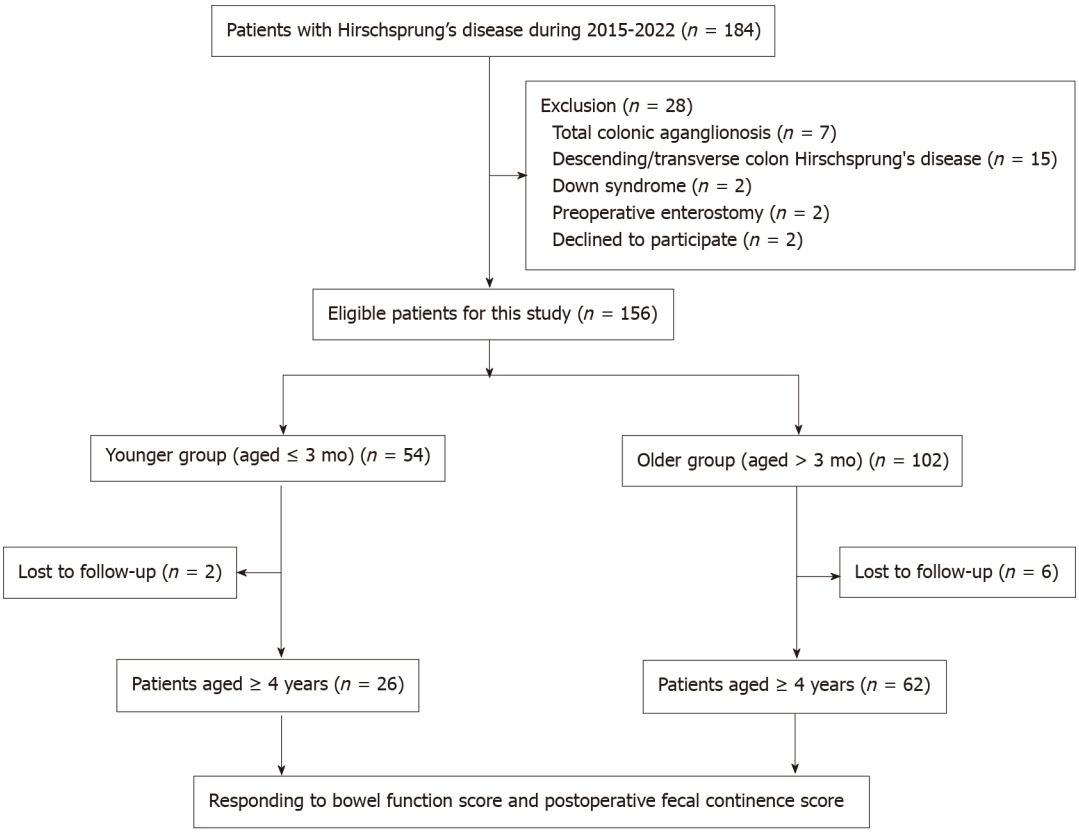
Statistical analysis

Categorical variables are presented as counts and percentages, while continuous variables are presented as the mean ± SD or median (range). The Kolmogorov–Smirnov test was used to assess the normality

Table 2 Scale for postoperative fecal continence score

Evaluation on the POFC scores	0	1	2
Frequency of motions (/day)	≥ 6	3-5	1-2
Severity of staining/soiling	Soiling	Staining	None
Severity of perianal erosion	Often	Occasionally	Nil
Anal shape	Prolapse needing surgery	Mucosa visible	Normal
Requirement for medications	Antidiarrheals	Laxatives/enemas	Nil
Sensation of rectal fullness	Not at all[1]	Occasionally	Always[2]
Ability to distinguish flatus from stool	Not at all[1]	Occasionally	Always[2]

[1]Full awareness or ability to distinguish less than once a week.
[2]Full awareness or ability to distinguish at least 4 out of 5 times (more than 80%).
POFC: postoperative fecal continence.



DOI: 10.3748/wjg.v29.i23.3715 **Copyright** ©The Author(s) 2023.

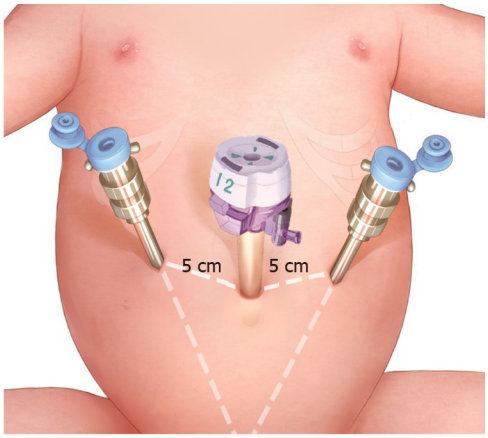
Figure 1 Flowchart of patient selection.

distribution of the data. To evaluate the differences between groups, the chi-square test or Fisher exact test was used to analyze categorical variables, and the Mann-Whitney U test was used to compare continuous variables because the data did not meet the normal distribution criteria. IBM SPSS Statistics version 26.0 was used for statistical analysis. A P value of < 0.05 was considered indicative of statistical significance.

RESULTS

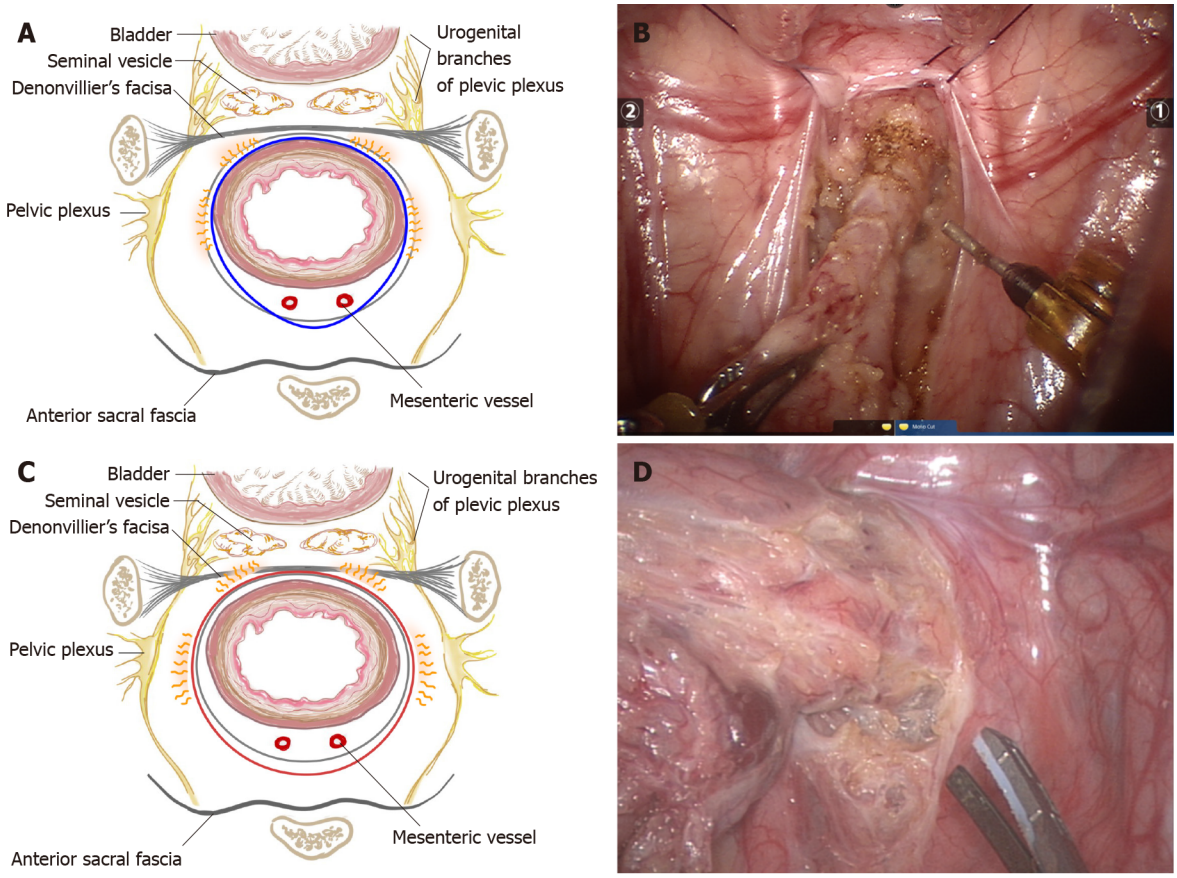
Patient demographics and operative data

A total of 184 participants were assessed for eligibility, and 156 patients were finally enrolled in this multicenter prospective study (Figure 1). The demographics and operative outcomes are shown in



DOI: 10.3748/wjg.v29.i23.3715 **Copyright** ©The Author(s) 2023.

Figure 2 Trocar site in robotic-assisted proctosigmoidectomy. There are three trocar ports, including a straight-cut umbilical trocar and two 8 mm working trocars located 5 cm from the umbilical trocar on either side.



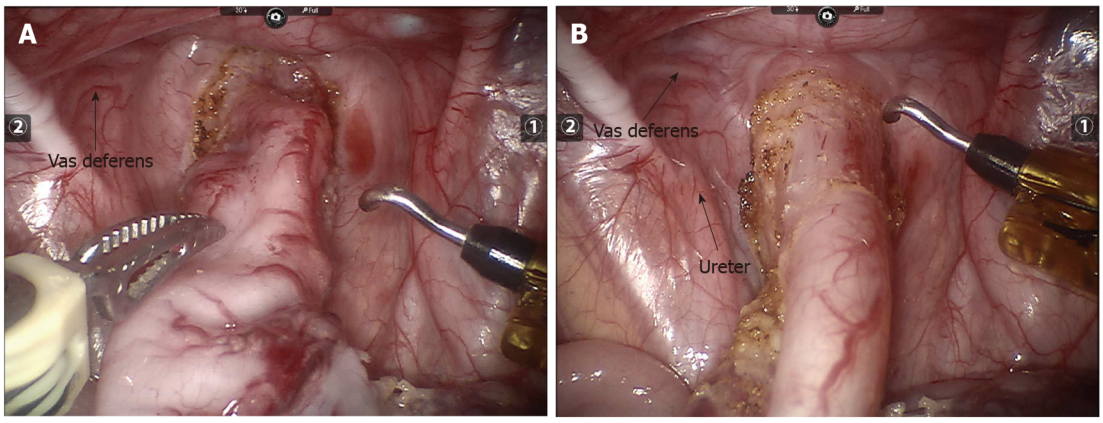
DOI: 10.3748/wjg.v29.i23.3715 **Copyright** ©The Author(s) 2023.

Figure 3 Diagram of pelvic dissection planes and intraoperative images of pelvic dissection. A: Pelvic dissection plane of robotic-assisted proctosigmoidectomy is under the serosa of the rectum or proper rectal fascia extended serous layer below the peritoneal reflection; B: Pelvic dissection under robotic endoscopy; C: Pelvic dissection plane of conventional laparoscopic Soave surgery is performed tightly around the rectal wall; D: Pelvic dissection under laparoscopy.

Table 3. No conversions or intraoperative complications occurred. The median age at surgery was 9.50 (range: 0.60-132.00) mo, and the weight was 9.09 ± 3.68 kg. The total operative time was 155.22 ± 16.77 min, and the robotic console time was 58.01 ± 7.71 min. The anal traction time was 45.28 ± 8.15 min, which included 15.21 ± 2.67 min for transanal dissection and 30.01 ± 5.82 min for anastomosis. The length of the removed bowel was 15.50 ± 5.23 cm, and the pelvic dissection depth under endoscopy was 4.50 ± 0.47 cm. The intraoperative estimated blood loss was 5.01 ± 1.81 mL.

Table 3 Operative parameters of patients

Parameter	*n* (%) or mean ± SD/median (range)
Age at surgery (month)	9.50 (0.60-132.00)
≤ 1 mo	4 (2.56%)
≤ 3 mo	50 (32.05%)
≤ 1 yr	77 (49.36%)
≤ 3 yr	16 (10.26%)
> 3 yr	9 (5.77%)
Level of aganglionosis	
Sigmoid colon	29 (32.95%)
Upper rectum	39 (44.32%)
Lower rectum	20 (22.73%)
Weight at surgery (kg)	9.09 ± 3.68
Operative time (min)	155.22 ± 16.77
Console time (min)	58.01 ± 7.71
Anal traction time (min)	45.28 ± 8.15
Transanal dissection time (min)	15.21 ± 2.67
Anastomosis time	30.01 ± 5.82
Estimated blood loss (mL)	5.01 ± 1.81
Pelvic dissection depth (cm)	4.50 ± 0.47
Length of the removed bowel (cm)	15.50 ± 5.23
Conversion	0 (0)
Intraoperative complications	0 (0)



DOI: 10.3748/wjg.v29.i23.3715 **Copyright** ©The Author(s) 2023.

Figure 4 The pelvic depth in robotic vision before and after pulling the rectum cranially; the depth becomes shallower after pulling. A: Before pulling; B: After pulling.

Postoperative outcomes

Postoperative outcomes are detailed in Table 4. The hospital stay was 7.25 ± 1.67 d, and the median follow-up duration was 44.00 (range: 6.00-78.00) mo. Eight patients were lost to follow-up one year after surgery. Postoperative complications were assessed in accordance with the Classification of Surgical Complications[11]. The postoperative 30-d complications included Clavien–Dindo grade II complications in two patients with wound infections, two patients with lung infections, six patients with enterocolitis, and thirteen patients with perianal dermatitis, all of whom were corrected by conservative treatment. One patient exhibited a Clavien–Dindo grade IIIa complication (anastomotic leakage treated

Table 4 Postoperative outcomes of patients

Parameter	*n* (%) or mean ± SD /median (range)
Hospital stay (day)	7.25 ± 1.67
Follow-up time (month)	44.00 (6.00-78.00)
Outcomes within postoperative 30 d	
Omental hernia	1 (0.64%)
Wound infections	2 (1.28%)
Lung infections	2 (1.28%)
Perianal dermatitis	13 (8.33%)
Uroschesis	0 (0)
Urinary incontinence	0 (0)
Anastomotic leakage	1 (0.64%)
Enterocolitis	6 (3.85%)
Cuff abscess	0 (0)
Post 30-d complications	
Perianal dermatitis	0 (0)
Anastomotic strictures	2 (1.28%)
Sphincter spasm	0 (0)
Enterocolitis	16 (10.26%)
Soiling	7 (4.49%)
Staining	18 (11.54%)
Constipation	4 (2.56%)
Perianal dermatitis	1 (0.64%)

by resuturing with presacral drainage[12]), and one patient had a Clavien–Dindo grade IIIb complication (omental hernia requiring surgical correction). There was no uroschesis, urinary incontinence, or cuff abscess. Post-30-d complications included Clavien–Dindo grade I complications, namely, seven soilings (received bowel habit training) and eighteen stainings (no change of underwear required) as well as Clavien–Dindo grade II complications, namely, two cases of anastomotic strictures (underwent anal dilation treatment without anesthesia), sixteen cases of enterocolitis (received rectal decompression, irrigation, and broad-spectrum antibiotics), four cases of constipation (received a laxative and enema) and one case of perianal dermatitis (received topical medication).

Normal stool frequency and enterocolitis at 1-6 years after surgery

As listed in Table 5, we divided follow-up into four phases: ≤ 1 year, 1 < years ≤ 2, 2 < years ≤ 4, and 4 < years ≤ 6, with further analysis of short- to medium-term stool frequency and enterocolitis. The incidence of normal stool frequency increased steadily while the enterocolitis rate decreased gradually over time; the overall normal stool frequency rate increased from 55.13% to 89.06% under diet control (younger group: 53.70% to 86.36%, older group: 55.88% to 90.48%) (Figure 6A) and the overall enterocolitis rate declined from 10.26% to 4.69% (younger group: 11.11% to 4.55%, older group: 9.8% to 4.76%) (Figure 6B).

BFS and POFC score in the assessment of medium-term functional outcomes

The BFS and POFC score are shown in Table 6. Eighty-eight patients aged ≥ 4 years were evaluated with two scoring systems during follow-up. The bowel functional result was good (BFS ≥ 17) in 66 patients (75.00%), moderate (12 ≤ BFS ≤ 16) in 14 patients (15.91%), and poor (BFS < 12) in 8 patients (9.09%). The total BFS was 17.32 ± 2.63, with satisfactory scores for each item. The POFC score at 4, 5 and 6 years of age postoperatively demonstrated a promising trend annually, with values of 10.95 ± 1.04, 11.48 ± 0.72, and 11.94 ± 0.81, respectively (Figure 6C).

Comparison of efficacy between patients aged ≤ 3 mo and aged > 3 mo at surgery

The outcomes comparing normal stool frequency and enterocolitis are shown in Table 5. The comparison results of postoperative complications are detailed in Table 7, while the comparison results

Table 5 Normal stool frequency and enterocolitis 1-6 years after surgery

	Younger group				Older group				*P* value	Total			
	≤ 1 yr	1 < yr ≤ 2	2 < yr ≤ 4	4 < yr ≤ 6	≤ 1 yr	1 < yr ≤ 2	2 < yr ≤ 4	4 < yr ≤ 6		≤ 1 yr	1 < yr ≤ 2	2 < yr ≤ 4	4 < yr ≤ 6
	n = 54	*n* = 48	*n* = 38	*n* = 22	*n* = 102	*n* = 91	*n* = 74	*n* = 42		*n* = 156	*n* = 139	*n* = 112	*n* = 64
Normal stool frequency, *n* (%)	29 (53.70%)	34 (70.83%)	30 (78.95%)	19 (86.36%)	57 (55.88%)	67 (73.63%)	61 (82.43%)	38 (90.48%)	0.80, 0.73, 0.66, 0.94	86 (55.13%)	101 (72.66%)	91 (81.25%)	57 (89.06%)
Enterocolitis, *n* (%)	6 (11.11%)	5 (10.42%)	3 (7.89%)	1 (4.55%)	10 (9.80%)	7 (7.69%)	4 (5.41%)	2 (4.76%)	0.80, 0.82, 0.92, 1.00	16 (10.26%)	12 (8.63%)	7 (6.25%)	3 (4.69%)

of BFS and POFC scores are shown in Table 8. Due to the small number of neonates in this series, we carried out a subgroup analysis to assess defecation function in younger infants, grouping the patients by age into ≤ 3 mo (younger group, n = 54) and > 3 mo (older group, n = 102). There was no significant difference in postoperative complication rates, BFSs (younger group: 17.19 ± 2.87, older group: 17.37 ± 2.54) or POFC scores at 4, 5 and 6 years of age postoperatively (younger group: 10.70 ± 0.99, 11.38 ± 0.62, 11.71 ± 0.76; older group: 11.07 ± 1.05, 11.52 ± 0.76, 12.00 ± 0.83) between the two groups (Figure 6C).

DISCUSSION

Robotic procedures are rapidly replacing open or laparoscopic procedures for the adult population in challenging procedures, such as operations for rectal and prostate cancer[2,3]. Nevertheless, the adoption of robots in pediatric surgery is low. Robotic surgery failed to show substantial benefits in studies comparing it to laparoscopic surgery because the procedures were initially used for less complex operations, such as the Nissen fundoplication[13]. In technically demanding situations, the application of robots for abdominal surgeries in children is relatively limited. Furthermore, only a few studies have revealed the feasibility of robotic-assisted surgery for HSCR, and the patient numbers were too small to generalize the application of robotic surgery in this field[14-17]. There is still a lack of studies involving large samples and long follow-up on functional outcomes. To our knowledge, 156 consecutive HSCR children who received RAPS represent the largest series in the literature. Long-segmental HSCR, total colonic aganglionosis, and trisomy 21 have been demonstrated to negatively affect the prognosis of HSCR patients[18-20]. Aiming to focus on the effect of surgical techniques on the postoperative outcomes of HSCR, we excluded these influencing factors and performed RAPS only on children with rectosigmoid HSCR.

The core of the original Soave procedure is pelvic endorectal dissection under the mucosa, but the mucosa is easily ruptured, resulting in pelvic contamination or mucosal residue. This explains the high rate of muscular sleeve infection following surgery in that era[4]. Pelvic endorectal dissection is a determining step in minimally invasive surgery for HSCR. Laparoscopic surgery facilitates tissue dissection in narrow spaces, and the technique still follows the concept of the original Soave procedure for nerve sparing. However, stiff laparoscopic instruments and unstable vision make submucosal rectal dissection more challenging, resulting in a higher mucosa rupture rate. Instead, extrarectal dissection is performed tightly around the rectal wall to 1-2 cm below the peritoneal reflection, and then a long-

Table 6 Bowel function scores and postoperative fecal continence scores among 88 patients aged 4 years or older

Parameter	Total (*n* = 88)
Bowel function score (Mean score ± SD)/*n* (%)	
Feels the urge to defecate	
Always	66 (75.00%)
Most of the time	19 (21.59%)
Uncertain	3 (3.41%)
Absent	0 (0)
Mean score ± SD	2.72 ± 0.52
Ability to hold back defecation	
Always	63 (71.59%)
Problems less than once a week	17 (19.32%)
Weekly problems	8 (9.09%)
No voluntary control	0 (0)
Mean score ± SD	2.63 ± 0.65
Normal defecation frequency	55 (62.50%)
Mean score ± SD	1.63 ± 0.49
Fecal soiling	
Never	32 (36.36%)
Staining < 1/wk	42 (47.73%)
Frequent soiling, change of underwear required	14 (15.91%)
Daily soiling, protective aids required	0 (0)
Mean score ± SD	2.23 ± 0.69
Fecal accidents	
Never	63 (71.59%)
Less than once a week	18 (20.45%)
Weekly accidents, protective aids often required	6 (6.82%)
Daily, aids required day and night	1 (1.14%)
Mean score ± SD	2.63 ± 0.67
Constipation	
No constipation	82 (93.18%)
Manageable with diet	0 (0)
Manageable with laxatives	4 (4.55%)
Manageable with enemas	2 (2.27%)
Mean score ± SD	2.84 ± 0.60
Social problems	
No social problems	61 (69.32%)
Sometimes (fouls odors)	18 (20.45%)
Problems causing restrictions in social life	9 (10.23%)
Major social/psychosocial problems	0 (0)
Mean score ± SD	2.59 ± 0.67
Total score	17.32 ± 2.63
Good bowel function (total score ≥ 17)	66 (75.00%)

Moderate bowel function (12 ≤ total score ≤ 16)	14 (15.91%)
Poor bowel function (total score < 12)	8 (9.09%)
Postoperative fecal incontinence scores (Mean score ± SD)	
Aged ≥ 4 years (n = 88)	10.95 ± 1.04
Aged ≥ 5 years (n = 60)	11.48 ± 0.72
Aged ≥ 6 years (n = 34)	11.94 ± 0.81

Table 7 Comparison of postoperative outcomes between the younger group and the older group

Parameter	Younger group (n = 54)	Older group (n = 102)	P value
Outcomes within postoperative 30 d, n (%)			
Omental hernia	1 (1.85%)	0 (0)	0.35
Wound infections	1 (1.85%)	1 (0.98%)	1.00
Lung infections	2 (3.70%)	0 (0)	0.24
Perianal dermatitis	5 (9.26%)	8 (7.84%)	1.00
Uroschesis	0 (0)	0 (0)	-
Urinary incontinence	0 (0)	0 (0)	-
Anastomotic leakage	1 (1.85%)	0 (0)	0.35
Enterocolitis	4 (7.41%)	2 (1.96%)	0.21
Cuff abscess	0 (0)	0 (0)	-
Post-30-d complications, n (%)			
Perianal dermatitis	0 (0)	0 (0)	-
Anastomotic strictures	1 (1.85%)	1 (0.98%)	1.00
Sphincter spasm	0 (0)	0 (0)	-
Enterocolitis	6 (11.11%)	10 (9.80%)	0.80
Soiling	3 (5.56%)	4 (3.92%)	0.95
Staining	7 (12.96%)	11 (10.78%)	0.69
Constipation	1 (1.85%)	3 (2.94%)	1.00
Perianal dermatitis	1 (1.85%)	0 (0)	0.35

distance submucosal dissection is conducted through the anus as in Georgeson's technique (Figure 3C and D) [21]. For selected patients, a totally transanal endorectal technique with submucosal dissection can even be performed as in Torre's technique[22]. These procedures have been demonstrated to provide better short-term outcomes than open surgery, with similar long-term outcomes[6,23,24]. Nonetheless, some studies have found that minimally invasive surgery, particularly totally transanal surgery that requires more anal dissection, results in poorer long-term defecation function than open surgery, especially in neonates[7,25,26]. This is probably a result of the technique's increased risk of anal sphincter traction/injury[27]. Therefore, we hypothesized that RAPS could reduce these risks to support better long-term bowel function for patients.

Herein, the primary strength of our robotic-assisted technique is that a new endorectal dissection layer (outside the longitudinal muscle) can be established. This potential gap between anatomical structures exists objectively[28]. The new layer is farther away from the urinal nerves on both sides of the rectum and the sexual nerves ahead of the Denonvillier's fascia[29]. A diagram of the pelvic dissection layer is shown in Figure 3A. The robotic system provides a magnified 3D image, stable maneuverability, and articulated movement in the narrow area *via* small incisions. Another major advantage is the image stability from robotic arm support as minor camera movements can cause image shifting. These merits facilitate ideal identification of the subserosa and precise rectum dissection, thus guaranteeing nerve-sparing. In addition, the rectum with intact longitudinal and circular muscles can be pulled strongly and is less prone to rupture; thus, the surgeon is able to pull the rectum cranially to make the pelvis shallower (Figure 4), allowing the dissection to nearly reach the dentate line (Figure 3B). Extensive intra-abdominal endorectal dissection would result in less need for transanal dissection and

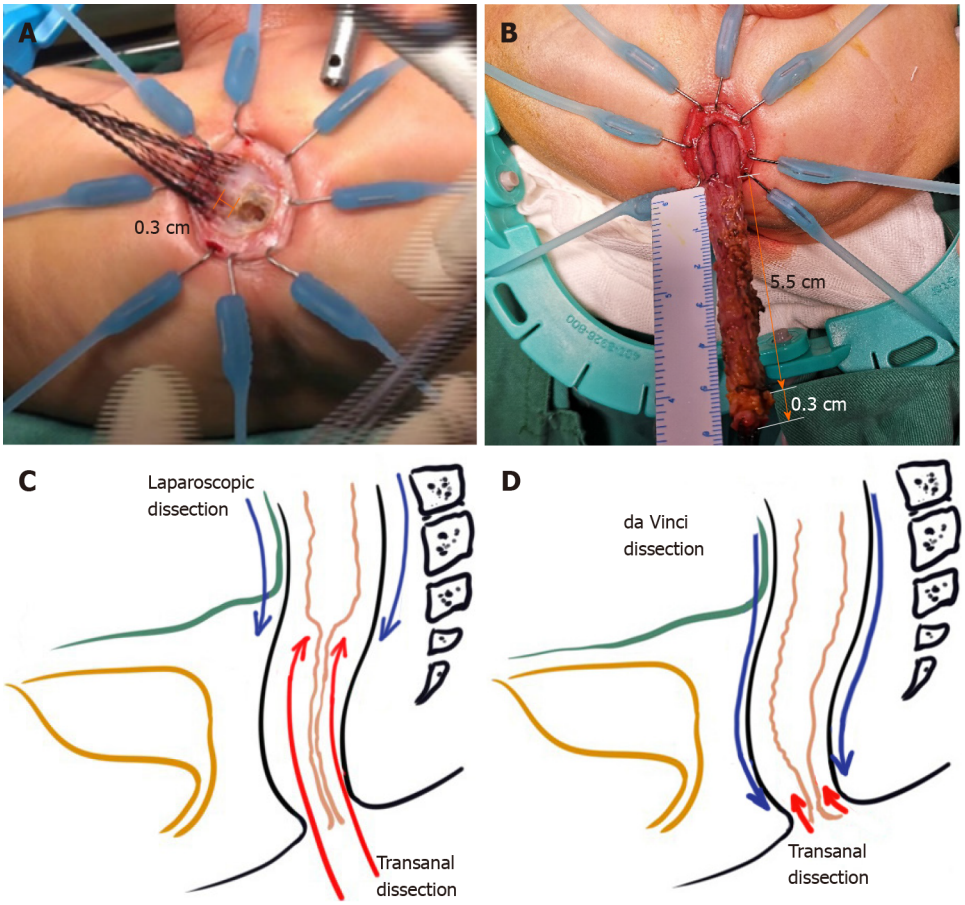
Table 8 Bowel function scores and postoperative fecal incontinence scores among patients aged 4 years or older between the younger group and the older group

Parameters	Younger group (*n* = 26)	Older group (*n* = 62)	*P* value
Bowel function scores (Mean score ± SD)			
Feels the urge to defecate	2.65 ± 0.63	2.74 ± 0.48	0.68
Ability to hold back defecation	2.58 ± 0.70	2.65 ± 0.63	0.71
Normal defecation frequency	1.69 ± 0.47	1.60 ± 0.49	0.40
Fecal soiling	2.19 ± 0.63	2.24 ± 0.72	0.67
Fecal accidents	2.58 ± 0.81	2.65 ± 0.60	0.98
Constipation	2.81 ± 0.69	2.85 ± 0.57	0.82
Social problems	2.62 ± 0.64	2.58 ± 0.69	0.93
Total bowel function score	17.19 ± 2.87	17.37 ± 2.54	0.90
Postoperative fecal incontinence scores (Mean score ± SD)			
Aged ≥ 4 yr	10.70 ± 0.99	11.07 ± 1.05	0.16
Aged ≥ 5 yr	11.38 ± 0.62	11.52 ± 0.76	0.46
Aged ≥ 6 yr	11.71 ± 0.76	12.00 ± 0.83	0.35

simpler transanal procedures, thus permitting minor or no sphincter damage. Figure 5C and D show a comparison of the length of endorectal dissection and transanal dissection between two minimally invasive approaches. As our results show, the pelvic dissection could reach a depth of 4.50 ± 0.47 cm, so the length of the rectum dissected transanally was greatly shortened to 0.20-0.40 cm (Figure 5B). This reduces the time and intensity of sphincter traction. As reported, prolonged transanal dissection is prone to sphincter traction/injury[18,30]. Hence, robotic practice in pelvic rectal dissection may offer an excellent surgical tool.

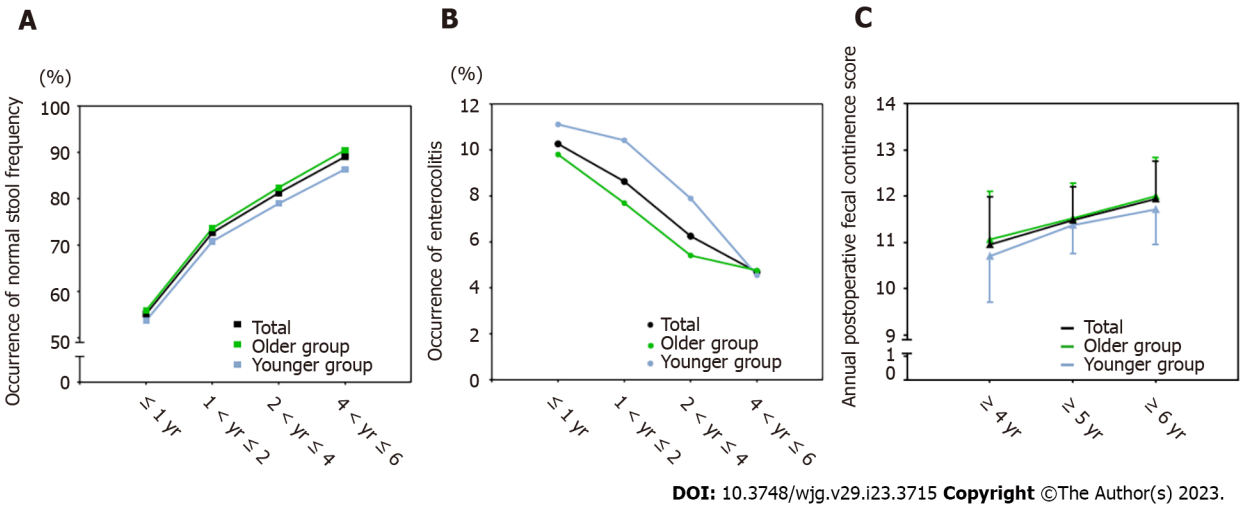
Due to the additional docking and setting time of the robotic arms, the total operation time of robotic procedures is generally longer than that of open or laparoscopic procedures[15,31]. In our series, however, the operative time was 155.22 ± 16.77 min and was comparable to that of laparoscopic surgery, which varied from 94.00 to 294.00 min in previous large-sample studies[6,18,32-36]. Moreover, our results revealed that postoperative complication rates were similar or even lower than those of transanal or laparoscopic approaches[18,32-34]. There were no cuff abscesses in our series. This is related to precise and complete dissection of the rectum outside the longitudinal muscle up to the dentate line, preventing mucosal tube injury and ensuring no residual rectal mucosa. Previous studies have shown that the incidence of urinary incontinence in HSCR patients postoperatively ranges from 2.70%-22.00% [37-41], and urine retention ranges from 1.04%-6.67%[42-44]. Urinary complications following pelvic procedures may be caused by direct damage or indirect thermal radiation injury to the nerve endings controlling voiding. No uroschesis or urinary incontinence occurred after removal of the urinary catheter 24-48 h after surgery in any of the patients. This highlights the most obvious advantage of SNS-RAPS, which is the precise safeguarding of the urinal nerve around the rectum. Following this logic, good short-term bladder nerve protection after RAPS could indirectly predict better long-term defecation and sexual nerve function.

Postoperative bowel function and continence are the most important criteria for evaluating the effectiveness of SNS-RAPS. BFS was used for a comprehensive assessment of defecation, soiling, constipation, and social problems. Previous studies evaluating long-term outcomes (follow-up ranged from 9.5 to 28 years) after open, laparoscopic or transanal approaches have shown that 88.00% to 89.00% of HSCR patients obtained moderate-to-good bowel function (good: BFS ≥ 17, 52.00%-63.00%; moderate: 12 ≤ BFS ≤ 16, 26.00%-36.00%)[7,45], with an overall score of 15.00 to 17.10[7,9,18,45-47]. One clinical trial even found that neonates with HSCR achieved a BFS of 17.44 for long -segment HSCR and 19.06 for short-segment HSCR after a transanal procedure (follow-up for more than 8 years)[48]. Our medium-term findings showed an overall BFS of 17.32 ± 2.63 and that 90.91% of patients achieved moderate-to-good bowel function (good: 75.00%; moderate: 15.91%), which was comparable to or better than the long-term results of previous studies. As studies have shown, postoperative bowel function improves with age[8, 46], so we predict that our series of patients will have better long-term bowel function. Furthermore, we used the POFC score to analyze fecal incontinence, reflecting the role of SNS-RAPS in nerve and sphincter protection[8]. The total POFC score gradually improved and was satisfactory in patients at 4, 5 and 6 years of age following surgery (10.95 ± 1.04, 11.48 ± 0.72 and 11.94 ± 0.81), representing a result similar to or superior to that of laparoscopic operation (8.60-11.30)[8,49]. Postoperative functional results are strongly related to long-term quality of life (QoL)[9,46,47]. Satisfactory BFS and POFC scores in this



DOI: 10.3748/wjg.v29.i23.3715 **Copyright** ©The Author(s) 2023.

Figure 5 Comparison of two minimally invasive approaches and dissection length measurement of robotic-assisted proctosigmoidectomy. A: The transanal Soave anastomosis procedure is performed by making a circular incision 0.5-1 cm from the dentate line and dividing the mucosa upward by 0.2-0.4 cm; B: The length of pelvic dissection was 5.5 cm and the length of transanal dissection was 0.3 cm of robotic-assisted proctosigmoidectomy; C: The length of endorectal dissection and transanal dissection in the laparoscopic approach; D: The length of endorectal dissection and transanal dissection in the robotic approach.



DOI: 10.3748/wjg.v29.i23.3715 **Copyright** ©The Author(s) 2023.

Figure 6 Short- to medium-term outcomes of robotic-assisted proctosigmoidectomy. A: Occurrence of normal stool frequency at 1-6 years after surgery; B: Occurrence of enterocolitis at 1-6 years after surgery; C: Annual postoperative fecal continence score analysis among patients aged 4 years or more.

series suggested that patients will achieve good long-term QoL.

Researchers in previous studies have mixed opinions on the efficacy in younger infants, especially neonates, compared with that in older children[49,50]. Although its appropriateness for younger infants with HSCR is debatable, robotic surgery could be successfully utilized for other diseases in the neonatal period[51]. We have gained experience in robotic surgery for these disorders and successfully applied

robotic surgery for neonates and infants with HSCR. As younger infants have a narrower pelvis and more compact structures than older children, the distance between the rectum and the surrounding structures is smaller. Moreover, younger age is associated with more fragile tissue that is vulnerable to operative injury[52]. These features increase the risk of injuring perirectal neurovascular tissues and sphincters during laparoscopic procedures, but the robotic system supplies a stable magnified 3D surgical field and precise rectal dissection to avoid the risk of disruption to the perirectal tissues. We found that HSCR patients in the younger group (aged ≤ 3 mo) and older group (aged > 3 mo) exhibited comparable complication rates, BFS and POFC scores. These data demonstrated that SNS-RAPS is feasible for HSCR patients aged ≤ 3 mo, and its efficacy was comparable to that in the older group. This also indicated that SNS-RAPS has better efficacy than previously reported open and laparoscopic procedures when considered from another perspective. Although totally transanal surgery was an option for 22.73% of patients with lower rectum HSCR in this study, our RAPS could reduce the time and intensity of sphincter traction and provide better outcomes. Taken together, our findings further support the view that the protection afforded by RAPS to the anal sphincter and perirectal nerves is no worse than other approaches and that RAPS is a preferred option for HSCR.

Although our study demonstrated favorable outcomes for RAPS, the limitations include only short- to medium-term outcomes and the absence of comparative data with other approaches. Therefore, a long-term follow-up and comparative trial should be performed to evaluate the effect of SNS-RAPS on HSCR. Currently, assessing long-term outcomes is not an option because SNS-RAPS has been used for less than 10 years. We intend to perform this clinical trial in the next several years. Moreover, the currently documented drawbacks of robotic surgery are longer operative time, expensive costs and oversized robotic devices for infants and neonates, creating economic and technical constraints. With the further advancement of pediatric robot devices, the reduction in surgical costs, and the improvement in surgeons' skills, the application of robots in pediatric surgery will mature. If surgery is to provide less pain and more effective therapy, then minimally invasive procedures achieved *via* robots that share the advantages of open or laparoscopic procedures may offer the answer.

CONCLUSION

SNS-RAPS is a safe and effective option for children of all ages with HSCR. The robotic platform can be utilized to further minimize surgical damage to the perirectal neurovascular tissue and anal sphincter, contributing to better bowel and urination function.

ARTICLE HIGHLIGHTS

Research background

Robotic-assisted surgery has been gradually introduced and applied to treat children with Hirschsprung's disease (HSCR). However, few studies have been conducted to evaluate its safety and efficacy for HSCR treatment.

Research motivation

We aimed to investigate the medium-term outcomes of robotic-assisted surgery for treating HSCR.

Research objectives

We aimed to analyze the feasibility and efficacy of robotic-assisted proctosigmoidectomy (RAPS) with sphincter- and nerve-sparing surgery (SNS) in the treatment of HSCR.

Research methods

We conducted a multicenter prospective study of 156 infants with rectosigmoid HSCR who underwent SNS-RAPS and divided them by age into a younger group (aged ≤ 3 mo) and an older group (aged > 3 mo) for comparison. Intraoperative data, postoperative complications, and medium-term outcomes were recorded and analyzed. In patients aged ≥ 4 years, the bowel function score (BFS) was used to assess overall bowel function, and the postoperative fecal continence (POFC) score was used to evaluate SNS-related incontinence.

Research results

A total of 156 patients underwent successful SNS-RAPS, with 25 complications within 30 d and 48 post-30-d complications after surgery. For children aged ≥ 4 years, the overall BFS was 17.32 ± 2.63 and 90.91% of patients showed moderate-to-good bowel function, while the POFC score increased annually from 4 to 6 years old (4 years old: 10.95 ± 1.04, 5 years old: 11.48 ± 0.72, 6 years old: 11.94 ± 0.81). There were no significant differences between the younger and older groups in postoperative complications

and POFC score.

Research conclusions

SNS-RAPS is a safe and effective alternative treatment for children of all ages with HSCR. It provides the advantage of further minimizing damage to sphincters and perirectal nerves, thus providing better continence function.

Research perspectives

Robotic-assisted surgery is beneficial for treating HSCR in infants and young children.

ACKNOWLEDGEMENTS

We are grateful to Professor Ping Yin for the statistical evaluation.

FOOTNOTES

Author contributions: Zhang MX, Zhang X, Chang XP, and Tang ST contributed to conceptualization and design; Zhang MX, Zhang X, Chang XP, Cao GQ, Li S, Chi SQ, Wan L, Zeng JX, and Bian HQ contributed to material preparation, data acquisition, and analysis; Zhang MX, Zhang X, and Chang XP contributed equally to this study; All authors contributed to writing-draft manuscript and writing-revision and approved to submit the final version.

Supported by the National Health and Family Planning of China, No. 201402007; and the National Natural Science Foundation of China, No. 81873848 and No. 82170528.

Institutional review board statement: This study was approved by the Ethics Committee at three centers: Union Hospital, Tongji Medical College, Huazhong University of Science and Technology; Guangzhou Women and Children's Medical Center, Guangzhou Medical University; and Wuhan Children's Hospital, Tongji Medical College, Huazhong University of Science and Technology.

Clinical trial registration statement: The clinical trial is registered in the Chinese Clinical Trial Registry (Registration ID: ChiCTR2000035220). Details are available at https://www.chictr.org.cn/showproj.aspx?proj=41379.

Informed consent statement: All study participants, or their legal guardians, provided written consent prior to study enrollment.

Conflict-of-interest statement: All the authors report no relevant conflicts of interest for this article.

Data sharing statement: There is no additional data available.

CONSORT 2010 statement: The authors have read the CONSORT 2010 Statement, and the manuscript was prepared and revised according to the CONSORT 2010 Statement.

Open-Access: This article is an open-access article that was selected by an in-house editor and fully peer-reviewed by external reviewers. It is distributed in accordance with the Creative Commons Attribution NonCommercial (CC BY-NC 4.0) license, which permits others to distribute, remix, adapt, build upon this work non-commercially, and license their derivative works on different terms, provided the original work is properly cited and the use is non-commercial. See: https://creativecommons.org/Licenses/by-nc/4.0/

Country/Territory of origin: China

ORCID number: Meng-Xin Zhang 0000-0001-9622-4882; Xi Zhang 0000-0001-8159-0855; Xiao-Pan Chang 0000-0002-6901-5716; Ji-Xiao Zeng 0000-0003-4854-4966; Hong-Qiang Bian 0000-0003-2417-1560; Guo-Qing Cao 0000-0002-1267-9714; Shuai Li 0000 -0001-7585-018X; Shui-Qing Chi 0000-0002-7537-0255; Ying Zhou 0000-0002-9257-0523; Li-Ying Rong 0000-0001-6670-050X; Li Wan 0000-0003-2839-2475; Shao-Tao Tang 0000-0002-1851-0610.

S-Editor: Li L
L-Editor: A
P-Editor: Li Li

REFERENCES

1 **Ahmad H**, Shaul DB. Pediatric colorectal robotic surgery. Semin Pediatr Surg 2023; 32:151259 [PMID: 36739693 DOI:

10.1016/j.sempedsurg.2023.151259]
2 **Crippa J**, Grass F, Dozois EJ, Mathis KL, Merchea A, Colibaseanu DT, Kelley SR, Larson DW. Robotic Surgery for Rectal Cancer Provides Advantageous Outcomes Over Laparoscopic Approach: Results From a Large Retrospective Cohort. *Ann Surg* 2021; **274**: e1218-e1222 [PMID: 32068552 DOI: 10.1097/SLA.0000000000003805]
3 **Stolzenburg JU**, Holze S, Arthanareeswaran VK, Neuhaus P, Do HM, Haney CM, Dietel A, Truss MC, Stützel KD, Teber D, Hohenfellner M, Rabenalt R, Albers P, Mende M. Robotic-assisted Versus Laparoscopic Radical Prostatectomy: 12-month Outcomes of the Multicentre Randomised Controlled LAP-01 Trial. *Eur Urol Focus* 2022; **8**: 1583-1590 [PMID: 35216946 DOI: 10.1016/j.euf.2022.02.002]
4 **Langer JC**, Seifert M, Minkes RK. One-stage Soave pull-through for Hirschsprung's disease: a comparison of the transanal and open approaches. *J Pediatr Surg* 2000; **35**: 820-822 [PMID: 10873018 DOI: 10.1053/jpsu.2000.6849]
5 **Tian Y**, Shi T, Wang F, Wu Y. Difference of efficacy between Laparoscopic Modified Soave operation and Open Radical Resection in the treatment of Hirschsprung's disease. *Pak J Med Sci* 2017; **33**: 1385-1389 [PMID: 29492064 DOI: 10.12669/pjms.336.13220]
6 **Kubota A**, Kawahara H, Okuyama H, Oue T, Tazuke Y, Okada A. Clinical outcome of laparoscopically assisted endorectal pull-through in Hirschsprung's disease: comparison of abdominal and perineal approaches. *J Pediatr Surg* 2004; **39**: 1835-1837 [PMID: 15616944 DOI: 10.1016/j.jpedsurg.2004.08.015]
7 **Neuvonen MI**, Kyrklund K, Rintala RJ, Pakarinen MP. Bowel Function and Quality of Life After Transanal Endorectal Pull-through for Hirschsprung Disease: Controlled Outcomes up to Adulthood. *Ann Surg* 2017; **265**: 622-629 [PMID: 28169931 DOI: 10.1097/SLA.0000000000001695]
8 **Miyano G**, Koga H, Okawada M, Doi T, Sueyoshi R, Nakamura H, Seo S, Ochi T, Yamada S, Imaizumi T, Lane GJ, Okazaki T, Urao M, Yamataka A. Rectal mucosal dissection commencing directly on the anorectal line *vs* commencing above the dentate line in laparoscopy-assisted transanal pull-through for Hirschsprung's disease: Prospective medium-term follow-up. *J Pediatr Surg* 2015; **50**: 2041-2043 [PMID: 26386879 DOI: 10.1016/j.jpedsurg.2015.08.022]
9 **Jarvi K**, Laitakari EM, Koivusalo A, Rintala RJ, Pakarinen MP. Bowel function and gastrointestinal quality of life among adults operated for Hirschsprung disease during childhood: a population-based study. *Ann Surg* 2010; **252**: 977-981 [PMID: 21107107 DOI: 10.1097/SLA.0b013e3182018542]
10 **Teitelbaum DH**, Coran AG. Enterocolitis. *Semin Pediatr Surg* 1998; **7**: 162-169 [PMID: 9718654 DOI: 10.1016/S1055-8586(98)70012-5]
11 **Dindo D**, Demartines N, Clavien PA. Classification of surgical complications: a new proposal with evaluation in a cohort of 6336 patients and results of a survey. *Ann Surg* 2004; **240**: 205-213 [PMID: 15273542 DOI: 10.1097/01.sla.0000133083.54934.ae]
12 **Chi S**, Guo J, Zhang X, Li K, Xu P, Cao G, Li S, Tang ST. Resuturing Without Enterostomy for the Treatment of Early-Stage Anastomotic Leaks After Laparoscopic Soave Procedure in Hirschsprung's Disease. *J Laparoendosc Adv Surg Tech A* 2020; **30**: 1295-1300 [PMID: 33181061 DOI: 10.1089/lap.2020.0640]
13 **Markar SR**, Karthikesalingam AP, Hagen ME, Talamini M, Horgan S, Wagner OJ. Robotic vs. laparoscopic Nissen fundoplication for gastro-oesophageal reflux disease: systematic review and meta-analysis. *Int J Med Robot* 2010; **6**: 125-131 [PMID: 20506440 DOI: 10.1002/rcs.309]
14 **Quynh TA**, Hien PD, Du LQ, Long LH, Tran NTN, Hung T. The follow-up of the robotic-assisted Soave procedure for Hirschsprung's disease in children. *J Robot Surg* 2022; **16**: 301-305 [PMID: 33843006 DOI: 10.1007/s11701-021-01238-z]
15 **Pini Prato A**, Arnoldi R, Dusio MP, Cimorelli A, Barbetta V, Felici E, Barbieri P, Barbero S, Carlini C, Petralia P, Mattioli G, Roveta A, Maconi A. Totally robotic soave pull-through procedure for Hirschsprung's disease: lessons learned from 11 consecutive pediatric patients. *Pediatr Surg Int* 2020; **36**: 209-218 [PMID: 31659436 DOI: 10.1007/s00383-019-04593-z]
16 **Delgado-Miguel C**, Camps JI. Robotic Soave pull-through procedure for Hirschsprung's disease in children under 12-months: long-term outcomes. *Pediatr Surg Int* 2022; **38**: 51-57 [PMID: 34557957 DOI: 10.1007/s00383-021-05018-6]
17 **Li W**, Lin M, Hu H, Sun Q, Su C, Wang C, Li Y, Chen J, Luo Y. Surgical Management of Hirschsprung's Disease: A Comparative Study Between Conventional Laparoscopic Surgery, Transumbilical Single-Site Laparoscopic Surgery, and Robotic Surgery. *Front Surg* 2022; **9**: 924850 [PMID: 35860198 DOI: 10.3389/fsurg.2022.924850]
18 **Bjørnland K**, Pakarinen MP, Stenstrøm P, Stensrud KJ, Neuvonen M, Granström AL, Graneli C, Pripp AH, Arnbjörnsson E, Emblem R, Wester T, Rintala RJ; Nordic Pediatric Surgery Study Consortium. A Nordic multicenter survey of long-term bowel function after transanal endorectal pull-through in 200 patients with rectosigmoid Hirschsprung disease. *J Pediatr Surg* 2017; **52**: 1458-1464 [PMID: 28094015 DOI: 10.1016/j.jpedsurg.2017.01.001]
19 **Sakurai T**, Tanaka H, Endo N. Predictive factors for the development of postoperative Hirschsprung-associated enterocolitis in children operated during infancy. *Pediatr Surg Int* 2021; **37**: 275-280 [PMID: 33245447 DOI: 10.1007/s00383-020-04784-z]
20 **Morabito A**, Lall A, Gull S, Mohee A, Bianchi A. The impact of Down's syndrome on the immediate and long-term outcomes of children with Hirschsprung's disease. *Pediatr Surg Int* 2006; **22**: 179-181 [PMID: 16362310 DOI: 10.1007/s00383-005-1617-0]
21 **Georgeson KE**, Fuenfer MM, Hardin WD. Primary laparoscopic pull-through for Hirschsprung's disease in infants and children. *J Pediatr Surg* 1995; **30**: 1017-21; discussion 1021 [PMID: 7472924 DOI: 10.1016/0022-3468(95)90333-X]
22 **De la Torre-Mondragón L**, Ortega-Salgado JA. Transanal endorectal pull-through for Hirschsprung's disease. *J Pediatr Surg* 1998; **33**: 1283-1286 [PMID: 9722005 DOI: 10.1016/S0022-3468(98)90169-5]
23 **Chen Y**, Nah SA, Laksmi NK, Ong CC, Chua JH, Jacobsen A, Low Y. Transanal endorectal pull-through *vs* transabdominal approach for Hirschsprung's disease: a systematic review and meta-analysis. *J Pediatr Surg* 2013; **48**: 642-651 [PMID: 23480925 DOI: 10.1016/j.jpedsurg.2012.12.036]
24 **Zhang S**, Li J, Wu Y, Hu Y, Duan C, Wang M, Gai Z. Comparison of Laparoscopic-Assisted Operations and Laparotomy Operations for the Treatment of Hirschsprung Disease: Evidence From a Meta-Analysis. *Medicine (Baltimore)* 2015; **94**: e1632 [PMID: 26426651 DOI: 10.1097/MD.0000000000001632]

25 **El-Sawaf MI**, Drongowski RA, Chamberlain JN, Coran AG, Teitelbaum DH. Are the long-term results of the transanal pull-through equal to those of the transabdominal pull-through? A comparison of the 2 approaches for Hirschsprung disease. *J Pediatr Surg* 2007; **42**: 41-7; discussion 47 [PMID: 17208539 DOI: 10.1016/j.jpedsurg.2006.09.007]

26 **Stensrud KJ**, Emblem R, Bjørnland K. Anal endosonography and bowel function in patients undergoing different types of endorectal pull-through procedures for Hirschsprung disease. *J Pediatr Surg* 2015; **50**: 1341-1346 [PMID: 25783406 DOI: 10.1016/j.jpedsurg.2014.12.024]

27 **Stensrud KJ**, Emblem R, Bjørnland K. Functional outcome after operation for Hirschsprung disease--transanal *vs* transabdominal approach. *J Pediatr Surg* 2010; **45**: 1640-1644 [PMID: 20713213 DOI: 10.1016/j.jpedsurg.2010.02.065]

28 **Zhang C**, Ding ZH, Li GX, Yu J, Wang YN, Hu YF. Perirectal fascia and spaces: annular distribution pattern around the mesorectum. *Dis Colon Rectum* 2010; **53**: 1315-1322 [PMID: 20706076 DOI: 10.1007/DCR.0b013e3181e74525]

29 **He M**, Muro S, Akita K. Positional relationship between the lateral border of Denonvilliers' fascia and pelvic plexus. *Anat Sci Int* 2022; **97**: 101-109 [PMID: 34529236 DOI: 10.1007/s12565-021-00629-4]

30 **Pratap A**, Gupta DK, Shakya VC, Adhikary S, Tiwari A, Shrestha P, Pandey SR, Yadav RK. Analysis of problems, complications, avoidance and management with transanal pull-through for Hirschsprung disease. *J Pediatr Surg* 2007; **42**: 1869-1876 [PMID: 18022438 DOI: 10.1016/j.jpedsurg.2007.07.017]

31 **D'Annibale A**, Morpurgo E, Fiscon V, Trevisan P, Sovernigo G, Orsini C, Guidolin D. Robotic and laparoscopic surgery for treatment of colorectal diseases. *Dis Colon Rectum* 2004; **47**: 2162-2168 [PMID: 15657669 DOI: 10.1007/s10350-004-0711-z]

32 **Karlsen RA**, Hoel AT, Fosby MV, Ertresvåg K, Austrheim AI, Stensrud KJ, Bjørnland K. Comparison of clinical outcomes after total transanal and laparoscopic assisted endorectal pull-through in patients with rectosigmoid Hirschsprung disease. *J Pediatr Surg* 2022; **57**: 69-74 [PMID: 35123788 DOI: 10.1016/j.jpedsurg.2022.01.011]

33 **van de Ven TJ**, Sloots CE, Wijnen MH, Rassouli R, van Rooij I, Wijnen RM, de Blaauw I. Transanal endorectal pull-through for classic segment Hirschsprung's disease: with or without laparoscopic mobilization of the rectosigmoid? *J Pediatr Surg* 2013; **48**: 1914-1918 [PMID: 24074667 DOI: 10.1016/j.jpedsurg.2013.04.025]

34 **Aubdoollah TH**, Li K, Zhang X, Li S, Yang L, Lei HY, Dolo PR, Xiang XC, Cao GQ, Wang GB, Tang ST. Clinical outcomes and ergonomics analysis of three laparoscopic techniques for Hirschsprung's disease. *World J Gastroenterol* 2015; **21**: 8903-8911 [PMID: 26269680 DOI: 10.3748/wjg.v21.i29.8903]

35 **Tang ST**, Wang GB, Cao GQ, Wang Y, Mao YZ, Li SW, Li S, Yang Y, Yang J, Yang L. 10 years of experience with laparoscopic-assisted endorectal Soave pull-through procedure for Hirschsprung's disease in China. *J Laparoendosc Adv Surg Tech A* 2012; **22**: 280-284 [PMID: 22449115 DOI: 10.1089/lap.2011.0081]

36 **Wang YJ**, He YB, Chen L, Lin Y, Liu MK, Zhou CM. Laparoscopic-assisted Soave procedure for Hirschsprung disease: 10-year experience with 106 cases. *BMC Surg* 2022; **22**: 72 [PMID: 35219304 DOI: 10.1186/s12893-022-01528-9]

37 **Boemers TM**. Urinary incontinence and vesicourethral dysfunction in pediatric surgical conditions. *Semin Pediatr Surg* 2002; **11**: 91-99 [PMID: 11973761 DOI: 10.1053/spsu.2002.31807]

38 **Ieiri S**, Nakatsuji T, Akiyoshi J, Higashi M, Hashizume M, Suita S, Taguchi T. Long-term outcomes and the quality of life of Hirschsprung disease in adolescents who have reached 18 years or older--a 47-year single-institute experience. *J Pediatr Surg* 2010; **45**: 2398-2402 [PMID: 21129554 DOI: 10.1016/j.jpedsurg.2010.08.040]

39 **Granström AL**, Danielson J, Husberg B, Nordenskjöld A, Wester T. Adult outcomes after surgery for Hirschsprung's disease: Evaluation of bowel function and quality of life. *J Pediatr Surg* 2015; **50**: 1865-1869 [PMID: 26164226 DOI: 10.1016/j.jpedsurg.2015.06.014]

40 **Allin BSR**, Opondo C, Bradnock TJ, Kenny SE, Kurinczuk JJ, Walker GM, Knight M; NETS2HD collaboration. Outcomes at five to eight years of age for children with Hirschsprung's disease. *Arch Dis Child* 2020; **106**: 484-490 [PMID: 33139346 DOI: 10.1136/archdischild-2020-320310]

41 **Fuchs O**, Booss D. Rehbein's procedure for Hirschsprung's disease. An appraisal of 45 years. *Eur J Pediatr Surg* 1999; **9**: 389-391 [PMID: 10661849 DOI: 10.1055/s-2008-1072289]

42 **Wang G**, Sun XY, Wei MF, Weng YZ. Heart-shaped anastomosis for Hirschsprung's disease: Operative technique and long-term follow-up. *World J Gastroenterol* 2005; **11**: 296-298 [PMID: 15633236 DOI: 10.3748/wjg.v11.i2.296]

43 **Wang M**, Pang W, Zhou L, Ma J, Xie S. Effect of Transumbilical Single-Port Laparoscopic-Assisted Duhamel Operation on Serum CRP and IL-6 Levels in Children with Hirschsprung's Disease. *J Healthc Eng* 2022; **2022**: 8349851 [PMID: 35281524 DOI: 10.1155/2022/8349851]

44 **Ateş O**, Hakgüder G, Kart Y, Olguner M, Akgür FM. The effect of dilated ganglionic segment on anorectal and urinary functions during 1-stage transanal endorectal pull through for Hirschsprung's disease. *J Pediatr Surg* 2007; **42**: 1271-1275 [PMID: 17618894 DOI: 10.1016/j.jpedsurg.2007.02.020]

45 **Davidson JR**, Kyrklund K, Eaton S, Pakarinen MP, Thompson DS, Cross K, Blackburn SC, De Coppi P, Curry J. Long-term surgical and patient-reported outcomes of Hirschsprung Disease. *J Pediatr Surg* 2021; **56**: 1502-1511 [PMID: 33706942 DOI: 10.1016/j.jpedsurg.2021.01.043]

46 **Stenström P**, Brautigam M, Borg H, Graneli C, Lilja HE, Wester T. Patient-reported Swedish nationwide outcomes of children and adolescents with total colonic aganglionosis. *J Pediatr Surg* 2017; **52**: 1302-1307 [PMID: 27912975 DOI: 10.1016/j.jpedsurg.2016.11.033]

47 **Xiong X**, Chen X, Wang G, Feng J. Long term quality of life in patients with Hirschsprung's disease who underwent heart-shaped anastomosis during childhood: A twenty-year follow-up in China. *J Pediatr Surg* 2015; **50**: 2044-2047 [PMID: 26423683 DOI: 10.1016/j.jpedsurg.2015.08.027]

48 **Zhang Y**, Liu Z, Li S, Yang S, Zhao J, Yang T, Chen Y, Guo W, Hou D, Li Y, Huang J. One-stage transanal endorectal pull-through for Hirschsprung disease: experience with 229 neonates. *Pediatr Surg Int* 2022; **38**: 1533-1540 [PMID: 36030350 DOI: 10.1007/s00383-022-05198-9]

49 **Yamataka A**, Kaneyama K, Fujiwara N, Hayashi Y, Lane GJ, Kawashima K, Okazaki T. Rectal mucosal dissection during transanal pull-through for Hirschsprung disease: the anorectal or the dentate line? *J Pediatr Surg* 2009; **44**: 266-9; discussion 270 [PMID: 19159754 DOI: 10.1016/j.jpedsurg.2008.10.054]

50 **Lu C**, Hou G, Liu C, Geng Q, Xu X, Zhang J, Chen H, Tang W. Single-stage transanal endorectal pull-through procedure

for correction of Hirschsprung disease in neonates and nonneonates: A multicenter study. *J Pediatr Surg* 2017; **52**: 1102-1107 [PMID: 28185631 DOI: 10.1016/j.jpedsurg.2017.01.061]

51 **Meehan JJ**, Sandler A. Robotic repair of a Bochdalek congenital diaphragmatic hernia in a small neonate: robotic advantages and limitations. *J Pediatr Surg* 2007; **42**: 1757-1760 [PMID: 17923210 DOI: 10.1016/j.jpedsurg.2007.06.013]

52 **Onishi S**, Kaji T, Nakame K, Yamada K, Murakami M, Sugita K, Yano K, Matsui M, Nagano A, Harumatsu T, Yamada W, Matsukubo M, Muto M, Ieiri S. Optimal timing of definitive surgery for Hirschsprung's disease to achieve better long-term bowel function. *Surg Today* 2022; **52**: 92-97 [PMID: 34383138 DOI: 10.1007/s00595-021-02356-9]

World Journal of Gastroenterology

Submit a Manuscript: https://www.f6publishing.com

World J Gastroenterol 2023 June 21; 29(23): 3733-3747

DOI: 10.3748/wjg.v29.i23.3733

ISSN 1007-9327 (print) ISSN 2219-2840 (online)

SYSTEMATIC REVIEWS

Paradoxical association between dyspepsia and autoimmune chronic atrophic gastritis: Insights into mechanisms, pathophysiology, and treatment options

Roberta Elisa Rossi, Alessandra Elvevi, Valentina Sciola, Francesco Vito Mandarino, Silvio Danese, Pietro Invernizzi, Sara Massironi

Specialty type: Gastroenterology and hepatology

Provenance and peer review: Invited article; Externally peer reviewed.

Peer-review model: Single blind

Peer-review report's scientific quality classification

Grade A (Excellent): 0
Grade B (Very good): B, B
Grade C (Good): C, C
Grade D (Fair): 0
Grade E (Poor): 0

P-Reviewer: Baryshnikova NV, Russia; Cheng H, China; Huang YQ, China; Jia J, China

Received: March 21, 2023
Peer-review started: March 21, 2023
First decision: April 12, 2023
Revised: April 23, 2023
Accepted: May 6, 2023
Article in press: May 6, 2023
Published online: June 21, 2023

Roberta Elisa Rossi, Gastroenterology and Endoscopy Unit, IRCCS Humanitas Research Hospital, Rozzano 20089, Milan, Italy

Alessandra Elvevi, Pietro Invernizzi, Sara Massironi, Gastroenterology Unit, Fondazione IRCCS San Gerardo dei Tintori, Monza 20900, Italy and Department of Medicine and Surgery, University of Milano-Bicocca, Monza 20900, Italy

Valentina Sciola, Gastroenterology and Endoscopy Unit, Fondazione IRCCS Ca' Granda Ospedale Maggiore Policlinico, Milano 20100, Italy

Francesco Vito Mandarino, Silvio Danese, Department of Gastroenterology and Endoscopy, IRCCS Ospedale San Raffaele, Milan 20132, Italy

Silvio Danese, School of Medicine, Vita-Salute San Raffaele University, Milan 20132, Italy

Corresponding author: Sara Massironi, MD, PhD, Chief Physician, Doctor, Medical Assistant, Research Scientist, Division of Gastroenterology, Fondazione IRCCS San Gerardo dei Tintori, Via Pergolesi, 33, Monza 20900, Italy. sara.massironi@libero.it

Abstract

BACKGROUND

Autoimmune gastritis (AIG) is a progressive, chronic, immune-mediated inflammatory disease characterized by the destruction of gastric parietal cells leading to hypo/anacidity and loss of intrinsic factor. Gastrointestinal symptoms such as dyspepsia and early satiety are very common, being second in terms of frequency only to anemia, which is the most typical feature of AIG.

AIM

To address both well-established and more innovative information and knowledge about this challenging disorder.

METHODS

An extensive bibliographical search was performed in PubMed to identify guidelines and primary literature (retrospective and prospective studies, systematic reviews, case series) published in the last 10 years.

RESULTS
A total of 125 records were reviewed and 80 were defined as fulfilling the criteria.

CONCLUSION
AIG can cause a range of clinical manifestations, including dyspepsia. The pathophysiology of dyspepsia in AIG is complex and involves changes in acid secretion, gastric motility, hormone signaling, and gut microbiota, among other factors. Managing dyspeptic symptoms of AIG is challenging and there are no specific therapies targeting dyspepsia in AIG. While proton pump inhibitors are commonly used to treat dyspepsia and gastroesophageal reflux disease, they may not be appropriate for AIG. Prokinetic agents, antidepressant drugs, and non-pharmacological treatments may be of help, even if not adequately evidence-based supported. A multidisciplinary approach for the management of dyspepsia in AIG is recommended, and further research is needed to develop and validate more effective therapies for dyspepsia.

Key Words: Dyspepsia; Dyspeptic symptoms; Gastro-intestinal symptoms; Autoimmune gastritis; Chronic autoimmune atrophic gastritis; Treatment

©The Author(s) 2023. Published by Baishideng Publishing Group Inc. All rights reserved.

Core Tip: The management of dyspepsia in patients with autoimmune gastritis (AIG), a chronic, immune-mediated disease, remains a challenge, as it can overlap with functional dyspepsia and gastroesophageal reflux disease. Currently, there are no specific therapies. A tailored treatment approach based on a better understanding of putative pathogenic mechanisms underlying symptoms is needed. Prokinetic agents, antidepressant drugs, and non-pharmacological treatments may be helpful, although not adequately evidence-based supported. As a future perspective, targeting dyspepsia in AIG based on changes in the microbiota and advanced endoscopic techniques to treat severe dyspeptic symptoms might be an area of ongoing research.

Citation: Rossi RE, Elvevi A, Sciola V, Mandarino FV, Danese S, Invernizzi P, Massironi S. Paradoxical association between dyspepsia and autoimmune chronic atrophic gastritis: Insights into mechanisms, pathophysiology, and treatment options. *World J Gastroenterol* 2023; 29(23): 3733-3747
URL: https://www.wjgnet.com/1007-9327/full/v29/i23/3733.htm
DOI: https://dx.doi.org/10.3748/wjg.v29.i23.3733

INTRODUCTION

Autoimmune gastritis (AIG) is an immune-mediated disease targeting the H+/K+ ATPase proton pump in the parietal cells, which are responsible for the secretion of gastric acid and intrinsic factor[1]. The pathogenesis of AIG involves the activation of both T and B lymphocytes, which infiltrate the gastric mucosa and destroy the parietal cells[1-5], leading to hypochloridria and vitamin B12 deficiency.

Symptoms of AIG can be nonspecific, with patients presenting with no or vague symptoms, including postprandial fullness, early satiation, abdominal pain, bloating[6], as well as epigastric pain. Therefore, the diagnosis of AIG can be challenging, as many of these symptoms overlap with other digestive disorders, mainly functional dyspepsia (FD) and gastroesophageal reflux disease (GERD). This overlap in clinical symptoms and characteristics can pose diagnostic challenges between AIG and FD, which share some common characteristics, including clinical symptoms, as well as a higher prevalence among women. Moreover, some patients may present with atypical symptoms, such as fatigue, joint pain, or skin rashes, which can further overlap with functional symptoms. Distinguishing between AIG and GERD can be even more challenging. While the pathophysiological mechanisms underlying GERD and AIG are different, they can present with similar abdominal symptoms, such as epigastric pain, heartburn, and nausea, which may pose diagnostic challenges, particularly in patients with atypical symptoms.

The pathophysiological mechanisms underlying clinical symptoms in AIG are poorly understood.

Appropriate evaluation, including endoscopy, is therefore required to differentiate these entities; indeed, based on the Rome Global Epidemiology Study, the diagnosis of FD requires the absence of organic, systemic, or metabolic disease upon routine investigation, including endoscopy[7,8].

It is therefore important to understand the different pathogenesis of symptoms in AIG, GERD, and FD, as the management of these conditions can be very different. This is particularly important when prescribing empirically proton pump inhibitors (PPIs) based therapies, which are often considered to be

the first-line therapy for GERD and are often used to manage symptoms of FD. Conversely, in AIG, a condition of hypochlorhydria, PPI therapy could further reduce acid secretion, stimulate gastrin hypersecretion, and further induce enterochromaffin-like (ECL) cell hyperplasia. As a result, the use of PPIs in patients with AIG is generally not indicated.

Therefore, accurate diagnosis and differentiation between these conditions are crucial to avoid inappropriate or potentially harmful management strategies. Understanding the pathophysiology of each condition can also guide the choice of appropriate treatments, including lifestyle modifications, dietary changes, and medication management.

In this review, we will discuss the putative pathogenic mechanisms underlying symptom generation in AIG, their clinical implications, and the current management strategies for this complex and multifaceted disease.

MATERIALS AND METHODS

An extensive bibliographical search was performed in PubMed to identify guidelines and primary literature (retrospective and prospective studies, systematic reviews, case series) published in the last 10 years, using both medical subject heading terms and free-language keywords: Dyspepsia; dyspeptic symptoms; gastro-intestinal symptoms; chronic autoimmune atrophic gastritis; diagnosis; treatment. The reference lists from the studies returned by the electronic search were manually searched to identify further relevant reports. The reference lists from all available review articles, primary studies, and proceedings of major meetings were also considered. Articles published as abstracts were included, whereas non-English language papers were excluded.

RESULTS

A total of 125 records were reviewed and 80 were defined as fulfilling the criteria for final consideration. Figure 1 presents the flow chart showing the process of study selection.

DISCUSSION

Dyspepsia in autoimmune gastritis: clinical manifestations and pathophysiological mechanisms

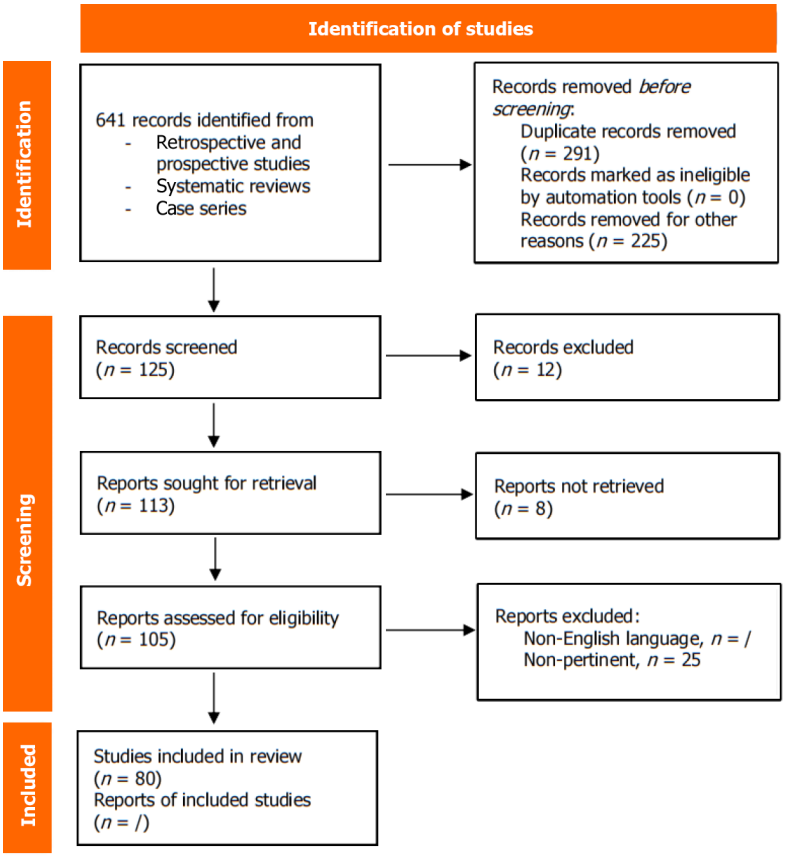
The spectrum of clinical manifestations in AIG is wide but often nonspecific[9,10]. Classical manifestations of AIG include pernicious anemia due to vitamin B12 deficiency, which can cause fatigue, weakness, and shortness of breath. Other hematological anomalies comprise micro/normocytic anemia due to the coexistence of iron deficiency anemia[9,11]. Neurological symptoms such as tingling, numbness, or weakness in the limbs, are due to vitamin B12 deficiency and are characterized by neuronal damage with peripheral neuropathy, myelopathy, and autonomic dysfunction[12,13]. Furthermore, psychiatric alterations have been reported such as depression, cognitive impairment, and psychosis[14,15]. As AIG is often associated with other autoimmune conditions, patients may also present with symptoms related to those conditions, such as joint pain, skin rashes, or thyroid dysfunction[16]. Also, the impaired absorption of other vitamins, such as 25-OH-vitamin D, or micronutrients, such as calcium, due to gastric hypo- or achlorhydria, has been hypothesized to be a predisposing factor also for the development of osteoporosis which can be a possible further extra gastrointestinal (GI) manifestation in AIG patients[17-19].

However, these manifestations usually characterize severe or long-standing disease.

In the early stages of AIG, patients may not present with these specific symptoms, and the patients may begin to experience non-specific GI symptoms such as upper abdominal discomfort, bloating, and nausea[11]. Focusing on GI symptoms, even if AIG is generally regarded as a silent disease, some recent studies highlight a not negligible percentage of patients who report upper GI discomfort mainly characterized by dyspeptic and/or GERD symptoms[20] and as in FD, dyspeptic symptoms may manifest as postprandial distress syndrome (PDS) with early satiation and/or postprandial fullness or as epigastric pain syndrome (EPS).

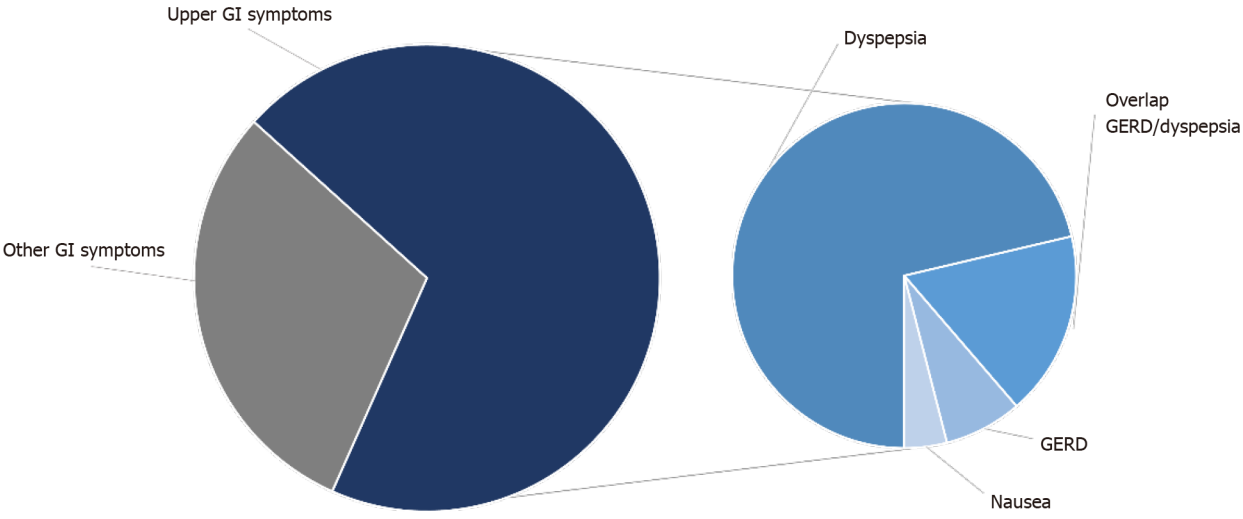
Indeed, according to both data from literature and real-life clinical practice, dyspepsia is frequently reported by AIG patients, which represents a challenge for their proper management.

In the cross-sectional study by Carabotti *et al*[21], more than half of the patients affected by AIG (56.7%, 215 out of 397) reported GI symptoms with a prevalence of upper GI symptoms (69.8%) including dyspepsia (71.2%), described as postprandial fullness, early satiety and/or epigastric pain, GERD related symptoms (7.2%) such as heartburn and/or regurgitation, overlap dyspepsia-GERD symptoms (17.2%) and nausea and vomiting (3.8%). Moreover, 15.8% of the patients enrolled in this study also reported lower irritable bowel syndrome (IBS) -like GI symptoms with overlapping of upper and lower GI symptoms in 14.4% of the patients (Figure 2).



DOI: 10.3748/wjg.v29.i23.3733 **Copyright** ©The Author(s) 2023.

Figure 1 Flow chart showing the process of study selection.



DOI: 10.3748/wjg.v29.i23.3733 **Copyright** ©The Author(s) 2023.

Figure 2 More common gastrointestinal symptoms seen in patients with autoimmune gastritis. GERD: Gastroesophageal reflux disease; GI: Gastrointestinal.

Dyspepsia, meant either as EPS or PDS, together with GERD symptoms such as acid regurgitation and heartburn, are reported as the most frequent symptoms also in the paper by Miceli *et al*[22] with a prevalence of 52.4% and 36.3%, respectively in the study population of 99 AIG patients. Contextually, weight loss and nausea are referred to approximately a quarter of patients (28.3% and 22.2%, respectively), while vomiting and dysphagia are in a lower percentage (9.1% and 3%, respectively).

According to another study[23], including a cohort of 54 patients with AIG, 70% were symptomatic for one or more upper GI symptoms, particularly a quarter of patients referred at least one typical GERD symptom such as regurgitation (18.5%) or heartburn (9%), while a major percentage complained

of atypical GERD symptoms including cough (29.6%), non-cardiac chest pain (22.2%) and dysphagia (14.8%).

As far as GERD symptom is concerned, in the prospective observational study published by Tenca *et al*[24], the prevalence of GERD has been investigated in a cohort of 41 AIG patients, 28 of whom with upper GI symptoms (53% GERD-related, 47% dyspepsia-like). The authors found that 24% of patients had GERD at multichannel intraluminal impedance-pH (MII-pH) monitoring mostly defined as non-acidic reflux, hypothesizing that non-acidic reflux could play a key role in the pathogenesis of the upper GI clinical manifestations. Consistent with the data above, those from the observational prospective study by Pilotto *et al*[25] confirm that among the group of AIG patients complaining of reflux symptoms (38/172, 22%) only 2 patients had documented GERD while 9 patients (24.7%) had reflux hypersensitivity predominantly related to non-acid-reflux (6/9 patients). The remaining 27 patients didn't have alterations at MII-pH but six of them had a major motility disorder. Therefore, the presence of upper GI symptoms appears to be paradoxical as AIG is typically characterized by gastric mucosal atrophy with resulting hypochlorhydria and alkaline gastric pH.

The pathophysiological mechanisms underlying GI symptoms in AIG are poorly understood. Several mechanisms have been hypothesized. The hypochlorhydria resulting from gastric oxyntic atrophy may contribute to dyspeptic symptoms[5], even if other mechanisms may be responsible, such as delayed gastric emptying[26,27], visceral hypersensitivity, and hormonal effects. Delayed gastric emptying may occur due to reduced acid secretion, which can lead to incomplete homogenization of gastric contents with macroscopic residues of undigested food and altered peristalsis, giving feelings of fullness, bloating, and discomfort after eating.

However, in patients with AIG, delayed gastric emptying has been described with elevated circulating gastrin levels and increase in parallel with the degree of the atrophy of the gastric mucosa, affecting gastric emptying T ½ time[27]. Visceral hypersensitivity is an important candidate pathogenic mechanism for several disorders characterized by dyspepsia, even if only a few studies are available for AIG patients[26]. Moreover, some gut hormones such as motilin and ghrelin levels were significantly decreased in AIG subjects with delayed gastric emptying and deranged autonomic function[26], suggesting their potential role in the delayed gastric emptying observed in these subjects. Additionally, the loss of intrinsic factor may result in impaired absorption of nutrients such as iron and vitamin B12, which can contribute to fatigue and other symptoms. Also, low-grade chronic inflammation associated with AIG could contribute to the development of dyspepsia, in parallel to what is described for low-grade bowel inflammation with increased numbers of submucosal mast cells and lymphocytes reported in IBS[28]. Finally, chronic inflammation associated with AIG together with impaired gastric acid secretion may cause changes in the gut microbiota, and this may contribute to the development of dyspeptic symptoms; however, further research is needed to better understand the pathophysiological mechanisms underlying dyspeptic symptoms in AIG and to develop more effective treatments for this condition. It is also important to remember that abnormal thyroid function, which is quite commonly associated with AIG, has been blamed for gastric dysmotility and dyspeptic symptoms[29], which is another possible cause of dyspepsia in AIG patients. However, it is difficult to understand whether the dyspepsia observed in AIG patients is the direct result of abnormal thyroid function or is caused by AIG itself or by a combination of these two autoimmune diseases. Table 1 summarizes the most frequent upper GI symptoms reported by AIG patients together with the underlying pathophysiological mechanisms.

Diagnostic work-up of dyspepsia in AIG

According to recent guidelines on the management of dyspepsia[30-32], upper GI endoscopy [esophagogastroduodenoscopy (EGDs)] is a key test to identify any organic disease of the upper digestive tract (*i.e.*, peptic ulcer, neoplasm), which may explain dyspeptic symptoms. Since EGDs is an invasive and expensive test and most patients with dyspepsia have FD[32], the American and British guidelines suggest limiting the use of EGDs to patients with suspected organic disease. Both the American and the British guidelines[30,32] as well as a recent evidence-based revision of the existing guidelines[31] suggest screening patients for past medical history and family history, medications, previous examinations, presence of *Helicobacter pylori* (*H. pylori*) infection, age, alarm symptoms and signs (*i.e.* anemia or bleeding, weight loss, age > 55 years, recurrent vomiting, dysphagia or odynophagia, fever). When one of the aforementioned alarm symptoms or signs is present, EGDs is mandatory to exclude or confirm an organic disease. If EGDs is negative for esophago-gastric diseases, an abdominal computed tomography -scan is suggested in order to exclude pancreatic, liver, or biliary tract cancers[32]. Distinguishing between AIG and FD in patients with dyspeptic symptoms may result difficult, as the two conditions can produce similar symptoms[20,21]. However, certain factors such as a medical history of autoimmune disease, anemia (including microcytic and macrocytic), vitamin B12 deficiency, and positivity for anti-parietal cells antibodies should raise clinical suspicion of AIG. In such cases, it is important to perform an EGDs to confirm the diagnosis, stage the disease, and evaluate for possible pre-cancerous lesions[33]. According to international guidelines[33], gastric biopsies should be picked up according to Sidney protocol. The protocol requires 5 gastric biopsies, which should be placed in separately labeled jars: 2 from the antrum along the lesser and greater curvature, within 2-3 cm of the pylorus; 2 from the gastric corpus (including 1 from the lesser curvature at 4 cm proximal to the incisura angularis and the

Table 1 Reported upper gastrointestinal symptoms and the underlying pathophysiological mechanisms in patients with autoimmune atrophic gastritis

Clinical manifestation	Pathophysiological mechanisms
Dyspeptic symptoms	
Postprandial fullness; Early satiety; Epigastric pain	Hypochlorhydria. Delayed gastric emptying due to: Hormonal effects (ghrelin, motilin); Reduced acid secretion. Visceral hypersensitivity. Low-grade chronic inflammation. Changes in the gut microbiota
Typical GER like symptoms	
Heartburn; Regurgitation	Non-acid reflux; Delayed gastric emptying; Visceral hypersensitivity; Changes in the gut microbiota
Atypical GERD-like symptoms	
Cough; Non-cardiac chest pain; Dysphagia	Delayed gastric emptying; Visceral hypersensitivity
Overlap dyspepsia-GER like symptoms	As above
Vomiting	Delayed gastric emptying; Visceral hypersensitivity
Nausea	Delayed gastric emptying
Fatigue	Impaired absorption of iron and vitamin B12

GER: Gastro-esophageal reflux; GERD: Gastroesophageal reflux disease.

other from the middle portion of the greater curvature of the gastric body at 8 cm from the cardia), and 1 from the incisura angularis[34]. Severity and topographic distribution of atrophic lesions should be reported according to Operative Link for Gastritis Assessment (OLGA)[35] and Operative Link for Gastric Intestinal Metaplasia Assessment (OLGIM)[36]. By following this protocol, it is less likely to miss the diagnosis of AIG. Moreover, OLGA e OLGIM scores are then used to determine whether endoscopic surveillance is needed and its frequency. Conversely, if there is no suspicion of organic disease, FD could be diagnosed. However, even in these cases, both the American and British guidelines[30,32] suggest testing dyspeptic patients for *H. pylori* with non-invasive tests (*i.e.* fecal antigen or carbon-urea breath testing) and treating the infected ones accordingly, as *H. pylori* infection is considered to be an etiologic factor of dyspepsia in 5% of dyspeptic patients[37].

In case of PDS, with dyspeptic symptoms that recall altered gastric emptying, gastric emptying scintigraphy (GES) is a useful tool to explore impaired (rapid or delayed) gastric dysmotility. Briefly, the test consists of a standard meal, which is marked with Technetium (Tc)-99m; after food ingestion, imaging is performed in the anterior and posterior projections at only four-time points (0, 1, 2, and 4 h). Delayed gastric emptying is determined to be > 90% at 1 h, > 60% at 2 h, and > 10% gastric retention at 4 h. Conversely, rapid gastric emptying is determined to be < 30% at 1 h[38]. While GES performs well in diagnosing gastroparesis[39], it is not reliable for the diagnosis of FD, which is supposed to be a lighter spectrum of the same gastric disorders[40], and no specific studies exist for AIG, therefore further studies are needed to clarify this item[39]. However, this technique can be time-consuming, as the test requires imaging at set intervals over several hours, it involves radiation exposure from the radioactive material in the meal and, as for FD, also in the case of AIG, it may not be reliable, as there is only a milder form of a gastric motility disorder. Moreover, it appears to have limited therapeutic implications, as it may suggest treating the patient with prokinetic drugs at most, which can also be done ex adjuvantibus**.** Recently, the wireless motility capsule (WMC) has been introduced, in order to simultaneously assess both regional and whole gut transit[41,42]. Ingestion of this non-digestible capsule that simultaneously measures luminal temperature, pH, and pressure facilitates the measurement of the gastric, small bowel, and colonic transit times. Approved by the United States Food and Drug Administration for the evaluation of gastroparesis and slow colonic transit, WMC should be considered in suspected GI motility disorders as it provides a single study capable of simultaneously assessing for regional, multi-regional, or generalized motility disorders[43]. Triadafilopoulos *et al*[43] suggested a potential WMC role in AIG diagnosis since it is able to register intragastric pH (usually > 6) and eventually associated dysmotility[43]. However, as for GES, even for WMC at present, considering the limited availability of prokinetic drugs, therapeutic implications are limited. Finally, a recent physiologic tool has been proposed to assess the functionality of the pyloric sphincter. The functional luminal imaging probe known as EndoFlip® is a 240-cm catheter with impedance electrodes at its distal end[44,45], that is used to assess the functionality of the pyloric sphincter. The device is placed in the pylorus either through the endoscope, under endoscopic visualization[45], or either by fluoroscopy guidance[46]. After positioning the device, the balloon is filled to set volumes of 10, 20, 30, 40, and 50 mL using a stepwise protocol, and the cross-sectional area (CSA), bag pressure, and distensibility index are recorded. The pyloric distensibility index (P-DI) is calculated in the zone with the narrowest CSA

with the corresponding intra-bag pressure[46]. A decreased P-DI has been observed in patients with gastroparesis[47], and also in patients with chronic nausea and vomiting without delayed gastric emptying, suggesting that pyloric dysfunction could explain "gastroparesis-like" symptoms in this group of patients[48]. However, normal and pathological values still need to be confirmed.

As mentioned above, GERD symptoms are frequently reported by AIG patients[24,25]. According to recent guidelines[49] and Lyon consensus[50], GERD is usually a clinical diagnosis, based on patients' symptoms (typical GERD symptoms, pyrosis, and acidic regurgitation) and empiric proton pump inhibitors (PPIs) treatment response (*i.e.* single dose for 4-8 wk).

Since AIG patients are supposed to have a higher intragastric pH (registered in one study, being median intragastric pH of 6.2 (4.6-7.0)[24], due to parietal cells atrophy, it may be surprising that AIG patients complain of GERD symptoms. A previous paper by Tenca *et al*[24] registered that 15 out of 41 AIG patients had GERD symptoms. Among them, acidic reflux, recorded by MII-pH monitoring, had a minor role, being present in one patient only. This could be explained by the residual production of acid from partially atrophic mucosa. Non-acidic reflux was instead more frequent, being present in 22% of the AIG population studied. It is common knowledge that non-acidic reflux can give rise to typical or atypical GERD symptoms[51-53].

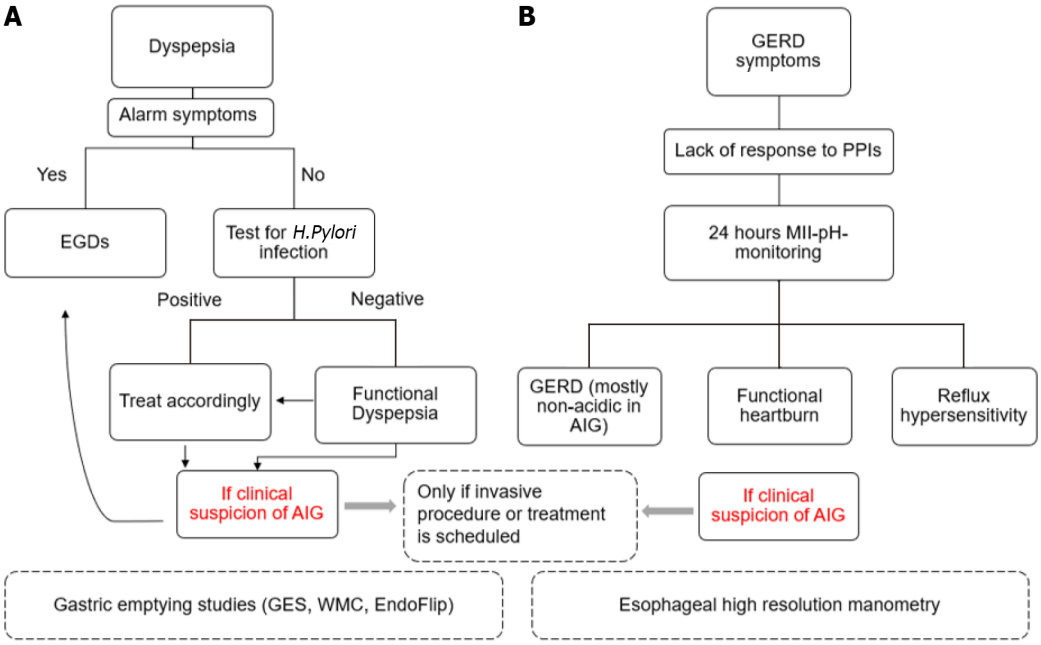
Moreover, it could be useful to study these patients with MII-pH-monitoring, which is able to identify acidic, weakly acidic, and non-acidic reflux events. The observation of a role of GERD in these patients' symptoms independently of acid is clinically relevant because it can guide their management. These patients may benefit from drugs that lower their visceral sensitivity (*i.e.*, tricyclic antidepressants and selective serotonin reuptake inhibitors)[7,54]. Furthermore, for those with severe drug-unresponsive symptoms anti-reflux surgery is an option[55,56]. Another study by Pilotto *et al*[25] characterizes AIG patients according to their GERD symptoms and MII-pH-monitoring results. Similarly, Tenca *et al*[24] found pathologic esophageal acid exposure in two out of 38 patients reporting GERD symptoms. On the contrary, a great part of them (30 out of 38 patients) had an increased number of non-acidic reflux episodes. Combining symptoms and MII-pH-monitoring results, the Authors classified AIG patients as having GERD (5%), functional heartburn (50%), and reflux hypersensitivity (24%). Interestingly, the Authors studied AIG patients with high-resolution esophageal manometry (HRM) and found that 37% of AIG patients had various motility disorders, including 8 minor disorders (n = 7 weak peristalsis and n = 1 hypertensive peristalsis), and 6 major disorders (n = 6 EGJ outflow obstruction) according to Chicago classification v 3.0[57]. Whether these manometric findings correlate with AIG is still debated. Similarly, the role of HRM in the diagnostic work-up of these patients remains unclear. MII-pH-monitoring could also have a role in the diagnosis of dyspepsia. It is known from the literature that epigastric pain is often more frequent in patients with pathologic MII-pH-monitoring[58]. In the population studied by Tenca *et al*[24], two dyspeptic patients showed a positive correlation between epigastric pain and non-acidic reflux. A possible diagnostic algorithm is represented in Figure 3.

In summary, dyspeptic symptoms and GERD are common in AIG patients; the diagnostic algorithm provides an EGDs study as the first diagnostic test to exclude organic disease and to confirm AIG diagnosis. If GERD symptoms are present, MII-pH-monitoring is useful to measure the entity of reflux and to classify patients (GERD, functional heartburn, hypersensitive esophagus) and treat them accordingly. Moreover, it could be useful in dyspepsia diagnosis. Esophageal motility tests, as well as gastric emptying tests, could have a role in AIG patients but further studies are needed to clarify these items.

Treatment

Dyspepsia is a common symptom in AIG and its management can be challenging, as the pathophysiology underlying dyspeptic symptoms in AIG is multifactorial. However, this issue is still understudied, and more research is needed to better understand the mechanisms of dyspepsia in AIG and to develop effective treatments tailored to the individual patient's symptoms and underlying pathophysiology. Indeed, although the primary goal of AIG treatment is to address vitamin deficiencies and prevent and monitor for gastric neoplasms, effectively managing common and difficult-to-treat symptoms like dyspepsia is crucial for improving patients' quality of life.

As a matter of fact, according to available guidelines[10], there is poor evidence regarding the best treatment options for dyspeptic symptoms in patients with AIG, also considering that PPIs are not indicated in this subset of patients who are typically hypochlorhydric. Despite this, several AIG patients referring dyspeptic symptoms are often prescribed PPIs by General Practitioners or gastroenterologists with no or low knowledge of this disease. The use of PPIs in this subgroup of patients should be discouraged for two main reasons. Firstly, AIG is characterized by a suppressed gastric acid secretion and consequent hypochlorhydria, thus treatment with antisecretory drugs is generally ineffective as already reported[24,59] taking into account that these patients refer reflux-like symptoms whose nature is non-acid. Secondly, and far more important, the long-term use of PPIs has been reported to be associated with the development or progression of gastric pre-malignant lesions. Of note, as already reported[60], the long-term treatment with PPIs which is responsible for increased levels of serum gastrin seems to be linked to a higher risk of progression of ECL-cell hyperplasia which precedes the development of gastric type 1 neuroendocrine neoplasm[61]; however, no clear-cut evidence was found between PPI therapy and increased progression of AIG or intestinal metaplasia[60].



DOI: 10.3748/wjg.v29.i23.3733 **Copyright** ©The Author(s) 2023.

Figure 3 Possible diagnostic algorithm for dyspepsia or gastroesophageal reflux disease -like symptoms in autoimmune atrophic gastritis. A: Dyspeptic symptoms; B: Gastroesophageal reflux disease symptoms. AIG: Autoimmune gastritis; EGDs: Esophagogastroduodenoscopy; GERD: Gastroesophageal reflux disease; GI: Gastrointestinal; *H. pylori*: *Helicobacter pylori*; PPIs: Proton pump inhibitors.

Initial management of dyspepsia in AIG may involve dietary modifications, such as avoiding trigger foods or eating smaller, more frequent meals. Patients may also benefit from lifestyle modifications, such as weight loss or stress reduction techniques, even if these procedures are not evidence-supported.

It is important to highlight that patients with AIG often have evidence of current or prior *H. pylori* infection[62]. Therefore, it is important to test these patients for *H. pylori* and, if positive, to eradicate it according to guidelines that suggested the "Test and treat" strategy[63]. Of note, *H. pylori* eradication appears to reduce the risk of gastric cancer[64]. In the specific setting of AIG, according to a randomized double-blinded placebo-controlled trial[65], that compared triple eradication therapy for *H. pylori* with placebo in histologically diagnosed AIG patients, at 3-years follow-up dyspeptic symptoms scores improved significantly in the patients in whom *H. pylori* had been eradicated. Similar findings were reported by another recent study[66], which showed that the beneficial effect of *H. pylori* eradication treatment on dyspeptic symptoms lasted until one year after treatment, being associated with a higher pretreatment symptom score and age inferior to 70 years old. Obviously, the benefit of *H. pylori* eradication in AIG patients is further increased by the fact that *H. pylori* more that autoimmunity per se, is linked to the risk of evolution towards dysplasia and gastric cancer in AIG, as recently described[1].

In addition to *H. pylori* eradication, several treatment options[67] have been investigated for their efficacy in managing dyspeptic symptoms in AIG. These treatments include prokinetic agents, neuromodulators, and herbal agents, as well as non-pharmacological treatments such as acupuncture, cognitive-behavioral therapy, and hypnotherapy. However, the evidence regarding their effectiveness is conflicting also taken into account the lack of dedicated prospective studies exploring the efficacy of prokinetics and neuromodulators in this specific setting of patients, making the management of AIG patients experiencing dyspeptic symptoms very challenging. Medications such as prokinetic agents including metoclopramide or domperidone may be used to improve gastric motility and reduce symptoms of bloating and nausea in patients with predominantly PDS symptoms. For patients presenting with EPS symptoms, a rational approach could therefore be to guide therapy based on the altered pathophysiological mechanism. As mentioned before, 24-h MII-pH-monitoring may be a useful tool to classify AIG patients having GERD symptoms. If MII-pH-monitoring found true acidic GERD, PPIs treatment could have a role. Being this an extremely rare condition, there are no clear-cut recommendations on treatment dosage and duration. Conversely, if MII-pH-impedance diagnoses a non-acidic reflux disease, as well as functional heartburn and reflux hypersensitivity, these patients may benefit from drugs that lower their visceral sensitivity (*i.e.* tricyclic antidepressants and selective serotonin reuptake inhibitors)[7,54]. Moreover, patients who did not respond to medical treatment as well as patients with a high burden of non-acidic reflux, may benefit from anti-reflux surgery[55,56].

In cases where dyspepsia is associated with underlying anxiety or depression, treatment with antidepressants or anxiolytics may be warranted[7,54]. However, future research is needed to identify more effective treatments for dyspepsia in AIG and to better understand the underlying mechanisms that drive dyspeptic symptoms in this condition.

Furthermore, a known consequence of atrophic gastritis-related hypochlorhydria and/or achlorhydria is a change in the gastric microbiome composition. However, there are currently no specific therapies targeting dyspepsia in AIG based on changes in the microbiota, even if an abnormally elevated presence of endoluminal bacteria which produce acetaldehyde from glucose metabolism has been described[68]. Again, according to some authors[69,70], L-cysteine, a non-essential amino acid, can modify the microenvironment of the achlorhydric stomach by both inactivating acetaldehyde and promoting recovery of gastric function[71,72]; furthermore, there is some anecdotal evidence that L-cysteine might improve functional symptoms often associated with atrophic gastritis. Based on these observations, Di Mario *et al*[73] recently conducted a study including a total of 330 patients with atrophic gastritis (both autoimmune or *H. pylori*-related), who were divided into two groups, treated with long-term L-cysteine and no specific treatment, respectively, and reported a significant improvement in the symptom scores of patients treated with L-cysteine when compared to the non-treated group. Of note, symptom improvement lasted all the two years of the follow-up. One limitation of this study is the inclusion of different etiologies from atrophic gastritis, which might be responsible for a certain grade of heterogeneity. While research into the gut microbiota and its role in AIG is ongoing[74,75], some studies suggest that probiotics and prebiotics may have a role in modulating the gut microbiota and reducing symptoms in patients with dyspepsia, including those with AIG[76,77]. Overall, while the potential for microbiota-based therapies in managing dyspepsia in AIG is promising, further research is needed to develop and validate such approaches.

Finally, further treatment may be available in the near future. Gastric per-oral endoscopic myotomy (G POEM) is a novel endoscopic procedure that has shown promising results in the management of refractory gastroparesis[78]. This technique has received increasing attention and emerged as a promising treatment for refractory gastroparesis, targeting the pylorus[79], as a result of the use of new tools to identify pyloric dysfunction in routine care, including functional luminal impedance planimetry (FLIP). The procedure involves creating a myotomy or an incision in the inner lining of the stomach, thereby allowing for better gastric emptying. Since AIG patients with PDS may have the same functional dysfunction of patients affected by gastroparesis, both from a pathophysiological and clinical point of view, G POEM may represent a feasible treatment for AIG patients with severe dyspeptic symptoms, which did not respond to medical treatment. Even if it is considered a safe procedure, a potential concern associated with G POEM is the risk of complications, such as bleeding, perforation, and infection[80]. Additionally, the long-term outcomes of G POEM are still unclear, and more studies are needed to assess its durability and impact on patient quality of life. Recently, Mandarino *et al*[81] found that a lower Intragastric Meal Distribution at pre-intervention gastric emptying study, which indicates antral food retention, could be associated with post-procedural functional success, defined as a decrease of more than 30% 2-h retention. However, further data are needed to establish long-term efficacy of endoscopic pyloromyotomy, especially in the management of dyspeptic AIG patients.

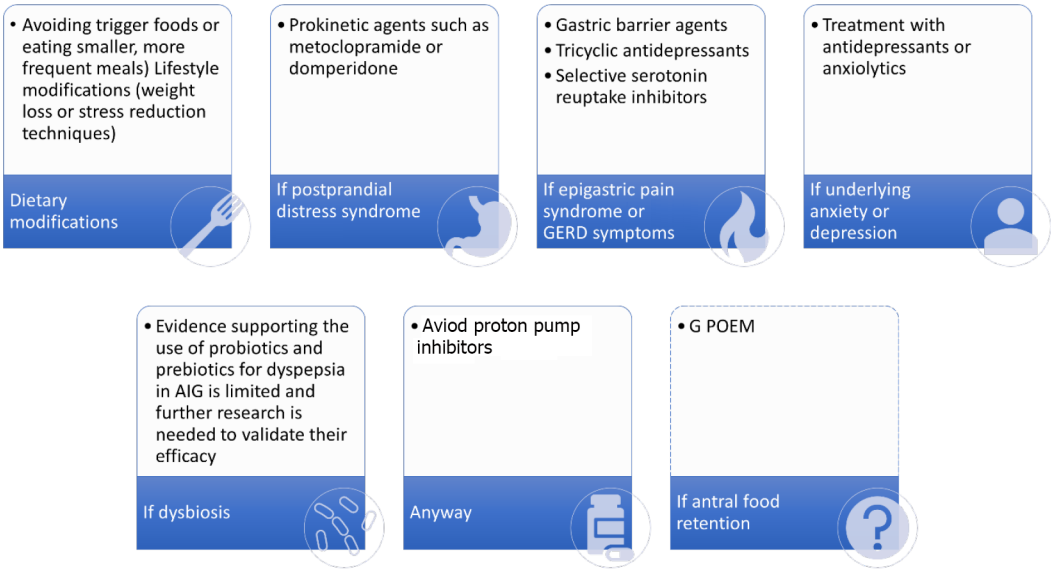
CONCLUSION

AIG can cause a range of clinical manifestations, including dyspepsia. Accurate diagnosis and appropriate management of dyspepsia in AIG are important to improve the patient's quality of life, as well as to prevent and monitor for potential complications such as vitamin deficiencies and gastric neoplasms. The pathophysiology of dyspepsia in AIG is complex and involves changes in acid secretion, gastric motility, hormone signaling, and gut microbiota, among other factors. Specifically, investigating the role of visceral hypersensitivity, impaired gastric accommodation, and impaired gastric motility in AIG-related dyspepsia may help to identify new targets for treatment.

Managing dyspeptic symptoms of AIG is challenging and there are no specific therapies targeting dyspepsia in AIG. While PPIs are commonly used to treat dyspepsia and GERD, they may not be appropriate for AIG, as the condition is already characterized by hypochlorhydria. Instead, prokinetic agents, antidepressant drugs, and non-pharmacological treatments may be of help, even if not adequately evidence-based supported.

Targeting dyspepsia in AIG based on changes in the microbiota is an area of ongoing research and some studies suggest that probiotics and prebiotics may have a role in reducing symptoms. G POEM may represent a feasible treatment for AIG patients with severe dyspeptic symptoms, even if more research is needed to establish its safety and efficacy in this specific setting of patients. Figure 4 summarizes the possible therapeutic approaches for dyspeptic or with GERD-like symptoms in patients with AIG.

Overall, a multidisciplinary approach for the management of dyspepsia in AIG is recommended, and further research is needed to develop and validate more effective therapies for dyspepsia in AIG, as well as to better understand the underlying pathophysiology of the disease; GERD: Gastroesophageal reflux disease.



DOI: 10.3748/wjg.v29.i23.3733 **Copyright** ©The Author(s) 2023.

Figure 4 Therapeutic approaches for dyspeptic or with gastroesophageal reflux disease -like symptoms in patients with autoimmune gastritis. AIG: Autoimmune gastritis; G POEM: Gastric per-oral endoscopic myotomy; GERD: Gastroesophageal reflux disease.

ARTICLE HIGHLIGHTS

Research background

Gastrointestinal symptoms such as dyspepsia and early satiety are very common in autoimmune gastritis (AIG), being second in terms of frequency only to anemia, which is the most typical feature of AIG. Understanding the pathophysiology of each condition can also guide the choice of appropriate treatments, including lifestyle modifications, dietary changes, and medication management.

Research motivation

The management of dyspepsia in patients with AIG, a chronic, immune-mediated disease, remains a challenge, as it can overlap with functional dyspepsia and gastroesophageal reflux disease. Currently, there are no specific therapies. A tailored treatment approach based on a better understanding of putative pathogenic mechanisms underlying symptoms is needed.

Research objectives

In this review, we will discuss the putative pathogenic mechanisms underlying symptom generation in AIG, their clinical implications, and the current management strategies for this complex and multi-faceted disease.

Research methods

An extensive bibliographical search was performed in PubMed to identify guidelines and primary literature (retrospective and prospective studies, systematic reviews, case series) published in the last 10 years, using both medical subject heading terms and free-language keywords: Dyspepsia; dyspeptic symptoms; gastro-intestinal symptoms; chronic autoimmune atrophic gastritis; diagnosis; treatment.

Research results

A total of 125 records were reviewed and 80 were defined as fulfilling the criteria.

Research conclusions

AIG can cause a range of clinical manifestations, including dyspepsia. The pathophysiology of dyspepsia in AIG is complex and involves changes in acid secretion, gastric motility, hormone signaling, and gut microbiota, among other factors. Managing dyspeptic symptoms of AIG is challenging and currently, there are no specific therapies. A tailored treatment approach based on a better understanding of putative pathogenic mechanisms underlying symptoms is needed. While proton pump inhibitors are commonly used to treat dyspepsia and GERD, they may not be appropriate for AIG. Prokinetic agents, antidepressant drugs, and non-pharmacological treatments may be of help, even if not adequately evidence-based supported. A multidisciplinary approach for the management of dyspepsia in AIG is recommended, and further research is needed to develop and validate more effective therapies for dyspepsia.

Research perspectives

As a future perspective, targeting dyspepsia in AIG based on changes in the microbiota and advanced endoscopic techniques to treat severe dyspeptic symptoms might be an area of ongoing research.

FOOTNOTES

Author contributions: Massironi S conceived the idea for the review; Rossi RE, Elvevi A, Sciola V, and Mandarino FV conducted the literature search; Rossi RE, Elvevi A, and Sciola V screened the articles for inclusion and exclusion criteria; Rossi RE, Sciola V, and Elvevi A wrote the initial draft of the manuscript; Massironi S, Mandarino FV, Danese S, and Invernizzi P contributed to revising the manuscript critically for important intellectual content and finally all authors approved the final version for submission.

Conflict-of-interest statement: All the authors declare no conflict of interests for this article.

PRISMA 2009 Checklist statement: The authors have read the PRISMA 2009 Checklist, and the manuscript was prepared and revised according to the PRISMA 2009 Checklist.

Open-Access: This article is an open-access article that was selected by an in-house editor and fully peer-reviewed by external reviewers. It is distributed in accordance with the Creative Commons Attribution NonCommercial (CC BY-NC 4.0) license, which permits others to distribute, remix, adapt, build upon this work non-commercially, and license their derivative works on different terms, provided the original work is properly cited and the use is non-commercial. See: https://creativecommons.org/Licenses/by-nc/4.0/

Country/Territory of origin: Italy

ORCID number: Roberta Elisa Rossi 0000-0003-4208-4372; Alessandra Elvevi 0000-0001-9841-2051; Francesco Vito Mandarino 0000-0002-9931-7221; Silvio Danese 0000-0001-7341-1351; Pietro Invernizzi 0000-0003-3262-1998; Sara Massironi 0000-0003-3214-8192.

S-Editor: Liu JH
L-Editor: A
P-Editor: Yuan YY

REFERENCES

1 **Rugge M**, Bricca L, Guzzinati S, Sacchi D, Pizzi M, Savarino E, Farinati F, Zorzi M, Fassan M, Dei Tos AP, Malfertheiner P, Genta RM, Graham DY. Autoimmune gastritis: long-term natural history in naïve Helicobacter pylori-negative patients. *Gut* 2023; **72**: 30-38 [PMID: 35772926 DOI: 10.1136/gutjnl-2022-327827]
2 Autoimmune gastritis. *Nat Rev Dis Primers* 2020; **6**: 57 [PMID: 32647157 DOI: 10.1038/s41572-020-0198-5]
3 **Massironi S**, Zilli A, Elvevi A, Invernizzi P. The changing face of chronic autoimmune atrophic gastritis: an updated comprehensive perspective. *Autoimmun Rev* 2019; **18**: 215-222 [PMID: 30639639 DOI: 10.1016/j.autrev.2018.08.011]
4 **Lenti MV**, Annibale B, Di Sabatino A, Lahner E. Editorial: Dissecting the immunological, pathological, and clinical aspects of autoimmune gastritis and its neoplastic complications. *Front Immunol* 2022; **13**: 1070250 [PMID: 36389672 DOI: 10.3389/fimmu.2022.1070250]
5 **Neumann WL**, Coss E, Rugge M, Genta RM. Autoimmune atrophic gastritis--pathogenesis, pathology and management. *Nat Rev Gastroenterol Hepatol* 2013; **10**: 529-541 [PMID: 23774773 DOI: 10.1038/nrgastro.2013.101]
6 **Hall SN**, Appelman HD. Autoimmune Gastritis. *Arch Pathol Lab Med* 2019; **143**: 1327-1331 [PMID: 31661309 DOI: 10.5858/arpa.2019-0345-RA]
7 **Broeders BWLCM**, Carbone F, Balsiger LM, Schol J, Raymenants K, Huang I, Verheyden A, Vanuytsel T, Tack J. Review article: Functional dyspepsia-a gastric disorder, a duodenal disorder or a combination of both? *Aliment Pharmacol Ther* 2023; **57**: 851-860 [PMID: 36859629 DOI: 10.1111/apt.17414]
8 **Wauters L**, Dickman R, Drug V, Mulak A, Serra J, Enck P, Tack J; ESNM FD Consensus Group, Accarino A, Barbara G, Bor S, Coffin B, Corsetti M, De Schepper H, Dumitrascu D, Farmer A, Gourcerol G, Hauser G, Hausken T, Karamanolis G, Keszthelyi D, Malagelada C, Milosavljevic T, Muris J, O'Morain C, Papathanasopoulos A, Pohl D, Rumyantseva D, Sarnelli G, Savarino E, Schol J, Sheptulin A, Smet A, Stengel A, Storonova O, Storr M, Törnblom H, Vanuytsel T, Velosa M, Waluga M, Zarate N, Zerbib F. United European Gastroenterology (UEG) and European Society for Neurogastroenterology and Motility (ESNM) consensus on functional dyspepsia. *United European Gastroenterol J* 2021; **9**: 307-331 [PMID: 33939891 DOI: 10.1002/ueg2.12061]
9 **Rustgi SD**, Bijlani P, Shah SC. Autoimmune gastritis, with or without pernicious anemia: epidemiology, risk factors, and clinical management. *Therap Adv Gastroenterol* 2021; **14**: 17562848211038771 [PMID: 34484423 DOI: 10.1177/17562848211038771]
10 **Lahner E**, Zagari RM, Zullo A, Di Sabatino A, Meggio A, Cesaro P, Lenti MV, Annibale B, Corazza GR. Chronic atrophic gastritis: Natural history, diagnosis and therapeutic management. A position paper by the Italian Society of Hospital Gastroenterologists and Digestive Endoscopists [AIGO], the Italian Society of Digestive Endoscopy [SIED], the

Italian Society of Gastroenterology [SIGE], and the Italian Society of Internal Medicine [SIMI]. *Dig Liver Dis* 2019; **51**: 1621-1632 [PMID: 31635944 DOI: 10.1016/j.dld.2019.09.016]

11 **Rodriguez-Castro KI**, Franceschi M, Noto A, Miraglia C, Nouvenne A, Leandro G, Meschi T, De' Angelis GL, Di Mario F. Clinical manifestations of chronic atrophic gastritis. *Acta Biomed* 2018; **89**: 88-92 [PMID: 30561424 DOI: 10.23750/abm.v89i8-S.7921]

12 **Yang GT**, Zhao HY, Kong Y, Sun NN, Dong AQ. Correlation between serum vitamin B12 level and peripheral neuropathy in atrophic gastritis. *World J Gastroenterol* 2018; **24**: 1343-1352 [PMID: 29599609 DOI: 10.3748/wjg.v24.i12.1343]

13 **O'Leary F**, Samman S. Vitamin B12 in health and disease. *Nutrients* 2010; **2**: 299-316 [PMID: 22254022 DOI: 10.3390/nu2030299]

14 **Wu H**, Liang G, Kong M, Zhang Y, Zhou Y, Han J, Hu X, Li Y, Zhan Q, Chen S, Du Y, Chen W. The status and risk factors for anxiety/depression in patients with atrophic chronic gastritis: a cross-sectional study. *Ann Palliat Med* 2022; **11**: 3147-3159 [PMID: 36096741 DOI: 10.21037/apm-22-730]

15 **Miceli E**, Brondino N, Lenti MV, Di Stefano M, Staiani M, Zugnoni F, Pisati M, Caccia Dominioni C, Corazza GR, Politi P, Di Sabatino A. Impaired Quality of Life in Patients with Autoimmune Atrophic Gastritis. *Dig Dis Sci* 2021; **66**: 3322-3329 [PMID: 33098024 DOI: 10.1007/s10620-020-06656-x]

16 **Utiyama SRR**, De Bem RS, Skare TL, De Carvalho GA, Teixeira LM, Bertolazo M, Ioshii SO, Nisihara R. Anti-parietal cell antibodies in patients with autoimmune thyroid diseases. *J Endocrinol Invest* 2018; **41**: 523-529 [PMID: 28929353 DOI: 10.1007/s40618-017-0755-2]

17 **Kim HW**, Kim YH, Han K, Nam GE, Kim GS, Han BD, Lee A, Ahn JY, Ko BJ. Atrophic gastritis: a related factor for osteoporosis in elderly women. *PLoS One* 2014; **9**: e101852 [PMID: 25003598 DOI: 10.1371/journal.pone.0101852]

18 **Goerss JB**, Kim CH, Atkinson EJ, Eastell R, O'Fallon WM, Melton LJ 3rd. Risk of fractures in patients with pernicious anemia. *J Bone Miner Res* 1992; **7**: 573-579 [PMID: 1615763 DOI: 10.1002/jbmr.5650070514]

19 **Massironi S**, Cavalcoli F, Zilli A, Del Gobbo A, Ciafardini C, Bernasconi S, Felicetta I, Conte D, Peracchi M. Relevance of vitamin D deficiency in patients with chronic autoimmune atrophic gastritis: a prospective study. *BMC Gastroenterol* 2018; **18**: 172 [PMID: 30409113 DOI: 10.1186/s12876-018-0901-0]

20 **Lenti MV**, Rugge M, Lahner E, Miceli E, Toh BH, Genta RM, De Block C, Hershko C, Di Sabatino A. Autoimmune gastritis. *Nat Rev Dis Primers* 2020; **6**: 56 [PMID: 32647173 DOI: 10.1038/s41572-020-0187-8]

21 **Carabotti M**, Lahner E, Esposito G, Sacchi MC, Severi C, Annibale B. Upper gastrointestinal symptoms in autoimmune gastritis: A cross-sectional study. *Medicine (Baltimore)* 2017; **96**: e5784 [PMID: 28072728 DOI: 10.1097/MD.0000000000005784]

22 **Miceli E**, Lenti MV, Padula D, Luinetti O, Vattiato C, Monti CM, Di Stefano M, Corazza GR. Common features of patients with autoimmune atrophic gastritis. *Clin Gastroenterol Hepatol* 2012; **10**: 812-814 [PMID: 22387252 DOI: 10.1016/j.cgh.2012.02.018]

23 **Carabotti M**, Esposito G, Lahner E, Pilozzi E, Conti L, Ranazzi G, Severi C, Bellini M, Annibale B. Gastroesophageal reflux symptoms and microscopic esophagitis in a cohort of consecutive patients affected by atrophic body gastritis: a pilot study. *Scand J Gastroenterol* 2019; **54**: 35-40 [PMID: 30638085 DOI: 10.1080/00365521.2018.1553062]

24 **Tenca A**, Massironi S, Pugliese D, Consonni D, Mauro A, Cavalcoli F, Franchina M, Spampatti M, Conte D, Penagini R. Gastro-esophageal reflux and antisecretory drugs use among patients with chronic autoimmune atrophic gastritis: a study with pH-impedance monitoring. *Neurogastroenterol Motil* 2016; **28**: 274-280 [PMID: 26568317 DOI: 10.1111/nmo.12723]

25 **Pilotto V**, Maddalo G, Orlando C, Fassan M, Rugge M, Farinati F, Savarino EV. Objective Evidence of Gastro-Esophageal Reflux Disease is Rare in Patients with Autoimmune Gastritis. *J Gastrointestin Liver Dis* 2021; **30**: 30-36 [PMID: 33723550 DOI: 10.15403/jgld-3033]

26 **Kalkan Ç**, Soykan I. The Relations Among Serum Ghrelin, Motilin and Gastric Emptying and Autonomic Function in Autoimmune Gastritis. *Am J Med Sci* 2018; **355**: 428-433 [PMID: 29753372 DOI: 10.1016/j.amjms.2017.12.021]

27 **Kalkan Ç**, Soykan I, Soydal Ç, Özkan E, Kalkan E. Assessment of Gastric Emptying in Patients with Autoimmune Gastritis. *Dig Dis Sci* 2016; **61**: 1597-1602 [PMID: 26725066 DOI: 10.1007/s10620-015-4021-1]

28 **Bashashati M**, Moossavi S, Cremon C, Barbaro MR, Moraveji S, Talmon G, Rezaei N, Hughes PA, Bian ZX, Choi CH, Lee OY, Coëffier M, Chang L, Ohman L, Schmulson MJ, McCallum RW, Simren M, Sharkey KA, Barbara G. Colonic immune cells in irritable bowel syndrome: A systematic review and meta-analysis. *Neurogastroenterol Motil* 2018; **30** [PMID: 28851005 DOI: 10.1111/nmo.13192]

29 **Daher R**, Yazbeck T, Jaoude JB, Abboud B. Consequences of dysthyroidism on the digestive tract and viscera. *World J Gastroenterol* 2009; **15**: 2834-2838 [PMID: 19533804 DOI: 10.3748/wjg.15.2834]

30 **Moayyedi P**, Lacy BE, Andrews CN, Enns RA, Howden CW, Vakil N. ACG and CAG Clinical Guideline: Management of Dyspepsia. *Am J Gastroenterol* 2017; **112**: 988-1013 [PMID: 28631728 DOI: 10.1038/ajg.2017.154]

31 **Miwa H**, Nagahara A, Asakawa A, Arai M, Oshima T, Kasugai K, Kamada K, Suzuki H, Tanaka F, Tominaga K, Futagami S, Hojo M, Mihara H, Higuchi K, Kusano M, Arisawa T, Kato M, Joh T, Mochida S, Enomoto N, Shimosegawa T, Koike K. Evidence-based clinical practice guidelines for functional dyspepsia 2021. *J Gastroenterol* 2022; **57**: 47-61 [PMID: 35061057 DOI: 10.1007/s00535-021-01843-7]

32 **Black CJ**, Paine PA, Agrawal A, Aziz I, Eugenicos MP, Houghton LA, Hungin P, Overshott R, Vasant DH, Rudd S, Winning RC, Corsetti M, Ford AC. British Society of Gastroenterology guidelines on the management of functional dyspepsia. *Gut* 2022; **71**: 1697-1723 [PMID: 35798375 DOI: 10.1136/gutjnl-2022-327737]

33 **Shah SC**, Piazuelo MB, Kuipers EJ, Li D. AGA Clinical Practice Update on the Diagnosis and Management of Atrophic Gastritis: Expert Review. *Gastroenterology* 2021; **161**: 1325-1332.e7 [PMID: 34454714 DOI: 10.1053/j.gastro.2021.06.078]

34 **Dixon MF**, Genta RM, Yardley JH, Correa P. Classification and grading of gastritis. The updated Sydney System. International Workshop on the Histopathology of Gastritis, Houston 1994. *Am J Surg Pathol* 1996; **20**: 1161-1181 [PMID: 8827022 DOI: 10.1097/00000478-199610000-00001]

35 **Rugge M**, Meggio A, Pennelli G, Piscioli F, Giacomelli L, De Pretis G, Graham DY. Gastritis staging in clinical practice: the OLGA staging system. *Gut* 2007; **56**: 631-636 [PMID: 17142647 DOI: 10.1136/gut.2006.106666]

36 **Capelle LG**, de Vries AC, Haringsma J, Ter Borg F, de Vries RA, Bruno MJ, van Dekken H, Meijer J, van Grieken NC, Kuipers EJ. The staging of gastritis with the OLGA system by using intestinal metaplasia as an accurate alternative for atrophic gastritis. *Gastrointest Endosc* 2010; **71**: 1150-1158 [PMID: 20381801 DOI: 10.1016/j.gie.2009.12.029]

37 **Moayyedi P**, Forman D, Braunholtz D, Feltbower R, Crocombe W, Liptrott M, Axon A. The proportion of upper gastrointestinal symptoms in the community associated with Helicobacter pylori, lifestyle factors, and nonsteroidal anti-inflammatory drugs. Leeds HELP Study Group. *Am J Gastroenterol* 2000; **95**: 1448-1455 [PMID: 10894577 DOI: 10.1111/j.1572-0241.2000.2126_1.x]

38 **Abell TL**, Camilleri M, Donohoe K, Hasler WL, Lin HC, Maurer AH, McCallum RW, Nowak T, Nusynowitz ML, Parkman HP, Shreve P, Szarka LA, Snape WJ Jr, Ziessman HA; American Neurogastroenterology and Motility Society and the Society of Nuclear Medicine. Consensus recommendations for gastric emptying scintigraphy: a joint report of the American Neurogastroenterology and Motility Society and the Society of Nuclear Medicine. *J Nucl Med Technol* 2008; **36**: 44-54 [PMID: 18287197 DOI: 10.2967/jnmt.107.048116]

39 **Camilleri M**, Kuo B, Nguyen L, Vaughn VM, Petrey J, Greer K, Yadlapati R, Abell TL. ACG Clinical Guideline: Gastroparesis. *Am J Gastroenterol* 2022; **117**: 1197-1220 [PMID: 35926490 DOI: 10.14309/ajg.0000000000001874]

40 **Pasricha PJ**, Grover M, Yates KP, Abell TL, Bernard CE, Koch KL, McCallum RW, Sarosiek I, Kuo B, Bulat R, Chen J, Shulman RJ, Lee L, Tonascia J, Miriel LA, Hamilton F, Farrugia G, Parkman HP; National Institute of Diabetes and Digestive and Kidney Diseases/National Institutes of Health Gastroparesis Clinical Research Consortium. Functional Dyspepsia and Gastroparesis in Tertiary Care are Interchangeable Syndromes With Common Clinical and Pathologic Features. *Gastroenterology* 2021; **160**: 2006-2017 [PMID: 33548234 DOI: 10.1053/j.gastro.2021.01.230]

41 **Lee YY**, Erdogan A, Rao SS. How to assess regional and whole gut transit time with wireless motility capsule. *J Neurogastroenterol Motil* 2014; **20**: 265-270 [PMID: 24840380 DOI: 10.5056/jnm.2014.20.2.265]

42 **Saad RJ**. The Wireless Motility Capsule: a One-Stop Shop for the Evaluation of GI Motility Disorders. *Curr Gastroenterol Rep* 2016; **18**: 14 [PMID: 26908282 DOI: 10.1007/s11894-016-0489-x]

43 **Triadafilopoulos G**, Lombard C. Use of the Wireless Motility Capsule in the Diagnosis of Gastric Hypochlorhydria: pHinding Extra Value. *Dig Dis Sci* 2021; **66**: 1442-1445 [PMID: 32974808 DOI: 10.1007/s10620-020-06605-8]

44 **Gourcerol G**, Tissier F, Melchior C, Touchais JY, Huet E, Prevost G, Leroi AM, Ducrotte P. Impaired fasting pyloric compliance in gastroparesis and the therapeutic response to pyloric dilatation. *Aliment Pharmacol Ther* 2015; **41**: 360-367 [PMID: 25523288 DOI: 10.1111/apt.13053]

45 **Malik Z**, Sankineni A, Parkman HP. Assessing pyloric sphincter pathophysiology using EndoFLIP in patients with gastroparesis. *Neurogastroenterol Motil* 2015; **27**: 524-531 [PMID: 25712043 DOI: 10.1111/nmo.12522]

46 **Wuestenberghs F**, Gourcerol G. Pyloric distensibility in health and disease. *Am J Physiol Gastrointest Liver Physiol* 2021; **321**: G133-G138 [PMID: 34160292 DOI: 10.1152/ajpgi.00460.2020]

47 **Desprez C**, Chambaz M, Melchior C, Basile P, Prevost G, Jacques J, Leroi AM, Gourcerol G. Assessment of pyloric sphincter distensibility and pressure in patients with diabetic gastroparesis. *Neurogastroenterol Motil* 2021; **33**: e14064 [PMID: 33314491 DOI: 10.1111/nmo.14064]

48 **Snape WJ**, Lin MS, Agarwal N, Shaw RE. Evaluation of the pylorus with concurrent intraluminal pressure and EndoFLIP in patients with nausea and vomiting. *Neurogastroenterol Motil* 2016; **28**: 758-764 [PMID: 26813266 DOI: 10.1111/nmo.12772]

49 **Yadlapati R**, Gyawali CP, Pandolfino JE; CGIT GERD Consensus Conference Participants. AGA Clinical Practice Update on the Personalized Approach to the Evaluation and Management of GERD: Expert Review. *Clin Gastroenterol Hepatol* 2022; **20**: 984-994.e1 [PMID: 35123084 DOI: 10.1016/j.cgh.2022.01.025]

50 **Gyawali CP**, Kahrilas PJ, Savarino E, Zerbib F, Mion F, Smout AJPM, Vaezi M, Sifrim D, Fox MR, Vela MF, Tutuian R, Tack J, Bredenoord AJ, Pandolfino J, Roman S. Modern diagnosis of GERD: the Lyon Consensus. *Gut* 2018; **67**: 1351-1362 [PMID: 29437910 DOI: 10.1136/gutjnl-2017-314722]

51 **Vela MF**, Camacho-Lobato L, Srinivasan R, Tutuian R, Katz PO, Castell DO. Simultaneous intraesophageal impedance and pH measurement of acid and nonacid gastroesophageal reflux: effect of omeprazole. *Gastroenterology* 2001; **120**: 1599-1606 [PMID: 11375942 DOI: 10.1053/gast.2001.24840]

52 **Sifrim D**, Dupont L, Blondeau K, Zhang X, Tack J, Janssens J. Weakly acidic reflux in patients with chronic unexplained cough during 24 hour pressure, pH, and impedance monitoring. *Gut* 2005; **54**: 449-454 [PMID: 15753524 DOI: 10.1136/gut.2004.055418]

53 **de Bortoli N**, Martinucci I, Savarino E, Franchi R, Bertani L, Russo S, Ceccarelli L, Costa F, Bellini M, Blandizzi C, Savarino V, Marchi S. Lower pH values of weakly acidic refluxes as determinants of heartburn perception in gastroesophageal reflux disease patients with normal esophageal acid exposure. *Dis Esophagus* 2016; **29**: 3-9 [PMID: 25212408 DOI: 10.1111/dote.12284]

54 **Viazis N**, Karamanolis G, Vienna E, Karamanolis DG. Selective-serotonin reuptake inhibitors for the treatment of hypersensitive esophagus. *Therap Adv Gastroenterol* 2011; **4**: 295-300 [PMID: 21922028 DOI: 10.1177/1756283X11409279]

55 **Mainie I**, Tutuian R, Shay S, Vela M, Zhang X, Sifrim D, Castell DO. Acid and non-acid reflux in patients with persistent symptoms despite acid suppressive therapy: a multicentre study using combined ambulatory impedance-pH monitoring. *Gut* 2006; **55**: 1398-1402 [PMID: 16556669 DOI: 10.1136/gut.2005.087668]

56 **del Genio G**, Tolone S, del Genio F, Aggarwal R, d'Alessandro A, Allaria A, Rossetti G, Brusciano L, del Genio A. Prospective assessment of patient selection for antireflux surgery by combined multichannel intraluminal impedance pH monitoring. *J Gastrointest Surg* 2008; **12**: 1491-1496 [PMID: 18612705 DOI: 10.1007/s11605-008-0583-y]

57 **Kahrilas PJ**, Bredenoord AJ, Fox M, Gyawali CP, Roman S, Smout AJ, Pandolfino JE; International High Resolution Manometry Working Group. The Chicago Classification of esophageal motility disorders, v3.0. *Neurogastroenterol Motil* 2015; **27**: 160-174 [PMID: 25469569 DOI: 10.1111/nmo.12477]

58 **Tack J**, Caenepeel P, Arts J, Lee KJ, Sifrim D, Janssens J. Prevalence of acid reflux in functional dyspepsia and its

association with symptom profile. *Gut* 2005; **54**: 1370-1376 [PMID: 15972301 DOI: 10.1136/gut.2004.053355]

59 **Lahner E**, Carabotti M, Annibale B. Treatment of Helicobacter pylori infection in atrophic gastritis. *World J Gastroenterol* 2018; **24**: 2373-2380 [PMID: 29904244 DOI: 10.3748/wjg.v24.i22.2373]

60 **Song H**, Zhu J, Lu D. Long-term proton pump inhibitor (PPI) use and the development of gastric pre-malignant lesions. *Cochrane Database Syst Rev* 2014; CD010623 [PMID: 25464111 DOI: 10.1002/14651858.CD010623.pub2]

61 **Cavalcoli F**, Zilli A, Conte D, Ciafardini C, Massironi S. Gastric neuroendocrine neoplasms and proton pump inhibitors: fact or coincidence? *Scand J Gastroenterol* 2015; **50**: 1397-1403 [PMID: 26059834 DOI: 10.3109/00365521.2015.1054426]

62 **Annibale B**, Lahner E, Santucci A, Vaira D, Pasquali A, Severi C, Mini R, Figura N, Delle Fave G. CagA and VacA are immunoblot markers of past Helicobacter pylori infection in atrophic body gastritis. *Helicobacter* 2007; **12**: 23-30 [PMID: 17241297 DOI: 10.1111/j.1523-5378.2007.00467.x]

63 **Collin A**, Mion F, Kefleyesus A, Beets C, Jaafari N, Boussageon R. Critical appraisal of international guidelines for the management of Helicobacter pylori infection in case of dyspepsia. *Helicobacter* 2023; **28**: e12952 [PMID: 36897573 DOI: 10.1111/hel.12952]

64 **Kato M**, Hayashi Y, Nishida T, Oshita M, Nakanishi F, Yamaguchi S, Kitamura S, Nishihara A, Akasaka T, Ogiyama H, Nakahara M, Yamada T, Kishida O, Yamamoto M, Shimayoshi A, Tsujii Y, Kato M, Shinzaki S, Iijima H, Takehara T. Helicobacter pylori eradication prevents secondary gastric cancer in patients with mild-to-moderate atrophic gastritis. *J Gastroenterol Hepatol* 2021; **36**: 2083-2090 [PMID: 33403702 DOI: 10.1111/jgh.15396]

65 **Kamada T**, Haruma K, Hata J, Kusunoki H, Sasaki A, Ito M, Tanaka S, Yoshihara M. The long-term effect of Helicobacter pylori eradication therapy on symptoms in dyspeptic patients with fundic atrophic gastritis. *Aliment Pharmacol Ther* 2003; **18**: 245-252 [PMID: 12869086 DOI: 10.1046/j.1365-2036.2003.01669.x]

66 **Yamada S**, Tomatsuri N, Kawakami T, Nakatsugawa Y, Nishimura T, Fujii H, Sato H, Okuyama Y, Kimura H, Yoshida N. Helicobacter pylori Eradication Therapy Ameliorates Latent Digestive Symptoms in Chronic Atrophic Gastritis. *Digestion* 2018; **97**: 333-339 [PMID: 29587295 DOI: 10.1159/000486618]

67 **Masuy I**, Van Oudenhove L, Tack J. Review article: treatment options for functional dyspepsia. *Aliment Pharmacol Ther* 2019; **49**: 1134-1172 [PMID: 30924176 DOI: 10.1111/apt.15191]

68 **Jokelainen K**, Siitonen A, Jousimies-Somer H, Nosova T, Heine R, Salaspuro M. In vitro alcohol dehydrogenase-mediated acetaldehyde production by aerobic bacteria representing the normal colonic flora in man. *Alcohol Clin Exp Res* 1996; **20**: 967-972 [PMID: 8892513 DOI: 10.1111/j.1530-0277.1996.tb01932.x]

69 **Linderborg K**, Marvola T, Marvola M, Salaspuro M, Färkkilä M, Väkeväinen S. Reducing carcinogenic acetaldehyde exposure in the achlorhydric stomach with cysteine. *Alcohol Clin Exp Res* 2011; **35**: 516-522 [PMID: 21143248 DOI: 10.1111/j.1530-0277.2010.01368.x]

70 **Maejima R**, Iijima K, Kaihovaara P, Hatta W, Koike T, Imatani A, Shimosegawa T, Salaspuro M. Effects of ALDH2 genotype, PPI treatment and L-cysteine on carcinogenic acetaldehyde in gastric juice and saliva after intragastric alcohol administration. *PLoS One* 2015; **10**: e0120397 [PMID: 25831092 DOI: 10.1371/journal.pone.0120397]

71 **Hellström PM**, Hendolin P, Kaihovaara P, Kronberg L, Meierjohann A, Millerhovf A, Paloheimo L, Sundelin H, Syrjänen K, Webb DL, Salaspuro M. Slow-release L-cysteine capsule prevents gastric mucosa exposure to carcinogenic acetaldehyde: results of a randomised single-blinded, cross-over study of Helicobacter-associated atrophic gastritis. *Scand J Gastroenterol* 2017; **52**: 230-237 [PMID: 27806647 DOI: 10.1080/00365521.2016.1249403]

72 **Crafa P**, Di Mario F, Grillo S, Landi S, Franceschi M, Rodriguez-Castro K, Tursi A, Brandimarte G, Franzoni L. Recovery of gastric function in patients affected by chronic atrophic gastritis using l-cysteine (Acetium®): one year survey in comparison with a control group. *Acta Biomed* 2022; **93**: e2022184 [PMID: 35775759 DOI: 10.23750/abm.v93i3.12812]

73 **Di Mario F**, Rodriguez-Castro KI, Franceschi M, Landi S, Grillo S, Franzoni L, Russo M, Brandimarte G, Tursi A, Crafa P. Improvement of Symptoms in Patients Affected by Chronic Atrophic Gastritis Using L-Cysteine (Acetium®). *Dig Dis* 2023; **41**: 198-205 [PMID: 36423587 DOI: 10.1159/000528168]

74 **Conti L**, Borro M, Milani C, Simmaco M, Esposito G, Canali G, Pilozzi E, Ventura M, Annibale B, Lahner E. Gastric microbiota composition in patients with corpus atrophic gastritis. *Dig Liver Dis* 2021; **53**: 1580-1587 [PMID: 34116969 DOI: 10.1016/j.dld.2021.05.005]

75 **Parsons BN**, Ijaz UZ, D'Amore R, Burkitt MD, Eccles R, Lenzi L, Duckworth CA, Moore AR, Tiszlavicz L, Varro A, Hall N, Pritchard DM. Comparison of the human gastric microbiota in hypochlorhydric states arising as a result of Helicobacter pylori-induced atrophic gastritis, autoimmune atrophic gastritis and proton pump inhibitor use. *PLoS Pathog* 2017; **13**: e1006653 [PMID: 29095917 DOI: 10.1371/journal.ppat.1006653]

76 **Rajilic-Stojanovic M**, Figueiredo C, Smet A, Hansen R, Kupcinskas J, Rokkas T, Andersen L, Machado JC, Ianiro G, Gasbarrini A, Leja M, Gisbert JP, Hold GL. Systematic review: gastric microbiota in health and disease. *Aliment Pharmacol Ther* 2020; **51**: 582-602 [PMID: 32056247 DOI: 10.1111/apt.15650]

77 **Lahner E**, Conti L, Annibale B, Corleto VD. Current Perspectives in Atrophic Gastritis. *Curr Gastroenterol Rep* 2020; **22**: 38 [PMID: 32542467 DOI: 10.1007/s11894-020-00775-1]

78 **Gregor L**, Wo J, DeWitt J, Yim B, Siwiec R, Nowak T, Mendez M, Gupta A, Dickason D, Stainko S, Al-Haddad M. Gastric peroral endoscopic myotomy for the treatment of refractory gastroparesis: a prospective single-center experience with mid-term follow-up (with video). *Gastrointest Endosc* 2021; **94**: 35-44 [PMID: 33373646 DOI: 10.1016/j.gie.2020.12.030]

79 **Soliman H**, Gourcerol G. Targeting the pylorus in gastroparesis: From physiology to endoscopic pyloromyotomy. *Neurogastroenterol Motil* 2023; **35**: e14529 [PMID: 36594414 DOI: 10.1111/nmo.14529]

80 **Ichkhanian Y**, Vosoughi K, Aghaie Meybodi M, Jacques J, Sethi A, Patel AA, Aadam AA, Triggs JR, Bapaye A, Dorwat S, Benias P, Chaves DM, Barret M, Law RJ, Browers N, Pioche M, Draganov PV, Kotzev A, Estremera F, Albeniz E, Ujiki MB, Callahan ZM, Itani MI, Brewer OG, Khashab MA. Comprehensive Analysis of Adverse Events Associated with Gastric Peroral Endoscopic Myotomy: An International Multicenter Study. *Surg Endosc* 2021; **35**: 1755-1764 [PMID: 32328824 DOI: 10.1007/s00464-020-07570-z]

81 **Mandarino FV**, Testoni SGG, Barchi A, Pepe G, Esposito D, Fanti L, Viale E, Biamonte P, Azzolini F, Danese S. Gastric emptying study before gastric peroral endoscopic myotomy (G-POEM): can intragastric meal distribution be a predictor of success? *Gut* 2023; **72**: 1019-1020 [PMID: 35697421 DOI: 10.1136/gutjnl-2022-327701]



Published by **Baishideng Publishing Group Inc**
7041 Koll Center Parkway, Suite 160, Pleasanton, CA 94566, USA
Telephone: +1-925-3991568
E-mail: bpgoffice@wjgnet.com
Help Desk: https://www.f6publishing.com/helpdesk
https://www.wjgnet.com



© 2023 Baishideng Publishing Group Inc. All rights reserved.

ISSN 1007-9327 (print)
ISSN 2219-2840 (online)

World Journal of *Gastroenterology*

World J Gastroenterol 2023 June 28; 29(24): 3748-3931



Published by Baishideng Publishing Group Inc

World Journal of Gastroenterology

Contents Weekly Volume 29 Number 24 June 28, 2023

MINIREVIEWS

3748 Vascular endothelial growth factor protein and gene delivery by novel nanomaterials for promoting liver regeneration after partial hepatectomy

Jin Y, Guo YH, Li JC, Li Q, Ye D, Zhang XX, Li JT

3758 Current status and future perspectives for the treatment of resectable locally advanced esophagogastric junction cancer: A narrative review

Shoji Y, Koyanagi K, Kanamori K, Tajima K, Ogimi M, Yatabe K, Yamamoto M, Kazuno A, Nabeshima K, Nakamura K, Nishi T, Mori M

ORIGINAL ARTICLE

Basic Study

3770 Mechanism of ELL-associated factor 2 and vasohibin 1 regulating invasion, migration, and angiogenesis in colorectal cancer

Feng ML, Sun MJ, Xu BY, Liu MY, Zhang HJ, Wu C

3793 Transcriptome sequencing and experiments reveal the effect of formyl peptide receptor 2 on liver homeostasis

Liu H, Sun ZY, Jiang H, Li XD, Jiang YQ, Liu P, Huang WH, Lv QY, Zhang XL, Li RK

Retrospective Cohort Study

3807 Prediction of lymph node metastasis in early gastric signet-ring cell carcinoma: A real-world retrospective cohort study

Yang JJ, Wang XY, Ma R, Chen MH, Zhang GX, Li X

3825 Regional variation in routes to diagnosis of cholangiocarcinoma in England from 2006 to 2017

Zalin-Miller A, Jose S, Knott C, Paley L, Tataru D, Morement H, Toledano MB, Khan SA

3843 Effect of lifestyle modification on hepatocellular carcinoma incidence and mortality among patients with chronic hepatitis B

Park Y, Kang D, Sinn DH, Kim H, Hong YS, Cho J, Gwak GY

Retrospective Study

3855 Comparison and development of machine learning for thalidomide-induced peripheral neuropathy prediction of refractory Crohn's disease in Chinese population

Mao J, Chao K, Jiang FL, Ye XP, Yang T, Li P, Zhu X, Hu PJ, Zhou BJ, Huang M, Gao X, Wang XD

Clinical Trials Study

3871 Stereotactic body radiotherapy combined with sintilimab in patients with recurrent or oligometastatic hepatocellular carcinoma: A phase II clinical trial

Chen YX, Yang P, Du SS, Zhuang Y, Huang C, Hu Y, Zhu WC, Yu YY, Liu TS, Zeng ZC

World Journal of Gastroenterology

Weekly Volume 29 Number 24 June 28, 2023

Contents

Observational Study

3883 Non-exposed endoscopic wall-inversion surgery with one-step nucleic acid amplification for early gastrointestinal tumors: Personal experience and literature review

Crafa F, Vanella S, Morante A, Catalano OA, Pomykala KL, Baiamonte M, Godas M, Antunes A, Costa Pereira J, Giaccaglia V

SCIENTOMETRICS

3899 Immunological factors in cirrhosis diseases from a bibliometric point of view

Zhang D, Liu BW, Liang XQ, Liu FQ

CASE REPORT

3922 Treatment of colonic varices and gastrointestinal bleeding by recanalization and stenting of splenic-vein-thrombosis: A case report and literature review

Füssel LM, Müller-Wille R, Dinkhauser P, Schauer W, Hofer H

ABOUT COVER

Editorial Board Member of *World Journal of Gastroenterology*, Mostafa Mohamed Sira, BM BCh, MD, MSc, PhD, Professor, Department of Pediatric Hepatology, Gastroenterology and Hepatology. National Liver Institute, Menoufia University, Shebin El-koom 32511, Menoufia, Egypt. msira@liver.menofia.edu.eg

AIMS AND SCOPE

The primary aim of *World Journal of Gastroenterology* (*WJG*, *World J Gastroenterol*) is to provide scholars and readers from various fields of gastroenterology and hepatology with a platform to publish high-quality basic and clinical research articles and communicate their research findings online. *WJG* mainly publishes articles reporting research results and findings obtained in the field of gastroenterology and hepatology and covering a wide range of topics including gastroenterology, hepatology, gastrointestinal endoscopy, gastrointestinal surgery, gastrointestinal oncology, and pediatric gastroenterology.

INDEXING/ABSTRACTING

The *WJG* is now abstracted and indexed in Science Citation Index Expanded (SCIE, also known as SciSearch®), Current Contents/Clinical Medicine, Journal Citation Reports, Index Medicus, MEDLINE, PubMed, PubMed Central, Scopus, Reference Citation Analysis, China National Knowledge Infrastructure, China Science and Technology Journal Database, and Superstar Journals Database. The 2022 edition of Journal Citation Reports® cites the 2021 impact factor (IF) for *WJG* as 5.374; IF without journal self cites: 5.187; 5-year IF: 5.715; Journal Citation Indicator: 0.84; Ranking: 31 among 93 journals in gastroenterology and hepatology; and Quartile category: Q2. The *WJG*'s CiteScore for 2021 is 8.1 and Scopus CiteScore rank 2021: Gastroenterology is 18/149.

RESPONSIBLE EDITORS FOR THIS ISSUE

Production Editor: *Yu-Xi Chen*; **Production Department Director:** *Xu Guo*; **Editorial Office Director:** *Jia-Ru Fan*.

NAME OF JOURNAL
World Journal of Gastroenterology

ISSN
ISSN 1007-9327 (print) ISSN 2219-2840 (online)

LAUNCH DATE
October 1, 1995

FREQUENCY
Weekly

EDITORS-IN-CHIEF
Andrzej S Tarnawski

EDITORIAL BOARD MEMBERS
http://www.wjgnet.com/1007-9327/editorialboard.htm

PUBLICATION DATE
June 28, 2023

COPYRIGHT
© 2023 Baishideng Publishing Group Inc

INSTRUCTIONS TO AUTHORS
https://www.wjgnet.com/bpg/gerinfo/204

GUIDELINES FOR ETHICS DOCUMENTS
https://www.wjgnet.com/bpg/GerInfo/287

GUIDELINES FOR NON-NATIVE SPEAKERS OF ENGLISH
https://www.wjgnet.com/bpg/gerinfo/240

PUBLICATION ETHICS
https://www.wjgnet.com/bpg/GerInfo/288

PUBLICATION MISCONDUCT
https://www.wjgnet.com/bpg/gerinfo/208

ARTICLE PROCESSING CHARGE
https://www.wjgnet.com/bpg/gerinfo/242

STEPS FOR SUBMITTING MANUSCRIPTS
https://www.wjgnet.com/bpg/GerInfo/239

ONLINE SUBMISSION
https://www.f6publishing.com

© 2023 Baishideng Publishing Group Inc. All rights reserved. 7041 Koll Center Parkway, Suite 160, Pleasanton, CA 94566, USA
E-mail: bpgoffice@wjgnet.com https://www.wjgnet.com

World Journal of Gastroenterology

Submit a Manuscript: https://www.f6publishing.com

World J Gastroenterol 2023 June 28; 29(24): 3748-3757

DOI: 10.3748/wjg.v29.i24.3748

ISSN 1007-9327 (print) ISSN 2219-2840 (online)

MINIREVIEWS

Vascular endothelial growth factor protein and gene delivery by novel nanomaterials for promoting liver regeneration after partial hepatectomy

Yun Jin, Ying-Hao Guo, Jia-Cheng Li, Qi Li, Dan Ye, Xiao-Xiao Zhang, Jiang-Tao Li

Specialty type: Gastroenterology and hepatology

Provenance and peer review: Invited article; Externally peer reviewed.

Peer-review model: Single blind

Peer-review report's scientific quality classification

Grade A (Excellent): 0
Grade B (Very good): B
Grade C (Good): C, C
Grade D (Fair): 0
Grade E (Poor): 0

P-Reviewer: Fereydouni N, Iran; Huan C, United States; Kordzaia D, Georgia

Received: April 3, 2023
Peer-review started: April 3, 2023
First decision: May 4, 2023
Revised: May 13, 2023
Accepted: June 2, 2023
Article in press: June 2, 2023
Published online: June 28, 2023

Yun Jin, Ying-Hao Guo, Qi Li, Dan Ye, Xiao-Xiao Zhang, Jiang-Tao Li, Department of Hepatopancreatobiliary Surgery, The Second Affiliated Hospital, College of Medicine, Zhejiang University, Hangzhou 310009, Zhejiang Province, China

Jia-Cheng Li, Department of General Surgery, Yuhuan Second People's Hospital, Taizhou 317600, Zhejiang Province, China

Corresponding author: Jiang-Tao Li, FACS, MD, Chief Doctor, Professor, Department of Hepatopancreatobiliary Surgery, The Second Affiliated Hospital, College of Medicine, Zhejiang University, No. 88 Jiefang Road, Hangzhou 310009, Zhejiang Province, China. zrljt@zju.edu.cn

Abstract

Partial hepatectomy (PH) can lead to severe complications, including liver failure, due to the low regenerative capacity of the remaining liver, especially after extensive hepatectomy. Liver sinusoidal endothelial cells (LSECs), whose proliferation occurs more slowly and later than hepatocytes after PH, compose the lining of the hepatic sinusoids, which are the smallest blood vessels in the liver. Vascular endothelial growth factor (VEGF), secreted by hepatocytes, promotes LSEC proliferation. Supplementation of exogenous VEGF after hepatectomy also increases the number of LSECs in the remaining liver, thus promoting the reestablishment of the hepatic sinusoids and accelerating liver regeneration. At present, some shortcomings exist in the methods of supplementing exogenous VEGF, such as a low drug concentration in the liver and the reaching of other organs. Moreover, VEGF should be administered multiple times and in large doses because of its short half-life. This review summarized the most recent findings on liver regeneration and new strategies for the localized delivery VEGF in the liver.

Key Words: Liver regeneration; Vascular endothelial growth factor; Nano materials; Liver resection

©The Author(s) 2023. Published by Baishideng Publishing Group Inc. All rights reserved.

Core Tip: Low regenerative ability of the liver remaining after partial hepatectomy may lead to serious complications including liver failure. The proliferation of liver sinusoidal endothelial cells (LSECs) is slower and occurs later compared to that of hepatocytes, leading to a delayed recovery of the hepatic sinusoids and impaired liver regeneration. Hepatocytes secrete vascular endothelial growth factor (VEGF) that promotes the proliferation of LSECs, and supplementation of exogenous VEGF after hepatectomy also increases the number of LSECs in the remaining liver, thus promoting the reestablishment of the hepatic sinusoids and accelerating liver regeneration. This review summarized the most recent findings on liver regeneration and new strategies for the localized delivery in the liver.

Citation: Jin Y, Guo YH, Li JC, Li Q, Ye D, Zhang XX, Li JT. Vascular endothelial growth factor protein and gene delivery by novel nanomaterials for promoting liver regeneration after partial hepatectomy. *World J Gastroenterol* 2023; 29(24): 3748-3757
URL: https://www.wjgnet.com/1007-9327/full/v29/i24/3748.htm
DOI: https://dx.doi.org/10.3748/wjg.v29.i24.3748

INTRODUCTION

Approximately 300 million people in China are suffering from liver diseases[1]. Liver cancer originates from hepatitis B in 80% of patients, and the incidence and mortality of liver cancer account for more than 50% of worldwide, making liver cancer the second leading cause of death in China[2]. Surgery remains the primary treatment option for liver cancer, but only 15% of patients can undergo this procedure[3]. Insufficient residual liver volume is the primary reason why about 30% of patients are ineligible for surgery[4], thus, becoming the main factor limiting the safe implementation of major liver resection. Therefore, there is an urgent need to improve the regenerative capacity of the liver and promote liver function after partial hepatectomy (PH).

SCHEMATIC DESCRIPTION OF LIVER REGENERATION AFTER PH

The proliferation time of each cell type in the liver after PH is different[5]. Hepatocytes begin to proliferate within a few hours after PH and reach a peak at 24 h. The proliferation of liver sinusoidal endothelial cells (LSECs) is slower and later compared to that of hepatocytes. Indeed, they start to proliferate at 36 h after PH and reach the peak at 96 h[6]. In the first 72 h after PH, the hepatic plate becomes wider, the proportion of LSECs decreased due to the rapid proliferation of hepatocytes, and the density of the liver sinusoid is temporarily reduced. This leads to hypoxia in some areas of the liver, inducing the secretion of vascular endothelial growth factor (VEGF) by the hepatocyte. VEGF is a vital regulator inducing the proliferation, mobilization, engraftment and differentiation of bone marrow progenitor cells of LSECs (BM SPCs), which is the main of renew LSECs[7]. BM SPCs have a high expression of hepatocyte growth factor (HGF) that promotes hepatocyte proliferation. The different proliferation time of the different cell types in the liver leads to their interaction to complete liver regeneration[7-9].

The regeneration of the liver after PH is a complex process that involves various types of cells and signaling pathways. Hepatocytes highly expressing VEGF are mainly located around the portal vein, and LSECs have the highest proliferation ability also around the portal vein after PH. Inhibition of VEGF significantly impairs the proliferation of hepatocytes and LSECs, while exogenous VEGF significantly promotes their proliferation, suggesting that VEGF promotes the proliferation of hepatocytes by acting on LSECs[10]. Moreover, LSECs regulate the expression of stromal cell-derived factor 1 (SDF-1) after PH, which leads to the recruitment and mobilization of chemokine receptor 7^+ ($CXCR7^+$) BM SPCs into the circulation. Furthermore, CXCR7+ BM SPCs are recruited to the liver and eventually differentiated into mature LSECs, being involved in the reconstruction of the hepatic sinusoids and the promotion of liver regeneration[11]. *In vitro* and *in vivo* studies demonstrated that the expression of CXCR7 receptor and downstream paracrine factor HGF in the microenvironment is regulated by a unique transcriptional regulator called inhibitor of DNA binding 1 (Id1)[12]. The regeneration and repair response in the liver when injured is regulated by the activation of the intrahepatic CXCR7-Id1-HGF/Wnt2 pathway[13]. Therefore, our hypothesis is that VEGF changes the guiding microenvironment through the SDF-1/CXCR7 pathway, activates Id-1 in LSECs, and up-regulates the expression of HGF and Wnt2 to reprogram the microenvironment during liver regeneration (Figure 1).

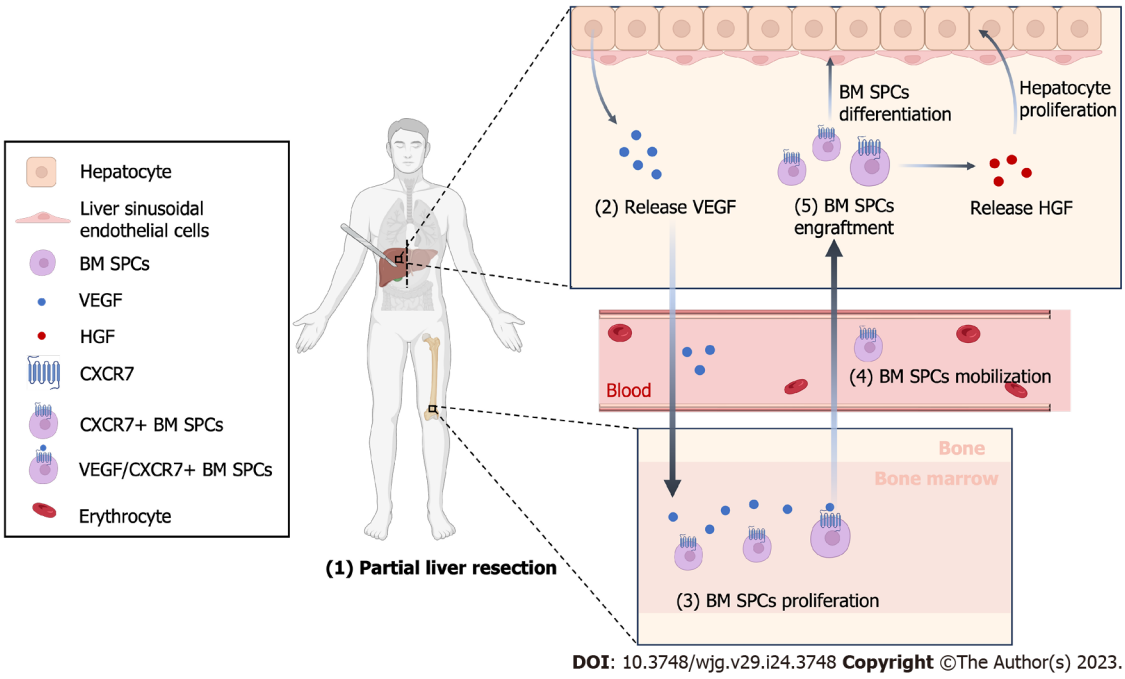


Figure 1 Schematic Illustration of liver after partial hepatectomy. After partial hepatectomy, hepatocytes begin to proliferate and release vascular endothelial growth factor, which promotes the proliferation of bone marrow-derived progenitor cells (BM SPCs) and reconstruction of hepatic sinusoids. BM SPCs secrete hepatocyte growth factor, which provides positive feedback and promotes hepatocytes proliferation. This figure was created with BioRender (BioRender.com). VEGF: Vascular endothelial growth factor; HGF: Hepatocyte growth factor; BM SPCs: Bone marrow-derived progenitor cells.

IMMUNITY AND LIVER REGENERATION

Liver regeneration is a complex process that involves multiple factors closely related to the immune response, which plays a critical role in tissue regeneration[14,15]. Following liver resection or injury, hypoxia occurs in certain liver areas, leading to hepatocyte apoptosis and release of apoptotic extracellular vesicles (aEVs). These aEVs are mainly cleared and phagocytosed by immune cells, while the main factor performing phagocytosis is still controversial. Some studies suggest that these aEVs are phagocytosed by Kupffer cells (KCs). KCs, the resident macrophages in the liver, are necessary for the emergence of liver progenitor-like cells (LPLCs), which are a source of newly regenerated hepatocytes under injury, as demonstrated by a mouse model of macrophage specific knockout[16]. KCs secrete inflammatory cytokines such as interleukin (IL)-6 and tumor necrosis factor (TNF)-α, which are crucial early signals to start regeneration[17]. While other studies demonstrated that hepatocytes are reborn from pre-existing hepatocytes[18], aEVs in the liver are mainly cleared and phagocytosed by circulating neutrophils rather than by phagocytes such as KCs[8,19]. Massive cell apoptosis after PH inhibits the phagocytic activity of immune cells resident in the liver[14]. At this time, circulating neutrophils are recruited and responsible for the phagocytosis and clearance of aEVs. Neutrophils phagocytose aEVs secreted by apoptotic hepatic cells and then, they released multiple growth factors including HGF and VEGF to regulate the proliferation of hepatic cells. Liver regeneration decreases under the specific condition of neutrophil exhaustion, and liver function recovery is also delayed[8]. Liver regeneration and immunity are closely related, and further studies should focus more on them, including the role of efferocytosis and metabolism.

RELATIONSHIP BETWEEN VEGF AND LIVER REGENERATION

VEGF belongs to a class of peptides with heparin-binding activity connected by a disulfide bond through a cysteine residue[20]. It is a potent mitogen for endothelial cells by directly acting on their specific surface receptors to exert its biological effects. The asynchronous proliferation of hepatocytes and LSECs delays the regeneration of new liver sinusoids, causing an insufficient liver regeneration in the early postoperative period (within 72 h)[21,22]. Therefore, this early period after PH is the most important period in which VEGF promotes liver regeneration. Endothelial cells under the action of VEGF migrate, proliferate and form tubular protrusions, eventually forming a network structure of arteries and veins, also increasing vascular permeability[23].

Exogenous VEGF promotes LSEC proliferation, but only in a dose-dependent manner, meaning that only above a certain dose of VEGF the proliferation of LSECs is promoted[24]. *In vitro* studies

demonstrated that the addition of VEGF to the culture medium of primary cultured LSECs promotes cell proliferation, while the group without VEGF showed a significantly less number of LSECs at 48 h than that at 16 h, and no significant difference was observed before and after the addition of 10 ng/mL VEGF. However, the number of LSECs at 48 h after the addition of 100 ng/mL VEGF is significantly higher than that at 16 h. Scanning electron microscopy showed that the window structure of LSECs gradually decreases with the increasing of time in the group without VEGF. LSECs in the liver are typically characterized by the presence of pores (fenestrae). These pores in the group with 10 ng/mL VEGF treatment are basically stable, and the number and size of this pores are significantly increased compared with those in the previous two groups. This indicated that VEGF promotes the proliferation of LSECs in a dose-dependent manner, with only a certain dose of VEGF promoting cell proliferation and exerting its function[24].

INTRAVENOUS INJECTION OF EXOGENOUS VEGF

Intravenous (IV) injection of exogenous VEGF is an proven method to induce the regeneration of the liver[25]. Indeed, it promotes the postoperative regeneration of the remaining liver after the detection of the PCNA index of hepatocytes in mice. The results showed that exogenous VEGF intervention significantly stimulates the proliferation of the remaining hepatocytes and promotes postoperative liver regeneration[26]. Another study also used tail vein injection of exogenous VEGF and *in vivo* microscopy to demonstrate that VEGF is involved in the regeneration after the removal of two-thirds of the liver [27]. The results showed that exogenous VEGF increases the hepatic vascular density, vascular diameter, and liver weight ratio as well as it enhances the proliferation of hepatocyte. Nevertheless, abnormal liver function and inhibition of hepatocyte proliferation are observed when endogenous VEGF is antagonized. However, the treatment with exogenous VEGF is not effective on liver regeneration when 90% of the liver is resected, as demonstrated by a rat resection model, suggesting that proliferation is also related to the degree of liver resection[28]. Although the administration of drugs through IV injection allows a certain degree of liver regeneration, the effective concentration of VEGF in the liver is insufficient due to its short half-life, uptake by other organs and tissues, and abundant hepatic blood flow[29]. Therefore, other efficient and safe liver-targeted drug delivery systems should be designed to overcome these shortcomings.

VEGF RELEASE BY NANOFIBERS

Electrospun nanofibers

The IV delivery of exogenous VEGF increases the content of VEGF only transiently, and long-term high concentrations in the liver cannot be achieved due to the abundant blood flow in the liver. Moreover, the short half-life of VEGF *in vivo* makes it difficult to achieve a constant effective concentration with a single injection, necessitating repeated injections that increase the complexity of treatment. Therefore, a controllable release nano-matrix membrane loaded with exogenous VEGF was designed and prepared to overcome the shortcomings, which was implanted into the residual liver wound after surgery to realize a targeted delivery of drugs by a local controlled release of VEGF.

The electrospinning technology is a universal and effective method for preparing nanoscale polymer fibers, and its principle is as follows: A polymer solution is connected with a high-voltage power supply through a wire, a receiving plate is grounded, and static electricity exists between the polymer solution and the receiving plate. The continuous increase of the voltage, the polymer solution gradually overcomes the surface tension and is ejected through a nozzle when the electrostatic action is greater than the cohesive force of the polymer flow, and the polymer is split into a fine polymer flow before reaching the collecting plate. The nanoscale polymer fibers in the form of a nonwoven fabric are thus obtained on the receiving sheet[30]. Nano-sized polymer fibers become a hot research topic in polymer material science in recent years due to their rapid preparation and their application in medical field is increasing and becoming mature.

Our research group previously developed a novel electrospun nanofiber loaded with VEGF, and thin layers of collagen were used as support to wrap the nanofiber between two layers of collagen to make a membrane-like structure. Collagen improves the stiffness of the fiber and confers a hemostatic function, which is beneficial to the fixation of the material at the implantation site. After the surgery, the fiber is directly covered on the liver wound surface, and the exogenous VEGF in the nanofiber in the local liver is continuously and efficiently controlled to form a microenvironment with effective VEGF concentration. This approach allows the proliferation of LSECs early after surgery, with an early promotion of liver regeneration[31]. The biodegradable biocompatible polymer and collagen used to make the nanofiber is approved by FDA of the United States and has a long-term traceable biological safety. The results showed that this new method of controlled release of VEGF through nanofibers significantly promotes the proliferation of the remaining hepatocytes at 48 and 72 h after surgery. The expression of

endogenous VEGF in the liver is also higher than that in the control group without nanofibers. The above results confirmed that biodegradable nanofibers represent a convenient and effective method for the release of VEGF specifically in the postoperative residual liver to effectively promote liver regeneration[31].

Hydrogel nanofiber technology

Electrospun nanofibers have some limitations in loading growth factors due to the high shear rate (10^5 to 10^6 s-1) of the polymer solution and the use of organic solvents. Moreover, the electrospinning of water-soluble polymers is difficult. These limitations make difficult the maintenance of an efficient activity of growth factors during the manufacturing process. Therefore, our research group prepared polymer composite hydrogel fibers by stretching the water-soluble polymer solution under the combined action of an electric field force and mechanical force[32]. The diameter and composition of the hydrogel fiber is realized by adjusting the components, concentration and stretching conditions of the polymer aqueous solution[33]. An important feature of this method is that the molecular chains in the fiber bundles are oriented using an electric field and a unidirectional mechanical tension. natural or synthetic polymer aqueous solutions were originally used to spin various hydrogel fibers, including alginate, collagen, fibrin, and hyaluronic acid. More importantly, this method without the use of organic solvents allows the formation of multilayered (core-shell) fibers that encapsulate growth factors in hydrogel fibers with a small impact on their bioactivity (Figure 2)[32]. In addition, the release rate of growth factors is controlled by adjusting the fiber composition and the degree of crosslinking, as well as the properties of the composite. The treatment with VEGF loaded with hydrogels accelerates the recovery of liver function after surgery in a rat model of 70% PH, and the peak value of alanine aminotransferase (ALT) and aspartate aminotransferase (AST) was 12 h earlier than that in the control group without hydrogels. Hepatocyte proliferation was also increased[34].

Retrograde intrabiliary infusion of VEGF nanoparticles

All parenchymal cells in the remaining liver after PH develop a proliferative potential, not just an exophytic growth from the wound site. Although the strategy of releasing VEGF from nanofiber results in the local release of growth factors onto the wound surface, the concentration of VEGF inside the liver decreases when the VEGF penetrate into the liver from the liver wound surface, so that the stimulation of VEGF on the cells in the liver is not uniform. Therefore, all cells in the residual liver should be stimulated by VEFG to effectively accelerate the regeneration of the residual liver and the recovery of liver function. Hence, it is necessary to design a new strategy to obtain a wide distribution of growth factors in the liver, allow their efficient uptake by intrahepatic cells, and realize high activity and low clearance rate in the liver.

The ultrastructural surface area of the hepatic biliary system is enormous, and the biliary system provides a surface in direct contact with almost all hepatocytes[35]. In addition, there are no KCs in the intrahepatic biliary system, thus, the non-specific phagocytosis of exogenous molecules by KCs is avoided and the immune inflammatory response of the body is reduced. The large volume of the intrahepatic bile duct makes the intrahepatic biliary system more distensible and able to tolerate the retrograde injection of a certain volume of fluid. Therefore, retrograde intrabiliary infusion (RII) has become a new way to perform a targeted delivery of drugs into the liver[36-38].

Administration of the VEGF gene has some advantages compared with the administration of the VEGF protein: Gene administration induces the transient expression of growth factor in hepatocytes, which is the ideal manner to realize an administration in the full residual liver. Although the conventional transgenic viral vectors effectively transfer the target gene into the parenchymal cells of liver, the side effects and immune responses induced by viruses limit their clinical application. Non-viral gene vectors have the advantages of diverse design, simple synthesis, storage stability, flexibility of the transgene length, low toxicity, and low immune response. In addition, the transfection of a non-viral gene vector is suitable for the transient expression of growth factors in liver regeneration.

At present, researchers have successfully prepared a variety of biodegradable nanoparticle systems for gene delivery[39-41]. Chitosan is a natural polysaccharide with good biodegradability, biocompatibility, anti-inflammatory effects, and its polycation structure confers many excellent properties in drug and gene delivery. Furthermore, the cationic structure of chitosan allows higher entrapment efficiency and loading of drugs, especially negatively charged genes. Finally, positively charged chitosan nanoparticles enhance the cellular uptake thanks to their slightly negatively charged cell membrane surface[42-44]. Ultra-pure, narrow molecular weight fully characterized chitosan is now available, and therefore, it is almost reaching the approval as a vector material than other gene vectors.

Previous studies demonstrated that chitosan-DNA nanoparticles (150-300 nm) achieve high transfection efficiency *in vivo* in rat hepatocytes after RII. The expression of transgenic proteins began at 12 h, peaks at 3 d after injection, and gradually declines after 14 d. Liver function analysis and histopathological examination show that the approach of using RII of nanoparticles does not produce significant toxic reactions and damage to the liver and bile ducts[45-47]. The expression of transgenic proteins in the kidney, lung, spleen and heart is almost negligible compared with their expression in the liver, which proves that this method results in a local high-efficiency and specific expression of the introduced gene in the liver. Therefore, RII is the best approach for gene delivery in the liver.

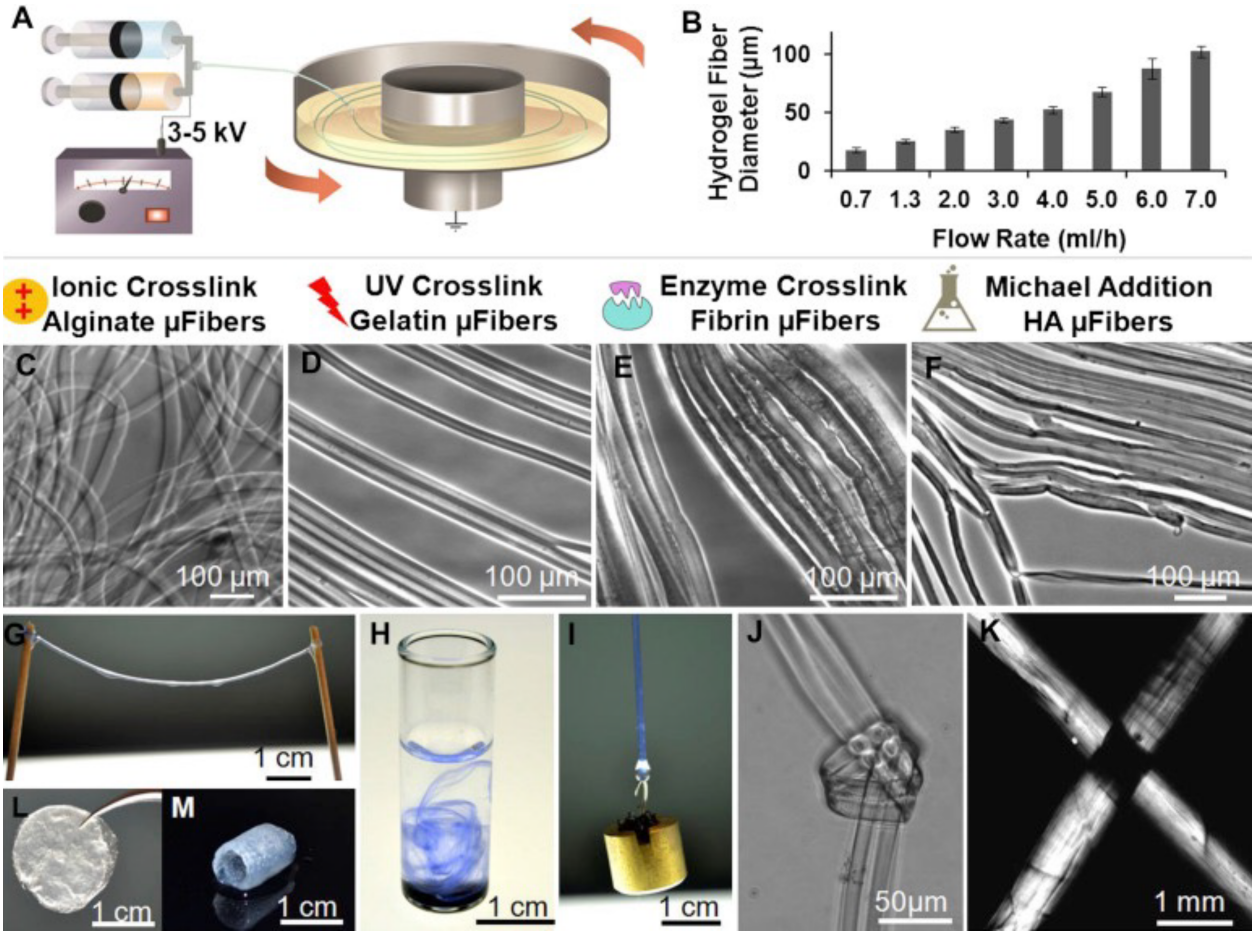


Figure 2 Preparation of hydrogel nanofiber. A: Illustration of the electrostretching setup; B: Effect of alginate solution feeding rate on the diameter of hydrogel microfibres; C-F: Various crosslinking mechanisms have been employed to crosslink alginate, gelatin, fibrin and hyaluronic acid hydrogel microfibers; G: Hydrogel microfibres of any desired length can be prepared; H: When dispersed in water, alginate hydrogel fibres formed a loose network of hydrogel fibres; I: A 10-g metal pillar was lifted with an alginate hydrogel microfibre bundle; J and K: A micro-knot was made with two alginate hydrogel microfibres; L and M: Beyond microfibre bundles, these hydrogel microfibres can also be fabricated into other forms like fibrous films (L) and self-supporting hydrogel tubes (M). Reproduced with permission [32]. Citation: Zhang S, Liu X, Barreto-Ortiz SF, Yu Y, Ginn BP, DeSantis NA, Hutton DL, Grayson WL, Cui FZ, Korgel BA, Gerecht S, Mao HQ. Creating polymer hydrogel microfibres with internal alignment *via* electrical and mechanical stretching. *Biomaterials* 2014; 35: 3243-3251. Copyright© The Authors 2013, Published by Elsevier Ltd.

Polycation-DNA nanoparticles are prepared by routine method, which consists of a mechanical mix polycations and plasmid DNA, but this assembly process is subjected to a variety of interference by kinetic factors during the preparation (about tens of milliseconds), easily leading to low homogeneity and unstable properties of nanoparticles. Therefore, our co-investigators developed a rapid nanocomposite method called flash nano-complexation to solve this technical problem, protecting plasmid DNA and working at very high flow rates inside a confined impact jet reactor. The polycationic solution reduces the mixing time of the two substances to approximately 10 milliseconds, avoiding significant folding denaturation of the plasmid DNA[48]. Uniform size, homogeneous properties and controllable oral plasmid DNA nanoparticles are prepared by this innovative method, and successfully used in the treatment of diabetes (Figure 3)[49]. Our group prepared VEGF-chitosan-DNA nanoparticles for RII in rats subjected to 70% hepatectomy and acute liver injury induced by acetaminophen. The preliminary results show that these nanoparticles promote the recovery of liver function and liver regeneration after PH.

LIMITATION AND FUTURE OUTLOOK

A precise spatio-temporal regulation of VEGF level is necessary for the proper functioning of the vascular system. VEGF plays a pivotal role in angiogenesis during embryonic development, tissue regeneration, and wound healing. However, VEGF is also a key mediator of angiogenesis in tumors. It can upregulate the expression of VEGF under various conditions, such as oncogene expression, multiple growth factors, and hypoxia, thereby promoting angiogenesis, which is essential for the development and growth of tumor[50]. In most solid tumors, VEGF is overexpressed. The abnormal expression of

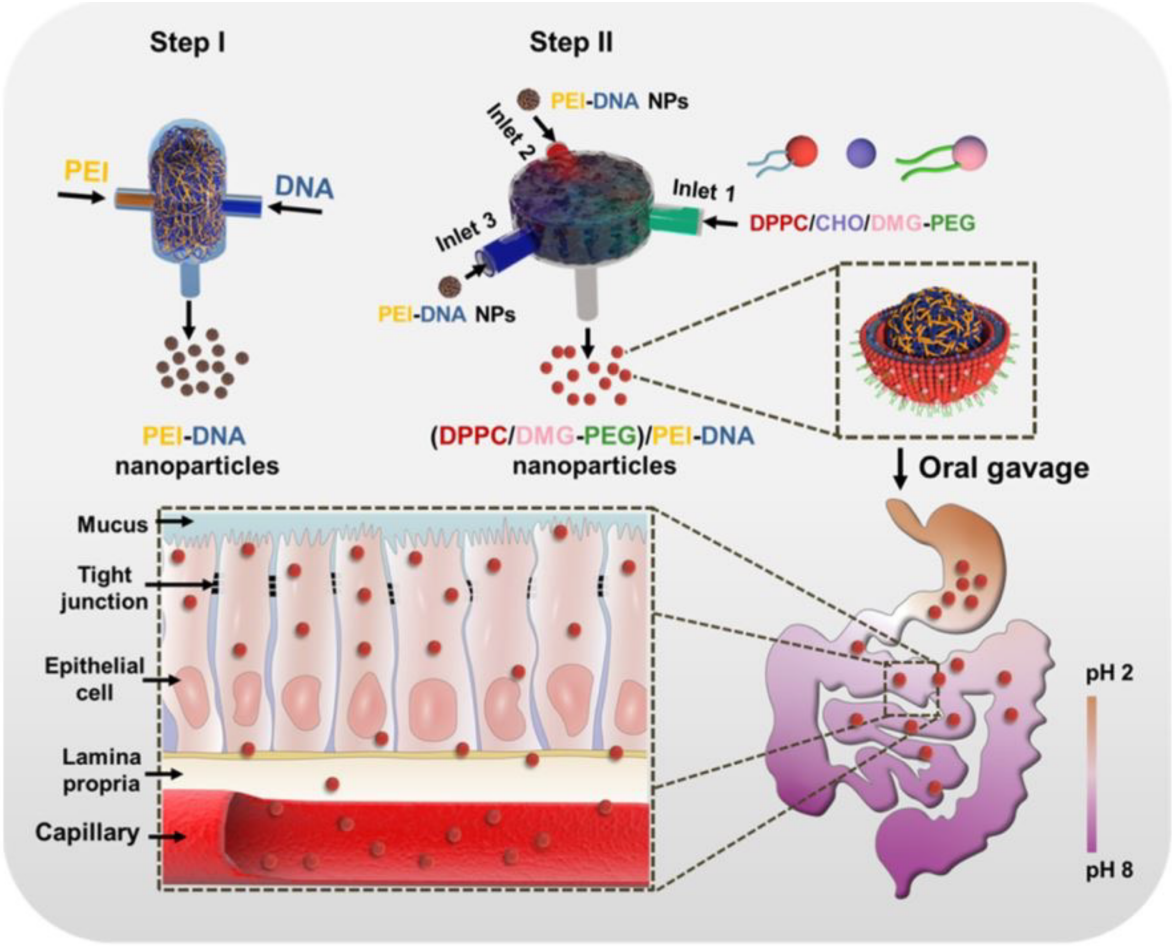


Figure 3 Illustration of PEI-DNA nanoparticle preparation *via* flash nanocomplexation and the proposed trafficking steps along the GI tract. Reproduced with permission[49]. Citation: Nie T, He Z, Zhou Y, Zhu J, Chen K, Liu L, Leong KW, Mao HQ, Chen Y. Surface Coating Approach to Overcome Mucosal Entrapment of DNA Nanoparticles for Oral Gene Delivery of Glucagon-like Peptide 1. *ACS Appl Mater Interfaces* 2019; 11: 29593-29603. Copyright© The Authors 2019. Published by American Chemical Society.

VEGF leads to the formation of a new vascular system in and around the tumor. These tumor vessels, formed under the action of VEGF, are structurally and functionally abnormal, thus promoting tumor growth. Given the central role of VEGF in tumor angiogenesis, it represents a rational target for anti-tumor therapy[51]. Therefore, by downregulating the VEGF signal in the tumor, the vascular system returns to a "normal" state. This "normalized" vascular system increases tumor oxygenation and improves drug permeability, leading to a better therapeutic response[52]. Therefore, in the future, we need to more accurately evaluate the VEGF of the recipient tissue and balance between promoting regeneration and inhibiting tumor.

CONCLUSION

VEGF is an important growth factor promoting angiogenesis and tissue regeneration, but it also promotes tumor growth depending on its expression. This contradiction reflects the complex role of VEGF in regulating cell growth and apoptosis[53]. Therefore, more studies are needed to better control VEGF expression to avoid the promotion of tumor growth and to promote tissue regeneration[54].

In the future, the administration of exogenous VEGF might become a potential treatment to promote liver regeneration after liver injury. However, the current intervention methods to administer exogenous VEGF are still limited, and the efficiency needs to be improved. Locally controlled-release VEGF by nanofibers and retrograde injection of VEGF-DNA-chitosan nanoparticles through bile ducts can promote residual liver regeneration, providing an alternative drug delivery mode in clinical practice.

ACKNOWLEDGEMENTS

The authors would like to thank Prof. Mao HQ (Johns Hopkins University), Dr. He ZY (Ocean University of China) and Dr. Nie TQ (Sun Yat-sen University) for the valuable supports.

FOOTNOTES

Author contributions: Jin Y and Guo YH wrote the paper; Jin Y and Li JT conceived and designed the study; Li JC, Li Q and Li JT reviewed and edited the manuscript; Ye D and Zhang XX created figures; all authors read and approved the manuscript; Jin Y and Guo YH contributed equally to this work.

Supported by the Natural Science Foundation of Zhejiang Province, No. LQ21H030005.

Conflict-of-interest statement: We declare that we have no conflict of interest to this work.

Open-Access: This article is an open-access article that was selected by an in-house editor and fully peer-reviewed by external reviewers. It is distributed in accordance with the Creative Commons Attribution NonCommercial (CC BY-NC 4.0) license, which permits others to distribute, remix, adapt, build upon this work non-commercially, and license their derivative works on different terms, provided the original work is properly cited and the use is non-commercial. See: https://creativecommons.org/Licenses/by-nc/4.0/

Country/Territory of origin: China

ORCID number: Yun Jin 0000-0002-3073-4043; Ying-Hao Guo 0000-0001-7544-4608; Jia-Cheng Li 0009-0007-1545-512X; Dan Ye 0000-0002-3035-4286; Xiao-Xiao Zhang 0000-0002-8566-2147; Jiang-Tao Li 0000-0001-7538-2910.

S-Editor: Yan JP
L-Editor: A
P-Editor: Yan JP

REFERENCES

1 **Wang FS**, Fan JG, Zhang Z, Gao B, Wang HY. The global burden of liver disease: the major impact of China. *Hepatology* 2014; **60**: 2099-2108 [PMID: 25164003 DOI: 10.1002/hep.27406]
2 **Baecker A**, Liu X, La Vecchia C, Zhang ZF. Worldwide incidence of hepatocellular carcinoma cases attributable to major risk factors. *Eur J Cancer Prev* 2018; **27**: 205-212 [PMID: 29489473 DOI: 10.1097/CEJ.0000000000000428]
3 **Marrero JA**, Ahn J, Rajender Reddy K; Americal College of Gastroenterology. ACG clinical guideline: the diagnosis and management of focal liver lesions. *Am J Gastroenterol* 2014; **109**: 1328-47; quiz 1348 [PMID: 25135008 DOI: 10.1038/ajg.2014.213]
4 **Chan A**, Kow A, Hibi T, Di Benedetto F, Serrablo A. Liver resection in Cirrhotic liver: Are there any limits? *Int J Surg* 2020; **82S**: 109-114 [PMID: 32652296 DOI: 10.1016/j.ijsu.2020.06.050]
5 **Michalopoulos GK**, DeFrances MC. Liver regeneration. *Science* 1997; **276**: 60-66 [PMID: 9082986 DOI: 10.1126/science.276.5309.60]
6 **Gadd VL**, Aleksieva N, Forbes SJ. Epithelial Plasticity during Liver Injury and Regeneration. *Cell Stem Cell* 2020; **27**: 557-573 [PMID: 32971004 DOI: 10.1016/j.stem.2020.08.016]
7 **DeLeve LD**. Liver sinusoidal endothelial cells and liver regeneration. *J Clin Invest* 2013; **123**: 1861-1866 [PMID: 23635783 DOI: 10.1172/JCI66025]
8 **Brandel V**, Schimek V, Göber S, Hammond T, Brunnthaler L, Schrottmaier WC, Mussbacher M, Sachet M, Liang YY, Reipert S, Ortmayr G, Pereyra D, Santol J, Rainer M, Walterskirchen N, Ramos C, Gerakopoulos V, Rainer C, Spittler A, Weiss T, Kain R, Messner B, Gruenberger T, Assinger A, Oehler R, Starlinger P. Hepatectomy-induced apoptotic extracellular vesicles stimulate neutrophils to secrete regenerative growth factors. *J Hepatol* 2022; **77**: 1619-1630 [PMID: 35985549 DOI: 10.1016/j.jhep.2022.07.027]
9 **Michalopoulos GK**, Bhushan B. Liver regeneration: biological and pathological mechanisms and implications. *Nat Rev Gastroenterol Hepatol* 2021; **18**: 40-55 [PMID: 32764740 DOI: 10.1038/s41575-020-0342-4]
10 **Taniguchi E**, Sakisaka S, Matsuo K, Tanikawa K, Sata M. Expression and role of vascular endothelial growth factor in liver regeneration after partial hepatectomy in rats. *J Histochem Cytochem* 2001; **49**: 121-130 [PMID: 11118484 DOI: 10.1177/002215540104900112]
11 **DeLeve LD**, Wang X, Wang L. VEGF-sdf1 recruitment of CXCR7+ bone marrow progenitors of liver sinusoidal endothelial cells promotes rat liver regeneration. *Am J Physiol Gastrointest Liver Physiol* 2016; **310**: G739-G746 [PMID: 26939868 DOI: 10.1152/ajpgi.00056.2016]
12 **Ding BS**, Cao Z, Lis R, Nolan DJ, Guo P, Simons M, Penfold ME, Shido K, Rabbany SY, Rafii S. Divergent angiocrine signals from vascular niche balance liver regeneration and fibrosis. *Nature* 2014; **505**: 97-102 [PMID: 24256728 DOI: 10.1038/nature12681]
13 **Shido K**, Chavez D, Cao Z, Ko J, Rafii S, Ding BS. Platelets prime hematopoietic and vascular niche to drive angiocrine-mediated liver regeneration. *Signal Transduct Target Ther* 2017; **2**: 16044-16044 [PMID: 29201496 DOI:

10.1038/sigtrans.2016.44]
14 **Di-Iacovo N**, Pieroni S, Piobbico D, Castelli M, Scopetti D, Ferracchiato S, Della-Fazia MA, Servillo G. Liver Regeneration and Immunity: A Tale to Tell. *Int J Mol Sci* 2023; **24** [PMID: 36674692 DOI: 10.3390/ijms24021176]
15 **Ben-Moshe S**, Veg T, Manco R, Dan S, Papinutti D, Lifshitz A, Kolodziejczyk AA, Bahar Halpern K, Elinav E, Itzkovitz S. The spatiotemporal program of zonal liver regeneration following acute injury. *Cell Stem Cell* 2022; **29**: 973-989.e10 [PMID: 35659879 DOI: 10.1016/j.stem.2022.04.008]
16 **Li L**, Cui L, Lin P, Liu Z, Bao S, Ma X, Nan H, Zhu W, Cen J, Mao Y, Jiang L, Nie Y, Ginhoux F, Li Y, Li H, Hui L. Kupffer-cell-derived IL-6 is repurposed for hepatocyte dedifferentiation *via* activating progenitor genes from injury-specific enhancers. *Cell Stem Cell* 2023; **30**: 283-299.e9 [PMID: 36787740 DOI: 10.1016/j.stem.2023.01.009]
17 **Peng WC**, Logan CY, Fish M, Anbarchian T, Aguisanda F, Álvarez-Varela A, Wu P, Jin Y, Zhu J, Li B, Grompe M, Wang B, Nusse R. Inflammatory Cytokine TNFα Promotes the Long-Term Expansion of Primary Hepatocytes in 3D Culture. *Cell* 2018; **175**: 1607-1619.e15 [PMID: 30500539 DOI: 10.1016/j.cell.2018.11.012]
18 **Pu W**, Zhu H, Zhang M, Pikiolek M, Ercan C, Li J, Huang X, Han X, Zhang Z, Lv Z, Li Y, Liu K, He L, Liu X, Heim MH, Terracciano LM, Tchorz JS, Zhou B. Bipotent transitional liver progenitor cells contribute to liver regeneration. *Nat Genet* 2023; **55**: 651-664 [PMID: 36914834 DOI: 10.1038/s41588-023-01335-9]
19 **Selzner N**, Selzner M, Odermatt B, Tian Y, Van Rooijen N, Clavien PA. ICAM-1 triggers liver regeneration through leukocyte recruitment and Kupffer cell-dependent release of TNF-alpha/IL-6 in mice. *Gastroenterology* 2003; **124**: 692-700 [PMID: 12612908 DOI: 10.1053/gast.2003.50098]
20 **Apte RS**, Chen DS, Ferrara N. VEGF in Signaling and Disease: Beyond Discovery and Development. *Cell* 2019; **176**: 1248-1264 [PMID: 30849371 DOI: 10.1016/j.cell.2019.01.021]
21 **Hu J**, Srivastava K, Wieland M, Runge A, Mogler C, Besemfelder E, Terhardt D, Vogel MJ, Cao L, Korn C, Bartels S, Thomas M, Augustin HG. Endothelial cell-derived angiopoietin-2 controls liver regeneration as a spatiotemporal rheostat. *Science* 2014; **343**: 416-419 [PMID: 24458641 DOI: 10.1126/science.1244880]
22 **Ding BS**, Nolan DJ, Butler JM, James D, Babazadeh AO, Rosenwaks Z, Mittal V, Kobayashi H, Shido K, Lyden D, Sato TN, Rabbany SY, Rafii S. Inductive angiocrine signals from sinusoidal endothelium are required for liver regeneration. *Nature* 2010; **468**: 310-315 [PMID: 21068842 DOI: 10.1038/nature09493]
23 **Dvorak HF**, Brown LF, Detmar M, Dvorak AM. Vascular permeability factor/vascular endothelial growth factor, microvascular hyperpermeability, and angiogenesis. *Am J Pathol* 1995; **146**: 1029-1039 [PMID: 7538264]
24 **Funyu J**, Mochida S, Inao M, Matsui A, Fujiwara K. VEGF can act as vascular permeability factor in the hepatic sinusoids through upregulation of porosity of endothelial cells. *Biochem Biophys Res Commun* 2001; **280**: 481-485 [PMID: 11162543 DOI: 10.1006/bbrc.2000.4148]
25 **Rizvi F**, Everton E, Smith AR, Liu H, Osota E, Beattie M, Tam Y, Pardi N, Weissman D, Gouon-Evans V. Murine liver repair *via* transient activation of regenerative pathways in hepatocytes using lipid nanoparticle-complexed nucleoside-modified mRNA. *Nat Commun* 2021; **12**: 613 [PMID: 33504774 DOI: 10.1038/s41467-021-20903-3]
26 **Assy N**, Spira G, Paizi M, Shenkar L, Kraizer Y, Cohen T, Neufeld G, Dabbah B, Enat R, Baruch Y. Effect of vascular endothelial growth factor on hepatic regenerative activity following partial hepatectomy in rats. *J Hepatol* 1999; **30**: 911-915 [PMID: 10365820 DOI: 10.1016/s0168-8278(99)80147-0]
27 **Bockhorn M**, Goralski M, Prokofiev D, Dammann P, Grünewald P, Trippler M, Biglarnia A, Kamler M, Niehues EM, Frilling A, Broelsch CE, Schlaak JF. VEGF is important for early liver regeneration after partial hepatectomy. *J Surg Res* 2007; **138**: 291-299 [PMID: 17275844 DOI: 10.1016/j.jss.2006.07.027]
28 **Bockhorn M**, Schöllmann S, Opitz B, Sotiropoulos GC, Sheu SY, Niehaus E, Trippler M, Frilling A, Broelsch CE, Schlaak JF. Vascular endothelial growth factor does not improve liver regeneration and survival after 90% subtotal liver resection. *Hepatol Res* 2007; **37**: 353-359 [PMID: 17441808 DOI: 10.1111/j.1872-034X.2007.00047.x]
29 **Wei S**, Li Z, Shi Q, Luan X, Yuan X, Li Y, Guo C, Wu X, Shi C, Di G. Collagenbinding vascular endothelial growth factor (CBDVEGF) promotes liver regeneration in murine partial hepatectomy. *Mol Med Rep* 2022; **26** [PMID: 36069236 DOI: 10.3892/mmr.2022.12842]
30 **Jin L**, Wang T, Zhu ML, Leach MK, Naim YI, Corey JM, Feng ZQ, Jiang Q. Electrospun fibers and tissue engineering. *J Biomed Nanotechnol* 2012; **8**: 1-9 [PMID: 22515089 DOI: 10.1166/jbn.2012.1360]
31 **Yu YQ**, Jiang XS, Gao S, Ma R, Jin Y, Jin X, Peng SY, Mao HQ, Li JT. Local delivery of vascular endothelial growth factor *via* nanofiber matrix improves liver regeneration after extensive hepatectomy in rats. *J Biomed Nanotechnol* 2014; **10**: 3407-3415 [PMID: 26000399 DOI: 10.1166/jbn.2014.1872]
32 **Zhang S**, Liu X, Barreto-Ortiz SF, Yu Y, Ginn BP, DeSantis NA, Hutton DL, Grayson WL, Cui FZ, Korgel BA, Gerecht S, Mao HQ. Creating polymer hydrogel microfibres with internal alignment *via* electrical and mechanical stretching. *Biomaterials* 2014; **35**: 3243-3251 [PMID: 24439410 DOI: 10.1016/j.biomaterials.2013.12.081]
33 **Li Z**, Zhao Y, Ouyang X, Yang Y, Chen Y, Luo Q, Zhang Y, Zhu D, Yu X, Li L. Biomimetic hybrid hydrogel for hemostasis, adhesion prevention and promoting regeneration after partial liver resection. *Bioact Mater* 2022; **11**: 41-51 [PMID: 34938911 DOI: 10.1016/j.bioactmat.2021.10.001]
34 **Jin Y**, Zhang XX, Yang JJ, Qian CM, Zhou JL, Yu YQ, Zhou DE, Wang L, Peng SY, Mao HQ. A novel strategy for locally deliver VEGF by nanofiber mesh for improving liver regeneration. *HPB* 2016; **18**: e290-e291 [DOI: 10.1016/j.hpb.2016.02.743]
35 **Trefts E**, Gannon M, Wasserman DH. The liver. *Curr Biol* 2017; **27**: R1147-R1151 [PMID: 29112863 DOI: 10.1016/j.cub.2017.09.019]
36 **Dai H**, Jiang X, Leong KW, Mao HQ. Transient depletion of kupffer cells leads to enhanced transgene expression in rat liver following retrograde intrabiliary infusion of plasmid DNA and DNA nanoparticles. *Hum Gene Ther* 2011; **22**: 873-878 [PMID: 21091274 DOI: 10.1089/hum.2010.146]
37 **Narmada BC**, Kang Y, Venkatraman L, Peng Q, Sakban RB, Nugraha B, Jiang X, Bunte RM, So PT, Tucker-Kellogg L, Mao HQ, Yu H. Hepatic stellate cell-targeted delivery of hepatocyte growth factor transgene *via* bile duct infusion enhances its expression at fibrotic foci to regress dimethylnitrosamine-induced liver fibrosis. *Hum Gene Ther* 2013; **24**: 508-519 [PMID: 23527815 DOI: 10.1089/hum.2012.158]

38 **Dai C**, Wang M, Zhao L, Xu C, Huang J, Fan Z. Liver gene transfection by retrograde intrabiliary infusion facilitated by temporary biliary obstruction. *J Gene Med* 2020; **22**: e3144 [PMID: 31742830 DOI: 10.1002/jgm.3144]

39 **Mao HQ**, Roy K, Troung-Le VL, Janes KA, Lin KY, Wang Y, August JT, Leong KW. Chitosan-DNA nanoparticles as gene carriers: synthesis, characterization and transfection efficiency. *J Control Release* 2001; **70**: 399-421 [PMID: 11182210 DOI: 10.1016/s0168-3659(00)00361-8]

40 **Roy K**, Mao HQ, Huang SK, Leong KW. Oral gene delivery with chitosan--DNA nanoparticles generates immunologic protection in a murine model of peanut allergy. *Nat Med* 1999; **5**: 387-391 [PMID: 10202926 DOI: 10.1038/7385]

41 **Mao HQ**, Leong KW. Design of polyphosphoester-DNA nanoparticles for non-viral gene delivery. *Adv Genet* 2005; **53**: 275-306 [PMID: 16240998]

42 **Cao Y**, Tan YF, Wong YS, Liew MWJ, Venkatraman S. Recent Advances in Chitosan-Based Carriers for Gene Delivery. *Mar Drugs* 2019; **17** [PMID: 31242678 DOI: 10.3390/md17060381]

43 **Zhang E**, Xing R, Liu S, Qin Y, Li K, Li P. Advances in chitosan-based nanoparticles for oncotherapy. *Carbohydr Polym* 2019; **222**: 115004 [PMID: 31320066 DOI: 10.1016/j.carbpol.2019.115004]

44 **Ashrafizadeh M**, Ahmadi Z, Mohamadi N, Zarrabi A, Abasi S, Dehghannoudeh G, Tamaddondoust RN, Khanbabaei H, Mohammadinejad R, Thakur VK. Chitosan-based advanced materials for docetaxel and paclitaxel delivery: Recent advances and future directions in cancer theranostics. *Int J Biol Macromol* 2020; **145**: 282-300 [PMID: 31870872 DOI: 10.1016/j.ijbiomac.2019.12.145]

45 **Dai H**, Jiang X, Tan GC, Chen Y, Torbenson M, Leong KW, Mao HQ. Chitosan-DNA nanoparticles delivered by intrabiliary infusion enhance liver-targeted gene delivery. *Int J Nanomedicine* 2006; **1**: 507-522 [PMID: 17369870 DOI: 10.2147/nano.2006.1.4.507]

46 **Jiang X**, Ren Y, Williford JM, Li Z, Mao HQ. Liver-targeted gene delivery through retrograde intrabiliary infusion. *Methods Mol Biol* 2013; **948**: 275-284 [PMID: 23070777 DOI: 10.1007/978-1-62703-140-0_19]

47 **Jiang X**, Dai H, Leong KW, Goh SH, Mao HQ, Yang YY. Chitosan-g-PEG/DNA complexes deliver gene to the rat liver *via* intrabiliary and intraportal infusions. *J Gene Med* 2006; **8**: 477-487 [PMID: 16389625 DOI: 10.1002/jgm.868]

48 **Liu HW**, Hu Y, Ren Y, Nam H, Santos JL, Ng S, Gong L, Brummet M, Carrington CA, Ullman CG, Pomper MG, Minn I, Mao HQ. Scalable Purification of Plasmid DNA Nanoparticles by Tangential Flow Filtration for Systemic Delivery. *ACS Appl Mater Interfaces* 2021; **13**: 30326-30336 [PMID: 34162211 DOI: 10.1021/acsami.1c05750]

49 **Nie T**, He Z, Zhou Y, Zhu J, Chen K, Liu L, Leong KW, Mao HQ, Chen Y. Surface Coating Approach to Overcome Mucosal Entrapment of DNA Nanoparticles for Oral Gene Delivery of Glucagon-like Peptide 1. *ACS Appl Mater Interfaces* 2019; **11**: 29593-29603 [PMID: 31348859 DOI: 10.1021/acsami.9b10294]

50 **Ferrara N**, Gerber HP, LeCouter J. The biology of VEGF and its receptors. *Nat Med* 2003; **9**: 669-676 [PMID: 12778165 DOI: 10.1038/nm0603-669]

51 **Yang Y**, Cao Y. The impact of VEGF on cancer metastasis and systemic disease. *Semin Cancer Biol* 2022; **86**: 251-261 [PMID: 35307547 DOI: 10.1016/j.semcancer.2022.03.011]

52 **Jain RK**. Normalization of tumor vasculature: an emerging concept in antiangiogenic therapy. *Science* 2005; **307**: 58-62 [PMID: 15637262 DOI: 10.1126/science.1104819]

53 **Eelen G**, Treps L, Li X, Carmeliet P. Basic and Therapeutic Aspects of Angiogenesis Updated. *Circ Res* 2020; **127**: 310-329 [PMID: 32833569 DOI: 10.1161/CIRCRESAHA.120.316851]

54 **Ahmad A**, Nawaz MI. Molecular mechanism of VEGF and its role in pathological angiogenesis. *J Cell Biochem* 2022; **123**: 1938-1965 [PMID: 36288574 DOI: 10.1002/jcb.30344]

World Journal of Gastroenterology

Submit a Manuscript: https://www.f6publishing.com

World J Gastroenterol 2023 June 28; 29(24): 3758-3769

DOI: 10.3748/wjg.v29.i24.3758

ISSN 1007-9327 (print) ISSN 2219-2840 (online)

MINIREVIEWS

Current status and future perspectives for the treatment of resectable locally advanced esophagogastric junction cancer: A narrative review

Yoshiaki Shoji, Kazuo Koyanagi, Kohei Kanamori, Kohei Tajima, Mika Ogimi, Kentaro Yatabe, Miho Yamamoto, Akihito Kazuno, Kazuhito Nabeshima, Kenji Nakamura, Takayuki Nishi, Masaki Mori

Specialty type: Gastroenterology and hepatology

Provenance and peer review: Invited article; Externally peer reviewed.

Peer-review model: Single blind

Peer-review report's scientific quality classification

Grade A (Excellent): 0
Grade B (Very good): B
Grade C (Good): C, C
Grade D (Fair): 0
Grade E (Poor): 0

P-Reviewer: Edholm D, Sweden; Li J, China; Molinari C, Italy

Received: March 28, 2023
Peer-review started: March 28, 2023
First decision: May 12, 2023
Revised: May 21, 2023
Accepted: June 2, 2023
Article in press: June 2, 2023
Published online: June 28, 2023

Yoshiaki Shoji, Kazuo Koyanagi, Kohei Kanamori, Kohei Tajima, Mika Ogimi, Kentaro Yatabe, Miho Yamamoto, Akihito Kazuno, Kazuhito Nabeshima, Kenji Nakamura, Takayuki Nishi, Masaki Mori, Department of Gastroenterological Surgery, Tokai University School of Medicine, Isehara 259-1193, Japan

Corresponding author: Kazuo Koyanagi, FACS, MD, PhD, Chairman, Professor, Department of Gastroenterological Surgery, Tokai University School of Medicine, 143, Shimokasuya, Isehara 259-1193, Japan. kkoyanagi@tsc.u-tokai.ac.jp

Abstract

Incidence rates for esophagogastric junction cancer are rising rapidly worldwide possibly due to the economic development and demographic changes. Therefore, increased attention has been paid to the prevention, diagnosis, and the treatment of esophagogastric junction cancer. Although there are discrepancies in the treatment strategy between Asian and Western countries, surgery remains the mainstay of treatment for esophagogastric junction cancer. Recent developments of perioperative multidisciplinary treatment may lead to better therapeutic effect, higher complete resection rate, and better control of the residual diseases, thus result in prolonged prognosis. In this review, we will focus on the treatment of locally advanced resectable esophagogastric junction cancer, and discuss the current status and future perspectives of the perioperative treatment including chemotherapy, radiation therapy, and immunotherapy, as well as the surgical strategy. Better understanding of the latest treatment strategy and future overlook may enable to standardize and individualize the treatment for esophagogastric junction cancer, thus leading to better prognosis for those patients.

Key Words: Esophagogastric junction cancer; Perioperative therapy; Neoadjuvant therapy; Surgery; Multidisciplinary treatment

©The Author(s) 2023. Published by Baishideng Publishing Group Inc. All rights reserved.

Core Tip: In recent years, increased attention has been paid to the prevention, diagnosis, and the treatment of esophagogastric junction cancer. Recent developments of perioperative multidisciplinary treatment led to increased patient outcomes. In this review, we will focus on the current status and future perspectives of the perioperative treatment including chemotherapy, radiation therapy, targeted therapy, and immunotherapy, as well as the surgical strategy for locally advanced esophagogastric adenocarcinoma. Better understanding of the latest treatment strategy and future overlook may lead to better prognosis for the patients.

Citation: Shoji Y, Koyanagi K, Kanamori K, Tajima K, Ogimi M, Yatabe K, Yamamoto M, Kazuno A, Nabeshima K, Nakamura K, Nishi T, Mori M. Current status and future perspectives for the treatment of resectable locally advanced esophagogastric junction cancer: A narrative review. *World J Gastroenterol* 2023; 29(24): 3758-3769
URL: https://www.wjgnet.com/1007-9327/full/v29/i24/3758.htm
DOI: https://dx.doi.org/10.3748/wjg.v29.i24.3758

INTRODUCTION

Incidence rates for esophagogastric junction (EGJ) cancer, especially EGJ adenocarcinoma (EGJAC) are rising rapidly worldwide possibly due to increased excess body weight, increasing gastroesophageal reflux disease, and decreasing levels of chronic infection with *Helicobacter pylori*[1,2]. These trends are predicted to continue, thus leading to increased incidence of EGJAC[1]. Treatment strategy for resectable locally advanced EGJAC differ from country to country, where perioperative therapy combined with surgery has been the standard of care for locally advanced EGJAC in the western countries[3,4], whereas surgery with or without adjuvant chemotherapy has been widely accepted in Japan since the significance of preoperative therapy has not yet been established[5]. Nevertheless, surgery remain the mainstay of treatment for locally advanced EGJAC, and therefore, there is an emerging need for the development of surgical approach, as well as other treatment modalities including chemotherapy, radiation therapy, and immunotherapy in order to improve patient outcomes.

Due to its unique anatomical location, optimal surgical strategy for EGJAC have long been questioned, and different opinions have been proposed between gastrointestinal and thoracic surgeons. Siewert type I tumors, which the tumor epicenter is located between 1cm to 5 cm above the EGJ, have usually been treated as esophageal cancer, whereas Siewert type III tumors, which is located between 2 cm to 5 cm below the EGJ, have generally been treated as gastric cardia cancer. Surgical procedure for Siewert type II tumors (1 cm above to 2 cm below EGJ) have been selected by individual surgeons or institutional preferences. Recent retrospective and prospective studies have unveiled the lymphatic flow for EGJ cancers[6,7], and thereby a standardized surgical strategy have been proposed. Another critical surgical issue during EGJ cancer treatment is the reconstruction method, which have long been related to high anastomotic complication rates[8]. Recent inventions and improvement of anastomotic methods [9-11] have enabled a safe esophagogastric anastomosis with less incidence of anastomotic leakage and gastroesophageal reflux.

Researchers have focused on the development of more intensive perioperative therapy to overcome the poor prognosis of advanced EGJ cancers. Preoperative chemotherapy or chemoradiotherapy have been utilized in the western countries[3,4], however, question remains whether which is the best treatment option. In recent years, immunotherapy has received particular attention in the treatment of EGJ cancers. Adjuvant checkpoint inhibitor immunotherapy is now the standard of care for EGJ cancer patients who received neoadjuvant chemoradiotherapy and had residual pathological disease after curative resection[12]. Recent studies have unveiled the efficacy of immunochemotherapy in neoadjuvant settings[13,14].

In this review, we will focus on locally advanced resectable EGJAC, and discuss the current clinical practice, ongoing clinical trials, and future perspectives of multidisciplinary treatment options for EGJAC.

STANDARDIZING THE SURGICAL PROCEDURE FOR EGJAC

Mediastinal lymph node dissection

The initial study to demonstrate the frequency of lymph node (LN) metastasis for EGJAC was reported by Rüdiger Siewert *et al*[15] in 2000. In this retrospective single-center study, 1002 patients with EGJAC underwent either transthoracic esophagectomy or transhiatal extended gastrectomy depending on the tumor location. Among the 271 patients with carcinoma of the cardia arising immediately at the esophagogastric junction (defined as Type II in the literature), 29 (15.6%) patients had lower mediastinal

lymph node metastasis. In another single center study by Pedrazzani *et al*[16], nodal involvement of 143 patients with locally advanced EGJAC were analyzed. In this study, middle/Lower mediastinal LN dissection was performed in 70%-85% of the patients with Siewert type I tumor, whereas the dissection rate was only 3.3%-35.5% for the patients with Siewert type III tumor. Middle and/or lower mediastinal LN metastasis was observed in 46.2%, 29.5%, and 9.3% for Siewert type I, II, and III tumors, respectively.

In 2017, Yamashita *et al*[6] conducted a questionnaire-based national retrospective study in Japan to define the optimal extent of LN dissection for EGJ cancers[6]. In this study, EGJ cancer was defined as having its tumor epicenter within 2 cm above or below EGJ according to the definition promulgated by the Japanese Gastric Cancer Association[17] and the Japanese Esophageal Society[18], and patients with tumors ≤ 4 cm were considered eligible. In total, 1560 patients with Siewert Type I/II EGJAC were enrolled. The estimated survival benefit by LN dissection was high for the abdominal LN along the lesser curvature, right and left cardia, and the left gastric artery, however, optimal extent of the mediastinal LN dissection could not be determined due to the low rate of upper/middle mediastinal LN dissection, which was below 20%. To further determine the value of mediastinal LN dissection in EGJ cancers, Kurokawa *et al*[7] reported the results of a prospective multicenter study in 2021[7], in which cT2-T4 cancers located within 2 cm of the EGJ were enrolled. Upper mediastinal LN dissection was performed for patients with esophageal invasion > 3 cm, whereas patients with esophageal invasion ≤ 3 cm underwent lower mediastinal LN dissection only. Within the 98 patients who had esophageal invasion > 3 cm (67 EGJAC and 31 esophageal squamous cell carcinomas, ESCC), rate of right recurrent laryngeal nerve LN metastasis was 10.7% (3/28) when the length of esophageal invasion exceeded 4 cm. As a result, surgical algorithm for EGJ cancers was proposed, and upper mediastinal LN dissection was recommended for advanced EGJ cancer patients with esophageal invasion > 4 cm and clinically positive LN in the upper/middle mediastinal field[19].

One of the unique features of these Japanese studies is that squamous cell carcinomas located within 2 cm of the EGJ are included, and are analyzed along with EGJAC. In Japan, regardless of histological type, tumors within 2 cm of the EGJ are classified as "EGJ cancers" according to the Nishi classification [17], possibly due to the high incidence of ESCC, whereas only adenocarcinomas have been regarded as EGJ cancers in the western countries. The difference in the definition of EGJ cancer have caused the difference in the treatment, including surgery and chemo (radio)therapy for tumors of the EGJ between countries. In the former study[7], rate of upper-mediastinal LN metastasis was similar between adenocarcinomas and squamous cell carcinomas for tumors within 2 cm of the EGJ, suggesting that similar surgical strategy may be applied regardless of histological type. Although further studies are needed to determine the optimal extent of LN dissection for tumors with greater esophageal invasion.

Some issues remain unsolved. First, is the difficulty to accurately measure the distance from the EGJ to the tumor proximal margin in patients with large tumors, circumferential tumors, and hiatal hernia. Therefore, extent of mediastinal LN dissection may not be determined preoperatively for such patients. Second, as mentioned above, EGJ tumors with long esophageal invasion, usually classified as Siewert type I, were excluded in recent studies. In our institute, 35 patients with Siewert type I EGJAC underwent curative resection including upper-mediastinal LN dissection between 2007 to 2022 (Tables 1 and 2). The rate for upper/middle/Lower mediastinal LN metastasis for the patients were 31.4%/29.4%/34.4%, respectively, suggesting the high incidence of mediastinal LN metastasis, and the importance of mediastinal LN dissection for those patients. However, survival benefit for mediastinal LN dissection for EGJAC remain unclear. In 2020, CARDIA-trial, a multinational, multicenter, randomized clinical trial which aimed to show the superiority of transthoracic esophagectomy with mediastinal LN dissection against transhiatal extended gastrectomy regarding overall survival (OS) was proposed, and is now undergoing[20]. To determine the value of mediastinal LN dissection, the results of this study and the survival analysis of the recent prospective study[7] is awaited.

Minimal-required proximal margin length

Negative surgical margin, as well as an adequate LN dissection, is essential to achieve curative resection in the surgical treatment for EGJAC. Although, especially during transhiatal approach, excessive proximal margin may lead to severe difficulty in anastomosis, thus result in higher complication rate. In 2013, Mine *et al*[21] reported the results of a single-center retrospective study which analyzed the proximal margin length of the 140 patients who underwent surgery for Siewert type II and III EGJAC. Patients with gross proximal margins greater than 20 mm had better survival outcomes than those shorter than 20 mm, and further, gross proximal margin ≤ 20 mm (hazard ratio (HR), 3.56; 95%CI: 1.39-9.14; P = 0.008) as well as pathological node status (HR, 1.76; 95%CI: 1.08-2.86; P = 0.024) were independent prognostic factors by multivariable analysis. Another recent study[22] retrospectively analyzed the proximal margin length in resected specimens for 289 EGJ/gastric cancer with gross esophageal invasion. Maximum length of discrepancy between the gross and pathological proximal boundary of the tumor was 15 mm for superficial growth type and 20 mm for expansive growth type tumors, respectively. These two studies indicate that 20 mm may be a sufficient proximal margin for advanced EGJAC, however, since proximal margins were measured in resected specimens in both studies, preoperative measures to decide the resection line remain unclear. Further, optima proximal margin for cases after preoperative therapy needs to be further studied.

Table 1 Patients with Siewert type I esophagogastric junction adenocarcinoma who underwent surgery at our institute

n	35
Male	34 (97.1%)
Age (yr)	67 (42-79)
Field of LN dissection 2/3	2/33
Open/MIE/Robot assisted	6/24/5
Preoperative chemotherapy	4 (11.4%)
Tumor size (mm)	35.3 (9-110)
Esophageal invasion length (mm)	30 (18-110)
pT 1a/1b/2/3/4a/4b[1]	4/10/3/18/0/0
pN 0/1/2/3[1]	15/4/4/12
pM 0/1[1]	30/5
pStage IA/IB/IIA/IIB/IIIA/IIIB/IVA/IVB[1]	3/7/2/6/0/4/8/5
Upper mediastinal LN metastasis	11/35 (31.4%)
Middle mediastinal LN metastasis	10/34 (29.4%)
Lower mediastinal LN metastasis	11/32 (34.4%)
Recurrence	14 (40.0%)
Site of recurrence[2]	
Liver	5
Adrenal gland	5
Distant LN	3
Peritoneum	2
Bone	2
Pleura	1
Pancreas	1

[1]Classified by the 8th edition of the Union for International Cancer Control (UICC)-Tumor Node Metastasis (TNM) classification.
[2]Including overlapped cases.
EGJAC: Esophagogastric adenocarcinoma; LN: Lymph node; MIE: Minimally invasive esophagectomy.

Reconstruction to prevent anastomotic complications

As a result of Japanese nationwide retrospective and prospective studies[6,7], LN along the distal portion of the stomach were much less often metastatic compared to LN along the right and left cardia, lesser curvature, and the left gastric artery for Siewert type II EGJAC. Therefore, the distal portion of the stomach does not need to be necessarily removed for Siewert type II EGJAC smaller than 4 cm, and proximal gastrectomy or total gastrectomy combined with distal esophagectomy is selected according to oncological status, patient condition, or institutional preference. According to a meta-analysis which compared proximal *vs* total gastrectomy for proximal early gastric cancer[23], proximal gastrectomy was superior to total gastrectomy in terms of operation time, intraoperative blood loss, and long-term nutritional status. Although, proximal gastrectomy followed by esophagogastrostomy was associated with a higher incidence of anastomotic complications such as stenosis and reflux esophagitis, as have been reported elsewhere[24,25]. In a prospective nationwide multicenter study in Japan[8], anastomotic leakage was observed in 12.2% of the 225 patients after transhiatal esophagectomy, and further, six patients suffered Clavien-Dindo (CD) grade IV or above anastomotic leakage where none of the patients after transthoracic esophagectomy hade leakage ≥ CD grade IV. Recently, novel surgical techniques, such as double-flap technique[11,26] and side overlap esophagogastrostomy[9,10] have been developed during gastric cancer surgery, and been introduced to EGJ cancers in order to overcome these anastomotic complications. Researchers have reported favorable results regarding anastomotic complications; however, these techniques require a more complex intracorporeal suturing technique and longer duration of surgery especially when performed for EGJ cancers which often requires intrathoracic anastomosis. Further investigation may be required for a higher level of evidence.

Table 2 Details of the mediastinal lymph node metastasis for the patients in Table 1

LN location		Metastasis rate (%)	
Upper mediastinum	Upper thoracic paraesophageal LN	8.5	(3/35)
	Left recurrent nerve LN	15.2	(5/33)
	Right recurrent nerve LN	20.6	(7/34)
	Left trachebronchial LN	17.4	(4/23)
Meddle mediastinum	Subcranial LN	18.2	(6/33)
	Middle thoracic paraesophageal LN	20.0	(7/35)
	Left main bronchus LN	12.9	(4/31)
	Right main bronchus LN	16.2	(5/31)
Lower mediastinum	Lower thoracic paraesophageal LN	17.1	(6/35)
	Supradiaphragmatic LN	13.3	(4/30)
	Posterior mediastinal LN	17.2	(5/29)

Number of patients with metastasis/number of patients who underwent lymph node dissection is indicated in each parenthesis. LN: Lymph node.

Minimally invasive surgery for EGJ cancers

Although none of the clinical trials specifically focusing on EGJ cancers have been conducted, several studies have demonstrated the safety and efficacy of minimally invasive surgery for esophageal/gastric cancer, which may also be applied to EGJ cancers. In 2012, Biere *et al*[27] reported the results of a multicenter, open-label, randomized control trial which aimed to demonstrate the safety of minimally invasive esophagectomy (MIE) verses open esophagectomy (OE) for patients with esophageal/EGJ cancers[27]. Patients in the study received preoperative therapy consisting of paclitaxel plus carboplatin plus concurrent radiotherapy of 41.4 Gy, followed by esophagectomy with two-field LN dissection, 6-8 wk after preoperative therapy. Within the 56 and 59 patients who were assigned to OE and MIE, respectively, OE group had more in-hospital pulmonary infection compared to MIE group (relative risk, 0.35; 95%CI: 0.16-0.78, P = 0.005), demonstrating the short-term benefits of MIE. Favorable short-term results regarding cardiopulmonary complications, postoperative pain, quality of life, and postoperative functional recovery were also reported in a single-center randomized trial comparing robot-assisted minimally invasive esophagectomy (MIE) *vs* OE for intrathoracic esophageal cancer (ROBOT trial)[28]. In the follow up study of ROBOT trial[29], long-term outcomes of the 112 patients including 40 EGJ cancer patients were analyzed. Comparable 5-year OS (41% *vs* 40%, P = 0.827) and disease-free survival (DFS, 42% *vs* 43%, P = 0.749) rates were observed for patients after RAMIE *vs* OE, respectively.

Regarding gastrectomy, the short-term surgical outcomes of a single-center non-inferiority randomized trial for laparoscopic *vs* open gastrectomy was reported in 2018[30]. In this study, 328 patients with cT2-3N0-3M0 gastric cancer, including 70 upper-third gastric cancer underwent open or laparoscopic total (33.5%), proximal (5.6%), and distal (60.9%) gastrectomy with D2 LN dissection depending on the tumor location. Overall complication rate was similar (laparoscopic, 11.7%; open, 14.4%; P = 0.512) between the groups, suggesting the feasibility of laparoscopic gastrectomy for advanced cancers.

Although evidence is lacking, especially for the oncological safety of minimally invasive transhiatal lower esophagectomy, minimally invasive surgery for EGJ cancer have been performed worldwide and is expanding rapidly. Surgeons must carefully decide the indication of minimally invasive surgery according to each patients general and oncological condition. In order to determine the superiority of robot-assisted over laparoscopic/thoracoscopic surgeries, results of ongoing studies[31] are awaited.

OPTIMAL PERIOPERATIVE TREATMENT FOR EGJAC

Neoadjuvant chemotherapy or chemoradiotherapy, which is the best choice?

Due to the poor survival outcome, researchers have focused on the development of more intensive preoperative treatment for advanced EGJAC. However, development and research for new therapeutic strategy has yet to be unified between Western and Asian countries. In addition, since EGJAC has been recognized as esophageal or gastric cancer until recently, various theories abound, and the optimal treatment option remain unclear.

In the Western countries, pre- and postoperative combination of docetaxel, oxaliplatin, leucovorin, and fluorouracil (FLOT) is now regarded as the standard treatment for locally advanced gastric cancer and EGJAC as a result of the FLOT4 trial[3]. For the 716 patients with cT2-4 cN+ gastric or EGJ cancer, median OS was 50 mo (95%CI: 38.33 to not reached), and pathological complete response (pCR) rate was 16% (95%CI: 10%-23%) after FLOT therapy[32], which were both significantly increased compared to conventional ECF/ECX therapy in this study. Subgroup analysis revealed that the effect of FLOT was similar between gastric and EGJ cancers. Another standard preoperative therapy for EGJ cancers in the Western countries is chemoradiotherapy as a result of the CROSS trial[4,33]. In this study, 368 patients with cT1N1 or cT2-3N0-1 esophageal or EGJ caner were either enrolled to surgery alone or neoadjuvant chemoradiotherapy followed by surgery. The chemoradiotherapy consisted of carboplatin, paclitaxel, and concurrent radiotherapy of 41.4 Gy. Within the 368 patients, results of the 366 patients were analyzed, and 88 (24%) of those patients had EGJAC. Median OS for the neoadjuvant therapy group was 48.6 (95%CI: 32.1-65.1) months, which was significantly longer than the surgery alone group. A pCR was achieved in 47 of the 161 patients (29%) who underwent resection after chemoradiotherapy.

In Korea, a phase III PRODIGY study[34] was designed to demonstrate the superiority of neoadjuvant docetaxel, oxaliplatin, and S-1 triplet therapy (DOS) followed by surgery and adjuvant S-1, *vs* conventional adjuvant S-1 after surgery in patients with gastric cancer and EGJAC. Neoadjuvant therapy was administered for 238 patients with cT2-3N+ and cT4 patients. Three-year progression-free survival (PFS) rate was 66.3% *vs* 60.2% (HR, 0.70; 95%CI: 0.52–0.95; P = 0.023) in the neoadjuvant group compared to surgery-first group. Neoadjuvant therapy led to pCR rate of 10.4%. As a result, preoperative DOS therapy is now considered as one of the standard treatment options in selected countries, however, OS was not significantly different between the two groups possibly because of the study setting, and the standard therapy for EGJAC is still questioned due to the relatively small population of EGJAC in this study (Table 3).

Thus far, several trials compared the therapeutic effect of preoperative chemoradiotherapy *vs* chemotherapy for EGJ cancers. In the NeoRes trial[35,36], patients with cT1N+ or cT2-3 esophageal or EGJ cancer were either randomized to neoadjuvant chemotherapy consisting of cisplatin plus fluorouracil, or the same chemotherapeutic regimen plus concurrent radiation therapy of 40 Gy. In this study, neoadjuvant chemoradiotherapy have achieved higher pCR rate (24% *vs* 8%) and R0 resection rate (76% *vs* 64%) when compared to neoadjuvant chemotherapy, however, three-year OS rates were equivalent between the groups (HR, 1.09; 95%CI: 0.73–1.64; P = 0.77). In another prospective randomized phase III trial[37], patients with cT3-4 EGJAC received either three courses of neoadjuvant triplet therapy (cisplatin, fluorouracil, and leucovorin, PLF) or two courses of PLF plus combined chemoradiotherapy consisting of cisplatin, etoposide, and concurrent radiation of 30 Gy. Within the evaluated 119 patients, high in-hospital mortality rate after neoadjuvant chemoradiotherapy (10.2%) compared to chemotherapy (3.8%) was observed, however, three-year OS rates were relatively higher in the neoadjuvant chemoradiotherapy group (47.4% *vs* 27.7%, HR, 0.67; 95%CI: 0.41–1.07; P = 0.07, Table 4). In 2021, preliminary results of a phase III study, which aimed to compare CROSS *vs* FLOT or MAGIC (epirubicin, cisplatin/oxaliplatin, and 5-fuluorouracil/capecitabine) regimen in terms of OS for esophagus and EGJ cancer were reported (Neo-AEGIS trial)[38]. Within the 362 evaluable patients, at a median follow up of 24.5 (1-92) mo, the 3-year estimated survival probability was equivalent between CROSS and MAGIC/FLOT arm (HR, 1.02; 95%CI: 0.74-1.42).

As shown, accumulated evidence has shown that neoadjuvant therapy may improve survival for patients with EGJAC, however, various issues remain unclear. First, is the ideal chemotherapeutic regimen for neoadjuvant treatment. The Japan Clinical Oncology Group (JCOG) is now planning a nationwide prospective study directly comparing DOS *vs* FLOT regimen as neoadjuvant treatment in EGJAC. Second, is the efficacy by the addition of radiotherapy to chemotherapy, since none of the previous studies used the current standard chemotherapeutic regimen for the chemoradiotherapy arm. Although the superiority of chemoradiotherapy have not yet been demonstrated, neoadjuvant chemoradiotherapy may be of utility in cases such as borderline resectable EGJAC because of the relatively high pCR rate. Finally, the safety of radiation therapy is a critical issue, and needs to be further discussed. Currently, a randomized phase III RACE[39] trial, which aimed to compare perioperative chemotherapy *vs* chemoradiotherapy (FLOT *vs* FLOT based chemoradiotherapy including concurrent radiation of 45 Gy) in terms of PFS in undergoing, and the results are awaited.

Immune checkpoint inhibitor immunotherapy, a paradigm shift in cancer treatment

Recent advances of immunotherapeutic agents, especially immune checkpoint inhibitors (ICI), have dramatically improved the treatment outcomes in several cancer types. In esophageal, gastric, and EGJ cancers, anti-PD-1 antibody (nivolumab/pembrolizumab) and anti-CTLA-4 antibody (ipilimumab) have already been regarded as one of the standard treatment options for unresectable/recurrent tumors[40-43]. In a recent phase II trial[13], the neoadjuvant combination of ICI and chemotherapy was investigated in locally advanced gastric and EGJ cancers. Thirty-six patients with cT3-4N+ diseases including 19 patients with EGJAC received capecitabine and simultaneous radiotherapy for 5 wk, sandwiched by a 21-d cycle of oxaliplatin plus capecitabine twice daily (days 1-14) followed by surgery. Anti-PD-1 antibody camrelizumab (day 1) was given for 5 cycles since initiating chemotherapy. The primary endpoint pCR rate was 33.3% (95%CI: 18.6-51.0), and patients with < 10% residual tumor cells/R0

Table 3 Clinical trials of neoadjuvant therapy for esophagogastric junction cancer included in this review

Study name	FLOT4[3,32]	CROSS[4,33]	PRODIGY[34]
Ref.	Al-Batran *et al*[3,32]	Shapiro *et al*[33], van Hagen *et al*[4]	Kang *et al*[34]
Year	2016/2019	2012/2015	2021
Study design	Phase II/III	Phase III	Phase III
Eligible patients	cT2-4 and/or cN+, cM0	cT1N+ or cT2-3, cM0	cT2-3N+ or cT4, cM0
	Gastric or EGJ cancer	Esophageal or EGJ cancer	Gastric or EGJ cancer
Experimental arm	FLOT	CBDCA + PTX + RT	DOS + adjuvant S1
Control arm	ECF/ECX	Surgery alone	Adjuvant S1
Total number of patients	716	366	484
EGJ cancer patients	56%	24%	6%
Primary outcome	OS	OS	Progression free survival
OS	50 *vs* 35 mo	48.6 *vs* 24.0 mo	NA
pCR rate	16% *vs* 6%	29%	10.40%
R0 resection rate	85% *vs* 78%	92% *vs* 69%	89% *vs* 84%
Special notes	Effective for EGJ cancer		Progression free survival, 66.3 months *vs* 60.2 months. Equivalent OS. Small population of EGJ cancer patients (27 patients)

EGJ: Esophagogastric junction; pCR: Pathological complete response; FLOT: 5-fluorouracil + leucovorin + oxaliplatin + docetaxel; ECF: Epirubicin + cisplatin + 5-fluorouracil; ECX: Epirubicin + cisplatin + capecitabine; CBDCA: Carboplatin; PTX: Paclitaxel; RT: Radiation therapy; DOS: Docetaxel + oxaliplatin + S-1; NA: Not available; OS: Overall survival.

resection rates were 44.4%/91.7%, respectively. Two-year PFS and OS rates were 66.9% and 76.1%, respectively in this study. In another phase II study[14], neoadjuvant nivolumab once every two weeks, 6 cycles, and ipilimumab once every six weeks, 2 cycles, followed by surgery and adjuvant nivolumab once every four weeks (nine injections) were administered in 32 patients with locally advanced resectable, deficient mismatch repair (dMMR)/microsatellite instability-high (MSI-H), cT2-4 gastric (16 patients) and GEJ cancer (16 patients). Twenty-nine patients who received surgery all had an R0 resection, and 17 (58.6%; 90%CI, 41.8-74.1) had pCR. Of those 29 patients with surgery, 23 received adjuvant nivolumab. At database lock (median follow-up, 14.9 mo), no patient had relapse and one died without relapse. Combination of ICI and chemotherapy with or without concurrent radiotherapy may exhibit promising pathological response with tolerable toxicity in patients with locally advanced EGJAC, and future phase III trials to demonstrate the safety and efficacy are awaited (Table 5).

Future of targeted therapy

In 2022, the results of the NRG Oncology/RTOG 1010 study[44], a multicenter randomized phase III trial which aimed to demonstrate the impact of monoclonal anti-HER2 (ERBB2) antibody trastuzumab with trimodality treatment for esophageal adenocarcinoma with HER2 expression was reported. In this study, patients with HER2 positive cT1N1-2 or cT2-3N0-2 diseases were either assigned to weekly intravenous paclitaxel and carboplatin for 6 wk with radiotherapy of 50.4 Gy followed by surgery, with or without intravenous trastuzumab for 5 wk during chemoradiotherapy, once preoperatively, and every 3 wk for 13 treatments starting 21-56 d after surgery. In total, 203 patients were included, and the median DFS (primary endpoint) was 19.6 mo and 14.2 mo for chemoradiotherapy with trastuzumab and chemoradiotherapy alone, respectively (HR, 0·99; 95%CI: 0.71-1.39; P = 0.97) (Table 5). Although addition of trastuzumab did not lead to increased toxicities, the study failed to demonstrate survival benefits, suggesting that combination with other chemotherapeutic agents or other drugs targeting HER2 may be necessary for the treatment of HER2 positive EGJAC. Currently, the treatment effect of an antibody-drug conjugate trastuzumab deruxtecan (T-DXd) against HER2 positive gastric and EGJ adenocarcinoma is tested under a phase II study in Japan (EPOC2003 study)[45]. In a recent analysis utilizing the Cancer Genome Atlas (TGCA)[46], EGJAC was classified into esophageal adenocarcinoma like and gastric adenocarcinoma like EGJAC according to the 400-gene classifier. Esophageal adenocarcinoma like EGJAC have shown significantly higher copy number amplification of ERBB2, as well as an increased protein expression of ERBB2 and EGFR, suggesting that the molecular characterization of EGJAC may enable to select patients who will benefit by ERBB2/EGFR blockade. Agents targeting vascular endothelial growth factor (VEGF) might also be future candidates for neoadjuvant therapy[47],

Table 4 Clinical trials comparing neoadjuvant chemotherapy versus chemoradiotherapy for esophagogastric junction cancer included in this review

Study name	NeoRes[35,36]	POET[37]	Neo-AEGIS[38]
Ref.	Klevebro *et al*[35,36]	Stahl *et al*[37]	John *et al*[38]
Year	2015/2016	2009	2021
Study design	Randomized phase II	Phase III	Phase III
Eligible patients	cT1N+ or cT2-3, M0	cT3-4, M0	cT2-3N0-3M0
	Esophageal or EGJ cancer	EGJ cancer	Esophageal or EGJ cancer
Experimental arm	CF + RT	PLF + RT	CROSS
Control arm	CF	PLF	MAGIC/FLOT
Total number of patients	181	119	377
EGJ cancer patients	17%	100%	NA
Primary outcome	pCR	OS	OS
OS	NA	33 *vs* 21 mo	NA
pCR rate	24% *vs* 8%	15.6% *vs* 2.0%	NA
R0 resection rate	76% *vs* 64%	69.5% *vs* 71.5%	NA
Special notes	Equivalent 3-year OS	Study closed early due to low accrual, high in-hospital mortality after chemoradiotherapy	Equivalent 3-year estimated survival probability

EGJ: Esophagogastric junction; pCR: Pathological complete response; CF: Cisplatin + 5-fluorouracil; RT: Radiation therapy; PLF: Paclitaxel + leucovorin + 5-fluorouracil; CROSS: Carboplatin + paclitaxel + radiation therapy; MAGIC: Epirubicin + cisplatin (oxaliplatin) + 5-fluorouracil; FLOT: 5-fluorouracil + leucovorin + oxaliplatin + docetaxel; NA: Not available; OS: Overall survival.

Table 5 Clinical trials of neoadjuvant immunotherapy/targeted therapy for esophagogastric junction cancer included in this review

Study name	Neo-PLANET[13]	NEONIPIGA[14]	NRG Oncology/RTOG 1010[44]
Ref.	Tang *et al*[13]	Andre *et al*[14]	Safran *et al*[44]
Yr	2022	2023	2022
Study design	Phase II	Phase II	Phase III
Eligible patients	cT3-4N+, M0	cT2-4, M0, dMMR/MSI-H	cT1N1-2 or cT2-3N0-2 HER2 positive
	Gastric or EGJ cancer	Gastric or EGJ cancer	Esophageal adenocarcinoma
Experimental arm	Camrelizumab plus chemoradiotherapy	Nivolumab plus ipilimumab	Trastuzumab plus chemoradiotherapy
Control arm	NA	NA	Chemoradiotherapy
Total number of patients	36	29	203
EGJ cancer patients	53.80%	50.00%	NA
Primary endpoint	pCR	pCR	Disease-free survival
OS	NA	NA	38.5 *vs* 38.9 mo
pCR rate	33.30%	58.60%	27% *vs* 29%
R0 resection rate	91.70%	100%	98% *vs* 100%
Special notes	Two-year OS, 76.2%		Disease-free survival, 19.6 *vs* 14.2 mo

EGJ: Esophagogastric junction; pCR: Pathological complete response; NA: Not available; OS: Overall survival.

and should be further discussed.

Is adjuvant therapy needed?

In Japan, EGJAC has usually been treated as gastric cancer, and the same agents have been administered

as adjuvant therapy for both cancer types. In the CLASSIC trial[48,49] which investigated the effect of adjuvant capecitabine plus oxaliplatin for pStage II-III gastric or EGJ adenocarcinoma, a trend toward improving OS was shown in the small subset of patients with EGJAC (24 patients, HR, 0.63; 95%CI: 0.09–4.45). In another randomized controlled phase III trial JACCRO CG-07[50,51], the effect of S-1 plus DOS over S-1 alone was demonstrated for pStage III gastric cancer, however, the study included only eight EGJAC patients. Although sufficient analysis for EGJAC alone could not be performed due to the small sample size, with the results against gastric adenocarcinomas, capecitabine plus oxaliplatin, S-1 plus DOS, or S-1 monotherapy[52] have been regarded as the standard adjuvant therapy for EGJAC.

In the recent CheckMate 577 study[12], the value of adjuvant ICI (nivolumab) was evaluated in patients with ypStage II-III esophageal or EGJ cancers after neoadjuvant chemoradiotherapy. A total of 794 patients, which included 319 (40.2%) EGJAC, after curative resection were either postoperatively randomized to receive nivolumab adjuvant therapy or placebo. Median DFS was 22.4 and 11.0 mo for nivolumab group and placebo group, respectively (HR, 0.69; 95%CI: 0.56–0.86; $P < 0.001$), which demonstrated the impact of adjuvant ICI. However, in the subgroup analysis, adjuvant nivolumab could not show prognostic advantages during EGJAC (HR, 0.87; 95%CI: 0.63–1.21). Value of adjuvant therapy for EGJAC, especially for patients after neoadjuvant chemotherapy, remain unclear. The ideal regimen, and further, whether adjuvant treatment is needed, should be further investigated.

CONCLUSION

Recent development of the perioperative treatment has improved therapeutic effect for EGJAC, and further, novel immunochemotherapeutic strategies have high expectations to further improve survival outcomes for the patients. Previous studies have enabled to standardize the surgical procedure for EGJAC, and novel surgical techniques have improved the safety of operation. Since the incidence of EGJAC are rising rapidly worldwide, there is an urgent need to accumulate new evidence and to unify the treatment strategy globally. Although multiple issues remain unclear, ongoing clinical trials included in this review may further contribute to improving outcomes for patients with EGJAC.

FOOTNOTES

Author contributions: Shoji Y and Koyanagi K contributed to Conceptualization; Shoji Y contributed to writing and original draft preparation; Kanamori K, Tajima K, Ogimi M, Yatabe K, Yamamoto M, Kazuno A, Nabeshima K, Nakamura K and Nishi T contributed to investigation; Koyanagi K and Mori M contributed to supervision; All authors have read and agreed to the published version of the manuscript.

Conflict-of-interest statement: All the authors report no relevant conflicts of interest for this article.

Open-Access: This article is an open-access article that was selected by an in-house editor and fully peer-reviewed by external reviewers. It is distributed in accordance with the Creative Commons Attribution NonCommercial (CC BY-NC 4.0) license, which permits others to distribute, remix, adapt, build upon this work non-commercially, and license their derivative works on different terms, provided the original work is properly cited and the use is non-commercial. See: https://creativecommons.org/Licenses/by-nc/4.0/

Country/Territory of origin: Japan

ORCID number: Yoshiaki Shoji 0000-0003-3074-1398; Kazuo Koyanagi 0000-0002-8010-8630.

Corresponding Author's Membership in Professional Societies: The Japanese Society of Gastroenterology.

S-Editor: Li L
L-Editor: A
P-Editor: Zhao S

REFERENCES

1 **Sung H**, Ferlay J, Siegel RL, Laversanne M, Soerjomataram I, Jemal A, Bray F. Global Cancer Statistics 2020: GLOBOCAN Estimates of Incidence and Mortality Worldwide for 36 Cancers in 185 Countries. *CA Cancer J Clin* 2021; **71**: 209-249 [PMID: 33538338 DOI: 10.3322/caac.21660]

2 **Arnold M**, Laversanne M, Brown LM, Devesa SS, Bray F. Predicting the Future Burden of Esophageal Cancer by Histological Subtype: International Trends in Incidence up to 2030. *Am J Gastroenterol* 2017; **112**: 1247-1255 [PMID: 28585555 DOI: 10.1038/ajg.2017.155]

3 **Al-Batran SE**, Homann N, Pauligk C, Goetze TO, Meiler J, Kasper S, Kopp HG, Mayer F, Haag GM, Luley K, Lindig U,

Schmiegel W, Pohl M, Stoehlmacher J, Folprecht G, Probst S, Prasnikar N, Fischbach W, Mahlberg R, Trojan J, Koenigsmann M, Martens UM, Thuss-Patience P, Egger M, Block A, Heinemann V, Illerhaus G, Moehler M, Schenk M, Kullmann F, Behringer DM, Heike M, Pink D, Teschendorf C, Löhr C, Bernhard H, Schuch G, Rethwisch V, von Weikersthal LF, Hartmann JT, Kneba M, Daum S, Schulmann K, Weniger J, Belle S, Gaiser T, Oduncu FS, Güntner M, Hozaeel W, Reichart A, Jäger E, Kraus T, Mönig S, Bechstein WO, Schuler M, Schmalenberg H, Hofheinz RD; FLOT4-AIO Investigators. Perioperative chemotherapy with fluorouracil plus leucovorin, oxaliplatin, and docetaxel versus fluorouracil or capecitabine plus cisplatin and epirubicin for locally advanced, resectable gastric or gastro-oesophageal junction adenocarcinoma (FLOT4): a randomised, phase 2/3 trial. *Lancet* 2019; **393**: 1948-1957 [PMID: 30982686 DOI: 10.1016/S0140-6736(18)32557-1]

4 **van Hagen P**, Hulshof MC, van Lanschot JJ, Steyerberg EW, van Berge Henegouwen MI, Wijnhoven BP, Richel DJ, Nieuwenhuijzen GA, Hospers GA, Bonenkamp JJ, Cuesta MA, Blaisse RJ, Busch OR, ten Kate FJ, Creemers GJ, Punt CJ, Plukker JT, Verheul HM, Spillenaar Bilgen EJ, van Dekken H, van der Sangen MJ, Rozema T, Biermann K, Beukema JC, Piet AH, van Rij CM, Reinders JG, Tilanus HW, van der Gaast A; CROSS Group. Preoperative chemoradiotherapy for esophageal or junctional cancer. *N Engl J Med* 2012; **366**: 2074-2084 [PMID: 22646630 DOI: 10.1056/NEJMoa1112088]

5 **Kitagawa Y**, Uno T, Oyama T, Kato K, Kato H, Kawakubo H, Kawamura O, Kusano M, Kuwano H, Takeuchi H, Toh Y, Doki Y, Naomoto Y, Nemoto K, Booka E, Matsubara H, Miyazaki T, Muto M, Yanagisawa A, Yoshida M. Esophageal cancer practice guidelines 2017 edited by the Japan Esophageal Society: part 1. *Esophagus* 2019; **16**: 1-24 [PMID: 30171413 DOI: 10.1007/s10388-018-0641-9]

6 **Yamashita H**, Seto Y, Sano T, Makuuchi H, Ando N, Sasako M; Japanese Gastric Cancer Association and the Japan Esophageal Society. Results of a nation-wide retrospective study of lymphadenectomy for esophagogastric junction carcinoma. *Gastric Cancer* 2017; **20**: 69-83 [PMID: 27796514 DOI: 10.1007/s10120-016-0663-8]

7 **Kurokawa Y**, Takeuchi H, Doki Y, Mine S, Terashima M, Yasuda T, Yoshida K, Daiko H, Sakuramoto S, Yoshikawa T, Kunisaki C, Seto Y, Tamura S, Shimokawa T, Sano T, Kitagawa Y. Mapping of Lymph Node Metastasis From Esophagogastric Junction Tumors: A Prospective Nationwide Multicenter Study. *Ann Surg* 2021; **274**: 120-127 [PMID: 31404008 DOI: 10.1097/SLA.0000000000003499]

8 **Mine S**, Kurokawa Y, Takeuchi H, Terashima M, Yasuda T, Yoshida K, Yabusaki H, Shirakawa Y, Fujitani K, Sano T, Doki Y, Kitagawa Y. Postoperative complications after a transthoracic esophagectomy or a transhiatal gastrectomy in patients with esophagogastric junctional cancers: a prospective nationwide multicenter study. *Gastric Cancer* 2022; **25**: 430-437 [PMID: 34590178 DOI: 10.1007/s10120-021-01255-9]

9 **Yamashita Y**, Tatsubayashi T, Okumura K, Miyamoto T, Ueno K. Modified side overlap esophagogastrostomy after laparoscopic proximal gastrectomy. *Ann Gastroenterol Surg* 2022; **6**: 594-599 [PMID: 35847432 DOI: 10.1002/ags3.12549]

10 **Yamashita Y**, Yamamoto A, Tamamori Y, Yoshii M, Nishiguchi Y. Side overlap esophagogastrostomy to prevent reflux after proximal gastrectomy. *Gastric Cancer* 2017; **20**: 728-735 [PMID: 27942874 DOI: 10.1007/s10120-016-0674-5]

11 **Shoji Y**, Nunobe S, Ida S, Kumagai K, Ohashi M, Sano T, Hiki N. Surgical outcomes and risk assessment for anastomotic complications after laparoscopic proximal gastrectomy with double-flap technique for upper-third gastric cancer. *Gastric Cancer* 2019; **22**: 1036-1043 [PMID: 30838469 DOI: 10.1007/s10120-019-00940-0]

12 **Kelly RJ**, Ajani JA, Kuzdzal J, Zander T, Van Cutsem E, Piessen G, Mendez G, Feliciano J, Motoyama S, Lièvre A, Uronis H, Elimova E, Grootscholten C, Geboes K, Zafar S, Snow S, Ko AH, Feeney K, Schenker M, Kocon P, Zhang J, Zhu L, Lei M, Singh P, Kondo K, Cleary JM, Moehler M; CheckMate 577 Investigators. Adjuvant Nivolumab in Resected Esophageal or Gastroesophageal Junction Cancer. *N Engl J Med* 2021; **384**: 1191-1203 [PMID: 33789008 DOI: 10.1056/NEJMoa2032125]

13 **Tang Z**, Wang Y, Liu D, Wang X, Xu C, Yu Y, Cui Y, Tang C, Li Q, Sun J, Zhang Q, Ji Y, Ma G, Li H, Shen Z, Shen K, Zheng R, Hou Z, Liu T, Wang J, Sun Y. The Neo-PLANET phase II trial of neoadjuvant camrelizumab plus concurrent chemoradiotherapy in locally advanced adenocarcinoma of stomach or gastroesophageal junction. *Nat Commun* 2022; **13**: 6807 [PMID: 36357415 DOI: 10.1038/s41467-022-34403-5]

14 **André T**, Tougeron D, Piessen G, de la Fouchardière C, Louvet C, Adenis A, Jary M, Tournigand C, Aparicio T, Desrame J, Lièvre A, Garcia-Larnicol ML, Pudlarz T, Cohen R, Memmi S, Vernerey D, Henriques J, Lefevre JH, Svrcek M. Neoadjuvant Nivolumab Plus Ipilimumab and Adjuvant Nivolumab in Localized Deficient Mismatch Repair/Microsatellite Instability-High Gastric or Esophagogastric Junction Adenocarcinoma: The GERCOR NEONIPIGA Phase II Study. *J Clin Oncol* 2023; **41**: 255-265 [PMID: 35969830 DOI: 10.1200/JCO.22.00686]

15 **Rüdiger Siewert J**, Feith M, Werner M, Stein HJ. Adenocarcinoma of the esophagogastric junction: results of surgical therapy based on anatomical/topographic classification in 1,002 consecutive patients. *Ann Surg* 2000; **232**: 353-361 [PMID: 10973385 DOI: 10.1097/00000658-200009000-00007]

16 **Pedrazzani C**, de Manzoni G, Marrelli D, Giacopuzzi S, Corso G, Minicozzi AM, Rampone B, Roviello F. Lymph node involvement in advanced gastroesophageal junction adenocarcinoma. *J Thorac Cardiovasc Surg* 2007; **134**: 378-385 [PMID: 17662776 DOI: 10.1016/j.jtcvs.2007.03.034]

17 **Japanese Gastric Cancer Association**. Japanese classification of gastric carcinoma: 3rd English edition. *Gastric Cancer* 2011; **14**: 101-112 [PMID: 21573743 DOI: 10.1007/s10120-011-0041-5]

18 **Japan Esophageal Society**. Japanese Classification of Esophageal Cancer, 11th Edition: part I. *Esophagus* 2017; **14**: 1-36 [PMID: 28111535 DOI: 10.1007/s10388-016-0551-7]

19 **Japanese Gastric Cancer Association**. Japanese Gastric Cancer Treatment Guidelines 2021 (6th edition). *Gastric Cancer* 2023; **26**: 1-25 [PMID: 36342574 DOI: 10.1007/s10120-022-01331-8]

20 **Leers JM**, Knepper L, van der Veen A, Schröder W, Fuchs H, Schiller P, Hellmich M, Zettelmeyer U, Brosens LAA, Quaas A, Ruurda JP, van Hillegersberg R, Bruns CJ. The CARDIA-trial protocol: a multinational, prospective, randomized, clinical trial comparing transthoracic esophagectomy with transhiatal extended gastrectomy in adenocarcinoma of the gastroesophageal junction (GEJ) type II. *BMC Cancer* 2020; **20**: 781 [PMID: 32819399 DOI: 10.1186/s12885-020-07152-1]

21 **Mine S**, Sano T, Hiki N, Yamada K, Kosuga T, Nunobe S, Yamaguchi T. Proximal margin length with transhiatal

gastrectomy for Siewert type II and III adenocarcinomas of the oesophagogastric junction. *Br J Surg* 2013; **100**: 1050-1054 [PMID: 23754647 DOI: 10.1002/bjs.9170]

22 **Koterazawa Y**, Ohashi M, Hayami M, Makuuchi R, Ida S, Kumagai K, Sano T, Nunobe S. Required esophageal resection length beyond the tumor boundary to ensure a negative proximal margin for gastric cancer with gross esophageal invasion or esophagogastric junction cancer. *Gastric Cancer* 2023; **26**: 451-459 [PMID: 36725762 DOI: 10.1007/s10120-023-01369-2]

23 **Xu Y**, Tan Y, Wang Y, Xi C, Ye N, Xu X. Proximal versus total gastrectomy for proximal early gastric cancer: A systematic review and meta-analysis. *Medicine (Baltimore)* 2019; **98**: e15663 [PMID: 31083268 DOI: 10.1097/MD.0000000000015663]

24 **An JY**, Youn HG, Choi MG, Noh JH, Sohn TS, Kim S. The difficult choice between total and proximal gastrectomy in proximal early gastric cancer. *Am J Surg* 2008; **196**: 587-591 [PMID: 18519129 DOI: 10.1016/j.amjsurg.2007.09.040]

25 **Ronellenfitsch U**, Najmeh S, Andalib A, Perera RM, Rousseau MC, Mulder DS, Ferri LE. Functional outcomes and quality of life after proximal gastrectomy with esophagogastrostomy using a narrow gastric conduit. *Ann Surg Oncol* 2015; **22**: 772-779 [PMID: 25212836 DOI: 10.1245/s10434-014-4078-7]

26 **Hayami M**, Hiki N, Nunobe S, Mine S, Ohashi M, Kumagai K, Ida S, Watanabe M, Sano T, Yamaguchi T. Clinical Outcomes and Evaluation of Laparoscopic Proximal Gastrectomy with Double-Flap Technique for Early Gastric Cancer in the Upper Third of the Stomach. *Ann Surg Oncol* 2017; **24**: 1635-1642 [PMID: 28130623 DOI: 10.1245/s10434-017-5782-x]

27 **Biere SS**, van Berge Henegouwen MI, Maas KW, Bonavina L, Rosman C, Garcia JR, Gisbertz SS, Klinkenbijl JH, Hollmann MW, de Lange ES, Bonjer HJ, van der Peet DL, Cuesta MA. Minimally invasive versus open oesophagectomy for patients with oesophageal cancer: a multicentre, open-label, randomised controlled trial. *Lancet* 2012; **379**: 1887-1892 [PMID: 22552194 DOI: 10.1016/S0140-6736(12)60516-9]

28 **van der Sluis PC**, van der Horst S, May AM, Schippers C, Brosens LAA, Joore HCA, Kroese CC, Haj Mohammad N, Mook S, Vleggaar FP, Borel Rinkes IHM, Ruurda JP, van Hillegersberg R. Robot-assisted Minimally Invasive Thoracolaparoscopic Esophagectomy Versus Open Transthoracic Esophagectomy for Resectable Esophageal Cancer: A Randomized Controlled Trial. *Ann Surg* 2019; **269**: 621-630 [PMID: 30308612 DOI: 10.1097/SLA.0000000000003031]

29 **de Groot EM**, van der Horst S, Kingma BF, Goense L, van der Sluis PC, Ruurda JP, van Hillegersberg R. Robot-assisted minimally invasive thoracolaparoscopic esophagectomy versus open esophagectomy: long-term follow-up of a randomized clinical trial. *Dis Esophagus* 2020; **33** [PMID: 33241302 DOI: 10.1093/dote/doaa079]

30 **Shi Y**, Xu X, Zhao Y, Qian F, Tang B, Hao Y, Luo H, Chen J, Yu P. Short-term surgical outcomes of a randomized controlled trial comparing laparoscopic versus open gastrectomy with D2 lymph node dissection for advanced gastric cancer. *Surg Endosc* 2018; **32**: 2427-2433 [PMID: 29234941 DOI: 10.1007/s00464-017-5942-x]

31 **Tagkalos E**, van der Sluis PC, Berlth F, Poplawski A, Hadzijusufovic E, Lang H, van Berge Henegouwen MI, Gisbertz SS, Müller-Stich BP, Ruurda JP, Schiesser M, Schneider PM, van Hillegersberg R, Grimminger PP. Robot-assisted minimally invasive thoraco-laparoscopic esophagectomy versus minimally invasive esophagectomy for resectable esophageal adenocarcinoma, a randomized controlled trial (ROBOT-2 trial). *BMC Cancer* 2021; **21**: 1060 [PMID: 34565343 DOI: 10.1186/s12885-021-08780-x]

32 **Al-Batran SE**, Hofheinz RD, Pauligk C, Kopp HG, Haag GM, Luley KB, Meiler J, Homann N, Lorenzen S, Schmalenberg H, Probst S, Koenigsmann M, Egger M, Prasnikar N, Caca K, Trojan J, Martens UM, Block A, Fischbach W, Mahlberg R, Clemens M, Illerhaus G, Zirlik K, Behringer DM, Schmiegel W, Pohl M, Heike M, Ronellenfitsch U, Schuler M, Bechstein WO, Königsrainer A, Gaiser T, Schirmacher P, Hozaeel W, Reichart A, Goetze TO, Sievert M, Jäger E, Mönig S, Tannapfel A. Histopathological regression after neoadjuvant docetaxel, oxaliplatin, fluorouracil, and leucovorin versus epirubicin, cisplatin, and fluorouracil or capecitabine in patients with resectable gastric or gastro-oesophageal junction adenocarcinoma (FLOT4-AIO): results from the phase 2 part of a multicentre, open-label, randomised phase 2/3 trial. *Lancet Oncol* 2016; **17**: 1697-1708 [PMID: 27776843 DOI: 10.1016/S1470-2045(16)30531-9]

33 **Shapiro J**, van Lanschot JJB, Hulshof MCCM, van Hagen P, van Berge Henegouwen MI, Wijnhoven BPL, van Laarhoven HWM, Nieuwenhuijzen GAP, Hospers GAP, Bonenkamp JJ, Cuesta MA, Blaisse RJB, Busch ORC, Ten Kate FJW, Creemers GM, Punt CJA, Plukker JTM, Verheul HMW, Bilgen EJS, van Dekken H, van der Sangen MJC, Rozema T, Biermann K, Beukema JC, Piet AHM, van Rij CM, Reinders JG, Tilanus HW, Steyerberg EW, van der Gaast A; CROSS study group. Neoadjuvant chemoradiotherapy plus surgery versus surgery alone for oesophageal or junctional cancer (CROSS): long-term results of a randomised controlled trial. *Lancet Oncol* 2015; **16**: 1090-1098 [PMID: 26254683 DOI: 10.1016/S1470-2045(15)00040-6]

34 **Kang YK**, Yook JH, Park YK, Lee JS, Kim YW, Kim JY, Ryu MH, Rha SY, Chung IJ, Kim IH, Oh SC, Park YS, Son T, Jung MR, Heo MH, Kim HK, Park C, Yoo CH, Choi JH, Zang DY, Jang YJ, Sul JY, Kim JG, Kim BS, Beom SH, Cho SH, Ryu SW, Kook MC, Ryoo BY, Yoo MW, Lee NS, Lee SH, Kim G, Lee Y, Lee JH, Noh SH. PRODIGY: A Phase III Study of Neoadjuvant Docetaxel, Oxaliplatin, and S-1 Plus Surgery and Adjuvant S-1 Versus Surgery and Adjuvant S-1 for Resectable Advanced Gastric Cancer. *J Clin Oncol* 2021; **39**: 2903-2913 [PMID: 34133211 DOI: 10.1200/JCO.20.02914]

35 **Klevebro F**, Alexandersson von Döbeln G, Wang N, Johnsen G, Jacobsen AB, Friesland S, Hatlevoll I, Glenjen NI, Lind P, Tsai JA, Lundell L, Nilsson M. A randomized clinical trial of neoadjuvant chemotherapy versus neoadjuvant chemoradiotherapy for cancer of the oesophagus or gastro-oesophageal junction. *Ann Oncol* 2016; **27**: 660-667 [PMID: 26782957 DOI: 10.1093/annonc/mdw010]

36 **Klevebro F**, Johnsen G, Johnson E, Viste A, Myrnäs T, Szabo E, Jacobsen AB, Friesland S, Tsai JA, Persson S, Lindblad M, Lundell L, Nilsson M. Morbidity and mortality after surgery for cancer of the oesophagus and gastro-oesophageal junction: A randomized clinical trial of neoadjuvant chemotherapy vs. neoadjuvant chemoradiation. *Eur J Surg Oncol* 2015; **41**: 920-926 [PMID: 25908010 DOI: 10.1016/j.ejso.2015.03.226]

37 **Stahl M**, Walz MK, Stuschke M, Lehmann N, Meyer HJ, Riera-Knorrenschild J, Langer P, Engenhart-Cabillic R, Bitzer M, Königsrainer A, Budach W, Wilke H. Phase III comparison of preoperative chemotherapy compared with chemoradiotherapy in patients with locally advanced adenocarcinoma of the esophagogastric junction. *J Clin Oncol* 2009;

27: 851-856 [PMID: 19139439 DOI: 10.1200/JCO.2008.17.0506]

38 **Reynolds JV**, Preston SR, O'Neill B, Lowery MA, Baeksgaard L, Crosby T, Cunningham M, Cuffe S, Griffiths GO, Roy R, Falk S, Hanna G, Bartlett FR, Parker I, Alvarez-Iglesias A, Nilsson M, Piessen G, Risum S, Ravi N, McDermott RS. Neo-AEGIS (Neoadjuvant trial in Adenocarcinoma of the Esophagus and Esophago-Gastric Junction International Study): Preliminary results of phase III RCT of CROSS vs perioperative chemotherapy (Modified MAGIC or FLOT protocol). (NCT01726452). *Journal of Clinical Oncology***39** (15_suppl): 4004 [DOI: 10.1200/JCO.2021.39.15_suppl.4004]

39 **Lorenzen S**, Biederstädt A, Ronellenfitsch U, Reißfelder C, Mönig S, Wenz F, Pauligk C, Walker M, Al-Batran SE, Haller B, Hofheinz RD. RACE-trial: neoadjuvant radiochemotherapy versus chemotherapy for patients with locally advanced, potentially resectable adenocarcinoma of the gastroesophageal junction - a randomized phase III joint study of the AIO, ARO and DGAV. *BMC Cancer* 2020; **20**: 886 [PMID: 32933498 DOI: 10.1186/s12885-020-07388-x]

40 **Doki Y**, Ajani JA, Kato K, Xu J, Wyrwicz L, Motoyama S, Ogata T, Kawakami H, Hsu CH, Adenis A, El Hajbi F, Di Bartolomeo M, Braghiroli MI, Holtved E, Ostoich SA, Kim HR, Ueno M, Mansoor W, Yang WC, Liu T, Bridgewater J, Makino T, Xynos I, Liu X, Lei M, Kondo K, Patel A, Gricar J, Chau I, Kitagawa Y; CheckMate 648 Trial Investigators. Nivolumab Combination Therapy in Advanced Esophageal Squamous-Cell Carcinoma. *N Engl J Med* 2022; **386**: 449-462 [PMID: 35108470 DOI: 10.1056/NEJMoa2111380]

41 **Sun JM**, Shen L, Shah MA, Enzinger P, Adenis A, Doi T, Kojima T, Metges JP, Li Z, Kim SB, Cho BC, Mansoor W, Li SH, Sunpaweravong P, Maqueda MA, Goekkurt E, Hara H, Antunes L, Fountzilas C, Tsuji A, Oliden VC, Liu Q, Shah S, Bhagia P, Kato K; KEYNOTE-590 Investigators. Pembrolizumab plus chemotherapy versus chemotherapy alone for first-line treatment of advanced oesophageal cancer (KEYNOTE-590): a randomised, placebo-controlled, phase 3 study. *Lancet* 2021; **398**: 759-771 [PMID: 34454674 DOI: 10.1016/S0140-6736(21)01234-4]

42 **Janjigian YY**, Shitara K, Moehler M, Garrido M, Salman P, Shen L, Wyrwicz L, Yamaguchi K, Skoczylas T, Campos Bragagnoli A, Liu T, Schenker M, Yanez P, Tehfe M, Kowalyszyn R, Karamouzis MV, Bruges R, Zander T, Pazo-Cid R, Hitre E, Feeney K, Cleary JM, Poulart V, Cullen D, Lei M, Xiao H, Kondo K, Li M, Ajani JA. First-line nivolumab plus chemotherapy versus chemotherapy alone for advanced gastric, gastro-oesophageal junction, and oesophageal adenocarcinoma (CheckMate 649): a randomised, open-label, phase 3 trial. *Lancet* 2021; **398**: 27-40 [PMID: 34102137 DOI: 10.1016/S0140-6736(21)00797-2]

43 **Kang YK**, Chen LT, Ryu MH, Oh DY, Oh SC, Chung HC, Lee KW, Omori T, Shitara K, Sakuramoto S, Chung IJ, Yamaguchi K, Kato K, Sym SJ, Kadowaki S, Tsuji K, Chen JS, Bai LY, Oh SY, Choda Y, Yasui H, Takeuchi K, Hirashima Y, Hagihara S, Boku N. Nivolumab plus chemotherapy versus placebo plus chemotherapy in patients with HER2-negative, untreated, unresectable advanced or recurrent gastric or gastro-oesophageal junction cancer (ATTRACTION-4): a randomised, multicentre, double-blind, placebo-controlled, phase 3 trial. *Lancet Oncol* 2022; **23**: 234-247 [PMID: 35030335 DOI: 10.1016/S1470-2045(21)00692-6]

44 **Safran HP**, Winter K, Ilson DH, Wigle D, DiPetrillo T, Haddock MG, Hong TS, Leichman LP, Rajdev L, Resnick M, Kachnic LA, Seaward S, Mamon H, Diaz Pardo DA, Anderson CM, Shen X, Sharma AK, Katz AW, Salo J, Leonard KL, Moughan J, Crane CH. Trastuzumab with trimodality treatment for oesophageal adenocarcinoma with HER2 overexpression (NRG Oncology/RTOG 1010): a multicentre, randomised, phase 3 trial. *Lancet Oncol* 2022; **23**: 259-269 [PMID: 35038433 DOI: 10.1016/S1470-2045(21)00718-X]

45 **Takahari D**, Kawazoe A, Machida N, Minashi K, Yamagata Y, Hara H, Wakabayashi M, Komura Y, Sato A, Kuwata T, Kojima M, Shitara K. Phase 2 study of trastuzumab deruxtecan in the neoadjuvant treatment for patients with HER2-positive gastric and gastroesophageal junction adenocarcinoma (EPOC2003). *Journal of Clinical Oncology***40** (16_suppl): TPS4161-TPS [DOI: 10.1200/JCO.2022.40.16_suppl.TPS4161]

46 **Suh YS**, Na D, Lee JS, Chae J, Kim E, Jang G, Lee J, Min J, Ock CY, Kong SH, George J, Zhang C, Lee HJ, Kim JI, Kim SJ, Kim WH, Lee C, Yang HK. Comprehensive Molecular Characterization of Adenocarcinoma of the Gastroesophageal Junction Between Esophageal and Gastric Adenocarcinomas. *Ann Surg* 2022; **275**: 706-717 [PMID: 33086305 DOI: 10.1097/SLA.0000000000004303]

47 **Yang YM**, Hong P, Xu WW, He QY, Li B. Advances in targeted therapy for esophageal cancer. *Signal Transduct Target Ther* 2020; **5**: 229 [PMID: 33028804 DOI: 10.1038/s41392-020-00323-3]

48 **Bang YJ**, Kim YW, Yang HK, Chung HC, Park YK, Lee KH, Lee KW, Kim YH, Noh SI, Cho JY, Mok YJ, Ji J, Yeh TS, Button P, Sirzén F, Noh SH; CLASSIC trial investigators. Adjuvant capecitabine and oxaliplatin for gastric cancer after D2 gastrectomy (CLASSIC): a phase 3 open-label, randomised controlled trial. *Lancet* 2012; **379**: 315-321 [PMID: 22226517 DOI: 10.1016/S0140-6736(11)61873-4]

49 **Noh SH**, Park SR, Yang HK, Chung HC, Chung IJ, Kim SW, Kim HH, Choi JH, Kim HK, Yu W, Lee JI, Shin DB, Ji J, Chen JS, Lim Y, Ha S, Bang YJ; CLASSIC trial investigators. Adjuvant capecitabine plus oxaliplatin for gastric cancer after D2 gastrectomy (CLASSIC): 5-year follow-up of an open-label, randomised phase 3 trial. *Lancet Oncol* 2014; **15**: 1389-1396 [PMID: 25439693 DOI: 10.1016/S1470-2045(14)70473-5]

50 **Yoshida K**, Kodera Y, Kochi M, Ichikawa W, Kakeji Y, Sano T, Nagao N, Takahashi M, Takagane A, Watanabe T, Kaji M, Okitsu H, Nomura T, Matsui T, Yoshikawa T, Matsuyama J, Yamada M, Ito S, Takeuchi M, Fujii M. Addition of Docetaxel to Oral Fluoropyrimidine Improves Efficacy in Patients With Stage III Gastric Cancer: Interim Analysis of JACCRO GC-07, a Randomized Controlled Trial. *J Clin Oncol* 2019; **37**: 1296-1304 [PMID: 30925125 DOI: 10.1200/JCO.18.01138]

51 **Kakeji Y**, Yoshida K, Kodera Y, Kochi M, Sano T, Ichikawa W, Lee SW, Shibahara K, Shikano T, Kataoka M, Ishiguro A, Ojima H, Sakai Y, Musha N, Takase T, Kimura T, Takeuchi M, Fujii M. Three-year outcomes of a randomized phase III trial comparing adjuvant chemotherapy with S-1 plus docetaxel versus S-1 alone in stage III gastric cancer: JACCRO GC-07. *Gastric Cancer* 2022; **25**: 188-196 [PMID: 34351555 DOI: 10.1007/s10120-021-01224-2]

52 **Sasako M**, Sakuramoto S, Katai H, Kinoshita T, Furukawa H, Yamaguchi T, Nashimoto A, Fujii M, Nakajima T, Ohashi Y. Five-year outcomes of a randomized phase III trial comparing adjuvant chemotherapy with S-1 versus surgery alone in stage II or III gastric cancer. *J Clin Oncol* 2011; **29**: 4387-4393 [PMID: 22010012 DOI: 10.1200/JCO.2011.36.5908]

World Journal of Gastroenterology

Submit a Manuscript: https://www.f6publishing.com

World J Gastroenterol 2023 June 28; 29(24): 3770-3792

DOI: 10.3748/wjg.v29.i24.3770

ISSN 1007-9327 (print) ISSN 2219-2840 (online)

ORIGINAL ARTICLE

Basic Study

Mechanism of ELL-associated factor 2 and vasohibin 1 regulating invasion, migration, and angiogenesis in colorectal cancer

Ming-Liang Feng, Ming-Jun Sun, Bo-Yang Xu, Meng-Yuan Liu, Hui-Jing Zhang, Can Wu

Specialty type: Oncology

Provenance and peer review: Unsolicited article; Externally peer reviewed.

Peer-review model: Single blind

Peer-review report's scientific quality classification

Grade A (Excellent): 0
Grade B (Very good): B
Grade C (Good): C, C
Grade D (Fair): 0
Grade E (Poor): 0

P-Reviewer: Cabezuelo AS, Spain; Ekine-Afolabi B, United Kingdom; Solimando AG, Italy

Received: January 18, 2023
Peer-review started: January 18, 2023
First decision: March 26, 2023
Revised: April 8, 2023
Accepted: May 12, 2023
Article in press: May 12, 2023
Published online: June 28, 2023

Ming-Liang Feng, Ming-Jun Sun, Bo-Yang Xu, Meng-Yuan Liu, Hui-Jing Zhang, Can Wu, Department of Endoscopy, The First Hospital Affiliated to China Medical University, Shenyang 110001, Liaoning Province, China

Corresponding author: Can Wu, PhD, Associate Research Scientist, Attending Doctor, Department of Endoscopy, The First Hospital Affiliated to China Medical University, No. 155 Nanjing North Street, Shenyang 110000, Liaoning Province, China. wucanydyy@163.com

Abstract

BACKGROUND

As a novel endogenous anti-angiogenic molecule, vasohibin 1 (VASH1) is not only expressed in tumor stroma, but also in tumor tissue. Moreover, studies have shown that VASH1 may be a prognostic marker in colorectal cancer (CRC). Knockdown of VASH1 enhanced transforming growth factor-β1 (TGF-β1)/Smad3 pathway activity and type I/III collagen production. Our previous findings suggest that ELL-associated factor 2 (EAF2) may play a tumor suppressor and protective role in the development and progression of CRC by regulating signal transducer and activator of transcription 3 (STAT3)/TGF-β1 signaling pathway. However, the functional role and mechanism of VASH1-mediated TGF-β1 related pathway in CRC has not been elucidated.

AIM

To investigate the expression of VASH1 in CRC and its correlation with the expression of EAF2. Furthermore, we studied the functional role and mechanism of VASH1 involved in the regulation and protection of EAF2 in CRC cells *in vitro*.

METHODS

We collected colorectal adenocarcinoma and corresponding adjacent tissues to investigate the clinical expression of EAF2 protein and VASH1 protein in patients with advanced CRC. Following, we investigated the effect and mechanism of EAF2 and VASH1 on the invasion, migration and angiogenesis of CRC cells *in vitro* using plasmid transfection.

RESULTS

Our findings indicated that EAF2 was down-regulated and VASH1 was up-regulated in advanced CRC tissue compared to normal colorectal tissue. Kaplan-Meier survival analysis showed that the higher EAF2 Level group and the lower VASH1 Level group had a higher survival rate. Overexpression of EAF2 might

inhibit the activity of STAT3/TGF-β1 pathway by up-regulating the expression of VASH1, and then weaken the invasion, migration and angiogenesis of CRC cells.

CONCLUSION

This study suggests that EAF2 and VASH1 may serve as new diagnostic and prognostic markers for CRC, and provide a clinical basis for exploring new biomarkers for CRC. This study complements the mechanism of EAF2 in CRC cells, enriches the role and mechanism of CRC cell-derived VASH1, and provides a new possible subtype of CRC as a therapeutic target of STAT3/TGF-β1 pathway.

Key Words: ELL-associated factor 2; Vasohibin 1; Transforming growth factor-β1; Signal transducer and activator of transcription 3; Colorectal cancer; Angiogenesis

©The Author(s) 2023. Published by Baishideng Publishing Group Inc. All rights reserved.

Core Tip: Endothelial cell-derived vasohibin 1 (VASH1) can regulate tumor angiogenesis and lymphangiogenesis, and tumor cell-derived VASH1 also has a potential functional role in inhibiting cancer cell proliferation and invasion. Knockdown of VASH1 enhanced transforming growth factor beta 1 (TGF-β) /Smad3 pathway activity and type I/III collagen production. Our previous findings suggest that ELL-associated factor 2 (EAF2) may play a tumor suppressor and protective role in the development and progression of colorectal cancer (CRC) by regulating signal transducer and activator of transcription 3 (STAT3)/TGF-β1 signaling pathway. In this study, we found that EAF2 was down-regulated and VASH1 was up-regulated in advanced CRC tissue compared to normal colorectal tissue by immunohistochemistry and Western blot. And the expression levels of EAF2 and VASH1 were positively correlated in advanced CRC tissue. Furthermore, *in vitro* cellular mechanism studies suggest that overexpression of EAF2 may inhibit the activity of STAT3/TGF-β1 pathway by up-regulating the expression of VASH1, thereby attenuating the invasion, migration and angiogenesis of CRC cells. This study provides new ideas and theoretical basis for the development of new diagnostic markers for CRC and the exploration of the mechanism of targeted therapy.

Citation: Feng ML, Sun MJ, Xu BY, Liu MY, Zhang HJ, Wu C. Mechanism of ELL-associated factor 2 and vasohibin 1 regulating invasion, migration, and angiogenesis in colorectal cancer. *World J Gastroenterol* 2023; 29(24): 3770-3792

URL: https://www.wjgnet.com/1007-9327/full/v29/i24/3770.htm

DOI: https://dx.doi.org/10.3748/wjg.v29.i24.3770

INTRODUCTION

The diagnosis and treatment of colorectal cancer (CRC) have greatly improved in recent years, and its incidence and mortality have steadily decreased by about 1.7% and 3.2% per year respectively[1]. This has benefited from the continuous in-depth research on the pathogenesis of CRC, especially the application of protein molecular markers and targeted therapy. However, the pathogenesis of CRC has not been fully elucidated, and its diagnosis and treatment remain a major challenge in clinical work. Malignant tumor metastasis is one of the main factors leading to poor survival of patients with CRC[2]. Therefore, there is an urgent need to clarify the potential mechanisms of invasion and metastasis of CRC and explore new therapeutic targets.

Current studies have shown that not only the proliferation, invasion, and metastasis of cancer cells themselves contribute to the growth, progression, and distant metastasis of CRC, but tumor microenvironmental factors such as tumor angiogenesis also play a crucial role. As a novel endogenous anti-angiogenic molecule, vasohibin 1 (VASH1) increased ΔY-tubulin level to attenuate endocytosis of vascular endothelial growth factor (VEGF) receptor 2 and fibroblast growth factor (FGF) receptor 1, resulting in suppressing pro-angiogenic factor-induced endothelial cells migration[3]. Several studies have shown that the expression of VASH1 in tumor tissue and stroma can be used as a new molecular marker for tumor prognosis. In addition, cancer cell-derived VASH1 regulates tumor growth and metastasis both *in vitro* and *in vitro*[4-6]. And studies have shown that VASH1 may be a marker for the prognosis of CRC[7-9]. It has been suggested that stroma VASH1 Level is negatively correlated with tumor size, clinical stage, and distant metastasis in colon cancer patients[8]. Whereas, other studies have suggested that the overall survival (OS) of patients with high VASH1 expression in CRC tissue are significantly lower than those with low VASH1 expression[9]. To date, the expression of VASH1 in CRC

cancer tissue and cancer cells remains controversial, the effect and mechanism of cancer cell-derived VASH1 have not been clarified.

Ingenuity Pathway Analysis showed that transforming growth factor (TGF)-β/SMAD signaling pathway was one of the most common mutated pathways in CRC metastasis[10]. Knockdown of VASH1 enhanced Smad3 phosphorylation and type I/III collagen production in renal fibroblasts stimulated by TGF-β[11]. What's more, inhibition of VASH1 in islet β cells can activate GF-β1 pathway and promote insulin resistance in gestational diabetes mellitus patients[12]. TGF-β1 is abundantly expressed in the tumor microenvironment of a variety of human tumors, which is an important molecular pathway connecting tumor cells with the surrounding microenvironment and leading to resistance to checkpoint blockade therapy[13]. More notably, blockade of TGF-β1 signaling is a strategic approach to treat CRC tumor metastasis[14]. Nevertheless, whether CRC cell-derived VASH1 regulates TGF-β1 related pathways in tumor development has not been investigated.

Androgen-responsive protein ELL-associated factor 2 (EAF2) has been shown to inhibit the growth of tumor size in prostate cancer models *in vivo*[15], and inhibit the proliferation and migration of prostate cancer cells *in vitro*[16]. Recent studies have found that EAF2 acts as a tumor suppressor in a variety of malignant tumors, such as renal cancer cells, human liver cancer cells and breast cancer cells[17,18]. In-depth mechanistic studies showed that EAF2 was involved in the regulation of cancer cell function by attenuating TGF-β1-induced G1 phase cell cycle arrest and cell migration[18]. In addition, silencing of EAF2 expression could modulate the cytotoxic response to statins in HCT-116 cells[19]. Our previous findings suggested that EAF2 may play a tumor suppressor and protective role in the development and progression of CRC by regulating STAT3/TGF-β1 signaling pathway[20]. Therefore, we ventured to speculate whether the mechanism of VASH1 in CRC was related to the EAF2-mediated TGF-β1 pathway.

In this study, we aimed to investigate the expression of VASH1 in CRC and its correlation with the expression of EAF2. To further explore the functional role and mechanism of VASH1-mediated TGF-β1 related pathway in CRC cells. To investigate whether VASH1 is involved in the regulation and protection of EAF2 in CRC cells by regulating STAT3/TGF-β1 signaling pathway. It provides a clinical basis for discovering new clinical diagnostic and prognostic markers of CRC, and a theoretical basis for elucidating its development mechanism and exploring new molecular targeted therapy.

MATERIALS AND METHODS

CRC patients and tissue samples

A total of 120 cases of colorectal adenocarcinoma and corresponding adjacent tissues were collected at the First Hospital of China Medical University from 2012 to 2017. Patients who received preoperative radiotherapy or chemotherapy were excluded. The American Joint Committee on Cancer/Union for International Cancer Control 8th edition TNM staging system was used for tumor staging. The study was approved by the institutional review board of the First Affiliated Hospital of China Medical University (registration number 2021-68-2, informed consent waived).

Cell culture

We cultured NCM460 and CRC cell lines (SW480, RKO, HCT116, HT29, and LoVo) (Chinese Academy of Sciences, Shanghai, China) with PMIS 1640 medium (Gibco, Grand Island, NY, United States) containing 10% fetal bovine serum (FBS; Gibco, Grand Island, NY, United States) in a humidified incubator at 37 °C with 5% CO_2. And we treated CRC cells with 5 ng/mL recombinant human TGF-β1 protein (100-21, PeproTech, United States) for 24 h. Human Umbilical Vein Endothelial Cells (HUVECs, Chinese Academy of Sciences, Shanghai, China) were cultured with DMEM medium (Gibco, Grand Island, NY, United States) containing 10% FBS (Gibco, Grand Island, NY, United States) in a humidified incubator at 37 °C and 5% CO_2.

Cell transfection

Gene transfection plasmids designed and synthesized by GeneChem (Shanghai, China) were used to treat CRC cells, including overexpressing human EAF2 plasmid (GenBank No. NM_018456), overexpressing human VASH1 plasmid (GenBank No. NM_014909), silencing human STAT3 plasmids (GenBank registration No. NM_139276) and silencing VASH1 plasmids (GenBank No. NM_014909). Table 1 Lists three gene-silencing plasmids targeting human STAT3 plasmids and three targeting human VASH1 plasmids. Lipofectamine 2000 Kit (Invitrogen, Carlsbad, CA, United States) was used to transfect plasmids into CRC cells for cell transfection.

Immunohistochemistry

Tissue blocks were fixed and serially sectioned. Antigen repair was performed with citric acid or repair solution, and endogenous peroxidase was blocked with hydrogen peroxide (3%). Rabbit anti-EAF2 monoclonal antibody (1:200 dilution, ab237753) (Abcam, United Kingdom) and rabbit anti-VASH1

Table 1 Gene sequences used for transfection

Gene	Sequences	
STAT3-siRNA	siRNA-S1-a	5′-CCG GGC TGA CCA ACA ATC CCA AGA ACT CGA GTT CTT GGG ATT GTT GGT CAG CTT TTT G-3′
	siRNA-S1-b	5′-AAT TCA AAA AGC TGA CCA ACA ATC CCA AGA ACT CGA GTT CTT GGG ATT GTT GGT CAG C-3′
	siRNA-S2-a	5′-CCG GGC ACA ATC TAC GAA GAA TCA ACT CGA GTT GAT TCT TCG TAG ATT GTG CTT TTT G-3′
	siRNA-S2-b	5′- AAT TCA AAA AGC ACA ATC TAC GAA GAA TCA ACT CGA GTT GAT TCT TCG TAG ATT GTG C-3′
	siRNA-S3-a	5′- CCG GGC TGA AAT CAT CAT GGG CTA TCT CGA GAT AGC CCA TGA TGA TTT CAG CTT TTT G-3′
	siRNA-S3-b	5′- AAT TCA AAA AGC TGA AAT CAT CAT GGG CTA TCT CGA GAT AGC CCA TGA TGA TTT CAG C-3′
VASH1-siRNA	siRNA-V1-a	5′-CCG GCT GCC AAT CAA ATG CCT GGA ACT CGA GTT CCA GGC ATT TGA TTG GCA GTT TTT G -3′
	siRNA-V1-b	5′-AAT TCA AAA ACT GCC AAT CAA ATG CCT GGA ACT CGA GTT CCA GGC ATT TGA TTG GCA G -3′
	siRNA-V2-a	5′-CCG GGA GCT GCA GTA CAA TCA CAC ACT CGA GTG TGT GAT TGT ACT GCA GCT CTT TTT G-3′
	siRNA-V2-b	5′-AAT TCA AAA AGA GCT GCA GTA CAA TCA CAC ACT CGA GTG TGT GAT TGT ACT GCA GCT C-3′
	siRNA-V3-a	5′-CCG GCA CAG GAC ATA GTG GTG CTT TCT CGA GAA AGC ACC ACT ATG TCC TGT GTT TTT G-3′
	siRNA-V3-b	5′-AAT TCA AAA ACA CAG GAC ATA GTG GTG CTT TCT CGA GAA AGC ACC ACT ATG TCC TGT G -3′

STAT3: Signal transducer and activator of transcription 3; VASH1: Vasohibin 1.

polyclonal antibody (5 μg/mL) (Abcam, United Kingdom) were then incubated overnight at 4 °C. Subsequently, secondary antibodies were incubated at 37 °C for 40 min. The stains were stained with diamine benzidine and counterstained with hematoxylin. Finally, the slices are air-dried, dehydrated and installed.

Slides were read in a double-blind manner by two experienced pathologists. The final staining score is the proportion score multiplied by the intensity score. Five 200 × high-power fields were randomly selected for each section, and the intensity of immunostaining was classified into four categories: 0 (negative immunostaining), 1 (weak immunostaining), 2 (moderate immunostaining), and 3 (strong immunostaining). The percentage of positive cells was also counted: 0 (positive cells < 5%); 1 (5%-25% positive cells), 2 (26%-50% positive cells), 3 (51%-75% positive cells), and 4 (> 75% positive cells).

Western blot assay

Tissues and cells were lysed with RIPA lysates containing PMSF protease inhibitors. Protein was extracted and assayed by BCA kit (Beyotime Institute of Biotechnology, China). Equal amounts of proteins (50 μg per sample) were separated by 10% sodium dodecyl sulfate/polyacrylamide gel electrophoresis (SDS/PAGE) at 80 V and then transferred to polyvinylidene difluoride (PVDF) membranes at a constant current of 200 mA. PVDF membranes were incubated with primary antibodies overnight at 4 °C. Primary antibodies to EAF2 (ab151692), VASH1 (ab176114) (Abcam, United Kingdom), TGF-β1 (#3709), phospho-STAT3 (Tyr705) (#9145), and STAT3 (#30835) (Cell Signaling, Danvers, MA, United States) were used at a 1:1000 dilution ratio and normalized to a 1:1000 dilution ratio for GAPDH (FL-335) (Santa Cruz, CA, United States). The PVDF membranes were further incubated with secondary antibody (1:5000) for 2 h at 37 °C. The immunoreactive bands were washed with PBS and detected by the Microchemi 4.2 bioimaging system using ECL-Plus chemiluminescence detection HRP reagent (Beyotime Institute of Biotechnology, China). ImageJ software was used to analyze the gray value of the Western blot results. The experiment was repeated at least 3 times under the same experimental conditions (Supplementary Figure 1).

Transwell invasion and migration assay

Matrigel (BD Biosciences, San Diego, CA, United States) was diluted in serum-free medium at 1:8 and spread in an 8-μM transwell chamber (3422, Corning, NY, United States) at 37 °C for 6 h. After the matrix gel for invasion assay was successfully prepared, 4 × 10^4 cells/well were diluted with 200 μL serum-free medium and inoculated into the upper chamber of 8-μM transwell chamber (3422), and 600 μL medium containing 20% FBS was added to the lower chamber.

In the transwell migration experiment, 2 × 10^5 cells/well diluted with 200 μL serum-free medium were inoculated into the upper chamber of Matrigel-free transwell chamber (3422) with a diameter of 8 μM, and 600 μL culture medium containing 10% FBS was injected into the lower chamber.

The chambers were collected after incubation for 72 h at 37 °C under constant temperature regulation. The chamber filters were fixed with methanol after removing the cells that were not invaded or migrated on the inner surface of the chamber filters. Cells that had been invaded or migrated on the fixed filter membrane were further stained with 0.1% crystal violet. The filter membrane was then

removed from the chamber and fixed. Finally, the invasive and metastatic cells were counted in 5 randomly selected fields under a light microscope (200 ×). Repeat the experiment at least 3 times under the same experimental conditions.

Wound healing assay

Cells were seeded in 6-well plates at 2 × 10^5 cells/well. When the cell confluence reached 90%, a 200 μL pipette tip was used to scratch the wound. Incubation was continued with medium containing 2% serum after gentle washing. The scratch wounds of five regions were selected and photographed (40 ×) at 0 h, 6 h, 12 h, 24 h, 48 h, and 72 h, respectively. The ImageJ software was used to measure the wound area. Repeat the experiment at least 3 times under the same experimental conditions.

Tube formation assay

Undiluted Matrigel (BD Biosciences) was plated in 96-well plates and incubated at 37 °C for 1 h in preparation for tube formation experiments. RKO cells were treated with TGF-β1 recombinant protein or EAF2 overexpression plasmid or VASH1 overexpression plasmid, and then conditioned medium was collected for later use. HUVECs were suspended with the collected conditioned medium and seeded in Matrigel coated 96-well plates at a density of 1.0 × 10^4 cells/well, and then incubated at 37 °C in an incubator containing 5% CO_2. After 6 h, the best tube formation was observed under inverted microscope (100 ×). Finally, the images were analyzed using the angiogenesis analyzer developed by Image J software to evaluate branch points. The experiment was repeated at least 3 times under the same experimental conditions.

HUVEC transwell migration assay

A total of 1 × 10^5 HUVECs were diluted with 200 μL serum-free medium and seeded into the upper chamber of Matrigel-free transwell chamber (3422) with a diameter of 8 μM. Conditioned medium was collected from RKO cells treated with TGF-β1 recombinant protein or EAF2 overexpression plasmid or VASH1 overexpression plasmid and placed in the lower chamber.

The chambers were collected after incubation for 6 h at 37 °C under constant temperature regulation. The chamber filters were fixed with methanol after removing the cells that were not invaded or migrated on the inner surface of the chamber filters. Cells that had been invaded or migrated on the fixed filter membrane were further stained with 0.1% crystal violet. The filter membrane was then removed from the chamber and fixed. Finally, the invasive and metastatic cells were counted in 5 randomly selected fields under a light microscope (200 ×). Repeat the experiment at least 3 times under the same experimental conditions.

HUVEC scratch assay

A total of 2 × 10^5 HUVECs/well was seeded in 6-well plates. When the cells reached about 90% confluence, a 200 μL tip was used for scratch. The cells were then washed three times with PBS and the incubation was continued with 2 mL of conditioned medium collected from RKO cells treated with TGF-β1 recombinant protein or EAF2 overexpression plasmid or VASH1 overexpression plasmid. Five areas (40 ×) were selected and photographed under a microscope at 0 h, 12 h, and 24 h time points. The ImageJ software was used to measure the wound area. The experiment was repeated at least 3 times under the same experimental conditions.

Statistical analysis

SPSS software (Version 26) was used for statistical analysis of the result data. Wilcoxon signed-rank test and Spearman rank correlation analysis were used to evaluate the expression of EAF2 and VASH1 and their correlation. Pearson's chi-square test was used to evaluate the correlation between proteins expression in tissues and clinicopathological parameters. All data were expressed as mean ± SD. Kaplan-Meier method and Log-rank tests were used for survival analysis. Student's t test was used for comparison between two groups, and one-way analysis of variance was used for comparison between three or more groups. One-way analysis of variance and Bonferroni test were used for statistical analysis. All P values were two-sided. A value of $P < 0.05$ was considered statistically significant.

RESULTS

Protein expression of EAF2 and VASH1 in CRC tissue

Immunohistochemical analysis was performed on paired adenocarcinoma and paracancerous tissues. The results of semi-quantitative analysis showed that the median score of EAF2 was 4.0 points in adenocarcinoma tissue and 7.2 points in paired paracancer tissue, with a median difference of -2.0 points. Wilcoxon signed-rank test showed that the expression level of EAF2 protein in adenocarcinoma tissue was significantly lower than that in paracancerous tissue ($Z = -5.843$, $P < 0.001$). Meanwhile, the median score of VASH1 was 12.0 points in adenocarcinoma tissue and 5.0 points in paired non-cancer

tissue, with a median difference of 6.0 points. The results of Wilcoxon signed-rank test showed that the expression of VASH1 protein in adenocarcinoma tissue was significantly higher than that in paracancerous tissue (Z = -8.594, P < 0.001). In addition, Spearman's rank correlation analysis showed that the expression of EAF2 and VASH1 protein in colorectal adenocarcinoma tissue was significantly positively correlated (r = 0.208, P = 0.022). Besides, localization analysis showed that EAF2 and VASH1 proteins were mainly located in the cytoplasm of colon epithelial cells (Figure 1A).

Not only that, Western blot was used to detect the protein expression of EAF2 and VASH1 in 8 paired fresh colorectal adenocarcinoma tissue and adjacent normal tissue. Compared with adjacent normal tissue, EAF2 protein expression was significantly lower (P = 0.023), while VASH1 protein expression was significantly higher (P < 0.001) in colorectal adenocarcinoma tissues (Figure 1B).

Association of EAF2 and VASH1 expression with clinicopathological parameters and the survival analysis in advanced CRC patients

The semi-quantitative immunohistochemical results of EAF2 and VASH1 in CRC patients were analyzed by ROC curve and the Youden index was determined. The results suggested that the cut-off value delimiting high and low expression of EAF2 (dependent variable is non-cancer) was 6.2 points (P < 0.001), and the cut-off value delimiting high and low expression of VASH1 (dependent variable is cancer, P < 0.01 indicated that it was significant for the diagnosis of tumor) was 8.5 points (P < 0.001). In this study, 100 of 120 CRC tissues were found to have EAF2 Low-expression and 84 were found to have VASH1 high-expression.

After defining the high and low expression of EAF2 and VASH1 proteins in colorectal adenocarcinoma tissues, the relationship between them and major clinicopathological features was further analyzed. We found that EAF2 protein was negatively correlated with angiolymphatic and/or perineural invasion (r = -0.180, P = 0.049), tumor stage (r = -0.194, P = 0.034), distant metastasis (r = -0.244, P = 0.007), and CEA (r = -0.211, P = 0.021), as well as positively correlated with the degree of differentiation (r = 0.225, P = 0.013) (Table 2). VASH1 protein was positively correlated with degree of differentiation (r = 0.186, P = 0.042), angiolymphatic and/or perineural invasion (r = 0.249, P = 0.006), distant metastasis (r = 0.190, P = 0.037), but not with other clinical characteristics (Table 2).

Furthermore, Kaplan-Meier survival analysis and Log-rank test showed that the survival rate of EAF2High group was higher than that of EAF2Low group (P = 0.016), and the survival rate of VASH1Low group was higher than that of VASH1High group (P = 0.047) (Figure 2).

Cox proportional-hazards model was used to analyze the influencing factors of OS in patients with advanced CRC. By univariate analysis, we found angiolymphatic and/or perineural invasion (P < 0.001), tumor stage (P < 0.001), tumor invasion depth (P < 0.001), lymph node status (P < 0.001), distant metastasis (P < 0.001) and EAF2 protein expression level (P = 0.024), p53 protein expression level (P = 0.048) were significantly associated with OS (Table 3). Confounding factors were further adjusted to evaluate the independent prognostic factors of OS in patients with advanced CRC. The clinicopathological features with P < 0.300 in the univariate analysis were included in the multivariate analysis, and the results suggested that, angiolymphatic and/or perineural invasion (P = 0.033), distal metastasis (P < 0.001), CEA protein expression (P = 0.004), p53 protein expression level (P = 0.048) were independent prognostic factors for OS (Table 3).

VASH1 overexpression inhibited STAT3/TGF-β1 pathway activity in RKO

Normal colorectal epithelial cells (NCM460) and a variety of human CRC cell lines (SW480, RKO, HCT116, HT29, and LoVo) were cultured *in vitro*. Western blot assay showed that, compared with NCM460 cells, VASH1 protein levels were increased to varying degrees in human CRC cell lines (Figure 3), and the expression was upregulated 2.336-fold in RKO cells (P = 0.002).

In addition, the expression level of phosphorylated STAT3 (Tyr705) (P < 0.001) and TGF-β1 protein (P < 0.001) in RKO were significantly higher than those in normal colorectal epithelial cells (NCM460). And then we suppressed STAT3 phosphorylation by transfecting RKO cells with silencing plasmid. In this study, RKO cells were transfected with three different STAT3 siRNAs (STAT3-si1, STAT3-si2, and STAT3-si3) targeting the STAT3 gene (Figure 4A). When compared to the control group (RKO-C), transfection with the three different STAT3-siRNAs decreased phosphorylated STAT3 expression. Additionally, STAT3-si2 was the most efficient, with a reduction of 61.8% in phosphorylated STAT3 expression (P < 0.001) (Figure 4A). Further study showed that when STAT3-si2 was transfected to silence STAT3, the expression of TGF-β1 protein in RKO was significantly lower than that in the normal control group (Figure 4B).

We used gene transfection technique to overexpress or silence the VASH1 gene in RKO cells and determined the activity and expression of STAT3/TGF-β1 signaling pathway. The results showed that overexpression of VASH1 (with 1.906-fold higher, P < 0.001, Figure 5B) significantly inhibited STAT3 phosphorylation (Tyr705) as well as TGF-β1 protein expression (Figure 5B). What's more, we transfected RKO cells with three different VASH1 siRNAs (VASH1-si1, VASH1-si2, and VASH1-si3) targeting the VASH1 gene (Figure 5A). When compared to the control group (RKO-C), transfection with the three different VASH1-siRNAs decreased VASH1 protein expression. Additionally, VASH1-si1 was the most efficient, with a reduction of 64.02% in VASH1 protein expression (P < 0.001) (Figure 5A). As a result,

Table 2 Baseline characteristics of patients with advanced colorectal cancer and the correlation with immunohistochemical expression of ELL-associated factor 2 and vasohibin 1

Clinicopathologic characteristics	Cases, *n* (%)	EAF2		*P* value	VASH1		*P* value
		Low (*n* = 100)	High (*n* = 20)		Low (*n* = 36)	High (*n* = 84)	
Age (yr)				0.569			0.248
< 61 (median)	44.17	43	10		13	40	
≥ 61	55.83	57	10		23	44	
Gender				0.935			0.843
Male	54.17	54	11		20	45	
Female	45.83	46	9		16	39	
Tumor site				0.657			0.515
Colon	29.17	30	5		9	26	
Rectum	70.83	70	15		27	58	
Size of the tumor, cm				0.250			0.689
≤ 4	41.67	44	6		16	34	
> 4	58.33	56	14		20	50	
Histological type				0.695			0.566
Mucinous	21.67	21	5		9	17	
Non-mucinous	78.33	79	15		27	67	
Degree of differentiation				0.013			0.042
Well/moderately differentiated	64.17	69	8		28	49	
Poor/mucinous differentiated	35.83	31	12		8	35	
Angiolymphatic and/or perineural invasion				0.049			0.006
Absent	45.00	41	13		23	31	
Present	55.00	59	7		13	53	
TNM				0.034			0.068
I-II	48.33	44	14		22	36	
III-IV	51.67	56	6		14	48	
Tumor invasion depth				0.219			0.084
T2-T3	57.50	55	14		25	44	
T4	42.50	45	6		11	40	
Lymph node status				0.073			0.095
N0	46.67	43	13		21	35	
N1-N2	53.33	57	7		15	49	
Distant metastasis				0.007			0.037
Absent	70.00	65	19		30	54	
Present	30.00	35	1		6	30	
CEA				0.021			0.874
Normal	56.67	52	16		20	48	
High	43.33	48	4		16	36	
CA19-9				0.321			0.809
Normal	40.00	38	10		15	33	

High	60.00	62	10		21	51	
P53				0.219			0.905
Normal	42.50	40	11		15	36	
High	57.50	60	9		21	48	
CDX2				0.224			0.921
Normal	20.00	18	6		7	17	
High	80.00	82	14		29	67	

EAF2: ELL protein-associated factor 2; TNM: Tumor-node-metastasis; CEA: Carcinoembryonic antigen; CA19-9: Carbohydrate antigen 19-9; VASH1: Vasohibin 1.

Table 3 Univariate and multivariate survival analysis of overall survival for colorectal cancer by Cox regression.

Variables	Univariate analysis			Multivariate analysis		
	HR	95%CI	*P* value	HR	95%CI	*P* value
Age (yr) (≥ 61/< 61)	1.703	0.969-2.991	0.064	1.413	0.764-2.613	0.270
Gender (female/male)	0.962	0.561-1.651	0.890			
Tumor site (colon/rectum)	1.410	0.798-2.492	0.237	1.211	0.638-2.298	0.558
Size of the tumor, cm (> 4/≤ 4)	0.777	0.446-1.356	0.375			
Histological type (mucinous/non-mucinous)	1.218	0.612-2.424	0.574			
Degree of differentiation (poor/mucinous, well/moderate)	0.917	0.523-1.608	0.761			
Angiolymphatic and/or perineural invasion (present/absent)	0.209	0.107-0.408	< 0.001	0.255	0.072-0.898	0.033
Tumor stage (III-IV/I-II)	0.240	0.128-0.450	< 0.001	1.455	0.339-6.256	0.614
Tumor invasion depth (T4/T2-T3)	0.353	0.202-0.614	< 0.001	0.547	0.225-1.331	0.184
Lymph node status (N1-N2/N0)	0.288	0.155-0.532	< 0.001	2.150	0.511-9.038	0.296
Distant metastasis (present/absent)	0.161	0.091-0.284	< 0.001	0.200	0.090-0.444	< 0.001
EAF2 (low/high)	3.244	1.170-8.999	0.024	2.049	0.698-6.014	0.191
VASH1 (high/low)	0.518	0.266-1.007	0.052	0.785	0.389-1.584	0.499
CEA (high/low)	1.590	0.906-2.790	0.106	2.506	1.336-4.702	0.004
CA19-9 (high/low)	0.817	0.466-1.433	0.481			
P53 (high/low)	0.558	0.313-0.994	0.048	0.545	0.299-0.995	0.048
CDX2 (high/low)	0.705	0.332-1.495	0.362			

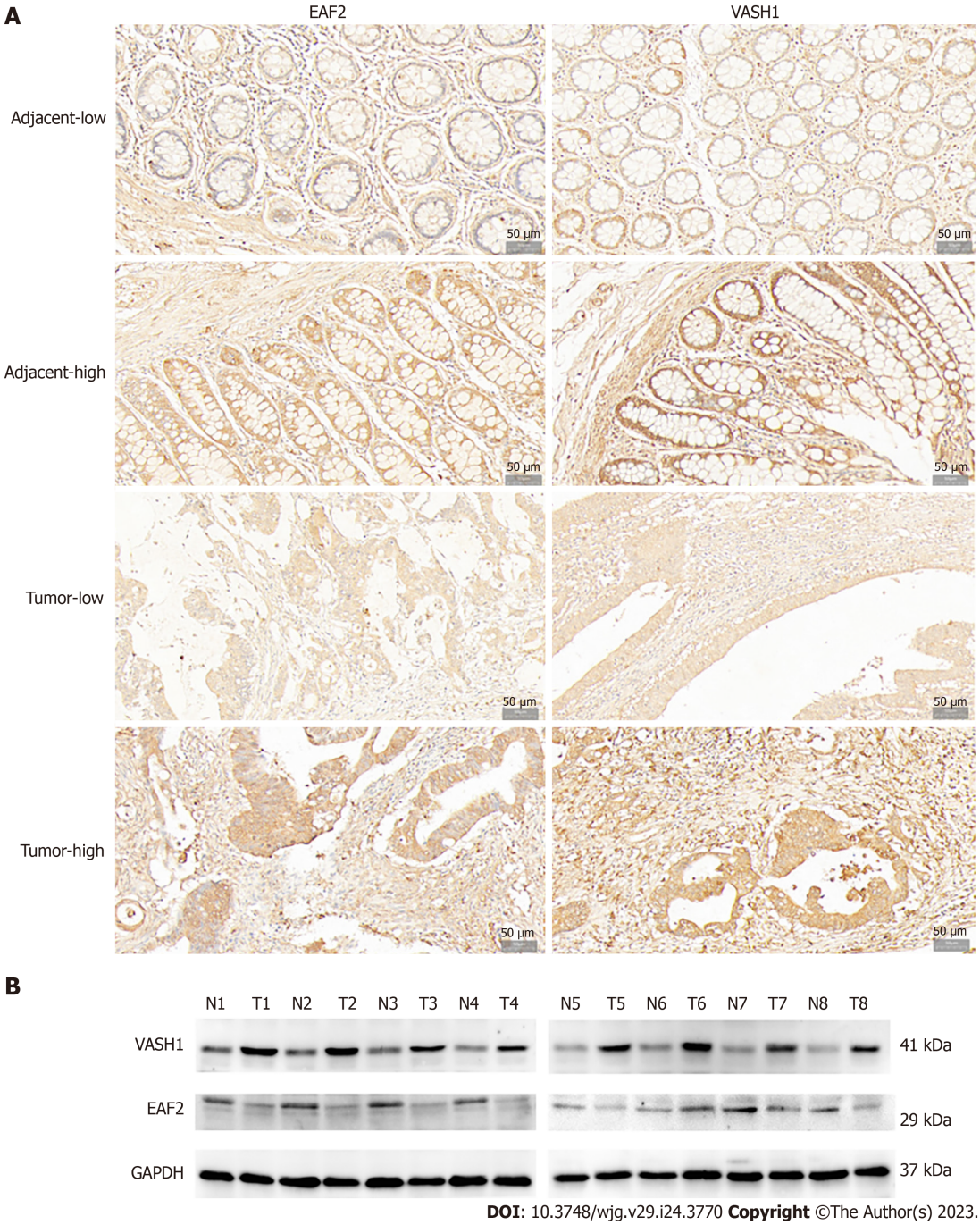
HR: Hazard ratio; CI: Confidence interval; EAF2: ELL protein-associated factor 2; CEA: Carcinoembryonic antigen; CA19-9: Carbohydrate antigen 19-9.

transfection with VASH1 siRNA significantly promoted STAT3 phosphorylation (Figure 5B, $P < 0.001$). However, when RKO cells were transfected with STAT3 siRNA, the expression level of VASH1 protein was not significantly different from that of RKO control group (Figure 4B). Treatment of RKO cells with exogenous TGF-β1 recombinant protein did not affect the expression of VASH1 protein (Figure 4B).

EAF2 overexpression inhibited STAT3/TGF-β1 pathway activity in RKO

Meanwhile, Western blot results also showed that the expression levels of EAF2 protein in human CRC cell lines (SW480, RKO, HCT116, HT29, and LoVo) were decreased to varying degree compared with NCM460 cells (Figure 3), and the decrease was 82.7% in RKO cells ($P < 0.001$). Therefore, we transfected RKO cells with EAF2 overexpression plasmid *in vitro* to investigate the potential function and molecular mechanism of EAF2 in CRC cells.

Transfecting RKO cells with EAF2 overexpression plasmids significantly upregulated the expression of EAF2 protein (with 2.1-fold higher, $P < 0.001$, Figure 5B). At the same time, we also found that the levels of phosphorylated STAT3 (Tyr705) protein and TGF-β1 protein were significantly decreased in RKO cells transfected with EAF2 overexpression plasmids compared with RKO control group.



DOI: 10.3748/wjg.v29.i24.3770 **Copyright** ©The Author(s) 2023.

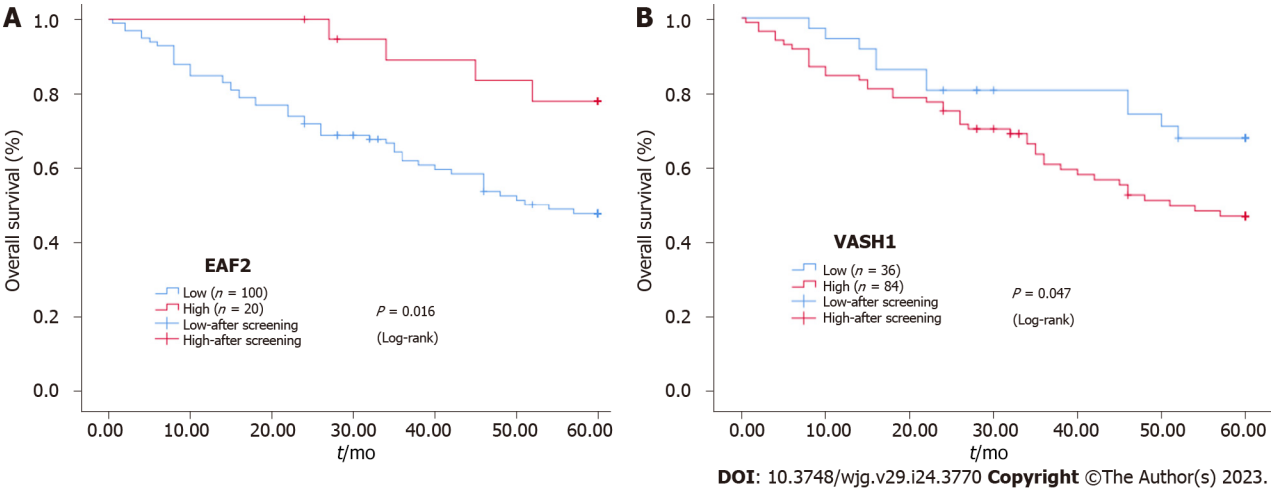
Figure 1 Expression of ELL-associated factor 2 and Vasohibin 1 proteins in tissues of patients with advanced colorectal cancer. A: Representative immunohistochemical staining of ELL-associated factor 2 (EAF2) and vasohibin 1 (VASH1) in colorectal adenocarcinoma tissue and the adjacent non-cancerous tissue (magnification 200 ×); B: The protein bands of EAF2 and VASH1 in 8-matched pairs of colorectal adenocarcinoma tissue and adjacent tissue were detected by Western blot assay. EAF2: ELL-associated factor 2; VASH1: Vasohibin 1; GAPDH: Glyceraldehyde-3-phosphate dehydrogenase; T: Colorectal adenocarcinoma tissue; N: Adjacent non-tumor tissue.

However, silencing STAT3 gene or exogenous TGF-β1 recombinant protein did not affect EAF2 protein expression in RKO cells (Figure 4B).

EAF2 overexpression or VASH1 overexpression inhibited biological function of RKO through STAT3/TGF-β1 pathway

Subsequently, we preliminarily explored the regulatory effects of EAF2 and VASH1 proteins on the biological function of RKO cells through the STAT3/TGF-β1 pathway *in vitro*, in an attempt to provide a scientific basis for exploring the role of EAF2 and VASH1 in CRC.

Transwell invasion assay of matrigel envelope showed that the invasion ability of RKO cells was significantly weakened after transfection of EAF2 overexpression plasmids (Figure 6A, $P < 0.001$). In transwell migration assay, RKO cells transfected with EAF2 overexpressing plasmids showed a



DOI: 10.3748/wjg.v29.i24.3770 **Copyright** ©The Author(s) 2023.

Figure 2 Kaplan-Meier survival curves. A and B: Kaplan-Meier survival curves for the protein expression of ELL-associated factor 2 and vasohibin 1 in colorectal cancer tissue. EAF2: ELL-associated factor 2; VASH1: Vasohibin 1.

significantly reduced migration ability compared with the control group (Figure 6A, $P < 0.001$). Consistent with this, overexpression of EAF2 also significantly reduced the scratch healing ability of RKO cells (Figure 6B, $P < 0.001$). Our treatment of RKO cells with exogenous TGF-β1 recombinant protein significantly promoted the transwell invasion, transwell migration, and scratch healing abilities of RKO cells (Figure 6). More importantly, when the RKO cells transfected with EAF2 overexpression plasmids were treated with TGF-β1 recombinant protein for 24 h, it was found that the transwell invasion, transwell migration and scratch healing abilities of the RKO cells inhibited by EAF2 overexpression were reversed by TGF-β1 recombinant protein (Figure 6).

Furthermore, the RKO cells were transfected with VASH1 overexpression plasmids for transwell invasion assay, transwell migration assay and wound healing assay. Combining the results of Matrigel-coated transwell invasion assay, transwell migration assay and wound healing assay, it was found that compared with RKO control group, RKO cells overexpressing VASH1 protein showed lower transwell invasion, transwell migration, and scratch healing abilities (Figure 7, $P < 0.001$). It was also of concern to us that the transwell invasion, transwell migration, and scratch healing of RKO cells transfected with VASH1 overexpression plasmids could be reversed after 24 h treatment with TGF-β1 recombinant protein (Figure 7, $P < 0.001$).

EAF2 overexpression or VASH1 overexpression inhibited CRC angiogenesis through STAT3/TGF-β1 pathway

Conditioned medium from RKO cells treated with TGF-β1 recombinant protein, EAF2-overexpressed plasmids, or VASH1-overexpressed plasmids was collected to treat HUVECs, respectively. Following, we further examined the tube formation and migration ability of HUVECs. In this study, the potential effects and mechanisms of EAF2 and VASH1 on CRC angiogenesis were investigated *in vitro*.

Tube formation assay showed that the tubular ability of HUVECs treated with the conditioned medium from RKO cells transfected with EAF2-overexpressed plasmids (EAF2-OV group) was significantly lower than that in the control group (RKO-C group), in which HUVECs were treated by conditioned medium from RKO cells grown in medium containing 10% serum. From the results of transwell migration assay and scratch assay, we also found that the migration ability of HUVECs in EAF2-OV group was significantly lower than that in RKO-C group (Figure 8, $P < 0.001$). In addition, the tube formation and invasion ability of HUVECs in the RKO + T group cultured with conditioned medium collected from RKO cells treated with exogenous TGF-β1 recombinant protein were significantly increased compared with those in the RKO-C group (Figure 8, $P < 0.001$). HUVECs were further cultured with conditioned medium from RKO cells in the EAF2-OV + T group, which were transfected with EAF2-overexpressed plasmids and treated with TGF-β1 recombinant protein for 24 h. The results of tube formation assay, transwell migration assay and scratch assay showed that TGF-β1 recombinant protein could reverse the inhibitory effect of EAF2 overexpression in RKO cells on tube formation and migration of HUVECs (Figure 8, $P < 0.001$).

At the same time, we treated HUVECs for 24 h with conditioned medium from RKO cells in the VASH1-OV group, which were transfected with VASH1-overexpressed plasmids, to investigate the role and mechanism of CRC cell-derived VASH1 in CRC angiogenesis. Then, the tube formation assay showed that the tubular ability of HUVECs in the VASH1-OV group was significantly lower than that in the control group (RKO-C group) (Figure 9, $P < 0.001$). The results of migration experiment and scratch experiment showed that the migration ability of HUVECs in VASH1-OV group was significantly lower than that in RKO-C group (Figure 9, $P < 0.001$). After treating RKO cells transfected with VASH1

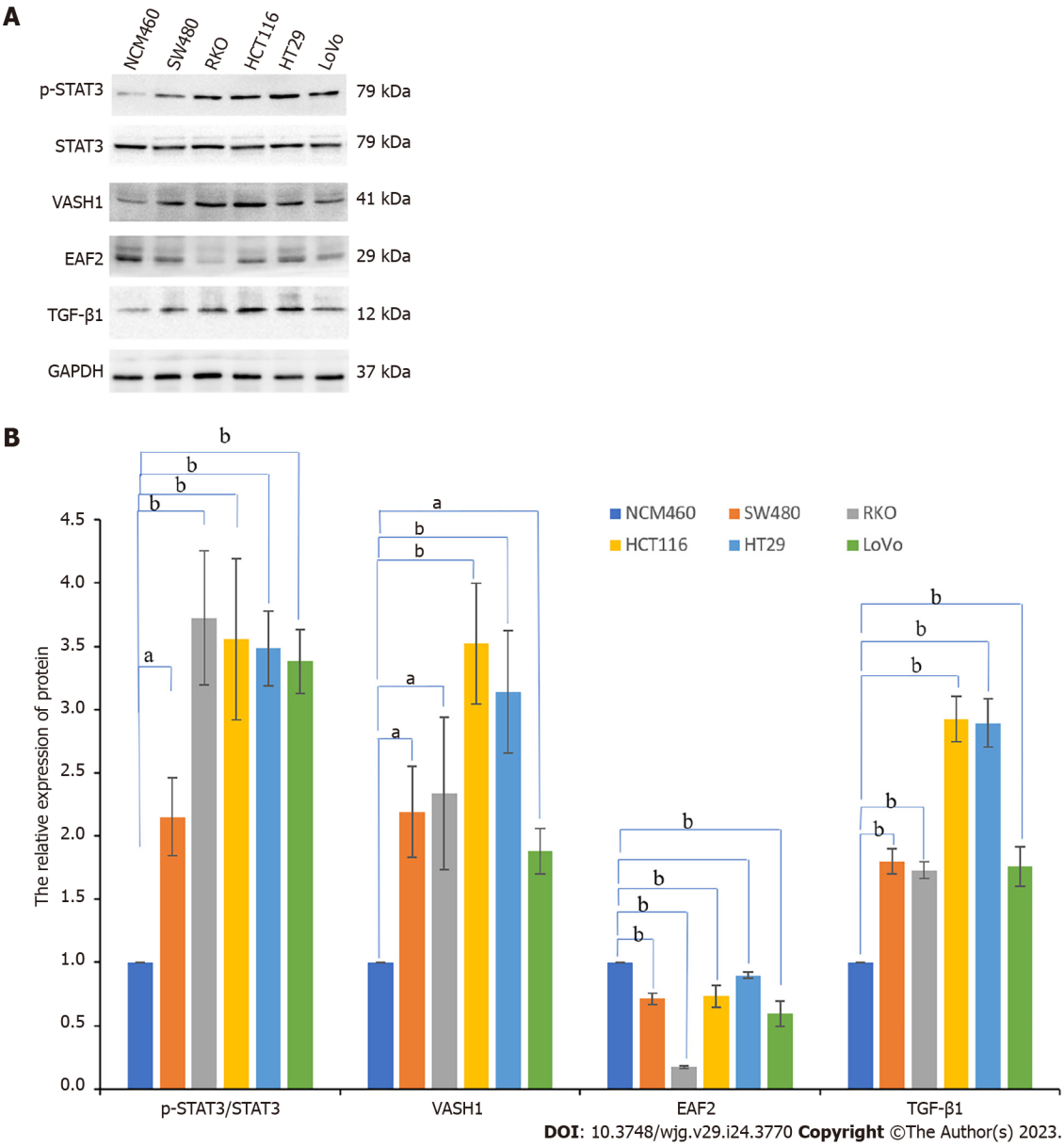


Figure 3 Protein expression of pathway-related factors in a variety of human colorectal cancer cells and colorectal epithelial cells. A and B: The protein bands of ELL-associated factor 2, vasohibin 1, phosphorylated-signal transducer and activator of transcription 3, and transforming growth factor-β1 in colorectal cancer cell lines (SW480, RKO, HCT116, HT29, and LoVo) and normal colorectal epithelial cells (NCM460) by Western blot assay and the corresponding data. $^{a}P < 0.05$, $^{b}P < 0.001$. EAF2: ELL-associated factor 2; VASH1: Vasohibin 1; p-STAT3: Phosphorylated-signal transducer and activator of transcription 3; TGF-β1: Transforming growth factor-β1.

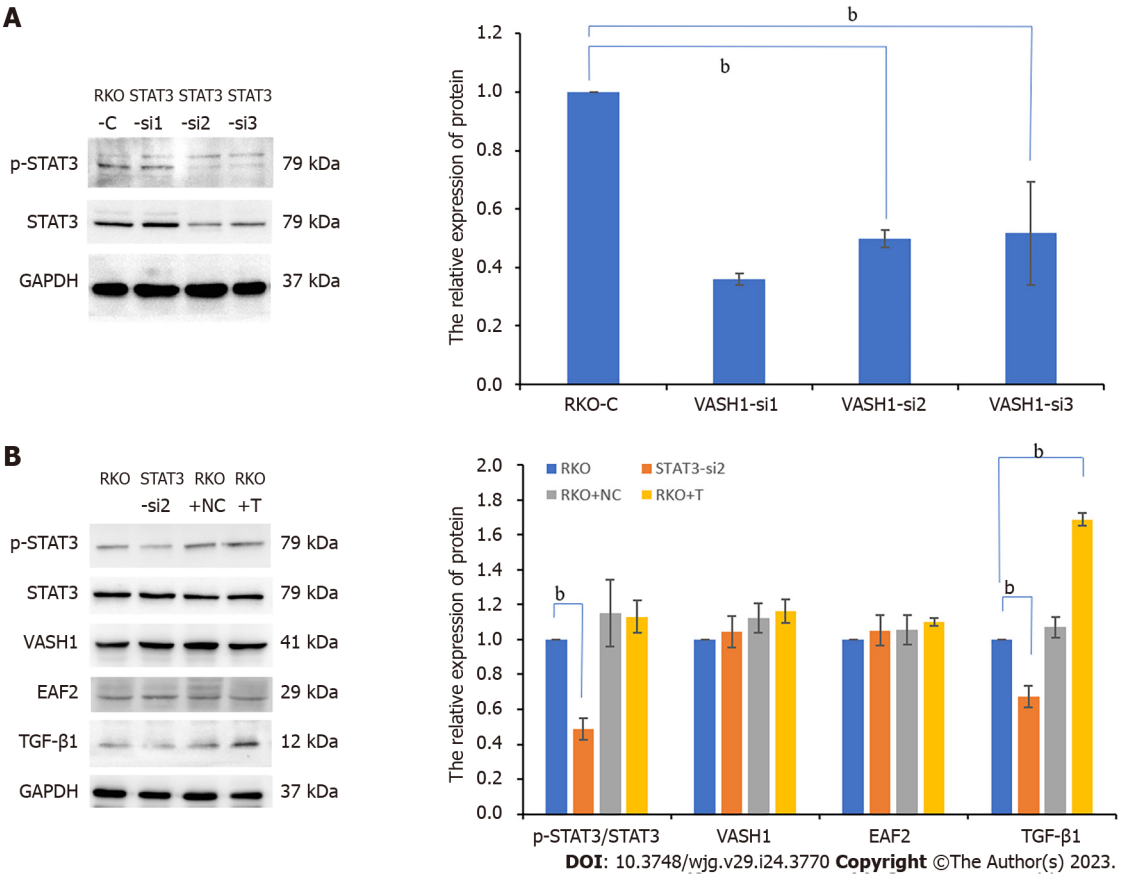
overexpression plasmid with TGF-β1 recombinant protein (VASH1-OV + T group), it was observed that the tube forming ability and migration ability of HUVECs were significantly increased (Figure 9, $P < 0.001$).

Overexpression of EAF2 up-regulated VASH1 to inhibit the activity of STAT3/TGF-β1 pathway

The previous results suggest that the expression levels of EAF2 and VASH1 proteins are positively correlated in CRC tissues. Therefore, it is of great significance to investigate whether there is a mutual regulatory effect between EAF2 and VASH1 in CRC cells.

Compared with RKO control group, transfection of the EAF2 overexpression plasmid significantly increased VASH1 protein expression in RKO cells (Figure 5B, $P = 0.001$). However, transfection of RKO cells with VASH1 overexpression plasmid or VASH1 siRNA did not significantly modulate the expression level of EAF2 protein (Figure 5B).

In the following experiments, we transfected the RKO cells with VASH1 siRNA to further determine whether VASH1 was involved in the activation of STAT3/TGF-β1 crosstalk pathway by overexpression of EAF2. The results showed that silencing VASH1 reversed the STAT3/TGF-β1 signaling pathway inhibited by EAF2 overexpression (Figure 10).



DOI: 10.3748/wjg.v29.i24.3770 **Copyright** ©The Author(s) 2023.

Figure 4 Silencing signal transducer and activator of transcription 3 phosphorylation significantly inhibits the expression of transforming growth factor-β1 protein in RKO cells. A: The protein bands of phospho-signal transducer and activator of transcription 3 (STAT3) in RKO cells transfected with STAT3 siRNA plasmids by Western blot assay and the corresponding data; B: The protein bands of pathway-related factors in RKO cells treated with STAT3 siRNA or exogenous transforming growth factor-β1 recombinant protein by Western blot assay. $^{b}P < 0.001$. RKO-C: RKO cells were cultured in 1640 medium containing 10% fetal bovine serum (FBS). STAT3-si: RKO cells were transfected with STAT3 siRNA plasmids for 6 h and then cultured in 1640 medium containing 10% FBS for 24 h. RKO + NC: RKO cells were transfected empty vector for 6 h and then cultured in 1640 medium containing 10% FBS for 24 h. RKO + T: RKO cells were cultured for 24 h in 1640 medium containing 10% FBS in which 5 ng/mL TGF-β1 recombinant protein was added. VASH1: Vasohibin 1; STAT3: Signal transducer and activator of transcription 3; EAF2: ELL-associated factor 2; TGF-β1: Transforming growth factor-β1.

DISCUSSION

CRC metastasis is a dynamic process that undergoes detachment of the primary cancer, infiltration into adjacent tissues and blood/lymph circulation, and metastasis to distant CRC colony formation. The mechanism is complex and affected by many factors. Angiogenesis is an important link in the process of tumor occurrence, invasion and metastasis, which can meet the oxygen and nutrients needed for the survival and growth of tumor cells[21]. The revolution of targeted agents has brought new hope for the treatment of patients with advanced tumors. Checkpoint inhibitors can significantly inhibit tumors and even may cure them, but currently only 3.8% of metastatic CRC are available[22]. The identification of predictive biomarkers and the exploration of new molecular targets contribute to the improvement of clinical diagnosis and the development of new drugs for advanced CRC.

The androgen response gene EAF2, a member of the EAF family, has tumor suppressive properties in multiple organs, including liver, lung and prostate[15]. EAF2 protein is under-expressed in prostate cancer tissues, and knocking down EAF2 in prostate cancer cell lines can enhance proliferation, migration, and invasion. Prostatic luminal epithelial cells have the potential to develop prostatic intraepithelial neoplasia in the EAF2 knockout mouse model[23]. In addition, the high expression of EAF2 also indicates a better prognosis of skin cutaneous melanoma patients[24]. Recent studies have identified EAF2 inactivation in MSI-H CRC, and not only that, but also intratumor heterogeneity (ITH) of EAF2 frameshift mutations in CRC[25]. Our previous determination of EAF2 expression levels in CRC tissues suggested that EAF2 expression was significantly lower in cancer tissues than in adjacent normal tissues[20]. In addition, the level of EAF2 protein in CRC tissues was negatively correlated with distant metastasis and CEA expression level in patients with advanced CRC[20]. In the present study, we further expanded the clinical sample size and similarly found that EAF2 protein level was significantly lower in CRC tissue than in non-cancer tissue. Further correlation analysis showed that advanced CRC tissue with low EAF2 protein expression had poor angiolymphatic and/or perineural

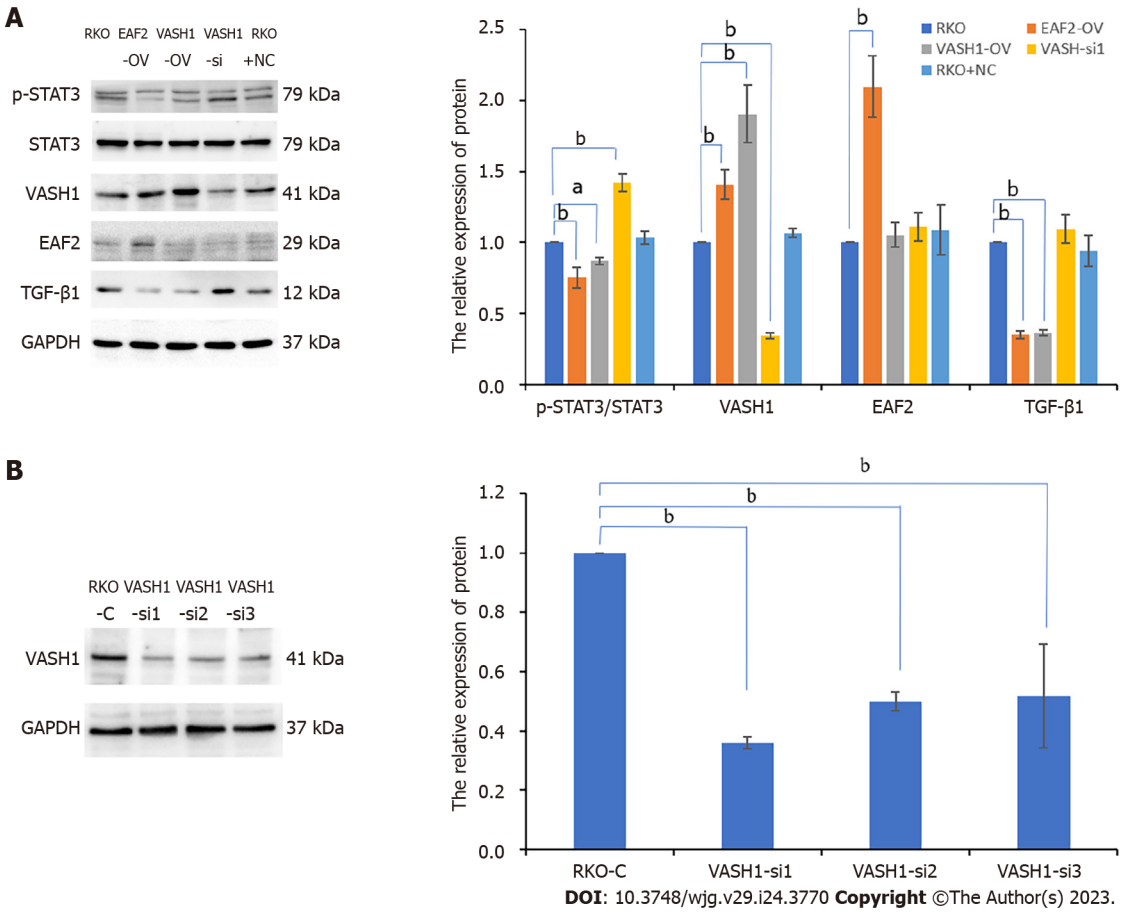


Figure 5 Overexpressing vasohibin 1 inhibits signal transducer and activator of transcription 3 phosphorylation (Tyr705) as well as transforming growth factor-β1 protein expression in RKO cells. A: The protein bands of pathway-related factors in RKO cells transfected with ELL-associated factor 2 (EAF2) overexpression plasmids, or vasohibin 1 (VASH1) overexpression plasmids, or VASH1 silencing plasmids by Western blot assay; B: The protein bands of VASH1 in RKO cells transfected with VASH1 siRNA plasmids by Western blot assay and the corresponding data. $^{a}P < 0.05$, $^{b}P < 0.001$. VASH1-si: RKO cells transfected with VASH1 siRNA plasmids for 6 h and then cultured in 1640 medium containing 10% fetal bovine serum (FBS) for 24 h. VASH1-OV: The group of RKO cells transfected with VASH1 overexpression plasmids for 6 h and then cultured in 1640 medium containing 10% FBS for 24 h. EAF2-OV: RKO cells transfected with EAF2 overexpression plasmids for 6 h and then cultured in 1640 medium containing 10% FBS for 24 h. VASH1: Vasohibin 1; EAF2: ELL-associated factor 2; TGF-β1: Transforming growth factor-β1.

invasion, poor TNM stage, poor distant metastasis, and high CEA protein expression compared with high EAF2. Meanwhile, advanced CRC tissue with high EAF2 protein expression had poor degree of differentiation compared with low EAF2. Therefore, by expanding the sample size, we still found that the expression level of EAF2 protein was lower in advanced CRC tissue. The results of Kaplan-Meier survival analysis were also consistent with previous studies[20], suggesting that the survival rate of the group with EAF2 high expression was higher than that of the group with EAF2 Low expression. These results further suggest that EAF2 protein expression in CRC tissues is closely related to tumor invasion and metastasis. EAF2 protein may be a new diagnostic and prognostic marker for CRC, and its low expression may be associated with poor prognosis of patients with advanced CRC. All these suggest that EAF2 may play a role in the occurrence and development of CRC, especially in the process of invasion and metastasis.

Vasohibin was originally identified and isolated as a novel angiogenesis inhibitor by microarray analysis of transcripts induced by VEGF in endothelial cells[26]. In addition, transfecting Lewis lung carcinoma (LLC) cells with vasohibin cDNA effectively inhibited tumor angiogenesis and tumor growth, indicating that vasohibin can act on endothelial cells from the outside[26]. VASH1, one of vasohibin family, is not only selectively expressed in endothelial cells under the induction of angiogenic growth factors (VEGF and FGF-2), which inhibits the migration, proliferation and tube formation of endothelial cells[26], but also expressed in tumor cells and tumor stroma, participating in the inhibition of tumor angiogenesis and prevention of tumor growth and metastasis[27,28]. Although previous studies have focused more on how endothelial cell-derived VASH1 regulates tumor angiogenesis and lymphangiogenesis[29], preliminary studies have also confirmed the potential functional role of tumor cell-derived VASH1 in inhibiting cancer cell proliferation and invasion[30,31]. It has also been shown that overexpression of VASH1 inhibits tumorigenesis and metastasis in a human colon cancer model [32]. However, the expression and function of VASH1 in CRC tissues and cells remain controversial,

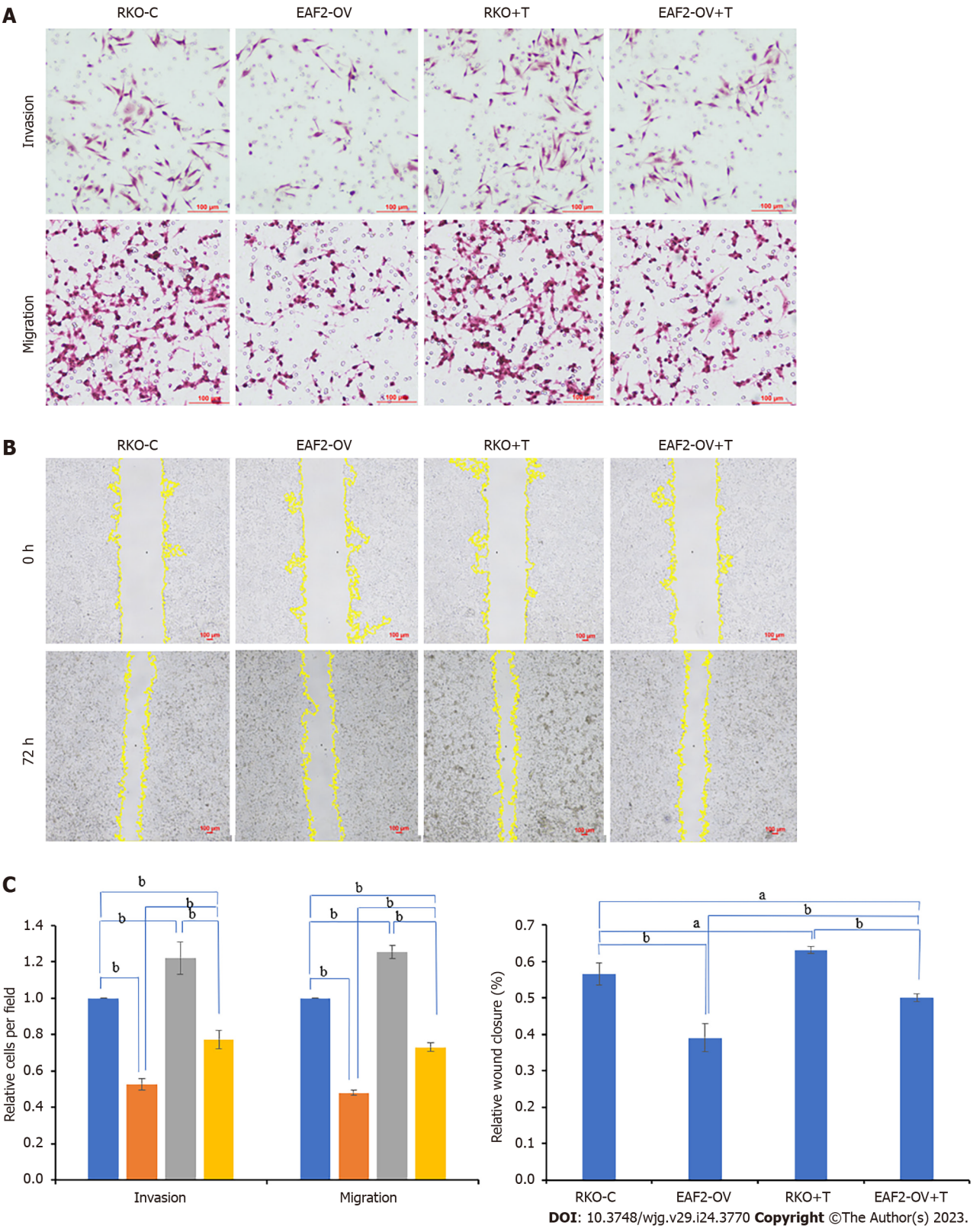


Figure 6 Overexpressing ELL-associated factor 2 inhibits the invasion and migration of RKO cells by suppressing transforming growth factor-β1 related pathway. A: The invasion and migration abilities were evaluated by the transwelll assay; B: The migration ability was analyzed by wound healing assay after 72 h; C: The results of migration and invasion abilities of RKO cells were measured using ImageJ software. $^{a}P < 0.05$, $^{b}P < 0.001$. ELL-associated factor 2 (EAF2)-OV + T: The group of RKO cells were transfected with EAF2 overexpression plasmids for 24 h and then cultured with 5 ng/mL transforming growth factor-β1 recombinant protein for 24 h. EAF2: ELL-associated factor 2.

and its direct effects on tumor cells and mechanisms remain to be elucidated.

Xiong *et al*[7] used RT-qPCR and Western blot to determine the RNA and protein expression levels of VASH1, and the results showed that VASH1 expression was significantly down-regulated in CRC

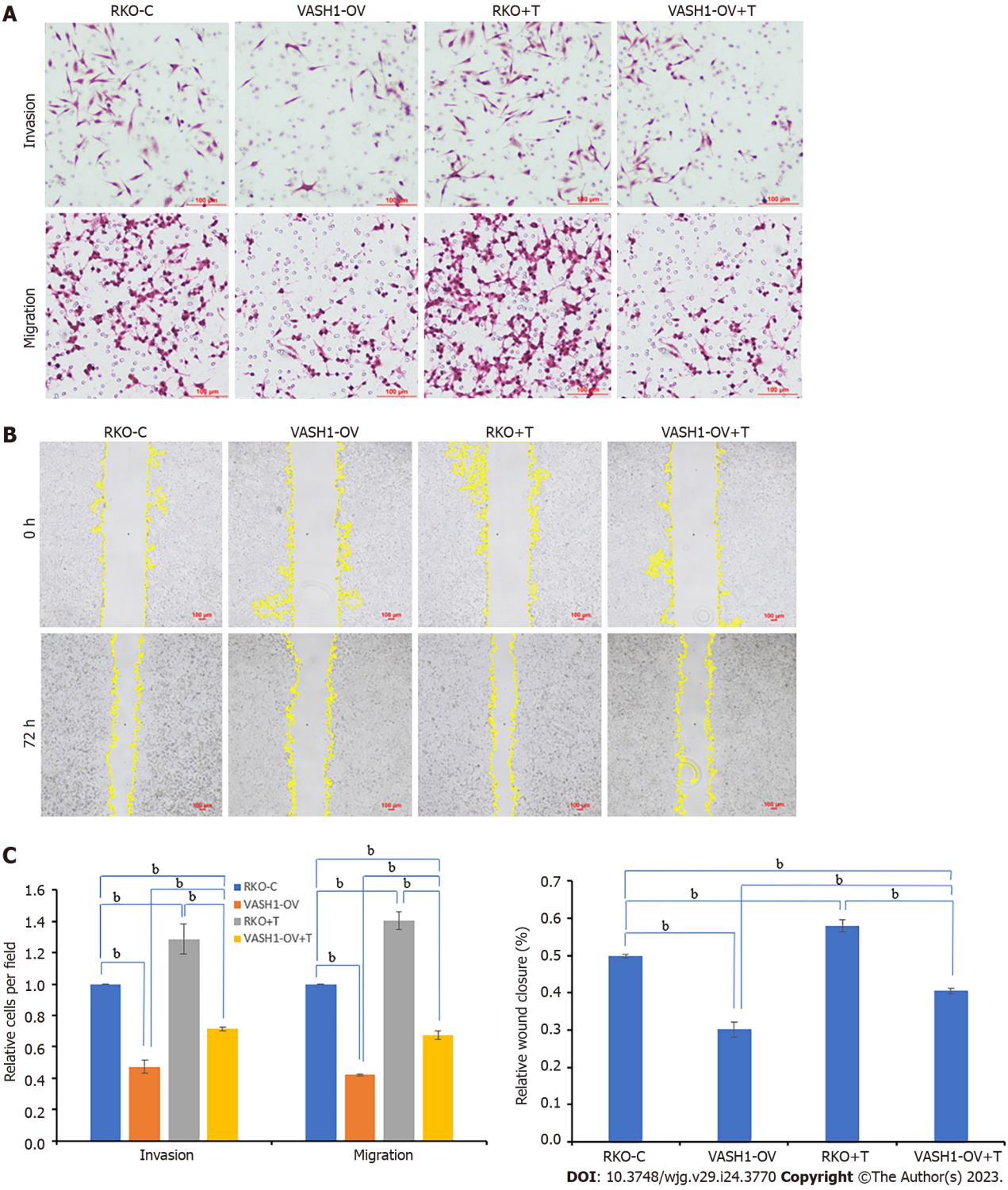
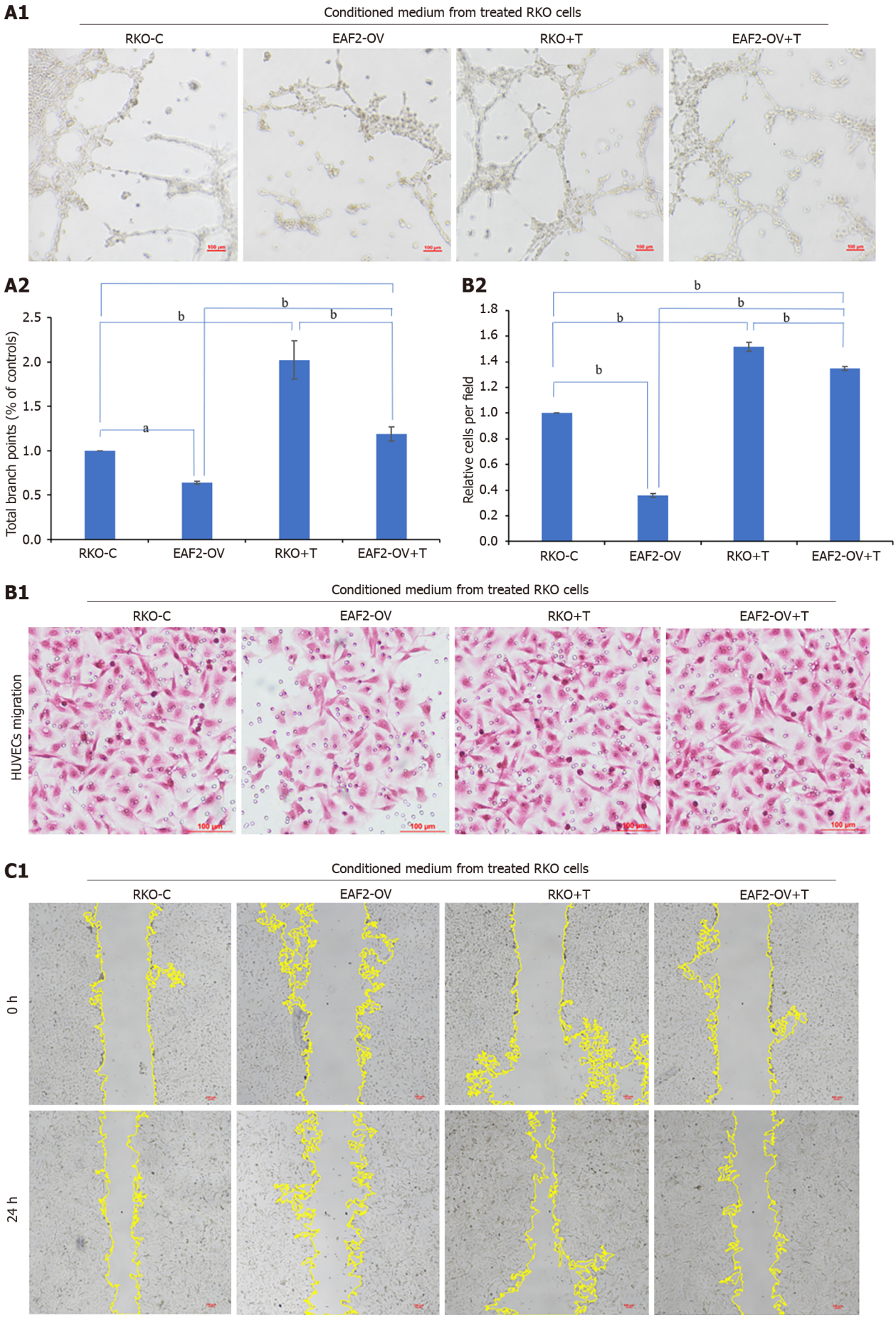
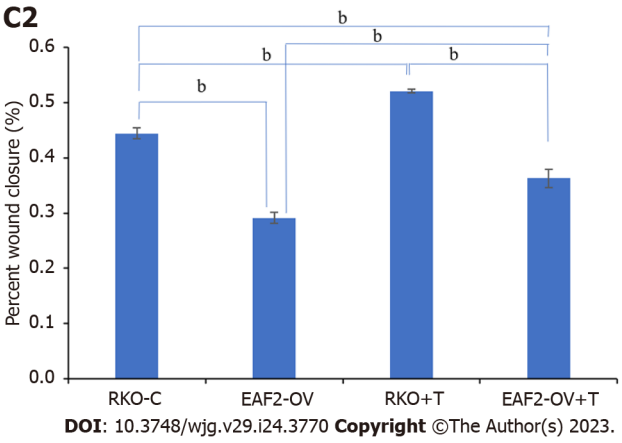


Figure 7 Overexpressing Vasohibin 1 inhibits the invasion and migration of RKO cells by suppressing transforming growth factor-β1 related pathway. A: The invasion and migration abilities were evaluated by the transwelll assay; B: The migration ability was analyzed by wound healing assay after 72 h; C: The results of migration and invasion abilities of RKO cells were measured using ImageJ software. $^{b}P < 0.001$. vasohibin 1 (VASH1)-OV + T: The group of RKO cells were transfected with VASH1 overexpression plasmids for 24 h and then cultured with 5 ng/mL transforming growth factor-β1 recombinant protein for 24 h. VASH1: Vasohibin 1.

tissues compared with adjacent normal tissues. However, through Western blot detection, Yan *et al*[9] found that the expression level of VASH1 protein in CRC tissue was significantly higher than that in adjacent normal tissues. Immunohistochemical analysis also indicated that 88.64% (117/132) of CRC tissue expressed VASH1 protein. Moreover, the expression of VASH1 protein and mRNA in colon cancer cell lines was significantly higher than that in normal colon mucosa cell lines. In this study, we also used immunohistochemistry and Western blot to detect the expression of VASH1 protein in advanced CRC tissue, and the results showed that the level of VASH1 protein in colorectal adenocar-


A1
Conditioned medium from treated RKO cells
RKO-C
EAF2-OV
RKO+T
EAF2-OV+T
A2
Total branch points (% of controls)
B2
Relative cells per field
B1
HUVECs migration
C1
0 h
24 h



DOI: 10.3748/wjg.v29.i24.3770 **Copyright** ©The Author(s) 2023.

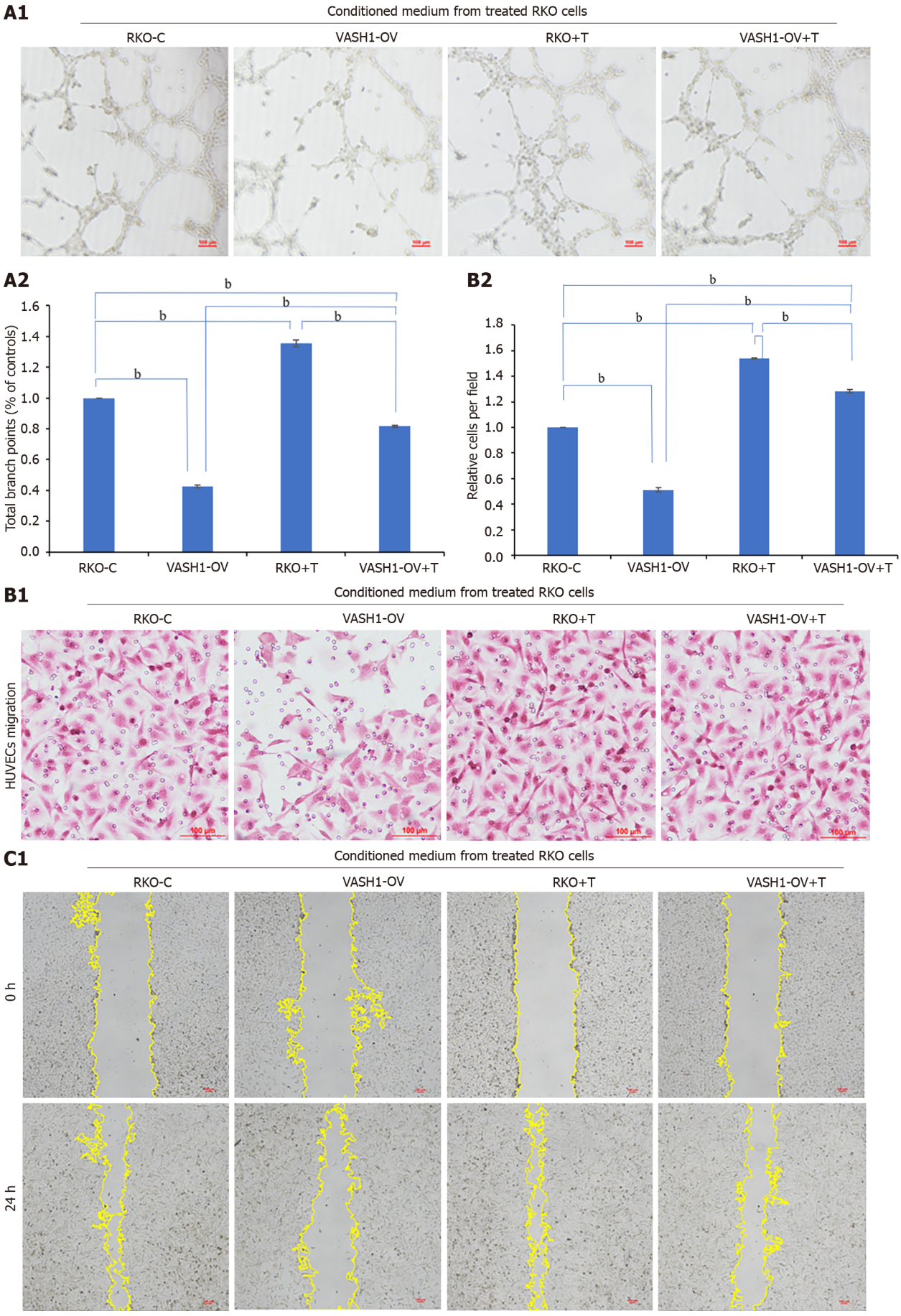
Figure 8 Overexpressing ELL-associated factor 2 inhibits tumor-induced angiogenesis in RKO cells *via* transforming growth factor-β1 related pathway. A: Conditioned medium from RKO cells transfected with ELL-associated factor 2-overexpressed plasmids or treated with transforming growth factor-β1 recombinant protein was collected to perform tube formation assay; B and C: The migration ability of Human Umbilical Vein Endothelial Cells was analyzed by transwell migration assay (B) and wound healing assay (C). And the results were measured by ImageJ software. $^{a}P < 0.05$, $^{b}P < 0.001$. EAF2: ELL-associated factor 2; TGF-β1: Transforming growth factor-β1.

cinoma tissue was significantly higher than that in paracancer tissues. In addition, our results found that advanced CRC tissue with high VASH1 protein expression had poor degree of differentiation, poor angiolymphatic and/or perineural invasion, poor distant metastasis compared with those with low VASH1. Kaplan-Meier survival analysis showed that the survival rate of patients with low VASH1 expression was higher than that of patients with high VASH1 expression. It is consistent with the findings of Yan *et al*[9], who showed that high VASH1 protein expression is an independent risk factor for worse OS and PFS. It is of great significance to further explore the function and mechanism of VASH1 protein in the occurrence and development of CRC, especially in the process of invasion and metastasis.

Univariate analysis showed that vascular lymphatic and/or neural invasion, tumor stage, depth of tumor invasion, lymph node status, distant metastasis, EAF2 protein expression level and p53 protein expression level were prognostic factors for the survival of patients with advanced CRC. However, multivariate analysis did not show that EAF2 or VASH1 expression levels were an independent prognostic factor for survival in patients with advanced CRC. More cases and more comprehensive clinical studies are needed to clarify the clinical significance of EAF2 and VASH1 proteins in CRC. In addition, this study is the first to investigate the correlation between the expression of the tumor suppressor EAF2 and the anti-angiogenic factor VASH1 in CRC tissues. The expressions of EAF2 and VASH1 proteins in advanced CRC tissue are positively correlated. Immunohistochemical localization showed that EAF2 and VASH1 proteins were mainly expressed in the cytoplasm of CRC epithelial cells. Therefore, we also ventured to speculate whether EAF2 and VASH1 interact in the development of CRC.

And then, we conducted *in vitro* cell studies to investigate the role and potential mechanism of CRC cell-derived EAF2 and VASH1 protein. Western blot assay showed that EAF2 protein expression was down-regulated and VASH1 protein expression was up-regulated in RKO cells compared with normal colon epithelial cells *in vitro*. In addition, RKO cells overexpressing EAF2 protein expressed higher levels of VASH1 protein. These results suggest that EAF2 overexpression can up-regulate the expression of VASH1 protein in RKO cells. Further investigation of the potential mechanism of EAF2 and VASH1 in CRC cells may provide a research direction for exploring the role of EAF2 and VASH1 in CRC.

In parallel, our results also found that phospho-STAT3 (Tyr705) and TGF-β1 protein levels were significantly increased in RKO cells. TGF-β signaling participates in and promotes the development of metastatic CRC through multiple mechanisms[33,34]. TGF-β1 expression is also significantly increased in CRC tissue and in distant metastases of CRC[35]. Targeting TGF-β signaling is emerging as a new therapy for CRC metastasis[36]. Not only that, increased TGF-β expression specifically promotes endothelial cell angiogenesis induced by the human CRC cell line HT-29 by upregulating VEGF secretion[37]. STAT3 is also one of the main factors closely related to the occurrence and development of CRC, and is involved in tumor angiogenesis and lymphangiogenesis to promote the early occurrence of advanced CRC. Immunohistochemical evaluation of pSTAT3 in a study containing 724 CRC patients showed that pSTAT3 expression was significantly associated with high mortality and increased peritumoral lymphoid reaction[38]. What's more, TGF-β1 promotes CRC invasion by inducing EMT *via* Src/Annexin A2 (ANXA2)/STAT3 pathway[39]. We also found *in vitro* that silencing STAT3 phosphorylation significantly downregulated TGF-β1 protein expression in RKO cells. Therefore, exploring the regulatory proteins of STAT3/TGF-β1 pathway is helpful to find new therapeutic targets for CRC.


A1
Conditioned medium from treated RKO cells
RKO-C
VASH1-OV
RKO+T
VASH1-OV+T
A2
Total branch points (% of controls)
B2
Relative cells per field
b
RKO-C
VASH1-OV
RKO+T
VASH1-OV+T
B1
Conditioned medium from treated RKO cells
HUVECs migration
100 μm
C1
Conditioned medium from treated RKO cells
0 h
24 h

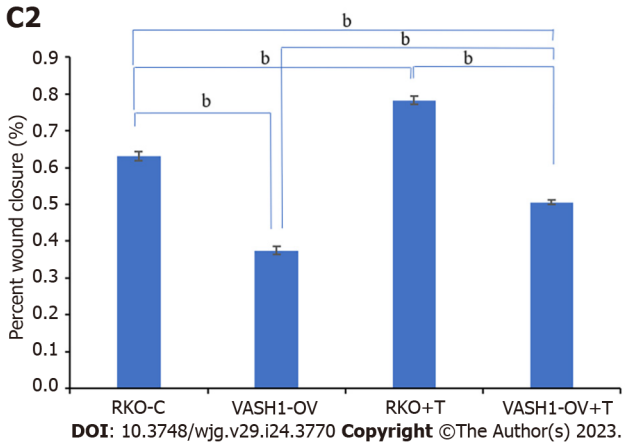


Figure 9 Overexpressing Vasohibin 1 inhibits tumor-induced angiogenesis in RKO cells *via* transforming growth factor-β1 related pathway. A: Conditioned medium from RKO cells transfected with VASH1-overexpressed plasmids or treated with transforming growth factor-β1 recombinant protein was collected to perform tube formation assay; B and C: The migration ability of Human Umbilical Vein Endothelial Cells was analyzed by transwell migration assay (B) and wound healing assay (C). And the results were measured by ImageJ software. $^{b}P < 0.001$. VASH1: Vasohibin 1; EAF2: ELL-associated factor 2.

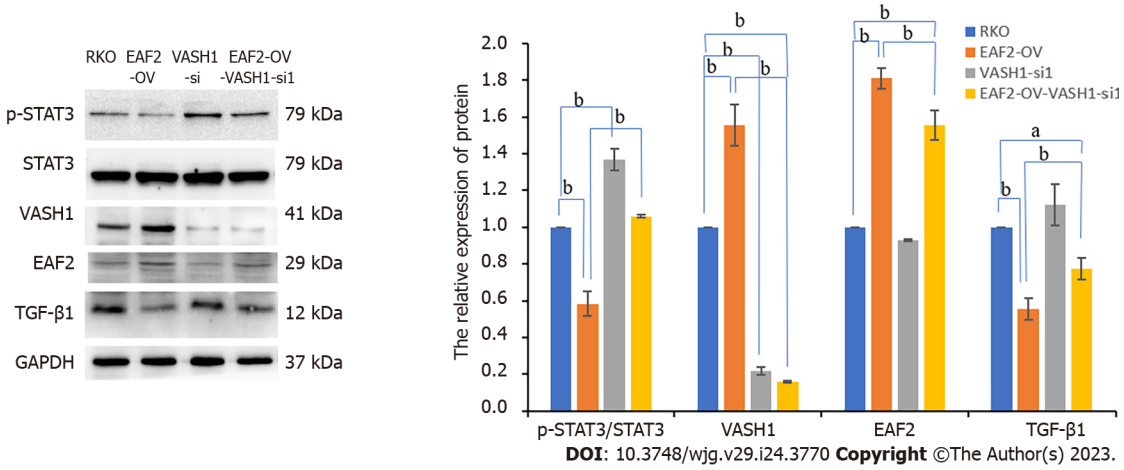
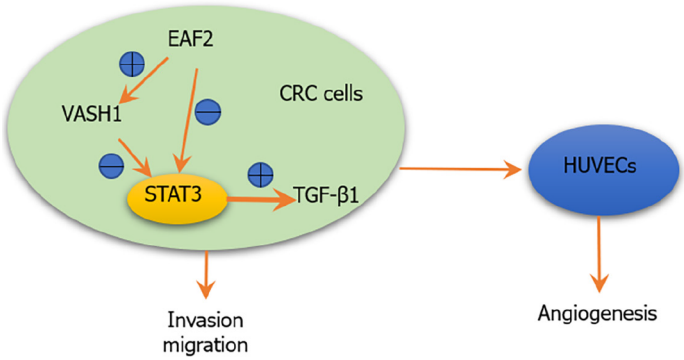


Figure 10 Silencing Vasohibin 1 reverses the signal transducer and activator of transcription 3/transforming growth factor-β1 pathway inhibited by ELL-associated factor 2 overexpression. $^{a}P < 0.05$, $^{b}P < 0.001$. ELL-associated factor 2 (EAF2)-OV- Vasohibin 1 (VASH1-si): The group of RKO cells transfected with EAF2 overexpression plasmids and VASH1 siRNA plasmids. VASH1: Vasohibin 1; EAF2: ELL-associated factor 2.

EAF2 has been shown to be a repressor of STAT3 signaling pathway in prostate cancer[40]. Down-regulation of EAF2 protein in human prostate cancer specimens correlated with the immunostaining of phosphorylated STAT3 (Tyr705), and knockdown of EAF2 gene induced STAT3 phosphorylation (Tyr705) in prostate cancer both *in vivo* and *in vitro*. Besides, EAF2 attenuates TGF-β1-induced G1 phase cell cycle arrest and cell migration in a variety of tumor cells[18]. Encouragingly, when we overexpressed EAF2 protein, the activity of STAT3/TGF-β1 pathway was inhibited in RKO cells. Furthermore, *in vitro* functional studies in CRC cells showed that overexpression of EAF2 inhibited not only the invasion and migration of RKO cells, but also the angiogenesis induced by RKO cells. However, the inhibitory effect of EAF2 overexpression on RKO cell function was reversed by recombinant TGF-β1 protein.

In this study we also found that overexpressing VASH1 protein in RKO cells significantly inhibited the activity of the STAT3/TGF-β1 pathway. More meaningfully, the silencing of VAH1 gene with variable activity in the STAT3/TGF-β1 pathway was reversed by overexpression of EAF2. It is suggested that CRC-derived VASH1 protein is involved in the EAF2-mediated STAT3/TGF-β1 pathway in CRC cells. Overexpression of VASH1 protein in colon cancer cells not only inhibited cancer cell growth and colony formation *in vitro*, but also inhibited tumor growth *in vivo*[8]. This is consistent with the results of our study, which revealed that overexpressing VASH1 protein inhibited RKO cell invasion, migration and angiogenesis. What's more, this effect was reversed by TGF-β1 recombinant protein. Similarly, VASH1 siRNA significantly increased the mobility of gastric cancer cell and endothelium cells vessel formation in Matrigel[41]. Hence, CRC cell-derived VASH1 may inhibit the invasion, migration and angiogenesis ability of RKO cells by inhibiting STAT3/TGF-β1 pathway. In



DOI: 10.3748/wjg.v29.i24.3770 **Copyright** ©The Author(s) 2023.

Figure 11 Schematic depiction of ELL-associated factor 2 and vasohibin 1 regulating the signal transducer and activator of transcription 3/ transforming growth factor-β1 signaling pathway in this study. Overexpression of ELL-associated factor 2 may inhibit the activity of signal transducer and activator of transcription 3/transforming growth factor-β1 pathway by up-regulating the expression of vasohibin 1, thereby inhibiting cell invasion, migration and angiogenesis. EAF2: ELL-associated factor 2; TGF-β1: Transforming growth factor-β1; STAT3: Signal transducer and activator of transcription 3; CRC: Colorectal cancer; HUVECs: Human umbilical vein endothelial cells; VASH1: Vasohibin 1.

addition, overexpression of EAF2 may inhibit the activity of STAT3/TGF-β1 pathway by up-regulating the expression of VASH1.

However, further studies are needed to clarify whether there is a direct effect of EAF2 on regulating VASH1 protein in CRC cells and the mechanism by which EAF2 and VASH1 regulate STAT3/TGF-β1 pathway. In addition, more objective and scientific experimental methods should be combined *in vivo* and *in vitro* to further comprehensively discuss and evaluate the functional effects of EAF2 and VASH1 on CRC, so as to make up for the limitations and one-sidedness of this study which only conducted *in vitro* invasion, migration and angiogenesis studies.

Moreover, in-depth study on the mechanism and methods of overexpressing EAF2 and VASH1 may provide new targets and ideas for the treatment of CRC. Deletion of EAF2 and Von Hippel-Lindau (VHL) produced a synergistic effect on angiogenesis in male fractional liver and prostate, accompanied by an increase in the expression of VHL target proteins hypoxia-inducible factor 1α and VEGF[42]. Further study on the effect and mechanism of EAF2-mediated VASH1 on endothelial cells in tumor microenvironment may help to elucidate the pathogenesis of CRC. Inhibition of cytotoxic T lymphocyte protein 4 can reactivate immune cells, especially T cells, in patients with CRC, thereby enhancing the ability of immune cells to fight tumors[43]. Regulatory T cells (Tregs) in tumor microenvironment can mediate mechanisms such as immune escape, and may also participate in the regulation of ovarian cancer angiogenesis through VEGFA and VASH1[44]. The synergistic effect of VASH1-related pathway anti-angiogenesis therapy and immunotherapy may become a new idea for CRC treatment.

CONCLUSION

In conclusion, our study found that EAF2 was down-regulated and VASH1 was up-regulated in advanced CRC tissue. Kaplan-Meier survival analysis showed that the high EAF2 Level group and the low VASH1 Level group had a higher survival rate. This study suggests that EAF2 and VASH1 may serve as new diagnostic and prognostic markers for CRC. What's more, overexpression of EAF2 protein or VASH1 protein in CRC cells inhibited STAT3/TGF-β1 pathway, and further inhibited invasion, migration and angiogenesis of CRC cells. Overexpression of EAF2 may provide tumor inhibition and protection against CRC by up-regulating VASH1 expression and inhibiting the activity of downstream STAT3/TGF-β1 pathway (Figure 11). This study provides new ideas and theoretical basis for the development of new diagnostic markers for CRC and the exploration of the mechanism of targeted therapy.

ARTICLE HIGHLIGHTS

Research background

More and more studies have suggested that the anti-angiogenic factor vasohibin 1 (VASH1) is not only expressed in the stroma of tumor cells, but also expressed in tumor cells. It also plays a certain role in the regulation of tumor growth, invasion and tumor microenvironment. Recent studies have found that ELL-associated factor 2 (EAF2) can mediate signal transducer and activator of transcription 3 (STAT3)/

transforming growth factor-β1 (TGF-β1) pathway to act on colorectal cancer (CRC). Knockdown of VASH1 enhanced TGF-β1/Smad3 pathway activity and type I/III collagen production.

Research perspectives

Further study on the effect and mechanism of EAF2-mediated VASH1 on endothelial cells in tumor microenvironment may help to elucidate the pathogenesis of CRC. The synergistic effect of VASH1-related pathway anti-angiogenesis therapy and immunotherapy may become a new idea for CRC treatment.

Research conclusions

This study suggests that EAF2 and VASH1 may serve as new diagnostic and prognostic markers for CRC. It complements the mechanism of EAF2 in CRC cells, enriches the role and mechanism of CRC cell-derived VASH1, and provides a new possible subtype of CRC as a therapeutic target of STAT3/TGF-β1 pathway.

Research results

Our findings indicated that EAF2 was down-regulated and VASH1 was up-regulated in advanced CRC tissue compared to normal colorectal tissue. Overexpression of EAF2 might inhibit the activity of STAT3/TGF-β1 pathway by up-regulating the expression of VASH1, thereby attenuating the invasion, migration and angiogenesis of CRC cells.

Research methods

We collected colorectal adenocarcinoma and corresponding adjacent tissues in patients with advanced CRC. Following, we investigated the effect and mechanism of EAF2 and VASH1 on the invasion, migration and angiogenesis of CRC cells *in vitro* using plasmid transfection.

Research objectives

To investigate the expression of VASH1 in CRC and its correlation with the expression of EAF2. Furthermore, we explored the functional role and mechanism of EAF2 and VASH1-mediated TGF-β1 related pathway in CRC cells.

Research motivation

Detection of EAF2 and VASH1 protein expression in CRC tissues may help to explore new diagnostic and prognostic markers for CRC. The study of the potential mechanism of EAF2 and VASH1 can provide new ideas for the treatment of CRC.

FOOTNOTES

Author contributions: Feng ML and Sun MJ designed the research study; Feng ML and Wu C performed the research; Zhang HJ and Liu MY contributed new reagents and analytic tools; Feng ML and Xu BY analyzed the data; Feng ML and Wu C wrote the manuscript; and all authors have read and approve the final manuscript.

Supported by the Natural Science Foundation of Liaoning Province, No. 2023-MS-149.

Institutional review board statement: The study was reviewed and approved by the institutional review board of the First Affiliated Hospital of China Medical University (approval No. 2021-68-2).

Informed consent statement: The informed consent was waived from the patients.

Conflict-of-interest statement: The authors declare that they have no conflict of interest.

Data sharing statement: Data can be acquired from the corresponding author.

Open-Access: This article is an open-access article that was selected by an in-house editor and fully peer-reviewed by external reviewers. It is distributed in accordance with the Creative Commons Attribution NonCommercial (CC BY-NC 4.0) license, which permits others to distribute, remix, adapt, build upon this work non-commercially, and license their derivative works on different terms, provided the original work is properly cited and the use is non-commercial. See: https://creativecommons.org/Licenses/by-nc/4.0/

Country/Territory of origin: China

ORCID number: Ming-Liang Feng 0000-0001-6624-9624; Ming-Jun Sun 0000-0003-0072-2575; Bo-Yang Xu 0000-0002-0435-7117; Meng-Yuan Liu 0000-0002-5058-1558; Hui-Jing Zhang 0000-0002-6322-2335; Can Wu 0000-0002-9532-8767.

S-Editor: Chen YL

L-Editor: A
P-Editor: Yu HG

REFERENCES

1 **Shaukat A**, Kahi CJ, Burke CA, Rabeneck L, Sauer BG, Rex DK. ACG Clinical Guidelines: Colorectal Cancer Screening 2021. *Am J Gastroenterol* 2021; **116**: 458-479 [PMID: 33657038 DOI: 10.14309/ajg.0000000000001122]
2 **Li X**, Wu Y, Tian T. TGF-β Signaling in Metastatic Colorectal Cancer (mCRC): From Underlying Mechanism to Potential Applications in Clinical Development. *Int J Mol Sci* 2022; **23** [PMID: 36430910 DOI: 10.3390/ijms232214436]
3 **Kobayashi M**, Wakabayashi I, Suzuki Y, Fujiwara K, Nakayama M, Watabe T, Sato Y. Tubulin carboxypeptidase activity of vasohibin-1 inhibits angiogenesis by interfering with endocytosis and trafficking of pro-angiogenic factor receptors. *Angiogenesis* 2021; **24**: 159-176 [PMID: 33052495 DOI: 10.1007/s10456-020-09754-6]
4 **Tamaki K**, Moriya T, Sato Y, Ishida T, Maruo Y, Yoshinaga K, Ohuchi N, Sasano H. Vasohibin-1 in human breast carcinoma: a potential negative feedback regulator of angiogenesis. *Cancer Sci* 2009; **100**: 88-94 [PMID: 19037993 DOI: 10.1111/j.1349-7006.2008.01015.x]
5 **Zhao G**, Yang Y, Tang Y, Han R, Sun Y. Reduced expression of vasohibin-1 is associated with clinicopathological features in renal cell carcinoma. *Med Oncol* 2012; **29**: 3325-3334 [PMID: 22865127 DOI: 10.1007/s12032-012-0313-x]
6 **Kosaka T**, Miyazaki Y, Miyajima A, Mikami S, Hayashi Y, Tanaka N, Nagata H, Kikuchi E, Nakagawa K, Okada Y, Sato Y, Oya M. The prognostic significance of vasohibin-1 expression in patients with prostate cancer. *Br J Cancer* 2013; **108**: 2123-2129 [PMID: 23591203 DOI: 10.1038/bjc.2013.169]
7 **Xiong HL**, Zhong XH, Guo XH, Liao HJ, Yuan X. circASS1 overexpression inhibits the proliferation, invasion and migration of colorectal cancer cells by regulating the miR-1269a/VASH1 axis. *Exp Ther Med* 2021; **22**: 1155 [PMID: 34504600 DOI: 10.3892/etm.2021.10589]
8 **Liu S**, Han B, Zhang Q, Dou J, Wang F, Lin W, Sun Y, Peng G. Vasohibin-1 suppresses colon cancer. *Oncotarget* 2015; **6**: 7880-7898 [PMID: 25797264 DOI: 10.18632/oncotarget.3493]
9 **Yan Y**, Shen Z, Ye Y, Jiang K, Zhang H, Shen C, Mustonen H, Puolakkainen P, Wang S. A novel molecular marker of prognosis in colorectal cancer: Vasohibin-1. *Med Oncol* 2014; **31**: 816 [PMID: 24366689 DOI: 10.1007/s12032-013-0816-0]
10 **Fang W**, Radovich M, Zheng Y, Fu CY, Zhao P, Mao C, Zheng S. 'Druggable' alterations detected by Ion Torrent in metastatic colorectal cancer patients. *Oncol Lett* 2014; **7**: 1761-1766 [PMID: 24932229 DOI: 10.3892/ol.2014.2047]
11 **Watatani H**, Maeshima Y, Hinamoto N, Yamasaki H, Ujike H, Tanabe K, Sugiyama H, Otsuka F, Sato Y, Makino H. Vasohibin-1 deficiency enhances renal fibrosis and inflammation after unilateral ureteral obstruction. *Physiol Rep* 2014; **2** [PMID: 24973329 DOI: 10.14814/phy2.12054]
12 **Tang XW**, Qin QX. miR-335-5p induces insulin resistance and pancreatic islet β-cell secretion in gestational diabetes mellitus mice through VASH1-mediated TGF-β signaling pathway. *J Cell Physiol* 2019; **234**: 6654-6666 [PMID: 30341900 DOI: 10.1002/jcp.27406]
13 **Martin CJ**, Datta A, Littlefield C, Kalra A, Chapron C, Wawersik S, Dagbay KB, Brueckner CT, Nikiforov A, Danehy FT Jr, Streich FC Jr, Boston C, Simpson A, Jackson JW, Lin S, Danek N, Faucette RR, Raman P, Capili AD, Buckler A, Carven GJ, Schürpf T. Selective inhibition of TGFβ1 activation overcomes primary resistance to checkpoint blockade therapy by altering tumor immune landscape. *Sci Transl Med* 2020; **12** [PMID: 32213632 DOI: 10.1126/scitranslmed.aay8456]
14 **Villalba M**, Evans SR, Vidal-Vanaclocha F, Calvo A. Role of TGF-β in metastatic colon cancer: it is finally time for targeted therapy. *Cell Tissue Res* 2017; **370**: 29-39 [PMID: 28560691 DOI: 10.1007/s00441-017-2633-9]
15 **Xiao W**, Zhang Q, Habermacher G, Yang X, Zhang AY, Cai X, Hahn J, Liu J, Pins M, Doglio L, Dhir R, Gingrich J, Wang Z. U19/Eaf2 knockout causes lung adenocarcinoma, B-cell lymphoma, hepatocellular carcinoma and prostatic intraepithelial neoplasia. *Oncogene* 2008; **27**: 1536-1544 [PMID: 17873910 DOI: 10.1038/sj.onc.1210786]
16 **Guo W**, Keener AL, Jing Y, Cai L, Ai J, Zhang J, Fisher AL, Fu G, Wang Z. FOXA1 modulates EAF2 regulation of AR transcriptional activity, cell proliferation, and migration in prostate cancer cells. *Prostate* 2015; **75**: 976-987 [PMID: 25808853 DOI: 10.1002/pros.22982]
17 **Zang Y**, Dong Y, Yang D, Xue B, Li F, Gu P, Zhao H, Wang S, Zhou S, Ying R, Wang Z, Shan Y. Expression and prognostic significance of ELL-associated factor 2 in human prostate cancer. *Int Urol Nephrol* 2016; **48**: 695-700 [PMID: 26895851 DOI: 10.1007/s11255-015-1210-y]
18 **Liu X**, Chen Z, Ouyang G, Song T, Liang H, Liu W, Xiao W. ELL Protein-associated Factor 2 (EAF2) Inhibits Transforming Growth Factor β Signaling through a Direct Interaction with Smad3. *J Biol Chem* 2015; **290**: 25933-25945 [PMID: 26370086 DOI: 10.1074/jbc.M115.663542]
19 **Savas S**, Azorsa DO, Jarjanazi H, Ibrahim-Zada I, Gonzales IM, Arora S, Henderson MC, Choi YH, Briollais L, Ozcelik H, Tuzmen S. NCI60 cancer cell line panel data and RNAi analysis help identify EAF2 as a modulator of simvastatin and lovastatin response in HCT-116 cells. *PLoS One* 2011; **6**: e18306 [PMID: 21483694 DOI: 10.1371/journal.pone.0018306]
20 **Feng ML**, Wu C, Zhang HJ, Zhou H, Jiao TW, Liu MY, Sun MJ. Overexpression of ELL-associated factor 2 suppresses invasion, migration, and angiogenesis in colorectal cancer. *World J Gastrointest Oncol* 2022; **14**: 1949-1967 [PMID: 36310706 DOI: 10.4251/wjgo.v14.i10.1949]
21 **Wang R**, Ma Y, Zhan S, Zhang G, Cao L, Zhang X, Shi T, Chen W. B7-H3 promotes colorectal cancer angiogenesis through activating the NF-κB pathway to induce VEGFA expression. *Cell Death Dis* 2020; **11**: 55 [PMID: 31974361 DOI: 10.1038/s41419-020-2252-3]
22 **Akagi K**, Oki E, Taniguchi H, Nakatani K, Aoki D, Kuwata T, Yoshino T. Real-world data on microsatellite instability status in various unresectable or metastatic solid tumors. *Cancer Sci* 2021; **112**: 1105-1113 [PMID: 33403729 DOI:

10.1111/cas.14798]
23 **Pascal LE**, Rigatti LH, Ai J, Zhang A, Zhou J, Nelson JB, Wang Z. EAF2 loss induces prostatic intraepithelial neoplasia from luminal epithelial cells in mice. *Am J Clin Exp Urol* 2020; **8**: 18-27 [PMID: 32211450]
24 **Han W**, Shen GL. Systematic expression analysis of EAF family reveals the importance of EAF2 in melanoma. *Int Immunopharmacol* 2020; **88**: 106958 [PMID: 33182068 DOI: 10.1016/j.intimp.2020.106958]
25 **Jo YS**, Kim SS, Kim MS, Yoo NJ, Lee SH. Candidate Tumor Suppressor Gene EAF2 is Mutated in Colorectal and Gastric Cancers. *Pathol Oncol Res* 2019; **25**: 823-824 [PMID: 30088132 DOI: 10.1007/s12253-018-0461-1]
26 **Watanabe K**, Hasegawa Y, Yamashita H, Shimizu K, Ding Y, Abe M, Ohta H, Imagawa K, Hojo K, Maki H, Sonoda H, Sato Y. Vasohibin as an endothelium-derived negative feedback regulator of angiogenesis. *J Clin Invest* 2004; **114**: 898-907 [PMID: 15467828 DOI: 10.1172/JCI21152]
27 **Heishi T**, Hosaka T, Suzuki Y, Miyashita H, Oike Y, Takahashi T, Nakamura T, Arioka S, Mitsuda Y, Takakura T, Hojo K, Matsumoto M, Yamauchi C, Ohta H, Sonoda H, Sato Y. Endogenous angiogenesis inhibitor vasohibin1 exhibits broad-spectrum antilymphangiogenic activity and suppresses lymph node metastasis. *Am J Pathol* 2010; **176**: 1950-1958 [PMID: 20133819 DOI: 10.2353/ajpath.2010.090829]
28 **Ito S**, Miyashita H, Suzuki Y, Kobayashi M, Satomi S, Sato Y. Enhanced cancer metastasis in mice deficient in vasohibin-1 gene. *PLoS One* 2013; **8**: e73931 [PMID: 24066086 DOI: 10.1371/journal.pone.0073931]
29 **Miyashita H**, Watanabe T, Hayashi H, Suzuki Y, Nakamura T, Ito S, Ono M, Hoshikawa Y, Okada Y, Kondo T, Sato Y. Angiogenesis inhibitor vasohibin-1 enhances stress resistance of endothelial cells *via* induction of SOD2 and SIRT1. *PLoS One* 2012; **7**: e46459 [PMID: 23056314 DOI: 10.1371/journal.pone.0046459]
30 **Ye J**, Huang X, Hsueh EC, Zhang Q, Ma C, Zhang Y, Varvares MA, Hoft DF, Peng G. Human regulatory T cells induce T-lymphocyte senescence. *Blood* 2012; **120**: 2021-2031 [PMID: 22723548 DOI: 10.1182/blood-2012-03-416040]
31 **Peng G**, Guo Z, Kiniwa Y, Voo KS, Peng W, Fu T, Wang DY, Li Y, Wang HY, Wang RF. Toll-like receptor 8-mediated reversal of CD4+ regulatory T cell function. *Science* 2005; **309**: 1380-1384 [PMID: 16123302 DOI: 10.1126/science.1113401]
32 **Kern J**, Bauer M, Rychli K, Wojta J, Ritsch A, Gastl G, Gunsilius E, Untergasser G. Alternative splicing of vasohibin-1 generates an inhibitor of endothelial cell proliferation, migration, and capillary tube formation. *Arterioscler Thromb Vasc Biol* 2008; **28**: 478-484 [PMID: 18187668 DOI: 10.1161/ATVBAHA.107.160432]
33 **Haque S**, Morris JC. Transforming growth factor-β: A therapeutic target for cancer. *Hum Vaccin Immunother* 2017; **13**: 1741-1750 [PMID: 28575585 DOI: 10.1080/21645515.2017.1327107]
34 **Colak S**, Ten Dijke P. Targeting TGF-β Signaling in Cancer. *Trends Cancer* 2017; **3**: 56-71 [PMID: 28718426 DOI: 10.1016/j.trecan.2016.11.008]
35 **Stanilova S**, Stanilov N, Julianov A, Manolova I, Miteva L. Transforming growth factor-β1 gene promoter -509C/T polymorphism in association with expression affects colorectal cancer development and depends on gender. *PLoS One* 2018; **13**: e0201775 [PMID: 30071009 DOI: 10.1371/journal.pone.0201775]
36 **Xie F**, Ling L, van Dam H, Zhou F, Zhang L. TGF-β signaling in cancer metastasis. *Acta Biochim Biophys Sin (Shanghai)* 2018; **50**: 121-132 [PMID: 29190313 DOI: 10.1093/abbs/gmx123]
37 **Yang L**, Hu S, Tan J, Zhang X, Yuan W, Wang Q, Xu L, Liu J, Liu Z, Jia Y, Huang X. Pregnancy-specific glycoprotein 9 (PSG9), a driver for colorectal cancer, enhances angiogenesis *via* activation of SMAD4. *Oncotarget* 2016; **7**: 61562-61574 [PMID: 27528036 DOI: 10.18632/oncotarget.11146]
38 **Kaartinen V**, Voncken JW, Shuler C, Warburton D, Bu D, Heisterkamp N, Groffen J. Abnormal lung development and cleft palate in mice lacking TGF-beta 3 indicates defects of epithelial-mesenchymal interaction. *Nat Genet* 1995; **11**: 415-421 [PMID: 7493022 DOI: 10.1038/ng1295-415]
39 **Rocha MR**, Barcellos-de-Souza P, Sousa-Squiavinato ACM, Fernandes PV, de Oliveira IM, Boroni M, Morgado-Diaz JA. Annexin A2 overexpression associates with colorectal cancer invasiveness and TGF-ß induced epithelial mesenchymal transition *via* Src/ANXA2/STAT3. *Sci Rep* 2018; **8**: 11285 [PMID: 30050103 DOI: 10.1038/s41598-018-29703-0]
40 **Pascal LE**, Wang Y, Zhong M, Wang D, Chakka AB, Yang Z, Li F, Song Q, Rigatti LH, Chaparala S, Chandran U, Parwani AV, Wang Z. EAF2 and p53 Co-Regulate STAT3 Activation in Prostate Cancer. *Neoplasia* 2018; **20**: 351-363 [PMID: 29518696 DOI: 10.1016/j.neo.2018.01.011]
41 **Shen Z**, Yan Y, Ye C, Wang B, Jiang K, Ye Y, Mustonen H, Puolakkainen P, Wang S. The effect of Vasohibin-1 expression and tumor-associated macrophages on the angiogenesis in vitro and in vivo. *Tumour Biol* 2016; **37**: 7267-7276 [PMID: 26666821 DOI: 10.1007/s13277-015-4595-4]
42 **Pascal LE**, Ai J, Rigatti LH, Lipton AK, Xiao W, Gnarra JR, Wang Z. EAF2 loss enhances angiogenic effects of Von Hippel-Lindau heterozygosity on the murine liver and prostate. *Angiogenesis* 2011; **14**: 331-343 [PMID: 21638067 DOI: 10.1007/s10456-011-9217-1]
43 **Derakhshani A**, Hashemzadeh S, Asadzadeh Z, Shadbad MA, Rasibonab F, Safarpour H, Jafarlou V, Solimando AG, Racanelli V, Singh PK, Najafi S, Javadrashid D, Brunetti O, Silvestris N, Baradaran B. Cytotoxic T-Lymphocyte Antigen-4 in Colorectal Cancer: Another Therapeutic Side of Capecitabine. *Cancers (Basel)* 2021; **13** [PMID: 34067631 DOI: 10.3390/cancers13102414]
44 **Qiao S**, Hou Y, Rong Q, Han B, Liu P. Tregs are involved in VEGFA/ VASH1-related angiogenesis pathway in ovarian cancer. *Transl Oncol* 2023; **32**: 101665 [PMID: 37018867 DOI: 10.1016/j.tranon.2023.101665]

World Journal of Gastroenterology

Submit a Manuscript: https://www.f6publishing.com

World J Gastroenterol 2023 June 28; 29(24): 3793-3806

DOI: 10.3748/wjg.v29.i24.3793

ISSN 1007-9327 (print) ISSN 2219-2840 (online)

ORIGINAL ARTICLE

Basic Study

Transcriptome sequencing and experiments reveal the effect of formyl peptide receptor 2 on liver homeostasis

Hui Liu, Ze-Yu Sun, Hua Jiang, Xu-Dong Li, Yong-Qiang Jiang, Peng Liu, Wen-Hua Huang, Qing-Yu Lv, Xiang-Lilan Zhang, Rong-Kuan Li

Specialty type: Gastroenterology and hepatology

Provenance and peer review: Unsolicited article; Externally peer reviewed.

Peer-review model: Single blind

Peer-review report's scientific quality classification
Grade A (Excellent): 0
Grade B (Very good): B, B
Grade C (Good): 0
Grade D (Fair): 0
Grade E (Poor): 0

P-Reviewer: Heij LR, Germany; Kuboki S, Japan

Received: April 18, 2023
Peer-review started: April 18, 2023
First decision: April 26, 2023
Revised: May 4, 2023
Accepted: May 22, 2023
Article in press: May 22, 2023
Published online: June 28, 2023

Hui Liu, Department of Gastroenterology, Second Hospital of Dalian Medical University, Dalian 116000, Liaoning Province, China

Ze-Yu Sun, Hua Jiang, Yong-Qiang Jiang, Peng Liu, Wen-Hua Huang, Qing-Yu Lv, Xiang-Lilan Zhang, State Key Laboratory of Pathogen and Biosecurity, Institute of Microbiology and Epidemiology, Academy of Military Medical Sciences, Beijing 100071, China

Xu-Dong Li, Microbiology Teaching and Research Office, Anhui Medical University, Hefei 230032, Anhui Province, China

Rong-Kuan Li, Department of Infectious Diseases, Second Hospital of Dalian Medical University, Dalian 116000, Liaoning Province, China

Corresponding author: Rong-Kuan Li, MD, Chief Doctor, Department of Infectious Diseases, Second Hospital of Dalian Medical University, No. 467 Zhongshan Road, Shahekou District, Dalian 116000, Liaoning Province, China. dalianlrk1@163.com

Abstract

BACKGROUND

Formyl peptide receptor 2 (Fpr2) is an important receptor in host resistance to bacterial infections. In previous studies, we found that the liver of $Fpr2^{-/-}$ mice is the most severely damaged target organ in bloodstream infections, although the reason for this is unclear.

AIM

To investigate the role of Fpr2 in liver homeostasis and host resistance to bacterial infections.

METHODS

Transcriptome sequencing was performed on the livers of $Fpr2^{-/-}$ and wild-type (WT) mice. Differentially expressed genes (DEGs) were identified in the $Fpr2^{-/-}$ and WT mice, and the biological functions of DEGs were analyzed by Gene Ontology (GO) and Kyoto Encyclopedia of Genes and Genomes (KEGG) enrichment analysis. Quantitative real time-polymerase chain reaction (qRT-PCR) and western blot (WB) analyses were used to further validate the expression levels of differential genes. Cell counting kit-8 assay was employed to investigate cell survival. The cell cycle detection kit was used to measure the distribution of

cell cycles. The Luminex assay was used to analyze cytokine levels in the liver. The serum biochemical indices and the number of neutrophils in the liver were measured, and hepatic histopathological analysis was performed.

RESULTS

Compared with the WT group, 445 DEGs, including 325 upregulated genes and 120 downregulated genes, were identified in the liver of Fpr2$^{-/-}$ mice. The enrichment analysis using GO and KEGG showed that these DEGs were mainly related to cell cycle. The qRT-PCR analysis confirmed that several key genes (*CycA*, *CycB1*, *Cdc20*, *Cdc25c*, and *Cdk1*) involved in the cell cycle had significant changes. The WB analysis confirmed a decrease in the expression of CDK1 protein. WRW4 (an antagonist of Fpr2) could inhibit the proliferation of HepG2 cells in a concentration dependent manner, with an increase in the number of cells in the G0/G1 phase, and a decrease in the number of cells in the S phase. Serum alanine aminotransferase levels increased in Fpr2$^{-/-}$ mice. The Luminex assay measurements showed that interleukin (IL)-10 and chemokine (C-X-C motif) ligand (CXCL)-1 levels were significantly reduced in the liver of Fpr2$^{-/-}$ mice. There was no difference in the number of neutrophils, serum C-reactive protein levels, and liver pathology between WT and Fpr2$^{-/-}$ mice.

CONCLUSION

Fpr2 participates in the regulation of cell cycle and cell proliferation, and affects the expression of IL-10 and CXCL-1, thus playing an important protective role in maintaining liver homeostasis.

Key Words: Cell cycle; Cell proliferation; Cdk1; Differentially expressed genes; Formyl peptide receptor 2; RNA-sequencing

©The Author(s) 2023. Published by Baishideng Publishing Group Inc. All rights reserved.

Core Tip: Formyl peptide receptor 2 (Fpr2) is an important receptor in host resistance to bacterial infection. After Fpr2 deletion, the pathways involved in the cell cycle are affected, the expression of Cdk1 is downregulated, the proliferation activity of HepG2 cells is reduced, and the distribution of cell cycle is abnormal. After Fpr2 deletion, the permeability of the hepatocyte membrane increases, and the expression of interleukin-10 and Chemokine (C-X-C motif) ligand-1 decreases. These changes reflect the important protective effect of Fpr2 in maintaining liver homeostasis.

Citation: Liu H, Sun ZY, Jiang H, Li XD, Jiang YQ, Liu P, Huang WH, Lv QY, Zhang XL, Li RK. Transcriptome sequencing and experiments reveal the effect of formyl peptide receptor 2 on liver homeostasis. *World J Gastroenterol* 2023; 29(24): 3793-3806
URL: https://www.wjgnet.com/1007-9327/full/v29/i24/3793.htm
DOI: https://dx.doi.org/10.3748/wjg.v29.i24.3793

INTRODUCTION

The liver plays an important role in human metabolism and immune homeostasis. Liver dysfunction and liver failure can directly lead to the progression of sepsis and death of patients. Pre-existing liver dysfunction is a risk factor for the progression of infection to sepsis[1]. The liver is an important organ that collects blood from the intestine *via* the portal vein. Once the intestinal barrier becomes dysfunctional, the liver is the first organ to encounter bacteria. The liver collects blood through the hepatic artery, so it is also an important organ involved in the removal of bacteria from the bloodstream in systemic infection[2,3].

As an organ mainly responsible for blood detoxification, the liver plays a key role in removing bacteria and toxins during sepsis. After intravenous injection, the liver captures 65% of bacteria in 10 min and over 80% in 6 h[4]. Two methods of liver clearance have been identified: Rapid and slow. The rapid clearance mainly relies on Kupffer cells to remove bacteria and does not depend on complement-mediated opsonophagocytosis or platelet combinations. The slow clearance ensures that the host not only removes a sufficient number of bacteria to prevent infection and damage but also maintains sufficient bacteria to induce host adaptive immunity. In addition to mesenteric lymph nodes, the liver is another important firewall against bacterial infections in the body[2,5,6].

Formyl peptide receptors (FPRs) are G-protein-coupled receptors that play an important role in host defense and inflammation. The most important biological activity of FPRs is the induction of leukocyte

chemotaxis in infected or injured areas. In addition to chemotaxis, FPRs also mediate phagocytosis, production of reactive oxygen species, and production of various cytokines/chemokines. According to sequence similarity, FPRs are divided into three family members: FPR1, ALX/FPR2, and FPR3. Based on the ability of FPRs to recognize bacterial formylated peptides, they are considered to play an important role in host defense against microbial invasion.

Initially, research on FPRs mainly focused on regulating inflammation, but increasing evidence demonstrated that FPRs can also regulate the host's defense process, including regulating the activation of neutrophils and dendritic cells and participating in host resistance to bacterial infection, tissue damage, and wound healing[7]. Liu *et al*[8] reported that during *Listeria monocytogenes* (*Listeria*) infection, FPRs can quickly recruit the first wave of neutrophils into the infected liver, followed by the second wave of neutrophil accumulation mediated by CXCR2. This discovery challenges the previously reported pattern of host defense against *Listeria*, that is, the receptor toll-like receptor 2 on the host cell is activated by bacterial lipoprotein, and then CXCR2 ligand is produced to induce neutrophil accumulation[9]. In sepsis, the biased expression of chemokine receptors CC chemokine receptor 5 (CCR5) and FPR2 in human and mouse neutrophils leads to the movement of neutrophils guided by CCR5 to aseptic tissue sites, whereas polymorphonuclear neutrophils guided by FPR2 to bacterial infection sites are significantly reduced[10]. Thus, inflammatory but non-functional neutrophils may increase the host's morbidity and mortality, which may be related to infectious injury[11]. The above findings emphasize the importance of FPRs in the host defense against microorganisms.

Our previous research revealed that in group B streptococcus infection, Fpr2 activated the downstream key signal molecules and produced chemokine (C-X-C motif) ligand (CXCL)1/2 to attract neutrophils, indicating that Fpr2, as a chemotactic receptor, could not only attract neutrophils directly, but also indirectly control neutrophil chemotaxis by regulating the production of chemokines to resist infection[12]. The liver is the most important organ in the removal of bacteria, and Fpr2 is an important receptor involved in resisting bacterial infection. However, the effect of Fpr2 on the liver homeostasis remains unclear. In the present study, we evaluated the liver of Fpr2 knockout and wild-type (WT) mice in terms of transcriptome sequencing, histology, immunity, and biochemistry to understand the reason for the antibacterial activity of Fpr2.

MATERIALS AND METHODS

Mice

$Fpr2^{-/-}$ (Fpr2 knockout) mice were purchased from Cyagen Biosciences (Guangzhou, China), who created this model according to previously reported methods[12]. The WT C57BL/6 mice (6-8 wk, 18-20 g body weight) were purchased from Charles River (Beijing, China). These mice were bred in the animal center of the Academy of Military Medical Sciences under specific pathogen free conditions. The animals were acclimatized to laboratory conditions (23 °C, 12 h/12 h light/dark, 50% humidity, and ad libitum access to food and water) for 2 wk, prior to experimentation. All animals were euthanized by isoflurane inhalation for tissue collection. The animal protocol was designed to minimize pain or discomfort to the animals. This research was conducted in compliance with the guidelines for laboratory animal care approved in China. All experimental procedures were approved by the Animal Ethics Committee of the Academy of Military Medical Sciences.

Cell culture

The HepG2 cell line was cultured in a high-glucose DMEM medium (Gibco, Rockville, MD, United States) supplemented with 10% fetal bovine serum (Gibco, Rockville, MD, United States). Cell counting kit-8 (CCK8; APExBIO, United States) assay was employed to investigate cell survival following the manufacturer's instructions. In brief, HepG2 cells were plated in 96-well plates at a density of 3×10^3 cells/well. On the second day, cells were treated with different concentrations of WRW4 [Sangon Biotech (Shanghai) Co., Ltd. China] for 24 h. Then, 10 μL CCK-8 was added to each well and cells were incubated at 37 °C for 2 h. Absorbance was measured at 450 nm using a microplate spectrophotometer (Molecular Devices LLC, Sunnyvale, CA, United States).

The cell cycle detection kit (KeyGEN BioTECH, Nanjing, China) was used to measure the distribution of cell cycles. HepG2 cells were plated in 6-well plates and treated with WRW4 (1 μM) for 24 h. Dimethyl sulfoxide used as a control to dissolve WRW4. Next, cells were collected, washed, and fixed overnight at 4 °C in 70% ethanol. The samples were then incubated with RNase A and propidium in the dark for 30 min and cell cycle distribution was analyzed using flow cytometry.

Total RNA isolation and cDNA library construction

The mice were sacrificed after anesthesia, and the liver was taken for subsequent RNA sequencing. RNA extraction, library preparation, DNA sequencing, and result analysis were conducted by Nevogene Co., Ltd (Beijing, China). Briefly, total RNA was extracted using TRIzol reagent (Invitrogen, Shanghai, China). RNA integrity was assessed using the RNA Nano 6000 Assay Kit on a Bioanalyzer 2100 system (Agilent Technologies, CA, United States).

To select cDNA fragments of 370-420 bp, the library fragments were purified with the AMPure XP system (Beckman Coulter, Beverly, United States). Polymerase chain reaction (PCR) was performed using Phusion High-Fidelity DNA polymerase, Universal PCR primers, and Index (X) Primer. Finally, PCR products were purified (AMPure XP system), and library quality was assessed on the Agilent Bioanalyzer 2100 system. Clustering of the index-coded samples was performed on a cBot Cluster Generation System using TruSeq PE Cluster Kit v3-cBot-HS (Illumina). The library preparations were sequenced on an Illumina Novaseq platform, and 150 bp paired-end reads were generated.

Sequence read quality control, mapping, and counting

After data cleaning (to obtain clean reads with high quality), reads were mapped to the reference genome. Reference genome and gene model annotation files were downloaded from the genome website directly. The index of the reference genome was built using Hisat2 v2.0.5, and paired-end clean reads were aligned to the reference genome using Hisat2 v2.0.5. FeatureCounts v1.5.0-p3 was used to count the number of reads mapped to each gene. Fragments per kilobase millions of each gene were calculated based on the length of the gene and the read counts were mapped to the respective genes.

Differential expression analysis and quantitative real time-PCR validation

Differential expression analysis of the two groups (four biological replicates per group) was performed using the DESeq2 R package (1.20.0). Genes with an adjusted $P < 0.05$ found by DESeq2 were assigned as differentially expressed. Quantitative real time-PCR (qRT-PCR) analysis further validated gene expression patterns. The primers used for qRT-PCR analysis were listed in Table 1.

Enrichment analysis of differentially expressed genes

Gene Ontology (GO) and Kyoto Encyclopedia of Genes and Genomes (KEGG) enrichment analysis of differentially expressed genes (DEGs) were implemented using the ClusterProfiler R package, in which gene length bias was corrected. GO terms with a corrected $P < 0.05$ were considered significantly enriched by DEGs. The ClusterProfiler R package was used to test the statistical significance of DEGs in KEGG enrichment pathways.

Western blotting

The liver tissues were taken and washed three times with phosphate buffer solution, then stored at -80 °C. Total proteins were extracted from the liver using RIPA buffer (Beyotime, Nantong, China), and the concentrations were estimated using the bicinchoninic acid protein assay kit (Pierce, Rockford, IL, United States). Next, 30 μg of protein was separated by sodium dodecyl-sulfate polyacrylamide gel electrophoresis on a 10% gel and transferred to PVDF membranes. The membranes were blocked in 3% nonfat dry milk and then probed with anti-CDK1 antibody (1:2000 dilution; ab32094; Abcam, Cambridge, MA, United States), and anti-beta actin antibody (1:3000; ab8227; Abcam, Cambridge, MA, United States) overnight at 4 °C. On the next day, membranes were incubated with appropriate secondary antibody for 1 h at room temperature. The protein bands were visualized using Amersham Hyperfilm™ ECL reagent (Thermo Fisher Scientific, MA, United States).

Cytokine measurements by the Luminex assay

Fresh liver tissues from the mice were weighed and homogenized. Concentrations of cytokines in the supernatants of the liver were measured by multiplexed Luminex xMAP assay (Cytokine & Chemokine 36-Plex Mouse ProcartaPlex™ Panel 1A; Thermo Fisher Scientific, MA, United States), according to the manufacturer's instructions.

Flow cytometry

The liver tissue was digested into single-cell suspension using type IV collagenase (Sigma-Aldrich, United States). The number of leukocytes in the liver were determined using a BD TruCount system (BD Biosciences, United States). The cells were stained with FITC-anti-mouse Ly6G (Biolegend, San Diego, CA, United States), PerCP-anti-mouse CD45 (Biolegend, San Diego, CA, United States), and PE-anti-mouse CD11b (Biolegend, San Diego, CA, United States) antibodies. All of the above-stained cells were assayed using a BD FACSVerse flow cytometer and data were analyzed using FlowJo software.

Determination of serum biochemical indexes

The blood from mice was collected, and serum was separated by centrifugation (4 °C, 3000 rpm, 10 min). A total of 200 μL serum was obtained and sent to the experimental animal center of the Academy of Military Medical Sciences for the determination of liver biochemical indexes.

Liver histopathology

The liver tissue of mice was fixed with 4% formaldehyde, paraffin sections were prepared, stained with hematoxylin and eosin, and observed and photographed with an Olympus camera system. The image magnifications were 200 × and 400 ×.

Table 1 List of primers used in the study

Primer	Sequences (5' to 3')
CycA-F	GCCTTCACCATTCATGTGGAT
CycA-R	TTGCTCCGGGTAAAGAGACAG
CycB1-F	AGAGCTATCCTCATTGACTGGC
CycB1-R	AACATGGCCGTTACACCGAC
Cdk1-F	AGAAGGTACTTACGGTGTGGT
Cdk1-R	GAGAGATTTCCCGAATTGCAGT
Cdc25c-F	GTTTCAGCACCCAGTTTTAGGT
Cdc25c-R	AGAATGCTTAGGTTTGCCGAG
Cdc20-F	TTCGTGTTCGAGAGCGATTTG
Cdc20-R	ACCTTGGAACTAGATTTGCCAG
Mps1-F	GCAGTGTGACGATTGATTCCA
Mps1-R	TCGGCACAGATTTTAGACAAGC
GAPDH-F	CATGGCCTTCCGTGTTCCTA
GAPDH-R	GCGGCACGTCAGATCCA

Statistical analysis

All data were analyzed using GraphPad Prism (version 8.0; GraphPad Software, La Jolla, CA, United States). Differences between the groups were calculated using an unpaired *t*-test and a log-rank test. Data were shown as mean ± SD. Differences were considered statistically significant at $P < 0.05$.

RESULTS

Identification of DEGs and their GO and KEGG pathway analysis

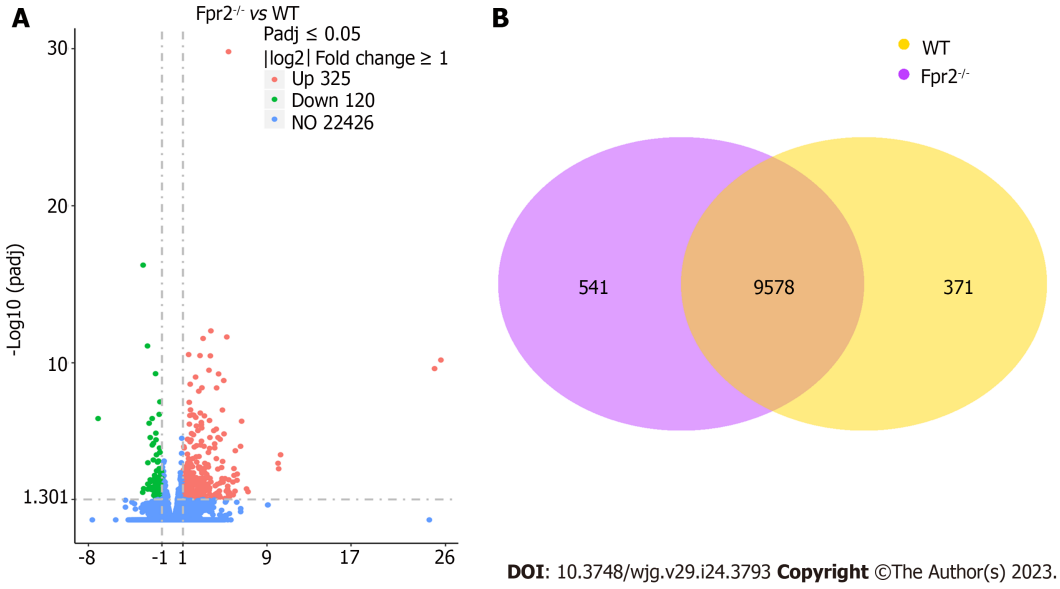
We used RNA-sequencing to analyze the liver transcriptome of $Fpr2^{-/-}$ mice and compared it with that of WT mice to determine DEGs. Taking $|\log2(\text{fold change})| \geq 1$ and padj ≤ 0.05 as criteria, compared with the WT group, 445 DEGs, including 325 upregulated genes and 120 downregulated genes, were identified in $Fpr2^{-/-}$ mice (Figure 1A). Venn diagram analysis showed that 9578 genes showed identical expression between $Fpr2^{-/-}$ and WT mice. On the other hand, 541 and 371 specific genes were expressed in $Fpr2^{-/-}$ and WT mice, respectively (Figure 1B).

According to the results of the enrichment analysis, 179 GO terms were obtained, including 136 biological processes (BPs), 25 cell component (CC), and 18 molecular function (MF) terms. The results showed that the DEGs were mainly annotated to the cell cycle (Figure 2A). Further GO enrichment analysis of upregulated DEGs showed that a total of 156 GO terms were obtained, including 121 BPs, 25 CC, and 10 MF terms. The BP terms were significantly enriched in mitotic sister chromatid segregation, chromosome segregation, sister chromatid segregation, and nuclear chromosome segregation. The CC terms were significantly enriched in chromosomes, centromeric regions, spindles, mitotic spindles, kinetochores, condensed chromosomes, centromeric regions, and chromosomal regions. The MF terms were significantly enriched in microtubule binding, tubulin binding, and microtubule motor activity (Figure 2B). The results of the GO analysis suggest that the upregulated DEGs are significantly enriched in many phases of cell division. In addition, GO analysis of downregulated DEGs revealed that BP terms were significantly enriched in many BPs related to liver function, such as organic hydroxy compound metabolic process, organic hydroxy compound biosynthetic process, steroid metabolic process, positive regulation of alcohol biosynthetic process, cellular hormone metabolic process, G-protein coupled receptor signaling pathway, and coupled to cyclic nucleotide second messenger (Figure 2C).

Four pathways with significant differences obtained based on KEGG analysis are listed in Table 2. These pathways included cell cycle, neuroactive ligand-receptor interaction, oocyte meiosis, and progesterone-mediated oocyte maturation (Figure 3). Both GO function analysis and KEGG pathway enrichment analysis showed that core DEGs mainly regulated the cell cycle of the liver tissue in Fpr2-deficient mice, which revealed that Fpr2 deficiency may cause cell division cycle disorder to some extent.

Table 2 Kyoto Encyclopedia of Genes and Genomes pathway significant enrichment analysis

Term	Description	Sample number	*P* value	Gene_name
mmu04110	Cell cycle	16/182	0.00009	Cdc20 Ccnb1 Ccnb2 Plk1 Ccna2 Ttk Mad2l1 Wee1 Bub1b Cdk1 Mcm5 Cdkn1a Cdc25c Mcm2 Espl1 Bub1
mmu04080	Neuroactive ligand-receptor interaction	16/182	0.00079	Fpr2 Mtnr1a Gzma P2ry1 Lpar2 Chrna4 Grid1 Gabra3 Adcyap1r1 Vipr1 Calcrl Pth1r Ednra Hcrtr2 Gpr35 P2ry13
mmu04114	Oocyte meiosis	13/182	0.00079	Cdc20 Ccnb1 Ccnb2 Plk1 Mad2l1 Camk2b Adcy1 Ar Cdk1 Cdc25c Adcy7 Espl1 Bub1
mmu04914	Progesterone-mediated oocyte maturation	11/182	0.00132	Ccnb1 Ccnb2 Plk1 Ccna2 Kif22 Mad2l1 Adcy1 Cdk1 Cdc25c Adcy7 Bub1



DOI: 10.3748/wjg.v29.i24.3793 **Copyright** ©The Author(s) 2023.

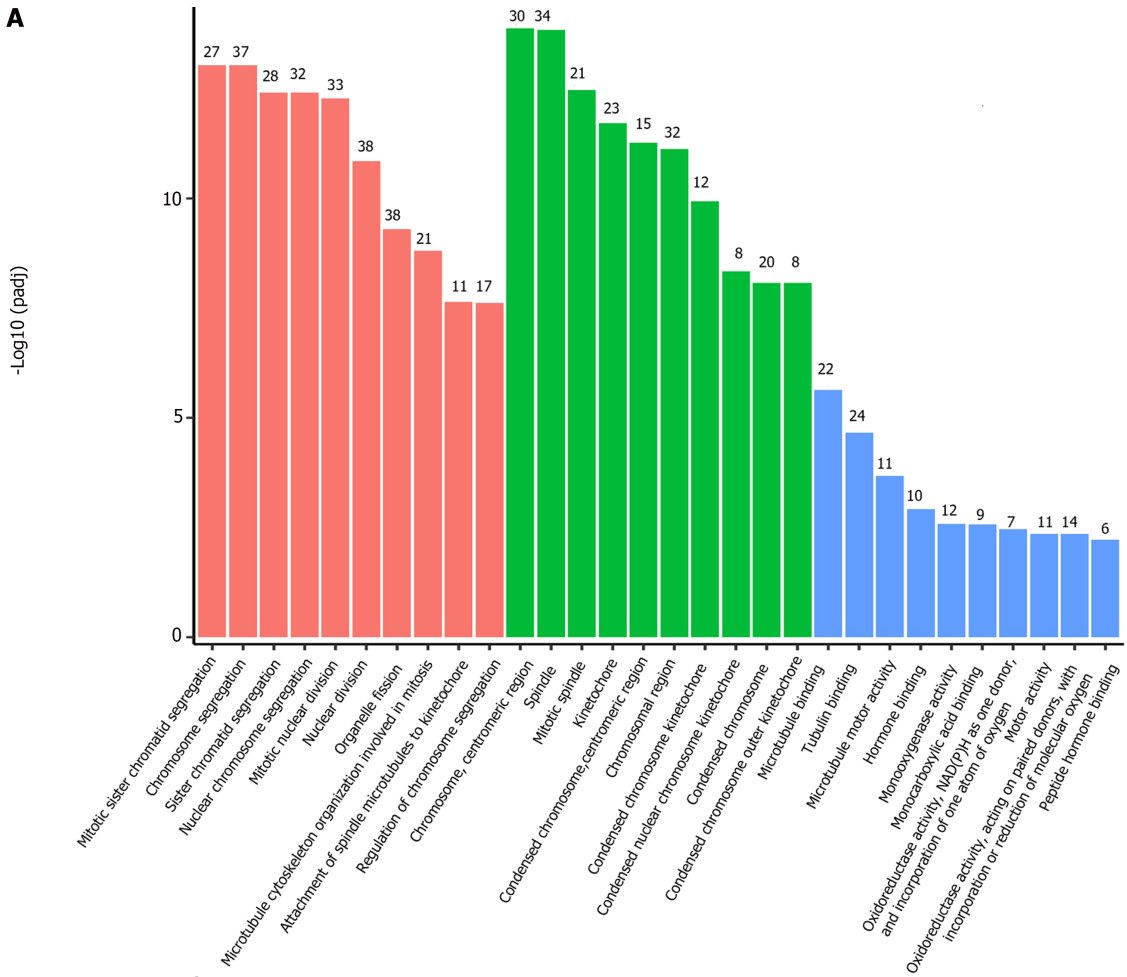
Figure 1 RNA-sequencing analysis of distributions of all differentially expressed genes. A: Volcano map of the distributions of all differentially expressed genes in formyl peptide receptor 2 (Fpr2)$^{-/-}$ and wild-type (WT) mice (n = 4). Red, green, and blue colors respectively represent upregulated genes, downregulated genes, and genes with no difference in expression; B: Venn diagram of gene counts expressed in the Fpr2$^{-/-}$ and WT mice (n = 4). 9578 genes show identical expression between Fpr2$^{-/-}$ and WT mice. 541 and 371 specific genes are expressed in Fpr2$^{-/-}$ and WT mice, respectively. Fpr2: Formyl peptide receptor 2; WT: Wild-type.

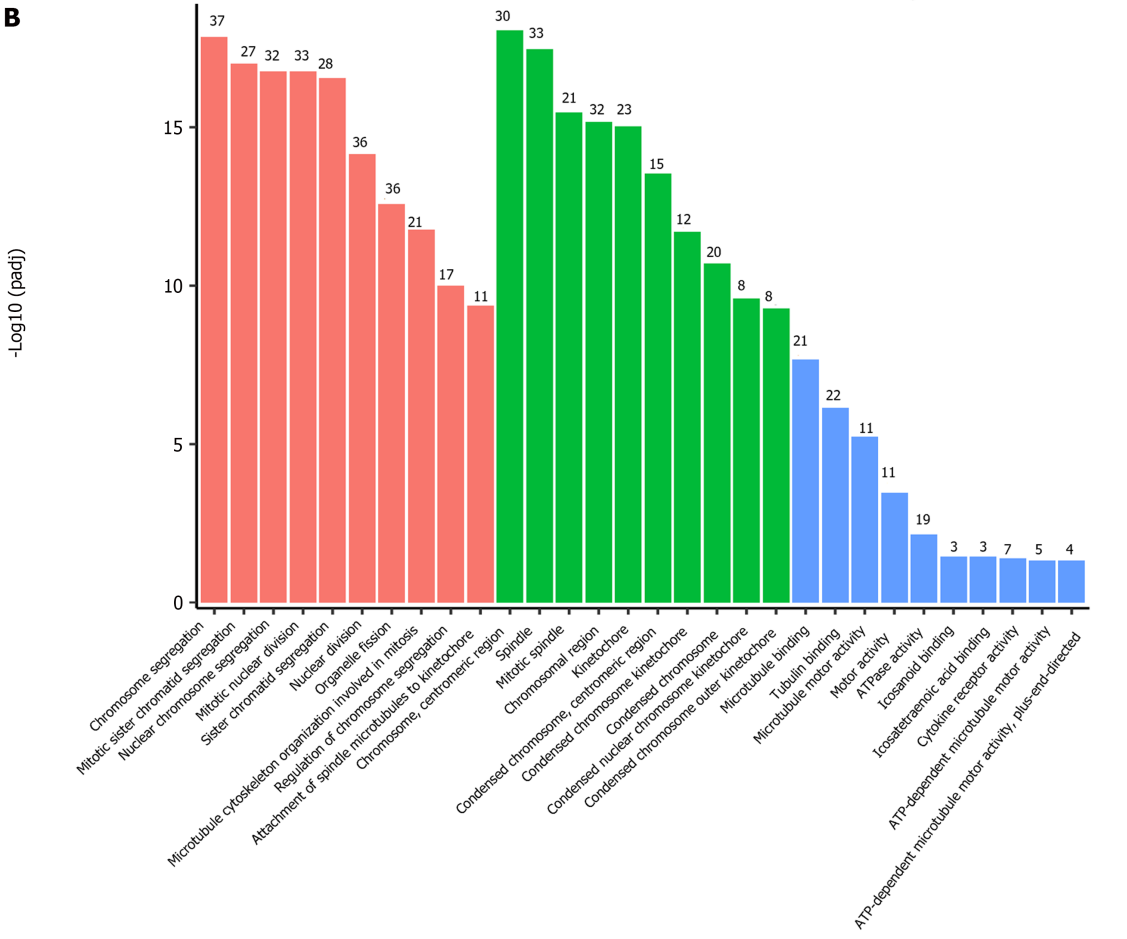
Fpr2 participated in the regulation of cell cycle

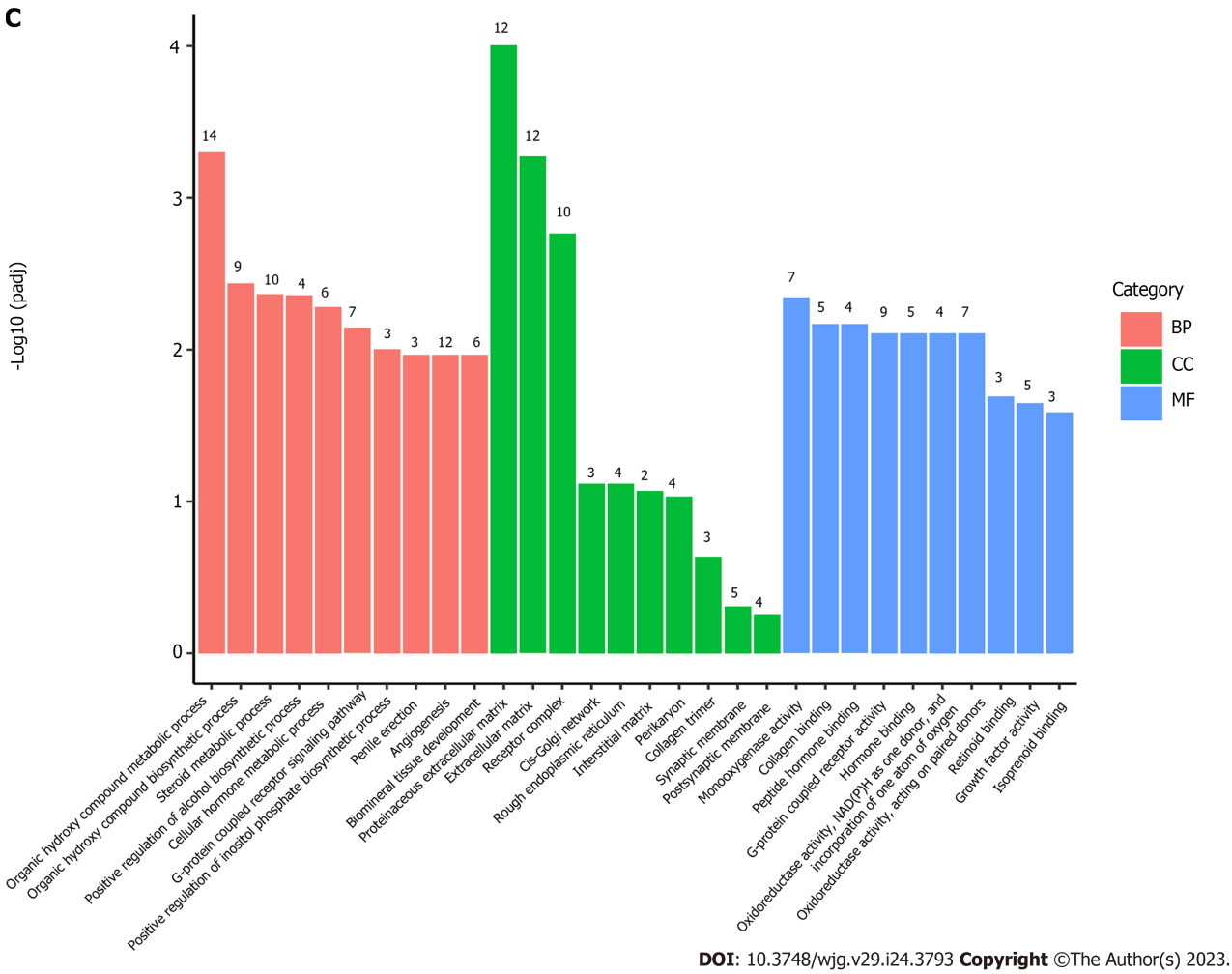
To further validate the results of RNA-sequencing, we selected several key genes *CycA*, *CycB1*, *Cdc20*, *Cdc25c*, *Mps1*, and *Cdk1*, which are closely related to the cell cycle, for qRT-PCR analysis. The results showed that the expression of *CycA*, *CycB1*, *Cdc20*, and *Cdc25c* was upregulated (Figure 4A), while the expression of *Cdk1* was downregulated in the Fpr2$^{-/-}$ mice (Figure 4B). There was no significant difference in the expression of *Mps1* between Fpr2$^{-/-}$ and WT mice (Figure 4A). The WB analysis further confirmed a decrease in CDK1 expression (Figure 4B). To clarify the impact of Fpr2 deficiency on liver cell proliferation, WRW4, an antagonist of Fpr2, was used to inhibit Fpr2 in the liver cells. CCK-8 further clarified the effect of different concentrations of WRW4 on the proliferation of HepG2 cells. Figure 4C indicates that WRW4 at all concentrations (0.125 μM, 0.25 μM, 0.5 μM, 1.0 μM, and 2.0 μM) inhibited the proliferation of HepG2 cells in a concentration dependent manner. WRW4 at 1 μM was used to analyze the distribution of cell cycles. Flow cytometry analysis showed that the number of cells in G0/G1 phase increased, and the number of cells in S phase decreased (Figure 4D). From the above analysis, it can be surmised that when Fpr2 is absent, some genes involved in cell cycle regulation are affected and these may inhibit cell proliferation by blocking the cell cycle.

Fpr2 maintained the stability of liver cell membrane

Considering that the lack of Fpr2 can lead to disruption of the liver cell cycle, we tested biochemical indicators that reflect liver function. Biochemical indicators related to liver function include determination of the levels of alanine transaminase (ALT), aspartate transaminase (AST), alkaline phosphatase (ALP), lactate dehydrogenase (LDH) and albumin (ALB). In Fpr2$^{-/-}$ mice, we detected higher levels of serum ALT and LDH compared to those in the WT mice, with no significant changes in AST, ALP, and


A
-Log10 (padj)
0
5
10
27 37 28 32 33 38 38 21 11 17 30 34 21 23 15 32 12 8 20 8 22 24 11 10 12 9 7 11 14 6
Mitotic sister chromatid segregation
Chromosome segregation
Sister chromatid segregation
Nuclear chromosome segregation
Mitotic nuclear division
Nuclear division
Organelle fission
Microtubule cytoskeleton organization involved in mitosis
Attachment of spindle microtubules to kinetochore
Regulation of chromosome segregation
Chromosome, centromeric region
Spindle
Mitotic spindle
Kinetochore
Condensed chromosome,centromeric region
Chromosomal region
Condensed chromosome kinetochore
Condensed nuclear chromosome kinetochore
Condensed chromosome
Condensed chromosome outer kinetochore
Microtubule binding
Tubulin binding
Microtubule motor activity
Hormone binding
Monooxygenase activity
Monocarboxylic acid binding
Oxidoreductase activity, NAD(P)H as one donor, and incorporation of one atom of oxygen
Motor activity
Oxidoreductase activity, acting on paired donors, with incorporation or reduction of molecular oxygen
Peptide hormone binding


B
-Log10 (padj)
0
5
10
15
37 27 32 33 28 36 36 21 17 11 30 33 21 32 23 15 12 20 8 8 21 22 11 11 19 3 3 7 5 4
Chromosome segregation
Mitotic sister chromatid segregation
Nuclear chromosome segregation
Mitotic nuclear division
Sister chromatid segregation
Nuclear division
Organelle fission
Microtubule cytoskeleton organization involved in mitosis
Regulation of chromosome segregation
Attachment of spindle microtubules to kinetochore
Chromosome, centromeric region
Spindle
Mitotic spindle
Chromosomal region
Kinetochore
Condensed chromosome, centromeric region
Condensed chromosome kinetochore
Condensed chromosome
Condensed nuclear chromosome kinetochore
Condensed chromosome outer kinetochore
Microtubule binding
Tubulin binding
Microtubule motor activity
Motor activity
ATPase activity
Icosanoid binding
Icosatetraenoic acid binding
Cytokine receptor activity
ATP-dependent microtubule motor activity
ATP-dependent microtubule motor activity, plus-end-directed



DOI: 10.3748/wjg.v29.i24.3793 **Copyright** ©The Author(s) 2023.

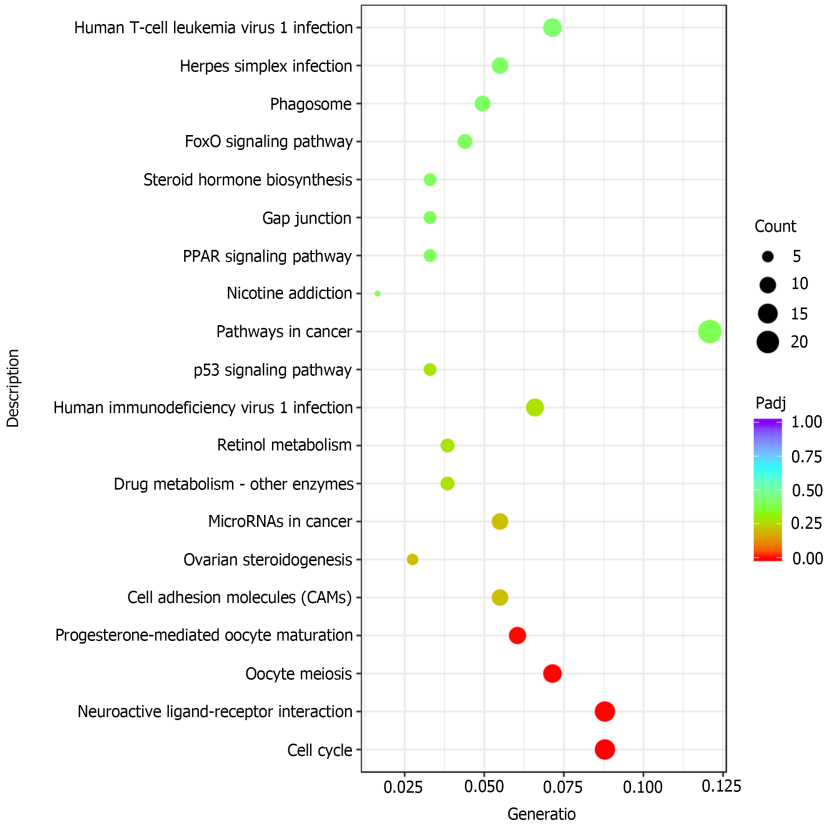
Figure 2 Gene Ontology pathway enrichment analysis of differentially expressed genes. The bar graph shows the top 10 (red for biological processes, green for cellular component and blue for molecular function) enriched Gene Ontology pathways. A: Gene Ontology (GO) pathway enrichment analysis of all differentially expressed genes (DEGs); B: GO pathway enrichment analysis of upregulated DEGs; C: GO pathway enrichment analysis of downregulated DEGs. BP: Biological process; CC: Cellular component; MF: Molecular function.

ALB in both mice (Figure 5). When the permeability of the liver cell membrane changes, ALT overflows from the cells into the bloodstream. Therefore, the increase of serum ALT in Fpr2$^{-/-}$ mice suggest that the stability of liver cell membrane is affected.

Fpr2 regulated the expression of interleukin-10 and CXCL-1

In the GO analysis, in addition to cell cycle, ERK1 and ERK2 cascade, myeloid leukocyte activation, and positive regulation of myeloid leukocyte differentiation were also significantly enriched in BP terms, and G-protein coupled receptor activity was significantly enriched in MF terms. These results prompted us to consider whether disruptions in the cell cycle and cell membrane stability may cause inflammation. The Luminex assay was performed to measure the cytokine levels in the liver. The results indicated that in addition to the increased levels of interferon gamma, the levels of interleukin (IL)-4, IL-6, IL-9, IL-12, IL-17A, IL-22, IL-23, IL-27, monocyte chemoattractant protein (MCP)-1, MCP-3, macrophage inflammatory protein (MIP)-1α, MIP-1β, MIP-2, CXCL10, Eotaxin, and tumor necrosis factor-α were decreased at different degrees in the Fpr2$^{-/-}$ mice (Figure 6). The decreases in IL-10, IL-18, and CXCL-1 levels were statistically significant.

Based on the above results, the inflammatory status of the liver was further evaluated. We measured the C-reactive protein (CRP) levels in the peripheral blood and the number of neutrophils in the liver and performed histopathological analysis of the liver. The results showed that there was no significant difference in the CRP levels and the number of neutrophils in the liver between WT and Fpr2 $^{-/-}$ mice (Figures 7A and B), and there was no inflammatory cell infiltration in the histopathology of the liver (Figure 7C). The above results indicate that although the absence of Fpr2 can affect the cell cycle and membrane stability, it does not cause significant inflammation in the liver.



DOI: 10.3748/wjg.v29.i24.3793 **Copyright** ©The Author(s) 2023.

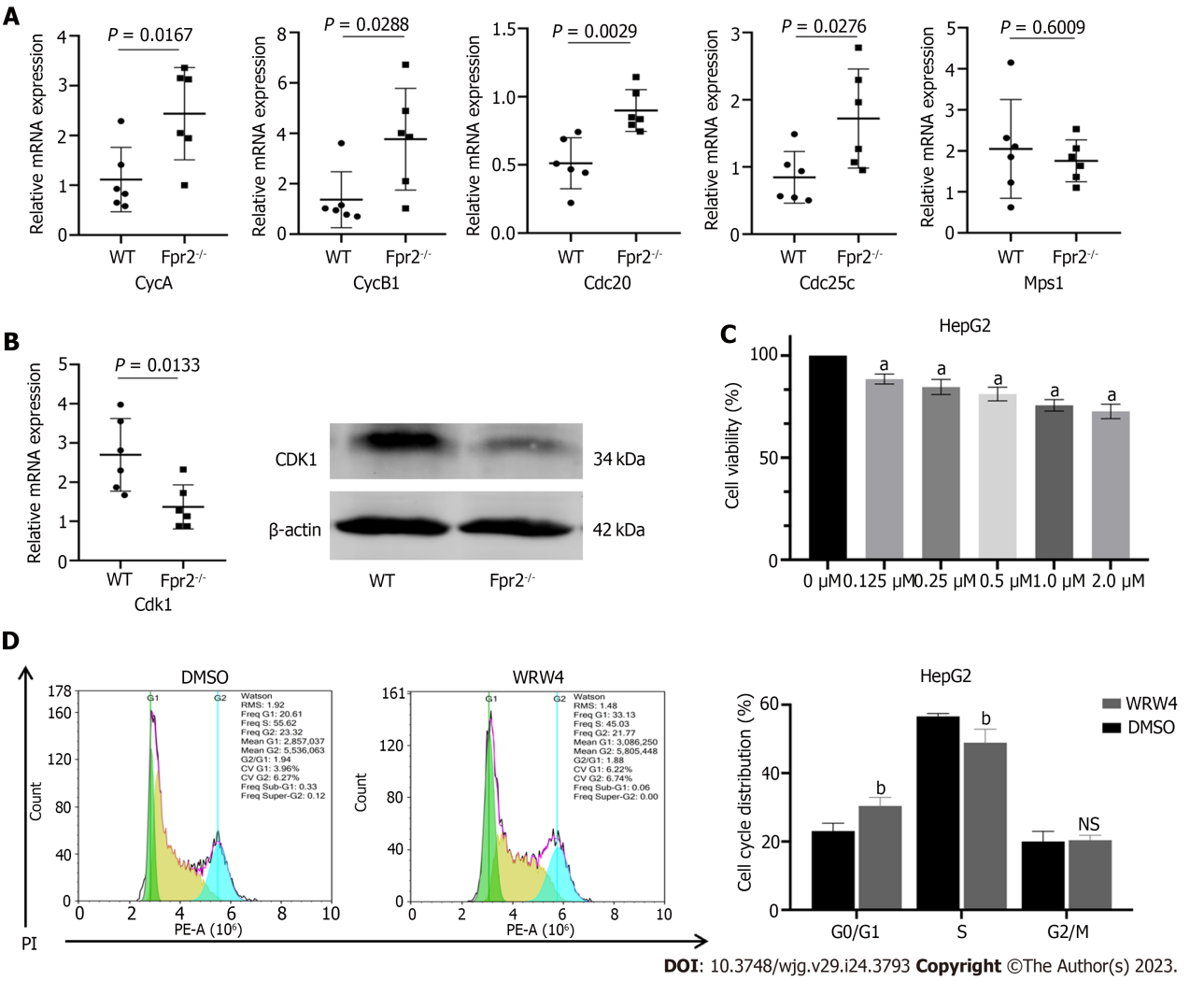
Figure 3 Significant enrichment of Kyoto Encyclopedia of Genes and Genomes pathways with differentially expressed genes. The size of the bubble indicates the enrichment score, and the color indicates the significance of the enrichment.

DISCUSSION

In this study, we focused on the effects of Fpr2 on liver homeostasis in mice. According to the results of RNA-sequencing, the deletion of Fpr2 mainly affects the cell cycle of the liver, which is clearly manifested by the significant changes in the expression of several key genes during cell division and enrichment of several related pathways of the cell cycle. The influence of Fpr2 deletion on the cell cycle may be multifaceted. From the perspective of function, DEGs contain many key genes in each stage of the cell cycle (*CycA*, *CycB*, *Cdk1*) and important cell cycle regulatory genes (*Cdc25*, *Cdc20*). In terms of distribution, DEGs are distributed in processes related to spindles, chromatin, and kinetochores. Cdk1 is essential for G1/S and G2/M phase transitions of eukaryotic cell cycle[13]. In $Fpr2^{-/-}$ mice, the expression level of Cdk1 is decreased. When FPR2 of HepG2 cells is blocked by WRW4, the cell proliferation activity decreased, the number of cells in G0/G1 phase increased, and the number of cells in S phase decreased, which indicates that FPR2 can affect cell proliferation by blocking cell cycle.

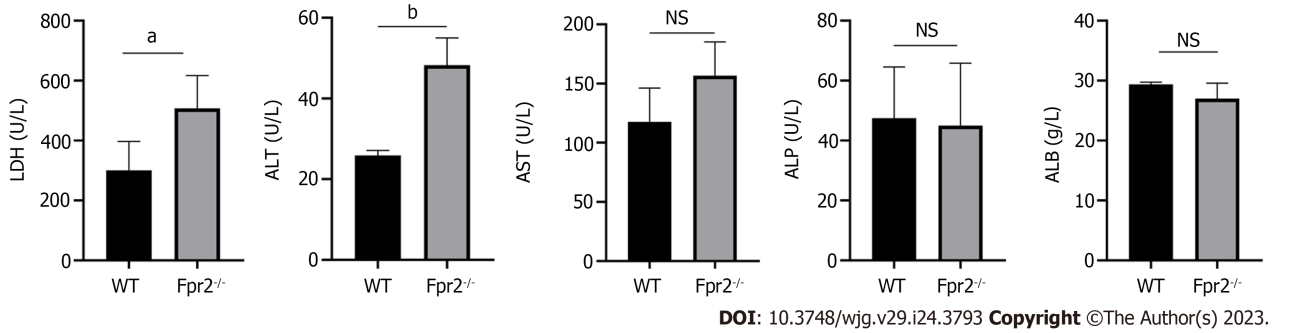
Most research on FPR2 has focused on its role in the regulation of immune cells in inflammation. Recently, it has also been reported that FPR2 is involved in regulating the migration and proliferation of many types of stem cells. Han *et al*[14] found that the proliferation of hair follicle stem cells and dermal papilla cells in $Fpr2^{-/-}$ mice was significantly reduced, which induced hair loss. Chen *et al*[15] found that $Fpr2^{-/-}$ mice displayed shortened colonic crypts and reduced acute inflammatory responses. This is because intestinal commensal bacteria mediate the proliferation and renewal of epithelial cells through Fpr2. In the present study, we found that the absence of this receptor in liver cells caused abnormal cell cycle. These findings provide evidence for the new function of Fpr2.

Although we found that Fpr2 deficiency can lead to abnormal liver cell cycle and membrane permeability, the infiltration of inflammatory cells in the liver was not observed when probed further. This is consistent with the fact that mice can still grow and reproduce normally with Fpr2 deficiency and do not die due to infection. Therefore, we speculate that these abnormal manifestations after Fpr2 deficiency may be offset by certain protective factors in the body. However, based on our previous research[12], the ability of $Fpr2^{-/-}$ mice to control infection was significantly lower than that of WT mice in the event of bacterial infections, with the liver becoming a severely damaged target organ. Therefore, our current findings may provide an explanation that the imbalance of cellular homeostasis caused by Fpr2 deficiency leads to insufficient defense function of the liver when encountering bacterial infections, making it a target organ for infection damage.



DOI: 10.3748/wjg.v29.i24.3793 **Copyright** ©The Author(s) 2023.

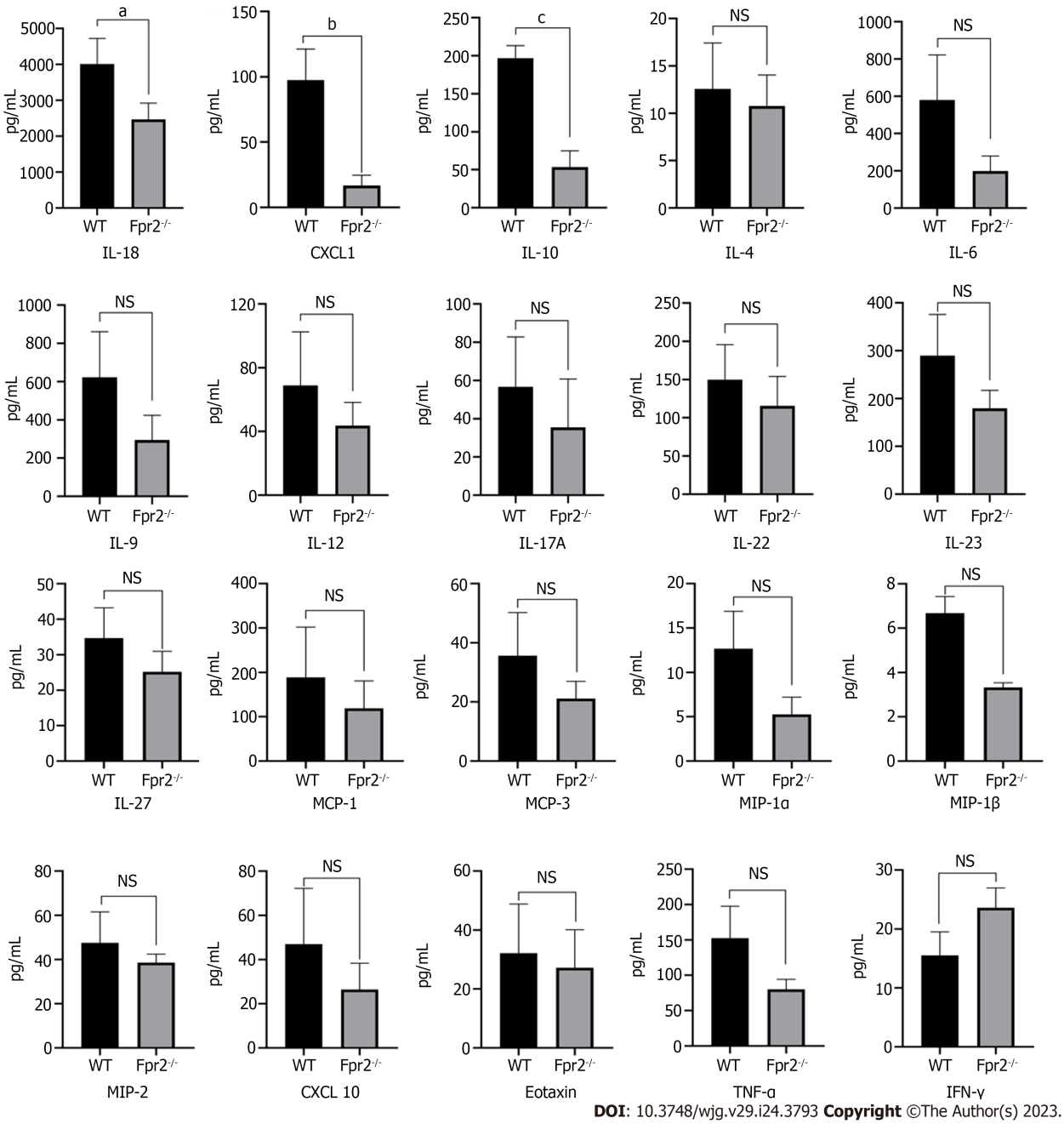
Figure 4 The effect of formyl peptide receptor 2 deletion on cell cycle. A: Quantitative real time-polymerase chain reaction (qRT-PCR) validates the expression of key cell cycle genes regulated by formyl peptide receptor 2 (Fpr2), including *CycA*, *CycB1*, *Cdc20*, *Cdc25c*, and *Mps1* (n = 6). P values are indicated on the graphs; B: qRT-PCR and western blot analyses are used to validate the changes in expression of CDK1; C: The effect of different concentrations of WRW4 on the proliferation activity of HepG2 cells detected by CCK-8 (n = 5); D: The cell cycle distribution of HepG2 cells treated with WRW4 (1 μM) and dimethyl sulfoxide determined by flow cytometry (n = 3). Data are shown as mean ± SD. [a]P < 0.0001 *vs* the 0 μM group; [b]P < 0.05 *vs* the dimethyl sulfoxide group; NS: No significant; Fpr2: Formyl peptide receptor 2; WT: Wild-type; DMSO: Dimethyl sulfoxide.



DOI: 10.3748/wjg.v29.i24.3793 **Copyright** ©The Author(s) 2023.

Figure 5 Liver function test in serum of wild-type and formyl peptide receptor 2$^{-/-}$ mice (n = 4). The values are expressed as g/L for albumin levels, and U/L for alanine transaminase, lactate dehydrogenase, aspartate transaminase, and alkaline phosphatase levels. Data are expressed as mean ± SD. [a]P < 0.05, [b] P < 0.01 *vs* the wild-type group; NS: No significant; ALB: Albumin; ALP: Alkaline phosphatase; ALT: Alanine transaminase; AST: Aspartate transaminase; LDH: Lactate dehydrogenase; Fpr2: Formyl peptide receptor 2; WT: Wild-type.

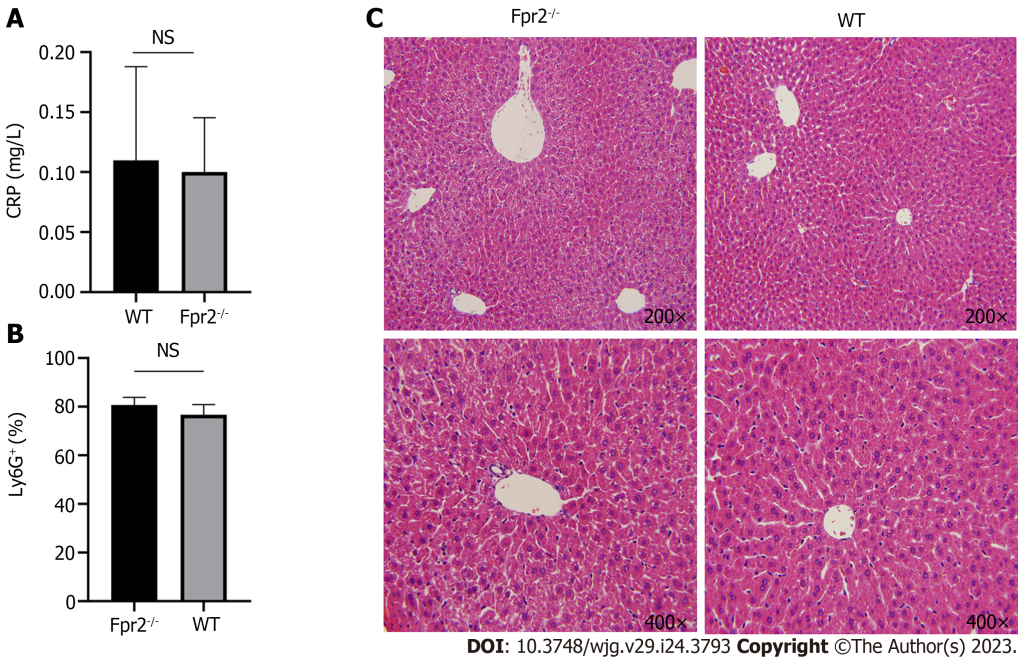
The levels of IL-10 and CXCL-1 were significantly reduced in the liver of Fpr2$^{-/-}$ mice. IL-10 is an important anti-inflammatory factor that can resist the pro-inflammatory effects of other cytokines, thus controlling inflammation. The anti-inflammatory reaction mediated by IL-10 is a fundamental



DOI: 10.3748/wjg.v29.i24.3793 **Copyright** ©The Author(s) 2023.

Figure 6 Luminex assay analyses cytokines/chemokines concentration in liver of wild-type and formyl peptide receptor 2$^{-/-}$ mice (n = 3). Mean concentration values are shown as normalized to tissue weight. Data are expressed as mean ± SD. $^{a}P < 0.05$, $^{b}P < 0.01$, $^{c}P < 0.001$ *vs* the wild-type group; NS: No significant; CXCL: Chemokine (C-X-C motif) ligand; IFN-γ: Interferon gamma; IL: Interleukin; MCP: Monocyte chemoattractant protein; MIP: Macrophage inflammatory protein; TNF: Tumor necrosis factor; Fpr2: Formyl peptide receptor 2; WT: Wild-type.

homeostatic mechanism that controls the degree and duration of inflammation. IL-10 is an important factor in maintaining immunological tolerance in the liver[16]. IL-10 also plays an important role in liver regeneration and repair[17]. In addition, various cells, such as hepatocytes, endothelial cells, Kupffer cells, and hepatic stellate cells, are involved in the production of IL-10[18]. CXCL-1 is an important chemokine in neutrophils. Our previous research found that the loss of Fpr2 leads to a decrease in the recruitment of neutrophils and weakening of the host's early immune response when resisting infection with *Streptococcus lactis*[12]. Therefore, the decline in repair ability and the decrease in chemotaxis to neutrophils may be another reason why Fpr2$^{-/-}$ mice are seriously injured when infected by bacteria. IL-18 was first discovered in Kupffer cells as a pro-inflammatory factor[19,20]. In Fpr2$^{-/-}$ mice, we observed a decrease in the levels of anti-inflammatory factor IL-10 and pro-inflammatory factor IL-18, and also observed varying degrees of decreases in the levels of other interleukin members, tumor necrosis factors, and chemokines. Considering the cell cycle disruption caused by Fpr2 deficiency, we postulate that the impact of Fpr2 deficiency on cell cycle may interfere with cytokine synthesis, although further validation is needed to test this hypothesis. In short, Fpr2 plays an important role in maintaining liver



DOI: 10.3748/wjg.v29.i24.3793 **Copyright** ©The Author(s) 2023.

Figure 7 Evaluation of liver inflammation status. A: Serum C-reactive protein level in wild-type (WT) and formyl peptide receptor 2 (Fpr2)$^{-/-}$ mice (n = 4); B: Flow cytometry analysis of the number of neutrophils (% of Ly6G^{+} cells) in the liver of WT and Fpr2$^{-/-}$ mice (n = 3); C: Representative images of hematoxylin-eosin staining of liver tissue sections of Fpr2$^{-/-}$ and WT mice. The image magnification is 200 × and 400 ×. NS: No significant difference. Fpr2: Formyl peptide receptor 2; WT: Wild-type; CRP: C-reactive protein.

homeostasis, which may help the body resist bacterial infections.

Some limitations of this study should be noted. First, we used an immortal liver cell line for our study. Recent studies have reported that mature liver cells located in the middle region of liver lobules are the main contributors to the production of new cells in the entire liver[21,22]. Therefore, it is necessary to further evaluate the regulatory effect of Fpr2 on cell cycle using primary liver cells. Second, further research is required to establish whether Fpr2 regulates cell cycle directly or indirectly.

CONCLUSION

Fpr2 plays an important role in maintaining liver homeostasis by participating in cell cycle regulation. Fpr2 may play a positive role in liver tissue repair and neutrophil chemotaxis by regulating the expression of IL-10 and CXCL-1. Our results provide a basis and novel perspective for further understanding the functional diversity of Fpr2.

ARTICLE HIGHLIGHTS

Research background

Formyl peptide receptor 2 (Fpr2) plays an important role in host's defense and inflammatory response, as it can help the body control bacterial infections. Studies have found that in Fpr2$^{-/-}$ mice, the liver is the most severely damaged target organ in bloodstream infections. However, the reason for this is unclear.

Research motivation

To verify the role of Fpr2 in liver homeostasis, to provide new clues for the decreased ability of the liver to clear bacteria after Fpr2 deficiency, and to provide new ideas for future drug research and development.

Research objectives

To investigate the role of Fpr2 in liver homeostasis.

Research methods

The differentially expressed genes (DEGs) in Fpr2$^{-/-}$ and wild-type (WT) mice were determined by transcriptome sequencing, and the biological functions of DEGs were analyzed by Gene Ontology (GO)

and Kyoto Encyclopedia of Genes and Genomes (KEGG) enrichment analysis. Quantitative real-time polymerase chain reaction (qRT PCR) and western blot (WB) were used to further validate the expression levels of differential genes. The Cell Counting Kit-8 assay was used to study cell proliferation. A cell cycle detection kit was used to measure the distribution of cell cycles. Luminex assay was used to analyze cytokine levels in the liver. A fully automated biochemical analyzer was used to detect the levels of serum biochemical indicators and C-reactive protein in WT and Fpr2$^{-/-}$ mice. The number of neutrophils in the liver was detected by flow cytometry. The histopathology of the liver was analyzed by hematoxylin-eosin staining.

Research results

Transcriptome sequencing showed that, compared with WT group, 445 genes in the liver of Fpr2$^{-/-}$ mice had significant changes in the expression level, including 325 upregulated genes and 120 downregulated genes. The functional enrichment analysis of GO and KEGG indicated that these DEGs were mainly related to cell cycle. qRT-PCR validated that after Fpr2 deletion, the expression levels of *CycA*, *CycB1*, *Cdc20*, and *Cdc25c* genes were upregulated. Both qRT-PCR and WB confirmed a decrease in the expression of CDK1. WRW4 (an antagonist of Fpr2) could inhibit the proliferation of HepG2 cells in a concentration dependent manner. The levels of serum alanine aminotransferase levels increased in Fpr2$^{-/-}$ mice with statistical significance. Luminex assay measurements showed that the expression levels of interleukin (IL)-10, IL-18, and CXCL-1 were significantly reduced in the liver of Fpr2$^{-/-}$ mice.

Research conclusions

Fpr2 may exert a protective effect on the liver by participating in the regulation of cell cycle and proliferation, as well as affecting the expression of IL-10 and CXCL-1.

Research perspectives

Fpr2 plays an important role in maintaining liver homeostasis, and its agonist may be a potential drug against bacterial infection.

FOOTNOTES

Author contributions: Li RK designed the research; Liu H wrote the manuscript; Jiang H, Sun ZY, and Li XD conducted experiments; Liu P, Huang WH, and Lv QY analyzed the data and drew pictures; Jiang YQ and Zhang XL revised the manuscript content; all authors approved the final version of the article.

Supported by the State Key Laboratory of Pathogen and Biosecurity, No. SKLPBS2119 and SKLPBS2212; and the Medical Science Research Project of Dalian, No. 2112015.

Institutional animal care and use committee statement: The animal study was reviewed and approved by the animal center of the Academy of Military Medical Sciences. The protocol for animal handling and experiment was approved by the Institutional Review Board of Academy of Military Medical Science (No: IACUC-DWZX-2022-052).

Conflict-of-interest statement: All the authors report no relevant conflicts of interest for this article.

Data sharing statement: The datasets presented in this study can be found in online repositories. The names of the repository/repositories and accession number(s) can be found below: https://www.ncbi.nlm.nih.gov/, PRJNA923726.

ARRIVE guidelines statement: The authors have read the ARRIVE guidelines, and the manuscript was prepared and revised according to the ARRIVE guidelines.

Open-Access: This article is an open-access article that was selected by an in-house editor and fully peer-reviewed by external reviewers. It is distributed in accordance with the Creative Commons Attribution NonCommercial (CC BY-NC 4.0) license, which permits others to distribute, remix, adapt, build upon this work non-commercially, and license their derivative works on different terms, provided the original work is properly cited and the use is non-commercial. See: https://creativecommons.org/Licenses/by-nc/4.0/

Country/Territory of origin: China

ORCID number: Hui Liu 0000-0003-4721-560X; Ze-Yu Sun 0009-0007-2720-5750; Hua Jiang 0000-0002-2769-1783; Xu-Dong Li 0009-0007-4750-0212; Yong-Qiang Jiang 0000-0001-7587-830X; Peng Liu 0000-0001-9948-0259; Wen-Hua Huang 0000-0003-4687-2755; Qing-Yu Lv 0009-0000-3620-8522; Xiang-Lilan Zhang 0000-0002-4946-4880; Rong-Kuan Li 0009-0006-9302-7000.

S-Editor: Wang JJ
L-Editor: A

P-Editor: Cai YX

REFERENCES

1 **Yan J**, Li S. The role of the liver in sepsis. *Int Rev Immunol* 2014; **33**: 498-510 [PMID: 24611785 DOI: 10.3109/08830185.2014.889129]

2 **Llorente C**, Schnabl B. Fast-Track Clearance of Bacteria from the Liver. *Cell Host Microbe* 2016; **20**: 1-2 [PMID: 27414492 DOI: 10.1016/j.chom.2016.06.012]

3 **Seki E**, Schnabl B. Role of innate immunity and the microbiota in liver fibrosis: crosstalk between the liver and gut. *J Physiol* 2012; **590**: 447-458 [PMID: 22124143 DOI: 10.1113/jphysiol.2011.219691]

4 **Gonnert FA**, Kunisch E, Gajda M, Lambeck S, Weber M, Claus RA, Bauer M, Kinne RW. Hepatic Fibrosis in a Long-term Murine Model of Sepsis. *Shock* 2012; **37**: 399-407 [PMID: 22266973 DOI: 10.1097/SHK.0b013e31824a670b]

5 **Broadley SP**, Plaumann A, Coletti R, Lehmann C, Wanisch A, Seidlmeier A, Esser K, Luo S, Rämer PC, Massberg S, Busch DH, van Lookeren Campagne M, Verschoor A. Dual-Track Clearance of Circulating Bacteria Balances Rapid Restoration of Blood Sterility with Induction of Adaptive Immunity. *Cell Host Microbe* 2016; **20**: 36-48 [PMID: 27345696 DOI: 10.1016/j.chom.2016.05.023]

6 **Wood NJ**. Liver: the liver as a firewall--clearance of commensal bacteria that have escaped from the gut. *Nat Rev Gastroenterol Hepatol* 2014; **11**: 391 [PMID: 24935420 DOI: 10.1038/nrgastro.2014.90]

7 **Zhang M**, Gao JL, Chen K, Yoshimura T, Liang W, Gong W, Li X, Huang J, McDermott DH, Murphy PM, Wang X, Wang JM. A Critical Role of Formyl Peptide Receptors in Host Defense against Escherichia coli. *J Immunol* 2020; **204**: 2464-2473 [PMID: 32221037 DOI: 10.4049/jimmunol.1900430]

8 **Liu M**, Chen K, Yoshimura T, Liu Y, Gong W, Wang A, Gao JL, Murphy PM, Wang JM. Formylpeptide receptors are critical for rapid neutrophil mobilization in host defense against Listeria monocytogenes. *Sci Rep* 2012; **2**: 786 [PMID: 23139859 DOI: 10.1038/srep00786]

9 **Chen K**, Bao Z, Gong W, Tang P, Yoshimura T, Wang JM. Regulation of inflammation by members of the formyl-peptide receptor family. *J Autoimmun* 2017; **85**: 64-77 [PMID: 28689639 DOI: 10.1016/j.jaut.2017.06.012]

10 **Gobbetti T**, Coldewey SM, Chen J, McArthur S, le Faouder P, Cenac N, Flower RJ, Thiemermann C, Perretti M. Nonredundant protective properties of FPR2/ALX in polymicrobial murine sepsis. *Proc Natl Acad Sci U S A* 2014; **111**: 18685-18690 [PMID: 25512512 DOI: 10.1073/pnas.1410938111]

11 **Diao N**, Zhang Y, Chen K, Yuan R, Lee C, Geng S, Kowalski E, Guo W, Xiong H, Li M, Li L. Deficiency in Toll-interacting protein (Tollip) skews inflamed yet incompetent innate leukocytes *in vivo* during DSS-induced septic colitis. *Sci Rep* 2016; **6**: 34672 [PMID: 27703259 DOI: 10.1038/srep34672]

12 **Sun Z**, Huang W, Zheng Y, Liu P, Yang W, Guo Z, Kong D, Lv Q, Zhou X, Du Z, Jiang H, Jiang Y. Fpr2/CXCL1/2 Controls Rapid Neutrophil Infiltration to Inhibit Streptococcus agalactiae Infection. *Front Immunol* 2021; **12**: 786602 [PMID: 34899755 DOI: 10.3389/fimmu.2021.786602]

13 **Krek W**, Nigg EA. Differential phosphorylation of vertebrate p34cdc2 kinase at the G1/S and G2/M transitions of the cell cycle: identification of major phosphorylation sites. *EMBO J* 1991; **10**: 305-316 [PMID: 1846803 DOI: 10.1002/j.1460-2075.1991.tb07951.x]

14 **Han J**, Lee C, Jung Y. Deficiency of Formyl Peptide Receptor 2 Retards Hair Regeneration by Modulating the Activation of Hair Follicle Stem Cells and Dermal Papilla Cells in Mice. *Dev Reprod* 2021; **25**: 279-291 [PMID: 35141453 DOI: 10.12717/DR.2021.25.4.279]

15 **Chen K**, Liu M, Liu Y, Yoshimura T, Shen W, Le Y, Durum S, Gong W, Wang C, Gao JL, Murphy PM, Wang JM. Formylpeptide receptor-2 contributes to colonic epithelial homeostasis, inflammation, and tumorigenesis. *J Clin Invest* 2013; **123**: 1694-1704 [PMID: 23454745 DOI: 10.1172/JCI65569]

16 **Nguyen NT**, Umbaugh DS, Sanchez-Guerrero G, Ramachandran A, Jaeschke H. Kupffer cells regulate liver recovery through induction of chemokine receptor CXCR2 on hepatocytes after acetaminophen overdose in mice. *Arch Toxicol* 2022; **96**: 305-320 [PMID: 34724096 DOI: 10.1007/s00204-021-03183-0]

17 **Yin S**, Wang H, Park O, Wei W, Shen J, Gao B. Enhanced liver regeneration in IL-10-deficient mice after partial hepatectomy *via* stimulating inflammatory response and activating hepatocyte STAT3. *Am J Pathol* 2011; **178**: 1614-1621 [PMID: 21435447 DOI: 10.1016/j.ajpath.2011.01.001]

18 **Wan S**, LeClerc JL, Schmartz D, Barvais L, Huynh CH, Devière J, DeSmet JM, Vincent JL. Hepatic release of interleukin-10 during cardiopulmonary bypass in steroid-pretreated patients. *Am Heart J* 1997; **133**: 335-339 [PMID: 9060803 DOI: 10.1016/s0002-8703(97)70229-1]

19 **Abbate A**, Toldo S, Marchetti C, Kron J, Van Tassell BW, Dinarello CA. Interleukin-1 and the Inflammasome as Therapeutic Targets in Cardiovascular Disease. *Circ Res* 2020; **126**: 1260-1280 [PMID: 32324502 DOI: 10.1161/CIRCRESAHA.120.315937]

20 **Dinarello CA**. The IL-1 family of cytokines and receptors in rheumatic diseases. *Nat Rev Rheumatol* 2019; **15**: 612-632 [PMID: 31515542 DOI: 10.1038/s41584-019-0277-8]

21 **He L**, Pu W, Liu X, Zhang Z, Han M, Li Y, Huang X, Han X, Liu K, Shi M, Lai L, Sun R, Wang QD, Ji Y, Tchorz JS, Zhou B. Proliferation tracing reveals regional hepatocyte generation in liver homeostasis and repair. *Science* 2021; **371** [PMID: 33632818 DOI: 10.1126/science.abc4346]

22 **Wei Y**, Wang YG, Jia Y, Li L, Yoon J, Zhang S, Wang Z, Zhang Y, Zhu M, Sharma T, Lin YH, Hsieh MH, Albrecht JH, Le PT, Rosen CJ, Wang T, Zhu H. Liver homeostasis is maintained by midlobular zone 2 hepatocytes. *Science* 2021; **371** [PMID: 33632817 DOI: 10.1126/science.abb1625]

World Journal of Gastroenterology

Submit a Manuscript: https://www.f6publishing.com

World J Gastroenterol 2023 June 28; 29(24): 3807-3824

DOI: 10.3748/wjg.v29.i24.3807

ISSN 1007-9327 (print) ISSN 2219-2840 (online)

ORIGINAL ARTICLE

Retrospective Cohort Study

Prediction of lymph node metastasis in early gastric signet-ring cell carcinoma: A real-world retrospective cohort study

Jia-Jia Yang, Xiao-Yong Wang, Rui Ma, Mei-Hong Chen, Guo-Xin Zhang, Xuan Li

Specialty type: Gastroenterology and hepatology

Provenance and peer review: Unsolicited article; Externally peer reviewed.

Peer-review model: Single blind

Peer-review report's scientific quality classification

Grade A (Excellent): 0
Grade B (Very good): B, B
Grade C (Good): 0
Grade D (Fair): 0
Grade E (Poor): 0

P-Reviewer: Dimofte GM, Romania; Muguruma N, Japan

Received: February 2, 2023
Peer-review started: February 2, 2023
First decision: March 20, 2023
Revised: March 30, 2023
Accepted: May 16, 2023
Article in press: May 16, 2023
Published online: June 28, 2023

Jia-Jia Yang, Mei-Hong Chen, Guo-Xin Zhang, Xuan Li, Department of Gastroenterology, The First Affiliated Hospital of Nanjing Medical University, Nanjing 210029, Jiangsu Province, China

Xiao-Yong Wang, Department of Gastroenterology, The Affiliated Changzhou No. 2 People's Hospital of Nanjing Medical University, Changzhou 213000, Jiangsu Province, China

Rui Ma, Department of Nursing, Jiangsu Health Vocational College, Nanjing 211800, Jiangsu Province, China

Corresponding author: Xuan Li, PhD, Attending Doctor, Department of Gastroenterology, The First Affiliated Hospital of Nanjing Medical University, No. 300 Guangzhou Road, Nanjing 210029, Jiangsu Province, China. lixuan20091225@163.com

Abstract

BACKGROUND

Signet-ring cell carcinoma (SRCC) was previously thought to have a worse prognosis than other differentiated gastric cancer (GC), however, recent studies have shown that the prognosis of SRCC is related to pathological type. We hypothesize that patients with SRCC and with different SRCC pathological components have different probability of lymph node metastasis (LNM).

AIM

To establish models to predict LNM in early GC (EGC), including early gastric SRCC.

METHODS

Clinical data from EGC patients who had undergone gastrectomy at the First Affiliated Hospital of Nanjing Medical University from January 2012 to March 2022 were reviewed. The patients were divided into three groups based on type: Pure SRCC, mixed SRCC, and non-signet ring cell carcinoma (NSRC). The risk factors were identified through statistical tests using SPSS 23.0, R, and EmpowerStats software.

RESULTS

A total of 1922 subjects with EGC were enrolled in this study, and included 249 SRCC patients and 1673 NSRC patients, while 278 of the patients (14.46%) presented with LNM. Multivariable analysis showed that gender, tumor size,

depth of invasion, lymphovascular invasion, ulceration, and histological subtype were independent risk factors for LNM in EGC. Establishment and analysis using prediction models of EGC showed that the artificial neural network model was better than the logistic regression model in terms of sensitivity and accuracy (98.0% *vs* 58.1%, $P = 0.034$; 88.4% *vs* 86.8%, $P < 0.001$, respectively). Among the 249 SRCC patients, LNM was more common in mixed (35.06%) rather than in pure SRCC (8.42%, $P < 0.001$). The area under the ROC curve of the logistic regression model for LNM in SRCC was 0.760 (95%CI: 0.682-0.843), while the area under the operating characteristic curve of the internal validation set was 0.734 (95%CI: 0.643-0.826). The subgroups analysis of pure types showed that LNM was more common in patients with a tumor size > 2 cm (OR = 5.422, $P = 0.038$).

CONCLUSION

A validated prediction model was developed to recognize the risk of LNM in EGC and early gastric SRCC, which can aid in pre-surgical decision making of the best method of treatment for patients.

Key Words: Early gastric cancer; Signet-ring cell carcinoma; Lymph node metastasis; Nomogram; Prediction model

©The Author(s) 2023. Published by Baishideng Publishing Group Inc. All rights reserved.

Core Tip: By establishing and comparing prediction models of lymph node metastasis (LNM) in early gastric cancer, we found that artificial neural network model was better than logistic regression model in sensitivity and accuracy. Among 249 signet-ring cell carcinoma (SRCC) patients, LNM was more common in mixed than in pure SRCC. A validated prediction model was also developed to recognize the risk for LNM in early gastric SRCC, which can be used to help make decisions regarding treatment of patients before performing surgery.

Citation: Yang JJ, Wang XY, Ma R, Chen MH, Zhang GX, Li X. Prediction of lymph node metastasis in early gastric signet-ring cell carcinoma: A real-world retrospective cohort study. *World J Gastroenterol* 2023; 29(24): 3807-3824

URL: https://www.wjgnet.com/1007-9327/full/v29/i24/3807.htm

DOI: https://dx.doi.org/10.3748/wjg.v29.i24.3807

INTRODUCTION

According to the latest global cancer statistics, gastric cancer is considered to be the fifth leading type of cancer and the fourth leading cause of cancer-related deaths worldwide[1]. However, the progression of diagnostic methods has led to early gastric cancer (EGC) being more easily detectable[2]. Our previous study revealed that the rate of EGC diagnosis was 10.0%, while the rate of lymph node metastasis (LNM) in EGC was 12.3%[3]. EGC can be treated using surgical therapy with a 5-year survival rate of 80%-100%[4], and can also be resected *via* endoscopic resection, which is recommended as an effective method of treatment for EGC. Endoscopic submucosal dissection (ESD) can effectively improve the prognosis of patients[5]. Clinical decision of endoscopic *vs* surgical resection for EGC relies on the accurate assessment of the risk of LNM[6]. LNM mainly depends on tumor size, depth of invasion, and histological type[7].

Signet ring cell carcinoma (SRCC) is a common histological type with dismal prognosis[8] that predominantly consists of cells with poor cohesiveness with the predominance of cells in the signet ring. Among gastric cancer cases, the incidence of SRCC has increased and is reported to vary from 8.7% to 23.4%[9-11], while the behavior of SRCC in gastric cancer is controversial. In advanced gastric cancer, SRCC is considered to be a more severe invasive type with a higher level of peritoneal dissemination and a similar or worse prognosis than non-signet ring cell carcinoma (NSRC)[5,12,13]. However, it has been reported that the behavior of early SRCC may be equivalent to, or more favorable than other types of EGC due to its lower probability of LNM[14,15], suggesting that less invasive surgery is suitable. In addition, only few reports have been published on risk factors for LNM in early SRCC and the clinicopathological differences between pure and mixed SRCC.

Therefore, the objectives of this research study were to: (1) To identify the factors that can predict LNM in EGC to establish suitable models; and (2) to investigate the differences between pure and mixed SRCC to identify factors that can predict LNM in EGC with a signet-ring cell histology.

MATERIALS AND METHODS

Patients

We examined the retrospective clinical information of patients who had undergone surgery at the First Affiliated Hospital of Nanjing Medical University, Nanjing, China, from January 2012 to March 2022. A total of 1922 patients were enrolled. The eligibility criteria used is illustrated in the flow diagram shown in Figure 1. Standard gastrectomy was the principal surgical procedure performed with a curative intent. Only patients who did not receive preoperative therapy were included in the study. The exclusion criteria were as follows: (1) pT2-4 gastric cancer identified using histopathological examination after radical gastrectomy; (2) high-grade dysplasia of the gastric mucosa; (3) a lack of lymphadenectomy; (4) cancer treated using neoadjuvant chemotherapy, (5) multiple gastric cancers; and (6) stump gastric cancer.

Gross and histopathological evaluation

All resected tumors samples made into 2-mm-thick slices, stained with hematoxylin and eosin (H&E) and immunohistochemical staining, and assessed by qualified pathologists at the institution using World Health Organization (WHO) diagnostic criteria. Based on this, the patients were divided into 3 groups: (1) Pure SRCC (p-SRCC), which is defined as having a predominant component (> 50%) isolated carcinoma cells containing intracytoplasmic mucin16; (2) mixed SRCC (m-SRCC), which is defined as adenocarcinoma with a minor component (10-50%) of isolated carcinoma cells containing intracytoplasmic mucin; and (3) NSRC. Identification of risk factors associated with LNM in patients with EGC were conducted by comparing the clinicopathological characteristics of the patients and the gross findings of cancer lesions, including the age and gender, tumor size, location and macroscopic type, lymphovascular invasion (LVI), LNM, depth of invasion, perineural invasion, histological type, and ulceration during surgery. The patients were also divided into 5 macroscopic type groups: Protruded (I), elevate (IIa), flat (IIb), depressed (IIc), and excavated (III). As for the location of lesion, we divided the stomach into five sections: cardia, fundus, body, antrum, and angle.

LNM was determined based on the indications for ESD recommended by the Japanese Gastric Cancer Association. Based on the guidelines for ESD and endoscopic mucosal resection for EGC (2nd edition) [16], the absolute indications for endoscopic treatment are as follows: (1) Differentiated intramucosal carcinoma with a maximum diameter of ≤ 2 cm and without ulcerative lesions; (2) differentiated intramucosal carcinoma with a maximum diameter of > 2 cm and without ulcerative lesions; (3) cT1a with a diameter of ≤ 3 cm and ulceration [UL (+)]; and (4) undifferentiated intramucosal carcinoma with a maximum diameter of ≤ 2 cm and without ulcerative lesions. The terminology used in this study is based on the Japanese classification of gastric carcinoma.

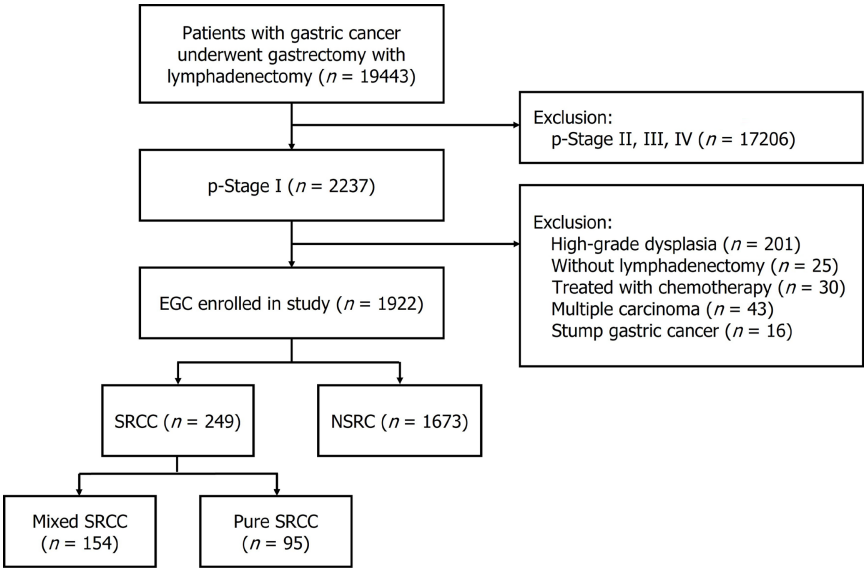
Development of a predictive model for LNM

Variables that are significantly associated with LNM ($P < 0.05$) were identified as candidate variables for the artificial neural network (ANN) model and multivariate logistic regression (LR). A random sample of 75% of all EGC patients were assigned to the training set, while the remaining 25% were used as internal validation of the LR model. The cut-off value was determined using ROC curves, which were then used to evaluate the discriminatory ability of the model. Then, a backward step-down selection process, with a maximum threshold of $P < 0.05$, was used for the final LR model selection of the nomogram. Bootstrapping using 2000 replications was conducted for internal validation.

In the ANN model, a total of 13 neural nodes were used as input layers. There were five neural nodes in the hidden layer, while the hyperbolic tangent transfer function was adopted. Two of the neural nodes in the output layer were LNM or not. The softmax transfer function was used as the transfer function. All samples were randomly assigned to the training group and the verification group at a ratio of 7:3. The training group was used to train the neural network. The verification group was used to evaluate the final neural network, and to construct the topological hierarchical structure of the neural network model. The final neural network fitting results were represented using the normalized importance percentage graph and a bar diagram was drawn. Finally, the area under the operating characteristic curve (AUC) of the recipients of the two models were calculated to compare and evaluate diagnostic accuracy using the chi-square test.

Statistical analysis

Continuous variables were converted to binary variables, and the cut-off point of age was determined by maximizing the sum of sensitivity and specificity after spline smoothing, which was found to be 65 years. Categorical variables are displayed as a percentage. Univariable analysis was performed to identify risk factors associated with LNM using various statistical tests, including the student *t*-test, Chi-square test, or the Fisher exact test. Multivariable analysis only included variables with a $P < 0.05$ in the univariate analysis. The results are shown as an odds ratio (OR), 95% confidence interval (CI), and a *P* value. The multivariate LR model was used to identify independent factors associated with LNM. Calibration of the model was assessed using the Hosmer-Lemeshow nomogram and ROC curve goodness-of-fit test. R (http://www.R-project.org) and EmpowerStats software (www.em-



DOI: 10.3748/wjg.v29.i24.3807 **Copyright** ©The Author(s) 2023.

Figure 1 Flow diagram showing the study design and population. EGC: Early gastric cancer; SRCC: Signet ring cell carcinoma; NSRC: Non-signet ring cell carcinoma.

powerstats.com, X&Y solutions, Inc. Boston, MA, United States) was used to determine the nomogram and ROC curve. The ANN model and further statistical analyses were performed using IBM SPSS Statistics for Windows v.23.0 software. A P value of < 0.05 was used to indicate statistical significance.

RESULTS

Clinicopathological features of patients with EGC

Among the 1922 patients enrolled, 249 patients were with SRCC and 1673 patients were with NSRC, and their outcomes are reported in Figure 1. The clinicopathological characteristics of SRCC and NSRC are described in Table 1. For patients with SRCC, the mean age was 53.14 ± 10.03, the male-to-female ratio was 1.15:1 (133/116), and the mean lesion size was 2.14 ± 1.43 cm. For patients with NSRC, the mean age was 57.01 ± 11.78, the male-to-female ratio was 2.85:1 (1238/435), and the mean lesion size was 1.89 ± 1.22 cm. When the patients were divided into five groups based on location, a majority of the EGCs were found to be in the gastric antrum and angle (n = 1189, 61.86%). There was a significant difference in SRCC and NSRC (P < 0.001) based on location. Most tumors were depressed (IIc), followed by flat (IIb) and elevated (IIa), protruded and excavated, which were in the minority, but no statistical significance was found based on macroscopic type between SRCC and NSRC (P = 0.105). Mucosa invasion occurred in 59.84% of (n = 149) SRCC, while submucosa invasion was observed more often in NSRC (n = 865, 51.70%). LVI was identified in 136 patients, among which 18 were diagnosed with SRCC and 118 were NSRC. LNM was identified in 278 patients, in which 62 were SRCC patients and 216 were NSRC patients. A total of 22 EGCs occurred with perineural invasion, of which 7 were SRCC and 15 were NSRC. Ulceration was identified in 701 patients, in which 74 (29.72%) were diagnosed with SRCC and 627 (37.48%) with NSRC. Overall, these results showed significant differences in age, gender, tumor size, LNM, depth of invasion, perineural invasion, tumor location, and ulceration between SRCC and NSRC.

Risk factors of LNM in EGC as shown through the univariate and multivariate analyses

In the univariate analysis, LNM was significantly associated with age (P = 0.015), gender (P < 0.001), tumor size (P < 0.001), macroscopic type (P = 0.008), depth of invasion (P < 0.001), LVI (P < 0.001), perineural invasion (P < 0.001), tumor location (P = 0.001), ulceration (P < 0.001) and histological subtype (P < 0.001). The multivariable analysis showed that being female (OR = 1.912, P < 0.001), tumor size (> 2 cm) (OR = 1.875, P = 0.001), submucosal invasion (OR = 3.340, P < 0.001), LVI (OR = 6.682, P < 0.001), the presence of ulcers (OR = 1.695, P = 0.001), and the pathological pattern of mixed SRCC (OR = 4.595, P < 0.001) were independent predictors of LNM in EGC (Table 2).

Comparison of clinical models of LNM in EGC

The LR model nomogram revealed that LVI had the greatest impact on scoring, followed by histological subtype and depth of invasion. The effects of gender, tumor size, and ulceration on model performance

Table 1 Clinical characteristics in patients with early gastric cancer

	SRCC	NSRC	*P* value
	n = 249, *n* (%)	*n* = 1673, *n* (%)	
Age (yr)	53.14 ± 10.03	57.01 ± 11.78	< 0.001
≤ 65	161 (64.66)	634 (37.90)	
> 65	88 (35.34)	1039 (62.10)	
Gender			< 0.001
Male	133 (53.41)	1238 (74.00)	
Female	116 (46.59)	435 (26.00)	
Location			< 0.001
Cardia	11 (4.42)	235 (14.05)	
Fundus	5 (2.01)	143 (8.55)	
Body	43 (17.27)	296 (17.69)	
Antrum	129 (51.81)	641 (38.31)	
Angle	61 (24.50)	358 (21.40)	
Macroscopic type			0.105
Protruded (0-I)	3 (1.20)	27 (1.61)	
Elevated (0-IIa)	11 (4.42)	128 (7.65)	
Flat (0-IIb)	52 (20.88)	353 (21.10)	
Depressed (0-IIc)	178 (71.49)	1076 (64.32)	
Excavated (0-III)	5 (2.01)	89 (5.32)	
Tumor size (cm)	2.14 ± 1.43	1.89 ± 1.22	0.001
≤ 2	139 (55.82)	1124 (67.18)	
> 2	110 (44.18)	549 (32.82)	
Ulceration			0.027
UL (-)	175 (70.28)	1046 (62.52)	
UL (+)	74 (29.72)	627 (37.48)	
Depth of invasion			0.001
M	149 (59.84)	808 (48.30)	
SM	100 (40.16)	865 (51.70)	
LVI			1
Absence	231 (92.77)	1555 (92.95)	
Presence	18 (7.23)	118 (7.05)	
Perineural invasion			0.041
Absence	242 (97.19)	1658 (99.10)	
Presence	7 (2.81)	15 (0.90)	
LNM			< 0.001
Absence	187 (75.10)	1457 (87.09)	
Presence	62 (24.90)	216 (12.91)	

SRCC: Signet-ring cell carcinoma; NSRC: Non-signet ring cell carcinoma; LVI: Lymphovascular invasion; LNM: Lymph node metastasis; M: Mucosal; SM: Submucosal; UL (-): Ulcer or ulcer scar is absent; UL (+): Ulcer or ulcer scar is present.

Table 2 Logistic regression analysis of the risk factors of lymph node metastasis in early gastric cancer

	LNM		Univariate	Multivariate analysis		
	Present	Absent	*P* value	OR	95%CI	*P* value
Total	278	1644				
Age			0.015			
≤ 65	135	660				
> 65	143	984				
Gender			< 0.001			
Male	160	1211		1		
Female	118	433		1.912	1.392-2.626	< 0.001
Location			0.001			
Cardia	17	229				
Fundus	9	139				
Body	45	294				
Antrum	141	629				
Angle	66	353				
Macroscopic type			0.008			
Protruded (0-I)	9	21				
Elevated (0-IIa)	16	123				
Flat (0-IIb)	37	368				
Depressed (0-IIc)	201	1053				
Excavated (0-III)	15	79				
Tumor size (cm)			< 0.001			
≤ 2	134	1129		1		
> 2	144	515		1.875	1.260-2.417	0.001
Ulceration			< 0.001			
UL (-)	134	1087		1		
UL (+)	144	557		1.695	1.246-2.306	0.001
Depth of invasion			< 0.001			
M	54	903		1		
SM	224	741		3.34	2.156-5.174	< 0.001
LVI			< 0.001			
Absence	199	1587		1		
Presence	79	57		6.682	4.358-10.245	< 0.001
Perineural invasion			< 0.001			
Absence	262	1638				
Presence	16	6				
Histological type						
Pure SRCC	8	87	< 0.001	1		< 0.001
NSRC	216	1457		2.619	1.454-3.598	0.894
Mixed SRCC	54	100		4.595	2.654-6.954	< 0.001

SRCC: Signet-ring cell carcinoma; NSRC: Non-signet ring cell carcinoma; M: Mucosal; SM: Submucosal; LVI: Lymphovascular invasion; LNM: Lymph

node metastasis; UL (-): Ulcer or ulcer scar is absent; UL (+): Ulcer or ulcer scar is present.

were also significant. Each level of the variable was summed using the total score based on the point scale and was positioned on the total score scale to determine the corresponding LNM probability for each patient (Figure 2). This predictive model demonstrated that the AUC was 0.797 with 95%CI: 0.776-0.818. Following 2000 bootstrap repetitions, the AUC of the internal validation in the training set was 0.816 (95%CI: 0.794-0.839).

We also established an ANN model and assessed its ability by comparing it with a traditional LR model to predict the risk of LNM in EGC patients (Figure 3) presents the structure of the established ANN model and was influenced by 6 significant predictors: Gender, tumor size, submucosal invasion, LVI, histological type and ulceration, and histological type revealed the greatest impact on scoring, followed by the depth of invasion and LVI, while ulceration accounted for the least but still exerted a significant effect. The predictive model demonstrated an AUC of 0.878 with a 95%CI of 0.862-0.893.

In addition, differences between ANN and the multivariate LR model were further compared based on sensitivity, specificity, positive predictive value, negative predictive value, accuracy, and AUC according to the actual rate of LNM confirmed pathologically. Table 3 shows the classification distribution of the two models. The sensitivity and accuracy of the ANN model (96.4% *vs* 58.3%, $P = 0.034$, 88.2% *vs* 86.7%, $P < 0.001$) and the AUC (0.878 *vs* 0.797, $P < 0.001$; 0.899 *vs* 0.816, $P < 0.001$; respectively) were better than that of the multivariate LR model in the training and validation sets (Figure 4). The specificity (88.0% *vs* 88.8%, $P < 0.001$) and positive predictive value (19.4% *vs* 27.7%, $P < 0.001$) was inferior to that of the multivariate LR model. There was no difference in the negative predictive value between the two groups (99.9% *vs* 96.7%, $P = 0.202$). The comparisons of the diagnostic assessment are listed in Table 4.

Comparison of the clinicopathological features of pure SRCC and mixed SRCC

As shown in Table 5, differences in the clinicopathological characteristics between pure SRCC (p-SRCC) and mixed SRCC (m-SRCC) patients were significant based on the following factors: (1) Age was younger in the p-SRCC (73.68%) patients than in the m-SRCC (59.09%) group ($P = 0.037$); (2) m-SRCC patients were more likely to show invasion into the SM layer, compared with p-SRCC (49.35% *vs* 25.26%, $P < 0.001$); (3) LVI resulted in a significantly higher proportion of cases in the m-SRCC (11.69% *vs* 0.00%, $P = 0.002$) group; (4) LNM was much more frequent in the m-SRCC group (35.06% *vs* 8.42%, $P < 0.001$) than in the p-SRCC group. We also found that ulcers were more likely to be present in the m-SRCC group than in the p-SRCC group, although the difference was no statistically significant. There were no significant differences in the other characteristics between the p-SRCC and m-SRCC groups.

Risk factors for LNM in early SRCC as shown by the univariate and multivariate analyses

The univariate analyses demonstrated that the depth of invasion (M and SM), histological type and LVI differed significantly between patients with and without LNM in early SRCC patients. More frequent ulceration was observed in LNM positive SRCC patients, although the difference was not statistically significant. Based on the stepwise multivariate analysis, the significant independent risk factors for LNM in early SRCC were SM invasion (OR = 2.615, $P = 0.008$), LVI (OR = 14.903, $P = 0.001$), and a pathological pattern of mixed SRCC (OR = 1.982, $P = 0.043$). The independent risk factors are listed in Table 6. In addition, we also performed a risk analysis for LNM in SRCC limited to the mucosa and in SRCC with different histological types (p-SRCC and m-SRCC). In SRCC limited to the mucosa (Table 7), histological type ($P = 0.010$) and LVI ($P = 0.016$) were significantly different between patients with and without LNM, and the multivariate analysis showed that the pathological pattern of mixed SRCC (OR = 4.557, $P = 0.023$) was an independent predictor of LNM. In m-SRCC (Table 8), the univariate analyses showed that depth of invasion (M and SM) ($P = 0.004$) and LVI ($P < 0.001$) were risk factors for LNM, and that LVI (OR = 16.173, $P = 0.001$) was a significant independent risk factor for LNM. In p-SRCC, the analyses showed that patients with a tumor size that exceeded 2 cm ($P = 0.014$) and submucosal infiltration ($P=0.045$) were at a greater risk of LNM, indicating that tumor size > 2 cm (OR = 5.422, $P = 0.038$) is a significant independent risk factor for LNM (Table 8).

Clinical model of LNM in early SRCC

A preoperative predictive nomogram containing important risk factors related to early gastric SRCC LNM was constructed based on the LR model. All parameters of the clinicopathological risk factors of LNM in early gastric SRCC in the univariate analysis were included in the multivariable analysis. The nomogram revealed that LVI had the greatest impact on scoring, followed by invasion depth, and histological subtype (Figure 5). The equation stepwise selected prediction model from observed data included total risk points of LNM = -3.24513 + 0.93264*DEPTH + 2.86614*LVI + 0.42064* HISTOLOGICAL. This predictive model demonstrated an area under the curve (AUC) of 0.760 with a 95%CI of 0.682-0.843 (Figure 6A), while the AUC of internal validation was 0.734 (95%CI: 0.643-0.826) (Figure 6B). In the calibration plots, the bias-corrected line was calculated using 2000 bootstrapping

Table 3 The Classification of the artificial neural network model and logistic regression model

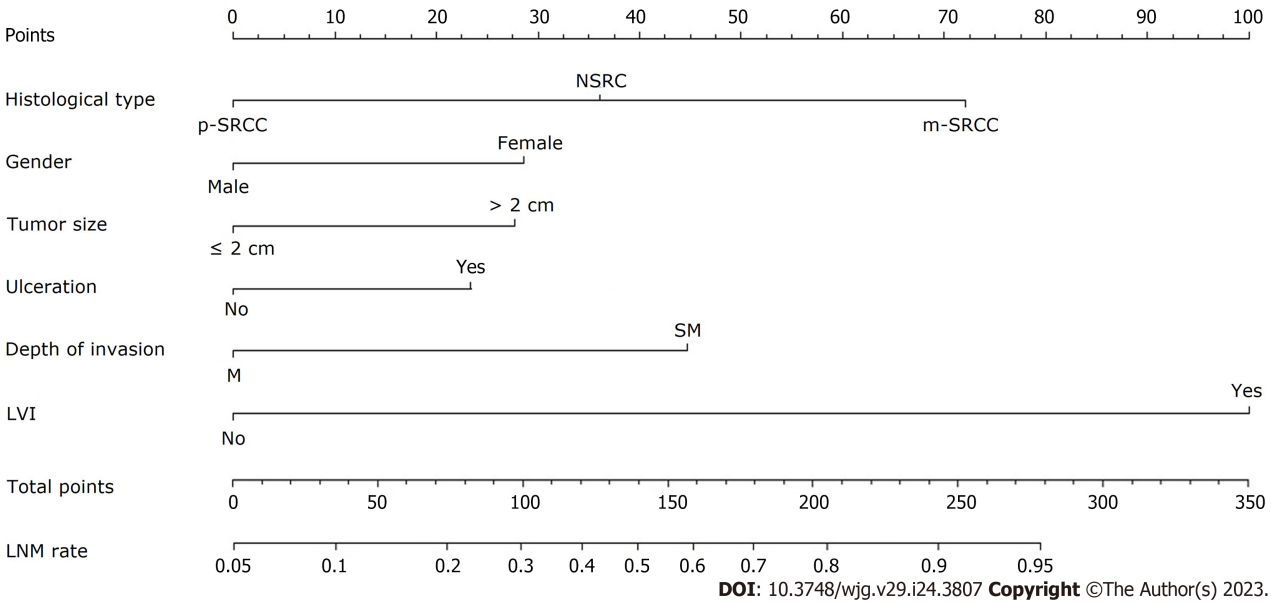
Models	Predicted results	Pathological diagnosis		
		+	-	Percent correct
LR	+	77	55	58.3%
	-	201	1589	88.8%
	Percent correct	27.7%	96.7%	86.7%
ANN	+	54	2	96.4%
	-	224	1642	88.0%
	Percent correct	19.4%	99.9%	88.2%

LR: Logistic regression; ANN: Artificial neural network.

Table 4 Comparison of artificial neural network model and logistic regression model for predicting lymph node metastasis

Diagnostic Index	LR model, (%, 95%CI)	ANN model (%, 95%CI)	*P* value
Sensitivity	58.3% (48.6-67.1%)	96.4% (87.8-99.9%)	0.034
Specificity	88.8% (87.2-90.4%)	88.0% (86.4-89.6%)	< 0.001
PPV	27.7% (22.3-33.9%)	19.4% (14.9-25.2%)	< 0.001
NPV	96.7% (95.6-97.5%)	99.9% (99.6-1.000%)	0.202
Accuracy	86.7% (85.1-88.2%)	88.2% (86.8-89.8%)	< 0.001
AUC	0.797 (0.776-0.818)	0.878 (0.862-0.893)	< 0.001

PPV: Positive predictive value; NPV: Negative predictive value; AUC: Area under the curve.



DOI: 10.3748/wjg.v29.i24.3807 **Copyright** ©The Author(s) 2023.

Figure 2 Nomogram for predicting lymph node metastasis in early gastric cancer patients. The factors of histological type, gender, tumor size, ulceration, depth of invasion and lymphovascular invasion were included in the model. p-SRCC: Pure signet-ring cell carcinoma; NSRC: Non-signet ring cell carcinoma; m-SRCC: Mixed signet-ring cell carcinoma; M: Mucosal; SM: Submucosal; LVI: Lymphovascular invasion; LNM: Lymph node metastasis.

iterations were indistinguishable and nearly approached the ideal line, while the 95%CI of the prediction model was also relatively accurate (Figure 6C). Therefore, the predictive power of the model was found to be good.

Table 5 Clinical characteristics in patients with pure signet-ring cell carcinoma and mixed signet-ring cell carcinoma

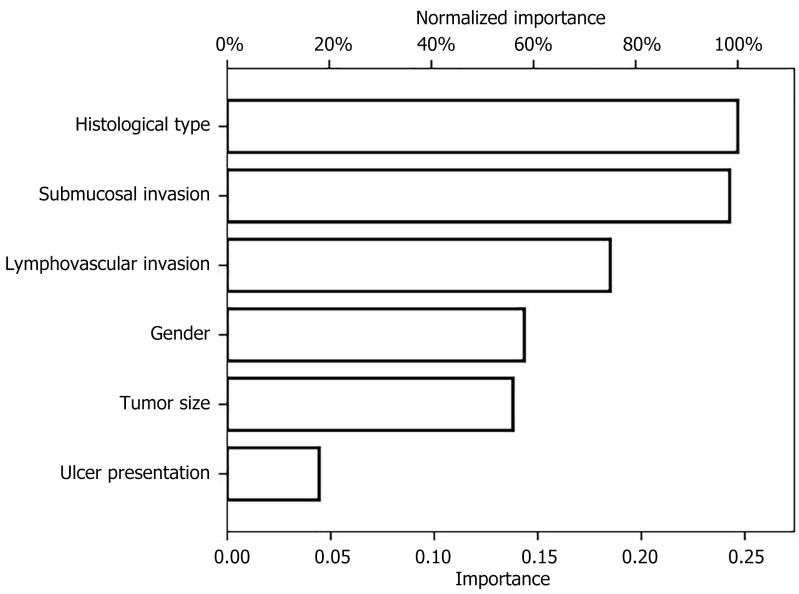
Variable	Pure SRCC	Mixed SRCC	*P* value
	n = 95, *n* (%)	*n* = 154, *n* (%)	
Age (yr)			0.037
≤ 65	70 (73.68)	91 (59.09)	
> 65	25 (26.32)	63 (40.91)	
Gender			0.131
Male	46 (48.42)	87 (56.49)	
Female	49 (51.58)	67 (43.51)	
Location			0.255
Cardia	4 (4.21)	7 (4.55)	
Fundus	2 (2.11)	3 (1.95)	
Body	13 (13.68)	30 (19.48)	
Antrum	51 (53.68)	78 (50.65)	
Angle	25 (26.32)	36 (23.38)	
Macroscopic type			0.152
Protruded (0-I)	1 (1.05)	2 (1.30)	
Elevated (0-IIa)	5 (5.26)	6 (3.90)	
Flat (0-IIb)	23 (24.21)	29 (18.83)	
Depressed (0-IIc)	65 (68.42)	113 (73.38)	
Excavated (0-III)	1 (1.05)	4 (2.60)	
Tumor size (cm)			0.126
≤ 2	60 (63.16)	79 (51.30)	
> 2	35 (36.84)	75 (48.70)	
Ulceration			0.051
UL (-)	75 (78.95)	100 (64.94)	
UL (+)	20 (21.05)	54 (35.06)	
Depth of invasion			< 0.001
M	71 (74.74)	78 (50.65)	
SM	24 (25.26)	76 (49.35)	
LVI			0.002
Absence	95 (100.00)	136 (88.31)	
Presence	0 (0.00)	18 (11.69)	
Perineural invasion			0.420
Absence	94 (98.95)	148 (96.10)	
Presence	1 (1.05)	6 (3.90)	
LNM			< 0.001
Absence	87 (91.58)	100 (64.94)	
Presence	8 (8.42)	54 (35.06)	

SRCC: Signet-ring cell carcinoma; M: Mucosal; SM: Submucosal; LNM: Lymph node metastasis; LVI: Lymphovascular invasion; UL (-): Ulcer or ulcer scar is absent; UL (+): Ulcer or ulcer scar is present.

Table 6 Logistic regression analysis of the risk factors of lymph node metastasis in signet-ring cell carcinoma

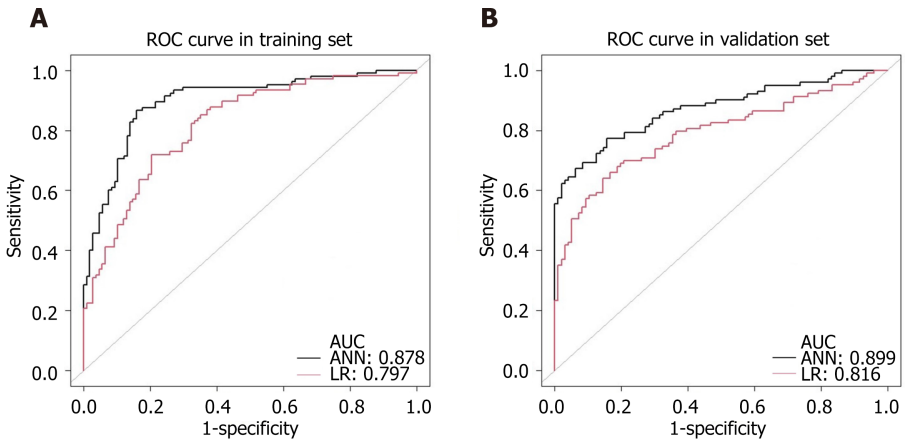
	LNM		Univariate	Multivariate analysis		
	Present	Absent	*P* value	OR	95%CI	*P* value
Total	62	187				
Age			0.617			
≤ 65	41	120				
> 65	21	67				
Gender			0.639			
Male	32	101				
Female	30	86				
Location			0.544			
Cardia	2	9				
Fundus	1	4				
Body	10	33				
Antrum	33	96				
Angle	16	45				
Macroscopic type			0.209			
Protruded (0-I)	0	3				
Elevated (0-IIa)	1	10				
Flat (0-IIb)	13	39				
Depressed (0-IIc)	46	132				
Excavated (0-III)	2	3				
Tumor size (cm)			0.351			
≤ 2	30	109				
> 2	32	78				
Ulceration			0.06			
UL (-)	37	128				
UL (+)	25	46				
Depth of invasion			< 0.001			
M	20	129		1		
SM	42	58		2.615	1.282-5.334	0.008
LVI			< 0.001			
Absence	46	185		1		
Presence	16	2		14.903	3.143-70.680	0.001
Perineural invasion			0.146			
Absence	58	184				
Presence	4	3				
Histological type			< 0.001			
Pure SRCC	8	87		1		
Mixed SRCC	54	100		1.982	0.923-4.237	0.043

SRCC: Signet-ring cell carcinoma; M: Mucosal; SM: Submucosal; LNM: Lymph node metastasis; LVI: Lymphovascular invasion; UL (-): Ulcer or ulcer scar is absent; UL (+): Ulcer or ulcer scar is present.



DOI: 10.3748/wjg.v29.i24.3807 **Copyright** ©The Author(s) 2023.

Figure 3 Artificial neural network model for predicting lymph node metastasis in early gastric cancer patients. This model consists of six parameters: histological type, submucosal invasion, lymphovascular invasion, gender, tumor size and ulcer presentation.



DOI: 10.3748/wjg.v29.i24.3807 **Copyright** ©The Author(s) 2023.

Figure 4 Receiver-operating characteristic curves of the established models for predicting lymph node metastasis in early gastric cancer. The black and the red curve represent the development data of the artificial neural network and logistic regression model, respectively. A: Comparison of receiver-operating characteristic (ROC) plot in the training set, the area under the curve (AUC) was 0.878 *vs* 0.797, $P < 0.001$; B: Comparison of ROC plot in the validation set, the AUC was 0.899 *vs* 0.816, $P < 0.001$. ROC: Receiver-operating characteristic; AUC: Area under the curve; ANN: Artificial neural network; LR: Logistic regression.

Positive LNM results in early SRCC based on the indications for ESD

In the p-SRCC group, the LNM rate of patients with an expanded indication was 2.44% (1/41), and that of patients out of indication was 12.96% (7/54). In the m-SRCC group, the LNM rate in patients with an expanded indication was 16.13% (5/31), and in patients out of indication was 36.59% (45/123). The LNM rate between the expanded indication and out of indication patients in the m-SRCC group was statistically significantly different ($P = 0.048$), while there was no statistical difference in the p-SRCC group ($P = 0.132$). Among all 228 patients, the LNM rate between the expanded indication (6/72, 8.33%) and the out of indication (52/177, 29.38%) patients was statistically significantly different ($P = 0.001$) (Table 9).

DISCUSSION

As the fifth most common type of cancer worldwide, gastric cancer is a significant threat to human

Table 7 Logistic regression analysis of the risk factors of lymph node metastasis in signet-ring cell carcinoma limited in mucosal

	LNM		Univariate	Multivariate analysis		
	Present	Absent	*P* value	OR	95%CI	*P* value
Total	20	129				
Age			0.195			
≤ 65	10	80				
> 65	10	49				
Gender			0.306			
Male	9	77				
Female	11	52				
Tumor size (cm)			0.123			
≤ 2	8	78				
> 2	12	51				
Macroscopic type			0.209			
Protruded (0-I)	0	2				
Elevated (0-IIa)	0	7				
Flat (0-IIb)	4	27				
Depressed (0-IIc)	15	91				
Excavated (0-III)	1	2				
LVI			0.016			
Absence	18	129				
Presence	2	0				
Perineural invasion			-			
Absence	20	129				
Presence	0	0				
Location			0.688			
Cardia	1	6				
Fundus	0	3				
Body	3	23				
Antrum	11	66				
Angle	5	31				
Ulceration			1			
UL (-)	15	101				
UL (+)	3	28				
Histological type			0.01			
Pure SRCC	3	66		1		
Mixed SRCC	17	63		4.557	1.235-16.820	0.023

SRCC: Signet-ring cell carcinoma; LNM: Lymph node metastasis; LVI: Lymphovascular invasion; UL (-): Ulcer or ulcer scar is absent; UL (+): Ulcer or ulcer scar is present.

health. Recently, its incidence (mainly of the intestinal type) has declined in Asia, which may be associated with an increase in focus on and treatment using Helicobacter pylori in Asia. However, the incidence of SRCC is rising and needs more attention. The biological behavior of a case is very important when assessing whether ESD is feasible or not. However, the characteristics of early gastric SRCC, including LNM, clinicopathological features and prognosis, are still disputable[9,10,12].

Table 8 Logistic regression analysis of the risk factors of lymph node metastasis in pure and mixed signet-ring cell carcinoma

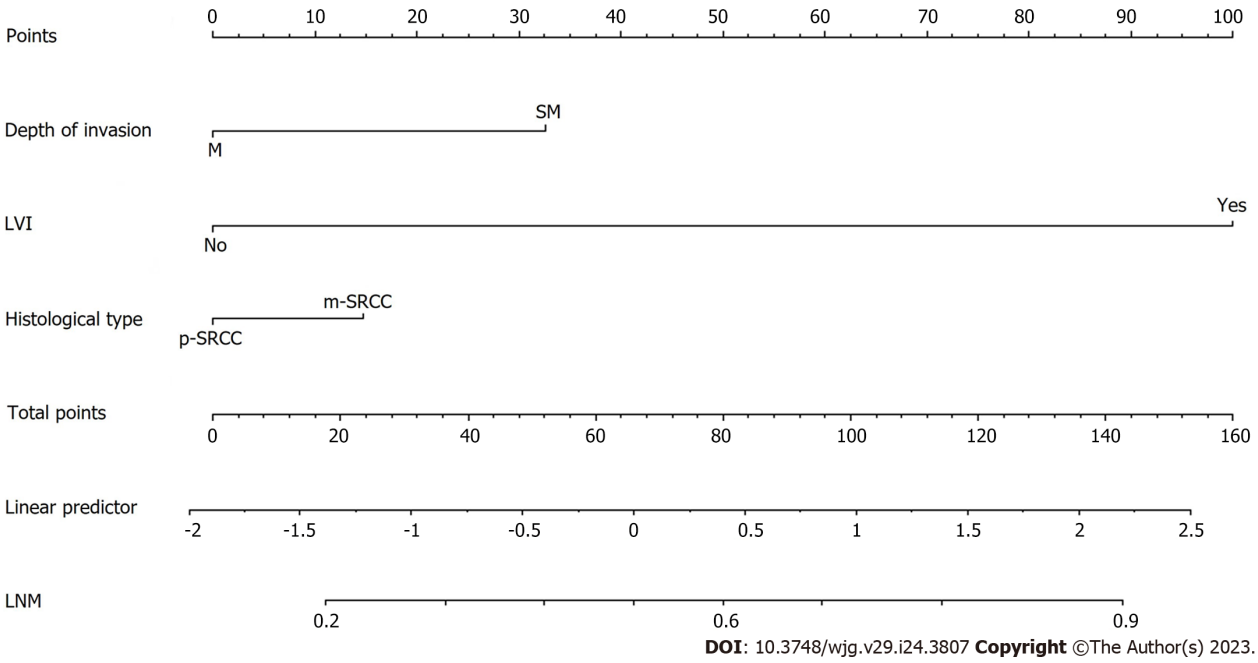
	LNM				Univariate		Multivariate analysis	
	Present		Absent		*P* value		OR, 95%CI, *P* value	
	Pure	Mixed	Pure	Mixed	Pure	Mixed	Pure	Mixed
Total	8	54	87	100				
Age					1	1		
≤ 65	7	33	58	63				
> 65	1	21	29	37				
Gender					1	0.377		
Male	3	29	39	62				
Female	5	25	48	38				
Location					0.706	0.412		
Cardia	0	2	4	5				
Fundus	0	1	2	2				
Body	1	9	12	21				
Antrum	5	28	46	50				
Angle	2	14	23	22				
Macroscopic type					0.788	0.314		
Protruded (0-I)	0	0	1	2				
Elevated (0-IIa)	0	1	5	5				
Flat (0-IIb)	3	10	20	19				
Depressed (0-IIc)	4	42	61	71				
Excavated (0-III)	1	1	0	3				
Tumor size (cm)					0.014	0.751		
≤ 2	4	26	56	53			1	
> 2	4	28	31	47			5.422 (1.095-26.856), 0.038	
Ulceration					1	0.189		
UL (-)	6	31	69	69				
UL (+)	2	23	18	31				
Depth of invasion					0.045	0.004		
M	3	17	70	59				1
SM	5	37	17	41				2.395 (0.891-4.998), 0.054
LVI					-	< 0.001		
Absence	8	38	87	98				1
Presence	0	16	0	2				16.173 (4.085-76.619), 0.001
Perineural invasion					1	0.376		
Absence	8	50	86	98				
Presence	0	4	1	2				
Mixed component						0.458		
Differentiated	-	1	-	7				
Undifferentiated	-	30	-	58				
Mixed	-	23	-	35				

M: Mucosal; SM: Submucosal; LNM: Lymph node metastasis; LVI: Lymphovascular invasion; UL (-): Ulcer or ulcer scar is absent; UL (+): Ulcer or ulcer scar is present.

Table 9 Lymph node metastasis in early gastric signet-ring cell carcinoma according to therapeutic criteria

	Meet expanded ESD indication			Beyond expanded ESD indication			*P* value
	Total	LNM (+)	LNM (-)	Total	LNM (+)	LNM (-)	
p-SRCC	41	1	40	54	7	47	0.132
m-SRCC	31	5	26	123	45	78	0.048
Total	72	6	66	177	52	125	0.001

ESD: Endoscopic submucosal dissection; p-SRCC: Pure signet-ring cell carcinoma; m-SRCC: Mixed signet-ring cell carcinoma; LNM: Lymph node metastasis.

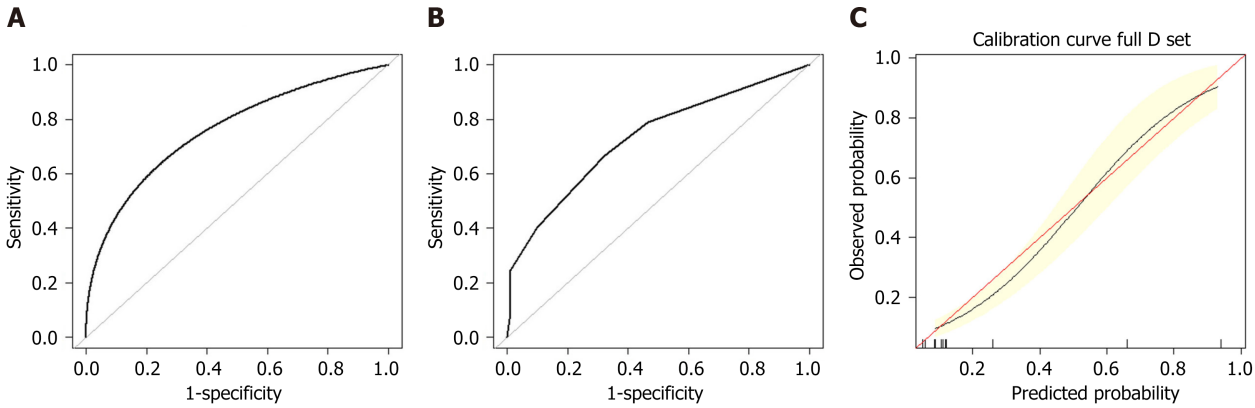


DOI: 10.3748/wjg.v29.i24.3807 **Copyright** ©The Author(s) 2023.

Figure 5 Nomogram for predicting lymph node metastasis in early signet-ring cell carcinoma patients. The factors of histological type, depth of invasion and lymphovascular invasion were included in the model. M: Mucosal; SM: Submucosal; LVI: Lymphovascular invasion; p-SRCC: Pure signet-ring cell carcinoma; m-SRCC: Mixed signet-ring cell carcinoma; LNM: Lymph node metastasis.

Numerous reports have identified SRCC as an independent predictor of poor prognosis due to its specific characteristics, such as the high incidence of LNM, as well as the high rate of peritoneal carcinomatosis[17,18], and low sensitivity to chemotherapy[19], especially as the vast majority of these tumors are diagnosed at an advanced stage. Several studies have reported that tumors with a diameter > 2 cm, submucous infiltration, and lymphatic vascular infiltration are risk factors and independent risk factors for LNM in early gastric SRCC[19]. Huh *et al*[11] and Japanese Gastric Cancer Association[20] showed that the LNM rate was higher in early mixed SRCC than in early pure SRCC, and that mixed SRCC was more aggressive than pure SRCC. To reach an agreement on the treatment options for EGC and early gastric SRCC, these aspects need to be further explored.

A previous study found that being male, age, depressed type, submucosal invasion, LVI, and tumor location were independent risk factors for LNM in EGC[3]. Oh *et al*[21] demonstrated that in patients with EGC without LVI, a tumor size of > 3 cm, submucosal invasion, and undifferentiated histological type were significant risk factors for LNM. In our research study, the incidence of LNM was 14.46%, which is similar to that of previous studies[9,10,13,22-24], and we found that patients of EGC in younger (≤ 60), female, tumor size >2cm, with elevated macroscopic type, submucosal invasion, LVI, perineural invasion, tumor located in the gastric antrum and angle, ulceration, and a pathological pattern of mixed SRCC are more likely to have LNM, and all factors were statistically different. In the multivariate



DOI: 10.3748/wjg.v29.i24.3807 **Copyright** ©The Author(s) 2023.

Figure 6 Assessment of the nomogram for predicting lymph node metastasis in the training set and validation set. A: Receiver-operating characteristic receiver-operating characteristic (ROC) plot in the training set. The area under the curve (AUC) of the ROC was 0.760 (95%CI: 0.682-0.843); B: ROC plot in the validation set. The AUC of the ROC was 0.734 (95%CI: 0.643-0.826); C: Calibration plot in the training set. After 2000 repetitions, the bootstrap-corrected calibration curve (black line) lay close to the ideal reference line (red line), which demonstrated a perfect agreement between the predicted and actual outcomes (mean absolute error 0.012).

analysis, being female, tumor size of > 2 cm, with submucosal invasion, LVI, ulceration, and mixed SRCC were independent predictors of LNM in EGC.

Since SRCC shows different clinicopathological and biological characteristics, compared to NSRC, there are only a few studies that have previously reported on it. Therefore, we analyzed the clinicopathological and biological characteristics of SRCC, including pure-SRCC, mixed-SRCC, and SRCC limited to the mucosa in our research. By comparing the clinicopathological features of patients with NSRC and SRCC, we observed that patients with SRCC were of a younger age, were usually female, and showed fewer lesions in the upper section of the stomach with remarkable statistics differences. With respect to the risk factors for LNM in SRCC, our findings demonstrated that patients with a mixed type, submucosal invasion, and higher LVI are more likely to experience LNM. At the same time, we found that the mixed type was the only independent risk factor for LNM in patients with SRCC limited to the mucosa, which is consistent with the multivariable analysis of LNM in patients with mixed SRCC. In addition, the LNM rate in m-SRCC patients with an expanded ESD indication had a higher LNM rate than p-SRCC patients, and the difference was statistically significant. Therefore, for early gastric m-SRCC patients, caution should be exercised when selecting ESD treatment when the lesion exceeds the mucosal layer. For early gastric m-SRCC patients, a tumor size of > 2 cm was independent risk factor for LNM.

At present the predictive probability of LNM has not been clearly defined, and the clinical diagnosis of gastric LNM in EGC is still challenging. Quantitative predictive models are beneficial for both clinicians and patients in making more objective decisions regarding treatment options. The optimal threshold depends on the extent to which the patient or clinician rejects the risk. It is widely known that LR is a simple machine learning algorithm used for binary classification tasks. Neural networks are similar to a LR and can be referred to as a generalized LR. The neural network has advantages over LR models: the hidden layers facilitate the discovery of more complex and non-linear associations of variables. In our research study, we established two models: the ANN and LR model (nomogram) of LNM in EGC, and the LR model (nomogram) of LNM in early gastric SRCC patients. The ANN model and LR model both showed satisfactory performance through internal cross-validation. The methods of assessing diagnostic test accuracy were further used for model comparison. Then, we found that the ANN model of LNM in EGC performed better than the LR model with a significantly higher level of sensitivity, accuracy, and AUC. There were also some differences in the proportion of each risk factor in these two models of EGC. In the nomogram, LVI was dominant, and it was assigned 100 points; while in the ANN, the histological subtype was the most important risk factor, and it was assigned 100%. In addition, we established a nomogram of LNM in early gastric SRCC. In the nomogram, LVI was assigned 100 points; while, submucosal invasion was assigned 32.5 points, and mixed type SRCC was assigned 15 points. The potential of LNM gradually increased along with point accumulation. Our nomogram could predict the potential of LNM in every individual patient, which may help clinicians make informed and customized decisions that guide clinical treatment. Since only a few independent risk factors of LNM were obtained from the multivariate analysis, the ANN model cannot be further established in SRCC patients.

Our ANN and nomogram may serve as effective tools for predicting the incidence of LNM in Chinese patients with EGC, including early gastric SRCC, which may lead to improved selection of appropriate treatments methods. However, there are still several limitations in our study. Firstly, we utilized single-center, retrospective data to build and validate the predictive model. Secondly, we confirmed the

predictability of the model only using internal validation. However, it is necessary to conduct external validation to demonstrate the accuracy of these models. Thirdly, only a limited number of participants were included in this study, which may lead to a statistical analysis bias. Finally, we did not develop a specific cut-off value for LNM for each of the different methods of treatment available for patients with EGC or early gastric SRCC. Hence, further multicenter, large-sample clinical studies that can help establish additional risk factors for LNM in EGC or early gastric SRCC are still necessary.

CONCLUSION

In conclusion, we constructed an ANN model and a nomogram to predict the probability of LNM in patients with EGC. The ANN model was better than the LR model nomogram in terms of sensitivity and accuracy. We constructed a nomogram for LNM in SRCC as well. These models can be used not only for preoperative evaluation to determine whether standard radical gastrectomy is needed for patients with EGC or early gastric SRCC patients at a high risk of LNM, but also for intraoperative evaluation to determine whether radical lymphadenectomy is necessary.

ARTICLE HIGHLIGHTS

Research background

Signet-ring cell carcinoma (SRCC) has shown discriminative biological characteristics compared with adenocarcinoma, and the behavior of SRCC in gastric cancer is controversial. In this study, we recognize the risk of lymph node metastasis (LNM) in early gastric SRCC, which can aid in pre-surgical decision making of the best method of treatment for patients.

Research motivation

At present the predictive probability of LNM has not been clearly defined, and the clinical diagnosis of gastric LNM in early gastric cancer (EGC) and early gastric SRCC is still challenging. Quantitative predictive models are beneficial for both clinicians and patients in making more objective decisions regarding treatment options.

Research objectives

We aimed to establish models to predict LNM in EGC, including early gastric SRCC, which can aid in pre-surgical decision making of the best method of treatment for patients.

Research methods

We examined the retrospective large-sample clinical information of patients who had undergone surgery, by comparing the clinicopathological features of patients with non-signet ring cell carcinoma and SRCC. Variables that are significantly associated with LNM were identified as candidate variables for the artificial neural network (ANN) model and multivariate logistic regression.

Research results

Our ANN and nomogram may serve as effective tools for predicting the incidence of LNM in Chinese patients with EGC, including early gastric SRCC, which may lead to improved selection of appropriate treatments methods.

Research conclusions

With respect to the risk factors for LNM in SRCC, our findings demonstrated that patients with a mixed type, submucosal invasion, and higher LVI are more likely to experience LNM. At the same time, we found that the mixed type was the only independent risk factor for LNM in patients with SRCC limited to the mucosa, which is consistent with the multivariable analysis of LNM in patients with mixed SRCC.

Research perspectives

Further multicenter, large-sample clinical and randomized controlled studies that can help establish additional risk factors for LNM in EGC or early gastric SRCC are still necessary.

FOOTNOTES

Author contributions: Yang JJ, Wang XY, Ma R and Chen MH contributed equally to this work; Yang JJ and Wang XY designed the research study and performed the research; Ma R and Chen MH contributed new reagents and analytic tools; Yang JJ, Wang XY, Ma R and Chen MH analyzed the data and wrote the manuscript; all authors have read and

approve the final manuscript.

Supported by National Natural Science Foundation of China, No. 82200625 and No. 82100595; Youth Talent Development Program, No. YNRCQN0313; Young Scholar Fostering Fund of the First Affiliated Hospital of Nanjing Medical University, No. PY2021023; Top Talent of Changzhou "The 14th Five-Year Plan" High-Level Health Talents Training Project, No. 2022CZBJ051; and Natural Science Foundation of Jiangsu Province, China, No. BK20210958.

Institutional review board statement: The study was reviewed and approved by the Medical Ethics Committee of the First Affiliated Hospital of Nanjing Medical University and the Affiliated Changzhou No. 2 People's Hospital of Nanjing Medical University (Approval No. 2021KY311-01).

Informed consent statement: All study participants, or their legal guardian, provided informed written consent prior to study enrollment.

Conflict-of-interest statement: The authors declare that they have no conflict of interest.

Data sharing statement: No additional data are available.

STROBE statement: The authors have read the STROBE Statement—checklist of items, and the manuscript was prepared and revised according to the STROBE Statement—checklist of items.

Open-Access: This article is an open-access article that was selected by an in-house editor and fully peer-reviewed by external reviewers. It is distributed in accordance with the Creative Commons Attribution NonCommercial (CC BY-NC 4.0) license, which permits others to distribute, remix, adapt, build upon this work non-commercially, and license their derivative works on different terms, provided the original work is properly cited and the use is non-commercial. See: https://creativecommons.org/Licenses/by-nc/4.0/

Country/Territory of origin: China

ORCID number: Jia-Jia Yang 0000-0002-1293-6506; Xiao-Yong Wang 0000-0002-4013-7402; Guo-Xin Zhang 0000-0002-2803-2653; Xuan Li 0000-0003-2703-1950.

S-Editor: Yan JP
L-Editor: A
P-Editor: Chen YX

REFERENCES

1 **Sung H**, Ferlay J, Siegel RL, Laversanne M, Soerjomataram I, Jemal A, Bray F. Global Cancer Statistics 2020: GLOBOCAN Estimates of Incidence and Mortality Worldwide for 36 Cancers in 185 Countries. *CA Cancer J Clin* 2021; **71**: 209-249 [PMID: 33538338 DOI: 10.3322/caac.21660]
2 **Park CH**, Song KY, Kim SN. Treatment results for gastric cancer surgery: 12 years' experience at a single institute in Korea. *Eur J Surg Oncol* 2008; **34**: 36-41 [PMID: 17442532 DOI: 10.1016/j.ejso.2007.03.004]
3 **Li X**, Liu S, Yan J, Peng L, Chen M, Yang J, Zhang G. The Characteristics, Prognosis, and Risk Factors of Lymph Node Metastasis in Early Gastric Cancer. *Gastroenterol Res Pract* 2018; **2018**: 6945743 [PMID: 29853864 DOI: 10.1155/2018/6945743]
4 **Smith DD**, Schwarz RR, Schwarz RE. Impact of total lymph node count on staging and survival after gastrectomy for gastric cancer: data from a large US-population database. *J Clin Oncol* 2005; **23**: 7114-7124 [PMID: 16192595 DOI: 10.1200/JCO.2005.14.621]
5 **Gotoda T**, Yamamoto H, Soetikno RM. Endoscopic submucosal dissection of early gastric cancer. *J Gastroenterol* 2006; **41**: 929-942 [PMID: 17096062 DOI: 10.1007/s00535-006-1954-3]
6 **Hu Q**, Dekusaah R, Cao S, Pang T, Wang Y, Zhang B, Lv Y, Zhang X, Ling T, Zhuge Y, Wang L, Zou X, Zhang W, Huang Q, Xu G. Risk Factors of Lymph Node Metastasis in Patients with Early Pure and Mixed Signet Ring Cell Gastric Carcinomas. *J Cancer* 2019; **10**: 1124-1131 [PMID: 30854120 DOI: 10.7150/jca.29245]
7 **Hirasawa T**, Gotoda T, Miyata S, Kato Y, Shimoda T, Taniguchi H, Fujisaki J, Sano T, Yamaguchi T. Incidence of lymph node metastasis and the feasibility of endoscopic resection for undifferentiated-type early gastric cancer. *Gastric Cancer* 2009; **12**: 148-152 [PMID: 19890694 DOI: 10.1007/s10120-009-0515-x]
8 **Fléjou JF**. [WHO Classification of digestive tumors: the fourth edition]. *Ann Pathol* 2011; **31**: S27-S31 [PMID: 22054452 DOI: 10.1016/j.annpat.2011.08.001]
9 **Zhang M**, Zhu G, Zhang H, Gao H, Xue Y. Clinicopathologic features of gastric carcinoma with signet ring cell histology. *J Gastrointest Surg* 2010; **14**: 601-606 [PMID: 20033340 DOI: 10.1007/s11605-009-1127-9]
10 **Chiu CT**, Kuo CJ, Yeh TS, Hsu JT, Liu KH, Yeh CN, Hwang TL, Jan YY, Lin CJ. Early signet ring cell gastric cancer. *Dig Dis Sci* 2011; **56**: 1749-1756 [PMID: 21104129 DOI: 10.1007/s10620-010-1487-8]
11 **Huh CW**, Jung DH, Kim JH, Lee YC, Kim H, Yoon SO, Youn YH, Park H, Lee SI, Choi SH, Cheong JH, Noh SH. Signet ring cell mixed histology may show more aggressive behavior than other histologies in early gastric cancer. *J Surg Oncol* 2013; **107**: 124-129 [PMID: 22991272 DOI: 10.1002/jso.23261]

12 **Kunisaki C**, Shimada H, Nomura M, Matsuda G, Otsuka Y, Akiyama H. Therapeutic strategy for signet ring cell carcinoma of the stomach. *Br J Surg* 2004; **91**: 1319-1324 [PMID: 15376179 DOI: 10.1002/bjs.4637]

13 **Endoscopic Classification Review Group**. Update on the paris classification of superficial neoplastic lesions in the digestive tract. *Endoscopy* 2005; **37**: 570-578 [PMID: 15933932 DOI: 10.1055/s-2005-861352]

14 **Yokota T**, Kunii Y, Teshima S, Yamada Y, Saito T, Kikuchi S, Yamauchi H. Signet ring cell carcinoma of the stomach: a clinicopathological comparison with the other histological types. *Tohoku J Exp Med* 1998; **186**: 121-130 [PMID: 10223615 DOI: 10.1620/tjem.186.121]

15 **Gronnier C**, Messager M, Robb WB, Thiebot T, Louis D, Luc G, Piessen G, Mariette C; FREGAT working group-FRENCH. Is the negative prognostic impact of signet ring cell histology maintained in early gastric adenocarcinoma? *Surgery* 2013; **154**: 1093-1099 [PMID: 24075273 DOI: 10.1016/j.surg.2013.05.020]

16 **Ono H**, Yao K, Fujishiro M, Oda I, Uedo N, Nimura S, Yahagi N, Iishi H, Oka M, Ajioka Y, Fujimoto K. Guidelines for endoscopic submucosal dissection and endoscopic mucosal resection for early gastric cancer (second edition). *Dig Endosc* 2021; **33**: 4-20 [PMID: 33107115 DOI: 10.1111/den.13883]

17 **Piessen G**, Messager M, Leteurtre E, Jean-Pierre T, Mariette C. Signet ring cell histology is an independent predictor of poor prognosis in gastric adenocarcinoma regardless of tumoral clinical presentation. *Ann Surg* 2009; **250**: 878-887 [PMID: 19855261 DOI: 10.1097/SLA.0b013e3181b21c7b]

18 **Otsuji E**, Yamaguchi T, Sawai K, Takahashi T. Characterization of signet ring cell carcinoma of the stomach. *J Surg Oncol* 1998; **67**: 216-220 [PMID: 9579367 DOI: 10.1002/(sici)1096-9098(199804)67:4<216::aid-jso2>3.0.co;2-b]

19 **Messager M**, Lefevre JH, Pichot-Delahaye V, Souadka A, Piessen G, Mariette C; FREGAT working group - FRENCH. The impact of perioperative chemotherapy on survival in patients with gastric signet ring cell adenocarcinoma: a multicenter comparative study. *Ann Surg* 2011; **254**: 684-93; discussion 693 [PMID: 22005144 DOI: 10.1097/SLA.0b013e3182352647]

20 **Japanese Gastric Cancer Association**. Japanese classification of gastric carcinoma: 3rd English edition. *Gastric Cancer* 2011; **14**: 101-112 [PMID: 21573743 DOI: 10.1007/s10120-011-0041-5]

21 **Oh YJ**, Kim DH, Han WH, Eom BW, Kim YI, Yoon HM, Lee JY, Kim CG, Kook MC, Choi IJ, Kim YW, Ryu KW. Risk factors for lymph node metastasis in early gastric cancer without lymphatic invasion after endoscopic submucosal dissection. *Eur J Surg Oncol* 2021; **47**: 3059-3063 [PMID: 33934939 DOI: 10.1016/j.ejso.2021.04.029]

22 **Kim DY**, Park YK, Joo JK, Ryu SY, Kim YJ, Kim SK, Lee JH. Clinicopathological characteristics of signet ring cell carcinoma of the stomach. *ANZ J Surg* 2004; **74**: 1060-1064 [PMID: 15574148 DOI: 10.1111/j.1445-1433.2004.03268.x]

23 **Hyung WJ**, Noh SH, Lee JH, Huh JJ, Lah KH, Choi SH, Min JS. Early gastric carcinoma with signet ring cell histology. *Cancer* 2002; **94**: 78-83 [PMID: 11815962 DOI: 10.1002/cncr.10120]

24 **Henson DE**, Dittus C, Younes M, Nguyen H, Albores-Saavedra J. Differential trends in the intestinal and diffuse types of gastric carcinoma in the United States, 1973-2000: increase in the signet ring cell type. *Arch Pathol Lab Med* 2004; **128**: 765-770 [PMID: 15214826 DOI: 10.5858/2004-128-765-DTITIA]

World Journal of Gastroenterology

Submit a Manuscript: https://www.f6publishing.com

World J Gastroenterol 2023 June 28; 29(24): 3825-3842

DOI: 10.3748/wjg.v29.i24.3825

ISSN 1007-9327 (print) ISSN 2219-2840 (online)

ORIGINAL ARTICLE

Retrospective Cohort Study

Regional variation in routes to diagnosis of cholangiocarcinoma in England from 2006 to 2017

Amy Zalin-Miller, Sophie Jose, Craig Knott, Lizz Paley, Daniela Tataru, Helen Morement, Mireille B Toledano, Shahid A Khan

Specialty type: Gastroenterology and hepatology

Provenance and peer review: Unsolicited article; Externally peer reviewed.

Peer-review model: Single blind

Peer-review report's scientific quality classification
Grade A (Excellent): A
Grade B (Very good): 0
Grade C (Good): C
Grade D (Fair): 0
Grade E (Poor): 0

P-Reviewer: Lee H, South Korea; Yildiz K, Turkey

Received: March 20, 2023
Peer-review started: March 20, 2023
First decision: April 27, 2023
Revised: May 5, 2023
Accepted: May 25, 2023
Article in press: May 25, 2023
Published online: June 28, 2023

Amy Zalin-Miller, Sophie Jose, Craig Knott, Department of Analytics, Health Data Insight CIC, Cambridge CB21 5XE, United Kingdom

Amy Zalin-Miller, Sophie Jose, Craig Knott, Lizz Paley, Daniela Tataru, National Disease Registration Service, NHS England, London E14 4PU, United Kingdom

Helen Morement, CEO, AMMF, London CM24 1QW, United Kingdom

Mireille B Toledano, MRC Centre for Environment and Health, School of Public Health, Imperial College London, London SW7 2BX, United Kingdom

Shahid A Khan, Liver Unit, Division of Digestive Diseases, Imperial College London, London W21NY, United Kingdom

Corresponding author: Amy Zalin-Miller, MSc, Senior Researcher, Department of Analytics, Health Data Insight CIC, Capital Park, Fulbourn, Cambridge CB21 5XE, United Kingdom. amy.zalin@nhs.net

Abstract

BACKGROUND

Incidence of cholangiocarcinoma (CCA) is rising, with overall prognosis remaining very poor. Reasons for the high mortality of CCA include its late presentation in most patients, when curative options are no longer feasible, and poor response to systemic therapies for advanced disease. Late presentation presents a large barrier to improving outcomes and is often associated with diagnosis *via* mergency presentation (EP). Earlier diagnoses may be made by Two Week Wait (TWW) referrals through General practitioner (GP). We hypothesise that TWW referrals and EP routes to diagnosis differ across regions in England.

AIM

To investigate routes to diagnosis of CCA over time, regional variation and influencing factors.

METHODS

We linked patient records from the National Cancer Registration Dataset to Hospital Episode Statistics, Cancer Waiting Times and Cancer Screening Programme datasets to define routes to diagnosis and certain patient character-

istics for patients diagnosed 2006-2017 in England. We used linear probability models to investigate geographic variation by assessing the proportions of patients diagnosed *via* TWW referral or EP across Cancer Alliances in England, adjusting for potential confounders. Correlation between the proportion of people diagnosed by TWW referral and EP was investigated with Spearman's correlation coefficient.

RESULTS

Of 23632 patients diagnosed between 2006-2017 in England, the most common route to diagnosis was EP (49.6%). Non-TWW GP referrals accounted for 20.5% of diagnosis routes, 13.8% were diagnosed by TWW referral, and the remainder 16.2% were diagnosed *via* an 'other' or Unknown route. The proportion diagnosed *via* a TWW referral doubled between 2006-2017 rising from 9.9% to 19.8%, conversely EP diagnosis route declined, falling from 51.3% to 46.0%. Statistically significant variation in both the TWW referral and EP proportions was found across Cancer Alliances. Age, presence of comorbidity and underlying liver disease were independently associated with both a lower proportion of patients diagnosed *via* TWW referral, and a higher proportion diagnosed by EP after adjusting for other potential confounders.

CONCLUSION

There is significant geographic and socio-demographic variation in routes to diagnosis of CCA in England. Knowledge sharing of best practice may improve diagnostic pathways and reduce unwarranted variation.

Key Words: Cholangiocarcinoma; Route to diagnosis; Two Week Wait; Emergency presentation; Regional variation

©The Author(s) 2023. Published by Baishideng Publishing Group Inc. All rights reserved.

Core Tip: We investigated changes to routes to diagnosis for cholangiocarcinoma patients across England's 21 regional Cancer Alliances over a 12-year period, and factors associated with differences. We found almost half (49.6%) of 23632 patients in the study were diagnosed *via* emergency presentation, a route associated with late presentation, advanced disease and poorer outcomes. Those diagnosed by Two Week Wait referral through a primary care doctor, where earlier diagnoses are possible, increased from 9.8-19.8% from 2006-2017, still considered low. Significant regional variation was found, alongside the discovery that age, comorbidities and underlying liver disease had independent associations with their routes to diagnosis.

Citation: Zalin-Miller A, Jose S, Knott C, Paley L, Tataru D, Morement H, Toledano MB, Khan SA. Regional variation in routes to diagnosis of cholangiocarcinoma in England from 2006 to 2017. *World J Gastroenterol* 2023; 29(24): 3825-3842

URL: https://www.wjgnet.com/1007-9327/full/v29/i24/3825.htm

DOI: https://dx.doi.org/10.3748/wjg.v29.i24.3825

INTRODUCTION

Cholangiocarcinoma (CCA) comprise a group of malignancies arising from the epithelium of the biliary tree within or outside the hepatic parenchyma. Globally CCA are the commonest biliary malignancy, and those arising within the liver parenchyma are the second most common primary hepatic malignancy[1]. CCA are sub-classified depending on their anatomical location within the biliary tree. Intrahepatic CCA (iCCA) arise within the hepatic parenchyma itself, anatomically above the second-order bile ducts. Extrahepatic CCA (eCCA) arise more distally and are further sub-divided into perihilar CCA and distal CCA, with the latter originating between the cystic duct and ampulla of Vater[1,2].

Studies over the past few decades have consistently reported an increasing incidence in CCA globally. These studies have utilised both international and national datasets, including data collections available through the World Health Organisation, United States cancer registries, and European cancer registries[3-6]. These studies indicate a long-running increase in the global incidence of CCA, together with a general trend of rising iCCA mortality rates but stable or decreasing eCCA mortality. The reasons for these trends remain unclear. The overall prognosis for all CCA is poor, with a 5-year overall survival of less than 10%[1]. Reasons for the high mortality of CCA include its late presentation in most patients, when the only curative option, surgery, is no longer feasible, and poor response to systemic therapies

for advanced disease[2]. Late presentation therefore presents a large barrier to preserving effective/curative treatment options and improving outcomes. Overcoming late presentation is difficult due to: The disease's largely sporadic nature, wherein most patients have no known pre-existing risk factors; a lack of effective diagnostic screening tools and an asymptomatic early disease phase. Late presentation is therefore often associated with diagnosis *via* an emergency route. It is well recognised the cancers with high rates of emergency presentation (EP) are associated with poorer outcomes[7]. This is one of the reasons behind the creation of the United Kingdom's National Health Service Urgent Two Week Waitreferral system (TWW), whereby a primary care doctor (General practitioner, GP) can ask the hospital for an urgent appointment to investigate for the presence of cancer, depending on specified symptom and laboratory test criteria. However the role of the TWW referral system toward achieving earlier diagnosis and therefore better outcomes may be limited for cancers such as CCA that are characterised by vague and non-specific symptoms that fall outside of specified referral criteria, which has led to the recent roll out of rapid diagnostic centres to provide a way for GPs to directly request diagnostic investigations of such symptoms[8,9]. Variation in the rates of TWW referrals and EP has been shown across English regions for all cancers[10]. We hypothesise that TWW referrals and EP for CCA differ across regions in England. To our knowledge there are no published studies analysing the pattern of routes to diagnosis for CCA. The aims of this study were to examine routes to diagnosis for CCA at a national level in England, to ascertain if these have changed over time and if regional variations exist and to determine which factors might influence any variation.

MATERIALS AND METHODS

Data used were obtained from the National Cancer Registration Dataset (NCRD) [AV2018][11]. Linked patient records from Hospital Episode Statistics (HES), Cancer Waiting Times and Cancer Screening Programme datasets were used to define Routes to Diagnosis and certain patient characteristics[12]. A CCA cohort was defined based upon the topographical and histological International Classification of Disease (ICD) codes to define the following tumours: Intrahepatic iCCA ICD10 C22.1; eCCA ICD10 C24.0; other CCA ICD10 C220, C222, C223, C224, C227, C229 with ICD-O2 8160 and ICD10 C248-249 (Table 1). Malignant neoplasm of liver and intrahepatic bile ducts ICD10 C220, C222, C223, C224, C227, C229 with an ICD-O2 8160 morphology were included in the study to capture CCA tumours which may have been miscoded. Patients were selected if residents in England and diagnosed between 2006 and 2017. For patients with multiple CCA diagnoses during this period, the first registered tumour was selected. Further inclusion criteria recorded were male or female gender, and age at diagnosis between 0 and 200 years following the National Cancer Registration and Analysis Service's Standard Operating Procedure[13].

Geographic variation in routes to diagnosis was analysed at the Cancer Alliance level according to 21 regions defined in 2020 for England[14]. The Cancer Alliance for each patient was assigned according to the main residence of the patient on the date of diagnosis. Patient characteristics identified a priori as possible confounding variables were: Gender (male/female); age at diagnosis (0-44/45-54/55-64/65-74/75-84/85+ years); income deprivation (quintiles)[15]; year of diagnosis; tumour sub-type (iCCA/eCCA/other); tumour morphology (adenocarcinoma/other); Charlson Comorbidity Index (CCI) (score 0/1/2/ > 2)[16]; underlying liver disease (yes/no)[17]. Underlying liver disease was identified by searching diagnostic codes in HES Admitted Patient Care (APC) episodes from 5 years before to 1 year after diagnosis indictive of chronic hepatitis C or B virus, primary biliary cholangitis, autoimmune hepatitis, haemochromatosis, alcoholic liver disease, or non-alcoholic liver disease (NAFLD). NAFLD was defined as Fatty (change of) liver, not elsewhere classified, or by the presence of cirrhosis (defined using a published algorithm[17]) combined with obesity or diabetes without the presence of any other underlying liver disease.

Routes to diagnosis were defined based on an established algorithm[12] and categorised as follows: Urgent GP TWW referral for suspected cancer; Other GP referral; EP; Other (includes Outpatient, Inpatient and Death Certificate Only routes); Unknown. The proportion of people diagnosed *via* TWW referral and EP were the outcomes of interest for the main analyses.

Statistical Analyses

The proportion of people diagnosed *via* each of five routes to diagnosis was described for all *a priori* patient and tumour characteristics. χ^2 tests were used to assess the statistical significance of any unadjusted variation in proportions diagnosed *via* TWW referral (vs any other route) or EP (vs any other route).

Linear probability models were then performed to assess the proportions of patients diagnosed *via* TWW referral or EP after adjustment for potential confounders. For these, two binary outcome variables were created (TWW referral *vs* other diagnosis routes; EP *vs* other diagnosis routes) and three models run on each with increasing levels of covariate adjustment:

Model 1 (unadjusted): A model that included only Cancer Alliance as the independent variable.

Table 1 Definition of cholangiocarcinoma: World Health Organization International Classification of Diseases codes included

Sub-type	ICD10 topography code	ICDO2 histology code
Intrahepatic (iCCA)	C221 (Intrahepatic bile duct carcinoma)	All
Extrahepatic (eCCA)	C240 (Extrahepatic bile duct carcinoma)	All
CCA other	C248 (Overlapping lesion of biliary tract), C249 (Biliary tract, unspecified)	All
	C220, C222, C223, C224, C227, C229	8160

iCCA: Intrahepatic cholangiocarcinoma; eCCA: Extrahepatic cholangiocarcinoma; CCA: Cholangiocarcinoma; ICD: International Classification of Disease; ICDO2: International Classification of Disease second edition.

Model 2 (demographic-adjusted): A model that included Cancer Alliance as well as patient age, gender and income deprivation quintile.

Model 3 (maximally-adjusted): A model that additionally included all patient and tumour characteristics.

Weighted effect coding was applied to the estimates generated by each linear probability model so that they became interpretable as percentage-point deviations from the sample mean[18]. Results from the linear probability models are presented as funnel plots with significance threshold lines denoting two and three SD from the sample mean, being approximately equivalent to 95.0% and 99.7% confidence intervals, respectively. The correlation between the proportion of people diagnosed by TWW referral and EP was investigated with Spearman's correlation coefficient on the results from Model 3.

A sensitivity analysis was also run on both binary outcome variables, equal to Model 3 with additional adjustment for the stage at diagnosis. This analysis was applied to a subgroup of the cohort who were diagnosed between 2014-2017 (covering the year from which staging data completeness improved in the NCRD) and had a known stage at diagnosis. The stage at diagnosis was not included in the main analysis due to the high proportion of missing data (72.1%) for this variable. Model 3 was repeated in this subgroup to determine how reducing the cohort impacted on model estimates before the stage was additionally adjusted for in this group.

RESULTS

There were 23632 people diagnosed with CCA in England between 2006 and 2017 (Figure 1). Of these, 22.2% were aged under 65 years at diagnosis (Figure 2) and 51.5% were women. The majority were diagnosed with an iCCA (75.0%). Over a quarter (26.0%) had at least one comorbidity on the CCI and 7% were classified as having underlying liver disease. The largest proportion of diagnoses was situated in the West Midlands Cancer Alliance (10.9%), with the smallest in North Central London Cancer Alliance (1.7%) (Table 2).

The most common route to diagnosis was EP (49.6%). Non-TWW GP referrals accounted for 20.5% of diagnosis routes, 13.8% were diagnosed by TWW referral, and the remainder 16.2% were diagnosed *via* an 'other' or Unknown route. The proportion of people diagnosed *via* a TWW referral doubled between 2006 and 2017, rising from 9.9% to 19.8% (Figure 3). Conversely, the proportion of people diagnosed *via* EP declined, falling from 51.3% to 46.0%, as did the proportion diagnosed *via* 'other' routes, from 17.0% to 10.9%.

Geographic Variation in TWW referral

Variation in unadjusted proportions of patients diagnosed *via* a TWW referral was observed across the Cancer Alliances ranging from 8.4% to 18.9% (Supplementary Table 1; $P < 0.001$, Figure 4). In a linear probability model that included only Cancer Alliance, the proportion diagnosed *via* TWW referral was more than two SD higher than the sample mean in three Cancer Alliances (equating to statistically significant variation at the 5% significance level), but more than two SD lower than average for six Cancer Alliances (Table 3; Model 1 and Figure 5A). This finding remained present after adjustment for demographic factors (Table 3; Model 2) and adjustment for all patient and tumour characteristics being considered (Table 3; Model 3 and Figure 5B).

Geographic Variation in EP

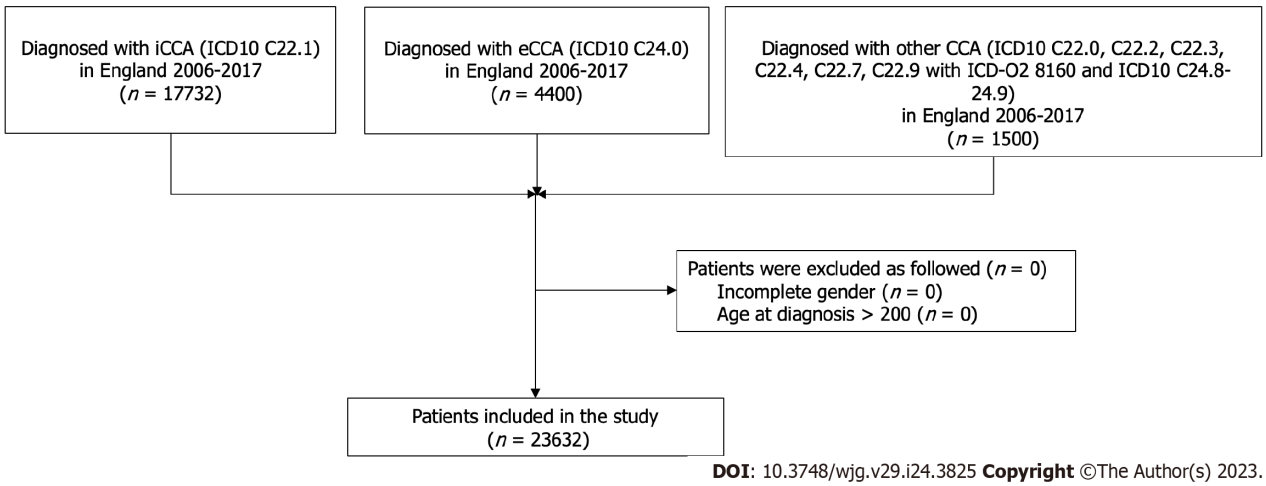
Variation in unadjusted proportions of patients diagnosed *via* EP was observed across the Cancer Alliances, ranging from 38.1% to 58.9% (Supplementary Table 1; $P < 0.001$, Figure 4). There was wider variation in the proportion diagnosed by EP across the nation than was observed for TWW referral route in Figure 4, with a larger number of Cancer Alliances showing statistically significant variation

Table 2 Cohort description

Characteristics		Patients, *n* (%)
Total patients (*n*, %)[1]		23632 (100.0)
Age at diagnosis (yr)	0-44	488 (2.1)
	45-54	1282 (5.4)
	55-64	3466 (14.7)
	65-74	6315 (26.7)
	75-84	7606 (32.2)
	> 84	4475 (18.9)
Gender	Male	11466 (48.5)
	Female	12166 (51.5)
Yr of diagnosis	2006	1585 (6.7)
	2007	1540 (6.5)
	2008	1732 (7.3)
	2009	1867 (7.9)
	2010	1952 (8.3)
	2011	1977 (8.4)
	2012	1997 (8.5)
	2013	2110 (8.9)
	2014	2060 (8.7)
	2015	2217 (9.4)
	2016	2262 (9.6)
	2017	2333 (9.9)
Stage at diagnosis	1	377 (1.6)
	2	873 (3.7)
	3	430 (1.8)
	4	4918 (20.8)
	Unstaged	17034 (72.1)
Tumour sub-type	CCA Other	1500 (6.3)
	eCCA	4400 (18.6)
	iCCA	17732 (75.0)
Tumour morphology	Adenomas and adenocarcinomas	21831 (92.4)
	Other	1801 (7.6)
English Index of Multiple Deprivation, income component	Quintile 1 (least deprived)	4491 (19.0)
	Quintile 2	4966 (21.0)
	Quintile 3	4823 (20.4)
	Quintile 4	4742 (20.1)
	Quintile 5 (most deprived)	4610 (19.5)
Charlson Comorbidity Index	0	17491 (74.0)
	1	2906 (12.3)
	2	1630 (6.9)
	3 +	1605 (6.8)
Underlying liver disease	No	21967 (93.0)

	Yes	1665 (7.0)
Cancer Alliance at diagnosis	Cheshire and Merseyside	1218 (5.2)
	East Midlands	2164 (9.2)
	East of England - North	1298 (5.5)
	East of England - South	1352 (5.7)
	Greater Manchester	1278 (5.4)
	Humber, Coast and Vale	862 (3.6)
	Kent and Medway	664 (2.8)
	Lancashire and South Cumbria	853 (3.6)
	North Central London	408 (1.7)
	North East London	498 (2.1)
	North West and South West London	1109 (4.7)
	Northern	1835 (7.8)
	Peninsula	950 (4.0)
	Somerset, Wiltshire, Avon and Gloucestershire	1191 (5.0)
	South East London	497 (2.1)
	South Yorkshire and Bassetlaw	655 (2.8)
	Surrey and Sussex	1354 (5.7)
	Thames Valley	590 (2.5)
	Wessex	1225 (5.2)
	West Midlands	2573 (10.9)
	West Yorkshire and Harrogate	1058 (4.5)

[1]The cohort contains cholangiocarcinoma patients diagnosed between January 2006 and December 2017 inclusive. If a patient received two cholangiocarcinoma diagnoses in the study time, their first cohort-relevant tumour was selected.
iCCA: Intrahepatic cholangiocarcinoma; eCCA: Extrahepatic cholangiocarcinoma; CCA: Cholangiocarcinoma; ICD: International Classification of Disease.



DOI: 10.3748/wjg.v29.i24.3825 **Copyright** ©The Author(s) 2023.

Figure 1 Flow diagram of eligible patients. iCCA: Intrahepatic cholangiocarcinoma; eCCA: Extrahepatic cholangiocarcinoma; CCA: Cholangiocarcinoma; ICD: International Classification of Disease.

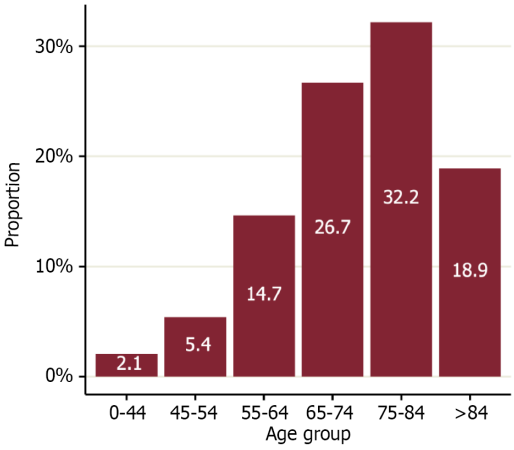
from the sample mean (Figure 6). In a linear probability model that included Cancer Alliance as the only independent variable, the proportion of patients diagnosed *via* EP was more than two SD below the sample mean for five Cancer Alliances. The proportion diagnosed *via* EP route was more than two SD higher than the sample mean for six Cancer Alliances (Table 4 and Figure 6A). In a model that additionally adjusted for demographics (Table 4; Model 2), four Cancer Alliances that varied

Table 3 Estimated proportions diagnosed *via* Two Week Wait referral (as opposed to any other route): Results from linear probability models

	Model 1: Unadjusted		Model 2: Demographic-adjusted[1]		Model 3: Adjusted[2]	
	Estimate	95%CI	Estimate	95%CI	Estimate	95%CI
Population average (intercept)	13.77	13.33-14.20	13.77	13.33-14.20	13.77	13.33-14.20
Cheshire and Merseyside	-4.16	-5.79--2.53	-4.08	-5.72--2.45	-3.66	-5.28--2.04
East Midlands	1.25	-0.18-2.68	1.07	-0.35-2.50	1.02	-0.38-2.43
East of England -North	1.87	-0.04-3.79	1.83	-0.09-3.75	1.71	-0.20-3.62
East of England -South	-2.67	-4.31--1.03	-2.85	-4.49--1.21	-3.01	-4.64--1.38
Greater Manchester	-2.11	-3.83--0.39	-1.92	-3.65--0.19	-1.78	-3.50--0.06
Humber, Coast and Vale	2.13	-0.26-4.52	1.93	-0.46-4.33	2.06	-0.31-4.43
Kent and Medway	-1.72	-4.17-0.73	-1.55	-3.98-0.89	-1.80	-4.24-0.64
Lancashire and South Cumbria	1.36	-1.00-3.72	1.37	-0.99-3.72	1.49	-0.84-3.82
North Central London	-4.70	-7.48--1.91	-4.57	-7.36--1.78	-4.48	-7.27--1.68
North East London	-1.92	-4.74-0.90	-1.32	-4.14-1.51	-1.04	-3.84-1.76
North West and South West London	-5.38	-6.99--3.77	-5.15	-6.76--3.53	-4.91	-6.51--3.30
Northern	3.62	1.97-5.27	3.6	1.94-5.25	3.66	2.02-5.30
Peninsula	-0.40	-2.52-1.73	-0.39	-2.52-1.74	-0.64	-2.76-1.49
Somerset, Wiltshire, Avon and Gloucestershire	1.18	-0.79-3.15	1.03	-0.94-2.99	1.18	-0.76-3.13
South East London	-0.49	-3.44-2.47	-0.02	-2.97-2.93	0.27	-2.67-3.20
South Yorkshire and Bassetlaw	1.50	-1.21-4.22	1.82	-0.89-4.54	1.93	-0.76-4.63
Surrey and Sussex	-0.99	-2.72-0.74	-1.20	-2.94-0.54	-1.41	-3.15-0.34
Thames Valley	0.81	-2.00-3.63	0.45	-2.37-3.27	0.30	-2.48-3.09
Wessex	5.17	3.05-7.30	4.89	2.76-7.02	4.73	2.63-6.83
West Midlands	-1.37	-2.58--0.16	-1.30	-2.51--0.09	-1.55	-2.76--0.35
West Yorkshire and Harrogate	2.68	0.50-4.86	2.91	0.73-5.08	3.12	0.96-5.28
Age 0-44	-8.44	-10.44--6.43	-7.76	-9.77--5.75	-8.76	-10.78--6.74
Age 45-54	-1.13	-2.90-0.65	-0.84	-2.62-0.93	-1.37	-3.14-0.40
Age 55-64	1.12	0.03-2.21	1.25	0.16-2.33	1.03	-0.06-2.13
Age 65-74	2.32	1.57-3.08	2.29	1.53-3.05	2.16	1.41-2.91
Age 75-84	0.42	-0.22-1.06	0.33	-0.31-0.97	0.56	-0.08-1.20
Age 85+	-3.62	-4.44--2.80	-3.67	-4.50--2.84	-3.46	-4.30--2.61
Female	-0.17	-0.60-0.26	0.04	-0.39-0.46	-0.27	-0.70-0.16
Male	0.18	-0.27-0.63	-0.04	-0.49-0.42	0.29	-0.17-0.74
Quintile 1 (least deprived)	0.91	-0.02-1.83	0.74	-0.20-1.67	0.42	-0.51-1.35
Quintile 2	0.59	-0.27-1.46	0.49	-0.38-1.35	0.28	-0.57-1.14
Quintile 3	0.29	-0.58-1.17	0.32	-0.56-1.20	0.33	-0.55-1.20
Quintile 4	-0.44	-1.31-0.43	-0.31	-1.18-0.56	-0.20	-1.06-0.67
Quintile 5 (most deprived)	-1.38	-2.24--0.52	-1.26	-2.15--0.37	-0.86	-1.74-0.03
2006	-3.86	-5.30--2.42			-4.4	-5.84--2.97
2007	-3.64	-5.11--2.16			-4.17	-5.64--2.69
2008	-3.31	-4.72--1.91			-3.90	-5.29--2.51

2009	-2.84	-4.21--1.47	-3.07	-4.44--1.69
2010	-1.93	-3.31--0.55	-2.15	-3.53--0.77
2011	-1.98	-3.35--0.61	-2.12	-3.49--0.75
2012	0.66	-0.82-2.13	0.73	-0.72-2.18
2013	1.07	-0.37-2.51	1.13	-0.30-2.56
2014	0.22	-1.21-1.65	0.54	-0.88-1.96
2015	2.52	1.07-3.97	3.00	1.57-4.44
2016	2.99	1.54-4.44	3.39	1.95-4.82
2017	6.04	4.52-7.55	6.42	4.92-7.93
Adenomas and adenocarcinomas	0.20	0.08-0.32	0.04	-0.08-0.16
Other morphology	-2.44	-3.86--1.02	-0.49	-1.99-1.02
eCCA	-0.38	-1.29-0.53	-0.52	-1.45-0.40
iCCA	0.12	-0.13-0.37	0.07	-0.19-0.33
Other subtype	-0.30	-1.97-1.38	0.72	-0.97-2.42
Charlson 0	1.64	1.40-1.87	1.68	1.44-1.92
Charlson 1	-2.93	-4.00--1.85	-2.88	-3.95--1.81
Charlson 2	-4.87	-6.23--3.51	-5.03	-6.40--3.67
Charlson 3 +	-7.60	-8.78--6.42	-7.98	-9.19--6.77
Liver disease -No	0.32	0.22-0.43	0.34	0.23-0.44
Liver disease -Yes	-4.28	-5.65--2.90	-4.44	-5.86--3.02

[1]Adjustment for: Age, gender, income deprivation quintile.
[2]Adjustment for: Age, gender, income deprivation quintile, Charlson comorbidity index, underlying liver disease at diagnosis, diagnosis year, tumour morphology, tumour sub-type.
Apart from intercept, estimates represent the percentage-point difference from the weighted cohort average probability of each route. If 95%CI does not contain zero, the percentage-point difference from average will be more than 2 SD and indicates variation that is unlikely to be due to chance. Bold indicates a difference that is > 2 SD above or below average. iCCA: Intrahepatic cholangiocarcinoma; eCCA: Extrahepatic cholangiocarcinoma.



DOI: 10.3748/wjg.v29.i24.3825 **Copyright** ©The Author(s) 2023.

Figure 2 Age at diagnosis for cholangiocarcinoma cohort diagnosed in England 2006-2017.

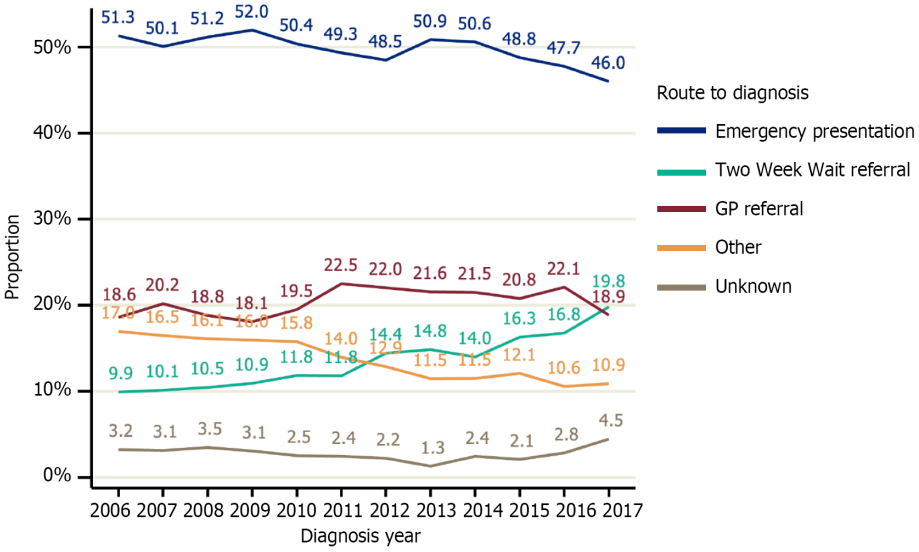
significantly from the sample mean in unadjusted analyses were no longer outliers. However, one further Cancer Alliance became an outlier from the sample mean after this adjustment. Further adjustment for patient and tumour characteristics had no apparent effect on the variation observed relative to the demographic-adjusted model (Table 4; Model 3 and Figure 6B). Five Cancer Alliances had a proportion of EP that was more than two SD higher than the sample mean and three had a proportion of EP that was more than two SD lower.

Table 4 Estimated proportions diagnosed *via* emergency presentation (as opposed to any other route): Results from linear probability models

	Model 1: Unadjusted		Model 2: Demographic-adjusted[1]		Model 3: Adjusted[2]	
	Estimate	95%CI	Estimate	95%CI	Estimate	95%CI
Population average (intercept)	49.57	(48.94, 50.21)	49.57	(48.95, 50.20)	49.57	(48.95, 50.19)
Cheshire and Merseyside	2.81	(0.08, 5.54)	2.39	(-0.31, 5.10)	2.26	(-0.44, 4.96)
East Midlands	-2.30	(-4.3, -0.29)	-1.76	(-3.74, 0.22)	-1.69	(-3.66, 0.29)
East of England -North	1.81	(-0.83, 4.46)	1.79	(-0.82, 4.40)	2.35	(-0.26, 4.97)
East of England -South	1.46	(-1.12, 4.05)	2.55	(0.00, 5.10)	2.82	(0.27, 5.38)
Greater Manchester	5.36	(2.70, 8.01)	4.59	(1.96, 7.22)	4.75	(2.12, 7.39)
Humber, Coast and Vale	3.44	(0.17, 6.72)	3.57	(0.37, 6.78)	3.50	(0.29, 6.71)
Kent and Medway	-1.98	(-5.73, 1.77)	-2.78	(-6.42, 0.85)	-2.66	(-6.29, 0.97)
Lancashire and South Cumbria	2.83	(-0.46, 6.12)	2.59	(-0.63, 5.82)	2.32	(-0.90, 5.54)
North Central London	-1.29	(-6.11, 3.53)	-1.97	(-6.77, 2.83)	-1.82	(-6.60, 2.97)
North East London	4.85	(0.51, 9.18)	3.44	(-0.89, 7.77)	3.32	(-1.02, 7.66)
North West and South West London	0.02	(-2.85, 2.90)	0.47	(-2.35, 3.28)	0.58	(-2.24, 3.40)
Northern	-0.53	(-2.72, 1.67)	-1.26	(-3.43, 0.91)	-1.34	(-3.51, 0.82)
Peninsula	-11.47	(-14.5, -8.44)	-12.11	(-15.12, -9.09)	-12.44	(-15.44, -9.44)
Somerset, Wiltshire, Avon and Gloucestershire	0.39	(-2.38, 3.15)	1.32	(-1.39, 4.03)	0.61	(-2.10, 3.32)
South East London	2.74	(-1.61, 7.10)	2.78	(-1.51, 7.07)	2.53	(-1.77, 6.82)
South Yorkshire and Bassetlaw	9.36	(5.64, 13.08)	7.67	(3.99, 11.34)	7.74	(4.06, 11.41)
Surrey and Sussex	-3.41	(-5.99, -0.83)	-2.08	(-4.61, 0.45)	-1.97	(-4.49, 0.56)
Thames Valley	-3.81	(-7.79, 0.17)	-1.23	(-5.16, 2.70)	-1.67	(-5.57, 2.22)
Wessex	-3.86	(-6.58, -1.14)	-2.94	(-5.61, -0.27)	-3.39	(-6.04, -0.73)
West Midlands	-2.16	(-3.98, -0.34)	-2.80	(-4.58, -1.02)	-2.58	(-4.36, -0.79)
West Yorkshire and Harrogate	5.15	(2.22, 8.09)	4.33	(1.45, 7.21)	4.56	(1.68, 7.43)
Age 0-44	-5.72	(-10.09, -1.35)	-6.46	(-10.82, -2.10)	-5.66	(-10.06, -1.27)
Age 45-54	-8.39	(-11.01, -5.76)	-8.83	(-11.44, -6.23)	-8.16	(-10.78, -5.53)
Age 55-64	-10.85	(-12.35, -9.35)	-10.98	(-12.47, -9.49)	-10.46	(-11.97, -8.95)
Age 65-74	-6.82	(-7.86, -5.77)	-6.61	(-7.65, -5.57)	-6.32	(-7.36, -5.28)
Age 75-84	3.66	(2.74, 4.58)	3.65	(2.74, 4.56)	3.35	(2.44, 4.27)
Age 85+	14.83	(13.56, 16.10)	14.87	(13.59, 16.14)	14.28	(12.98, 15.57)
Female	1.91	(1.29, 2.53)	0.94	(0.32, 1.55)	1.11	(0.49, 1.72)
Male	-2.02	(-2.68, -1.37)	-0.99	(-1.64, -0.34)	-1.17	(-1.83, -0.52)
Quintile 1 (least deprived)	-4.93	(-6.24, -3.62)	-4.91	(-6.21, -3.60)	-4.61	(-5.92, -3.31)
Quintile 2	-2.69	(-3.93, -1.46)	-2.65	(-3.87, -1.43)	-2.50	(-3.71, -1.28)
Quintile 3	-0.66	(-1.92, 0.60)	-0.44	(-1.69, 0.80)	-0.41	(-1.65, 0.83)
Quintile 4	3.11	(1.84, 4.38)	3.00	(1.74, 4.25)	2.86	(1.61, 4.11)
Quintile 5 (most deprived)	5.20	(3.91, 6.49)	5.02	(3.70, 6.33)	4.67	(3.36, 5.99)
2006	1.72	(-0.66, 4.10)			1.85	(-0.49, 4.19)
2007	0.49	(-1.92, 2.91)			1.40	(-0.98, 3.79)
2008	1.58	(-0.68, 3.85)			2.50	(0.28, 4.71)

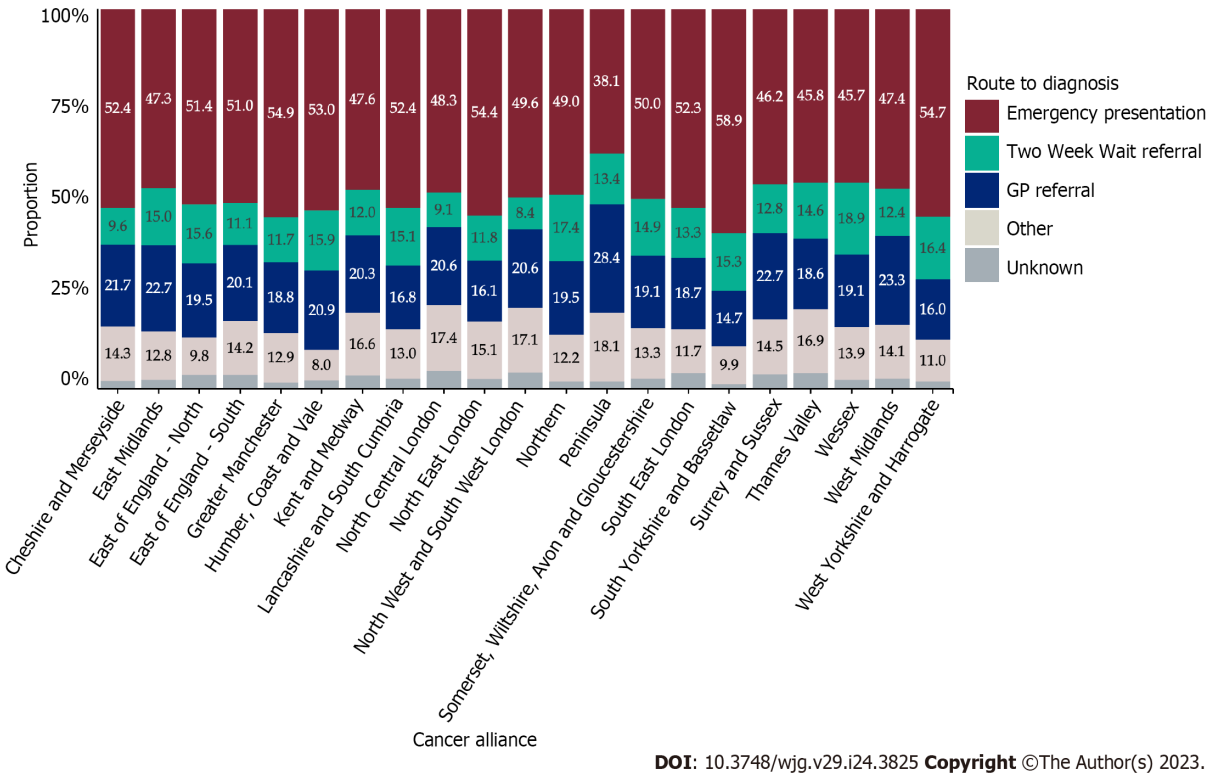
2009	2.38	(0.21, 4.56)	2.47	(0.33, 4.61)
2010	0.79	(-1.34, 2.91)	0.64	(-1.43, 2.71)
2011	-0.26	(-2.37, 1.85)	-0.05	(-2.13, 2.02)
2012	-1.10	(-3.20, 1.00)	-1.38	(-3.42, 0.66)
2013	1.28	(-0.76, 3.32)	1.24	(-0.74, 3.22)
2014	1.01	(-1.05, 3.07)	0.32	(-1.70, 2.33)
2015	-0.81	(-2.79, 1.17)	-1.37	(-3.31, 0.57)
2016	-1.83	(-3.79, 0.13)	-2.22	(-4.15, -0.30)
2017	-3.58	(-5.50, -1.66)	-3.27	(-5.16, -1.38)
Adenomas and adenocarcinomas	-0.56	(-0.74, -0.37)	-0.38	(-0.58, -0.19)
Other morphology	6.73	(4.52, 8.93)	4.64	(2.31, 6.97)
eCCA	-3.41	(-4.74, -2.08)	-2.84	(-4.16, -1.53)
iCCA	0.80	(0.43, 1.17)	0.81	(0.44, 1.18)
Other subtype	0.56	(-1.89, 3.01)	-1.26	(-3.74, 1.22)
Charlson 0	-2.09	(-2.46, -1.71)	-1.28	(-1.66, -0.90)
Charlson 1	3.97	(2.27, 5.67)	1.95	(0.29, 3.62)
Charlson 2	5.21	(2.88, 7.55)	2.74	(0.45, 5.02)
Charlson 3 +	10.24	(7.92, 12.56)	7.63	(5.31, 9.95)
Liver disease -No	0.07	(-0.11, 0.24)	-0.19	(-0.36, -0.01)
Liver disease -Yes	-0.86	(-3.18, 1.45)	2.45	(0.10, 4.70)

[1]Adjustment for: Age, gender, income deprivation quintile.
[2]Adjustment for: Age, gender, income deprivation quintile, Charlson comorbidity index, underlying liver disease at diagnosis, diagnosis year, tumour morphology, tumour sub- type.
Apart from intercept, estimates represent the percentage- point difference from the weighted cohort average probability of each route. If 95%CI does not contain zero, the percentage- point difference from average will be more than 2 SD and indicates variation that is unlikely to be due to chance. Bold indicates a difference that is > 2 SD above or below average. iCCA: Intrahepatic cholangiocarcinoma; eCCA: Extrahepatic cholangiocarcinoma.



DOI: 10.3748/wjg.v29.i24.3825 **Copyright** ©The Author(s) 2023.

Figure 3 Routes to diagnosis of cholangiocarcinoma patients in England, 2006-2017. GP: General practitioner.



DOI: 10.3748/wjg.v29.i24.3825 **Copyright** ©The Author(s) 2023.

Figure 4 Routes to diagnosis according to Cancer Alliance of residence at diagnosis. GP: General practitioner.

There was no strong correlation (P = 0.2) between the proportion of people diagnosed *via* TWW referral and the proportion of EP across the Cancer Alliances; only one of three Cancer Alliances with a higher than average proportion of TWW referral routes had a lower than average proportion of EP. Two of six Cancer Alliances with a lower than average proportion of TWW referral routes had a higher than average proportion of EP.

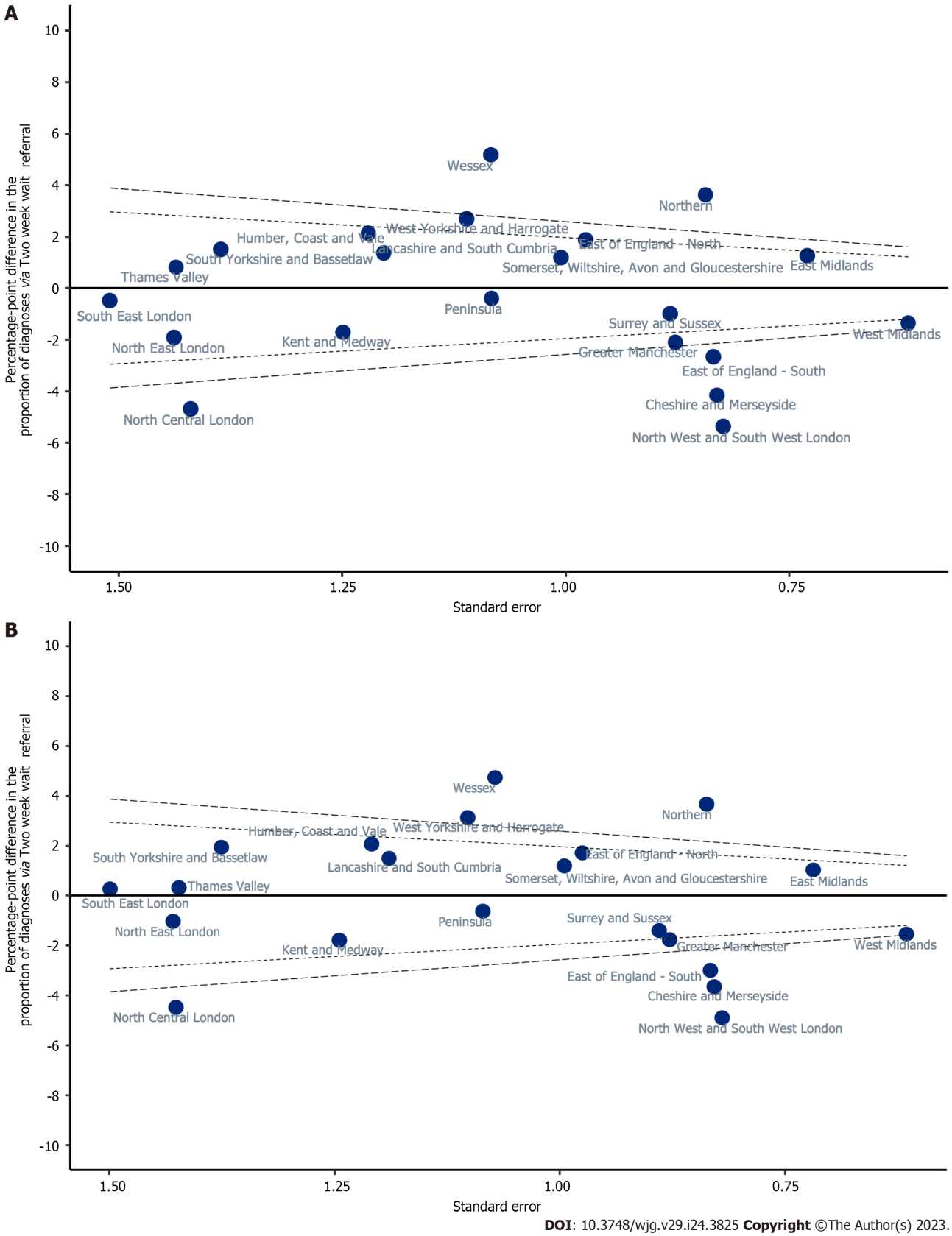
Associations with patient and tumour characteristics

A summary of all univariable associations between the route to diagnosis and patient and tumour characteristics is provided in Supplementary Table 1, with estimated proportions diagnosed *via* TWW referrals and EP in Tables 3 and 4. The lowest proportion diagnosed by TWW referral was observed in the 0-44 years age group [5.3%; unadjusted percentage point difference from average (pp) = -8.44 (95%CI: -10.44 to -6.43)], but the relationship with age was an inverted u-shape, with those aged over 84 years also having a lower proportion of TWW referral routes than average [unadjusted pp = -3.62 (95%CI: -4.44 to -2.80)]. Age remained associated with the proportion diagnosed *via* TWW referral in a model that included all other cofactors of interest (Model 3; Table 3). Likewise, the presence of comorbidity on the CCI and the presence of underlying liver disease were each independently associated with a lower proportion of people being diagnosed *via* a TWW referral (Model 3; Table 3).

A greater-than-average proportion of EP diagnosis routes was observed for females, those aged over 84 years, those who were more deprived, those with more comorbidities, intrahepatic tumour types and non-adenocarcinoma morphology (Supplementary Table 1; all P < 0.001). These associations remained present in an analysis that adjusted for all other factors of interest (Table 4; Model 3). Age above 84 [pp = 14.28 (95%CI: 12.98 to 15.57)] years and a CCI of 3 or more [pp = -7.98 (95%CI: -9.19 to -6.77)] showed the largest effect on the proportion of EP. Underlying liver disease was only associated with a higher proportion of EP after adjustment for other patients and tumour characteristics (Table 4).

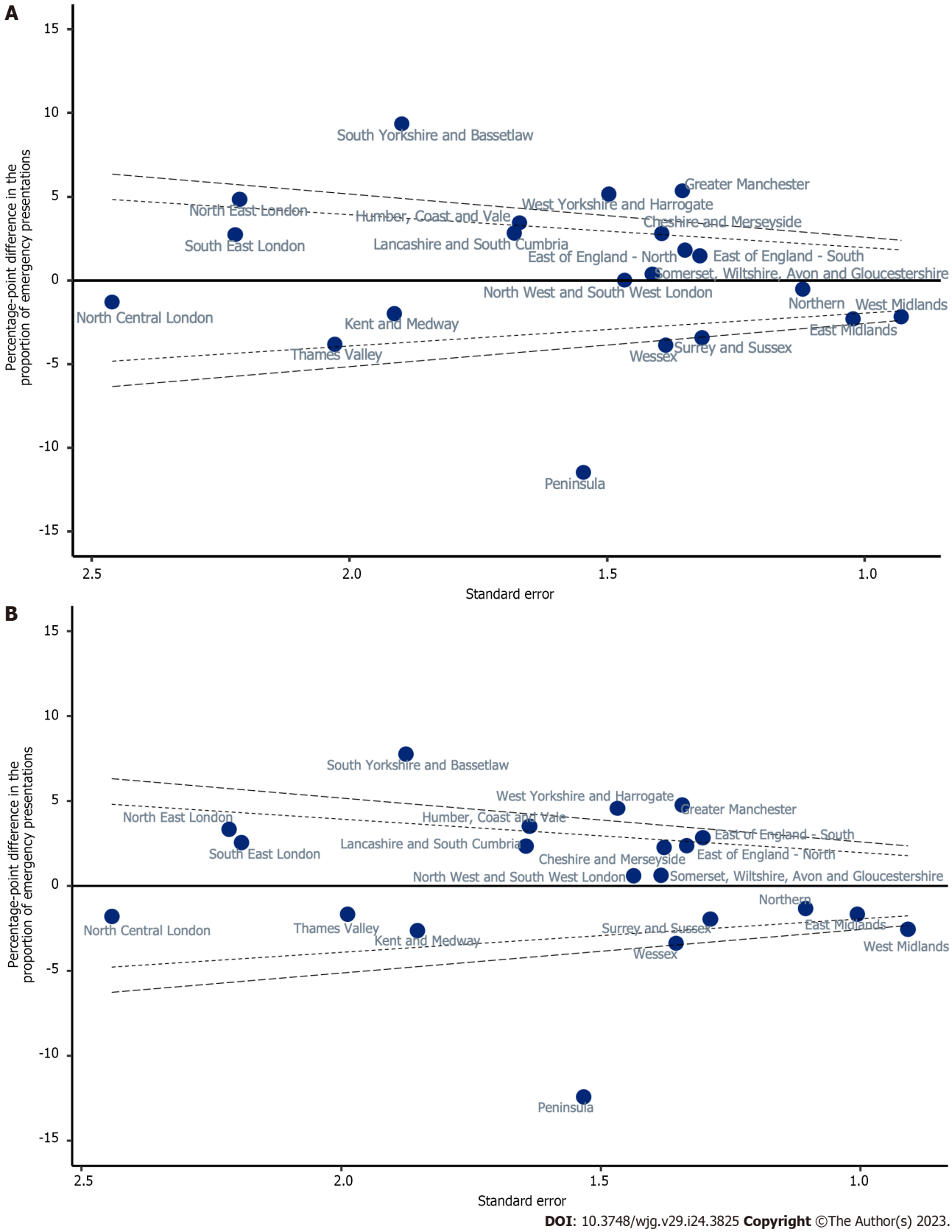
Sensitivity Analysis

A subgroup of 8872 people were diagnosed with CCA between 2014 and 2017, of whom 4832 (54.5%) had a known stage at diagnosis and were included in the sensitivity analysis. The proportion of people staged varied by Cancer Alliance, from 36.7% to 74.7% (P < 0.001). Those with unknown stage at diagnosis were more likely to be older, diagnosed in an earlier year of the study period, have a high comorbidity score and an 'other' tumour subtype or morphology (all P < 0.001). For both diagnosis routes, fewer Cancer Alliances showed significant variation from the sample mean than in the main results following adjustment to all a priori confounders (Tables 3 and 4; Model 3). Upon further adjustment for stage at diagnosis, the variation observed across the Cancer Alliances was not attenuated (results not shown).



DOI: 10.3748/wjg.v29.i24.3825 **Copyright** ©The Author(s) 2023.

Figure 5 Proportion of people diagnosed *via* a Two Week Wait referral in each Cancer Alliance: Results from linear probability model. A: Unadjusted estimates. Inner dashed line = 2 SD difference from average. Outer dashed line = 3 SD difference from average; B: Adjusted estimates. Inner dashed line = 2 SD difference from average. Outer dashed line = 3 SD difference from average. Adjustment for: age, gender, income deprivation quintile, Charlson comorbidity index, underlying liver disease, diagnosis year, tumour morphology and sub-type.



DOI: 10.3748/wjg.v29.i24.3825 **Copyright** ©The Author(s) 2023.

Figure 6 Proportion of people diagnosed *via* an emergency presentation in each Cancer Alliance: Results from linear probability models. A: Unadjusted estimates. Inner dashed line = 2 SD difference from average. Outer dashed line = 3 SD difference from average; B: Adjusted estimates. Inner dashed line = 2 SD difference from average. Outer dashed line = 3 SD difference from average. Adjustment for: Age, gender, income deprivation quintile, Charlson comorbidity index, underlying liver disease, diagnosis year, tumour morphology and sub-type.

DISCUSSION

This study examined changes to routes to diagnosis for CCA across all of England's 21 regional Cancer Alliances over a 12-year period. We found significant variation in the proportion of patients diagnosed by EP and *via* TWW referral across regions. Exploration of factors contributing to regional differences revealed associations between diagnosis route and gender, the burden of comorbidity, deprivation, age at diagnosis and CCA sub-type. It is worth noting that although CCA is often deemed a cancer of the elderly, 22% of cases during the period under study were under 65 years old. The majority of CCA cases were recorded as intrahepatic, but due to the lack of historic codes specifically for peri-hilar CCA, there remains some controversy regarding the true proportional breakdown with nationally recorded numbers of the three anatomical variants of CCA[1,2]. The most common route to diagnosis was EP, in keeping with the typically late presentation of patients with CCA due to the lack of obvious early symptoms, a targetable screening population and accurate diagnostic screening tests.

The significant variation by Cancer Alliance in the proportions diagnosed *via* TWW referral and EP was found after controlling for a range of patient and tumour characteristics. This indicates there are marked differences in the routes that lead individuals to a diagnosis of CCA between Cancer Alliances in England, beyond what would be expected due to chance. The regional variation we found does not appear to be explained by case-mix, in so far as we could adjust for it. Although this variation is unlikely to be random, residual confounding could remain. For example, it was not possible to account for symptoms present prior to diagnosis or health seeking behaviour which might determine how and where people will present for care. Regions found to have higher than average EP or lower than average TWW may want to investigate why. It is possible that this reflects genuine differences in established diagnostic pathways from primary care to secondary care across regions, or different levels of expertise and knowledge of biliary tract cancers in primary care. There was more geographic variation in the proportion of EP routes for extrahepatic than for intrahepatic tumours. Possible reasons for why there might be more variation in diagnostic pathways could relate to symptom profile or other factors. It was not always the case that Cancer Alliances with significantly higher proportion of TWW have a lower proportion of EP. This suggests that for some areas 'additional' TWWs above average are in people who would otherwise have been diagnosed *via* other routes as well as *via* EP. Increases over time in the proportion of TWW were also not matched by decreases in EP alone, but also by decreases in the proportion diagnosed *via* 'other' routes. A lack of direct relationship between TWW and EP may suggest that a significant proportion of people who present as an emergency either would not meet the criteria for a TWW referral or do not interact with their GP at all prior to their diagnosis, limiting the potential for this diagnostic pathway to prevent EPs. The overall proportion of diagnoses *via* the TWW pathway did double from 9.8% to 19.8% during the study period, but this still remains low. Whilst consistent and high-quality implementation of the TWW pathway across all regions is vital to avoid disparities in care, there may also be a need to look to other techniques, particularly at primary care level, in order to further improve the early diagnosis rate specific for CCA in the UK. For example, there may be benefits for screening in patients known to be at high risk of CCA, such as patients with primary sclerosing cholangitis[19]; and the development and validation of novel diagnostic biomarkers remains an active and important area of CCA research[20].

As deprivation increased, so did the proportion diagnosed by EP, corresponding with a reduction in diagnoses by TWW referral. The association between deprivation and primary care services is complex and multi-factorial, relating both to levels of engagement with healthcare services and the availability and quality of primary care services in deprived areas[21-24]. CCA cases were also more likely to present *via* EP if they were female and the reasons for this are difficult to ascertain. That being female, deprived or elderly was associated with a higher risk of EP requires further exploration to ensure groups are not disadvantaged due to their inherent characteristics, which may not necessarily be specific to CCA.

As age at diagnosis increased, so did the proportion diagnosed by EP. Patients who are older may be more likely to excuse vague or non-specific symptoms of CCA as being down to ageing and be less likely to seek healthcare. Another possibility is that they may be less able to seek it. Similarly, CCA patients were less likely to present *via* the TWW pathway if they were over 84 years old, and had co-morbidities and/or underlying liver disease.

CCA cases were more likely to present *via* EP if the CCA was intrahepatic. This may be explained by the fact that iCCA more often presents with non-specific symptoms than eCCA, which can cause obstructive jaundice[1]. People with more specific symptoms may be more likely to seek healthcare sooner, potentially resulting in fewer diagnosed *via* EP.

Although a more limited cohort with staging data available was analysed (diagnosed 2014-2017), adjusting for stage at diagnosis did not explain geographic variation observed after controlling for other patient and tumour characteristics. The 2014-2017 cohort with complete staging data was shown to differ from the full 2006-2017 cohort, with a lower proportion diagnosed by EP, and a higher proportion diagnosed by TWW referral, which could suggest slightly better-managed diagnostic pathways in patients with complete staging data.

It is important to note that a large proportion of stage (72.1%) and performance status (89.4%) data is missing for CCA patients in the NCRD from 2006-2017, which is a limitation of this study. It is unknown if the stage of diagnosis is not known, not recorded, or missing only from the data feeds and submissions used to form the NCRD. Performance status was added to the Cancer Outcomes and Services data collection in 2013, so is only available for patients diagnosed after this. Missingness of performance status remains high (77.5%) even when restricting the cohort to 2013-2017. The completeness of CCA staging information was also variable across Cancer Alliances. Though stage completeness improved in more recent years (from 44% in 2014 to 64% in 2017), these are higher proportions of missing data compared to other tumour types. For example, 89% of colon cancers diagnosed in 2017 were staged, as were 81% of pancreas cancers[25]. Where stage at diagnosis was known, a high proportion were at an advanced disease stage. This reveals a need to publicise the value of this data and encourage the completion of these fields across all providers within Cancer Alliances, so future CCA research can monitor and adjust for these key prognostic factors for treatment options and patient outcomes.

Strengths of the study include that this was a population level analysis, and to our knowledge is the first study analysing routes to diagnosis for CCA across geographic regions and factors associated with this.

Our study does have some inherent limitations. Some of the observed geographic differences may be attributable to residual confounding that cannot be fully accounted for in the current analysis, rather than disparities in clinical practice. For example, it is not known what symptoms patients experienced leading up to their diagnosis of cancer. There is likely a significant role of patient health-seeking behaviour in these outcomes of interest particularly. It is not known from the data available whether individuals presented to their GP to seek advice prior to their diagnosis.

The study only included CCA patients diagnosed in England and therefore, without further research, it is unknown if our findings can be applied to other countries.

Regarding the identification of underlying liver disease, HES APC episodes from 5 years before to 1 year after diagnosis were searched for relevant diagnostic codes. The patient must therefore have had an inpatient episode where their underlying liver disease was documented. Patients may only spend time in the hospital towards the end of their disease and could be treated in outpatient or primary care prior to that. Therefore, the study is likely to have identified more serious cases of underlying liver disease only and may underestimate the burden by missing diagnoses or treatment exclusively documented in outpatient or primary care settings.

CONCLUSION

In conclusion, it would be preferable to reduce the amount of CCA presentations diagnosed by emergency and promote better managed diagnosis pathways earlier in the disease to improve outcomes. Whilst it is possible that the geographic variation observed may be explained by factors that we are unable to account for in the present analysis, these findings provide a signal that further research is necessary to identify and address the complex and multifactorial nature of the observed geographic differences, including potential differences in clinical practice, healthcare access, and socioeconomic factors across different regions in England. It is possible that variation in routes to the diagnosis of CCA by patient demographic factors could reflect genuine differences in practice and recognition of relevant cancer symptoms in a primary care setting, and that certain groups are disadvantaged when it comes to CCA diagnosis. Where variation exists, there may be opportunities for knowledge sharing of good practice to improve diagnostic pathways, such as education or awareness campaigns to increase public and clinician understanding of the common symptoms of CCA and increase diagnoses made by TWW urgent GP referrals. However, this may only improve things so far in a disease that often has no or non-specific symptoms, in which case there may also be a role for screening strategies and non-specific symptom diagnosis clinics.

ARTICLE HIGHLIGHTS

Research background

Cholangiocarcinoma (CCA), a cancer with rising incidence and poor survival, is often diagnosed late. Treatment options are limited for late stage patients. The only curative treatment for CCA is surgery, which is not feasible in patients with advanced disease, and response to systemic therapies at later stage is poor.

Research motivation

Late stage diagnosis presents a large barrier to improving outcomes for patients with CCA. Being diagnosed *via* an emergency presentation (EP) route is associated with later stage diagnoses, whereas

earlier diagnoses may be made *via* the Two Week Wait (TWW) referral route through primary care clinicians. Geographic variation in the proportion of patients diagnosed *via* these routes is important to understand and explore, as some regions may be diagnosing patients *via* better managed and less urgent routes at an earlier stage. Reasoning and learning behind such variation could be shared to improve CCA patients' prognoses.

Research objectives

We aimed to investigate routes to diagnosis of CCA over time, regional variation across England and influencing factors to understand if TWW referrals and EP routes to diagnosis differ across regions in England as we hypothesised.

Research methods

We conducted a retrospective cohort study including patients diagnosed with CCA from 2006-2017 in England. We linked electronic patient records to define routes to diagnosis and patient and tumour characteristics. We used linear probability models to investigate geographic variation in the proportions of patients diagnosed *via* TWW referral or EP across regions in England, adjusting for potential confounders.

Research results

Almost half of CCA patients in England from 2006-2017 were diagnosed *via* EP (49.6%), with just 13.8% diagnosed *via* TWW referrals. The proportion diagnosed *via* TWW referral doubled between 2006-2017 rising from 9.9% to 19.8%. Statistically significant variation in both the proportions diagnosed *via* a TWW referral and EP route was found across regions in England. Age, presence of comorbidities and underlying liver disease were independently associated with lower proportions of patients diagnosed *via* TWW referral and a higher proportion diagnosed *via* EP.

Research conclusions

We found significant geographic and socio-demographic variation in routes to diagnosis of CCA in England.

Research perspectives

There may be opportunities for knowledge sharing of good practice to improve diagnostic pathways where variation exists, such as education or awareness campaigns to increase public and clinician understanding of the common symptoms of CCA and increase diagnoses made by TWW urgent GP referrals. Further research is also warranted to identify and address the complex and multifactorial nature of the observed geographic differences, alongside exploring screening strategies and non-specific symptom diagnosis clinics as CCA often has no or non-specific symptoms.

ACKNOWLEDGEMENTS

This work uses data that has been provided by patients and collected by the NHS as part of their care and support. The data are collated, maintained and quality assured by the National Disease Registration Service, which is part of NHS England. Mireille B Toledano and Shahid Khan are additionally grateful for infrastructure support from the United Kingdom National Institutes for Health Research (NIHR) Biomedical Research Centre at Imperial College London. Mireille B Toledano's Chair is supported in part by a donation from Marit Mohn to Imperial College London to support Population Child Health through the Mohn Centre for Children's Health and Wellbeing.

FOOTNOTES

Author contributions: Zalin-Miller A, Jose S, Morement H and Khan SA designed the study; Zalin-Miller A, Jose S and Khan SA wrote the manuscript; Knott C, Paley L and Toledano MB advised on the study; Knott C, Paley L, Tataru D, Morement H and Toledano MB reviewed the results and manuscript.

Supported by AMMF – The Cholangiocarcinoma Charity.

Institutional review board statement: Consent for this study was given by the National Disease Registration Service Project Proposal Panel in NHS England.

Conflict-of-interest statement: Zalin-Miller A reports grants from AMMF, during the conduct of the study.

Data sharing statement: The data that support the findings of this study are available from NHS England, but restrictions apply to the availability of these data as they are not publicly available.

STROBE statement: The authors have read the STROBE Statement – checklist of items, and the manuscript was prepared and revised according to the STROBE Statement – checklist of items.

Open-Access: This article is an open-access article that was selected by an in-house editor and fully peer-reviewed by external reviewers. It is distributed in accordance with the Creative Commons Attribution NonCommercial (CC BY-NC 4.0) license, which permits others to distribute, remix, adapt, build upon this work non-commercially, and license their derivative works on different terms, provided the original work is properly cited and the use is non-commercial. See: https://creativecommons.org/Licenses/by-nc/4.0/

Country/Territory of origin: United Kingdom

ORCID number: Amy Zalin-Miller 0000-0002-3123-3566; Sophie Jose 0000-0002-3536-4344; Craig Knott 0000-0002-8593-6216; Lizz Paley 0000-0002-3879-5377; Daniela Tataru 0009-0002-2655-4717; Helen Morement 0000-0001-6141-2816; Mireille B Toledano 0000-0001-5695-6210; Shahid A Khan 0000-0003-2538-0911.

S-Editor: Li L
L-Editor: A
P-Editor: Zhang XD

REFERENCES

1 **Banales JM**, Marin JJG, Lamarca A, Rodrigues PM, Khan SA, Roberts LR, Cardinale V, Carpino G, Andersen JB, Braconi C, Calvisi DF, Perugorria MJ, Fabris L, Boulter L, Macias RIR, Gaudio E, Alvaro D, Gradilone SA, Strazzabosco M, Marzioni M, Coulouarn C, Fouassier L, Raggi C, Invernizzi P, Mertens JC, Moncsek A, Rizvi S, Heimbach J, Koerkamp BG, Bruix J, Forner A, Bridgewater J, Valle JW, Gores GJ. Cholangiocarcinoma 2020: the next horizon in mechanisms and management. *Nat Rev Gastroenterol Hepatol* 2020; **17**: 557-588 [PMID: 32606456 DOI: 10.1038/s41575-020-0310-z]

2 **Brindley PJ**, Bachini M, Ilyas SI, Khan SA, Loukas A, Sirica AE, Teh BT, Wongkham S, Gores GJ. Cholangiocarcinoma. *Nat Rev Dis Primers* 2021; **7**: 65 [PMID: 34504109 DOI: 10.1038/s41572-021-00300-2]

3 **Patel T**. Worldwide trends in mortality from biliary tract malignancies. *BMC Cancer* 2002; **2**: 10 [PMID: 11991810 DOI: 10.1186/1471-2407-2-10]

4 **Bertuccio P**, Bosetti C, Levi F, Decarli A, Negri E, La Vecchia C. A comparison of trends in mortality from primary liver cancer and intrahepatic cholangiocarcinoma in Europe. *Ann Oncol* 2013; **24**: 1667-1674 [PMID: 23378539 DOI: 10.1093/annonc/mds652]

5 **Bertuccio P**, Malvezzi M, Carioli G, Hashim D, Boffetta P, El-Serag HB, La Vecchia C, Negri E. Global trends in mortality from intrahepatic and extrahepatic cholangiocarcinoma. *J Hepatol* 2019; **71**: 104-114 [PMID: 30910538 DOI: 10.1016/j.jhep.2019.03.013]

6 **West J**, Wood H, Logan RF, Quinn M, Aithal GP. Trends in the incidence of primary liver and biliary tract cancers in England and Wales 1971-2001. *Br J Cancer* 2006; **94**: 1751-1758 [PMID: 16736026 DOI: 10.1038/sj.bjc.6603127]

7 **McPhail S**, Elliss-Brookes L, Shelton J, Ives A, Greenslade M, Vernon S, Morris EJ, Richards M. Emergency presentation of cancer and short-term mortality. *Br J Cancer* 2013; **109**: 2027-2034 [PMID: 24045658 DOI: 10.1038/bjc.2013.569]

8 **Redaniel MT**, Ridd M, Martin RM, Coxon F, Jeffreys M, Wade J. Rapid diagnostic pathways for suspected colorectal cancer: views of primary and secondary care clinicians on challenges and their potential solutions. *BMJ Open* 2015; **5**: e008577 [PMID: 26493457 DOI: 10.1136/bmjopen-2015-008577]

9 **Dolly SO**, Jones G, Allchorne P, Wheeler D, Ali S, Mukadam Y, Zheng S, Rahman L, Sindhar J, Moss CL, Harari D, Van Hemelrijck M, Cunliffe A, De Michele LV. The effectiveness of the Guy's Rapid Diagnostic Clinic (RDC) in detecting cancer and serious conditions in vague symptom patients. *Br J Cancer* 2021; **124**: 1079-1087 [PMID: 33402736 DOI: 10.1038/s41416-020-01207-7]

10 **National Cancer Registration and Analysis Service**. Routes to Diagnosis, 2018. [cited 13 May 2023]. Available from: https://digital.nhs.uk/data-and-information/publications/statistical/routes-to-diagnosis/2018

11 **Henson KE**, Elliss-Brookes L, Coupland VH, Payne E, Vernon S, Rous B, Rashbass J. Data Resource Profile: National Cancer Registration Dataset in England. *Int J Epidemiol* 2020; **49**: 16-16h [PMID: 31120104 DOI: 10.1093/ije/dyz076]

12 **Elliss-Brookes L**, McPhail S, Ives A, Greenslade M, Shelton J, Hiom S, Richards M. Routes to diagnosis for cancer - determining the patient journey using multiple routine data sets. *Br J Cancer* 2012; **107**: 1220-1226 [PMID: 22996611 DOI: 10.1038/bjc.2012.408]

13 **National Cancer Registration and Analysis Service**. National Cancer Registration and Analysis Service's Cancer Analysis System SOP#1 Counting cancer cases. [cited 13 May 2023]. Available from: https://www.cancerdata.nhs.uk/getdataout/GDO_0024/CAS_SOP_Counting_cancer_cases.pdf

14 **NHS England**. Cancer Alliances - improving care locally. [cited 13 May 2023]. Available from: https://www.england.nhs.uk/cancer/cancer-alliances-improving-care-locally/

15 **Smith T**, Noble M, Noble S, Wright G, McLennan D, Plunkett E. The English Indices of Deprivation 2015, Technical report, in Department for Communities and Local Government, 2015. [cited 13 May 2023]. Available from: https://assets.publishing.service.gov.uk/government/uploads/system/uploads/attachment_data/file/464485/English_Indices_of_Deprivation_2015_-_Technical-Report.pdf

16 **Crooks CJ**, West J, Card TR. A comparison of the recording of comorbidity in primary and secondary care by using the Charlson Index to predict short-term and long-term survival in a routine linked data cohort. *BMJ Open* 2015; **5**: e007974

[PMID: 26048212 DOI: 10.1136/bmjopen-2015-007974]

17 **Driver RJ**, Balachandrakumar V, Burton A, Shearer J, Downing A, Cross T, Morris E, Rowe IA. Validation of an algorithm using inpatient electronic health records to determine the presence and severity of cirrhosis in patients with hepatocellular carcinoma in England: an observational study. *BMJ Open* 2019; **9**: e028571 [PMID: 31292182 DOI: 10.1136/bmjopen-2018-028571]

18 **Te Grotenhuis M**, Pelzer B, Eisinga R, Nieuwenhuis R, Schmidt-Catran A, Konig R. When size matters: advantages of weighted effect coding in observational studies. *Int J Public Health* 2017; **62**: 163-167 [PMID: 27796415 DOI: 10.1007/s00038-016-0901-1]

19 **Chascsa DM**, Lindor KD. Cancer risk, screening and surveillance in primary sclerosing cholangitis. *Minerva Gastroenterol Dietol* 2019; **65**: 214-228 [PMID: 31220911 DOI: 10.23736/S1121-421X.19.02586-8]

20 **Neal RD**, Johnson P, Clarke CA, Hamilton SA, Zhang N, Kumar H, Swanton C, Sasieni P. Cell-Free DNA-Based Multi-Cancer Early Detection Test in an Asymptomatic Screening Population (NHS-Galleri): Design of a Pragmatic, Prospective Randomised Controlled Trial. *Cancers (Basel)*14(19):4818. [PMID: 36230741 DOI: 10.3390/cancers14194818]

21 **Maheswaran R**, Pearson T, Jordan H, Black D. Socioeconomic deprivation, travel distance, location of service, and uptake of breast cancer screening in North Derbyshire, UK. *J Epidemiol Community Health* 2006; **60**: 208-212 [PMID: 16476749 DOI: 10.1136/jech.200X.038398]

22 **Parsons J**, Bryce C, Atherton H. Which patients miss appointments with general practice and the reasons why: a systematic review. *Br J Gen Pract* 2021; **71**: e406-e412 [PMID: 33606660 DOI: 10.3399/BJGP.2020.1017]

23 **NHS Digital**. A&E attendances twice as high for people in the most deprived areas as in the least deprived. [cited 13 May 2023]. Available from: https://digital.nhs.uk/news/2019/ae-attendances-twice-as-high-for-people-in-the-most-deprived-areas-as-in-the-least-deprived?msclkid=5453cc7ecfb611eca5d3a808deeb1be8

24 **The Health Foundation**. Level or not? Comparing general practice in areas of high and low socioeconomic deprivation in England, 2021. [cited 13 May 2023]. Available from: https://reader.health.org.uk/Level-or-not

25 **National Disease Registration Service**. Staging Data in England, 2020. [cited 13 May 2023]. Available from: https://www.cancerdata.nhs.uk/stage_at_diagnosis

World Journal of Gastroenterology

Submit a Manuscript: https://www.f6publishing.com

World J Gastroenterol 2023 June 28; 29(24): 3843-3854

DOI: 10.3748/wjg.v29.i24.3843

ISSN 1007-9327 (print) ISSN 2219-2840 (online)

ORIGINAL ARTICLE

Retrospective Cohort Study

Effect of lifestyle modification on hepatocellular carcinoma incidence and mortality among patients with chronic hepatitis B

Yewan Park, Danbee Kang, Dong Hyun Sinn, Hyunsoo Kim, Yun Soo Hong, Juhee Cho, Geum-Youn Gwak

Specialty type: Gastroenterology and hepatology

Provenance and peer review: Unsolicited article; Externally peer reviewed.

Peer-review model: Single blind

Peer-review report's scientific quality classification

Grade A (Excellent): 0
Grade B (Very good): B
Grade C (Good): C, C, C, C
Grade D (Fair): 0
Grade E (Poor): 0

P-Reviewer: Amin A, United Arab Emirates; Luo Y, China; Tai DI, Taiwan

Received: April 10, 2023
Peer-review started: April 10, 2023
First decision: April 28, 2023
Revised: May 13, 2023
Accepted: May 24, 2023
Article in press: May 24, 2023
Published online: June 28, 2023

Yewan Park, Department of Internal Medicine, Kyung Hee University Hospital, Seoul 02447, South Korea

Yewan Park, Dong Hyun Sinn, Department of Digital Health, SAIHST, Sungkyunkwan University, Seoul 06355, South Korea

Danbee Kang, Juhee Cho, Department of Clinical Research Design and Evaluation, SAIHST, Sungkyunkwan University, Seoul 06355, South Korea

Danbee Kang, Hyunsoo Kim, Juhee Cho, Center for Clinical Epidemiology, Samsung Medical Center, Sungkyunkwan University, Seoul 06351, South Korea

Dong Hyun Sinn, Geum-Youn Gwak, Department of Medicine, Samsung Medical Center, Sungkyunkwan University School of Medicine, Seoul 06351, South Korea

Yun Soo Hong, Juhee Cho, Departments of Epidemiology and Medicine, and Welch Center for Prevention, Epidemiology and Clinical Research, Johns Hopkins Medical Institutions, Baltimore, MD 21287, United States

Corresponding author: Danbee Kang, PhD, Professor, Department of Clinical Research Design and Evaluation, SAIHST, Sungkyunkwan University, 25-2 Sungkyunkwan-ro, Jongno-gu, Seoul 06355, South Korea. dbee.kang@gmail.com

Abstract

BACKGROUND

Research exploring the influence of healthier lifestyle modification (LSM) on the risk of hepatocellular carcinoma (HCC) in patients with chronic hepatitis B (CHB) is limited.

AIM

To emulate a target trial to determine the effect of LSM on HCC incidence and mortality among patients with CHB by large-scale population-based observational data.

METHODS

Among the patients with CHB enrolled in the Korean National Health Insurance Service between January 1, 2009, and December 31, 2017, those aged ≥ 20 years who drank alcohol, smoked cigarettes, and were sedentary were analyzed. Exposure included at least one LSM, including alcohol abstinence, smoking

cessation, and regular exercise. The primary outcome was HCC development, and the secondary outcome was liver-related mortality. We used 2:1 propensity score matching to account for covariates.

RESULTS

With 48766 patients in the LSM group and 103560 in the control group, the adjusted hazard ratio (HR) for incident HCC and liver-related mortality was 0.92 [95% confidence interval (CI): 0.87-0.96] and 0.92 (95%CI: 0.86-0.99) in the LSM group, respectively, compared with the control group. Among the LSM group, the adjusted HR (95%CI) for incident HCC was 0.84 (0.76-0.94), 0.87 (0.81-0.94), and 1.08 (1.00-1.16) for alcohol abstinence, smoking cessation, and regular exercise, respectively. The adjusted HR (95%CI) for liver-related mortality was 0.92 (0.80-1.06), 0.81 (0.72-0.91), and 1.15 (1.04-1.27) for alcohol abstinence, smoking cessation, and regular exercise, respectively.

CONCLUSION

LSM lowered the risk of HCC and mortality in patients with CHB. Thus, active LSM, particularly alcohol abstinence and smoking cessation, should be encouraged in patients with CHB.

Key Words: Lifestyle modification; Chronic hepatitis B; Hepatocellular carcinoma; Cancer; Mortality

©The Author(s) 2023. Published by Baishideng Publishing Group Inc. All rights reserved.

Core Tip: Unhealthy behaviors, including smoking, sedentary lifestyle, or alcohol drinking, are known to have adverse effect on the outcome among chronic hepatitis B (CHB) patients. However, there are limited data on the effect of healthier lifestyle modification (LSM), including quitting smoking, regular exercise, and quitting drinking, on the risk of hepatocellular carcinoma (HCC) in CHB patients. In this first hypothetical randomized trial, we demonstrated that the LSM lowers the risk of developing HCC by using the nationwide database. The findings of this study highlight the necessity for active counseling and therapeutic intervention for LSM in CHB patients.

Citation: Park Y, Kang D, Sinn DH, Kim H, Hong YS, Cho J, Gwak GY. Effect of lifestyle modification on hepatocellular carcinoma incidence and mortality among patients with chronic hepatitis B. *World J Gastroenterol* 2023; 29(24): 3843-3854

URL: https://www.wjgnet.com/1007-9327/full/v29/i24/3843.htm

DOI: https://dx.doi.org/10.3748/wjg.v29.i24.3843

INTRODUCTION

Chronic hepatitis B virus (HBV) infection is the leading cause of hepatocellular carcinoma (HCC) and accounts for 56% of all cases[1,2]. Despite the introduction of neonatal immunization to prevent vertical transmission and antiviral medications with high genetic barrier, the risk of HCC remains high[3]. Thus, ongoing efforts are being made to further decrease the global health burden of chronic hepatitis B (CHB) with modifiable risk factors.

Mounting evidence indicates that not only viral factors but also host factors, such as alcohol consumption, smoking, and obesity, and diet influence the prognosis of patients with CHB[4-7]. Alcohol drinking was associated with increased risk of HCC[8] and mortality[9]. A meta-analysis reported that smoking elevated the risk of HCC by 1.44 times through an additive interaction[10], and a recent prospective cohort study on patients with diabetes and CHB showed pack per year dose responsiveness [7]. Insulin resistance[11] and central obesity[12] increase the incidence of liver cancer in patients with CHB. In contrast, increased physical activity can lower the incidence of liver cancer[13]. Correspondingly, few studies have evaluated whether the modification on behavioral risk factors reduces the incidence of HCC, although studies have demonstrated that the risk of developing HCC increases with unhealthy behavior[14]. A meta-analysis attempted to confirm whether alcohol abstinence prevents HCC; however, reliable results were not obtained owing to the lack of quality studies[14]. Evidence from observational studies and meta-analyses suggests that coffee consumption can reduce the incidence of HCC including in patients with CHB[15,16]. Furthermore, several studies have demonstrated that food-derived components may have a positive impact on the progression of liver fibrosis[17,18] and the treatment of HCC[19-21]. Randomized controlled trials (RCTs) are required to confirm the benefits of modifying behavioral risk factors for HCC in patients with CHB. However, no RCT on patients with CHB has evaluated the impact of lifestyle modifications (LSM) on the incidence of

HCC. This might be because RCTs require enormous resources and time, including medical care, patient participation, human resources, and time to observe events.

An emulated target trial using observational data can help avoid methodological pitfalls in observational studies[22]. It can yield the same estimated effects as that of an RCT if the emulation is successful [23]. HBV infection is the most common cause of HCC in South Korea[24]. South Korea has government-mandated universal health insurance coverage for the entire population[25]. The Korean National Health Insurance Service (K-NHIS) claims database includes information on disease and treatment, as well as health behaviors. Thus, we conducted an emulation trial to determine the effect of LSM on HCC incidence and mortality among patients with CHB using nationwide registry data.

MATERIALS AND METHODS

Data sources and study population

We performed a sequential trial emulation study using the K-NHIS database. The K-NHIS database represents the entire South Korean population. The K-NHIS claims database contains information on demographics, medical treatment, procedures, prescription drugs, diagnostic codes, and hospital use. Diagnoses in the K-NHIS database were based on the International Classification of Diseases, 10th revision (ICD-10). In addition, the K-NHIS claims database includes data from the National Health Screening Examination (NHSE), which is a standardized health screening program provided to all insured persons every 2 years[26]. The NHSE includes a self-administered questionnaire on medical history and health behaviors; including smoking, drinking, and physical activity; anthropometric measurements; and laboratory tests. The participation rate of the NHSE in the target population is approximately 76%. The use of the K-NHIS database was approved by the NHIS Review Committee (protocol number: NHIS-2021-1-575). All patients received an anonymous identification code in the K-NHIS data to protect the patients' information and identity.

This study included participants aged ≥ 20 years with CHB, which was defined as the presence of HBV (B18.0, B18.1, B18.10, B18.18, or Z22.5) codes in any claim or presented in a death certificate during the study period. We restricted participants to those who were drinking, smoking, and did not exercise regularly during the health screening exam between January 1, 2009, and December 31, 2017, as our study aimed to evaluate the benefits of LSM. We then selected participants who had at least one additional health screening examination to evaluate changes in lifestyle (baseline). We excluded participants with a history of cancer, human immunodeficiency virus (HIV) infection (ICD-10 codes: B20, B21, B22, and B24), hepatitis C virus (HCV) infection (ICD 10 code: B18.2), liver cirrhosis (ICD-10 codes: K70.2, K70.3, K71.7, K76.1, and K74), jaundice (ICD-10 code: R17), ascites (ICD-10 code: R18), and hepatic failure (ICD-10 code: K720). Furthermore, we excluded participants who developed cancer or died within the first month of follow-up to minimize potential reverse causality. We also excluded those with missing data for matching variables. The Institutional Review Board of Samsung Medical Center approved the study and waived the requirement for informed consent because the K-NHIS data were de-identified.

Measurements

The main exposure was LSM including alcohol abstinence, smoking cessation, and regular exercise. The NHSE used standardized questionnaires to obtain information on alcohol drinking, smoking, and exercise. For the information on smoking status, participants were asked if they had ever smoked at least 100 cigarettes in their lifetime, based on the World Health Organization definition. Ever smokers were then asked regarding the duration of smoking and the mean number of cigarettes smoked per day. For drinking, participants were asked for the frequency (number of days per week) and quantity (amount of standard unit per occasion) of alcohol consumption. A standard unit was defined as a specialized cup for each type of alcohol such as beer, wine, Korean traditional alcohol (soju), or whisky. One standard unit contains roughly 8 g of ethanol in Korea, although different drinks can have very different alcohol content. The weekly amount of alcohol consumption was calculated by multiplying these two values. Alcohol intake was categorized into none, moderate (< 40 g/d in women and < 60 g/d in men), and heavy (≥ 40 g/d in women and ≥ 60 g/d in men). The exercise questionnaire used a 7-d recall method. The questionnaire was similar to the International Physical Activity Questionnaire (IPAQ)-Short form, which was modified by the Korean NHIS (see Supplementary Figure 1). The questionnaire consisted of the following three questions: (1) How many days in the past week did you engage in vigorous activities that made you breathe much harder than normal for at least 20 min per day (*e.g.*, running, aerobics, fast biking, climbing, *etc.*)? (2) How many days in the past week did you engage in moderate activities that made you breathe somewhat harder than normal for at least 30 min per day (*e.g.*, fast walking, doubles tennis, riding a bicycle at a normal speed, mopping, *etc.*)? and (3) How many days in the past week did you engage in light activities, such as walking for at least 30 min per day, adding up to a total of at least 30 min per day (*e.g.*, walking to and from work or for leisure, light household chores, *etc.*)? This questionnaire has been widely used in previous studies. The main exposure was regular physical activity, which was defined as vigorous physical activity for ≥ 3 d per

week (at least 60 min per week) or moderate physical activity for ≥ 5 d per week (at least 150 min per week).

The primary endpoint was the development of HCC. HCC was defined as the presence of a cancer-specific insurance claim code (V193 code) with the C22.0 code, which is ICD-10 code for HCC. The secondary endpoint was liver-related mortality. Vital status and cause of death were obtained from death certificates collected by the Statistics Korea at the Ministry of Strategy and Finance of South Korea [27]. We considered it a liver-related death if the patients had liver cancer (C22) or liver disease (B15–B19, K70–K75) codes for the cause of death. We also included the development of all types of cancer, extrahepatic cancer, and all-cause mortality as the endpoints.

We included age, sex, body mass index (BMI), liver enzymes [aspartate aminotransferase (AST), alanine aminotransferase (ALT), and γ-glutamyl transferase (GGT)], comorbidities, and antiviral medications at baseline as covariates. Daily alcohol consumption, drinking status, smoking status, and level of physical activity at the time of inclusion were also analyzed.

Assigned groups and follow-up

We emulated a pragmatic sequence of trials by aligning the eligibility window, group assignment, and start of follow-up between study arms[28]. We identified patients with CHB who met the eligibility criteria on the day of health-screening visits to emulate a trial of the effectiveness of LSM on clinical outcomes in patients with CHB. We repeated the enrollment process for all available health screening visits. Each participant could contribute as an eligible individual to as many trials as possible. The emulation of sequential trials is a valid and efficient procedure if participants meet the eligibility criteria at several time points[29]. The participants were then reclassified into two groups according to LSM at the visit. In all trials, participants were followed from baseline until the development of HCC, death, or December 2019, whichever occurred first.

Furthermore, propensity score (PS) matching was performed to minimize the potential impact of confounders on outcomes. We conducted multivariable logistic regression using the following covariates: Age, BMI, AST, ALT, GGT, presence of hypertension, diabetes, myocardial infarction, congestive heart failure, cerebrovascular accident, whether the participant took antiviral medications at the current health screening visit, drinking status (moderate or heavy), smoking status, daily alcohol consumption, and physical activity status (not at all or a little) at the previous health screening visit to estimate the PS for the LSM group. Furthermore, if a patient had health screenings at different time points, we followed them from the date of their first screening, and then the time since the previous exam was included in the matching variables. Matching was performed using a greedy algorithm (caliper = 0.1). The control group was matched 2:1 with the LSM group in each trial. The covariate variables were updated at the start of each trial in the analysis. The covariates were updated over time following the sequential target emulate trial methods. This methodological strategy aligned the assessment of eligibility criteria, treatment assignment, and starting of follow-up, thus removing any immortal-time bias related to the delay between the health screening visit and adoption of healthy behaviors on clinical outcomes. We pooled data from all trials into a single model and included the day of the trial's baseline in the analysis.

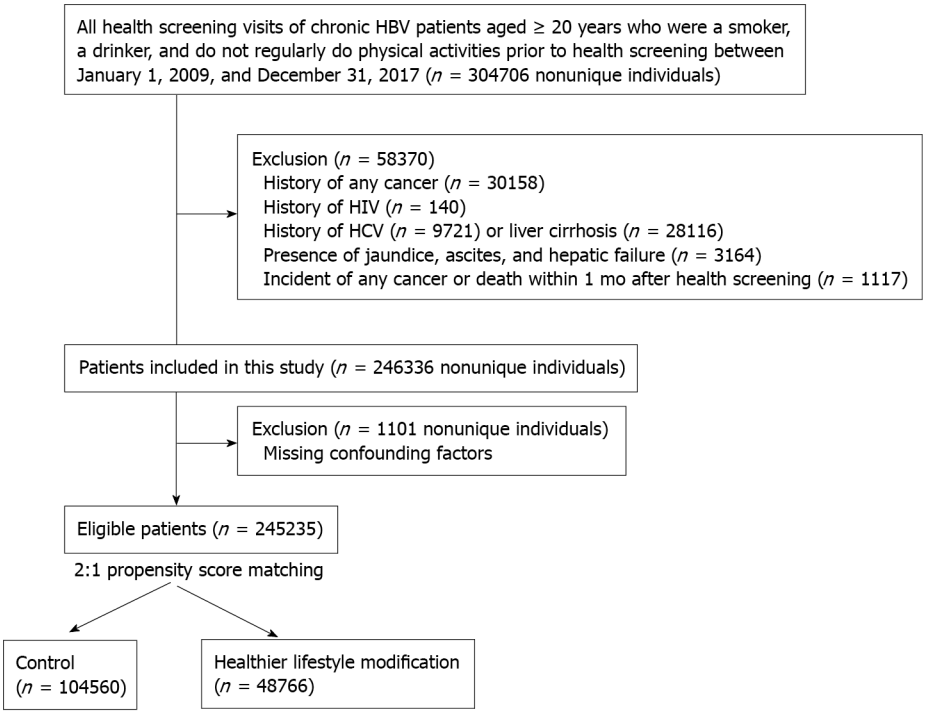
Statistical analysis

The primary analysis was intention-to-treat analysis. Cumulative incidence of each outcome was estimated using the Kaplan-Meier method, and log rank tests were used to evaluate differences between the groups. We calculated hazard ratios (HR) with 95% confidence intervals (CI) for incidence of clinical outcome using a Cox regression model. Covariates with SMD > 0.1, which can provide evidence of an imbalance between matched groups, were adjusted for survival analysis.

We examined the proportional hazards assumption using plots of the log(-log) survival function and Schoenfeld residuals. All *P* values were two-sided, and a *P* value < 0.05 was considered as significant. Analyses were performed using of SAS® Visual Analytics (SAS Institute Inc., United States) and R 4.1.2 (R Foundation for Statistical Computing, Vienna, Austria).

RESULTS

Of the 304706 potential person-trials, we excluded participants with a history of any cancer (*n* = 30158), HIV (*n* = 140), HCV (*n* = 9721) infection, or liver cirrhosis (*n* = 28116). We also excluded participants who had jaundice, ascites, or hepatic failure (*n* = 3164) and 1117 participants who developed cancer or died within the first month of follow-up. Thus, 246336 person-trials met the eligibility criteria; however, 1101 person-trials were excluded because of missing data on confounding factors. Therefore, the final sample size included 245235 person-trials. Among them, we selected two person-trials for the control group per LSM person-trial. Thus, we obtained a control group of 104560 person-trials matched with 48766 person-trials from the LSM group (Figure 1). In the LSM group, 33.7%, 29.6%, and 16.9% of participants belonged to the quitting smoking (QS), regular exercise (RE), and quitting drinking (QD) groups, respectively. In addition, 1.5% of the participants belonged to the QD + QS + RE group.



DOI: 10.3748/wjg.v29.i24.3843 **Copyright** ©The Author(s) 2023.

Figure 1 Flow chart of study participants. HBV: Hepatitis B virus; HIV: Human immunodeficiency virus; HCV: Hepatitis C virus.

The mean age of the study participants was 50 years, and 95% of them were men (Table 1). All SMDs of the difference between the control and LSM groups were less than 0.1, except for age and sex (Figure 2). The LSM group was more likely to be older and female compared with the control group.

During follow-up, 14401 participants developed cancer, and 50.8% of the incident cancers were HCC. The fully adjusted HR for incident HCC comparing LSM group to the control group was 0.92 (95%CI: 0.87-0.96). The association between LSM and HCC was consistent in all subgroups analyzed, except for sex (Table 2). The QD (HR = 0.84, 95%CI: 0.76-0.94) and QS groups (HR = 0.87, 95%CI: 0.81-0.94) showed a beneficial effect on reducing incident HCC compared with the control group when we subcategorized LSM. The fully adjusted HR for incident all cancer and extrahepatic cancer comparing the LSM group to the control group was 0.93 (95%CI: 0.90-0.97) and 0.96 (95%CI: 0.91-1.01), respectively (Table 2).

During the follow-up period, 6833 participants died, and 52.8% were liver-related death. The LSM group had a significantly lower risk of liver-related death compared with the control group over the entire period. The fully adjusted HR for all-cause mortality, when comparing the LSM group with the control group, was 0.94 (95%CI: 0.90-0.99) (Table 3). The fully adjusted HR for liver-related mortality, when comparing the LSM group with the control group, was 0.92 (95%CI: 0.86-0.99) (Table 3).

DISCUSSION

This study demonstrated that LSM is associated with a reduced incidence of HCC and liver-related mortality in patients with CHB. Specifically, alcohol abstinence and smoking cessation were associated with a reduced incidence of HCC, while smoking cessation was associated with reduced liver-related and all-cause mortality.

We included patients with CHB who drank, smoked, and did not exercise regularly. As the risk of developing HCC increases with the presence of more behavioral risk factors[30], the participants of this study are expected to have the poorest prognosis. We found that the risk of HCC was reduced by 8% with the adoption of one LSM. Specifically, the risk was reduced by 16%, 13%, and -8% with alcohol abstinence, smoking cessation, and regular exercise, respectively. Risk was reduced by 21% when all LSM components were adopted. These findings strongly suggest that patients with CHB should be encouraged to adopt healthier lifestyles, particularly alcohol abstinence and smoking cessation.

To date, little is known regarding the effects of LSM on HCC and liver-related mortality in patients with CHB. Alcohol consumption increases the incidence of HCC[31,32]. A meta-analysis on the effect of alcohol abstinence in patients with CHB predicted that limiting alcohol consumption would have a protective effect against the development of HCC even though quality research has not been conducted [14]. Abstinence is believed to counteract some effects of alcohol. Drinking upregulates cytochrome P450 2E1 (CYP2E1), which promotes the generation of reactive oxygen species and electrolyte leakage in the

Table 1 Baseline characteristics

	Control (*n* = 104560)	LSM (*n* = 48766)	SMD
Age, yr	50.1 (7.4)	51.4 (8.0)	0.122
Sex			-0.133
Male	100642 (96.3)	45496 (93.3)	
Female	3918 (3.7)	3270 (6.7)	
BMI			
Underweight (< 18.5 kg/m^2)	2017 (1.9)	860 (1.8)	0.028
Normal (18.5-23 kg/m^2)	34098 (32.6)	15065 (30.9)	-0.012
Obesity (23-25 kg/m^2)	27019 (25.8)	12856 (26.4)	-0.037
Overweight (> 25 kg/m^2)	41413 (39.6)	19976 (41.0)	0.012
Unknown	13 (0.0) 0.012	9 (0.0)	0.005
Daily alcohol consumption[1], g/d	28.8 (27.1)	26.3 (27.5)	-0.064
Drinking status[1]			
Moderate	92707 (88.7)	43734 (89.7)	0.097
Heavy	11853 (11.3)	5032 (10.3)	-0.033
Smoking[1], pack-year	19.1 (11.8)	18.2 (12.9)	-0.052
Physical activity status[1]			0.051
Not at all	56184 (53.7)	24967 (51.2)	
A little	48376 (46.3)	23799 (48.8)	
AST, U/L	38.0 (49.6)	37.3 (45.8)	-0.009
ALT, U/L	40.8 (60.8)	40.3 (59.6)	-0.006
GGT, U/L	76.6 (91.8)	69.5 (94.2)	-0.046
Hypertension (%)	27297 (26.1)	14145 (29.0)	0.065
Diabetes (%)	22475 (21.5)	11712 (24.0)	0.06
Myocardial infarction (%)	838 (0.8)	537 (1.1)	0.031
Congestive heart failure (%)	2142 (2.0)	1288 (2.6)	0.039
Cerebrovascular accident (%)	5150 (4.9)	3145 (6.4)	0.066
Renal disease (%)	867 (0.8)	515 (1.1)	0.023
Antiviral medications (%)	896 (0.9)	533 (1.1)	-0.024

[1]At the time of inclusion.

Values were presented *n* (%) or mean (SD). LSM: Lifestyle modification; SMD: Standard mean difference; BMI: Body mass index; AST: Aspartate aminotransferase; ALT: Alanine aminotransferase; GGT: γ-glutamyl transferase.

mitochondrial respiratory chain[33]. After 3 d of abstinence, the levels of CYP2E1 have been shown to decrease rapidly, corroborating our findings[34].

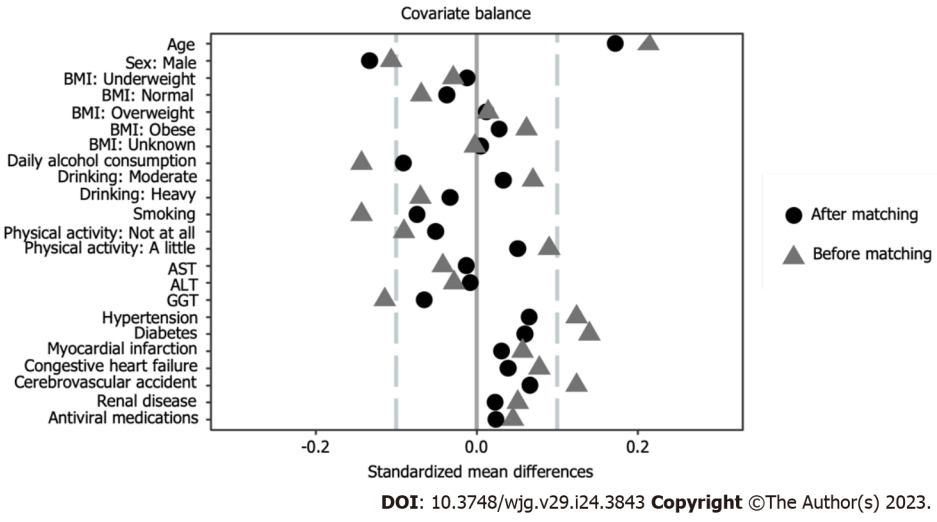
Smoking is another important risk factor for HCC development from the host side. In 2010, the Surgeon General's report expanded the list of smoking-related cancers to include HCC[35]. Few studies have demonstrated the effects of smoking cessation, although smoking is widely acknowledged as a risk factor for HCC. Two prospective observational studies examined the incidence of HCC, ALT elevation, and fibrosis score; however, no statistically significant results were obtained whether smoking cessation had a positive effect on the liver[36,37]. Conversely, a retrospective pooled cohort study of patients with CHB found that as the number of years of smoking cessation increased in ex-smokers, the rate of ALT elevation decreased. This effect is particularly potent after > 10 years of smoking cessation[38]. Previous research has provided an explanation on why smoking cessation reduces HCC. The ability of natural killer cells to stop HBV replication is known to be decreased by smoking, and notably, this effect is restored 1 mo after quitting smoking[39].

Table 2 Hazard ratios for incident cancer according to lifestyle modification

	No. of case (100 persons year)	HR (95%CI)
Hepatocellular carcinoma		
Control (*n* = 104560)	5031 (0.8)	Reference
LSM[1] (*n* = 48766)	2296 (0.8)	0.92 (0.87-0.96)
QD (*n* = 8224)	371 (0.7)	0.84 (0.76-0.94)
QS (*n* = 16423)	695 (0.7)	0.87 (0.81-0.94)
RE (*n* = 14457)	799 (0.9)	1.08 (1.00-1.16)
QD + QS + RE (*n* = 686)	31 (0.7)	0.79 (0.55-1.12)
All cancer		
Control (*n* = 104560)	9691 (1.6)	Reference
LSM (*n* = 48766)	4710 (1.6)	0.93 (0.90-0.97)
QD (*n* = 8224)	826 (1.7)	0.92 (0.86-0.99)
QS (*n* = 16423)	1411 (1.5)	0.89 (0.84-0.94)
RE (*n* = 14457)	1506 (1.8)	1.04 (0.99-1.10)
QD + QS + RE (*n* = 686)	70 (1.7)	0.85 (0.67-1.07)
Extrahepatic cancer		
Control (*n* = 104560)	4660 (0.8)	Reference
LSM (*n* = 48766)	2414 (0.8)	0.96 (0.91-1.01)
QD (*n* = 8224)	455 (0.9)	1.01 (0.92-1.11)
QS (*n* = 16423)	716 (0.8)	0.91 (0.84-0.99)
RE (*n* = 14457)	707 (0.8)	1.00 (0.93-1.09)
QD + QS + RE (*n* = 686)	39 (0.9)	0.91 (0.67-1.25)

[1]Lifestyle modification is quitting drinking or quitting smoking or regular exercise.

HR: Hazard ratio; CI: Confidence interval; LSM: Lifestyle modification; QD: Quitting drinking; QS: Quitting smoking; RE: Regular exercise.



DOI: 10.3748/wjg.v29.i24.3843 **Copyright** ©The Author(s) 2023.

Figure 2 Covariate balance check. AST: Aspartate aminotransferase; ALT: Alanine aminotransferase; CCT: γ-glutamyl transferase; BMI: Body mass index.

Some findings regarding the effect of exercise on HCC in patients with CHB are inconsistent, although the preventive effect of exercise on liver-related outcomes in patients with non-alcoholic fatty liver is well established. A study of patients with CHB revealed that exercise reduces the risk of HCC overall, whereas physical activity of ≥ 1500 MET-min/week increases the risk of HCC in patients with

Table 3 Hazard ratios for mortality according to lifestyle modification

	No. of case (100 persons year)	HR (95%CI)
Liver-related mortality		
Control (*n* = 104560)	2458 (0.4)	Reference
LSM[1] (*n* = 48766)	1150 (0.4)	0.92 (0.86-0.99)
QD (*n* = 8224)	203 (0.4)	0.92 (0.80-1.06)
QS (*n* = 16423)	319 (0.3)	0.81 (0.72-0.91)
RE (*n* = 14457)	422 (0.5)	1.15 (1.04-1.27)
QD + QS + RE (*n* = 686)	17 (0.4)	0.85 (0.53-1.37)
All-cause mortality		
Control (*n* = 104560)	4539 (0.7)	Reference
LSM (*n* = 48766)	2294 (0.7)	0.94 (0.90-0.99)
QD (*n* = 8224)	451 (0.9)	1.04 (0.94-1.15)
QS (*n* = 16423)	588 (0.6)	0.78 (0.72-0.85)
RE (*n* = 14457)	772 (0.9)	1.11 (1.03-1.20)
QD + QS + RE (*n* = 686)	38 (0.9)	0.91 (0.66-1.25)

[1]Lifestyle modification is quitting drinking or quitting smoking or regular exercise.

HR: Hazard ratio; CI: Confidence interval; LSM: Lifestyle modification; QD: Quitting drinking; QS: Quitting smoking; RE: Regular exercise.

liver cirrhosis[13]. In addition, in a multinational cohort study, the effect of exercise on HCC prevention was not statistically significant in the sub-analysis of patients with CHB[40]. In our study, unlike alcohol abstinence and smoking cessation, regular exercise did not have a beneficial effect on HCC prevention or mortality. However, in this study, we had no detailed information on exercise, such as intensity or reason for exercise. Future studies are required to determine the effect of exercise and its type on HCC and the dose relationship in patients with CHB.

This study had several limitations. First, because this was a retrospective study, inevitable problems were encountered. Exclusion criteria were established to identify individuals who were expected to sustain their health status for an extended length of time at baseline. Nonetheless, the issue of reverse causation may remain. The K-NHIS does not provide information on the reasons for changing health behaviors. Consequently, sick quitter bias may arise in which people abstain from drinking or smoking because their health deteriorates to the point that they no longer find drinking or smoking enjoyable [41]. We further excluded participants who developed cancer or died within the first month of follow-up from baseline to minimize potential reverse causality. Second, our study used a self-report questionnaire to assess health behaviors. People might overreport or underreport health behaviors that would affect the results[42,43]. However, the NHSE uses a standardized questionnaire to assess health behaviors. Third, quantitative guidance for HCC risk and mortality reduction could not be offered because the dose- and time-effect linkages of LSM were not determined in this study. In addition, patients' assigned groups during the study might have changes, which could potentially underestimate the association between LSM and outcomes. However, additional biases in the analysis could have been introduced as some patients did not participate in the next health screening visit. Therefore, we performed target trial emulation to reduce selection bias and provide more robust estimates of treatment effects. Specifically, we were able to allocate the two groups at the "beginning" of induction, before subsequently emulating the randomization process using coarsened exact matching, through simultaneous determination of eligibility and assigning two arms. Fourth, we lacked several important variables for the outcome of CHB, for example, the degree of liver fibrosis and hepatitis B viral load. However, the administration of antiviral agents in Korea is subject to a reimbursement policy based on the presence of liver cirrhosis, elevated AST or ALT levels, and DNA levels. In this study, we attempted to partially account for liver fibrosis and DNA levels *via* adjusting for whether or not the patient received antiviral treatment. We were able to allocate the two groups at the "beginning" of induction, before subsequently emulating the randomization process using coarsened exact matching, through simultaneous determination of eligibility and assigning two arms.

CONCLUSION

In conclusion, LSM, particularly alcohol abstinence and smoking cessation, was associated with a reduced incidence of HCC in patients with CHB. Smoking cessation is also associated with reduced liver-related and all-cause mortality. Thus, active LSM should be encouraged in patients with CHB. A prospective study is required to confirm the results of this study and establish the dose and time effects of LSM in this population.

ARTICLE HIGHLIGHTS

Research background

Despite various efforts to reduce the incidence of hepatocellular carcinoma (HCC) in patients with chronic hepatitis B (CHB), it remains a persistent issue. Reports suggest that host factors such as alcohol consumption, smoking, and obesity, in addition to viral factors, contribute to the development of HCC.

Research motivation

Few studies have investigated the impact of lifestyle modifications (LSM) on reducing the incidence of HCC and liver-related mortality in patients with CHB.

Research objectives

This study used a nationwide database in Korea to investigate whether improvements in at least one of the following lifestyle factors - drinking, smoking, and sedentary behavior - were associated with reductions in HCC incidence and liver-related mortality in patients with CHB.

Research methods

We analyzed patients with CHB who participated in the Korean National Health Insurance Service and who drank alcohol, smoked cigarettes, and were sedentary. Target trial emulation was used and covariates were adjusted through 2:1 propensity score matching.

Research results

With 48766 patients in the LSM group and 103560 in the control group, the LSM group had a lower adjusted hazard ratio for incident HCC and liver-related mortality compared to the control group. Within the LSM group, alcohol abstinence and smoking cessation were associated with lower adjusted hazard ratios for both outcomes.

Research conclusions

LSM, specifically alcohol abstinence and smoking cessation, were associated with a decreased risk of HCC in patients with CHB.

Research perspectives

The findings of this study suggest a need for active counseling for LSM in CHB patients, particularly alcohol abstinence and smoking cessation. Further investigation through a well-designed prospective cohort study is necessary to confirm these results.

FOOTNOTES

Author contributions: Park Y, Kang D, Cho J, and Gwak GY contributed to the study design; Kang D and Kim H contributed to the data collection and statistical analysis; Park Y and Kang D contributed to the drafting of the manuscript; Sinn DH, Hong YS, Cho J, and Gwak GY contributed to the critical review of the manuscript; Sinn DH, Cho J, and Gwak GY contributed to the study supervision; all the authors have full access to all of the data and take responsibility for the integrity of the data and accuracy of the data analysis.

Institutional review board statement: The use of the K-NHIS database was approved by the NHIS Review Committee (protocol number: NHIS-2021-1-575).

Informed consent statement: The institutional review board of Samsung Medical Center waived the requirement for informed consent for use of de-identified data. (Protocol number: SMC-2020-05-095).

Conflict-of-interest statement: All authors have nothing to disclose.

Data sharing statement: The corresponding author may provide data upon receipt of reasonable requests. However, due to restriction on information disclosure by the Korean National Insurance Service, data availability may be

limited.

STROBE statement: The authors have read the STROBE Statement—checklist of items, and the manuscript was prepared and revised according to the STROBE Statement—checklist of items.

Open-Access: This article is an open-access article that was selected by an in-house editor and fully peer-reviewed by external reviewers. It is distributed in accordance with the Creative Commons Attribution NonCommercial (CC BY-NC 4.0) license, which permits others to distribute, remix, adapt, build upon this work non-commercially, and license their derivative works on different terms, provided the original work is properly cited and the use is non-commercial. See: https://creativecommons.org/Licenses/by-nc/4.0/

Country/Territory of origin: South Korea

ORCID number: Yewan Park 0000-0003-2560-7346; Danbee Kang 0000-0003-0244-7714; Dong Hyun Sinn 0000-0002-7126-5554; Hyunsoo Kim 0000-0001-5241-289X; Yun Soo Hong 0000-0002-2438-5641; Juhee Cho 0000-0001-9081-0266; Geum-Youn Gwak 0000-0002-6453-3450.

S-Editor: Yan JP
L-Editor: A
P-Editor: Yan JP

REFERENCES

1 **Rumgay H**, Arnold M, Ferlay J, Lesi O, Cabasag CJ, Vignat J, Laversanne M, McGlynn KA, Soerjomataram I. Global burden of primary liver cancer in 2020 and predictions to 2040. *J Hepatol* 2022; **77**: 1598-1606 [PMID: 36208844 DOI: 10.1016/j.jhep.2022.08.021]
2 **Maucort-Boulch D**, de Martel C, Franceschi S, Plummer M. Fraction and incidence of liver cancer attributable to hepatitis B and C viruses worldwide. *Int J Cancer* 2018; **142**: 2471-2477 [PMID: 29388206 DOI: 10.1002/ijc.31280]
3 **Korean Association for the Study of the Liver (KASL)**. KASL clinical practice guidelines for management of chronic hepatitis B. *Clin Mol Hepatol* 2019; **25**: 93-159 [PMID: 31185710 DOI: 10.3350/cmh.2019.1002]
4 **Jachs M**, Tillmann HL. It's not all about the virus-On the importance of modifiable lifestyle factors in the development of hepatocellular carcinoma in chronic hepatitis B. *Hepatology* 2023; **77**: 352-354 [PMID: 36114783 DOI: 10.1002/hep.32798]
5 **Wu S**, Zhou J, Wu X, Sun Y, Wang B, Kong Y, Zhan S, Jia J, Yang HI, You H. Comparative Performance of 14 HCC Prediction Models in CHB: A Dynamic Validation at Serial On-Treatment Timepoints. *Am J Gastroenterol* 2022; **117**: 1444-1453 [PMID: 35973147 DOI: 10.14309/ajg.0000000000001865]
6 **Jee SH**, Ohrr H, Sull JW, Samet JM. Cigarette smoking, alcohol drinking, hepatitis B, and risk for hepatocellular carcinoma in Korea. *J Natl Cancer Inst* 2004; **96**: 1851-1856 [PMID: 15601641 DOI: 10.1093/jnci/djh334]
7 **Mak LY**, Hui RW, Lee CH, Mao X, Cheung KS, Wong DK, Lui DT, Fung J, Yuen MF, Seto WK. Glycemic burden and the risk of adverse hepatic outcomes in patients with chronic hepatitis B with type 2 diabetes. *Hepatology* 2023; **77**: 606-618 [PMID: 36130882 DOI: 10.1002/hep.32716]
8 **Ikeda K**, Saitoh S, Suzuki Y, Kobayashi M, Tsubota A, Koida I, Arase Y, Fukuda M, Chayama K, Murashima N, Kumada H. Disease progression and hepatocellular carcinogenesis in patients with chronic viral hepatitis: a prospective observation of 2215 patients. *J Hepatol* 1998; **28**: 930-938 [PMID: 9672166 DOI: 10.1016/s0168-8278(98)80339-5]
9 **Sinn DH**, Kang D, Guallar E, Chang Y, Ryu S, Zhao D, Hong YS, Cho J, Gwak GY. Alcohol Intake and Mortality in Patients With Chronic Viral Hepatitis: A Nationwide Cohort Study. *Am J Gastroenterol* 2021; **116**: 329-335 [PMID: 33038136 DOI: 10.14309/ajg.0000000000000966]
10 **Chuang SC**, Lee YC, Hashibe M, Dai M, Zheng T, Boffetta P. Interaction between cigarette smoking and hepatitis B and C virus infection on the risk of liver cancer: a meta-analysis. *Cancer Epidemiol Biomarkers Prev* 2010; **19**: 1261-1268 [PMID: 20447919 DOI: 10.1158/1055-9965.EPI-09-1297]
11 **Kim JH**, Sinn DH, Gwak GY, Kang W, Paik YH, Choi MS, Lee JH, Koh KC, Paik SW. Insulin resistance and the risk of hepatocellular carcinoma in chronic hepatitis B patients. *J Gastroenterol Hepatol* 2017; **32**: 1100-1106 [PMID: 27862289 DOI: 10.1111/jgh.13647]
12 **Fan R**, Niu J, Ma H, Xie Q, Cheng J, Rao H, Dou X, Xie J, Zhao W, Peng J, Gao Z, Gao H, Chen X, Chen J, Li Q, Tang H, Zhang Z, Ren H, Cheng M, Liang X, Zhu C, Wei L, Jia J, Sun J, Hou J; Chronic Hepatitis B Study Consortium. Association of central obesity with hepatocellular carcinoma in patients with chronic hepatitis B receiving antiviral therapy. *Aliment Pharmacol Ther* 2021; **54**: 329-338 [PMID: 34157146 DOI: 10.1111/apt.16469]
13 **Chun HS**, Park S, Lee M, Cho Y, Kim HS, Choe AR, Kim HY, Yoo K, Kim TH. Association of Physical Activity with the Risk of Hepatocellular Carcinoma in Patients with Chronic Hepatitis B. *Cancers (Basel)* 2021; **13** [PMID: 34298640 DOI: 10.3390/cancers13143424]
14 **Heckley GA**, Jarl J, Asamoah BO, G-Gerdtham U. How the risk of liver cancer changes after alcohol cessation: a review and meta-analysis of the current literature. *BMC Cancer* 2011; **11**: 446 [PMID: 21995442 DOI: 10.1186/1471-2407-11-446]
15 **Gelatti U**, Covolo L, Franceschini M, Pirali F, Tagger A, Ribero ML, Trevisi P, Martelli C, Nardi G, Donato F; Brescia HCC Study Group. Coffee consumption reduces the risk of hepatocellular carcinoma independently of its aetiology: a case-control study. *J Hepatol* 2005; **42**: 528-534 [PMID: 15868652 DOI: 10.1016/j.jhep.2004.11.039]

16 **Bravi F**, Tavani A, Bosetti C, Boffetta P, La Vecchia C. Coffee and the risk of hepatocellular carcinoma and chronic liver disease: a systematic review and meta-analysis of prospective studies. *Eur J Cancer Prev* 2017; **26**: 368-377 [PMID: 27111112 DOI: 10.1097/CEJ.0000000000000252]

17 **Hamza AA**, Lashin FM, Gamel M, Hassanin SO, Abdalla Y, Amin A. Hawthorn Herbal Preparation from Crataegus oxyacantha Attenuates In Vivo Carbon Tetrachloride -Induced Hepatic Fibrosis *via* Modulating Oxidative Stress and Inflammation. *Antioxidants (Basel)* 2020; **9** [PMID: 33255507 DOI: 10.3390/antiox9121173]

18 **El-Dakhly SM**, Salama AAA, Hassanin SOM, Yassen NN, Hamza AA, Amin A. Aescin and diosmin each alone or in low dose- combination ameliorate liver damage induced by carbon tetrachloride in rats. *BMC Res Notes* 2020; **13**: 259 [PMID: 32460808 DOI: 10.1186/s13104-020-05094-2]

19 **Abdu S**, Juaid N, Amin A, Moulay M, Miled N. Effects of Sorafenib and Quercetin Alone or in Combination in Treating Hepatocellular Carcinoma: In Vitro and In Vivo Approaches. *Molecules* 2022; **27** [PMID: 36432184 DOI: 10.3390/molecules27228082]

20 **Nelson DR**, Hrout AA, Alzahmi AS, Chaiboonchoe A, Amin A, Salehi-Ashtiani K. Molecular Mechanisms behind Safranal's Toxicity to HepG2 Cells from Dual Omics. *Antioxidants (Basel)* 2022; **11** [PMID: 35740022 DOI: 10.3390/antiox11061125]

21 **Al-Dabbagh B**, Elhaty IA, Murali C, Madhoon AA, Amin A. Salvadora persicat; (Miswak): Antioxidant and Promising Antiangiogenic Insights. *Am J Plant Sci* 2018; **9**: 1228-1244 [DOI: 10.4236/ajps.2018.96091]

22 **Cheol Seong S**, Kim YY, Khang YH, Heon Park J, Kang HJ, Lee H, Do CH, Song JS, Hyon Bang J, Ha S, Lee EJ, Ae Shin S. Data Resource Profile: The National Health Information Database of the National Health Insurance Service in South Korea. *Int J Epidemiol* 2017; **46**: 799-800 [PMID: 27794523 DOI: 10.1093/ije/dyw253]

23 **Chun CB**, Kim SY, Lee JY, Lee SY. Republic of Korea. Health system review. Health Systems in Transition 2009; 11

24 **Lee J**, Lee JS, Park SH, Shin SA, Kim K. Cohort Profile: The National Health Insurance Service-National Sample Cohort (NHIS-NSC), South Korea. *Int J Epidemiol* 2017; **46**: e15 [PMID: 26822938 DOI: 10.1093/ije/dyv319]

25 **Shin DW**, Cho B, Guallar E. Korean National Health Insurance Database. *JAMA Intern Med* 2016; **176**: 138 [PMID: 26747667 DOI: 10.1001/jamainternmed.2015.7110]

26 **García-Albéniz X**, Hsu J, Bretthauer M, Hernán MA. Effectiveness of Screening Colonoscopy to Prevent Colorectal Cancer Among Medicare Beneficiaries Aged 70 to 79 Years: A Prospective Observational Study. *Ann Intern Med* 2017; **166**: 18-26 [PMID: 27669524 DOI: 10.7326/M16-0758]

27 **Caniglia EC**, Rojas-Saunero LP, Hilal S, Licher S, Logan R, Stricker B, Ikram MA, Swanson SA. Emulating a target trial of statin use and risk of dementia using cohort data. *Neurology* 2020; **95**: e1322-e1332 [PMID: 32753444 DOI: 10.1212/WNL.0000000000010433]

28 **Hernán MA**, Sauer BC, Hernández-Díaz S, Platt R, Shrier I. Specifying a target trial prevents immortal time bias and other self-inflicted injuries in observational analyses. *J Clin Epidemiol* 2016; **79**: 70-75 [PMID: 27237061 DOI: 10.1016/j.jclinepi.2016.04.014]

29 **European Association for the Study of the Liver**. EASL 2017 Clinical Practice Guidelines on the management of hepatitis B virus infection. *J Hepatol* 2017; **67**: 370-398 [PMID: 28427875 DOI: 10.1016/j.jhep.2017.03.021]

30 **Luu HN**, Behari J, Goh GB, Wang R, Jin A, Thomas CE, Clemente JC, Odegaard AO, Koh WP, Yuan JM. Composite Score of Healthy Lifestyle Factors and Risk of Hepatocellular Carcinoma: Findings from a Prospective Cohort Study. *Cancer Epidemiol Biomarkers Prev* 2021; **30**: 380-387 [PMID: 33187965 DOI: 10.1158/1055-9965.EPI-20-1201]

31 **Terrault NA**, Lok ASF, McMahon BJ, Chang KM, Hwang JP, Jonas MM, Brown RS Jr, Bzowej NH, Wong JB. Update on prevention, diagnosis, and treatment of chronic hepatitis B: AASLD 2018 hepatitis B guidance. *Hepatology* 2018; **67**: 1560-1599 [PMID: 29405329 DOI: 10.1002/hep.29800]

32 **Seitz HK**, Bataller R, Cortez-Pinto H, Gao B, Gual A, Lackner C, Mathurin P, Mueller S, Szabo G, Tsukamoto H. Alcoholic liver disease. *Nat Rev Dis Primers* 2018; **4**: 16 [PMID: 30115921 DOI: 10.1038/s41572-018-0014-7]

33 **Purohit V**, Rapaka R, Kwon OS, Song BJ. Roles of alcohol and tobacco exposure in the development of hepatocellular carcinoma. *Life Sci* 2013; **92**: 3-9 [PMID: 23123447 DOI: 10.1016/j.lfs.2012.10.009]

34 **Oneta CM**, Lieber CS, Li J, Rüttimann S, Schmid B, Lattmann J, Rosman AS, Seitz HK. Dynamics of cytochrome P4502E1 activity in man: induction by ethanol and disappearance during withdrawal phase. *J Hepatol* 2002; **36**: 47-52 [PMID: 11804663 DOI: 10.1016/s0168-8278(01)00223-9]

35 How Tobacco Smoke Causes Disease: The Biology and Behavioral Basis for Smoking-Attributable Disease: A Report of the Surgeon General. Atlanta (GA): Centers for Disease Control and Prevention (US); 2010 [PMID: 21452462]

36 **Tran TXM**, Kim S, Song H, Park B. Longitudinal Changes in Smoking Habits in Women and Subsequent Risk of Cancer. *Am J Prev Med* 2022; **63**: 894-903 [PMID: 36050198 DOI: 10.1016/j.amepre.2022.07.001]

37 **Brahmania M**, Liu S, Wahed AS, Yim C, Hansen BE, Khalili M, Terrault NA, Lok AS, Ghany M, Wang J, Wong D, Janssen HLA; Hepatitis B Research Network. Alcohol, tobacco and coffee consumption and liver disease severity among individuals with Chronic Hepatitis B infection in North America. *Ann Hepatol* 2020; **19**: 437-445 [PMID: 32139262 DOI: 10.1016/j.aohep.2020.01.005]

38 **Wang YH**, Chuang YH, Wu CF, Jan MC, Wu WJ, Lin CL, Liu CJ, Yang YC, Chen PJ, Lin SM, Tsai MH, Huang YW, Yu MW. Smoking and Hepatitis B Virus-Related Hepatocellular Carcinoma Risk: The Mediating Roles of Viral Load and Alanine Aminotransferase. *Hepatology* 2019; **69**: 1412-1425 [PMID: 30382583 DOI: 10.1002/hep.30339]

39 **Meliska CJ**, Stunkard ME, Gilbert DG, Jensen RA, Martinko JM. Immune function in cigarette smokers who quit smoking for 31 days. *J Allergy Clin Immunol* 1995; **95**: 901-910 [PMID: 7722172 DOI: 10.1016/s0091-6749(95)70135-4]

40 **Baumeister SE**, Schlesinger S, Aleksandrova K, Jochem C, Jenab M, Gunter MJ, Overvad K, Tjønneland A, Boutron-Ruault MC, Carbonnel F, Fournier A, Kühn T, Kaaks R, Pischon T, Boeing H, Trichopoulou A, Bamia C, La Vecchia C, Masala G, Panico S, Fasanelli F, Tumino R, Grioni S, Bueno de Mesquita B, Vermeulen R, May AM, Borch KB, Oyeyemi SO, Ardanaz E, Rodríguez-Barranco M, Dolores Chirlaque López M, Felez-Nobrega M, Sonestedt E, Ohlsson B, Hemmingsson O, Werner M, Perez-Cornago A, Ferrari P, Stepien M, Freisling H, Tsilidis KK, Ward H, Riboli E, Weiderpass E, Leitzmann MF. Association between physical activity and risk of hepatobiliary cancers: A multinational cohort study. *J Hepatol* 2019; **70**: 885-892 [PMID: 30582978 DOI: 10.1016/j.jhep.2018.12.014]

41 **Wannamethee G**, Shaper AG. Men who do not drink: a report from the British Regional Heart Study. *Int J Epidemiol* 1988; **17**: 307-316 [PMID: 3403125 DOI: 10.1093/ije/17.2.307]
42 **Stockwell T**, Zhao J, Greenfield T, Li J, Livingston M, Meng Y. Estimating under- and over-reporting of drinking in national surveys of alcohol consumption: identification of consistent biases across four English-speaking countries. *Addiction* 2016; **111**: 1203-1213 [PMID: 26948693 DOI: 10.1111/add.13373]
43 **Kim Y**, Choi YJ, Oh SW, Joh HK, Kwon H, Um YJ, Ahn SH, Kim HJ, Lee CM. Discrepancy between Self-Reported and Urine-Cotinine Verified Smoking Status among Korean Male Adults: Analysis of Health Check-Up Data from a Single Private Hospital. *Korean J Fam Med* 2016; **37**: 171-176 [PMID: 27274388 DOI: 10.4082/kjfm.2016.37.3.171]

World Journal of Gastroenterology

Submit a Manuscript: https://www.f6publishing.com

World J Gastroenterol 2023 June 28; 29(24): 3855-3870

DOI: 10.3748/wjg.v29.i24.3855

ISSN 1007-9327 (print) ISSN 2219-2840 (online)

ORIGINAL ARTICLE

Retrospective Study

Comparison and development of machine learning for thalidomide-induced peripheral neuropathy prediction of refractory Crohn's disease in Chinese population

Jing Mao, Kang Chao, Fu-Lin Jiang, Xiao-Ping Ye, Ting Yang, Pan Li, Xia Zhu, Pin-Jin Hu, Bai-Jun Zhou, Min Huang, Xiang Gao, Xue-Ding Wang

Specialty type: Gastroenterology and hepatology

Provenance and peer review: Unsolicited article; Externally peer reviewed.

Peer-review model: Single blind

Peer-review report's scientific quality classification

Grade A (Excellent): 0
Grade B (Very good): B, B
Grade C (Good): 0
Grade D (Fair): 0
Grade E (Poor): 0

P-Reviewer: Muneer A, Malaysia; Patel J, United States

Received: April 5, 2023
Peer-review started: April 5, 2023
First decision: April 21, 2023
Revised: May 7, 2023
Accepted: May 23, 2023
Article in press: May 23, 2023
Published online: June 28, 2023

Jing Mao, Fu-Lin Jiang, Ting Yang, Pan Li, Bai-Jun Zhou, Min Huang, Xue-Ding Wang, Institute of Clinical Pharmacology, School of Pharmaceutical Sciences, Sun Yat-sen University, Guangzhou 510006, Guangdong Province, China

Jing Mao, Ting Yang, Pan Li, Min Huang, Xue-Ding Wang, Guangdong Provincial Key Laboratory of New Drug Design and Evaluation, Sun Yat-sen University, Guangzhou 510006, Guangdong Province, China

Kang Chao, Xia Zhu, Pin-Jin Hu, Xiang Gao, Department of Gastroenterology, The Sixth Affiliated Hospital, Sun Yat-sen University, Guangzhou 510006, Guangdong Province, China

Xiao-Ping Ye, Department of Pharmacy, Guangdong Women and Children Hospital, Guangzhou 510000, Guangdong Province, China

Corresponding author: Xue-Ding Wang, PharmD, Professor, Teacher, Institute of Clinical Pharmacology, School of Pharmaceutical Sciences, Sun Yat-sen University, No. 132 Waihuan Dong Road, Guangzhou 510006, Guangdong Province, China. wangxd@mail.sysu.edu.cn

Abstract

BACKGROUND

Thalidomide is an effective treatment for refractory Crohn's disease (CD). However, thalidomide-induced peripheral neuropathy (TiPN), which has a large individual variation, is a major cause of treatment failure. TiPN is rarely predictable and recognized, especially in CD. It is necessary to develop a risk model to predict TiPN occurrence.

AIM

To develop and compare a predictive model of TiPN using machine learning based on comprehensive clinical and genetic variables.

METHODS

A retrospective cohort of 164 CD patients from January 2016 to June 2022 was used to establish the model. The National Cancer Institute Common Toxicity Criteria Sensory Scale (version 4.0) was used to assess TiPN. With 18 clinical features and 150 genetic variables, five predictive models were established and

evaluated by the confusion matrix receiver operating characteristic curve (AUROC), area under the precision-recall curve (AUPRC), specificity, sensitivity (recall rate), precision, accuracy, and F1 score.

RESULTS

The top-ranking five risk variables associated with TiPN were interleukin-12 rs1353248 [P = 0.0004, odds ratio (OR): 8.983, 95% confidence interval (CI): 2.497-30.90], dose (mg/d, P = 0.002), brain-derived neurotrophic factor (BDNF) rs2030324 (P = 0.001, OR: 3.164, 95%CI: 1.561-6.434), BDNF rs6265 (P = 0.001, OR: 3.150, 95%CI: 1.546-6.073) and BDNF rs11030104 (P = 0.001, OR: 3.091, 95%CI: 1.525-5.960). In the training set, gradient boosting decision tree (GBDT), extremely random trees (ET), random forest, logistic regression and extreme gradient boosting (XGBoost) obtained AUROC values > 0.90 and AUPRC > 0.87. Among these models, XGBoost and GBDT obtained the first two highest AUROC (0.90 and 1), AUPRC (0.98 and 1), accuracy (0.96 and 0.98), precision (0.90 and 0.95), F1 score (0.95 and 0.98), specificity (0.94 and 0.97), and sensitivity (1). In the validation set, XGBoost algorithm exhibited the best predictive performance with the highest specificity (0.857), accuracy (0.818), AUPRC (0.86) and AUROC (0.89). ET and GBDT obtained the highest sensitivity (1) and F1 score (0.8). Overall, compared with other state-of-the-art classifiers such as ET, GBDT and RF, XGBoost algorithm not only showed a more stable performance, but also yielded higher ROC-AUC and PRC-AUC scores, demonstrating its high accuracy in prediction of TiPN occurrence.

CONCLUSION

The powerful XGBoost algorithm accurately predicts TiPN using 18 clinical features and 14 genetic variables. With the ability to identify high-risk patients using single nucleotide polymorphisms, it offers a feasible option for improving thalidomide efficacy in CD patients.

Key Words: Thalidomide-induced peripheral neuropathy; Refractory Crohn's disease; Neurotoxicity prediction models; Machine learning; Gene polymorphisms

©The Author(s) 2023. Published by Baishideng Publishing Group Inc. All rights reserved.

Core Tip: Thalidomide-induced peripheral neuropathy (TiPN) is a life-threatening condition in Crohn's disease and has a high incidence in Asia. However, there are no effective medical interventions for TiPN. Here, we established a predictive model using machine learning and identified genes closely related to TiPN occurrence. We have found that extreme gradient boosting algorithm can sensitively identify patients who are prone to TiPN, which is useful for doctors to adjust the thalidomide therapy.

Citation: Mao J, Chao K, Jiang FL, Ye XP, Yang T, Li P, Zhu X, Hu PJ, Zhou BJ, Huang M, Gao X, Wang XD. Comparison and development of machine learning for thalidomide-induced peripheral neuropathy prediction of refractory Crohn's disease in Chinese population. *World J Gastroenterol* 2023; 29(24): 3855-3870
URL: https://www.wjgnet.com/1007-9327/full/v29/i24/3855.htm
DOI: https://dx.doi.org/10.3748/wjg.v29.i24.3855

INTRODUCTION

Thalidomide is widely used in refractory Crohn's disease (CD) patients, with a remission rate of 40%-70%[1,2]. However, the clinical application of thalidomide is limited by its side effects, especially peripheral neuropathy. A large individual difference (20%-75%) was found in the incidence of peripheral nerve lesions[3]. If neurotoxicity occurs during the treatment, reduction or cessation is needed to avoid further neurotoxicity. This may lead to treatment failure[4]. The nerve lesions after withdrawal may worsen for several months, recovery can be slow and incomplete, and the resulting neurotoxicity profoundly affects quality of life[5]. Hence, developing a predictive model for thalidomide-induced peripheral neuropathy (TiPN) and identifying related factors that can accurately predict peripheral neuropathy are important.

Thalidomide is a small molecule with immunomodulatory activity[4]. Numerous clinical studies have confirmed that thalidomide is effective for treatment of CD, especially in patients with hormone intolerance, lack of efficacy of azathioprine/6-mercaptopurine, and biological treatment failure[6,7], It brings hope to patients with refractory CD, which can reduce economic and healthcare costs because of its low price from the perspective of pharmacoeconomics. A retrospective multicenter observational

study showed that the proportion of adults with refractory CD from whom thalidomide was withdrawn because of toxicity alone was up to 46% at 2 years[7], which affected maintenance of remission in nearly half of patients treated with thalidomide. TiPN may appear primarily as sensory peripheral nerve lesions and may differ in symptoms, including paralysis, sensory disturbance, sensory abnormalities, hyperalgesia and severe pain[8]. The empiric identification of agents and interventions to mitigate TiPN has been disappointing, and presently there is no intervention available for prevention except dose management. Although electrophysiological monitoring has been used in patients prescribed thalidomide, it provides no clear benefit for the occurrence of neuropathy compared to clinical assessment[3,9].

Few researchers have studied risk factors related to TiPN[10,11], and most studies have been conducted in chemotherapy patients. Szudy-Szczyrek *et al*[12] used serum brain-derived neurotrophic factor (BDNF) concentration as an indicator of polyneuropathy, which did not accurately reflect nerve damage and the results could not be generalized due to small number of patients. Only a limited number of molecular genetic studies in TiPN have been conducted, but none has discussed the association between genetic factors and TiPN in patients with CD. TiPN is thought to be a dose-limiting toxicity[13], and the therapeutic dose of thalidomide between chemotherapy and CD patients can differ by up to 10 times[14]. Thus, the existing findings are probably not fully representative of patients with CD.

The neurotoxic mechanism of thalidomide is still unclear[15]. Some hypotheses and treatment directions for TiPN have appeared. Thalidomide exhibits an antiangiogenic effect, which is considered to cause secondary ischemia and hypoxia of nerve fibers, which may lead to ischemia-related neuropathy. Vascular endothelial growth factor gene therapy in animals with TiPN led to obvious improvement in vascular recovery[16,17]. In addition, neuronal susceptibility can be increased by the dysregulation of neurotrophic factors through immunomodulatory mechanisms[18]. Tonello *et al*[19] analyzed dorsal root ganglion tissues from their animal experiments. Matrix metalloproteinase (MMP)9 monoclonal antibody significantly decreased oxidative stress and affected the expression of neuroinflammatory mediators, suggesting that MMP9 acts on peripheral nerve lesions. Thalidomide metabolites are considered to cause neuronal damage through reactive oxidative species causing damage to DNA[20]. BDNF is the only neurotrophic factor expressed during most peripheral damaged sensory neurons. It has been proven to be an effective regulator of regeneration-related gene expression in the peripheral and central nervous systems[21,22]. Additionally, Navia-Pelaez *et al*[23] observed the induction of mouse neuralgia by ATP binding cassette transporter (ABC)A1/ATP binding cassette transporter (ABC)G1 knockdown, which prevented apolipoprotein A-I binding protein from reversing peripheral neuropathy allodynia[23]. Johnson *et al*[9] reported that gene polymorphisms of ABCA1 had a significant association with thalidomide-related neuropathy[9]. Interleukin (IL)-12 was upregulated in MPTP-intoxicated mice[24]. In the patients who received CTL019, IL-2 level in those with neurotoxicity was higher than in those without neurotoxicity[25]. Zhang *et al*[26] supported IL-12 cytokine profiles as indicators of neurotoxicity[26]. Few studies have demonstrated a relationship between cumulative dose and TiPN[27,28]. The gene polymorphisms of transcriptional regulators, inflammatory cytokines and transporters may have an important impact on individual differences in TiPN. These genetic factors may adequately explain the neurotoxicity with clinical variables.

Therefore, an accurate model for identifying TiPN with comprehensive clinical and genetic variables is required in patients with CD. In recent years, powerful data mining and computing have encouraged a growing use of machine learning in the medical field, including diagnosis, treatment, prognostic data classification, and regression[29-31]. Tao *et al*[32] generated a predictive model for clinical response in patients with rheumatoid arthritis using a multiomics approach and machine learning, with a predictive accuracy > 85%[32]. Mo *et al*[33] developed a Tacrolimus nephrotoxicity predictive model in nephrotic syndrome using machine learning algorithms with clinical and genetic variables, and 78% were accurately identified[33]. To date, there is no predictive model for CD patients generated by machine learning.

The aim of this study was to develop a sensitive and accurate TiPN predictive model based on clinical and genetic variables, which is beneficial for the treatment of thalidomide.

MATERIALS AND METHODS

Study population

A total of 164 CD patients diagnosed according to the criteria of Lennard-Jones were randomly recruited from the Sixth Affiliated Hospital of Sun Yat-sen University from January 2016 to June 2022. The patients treated with thalidomide at any course of their disease were considered eligible for the study. The inclusion criteria were: (1) Diagnosis of CD; (2) CD activity index > 150 points, with endoscopically active lesions; and (3) refractory or intolerant to immunosuppressive drugs or biological agents which are used in current treatment. The exclusion criteria were: (1) fiber stenosis caused by gastrointestinal obstruction symptoms; (2) fistula, excluding anal fistula; (3) pregnancy or lactation; (4) fertility program during the study; (5) less than eight weeks of biologic treatment after last IFX; (6) central or peripheral

nervous disease; (7) abnormal liver and renal function; (8) heart dysfunction; (9) malignant tumor; and (10) active tuberculosis.

Ethical approval was obtained by the Ethics Committee of the Sixth Affiliated Hospital of Sun Yat-Sen University, Guangzhou, China. This study was registered at the Clinical Trial Registry (Registration Number: NCT02956538). Written informed consent was obtained from all participants. Blood samples were collected from all recruited patients.

Assessment of neurotoxicity

For the neurophysiological assessment, the same methods were used throughout the whole process of observation to minimize any potential bias. For the clinical assessment, the National Cancer Institute Common Toxicity Criteria Sensory Scale (version 4.0, 2009) was used. Details of thalidomide administered to each patient were acquired directly from the medical records of the patients. Meanwhile, patients without blood samples or intact clinical data were excluded.

Clinical variables

In order to adjust the influence of clinical variables on TiPN, 18 types of baseline clinical variables were collected, including demographic data (weight, age, *etc.*), inflammatory indexes (C-reactive protein, erythrocyte sedimentation rate, *etc.*), hepatic function (alanine aminotransferase, aspartate aminotransferase, *etc.*), and routine blood examination. Supplementary Table 1 shows the full names and local abbreviations of clinical characteristics.

Single nucleotide polymorphism selection and genotyping

We performed comprehensive detection of genetic variables (single nucleotide polymorphisms; SNPs), including genes related to thalidomide pharmacokinetic/pharmacodynamic pathways, metabolic enzymes, transcriptional regulators, nerve growth factors, inflammatory cytokines, *etc.* Details of the selection steps of these genes (SNPs) were as follows. (1) The physical position of these genes was obtained through the human Ensembl GRCh37 database (http://asia.ensembl.org/Homo_sapiens/Info/Index). In the VCF to PED Converter window (http://grch37.ensembl.org/Homo_sapiens/Tools/VcftoPed), positions of genes were entered, the Chinese Han population in Beijing was selected, and then, PED and info file for the SNPs of these genes were download; and (2) Haploview software for entry criterion was set (minor allele frequency > 5%, $r^2 < 0.8$, min genotype > 75%, and Hardy–Weinberg equilibrium > 0.05) to obtain the tag-SNP. Ultimately, 150 genetic variables met the above standards. DNA analysis was performed by collecting 5-mL peripheral blood samples. DNA extraction from whole blood was performed using Genomic Blood DNA Extraction Kit (DP304, Tiangen, Beijing, China). Nanodrop 2000C (Thermo Scientific, Fitchburg, WI, United States) was used for the detection of DNA concentration.

The published polymerase chain reaction-restriction fragment length polymorphism method was used for the detection of all SNPs[34,35], and 150 SNPs were detected by Agena Bioscience MassARRAY (Agena Bioscience, San Diego, CA, United States).

Machine learning

Single-sample Kolmogorov-Smirnov tests were carried out to test the distribution of continuous variables. Data were shown as median (range) or mean ± SD, according to the data type.

Based on clinical and genetic variables, a predictive model for TiPN in CD patients was developed using a series of machine learning methods. We implement machine learning as a three-step process, data preprocessing, feature selection, and model generation and verification. To evaluate the performance of the model generation, a fivefold cross-verification was performed. The evaluation indicators used included confusion matrix, receiver operating characteristic (ROC) curve, precision recall (PR) curve, specificity, sensitivity, precision, accuracy and F1 core. Figure 1 shows the workflow for machine learning.

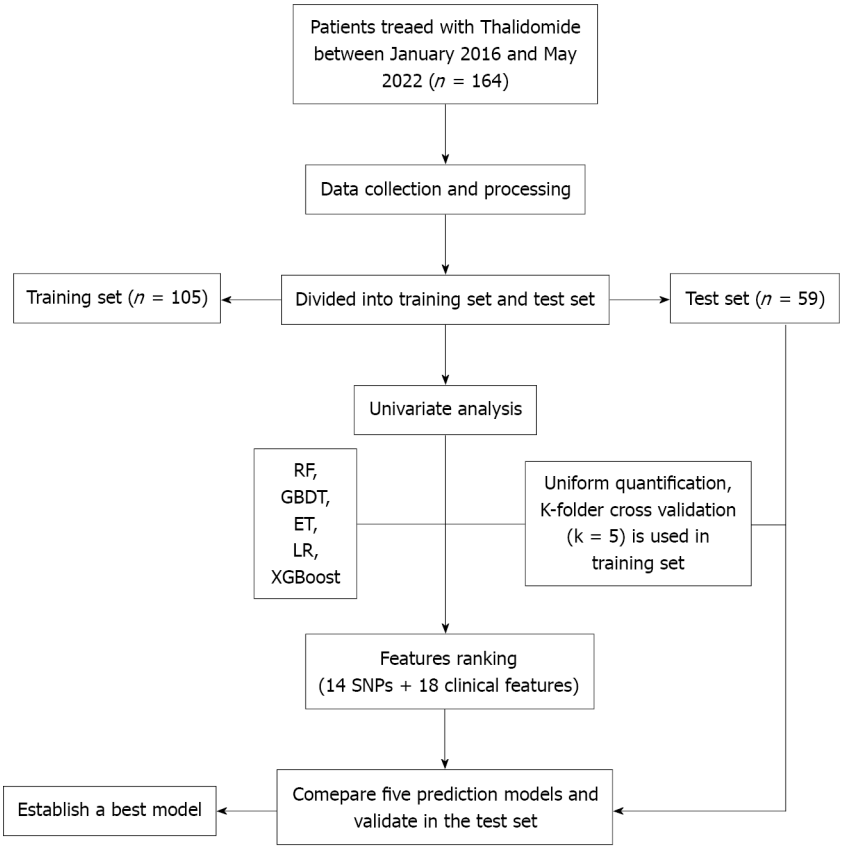
The *t*-test and nonparametric Mann–Whitney *U* test were used to analyze continuous variables while categorical variables were analyzed by χ^2 test. Machine learning techniques were performed in Python 3.7.13. GraphPad Prism version 8 (GraphPad, San Diego, CA, United States) was used for graphic analysis. $P < 0.05$ was considered to be a statistically significant difference.

Data preprocessing

Features with missing rates > 30% were removed after the collection of variables was finished. The missing value of a continuous variable was filled with an average value, and the classification variable was processed by removing the missing value. The continuous variables were uniform quantized by minimum-maximum normalization, and the categorical variables were represented using dummy variables. The range of each clinical data set is shown in Supplementary Table 1.

Feature selection

Univariate analysis was used to evaluate the relationship between each variable and TiPN. SNPs with weak effects ($P > 0.1$) were eliminated. In order to reduce the model complexity, clinical variables were



DOI: 10.3748/wjg.v29.i24.3855 **Copyright** ©The Author(s) 2023.

Figure 1 Flow chart display. Flow chart showing the process of model generation validation of the model. RF: Random forest; GBDT: Gradient boosting decision tree; ET: Extremely randomized trees; LR: Logistic regression; XGBoost: Extreme gradient boosting.

uniformly quantified into 11 categorical variables [0, 0.1, 0.2, ..., 1], since the dataset included both categorical variables (*e.g.* gender, polymorphisms and outcomes) and continuous variables (*e.g.* drug dose, age and clinical tests). To improve robustness and accuracy of the prediction of our approach, the dataset was reiterated 1000 times, resulting in different test sets, which were used to select model hyperparameters. Five models were established to predict TiPN development, named extreme gradient boosting (XGBoost), gradient boosting decision tree (GBDT), extremely random tree (ET), random forest (RF) and logistic regression (LR) model. The paramount variables of all these models are ranked by information gain[36].

Model development and validation

One hundred and sixty-four patients were randomly divided into training (80%) and testing (20%) data sets[37,38]. The Synthetic Minority Oversampling Technique (SMOTE) algorithm was combined in the training set and the test set to deal with the data imbalance. The five predictive models were trained using k folder cross-validation (k = 5). Through implementation and comparison, we avoided merging plans and improved the generalization performance of these models.

XGBoost, ET, GBDT, RF and LR algorithms were used to analyze the feature set and to generate neurotoxicity prediction models. To guarantee the robust stability of these computational models, the dataset was randomly divided 1000 times to obtain different training sets to test the hyperparameter for each group. Taking XGBoost as an example, the main hyperparameter included learning rate, maximum depth, estimators, and eta. The performance of the tested classification algorithm was evaluated and compared based on the area under the ROC curve, area under the PR curve, specificity, sensitivity (recall), precision, accuracy, and F1 score.

Bioinformatics analysis

The effects of expression quantitative trait loci (eQTLs) on the top-four gene expressions were examined with the Genotype-Tissue Expression (GTEx) database. https://www.gtexportal.org/home/.

RESULTS

Patient characteristics

A total of 164 patients with CD were collected in this study, including 119 men and 45 women. The average age of the patients was 34.3 ± 12.7 years. Median dose of thalidomide was 1.5 mg/kg/d (range 0.3-2.9). TiPN was observed in 59 patients (36%) during follow-up. Median duration of thalidomide treatment was 17.2 mo (range 1-60). We collected 18 baseline variables and 150 genetic variables (Supplementary Table 2) of the patients. Table 1 shows the baseline characteristics of the patients. The genotype coincided with Hardy Weinberg equilibrium.

Feature selection

In the univariate analysis, variables that had a significant impact on TiPN included *IL-12* rs1353248 (P = 0.0004), *BDNF* rs2030324 (P = 0.001), *BDNF* rs6265 (P = 0.001), and dose (P = 0.002), *ABCA1* rs10991419 (P = 0.002). After removing genetic variables with low correlation (P > 0.1), 14 SNPs and 18 clinical variables were included in the following analysis (Table 2 and Supplementary Table 1).

Identification of appropriate biomarkers that distinguished the neurotoxic symptom group from the well-tolerated group was deemed important, which helped in exploring disease biomarkers and understanding pathogenesis. After the data transformation, models were generated using ET, GBDT, RF, XGBoost and LR, and the feature importance scores were used to rank all the features. The higher the information gain value, the more significant the variable became (Figure 2). By ranking each feature, the top five ranked features were *IL-12* rs1353248, dose (mg/d), *BDNF* rs6265, *BDNF* rs2030324 and *BDNF* rs11030104. *IL-12* rs1353248 was found to have the highest predictive variable importance for TiPN, followed by thalidomide daily dose, rs6265, rs2030324 and rs11030104. Figure 3 shows the four genetic variables and the occurrence of TiPN. Patients with *BDNF* rs2030324_AG, *BDNF* rs6265_CT, *BDNF* rs11030104_AG, and *IL-12* rs1353248_TT genotypes were more likely to have TiPN; patients with BDNF rs2030324_AG genotype had more neurotoxicity than patients with AA+GG; CT genotype carriers of *BDNF* rs6265 had higher neurotoxicity than CC+TT carriers; neurotoxicity in carriers of *BDNF* rs11030104_AG was more than in patients with AA+GG genotype; and patients with *IL-12* rs1353248_TT genotype had more neurotoxicity than those who carried CT+CC. Additionally, we noticed that there were three SNPs derived from the same gene, which suggested that BDNF played a significant role in neurotoxicity.

Functional consequences of the top four SNPs

The GTEx eQTL database was used to examine the functional consequences of the top four SNPs. The results suggested that four variants, rs1353248 (chr3_159905770, $P = 8.52 \times 10^{-4}$), rs6265 (chr11_27658369, $P = 1.07 \times 10^{-4}$), rs2030324 (chr11_27705368, $P = 9.2 \times 10^{-11}$), rs11030104 (chr11_27662970, $P = 2.76 \times 10^{-5}$) could affect IL-12 and BDNF gene expression on human nerve tibial tissue (Figure 4). The expression levels of the BDNF gene were reduced in rs6265CT and rs11030104AG, with a significant reduction in the rs6265CT genotype. Additionally, the expression levels of the *IL-12* gene were significantly decreased in the rs1353248TT. The results showed a similar trend, indicating that these four loci may play an important biological role in peripheral neurotoxicity and have potential for the prediction of TiPN (Figure 3). Further investigation into their biological functions is warranted.

Comparison of five algorithms in the training set

Using k-fold cross-validation (k = 5) in the training set, we identified all possible parameter combinations identified by random grid search. The evaluation indicators used included confusion matrix, ROC curve, PR curve, specificity, sensitivity, precision, accuracy and F1 core. The average ROC curve, PR curve and 95% confidence interval (CI) are shown in Figure 5. Here, the ROC curves of four models were > 0.90, the PR curve of the LR model was 0.874, and the remainder were > 0.97. In addition, these models exhibited different performances (Table 3). The ET model obtained the highest ROC curve (0.999) but had the lowest specificity rate of 0.471. The RF model obtained a high ROC curve (0.996) and a common precision (0.769) compared with XGBoost and GBDT. The results indicated that XGBoost and GBDT had superior performance, and the precision, specificity, accuracy and F1 scores were above 0.90, 0.82, 0.88 and 0.87, respectively.

To evaluate the importance of genetic variables or clinical features in five models, we used 14 SNPs, 18 clinical features, and three top five ranked features included in five models of the other three round workouts with similar analytic approach. The results indicated that by including 18 clinical features, ROC curves were 0.759–0.999, and PRC curves were 0.602–0.998 (Supplementary Figure 1). The ET model showed the best sensitivity (1.0) but had the lowest precision (0.431) and specificity rate (0.262). The precision, specificity, accuracy, and F1 were low for LR and RF models (Supplementary Table 3). Additionally, with only input of the 14 SNPs, the models achieved better performance than the clinical features. The ROC curve and PR curve of XGBoost, ET, GBDT, and RF models were > 0.90 (Supplementary Figure 2); the precision, sensitivity, specificity, accuracy and F1 score of XGBoost and GBDT were > 0.90 (Supplementary Table 4). These results indicated that genetic variables were more important in predicting TiPN than clinical features.

Table 1 Patients characteristics

Characteristics	Values (*n* = 164)
Male/Female	119/45
Age (yr)	34.3 ± 12.7
Thalidomide dosage mg/kg/d	1.5 (0.3-2.9)
White blood cell (10^9/L)	6.2 ± 2.7
Peripheral neuropathy	59 (36%)
Duration of thalidomide treatment (m)	17.2 (1-60)

Data are presented as median with range, mean ± SD or amount.

Table 2 Univariate analyses of factors associated with thalidomide-induced peripheral neuropathy

SNP	Gene	Minor allele	Main allele	OR	95%CI	*P* value
rs1353248	*IL-12*	T	C	8.983	2.497-30.90	0.0004
rs6265	*BDNF*	T	C	3.150	1.546-6.073	0.001
rs2030324	*BDNF*	G	A	3.164	1.561-6.434	0.001
rs11030104	*BDNF*	G	A	3.091	1.525-5.960	0.001
rs10991419	*ABCA1*	T	C	3.833	1.521-8.926	0.002
rs7795841	*ABCB1*	G	T	4.333	1.371-13.39	0.014
rs2575876	*ABCA1*	A	G	2.559	1.306-5.209	0.007
rs3918249	*MMP9*	T	C	3.800	1.208-10.50	0.016
rs7795846	*ABCB1*	A	G	3.690	1.155-10.25	0.020
rs62447181	*IKZF1*	A	G	2.933	0.763-9.514	0.096
rs11030100	*BDNF*	G	T	2.205	1.074-4.430	0.030
rs2777795	*ABCA1*	A	G	1.830	0.793-4.114	0.09
rs12718731	*IKZF1*	G	A	2.471	0.686-8.328	0.1
rs34165419	*ABCA1*	T	C	2.564	0.664-10.41	0.1

CI: Confidence interval; OR: Odds ratio; TiPN: Thalidomide-induced peripheral neuropathy; BDNF: Brain-derived neurotrophic factor; IL: Interleukin; SNP: Single nucleotide polymorphisms.

Table 3 Performance of the models for training set (all features)

Model	Precision	Sensitivity	Specificity	Accuracy	AUROC	F1 score
XGBoost	0.904	1	0.94	0.962	0.988	0.949
ET	0.526	1	0.471	0.667	0.999	0.69
GBDT	0.952	1	0.971	0.981	1	0.976
LR	0.613	0.95	0.647	0.759	0.907	0.745
RF	0.769	1	0.824	0.889	0.996	0.87

AUROC: Area under the receiver operating characteristic; XGBoost: Extreme gradient boosting; ET: Extremely random trees; GBDT: Gradient boosting decision tree; LR: Logistic regression; RF: Random forest.

When including the top five ranked features, the ROC curve for the four models was > 0.82, The LR model only achieved a low value (0.72). The PRC curve of the LR model was 0.578, and the remainders were > 0.72. The XGBoost showed the highest PR curve (0.803, 95%CI: 0.697–0.871) and accuracy (0.718).

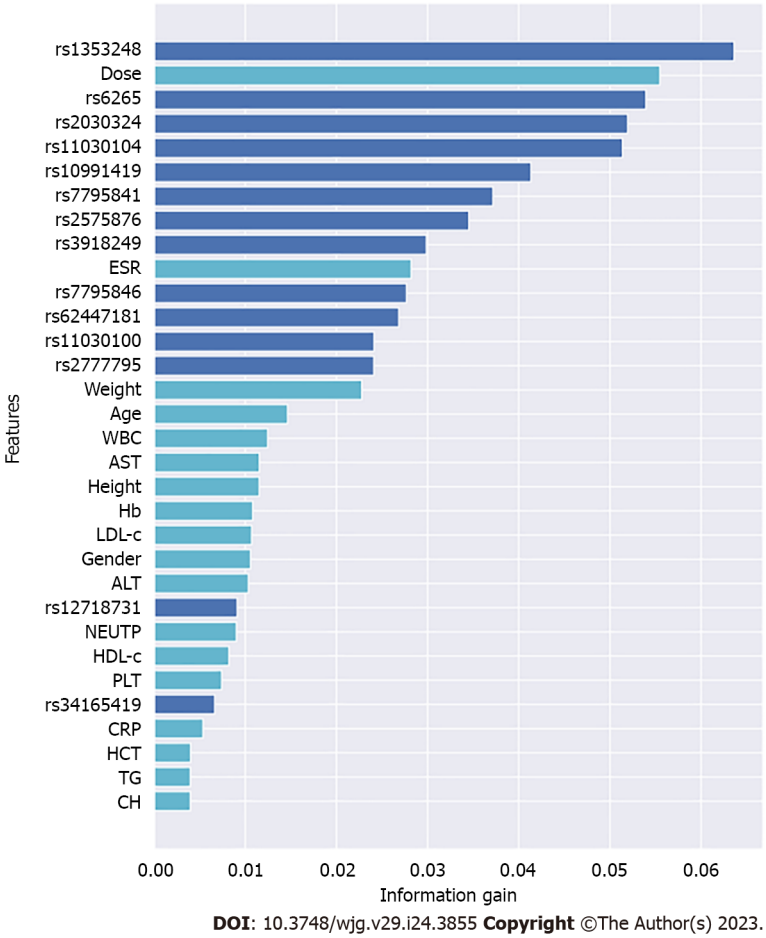


Figure 2 Information gain values of the features. The higher the information gain value, the more important the variable. Therefore, these five variables (rs1353248, dose, rs6265, rs2030324, rs11030104) are the optimal feature set.

The GBDT obtained the highest ROC curve (0.88, 95%CI: 0.804-0.956). However, F1 score was < 0.70 for all models (Supplementary Figure 3 and Supplementary Table 5). The findings indicated that integration with genetic features and clinical data may be refining the performance of prediction models.

Validation of the five algorithms in the test set

Five algorithms in the test set were verified based on training results. The performance of five prediction models based on the 18 clinical features and 14 SNPs were: Precision 0.625-0.8, sensitivity 0.667-1.0, specificity 0.667-0.889, accuracy 0.733-0.818, and F1 score 0.714-0.8 (Table 4). The average area of the ROC and PR curves was 0.741-0.907 and 0.718-0.864, respectively (Figure 6). The models generated by the XGBoost algorithm had the best overall predictive power and the highest specificity (0.857), accuracy (0.818) and PR curve (0.864, 95%CI: 0.828-1.011); the ROC curve was (0.889, 95%CI: 0.757-1.021), and the remaining values for precision, sensitivity and F1 score were > 0.75. The RF acquired the highest ROC curve (0.907, 95%CI: 0.731-1.084), and the ET and GBDT achieved the best F1 score, but all three had the lowest specificity (0.667).

We validated only 14 genetic variables, 18 clinical variables and the top five ranked features in five models. All these models behaved poorly with the 18 clinical features (Supplementary Table 6), while the sensitivity score was > 0.83 for four models (XGBoost, ET, GBDT and RF). The performance of the overall value of the ROC curve (0.528-0.718) was higher than the PR curve (0.359-0.556) (Supplementary Figure 4).

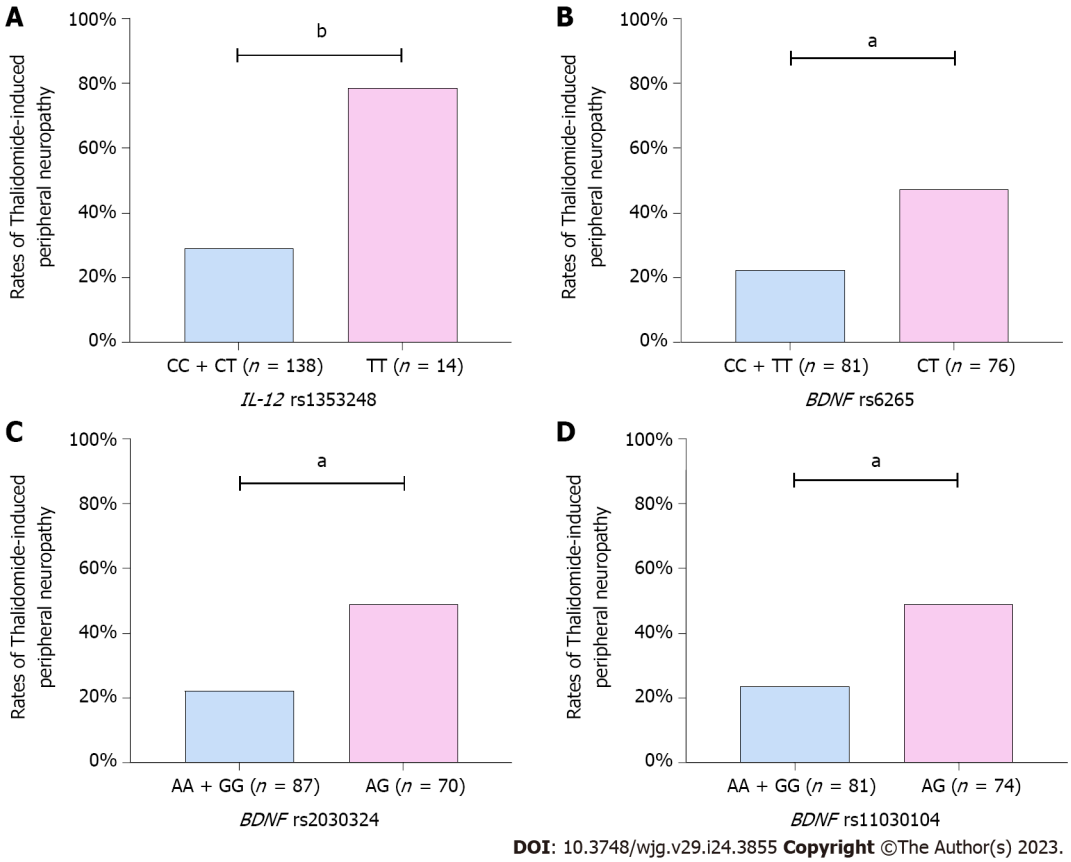
When only 14 SNPs were considered, the ROC curve of XGBoost and RF were up to 0.802 and 0.907; the PRC curve was > 0.70 for the four models (XGBoost, ET, GBDT and RF) (Supplementary Figure 5), with accuracy, precision, sensitivity, specificity and F1 score above 0.73, 0.66, 0.66, 0.77 and 0.66, respectively (Supplementary Table 7). The LR had the lowest ROC curve (0.722) and PR curve (0.601).

Considering only the top five ranked features, the ROC and PR curves were > 0.79 and > 0.73 for all these models, respectively (Supplementary Figure 6). XGBoost had the best overall predictive power and highest specificity (0.857), sensitivity (0.833), accuracy (0.848) and F1 score (0.8). The LR had the lowest accuracy (0.552), specificity (0.316) and precision (0.435) (Supplementary Table 8).

Table 4 Performance of the models for testing set (all features)

Model	Precision	Sensitivity	Specificity	Accuracy	AUROC	F1 score
XGBoost	0.75	0.75	0.857	0.818	0.889	0.75
ET	0.667	1	0.667	0.8	0.833	0.8
GBDT	0.667	1	0.667	0.8	0.87	0.8
LR	0.8	0.667	0.889	0.8	0.741	0.727
RF	0.625	0.833	0.667	0.733	0.907	0.714

AUROC: Area under the receiver operating characteristic; XGBoost: Extreme gradient boosting; ET: Extremely random trees; GBDT: Gradient boosting decision tree; LR: Logistic regression; RF: Random forest.



DOI: 10.3748/wjg.v29.i24.3855 **Copyright** ©The Author(s) 2023.

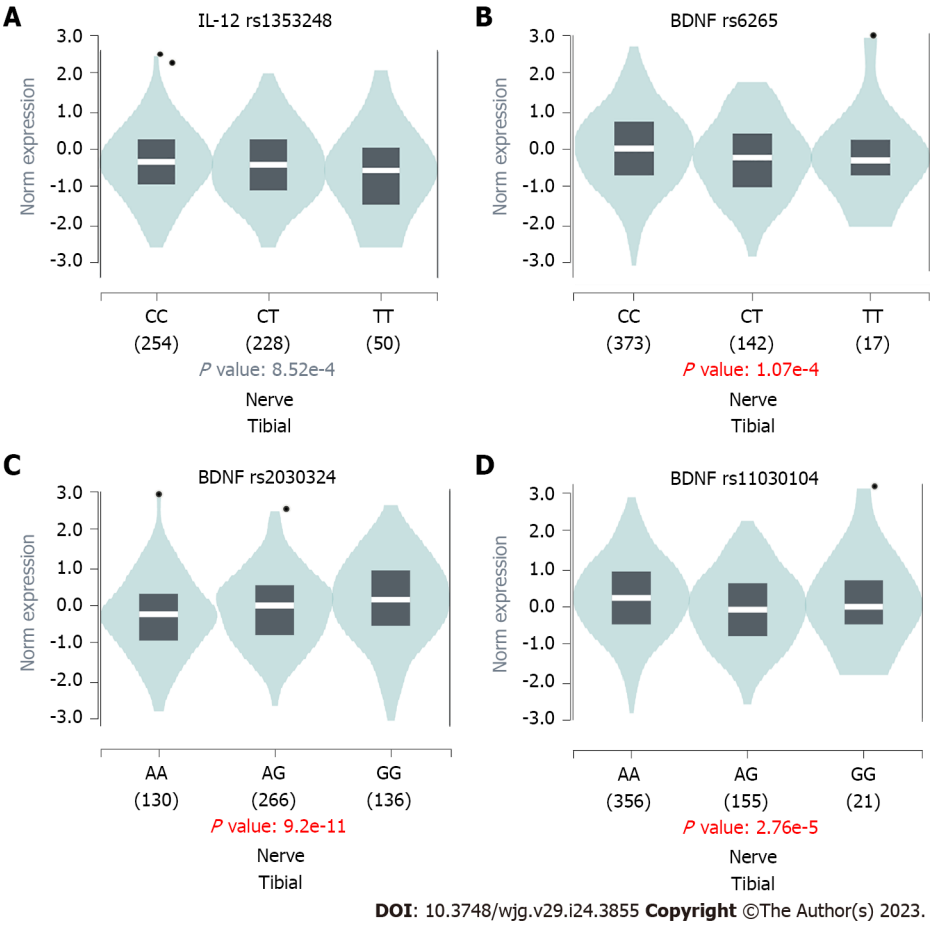
Figure 3 The correlation between the optimal variables and thalidomide-induced peripheral neuropathy. Illustrate patients with interleukin-12 rs1353248_TT, brain-derived neurotrophic factor (BDNF) rs2030324_AG, BDNF rs6265_CT, and BDNF rs11030104_AG, genotypes are more likely to have thalidomide-induced peripheral neuropathy than non-carriers. A: IL-12; B-D: BDNF. [a]$P < 0.01$, [b]$P < 0.001$. BDNF: Brain-derived neurotrophic factor; IL: Interleukin.

DISCUSSION

Thalidomide leads to well-documented adverse effects in some patients, and drug discontinuation derived from neurotoxicity alone was up to 46%[2,36]. However, it is still unclear to predict TiPN risk in Chinese people by combining genetic polymorphism and clinical factors.

So far, there have been few studies on the risk factors of TiPN in patients with CD. As far as we know, only Bramuzzo *et al*[28] developed a model to identify genetic variables using LR to predict the occurrence of TiPN in children. They found that polymorphisms in *ICAM1* and *SERPINB2* were protective factors. However, genetic tests were used only in a few patients and the survey variables were not sufficient. The LR method also reduced the predictive performance of the model[28].

In comparison with traditional statistical methods, based on the previous studies, machine learning can generate models of higher predicted performance by handling more complex data, which may achieve higher accuracy and improved generalization[37,38]. With the rapid increase in artificial intelligence, machine learning methods are widely applied in the field of disease diagnosis and



DOI: 10.3748/wjg.v29.i24.3855 **Copyright** ©The Author(s) 2023.

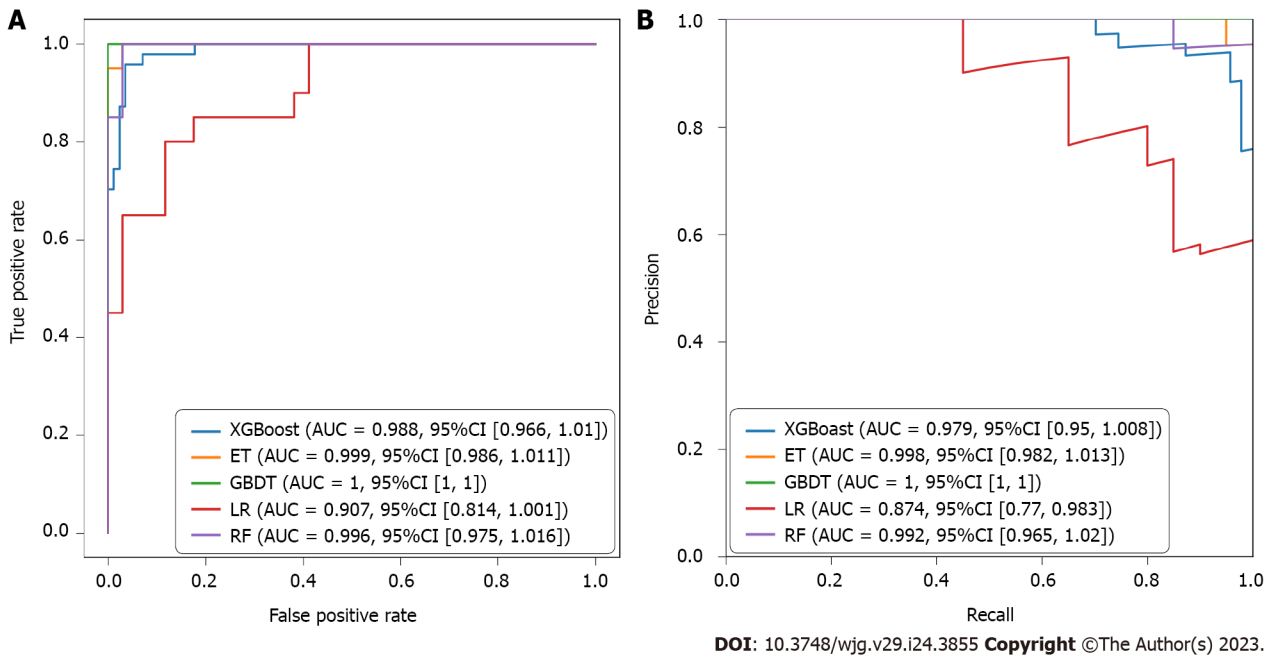
Figure 4 Examination of consequences between the top four single nucleotide polymorphisms and gene expression in nerve tibial tissue. Patients with interleukin (IL)-12 rs1353248_TT (chr3_159905770, $P = 8.52 \times 10^{-4}$), brain-derived neurotrophic factor (BDNF) rs6265_CT (chr11_27658369, $P = 1.07 \times 10^{-4}$) BDNF rs2030324_AG (chr11_27705368, $P = 9.2 \times 10^{-11}$), and BDNF rs11030104_AG (chr11_27662970, $P = 2.76 \times 10^{-5}$). A: IL-12; B-D: BDNF. The expression levels of the BDNF gene were reduced in rs6265CT and rs11030104AG. Additionally, the expression levels of the IL-12 gene were significantly decreased in the rs1353248TT. BDNF: Brain-derived neurotrophic factor; IL: Interleukin.

prediction[39-41]. Not only this, the method based on machine learning no longer requires strong assumptions about basic mechanisms such as image classification[40] and speech recognition[42], which have achieved cutting-edge predictive capabilities.

We developed a model for predicting TiPN in Chinese people using machine learning (XGBoost, ET, GBDT, RF and LR) based on genetic and clinical variables for the first time. As a result of the comprehensive evaluation, the model generated by the XGBoost algorithm reached the optimum prediction ability, which could accurately distinguish 88.9% of patients (Table 4), this was consistent with the results of other relevant studies[43,44]. By ranking each feature, rs1353248, rs6265, rs2030324 and rs11030104, and drug dose had the top five effects on TiPN. We showed that machine learning methods were superior to traditional statistical methods, and compared with two recently published studies on other diseases[45,46], our XGBoost model yielded higher ROC-AUC and PRC-AUC scores. Furthermore, the significant aspect of the XGBoost model is that TiPN can be identified at a high probability early in the disease course and may significantly improve the treatment outcome.

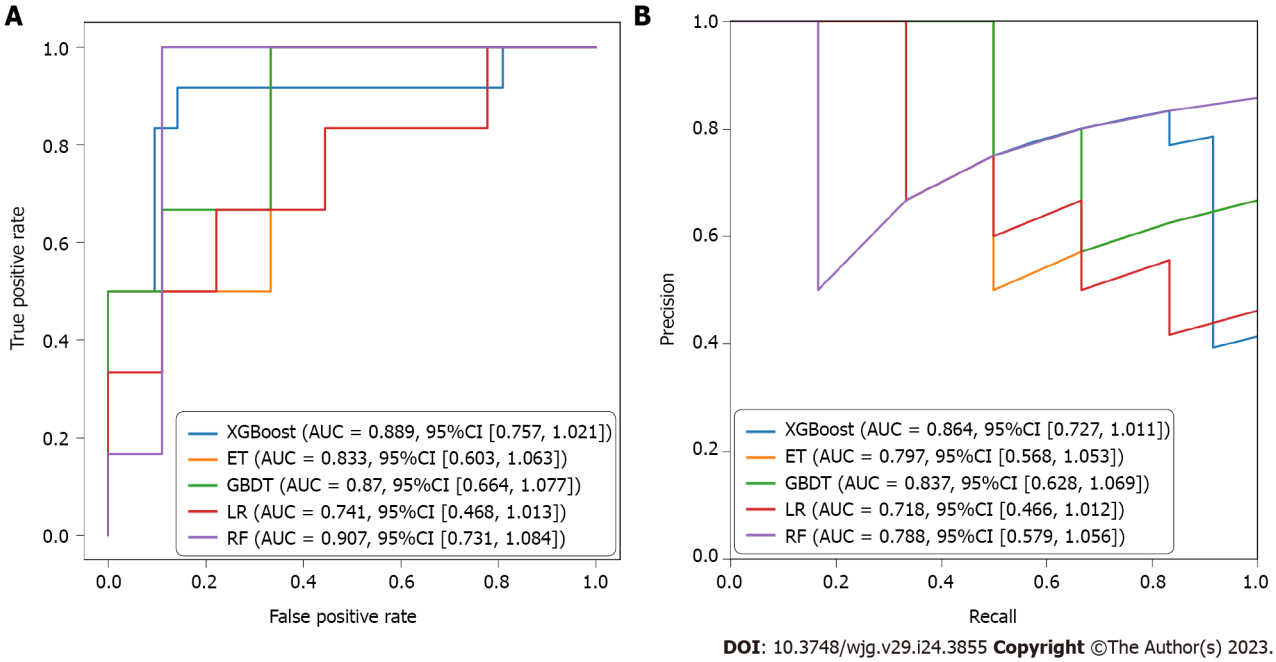
We applied an additional analysis by inputting SNPs, clinical variables, and the top five ranked features investigate whether there was any impact on model performance. As a result, all the models performed well when including SNPs and the top five features, near the level of all features combining 18 clinical variables and 14 SNPs in the models. Taken together with the ROC and PR curves, these results showed that genetic variables had a more important role than clinical variables in predicting TiPN occurrence, while in combination with clinical data, they markedly improved the model, suggesting that integration with genetic features and clinical data refined the predictive models.

Among the four SNPs, we focused mainly on *BDNF* and *IL-12* according to the ranked results. So far, the relationship between SNPs of the *IL-12* gene and the risk of TiPN has not been studied. To our knowledge, only one genome-wide association study has reported that *IL-12* rs1353248 had strong relevance to celiac disease[47]. In our study, *IL-12* rs1353248 had distinct relevance to TiPN, indicating a new and genetically relevant connection between genetic determinants of IL-12 and TiPN risk.



DOI: 10.3748/wjg.v29.i24.3855 **Copyright** ©The Author(s) 2023.

Figure 5 Evaluation of the predictive models. Average area under the receiver operating characteristic curve and precision recall curve of the five models in the training set. A: Receiver operating characteristic curve (training set); B: Precision-recall curve (training set). Average area and 95% confidence intervals of different predictive models are displayed in the box. XGBoost: Extreme gradient boosting; ET: Extremely random trees; GBDT: Gradient boosting decision tree; LR: Logistic regression; RF, random forest; CI: Confidence interval.



DOI: 10.3748/wjg.v29.i24.3855 **Copyright** ©The Author(s) 2023.

Figure 6 Validation of the training set. The picture shows average area under the receiver operating characteristic curve and precision recall curve of the five models in the test set. A: Receiver operating characteristic curve (testing set); B: Precision-recall curve (testing set). AUC: Area under the curve; CI: Confidence interval; XGBoost: Extreme gradient boosting; ET: Extremely random trees; GBDT: Gradient boosting decision tree; LR: Logistic regression; RF: Random forest; CI: Confidence interval.

BDNF plays a significant role in neuronal differentiation, survival, and synaptic plasticity. BDNF protein levels in fibromyalgia patients are significantly elevated. Similar to our research, Park *et al*[48] found that *BDNF* rs11030104_GG had a protective effect against fibromyalgia compared with *BDNF* rs11030104_AG in a multicenter prospective study of the Korean population[46]. In addition, *BDNF* rs6265 SNP has been widely studied for its role in the regulation of neuronal survival, differentiation, and plasticity[49-52]. Xie *et al*[53] revealed that rs2030324_CT and rs6265_AG were associated with

amnestic mild cognitive impairment[53]. The effects of *BDNF* rs6265 polymorphism have been widely studied in animal models. In adult male mice, the *BDNF* Val66Met polymorphism impaired sports training-induced synaptic plasticity and beneficial behavior[54]. We reported similar findings, with *BDNF* rs6265_CT and *BDNF* rs2030324_AG being risk factors for TiPN. We suggest that heterozygotes for this gene impair neuronal activity, which is potentially involved in the perception of neuropathy symptoms. It can be speculated that mutation of the T allele of rs6265, G allele of rs2030324 and rs11030104 has a major impact on the expression levels of this gene according to the GTEx databases, and the mechanism of action merits further, in-depth investigation. In the Israeli population with lymphoma and myeloma, the severity and persistence of chemotherapy-induced peripheral neuropathy were markedly higher in the carriers of the Val/Val genotype than in patients with the Val/Met and Met/Met genotypes[50], which is different from our results. This difference may be due to the fact that the two research results are inherently different and difficult to compare directly. However, it suggests that the risk of neurotoxicity differs in different human populations according to the National Center for Biotechnology Information (NCBI, https://www.ncbi.nlm.nih.gov/) and China Metabolic Analytics Project (http://www.mbiobank.com/). It is noteworthy that the mutation rate of rs6265 and rs11030104 in Asian populations is as high as 49%, while in European and American populations, the mutation rate of these loci does not exceed 22%. This indicates that a higher number of individuals in Asian populations may be susceptible to TiPN, and these two loci are of predictive significance in Asian populations.

In addition to SNP-based correlation analysis, we considered 18 clinical features that may be related to the development of TiPN. In the training set, five models (LR, RF, ET, GBDT and XGBoost) were constructed to predict the TiPN risk including 14 SNPs and 18 clinical features. Considered collectively, the XGBoost model obtained the optimum performance in all functional training and test sets. As a result of predicting the characteristic importance using the XGBoost model, the dose was found to be the second most important factor. This finding was in line with previous reports[13,55]. In addition, the prospective study on 135 patients with skin disease showed that the incidence rate of TiPN was 11% (4/35) with a dose of 25-50 mg/d, 29% (11/38) with 50-75 mg/d, and 48% (19/40) with 75-100 mg/d. The incidence of neurotoxicity was three times higher in patients taking higher doses than in those taking lower doses. Similar trends were found in this study, the incidence rate of TiPN was 18% (9/49) with 25-50 mg/d, 33% (14/43) with 50-75 mg/d, and 49% with > 75 mg/d.

There were some limitations to our study. First, the sample size was small because it was a single-center trial. To improve the generalization and robustness of our predictive model, we reiterated this random procedure 1000 times. Second, clinical measures like peripheral nerve injury severity, presence of current therapy, duration and cumulative dose were not specified by the initial protocol design. Third, a limited number of SNPs and genes were selected for examination because of cost constraints, and more SNPs remain to be found.

Interventions may be a key adjunct to reducing the incidence of TiPN in future treatment. This is the first study to use cutting-edge machine learning to establish and validate a TiPN predictive model using comprehensive genetic and clinical variables. Genes encoding inflammatory cytokines, growth of nerve fibers, and enzymes involved in ubiquitination were also screened out. These SNPs are closely related to the occurrence and development of TiPN. The results suggest that SNPs are important to fully predict TiPN. Through the prediction of this model, physicians can assess the possibility of TiPN in CD patients, which contributes to the rational use, timely intervention after administration, and avoidance of peripheral nerve damage. These findings are important for the management of CD patients with thalidomide.

CONCLUSION

In this study, the XGBoost algorithm exhibited a high degree of accuracy in predicting TiPN by utilizing 18 clinical features and 14 genetic variables. Furthermore, it can identify high-risk patients through SNPs. This suggests that XGBoost may offer a feasible option for improving thalidomide efficacy in CD patients.

ARTICLE HIGHLIGHTS

Research background

Thalidomide-induced peripheral neuropathy (TiPN), a life-threatening condition in Crohn's disease (CD), has a high incidence in Asia. However, there are no effective medical interventions for TiPN.

Research motivation

Can we develop a predictive model of TiPN combining genetic and clinical variables? Which variable affects TiPN more?

Research objectives

To establish an optimal model using clinical variables and genotypes to predict TiPN and improve the safety for the thalidomide treatment.

Research methods

A total of 164 patients diagnosed with CD at the Sixth Affiliated Hospital of the Sun Yat-Sen University were included in this study. Peripheral blood was collected from the patients to detect the genotypes at School of Pharmaceutical Sciences, Sun Yat-Sen University. The X^2 method or Single-sample Kolmogorov–Smirnov test was used to determine the association of TiPN with 18 clinical features and 150 genetic variables. Five predictive models were established and evaluated by the confusion matrix receiver operating characteristic curve (AUROC), area under the precision-recall curve (AUPRC), specificity, sensitivity (recall rate), precision, accuracy, and F1 score.

Research results

TiPN was observed in 59 individuals. Among the five models, extreme gradient boosting (XGBoost) algorithm exhibited the best predictive performance with the highest specificity (0.857), accuracy (0.818), AUPRC (0.86) and AUROC (0.89) after evaluation. The top-ranking five risk variables associated with TiPN were interleukin-12 rs1353248 [P = 0.0004, odds ratio (OR): 8.983, 95% confidence interval (CI): 2.497-30.90), dose (mg/d, P = 0.002), brain-derived neurotrophic factor (BDNF) rs2030324 (P = 0.001, OR: 3.164, 95%CI: 1.561-6.434), BDNF rs6265 (P = 0.001, OR: 3.150, 95%CI: 1.546-6.073) and BDNF rs11030104 (P = 0.001, OR: 3.091, 95%CI: 1.525-5.960).

Research conclusions

The XGBoost algorithm accurately predicts TiPN using 18 clinical features and 14 genetic variables. It is able to identify high-risk patients using single nucleotide polymorphisms.

Research perspectives

Applying the machine learning to adjust thalidomide therapies based on these specific genotypes is recommended before the thalidomide treatment.

ACKNOWLEDGEMENTS

We thank the physicians and nurses from department of gastroenterology for their cooperation in this study.

FOOTNOTES

Author contributions: Mao J, Chao K, Zhu X, and Wang XD designed the study; Mao J and Zhou BJ performed the experiments; Chao K, Gao X, Yang T and Li P enrolled the patients and collected the clinical data; Mao J and Ye XP performed the machine learning analyses; Huang M and Hu PJ supervised the study; Mao J and Wang XD wrote the manuscript.

Supported by National Natural Science Foundation of China, No. 81973398, No. 81730103, No. 81573507 and No. 82020108031; The National Key Research and Development Program, No. 2017YFC0909300 and No. 2016YFC0905001; Guangdong Provincial Key Laboratory of Construction Foundation, No. 2017B030314030 and No. 2020B1212060034; Science and Technology Program of Guangzhou, No. 201607020031; National Engineering and Technology Research Center for New Drug Druggability Evaluation (Seed Program of Guangdong Province), No. 2017B090903004; The 111 Project, No. B16047; China Postdoctoral Science Foundation, No. 2019M66324, No. 2020M683140 and No. 2020M683139; and Natural Science Foundation of Guangdong Province, No. 2022A1515012549 and No. 2023A1515012667.

Institutional review board statement: This study was reviewed and approved by the Ethics Committee of the Sixth Affiliated Hospital (No. E2016022), Sun Yat-Sen University, Guangzhou, China.

Informed consent statement: All study participants or their legal guardian provided informed written consent about personal and medical data collection prior to study enrolment.

Conflict-of-interest statement: The authors declare that the research was conducted in the absence of any commercial or financial relationships that could be construed as a potential conflict of interest.

Data sharing statement: Technical appendix, statistical code, and dataset available from the corresponding author at wangxd@mail.sysu.edu.cn consent was not obtained but the presented data are anonymized and risk of

identification is low.

Open-Access: This article is an open-access article that was selected by an in-house editor and fully peer-reviewed by external reviewers. It is distributed in accordance with the Creative Commons Attribution NonCommercial (CC BY-NC 4.0) license, which permits others to distribute, remix, adapt, build upon this work non-commercially, and license their derivative works on different terms, provided the original work is properly cited and the use is non-commercial. See: https://creativecommons.org/Licenses/by-nc/4.0/

Country/Territory of origin: China

ORCID number: Jing Mao 0009-0004-8412-033X; Kang Chao 0000-0002-1647-0563; Fu-Lin Jiang 0000-0002-0918-805X; Xiao-Ping Ye 0009-0000-9593-2326; Ting Yang 0000-0001-5875-5906; Pan Li 0000-0002-2819-4439; Xia Zhu 0000-0001-8893-0875; Pin-Jin Hu 0000-0001-7477-762X; Bai-Jun Zhou 0009-0007-0296-0020; Min Huang 0000-0002-2844-5680; Xiang Gao 0000-0003-4309-0600; Xue-Ding Wang 0000-0002-3580-9155.

S-Editor: Fan JR
L-Editor: A
P-Editor: Fan JR

REFERENCES

1 **Lazzerini M**, Martelossi S, Magazzù G, Pellegrino S, Lucanto MC, Barabino A, Calvi A, Arrigo S, Lionetti P, Lorusso M, Mangiantini F, Fontana M, Zuin G, Palla G, Maggiore G, Bramuzzo M, Pellegrin MC, Maschio M, Villanacci V, Manenti S, Decorti G, De Iudicibus S, Paparazzo R, Montico M, Ventura A. Effect of thalidomide on clinical remission in children and adolescents with refractory Crohn disease: a randomized clinical trial. *JAMA* 2013; **310**: 2164-2173 [PMID: 24281461 DOI: 10.1001/jama.2013.280777]

2 **Peng X**, Lin ZW, Zhang M, Yao JY, Zhao JZ, Hu PJ, Cao Q, Zhi M. The efficacy and safety of thalidomide in the treatment of refractory Crohn's disease in adults: a double-center, double-blind, randomized-controlled trial. *Gastroenterol Rep (Oxf)* 2022; **10**: goac052 [PMID: 36284737 DOI: 10.1093/gastro/goac052]

3 **Mileshkin L**, Stark R, Day B, Seymour JF, Zeldis JB, Prince HM. Development of neuropathy in patients with myeloma treated with thalidomide: patterns of occurrence and the role of electrophysiologic monitoring. *J Clin Oncol* 2006; **24**: 4507-4514 [PMID: 16940275 DOI: 10.1200/JCO.2006.05.6689]

4 **Franks ME**, Macpherson GR, Figg WD. Thalidomide. *Lancet* 2004; **363**: 1802-1811 [PMID: 15172781 DOI: 10.1016/S0140-6736(04)16308-3]

5 **Selvy M**, Kerckhove N, Pereira B, Barreau F, Nguyen D, Busserolles J, Giraudet F, Cabrespine A, Chaleteix C, Soubrier M, Bay JO, Lemal R, Balayssac D. Prevalence of Chemotherapy-Induced Peripheral Neuropathy in Multiple Myeloma Patients and its Impact on Quality of Life: A Single Center Cross-Sectional Study. *Front Pharmacol* 2021; **12**: 637593 [PMID: 33967771 DOI: 10.3389/fphar.2021.637593]

6 **Yang C**, Singh P, Singh H, Le ML, El-Matary W. Systematic review: thalidomide and thalidomide analogues for treatment of inflammatory bowel disease. *Aliment Pharmacol Ther* 2015; **41**: 1079-1093 [PMID: 25858208 DOI: 10.1111/apt.13181]

7 **Simon M**, Pariente B, Lambert J, Cosnes J, Bouhnik Y, Marteau P, Allez M, Colombel JF, Gornet JM. Long-term Outcomes of Thalidomide Therapy for Adults With Refractory Crohn's Disease. *Clin Gastroenterol Hepatol* 2016; **14**: 966-972.e2 [PMID: 26598226 DOI: 10.1016/j.cgh.2015.10.034]

8 **Mlak R**, Szudy-Szczyrek A, Mazurek M, Szczyrek M, Homa-Mlak I, Mielnik M, Chocholska S, Jankowska-Łęcka O, Małecka-Massalska T, Hus M. Polymorphisms in the promotor region of the CRBN gene as a predictive factor for peripheral neuropathy in the course of thalidomide-based chemotherapy in multiple myeloma patients. *Br J Haematol* 2019; **186**: 695-705 [PMID: 31115923 DOI: 10.1111/bjh.15972]

9 **Johnson DC**, Corthals SL, Walker BA, Ross FM, Gregory WM, Dickens NJ, Lokhorst HM, Goldschmidt H, Davies FE, Durie BG, Van Ness B, Child JA, Sonneveld P, Morgan GJ. Genetic factors underlying the risk of thalidomide-related neuropathy in patients with multiple myeloma. *J Clin Oncol* 2011; **29**: 797-804 [PMID: 21245421 DOI: 10.1200/JCO.2010.28.0792]

10 **Felipez LM**, Gokhale R, Tierney MP, Kirschner BS. Thalidomide use and outcomes in pediatric patients with Crohn disease refractory to infliximab and adalimumab. *J Pediatr Gastroenterol Nutr* 2012; **54**: 28-33 [PMID: 21681114 DOI: 10.1097/MPG.0b013e318228349e]

11 **García-Sanz R**, Corchete LA, Alcoceba M, Chillon MC, Jiménez C, Prieto I, García-Álvarez M, Puig N, Rapado I, Barrio S, Oriol A, Blanchard MJ, de la Rubia J, Martínez R, Lahuerta JJ, González Díaz M, Mateos MV, San Miguel JF, Martínez-López J, Sarasquete ME; GEM (Grupo Español de MM)/PETHEMA (Programa para el Estudio de la Terapéutica en Hemopatías Malignas) cooperative study group. Prediction of peripheral neuropathy in multiple myeloma patients receiving bortezomib and thalidomide: a genetic study based on a single nucleotide polymorphism array. *Hematol Oncol* 2017; **35**: 746-751 [PMID: 27605156 DOI: 10.1002/hon.2337]

12 **Szudy-Szczyrek A**, Mlak R, Bury-Kamińska M, Mielnik M, Podgajna M, Kuśmierczuk K, Mazurek M, Homa-Mlak I, Szczyrek M, Krawczyk J, Małecka-Massalska T, Hus M. Serum brain-derived neurotrophic factor (BDNF) concentration predicts polyneuropathy and overall survival in multiple myeloma patients. *Br J Haematol* 2020; **191**: 77-89 [PMID: 32567687 DOI: 10.1111/bjh.16862]

13 **Stage TB**, Hu S, Sparreboom A, Kroetz DL. Role for Drug Transporters in Chemotherapy-Induced Peripheral Neuropathy.

Clin Transl Sci 2021; **14**: 460-467 [PMID: 33142018 DOI: 10.1111/cts.12915]

14 **Islam B**, Lustberg M, Staff NP, Kolb N, Alberti P, Argyriou AA. Vinca alkaloids, thalidomide and eribulin-induced peripheral neurotoxicity: From pathogenesis to treatment. *J Peripher Nerv Syst* 2019; **24** Suppl 2: S63-S73 [PMID: 31647152 DOI: 10.1111/jns.12334]

15 **Zajączkowska R**, Kocot-Kępska M, Leppert W, Wrzosek A, Mika J, Wordliczek J. Mechanisms of Chemotherapy-Induced Peripheral Neuropathy. *Int J Mol Sci* 2019; **20** [PMID: 30909387 DOI: 10.3390/ijms20061451]

16 **Bartlett JB**, Dredge K, Dalgleish AG. The evolution of thalidomide and its IMiD derivatives as anticancer agents. *Nat Rev Cancer* 2004; **4**: 314-322 [PMID: 15057291 DOI: 10.1038/nrc1323]

17 **Kirchmair R**, Tietz AB, Panagiotou E, Walter DH, Silver M, Yoon YS, Schratzberger P, Weber A, Kusano K, Weinberg DH, Ropper AH, Isner JM, Losordo DW. Therapeutic angiogenesis inhibits or rescues chemotherapy-induced peripheral neuropathy: taxol- and thalidomide-induced injury of vasa nervorum is ameliorated by VEGF. *Mol Ther* 2007; **15**: 69-75 [PMID: 17164777 DOI: 10.1038/sj.mt.6300019]

18 **Keifer JA**, Guttridge DC, Ashburner BP, Baldwin AS Jr. Inhibition of NF-kappa B activity by thalidomide through suppression of IkappaB kinase activity. *J Biol Chem* 2001; **276**: 22382-22387 [PMID: 11297551 DOI: 10.1074/jbc.M100938200]

19 **Tonello R**, Lee SH, Berta T. Monoclonal Antibody Targeting the Matrix Metalloproteinase 9 Prevents and Reverses Paclitaxel-Induced Peripheral Neuropathy in Mice. *J Pain* 2019; **20**: 515-527 [PMID: 30471427 DOI: 10.1016/j.jpain.2018.11.003]

20 **Wani TH**, Chakrabarty A, Shibata N, Yamazaki H, Guengerich FP, Chowdhury G. The Dihydroxy Metabolite of the Teratogen Thalidomide Causes Oxidative DNA Damage. *Chem Res Toxicol* 2017; **30**: 1622-1628 [PMID: 28745489 DOI: 10.1021/acs.chemrestox.7b00127]

21 **Kobayashi NR**, Fan DP, Giehl KM, Bedard AM, Wiegand SJ, Tetzlaff W. BDNF and NT-4/5 prevent atrophy of rat rubrospinal neurons after cervical axotomy, stimulate GAP-43 and Talpha1-tubulin mRNA expression, and promote axonal regeneration. *J Neurosci* 1997; **17**: 9583-9595 [PMID: 9391013 DOI: 10.1523/JNEUROSCI.17-24-09583.1997]

22 **Wu Y**, Shen Z, Xu H, Zhang K, Guo M, Wang F, Li J. BDNF Participates in Chronic Constriction Injury-Induced Neuropathic Pain *via* Transcriptionally Activating P2X(7) in Primary Sensory Neurons. *Mol Neurobiol* 2021; **58**: 4226-4236 [PMID: 33963520 DOI: 10.1007/s12035-021-02410-0]

23 **Navia-Pelaez JM**, Choi SH, Dos Santos Aggum Capettini L, Xia Y, Gonen A, Agatisa-Boyle C, Delay L, Gonçalves Dos Santos G, Catroli GF, Kim J, Lu JW, Saylor B, Winkels H, Durant CP, Ghosheh Y, Beaton G, Ley K, Kufareva I, Corr M, Yaksh TL, Miller YI. Normalization of cholesterol metabolism in spinal microglia alleviates neuropathic pain. *J Exp Med* 2021; **218** [PMID: 33970188 DOI: 10.1084/jem.20202059]

24 **Birla H**, Rai SN, Singh SS, Zahra W, Rawat A, Tiwari N, Singh RK, Pathak A, Singh SP. Tinospora cordifolia Suppresses Neuroinflammation in Parkinsonian Mouse Model. *Neuromolecular Med* 2019; **21**: 42-53 [PMID: 30644041 DOI: 10.1007/s12017-018-08521-7]

25 **Gofshteyn JS**, Shaw PA, Teachey DT, Grupp SA, Maude S, Banwell B, Chen F, Lacey SF, Melenhorst JJ, Edmonson MJ, Panzer J, Barrett DM, McGuire JL. Neurotoxicity after CTL019 in a pediatric and young adult cohort. *Ann Neurol* 2018; **84**: 537-546 [PMID: 30178481 DOI: 10.1002/ana.25315]

26 **Zhang B**, Kopper TJ, Liu X, Cui Z, Van Lanen SG, Gensel JC. Macrolide derivatives reduce proinflammatory macrophage activation and macrophage-mediated neurotoxicity. *CNS Neurosci Ther* 2019; **25**: 591-600 [PMID: 30677254 DOI: 10.1111/cns.13092]

27 **Cavaletti G**, Beronio A, Reni L, Ghiglione E, Schenone A, Briani C, Zara G, Cocito D, Isoardo G, Ciaramitaro P, Plasmati R, Pastorelli F, Frigo M, Piatti M, Carpo M. Thalidomide sensory neurotoxicity: a clinical and neurophysiologic study. *Neurology* 2004; **62**: 2291-2293 [PMID: 15210898 DOI: 10.1212/wnl.62.12.2291]

28 **Bramuzzo M**, Stocco G, Montico M, Arrigo S, Calvi A, Lanteri P, Costa S, Pellegrino S, Magazzù G, Barp J, Ghione S, Lionetti P, Zuin G, Fontana M, Di Chio T, Maggiore G, Lazzerini M, Lucafò M, Udina C, Pellegrin MC, Chicco A, Carrozzi M, Decorti G, Ventura A, Martelossi S. Risk Factors and Outcomes of Thalidomide-induced Peripheral Neuropathy in a Pediatric Inflammatory Bowel Disease Cohort. *Inflamm Bowel Dis* 2017; **23**: 1810-1816 [PMID: 28817461 DOI: 10.1097/MIB.0000000000001195]

29 **Tang J**, Liu R, Zhang YL, Liu MZ, Hu YF, Shao MJ, Zhu LJ, Xin HW, Feng GW, Shang WJ, Meng XG, Zhang LR, Ming YZ, Zhang W. Application of Machine-Learning Models to Predict Tacrolimus Stable Dose in Renal Transplant Recipients. *Sci Rep* 2017; **7**: 42192 [PMID: 28176850 DOI: 10.1038/srep42192]

30 **Alabi RO**, Mäkitie AA, Pirinen M, Elmusrati M, Leivo I, Almangush A. Comparison of nomogram with machine learning techniques for prediction of overall survival in patients with tongue cancer. *Int J Med Inform* 2021; **145**: 104313 [PMID: 33142259 DOI: 10.1016/j.ijmedinf.2020.104313]

31 **Lu RY**, Bagdasarova Y, Lee AY. Machine Learning-Based Anomaly Detection Techniques in Ophthalmology. *JAMA Ophthalmol* 2022; **140**: 189-190 [PMID: 34967861 DOI: 10.1001/jamaophthalmol.2021.5555]

32 **Tao W**, Concepcion AN, Vianen M, Marijnissen ACA, Lafeber FPGJ, Radstake TRDJ, Pandit A. Multiomics and Machine Learning Accurately Predict Clinical Response to Adalimumab and Etanercept Therapy in Patients With Rheumatoid Arthritis. *Arthritis Rheumatol* 2021; **73**: 212-222 [PMID: 32909363 DOI: 10.1002/art.41516]

33 **Mo X**, Chen X, Ieong C, Zhang S, Li H, Li J, Lin G, Sun G, He F, He Y, Xie Y, Zeng P, Chen Y, Liang H, Zeng H. Early Prediction of Clinical Response to Etanercept Treatment in Juvenile Idiopathic Arthritis Using Machine Learning. *Front Pharmacol* 2020; **11**: 1164 [PMID: 32848772 DOI: 10.3389/fphar.2020.01164]

34 **Li JL**, Wang XD, Chen SY, Liu LS, Fu Q, Chen X, Teng LC, Wang CX, Huang M. Effects of diltiazem on pharmacokinetics of tacrolimus in relation to CYP3A5 genotype status in renal recipients: from retrospective to prospective. *Pharmacogenomics J* 2011; **11**: 300-306 [PMID: 20514078 DOI: 10.1038/tpj.2010.42]

35 **Zhang Y**, Li JL, Fu Q, Wang XD, Liu LS, Wang CX, Xie W, Chen ZJ, Shu WY, Huang M. Associations of ABCB1, NFKB1, CYP3A, and NR1I2 polymorphisms with cyclosporine trough concentrations in Chinese renal transplant recipients. *Acta Pharmacol Sin* 2013; **34**: 555-560 [PMID: 23503472 DOI: 10.1038/aps.2012.200]

36 **Noh B**, Yoon H, Youm C, Kim S, Lee M, Park H, Kim B, Choi H, Noh Y. Prediction of Decline in Global Cognitive

Function Using Machine Learning with Feature Ranking of Gait and Physical Fitness Outcomes in Older Adults. *Int J Environ Res Public Health* 2021; **18** [PMID: 34769864 DOI: 10.3390/ijerph182111347]

37 **Kruppa J**, Ziegler A, König IR. Risk estimation and risk prediction using machine-learning methods. *Hum Genet* 2012; **131**: 1639-1654 [PMID: 22752090 DOI: 10.1007/s00439-012-1194-y]

38 **Seo H**, Badiei Khuzani M, Vasudevan V, Huang C, Ren H, Xiao R, Jia X, Xing L. Machine learning techniques for biomedical image segmentation: An overview of technical aspects and introduction to state-of-art applications. *Med Phys* 2020; **47**: e148-e167 [PMID: 32418337 DOI: 10.1002/mp.13649]

39 **Ksenofontov AA**, Lukanov MM, Bocharov PS. Can machine learning methods accurately predict the molar absorption coefficient of different classes of dyes? *Spectrochim Acta A Mol Biomol Spectrosc* 2022; **279**: 121442 [PMID: 35660154 DOI: 10.1016/j.saa.2022.121442]

40 **Alam M**, Le D, Lim JI, Chan RVP, Yao X. Supervised Machine Learning Based Multi-Task Artificial Intelligence Classification of Retinopathies. *J Clin Med* 2019; **8** [PMID: 31216768 DOI: 10.3390/jcm8060872]

41 **Chen J**, Remulla D, Nguyen JH, Dua A, Liu Y, Dasgupta P, Hung AJ. Current status of artificial intelligence applications in urology and their potential to influence clinical practice. *BJU Int* 2019; **124**: 567-577 [PMID: 31219658 DOI: 10.1111/bju.14852]

42 **Zhang L**, Zhao Z, Ma C, Shan L, Sun H, Jiang L, Deng S, Gao C. End-to-End Automatic Pronunciation Error Detection Based on Improved Hybrid CTC/Attention Architecture. *Sensors (Basel)* 2020; **20** [PMID: 32218379 DOI: 10.3390/s20071809]

43 **Mo X**, Chen X, Li H, Li J, Zeng F, Chen Y, He F, Zhang S, Pan L, Zeng P, Xie Y, Huang M, He Y, Liang H, Zeng H. Early and Accurate Prediction of Clinical Response to Methotrexate Treatment in Juvenile Idiopathic Arthritis Using Machine Learning. *Front Pharmacol* 2019; **10**: 1155 [PMID: 31649533 DOI: 10.3389/fphar.2019.01155]

44 **Lee HC**, Yoon SB, Yang SM, Kim WH, Ryu HG, Jung CW, Suh KS, Lee KH. Prediction of Acute Kidney Injury after Liver Transplantation: Machine Learning Approaches vs. Logistic Regression Model. *J Clin Med* 2018; **7** [PMID: 30413107 DOI: 10.3390/jcm7110428]

45 **Mo X**, Chen X, Ieong C, Gao X, Li Y, Liao X, Yang H, Li H, He F, He Y, Chen Y, Liang H, Huang M, Li J. Early Prediction of Tacrolimus-Induced Tubular Toxicity in Pediatric Refractory Nephrotic Syndrome Using Machine Learning. *Front Pharmacol* 2021; **12**: 638724 [PMID: 34512318 DOI: 10.3389/fphar.2021.638724]

46 **Ma X**, Wu Y, Zhang L, Yuan W, Yan L, Fan S, Lian Y, Zhu X, Gao J, Zhao J, Zhang P, Tang H, Jia W. Comparison and development of machine learning tools for the prediction of chronic obstructive pulmonary disease in the Chinese population. *J Transl Med* 2020; **18**: 146 [PMID: 32234053 DOI: 10.1186/s12967-020-02312-0]

47 **Trynka G**, Hunt KA, Bockett NA, Romanos J, Mistry V, Szperl A, Bakker SF, Bardella MT, Bhaw-Rosun L, Castillejo G, de la Concha EG, de Almeida RC, Dias KR, van Diemen CC, Dubois PC, Duerr RH, Edkins S, Franke L, Fransen K, Gutierrez J, Heap GA, Hrdlickova B, Hunt S, Plaza Izurieta L, Izzo V, Joosten LA, Langford C, Mazzilli MC, Mein CA, Midah V, Mitrovic M, Mora B, Morelli M, Nutland S, Núñez C, Onengut-Gumuscu S, Pearce K, Platteel M, Polanco I, Potter S, Ribes-Koninckx C, Ricaño-Ponce I, Rich SS, Rybak A, Santiago JL, Senapati S, Sood A, Szajewska H, Troncone R, Varadé J, Wallace C, Wolters VM, Zhernakova A; Spanish Consortium on the Genetics of Coeliac Disease (CEGEC); PreventCD Study Group; Wellcome Trust Case Control Consortium (WTCCC), Thelma BK, Cukrowska B, Urcelay E, Bilbao JR, Mearin ML, Barisani D, Barrett JC, Plagnol V, Deloukas P, Wijmenga C, van Heel DA. Dense genotyping identifies and localizes multiple common and rare variant association signals in celiac disease. *Nat Genet* 2011; **43**: 1193-1201 [PMID: 22057235 DOI: 10.1038/ng.998]

48 **Park DJ**, Kim SH, Nah SS, Lee JH, Kim SK, Lee YA, Hong SJ, Kim HS, Lee HS, Kim HA, Joung CI, Lee SS. Association between brain-derived neurotrophic factor gene polymorphisms and fibromyalgia in a Korean population: a multicenter study. *Arthritis Res Ther* 2018; **20**: 220 [PMID: 30285822 DOI: 10.1186/s13075-018-1726-5]

49 **Huang R**, Huang J, Cathcart H, Smith S, Poduslo SE. Genetic variants in brain-derived neurotrophic factor associated with Alzheimer's disease. *J Med Genet* 2007; **44**: e66 [PMID: 17293537 DOI: 10.1136/jmg.2006.044883]

50 **Azoulay D**, Giryes S, Nasser R, Sharon R, Horowitz NA. Prediction of Chemotherapy-Induced Peripheral Neuropathy in Patients with Lymphoma and Myeloma: the Roles of Brain-Derived Neurotropic Factor Protein Levels and A Gene Polymorphism. *J Clin Neurol* 2019; **15**: 511-516 [PMID: 31591840 DOI: 10.3988/jcn.2019.15.4.511]

51 **Egan MF**, Kojima M, Callicott JH, Goldberg TE, Kolachana BS, Bertolino A, Zaitsev E, Gold B, Goldman D, Dean M, Lu B, Weinberger DR. The BDNF val66met polymorphism affects activity-dependent secretion of BDNF and human memory and hippocampal function. *Cell* 2003; **112**: 257-269 [PMID: 12553913 DOI: 10.1016/s0092-8674(03)00035-7]

52 **Ng T**, Teo SM, Yeo HL, Shwe M, Gan YX, Cheung YT, Foo KM, Cham MT, Lee JA, Tan YP, Fan G, Yong WS, Preetha M, Loh WJ, Koo SL, Jain A, Lee GE, Wong M, Dent R, Yap YS, Ng R, Khor CC, Ho HK, Chan A. Brain-derived neurotrophic factor genetic polymorphism (rs6265) is protective against chemotherapy-associated cognitive impairment in patients with early-stage breast cancer. *Neuro Oncol* 2016; **18**: 244-251 [PMID: 26289590 DOI: 10.1093/neuonc/nov162]

53 **Xie B**, Liu Z, Liu W, Jiang L, Zhang R, Cui D, Zhang Q, Xu S. DNA Methylation and Tag SNPs of the BDNF Gene in Conversion of Amnestic Mild Cognitive Impairment into Alzheimer's Disease: A Cross-Sectional Cohort Study. *J Alzheimers Dis* 2017; **58**: 263-274 [PMID: 28387675 DOI: 10.3233/JAD-170007]

54 **Ieraci A**, Madaio AI, Mallei A, Lee FS, Popoli M. Brain-Derived Neurotrophic Factor Val66Met Human Polymorphism Impairs the Beneficial Exercise-Induced Neurobiological Changes in Mice. *Neuropsychopharmacology* 2016; **41**: 3070-3079 [PMID: 27388329 DOI: 10.1038/npp.2016.120]

55 **Bastuji-Garin S**, Ochonisky S, Bouche P, Gherardi RK, Duguet C, Djerradine Z, Poli F, Revuz J; Thalidomide Neuropathy Study Group. Incidence and risk factors for thalidomide neuropathy: a prospective study of 135 dermatologic patients. *J Invest Dermatol* 2002; **119**: 1020-1026 [PMID: 12445187 DOI: 10.1046/j.1523-1747.2002.19502.x]

World Journal of Gastroenterology

Submit a Manuscript: https://www.f6publishing.com

World J Gastroenterol 2023 June 28; 29(24): 3871-3882

DOI: 10.3748/wjg.v29.i24.3871

ISSN 1007-9327 (print) ISSN 2219-2840 (online)

ORIGINAL ARTICLE

Clinical Trials Study

Stereotactic body radiotherapy combined with sintilimab in patients with recurrent or oligometastatic hepatocellular carcinoma: A phase II clinical trial

Yi-Xing Chen, Ping Yang, Shi-Suo Du, Yuan Zhuang, Cheng Huang, Yong Hu, Wen-Chao Zhu, Yi-Yi Yu, Tian-Shu Liu, Zhao-Chong Zeng

Specialty type: Gastroenterology and hepatology

Provenance and peer review: Unsolicited article; Externally peer reviewed.

Peer-review model: Single blind

Peer-review report's scientific quality classification

Grade A (Excellent): 0
Grade B (Very good): B
Grade C (Good): C
Grade D (Fair): 0
Grade E (Poor): 0

P-Reviewer: Lykoudis PM, United Kingdom; Manfredi S, France

Received: March 26, 2023
Peer-review started: March 26, 2023
First decision: April 26, 2023
Revised: May 6, 2023
Accepted: May 30, 2023
Article in press: May 30, 2023
Published online: June 28, 2023

Yi-Xing Chen, Ping Yang, Shi-Suo Du, Yuan Zhuang, Yong Hu, Wen-Chao Zhu, Zhao-Chong Zeng, Department of Radiation Oncology, Zhongshan Hospital, Fudan University, Shanghai 200032, China

Cheng Huang, Liver Cancer Institute, Zhongshan Hospital, Fudan University, Shanghai 200032, China

Yi-Yi Yu, Tian-Shu Liu, Department of Medical Oncology, Zhongshan Hospital, Fudan University, Shanghai 200032, China

Corresponding author: Zhao-Chong Zeng, PhD, Professor, Department of Radiation Oncology, Zhongshan Hospital, Fudan University, No. 180 Fenglin Road, Xuhui District, Shanghai 200032, China. zeng.zhaochong@zs-hospital.sh.cn

Abstract

BACKGROUND

Stereotactic body radiotherapy (SBRT) and programmed cell death 1 inhibitors have shown potential in treating hepatocellular carcinoma (HCC) in retrospective studies.

AIM

To evaluate the efficacy of combining SBRT with sintilimab for patients with recurrent or oligometastatic HCC.

METHODS

This trial involved patients with recurrent or oligometastatic HCC intravenously treated with SBRT plus sintilimab every 3 wk for 12 mo or until disease progression. The primary endpoint was progression-free survival (PFS).

RESULTS

Twenty-five patients were enrolled from August 14, 2019, to August 23, 2021. The median treatment duration was 10.2 (range, 0.7-14.6) months. SBRT was delivered at a median dose of 54 (range, 48-60) Gy in 6 (range, 6-10) fractions. The median follow-up time was 21.9 (range, 10.3-39.7) mo, and 32 targeted lesions among 25 patients were evaluated for treatment response according to the Response

Evaluation Criteria in Solid Tumors version 1.1. The median PFS was 19.7 mo [95% confidence interval (CI): 16.9-NA], with PFS rates of 68% (95%CI: 52-89) and 45.3% (95%CI: 28-73.4) at 12 and 24 mo, respectively. The median overall survival (OS) was not reached, with OS rates of 91.5% (95%CI: 80.8-100.0) and 83.2% (95%CI: 66.5-100.0) at 12 and 24 mo, respectively. The 1- and 2-year local control rate were 100% and 90.9% (95%CI: 75.4%-100.0%), respectively. The confirmed objective response rate and disease control rate was 96%, and 96%, respectively. Most adverse events were graded as 1 or 2, and grade 3 adverse events were observed in three patients.

CONCLUSION

SBRT plus sintilimab is an effective, well-tolerated treatment regimen for patients with recurrent or oligometastatic HCC.

Key Words: Stereotactic body radiotherapy; Programmed cell death 1; Sintilimab; Hepatocellular carcinoma; Efficacy and safety

©The Author(s) 2023. Published by Baishideng Publishing Group Inc. All rights reserved.

Core Tip: In this single-arm phase II trial, stereotactic body radiotherapy (SBRT) plus sintilimab showed outstanding progression-free survival and objective response rate in the treatment of recurrent or oligometastatic hepatocellular carcinoma. Moreover, the combined use of SBRT and sintilimab is safe and tolerable. Patients can recover rapidly from radiotherapy-induced decreases in lymphocyte counts. This result suggests that SBRT combined with sintilimab may be a new treatment option for patients with recurrent or oligometastatic hepatocellular carcinoma.

Citation: Chen YX, Yang P, Du SS, Zhuang Y, Huang C, Hu Y, Zhu WC, Yu YY, Liu TS, Zeng ZC. Stereotactic body radiotherapy combined with sintilimab in patients with recurrent or oligometastatic hepatocellular carcinoma: A phase II clinical trial. *World J Gastroenterol* 2023; 29(24): 3871-3882
URL: https://www.wjgnet.com/1007-9327/full/v29/i24/3871.htm
DOI: https://dx.doi.org/10.3748/wjg.v29.i24.3871

INTRODUCTION

Liver cancer is the sixth most prevalent cancer, with the fourth highest mortality rate. China accounts for nearly half of all hepatocellular carcinoma (HCC) cases globally[1,2]. Surgery is an important curative therapy for HCC. The 5-year recurrence rate of HCC has reached 60%-70% after surgical resection and active postoperative management[3-5]. In addition to intrahepatic recurrence, the most common sites of metastasis are the lung, lymph node, and bone[6]. Oligometastasis is defined as a transition point between localized disease and widespread metastasis and has been applied to several solid tumors[7]. Although systemic treatment is the standard of care for patients with HCC presenting with extrahepatic metastases, effective treatments for oligometastatic HCC remain unknown[8]. Studies have demonstrated the efficacy of stereotactic body radiotherapy (SBRT) for HCC, with a high local control rate and acceptable toxicity[9-11]. However, the treatment effect of SBRT is determined by lesions in the irradiated field. Therefore, the development of additional treatment regimens to further reduce the recurrence out of the radiation volume and improve the prognosis of HCC is urgently required.

The combination of programmed cell death 1 (PD-1) inhibitors and targeted antiangiogenic treatment is considered the standard first-line treatment regimen for advanced HCC[12,13]. Immunotherapy, as a systematic treatment, has a long tail effect. It can provide a lasting survival benefit by generating memory T cells and exercise better control of tumor cells throughout the body[14]. The upregulation of programmed death ligand-1 (PD-L1) is associated with radioresistance in patients with HCC after radiotherapy, and the use of PD-1/PD-L1 inhibitors can kill tumor cells through the immune response effect. Thus, the recurrence rate can be further reduced owing to the potential synergistic effect of combined radiotherapy and PD-1 inhibitors[15,16].

Sintilimab is a highly selective, fully human immunoglobulin G4 monoclonal antibody against PD-1, and the combined use of sintilimab and bevacizumab is the first-line treatment for advanced HCC in China[13]. A retrospective cohort study included 76 patients with intermediate-stage HCC who presented with trans-arterial chemoembolization (TACE) refractoriness and found that progression-free survival (PFS) and overall survival (OS) were improved after the use of SBRT combined with a PD-1 inhibitor[17], but these results were not verified in clinical trials. Thus, the current phase II trial aimed to

assess the efficacy and safety of SBRT plus sintilimab in patients with recurrent or oligometastatic HCC.

MATERIALS AND METHODS

Study design and participants

This was a single-arm, open-label, single-center, phase II trial registered with ClinicalTrials.gov (NCT03857815). This study enrolled adult patients (aged between 18 and 75 years) with diagnostic criteria for HCC between August 14, 2019, and August 23, 2021, at Zhongshan Hospital, Fudan University. Patients with Child–Pugh A and an Eastern Cooperative Oncology Group performance status (ECOG PS) of 0–1 were eligible for this study. Other main inclusion criteria were as follows: (1) Patients with the number of lesions between one and five, which is suitable for SBRT; (2) patients without a history of radiotherapy; and (3) patients with adequate hematological and organ functions. Patients presenting with fibrolamellar HCC, sarcomatoid HCC, and cholangiocarcinoma and with a history of liver transplantation and other acute or chronic conditions were ineligible. The eligibility criteria are detailed in the study protocol and are shown in the supplementary file.

The Medical Ethics Committee of Zhongshan Hospital, Fudan University, approved this study (B2019-010R), which was conducted in accordance with the standards of Good Clinical Practice and the Declaration of Helsinki and Istanbul. All patients consented to participate after being informed of the study's purpose.

All authors had access to the study data and reviewed and approved the final manuscript.

Treatment and assessments

After enrollment, all patients underwent SBRT combined with sintilimab for 12 mo or until disease progression. For SBRT, the gross tumor volume (GTV) was defined as computed tomography (CT), magnetic resonance imaging (MRI), or CT/MRI/positron emission tomography fusion images, and all lesions were included. The internal target volume (ITV) was constructed based on four-dimensional CT to delineate the GTV of each time phase and was generated. The planning target volume was defined as the ITV plus a margin of 3 mm. The patients underwent daily on-board megavoltage CT for imaging guidance. The patients received a total dose of 48–60 Gy in 5–10 fractions 5 times per week. Patients received 200 mg sintilimab intravenously once every 3 wk for 12 mo or until disease progression. Tumor imaging assessments were performed every 6 wk (± 7 d) from the first day of sintilimab treatment and every 12 wk (± 7 d) after 48 wk. After the initial evaluation of imaging progression by the investigator, if the participant was clinically stable, medication was continued, and imaging was repeated 4-6 wk later to confirm disease progression, or treatment was continued if no progression was confirmed.

Endpoints

The primary endpoint was PFS, which was defined as the time from the start of treatment to the date of progressive disease or death, whichever occurred first. The secondary endpoints included OS (the time from receipt of the study drug to death), local control rate, objective response rate [ORR, the proportion of patients who achieved complete response (CR) or partial response (PR) as their best overall response (BOR)], disease control rate (DCR, the proportion of patients who achieved CR, PR, or stable disease as their BOR), and adverse events. All outcomes were assessed by blinded independent central reviewers and investigators according to the Response Evaluation Criteria in Solid Tumors (RECIST) version 1.1. The details of the adverse event assessment are shown in the study protocol.

Statistical analysis

With reference to historical controls[18], patients with HCC with oligometastases or recurrence were treated with SBRT, with a median PFS period of approximately 8 mo. Assuming a median PFS period of 14.8 mo with SBRT plus sintilimab, a sample size of 25 patients would be required to provide a power of 80% with a one-sided alpha level of 0.05, assuming a drop rate of 10%. The Kaplan-Meier method was used for survival analysis. Descriptive summaries were provided for all other efficacy and safety endpoints. Unpaired T Test was used to explore the differences in the counts of biomarkers between groups. The *P* values for biomarkers between groups were two-sided, with $P < 0.05$ being considered statistically significant. Statistical analyses were performed using R 4.0.5.

RESULTS

Patient characteristics of treatment

The baseline characteristics of the enrolled patients are shown in Table 1. Twenty-five patients were enrolled in this study. Twenty-four (96%) patients were infected with hepatitis B. The liver function of all patients was Child-Pugh class A. Nineteen (76%) patients had intrahepatic recurrence, 6 (24%) patients showed extrahepatic recurrence, and 2 patients showed both intra- and extrahepatic

Table 1 Patient demographics and baseline clinical characteristics

Characteristics	*n* = 25
Age, years, median (range)	64 (33-71)
Male sex, *n* (%)	24 (96)
Etiology, *n* (%)	
Hepatitis B infection	24 (96)
Others	1 (4)
ECOG performance status, *n* (%)	
0	19 (76)
1	6 (24)
Child-Pugh class A, *n* (%)	25 (100)
BCLC C stage, *n* (%)	25 (100)
Site of recurrence, *n* (%)	
Intrahepatic	19 (76)
Extrahepatic	6 (24)
Both Intra-Extrahepatic	2 (8)
Target tumor size, cm, median (range)	2.0 (1.0-7.4)
Tumor number, *n* (%)	
1	19 (76)
2	5 (25)
3	1 (4)
Serum AFP ≥ 400 ng/mL, *n* (%)	3 (12)
Prior therapy, *n* (%)	
Surgery	17 (68)
Ablation	9 (36)
TACE	13 (52)

AFP: α-fetoprotein; BCLC: Barcelona Clinic Liver Cancer; ECOG: Eastern Cooperative Oncology Group; TACE: Trans-arterial chemoembolization.

recurrences. Tumors 1, 2, and 3 were reported in 19, 5, and 1 patient(s), respectively. All the patients underwent surgery, ablation, or TACE previously. The median treatment duration was 10.2 (range, 0.7-14.6) months, and SBRT was delivered at a median dose of 54 (range, 48–60) Gy in 6 (range, 6–10) fractions.

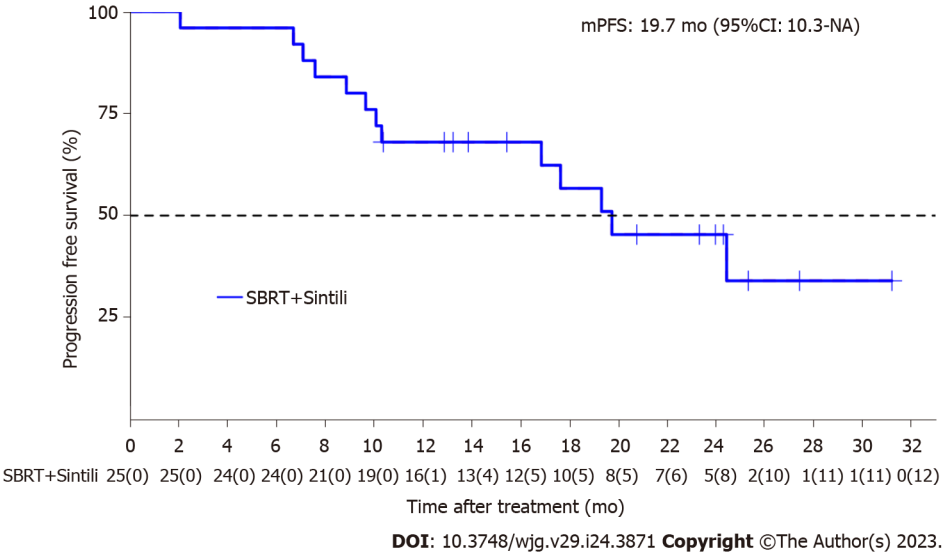
Efficacy

The median follow-up time was 21.9 (range, 10.3–39.7) months, and 32 lesions in 25 patients were evaluated for treatment response according to RECIST version 1.1. The median PFS period was 19.7 [95% confidence interval (CI): 16.9-NA; Figure 1] mo, and the PFS rates at 12 and 24 mo were 68% (95%CI: 52-89) and 45.3% (95%CI: 28-73.4), respectively.

The median OS was not reached, and three events of death were observed, with 91.5% (95%CI: 80.8-100.0) and 83.2% (95%CI: 66.5-100.0) OS rates at 12 and 24 mo, respectively. Moreover, the 1- and 2-year local control rates were 100% and 90.9% (95%CI: 75.4%-100.0%), respectively (Table 2). The ORR was 96% (24/25) according to RECIST version 1.1, with 17 achieving CR and 7 achieving PR after sintilimab plus SBRT therapy. After one cycle of treatment, all target liver lesions disappeared, although new lesions appeared in the lungs of one patient, which was judged as PD. The best change in the target tumor size is shown in Figure 2A. One patient achieved PR after two cycles of sintilimab plus SBRT therapy. However, the patient underwent a self-determined liver transplant (protocol violation reported) and died 5 mo after surgery due to liver failure caused by liver transplantation (Figure 2B). Similarly, the DCR for patients with HCC treated with SBRT combined with sintilimab was 96% (Table 2). The median time to response was 2.1 (range, 0.9-6.6) months for the 24 responders, whereas the median duration of response was 16.9 mo (95%CI: 8.18-NA).

Table 2 Summary of radiographic response per response evaluation criteria in solid tumors version 1.1

Variable	*n* = 25
Best overall response, *n* (%)	
Complete response	17 (68)
Partial response	7 (28)
Stable disease	0
Progressive disease	1 (4)
Objective response rate, *n* (%)	24 (96)
Disease control rate, *n* (%)	24 (96)
1 yr local control rate, *n* (%)	25 (100)



DOI: 10.3748/wjg.v29.i24.3871 **Copyright** ©The Author(s) 2023.

Figure 1 Kaplan-Meier analysis of median progression-free survival according to the response evaluation criteria in solid tumors version 1.1. mPFS: Median progression-free survival; SBRT: Stereotactic body radiotherapy.

Safety

All the patients received at least one dose of the study treatment and were included in the safety analysis. The details of the adverse events in patients with HCC treated with SBRT combined with sintilimab are shown in Table 3. In total, 22 (88.0%) patients reported treatment-related adverse events (TRAEs), and grade 1 and 2 adverse events were observed in 17 (68%) and 14 (56%) patients, respectively. The most common TRAE was decreased lymphocyte count (probably caused by radiotherapy). The lymphocyte count decreased significantly after the second treatment (Supplementary Figure 1). However, the lymphocyte counts gradually returned to baseline after the third treatment session. Grade 3 TRAEs, including increased gamma-glutamyl transpeptidase level, decreased platelet count, and myositis, were observed in 3 (12%) patients. No grade 4 or 5 TRAEs were observed.

Four patients presented with serious adverse events. One patient had grade 1 myocarditis, possibly due to immunotherapy; one had grade 2 immune pneumonia; and one patient had viral hepatitis, which was evaluated to be independent of the treatment regimen. One patient experienced upper gastrointestinal bleeding owing to cirrhosis of liver. All four patients recovered after medical treatment. The study treatment was interrupted due to emergent adverse events in 3 (12%) of the 25 patients, including 1 patient with myocarditis, 1 with upper gastrointestinal bleeding, and 1 with arthritis. Patients should continue treatment after recovery from adverse reactions; however, all three patients refused to resume use. Permanent discontinuation due to adverse events occurred in three patients, including one patient with pneumonia (grade 2), one with elevated bilirubin level (grade 3), and one with ascites (grade 2).

Table 3 Treatment-related adverse events

Treatment-related adverse events	Any grade	Grade 1	Grade 2	Grade 3
All adverse events, *n* (%)	22 (88)	17 (68)	14 (56)	3 (12)
Decreased lymphocyte count	14 (56)	7 (28)	7 (28)	0
Increased GGT	7 (28)	3 (12)	3 (12)	1 (4)
Decreased platelet count	5 (20)	0	4 (16)	1 (4)
Increased blood bilirubin	5 (20)	4 (16)	1 (4)	0
Rash	4 (16)	2 (8)	2 (8)	0
Increased ALT	2 (8)	1 (4)	1 (4)	0
Increased AST	2 (8)	2 (8)	0	0
Myositis	2 (8)	0	1 (4)	1 (4)
Abnormal liver function	2 (8)	1 (4)	1 (4)	0
Paronychia	2 (8)	2 (8)	0	0
Jaundice	2 (8)	0	2 (8)	0
Decreased white blood cell count	1 (4)	1 (4)	0	0
Decreased neutrophil count	1 (4)	1 (4)	0	0
Ascites	1 (4)	0	1 (4)	0
Arthritis	1 (4)	0	1 (4)	0
Pneumonia	1 (4)	0	1 (4)	0
Myocarditis	1 (4)	1 (4)	0	0
Dry eye	1 (4)	1 (4)	0	0

GGT: Gamma-glutamyl transpeptidase; ALT: Alanine aminotransferase; AST: Aspartate aminotransferase.

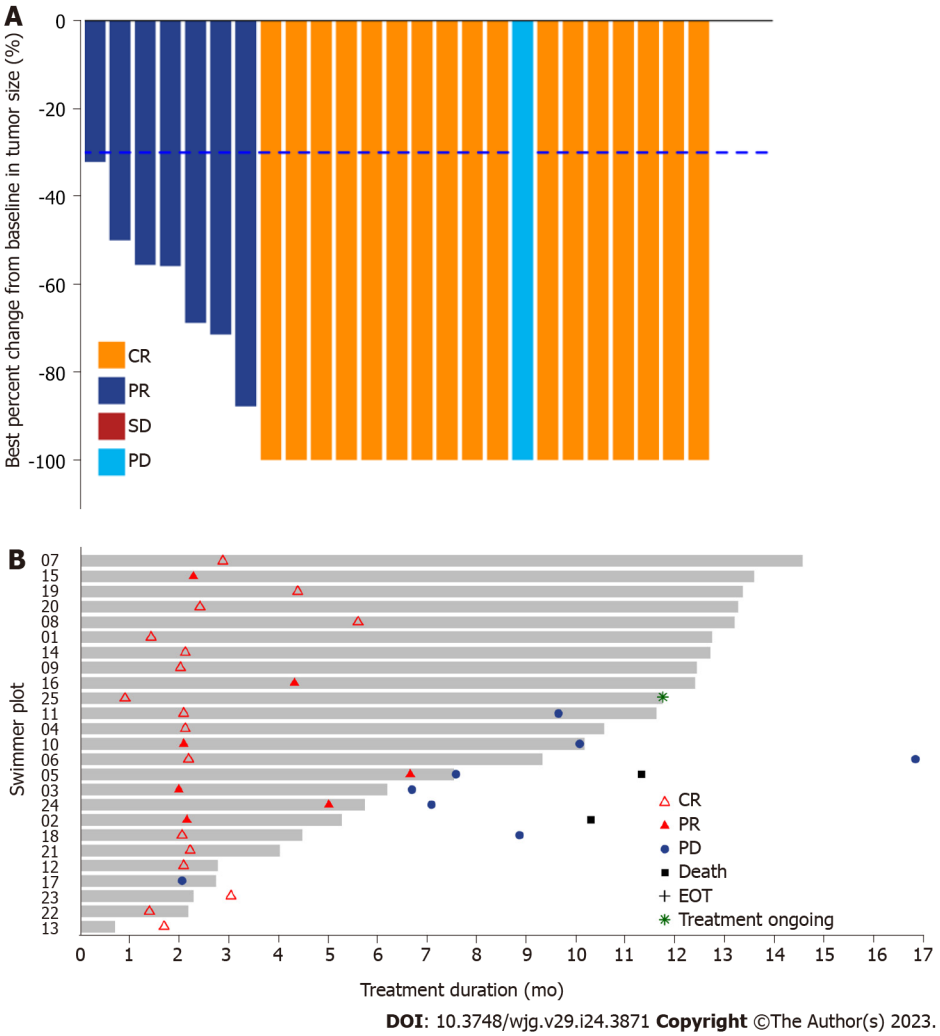
Exploration of biomarkers

This study also explored biomarkers that could be used to predict efficacy. In this study, blood samples from patients after each treatment were collected and analyzed for lymphocyte counts and their subset populations [CD19+ B cells, CD3+, CD4+, CD8+ T cells, and CD15+CD56+ natural killer (NK) cells] by flow cytometry. The median PFS period (19.7 mo) was applied as a cutoff value, and there were no significant differences between PFS ≥ 19.7 and PFS < 19.7 mo for lymphocyte count, CD19+ B, CD3+, CD4+, CD8+ T, and CD15+CD56+ NK cells at baseline. PFS period ≥ 19.7 mo was associated with higher lymphocyte counts and CD3+, CD4+, CD8+ T, and CD15+CD56+ NK cells compared to PFS period < 19.7 mo after three treatments. These significant differences persisted after the four treatments, except for CD8+ T cells. Furthermore, the difference between PFS ≥ 19.7 and PFS < 19.7 mo after five treatments disappeared for most biomarkers, whereas significant differences remained for lymphocyte count and CD19+ B cells. Finally, PFS ≥ 19.7 mo persisted and was associated with elevated number of CD19+ B cells (Figure 3).

DISCUSSION

To the best of our knowledge, this is the first prospective study of SBRT in combination with PD-1 inhibitor for recurrent or oligometastatic HCC. This study demonstrated that SBRT delivered at a median dose of 54 Gy in 6 fractions plus sintilimab achieved a remarkable PFS period of 19.7 mo and an outstanding ORR of 96% in such patients. Although the median OS was not reached, the OS rates at 12 and 24 mo were 91.5% and 83.2%, respectively. Moreover, the local control rates at 12 and 24 mo were 100% and 90.9%, respectively, whereas the DCR after treatment was 96%. Furthermore, TRAEs in most patients were mild and well tolerated.

The enrolled patients in our study were diagnosed with recurrent or oligometastatic HCC and belonged to the advanced-stage HCC population. Currently, the standard systemic treatment for advanced HCC is PD-1/PD-L1 inhibitors in combination with bevacizumab, such as sintilimab plus bevacizumab and atezolizumab plus bevacizumab. The median PFS period of the experimental groups in Orient-32 and Imbrave150 were 4.6 and 6.8 mo, respectively[13,19]. In our study, 19.7 mo of median

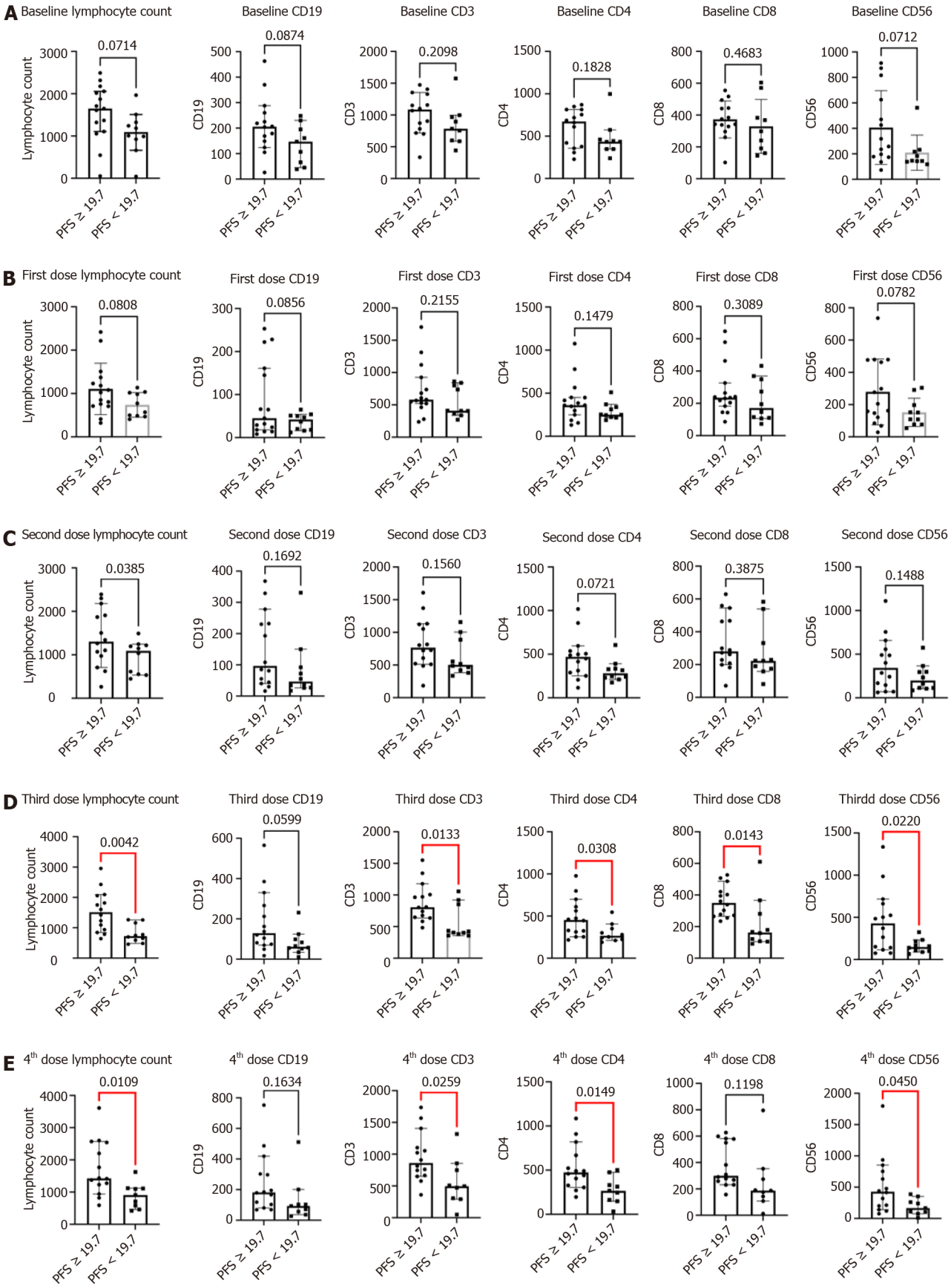


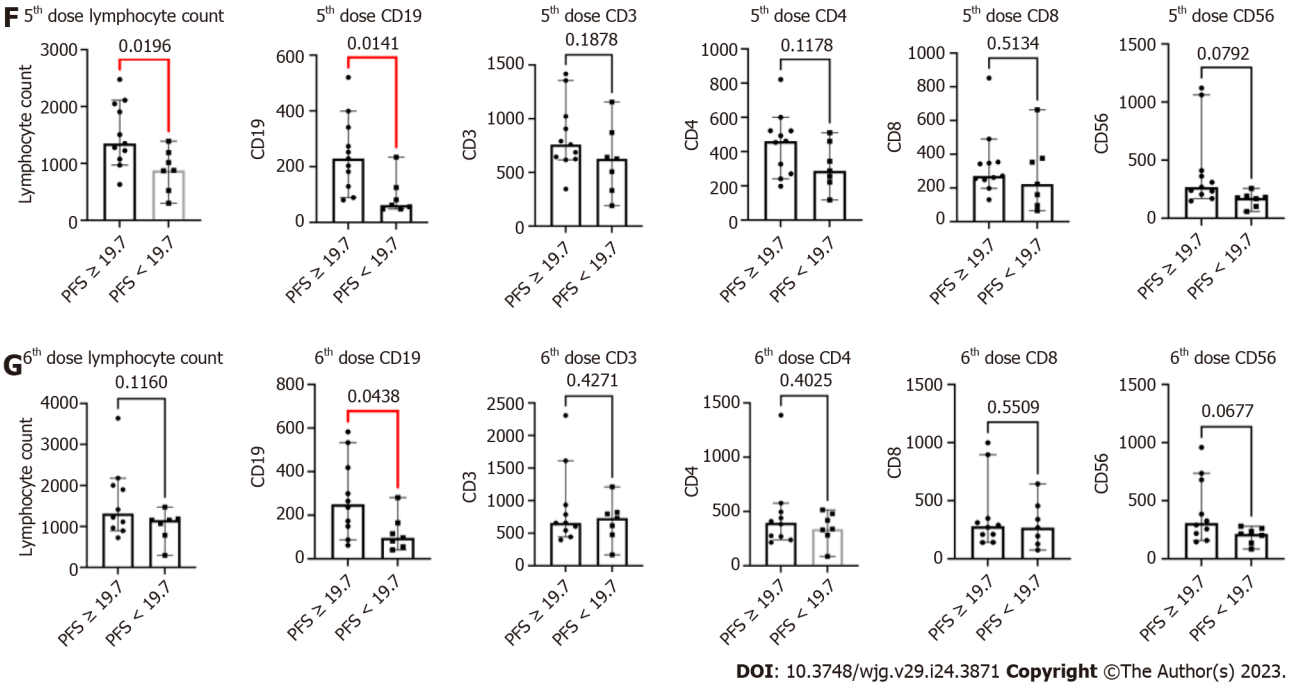
DOI: 10.3748/wjg.v29.i24.3871 **Copyright** ©The Author(s) 2023.

Figure 2 Radiographic responses to stereotactic body radiotherapy plus sintilimab. A: Waterfall plots of the proportion of patients with an overall response according to the response evaluation criteria in solid tumors version 1.1; B: The swimmer plot shows the treatment duration for patients receiving stereotactic body radiotherapy and sintilimab. CR: Complete response; PR: Partial response; PD: Progressive disease; EOT: End-of-treatment; SD: Stable disease.

PFS (mPFS) period showed a beneficial tendency with SBRT and sintilimab. Notably, the population characteristics of our study were different from these two phase-III studies. The proportion of patients with vessel invasion or extrahepatic metastasis was > 60% in both Orient-32 and Imbrave150. Moreover, patients accounted for approximately 40% of the total population with both ECOG PS of 1 andα-fetoprotein (AFP) ≥ 400 ng/mL. However, patients with few metastases or relapses were enrolled in our study, and the median number of metastases was 1. Additionally, most of them had ECOG PS 0 (76%), and patients with AFP ≥ 400 ng/mL only accounted for 12%. Given the above, the high proportion of patients with good physical condition and the low proportion of patients with AFP ≥ 400 ng/mL could be explained by the remarkable mPFS period in this study. Moreover, it can also be considered the main possible reason that patients with recurrent or oligometastatic HCC (tumor lesions ≤ 5) benefit from combination therapy of SBRT plus immunotherapy.

Oligometastasis was defined as ≤ 5 metastatic lesions, and SBRT was recommended for patients with oligometastasis and many other cancers. However, no prospective clinical studies have reported the treatment strategies for patients with recurrent or oligometastatic HCC. Several retrospective clinical studies on patients with recurrent or oligometastatic HCC demonstrated that after SBRT, the 1-year OS and local control rates were 55%-84% and 77%-94%, respectively[5,20-23]. In the current study, the 1-year OS and local control rates were 91.5% and 100%, respectively. Although comparisons between studies need to be made cautiously, in terms of benefit trends, it seems that SBRT plus sintilimab has more survival benefits. This encouraging therapeutic effect can be interpreted as radiation activating the immune system by inducing tumor cell death, which can promote cytokine release and damage-associated molecular patterns. The tumor-specific T lymphocytes are then primed and trafficked into the tumor microenvironment, which can enhance the efficacy of PD-1 inhibitors[24]. Another retrospective study of SBRT plus PD-1 inhibitors for patients with Barcelona Clinic Liver Cancer intermediate-stage HCC with a median PFS period of up to 19.6 mo also verified the combination efficacy[17]. It should be emphasized that this retrospective study included patients with intermediate-stage HCC, which theoret-


A
Baseline lymphocyte count
0.0714
Baseline CD19
0.0874
Baseline CD3
0.2098
Baseline CD4
0.1828
Baseline CD8
0.4683
Baseline CD56
0.0712
B
First dose lymphocyte count
0.0808
First dose CD19
0.0856
First dose CD3
0.2155
First dose CD4
0.1479
First dose CD8
0.3089
First dose CD56
0.0782
C
Second dose lymphocyte count
0.0385
Second dose CD19
0.1692
Second dose CD3
0.1560
Second dose CD4
0.0721
Second dose CD8
0.3875
Second dose CD56
0.1488
D
Third dose lymphocyte count
0.0042
Third dose CD19
0.0599
Third dose CD3
0.0133
Third dose CD4
0.0308
Third dose CD8
0.0143
Thirdd dose CD56
0.0220
E
4th dose lymphocyte count
0.0109
4th dose CD19
0.1634
4th dose CD3
0.0259
4th dose CD4
0.0149
4th dose CD8
0.1198
4th dose CD56
0.0450
Lymphocyte count
CD19
CD3
CD4
CD8
CD56
PFS ≥ 19.7
PFS < 19.7



DOI: 10.3748/wjg.v29.i24.3871 **Copyright** ©The Author(s) 2023.

Figure 3 Biomarker analysis. A: Baseline: Progression-free survival (PFS) ≥ 19.7 *vs* PFS < 19.7; B: 1st Dose: PFS ≥ 19.7 *vs* PFS < 19.7; C: 2nd Dose: PFS ≥ 19.7 *vs* PFS < 19.7; D: 3rd Dose: PFS ≥ 19.7 *vs* PFS < 19.7; E: 4th Dose: PFS ≥ 19.7 *vs* PFS < 19.7; F: 5th Dose: PFS ≥ 19.7 *vs* PFS < 19.7; G: 6th Dose: PFS ≥ 19.7 *vs* PFS < 19.7. PFS: Progression-free survival.

ically represent a better prognosis.

In addition, our study reported that the ORR after sintilimab and SBRT was 96%, and only one patient had liver lesions that disappeared with pulmonary metastasis. In previous retrospective studies on HCC with recurrence or oligometastases, the ORR of SBRT in this subset was 59%-85%. The authors clearly stated that out-of-field recurrence was the major cause of disease progression[5,20-23]. Sintilimab, as a systemic immunotherapy, can inhibit tumor cell escape and reactivate T cells, thereby reducing out-field recurrence.

In terms of safety, the combination of sintilimab and SBRT was well tolerated. Most TRAEs were of grades 1-2. Grade 3 TRAEs were observed in only 12% of the patients. A decreased lymphocyte count a common AE associated with radiotherapy. The results of monitoring changes in lymphocyte counts showed that decreased lymphocyte counts gradually recovered, and previous reports indicated that recovery from reduced lymphocyte count is faster in patients with HCC treated with SBRT than in those treated with conventional RT.

Biomarker-related analyses have mainly explored the relevance of lymphocytes and their subsets to efficacy. The results showed that patients with a longer PFS had higher lymphocyte counts and CD19+ B, CD3+, CD4+, CD8+ T, and CD15+CD56+ NK cells after four to five prior therapies. This is consistent with the result of a previous biomarker explorative study on SBRT for lung cancer, suggesting that lymphocyte counts and subsets can be potential biomarkers for predicting efficacy[25]. The significant difference gradually disappeared after the fifth to sixth treatments, which is likely related to the reduced sample size due to the increasing number of patients with disease progression and loss of follow-up. This needs to be confirmed in further studies with larger sample sizes.

This study has some limitations. The current study was designed as a phase II trial with no parallel control group. Moreover, the sample size was small, and stratified analyses according to patient characteristics were not performed. Finally, the history of prior therapy varied across the enrolled patients, which could have affected the prognosis of HCC.

CONCLUSION

In this single-arm phase II trial, SBRT plus sintilimab showed outstanding PFS and ORR in the treatment of recurrent or oligometastatic HCC. Moreover, the combined use of SBRT and sintilimab is safe and tolerable. Patients can recover rapidly from radiotherapy-induced decreases in lymphocyte counts. Considering mostly included patients (96%) infected with hepatitis B, this result suggests that SBRT combined with sintilimab may be a new treatment option for patients with recurrent or oligometastatic HCC and infected with hepatitis B. Further large-scale, parallel-control randomized controlled trials should be conducted to compare the effects of SBRT plus sintilimab with other

treatments, including SBRT without immunotherapy or radioembolization delivers doses to the tumor greater than 100 Gy.

ARTICLE HIGHLIGHTS

Research background

Hepatocellular carcinoma (HCC) accounts for the third-leading cause of cancer-related deaths, and only 30%-40% of patients were diagnosed at early stages. The oligometastatic HCC indicated the metastasis of HCC was not widespread, and some patients may obtain benefits for curative treatments.

Research motivation

Stereotactic body radiotherapy (SBRT) and programmed cell death 1 (PD-1) inhibitors are widely used for HCC, whether the use of SBRT combined with a PD-1 inhibitor could offer superior benefits for oligometastatic HCC remained unclear.

Research objectives

To assess the efficacy and safety of combining SBRT with sintilimab for patients with recurrent or oligometastatic HCC.

Research methods

Patients with recurrent or oligometastatic HCC were involved and treated with combining SBRT with sintilimab for 12 mo or disease progression. The primary endpoint was progression-free survival (PFS), while the secondary endpoints included overall survival (OS), local control rate, objective response rate (ORR), disease control rate (DCR), and adverse events.

Research results

The median PFS was 19.7 mo [95% confidence interval (CI): 16.9-NA], while the median OS was not reached. Moreover, the 1- and 2-year local control rate were 100% and 90.9% (95%CI: 75.4%-100.0%), while the ORR and DCR were 96%, and 96%, respectively. Only 3 patients reported grade 3 adverse events, including increased gamma-glutamyl transpeptidase level, decreased platelet count, and myositis.

Research conclusions

SBRT plus sintilimab can serve as an effective, well-tolerated treatment regimen for patients with recurrent or oligometastatic HCC.

Research perspectives

Further large-scale, parallel-control randomized controlled trials should be performed to verify the therapeutic effects of SBRT plus sintilimab for patients with recurrent or oligometastatic HCC.

FOOTNOTES

Author contributions: Zeng ZC, Liu TS, Chen YX, Du SS, and Yu YY contributed to the conception and study design; Chen YX, Yang P, Zhuang Y, Huang C, Hu Y, and Zhu WC contributed to the investigation and data curation; Chen YX, Zeng ZC, and Liu TS performed the data analysis and interpretation; Chen YX wrote the original draft; Zeng ZC, Liu TS, Chen YX, and Du SS wrote the review and editing; Liu TS and Zeng ZC contributed equally to this work. All authors reviewed and approved the final draft of the manuscript.

Supported by The Ministry of Science and Technology of The People's Republic of China, No. 2022YFC2503700, and No. 2022YFC2503704.

Institutional review board statement: The Medical Ethics Committee of Zhongshan Hospital, Fudan University, approved this study (B2019-010R), which was conducted in accordance with the standards of Good Clinical Practice and the Declaration of Helsinki. All patients consented to participate after being informed of the study's purpose.

Clinical trial registration statement: This was a single-arm, open-label, single-center, phase II trial registered with ClinicalTrials.gov (NCT03857815).

Informed consent statement: All patients consented to participate after being informed of the study's purpose.

Conflict-of-interest statement: The authors declare that they have no conflict of interest.

Data sharing statement: The datasets used and/or analysed during the current study are available from the corresponding author on reasonable request.

CONSORT 2010 statement: The authors have read the CONSORT 2010 statement, and the manuscript was prepared and revised according to the CONSORT 2010 statement.

Open-Access: This article is an open-access article that was selected by an in-house editor and fully peer-reviewed by external reviewers. It is distributed in accordance with the Creative Commons Attribution NonCommercial (CC BY-NC 4.0) license, which permits others to distribute, remix, adapt, build upon this work non-commercially, and license their derivative works on different terms, provided the original work is properly cited and the use is non-commercial. See: https://creativecommons.org/Licenses/by-nc/4.0/

Country/Territory of origin: China

ORCID number: Yi-Xing Chen 0000-0001-5523-2843; Shi-Suo Du 0000-0001-5477-5141; Cheng Huang 0000-0003-1348-6268; Yi-Yi Yu 0000-0002-8444-0235; Tian-Shu Liu 0000-0001-5523-2881; Zhao-Chong Zeng 0000-0002-5736-1363.

S-Editor: Fan JR
L-Editor: A
P-Editor: Liu JH

REFERENCES

1 **Sung H**, Ferlay J, Siegel RL, Laversanne M, Soerjomataram I, Jemal A, Bray F. Global Cancer Statistics 2020: GLOBOCAN Estimates of Incidence and Mortality Worldwide for 36 Cancers in 185 Countries. *CA Cancer J Clin* 2021; **71**: 209-249 [PMID: 33538338 DOI: 10.3322/caac.21660]

2 **Siegel RL**, Miller KD, Fuchs HE, Jemal A. Cancer statistics, 2022. *CA Cancer J Clin* 2022; **72**: 7-33 [PMID: 35020204 DOI: 10.3322/caac.21708]

3 **Zou H**, Zhu CZ, Wang C, Wang ZS, Ma X, Han B, Wu LQ. Recurrence of Barcelona Clinic Liver Cancer Stage A Hepatocellular Carcinoma After Hepatectomy. *Am J Med Sci* 2017; **354**: 262-267 [PMID: 28918833 DOI: 10.1016/j.amjms.2017.05.014]

4 **Lee SU**, Yoon SM, Cheng JC, Kim TH, Kim BH, Park JH, Jung J, Tsai CL, Chiang Y, Park JW. Multi-Institutional Retrospective Study of Radiotherapy for Hepatocellular Carcinoma in the Caudate Lobe. *Front Oncol* 2021; **11**: 646473 [PMID: 33718247 DOI: 10.3389/fonc.2021.646473]

5 **Yao E**, Chen J, Zhao X, Zheng Y, Wu X, Han F, Huang H, Liang P, Liu J, Wu F, Lin L. Efficacy of Stereotactic Body Radiotherapy for Recurrent or Residual Hepatocellular Carcinoma after Transcatheter Arterial Chemoembolization. *Biomed Res Int* 2018; **2018**: 5481909 [PMID: 29687004 DOI: 10.1155/2018/5481909]

6 **Li C**, Wang H, Chen R, Zhang H, Xu Y, Zhang B, Li Y, Zhang C, Yang Y, Wang X, Li X. Outcomes and recurrence patterns following curative hepatectomy for hepatocellular carcinoma patients with different China liver cancer staging. *Am J Cancer Res* 2022; **12**: 907-921 [PMID: 35261811]

7 **Weichselbaum RR**, Hellman S. Oligometastases revisited. *Nat Rev Clin Oncol* 2011; **8**: 378-382 [PMID: 21423255 DOI: 10.1038/nrclinonc.2011.44]

8 **Nowak AK**, Chow PK, Findlay M. Systemic therapy for advanced hepatocellular carcinoma: a review. *Eur J Cancer* 2004; **40**: 1474-1484 [PMID: 15196530 DOI: 10.1016/j.ejca.2004.02.027]

9 **Kang JK**, Kim MS, Cho CK, Yang KM, Yoo HJ, Kim JH, Bae SH, Jung DH, Kim KB, Lee DH, Han CJ, Kim J, Park SC, Kim YH. Stereotactic body radiation therapy for inoperable hepatocellular carcinoma as a local salvage treatment after incomplete transarterial chemoembolization. *Cancer* 2012; **118**: 5424-5431 [PMID: 22570179 DOI: 10.1002/cncr.27533]

10 **Andolino DL**, Johnson CS, Maluccio M, Kwo P, Tector AJ, Zook J, Johnstone PA, Cardenes HR. Stereotactic body radiotherapy for primary hepatocellular carcinoma. *Int J Radiat Oncol Biol Phys* 2011; **81**: e447-e453 [PMID: 21645977 DOI: 10.1016/j.ijrobp.2011.04.011]

11 **Bujold A**, Massey CA, Kim JJ, Brierley J, Cho C, Wong RK, Dinniwell RE, Kassam Z, Ringash J, Cummings B, Sykes J, Sherman M, Knox JJ, Dawson LA. Sequential phase I and II trials of stereotactic body radiotherapy for locally advanced hepatocellular carcinoma. *J Clin Oncol* 2013; **31**: 1631-1639 [PMID: 23547075 DOI: 10.1200/JCO.2012.44.1659]

12 **Finn RS**, Ryoo BY, Merle P, Kudo M, Bouattour M, Lim HY, Breder V, Edeline J, Chao Y, Ogasawara S, Yau T, Garrido M, Chan SL, Knox J, Daniele B, Ebbinghaus SW, Chen E, Siegel AB, Zhu AX, Cheng AL; KEYNOTE-240 investigators. Pembrolizumab As Second-Line Therapy in Patients With Advanced Hepatocellular Carcinoma in KEYNOTE-240: A Randomized, Double-Blind, Phase III Trial. *J Clin Oncol* 2020; **38**: 193-202 [PMID: 31790344 DOI: 10.1200/JCO.19.01307]

13 **Ren Z**, Xu J, Bai Y, Xu A, Cang S, Du C, Li Q, Lu Y, Chen Y, Guo Y, Chen Z, Liu B, Jia W, Wu J, Wang J, Shao G, Zhang B, Shan Y, Meng Z, Gu S, Yang W, Liu C, Shi X, Gao Z, Yin T, Cui J, Huang M, Xing B, Mao Y, Teng G, Qin Y, Xia F, Yin G, Yang Y, Chen M, Wang Y, Zhou H, Fan J; ORIENT-32 study group. Sintilimab plus a bevacizumab biosimilar (IBI305) versus sorafenib in unresectable hepatocellular carcinoma (ORIENT-32): a randomised, open-label, phase 2-3 study. *Lancet Oncol* 2021; **22**: 977-990 [PMID: 34143971 DOI: 10.1016/S1470-2045(21)00252-7]

14 **Chen H**, Li Z, Qiu L, Dong X, Chen G, Shi Y, Cai L, Liu W, Ye H, Zhou Y, Ouyang J, Cai Z, Liu X. Personalized neoantigen vaccine combined with PD-1 blockade increases CD8(+) tissue-resident memory T-cell infiltration in

preclinical hepatocellular carcinoma models. *J Immunother Cancer* 2022; **10** [PMID: 36113894 DOI: 10.1136/jitc-2021-004389]

15 **Li W**, Yan J, Tian H, Li B, Wang G, Sang W, Zhang Z, Zhang X, Dai Y. A platinum@polymer-catechol nanobraker enables radio-immunotherapy for crippling melanoma tumorigenesis, angiogenesis, and radioresistance. *Bioact Mater* 2023; **22**: 34-46 [PMID: 36203954 DOI: 10.1016/j.bioactmat.2022.09.006]

16 **Kreidieh M**, Zeidan YH, Shamseddine A. The Combination of Stereotactic Body Radiation Therapy and Immunotherapy in Primary Liver Tumors. *J Oncol* 2019; **2019**: 4304817 [PMID: 31182960 DOI: 10.1155/2019/4304817]

17 **Xiang YJ**, Wang K, Zheng YT, Feng S, Yu HM, Li XW, Cheng X, Cheng YQ, Feng JK, Zhou LP, Meng Y, Zhai J, Shan YF, Cheng SQ. Effects of Stereotactic Body Radiation Therapy Plus PD-1 Inhibitors for Patients With Transarterial Chemoembolization Refractory. *Front Oncol* 2022; **12**: 839605 [PMID: 35387113 DOI: 10.3389/fonc.2022.839605]

18 **Huang WY**, Jen YM, Lee MS, Chang LP, Chen CM, Ko KH, Lin KT, Lin JC, Chao HL, Lin CS, Su YF, Fan CY, Chang YW. Stereotactic body radiation therapy in recurrent hepatocellular carcinoma. *Int J Radiat Oncol Biol Phys* 2012; **84**: 355-361 [PMID: 22342300 DOI: 10.1016/j.ijrobp.2011.11.058]

19 **Finn RS**, Qin S, Ikeda M, Galle PR, Ducreux M, Kim TY, Kudo M, Breder V, Merle P, Kaseb AO, Li D, Verret W, Xu DZ, Hernandez S, Liu J, Huang C, Mulla S, Wang Y, Lim HY, Zhu AX, Cheng AL; IMbrave150 Investigators. Atezolizumab plus Bevacizumab in Unresectable Hepatocellular Carcinoma. *N Engl J Med* 2020; **382**: 1894-1905 [PMID: 32402160 DOI: 10.1056/NEJMoa1915745]

20 **Gerum S**, Heinz C, Belka C, Walter F, Paprottka P, De Toni EN, Roeder F. Stereotactic body radiation therapy (SBRT) in patients with hepatocellular carcinoma and oligometastatic liver disease. *Radiat Oncol* 2018; **13**: 100 [PMID: 29843752 DOI: 10.1186/s13014-018-1048-4]

21 **Matoba M**, Tsuchiya H, Kondo T, Ota K. Stereotactic body radiotherapy delivered with IMRT for oligometastatic regional lymph node metastases in hepatocellular carcinoma: a single-institutional study. *J Radiat Res* 2020; **61**: 776-783 [PMID: 32845298 DOI: 10.1093/jrr/rraa067]

22 **Su TS**, Liang P, Lu HZ, Liang J, Gao YC, Zhou Y, Huang Y, Tang MY, Liang JN. Stereotactic body radiation therapy for small primary or recurrent hepatocellular carcinoma in 132 Chinese patients. *J Surg Oncol* 2016; **113**: 181-187 [PMID: 26799260 DOI: 10.1002/jso.24128]

23 **Jo IY**, Park HC, Kim ES, Yeo SG, Kim M, Seong J, Kim JW, Kim TH, Yoon WS, Jeong BK, Kim SH, Lee JH. Stereotactic ablative radiotherapy for pulmonary oligometastases from primary hepatocellular carcinoma: a multicenter and retrospective analysis (KROG 17-08). *Jpn J Clin Oncol* 2022; **52**: 616-622 [PMID: 35311896 DOI: 10.1093/jjco/hyac028]

24 **Romano E**, Honeychurch J, Illidge TM. Radiotherapy-Immunotherapy Combination: How Will We Bridge the Gap Between Pre-Clinical Promise and Effective Clinical Delivery? *Cancers (Basel)* 2021; **13** [PMID: 33530329 DOI: 10.3390/cancers13030457]

25 **Liu C**, Hu Q, Xu B, Hu X, Su H, Li Q, Zhang X, Yue J, Yu J. Peripheral memory and naïve T cells in non-small cell lung cancer patients with lung metastases undergoing stereotactic body radiotherapy: predictors of early tumor response. *Cancer Cell Int* 2019; **19**: 121 [PMID: 31080362 DOI: 10.1186/s12935-019-0839-5]

World Journal of Gastroenterology

Submit a Manuscript: https://www.f6publishing.com

World J Gastroenterol 2023 June 28; 29(24): 3883-3898

DOI: 10.3748/wjg.v29.i24.3883

ISSN 1007-9327 (print) ISSN 2219-2840 (online)

ORIGINAL ARTICLE

Observational Study

Non-exposed endoscopic wall-inversion surgery with one-step nucleic acid amplification for early gastrointestinal tumors: Personal experience and literature review

Francesco Crafa, Serafino Vanella, Aristide Morante, Onofrio A Catalano, Kelsey L Pomykala, Mario Baiamonte, Maria Godas, Alexandra Antunes, Joaquim Costa Pereira, Valentina Giaccaglia

Specialty type: Surgery

Provenance and peer review: Invited article; Externally peer reviewed.

Peer-review model: Single blind

Peer-review report's scientific quality classification

Grade A (Excellent): 0
Grade B (Very good): 0
Grade C (Good): C, C
Grade D (Fair): 0
Grade E (Poor): 0

P-Reviewer: Goto O, Japan; Guo X, China

Received: March 25, 2023
Peer-review started: March 25, 2023
First decision: April 21, 2023
Revised: May 11, 2023
Accepted: May 31, 2023
Article in press: May 31, 2023
Published online: June 28, 2023

Francesco Crafa, Serafino Vanella, Mario Baiamonte, Maria Godas, Division of General and Surgical Oncology, St. Giuseppe Moscati Hospital, Center of National Excellence and High Specialty, Avellino 83100, Italy

Aristide Morante, Division of Gastorenterology and Endoscopy, St. Giuseppe Moscati Hospital, Center of National Excellence and High Specialty, Avellino 83100, Italy

Onofrio A Catalano, Department of Radiology, Athinoula A Martinos Center for Biomedical Imaging, Massachusetts General Hospital, Harvard Medical School, Boston, MA 02114, United States

Kelsey L Pomykala, Department of Nuclear Medicine, Department of Radiological Sciences, University Hospital Essen, University of Duisburg-Essen, Essen 45141, Germany

Alexandra Antunes, Joaquim Costa Pereira, Department of General Surgery, Braga Hospital, Braga 4710-243, Portugal

Valentina Giaccaglia, Department of Surgery, Medclinic City Hospital, Dubai 505004, United Arab Emirates

Corresponding author: Serafino Vanella, MD, PhD, Doctor, Surgeon, Surgical Oncologist, Division of General and Surgical Oncology, St. Giuseppe Moscati Hospital, Center of National Excellence and High Specialty, C/da Amoretta, Avellino 83100, Italy. nekroma@yahoo.it

Abstract

BACKGROUND

Laparoscopic and endoscopic cooperative surgery is a safe, organ-sparing surgery that achieves full-thickness resection with adequate margins. Recent studies have demonstrated the safety and efficacy of these procedures. However, these techniques are limited by the exposure of the tumor and mucosa to the peritoneal cavity, which could lead to viable cancer cell seeding and the spillage of gastric juice or enteric liquids into the peritoneal cavity. Non-exposed endoscopic wall-inversion surgery (NEWS) is highly accurate in determining the resection margins to prevent intraperitoneal contamination because the tumor is inverted into the visceral lumen instead of the peritoneal cavity. Accurate intraoperative asse-

ssment of the nodal status could allow stratification of the extent of resection. One-step nucleic acid amplification (OSNA) can provide a rapid method of evaluating nodal tissue, whilst near-infrared laparoscopy together with indocyanine green can identify relevant nodal tissue intraoperatively.

AIM

To determine the safety and feasibility of NEWS in early gastric and colon cancers and of adding rapid intraoperative lymph node (LN) assessment with OSNA.

METHODS

The patient-based experiential portion of our investigations was conducted at the General and Oncological Surgery Unit of the St. Giuseppe Moscati Hospital (Avellino, Italy). Patients with early-stage gastric or colon cancer (diagnosed *via* endoscopy, endoscopic ultrasound, and computed tomography) were included. All lesions were treated by NEWS procedure with intraoperative OSNA assay between January 2022 and October 2022. LNs were examined intraoperatively with OSNA and postoperatively with conventional histology. We analyzed patient demographics, lesion features, histopathological diagnoses, R0 resection (negative margins) status, adverse events, and follow-up results. Data were collected prospectively and analyzed retrospectively.

RESULTS

A total of 10 patients (5 males and 5 females) with an average age of 70.4 ± 4.5 years (range: 62-78 years) were enrolled in this study. Five patients were diagnosed with gastric cancer. The remaining 5 patients were diagnosed with early-stage colon cancer. The mean tumor diameter was 23.8 ± 11.6 mm (range: 15-36 mm). The NEWS procedure was successful in all cases. The mean procedure time was 111.5 ± 10.7 min (range: 80-145 min). The OSNA assay revealed no LN metastases in any patients. Histologically complete resection (R0) was achieved in 9 patients (90.0%). There was no recurrence during the follow-up period.

CONCLUSION

NEWS combined with sentinel LN biopsy and OSNA assay is an effective and safe technique for the removal of selected early gastric and colon cancers in which it is not possible to adopt conventional endoscopic resection techniques. This procedure allows clinicians to acquire additional information on the LN status intraoperatively.

Key Words: Laparoscopic and endoscopic cooperative surgery; Non-exposed endoscopic wall inversion surgery; Early gastric cancer; Early colorectal cancer; Sentinel lymph node; One-step nucleic acid amplification; Endoscopic full-thickness resection

©The Author(s) 2023. Published by Baishideng Publishing Group Inc. All rights reserved.

Core Tip: The treatment efficacy of non-exposed endoscopic wall-inversion surgery combined with sentinel lymph node (LN) biopsy and intraoperative one-step nucleic acid amplification assay remains to be fully evaluated in early gastric and colon cancers. The patients included in the experiential portion of our investigations were diagnosed with early gastric and colon cancers that were not amenable to conventional endoscopic resection techniques. We found that this approach provides essential details on LN status intraoperatively and we discuss the related literature to help guide future research studies and clinical care.

Citation: Crafa F, Vanella S, Morante A, Catalano OA, Pomykala KL, Baiamonte M, Godas M, Antunes A, Costa Pereira J, Giaccaglia V. Non-exposed endoscopic wall-inversion surgery with one-step nucleic acid amplification for early gastrointestinal tumors: Personal experience and literature review. *World J Gastroenterol* 2023; 29(24): 3883-3898

URL: https://www.wjgnet.com/1007-9327/full/v29/i24/3883.htm

DOI: https://dx.doi.org/10.3748/wjg.v29.i24.3883

INTRODUCTION

The most effective treatment for patients with resectable gastrointestinal submucosal tumors (SMTs), including gastrointestinal stromal tumors[1-4] and early gastrointestinal cancer[5], is complete surgical

resection. Segmental resection is acceptable based on oncologic principles[6-8]. Endoscopic submucosal dissection (ESD) is a well-studied treatment for adenomas and early cancer of the gastrointestinal tract [9]. In some cases, it has low rates of microscopic resections with a negative margin (R0). ESD in lesions involving the muscularis propria remains controversial due to the increased risk of perforation[10-13]. Adverse events have also been described in lesions located in anatomical positions that are difficult to access.

Previous studies reported that laparoscopic wedge resection for gastric submucosal tumors (SMTs) was oncologically feasible and safe with a decrease in blood loss and length of hospital stay[14-16] compared to other classic gastric resections. Using the conventional laparoscopic approach, it is difficult to establish the exact line of resection for intraluminally developing gastrointestinal tumors. With limited or overabundant resections, there is a risk of having postoperative functional problems or infiltrated resection margins with postoperative recurrence[17,18]. Endoscopic control of the resection margin is essential for safe local resection in early gastrointestinal cancers[19]. Narrow-band imaging (NBI) is a digital optical method of image-enhanced endoscopy that enhances the vessel and surface structure of colorectal lesions using 415 nm and 540 nm wavelength filters[20-22]. Several NBI classifications for colorectal lesions have been proposed. These classifications were unified as the NBI International Colorectal Endoscopic (NICE) classification for non-magnifying endoscopy in 2009 and the Japan NBI Expert Team (JNET) classification for magnifying endoscopy in 2014[20,23-27].

NICE was divided into three groups based on histology: Hyperplastic or sessile serrated polyp (type 1), adenoma (type 2), and deep submucosal invasive cancer (type 3). There are also three criteria: Surface pattern, vase pattern and colour[26,27]. The Japanese endoscopists separated the type 2 NICE category into type 2A (low-grade adenoma) and type 2B (high-grade adenoma and submucosal cancer) using magnifying endoscopy. They developed the JNET classification as an advanced version of the NICE classification. When magnifying endoscopy is available, the JNET classification is better at selecting the correct therapeutic strategy based on precise diagnosis[20].

To overcome the limitations of endoscopic resections and wedge resections, Hiki *et al*[28] combined the ESD technique to properly determine the resection margin with laparoscopic full-thickness excision, developing a hybrid technique of laparoscopic endoscopic cooperative surgery (LECS). The LECS allows to preserve the vascularization, the innervation of the wall, and the organs' functionality with a better postoperative quality of life for the patient.

To expand the indication of LECS, some modified LECS procedures were developed, such as non-exposed endoscopic wall-inversion surgery (NEWS)[29-36]. Currently, the LECS, already widely studied for stomach lesions, is also used for lesions of other organs, such as the duodenum[37], the rectum and the colon[38,39]. This technique allows the lesion to be approached simultaneously from the inside endoscopically and externally laparoscopically, allowing a limited resection that respects oncological principles[40-44].

Diagnostic imaging assessment of lymphadenopathy in gastric and colorectal cancers (CRCs) is challenging. Individual imaging modalities face specific intrinsic limitations, which negatively impact detection and it does not allow a correct evaluation of important lymph node (LN) details. Therefore we only have the size criterion available to determine lymphadenopathies[45]. A new semi-automated diagnostic method called one-step nucleic acid amplification (OSNA) has been developed to detect LN metastases. OSNA is based on reverse transcription–loop-mediated isothermal amplification[46,47] to amplify cytokeratin 19 (*CK19*) mRNA. The OSNA test has been used successfully in numerous malignancies[48]. Yaguchi *et al*[49] defined the CK19 mRNA cutoff to identify LN metastases with OSNA assay in gastric cancer[49-52]. Kumagai *et al*[50] showed that OSNA could be advantageously used to diagnose LN metastases in advanced gastric cancer.

CK19 is an epithelial marker. When it is identified in LNs from patients with CRC, it is highly suggestive of LN metastases[53-55]. The OSNA assay can assess LN metastasis in various cancers expressing CK19, including sentinel LNs in breast cancer and other cancers[56-59].

In this study, we determined the safety and feasibility of NEWS in early gastric and colon cancers and adding rapid intraoperative LN assessment with OSNA.

MATERIALS AND METHODS

A cohort study approach was taken, relying on data from a prospectively maintained database of consecutive patients undergoing elective NEWS for early gastric and colon cancers at St. Giuseppe Moscati Hospital of Avellino, Italy. The database included preoperative, intraoperative and postoperative data. Inclusion criteria were: (1) Adult age; (2) diagnosis with early gastric or colon cancer; and (3) eligibility for the NEWS procedure. Exclusion criterion was: Allergy to indocyanine green (ICG). In total, 10 patients were included in this study.

This study was carried out in continuity with our previous study[59] and conducted according to the ethical principles of the Institution following the Declaration of Helsinki and with approval by the Institutional Review Board of the St. Giuseppe Moscati Hospital (Approval No. 201801). Written informed consent was granted by study participants for the publication of this article.

Surgical-endoscopic technique and histopathological evaluation

Immediately after access to the abdominal cavity by laparotomy or laparoscopy, a flexible endoscope was passed to the tumor site (Figure 1) to allow a 0.5 mL submucosal injection of ICG (2.5–5.0 mg/mL) at four points around the tumor (Figure 2). The nodal basin was then examined under near-infrared (NIR) illumination (Karl Storz SE & Co., Tuttlingen, Germany). In the case of the stomach, we proceeded to the exeresis of identifiable nodes at one or two nodal basins (Figure 3). In contrast, in the case of the colon, any identifiable sentinel LNs were excised and submitted immediately to the pathology department. LNs harvested in this way were cleaned of fat. LNs weighing between 0.05 g and 0.60 g or with a cross diameter of less than 8 mm were exclusively processed using the OSNA technique. LNs weighing more than 0.60 g or with diameter over 8 mm were dissected and analyzed using the OSNA technique and hematoxylin and eosin (H&E). In the latter case, LNs were divided at 2-mm intervals, and nonadjacent blocks were alternatively subjected to definitive histopathological examination with H&E or OSNA. Our technique for preparation of materials for OSNA and interpretation of results has already been described in our previous study[59] (Figure 4). The patient's total tumor load (TTL) resulted from the sum of all *CK19* mRNA tumor copies/μL of each LN.

OSNA results with *CK19* mRNA above 250 copies/μL were designated positive, and those with fewer than 250 copies/μL were considered negative[59]. The result of the sentinel LN analysis was intraoperatively communicated to the surgeon. All patients underwent the NEWS procedure.

In this procedure, mucosal markings are placed around the tumor followed by serosal markings *via* laparoscope under endoscopic navigation. A longitudinal seromuscular incision is performed laparoscopically around the serosal markings, taking special care not to create a full-thickness opening in the wall. The pending vessels of the submucosa are coagulated laparoscopically. The seromuscular layers are sutured transversely (Figure 5) to avoid postoperative strictures, particularly in patients with colon cancer, and the lesion is inserted into the inside of the lumen. Finally, circumferential mucosal and submucosal tissue incisions are made endoscopically around the inverted tumor (Figure 6). The resected tumor is retrieved, and the mucosal defect is sutured with several endoscopic clips.

Patients with early gastric cancer and early colon cancer were encouraged to begin drinking and eating on postoperative day 1 after the NEWS procedure. If the postoperative course was uneventful, then patients could be discharged on postoperative day 1 or 2.

Subsequently, the records of each patient were discussed in a multidisciplinary conference with surgeons, pathologists, and oncologists, considering the definitive examination of the surgical specimen and the result of the sentinel LN analysis. The final histology of the surgical specimen and harvested LNs were always concluded based on the H&E analysis.

RESULTS

A total of 10 patients (5 males and 5 females) with an average age of 70.4 ± 4.5 years (range: 62-78 years) were observed in this study. Five patients were diagnosed with early-stage gastric cancer, and five patients were diagnosed with early-stage colon cancer. The mean tumor diameter was 23.8 ± 11.6 mm (range: 15-36 mm). The patient characteristics are shown in Table 1.

The NEWS procedure was successful in all cases. The mean procedure time was 111.5 ± 10.7 min (range: 80-145 min). The OSNA assay revealed no LN metastases in any patient. The diagnostic accuracy in predicting the LN status based on the sentinel LN concept by OSNA compared with the postoperative histological examination was 100%. Complete histological resection (R0) was achieved in 9 (90.0%) patients. The average post-procedure length of hospitalization was 3.1 ± 4.8 d (range: 1-8 d). There was no recurrence during the follow-up. The mean follow-up was 6.3 ± 4.2 mo.

There was only 1 patient who experienced a complication. In the gastric cancer group, 1 patient was treated conservatively for intrabdominal fluid collection (Table 2). One patient who underwent the removal of a lesion affecting the proximal transverse colon presented positive focal margins after histological examination. Therefore, he underwent a right hemicolectomy. The definitive histological examination showed no residual tumor foci or LN metastases (Table 3).

The average LN count was 2.5 ± 2.2, ranging from 1 to 5 nodes per patient. Five patients had early gastric cancer, and five had early CRC confirmed by final histology.

DISCUSSION

In this article, we investigated the possibility of adding to the NEWS (for early gastrointestinal cancers) an intraoperative study of LNs using fluorescence and ICG to identify the LN basin of the tumor and OSNA for the analysis of the excised LNs. We also performed a literature review on the use of NEWS in early gastrointestinal cancers, on sentinel LN and LN basin studies in gastric and colonic cancers, and on the intraoperative use of OSNA.

Table 1 Patient demographics and clinical results

Variables	Results
Sex	
Male	5 (50)
Female	5 (50)
Age	70.4 ± 4.5 (62-78)
BMI	23.7 ± 2.1 (20.2-26.5)
ASA physical status classification	
I	0
II	5
III	5
IV	0
V	0
Tumor size in mm	23.8 ± 11.6 (10-36)
Tumor location	
Stomach	5
Colon	5
Operation time in min	111.5 ± 10.7 (80-145)
Negative margin	9/10
Number of nodes	2.5 ± 2.2 (1-5)
Postoperative complications	1/10
Recurrence	0
Follow-up period in mo	6.3 ± 4.2

Data are presented as *n*, *n*/total, *n* (%), or mean ± SD (range). All patients were included in the evaluations. ASA: American Society of Anesthesiologists; BMI: Body mass index.

Table 2 Tumor size, number of retrieved lymph nodes, and clinical and anatomical parameters of the gastric lesions

Variables	Results
Number	5
Tumor size in mm	23.5 ± 12.1 (10-36)
Primary site	
Body	3 (60)
Antrum	2 (40)
Operation time in min	110.5 ± 10.9 (80-145)
Complete resection	5/5
Complications	1/5
Number of lymph nodes	2.6 ± 2.2 (1-4)
Length of hospitalization in d	3.6 ± 4.2 (1-8)
Recurrence	0

Data are presented as *n*, *n*/total, *n* (%), or mean ± SD (range). All patients were included in the evaluations.

NEWS in early gastrointestinal cancers

NEWS has been reported as a novel full-thickness resection technique without wall perforation. It is primarily used to treat early gastrointestinal cancer[30,32-34,60,61]. An advantage of NEWS is that all the gastric or intestinal layers can be resected precisely under direct visualization by laparoscopy and endoscopy. As a result, wall resection is limited and oncological principles are respected. The size of the tumor is one of the main limitations of NEWS. Lesion size should be 30 mm or less as the resected specimen is retrieved perorally or transanally. The LECS concept initially adopted for gastric lesions can also be applied to colorectal tumors[38]. The appropriate indications of LECS for colorectal tumors are: (1) Intramucosal carcinoma (Tis) and adenoma with high-grade atypia accompanied by a severe degree of fibrosis in the submucosal layer (tumor recurrence after endoscopic or surgical resection); (2) Tis and adenoma with high-grade atypia involving the appendix or diverticulum; or (3) intraluminal or intramural growth-type SMTs. LECS for the colon is a safe and feasible procedure[62,63]. LECS for colorectal tumors has a 0% rate for either residual or local recurrence.

Currently, modified LECS procedures can be applied to cases of early gastrointestinal cancer (within the indication for endoscopic mucosal resection/ESD) that would be technically difficult to treat with endoscopic mucosal resection/ESD. Innovative organ-preserving procedures such as transanal minimally invasive surgery, LECS, and modified LECS allow adequate resection of early-stage tumors without extensive interventions[64].

Sentinel LN and nodal basin

The LN stage remains crucial for oncological treatments. Identifying LN metastases in gastric or CRC is still unsatisfactory despite improvements in imaging techniques[65-67]. Sentinel LN biopsy for early gastric cancer is reportedly helpful when deciding whether to perform LN dissection, and LECS combined with sentinel LN dissection has been attempted for early gastric cancer as well[31,68-70]. The sentinel LN is the first LN that receives lymphatic drainage from the primary tumor and is a predictor of the pathological status of all other LNs. Miwa[71] studied lymphatic basin dissection in gastric cancer as a method of sentinel LN biopsy. The specific lymphatic system for gastric cancer is stained by a dye tracer injected near the gastric lesion and drained into the lymphatic system. The lymphatic system is then dissected en bloc, and the sentinel LN analysis is performed.

Multiple reports have investigated lymphatic basin dissection as a specific sentinel LN biopsy in stomach cancer[72-75]. The lymphatic basin identified by dye mapping is excised en bloc, and sentinel LNs are analyzed ex vivo after dissection of the basin and sent for rapid intraoperative diagnosis. If, after sentinel LN biopsy, a positive LN is found, D2 gastrectomy is added. If LNs are negative for metastases, further dissection is avoided, gastric vasculature outside the basin is preserved, and the gastric resection area is minimized[76-79].

In recent years, a number of clinical trials in Japan and South Korea have shown that the safety and therapeutic effect of sentinel LN navigation surgery in early gastric cancer are acceptable[74,80-84]. A multicenter study in Japan showed that the detection rate of sentinel LNs in early gastric cancer reached 97.5%, with 93% sensitivity and 99% accuracy[75]. A multicenter randomized controlled trial (SENORITA) conducted in South Korea showed that the sentinel LN biopsy group did not have non-inferiority to the radical gastrectomy group for 3-year disease-free survival. However, the 3-year disease-free survival and 3-year overall survival rates did not differ after rescue surgery in recurrence/metachronous gastric cancer cases. The sentinel LN biopsy group had a better long-term quality of life and nutrition than the radical gastrectomy group[76,77].

Goto *et al*[34] reported the use of NEWS for early gastric cancer in combination with sentinel LN navigation surgery (SNNS). The lymphatic basin is an essential concept in SNNS.

OSNA in gastric cancer and CRC

Recent developments in the OSNA test allow for rapidly identifying metastases over the entire LN. The OSNA assay, already extensively studied in breast cancer[56], is under evaluation as an alternative diagnostic test for identifying secondary localizations of sentinel LNs in gastric cancer[65]. In the study by Yaguchi *et al*[49], the agreement rate between the OSNA test and H&E stain was 94.4%, and the sensitivity and specificity were 88.9 and 96.8%, respectively, when the CK19 mRNA cutoff value is 250 copies/μL. The multicenter study by Kumagai *et al*[50] showed that the OSNA test has the same precision as the 2 mm interval histological examination in detecting LN metastases in the case of stomach cancer. Shoji *et al*[85] showed that single-tracer sentinel LN mapping by ICG fluorescence imaging with intraoperative diagnosis by OSNA assay is feasible and safe.

Joosten *et al*[86] in 1999 introduced the concept of sentinel LN in the CRC to reduce false negative results and study the importance of LN involvement. The main advantage of sentinel LN mapping in CRC is identifying nodes with an increased risk of metastasis so that they undergo further testing.

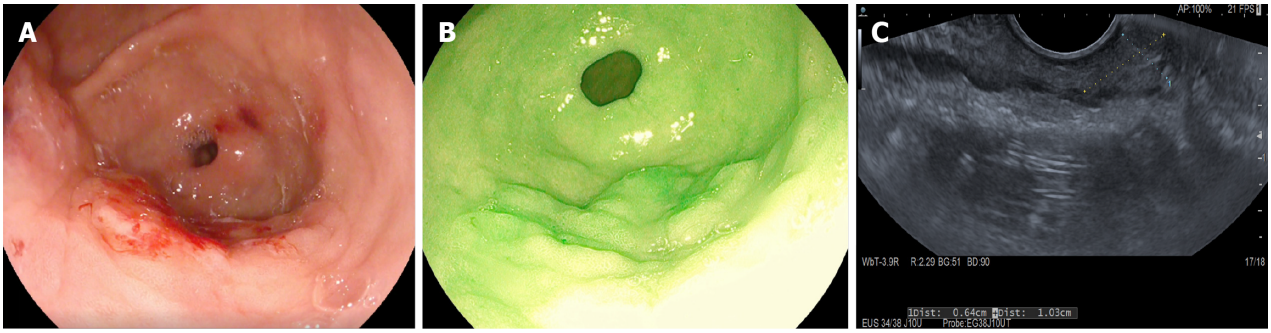
The OSNA test can also detect colorectal metastases in LNs based on *CK19* levels within 20 min of removal[87-89]. Until recently, it was predominantly used to evaluate the entire LN basin, but its rapidity could make it a functional intraoperative test to guide decision-making.

Vogelaar *et al*[90] compared OSNA with a single H&E stain and multilevel fine pathology (immunohistochemistry with pan-cytokeratin antibody staining) to identify metastases in the sentinel LN of

Table 3 Tumor size, number of retrieved lymph nodes, and clinical and anatomical parameters of the colonic lesions

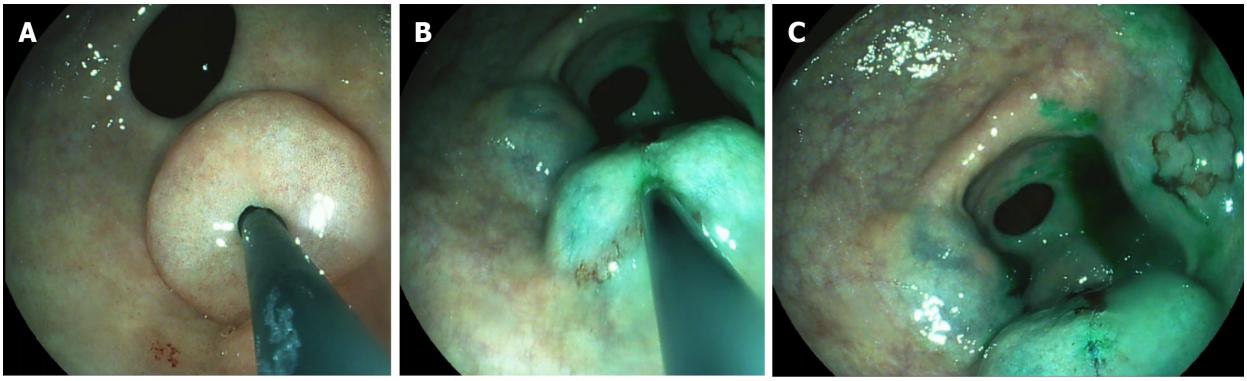
Variables	Results
Tumor number	5
Tumor size in mm	24.0 ± 10.6 (18-35)
Primary site	
Right colon	2 (40)
Left colon	3 (60)
Operation time in min	112.5 ± 10.6 (105-120)
Complete resection	4/5
Complications	0/5
Number of lymph nodes	2.4 ± 2.7 (1-5)
Length of hospitalization in d	2.3 ± 1.7 (1-4)
Recurrence	0

Data are presented as *n*, *n*/total, *n* (%), or mean ± SD (range). All patients were included in the evaluations.



DOI: 10.3748/wjg.v29.i24.3883 **Copyright** ©The Author(s) 2023.

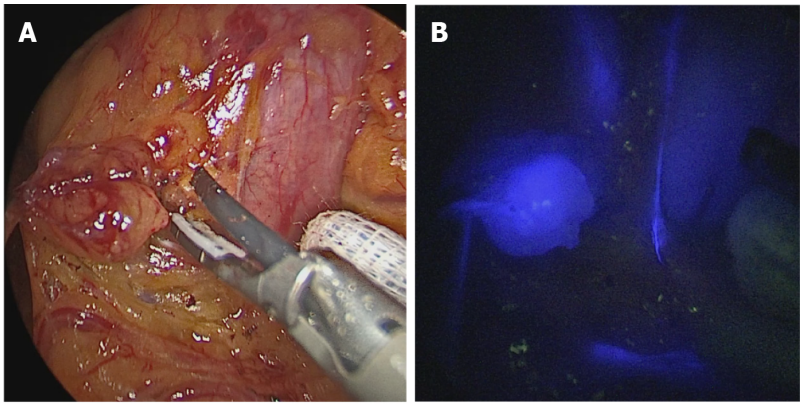
Figure 1 Preoperative endoscopy of prepyloric early gastric cancer. A: Endoscopy; B: Virtual chromoendoscopy; C: Endoscopic ultrasound.



DOI: 10.3748/wjg.v29.i24.3883 **Copyright** ©The Author(s) 2023.

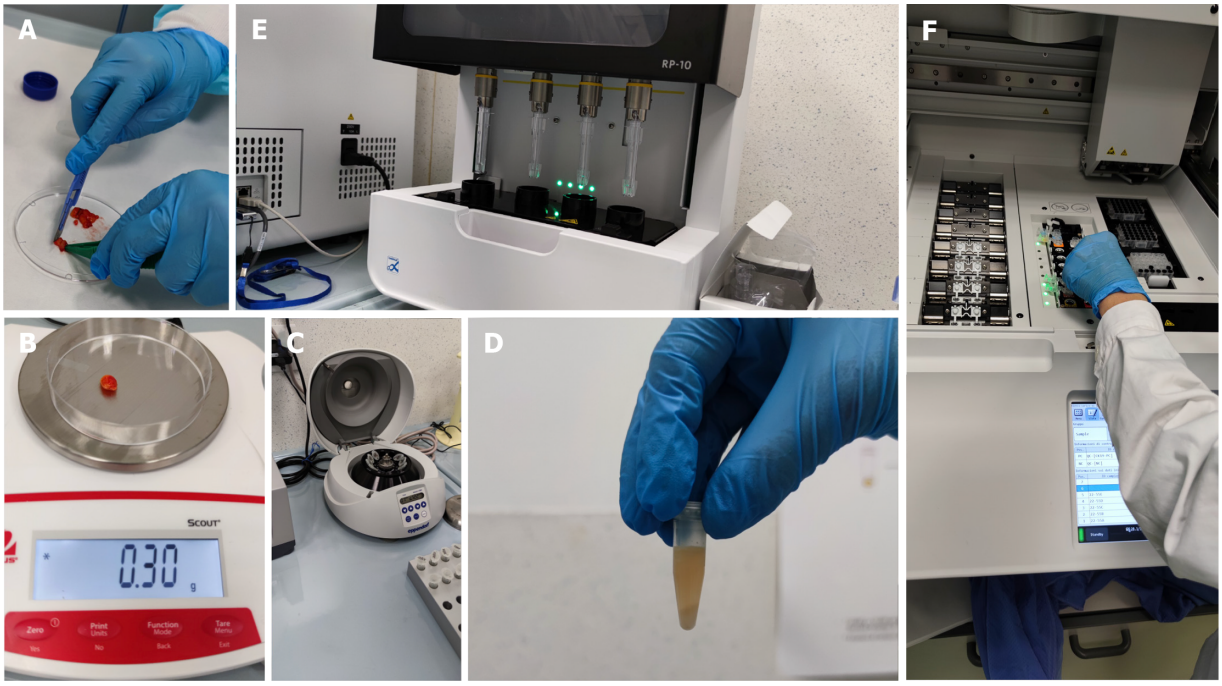
Figure 2 Endoscopic injection of indocyanine green at cardinal points 1 cm from the margins of a prepyloric early gastric cancer lesion. A: First injection of indocyanine green (ICG); B: Second injection of ICG; C: Cardinal points of the lesion injected with ICG.

colon cancer patients. OSNA and fine pathological examination were superior to a single H&E stain. Additionally, combining the two methods observed a 46.5% upstaging rate. The study by Yamamoto *et al*[91] shows that if the sum of CK19 mRNA is higher, the number of histologically positive LNs increases. The median CK19 mRNA value was significantly lower if there were fewer than three metastatic regional LNs than in patients with more than four positive LNs.



DOI: 10.3748/wjg.v29.i24.3883 **Copyright** ©The Author(s) 2023.

Figure 3 Sentinel lymph node biopsy. A: Level 4 d node; B: Level 4 d fluorescent node with near-infrared vision.

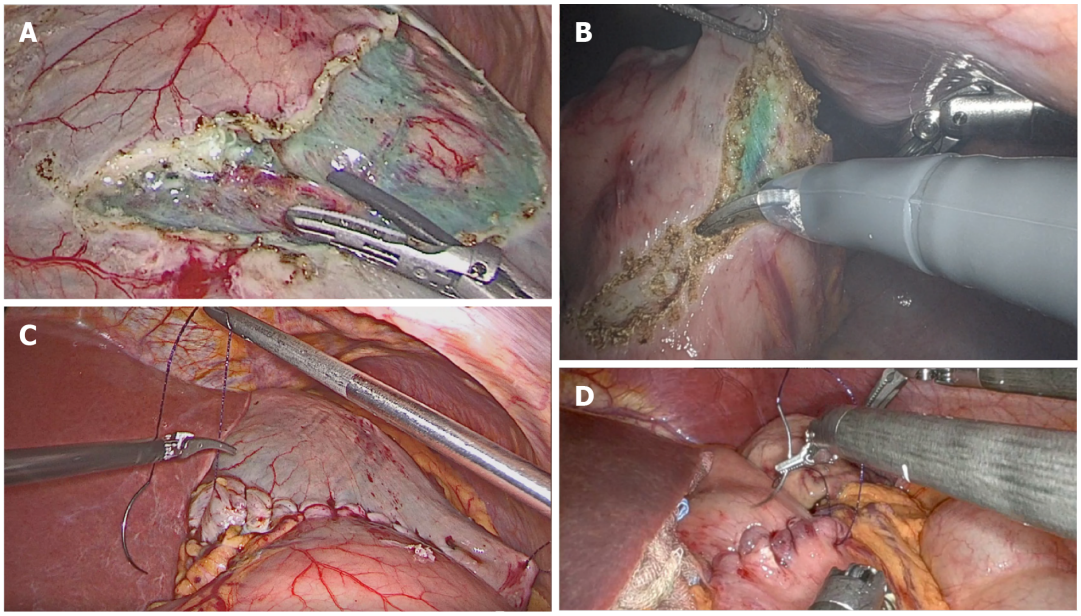


DOI: 10.3748/wjg.v29.i24.3883 **Copyright** ©The Author(s) 2023.

Figure 4 One-step nucleic acid amplification assay. A-F: Lymph nodes were prepared and placed in homogenized lysis buffer (Lynorhag; Sysmex) and then centrifuged. *CK19* mRNA was extracted from the lysate and analyzed by reverse transcription-loop-mediated isothermal amplification in the RD-100i system (Sysmex) using the Lynoamp (Sysmex) reagent kit[59].

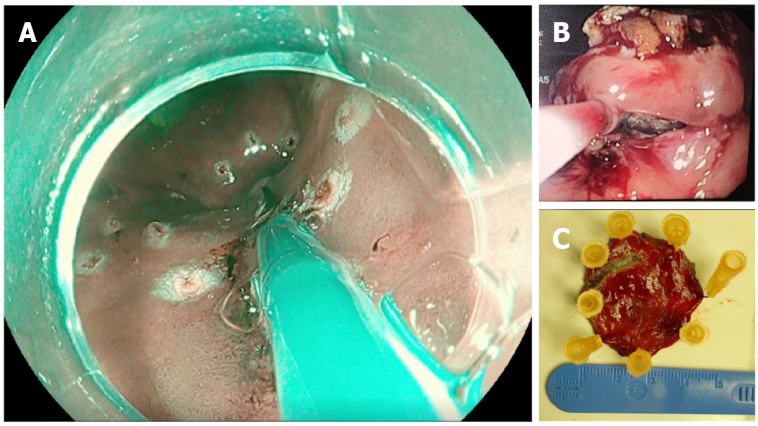
The median TTL values of pN0, pN1 (1-3 LN positive), and pN2 (4 or more LN positive) were 1550 copies/μL (300-320000 copies/μL), 24050 copies/μL (250-890000 copies/μL) and 90600 copies/μL (7700-1635100 copies/μL), respectively. The TTL increases with the advancing LN stage. In the study by Aldecoa *et al*[92], TTL correlated with pT stage ($P = 0.01$) and tumor size ($P < 0.01$) in low-grade tumors. In this study, classic high-risk factors correlated with TTL in patients with stage I-II colon cancer. These results showed that the sum of CK19 mRNA obtained by the OSNA method is comparable with the current pathology diagnosis system. These studies pave the way for a new molecular staging using OSNA based on the amount of CK19mRNA rather than the number of LN metastases. Furthermore, TTL has been suggested to be related to a poor prognosis, worse disease-free survival, and other CRC risk factors[45,93,94], such as pN, pT, tumor grade, male sex, tumor size, and lymph vascular invasion.

In the literature, the association between the use of fluorescence to search for colorectal LNs and the use of OSNA to provide an accurate and rapid assessment of the oncological status of these specific LNs has been shown, which can give information on the entire LN basin. In the study by Shimada *et al*[58], there is a high agreement between OSNA and histopathology. For this reason, the OSNA test can be considered a convenient, objective and valuable alternative to the current pathological method for detecting LN metastases.



DOI: 10.3748/wjg.v29.i24.3883 **Copyright** ©The Author(s) 2023.

Figure 5 Laparoscopic and robotic surgical incision and reconstruction of the external gastric wall. A and B: Incision, representative views; C and D: Reconstruction, representative views.



DOI: 10.3748/wjg.v29.i24.3883 **Copyright** ©The Author(s) 2023.

Figure 6 Endoscopic full thickness resection of early gastric cancer using the non-exposed endoscopic wall-inversion surgery procedure. A: Mucosal markings placed around the tumor; B: Endoscopic incision of the internal layers of the gastric wall; C: Specimen.

Some studies have used intraoperative OSNA testing to evaluate its diagnostic accuracy and elapsed time between surgery and postoperative adjuvant chemotherapy[59,95,96]. A rapid intraoperative test, such as OSNA (which takes approximately 40 min[95]), to obtain information on the status of LNs in the tumor drainage basin can overcome the limitations of preoperative imaging in clinically LN-negative patients. The OSNA test, thanks to its intraoperative diagnostic accuracy and rapidity, may be indispensable for safely performing minimal resections in patients with early-stage gastrointestinal cancer. With more experience using this technology and further refinement of the technique, ICG analysis could be used in conjunction with OSNA intraoperatively to identify LN metastases, which would influence surgical decision-making.

In our previous study[37] we described the advantages and limitations of the OSNA technique. Some authors have proposed that positive *CK19* on immunohistochemistry in primary tumors should be a prerequisite for OSNA use[37,73].

To our knowledge, this is the first study investigating the utility of intraoperative OSNA testing in the assessment of sentinel LN in patients with early-stage gastrointestinal cancer undergoing the NEWS procedure.

Study limitations

This article included a single-center pilot study. As such, the number of patients collected was small and

the selected patients did not have LN metastases. Therefore, it was not possible to validate the sentinel LN technique.

At present, two methods are predominantly used in the detection of sentinel LNs; it involves injecting a radioisotope with a gamma probe or a dye. Hot LNs are identified by radioisotope uptake, and sentinel LNs are colored blue or green by dye after injection around the tumor with a radioisotope colloid or dye. The currently established double-tracer method (dye and radioisotope tracers) described in several studies[97-99] appears to increase the sensitivity of identifying true sentinel LNs. We used only one tracer method in this study. ICG has hypoallergenic potential, deep detection depth, high sensitivity, and stable signal. Furthermore, tight regulation and costs of radioactive substances limit the widespread use of the probe-guided method.

The SNNS concept has been established in early gastric cancer but is still controversial in CRC. Colorectal sentinel LN basins are still not well defined. The usefulness of sentinel LN basin dissection for curative resection needs to be investigated. In this situation, the effectiveness of SNNS combined with OSNA could not be determined in CRC.

CONCLUSION

NEWS is a feasible and safe technique for organ-sparing surgery in selected patients in centers with a high experience in endoscopy, laparoscopy, and robotic surgery. ICG-NIR lymphangiography in combination with sentinel LN OSNA analysis is feasible and may allow intraoperative prediction of LN status in patients with early colon or gastric cancer treated with the NEWS procedure. Furthermore, its implementation allows more precise staging. ICG-NIR lymphangiography and OSNA could be used to plan personalized surgery and lymphadenectomy in patients with early-stage cancers. Prospective multicenter studies with large populations of patient cohorts are needed to provide definitive conclusions.

ARTICLE HIGHLIGHTS

Research background

There are more and more studies in the literature concerning endoscopic and surgical resections for organ preservation in early gastrointestinal neoplasms, respecting oncological principles. Lymph node (LN) study with one-step nucleic acid amplification (OSNA) is also the subject of numerous studies.

Research motivation

Organ-sparing endoscopic and imaging techniques do not currently allow for an accurate LN study. Using LN biopsy with rapid intraoperative results during the laparoscopic and endoscopic cooperative approach can add important information.

Research objectives

This article aims to stimulate studies that can add further information on LN status in patients with early gastrointestinal cancer, which, if treated only with endoscopic technique or with modified Laparoscopic and endoscopic cooperative surgery, would have no additional information on LN status beyond radiological ones. However, our study is the first to evaluate the utility of intraoperative OSNA assay in assessing SN in patients with early-stage gastrointestinal cancer undergoing the Non-exposed endoscopic wall-inversion surgery (NEWS).

Research methods

This pilot study with a literature review is based on data collected prospectively from a database of patients undergoing elective NEWS for early gastrointestinal cancer at St. Giuseppe Moscati Hospital of Avellino, Italy. The database included preoperative, operative, and postoperative data. Inclusion criteria included adult patients with early gastric and colonic cancer eligible for the NEWS procedure. Exclusion criteria included participants with an allergy to any indocyanine green (ICG).

Research results

A total of 10 patients were enrolled in this study, which included 5 gastric and 5 colonic early-stage cancers. The NEWS procedure was successful in all cases. The OSNA assay revealed no LN metastasis in all patients. The diagnostic accuracy in predicting the LN status based on the SN concept by OSNA compared with the postoperative histological examination was 100%. Histologically complete resection (R0) was achieved in 9 (90.0%) patients. There was no recurrence during the follow-up. An intrabdominal fluid collection treated conservatively was observed in 1 (10.0%) patient of the gastric group. One patient who underwent the removal of a lesion affecting the proximal transverse colon presented

positive focal margins on a definitive histological examination. Therefore he subsequently underwent a right hemicolectomy. The definitive histological examination showed no residual tumour foci or LN metastases.The mean follow-up was 6.3 ± 4.2 mo. There was no recurrence during the follow-up period. Ours is a single-centre pilot study. The number of patients collected is small. The selected patients were all patients without LN metastasis; therefore, it is not possible to validate the sentinel node technique.

Research conclusions

Our study is the first to analyze the utility of intraoperative OSNA assay in sentinel node and nodal basin assessment in patients with early-stage gastrointestinal cancer undergoing the NEWS procedure. NEWS is a feasible and safe technique for organ-sparing surgery in selected patients. Additionally, implementing the NEWS association with the intraoperative study with OSNA will allow for more precise staging.

Research perspectives

OSNA and ICG near-infrared lymphangiography could be used to develop customized surgery and lymphadenectomy in patients with early cancers. Prospective multicenter studies with large populations of patient cohorts are needed to provide definitive conclusions.

ACKNOWLEDGEMENTS

We thank the colleagues of the Department of Surgery and Histopathology of the "San Giuseppe Moscati" Hospital of National Importance and High Specialty for carefully reading and revising the manuscript.

FOOTNOTES

Author contributions: Crafa F wrote and edited the manuscript and collected the clinical data; Vanella S reviewed the discussion in the manuscript; Baiamonte M, Catalano OA, Pomykala KL, Godas M, Antunes A, Costa Pereira J, and Giaccaglia V revised the manuscript for important intellectual content and provided recommendations for the clinical diagnosis paragraph; All authors read and approved the final manuscript.

Institutional review board statement: This study was conducted according to the ethical principles of the Institution following the Declaration of Helsinki and with approval by the Institutional Review Board of the St. Giuseppe Moscati Hospital, No. 201801.

Informed consent statement: All study participants or their legal guardian provided informed written consent about personal and medical data collection prior to study enrolment.

Conflict-of-interest statement: All the authors report no relevant conflicts of interest for this article.

Data sharing statement: Dataset available from the corresponding author at nekroma@yahoo.it. Participants gave informed consent for data sharing.

STROBE statement: The authors have read the STROBE Statement—checklist of items, and the manuscript was prepared and revised according to the STROBE Statement—checklist of items.

Open-Access: This article is an open-access article that was selected by an in-house editor and fully peer-reviewed by external reviewers. It is distributed in accordance with the Creative Commons Attribution NonCommercial (CC BY-NC 4.0) license, which permits others to distribute, remix, adapt, build upon this work non-commercially, and license their derivative works on different terms, provided the original work is properly cited and the use is non-commercial. See: https://creativecommons.org/Licenses/by-nc/4.0/

Country/Territory of origin: Italy

ORCID number: Francesco Crafa 0000-0002-2038-625X; Serafino Vanella 0000-0002-6599-8225; Onofrio A Catalano 0000-0001-7733-4138; Kelsey L Pomykala 0000-0001-8922-9597; Mario Baiamonte 0000-0001-8323-8118; Maria Godas 0000-0002-3777-5788.

S-Editor: Fan JR
L-Editor: A
P-Editor: Zhang XD

REFERENCES

1 **Koo DH**, Ryu MH, Kim KM, Yang HK, Sawaki A, Hirota S, Zheng J, Zhang B, Tzen CY, Yeh CN, Nishida T, Shen L, Chen LT, Kang YK. Asian Consensus Guidelines for the Diagnosis and Management of Gastrointestinal Stromal Tumor. *Cancer Res Treat* 2016; **48**: 1155-1166 [PMID: 27384163 DOI: 10.4143/crt.2016.187]

2 **Nishida T**, Hirota S, Yanagisawa A, Sugino Y, Minami M, Yamamura Y, Otani Y, Shimada Y, Takahashi F, Kubota T; GIST Guideline Subcommittee. Clinical practice guidelines for gastrointestinal stromal tumor (GIST) in Japan: English version. *Int J Clin Oncol* 2008; **13**: 416-430 [PMID: 18946752 DOI: 10.1007/s10147-008-0798-7]

3 **Iwahashi M**, Takifuji K, Ojima T, Nakamura M, Nakamori M, Nakatani Y, Ueda K, Ishida K, Naka T, Ono K, Yamaue H. Surgical management of small gastrointestinal stromal tumors of the stomach. *World J Surg* 2006; **30**: 28-35 [PMID: 16369707 DOI: 10.1007/s00268-005-7944-4]

4 **Onimaru M**, Inoue H, Ikeda H, Abad MRA, Quarta Colosso BM, Shimamura Y, Sumi K, Deguchi Y, Ito H, Yokoyama N. Combination of laparoscopic and endoscopic approaches for neoplasia with non-exposure technique (CLEAN-NET) for gastric submucosal tumors: updated advantages and limitations. *Ann Transl Med* 2019; **7**: 582 [PMID: 31807563 DOI: 10.21037/atm.2019.09.19]

5 The Paris endoscopic classification of superficial neoplastic lesions: esophagus, stomach, and colon: November 30 to December 1, 2002. *Gastrointest Endosc* 2003; **58**: S3-43 [PMID: 14652541 DOI: 10.1016/s0016-5107(03)02159-x]

6 **Clavien PA**, Barkun J, de Oliveira ML, Vauthey JN, Dindo D, Schulick RD, de Santibañes E, Pekolj J, Slankamenac K, Bassi C, Graf R, Vonlanthen R, Padbury R, Cameron JL, Makuuchi M. The Clavien-Dindo classification of surgical complications: five-year experience. *Ann Surg* 2009; **250**: 187-196 [PMID: 19638912 DOI: 10.1097/SLA.0b013e3181b13ca2]

7 **Goh C**, Burke JP, McNamara DA, Cahill RA, Deasy J. Endolaparoscopic removal of colonic polyps. *Colorectal Dis* 2014; **16**: 271-275 [PMID: 24308442 DOI: 10.1111/codi.12512]

8 **Nakajima T**, Saito Y, Tanaka S, Iishi H, Kudo SE, Ikematsu H, Igarashi M, Saitoh Y, Inoue Y, Kobayashi K, Hisasbe T, Matsuda T, Ishikawa H, Sugihara K. Current status of endoscopic resection strategy for large, early colorectal neoplasia in Japan. *Surg Endosc* 2013; **27**: 3262-3270 [PMID: 23508817 DOI: 10.1007/s00464-013-2903-x]

9 **Chung IK**, Lee JH, Lee SH, Kim SJ, Cho JY, Cho WY, Hwangbo Y, Keum BR, Park JJ, Chun HJ, Kim HJ, Kim JJ, Ji SR, Seol SY. Therapeutic outcomes in 1000 cases of endoscopic submucosal dissection for early gastric neoplasms: Korean ESD Study Group multicenter study. *Gastrointest Endosc* 2009; **69**: 1228-1235 [PMID: 19249769 DOI: 10.1016/j.gie.2008.09.027]

10 **Chun SY**, Kim KO, Park DS, Lee IJ, Park JW, Moon SH, Baek IH, Kim JH, Park CK, Kwon MJ. Endoscopic submucosal dissection as a treatment for gastric subepithelial tumors that originate from the muscularis propria layer: a preliminary analysis of appropriate indications. *Surg Endosc* 2013; **27**: 3271-3279 [PMID: 23519491 DOI: 10.1007/s00464-013-2904-9]

11 **He Z**, Sun C, Wang J, Zheng Z, Yu Q, Wang T, Chen X, Liu W, Wang B. Efficacy and safety of endoscopic submucosal dissection in treating gastric subepithelial tumors originating in the muscularis propria layer: a single-center study of 144 cases. *Scand J Gastroenterol* 2013; **48**: 1466-1473 [PMID: 24131359 DOI: 10.3109/00365521.2013.845796]

12 **Białek A**, Wiechowska-Kozłowska A, Pertkiewicz J, Polkowski M, Milkiewicz P, Karpińska K, Ławniczak M, Starzyńska T. Endoscopic submucosal dissection for treatment of gastric subepithelial tumors (with video). *Gastrointest Endosc* 2012; **75**: 276-286 [PMID: 22032850 DOI: 10.1016/j.gie.2011.08.029]

13 **Guo JT**, Zhang JJ, Wu YF, Liao Y, Wang YD, Zhang BZ, Wang S, Sun SY. Endoscopic full-thickness resection using an over-the-scope device: A prospective study. *World J Gastroenterol* 2021; **27**: 725-736 [PMID: 33716450 DOI: 10.3748/wjg.v27.i8.725]

14 **Choi SM**, Kim MC, Jung GJ, Kim HH, Kwon HC, Choi SR, Jang JS, Jeong JS. Laparoscopic wedge resection for gastric GIST: long-term follow-up results. *Eur J Surg Oncol* 2007; **33**: 444-447 [PMID: 17174060 DOI: 10.1016/j.ejso.2006.11.003]

15 **Matsuhashi N**, Osada S, Yamaguchi K, Okumura N, Tanaka Y, Imai H, Sasaki Y, Nonaka K, Takahashi T, Futamura M, Yoshida K. Long-term outcomes of treatment of gastric gastrointestinal stromal tumor by laparoscopic surgery: review of the literature and our experience. *Hepatogastroenterology* 2013; **60**: 2011-2015 [PMID: 24719942]

16 **Melstrom LG**, Phillips JD, Bentrem DJ, Wayne JD. Laparoscopic versus open resection of gastric gastrointestinal stromal tumors. *Am J Clin Oncol* 2012; **35**: 451-454 [PMID: 21552096 DOI: 10.1097/COC.0b013e31821954a7]

17 **Matsuda T**, Hiki N, Nunobe S, Aikou S, Hirasawa T, Yamamoto Y, Kumagai K, Ohashi M, Sano T, Yamaguchi T. Feasibility of laparoscopic and endoscopic cooperative surgery for gastric submucosal tumors (with video). *Gastrointest Endosc* 2016; **84**: 47-52 [PMID: 26684599 DOI: 10.1016/j.gie.2015.11.040]

18 **Hu J**, Or BH, Hu K, Wang ML. Comparison of the post-operative outcomes and survival of laparoscopic versus open resections for gastric gastrointestinal stromal tumors: A multi-center prospective cohort study. *Int J Surg* 2016; **33** Pt A: 65-71 [PMID: 27475743 DOI: 10.1016/j.ijsu.2016.07.064]

19 **Eisenberg D**, Bell R. Intraoperative endoscopy: a requisite tool for laparoscopic resection of unusual gastrointestinal lesions--a case series. *J Surg Res* 2009; **155**: 318-320 [PMID: 19482295 DOI: 10.1016/j.jss.2008.06.046]

20 **Sano Y**, Teramoto A, Iwatate M. Magnifying Endoscopy: Image-Enhanced Endoscopy Focused on JNET Classification—Narrow-Band Imaging (NBI). In: Tanaka, S., Saitoh, Y. (eds) Endoscopic Management of Colorectal T1(SM) Carcinoma. Singapore: Springer; 2020: 17-23

21 **Yang Q**, Liu Z, Sun H, Jiao F, Zhang B, Chen J. A narrative review: narrow-band imaging endoscopic classifications. *Quant Imaging Med Surg* 2023; **13**: 1138-1163 [PMID: 36819279 DOI: 10.21037/qims-22-728]

22 **Gono K**, Obi T, Yamaguchi M, Ohyama N, Machida H, Sano Y, Yoshida S, Hamamoto Y, Endo T. Appearance of enhanced tissue features in narrow-band endoscopic imaging. *J Biomed Opt* 2004; **9**: 568-577 [PMID: 15189095 DOI: 10.1117/1.1695563]

23 **Sano Y**, Horimatsu T, Fu KI, Katagiri A, Muto M, Ishikawa H. Magnifying observation of microvascular architecture of colorectal lesions using a narrow-band imaging system. *Dig Endosc* 2006; **18**: S44-S51 [DOI:

10.1111/j.1443-1661.2006.00621.x]

24 **Sano Y**, Tanaka S, Kudo SE, Saito S, Matsuda T, Wada Y, Fujii T, Ikematsu H, Uraoka T, Kobayashi N, Nakamura H, Hotta K, Horimatsu T, Sakamoto N, Fu KI, Tsuruta O, Kawano H, Kashida H, Takeuchi Y, Machida H, Kusaka T, Yoshida N, Hirata I, Terai T, Yamano HO, Kaneko K, Nakajima T, Sakamoto T, Yamaguchi Y, Tamai N, Nakano N, Hayashi N, Oka S, Iwatate M, Ishikawa H, Murakami Y, Yoshida S, Saito Y. Narrow-band imaging (NBI) magnifying endoscopic classification of colorectal tumors proposed by the Japan NBI Expert Team. *Dig Endosc* 2016; **28**: 526-533 [PMID: 26927367 DOI: 10.1111/den.12644]

25 **Iwatate M**, Sano Y, Tanaka S, Kudo SE, Saito S, Matsuda T, Wada Y, Fujii T, Ikematsu H, Uraoka T, Kobayashi N, Nakamura H, Hotta K, Horimatsu T, Sakamoto N, Fu KI, Tsuruta O, Kawano H, Kashida H, Takeuchi Y, Machida H, Kusaka T, Yoshida N, Hirata I, Terai T, Yamano HO, Nakajima T, Sakamoto T, Yamaguchi Y, Tamai N, Nakano N, Hayashi N, Oka S, Ishikawa H, Murakami Y, Yoshida S, Saito Y; Japan NBI Expert Team (JNET). Validation study for development of the Japan NBI Expert Team classification of colorectal lesions. *Dig Endosc* 2018; **30**: 642-651 [PMID: 29603399 DOI: 10.1111/den.13065]

26 **Hewett DG**, Kaltenbach T, Sano Y, Tanaka S, Saunders BP, Ponchon T, Soetikno R, Rex DK. Validation of a simple classification system for endoscopic diagnosis of small colorectal polyps using narrow-band imaging. *Gastroenterology* 2012; **143**: 599-607.e1 [PMID: 22609383 DOI: 10.1053/j.gastro.2012.05.006]

27 **Hayashi N**, Tanaka S, Hewett DG, Kaltenbach TR, Sano Y, Ponchon T, Saunders BP, Rex DK, Soetikno RM. Endoscopic prediction of deep submucosal invasive carcinoma: validation of the narrow-band imaging international colorectal endoscopic (NICE) classification. *Gastrointest Endosc* 2013; **78**: 625-632 [PMID: 23910062 DOI: 10.1016/j.gie.2013.04.185]

28 **Hiki N**, Yamamoto Y, Fukunaga T, Yamaguchi T, Nunobe S, Tokunaga M, Miki A, Ohyama S, Seto Y. Laparoscopic and endoscopic cooperative surgery for gastrointestinal stromal tumor dissection. *Surg Endosc* 2008; **22**: 1729-1735 [PMID: 18074180 DOI: 10.1007/s00464-007-9696-8]

29 **Nunobe S**, Hiki N, Gotoda T, Murao T, Haruma K, Matsumoto H, Hirai T, Tanimura S, Sano T, Yamaguchi T. Successful application of laparoscopic and endoscopic cooperative surgery (LECS) for a lateral-spreading mucosal gastric cancer. *Gastric Cancer* 2012; **15**: 338-342 [PMID: 22350555 DOI: 10.1007/s10120-012-0146-5]

30 **Goto O**, Mitsui T, Fujishiro M, Wada I, Shimizu N, Seto Y, Koike K. New method of endoscopic full-thickness resection: a pilot study of non-exposed endoscopic wall-inversion surgery in an ex vivo porcine model. *Gastric Cancer* 2011; **14**: 183-187 [PMID: 21394421 DOI: 10.1007/s10120-011-0014-8]

31 **Goto O**, Takeuchi H, Kawakubo H, Sasaki M, Matsuda T, Matsuda S, Kigasawa Y, Kadota Y, Fujimoto A, Ochiai Y, Horii J, Uraoka T, Kitagawa Y, Yahagi N. First case of non-exposed endoscopic wall-inversion surgery with sentinel node basin dissection for early gastric cancer. *Gastric Cancer* 2015; **18**: 434-439 [PMID: 25087058 DOI: 10.1007/s10120-014-0406-7]

32 **Mitsui T**, Goto O, Shimizu N, Hatao F, Wada I, Niimi K, Asada-Hirayama I, Fujishiro M, Koike K, Seto Y. Novel technique for full-thickness resection of gastric malignancy: feasibility of nonexposed endoscopic wall-inversion surgery (news) in porcine models. *Surg Laparosc Endosc Percutan Tech* 2013; **23**: e217-e221 [PMID: 24300935 DOI: 10.1097/SLE.0b013e31828e3f94]

33 **Mitsui T**, Niimi K, Yamashita H, Goto O, Aikou S, Hatao F, Wada I, Shimizu N, Fujishiro M, Koike K, Seto Y. Non-exposed endoscopic wall-inversion surgery as a novel partial gastrectomy technique. *Gastric Cancer* 2014; **17**: 594-599 [PMID: 23974429 DOI: 10.1007/s10120-013-0291-5]

34 **Goto O**, Takeuchi H, Kawakubo H, Matsuda S, Kato F, Sasaki M, Fujimoto A, Ochiai Y, Horii J, Uraoka T, Kitagawa Y, Yahagi N. Feasibility of non-exposed endoscopic wall-inversion surgery with sentinel node basin dissection as a new surgical method for early gastric cancer: a porcine survival study. *Gastric Cancer* 2015; **18**: 440-445 [PMID: 24619187 DOI: 10.1007/s10120-014-0358-y]

35 **Inoue H**, Ikeda H, Hosoya T, Yoshida A, Onimaru M, Suzuki M, Kudo SE. Endoscopic mucosal resection, endoscopic submucosal dissection, and beyond: full-layer resection for gastric cancer with nonexposure technique (CLEAN-NET). *Surg Oncol Clin N Am* 2012; **21**: 129-140 [PMID: 22098836 DOI: 10.1016/j.soc.2011.09.012]

36 **Kikuchi S**, Nishizaki M, Kuroda S, Tanabe S, Noma K, Kagawa S, Shirakawa Y, Kato H, Okada H, Fujiwara T. Nonexposure laparoscopic and endoscopic cooperative surgery (closed laparoscopic and endoscopic cooperative surgery) for gastric submucosal tumor. *Gastric Cancer* 2017; **20**: 553-557 [PMID: 27599829 DOI: 10.1007/s10120-016-0641-1]

37 **Irino T**, Nunobe S, Hiki N, Yamamoto Y, Hirasawa T, Ohashi M, Fujisaki J, Sano T, Yamaguchi T. Laparoscopic-endoscopic cooperative surgery for duodenal tumors: a unique procedure that helps ensure the safety of endoscopic submucosal dissection. *Endoscopy* 2015; **47**: 349-351 [PMID: 25479560 DOI: 10.1055/s-0034-1390909]

38 **Fukunaga Y**, Tamegai Y, Chino A, Ueno M, Nagayama S, Fujimoto Y, Konishi T, Igarashi M. New technique of en bloc resection of colorectal tumor using laparoscopy and endoscopy cooperatively (laparoscopy and endoscopy cooperative surgery - colorectal). *Dis Colon Rectum* 2014; **57**: 267-271 [PMID: 24401891 DOI: 10.1097/DCR.0000000000000049]

39 **Hiki N**, Nunobe S. Laparoscopic endoscopic cooperative surgery (LECS) for the gastrointestinal tract: Updated indications. *Ann Gastroenterol Surg* 2019; **3**: 239-246 [PMID: 31131352 DOI: 10.1002/ags3.12238]

40 **Ntourakis D**, Mavrogenis G. Cooperative laparoscopic endoscopic and hybrid laparoscopic surgery for upper gastrointestinal tumors: Current status. *World J Gastroenterol* 2015; **21**: 12482-12497 [PMID: 26604655 DOI: 10.3748/wjg.v21.i43.12482]

41 **ESMO / European Sarcoma Network Working Group**. Gastrointestinal stromal tumors: ESMO Clinical Practice Guidelines for diagnosis, treatment and follow-up. *Ann Oncol* 2012; **23** Suppl 7: vii49-vii55 [PMID: 22997454 DOI: 10.1093/annonc/mds252]

42 **Yada T**, Yokoi C, Uemura N. The current state of diagnosis and treatment for early gastric cancer. *Diagn Ther Endosc* 2013; **2013**: 241320 [PMID: 23533320 DOI: 10.1155/2013/241320]

43 **Aisu Y**, Yasukawa D, Kimura Y, Hori T. Laparoscopic and endoscopic cooperative surgery for gastric tumors: Perspective for actual practice and oncological benefits. *World J Gastrointest Oncol* 2018; **10**: 381-397 [PMID: 30487950 DOI: 10.4251/wjgo.v10.i11.381]

44 **Tamegai Y**, Fukunaga Y, Suzuki S, Lim DNF, Chino A, Saito S, Konishi T, Akiyoshi T, Ueno M, Hiki N, Muto T. Laparoscopic and endoscopic cooperative surgery (LECS) to overcome the limitations of endoscopic resection for colorectal tumors. *Endosc Int Open* 2018; **6**: E1477-E1485 [PMID: 30574538 DOI: 10.1055/a-0761-9494]

45 **Crafa F**, Vanella S, Catalano OA, Pomykala KL, Baiamonte M. Role of one-step nucleic acid amplification in colorectal cancer lymph node metastases detection. *World J Gastroenterol* 2022; **28**: 4019-4043 [PMID: 36157105 DOI: 10.3748/wjg.v28.i30.4019]

46 **Güller U**, Zettl A, Worni M, Langer I, Cabalzar-Wondberg D, Viehl CT, Demartines N, Zuber M. Molecular investigation of lymph nodes in colon cancer patients using one-step nucleic acid amplification (OSNA): a new road to better staging? *Cancer* 2012; **118**: 6039-6045 [PMID: 22684906 DOI: 10.1002/cncr.27667]

47 **Notomi T**, Okayama H, Masubuchi H, Yonekawa T, Watanabe K, Amino N, Hase T. Loop-mediated isothermal amplification of DNA. *Nucleic Acids Res* 2000; **28**: E63 [PMID: 10871386 DOI: 10.1093/nar/28.12.e63]

48 **Tamaki Y**. One-step nucleic acid amplification (OSNA): where do we go with it? *Int J Clin Oncol* 2017; **22**: 3-10 [PMID: 27549784 DOI: 10.1007/s10147-016-1030-9]

49 **Yaguchi Y**, Sugasawa H, Tsujimoto H, Takata H, Nakabayashi K, Ichikura T, Ono S, Hiraki S, Sakamoto N, Horio T, Kumano I, Otomo Y, Mochizuki H, Yamamoto J, Hase K. One-step nucleic acid amplification (OSNA) for the application of sentinel node concept in gastric cancer. *Ann Surg Oncol* 2011; **18**: 2289-2296 [PMID: 21301968 DOI: 10.1245/s10434-011-1591-9]

50 **Kumagai K**, Yamamoto N, Miyashiro I, Tomita Y, Katai H, Kushima R, Tsuda H, Kitagawa Y, Takeuchi H, Mukai M, Mano M, Mochizuki H, Kato Y, Matsuura N, Sano T. Multicenter study evaluating the clinical performance of the OSNA assay for the molecular detection of lymph node metastases in gastric cancer patients. *Gastric Cancer* 2014; **17**: 273-280 [PMID: 23743877 DOI: 10.1007/s10120-013-0271-9]

51 **Pimentel-Nunes P**, Dinis-Ribeiro M, Ponchon T, Repici A, Vieth M, De Ceglie A, Amato A, Berr F, Bhandari P, Bialek A, Conio M, Haringsma J, Langner C, Meisner S, Messmann H, Morino M, Neuhaus H, Piessevaux H, Rugge M, Saunders BP, Robaszkiewicz M, Seewald S, Kashin S, Dumonceau JM, Hassan C, Deprez PH. Endoscopic submucosal dissection: European Society of Gastrointestinal Endoscopy (ESGE) Guideline. *Endoscopy* 2015; **47**: 829-854 [PMID: 26317585 DOI: 10.1055/s-0034-1392882]

52 **Maehata T**, Goto O, Takeuchi H, Kitagawa Y, Yahagi N. Cutting edge of endoscopic full-thickness resection for gastric tumor. *World J Gastrointest Endosc* 2015; **7**: 1208-1215 [PMID: 26566427 DOI: 10.4253/wjge.v7.i16.1208]

53 **Schem C**, Maass N, Bauerschlag DO, Carstensen MH, Löning T, Roder C, Batic O, Jonat W, Tiemann K. One-step nucleic acid amplification-a molecular method for the detection of lymph node metastases in breast cancer patients; results of the German study group. *Virchows Arch* 2009; **454**: 203-210 [PMID: 19101726 DOI: 10.1007/s00428-008-0703-9]

54 **Tsujimoto M**, Nakabayashi K, Yoshidome K, Kaneko T, Iwase T, Akiyama F, Kato Y, Tsuda H, Ueda S, Sato K, Tamaki Y, Noguchi S, Kataoka TR, Nakajima H, Komoike Y, Inaji H, Tsugawa K, Suzuki K, Nakamura S, Daitoh M, Otomo Y, Matsuura N. One-step nucleic acid amplification for intraoperative detection of lymph node metastasis in breast cancer patients. *Clin Cancer Res* 2007; **13**: 4807-4816 [PMID: 17699859 DOI: 10.1158/1078-0432.CCR-06-2512]

55 **Visser M**, Jiwa M, Horstman A, Brink AA, Pol RP, van Diest P, Snijders PJ, Meijer CJ. Intra-operative rapid diagnostic method based on CK19 mRNA expression for the detection of lymph node metastases in breast cancer. *Int J Cancer* 2008; **122**: 2562-2567 [PMID: 18324628 DOI: 10.1002/ijc.23451]

56 **Tamaki Y**, Akiyama F, Iwase T, Kaneko T, Tsuda H, Sato K, Ueda S, Mano M, Masuda N, Takeda M, Tsujimoto M, Yoshidome K, Inaji H, Nakajima H, Komoike Y, Kataoka TR, Nakamura S, Suzuki K, Tsugawa K, Wakasa K, Okino T, Kato Y, Noguchi S, Matsuura N. Molecular detection of lymph node metastases in breast cancer patients: results of a multicenter trial using the one-step nucleic acid amplification assay. *Clin Cancer Res* 2009; **15**: 2879-2884 [PMID: 19351770 DOI: 10.1158/1078-0432.CCR-08-1881]

57 **Castellano I**, Macrì L, Deambrogio C, Balmativola D, Bussone R, Ala A, Coluccia C, Sapino A. Reliability of whole sentinel lymph node analysis by one-step nucleic acid amplification for intraoperative diagnosis of breast cancer metastases. *Ann Surg* 2012; **255**: 334-342 [PMID: 21975319 DOI: 10.1097/SLA.0b013e31823000ed]

58 **Shimada A**, Takeuchi H, Nishi T, Mayanagi S, Fukuda K, Suda K, Nakamura R, Wada N, Kawakubo H, Nakahara T, Kameyama K, Kitagawa Y. Utility of the one-step nucleic acid amplification assay in sentinel node mapping for early gastric cancer patients. *Gastric Cancer* 2020; **23**: 418-425 [PMID: 31667687 DOI: 10.1007/s10120-019-01016-9]

59 **Esposito F**, Noviello A, Moles N, Coppola Bottazzi E, Baiamonte M, Macaione I, Ferbo U, Lepore M, Miro A, Crafa F. Sentinel Lymph Node Analysis in Colorectal Cancer Patients Using One-Step Nucleic Acid Amplification in Combination With Fluorescence and Indocyanine Green. *Ann Coloproctol* 2019; **35**: 174-180 [PMID: 31487764 DOI: 10.3393/ac.2018.07.21.1]

60 **Min JS**, Seo KW, Jeong SH. Choice of LECS Procedure for Benign and Malignant Gastric Tumors. *J Gastric Cancer* 2021; **21**: 111-121 [PMID: 34234973 DOI: 10.5230/jgc.2021.21.e21]

61 **Matsuda T**, Nunobe S, Ohashi M, Hiki N. Laparoscopic endoscopic cooperative surgery (LECS) for the upper gastrointestinal tract. *Transl Gastroenterol Hepatol* 2017; **2**: 40 [PMID: 28616596 DOI: 10.21037/tgh.2017.03.20]

62 **Lee SW**, Garrett KA, Shin JH, Trencheva K, Sonoda T, Milsom JW. Dynamic article: long-term outcomes of patients undergoing combined endolaparoscopic surgery for benign colon polyps. *Dis Colon Rectum* 2013; **56**: 869-873 [PMID: 23739193 DOI: 10.1097/DCR.0b013e3182821e58]

63 **Yan J**, Trencheva K, Lee SW, Sonoda T, Shukla P, Milsom JW. Treatment for right colon polyps not removable using standard colonoscopy: combined laparoscopic-colonoscopic approach. *Dis Colon Rectum* 2011; **54**: 753-758 [PMID: 21552062 DOI: 10.1007/DCR.0b013e3182108289]

64 **deBeche-Adams T**, Hassan I, Haggerty S, Stefanidis D. Transanal Minimally Invasive Surgery (TAMIS): a clinical spotlight review. *Surg Endosc* 2017; **31**: 3791-3800 [PMID: 28656337 DOI: 10.1007/s00464-017-5636-4]

65 **Sakuragi M**, Togashi K, Konishi F, Koinuma K, Kawamura Y, Okada M, Nagai H. Predictive factors for lymph node metastasis in T1 stage colorectal carcinomas. *Dis Colon Rectum* 2003; **46**: 1626-1632 [PMID: 14668587 DOI: 10.1007/BF02660767]

66 **Dighe S**, Purkayastha S, Swift I, Tekkis PP, Darzi A, A'Hern R, Brown G. Diagnostic precision of CT in local staging of

colon cancers: a meta-analysis. *Clin Radiol* 2010; **65**: 708-719 [PMID: 20696298 DOI: 10.1016/j.crad.2010.01.024]

67 **Choi AH**, Nelson RA, Schoellhammer HF, Cho W, Ko M, Arrington A, Oxner CR, Fakih M, Wong J, Sentovich SM, Garcia-Aguilar J, Kim J. Accuracy of computed tomography in nodal staging of colon cancer patients. *World J Gastrointest Surg* 2015; **7**: 116-122 [PMID: 26225194 DOI: 10.4240/wjgs.v7.i7.116]

68 **Takeuchi H**, Goto O, Yahagi N, Kitagawa Y. Function-preserving gastrectomy based on the sentinel node concept in early gastric cancer. *Gastric Cancer* 2017; **20**: 53-59 [PMID: 27714472 DOI: 10.1007/s10120-016-0649-6]

69 **Eom BW**, Kim CG, Kook MC, Yoon HM, Ryu KW, Kim YW, Rho JY, Kim YI, Lee JY, Choi IJ. Non-exposure Simple Suturing Endoscopic Full-thickness Resection with Sentinel Basin Dissection in Patients with Early Gastric Cancer: the SENORITA 3 Pilot Study. *J Gastric Cancer* 2020; **20**: 245-255 [PMID: 33024581 DOI: 10.5230/jgc.2020.20.e22]

70 **Kim SG**, Eom BW, Yoon HM, Kim CG, Kook MC, Kim YW, Ryu KW. Recent updates and current issues of sentinel node navigation surgery for early gastric cancer. *Chin J Cancer Res* 2021; **33**: 142-149 [PMID: 34158734 DOI: 10.21147/j.issn.1000-9604.2021.02.02]

71 **Miwa K**. [Sentinel node concept and its application for cancer surgery]. *Nihon Geka Gakkai Zasshi* 2000; **101**: 307-310 [PMID: 10773998]

72 **Kinami S**, Nakamura N, Tomita Y, Miyata T, Fujita H, Ueda N, Kosaka T. Precision surgical approach with lymph-node dissection in early gastric cancer. *World J Gastroenterol* 2019; **25**: 1640-1652 [PMID: 31011251 DOI: 10.3748/wjg.v25.i14.1640]

73 **Kinami S**, Fujimura T, Ojima E, Fushida S, Ojima T, Funaki H, Fujita H, Takamura H, Ninomiya I, Nishimura G, Kayahara M, Ohta T, Yoh Z. PTD classification: proposal for a new classification of gastric cancer location based on physiological lymphatic flow. *Int J Clin Oncol* 2008; **13**: 320-329 [PMID: 18704632 DOI: 10.1007/s10147-007-0755-x]

74 **Kinami S**, Nakamura N, Miyashita T, Kitakata H, Fushida S, Fujimura T, Iida Y, Inaki N, Ito T, Takamura H. Life prognosis of sentinel node navigation surgery for early-stage gastric cancer: Outcome of lymphatic basin dissection. *World J Gastroenterol* 2021; **27**: 8010-8030 [PMID: 35046627 DOI: 10.3748/wjg.v27.i46.8010]

75 **Kitagawa Y**, Takeuchi H, Takagi Y, Natsugoe S, Terashima M, Murakami N, Fujimura T, Tsujimoto H, Hayashi H, Yoshimizu N, Takagane A, Mohri Y, Nabeshima K, Uenosono Y, Kinami S, Sakamoto J, Morita S, Aikou T, Miwa K, Kitajima M. Sentinel node mapping for gastric cancer: a prospective multicenter trial in Japan. *J Clin Oncol* 2013; **31**: 3704-3710 [PMID: 24019550 DOI: 10.1200/JCO.2013.50.3789]

76 **Kim YW**, Min JS, Yoon HM, An JY, Eom BW, Hur H, Lee YJ, Cho GS, Park YK, Jung MR, Park JH, Hyung WJ, Jeong SH, Kook MC, Han M, Nam BH, Ryu KW. Laparoscopic Sentinel Node Navigation Surgery for Stomach Preservation in Patients With Early Gastric Cancer: A Randomized Clinical Trial. *J Clin Oncol* 2022; **40**: 2342-2351 [PMID: 35324317 DOI: 10.1200/JCO.21.02242]

77 **An JY**, Min JS, Hur H, Lee YJ, Cho GS, Park YK, Jung MR, Park JH, Hyung WJ, Jeong SH, Kim YW, Yoon HM, Eom BW, Kook MC, Han MR, Nam BH, Ryu KW; SEntinel Node ORIented Tailored Approach (SENORITA) Study Group. Laparoscopic sentinel node navigation surgery versus laparoscopic gastrectomy with lymph node dissection for early gastric cancer: short-term outcomes of a multicentre randomized controlled trial (SENORITA). *Br J Surg* 2020; **107**: 1429-1439 [PMID: 32492186 DOI: 10.1002/bjs.11655]

78 **Huang Y**, Pan M, Deng Z, Ji Y, Chen B. How useful is sentinel lymph node biopsy for the status of lymph node metastasis in cT1N0M0 gastric cancer? A systematic review and meta-analysis. *Updates Surg* 2021; **73**: 1275-1284 [PMID: 33723712 DOI: 10.1007/s13304-021-01026-2]

79 **Ohi M**, Toiyama Y, Omura Y, Ichikawa T, Yasuda H, Okugawa Y, Fujikawa H, Okita Y, Yoshiyama S, Hiro J, Araki T, Kusunoki M. Possibility of limited gastrectomy for early gastric cancer located in the upper third of the stomach, based on the distribution of sentinel node basins. *Surg Today* 2019; **49**: 529-535 [PMID: 30684050 DOI: 10.1007/s00595-019-1768-6]

80 **Isozaki H**, Matsumoto S, Murakami S. Survival outcomes after sentinel node navigation surgery for early gastric cancer. *Ann Gastroenterol Surg* 2019; **3**: 552-560 [PMID: 31549015 DOI: 10.1002/ags3.12280]

81 **Takahashi N**, Nimura H, Fujita T, Mitsumori N, Shiraishi N, Kitano S, Satodate H, Yanaga K. Laparoscopic sentinel node navigation surgery for early gastric cancer: a prospective multicenter trial. *Langenbecks Arch Surg* 2017; **402**: 27-32 [PMID: 27999935 DOI: 10.1007/s00423-016-1540-y]

82 **Feng M**, Wei J, Ji K, Zhang Y, Yang H, Wu X, Zhang J, Bu Z, Ji J. Characteristics of lymph node stations/basins metastasis and construction and validation of a preoperative combination prediction model that accurately excludes lymph node metastasis in early gastric cancer. *Chin J Cancer Res* 2022; **34**: 519-532 [PMID: 36398119 DOI: 10.21147/j.issn.1000-9604.2022.05.11]

83 **Arigami T**, Natsugoe S, Uenosono Y, Mataki Y, Ehi K, Higashi H, Arima H, Yanagida S, Ishigami S, Hokita S, Aikou T. Evaluation of sentinel node concept in gastric cancer based on lymph node micrometastasis determined by reverse transcription-polymerase chain reaction. *Ann Surg* 2006; **243**: 341-347 [PMID: 16495698 DOI: 10.1097/01.sla.0000201453.65534.f1]

84 **Shimizu Y**, Takeuchi H, Sakakura Y, Saikawa Y, Nakahara T, Mukai M, Kitajima M, Kitagawa Y. Molecular detection of sentinel node micrometastases in patients with clinical N0 gastric carcinoma with real-time multiplex reverse transcription-polymerase chain reaction assay. *Ann Surg Oncol* 2012; **19**: 469-477 [PMID: 22065193 DOI: 10.1245/s10434-011-2122-4]

85 **Shoji Y**, Kumagai K, Kamiya S, Ida S, Nunobe S, Ohashi M, Yoshimizu S, Horiuchi Y, Yoshio T, Ishiyama A, Hirasawa T, Osako T, Yamamoto N, Fujisaki J, Sano T, Hiki N. Prospective feasibility study for single-tracer sentinel node mapping by ICG (indocyanine green) fluorescence and OSNA (one-step nucleic acid amplification) assay in laparoscopic gastric cancer surgery. *Gastric Cancer* 2019; **22**: 873-880 [PMID: 30603913 DOI: 10.1007/s10120-018-00919-3]

86 **Joosten JJ**, Strobbe LJ, Wauters CA, Pruszczynski M, Wobbes T, Ruers TJ. Intraoperative lymphatic mapping and the sentinel node concept in colorectal carcinoma. *Br J Surg* 1999; **86**: 482-486 [PMID: 10215818 DOI: 10.1046/j.1365-2168.1999.01051.x]

87 **Croner RS**, Schellerer V, Demund H, Schildberg C, Papadopulos T, Naschberger E, Stürzl M, Matzel KE, Hohenberger W, Schlabrakowski A. One step nucleic acid amplification (OSNA) - a new method for lymph node staging in colorectal

carcinomas. *J Transl Med* 2010; **8**: 83 [PMID: 20819209 DOI: 10.1186/1479-5876-8-83]

88 **Yamamoto H**, Sekimoto M, Oya M, Yamamoto N, Konishi F, Sasaki J, Yamada S, Taniyama K, Tominaga H, Tsujimoto M, Akamatsu H, Yanagisawa A, Sakakura C, Kato Y, Matsuura N. OSNA-based novel molecular testing for lymph node metastases in colorectal cancer patients: results from a multicenter clinical performance study in Japan. *Ann Surg Oncol* 2011; **18**: 1891-1898 [PMID: 21290195 DOI: 10.1245/s10434-010-1539-5]

89 **Yamamoto N**, Daito M, Hiyama K, Ding J, Nakabayashi K, Otomo Y, Tsujimoto M, Matsuura N, Kato Y. An optimal mRNA marker for OSNA (One-step nucleic acid amplification) based lymph node metastasis detection in colorectal cancer patients. *Jpn J Clin Oncol* 2013; **43**: 264-270 [PMID: 23293371 DOI: 10.1093/jjco/hys227]

90 **Vogelaar FJ**, Reimers MS, van der Linden RL, van der Linden JC, Smit VT, Lips DJ, van de Velde CJ, Bosscha K. The diagnostic value of one-step nucleic acid amplification (OSNA) for sentinel lymph nodes in colon cancer patients. *Ann Surg Oncol* 2014; **21**: 3924-3930 [PMID: 24912612 DOI: 10.1245/s10434-014-3820-5]

91 **Yamamoto H**, Tomita N, Inomata M, Furuhata T, Miyake Y, Noura S, Kato T, Murata K, Hayashi S, Igarashi S, Itabashi M, Kameoka S, Matsuura N. OSNA-Assisted Molecular Staging in Colorectal Cancer: A Prospective Multicenter Trial in Japan. *Ann Surg Oncol* 2016; **23**: 391-396 [PMID: 26438440 DOI: 10.1245/s10434-015-4880-x]

92 **Aldecoa I**, Atares B, Tarragona J, Bernet L, Sardon JD, Pereda T, Villar C, Mendez MC, Gonzalez-Obeso E, Elorriaga K, Alonso GL, Zamora J, Planell N, Palacios J, Castells A, Matias-Guiu X, Cuatrecasas M. Molecularly determined total tumour load in lymph nodes of stage I-II colon cancer patients correlates with high-risk factors. A multicentre prospective study. *Virchows Arch* 2016; **469**: 385-394 [PMID: 27447172 DOI: 10.1007/s00428-016-1990-1]

93 **Itabashi M**, Yamamoto H, Tomita N, Inomata M, Murata K, Hayashi S, Miyake Y, Igarashi S, Kato T, Noura S, Furuhata T, Ozawa H, Takemasa I, Yasui M, Takeyama H, Okamura S, Ohno Y, Matsuura N. Lymph Node Positivity in One-Step Nucleic Acid Amplification is a Prognostic Factor for Postoperative Cancer Recurrence in Patients with Stage II Colorectal Cancer: A Prospective, Multicenter Study. *Ann Surg Oncol* 2020; **27**: 1077-1083 [PMID: 31722072 DOI: 10.1245/s10434-019-07971-y]

94 **Rakislova N**, Montironi C, Aldecoa I, Fernandez E, Bombi JA, Jimeno M, Balaguer F, Pellise M, Castells A, Cuatrecasas M. Lymph node pooling: a feasible and efficient method of lymph node molecular staging in colorectal carcinoma. *J Transl Med* 2017; **15**: 14 [PMID: 28088238 DOI: 10.1186/s12967-016-1114-3]

95 **Snook KL**, Layer GT, Jackson PA, de Vries CS, Shousha S, Sinnett HD, Nigar E, Singhal H, Chia Y, Cunnick G, Kissin MW; OSNA Study Group. Multicentre evaluation of intraoperative molecular analysis of sentinel lymph nodes in breast carcinoma. *Br J Surg* 2011; **98**: 527-535 [PMID: 21656717 DOI: 10.1002/bjs.7347]

96 **Marhic A**, Tremblay JF, Kaci R, André T, Eveno C, Pocard M. Molecular analysis of sentinel lymph node in colon carcinomas by one-step nucleic acid amplification (OSNA) reduces time to adjuvant chemotherapy interval. *Dig Liver Dis* 2017; **49**: 924-928 [PMID: 28668271 DOI: 10.1016/j.dld.2017.05.017]

97 **Li Z**, Li X, Zhu X, Ai S, Guan W, Liu S. Tracers in Gastric Cancer Surgery. *Cancers (Basel)* 2022; **14** [PMID: 36497216 DOI: 10.3390/cancers14235735]

98 **Eom BW**, Yoon HM, Min JS, Cho I, Park JH, Jung MR, Hur H, Kim YW, Park YK, Nam BH, Ryu KW; Sentinel Node Oriented Tailored Approach (SENORITA) Study Group. Prospective Multicenter Feasibility Study of Laparoscopic Sentinel Basin Dissection after Endoscopic Submucosal Dissection for Early Gastric Cancer: SENORITA 2 Trial Protocol. *J Gastric Cancer* 2019; **19**: 157-164 [PMID: 31245160 DOI: 10.5230/jgc.2019.19.e12]

99 **Ichikura T**, Chochi K, Sugasawa H, Yaguchi Y, Sakamoto N, Takahata R, Kosuda S, Mochizuki H. Individualized surgery for early gastric cancer guided by sentinel node biopsy. *Surgery* 2006; **139**: 501-507 [PMID: 16627059 DOI: 10.1016/j.surg.2005.09.005]

World Journal of Gastroenterology

Submit a Manuscript: https://www.f6publishing.com

World J Gastroenterol 2023 June 28; 29(24): 3899-3921

DOI: 10.3748/wjg.v29.i24.3899

ISSN 1007-9327 (print) ISSN 2219-2840 (online)

SCIENTOMETRICS

Immunological factors in cirrhosis diseases from a bibliometric point of view

Dan Zhang, Bo-Wen Liu, Xiao-Qing Liang, Fu-Quan Liu

Specialty type: Gastroenterology and hepatology

Provenance and peer review: Unsolicited article; Externally peer reviewed.

Peer-review model: Single blind

Peer-review report's scientific quality classification

Grade A (Excellent): 0
Grade B (Very good): B, B
Grade C (Good): 0
Grade D (Fair): 0
Grade E (Poor): 0

P-Reviewer: Navarro-Alvarez N, Mexico; Paparoupa M, Germany

Received: April 9, 2023
Peer-review started: April 9, 2023
First decision: May 12, 2023
Revised: May 20, 2023
Accepted: May 24, 2023
Article in press: May 24, 2023
Published online: June 28, 2023

Dan Zhang, Bo-Wen Liu, Fu-Quan Liu, Department of Interventional Therapy, Beijing Shijitan Hospital, Capital Medical University, Beijing 100038, China

Xiao-Qing Liang, Department of Oncology, Beijing Shijitan Hospital, Capital Medical University, Beijing 100038, China

Corresponding author: Fu-Quan Liu, MM, Chief Doctor, Doctor, Professor, Department of Interventional Therapy, Beijing Shijitan Hospital, Capital Medical University, No. 10 Tieyi Road, Yangfangdian Street, Haidian District, Beijing 100038, China. liufuquan@ccmu.edu.cn

Abstract

BACKGROUND

Cirrhosis results from persistent liver injury that leads to liver fibrosis. Immunological factors play important regulatory roles in the development and progression of cirrhosis. Bibliometrics is one of the most commonly used methods for systematic evaluation of a field of study. To date, there are no bibliometric studies on the role of immunological factors in cirrhosis.

AIM

To provide a comprehensive overview of the knowledge structure and research hotspots of immunological factors in cirrhosis.

METHODS

We retrieved publications related to immunological factors in cirrhosis between 2003 to 2022 from the Web of Science Core Collection database on December 7, 2022. The search strategy was TS = ((Liver Cirrhosis OR hepatic cirrhosis OR liver fibrosis) AND (Immunologic* Factor* OR Immune Factor* OR Immunomodulator* OR Biological Response Modifier* OR Biomodulator*)). Only original articles and reviews were included. A total of 2873 publications were analyzed using indicators of publication and citation metrics, countries, institutes, authors, journals, references, and keywords by CiteSpace and VOSviewer.

RESULTS

A total of 5104 authors from 1173 institutions across 51 countries published 2873 papers on cirrhosis and immunological factors in 281 journals. In the past 20 years, the increasing number of related annual publications and citations indicates that research on immunological factors in cirrhosis has become the focus of attention and has entered a period of accelerated development. The United States (781/27.18%), China (538/18.73%), and Germany (300/10.44%) were the leading

countries in this field. Most of the top 10 authors were from the United States (4) and Germany (3), with Gershwin ME contributing the most related articles (42). *World Journal of Gastroenterology* was the most productive journal, whereas *Hepatology* was the most co-cited journal. Current research hotspots regarding immunological factors in cirrhosis include fibrosis, cirrhosis, inflammation, liver fibrosis, expression, hepatocellular carcinoma, activation, primary biliary cirrhosis, disease, and hepatic stellate cells. Burst keywords (*e.g.*, epidemiology, gut microbiota, and pathways) represent research frontiers that have attracted the interest of researchers in recent years.

CONCLUSION

This bibliometric study comprehensively summarizes the research developments and directions of immunological factors in cirrhosis, providing new ideas for promoting scientific research and clinical applications.

Key Words: Immunological factors; Cirrhosis; CiteSpace; VOSviewer; Bibliometrics; Visualization

©The Author(s) 2023. Published by Baishideng Publishing Group Inc. All rights reserved.

Core Tip: Over the last 20 years, 5104 authors from 1173 institutions in 51 countries have published 2873 papers on cirrhosis and immunological factors in 281 journals. Immune dysfunction, gut microbiota, epidemiology, mouse model, pathway, obesity, extracellular vesicles, bile acids, and the extracellular matrix are currently at the frontiers of research on immunological factors in cirrhosis. It is notable that in addition to focusing on basic research, we should also pay attention to the translation and application of the research results.

Citation: Zhang D, Liu BW, Liang XQ, Liu FQ. Immunological factors in cirrhosis diseases from a bibliometric point of view. *World J Gastroenterol* 2023; 29(24): 3899-3921
URL: https://www.wjgnet.com/1007-9327/full/v29/i24/3899.htm
DOI: https://dx.doi.org/10.3748/wjg.v29.i24.3899

INTRODUCTION

Hepatic cirrhosis is defined as extensive fibrosis, pseudolobules, and distortion of the hepatic vascular architecture due to various chronic liver diseases[1]. Patients with compensated cirrhosis are asymptomatic, whereas severely impaired liver function and portal hypertension are common in the decompensated stage. Patients with decompensated cirrhosis often have complications such as ascites, bleeding esophageal varices, hepatic encephalopathy, and hepatorenal syndrome, which may eventually progress to multi-organ failure and death. Cirrhosis has a diverse etiology and can be caused by chronic liver injury, progressing to inflammation and liver fibrosis with fibrous septa and regenerative nodules[2]. Subsequently, the liver structures may collapse, resulting in distortion of the liver parenchyma and vascular structures. Progressive fibrosis and cirrhosis subsequently lead to a decrease in the metabolic and synthetic functions of the liver, causing elevated bilirubin levels, decreased production of coagulation factors and thrombopoietins, splenic platelet retention, elevated portal vein pressure, and the development of ascites and esophageal varices[3]. Viral hepatitis [hepatitis B virus (HBV) infection and HCV infection], alcoholic and non-alcoholic fatty liver diseases are the most common identifiable causes[4].

Liver inflammation and immune responses are the key factors in the pathogenesis of cirrhosis. The immune system triggers inflammation during hepatic fibrosis and is involved in wound healing and tissue repair. Various cells in the liver, such as sinusoidal endothelial cells, intravascular liver-resident macrophages (Kupffer cells), and dendritic cells (DCs), are capable of antigen presentation and produce cytokines and chemokines[5]. Following liver injury, infiltrating immune cells promote the liver fibrosis cascade by secreting pro-inflammatory cytokines such as tumor necrosis factor alpha (TNF-α), interleukin-6 (IL-6), and chemokine 4 (CCL4). These cytoplasmic factors mediate interactions between immune cells and hepatic stellate cells (HSC), leading to HSC activation and fibroblast transdifferentiation. Immune-related genes are vitally important in immune infiltration and response[6]. These results indicate that immunological factors play a complex and important role in cirrhosis, and analysis of the results obtained in this area can help us estimate the trends of cirrhosis-related immunological factors and guide experimental strategies and funding decisions.

Bibliometrics, which applies mathematical and statistical methods to the study of books and other media, is one of the most commonly used methods for the systematic evaluation of a field of study. It can be used not only for qualitative and quantitative analysis in research on countries, regions,

institutions, authors, co-cited authors, journals, references, and keywords, but also to describe and predict research hotspots and trends in specific fields[7]. Over the years, many scholars have applied bibliometric analyses to various fields of medicine, including cardiovascular diseases[8], respiratory diseases[9], obstetrical and gynecological diseases[10], psychiatric diseases[11], dermatological diseases [12], and biologic signaling[13]. To the best of our knowledge, bibliometric analyses of immunological factors in non-small cell lung cancer[14], cardiovascular diseases[15], and cancer[16] have been conducted by related scholars. Recent studies have shown that immunomodulators are a promising treatment option for cirrhosis. Therefore, we performed a bibliometric study of immunological factors in cirrhosis based on published data using CiteSpace and VOSviewer, two commonly used scientometric software packages, to create knowledge maps and explore the evolution and development trends of hotspots in this field. Microsoft Office Excel 2019 was used to perform a quantitative analysis of the publications and citations.

MATERIALS AND METHODS

Data source and retrieval strategy

We used the Web of Science Core Collection (WoSCC) developed by Thomson Scientific to extract relevant literature on cirrhosis and immunological factors published between January 2003 and November 2022. To avoid citation fluctuations due to rapid updates, literature searches were conducted within 1 d (December 7, 2022). The search strategy was TS = ((Liver Cirrhosis OR hepatic cirrhosis OR liver fibrosis) AND (Immunologic* Factor* OR Immune Factor* OR Immunomodulator* OR Biological Response Modifier* OR Biomodulator*)). A total of 2896 publications was obtained. Among various publication types, only original articles and reviews were included. Finally, only 2873 publications that met the inclusion criteria were included in the bibliometric analyses. The detailed screening process is illustrated in Figure 1.

Data analysis and visualization

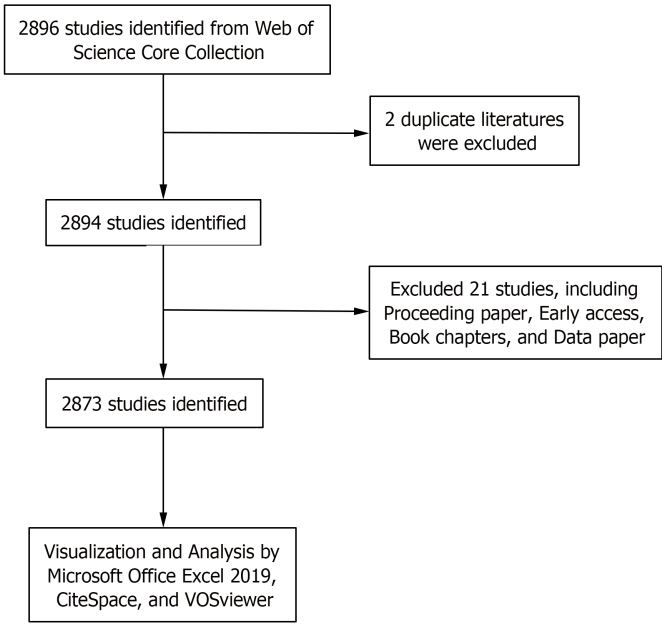
CiteSpace software was developed by Professor Chaomei Chen for bibliometric and visual analyses. Specifically, it explores collaborations, structures, hotspots, and frontiers in a research field and presents trends in a discipline or field of knowledge over time in a visual and intuitive form. Nodes with high centrality, highlighted by purple rings, are often considered hotspots or turning points in a research field. The thickness of the purple ring indicates the strength of its centrality; the thicker it is, the stronger its centrality[17]. Cluster analysis of keywords can be used to identify important regions of research on immunological factors in cirrhosis by classifying keywords. In addition, the variant word indicates a sudden growth of hotspots in the field and also shows the future trend of the topic[18]. A high mutation value indicated a large variation in size. Keywords and reference mutations can be used to identify new research trends in immunological factors associated with liver cirrhosis. Therefore, we used CiteSpace (version 6.1. R3) for the collaborative network analysis (country/region, institution, author, and journal), co-citation analysis (author, journal, and reference), dual mapping, and citation burst detection of references and keywords.

We constructed bibliometric maps using the VOSviewer software developed by Leiden University to obtain more comprehensive information about the results based on co-citation and co-occurrence. VOSviewer excels in map creation and presents bibliometric maps in different ways, including network, overlay, and density maps, each focusing on various aspects. The color of the nodes represents different times or clusters, the size of the nodes indicates the number of publications, and the thickness of the lines represents the strength of the relationship[19]. In our study, VOSviewer (version 1.6.18) performed the following analyses: Country and institution, authors, co-cited authors, and keywords.

RESULTS

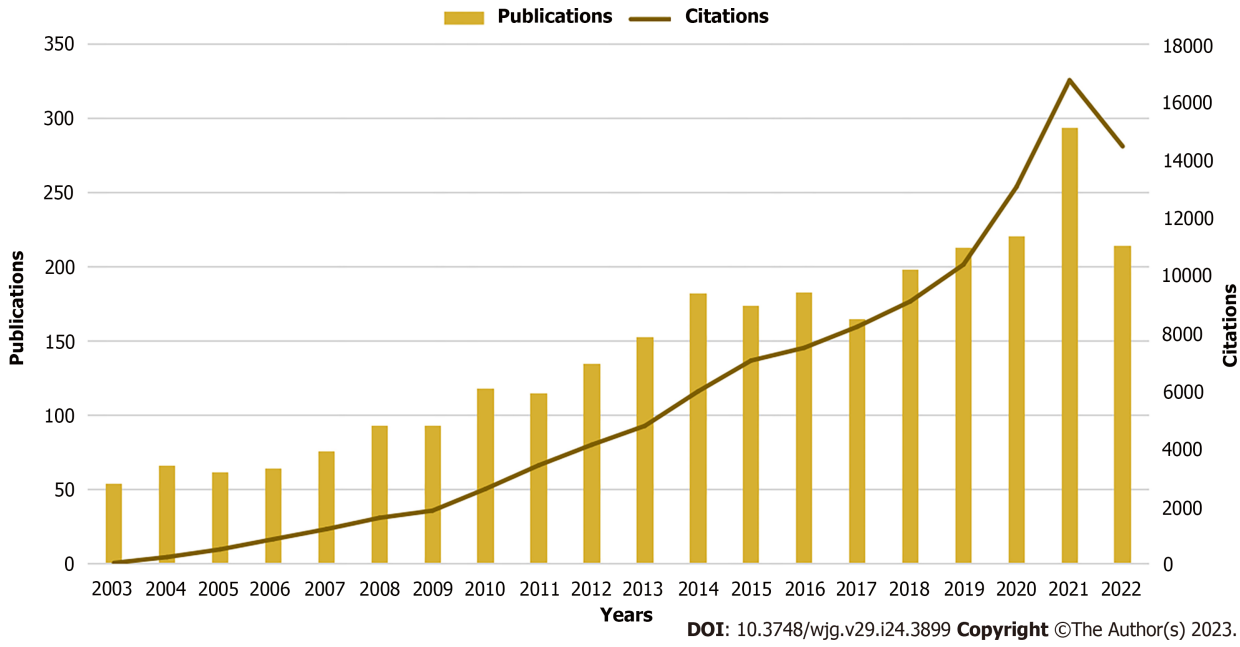
Temporal distribution map of publications and citations

From 2003 to 2022, publications on immunological factors in cirrhosis included 1906 original articles and 967 reviews, showing a constantly increasing trend (Figure 2). From 2003 to 2014, the number of annual publications in this field steadily increased. Annual publications started with over 100 and 182 articles published in 2010 (n = 118) and 2014, respectively. Annual publications fluctuated slightly between 2014 and 2017 and gradually increased from 2018 to 2021. Subsequently, it increased significantly and peaked in 2021 (n = 294). The number of citations increased rapidly annually and exhibited a continuously rising trend. The upward trend in annual publications and citations indicates that research on immunological factors in cirrhosis has become a focus of attention and has entered a period of accelerated development.



DOI: 10.3748/wjg.v29.i24.3899 **Copyright** ©The Author(s) 2023.

Figure 1 Flowchart of the screening process.



DOI: 10.3748/wjg.v29.i24.3899 **Copyright** ©The Author(s) 2023.

Figure 2 Temporal distribution map of publications and citations.

Publications were from 51 countries and 1173 institutions. As shown in Tables 1 and 2, we ranked the 10 high-productivity countries/regions and institutions. The United States (781/27.18%), China (538/18.73%), and Germany (300/10.44%) published the most articles, accounting for more than half of the total number of studies reported, indicating a high interest in studying immunological factors in cirrhosis. This was followed by Italy (259/9.01%) and Japan (192/6.68%). Subsequently, we constructed collaborative networks based on the publications and relationships in each country (Figure 3). It is noteworthy that there are many active collaborations among different countries (Figure 3A). For example, the United States has actively cooperated with China, Italy, Germany, England, Japan, France, and Australia; China has collaborated closely with the United States, Japan, Germany, Italy, England, Canada, and Australia; and Germany has collaborated with the United States, Switzerland, France, the Netherlands, Australia, China, and Spain. The top 10 institutions are distributed across five countries, with half in the United States. The University of California, Davis (65, 2.26%) led the publications, followed by the Mayo Medical Center (47, 1.64%) and Zhejiang University (44, 1.53%). We also observed

Table 1 Publications in the 10 most productive countries/regions

Rank	Country/region	Year	Count (%)	Centrality
1	United States	2003	781 (27.18%)	0.36
2	China	2003	538 (18.73%)	0.06
3	Germany	2003	300 (10.44%)	0.17
4	Italy	2003	259 (9.01%)	0.19
5	Japan	2003	192 (6.68%)	0.03
6	England	2003	186 (6.47%)	0.20
7	Spain	2003	157 (5.46%)	0.09
8	France	2003	132 (4.59%)	0.17
9	Australia	2004	85 (2.96%)	0.12
10	Canada	2003	84 (2.92%)	0.12

Table 2 Publications in the 10 most productive institutions

Rank	Institution	Year	Count (%)	Centrality
1	Univ Calif Davis (United States)	2004	65 (2.26%)	0.12
2	Mayo Clin (United States)	2007	47 (1.64%)	0.02
3	Zhejiang Univ (China)	2011	44 (1.53%)	0.01
4	Univ Birmingham (England)	2009	38 (1.32%)	0.04
5	Univ Calif San Diego (United States)	2009	28 (0.97%)	0.07
6	Yale Univ (United States)	2007	26 (0.90%)	0.06
7	Inst Salud Carlos III (Spain)	2008	25 (0.87%)	0.06
8	Univ Milan (Italy)	2004	24 (0.84%)	0.06
9	Univ Barcelona (Spain)	2003	23 (0.80%)	0.03
10	Emory Univ (United States)	2006	23 (0.80%)	0.05

a network diagram of institutional collaboration in research on immunological factors in cirrhosis (Figure 4A). The figure shows a very close cooperation among the University of California, Davis, University of Milan, Monash University, Emory University, and Mayo Clinic, and a more active collaboration between Zhejiang University, Emory University, and the University of Science and Technology of China. In addition, several countries and affiliations, including the United States (0.36), England (0.20), Italy (0.19), Germany (0.17), France (0.17), Canada (0.12), Australia (0.12), Egypt (0.11), and the University of California, Davis (0.12) showed high centrality, circled in purple in Figure 3B and Figure 4B, respectively. An article with high centrality could be a transformative discovery. These findings suggest that these countries and institutions play key roles in the study of immunological factors associated with cirrhosis. Notably, despite their high volume of publications, China and Japan might not provide scientists with the same level of novel insights compared to countries with high centrality.

Analysis of authors and co-cited authors

A total of 5104 authors participated in the study on the immunological factors associated with cirrhosis. The top 10 high-producing authors are listed in Table 3. As shown in Figure 5A, a larger font size and higher yellow opacity indicate more publications. Gershwin ME from the University of California Davis was the most productive author, with 42 publications, followed by Tacke *et al*[20] (n = 27) and Trautwein *et al*[21] (n = 20) from the University Hospital Aachen. Most of the top 10 authors were from the United States (4), and Germany (3). As shown in Figure 5B, there are collaborations between different authors; however, it is noteworthy that the centrality is low (≤ 0.02), which means that various authors have little influence on each other's research. All the top 10 co-cited authors had more than 100 co-citations (Table 3). As shown in Figure 6A, a larger font size and a higher yellow opacity imply a higher citation frequency. Friedman, from the Icahn School of Medicine, had the highest number of co-citations (n = 337). The next most cited were Bataller (n = 235) from Pittsburgh Liver Research and Seki (

Table 3 Top 10 authors and co-cited authors

Rank	Author	Count (%)	Centrality	Co-cited author	Co-citation	Centrality
1	Gershwin M Eric (United States)	42 (1.46%)	0.02	Friedman Scott L (United States)	337	0.05
2	Tacke Frank (Germany)	27 (0.94%)	0.01	Bataller Ramon (United States)	235	0.06
3	Trautwein Christian (Germany)	20 (0.70%)	0.01	Seki Ekihiro (United States)	204	0.05
4	Weiskirchen Ralf (Germany)	13 (0.45%)	0	Tilg Herbert (Austria)	141	0.07
5	Hirschfield Gideon M (Canada)	11 (0.38%)	0.01	Wynn Tomas A (United States)	140	0.02
6	Friedman Scott L (United States)	9 (0.31%)	0	Albillos Agustín (Spain)	128	0.01
7	Such Jose (Spain)	9 (0.31%)	0	Szabo Gyongyi (United States)	126	0.04
8	Szabo Gyongyi (United States)	8 (0.28%)	0	Gao Bin (United States)	125	0.08
9	Invernizzi Pietro (Italy)	8 (0.28%)	0	Hirschfield Gideon M (Canada)	120	0.09
10	Czaja Albert J (United States)	8 (0.28%)	0	Li J (China)	116	0.02

n = 204) from the Cedars-Sinai Medical Center. More than half (*n* = 6) of the top 10 co-cited authors were from the United States. As shown in Figure 6B, there was active cooperation between the different authors.

Analysis of journals and co-cited journals

The most influential journals on research on immunological factors in cirrhosis are listed in Table 4. A total of 2873 articles were published in 281 journals. The *World Journal of Gastroenterology* was the most frequently published journal (*n* = 113), followed by *Hepatology* (*n* = 109) and *Frontiers in Immunology* (*n* = 73). Among the top 10 journals, six belonged to *Journal Citation Reports* (JCR) Q1, and eight had impact factors (*IF*) of > 5. Among the co-cited journals, 12 had > 1000 citations. *Hepatology* was ranked first with 2409 citations, followed by the *Journal of Hepatology* (2124 citations) and *Gastroenterology* (1988 citations). Eight of the top 10 co-cited journals belonged to JCR Q1, and eight journals had *IF* > 10, including two journals with *IF* above 100. We analyzed the published and co-cited journals using a journal dual-map overlay, as shown in Figure 7. The cited and co-cited journals are located on the left and right sides of the graph, respectively. Different colored paths indicate the cited relationships. We identified two orange and green citation paths. Studies published in the Molecular/Biology/Clinics and Health/Nursing/Medicine journals were mainly cited in the Molecular/Biology/Immunology and Medicine/Medical/Clinical journals.

Analysis of co-cited references and reference bursts

The top 10 co-cited references are listed in Table 5, all of which were co-cited at least 31 times. A reference co-citation network was mapped (Figure 8A). The link between two nodes implies that they are cited in a publication. The node size indicates the co-citations of the references. A node with a purple ring represents a higher centrality. The article with the most co-citations was by Tsuchida *et al*[22], which revealed that HSC activation is regulated by multiple mechanisms, including autophagy, endoplasmic reticulum stress, oxidative stress, retinol and cholesterol metabolism, epigenetic and receptor-mediated signaling, and extracellular signals from resident and inflammatory cells, which play an essential role in the development of liver fibrosis. The second study, published by Albillos *et al*[23] in 2014, revealed that immunodeficiency in cirrhosis is induced by local immune surveillance, functional impairment of the liver, reduction of pattern recognition receptors, and damage at the systemic level of immune response cell function. The third article[24] published in the *Journal of Hepatology* by the European Association for the Study of the Liver, provided validated recommendations for the optimal management of HBV infection. Among the top 10 articles, research by Heymann *et al*[5] possessed a high centrality (0.14), indicating that the article is influential. It illustrated that the liver can rapidly activate immunity, and the final outcome of the intrahepatic immune response depends on the functional versatility of macrophages and DCs and the balance between the pro- and anti-inflammatory T cell populations. CiteSpace provides citation bursts that imply significant changes in reference citations over time. References with citation bursts have frequently been cited by researchers in recent years to represent emerging topics in specific research field[25]. Figure 8B shows the 25 most cited references with the strongest bursts. The most-cited study was by Albillos *et al*[23], with a strength of 18.92. Tsuchida *et al*[22] also reported a large burst. These are representative articles on the immunological factors involved in cirrhosis.

Analysis of research hotspots and frontiers

As shown in Table 6, the most frequently cited keywords for immunological factors in cirrhosis in the

Table 4 Top 10 journals and co-cited journals for research of immunological factors in cirrhosis

Rank	Journal	Count (%)	*IF* (2021)	JCR	Co-cited Journal	Citation	*IF* (2021)	JCR
1	*World Journal of Gastroenterology*	113 (3.928%)	5.374	Q2	*Hepatology*	2409	17.298	Q1
2	*Hepatology*	109 (3.790%)	17.298	Q1	*Journal of Hepatology*	2124	30.083	Q1
3	*Frontiers in immunology*	73 (2.540%)	8.786	Q1	*Gastroenterology*	1988	33.883	Q1
4	*Journal of Hepatology*	70 (2.430%)	30.083	Q1	*Gut*	1369	31.793	Q1
5	*Liver International*	59 (2.050%)	8.754	Q1	*Journal Of Clinical Investigation*	1301	19.456	Q1
6	*PLoS One*	57 (1.980%)	3.752	Q2	*Journal Of Immunology*	1280	5.426	Q2
7	*International Journal of Molecular Sciences*	46 (1.600%)	6.208	Q1	*The New England Journal of Medicine*	1240	176.079	Q1
8	*Gastroenterology*	35 (1.220%)	33.883	Q1	*Proceedings of the National Academy of Sciences of the United States of America*	1221	12.779	Q1
9	*Seminars in Liver Disease*	32 (1.110%)	6.512	Q2	*PLoS One*	1183	3.752	Q2
10	*Hepatology Research*	30 (1.040%)	4.942	Q2	*Lancet*	1153	202.731	Q1

IF: Impact factors; JCR: Journal Citation Reports.

Table 5 Top 10 co-cited references on research of immunological factors in cirrhosis

Rank	Reference	Year	Journal	Citation	Centrality
1	Mechanisms of hepatic stellate cell activation	2017	*Nature Reviews Gastroenterology & Hepatology*	50	0.03
2	Cirrhosis-associated immune dysfunction: Distinctive features and clinical relevance	2014	*Journal of Hepatology*	46	0.02
3	EASL 2017 Clinical Practice Guidelines on the management of hepatitis B virus infection	2017	*Journal of Hepatology*	35	0.03
4	Acute-on-chronic liver failure is a distinct syndrome that develops in patients with acute decompensation of cirrhosis	2013	*Gastroenterology*	35	0.03
5	Global cancer statistics 2018: GLOBOCAN estimates of incidence and mortality worldwide for 36 cancers in 185 countries	2018	*CA: A Cancer Journal for Clinicians*	33	0.02
6	Nivolumab in patients with advanced hepatocellular carcinoma (CheckMate 040): An open-label, non-comparative, phase 1/2 dose escalation and expansion trial	2017	*Lancet*	33	0.04
7	Immunology in the liver-from homeostasis to disease	2016	*Nature Reviews Gastroenterology & Hepatology*	32	0.14
8	Systemic inflammation in decompensated cirrhosis: Characterization and role in acute-on-chronic liver failure	2016	*Hepatology*	31	0.07
9	Primary biliary cirrhosis associated with HLA, IL12A, and IL12RB2 variants	2009	*The New England Journal of Medicine*	31	0.02
10	TLR4 enhances TGF-beta signaling and hepatic fibrosis	2007	*Nature Medicine*	31	0.06

last 20 years were fibrosis (428), cirrhosis (423), inflammation (384), liver fibrosis (381), expression (340), hepatocellular carcinoma (HCC) (309), activation (234), primary biliary cirrhosis (PBC) (232), disease (231), and HSC (228). These keywords reflect the research hotspots in this field. Among the 10689 keywords, the minimum number of repetitions was set to 20 and 288 eligible keywords were selected for VOSviewer visualization and analysis (Figure 9). The keyword clusters describe the internal knowledge structure of the research field[7]. The immunological factors associated with cirrhosis were divided into five clusters (Figure 9A). Cluster 1 (red) focused on the progression and treatment strategies for cirrhosis. Cluster 2 (green) includes the mechanisms and primary immune cells involved

Table 6 Top 20 keywords on research of immunological factors in cirrhosis

Rank	Keyword	Occurrences	Total link strength	Rank	Keyword	Occurrences	Total link strength
1	Fibrosis	428	2558	11	Liver	225	1276
2	Cirrhosis	423	2483	12	Risk factors	221	1200
3	Inflammation	384	2438	13	Infection	184	1123
4	Liver fibrosis	381	2290	14	Necrosis factor alpha	160	1001
5	Expression	340	1884	15	T cells	155	923
6	Hepatocellular carcinoma	309	1895	16	Cells	143	770
7	Activation	234	1421	17	Regulatory t cells	140	863
8	Primary biliary cirrhosis	232	1268	18	Liver cirrhosis	133	770
9	Disease	231	1355	19	Growth factor beta	130	834
10	Hepatic stellate cells	228	1525	20	Oxidative stress	129	836

in cirrhosis. Cluster 3 (blue) mainly focused on the diagnosis and prognosis of cirrhosis. Cluster 4 (yellow) centered on the pathological mechanisms of immune inflammation. Cluster 5 (purple) mainly consisted of various chronic liver diseases that cause liver injury. Figure 9B shows the co-occurrence of keywords by the average publication year (APY). Circles in different colors indicate the APY of the study, and those closer to yellow represent more recent years. Therefore, changes in research hotspots during a given period can be observed directly. The most recent keywords were extracellular vesicles (EVs) (cluster 2, APY: 2019.55), followed by tumor microenvironment (cluster 2, APY: 2019.43), PBC (cluster 5, APY: 2019.33), nafld (cluster 4, APY: 2019.19), and gut microbiota (cluster 4, APY: 2019.17). This indicates that EVs, the tumor microenvironment, PBC, nonalcoholic fatty liver disease, and gut microbiota have interested researchers. Additionally, we used CiteSpace for keyword–citation burst detection. There are 25 keywords had strong bursts, as shown in Figure 9C. Human immunodeficiency virus ranked first, with the strongest burst (strength = 11.59). Immune dysfunction, gut microbiota, epidemiology, mouse models, pathways, obesity, EVs, bile acids, and the extracellular matrix (ECM) are the current research frontiers of immunological factors in cirrhosis and have been in an explosive period.

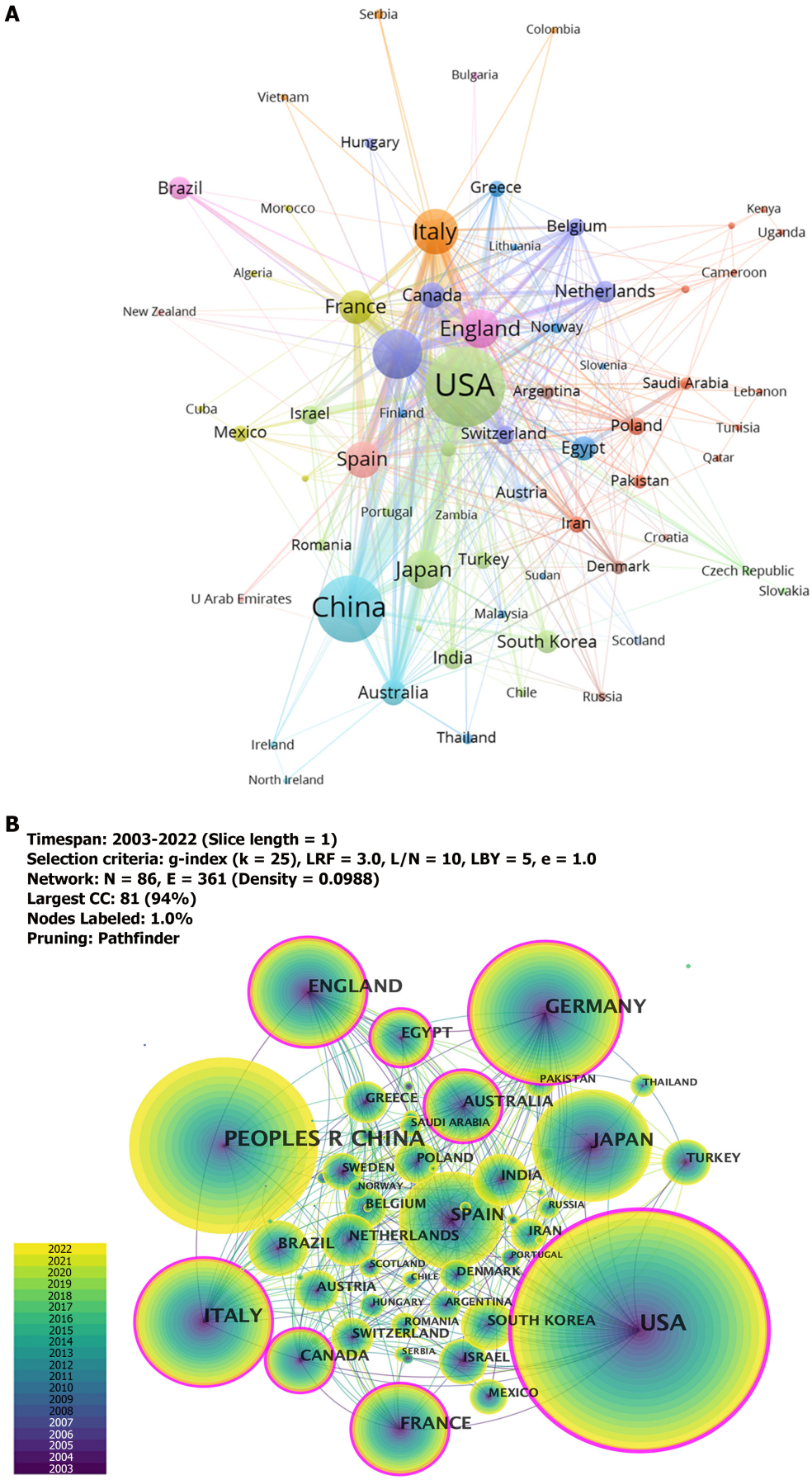
DISCUSSION

General information

According to the WoSCC database, as of December 7, 2022, 5104 authors from 1173 institutions in 51 countries have published 2873 papers on cirrhosis and immunological factors in 281 journals. Our study analyzed the literature on immunological factors in cirrhosis using CiteSpace and VOSviewer to review research results and progress. Basic information, including annual publications, countries, institutions, authors, journals, references, and keywords, was quantitatively analyzed. There is a gradual increase in publications and citations on the immunological factors of cirrhosis. More citations of a paper indicate higher quality and greater impact. The number of citations in the field has increased annually, with an accelerating trend in the later half of the period reflecting the speed and progress of the research field. This indicates that research in this field has been in an explosive period, with increasing attention from scholars.

The United States, China, and Germany are the main countries that have studied the immunological factors associated with cirrhosis. Japan, Australia, France, and United States have relatively well-researched studies on immunological factors in cirrhosis. Of the top 10 institutions, five are in the United States, two in Spain, and one each in China, England, and Italy. Davis University of California has the most publications in this field. Close collaboration between countries and institutions helps to overcome scientific difficulties and promote research on immunological factors in cirrhosis.

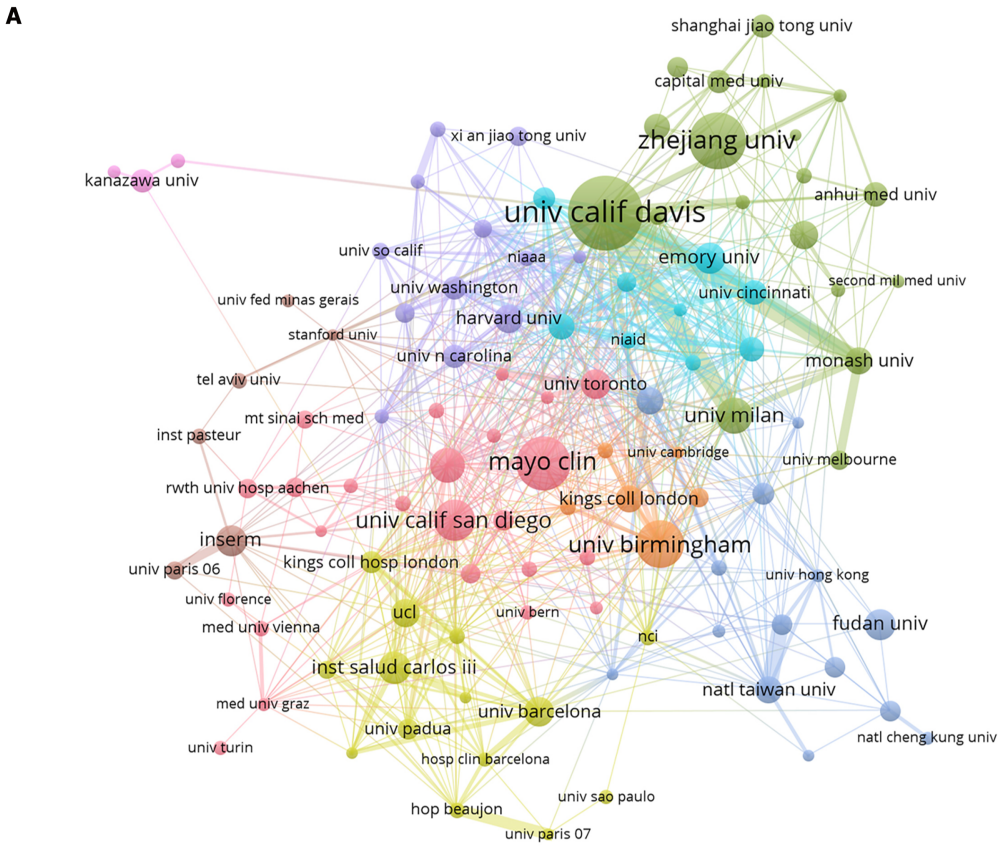
Gershwin ME from the United States published the most articles (42, 1.46%), followed by Tacke *et al* [20] (27, 0.94%) and Trautwein *et al*[21] (20, 0.70%) from Germany. These three authors have made outstanding contributions to the field of immunological factors in cirrhosis. Gershwin explained the immune response mechanisms in the liver[26] and elucidated the regulatory mechanisms of liver fibrosis from an immunological perspective[27,28]. They then explored the relationship between the gut microbiota and autoimmune liver disease and concluded that the gut-liver axis involves multiple inflammatory cell types, cytokines, chemokines, and other molecules that lead to the disruption of normal liver structure[29]. Tacke *et al*[20] researched the role of macrophages in liver fibrosis, the polarization and function of which can be further determined by specific environmental signals,

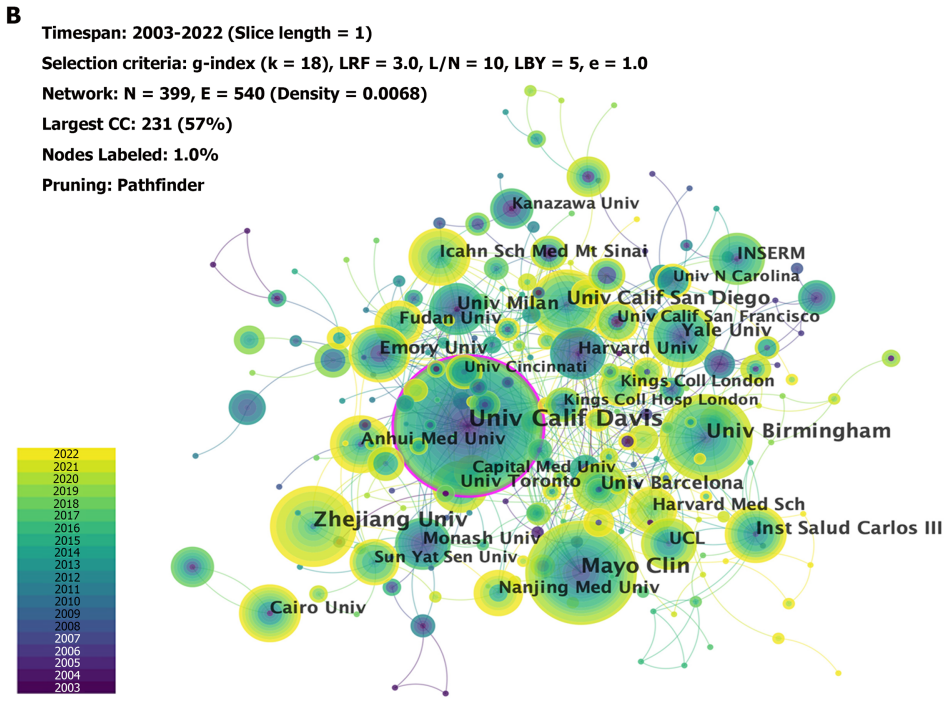


DOI: 10.3748/wjg.v29.i24.3899 **Copyright** ©The Author(s) 2023.

Figure 3 Cooperation map of countries/regions in immunological factors in cirrhosis. A: A visual map for VOSviewer network; B: A visual map for

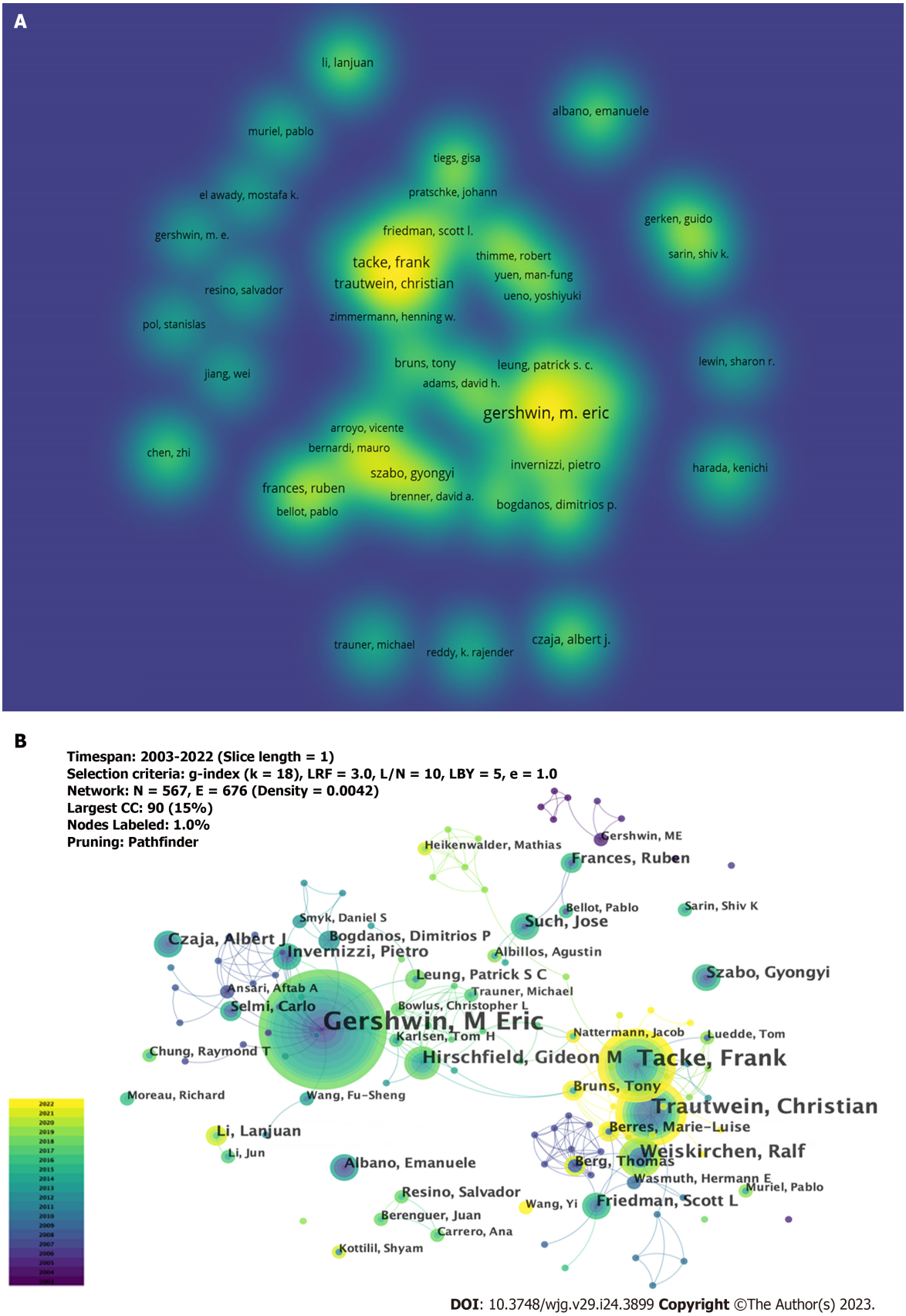
CiteSpace network. The size of the node reflects the frequencies, and the links indicate the collaboration relationships. The outermost purple ring represents the centrality level, and the nodes with high centrality are considered to be the key points in the research field.





DOI: 10.3748/wjg.v29.i24.3899 **Copyright** ©The Author(s) 2023.

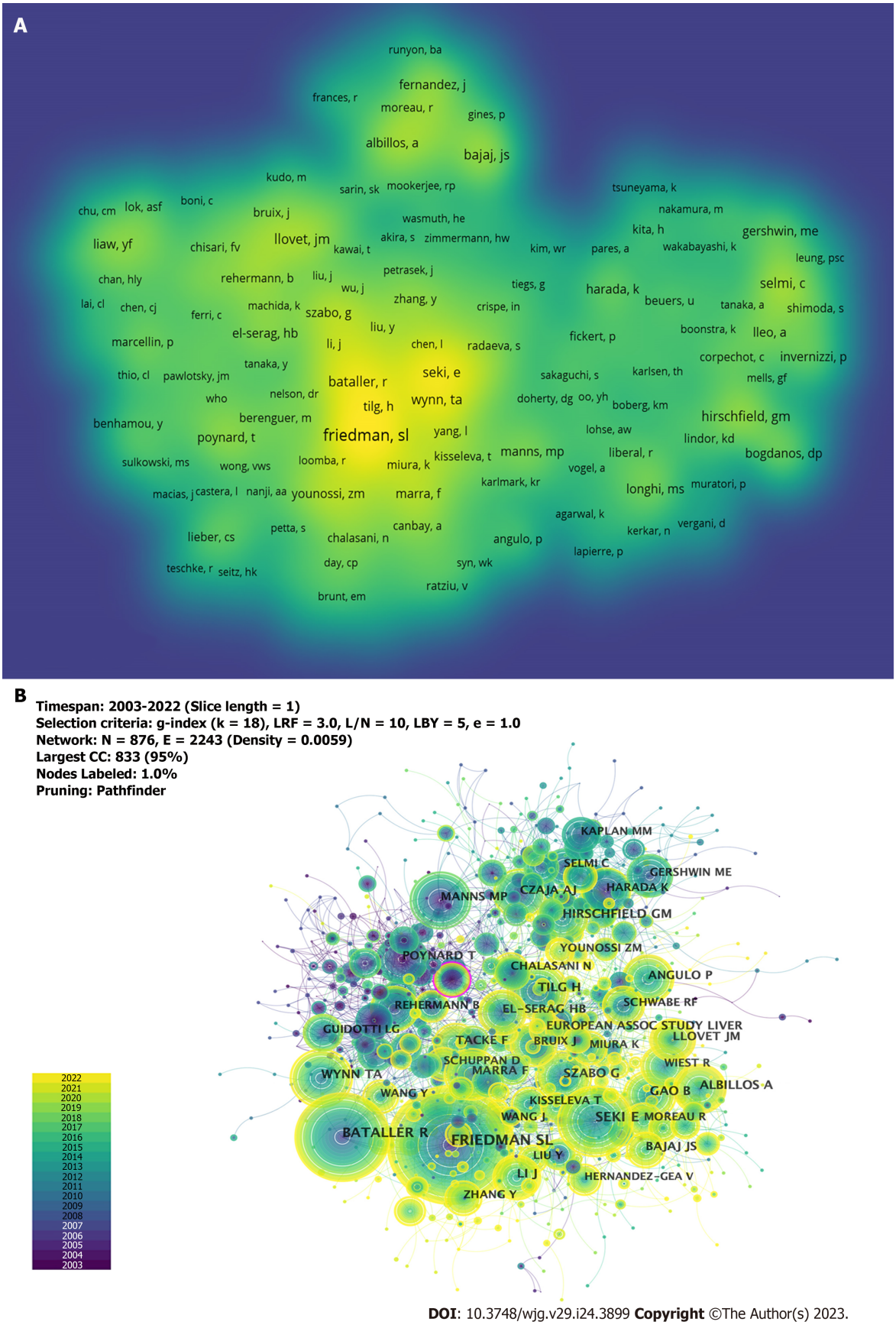
Figure 4 Cooperation map of institutions in immunological factors in cirrhosis. A: A visual map for VOSviewer network; B: A visual map for CiteSpace network.



DOI: 10.3748/wjg.v29.i24.3899 **Copyright** ©The Author(s) 2023.

Figure 5 The visualization of authors. A: A density map; B: A cooperation map.

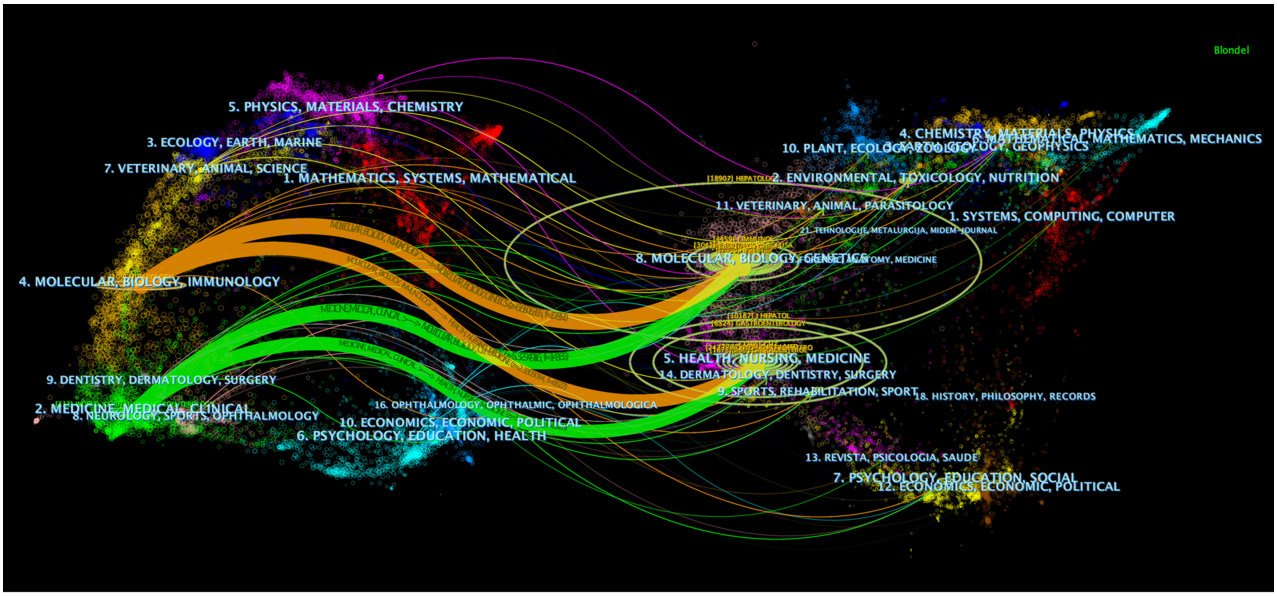
presenting with tissue recovery following liver injury or infection, or the progression of liver disease, conversely[30]. They found that infiltrating Ly-6C$^+$ MoMFs are associated with chronic inflammation and fibrosis[20]. They considered hepatic macrophages to be effective therapeutic targets and searched for new treatments[31]. Two study elaborated on the importance of chemokines in liver diseases and



DOI: 10.3748/wjg.v29.i24.3899 **Copyright** ©The Author(s) 2023.

Figure 6 The visualization of co-cited authors. A: A density map; B: A cooperation map.

highlighted their potential to intervene in inflammation and fibrosis[32,33]. They proposed that canicriviroc treatment significantly reduced hepatic Ly-6C$^+$ MoMF recruitment, confirming its therapeutic potential in patients with nonalcoholic steatohepatitis (NASH)[34]. They also found that



DOI: 10.3748/wjg.v29.i24.3899 **Copyright** ©The Author(s) 2023.

Figure 7 The dual-map overlay of journals in immunological factors in cirrhosis.

NOD-like receptor protein 3 activation was relevant to disease activity in patients with PBC[35].

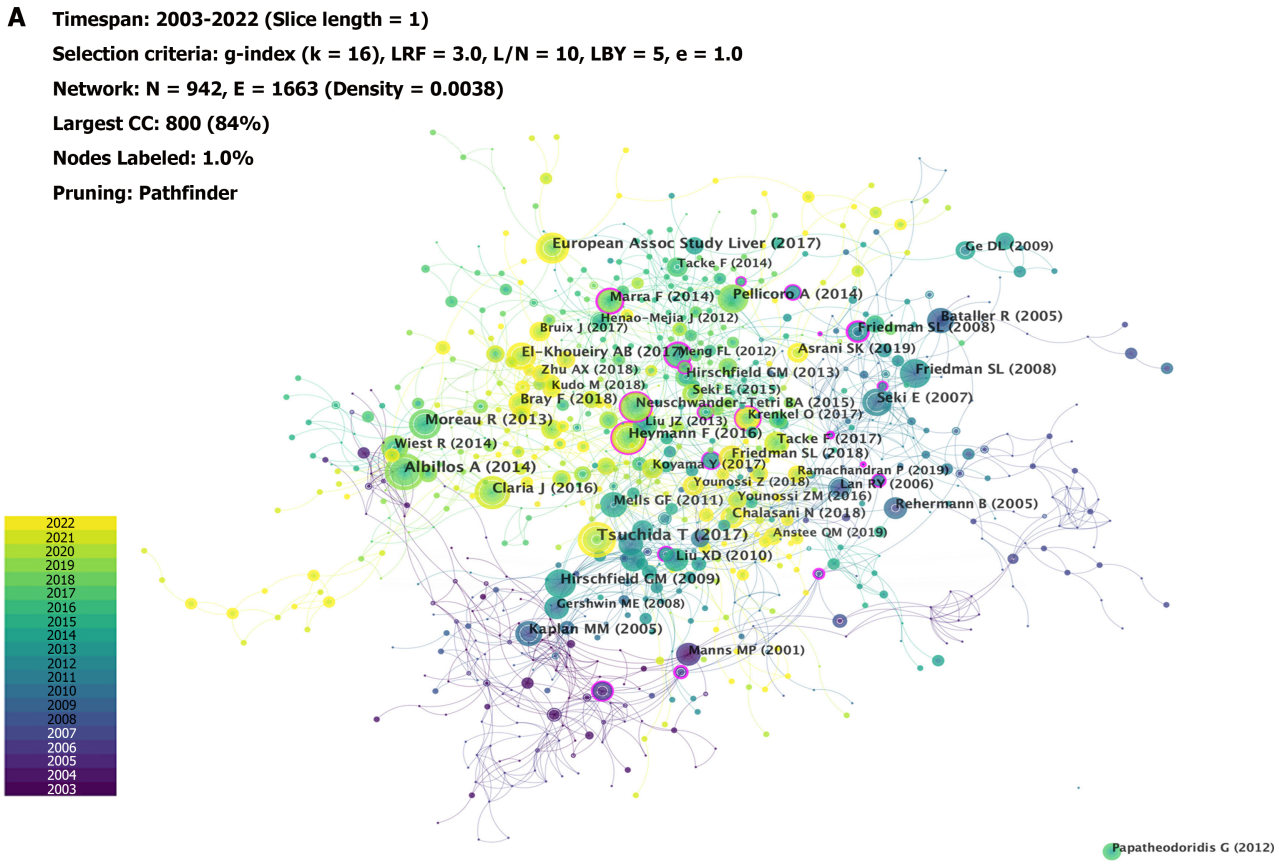
Of the top 10 journals, six were in the Q1 JCR division and eight in the *IF* > 5. Most studies on immunological factors in cirrhosis were published in the *World Journal of Gastroenterology* (113, *IF* = 5.374, Q2), followed by *Hepatology* (109, *IF* = 17.298, Q1), and *Frontiers in Immunology* (73, *IF* = 8.786, Q1). These journals are the most popular in this research field. Eight of the top 10 co-cited journals were located in the Q1 JCR division, and eight had IF above 10, including two journals with IF above 100. The top three co-cited journals were *Hepatology* (2409, *IF* = 17.298, Q1), *Journal of Hepatology* (2124, *IF* = 30.083, Q1), and *Gastroenterology* (1988, *IF* = 33.883, Q1). These findings indicate that many high-quality and influential journals are interested in studying cirrhosis and its immunological factors. Figure 7 reveals that papers published in molecular, biology, clinical, health, nursing, and medicine journals are mainly cited in Molecular, Biology, Immunology, and Medicine, Medical, Clinical journals. This implies that current research on cirrhosis and immunological factors is mainly focused on basic research and translational medicine.

Knowledge base

We can observe the research base in the field of immunological factors in liver cirrhosis by analyzing the co-cited references. The most co-cited was "Mechanisms of hepatic stellate cell activation" published in *Nature Reviews Gastroenterology & Hepatology* by Tsuchida *et al*[22] in 2017, followed by "Cirrhosis-associated immune dysfunction: Distinctive features and clinical relevance" by Albillos *et al*[23], and "EASL 2017 Clinical Practice Guidelines on the management of HBV infection" by European Association for the Study of the Liver. The top 10 co-cited references were all cited 30 times at least, mainly involving the immunoinflammatory mechanisms of cirrhosis and liver fibrosis. Liver fibrosis is a dynamic process caused by chronic liver injury. The inflammatory response in the liver is initiated by danger-associated molecular patterns, Toll-like receptors (TLRs) signaling, or inflammatory vesicle activation[5]. HSC activation is the central driver of liver fibrosis[22]. The activation of hepatic macrophages (Kupffer cells) and resident mast cells promotes tissue injury by producing pro-inflammatory and vascular-permeable mediators, which induce the accumulation of neutrophils, lymphocytes, eosinophils, and monocytes in the liver[36]. Systemic inflammation, the main driver of acute-on-chronic liver failure (ACLF), affects the function of somatic tissues and alters the clinical manifestations of cirrhosis[37]. The immune response pattern changes from a proinflammatory phenotype in patients with stable decompensated cirrhosis to an immunodeficient phenotype in patients with severely decompensated cirrhosis and extrahepatic organ failure[23].

Hotspots and frontiers

In the study of immunological factors in cirrhosis, high-frequency keywords were mainly fibrosis (428), cirrhosis (423), inflammation (384), liver fibrosis (381), expression (340), HCC (309), activation (234), PBC (232), disease (231), and HSC (228), which are the hot topics of research in this field. Systemic inflammation is a crucial mechanism in the progression of cirrhosis to the decompensated stage and is a common pathophysiological mechanism underlying the clinical features of acutely decompensated cirrhosis, such as ascites, encephalopathy, gastrointestinal bleeding, bacterial infection, and extrahepatic



B

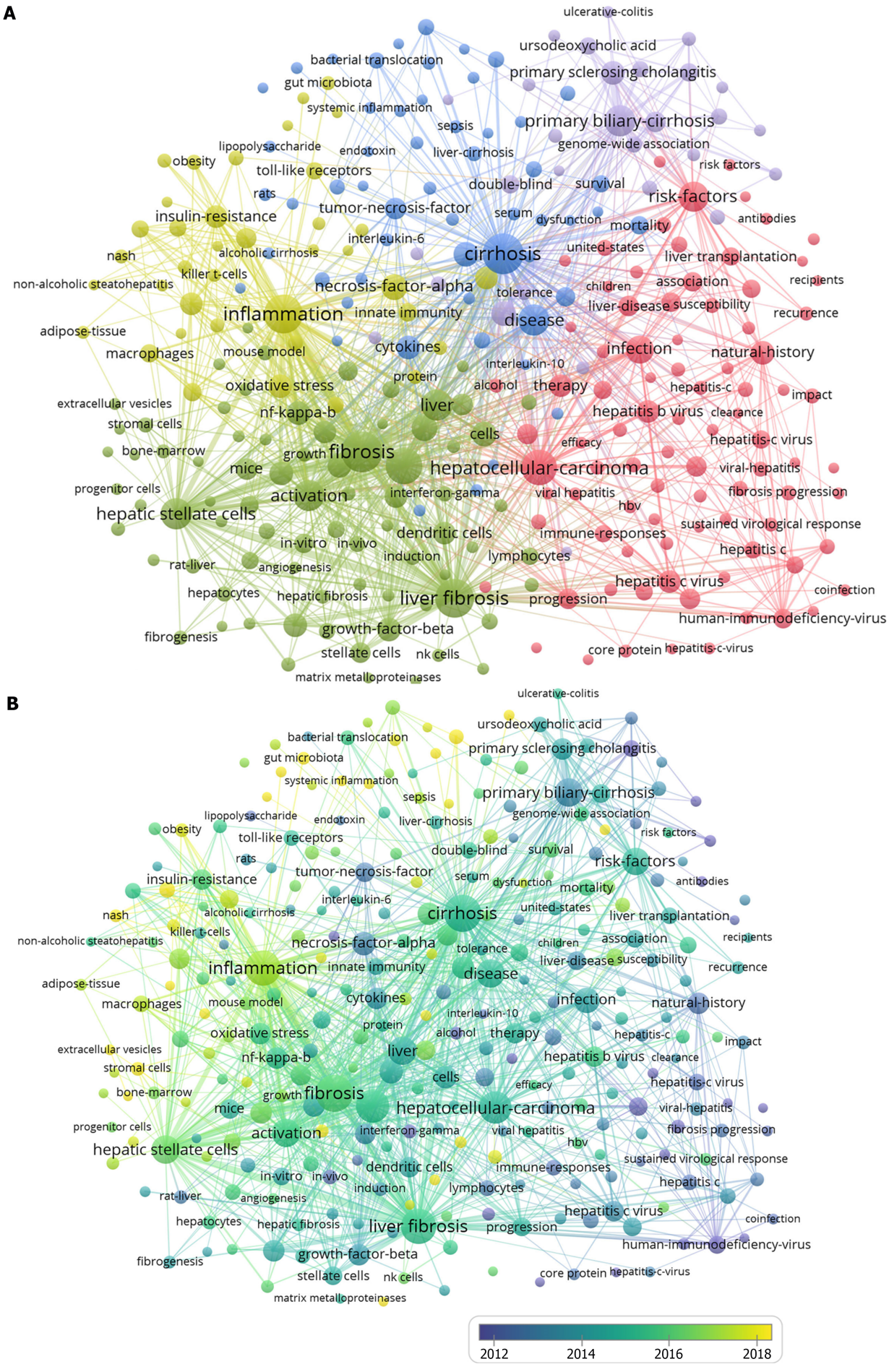
Top 25 references with the strongest citation bursts

References	Year	Strength	Begin	End	2003-2022
Manns MP, 2001, LANCET, V358, P958, DOI 10.1016/S0140-6736(01)06102-5, DOI	2001	12.6	2003	2006	
Bataller R, 2005, J CLIN INVEST, V115, P209, DOI 10.1172/JCI200524282, DOI	2005	15.28	2006	2010	
Rehermann B, 2005, NAT REV IMMUNOL, V5, P215, DOI 10.1038/nri1573, DOI	2005	12.63	2006	2010	
Kaplan MM, 2005, NEW ENGL J MED, V353, P1261, DOI 10.1056/NEJMra043898, DOI	2005	15.8	2007	2010	
Lan RY, 2006, HEPATOLOGY, V43, P729, DOI 10.1002/hep.21123, DOI	2006	10.54	2007	2011	
Seki E, 2007, NAT MED, V13, P1324, DOI 10.1038/nm1663, DOI	2007	16.44	2009	2012	
Friedman SL, 2008, GASTROENTEROLOGY, V134, P1655, DOI 10.1053/j.gastro.2008.03.003, DOI	2008	13.73	2009	2013	
Friedman SL, 2008, PHYSIOL REV, V88, P125, DOI 10.1152/physrev.00013.2007, DOI	2008	11.35	2009	2013	
Hirschfield GM, 2009, NEW ENGL J MED, V360, P2544, DOI 10.1056/NEJMoa0810440, DOI	2009	13.9	2010	2014	
Ge DL, 2009, NATURE, V461, P399, DOI 10.1038/nature08309, DOI	2009	10.29	2010	2014	
Liu XD, 2010, NAT GENET, V42, P658, DOI 10.1038/ng.627, DOI	2010	12.49	2012	2015	
Mells GF, 2011, NAT GENET, V43, P329, DOI 10.1038/ng.789, DOI	2011	12.01	2012	2015	
Albillos A, 2014, J HEPATOL, V61, P1385, DOI 10.1016/j.jhep.2014.08.010, DOI	2014	18.92	2015	2019	
Moreau R, 2013, GASTROENTEROLOGY, V144, P1426, DOI 10.1053/j.gastro.2013.02.042, DOI	2013	16.51	2015	2018	
Pellicoro A, 2014, NAT REV IMMUNOL, V14, P181, DOI 10.1038/nri3623, DOI	2014	12.29	2015	2019	
Marra F, 2014, GASTROENTEROLOGY, V147, P577, DOI 10.1053/j.gastro.2014.06.043, DOI	2014	11.14	2016	2019	
Neuschwander-Tetri BA, 2015, LANCET, V385, P956, DOI 10.1016/S0140-6736(14)61933-4, DOI	2015	10.96	2016	2020	
Heymann F, 2016, NAT REV GASTRO HEPAT, V13, P88, DOI 10.1038/nrgastro.2015.200, DOI	2016	11.62	2017	2022	
Claria J, 2016, HEPATOLOGY, V64, P1249, DOI 10.1002/hep.28740, DOI	2016	11.25	2017	2022	
Tsuchida T, 2017, NAT REV GASTRO HEPAT, V14, P397, DOI 10.1038/nrgastro.2017.38, DOI	2017	15.75	2018	2022	
European Assoc Study Liver, 2017, J HEPATOL, V67, P370, DOI 10.1016/j.jhep.2017.03.021, DOI	2017	10.98	2018	2022	
El-Khoueiry AB, 2017, LANCET, V389, P2492, DOI 10.1016/S0140-6736(17)31046-2, DOI	2017	12.33	2019	2022	
Bray F, 2018, CA-CANCER J CLIN, V68, P394, DOI 10.3322/caac.21492, DOI	2018	12.33	2019	2022	
Koyama Y, 2017, J CLIN INVEST, V127, P55, DOI 10.1172/JCI88881, DOI	2017	10.29	2019	2022	
Asrani SK, 2019, J HEPATOL, V70, P151, DOI 10.1016/j.jhep.2018.09.014, DOI	2019	10.85	2020	2022	

DOI: 10.3748/wjg.v29.i24.3899 **Copyright** ©The Author(s) 2023.

Figure 8 Analysis of references in immunological factors in cirrhosis. A: References co-citation network; B: Top 25 references with strong citation bursts. A red bar indicates high citations in that year.

organ failure[38]. IL-6, TNF-α, and transforming growth factor beta (TGF-β) are key pro-inflammatory and pro-fibrotic cytokines that drive liver fibrosis[39]. A recent study found that under pathological conditions, TGF-β overexpression leads to epithelial mesenchymal-mesenchymal transition, ECM deposition, and cancer-associated fibroblast formation, resulting in fibrotic disease and cancer[40].


A
ulcerative-colitis
ursodeoxycholic acid
bacterial translocation
primary sclerosing cholangitis
gut microbiota
systemic inflammation
primary biliary-cirrhosis
sepsis
genome-wide association
lipopolysaccharide
endotoxin
liver-cirrhosis
risk factors
obesity
toll-like receptors
double-blind
survival
rats
risk-factors
tumor-necrosis-factor
serum
dysfunction
antibodies
insulin-resistance
mortality
interleukin-6
united-states
nash
alcoholic cirrhosis
cirrhosis
liver transplantation
killer t-cells
children
association
recipients
non-alcoholic steatohepatitis
necrosis-factor-alpha
tolerance
liver-disease susceptibility
inflammation
innate immunity
disease
recurrence
adipose-tissue
cytokines
infection
natural-history
macrophages
mouse model
interleukin-10
protein
alcohol
therapy
hepatitis-c
impact
oxidative stress
extracellular vesicles
nf-kappa-b
liver
hepatitis b virus
clearance
stromal cells
cells
efficacy
hepatitis-c virus
bone-marrow
growth
fibrosis
hepatocellular-carcinoma
viral-hepatitis
mice
progenitor cells
interferon-gamma
viral hepatitis
fibrosis progression
activation
hbv
hepatic stellate cells
sustained virological response
dendritic cells
immune-responses
in-vitro
in-vivo
hepatitis c
induction
lymphocytes
rat-liver
angiogenesis
hepatitis c virus
coinfection
hepatocytes
hepatic fibrosis
liver fibrosis
progression
human-immunodeficiency-virus
fibrogenesis
growth-factor-beta
stellate cells
nk cells
core protein
hepatitis-c-virus
matrix metalloproteinases
B
2012
2014
2016
2018

C

Top 25 keywords with the strongest citation bursts

Keywords	Year	Strength	Begin	End	2003-2022
Chronic hepatitis c	2003	8.53	2003	2012	
Immune response	2003	8.09	2003	2007	
Interferon alpha	2003	7.42	2003	2013	
Chronic active hepatiti	2003	6.81	2003	2010	
human immunodeficiency virus	2004	11.59	2004	2014	
Peripheral blood	2004	6.55	2004	2010	
Core protein	2004	6.27	2004	2013	
Molecular mimicry	2004	6.08	2004	2010	
Necrosis factor alpha	2003	8.78	2005	2007	
Virus infection	2003	7.37	2005	2016	
T cell response	2006	7.13	2006	2014	
Primary biliary cirrhosis	2003	9.89	2008	2012	
Antimitochondrial antibody	2008	6.63	2008	2014	
Natural history	2003	6.27	2008	2010	
Lymphocyte	2004	7.18	2009	2013	
Genome wide association	2011	8.28	2013	2017	
Immune dysfunction	2016	6.15	2016	2022	
Gut microbiota	2017	7.71	2017	2022	
Epidemiology	2018	8.24	2018	2022	
Mouse model	2016	6.15	2018	2022	
Pathway	2012	6.61	2019	2022	
Obesity	2019	6.22	2019	2022	
Extracellular vesicle	2017	6.41	2020	2022	
Bile acid	2011	6.32	2020	2022	
Extracellular matrix	2007	6.06	2020	2022	

DOI: 10.3748/wjg.v29.i24.3899 **Copyright** ©The Author(s) 2023.

Figure 9 Analysis of Keywords in immunological factors in cirrhosis. A: The cluster of keywords; B: Keyword co-occurrence network. Keywords in yellow appeared later than that in blue; C: Top 25 keywords with the strongest citation bursts.

Toxins such as alcohol, steatosis, or viral infection can trigger inflammation, and the inflammatory cytokine IL-17 drives HSC and Kupffer cells to produce pro-fibrotic IL-6, TNF-α, and TGF-β[41]. A previous study[42] demonstrated that albumin binds and activates many inflammatory promoters in decompensated cirrhosis and that high doses of albumin have significant immunomodulatory effects. However, the anti-inflammatory effects of albumin in cirrhosis require further investigation. This evidence suggests the potential value of anti-inflammatory agents in the treatment of cirrhosis. Approximately 90% of HCC cases occur in a cirrhotic setting, but less than 5% of patients progress to HCC each year[43]. Cancer-associated fibroblasts, which may originate from HSC, are critical for hepatocarcinogenesis. After being activated to become myofibroblasts producing the ECM, they can interact with cancer cells, contributing to the growth and invasion of HCC[44]. PBC is characterized by a loss of immune tolerance in biliary epithelial cells, and the interdependence of biliary tract injury, cholestasis, and progressive hepatic fibrosis has become a major disease worldwide[45]. PBC is considered an autoimmune disease with a specific autoantibody, antimitochondrial antibody, and the establishment of ursodeoxycholic acid as a first-line therapeutic agent has significantly reduced disease progression in cirrhosis[46]. In patients with PBC who did not respond adequately to ursodeoxycholic acid alone, besides ursodeoxycholic acid, we also treated them with bezafibrate; however, its effect on liver transplantation and death needs to be clarified by further studies[47]. Liver fibrosis is an advanced stage of chronic liver disease that develops from a variety of diseases, such as chronic hepatitis virus infection (HBV and HCV), NASH, PBC, primary sclerosing vasculitis, autoimmune hepatitis, Wilson's disease, and hemochromatosis[48]. Researches on the pathogenesis and targeted agent of PBC have excited particular concern in recent years[49,50]. The crucial role and activation mechanisms of HSC in cirrhosis have been extensively elaborated in detail[22,51,52]. Paracrine signals from damaged epithelial cells, fibrotic microenvironment, dysregulation of immune and systemic metabolism, dysregulated intestinal microecology, and hepatitis virus products can directly or indirectly activate HSC[51]. The clearance of HSC, including apoptosis, senescence, and return to an inactivated state, has been fully elucidated[22].

In conclusion, these findings reveal the remarkable complexity and plasticity of HSC activation. The modulation of HSC provides vital value for developing therapeutic strategies for cirrhosis.

The keywords that have exploded in recent years are immune dysfunction, gut microbiota, epidemiology, mouse models, pathways, obesity, EVs, bile acid, and ECM, representing the current frontiers of research on immunological factors in cirrhosis. In hepatic fibrosis, the immune system is involved in wound healing and tissue repair by triggering inflammation. Immune cells regulate the progression and regression of liver fibrosis. Various immune cells participate in the regulation of liver fibrosis, including innate immune cells (monocytes, macrophages, and DCs), adaptive immune cells (T cells and B cells), and various cytokines. Following liver injury, infiltrating immune cells are recruited to the site of the injured hepatocytes and participate in the liver fibrosis cascade by secreting proinflammatory cytokines such as TNF-α, IL-6, and CCL4[39]. As the first line of defense against pathogens, Kupffer cells are activated by LPS, the complement system, and other pathogen-associated molecular patterns *via* the expression of TLRs, including TLR2, TLR3, and TLR4, to recognize microbial antigens and signals from damaged hepatocytes. Cytoplasmic division generated by Kupffer cells in response to TLR signaling subsequently recruits and activates neutrophils[6]. DCs present antigens, control subsequent T cell differentiation, and regulate T cell responses[53]. Systemic inflammation and immunodeficiency have been identified as two critical factors in cirrhosis-associated immune dysfunction, with the most severe immune changes being more common in ACLF[54]. The pathophysiology of ACLF involves persistent inflammation, immune dysregulation, systemic inflammatory response syndrome, and subsequent sepsis due to immune paralysis[55,56]. Two main types of systemic immune alterations are typical in cirrhosis: On the one hand, cirrhosis-associated immune dysfunction results in immunodeficiency; on the other hand, persistent under-stimulation of immune cells leads to systemic inflammation[53]. Immunodeficiency in cirrhosis results from the structural distortion of the liver parenchyma and functional impairment of circulating immune cells. It can increase the risk of bacterial infection at any stage of liver disease and may lead to acute decompensation and acute or chronic liver failure, which are associated with high short-term mortality [36,37]. Inflammatory factors play an essential role in immune regulation. Further regulation of relevant immune cells and cytokines to control inflammation and block critical targets of the immune-inflammatory response can delay and inhibit the onset and progression of cirrhosis. Gut microbiota is involved in maintaining the balance of the immune system and preventing autoimmunity[57]. In chronic liver disease, the adhesion of pathogenic bacteria to mucosal surfaces and barrier damage are central to the initiation of mucosal immunity[58]. Microbial products (especially LPSs), as pathogen-associated molecular patterns, can be transferred from the gut to the liver, bind to TLR, activate Kupffer cells, stimulate immune responses, and produce inflammatory cytokines (*e.g.*, IL-1β and TNF) and reactive oxygen species[57,59]. The gut microbiota can lead to systemic inflammation either directly through translocation or indirectly through its metabolic pathways, resulting in the progression of decompensated cirrhosis and ACLF[60]. Thus, regulation of the gut microbiome contributes to the development of cirrhosis[57]. Summarizing the epidemiological features of cirrhosis will be beneficial for providing clinical guidance and assistance. Globally, approximately 1 million people die annually from cirrhosis, the 11th most common cause of death, which is widely prevalent in low-, middle-, and high-income countries and is associated with high morbidity and mortality[1]. In 2019, an estimated 25% of global deaths from cirrhosis were alcohol-related[61]. Epidemiology-related recognition remains a hot topic and a frontier for future research. Various mouse models of liver fibrosis are often used in cirrhosis research, and the most commonly used are the toxic, biliary, and metabolic liver fibrosis models[62,63]. Recent studies on the mechanisms and pathways involved in hepatic fibrosis and cirrhosis have yielded promising results. The study of related pathways may shed light on the regulation of liver fibrosis and potential targets for therapy. For example, TGF-βpromotes liver fibrosis by activating Sma- and Mad-associated protein 3, intracellular IL-37 downregulates liver inflammation and fibrosis by interacting with Smad3[64], and curcumin inhibits liver fibrosis by activating autophagy to suppress TGF-β/Smad signaling, thereby inhibiting epithelial-mesenchymal transition and ECM production[65]. A study by Kong *et al*[66] showed that ferritin phagocytosis-mediated iron sagging in HSC is responsible for the antifibrotic effect induced by artesunate, which provides new clues for further pharmacological studies of artesunate. Zhang *et al*[67] found that melanoma differentiation-associated gene 5 effectively inhibits hepatic lipid accumulation and metabolic disorders by blocking the N-terminal dimerization of apoptosis signal-regulating kinase 1. Regardless of the etiology of the disease, obesity is an independent risk factor for hepatic decompensation[68]. Statistically, 20% of patients with NASH progress to cirrhosis and have an increased risk of developing HCC[69]. Dyslipidemia significantly contributes to cardiovascular-related mortality and morbidity in patients with NASH. Efluxifermin has been shown to remarkably reduce hepatic lipids and is usually safe and tolerated in patients with NASH (F1-F3) fibrosis, suggesting that efluxifermin may alter the progression of NASH[70]. However, further studies are required to investigate the specific mechanisms and effects. Numerous studies have been conducted on the potential role of EVs as biomarkers of liver diseases. EVs are significantly involved in intercellular communication by delivering different cargo and acting as vital cell-derived particles in the progression of liver injury and fibrosis, helping predict complications and mortality, detect early HCC, and predict the outcome of acute liver failure[71]. In the treatment of cirrhosis, EVs play a crucial role in anti-inflammatory mechanisms. For example, lipotoxic EVs mediate

the adhesion of monocytes to liver sinusoidal endothelial cells mainly through an ITGβ1-dependent mechanism, and ITGβ1 exhibits an inflammatory inhibitory effect in a mouse model of NASH; however, further studies are needed to determine whether a similar therapeutic effect exists in human patients [62]. Gao *et al*[72] demonstrated that Src-homology 2 domain protein phosphatase 2 in HSC promotes the release of fibrotic EVs by inhibiting autophagy and Rho-associated protein kinase 1, and activating the mammalian target of the rapamycin pathway, which provides a new idea for a new target for liver fibrosis treatment. However, the exact mechanism of action of the autophagy-dependent EVs requires further investigation. A previous study[73] found that EVs released from a stem cell-like population derived from the human adult liver demonstrated antifibrotic and anti-inflammatory effects in an immunocompromised NASH mouse model, providing new clues for the treatment of cirrhosis. The role of bile acids in hepatic cirrhosis is receiving increasing attention. Bile acids can alter the microbiome and liver regeneration, and chronic cholestasis in PBC caused by the bile acid-affected microbiome can reversely lead to liver injury, creating a vicious cycle of chronic liver injury[46]. It was reported that cholesterol ameliorates bile acid toxicity in mouse models of NASH and fibrosis by inducing Nrf-2 and HIF-1α-dependent hepatocyte proliferation and liver regeneration[63]. One study[74] found that antagonizing TGR5 or inhibiting ERK1/2 and p38MAPK signaling may contribute to the prevention or reversal of liver fibrosis by reducing the hepatic concentrations of conjugated 12α-OH-bile acids. Salhab *et al*[75] found that the sodium+/taurocholate co-transporting polypeptide is a membrane transporter protein that affects the enterohepatic circulation of bile acids and that sodium+/taurocholate co-transporting polypeptide blockers can prevent the development of hepatic fibrosis. These findings provide further directions for specific targeted therapies for cirrhosis. The role of bile acids in the pathogenesis of cirrhosis is extremely complex and influenced by many mechanisms of interaction. Substantial research is required to determine their specific roles. ECM has also been one of the keywords of the outbreak in recent years. Liver fibrosis and cirrhosis are characterized by the abnormal deposition of ECM proteins. Alterations in ECM composition are critical for tissue repair, remodeling, and cellular responses to fibrosis[76]. A previous study[77] reported that surface-active vesicle-based ECM therapeutics can also treat liver fibrosis. Studying the interactions between fibroblasts, ECM, and inflammation may provide new avenues for identifying new therapeutic targets for cirrhosis[78]. To date, it is not fully understood how the ECM is dynamically remodeled during the development of cirrhosis, and whether ECM signaling has a predictive value for the prognosis of early cirrhosis still needs to be studied on a large scale[79].

Advantages and shortcomings

Based on bibliometric analysis and literature visualization, the hotspots, evolutionary processes, and developmental trends of research on immunological factors in cirrhosis are presented visually, providing further insight into the current status and future perspectives compared to traditional reviews. Meanwhile, VOSviewer and CiteSpace have been used extensively for bibliometric analyses; therefore, our data analysis process was relatively objective and reliable. However, this study had some limitations. First, we retrieved publications and data from WoSCC; despite our efforts to obtain the most comprehensive literature, some articles were not included in the analysis, which may have led to bias. Second, owing to the time lag, some newly published high-quality papers did not receive sufficient citations and therefore could not be included in the analysis.

CONCLUSION

Immunological factors associated with cirrhosis have important research and application prospects. With the rapid increase in the number of studies, the study of immunological factors in cirrhosis has attracted great interest from researchers worldwide. The United States and China are the leading countries, and there is close cooperation between various countries and institutions. Current research hotspots regarding immunological factors in cirrhosis include fibrosis, cirrhosis, inflammation, liver fibrosis, expression, HCC, activation, PBC, disease, and HSCs. Immune dysfunction, gut microbiota, epidemiology, mouse model, pathway, obesity, EVs, bile acids, and the ECM are currently at the frontier of research on immunological factors in cirrhosis. It is notable that in addition to focusing on basic research, we should also pay attention to the translation and application of the research results.

ARTICLE HIGHLIGHTS

Research background

Cirrhosis is deemed a systemic disease associated with the immune system resulting from a persistent liver injury leading to liver fibrosis. Immunological factors play important regulatory roles in the development and progression of cirrhosis.

Research motivation

Bibliometrics is one of the most used methods for the systematic evaluation of a field of study. To date, no bibliometric studies have been conducted on the role of immunological factors in cirrhosis. A statistical analysis conducted by a bibliometric method may provide a more comprehensive understanding and assessment of the hot spots and trends in research on immunological factors in cirrhosis disease.

Research objectives

To provide a comprehensive overview of the knowledge structure and research hotspots of immunological factors in cirrhosis, which can help scholars quickly understand the research status and provide new ideas and directions for studying immunological factors in cirrhosis.

Research methods

We retrieved publications related to immunological factors in cirrhosis between 2003 to 2022 from the Web of Science Core Collection (WoSCC) database on December 7, 2022. The search strategy was TS = ((Liver Cirrhosis OR hepatic cirrhosis OR liver fibrosis) AND (Immunologic* Factor* OR Immune Factor* OR Immunomodulator* OR Biological Response Modifier* OR Biomodulator*)). Only original articles and reviews were included. A total of 2873 publications were analyzed using indicators of publication and citation metrics, countries, institutes, authors, journals, references, and keywords by CiteSpace and VOSviewer.

Research results

A total of 5104 authors from 1173 institutions across 51 countries published 2873 papers on cirrhosis and immunological factors in 281 journals. In this article, we explored and analyzed research in this field according to country, journal, author, and other relevant factors. Current research hotspots in this field include fibrosis, cirrhosis, inflammation, liver fibrosis, expression, hepatocellular carcinoma, activation, primary biliary cirrhosis, disease, and hepatic stellate cells. Burst keywords (*e.g.*, epidemiology, gut microbiota, and pathways) represent research frontiers that have attracted the interest of researchers in recent years.

Research conclusions

We used bibliometrics, a relatively new literature research method, to analyze the knowledge structure and hotspots of research in the field, providing new ideas for promoting scientific research and clinical applications.

Research perspectives

Burst keywords, including immune dysfunction, gut microbiota, epidemiology, mouse models, pathways, obesity, extracellular vesicles, bile acids, and the extracellular matrix, represent the current frontiers of research on immunological factors in cirrhosis.

FOOTNOTES

Author contributions: Zhang D designed and performed the research; Zhang D, Liu BW, and Liang XQ did statistical analysis; Liu FQ reviewed and revised the manuscript; and all authors have read and approved the final manuscript.

Supported by the National Multi-Center Clinical Research Project of Peking University First Hospital, No. 2022CR57.

Conflict-of-interest statement: The authors declare that they have no conflict of interest.

PRISMA 2009 Checklist statement: The authors have read the PRISMA 2009 Checklist, and the manuscript was prepared and revised according to the PRISMA 2009 Checklist.

Open-Access: This article is an open-access article that was selected by an in-house editor and fully peer-reviewed by external reviewers. It is distributed in accordance with the Creative Commons Attribution NonCommercial (CC BY-NC 4.0) license, which permits others to distribute, remix, adapt, build upon this work non-commercially, and license their derivative works on different terms, provided the original work is properly cited and the use is non-commercial. See: https://creativecommons.org/Licenses/by-nc/4.0/

Country/Territory of origin: China

ORCID number: Dan Zhang 0000-0003-1478-0338; Bo-Wen Liu 0000-0001-8837-7870; Xiao-Qing Liang 0000-0003-1992-9592; Fu-Quan Liu 0000-0003-1972-7712.

S-Editor: Chen YL

L-Editor: A
P-Editor: Cai YX

REFERENCES

1 **Ginès P**, Krag A, Abraldes JG, Solà E, Fabrellas N, Kamath PS. Liver cirrhosis. *Lancet* 2021; **398**: 1359-1376 [PMID: 34543610 DOI: 10.1016/S0140-6736(21)01374-X]
2 **Roehlen N**, Crouchet E, Baumert TF. Liver Fibrosis: Mechanistic Concepts and Therapeutic Perspectives. *Cells* 2020; **9** [PMID: 32260126 DOI: 10.3390/cells9040875]
3 **Engelmann C**, Clària J, Szabo G, Bosch J, Bernardi M. Pathophysiology of decompensated cirrhosis: Portal hypertension, circulatory dysfunction, inflammation, metabolism and mitochondrial dysfunction. *J Hepatol* 2021; **75** Suppl 1: S49-S66 [PMID: 34039492 DOI: 10.1016/j.jhep.2021.01.002]
4 **Fortea JI**, Crespo J, Puente Á. Cirrhosis, a Global and Challenging Disease. *J Clin Med* 2022; **11** [PMID: 36362738 DOI: 10.3390/jcm11216512]
5 **Heymann F**, Tacke F. Immunology in the liver--from homeostasis to disease. *Nat Rev Gastroenterol Hepatol* 2016; **13**: 88-110 [PMID: 26758786 DOI: 10.1038/nrgastro.2015.200]
6 **Liu Y**, Dong Y, Wu X, Wang X, Niu J. Identification of Immune Microenvironment Changes and the Expression of Immune-Related Genes in Liver Cirrhosis. *Front Immunol* 2022; **13**: 918445 [PMID: 35903097 DOI: 10.3389/fimmu.2022.918445]
7 **Hou J**, Su H, Kuang X, Qin W, Liu K, Pan K, Zhang B, Yang S, Peng X, Nie X, Hua Q. Knowledge Domains and Emerging Trends of Osteoblasts-Osteoclasts in Bone Disease From 2002 to 2021: A Bibliometrics Analysis and Visualization Study. *Front Endocrinol (Lausanne)* 2022; **13**: 922070 [PMID: 35937845 DOI: 10.3389/fendo.2022.922070]
8 **Devos P**, Menard J. Bibliometric analysis of research relating to hypertension reported over the period 1997-2016. *J Hypertens* 2019; **37**: 2116-2122 [PMID: 31136459 DOI: 10.1097/HJH.0000000000002143]
9 **Zheng MQ**, Li XX, Xu R, Liu S, Rui ZY, Guo ZY, Chen D. Bibliometric analysis of tuberculosis molecular epidemiology based on CiteSpace. *Front Public Health* 2022; **10**: 1040176 [PMID: 36483245 DOI: 10.3389/fpubh.2022.1040176]
10 **Brandt JS**, Hadaya O, Schuster M, Rosen T, Sauer MV, Ananth CV. A Bibliometric Analysis of Top-Cited Journal Articles in Obstetrics and Gynecology. *JAMA Netw Open* 2019; **2**: e1918007 [PMID: 31860106 DOI: 10.1001/jamanetworkopen.2019.18007]
11 **Barboza-Palomino M**, Salas G, Vega-Arce M, Caycho-Rodríguez T, Ventura-León J, Flores-Kanter PE, Salas-Blas E, Landa-Barzola M, López-López W. Thirty Years of Psicothema: A Bibliometric Analysis (1989-2018). *Psicothema* 2020; **32**: 459-468 [PMID: 33073751 DOI: 10.7334/psicothema2020.145]
12 **Gantenbein L**, Arora P, Navarini A, Brandt O, Mueller SM. Global publication productivity in dermatology: a bibliometric description of the past and estimation of the future. *J Eur Acad Dermatol Venereol* 2021; **35**: 1424-1433 [PMID: 33656185 DOI: 10.1111/jdv.17196]
13 **Tárnok A**. Bibliometric news and more about signal transduction and disease. *Cytometry A* 2021; **99**: 764-765 [PMID: 34323357 DOI: 10.1002/cyto.a.24486]
14 **Huang YJ**, Huang CJ. Construction of a 5 immune-related lncRNA-based prognostic model of NSCLC *via* bioinformatics. *Medicine (Baltimore)* 2021; **100**: e27222 [PMID: 34664861 DOI: 10.1097/MD.0000000000027222]
15 **Xu X**, Wang Y, Li Y, Zhang B, Song Q. The Future Landscape of Macrophage Research in Cardiovascular Disease: A Bibliometric Analysis. *Curr Probl Cardiol* 2022; **47**: 101311 [PMID: 35810847 DOI: 10.1016/j.cpcardiol.2022.101311]
16 **Liu B**, He X, Wang Y, Huang JW, Zheng YB, Li Y, Lu LG. Bibliometric Analysis of γδ T Cells as Immune Regulators in Cancer Prognosis. *Front Immunol* 2022; **13**: 874640 [PMID: 35493488 DOI: 10.3389/fimmu.2022.874640]
17 **Liu S**, Sun YP, Gao XL, Sui Y. Knowledge domain and emerging trends in Alzheimer's disease: a scientometric review based on CiteSpace analysis. *Neural Regen Res* 2019; **14**: 1643-1650 [PMID: 31089065 DOI: 10.4103/1673-5374.255995]
18 **Lin J**, Ling F, Huang P, Chen M, Song M, Lu K, Wang W. The Development of GABAergic Network in Depression in Recent 17 Years: A Visual Analysis Based on CiteSpace and VOSviewer. *Front Psychiatry* 2022; **13**: 874137 [PMID: 35664493 DOI: 10.3389/fpsyt.2022.874137]
19 **Chen P**, Zhong C, Jin S, Zhang Y, Li Y, Xia Q, Cheng J, Fan X, Lin H. Global Trends in Research of Lipid Metabolism in T lymphocytes From 1985 to 2022: A Bibliometric Analysis. *Front Immunol* 2022; **13**: 884030 [PMID: 35720273 DOI: 10.3389/fimmu.2022.884030]
20 **Tacke F**, Zimmermann HW. Macrophage heterogeneity in liver injury and fibrosis. *J Hepatol* 2014; **60**: 1090-1096 [PMID: 24412603 DOI: 10.1016/j.jhep.2013.12.025]
21 **Trautwein C**, Friedman SL, Schuppan D, Pinzani M. Hepatic fibrosis: Concept to treatment. *J Hepatol* 2015; **62**: S15-24 [PMID: 25920084 DOI: 10.1016/j.jhep.2015.02.039]
22 **Tsuchida T**, Friedman SL. Mechanisms of hepatic stellate cell activation. *Nat Rev Gastroenterol Hepatol* 2017; **14**: 397-411 [PMID: 28487545 DOI: 10.1038/nrgastro.2017.38]
23 **Albillos A**, Lario M, Álvarez-Mon M. Cirrhosis-associated immune dysfunction: distinctive features and clinical relevance. *J Hepatol* 2014; **61**: 1385-1396 [PMID: 25135860 DOI: 10.1016/j.jhep.2014.08.010]
24 **European Association for the Study of the Liver**. EASL 2017 Clinical Practice Guidelines on the management of hepatitis B virus infection. *J Hepatol* 2017; **67**: 370-398 [PMID: 28427875 DOI: 10.1016/j.jhep.2017.03.021]
25 **Wu F**, Gao J, Kang J, Wang X, Niu Q, Liu J, Zhang L. Knowledge Mapping of Exosomes in Autoimmune Diseases: A Bibliometric Analysis (2002-2021). *Front Immunol* 2022; **13**: 939433 [PMID: 35935932 DOI: 10.3389/fimmu.2022.939433]
26 **Selmi C**, Mackay IR, Gershwin ME. The immunological milieu of the liver. *Semin Liver Dis* 2007; **27**: 129-139 [PMID: 17520513 DOI: 10.1055/s-2007-979466]

27 **Tanaka H**, Leung PS, Kenny TP, Gershwin ME, Bowlus CL. Immunological orchestration of liver fibrosis. *Clin Rev Allergy Immunol* 2012; **43**: 220-229 [PMID: 22695942 DOI: 10.1007/s12016-012-8323-1]

28 **Hirschfield GM**, Gershwin ME. The immunobiology and pathophysiology of primary biliary cirrhosis. *Annu Rev Pathol* 2013; **8**: 303-330 [PMID: 23347352 DOI: 10.1146/annurev-pathol-020712-164014]

29 **Ma HD**, Wang YH, Chang C, Gershwin ME, Lian ZX. The intestinal microbiota and microenvironment in liver. *Autoimmun Rev* 2015; **14**: 183-191 [PMID: 25315744 DOI: 10.1016/j.autrev.2014.10.013]

30 **Krenkel O**, Tacke F. Liver macrophages in tissue homeostasis and disease. *Nat Rev Immunol* 2017; **17**: 306-321 [PMID: 28317925 DOI: 10.1038/nri.2017.11]

31 **Wen Y**, Lambrecht J, Ju C, Tacke F. Hepatic macrophages in liver homeostasis and diseases-diversity, plasticity and therapeutic opportunities. *Cell Mol Immunol* 2021; **18**: 45-56 [PMID: 33041338 DOI: 10.1038/s41423-020-00558-8]

32 **Wasmuth HE**, Tacke F, Trautwein C. Chemokines in liver inflammation and fibrosis. *Semin Liver Dis* 2010; **30**: 215-225 [PMID: 20665374 DOI: 10.1055/s-0030-1255351]

33 **Sahin H**, Trautwein C, Wasmuth HE. Functional role of chemokines in liver disease models. *Nat Rev Gastroenterol Hepatol* 2010; **7**: 682-690 [PMID: 20975742 DOI: 10.1038/nrgastro.2010.168]

34 **Krenkel O**, Puengel T, Govaere O, Abdallah AT, Mossanen JC, Kohlhepp M, Liepelt A, Lefebvre E, Luedde T, Hellerbrand C, Weiskirchen R, Longerich T, Costa IG, Anstee QM, Trautwein C, Tacke F. Therapeutic inhibition of inflammatory monocyte recruitment reduces steatohepatitis and liver fibrosis. *Hepatology* 2018; **67**: 1270-1283 [PMID: 28940700 DOI: 10.1002/hep.29544]

35 **Frissen M**, Liao L, Schneider KM, Djudjaj S, Haybaeck J, Wree A, Rolle-Kampczyk U, von Bergen M, Latz E, Boor P, Trautwein C. Bidirectional Role of NLRP3 During Acute and Chronic Cholestatic Liver Injury. *Hepatology* 2021; **73**: 1836-1854 [PMID: 32748971 DOI: 10.1002/hep.31494]

36 **Bernsmeier C**, van der Merwe S, Périanin A. Innate immune cells in cirrhosis. *J Hepatol* 2020; **73**: 186-201 [PMID: 32240716 DOI: 10.1016/j.jhep.2020.03.027]

37 **Clària J**, Stauber RE, Coenraad MJ, Moreau R, Jalan R, Pavesi M, Amorós À, Titos E, Alcaraz-Quiles J, Oettl K, Morales-Ruiz M, Angeli P, Domenicali M, Alessandria C, Gerbes A, Wendon J, Nevens F, Trebicka J, Laleman W, Saliba F, Welzel TM, Albillos A, Gustot T, Benten D, Durand F, Ginès P, Bernardi M, Arroyo V; CANONIC Study Investigators of the EASL-CLIF Consortium and the European Foundation for the Study of Chronic Liver Failure (EF-CLIF). Systemic inflammation in decompensated cirrhosis: Characterization and role in acute-on-chronic liver failure. *Hepatology* 2016; **64**: 1249-1264 [PMID: 27483394 DOI: 10.1002/hep.28740]

38 **Arroyo V**, Angeli P, Moreau R, Jalan R, Clària J, Trebicka J, Fernández J, Gustot T, Caraceni P, Bernardi M; investigators from the EASL-CLIF Consortium, Grifols Chair and European Foundation for the Study of Chronic Liver Failure (EF-Clif). The systemic inflammation hypothesis: Towards a new paradigm of acute decompensation and multiorgan failure in cirrhosis. *J Hepatol* 2021; **74**: 670-685 [PMID: 33301825 DOI: 10.1016/j.jhep.2020.11.048]

39 **Kisseleva T**, Brenner D. Molecular and cellular mechanisms of liver fibrosis and its regression. *Nat Rev Gastroenterol Hepatol* 2021; **18**: 151-166 [PMID: 33128017 DOI: 10.1038/s41575-020-00372-7]

40 **Peng D**, Fu M, Wang M, Wei Y, Wei X. Targeting TGF-β signal transduction for fibrosis and cancer therapy. *Mol Cancer* 2022; **21**: 104 [PMID: 35461253 DOI: 10.1186/s12943-022-01569-x]

41 **Keenan BP**, Fong L, Kelley RK. Immunotherapy in hepatocellular carcinoma: the complex interface between inflammation, fibrosis, and the immune response. *J Immunother Cancer* 2019; **7**: 267 [PMID: 31627733 DOI: 10.1186/s40425-019-0749-z]

42 **Fernández J**, Clària J, Amorós A, Aguilar F, Castro M, Casulleras M, Acevedo J, Duran-Güell M, Nuñez L, Costa M, Torres M, Horrillo R, Ruiz-Del-Árbol L, Villanueva C, Prado V, Arteaga M, Trebicka J, Angeli P, Merli M, Alessandria C, Aagaard NK, Soriano G, Durand F, Gerbes A, Gustot T, Welzel TM, Salerno F, Bañares R, Vargas V, Albillos A, Silva A, Morales-Ruiz M, Carlos García-Pagán J, Pavesi M, Jalan R, Bernardi M, Moreau R, Páez A, Arroyo V. Effects of Albumin Treatment on Systemic and Portal Hemodynamics and Systemic Inflammation in Patients With Decompensated Cirrhosis. *Gastroenterology* 2019; **157**: 149-162 [PMID: 30905652 DOI: 10.1053/j.gastro.2019.03.021]

43 **Garrido A**, Djouder N. Cirrhosis: A Questioned Risk Factor for Hepatocellular Carcinoma. *Trends Cancer* 2021; **7**: 29-36 [PMID: 32917550 DOI: 10.1016/j.trecan.2020.08.005]

44 **Baglieri J**, Brenner DA, Kisseleva T. The Role of Fibrosis and Liver-Associated Fibroblasts in the Pathogenesis of Hepatocellular Carcinoma. *Int J Mol Sci* 2019; **20** [PMID: 30959975 DOI: 10.3390/ijms20071723]

45 **Gulamhusein AF**, Hirschfield GM. Primary biliary cholangitis: pathogenesis and therapeutic opportunities. *Nat Rev Gastroenterol Hepatol* 2020; **17**: 93-110 [PMID: 31819247 DOI: 10.1038/s41575-019-0226-7]

46 **Tanaka A**. Current understanding of primary biliary cholangitis. *Clin Mol Hepatol* 2021; **27**: 1-21 [PMID: 33264835 DOI: 10.3350/cmh.2020.0028]

47 **Corpechot C**, Chazouillères O, Rousseau A, Le Gruyer A, Habersetzer F, Mathurin P, Goria O, Potier P, Minello A, Silvain C, Abergel A, Debette-Gratien M, Larrey D, Roux O, Bronowicki JP, Boursier J, de Ledinghen V, Heurgue-Berlot A, Nguyen-Khac E, Zoulim F, Ollivier-Hourmand I, Zarski JP, Nkontchou G, Lemoinne S, Humbert L, Rainteau D, Lefèvre G, de Chaisemartin L, Chollet-Martin S, Gaouar F, Admane FH, Simon T, Poupon R. A Placebo-Controlled Trial of Bezafibrate in Primary Biliary Cholangitis. *N Engl J Med* 2018; **378**: 2171-2181 [PMID: 29874528 DOI: 10.1056/NEJMoa1714519]

48 **Parola M**, Pinzani M. Liver fibrosis: Pathophysiology, pathogenetic targets and clinical issues. *Mol Aspects Med* 2019; **65**: 37-55 [PMID: 30213667 DOI: 10.1016/j.mam.2018.09.002]

49 **Shah RA**, Kowdley KV. Current and potential treatments for primary biliary cholangitis. *Lancet Gastroenterol Hepatol* 2020; **5**: 306-315 [PMID: 31806572 DOI: 10.1016/S2468-1253(19)30343-7]

50 **Mayo MJ**. Mechanisms and molecules: What are the treatment targets for primary biliary cholangitis? *Hepatology* 2022; **76**: 518-531 [PMID: 35152430 DOI: 10.1002/hep.32405]

51 **Higashi T**, Friedman SL, Hoshida Y. Hepatic stellate cells as key target in liver fibrosis. *Adv Drug Deliv Rev* 2017; **121**: 27-42 [PMID: 28506744 DOI: 10.1016/j.addr.2017.05.007]

52 **Friedman SL**, Pinzani M. Hepatic fibrosis 2022: Unmet needs and a blueprint for the future. *Hepatology* 2022; **75**: 473-488 [PMID: 34923653 DOI: 10.1002/hep.32285]

53 **Lurje I**, Hammerich L, Tacke F. Dendritic Cell and T Cell Crosstalk in Liver Fibrogenesis and Hepatocarcinogenesis: Implications for Prevention and Therapy of Liver Cancer. *Int J Mol Sci* 2020; **21** [PMID: 33036244 DOI: 10.3390/ijms21197378]

54 **Albillos A**, Martin-Mateos R, Van der Merwe S, Wiest R, Jalan R, Álvarez-Mon M. Cirrhosis-associated immune dysfunction. *Nat Rev Gastroenterol Hepatol* 2022; **19**: 112-134 [PMID: 34703031 DOI: 10.1038/s41575-021-00520-7]

55 **Arroyo V**, Moreau R, Jalan R. Acute-on-Chronic Liver Failure. *N Engl J Med* 2020; **382**: 2137-2145 [PMID: 32459924 DOI: 10.1056/NEJMra1914900]

56 **Sarin SK**, Choudhury A. Acute-on-chronic liver failure: terminology, mechanisms and management. *Nat Rev Gastroenterol Hepatol* 2016; **13**: 131-149 [PMID: 26837712 DOI: 10.1038/nrgastro.2015.219]

57 **Lee NY**, Suk KT. The Role of the Gut Microbiome in Liver Cirrhosis Treatment. *Int J Mol Sci* 2020; **22** [PMID: 33379148 DOI: 10.3390/ijms22010199]

58 **Tranah TH**, Edwards LA, Schnabl B, Shawcross DL. Targeting the gut-liver-immune axis to treat cirrhosis. *Gut* 2021; **70**: 982-994 [PMID: 33060124 DOI: 10.1136/gutjnl-2020-320786]

59 **Campana L**, Esser H, Huch M, Forbes S. Liver regeneration and inflammation: from fundamental science to clinical applications. *Nat Rev Mol Cell Biol* 2021; **22**: 608-624 [PMID: 34079104 DOI: 10.1038/s41580-021-00373-7]

60 **Trebicka J**, Bork P, Krag A, Arumugam M. Utilizing the gut microbiome in decompensated cirrhosis and acute-on-chronic liver failure. *Nat Rev Gastroenterol Hepatol* 2021; **18**: 167-180 [PMID: 33257833 DOI: 10.1038/s41575-020-00376-3]

61 **Huang DQ**, Mathurin P, Cortez-Pinto H, Loomba R. Global epidemiology of alcohol-associated cirrhosis and HCC: trends, projections and risk factors. *Nat Rev Gastroenterol Hepatol* 2023; **20**: 37-49 [PMID: 36258033 DOI: 10.1038/s41575-022-00688-6]

62 **Guo Q**, Furuta K, Lucien F, Gutierrez Sanchez LH, Hirsova P, Krishnan A, Kabashima A, Pavelko KD, Madden B, Alhuwaish H, Gao Y, Revzin A, Ibrahim SH. Integrin β(1)-enriched extracellular vesicles mediate monocyte adhesion and promote liver inflammation in murine NASH. *J Hepatol* 2019; **71**: 1193-1205 [PMID: 31433301 DOI: 10.1016/j.jhep.2019.07.019]

63 **Kaminsky-Kolesnikov Y**, Rauchbach E, Abu-Halaka D, Hahn M, García-Ruiz C, Fernandez-Checa JC, Madar Z, Tirosh O. Cholesterol Induces Nrf-2- and HIF-1α-Dependent Hepatocyte Proliferation and Liver Regeneration to Ameliorate Bile Acid Toxicity in Mouse Models of NASH and Fibrosis. *Oxid Med Cell Longev* 2020; **2020**: 5393761 [PMID: 32566088 DOI: 10.1155/2020/5393761]

64 **Mountford S**, Effenberger M, Noll-Puchta H, Griessmair L, Ringleb A, Haas S, Denk G, Reiter FP, Mayr D, Dinarello CA, Tilg H, Bufler P. Modulation of Liver Inflammation and Fibrosis by Interleukin-37. *Front Immunol* 2021; **12**: 603649 [PMID: 33746950 DOI: 10.3389/fimmu.2021.603649]

65 **Kong D**, Zhang Z, Chen L, Huang W, Zhang F, Wang L, Wang Y, Cao P, Zheng S. Curcumin blunts epithelial-mesenchymal transition of hepatocytes to alleviate hepatic fibrosis through regulating oxidative stress and autophagy. *Redox Biol* 2020; **36**: 101600 [PMID: 32526690 DOI: 10.1016/j.redox.2020.101600]

66 **Kong Z**, Liu R, Cheng Y. Artesunate alleviates liver fibrosis by regulating ferroptosis signaling pathway. *Biomed Pharmacother* 2019; **109**: 2043-2053 [PMID: 30551460 DOI: 10.1016/j.biopha.2018.11.030]

67 **Zhang X**, Yang H, Zeng S, Tian S, Hu S, Yang L, Ma T, Liu Z, Wan J, Zhong Y, Li H. Melanoma differentiation-Associated gene 5 protects against NASH in mice. *Hepatology* 2022; **75**: 924-938 [PMID: 34482560 DOI: 10.1002/hep.32139]

68 **El-Sherif O**, Armstrong MJ. Peculiarities of Cirrhosis due to Nonalcoholic Steatohepatitis (NASH). *Semin Liver Dis* 2020; **40**: 1-10 [PMID: 31537030 DOI: 10.1055/s-0039-1697616]

69 **Sheka AC**, Adeyi O, Thompson J, Hameed B, Crawford PA, Ikramuddin S. Nonalcoholic Steatohepatitis: A Review. *JAMA* 2020; **323**: 1175-1183 [PMID: 32207804 DOI: 10.1001/jama.2020.2298]

70 **Harrison SA**, Ruane PJ, Freilich BL, Neff G, Patil R, Behling CA, Hu C, Fong E, de Temple B, Tillman EJ, Rolph TP, Cheng A, Yale K. Efruxifermin in non-alcoholic steatohepatitis: a randomized, double-blind, placebo-controlled, phase 2a trial. *Nat Med* 2021; **27**: 1262-1271 [PMID: 34239138 DOI: 10.1038/s41591-021-01425-3]

71 **Thietart S**, Rautou PE. Extracellular vesicles as biomarkers in liver diseases: A clinician's point of view. *J Hepatol* 2020; **73**: 1507-1525 [PMID: 32682050 DOI: 10.1016/j.jhep.2020.07.014]

72 **Gao J**, Wei B, de Assuncao TM, Liu Z, Hu X, Ibrahim S, Cooper SA, Cao S, Shah VH, Kostallari E. Hepatic stellate cell autophagy inhibits extracellular vesicle release to attenuate liver fibrosis. *J Hepatol* 2020; **73**: 1144-1154 [PMID: 32389810 DOI: 10.1016/j.jhep.2020.04.044]

73 **Bruno S**, Pasquino C, Herrera Sanchez MB, Tapparo M, Figliolini F, Grange C, Chiabotto G, Cedrino M, Deregibus MC, Tetta C, Camussi G. HLSC-Derived Extracellular Vesicles Attenuate Liver Fibrosis and Inflammation in a Murine Model of Non-alcoholic Steatohepatitis. *Mol Ther* 2020; **28**: 479-489 [PMID: 31757759 DOI: 10.1016/j.ymthe.2019.10.016]

74 **Xie G**, Jiang R, Wang X, Liu P, Zhao A, Wu Y, Huang F, Liu Z, Rajani C, Zheng X, Qiu J, Zhang X, Zhao S, Bian H, Gao X, Sun B, Jia W. Conjugated secondary 12α-hydroxylated bile acids promote liver fibrogenesis. *EBioMedicine* 2021; **66**: 103290 [PMID: 33752128 DOI: 10.1016/j.ebiom.2021.103290]

75 **Salhab A**, Amer J, Lu Y, Safadi R. Sodium(+)/taurocholate cotransporting polypeptide as target therapy for liver fibrosis. *Gut* 2022; **71**: 1373-1385 [PMID: 34266968 DOI: 10.1136/gutjnl-2020-323345]

76 **de Castro Brás LE**, Frangogiannis NG. Extracellular matrix-derived peptides in tissue remodeling and fibrosis. *Matrix Biol* 2020; **91-92**: 176-187 [PMID: 32438055 DOI: 10.1016/j.matbio.2020.04.006]

77 **Geervliet E**, Moreno S, Baiamonte L, Booijink R, Boye S, Wang P, Voit B, Lederer A, Appelhans D, Bansal R. Matrix metalloproteinase-1 decorated polymersomes, a surface-active extracellular matrix therapeutic, potentiates collagen degradation and attenuates early liver fibrosis. *J Control Release* 2021; **332**: 594-607 [PMID: 33737203 DOI: 10.1016/j.jconrel.2021.03.016]

78 **Moretti L**, Stalfort J, Barker TH, Abebayehu D. The interplay of fibroblasts, the extracellular matrix, and inflammation in

scar formation. *J Biol Chem* 2022; **298**: 101530 [PMID: 34953859 DOI: 10.1016/j.jbc.2021.101530]

79 **Wu Y**, Cao Y, Xu K, Zhu Y, Qiao Y, Wu Y, Chen J, Li C, Zeng R, Ge G. Dynamically remodeled hepatic extracellular matrix predicts prognosis of early-stage cirrhosis. *Cell Death Dis* 2021; **12**: 163 [PMID: 33558482 DOI: 10.1038/s41419-021-03443-y]

World Journal of Gastroenterology

Submit a Manuscript: https://www.f6publishing.com

World J Gastroenterol 2023 June 28; 29(24): 3922-3931

DOI: 10.3748/wjg.v29.i24.3922

ISSN 1007-9327 (print) ISSN 2219-2840 (online)

CASE REPORT

Treatment of colonic varices and gastrointestinal bleeding by recanalization and stenting of splenic-vein-thrombosis: A case report and literature review

Lisa-Michaela Füssel, Rene Müller-Wille, Patrick Dinkhauser, Walter Schauer, Harald Hofer

Specialty type: Gastroenterology and hepatology

Provenance and peer review: Unsolicited article; Externally peer reviewed.

Peer-review model: Single blind

Peer-review report's scientific quality classification

Grade A (Excellent): A
Grade B (Very good): B
Grade C (Good): 0
Grade D (Fair): 0
Grade E (Poor): 0

P-Reviewer: Ding WW, China; Protopapas AA, Greece

Received: February 1, 2023
Peer-review started: February 1, 2023
First decision: April 14, 2023
Revised: April 27, 2023
Accepted: May 24, 2023
Article in press: May 24, 2023
Published online: June 28, 2023

Lisa-Michaela Füssel, Patrick Dinkhauser, Harald Hofer, Department of Internal Medicine I, Gastroenterology and Hepatology, Klinikum Wels-Grieskirchen, Wels 4600, Austria

Rene Müller-Wille, Department of Radiology, Klinikum Wels-Grieskirchen, Wels 4600, Austria

Walter Schauer, Department of Abdominal Surgery, Klinikum Wels-Grieskirchen, Wels 4600, Austria

Corresponding author: Harald Hofer, MD, Professor, Department of Internal Medicine I, Gastroenterology and Hepatology, Klinikum Wels-Grieskirchen, Grieskirchnerstraße 42, Wels 4600, Austria.harald.hofer@klinikum-wegr.at

Abstract

BACKGROUND

Splenic vein thrombosis is a known complication of pancreatitis. It can lead to increased blood flow through mesenteric collaterals. This segmental hypertension may result in the development of colonic varices (CV) with a high risk of severe gastrointestinal bleeding. While clear guidelines for treatment are lacking, splenectomy or splenic artery embolization are often used to treat bleeding. Splenic vein stenting has been shown to be a safe option.

CASE SUMMARY

A 45-year-old female patient was admitted due to recurrent gastrointestinal bleeding. She was anemic with a hemoglobin of 8.0 g/dL. As a source of bleeding, CV were identified. Computed tomography scans revealed thrombotic occlusion of the splenic vein, presumably as a result of a severe acute pancreatitis 8 years prior. In a selective angiography, a dilated mesenterial collateral leading from the spleen to enlarged vessels in the right colonic flexure and draining into the superior mesenteric vein could be confirmed. The hepatic venous pressure gradient was within normal range. In an interdisciplinary board, transhepatic recanalization of the splenic vein *via* balloon dilatation and consecutive stenting, as well as coiling of the aberrant veins was discussed and successfully performed. Consecutive evaluation revealed complete regression of CV and splenomegaly as well as normalization of the red blood cell count during follow-up.

CONCLUSION

Recanalization and stenting of splenic vein thrombosis might be considered in

patients with gastrointestinal bleeding due to CV. However, a multidisciplinary approach with a thorough workup and discussion of individualized therapeutic strategies is crucial in these difficult to treat patients.

Key Words: Pancreatitis-induced splenic vein thrombosis; Gastrointestinal hemorrhage; Colonic varices; Splenic vein stenting; Segmental/sinistral hypertension; Case report

©The Author(s) 2023. Published by Baishideng Publishing Group Inc. All rights reserved.

Core Tip: Splenic vein thrombosis (SVT) is a complication of pancreatitis and can lead to development of varices with a high risk of gastrointestinal bleeding. While clear guidelines are lacking, splenectomy or splenic artery embolization are often employed. We present a rare case of recurrently bleeding colonic varices (CV) due to pancreatitis-induced (PI) SVT. In an interdisciplinary board, transhepatic recanalization of the splenic vein and consecutive stenting, as well as coiling of aberrant veins was decided and successfully performed. Follow-up revealed complete regression of varices. According to our knowledge, there is no case report in English literature describing stenting of PISVT in a patient with CV.

Citation: Füssel LM, Müller-Wille R, Dinkhauser P, Schauer W, Hofer H. Treatment of colonic varices and gastrointestinal bleeding by recanalization and stenting of splenic-vein-thrombosis: A case report and literature review. *World J Gastroenterol* 2023; 29(24): 3922-3931
URL: https://www.wjgnet.com/1007-9327/full/v29/i24/3922.htm
DOI: https://dx.doi.org/10.3748/wjg.v29.i24.3922

INTRODUCTION

Gastrointestinal bleeding due to colonic varices (CV) is rare but can be severe[1,2]. CV may be caused by thrombosis of the splenic vein. In our patient this was due to an episode of acute pancreatitis. Moreover, treatment is challenging, and a multidisciplinary individualized approach is warranted in these patients. Cases are rare and clear guidelines for management are lacking, as the available data is heterogenous and case numbers for interventional recanalization are low. Therefore, we present a patient with CV due to pancreatitis-induced splenic vein thrombosis (PISVT) and summarize the clinical features, treatment options and available data in the current literature.

SVT

The splenic vein is located at the posterior surface of the pancreas and is fed by tributaries from the spleen, the inferior mesenteric vein, the short gastric veins, the left gastroepiploic vein and pancreatic veins[2]. Isolated obstruction can occur as a result of external compression due to malignancy, retroperitoneal disease or splenic artery aneurysms[2,3]. In addition, SVT can be associated with a variety of diseases shown in Table 1[2,4,5].

PISVT

The predominant cause in approximately 50%-60% of isolated SVT is acute or chronic pancreatitis[5,6]. While Butler *et al*[7] yielded an overall incidence of PISVT of 14.1% in patients with pancreatitis (22.6% in acute and 12.4% in chronic pancreatitis), a meta-analysis including over 10000 patients reported the pooled prevalence of SVT in pancreatitis to be as high as 11.2%[7,8]. Thrombosis is a consequence of the associated inflammatory process of the pancreas, fostered by endothelial damage, the release of prothrombotic cytokines and vein compression due to edema, lymphadenopathy or pseudocysts causing stasis of blood flow[6]. However, it is still unclear if the risk of thrombosis correlates with the severity of pancreatitis[2,8]. Since PISVT is mainly diagnosed after the acute phase, recurrent indolent episodes of pancreatitis could play a major role in its development[6]. The diagnosis can be challenging as the accuracy of doppler sonography to diagnose SVT is low due to the small size, the location of the splenic vein and the presence of adjacent collaterals[6]. In addition, the incidence of compensatory splenomegaly in SVT was reported at 51.9%, rendering it unreliable for diagnosis[8]. Additionally, D-dimer levels can be elevated in SVT, but are also unspecific[4]. The diagnostic test of choice to assess the presence of SVT is late-phase celiac angiography [computed tomography (CT) or magnetic resonance imaging][6]. Ultimately, the gold standard to confirm SVT is selective angiography of the splenic artery with lacking drainage *via* the splenic vein[6]. Clinical symptoms of SVT are nonspecific and include abdominal pain and nausea[4]. Historically, patients with SVT were commonly described to present with acute bleeding, thereby overestimating the risk for hemorrhage, which has since been thought to

Table 1 Possible etiologies of splenic vein thrombosis[2,4,5]

Pancreatic diseases[1]	Carcinoma
	All forms of pancreatitis
	Pseudocysts
	Abscess
	Pancreas divisum
Liver diseases	Liver cirrhosis
	Budd-Chiari syndrome
Coagulation disorders	Thrombocythemia
	Deficiency of antithrombin III, Protein S or C
	Antiphospholipid syndrome
	Mutation of factor V
	Myeloproliferative disorders
Inflammatory disorders	Autoimmune disease
	Inflammatory bowel disease
	Intraabdominal inflammation
Others	Prior abdominal surgery
	Hormonal therapy
	Paroxysmal nocturnal hemoglobinuria
	Bechet's disease
	Retroperitoneal fibrosis
	Tuberculous adenitis

[1]Most common due to local proximity.

be about 4%-17%[9,10]. Due to a broader availability and improvement of imaging, at present the majority of cases are diagnosed at an asymptomatic state[8].

Segmental Hypertension

PISVT can lead to increased blood flow through splenoportal, gastroepiploic or mesenteric collaterals creating a localized form of venous hypertension referred to as "segmental", "sinistral" or "linear hypertension"[8]. This results in the development of varices in the area decompressing the corresponding segment and entails an increased risk of severe hemorrhage[2]. Frequently, the short gastric veins collateralize through portosystemic esophageal veins to the azygos system leading to esophageal varices[11]. Other pathways decompress the short gastric veins *via* the coronary vein into the portal vein or *via* the gastroepiploic arcade into the vena mesenterica superior creating gastric varices[11]. Another path runs along the left gastroepiploic vein to the left colic and inferior mesenteric vein[11]. Furthermore, collateral channels along intercostal and diaphragmatic veins draining into the vena cava inferior and a pathway *via* the adrenal vein into the renal vein have been described[11]. Segmental hypertension occurred in 12.5% in acute pancreatitis and in 2.7% in chronic pancreatitis[10,12]. Identified risk factors for the development of PISVT in pancreatitis were smoking, alcohol consumption, hypertriglyceridemia, diabetes, recurrent acute pancreatitis, infection of necrosis and pseudocysts[10,12]. Gastrointestinal varices are found in 53% of PISVT and are gastric in the majority (77.3%) of cases [8]. This is especially relevant as the rate of bleeding in patients with PISVT was reported to be 12.3% [8]. In case of varices the bleeding rate was at 19.1% and seemed to be higher in alcoholic than in non-alcoholic pancreatitis[12,13].

CV

CV associated with PISVT are very rare, data is scarce and only a few case reports exist[1,14-17]. In these cases, splenectomy was performed to manage bleeding and decompress the varices. The incidence rate of CV in general is estimated at 0.07%[3,18]. Causes of CV include liver cirrhosis (as the most frequent etiology), congestive heart failure, porto-mesenteric thrombosis, post-operative adhesions, inherited vascular anomalies (*e.g.*, Klippel-Trenaunay-Weber syndrome) and idiopathic varices[18,19]. Diagnosis

is primarily established *via* colonoscopy, although selective mesenteric angiography is the gold standard, as varices can be missed when flattened with insufflation and in hypotensive patients, especially if active bleeding is present[3]. Ectopic varices are reported to be more prone to bleeding and can have a mortality rate as high as 40%[20]. CV are rarer than small bowel and rectal varices; in one recent study only 3.5% of ectopic varices were situated in the colon[18,21].

CASE PRESENTATION

Chief complaints

We present a 45-year-old female who was admitted to the hospital due to recurrent hematochezia.

History of present illness

She denied abdominal pain, weight loss, fever or night sweats and there was no history of malignancy or inflammatory bowel disease.

History of past illness

Patient history included alcohol misuse, bipolar disorder, arterial hypertension, cholecystolithiasis, pancreatic insufficiency and an episode of severe acute pancreatitis 8 years prior, which required intensive care treatment.

Personal and family history

Family history for gastrointestinal disease, tumor or bleeding was negative.

Physical examination

On presentation, abdominal examination was unremarkable and vital signs were stable.

Laboratory examinations

Blood work showed anemia with a hemoglobin of 8 g/dL (12-15.4 g/dL), a mean corpuscular volume of 70 fL (80-99 fL) and a mean corpuscular hemoglobin of 22 pg (27-33.5 pg) while coagulation parameters were within normal range.

Imaging examinations

Gastroscopy revealed reflux esophagitis of grade A and a mild duodenitis. There was no evidence for varices or ulcers. During colonoscopy, largely dilated and tortuous varices spreading from the right transverse colon to just underneath the right colonic flexure were diagnosed (Figure 1). There was no active bleeding. A CT angiography confirmed an extensive venous convolute at the right colonic flexure and evidenced an aberrant mesenteric collateral coming from the splenic hilum as its feeding vein (Figure 2). The varices' draining vein could be identified and lead to the superior mesenteric vein. In addition, splenomegaly (15 cm) and thrombotic occlusion of the splenic vein were diagnosed, while the portal vein and superior mesenteric vein were perfused regularly.

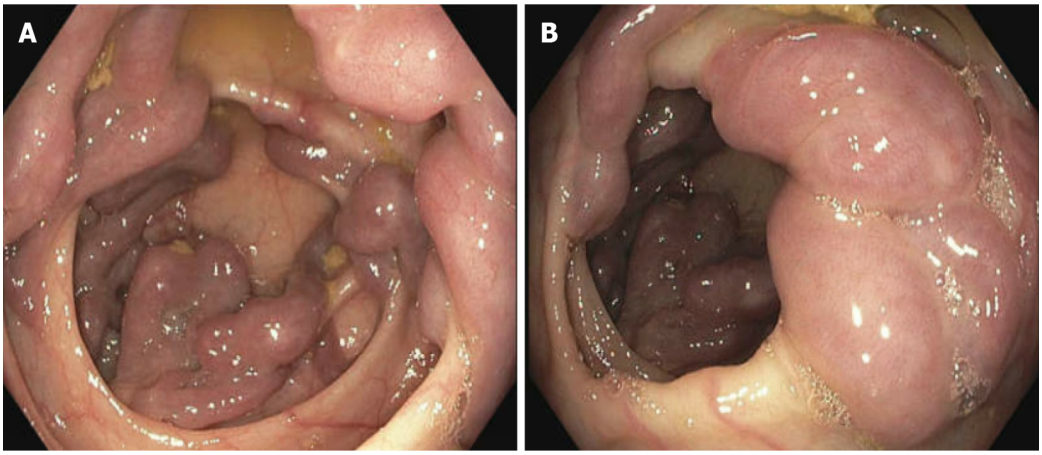
Selective angiography of the spleen *via* the femoral artery observed a long-segment occlusion of the splenic vein up to the confluence of the portal vein. It confirmed the findings of the CT angiography and noted that almost the entire venous drainage of the spleen occurred *via* mesenteric collaterals (Figure 2). Simultaneously, an arterio-portal fistula was ruled out. There was no evidence of liver cirrhosis or portal hypertension. Laboratory investigations showed transaminases, albumin and coagulation parameters within normal range. Platelets were slightly decreased due to splenomegaly. Transient elastography showed a value of 7.5 kPa and the hepatic venous pressure gradient was normal (3 mmHg).

FINAL DIAGNOSIS

Presumably, the splenic vein thrombosis was a result of the reported acute severe pancreatitis 8 years prior. Consequently, we postulated that PISVT prompted the formation of collaterals which lead to CV and gastrointestinal bleeding.

TREATMENT

In an interdisciplinary board, interventional transhepatic recanalization of the splenic vein *via* balloon dilatation and consecutive stenting, as well as coiling of the aberrant mesenteric veins under general anesthesia was planned. The splenic artery was cannulated *via* the femoral artery and a microcatheter was used to reach the splenic hilus and monitor venous drainage during the procedure (Figure 3A).



DOI: 10.3748/wjg.v29.i24.3922 **Copyright** ©The Author(s) 2023.

Figure 1 Dilated and tortuous colonic varices on endoscopy without active bleeding. A: Right transverse colon; B: Right colonic flexure.

Subsequently, right portal vein access was obtained transhepatically, a 6-French vascular sheath (Biotronik®, Berlin, Germany) was placed and a contrast venogram showed the expected occlusion of the splenic vein measuring 8 cm (Figure 3B and C). The aberrant vein feeding the varices was contrasted (Figure 3D). The obstructed vein was successfully cannulated using a 5-MP catheter and a Progreat-microcatheter (Terumo Interventional Systems, Somerset, NJ, United States). After crossing the occlusion, balloon angioplasty with a 3 mm × 12 mm and a 5 mm × 40 mm percutaneous transluminal angioplasty balloon was performed and was followed by deployment of two overlapping stentgrafts (8 mm × 57mm and 8 mm × 37 mm, BeGraft, Bentley), achieving successful recanalization of the splenic vein (Figure 3E and F). A follow-up venography confirmed restoration of antegrade flow. Afterwards, the dilated mesenteric collateral vein leading from the splenic hilum to the colon was cannulated *via* stentgrafts and a distal and proximal embolization by the deployment of multiple coils (Boston Scientific Interlock®; Marlborough, MA, United States) was performed (Figure 3G). A small gastral aberrant vein was also coiled. Follow-up angiography demonstrated patent stentgrafts allowing complete drainage of the spleen through the splenic vein (Figure 3H). The transhepatic access tract was occluded by means of gelfoam slurry (EmboCubes®; Merit Medical, South Jordan, UT, United States) and the femoral access using AngioSeal® (Terumo Interventional Systems).

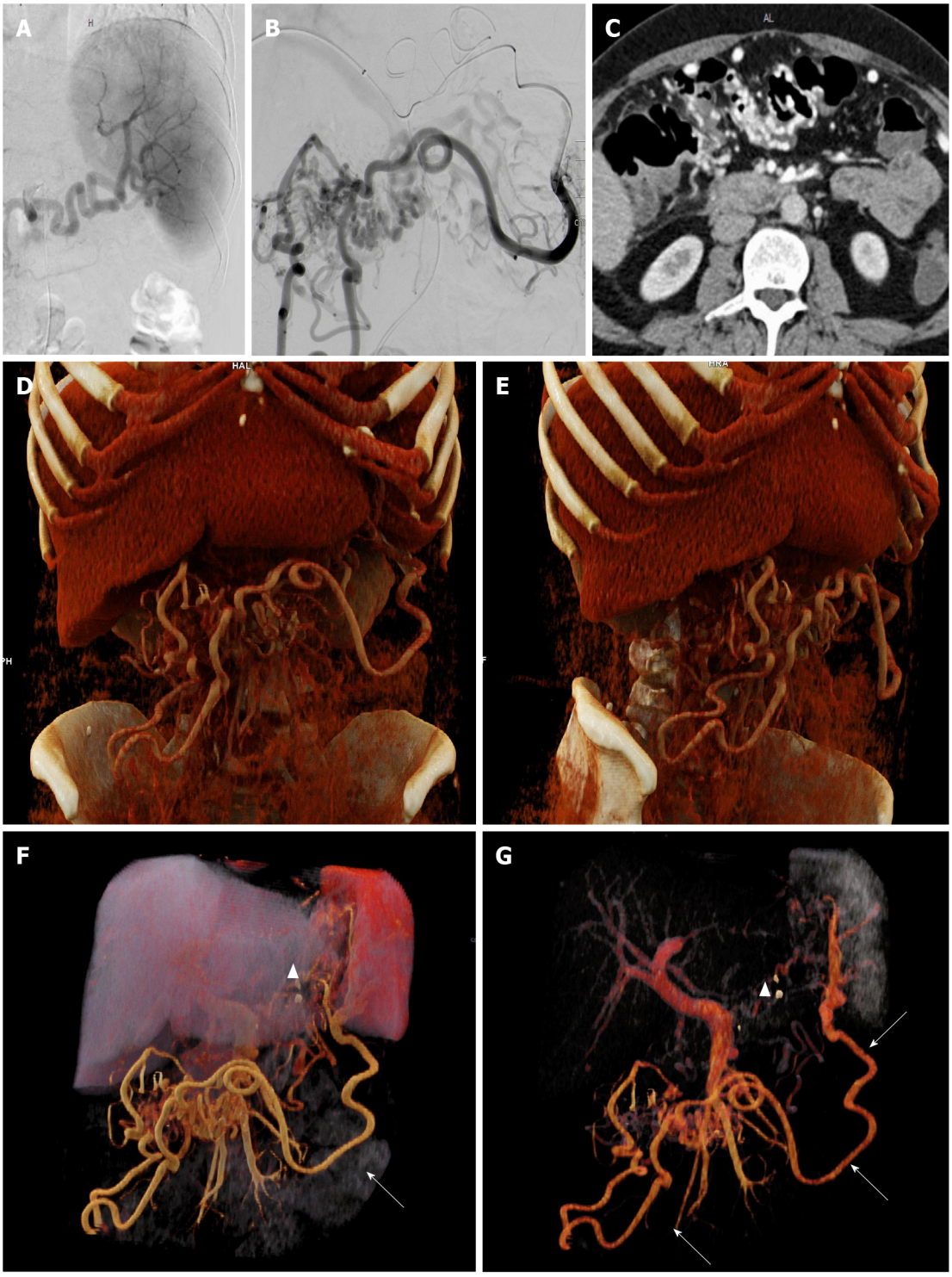
OUTCOME AND FOLLOW-UP

A consecutive Doppler examination revealed antegrade perfusion of the splenic vein and regression of splenomegaly (1 d post-recanalization 15 cm, after 4 d 13 cm). At follow-up 2 mo later, lab results found a normalization of red blood cell count (hemoglobin 12.1 g/dL) and a colonoscopy confirmed drastic regression of CV with few residual veins in the right colonic flexure (Figure 4A). One year post-intervention, hemoglobin was at 13.2 g/dL, the spleen measured 11.5 cm, the splenic vein stent was patent with orthograde perfusion on duplex sonography and residual veins had completely disappeared (Figure 4B).

DISCUSSION

Gastrointestinal bleeding due to CV caused by PISVT is rare and difficult to treat[1,14-17]. Time from the onset of pancreatitis to the detection of SVT is highly variable ranging between 10 d and 9 years[10]. In our patient, there was an 8 year gap between the episode of pancreatitis and diagnosis of PISVT.

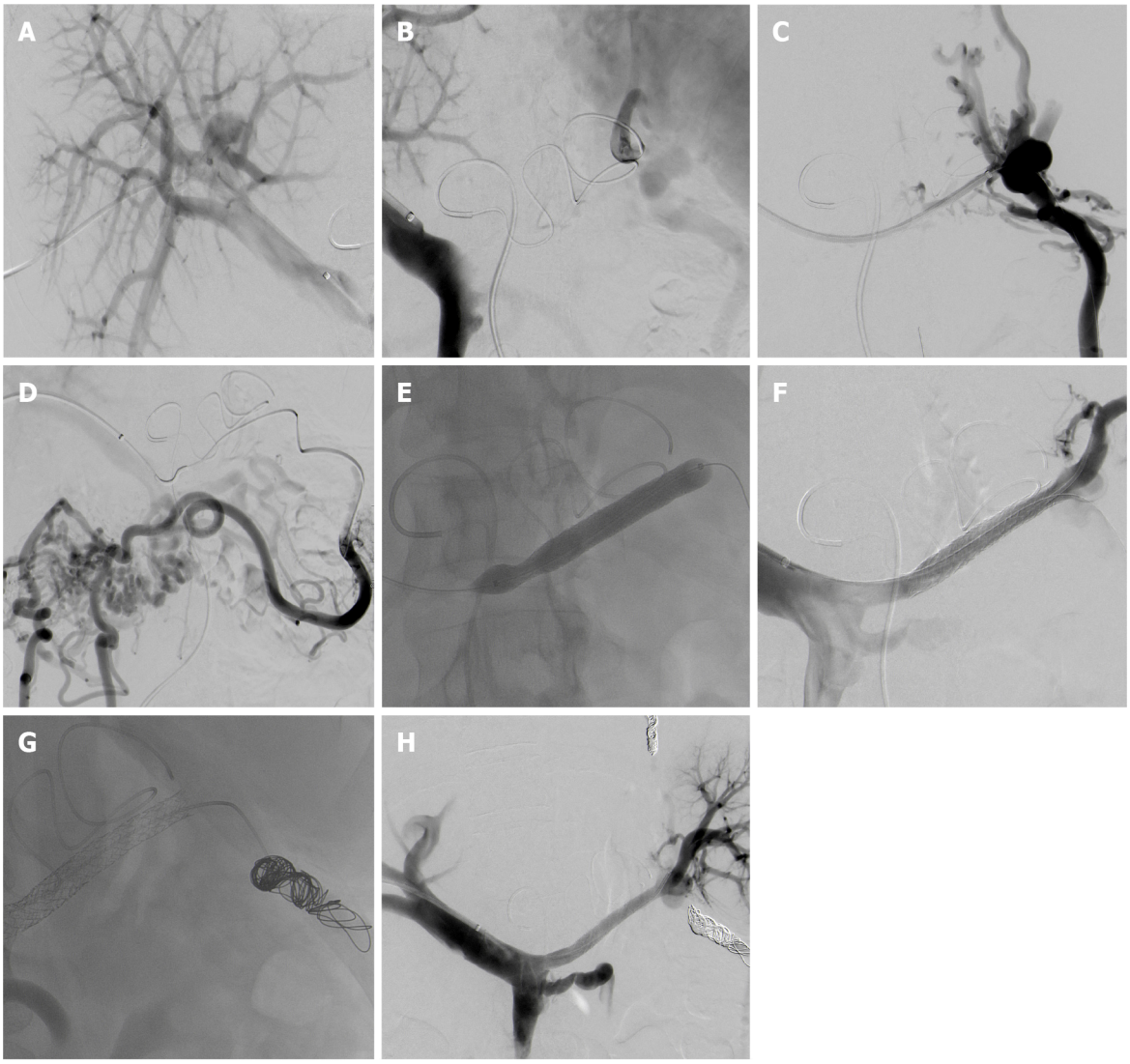
Due to limited data, clear guidelines for the treatment of CV are lacking. The use of non-selective beta-blockers for bleeding prophylaxis has been recommended with a low quality of evidence[22,23]. Conservative treatment also includes iron supplements and avoiding constipation[24]. The use of anticoagulation (AC) in chronic SVT with collaterals is controversial and dependent on etiology, risk of recurrence, progression and hemorrhage[5]. Considering the low rate of recanalization as well as the substantial bleeding risk if varices are present, an individualized risk assessment is necessary[4,5,10]. In our case, AC was not viable due to ongoing intermittent bleeding. However, our patient had suffered from acute pancreatitis previously and AC might be beneficial in acute pancreatitis to avoid SVT[25]. In acute pancreatitis and PISVT, data on AC are conflicting regarding recanalization and bleeding rate[10,26-28].



DOI: 10.3748/wjg.v29.i24.3922 **Copyright** ©The Author(s) 2023.

Figure 2 Angiography images and computed tomography images. A: Angiography of splenic artery; B: Angiography of the mesenterial vein draining the spleen; C: Computed tomography (CT)-angiography showing colonic varices; D-G: 3D-Reconstruction of CT imaging. 3D-Reconstruction with the thrombosis of the splenic vein (arrowhead) and collateral vessels to the colon indicated by arrows.

Endoscopic therapies such as variceal ligation, injection of cyanoacrylate or sclerotherapy may be performed for bleeding control in localized varices, but success depends on the location and expansion of the varices[2,18,23]. In addition, these techniques do not treat the underlying cause, thereby resulting in high re-bleeding rates[2,23]. In the setting of portal hypertension, transjugular intrahepatic portosystemic shunt (TIPS) is an option and achieved 100% initial hemostasis in ectopic variceal bleeding, with a subsequent re-bleeding rate of 21%[29]. Nevertheless, TIPS is not expedient in segmental hypertension when portal pressure and hepatic function are normal[2,23]. Another option to manage CV is embolization of the feeding veins[23,29]. Complications are rare and include post-embolization syndrome, infection, vessel injury and thromboembolism[30]. Embolization represents



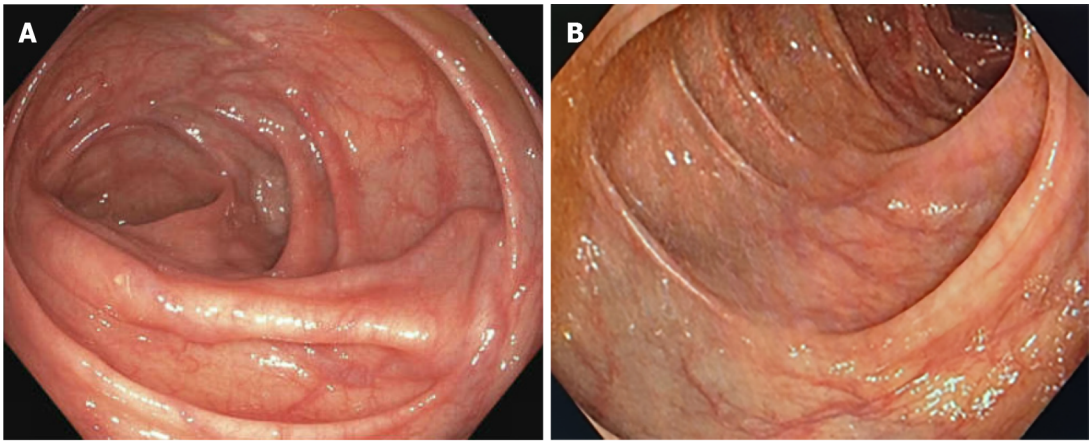
DOI: 10.3748/wjg.v29.i24.3922 **Copyright** ©The Author(s) 2023.

Figure 3 Angiography images. A: Right portal vein access; B: Simultaneously performed direct portography and indirect mesentericography *via* the splenic artery showing complete obstruction of the splenic vein; C: Successful cannulation of the obstructed splenic vein (SV); D: Phlebography of the colonic varices (CV) arising from the splenic hilum; E: Recanalization of the SV using balloon and stentgrafts; F: Successful recanalization of the SV; G: Coiling of the aberrant vein feeding the CV; H: Patent stentgraft with drainage of the spleen through the splenic vein.

another short-term therapy with a high rate of successful bleeding control, but does not influence portal pressure, thus entailing high re-bleeding rates[23].

Surgical treatment, as for example, colon resection, can be required in cases of uncontrolled bleeding or when extensive varices are present[24]. Surgical devascularization, shunt procedures or other local therapy depending on the underlying etiology have been reported[23,29]. Historically, the surgical treatment of choice for PISVT is splenectomy, which eliminates the collateral outflow[6,31]. In patients with hemorrhage unresponsive to conservative management or a history of bleeding, it is still the treatment of choice[2]. However, considering the reported lack of progression and rarity of hemorrhage in patients with asymptomatic varices, as well as operative risk, risk of postoperative infection and portal vein thrombosis, "prophylactic splenectomy" in patients without evidence of bleeding remains controversial[2,6,11,31]. Splenic artery embolization (SAE) resulting in splenic infarction represents an option, although the risk of splenic abscess and intervention associated morbidity is considerable[2,6].

Reports on splenic vein recanalization and thereby minimizing blood flow to collaterals in segmental hypertension are scarce[11]. A retrospective study of endovascular splenic vein recanalization in patients with SVT by a transjugular approach achieved success in 8 of 11 cases[32]. Another study reported effective splenic vein stenting in 3 patients using a transhepatic approach[33]. Recently, Liu *et al*[34] compared 9 patients with splenic vein stenting, 12 cases of splenectomy and 12 patients with conservative treatment in PISVT and there were no recurrent bleeding or major complications in the interventional group[34]. Stent patency was 100% and PISVT receded significantly[34]. Furthermore, a retrospective analysis comparing splenic vein stenting and SAE in SVT related bleeding found significantly less re-bleeding in the recanalization group[35].



DOI: 10.3748/wjg.v29.i24.3922 **Copyright** ©The Author(s) 2023.

Figure 4 Follow-up colonoscopy. A: Right colonic flexure 2 mo after intervention; B: Transverse colon 1 year after intervention.

In our patient, endoscopic treatment and TIPS were not viable options due to the localization, size and extension of the varices and absence of portal hypertension. Embolization alone, balloon-occluded retrograde transvenous obliteration (commonly referred to as BRTO) or segmental colonic resection were considered as short-term options, but were unlikely to prevent future bleeding because of potential collateral development. Moreover, splenectomy to alleviate the segmental hypertension was discussed, but as the patient was stable and preferred a less invasive alternative, we opted to perform transhepatic recanalization of the splenic vein and consecutive stenting, as well as coiling of the feeding veins. Splenic vein stenting has been shown to be a safe option[32,33]. According to our knowledge, there is no case report in the English literature describing recanalization and stenting of PISVT in a patient with CV. We found two case reports using recanalization and stenting in superior mesenteric vein thrombosis – one in hepatitis with CV and one in PISVT and associated duodenal varices with excellent results[18,36]. Also, there is a case report of successful splenic vein stenting in PISVT with gastric varices[11]. In the current case, we describe a successful transhepatic endovascular recanalization and stenting of a fully occluded splenic vein and embolization of aberrant veins in the setting of PISVT and CV with gastrointestinal bleeding. It can be argued, that coiling of the dilated aberrant veins leads to faster recompensation but may increase risk of splenic rupture in acute stent failure[35].

CONCLUSION

In summary, splenic vein recanalization seems to be an effective and safe procedure to resolve variceal complications in PISVT. An interdisciplinary discussion of potential therapeutic options is crucial as the available experience is important and an individualized approach to these patients is mandatory.

FOOTNOTES

Author contributions: Füssel LM and Hofer H performed the research and drafting of the manuscript; Dinkhauser P, Müller-Wille R and Schauer W did a critical revision of the manuscript for important intellectual content; Füssel LM and Müller-Wille R performed image editing; All authors have read and approved the final manuscript.

Informed consent statement: Informed written consent was obtained from the patient for publication of this report and any accompanying images.

Conflict-of-interest statement: All the authors report having no relevant conflicts of interest for this article.

CARE Checklist (2016) statement: The authors have read CARE Checklist (2016), and the manuscript was prepared and revised according to CARE Checklist (2016).

Open-Access: This article is an open-access article that was selected by an in-house editor and fully peer-reviewed by external reviewers. It is distributed in accordance with the Creative Commons Attribution NonCommercial (CC BY-NC 4.0) license, which permits others to distribute, remix, adapt, build upon this work non-commercially, and license their derivative works on different terms, provided the original work is properly cited and the use is non-commercial. See: https://creativecommons.org/Licenses/by-nc/4.0/

Country/Territory of origin: Austria

ORCID number: Lisa-Michaela Füssel 0000-0003-2928-6738; Rene Müller-Wille 0000-0003-3437-2817; Patrick Dinkhauser 0000-0003-4785-0873; Harald Hofer 0000-0002-2786-7689.

S-Editor: Li L
L-Editor: Filipodia
P-Editor: Li L

REFERENCES

1 **Kitagawa S**, Sato T, Hirayama A. Colonic Varices Due to Chronic Pancreatitis: A Rare Cause of Lower Gastrointestinal Bleeding. *ACG Case Rep J* 2015; **2**: 168-170 [PMID: 26157952 DOI: 10.14309/crj.2015.43]
2 **Köklü S**, Coban S, Yüksel O, Arhan M. Left-sided portal hypertension. *Dig Dis Sci* 2007; **52**: 1141-1149 [PMID: 17385040 DOI: 10.1007/s10620-006-9307-x]
3 **Dina I**, Braticevici CF. Idiopathic colonic varices: case report and review of literature. *Hepat Mon* 2014; **14**: e18916 [PMID: 25147571 DOI: 10.5812/hepatmon.18916]
4 **Valeriani E**, Riva N, Di Nisio M, Ageno W. Splanchnic Vein Thrombosis: Current Perspectives. *Vasc Health Risk Manag* 2019; **15**: 449-461 [PMID: 31695400 DOI: 10.2147/VHRM.S197732]
5 **Thatipelli MR**, McBane RD, Hodge DO, Wysokinski WE. Survival and recurrence in patients with splanchnic vein thromboses. *Clin Gastroenterol Hepatol* 2010; **8**: 200-205 [PMID: 19782767 DOI: 10.1016/j.cgh.2009.09.019]
6 **Weber SM**, Rikkers LF. Splenic vein thrombosis and gastrointestinal bleeding in chronic pancreatitis. *World J Surg* 2003; **27**: 1271-1274 [PMID: 14502405 DOI: 10.1007/s00268-003-7247-6]
7 **Butler JR**, Eckert GJ, Zyromski NJ, Leonardi MJ, Lillemoe KD, Howard TJ. Natural history of pancreatitis-induced splenic vein thrombosis: a systematic review and meta-analysis of its incidence and rate of gastrointestinal bleeding. *HPB (Oxford)* 2011; **13**: 839-845 [PMID: 22081918 DOI: 10.1111/j.1477-2574.2011.00375.x]
8 **Xu W**, Qi X, Chen J, Su C, Guo X. Prevalence of Splanchnic Vein Thrombosis in Pancreatitis: A Systematic Review and Meta-Analysis of Observational Studies. *Gastroenterol Res Pract* 2015; **2015**: 245460 [PMID: 26451142 DOI: 10.1155/2015/245460]
9 **Heider TR**, Azeem S, Galanko JA, Behrns KE. The natural history of pancreatitis-induced splenic vein thrombosis. *Ann Surg* 2004; **239**: 876-80; discussion 880 [PMID: 15166967 DOI: 10.1097/01.sla.0000128685.74686.1e]
10 **Li H**, Yang Z, Tian F. Clinical Characteristics and Risk Factors for Sinistral Portal Hypertension Associated with Moderate and Severe Acute Pancreatitis: A Seven-Year Single-Center Retrospective Study. *Med Sci Monit* 2019; **25**: 5969-5976 [PMID: 31400275 DOI: 10.12659/MSM.916192]
11 **El Kininy W**, Kearney L, Hosam N, Broe P, Keeling A. Recurrent variceal haemorrhage managed with splenic vein stenting. *Ir J Med Sci* 2017; **186**: 323-327 [PMID: 26911860 DOI: 10.1007/s11845-016-1420-z]
12 **Ru N**, He CH, Ren XL, Chen JY, Yu FF, Yan ZJ, Guo JY, Zhu JH, Wang YC, Qian YY, Pan J, Hu LH, Li ZS, Zou WB, Liao Z. Risk factors for sinistral portal hypertension and related variceal bleeding in patients with chronic pancreatitis. *J Dig Dis* 2020; **21**: 468-474 [PMID: 32584511 DOI: 10.1111/1751-2980.12916]
13 **Anand A**, Gunjan D, Agarwal S, Kaushal K, Sharma S, Gopi S, Mohta S, Madhusudhan KS, Singh N, Saraya A. Vascular complications of chronic pancreatitis: A tertiary center experience. *Pancreatology* 2020; **20**: 1085-1091 [PMID: 32800648 DOI: 10.1016/j.pan.2020.07.005]
14 **Burbige EJ**, Tarder G, Carson S, Eugene J, Frey CF. Colonic varices. A complication of pancreatitis with splenic vein thrombosis. *Am J Dig Dis* 1978; **23**: 752-755 [PMID: 685944 DOI: 10.1007/BF01072365]
15 **Alarco HA**, Gómez Rodríguez-Bethencourt MA, Díaz H, Pérez Palma J, Minguillón A, Bordallo A, González Hermoso F. [Colonic lesion caused by acute pancreatitis. Use of minimal catheter jejunostomy. Apropos of 6 cases]. *Rev Esp Enferm Apar Dig* 1989; **75**: 465-469 [PMID: 2669046]
16 **Fracasso P**, Caviglia R, Grassi A, Lapenta R, Stigliano V, Casole P, Casale V. [Colonic varices secondary to recurrent acute pancreatitis]. *Minerva Gastroenterol Dietol* 1993; **39**: 191-193 [PMID: 8161618]
17 **Van Wijngaarden P**, Van der Wiel HE, Tetteroo GW, Bode WA. A patient with gastric fundal varices and colonic varices due to splenic vein thrombosis. *Neth J Med* 1997; **51**: 187-191 [PMID: 9455099 DOI: 10.1016/s0300-2977(97)00062-4]
18 **Naffouj S**, Al-Shammari M, Salgia R. Treatment of colonic varices with a superior mesenteric venous stent: a case report describing a unique approach. *Gastroenterol Rep (Oxf)* 2021; **9**: 597-600 [PMID: 34925858 DOI: 10.1093/gastro/goab003]
19 **Krishna RP**, Singh RK, Ghoshal UC. Recurrent lower gastrointestinal bleeding from idiopathic ileocolonic varices: a case report. *J Med Case Rep* 2010; **4**: 257 [PMID: 20698946 DOI: 10.1186/1752-1947-4-257]
20 **Saad WE**, Lippert A, Saad NE, Caldwell S. Ectopic varices: anatomical classification, hemodynamic classification, and hemodynamic-based management. *Tech Vasc Interv Radiol* 2013; **16**: 158-175 [PMID: 23830673 DOI: 10.1053/j.tvir.2013.02.004]
21 **Watanabe N**, Toyonaga A, Kojima S, Takashimizu S, Oho K, Kokubu S, Nakamura K, Hasumi A, Murashima N, Tajiri T. Current status of ectopic varices in Japan: Results of a survey by the Japan Society for Portal Hypertension. *Hepatol Res* 2010; **40**: 763-776 [PMID: 20649816 DOI: 10.1111/j.1872-034X.2010.00690.x]
22 **Simonetto DA**, Singal AK, Garcia-Tsao G, Caldwell SH, Ahn J, Kamath PS. ACG Clinical Guideline: Disorders of the Hepatic and Mesenteric Circulation. *Am J Gastroenterol* 2020; **115**: 18-40 [PMID: 31895720 DOI: 10.14309/ajg.0000000000000486]
23 **Helmy A**, Al Kahtani K, Al Fadda M. Updates in the pathogenesis, diagnosis and management of ectopic varices. *Hepatol Int* 2008; **2**: 322-334 [PMID: 19669261 DOI: 10.1007/s12072-008-9074-1]

24 **Akküçük S**, Aydoğan A, Paltacı İ, Temiz M. Diffuse idiopathic varices in the colon characterized by lower gastrointestinal bleeding. *Ulus Cerrahi Derg* 2014; **30**: 109-111 [PMID: 25931906 DOI: 10.5152/UCD.2014.1814]

25 **Zhou J**, Zhang H, Mao W, Ke L, Li G, Ye B, Zhang J, Lin J, Gao L, Tong Z, Li W. Efficacy and Safety of Early Systemic Anticoagulation for Preventing Splanchnic Thrombosis in Acute Necrotizing Pancreatitis. *Pancreas* 2020; **49**: 1220-1224 [PMID: 32898006 DOI: 10.1097/MPA.0000000000001661]

26 **Vadlamudi RS**, Matli VVK, Thoguluva Chandrasekar V, Kalakonda A, Rawlins SR. Chemoprophylaxis to Prevent Deep Venous Thrombosis in Patients Hospitalized for Pancreatitis: Beneficial or Harmful? *Cureus* 2021; **13**: e19645 [PMID: 34956767 DOI: 10.7759/cureus.19645]

27 **Hajibandeh S**, Hajibandeh S, Agrawal S, Irwin C, Obeidallah R, Subar D. Anticoagulation Versus No Anticoagulation for Splanchnic Venous Thrombosis Secondary to Acute Pancreatitis: Do We Really Need to Treat the Incidental Findings? *Pancreas* 2020; **49**: e84-e85 [PMID: 33003093 DOI: 10.1097/MPA.0000000000001644]

28 **Sissingh NJ**, Groen JV, Koole D, Klok FA, Boekestijn B, Bollen TL, van Santvoort HC, Verdonk RC, Bonsing BA, van Eijck CHJ, van Hooft JE, Mieog JSD; Dutch Pancreatitis Study Group. Therapeutic anticoagulation for splanchnic vein thrombosis in acute pancreatitis: A systematic review and meta-analysis. *Pancreatology* 2022; **22**: 235-243 [PMID: 35012902 DOI: 10.1016/j.pan.2021.12.008]

29 **Sarin SK**, Kumar CKN. Ectopic varices. *Clin Liver Dis (Hoboken)* 2012; **1**: 167-172 [PMID: 31186880 DOI: 10.1002/cld.95]

30 **Ohs Z**, Jones M, Sharma N, Loveridge K. Percutaneous Transhepatic Embolization of Ectopic Varices in a Patient With Portal Hypertension Presenting With Hemorrhagic Shock. *Cureus* 2021; **13**: e18209 [PMID: 34589375 DOI: 10.7759/cureus.18209]

31 **Pandey V**, Patil M, Patel R, Chaubal A, Ingle M, Shukla A. Prevalence of splenic vein thrombosis and risk of gastrointestinal bleeding in chronic pancreatitis patients attending a tertiary hospital in western India. *J Family Med Prim Care* 2019; **8**: 818-822 [PMID: 31041207 DOI: 10.4103/jfmpc.jfmpc_414_18]

32 **Luo X**, Nie L, Wang Z, Tsauo J, Tang C, Li X. Transjugular endovascular recanalization of splenic vein in patients with regional portal hypertension complicated by gastrointestinal bleeding. *Cardiovasc Intervent Radiol* 2014; **37**: 108-113 [PMID: 23636249 DOI: 10.1007/s00270-013-0625-z]

33 **Stein M**, Link DP. Symptomatic spleno-mesenteric-portal venous thrombosis: recanalization and reconstruction with endovascular stents. *J Vasc Interv Radiol* 1999; **10**: 363-371 [PMID: 10102204 DOI: 10.1016/s1051-0443(99)70044-8]

34 **Liu J**, Wang Q, Ding X, Liu Q, Huang W, Gu J, Wang Z, Wu W, Wu Z. The clinical applicability of percutaneous splenic vein stent implantation for pancreatic portal hypertension. *BMC Gastroenterol* 2022; **22**: 136 [PMID: 35337294 DOI: 10.1186/s12876-022-02214-z]

35 **Wei B**, Zhang L, Tong H, Wang Z, Wu H. Retrospective Comparison of Clinical Outcomes Following Splenic Vein Stenting and Splenic Arterial Embolization in Sinistral Portal Hypertension-Related Gastrointestinal Bleeding. *AJR Am J Roentgenol* 2021; **216**: 1579-1587 [PMID: 32845712 DOI: 10.2214/AJR.20.23859]

36 **Bhat AP**, Davis RM, Bryan WD. A rare case of bleeding duodenal varices from superior mesenteric vein obstruction - treated with transhepatic recanalization and stent placement. *Indian J Radiol Imaging* 2019; **29**: 313-317 [PMID: 31741602 DOI: 10.4103/ijri.IJRI_21_19]



Published by **Baishideng Publishing Group Inc**
7041 Koll Center Parkway, Suite 160, Pleasanton, CA 94566, USA
Telephone: +1-925-3991568
E-mail: bpgoffice@wjgnet.com
Help Desk: https://www.f6publishing.com/helpdesk
https://www.wjgnet.com



© 2023 Baishideng Publishing Group Inc. All rights reserved.